



physics abstracts

Q
1
53
Vol. 72
1969
Subject index
Pg. 2

20 Oct 71

An INSPEC Publication
The Institution of
Electrical Engineers

LY-DECEMBER 1969

SEP 16 1970

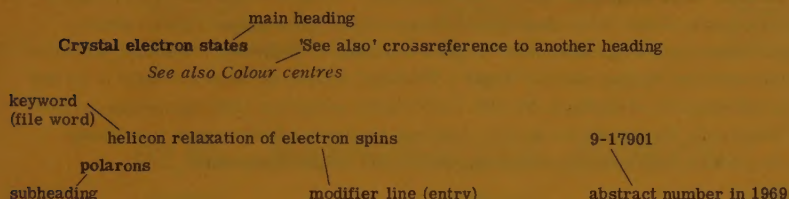
PART II SUBJECT INDEX NUMBER

SUBJECT INDEX – PART II

INTRODUCTION

The entries in this index refer to the abstracts by their serial number, not by the page number. The entries are grouped under headings (printed in bold type, e.g. "**Algebra**"). If a heading for a particular subject does not appear, the subject may be in the form of a cross-reference to another heading, perhaps of a more general nature. Many of the headings are subdivided by the use of subheadings, which are indented (i.e. printed slightly to the right) and commence with a small letter.

The information contained in the subject index is illustrated by following example:



Associated with the subheading "polarons" is a 'See' crossreference as follows:

Polarons See *Crystal electron states/polarons*

This means that for papers on "polarons" the reader should consult the subheading "polarons" of "Crystal electron states" as displayed above.

ARRANGEMENT OF HEADINGS AND SUBHEADINGS

The headings and crossreferences are arranged throughout the index in alphabetical order according to the "word by word" system. The subheadings are themselves arranged in alphabetical order under their respective headings.

ARRANGEMENT OF ENTRIES UNDER HEADINGS

Entries are arranged in four distinct groups as follows:

- First group: arabic numerals
- Second group: English alphabet (A-Z), roman numerals, Greek alphabet (excluding elementary particles)
- Third group: elementary particle symbols i.e. Greek and English alphabet e.g. μ (muon), p (proton)
- Fourth group: chemical formulae (including entries beginning with nuclei, e.g. ^{57}Fe)

CLASSIFIED LIST OF SUBJECT INDEX HEADINGS

In this list the headings are not arranged in alphabetical order, but are grouped into sections by subject, on the same basis as the arrangement in the fortnightly issues of Physics Abstracts. By using this list the reader can quickly determine all the headings which are appropriate to his subject, and then they can easily be found in the main index in their alphabetical position.

HEADINGS WITH NO ENTRIES

All the headings in current use in a given year are printed, even those for which there are no abstracts to be recorded. The latter are followed by the announcement "No entries". This confirms that these headings have not been dropped from the index, and entries may appear under them in subsequent issues.

NUCLEI, ELEMENTS, COMPOUNDS AND OTHER SUBSTANCES

Abstracts on nuclei whose mass number (or mass number range) is given are listed under a set of headings which begin "Nuclei with. . . " e.g. Nuclei with $6 \leq A \leq 19$ where A is the mass number.

The names of elements, their compounds, a few compounds of special interest (e.g. "Ruby", "Water") and a few common materials (e.g. "Wood", "Paper") are included as headings or sub-headings (e.g. "barium titanate" under "Barium compounds"). Under these, as well as under the appropriate "subject" headings, are listed any abstracts which contain significant physical information about the element, compound or substance named.

Inorganic compounds of the elements are listed under the first element in the chemical formula, and all the compounds of a given element are grouped under a single heading (e.g. "Sodium compounds"). Alloys are listed under compounds of the named constituents e.g. Au-Ag alloys under "Gold compounds" and "Silver compounds". There are also four special headings for the common alloys: "Aluminium alloys", "Copper alloys", "Iron alloys", "Nickel alloys". Organic compounds are grouped under "Organic compounds", "Polymers", "Plastics" and under special substance headings such as "Paper", "Proteins", etc.; all the latter are listed at the end of the classified list of headings. Metallic co-ordination compounds when regarded as inorganic are listed under the appropriate metallic compound heading (not under organic compounds) e.g. Ni complex, bis(dimethylglyoximate)nickel(II) under "Nickel compounds"

CLASSIFIED LIST OF SUBJECT INDEX HEADINGS

The headings are grouped into sections on the same basis as the arrangement of the abstracts in the fortnightly issues of Physics Abstracts. A summary of the layout of these sections (these are actually further subdivided), is given below. Each section lists the headings which concern its subject and it follows that many of the headings are listed in several places.

SUBJECT SECTIONS

- 01.00 GENERAL
- 02.00 MATHEMATICAL PHYSICS
- 03.00 MECHANICS. ELASTICITY. VIBRATION.ACOUSTICS
- 04.00 HEAT. THERMODYNAMICS
- 05.00 ELECTROMAGNETISM
- 06.00 ELECTRODYNAMICS & PARTICLE OPTICS
- 07.00 QUANTUM ELECTRONICS. QUANTUM OPTICS
- 08.00 OPTICS
- 09.00 QUANTUM FIELD THEORY
- 10.00 ELEMENTARY PARTICLES
- 11.00 ELEMENTARY PARTICLE & NUCLEAR MEASUREMENT
- 12.00 NUCLEAR PHYSICS
- 13.00 ATOMIC & MOLECULAR PHYSICS
- 14.00 FLUIDS
- 15.00 CHANGE OF STATE
- 16.00 SOLID-STATE STRUCTURE & MECHANICAL PROPERTIES
- 17.00 SOLID-STATE ELECTRICAL & MAGNETIC PROPERTIES
- 18.00 SOLID-STATE SPECTROSCOPY & OPTICAL PROPERTIES
- 19.00 PHYSICAL CHEMISTRY
- 20.00 GEOPHYSICS
- 21.00 ASTROPHYSICS
- 22.00 BIOPHYSICS
- 23.00 LABORATORY & EXPERIMENTAL TECHNIQUES

01.00 GENERAL

Biographies
Collections of physical data
History

Laboratories
Laboratory apparatus and technique

Nomenclature and symbols
Physics

Physics fundamentals
Reviews

01.10 EDUCATION

Biographies
History
Laboratories

Laboratory apparatus and technique
Physics

Physics fundamentals
Reviews
Teaching demonstrations

01.20 UNITS. MEASUREMENT AND METROLOGY

Acceleration measurement
Anemometers
Angle measurement
Angular velocity measurement
Area measurement
Balances
Constants
Density measurement

Dimensions
Force measurement
Instruments
Interferometry
Length measurement
Manometers
Measurement errors
Mechanical measurement

Micrometry
Nomenclature and symbols
Particle size
Pressure measurement
Recording
Standards
Strain gauges
Stroboscopes

Surface measurement
Thickness measurement
Time interval measurement
Time measurement
Units
Vapour pressure measurement
Velocity measurement
Volume measurement

02.00 MATHEMATICAL PHYSICS

Algebra
Differential equations
Equations
Field theory, classical
Fluctuations
Fourier analysis
Functions

Geometry
Green's function methods
Group theory
Hysteresis
Information theory
Integral equations
Integrals

Mathematics
Matrices
Probability
Radiation
Relaxation
Series
Space-time configurations

Statistical analysis/applications
Tensors
Transformations, mathematical
Vectors
Waves

02.10 GRAVITATION AND RELATIVITY

Gravitation
Gravitational waves

Relativity/
general
special
unified field theories
Space-time configurations

02.20 QUANTUM THEORY

Collision processes
Dispersion relations
Indeterminacy
Parity
Quantum electrodynamics

Quantum theory/
application methods
quantization
wave equations
Scattering

02.30 STATISTICAL PHYSICS

Brownian motion
Electron gas
Fluctuations
Hysteresis
Information theory
Kinetic theory

Lattices, theory and statistics
Many-body problems
Probability
Quantum fluids/
boson systems
fermion systems

Quantum theory
Radiation
Radiative transfer
Random processes
Relaxation
Statistical analysis/

applications
Statistical mechanics/
quantum
Thermodynamics
Transport processes

02.40 MATHEMATICAL METHODS

Calculation
Graphs
Nomograms

Statistical analysis
applications
Tables, mathematical

03.00 MECHANICS. ELASTICITY. VIBRATION. ACOUSTICS

Oscillations
Vibrations
Waves

03.10 MECHANICS

Ballistics
Centrifuges
Dynamics
Friction
Gravitation
Gyroscopes
Impact
Kinematics

Mechanics
Pendulums
Pressure
Rockets
Rotating bodies
Torsion
Velocity

03.15 RHEOLOGY, ELASTICITY AND PLASTICITY

Bending
Compressibility
Damping
Deformation
Elastic deformation
Elasticity
Photoelasticity
Plastic deformation

Plasticity
Relaxation
Rheology
Stress analysis
Stresses, internal
Thermoelasticity
Viscoelasticity

03.30 VIBRATIONS AND ELASTIC WAVES

Damping
Elastic waves
Magnetoelastic waves
Membranes

Oscillations
Piezoelectric oscillations
Relaxation
Resonators

Seismic waves
Shock waves/
effects
Vibrating bodies

Vibrations/
excitation
measurement
Waves

03.40 ACOUSTICS

Absorption/ acoustic waves acoustic waves, ultrasonic	Atmospheric acoustics Biological effects of radiations Chemical effects of radiations/ acoustic waves	Interferometers/ acoustic waves Interferometry/ acoustic waves	Scattering/ acoustic waves acoustic waves, ultrasonic
Acoustic analysis Acoustic generators Acoustic impedance Acoustic radiators Acoustic receivers Acoustic resonators Acoustic streaming Acoustic wave propagation/ ultrasonic	Diffraction/ acoustic waves acoustic waves, ultrasonic Diffusion/ acoustic waves Dispersion, acoustic/ ultrasonic	Magnetoacoustic effects Microphones Musical instruments Noise/ acoustic Noise abatement Physical effects of radiations Radiation pressure Recording Reflection/ acoustic waves acoustic waves, ultrasonic	Schlieren systems Sound ranging Sound reproduction Speech Stroboscopes Transducers Transmission/ acoustic waves acoustic waves, ultrasonic
Acoustic waves/ effects Acoustical laboratories Acoustical measurement Acoustics/ musical Acoustoelectric effects Architectural acoustics	Doppler effect Echo Helium/ liquid, sound propagation Holography Intensity measurement/ acoustics Interference/ acoustic waves	Refraction/ acoustic waves acoustic waves, ultrasonic Reverberation	Ultrasonics Velocity/ acoustic waves acoustic waves, ultrasonic Velocity measurement/ acoustic waves acoustic waves, ultrasonic

03.50 SHOCK WAVES

Detonation Explosions/ nuclear	Schlieren systems Shock tubes Shock waves/ effects Supersonic flow
--------------------------------------	--

04.00 HEAT AND THERMODYNAMICS

Bolometers Calorimeters Calorimetry Combustion Conductivity, thermal Convection Cooling Emissivity Entropy/ properties of substances	Equations of state/ gases liquids solids Flames Heat Heat conduction Heat transfer Heat treatment Heating	High-temperature phenomena and effects Joule-Thomson effect Latent heat Pyrometers Radiation/ heat Radiation detectors Radiation pressure Radiation transfer Specific heat Temperature	Temperature distribution Temperature measurement/ spectral methods Thermal expansion Thermal measurement Thermocouples Thermodynamic properties Thermodynamics/ applications Thermometers/ resistance Thermostats
---	--	---	--

05.00 ELECTROMAGNETISM

Eddy-currents
Electromagnetism
Electromagnetic fields
Electromotive force
Inductance

05.10 ELECTROMAGNETIC WAVES AND OSCILLATIONS

Absorption/ electromagnetic waves Amplifiers Diffraction/ electromagnetic waves Diffusion/ electromagnetic waves Doppler effect Electromagnetic oscillations	Electromagnetic wave propagation/ atmosphere ionosphere guided waves Electromagnetic waves/ radiators Interference/ electromagnetic waves	Interferometers/ electromagnetic waves Interferometry/ electromagnetic waves Light/ electromagnetic theory Microwave techniques and devices	Plasma/ electromagnetic wave propagation Radiation Reflection/ electromagnetic waves Refraction/ electromagnetic waves Scattering/ electromagnetic waves
--	--	--	--

05.20 RADIOFREQUENCY SPECTROSCOPY. MAGNETIC RESONANCES

Antiferromagnetic resonance Cyclotron resonance Ferrimagnetic resonance Ferromagnetic relaxation Ferromagnetic resonance	Magnetic resonance and relaxation Nuclear magnetic resonance and relaxation/ measurement	Nuclear quadrupole resonance Paramagnetic resonance and relaxation/ measurement	Spectra Spectrometers, radio frequency Spectroscopy, radio frequency
--	---	--	--

05.30 ELECTRICAL QUANTITIES AND THEIR MEASUREMENT. CIRCUITS

Acoustoelectric effects	Electric fields/ effects	Ferroelectric phenomena	Piezoelectric oscillations
Amplifiers	Electric strength	Fluctuations	Piezoelectricity
Breakdown, electric	Electrical machines	Hall effect	Piezoresistance
Circuits	Electrical measurement	High-voltage techniques	Plasma/ diagnostics
Conductivity, electrical/ measurement	Electrical properties of sub- stances	Hysteresis	Pyroelectricity
Contacts, electrical	Electrokinetic effects	Image convertors and amplifiers	Rectifiers
Counting circuits	Electroluminescence	Inductance	Relaxation
Current, electrical	Electromotive force	Magnetoelectric effects	Semiconductors
Dielectric devices	Electron gas	Magnetoresistance	Skin effect
Dielectric measurement	Electrons	Noise, electrical	Space charge
Dielectric phenomena	Electro-optical effects	Oscillators	Superconductivity
Eddy-currents	Electrophoresis	Photoconductivity	Thermoelectricity
Electrets	Electrostatics	Photoelectricity	Triboelectricity
Electric charge	Electrostriction	Photoelectromagnetic effects	
		Photovoltaic effects	

05.35 DIRECT CONVERSION

Electricity, direct conversion/
fuel cells
magnetohydrodynamics
solar cells
thermionic

05.40 MAGNETISM

Antiferromagnetism	Gyromagnetic effect	Magnetic resonance and relaxa- tion	Magneto-optical effects
Compasses	Gyromagnetic ratio	Magnetism	Magnetoresistance
de Haas-van Alphen effect	Hall effect	Magnetization process	Magnetostriction
Diamagnetism	Magnetic devices	Magnetization state	Magnetochemical effects
Ferrimagnetism	Magnetic field measurement	Magnetoacoustic effects	Magnets
Ferromagnetism/ spin-wave theory	Magnetic fields/ effects	Magnetoelastic effects	Paramagnetism
Films, solid/ magnetic properties	Magnetic measurement	Magnetomechanical effects	Storage devices

06.00 ELECTRODYNAMICS AND PARTICLE OPTICS

Electrodynamics	Particle optics
Energy loss of particles	Particle velocity analysis
Particle beams	Scattering, particles

06.10 ELECTRON BEAMS, ELECTRON OPTICS AND TUBES

Electron beams/ effects	Electron microscopes	Electrons/ absorption	Fluctuations
Electron diffraction	Electron microscopy	ionization	Gas-discharge tubes
Electron gas	Electron optics	radiation	Image convertors and amplifiers
Electron lenses/ electrostatic magnetic	Electron tubes	scattering	Noise, electrical
			Photomultipliers
			Space charge

06.20 ION BEAMS, ION OPTICS AND SOURCES

Ion beams/ effects	Ion velocity
Ion microscopes	Ions/ recombination
Ion optics	scattering
Ion sources	Sputtering

07.00 QUANTUM ELECTRONICS AND QUANTUM OPTICS

Light/
coherence
Optical pumping
Photons
Quantum optics

07.10 MASERS

Amplifiers
Masers
Optical pumping

07.20 LASERS

Amplifiers
Lasers
Light/
coherence
Optical pumping
Resonators

07.23 Gas and Liquid Lasers

Amplifiers
Lasers/
gaseous
liquid
Light/
coherence
Optical pumping

07.25 Solid Lasers

Amplifiers
Lasers/
semiconductor
solid

Light/
coherence
Optical pumping

07.27 Laser Beam Optics

Holography
Laser beams/
applications
effects

Light/
coherence
modulation

08.00 OPTICS

Doppler effect
Electro-optical effects
Light/
electromagnetic theory
modulation

Light sources
Nonlinear optics
Optics

Photons
Photophoresis
Radiation

Radiation pressure
Velocity/
light
Velocity measurement/
light

08.10 GEOMETRICAL OPTICS

Aberrations, optical
Dispersion, optical
Lenses/
aspherical
photographic

Mirrors
Optical images
Optical systems
Optics/
geometrical

Prisms, optical
Reflection/
light
Refraction/
light

Refractive index/
light
Resolving power, optics
Schlieren systems

08.20 PHYSICAL OPTICS

Absorption/
light
Diffraction/
light
Diffraction gratings
Diffusion/
light
Dispersion, optical
Doppler effect
Double refraction/
flow
mechanical

Electro-optical effects
Filters, optical
Holography
Interference/
light
Interferometers/
light
Interferometry/
light
Magneto-optical effects
Optical constants
Optical films

Optical pumping
Optical rotation
Photoelasticity
Pleochroism
Polarimeters
Polarized light
Reflection/
light
Reflectivity

Refraction/
light
Refractive index/
light
Scattering/
light
Transmission/
light
Transparency

08.30 PHOTOMETRY. CALORIMETRY

Bolometers
Brightness
Colorimetry
Colour

Densitometry
Emissivity
Illumination

Photometers
Photometry/
light sources

Pyrometers
Radiation detectors

08.40 INSTRUMENTAL OPTICS

Aberrations, optical
Dispersion, optical
Fibres/
optical
Films/
liquid
Films, solid/
optical properties
Filters, optical
Glass
Image convertors and amplifiers

Lasers/
gaseous
solid
Lenses/
aspherical
photographic
Light sources
Luminescent devices
Microscopes
Microscopy
Mirrors

Optical constants
Optical images
Optical instrument testing
Optical instruments
Optical materials
Optical systems
Prisms, optical
Projectors, optical
Quartz
Reflection/
light

Refraction/
light
Refractive index/
light
Refractive index measurement
Refractometers
Resolving power, optics
Schlieren systems
Stroboscopes
Telescopes

08.45 Spectroscopy

Astronomical spectra
Atmospheric spectra
Monochromators
Spectral line breadth

Spectrochemical analysis
Spectrometers/
accessories
Spectrophotometers

Spectrophotometry
Spectroscopy/
light sources
Stark effect

Temperature measurement/
spectral methods
Zeeman effect

08.50 PHOTOGRAPHY

Cameras
Cinematography
Densitometry
Lenses/
photographic

Light sources
Nuclear track emulsions
Photographic materials/
sensitivity

Photographic process/
development
Photography/
applications
colour
high-speed
Radiography

09.00 QUANTUM FIELD THEORY

Current algebra	Nuclear forces
Dispersion relations	Parity
Field theory, quantum/interactions	Quantum electrodynamics
interactions, strong	Quantum theory/
interactions, weak	application methods
meson field	quantization
quantization	wave equations
scattering	S-matrix theory
	Scattering

10.00 ELEMENTARY PARTICLES

Bosons	Gravitons	Particle velocity analysis	Strange particles
Elementary particles	Parity	Quarks	Synchrotron radiation
Fermions	Energy loss of particles		

10.10 ELEMENTARY PARTICLE THEORY

Bosons	Elementary particles/interactions	Fermions
Current algebra	interactions, strong	Nuclear forces
Dispersion relations	interactions, weak	Parity
	scattering	S-matrix theory
	symmetry	Strange particles
	theory	

10.20 PHOTONS, GAMMA-RAYS AND X-RAYS

Bremsstrahlung	Gamma-rays/absorption	Mössbauer effect	X-ray absorption
Cherenkov radiation	angular distribution	Photons/interactions	X-ray diffraction
Compton effect	detection, measurement	polarization	X-ray measurement
Gamma-ray spectrometers	effects	scattering	X-ray reflection
	scattering	Synchrotron radiation	X-ray scattering
			X-rays/effects

10.30 LEPTONS

Leptons

10.33 Neutrinos

Neutrinos and antineutrinos

10.35 Electrons

Beta-ray spectra/conversion electrons	Electron theory
Beta-ray spectrometers	Electrons/absorption
Beta-rays/absorption	interactions
angular distribution	ionization
detection, measurement	radiation
effects	scattering
polarization	scattering, electron-proton
scattering	Positronium
Electron pairs/annihilation	Positrons
production	Synchrotron radiation

10.37 Muons

Muons/capture
decay
detection, measurement

Muons/interactions
production
scattering
Muonium

10.40 HADRONS

Hadrons/current
decay
Quarks

10.41 Hadron interactions

Hadrons/interactions

10.42 Hadron scattering

Hadrons/scattering

10.45 Mesons

Mesons/absorption
capture
decay
detection, measurement
effects

Mesons/interactions
magnetic moment
mass
production
scattering
spin and parity

10.46 Kaons

decay
interactions

production
scattering

10.47 Pions

Pions/decay
interactions
interactions, pion-nucleon
interactions, pion-pion
interactions, pion-proton

Pions/production
scattering
scattering, pion-nucleon
scattering, pion-pion
scattering, pion-proton

10.48 Meson Resonances

Mesons/resonances

10.51 Baryons

Baryons/interactions
scattering

10.52 Nucleons

Nuclear forces
Nucleons and antinucleons/antinucleons
interactions
interactions, nucleon-nucleon
scattering
scattering, nucleon-nucleon

10.53 Protons	10.54 Neutrons	10.56 Hyperons	10.58 Baryon Resonances
Proton spectra Protons and antiprotons/ absorption angular distribution antiprotons detection, measurement effects interactions interactions, proton-proton magnetic moment polarization production scattering scattering, proton-deuteron scattering, proton-proton	Neutron diffraction Neutron spectra Neutron spectrometers Neutrons and antineutrons/ absorption angular distribution detection, measurement diffusion effects interactions moderation polarization production reflection scattering scattering, neutron-proton	Hypernuclei Hyperons/ absorption capture decay detection, measurement effects interactions magnetic moment mass production resonances scattering spin and parity Strange particles	Baryons/ resonances Hyperons/ resonances Nucleons

10.60 COMPOSITE PARTICLES

Composite particles

10.63 Deuterons	10.65 Tritons	10.67 Alpha-particles and He ³
Deuterons/ effects interactions photodisintegration polarization scattering	Tritons/ interactions scattering	Alpha-particle spectrometers Alpha-particles/ absorption angular distribution detection, measurement effects interactions scattering Helium-3 interactions scattering

10.70 COSMIC RAYS

Cosmic rays/ absorption apparatus composition alpha-particles and helium nuclei deuterons electrons mesons muons neutrinos neutrons nucleons photons protons X-rays	effects and interactions origin primary showers and bursts variation
---	--

11.00 ELEMENTARY PARTICLE AND NUCLEAR MEASUREMENT

11.10 APPARATUS. DETECTORS AND DETECTOR CIRCUITS

Alpha-particle spectrometers Amplifiers Beta-ray spectrometers Counters/ accessories Cherenkov crystal Geiger operation technique proportional scintillation semiconductor spark statistical analysis	Counting circuits Dosimetry Gamma-ray spectrometers Ionization chambers Neutron spectrometers Nuclear bombardment targets Particle accelerators	Particle detectors Particle optics Particle spectrometers Particle velocity analysis Photomultipliers Radioactivity measurement/ apparatus
--	---	--

11.15 Track Visualization

Bubble chambers Cloud chambers	Energy loss of particles Luminescence chambers	Nuclear track emulsions Particle tracks	Particle track visualization Spark chambers
-----------------------------------	---	--	--

11.20 PARTICLE ACCELERATORS

High-voltage techniques Ion sources	Particle accelerators/ accessories betatrons cyclotrons linear synchrotrons
--	--

12.00 NUCLEAR PHYSICS

Nuclear physics

12.10 NUCLEAR STRUCTURE AND ENERGY LEVELS

Beta-ray spectra/ conversion electrons	Mössbauer effect	Nuclei with $A \leq 5$	Nucleus/ electric moment
Gamma-ray spectra	Nuclear excitation	Nuclei with $6 \leq A \leq 10$	energy level transitions
Gamma-rays/ angular distribution	Nuclear forces	Nuclei with $20 \leq A \leq 49$	energy levels
internal conversion	Nuclear isomerism	Nuclei with $50 \leq A \leq 89$	magnetic moment
Gyromagnetic ratio	Nuclear magnetic resonance and relaxation	Nuclei with $90 \leq A \leq 149$	models
Hypernuclei	Nuclear polarization	Nuclei with $150 \leq A$	size
			spin and parity
			theory

12.20 NUCLEAR DECAY AND RADIOACTIVITY

Alpha-particles	Beta-ray spectrometers	Dosimetry	Nuclear bombardment targets
Alpha-particle spectra	Beta-rays/ absorption	Fallout	Physical effects of radiations
Alpha-particle spectrometers	angular distribution	Gamma-ray spectra	Radiation monitoring
Alpha-particles/ absorption	detection, measurement	Gamma-ray spectrometers	Radiation protection
angular distribution	effects	Gamma-rays/ absorption	Radioactive dating
detection, measurement	polarization	angular distribution	Radioactive tracers
effects	scattering	detection, measurement	Radioactivity/ decay periods
scattering	Biological effects of radiations	effects	decay schemes
Beta-decay theory	Chemical effects of radiations/ ionizing radiations	internal conversion	electron capture
Beta-ray spectra/ conversion electrons		scattering	Radioactivity measurement/ apparatus
		Nuclear decay theory	Radiochemistry

12.30 NUCLEAR REACTIONS AND SCATTERING

Chemical analysis/ by nuclear reactions	Nuclear reactions and scattering due to/ alpha-particles	Nuclear spallation
Collision processes	cosmic rays	Nuclei with $A \leq 5$
Nuclear bombardment targets	deuterons	Nuclei with $6 \leq A \leq 19$
Nuclear excitation	electrons	Nuclei with $20 \leq A \leq 49$
Nuclear forces	helium-3	Nuclei with $50 \leq A \leq 89$
Nuclear reactions and scatter- ing/ chemical effects	hyperons	Nuclei with $90 \leq A \leq 149$
high energy $\geq 1\text{GeV}$	mesons	Nuclei with $150 \leq A$
	muons	Radiation monitoring
	neutrinos	Radiation protection
	neutrons	Scattering, particles
	nuclei of $Z > 2$	
	nucleons	
	photons	
	protons	
	tritons	

12.39 Nuclear fission and fusion

Explosions/ nuclear	Nuclear fission/ products uranium	Nuclear fusion	Plasma
		Nucleons	Thermonuclear reactions

12.40 NUCLEAR POWER STUDIES

12.43 Neutron Transport Theory

Neutrons and antineutrons/ absorption	Nuclear fission/ products uranium
angular distribution	Nuclear fusion
detection measurement	Nuclear reactions
diffusion	Thermonuclear reactions
effects	
interactions	
moderation	
polarization	
production	
reflection	
scattering	

12.47 Nuclear Reactors

Biological effects of radiations	Nuclear reactors, fission/ materials
Chemical analysis/ by nuclear reactions	operation
Chemical effects of radiations/ ionizing radiations	theory
Dosimetry	Nuclear reactors, fusion
Nuclear fission/ products	Physical effects of radiations
uranium	Plasma/ devices
Nuclear fusion	Radiation monitoring
Nuclear reactions/ chemical effects	Radiation protection
	Radiochemistry
	Thermonuclear reactions

13.00 ATOMIC AND MOLECULAR PHYSICS

Collision processes
Orbital calculation methods
Quantum theory

13.10 MASS SPECTROMETERS

Mass spectra	Mass spectrometers/ accessories applications
--------------	--

13.20 ATOMS

Atomic beams
Atomic mass and weight
Atoms
 electron scattering
 excitation
 magnetic moment
 structure
Charge exchange
Collision processes/
 atoms

Electron emission
 photoelectric
Elements
 origin
 relative abundances
Exchange interactions
Gyromagnetic ratio
Helium/
 gas

Hydrogen/
 ions
 neutral atoms
Ionization potential
Luminescence
 gases
Optical pumping
Orbital calculation methods
Periodic system

Spectra
 atoms
Spectral line breadth
Stark effect
X-ray spectra
 absorption
 emission
Zeeman effect

13.25 Isotopes

Isotope effects
Isotope exchanges
Isotope separation
Isotopes
 detection
 relative abundances
Mass spectra

Mass spectrometers/
 applications
Radioactive dating
Radioactive tracers
Radiochemistry
Tracers

13.27 Mesic and Muonic Atoms

Atoms, mesic and muonic

13.30 MOLECULES

Bonds
Chemical shift
Chemical structure
Exchange interactions
Isomerism
Jahn-Teller effect
Luminescence/
 gases
Magnetic resonance and relaxa-
 tion
Molecular weight

Molecules/
 configuration and dimensions
 inorganic
 organic
excitation
internal mechanics
electronic structure
electronic structure, inorganic
electronic structure, organic
nuclear coupling
relaxation
rotation
vibration
moments

Nuclear magnetic resonance and
 relaxation
Nuclear quadrupole resonance
Optical pumping
Orbital calculation methods
Paramagnetic resonance and
 relaxation
Scattering/
 light
 light, Brillouin spectra
 light, Raman spectra
 light, Raman spectra, inorganic^c
 light, Raman spectra, organic

Spectra/
 inorganic molecules
 diatomic
 diatomic, radiofrequency
 polyatomic
 polyatomic, radio-frequency
inorganic liquids and solutions
inorganic solids
 radiofrequency
 molecules
organic molecules and
 substances
infrared
 radiofrequency
Spectral line breadth
Stark effect
Valency
Zeeman effect

13.34 Dissociation. Free radicals

Association/
 gases
Free radicals
Heat of dissociation

Molecules/
 dissociation
 dissociation energies

13.35 Macromolecules

Association
Heat of formation
Isomerism
Macromolecules

Molecules/
 configuration and dimensions,
 macromolecules
Polymers
Proteins

13.36 Mesic and Muonic Molecules

Molecules, mesic and muonic

13.37 Intermolecular mechanics

Charge exchange
Collision processes/
 molecules

Molecular beams
Molecules/
 intermolecular mechanics

14.00 FLUIDS

Boundary layers
Flow/
 two-phase
Fluids
Hydrodynamics
Hydrostatics

Oscillations
Turbulence
Viscosity
Vortices
Waves

14.10 MAGNETOHYDRODYNAMICS

Magnetohydrodynamics
Shock waves/
 effects
Turbulence

14.20 PLASMA

Discharges, electric/
 glows
 high-frequency
Nuclear fusion
Nuclear reactors, fusion

Plasma/
 collison processes
 electromagnetic waves
 magnetohydrodynamics
production
shock waves

Shock waves/
 effects
Space charge/
 gas
Thermonuclear reactions

14.24 Plasma Confinement, Devices and Measurements

Plasma/
confinement
devices
diagnostics

14.26 Plasma Oscillations and Stability

Plasma/
magnetohydrodynamics
oscillations
stability

14.30 IONIZATION

Charge exchange	Ionization potential	Photoionization/
Dissociation	Ionization, surface	gases
Ion velocity	Ions/	Shock waves/
Ionization/	recombination	effects
gases	scattering	Space charge/
		gas

14.40 ELECTRIC DISCHARGES

Arcs, electric	Discharges, electric/	Lightning
Breakdown, electric/	glows	Sparks, electric
gases	high frequency	Sputtering
Corona, electric discharge	Gas-discharge tubes	

14.50 MECHANICS OF GASES

Acoustic streaming	Diffusion in gases/	Hygrometers	Turbulence
Aerodynamics	thermal	Jets	Viscometers
Anemometers	Flow/	Manometers	Viscosity/
Compressibility/	gases	Moisture	gases
gases	two-phase	Pressure	Vortices
Condensation	Flowmeters	Pumps	Waves
Density/	Gases	Radiation pressure	
gases	Humidity	Supersonic flow	

14.60 GASEOUS STATE

Absorption/	Diffusion/	Molecules/	Sorption
acoustic waves	acoustic waves	intermolecular mechanics	Specific heat/
acoustic waves, ultrasonic	electromagnetic waves	Nuclear magnetic resonance and	gases
electromagnetic waves	light	relaxation	Spectra
light	Electrical properties of sub-	Nuclear quadrupole resonance	Statistical mechanics
Association/	stances	Optical properties of substances	Thermoluminescence
gases	Electroluminescence	Paramagnetic resonance and	Transmission/
Breakdown, electric/	Equations of state/	relaxation	acoustic waves
gases	gases	Reflection/	acoustic waves, ultrasonic
Conductivity, electrical/	Gases	acoustic waves	light
gases	Helium/	acoustic waves, ultrasonic	Velocity/
measurement	gas	electromagnetic waves	acoustic waves
Conductivity, thermal/	Interference/	light	acoustic waves, ultrasonic
gases	acoustic waves	Refraction/	
measurement	Joule-Thomson effect	acoustic waves	
Dielectric properties of sub-	Kinetic theory/	acoustic waves, ultrasonic	
stances/	gases	electromagnetic waves	
gases	Lasers/	light	
Diffraction/	gaseous	Scattering/	
acoustic waves	Luminescence/	acoustic waves	
acoustic waves, ultrasonic	gases	acoustic waves, ultrasonic	
electromagnetic waves	Magnetic resonance and relaxation	electromagnetic waves	
light		light	

14.65 Viscosity and Diffusion of Gases

Diffusion in gases/	Transport processes
thermal	Viscosity/
	gases

14.70 MECHANICS OF LIQUIDS

Acoustic streaming	Drops	Hydrodynamics	Schlieren systems
Bubbles	Elasticity/ liquids	Hydrostatics	Sprays
Capillarity	Emulsions	Jets	Surface energy
Cavitation	Films/ liquid	Liquid oscillations	Surface tension
Compressibility/ liquids	Filters	Liquid waves/ surface	Surface tension measurement
Density/ liquids	Flow/ liquids	Lubrication	Thixotropy
Diffusion in liquids thermal	two-phase	Moisture	Turbulence
Double refraction/ flow	Flowmeters	Pressure	Viscometers
	Foams	Pumps	Viscosity/ liquids
		Radiation pressure	Vortices
		Rheology	Wetting

14.80 LIQUID STATE

Liquids
Liquid metals

14.82 Theory and Structure of Liquids and Solutions

Association/ liquids	Films/ liquid	Neutron diffraction examination of materials	Solutions
Electron diffraction examination of materials	Heat of solution	Neutrons and antineutrons/ scattering	X-ray examination of materials/ liquids
Equations of state/ liquids	Liquid crystals	Polymers	
	Liquids/ structure theory	Solubility	

14.83 Viscosity, Surface tension and Diffusion

Diffusion in liquids/ thermal	Membranes	Surface tension	Viscosity/ liquids
Filters	Osmosis	Surface tension measurement	
	Sorption	Transport processes	

14.85 Thermal properties of Liquids

Conductivity, thermal/ liquids measurement	Heat of solution	Thermal expansion
	Specific heat/ liquids	Thermodynamic properties

14.86 Acoustical Properties of Liquids

Absorption/ acoustic waves acoustic waves, ultrasonic	Diffusion/ acoustic waves	Refraction/ acoustic waves	Transmission/ acoustic waves
Acoustic wave propagation/ ultrasonic	Interference/ acoustic waves	acoustic waves, ultrasonic	acoustic waves, ultrasonic
Diffraction/ acoustic waves	Reflection/ acoustic waves	Scattering/ acoustic waves	Velocity/ acoustic waves
acoustic waves, ultrasonic	acoustic waves, ultrasonic	acoustic waves, ultrasonic	acoustic waves, ultrasonic

14.87 Optical Properties of Liquids

Absorption/ electromagnetic waves	Double refraction	Refraction/ electromagnetic waves	Spectra/ inorganic liquids and solutions
light	flow	light	Thermoluminescence
Chemical shift	Electroluminescence	Scattering/ electromagnetic waves	Transmission/ light
Diffraction/ electromagnetic waves	Luminescence/ liquids and solutions	light	
light	Optical pumping	light, Brillouin spectra	
Diffusion/ electromagnetic waves	Optical properties of substs.	light, Raman spectra	
light	Reflection/ electromagnetic waves	light, Raman spectra, inorganic	
	light	light, Raman spectra, organic	

14.88 Electrical and Magnetic properties of Liquids

Absorption/ electromagnetic waves	Dielectric properties of substs./ liquids and solutions	Metals
Breakdown, electric/ liquids	Electrical properties of substs.	Nuclear magnetic resonance and relaxation
Conductivity, electrical/ liquids	Ionization, liquids	Nuclear quadrupole resonance
liquids, electrolytic measurement	Liquid metals	Paramagnetic resonance and relaxation
	Magnetic properties of substs.	Semiconducting materials
	Magnetic resonance and relaxa- tion	Semiconductors

14.90 DISPERSIONS AND COLLOIDS

Aerosols
Centrifuges
Colloids
Disperse systems
Electrophoresis

Emulsions
Filters
Foams
Gels
Heat of solution

Membranes
Osmosis
Particle size
Precipitation
Sedimentation

Sols
Solubility
Solutions
Surface phenomena
Suspensions
Thixotropy

14.95 LIQUID HELIUM

Helium/
liquid
liquid, sound propagation
solid

Quantum fluids/
boson systems
fermion systems

15.00 CHANGE OF STATE

Boiling
Boiling point
Condensation
Critical constants, thermal
Distillation
Drying

Equations of state
gases
liquids
solids
Evaporation
Freezing
Heat of fusion

Heat of sublimation
Heat of transformation
Heat of vaporization
Humidity
Liquefaction, gases
Melting
Melting point

Phase equilibrium
Phase transformations
Sublimation
Supercooling
Vapour pressure
Vapour pressure measurement
Vaporization

16.00 SOLID STATE STRUCTURE AND MECHANICAL PROPERTIES

Crystal properties
Equations of state/
solids

Solids/
structure
theory

16.10 NON-CRYSTALLINE STATE

Amorphous state
Glass

Plastics
Polymers

Rubber
Vitreous state

Waxes

16.20 SURFACE AND INTERFACE PHENOMENA

Surface energy
Surface measurement

Surface phenomena
Surface structure

16.23 Films

Crystals/
growth
Epitaxy
Evaporation

Films, solid/
electrical properties
magnetic properties
optical properties
Sputtering
Sublimation

16.25 Adsorption

Adsorbed layers
Adsorption

Heat of adsorption
Sorption

16.30 CRYSTALLOGRAPHY

Bonds
Charge compensation
Crystal chemistry
Crystal properties
Crystallography

Crystals/
etching
faces
orientation
twinning

Isomorphism
Minerals
Polymorphism
Solids/
structure
Surface structure

16.33 Crystal growth

Crystallization
Crystals/
growth
whiskers

Epitaxy
Zone melting and refining

16.35 Crystal Structures, Techniques and Apparatus

Alloys	Electron diffraction crystal- lography	Microscopy	X-ray crystallography/ apparatus
Amorphous state	Electron diffraction examination of materials	Neutron diffraction crystal- lography	calculation apparatus
Crystal structure/ microstructure	Electron microscope examination of materials	Neutron diffraction examination of materials	calculation methods
Crystal structure, atomic/ alloys	Electron microscopy	Particle size	technique
elements	Fibres	Polymers	X-ray diffraction
inorganic compounds	Granular structure	Porous materials	X-ray examination of materials
organic compounds	Ion microscopes	Powders	microstructure
Density/ solids	Metallurgy	Radiography	molecular structure
		Surface structure	X-ray measurement
		X-ray absorption	X-ray monochromators
			X-ray reflection
			X-ray scattering
			X-ray tubes

16.40 DEFECT PROPERTIES OF SOLIDS

Cold working	Crystal structure	Electron microscope examina- tion of materials	Plastic deformation
Creep	Crystals	Heat treatment	Plastic flow
Crystal imperfections	etching	alloys	Slip
dislocations	twinning	Internal friction	Stresses, internal
impurities	Deformation	Neutron diffraction examination of materials	Work hardening
interstitials	Elastic deformation		X-ray examination of materials/ microstructure
vacancies	Electron diffraction examination of materials		

16.45 Colour centres

Absorption/ light	Colour centres
	X-rays/ effects

16.50 DIFFUSION IN SOLIDS

Diffusion in solids/ thermal	Permeability, mechanical
---------------------------------	--------------------------

16.60 MECHANICAL PROPERTIES OF SOLIDS

Abrasion	Elastic fatigue	Lubrication	Plasticity
Bending	Elastic limit	Magnetoelastic waves	Rheology
Brittleness	Elastic relaxation	Magnetomechanical effects	Slip
Compressibility	Elasticity	Mechanical properties of sub- stances	Strain gauges
Cracks	Fracture	Mechanical strength/ compressive	Stress analysis
Creep	Friction	shear	Stress effects
Deformation	Hardness	tensile	Stress/strain relations
Density/ solids	High-pressure phenomena and effects	Photoelasticity	Stresses, internal
Elastic constants/ measurement	Hysteresis	Plastic deformation	Thermoelasticity
Elastic deformation	Impact	Plastic flow	Thixotropy
	Internal friction		Torsion
			Viscoelasticity
			Wear

16.65 Metallurgy. Phase transformations

Adhesion	Forming processes	Phase transformations/ solid-state	Precipitation
Ageing	Heat treatment/ alloys	Physical effects of radiations	Sintering
Alloys	Metallurgy	Polymorphism	Solid solutions
Cold working	Phase equilibrium	Powders	Solubility
Corrosion			Work hardening

16.70 LATTICE MECHANICS

Crystals/ lattice mechanics	Mössbauer effect
--------------------------------	------------------

16.80 ACOUSTICAL PROPERTIES OF SOLIDS

Absorption/ acoustic waves	Dispersion, acoustic/ ultrasonic	Refraction/ acoustic waves	Transducers
acoustic waves, ultrasonic	Magnetoacoustic effects	acoustic waves, ultrasonic	Transmission/ acoustic waves
Acoustic wave propagation/ ultrasonic	Reflection/ acoustic waves	Scattering/ acoustic waves	acoustic waves, ultrasonic
Acoustoelectric effects	acoustic waves, ultrasonic	acoustic waves, ultrasonic	Velocity/ acoustic waves
Acousto-optical effects			acoustic waves, ultrasonic
Diffraction/ acoustic waves			
acoustic waves, ultrasonic			

16.90 THERMAL PROPERTIES OF SOLIDS

Conductivity thermal/ measurement solids	Equations of state/ solids	Specific heat/ solids
	Heat conduction	Thermal expansion
		Thermodynamic properties

16.95 RADIATION INTERACTION WITH SOLIDS

Acoustic waves/ effects	Electron beams/ effects	Ion beams/ effects	Physical effects of radiations
Alpha-particles/ effects	Energy loss of particles	Mesons/ effects	Protons and antiprotons/ effects
Beta-rays/ effects	Gamma-rays/ effects	Neutrons and antineutrons/ effects	Sputtering
Deuterons/ effects	Hyperons/ effects		X-rays/ effects

17.00 SOLID STATE ELECTRICAL AND MAGNETIC PROPERTIES

Crystals/
internal fields

17.10 ELECTRON STATES IN SOLIDS

Crystal electron states band structure excitons Fermi level Fermi surface impurity states and effects plasma polarons surface transport processes	Crystal properties Cyclotron resonance de Haas-van Alphen effect Electron beams/ effects Electron gas Electron pairs/ annihilation	Electrons absorption radiation scattering Hall effect Kondo effect Magnetoacoustic effects Magnetoresistance	Metals/ theory Piezoresistance Skin effect Solids/ theory Surface phenomena
--	---	---	---

17.20 ELECTRICAL PROPERTIES OF SOLIDS

Acoustoelectric effects Conductivity, electrical/ measurement solids Contacts, electrical	Crystal electron states Eddy-currents Electrical properties of substs. Electron gas Electro-optical effects	Films, solid/ electrical properties Fluctuations Hall effect Magnetoelectric effects	Magnetoresistance Magnetothermal effects Noise, electrical Piezoelectricity Piezoresistance Space charge
---	---	--	---

17.22 Metallic Conducting Properties

Electron gas Hall effect Magnetoelectric effects Magnetoresistance	Metals/ theory Piezoresistance Semimetals Skin effect
---	---

17.24 Superconducting Properties

Storage devices Superconducting devices Superconducting magnets	Superconducting materials/ lead niobium Superconductivity/ type II
---	--

17.26 Semiconducting Properties

Acoustoelectric effects Contacts, electrical Electron gas Electro-optical effects Fluctuations Hall effect Magnetoelectric effects Magnetoresistance Magnetothermal effects Noise, electrical	Piezoelectricity Piezoresistance Semiconductors Space charge Semiconducting materials/ gallium arsenide germanium indium antimonide silicon
--	---

17.28 Semiconductor and Interface devices

Microwave techniques and devices Rectifiers	Semiconductor devices/ diodes junctions transistors tunnel and interface devices Storage devices
---	---

17.29 Dielectric Properties

Breakdown, electric/ solids Contacts, electrical Dielectric devices Dielectric measurement Dielectric phenomena	Dielectric properties of substs./ solids Electrets Electric charge Electric fields Electric strength	Electrostriction Ferroelectric materials/ barium titanate Ferroelectric phenomena Hysteresis Ionic conduction, solids Piezoelectric oscillations	Piezoelectricity Pyroelectricity Relaxation Rochelle salt Space charge/ solid Triboelectricity
--	---	--	--

17.40 THERMOELECTROMAGNETIC PROPERTIES

Magnetolectric effects Magnetothermal effects	Thermocouples Thermoelectricity
--	------------------------------------

17.50 PHOTOELECTRIC PROPERTIES

Photoconducting devices Photoconductivity	Photoelectricity Photoelectromagnetic effects	Photovoltaic effects
--	--	----------------------

17.52 ELECTRON AND ION EMISSION BY SOLIDS

Cathodes/ oxide	Ion emission/ secondary
Electron emission	thermionic
field emission	Ionization/ solids
photoelectric	Ionization, surface
secondary	Work function
thermionic	

17.60 MAGNETIC PROPERTIES OF SOLIDS

Antiferromagnetism	Films, solid/ magnetic properties	Magnetic properties of substs.	Magnetoacoustic effects
de Haas-van Alphen effect	Gyromagnetic ratio	antiferromagnetic	Magnetoelastic waves
Diamagnetism	Hall effect	diamagnetic	Magnetolectric effects
Electron diffraction examination of materials	Hysteresis	ferrimagnetic	Magneto-optical effects
Electron microscope examination of materials	Kondo effect	ferromagnetic	Magneto-resistance
Exchange interactions	Magnetic devices	paramagnetic	Magnetostriction
Ferrimagnetism	Magnetic fields/ effects	transitions	Magneto-thermal effects
Ferrites	Magnetic properties of dissolved atoms in dilute alloys	Magnetism	Neutron diffraction examination of materials
Ferromagnetism/ spin-wave theory		Magnetization process	Paramagnetism
		Magnetization state/ domains	Zeeman effect

17.62 Paramagnetic Properties

Magnetic properties of sub-
stances/
paramagnetic
Paramagnetism

17.64 Ferromagnetic Properties

Exchange interactions
Ferromagnetism/
spin-wave theory
Films, solid/
magnetic properties
Hysteresis
Magnetic devices

Magnetic properties of sub-
stances/
ferromagnetic
Magnetization process
Magnetization state/
domains
Storage devices

17.66 Ferrimagnetic Properties. Ferrites

Exchange interactions
Ferrimagnetism
Ferrites
Hysteresis
Magnetic devices

Films, solid/
magnetic properties
Magnetic properties of sub-
stances/
ferrimagnetic
Storage devices

17.68 Antiferromagnetic Properties

Antiferromagnetism
Exchange interactions

Magnetic properties of sub-
stances/
antiferromagnetic

17.69 Magnetic Relaxation Phenomena

Ferromagnetic relaxation
Magnetic resonance and relaxa-
tion

Nuclear magnetic resonance and
relaxation
Paramagnetic resonance and
relaxation

18.00 SOLID STATE SPECTROSCOPY AND OPTICAL PROPERTIES

Chemical shift Crystal field theory	Crystals/ hyperfine field interactions	Jahn-Teller effect Nuclear polarization
--	---	--

18.10 OPTICAL PROPERTIES OF SOLIDS

Absorption/ electromagnetic waves	Electromagnetic wave propaga- tion	Optical constants	Refraction/ electromagnetic waves
light	Electro-optical effects	Optical materials	light
Acousto-optical effects	Emissivity	Optical properties of substances	Refractive index/ light
Diffraction/ electromagnetic waves	Films, solid/ optical properties	Optical pumping	Scattering/ electromagnetic waves
light	Interference/ light	Optical rotation	light
Diffusion/ electromagnetic waves	Lasers/ solid	Photoelasticity	Transmission/ light
light	Magneto-optical effects	Pleochroism	light
Dispersion, optical	Nonlinear optics	Polarized light	Transparency
Double refraction/ mechanical		Reflection/ electromagnetic waves	Velocity/ light
		light	
		Reflectivity	

18.20 MÖSSBAUER SPECTRA OF SOLIDS

Crystals/
hyperfine field interactions
internal fields
Mössbauer effect

18.30 OPTICAL SPECTRA OF SOLIDS

Crystals/ hyperfine field interactions	Scattering/ electromagnetic waves	Spectra/ inorganic solids	Spectral line breadth
Reflection/ electromagnetic waves	light	inorganic solids, radio frequency	Stark effect
light	light, Brillouin spectra	organic molecules and sub- stances	X-ray spectra/ absorption
Reflectivity	light, Raman spectra, inorganic	organic molecules and sub- stances, infrared	emission
	light, Raman spectra, organic	organic molecules and sub- stances, radio frequency	Zeeman effect

18.40 LUMINESCENCE SPECTRA OF SOLIDS

Colour centres	Luminescence/ solids, inorganic
Counters/ scintillation	solids, organic
Electroluminescence	Luminescent devices
	Thermoluminescence

18.50 MAGNETIC RESONANCES IN SOLIDS

Crystals/ hyperfine field interactions	Cyclotron resonance	Ferromagnetic resonance	Magnetoelastic waves
Antiferromagnetic resonance	Ferrimagnetic resonance	Gyromagnetic ratio	Magnetomechanical effects
	Ferromagnetic relaxation	Magnetic resonance and relaxa- tion	Optical pumping

18.52 Paramagnetic Resonances and Relaxation

Crystals/ hyperfine field interactions	Paramagnetic resonance and relaxation/ measurement
---	--

18.54 Nuclear Magnetic Resonance and Relaxation

Crystals/ hyperfine field interactions	Nuclear magnetic resonance and relaxation/ measurement
	Nuclear quadrupole resonance

19.00 PHYSICAL CHEMISTRY

Atomic mass and weight	Distillation	Laboratory app. and technique	Precipitation
Balances	Elements/ origin	Macromolecules	Pumps
Bonds	relative abundances	Molecular weight	Quantum chemistry
Centrifuges	Filters	Molecular weight determination	Sedimentation
Chemical structure	Isomerism	Periodic system	Valency
Chemical technology		Physical chemistry	

19.10 THERMOCHEMISTRY AND REACTIONS

Association	Crystal chemistry	Heat of adsorption	Phase equilibrium
gases	Detonation	Heat of combination	Phase transformations
liquids	Dissociation	Heat of dissociation	Polymerization
Catalysis	Exchanges, chemical	Heat of formation	Polymers
Chemical reactions	Explosions	Heat of reaction	Reaction kinetics
Combustion	Flames	Isotope exchanges	Sorption

19.15 Oxidation and Corrosion

Corrosion
Oxidation

19.20 ELECTROCHEMISTRY

Conductivity, electrical/ liquids, electrolytic	Electrochemistry electrodes	Electrolysis	Ion velocity/ electrolytic
Dissociation/ electrolytic	Electrokinetic effects	Electrolytic deposition	Ions, electrolytic
		Electrophoresis	

19.30 PHOTOCHEMISTRY AND RADIOCHEMISTRY

Chemical effects of radiations/ acoustic waves	Nuclear reactions and scattering/ chemical effects
ionizing radiations	Photochemistry
	Radiochemistry

19.40 PHYSICAL METHODS OF CHEMICAL ANALYSIS

Chemical analysis/ adsorption by mass spectrometry by nuclear reactions electrochemical radioactive X-ray	Chromatography Radioactive tracers Spectrochemical analysis Tracers
---	--

20.00 GEOPHYSICS

Earth/ age composition electricity heat rotation	Geodesy Geophysical prospecting Geophysics Glaciers	Gravity Minerals Oceanography Radioactive dating	Radioactivity Seawater Seismic waves Seismology Soil
---	--	---	--

20.10 ATMOSPHERE

Anemometers Atmosphere/ composition humidity movements precipitation radioactivity structure temperature thermodynamics Atmospheric acoustics	Atmospheric electricity Atmospheric optics Atmospheric pressure and density Atmospheric spectra Atmospherics Clouds Condensation Electromagnetic wave propaga- tion/ atmosphere	Evaporation Fallout Fog Humidity Hygrometers Ice Lightning Meteorological instruments Meteorology Rain	Rockets Satellites, artificial Sky brightness Snow Sunlight Thunderstorms Twilight Wind
---	---	---	--

20.20 UPPER ATMOSPHERE

Airglow Atmosphere/ composition movements radiation belts radioactivity structure temperature thermodynamics upper	Atmospheric electricity Atmospheric optics Atmospheric pressure and density Atmospheric spectra Atmospherics	Aurora Fallout Ionization, atmosphere Magnetosphere Meteors Rockets	Satellites, artificial Sky brightness Sunlight Twilight Zodiacal light
---	---	--	--

20.30 IONOSPHERE

Atmospherics Aurora	Electromagnetic wave propaga- tion/ ionosphere	Ionization, atmosphere Ionosphere Ionosphere measuring apparatus
------------------------	--	--

20.35 D, E and F-regions

Ionosphere/
D-region
E-region
F-region

20.40 GEOMAGNETISM

Compasses Earth/ magnetic field magnetic field, variations	Magnetic storms Rock magnetism
---	-----------------------------------

20.50 SPACE RESEARCH TECHNIQUES

Rockets Satellites, artificial	Space research Space vehicles/ instrumentation
-----------------------------------	--

21.00 ASTROPHYSICS

Astronomical observations Astronomical spectra Astronomy and astrophysics	Celestial mechanics Cosmic rays Cosmology	Elements/ origin relative abundances	Gravitation Interstellar matter
---	---	--	------------------------------------

21.10 GALAXIES

Cosmic radiations, r.f.
Galaxies/
the Galaxy

Magnetohydrodynamics
Nebulae

21.20 STARS

Interstellar matter
Magnetohydrodynamics
Novae

Stars/
composition
evolution
magnetism
radiation
spectra
structure
Thermonuclear reactions

21.30 RADIOSOURCES, X-RAY AND GAMMA-RAY SOURCES

Cosmic radiations, r.f.
Quasars
X and gamma-ray astronomy

21.40 SOLAR SYSTEM

Comets
Cosmic rays
Earth/
rotation
Gravitation
Interplanetary magnetic field

Interplanetary matter
Meteorites
Meteors
Moon
Planets
Solar system

21.45 Sun

Cosmic rays
Sun/
corona
eclipses
flares
magnetism
prominences
radiation
radiation, corpuscular
radiation, r.f.
spectra

Sunspots
Zodiacal light

21.60 ASTRONOMICAL TECHNIQUES

Astronomical instruments
Astronomical observations

Astronomy and astrophysics
Radioastronomy

Telescopes/
astronomical

22.00 BIOPHYSICS

Biophysics

22.10 HEALTH AND MEDICAL PHYSICS

Biological effects of radiations
Biological technique and instruments

Blood
Dosimetry
Medical science

Physiology
Proteins
Radiation protection

Radiography
Zoology

22.20 HEARING AND SPEECH

Ear
Hearing
Noise/
acoustic
Speech

22.30 VISION

Eye
Colour vision
Vision

23.00 LABORATORY AND EXPERIMENTAL TECHNIQUES

Biological technique and instruments
Calculating apparatus/
analogue apparatus
digital computers
digital computer programmes

Chemical technology
Heat treatment/
alloys
Laboratory apparatus and technique
Leak detection

Materials
Metallurgy
Zone melting and refining

23.10 HIGH AND LOW TEMPERATURE TECHNIQUES

Cryostats
High-temperature phenomena and effects

Joule-Thomson effect
Liquefaction, gases
Low-temperature phenomena

Low-temperature production
Low-temperature technique
Magnetic cooling

23.20 HIGH PRESSURE TECHNIQUES

High-pressure phenomena and effects

23.30 VACUUM TECHNIQUES

Leak detection
Manometers
Seals
Sputtering

Vacuum apparatus
Vacuum gauges
Vacuum pumps
Vacuum technique

23.40 X-RAY TUBES AND TECHNIQUES

Dosimetry
High-voltage techniques
Radiation monitoring
Radiation protection
Radiography

X-ray absorption
X-ray diffraction
X-ray examination of materials
X-ray measurement
X-ray monochromators

X-ray reflection
X-ray scattering
X-ray spectra/
absorption
emission

X-ray spectrometers
X-ray spectroscopy
X-ray tubes
X-rays/
effects

Chemical elements and inorganic compounds

All the chemical elements are listed by name, followed by their compounds, e.g. "Cadmium", "Cadmium compounds".

"Hydrogen" is subdivided by the subheadings "neutral atoms", "neutral molecules" and "ions". "Deuterium" and "Tritium" are independent headings. "Hydrogen compounds" is supplemented by "Ice", "Steam" and "Water".

"Oxygen" is supplemented by "Ozone" and "Carbon" is supplemented by "Diamonds" and "Graphite"

The following inorganic compounds are further subdivided by subheadings as shown:-

Barium compounds/ barium titanate*	Nitrogen compounds/ ammonia
Cadmium compounds/ cadmium sulphide	ammonium compounds
Calcium compounds/ calcium fluoride	Potassium compounds/ potassium bromide
Gallium compounds/ gallium arsenide†	potassium chloride
Indium compounds/ indium antimonide†	Sodium compounds/ sodium chloride
Lithium compounds/ lithium fluoride	Zinc compounds/ zinc sulphide

* Ferroelectric properties are listed under "Ferroelectric materials/barium titanate"

† Semiconducting properties are listed under the corresponding subheadings of "Semiconducting materials"

Organic compounds

Organic compounds are grouped under headings "Organic compounds", "Polymers", "Plastics", "Proteins". "Rochelle salt" is an independent heading.

Co-ordination compounds

Metallic co-ordination compounds are regarded as inorganic with a few exceptions and are indexed under the appropriate metallic compound heading, (not under organic compounds) e.g. Ni complex, bis (dimethylglyoximate) nickel (II) under Nickel compounds.

Substance groups

In addition there are the following headings for groups of elements, compounds or substances:-

Actinides	Metals
Actinide compounds	Minerals
Alkali metals	Rare-earth metals
Alkali-metal compounds/ halides	Rare-earth compounds
Alkaline-earth metals	Semiconductors
Alkaline-earth compounds	Semiconducting materials/ gallium arsenide§
Ferrites	germanium§
Ferroelectric materials/ barium titanate†	indium antimonide§
Garnets	silicon§
Halogens	Superconducting materials/ lead
Inert gases	niobium
	Transition metals
	Transition-metal compounds

† Used for ferroelectric properties only

§ Used for semiconducting properties only

|| Used for superconducting properties only

Alloys

General papers on alloys are indexed under "Alloys". Alloys of specified composition are listed under, either

- (i) special alloy headings (there are five of them: "Aluminium alloys", "Copper alloys", "Iron alloys", "Nickel alloys", "Steel"), e.g. Al-Ni alloys under "Aluminium alloys", and "Nickel alloys".
- (ii) compounds of the named elements, e.g. Mn-Zn alloys under "Manganese compounds" and "Zinc compounds". Silicon-iron under "Iron alloys" and "Silicon compounds".

Special substances and materials

There are also the following special headings for certain common substances:-

Air	Paper
Blood	Porous materials
Ceramics	Powders
Clay	Quartz
Coal	Rubber
Concrete	Ruby
Fibres	Sand
Gelatin	Seawater
Glass	Soil
Mica	Waxes
Optical materials	Wood

4 π counters

No entries

Abacs *see* **Nomograms****Aberrations, optical***see also* **Electron lenses; Ion optics; Optical instrument testing; Optics/geometrical; Particle optics**

achromatism, F and C, mean reference wavelength standards, formulae 9-25375

astigmatism, Fresnel lenses, expression 9-27371

astigmatism of first-order ray pencil, rel. to consistency of results 9-25338

astigmatism of eye, statistical data and interpretation 9-31711

balancing merit function in automatic lens design, use of modulation transfer function 9-45980

chromatic, correction rel. white modulation transfer function 9-22445

chromatic, in quadrupole and octopole electron lenses 9-47900

coefficients, rel. Eikonal 9-25185

complex systems, automatic correction 9-36344

in composite systems, automatic correction 9-34217

correction in symmetric eyepieces 9-36339

diffraction images of coherently illuminated objects 9-34207

electron, in axisymmetric probe system, 3rd and 5th order correction 9-43851

electron lenses, axisymmetric single, spherical aberration meas. 9-36259

in electron lenses, mag., 5th order spherical 9-41857

electron opt. system, design for minimum 3rd order aberrations 9-38353

electrostatic quadrupole lens, field asymmetries effect 9-31915

eye, resolving power dependence on various combinations 9-27129

F and C achromatism, mean reference wavelength standards, formulae 9-25375

in film solar energy concentrator 9-31996

geometrical, in Manenc's double focusing method 9-37121

hologram imaging by ray tracing, evaluation 9-36323

holographic double image elimination using single sideband waves 9-40367

in holography, scanning obs. 9-31979

images of single and double mirrors 9-36336

interferometers, Fabry-Perot, used as filters 9-48105

lens, spot diagram generator for testing 9-22467

minimal astigmatism surfaces, calc. 9-36346

mirror systems, single and double, theory 9-40375

modulation transfer factor for instrument made stigmatic by deposition of dielec. thin film on lens 9-46009

primary, of single lens positive systems 9-29450

spectrograph, Czerny-Turner, coma width of meridional image 9-46024

spherical, 7th order, optimum corrections 9-22443

spherical, correction in two mirror system 9-32002

spherical, correction using Hoppe zoneplate 9-22441

spherical, optical transfer function, 3rd and 5th order determ. 9-22468

spherical, zero 3rd order in 2 surface refracting systems 9-40376

spherical and chromatic in electron microscopes, correction using mirror with superimposed mag. field 9-25188

spherical of triplet photographic objectives 9-31999

stellar interferometer fringe visibility, non-monochromaticity effect 9-48090

third-order coeff. partial derivatives, evaluation 9-31998

wave, effect on modulation transfer function of optical systems 9-27364

wave-aberration difference function variance magnitude, correlation with relative modulation function 9-36347

Abrasion*see also* **Hardness; Wear**

semiconductor polishing, optimum abrasive sizes for minimizing times taken 9-30883

Mo as-grown single cryst., effect on dislocation struct. 9-42836

Absorption*see also* **Alpha-particles; Beta-rays; Cosmic rays; Electrons; Gamma-rays; Hyperons; Mesons; Neutrons and antineutrons; Protons and antiprotons; and also Sorption; X-ray absorption**

impurity center in crystals, effect of vibrational mixing of two close-lying levels 9-28677

partially cryst. materials, microwave and far i.r., phonon density distrib. and multiphonon effects obs. 9-35263

plasma radiation, transverse and longitudinal 9-28001

of thermal rad., effect on subsonic gas flow 9-32720

YFe garnet single crystal, resonant, of elastic waves, in absence of external mag. field 9-30649

GaAs, substitutional Cu impurities, electroabsorption study 9-35413

N by liquid iron from a plasma 9-46455

acoustic waves*see also* **Noise abatement; Transmission/acoustic waves**

in air, free, generation of pulses with finite amplitude, pulse source behaviour and peak press. relationship 9-32735

butanols, 10-300 kHz, relax. obs., reson. reverberation method 9-28123

conductors, thin, in mag. field, sensitivity to electron scatt. 9-24029

dielectric, phonon absorpt., theory 9-48954

diffraction corrections from mean pressure acting on transducer as function of radiator and receiver dimensions 9-22250

by elastomers, in reson. absorbers for waterborne sound, props. 9-36180

ferroelectric cryst., KH₂PO₄-type, critical anomaly of sound attenuation 9-39693

freshwater (Lake Superior), l.f. sound, comparison with seawater results 9-28124

in gases, low pressure, confined to tubes of circular cross section 9-46571

glass fiber, effect of cloth covers 9-39516

in liquid metals, obs. from melting point to 900-1000°C 9-30395

metal, in quantizing mag. field for open trajectory case, giant oscillations 9-39517

metal plates, e.m. excitation of resonances, surface impedance singularity meas. 9-48957

metals, structural realignment effects from meas. in molten semimetals from melting to 900°C 9-30394

MgO, paramag. reson. interpret. taking account of Jahn-Teller effect 9-24346

paper, onionskin, decoupling props. 9-46991

quartz, attenuation of u.h.f. waves, phonon interactions contrib. 9-48947

rutile, reduced, microwave relaxation 9-35280

sawtooth, guided, weak, decay inside tubes 9-45854

semiconductor, attenuation temp. dependence rel. to electron-phonon expt. investigation 9-33294

Absorption continued**acoustic waves continued**

semimetals, giant oscillations, ang. depend. of amplitude 9-48955

semimetals, molten, from melting to 900°C 9-30394

solutions, liq., additional absorpt. due to conc. fluctuations, calc. 9-28119

toluene, 10-300kHz, relax. obs., reson. reverberation method 9-28123

waterborne, fluid damped resonance-absorbers 9-41826

waterborne, reson. absorbers containing elastomers, props. 9-36180

BaTiO₃, displacive-type ferroelec., attenuation near Curie point, anomalous behaviour 9-35277

Ca-Bi-V-ferrite, attenuation decrement 9-37346

CdS, semicond., parametric amplification of shear waves 9-37343

Ga plates, e.m. excitation of resonances, surface impedance singularity meas. 9-48957

³He liq., coeffs. and relax. times 9-30445

InSb, longit. magnetoacoustic absorpt. Landau levels effects 9-26420

KH₂PO₄-type ferroelec. cryst., critical anomaly of sound attenuation 9-39693LiNbO₃:MgO single cryst., doping eff. on attenuation 9-37334LiTaO₃:MgO single cryst., doping eff. on attenuation 9-37334MgAl₂O₄:Fe²⁺, attenuation of shear waves 9-37335MgO:Fe²⁺, attenuation at 1.5°K 9-37315SrTiO₃, displacive-type ferroelec., attenuation near Curie point, anomalous behaviour 9-35277

YFe garnet rods, transversally magnetised, resonance absorption of longitudinal phonons 9-28421

ZnO:Cu, microwave amplification 9-37344

acoustic waves, ultrasonicalkali halides containing CN⁻, attenuation and velocity 9-37329

alkali-borosilicate glass, rel. to spectrum of relaxation times and fluctuation theory 9-26096

antiferromagnetic systems, attenuation at low temp. 9-49198

attenuation in solids, intrinsic and extrinsic mechanisms 9-37330

attenuation near mag. critical pts. spin-lattice relax. and spin thermal conduction effects 9-44820

benzene, determ. from Brillouin line breadth 9-44560

biological materials, thermal effects 9-47698

bitumens in rubber transition zone 9-30450

t-butyl alcohol-water soln., soln., comparison with methyl cyanide-water 9-42651

CaF₂:U⁴⁺, spin-phonon interaction from u.s. paramag. resonance 9-33623

carbon tetrachloride, determ. from Brillouin line breadth 9-44560

carboxylic acids, dilute, aqueous, at 5.04 MHz, effect on dissociation 9-48695

coupling losses 9-48956

crystals, uniaxial, travelling-wave photoelastic amplification, laser pump use 9-37341

dextran, aq. solns. 9-42653

dextran, aqueous soln., relaxation behaviour obs. 9-36874

diffraction effects in measurement 9-47822

ferroelectric solid solns. with perovskite struct., temp. depend. 9-41084

ferroelectrics, KDP-type, anomalous attenuation near the Curie point 9-49140

ferromagnetic systems, attenuation at low temp. 9-49198

1-fluoro-1, 1, 2, 2-tetrachloroethane, relax. and internal rot. 9-27896

group III-V cpds., nuclear acoustic resonance meas., of gradient-elastic tensors 9-23851

Heisenberg magnets, attenuation, heuristic improvement 9-41087

laurylpyridinium bromide (iodide), u.s. vib. potentials as function of conc. 9-48694

liquid metals, dense-gas formulation 9-34902

liquids, associated, pressure depend. of absorpt. coeff. 9-36870

liquids, excitation by impact of cyl. projectiles, visualiz. and opt. meas. presentation in slow motion 9-36872

liquids, new theory of compressional relaxation with vib. point as group of mols. 9-30389

magnetoacoustic attenuation, deformation-potential theory 9-46995

metals, attenuation by magnetic surface states 9-28418

methyl cyanide-water soln., study and comparison with t-butyl alcohol-water soln. 9-42651

Mossbauer eff. meas. 9-37697

polyethylene glycol soln., relaxation behaviour obs. 9-36874

pulse echo attenuation and phase shift meas. method, in presence of noise 9-29273

quantum oscillations, giant, rel. to electron mean free paths study 9-37388

rare earth metals, expression for acoustic paramag. reson. 9-41422

rare earths, attenuation at mag. phase transitions, freq. and temp. depend. 9-48958

recorder, logarithmic, high sensitivity, for attenuation studies 9-38299

ruby, attenuation of longit. waves of microwave freqs. temp. depend. 9-39518

semiconductor, attenuation decrement calc., in uniform electric fields 9-41085

semiconductors, piezoelectric, non-linear effects in u.s. amplification 9-46994

semiconductors, propagation in h.f. electric field, re-derivation of dispersion relationship 9-41086

semiconductors with screened deform., piezoelec. interactions and many-valley band struct., hypersound absorpt. 9-48952

semimetal, attenuation decrement calc., attenuation decrement calc. in uniform electric fields 9-41085

sodium laurylsulphate solns., u.s. vib. potentials as function of conc. 9-48694

solids, crystalline, ultrasonic and extrinsic attenuation mechanisms 9-37331

solids, excitation by impact of cyl. projectiles, visualiz. and opt. meas. presentation in slow motion 9-36872

three-phonon interactions in single-crystals, theory 9-42942

travelling-wave photoelastic amplification in uniaxial cryst., use of laser pump 9-37341

1,1,2-trichloroethane, u.s. relax. and vol. change during internal rot. 9-42652

u.p.r. analogue of ENDOR, technique 9-29351

urea, aq. solns. 9-30400

water, for size distrib. of gas bubbles determ. 9-46607

water-methyl cyanide soln., study and comparison with t-butyl alcohol-water soln. 9-42651

Ag thin films, hypersonic attenuation 8.4-10.0GHz 9-44821

Absorption continued**acoustic waves, ultrasonic continued**

- Al, attenuation due to dislocations as function of strain and temp. 9-37332
- Al₂O₃:Fe³⁺ single crystal, paramagnetic relax. absorpt. of hypersound 9-33172
- Al₂O₃, non-collinear attenuation of transverse waves at low temp., temp. depend. 9-39519
- Al₂O₃ attenuation of longit. waves of microwave freqs., temp. depend. 9-39518
- AlSb, nuclear acoustic resonance meas. of gradient-elastic tensors 9-23851
- (Ba,Sr)TiO₃ solid solns., polycrystalline, temp. depend. 9-41084
- BaF₂, normal mode frequencies volume dependencies, calc. for non-dispersive modes 9-33016
- CS₂, determ. from Brillouin line breadth 9-44560
- CaF₂, normal mode frequencies volume dependencies, calc. for non-dispersive modes 9-33016
- Cd, normal and supercond., attenuation rel. to Fermi surface and deform. parameter 9-37338
- Cd, quantum oscillations, rel. to Fermi surface 9-44822
- Cd, resonance oscillations due to orbits on Fermi surface 9-30772
- CdS, attenuation obs. via acoustoelec. effect, pulsed u.s. meas. 9-24031
- CdS, parametric amplification of u.s. waves 9-37342
- CdSe cryst., attenuation of transverse waves, action of photons 9-28420
- CoO, attenuation near antiferromag. critical pt. 9-44823
- CoSO₄ in soln., obs. and calc. of reaction rate 9-30397
- CuSO₄ solutions in glycol-water mixtures, as function of temp. 9-34903
- EuO, attenuation, temp. and mag. field depend. 9-44824
- EuO, near mag. phase transition, vel. change with const. attenuation 9-24030
- α -Fe, attenuation obs. at 31 and 60 MHz, diffusion coeff. of carbon determ. 9-37196
- GaSb, nuclear acoustic resonance meas. of gradient-elastic tensors 9-23851
- GaSs, nuclear acoustic resonance meas. of gradient-elastic tensors 9-23851
- He liquid, 1 GHz attenuation obs. 9-23561
- Hg, liquid, dense-gas formulation 9-34902
- HgTe single crystals, 10-300 MHz, 1.2° to 380°K 9-42958
- In, attenuation in normal and superconductivity states, non-free-electron behaviour 9-26417
- In, shear-wave attenuation amplitude dependence near T_c 9-26418
- InAs, nuclear acoustic resonance meas. of gradient-elastic tensors 9-23851
- n-InSb:Ge, amplitude-depend. attenuation at liq.-He temp. 9-44825
- InSb, nuclear acoustic resonance meas. of gradient-elastic tensors 9-23851
- KCl, KBr and KI containing CN⁻, attenuation and velocity 9-37329
- KTaO₃, attenuation, temp. and freq. depend., interpret. w.r.t. soft optic phonon mode interact. 9-37328
- KTaO₃, attenuation by interaction with soft optic mode 9-24025
- LiCl in alcohol soln., relax. curves at 25°C rel. to ion assoc. and dissociation 9-23493
- LiNbO₃, microwave pulses, spatial intensity distrib., attenuation coeff., Brillouin scatt. obs. 9-35278
- LiTaO₃, microwave attenuation 9-44826
- Mg alloys, effect of decomposition of the supersaturated solid soln. on attenuation 9-46990
- MnF₂, attenuation meas. at 10-30 MHz for mag.-phase diagram 9-41339
- MnF₂ attenuation at mag. phase transitions freq. and temp. depend 9-48958
- MnSO₄ mixture in H₂O-ethylene glycol, 3 MHz to 330 MHz 9-39097
- Mo crystal irradiated with u.s. of 150 W/cm², attenuation of u.s. between 5-30 Mc/s 9-40952
- (NH₄)₂SO₄, meas. for suspension concentration 9-32802
- NaCl containing CN⁻, attenuation and u.s. velocity 9-37329
- NaNO₂, attenuation near critical pts. 9-44827
- Nb, mixed state, 10GHz hypersonic waves, 1.3°K 9-35279
- Nb single crystals, attenuation, eff. of O additions, 4.2° to 313°K 9-30634
- Nd, attenuation, 4.2-300°K, elastic moduli, correl. with antiferromag. transitions 9-35146
- NiSO₄ in soln., obs. and calc. of reaction rate 9-30397
- Pb, superconducting, u.s. shear-wave attenuation 9-24026
- Pb single cryst., dislocation damping, temp. and freq. depend 9-41089
- Pr, attenuation, 4.2-300°K, elastic moduli, correl. with antiferromag. transitions 9-35146
- Pu-Al delta-stabilized alloys, attenuation temp. depend 9-37224
- Pu-Ce delta-stabilized alloys, attenuation, temp. depend 9-37224
- RbMnF₃, antiferromagnetic, frequency-depend. due to resonant acoustic coupling to ⁸⁵Mn nucleus 9-46993
- RbMnF₃ attenuation at mag. phase transitions freq. and temp. depend 9-48958
- SbSI, damping as function of illumination, near phase transition temp. 9-46992
- SbSI coefficient and velocity of 10-30 Mc/s, temp. depend., 16-24°C 9-42960
- Sm, attenuation, 4.2-300°K, elastic moduli, correl. with antiferromag. transitions 9-35146
- Sn, in supercond. transition rel. to cryst. orientation 9-37336
- SrTiO₃, pseudo-cubic, anomalous hypersonic absorpt. 9-37337
- TiO₂ rutile, temp. and freq. depend. of acoustic microwave absorption 9-30773
- Zn, normal and supercond., attenuation rel. to Fermi surface and deform. parameter 9-37338
- Zn, quantum oscillations, rel. to Fermi surface 9-44822
- Zn crystals, dislocation contrib. to u.s. attenuation 9-39521
- Zn single cryst., attenuation at low temp. 9-33174
- ZnO:Li, u.s. wave attenuation, temp. and freq. depend. 9-37339
- ZnO, attenuation of compressional and shear piezoelectrically active waves, freq. depend. 9-37340
- ZnSO₄ mixture in H₂O-ethylene glycol, 3 MHz to 330 MHz 9-39097

electromagnetic waves

see also *Spectra (radiofrequency subheadings)*

- atmosphere, meas. at 31.9 cm wavelength 9-31330
- auroral, electron density observations radio communication problems 9-33839
- auroral, near S. Geomag. Pole, rel. to mag. activity 9-35856
- auroral for distances over 4000 km, simplified calc. 9-35857

Absorption continued**electromagnetic waves continued**

- auroral type, in mag. conjugated regions 9-35861
- cosmic noise, by ionospheric, sudden increases 9-45524
- of cosmic radio noise by ionosphere, 1959-65 obs. 9-40070
- crystal, by local centers near exciton zone, level shift and band width 9-28708
- D-region, lunar tides study by absorption analysis 9-37980
- dielectric media on opaque substrate 9-26671
- dissipation function by the invariant imbedding eqn. 9-45583
- dissociation of molecules by absorption of line radiation 9-27921
- gas, meas. from acoustic wave prod. 9-28077
- high latitudes, normal and abnormal absorptions 9-33788
- ice I, microwave 9-45264
- by impurity polarons, polarization mechanism 9-31096
- ionosphere, at different frequencies, lunar variation 9-37970
- ionosphere, effect on mid-latitude geomag. pulsation correlations 9-35900
- ionospheric radiowave absorption in broken terrain, meas. 9-45525
- liquid, variation due to continuous distrib. of resonances, Debye and Gaussian type 9-32782
- metal, rel. to surface roughness 9-45268
- nonpolar gases, microwave, press.-induced 9-30350
- plasma, anomalous dispersion region, analysis 9-48564
- plasma, collisionless, anomalous absorpt. of powerful wave 9-46486
- polar cap absorption, characteristics 9-33787
- polar cap absorption, v.l.f. records 9-33840
- polar molecules in nonpolar solvents, dielectric absorpt. meas. of molecular relaxation 9-23088
- radio, by water vapour in atmosphere of Venus and of Mars 9-47676
- radiowaves, l.f., in ionosphere, calc. 9-31387
- resonant, applic. of perturbation method in wave mechanics 9-38230
- solar, by various building materials 9-33542
- solar radiation integral coeff. determ., review 9-41841
- stimulated thermal emission, critical absorption coeff. calc. 9-43814
- surface layer, rel. to elastic-plastic wave generation 9-45846
- v.l.f. radiowaves in ionosphere, validity of f cos i theorem 9-43447
- BaTiO₃, microwave-absorption fluctuations at Curie temp. 9-28559
- BaTiO₃, microwave absorpt. by free carriers 9-31101
- Bi, r.f. size effect in determ. skin depth 9-24110
- HNO₃ in atmosphere, upper, solar i.r. absorption balloon obs. 9-47530
- r.f. size effect in determ. skin depth 9-24110
- Zn, supercond., microwave absorpt., mag. field depend. 9-47094
- light**
- see also *Atmospheric optics; Densitometry; Films, solid/optical properties; Filters, optical; Optical constants; Pleochroism; Transmission/light; Spectra*
- A²BC² semiconductor cpds., edge spectra, peculiarities 9-37715
- absorption term, bichromatic differential 9-32033
- alkali, halides: Ni(Cu), rel. to coordination props. 9-33548
- alkali chloride solid solns., fund. absorpt. in extreme u.v. 9-35662
- alkali halide crystals, U bands, band shape and phonon broadening 9-46830
- alkali halides, direct band due to OH ion 9-43236
- alkali halides, F⁺ centre obs., polaron model applic. 9-44716
- alkali halides, l.r. meas. rel. to anharmonicity 9-47348
- alkali halides, OH⁻ doped, l.r. stretching band obs. 9-24403
- alkali halides, spectra of aggregate centres fine struct. and oscillatory effect obs. 9-39370
- alkali halides, two-photon spectroscopy 9-47349
- alkali halides, u.v. spectra of Ag⁺, Cu⁺ and Ti⁴⁺ centres, band electronic fine struct. obs. 9-43237
- alkali metals, optical conductivity, Mayer-Naby peak 9-28679
- alkali-halide crystals with defects, i.r. absorption obs. 9-33568
- alkali-halides U₂ centres, effect of external stresses 9-49251
- alkaline earth oxides and fluorides, F⁺ and F⁺ transitions Mollwo-Ivey plots 9-35108
- alkaline earth tungstates, Bi doped, u.v.-induced colouration, darkening and fading processes 9-45282
- aluminum-boro-phosphate glasses, spectra of Mo⁴⁺ 9-47350
- anthracene: tetracene radiation damage rel. to optical absorption 9-26747
- anthracene, two-photon, energy depend. 9-39795
- anthracene in benzene, toluene, from dispersion obs. 185, 250 nm 9-34912
- anthracene solidified vitreous solns., spectra, aggregates existence obs 9-46701
- antiferromagnetic semiconductors, rel. to magnon drag contrib. to transport props. 9-24332
- attenuation function in reflection from inhomogeneous layer 9-45990
- band filling in semiconductors, saturated 9-24167
- beams in liquids, thermal blooming and instability 9-26099
- benzene crystals, doped, spectra of localized exciton states 9-31112
- blood, parameters 9-47694
- broad-spectrum radiation, coeff. and kinetics determ. 9-22448
- n-butane, cross-sections and photoionization yields, isotope effects 9-30298
- CdS photodesorption, effect on rectification props. of high-resistance barrier layer 9-39640
- coals and soots, absorpt. index, i.r. region 9-24357
- colloid, capillary-porous, rad. energy abs. and rad. distrib. 9-23546
- crystals, i.r., and combinational scattering, selection rules 9-41371
- crystals, i.r. lines due to lattice vibr. modes, temp. depend. 9-33157
- crystals, non-conducting, interband absorpt. change in elec. field, Stark effect obs. 9-33547
- 9-cyanoanthracene, polarized u.v. spectrum at 4.2°K 9-33566
- cyanol-(9) anthracene vitreous solns., spectra, aggregates struct. obs. 9-46702
- diamond, substitutional N donor obs. 9-37401
- diamonds, effect of heat and pressure treatment 9-26366
- by diatomic molecules at high temp., continuous 9-23170
- 9,10-dichloroanthracene, Urbach rule and long-wave tail of exciton band 9-39849
- 9,10-dichloroanthracene with chlorinil, spectra 9-30073
- 5,10-dihydrophenazine, near-u.v. absorpt. spectrum 9-32508
- discharge plasma, coefficient meas. using laser pulses 9-28000
- ethylene, cross-sections and photoionization yields, isotope effects 9-30298
- from excited levels, low-temp. suppression 9-29907
- excitonic, in high mag. fields 9-43232
- film, absorbance at surface opposite surface of incidence 9-49237

Absorption continued

- light continued
 by film in standing wave 9-41360
 fluoroplastic, F32L, film 9-43136
 gas, resonance absorpt. saturation, spatial effects 9-39054
 gases, far u.v. coeffs. meas. 9-28078
 gases, small absorpt. coeffs. meas. using Fabry-Perot interferometer 9-29465
 glass, barium silicate containing Ti, gamma-induced absorpt. effect of TiO_2 increase 9-37693
 glasses, chalcogenide 9-30956
 Glasses, $\text{K}_2\text{O-PbO-SiO}_2$, spectra 9-31129
 glasses, $\text{K}_2\text{O-PbO-SiO}_2$, spectra 9-31129
 graphite, Rosseland and Planck mean absorpt. coeffs. 9-49548
 grazing incidence on ellipsoidal Earth, generalization of Chapman's theory 9-41522
 group II-VI compounds, spectra near fundamental band edge 9-37708
 group IV and V boron hydrides, i.r. spectra 9-42381
 ice, far-i.r. spectra of orientally-ordered and disordered phases 9-33557
 ice, Rosseland and Planck mean absorpt. coeffs. 9-49548
 ice I, i.r. 9-45264
 impurity absorption, long-wavelength edge shape, Green's function investigation 9-45310
 impurity absorption in ionic crystals, anharmonic effects due to weak vibrational-electronic coupling 9-33574
 impurity atoms, two-electron-eigenstates of (sp) ^3P multiplet and phonon-induced optical transitions 9-41372
 impurity centres, electron-vib. spectrum, band broadening mechanisms 9-26730
 by impurity centres in solids, spectra shape and Urbach's rule 9-33546
 impurity spectra, connection with electronic excitation transfer processes 9-33220
 impurity spectra of solids, applic. to metal-ion activated alkali halide phosphors 9-31098
 impurity spectra of solids, theory 9-31097
 interstellar, in IC 1805 region, spectrophotometric obs. 9-47650
 interstellar spectra, A4430, image tube obs. 9-27025
 i.r., true freq. determ. from internal refl. spectroscopy 9-37713
 laser beams in liquids, thermal defocusing, time dependence experiment 9-26100
 laser signals, by atmospheric gases 9-47549
 liquids, organic, temp. depend. cell for meas. 9-28130
 metal films, self-supporting, covered by oxide layers, eff. of plasma oscils. 9-26672
 methane, coeff., far u.v. obs. 9-28078
 methane, Stark effect of absorpt. line, maser obs. 9-34678
 mists, volume attenuation coeff., 0.3 to 2.5 μ wavelength 9-44526
 molecular cryst., exciton phenomena, book 9-49005
 molecular crystals, exciton-phonon interaction influence on bands 9-43234
 molecular crystals with defect levels, intensity, and polarization ratio 9-33541
 nitrate glass, Co (II)-doped, rel. to Co coordination 9-26735
 organic dye absorbers, ruby laser, fluorescence decay times, recovery times and nonlinearities 9-26113
 ozone, liq., i.r. spectra 9-46641
 by particles with small real refr. index 9-34200
 phosphors, colour centres, wavelength depend. of loss in luminous efficiency after u.v. and X-irrad. 9-28721
 photochromic spiropyran layers, coloration by u.v. laser radiation 9-27916
 photoionization of large radius excitons, accompanied by carrier transfer to a different band 9-37410
 phthalocyanine dyes, fluorescence decay times, recovery times and nonlinearities 9-26113
 phytochrome systems, mol. mechanism 9-40618
 piezospectroscopic effects on bands, using device meas. linear dichroism 9-46010
 plasma, laser radiation, transparency effect 9-25888
 plasma, laser-produced on solid surface 9-38983
 polarization due to donor-acceptor associates, wurtzite type cry. 9-33544
 polarizing pile of dielectric plates, optical characters. 9-29472
 polymer films, synthesized, vacuum u.v. spectra, electr. struct. obs. 9-31116
 polymers in methylene series, i.f. spectra 9-48525
 polymethine cyanine dyes, fluorescence decay times, recovery times and nonlinearities 9-26113
 polynucleotides, homogeneous, vacuum u.v. spectra, rel. to electronic structure 9-26750
 polystyrene film 9-43136
 powder and massive substance, rel. between spectra 9-39829
 powdered ionic crystals, i.r. freqs., interpretation 9-31111
 pyrazine, $^3\text{B}_{2u}(\pi-\pi^*)$ - A_{1g} spectra, excitonic struct. 9-47405
 pyrographite, absorpt. index, i.r. region 9-24357
 radiation laws rel. to gross and net absorpt. 9-48087
 rhodopsin systems, mol. mechanism 9-40618
 rosin films, spectral characters. of light sensitive volume changes 9-28698
 ruby, multiplet impurity bands, method of moments applic. to calc. 9-45313
 saturable, spectroscopic exptl. methods 9-23009
 secondary beam, laser-induced in mol. liquid, obs. 9-32506
 semiconductor, impure, internal electric fields effects 9-24402
 semiconductor, induced absorpt. by nonequil. holes, effect on two-phonon photoconductivity 9-39708
 semiconductor, optical mixing by mobile carriers 9-44952
 semiconductor subject to intense laser beam while in strong magnetic field 9-39828
 semiconductor surface, coeff. behaviour 9-39827
 semiconductors, absorpt. coeff. at low-temp., indirect two-photon transitions 9-37714
 semiconductors, by free electrons, two-photon coeff. 9-31095
 semiconductors, impurity line shapes, effect of resonant phonon interactions 9-26741
 semiconductors, nonlinear, and restriction of light intensity 9-26685
 solid, meas., elimination of surface refl. effects 9-33519
 solids, effect of spatially dependent perturbations 9-24396
 spatial resolution of volume emission coefficient in self-absorbing sources 9-32040
 stilbene crystal, 2-photon, depend. on polarization 9-24375
 stimulated thermal emission, critical absorption coeff. calc. 9-43814

Absorption continued

- light continued
 stimulated thermal Rayleigh scattering in fluids 9-25309
 tetracyanoquinodimethan, coeff. calc. from reflection and transmission meas. 9-39796
 tetraphenylhydrazine, diphenylamino radical dimer as colour centre 9-42855
 thin layer on metal surface, reflection determ. of i.r. spectrum 9-35648
 transition metals, spectra in 3p transition region 9-33561
 in turbid media, new equation 9-36363
 ultraviolet spectra, polyvinyl alcohol films 9-35669
 Urbach's rule impurity absorption for insulators and semiconductors 9-45310
 water vapour, background near 3811 cm^{-1} 9-38845
 water vapour rel. to atm. anomalous absorpt., $337, 311\text{ }\mu\text{m}$ 9-47547
 Ag halide vapours, u.v. cross-sections 9-46376
 Ag halides, induced i.r. absorpt. due to bound polarons 9-46829
 Ag halides, induced i.r. due to excitons generated by band-to-band excitation 9-39830
 Ag halides, spectra of aggregate centres, fine struct. and oscillatory effect obs. 9-39370
 Ag halides, spectra of aggregate centres, fine struct. and oscillatory effect obs. 9-39370
 Ag thin films, abnormal absorpt. in vacuum and gas atmosphere 9-47347
 AgBr, absorpt. edge press. shifts 9-45312
 AgBr, brominated, acceptor ionization energy of neutral Ag vacancies obs. 9-41373
 AgBr, piezo-optic study of exciton and polaron states 9-39814
 AgCl, absorpt., edge press. shifts 9-45312
 AgCl, exciton-phonon coupling effects in spectrum 9-39831
 Al-Zn-Mg 1 type alloy, blue tint of glossy anodized extruded profiles 9-39833
 Al, L shell contrib. to total cross-section 9-45314
 Al SiO_2 -coated, solar absorptivity 9-37373
 Al $_2\text{O}_3\text{:Ti(V, Cr)}$, far-i.r. spectra in applied mag. field, Zeeman splitting of lines, single d electrons obs. 9-31100
 AlN, microcryst., i.r., surface modes and finite size effects obs. 9-37717
 Ar, liq., with Xe and Kr doping far i.r. absorpt. 9-34908
 β -B, rhombic, lattice vibr. spectrum, band edge and free carrier absorpt. 9-39834
 $\text{Ba}_2\text{NaNb}_2\text{O}_{15}\text{:Pt}^{4+}, \text{Ir}^{4+}$, defect-induced absorpt. at $5300\text{ }\text{\AA}$ 9-28651
 $\text{Ba}_2\text{Zn}_2\text{Fe}_{12}\text{O}_{22}$ hexagonal ferrite, and Faraday rotation, 300°K , 1 to $8\text{ }\mu$ 9-45277
 $\text{BaFe}_{12}\text{O}_{22}$ hexagonal ferrite, and Faraday rotation, 300°K , 1 to $8\text{ }\mu$ 9-45277
 $\text{Bi}_2\text{O}_3\text{:TeO}_2$ films 9-35649
 C and coals, absorpt. index, i.r. region 9-24357
 CO_2 , coeff., far u.v. obs. 9-28078
 $\text{CO}_2 \ll \text{P}_{36} \gg$ absorpt. ray anomalies for $\nu_3\text{-}\nu_1$ transition, laser source spectroscopy obs. 9-46359
 CO_2 laser i.r. beam in liquids, thermal self-defocusing 9-26108
 CO_2 laser radiation, P(20) line 9-33772
 CO i.r. down to 113°K 9-32471
 $\text{Ca}_{10}(\text{PO}_3)_6\text{F}_2$, specific absorpt. from OH and oxide ion impurities 9-40933
 $\text{CaF}_2\text{:Dy}^{3+}$, transition time for transfer of Dy^{2+} ions in band 9-47351
 $\text{CaF}_2\text{:GdF}_3$ mixed cryst., Gd^{3+} spectra, energy levels obs. 9-35660
 $\text{CaF}_2\text{:Nd}^{3+}$ at liquid oxygen temp., Nd^{3+} spectra 9-47352
 $\text{CaF}_2\text{:Sm}^{3+}$ crystal, coeff. for charact. freqs. 9-37704
 $\text{CaF}_2\text{:Yb}^{3+}$, Zeeman effect rel. to different site symmetries of Yb^{3+} 9-31103
 $\text{CaF}_2\text{:R}^{3+}, \text{H}^-$ (R=rare earth), i.r. spectra obs. 9-47353
 CaO:Bi , Zeeman splitting of spectral lines 9-33549
 CaO , F^+ and F^+ centres obs. 9-45382
 $\text{CaWO}_4\text{:Nd}^{3+}$, polarized absorpt. obs. of $^4\text{I}_{9/2}\text{-}^2\text{P}_{1/2}$ transition, assignments of ground-state sub-levels 9-39805
 $\text{CaWO}_4\text{:Nd}^{3+}$ at liquid oxygen temp., Nd^{3+} spectra 9-47352
 $\text{CaWO}_4\text{:Tb}^{3+}$, spectra rel. to crystal field parameters 9-33550
 Cd,Hg-xTe alloy, rel. to electronic props. in vicinity of semimetal-semiconductor transition 9-49078
 $\text{CdCl}_2\text{:Ag}$, irrad., band and bleaching obs. 9-49272
 $\text{CdCr}_2\text{S}_4(\text{Se})$ ferromagnetic semiconductor, edge shift, exchange restriction rel. to mechanism 9-45155
 $\text{CdF}_2\text{:Y}$, i.r. band donor conc. and temp. depend. rel. to trapped electron transitions 9-47354
 CdO films, effect of lattice vibrations 9-35613
 CdS , intrinsic, associated with longitudinal optical-phonon assisted 'direct' exciton creation 9-37719
 CdS , spectra, rel. to exciton-phonon interaction 9-37709
 CdS , thin films on Al, peaks in i.r. reflectivity spectra 9-26733
 CdS absorpt., edge, surface effects 9-45316
 CdS films, spectrum, intense ruby laser radiation effect 9-35652
 CdS plastically deformed single cryst., spectra depend. on dislocation density 9-35644
 CdS single cryst., absorpt. spectrum, internal photoeff. in exciton region 9-26603
 CdS single cryst., spectra, intrinsic excitonic correl. with photoconductivity 9-35503
 CdS(Se) , electroabsorption spectrum in exciton region, band structure 9-35625
 CdSe , and emission spectra of bound exciton complexes, 4.2°K 9-37718
 CdSe , structure of absorption edge 9-47355
 n-CdTe:Br , i.r. spectrum 9-26734
 CdTe , i.r., of Be 9-45317
 CdTe , i.r., of Be 9-45318
 CdTe , structure of absorption edge 9-47355
 CdTe films, high elec. fields effects 9-41376
 $\text{CoCl}_2\cdot 2\text{H}_2\text{O}$, antiferromag., far-i.r. mag. reson. absorpt., clustered multipole states obs. 9-33483
 CoF_2 , antiferromagnetic, far i.r. expts., rel. to magnon-optical phonon interaction, temp. depend. 9-47356
 Cr , spectra, 293 and 420°K rel. to mag. props. 9-24359
 Cr_2O_3 , spectrum of excitons, mag. Davydov splittings 9-33552
 Cr and alloys, rel. to itinerant antiferromag. optical and pressure effects 9-45213
 Cs-Ar low-pressure discharge, radial and axial Cs-atom distrib., spectra 9-34801
 $\text{Cs}_2\text{UO}_2\text{Cl}_4\text{:NpO}_2^{2+}$ spectrum, energy level obs. 9-33553
 CsBr , i.r., by U centres 9-26294
 CsCl , i.r., by U centres 9-26294

Absorption continued
light continued

- CsF, F band, temp. depend., mag. circular dichroism and stress-induced behaviour 9-39374
 CsI:Li⁺(Na⁺,K⁺,Rb⁺,Tl⁺) impurity induced far i.r. absorpt. 9-37720
 CsI, i.r., by U centres 9-26294
 CsI thin film, far u.v. absorption spectrum obs. and interpreted 9-37730
 Cu-Ni alloys, i.r. and reflectivity meas. rel. to virtual bound state 9-45269
 Cu₂O, electro-optical absorpt. due to 1s exciton 9-49275
 Cu₂O, exciton line at $\lambda_2=5817 \text{ \AA}$ 9-33235
 Cu₂O, quenched, spectra 9-28683
 Cu₂O, spectrum contour, line broadening and asymmetry w.r.t. exciton-phonon interac. 9-35656
 Cu₂S films, and prep. 9-46727
 Cu₂S films, constant variation for forbidden band width 9-44949
 Cu complex, diphenyl sulphoxide perchlorate, solvent eff. studies 9-24488
 Cu i.r., and reflectivity meas., rel. to virtual bound state 9-45269
 CuCl, spectrum, study of lines ν_4 (25571.5 cm⁻¹) and ν_5 (25501 cm⁻¹), 4.2°K 9-49274
 D₂S, spectra, far i.r. 9-27858
 DCl cry., i.r. spectrum 9-47360
 DyAl garnet, antiferromag., spectrum, Monte Carlo calc. rel. to interpret. 9-24408
 ErFe garnet, spectra at 4.2°, 20° and 62°K, mag. moment and G-factor determ. 9-45319
 ErFeO₃, effect of Y and Bi substitution 9-45061
 Eu chalcogenides, absorpt. edge press. depend. 9-37722
 EuCl₃ aq. soln., Cotton-Mouton effect through absorpt. band 9-39100
 F, u.v., colour centre form, e.s.r. identification of Y impurity 9-40971
 Fe, ferromag., interband, freq. dispersion 9-39836
 Ga, thin film, in different gaseous media, displacement of abnormal absorpt. band 9-45265
 GaAs:Si, compensated, local mode absorpt. and defects 9-47357
 n-GaAs, coeff., by acoustoelastic domains at anode, room temp. 9-37724
 GaAs, energy gap temp. dependence, 300-973°K 9-43249
 GaAs, high resistivity, for i.r. at 82°K 9-49276
 GaAs_{1-x}P_x solid solutions, spectra, temp. depend. 9-33554
 GaAs₂P_{1-x}, low-level interval absorpt. 9-47358
 GaAs diode laser in gas laser resonator, i.r. absorpt. by non equilibrium carriers 9-38383
 GaP, energy gap temp. dependence, 297-1273°K 9-43249
 GaP, i.r., localized vibrational modes of impurities 9-35657
 GaP electrodes, redox processes, photoexcitation obs. of charge transfer 9-30990
 GaP films, vacuum-deposited, absorpt.-edge shifts rel. to structural props. 9-42719
 GaSe spectra for Br impurity effect on energy structure 9-35412
 GdCrO₃, and fluorescence spectrum of Cr³⁺ magnon-assisted 9-49321
 GdF₃, Gd³⁺ spectra, energy levels obs. 9-35660
 GdFe garnet, spectra, 2000-5000 Å 9-35658
 Ge:Au, i.r. absorpt. rel. to hole transitions from impurity levels to valence band 9-44981
 Ge:Bi, i.r. absorpt. rel. to hole transitions from impurity levels to valence band 9-44981
 Ge:Sb far i.r. spectra, excitation lines shift, conc. depend. 9-35659
 Ge, for i.r. studies on shallow impurity states under elec. breakdown 9-28517
 Ge amorphous, sharp absorption edge at 0.5 eV 9-31106
 H₂O, between 0.5 and 36 cm⁻¹, line parameters 9-34620
 H₂S, spectra far i.r. 9-27858
 He-Ne laser Brewster angle attenuator within laser cavity, eqns. of polarization and attenuation 9-31969
 He liquid, of u.v. radiation 9-44565
 Hg_{1-x}Cd_xTe alloys, intrinsic meas., comparison with photoconductivity obs. 9-41266
 HgCr₂Se₄, ferromag., band gap obs. 9-44961
 HgI₂ vapour 9-42612
 HgS, fundamental edge 9-47361
 α -HgS, spectra meas. rel. to valence band splitting 9-28448
 In, thin film, in different gaseous media, displacement of abnormal absorpt. band 9-45265
 InSb, donor-impurity excitation spectra in high mag. fields 9-45320
 n-InSb, i.r. obs. of combined reson. 9-47115
 InSb, induced absorpt. by nonequil. holes, effect on two-photon photoconductivity 9-39708
 InSb_{1-x}Bi_x alloys, optical gap obs. 9-43240
 p-InSb film, fundamental absorpt. edge, at 90 and 300°K, 120-370 Å thick 9-41379
 InTe layers, tetragonal phase, coeff. w.r.t. wavelength meas. 9-41200
 K, atomic spectrum, shift and splitting in laser beam radiation field 9-29937
 K, electron-electron interaction effects 9-49279
 K₂CoF₄ two-dimensional antiferromagnet, 4.2° to 300°K 9-45321
 K₂CsSb photocathode, energy band scheme 9-28584
 K₂O-PbO-SiO₂ glasses, spectra 9-31129
 KBr:Cd, F centres formation obs., correl. with thermoluminesc. 9-33606
 KBr:Ti⁴⁺, band shifts under influence of uniaxial compressive stress 9-31075
 KBr:Zn, F centres formation obs., correl. with thermoluminesc. 9-33606
 KBr-KCl solid solution film, fundamental spectra 9-28685
 KBr-NaBr solid solution film, fundamental spectra 9-28685
 KBr-RbBr solid solution film, fundamental spectra 9-28685
 KBr, F-centre prod. by two-photon absorpt., quantum efficiency 9-44719
 KBr, F centre, lattice and electronic, rel. to lattice dynamics 9-35118
 KBr, F centre spin-lattice relax., theory and meas., 0-50 kG 9-24342
 KBr, i.r., of Li⁺, particle in curved box model 9-47364
 KCl:Ag⁺, stress-induced dichroism in u.v. bands, temp. depend. 9-45322
 KCl:Ca, F centres obs. 9-37191
 KCl:Ca(Cd, Mn, Pb), growth of F and M bands, impurity eff. 9-28686
 KCl:Mg, additively coloured, spectrum obs. 9-48868
 KCl:Mn, optical density under F-band, var. with time, room temp. 9-28303
 KCl:Pb²⁺, spectra, effect of vacancy pairs aggregation 9-31108
 KCl:Ti⁴⁺, band shift under influence of uniaxial compressive stress 9-31075
 KCl, attenuation by colloidal K particles, spectral dependence of coeffs. 9-49278
 KCl, F centre, lattice and electronic, rel. to lattice dynamics 9-35118
 KCl, F centres obs. 9-37191

Absorption continued
light continued

- KCl, simultaneous optical bleaching and X-irrad., e.s.r. obs. 9-42848
 KCl, U₂ centre, continuum theory 9-41380
 KCl, u.v., effect on V₂ centre reorientation 9-35113
 KCl containing NO₃⁻, CO₃²⁻ and SO₄²⁻, i.r. spectra of ion vibrs. 9-41382
 KCl single cryst., conductivity and energy loss spectra, temp. depend. 9-33559
 KClO₃, X-irrad. at low temp., and e.p.r. of ClO₂, ($\Delta M_3=1$, $\Delta M_1=\pm 1$ or ± 2) 9-49352
 KI:(Ga³⁺)₂ spectra, bands due to ion centers obs., electr. struct. 9-35111
 KI:(In³⁺)₂ spectra, bands due to ion centers obs., electr. struct. 9-35111
 KI:Ti⁴⁺, band shifts under influence of uniaxial compressive stress 9-31075
 KI:(Ti⁴⁺)₂ spectra, bands due to ion centers obs., electr. struct. 9-35111
 KI, F centre, lattice and electronic, rel. to lattice dynamics 9-35118
 KI thin film, far u.v. absorption spectrum obs. and interpreted 9-37730
 KMnF₃ single crystal slab, multiple magnons in spectra 9-45326
 Ki, F-centre prod. by two-photon absorpt., quantum efficiency 9-44719
 Ki, F-centre spin-lattice relax., theory and meas., 0-50 kG 9-24342
 La glass, effect of coloration impurities Nd³⁺, Pr³⁺, Cr³⁺, Cu²⁺, Fe³⁺, Ni²⁺, Co²⁺, Mn²⁺ and Ce³⁺ 9-24372
 LaF₃, Gd³⁺ spectra, energy levels obs. 9-35660
 La_{0.5}Fe_{0.5}O₄ spinel ferrite, and Faraday rotation, 300°K, 1 to 8 μ 9-45277
 LiF:H⁺ (D⁺), i.r. absorption due to localized vibrations of ions 9-30619
 LiF, F-band formed by radiation with reactor neutrons and γ 9-35114
 LiF, irradiated, Y-absorpt. band obs. 9-37726
 LiF, N-region absorpt. at 3°K 9-28688
 LiF, TLD, correl. with thermoluminesc. 9-45323
 LiF crystal opt. props. determ., 2-25 μ 9-24373
 LiF with MgF₂ and MgO impurities, spectra 9-41383
 LiNbO₃Cr³⁺ single crystal, rel. to dichroism 9-39803
 LiYF₄:Er³⁺ spectra, Er³⁺ energy levels 9-31107
 LuCrO₃ and fluorescence spectrum of Cr³⁺ magnon assisted 9-49321
 (Mg, Fe):SiO₂, olivine, spectra, 1.7° to 290°K 9-45324
 MgF₂:Co²⁺, far-i.r. spectra, exchange interactions obs. 9-41384
 MgF₂ single crystal, cluster, F- and M-centres due to electron- and neutron-irrad. 9-35117
 MgFe₂O₄ spinel ferrite, and Faraday rotation, 300°K, 1 to 8 μ 9-45277
 MgO, electron irrad., neutron irrad. and additively coloured crystals, zero-phonon line study 9-45325
 MgO, F-band, paramagnetic Faraday-rotation pattern, 1.8°K 9-35116
 MgO single crystal, electron and neutron irrad., colouration and flow stress 9-33099
 Mn₂Fe_{3-x}O₄ ferrites, cubic and tetragonal, i.r. spectra, lattice vibrs. classification and band splitting obs. 9-39841
 MnF₂:Fe²⁺, near i.r. 9-49280
 MnF₂, spectrum, magnon sidebands obs. 9-35661
 MnF₂ single crystal slab, multiple magnons in spectra 9-45326
 MnO, crystal field transition intensities rel. to antiferromag. 9-45252
 MnO, spectra of crystal-field transitions 9-39840
 MnO, spectrum, 300-1.7°K 9-47365
 α -MnS, crystal field transition intensities rel. to antiferromag. 9-45252
 α -MnS, single cryst., spectra, fine struct. 9-43241
 MnTe, rel. to magnon drag contrib. to transport props. 9-24332
 α -MoTe₂ single cryst., photovoltaic spectral distrib. 9-33411
 N₂O, linewidths for 2224 cm⁻¹ band 9-42406
 NH₃ i.r. absorptance, 20 to 35 μ 9-40598
 NH₃OHCl, X-irrad., optical conversion of V₂ centres 9-32995
 NH₃-N mixture, i.r., 20 to 35 μ 9-40598
 NY₂ClO₄, u.v. photon induced colour centres 9-42853
 Na-NaCl system, attenuation coeffs. calc. 9-39790
 Na, electron-electron interaction effects 9-49279
 Na, liquid, plasmon effect 9-44572
 Na, in near i.r. calc. 9-24414
 Na thin films, anomalous absorpt., rel. to bulk metal and effect of temp. 9-35631
 NaBa₂Nb₂O₁₅, spectra, H impurity content obs. 9-41374
 NaCl:Ca²⁺, OH⁻, impurity assoc. effects 9-37728
 NaCl:Cu, additively coloured with Na vapour, colloidal absorpt. bands 9-32998
 NaCl:Cu²⁺, i.r. obs., resonant mode broadening 9-33164
 NaCl:Cu²⁺, stress-induced dichroism in u.v. bands, temp. depend. 9-45322
 NaCl:Pb²⁺, spectra, effect of vacancy pairs aggregation 9-31108
 NaCl, charged F-aggregate centres obs. 9-35119
 NaCl, F centre, lattice and electronic, rel. to lattice dynamics 9-35118
 NaCl, irrad., colour centre conc. rel. to stored energy and release 9-46839
 NaF:H⁺ (D⁺), i.r. absorption due to localized vibrations of ions 9-30619
 NaF, R-band, decrease due to uniaxial plastic deformation of γ -irrad. crystals 9-26297
 NaHSO₄-KHSO₄ melt and glass, Mo V spectrum 9-37729
 NaI thin film, far u.v. absorption spectrum obs. and interpreted 9-37730
 NaNO₂, ferroelec. far i.r. abs., temp. depend. 9-33163
 NbO vapour deposited films, fundamental edge and coefficient 9-30958
 Nd glass during pumping rel. to activator content 9-48029
 Ni₃B₂O₁₃X (W=Cl, Br, I), ferroelec., characts., and crystal field 9-45259
 Ni i.r. and reflectivity meas., rel. to virtual bound state 9-45269
 β -NiAl, band struct. obs. 9-47367
 NiFe₂O₄ spinel ferrite, and Faraday rotation, 300°K, 1 to 8 μ 9-45277
 O₂ coefficient near 1215 Å, and rel. to press. (100 to 760 torr) 9-34638
 O₂ Lyman-alpha spectra, 9-23061
 O i.r. vibration spectrum, effect of precip. of solid solution of Au in Si 9-45315
 PbI₂, electroabsorption in exciton region 9-33539
 PbO, yellow, in polarized light 9-49284
 PbS and PbSe, direct-transition, from relativistic augmented-plane-wave functions 9-41387
 PbTe, direct-transition, from relativistic augmented-plane-wave functions 9-41387
 RbMgF₃-RbCoF₃ ferrimags, 9-47274
 RbMgF₃-RbCoF₃ system, ferrimagnetic single crystals, and mag. props. 9-45186
 RbMnF₃, spectra, thermal shift and broadening of 3975 Å line 9-39844
 RbMnF₃, spectra, thermal shift and broadening of 3975 Å line 9-39845
 S, orthorhombic, in vacuum u.v. 9-37682
 SF₆, i.r. laser rad., saturation rel. to press. and buffer gases 9-48480

Absorption continued**light continued**

- SF₆, narrow reson. in Doppler line of rot.-vibr. transitions of ν_1 band by CO₂-laser emission method 9-46375
 SF₆ gas, transmission of coherent optical pulses 9-46574
 SF₆ mol., of CO₂ laser rad., vibr. excitation 9-25750
 SbSI, ferroelec., anomalous shift of edge near transition point, Kern-Harbecke effect 9-26591
 Se-Te solid solns., edge absorpt. and band gap obs. 9-43250
 Se, amorphous, edge displacement under influence of elec. field 9-35618
 α -Se, monoclinic cryst., comparison in solns. 9-39846
 Se, thin single crystals, spectra near fundamental edge 9-28692
 Se, trigonal, exponential absorpt. edge rel. to crystal orientation w.r.t. incident light 9-41388
 Si:B, i.r. absorpt. rel. to hole transitions from impurity levels to valence band 9-44981
 Si:Bi, impurity line shapes, effect of resonant phonon interactions 9-26741
 Si-containing alloys, i.r. spectra of inclusions 9-35213
 Si, edge modification by radiation-induced defects 9-47132
 Si containing C isotopes, vibr. absorpt. of C and C-O complexes 9-41390
 Si on sapphire film, rel. to thickness and doping density 9-37545
 n-SiC (α (6H) crystals, optical absorpt. in 0.6 μ range from 80 to 1100°K 9-43243
 SiO₂, natural, electron irradi., 'A' band and absorpt. in near i.r. correl. 9-41391
 SiO₂, Rosseland and Planck mean absorpt. coeffs. 9-49548
 Sm activated, quartz glass 9-41407
 SnI₂ and SnI₄ vapour 9-42612
 SrF₂:Nd³⁺, spectra rel. to photoreduction of Nd³⁺ to Nd²⁺ 9-31960
 SrO, additive coloration, absorpt. band and F' centres obs. 9-44721
 SrTiO₃:Cr³⁺(Mn⁴⁺), spectrum obs. 9-26743
 SrTiO₃, coloration by elec. field at 20 V/mm, 100-165°C 9-40976
 Ta-N film, meas. rel. to N content and lattice structure 9-23625
 Tb(OH) ferromagnetic, spectrum rel. to low temp. mag. and thermal props. 9-47401
 ThO₂:Np⁴⁺, spectral analysis of crystal field splitting of J levels 9-35665
 Ti halide vapours, u.v. cross-sections 9-46376
 TiBr₃, absorpt. edge press. shifts 9-45312
 TiCl₃, absorpt. edge press. shifts 9-45312
 TiI films, strain-reduced, exciton-longit. optical phonon coupled state side-band obs. 9-43219
 Xe plasma in continuum, obs. 9-34766
 Y₂O₃:Eu³⁺, spectrum, 'F'₆→'D'₂ transition due to S₆ Eu³⁺ 9-33562
 Y₃Al₅O₁₂, 10- to 55000 cm⁻¹ wave no. 9-35666
 YCrO₃, and fluorescence spectrum of Cr³⁺ magnon-assisted 9-49321
 YFe garnet, energy levels of Ho³⁺ 9-45331
 YGa garnet, energy levels of Ho³⁺ 9-45331
 YVO₄:Nd³⁺, and luminescence and stimulated emission spectra 9-26746
 ZnAl₂O₄, of Cr³⁺ and Fe³⁺, rel. to single-ion mag. interactions 9-45080
 ZnGa₂O₄, of Cr³⁺ and Fe³⁺, rel. to single-ion mag. interactions 9-45080
 ZnO, intrinsic, associated with longitudinal optical-phonon assisted 'direct' exciton creation 9-37719
 ZnP₂, coefficient rel. to photon energy, 1.2 to 2.0 eV 9-35609
 ZnS:Cu, Zeeman effect in 1.44 μ m line 9-24417
 ZnS, spectra of single crystals grown from Ga and In melts, absorption and emission 9-37095
 ZnS epitaxial films, spectrum obs., edge spreading 9-37684
 ZnS epitaxial films, spectrum obs., edge spreading 9-37684
 p-ZnSe:Cu, investig. of imperfections responsible 9-49164
 ZnTe, exciton interpretation of spectra 9-37733
 ZnTe, semicond., interpretation in quantum mech. model, visible band role in nonlinear Pockels' coeff. derivation 9-39811
 ZnWO₄:Co(Ni), spectra 9-37731
 ZnWO₄:Cr³⁺, exp. obs. 9-33563

Abundance ratio see *Elements/relative abundances; Isotopes/relative abundances*

Acceleration see *Dynamics; Kinematics*

Acceleration measurement

see also *Velocity measurement*

- accelerometer axial testing of roller bearings for noise qualities determ. 9-29299
 Atwood's machine, a simple frictionless rotation-free one 9-36101
 g measurement by free fall, apparatus 9-22032
 gravity, laser-interferometer method 9-45730

Accelerators see *Particle accelerators*

Accommodation coefficient see *Gases; Kinetic theory/gases; Surface phenomena*

Acids, inorganic see *Individual compounds, and Hydrogen compounds*

Acids, organic see *Organic compounds*

Acoustic amplification in solids see *Acoustoelectric effects*

Acoustic analysis

- air nuclei distribution determination for cavitation in water 9-22264
 energy-equivalent continuous sound level traffic noise, from street 9-34085
 far-field intensity prediction for partially coherent sound fields from near-field measurements 9-41823
 image reconstruct. from sampled sound-wave hologram 9-34086
 linear distributed system response to homogeneous random field, fast Fourier transform applic. 9-45847
 musical intervals, expt. determ. using 'visible speech' method 9-36185
 noise, Gaussian, white, detect. of known signal 9-29303
 noise, Gaussian, white, detect. of known signal 9-29304
 periodicity of complex signal, meas. method based on time envelope shape 9-38304
 plane sawtooth waves decay inside tubes 9-45854
 waveguides, cylindrical, asymmetries 9-45855

Acoustic field see *Acoustic radiators; Acoustics; Intensity measurement/acoustics*

Acoustic generators

see also *Musical instruments*

- boundary layers, turbulent, influence of an elastic plate on radiation 9-45861
 cavitation void, effect of gas diffusion into cavity on radiation 9-28087
 electrical machines, radiated acoustic power calc. method 9-36172
 electrostrictive mixing of light beams, difference freq. prod. 9-34083
 exploding wire, high intensity underwater sound impulse generation 9-29283

Acoustic generators continued

- organ pipe, using transmission line theory, analysis 9-43790
 piezoelectric transducers, non-uniform, elimination of resonant behaviour 9-34082
 Saturn V, lunar space vehicle (1967), infrasound emission soon after launch 9-27228
 semiconductors, piezoelec., and semi metals, by drifting supersonic carrier fluxes 9-30774
 sound generation by turbulence and surfaces in arbitrary motion 9-25104

Acoustic impedance

- array, periodic, linear, extended, radiation impedance and gain calc. 9-22253
 films, thin, meas. tech. 9-37323
 stilbene, high temp. material for acoustic bonding 9-26416
 Sn, surface impedance behaviour on e.m. excitation of standing wave and quantum oscillations obs. 9-46987

Acoustic mode, crystals see *Crystals/lattice mechanics*

Acoustic paramagnetic resonance see *Paramagnetic resonance and relaxation*

Acoustic radiators

see also *Doppler effect*

- array, periodic, linear, extended, radiation impedance and gain calc. 9-22253
 array, periodic, plane infinite, near field calc. 9-22248
 excitation of mechanical vibrations in nearby structures, theory 9-29239
 gas subject to microwaves as detector and for gas studies 9-28077
 line source near interface between two fluids, exact transient soln., weak shocks onset 9-29266
 loudspeaker, air modulated, performance, theor. analysis 9-29285
 loudspeaker, electrodynamic, secondary resonances of conical diaphragm 9-36182
 magnetostrictors, high power, sound output and efficiency, nonlinear design technique 9-29281
 phase difference from receiver, due to motion of medium 9-25097
 piston in nonrigid baffle, radiation impedance, numerical evaluation 9-29282
 plane boundaries, farfield radiation evaluation, operational method for integral equations soln. 9-27224
 rockbursts and earthquakes, pre-occurrence study 9-47498
 spherical, field at finite distances, Kirchhoff integral computation 9-25095
 spherical, slightly convex, analysis in Kirchhoff approx. 9-36174
 spherical, slightly convex, analysis in Kirchhoff approx. 9-22251
 underwater, liq. modulation, speech communication device 9-27231

Acoustic receivers

see also *Microphones*

- adaptive optimum detect. theory, appl. to recurrence phenomena in noise 9-29287
 bolometric detection of hypersound, 3 GHz and 3.7°K 9-45863
 endfire array, resonant transducer element design 9-29288
 hydrophones, optimum passive bearing estimation is spatially incoherent noise environment 9-43789
 multibeam arrays, directivity, effect of electroacoustic transducer acoustic interaction 9-47827
 phase difference from source, due to motion of medium 9-25097
 signal detect., known, in non-Gaussian noise process 9-29300
 steered beam analysis using shaded linear array 9-29289

Acoustic resonators

- cavity with small aperture, soln. and equiv. circuit 9-22260
 Helmholtz, appl. of cavity with small aperture soln. 9-22260
 Helmholtz, in toroidal microphone as l.f. compensator 9-43788
 Helmholtz, pulsating combustion chambers 9-45838

Acoustic streaming

- in cavitation zone, flow vel. calc. 9-23427
 about spherical obstacles, small, theory 9-25096

Acoustic transducers see *Transducers*

Acoustic wave propagation

see also *Absorption/acoustic waves; Dispersion/acoustic; Doppler effect Helium/liquid, sound propagation; Shock waves; Velocity/acoustic waves*

- in air, free, generation of pulses with finite amplitude, pulse source behaviour and peak press. relationship 9-32735
 atmosphere, acoustic-gravity waves, multilayer approximation 9-41539
 in atmosphere, non-gray radiating 9-26914
 in atmosphere, three transmission anomalies with explanations 9-28902
 benzene-carbon disulphide solns., acoustic relax. obs. and its mechanisms 9-46632
 in channel with range depend. sand speed 9-27226
 in classical fluid, particular soln. of Enskog eqn. 9-44395
 confined beams in nonlinear media without absorpt., equation 9-45848
 creeping and circumferential surface waves 9-45852
 creeping and circumferential surface waves 9-45851
 creeping waves, theory and expt. 9-47823
 near critical point of liquid-vapour system 9-40824
 crystal at liquid-solid transition at T=0, sound wave 9-35273
 crystals, 1-dimen., theory of zero, first and second sound 9-39515
 crystals, energy propag. in cubic, tetragonal and quadratic systems, directions obs. 9-41083
 by dislocation passing through elastic modulus discontinuity plane 9-37353
 distortionsless propag. of one dimen. longit. motion, definition of linear medium 9-38297
 elastic solids, mag. field depend. of stiffness and attenuation 9-35283
 exploding wire, high intensity underwater sound impulse generation 9-29283
 fluids, finite amplitude plane waves, weak-shock approach 9-29309
 in gas, diatomic, kinetic description for plane waves 9-26033
 in gas, effect of mol. dissociation and radiative beat transfer 9-48663
 gas, rarefied, kinetic theory 9-30348
 gases, relaxation time determ. from config. of effective Mach line 9-46570
 in glass, rarefied, free molecule expansion polynomials 9-44525
 glass, T-40, 3rd order elastic const. meas. 9-35141
 Huygen's principle extension, inhomogeneous medium 9-45849
 hydroacoustic signals from CHASE V explosion of Cape Mendocino 9-29268
 impulsive, in fluid sphere of variable internal friction 9-38298
 inhomogeneous media, sound absorpt. associated with heat transfer 9-28119
 inhomogeneous weighty absorbing medium, Huygens sources 9-45850

Acoustic wave propagation continued

- ion, in collision-free, gravity-supported plasma, Landau damping 9-46525
- ion, in plasma, of long wavelength, Landau damping 9-25920
- ionosphere, Faraday rot. obs. from satellite 9-33827
- line source near interface between two fluids, exact transient soln., weak shocks onset 9-29266
- linear medium, definition for one dimen. longit. motion 9-38297
- linearised, in atmosphere, numerical model 9-37931
- liquids, classical, existence of zero sound 9-32761
- liquids, classical, zero sound dispersion law 9-28121
- liquids, thermally relaxing, pulse distortion 9-30392
- magnetic and piezoelec. media, geometrical optics 9-27227
- modulation, acoustic, of large amplitude waves 9-45859
- nonlinear phenomena using optical Bragg diffraction 9-26414
- ocean surface channel propag., surface coupled losses 9-31281
- in oceans, in presence of stochastic boundaries, theory 9-36873
- partially ionized plasma, modulation of discharge parameters 9-36765
- periodic wall-structure, propagation in duct 9-34081
- phase difference between oscillations of sound source and receiver, motion of medium influence 9-25097
- piezoelectric and mag. media, geometrical optics 9-27227
- piezoelectric plates, infinite, simple modes 9-22247
- piezoelectric substrates, surface waves 9-37320
- piezosemiconductors, acoustic wave generation 9-28419
- plasma, in elec. disturbance near-field 9-32656
- pressure wave in gas-liquid system with large void fraction 9-28122
- Pyrex, 3rd.order elastic const. meas. 9-35141
- quartz, cryst., surface waves, 30-800 MHz 9-37319
- α -quartz, surface wave mixing, obs. 9-48950
- in radnom medium, general method for velocity and attenuation determ. 9-36119
- rotational flow at rest at infinity, unsteady, sound generation 9-27949
- second sound detection by scattering piezosecond laser pulses 9-24022
- semiconductor electron-phonon expt. investigation 9-33294
- semimetals, giant sound absorption oscillations, rel. to ang. depend. of amplitude 9-48955
- through shells, thick, uniform spherical radiation 9-29265
- silica, vitreous, 3rd.order elastic const. meas. 9-35141
- past sinusoidal surface, acoustic field analysis 9-29267
- sound generation by turbulence and surfaces in arbitrary motion 9-25104
- spectrum broadening due to ocean wave interference 9-29269
- spherical, with energy losses due to cavitation 9-36867
- spherical radiation, uniform, propag. through thick shells 9-29265
- surface waves on solids, attenuation due to interaction with phonons 9-28416
- through system undergoing phase transformations 9-29270
- temperature and wind stratified atmosphere 9-26915
- undersea, effects of various parameters 9-37899
- undersea, shallow, 1120 Hz signal monitored by hydrophones 5000 ft. away, fluctuations 9-26097
- underwater, computer predictive model 9-45860
- underwater, high intensity impulse generation by exploding wire 9-29283
- viscoelastic material, solns. from superposition principle 9-27208
- water, shallow, isovelocity, normal mode propag. 9-30390
- wave difference equations, computer soln. 9-45860
- waveguide, nonuniform cross section, mode conversion energy 9-36176
- in waveguides, curvilinear analysis of normal modes 9-22252
- waveguides, cylindrical, asymmetries 9-45855
- Ag_3AsS_3 9-30770
- Ar, liquid, zero sound dispersion law 9-28121
- LiNbO_3 , surface wave propagation losses, microwave frequency 9-33173
- LiNbO_3 , surface wave piezoelec. coupling across air gap 9-26594
- Sn, e.m. excitation 9-42956
- Sn, surface impedance behaviour on e.m. excitation of standing wave and quantum oscillations obs. 9-46987
- YFe garnet films, epitaxial, on YAl garnet and GdGa garnet, microwave phonon generation 9-44816

ultrasonic

- biological materials, thermal effects 9-47698
- bolometric detection of hypersound, 3 GHz and 3.7K 9-45863
- characteristics for ranging in air 9-33800
- crystals, analogies with propag. of light waves 9-37325
- in elastic materials, non-homogeneously and dynamically deformed isotropic 9-36177
- evanescent waves, exptl. detection by Bragg diff. 9-36175
- gas binary mixtures, components of diff. mol. wt. 9-26012
- impact excited waves in plane solid sheets, visualization techniques 9-34057
- light diffraction by u.s. standing wave, spectrum analysis by holographic method 9-36320
- liquids, hypersonic relax., temp. coeff. 9-30393
- liquids and solids, meas. methods 9-30768
- magnetostrictive stimulation of domain walls 9-41319
- microwave frequencies, interactions with crystal lattice 9-33170
- mixed salt solutions, concentration depend. rel. to complex formation 9-23491
- modulation of light by u.s. progressive waves 9-34187
- pentachlorobiphenyl, detect. of vitrons at 40 MHz 9-39098
- 1,2-propylene glycol, liq., hypersound propag. obs. from stimulated Mandelstam-Brillouin scatt. 9-30399
- quartz, interaction of two collinear longit. waves 9-46986
- radiator focusing, 60 MHz, using CdS crystal 9-22266
- random medium, covariance between acoustic signals travelling diverging paths 9-27225
- in rock, meas. using automatic pulse system 9-37884
- salol, liq., transversal hypersound propag. and Rayleigh line using fine struct. 9-44573
- solids, optical imaging of multiple microwave u.s. beams by Bragg diff. 9-36189
- solids at high temp., Au-In alloy use as bonding material 9-46983
- superconductors, propag. in magnetically induced structures 9-37464
- triacetin, liq., hypersound propag. obs. from stimulated Mandelstam-Brillouin scatt. 9-30399
- velocities in resonance absorption region, low-pulse, 10 GHz 9-25098
- EuO, attenuation, temp. and mag. field depend. 9-44824
- InSb , generation using ^{115}In spin system 9-46984
- KH_2PO_4 , near ferroelec. phase transition, elastic anomaly and polarization relax. time obs. 9-48949

Acoustic wave propagation continued
ultrasonic continued

- LiNbO_3 , mixing of two longit. waves of different freqs. along (001) direction 9-42959
 - MgF_2 , ceramic, hot-pressed, shear wave meas. 9-46983
 - MnCO_3 , antiferromag., hypersound propag., birefringence obs. 9-46985
- Acoustic waves**
- see also *Diffraction; Interference, etc.; Elastic waves; Shock waves; Ultrasonics*
 - arc plasma in mag. field, low press., ion-sonic vibrations 9-42550
 - atmospheric upward travelling due to earthquake May 1968, Japan 9-43355
 - auroral infrasonic, morphology rel. to supersonic motion distribution 9-41564
 - dielectric crystals, second sound and phonon Poiseville flow, effect of Umklapp-processes 9-46968
 - energy flux from unit area downstream of shock- turbulence interaction 9-34825
 - field theory, finite amplitude, equation of state using volumetric strain 9-36173
 - generation by temp. modulation of plasma 9-23303
 - generation in GaAs, subharmonic 9-30908
 - generation in metals electromagnetically 9-39513
 - gravity, single perturbation analysis 9-31854
 - gravity-, in ionos. F region, ion drag effect on propag. 9-43471
 - h.f. in ideal gases with internal dissipation 9-26031
 - ion-sound, stationary in plasma stream 9-44403
 - ionic crystals, long-wave oscillations 9-26407
 - Kundt's tube, temp. distrib., thermistor obs. 9-45723
 - magnetosonic rays in magnetosphere 9-37934
 - in metals, generation by e.m. radiation 9-26422
 - in piezo-semiconductors, amplification, effects of inhomogeneities 9-48953
 - production by shock-turbulence interaction, expt. 9-42602
 - production of compressional waves in metals in static mag. fields, e.m. generation 9-37322
 - reflection from vacuum-piezoelectric crystal boundary 9-44819
 - relation with neutron waves 9-29860
 - in semiconductors, nonlinear interaction, theory 9-41088
 - in spin-phonon system, thermal noise analysis 9-30760
 - underwater, wavefront variations caused by internal waves 9-30391
 - u.s., oscillations in magnetized media 9-44814
 - in GaAs, subharmonic generation 9-30908
 - He cryogenic plasma, excitation and damping of oscillations 9-48606
 - InSb , generation of ultrasound using ^{115}In spin system 9-46984
 - InSb , high mobility, sound wave amplification, 0.5-2 GHz 9-39522
 - Ne ionic, rel. to moving striations 9-48636
- effects**
- see also *Chemical effects of radiations/acoustic waves*
 - aerosol generators, u.s. concentrators, design parameters 9-29291
 - aerosols, in sound field, particle interactions regularities, expt. and theory 9-26138
 - amplification with piezoelec. plate coupled to n-Si 9-26419
 - beams, uniform, response to homogeneous random press. fields 9-29247
 - Bragg diffraction of laser beam, relative efficiency as function of interaction geometry 9-34211
 - breakdown, microwave, of low pressure gases, resonant sound pressure meas. 9-32707
 - bubble growth kinetics in acoustic field, effect of surface active substances 9-46601
 - cavitation bubble dynamics in 20.5 KHz u.s. field 9-34855
 - cavitation in liquids, dimensions smaller than wavelength, cinecamera study 9-23488
 - crystal nucl. mag. energy levels in rotating frame, excitation 9-35601
 - dialysis, effect of ultrasound on diffusion rate 9-34893
 - diffusion, convective, liq.-solid interface, accel. by u.s. sound field 9-23615
 - electrodeposition of metal in sound field, localization of deposit 9-47469
 - flow, viscous fluid, interaction with intense acoustic fields 9-32578
 - fountain, u.s. in liqs. influence of static press. on height 9-23490
 - hailstones, induction of cavitation by u.s. waves 9-45491
 - holographic image by electronic means 9-27230
 - holographic imaging 9-48058
 - hydrolysis of sucrose solns., non-cavitating ultrasound 9-37821
 - ionosphere, F region, elec. field excitation 9-43468
 - ionosphere, ionization velocity effect of polarization field 9-41578
 - ionosphere decametric wave Doppler effect 9-41574
 - laser, ruby, u.s. modulation 9-48072
 - light diffraction in anisotropic media, modified Bragg formalism 9-27387
 - liquids, atomization, mechanism 9-46626
 - magnetostrictive stimulation of domain walls by u.s. 9-41319
 - Mossbauer line narrowing by u.s. vibrations with decaying amplitudes 9-26717
 - organic liquids, ultrasound effect on viscosity 9-42637
 - phonic desorption of impurities from walls of a vacuum vessel 9-40217
 - plasma, ion acoustic, transient sheath formation 9-23304
 - polystyrene, effect of ultrasound on stressed state 9-46880
 - rod, linearly elastic, semi infinite, response to time varying press. applied at end 9-29248
 - shell, spherical, elastic, transient interaction with plane pulse waves 9-22254
 - shells, spherical, submerged, h.f. response to radial point force 9-25102
 - solubility of gases in liq., reduction in sound fields, mechanism 9-46612
 - toluene, ultrasound effect on viscosity 9-42637
 - triglycine sulphate, polarization switching processes, effect of u.s. vibrations 9-47183
 - u.s. modulation of light, theory and expt. 9-32021
 - Al_2O_3 , double ^{51}Cr - ^{27}Al acousto-nuclear mag. reson., 4.2K 9-49359
 - Al single crystal, plasticity and elec. cond. macroscopic effects 9-46928
 - Au sol, u.s. induced birefringence 9-36908
 - CdS, current oscill. stimulated by external u.s. signal 9-48965
 - CdS, on conductivity at 10-45 MHz 9-39619
 - Cu, u.s. hardening at 90K, influence of pre-annealing at room temp. 9-28374
 - Cu electrode, electrodeposition and dissolution in standing wave sound field 9-47468
 - n-GaAs, donor ionization, h.f. phonon generation and detection 9-39520
 - NaCl single crystal, excitation of Na nucl. mag. energy levels in rotating frame 9-35601
 - n-Si coupled to piezoelec. plate, amplification 9-26419

Acoustical laboratories

No entries

Acoustical measurement

see also *Interferometry/acoustic waves; and under separate subjects e.g. Intensity measurement/acoustics*
 cables, mechanical, in oceanic engineering, acoustic structural failure detec. method 9-38302
 crystals with zero defectons, props. 9-40927
 filter characteristics expt. determination, for use in pulsating gas flows 9-43794
 Mossbauer effect appl. 9-34088
 musical intervals, expt. determ. using 'visible speech' method 9-36185
 oceanographic 9-24631
 polymers, liquid, rheological properties 9-36835
 pulse-echo, of U.S. velocity and absorption in liquids, computer program for data reduction 9-42649
 sonometer for musical expts. 9-36186
 ultrasonic rel. in liq., semi-automatic meas. method 9-46630
 u.s. pulses in liquids and solids, methods 9-30768

Acoustics

see also *Acoustic resonators; Architectural acoustics; Atmospheric acoustics; Hearing; Noise/acoustic; Sound reproduction; Speech; Ultrasonics; Vibrations*

bond, acoustic, for mercury, low temp. 9-31722
 cavitation fields, control 9-36833
 computers, digital, use in acoustic research 9-29260
 holography, image distortion in reconstructions from phase-only holograms 9-36192
 holography, non-time-averaged instantaneous 9-36193
 holography, phase-only 9-29440
 holography techniques and applications 9-48067
 integral equations in radiation problems, nonexistence and nonuniqueness failures 9-29263
 integral formulation, improved, of radiation problems 9-29264
 lenses, imaging charact. 9-36196
 musical, octave notation, need for conformity 9-29290
 openings, annular baffled, radiation efficiency of higher order modes 9-41822
 openings, baffled, acoustic props. at l.f. 9-41821
 sound intensity estimations, comparison of two methods 9-29262
 stereophony, head orientated, efficiency 9-41820

musicalsee also *Musical instruments*

No entries

Acousto-optical effects

castor oil, acoustically induced birefringence study 9-23495
 elastic second harmonic generation by u.s. waves, Bragg diffraction study 9-26679
 gas acoustic pulse prod. on absorpt. of microwaves, as detector and for gas analysis 9-28077
 light beam traversing plane piston transducer's sound field, integrated optical effect. 9-22249
 radiation behind shock wave in simulated Martian atmosphere 9-23385
 radiation detectors in gas analysers, sensitivity and selectivity 9-37851
 tuning, optical, parametric oscillators 9-25232
 wideband deflectors using acoustic beam steering 9-36188
 CdS, stimulated Brillouin scattering, threshold and direction control 9-48960
 α -HIO₃ soln. grown crystal, acousto-opt. device applic. 9-37326
 PbMoO₄ crystal, melt grown 9-49254

Acoustoelasticity see *Elasticity***Acoustoelectric effects**

amplification of acoustic wave in piezoelectric semiconductor, analysis using root-locus techniques 9-28423
 amplification of transverse u.s. waves by CdS 9-47824
 device operation modes and basic physics of acoustoelectrics 9-41245
 domains propag. in piezoelec. III-V semicond., evolution 9-37349
 geometrical optics of acoustic waves in piezoelec. media 9-27227
 interaction at large amplitude, saturation mechanism 9-35284
 liquid, electroacoustic wave dynamics 9-40788
 liquids, electroacoustic wave, solitary, stability 9-42648
 parametric amplification of u.s. waves 9-37342
 phonon generation observed in X-ray diffraction microscopy 9-46997
 piezo-semiconductors, static domain 9-37350
 piezoelectric III-V semicond., evolution of propag. acoustoelec. domains 9-37349
 piezoelectric materials, nonuniform, sound generation 9-37348
 piezoelectric semicond., amplification under large signal conditions 9-33177
 piezoelectric semiconductor transducers, modification of energy conversion process by effects due to carriers 9-34084
 piezoelectric semiconductors, nonlinear limiting of acoustic wave amplification 9-28422
 plasma, electroacoustic wave dynamics 9-40788
 plasma, noise radiation at reson. freq. 9-44423
 quartz, Bechmann's number for harmonic overtones of thickness-shear vibs. 9-31848
 semiconductor, coupling coeff. temp. dependence rel. to electron-phonon expt. investigation 9-33294
 semiconductor, nonpiezoelectric, with ambipolar conduction, amplification by elec. field 9-33175
 semiconductor, piezoelec. domain theory, nonlinear interactions 9-48963
 semiconductor, piezoelectric, domain theory, linear regime 9-48962
 semiconductor, piezoelectric, domain theory, soln. 9-48964
 semiconductor, rel. to non-linear effects in u.s. amplification 9-37347
 semiconductor, shock strained, Boltzmann equation and wave-particle drag 9-37513
 semiconductor crystals with high permittivity, waves interaction with carriers 9-28424
 semiconductor u.s. absorpt. in uniform elec. field 9-41085
 semiconductors, nonlinear theory of acoustic wave interac. 9-37351
 semiconductors, piezoelec., amplification under large signal conditions 9-33177
 semiconductors, piezoelec., amplification and generation of acoustic waves 9-30774
 semiconductors, piezoelec., static domain 9-37350
 semiconductors, piezoelec. III-V, evolution of propag. domains 9-37349
 semiconductors with arbitrary degree of degeneracy, u.s. amplification 9-35281

Acoustoelectric effects continued

semimetal u.s. absorpt. in uniform elec. field 9-41085
 semimetals, amplification and generation of acoustic waves 9-30774
 skin-effect acoustic generation in conductors, approx. theory 9-42962
 static domain in piezo-semicond. 9-37350
 surface waves in piezoelec. or conducting solids 9-28425
 Bi, acoustomagnetoec. effect meas. rel. to electron-hole recombination temp. dependence, 2-50°K 9-35306
 CdS, acoustic shear-waves generated by supersonic electrons, Brillouin scattering study 9-46996
 CdS, after-sounding effect 9-37522
 CdS, current oscills. stimulated by external u.s. signal 9-48965
 CdS, domain form., Brillouin scatt. obs. 9-43055
 CdS, domain formation at high elec. fields 9-46998
 CdS, phonon frequency spectra of travelling acoustoelectric domains 9-26421
 CdS, phonon generation observed in X-ray diffraction microscopy 9-46997
 CdS, phonon spectra of acoustic domains 9-37312
 CdS, photocond., conductivity variation of non-ohmic behaviours 9-43053
 CdS, pulsed u.s. meas. rel. to attenuation and trapping obs. 9-24031
 n-CdS, second sound-acoustic electron-wave interaction, effect on distributed acoustic amplification 9-30775
 CdS, semicond., acoustic domains, Brillouin scatt. meas. 9-35397
 CdS, semicond., parametric amplification of acoustic shear waves 9-37343
 CdS, u.s. amplification with continuous drift field at 20°C 9-35282
 CdS photoconductive single cryst., electromech. coupling const. correl. with resistivity inhomogeneities 9-35502
 CdS second current saturation of non-ohmic behaviour 9-47107
 CdS semicond. tapered samples, acoustic domain studies 9-37521
 CdS thin-film transducer, U.S. transverse wave amplification 9-47824
 CdSe, after-sounding effect 9-37522
 CdSe, current fluctuations, spectral power 9-33296
 CdSe, rel. to current saturation and oscillation mechanism 9-26543
 CdSe, photoconducting, amplification, and acoustic noise 9-33176
 CdSe 9-47103
 n-GaAs, acoustoelec. domains, Brillouin scatt. studies 9-37352
 GaAs, current instability and threshold field under acoustic amplification 9-28499
 GaAs, current saturation induced by sound amplification, nonlinear theory 9-47111
 GaAs, domain motion rel. to current oscillations 9-35399
 GaAs, domains, Brillouin scatt. obs. 9-44958
 n-GaAs, domains, rel. to modulation of near i.r. radiation, room temp. 9-37724
 n-GaAs, generation and detection of 10¹² Hz phonons 9-49083
 n-GaAs, instabilities rel. to inhomogeneities of Ohmic resistivity, from optical probing 9-49080
 GaAs, interaction, piezoelec. elastic anisotropy effects 9-41090
 n-GaAs, microwave emission study of acoustic freqs. in acoustoelec. domains 9-48966
 n-GaAs, second sound-acoustic electron-wave interaction, effect on distributed acoustic amplification 9-30775
 GaAs, subsonic acoustic domain 9-24032
 GaAs, trap-controlled bunching of electrons in acoustoelec. domains 9-44976
 n-InSb, amplification in transverse mag. field 9-24028
 n-InSb, decay of domain and microwave emission 9-35402
 n-InSb, microwave emission enhanced by acoustic cyclotron resonance 9-48967
 ZnO, acoustic shear-waves generated by supersonic electrons, Brillouin scattering study 9-46996
 ZnO single crystals, high electric field effects 9-47116

Acoustomagnetic effects see *Magnetoacoustic effects***Actinide compounds**

No entries

Actinides

No entries

Actinium

No entries

Actinium compounds

No entries

Actinometry see *Photometry***Activation analysis** see *Chemical analysis/by nuclear reactions***Active nitrogen** see *Nitrogen***Active oxygen** see *Oxygen***Adhesion**

acoustic bond for mercury, low temp. 9-31722
 cements for chemical bonding of alumina powders 9-35229
 diamond-metal interaction 9-23930
 elastic contact of two rough cylinders 9-36156
 epoxy resin, use at low temp. 9-26382
 glass substrate-Au film, adherent intermediate layer, mechanism determ. 9-39480
 glass to metal, effect of ultrasonic vibration 9-28388
 kinetic, theory interpretation for slider on moving disc 9-44797
 metal/alumina interfaces, corals. with strengths 9-23903
 plastic, use at low temp. 9-26382
 polyethylene, yield strength 9-30734
 polyethylene-stainless-steel lap joints, yield strength 9-30734
 powder particles, electrostatic contact. 9-44798
 punch in contact with elastic half-space rocking and translation parallel to plane, soln. 9-38279
 solid surfaces, clean, investig. methods 9-28203
 spheres, two, due to liquid 9-37297
 steel, of Al chemically vapour deposited coating 9-28376
 thermal characteristics of adhesives 9-37364
 varnish, use at low temp. 9-26382
 viscoelastic materials, to rigid substrates, peeling force meas. 9-35239
 Au/Au contacts, w.r.t. contact resistance 9-33132
 Au/Pt group metal contacts, w.r.t. contact resistance 9-33132
 Fe, chemisorbed film effects 9-37272
 Ge surface, variation when modified by alkylchlorosilane 9-48924
 Pt/Pt contacts, w.r.t. contact resistance 9-33132
 Si oxidized substrate-Au film, adherent intermediate layer, mechanism determ. 9-39480

Adiabatic demagnetization *see* **Magnetic cooling**

Adion *see* **Adsorption**

ADP (ammonium dihydrogen phosphate) *see* **Nitrogen compounds/ammonium compounds**

Adsorbed layers

- condensation, lateral intermol. force constant determ. 9-23593
Fermi atoms adsorbed on substrate at low temp., specific heat 9-46730
gases on C surface, condensation 9-23592
immobile films formed by dissociative chemisorption 9-26816
i.r. spectra of adsorbed molecules, review 9-42367
on metal surfaces secondary electron emission following bombardment by atomic and molecular beams 9-31007
molecular complexes on active substrates, dissoc. equil., refl. meas. 9-39166
monomer cluster distrib. on one-dimens. lattice, matrix method calcs. 9-34997
polymer spheres in monolayer, crystal structure demonstration by laser light diff. 9-47712
protein, film hysteresis and stress-relax. 9-23450
pyridine on porous glass, i.r. spectra 9-26196
radiolysis 9-24591
surface layer on model cryst., influence on vibr. props. 9-37311
tunneling of field emitted electrons from W, through Zr and χ -N 9-30960
water, effect on wetting props. of borosilicate glass, quartz and sapphire by hydrophobic liq. 9-34978
water on metal surfaces, effect on critical surface tension of wetting 9-23437
weighting, automatic apparatus 9-38189
Al, or C or O, identification of contamination by nuclear reaction analysis 9-26178
Au on KCl crystal, surface diffusion, 130-500°C 9-40848
BaO by GaAs, eff. on photoelec. emission from GaAs 9-26614
CO chemisorbed on Rh, Ir and Pt, i.r. spectra, temp. effect 9-43325
CO on metal films, i.r. absorption spectra 9-26193
Cs by GaAs, eff. on photoelec. emission from GaAs 9-26614
Cs on W, decay rate of surface plasmons 9-32849
on Fe, chemisorbed films effect on friction and adhesion props. 9-37272
H₂O, dielectric props., changes during adsorption by solids 9-48716
He superfluid, third-sound obs. 9-34946
⁴He monolayer, quantum theory 9-23557
N₂O on silica gel and Zirconia, radiolysis 9-24591
 χ -N on W, tunneling of field emitted electrons 9-30960
PbS polycrystalline film, chemisorbed O, effect on photocond. props. 9-37622
W, of metals, cluster form of diffusing atoms 9-40851
W, of U, to twelve monolayers, work function rel. to deposit growth 9-32850
Zr on W, tunneling of field emitted electrons 9-30960

Adsorption

- see also* **Chemical analysis/adsorption; Chromatography; Films**
Heat of adsorption; Sorption
adatom interactions, indirect, through AB-type cryst., rel. to surface states 9-34998
c blacks, surface area and porosity eval. 9-23645
Ceto alloy, effect of Ti additive 9-36965
cluster distrib. on one-dimens. lattice, matrix method calcs. 9-34997
field-emission examination technique 9-41277
gas mixtures, thermodynamic approach 9-34996
gas-solid interactions at ultra-high vacuum 9-39152
glass, of benzoic acid, rate and magnitude meas. 9-30502
graphite, of Ar, fourth-order interaction using third virial coeff. of 2-dimens. Lennard-Jones gas 9-42605
graphite, of He and Ne atoms, quasiharmonic freq. shifts. 9-48769
graphite, of I, and desorp., in vacuum and Ar, 27-1100°C 9-28221
interface reactions, press. effects 9-24531
ion desorption, electron-induced, from Pt, Pt-Ir, Mb; u.h.v. gauge, mass spectrometric investigation 9-38178
isotherms determ., volumetric method 9-39165
localized vibration mode, modification of energy and preexponential factor 9-48768
low vapour pressure materials, i.r. spectroscopy 9-36383
metals, of CO, i.r. spectra obs., effect of other gases 9-35002
molecular complexes on active substrates, dissoc. equil., refl. meas. 9-39166
molecular sieve, struct. of adsorbed NO 9-39167
physical, virial expansion treatment 9-40847
polymer chain, conformation 9-30503
polymers, of water vapour 9-42736
Pyrex, of N at very low pressure 9-36969
rubber, gas desorption and permeability in vacuum 9-39178
silica, microporous, prep. by freeze-thawing technique 9-46732
silica gel, fibrous, of aliphatic normal alcohol monolayer 9-23649
silica gel, mag. susceptibility of adsorbed NO mols. 9-44631
silica gel, role of surface hydroxyls 9-48723
silica gel, H-bonding in interaction of adsorbed mols. with surface OH groups 9-23650
silica glass, of water vapour 9-42736
for solid bodies in non-corrosive liquids, effect on mechanical props 9-44629
steel, stainless, of H₂ and H₂-Ar exchange 9-39170
sticking coeff. and desorption rate variations during condensed gas layer growth on liq. He cooled surfaces 9-48770
in upper atmosphere density meas. 9-45503
water vapour, as pore struct. analysis method, t-curves 9-35052
zeolite X and Y, sodium cation adsorption sites 9-24521
zeolite Y, of aromatic hydrocarbons, i.r. spectroscopy rel. to surface interactions 9-24520
zeolite Y, of pyridine, i.r. spectroscopy rel. to adsorbent surface props. 9-24519
zeolites, effect of sorbed mols. on quadrupole coupling constants of ²³Na and ²⁷Al 9-43300
 γ -Al₂O₃, of pyridine, active centres nature, i.r. obs. 9-26192
Ar, of H, influence of temp. history, ⁹K 9-36966
Ar (100) sfacc, adsorp. and diffusion of Ar atoms on three possible structs. 9-35000
Au of Co and H₂, spectroscopic obs. 9-35001
Ba thin film, Ar desorption, temp. dependence 9-40849
Be, adsorption of N, H, O, CO on thick film obs. 9-36964
CdI₂ of organic mols., stimulation and extinction of excitonic transitions 9-26194

Adsorption continued

- CdS, of oxygen in dark and photoadsorption, LEED obs. 9-28211
CdSe films, of O, rel. to simultaneous variation of conductivity and space charge region 9-30905
Cr, gettering effect, detection during evaporation and condensation in vacuum 9-30457
CuI absorption edge, donor-acceptor interactions and adsorption of organic mols. 9-25739
CuI of organic mols., stimulation and extinction of excitonic transitions 9-26194
D₂, sticking coeff. and desorption rate changes with condensation conditions and history of layers 9-48770
Fe thin coatings, of Hg, effect on elec. cond. 9-37428
n-, α -Ga₂O₃ of O, effect on elec. conductivity 9-49081
Ge, of CO, effect on donor and acceptor character of surface states 9-43074
n-Ge, of Hz effect on elec. props. 9-39642
Ge, studies of internal recontacted splits 9-42846
H-Ni system, desorption kinetics for binding states 9-23646
H₂, sticking coeff. and desorption rate changes with condensation conditions and history of layers 9-48770
H₂ on silica-supported Pt and silica, i.r. spect. study 9-30044
H on glass surfaces, 300-500°K 9-40850
HgI₂ of organic mols., stimulation and extinction of excitonic transitions 9-26194
Kr, on cleaved faces of adsorbents with lamellar struct., formation of first condensed layer 9-48776
LaBe cathode poisoning 9-42731
LiF films, u.v. spectra of adsorbed Xe and CO 9-44630
Mo(100), adsorp. of O₂, low-energy electron diff. 9-42732
NaCl, colour centres due to ⁶⁰Co- γ -irrad. effect of gas adsorp. 9-48869
NaCl pellets, octahedral, of urea and PbCl₂ 9-48771
NaY zeolite, adsorbed anthracene mol. state, luminesc. obs. 9-28222
Ni, of O, S, and Se whose structure is examined by ion neutralization spectroscopy 9-32484
Ni (100), of N₂O, NO and CO₂, interactions and effect on work function 9-35003
Ni ultraclean thin films, of gases, compressive intrinsic stress release obs. 9-44758
PbTe, of polar mols. rel. to surface charge distrib. exam. 9-39173
Pt-Al₂O₃ catalyst, surface transport of various gases 9-26195
Pt, of O₂, on oriented field emitters 9-23648
Pt, phenomena, investig. by potentiostatic method 9-46731
SbSI, of O₂, eff. on elec. conductivity, photoconductivity and work function 9-30496
Si, of H rel. to atom recombination kinetics on differently oriented planes 9-36968
Si, studies of internal recontacted splits 9-42846
SiO₂ aerogels, adsorp. of Ar and N₂ 9-30498
SiO₂ gel, e.s.r. of adsorbed Cl atoms 9-39174
SiO₂ gel, e.s.r. of adsorbed Cl atoms 9-30497
Ti, of O₂, study at 273, 195 and 77°K 9-48772
Ti₂HgGeO₄·4H₂O, of water and Ti, n.m.r. obs. 9-33650
V(100), gas adsorp., low-energy electron diffraction 9-30500
W, adatom diffusion process for surface self-diffusion 9-44622
W, adsorbate effects on electron ejection by metastable atoms 9-31002
W, adsorp. and decomp. of NH₃ 9-48774
W, adsorp. and decomp. of NH₃ 9-48773
W, flash decomp. of adsorbed, acetylene, ethylene, ethane and methane 9-43327
W, O₂, rel. to thermal faceting of single cryst. 9-35012
W, of ³He, small energy accommodation coeffs., classical theory 9-35004
W, of CO, field emission from single planes 9-39176
W, of Cs on single-cryst. planes 9-39175
W, of H₂ and N₂ simultaneously at 300°K, obs. 9-23651
W, of methanol, photoelectron spectroscopy rel. to orbitals involved in bonding 9-44634
W, of O₂, N₂, H₂ and CO, surface potentials determ. 9-48775
W, of Sr, field emission 9-24251
W, oxygenated and carburized, of Ag and Au, lifetimes and binding energies 9-39177
W (100) surface, of O₂, N₂, CO₂ and H₂ rel. to work function changes 9-42734
W accommodation coeffs. of ⁴He and ³He on clean surface 9-30501
Xe, on cleaved faces of adsorbents with lamellar struct., formation of first condensed layer 9-48776
Zn, anisotropy of loss of strength 9-23911
ZnO, exposure to oxygen effect on LEED patterns 9-28211
ZnO, of H or O, rel. to poplar surface props. 9-42741
Zr, 2-d crystals on W and Nb, binding energy from temp. depend. of growth 9-23652

Aerials *see* **Electromagnetic waves/radiators**

Aerodynamics

- see also* **Flow/gases; Jets; Shock waves; Supersonic flow; Turbulence**
aerofoils, lift fluctuations due to gust parallel to undisturbed flow 9-26011
aerospace simulation, conference, Farmingdale, NY, USA (1969) 9-48652
air props. changed in neighbourhood of high speed vehicle 9-34822
airfoil, rotating, boundary layer theory for incompressible layer 9-26004
airfoils, thin, in nonequilibrium MGD, aligned magnetic field 9-27965
attachment line calc. and expt. in wind tunnel, for swept wing 9-39037
boundary layer near windward generator of cone, 3 dimens., with uniform mass transfer 9-26010
control surfaces at Mach 6, turbulent heat transfer 9-26006
convection boundary layer on plane vertical isothermal wall, stability criteria 9-25126
cylindrical shell, circumferentially travelling wave flutter, limiting amplitudes, nonlinear anal. 9-22243
design of body to produce specified sonic boom signature 9-26013
disc, rotating, free-flight stability modelling 9-40738
drag, forebody, minimization in supersonic flow 9-32727
flat plate, lift and drag at low Reynolds no., variational calc. 9-34817
flat plate unsteady boundary layer, incompress. laminar 9-30174
flow, separated, dividing streamline and momentum integral analysis, semi-empirical parameters 9-38944
flow around circular cone, non-linear equations soln., integral relations method 9-46562
flow fields, low density, quantitative visualization by electron beam excitation technique 9-48650

Aerodynamics continued

- flow over ridge, lee waves numerical cal. 9-43389
 flow over ridge, lee waves numerical calc. 9-37912
 gas binary mixtures, components of diff. mol. wt., two-temp. hydrodynamics 9-26012
 gases, rarefied stream, pressure measuring systems time delay 9-43715
 helicopter blade, flapping torsion flutter during forward flight 9-23387
 helicopter rotors, wind tunnel constraint effects 9-23389
 hypersonic flow around blunt body, heating theory 9-26007
 hypersonic laminar flow, boundary layer transition on blunted cones, heat transfer 9-36800
 hypersonic wake diagnostics, electrostatic probes, use and calibration 9-48649
 laminar wake, compressible, behind long, slender cylinder, theory and expt. 9-23381
 lift and stability of delta wings 9-32727
 nonplanar oscillating surface problem, used complex cross-flow representation 9-22229
 optical visualization of flow 9-46450
 oscillating foil in plunging or pitching modes, flow and lifting problem 9-23410
 overpressure peak at foot of vertical wall facing air blast 9-34823
 particle motion in wind tunnel 9-39040
 pressure transducer, pneumatically operated, calibrator 9-45731
 prismatic bodies, resistance coefficient, initial turbulence effect 9-44516
 rain gauges, airflow around 9-49445
 rarefied gases, kinetic theory, and gas-solid interaction, book 9-44519
 reverse transition criteria for turbulent boundary-layer flow 9-34824
 rotating cylinder in flow at slanting angle 9-39039
 roughness drag, heat transfer eff. 9-23386
 sails, 2-dimens., interaction for smoothly attached flow of inviscid, incompressible fluid 9-34827
 sandwich panels in supersonic gas flow, dynamic stability and vibrations 9-22231
 shock tubes for diffusor study 9-42599
 shock-turbulence interaction, acoustic waves production, experiment 9-42602
 skin friction, derivation of Karman-Schoenherr formula 9-28072
 skin friction balance 9-28069
 sonic boom, energy spectral density derivation 9-29308
 sonic boom, minimum shock strengths and overpressures eqn. for given conditions 9-40740
 sphere and core drag corrls. at hypersonic speeds 9-26005
 supersonic, holography 9-31985
 supersonic flow of viscous heat conducting gas, asymptotic damping of disturbances, second approx. derivation 9-23384
 surface, moving, pressure due to atmospheric turbulence 9-46560
 transonic, textbook, with theoretical aspects stressed 9-32726
 turbines, partial admission, losses 9-39038
 turbulent boundary layers on porous flat plate with injection 9-30330
 turbulent flow in low speed wind tunnel, diffusion characts. 9-36826
 wake, axisymmetric compressible, turbulent front struct. 9-28070
 wing oscillation in transonic flight, calc. of forces 9-23388
 wings of complex shape, flow charact., numerical analysis 9-42600

Aeronomy see *Atmosphere; Meteorology*

Aerosols

see also *Foams*

- α -active, charging by secondary e emission 9-26139
 atmosphere, absorption coeff., vertical statistical structure 9-24654
 atmospheric, concentration and size distribution determ. 9-41516
 atmospheric, effect on elec. field near ground 9-43398
 atmospheric, interaction with ground surface 9-35828
 atmospheric, reviewed 9-43385
 atmospheric, study by light scatt., photometric meas. 9-40053
 atmospheric, U.V. decomposition 9-24588
 atmospheric above 18000 ft., attenuation of downward solar radiative flux 9-41519
 atmospheric hygroscopic particles, effect on backscattered power of laser beam 9-41529
 droplet velocity rel. to concentration, Fabry-Perot laser interferometer obs. 9-42685
 generators, u.s. concentrators, design parameters 9-29291
 in ionosphere, lower, ion pair annihilation 9-43439
 in Jupiters atmosphere, effect on emitted polarised light 9-29068
 monodisperse, generation using disintegrated liquid jet 9-34933
 oil drops and smoke particles in gas having temp. gradient, random motion obs. 9-26022
 particle concentration and size distribution, determination, apparatus, patent 9-34934
 particle initial vel., dimensions eff. on trajectory, expt. and theory 9-30439
 particle size determ. using light scatt. counters, influence of refractive index 9-28889
 powder-gas, two-phase shock tube obs. of oscillator strengths 9-28161
 protein, electronic deposition of nebulized aerosol for e. microscopy 9-42686
 size classifier, sub-micron, calibration 9-34932
 size distribution from spectral attenuation meas. 9-36905
 solar beam attenuation at high altitudes 9-47544
 in sound field, particle interaction regularities, expt. and theory 9-26138
 spherical atmosphere, light scattering 9-37917
 stratosphere, spectral extinction coeff. statistical structure of vertical profile 9-40035
 stratospheric, infrared and lidar obs. 9-31297
 in troposphere and stratosphere 9-40014
 tropospheric and stratospheric concentration from daytime meas. of sky polarization 9-45490
 RnA and RnB, distrib. of decay products calc. in different shaped volumes of air 9-22761
 RnA and RnB, distrib. of decay products calc. in different shaped volumes of air 9-34424

Afterglow see *Discharges, electric*

Ageing

- alkali metal niobates based highly dense piezoelectric material 9-39676
 alloy E1437B, up to 20 hrs., 700-850°C, effect on fine structure in X-ray diff. exam. 9-41047
 binary solid solutions, coherence loss, X-ray exam. 9-30711
 Ferrovac E iron, strain ageing behaviour rel. to applied ageing stress and interstitial conc. in soln. 9-41050

Ageing continued

- martensite, C-bearing, kinetics 9-39462
 Ostwald ripening, volume diffusion-controlled, particle size distribution 9-39460
 permalloy films, anisotropy ageing, annealing obs. 9-37660
 polyethylene, high density, under mechanical stresses 9-46930
 steel, austenitic, strength and hardness, effect of previous deform. 9-33059
 steel, austenitic containing Al and Ti, soln.-treated, equil. precip. formed obs. by electron microscopy 9-46949
 steel, H-11, vacuum-melted, effect on mech. props. 9-46904
 steel, strain ageing effects on brittle cracking susceptibility 9-39439
 steel castings, 18-8 Mo stainless, high temp. strength obs. 9-44771
 steels, rel. to weldability 9-30713
 strain, influence of pair of edge dislocations in perpendicular slip planes 9-44786
 wire memories, DRO-plated, accelerated process rel. to life expectancy 9-43842
 -Co solid solutions, magnetic hysteresis depend. on ageing time 9-26622
 Al-(0.06 at.%) Si, Si atoms clustering, rel. to resist., 300°C 9-30712
 Al-(0.13 at.%) Si, Si atoms clustering rel. to resist., 300°C 9-30712
 Al-0.12 at. %Si, step aging, clustering of Si atoms, resistometric study 9-23940
 Al-Cu-Mg-Ag alloy, preageing effect on S precip. 9-48928
 Al-Cu-Mg alloys, preageing effect on S precip. 9-48928
 Al-Cu alloy θ' precipitate, as-aged, stacking faults 9-35098
 Al-(2.5 at.%) Cu-(1.2 at. %) Mg alloy, effect of Si on initial stages 9-48915
 Al-(4 at.%) Cu alloy, vacancies excess conc. and slow reaction mechanism obs. 9-48916
 Al-Mg-Si alloys containing Mg₂Si, 2-stage effect 9-39461
 Al-Mg-Zn alloy, dislocation distrib. influence on recrystn. 9-37276
 Al-Mg-Zn alloy, kinetics by hardness meas. 9-37280
 Al-(11 wt.%) Mg age-hardening alloy, deform. by hydrostatic extrusion effect on struct. and props. 9-41051
 Al-Mn-Zn alloys, effect on lattice parameters during pre-precipitation 9-41049
 Al-Zn-Mg alloys, effect of natural ageing and ageing between 100-340°C 9-37281
 Al-(40 wt.%) Zn, alloys, structural changes during ageing 9-23943
 Al-(40 at.%) Zn alloy, rel. to stacking fault formation 9-32979
 Al-Zn alloys, effect on tensile props. and hardness 9-37289
 Al-Zn alloys, X-ray study of spinodal structs. stability and decomp. 9-37290
 Al-(4.4 wt.%) Zn alloy, Be influence on elec. resistivity changes due to clustering 9-40932
 Al-Zr-Si alloys, age hardening, influence of Si 9-42910
 Al, quenched and aged, plastic flow mechanism, 86°K 9-48900
 Al-2at.% Zn-2at.% Mg alloy, reaging 9-41048
 BaTiO₃, tetragonal ferroelec., domain reactions 9-49142
 Be-(1.3 wt.%) Ni alloy, low-temp. and mixed ageing, struct. and hardness changes 9-39464
 Be sheet, rel. to ductility behaviour around transition temp. 9-26333
 Co-(7.45 at.%) Ti solid soln., γ -phase precip., neutron diff. and chem. analysis 9-41065
 Co alloys, high strength, patent 9-26377
 Cu-Be alloys, mechanisms at different temp. 9-37285
 Cu-Mn-Al struct. study by X-ray and neutron diff. anal. and electron microscope exam. 9-37293
 Cu-Ti-Al, Cu-Ti alloys, plastic deform. and recovery 9-37292
 Cu-Ti-Al alloys, struct. changes, electron microscope obs. 9-46938
 Cu-Ti alloys, struct. changes, electron microscope obs. 9-46938
 Cu(9.5 at.%) Be-(0.2 at.%) Zn, alloys, neutron irradiat., characts. from resistivity meas. 9-33115
 Cu-Ti alloys, kinetics, activation energies for decomposition 9-23941
 Fe-Al alloy, (FeMn); AlC precip. obs. 9-33139
 Fe-Mn-Ni alloys with Ti added 9-48917
 Fe-Ni-Mn-Ti martensitic alloys, hardness and pre-precip. stage obs. 9-37283
 Fe-Si, effect on texture form. during primary recrystn. 9-46921
 Fe alloys, low-C, martensite, rel. to thermomech. treatment 9-42912
 Fe-Ni alloys, martensite ageing at high temp., eff. of Co on hardening 9-23942
 Fe-(0.04 wt.%) C, quench aged, under cyclic straining, mech and microstruct. changes 9-33079
 Mg-Zn-Mn alloy, age hardening, patent 9-48942
 NaCl:BaCl₂ crystals, effect of dislocation density, elec. conductivity meas. at 550°C 9-46929
 Nb-(25 at.%) Ti-(10 at.%) Zr alloy, solution-treated, rel. to recrystallization 9-33122
 Nb, strain-ageing effects rel. to dislocation atmosphere formation 9-28381
 Nb, strain ageing, interstitial impurities obs. 9-35198
 Pb-base alloys, grain boundary precipitation during age hardening 9-39301
 Pt-Co alloys, rel. to coercive force increase 9-26372
 Ta, low temp. strain ageing, hardening obs. 9-44767

Air

see also *Atmosphere*

- acoustic plane wave propag. 9-26033
 aeration meas. by ¹⁰B(n, α)/Li reaction on methylboric acid label 9-24609
 afterglow, electron loss mechanisms 9-44505
 air-graphite suspensions, heat transfer agent, hydrodynamics, expt. 9-30437
 air-steam convection currents, u.s. anemometer design 9-36794
 breakdown, impulse, secondary leader channels obs. 9-44511
 breakdown, microwave, temp. depend. 9-32708
 breakdown at high elec. fields, delay time increases 9-44510
 bubble collapse and explosion initiation of AgN₃ and β -PbN₆ 9-28788
 compressed, injection of water, temp. levelling rel. to droplet size 9-23435
 conditioning and building cooling systems, conference 9-34094
 convection through section having parallel faces, one rotating about its axis 9-45877
 convective flow in enclosures, circular and rectangular, with localized heating from below 9-40746
 density at heights between 130-160 km, from anal. of orbit of 1968-59B satellite 9-47553
 dielectric const. of liquid at microwave frequencies in X-band 9-46647
 diffusion or organic and other vapours, coeff. meas. 9-30326
 discharge, impulsive, in axial rot. flow 9-25976

Air continued

- discharge, variation of striking and extinction voltages at low press 9-23358
 discharge at 7.5-20 cm gap distances 9-48623
 discharge in coaxial cavity, cyclotron resonance rel. to elec. field freq. 9-44499
 dissociating, collision integrals for components 9-23407
 electrical cond. and permittivity of weakly ionized air in mag. field, obs. 9-28080
 electrical conductivity, reduction due to pollution 9-41535
 electron beam absorpt., 20 to 50000 eV, and in plastic 9-37376
 fallout obs. (Jan.-June 1967) 9-31335
 flow, one dimensional at high temp. with heat exchange 9-23378
 flow, Reynolds similarity, exactness investigation 9-25996
 flow over ridge, lee waves numerical cal. 9-43389
 flow over ridge, lee waves numerical calc. 9-37912
 flow over water surface, turbulent heat transfer obs., temp. vel. depend 9-34837
 flow through collection of tubes, heat transfer 9-30327
 heated, basic radiative processes and spectral props. 9-23400
 heated integral props. for spectrum and intervals, 4000-20000°K 9-23401
 high speed flight effects on props. 9-34822
 impulse testing in nanosecond range, current and tension 9-42577
 influence on growth of Ag and Au films in ultra high vac. 9-34993
 injection into atmospheric burner, charact. indices 9-41842
 interaction with sea, atmospheric motion 9-26891
 interface with water, effect of hydration on CO₂ exchange 9-30453
 internal heat transfer inside heated porous mats 9-28074
 ionization, water vapour influence 9-46534
 ionization by alpha particles, effect on elec. conductivity 9-25966
 ionization relaxation behind shock waves 9-42560
 ionization relaxation zone length behind strong shock front 9-25961
 jet impinging on liquid surface, shape of cavities formed 9-40762
 liquid, dielectric const. at microwave frequencies in X-band 9-46647
 liquid, specific heat deriv. from molecular model 9-34869
 mass trajectories in free atmosphere, synthesis of general problem 9-47533
 molecular spectra, effect of halogen compounds 9-34629
 oxidation of graphite channel, kinetics and radial diffusional effects 9-26824
 plasma, emissivity meas., 110-300 nm, 2×10⁴⁰K and e density ~ 10¹⁷ cm⁻³ 9-48590
 plasma contrib. to emission by N⁻ 9-44442
 plasma flow behind shock wave, elec. conductivity 9-40669
 plasma radiative power, total, 250-700 n.m. obs. 9-30261
 pollution, particulate, in USA 9-43382
 pollution analysis by correlation spectrometer 9-33693
 propane-air flame, electrically augmented, temp. and heat transfer meas. in discharge zone 9-25131
 propane-air mixtures, constant volume, combustion, effect of containing wall linings 9-45881
 radiating power in range 0.2 to 3 μ at 10⁴K, 1 atm. 9-40753
 radiative heat transfer, end-wall, shock tube meas. 9-23395
 shock layer, radiative cooling and nongray self-absorpt. effects 9-23383
 shock waves, emission spectra and ionization temp. 9-36202
 spark breakdown, primary and secondary streamer dendrites 9-28051
 spark gap, dispersion of sparking voltage under high current successive discharges 9-48639
 sparks, 4-m length 9-46546
 spectral line half width, mean 9-36705
 subsonic flow in contraction section, flow field and heat transfer meas. 9-28065
 supercooled, water drop nucleation 9-26075
 thermal conductivity meas. at 35 and 90°C 9-36814
 turbulent jets, book 9-40737
 viscosity meas. by oscillating disc method, exp.6 exponential-6 potential preferred 9-36823
 water-air mixtures, concurrent flow down vertical pipes, expt. 9-26001
²¹⁰Pb, in surface air and precipitation, measurement 9-28900
 H₂-Ar air flames, turbulent, atoms fluoresc. power efficiencies, obs. 9-24601
 NO₂⁺ production 9-43387
 Rn decay products, transport in air 9-22762
 Rn decay products, transport in air 9-23237

Airglow

- see also *Atmospheric spectra; Aurora; Sky brightness, Twilight; Zodiacal light*
 burst, 2 components, Cosmos 92 obs. 9-43422
 clouds, noctilucous, exact identification w.r.t. auroral occurrences 9-31364
 clouds, noctilucous, freq. rel. to mesospheric circulation 9-31355
 clouds, noctilucous, geographical spread 9-41558
 clouds, noctilucous, obs. in Germany 9-41559
 dayglow, visible and ultraviolet, rocket observations 9-35843
 daytime, weak emissions, 6000-11500 Å, rocket obs. 9-45511
 emission in soft auroral zone 9-28926
 emission spectrum of night airglow, 2 to 4 μm 9-28922
 interferometric spectra, 1.2 to 1.6 μm 9-28923
 ionosphere, night, study using height model 9-31399
 i.r. day and night airglow, principal emission features 9-28921
 night, 5577 Å, atmospheric movement deductions 9-37954
 night, [OI]λ6300, Doppler shifts 9-45514
 night glow, emission spectrum, 2 to 4 μm 9-28922
 night-time, spectrum between 3 and 4 μm, obs. of OH, methane and CO₂ bands 9-24679
 nightglow, 6300 Å, comments on Barbier's intensity formula 9-33805
 nightglow 6300 Å enhancements rel. to F₂ height variations, obs. 9-41557
 nightglow H_α, rel to neutral H vertical distrib. in upper atm., obs. 9-26923
 nightglow intensity obs., rel. to ozone content and stratospheric temp. 9-41561
 photometer with improved red sensitivity 9-45512
 predawn enhancement of red line of atomic O over U.K. (1965-1968) 9-47562
 predawn photoelectron conjugate effects calc. 9-35866
 red line, predawn enhancement over U.K., (1965-1968) 9-47562
 Tunguska meteorite effects 9-26916
 u.v., of earth between 1100 and 3400 Å, spectrometer 9-37953
 N I forbidden lines in nightglow at mag. equator 9-33806

Airglow continued

- NO atmospheric, 60 to 96 km, evening twilight rocket obs. 9-31344
 O₂ atmospheric i.r. bands, temporal variations, balloon obs. 9-45509
 O 6300 Å emission in nightglow, post-midnight peak obs. and theory 9-40054
 O I forbidden lines in nightglow at mag. equator 9-33806
 O red-line emission, at night, total intensity formula 9-49472
 OH contamination of night obs. 9-41560
 OI 6300 Å twilight, enhancement rel. to latitude 9-28924
- Albedo** see *Cosmic rays; Earth; Neutrons and antineutrons/reflection; Nuclear reactors, fission*
- Alfven waves** see *Magnetohydrodynamics; Plasma/oscillations*
- Algebra**
 automorphism groups induced on lattices by interactions 9-45775
 Clifford algebra eqn., for spin-1/2 particles to Dirac-type form 9-48156
 continuum analogue of lattice gas 9-22113
 differential operators, second order ordinary, eigenvalues distrib. 9-31743
 Gell-Mann-Dashen type, skewsymmetric irreducible representations 9-47727
 Green-Volkov, irreducible representations in configuration space 9-32112
 Hermitian spaces, rel. to Jordan algebras, book 9-31745
 Hilbert spaces with kernel functions, theory and applics. 9-31744
 IO(n), class of representations 9-22059
 IU(n), class of representations 9-22059
 Jordan algebra, rel. to Hermitian spaces, book 9-31745
 Laguerre polynomials in analysis of neutron-wave propagation 9-22854
 Lie, algebraic, Gelfand-Kirillov conjecture on the Lie field 9-38198
 Lie, Semisimple, Clebsch-Gordon series, multiplicity, reduction to soln. of linear eqn. syst. 9-22058
 O(n,1), class of representations 9-22059
 quasi-unitary, attached to temperature states in statistical mechanics 9-22120
 quaternion soln. to Schwarzschild problem 9-31758
 of Regge pole tribes and observables 9-29558
 representation theory for field-type algebras 9-29171
 Riemann spaces, 4-dimensional, algebraic classification 9-38207
 symmetric spaces, compact, complete classification, book 9-31745
 topology applied to sintering process 9-23934
 U(n,1), class of representations 9-22059
 Volterra operators, applic. to viscoelasticity 9-22220
- Algol** see *Calculating apparatus/digital computer programmes*
- Algorithms** see *Calculation*
- Alignment** see *Mechanical measurement*
- Aliphatic compounds** see *Organic compounds*
- Alkali metal compounds**
 see also *the compounds of the individual metals*
 alkali dithioferates (III), Mossbauer spectra 9-43220
 alkali metals azides, new electronic and i.r. band after irradi., D_{3h} ion symmetry 9-27844
 alkali silicate glasses, internal friction, effect of second alkali addition 9-48886
 alloys, liquid, Knight shift, rel. to conc. 9-30429
 antimonide cathodes, cathodes, thermosensitive discontinuities and hystereses at high light intensities 9-39740
 azides, D_{3h} symmetry of ion, explanation of new electronic and i.r. band 9-27844
 borohydrides, n.m.r., internal rotations and phase transitions 9-43308
 chlorides, molten mixtures with InCl₃, Raman spectra 9-44570
 halide crystal lattice energy calc. 9-40852
 intermetallic cpds., D₁ struct. type 9-39243
 metaborates, i.r. spectra in solid Ar or Kr matrix 9-32463
 molybdate syst., glass formation 9-30454
 niobate-rare earth niobate solid soln., dielec. props. rel. to crystal chemistry 9-24210
 niobates based highly dense piezoelectric material 9-39676
 nitrates, electrical conductivity rel. to temp. in stable state and during phase transition 9-24115
 nitrates, molten i.r. absorpt. band shapes 9-30411
 nitrates, molten mixtures with AgNO₃ and TiNO₃, elec. cond. and density 9-23520
- halides**
 see also *the compounds of the individual metals*
 absorption band obs. due to OH ion 9-43236
 absorption spectra, u.v., of Ag⁺, Cu⁺ and Ti⁺ centres 9-43237
 aggregate centres, absorpt. spectra, oscillatory effect and fine struct. obs. 9-39370
 anharmonicity rel. to i.r. absorpt. 9-47348
 barrier for fast electrons, energy distribution 9-24074
 binding energy calc. for diatomic molecules 9-48452
 chemical interdiffusion coeff. 9-28311
 chlorides, aq. solns., nuclear spin-lattice relax. 9-44593
 chlorides, solid solns., fund. absorpt. in extreme u.v. 9-35662
 colour centre destruction due to radiation, domain subsystem behaviour 9-32989
 deformation potential determ. from piezobirefringence meas. 9-24364
 diatomic, interatomic forces and cohesive energies 9-28250
 dielectric loss, Maxwell-Wagner polarization 9-33371
 diffusion by divalent ions 9-28314
 dislocation etch figs., effect of neutron irradi. on dimensions 9-40945
 dislocation mobility, influence of lattice defects 9-39362
 dynamical matrix and three-body overlap forces, coupling coeffs. 9-39506
 electron-phonon interaction, transmission secondary emission 9-44868
 electron-phonon interaction second. electron transport 0.25-7.5 E_v 9-44867
 electronic polarizability of ions 9-31058
 F₃⁺ model of R⁺ centre, electronic states obs. 9-39369
 F⁺ centre, polaron model applic. for calc. of electronic and ionic polarization effects 9-44716
 F centre form. under electron irradi., saturation 9-48867
 F-centre prod. in mixed cryst., reduction due to disruption of replacement collision sequences 9-32991
 F-centres, Stark effect of relaxed excited states 9-24392
 f.c.c., mass transport 9-44729
 films, grown from melt, cell and platelet structure 9-23627
 force constants, mean-square quantities and bond energies, universal parameter 9-38840
 halides, thermal conductivity of solutions 9-36866

Alkali metal compounds continued

- halides continued
- hyperfine and superhyperfine interaction of stabilized Cu and Ag atoms, theoretical study 9-37792
- interaction with Pt electrodes, capacitance enhancement 9-49134
- interparticle distance correl. with interionic separation at melting point 9-35007
- ionic crystals, recombination luminescence investigated by EPR relaxation 9-33576
- ionic radii, calc. using repulsive energy method 9-35006
- ions, temp. parameters, Debye-Waller factors 9-30507
- iron fluorides, MFeF_3 (M = Na, K, Rb, Cs), crystal structures and mag. props. 9-35063
- Kerr effect, dynamic meas. 9-33514
- localised modes due to U-centres, freqs. 9-35265
- luminescence, doped with homologous anions and cations, nature of vibronic transitions 9-33580
- luminescence, O_2^- and S_2^- impurity centres obs. 9-39861
- luminescence, O_2^- impurity centres, effect of hydrostatic press. 9-39864
- luminescence, O_2^- impurity centres obs. 9-39862
- luminescence, O_2^- impurity centres obs., thermal quenching 9-39863
- luminescence centres in noble metal ion activated crystals, optical struct. 9-47387
- luminescence of O_2^- and S_2^- centres investigated 9-33591
- luminescence of rare earth ions 9-33592
- macrodefects, radiation produced, electron microscope investigation 9-32984
- metals, b.c.c., glide band broadening at yield point 9-32938
- mixed crystal of LiCl-RbCl type, optical vibrations 9-39512
- mixed crystals with thiourea, i.r. absorption spectra, interaction obs. 9-24420
- n.m.r. of aqueous solns., chem. shifts of ^{35}Cl , ^{81}Br and ^{127}I 9-34925
- n.q.r., quantum mechanical calculation 9-24514
- nucleation, transient, from aqueous supersaturated solns. 9-48810
- optical absorption of U-cent., effect of external stresses 9-49251
- optical props., XUV spectrophotometer 9-29485
- optical vibrations, influence of heavy impurities 9-39512
- phosphors, metal-ion activated, absorption spectra 9-31098
- photoconductivity, spin depend. 9-41257
- polar impurities motion, effect of localized lattice vibr. 9-33159
- polaron effective mass, translational energy depend., cyclotron reson. obs. 9-39573
- positron annihilation, in crystals, lifetime rel. to anion, void vols. 9-33239
- proton irradi., recoil radio-I species and annealing, obs. 9-28818
- R^+ centre, electronic states obs. and F_3^+ -model 9-39369
- radiation induced defects in whiskers, dependence on shape 9-32941
- Raman spectra and i.r. absorption obs., with defects 9-33568
- Reststrahlen frequency in ionic crystals 9-30756
- Schottky defect formation energy 9-48849
- scintillation crystals, impurity- centre distrib. laws, crystallochem. analysis 9-23798
- scintillators, thermoluminescence, effect of elec. field 9-45354
- self-trapping of excitons, optical phenomena 9-33589
- stopping power, extrapolated range and degradation spectrum of low energy electrons 9-33211
- stress relaxation, dislocations mechanism, -196°C 150°C 9-33026
- as substrates for evaporated f.c.c. metals, epitaxy modifications due to electron bombardment 9-46760
- surface phenomena, decoration method with electron microscopy 9-23619
- surface phenomena and dislocations 9-23618
- surface tension and energy of (100) face 9-30478
- surface topography change due to temp. effects (thermal attack) 9-30477
- thermal cond. meas. 60°K - 100°K , device 9-30790
- thermal conductivity of solutions 9-36866
- triboluminescence 9-43268
- two-photon absorpt. spectroscopy 9-47349
- U bands, band shape and phonon broadening 9-46830
- u.s. attenuation and velocity in crystal containing CN^- 9-37329
- V_k -centres, stability calc., model 9-42847
- vapour, absorption spectra bands obs., ν_2 bending vib assignment 9-23037
- zone refining techniques, review 9-23674
- Ag^+ centres excitation and emission spectra, hydrostatic press. effect 9-41401
- Ag^+ doped, Ag^- mag. circular dichroism obs. 9-33508
- Cd centres obs. 9-40970
- Co doped, absorption and i.r. emission 9-33548
- Cu^+ centres excitation and emission spectra, hydrostatic press. effect 9-41401
- Eu^{2+} and Sm^{2+} doped, zero-phonon transitions 9-37716
- KCl, M-centre singlet-triplet splitting, calc. 9-35107
- KCl.KBr-Tl crystal, symmetry of Tl centres 9-42852
- Ni dopes, absorption and i.r. emission 9-33548
- OH^- doped, i.r. stretching band absorpt. obs. 9-24403
- P activated, luminescence obs. 9-33583
- Sm^{2+} defect vibronic side bands calc. 9-49285

Alkali metals

- see also the individual metals
- in arc, effect on cathode spot damage 9-30322
- atom, excitation by electron impact 9-44278
- atom, hyperfine structure, theoretical analysis 9-34546
- atom in excited state, van der Waals const. with inert gases 9-36677
- atom interactions with atoms and non-reactive diatomic mols., cross sections and van der Waals constants 9-42342
- atom scatt. spin-exchange cross-sections calc. 9-22984
- atomic beams reaction with triat. halide mols. 9-25795
- atoms, elastic collisions, effect of spin-orbit coupling 9-38793
- atoms, electronic dipole polarizabilities calc. 9-40545
- atoms, excitation transfer in collisions between identical atoms 9-42339
- atoms, excited, scattering by inert gas atoms, collision induced transitions, calcs. 9-40556
- compressibility, shock wave and static data 9-46882
- conductivity, thermal and elec., rel. comparison with Cu 9-24060
- in discharge, spectrochem. analysis by introducing oxides of Co, Ti and V 9-31229
- electric arc, admixture with arbitrary gas, magnetic holding 9-25989
- electrical and thermal resistivities, temp. depend. using Sharma-Joshi model 9-42995
- electrical resistivities up to pressures of 600 kbar 9-30841

Alkali metals continued

- electron-phonon interactions, anisotropy 9-37389
- Fermi surface, rel. to electron-ion interaction 9-26478
- films and wires resistivity, effect of electron-electron scattering 9-37435
- heat of vaporization and critical parameters 9-40828
- interatomic potential between alkali ions and rare-gas atoms using charge-transfer and Firsov's theory 9-25711
- ionization, cross section calc. from atomic shell structure 9-23341
- ions, hydrated, in aqueous soln., nuclear magnetic shielding 9-32797
- liquid, isothermal compressibility and structure function determ. 9-23465
- liquid, plugging meter, expld. continuous- indication, for impurity monitoring 9-24991
- liquid, thermoelectric powers, changes at melting point 9-40802
- liquids, atomic heat conduction 9-39111
- magnetoplasma, electron temp. eff. on i.f. oscillations 9-42544
- metal- NH_3 solns., unpaired electron spin correl. times 9-44587
- molecules, energies of electronic transitions, estimation by new method 9-30015
- optical conductivity, Mayer-Naby peak, transition from Fermi sea to Brillouin zone boundaries 9-28679
- photo-enhanced electron emission into anthracene, trapping obs. 9-33232
- plasma, dilute computation of thermo props. 9-36755
- plasma, oscillations, noise due to radial electric field 9-28029
- plasma, quadrupole transitions in diagnostics 9-23320
- Raman scattering of light by spin waves 9-37738
- reactive, protection of solid samples for X-ray diff. 9-46767
- scattering of thermal energy atoms by halogen atoms mols., cross section, curve crossing eff. 9-29969
- solid, electron-phonon interactions, transport processes 9-30814
- spin relaxation, optical obs. in buffer gas 9-29942
- superconductivity 9-43031
- thermal resistance determ. using free electron approx. and Krebs mode 9-24062
- thermoelectric power parameter rel. to volume depend. electron-lattice interaction 9-33402
- vacancy relax. and migration energy, lattice dynamical calc. 9-23792
- vapour h.f. spectrum, saturation eff. of Zeeman transitions 9-27806
- vapours, sensitized fluorescence 9-29971
- vapours, thermal cond. determ. by dilatometric method 9-26029
- work function, correlation energy contribution using pseudopotential model 9-35515

Alkaline earth compounds

- see also the compounds of the individual metals
- aluminates, flame spectroscopy, thermodynamic stability 9-33692
- borate-phosphates: Eu^{2+} , luminescence 9-35678
- chalcogenides, point defect form. energy calc. 9-44688
- fluorides, F and F^+ colour centre transitions Mollwo-Ivey plots 9-35108
- fluorides, H and F bands 9-28302
- fluorides, self-trapped hole and exciton obs. 9-46831
- fluorides, V_k centres, opt. and e.p.r. spectra, eff. of polarized bleaching light 9-23826
- oxides, electronic states of defects 9-44689
- oxides, F and F^+ colour centre transitions Mollwo-Tlvey plots 9-35108
- oxides, flame spectroscopy, thermodynamic stability 9-33692
- sulphide phosphors, electroluminescent cell construction and characteristics for brightness, variation with frequency and voltage 9-47417
- tungstates, Bi doped, u.v.-induced colouration, darkening and fading processes 9-45282
- uranates, crystal structure and refinement, neutron powder diff. data 9-39253

Alkaline earth metals

- see also the individual metals
- superconductivity 9-43031

Allotropes see Phase transformations; Polymorphism

Alloys

- see also Ageing; Crystal structure, atomic/alloys; Heat treatment/alloys; Solid solutions; Steel; and under alloys or compounds of the named elements. Alloys such as AuCu , Au-Cu , Au-Cu-Zn are indexed under compounds of the named elements, i.e. Gold compounds, Copper alloys, Zinc compounds in these examples
- ageing, X-ray diff. eff. rel. to elastic lattice distortion 9-23746
- austenitic, helium gas bubbles effect on creep ductility 9-41021
- B2 type, faulting energy created by slip 9-42841
- b.c.c., short-range order, equilibria and kinetics 9-41054
- binary, cylindrical rods, cond. distrib. after zone melting from variable length of melted zone 9-39470
- binary, ferromagnetic, inter band optical transitions investigation, low temp. magneto-optic meas. 9-41136
- binary, generalised spherical model 9-24292
- binary, long-period superlattice structure, electronic states 9-30818
- binary, of transition elements, non-collinear mag. structures 9-45056
- binary, partially ordered, energy bands using Green's function 9-48990
- binary, pile-up of dislocations 9-42823
- binary, solidification in presence of heat flow, interface distrib. coeffs. 9-37100
- binary, thin films, effective surface diffusion coeffs., vol. diffusion effect in electron diff. obs. 9-39379
- binary pnictides, with marcasite type struct., mag. props. 9-31016
- binding energy, exothermic, explanation w.r.t. electron effects 9-39180
- brass-like close-packed, stacking-sequences, energetic significance 9-28249
- Ceto, adsorption rel. to Ti additive 9-36965
- chemical compatibility with PbTe and ZnTe thermoelec. materials 9-26808
- corrosion protection by anodic metal dispersion, patent 9-23946
- dilute, elec. resistivities and Matthiessen's rule deviations 9-37432
- dilute, Fermi surface topology from supercond. transition temp. dependence 9-47043
- dilute, impurity X-ray spectrum, effect of localized states 9-49301
- dilute, magnetic, electron-electron interaction and supercond. above Kondo temp. 9-44925
- dilute, magnetic, Kondo spin-compensated state, range and spatial variation 9-33429
- dilute, magnetic ground state energy calc. by Nagaoka-Suhl theory 9-45052
- dilute, screening, nonlinear Thomas-Fermi eqn. soln. 9-47019
- dilute binary, freezing, interface stability 9-23582
- dilute binary, nonlinear stability investig. of moving solid-liq. interface 9-36920

Alloys continued

- dilute magnetic; thermopower, electrical and thermal resistivity calc. by Suhl-Nagaoka theory 9-45051
- dilute magnetic, dielectric const. calc. 9-39667
- dilute magnetic, nuclear spin relax. mechanism 9-24338
- dilute solutions, equations of general appl. 9-42915
- dilute solutions, equations of general appl. 9-42914
- dilute solutions, equations of general applic. 9-42913
- disordered, pair effects and self-consistent corrections 9-46816
- disordered, phonon freq. spectra, interpolation formula 9-44807
- disordered substitutional, electronic props., analysis from simple model 9-26476
- elastically inhomogeneous, dislocation model of strength 9-39430
- electrical resistivity meas. applic. to metallurgical processes analysis 9-46932
- evaporation on hot metal filaments, emission of electrons 9-35204
- f.c.c., and related superlattices, passing dislocations 9-39360
- f.c.c. ferromagnetic, magnetic lag and anisotropy due to interstitials 9-45130
- f.c.c. ternary, order-disorder critical temp., conc. depend. 9-28401
- formation between low and high melting pt. metals by reduction of volatile halides 9-39466
- grain-boundary precipitates, growth 9-35101
- high resistivity, Peltier meas. technique below 4°K 9-30983
- impurity zone in a binary model, Green function and energy spectrum evaluation 9-37163
- inhomogeneous, electron energy loss meas., effect of elastic constraints 9-48978
- internal friction due to precipitation 9-33021
- Knight shifts, solvent, origin and nonlinear effects 9-33642
- liquid, excess volume analysis 9-39471
- liquid, Knight shift calc. from pseudopotential formalism 9-23532
- liquid, Percus-Yevick Partial structure factors 9-40768
- magnetic, dilute, fluctuation theory of Kondo effect 9-41288
- magnetic, dilute, frequency depend. elec. cond. 9-47064
- magnetic, dilute, spin correlation between mag. impurity and conduction electrons 9-31021
- magnetic, dilute, spin correlation function perturbation calc. 9-28591
- metallic, emission processes, vibrational character due to electric spark 9-45311
- noble metal, α -phase, Debye charact. temp. 9-44836
- noble metal, long period structs. 9-23745
- nucleation phenomena in liq. to solid transform. 9-48736
- ordering, early stages, applic. of model for diffusion on cubic lattices 9-30622
- ordering strains, relief by twinning 9-35252
- with paramagnetic impurities, gapless superconductivity region 9-43033
- phonon conductivity determ. from expt. data 9-39535
- phonon scattering by Cottrell atmospheres surrounding dislocations 9-46966
- plastic flow stress, temp. and strain rate depend., 150° to 250°K 9-33044
- quaternary systems, temp.-conc. sections along curves or surfaces where a melt is saturated w.r.t. 2 phases 9-39130
- quenched dilute, non-equilib. segregation of impurities, model rel. to grain boundary hardening 9-48919
- rate processes, effects of radiation 9-24068
- Saxon-Hutner theorem proof for 1-dimens. general alloys 9-42989
- semiconductor, polyphase, thermoelec. props. 9-37609
- single cryst. growth stationary mould solidification technique 9-32877
- stacking fault energies, precise determination 9-32976
- substitutional, serrated yielding 9-39411
- super-strength, mechanical props., high temp. 9-33056
- super-strength, resistivity and mech. props., review 9-33179
- superconducting, dynamic props. in critical region in strong alternating fields 9-30864
- superconducting, with rigidly pinned vortex lattice, temp. depend. of critical current 9-47080
- superdislocations, line tension calcs. rel. to antiphase boundary energy 9-46819
- superplasticity of certain metal alloys, popular article 9-48903
- ternary, liquid systems, miscibility calcs. 9-46614
- ternary systems, temp.-conc. sections along curves or surfaces where a melt is saturated w.r.t. 2 phases 9-39130
- thermodynamic activities calc. using point defect conc. 9-30714
- thermoelectric power expressions for dilute magnetic alloys 9-33401
- Thomas-Fermi model, electron cloud of solvent and solute atoms in crystal lattice 9-40898
- transition element binary, non-collinear mag. structures 9-45056
- transition metals, IIIA-VIA groups, binary, relations of constitutional diagrams 9-39469
- transport coeffs. meas. w.r.t. temp. 9-41157
- twin boundaries, coherent, free energy and surface free energy 9-44714
- two-phase; microstructural development during liquid-phase sintering 9-42919
- two-phase sintered, crack formation 9-42902
- Volume changes on alloying, applic. of excess vol. method to liquids and solids 9-39471
- C fibre reinforcement, popular article 9-46944
- CSiCl-type ordered, vacancy distrib. 9-30585
- Ni-Co films, electrolytically deposited, magnetocryst. anisotropy 9-41323
- Si-containing, inclusions, i.r. absorpt. obs. 9-35213

Alnico alloys *see Nickel alloys***Alpha decay** *see Nuclear decay theory; Radioactivity/decay periods; Radio-activity/decay schemes***Alpha-particle model** *see Nucleus/models***Alpha-particle spectra**

- see also Nuclear decay theory*
- A=104, isotope production from ^{249}Cf , $^{12,13}\text{C}$; α emission, isotope identification 9-42219
- transition cross sections in residual nucleus for (n,α) , $E_n=14.6$ MeV 9-27724
- $^{235}\text{U}(n,\alpha)^{232}\text{Th}$, meas. of low energy part 9-22800
- ^{256}Lw , emission, 8.3-8.5 MeV, review 9-36584
- ^{206}Ra to ^{214}Ra isotope decay props. determ. 9-27645
- ^{247}Bk - ^{243}Am , levels spin and parity determ. 9-27651
- $^9\text{Be}(n,\alpha)^6\text{He}$, ^6He excited states obs. 9-32306
- $^{11}\text{B}(p,\alpha)$, ^{12}C resonances shape spin and parity depend., $E_p=0.15$ -4 MeV 9-25625

Alpha-particle spectrometers

- semiconductor, high resolution, rapid source prep. technique 9-27586
- semiconductor detectors, design 9-34356
- ^{227}Th decay meas. attachment for separation of decay product background 9-22752

Alpha-particles

- see also Cosmic rays/alpha-particles and helium nuclei; Radioactivity*
- cluster structure of nuclei 9-48271
- configuration-space states of arbitrary symmetry, translationally invariant 9-48213
- form factor, symmetric harmonic-oscill. states in config. space 9-38600
- four-body correlation and reduced width in heavy nuclei 9-34410
- production by 28.5 BeV proton bombard. of BeO 9-32345
- ^{252}Cf fission KX-rays emitted in association with long-range α , rel. to emission products 9-38727
- ^4He , first excited state 0^+ 9-27739
- from Pu isotopes, ratio with photons 9-25604

absorption

No entries

angular distribution

- $^{12}\text{C}(\alpha,\alpha)^{12}\text{C}$, $E_\alpha=20$ -24 MeV, obs. 9-22810

detection, measurement

- see also Alpha-particle spectrometers+ Dosimetry; Particle detectors; Radioactivity measurement*
- calorimeter for low-power sources 9-29664
- Geiger counter 9-29652
- scintillation counter, design of specimen holder 9-44085
- with spark counter 9-22664
- track, pattern recording using cellulose nitrate plastic, crystal scatt. appl. 9-42763
- ^{227}Th attachment to a α spectrometer for separation of effects due to decay products 9-22752

effects

- see also Nuclear reactions and scattering due to alpha-particles*
- calcite, thermoluminescence mechanisms following α and reactor irradiation 9-31147
- cementite, thermal stability 9-47000
- methane, ion-mol. reactions 9-45428
- Al, irradi., internal friction peaks ascribed to reorientation of interstitial clusters 9-39398
- Al film, prod. of secondary electrons, energy spectrum 9-49177
- Ar luminescence, α -particle induced, in elec. field 9-42328
- H_2O vapour, ion-mol. reactions 9-45428
- LiF irradi., Y-absorpt. band obs. 9-37726
- S, of orthorhombic S at 77°K, prod. of unstable form. 9-30747
- P-Si, irradiated, energy spectra of radiation defects 9-30589
- UO_2 , irradi., rel. to ^{238}U fission, shadow pattern agn. distrib. of fragments 9-40524
- ZnS:Ag scintillation decay 9-47410

interactions

- cluster model, α -particles, role of Pauli principle 9-32297
- photodisintegration, tensor forces and vel. depend. potential for cross section calc. 9-38601
- potential in composite particles, repulsive core and Pauli principle 9-34375

scattering

- cluster model, α -particles, role of Pauli principle 9-32297
- inconsistency in analysis 9-22640
- X-ray emission spectra excited by α -bombardment, cross-section meas. for various atoms 9-46267
- α - α , d-wave phase shift rel. to ^8Be 2^+ states 9-40473
- α d, elastic, distortion effects 9-44066
- e, elastic form factor calc. 9-25615
- e, quasi-elastic scatt., e-N McVoy and Van Hove treatment 9-25614
- π - α , differential cross section meas., phase-shift analysis, π e.m. radius determ., $E_\pi=51$ -75 MeV 9-38521
- π α cross section determ., Coulomb interference corrections determ. 9-38522

Altimeters *see Length measurement***Aluminium**

- absorption, total cross-section, L shell contrib. 9-45314
- adhesion of chemically vapour deposited coating to steel 9-28376
- anharmonic phonon widths, shifts and dispersion curves, wave number depend. 9-35266
- annealing processes in cold-worked foils, h.v. electron microscope obs. 9-42909
- anodized layer, elec. output during shock-wave loading 9-24117
- atmospheric corrosion, eff. of initial weather conditions 9-24568
- atom, Raman and Rayleigh scattering cross sections 9-25690
- atom form factor determ. by high voltage e. diff. 9-23722
- atom series perturbations and oscillator strengths, ^2D series, Hartree-Fock approx. 9-22939
- band theory, constant-energy surfaces, Korringa-Kohn-Rostoker calcs. 9-26479
- bicrystal, grain boundary sliding rel. to deform. 9-46888
- binding energy, single-orthogonalized-plane-wave, Hartree-Fock calc. 9-24081
- in clinopyroxenes, total content rel. to value of lattice parameter b 9-30554
- co-ordination no. in titanobarium glass and ceramic, from X-ray emission spectra 9-41398
- coating on ground pyrex, reflection diffusion rel. to incidence angle 9-48080
- cold-worked, Debye-Scherrer line broadening meas. 9-46776
- contact. pot., stress induced shifts, obs. 9-43019
- corrosion, anaerobic, by sulphate-reducing bacterial 9-24567
- corrosion, atmospheric results of 6 year exposure tests 9-24571
- corrosion, atmospheric weathering tests, 7-year data 9-24569
- corrosion, literature review 9-26828
- crack growth during fatigue, effect of air pressure 9-46906
- crater formation by Fe microspheres at 0.5 to 10 km/sec. 9-30700
- creep, stacking fault energy effect 9-39421
- Creep with incremental stress variation 9-39422
- crystals, (p,α) reaction, α -particle track recording using cellulose nitrate plastic 9-42763
- damping in plastic deformation, amplitude depend. and dislocation effects 9-30661
- Debye-Waller factors, temp. depend. 9-35261

Aluminium continued

- deformation of 1100 Al under u.s. vib., isothermal recrystallization kinetics investig. 9-37238
- depth distributions, low-energy, obtained by sputtering 9-47013
- determination in presence of fluoride by emission spectroscopy 9-37856
- diffusion in n-SiC:N in prep. of electroluminesc. diodes, anomalous nature 9-37776
- diffusion in SiC, by heating 59 1800-2400°C for 2-30 hours 9-33009
- dislocation configurations at 350°C, X-ray topographical investig. 9-46820
- dislocation configurations in single cryst. produced by annealing in air and vacuum, comparison 9-37171
- dislocation motion in plastic flow during tensile or creep tests 9-30675
- dynamic stress-strain release paths up to 200kb 9-39405
- elastic modul, high temp. 9-37219
- electrical resistivity, effect of grain boundaries, 4.2° to 77°K 9-30849
- electron emission, secondary, produced by relativistic primary electrons in high elec. fields 9-31009
- electron energy loss spectra in i.r. region 9-28441
- electron irradi., factors affecting energy-range relation 9-35302
- electron irradiation damage obs. 9-42805
- electron maximum range, 15, 4.1 and 9.8 MeV, exptl. determ. 9-26470
- electrons, high energy, measured energy loss 9-39551
- emittance at cryogenic temp., cyclic incident radiation technique 9-24064
- EPR of Cr³⁺ with and without doping 9-37796
- extrusions, microstruct. 9-39252
- fatigue props. in vacuum, defect substruct. distrib. and crack propag. obs. 9-28364
- f.c.c. polycrystalline, flow stress and microstructure after shock-relief deformation 9-23879
- Fermi momentum determ. from annihilation spectra, valence electrons calc. 9-33229
- fibres, mechanical damage accumulation under static load 9-33039
- film, deposition by vacuum evaporation, effect of electric field on critical thickness 9-32838
- film, evaporated, intrinsic tensile stress meas., temp. depend. 9-37233
- film, internal friction for attenuation of mechanical oscillations 9-23856
- film, secondary electrons, energy spectrum, prod. by α particles and fission fragments 9-49177
- film, thin, photoelec. emission rel. u.v. polarization and angle of incidence 9-31072
- film in vac., photoelectric yield, plasma resonance obs., light irradiation 9-41282
- films, conductivity, rel. to thickness 9-49023
- films, electrical conductivity of single- and polycrystals, thickness and temp. dependence 9-44905
- films, electron energy-loss spectra, convolution effects by electron transmission 9-47015
- films, growth, elec. field effect on form. and substruct. 9-48762
- films, supercond., dirty, Knight shift, BCS-Yosida depend. 9-45394
- films, thin, thermal cycling effect on surface hillocks prod. by annealing 9-30705
- films evap. on air-cleaved NaCl, electron microscope obs. of structure 9-26185
- films of fine smoke cryst., enhanced superconductivity 9-33270
- films on W(110) face, (structure from LEED obs. 9-26184
- films r.f. sputter-thinned, resistivity 9-24123
- flow-stress relation to strain and strain-rate, drop-hammer test 9-39406
- foil, insulating material for space flight, outgassing behaviour 100-1800°F obs. 9-38173
- foil bremsstrahlung, spectrometer for meas. using Compton eff. 9-46133
- foil target, attenuation of heavy ions, obs. 9-28440
- foils, cold-worked, annealing processes, h.v. electron microscope obs. 9-42909
- foils, fatigued, surface deformation markings, direct correlation of dislocation structures 9-23878
- forbidden transitions in isoelectronic sequence, relative line strengths 9-36653
- force-const. changes effect on coherent neutron scatt. rel. to vibr. props. 9-42953
- freezing from plane chill, analytical solutions, exact. and approx., comparison 9-39135
- gamma ray scatt., 145 keV, differential elastic scatt. X-section 9-46263
- Gibbs free energy of self and impurity diffusion 9-33001
- grain boundary sliding in bicrystals rel. to deform. 9-46888
- granular films, superconducting fluctuations in 3-d regime causing excess conductivity 9-26527
- Hall coeff., accurate determ. from helicon waves and surface mode loss 9-24124
- Hall coeff., depend. on cryst. orientation 9-35334
- Hall field reversal, rel. to band relax. times and temp. depends. 9-37438
- Hartree-Fock calc. of single-orthogonalized- plane-wave binding energy 9-24081
- internal friction peaks after α -irrad. ascribed to reorientation of interstitial clusters 9-39398
- ion irradiated, vacancy clusters 9-28279
- ionization by H, He ions, cross section and K-shell X-ray yield meas., E=25-200 keV 9-22940
- K-ionization by e impact, cross section anomalies obs. 3-20 keV 9-46291
- Laue diffraction patterns, study using cascaded image intensifier 9-48821
- LEED beam scattering, non-specular by (100) face 9-46778
- liquid, pair correlation fn. and pair potential 9-44546
- magnetoresistance, Kohler rule validity for neutron-irrad. cryst. at 4.2K 9-44906
- metallization of plastic dielectrics for capacitors 9-39698
- in minerals X-ray K spectra obs., chemical bonds covalence and ionicity determ. 9-37741
- mirror protection from Hg acetate corrosion 9-33672
- mirror with MgF₂ coating, for space flight, degradation due to condensation and u.v. irrad. 9-40111
- mirrors, LiF coated, highest reflectance in vacuum ultraviolet 9-32011
- m.i.s. system, I-V characts. 9-44997
- molten, density and surface energy polytherms 9-40781
- molten, solubility of AlP, 900°-1200°C 9-30372
- molten, wetting of sapphire, ruby and recrystallized alumina 9-34977
- n.m.r. lines quadrupole broadening w.r.t. plastic deform., dislocations density obs. 9-35723
- notched columns with fixed ends, failure under load 9-48906
- optically excited plasma resonance 9-48591
- oscillatory wire drawing, reduced stress and friction 9-37286

Aluminium continued

- oxidation of fine wires, mech. effects during growth of anodic oxide films 9-31192
- oxidation rate, infl. of light, estimation of Al₂O₃ film band structure 9-31000
- phonons, anharmonic effects, wave number depend. of widths, shifts and dispersion curves 9-35266
- pit formation during heat treatment of single crystals 9-32946
- plasma, laser produced, microwave diagnostics 9-23319
- plasma, spectra for excitation by ruby laser 9-38781
- plasma, emission lines, 5000 to 100000°K 9-40675
- plasma due to exploding wire in vacuum, opt. and spectral props. 9-44440
- plasma prod. by laser impact on Al target, u.v. emission spectrum obs. 9-36769
- plasmons radiation, 10.1 eV peak, due to 50 keV electron irradiation 9-41146
- plastic behaviour of polycryst. on tensile deform. 9-41014
- plastic flow mechanism in quenched and aged sample, 86°K 9-48900
- plates, temp. depend. of sound vel. 9-46988
- polycrystal, effect of orientation-dependent solidification 9-46931
- powder-oxygen mixtures, detonation investigation 9-27234
- powders, sintering n.m.r. obs. of cryst. lattice distortions rel. to oxidation 9-47442
- proton channeling, determ. of energy loss in single crystal 9-30801
- proton energy losses 9-30807
- quenched, faulted dislocation loops annealing behaviour 9-39451
- quenched, internal friction and vacancy migration 9-46809
- quenched and aged, plastic flow mechanism, 86°K 9-48900
- radiative Auger effect, simultaneous emission of X-ray photon and L-shell electron 9-40553
- recrystallization kinetics of 1100 Al after deform. under u.s. vib. 9-37238
- recrystallization of single cryst. after pt. deform. 9-42908
- reflector in fast reactor critical expt., meas. and analysis 9-29883
- reinforced with SiO₂ fibre, eff. of irradiation on strength 9-26338
- resistivity, low temp., quadratic temp. depend. 9-37437
- shielding studies for 10 MeV gamma rays 9-22528
- single crystal, yield, plasticity and elec. cond., macrosound and n effects 9-46928
- sintered powders, control of fretting wear 9-41035
- sintering powders, n.m.r. obs. of crystal lattice distortions rel. to oxidation 9-47442
- slip, coarse, model of crack formation and propag., rel. to fatigue 9-48904
- solid and liquid equations of state calc. from low temp. mechanical obs. 9-39090
- solubility of AlP, rel. to temp., for crystal growth 9-37025
- solubility of Fe, enhanced value obtained by rapid quenching 9-42916
- spall layer thickness from fracture criterion 9-33063
- spherical cap, impact tests on liquid, study of parameter significance 9-22186
- sputtering of U in-reactor, subsequent irrad. for fission fragment track etching and obs. 9-34489
- stopping power for 0.6-2.4 MeV protons 9-33212
- strain hardening and softening by cycles of plastic deform. 9-23867
- strengthening by 3D network of Al₂O₃ part. 9-26337
- stress/strain diagram rel. to stress rate in elastic range 9-41008
- superconductivity, critical temp., hydrostatic press. effect 9-37467
- superconducting, lifetime of excitations, calc. 9-44935
- superconducting, quasiparticle recombination rate, calc. 9-44934
- superconducting films, dirty Knight shift BCS-Yosida depend. 9-45394
- superconducting films, granular, transition temp. enhancement 9-24149
- superconducting granular films, microwave conductivity 9-37466
- superconducting temp. enhancement for very thin films 9-30869
- superconducting thin films, microwave conductivity 9-28481
- superconducting thin films, strain effect on T_c 9-41177
- superconductivity enhancement in films of fine smoke cryst. 9-33270
- superconductivity enhancement mechanism in granular films, expt. evidence 9-24150
- surface contamination by C and O, nuclear reaction analysis 9-26178
- surface layer stress, effect on fatigue resistance and brittle fracture 9-23880
- surface microrrelief changes due to cyclic straining X-ray diff. method obs. 9-46777
- target, 70GeV proton bombard, search for quarks 9-34259
- tensile strength and cell struct. rel. to hydrostatic extrusion 9-41029
- thermal conductivity, 78 to 373°K, apparatus descrip. 9-26439
- thermal diffusivity from linear dimens. changes 9-41097
- thermal fractional expansion 9-42971
- u.s. wave attenuation due to dislocations as function of strain and temp. 9-37332
- water laminations, fast neutron spectrum obs. 9-22896
- wires, crystallite orientation changes during 1% plastic deformation 9-35170
- work function, correlation energy contribution using pseudopotential model 9-35515
- X-ray K spectra obs. in minerals, chemical bonds covalence and ionicity determ. 9-37741
- X-ray scatt. factors, absolute meas. from transmission meas. on powder samples 9-28254
- γ reflected, polarization deduced from Mossbauer spectrum 9-30532
- ρ , range and ionization energy losses, Bragg's curve method meas., E_p=100-660 MeV 9-33213
- Al/As-S glass, composite system, bonding mechanism 9-32852
- Al-Al₂O₃-Au(Ag) structure, I-V characts. 9-30954
- Al-Al₂O₃-Bi-I-Sb₂ film junctions, oscillatory effects on electron tunnelling 9-39657
- Al-Al₂O₃ triodes, hot-electron transport 9-49128
- Al-Al₂O₃-ZnTe, I-V characts. of tunnelling junction 9-33357
- Al-GaSe-Au struct., carrier transport 9-41228
- Al-I-M films, (M=Ni, Pd, NiPd alloys, Fe, Gd) electron tunnelling, rel. to spin wave excitation 9-44995
- Al-Si₃N₄-Si structure, prep. and elec. props. 9-43097
- Al, fatigue crack initiation and propag., correlation, effect of substruct. 9-30685
- Al³⁺, isoelectronic series, theoretical ionization energies and oscillator strengths 9-22927
- Al atomic scatt. factors from thermal diffuse intensities meas. 9-32900
- Al films, granular, microwave conductivity in supercond. transition region 9-26504

Aluminium continued

- Al I, $3s^2 3d^2 D_{5/2}$ and $^3D_{3/2}$ hyperfine structure, Stark effect investigations 9-40539
 Al I to III, singlets and multiplets, mean lives 9-46290
 Al cold-rolled, yield strength determ. 9-28342
 Al-Al₂O₃-Al thin films, noise meas. to verify tunnelling 9-33356
 Cd-Al₂O₃-Al supercond. junctions, electron tunnelling charact. 9-37497
 n-Cd_{1-x}Mg_xTe:Al mixed cryst., elec. props. 9-43054
 n-CdTe:Al, heat treated, multiply charged acceptors, photo-Hall effect obs. 9-49075
 CoO:Al, self-diffusion of ^{18}O 9-49082
 films, epitaxial, nucleation and growth struct. on NaCl substrates 9-36945
 films, evap., electron diff. intensities variation with energy loss 9-35053
 Si:Al, electron-irrad., defects effect on photoconductivity spectra 9-44985
 SiO₂-coated, reflectance, solar absorptivity and thermal emissivity 9-37373
 spectral lines, Stark broadening and displacement rel. plasma high temp. meas. 9-25913
 Ta-Al point contacts, radiative emission at Ta energy gap freq. 9-25300
 in U alloys, determ. by atomic absorption spectroscopy 9-26839

Aluminium alloys

see also *Aluminium compounds*

- Alnico, Ti bearing, mag. props. rel. to structure 9-24310
 atmospheric corrosion, eff. of initial weather conditions 9-24568
 atmospheric stress corrosion testing 9-37827
 composition effects on X-ray transmission thickness gauging 9-39156
 corrosion, atmospheric results of 6 year exposure tests 9-24571
 corrosion cracking, stress conc. influence 9-44778
 corrosion tests for architectural purposes on hard-rolled alloys 9-24570
 cylinder, ductility under explosive loading cond., strain at fracture 9-30660
 deformation instability, strain-induced 9-26326
 dilute, ^{27}Al n.m.r. relax. rel. to atomic diffusion 9-47443
 Duralumin, plastic deform., stress reduction on applic. of oscillatory energy 9-37286
 duraluminium, plastically deformed at 77°K, recovery of elec. resistivity 9-39581
 fatigue, low-endurance, studies under cyclic torsion 9-23860
 fatigue crack propag., microfractographic investig. 9-33080
 fatigue properties, variations with batches 9-23855
 fatigue props. of machine cut, unnotched specimens, cut depth effect 9-33074
 fretting fatigue prevention 9-42898
 hard-rolled, corrosion tests for architectural purposes 9-24570
 high strength, metallurgical treatment, patent 9-26376
 mechanical properties, effect of low temps. 9-23905
 porosity, depend. on grain size and composition 9-28393
 specific heat of six commercial alloys, 1.6 to 4°K 9-35293
 stress corrosion cracks, detection using Rayleigh waves 9-42704
 stress-corrosion induced prop. changes, nondestructive eval. 9-26829
 tensile strength and cell struct. rel. to hydrostatic extrusion 9-41029
 tensile strength during atmospheric corrosion test 9-37828
 thermal conductivity meas. apparatus at cryogenic temps. 9-26454
 thickness gauging by X-ray transmission, composition effects 9-39156
 AL-10wt.%Pu, fuel elements, injection casting in Pyrex molds, and encapsulating in Zircaloy 9-22897
 Ag-(0.2-0.4 at.%)Al, oxidized, internal friction meas. 9-48885
 Al-alumina, slip bands and glide planes 9-37246
 Al-(0.06 at.%) Si, resist. rel. to Si atoms clustering in ageing, 300°C 9-30712
 Al-(0.13 at.%) Si, resist. rel. to Si atoms clustering in ageing, 300°C 9-30712
 Al-(18wt.%)Ag, dissolution kinetics of precipitate, depend. on growth mode 9-30749
 Al-(15wt.%)Ag, growth of h.c.p. γ plates, mechanism, e microscopy 9-30738
 Al-(1 at.%) Ag, dissociated prismatic dislocation loops, model verification 9-35091
 Al-Ag, δ phase formation, small angle X-ray diffraction study 9-23947
 Al-Ag, internal friction peaks due to γ' phase precipitation 9-35152
 Al-Ag, strength increase by strain-induced solute disposition stability control, eff. of additions 9-28360
 Al-Ag dilute, impurity resistance, 1.2° to 300°K 9-30840
 Al-Ag dilute solid solutions, vibrational entropy, electronic influences 9-39508
 Al-Al₂O₃, creep behaviour, 450°C, rel. to crack formation 9-46898
 Al-Al₂O₃, sintered two-phase, crack formation 9-42902
 Al-Au dilute, impurity resistance, 1.2° to 300°K 9-30840
 Al-Au thin films, diffusion anomalies 9-35123
 Al-Bi system, phase equi. obs., thermodynamic props. 9-46679
 Al-0.12 at. %Si dil. alloy, clustering of Si atoms during step aging 9-23940
 Al-Cr dil. solid soln., mag. susceptibility and sp. ht. w.r.t. localized d-state props. 9-33269
 Al-Cu-Ag, resistivity changes rel. to growth and dissolution of Ag-rich zones and vacancies 9-46758
 Al-Cu-Cr supersaturated solid solns., kinetics of decomp. 9-46937
 Al-Cu-Mg-Ag, S precip. obs. 9-48928
 Al-Cu-Mg, S precip. obs. 9-48928
 Al-(4 at.%)Cu, vacancies excess conc. during ageing and slow reaction mechanism obs. 9-48916
 Al-(4 at.%) Cu, grain-boundary precipitates, growth 9-35101
 Al-(4wt.%)Cu, transition precipitate structures formation, effect of cyclic straining 9-39490
 Al-Cu, binding free energy bet. vacancies and second solute atom 9-23793
 Al-Cu, dilute, thermopower, temp. and size depend. 9-43123
 Al-Cu, molten, wetting of sapphire, ruby and recrystallized alumina 9-34977
 Al-Cu θ' precipitate, stacking faults, electron microscope exam. 9-35098
 Al-(2.5 at.%)Cu-(1.2 at.%)Mg, ageing, Si effect on initial stages 9-48915
 Al-(4.3 wt.%)Cu, precip., effect of pressure 9-42917
 Al-CuAl₂ eutectic, directionally frozen, structure 9-39250
 Al-CuAl₂ eutectic, lattice rotations 9-39251
 Al-(68.9 at.%)Fe, galvanomagnetic effect, longitudinal 9-24278
 Al-Fe, dilute, thermopower, temp. and size depend. 9-43123
 Al-In system, phase equi. obs., thermodynamic props. 9-46679
 Al-Li, charact. temp., Young's modulus, linear expansion coeff., variation with Li conc. 9-39395

Aluminium alloys continued

- Al-Mg-Si, electron microscope images, quality deterioration with specimen thickness, 50-100 KeV 9-23747
 Al-Mg-Si, recrystn. behaviour, influence of precipitates 9-39452
 Al-Mg-Si containing Mg₂Si, 2-stage ageing effect 9-39461
 Al-Mg-Zn, ageing and plastic deform. 9-37280
 Al-Mg-Zn, recrystn., dislocation arrangement influence 9-37276
 Al-Mg-Zn pre-precipitation, lattice parameters rel. to ageing 9-41049
 Al-(11 wt.%)Mg, alloys, age-hardening, deform. by hydrostatic extrusion, effect on struct. and props. 9-41051
 Al-Mg, stress-induced knitting of dislocation networks with four-fold nodes 9-44706
 Al-(0.5 at.%)Mg, quenched, hardening mechanism at 86°K 9-30699
 Al-Mn, dilute, n.m.r., low temp. phen., impurity obs. 9-28754
 Al-Mn dil. solid soln., mag. susceptibility and sp. ht. w.r.t. localized d-state props. 9-33269
 Al-Ni, molten, wetting of sapphire, ruby and recrystallized alumina 9-34977
 Al-(20wt.%)Si, primary Si spherulite growth and morphology 9-23775
 Al-Si, dilute, cold-worked, isochronal annealing obs., recovery process 9-33104
 Al-Si, subeutectic, thermal stresses calc. by phase suspension model 9-23948
 Al-Si eutectic, banding explanation 9-44613
 Al-Ta, dil., ^{27}Al n.m.r. rel. to impurity-disloc. effects 9-24504
 Al-(0.22at.%)Ti, lattice parameter comp. depend. 9-42918
 Al-V dil. solid soln. mag. susceptibility and sp. ht. w.r.t. localized d-state props. 9-33269
 Al-Zn-Mg-Cu, deformed, substructure and susceptibility to intergranular stress corrosion cracking 9-23811
 Al-Zn-Mg, fatigue props., effect of shot peening 9-26315
 Al-Zn-Mg, preprecip., hardness and small-angle X-ray scatt. meas. 9-23979
 Al-Zn-Mg, weldable, stress-corrosion resistance, effect of quench rate, rel. to microstruct. changes 9-46919
 Al-Zn-Mg 1 type blue tint of glossy anodized extruded profiles 9-39833
 Al-Zn-Mg properties rel. to natural ageing and ageing between 100-340°C 9-37281
 Al-Zn-Mg precipitation near grain boundaries 9-39489
 Al-(40 at.%)Zn, aged at 240° to 250°C, stacking fault formation 9-32979
 Al-(10 wt.%)Zn, irradiated at 78°K, pre-precipitation rate 9-30715
 Al-(30 at.%)Zn, side-bands in Debye-Scherrer patterns 9-46936
 Al-(40 wt.%)Zn, structural changes during ageing 9-23943
 Al-Zn, spinodal decomposition effect on yield and tensile strengths and ductility 9-37289
 Al-Zn, spinodal struct. decomp. by Zn precip., dislocation struct. 9-37291
 Al-Zn, spinodal structures, study by X-ray diff., stability and breakdown during ageing 9-37290
 Al-Zn dilute solid solutions, vibrational entropy, electronic influences 9-39508
 Al-Zn eutectoid, superplastic behaviour, rel. to grain boundary sliding and grain rotation 9-23900
 Al-Zn solid soln. and precip. hardened alloy cryst., plastically deformed, dislocation distrib. 9-39364
 Al-(4.4 wt.%)Zn, Be atoms influence on elec. resistivity changes due to clustering 9-40932
 Al-(6wt.%)Zn-(2wt.%)Mg, precipitate nature and morphology 9-28390
 Al-Zr-Si, recrystn. and age hardening, influence of Si 9-42910
 Al-(0.5wt.%)Zr, precipitation eff. on plastic deformation and recrystallization 9-44794
 Al-Zr, quenched, superheating melt effect on struct. and props. 9-39450
 Al-(3-15wt.%)mg, dislocation structure by X-ray diff. and electron microscopy 9-40946
 Al-(0.3-0.4 wt.%) Cu bicrystal, grain boundary sliding rel. to deform. 9-46888
 (1-x)Al_{1-x}LiO₂-xGeAlLiO₄ solid soln., spinel phase, stability domain boundaries 9-33119
 Al-Ga_{1-x}As_xSi electroluminesc. diodes, props. and efficiency 9-37775
 Al-Ga_{1-x}As solid solns. with forbidden band width gradient, recomb. radiation 9-47389
 Al1.5wt.%Mn, Aluman, laser microprobe analysis, impurity emission rel. to matrix effects, obs. 9-24604
 AlMn supercond. critical temp., effect of Mn 9-24134
 AlZnMg 1, annealing effect on microstruct., susceptibility to stress and layer corrosion 9-46779
 Al-2at.%Zn-2at.%Mg, reversion reaging 9-41048
 Al-(2wt.%)Cu, solid-liquid interface, microstructure and composition variation 9-34961
 Be-vacancy interactions 9-44692
 Be vacancy interactions 9-44691
 Co-(42-54 at.%)Al alloys, electric and mag. props. 9-47069
 Co-Al local moment formation and resistivity minima 9-44908
 Co-Ni-Al-Cu-Nb-Fe, magnetostruct. analysis 9-47251
 Co-Ni-Al-Cu-Ti-Fe, magnetostruct. analysis 9-47251
 Cu-(14.5 wt.%)Al-(3.5 at.%)Ni with thermoelectric martensite, internal friction, amplitude depend. 9-42869
 Cu-Al-Fe-Ni aluminium bronzes, ductility rel. to microstructure, 20-800°C 9-23894
 Cu-(5 wt.%)Al, tensile deformation at room temperature 9-30680
 Cu-(16 at.%)Al, short-range ordering kinetics 9-33120
 Cu-Al, dislocation phonon scattering values from thermal conductivity and dislocation density meas. 9-41078
 Cu-Al, latent hardening rel. to composition and prestrain 9-41015
 Cu-Al, martensitically transformed, Young's mod., yield stress and plastic deform. 9-35172
 Cu-Al, quenched, Frank dislocations dissociate, e diff. obs. 9-40959
 α -Cu-Al, short-range ordered state and stable superlattice phase obs. 9-39275
 Cu-(16 at.%)Al solid soln., high temp. creep behaviour 9-33043
 Cu-Al dislocation loops, complex Frank, stacking fault steps form. rel. to fault climb 9-40943
 Cu-Al films, effective surface diffusion coeffs., vol. diffusion effect in electron diff. obs. 9-39379
 Cu-Al martensite cryst. struct. stability, solute content effect 9-42929
 Cu-Al solid solns., stacking fault energy influence on high temp. creep 9-42886
 Cu-Al solid solns., stacking fault energy influence on high temp. creep 9-42887

Aluminium alloys continued

- Cu-(0.2 wt.%)Al, internally oxidised, effect of Si additions on mech. props. 9-46903
 Cu-(15 at.%) Al, Shockley partial dislocations, unstable directions 9-35093
 Cu-Mn-Al struct. study by X-ray and neutron diffraction anal. and electron microscope exam. 9-37293
 Cu-Ti-Al, decomp. and recovery after low-temp. ageing 9-37292
 Cu-Ti-Al, decomp. nature, struct. changes on ageing electron microscopy 9-46938
 Cu-Ti-Al, dispersion-hardened, mechanical twinning 9-23926
 Cu-(15 at.%)Al deformed cryst., lattice thermal conductivity 9-35291
 dAl-(1 wt.%)Cd, pre-precipitation, rel. to recovery after quenching and cold-washing 9-23936
 Fe-(25 at.%)Al, electron microscopy investig., one- and two-phase struct. obs., magnetiz. and magnetocrystalline anisotropy 9-26648
 Fe-(40 at.%)Al, ordering and struct. distortions, X-ray diffraction obs. 9-42784
 Fe-Al, domain structure and short range order, depend. on Al conc. 9-23757
 Fe-Al, Mossbauer effect following n capture, recoil effects obs. 9-43224
 Fe-Al, phase relations, X-ray diffraction obs. 9-44664
 Fe-Al, short-range order, X-ray diffuse scattering obs. 9-44665
 α -Fe-Al, superlattice phases, equilibria and transforms 9-46952
 Fe-Al, X-ray K-absorption edges of Fe, position investig. 9-33571
 Fe-Al ageing, precip. of (FeMn)₃AlC 9-33139
 Fe-Al Fe-rich, transf. diagram construct., electron microscope applic. 9-33131
 Fe-Al single crystal, mag. anisotropy and order 9-47252
 Fe-Al single crystal, mag. susceptibility superimposed on saturation magnetization 9-47258
 Fe-Al system intermetallics, microhardness, strength, elec. resistivity, thermal expansion, Fe diffusion coeffs. 9-46890
 Fe-Ni-Al-Co-Ti alloys, thermomech. treatment effect on mag. props. 9-47259
 Fe-Ni-Al, b.c.c., mag. moment behaviour rel. to composition changes 9-24274
 Fe-Ni-Al, decomp. of supersaturated solid solns., elastic stresses effect 9-39475
 Fe-(2 wt.%)Si, Ge effect on internal oxidation 9-46740
 Ge-Al alloy dot on n-type Ge, h.f. tunnel diode, low resistance, capacitance, prod., patent 9-30946
 Ge alloying of thin Al film, obs. 9-33116
 La_{1-x}Ce_xAl₃, supercond. transition temp., eff. of press. 9-28477
 La_{1-x}Gd_xAl₃, supercond. transition temp., eff. of press. 9-28477
 Li-Al, lattice parameters 9-42789
 Mg-Al-Zr-Be, correlation of orientation and polarized etching, facets 9-39186
 Mg-Al eutectic, superplastic deform. mechanism 9-42883
 Mg-(5 at.%)Li-(1.5 at.%)Al, plastic deform. during rolling, mechanism 9-33035
 MnAlGe, ternary alloy, magnetic structure by neutron and X-ray diffraction 9-35560
 Nb-Al positron annihilation, critical temp. eqn. parameters 9-39598
 Ni-(49-51 at.%)Al, electric and mag. props. 9-47069
 Ni-(1.8 at.%)Al, creep rate, 700°C, effect of ultrasonic vibrations 9-33047
 Ni-Al-Sc system, phase equilibria and solubility limits in Ni-rich region 9-30720
 Ni-Al, γ phase, coherent solubilities 9-28403
 Ni-Al, shear stress, critical, temperature dependence 9-23908
 Ni₃Al single-cryst. elastic consts. 9-35140
 Ni₃(TiAl), hardened by coherent and ordered precip., yielding 9-39408
 β -NiAl, optical props. and energy band struct. 9-47367
 Pu-Al, diffusion in stabilized δ -Pu 9-28323
 Pu-Al, electron microprobe anal. 9-49400
 Pu-Al delta-stabilized elastic and anelastic behaviour at low temp. 9-37224
 Ti-(5 wt.%)Al-(2.5 wt.%)Sn fracture toughness and mech. props. at cryogenic temps. 9-37253
 Ti-(6 at.%)Al-(4 at.%)V, plane-strain cyclic and sustained load flow growth charact. 9-30722
 Ti-(8 wt.%)Al-(4 wt.%)Co, heat treatment rel. to mech. props. 9-40994
 Ti-(8 wt.%)Al-(4 wt.%)Co, mech. props. and structure 9-23956
 Ti-(8 wt.%)Al-(4 wt.%)Co, microstruct. and heat treatment rel. to mech. props. 9-44747
 Ti-(6 wt.%)Al-(4 wt.%)V, surface treatment for impact fatigue and wear resistance 9-37259
 Ti-(6 wt.%)Al-(4 wt.%)V, two-phase microstructures, toughness 9-37251
 Ti-Al-Co system, diagram for Ti-rich corner, struct. obs. 9-40919
 Ti-(8wt.%)Al-(1wt.%)Mo-(1wt.%)V sheet, hot-salt-stress-corrosion cracking and effect on tensile props. 9-23923
 Ti-Al, equilib. diagram, study on Ti-rich region 9-26381
 Ti-Al, Ti₃Al precip., particle size line broadening 9-28400
 Ti₃Al ordered and disordered alloys, low temp. electronic sp. ht. coeff. 9-30751
 Zn-Al, liquid, density meas. up to 700°C 9-30375
 Zn-Al, superplasticity 9-26330

Aluminium compounds

see also *Aluminium alloys; Ruby*

- Al₂O₃ sprayed coating, elec. insulation rel. gas-flame deposition process in Ar with Cs admixture 9-24211
 alumina, cryochem. method for prep. 9-33125
 alumina, fabrication with good surface finish by electrophoretic deposition 9-35219
 alumina, polycrystalline, compressive creep characts. 9-37244
 alumina, recrystallized, wetting by molten Al, alloys, Cu and Au, contact angle meas., sessile drop technique 9-34977
 alumina, thin wall capillary tubes, fabrication by vapour deposition 9-35220
 alumina particles dispersed in Al matrix, electron diffraction contrast obs. 9-32890
 alumina powders, binary mixtures, sintering kinetics 9-35230
 alumina powders, cements for chemical bonding 9-35229
 alumina powders, hot-pressing technique 9-35201
 alumina strengthening by glazing and quenching 9-23935
 alumina trichites, prod. and props. 9-35016
 alumina whiskers/Ni composites, electron microscope obs. 9-33169
 alumina/metal interfaces, room-temp. strengths, correls. with phys. props. 9-23903

Aluminium compounds continued

- aluminoboro-phosphate glasses, absorpt. and fluoresc. spectra of Mo³⁺ 9-47350
 carbides, heat of formation 9-49369
 corundum, e.p.r. of Fe³⁺, angular dependence obs. 9-47428
 corundum, hyperfine structure of ⁵⁷Fe, stabilization eff. 9-26719
 corundum crystal, light scatt. effects 9-33522
 corundum with paramagnetic ion impurities, electron states group theoretical classification 9-28443
 faujasite, dehydrated La-exchanged, position of mols and cations at 420°C 9-32899
 faujasite, hydrated Ca-exchanged, positions of cations and molecules 9-30556
 fluorescence spectra, K α satellites 9-49327
 garnets, rare earth, i.r. lattice spectra 9-47338
 leucosapphire, i.r. refl. spectrum, 5-25 μ 9-28669
 methylammonium alum., elementary cell parameters in phases I and II, temp. depend. 9-42927
 montmorillonite aqueous gels, n.m.r. 9-23553
 muscovite, dislocation planes, electron microscopy 9-23748
 oxide anodic films, mech. effects during growth on fine wires 9-31192
 sapphire, Czochralski, dislocation reactions and cavities in veiled region 9-35092
 sapphire, epitaxy of Si single crystal film 9-34990
 sapphire, filamentary damage formation by laser beam 9-48847
 sapphire, gas phase etching by fluorinated hydrocarbons 9-36987
 sapphire, heat pulse expts. for low temp. thermal transport 9-26438
 sapphire, orientation selection as substrate for Si films 9-23658
 sapphire, temp. distrib. for values of reflection coeff. 9-42964
 sapphire, wetting by Cu-O liquid alloys 9-26179
 sapphire, wetting by hydrophobic liqs., effect of adsorbed water 9-34978
 sapphire, wetting by molten Al, alloys, Cu and Au, contact angle meas., sessile drop technique 9-34977
 sapphire single crystal, high-temp. creep, rel. to dislocation climb 9-30658
 sapphire single crystals, obs. of thermally emitted phonons 9-30761
 sapphire whiskers, tensile strength, temp. depend. 9-35180
 sapphire-sapphire contact, thermal resistance 9-39544
 ultramarines, e.p.r. investigation of S radicals 9-36727
 zeolite, La-exchanged type X, cations and mol. positions at 25, 425 and 735°C 9-39249
 Al-(18wt.%)Ag alloys, dissolution kinetics of precipitate, depend. on growth mode 9-30749
 Al-Al₂O₃ films, photoemission in vacuum u.v. 9-37632
 Al-Al₂O₃ triodes, hot-electron transport 9-49128
 Al-I-Bi tunnel junctions, pressure effects up to 30 kbar, 77°K 9-37556
 β -Al-Mg, electron diffraction, transmission and reflection study 9-26222
 Al-O system, existence of suboxides and P-T-x diagram 9-26158
 γ -Al₂O₃ i.r. spectrum, absorption band 1370-1390 cm⁻¹ 9-49270
 Al₂-Cr₂BeO₄, alexandrite, anti-phase boundaries electron microscopy obs. 9-35104
 Al₂O₃ in k feldspar glass, glass, surface features meas. by molec. emission 9-42709
 Al₂O₃:Cr³⁺, pin-phonon interaction in ext. elec. fields 9-45243
 Al₂O₃:Cr(Fe,Mn,V) single cryst., low temp. thermal conductivity meas. 9-35086
 Al₂O₃:Fe³⁺ single crystal, paramagnetic relax. absorpt. of hypersound 9-33172
 Al₂O₃:Ti(V,Cr) far i.r. absorpt. spectrum in applied mag. field, Zeeman splitting of lines, single d electron obs. 9-31100
 Al₂O₃/Y₂Al₂O₇ system, eutectic solidification 9-34960
 Al₂O₃:Fe₂O₃:SiO₂-CaO system hydraulic strength 9-23907
 Al₂O₃:Fe₂O₃:SiO₂-CaO system, hydraulic strength 9-23907
 Al₂O₃:PbO-B₂O₃ system glasses, spinodal decomposition 9-39492
 Al₂O₃-Y₂Al₂O₇ system, eutectic point position, microstruct. obs. 9-35254
 Al₂O₃, active, η -type prod. by plasma jet treatment of aluminium hydroxide 9-46945
 Al₂O₃, brittle fracture below 1000°C 9-33084
 Al₂O₃, corundum, impurity-doped, decorated disloc. movements during annealing 9-37172
 α -Al₂O₃, diffusion of B-active fission products, obs. 9-30623
 Al₂O₃, double ⁵³Cr-²⁷Al acousto-nuclear mag. reson., 4.2°K 9-49359
 Al₂O₃, hot-pressing, effects of gaseous impurities 9-35202
 Al₂O₃, ht. capacity, 300-1100°K 9-35285
 Al₂O₃, lattice energies, heat of atomization, bond energy and dissociation energies, rel. to fund. props. 9-30494
 β -Al₂O₃, lattice self-potentials and Madelung const. 9-36974
 Al₂O₃, microwave dielectric constant, 375 kb 9-28547
 α -Al₂O₃, neutron damage 9-23810
 Al₂O₃, neutron irradiat., e.p.r. spectrum of triplet (S=Z) state defect 9-44689
 Al₂O₃, non-collinear acoustic attenuation of transverse waves, temp. depend. 9-39519
 α -Al₂O₃, phosphoresc. and thermoluminesc., activation energies 9-39889
 γ -Al₂O₃, pyridine absorpt., active centres nature, i.r. obs. 9-26192
 Al₂O₃, recrystallization kinetics during sintering 9-33105
 Al₂O₃, sapphire, Young's modulus at high temp., u.s. meas. 9-42966
 Al₂O₃, self-supporting films, thermal conductivity 9-39543
 Al₂O₃, sintered alumina, effects of Mn and Na additions on glow curve 9-28728
 Al₂O₃, surface diffusion, obs. review 9-37198
 Al₂O₃, thermal conductivity meas. 9-37365
 Al₂O₃, volume change on freezing 9-40820
 Al₂O₃, X-ray determ. of electron band structure 9-30811
 α - and γ -Al₂O₃, X-ray spectral investigation of chemical bonding 9-49304
 Al₂O₃:3H₂O two types treated by N, Ar plasma jets to produce active η -alumina 9-46945
 Al₂O₃ (sapphire), heat pulse expts. for low temp. thermal transport 9-26438
 Al₂O₃ (sapphire), orientation selection as substrate for Si films 9-23658
 Al₂O₃ added to borolanthanum glasses, immiscibility and catalytic crystallization 9-34971
 Al₂O₃ anode films, photoluminescence 9-49330
 Al₂O₃ attenuation of u.s. longit. waves at microwave freqs. temp. depend. 9-39518
 Al₂O₃ bicrystals, [110] tilt boundaries, relative grain boundary energy and surface diffusion coeff. 9-26290
 α -Al₂O₃ corundum, heat capacity, 2-25 K 9-44833
 Al₂O₃ film, band structure parameters, estimation from light infl. on Al oxidation rate 9-31000

Aluminium compounds continued

- Al₂O₃ film growth kinetics on Cu-Al alloys 9-23635
 Al₂O₃ irregular cryst., sintering under high press. 9-30728
 Al₂O₃ particles-Cu matrix interface, generation of dislocations, local shear stresses 9-30611
 Al₂O₃ polycrystals, elastic moduli, isotropic, pressure and temp. derivatives 9-46863
 Al₂O₃ reflector in fast reactor critical expt., meas. and analysis 9-29883
 Al₂O₃ specific heat review 9-37355
 α -Al₂O₃ symmetry props. of normal modes of vib., group theory anal. 9-39507
 Al₂O₃ thin film, O K-shell X-ray prod. by 20–100 keV protons 9-24073
 Al₂O₃ thin foils, small-angle scatt. of ³⁵S and ¹⁶O beams 9-35298
 Al₂O₃-SiO₂ system, immiscibility, metastable glass-in-glass separation and crystn. nucleation 9-32826
 Al₂Th₃ superconductivity rel. to Si₂U₃-type structure 9-39596
 Al₂N₄ anisotropic growth, neutron irradi. 9-40857
 Al₂N₃ susceptibility temp. dependence 9-28616
 Al₂Ga_{1-x}As injection lasers, charact. 9-27335
 Al₂Ga_{1-x}As:Si electroluminesc. diodes, props. and efficiency 9-37775
 Al₂Ga_{1-x}P diodes prep. by liq. phase epitaxy, electroluminesc. obs. 9-47413
 AlF₃ crystal growth from low melting flux 9-39207
 AlF₃ modifications, ¹⁹F n.m.r. chem. shift 9-48453
 AlN, effect on primary recrystallization textures in cold-rolled-(110)[001]-oriented single crystals of Fe-(3 wt.%)Si 9-44784
 AlN, energy band structure, orthogonalized plane wave method 9-26480
 AlN, hardness, infl. of highstatic and dynamic pressure 9-26361
 AlN, microcryst., I.r. absorpt., surface modes and finite size effects obs. 9-37717
 AlN, phonon structure of Mn⁴⁺ activator centres 9-24010
 AlN, positron annihilation 9-30830
 AlN films grown by reactive sputtering, dielectric props. 9-37575
 AlN refractory, melting technique 9-34955
 AlO, visible region spectrum, new bands 9-46354
 α -AlOOH:Fe²⁺ e.p.r. spectrum, theoretical and expt. obs. of low-symmetry effects 9-41427
 AlP, solubility in Al, rel. to temp., for crystal growth 9-37025
 AlP, solubility in molten Al, 900^o-1200^oC 9-30372
 AlP, vaporization 9-36927
 AlSb, chemical and isoconcentration diffusion of Zn, Longini's interstitial/substitutional model 9-35125
 AlSb, chemical and isoconcentration diffusion of Zn, conc. depend. 9-35124
 AlSb, gradient-elastic tensor determ by nuclear acoustic resonance 9-23851
 AlSb semiconducting films, condensation 9-28487
 AlSe, electronic band system obs. in thermal emission 9-42380
 CaF₂-AlF₃ system, phase diagram, DTA and X-ray powder obs. 9-44805
 Cd-Al₂O₃-Al supercond. junctions, electron tunnelling charact. 9-37497
 Cr-Al acetylacetonate mixed single crystals, spin-lattice relax. props. 9-49227
 Cu-Al:Fe dilute alloy, specific heat 1.2^o to 14^oK 9-47001
 Fe-Al alloy, Fe-rich nuclear transverse relaxation times of ⁵⁷Fe, Suhl-Nakamura interaction 9-45240
 GaAs-AlAs diffused diodes, injection electroluminesc. 9-37780
 Ge-Al₂O₃-In₂O₃ heterojunctions, switching effect 9-47141
 MgO-Al₂O₃:Cr³⁺ absorption and fluorescence spectra 9-26778
 PbF₂-AlF₃ system, phase diagram, DTA and X-ray powder obs. 9-44805
 xSiO₂-(1-x)Al₂O₃:Eu²⁺ phosphors, luminesc. 9-47390
 Ti-(6 wt.%)Al-(4wt.%)V alloy, stress-corrosion cracking in anhydrous methanol, mechanism 9-48894
 U-Al₂-Al₂Mo₃ Mo system, melting equil. 9-39133
 Zr-Al, N diffusion, pumping speed meas., 10⁻⁶-1 Torr, 300 and 500^oC 9-37197

Americium

- electrodeposition by mol. plating method 9-43331
 magnetic hyperfine coupling at low temp 9-47334
²⁴³Am, separation from ²⁴⁴Cm by precipitation of K₃AmO₂(CO₃)₂ 9-26802

Americium compounds

- Am-Be neutron spectrum, calc. and expt. 9-22629
 AmF₃ Mossbauer spectrum of ²⁴³Am 9-44167
 AmO₂, Mossbauer spectrum of ²⁴³Am 9-44167
 AmO₂F₂, lattice constants 9-23749

Ammonia *see Nitrogen compounds/ammonia***Ammonium compounds** *see Nitrogen compounds/ammonium compounds***Amorphous state**

- see also Vitreous state*
 aromatic, polyesters, and polyamides, solubility and heat resistance 9-28191
 butadienenitrile rubbers, NMR, light scattering study of structure, vulcanization character 9-23789
 chalcogenide semiconductor films, conduction and elec. switching 9-28491
 irradiation target, penetration range of ions 9-42983
 Madelung const. and dispersion 9-42705
 of poly- ϵ -methylcaprolactam 9-32551
 polyethylene-polyisobutene mixtures, struct., X-ray obs. 9-30474
 polymers, high, linear, orientation anisotropy of heat conductivity 9-35292
 polymers, reversible deformation, singularities in development curve 9-26331
 polymethylmethacrylates, orientation anisotropy of heat conductivity 9-35292
 polypropylene, crystallinity influence on relax., phenomena 9-34974
 polystyrenes, orientation anisotropy of heat conductivity 9-35292
 semiconducting alloys, band model 9-33316
 semiconductors, popular review 9-44948
 solid, vibrational props., Greens functions 9-33219
 stopping of kV ions by elastic collisions 9-36678
 vibration spectrum, calc. by variational method 9-42941
 As, dimensions of struct. element of lattice from X-ray intensity curves 9-32824
 As₂S₃, refr. index, 0.6-2 μ 9-39797
 CdGeAs₂, semicond., thermal conductivity, phonons mean free path from Debye model 9-37367

Amorphous state continued

- Co-P alloys, amorphous layers, low coercive force characterisation 9-24311
 Fe-P alloys, amorphous layers, low coercive force characterisation 9-24311
 Fe₅₀P₁₃C₇ ferromag. alloy, resistivity minimum 9-37429
 Fe₅₀P₁₃C₇ ferromag. alloy, Hall effect 9-39578
 Ge-MgSb₂ films, reordering diffusion process under annealing 9-34985
 Ge sharp optical absorption edge obs. at 0.5eV 9-31106
 Pd-Si based alloy glasses, form., stability and struct. 9-42706
 Se, dimensions of struct. element of lattice from X-ray intensity curves 9-32824
 Se, i.r. absorpt. and multiphonon processes 9-45330
 Se, transient photoconductivity 9-37909
 Si thin film deposition by electron irradi. of tetramethylsilane, electron diff. and microscopy obs. 9-44628
 SiO₂ films, anodic growth, dielec. breakdown and carrier transport 9-45006

Amplifiers

- beam-plasma system, parametric amplification 9-42503
 Brillouin, stimulated, transient and steady gain, analysis 9-25206
 electroacoustic, root-locus analysis 9-28423
 e.s.r. two-transistor modulation amplifier 9-34127
 gas laser, polarization effects 9-25237
 helicon wave, for gain in wave propag. in plasma, patent 9-48577
 laser, in homogeneously broadened, transient behaviour of ultrashort e.m. pulses 9-29399
 laser amplification and self excitation 9-40345
 laser power, using active medium left after separation for reference oscillator 9-27301
 laser system of glass and SeOCl₂ liquid lasers 9-31948
 maser, H, atomic jet populations meas. 9-45943
 operational, using junction f.e.t., low-noise, high input impedance 9-41864
 optical t.w., for ruby laser high-coherent output improvement 9-25286
 parametric, band extension using two uncoupled resonators 9-36248
 parametric, P-representation 9-34150
 power, use of regenerative laser amplifier with oscillator 9-25230
 preamplifiers, charge sensitive, for use with solid state detectors 9-29658
 radiation amplification by plasma jet 9-32633
 RC, time consts. used in proportional counter waveform attenuation 9-25510
 semiconductor travelling wave, loss characts. 9-47135
 solid-state, improvement for Dobson ozone spectrophotometer 9-41475
 superregenerative, laser application 9-36318
 CO₂-N₂-He, amplifier, laser time-depend processes 9-38372
 CO₂ laser, photo-induced current changes 9-47976
 CO₂ laser, rot. relax. and gain saturation 9-41895
 CdS, u.s. amplification with continuous drift field at 20^oC 9-35282
 CdS piezoelectric semiconducting crystal acoustic, temp. depend. of characts. 9-44815
 CdS piezoelectric semiconducting crystal acoustic, temp. depend. of characts. 9-44815
 CO₂ laser, 1 kW average power, with optical a.m. 9-25253
 GaAs diode-based injection quantum-amplifier 9-34178
 He-Ne laser, 3.39 μ , experimental study of polarization-dependent gain saturation and nonlinearity-induced anisotropy 9-22398

Analogue computers *see Calculating apparatus/analogue apparatus***Analysis** *see Chemical analysis; Statistical analysis***Anechoic rooms** *see Acoustical laboratories***Anelasticity** *see Internal friction***Anemometers**

- heterodyne experiments, low-frequency, Ar laser source assessment 9-47721
 sonic anemometer - thermometer for direct method of determ. turbulent transport of physical quantities 9-24644
 u.s. for air-steam convection currents meas. 9-36794

Angle measurement

- declination, precise method for tidal and crustal movement investigation 9-43363
 e.m. radiation, direction-finding, effect of diff. at perfectly conducting obstacles 9-29343
 films, cylindrical plated on nonferromag. wires, easy axis orientation 9-24306
 goniometer for ultra high vacuum 9-23643
 interferometer, modified design 9-32016
 phototeodolite, ballistic, multiple-frame camera 9-32089
 reflectometer, measurement of principal angle of incidence and principal azimuth of reflecting surface 9-32028
 sound ranging, azimuth and elevation errors for square array of microphones 9-29284
 spectrometer table, high precision, with removable arms 9-24479

Angular distribution *see Gamma-rays/angular distribution; Neutrons and anti-neutrons/angular distribution; Protons and anti-protons/angular distribution***Angular momentum theory** *see Quantum theory***Angular velocity measurement***see also Stroboscopes**No entries***Annealing** *see Heat treatment***Annihilation of electrons** *see Electron pairs/annihilation***Anodic films** *see Electrochemistry; Films, solid***Antennas** *see Electromagnetic waves/radiators***Antiferroelectric materials** *see Ferroelectric materials***Antiferromagnetic resonance**

- e.m. wave propag. in material showing resonance in submillimeter region 9-45375
 haematite, weakly ferromag., temp. depend. 9-39899
 spin-flop region, frequency depend. on metastable state existence 9-24479
 CoCO₃, splitting in spectrum at low frequencies 9-28741
 CuCl₂·2H₂O single crystal, at 1.57^oK and low frequency branch of spin wave 9-47425
 EuTe, linewidth, temp. depend. 9-45376
 FeCl₂, rel. to dipole absorpt. in far i.r. 9-35586
 LiMnPO₄ single cryst. 9-39900
 NaNiF₃ single crystal, reson. in wavelength range 1.2-10 mm, fields up to 150 kOe, temp. 77-150^oK 9-41421
 NiCl₂ single cryst. 9-47426

Antiferromagnetic resonance continuedYMnO₃ hexagonal, far i.r. 9-45377**Antiferromagnetism***see also Exchange interactions; Magnetic properties/antiferromagnetic in band model, rel. to Mott insulation and ordering 9-44883*

electron solid 9-41330

exchange integrals momentum dependence, eff. on Kondo temp. 9-31044
flopped antiferromagnet, excitation to electronic and nuclear spin waves 9-47282

Goldstone-type model with antiferromagnetic props. 9-25405

Heisenberg, 1/z expansion at low temp. 9-45201

Heisenberg antiferromagnet, with magnetic impurity, perturbed states 9-39761

Heisenberg magnets, spin pair correlation studied using thermal Green function method 9-33449

Heisenberg magnet, u.s. attenuation, heuristic improvement 9-41087

Heisenberg model, anisotropic, mag. order impossibility 9-41289

Heisenberg model, isotropic, with long-range interactions absence 9-49194

Heisenberg model of spin waves and thermodynamic props. 9-28637

Heisenberg quasi-two-dimensional, rel. to 3-dim. mag. systems 9-45098

Heisenberg spin chain with isotropic interac., energy spectrum of bound excited states 9-31046

impure antiferromagnets, zero-point spin deviation 9-28636

ising lattices with random arrangements of ferromag. and antiferromag. bonds 9-49200

Ising model, super-exchange, transition props. 9-49220

itinerant electron theory, effect of imperfect Fermi surface nesting 9-47278

itinerant-electron antiferromagnet, Cr-like model 9-47281

linear chain, in Fermi liquid theory calc. of sp. ht. and mag. susceptibility 9-49221

linear chain, infinite, Overhauser's spin-density- wave state, itinerant modes obs. 9-41331

magnon drag 9-24332

magnon energies, temp. depend theory 9-45200

magnon energies, time-depend., theory 9-35578

magnons, g factor renormalization 9-28603

perovskites, localized magnon and magnon-exciton interactions, theory 9-45198

phonon pumping of nuclear magnon pairs, with acoustic waves 9-33481

spin configurations in two sublattice slab 9-45205

spin deviation, zero-point, in impure antiferromagnets 9-28636

spin wave spectrum of metal 9-28638

spin waves, electronic and nuclear, excitation in flopped antiferromagnet 9-47282

spin-flipping, dynamical behaviour 9-47279

spin-flipping, numerical integration of phenomenological eqns. for orthorhombic and uniaxial systems 9-47280

spin-forbidden resonance energy transfer, mechanism 9-24323

spin-wave spectrum of split-band antiferromagnet deduced from spin susceptibility 9-35577

spinwaves, hydrodynamic theory 9-45203

spiral structures, spin wave resonance 9-37786

split-band model, eff. of impurities 9-31045

split-band model and superexchange theory comparison in insulator 9-43190

sublattice magnetization vector, dynamical behaviour 9-47280

sublattice magnetization vector, dynamical behaviour near spin-field critical field 9-47279

super-exchange Ising model, transition props. 9-49220

two-magnon inelastic scatt. of slow neutrons 9-43192

two-sub-lattice antiferromagnet, spin wave Green's function, reciprocal lattice sum evaluation for 10 points 9-28635

U.S. attenuation at low temp. 9-49198

CoCl₂·2H₂O magnon-phonon interaction, obs. in far i.r. 9-45077CoF₃, magnon-optical phonon interaction, temp. depend. 9-47356

Cr, itinerant spin-density excitation in light-scatt. obs. 9-47372

CsMnF₃ hexagonal nuclear and electronic spin-wave relax rate 9-45216FeCl₂·2H₂O magnon-phonon interaction, obs. in far i.r. 9-45077GdCrO₃ magnon assisted absorption and fluorescence spectrum of Cr³⁺ 9-49321K₂NiF₄ neutron scatt., two-dimen. Heisenberg antiferromagnet model 9-26660KMnF₃ single crystal slab, multiple magnons in absorpt. spectra in far i.r. and visible 9-45326LuCrO₃ magnon-assisted absorption and fluorescence spectrum of Cr³⁺ 9-49321MnF₂ single crystal slab, multiple magnons in absorpt. spectra in far i.r. and visible 9-45326RbMnF₃ localized magnon and magnon-exciton interactions, theory 9-45198Ti₂O₃, existence, rel. to metal-semiconductor transition 9-45236YcrO₃ magnon-assisted absorption and fluorescence spectrum of Cr³⁺ 9-49321**Antimony**

diffusion in Ag, intercryst., temp. depend. 9-46846

electrical resistivity, reluctance, Hall const., differential thermo-e.m.f., 300-750K 9-47076

electrotransfer in Bi 9-48873

Fermi surface, pressure-depend. meas. by de Haas-van Alphen eff. 9-30821

Fermi surface hydrostatic press. depend. 9-37409

fusion, enthalpy 9-30449

incorporation into BaTiO₃ lattice sites 9-36972

40 keV, bombardment of Si, effect on optical reflectivity 9-33506

liquid, ¹²¹Sb n.m.r. obs. 9-23534liquid, nuclear spin-lattice relax. of ¹²¹,¹²³Sb 9-26134

molten, electrical resistance meas. by rot. field method 9-39583

n.m.r. Knight shifts in rare-earth group-VA intermetallic cpds. 9-33648

Peltier coeff. at boundary between solid and liq. phases, determ. 9-45019

proton energy losses 9-30807

superconductivity under pressure 9-39602

thermal expansion, linear, 200° to 8°K, Gruneisen parameters 9-33189

vaporization, (111) cleavage face, pit growth at spiral dislocation site 9-30467

¹²³Sb, nuclear decay effects on electronic structure of decaying atom and its bonding in cpds. from Mossbauer meas. 9-38769¹²³Sb, thermomigration in Au 9-35126**Antimony continued**

Ge:Sb, far i.r. absorpt. spectra, excitation lines shift, conc. depend. 9-35659

Ge:Sb, Hall coeff. obs. of semicond.-to-metal transition rel. to impurity conc. 9-49095

n-Ge:Sb, microwave Faraday rot. 9-41355

in LaTe₂-LaSb₂, effect on resistivity and thermoelec. power 9-39639Sb³⁺ photochemical oxidation in HCl, LiCl soln., Bunsen-Roscoe law breakdown 9-29939Sb³⁺ solubility in Ca₁₀(PO₄)₆Cl₂ 9-42740**Antimony compounds**

pnictides, binary, with marcasite type struct. mag. props. 9-31016

Bi-Sb alloys, magnetoreflection obs. of band struct. 9-41162

Bi-Sb semiconducting alloys, magnetoresistance anomalies, 4.2° to 10°K 9-30890

Bi_{1-x}Sb_x, mag. susceptibility, elec. resistivity, Hall eff. and magnetoresistance 9-30842Bi₈₈Sb₁₂:Sn,Te alloy, thermoelectromag. props. 9-49154Bi₉₃Sb₇:Sn,Te alloy, thermoelectromag. props. 9-49154

BiSb alloys, emission of microwave radiation in weak electric field 9-31102

Ga_{1-x}In_xSb solid soln., growth and characterization using temp.-gradient zone melting 9-30719In-As-Sb phase diagrams, quasi-chem. equil. model 9-44610
InSb, YFe Garnet hybrid structure, interaction between spin waves and electrons 9-24320

Sb-Cs photoelement, spectral sensitivity rel. voltage changes 9-31006

Sb₂S₃, photoelec. props., effect of high hydrostatic pressure 9-28571Sb₂S₃, reflection and transmission spectra 9-39825Sb₂S₃, thermal conductivity, 700-1150°K 9-36864Sb₂S₃, transmission spectra, 0.4-0.06 eV 9-39825Sb₂S₃ ferroelectric semicond., pyrocurrents due to spontaneous polarization 9-41246Sb₂S₃ films, crystallization process, X-ray study 9-42726Sb₂S₃ single crystals, i.r. and thermal quenching effect on photocond. 9-49162Sb₂S₃ single crystals, optical props. in ferroelec. phase transition temp. range 9-45261Sb₂S₃, transmission spectra, 0.4-0.06 eV 9-39825Sb₂Se₃-Sb(Te) alloy, liquid thermal conductivity mechanisms 9-34900Sb₂Se₃, liquid, thermal conductivity mechanisms 9-34900Sb₂Se₃, photoelec. props., effect of high hydrostatic pressure 9-28571(Sb₂Te₃-Bi₂Te₃)-(Bi₂Te₃-Bi₂Se₃) thermocouple, transient response of thermoelec. coding 9-28569Sb₂Te₃, Peltier coeff. at boundary between solid and liq. phases, determ. 9-45019Sb₂Te₃, reflectivity spectra, 0.7 to 12.5eV 9-33538

Sb complex, tetraphenylantimony hydroxide, mol. structure, 3-dimens. X-ray diff. obs. 9-42418

SbCl₃, quadrupole spin-lattice relaxation time, two-freq. investig. method 9-45246SbF₃-H₂, methane mixtures photolysis, HF chem. laser emission, obs. 9-31944SbI₃:Cr³⁺, e.s.r. of Cr³⁺ single ions 9-24482SbI₃ in soln. and solid phases, Raman spectra 9-26758

SbO, fine structure analysis and isotope effect studies in B-X, C-X and D-X systems 9-23072

(SbO₃)³⁻ impurity in CaWO₄, phosphoresc. enhancement 9-39884SbS₄³⁻, orbital valence force field constants 9-32486SbSI, adsorption of O₂, eff. on elec. conductivity, photoconductivity and work function 9-30496

SbSI, damping of u.s. waves as function of illumination, near ferroelec. phase transition 9-46992

SbSI, dielec. props., temp. and hydrostatic pressure depend. 9-28565

SbSI, dielectric props., temp. and hydrostatic pressure depend., 30 to -60°C 9-43104

SbSI, ferroelec., Kern-Harbeck effect, effect of hydrostatic pressure 9-26591

SbSI, ferroelectric, dielectric constant, dynamical nonlinearity 9-35488

SbSI, oriented bifurrow cryst., growth and dielec. props. 9-48808

SbSI, paraelectric, nonlinear I-V charactrs. 9-28555

SbSI, phase transition near critical Curie pt., optical obs. 9-24221

SbSI, polarization, electrostriction and piezoelec. modulus 9-30974

SbSI absorption coefficient and velocity of 10-30 Mc/s u.s., temp. depend., 16-24°C 9-42960

SbSI ferroelectric, elec. field effect on phase boundaries 9-41250

SbSI ferroelectric props. 9-41245

SbSI phase transition, nonequilibrium carrier effects 9-24233

SbSI photopyro-effect 9-24243

Sn-Sb dil. alloys, internal friction anomalies near melting pt. 9-39399

Sn-(1.0-6.0wt.%)Sb alloys, Sn dendrite growth as function of supercooling 9-48815

Antineutrinos *see Neutrinos and antineutrinos***Antineutrons** *see Neutrons and antineutrons***Antinucleons** *see Nucleons and antinucleons***Antiparticles** *see corresponding particle***Antiphase domains** *see Alloys; Crystal structure/microstructure; Solids/structure***Antiprotons** *see Protons and antiprotons***Antireflection coatings** *see Films, solid/optical properties***Apodization** *see Optical images***Apparatus** *see Cosmic rays/apparatus; Instruments; Ionosphere measuring apparatus; Laboratory apparatus and technique; Radioactivity measurement/apparatus; Vacuum apparatus; X-ray crystallography/apparatus. Further entries describing apparatus for specific purposes are included under the headings of the appropriate subjects***Appearance potential** *see Ionization potential***Architectural acoustics***see also Echo; Noise abatement; Reverberation; Transmission/acoustic waves*

articulation tests in auditorium studies 9-29305

auditoria sound diffusion 9-34089

auditoriums, articulation tests 9-29305

concert hall acoustics, multimode transmission media frequency response 9-45864

diffusion of auditoria sound 9-34089

insulation between dwellings, physical and subjective obs. 9-41832

openings, baffled, acoustic props. at l.f. 9-41821

Architectural acoustics continued

- power injection and response in rooms and structures, statistical anal. 9-25106
- reading room, library and lecture room meas. 9-34090
- reverberation curve of several rooms, integrated tone burst obs. 9-36198
- rooms and structures, input power and response, statistical calcs. 9-25106
- Sabine's statistical room acoustics theory, improvement in differential formulation 9-36199
- statistical room acoustics as a problem of diffusion 9-36199
- transmission responses of multimode media, effect of frequency and space averaging 9-45864
- walls, solid and hollow, sound transmission, and rooms reverberation 9-25107

Arcs, electric

- a.c., oil-cooled, pyrolytic C growth 9-23364
- arbitrary gas mixed with alkali metal vapour, magnetic holding 9-25989
- arc-flow-electrode interacts in superimposed gas flow, symptomatic behaviour 9-23365
- atomic concentrations in interelectrode gap, determ. 9-48642
- cathode arc tracks, current density meas. 9-32711
- cathode spot retrograde motion, explanation based on ions movement near edge 9-42581
- characteristics correlation 9-28056
- in coaxial cylinders in transverse magnetic field 9-42584
- column with natural convection, theory 9-32714
- in crossed fields, elec. and mag., chain mechanism development 9-48641
- current intensity rel. to discharge gap length 9-49395
- d.c., for spectrography, anode and excitation conditions 9-30320
- d.c., in cylindrical channel, characts. calc. 9-32713
- d.c., in emission spectrography, selected buffer compounds influence 9-36382
- d.c. in vacuum ambient, electrode products analysis 9-34816
- discharge tube, rotation for plasma stabilization, patent 9-34790
- erosion rate at electrodes of an arc rotated by a transverse mag. field 9-42578
- filament type, with small cross section, temp. profile 9-42579
- formation under pulsating voltage between positive peak and plane in surrounding air 9-46548
- free-burning, with transverse and longit. blowing, charact. correlation 9-28057
- gas flow, Schlieren obs., properties of Ar laser 9-22384
- graphite electrode temp. meas. 9-30321
- high current, advantages for spectrochem. analysis of ashed biological materials 9-47477
- interaction with gas flow in constrictor, theory and experiment 9-40726
- ion source, vibrating contact arc, props. 9-27286
- lamp cathodes, l.p. and high-current energy balance 9-48640
- magnetically balanced, fluid mechanics in cross flows 9-25990
- melter, construction 9-33103
- metal and alloy ingress, effect of alkali elements and halogens 9-30322
- non-isothermal in local collision regime, theory 9-48633
- nonequilibrium, relax. method for determ. of nature of continuum 9-44512
- nonstationary, V-I charact. 9-42580
- plasma, high pressure, transport coeff. determ. 9-32635
- plasma, magnetic intensification of close cathode intensified spectral, lines 9-25988
- plasma in mag. field, low press. 9-42550
- positive column, power balance equation 9-42582
- production and investigation of high press. heavy current long arcs, apparatus 9-39033
- solar furnace, simulator with pyrometric chopper 9-40283
- source of low temp. plasma 9-40725
- spectrochemical analysis, servocontroller for sample vaporization 9-28827
- spectrochemical determ. of carbonate in bone 9-35759
- stationary in cross flow and transverse mag. field, analysis 9-46549
- temperature of positive column, calc. 9-42582
- temperature profile and radiation efficiency calc., relax. method 9-48643
- in thermionic convertor, ionization equilibrium 9-47893
- vacuum, d.c., anode voltage drop and spot formation 9-32712
- wall stabilized, axially symmetric, numerical descriptions 9-28058
- wall-stabilized, static, temp. depend. of radiated power density, elec. and thermal conductivity 9-36793
- Ar, energy fluxes to anode in MPD config. heat transfer mech. responsible 9-32610
- Ar, h.f. volt. oscills. and rel. anode thermal effects 9-23368
- Ar, hollow cathode, positive column props., 4 torr 9-25991
- Ar, low current d.c., temperature obs. 9-23366
- Ar, symptomatic behaviour in superimposed gas flow arc-flow-electrode interacts 9-23365
- Ar arc light intensity calib. 9-44269
- in Ar atmosphere with added K, weak current cylindrical, light probing 9-39034
- Ar column, cylindrically symmetrical, temp. field 9-25992
- Ar continuous spectrum nature, determ. using relax. method 9-44512
- Ar high press., elec., thermal and opt. props. 9-40727
- Ar II spectral transition probabilities, obs. 9-46292
- Ar Knudsen, plasma density and electron temperature 9-42585
- Ar steady, current 10 to 40 A, total radiation obs. 9-40672
- in Ar stream with Cs in mag. field 9-23367
- C, effect on electrode temperature 9-25993
- C electrode temp. meas. 9-30321
- C spectra line Stark broadening in arc plasma 9-44258
- Cs plasma, excitation temps. from relative intensities of spectrum transitions in arc 9-25707
- Cs thermal current, electronic contribution 9-44513
- Cs vapour, ionic composition of arc-discharge plasma 9-36759
- Cs vapour, ionic composition of arc-discharge plasma 9-36759
- H, vortex-cooled, H₂, H₂ Balmer line profiles obs. 9-27825
- H₂, symptomatic behaviour in superimposed gas flow arc-flow-electrode interacts 9-23365
- H₂ cascade arc, radial temp. distributions, meas. up to 27,000 °K 9-40728
- He-H₂ continuous spectrum nature, determ. using relax. method 9-44512
- He, symptomatic behaviour in superimposed gas flow arc-flow-electrode interacts 9-23365
- He continuous spectrum nature, determ. using relax. method 9-44512
- Hg-Cs vapour, nonequilibrium plasma obs. 9-38972

Arcs, electric continued

- Hg and Xe, high pressure, stabilized, radiation portion, indirect determination 9-30323
 - Hg plasma tube, electron density and temp., Langmuir probe analysis 9-42538
 - K i mol. % cone in various gases, temp. and radiation intensity distribution 9-42583
 - N₂ symptomatic behaviour in superimposed gas flow arc-flow-electrode interacts 9-23365
 - NH₃ energy fluxes to anode in MPD config. heat transfer mech. responsible 9-32610
 - Na, temp. profile and radiation efficiency calc., relax. method 9-48643
 - U matrix in air, d.c. arc plasma, temp., voltage and elec. field distrib. 9-25918
 - Xe, far i.r. emission meas. 9-28059
 - ZnSe, d.c., spectral anal. of excess Zn, comparison with hollow cathode 9-37859
- Area measurement**
No entries
- Area measurement, porous substances** *see Surface measurement*
- Argon**
- adsorption and diffusion on three structs. of Ar (100) surface 9-35000
 - adsorption of graphite, fourth-order interactions using third virial coeff. of 2-dimens. Lennard-Jones gas 9-42605
 - adsorption of H₂, influence of temp. history, 9°K 9-36966
 - adsorption on silica aerogels 9-30498
 - afterglow, electron temp. and density meas. 9-28048
 - afterglow plasma, electron temp. gradient, spatially nonuniform parameters effect on transport processes 9-34755
 - Ar⁺+D₂(or CD₄)+ArD⁺+D(or CD, deviations from stripping model 9-27944
 - Ar IIE, 4s levels new radiative lifetime values 9-25706
 - Ar-alcohol Geiger counter, photon spectrum in discharge obs. 9-25507
 - arc, cylindrically symmetrical column, temp. field 9-25992
 - arc, h.f. volt. oscills. and rel. anode thermal effects 9-23368
 - arc, hollow cathode, positive column props., 4 torr 9-25991
 - arc, low current d.c., temperature obs. 9-23366
 - arc discharge, nature of continuous spectrum, determ. using relax.-method 9-44512
 - arc light intensity calib. 9-44269
 - arc plasma jet temp. meas. at atm. pressure 9-30251
 - arc in superimposed gas flow, arc-flow-electrode interacts and mode behaviour 9-23365
 - arc with added K, weak current cylindrical, light probing 9-39034
 - arcs, high press. elec. thermal and opt. props. 9-40727
 - atmospheric, ³⁹Ar-activity, detection using proportional gas counter 9-45498
 - atom, dipole polarizabilities, elec., and dipole shielding factors from Hartree-Fock wave eqns. 9-44241
 - atom, electron scatt., neutral bremsstrahlung cross section, shock tube obs. 9-29965
 - atom, excitation, 0.15-1.0 MeV proton induced 9-42337
 - atom, highly ionized, spectrum in plasma focus discharge 9-42329
 - atom, mean excitation energies upper and lower bounds calc. 9-38779
 - atomic beam, preferential scatt. from LiF(001) surface 9-42714
 - atomic beam, shock tube drives, metastable atoms, obs. 9-44289
 - atoms, differential elastic scatt. of low-energy protons 9-44287
 - atoms, long-lived autoionization states, mass spectra 9-38782
 - atoms scattered from solid surface, spatial distribution of 0.30-0.54° eV gaseous atoms 9-27821
 - beams, monoenergetic, scattering heated Pt 9-44316
 - breakdown, dye laser-induced, wavelength dependence 9-46543
 - breakdown, microwave, temp. depend. 9-32708
 - breakdown pot. obs., secondary ionization coeffs. calc., mild steel electrodes 9-34811
 - collision, inelastic, with O⁺, energy transfer distrib. meas., 50-200 keV 9-46313
 - collision of Ar⁺ with Ar atoms, energy spectrum of released electrons, investg. 9-22983
 - collision with H₂, -ve charge prod. cross section determ., 50-1000 eV 9-27826
 - collision with incident beams of H, He, He⁺; electron and ion prod. cross section meas., 0.15-1.0 MeV 9-22982
 - compressed gas, thermal conductivity, concentric cylinder meas. method 9-26027
 - concentrations in the Pacific, comparison of data 9-45467
 - critical region P-V-T meas., isothermal compressibility and density, theory and expt. 9-28174
 - crystal growth, big, mosaic spread, thermal etching and preferential orientation obs. 9-40859
 - dense gas, self-diffusion obs. 9-36828
 - desorption from Ba thin film, temp. dependence 9-40849
 - desorption of ionically pumped gas from clean and metallized glass surfaces 9-30495
 - diffusion in benzene and CCl₄, open-tube obs. 9-30383
 - discharge, 1s and 2p level population, electronic temp., conc. meas., 9500 MHz 9-32702
 - discharge, decaying, e conc. by laser interferometry, 10⁻²-3 mm Hg 9-28050
 - discharge, ion laser, in vacuum u.v., spectroscopic studies 9-25242
 - discharge, medium press., effect of Hg vapour 9-23352
 - discharge, positive column contraction 9-48632
 - discharge, pulsed, e vel. distrib. and conc., 0.02 torr 9-28049
 - discharge, r.f., mass spectra obs. of ionic species 9-36787
 - discharge excitation source for solns. spectrochem. analysis, 2450 MHz 9-28822
 - discharge in coaxial cavity, cyclotron resonance rel. to elec. field freq. 9-44499
 - discharge positive column, light fluctuations correlation 9-34806
 - electron elastic scatt., phase shifts, isoelectronic sequence extrapolation techniques 9-29964
 - electron elastic scattering from ³p metastable state, calc. 9-46307
 - emissivity, temp. range 6000-12000°K for 1,10 and 100 cm layers 9-26035
 - equation of state, high-pressure fluid 9-42690
 - excited levels, mag.-reson. expts. 9-29955
 - excited state, repulsive interaction with He, Ne, Ar ground state atoms 9-29968
 - flow, in converging nozzle, continuum, slip and free mol. regimes 9-32722
 - flow boundary layer ≤ 1500°C, soft X ray absorption obs. 9-40735

Argon continued

- gas, diffusion of Cs and K vapours 9-39059
 Gas, second virial coeff. 9-34833
 gas behind shock wave, thermodynamic props. 9-38974
 gas laser simplified 9-22386
 gas target, traversed by He beam, charge equilb. fractions obs. 9-40559
 gas viscosity meas. pot. fitted 9-36823
 gas-liquid phases coexistence curves 9-46688
 heating of, with K admixture plasmatron 9-38993
 hypersonic shock wave, energy transfer mechanisms compared with air 9-46564
 hypersonic shock wave, mechanisms of energy transfer between different degrees of freedom 9-46564
 intermolecular pair potential 9-30339
 intermolecular potential calcs. rel. to thermal-diffusion column operation 9-34843
 inverse pinch, m.h.d. prod. of collisional shocks, characts. 9-46495
 ion, multiply-charged, population inversion, excitation mechanism 9-28041
 ion laser, c.w. parametric u.v. generation by ADP and KDP on cavity 9-27363
 ion laser, introductory paper 9-36288
 ion laser, miniature, for hologram reconstruction; design and charact. 9-47962
 ion laser, transitions, interaction mechanisms 9-29411
 ion laser, transverse modes of low order 9-36286
 ionically pumped, desorption from clean and metallized glass surfaces 9-30495
 ionized partially, elec. conductivity 9-26037
 ionizing, behind reflected shock wave, shock reflection process and thermal layer 9-48662
 ions, singly charged, long-lived autoionization states, mass spectra 9-38782
 isotherms to 10 kbar and 400°C 9-32732
 laser, construction and operational characts., plasma jet as cathode 9-40351
 laser, CW, fundamental TEM₀₀ mode intensity distrib. amplification saturation depend. 9-22385
 laser, gain saturation of 4880 Å line operating in single-freqs. state 9-25246
 laser, ion, discharge electron temp. and density, calc. 9-47960
 laser, line excitation threshold rel. to press., and unsaturated gain v.s. current 9-25247
 laser, self-focusing, thermal, transient and steady-state 9-22383
 laser, super-mode f.m., monochromatic generation at 5145 Å 9-27317
 laser, toroidal, inductively coupled r.f.-excited, with aperture-magnetic confinement 9-47961
 laser capillary discharge, radial distrib. of excited atoms and ions 9-36289
 laser in Schlieren study of gas flow in elec. arc or plasma 9-22384
 laser oscillator, ion-type, signal freq. spectrum when operating at 4880 Å 9-25248
 laser source for l.f. heterodyne anemometry 9-47721
 Laser vacuum ultraviolet perturbations spectroscopy 9-22382
 liquid, atomic overlap, neutron diff. obs. 9-34875
 liquid, compressibility and density up to 1000 kb/cm² 9-46593
 liquid, eqn. of state 9-39071
 liquid, equation of state and interatomic potential 9-28093
 liquid, shock compression applic. of significant structure theory 9-28095
 liquid, specific heat deriv. from molecular model 9-34869
 liquid, velocity autocorrelation function, hindered-translator model 9-22154
 liquid, with Xe and Kr doping far i.r. absorpt. 9-34908
 liquid 12-6 potential, Monte Carlo calc. 9-39070
 liquid and solid, refractive indices 9-44562
 liquid velocity autocorrelation function and neutron scatt. cross sections, calc. 9-34871
 liquid-gas phases coexistence curves 9-46688
 luminescence, α -particle induced, in elec. field 9-42328
 melting, Lindemann's law, calculations along melting line 9-28177
 metals strong emission line shifts in compressed Ar, obs. 9-48377
 metastable atoms, electron ejection from W surfaces 9-31001
 MPD arc config., energy fluxes to anode, heat transfer mech. responsible 9-32610
 Ne⁺, zNe⁺Ne⁺, Ne; 3-body conversion rate coeff., ion sampling in discharge positive column 9-46317
 optical pumping of ³P₂ state and subsequent collisional depolarization 9-22973
 optical pumping of atoms in ³P₂ metastable state 9-27814
 pair potential 9-48657
 perturbation theory, eqn. of state and free energy 9-46610
 phase transition study on Lennard-Jones potential 9-46687
 photo-ionization cross section in Hartree-Fock approx., calc. 9-40549
 plasma, afterglow, electron temp. gradient, spatially nonuniform parameters effect on transport processes 9-34755
 plasma, expansions in Laval nozzles, approximate calc. 9-46471
 plasma, impulse drivers, interactions with transverse magnetic field 9-30229
 plasma, induction coupled, modification of microcryst. particles passing through 9-37133
 plasma, NaK seeded, flowing, electron temp. meas. 9-27978
 plasma, strongly ionised, low press., prod. by microwaves 9-48592
 plasma, thermal induction, energy balance equation, analytical solution of Heller-Elenbaas equation 9-28004
 plasma, thermodynamic functions, approximate calc. 9-46464
 plasma, viscosity obs. to 12×10³K 9-38964
 plasma afterglow, in mag. field, microwave scattering and noise emission 9-48568
 plasma beam prod. in Laval nozzle, calcs. 9-39001
 plasma column, axial current density meas. 9-34768
 plasma flow in presence of boundary layer, volt amp. characts. 9-44426
 plasma highly ionized, magnetically confined column 9-25891
 plasma in homopolar rot. device, 10⁻² mm Hg, electron collision freq. and current growth 9-25857
 plasma in Knudsen arc, density and electron temperature 9-42585
 plasma jet, electron conc. 9-42522
 plasma pulsed discharge, spectral absorptivity calc. from radiance spectral density 9-23301
 plasma torch, induction, temp. and electron density distribution 9-25907
 positron annihilation, models 9-38785

Argon continued

- positron annihilation, rel. to applied elec. field and Ar density 9-38784
 quenching of excited mol. N₂ in yellow afterglow studies 9-39029
 quenching of Na 3p²P fluorescence 9-38780
 r.f. discharge in non-resonant mag. field, breakdown characts. 9-25986
 scattering of CsF molecules, cross sections and anisotropy parameters 9-44387
 shock wave precursor and trailing region, physical processes in argonlike gas 9-46553
 shock waves, spectral distrib. of u.v. and visible radiation 9-48654
 solid, diffusion coeff. determ. 9-44722
 solid, electron drift velocity saturation 9-26587
 solid, equilb. conc. of Ne and Kr atoms in (100) face 9-23616
 solid, self-diffusion vacancy mechanism, many-body effects 9-46693
 solid, wetting, critical surface tension and contact angle meas. 9-23451
 solids, specific heat meas., 0.4-12°K and extrapolation to 0°K 9-24041
 spark discharge channel, h.p. radiance saturation and afterglow emission 9-30314
 spark spectra in various gases, line intensities rel. to press. and Cu or graphite electrodes 9-36792
 spectra low press. gas-jet source, vacuum ultra-violet region 9-22941
 stopping power for ions (Z=3-13) 9-39014
 stream with Cs, arc in mag. field 9-23367
 supercooled, water drop nucleation 9-26075
 supersonic jets, intermolecular binding 9-23035
 thermal conductivity at high temp., meas. with hot wire cell 9-39096
 thermal conductivity calc. from shock heated gas heat transfer rates, 650-5000°K 9-26026
 thermal expansion coeff., Gruneisen parameter determ., 1-25K 9-41092
 thermal-diffusion column operation rel. to intermol. pot. calcs. 9-34843
 thermosphere, lower, conc. from mass spectrometer obs. 9-28906
 vapour press., correction of tables 9-39144
 between vertical concentric cylinders, heat transfer and end effects for various temp. differences 9-40749
 viscosity determ. 3500°-8500°K 9-26044
 X-ray K series excitation by e collision, 3-16 keV 9-34539
 Ar/Kr, solidified mixtures, lattice parameters rel. to Ar conc., e diff. study 9-28255
 Ar/Ne, solidified mixtures, e diff. study of crystallized phases 9-28255
 Ar-methane, phase diagram 9-44803
 Ar-Ar⁺ atomic solisition 0.5-6 MeV with large angle scatt., evidence for prod. of inner shell vacancies 9-32428
 Ar-H₂, collision, total cross-section, for particular rotational *j*, *m_j* state of H₂ molecule 9-27945
 Ar-Hg discharge, medium press., axial cataphoresis 9-48630
 Ar-Hg discharge positive column plasma, effect of cathode props. 9-48631
 Ar-Kr liq. mixtures, thermodynamic props., Monte Carlo calc. in isothermal-isobaric ensemble 9-32560
 Ar-Kr liq. mixtures, thermodynamic excess props., analysis 9-42646
 Ar-N solid mixtures, thermodynamic props. 9-39528
 Ar-ethyl alcohol two-phase flow, adiabatic, phase and vel. distrib., obs. 9-46558
 Ar-methane anisotropic intermolec. forces 9-38935
 Ar-water two-phase flow, adiabatic, phase and vel. distrib., obs. 9-46558
 Ar, Percus-Yevick approx. for truncated Lennard-Jones (12-6) potential 9-23210
 Ar⁺, dissociative recombination, electron-temp. dependence 9-34795
 Ar⁺ in Ar-Cs r.f. discharge, mass spectra obs. 9-36787
 Ar⁺-Ar charge-transfer cross-sections, oscillations 9-38791
 Ar⁺, sputtering probability of secondary W oxide ions 9-42982
 Ar⁺zAr→Ar⁺z, Ar; 3-body conversion rate coeff., ion sampling in discharge positive column 9-46317
 Ar⁺zAr→Ar⁺z, Ar; 3-body conversion rate coeff., ion sampling in discharge positive column 9-46317
 Ar⁺ electron beam ionization, obs. near threshold 9-25963
 Ar⁺ in Ar-Cs r.f. discharge, mass spectra obs. 9-36787
 Ar⁺ ions, collisions with surface Cu atoms, charge exchange of scattered ions 9-48418
 Ar⁺ laser, 4880Å, single pass gain as function of discharge current 9-45949
 Ar⁺ on K, Rb, Cs; total charge-transfer cross section meas., 10-1500 eV 9-46316
 Ar⁺ scatt., large-angle obs. of Au crystal surfaces 9-48748
 Ar⁺-Ar collisions, 100-400 keV, emission cross sections from excitation, Doppler shift anal. 9-44280
 Ar⁺+Ar excitation resonances for production of metastable atoms 9-34560
 Ar⁺+CH₄→Ar+CH₃⁺+H→Ar+CH₂⁺+H₂, 1.5-4.2 eV range, mechanism 9-39936
 Ar⁺+D₂→ArD⁺+D reaction crossed-beam technique appl. 9-41442
 Ar I 7635.10 Å emission profile and self-absorpt. correction, obs. 9-48386
 Ar I lines in near i.r., transition probabilities 9-46293
 Ar I radiation lifetimes and transition probabilities meas., delayed coincidence method 9-22942
 Ar II, decay of 4p¹¹D^{3/2} level, absolute meas. by correlation of photons emitted in cascade 9-46294
 Ar II, III, IV, cascade-free transitions, radiative lifetimes 9-25691
 Ar II d.c. laser, perturbation spectroscopy, 3p¹[4p] 4p level transition 9-25244
 Ar II ions, widths and shifts of spectral lines, calc. 9-44250
 Ar II laser, saturation phenom. from amplification coeff. and rad. intensity 9-36287
 Ar II optical transition probabilities, arc obs. 9-46292
 Ar II radiative lifetimes for transitions in 1900-4500 Å range 9-32407
³⁹Ar in stone and iron meteorites 9-24888
 ArI excitation and population inversion 9-29921
 ArIII, excited level lifetime 9-34559
 ArIII in quasi c.w. ion laser, o/p at 3638 and 3511 Å 9-25233
 CO₂-Ar mixtures, influence of dimers on thermal diff. factor 9-36686
 CO₂-Kr mixtures, influence of dimers on thermal diff. factor 9-36686
 CO₂-Ar mixtures, desorption rates from silica gel at various temps. 9-46663
 Cr I emission line shifts in compressed Ar, 3014-5328 Å 9-48390
 Cs I spectrum, 4555 Å line broadening 9-34535
 H-Ar atomic collision, free scatt. model for e loss 9-46310
 H exchange and adsorption on stainless steel 9-39170
 He-Ar discharge electron energy distrib. functions electron mobilities and collision rates calc. 9-48621
 He-Ar mixtures, influence of dimers on thermal diff. factor 9-36686

Argon continued

- K-Ar collisions, cross-sections 9-27823
 Kr-Ar liq. mixtures, thermodynamic excess props., analysis 9-42646
 Kr-Ar simple liquid mixtures, shear viscosity 9-36851
 Ne-Ar mixed gas mixtures, generated by fission fragments, electron density 9-34751
 neutral number densities in thermosphere, lower, day-night vars. 9-26920
 Ni I emission line shifts in compressed Ar, 3050-3619 Å 9-48390
 O₂-Ar mixture, vibrational excitation of diatomic mols. by atom collision, calc. 9-40588
 O₂-Ar solid mixtures, mag. props. of O₂ molecules 9-45231
 O(¹D)-Ar interaction, electronic de-excitation of O(¹D) during vacuum u.v. photolysis of O₂ 9-35755
 photoionization continua, 40-60 Å region, discrete structure 9-34531

Argon compounds

- He cpds., mixture, thermal conductivity calc. from shock heated gas transfer rates, 650-5000 °K 9-26026
 Ar-Cs r.f. discharge, mass spectra obs. of ionic species 9-36787
 Ar-He mixture, thermal conductivity calc. from shock heated gas heat transfer rates, 650-5000 °K 9-26026
 Ar-He plasma jet, electron conc. 9-42522
 Cs-Ar low-press. discharge, Cs depletion in positive column 9-34802
 Cs-Ar low-press. discharge, radial and axial Cs-atom distrib., absorpt. spectra obs. 9-34801
 H₂-Ar-air flames, turbulent, atoms fluoresc. power efficiencies, obs. 9-24601

Aromatic compounds *see Organic compounds***Arsenic**

- amorphous, X-ray intensity curves rel. to dimensions of struct. element 9-32824
 atomic spectrum, bibliography 9-38765
 crystal structure determ. at 4.2, 78 and 299°K 9-39254
 diffusion in Si, isoconcentration studies 9-37208
 diffusion in Si using AsH₃ 9-28324
 Fermi surface, de Haas-Shubnikov effect obs. 9-43024
 growth, hydrothermal 9-37027
 implantation in silicon, range 9-44856
 impurities in Ni alloys and steels, determ. 9-28830
 magneto-acoustic attenuation, giant quantum oscillations, spin splitting 9-35335
 magnetoreflexion, i.r., obs. on trigonal face rel. to band parameters 9-47320
 magnetoresistance, de Haas-Shubnikov oscillations, Fermi surface obs. 9-43024
 magnetoresistance tensor, low field, Fermi surface carrier density and mobility determ., 77-305°K 9-35311
 n.m.r. Knight shifts in rare-earth group-VA intermetallic cpds. 9-33648
 superconductivity search 9-39602
 vaporization, (111) cleavage face, pit growth at spiral dislocation site 9-30467
 p-Ge:GaAs, radiative recomb., influence of local pot. fluctuations, low-temp. 9-39867
 Ge-As solid solution, new phase precipitation mechanism 9-35243
 n-Si:As, photomagnetoelc. and photoconductive effects, low temp. 9-39723

Arsenic compounds

- arsenates, electro-optic parameter in 400-700 nm range at room temperature 9-31086
 As-S glass/Al composite system, bonding mechanism 9-32852
 chalcogenide glasses, elec. conductivity and opt. absorpt. 9-30956
 infrared and Raman spectra 9-36695
 pnictides, binary, with marcasite type struct. mag. props. 9-31016
 As-Se alloy system, transient photoconductivity 9-39709
 As-Se system, laser-induced vaporization, mass spectra 9-28187
 As₂S₃ Raman spectra 9-31117
 As₂S₃ conductivity, effect of Ag and Cu impurities 9-33295
 As₂S₃ films, e bombardment conductivity, columnar ionization 9-33369
 As₂S₃, amorphous, refr. index, 0.6-2 μ 9-39797
 As₂Se₃ amorphous films, drift mobility of carriers, hopping conduction 9-26474
 As₂Se₃ single crystal growth 9-23678
 As₂SeTe₂ semiconductor diode switching, filamentary conduction 9-35449
 As₂Te₃-SnTe quasibinary system, investig. 9-42920
 As₂S₄ Raman spectra 9-31117
 AsF₃, liquid and solid, molecular motion and ¹⁹F spin-lattice relaxation time 9-44594
 AsH₃, i.r. spectra, effect of accidental Coriolis-type reson. 9-34608
 AsH₃ vibration-rotation bands in 2 μ region 9-25731
 AsO₂²⁻, e.s.r. in p-irrad. calcite 9-39903
 AsO₂²⁻, non-linear polarizabilities 9-35611
 (AsO₄)³⁻ impurity in CaWO₄, phosphoresc. enhancement 9-39884
 AsO₄³⁻, rotational analysis of A-X bands 9-46355
 AsO mol., u.v. spectrum, electronic band systems obs. 9-46356
 AsO molecule, emission spectrum bands 9-48454
 AsS₄³⁻, orbital valence force field constants 9-32486
 Ge-As solid soln., defects during precip., nature 9-44682
 In-As-Sb phase diagrams, quasi-chem. equil. model 9-44610
 In-Ga-As phase diagram, quasi-chem. equil. model 9-44610

Assistors *see Conductivity, electrical; Semiconducting devices***Association**

- carbon tetrachloride, equilibria of assoc. bet. pyridine deriv. and alcohols 9-23106
 dye molecules, effect of binary solvents 9-27922
 ethanol, isotopic 9-38892
 ethylene, polymerization induced by Co⁶⁰ γ obs. 9-33665
 tetrolonitrile, polymerization and preparation 9-33667
 Rb-rare gas mol. formation, Rb polarized atom relaxation in rare gas, theory 9-32534

ASES

- alcohols, vapour phase 9-23507
 methanol, self-assoc. from n.m.r. meas. 9-48500
 methanol-trimethylamine mixtures, from n.m.r. meas. 9-48500
 Na⁺ atmospheric formation rate rel. to press. 9-28910
 water clusters in vapour phase 9-44616
 Na⁺ formation in atmosphere 9-28909

liquids

- see also Colloids*
 alcohol, solvation to radical ions, e.p.r. study 9-34880

Association continued**liquids continued**

- alcohols, in soln. 9-23507
 counterions to polyelectrolytes in soln. 9-44552
 counterions to polyelectrolytes in soln. 9-42642
 fluorenone ketyl, existence of paramagnetic and diamagnetic ion clusters 9-34923
 N(4)-hydroxycytosines, H-bond assoc. with purines 9-42635
 trihalomethane-halide ion complexes in soln. 9-23537
 BeSO₄, ion-assoc. process, nature of, u.s. absorpt. studies 9-23460
 Co(II) chloride solns. in water and alcohols, X-ray diffr. 9-44548
 CsCl aqueous soln., const. from elec. cond. data 9-48717
 KCl aqueous soln., const. from elec. cond. data 9-48717
 LiCl aqueous soln., const. from elec. cond. data 9-48717

Astatine

- No entries

Astatine compounds

- No entries

Asteroids *see Planets; Solar system***Astigmatism** *see Aberrations, optical***Astronautics** *see Space research***Astronomical instruments**

- see also Radioastronomy; Telescopes/astronomical*
 'seeing', meas. in solar observation instruments 9-36038
 anastigmats, flat-field, distortion-free 9-29108
 cameras, satellite tracking, three East German instruments 9-27115
 Culgoora solar observatory, optical programme 9-36030
 glass filters, flatness required for accurate image positions, quantitative meas. 9-27114
 high-dispersion i.r. image-tube spectroscopy with small telescope 9-31683
 image intensifier systems, review 9-24937
 image tube, Lenard-window, construction and results 9-45695
 intensity interferometer app. 9-45998
 i.r. flux collectors 9-45694
 i.r. region, instrumental features and problems, thermal and background adiation 9-47689
 Liege solar atlas, instrumental profile 9-41685
 mosaic prism for star field photometric calibration 9-24936
 narrow slit in photometry for brightness meas. of stellar systems 9-43685
 photogrammetric parameters of cameras for stellar photographs 9-41713
 photometer, stellar, synchronous three colour 9-31681
 photometers, current-to-frequency converter which works directly with photomultiplier currents 9-45696
 plates, astronomical, device for comparing 9-31682
 reflecting astrolabe, 25 cm aperture 9-33961
 review and forecast 9-31680
 r.f. digital autocorrelation spectrometer, description 9-45692
 solar filter, series of Fabry-Perot interferometers 9-36037
 spectral-line receiver, multi-channel, for radioastron. 9-31676
 spectrographs on telescopes, research possibilities with moderate dispersion 9-31677
 spectroheliograph, rocket-borne, for Mg II line at 2802.7 Å 9-36396
 spectrohelioscope for the amateur 9-24934
 spectrometer, 33-channel photoelectric; design 9-33960
 spectrometer, double-pass, performance on observing Arcturus spectrum 9-41639
 spectrophotometers, instrument profile effects, reference to the Arcturus Atlas 9-41638
 Stonyhurst discs, construction details 9-24935
 Utrecht Solar Atlas, instrumental profile 9-41686
 vectormagnetograph, simul. direction meas., calibration techniques 9-31684
 X-ray objectives, design and manufacture 9-29140
 Zenith mirror 9-48102

Astronomical observations*see also Radioastronomy*

- 1967, activity in photosphere, (1967) 9-31651
 aberration const. meas. from radial speed optical obs. of Mercury 9-47687
 absorption effects in photoelec. photometry of bright stars due to interplanetary dust 9-27091
 aircraft obs. of solar eclipses 9-45687
 astronomical unit, determ. from galactic H line source (r.f.) radial vel. meas 9-29100
 astronomical unit, radio determ. method, agreement with dynamical method 9-47688
 astronomical unit, radio determ. method, agreement with dynamical method 9-43686
 binaries, eclipse observations 9-45629
 BL Tel, eclipsing variable 9-45630
 B-V photometry, for metal abundance deriv. by colour difference, in G8-K2 giants 9-27012
 cartographic gridding of photographs received from Zond-3 9-43684
 catalogue of the positions and proper motions of stars between declinations -35° and -40° 9-28998
 collection and cataloging of data 9-28977
 cosmological theory 9-26977
 Crab Nebula, of optical flashes 9-40132
 Crab Nebula pulsar, television detection of optical pulses 9-43591
 Crab pulsar, linear and circular polarization meas. 9-43596
 Crab pulsar, search for nanosecond optical pulses 9-41668
 Delta Scuti type variable, observations of five by photometry 9-45626
 far i.r. sky survey using balloon-borne instrument 9-29102
 high-dispersion i.r. image-tube spectroscopy with small telescope 9-31683
 Icarus, asteroid, Belgian obs. 9-31605
 i.r. astronomy, conference 9-29101
 i.r. object in region of IC 1805, obs. 9-27027
 Jupiter red spot visibility, correl. with redspot activity 9-47672
 latitudes determination and their computer programs 9-27110
 mapping sky in i.r. using E.S.R.O. satellite 9-29106
 millimetre and submillimetre astronomy 9-29104
 night sky background, near i.r., rocket-borne telescope and ground-based equipment obs. 9-29103
 observatories, two, non-polar low freq. latit. variations, investigation 9-24931
 occultation of radio sources by the sun, refraction and scatt due to corona 9-31564
 occultation of stars, photometrical observation from the moon 9-31674

Astronomical observations continued

- optical pulsar in Crab Nebula, light curve shape rel. to colour and polarization 9-45644
 parallax, stellar, no need for corrections suns gravitational eff. 9-31673
 parallax obs. of six stars using two different refractors discrepancies 9-40193
 photographic plate meas., influence of centering error 9-47686
 polarization and extinction, interstellar, wavelength depend., correl. 9-31534
 pulsar in Crab Nebula, optical pulse meas. rel. to wavelength independ. of velocity of light 9-41665
 pulsar NP 0532, confirmation of strong light flashes 9-41658
 pulsar NP 0532, discovery of strong light flashes 9-43590
 pulsar NP 0532, optical and radio meas. showing simultaneous emission of pulses 9-47657
 pulsar NP 0532, strong pulsed X-ray signals, comparison with optical pulses 9-43605
 pulsar PSR 0833-45, search for optical radiation 9-45645
 radar observation of planets, introductory paper 9-24932
 radar time of flight obs. to Venus 9-27082
 red-shifts, emission and absorpt. of quasars and related objects 9-41653
 resolution of solar granules 9-36062
 satellites, artificial, optical tracking 9-28973
 Saturn, photometry of ring disappearance in 1966, condensation obs. 9-24867
 SCO X-1 X-ray source, long term periodicity in optical intensity 9-43607
 southern radio sources, 123 obs. of brightness distribution by interferometric methods 9-43580
 spectrophotometric gradients of galaxies 9-24750
 star and planet coincidence errors rel. to telescope parameters, expt. 9-40195
 star transit obs. complete reduction by computer 9-33956
 of star transits 9-45688
 stars, flare, multiple exposure photographic techniques 9-27035
 stars from outside Earth's atm, absence of twinkling, implications 9-41641
 stellar diameter meas. from apparent angular diameter and occultation by moon 9-24775
 stellar radial vels., microphotometer meas. technique 9-31671
 stellar spectrophotometry, instrument profile effects, reference to the Arcturus Atlas 9-41638
 stellary evolution, comparison with theory 9-31533
 submillimetre astronomy, results and prospects 9-29105
 temperature fluctuations in atmosphere, depend. on telescope positioning 9-31675
 U.B.V. system, corrected response curves, new parameters, revision of V magnitude 9-40146
 Vela pulsar, search for optical pulsations 9-43594
 Vela pulsar, visible brightness meas. 9-43596
 VRO 42 22 01 radio source, interferometric obs. for linear and circular polarizations 9-45648
 water, interstellar, detection by its microwave rad. 9-41649
 X-ray, review of technique 9-29107
 H, neutral, absorpt. rel. to pulsar distances 9-41663
 H II minor southern galactic regions 9-24758

Astronomical spectra

- see also Atmospheric spectra; Cosmic radiations, radio-frequency; Stars/spectra; Sun/spectra; and other individual astronomical bodies*
 absorption band, (4430Å), asymm. profiles meas., electronographic method 9-29035
 analysis of observations, comparison of procedures 9-31617
 extragalactic radio spectrum, obs. of background rad. in isotropic world models 9-26979
 interstellar band absorpt., possibly due to supanova dust 9-43578
 of interstellar matter, absorption book 9-24741
 Mars, visible and i.r., rel. to comp. of surface mats. by laboratory comparisons 9-41678
 nebulae, planetary, visual line strengths, short-term variations 9-27001
 night sky, Balmer line emission, intensity and radial vel. 9-38028
 planetary nebula IC 4642, line intensity var., expt. and comments 9-41628
 pulsar NP 0532, confirmation of strong light flashes 9-41658
 pulsar NP 0532, discovery of strong light flashes 9-43590
 quasar red-shift anal., using combined grav. and cosmological factors 9-43583
 radiation transfer in a spectral line nonlinear, nonstationary problem 9-43924
 red shift, large, in models of clusters of point masses 9-45584
 red shift and Evershed velocity obs. in sunspots 9-33954
 relativistic, Doppler eff. in spectral lines, ambiguity 9-22436
 resonance line radiative transfer from a point on the boundary of a half-space 9-44272
 U.B.V. system, corrected response curves, new parameters, revision of V magnitude 9-40146
 u.v. and forbidden line intensities 9-25685
 u.v. radiation below 1215Å, flux density rel. to absorpt. by H in interstellar grains 9-43576
 H₂ electronic transition moments for Lyman band 9-24810
 H interstellar clouds, i.r. emission after cloud collision, rel. to abundance of H₂ 9-24816
 H₂ night sky emission line, intensity and radial vel. 9-38028

Astronomical telescopes *see Radioastronomy; Telescopes/astronomical***Astronomy and astrophysics**

- see also Cosmology; Radioastronomy*
 alphabetical dictionary of terms 9-33882
 annual review 9-24720
 astrodynamics, applic. to upper atmosphere 9-40043
 blackbody radiation, covariant; 3°K radiation field 9-33886
 book, introductory for the general reader 9-43504
 classical, rel. to celestial mechanics 9-40118
 computer applications 9-40196
 conference, Arcetri (1964) 9-40112
 conference, Bologna (1965) 9-45580
 constants in 1964 new I.A.U. system 9-41618
 cosmic objects, various, role of multiple 'Compton', energy losses of energetic electrons 9-47610
 data, collection and cataloging 9-28977
 distance estimates for pulsars, comments on methods 9-45641
 dynamic systems, mass rel. to average velocity dispersion 9-41616
 education of astronomers in Britain 9-25016

Astronomy and astrophysics continued

- e.m. wave 'swinging' by generated Compton effect, source of radio emission 9-24717
 extragalactic research, review 9-40194
 Hale's solar work 9-22028
 interstellar magnetic field, determ. by Zeeman effect meas. in HI clouds 9-36002
 introductory book 9-31485
 i.r. astronomy, conference 9-29101
 i.r. region, instrumental features and problems, thermal and background adiation 9-47689
 Italian Astron. Soc. reunion, Bologna (1965), opening address 9-45581
 light scatt. in semi-infinite medium asymptotic formula 9-45595
 magnetic fields, weak, amplification in turbulent flow, calc. 9-48541
 manned satellites, programme plan 9-38025
 Mount Wilson and Palomar observatory, solar research, apparatus 9-31484
 nebulae, history of their obs. 9-22027
 nebulae observations by four 16th-17th century astronomers 9-34000
 observatory, high altitude, at Boulder, Co., USA 9-36074
 plasma motion in time depend. mag. field 9-42490
 plasma radiation mechanism 9-41617
 pulsar distance calcs., effect of electron density along line of sight 9-45605
 pulsar producing events, frequency estimation from period change of Crab Nebula pulsar 9-40165
 radiative transfer in inhomogeneous atm. by coherent scatt. and gray absorpt. 9-47791
 radio recomb. line spectroscopy application 9-27109
 random force and its time derivative, numerical tables 9-47621
 research reports from German Democratic Republic (1967) 9-24718
 three-body problem, periodic orbits, asymptotic soln. 9-26972
 universe rot., discussion 9-24721

Atmosphere

- see also Air; Electromagnetic wave propagation/atmosphere; Ionosphere*
 aerosol absorption coeff., vertical statistical structure 9-24654
 atomic physics textbook 9-48371
 auroral electrons, intense radio noise generation by Cherenkov rad. 9-40076
 boundary layer, models, finite-difference methods. 9-24678
 cloudy sky, heat influx 9-31289
 conductive, turbulence 9-43388
 diffusion, lateral rel. to finite time of admixture injection 9-40020
 Ekman layer, development at leading edge 9-28860
 explosions, propag. energy 9-31409
 Hadley cell, directness in question 9-24652
 height and turbulent flow field depend., surface boundary layer 9-37909
 height of, sea level press. and upper air temp. rel. muon obs. 9-31467
 ice crystals, velocity and growth rate for 1 min. after nucleation in fog 9-41511
 interaction with micrometeoroids 9-43633
 interhemispheric angular momentum transfer, comparison with hemispheric contents of ang. momentum 9-40023
 inversion above heated ground, simulation by non-steady penetrative convection in water 9-34896
 ion distrib., depend. on meteor ionization determ. 9-31621
 Jupiter, minor constituents 9-24854
 local cooling ice nucleation model 9-28866
 macroturbulent horizontal exchange, coefficient 9-24651
 night sky radiation, variations between 1 and 2 µm, continuously recording radiometer design 9-33807
 numerical model, LAM code, tidal effects 9-33767
 oscillation theory, response curves 9-31303
 planets, rot. and non-rot., Hadley regime props. 9-38068
 radiation, Kew Observatory work review 9-47545
 radiation, net, study over five years, Delhi, India 9-28883
 radiation flux, upward, computations 9-31318
 Rayleigh, light emerging from top colorimetric description 9-28884
 remote electromagnetic probing, wave propagation theory 9-31872
 remote sensing using radiometric techniques at microwave frequencies review 9-33780
 rossby wave packets, resonantly interacting triad, longterm behaviour and zonal flows 9-33756
 rotating differentially heated fluid, amplitude vacillation characteristics determined by multi-probe technique 9-27947
 sea interaction, macroscale, model 9-43378
 sensing, remote of inhomogeneities using microwave and i.r. 9-33781
 stellar magnitude extinction rel. to density 9-33905
 stratospheric data collection 9-40004
 stratospheric turbidity rel. to sky polarization at sunset 9-43396
 surface layer, turbulent heat and momentum flux spectra 9-40005
 thermalgeostrophic, response to tidal oscillations 9-41496
 tropical stratosphere, Kelvin waves, observational evidence 9-24671
 troposphere, const. related to variations of solar wind velocities 9-45480
 troposphere, const. related to variations of solar wind velocities 9-28859
 troposphere, vertical exchanges of artificial aerosols 9-47534
 tropospheric and ground effects on solar radio meas. at 7 GHz 9-24664
 tropospheric radio signals diffraction phenomena 9-37926
 turbulence, clear air in tropopause, energy dissipation 9-47535
 turbulence spectrum in stable and convective layers 9-45488
 two-layered, diffuse refl. and transmission of rad. from scatt. and transmission functions 9-24662
 Venus, appl. theory growth curve and phase effects in cloudy atmosphere 9-38077
 Venus, chemical composition based on Venera 4 obs. 9-24868
 Venus, optical and radio refraction 9-38065
 Venus, radar signal absorption 9-38072
 Venus, radiative transfer rel. 8-14 µm limb darkening 9-24874
 Venus, review 9-24875
 Venus, spectral search for minor constituents 9-24873
 Venus, two component model, H and H₂ 9-24870
 Venus, water vapour escape mechanism, comparison with Earth's 9-24876
 waves, charact., generating influences and eigenvalues 9-31349
³⁹Ar activity, detection using proportional gas counter 9-45498
 O₃ in stratosphere, perturbations during solar eclipse (12 Nov 1966) 9-31294

composition

- aerosol, props. reviewed 9-43385
 aerosols., U.V. decomposition 9-24588

Atmosphere continued**composition continued**

- analysis, electrochem. concentration cells 9-41457
 Arctic, concentrations of CO and organic gases 9-43386
 distortions of image and spectrum of a star 9-24786
 electron density distribution, above winter Pole 9-31418
 ion conc. profiles rel. to F1 layer formation 9-31439
 ionic, distribution of, rel. to temp. determ. 9-43445
 ionosphere measurements using r.f. probe 9-26943
 ions, light, abundance obs. by OGO, interpretation 9-41546
 meas. spectrometer, sweeping, for neutral and positive ion concentration meas., design 9-35835
 mesosphere and lower thermosphere, vertical eddy transport eff. 9-35833
 meteor dust concentration and collection 9-43384
 neutral particles at 110 to 160 km, obs. 9-45500
 ozone, horiz. and vertical distrib., special cases 9-41487
 ozone, photochemical 9-24641
 ozone, total characts. and station network effectiveness 9-41492
 ozone concentration above 40 km, anomaly 9-41494
 ozone content, rel. to nightglow intensity 9-41561
 ozone determ. from 1043 cm⁻¹ spectra by satellites 9-41490
 ozone distribution, estimation by inverting radiative transfer equations for sure molecular scattering 9-28870
 ozone meridional distrib., chem., atm. and solar effects 9-41485
 ozone optical sonde with simultaneous meas. 9-41474
 ozone photochem., 30 to 35 km, parameters determ. 9-41491
 ozone production by silent discharges 9-41544
 ozone sensors, Brewer-Mast, accuracy 9-41476
 ozone total obs., computer evaluation 9-41493
 ozone vertical distrib., comparison of Umkehr and electrochem. sonde obs. 9-41488
 ozone vertical distrib., simultaneous Umkehr obs. with two Dobson photometers 9-41489
 ozone vertical distrib. from 9.6 μ emission and absorpt. spectra 9-41486
 ozone vertical distrib. in upper stratosphere, satellite obs. 9-41545
 particulate pollution in USA 9-43382
 pollution analysis by correlation spectrometer 9-33693
 pollution-induced decrease of elec. conductivity 9-41535
 stratospheric aerosol, investigation by infrared and lidar techniques 9-31297
 thermosphere, lower, composition, from mass spectrometric obs. (Summer 1967) 9-28906
 thermosphere, midlatitude 150 to 450 km, N₂, O₂ and He concentration and temp. 9-28905
 upper, Tunguska meteorite effects rel. to airglow and cond. 9-26916
 Venus, sources of HCl and HF 9-24880
 water cluster ions in ionospheric D region, origin due to vapour reactions, lab. obs. 9-43457
 water molecule dimers, presence shown by maser and interferometer expts. 9-33755
¹³¹I conc. in biosphere in 1968, meas. by thyroid testing 9-43405
 Ar, He number densities, lower thermosphere, day-night vars. 9-26920
 CO₂ conc. in upper troposphere and lower stratosphere, continuous meas. 9-40015
 Ca⁺ abundance, obs. and theory of origin 9-35832
 Fe⁺, Mg⁺, Ca⁺ and K⁺ ions, measurements of reactions with ozone 9-40044
 H, neutral, in exosphere and thermosphere, vertical distrib., airglow H _{α} obs. 9-26923
 H₂O vapour in troposphere, surface evaporation minus precipitation 9-49450
 H in thermosphere and exosphere, vertical profiles giving more consistent results 9-33803
 HNO₃ solar i.r. absorption, balloon obs. 9-47530
 He⁺ concentration at 1000-1200 km, cosmos 5 obs. 9-45505
 He escape, nonthermal process 9-45504
³He loss and production 9-43410
 K abundance, obs. and theory of origin 9-35832
 Li abundance, obs. and theory of origin 9-35832
 N₂ beam sputtering of Ag and Au deposits on satellites, rel. to surface binding energy 9-24076
 N₂ predissociation, influence on atomic N production 9-28908
 N number densities, lower thermosphere, day-night vars. 9-26920
 N⁺ formation in nitrogen 9-28909
 N⁺ formation rate rel. to press. 9-28910
 N absorption, effect on composition meas. 9-28907
 N night-time density, 120 to 230 km, computation 9-41543
 NO₂⁺ production in air 9-43387
 NO 60 to 96 km, evening twilight rocket obs. 9-31344
 NO night-time density, 120 to 230 km, computation 9-41543
 Na, night time abundance and distrib., meas. by tuned laser radar 9-49466
 Na abundance, obs. and theory of origin 9-35832
 O₂ number densities, lower thermosphere day-night vars. 9-26920
 O₂ densities, 100 to 130 km at night 9-43411
 O₂ density, rocket obs. of solar u.v. and X-ray absorp. 9-31346
 O₂ mol., density in thermosphere Ariel III obs. 9-47554
 O₂ layer, u.v. spectra of reflected solar light, obs. from space 9-40033
 O₂ photochemistry in presence of water vapour 9-31298
 O₂ planetary distribution, satellite u.v. spectral obs. 9-40013
 O₂ in stratosphere, effect on twilight polarization 9-41556
 O₂ stratospheric concentration rel. to photochemical processes 9-47532
 O₂ unsteady regime, short period vars. 9-31296
 O₂ vertical distribution, upper layers from satellite obs. of scattered u.v. 9-40012
 O⁺ concentration at 1000-1200 km, cosmos 5 obs. 9-45505
 O absorption, effect on composition meas. 9-28907
 O atomic, in mesosphere, polar at night, distribution 9-31343
 Rn, equilibrium with short lived decay products at 2m above ground 9-47552

humidity

see also *Humidity*

- concentration and movement, aerial sensing equipment and techniques 9-35810
 dew point dynamic determ. method suitable for use on radiosondes 9-26895
 dispersion calculated for water vapour 9-33774
 infrared spectral meas., profiles estimation 9-47531
 near-surface layer, rel. to turbulence parameters 9-24643
 stratosphere from solar absorption spectra 9-24642

Atmosphere continued**humidity continued**

- vertical profile remote probing using acoustic waves 9-33798
ionization see *Atmospheric electricity; Ionization, atmosphere; Ionosphere*
movements
 see also *Wind*
 acoustic gravity wave propag. in ionos. F region, ion drag effect 9-43471
 air mass exchange, use of presence of ³¹P 9-45499
 air mass trajectories, synthesis of general problem 9-47533
 air-sea interaction 9-26891
 angular momentum transfer between hemispheres, comparison with hemispheric contents 9-40023
 baroclinic zonal flow waves, effect of horizontal shear on structure 9-41499
 Benard convection problem with vertically varying exchange processes 9-41481
 boundary layers, two dimensional time dependent numerical model 9-43391
 buoyant jets, phase space solution 9-24650
 circulation, cycle of oscill., solar activity effects 9-31300
 circulation, differentially heated rotating annulus model 9-28872
 circulation, equatorial, group invariant solns. of equations 9-35813
 circulation, general, intensity estimation 9-49451
 convective spherical shell, rotating 9-26922
 cumulus dynamics, thermodynamic equation 9-41508
 currents along mag. field lines, and directional hydromag. emission 9-40061
 currents rel. to mesoscale disturbances, stability 9-40021
 deductions from 5577 Å nightglow 9-37954
 diffusion from linear source in surface layer 9-35815
 dynamics of ultra-long waves, influence of large scale heat sources 9-33762
 eddy fluxes, meas. in lower atmosphere 9-24647
 equations of motion in spectral form 9-24649
 flow in lower layer of marine atm. 9-40017
 flow over ridge, lee waves numerical calc. 9-37912
 flow over ridge, lee waves numerical calc. 9-43389
 friction of air currents over inhomogeneous soils 9-31301
 geostrophic wind field, northern hemisphere, zonal harmonic analysis 9-33765
 gravity waves, internal, ray tracing 9-42478
 gravity waves, ionospheric F region during mag. storm 9-49505
 helical circulations in planetary boundary layer, Lagrangian study 9-26921
 hurricanes, thermodynamics, recent advances in theoretical studies 9-31309
 hydrodynamic instability and energy conversion in quasi-geostrophic model, numerical solns. 9-41497
 interaction with ocean, computations of basic parameters 9-28861
 interatmospheric level exchange at altitudes below 35 km 9-49480
 ionosphere, E region, wind driven instability 9-49501
 ionosphere, lower, tidal semi-diurnal winds, seasonal phase changes 9-49491
 ionospheric wind dynamics 9-40077
 large-scale, nonlinear aspects, effects of interactions upon growth of baroclinic waves 9-33763
 lee waves in stratified flow over semi-elliptical obstacle 9-34730
 lee waves in stratified flow over obstacle, perturbation approx. 9-34731
 mesoscale mountain waves 9-35811
 mesospheric circulation rel. to noctilucent cloud freq. 9-31355
 N. Hemisphere W-E wind, latit. profile and atm. angular momentum 9-47537
 negative viscosity phenomena book 9-32564
 ozone dynamics 9-41495
 planetary boundary layer flow with neutral thermal stability, wind spiral model 9-41501
 planetary wave-zonal flow interaction 9-28871
 planetary waves 9-35812
 quasi-geostrophic flow, stability 9-24646
 rossby wave packets, resonantly interacting triad, longterm behaviour and zonal flows 9-33756
 Rossby waves, planetary, vertical propag. with Newtonian cooling 9-31302
 Rossby waves, time periodic, effect of random currents 9-43377
 sea-air interactions, long range prediction of large scale motion, simplified model 9-24648
 semi-diurnal oscillations, hypothesis of autobarotropic fluid on rotating earth 9-45486
 shear flow with friction, vortices and circulating cylinder motions 9-41500
 stratosphere, wind during solar eclipse (12 Nov 1966) 9-31294
 stratospheric wind observations in tropics 9-31311
 surface boundary layer, turbulent flow field, micrometeorology 9-37909
 suspension in lowest boundary layers, turbulent nonadiabatic diffusion 9-31304
 thermosphere, mid-latitude, continuity of motion 9-49467
 tidal, at 90 to 120 km height, theory and analysis of experimental data 9-41548
 tidal theory with Newtonian cooling 9-26896
 tide, antisymmetric diurnal, oscillatory modes 9-35837
 tide, rotation of horizontal velocity vector 9-35838
 tropical Hadley cell circulation, annual and biennial modulations 9-45485
 troposphere, disturbances correl. with geomag. variations 9-45487
 troposphere, vertical exchanges of artificial aerosols 9-47534
 turbopause, short period vertical movements 9-49492
 turbulence, diffusion calculations using Richardson's number and eddy diffusivity 9-43392
 turbulence, optical strength, remote probing using stellar scintillations 9-33758
 turbulence, remote probing using fluctuations of focused beam wave, theory 9-33757
 turbulence in boundary layer above steppe and sea 9-37911
 turbulence parameters, meas. in near-surface layer 9-24643
 turbulence remote probing using acoustic waves 9-33798
 turbulence spectra 9-33760
 turbulence with thermal stratification, spectral characts. 9-45484
 turbulent heat and moisture fluxes, and turbulent friction stress, from profile obs. 9-40016

Atmosphere continued
movements continued

- turbulent region of boundary layer, influence of baroclinicity and nonstationarity 9-40018
- turbulent transfer processes, new system for meas. 9-24644
- upper, tides and gravity waves, meas. 9-31348
- vertical, distribution, rel. to cloud front system 9-35817
- vertical, ionized formations in ionos., spatial distributions 9-40079
- vortices, mesoscale with vertical axis, non-stationary problem 9-35814
- waves, characteristic parameters 9-40022
- waves, internal gravity for inhomogeneous atmosphere 9-40019
- westerly wind field, small-scale eddy momentum and heat diffusion processes 9-41498
- wind and temperature-stratified, vertical energy flux due to ground disturbance 9-35816
- zonal flows, hydrodynamic instability charact., quasi-geostrophic model 9-43390
- zonal flows from resonantly interacting triad of rossby wave packets 9-33756
- zonal winds at 200 mb level, rel. to month and latitude 9-41505

precipitation

- see also Ice; Rain; Snow*
- actual and computer-calculated, comparison 9-41518
- aerosols, concentration and size distribution determ. 9-41516
- aerosols, tropospheric and stratospheric concentration from daytime meas. of sky polarization 9-45490
- artificial modification 9-43393
- auroral particles, implications for high latitude communications 9-33815
- clouds, precipitating, properties meas. by weather radar, feasibility 9-33752
- electron, following SSC, balloon obs. 9-35903
- frontal, warm, advected changes in melting layer height 9-47542
- hail prevention and stat. evaluation of effects 9-47539
- hailstones, brake-up induced by u.s. waves 9-45491
- ice agglomeration into T formation, lab. expt. 9-41512
- as noise source in cm. range 9-31316
- pairs of drops raised to equal and opposite potentials, comments 9-26899
- particle growth, motion and concentration in convective storm 9-41513
- particles, rel. to ice sphere charging 9-41534
- rainfall onset rel. to ice nuclei 9-41517
- relation to potential gradient, space charge and conduction current, aircraft soundings 9-26906
- snowflakes and raindrops on mountain slope, size distribution 9-41514
- space charge, artificial, effects 9-43399
- spherical cap approximation, validity in heterogeneous nucleation 9-28875
- velocity, Doppler radar determ. 9-41507
- water droplets in free fall, freezing and shattering phenom. 9-28181
- ²¹⁰Pb, in surface air and precipitation, measurement 9-28900
- Agl crystals, ice and water nucleation 9-41510

radiation belts

- artificial, 1962 Jul.9, satellite obs. 9-37966
- axisymmetric, mag. field and energy 9-28935
- bimodal diffusion, trapped particle energy spectra 9-41572
- diffusion, radial, and precipitation loss 9-37950
- electron acceleration in outer zone, morphology 9-43434
- electron diffusion, radial at low L values 9-28938
- electrons, 10-100 keV trapped, Explorer obs. 9-37968
- electrons, 1.76<L<5, radial diffusion coeff. 9-24682
- formation, possible mechanisms, review 9-37963
- geomagnetic closed field lines, high-latitude limit 9-35873
- inner, charged particle fluxes prior to 9 July 1962 nuclear explosion 9-33824
- inner, electron fluxes and energies due to Starfish explosion, obs. (1965) 9-26934
- inner, non-adiabatic particle losses 9-40066
- and magnetosphere, book 9-24683
- rel. to magnetospheric convection 9-37951
- magnetospheric trapped radiation inward diffusion, effect of convection electric fields 9-43435
- nucleon flux intensities, calculated specific yield functions for neutrons monitors 9-29634
- outer, diffusion of equatorial particles 9-45517
- outer, electron intensities during mag. storms, obs. 9-43434
- outer, energetic electrons during mag. bays 9-31381
- outer, particle dynamics, review 9-37964
- outer, particle flux obs., review 9-37965
- outer, processes determ. from rel. between mag. activity and v.l.f. emissions 9-40102
- outer, relativistic electron radial diffusion spectra 9-33825
- outer, total ionization measurements by POGO, ion chamber experiment 9-40067
- outer electron flux, drift periodic echoes 9-28937
- outer electrons of energy >100 keV, radial diffusion 9-40064
- outer protons, cyclotron instability 9-40065
- outer zone, omnidirectional electron intensity contours, obs. 9-37962
- particles, enhancement of electron concentration of F2-region 9-40092
- proton belt, bimodal diffusion 9-41571
- proton dynamics 9-31380
- proton spectra, 2<L<3, obs. 9-35860
- protons, 100 keV-10 MeV trapped, Explorer obs. 9-37968
- protons, interactions with hydromag. waves 9-31379
- ring current, self consistent, from non-linear symmetric inflation of a mag. dipole 9-45518
- ring current belt, non uniform growth, effect of magnetospheric substorms 9-31378
- ring current particle distributions from mag. obs. 9-26933
- synchrotron radiation from trapped electrons above auroral zones 9-37961
- trapped particles, bounce resonant scattering 9-28936
- trapped particles, Telstar 1 and Explorer 15 obs. 9-37967
- Van Allen, upper bounds for total particle energy 9-46501
- V.L.F. chorus, interpretation 9-40068

radioactivity

- see also Fallout*
- data, at Dourbes (Belgium), during April (1968) 9-49509
- debris from Chinese sixth nuclear test, activity meas. in Sweden 9-49458
- measurements in Finland, tables grouped according to fractions of aerosol beta activity 9-31334
- natural, electrical and neutral carriers 9-24667

Atmosphere continued**radioactivity continued**

- neutron flux induced by solar neutrons, calc. 9-35829
 - neutron flux produced by cosmic ray interactions, atmospheric depth function 9-47551
 - neutron spatial and time distrib. 10-1000 m above earth's surface 9-37929
 - raindrops, results of measurements 9-28899
 - show neutron density distrib. in minimum solar activity years, obs. 9-25496
 - surface layer, gamma field variation 9-31333
 - ²¹⁰Pb, in surface air and precipitation, measurement 9-28900
 - ²²⁶Rn (thoron) meas. of turbulent diffusion 9-37930
 - ¹³¹I conc. in biosphere in 1968, meas. by thyroid testing 9-43405
 - ²¹²Bi meas. and geophysical applications 9-24670
 - ²¹²Pb (Th B) meas. of turbulent diffusion 9-37930
 - ²¹²Pb meas. and geophysical applications 9-24670
 - ⁴¹Ar oven reactor core and in exhaust air, IRT-1000 Sofia 9-22875
 - ¹⁴C in CO₂, apparatus for preparation and activity meas. 9-26912
 - ¹⁴C particulate tracers of stratospheric motion 9-28896
 - ³P prod. as air mass exchange indicator 9-45499
 - Rn, equilibrium with short lived decay products at 2m above ground 9-47552
 - Rn daughter products, systematic errors in meas. by filter method 9-40042
 - Rn decay products, transport proc. in air 9-32327
 - Rn decay products transport proc. in air 9-22762
 - Rn meas. method and its validity 9-41538
 - RnA and RnB, distrib. of decay products calc. in different shaped volumes of air 9-22761
 - RnA and RnB, distrib. of decay products calc. in different shaped volumes of air 9-34424
 - Sr⁹⁰, stratospheric residence time and interhemispheric mixing from fallout in rain 9-40041
 - ⁹⁰Sr particulate tracers of stratospheric motion 9-28896
- structure**
- aerosol vertical distribution 9-40014
 - clear remote probing with radar features of structures observed 9-33783
 - Ekman layer, cloud diffusion calc. 9-41509
 - interfacial water structure studies 9-31299
 - lower, remote probing using acoustic wave 9-33798
 - lower acoustic sounding experiments, interpretation of data 9-33799
 - multilayer approx. use in acoustic gravity wave propag. calc. 9-41539
 - probing, multifrequency, accuracy limitation 9-33751
 - remote sensing using Rake tropospheric scatter technique, experimental data 9-33784
 - remote sensing using Rake tropospheric scatter technique, interpretation of experimental data 9-33785
 - stratification, large-scale, effect of convective clouds 9-33770
 - stratospheric dust striations 9-31295
 - troposphere, inversion layer study by simultaneous lidar and refractometer soundings 9-43380
 - O₃ layer disturbance, height determ. 9-43383
- temperature**
- air-ocean interface, heat flux and temp. variation 9-47528
 - airborne surface measurements, influence of air layer between target and radiometer 9-33754
 - annual variation in lower tropical stratosphere 9-28867
 - convective spherical shell, rotating 9-26922
 - Doppler, 6300 Å interferometric obs. (30 Oct-2 Nov 1968) 9-49459
 - fluctuation, depend. on telescope optimum positioning 9-31675
 - forecasting of night minimum at surface 9-49448
 - interferometric thermometer for air temp., 25-30 km 9-37910
 - inversion, location and intensity remote probing using acoustic waves 9-33798
 - inversions, low-level midday, development 9-31291
 - ionos. F layer, electron temp. 120 to 630 km 9-45544
 - ionosphere, night over Arecibo 9-24685
 - ionosphere E region, radar scatter obs. rel. to possible tidal heating 9-43462
 - ionosphere F1, form thickness parameter IGY and IQSY 9-43469
 - ionosphere F region, fine structure obs. 9-31440
 - ionospheric topside ion and electron temp. rel. to concentration profiles 9-43449
 - kinetic, rel. to rotational and oscillational temps. from O₂ spectrum 9-26893
 - large-scale heat sources, influence on dynamics of ultra-long waves 9-33762
 - local cooling resulting from dissolution of soluble ice nuclei, laboratory study 9-28863
 - near-surface layer, rel. to turbulence parameters 9-24643
 - neutral, electron and ion from composition distribution 9-43445
 - neutral particles at 110 to 160 km. obs. 9-45500
 - oscillations spectra for near-water layer 9-40008
 - profile determ., statistical regularization 9-40009
 - profiles, vertical, statistical determ. from i.r. satellite obs. 9-45482
 - radiative transfer of heat, solution to integral equations 9-31293
 - statistics, effect of vertical line averaging 9-33753
 - stratosphere, Antarctic warming effect of solar corpuscular rad. (Spring 1963) 9-41484
 - stratosphere, during solar eclipse (12 Nov 1966) 9-31294
 - stratosphere, ozone and temp. vertical profiles 9-41540
 - stratosphere, rel. to nightglow intensity 9-41561
 - surface and mid-troposphere, rel. to water vapour 9-49450
 - thermal interactions with earth, propagation of diurnal temperature waves 9-24640
 - thermosphere, 150-300 km, 1964-5 satellite obs. 9-31342
 - thermosphere, midlatitude 150 to 450 km N₂, O₂ and He 9-28905
 - thermosphere shape parameter, probe obs. 9-49493
 - thermospheric structure and vars. 9-49460
 - topside ionosphere, latitudinal temperature structure 9-26944
 - tropical Hadley cell circulation, annual and biennial modulations 9-45485
 - troposphere, vars. of value calc. from aircraft rad. obs. 9-40007
 - tropospheric soundings at 5 levels, in 15μ CO₂ band 9-41483
 - turbulent heat flux patterns, winter, over N.Atlantic 9-31290
 - upper atm. variations with height, optical meas. using space vehicles 9-41542
 - virtual, moist-adiabatic vertical gradient 9-49447
 - winter, correl. with autumn rainfall 9-31287
 - from BaO spectra recorded in Ba release expts. 9-26917

Atmosphere continued
temperature continued

- He⁺ at 1000-1200km, cosmos 5 obs. 9-45505
rel. to O₂ B-band line parameters 9-40011
O₃, effective, estimation during disturbance 9-43383
O₃, layer stationary regime effective temp. vars. day and night 9-40006
O₃ determ. from solar spectrum obs. 9-31288
O⁺ at 1000-1200km, cosmos 5 obs. 9-45505

thermodynamics

- cloudy sky, heat influx 9-31289
convection anelastic approximation thermal 9-41482
cumulus dynamics equation 9-41508
cyclones, developing, energy conversions 9-49449
diurnal thermal wave in non-grey atmosphere 9-28865
enthalpy rel. to total potential energy in horizontally finite column 9-47529
hurricanes, recent advances in theoretical studies 9-31309
protonosphere night cooling 9-26918
radiation heat balance, sea-sky, obs. 9-31317
Rossby waves, planetary, vertical propag. through atmosphere with Newtonian cooling 9-31302
troposphere, inversion layer study by simultaneous lidar and refractometer soundings 9-43380
turbulent flux near ground, negligible third moment term 9-31292
variations in troposphere and lower stratosphere, interrelationships 9-43381
volume free energy associated with soluble ice nuclei 9-28868
radiative terms in thermal conduction equation arising from O and CO net emission 9-26894

upper

see also *Magnetosphere*

- astrodynamics application 9-40043
auroral electron precip., presence of mono-energetic beams 9-49475
CENFAM multistation radar system, receiving apparatus 9-41614
CENFAM Project for multistation radar system 9-41613
conference, Bologna (1965) 9-45580
cosmic ray neutrons, atmosphere and earth leakage flux, balloon obs. (1966) 9-38602
density at 275 km, satellite drag obs. 9-49462
density meas., roles of kinetic theory and gas-surface interactions 9-45503
density probe, 130 to 160 km, from satellite orbit 9-31339
density shifts, systematic analysis rel. to reference models 9-28903
density variation, 33-month periodicity 9-28904
density variations at heights 140-180 km, July to Nov. 1968 9-43408
density vars., semi-annual, review 9-49461
electrojet, equatorial in Pacific, N-S cross sections and effect of solar eclipse 9-37960
electron bursts, field aligned high latitude, OGO 4 obs. 9-40062
electron cooling by O₂ vibrational excitation 9-43444
electron density distribution, above winter Pole 9-31418
exospheric plasma, trans-polar, unified model 9-37940
gas clouds, moving, flow fields 9-28063
gas-surface energy transfer, satellite experiment 9-35831
geomagnetic tail, current sheet waves damping by radiation 9-47560
geomagnetic tail, e.m. noise in current sheet 9-47559
heating, rel. to geomag. perturbations 9-41601
heating, transient, response 9-41541
heterosphere, density variations 9-45501
ion and electron cone during an aurora 9-33813
ion-exosphere model for variable baropause conditions 9-26927
ionisation, recombination and charge transfer during an aurora 9-33813
ionization by satellite 9-31353
i.r. scattering observations 9-47561
magnetosphere and radiation belts, book 9-24683
magnetosphere asymmetric inflation rel. to auroras 9-26929
magnetosphere boundary distance rel. to geomag. field non-dipole component, IMP-1 obs. 9-26924
measurement, rocket-released magnetometer, construction and preliminary results 9-41593
mesosphere and lower thermosphere, vertical eddy transport off on composition 9-35833
meteor streams, mass influx and penetration rate 9-31619
MHD waves, excitation by finite source 9-49470
neutral, 110 to 160 km altitude, density, composition and temperature 9-45500
neutral winds, 150-400 km, calc. 9-40045
ozone layer photochemistry 9-35834
phenomena related to geomag. field vars. 9-47591
planetary exosphere, lateral transport He 9-29059
planetary exosphere, rotating neutral, model 9-47670
plasma, transpolar exospheric, plasmasphere termination 9-28915
polar substorms study, review, book 9-24676
protonosphere, night cooling 9-40049
protonosphere night cooling 9-26918
ring currents, Vlasov-equation study 9-47567
scintillation boundary for satellite radio signals 9-31391
stratosphere, ozone and temp. vertical profiles 9-41540
stratosphere, ozone vertical distrib. satellite obs. 9-41545
temperature meas., tungsten wire sensor 9-43409
thermosphere, lower, composition from mass spectrometric obs. (Summer 1967) 9-28906
thermosphere, mid-latitude, continuity of motion 9-49467
thermosphere, mol. o density, Ariel III obs. 9-47554
thermosphere, temp. and density 150-300 km, 1964-5 satellite obs. 9-31342
thermosphere, temp. and density semiannual variations, influence of interstellar matter 9-24812
thermosphere, wave propag., Explorer 32 obs. 9-28912
tidal, at 90 to 120 km height, theory and analysis of experimental data 9-41548
tide, antisymmetric diurnal, oscillatory modes 9-35837
tide, rotation of horizontal velocity vector 9-35838
tides and gravity waves, meas. 9-31348
Tunguska meteorite effects rel. to airglow and cond. 9-26916
turbosphere, altitude var. of turbulence field 9-35836
turbulence, 80 to 100 km, internal scale determ. from structure function of inhomogeneities 9-31347
twilight phenomena, use in exploration 9-49474
Venus, CO₂ model 9-24872

Atmosphere continued
upper continued

- Venus, review 9-24871
Venus, structure 9-38074
vertical energy flux due to ground disturbance 9-35816
wave obs. from separate sites, cross spectra, effect of bandwidth on interpretation 9-28947
wind obs. by means of meteor trails 9-41547
winds, irregular, near 100 km altitude 9-28911
Ca⁺ abundance, obs. and theory of origin 9-35832
H₂, neutral, in exosphere and thermosphere, vertical distrib., airglow H₂ obs. 9-26923
HNO₃ solar i.r. absorption, balloon obs. 9-47530
He⁺ and O⁺, conc. and temp. 1000-1200km, cosmos 5 obs. 9-45505
He flux, lower thermosphere 9-31345
K abundance, obs. and theory of origin 9-35832
Li abundance, obs. and theory of origin 9-35832
N₂ beam sputtering of Ag and Au deposits on satellites, rel. to surface binding energy 9-24076
N night-time density, 120 to 230 km, computation 9-41543
NO night-time density, 120 to 230 km, computation 9-41543
Na abundance, obs. and theory of origin 9-35832
O₂ distrib. at 100-150 km, Woomea 9-37932
OH emission, as function of solar cycle, seasons and geomag. disturbances 9-45508

Atmospheric acoustics

- acoustic gravity wave propag., use of multilayer approximation 9-41539
echo sounding of lower atmosphere interpretation of experimental data in terms of atmospheric structure 9-33799
infrasonic missile noise, long range supersonic propag. 9-31337
ion-acoustic waves modified by gravity 9-31336
linearised waves, numerical model 9-37931
nonlinear propagation theory, expt. verification from chemical shot signals 9-43404
ray tracing using shifting coordinate system 9-43407
remote probing of structure 9-33798
temperature and wind stratified atmosphere, acoustic-gravity wave propagation 9-26915
transmission anomalies, three, with explanations 9-28902
ultrasonic propagation characteristics for ranging 9-33800
wave propagation in non-gray radiating atmosphere 9-26914

Atmospheric disturbances see *Atmosphere/movements; Thunderstorms***Atmospheric duct** see *Electromagnetic wave propagation***Atmospheric electricity**

- see also *Atmosphere/radioactivity; Atmospherics; Aurora; Electromagnetic wave propagation/atmosphere; Ionization, atmosphere; Lightning; Thunderstorms*
air-earth current density, global diurnal vars. 9-28891
auroral electrojet, enhanced conductivity of ionosphere, with impressed primary electric field 9-40056
charge separation in melting ice particles 9-31326
cloud charging and precipitation, effect of artificial space charge 9-43399
clouds, manipulation for weather control 9-28862
conductivity decrease due to pollution 9-41535
currents, Birkeland field aligned at auroral latitudes 9-28934
data, at Dourbes (Belgium), during April (1968) 9-49509
double diurnal vertical gradient oscillation 9-24637
electrojet equatorial, current distrib. in vicinity by Stening equivalent circuit 9-47568
electrojet, equatorial, e.m. induction of Earth currents, simple relations 9-45460
electrojet, equatorial, non-2-stream irregularities 9-43432
electrojet, equatorial in Pacific and effect of solar eclipse 9-37960
electrojet, night equatorial, electron drift vel. v.h.f. radar obs. 9-31377
electrojet, polar, rel. to geomag. S₂ variation 9-35904
electrojet equatorial with meridional current system, model 9-49479
electrojet probe 9-24681
electrojet stations, SCs and SIs in magnetic field equatorial, India 9-28962
electron fluxes, soft, intense, equatorial 9-40063
equatorial electrojet, electron density irregularity, observation and interpretation 9-26932
field, stationary distribution in near-ground layer 9-49454
field in ground layer 9-35825
field near ground, effect of aerosol 9-43398
generation processes and other phenomena, review of recent investigations 9-31327
global current flow, area averaging 9-49455
ice sphere charging due to rotation through cloud or precipitation particles 9-41534
ion and electron heating by auroral fields 9-33823
ionosphere and magnetosphere currents, models 9-35858
low shock, electrical cond. from macroscopic eqn. 9-47556
magnetosphere, currents along mag. field lines 9-31375
magnetospheric currents due to ionos. dynamo action 9-31376
magnetospheric electric field estimation from micropulsation freq. drift 9-31354
point discharge, pulse tech. for meas. using electrodes capacitively coupled with spruce tree 9-45496
point discharge current meter 9-49456
proton cyclotron harmonic waves, electrostatic, from e.l.f. data, Alouette 2 obs. 9-49478
ring current belt, non uniform growth, effect of magnetospheric substorms 9-31378
ring current effects rel. to auroral substorm activity 9-43433
ring current rel. to auroral oval position 9-43431
ring currents, Vlasov-equation study 9-47567
ring currents measurable at low latitude stations 9-47589
space charge, artificial, effect on atm. electrification, cloud charging and precipitation 9-43399
space charge, pot. gradient and conduction current rel. to precipitation 9-26906
surge of auroral electrojet westward travelling March 3, 1968, absence of H₂ emission 9-47569
thunderbolts, historical examination, book 9-33778
thunderclouds, elec. field and conductivity obs. 9-31324
upper, electrical nature, review 9-35859
water drops, collisional charging wind tunnel expt. 9-31325
waves, e.s., particle acceleration in d.c. magnetic field 9-28023

Atmospheric optics

- see also *Airglow; Sky brightness; Sunlight; Twilight*
 absorption and opacity from auroral obs. 9-33820
 absorption of grazing incidence radiation, Chapman's theory generalized to ellipsoidal Earth 9-41522
 absorption of laser signals by atmospheric gases 9-47549
 aerosol absorption coeff., vertical statistical structure 9-24654
 aerosol particle size determ. using light scatt. counters, influence of refractive index 9-28889
 aerosol study by light scatt., photometric meas. 9-40053
 albedo vars., calc. from satellite obs. 9-43395
 albedo vats., calc. from satellite obs. 9-37914
 atmosphere-ocean system, radiative transfer 9-36149
 backscattering of light pulses by turbid medium, effect of phase function at forward angle 9-41530
 beams, narrow collimated multiply scattered, luminence rel. to beam and receiver diameter 9-40032
 coherence degradation in random media 9-22366
 coherence function, 4th order, propag. in random medium 9-45988
 density determ. using satellite, accuracy of phase and angle refraction meas. 9-24639
 density vertical distrib., near u.v., satellite obs. 9-41525
 depolarization, polarimeter and obs. 9-48093
 depolarization at 6328 Å due to atmospheric transmission 9-37916
 dispersion calculated for water vapour 9-33774
 fluorescence as noise source in laser backscatter expt. 9-37920
 Gaussian beam fluctuations in random medium, correls. 9-45987
 Glory phenomenon, scatt. of scalar wave by transparent sphere 9-29178
 green flash development with time, pictures from 10.6 km altitude 9-41521
 haze transparency, 0.37 to 1.0 μ 9-40037
 holographic image degradation 9-40366
 hygroscopic particles, effect on backscattered power of laser beam 9-41529
 image of sun on airborne ice crystals 9-33775
 incoherent objects seen through turbulent medium, detection and resolution 9-41531
 infrared measurements of atmospheric transmission at sea level 9-33771
 i.r. sky flux obs. and correl. with local conditions 9-41523
 laser beam, Gaussian in turbulent atmosphere, log-amplitude mean 9-47546
 laser beam attenuation and backscatter rel. to visibility 9-28885
 laser beam in turbulent air with Gaussian correl. refractive index fluctuations 9-31323
 laser beam in turbulent atmosphere, log-amplitude fluctuations 9-31320
 laser beam scintillation over for 1.2 km path at 0.632 and 10.6 μ 9-31973
 laser beam transmission 9-31322
 laser beams, 0.63 μ propag. in artificial fogs, wood smokes and model media 9-28886
 laser beams, pulsed and c.w., scintillation magnitude saturation in near-earth propag. 9-31968
 laser light scatt. by fogs and smokes, polarization 9-35824
 laser radiation backscatt. along oblique paths, calc. 9-33777
 laser signal absorption by atmospheric gases 9-47549
 log-amplitude variance for several propagation paths, meas. 9-31321
 micron wavelength propagation effects 9-37915
 model, with equilibrium radiance independent of height and no absorption 9-33776
 modulation transfer and phase structure functions in turbulent medium 9-44527
 mutual power spectrum expression, Beran result generalization 9-31319
 night vision systems, active, backscatter effects 9-26902
 objects illuminated by narrow beam in scatt. medium observation 9-37918
 optical characts., lzser obs. 9-40034
 polarization of diffusely refl. light 28 km. 3620-5990 Å 9-47548
 polarization of sky at sunset, neutral points, Mar-July (1968) 9-43396
 propagation in random media, ratio of short-time to long-time blur widths of images 9-26904
 radiance, earth-atmosphere 8-14 μ window rel. to altitude 9-28882
 Rainbow phenomenon, scatt. of scalar wave by transparent sphere 9-29178
 range of vision, instrumental meas. 9-41532
 Rayleigh atm., light emerging from top, colorimetric description 9-28884
 Rayleigh scattering, intensity of radiation 9-28933
 reflection and transmission functions of finite isotropically scatt. atmosphere 9-29531
 refractive index vertical spectra rel. to atm. stability 9-41526
 refractometer, lightweight, for field use 9-38407
 resolution, limiting, looking upward 9-26890
 scattered radiation during cloud formation, polarization and angular distribution changes 9-28887
 scattering, multiple, by cloudy and hazy planetary atmospheres 9-41527
 scattering by large water droplets 9-28888
 scattering in an aerosol spherical atmosphere 9-37917
 scattering of polarized light in slab of randomly oriented particles, symmetry relations 9-41528
 spherical wave propag. in turbulent media 9-40752
 submillimetre absorption, effects of isotopic and vib. excited forms of water vapour 9-44331
 sunspot obs. through water clouds 9-43397
 surface layer transparency, i.r. 9-40036
 transfer function of scatt. media 9-25366
 turbid medium illuminated by narrow beam, nonstationary light field 9-40039
 turbidity, role of condensation and dry aerosol particles 9-40037
 turbulence effect on laser beam, meas. 9-28890
 turbulence layers, twinkling range, 9-26905
 turbulent medium propag. 9-25350
 upper, infrared scattering observations 9-47561
 visibility in polarized light, horizontal range 9-40038
 visibility measurement using backscattered light 9-26903
 water-air interface, light field structure produced by emerging narrow beam 9-37919

Atmospheric pressure and density

- cyclone development, potential vorticity field 9-47536
 density., rocket obs. of solar u.v. and X-ray absorp. 9-31346
 density at 90 km, semi-annual variation 9-45502
 density between 130 and 160 km from analysis of orbit of 1968-59B satellite 9-47553

Atmospheric pressure and density continued

- density meas. of upper, roles of kinetic theory and gas-surface interactions 9-45503
 density near 100 Km, and diurnal variations, Thomson scatt. obs. 9-31340
 density variations at 140-180 km height, July to Nov. 1968 9-43408
 density varying exponentially with altitude, shock wave propag. from point explosion 9-34091
 double diurnal pressure oscillation 9-24637
 effect on horizontal pendulum oscillation period 9-40263
 fluctuations on mesoscale rel. to distance from jet stream core 9-28869
 forecast of press. field, use of dynamical eqns. 9-45481
 forecasting of barometric field, numerical, orographic and frictional effects 9-49446
 gauge, γ scatt., design by multivariable search method 9-24636
 ground-pressure waves from nuclear explosion, rel. to wind, models 9-24645
 heterosphere, density variations 9-45501
 kinetic theory and gas-surface interactions measurements of upper atmospheric density 9-26919
 neutral density 300-700 km, latitudinal vars. 9-49465
 neutral particles at 110 to 160 km. obs. 9-45500
 oscillations, microbarographic, due to nuclear explosions 9-33761
 oscillations spectra for near-water layer 9-40008
 pressure oscillation in 10-level model 9-33759
 pressure variation coeffs. computation from zonal current wave harmonic analysis 9-41502
 pressure waves coupled to Rayleigh waves from distant earthquake 9-28849
 radio occultation meas. from Mariner, effect of water vapour in on-board estimation 9-49464
 radio sensing using satellites, density obs. 9-33782
 satellite determ., accuracy of phase and angle refraction meas. 9-24639
 rel. to sea level forced oscils., S. Baltic 9-37900
 stratification (density) in near-water layer rel. to stress and heat exchange coeffs. 9-40010
 troposphere press. disturbances correl. with geomag. variations 9-45487
 upper, 275 km, satellite drag obs. 9-49462
 upper, semi-annual density vars., review 9-49461
 upper, systematic analysis of density shifts rel. to reference models 9-28903
 upper atmosphere, variation, 33-month periodicity 9-28904
 upper profile, 130 to 160 km, from satellite orbit data 9-31339
 zonal flows, hydrodynamic instability charact., quasi-geostrophic model 9-43390
 H density, effect of incoming interstellar H atoms 9-49463
 O₂ density distribution in 70 to 150 km regions, Y-ray and EUV photometric determination of latitudinal and temporal variations 9-31341
- Atmospheric spectra**
 see also *Atmospheric optics*
 9.6 μ emission and absorption, rel. to ozone vertical distrib. 9-41486
 aerosol extinction coeff., stratosphere, statistical structure of vertical profile 9-40035
 air glow, predawn, 6300 Å, obs. over U.K. (1965-1968) 9-47562
 airglow, daytime, weak emissions 6000-11500 Å 9-45511
 airglow, interferometric spectra, 1.2 to 1.6 μ m 9-28923
 aurora, O5577 Å lin transition probability lab. obs. 9-46282
 aurora, rocket obs. 9-33811
 aurora, spectroscopy and excitation mechanisms, review 9-31371
 aurora u.v. emission lines of O, N and N₂ 9-33817
 auroral glow at solar maximum and minimum, comparison 9-35852
 auroral green line transition probability, absolute lab. meas. 9-31373
 clouds, formation 9-37913
 green flash development with time, pictures from 10.6 km altitude 9-41521
 haze transparency, 0.37 to 1.0 μ 9-40037
 infrared spectral meas., relative humidity profiles estimation 9-47531
 i.r. day and night airglow, principal emission features 9-28921
 i.r. flux divergence, 12-44.44 μ spectral and vertical distribution 9-35822
 molecular lines in far absorpt. i.r. spectra, identification 9-31361
 night airglow, between 3 and 4 μ m, obs. of OH, methane and CO₂ bands 9-24679
 night airglow, emission spectrum, 2 to 4 μ m 9-28922
 nightglow 6300 Å enhancements rel. to F2 height variations, obs. 9-41557
 O₂ i.r. bands in airglow temporal variations, balloon obs. 9-45509
 ozone, coeffs. of absorption in Hartley band, verification 9-41524
 ozone determ. from 1043 cm⁻¹ spectra by satellites 9-41490
 radiation flux, upward, computations 9-31318
 refractive index and air vel., vertical, rel. to atm. stability 9-41526
 solar absorption, rel. to stratosphere humidity determ. 9-24642
 terrestrial outgoing radiation, Cosmos obs. 9-31314
 terrestrial radiation, 7-15 μ m, Cosmos 45 obs. 9-31315
 of turbulence 9-33760
 turbulence with thermal stratification, spectral characts. 9-45484
 u.v., of solar rad. reflected by ozonosphere, obs. from space 9-40033
 water vapour, absorption background near 3811 cm⁻¹ 9-38845
 water vapour absorption, strong and weak, radiation heat exchange determ. 9-24638
 water vapour rel. to anomalous absorpt., 337, 311 μ m 9-47547
 whistlers, 1-10 kHz, amplitude spectra 9-31386
 zenith twilight, second Umkehr obs. and interpretation 9-41555
 CO₂ band, 15 μ m, use in yroposphere temp. soundings 9-41483
 CO₂ laser radiation, absorption of P(20) line 9-33772
 H β emission in pulsating aurora 9-35853
 He I (1.083 μ) and I (5577 Å) in sunlit aurora, brightnesses rel. to primary e spectrum, obs. 9-47566
 N I ⁴S_{3/2}-²D_{3/2,3/2} transitions at night, permanent feature of upper atm. 9-33804
 NH₃ microwave emission in Sagittarius region, rel. to dust cloud conditions 9-43574
 NO lines in airglow burst, Cosmos 92 obs. 9-43422
 O₂, 1-1 and 2-0 bands, rel. to rotational, oscillational and kinetic temps. 9-26893
 O₂ electron transition probability in red 9-36706
 O₂ lines, spin-rotational, absorption coefficient in geomagnetic field 9-45495
 O₃, temp. determ. from solar spectrum obs. 9-31288
 O₃ u.v., reflection, satellite obs. 9-40013
 O 6300 Å emission in nightglow, post-midnight peak obs. and theory 9-40054

Atmospheric spectra continued

- O I (5577Å) and He I (1.083 μ) in sunlit aurora, brightnesses rel. to primary e spectrum, obs. 9-47566
OH band contamination of nightglow obs. 9-41560
OH emission in upper atmosphere during solar cycle, seasons and geomag. disturbances 9-45508

Atmospherics

- e.l.f. determination of lightning discharge characteristics 9-28893
ion cyclotron whistlers in cold collisional multicomponent plasma 9-40051
ionosphere effects during thunderstorms observations at site having collocated array of various types of sensors 9-33849
ionospheric and tropospheric propagation Doppler effects in satellite communications, computer program 9-45575
l.f. radiation from erratic lightning path 9-45497
from lightning and sources, distrib. Ariel III obs. 9-49457
magnetospheric, v.i.f. noise triggering by Morse dots at 14.7 kHz 9-43415
magnetospheric l.f. waves generated by lightning, ground transmitters and charged particles 9-37947
noise, cm. range, due to tropospheric thermal rad. and precipitation 9-31316
noise at 33.5 GHz, rel. to cloud attenuation 9-33779
noise bursts, h.f., pulse spacing 9-43401
propagation of slow tail portion 9-43437
radio noise, generation by Cherenkov rad. from auroral electrons 9-40076
radio noise measurements at 27 kHz, fixed stations in Europe 9-33786
radio noise of auroral origin 9-37955
substorms, successive v.l.f. and optical emissions 9-41533
sudden enhancement of effects subsequent to nuclear explosions in atmosphere 9-47550
sudden enhancements, IGY obs. 9-37923
v.h.f. hiss, equatorial 9-40063
v.l.f., medium latit., geomag. storm-time evolution, satellite obs. (May 25/26 1967) 9-37939
v.l.f. bursts, outer ionospheric, rel. to mag. activity 9-40071
v.l.f. chorus interpretation 9-40068
v.l.f. emissions, mid-latitude, rel. to mag. activity at conjugate points 9-40102
v.l.f. emissions from magnetosphere, properties 9-31360
v.l.f. hiss, equatorial 9-40063
v.l.f. whistlers, ionospherically propagating, cutoff 9-24688
whistler characts. change in disturbed mag. field of magnetosphere 9-45506
whistler duct drift across mag. shell, triggering of v.l.f. noise 9-43414
whistler mode V.L.F. signals, Magnetospheric amplification 9-26926
whistler recording, synoptic, at Durban during IGY and IQsy 9-28892
whistlers, amplitude spectra, 1-10 kHz 9-31386
whistlers, magnetospheric propag. 9-40046
whistlers, propagation theory rel. to delay and distortion in moving plasma 9-40297
whistlers and v.l.f., multichannel spectral analyser 9-26907
whistlers during solar min. 1965, obs. 9-43400
whistlers in cold plasma, amplitude dispersion and nonlinear instability 9-44433
whistlers in magnetosphere, cyclotron resonance amplification 9-41554

Atomic beams

see also *Particle velocity analysis*

- alkali ats. reaction with triat. halide mols. 9-25795
deflection at uncharged conducting surface 9-34575
frequency shift depend. on C field 9-22986
inert gas, reflection from high temp. W ribbon in low press. O or ethylene atm., obs. 9-40558
inert gases, metastable atoms, electron ejection from W surfaces 9-31002
magnetic reson. expt. for determ. of hyperfine structure of excited states 9-44252
neutral, 1-20 keV detector, patent 9-38795
scattering from plasmas, collective effects 9-25856
scattering of high-energy beams, determ. of atom-molecule potential-energy functions 9-38794
Ar, shock tube drives metastable atoms, obs. 9-44289
Ar metastable atoms, electron ejection from W surfaces 9-31001
Ar preferential scatt. from LiF(001) surface 9-42714
C II, C III radiative lifetimes of multiplets obs. by beam foil method 9-22943
Ca, (4s4p)¹P₁ state, coherence narrowing and shift of optical double reson. signals 9-29923
Cs, scatt. liq. HBr 9-42469
from Ge [100] surfaces, sputtered ejection pattern, temp. depend. 9-35301
H, emerging from C foil, periodic intensity fluctuations in Balmer spectrum 9-46332
H, hyperfine state selection by longitudinal periodic field mag. lens 9-29979
H, magnetic beam, magnetic separation and focalization, phase-space calc. method 9-27828
H, preparation for maser operation with unpolarized atoms 9-40338
H, thin-film detector using MoO₃ 9-22987
H+C₆D₆→HD+C₆D₅, translational-energy depend. 9-39944
He, fast metastable atoms, passing through H₂, He⁺ formation 9-29985
He, in H₂, N₂, Ne and Ar gases, charge equilb. fractions obs. 9-40559
He, scattering by CF₄, CHF₃ and CH₂F₂, determ. of atom-molecule potential-energy functions 9-38794
He isotopes, scatt. from Ag(111) surface 9-42713
He metastable atoms, electron ejection from W surfaces 9-31001
K, intense, used as source of polarized electrons 9-40459
K, scatt. by crossed molec. beams 9-42469
K gravitational deflection obs. 9-43725
K polarized, ionization "with u.v. light to produce polarized e beam 9-27282
Li, glory scatt. by fluorocarbons and hydrocarbons 9-42471
N, scattering, elastic, by NO and CO molecules, characts. 9-25712
Na-Cs interaction 9-25713
Ne, beam-foil excitation and 2000 to 6000 Å spectra 9-46320
O, scattering, elastic, by NO and CO molecules, characts. 9-25712
O, values of 4p²P levels using new high intensity spectroscopic source 9-42344
Rb, comparison meas. with UHV microbalance, quartz osc. and ionization foil 9-22988

Atomic beams continued

- W ribbon at high temp. in low pressure O or ethylene atmosphere, anomalous reflection of raregas atoms 9-40558

Atomic clocks see *Time measurement***Atomic frequency standards** see *Time measurement***Atomic mass and weight**

see also *Isotopes*; *Mass spectra*
No entries

Atomic orbitals see *Atoms/structure*; *Orbital calculation methods***Atomic scattering factors** see *Crystal structure, atomic*; *X-ray crystallography*; *X-ray scattering***Atomic spectra** see *Spectral/atoms***Atoms**

see also *Atoms, mesic and muonic*; *Collision processes/atoms*; *Elements*; *Nucleus*; *Positronium*

- alkali, charge exchange of protons 9-44254
alkali, electronic dipole polarizabilities calc. 9-40545
alkali, in excited states, van der Waals const. with inert gases 9-36677
alkali metal, ionization by slow electrons, role of incident wave distortion due static and polarization pot. 9-32689
alkali metal, spin relax. using optical methods, review 9-42332
arbitrary, soln. of Schrodinger eqn. 9-34510
atomic physics, college textbook 9-48370
autoionization states, variational-bound method, configurations superposition 9-22924
binding energy, photoelectron determ. 9-29961
bound state, Green's function in spherically symm. pot., phase integral approx. 9-38748
coherence of emitted radiation, effect of random motion 9-38747
Compton scatt. factors for aspherical free atoms 9-42340
Compton scatt. of X-rays from atomic electrons, generalized equation 9-46303
coordinate systems, relative, description of n particles 9-46255
d²-¹sp configuration coulomb interactions in L-S coupling 9-46270
dynamic polarizability bounds, complementary variational principles 9-32431
electron capture by halogens, calc. of photodetachment cross-section 9-27817
electron electric dipole moment, amplification 9-40534
electron spin-spin contact interaction, pⁿ configurations calc. 9-22935
electron sums over states and electron specific heat calc. 9-38750
electronegativity, quantum-thermodynamic defn. 9-44239
elements, collection of data, book 9-22026
e.m. interactions of elementary particles in the atom 9-44240
fractional parentage coeff., group theory reln. 9-36645
free, interaction, 2nd virial coeff. calc. 9-40744
group theory in atomic physics, review 9-46266
helium-like, multiconfiguration approximation 9-29916
interacting, resonance radiation 9-38789
interaction of three, rel. to 3rd virial coeff. calc. 9-40743
interaction with radiofrequency photons, absorption and scattering of optical photons 9-22969
ionization, maximum cross-sections 9-42335
ionization, multiple, by photons, probability calc. method 9-36673
ionization cross-section for Penning ionization 9-32688
lⁿ-l^m configuration coulomb interactions in L-S coupling 9-46270
Lennard-Jones params. of excited states, obs. 9-48528
matrix elements of operators between states of two degenerate levels 9-22929
in molecule, applic. of quantum-thermodynamic defn. of electronegativity 9-44239
moment distribution, case of wave functions with non-integer principal quantum number 9-27792
multipole dispersion interactions, inequalities 9-44285
perturbation theory geometric approximation, derivation 9-46264
polarized, relativistic dynamics 9-27793
potential, a new model for alkali ions that is applicable to matter 9-34518
properties, from Coulomb's Green function in perturbation theory 9-46262
radiation, conflict in predictions of Bohr's freq. law and Schrodinger's emission law 9-45769
in radiation field of the atom itself, semiclassical theory 9-38437
resonance luminescence capture, theory, role of Langmuir oscillations 9-22918
resonance radiative processes in strong field 9-48385
resonance theory of termolec. recomb. kinetics 9-48426
in solid, applic. of quantum-thermodynamic defn. of electronegativity 9-44239
spinning particle, classical treatment, book 9-41766
superradiant system, time depend. energy loss 9-38255
target for negative ions, charge exchange cross-section meas. 9-22980
transition operator in radiative damping theory 9-32399
uncoupled, 2nd virial coeff. dissociating gas 9-23391
van der Waals interactions between atoms, upper and lower bounds 9-42341
¹⁶⁶Er, nuc. hyperfine splitting, temp. depend., Mossbauer eff. obs. 9-24272
Ag, gamma ray scatt., 145 keV, differential elastic scatt. X-section 9-46263
Al, gamma ray scatt., 145 keV, differential elastic scatt. X-section 9-46263
Ar, metastable, prod. from ion-atom collisions 9-34560
Ar, photo-ionization cross section in Hartree-Fock approx., calc. 9-40549
Ar, scattered from solid surface, spatial distribution of 0.30-0.54 eV gaseous atoms 9-27821
C, correlation effects of non-closed shell many electron theory 9-38773
Cd photoelec. cross sections meas., E_p=280 keV 9-22945
Cu, gamma ray scatt., 145 keV, differential elastic scatt. X-section 9-46263
Cu, mean total γ cross-sections, 40-80 keV, analysis 9-22949
Cu photoelec. cross sections meas., E_p=280 keV 9-22945
Er³⁺(4f¹¹), spin-spin interactions determ. from matrix element expression 9-38774
Fe, gamma ray scatt., 145 keV, differential elastic scatt. X-section 9-46263
Fe I-III at up to 15000°K sums and distribution over electron states 9-38751
H-H spin exchange cross section using H maser 9-25716

Atoms continued

- H, 2s and 2p states, cross-sections for impact ionization 9-34583
 H Compton scattering on bound state, theory 9-32419
 H electron capture into n=6 level, by 5-70 keV protons in Mg vapour and Ne 9-46330
 H recomb. reaction, H ats. as third bodies 9-25786
 H+H+M→H₂+M, resonance theory of recombination kinetics 9-48426
 He, interatomic potentials 9-38801
 He, monoenergetic impact excitation at low energy, detection with SF₆ 9-29982
 He, variational calc. of correlation eff. on g.s. 9-22958
 He isoelectronic sequence, 2¹P and 2³P states Breit interaction, matrix elements 9-32437
 He quenching rate in He-Ne discharge He level population depend. on Ne atom conc. 9-25974
 Hg²⁺, nuclear quadrupole anti-shielding factor, calc. using three different wave-functions 9-34540
 Kr, effective radii in liquid from sound vel. isotherms obs. 9-30396
 Li, variational calc. of correlation eff. on g.s. 9-22958
 Li g.s. anal., spin orbitals and Fermi contact term 9-22959
 N, correlation effects of non-closed shell many electron theory 9-38773
 Nd ³⁺(4F), spin-spin interactions determ. from matrix element expression 9-38774
 Ne, 2-electron energies transformation props., inter-orbital correlation energies 9-38773
 O-, electrons photodetachment cross section, pseudopotential calc. method 9-46257
 O, correlation effects of non-closed shell many electron theory 9-38773
 O, London dispersion forces 9-25714
 Pb, gamma ray scatt., 145 keV, differential elastic scatt. X-section 9-46263
 Pb, mean total ν cross-sections, 40-80 keV, analysis 9-22949
 Pr³⁺(4f), spin-spin interactions determ. from matrix element expression 9-38774
⁸⁵Rb optical pumping in inert gases, excited state mixing obs. 9-34561
⁸⁷Rb optical pumping in inert gases, excited state mixing obs. 9-34561
 Sn, gamma ray scatt., 145 keV, differential elastic scatt. X-section 9-46263
 Sn, mean total ν cross-sections, 40-80 keV, analysis 9-22949
 Ta photoelec. cross sections meas., E_y=280 keV 9-22945
 Th I, Hartree-Fock solns. of Slater, configuration-interact. and dipole integrals 9-25700
 Tm³⁺(4f¹²), spin-spin interactions determ. from matrix element expression 9-38774
 W, mean total ν cross-sections, 40-80 keV, analysis 9-22949
 Xe, effective radii in liquid from sound vel. isotherms obs. 9-30396
 Zn isoelectronic series, oscillator strengths energy eigenvalues, mean radii, calcs. 9-44271

electron scattering

- alkali, excitation cross-sections 9-44278
 amplitude, exchange correction 9-46305
 Born approx. excitation cross sections, parameters and expressions 9-27818
 Born approximation, n th order appl. 9-48414
 channel coupling effects in elastic collisions 9-34565
 electron conductivity in high magnetic field meas., test-particle technique 9-22981
 electron optical phase contrast calcs. for ats. and at. groups 9-32893
 Fadeev eqns. used to determ. collision amplitudes 9-46311
 fast inelastic, quantum-mech. formulas 9-22533
 inelastic, anomaly-free variational method 9-22105
 inert gas, diffusion transport cross section 9-32273
 ionization of various ions, mass-sections obs. 9-46296
 ionization threshold region, insight by exam. of doubly excited states of compound ion 9-34582
 ions, positive, e collisions, scatt. matrix near reson., quantum defect theory 9-22979
 ions, positive, excitation by electrons, effective Gaunt factors 9-38778
 K-shell ionization, recal. of Burhops' results 9-46289
 long-range forces, nonadiabatic, general expression 9-32425
 Monte Carlo trajectory calc. of atomic excitation near ionization limit 9-32420
 non-adiabatic effects, distortion potential 9-38783
 phase shift depend. on energy and atomic no., E_e up to 2 Ry 9-46306
 photoionization cross section calc. 9-23339
 positive ions, asymptotic solns. of coupled eqns. 9-44283
 potential one-body suitable for Schrodinger equation 9-36676
 Rutherford scattering, complete correspondence identity for electron-proton system 9-41769
 Spectral line broadening, contrib. or radiation prod. by electrons 9-32403
 spin polarization of low-energy elastically scatt. electrons 9-34564
 Al K-ionization cross-section, anomalies obs. 3-20 keV 9-46291
 Ar, neutral bremsstrahlung cross section, shock tube obs. 9-29965
 Ar ²⁺ metastable state, elastic scatt. calc. 9-46307
 Ar elastic phase shifts, isoelectronic sequence extrapolation technique 9-29964
 Au, bremsstrahlung cross-section, 50-500 keV 9-22977
 Ba⁺ excitation of resonance transitions, emission cross section meas., crossed beam technique, 8-9 eV 9-27815
 C, shape resonance, cross section and collision strength determ. 9-38786
¹²C, root mean square charge radii 9-48415
 Cs generalized oscillator strengths 9-29963
 Cs vapour, momentum transfer cross section from drift vel. obs. 9-40554
 H-e⁺ scatt. resonance below positronium threshold, 3-body variational wave junc. converging expansion 9-46322
 H, ¹S-wave elastic scatt. zero-energy length determ. 9-32397
 H, 10-50 eV, excitation of 2p state, various resonances obs. 9-22994
 H, ang. distrib. meas., cf. Glauber theory prediction 9-38798
 H, elastic scatt. channel above 10 eV, calc. and obs. resonances, comparison 9-34581
 H, Fadeev eqns. used to determ. collision amplitudes 9-46311
 H, multiple solutions of Hartree-Fock equations 9-36682
 H, of e⁺ cross section for positronium formation 9-46064
 H, phase shift results for electron and positron, target atom distortion 9-22993
 H, small angle, elastic, low and high energy electrons, channel coupling effects 9-34565
 H, variational calcs. for resource widths by Bransden and Dalgarno method 9-44294
 H-, detachment by e impact 9-44293

Atoms continued

electron scattering continued

- He-e⁺ bound state search, 3-body variational wave junc. converging expansion 9-46322
 He, 100-400 eV, inclusion of adiabatic and nonadiabatic distortion eff. 9-23003
 He, ³1¹D, 4¹1¹F levels excited obs. 9-32441
 He, conductivity ratio meas. in microwave resonant cavity discharge, 2.7 GHz 9-23288
 He, elastic, ang. distrib., differential cross sections 9-34587
 He, elastic at 500eV, absolute differential cross sections 9-38800
 He, excitation by low energy electrons, cross section calc. 9-38853
 He, from ground state, elastic and inelastic, first Born approx. calc. 9-32422
 He, low energy scatt., reson. structure 9-42353
 He, oscillator strength for 1¹S→2¹P transition 9-29980
 He, resonant differential scatt. at ~19.3 eV 9-42352
 He⁺, ¹S and ³S elastic scatt., Rydberg state quantum defects calc. 9-32397
 He⁺Si metastable state, elastic scatt. calc. 9-46307
 He elastic phase shifts, isoelectronic sequence extrapolation technique 9-29964
 Hg, excitation, light emission obs. rel. to meas. of polarization of incident electron beam 9-44284
 Hg, excitation of metastable state 6³P₂ by electrons of 4-15 eV, obs. by secondary emission 9-32421
 Hg, large angle, elastic, low energy electrons, channel coupling effects 9-34565
 K, effect of long-range forces 9-27819
 Kr ²⁺ metastable state, elastic scatt. calc. 9-46307
 Kr conductivity ratio meas. in microwave resonant cavity discharge, 2.7 GHz 9-23288
 Li, 2s, 2p close-coupling eqns., soln. from threshold to 54.4 eV 9-48416
 N, low energy neutral bremsstrahlung cross section, shock tube obs. 9-32423
 N, shape resonance, cross section and collision strength determ. 9-38786
 N⁺, shape resonance, cross section and collision strength determ. 9-38786
¹⁴N, root mean square charge radii 9-48415
 Na, effect of long-range forces 9-27819
 Ne, from ground state, elastic and inelastic, first Born approx. calc. 9-32422
 Ne, neutral bremsstrahlung cross section, shock tube obs. 9-29965
 Ne ¹p₂ metastable state, elastic scatt. calc. 9-46307
 Ne conductivity ratio meas. in microwave resonant cavity discharge, 2.7 GHz 9-23288
 Ne elastic phase shifts, isoelectronic sequence extrapolation technique 9-29964
 O, low energy neutral bremsstrahlung cross section, shock tube obs. 9-32423
 O, shape resonance, cross section and collision strength determ. 9-38786
 O⁺, shape resonance, cross section and collision strength determ. 9-38786
 O²⁺ ³p₂ excitation by electron impact, ²D_{3/2}-²D_{5/2} transition, collision strengths resons. 9-34566
 O²⁺, shape resonance, cross section and collision strength determ. 9-38786
¹⁶O root mean square charge radii 9-48415
 Rb, low-energy, phase-shift calc. 9-22978
 Rb generalized oscillator strengths 9-29963
 Xe, neutral bremsstrahlung cross section, shock tube obs. 9-29965
 Xe ³P₂ metastable state, elastic scatt. calc. 9-46307
 Xe conductivity ratio meas. in microwave resonant cavity discharge, 2.7 GHz 9-23288
- excitation**
 alkali, by electron impact 9-44278
 alkali, depolarization cross sections significance from D₂ optical pumping 9-34558
 alkali atoms, excitation transfer in collisions between identical atoms 9-42339
 Ar excited state, repulsive interaction with ground state He, Ne, Ar atoms 9-29968
 Ar IIE, 4s levels new radiative lifetime values 9-25706
 atom-atom excitation cross-sections calc. by classical methods 9-44286
 Auger, by internal secondary electrons rel. to analytical spectroscopy 9-49401
 balance equation corrected for diffusion and collisions of first and second kind 9-46309
 by beam-foil collisions, oscills. in decay curves, explanation 9-42336
 decay curve oscills. in lifetime meas., interference between coherent emissions explanation 9-42336
 gamma source using ¹⁰B(n, α)⁷Li→⁷Li 9-29953
 Hanle eff., resonance fluorescence and interfering levels 9-25702
 He, 4¹P→4¹F collisional transfer 9-32441
 He, photoexcitation and photoionization, simultaneous, 186 Å obs. 9-23001
 heavy elements, L₂- and L₃-subshell fluorescence yields 9-34525
 hyperfine structure, atomic beam mag. reson. expt. 9-44252
 hyperfine structure, determ. from ground state population number changes 9-44252
 inert gas, ionized excited states formation through loss of metastable electron 9-34569
 inert gas excitation cross-sections, absolute determ. by electron collision 9-46298
 ionization, L- and M-shell, by heavy charged particles 9-34557
 ionization potentials, higher, for Z=31-92 9-44275
 ions, positive, excitation by electrons, effective Gaunt factors 9-38778
 isoelectronic atoms and ions, C-like to F-like, excitation and ionization energies calc. 9-44277
 K-shell ionization, recal. of Burhops' results 9-46289
 level calc. by many-electron pseudopotential formalism 9-32397
 level degeneracy effect on interaction between two travelling waves 9-42334
 level transitions rel. to electron energy distribution in low temp. plasma 9-40659
 many-electron atom, collective excitations, variational calc. 9-25704
 Monte Carlo trajectory calc. of atomic excitation near ionization limit 9-32420
 multiquantum transitions selection rules, laser beams applic. 9-22367

Atoms continued

- excitation continued
 perturbation study, 2-electron atoms, transition oscillator strength values 9-32417
 photoionization of heavy atoms, using nonrelativistic model with central pot. 9-44276
 radiation emission by extended syst. 9-38436
 radiation interaction with two level system 9-25701
 radiative Auger effect, simultaneous emission of X-ray photon and L-shell electron 9-40553
 radiative lifetime, effect of neighbouring identical atoms 9-36668
 radiative/nonradiative transitions rel. prob., light multiply ionized atoms 9-36667
 relaxation of multipole moment, collision induced, cross section determ. 9-32426
 resonance lines, modulation in spectral lamp by means of pulsating vapour cloud 9-31227
 resonance struct., analysis by quantum defect theory 9-22979
 resonant transfer and change in hyperfine state 9-22968
 structure and energy, all-external pair electron correlation and affinity determ. 9-32405
 superradiant system time depend. energy loss 9-38255
 ultrafine struct. in excited levels, meas. method 9-46269
 vapour under optical pumping, ang. charact. of ground state and rel. to absorpt. and dispersion props. 9-32416
 X-ray photon absorpt., Auger effect and radiative transfer formulae deduced 9-36672
 X-ray source in optically thick environment, physical conditions 9-36014
 X-ray source in optically thin environment, physical conditions 9-36013
¹⁵³Gd, ¹⁵⁷Gd, ^{4f}5d6s² 9D multiplets, hyperfine struct. meas. by atomic beam mag. reson., nuc. mom. calc. 9-22952
 Ag excited levels, electron bombardment excitation obs. 9-29955
 Al I to III, singlets and multiplets, mean lives 9-46290
 Al K-ionization cross-section, anomalies obs. 3-20 keV 9-46291
 Al radiative Auger effect, simultaneous emission of X-ray photon and L-shell electron 9-40553
 Ar, 0.15-1.0 MeV proton induced 9-42337
 Ar, mean energies upper and lower bounds calc. 9-38779
 Ar, population inversion in transitions of Ar III and Ar IV 9-28041
 Ar¹⁺-Ar collisions, 100-400 keV, emission cross sections, Doppler shift anal. 9-44280
 Ar and Kr, rel. to population inversion 9-29921
 Ar excited levels, mag.-reson. expts. 9-29955
 Ar I, transition probabilities for near i.r. lines 9-46293
 Ar I radiation lifetimes and transition probabilities meas., delayed coincidence method 9-22942
 Ar II, decay of 4p^{11/2}D_{3/2} level, absolute meas. by correlation of photons emitted in cascade 9-46294
 Ar II radiative lifetimes for transitions in 1900-4500 Å range 9-32407
 Ar K series by e collision, cross sections, 3-16 keV 9-34539
 Ar laser capillary discharge, radial distrib. of excited atoms and ions 9-36289
 Ar long-lived autoionization states, mass spectra 9-38782
 Ar* ioniz. of Hg 9-40709
 B III, mean lives of 2p²P levels, oscillator strengths 9-44256
 Ba⁺ electron impact, emission cross section, resonance transitions meas., crossed beam technique, 8-98 eV 9-27815
 Ba excited levels, electron bombardment excitation obs. 9-29955
 Be II, mean lives of 2p²P levels, oscillator strengths 9-44256
 Bi in pulsed discharge, generation spectra, obs. 9-25692
 C, in shock heated CO, CH₄ and CF₄ mixtures in Ar and Ne, rel. to 2478 Å line emission 9-48387
 C ions form. in He⁺-CO collisions 9-36724
 Cd at 5th p. level, Hertzian coherence conservation in sensitized fluoresc. 9-46275
 Cl, (3²P_{1/2}) and (3²P_{3/2}) states, kinetic spectroscopic studies in vac. u.v. 9-34534
 Cs depletion in positive column of Cs-Ar discharges 9-34802
 Cs I lines, electronic cross section meas. in gas discharge plasma 9-27816
 Cs II reson. lines in Cs⁺+He collision, threshold behaviour of cross-section 9-48419
 Cs impact ionization by electrons and protons, cross section obs. 9-34556
 Cs radial and axial distrib. in Cs-Ar low-press. discharges, absorpt. spectra obs. 9-34801
 Cs temperatures from relative intensities of spectrum transitions in arc plasma 9-25707
 Cu, electron impact, polarization of spectral lines w.r.t. electron energies in mag. field 9-29928
 Eu I oscillator strength, f-values determ. by hook method 9-34537
 F VI, 2p² 1D level, mean life 9-25708
 Ga mechanism of direct line fluorescence 9-48409
 GH, and deactivation of metastable atoms in 6thPo level 9-22971
 H-H collisions, excitation cross sections, impact parameter treatment, two-state approx. 9-42348
 H-H collisions, excitation cross sections, impact parameter treatment, four state approx. 9-44297
 H, by fast protons, asymptotic expressions for cross sections 9-34579
 H, electron scatt., 10-50 eV, resonance excitation and behaviour 9-22994
 H, fast atoms passing through He, first Born approx. cross sections for electron loss 9-48425
 H, from electron impact on hydrocarbons 9-23174
 H, levels between 9 and 23, from neutralization of accel. protons 9-46327
 H, mean energies upper and lower bounds calc. 9-38779
 H, metastable, prod. by e capture of p in He target 9-40562
 H, p impact ionization 9-38797
 H, two-photon ionization in ground state 9-34580
 H⁺, doubly excited states of high principle quantum number, implications for e-atom ionization 9-34582
 H⁺ ionization by e impact, computation 9-34577
 H⁺N₂→HN₂⁺, Balmer-α, N₂⁺(0,0) 1st v band photon emission, cross sections meas. 9-22985
 H and D, from electron impact on H₂ and D₂ 9-23168
 H excited atom ionization by collisions with H, Li, Na 9-22992
 H formation in proton charge exchange collisions with Na and Li 9-27813
 H in dissoc. of water vapour by electrons 9-30151
 H ionization, exchange cross sections 9-34578
 H level populations, double-resonance method 9-47925

Atoms continued

- excitation continued
 H(1s)+H(1s)→H(21m)+H(21m'), 6.25 KeV-3.0 MeV, cross-section calc. using impact-parameter method 9-46331
 He, 3^{1,3}D, 4^{1,3}F levels excited obs. 9-32441
 He, by electron impact, polarization of emitted light 9-29958
 He, by H₂⁺ and H₃⁺ ions, 1-150 keV, cross sections 9-48410
 He, by p of 7'S state, changes in wave function representation 9-32439
 He, fast atoms passing through H and He, first Born approx. cross section for electron loss 9-48425
 He, interaction of two metastable triplet atoms 9-48434
 He, laser transition spectra 9-48431
 He, mean energies upper and lower bounds calc. 9-38779
 He, transitions between doubly excited states and 2'S state, line strengths calc. 9-42350
 He ¹²p-1D by optical pumping, prob. calc. 9-23000
 He* (2'S), (2'S), ioniz. of Hg 9-40709
 He (2s²2p)³P cpd. state decay by 2-electron emission 9-40568
 He by protons and electrons 9-27829
 He collisions with metastable He, excitation transfer 9-29984
 He excitation by low-energy electrons, cross section calc. 9-38853
 He glow discharge, 2'S state decay by e collisions, obs. 9-34808
 He I, population in hollow cathode discharge 9-48635
 He in discharge plasma +ve column mechanism 9-25721
 He isoelectronic sequence, 2²P state, cross section depend. on singlet-triplet mixing 9-32437
 He metastable, collisions in afterglow plasma, He⁺ production 9-46336
 He metastable atoms, destruction in binary collisions 9-38802
 He metastable state transitions, computation of oscillator strengths 9-32440
 He neutral atom, by high energy p 9-38799
 He singlet states prod. by ion collisions relax. times of alignment 9-29983
 He, ultrafine struct. meas. in 1D levels 9-46269
 He + p charge-transfer collisions, polarization of Balmer-α radiation 9-22989
 Hg, by electron impact, rel. to meas. of polarization of incident electron beam 9-44284
 Hg, line shift by high power laser pulse 9-25709
 Hg, relative brightness and optical excitation functions meas. 9-29933
 Hg of metastable state, 6³P₂ by electrons of 4-15 eV, obs. by secondary emission 9-32421
 Hg vapour, double reson. expt., correlated intensity fluctuations 9-36670
 I, 5²P_{1/2}→5²P_{3/2} transition, generation termination mechanism 9-46295
 I(S²P_{1/2}), electr. excited, react. with Cl₂, Br₂, ICl and IBr, decay and rate consts. 9-43319
 In mechanism of direct line fluorescence 9-48409
 K(²P_{1/2}) + Rb(²S_{1/2})→K(²S_{1/2}) + Rb(²P_{1/2}) + ΔE, fluorescence detected, cross-section meas. 9-32429
 K impact ionization by electrons and protons, cross section obs. 9-34556
³⁹K 4³P_{3/2} state, hyperfine structure, atomic beam mag. reson. obs. 9-44252
 Kr, mean energies upper and lower bounds calc. 9-38779
 Kr 1236 Å resonance beam, disturbance by inert gases and H₂ 9-44265
 Kr long-lived autoionization states, mass spectra 9-38782
 Li, mag. hyperfine struct. and core polarization in excited states 9-34545
 Li, photoionization cross-section, many-body calc. 9-34571
 Li I, mean lives of 2p²P levels, oscillator strengths 9-44256
 Li photoionization cross section for base and 1st ten states 9-42338
 Li target, proton charge exchange collisions, H atom formation cross section 9-27813
 Li transition multipole matrix elements calc., hypervirial theorems 9-29895
 Mg radiative Auger effect, simultaneous emission of X-ray photon and L-shell electron 9-40553
 N(²D) deactivation in vac. u.v. photolysis of N₂O 9-49385
 N II excitation conditions in planetary nebulae 9-31514
 Na, impact ionization by electrons and protons, cross section obs. 9-34556
 Na target, proton charge exchange collisions, H atom formation cross section 9-27813
 Nd³⁺ in vitreous matrix, effective amplification section of 1.06 transition 9-48399
 Ne, by electron impact, pulsed super-emittance from 2p-1s transition, mechanism 9-29959
 Ne, collective excitations, variational calc. 9-25704
 Ne, by electron impact, and intensities of oscillators for $\bar{\Gamma}$ → $\bar{\Gamma}^*$ transition 9-36671
 Ne, hollow cathode discharge, balance eqn. for levels derivation 9-22961
 Ne, mean energies upper and lower bounds calc. 9-38779
 Ne, multi-ionized, transitions and decay meas. of levels 9-46299
 Ne, total cross section, determ. using Townsend's primary ionization coeff. 9-42561
 Ne 2p_{1/2} level, population relax. times, obs. using laser 9-46300
 Ne excited levels, mag.-reson. expts. 9-29955
 Ne excited state, repulsive interaction with ground state He, Ne, Ar atoms 9-29968
 Ne I 2s_{1/2} laser level transition probabilities and mean lives 9-48413
 Ne I J=1 levels, radiative lifetimes, branching ratios and oscillator strengths determ. 9-27812
 Ne I J=1 levels, radiative lifetimes, branching ratios and oscillator strengths determ. 9-40547
 Ne in plasma, level broadening due to interaction 9-23275
 Ne* ioniz. of Hg 9-40709
 O, rel. to ionosphere E, F₂ regions e-ion and neutral gas cooling 9-47581
 O⁺ 2p², by electron impact, ²D_{3/2}-²D_{5/2} transition, collision strengths resons. 9-34566
 O¹D, excited atoms, reaction with isobutane 9-24543
 O(¹D), production by vacuum u.v. photolysis and electronic de-excitation by inert gases 9-35755
 O²⁺, forbidden lines excitation, resons. in cross sections 9-22974
 O I, excitation conditions in planetary nebulae 9-31514
 O II to VI electronic states lifetime meas. by beam-foil technique 9-22975
 O V, 2p² 1D level, mean life 9-25708
 Rb impact ionization by electrons and protons, cross section obs. 9-34556
 Rb nonlinear hyperfine pressure shift induced by optical pumping 9-36664
 Rb optical pumping, transition probabilities between magnetic sublevels 9-46301
 Rb I, II, levels g factors spectral determ. 9-29944

Atoms continued**excitation continued**

- S II level excitation by beam-foil technique 9-48402
 S III, level excitation by beam-foil technique 9-48402
 S radiative Auger effect, simultaneous emission of X-ray photon and L-shell electron 9-40553
 Si radiative Auger effect, simultaneous emission of X-ray photon and L-shell electron 9-40553
 Tb³⁺, 4f-5d excitation energy in solids 9-49320
 Tl, ⁷S_{1/2} state, lifetime, depend on exciting conditions 9-29960
 Tl, depolarizing collision with inert gas, cross section meas. 9-22976
 Tl mechanisms of direct line fluorescence 9-48409
 Xe- I, radiative lifetimes and collision cross-sections for 16 states 9-48405
 Xe, 1295 Å resonance beam, disturbance by inert gases and H₂ 9-44265
 Xe, decays and Lande factors of 7p^{1/2}_{1/2} and 7p^{1/2}_{3/2} levels, mag. reson. meas. 9-46285
 Xe, photoionization, cross-sections for Xe⁺, Xe²⁺ and Xe³⁺ production, 28.83 eV 9-40551
 Xe excited levels, mag.-reson. expts. 9-29955
 Xe II radiative lifetimes for 6 excited states 9-48405
 Xe long-lived autoionization states, mass spectra 9-38782
 Yb³⁺ in silica glass laser, Cr³⁺ energy transfer mechanism, obs. 9-29430
 Zn, ³P, state, collision broadening of double resonance line empirical formula for resonance curve 9-34554
 Zn, energy transfer to 4¹D₂ level from 7³S level of Hg in discharge, process 9-48422

magnetic moment

- see also *Gyromagnetic ratio*
 spins of particles, orientation, in space 9-27047
 H, g-factor of e and p, relativistic treatment of shielding 9-46324
 H, mag. susceptibility in H maser 9-36268
 O, (2p³) ³P_{1,2} levels, precision calc. 9-36656

structure

see also *Nucleus; Spectra/atoms*

- alkali metal, shell structure in ionization cross section calc. 9-23341
 alkali metals, hyperfine structure, theoretical analysis 9-34546
 alkali metals, spin relaxation, optical obs. in buffer gas 9-29942
 comprehensive university level text book 9-32395
 configuration mixing in N=4 electron isoelectronic sequence 9-34521
 configurations 1s²2s²2p_n, SCF approx. of splittings for isoelectronic sequence Z=N+4, N+5,...20 9-38760
 configurations (d+s)ⁿ p, construction of their algebraic matrices 9-38749
 core and outer electron, correlation, in perturbation method 9-25684
 coupling, LS to LL for dⁿ config., transform. matrices 9-29910
 d, f and g electrons for atoms from Z=2 to Z=126, quantum no. calcs. 9-27800
 diamagnetic susceptibilities, Thomas-Fermi and Dirac eqns. calc. 9-42324
 dipole shielding tensor 9-48374
 dipole transition probabilities, corrections, struct. of perturbation series 9-48381
 eigenvalues, nonrelativistic, of some states of 3-10 electron atoms 9-40536
 electric dipole transitions, correlation effects and multiplet oscillator strengths 9-42323
 electron affinities of heavy elements 9-44274
 electron binding energies, relativistic calc. by modified Hartree-Fock Slater method 9-34529
 electron correlation, all-external pair, electron affinities and excitation energies prediction 9-32405
 electron correlation types in ground and excited configurations 9-32404
 electron density and potential, approx. behaviour 9-40535
 electron shell calc. by quantum field theory method 9-48380
 electron shells, equivalent, wave functions 9-29915
 electron spin density determ. using internal conversion 9-48383
 e.m. external radiation effect on energy levels of electron system 9-32402
 energy level calc. from exact propagator for electron in uniform strong elec. fields 9-29911
 energy levels of electron system, effect of external radiation 9-32402
 excited energy levels, Hanle effect, double reson. expts., level crossings and anticrossings, review 9-29908
 F core polarization and hyperfine structure calcs. 9-46273
 first-row atoms, spin-extended wavefunctions 9-34526
 frozen core approx. for systems with one valence electron in addition to filled shells, props. 9-22926
 gas, phonon echo polarization and amplitude 9-42327
 Gaussian expansions of atomic orbitals 9-38755
 Green's function for noninteracting particles 9-41735
 ground states in boron-like ions, perturbation treatment of Hartree-Fock equations 9-34520
 group II, collisions between identical atoms, transitions between fine structure component, cross sections 9-48382
 Hanle effect and developments for investigation of excited levels, review 9-29908
 Hartree-Fock, pressure calc. and virial theorem 9-39554
 Hartree-Fock approximation using harmonic oscillator functions 9-29918
 Hartree-Fock parameters in energy interactions, comprehensive calc. 9-34519
 Hartree-Fock wave functions and energies from perturbation theory 9-34524
 heavy atoms, screening effects on $\mu(0)^2$, *ab initio* calc. 9-34527
 helium-like, multiconfiguration approximation 9-29916
 Hulthen approximations to 1s and 2p orbitals 9-44245
 Hulthen type radial functions, generalized, as approximation to Hartree-Fock 2p functions 9-38752
 hydrogen wave functions describing levels with width 9-29977
 independent particle model, analytic 9-46265
 integrals containing r_0^2 correl. factors with unlinked indices 9-44246
 K₁ X-ray energies, π , μ , meas. for elements Z=3 to Z=6, including nuclear force shifts 9-27803
 L-S eigenfunctions, construction and use by a computer program 9-36655
 matrix elements for d_s config. in weak octahedral field 9-24348
 matrix elements of operators between two degenerate levels, calc. using field form of perturbation theory 9-44244
 model based on Hartree-Fock density distrib. 9-25687
 multiconfiguration self-consistent-field wavefunctions 9-22930

Atoms continued**structure continued**

- multilevel systems, transition rates 9-36644
 nuclear effective charge calc. from valence electron spectra 9-38761
 nuclear elec. quadrupole moment interac., sum rule for elec. field gradient 9-25688
 O, g(³P_{1,2}) precision calcs. 9-36656
 one-electron ion in uniform elec. field, high-order perturbation theory 9-34528
 one-photon corrections to interactions between atomic states 9-25680
 open shell type, approx. soln. of Hartree-Fock eqns. 9-38759
 optimized Gaussian basis SCF wavefunctions for first-row atoms 9-48375
 oscillator strengths, multiplet, calcs. and comparison with expts. 9-40537
 Pauling radii correlations with self-consistent field wave functions 9-22932
 phonon echo polarization and amplitude in gas medium 9-42327
 positive ions, Thomas-Fermi eqn., analytical solns. 9-29905
 proton pseudopotential form factor 9-48424
 pseudopotential calc., excited states, wavefunctions and oscillator strengths 9-27799
 r₁ Lie group applied to 2s²2pⁿ and 3s²3p³3dⁿ atomic configurations 9-27801
 rare-earth, Hartree-Fock wave functions, inaccuracies in use of explicit angular momentum coupling 9-34511
 screening consts. and transition energies 9-48373
 self-consistent field equation, deviation from spherical symmetry and calc. of expectation values 9-29914
 self-consistent field method, Hartree-Fock eqns., further approximation. 9-29913
 Slater integrals, energy-depend., from Hartree-Fock calcs. 9-48376
 spin degeneracy and stability of Hartree-Fock states 9-42317
 spin-spin interaction for fⁿ and fⁿ configs. 9-38753
 super heavy atoms, ground state, energy eigenvalues, spectrum energy predictions 9-22937
 Thomas-Fermi and Thomas-Fermi-Dirac eqns., analytical solns. 9-42324
 Thomas-Fermi eqn. for positive ions, analytical solns. 9-29905
 Thomas-Fermi equation, mathematical aspects 9-47726
 Thomas-Fermi potential in Schrodinger eqn. 9-25686
 Thomas-Fermi-Dirac and TFD-Gombas eqns., analytical solns. 9-38754
 transition probabilities, review of theory 9-27802
 two-centre Coulomb integrals, analytic expression 9-44236
 two-electron, lower bounds to eigenvalues 9-36131
 two-electron systems variational perturbation theory calculations 9-42326
 variational wavefunctions, sum rules 9-41758
 wavefunctions, spin-extended, for first-row atoms 9-34526
^{151,153}Eu, hyperfine struct. and nucl. quadrupole moment, spark spectrum 9-29929
²⁰¹Hg, 6³P₁ level, hyperfine struct. and Lande factor 9-29931
²³¹U ground ¹L₆ level, hyperfine struct., arc spectrum obs. 9-29952
^{199,200}Hg, 6³P₁, 6³D_{1,2} and 6³P₀, 6³D₂ transitions, hyperfine struct. 9-29932
¹⁹⁹Hg, 6³P₁ level, hyperfine struct. and Lande factor 9-29931
¹⁸⁹Os, hyperfine struct. and nucl. quadrupole moment, arc spectrum 9-29929
¹⁵⁹Tb, hyperfine struct. and g_J values of low levels 9-48403
¹²⁹Xe, hyperfine struct. of i.r. laser lines, interpretation on visible and i.r. 9-29954
 Ag excited levels, spectroscopic study by electron bombardment 9-29955
 Al²⁺ isoelectronic series, theoretical ionization energies and oscillator strengths 9-22927
 Ar, dipole polarizabilities, elec., and dipole shielding factors from Hartree-Fock wave eqns. 9-44241
 Ar, photo-ionization cross section in Hartree-Fock approx., calc. 9-40549
 Ar excited levels, mag.-reson. expts. 9-29955
 Ar III, excited level lifetime 9-34559
 B, core polarization and hyperfine structure calc. 9-46273
 B, g(²P_{1/2 3/2}) factors, calc. 9-36658
 B, g.s. first-order wave function, h.f.s. calc. 9-32408
 B, polarization wave functions for ground state 9-34532
 B²⁺, ²S, spin-optimized, self-consistent field wave function determ. 9-40544
 Ba excited levels, spectroscopic study by electron bombardment 9-29955
 Be, ¹S, spin-optimized, self-consistent field wave function determ. 9-40544
 Be, ¹S state, calc. in Hylleraas coordinates 9-32409
 Be, energy levels calc. using step-like model potential function and perturbation theory 9-44243
 Be, ground state energy, applic. of Hartree-Fock approximation using harmonic oscillator functions 9-29918
 Be⁺, ²S, spin-optimized, self-consistent field wave function determ. 9-40544
 Bi³⁺ in ZnS phosphor, electronic struct 9-24462
 C, g.s. first-order wave function, h.f.s. calc. 9-32408
 C, lowest ³P, ¹D, and ¹S states, multiconfig. Hartree-Fock calc. 9-25693
 C, polarization wave functions for ground state 9-34532
 C best-atom Slater orbitals, hybridized-promoted, total energies of states 9-48384
 C core polarization and hyperfine structure calc. 9-46273
 C II, C III radiative lifetimes of multiplets obs. by beam foil method 9-22943
 Ca, (4s4p)¹P₁ state, coherence narrowing and shift of optical double reson. signals 9-29923
 Ca I, distortion of the G²(3d4s) integral 9-29924
⁴³Ca, 4s4p¹P₁ state, hyperfine struct., level crossing meas. 9-29922
 Ce³⁺ in MeF₂ crystal, lowest Stark sublevels of 4f¹, 5d¹ configurations determ. 9-22947
 Cl, (³P_{1/2}) and (³P_{3/2}) states, kinetic spectroscopic studies in vac. u.v. 9-34534
 Co, 3d⁷ and 3d⁷4p config., calc. of energy spectra 9-38767
 Co, electronic configurations 9-25697
 Cr, electronic configurations 3d⁵ and 3d⁵4p, energy spectra, theoretical investig. 9-29940
 Cs, hyperfine freq., effects of molec. buffer gases 9-29948
 Cs, quenching of reson. radiation by He 9-42343
 Cu, A=63.65, ⁴F_{5/2} and ⁴P_{3/2} levels h.f.s. and g_J values meas., atomic-beam mag.-resonance method 9-32410
 Cu I, 3d⁹4s5s and 3d⁹4s4p configurations 9-42331

Atoms continued

structure continued

- Cu II $3d^{9}4s^1D$ and $3D$ levels, isotope shift w.r.t. specific-mass effect, exchange polarization of $3d$ -shell 9-29927
- Er³⁺, fluoresc. in SrF₂, quantum efficiencies and lifetimes 9-24453
- F, g.s. first-order wave function, h.f.s. calc. 9-32408
- F polarization wave functions for ground state 9-34532
- Fe, $3d^7$ and $3d^44p$ config., calc. of energy spectra 9-38767
- Fe, electronic configurations 9-25697
- Fe²⁺, $3d^44p$ config., energy spectrum 9-48397
- Fe²⁺, electronic struct. and quadrupole splittings in hemoglobin 9-42459
- Fe group, energy spectra of config. $3d^44p$ 9-48395
- Fe group, energy spectra of configs. $3d4s$, $3d^24s$, $3d^34s$, $3d^4s$, $3d^34s$ and $3d^44s$ 9-48393
- Fe group energy spectra of configs. $3d^44d$ and $3d^44d$ 9-48396
- Fe group isoelectronic series, energy spectra of configs. $3d^44s$, $3d^44s$ and $3d^44s$ 9-48394
- ⁵⁷Fe electron spin density determ. using internal conversion 9-48383
- Ga, A=67 and 72, hyperfine structure in $^2P_{1/2}$ and $^2P_{3/2}$ states 9-36661
- Ga V, elec. dipole transition configs. obs. 9-48398
- Gd³⁺, energy levels in CaF₂ 9-43238
- Gd³⁺ in aq. soln., electronic energy levels 9-26118
- Gd configuration identification using Zeeman effect 9-44262
- Ge VI, elec. dipole transition configs. obs. 9-48398
- H, $2S_{1/2}$ - $2P_{3/2}$ interval, meas. 9-25715
- H, Born-Oppenheimer treatment 9-46323
- H, dipole sum over Dirac states, relativistic corrections 9-44290
- H, $\Delta E_{\alpha-\beta}$ $2S_{1/2}$ - $2P_{3/2}$ separation meas. by atomic beam r.f. method 9-40561
- H, Gaussian-orbital approx. by minimization of variance 9-29974
- H, Lamb shift, time dependence of frequency in semiclassical theory 9-38437
- H, Lamb shifts obs. using spatially periodic potentials 9-42346
- H, proton pseudopotential form factor 9-48424
- H, wave functions describing levels with width 9-29977
- H⁺, doubly excited states of high principle quantum number, implications for e-atom ionization 9-34582
- H⁻, nonexistence of 1 sns autoionization states 9-44292
- H Green's function, reduced for ground state 9-46325
- ³H, spatial wave func. from symmetry reln. 9-25718
- He-like, $2p^2D$ and 3P weakly quantized states, Hartree-Fock eqn. perturbation treatment 9-32438
- He-like, Schrodinger eqn. for He, new coord. system 9-40567
- He-like systems, double perturbation theory 9-38756
- He, $1S^2$ - $2P^1$ transition, oscillator strength calc. using Hanle method 9-38776
- He, $2p^3D$ state, Hartree-Fock eqn. perturbation treatment 9-32438
- He, $7S$ state, changes in wave function representation 9-32439
- He, Hartree-Fock energies of $1S$ and $2S$ states 9-36684
- He, natural orbitals, direct calc. 9-38742
- He, oscillator strength for $1S^2$ - $2P^1$ transition 9-29980
- He dipole transition probabilities, corrections, struct. of perturbation series 9-48381
- He isoelectronic series, non-exponential orbital 9-48372
- He self-consistent field equation, deviation from spherical symmetry and calc. of expectation values 9-29914
- He transitions from ground to $3D$, $4P$ states, generalized oscillator strengths 9-46333
- ³He, spatial wave func. from symmetry reln. 9-25718
- ⁴He⁺, $4S_{1/2}$ and $4P_{1/2}$ levels, observation of resonance effect, in modulated fluorescent light 9-25720
- Hg of metastable state, 6^3P_2 by electrons of 4-15 eV, obs. by secondary emission 9-32421
- In I, hyperfine struct. of $5s^25d^3D_{3/2}$ and $5s^26d^3D_{3/2}$ states, Stark eff. investig. 9-29938
- K, octopole-allowed transitions in electron energy-loss spectra 9-40543
- K deformation of K, L and M due to interaction with optical electron 9-44268
- K I, $3p^43d$ configuration, intermediate coupling matrices, transitions obs. 9-32412
- Li, 2S and 2P spin-optimized, self-consistent field wave function determ. 9-40544
- Li, electron affinity 9-44281
- Li, energy levels calc. using step-like model potential function and perturbation theory 9-44243
- Li, mag. hyperfine struct. and core polarization in excited states 9-34545
- Li, variational calc. of ground state energy 9-46279
- Li h.f.s. $1,^2P^1$ calc. Brueckner-Goldstone theory 9-27810
- Li lowest-lying S^2 , $^4P^2$ states, decay to $^4P^0$ state identified in spectra 9-25698
- Li sequence, $2s$ - $2p$ and $3s$ - $3p$ dipole transition probabilities, calc. 9-34544
- Li sequence, relative and mass-polarization corrections, calc. of leading terms 9-34544
- Mg, dipole polarizabilities, elec., and dipole shielding factors from Hartree-Fock wave eqns. 9-44241
- Mg⁺ isoelectronic series, theoretical ionization energies and oscillator strengths 9-22927
- N, g.s. first-order wave function, h.f.s. calc. 9-32408
- N, polarization wave functions for ground state 9-34532
- N best-atom Slater orbitals, hybridized-promoted, total energies of states 9-48384
- N core polarization and hyperfine structure calc. 9-46273
- N g($^4S_{3/2}$), calc. to 1 ppm 9-36657
- Na, 4P state, in collision with He, behaviour of cross-section 9-29973
- Na, deformation of K, L and M due to interaction with optical electron 9-44268
- Na, isoelectronic series, theoretical ionization energies and oscillator strengths 9-22927
- Na, role in five-photon ionization 9-48412
- Na, spin-extended wavefunction 9-34547
- Na⁺, energy levels calc. using step-like model potential function and perturbation theory 9-44243
- Nd I, electronic configs. in arc spectrum, parametric calc. 9-29943
- Ne, absolute spontaneous transition probabilities 9-46281
- Ne, dipole polarizabilities, elec., and dipole shielding factors from Hartree-Fock wave eqns. 9-44241
- Ne, multi-ionized, transitions and decay meas. of levels 9-46299
- Ne, three electron correl. effects 9-38772
- Ne energy levels calc. using step-like model potential function and perturbation theory 9-44243

Atoms continued

structure continued

- Ne excited levels, mag.-reson. expts. 9-29955
- Nel, line strength transitions and coupling coeffs. 9-27811
- Ni, $3d^7$ and $3d^44p$ config., calc. of energy spectra 9-38767
- Ni, electronic configurations 9-25697
- Np⁴⁺, energy levels in PbMoO₄ 9-31110
- nuclear decay effects on electronic structure of decaying atom from Mossbauer meas. 9-38769
- N(v) relative intensities and exponential decay of $^2P_{3/2}$ and $^2P_{1/2}$ 9-44267
- O, g.s. first-order wave function, h.f.s. calc. 9-32408
- O, h.f.s. calc. from orbital, spin-dipolar and quadrupole interac. 9-22962
- O, polarization wave functions for ground state 9-34532
- O best-atom Slater orbitals, hybridized-promoted, total energies of states 9-48384
- O core polarization and hyperfine structure calc. 9-46273
- Pr III $4f^66s$, $4f^56s$, and $4f^66p$ configurations, level energies, interpretation 9-22964
- Rb, octopole-allowed transitions in electron energy-loss spectra 9-40543
- Sb, nuclear decay effects on electronic structure of decaying atom from Mossbauer meas. 9-38769
- Sm I spectrum, level lifetimes, Hanle effect meas. 9-29950
- Tb³⁺ in aq. soln., electronic energy levels 9-36886
- Te, nuclear decay effects on electronic structure of decaying atom from Mossbauer meas. 9-38769
- Ti, electronic configurations $3d^3$ and $3d^34p$, energy spectra, theoretical investig. 9-29940
- Tm I spectrum, level lifetimes and crossings, Hanle effect meas. 9-29950
- U II spark spectrum, A and B systems unification 9-29951
- V, electronic configurations $3d^3$ and $3d^34p$, energy spectra, theoretical investig. 9-29940
- Xe, decays and Lande factors of $7p[1/2]_1$ and $7p[1/2]_2$ levels, mag. reson. meas. 9-46285
- Xe excited levels, mag.-reson. expts. 9-29955
- Zn IV, elec. dipole transition configs. obs. 9-48398
- Atoms, mesic and muonic**
- deformed nuclei muonic atoms, exact calc. of eigenvalues 9-40570
- Dirac equations, coupled, solns. for deformed nuclei muonic atoms 9-40570
- mesoatomic processes and model of large mesic molecules 9-40571
- mesonic, validity of approximations used in calculations 9-46338
- muonic, interaction between atom and valence electron, hyperfine struct. 9-44302
- muonium mechanism of μ^+ depolarization in media with tensor relax. of muonium electron spin 9-29996
- nuclear charge distribution produced 9-38632
- plastics, scintillation, μ^+ depolarization, mag. field depend. 9-29995
- semiconductors, muonium mechanism of μ^+ depolarization 9-29996
- X-ray yields, K and L in low-Z atoms, discrepancies removed 9-46339
- $\alpha\pi\pi^-$, $\alpha\pi\pi^0$ atoms, K₊ metastable states 9-42357
- K⁺He, validity of DGBT formula 9-46338
- K⁺ capture meas. in heavy nuclei, implication of n halo 9-40516
- π -mesonic of light nuclei, simple empirical formula in place of DGBT approx. 9-46338
- ²³²Th, charge distrib., intrinsic quadrupole moment, radius studied by obs. of muonic X-rays 9-38677
- ²³⁸U charge distrib., intrinsic quadrupole moment, radius studied by obs. of muonic X-rays 9-38677
- B, K⁺ mesic X-ray yields 9-36685
- ⁹Be, K⁺ mesic X-ray yields 9-36685
- ¹²C, K⁺ mesic X-ray yields 9-36685
- Eu muonic atom isotopes, K and L x-rays meas. 9-29997
- ¹⁹F, $2p$ - $1s$ X-rays obs., $2p$ pionic levels population determ. 9-44301
- Ge single cryst., muonium depolarization processes 9-29994
- ⁷Li, K⁺ mesic X-ray yields 9-36685
- Lu muonic atom isotopes, K and L x-rays meas. 9-29997
- ¹⁴N, $2p$ - $1s$ X-rays obs., $2p$ pionic levels population determ. 9-44301
- ²²Na, $2p$ - $1s$ X-rays obs., $2p$ pionic levels population determ. 9-44301
- ¹⁶O, $2p$ - $1s$ X-rays obs., $2p$ pionic levels population determ. 9-44301
- ¹⁸O, $2p$ - $1s$ X-rays obs., $2p$ pionic levels population determ. 9-44301

Attenuation see Absorption

Auger effect see Atoms/excitation; Atoms, mesic and muonic; Radioactivity

Auger showers see Cosmic rays/showers and bursts

Aurora

see also Airglow; Atmospheric spectra

- 1966, Nov 19, spectroscopic obs. in visible and near u.v. 9-33820
- 1967, Feb 4, spectroscopic obs. in visible and near u.v. 9-33820
- absorption, auroral type, in mag. conjugated regions 9-35861
- absorption, electron density observations, radio communication problems 9-33839
- absorption for distances over 4000 km, simplified calc. 9-35857
- absorption occurrence patterns rel. to mag. KP vars. 9-43494
- absorption rel. to geomag. activity 9-31374
- absorption rel. to geomag. disturbance, diurnal pattern 9-31466
- absorption zone position, seasonal variations for mag. active periods 9-40060
- arcs, electron and proton motion along 9-43484
- arcs, quiet, homogeneous, Halley Bay obs. (1956-1965) 9-37956
- arcs, shift during polar mag. storm 9-31457
- backscatter v.h.f. bistatic communication 9-33792
- bursts periodicity rel. to seismic waves, obs. 9-26930
- charged particle flux, satellite and rocket obs. of fine structure 9-33810
- conjugacy, auroral and magnetic, hypotheses 9-40106
- conjugacy in magnetic disturbances March 1968 obs. 9-41565
- daytime, origin from magnetospheric tail, model 9-33808
- detection by high sensitivity, satellite-borne TV camera 9-33812
- diffuse radio, origin 9-33821
- disturbances, v.l.f. records 9-33840
- E-region, rocket obs. of electron densities 9-31424
- electrojet field heating of ions and electrons 9-33823
- electron and proton obs. (1964-7) 9-35848
- electron density and spectral emission, rocket obs. 9-33811
- electron energy and ang. distrib. obs., systematics 9-31365
- electron energy spectrum, extended to 45 eV 9-28929
- electron in-situ meas. limitations 9-41562
- electron low-energy spectra and pitch angle distrib., rocket obs. 9-40055
- electron precipitation, presence of mono-energetic beams 9-49475
- electron precipitation, low energy at high latitudes 9-43426

Aurora continued

- electron precipitation from plasma sheet 9-28928
 electron precipitation rel. magnetotail electron bursts 9-40048
 electron precipitations in and near auroral zone IQSY obs. 9-26931
 electron temp. and secondary distrib., rocket obs. 9-35850
 electrons, geomag. trapped, bounce resonant scattering 9-28927
 electrons, intense noise band generation by Cherenkov rad. 9-40076
 electrons, modulation at large distances from earth 9-28930
 electrons, parameter m by Stormer method 9-45516
 electrons, post substorm, flux magnitude rel. to pitch angle distribution 9-49477
 enhanced conductivity of ionosphere, with impressed primary electric field 9-40056
 equatorial electrojet region, Dst values 9-24707
 fine structure 9-45515
 glow spectra at solar maximum and minimum, comparison 9-35852
 green line excitation of atomic oxygen by N_2 ($A^3\Sigma_u^+$), rate const. calc. 9-43424
 injected particle energy 9-43484
 ion and electron concentrations, ionisation, recombination and charge transfer 9-33813
 ionosphere, ion-acoustic instabilities, effect of ion-neutral collisions 9-40057
 ionosphere, lower, electron concentration vs. height during periods of absorption 9-31402
 ionosphere above, instabilities 9-43451
 ionosphere D region, electrons, positive ions and particles >40 keV, rocket obs. 9-35881
 ionosphere latitudinal movements, scintillation meas. 9-41584
 ionospheric, anomalous radio absorption, characts. 9-43428
 low latitude and M-arcs 9-24813
 M arc, obs. at Moscow, USA 9-31368
 at magnetically conjugate stations, morphological similarities obs. 9-41563
 rel. to magnetospheric convection 9-37951
 measurements with rocket-borne photometers 9-31366
 midday, 13 Dec 1967, airborne obs. 9-40059
 morphological evolution, generalization of IUGG code 9-41568
 noise bands, 700 Hz near auroral zone 9-28944
 occurrence w.r.t. exact identification of noctilucent clouds 9-31364
 optical morphology, review 9-35847
 oval, magnetospheric tail field calc. 9-35845
 oval position rel. to ring current 9-43431
 ozone decrease in geomag. storm, X-ray ionization effect 9-41570
 particle, optical and electron content coordinated meas. 9-35849
 particle precipitation, implications for high latitude communications systems 9-33815
 particle precipitation, temporal and spatial variations rel. to drift wave model 9-31367
 periodicity attributable to Moon 9-33809
 polar, ESRO I/Aurora satellite expts. 9-33814
 polar, height distribution 145 to 180 km 9-31465
 polar, pre-IGY obs. statistical analysis 9-41569
 polar in diurnal hemisphere, hydromag. pressure model 9-41567
 polar night, atomic O formation in layer of max. intensity 9-31343
 rel. to polar substorms, expt. and theory review 9-37957
 precipitation boundary location calc. 9-37950
 primary electron energy spectra, rocket obs. 9-35851
 propagation, transauroral, induced phase perturbation, observed fine structure 9-40058
 proton and electron ovals, 55° to 78°N, 100°W 9-43425
 proton and electron precipitation, sounding rocket obs. 9-28928
 pulsating patches and flaring, obs. 9-47564
 pulsations, optical and X-ray, relative damping due to primary particle velocity dispersion 9-35846
 pulsations rel. to irregular geomag. field pulsation 9-43487
 radar, and ionospheric plasma instabilities, review 9-33822
 radio, 1295 MHz, afternoon obs. (1965) 9-28932
 radio, morphology of the southern auroral zone during IQSY 9-37959
 radio absorption near S. Geomag. Pole, rel. to mag. activity 9-35856
 radio aurora event, physical model 9-43427
 radio noise, origin of 9-37955
 radio noise on 28 Mc/s 9-47563
 radio research (1963-7), review 9-35854
 radio-, rate of occurrence in eastern Canada over eleven-year period, statistical charact. 9-24680
 related events in ring current and mag. storms 9-38001
 soft zone, latitude distribution of emissions 9-28926
 rel. to solar wind and magnetosphere inflation 9-26929
 spectra, green line transition probability, absolute lab. meas. 9-31373
 spectroscopy and excitation mechanisms, review 9-31371
 substorm activity rel. to sudden commencements, ring current effects and solar protons 9-43433
 surge of auroral electrojet westward travelling March 3, 1968, absence of H β emission 9-47569
 synchrotron radiation, r.f., from trapped electrons above auroral zones 9-37961
 type-B, green line suppression 9-37958
 universal instability rel. to periodic phenomena 9-31367
 universal instability role 9-41566
 visual, conjugacy during mag. quiet periods 9-28925
 visual observations, Canadian programme 9-35844
 v.l.f. continuous emission spectra, apparatus and methods 9-35855
 v.l.f. fields, elec. and mag., sounding rocket obs. (25 May 1968) 9-49476
 waves, infrasonic, morphology rel. to supersonic motion distribution 9-41564
 work of Birkeland and successors, historical review 9-33999
 X-ray intensity pulsations, rel. to auroral electrojet development 9-31369
 X-ray intensity pulsations rel. to electron precipitation 9-31370
 zone position, and arc azimuth diurnal pattern 9-43484
 H α emission, obs. using image intensifier and camera 9-31372
 H β and He I emission obs. 9-33819
 H emission, location midnight reversal 9-33816
 H α and O I ($\lambda 5777$) line intensities, proton and electron ovals, obs. 9-43425
 H β emission in pulsating aurora 9-35853
 He I (1.083μ) and O I ($\lambda 5777$) brightnesses rel. to primary e spectrum, sunlit aurora obs. 9-47566
 He twilight 10830 Å emission, identification and photometric obs. 9-31363

Aurora continued

- N_2 emission lines in u.v. spectrum 9-33817
 N^+ night time distrib., and auroral ionosphere $\lambda 5755$ emission 9-28931
 N emission lines in u.v. spectrum 9-33817
 O $_2$ dissociation and i.r. OH emission 9-33818
 O 5777 Å line transition probability lab. obs. 9-46282
 O emission lines in u.v. spectrum 9-33817
 O I 5777 and 6300 Å intensity ratio in quiet aurora 9-47565
 O I ($\lambda 5777$) and He I (1.083μ) brightnesses rel. to primary e spectrum, sunlit aurora obs. 9-47566
 O I (6300 Å) emission in F-region, mechanism 9-26952
 O I 6300 Å emission 9-28926
- Austenite** see Iron alloys; Steel
- Autoionization** see Ionization
- Avagadro's number** see Constants
- Axicons** see Lenses
- Backscattering** see Scattering, particles; and under 'scattering' subheadings of the appropriate particles
- Backward wave oscillations** see Electromagnetic oscillations; Electron tubes
- Balances**
 automatic, for high vacuum meas. 9-22040
 float, for determ. of mixture composition 9-34003
 sensitive, for very heavy loads, improvements and tests 9-29167
 surface, for press. meas. at oil-water or air-water interfaces 9-34006
 thermobalance protection from corrosive atmospheres 9-38190
 torsion, on moving bases for gravimetry 9-33703
 weighing in hermetically closed box with balance outside 9-45727
- Ballistics**
 see also Impact
 acceleration of solid particles by cumulative explosion 9-25064
 bow-and-arrow system, computer soln. of eqns. 9-38268
 exit trajectories, optimum, with specified transfer angle in inverse square gravitational field 9-29223
 gravitational fields produced by bullet in its motion in gun 9-29188
 holography and photography with laser beams 9-31986
 projectile hypersonic wake, l.p., Schlieren obs. 9-30331
 projectile impact on viscoplastic circular plate, finite deflection 9-25065
 slender body at supersonic speed, soln. for head-on collision with plane shock waves 9-25109
 sphere and core drag corrs. for hypersonic speeds 9-26005
- Band theory of solids** see Crystal electron states/band structure; Solids/theory
- Bardeen-Cooper-Schrieffer theory** see Nucleus/theory; Superconductivity
- Barium**
 coating on Mo and W surface, field-emitted electron energy distrib. 9-45031
 diffusion of H $_2$, 200 to 620°C, and solubility limit of BaH $_2$ 9-28315
 excited levels, spectroscopic study by electron bombardment 9-29955
 getter film in vacuum apparatus, activity determ., press. meas., pumping speed calc. 9-38169
 in meteorites and in terrestrial samples, isotopic analysis 9-45674
 in NH $_3$, conc. >6 MPM, electrical conductivity meas., 200-300°K 9-23521
 plasma, density meas. in low density range, rel. to verification of 'equilibrium' theory of Q-devices 9-28018
 plasma, diagnosis using tunable dye lasers 9-44463
 superconductivity under pressure at 1.3°K and 5°K 9-24146
 thin film, Ar desorption temp. dependence 9-40849
 vapour density 9-42702
 ^{133}Ba , 7.2 yr., Mossbauer effect 9-33525
 Ba $^+$ electron impact, emission cross section for excitation of resonance transitions meas., crossed beam technique, 8-98 eV 9-27815
 Ba I, resonance line broadening by inert gases, effective cross sections 9-48388
 Ba I, 6s 2 $^1\text{S}_0$, 6s5d $^1\text{D}_2$ photoionization cross sections, Many-Channel Quantum Defect calc. 9-48406
 Ba II lines emitted by discharge along surface of liquid jet, Stark width 9-40716
 Ba II spectrum, isotope shift meas., error sources and soln. 9-29987
- Barium compounds**
 BaO, spectra, recorded in Ba release expt. for atm. temp. determ. 9-26917
 kimrite, (hydrated feldspar), at. struct., satellite occurrence in inverse lattice 9-46782
 silicate glasses containing Ti, gamma-induced optical absorpt. 9-37693
 (Ba,Sr)TiO $_3$ solid soln., u.s. wave absorption and velocity, temp. depend. 9-41084
 Ba $_{0.75}\text{Ca}_{0.25}\text{Nb}_{26}\text{O}_{15}$:Nd $^{3+}$ 9-43203
 Ba $_{0.75}\text{Ca}_{0.25}\text{Nb}_{26}\text{O}_{15}$:Nd $^{3+}$ coherent emission obs. 9-26738
 Ba $_{1-x}\text{Ce}_{2n/3}\text{TiO}_3$:Fe semiconducting props., validity for Ba $_{1-x}\text{La}_{2n/3}\text{TiO}_3$ 9-37506
 Ba $_{1-x}\text{La}_{2n/3}\text{TiO}_3$ semiconducting props., validity from Ba $_{1-x}\text{Ce}_{2n/3}\text{TiO}_3$ data 9-37506
 Ba $_{1-x}\text{Sr}_x\text{O}_2\text{Nb}_2\text{O}_{15}$, ferroelec., spontaneous polarization, room-temp., pulsed-field method 9-35478
 Ba $_{1-x}\text{Sr}_x\text{Nb}_{1-2x}\text{Nb}_{15}\text{O}_{15}$, tetragonal, Curie temp., polarization, dielec. const., composition dependence 9-35480
 Ba $_{1-x}\text{Nb}_x\text{O}_{15}$ crystals, transparent, striation-free grown by Czochralski technique 9-39208
 Ba $_{1-x}\text{Nb}_x\text{O}_{15}$:Pt $^{4+}$, Ir $^{4+}$, optical defects 9-28651
 Ba $_{1-x}\text{Nb}_x\text{O}_{15}$, ferroelec., spontaneous polarization, room-temp., pulsed-field method 9-35478
 Ba $_{1-x}\text{Nb}_x\text{O}_{15}$, parametric oscillator, tunable, 13 W threshold power 9-25289
 Ba $_{1-x}\text{Nb}_x\text{O}_{15}$, single crystal and single domain, nonlinear optical props. study 9-26687
 Ba $_{1-x}\text{Nb}_x\text{O}_{15}$, tetragonal, optical nonlinearities and parametric emission 9-43202
 Ba $_{1-x}\text{Nb}_x\text{O}_{15}$ 0.53 μm source continuous, in 1.06 μm YAIG:Nd laser cavity 9-40362
 Ba $_{1-x}\text{Nb}_x\text{O}_{15}$ parametric emission, spontaneous, power and bandwidth 9-25198
 Ba $_{1-x}\text{Nb}_x\text{O}_{15}$ parametric oscillation and freq. doubling 9-37677
 Ba $_{1-x}\text{SiO}_x\text{-Ca}_x\text{SiO}_4$ system, fluorescence of Eu $^{2+}$, depend. on composition 9-28717
 Ba $_{1-x}\text{SiO}_x\text{-Sr}_x\text{SiO}_4$ system, fluorescence of Eu $^{2+}$, depend. on composition 9-28717

Barium compounds continued

- Ba₂ZnFe₁₂O₂₂ hexagonal ferrite, absorpt. and Faraday rotation, 300°K, 1 to 8 μ 9-45277
- Ba₂ZnFe₃O₆₀, and Mn substituted, single crystals, ferromag. reson. 9-45365
- Ba₄(Al₁₀)Na₂(-2₉)Nb₁₀O₃₀, ferroelec., cryst. struct. 9-46781
- Ba₄(Al₁₀)Na₂(-2₉)Nb₁₀O₃₀, crystallographic data and thermal expansion coeffs. 9-37134
- Ba₂Fe₂Zn₂O₂, numerical symbols for describing structure 9-40900
- (Ba₂Sr_{1-x})TiO₃ degenerate semiconductor, review of exptl. data on superconductivity 9-41179
- n-BaB₆ single cryst., conduction-e.s.r. 9-37793
- BaCl₂·H₂O and BaCl₂·D₂O systems, polymorphic and dehydration phase boundaries to 40 kbar 9-28171
- BaClF:Sm²⁺, fluoresc., temp. effects 9-41409
- Ba(ClO₄)₂·H₂O, neutron inelastic scatt. obs. of librational freqs. 9-42955
- BaD absorpt., 6100-7300 Å. 9-32465
- BaF₂:¹⁵¹Eu²⁺ hyperfine coupling const., temp. depend. 9-33496
- BaF₂:U³⁺, spin-lattice relaxation examined by paramagnetic resonance 9-35710
- BaF₂:U neutron-irrad. single cryst., diffusion of Kr and Xe 9-35127
- BaF₂, elastic constants pressure and temp. derivs. 9-33016
- BaF₂, etch patterns on matched cleavage faces, discrepancies rel. to stepped dislocations 9-37173
- BaF₂, h.f.s. consts. of V_K and V_L-centres, lattice vibr. influence 9-43274
- BaF₂, hyperfine interactions of H atoms, temp. depend. 9-31060
- BaF₂, neutron-irrad., e.s.r., F- and V-centres thermal stability obs. 9-43275
- BaF₂, structure factor determ. by elastic scatt. of neutrons, lattice vibrations correction 9-24014
- BaF₂, thermal ionization potentials of Nd²⁺, Dy²⁺, He²⁺ and Er²⁺ 9-46739
- BaF₂, vibr. atom, Edgeworth map. rel. to smearing function 9-42954
- BaF₂ center formation due to X-ray irradiation with and without H doping 9-26293
- BaF₂ crystal, i.r. absorption spectra meas., 50 μ 9-26740
- BaF₂ diffusion of ⁸⁹Sr, study of cation defects 9-39382
- BaF₂ M colour center, optical absorption 9-26292
- BaF₂ neutron-irrad. single cryst., diffusion of Kr and Xe 9-35127
- BaF₂ vapour, absorption spectra bands obs., ν_2 bending vib. assignment 9-23037
- BaFPO₃, n.m.r. chem. shift anisotropies 9-31169
- BaFe₁₂O₁₉, polycryst., mag. stiffness meas. 9-35571
- BaFe₁₂O₁₉ hexagonal ferrite, absorpt. and Faraday rotation, 300°K, 1 to 8 μ 9-45277
- BaFe₁₂O₁₉ single cryst. growth in solid state in polycrystalline aggregate 9-36996
- BaFe₁₂O₁₉ single crystal M₁ and K₁ as functions of temp. from mag. meas 9-47256
- BaFe₂₂O₁₉, magnetocryst. anisotropy consts. determ. by magnetization curves 9-43170
- BaGe₄O₉, crystal structure determ. 9-23751
- BaH₂, solubility limit in Ba, 200 to 620°C 9-28315
- BaLuF₃, Yb³⁺-Er³⁺ and Yb³⁺-Ho³⁺ ions, i.r. to visible conversion 9-49266
- BaM²⁺F₆(M=Mg, Co, Ni, Zn), ferroelectricity, spontaneous polarizations 9-45009
- BaMnF₄, antiferromag., spin- ρ transition 9-43193
- BaMnO₃ perovskite-like struct., phase transf. and stability relations at high press. 9-35241
- Ba(NO₃)₂·H₂O, n.q.r. of ¹⁴N, temp. depend. between 77°K and 300°K 9-37809
- BaO-Ar suspensions as closed-cycle MHD working fluids, coagulation 9-30436
- BaO-MgO-P₂O₅ system, luminescence of Eu²⁺ 9-31131
- BaO-SiO₂ glass films, two-phase structure development 9-26174
- BaO-TiO₂ glasses, splat-cooled, fourfold co-ordination of Ti ions 9-32827
- BaO, electrical conductivity, electric field effects 9-30833
- BaO, F-centre, e.s.r. obs. 9-35109
- BaO adsorbed layers on GaAs, eff. on GaAs photoelec. emission 9-26614
- BaO cathodoluminescence obs. 9-28731
- Ba(OD)₂·D₂O, i.r. absorpt. spectrum 9-33167
- BaOFe₂O₃, struct. and mag. props., X-ray and neutron diff., Mossbauer effect 9-47283
- Ba₂O₆·2H₂O, proton magnetic resonance obs. 9-24505
- BaSO₄:Pb luminesc. emission and quantum yield for X-ray excitation 9-49322
- BaSO₄-C-PbCrO₄, powder mixtures, diffuse reflectance 9-24360
- BaSO₄-SrSO₄-PbSO₄ system, subsolidus phase relations and lattice constants 9-23949
- BaSc₂Fe_{12-x}O₁₉ hexagonal ferrite single cryst., anomalous intensity distrib. in satellites in neutron diff. obs. 9-31043
- BaSc₂Fe_{12-x}O₁₉(M), helicoidal antiphase spin ordering, neutron diffraction 9-37663
- BaSnO₃-BaTiO₃-SrTiO₃ system solid solns. semiconducting props. 9-41192
- (BaSr)O cathodoluminescence obs. 9-28731
- BaSrO cathode in nonreactive atmosphere for gas laser use, properties 9-49171
- Ba(Ti,Zr)O₃ solid soln., u.s. wave absorption and velocity, temp. depend. 9-41084
- BaTiC₃-CdS boundary, photoeffects 9-43128
- BaTiO₃, dipolar fields and energy of 180° domains 9-28557
- BaVS₃, prep., props., crystal structure and refinement 9-39255
- BaWO₄:Er³⁺ e.p.r. spectrum, ground and first excited states of tetragonal Er³⁺ centres 9-41424
- BaYF₃, L_r-pumped visible and u.v. emission from Yb³⁺-Er³⁺ and Yb³⁺-Ho³⁺ ions, mechanisms 9-48110
- BaYF₃, Yb³⁺-Er³⁺ and Yb³⁺-Ho³⁺ ions, i.r. to visible conversion 9-49266
- BaZrO₃ cathode in reactive atmosphere for gas laser use, properties 9-49171
- BuO added to borolanthanum glasses, immiscibility and catalytic crystallization 9-34971
- NaCl:BaCl₂ crystals, dislocation density effect on ageing, elec. conductivity meas. at 550°C 9-46929
- NaCl-BaCl₂ single cryst. pulled from melt, oriented impurity precipitates 9-30601
- NaNbO₃-BaNb₂O₆ system, liquidus and solidus equil. 9-39503

Barium compounds continued**barium titanate**

see also Ferroelectric materials/barium titanate

- absolute reflectance spectra, 0.325-0.7 μ 9-33537
- atom. chain structure rel. to phase transition 9-32901
- BaTiO₃-SrTiO₃-BaSnO₃ system solid solns., semiconducting props. 9-41192
- ceramics, thermal conductivity influence of d.c. field in phase transition region 9-39545
- cubic-tetragonal transitions in high resistivity single cryst. 9-43115
- defect structure identification from i.r. spectra bands 9-35105
- dipole field correction due to lattice deformation 9-28558
- displacement correlation of Ti-ions, lattice dynamical model, anomalous X-ray scattering 9-35267
- dynamical, scattering and dielec. props. 9-49141
- ferroelectric domains boundaries, X-ray topography obs. 9-28556
- incorporation of Sb into lattice sites 9-36972
- lattice structure of (100) free surface 9-28210
- microwave absorption by free carriers 9-31101
- nucleation models for 1st-order transition front 9-42924
- Raman scattering by polaritons 9-35671
- rare-earth doping effects on elec. props. 9-39685
- reduced and reoxidized, phase comp. 9-42939
- semicond. acting properties due to doping, origin 9-39610
- surface state of single crystals, X-ray diff. study 9-39683
- tetragonal, ageing and domain reactions 9-49142
- tilt angles of twin components in various lattice planes, Berg-Barrett X-ray determ. 9-37145
- transistor, field, small control coercive field strength, composition, patent 9-30950
- BaTi_{1-x}Ni_xO₃ optical and dielectric props. in single crystals prep. from molten KF 9-41362
- BaTiO₃:Co, electromechanical props. 9-47171
- BaTiO₃-SrTiO₃ solid soln., dielec. const. reversible, depend. on field strength above Curie point 9-41239
- dielectric constant, reversible depend. on field strength above Curie point 9-41239

Barkhausen effect *see Magnetization process*

Barnett effect *see Gyromagnetic effect*

Baryons

see also Hyperons; Nucleons and antinucleons

- 35-plet of baryons, dibaryons, mass relations and decays 9-38555
- 'elastic', production by neutrinos 9-38556
- 1/2⁺, Hamiltonian, current algebra, radiative corrections and CP violation 9-36438
- baryon-antibaryon separation, occurrence in blackbody radiation at high temps. 9-42096
- considered as discrete quantized states of internal struct. of elementary particles 9-43980
- current, equal-time anticommutator structure in neutral pseudoscalar-meson theory 9-44001
- decay, leptonic, rel. to Cabibbo one-angle theory 9-40410
- decay, selection rules, the octet rule, review 9-40398
- decay of SU(3)' excited resonances 9-38592
- e.m. current and partial conservation of tensor current 9-48204
- e.m. mass difference among octet members, contrib. of decuplet states 9-36491
- empirical mass formula 9-25479
- I=0, Y=0, possible existence, search for in K⁻d interaction 9-42097
- isomultiplets, Regge sequences 9-40437
- leptonic decays, form factors 9-42098
- Low one-meson eqn. of static-baryon model, resonant soln. from fixed-point theorems 9-38552
- magnetic moments, e.m. mas splitting and Gell-Mann Okubo mass formula 9-25425
- magnetic moments, nonstatic relations in quark model 9-48205
- mass relations in SU(3)-octet, and decuplets 9-22616
- mass spectra from eigenfunctions of quark model 9-27546
- mass spectrum in strong-coupling model with O(3)⊗SU(2)⊗SU(3) symmetry 9-38553
- meson-baryon, decouplet superconvergence relations 9-42057
- meson-baryon coupling constants, sum rules 9-48135
- meson-baryon couplings, rescattering eff. in quark model 9-38500
- nucleons, classification by pattern recognition; mass, spin, isospin, parity and decay widths 9-34335
- P-wave, mag. moments, e.m. mass differences, Capps bootstrap model calc. 9-22617
- SU(3) multiplets and baryon wave eqns. from G=SO(6,1)×U(1) global dynamic unification group, mass formula 9-46070
- SU(3) structure of -ve parity states mass spectrum, decay sum rules studied 9-46113
- trajectories, Minami symmetry 9-32208
- B-B⁺ev⁻ correlation between spin of B⁺ and lepton momenta, weak magnetism term 9-38587

interactions

- baryon-antibaryon, by U_{6,6} peripheral absorpt. model 9-41996
- baryon-baryon, by U_{6,6} peripheral absorpt. model 9-41996
- baryon-baryon, multiprod. process cross-sections, asymptotic equalities 9-36459
- baryon-baryon, phase shift, scatt. length and effective ranges from Schrödinger eqn. potential 9-38554
- compressibility coeff., calc. from $\pi\pi$, K π and pp cross sections 9-44047
- meson-baryon, quark model with production of positive parity meson 9-46085

resonances

- 3/2⁻ baryon p octet to D-wave baryon pseudoscalar mes. composites decay modes, SU(3) symmetry breaking 9-29623
- capacity-constant shifts of N and Δ (1238) in bootstrap model, and e.m. mass 9-46115
- classification into broken SU(6)×O(3) scheme, using quark-diquark model 9-32227
- coupling regularities 9-32228
- decay, selection rules derived for SU(3)' excitation 9-38592
- decay rates calc. from unified static bootstrap model 9-25478
- e.m. decays and radiative width estimation by harmonic-oscillator model 9-38593
- energy relationships for resonance states 9-48177
- exotic, systematic description 9-22603

Baryons continued**resonances continued**

- harmonic-oscillator model for positive parity resonances, 1500-2000 MeV mass region 9-38591
 higher multiplets, suppression factor rel. to existence 9-22554
 $I=5/2$ nonstrange reson. of mass 1640 MeV/c², evidence against prod. 9-42114
 $I=1/2$, prod. in $pp \rightarrow p\pi N_{1/2}^*$, diffraction dissoc. react. mech. 9-27566
 $I=1/2$ production in $\pi^- d \rightarrow p\pi\pi^- \pi^+ \pi^-$, 1640 MeV/c², $M\pi=2.26$ GeV/c 9-27562
 isobar, 1470 MeV, $I=5/2$, $Y=1$, possible existence 9-42113
 $J=1/2$ reson. dominance model exam. of rel. bet. wide dispersion relation calc. of N mag. moments and g_M/g_N 9-22622
 mass, spin and parity, review 9-36498
 mass relationships for resonance states, empirical derivation 9-46084
 May 1966 classification 9-22633
 polarized target expts. 9-27535
 production 9-29622
 production cross-sections in p-p collisions at 4 GeV/c 9-38569
 review 9-42112
 review 9-36443
 spin, information from decay angles 9-44039
 spin and parity through spin-rotation parameter meas., method 9-22570
 unstable particles, mass distribution, admissibility conditions 9-22602
 $\Delta_{1236}(7/2, 3/2)$ static multipole moments from superconvergence in $N\gamma \rightarrow \Delta\pi$ 9-38595
 $\Delta(1238)$ isobar, photoproduction at photon energies below 1 GeV 9-22635
 Δ production from πN interaction, helicity amplitude reggeization, production cross section determ. 9-34304
 Δ Regge trajectory residue at $\alpha \Delta=1/2$, possible zero at wrong-signature sense-point 9-38594
 $\Delta(1238)$, production in 2.7 GeV/c π^+ interactions on deuterium 9-32186
 $pp \rightarrow \pi^+ p$ baryonic resonance contributions, quark model 9-29580
 $\Lambda_{1/2}(1385)$ mass predicted from $\pi \Lambda$ scatt. 9-42080
 $N-N^*(1236)$ transition form factors, asymptotic chiral symmetry predictions 9-27564
 $N-N^*(1236)$ transition form factors, asymptotic chiral symmetry predictions 9-29624
 $N_{1/2}^*$ prod. in $pp \rightarrow p\pi N_{1/2}^*$, diffraction dissoc. react. mech. 9-27566
 N_{33}^* production, Low equations, stability of solns. 9-41976
 N^*_{1236} isobars as $p\pi^+\pi^-$, in πp interac., 2-10 GeV 9-25487
 $N^*_{3/2}$ from πN , mass and width determ. from quantum field theory without cutoff 9-27565
 $N^*_{3/2}$ from πN , mass and width determ. from quantum field theory without cutoff 9-34336
 N^* and N^{*++} prod. in $K^- d \rightarrow K^- \pi^+ \pi^- p n$ reaction at 2.24 BeV/c 9-32178
 $N^* K^- \pi^+$ [(71 \pm 7)%], dominance in $K n \rightarrow K^- \pi^+ \pi^-$ reaction 9-32178
 N^{*++} , in $\pi^+ p \rightarrow \pi^+ N^{*++} \pi^0$ and $\pi^+ p \rightarrow \pi^+ N^{*++} w$ react., quark-model predictions for joint decay distrib., 8 GeV/c 9-38528
 N^{*++} production in channels by $\pi^+ p$ interactions, $E_\pi=8$ GeV/c 9-46099
 $N^*_{1/2}$, in mass range 1800-2200 MeV 9-44064
 N^* radiative width estimation by harmonic-oscillator model 9-38593
 $N^*(1236)$ double-reson. prod. in $K^+ p$ 9-42094
 $N^*(1236)$ isobar prod. and dominance in pp collisions, 4 GeV/c 9-38569
 $N^*(1400)$, evidence in 3.0 GeV/c K^+ interac. 9-27534
 $N^*(1470)$ prod. from $pd \rightarrow p\pi p\pi^+$ at 7.0 GeV/c 9-25486
 $N^*(1688)$ in d in pd scatt., cross section and peak determ., $E_p=1$ GeV 9-42103
 $N\pi^0$ vertices, vector and axial, form factor from Ward identity and sidewise dispersion relations 9-44063
 $\Pi^- \rightarrow Y^* K^+ K^-$ at 2 to 4 GeV/c, peripheral peaking in $Y_1^*(1385)$ ang. distrib. 9-25467
 $\pi\Delta(1236)$ scatt., sum rules in $O(3,1)$ dynamical group model 9-36499
 Y_0^* , role in K^- meson capture on complex nuclei 9-42293
 $Y_0^*(1520)$ prod. in $K^- n \rightarrow Y_0^*(1520)\pi^-$, react. at 3 GeV/c, decay branching ratios 9-38597
 $Y_1^*(1385)$ $\Sigma\pi$ coupling and superconvergence 9-40448
 Y^* , (1616), observation in $K^0 p \rightarrow \Lambda \pi^+$ 9-44065
 Y^* , (1700), observation in $K^0 p \rightarrow \Lambda \pi^+ \pi^0$ 9-44065
 Y^* production in $K^- n \rightarrow \Sigma^+ \pi^-$, 1600-1800 MeV 9-38596
 Y^* prod., one baryon exchange model appl. 9-25488
 Y^* production in $Y\pi\pi$ final states, from $K^- p$ interactions at 1.33 GeV/c 9-40447
 $Y^*(1385)BP$ coupling and superconvergence in $\bar{K}N \rightarrow K\Xi$ 9-22636
 Z^* , strangeness +1 baryon, search for in $\pi^+ p \rightarrow K^- Z^*$, 6, 8 GeV/c 9-22634
 in deuteron, dipole moment and D*-state components 9-34394
 $N(1470)$ Roper resonance existence in Dalitz 3-quark model 9-27563
 Y^* rel. to exchange degeneracy from FESR 9-43999

scattering

- baryon-baryon, high-energy polarizations, theory 9-27491
 baryon-baryon total cross-section prediction, CHKN model energy depend. 9-36490
 bootstrap model, unified static, for even- and odd-parity excited states 9-25478
 meson-baryon, backward differential cross section calc., N and Δ Regge trajectory exchange 9-27494
 meson-baryon, static, Cutkosky bootstrap eqns. for degenerate baryon mass. 9-38557
 meson-baryon, SU_3 , continuous moment sum rules saturation 9-46086
 meson-baryon $35/356$ low energy scatt., Lagrangian construction 9-38502
 meson-baryon scatt., superconvergent sum rules and J-plane singularities 9-29565
 meson-baryon total cross-section prediction, CHKN model energy depend. 9-36490
 quark model for baryon-baryon and baryon-antibaryon scattering 9-22559
 KB , interaction symmetry, B spin and isospin connection from unified static bootstrap model 9-25478
 πB , interaction symmetry, B spin and isospin connection from unified static bootstrap model 9-25478

Barysphere *see Earth***Bauschinger effect** *see Deformation***Bayard-Alpert gauges** *see Vacuum gauges***Bays** *see Earth/magnetic field; Magnetic storms***BCS theory** *see Nucleus/theory; Superconductivity***Bells** *see Musical instruments***Bending***see also Stress analysis; Torsion*

- assemblages, thin walled, consistent matrix formulation 9-45805
 beam, longitudinal bend-buckling 9-38274
 beams, prismatic with longitudinal cavities, membrane analogy 9-34064
 buckling, dynamic, of shallow truss, effect of plastic deform. 9-45827
 buckling, local, of thin flat-walled structures combined shear and stress: stability function 9-36158
 buckling, under arbitrary membrane loading, discrete element method applic. 9-38269
 cantilever, bend-twist buckling 9-38274
 cantilever beams, deflection under load, analytic, numerical and graphical solns. compared 9-38275
 cantilever stability under eccentric follower force, effect of warping rigidity 9-43778
 cylinders, orthotropic shallow-stiffened, instability 9-36161
 cylinders and cones, sandwich, subjected to axial compression 9-23872
 deflections of disk spring with frictional effect 9-27206
 elastic-plastic plates, impulsively loaded, waves 9-41796
 extension and flexure of flat plate, electrical analogue 9-27205
 fatigue of high strength deformed bars in reinforced concrete bridges 9-23854
 flexure of triangular sections subject to terminal loads 9-38284
 fracture, interpret. 9-26350
 frequencies of compressed beams 9-29250
 graphite, pyrolytic, flexural strength, post deposition high temp. treatment eff. 9-23906
 helicopter rotor blade airloads, bending moments and motions 9-25063
 large deflection behaviour of simply-supported inextensible uniform beam subjected to point loads 9-36159
 metal foils with oxidized stressed surface layer 9-31189
 moment equations for elliptical vacuum chamber 9-47708
 piezoelectric rectangular plate, theory 9-36160
 plate, elastic, transient plane wave propag., three-dimensional analysis methods applicability 9-45815
 plate theory, generalized two-dimensional 9-40268
 plates, buckling load calc. using finite element method 9-22235
 plates, triangular, explicit transverse stiffness and mass matrices 9-41791
 shell, circular cylindrical simply supported, subjected to uniform line load along a generator 9-25078
 shells, conical, orthotropic and isotropic, and buckling 9-47812
 of steel, case hardened, repeated 9-42892
 steel and concrete composite beam, partial interaction between elastically connected elements 9-26380
 stress distrib. around elliptic hole in cylindrical shell, axial tension 9-31812
 symmetric, three-layered, elastic plates with light rigid filler 9-25076
 unbending of cryst., diffusion "climb" mechanism 9-26324
 vibrations in bars, propag. 9-34079
 wire, plated, memory elements, rotational variations 9-48895
²³⁵U enriched tubes, buckling in light water 9-23913
 Al alloys, prevention of fretting fatigue 9-42898
 Bi whisker, rel. to resistance changes below 300°K 9-37453
 CdS elastic oscillations excited by elec. current 9-44763
 HfB₂, transverse bend strengths 9-35183
 In whisker, rel. to resistance changes below 8°K 9-37453
 KCl, straightening of bent crystal by diffusion annealing 9-42884
 NaCl, straightening of bent crystal by diffusion annealing 9-42884
 NaCl single crystal, moment, and dislocation and slip line formation, 300° to 1.4°K 9-33036
 Sn whisker, rel. to resistance changes below 20°K 9-37453
 UO₂ cermets from UO₂-Mo system, strength depend. on porosity and Mo content 9-35222
 Zn whisker, rel. to resistance changes below 6°K 9-37453
 ZrB₂, transverse bend strengths 9-35183

Bending of light *see Gravitation; Light***Berkelium**

No entries

Berkelium compounds

No entries

Beryllium

- 9-44243

- abundance in Ib supergiants and Cepheids 9-24796
 adsorption of N, H, O, CO on thick film obs. 9-36964
 anodic dissolution of polycrystalline material 9-24583
 atom, ¹S, spin-optimized, self-consistent field wave function determ. 9-40544
 atom, ¹S state, calc. in Hylleraas coordinates 9-32409
 atom, ground state energy, applic of Hartree-Fock approximation using harmonic oscillator functions 9-29918
 crystal structure, 77° to 300°K 9-32902
 diffusion in b.c.c. phase of Fe, temp. depend. 9-23839
 ductility behaviour around transition temp., effect of orientation, ageing and grain refinement 9-26333
 elastic shear constants, band structure contribution, model potential theory validity 9-30630
 electron emission, secondary, charact. energy losses 9-31008
 electron energy loss spectra in Li.r region 9-28441
 electron maximum range, 15 MeV, expl. determ. 9-26470
 evaporation by electron beam, controlling method 9-39145
 Fermi surface and press. depend. pseudopot. model, de Haas-van-Alphen effect obs. 9-43001
 foil, preparation for transmission electron microscopy using chemical saw 9-39256
 hexagonal, vibrational spectrum 9-42946
 irradiated, hot pressed, release of gas 9-37282
 isostatically hot-pressed, microyield and flow stress rel. to microstrain 9-35181
 isotopes formation cross section for proton spallation of ¹⁶O 9-44203
 magnetic breakdown and de Haas-van Alphen effect 9-39749
 metallographic preparation, microstructure, influence of improper preparation 9-39446
 microyield strength and flow stress, depend. on grain size, ht. treatment, temp. and impurity conc. 9-35181
 in minerals, spectrochem. analysis using C cavity electrodes, obs. 9-28828
 neutron irradi., impact resist., obs. 9-28368
 origin in solar system 9-36015
 phonon dispersion relations, pseudopotential calcs. 9-24011

Beryllium continued

- radiation damage mechanisms, eff. on macroscopic props., review 9-24069
 specific heat at low temps., rel. to impurities 9-24042
 superconducting transition temp. 9-35358
 target for 12.3 BeV/c p, cross-sections for prod of $\pi, \kappa, \rho, \bar{p}$ 9-38580
 thermal conductivity meas. for hot pressed block 9-37366
 u.v. spectrum, 2000-500 Å, auto-ionized line series 9-42330
 X-ray index of refraction of single crystal 9-39798
 X-ray scatt. spectra, Cu K α and β_1 rad. 9-45338
 n yields of a target following bombard. by 20 MeV ^3He , 14 MeV p and ^7Li
 MeV d 9-38607
 IN Al-(4.4 wt.%)Zn alloy, influence on elec. resistivity changes due to clustering 9-40932
 in Al alloys, interaction with vacancies 9-44691
 in Al alloys, interaction with vacancies 9-44692
 Be $^{+}$, ^4S , spin-optimized, self-consistent field wave function determ. 9-40544
 Be II, mean lives of $2p^2P^o$ levels, oscillator strengths 9-44256
 Be II lines in solar spectrum, isotropic wavelength shifts 9-27095
 ^7Be , K γ mesic X-ray yields 9-36685
 BeO, K emission spectra of Be 9-26761
 in CdTe, i.r. absorpt. 9-45317
 in CdTe, i.r. absorpt. 9-45318
 in Cu, bond const. variations 9-39181
 SiC:Be, luminesc. spectra rel. to Be conc., 77 to 500°K 9-28713

Beryllium compounds

- BeF $_2$ -LiF molten solns., viscosity and density 9-42639
 beryl, refr. index press. depend. 9-47317
 carbides, heat of formation 9-49369
 intermetallic, magnetic behaviour at 4.2°K, n.m.r. investigation 9-45396
 microstrain analysis of BeO single crystals, double-crystal X-ray diff. method 9-42765
 Am-Be neutron spectrum, calc. and expt. 9-22629
 Be-(1.3 wt.%)Ni alloy, low-temp. and mixed ageing, struct. and hardness changes 9-39464
 Be $_2$ Nb $_3$, superconductivity, rel. to Si $_2$ U $_3$ -type structure 9-39596
 Be $_2$ Ta $_3$, superconductivity rel. to Si $_2$ U $_3$ -type structure 9-39596
 Be $_2$ N $_2$, X-ray scatt. spectra, Cu K α and β_1 rad. 9-45338
 BeB $_2$ H $_8$, structure 9-44318
 BeCl and BeCl $_2$, dissociation energies 9-48511
 BeF, A $^2\Pi-X^2\Sigma$ syst., character analysis 9-23031
 BeF, Franck-Condon factors and r-centroids for bands of A $^2\Pi-X^2\Sigma$ syst. 9-46358
 BeF $_2$ -XF glass system with X-alkali ion, i.r. spectra 9-41375
 BeO, 28.5 BeV proton bombard., α prod. 9-32345
 BeO, exoelectron emission, self-excitation, diffusion controlled 9-26607
 BeO, K emission spectra of Be 9-26761
 BeO, normal modes of vibr., expt. and theory 9-42945
 BeO, radiation damage mechanisms, eff. on macroscopic props., review 9-24069
 BeO, thermal conductivity meas., heat losses in cut-bar apparatus 9-26441
 BeO, u.v. spectrum for reflectance and band struct. 9-28670
 BeO, wurtzite-type, 1st-order Raman scatt. 9-47373
 BeO, X-ray scatt. spectra, Cu K α and β_1 rad. 9-45338
 BeO assemblies, neutron population decay const., and thermal diffusion parameters 9-36629
 BeO assemblies, pulsed, decay curves in region of Corngold's limit 9-22909
 BeO in Be, influence of increased content on microyield strength 9-35181
 BeO powder, sintering to high density 9-35231
 BeO pulsed assemblies, calc. of buckling corresponding to λ^* 9-22894
 BeO pulsed assemblies, extrapolation distances rel. to buckling 9-22908
 BeO rapid fission factor determ. 9-34469
 BeO reflector in fast reactor critical expt., meas. and analysis 9-29883
 BeO thin foils, small-angle scatt. of ^{32}S AND ^{16}O beams 9-35298
 Be(OH) $_2$ powders, calcination process, electron microscope exam. 9-35221
 BeSO $_4$, ion-assoc. process, nature of, u.s. absorpt. studies 9-23460
 BeSO $_4$.4H $_2$ O, neutron inelastic scatt. obs. of librational freqs. 9-42955
 BeSO $_4$.4H $_2$ O, Raman and i.r. spectra 9-24423
 Co-Fe-Ba semi-hard mag. alloys, square hysteresis loop and low magnetstriction coercive force 9-45137
 Cu-(12.6wt.%) Be-(0.2wt.%) -(0.1wt.%) Zn alloy, Mossbauer eff. 9-45288
 Cu-Be-Co, dil., constitution and behaviour 9-39274
 Cu-Be, ageing investigations from sp. ht. meas. by an adiabatic calorimeter 9-37285
 Cu(9.5 at.%)Be-(0.2 at.%)Zn, alloys, neutron irradi., ageing characts. from resistivity meas. 9-33115
 Fe-Be alloys, magnetization and sp. ht. 9-45143
 Fe-Ni-Cr-Be alloy, precip. processes, transmission electron microscopy obs. 9-39498
 Mg-Al-Zr-Be, alloy, correlation of orientation and polarized etching facets 9-39186
 Pu-Be neutron spectrum, calc. and expt. 9-22629

Bessel functions *see Functions***Beta-decay theory**

- see also Nuclear decay theory*
 0 $^{+}$ -0 $^{+}$ superallowed transitions, *f*-values, neutron and proton density distributions 9-44172
 0 $^{+}$ -0 $^{+}$ nuclear beta transitions 9-29768
 0-0 transitions, analysis for information on axial current 9-36424
 for deformed nuclei, superfluid corrections 9-42240
 e.m. corrections, 2nd order, to G $_A$ /G $_V$ 9-38582
 Fermi matrix elements rel. to isospin purity 9-48310
 Fierz term, assessment from data obtained by 0 $^{+}$ -0 $^{+}$ transitions 9-48309
f-values of superallowed transitions and neutron and proton density distributions 9-44172
 Gamow-Teller transitions and M1 γ -rays meas., A=4N+2 nuclei, A \leq 30, sum rule proposal 9-29763
 mirror nuclei, *f* values for isospin doublets ang.momentum distrib. between orb. ang. mom. and spin 9-46220
 photon exchange effects, no contrib., conserved vector current theory applic. 9-42241
 probability, determining functions, values for electron β decay 9-46219
 N axial vector coupling const., quasi-indep. quark model calc. 9-27552

Beta-decay theory continued

- ^{113}Sn - ^{113}In , isomeric state half-life determ. form γ spectra 9-27630

Beta-ray spectra

see also Nuclear decay theory

- ^{150}Eu , β - γ circular polarization correl. meas. 9-46221
 ^{192}Ir , β - γ angular correl. studies on two cascades 9-34423
 $^{184\text{m}}\text{Re}$ - $^{184\text{m}}\text{W}$ decay, conversion electron spectra 9-40495
 ^{163}Er , conversion-electron spectra 9-38672
 ^{116}In , polarized, β decay anisotropy 9-44177
 ^{147}Gd - ^{147}Eu , decay, e- γ coincidence spectra 9-40492
 ^{169}Tm - ^{169}Er decay, e- γ coincidence spectra 9-40492
 ^{149}Tb , conversion electron spectrum 9-44180
 ^{61}Fe - ^{61}Co decay 9-44174
 $^{80\text{m}}\text{Br}$ decay, Kurie plots, transitions rel. intensities and energies 9-42216
 ^{96}Nb -Mo decays 9-44176
 ^{65}Ni , β - γ circular polarization correl. meas. 9-46221
 ^{32}P , and $4\pi\beta$ spectrometer characteristics 9-36511
 ^{48}Sc , β - γ circular polarization correl. meas. 9-46221

conversion electrons

L/K electron capture ratios in terms of internal conversion coeffs.

- 9-27672

from Mossbauer bombard. of a surface, used to study struct. 9-30476

- ^{210}Bi obs. with new β spectrometer 9-42130

- ^{160}Dy , internal particle parameters for several low-lying E2 transitions 9-29737

- ^{170}Lu decay, spectrum obs. 9-48317

- ^{221}Fr , low energy spectra, transition multipolarity, level obs. 9-32313

- ^{151}Gd decay, intensities obs. 9-48313

- ^{151}Gd - ^{151}Eu decay 9-42251

- ^{152}Gd , internal particle parameters for several low-lying E2 transitions 9-29737

- ^{192}Ir source, obs. with double-focusing sector-type spectrometer 9-38610

- ^{152}Sm , internal particle parameters for several low-lying E2 transitions 9-29737

- $^{123\text{m}}\text{Te}$, isomeric transitions 9-46205

- $^{124\text{b}}\text{Sb}$ decay, internal conversion coefficients 9-48292

- ^{204}Tl obs. with new β spectrometer 9-42130

- ^{155}Gd thermal n capture 9-32350

- ^{115}In , 35.6 keV transition, K-conversion coefficient meas. 9-42221

- $^{127\text{m}}\text{Te}$, isomeric transitions 9-46205

- ^{137}Cs source, obs. with double-focusing sector-type spectrometer 9-38610

- ^{198}Au source, obs. with double-focusing sector-type spectrometer 9-38610

- ^{158}Ho decay, $E\beta > 1000$ KeV 9-48314

- $^{199\text{m}}\text{Hg}$, conversion coefficients and fluorescence yields obs. 9-42255

- ^{159}Ho decay obs. 9-48315

- ^{57}Fe electron spin density determ. using internal conversion 9-48383

- ^{99}Mo - ^{99}Tc , K-shell conversion coeff. of 40.58 keV transition 9-29773

- ^{32}P obs. with new β -spectrometer 9-42130

- ^{48}Sc obs. with new β -spectrometer 9-42130

- Sn Mossbauer investigation of surface props. 9-30476

- ^{96}Tc - ^{96}Mo , energies and relative intensities 9-44175

Beta-ray spectrometers

- Auger e spectrometer for analysis of contaminants on the surface in ultrahigh vacuum work 9-39150
 backscatter gauge applic. protective film thickness meas. 9-39154
 calibration procedure for iron-free mag. electron spectrometer 9-22658
 Compton, used to determine γ spectrum 9-46133
 double focussing $\pi/2$, mag. field meas. and regulation by saturated Fe core transformer 9-46135
 double-focusing sector type, construction and application 9-38610
 double-focusing sector type, transfer matrix calc. 9-38609
 energy analyzer, fast recording electrostatic 9-25535
 for energy distribution of fast electrons after passing through barriers 9-24074
 magnetic, sector-focusing, optimization 9-44079
 retarding field analyzer for Auger electron spectroscopy using display LEED optics 9-32246
 retarding field energy analyzer, instrumental effects in He electron impact spectra meas. 9-34351
 Uppsala, Sweden, 50 cm Fe-free spectrometer, recent work 9-38608
 Si, 4π geometry, and ^{32}P spectrum measurement applic. 9-36511
 Si(Li), with 4π geometry 9-42130

Beta-rays

see also Electrons

No entries

absorption

see also Electrons/absorption

No entries

angular distribution

No entries

detection, measurement

see also Beta-ray spectrometers; Dosimetry; Particle detectors; Radioactivity measurement

autoradiography in the presence of latent image fading 9-48233

calorimeter for low-power sources 9-29664

flux recording inside β -emitting medium by G-M tube 9-25508

Geiger counter 9-29652

helicity new meas. method 9-43971

pulse shaping network, use in improving signal-to-noise ratios in β activity meas. 9-44170

showers, simulation using Monte Carlo programme 9-44070

β - γ emitter activity, coincidence method, automatic correction digital app. 9-22750

^{235}U , fission products, kinetic energy of β decay 9-22753

^{14}C activity on planar surface, scanning device 9-27593

NaI(Tl) scintillation counter efficiency by liq. β emitters activity obs. 9-22754

^{35}S activity on planar surface, scanning device 9-27593

effects

see also Electron beams/effects; Nuclear reactions and scattering due to electrons

CdS, semicond., beta-excitation, charge pulses obs. 9-33298

polarization

helicity new meas. method 9-43971

^{152}Eu , relative meas. 9-22759

Beta-rays continued**scattering**see also *Electrons/scattering*

No entries

Betatrions see *Particle accelerators/betatrions***Bethe-Salpeter equation** see *Field theory, quantum***Bethe-Uhlenbeck equations** see *Statistical mechanics***Bevatron** see *Particle accelerators***Binary stars** see *Stars***Binding energy, solid state** see *Bonds; Solids***Bingham plastics and solids** see *Rheology***Biographies**

Frocht, Max M., photoelasticity papers 9-41803

Hale's solar work 9-22028

Biological effects of radiations

acoustic thermal 9-47698

alga nitella flexilis, cell membrane resting pot., elec. stimulation threshold and resistance 9-31686

barley seeds, new class of radiobiological damage 9-29111

corneal damage thresholds for CO₂ laser radiation 9-43690corneal irradiation by CO₂ laser, anterior chamber meas. 9-47697

Dictyostelium discoideum, slime mold, gamma ray resistance 9-24938

electron fluence emitted from soft tissues following γ irradiation 9-24066

eye, human, laser damage threshold theory 9-45704

human thermal stresses in different climates, conference 9-34094

laser, model 9-49602

manned Earth satellites, Russian, absorbed radiation doses, obs. 9-45573

melanoma cells in vitro, ruby laser radiation effect 9-49603

music, rock-and-roll, damage risk, sound and spectrum obs. 9-24958

nucleons <400 MeV, absorbed dose calc. 9-24942

ocular hazards of lasers 9-45702

photosynthesis, meas. of radiant energy acting on plants 9-27122

plant leaves, spectral coeff. changes due to rad. 380-710nm, dynamics 9-38133

population exposure risk from re-entering isotopic power devices 9-28901

proteins, radical state prod., e.s.r. study and migration 9-24941

space flight permissible doses, substantiation 9-31687

on tissue, normal and turnover, high power Nd laser 9-49604

 π absorption in tissue-equivalent material 9-27123

Co isotopes, retention in rat 9-24949

Biological technique and instruments

blood flow determ. by conjunctival photography 9-49605

calorimeter, differential emissivity, for measuring radiant heat exchange of small animals 9-47691

cell elemental anal., spark cross-excitation for laser microprobe spectroscopy 9-47476

collimator, penetration eff. due to γ rad. coming through wall 9-24951

DEEPSTAR 4000 submersible for deep ocean obs. 9-37906

dielectrophoresis in lossy media, theory, applic. and usefulness 9-28145

neutron activation analysis of normal and atherosclerotic aortas 9-36080

radiographic display system, three-dimensional with full-color 9-49615

skin, internal reflection spectrochem. anal. 9-37853

solar therapy device with parabolocylindrical and spherical concentrators 9-32030

spectrochemical analysis of ashed materials, advantages of high current d.c. arc 9-47477

superconducting magnet system for intravascular navigation of catheter 9-35380

telecentric optical system for vocal cord cinematography 9-33964

thyroid testing of ¹³¹I conc. in biosphere in 1968 9-43405

X-ray meas. with inflated balloon ionization chamber 9-27152

Ge(Li) γ spectrometer for radionuclide counting 9-44081**Biology**see also *Medical science; Physiology; Zoology*

DNA in phages, filament struct. from lum. with orange acridine, obs. 9-27926

laser beam applications 9-49599

plant leaves, pigment movement due to light irradi., study by spectral coeff. changes 9-38133

Biophysics

adenosine triphosphate, storage by polyhydric compounds addition, patent 9-24939

biological particles, counting and sizing, optical method 9-47692

biomedical applications of holography, popular article 9-49598

biomolecules, photosensibilization, e.s.r. study of solvent effect 9-47472

biopolymer, n.m.r. study at high field strength, tech. and limitations 9-30155

blood optics, scattering and absorption constants 9-47694

chlorophyll solns., eff. of laser light on optical transmission coeff. 9-28131

collagen, molecular structure study from models 9-43689

creatine phosphokinase, storage by polyhydric compounds addition, patent 9-24939

Dictyostelium discoideum, slime mold, gamma ray resistance 9-24938

fucose-61-phosphate dehydrogenase, storage by polyhydric cpds. addition, patent 9-24939

glucose, storage by polyhydric compounds addition, patent 9-24939

heat and bladder, magnetically induced function 9-45698

human teeth, sound vel. 9-37327

intermolecular electron transfer theory of defence mechanisms 9-27117

mass spectrometers, respiratory specifications and design requirements 9-36649

membranes of 100 Å thickness elec. phenom. anal. by changes in absorpt. 9-47695

microorganisms orientation by e.m. fields, theory and experiment 9-47693

micro action, theory 9-41779

night-flying moths, h.f. dielectric waveguide on the antennae 9-33962

optics, X-ray and neutron activation analysis, forensic 9-25333

photosynthesis, exciton trapping, random walk problem 9-38244

photosynthesis, meas. of radiant energy acting on plants 9-27122

physics in biological sciences 9-29147

red blood cells squeezed through narrow capillary, model and soln. 9-22168

retinal and occipital potentials due to wavelength changes 9-31710

ribosomes, e. microscope exam., statistical anal. to determ. length 9-29110

ultrasonic diathermy 9-47698

Biophysics continued

virus suspension, absorption meas. with integrating photometer 9-31685

Si removal from ocean by biogenous deposits, total rate 9-33749

Biot-Savart law see *Electromagnetism***Birefringence** see *Double refraction***Blaschke**

Alfvén-wave propag. 9-24106

in alkaline earth tungstates, u.v.-induced colouration, fading and darkening processes obs. 9-45282

Bauschinger effect in twinning of crystals 9-42880

crystal, single, γ ray ang. distrib. prod. by positron annihilation, temp. effect 9-24113

cyclotron resonance, measured and calculated wave spectrum 9-49012

deformation potential for electrons and holes 9-37345

deformation potentials for electrons and holes 9-33252

diffusion coeffs., partial, from conc. meas. in zone of contact liq. layer with Cd and Sn, resp. 9-33003

diffusion in PbO evaporated thin films, autoradiographic exam. 9-26303

electrical conduction, size effect 9-33253

electrodifffusion in Hg and liq. Sn, effect of Tl, In and Sn additions 9-46623

electron emission, second., total yield and charact. energy losses 9-31008

electron mean free path, temp. depend. 9-30846

electron relax. time from magnetoacoustic oscillations and tilt effect 9-47072

electron relaxation time determ. from Alfvén waves absorpt in mag. field 9-37382

electrotransfer of small Sb and Zn impurities 9-48873

equilibrium boundaries, III-V and IV-V, from monitoring elec. resistance changes 9-41071

Fermi surface singularities, magnetoacoustic effect studies 9-39564

Fermi surfaces, DeHaas-van Alphen eff. studies 9-28446

film, complex impedance characteristics, 2-15 μ , equivalent circuit tested 9-37439

film, resistivity, anomalies 9-49020

film, thin, photoelectromagnetic effect meas. 9-47209

films, elec. conductivity and Hall effect, thickness dependence, 4.2°-300°K 9-33251

films, holograms with > 6% efficiencies and resolutions close to 1000 lines/mm 9-45970

films, orientation re. to substra e 9-44624

films, resistivity oscillations upon deform., 78° and 300°K 9-30845

films, size-quantized, magnetoresistance meas. rel. to non-extremal sections of Fermi surface 9-49021

films, thin, elec. conductivity and Hall effect, 4.2-300K 9-39582

galvanomagnetic coeffs., low-field, temp. depend. 9-49019

heat capacity, 1-30°K 9-47006

heat-transfer bonding betw. ceramic nuclear fuel and cladding 9-22892

impurities in Ni alloys and steels, determ. 9-28830

ionization multiplication M-shell vacancies arising from L-subshell vacancies 9-48407

Kerr polar effect, magneto-optical reson. obs. 9-47321

liquid, nuclear spin-lattice relax. of ²⁰⁹Pb 9-26134

magneto-optical reson., Kerr polar effect obs. 9-47321

magnetoacoustic attenuation, anisotropy of giant quantum. oscill. 9-37345

magnetoplasma waves, spatial dispersion effect on spectrum 9-30826

magnetoresistance, surface effect 9-30844

magnetoresistance anisotropy, carrier influence 9-41161

molten, electrical resistance meas. by rot. field method 9-39583

Nerst-Ettingshausen effect, anomalous, theoretical 9-47194

n.m.r. Knight shifts in rare-earth group-VA intermetallic cpds. 9-33648

nucleation, eff. of small addition of solute 9-28180

nucleation, NMR obs. 9-23583

nucleation, supercooling depend. on liq. drop size 9-28179

oxide films, orientation rel. to substrate 9-44624

photoelectromagnetic effect meas. in thin films 9-47209

proton energy losses 9-30807

resistance ratio in earth's mag. field, rel. to purity 9-33250

second-harmonic generation by damped Alfvén waves and helicons 9-41160

specific heat of metallic Bi, 0.05-0.8K, suppression of nuclear heat capacity 9-42967

spectrum in pulsed discharge, excitation and transitions, obs. 9-25692

substitution in rare earth orthoferrites, effect on mag. props. 9-32869

superconducting amorphous, phonon spectrum by electron tunneling 9-41076

superconducting film, transition temp. size dependence 9-30870

superconducting films, transition curves in perpendicular field, superconducting fluctuations 9-44931

surface tension, 1300-2200°K 9-28110

thermal expansion, down to 2°K 9-24054

thermal expansion, linear, 200° to 4.5°K, Gruneisen parameters 9-33189

thermo-e.m.f. and thermomag. props., 3° to 80°K 9-30984

thermoelectric power, anomalous behaviour at low temps. and high mag. field, theoretical 9-47193

whisker, elastically bent, resistance increase, below 300°K, rel. to electron mean free path meas. 9-37453

Bi:Ph, band structure from magnetoresistance and Hall eff. meas. 9-30843

Bi:Sn, distrib. coeff. and acceptor valency determ. 9-43002

Bi:Te, helicon dispersion relation, depend. on mass density 9-35395

Bi:Te, second-harmonic generation by damped Alfvén waves and helicons 9-41160

Bi:Te layered structure, helicon propag. rel. to carrier drift effects 9-43015

Bi, electron-hole recombination temp. dependence, 2-50°K 9-35306

Bi³⁺ in rare earth oxysulphates (Ln₂ SO₄), fluoresc., phosphors obs. 9-43258Bi³⁺ in Y₂O₃, Gd₂O₃ and Sc₂O₃, luminescence 9-31125Bi³⁺ in ZnS phosphor, electronic struct 9-24462

in GaP, impurity electronic trap, rel. to interimpurity recombinations 9-39866

in Na, molten, spin-flip scatt. of conduction electrons 9-32793

in Si, impurity absorpt. line shapes, effect of resonant phonon interactions 9-26741

Te-Bi photovoltaic eff. on contact of thin films 9-35511

Bismuth compounds

ferrite, mag.-acoustic resonance 9-37346

Ag-Bi eutectic, struct. of Ag-rich phase 9-37131

Bismuth compounds continued

- Al-Bi system, phase equil. obs., thermodynamic props. 9-46679
 Bi-Ag-Cs photocathode, spectral sensitivity rel. voltage changes 9-31006
 Bi-Sb alloys, magnetoreflection obs. of band struct. 9-41162
 Bi-Sb semiconducting alloys, magnetoresistance anomalies in strong mag. fields, 4.2° to 10°K 9-30890
 Bi-Sn alloys, crystal structure and superconducting props. under high pressures 9-23752
 Bi-Sn alloys, magnetoresistance anisotropy, carrier influence 9-41161
 Bi-Te alloys, nucleation, NMR obs. 9-23583
 Bi-50-60at%Te, phase characterization by X-ray diffr. patterns 9-28394
 Bi-Th system, Bi dissoc. press. 9-39937
 Bi_{0.37}Ca_{0.63}Fe_{2.65}V_{1.31}O₁₂ ferrogarnet, mag. anisotropy, -183° to 100°C 9-45131
 Bi_{1-x}Sb_x, mag. susceptibility, elec. resistivity, Hall eff. and magnetoresistance 9-30842
 Bi₁₂GeO₂₀, crystal prep. and optical transmission 9-40864
 Bi₁₂GeO₂₀, growth by Czochralski method, and props. 9-42751
 Bi₁₂GeO₂₀, piezoelec., elasto-optic matrix elements 9-33394
 Bi₁₂SiO₂₀, photoactivity and field-induced changes in optical rot. 9-35621
 Bi₁₂SiO₂₀, piezoelec., elasto-optic matrix elements 9-33394
 Bi₂K, supercond. transition temp. press. depend. 9-49048
 Bi₂O₃-TeO₂ films, optical absorption 9-35649
 δ-Bi₂O₃, cubic structure, electron diff. study 9-42783
 Bi₂O₃ layers, evaporated, prep., elec. and optical props. 9-39162
 Bi₂O₃-B₂O₃-(R₂O) glass systems, structure and props. 9-46698
 Bi₂Se₃, electrons effective mass depend. on carrier conc. 9-37390
 Bi₂Se₃, reflectivity spectra, 0.7 to 12.5eV 9-33538
 Bi₂Se₃ films, semiconducting properties 9-30889
 Bi₂Se₃ liquid, 700 to 1200°C in stationary state, thermal cond. 9-26094
 Bi₂Te₃-Bi₂Se₃ alloys, lattice thermal conductivity 9-41100
 Bi₂Te₃-Bi₂Se₃ pressed powder compacts, preferred orientation meas. by pulsed neutron diff. 9-32862
 Bi₂Te₃-(20 Mol.%)Bi₂Se₃ solid solns., thermoelec. props., conc. inhomogeneities influence 9-41252
 Bi₂Te₃, band structure, pseudopotential approach 9-44885
 Bi₂Te₃, lattice thermal conductivity 9-41100
 Bi₂Te₃, reflectivity spectra, 0.7 to 12.5eV 9-33538
 Bi₂Te₃ films, semiconducting properties 9-30889
 Bi₂GeO₁₂-Nd³⁺, electro-optic crystals, parametric oscills. of Nd³⁺ at room temp. 9-43203
 Bi₂GeO₁₂-Nd³⁺ coherent emission obs. 9-26738
 Bi₄(GeO₄)₃, Czochralski growth 9-23679
 Bi₄(GeO₄)₃, growth by Czochralski method, and props. 9-42751
 Bi₈₈Sb₁₂-Sn₁₂-Te alloy, thermoelectromag. props. 9-49154
 Bi₉₅Sb₅-Sn₁₂-Te alloy, thermoelectromag. props. 9-49154
 BiCaV ferrogarnet single crystal, rotatory mag. hysteresis losses 9-45136
 BiCrO₃, magnetic props. and crystal distortions 9-28608
 BiF, 2250A system, rotational structure 9-42383
 BiF, Franck-Condon factors and r-centroids for A-X₁ syst. 9-23074
 BiF₃, thermodynamic props. 9-30021
 BiFeO₃-Pb(Fe_{0.5}Nb_{0.5})₂ solid solution, spontaneous magnetic moment by neutron diffraction 9-33482
 BiFeO₃, atomic struct. 9-37135
 Bi₁₃Cr₁₄, e.s.r. of Cr³⁺ single ions and exchanged-coupled Cr³⁺ pairs 9-24482
 BiMn₂O₅, antiferromagnetic transitions rel. to mag. symmetry and ferroelec. 9-45208
 BiMnO₃, magnetic props. and crystal distortions 9-28608
 BiSb, orthorhombic needles growth, spectral transmission 570-650nm, 93-293°K, internal photoeffect, 293°K 9-32870
 BiSb alloys, emission of microwave radiation in weak electric field 9-31102
 Bi-(0.3 at.%)Sn alloy, isoenergetic surfaces struct. at L-maximum 9-35312
 In-Bi alloys, supercond., metastable states obs. 9-44938
 In-(3at.%)Bi magnetization curves, demagnetization coeff. dependence 9-26529
 InBi foil, effect of cold working on supercond. transition temp. 9-47078
 LiNbO₃:Nd³⁺, Tm³⁺, Ho³⁺ coherent emission obs. 9-26738
 Mg-Bi alloys, amorphous, prep. elec. conductivity and thermoelec. power 9-30851
 Pb-(0/25 wt.%)Bi, superconducting, surface-sheath nucleation field, temp. depend. 9-35366
 Pb-Bi alloys, d.h.c.p. phase form under h.p. 9-44802
 Pb-Bi eutectic, drop on stainless steel, surface tension and contact angle calc. from shape 9-34867
 Pb-(0-56.5at.%)Bi superconducting alloys, type I and II, rel. to mag. behaviour 9-43041
 Sn-Bi, thermal conductivity, solid and liquid states 9-24065
 Sn-(0.5-8.0)Bi alloys, Sn dendrite growth as function of supercooling 9-48815
 Ti-Pb-Bi alloys, superconductivity from tunneling meas. 9-24161

Bitter patterns *see Magnetization state/domains***Bitumen** *see Materials***Bloch walls** *see Ferromagnetism; Magnetization state/domains***Blood**

- aneurysms, intracranial occlusion by ferromag. thrombi 9-45699
 bubble dynamics, small insoluble gas bubble vibration characteristics 9-46603
 flow determ. by conjunctival photography 9-49605
 optical transmission for highly collimated light 9-45703
 Pu determination of contamination by anion exchange 9-29113
 vessel walls, piezoelec. eff. 9-38129

Boiling*see also Distillation*

- acetone, heat transfer depend. on e.m. field 9-23597
 application of rocket effect on bubbles 9-39068
 benzol, heat transfer depend. on e.m. field 9-23597
 binary mixtures, nucleate-type, study of local temp. fluctuations 9-26164
 bubble volume and dia. rel. to frequency 9-30459
 dielectric liquids, heat transfer, effect of elec. field 9-23596
 droplets evaporation rate, electrostatic force effects 9-34964
 ethanol, heat transfer depend. on e.m. field 9-23597
 ethyl alcohol growth on glass surface 9-30465
 film, laminar; boundary layer flows, heat transfer, phase flow and friction determ. 9-32816
 film boiling from elec. conducting wire to boiling water, heat transfer obs. at different pressures 9-30462

Boiling continued

- Freon 113 temp. profile of thermal sublayer on Cu horizontal surface during pool boiling 9-23598
 Freon 13, in critical region, by Pt wire, obs. 9-28186
 Freon-12, in region of centrifugal forces, heat transfer rel. to inertia over-loadings 9-23603
 heat transfer, effect of temp.-induced surface tension gradients 9-32776
 Hg, with thermal load up to 2×10⁶ Wm⁻² 9-44557
 immiscible liquid layers with simultaneous stirring, direct contact heat transfer 9-30461
 metals, analysis rel. to fast reactor safety 9-39142
 methanol, temp. profile of thermal sublayer on Cu horizontal surface during pool boiling 9-23598
 methanol temp. profile of thermal sublayer on Cu horizontal surface during pool boiling 9-23598
 mixture of liquids with widely different b.p. 9-23599
 natural convection, crisis mechanism, role of gas phase 9-23600
 nucleate, in liquid film, heating surface effects 9-36925
 pure liquid, nucleate, study of local temp. fluctuations 9-26164
 quartz layer, loss of u.v. transparency, causes 9-36880
 toluene, bubble growth on glass surface 9-30465
 water, heat transfer depend. on e.m. field 9-23597
 water, temp. profile of thermal sublayer on Cu horizontal surface during pool boiling 9-23598
 water, transient film boiling on horizontal submerged wire 9-28188
 CO₂ in critical region, by Pt wire, obs. 9-28186
 CaSO₄ aqueous solution, mass transfer characts. 9-23602
 D₂ moderator, local, risk study by heat exchanges with coolant channels 9-25673
 in He II heat induced counterflow, local 9-44609
 K in tubes, heat transfer coeffs. mean and local 9-23487
 K liquid, incipient superheat meas. 9-26165
 N₂, dispersed flow film boiling, expt and anal. 9-26166
 N₂, nucleate pool boiling rel. to surface roughness and material 9-28189

Boiling point

- refractory metal oxides, rel. to lattice energies and heat of atomization 9-30494
 solid and liquid elements, data 9-46689
 BiF₃, calculation 9-30021
 O, reproducibility, press.-temp. relation near 1 atm. 9-26168

Bolometers

- detector for very-far infrared, fast with high-responsivity, theory, construction and performance 9-40284
 hypersound detection, 3 GHz and 3.7°K 9-45863
 solid state, range i.r. to mm 9-41840
 superconducting, equiv. cct. 9-44947
 thermistor, for monochromatic light meas. 9-47832

Boltzmann equation *see Transport processes***Bonding of materials** *see Adhesion***Bonds***see also Molecules*

- acetaldehyde (-di), electro-optical props. of C=O, C-C and C-H bonds 9-27884
 acetylene, high content in polymerized dimethylvinylethynylcarbinol 9-24553
 alcohols, OH stretching freqs., influence of hydrogen bonding on anharmonicity 9-30070
 alkali halide cryst., diatomic, interatomic forces and cohesive energies 9-28250
 alkali halide diatomic molecules, binding energy calc. 9-48452
 alkali halides, interionic separation correl. with interparticle distance at m.p. 9-35007
 alkali halides, ionic radii deriv. using repulsive energy method 9-35006
 alkali halides, ions temp. parameters 9-30507
 alkali halides, lattice energy calc. 9-40852
 n-alkyl acid far i.r. spectra, H bond stretching vib. determ. 9-23087
 alkyl ammonia anions-nonyl alcohol H-bonds, i.r. obs. 9-27885
 allosteric enzymes. Monod-Wyman-Changeux, model, quaternary structure and cooperative ligand binding 9-34695
 alloys, electron effects w.r.t. exothermic binding energy 9-39180
 alternation in polyenes 9-44348
 amines, NH₂ group H bonding rel. to valence vibrs. 9-34653
 bis(diphenylmethyl) diselenide, X-ray analysis 9-39322
 chemical, influence on high-energy n cross-sections 9-30547
 chemical and ion valence from X-ray microanalysis of emission spectra fine structure 9-37739
 chemical for elements 12<Z≤18, from X-ray emission spectra 9-37740
 chloroform, interaction with electron-donor mol. 9-23518
 chloronitrobenzenes in THF, H bonding between aromatic ring hydrogens and the ether, evidence from u.v. spectra 9-30095
 citric acid, anhydrous, X-ray diffr. obs. 9-35074
 citric acid, anhydrous, X-ray diffr. obs. 9-44677
 covalence effects on second moments of e.s.r. absorpt. curves for complex ions 9-31167
 covalent bond formation, softness of acceptors and donors, classification 9-38818
 covalent-ionic transition in electronic nature of solids 9-39183
 cumene hydroperoxide solution, H-bonding investigated by i.r. absorpt. 9-27892
 cyclic molecules, superpositioning 9-26255
 dibromomethyl radical 9-44378
 dichloromethyl radical 9-46425
 2,4-dichlorophenyl methyl isopropylphosphoramidate, intermol. H-bonds rel. to n.m.r. asymmetry, obs. 9-27879
 3,5-dichlorosalicylaldehyde, intramolecular H, temp. depend. of chemical shifts of protons 9-34665
 dimethylglyoxime crystal, H bond distances and angles 9-40853
 4,5-dioxo-2-thioxo-1,3-dithiolan, β form 9-39328
 2,5-diphenyl-1,3,4-oxadiazol dioxo derivatives of scintillator activators, intermol. H-bonds, obs. 9-30414
 electric field gradients screening const. calc., rare earth ions 9-22955
 electron affinities of heavy elements 9-44274
 electronegativity in covalent systems, quantum dielec. theory, electronic dielectric constant 9-46735
 estriol, effect of differences in hydrogen bonding on molecular structure 9-39333
 ethyl cyanide, cylindrical symmetry about CN bond from hyperfine struct. exam. 9-38890

Bonds continued

- ethyl fluoride dissolved in nematic liq. cry., coupling const. absolute signs, NMR obs. 9-40613
ethylene thiourea, C=S bond force constant queried 9-30112
ethylenes, monosubstituted, J13- π coupling constants 9-27894
Fe (III) complexes, covalency 9-28225
fluorides, effective ionic radii 9-39182
glycine chelates, isomeric, far i.r. spectra, metal-O bond stretching vib. 9-27898
group IIB halides 9-40589
H-bond length, isotope effect 9-42370
halides, energies, force constants, mean-square quantities, universal parameter 9-38840
halogenated ethylenes, two-bond, C-proton coupling const. 9-44358
heterocyclic systems containing 2.41 and 2.64 Å sulphur-oxygen distances, Huckel calcs. 9-46378
homonuclear diatomic mols., bond order 9-42369
hydrazinium hydrogen oxalate, cryst., H-bond symmetry, D-substitution effects, obs. 9-24393
hydrides, second-row diatomic, molec. charge distrib. and binding 9-48464
hydrocarbons chemisorbed on metal surfaces 9-39948
hydrogen, bifurcated 9-23653
hydrogen bonding, influence on anharmonicity of OH stretching vibrations 9-30070
hydroxy crystals, evidence for non-H-bonded hydroxyl groups 9-42739
N(4)-hydroxycytosines, H-bond assoc. with purines 9-42635
1-(β -hydroxyethoxy)-2,4-dinitrobenzene, intermol. H bonding, NMR detect. 9-27900
inorganic binary compounds, correlation between bond energies and forbidden bands 9-48780
insulating cryst., lattice energy, pair pots. and ionic radii, use of models of forces between atoms 9-44635
interaction energy surfaces in dimers, determination for formic and acetic acid dimers 9-38822
interatomic binding energy in solids rel. to semiconduction 9-30894
iodomethanes, iodine bond hybridization, Mossbauer determ. 9-32519
ionic crystals, lattice self-potentials and Madelung const. 9-36973
ionic radii, radii, multivalent self-consistent set derivation 9-32854
ionicity, dielectric definition 9-38820
ligand field spectra, characterization by diffuse reflectance spectroscopy 9-37672
liquids, organic, cohesion energy-vol.-temp. relations, obs. 9-28094
London-van der Waals forces, pairwise additivity, Drude model calc. 9-28223
Madelung energies of centrosymmetric struct., direct summation, computerized procedure 9-30506
mercuric halide adducts of cyclic thio-ethers, Hg-S bond 9-30107
metal oxides, covalency 9-44637
metal-ligand σ and π bonding in pyridine complexes 9-23038
metals, interionic separation correl. with interparticle distance at m.p. 9-35007
metals, monovalent, cohesive energies from virial theorem applic. 9-39179
methanol and methanol-trimethylamine mixtures, H-bonding from n.m.r. meas. 9-48500
methyl compounds of some group I, II and III elements, factors by Huckel calc. 9-46403
methylolithium, from n.m.r. meas. 9-46405
N-methylthiourea in nonpolar and polar solvents, rot. barrier about C-N bond from n.m.r. meas. 9-46658
molecular, participation of d orbitals 9-40583
molecular crystals, dielectric constant formulation of long wave-length binding energy 9-35005
molecular overlap integrals involving f orbitals, potentials for numerical integration 9-32455
molecules, inactive, role of H bonding in optical activity 9-48700
organic cpds., inter- and intra-mol. H-bonding rel. to absorpt., fluoresce. band widths, obs. 9-23081
organophosphoryl compounds containing N-P and S-P bonds, hydrogen bonding ability 9-30138
oxide systems, effect of cationic field strengths in liquids 9-23579
oxides, O K-spectra, investigation of chem. bonding 9-49304
oxides effective ionic radii 9-39182
oxygen-tetrahedra cpds., geometric contrib. to non-linear polarizability 9-35611
 p - π conjugation, rel. to hybridization of AO of nonbonding pair of electrons 9-48485
pentafluorophenyl derivatives, π interactions and bonding in selected compounds 9-42435
phenol, OH stretching freqs., influence of hydrogen bonding on anharmonicity 9-30070
3-phenylisoxazolin-5-one, X-ray obs. 9-35077
3-phenylisoxazolin-5-one, X-ray obs. 9-42801
phosphates, crystalline condensed, dihedral angle determ. 9-40906
polyisoprene, polymerized on β -TiCl₃, i.r. obs. 9-27937
propanoic acid far i.r. spectra, H-bond stretching vib. determ. 9-23087
proton in H-bonds, lingering time in wells of double-minimum potential 9-23023
pyridine complexes of iodine monohalides, from Mossbauer effect of ¹²⁹I 9-34688
quartz, surface conc. of broken bonds on fresh face 9-46734
quinclidinyl benzoate hydrobromide 9-35078
refractory metal oxides, energy values and dissociation energies 9-30494
sandwich complexes, covalency 9-42420
semiconductors, diamond-type, covalency 9-30915
semiconductors and semimetals, configuration of bonding electrons causing excess entropy of fusion 9-28175
silica gel, H-bonding in interaction of adsorbed mols. with surface OH groups 9-23650
siliceous materials, surface conc. of broken bonds on fresh face 9-46734
silver nitrate adducts of cyclic thio-ethers, Ag-S bond 9-32512
stretching-energy curves from integral Hellmann-Feynman method 9-30012
succinic acid crystal, H bond strength and vibs. from i.r. and Raman spectra 9-35668
surface bonds of adsorbed species, orbitals involved study by photoelectron spectroscopy 9-44634
thio-ethers, cyclic, mercuric halide adducts, Hg-S bond 9-30107
thio-ethers, cyclic, silver nitrate adducts, Ag-S bond 9-32512

Bonds continued

- transition metal borides, theory test from heat capacity meas., 1.5-18°K 9-28445
transition metal carbides, binding energy shifts electron spectroscopic meas., charge transfer obs. 9-44636
transition-metal complexes 9-23744
treated in quantum mechanics textbooks 9-41756
triglycine sulphate, H-bond vibrations 9-32516
undecanoic acid far i.r. spectra, H-bond stretching vib. determ. 9-23087
valence-bond calcs. for electronic struct. of methylene 9-46404
valence-bond theory of contact nuclear spin-spin coupling by Penny-Dirac bond orders 9-46348
water, fraction of broken H bonds, rel. to structure 9-28099
water, H-bond energy for clusters in vapour phase 9-44616
water, H-bonding obs. from stimulated Raman spectrum 9-34911
¹¹⁹Sn monomeric and polymeric cpds., influence on temp. depend. of anisotropic Lamb-Mossbauer factor 9-27915
AgCl, ions deform., X-ray obs. 9-30507
Al/As-S glass, composite system, bonding mechanism 9-32852
Al, binding energy, single-orthogonalized- plane-wave, Hartree-Fock calc. 9-24081
 α - and γ -Al₂O₃, O K-spectra, investigation of chem. bonding 9-49304
As-O in tetrahedra AsO₄²⁻, geometric contrib. to non-linear polarizability 9-35611
BaTiO₃, oxygen nonstoichiometry and hydrogen bonds 9-35105
BiF₃, Bi-F bond energy, derivation and comparison with other group VA halides 9-30021
(CH₃)₃CX, C-X band bond lengthening, Lide effect 9-23139
CN chemisorbed on metal surfaces 9-39948
CO chemisorbed on metal surfaces 9-39948
CaSO₄·2H₂O, HDO mol. vibs. rel. to pot. environment, obs. 9-24391
Cl s orbitals in molecules, s character determ. from n.q.r. and BEEM 9-32454
CuCuCl₂, thermal and mag. obs. 9-24044
Cs-Mg solid solns., dilute, binding energy between dislocation and Mg atom 9-37175
Cu, force const. of Be impurity atoms, variations 9-39181
Cu and Sn, cohesion coeffs. of virgin surfaces, investig. methods 9-28203
Dy silicides and germanides, charact., Mossbauer effect obs. 9-37696
Eu silicides and germanides, charact., Mossbauer effect obs. 9-37696
Fe complex, bis-dithioacetate tetrachloro ferrate (II), FeII bonding, Mossbauer obs. 9-38842
Fe complex, tetramethyl ammonium liq. tetrachloro ferrate (II), to FeII bonding, 78°K Fe II bonding, Mossbauer obs. 9-38842
Fe(III)Cl₃, from solute structure obs. in methanol 9-34878
FeLiO₂, electrostatic energy, local displacement of ions and short-range order 9-48935
 β -Ga₂O₃, O K-spectra, investigation of chem. bonding 9-49304
GaAs, covalent charge transfer 9-33302
GaSb, covalent charge transfer 9-33302
GeO₂, ionic character of Ge-O from cryst. energy calcs. 9-30504
GeO₂, vitreous state, vibrational analysis using i.r. absorpt. and reflection spectra 9-28196
H-bond strengths, significance of i.r. freq. shifts 9-25726
H-bonded syst. in conc. soln. of NH₃ salts in liq. NH₃ and NH₄Cl, 3NH₃, i.r. spectra study 9-30042
H, between OH and nitro groups, i.r. spectra 9-23080
H, far-i.r. obs., vibr. assignments 9-32453
H, in Na ethyl sulphate monohydrate, Raman and i.r. spectra obs. 9-24431
H, mol. to metallic transition 9-42738
H₂B₂O₃, lengths, molecular-orbital treatment 9-39279
H₂Fe(CN)₆ cryst., H-bond obs. 9-23756
H bonding in methanol and methanol-trimethylamine mixtures, n.m.r. meas. 9-48500
H in BeSO₄·4H₂O, i.r. vib. spectra obs. 9-24423
HCN, lattice energies, high and low temp. forms, calc. as sum of long- and short-range interactions 9-30505
HCO₂ and DCO₂, O-H-O and O-D-O bonds 9-32908
HNO₃ and DNO₃, normal co-ord. treatment for physically true force const. in vapour and liquid states 9-46362
³He, binding energy at zero temp. 9-34939
Hf₂, e , density in H atom, theory and expt. 9-23759
In₂O₃, O K-spectra, investigation of chem. bonding 9-49304
InAs, covalent charge transfer 9-33302
KD₃(SeO₃)₂ ferroelec. single cryst., H-bond role in phase transition 9-32855
KH₂(SeO₃)₂, H-bond role, KD₃(SeO₃)₂ dielec. const. temp. depend. obs. 9-32855
Li₂RhH₃ (X=As), X-ray, neutron diff. and e.p.r. meas. 9-48834
LiD₃(SeO₃)₂ ferroelec. single cryst., H-bond network, deuteron mag. reson. obs. 9-33389
LiO₂, i.r. 9-43333
MnCl₄²⁻ tetrahedral complexes, covalent bonding 9-37799
MnCl₄²⁻ octahedral complexes, covalent bonding 9-37799
Mn(II) complexes of spin- $\frac{1}{2}$ with large ligand field splittings 9-41428
Na⁺, geometries by approx. SCF-MO theory which considers intermol. differential overlap 9-34637
NH₄F, N-H bond distances, neutron and X-ray diff. obs. 9-32923
Na, b.c.c. and h.c.p., binding energy 9-42737
Na[Cu(NH₃)₄][Cu(S₂O₃)₂] e.s.r. absorpt. curves, covalence effects on second moments 9-31167
Na energy, calc. 9-42950
NaCl, ions deform., X-ray obs. 9-30507
NaD₃(SeO₃)₂ ferroelec. single cryst. H-bond network, deuteron and ²³Na mag. reson. obs. 9-33392
NbO₂, collapse of long-range ordering of Nb-Nb w.r.t. phase transition 9-33143
O₄²⁻, O₄²⁻, geometries by approx. SCF-MO theory which considers intermol. differential overlap 9-34637
OH in mica, i.r. spectroscopic obs. 9-31099
P-F geminal coupling const., sign inversion 9-46412
P-F in tetrahedra PO₄²⁻, geometric contrib. to non-linear polarizability 9-35611
P₂O₁₀, P-O bond orders, vibr. obs. 9-27871
P₂O₆, P-O bond orders, vibr. obs. 9-27871
Pb complex, lead (II) O, O-diisopropylphosphorodithioate 9-42794
 α -Pb(N₃)₂, neutron diffraction structure study 9-39300
Pd complex, Pd(II)X₂Y₂(X=Cl, Br or I, Y=MeS₂P or MeAs), degree of π bonding in Pd-P and Pd-As bonds 9-30052

Bonds continued

- Pt complex, potassium amminotrichloroplatinate monohydrate, bond lengths 9-26244
 Pt complex, Pt(II)X₂Y₂(X=Cl, Br or I, Y=Me₃P or Me₃As), degree of π bonding in Pt-P and Pt-As bonds 9-30052
 Re(CO)₆⁺, Re-C bond strength, effect of charge on Re, degree of back-bonding estimation 9-32491
 S-O in tetrahedra SO₄²⁻, geometric contrib. to non-linear polarizability 9-35611
 SO₂ polymeric, potential energy calc. Van der Waals interac. 9-46736
 ScH₃NH₃, SCF calc. 9-42419
 α Sn, semicond., covalent bond in rel. to neutral pseudo atom concept 9-28507
 SnL₂ Mossbauer studies reveal nature of bond in molecular crystal 9-34643
 SnO₂, ionic character of Sn-O from cryst. energy calc. 9-30504
 ThC, chemical bonding and mag. susceptibility at various temp. 9-28224
 Ti cpds., binding energy shifts electron spectroscopic meas., charge transfer obs. 9-44636
 TiH₃F, SCF calc. 9-42419
 TiO₂, ionic character of Ti-O from cryst. energy calc. 9-30504
 UC, chemical binding effect on neutron scatt. of C atoms 9-23776
 V cpds., binding energy shifts electron spectroscopic meas., charge transfer obs. 9-44636
 V(CO)₆⁻, V-C bond strength, effect of charge on V, degree of back-bonding estimation 9-32491
 W, bonding of surface atoms 9-26181
 Y, lengths from K-absorpt. spectra 9-39859
 Yb silicides and germanides, charact., Mossbauer effect obs. 9-37696
 Zr, 2-d crystals on W and Nb, binding energy from temp. depend. of growth 9-23652

Bone *see* **Materials****Bootstrap theory** *see* **Elementary particles**; **Field theory**, **quantum****Bordoni effect** *see* **Acoustic wave propagation**/**ultrasonic**; **Damping**; **Internal friction****Boron**

- atom, core polarization and hyperfine structure calc. 9-46273
 atom, $g_2(2F_{1/2})$ factors, calc. 9-36658
 atom, hyperfine structure calc., g.s. first-order wave function 9-32408
 atom, polarization wave functions for ground state 9-34532
 carrier mobility, trapping levels and temp. depend. 9-28494
 diffusion in n-SiC:N in prep. of electroluminesc. diodes, anomalous nature 9-37776
 diffusion in Si 9-48877
 diffusion in Si, strain compensation rel. to dislocation generation obs. 9-46824
 diffusion through SiO₂ layers into Si 9-48876
 in enriched U soln., critical obs. 9-34498
 filament, vapour deposited on W, cracks rel. to chem. interaction 9-48866
 filament coated with SiC, tensile strengths after exposure to air 9-30679
 filaments, vapour-deposited, crystal structure 9-46780
 gaseous transport species deposition on Si 9-37534
 graphite:B, neutron irradi., effect of conc. on defect clustering, physical prop. meas. 9-30597
 graphite:B, neutron irradi., effect of conc. on interstitial loop nucleation 9-30596
 graphite:B, neutron irradi., effect of conc. on interstitial loop clustering, electron microscope obs. 9-30595
 implantation in silicon, range 9-44856
 isotope effect on ZrB₁₂ supercond. transition temp. 9-24132
 isotopes formation cross section for proton spallation of ¹⁶O 9-44203
 K-emission spectra of B 9-24436
 microcryst. particles modifications prod. by transit of induction coupled Ar plasma 9-37133
 neutron filter, spectrum-hardening, for fast flux testing in thermal reactor 9-36642
 origin in solar system 9-36015
 photoconductivity, single crystals and films 9-35500
 precipitation in silicon 9-37164
 solubility in α -SiC in SiC-B₂C system at approx. 2450°C 9-48939
 in steels, Mo, quenched and tempered, influence on carbide precip. 9-48931
 X-ray emission spectra in ultrasoft region, energy band structure determ. 9-37742
 X-ray scatt. spectra, Cu K α and β_1 rad. 9-45338
 β -B, rhombohedral, thermal conductivity, 80° to 1100°K, rel. to crystal struct. 9-44845
 B, thermally stimulated current, trapping processes obs. 9-43062
 B²⁺, ²⁵S, spin-optimized, self-consistent field wave function determ. 9-40544
 B²⁺, ²⁵S, spin-optimized, self-consistent field wave function determ. 9-40544
 B III, mean lives of 2p²P⁰ levels, oscillator strengths 9-44256
⁹Be, K-mesic X-ray yields 9-36685
 Ge:B, i.r. absorpt. rel. to hole transitions from impurity levels to valence band 9-44981
 Ge:B, i.r. absorpt. rel. to hole transitions from impurity levels to valence band 9-44981
 Po-B neutron source, scatt. in cylinder of water, distrib junction calc. 9-22841
 Si:B, electron-irrad., defects effect on photoconductivity spectra 9-44985
 Si:B, i.r. absorpt. rel. to hole transitions from impurity levels to valence band 9-44981
 Si:B, impurity-assisted intervalley electron scatt. 9-43076
 Si:B, quenched in defects, elec. and photo-conductivity obs. 9-39357

Boron compounds

- BAs, cubic; B contact with As vapour, 700-900°C, patent 9-23664
 borides, plasma refl. edge and u.v. reflectivity obs. 9-39802
 borohydrides of Li, Na and K, n.m.r., internal rotations and phase transitions 9-43308
 borolanthanum glass, immiscibility and catalytic crystallization, additions of various oxides 9-34971
 borosilicate, diffusion of Ag⁺ in elec. field, dendritic growth obs. 9-48872
 carbide-boride-graphite ceramics, fusion-cast, phase assemblages, microstruct. props. 9-30729
 halides, solid ¹¹B quadrupole coupling consts. 9-43296
 hydride derivatives of group IV and V, i.r. absorpt. spectra 9-42381
 mixed halides, ¹¹B-¹⁹F nmr coupling constant, rel. to ¹⁹F chemical shift 9-32464

Boron compounds continued

- soda-boric oxide glass, e.s.r. and optical spectra of Cu²⁺ 9-37800
 triphenylborate, i.r. spectra 9-23164
 B₂Cl₄, molec. struct. and internal rot., electron diff. 9-44319
 B₂H₆, B nuclear spin-lattice relax. 9-42681
 B₂H₆, comparison of struct. determ. by electron diff. and spectroscopy 9-36713
 B₂O₃-PbO-Al₂O₃ system glasses, spinodal decomposition 9-39492
 B₂O₃, K-emission spectra of B 9-24436
 B₂O₃, viscosity, pressure depend., 380° to 465°C 9-26084
 B₂O₃ formed from oxidation of boronated graphite 9-28795
 B₂O₃ mol. config. electron diff. obs. 9-23029
 B₂C, cry. growth and two-dimens. nucleation at screw dislocations, obs. 9-28290
 B₂C, K-emission spectra of B 9-24436
 B₂C absorbers, effective boundary conds. applic. to cluster control calcs. 9-22885
 B₂H₆, B nuclear spin-lattice relax. 9-42681
 BAs, orthorhombic; B contact with As vapour, 900-1200°C, patent 9-23664
 BF₃ counter bank, improved, mixer circuit for neutron time-of-flight meas. 9-29646
 BH, mol. props. and electronic structure in ground and excited states 9-38830
 BH, optical emission spectrum, Stark effect, X(¹ σ) and A(¹ π) dipole moments determ. 9-46357
 BH₃, dissociation energy 9-43314
 BH₃CO, pyrolysis energetics 9-43314
 BH₄⁻ vibrations characts. and forms 9-42382
 BN, corrosion and conductivity in cryolite-Al melts 9-28798
 BN, growth from metal solutions 9-37017
 BN, K-emission spectra of B 9-24436
 BN, pyrolytic, struct. transform. on annealing or hot working 9-41041
 BN X-ray determ. of electron band structure 9-30811
 BN X-ray emission spectra in ultrasoft region, energy diagrams determ. 9-37742
 BO α system, rotational analysis of 0,2 band 9-44317
 BP, X-ray determ. of electron band structure 9-30811
 BS molecule, ² Δ -A² Π ; and two ²S⁺-² Π transitions 9-30022
 B-S-C, solid soln. cathode for MHD, electron emissivity 9-24253
 Cl₃BN(CH₃), field gradient calc. 9-23030
 Cu-B alloy, dilute, formation of He bubbles on irradi., influence of precipitates 9-41116
 D₂BN(CH₃), d.m.r. 9-33643
 H₂BNH₂, field gradient calc. 9-23030
 Na-B-Si glass, spectra, Raman, c.p.r., i.r. and electronic 9-26757
 Ni-Ga-B dil. alloys, phase equl. during solidification 9-39136
 UO₂, 6% enriched, -0.05 wt% B₂C reactor fuel irradi. stability, 1000 and 5000 MWd/te burnup 9-32389
 ZnO-B₂O₃ syst., eutectic solidification forming lamellar glass-cryst. structures 9-36930

Bormann effect *see* **X-ray diffraction****Bose gas** *see* **Quantum fluids**/**boson systems****Bosons**

- see also* **Gravitons**; **Mesons**; **Photons**; **Quantum fluids**/**boson systems**; **Statistical mechanics**/**quantum**
 antiparticle concept rel. to relativistic scatt. 9-48147
 considered as discrete quantized states of internal struct. of elementary particles 9-43980
 cross-section, production, attempt to establish an upper limit, in 400 MeV mass region for neutral bosons 9-22573
 fields, under general class of cut-off interactions 9-22518
 higher multipoles, suppression factor rel. to existence 9-22554
 leptonic, contrib. to lepton magnetic moment by Yukawa-type interaction 9-34254
 many body problem with repulsive potential, quantum mechanical treatment 9-38456
 neutral, production cross-sections, attempt to establish an upper limit, in 400 MeV mass region 9-22573
 OBE mode of two and three π contrib. to N-N scatt. 9-44051
 octet mass formula deduced using SU(3)@SU(3) charge algebra 9-38540
 radiation in field of two plane linearly polarized e.m. waves moving towards each other 9-41851
 resonance, decay into two spin $\frac{1}{2}$ particles, analysis 9-32121
 resonances, a review 9-40432
 resonances, production cross-sections in p-p collisions at 4 GeV/c 9-38569
 resonances and their octets and singlets 9-22554
 resonating, mass, spins 9-29550
 spin zero boson-boson system of zero total mass, soln. cp Bethe-Salpeter eqn. 9-38449
 spinless, interacting, nonrelativistic quantum mech. in terms of currents 9-29532
 Wick theorem for boson system, allowing evaluation of time-ordered products of Heisenberg operators 9-46038
 zero-mass, soft coupling to other particles, S-matrix study 9-32115
 NN scatt. T=O state, one-boson exchange 9-32212
 W, 2-30 GeV production in neutrino beam 9-27450
 W, partial decay rate into two pseudoscalar mesons, pseudoscalar and vector meson, p+n 9-22607

Boundary layers

- atmosphere, models, finite-difference methods 9-24678
 atmosphere, turbulent nonadiabatic diffusion of suspensions 9-31304
 atmosphere, turbulent region, influence of baroclinicity and nonstationarity 9-40018
 atmosphere above steppe and sea, turbulence 9-37911
 atmospheric, two dimensional time dependent numerical model 9-43391
 compressible, near fixed wall, velocity overshoot from anal. of similar solutions 9-25809
 convection, free, flow past isothermal semi-infinite isothermal plate, asymptotic soln. for large Prandtl n.b. 9-30387
 convection, laminar, over heated surface, instability and disturbance amplification 9-34895
 convection, on plane vertical isothermal wall, stability criteria 9-25126
 convection at low Prandtl number, effects of transverse press. grad. and streamwise second derivs. 9-23481
 differential eqn., ordinary non-linear, soln. method 9-22049
 Ekman, atm. development at leading edge 9-28860
 Ekman, magnetic field effect 9-30194

Boundary layers continued

- Ekman composite, for flow induced by infinite rotating disk near stationary coax. disk 9-46431
 elastico-viscous fluid, fluctuating flow past porous wall with variable suction 9-34734
 electrode surface double layer, Poisson's eqn., uniform boundary functions for certain one-dimens. form 9-35752
 flow, asymptotic, non-Newtonian, with suction 9-23219
 flow, injection effects in high Prandtl number 9-27951
 flow around cylinder at Reynolds numbers 40, 200 and 500, numerical soln. 9-34848
 flow of radiating gas, limiting soln. 9-26002
 flow over heated vertical plate, effect of buoyancy forces 9-34729
 flow problem, mathematical similarity to conc.-dependent diffusion problem 9-38945
 fluid, viscoelastic, flow equations 9-36836
 gas, diatomic seeded, elec. props. 9-26036
 gas slip flow, soln. for general specular-diffuse boundary cond. in kinetic theory 9-40733
 heat conduction in solids, approximations 9-41094
 heat transfer from hypersonic, laminar flow to blunted cone 9-36800
 with injection, turbulence, calculation 9-42601
 laminar, flow studies for Mach nos. to 15 9-46433
 laminar, transient free convection heat transfer from vertical plate, eqns. 9-22291
 laminar compressible, flow soln. by quasilinearization 9-23371
 laminar compressible eqns., reverse flow solns. 9-32575
 laminar incompressible, effects of displacement thickness, longit. curvature, external shear and slip 9-34722
 laminar natural convection, stability 9-25811
 magnetic, non-viscous, in flow round dielectric body, with field originating in dielec. 9-25826
 magnetic non-viscous, non-stationary flow 9-30189
 MGD, similarity transformations 9-25838
 at MHD channel generator electrodes, rel. to efficiency 9-29366
 at MHD converted cold electrode, interacts. with basic flow, and effects 9-25167
 mixing of two parallel streams, laminar, displacement effects 9-36742
 multicomponent laminar, behaviour prediction using integral-matrix method 9-23216
 non-linear interaction of inertial modes, rel. to steady geostrophic circulation 9-46435
 non-stationary, near rotating disc 9-23220
 over porous plate with variable suction or injection velocity, heat and mass transfer 9-25998
 phase interface near critical point, effect of gravity on position 9-36859
 plate plane in supersonic flow field, vel. fluctuations 9-40636
 planetary, helical circulations, Lagrangian study 9-26921
 planetary flow with neutral thermal stability, wind spiral model 9-41501
 plasma, MGD, two-dimensional, similarity solutions 9-40654
 plasma, mobility-controlled, charge distrib. obs. by ion collection probe 9-25908
 plate, flat, impulsively started, fluid flow 9-34739
 polarization anal. in electroanalysis of two-dimens. laminar flow 9-47464
 reverse transition, special cases of general Reynolds-number criterion 9-34727
 reverse transition criteria for two-dimens. turbulent flow 9-34824
 on rotating airfoils, theory and soln. for incompressible layer 9-26004
 rotating cylinder of fluid, soln. of centrifugally driven thermal convection 9-34720
 rotating plate in elastico-viscous liq., flow reversal due to edge effects 9-39063
 roughness drag at Mach 3, heat transfer eff. 9-23386
 second harmonic generation at boundary of isotropic medium 9-22439
 shear flow instabilities in rotating systems 9-23233
 shear layer between two parallel streams in two-dimensional flow 9-23234
 shear layer effect on plane sound waves in fluid 9-45856
 in shock tube, dependence on shock strength 9-45868
 shock-induced on flat plate, heat transfer and transition to turbulence 9-40739
 stratified rotating fluid, time-depend. motion 9-46447
 stratified rotating fluid in spherical annulus of narrow gap, steady axially symmetric motion 9-46449
 temperature and electrode effects in MHD-generators 9-22330
 thermal, round rotating sphere, schlieren method study 9-29327
 three-dimensional, surface-vel. grad., meas. technique 9-30359
 transition on slender cone in hypersonic flow, circumferential nonuniform heating 9-44517
 transitions in supersonic aerodynamics 9-32727
 turbulent, 3-D, attachment line calc. and expt. in wind tunnel, for swept wing 9-39037
 turbulent, compressible, on flat plate with air injection, experiment 9-42586
 turbulent, compressible, study on coefficient of local skin friction 9-30181
 turbulent, compressible, with pressure gradient 9-23218
 turbulent, diffusion from line source 9-34842
 turbulent, on impermeable plate, heat transfer rel. to boundary conds. 9-27240
 turbulent, in tidal current, dynamics 9-39996
 turbulent, interaction with an oblique shock wave 9-22268
 turbulent, noise transmission from, through flexible plate into closed cavity 9-45866
 turbulent, pressure fluctuations resolution, effect of transducer size 9-45862
 turbulent, reversion to laminar flow in presence of severe favourable press. grad. 9-39036
 turbulent, three-dimensional, wall similarity 9-23217
 turbulent flow on smooth wall, effect of press. gradient on law of wall 9-34725
 turbulent patch formation in transition boundary layer 9-23425
 in vapour-gas mixture at tube wall behind shock wave 9-39140
 vehicle/water, nearfield flow noise generation 9-45865
 velocity gradients at surface, for flow round cylinder at Reynolds numbers 5×10^3 to 10^5 9-34847
 in vertical slot, stability of natural convection 9-40745
 in viscous liquid flow past body with mag. field in dirn of flow 9-28082
 viscous magnetospheric, analysis 9-33802
 at wall of converging funnel, velocity profiles for swirling flow 9-34846

Boundary layers continued

- water, liquid oscillation meas. by obs. tension in fibre suspended at right angles 9-32750
 water, turbulent thermal, study by forced convection 9-23424
 Ar gas flow, temp. $\leq 1500^\circ\text{C}$ press. 1 atm.; soft X ray absorption obs. 9-40735
Bragg reflection see *X-ray crystallography*
Brass see *Copper alloys*
Bravais lattice see *Crystal structure, atomic*
Breakdown, electric
 see also *Discharges, electric; Electric strength*
 insulator surfaces in vacuum, obs. 9-23360
 p/n planar junctions, breakdown voltage by SiO_2 diffusion masks 9-41223
 p-n junction, planar, breakdown voltage, increase using punch-through controlled surface 9-28525
 plasma, charged arc, in Cs vapour, spectral line intensity and complexity 9-38971
 plasma-electrode system, investig. 9-40724
 of teflon capacitors 9-37586
 time-lags, statistical distrib. by Townsend mechanism under high-energy particle irradi. 9-48637
 transistor, h.f. power, increased reverse voltage, patent 9-41226
 vacuum, between plane electrodes, with spontaneous pre-breakdown current increase 9-48638
 vacuum literature digest, 1967 9-33368
 voltage meas. between 2-cm brass spheres with gaps <0.005 cm, effect of irradiation 9-34813
 water, trigger spark-effect 9-32709
 CaF_2 capacitors 9-37586
 CeF_3 , CeO_2 capacitors 9-37586
 MgF_2 capacitors 9-37586
 SiO_2 capacitors 9-37586
 air, delay time increases at high elec. fields 9-44510
 air, impulse breakdown, secondary leader channels obs. 9-44511
 air, microwave breakdown temp. depend. 9-32708
 air, spark, primary and secondary streamer dendrites 9-28051
 air discharge at 7.5-20 cm gap distances 9-48623
 current, pre-breakdown in high vacuum, voltage dependence 9-44509
 diatomic, breakdown pot., secondary ionization coeffs., mild steel electrodes 9-34812
 h.f. pulsed, with nonuniform fields, variational prediction 9-30353
 laser beam-induced, bibliographical review 9-25985
 laser-induced, elec. field distrib. along beam axis 9-28055
 laser-induced, enhanced plasma heating at shock front 9-30233
 literature digest, 1967 9-33368
 microwave, at low pressure, acoustic measurements and convective effects 9-32707
 multiple-electrode (vacuum) gap characts., influence of low pressure hydrogen 9-41883
 optical, by laser operating in mode-synchronization regime 9-25984
 plane air-gap, field strength meas. rel. to additional space charges 9-23361
 polyatomic, breakdown pot., secondary ionization coeffs., mild steel electrodes 9-34812
 radiation-driven breakdown wave propagation, hydrodynamic model, ionization effects 9-42614
 spark gap in air, laser-produced, polarity effects 9-32706
 statistical investigation, medium pressures 9-30316
 in uniform field discharge gap, probability calcs. 9-39031
 u.v.-initiated directional breakdown 9-28052
 vacuum, in small gaps, photographic obs. 9-39030
 Ar, between mild steel coaxial cylinders, pot. obs., secondary ionization coeffs. calc. 9-34811
 Ar, laser induced, wavelength dependence, use of dye lasers 9-46543
 Ar, microwave breakdown temp. depend. 9-32708
 Ar, r.f. excited in non-resonant mag. field characts. 9-25986
 H, formative time lags 9-34814
 He, between mild steel coaxial cylinders, pot. obs., secondary ionization coeffs. calc. 9-34811
 He, laser-induced 9-48725
 He, laser induced, plasma development analysis 9-25844
 He, laser induced, time and space development of space parameters 9-28053
 He, laser prod., incident, light scatt. at breakdown front, mechanism 9-23362
 He, r.f. excited in non-resonant mag. field, characts. 9-25986
 He plasma, acoustic oscillations obs. at low temp. 9-39010
 Kr, between mild steel coaxial cylinders, pot. obs., secondary ionization coeffs. calc. 9-34811
 N_2 , elec. strength at elevated pressures and small gap spaces 9-42575
 N_2 , impulse breakdown, secondary leader channels obs. 9-44511
 N_2 , microwave breakdown temp. depend. 9-32708
 N_2 , under picosec. ruby-laser pulse, threshold depend. on press. 9-46544
 by Nd glass and ruby lasers, evidence for self-focusing 9-25983
 Ne, between mild steel coaxial cylinders, pot. obs., secondary ionization coeffs. calc. 9-34811
 Ne, r.f. excited in non-resonant mag. field, characts. 9-25986
 Xe, between mild steel coaxial cylinders, pot. obs., secondary ionization coeffs. calc. 9-34811
 Xe laser induced, wavelength dependence, use of dye lasers 9-46543
liquids
 compression headwaves, X-ray photography 9-32768
 of dielectric liquids book 9-34917
 electrocapillary discharge 9-23516
 literature digest, 1967 9-33368
 trigatron spark gap in liq. dielectrics, characts. 9-32789
 He laser-induced 9-48725
 N_2 , d.c. pre-breakdown phenom. using electron field emission from metal electrode 9-44581
 dielectric, research trends, review 9-30968
 fusain-argillite layers, disruption of stronger component 9-45004
 inception stresses in dielectric with air-filled cavity 9-35474
 literature digest, 1967 9-33368
 muscovite mica, correl, with high field conduction, barrier action mechanism obs. 9-37587
 mylar films, non-destructive breakdown 9-49139

Breakdown, electric continued
solids continued

- mylar films, non-destructive breakdown 9-47162
 p-n planar junction, breakdown voltage, increase using punch-through controlled surface 9-28525
 p-n stop junction, avalanche rel. to structural irregularities 9-43078
 polymer films, dielectric rel. to electromechanical deformation 9-43110
 polymethylmethacrylate, discharge development investig. 9-43109
 quartz, X-cut, and recovery under shock wave compression 9-47189
 rocksalt, thin films 9-33381
 semiconductor junction, avalanche current elec. suppression 9-41220
 semiconductor p-n junctions, Zener current meas. 9-28528
 Teflon capacitor studies 9-37586
 transistors, second, meas. 9-33280
 CaF₂ capacitor studies 9-37586
 CdS, photoluminesc. field quenching obs. 9-35703
 CeF₃, CeO₂ capacitor studies 9-37586
 Ge-Si-As-Te, glassy semiconductor films, mechanism 9-33305
 n-Ge, eff. of i.r. radiation, wavelength depend. 9-30926
 G, shallow impurity states, far i.r. absorpt. studies 9-28517
 n-Ge obs. 4.2° to 7.9°K 9-28512
 n-InSb, avalanches, higher conduction band minima and assoc. impurity levels obs. 9-41202
 MgF₂ capacitor studies 9-37586
 NaCl, plasma instability during breakdown, formation of gas bubbles 9-41235
 NaCl intrinsic to 240°, including thermal instability above 9-28554
 NaCl single crystal, discharge development investig. 9-43109
 Se rectifiers, critical voltage from I-V characts. under hydrostatic pressure 9-26564
 Si, three-point probe technique, theoretical model 9-30928
 Si n⁺-p-n structures, localization under emitter dip effect conditions 9-35441
 SiC epitaxial p-n junctions, avalanche breakdown 9-35442
 SiO₂ amorphous films, dielec., rel. to anodic growth conditions 9-45006
 SiO₂ pyrolytic films, nature, 77° to 223°K 9-33382
 SiO₂ in Si-SiO₂-Al structure, elec. strength rel. to thickness 9-35475
 SiO₂ capacitor studies 9-37586
 SiO films, pulse, tests and thermal and elec. props. obs. 9-45005
 SiO thin film, surface irregularities effect 9-41236

Breaking strength *see* Mechanical strength**Breeders** *see* Nuclear reactors, fission**Bremsstrahlung**

- see also* Electrons/radiation; Gamma-ray spectra; Gamma-rays;
 X-ray spectral emission; X-rays
 betatron, derivm. of time correlation component of intensity envelope 9-27603
 bremsstrahlung, cross section calc. using Sommerfeld-Maue eigenfunctions 9-38462
 cross section calc. using sum rules effect of velocity dependent forces 9-42008
 dipole and quadrupole, from electron plasma, calc. 9-30267
 energy spectrum, near asymptotic expression 9-38461
 enhanced, from isotropic, homogeneous plasma, calc. using distribution function 9-30268
 graviton bremsstrahlung and i.r. divergence 9-47743
 high energy, Poisson distrib. 9-36431
 interaction of p-quanta with complex nuclei for nuclear fission 9-22773
 intergalactic, non-thermal, rel. to diffuse X-ray background 9-24833
 inverse, cross-sections in screened potentials, classical calcs. 9-46271
 Linac thick-target spectra meas. with large NaI scintillation spectrometer 9-32276
 measurement with electron spectrometer using Compton eff. 9-46133
 monitor, ¹²C(p,X)Be reaction for high energy beam, E_p=0.4-0.9 GeV 9-27694
 monochromator for photon scatt. investig. 9-42007
 μ, for quantum electrodynamic testing 9-22540
 in nuclear reactions, direct 9-22771
 from plasma, relativistic correction 9-44435
 in plasma freq. region, calc. 9-36772
 production efficiency from internal target of electron synchrotron 9-25551
 proton-proton, 30-200 MeV, pot. model 9-46116
 radiation in field of O II and Ne II ions 9-30261
 solar, intensity depend. on heliographic longit. 9-43660
 tetatron plasma emission 9-23300
 β decay of ³²P, radiation spectra obs. 9-22532
 ep-*repp*, wide angle, differential cross section meas., E_e=1 GeV 9-36432
r pair calc. for hot degenerate electron gas Coulomb scatt. on nuclei 9-42009
 pp, 65 MeV obs. rel. to potential in nuclear matter 9-40444
 pp, noncoplanar, calc. at 48 and 30 MeV, using Hamada-Johnson potential 9-42100
 pp, rel. to off-energy-shell effects 9-38572
 Al foil measurement with electron spectrometer using Compton eff. 9-46133
 Ar neutral atom, radiative electron scatt., cross section obs. 9-29965
 Au, e. scatt. cross-section 50-500 keV 9-29277
 Au foil measurement with electron spectrometer using Compton eff. 9-46133
¹²C(e⁺,e⁺)C wide angle yield at 6.2°, E_e=9.5 GeV 9-25613
⁵⁵Fe electron capture decay, inner - bremsstrahlung spectrum endpoint, decay energy meas. 9-42244
¹H, p, p-p cross section, time of flight diff., E_p=10 MeV 9-29798
²⁴Mg(p,n)²³Mg, ²⁴Mg(p,n) 22Mg, yield curve analysis rel. to cross-section calc. 9-27698
 N₂ electron radiative scatt., low energy cross section 9-32423
 N electron radiative scatt., low energy cross section 9-32423
 N plasma continuum radiation, 975-37000 Å 9000-13500°K, 1, 2 atm. press. obs. 9-23302
 Ne neutral atom, radiative electron scatt., cross section obs. 9-29965
 O electron radiative scatt., low energy cross section 9-32423
 Xe neutral atom, radiative electron scatt., cross section obs. 9-29965

Brightness*see also* Illumination

- change, visibility in presence or absence of boundary 9-29128
 Earth, Cosmos 149 obs. 9-40029
 lunar, surface layer models 9-27074

Brillouin scattering *see* Scattering/light, Brillouin spectra**Brillouin zones** *see* Crystal electron states/band structure**Brittleness***see also* Breaking strength

- ceramics, static characts rel. to impact resistivity dynamic characts. 9-46905
 Inconel 625, n irradi., and creep strength, 650°C 9-37250
 overstressing to reduce subsequent brittle failure risks 9-33070
 stainless steels, irradi., rel. to He-filled deform. defects 9-37260
 steel, on ageing rel. to weldability 9-30713
 steel, austenitic, H-charged, embrittlement 9-33085
 steel, brittle fracture, statistical model 9-35186
 steel, brittle fracture with interaction between elastic crack and slip band, criterion 9-44779
 steel, n irradi., rel. to microstruct., theory 9-37261
 steel, neutron radiation embrittlement, choice of parameters for meas. 9-24071
 steel, neutron radiation embrittlement, choice of parameters for meas. 9-35299
 steel, susceptibility to brittle cracking, effects of residual stresses and strain ageing 9-39439
 steels, produced by boron-rich phase precip. from superheated austenite 9-41042
 strain-energy and size effects in brittle materials 9-28367
 Al₂O₃, fracture below 1000°C 9-33084
 Cr, pressurized at 10-25 kbars, ductile/brittle transition, dislocation distrib. change 9-39427
 Cu, irradi., rel. to He-filled deform. defects 9-37260
 Cu, Si hardened, irradi., rel. to He-filled deform. defects 9-37260
 Fe (49wt.%Cr) (2wt.%V), fracture slip mode effects 9-26356
 Fe, n irradi., rel. to microstruct., theory 9-37261
 Mo, annealed under high-vacuum 9-26367
 Mo, polycryst., ductile-brittle transition, temp. depend. on strain rate, neutron irradi., press. and grain size 9-30742
 Ni, inherent brittleness increase after oxidation 9-39424
 Ni, irradi., rel. to He-filled deform. defects 9-37260
 Ni alloy, precip.-hardened, irradi., rel. to He-filled deform. defects 9-37260
 Ti (6 wt.%Al) (4 wt.%V), stress-corrosion cracking as form of H embrittlement 9-48894
 W-Rh alloy, ductile-brittle transition temp. rel. to Rh conc., and fracture 9-39415
 W, polycryst. cast. brittle fracture stress. effect of temp. and pressurization 9-44757
 W single crystal, <100>axis fracture, 77°K 9-33095
 Zn in liquid Hg, fracture, effects of alloying 9-23916

Bromine

- atom recombination, thermal effects in flash photolysis 9-26835
 atomic spectrum, bibliography 9-38765
 crystal struct. at high-pressure 9-32903
 intercalation in graphite, induced dimensional variations 9-26223
 methanolic soln. for etching ZnSe 9-46750
 surface ionization, negative, on (100) face of Br 9-49179
 Br₂ liquid, i.r. absorption spectra temp. depend., induced dipole moment and correlation function determ. 9-42660
 Br+Cl→ClBr+Br reaction, energy disposal 9-39938
 Br₂l₂ liquid, i.r. absorption spectra temp. depend., induced dipole moment and correlation function determ. 9-42660
⁸¹Br in KBrO₃ and NaBrO₃, chemical shift meas. in presence of strong nuc. quadrupole couplings 9-26670
 in n-CdTe, i.r. absorpt. spectrum obs. of donor level in conduction band 9-26734

Bromine compounds

- α-antraquinone, cryst. and molecular struct. 9-42799
 bromide impurity diffusion in AgCl 9-40979
 ethyl bromide, effects on naphthalene luminesc. and absorpt., obs. 9-28138
 Br complex, Br-dioxane, use in obs. of Raman scatter of liqs. and solids prod. by laser 9-36883
 BrHBr⁺, i.r. spectra at 20°K 9-44320
 BrO free radical, microwave spectrum 9-44376

Brownian motion

- in ear, cochlear partition, estimates 9-31693
 in gas with temp. gradient, anisotropy, oil drop and smoke particle obs. 9-26022
 lattice-model polymer chains 9-34696
 magnetic field effect on particles with mag. mom. 9-27177
 momentum relax. time of particle, quantum corrections 9-43756
 polar fluid, dynamical Langevin eqn. 9-42472
 quantum particle, calc. of transition probabilities 9-34042
 random walk on lattices, calc. of first passage times 9-38244
 random walk problem for excitons in photosynthesis 9-38244
 rotary, of macromols. in soln., detect. by broadening of Rayleigh lines 9-39104
 u.s. relaxation in liq. expression for particle motion 9-30389
 Au crystallites on (100) KCl surface 9-37204

Brush discharges *see* Corona, electric discharge**Bubble chambers**

- Brookhaven Nat. Lab., 8-ft.-diam. 30 kG supercond. magnet construct, 9-37490
 conference, 1968 9-38604
 film measuring equipment employing high accuracy image plane digitizers 9-48230
 flying spot digitizer for automatic analysis of photographs 9-36535
 giant, charact., construct. and problems 9-38623
 photographic plates, automatic meas. 9-38624
 photography, reliability of Fraunhofer holograms 9-27600
 propane, as low level counter for H⁺ and C¹⁴ 9-36534
 propane, charact. 9-38623
 reaction channel separation at exposure to 2-10 GeV neutron beam 9-27599
 superconducting magnet, 8-ft.-diam. 30 kG, for Brookhaven Nat. Lab. 7ft. chamber 9-37490
 track, ionization meas. by Television Measuring Projector 9-25541
 H, giant, charact. 9-38623
 He, u.s. expansion techniques, test 9-34365
 Ne-H₂ track sensitive d target 9-25542
 Xe, accuracy for determ. of energy of γ 40-2400 MeV 9-22681

Bubblessee also *Foams*

- air, collapse and initiation of explosion of AgN_3 and $\beta\text{-PbN}_4$ 9-28788
 air, in high viscosity liq., cavitation and sonoluminescence obs. 9-36871
 air, on sea surface, contribution to acoustic reverberation 9-24610
 in blood, vibration characts. when subject to fluctuating press. 9-46603
 boiling crisis in natural convection, role of gas phase 9-23600
 bubbling column, local gas content meas. by elec. resistance of bubbling layer 9-23440
 cavitation, collapsing, temporal and spacial contours of press. pulse 9-42628
 cavitation, growth and oscills. in water-filled press. chamber, photographs and theory 9-42629
 cavitation bubble, dynamics, in 20.5 KHz u.s. field 9-34855
 cavitation noise associated with bubble collapse 9-23489
 ellipsoidal, in slightly viscous fluid, dissolution 9-38941
 ethyl alcohol, growth on glass surface during boiling 9-30465
 fission gas, growth in irradiated UO_2 9-28152
 gas, ascending in liq., behaviour of vol. and gas press., and gas diffusion 9-46606
 gas, flowing into fluid, speed 9-40766
 gas, formed by under-water explosion, gravitational effect on shape 9-46602
 gas, in water, size distrib. from sound attenuation obs. 9-46607
 gas, inert, hot, thermal stability in cool reactive liq. 9-28073
 gas, moving in inviscid liq. under sound press. change, dynamics 9-34865
 gas, solubility 9-48677
 gas bubbles in liquid, eqns. of motion 9-23442
 gas in elastomers, nucleation and growth 9-34972
 gas in gas-solid fluidized bed, interchange 9-40823
 gas in liquid, ascent, eff. of acoustic radiation pressure 9-23438
 generation of single bubbles, apparatus 9-26073
 growth kinetics in acoustic field, effect of surface active substances 9-46601
 inert gas, growth in solids, constant rate of gas generation 9-32823
 in liquids, eigenfreqs., approx. calc. method 9-36869
 in metal, surface plasma oscillations 9-39574
 plasma in crystal, form. by laser irradi., rel. to conduction band definition 9-26490
 plasma oscillations, surface 9-39574
 produced by Taylor instability of superposed fluids in cylindrical tube, motion 9-23441
 rocket effect, applications 9-39068
 spherical, in cavitation, effect of solid wall on closing 9-23428
 spherical, growth and dynamics on injection into liq. for cooling 9-26074
 surface tension, temperature dependent variations 9-32776
 in tektites and other natural glasses, gas content 9-46697
 toluene, growth on glass surface during boiling 9-30465
 two-dimensional, in slow viscous flows 9-23443
 vapour bubble growth on semi-infinite solid 9-28206
 vibration characteristics, insoluble gas bubbles in blood 9-46603
 volume and dia. rel. to frequency 9-30459
 volume change of rising bubble, rel. to velocity of rise and instantaneous mass transfer coeff. 9-26072
 water/air, parallel flow, exchange between phases 9-23224
 H liquid, stability of electronic bubbles 9-46608
 He, effect on creep ductility of an austenitic alloy 9-41021
 He, condensation of ^3He , rel. to creation of vortex rings 9-23558
 in NH_4Cl , sublimation mechanism of migration in temp. gradient 9-35134
 Na vapour bubbles in cold liquid, sudden collapse 9-23595
 Ne liquid, stability of electronic bubbles 9-46608
 in UO_2 , fission gas, irradi. stability, obs. 9-37187
 in UO_2 , irradiated, entrapment of fission gases rel. to re-solution process 9-28326
 in UO_2 , rel. to fission gas release, mobility, obs. 9-37190
 in UO_2 , stability in irradiation environment near 1000°C 9-34495
 in UO_2 , sublimation mechanism of migration in temp. gradient 9-35134

Burgers vector see *Crystal imperfections/dislocations***Cadmium**

- in alkali halides, electrolytically coloured, band obs. 9-40970
 atom, reson. line λ 3261 Å, press. effects obs. 9-48389
 atom, spectral line resonance broadening temp. dependence 9-40541
 atoms at 5^3P_1 level, depolarization effective cross-sections at collisions with rare gases and nitrogen 9-27822
 atoms excited at 5^3P_1 level, Hertzian coherence conservation in sensitized fluoresc. 9-46275
 compressibility, comparative with Cu and Pb at high press. 9-30655
 crater formation by Fe microspheres at 0.5 to 10 km/sec. 9-30700
 creep deform. of single crystal, at liq. He temp. 9-23895
 Debye temp. by X-ray reflections from powders 9-28428
 diamagnetic resonance in mag. field normal to surface 9-31019
 diffusion and electromigration in liq. Na 9-31201
 diffusion coeffs., partial, from conc. meas. in zone of contact liq. layer with Bi 9-33003
 diffusion in CdTe, 700-1000°C 9-37201
 diffusivity in Pb, mechanism 9-46855
 elastic shear constants, band structure contribution, model potential theory validity test 9-30630
 electronic density of states for liquid and solid, model-potential calcs. 9-26131
 epitaxial growth of electrodeposits on Cu single crystals 9-30490
 fatigue damage under cyclic stress, slip band extrusions and twin boundary filamentary growths 9-32981
 Hall resistivity and magnetoresistance rel. to small-angle intersheet scat. 9-26515
 Hall resistivity meas. below 77°K, scattering phenomenon 9-37440
 Hall Sondheimer resistivity oscillations, in single crystal 9-37441
 heat capacity, 1-30°K 9-47006
 internal friction anomalies near melting point 9-39399
 ion polarization via Penning collisions with optically pumped metastable He 9-38803
 Knight shift, temp. depend. calc. 9-33644
 laser, gaseous, isotope shifts and c.w. operation 9-29410
 n.m.r. in $\text{CdCr}_2(\text{Se}_4)$ rel. to transferred spin polarization 9-47444
 n.m.r. spin-echo meas. of spin-spin interactions 9-47445
 oxidized surface, work function, contact potential difference method 9-31000
 photoelec. cross sections meas., $E_p=280$ keV 9-22945
 pseudopotential, local, parameters 9-33221

Cadmium continued

- resonance line, λ 3261 Å, collision broadening by pressure of inert gases, temp. effects 9-40557
 resonance oscillations of u.s. absorption, due to orbits on fermi surface 9-30772
 sound velocity, mag. field dependence, in ultrapur material 9-35274
 Stark effect, shifts in 3P_1 excited states 9-36660
 sublimation, enthalpy and entropy correlation, torsional and Knudsen vapour pressure meas. methods 9-39146
 superconducting, intermediate isotope effect 9-44936
 superconducting transition temp. 9-35358
 surface free energy anisotropy, from equil. shapes of Ar bubbles 9-46717
 u.s. absorpt., quantum oscillations, rel. to Fermi surface 9-44822
 u.s. attenuation in normal and supercond. state 9-37338
 vapour, vacuum u.v. spectrum, absorpt. cross section obs. 9-22946
 ^{113}Cd resonance line, λ 3261 Å, temp. depend. of broadening effects 9-29934
 in AgCl single cryst., relax. of vacancy-dipoles 9-33372
 Cd-AlO_2 -Al supercond. junctions, electron tunnelling charact. 9-37497
 Cd^{2+} , solubility in NaCl crystals by ionic conductivity meas. 9-30626
 Cd^{2+} activator in alkali halide crystals, optical struct. of luminescence centres 9-47387
 Cd^{2+} in KCl, effect on F-centre mobility, 540-700°C 9-40972
 Cd II laser c.w. transition, 3250 Å 9-47983
 Cd whiskers, lattice imperf., X-ray diff. obs. 9-37109
 CdI absorption spectrum obs. in vacuum u.v. 9-27798
 n- CdTe :Cd, heat treated, multiply charged acceptors photo-Hall effect obs. 9-49075
 Fe-Cd couple, galvanic behaviour in NaHCO_3 , NaNO_3 and NaCl solns. 9-28811
 GaAs:Cd, electron-irrad., intrinsic and annealed, luminesc. 9-49316
 in GaAs, surface resistivity, average mobility and carrier conc. obs., post-implantation annealing depend. 9-33320
 Hall resistivity and magnetoresistance 9-41165
 In-Cd, band struct. effective mass meas. and applic. To electron-phonon interaction 9-47042
 in KBr, thermoluminesc. and optical absorpt., F centres formation 9-33606
 in KCl, impurity eff. on growth of F and M optical absorption bands 9-28686
 NaCl:Cd, Na^+ diffusion and ionic conductivity obs. 9-39672
 in NaCl, thermoluminesc. and F centres formation obs. 9-33606
 in Sn, lattice thermal conductivity, dopant-conc. dependence, rel. to normal and superconducting states 9-26452
 in Xe solid, absorption spectrum, multiplet struct. 9-22956

Cadmium compounds

- after-sounding effect 9-37522
 chalcogenides, e.p.r. of rare-earth ions, rel. to atomic environment 9-47430
 chalcogenides, solution growth using tin as solvent 9-37073
 focusing effect of d.c. driven plate 9-26707
 halides, vibr. spectra 9-40589
 (Hg,Cd)Te photodetectors for 1.5μ 9-49160
 phthalates, luminesc. 9-47399
 Ag-Cd alloys, activity meas., by atomic absorption 9-37855
 Ag-Cd β -phase alloys, order-disorder transf., Hall coeffs., elec. resistivity 9-35253
 α -Ag-Cd alloys, self-diffusion 9-33002
 Al(1 wt.%)Cd, alloy, pre-precipitation rel. to recovery after quenching and cold-washing 9-23936
 Au(46.1 at.%)Cd alloy, pseudo-elastic flow due to twinning surface dislocations 9-35156
 Au(46.1 at.%)Cd alloy, twinning surface dislocations, intrinsic resistive stress 9-35157
 Au(50 at.%)Cd alloy, plastic deformation influence on martensite transformation 9-34941
 (Ca, Cd) $_{10}(\text{PO}_4)_8\text{FCl}$ structural and optical props., Pb and Mn activated 9-47382
 Cd-Hg alloys, phase equil. and transform., thermodynamic investigations 9-48878
 Cd-Zn alloys, Hall resistivity meas., below 77°K, scattering phenomenon 9-37440
 Cd-Zr system, crystal structure of intermetallic compounds 9-39266
 $\text{Cd}_{0.9}\text{-xTe}$ graded-gap structures, photoelec. props. 9-49156
 $\text{Cd}_{1-x}\text{Mg}_x\text{Te}$ p-n junctions, prep. and electroluminescent props. 9-26569
 n- $\text{Cd}_{1-x}\text{Mg}_x\text{Te}$:Al mixed cryst., Hall coeff. and resistivity w.r.t. electron mobility, carrier conc. and donor ioniz. energy 9-43054
 $\text{Cd}_3\text{-xZn}_x\text{S}$, i.r. active lattice modes from reflectivity spectra 9-47343
 Cd_3As_2 -NiAs eutectic, Hall effect, conductivity and magnetoresistance meas. 9-41196
 $\alpha^{\text{Fe}}\text{-Cd}_3\text{As}_2$ crystal structures refinement 9-39262
 Cd_3As_2 , effective mass of electrons from thermoelectric power and Hall coeff. dates 9-35313
 Cd_3As_2 , Shubnikov-de Haas effect, Fermi surface form and non-parabolic model of conduction band obs. 9-41151
 n- Cd_3As_2 , thermal conductivity, electronic and lattice components at low temps. 9-33193
 Cd_3As_2 , thermal conductivity, 60° to 400°K 9-41101
 $\text{Cd}_3\text{Fe}_2\text{Ge}_2\text{O}_{12}$ paramagnetic garnet, Mossbauer spectra of ^{57}Fe , at room temp. 9-43221
 Cd_3P_2 , field emission anomalous temp. depend. 9-43139
 n- Cd_3P_2 , photoconductivity 9-39712
 n- Cd_3P_2 , recomb. radiation, optically excited, and stimulated emission, obs. 9-49312
 $\text{Cd}_3\text{Ca}_{1-x}\text{O}$ Reststrahlenbands and intrinsic absorption edge 9-47342
 $\text{Cd}_3\text{Hg}_{1-x}\text{Te}$ alloys, electronic props. in vicinity of semimetal-semiconductor transition 9-49078
 $\text{Cd}_3\text{Hg}_{1-x}\text{Te}$, cryst. growth from melt, and props. 9-46756
 $\text{Cd}_3\text{Hg}_{1-x}\text{Te}$, effective mass for composition range 0-30% 9-48995
 $\text{Cd}_3\text{Hg}_{1-x}\text{Te}$, growth and props. 9-37070
 $\text{Cd}_3\text{Hg}_{1-x}\text{Te}$, Shubnikov-de Haas effect 9-47061
 $\text{Cd}_3\text{Hg}_{1-x}\text{Te}$ alloys, photovoltaic effect assoc. with effective mass gradient 9-39730
 $\text{Cd}_3\text{Hg}_{1-x}\text{Te}$ cryst., prep. by vertical-zone melting method 9-46755
 $\text{Cd}_3\text{Mg}_{1-x}\text{Te}$ solid solns., fund. reflectivity spectrum, 1.5-4 eV, band struct. obs. 9-45306
 $\text{Cd}_2\text{Mg}_{1-x}\text{Te}$:Cl, double-acceptor defects and hole traps 9-41263
 $\text{Cd}_2\text{Zn}_{1-x}\text{S}$ mixed semicond. phonon vibr. spectrum 9-42947

Cadmium compounds continued

- Cd complex, bis(selenourea)cadmium (II) thiocyanate, X-ray powder data, i.r. spectra and crystal structure 9-26227
- Cd complexes with o-phenylenedibisdimethylarsine, i.r. spectra 9-23078
- CdBr₂, dissolution energy in KBr and Cd²⁺ assoc. with cation vacancy, rel. to low temp. cond. 9-35472
- CdCl₂:Ag, irradi., optical absorpt. and e.p.r. obs. 9-49272
- CdCr₂S₄, n.m.r. of ¹¹¹Cd, transferred spin polarization obs. 9-43297
- CdCr₂S₄, 3d transition metal ion substituted spinels, mag. props. 9-35551
- n-CdCr₂S₄ ferromagnetic semiconductor, magnetoresistance, effect of exchange interaction 9-44956
- CdCr₂S₄ ferromagnetic semiconductor, exchangestriction rel. to absorpt. edge shift 9-45155
- CdCr₂S₄(Se₄) chalcogenide spinels, hyperfine and exchange interac. systematics, n.m.r. 9-31170
- CdCr₂S₄(Se₄) n.m.r. of Cd, rel. to transferred spin polarization 9-47444
- CdCr₂S₄(Se₄) single crystals, growth 9-44646
- CdCr₂S₄(Se₄) spinels, ferromagnetic phase transitions, pressure depend 9-45119
- (1-x)CdCr₂S₄xCdCr₂Se₄, mixed ferromagnetic system, Curie temp., model 9-28609
- n-CdCr₂Se₄:In seebeck coeff., normal Hall coeff. and elec. resistivity 9-45018
- CdCr₂Se₄, n.m.r. of ¹¹¹Cd, transferred spin polarization obs. 9-43297
- CdCr₂Se₄, topochemical reactions, growth 9-23662
- CdCr₂Se₄ ferromagnetic semiconductor, exchangestriction rel. to absorpt. edge shift 9-45155
- CdF₂:Cr³⁺, e.p.r. 9-47385
- CdF₂:Eu²⁺, e.p.r. at 300, 77 and 1.5°K 9-28745
- CdF₂:V³⁺, V²⁺ optical spectra, EPR and ENDOR 9-47385
- CdF₂:Y, i.r. absorpt. and transport props. rel. to trapped electron theories 9-47354
- CdF₂:Y, semicond., resistivity and Hall coeff. 9-49077
- CdF₂, e.p.r. of Gd³⁺ 9-37795
- CdF₂, semiconducting, effective mass and scatt. mech. 9-41205
- CdFe₂O₄, electric field gradient sign at octahedral site from Mossbauer spectrum 9-35633
- CdFe₂O₄, oxygen parameter and degree of inversion, X-ray meas. 9-44660
- CdGa₂S₄, class $\bar{4}$, optical activity and rotatory power at 4872 Å 9-31074
- CdGa₂S₄, growth of single cryst. 9-35024
- CdGa₂S₄, non-enantiomorphous class $\bar{4}$, optical activity 9-49242
- CdGeAs₂, preparation by zone-melting method 9-37071
- CdGeAs₂ semicond. amorphous, thermal conductivity, phonons mean free path from Debye model 9-37367
- CdI, evidence for disloc. dislocations 9-48859
- CdI₂, photoconductivity spectral distribution 9-28576
- CdI₂, tilt boundaries of dislocations in single cryst. growth, arcs formation on X-ray photographs 9-30606
- CdI₂, tilt boundaries of dislocations in single cryst. growth, closed rings formation on X-ray photographs 9-30607
- CdI₂, adsorption of organic moles., stimulation and extinction of excitonic transitions 9-26194
- CdI in KI, thermoelec. power and ionic conductivity obs. 9-41253
- CdIn₂S₄/In₂S₃ mixed cryst., photoluminesc. w.r.t. struct. props. 9-33614
- CdIn₂S₄, growth of single cryst. 9-35024
- CdIn₂S₄, photoluminesc. w.r.t. struct. props. 9-33614
- Cd(NO₃)₂-glycine-water system, cpd. existence from viscometric and densimetric obs. 9-23461
- CdO-Cr₂O₃-O₂ system, phase equilibrium at high O pressures 9-28404
- CdO, i.r. absorpt. spectrum, phonon and polaron effects 9-24404
- CdO, optical properties, effect of lattice vibrations, 300° and 85°K 9-35613
- CdO, sublimation and optimum growth conditions of single cryst. 9-34967
- CdO films, d.c. reactive sputtered, electrical and optical props. 9-48756
- CdP₄, field emission 9-24249
- CdS (40 wt.%) ZnS:Cu electroluminescent cell, d.c., efficiency of i.r. emitting phosphors 9-41415
- CdS-Cu₂S heterojunctions in film photocells, charact. 9-46845
- CdS, parametric amplification of u.s. waves 9-37342
- CdS, u.s. amplification with continuous drift field at 20°C 9-35282
- CdS_{1-x}Se_x, g-factor of conduction band electrons 9-47040
- CdS_{1-x}CdSe_x, photocond. of cryst. excited by ruby laser 9-47199
- CdS_{1-x}Se_x mixed-crystal system, phonon freqs. from i.r. reflectance and transmittance spectra 9-46971
- CdS_{1-x}Se_x, refl. in fund absorpt. region, band struct. 9-47341
- CdS multiple-phonon-resonance Raman eff., rein. with fluorescent-emission spectrum 9-26754
- CdS multiple-phonon resonant Raman scatt., frequency spectra of higher orders 9-26753
- CdSb:Ag, effective mass of free holes from reflectivity meas. 9-39618
- p-CdSb, Hall coeff. and specific resistance rel. to temp. in strong elec. field 9-24174
- CdSb, magnetic susceptibility temp. and carrier conc. dependence, inequivalent valley model 9-26621
- CdSb, Peltier coeff. at boundary between solid and liq. phases, determ. 9-45019
- CdSe, acoustoelec. effects 9-47103
- CdSe, acoustoelectric current fluctuations, spectral power 9-33296
- CdSe, band structure, pseudopotential calc. 9-37404
- CdSe, bound exciton complexes, emission and absorpt. spectra, 4.2°K 9-37718
- CdSe, current saturation and oscillation, mechanism rel. to acoustoelec. eff. in piezoelec. mats. 9-26543
- CdSe, electroabsorption spectrum in exciton region, band structure 9-35625
- CdSe, electron-bombarded and u.v. radiation illum., electron-hole pair form. energy 9-47133
- CdSe, energy band models, self-consistent orthogonalized-plane-wave empirically refined orthogonalized-plane-wave calcs. 9-39567
- CdSe, growth of vapour phase deposits on single crystal substrates 9-46726
- CdSe, high-temp. defect equilibria, investigation by self-diffusion and electrical transport props. meas. 9-37200
- CdSe, I-V characts. of photo-current caused by trapping of carriers 9-26602
- CdSe, Γ -point valence band, spin-orbit corrections 9-37403
- CdSe, i.f. current noise illumination dependence 9-41260
- CdSe, optical absorption edge, structure 9-47355

Cadmium compounds continued

- CdSe, photoconducting, acoustic noise and sound amplification 9-33176
- CdSe, photoconducting, temp.-elec. instability 9-39711
- CdSe, recombination and luminescence processes in single crystals 9-37759
- CdSe, Se X-ray K-absorpt. edges, shifts 9-39858
- CdSe, synthesis and crystal growth 9-37074
- CdSe, valence band structure calc. 9-48994
- CdSe, Wannier exciton binding energy rel. to anisotropy 9-41137
- CdSe evaporated films, conductivity and Hall effect 9-33299
- CdSe film, change density reduction by surface alloying of In 9-33319
- CdSe films, interface-related elec. props. 9-30905
- CdSe films, props. of Au contacts 9-41211
- p-n-CdSe heterojunctions as photoelements, prep. 9-35505
- CdSe laser, electron beam pumped, high power and efficiency 9-34177
- CdSe photoconductivity, short-wavelength quenching eff. between 400 and 700 nm 9-37616
- CdSe piezoelec. semicond., attenuation of transverse u.s. waves 9-28420
- CdSe Schottky barriers, barrier heights rel. to preparation 9-24194
- CdSe textured films, recombination processes 9-31123
- CdSe thin film transistor 9-49125
- Cd(SeS) platelets, laser emissions, excited with mode-locked He-Ne laser 9-31950
- p-CdSiAs₂, conductivity, Hall effect mobility 9-44957
- CdSnAs₂ supercond. polymorph, high-pressure 9-41178
- n-CdTe:Br, i.r. absorpt. spectrum 9-26734
- CdTe:Co²⁺, electrically induced e.p.r. transitions 9-35711
- n-CdTe:In (Al, Cd), heat treated, multiply charged acceptors, photo-Hall effect obs. 9-49075
- CdTe:Yb,Er, effects of P and Li compensation on rare earth doping, e.p.r. study 9-47434
- CdTe-MgTe solid solution, new material for visible light-emitting diodes 9-47418
- CdTe-PbTe alloys, phase equilibria 9-42923
- CdTe, band structure determination using photoemission studies 9-37397
- CdTe, defect centres, electronic props. 9-49158
- CdTe, electro-optic props. rel. to modulation appls., 3.39 and 10.6 μ 9-49249
- CdTe, electrooptical effects between 20 to 120 micron range 9-28660
- CdTe, growth of single crystals by liquid encapsulation 9-37072
- CdTe, growth of vapour phase deposits on single crystal substrates 9-46726
- CdTe, Gunn effect 9-49090
- CdTe, i.r. absorpt. of Be 9-45318
- CdTe, i.r. absorpt. of Be 9-45317
- CdTe, γ detection props. 9-25523
- CdTe, optical absorption edge, structure 9-47355
- CdTe, photo- and cathode-luminescence 9-35699
- CdTe, photoluminescence, 20-80°K, fine structure of spectra 9-37760
- CdTe, self-diffusion of Cd, 700-1000°C 9-37201
- CdTe, spectrographic determination of In and Ga, use of alumina-cup electrode 9-35761
- CdTe APN films, photocurrent kinetics and relax. time 9-26601
- CdTe coaxial diode, construction and characts. 9-35443
- CdTe crystals, simultaneous growth with Te whiskers by vapour phase reaction 9-28232
- CdTe film, d.c. electromotive force caused by microwave field, investig. 9-30885
- CdTe film, elec. conductivity, investig. at microwave freq. 9-30904
- CdTe film, photovoltaic effect, anomalously high, nature 9-26605
- CdTe film photoc converters, props. 9-31903
- CdTe films, absorpt. spectra in high elec. fields 9-41376
- CdTe films, photosensitivity spectrum, influence of temp. 9-33535
- CdTe films, stimulated recrystn. rel. to cond. and hole mobility 9-39163
- CdTe films of anomalously high photovoltage, number of microphotoelements determ. 9-37613
- CdTe for gamma detection, between -100°C and +100°C 9-22671
- CdTe p-n junctions, capacitance charact. 9-47137
- CdTe thin-film photocells, fabrication 9-33413
- CdTe thin film, co-evaporated, nucleation and structure, influence of stoichiometric deviations 9-36949
- CdTiO-NaNbO₅ solid solns., struct. and dielec. props. 9-39695
- CdTiO₃-BaTiO₃ solid soln. single crystals, elec. props. 9-47172
- CdWO₄:Cu²⁺, e.p.r. spectra, linear elec. field effects 9-24486
- CdWO₄:Mn²⁺, e.p.r., spectrum, effect of external elec. field on hyperfine structure 9-31162
- CdWO₄-CaWO₄:Tb³⁺ system, luminesc. 9-39865
- Cte film heterojunction, photoelec effects 9-30988
- Hg-CdTe alloy system, magneto-optical effects, band struct. and cyclotron reson. obs. 9-35807
- (Hg,Cd)Te as i.r. detector material 9-47204
- Hg_{1-x}Cd_xTe alloys, 1 eV band gap, photoconductivity 9-41267
- Hg_{1-x}Cd_xTe alloys, photoconductivity and material parameters 9-41266
- In-Cd dil. alloy, Fermi surface topology from supercond. transition temp. dependence 9-47043
- Li-Cd alloys, lattice parameters 9-42789
- NaCl:CdCl₂, dipole aggregation, kinetics 9-39356
- p-PbTe-CdTe alloy, scattering of light-mass holes from magnetoresist. meas. 9-41206
- Sn-Cd eutectic, plane to clat transition on solidification 9-23585
- Sn-Cd lamellar eutectic, fault structure 9-28299
- n-Zn_{1-x}Cd_xO₂Sb effect of oxygen and conduction 9-49098
- ZnO-CdSe alloy systems, electroluminesc. 9-47415
- ZnS-CdS:Mn, u.v. and visible photoluminesc., i.r. reinforcement 9-47416

cadmium sulphide

- absorption edge 9-37719
- absorption edge, surface effects 9-45316
- acoustic shear-waves generated by supersonic electrons, Brillouin scattering study 9-46996
- acoustoelectric domain, light emissions obs. 9-45344
- acoustoelectric domain form., Brillouin scatt. obs. 9-43055
- acoustoelectric domain formation at high elec. fields 9-46998
- acoustoelectric effect, u.s. attenuation and trapping, pulsed u.s. meas. 9-24031
- acoustoelectric phonon generation observed in X-ray diffraction microscopy 9-46997
- after-sounding effect 9-37522
- Auger recomb. involving free and bound excitons 9-43252
- band structure, pseudopotential calc. 9-37404
- Brillouin scattering, stimulated, threshold and direction control 9-48960

Cadmium compounds continued**cadmium sulphide continued**

- carrier dragging due to laser rad. 9-28578
 carrier injection and field-induced excitation 9-43108
 carrier trapping effects resolving by use of supercond. cavities 9-41209
 ceramic photovoltaic solar cell, props. and model 9-25171
 conductivity, effect of u.s. waves in 10-45 MHz freq. range 9-39619
 creep, transient and steady state, effect of crystallographic orientation 9-42885
 crystal, double injected, transient elec. conduction processes 9-49074
 crystals compound, exciton photon transitions during ruby laser 2-photon excitation 9-49283
 current, space charge limited, in single crystals, temp. depend. 9-44955
 current oscill. stimulated by external u.s. signal 9-48965
 current saturation and oscillation, nonlinear theory 9-47105
 dark conductivity rel. to S vapour press. during heat treatments, 500 to 700°C 9-49076
 deformation potential constns. of wurtzite type 9-26498
 deposited on cleavage surfaces of NaCl, KCl, KBr, and on amorphous cellulose nitrate, structure 9-40840
 detector for observing Mossbauer effect 9-26716
 donor-acceptor pair lines 9-49273
 elastic bending oscills. in elec. conducting sample 9-44763
 electrical conductivity, frozen-in, extinction by elec. field 9-28577
 electric current rel. to temp. 9-37520
 electroabsorption spectrum in exciton region, band structure 9-35625
 electroluminescence in polycrystalline thin films, vacuum evaporated 9-31152
 electroluminescence in single crystals with electron and hole injecting electrodes 9-37777
 electron bombarded, i.r. attenuation of induced photocond. current 9-47198
 electron radiative capture by activated recombination r-centres, cross section determ., impurity photoeffect meas. 9-30798
 electron traps determ. from thermally-stimulated-current curves 9-41259
 electron-phonon packets, observation by microwave transmission and Brillouin scattering meas. 9-47106
 energy band models, self-consistent orthogonalized-plane-wave and empirically refined orthogonalized-plane-wave calcs. 9-39567
 epitaxial films, prod. by gas transport reactions 9-42722
 epitaxial growth of single cryst. layers on ZnS platelets 9-34988
 e.p.r. of photoinduced Cu and Ag centres 9-47433
 exciton absorpt. and photoconductivity correl. from spectra obs. 9-35503
 exciton and oscillatory photoconductive spectra 9-39713
 exciton dissociation, and photocarrier recomb. 9-41261
 exciton line widths and phonon interaction 9-37766
 exciton-phonon interaction 9-37709
 film on Al, i.r. reflectivity spectra showing absorption peaks 9-26733
 films, adsorption spectrum, intense ruby laser radiation effect 9-35652
 films, longit. cathode conductivity under e. bombardment 9-41155
 films, vacuum deposited, oriented crystallization 9-42724
 films on Ge plates, switching effect 9-43079
 growth from controlled atmospheres of constituent elements 9-37006
 growth from metallic solution 9-37031
 growth from vapour phase, model for existence of various crystal forms 9-39194
 growth of crystals from reacting solns. 9-37030
 growth of hollow conical single cryst. from vapour, struct. and defect obs. 9-35017
 growth of single crystals, controlled composition, from vapour phase 9-37005
 Hall and magnetoresistance coeff., elec. and mag. field depend. 9-33297
 heteroepitaxial, on GaAs, growth hillocks and cryst. structs. 9-48758
 high-field domains, transition between stationary and moving 9-33324
 hole injection by electrolytic contact 9-24172
 hole-trap depletion layer form. 9-41210
 holes two channel capture mechanism at sensitizing recomb. centres 9-41262
 imperfections in vapour-grown crystal 9-37174
 laser, electron beam pumped, high power and efficiency 9-34177
 laser, electron-pumped, 10 MW light emission 9-48038
 laser emission spectrum on excitation by e. bombardment, radiative recombination mechanism 9-24445
 lattice dynamics and properties 9-46972
 lattice scattering of electrons 9-47031
 layers, currents bounded by space charge 9-30906
 layers, thermally stimulated currents 9-30985
 l.f. photocurrent oscillations in cry. with induced neg. diff. conductivity 9-33407
 losing transitions 9-36312
 luminescence, dislocation effects 9-37771
 luminescence, from polariton inelastic scattering by longitudinal optical phonons 9-37757
 luminescence, stimulated exciton-photon, excitation by two- and three-photon absorpt. of giant laser pulse 9-45343
 luminescence of single cryst. alloyed with In and Ga impurities 9-37756
 magnetomicrowave effects at 38 GHz, charge carrier density control by photogeneration 9-30922
 metal-CdS contacts, work function at higher current densities 9-39733
 n-type, second sound-acoustic electron-wave interaction, effect on distributed acoustic amplification 9-30775
 neutron irradiation, high-energy, elec. changes and associated radioactive decay 9-47104
 n.m.r. of ^{113}Cd , spin-lattice relaxation time, 77-450°K 9-47298
 non-ohmic behaviour, current saturation study 9-24118
 nonstoichiometry of crystals grown by different methods 9-36978
 paramagnetic resonance of Fe^{3+} :Cu associated centres, 77°K 9-47432
 phonon frequency spectra of travelling acoustoelectric domains 9-26421
 phonon spectra of acoustic domains 9-37312
 phonon-assisted emission of free excitons 9-37765
 photocarrier recomb. and exciton dissociation 9-41261
 photoconductance comparison with e-conductance 9-37617
 photoconducting, conductivity variation of non-ohmic behaviours 9-43053
 photoconducting, non-equil. contact pot. difference on surface 9-33409
 photoconduction, generated by e beam 9-33408
 photoconductive single cryst., electroacoustic props. correl. with resistivity inhomogeneities 9-35502
 photoconductive spectra, oscillatory, and exciton spectra 9-39713

Cadmium compounds continued**cadmium sulphide continued**

- photoconductivity, phonon-assisted exciton transitions in spectral response 9-43127
 photoconductivity, residual, at room temp. 9-35504
 photoconductivity, saturation, and appearance of fast-decay photocurrents, under laser excitation 9-49157
 photoconductivity and intrinsic excitonic absorpt. correl. from spectra obs. 9-35503
 photoconductivity excitation spectra obs. in intrinsic absorpt. range near fund. edge, coeff. correl. 9-39710
 photoconductivity of cryst. excited by ruby laser 9-47199
 photoconductivity under i.r. irradiation 9-26600
 photoeffect, internal, in exciton region of absorpt. spectrum 9-26603
 photoelectronic behaviour in ambient-sensitive insulating layers 9-47200
 photoluminescence, low-temperature 9-49314
 photoluminescence field quenching at elec. breakdown 9-35703
 piezoelectric and elastic props., 1.5-300°K 9-33395
 piezoelectric semiconducting crystal acoustic amplifier, temp. depend. of characs. 9-44815
 plastically deformed single cryst., optical spectra depend. on dislocation density 9-35644
 radiative recombination on excitation by e. bombardment 9-24445
 Raman scatt., 1st-order 9-47373
 recombination and luminescence processes in single crystals 9-37759
 recombination processes under high excitation 9-37758
 rectification, voltage, high-resistance barrier layer, effect of various gaseous media at -20-80°C 9-39640
 resistivity inhomogeneities in single crystal 9-37507
 semicond., beta-excitation, charge pulses obs., carrier mobility and lifetimes, electron-hole prod. energy 9-33298
 semicond. tapered samples, acoustic domain studies 9-37521
 semiconducting, films, elec. cond. rel. to intercryst. barriers, >500 V cm^{-1} 9-26542
 semiconductor, acoustic domains, Brillouin scatt. meas. 9-35397
 sensitizing recomb. centres, two channel capture mechanism of holes 9-41262
 single crystal growth from vapour, whisker disloc. behaviour 9-46759
 spectra depend. on density of dislocations due to plastic flow 9-35644
 surface, {0001}, LEED obs. 9-28211
 surface trapping levels, discrete, detection 9-28575
 thermal conductivity of doped and pure single crystals, 1.4 to 80°K 9-35290
 thin layers, current fluctuations due to elastic waves 9-35396
 transducers, i.f., vapour deposition method 9-33984
 in u.s. focusing radiator 9-22266
 valence band structure, spin-orbit corrections 9-37403
 valence band structure calc. 9-48994
 work function of blocking Au contacts, reduction with increasing photocurrent 9-3732
 wurtzite structure, X-ray K-absorpt. of S. obs. 9-31121
 X-ray conductivity 9-24173
 zincblende structure, X-ray K-absorpt. of S. obs. 9-31121
 CdS:Ag electroluminescent cell, d.c., efficiency of i.r. emitting phosphors 9-41415
 CdS:Ag shear-mode-evaporated u.s. transducers, preparation 9-42957
 CdS:Pt. impurity photovoltaic effects, stimulation mechanism in i.r. spectral region 9-30997
 CdS:Se mixed alloy system, band structure, pseudopotential calc. 9-37404
 CdS-BaTiC₃ boundary, photoeffects 9-43128
 CdS-CdSe variable composition photoresistors 9-35501
 CdS-Cu₂S heterojunctions, photovoltaic effect study 9-24240
 CdS-Cu₂S heterojunctions, heat-treated, photovoltaic effect mechanism 9-39650
 CdS-SiO₂ film system, frozen-in conductivity extinction by elec. field 9-28577
 CdS, conductivity and luminescence induced by intensive electron bombardment, 300°K 9-30903
 α -CdS, refr. index press. depend. 9-47317
 CdS, trap conc. determ. by space charge currents 9-37402
 CdS- Se_{1-x} , photon-phonon interactions in Raman spectra 9-26752
 CdS second current saturation of non-ohmic behaviour 9-47107
 Cte film heterojunction, photoelec effects 9-30988
 Cu-doped sintered coordinate-sensitive photoresistor prep. 9-35513
 excitons, Wannier, binding energy rel. to anisotropy 9-41137
 iodine-doped, hollow crystals grown by vapour transport 9-39195
 single crystal, photo Hall mobility at high electric field, temperature dependence 9-28582
- Cesium**
 absorpt. lines, shift due to inert gas presence, obs. and model 9-29926
 absorption on W thermionic converter electrode rel. surface defects 9-24254
 acoustic velocity meas. in vapour 9-32736
 admixture in Ar gas-flame deposition of corundum, rel. to elec. insulation of coating 9-24211
 adsorbed layers on GaAs, eff. on GaAs photoelec. emission 9-26614
 adsorbed on W, electronic and lattice 9-32849
 adsorption on W single-cryst. planes 9-39175
 arc, electric, electronic contribution to thermal current 9-44513
 atom, 8521 Å line display utilizing swept GaAs laser 9-48408
 atom, electron impact, generalized oscillator strengths 9-29963
 atom, hyperfine freq., effects of molec. buffer gases 9-22948
 atom, impact ionization by electrons and protons, cross section obs. 9-34556
 atom, ionized, absorption spectra 9-44253
 atom, Rayleigh scattering cross section 9-25690
 atom in low pressure discharge, level population determ. 9-34536
 atomic beam, scatt. by HBr 9-42469
 atomic cluster, ionization pot. obs. 9-29956
 atomic spectrum, broadening and shift in the presence of Xe, CF₄ 9-46276
 atoms, ionization coeffs. determ. on W and Pt surfaces 9-45034
 band struct. and props. 9-48996
 charge-transfer cross section for He⁺ and Ar⁺ meas. 10-1500 eV 9-46316
 coating on Mo and W surface, field-emitted electron energy distrib. 9-45031
 condensed, elec. conduct. for temp. up to 1200°K 9-26130
 discharge, e drift vel. and energy distrib. function 9-39024
 discharge, electron density and drift vels. 9-46541

Caesium continued

- electrical conductivity up to 2000°C, 100 to 320 atm. 9-40801
 electrical resistance, temp. depend. 1.65-5°K and 14-20.4°K 9-28465
 electrical resistivity anomalous temp.-dependence at high pressure 9-24125
 electron density meas. under collision conditions, comparative study by Langmuir probe and spherical h.f. probe 9-46479
 equation of state to 23 kbar, 20-280K 9-40831
 g-factor meas., atomic structure parameters derived 9-29936
 gas, thermodynamic props. by X-ray analysis 9-26177
 gas-laser diagnostics of plasma 9-46510
 hyperfine interaction, relativistic analysis 9-24349
 ion, field emission from positive electrode 9-28583
 Knight shift, pressure depend. calc. 9-33647
 in NH₃, conc.>6 MPM, electrical conductivity meas., 200-300°K 9-23521
 plasma, e.m. wave propagation near hybrid ion-electron resonant freq. 9-23298
 plasma, mass spectrometer analysis of dominant ionic species 9-42485
 plasma, nonequilib., population of excited atomic states and ionization at low pressure 9-42484
 plasma, oscillations, noise due to radial elec. field obs. 9-28029
 plasma, thermally ionized, collisionless sheaths between field modified emitters and plasma 9-25893
 plasma, thermally ionized, large amplitude ion acoustic waves, collisionless damping 9-40701
 plasma, weakly ionized, helical instability onset 9-25959
 plasma diode, electron and ion oscillations, simultaneous excitation 9-25943
 plasma in arc, excitation temps. from relative intensities of spectrum transitions 9-25707
 plasma ionization and simultaneous free-electron Maxwellization 9-34750
 plasma thermionic discharge, electron energy distrib. 9-34756
 recovery from nuclear wastes by adsorp. on TiPO₄ and elution 9-24593
 resonance radiation, quenching by He 9-42343
 saturated vapour, press. determ. 9-42700
 scattering by alkali atom, spin-exchange cross section calc., partial-wave anal. 9-22984
 sorption on graphite, characts. at high temp. and low Cs pressures 9-39168
 Stark eff., 7P_{3/2} state hyperfine levels meas. 9-25694
 structure when molten, neutron beam exam. 9-39075
 sunspot abundance from sunspot spectra 9-31657
 thermionic diode, emitter and collector sheaths 9-34769
 vapour, electron-atom collisions momentum transfer cross section 9-40554
 vapour, ionic composition of arc-discharge plasma 9-36759
 vapour, speed-of-sound meas. 9-32736
 vapour diffusion in He and Ar 9-39059
^{131,132}Cs, isotope shifts w.r.t. ¹³³Cs by scanning level crossing signal 9-29990
^{1,33}Cs and ¹⁴¹N optically pumped, spin exchange 9-32418
¹³³Cs atom, self spin-exchange cross-sections meas. using microwave absorption between Zeeman sublevels 9-46314
¹³³Cs gamma spectrometry, airborne, use in global radioactive pollution meas. 9-37894
¹³³Cs in molten alkali nitrate salts, diffusion and conic mobility meas. 9-34891
 Cs-6^{3P_{3/2}} states distrib. due to sat. hydrocarbon collisions, eff. cross sections 9-44279
 Cs⁺ electronic dipole polarizabilities calc. 9-40545
 Cs⁺ in Ar-Cs r.f. discharge, mass spectra obs. 9-36787
 Cs⁺+He collision, threshold behaviour of the cross-section for excitation of Cs II reson. lines 9-48419
 Cs I lines electronic excitation cross section meas. in gas discharge plasma 9-27816
 Cs I spectrum, 4555 Å line broadening by Ar 9-34535
 Cs I spectrum, isotope shift meas., error sources and soln. 9-29987
 and Cu optically pumped spin exchange 9-40548
 p-GaSb, caesiating effect on photoemission 9-43145
 and Na atomic beams, interaction 9-25713
 on Ni, effect on photoemission from (111) surface 9-26617

Caesium compounds

- halides, F-centre emission energies and lifetimes 9-32999
 halides, photoionization, high temp. 9-44373
 halides, three-body interaction rel. to stability 9-24005
 targets for high energy p radiodiode recoils 9-49388
 Ar-Cs r.f. discharge, mass spectra obs. of ionic species 9-36787
 Cs-Ar low-press. discharge, Cs depletion in positive column 9-34802
 Cs-Ar low-press. discharge, radial and axial Cs-atom distrib., absorpt. spectra obs. 9-34801
 Cs₆, α-NiO₄, crystal structure 9-40905
 Cs₂BeF₄, n.m.r. of ¹⁹F, rel. to retarded motion of tetrahedral group BeF₄ 9-43298
 Cs₂MnCl₄.2H₂O, antiferromagnetic props. 9-24326
 Cs₂MnCl₄.2H₂O, antiferromag., n.m.r. obs. of mag. ordering 9-41333
 Cs₂Te photocathode photomultipliers, props. 9-25190
 Cs₂UO₂Cl₂:NpO₂²⁺, Np⁶⁺ e.p.r. spectrum, ²³⁷Np nucl. moment obs. 9-35712
 Cs₂UO₂Cl₂:NpO₂²⁺ absorpt. spectrum, energy level obs. 9-33553
 Cs₂O, CsOH and Cs₂O₃, oxidation products studied by differential thermal analysis 9-26609
 Cs₂Sb cathodes, photoemission, thermosensitive discontinuities and hysterises at high light intensities 9-39740
 Cs₂Sb photoelectron emission depth, spectral emission 9-43144
 CsBr, colour centres due to 380 keV e irradiat. at 80°K 9-46832
 CsBr, elec. cond. in H₂O-dioxane and H₂O-tetrahydrofuran mixtures 9-39114
 CsBr, ionic conductivity 9-33398
 CsBr, U centre i.r. absorpt. 9-26294
 CsBr₃, cryst. struct., X-ray diff. obs., Br⁻ and I⁻ systems comparison 9-35057
 CsBr in aqueous solution, ⁸¹Rb n.m.r. relaxation times 9-32799
 CsBr crystal, vibrations group theory analysis, wave vector group and phonon dispersion reln. 9-35268
 CsCl, colour centres due to 380 keV e irradiat. at 80°K 9-46832
 CsCl, neutron-irrad., rare gas diffusion, effect of α to β phase transform. 9-33004
 CsCl, U centre i.r. absorpt. 9-26294

Caesium compounds continued

- CsCl aqueous soln, dec. conductivity, 300-1000°C up to 12 kbar 9-48717
 CsCl structures, i.r. localized modes, shell models 9-23800
 CsCuCl₃, Cl³⁵ n.m.r. 9-45397
 CsCuCl₃, thermal and mag. study of bonding 9-24044
 CsF, F centre, optical absorpt. props. 9-39374
 CsF, in selected vib-rot. states, focused beam prod. 9-27849
 CsF, pulsed n.m.r. obs. of free-induction-decay curves of ¹⁹F and ¹³³Cs 9-35722
 CsF, scatt. by Ar and He, cross sections and anisotropy parameters 9-44387
 CsF attractive interaction with rare gases, anisotropy factor and scattering cross section 9-44390
 CsFeF₃, Mossbauer studies of ⁵⁷Fe hyperfine structure and magnetization meas. 9-45058
 CsI:Li⁺(Na⁺,K⁺,Rb⁺,Tl⁺) impurity induced far i.r. absorpt. 9-37720
 CsI-Tl electroluminescence intensity depend. on exciting voltage parameter 9-26783
 CsI, ¹³³Xe diffusion and trapping rel. to defects, obs. 9-37202
 CsI, diffusion of ¹³³Xe, use of fission recoil doping techniques 9-23837
 CsI, electrical conductivity, effect of divalent impurities rel. to temp. 9-33380
 CsI, energy bands calc. using Green's function method 9-43003
 CsI, even-parity X-exciton two-photon spectrum obs. 9-26736
 CsI, neutron-irrad., rare gas diffusion, effect of α to β phase transform. 9-33004
 CsI, U centre i.r. absorpt. 9-26294
 CsI thin film, far u.v. absorption spectrum obs. and interpreted 9-37730
 CsI(Na) scintillation pulse shape, decay time, response function to charged particles 9-22666
 CsMnCl₃, broadband fluoresc., temp. depend. 9-49319
 CsMnCl₃.2H₂O, mag. phase diagram 9-35534
 CsMnF₃, hexagonal antiferromag. nuclear and electronic spin-wave relax rate 9-45216
 CsMnF₃, magnon-phonon interaction and exchange consts. determ. 9-47286
 CsMnF₃, n.m.r., ⁵⁵Mn linewidth, field depend., 1.8 and 4.2°K 9-33649
 CsMnF₃ perovskite-like struct., phase transf. and stability relations at high press. 9-35241
 CsNO₃, pyroelectric props. rel. to crystal space group 9-30977
 CsNiCl₃, Cl³⁵ n.m.r. 9-45397
 CsNiF₃, high pressure forms 9-45059
 CsOH, vibr.-rot. interactions and struct. refinement 9-44325
 CsPbCl₃, crystal growth and phase transitions 9-39211
 CsPbCl₃, n.q.r. determ. of phase transitions 9-41058
 CsUO₂(NO₃):NpO₂²⁺, Np⁶⁺ e.p.r. spectrum, ²³⁷Np nucl. moment obs. 9-35712
 Cs₂[Zn(NO₃)₄], u.v., i.r. and Raman spectra 9-49288
 CsI, colour centres due to 380 keV e irradiat. at 80°K 9-46832
 K-Cs binary alloys, electron spin susceptibilities, Knight shift 9-39116
 Na-Cs binary alloys, electron spin susceptibilities, Knight shift 9-39116
 Rb-Cs binary alloys, electron spin susceptibilities, Knight shift 9-39116

Calcium

- atomic beam, coherence narrowing and shift of optical double reson. signals in (4s4p)¹P₁ state 9-29923
 autoionizing lines, oscillator strength obs. m shock tube 9-22944
 Ca²⁺ e.s.r. in NaCl and NaBr, paramag. centres prod., obs. 9-33633
 Debye-Waller factors, temp. depend. 9-35261
 ionized, solar H and K lines 9-31635
 isotopes, fractionation from precipitation of CaCO₃ 9-42356
 isotopes, search for natural variations in abundance 9-44299
 laser-pumped, abs. from excited states 9-46274
 in NH₃, conc.>6 MPM, electrical conductivity meas., 200-300°K 9-23521
 optical isotope shift, nucl. vol. and mass eff. 9-29988
 self-diffusion, and of low solubility impurities 9-23836
 solar chromospheric plages, decay curves 9-31652
 stable nuclides produced by cosmic rays in iron meteorites, surface ionization mass spectrometric obs. 9-40182
 Ca-exchanged hydrated faujasite, positions of cations and molecules 9-30556
 Ca⁺, earth's atmosphere, measurements of reaction with ozone 9-40044
 Ca⁺ concentration in Antarctic ice, obs. 9-33729
 Ca⁺ in upper atmosphere, abundance and theory of origin 9-35832
 Ca²⁺ diffusion in MgO 9-44739
 Ca²⁺ in KCl, elec. conductivity 9-47154
 Ca²⁺ in NaCl:OH⁻, impurity assoc. effects on optical absorpt. 9-37728
 Ca²⁺ X-ray K-absorpt. in CaS, obs. 9-24438
 Ca I, resonance line broadening by inert gases, effective cross-sections 9-48388
 Ca I distortion of the G²(3d4s) integral 9-29924
 Ca II, H and K line profiles in solar flares 9-36069
 Ca II, K line profile, comparison of models for chromosphere 9-31636
 Ca II forbidden resonance line in Arcturus spectrum 9-27013
 Ca II line in solar spectrum rel. to non-uniform model of chromosphere 9-36070
 Ca II transition, photospheric spectrum Fraunhofer line, photoelectric obs. 9-31653
 Ca XV, fine structure obs. 9-31628
⁴⁴Ca, 4s4p¹P₁ state, hyperfine struct., level crossing meas. 9-29922
 in KCl, F centres, e.s.r. and optical absorpt. obs. 9-37191
 in KCl, impurity eff. on growth of F and M optical absorption bands 9-28686
 NaCl:Ca, Na⁺ diffusion and ionic conductivity obs. 9-39672
 in NaCl, thermoluminesc. and F centres formation obs. 9-33606
 Pb-Ca battery grids, pressure cast, abnormal corrosion 9-28802

Calcium compounds

- apatite in aqueous soln., zeta potential, changes on addition of Ca and F 9-24584
 Ca-Yb system, solid state equil. by b.c.c. and f.c.c. solid solutions 9-30716
 CaFPO₄ spectroscopic props. and laser characts. 9-26673
 calcite, γ-irrad., e.s.r. of AsO₂²⁻ 9-39903
 calcium halophosphate luminescence, activated by Sb, temperature quenching 9-26780
 CaS phosphors, thermoluminescence and phosphorescence decay in rare earth activated 9-31146
 chlorapatite, pure and Sb-activated, chemistry and luminescence 9-24444
 complex, CuCl₂.CH₃CN, cryst. struct. 9-32910

Calcium compounds continued

- dolomite, cryst. defects, X-ray topographic obs. 9-32958
 fluorapatite, activated by rare earth, Mg lamp excitation, fluorescence spectra obs. 9-31133
 fluorapatite, Czochralski-growth 9-37069
 formate, crystalline, Raman spectra 9-47378
 gypsum, proton and deuteron magnetic resonance 9-28755
 gypsum, pulsed-n.m.r. line shapes, computation and analysis 9-43294
 gypsum, X-ray spectrochem. analysis, 2θ values 9-47484
 hydroxyapatite monocrystals, polarization anisotropy 9-30978
 limestones and marbles, compressional velocity data representation near Lambda transition 9-46884
 Perovskite cpds., prep., struct., phase transform. behaviour 9-33127
 phosphates, Sb-containing, chemistry and luminescence 9-24444
 silicates, surface charge on contact with NaOH electrolytic soln. 9-24581
 tartrate, nucleation and growth in gels 9-37029
 yugawaralite, $\text{Ca}_2\text{Al}_2\text{Si}_2\text{O}_{12}\cdot 8\text{H}_2\text{O}$, cryst. struct. 9-39258
 Ag-Ca alloys, phase diagram over whole composition range 9-48937
 Ca-Bi-V-ferrite, mag.-acoustic resonance 9-37346
 (Ca, Cd)(PO₄)₂FCI structural and optical props., Pb and Mn activated 9-47382
 Ca₁₀(PO₄)₆F₂, Czochralski-growth 9-37069
 Ca₁₀(PO₄)₆Cl₂, Sb³⁺ solubility 9-42740
 Ca₁₀(PO₄)₆F₂, O and oxide ion impurities giving rise to specific absorpt., fluoresc., and form. of colour and paramag. centres 9-40933
 Ca₁₀(PO₄)₆F₂ cryst. spectra, coupled PO₄³⁻ vib. 9-37317
 Ca₂B₁₂-xFe₂-V₂O₇, garnet, magneto-elastic coupling coeff. from ferro-mag. reson. method 9-37664
 Ca₂Al₂Si₂O₁₂·8H₂O, yugawaralite, cryst. struct. 9-39258
 Ca₂SiO₄-Ba₂SiO₄ system, fluorescence of Eu²⁺, depend. on composition 9-28717
 Ca₂SiO₄-Sr₂SiO₄ system, fluorescence of Eu²⁺, depend. on composition 9-28717
 Ca₂Fe₂Ge₂O₁₂ paramagnetic garnet, Mossbauer spectra of ⁵⁷Fe, at room temp. 9-43221
 Ca₂Fe₂Si₂O₁₂ garnet, paramagnetic Mossbauer spectra ⁵⁷Fe, at room temp. 9-43221
 Ca₃(Mn_{1-x}Al_x)₂[(SiO₄)₂(OH)₄], henritermierite, tetragonal hydrogarnet, cryst. struct. 9-32905
 Ca₃(Mn_{1-x}Al_x)₂[(SiO₄)₂(OH)₄], henritermierite, chem., spectrographic and microprobe obs. 9-32906
 Ca₃F(PO₄)₂, fluorapatite, dislocation arrangements 9-42826
 (Ca₃Sr_{1-x})TiO₃ degenerate semiconductor, review of expl. data on superconductivity 9-41179
 Ca complex 1,3-diphenylimidazole, crystal structure 9-30580
 CaAl₂O₄, high pressure transformations 9-44799
 CaB₂O₄, polymorphism 9-39260
 CaB₂O₄(III), high pressure phase, crystal structure 9-39259
 CaB₂O₄(IV) high pressure phase, structure of single crystal 9-39260
 n-CaB₆, polycryst., conduction e.s.r. 9-37793
 CaCO₃:Pb²⁺ e.p.r. at 77°K and 9.3 Gc/s 9-41425
 CaCO₃, calcite, Ca K-absorpt. fine structure obs. 9-24437
 CaCO₃, calcite, thermoluminescence mechanisms following α and reactor irradiation 9-31147
 CaCO₃, calcite tunable four-photon optical parametric noise, 4300-5860 Å 9-49253
 CaCO₃, fission fragment tracks, structure and healing 9-26467
 CaCO₃, self-diffusion of C and O by isotope exchange with CO₂ 9-46844
 CaCO₃, symmetry props. of normal modes of vib., group theory anal. 9-39507
 CaCO₃ precipitation, fractionation of Ca isotopes 9-42356
 CaCl₂ soln., diff. coeff. determ. by pulsation method 9-44555
 CaCo₄·2H₂O, limestone, Ca K-absorpt. fine structure obs. 9-24437
 CaF, Franck-Condon factors and r-centroids for A-X and B-X syst. 9-23074
 CaF₂:¹⁵¹Eu²⁺ hyperfine coupling const., temp. depend. 9-33496
 CaF₂:Dy²⁺ absorpt. band, transition time for transfer of Dy²⁺ ions 9-47351
 CaF₂:Eu²⁺ emission and excitation spectra, Eu-O complexes identification 9-47391
 CaF₂:Gd³⁺ spin-lattice coeffs. determ. 9-45380
 CaF₂:GdF₃ mixed cryst., Gd³⁺ absorpt. and fluoresc. spectra, energy levels obs. 9-35660
 CaF₂:Ho²⁺ (f-f) absorption spectrum obs. 9-28682
 CaF₂:Nd²⁺ (f-f) absorption spectrum obs. 9-28682
 CaF₂:Nd²⁺ ENDOR obs. of F- and H- interstitials 9-47449
 CaF₂:R³⁺, H- (R=rare earth), spectra 9-47353
 CaF₂:Sm²⁺ crystal laser, characts. 9-38380
 CaF₂:Tm²⁺ (f-f) absorption spectrum obs. 9-28682
 CaF₂:U³⁺, strongly polarized, e.p.r. population transfer among spin packets obs. 9-39901
 CaF₂:Yb³⁺, ENDOR on ¹⁷³Yb³⁺, electronic shielding by closed shells obs. 9-35731
 CaF₂-AlF₃ system, phase diagram, DTA and X-ray powder obs. 9-44805
 CaF₂, antiferromag. nucl. state prod. and obs. 9-45207
 CaF₂, ENDOR obs. of Gd³⁺, transferred hyperfine interaction 9-49363
 CaF₂, fluorite synthetic cryst., inhomogeneities, optical investig. 9-37165
 CaF₂, h.f.s. consts. of V_K- and V_L-centres, lattice vibrs. influence 9-43274
 CaF₂, luminesc., optical centres of Ho³⁺ 9-33579
 CaF₂, rare-earth doped, photo-reversible charge transfer 9-33406
 CaF₂, rare-earth doped, thermal conductivity in mag. fields 9-47008
 CaF₂, spin-lattice relax. times of Yb³⁺ by nucl. dynamic polarization 9-47297
 CaF₂ vapour, absorption spectra bands obs., ν_2 bending vib. assignment 9-23037
 CaF₂ crystals, tensile strength rel. to surface preparation 9-41027
 CaFe₂O₄ mag. peaks obs. using linear electron accelerator 9-42779
 Ca₄(H₂PO₄)₂·H₂O and deuterated analogue, H₂PO₄⁻ and H₂O vibrs., 4000-200 cm⁻¹ 9-44347
 CaK₂H(PO₄)₂, lattice parameters and space group determ. 9-30558
 CaMg(CO₃)₂, dolomite, Ca K-absorpt. fine structure obs. 9-24437
 CaMn₂O₄ antiferromagnetic transitions rel. to mag. symmetry and ferroelec. 9-45208
 Ca(NO₃)₂:KNO₃ glass-forming melts, high-press. elec. cond. 9-39113
 Ca(NbO₃)₂:Nd³⁺ crystal laser, stimulated radiation, 77 and 300°K 9-27332
 CaO:Bi, Zeeman, absorption and emission spectra 9-33549
 CaO:Gd³⁺, spin-lattice coeff. determ. from uniaxial stress effects on e.p.r. spectra 9-33492

Calcium compounds continued

- CaO:Ni²⁺, electronic absorption spectrum 9-28680
 CaO-Al₂O₃-Fe₂O₃-SiO₂ system, hydraulic strength 9-23907
 CaO-Mn₂O₃-ZnO-Fe₂O₃ system, phase diagram 9-46958
 CaO-Ta₂O₅ system, phase diagram, equilb. and melting points 9-39494
 CaO-ZrO₂ system, cubic phase existence, 1300° to 1700°C 9-23974
 CaO, e.s.r. of N centre due to neutron irradi. 9-37794
 CaO, electron-lattice interaction in F centre 9-44717
 CaO, F⁺ and F centres obs. in absorpt. spectrum, paramag. reson. linewidth and hyperfine interactions obs. 9-45382
 CaO, hot-pressing, effects of gaseous impurities 9-35202
 CaO, impurity effects, e.s.r. spectrum obs. 9-45381
 CaO, luminesc. from F and F⁺ centres 9-49311
 CaO, phonon dispersion curves 9-39509
 CaO, thermal expansion 12-300°K, deriv. from lattice parameter data. 9-28429
 CaO added to borolanthanum glasses, immiscibility and catalytic crystallization 9-34971
 CaO calcite, heavy particle tracks 9-41123
 CaO-SiO₂-2CaO-SiO₂-ZrO₂ system, phase equilibria 9-33147
 CaP₄O₁₁, unit cell, space group and other cryst. data 9-35055
 CaQO₄:Nd³⁺, visible absorption spectra of Nd³⁺ at liquid oxygen temp. 9-47352
 CaS:Cu, phosphoresc. decay curves and thermal glow curves, rel. to trap levels 9-35693
 CaS:Cu,Zr, phosphoresc. decay and thermoluminesc. rel. to trap levels 9-35694
 CaS, X-ray K-absorpt. of Ca²⁺ and S²⁻, obs. 9-24438
 CaS gas, A¹ Σ^+ -X¹ Σ^+ band rotational analysis, 1900°C, 6200-7200 Å 9-42389
 CaSO₄:Mn+impurity ions, thermoluminescent radiation dosimeter, preparation, patent 9-27596
 CaSO₄, e irradiated, luminesc. and exoelectronic emission 9-41402
 CaSO₄·2H₂O crystal, i.r. absorption, H bond vib. and electronic spectra 9-23799
 CaSO₄ aqueous solution, boiling, mass transfer characts. 9-23602
 CaSO₄(Mn) film phosphors for use in thermoluminescent dosimeters 9-27594
 CaSO₄·2H₂O, glass-reinforced plaster, fracture studies using scanning electron microscope 9-42894
 CaSO₄·2H₂O, gypsum, Ca K-absorpt. fine structure obs. 9-24437
 CaSO₄·2H₂O, HDO mol. vibrs. rel. to pot. environment, obs. 9-24391
 CaSO₄·2H₂O, neutron inelastic scatt. obs. of librational freqs. 9-42955
 CaSiO₃:Mn(Pb), excited by u.v., induction phenomena 9-49310
 CaSiO₃, high pressure polymorph, crystal structure 9-39261
 CaTiO₃:Fe-Mo, photochromic, photobleachable electron-beam-induced colouration 9-43201
 CaTiO₃-based binary solid solns., conc. depend. and temp. coeff. of dielec. const. 9-39663
 CaTiO₃-(Sr,Bi)₂TeO₃ system solid solns., dielec. props. 9-41231
 CaTiO₃, point defect diffusion coeffs. by analysis of transient elec. conductivity data 9-28317
 CaTiO₃, point defects formation, elec. conductivity and Seebeck coeff. study 9-28276
 CaTiSiO₃ grown by Czochralski method, struct. determ. 9-39209
 CaWO₄:Nd³⁺ solid laser, fundamental longitudinal modes exam. 9-22419
 CaWO₄:Nd³⁺, energy levels of Nd³⁺ and cryst. field parameters 9-49232
 CaWO₄:Na⁺, structure of stimulated emission bands 9-35650
 CaWO₄:Nd, imperfection assessment and control in crystals used for laser devices 9-37157
 CaWO₄:Nd³⁺, Faraday effect obs. of ⁴I_{9/2}-²P_{1/2} transition, assignments of ground-state sub-levels 9-39805
 CaWO₄:Nd³⁺ laser, stimulated emission cross-section meas. 9-41916
 CaWO₄:Tb³⁺, absorpt. and fluorescence spectra, 4.2-77°K, rel. to crystal field parameters 9-33550
 CaWO₄-CdWO₄:Tb³⁺ system, luminesc. 9-39865
 CaWO₄, by thermal conductivity and diffusivity meas. 9-26427
 CaWO₄, local trapping levels, thermal activation energies and recomb. kinetics, thermoluminesc. props. rel. to X-ray luminesc. props. 9-39890
 CaWO₄, luminesc. emission and quantum yield for X-ray excitation 9-49322
 CaWO₄, phosphoresc. enhancement by (AsO₄)³⁻, (SbO₄)³⁻ and Pb²⁺ impurities 9-39884
 CaWO₄, scheelite, crystal field calc. 9-43199
 CaWO₄ phosphors sintered in HCl stream, luminescence props. 9-28722
 CaWO₄ synthetic cryst., inhomogeneities, optical investig. 9-37165
 CaWO₄:Eu²⁺, crystal field splittings and hyperfine structure consts., 4.2 and 78°K 9-43200
 3Ca₃(PO₄)₂·Ca(F_{1-x}Cl_x)₂:Mn²⁺, synthetic, e.p.r. rel. to effect of incorp. of Cl on Mn²⁺ positions 9-47431
 GaAs_{1-x}P_x photoemissive, p-type, Cs activated, with high quantum yield for visible spectrum 9-49174
 La₂C₃, bicic. structure, superconducting over entire homogeneity range 9-33272

calcium fluoride

- Brillouin spectra, longit. hypersonic damping, obs. 9-26759
 CaF₄:U⁴⁺, spin-phonon interaction from u.s. paramag. resonance 9-33623
 centres trapped electron and H atom only prod. by X-rays when there is H doping 9-26293
 diffusion of ⁸⁹Sr, study of cation defects 9-39382
 elastic constants pressure and temp. derivs. 9-33016
 emissivity and thermal radiation, obs. 9-35651
 ENDOR obs. for Ce³⁺-H⁺ and Ce³⁺-F⁻, odd crystal field eff. 9-37808
 e.p.r. of Dy²⁺ at T=4.2°K in wavelength range 1.7-2.35 mm 9-33622
 fluoride, energy transfer from Gd³⁺ to Pr³⁺ from luminescence obs. 9-45341
 hyperfine interactions of H atoms, temp. depend. 9-31060
 impurity ions Ce³⁺ and Eu²⁺ in cubic centres, lattice distortion 9-26198
 ionic conductivity obs. with differing conc. of DyF₃, HoF₃ and TmF₃ 9-35470
 lattice self-potential and similarity of lattice and interstitial sites 9-36974
 M color center, structure, fluorescence lifetime and thermal orientation. 9-26292
 n.m.r., pulsed-, line shapes of crystals, computation and analysis 9-43294
 optical centres and interac. of Yb³⁺ ions 9-31091
 rare earths amounts used in activation, spectrochem. determination 9-33695
 rare-earth doped, thermal glow curves, analysis 9-47406
 spin-lattice coupling consts. for V³⁺ impurity ion 9-31054

Calcium compounds continued**calcium fluoride continued**

- thermal glow curves for rare-earth doped crystals 9-47406
 thermal ionization potentials of Nd^{2+} , Dy^{2+} , He^{2+} and Er^{2+} 9-46739
 thin film capacitor, break-down studies 9-37586
 X-ray diffraction profiles broadening due to pile irradiation 9-46784
 $^{171}\text{Yb}^{3+}$, ENDOR obs. 9-35732
 $^{173}\text{Yb}^{3+}$, ENDOR obs. 9-35732
 CaF_2 : rare earth ions, irradiated by X-rays antiresonance phenomena 9-49271
 CaF_2 : Ce^{3+} , presence of permanent dipoles 9-37166
 CaF_2 : Dy^{3+} , γ -irrad., thermally stimulated luminesc. 9-41411
 CaF_2 : Dy^{3+} , γ irradi., thermally stimulated luminesc. 9-41411
 CaF_2 : Dy^{3+} , e.p.r. at $T=4.2^\circ\text{K}$ in wavelength range 1.7-2.35 mm 9-33622
 CaF_2 : Dy^{3+} crystals, magneto-optical rotation in f-d-transitions 9-49247
 CaF_2 : Dy^{3+} , Ce^{3+} , Ce^{3+} codopant eff. on luminescence 9-35682
 CaF_2 : Dy^{3+} , I_8 quartet e.p.r. under uniaxial stress 9-39906
 CaF_2 : Dy^{3+} (Na^+) luminescence spectra, 4.2° and 77°K 9-33578
 CaF_2 : Eu^{2+} , c.s.r. effect of nearby Jahn-Teller tunneling level 9-45383
 CaF_2 : Eu^{2+} , spin-lattice coeff. determ. from uniaxial stress effects on e.p.r. spectra 9-33492
 CaF_2 : Gd^{3+} , crystal field splitting of $^6\text{P}_7$ and $^6\text{I}_7$ terms of Gd^{3+} 9-31056
 CaF_2 : Gd^{3+} , spin-lattice coeff. determ. from uniaxial stress effects on e.p.r. spectra 9-33492
 CaF_2 : Gd^{3+} , u.v. absorpt. spectrum 9-43238
 CaF_2 : Gd^{3+} , $^{76}\text{F}^{3+}$, cumulative luminesc., obs. 9-35683
 CaF_2 : Gd^{3+} lifetimes of levels, prob. of radiative transition, luminescence 9-28681
 CaF_2 : Ho^{3+} luminescence absorption and relaxation spectra 9-35681
 CaF_2 : NaF , electrical and mechanical relaxation 9-28548
 CaF_2 : Nd^{3+} , visible absorption spectra of Nd^{3+} at liquid oxygen temp. 9-47352
 CaF_2 : Sm^{2+} , fluoresc., temp. effects 9-41409
 CaF_2 : Sm^{2+} crystal, electron-vibrational transitions, rel. to laser spectrum 9-37704
 CaF_2 : Tb^{3+} , Yb^{3+} , luminescence, quanta summation processes 9-45342
 CaF_2 : Tm^{2+} acoustical phonon tunable detector 9-26403
 CaF_2 : Tm^{3+} anomalous population distrib. in optically excited metastable level 9-31161
 CaF_2 : Tr^{3+} (Tr^{3+} =trivalent rare-earth), thermodynamics of optical centres 9-30614
 CaF_2 : U^{3+} , spin-lattice relaxation examined by paramagnetic resonance 9-35710
 CaF_2 : Yb^{3+} , Zeeman effect in absorpt. spectra rel. to different site symmetries of Yb^{3+} 9-31103
 CaF_2 : SrF_2 : Nd^{3+} , stimulated emission from Nd^{3+} , luminescence of $^4\text{F}_{3/2} \rightarrow ^1\text{I}_{1/2}$ transition, 300°K 9-29426
 CaF_2 , H^- and D^- compensated tetragonal Ce^{3+} centres, ENDOR 9-39927
 CaF_2 : Y^{3+} , colour centre in γ -irrad. cryst. 9-39373
 elec. fields and polariz. prod. by defect charge density, lattice summations 9-33215
 Eu^{2+} doped, spin lattice relaxation time rel. to magnetic field, Faraday rot. obs. 9-49228
 NaCl , electrostatic pots. and spatial deriv. about pt. defects 9-33214

Calculating apparatus

- see also *Fourier analysis*; *X-ray crystallography/calculation apparatus*
 integrator, electronic, for magnetization meas. of low-volume superconductors 9-39591
 memory, plated-wire, mag.-field computation using integral/matrix-eqn. technique 9-43845
 particle, charged, spectra from low energy nuclear reaction, computer scanning method 9-27139
 RC-circuits, elec. simulation soln. of energy and mass transfer problems 9-27191
 γ spectra analysis, computer spectrum shifting and dead time correction 9-27140

analogue apparatus

see also *Nomograms*

- A/D converter with high speed and resolution 9-47705
 acoustic wave propagation underwater, computer predictive model 9-45860
 analogue-digital converter, fast, for pulse spectroscopy 9-29669
 computer for Fourier transform spectroscopy in far i.r. 9-36405
 coolant temperature calc. in double sided cooling of tubular fuel element 9-22865
 electrolytic trough for supercond. surface mag. field simulation 9-24130
 multiplier, two-pulse, for Vela 5 satellite E. de/dx particle identifier 9-38016
 optical computer for Fourier transform spectroscopy 9-29487

digital computer programmes

- angular correlation data acquisition, multi-parameter analysis 9-38160
 atmospheric ozone total obs. evaluation 9-41493
 atomic integrals 9-44246
 atomic L-S eigenfunctions, construction and use 9-36655
 burn-up-synthesis calcs., dynamic co-ord. functions used to save computer time 9-22862
 h.c.p. crystal freq. distrib. function calc., FORTRAN 9-33158
 crystal unit cell determ. from powder data, fully automatic program 9-48826
 curve fitting of Mossbauer spectra 9-42198
 for Diophantine eqn. soln., ALGOL 60 algorithm 9-29170
 Doppler error calc., ionospheric and tropospheric communication 9-45575
 electric and magnetic fields in uniform waveguide, computation 9-34125
 e.m. showers, simulation using Monte Carlo programme 9-44070
 for emission data evaluation of direct-reading emission spectrometer 9-46026
 e.p.r. spectrometer control 9-31881
 ESR spectra, program for calculation from parametric spin-Hamiltonian 9-36691
 FLUXPOS, for neutron spectra calc. in 80 MeV α bombard. of ^{181}Ta 9-34474
 FORTRAN program, and data, for resolving pulse height spectra 9-22173
 furnace, radiative heat transfer between gas and wall, Monte Carlo 3D analysis 9-34832
 for gas proportion counter analysis of proton recoil 9-22660

Calculating apparatus continued**digital computer programmes continued**

- Hamilton's least action principle, computer programme to produce graph to illustrate 9-36099
 harmonic analysis and correl. meas. of velocity fluctuations in grid turbulence 9-28066
 hypersonic near wake flow, FORTRAN program for calculation of solutions 9-40632
 ionospheric current systems analysis 9-38000
 i.r. spectrochemical analysis 9-41460
 i.r. specular reflectance to absorpt. spectrum, transformation 9-46020
 LAOCOON III, refining chemical shifts and coupling consts. of 1- and 2-methylbenzotriazole 9-30130
 liquid U.S. velocity, pulse-echo meas. 9-42649
 Lorentz-field amplification in bounded semiconductor 9-37502
 low-energy accelerator facility data acquisition and analysis, time-shared computer complex 9-36543
 mass spectrographic photoplates, quantitative interpretation 9-26838
 molecular i.r. spectra anal. 9-38895
 molecular struct. and props. computation 9-42372
 molecular vibrational analysis, G matrices calc. using KDF-9 Algol program 9-30016
 molecule kinematic coeffs., algorithm and tech. for matrix formation 9-36692
 Mossbauer spectra analysis, versatile program 9-49256
 Mossbauer spectra calc. for mixed polarity transitions 9-34386
 multicentre integrals, evaluation by polished brute-force techniques 9-44233
 multiprogrammed operating system for nuclear physics data acquisition 9-38163
 n.m.r., pulsed, line shapes of crystals 9-43294
 nuclear emission digitized video track scanning and analysis 9-36539
 in nuclear expts. control 9-40212
 nuclear physics lab. experiments monitoring and control 9-38165
 nuclear reaction cross-sections, synthetic, generation 9-27688
 nuclear reactor rod cluster, hydraulic and burnout characteristics subchannel anal. 9-22870
 nuclear research data acquisition system, on-line, with foreground and background operation 9-38161
 on-line, use in phys. expts. information processing 9-40212
 on-line for use with ΔE -E solid state detector 9-29657
 particle spectra produced in high-energy proton-proton collisions, calculation 9-36493
 for photographic emulsion calibration 9-43933
 plotting stereographic projections of cryst. structs. 9-48828
 polymers, electronic struct. 9-30153
 probability density calc. of ionospheric obs. 9-43770
 for quasars mean-suspended flux density values calc. 9-24821
 for radioactivity growth-decay data by least-squares method 9-38682
 resistance thermometers, calibration at low temperatures using ALGOL program 9-34103
 satellite, gravity gradient, for dynamic behaviour 9-26971
 search for extremum pressure in binary mixtures vapor-liquid critical states 9-34949
 sedimentation, anisotropy in packing of random spheres, simulation 9-30438
 sessile drops, for surface tension and contact angle calc. from shape 9-34867
 spark chamber, wire, on-line data analysis 9-36536
 spark chambers, wire, high-energy experiments, data acquisition, analysis and control, real time computer system 9-36537
 spectral data, compressed, extraction, models test 9-29135
 stress wave propag., two-dimens. in nonlinear media 9-41819
 for weather forecasting from data of atmospheric models 9-41479
 x-ray crystallography, method of alphabetic plotting of undistorted Fourier maps 9-39240
 X-ray scatt., small angle, collisional distortion calc. 9-46769
 X-ray scatt. data collimation corrections, FORTRAN IV 9-48827
 for X-ray spectrochem. analysis with multichannel quantometer 9-45433
 γ -ray spectra, analysis using photopeak method 9-48224
- digital computers**
- 3-D movies, computer generated, use of varifocal mirror 9-32073
 in acoustics, role played over past decade 9-29260
 amplitude spectra, preliminary processing on Minsk-2 computer using light-pencil oscillograph 9-42123
 application to algebraic ray tracing 9-36345
 application to rotational analysis of diatomic mol. spectra 9-38827
 applications to weather forecasting 9-41479
 astronomical applications 9-40196
 atmospheric precipitation, comparison of actual and computed values 9-41518
 of average transients to record ESR spectra of transient paramag. species 9-29350
 γ spectrometry data processing system for satellites 9-38018
 closed loop systems, performance improvement by non-uniform quantization of input 9-27138
 data collection interface of Brookhaven Nat. Lab. data acquisition and analysis complex 9-38164
 hologram generation and reconstruction 9-27357
 isotope reactor reactivity and rod symmetry control system appln. 9-36626
 lens transfer function meas. application 9-31997
 monochromator control, hardware 9-36397
 in nuclear expts. control 9-40212
 nuclear power plant applications 9-36625
 numerical approximation of integral eqn. rel. to soln. of time-invariant conservative fields 9-31751
 on-line, use in phys. expts. information processing 9-40212
 PDP7 used as 150000 channel analyzer 9-44092
 plasma experiments, fast numerical procedures 9-33980
 pulsars, weak, two methods for searching in radio noise of telescopes 9-43593
 radiation meas. 9-22649
 Sigma-7, use in nuclear physics lab. 9-38162
 simulation of plasma temporal echoes 9-46519
 simulation of sputtering 9-35296
 spectral analyser, algorithm 9-38166
 spectrometer design and manufacture, application 9-32060
 spectrometer experiment, improved computer version 9-43700
 stereoscopic drawing, degree of distortion 9-33981

Calculating apparatus continued
digital computers continued

- in X-ray crystallography, error evaluation cost aspects 9-23726
- NiO, catalytic activity, influence of metal support and u.v. irradi. 9-41446

Calculation

- see also *Graphs; Nomograms*
- algorithm for energy dissipation by normally incident monoenergetic electron beams 9-41121
- eigenfunction-expansion method for nonlinear boundary-value problems in 1- and 2D domains 9-22169
- neutron attenuation function, from exptl. curve 9-38729
- nonlinear boundary-value problems in 1- and 2D composite domains, general eigenfunction-expansion method 9-22169
- symmetry and local group structure of equations 9-25029

Calculus see *Differential equations; Integrals; Mathematics***Californium**

- fission source of heavy ions, attenuation in Al, Ag and Au foils 9-28440
- ²⁵²Cf as neutron source for radiography 9-42257
- ²⁵²Cf spontaneous decay rel. to supernovae brightness decreases 9-49559

Californium compounds

- CfOF cry. growth by hydrolysis of CfF X-ray diffraction study, structure determ. 9-26205

Calorimeters

- adiabatic for meas. of sp. ht. of Cu-Be alloys 9-37285
- for adiabatic meas. of specific heat at low temp. 9-25135
- alpha-ray low-power source meas. 9-29664
- beta-ray low-power source meas. 9-29664
- deformation, liq.-vapour, calibration technique 9-29331
- differential emissivity for measuring radiant heat exchange of small animals 9-47691
- heat loss compensated, design of core surrounded by heat jacket and shield 9-45886
- isothermal, CO₂/graphite rig radiation dose rate meas. 9-22915
- for laser (continuous) output power 9-43804
- for laser (pulse) output energy 9-43804
- X-ray total absorption 9-27151

Calorimetry

- see also *Heat of adsorption, etc; Specific heat*
- black body type, light pulses, energy measurement 9-34106
- for dielectric loss meas. at low temp. 9-33375
- high wattage, isothermal water-bath design and theory 9-29330
- microns, metal, refl. coeff. meas. 9-26701
- polypropylene, thermal behaviour of phases formed on pressure-crystallization from differential scanning calorimetry 9-46711
- thermister applic. high temp. mixture 9-22302
- Mo as reference substance, 1000-2850°K 9-37356

Cameras

- Chronolite, variable spark-gap with gas pressure chamber 9-32094
- fixed focus, lab. applications 9-46030
- foil-shutter multi-lens prototype 9-32084
- framing drum spectrograph 9-32069
- gamma, aperture indexed collimators 9-22650
- high-speed, continuous mirror scanning system 9-31995
- high-speed 70 mm drum type 9-29502
- high-speed continuous access framing, 45 ns exposure 9-32092
- high-speed rotating-prism, with registration sprocket 9-29503
- holographic, for recording interferograms 9-46032
- holographic, wide view-angle 9-41925
- Imacon system with image converter 9-32046
- image converter, for over-wide time intervals 9-32048
- image converter framing, tubes and recording systems 9-29480
- image converter, camera, functional influences on design 9-32047
- image converter, camera system for single photoelectron recording 9-34224
- image-intensifier framing, development 9-29478
- integral image, 1 ns exposure time 9-29499
- Kerr magneto-optic, nanosecond, for thin film magnetization config. on flux reversal 9-32082
- multiple-frame, as ballistic phototheodolite 9-32089
- multiple-spark with optical frame separation 9-32093
- PhC-1 high-speed, with high aperture ratio 9-29504
- pinhole, instrumentation for solar photography in extreme u.v. 9-43654
- ribbon-frame, high-speed drum shutter 9-32083
- rotating-mirror, continuous access for 250000 frames/sec. 9-32091
- satellite tracking, three East German instruments 9-27115
- Schmidt, image quality exam. using spot diagrams 9-49596
- smear, high-speed photography with pulsed laser 9-46034
- stereoscopic grid, high-speed photography 9-32081
- streak, attachments for stereoscopy, spectrography and image dissection 9-32090
- streak, rotating-mirror, problems in shock-wave compression photography 9-32087
- streak, time resolution meas. by pulsed laser diodes 9-32088
- strobe photos with 'Big Swinger' 9-46031
- Telford image converter, development 9-29479
- TV, high sensitivity, satellite-borne, for detection of auroras 9-33812
- u.s., solid state, design 9-34087

Candoluminescence see *Luminescence***Capillarity**

- see also *Bubbles; Drops; Films/liquid; Foams; Surface tension*
- capillary waves, longitudinal, experimental evidence 9-44542
- contact angle in thin liq. film, meas. technique 9-36839
- drop/surface shape on horizontal plane 9-30363
- flow technique rel. to surface tension of glasses 9-36854
- liquid surface shape in diverging circular tube 9-30363
- plaster moulds 9-30703
- pressure gradients during flow, threshold value determ. 9-23436
- static meniscus in vertical circular cylinder, for entire range of Bond nos. and contact angles 9-34885

Capture cross-sections see *Nuclear reactions and scattering and subheadings***Caratheodory's principle** see *Thermodynamics***Carbon**

- see also *Diamonds; Graphite*
- ¹²C and ¹³C substituted molcs., diffusion in liquids, isotope eff. 9-32777
- active, sorption and interact. of SO₂, 50 to 650°C, and regeneration of C 9-26806
- adsorbed gas condensation 9-23592
- in arc, d.c., atoms and ion persistent lines intensities calc. 9-24602

Carbon continued

- arc, effect on electrode temperature 9-25993
- atom, core polarization and hyperfine structure calc. 9-46273
- atom, correlation effects of non-closed shell many electron theory 9-38773
- atom, hyperfine structure calc., g.s. first-order wave function 9-32408
- atom, lowest ³P, ¹D, and ³S states, multiconfig. Hartree-Fock calc. 9-25693
- atom, polarization wave functions for ground state 9-34532
- atomic line emission at 2478 Å in shock heated CO, CH₄ and CF₄ mixtures in Ar and Ne 9-48387
- BaSO₄-C powder mixtures, diffuse reflectance 9-24360
- best-atom Slater orbital calcs., hybridized-promoted 9-48384
- burning in stars, conditions for explosive nucleosynthesis 9-49546
- c blacks, surface area and porosity eval. 9-23645
- CaCO₃, self diffusion in calcite by isotope exchange with CO₂ 9-46844
- cellulose char, e.p.r. parameters rel. to initial state and carbonization temp. 9-26810
- charcoal, oxidation kinetics in CO₂, 10⁻³ to 40 atm., 700 to 1300°C 9-41449
- colloidal suspensions in insulating liq., electrophoretic development of electrostatic charge images 9-44604
- crapitizing, formation by solidification from liq. or plastic state 9-48743
- deposition, effect of substrate structure 9-44625
- deposition from r.f. discharges in C containing gases, species involved obs. 9-23353
- diffusion coeff. in α -iron at 408° and 430°C, u.s. determ. 9-37196
- diffusion in Ta, Nb and V 9-35133
- diffusion into Re at high temp. 9-42966
- dimensional changes and creep, irradi. induced, rel. to strain and struct. 9-41022
- electrode temp. meas. for arcs in room air 9-30321
- electron scattering, shape resonance, cross section and collision strength determ. 9-38786
- epitaxy on diamond surface 9-35033
- e.s.r. black, heat treatment eff. on g-shift 9-24485
- excited ions form. in He⁺-CO collisions 9-36724
- fibre, polyacrylonitrile based, stress graphitization 9-39493
- fibre, preferred orientation effect on (h,k) interferences in electron diffraction 9-28259
- fibres, lattice vibrations along c-axis, neutron spectrometry 9-28414
- fibres, structure determ. by e.s.r., g values rel. to preferred orientation 9-32904
- fibres for reinforcing composite mats., popular article 9-46944
- film, evaporated, e.s.r., effect of water vapour 9-39904
- film, evaporated, graphitization under heat treatment, 1000° to 2200°C 9-39453
- film deposited on Ag, coherence 9-37112
- forbidden transitions in isoelectronic sequence, relative line strengths 9-36653
- gasification, catalysis 9-49377
- glassy, deformation-induced anisotropy 9-39147
- glassy, graphitization, role of strain 9-23980
- graphitized fibres, fine struct. 9-30557
- Hall coeff. and magnetoresistance in soft C, doped with acceptors, 2° to 300°K 9-41154
- Hall coefficient and magnetoresistance, 1.5° to 300°K 9-41153
- hard, partial graphitization above 2000°C, layer stacks and phases present 9-28396
- hot atom reaction with O₂, quantum chem. 9-24538
- ion, collisionally excited u.v. and forbidden lines, intensity calcs. 9-25685
- ion energy levels, radiative lifetimes 9-36659
- iron ore sinter mix, neutron carbon meter using inelastic scattering technique, design 9-33700
- metallic state existence of dynamically compressed samples 9-30847
- monofilaments, glassy, prep., struct. isotropy 9-28195
- in M.S.O. alloy, effect on mag. shunt props. 9-45050
- negative magnetoresistance due to diffuse scatt. at crystallite boundaries 9-24277
- negative magnetoresistance due to diffuse scatt. at crystallite boundaries 9-24277
- neutron scattering in UC, effect of chem. binding 9-23776
- non-graphitizable, X-ray small angle scattering, micropore system 9-37136
- non-graphitizing from polyacrylonitrile, random layers, profile anal. 9-28260
- optical const., i.r. region 9-24357
- plasma, line radiation energy, 10⁴ to 10⁵°K 9-40676
- proton energy losses 9-30807
- pyrocarbon-graphite composite mats. obtained by natural gas decomposition, n.irrad. effs. 9-28436
- pyrocarbons and graphite, g-factor and diamagnetic anisotropies, relationship 9-47228
- pyrolytic, B-doping effects on dynamic elastic moduli and internal friction 9-26320
- pyrolytic, basal plane distortion 9-39412
- pyrolytic, dimensions, effect of high neutron exposure 9-40992
- pyrolytic, growth in oil-cooled a.c. arcs 9-23364
- pyrolytic nuclear fuel coating technique 9-36633
- replica for electrical structure of Si p-n junction 9-32847
- replica for electrical surface relief of NaCl 9-32848
- replica of Ag substrate, evaporation of Au film 9-37112
- saccharose, (hard coke), heat treatment effects 9-37277
- soft, doped with acceptors, Hall coeff. and magnetoresistance, 2° to 300°K 9-41154
- solubility in solid Au, Cu and Ag 9-44788
- solubility in U, UC precipitation in U Mo 1.5% alloy 9-35260
- spectral lines in arc plasma, Stark broadening 9-44258
- sphere, pulsed with neutrons (14 MeV), time spectra of emitted neutrons 9-34479
- stacking faults, 001 reflections, analysis 9-37183
- in steel, effect on γ -martensite 9-37294
- stellar abundance in K grants 9-43528
- stress-graphitized pyrolytic, dynamic elastic mod. and internal friction 9-26320
- structure, vaporization, mech. props., growth and gasification studies, book 9-46695
- structure and mech. strengths of deposits, effect of deposition surface topography 9-26226

Carbon continued

- sublimation and self-diff., role in C-CO₂ interac., temp. >2000°K 9-28779
 surface distribution by ³He activation and autoradiography 9-26849
 thermal black, microstruct. study via oxidation 9-28258
 thermonuclear burning in stars, expt. investigation of ¹²C-¹²C reacts. 9-43540
 thermonuclear burning in stars, synthesis of elements and energy generation 9-40142
 thin foils, small-angle scatt. of ³⁵S and ¹⁶O beams 9-35298
 turbostratic, with B and Na doping, e.p.r. rel. to heat treatment 9-26791
 vaporization, heat of sublimation and vapour composition and pressure 9-48740
 vitreous, combustion kinetics in low O₂ press. 9-26815
 X-ray diffraction studies 9-48822
 X-ray emission K α band, in TiC, diamond and graphite 9-26762
 X-ray scatt. spectra, Cu K α and β rad. 9-45338
 p, range and ionization energy losses, Bragg's curve method meas., E₀=100-660 MeV 9-33213
 C-CO₂ interac., role of sublimation and self-diff., temp. >2000°K 9-28779
 C, pyrolytic, deposited in fluidized beds from hydrocarbons, comparison, 1200-1400°C 9-24536
 C₂ spectra of discharge, extension of (A³Π_g-x³Π_u) band system 9-34610
 C₂⁺, electronic states calc. 9-36696
 C₂, Hulburt-Hirschfelder calc. of r-centroid 9-30018
 C₂ line spectrum solar center-to-limb behaviour 9-31633
 C₂ molecules, photodissociation in comets' atmosphere 9-24882
 C₂⁺, C₂⁺, electronic struct., non-paired spatial orbital method 9-42388
 C deposition on Fe and Ni surfaces from methane, ethane and ethylene 9-24535
 C films, annealing, activation energies 9-23937
 C II, C III radiative lifetimes of multiplets obs. by beam foil method 9-22943
 C V, S and P state transitions, wavelength calc. and comparison with expt. 9-44257
 C V, S and P state transitions, wavelength calc. and comparison with expt. 9-40540
¹²C, K α mesic X-ray yields 9-36685
¹²C root mean square charge radii 9-48415
¹³C/¹²C isotope ratio of enriched ethyl acetate, meas. with gas density meter, method 9-34588
¹³C satellites in PMR spectrum of tetravinyltin, J_{13-C-H} coupling const. 9-27917
¹⁴C counting method in atm. CO₂ 9-26912
¹⁴C diffusion in Li/Na/KCO₃ near eutectic mixture 9-30625
¹⁴C diffusion in TiC_{0.67}, anomalous 9-46858
¹⁴C isotope enrichment by counter current electromigration 9-48439
 C+CO₂ rate constant at high temp. 9-26817
 C+N atom collisions, interaction potts. 9-38792
 in Fe, effect on ³⁵S mobility in grain boundaries 9-37203
 H-C plasma at 40 000°K and 70 atm., coeff. of continuous absorpt. calc. 9-44444
 PbCrO₄-C powder mixtures, diffuse reflectance 9-24360
 in Si, vibr. absorpt. 9-41390
 in Si epitaxial layers 9-46725
 SiO₂-C fibre reinforced, Young's modulus, rupture modulus and fracture toughness 9-44773
 in steel, spectroscopic examination using Ar discharge source 9-47480
 Th-C, superconducting energy gap, anisotropy changes 9-30879
 on W surfaces, FEM-LEED studies 9-35071

Carbon compounds

see also *Organic compounds*

- C-O-N-U system, phase relations at 1700°C 9-26400
 carbide-boride-graphite ceramics, fusion-cast, phase assemblages, microstruct. props. 9-30729
 carbonyls, mol. freq. vib. calc., spectroscopic and crystallographic study 9-30020
 CO₂ chemically derived in electric discharge, use in laser 9-43883
 CO₂ pulsed laser, excitation mechanisms 9-43880
 CS₂ solid polymer, structural and elec. props. investigation 9-34975
 metal carbides, refractory, surface layer fracture due to giant laser pulses 9-44774
 pyrocarbons, self-diffusion meas. 9-44730
 steel, 0.17%C induction hardened, fatigue strength rel. to microstruct. and surface residual stress, obs. 9-26347
 steel, 0.3%C, fatigue strength rel. to stress waveform, obs. 9-26346
 steel, Cr-Ni-Mo high C low alloy, fatigue strength rel. to hardness, obs. 9-26345
 α gas phase reaction rate data at high temperature 9-49373
 C/Cr/Ni/Si system, controlled solidification using monovariant eutectic reactions 9-36921
 C-N- α -Fe solid solution, permeability disaccommodation, -40°-+180°C 9-26322
 C-O complexes in Si, vibr. absorpt. 9-41390
 C₁FeCl₃, Mossbauer spectra, electron charge transfer and quadrupole splitting obs. 9-24378
 C₂ transition probabilities for Swan and Muliken bands 9-42384
 C₂O₂ photolysis at 1470 Å in presence of CH₃F 9-47473
 C₂FeCl₃, Mossbauer spectra, electron charge transfer and quadrupole splitting obs. 9-24378
 CaK, supercond. 9-49034
¹²C/¹³P mol., Franck-Condon factors and r-centroids for B²Σ⁺→A²Π_i band syst. 9-23033
 CCl₄, SAVE-CNDO theory, semi-empirical all valence electron, effective field gradient 9-42413
 CF₂, oscillator strengths, 2250-3000 Å absorpt. 9-27846
 CF₂ capillary, ion oscillations, intensity determination, first, second, third and fourth stages of ionization 9-25973
 (CH₃)CX, C-X band bond lengthening, Lide effect 9-23139
 CH line spectrum solar center-to-limb behaviour 9-31633
 CN, A³Π_{1/2} state, microwave-optical double reson. 9-34609
 CN, electron affinity and ht. of formation 9-30296
 CN, mag. dipole transitions between excited electronic states obs., 10.5-11.5 GHz 9-23036
 CN in KCl, splitting in impurity motional spectrum rel. to dielectric behaviour at low temp. 9-26583
 CN⁻ in RbCl, tunnel splitting of impurity motional ground states rel. to elec. cooling 9-27143
 CN absorption in nuclei of galaxies 9-31501

Carbon compounds continued

- CN group, electronic struct. 9-42386
 CN in KCl(KBr), phonon resonant scatt. 9-26408
 CN line spectrum solar center-to-limb behavior 9-31633
 CN mol., rot. transition by electron collisions 9-42465
 CN on metal surfaces, π -electron system and bond energies 9-39948
 CN red system, r-centroid calc. by Hulburt-Hirschfelder method 9-30018
 CN violet band system, electronic transition moment variation 9-38834
 CO/H₂ fuel cell mixtures, use of Pt-Ni catalysts as anodes 9-29365
 CO-N₂-He lasers, high power, high efficiency 9-22391
 CO₂-N₂-He laser power enhancement by noncontracted discharge 9-22390
 CO-O₂ mixtures, spin detonation anal. and shock wave confluences 9-34093
 CO-air-He, laser, Q switched, l to 7.7 kW peak powers 9-47952
 CO-chloromethane system, composition dependence of thermal diffusion factor 9-39058
 CO, adsorption and oxidation over Au, spectroscopic obs. 9-35001
 CO, adsorption by metals, i.r. spectra obs., effect of other gases 9-35002
 CO, adsorption obs. on thick Be film 9-36964
 CO, adsorption on Ge, effect on donor and acceptor character of surface states 9-43074
 CO, adsorption on W, and field emission 9-39176
 CO, chemisorption on Re 9-49376
 CO, diffusion in H₂O, coeffs., 10° to 60°C 9-26086
 CO, e impact excitation structure obs. at 2.3 eV., electron affinity 9-34612
 CO, electron-ion recombination, diffusion coeff., 775°K 9-48617
 CO, electron scatt., elastic at 500 eV, absolute differential cross sections 9-38800
 CO, enthalpy calc. from shock waves propagation, press., density, temp., and speed meas. 9-31850
 CO, foreign-gas broadening coeffs., rel. to N₂ 9-25736
 CO, isotope exchange in shock waves 9-49370
 CO, lattice vibrs. freq. distrib. and heat capacity meas., low temp. 9-41077
 CO, one-electron props. of near-Hartree-Fock wavefunctions 9-32514
 CO, reclassification of upper state of 3A bands 9-44322
 CO, resonant scatt. of electrons, ang. distrib. 9-27855
 CO₂-Ar, Kr mixtures, influence of dimers on dimers on thermal diff. factor 9-36686
 CO₂-C interac., role of sublimation and self-diff. of C, temp. >2000°K 9-28779
 CO₂-H₂O mixtures emissivity, analytical calc. 9-26028
 CO₂-He gas mixture, absolute viscosity determ. using 200 foot stainless steel capillary 9-36825
 CO₂-N₂-He-H₂O flowing laser, elec. discharge effect on mol. comp. 9-40352
 CO₂-N₂-He-H₂O glow discharge, spectra 2800-6500 Å, 3-7 torr 9-25979
 CO₂-N₂-He, laser amplifiers, time-depend. processes 9-38372
 CO₂-N₂-He glow discharge, spectra 2800-6500 Å, 3-7 torr 9-25979
 CO₂-N₂-He laser, electron energy distribution and vibrational excitation rates 9-27320
 CO₂-N₂-He laser, with flow, 10-120 Torr, continuous wave operation 9-47966
 CO₂-N₂-He laser, with confocal unstable resonator, properties 9-47973
 CO₂-N₂-He laser, with flow, kilowatt continuous wave 9-47967
 CO₂-N₂-He laser discharge current changes due to generation 9-47980
 CO₂-N₂, vibrational thermal relax. times, determ. by stopping point, fluorescent and spectrophotom. methods 9-48455
 CO₂-N₂ gas discharge, aimed depend. decay of CO₂ 00°1 level 9-34159
 CO₂-N₂ gas mixture, Prandtl number meas., thermal conductivity calc. 9-36816
 CO₂-N₂ molecular laser, central tuning dip on individual transitions 9-47999
 CO₂-N₂ reson. vibr. energy transfer between mode N₃ 9-30164
 CO₂-chloromethane system, composition dependence of thermal diffusion factor 9-39058
 CO₂, 10.6 μ m line, saturation of absorption 9-25733
 CO₂, absorpt. coeff., far u.v. obs. 9-28078
 CO₂, adsorption and interactions on Ni (100), effect on work function 9-35003
 CO₂, blue continuum emission, 1900-2400°K, shock tube study 9-38837
 CO₂, compressed gas, thermal conductivity, concentric cylinder meas. method 9-26027
 CO₂, current depend. decay of 00°1 level in pulsed CO₂-N₂ gas discharge 9-34159
 CO₂, dissoci. in positive column of glow discharge 9-38919
 CO₂, imprisoned 4.35 μ spontaneous emission, pressure depend. of decay rate 9-38833
 CO₂, internal energy meas. near critical point, gravity effect 9-36916
 CO₂, liq., specific heat calc. from molecular model of liquids 9-34869
 CO₂, metastable species prod. by electron excitation 9-32478
 CO₂, ν_3 spectral band near 2350 cm⁻¹ in night airglow 9-24679
 CO₂, oxidation of graphite and charcoal, kinetics, 10⁻³ to 40 atm., 700 to 1300°C 9-41449
 CO₂, pure or plus methane, radiolytic oxidation of graphite, thermal degassing studies 9-28220
 CO₂, radiolytic corrosion of graphite, effect of pore size variation on rate 9-41452
 CO₂, resonant scatt. of electrons, ang. distrib. 9-27855
 CO₂, second virial coeff. 9-34833
 CO₂, solid used to excite vibrating plates 9-29240
 CO₂, stimulated Rayleigh scatt., critical absorption coeffs. and anti-Stokes shift density depend. 9-46573
 CO₂, supercooled, water drop nucleation 9-26075
 CO₂, supersonic jets, intermolecular binding 9-23035
 CO₂, thermal relax. times of vibr. levels 9-42385
 CO₂, Venus atmosphere model 9-29070
 CO₂, Venus upper atmosphere 9-24871
 CO₂, vibrational-rotational transitions, eff. of collisions on saturation nature 9-44323
 CO₂, vibrational relax. freq. of asymmetric stretching mode 9-34611
 CO₂, $\ll P_{56} \gg$ absorpt. ray anomalies for ν_3 - ν_1 transition, laser source spectroscopy obs. 9-46359
 CO₂ 00°1-10°0 and 00°1-02°0 transitions amplification coeff., obs. 9-25255
 CO₂⁺, bombardment of D₂ gas, reaction kinetics 9-49374
 CO₂⁺-X²Π_g, sym. stretching quantum ν_1 and bending quantum ν_2 determ. 9-27845

Carbon compounds continued

- CO₂⁺[A²Π_g→X²Π_g] bands obs., excitation by neutral mol. photons 9-27845
 CO₂ 15 μ band narrow intervals, transfer function numerical modelling 9-38832
 CO₂ adsorbed on synthetic Linde type-A zeolite, dielec. props. 9-41233
 CO₂ adsorption on W(100) surface rel. to work function change 9-42734
 CO₂ band, 15 μ, use in yropospheric temp. soundings 9-41483
 CO₂ band, Venus, effect of cloud scattering 9-41679
 CO₂ chem. pumped DF laser 9-29412
 CO₂ conc. in upper troposphere and lower stratosphere, continuous meas. 9-40015
 CO₂ convective heat transfer in tube at supercritical press. 9-26023
 CO₂ coolant circuit in graphite-moderated nuclear reactor, patent 9-46250
 CO₂ discharges, h.f. at lower than atmospheric press. 9-36788
 CO₂ exchange at air-water interface, effect of hydration 9-30453
 CO₂ fluid, critical region, chemical pot. function of density and temp. 9-26155
 CO₂ folded laser, optimum transmission coeff. and power output 9-47978
 CO₂ gas viscosity meas. pot. fitted 9-36823
 CO₂ gaseous and condensed, isotropic fractionation, 220-303°K 9-23588
 CO₂ glow discharge, mass spectrometric sampling, constricted ion-getter pump, 50-1000 μ, 5-200 mA 9-36790
 CO₂ glow discharge, spectra 2800-6500 Å, 3-7 torr 9-25979
 CO₂ in laser, 00⁰1 population level meas. and obs. 9-43882
 CO₂ in laser, lifetime of 00⁰V levels rel. to discharge current and power dissipation 9-43881
 CO₂ in laser, population and gas temp. vs discharge current 9-47981
 CO₂ in laser discharge, dissociation 9-41899
 CO₂ in Venus upper atmosphere 9-38074
 CO₂ isotopes, partition functions calc. 9-32468
 CO₂ laser, damage to KBr windows by fracture and deform. 9-31943
 CO₂ laser, development for space applications survey 9-47982
 CO₂ laser, gain saturation and diffusion 9-47969
 CO₂ laser, inversion dependence on pump pulse repetition frequency 9-45952
 CO₂ laser, passive Q-switching using mixture of SF₆ and C₂F₃Cl 9-27319
 CO₂ laser, photo-induced current changes 9-47976
 CO₂ in laser, population of 00⁰1, 10⁰ and 02⁰ levels 9-45951
 CO₂ laser, Q-switched, peak power production 9-47970
 CO₂ laser, Q-switched pulses, frequency-swept, charact. 9-47968
 CO₂ laser, Q-switched pulsed discharge, properties dependent on different gas mixtures 9-41897
 CO₂ laser, rapid assembly method for tubes 9-34162
 CO₂ laser, repetitively pulsed and wavelength selective 9-25249
 CO₂ laser, sealed, power increase by gas rotation 9-31942
 CO₂ laser, single mode operation 9-29413
 CO₂ laser, spontaneous emission between 6000 and 9000 Å, spectra 9-47971
 CO₂ laser, transverse discharge configuration, gain charact. 9-47974
 CO₂ laser, vibr. temps. from visible sidlight emission, obs. 9-47977
 CO₂ laser amplifiers, rot. relax. and gain saturation 9-41895
 CO₂ laser beam corneal damage thresholds 9-38159
 CO₂ laser cavity Q switching 9-29414
 CO₂ laser freq. stabilization by absorpt. saturation of SF₆ obs. 9-46375
 CO₂ laser high peak power generation 9-41896
 CO₂ laser interferometer, transient low-density plasma meas. 9-40353
 CO₂ laser interferometer, plasma electron density meas. 9-23315
 CO₂ laser interferometry of rough surfaces 9-45993
 CO₂ laser levels relaxation times meas. by collisions with foreign gases 9-27321
 CO₂ laser plasma properties 9-47972
 CO₂ laser rad., SF₆ absorpt. and mol. vibr. induced 9-25750
 CO₂ laser radiation, atmospheric absorption of P(20) line 9-33772
 CO₂ lasers, gas temp. and electron density in discharge 9-25256
 CO₂ lasers, variable attenuator for 10.6-μ wavelength region 9-25316
 CO₂ lasers, vibration-rotation transitions for 00⁰1-10⁰ band, collision effects on saturation characteristics 9-22972
 CO₂ liq. in critical region boiling by Pt wire, obs. 9-28186
 CO₂ mol. gas, excited by fast electrons, glow spectra in i.r. region 9-38831
 CO₂ molecule, population inversion of energy levels rel. to energy of chem. reactions 9-48459
 CO₂ molecule, vibrational relaxation and population inversion in nonstationary conditions 9-48457
 CO₂ natural convective heat transfer, comparison with N₂O and chlorotrifluoromethane 9-28170
 CO₂ radiating power in range 0.2 to 3 μ at 10⁴K, 1 atm. 9-40753
 CO₂ rot. transition by collisions, relax. time calc. 9-44389
 CO₂ rotational constants, from meas. of cw beats in bulk GaAs between CO₂ vibrational-rotational lines 9-25737
 CO₂ spectral line strengths, P(20) and P(16) 9-42390
 CO₂ supercritical flow, turbulent vel. and temp. meas. 9-28172
 CO₂ thermal conductivity, vibrational relaxation eff. 9-36815
 CO₂ thermal disturbances, radiative decay 9-30343
 CO₂ Venus, upper atmosphere 9-24872
 CO₂ Venus emission, 8-13 μ spectra, telescope obs. 9-38075
 CO₂ vibr. excitation by dipole interaction with slow electrons 9-36697
 CO₂ vibrational thermal relax. times, determ. by stopping point, fluorescent and spectrophone methods 9-48455
 CO₂N₂He laser continuous, with high power density 9-45950
 CO₂-Xe-He laser, operated with Brewster angle windows, characteristics 9-25257
 CO₂+C rate constant at high temp. 9-26817
 CO₂(ν₃) vibrationally excited, deactivation by collisions with CO₂ or N₂ 9-42387
 CO₂²⁻ in KCl cryst., i.r. absorpt. spectra of ion vibr. 9-41382
 CO⁺ ion, new electr. band syst. assigned to ²Δ_g-A²Π_g transition 9-25738
 CO⁺+D₂(or CD₄)→COD⁺+D(or CD₃), deviations from stripping model 9-27944
 CO adsorbed on LiF films, u.v. spectra 9-44630
 CO adsorbed on metal films, i.r. absorption spectra 9-26193
 CO adsorption on W single crystal faces, surface potentials determ. 9-48775
 CO anodic oxidation in 6N KOH on Ni₃S₂ 9-31193
 CO chemisorbed on Rh, Ir and Pt, i.r. spectra, temp. effect 9-43325
 CO chemisorption on metal surfaces, π-electron system and bond energies 9-39948
 CO conc. in Arctic atmospheres 9-43386

Carbon compounds continued

- CO dissoci. in He⁺-CO collisions, excited C ions form. obs. 9-36724
 CO electronic transitions, pulsed laser action at cooling of gas 9-47979
 CO fundamental, ratio of collision cross-sections for self-broadening to foreign-gas broadening 9-25735
 CO i.r. absorptance down to 113°K 9-32471
 CO line spectrum solar center-to-limb behavior 9-31633
 CO mol., electron reson. scatt., elastic and inelastic channel obs. 9-23057
 CO mol., i.r. bands, self and foreign gas broadening effects, comparison 9-27848
 CO mol. gas, excited by fast electrons, glow spectra in i.r. region 9-38831
 CO molecules, rel. to scattering of O and N atoms 9-25712
 CO on Ni, desorption induced by photon radiation 2.1-4.8 eV 9-23647
 CO oxidation, photosensitized, of ZnO on Ag support 9-28796
 CO₂ fluid mixing laser system, gain meas. 9-22392
 CO₂ laser, rotational relaxation rate 9-22387
 CO₂ laser radiation, effects of wind on thermal defocusing 9-22424
 CO₂ lasers, inversion kinetics, use of pulse pumping combined with Q-switching 9-22389
 CO₂ lasers, mode competition for case of homogeneous line broadening 9-22375
 CO₂ lasers, spontaneous emission from discharges, spectroscopic investigation 9-22388
 COH⁺, protonated CO, non-empirical molecular orbital calc. of most stable configuration 9-34613
 COS, valence force consts., mean amplitudes of vibration, thermodynamic functions 9-23032
 CO+N₂O bimolec. reaction in single pulse shock tube 9-43321
 CO₂(001), deactivation rate determ. by meas. intensity of fluorescence radiation 9-25732
 CS, new band system in near u.v. region, seen in diffusion flames 9-48456
 CS₂-Ar, shock heated, emission spectrum rel. to CS₂ thermal decomp., obs. 9-35740
 CS₂, backward stimulated Raman scatt. 9-23504
 CS₂, cryst. struct., high-press. 9-32903
 CS₂, eff. on corrosion of tinplate 9-28803
 CS₂, hypersonic absorpt. determ. from Brillouin line breadth 9-44560
 CS₂, Raman scattering, backward-stimulated, investigation 9-26114
 CS₂, stimulated Brillouin scattering threshold and line shift, temp. dependence 9-26110
 CS₂, Kerr cells, laser internal microwave modulation 9-36285
 CS₂ mol. trapped, e and Rydberg transitions, u.v. obs. 9-32466
 CS₂ reaction with atomic O, e.s.r. detect. 9-24534
 CS₂ with large optical Kerr effect, subpicosecond pulse generation 9-48002
 CS₂ i.r. and Raman spectra 9-34614
 Cn polar mol., rotational transition by electron collisions, differential cross sections 9-46360
 Co₂-Ar mixtures, desorption rates from silica gel. at various temps. 9-46663
 Co₂-N₂-He discharge, lasing action influence on electron energy distrib. 9-34800
 Co₂-N binary syst., mass transfer cooling of flat plate, dissociation depend. 9-25789
 Co₂, deactivation of bending mode by H₂ and D₂ 9-23034
 Co₂ spectral lines, collision broadened, shapes 9-40590
 Co⁺, radiative lifetime of B²Σ⁺ state 9-44321
 Fe-C alloy, microcrack formation, statistical analysis 9-30694
 Fe-C alloy, shape strain for (225)_r martensitic transformation 9-28344
 Fe-C alloy, surface contamination during H₂ annealing 9-36938
 Fe-C alloys, oxidation at 500°C 9-31197
 Fe-C alloys, phase transform. singularities during tempering and cold plastic deform. 9-39496
 Fe-C martensite crystal, diffuse electron scattering due to short-range order 9-32912
 Fe(0.05 wt.%)C alloy, dislocation-interstitial interactions 9-30594
 Fe-Mn-C alloys, internal friction temp. dependence rel. to stress-induced ordering of C 9-23862
 Fe-Mn-C alloys, internal friction temp. dependence rel. to stress-induced ordering of C 9-23862
 Fe-Mn-C alloys, shape strain for (225)_r martensitic transformation 9-28344
 Fe-Ni-C alloy, shape strain for (259)_r martensitic transformation 9-28344
 Fe₈₀P₁₅C₅ alloy, amorphous ferromag., resistivity minimum 9-37429
 Fe₈₀P₁₅C₅ amorphous ferromag. alloy, Hall effect 9-39578
 Fe-≤(0.04 wt.%)C-, quench aged, under cyclic straining, mech and microstruct. changes 9-33079
 He*CO collisions, excited ions form. obs. 9-36724
 ICN, Fermi reson. const. 9-32467
 N₂-CO₂ supersonic expansion in Laval nozzle, CO₂ population inversion 9-48648
 Na-C-O system, three-phase equil., thermodynamic analysis 9-39127
 Ni-C eutectic alloy, flake graphite struct. and defects obs., microscopy 9-44671
 Ni-C solid solns., Curie temps and residual resistivities 9-44914
 OCS, Mag. susceptibility anisotropy and quadrupole moment 9-30046
 PCL⁺, SAVE-CNDO theory, semi-empirical all valence electron, effective field gradient 9-42413

Carbon tetrachloride (CCl₄) *see Organic compounds***Carcinotrons** *see Electromagnetic oscillations; Electron tubes***Carrier mobility** *see Crystal electron states/transport processes; Semiconductor materials; Semiconductors***Carrier scattering** *see Crystal electron states/transport processes; Semiconductor materials; Semiconductors***Catalysis**

- see also Reaction kinetics*
 benzalacetophenone-mesityl oxide reaction, Li-catalysed condensation, obs. 9-47461
 in copolymerization of ethylene, propylene and 4-vinylcyclohexane-1 9-31188
 diamond formation from graphite in presence of metals, catalytic behaviour of metallic intermediate cpds. 9-41064
 ethyl cinnamate-mesityl oxide reaction, Li-catalysed condensation, obs. 9-47461
 metal oxides, rel. to irradiation effects from e.s.r. obs. 9-35709
 i-propanol on Al oxides, catalytic decomposition, apparatus for obs. 9-37823
 propylene-1-d₁, thermal and NO catalyzed cis-trans isomerization 9-43328

Catalysis continued

- C gasification 9-49377
- on Ni-Al₂O₃, D exchange between H and H₂O vapour, obs. 9-28790
- Ni, interactions of N₂O, NO and CO₂ on adsorption 9-35003
- O atom exposure-depend. surface recomb. 9-28791
- Pt-Ni electrocatalysts for H₂/CO fuel cell anodes 9-29365
- α -SiC etching in H at high temp., susceptor material catalytic action 9-30514
- W, equilibration of ³⁰N₂ and ²⁸N₂ mixture, distrib. of active sites on surface 9-33662

Cataphoresis *see Electrophoresis***Cathode rays** *see Electron beams***Cathode-ray oscillographs** *see Electrical measurement***Cathode-ray tubes** *see Electron tubes***Cathodes***see also Electron emission*

- alkali-antimonide, photoemission, thermosensitive discontinuities and hystereses at high light intensities 9-39740
- in arc discharge, spot damage, effect of alkali element introduction 9-30322
- arc lamp, l.p. and high-current energy balance 9-48640
- arc track obs., current density meas. 9-32711
- cooled, in MHD generator, potential drop 9-22333
- crossed-wire system, rel. to elec. conduction in hexane and decane liqs. 9-40804
- destruction in vacuum impulse discharge 9-48620
- electron gun heated by electron bombardment, cathode temp. stabilization 9-40316
- erosion in spark discharge 9-43330
- erosion rate at electrodes of an arc rotated by a transverse mag. field 9-42578
- geoides, deviations from mean level in English Channel 9-24611
- glow space in hollow cathode, optical investigation 9-40719
- graphite, temp. meas. for arcs in room air 9-30321
- hollow, feeding cct. parameter changes rel. to discharge 9-48618
- metal, photoelec. yield in vacuum u.v., reproducibility and stability 9-26616
- Penning structure, axial electron flow with excess energy 9-25189
- photo, emitted, electron kinetic energy theory 9-41281
- photocathodes, prep. props. and uses, book 9-49173
- plasma jet, for Ar laser 9-40351
- plasma-electrode system, elec. breakdown, investig. 9-40724
- refractory materials condensation and evaporation in Cs arc effective heats 9-44513
- spot retrograde motion, explanation based on ions movement near edge 9-42581
- Zirconia, yttria-stabilized, conductivity obs. 9-33248
- electron guns, tip and needle types, high stability 9-25182
- Au contacts on CdS, reduction of work function with increasing photocurrent 9-39732
- C temp. meas. for arcs in room air 9-30321
- CdS films, longit. conductivity under e. bombardment 9-41155
- Cs₂Te, in photomultipliers, props. 9-25190
- Cs₂Sb, photoemission, thermosensitive discontinuities and hystereses at high light intensities 9-39740
- Cu, erosion in high current discharge and cathode spot temp., obs. 9-34798
- CuBe, photoelec. yield in vacuum u.v. 9-26616
- GaAs_{1-x}P_x photoemissive, p-type, C activated, with high quantum yield for visible spectrum 9-49174
- He-Ne laser, effect of temperature on illuminating power 9-29417
- LaB₆, poisoning 9-42731
- LiF, photoelec. yield in vacuum u.v., eff. of irrad. 9-26616
- MO spot fixator lifetime rel. to dispersion threshold 9-49169
- Ni, erosion in high current discharge and cathode spot temp., obs. 9-34798
- Ni spot fixator lifetime rel. to dispersion threshold 9-49169
- spot fixators, Ni and Mo, destruction mechanism 9-49169
- SrF₂, photoelec. yield in vacuum u.v. 9-26616
- W, erosion high current discharge and cathode spot temp., obs. 9-34798
- W, field emission, Ge coated surfaces with oxygen adsorption, electron emission charact. stability 9-45030
- W of variable current, plasmatoms, emission 9-43141
- ZnS films, longit. conductivity under e. bombardment 9-41155
- ZnSe films, longit. conductivity under e. bombardment 9-41155

oxide

- in arc discharges, effect of characteristics on positive column plasma 9-39028
- current extraction systems, electron energy distribution 9-41278
- dispersed Ni in coating, infl. on emission props. 9-24245
- emission distrib., surface, obs. 9-49172
- properties, effect on positive column plasma in Ar-Hg discharge 9-48631
- rare-earth metal cpds., preparation, coating techniques and properties 9-41279
- work function reduction, electric field effect 9-30999
- BaO, thermal conductivity meas. method 9-30794
- BaSrO, in nonreactive atmosphere for gas laser use, properties 9-49171
- BaZrO₃, in reactive atmosphere for gas laser use, properties 9-49171
- W oxides, thermionic emission properties 9-33419

Cathodoluminescence *see Luminescence***Causality** *see Physics fundamentals***Cavitation***see also Vortices*

- acoustic streaming flow vel. calc. 9-23427
- bubble dynamics in 20.5 KHz u.s. field 9-34855
- bubble growth and oscils. in water-filled press. chamber, photographs and theory 9-42629
- bubble in 205 KHz u.s. field 9-34855
- cement, wet, cavities on surface due to impinging air jet 9-40762
- control of cavitation fields 9-36833
- elementary zones, growth investigated with cinecamera 9-23488
- erosion, application of rocket effect on bubbles 9-39068
- erosion due to u.s. cavitation 9-34856
- erosion in non-aqueous liquid 9-36834
- glycerine in water, sonically induced, low level excitation of luminescence obs. 9-36871
- hailstones, induction of cavitation by u.s. waves 9-45491
- high-speed photographic obs. 9-32754
- inception in two-dimensional and periodical motion of hydrofoils 9-26062

Cavitation continued

- liquid, effect of elec. current on vortex street behind a cylinder 9-48676
- in liquids, collapse by elec. discharge 9-48675
- noise associated with bubble collapse 9-23489
- noise from rot. bars in water, spectra 9-26059
- in organic liquids, due to laser irradiation 9-48710
- pressure pulse of collapsing bubble, temporal and spacial contours 9-42628
- role in acoustic atomization of liquids 9-46626
- scale formulae for reaction type water turbines 9-34857
- solids, hydrogen penetration, a mechanism of cavitation damage ? 9-44746
- sonically induced, low level excitation of luminescence obs. 9-36871
- spherical cavity closing, effect of solid wall 9-23428
- spherical sound wave propagation, energy loss due to cavitation 9-36867
- ultrasonic, relaxation phenomena 9-46629
- u.s., true, absence of erosion, chemical effects, sonoluminesc., explanation 9-36832
- void, sound radiation, effect of gas diffusion into cavity 9-28087
- in water, acoustic method of determining the distribution of air nuclei responsible 9-22264
- water, cavities on surface due to impinging air jet 9-40762
- water, spherical empty cavity, collapsing, flow field behind 9-23429
- water, threshold lowering by fast neutron irradiation 9-46592
- in He II heat induced counterflow 9-44609
- KI, ultrasonic, relaxation phenomena 9-46629
- Ni, increase due to oxidation 9-39424
- Ta, hydrogen penetration, an mechanism of cavitation damage ? 9-44746

Cavity resonators *see Acoustic resonators; Electromagnetic oscillations***Celestial mechanics**

- ADS 11680, improved orbit 9-31551
- ADS 9392, improved orbit 9-29032
- asteroids in resonance with Jupiter, secular motion analysed 9-24850
- Barnard's star, alternate dynamical analysis 9-47633
- η Cas, orbit calc. 9-47634
- and classical astronomy 9-40118
- Darwin ellipsoids, congruent, synchronous coupled oscils., instabilities 9-49527
- deformable bodies, precession and nutation, equations 9-49528
- deformable bodies, precession and nutation, soln. to equations 9-47618
- dynamical systems with two degrees of freedom, second order stability 9-47617
- Earth velocity w.r.t. cosmic 3°K background radiation 9-45668
- earth-moon system, motion of small mass 9-43773
- Earth-to-Moon trajectories, asymptotic soln., errata and addenda 9-26970
- eclipses, book 9-33893
- equatorial co-ordinate system rel. to sidereal-diurnal variations of cosmic rays 9-35933
- estimation of trajectories and rotation in a central gravitational field 9-33892
- expanding universe, concentration of matter anal. via 'critical density ratio' 9-24737
- figure-eight periodic orbits, family generation in restricted three-body problem 9-26988
- force law K_c calc. using obs. of the A0-AZ NGP stars 9-28987
- galaxy, changes in shape and rotation due to stellar evaporation 9-31506
- Laplace theory, role of Callisto's evection principle 9-49526
- Newton's const. variation with gravitational potential, assumption and possible test 9-47620
- orbits, perfectly plane, determination 9-47619
- orbits, periodic, Trojan, for the reson. 1/12, 9-29069
- orbits asymptotic to periodic orbit, construction 9-28986
- perturbations in the solar system, elementary book 9-43512
- postgraduate level text 9-49529
- random force and its time derivative, numerical tables 9-47621
- rotational motion of triaxial rigid body orbiting oblate primary, first-order theory 9-31496
- satellite, ellipsoidal, under spheroidal planet and point sun gravitational attraction 9-24735
- satellite orbits, perturbations due to sun and moon 9-35940
- satellites, artificial, 16, orbital parameters and plots 9-45725
- self-gravitating system in uniform motion, gravitohydrodynamic instability criterion 9-24732
- self-gravitating systems; structure of galaxies 9-47622
- solar system, motion of planets and space probes, popular review articles, book 9-49574
- space probe orbital information on planet masses and lunar mascons, popular article 9-47607
- spheroidal expansions of rot. gas masses, gravitational instability, cosmogonic fragmentation mechanism 9-24733
- stability, local, of non-rot. system of particles in gravitational Einstein field 9-24734
- stability of galactic arm, Lagrange and Jacobi identities 9-31498
- stellar orbits in galactic plane, in generalized Kepler motion 9-24760
- Tau Persei, parallax and orbital motion, obs. (1945-64) 9-29030
- three-body problem, unrestricted, Hill stability 9-24736
- two rigid spheroids, restricted problem, 9-38036
- universe rot., discussion 9-24721

Cell model *see Liquids, theory***Centrifuges**

- in crystal growth 9-37022
- demonstration of force for students using candle flame 9-36102

Ceramics

- alumina, cryochem. method for prep. 9-33125
- alumina, thin wall capillary tubes, fabrication by vapour deposition 9-35220
- alumina strengthening by glazing and quenching 9-23935
- aqueous conductivity of unfired ceramic bodies, method 9-28387
- brittleness and impact resistance, comparison 9-46905
- carbide-boride-graphite, fusion-cast, phase assemblages, microstruct., props. 9-30729
- casting, u.s. 9-37275
- cements, high-temperature, compatibility expts. 9-23945
- crystal struct. defects and reactivity, effect of very high press. 9-30553
- defect structures review 9-30727
- densification by isostatic pressing technique 9-30726
- engineering, high-temp. 9-23960
- engineering and economy of industrial society 9-23959

Ceramics continued

- fabrication by electrophoretic deposition 9-35219
 fabrication problems, shaping and densification limitations 9-35215
 ferroelectric, permittivity var. with elec. field, applic. to parametron 9-30969
 ferroelectric, pyroelectric effect 9-39684
 ferroelectric, VK-2, VK-4 and VK-6 film Varikonds, nonlinear and switching props. 9-39675
 ferroelectric, with different types of crystal struct., orientational dielec. polarization calcs. 9-47163
 in fuel cells, molten-carbonate, use as insulators, electrodes and electrolyte diaphragms 9-31899
 glass, impact compressive strength determ. device 9-33031
 glass, transparent 9-49234
 glass-ceramics, optical, properties and applications 9-33500
 glass-crystal composites, strength rel. to shape of dispersed particles 9-48884
 glass/ceramic mats., two-phase, strengths, crack formation and stresses around part. obs. 9-30677
 impact resistance and brittleness, comparison 9-46905
 lenses for control of u.s. energy 9-36195
 magnesia, cryochrom. method for prep. 9-33125
 mechanical properties, strength and fracture behaviour 9-33011
 nuclear fuel, radiation effects, review 9-22902
 $\text{Pb}_{0.95}\text{Sr}_{0.05}(\text{Zr}_{0.55}\text{Ti}_{0.45})\text{O}_3 + 3\% \text{PbO}$ ferroelectric, internal friction 9-41004
 perlite, elastic constants rel. to porosity 9-30635
 piezoelec. plate coupled to N-Si acoustic wave amplification 9-26419
 piezoelectric, Na_2O , Li_2O , and Nb_2O_5 composition, patent 9-30725
 piezoelectric, props. rel. to orientational dielec. polarization 9-47187
 piezoelectric coeffs., accurate meas. method 9-37592
 polycrystalline, crack interaction with microstructure, monitoring technique 9-33091
 porcelain enamel slips, particle size determ. by composite method 9-23611
 powder compacted nuclear fuel, Bi heat-transfer bond to cladding 9-22892
 powders, vibration pressing 9-35217
 preparation, cryochrom. method 9-33125
 properties, practical limitations and industrial applications rel. to metals, book 9-23961
 quartz, strength as influenced by caking and crystn. 9-48908
 seal, ceramic-to-metal, formation, patent 9-24995
 seal, ceramic-to-metal conductive, composition, patent 9-24996
 silica, cryochrom. method for prep. 9-33125
 thermal diffusivity meas. by a modulated electron beam technique 9-48973
 thermal stress resistance and micromech. thermal stresses in porous, brittle mats. 9-48968
 thermomechanical processing 9-35216
 three-dimensional and stereo obs, using secondary electron emission mode of scanning microscope 9-32825
 titanate materials, lattice defects and colour centres 9-32942
 titanobarium, Ti valence and Al co-ordination no. determ. from X-ray emission spectra 9-41398
 toughness meas., rel. to work of fracture 9-37247
 tube fabrication, varying props., lab. technique 9-35218
 whitewares, quartz particle strain meas. by X-ray technique 9-23869
 zirconia, stabilized particles, prep. by sol-gel process 9-30731
 AlN refractory, melting technique 9-34955
 BaTiO_3 , absolute reflectance spectra, $0.325\text{--}0.7\ \mu$ 9-33537
 BaTiO_3 , irradiation effect on electrophysical props. 9-41238
 BaTiO_3 base, thermal conductivity influence of d.c. field in phase transition region 9-39545
 BaTiO_3 s.h.f. dispersion of dielec. constant in low-temp. phases 9-39687
 $\text{CuCr}_2\text{Se}_4\text{--Br}_2$ spinels, press. sintering 9-33126
 HfB₂, densification in high-press. hot-pressing, mechanisms 9-35223
 [(1-x)Li_{1-x}Ca]MnO₃, prep., struct., phase transform. behaviour 9-33127
 MgAl_2O_4 spinel, sintered, kinetics of formation 9-28389
 MgF_2 , hot-pressed, u.s. shear wave propag. meas. 9-46983
 $(\text{Na}_{1-x}\text{Li}_x)\text{NbO}_3$ solid solution, structure, dielectric and piezoelec. props. 9-26389
 $\text{Pb}_{1-x}\text{Zr}_x\text{TiO}$ transducer ceramic, mechanical loss, large amplitude static and dynamic stress effects. 9-39397
 PbTi_2O_7 pyrochlore, X-ray diff. pattern 9-40914
 Pb zirconate-titanate ceramics, optical and electrooptical properties, improvements 9-35485
 PbO-SiO_2 system, crystallization sequences in silica phase 9-26390
 PbTiO_3 glass, study of composites for homogeneous crystn. 9-46941
 $\text{Pb}(\text{Zr,Ti})\text{O}_3$ piezoelectric, adulterated, high-field losses 9-26585
 $\text{Pb}(\text{La}_{0.5}\text{M}^{3+}_{0.5})_{1-x}\text{Ti}_x\text{--xO}_3$, (M=V or Nb), props. rel. to composition 9-24220
 Pt-SiO cermet thin films, resistances obs. 9-47155
 Pu compounds, physical props., data manual 9-22907
 $\text{F}_2\text{O-C}$ fibre reinforced, Young's modulus, rupture modulus and fracture toughness 9-44773
 $\text{SrTiO}_3\text{:Zr}$, superconducting, effective masses determ. 9-26532
 $\text{SrTiO}_3\text{:Zr}$, superconducting, effective masses determ. 9-26532
 UO_2 -metal cermets, preparation and thermic conductivity 9-26455
 UO_2 cermet from $\text{UO}_2\text{-Mo}$ system, by particle coating and isostatic hot pressing 9-35222
 W-UO_2 cermet produced from coated particles, high temp. creep-rupture tests 9-23910
 $\text{Y}_2\text{O}_3\text{:ThO}$ sintered optical material, prep., props. and applic. 9-33501

Cherenkov radiation *see Cherenkov radiation***Cerium**

- Cv centre in MeF_2 type crystals, Stark structure of $5d^1$ config. 9-43228
 compressibility, adiabatic, low-temp. phase transform. effect 9-40997
 Debye temp., low-temp. phase transform. effect 9-40997
 elastic moduli, low-temp. phase transform. effect 9-40997
 garnet, Ce activated, fluorescence 9-26777
 IV, isotope shifts between ^{140}Ce and ^{142}Ce , obs. 9-34533
 position annihilation meas., γ - α phase transition obs. 9-46946
 X-ray determination in modular iron 9-35763
 X-ray structural analysis, transition to tetravalent state under press., 50 kbar 9-41072
 Ce-S solid solution, transition metal doped, thermal conductivity, temp. depend. 9-37368
 α , γ -Ce, band struct. 9-33230
 γ -, α -Ce, positron annihilation, phase obs. 9-46946

Cerium continued

- Ce₂, dissociation energy 9-48512
 $\text{Ce}^{3+}\text{-H}^-$, $\text{Ce}^{3+}\text{-F}^-$ ENDOR obs. in CaF_2 9-37808
 Ce^{3+} , dipolar-broadened electron resonance lines in $43\frac{1}{2}\text{.24H}_2\text{O}$, saturation, in presence of phonon bottleneck 9-49347
 Ce^{3+} , H⁻ and D⁻ compensated tetragonal centres in CaF_2 , ENDOR 9-39927
 Ce^{3+} impurities in CaF_2 , presence of permanent dipoles 9-37166
 Ce^{3+} impurity ions in cubic centres in CaF_2 , lattice distortion 9-26198
 Ce^{3+} in ag. soln., indirect determ. of short relax. time 9-30426
 Ce^{3+} in $\text{CaF}_2\text{:Dy}^{3+}$, codopant eff. on luminescence 9-35682
 Ce^{3+} in CaF_2 , thermal conductivity in mag. fields 9-47008
 Ce^{3+} in $\text{La}_2\text{Mg}_3(\text{NO}_3)_{12}$, Orbach relax. processes, T_1 and T_2 9-24492
 Ce^{3+} in $\text{La}_2\text{Mg}_3(\text{NO}_3)_{12}$, e.s.r. temp. dependence, T_1/T_2 ratios 9-24483
 Ce^{3+} in MeF_2 crystal, lowest Stark sublevels of $4f^1$, $5d^1$ configurations determ. 9-22947
 Ce^{3+} in rare earth oxysulphates (Ln_2SO_6), fluoresc., phosphors obs. 9-43258
 Ce^{3+} ions in disordered systems, e.p.r. line shapes 9-28742
 Ce^{4+} coloration impurity in lanthanum glass, effect on light absorption 9-24372
 Ce I, II, infrared lines, isotope shifts 9-29989
 Ce II solar lines, 4000 Å-4700 Å, non-coherent scatt. explanation 9-29089
 Ce II solar lines, reversal from absorpt. to emission 9-40187
 La-Ce Kondo superconductor, quasibound states obs. 9-33268
 in YPO_4 u.v. phosphor, sensitization by Th ions 9-31140
- Cerium compounds**
 hydrides, nonstoichiometric crysts., elec. resistivities 9-44907
 Ce-C system, vaporization thermodynamics 9-32821
 Ce-La alloys nondil., resistance minima, spin-compensated mag. state and Neel temp. obs. 9-35337
 Ce-Y alloys, nondil., resistance minima, spin-compensated mag. state and Neel temp. obs. 9-35337
 $\text{Ce}_2\text{Mg}_3(\text{NO}_3)_{12}\cdot 24\text{H}_2\text{O}$, obs. antiferromagnetic in mellekelvin range 9-45210
 $(\text{Ce}_{1-x}\text{La}_x)_2\text{Mg}_3(\text{NO}_3)_{12}\cdot 24\text{H}_2\text{O}$, dipolar-broadened electron resonance lines of Ce^{3+} ions, saturation, in presence of phonon bottleneck 9-49347
 γ -Ce alloys, Young's modulus anomalous decrease, low temp. 9-44751
 CeB_6 , antiferromagnetic, inverse susceptibility, theory 9-45209
 CeBr_3 , magnetic interaction tensors from adiabatic susceptibility meas. 9-47229
 CeC, stability 9-32490
 CeC_2 , heat of formation 9-32821
 CeCl_3 , electronic and phonon Raman effects, asymmetry 9-26755
 CeCl_3 , electronic Raman effect 9-24424
 CeCl_3 in aqueous soln., fluoresc. quenching by org. ligands 9-42665
 $\text{CeF}_3\text{:Nd}^{3+}$ oriented single cryst., far i.r. electr. and vibronic transitions 9-39843
 $\text{CeF}_3\text{:Nd}^{3+}$ single cryst., far i.r. electronic and vibronic transitions obs. 9-35653
 CeF_3 , CeO_2 thin film capacitor, break-down studies 9-37586
 CeF_3 , polarized i.r. reflectance, optical phonons and mag. symmetry 9-47345
 CeFeO_3 orthoferri, prop., mag. props., Mossbauer spectra 9-45055
 $\text{CeMg}(\text{NO}_3)_3$, ground-state g factor, mag. field depend. 9-43276
 $\text{CeMg}(\text{NO}_3)_3$, high field magnetization, calibration error correct. 9-43277
 $\text{CeMg}(\text{NO}_3)_3$ pure dipole-dipole system, entropy and susceptibility 9-45054
 $\text{CeO}_2\text{:Gd}^{3+}$, ENDOR obs. on ^{155}Gd and ^{157}Gd , nucl. mag. moments and hyperfine struct. anomaly obs. 9-35733
 $\text{CeO}_2\text{:Sm}$ luminescence centres investigated 9-33594
 CeO_2 , formation of trigonal Dy^{3+} , Er^{3+} and Yb^{3+} centres from charge compensation mechanical, ENDOR study 9-33652
 CeO_2 , growth of single cryst. from PbF_2 flux melts 9-35025
 CeO_2 and $\text{CeO}_2\text{:Gd}^{3+}$ single crystals, elec. conductivity, thermoelec. power and O diffusion coeff. 9-33246
 CeO_2 thin films, a.c. and d.c. behaviour 9-39664
 $\text{CeO}_2\text{-ZrO}_2$ binary system, solvated electron study 9-39957
 CeSi, cryst. struct. 9-32907
 La-Ce dilute alloy, Kondo superconductor, quasiband states 9-44941
 La-Ce dilute alloys, Kondo temp. determ. from thermoelec. power and resistivity meas. 9-43152
 La-Fe dilute solid solns. Kondo phenomenon 9-44913
 $\text{La}_{1-x}\text{Ce}_x\text{Al}_3$ alloys, supercond. transition temp., eff. of press. 9-28477
 $\text{La}_{1-x}\text{Ce}_x\text{In}$ alloys, supercond., transition temp. rel. to pressure, 0-23kbar 9-47090
 Pu-Ce delta-stabilized alloys elastic and anelastic behaviour at low temp. 9-37224
 δ -Pu (10 at %)Ce, thermal cond. in temp. range 75-300°K 9-41108

Cermets *see Ceramics; Metals***Change of state** *see Boiling; Condensation; Freezing; Melting; Phase transformations; Sublimation; Vaporization***Characteristic temperature** *see Specific heat***Charcoal** *see Carbon***Charge** *see Electric charge***Charge carriers** *see Crystal electron states; Semiconducting materials; Semiconductors***Charge compensation**

- group II-VI compounds, of ionized donor, e.p.r. monitoring 9-37531
 $\text{CaF}_2\text{:Eu}^{3+}$ emission and excitation spectra, Eu-O complexes identification 9-47391
 CdTe:Yb, Er, effects of P and Li compensation on rare earth doping, e.p.r. study 9-47434
 CeO_2 , mechanisms rel. to trigonal Dy^{3+} , Er^{3+} and Yb^{3+} centres, ENDOR studies 9-33652
 ZnSe:V, of ionized donor, e.p.r. monitoring 9-37531

Charge exchange

- alkali atoms, of protons rel. to internal shell electron capture 9-44254
 aromatic molecules, π - π^* charge-transfer states 9-32495
 atomic, quantum treatment in book on approximation methods 9-40242
 cross-sections, meas. 9-36781
 cross-sections, meas. 9-36782
 cross-sections at high energies, isotopic effect using H and D 9-30301
 in interaction pot. between alkali ions and rare gas atoms 9-25711
 ion charge transfer in gaseous discharges, review 9-32699
 ion-atom slow interchange reactions, temp. depend. 9-43312
 ion-molecule reactions, electron density rearrangement theory 9-28778

Charge exchange continued

- ions, negative, on atomic and molecular targets, cross-section meas. 9-22980
- methyl-pyridinium salts, anomalous charge transfer fluorescence 9-34679
- in night-time F region, nonlinear loss and decay 9-31443
- organic charge-transfer complexes, solid, electro-optical effect 9-45281
- in plasma, partially ionized, accidental resonance and ion momentum transfer 9-46467
- π - π^* transfer states in aromatic molecules 9-32495
- reactions with H₂, D₂ and He, producing H⁺ polarized beams 9-34585
- resonance and ion momentum transfer in partially ionized plasma 9-46467
- transition metal carbides, electron transfer, electron spectroscopic meas. 9-44636
- pn scatt., contrib. to amplitude from moving cuts 9-38578
- π - p to π -n, polarization meas. 9-27523
- π^+ scatt. by ¹²C- π ⁰, ¹³N cross section around 1st resonance in π -N system meas. 9-22807
- π^+ , π^0 on light nuclei, cross section calc. at (3,3) resonance 9-34302
- π^+ , single, rel. to spectroscopy of light nuclei 9-22715
- Ar⁺-Ar. oscillations in cross-sections 9-38791
- Ar⁺ ions, collisions with surface Cu atoms, charge exchange of scattered ions 9-48418
- Ar⁺+Ar excitation resonances for production of metastable atoms 9-34560
- Ar⁺+CH₄→Ar+CH₃⁺+H→Ar+CH₂⁺+H₂, 1.5-4.2 eV range, mechanism 9-39936
- Ar and H collision, -ve charge prod. cross section determ., 50-1000 eV 9-27826
- ¹¹B(π , π^0)¹²C single charge-exchange react., cross-section, E_π=80 to 200 MeV 9-25641
- C₁₂FeCl₃, electron charge transfer to Fe, Mossbauer spectra obs. 9-24378
- C₁₂FeCl₃, electron charge transfer to Fe, Mossbauer spectra obs. 9-24378
- Cs, He⁺ and Ar⁺ collisions, total charge-transfer cross section meas., 10-1500 eV 9-46316
- D₂ transfer reactions with CO₂⁺, D₂O⁺ and H₂S⁺, kinetics 9-49374
- D₂⁺-D₂(H₂) charge-exchange collisions, search for isotope effect 9-44295
- GaAs, covalent charge transfer 9-33302
- GaSb, covalent charge transfer 9-33302
- H₂⁺ collision with molecular gas, products obs. 9-22995
- H₂⁺-H₂ collisions, and vibrational excitations 9-23051
- H₂ and H collision, -ve charge prod. cross section determ., 50-1000 eV 9-27826
- H₂O⁺ vapour ions, transfer cross sections 9-25967
- H₂-He fast beam, He⁺ formation 9-29985
- H₃⁺ de-excitation by H₂, energy transfer 9-44494
- H⁺-H₂ interac., elementary processes 9-30165
- H⁺ collision with molecular gas, products obs. 9-22995
- H⁺ on all ground state atoms, 5-140KeV calc. of charge exchange ratio of excited to all captures 9-25717
- H⁺-D₂(H₂) charge-exchange collisions, search for isotope effect 9-44295
- H⁺+He(S²)→H(2S)+He⁺(S) cross section normalization 9-22996
- H atoms and ions, 5-70 keV, in Mg vapour, electron transfer cross-section meas. 9-22997
- H excited atoms, collisions with protons, resonance charge transfer, classical approx. 9-48428
- H excited atoms, collisions with protons, resonance charge transfer, quantal two-state approx. 9-48427
- H formation by proton bombard of Na and Li atoms 9-27813
- H ion beam, with H₂O mols., effective cross sections for energies 1 to 60 keV 9-44493
- He⁺ collision with molecular gas, products obs. 9-22995
- He²⁺+H(1s) collisions, resonance charge transfer 9-48435
- He and H collision, -ve charge prod. cross section determ., 50-1000 eV 9-27826
- ³He and ⁴He gases, proton bombardment, cross sections 9-48614
- He+p collisions, polarization of Balmer- α radiation 9-22989
- Hg⁺ in atomic Hg, charge-transfer cross sections 9-48420
- I ion beam in H₂, equilibrium charge state 9-46319
- InAs, covalent charge transfer 9-33302
- K, He⁺ and Ar⁺ collisions, total charge-transfer cross section meas., 10-1500 eV 9-46316
- Kr⁺, symmetric charge transfer, (²P_{1/2}→²P_{1/2}) 9-44261
- Li target, proton bomb., H atom formation cross section 9-27813
- ⁷Li(π , π^0)⁷B, double charge-exchange react., cross-section, E_π=80 to 200 MeV 9-25641
- N₂⁺+O₂→N₂+O₂⁺, in gas discharge in N₂-O₂ 9-30303
- N₂⁺+O₂→N₂+O₂⁺, energy depend. in thermal and low eV region 9-42565
- Na target, proton bomb., H atom formation cross section 9-27813
- Ne and H collision, -ve charge prod. cross section determ., 50-1000 eV 9-27826
- ¹⁴N(π , π^0)¹⁴O, 180 MeV obs. and comparison with calc. 9-22808
- Rb He⁺ and Ar⁺ collisions, total charge transfer cross section meas., 10-1500 eV 9-46316
- Ti cpds., electron transfer, electron spectroscopic meas. 9-44636
- V cpds., electron transfer electron spectroscopic meas. 9-44636
- Xe-methane, obs. by ion-cyclotron double reson. 9-44495
- Xe-methane system, using tandem mass spectrometer 9-42566
- Xe⁺, symmetric charge transfer, (²P_{1/2}→²P_{1/2}) 9-44261
- ⁹¹Zr(p,n)⁹¹Nb⁺, cross section calc. 9-40512

Chelates see *Molecules; Organic compounds. For inorganic chelates see under metal compound headings*

Chemical analysis

- see also *Spectrochemical analysis*
- aromatic hydrocarbon mixtures, by selective fluoresc. 9-24605
- atmospheric gas, electrochem. concentration cells 9-41457
- Auger e spectrometer for analysis of contaminants on the surface in ultrahigh vacuum work 9-39150
- Auger spectroscopy, excitation by internal secondary electrons 9-49401
- electron probe micro-analysis method for films <4μm 9-24607
- element composition by neutron resonance absorption and activation method 9-37844
- gases from acoustic pulse following microwave irradiation 9-28077
- grain size effect in low energy γ and X-ray scatt. 9-49399
- isotopic, of solid samples, improved mass spectrometry 9-29899
- lunar surface composition, direct methods for analysis 9-24836
- medical technology, book 9-41714
- meteorites (chondrites), K and Xe, isotopic composition 9-49393

Chemical analysis continued

- micas, kersantites, minettes and lamproites, composition and physical props. 9-32898
- microanalysis using monochromatic cathodoluminesc. image obs. in scanning electron microscope 9-43266
- microsampling by laser-microscope system 9-24594
- microscopy, chemical, in historical object examination 9-26846
- of mineral aggregates, fine-grained using electron microprobe scanning pictures 9-39971
- moisture probe, h.f., response to soluble salts 9-49389
- moussanite, PbFe₂(VO₄)(OH)₂, X-ray powder obs. 9-32925
- nuclear fuels, irradi., nondestructive assay methods 9-25676
- photomicrographs of inorg. crystal precipitations 9-41458
- polymers, trace contamination identification 9-49391
- Pueblito de Allende meteorite, for organic constituents 9-43638
- raguinite, giving a formula TlFeS₂ 9-30574
- refractory metal microsampling by laser-microscope system 9-24594
- steel, composition, thermoelec. determ. 9-37846
- steel, electron probe microanalysis 9-49398
- steels, C, Mn-containing, determ. of N content 9-46940
- water content in solids, determ. by neutron moderation 9-39972
- γ -ray transmission, monograph 9-37845
- ²³⁹Pu separation with strongly basic anion-exchange resin paper 9-28819
- Ba in meteorites and terrestrial samples, isotopic analyses 9-45674
- CdS, nonstoichiometry of crystals grown by different methods, gas chromatographic meas. 9-36978
- Co-(7.45 at.%)Fe solid soln., γ -phase precip. during ageing 9-41065
- Fe-Ni-Co alloys, complexometric determination of elements 9-45430
- H content in metals, n.m.r. determ. 9-43345
- O isotopic concentrations gradient determinations, ion mass analyzer 9-24596
- UO₂ fuel rods, irradi., isotopic distrib. of U and Pu, theory and expt. 9-25675
- YFe garnet single crystals, homogeneous distribution of gallium 9-36979
- adsorption**
- see also *Chromatography*
- i.r. absorption gas analyser, developments 9-28825
- weighing of adsorbed gases, automatic apparatus 9-38189
- by mass spectrometry**
- see also *Mass spectrometers/applications*
- Auger and photoelectron spectroscopy 9-29961
- diglycerides analysis by coupled mass spectrometry-gas chromatography 9-31221
- gas analysis by modulated molecular beam 9-24595
- high-resolution field ionization 9-29904
- Hull's equation, physical meaning of factor R 9-26836
- isotopic analysis by surface ionization technique, error analysis in double spiking methods 9-35757
- liquid impurity determination by spark-source spectroscopy 9-26837
- mass spectrographic photoplates, quantitative interpretation 9-26838
- methanol 9-31220
- micro-impurity analysis using energy focusing 9-47914
- polyamide (6 nylon) pyrolytic products, analysis 9-43347
- polyvinyl acetate pyrolytic products, analysis 9-43347
- residual gas analysis at high vacuum, fast spectrometer 9-24597
- single-stage, growth curve, by triple filament method 9-47475
- spark source spectrography, sources of error, evaluation 9-31218
- C deposition from r.f. discharges in C containing gases, ionic species involved obs. 9-23353
- Fe high purity, spark source analysis 9-31219
- Mo additive in TaO capacitor films 9-39968
- Pb, triple-filament analysis for calibration of mass spectrometer 9-47475
- Pu in neutron-irradiated UO₂, isotopic analysis 9-43346
- by nuclear reactions**
- activation analysis, non-destructive, total absorpt. peaks shift, effect on determ. accuracy 9-24608
- activation of 60 elements with fast neutrons, detection sensitivity 9-31236
- air, aeration meas. by labelling with methylboric acid and ⁶B(n, α)⁷Li reactions 9-24609
- core analysis by thermal neutron capture cross section, patent 9-33699
- element composition determ. from (n, γ) reaction emission 9-37865
- known and unknown samples, neutron activation analysis, patent 9-39973
- neutron activation, applic. to cystic fibrosis diagnosis 9-49608
- neutron activation, applic. to forensic science 9-27397
- neutron activation, forensic 9-25333
- neutron activation analysis of normal and atherosclerotic aortas 9-36080
- neutron carbon meter, inelastic scattering technique, design 9-33700
- neutron irradiation, flux variation compensation equipment, design and construction 9-35766
- peaks in non-destructive activation analysis, effect of shift on determ. accuracy 9-24608
- rare earth abundances in meteoritic chondrites, neutron activation analysis 9-29077
- separation methods in α activation anal. 9-49402
- ¹²⁵Sb-Be source of thermal neutrons, for precision anal. and tracer prod. 9-28834
- Al surface contamination by C or O 9-26178
- B(n, α)⁷Li, on methylboric acid label in air, meas. of aeration 9-24609
- Fe meteorites, trace element distrib., analytical methods 9-28835
- ⁵³Mn in meteoritic iron, neutron activation analysis 9-39974
- ¹⁶O(d,p)¹⁷O, surface impurities investigation 9-28836
- electrochemical**
- No entries
- radioactive**
- see also *Radiochemistry*
- lower limit of detection for very short-lived radioisotopes 9-25596
- moisture meas. by neutron moderation, depth and surface probes 9-35765
- organic cpds., labelled, new anal. method using interrupted elution 9-24600
- trace, multielement, sensitivity of suitable X-ray fluorescent spectrometer 9-26848
- ²³⁹Pu in waste drums, assay by intensity of 765 keV γ -line 9-37864
- C and O surface distribution by ³He activation and autoradiography surface 9-26849
- GaAs: Cd, meas. rel. to diffusion process of Cd 9-46852
- Li in various materials, by neutron activation 9-26850
- O in Ti and refractory metals, by neutron activation fast 9-26851

Chemical analysis continued
radioactive continued

- SiO₂ film on Si impurities 9-42814
U content of stone meteorites, by fission track method, and Pu-Xe decay intervals 9-45675

X-ray

- see also X-ray examination of materials*
diffraction equipment applic. to forensic science 9-27397
electron microbeam probe samples, colour photography appl. 9-31234
electron probe microanalysis, small sample mounting method 9-39970
electron probe microanalysis recent developments 9-39969
electron-probe microanalysis, X-ray prod. and electron scatt. predictions using Boltzmann eqn. 9-36092
elements in low at. no. matrices, sensitivity of radioisotope X-ray fluorescence spectrometer 9-49397
fluorescence, quantitative, X-ray tube spectral distribution 9-31232
fluorescence analyser using avalanche detector, planetary geochemical exploration 9-37863
fluorescence spectrometry, improved calc. methods 9-47482
fluorescent spectroscopy, calc. methods, empirical coeffs. and fundamental parameters 9-31233
forensic applic. 9-25333
grain size effect in low energy scatt. 9-49399
grain-size effect in nondispersive fluoresc. analysis, nomograms 9-28833
gypsum, 2 θ values up to 13 Å 9-47484
henritermicitic, Ca₃(Mn_{1-x}Al_x)₂(SiO₃)₂(OH)₄ 9-32906
inclusions, by colour X-ray images obtained with microprobe 9-48851
magnetite content of type I carbonaceous meteorite, by diffractometry 9-31622
metal oxides, fluoresc. analysis, use of thin metal film standards 9-47483
multichannel quantometer and computer program 9-45433
paintings, dating and analysis 9-28820
powder diffraction, quantitative comparison of patterns 9-24606
quartz crystal, 2 θ values up to 13 Å 9-47485
radioisotope fluorescence spectrometer with high-resolution semicond. detector, sensitivity 9-49397
rancierte 9-32922
spectrograph, total reflection, for fluorescent analysis of light elements 9-31235
trace elements, slope-ratio technique, matrix problems 9-37862
Ce determination in nodular iron 9-35763
Cr₂O₃, sintered, surface anal. for metal content by electron microprobe 9-37279
Fe-(40 at.%)Ni alloy oxidized at high temp., scale struct. and chem. composition 9-33669
Fe₂O₃, sintered, surface anal. for metal content by electron microprobe 9-37279
⁵⁵Fe radioisotope source 9-26847
Hf oxide (carbide chloride) mixture with Zr oxide (carbide, chloride) 9-41461
Pu-Al, alloys, by electron microprobe 9-49400
U isotopic analysis using X-ray fluorescence combined with α -activity meas. 9-24598
U isotopic analysis using X-ray fluorescence combined with A-activity meas. 9-33690
Zr oxide (carbide, chloride) mixture with Hf oxide (carbide, chloride) 9-41461

Chemical effects of radiations

- see also Nuclear reactions and scattering/chemical effects; Photochemistry*
adsorbed layers 9-24591
butanes, methyl-substituted, γ -irrad., free radical production 9-48499
copper acetate monohydrate, γ -irrad., conversion of Cu²⁺ to Cu⁺ 9-49386
cyclopentane, radiolysis, mass spectrometric investigation of products 9-24592
dibenzocyclohexadienyl radical in anthracene single crystal, radiation induced, ENDOR studies 9-39913
dosimetry by organic halide conductivity cell 9-29665
e.s.r. spectrometer for obs. of u.v. irradiation effects 9-33680
maleimide monomer-fluorene, radiation-induced polymerization 9-26821
mesitylene, e.s.r. study of radical formed on e. irradiation 9-42439
polyenes, photo and thermal isomerization mechanisms 9-35738
steel, mild, low temp. aqueous corrosion under reactor radiation 9-26826
thermal decomposition, review 9-24533
water radiolysis, nanosecond pulse expts., nonhomogeneous kinetics rel. to e(H₂O) behaviour 9-35756
H atoms, stability in irradiated aqueous solutions, e.s.r. study 9-39962
N₂O adsorbed on silica gel and zirconia, radiolysis 9-24591

acoustic waves

No entries

ionizing radiations

- L-alanine-1-¹³C, irrad. at low temp., e.s.r. 9-33686
alkali halide mixed crystals, γ -irrad., recoil radio-1 species, obs. 9-28818
alkanes, radiolysis, charge separation and ionic processes 9-31214
alkyl bromides, solid-phase radiolysis, e.p.r. of radicals 9-39912
anthracene-doped boric acid glass, spectra 9-42423
aromatic cpds. in halogenated liqs., molec. cations obs. by pulse radiolysis 9-31215
benzyl chloride in cyclohexane, gas-phase pulse radiolysis, benzyl radicals 9-43339
glycine hydrochloride, X-irrad., radical formation 9-43340
graphite, oxidation in CO₂ or CO₂ + methane, thermal degassing studies 9-28220
graphite, radiolytic corrosion by CO₂, effect of pore size variation on rate 9-41452
n-hydrocarbons, pairwise trapping of radicals, e.s.r. 9-45427
hydrocarbons, rate const. for scavenging of electrons in radiolysis 9-43341
hydroxyurea, X-irrad., e.s.r. of radical pairs 9-45426
ion-pair recomb. rates in liqs. of low dielec. const. 9-30425
methane, α -irrad., ion-mol. reactions 9-45428
naphthalene, triplet states in pulse radiolysis of gaseous mixtures with benzene 9-49387
neutralization of isolated ion pair in polar liqs. 9-42675
neutralization of isolated ion pair in polar liqs. 9-42674
polymers, pairwise trapping of radicals, e.s.r. 9-33687
polymethylmethacrylate, nanosec. pulse radiolysis 9-31216
polystyrene, nanosec. pulse radiolysis 9-31216

Chemical effects of radiations continued
ionizing radiations continued

- solvated electrons, yield in polar liqs. 9-42674
trapped dielectron, theory 9-46613
water vapour radiolysis by fission fragments, obs. 9-33684
Cr (III) tris acetylacetonate, n irrad., ⁵¹Cr species and annealing, obs. 9-28817
Fe(NH₄)₂(SO₄)₆·6H₂O: ⁵⁷Co²⁺, H₂O radiolysis by Auger e rel. to daughter Fe³⁺ stabilization, obs. 9-23801
H₂O radiolysis, charge separation and ionic processes 9-31214
H₂O vapour, α -irrad., ion-mol. reactions 9-45428
H₂O vapour, excited H atoms prod. by electron impact 9-30151
Hg, radioisotope enrichment by n irrad. of diphenylmercury solns. 9-37843
N₂O radiolysis with electron pulses, effect of temp. on yields 9-33685
NH₄ ClO₄, burning, alone and in fuel, eff. of ionizing radiations 9-28787
NO, pulse radiolysis, NO₂ and N₂O₃ prod. 9-45425
O₂, yield of O₃ in pulse radiolysis at v. high dose rate 9-39963
SiHF₃ matrix-isolation vac. u.v. photolysis 9-31211

Chemical equilibrium *see Chemical reactions***Chemical exchanges** *see Exchanges, chemical***Chemical kinetics** *see Reaction kinetics***Chemical reactions**

- see also Exchanges, chemical; Heat of formation; Heat of reaction; Oxidation; Photochemistry; Polymerization; Reaction kinetics*
activation energy, apparent, at high temp. 9-45418
aromatic stable radical intermediates in pyrolysis, e.s.r. 9-40604
bimolecular reactions, mol. beam investigation 9-25792
bimolecular reactions, theory 9-25793
binary gas mixture, rate effect on temp. and conc. distrib. 9-28777
body rotating in ionized air stream, destruction kinetics 9-47452
carbazole graphitization, enhancement by copolyolysis with aryne precursors, and enhanced graphitization 9-26811
CdCr₂Se₄, growth by topochemical reactions 9-23662
cellulose pyrolysis to char. e.p.r. parameters rel. to initial state 9-26810
ceramic-refractory metal compatibility in cermet production 9-23945
charge-transfer-complex formation, use of hexafluorobenzene and pentafluorobenzonitrile as acceptors 9-28784
chemisorptive luminesc. 9-43326
clays and seawater, equilibrium 9-45466
diamond formation from graphite in presence of metals, catalytic behaviour of metallic intermediate cpds. 9-41064
diamond-silicon interaction at high pressures and temps. 9-26807
dihydrothymine, radicals formed by H-atom bombard. 9-43324
dimerisation, interaction energy surfaces determination for formic and acetic acid dimers 9-38822
electrochemical 9-37840
electron transfer in polar liqs., radiationless transition probability 9-31182
enthalpy and entropy var., determination from exptl. equil. curves, method 9-37814
fluid filtration through porous media, porosity changes, simulation problems 9-38947
fluorene, graphitization enhancement by copolyolysis with aryne precursors 9-26811
fluoroaromatic cpds., mass spectral obs. 9-24532
flux-reaction technique for synthesizing inorg. cpds. 9-28234
in gas, reversible effect on shock initiated flow 9-48645
for gas flow visualization 9-32719
gaseous mixture, equilibrium study, Monte-Carlo method 9-39044
gases in discharge flow sys., at. and free radical conc. meas. 9-26805
glasses for optical fibres, compatibility definition and meas. 9-38412
graphite, neutron irradiated in CO₂, interstitial cpd. formation 9-28316
graphite reactivity to O, eff. of neutron bombardment 9-35743
graphite single cry. with H₂O vapour in He, rates, activation energy var., e. microscopic investig. 9-24537
hexafluorobenzene as acceptor in charge-transfer-complexes 9-28784
high temperature, bibliography 9-4718
hydrocarbon oil breakdown in a.c. arc, growth of pyrocarbon 9-23364
hydrolysis, sucrose solns., non-cavitating ultrasound effects 9-37821
intramolecular reaction spins, NMR Boltzmann eqn. 9-25727
ion-molecule, crossed-beam techniques 9-41442
i.r. emulsions, hypersensitization in water-alcohol soln. with 6% NH₃ 9-25390
materials, protection with polymer coating during X-ray exam. 9-46767
metal halides, volatile reduction, alloy form. between low and high melting p.t. metals 9-39466
metal oxides, first transition series, p-H₂ enrichment, hydrogen-deuterium equilibration 9-24524
metal oxides, ternary, crystal growth by chem. transport 9-36999
methane, α -irrad., ion-mol. reactions 9-45428
mixing, isotropic turbulent, under second-order reaction, Lagrangian history direct interaction equations 9-30171
mixing of liquids, rapid, energetic model 9-33656
monochloroethyl radicals, chemically activated, decomposition 9-39947
oxide powders, calcination process, electron microscope exam. 9-35221
pentafluorobenzonitrile as acceptor in charge-transfer-complexes 9-28784
i-propanol on Al oxides, catalytic decomposition, apparatus for obs. 9-37823
pyrolysis, internal reflection spectrochem. anal. 9-37853
pyrolysis, preparation of ATR i.r. spectrophotometric samples 9-36391
pyrolysis of acetylene over metals, rel. to growth of single-crystal graphite 9-39192
pyrrhotites of Pierreite (Hautes-Pyrenees), thermochem. obs. 9-33657
radical formation in organic solids by H-atom bombard., temp. effect 9-43324
with radical intermediates, high temp., rate eqns., consecutive-parallel and Rice-Herzfeld mechanisms 9-35739
rancierte, dehydration curve obs. 9-32922
reacting gas mixtures, transport coefficients by rigorous kinetic theory 9-26016
redox reaction due to photo-excited dye mols., rel. to Fermi level of dyes 9-41973
s-collidine impurity determination 9-35744
sapphire with liquid Cu-O alloys, interface reaction on wetting 9-26179
sphalerites of Pierreite (Hautes-Pyrenees), thermochem. obs. 9-33657
stability criteria in bimolecular systems 9-45411
thermal decomposition of irradiated materials, review 9-24533

Chemical reactions continued

- thermal decomposition prod. by fracture in brittle solids, direct obs. 9-30531
- thymine, radicals formed by H-atom bombard. 9-43324
- transition metal complexes, one and more step reactions, extension of Woodward-Hoffmann rules of stereoelectronic control 9-39932
- transport, for oxide single cryst. growth 9-44643
- transport processes, simplified models, review 9-37816
- transport reactions, theory 9-37817
- vapour transport react. for refractory cryst. prod., thermodynamic analysis 9-28231
- vulcanization character of two elastomers 9-23789
- Ag₂S formation, influence of AgBr surface structure on mechanism 9-37024
- AgTe monocrystral formation by transport reaction 9-42759
- Ar⁺+CH₄→Ar+CH₃⁺+H→Ar+CH₂⁺+H₂, 1.5-4.2 eV range, mechanism 9-39936
- Ar⁺+D₂→ArD⁺+D, crossed-beam technique application 9-41442
- B filament, vapour deposited, with W substrate rel. to cracking 9-48866
- Be(OH)₂ powders, calcination process, electron microscope exam. 9-35221
- C-CO₂, role of sublimation and self-diff. of C, temp.>2000°K 9-28779
- C-CO₂ gasification, catalysis by Fe, Co and Ni 9-49377
- C, gasification, and structure, vaporization, growth and mech. props. studies, book 9-46695
- C, pyrolytic, deposited in fluidized beds, from hydrocarbons, comparison, 1200-1400°C 9-24536
- C deposition from r.f. discharges in C containing gases, ionic species involved obs. 9-23353
- C deposition on Fe and Ni surfaces from methane, ethane and ethylene 9-24535
- CD₄+X⁺→CD₃⁺+XD⁺, deviations from stripping model 9-27944
- CH₃OH⁺+D₂ (or CD₄)→CH₃OHD⁺+D (or CD₃)⁺ stripping→complex transition 9-38936
- CO₂-C, role of sublimation and self-diff. of C, temp.>2000°K 9-28779
- CO₂ molecule, energy rel. to population inversion of energy levels 9-48459
- CS₂ thermal decomp., shock heated CS₂-Ar emission spectrum obs. 9-35740
- Cl+Br₂→ClBr+Br, energy disposal 9-39938
- Co₃O₄ transport by HCl gas, single cryst. growth obs. 9-32871
- Cu alloys, nitridation, internal 9-28384
- CuFe₂O₄-α-Fe₂O₃ mixture, reaction and phases formed on heating, rel. to Cu_{0.5}Fe_{1.5}O₄ spinel formation 9-30740
- D₂+X⁺→DX⁺, deviations from stripping model 9-27944
- H-F branched chain reaction based chem. laser 9-47984
- H₂ reactivity to atomic N and O 9-43317
- H₂ with graphite at 1900-2400°K 9-43315
- H₂O_(g)+HD_(g)→H₂O_(g)+HDO_(g), spectroscopic and statistical mechanics constants compared 9-28773
- H₂O vapour, α-irrad., ion-mol. reactions 9-45428
- H₂O vapour with graphite single cry., in He, rates, activation energy var., e. microscopic investig. 9-24537
- H at recomb. reaction, H ats. as third bodies 9-25786
- HCl formed by H atom reaction with Cl₂O, chemiluminesc. obs. 9-47453
- HY+X→HX+Y(X=F, Cl, Br, I), product energy from i.r. chemiluminescence, methods 9-41444
- H-X₂→HX+X (X=F, Cl, Br, I), product energy distrib. from i.r. chemiluminescence, methods 9-41444
- He(2³S) chemiluminesc. reactions with N₂, O₂, CO and CO₂ 9-43318
- I₂ reversible photodissoc. laser system 9-34166
- K+HBr(DBr)→KBr reactive collisions in crossed mol. beams, angular and vel. distrib. of KBr 9-35741
- MnCO₃-ZnO-Fe₂O₃ system, calcination 950-1100°C, Mn-Zn ferrite production 9-35742
- MoO₃ thermal decomp. and crystallographic shear planes form., obs. 9-35106
- N₂⁺+D₂→N₂D⁺+D, crossed-beam technique application 9-41442
- ³⁰N₂, ²⁸N₂ mixture equilibration by W catalysis, distrib. of active sites on W surface 9-33662
- NO titration method chemiluminesc., reacts. 9-41445
- N-NO₂→N₂O+O formation of N₂O in vibrational excitation determ. from i.r. emission 9-24539
- N-NO₂→NO+NO formation of NO vibrationally excited state, i.r. emission 9-24539
- Na₂S₂O₄ isothermal decomposition, concentration oscillations 9-24540
- NaCl, coloured and annealed, thermochem., rel. to colloid evolution 9-26296
- Nb hydriding process at high temp., lattice transforms and dissociation 9-31185
- Ni (100) surface, adsorption, interactions and decomposition of N₂O, NO and CO₂ 9-35003
- Ni single crystals, continuous hydrogenation effect on deform. 9-46892
- NiBr₂, thermal decomp., Ni platelets and whiskers growth obs. 9-35018
- Ni₂, thermal decomp., Ni platelets and whiskers growth obs. 9-35018
- NiO-Fe₂O₃, solid state in range 1100 to 1300°C, rate rel. to reaction layer thickness 9-37820
- O₂⁺+D₂, evidence of long-lived DO₂⁺ 9-47456
- O reactivity to graphite, eff. of neutron bombardment 9-35743
- PbO-Cr₂O₃-O₂ ternary system, and phase relations 9-28405
- PrP, transport reaction for growth 9-39197
- Pu oxides and Ta reactions at high temps. 9-28782
- Re, chemisorption of N₂ and CO 9-49376
- SO₂ with active C, 50 to 650°C, and regeneration of C 9-26806
- SiC film formation by reactive deposition and chem. conversion 9-42728
- SiC thermal reactions with oxides and compounds of Ti, Zr, V, Ta, Mo and W, X-ray exam of products 9-49372
- SiH₄-oxidant systems in SiO₂ film formation, study 9-23639
- Ta, hydriding process at high temp., lattice transforms and dissociation 9-31185
- ThO₂, gases, calcination process, electron microscope exam. 9-35221
- ThO₂ powders, calcination process, electron microscope exam. 9-35221
- ThP synthesis by reaction of Th with PH₃ gas 9-33123
- U oxides and Ta reactions at high temps. 9-28782
- UC, synthesis by reaction of dissolved U and suspended C in liq. Zn-Mg, and precipitation 9-36630
- UC_{1-x}O₂, thermochem. study rel. to heat of formation and heat capacity 9-28783
- UC preparation from UF₄, Al and graphite 9-28772
- W, adsorpt. and decomp. of NH₃ 9-48774

Chemical reactions continued

- W, adsorpt. and decomp. of NH₃ 9-48773
- W, chemisorptive luminesc. 9-43326
- ZnO, growth of single crystals by vapour phase reaction method 9-37012
- ZnTe, thermoelec. material, chemical compatibility with alloys 9-26808
- Chemical shift**
- adenosine 5'-monophosphate p.m.r. rel. to mol. struct., 100 MHz 9-32499
- adenosine 5'-triphosphate, p.m.r. rel. to mol. struct., 100 MHz 9-32499
- alkali halide aqueous solns., of ¹³Cl, ⁸¹Br and ¹²⁷I 9-34925
- alkali ions, hydrated, in aqueous soln. 9-32797
- alkyl substituent protons in alkylpyridines 9-38876
- amines, NH p shift in protonation and Co(III) coordination rel. to neighbouring mag. anisotropy 9-28155
- ammonium-¹⁵N mol., from heteronuc. double reson. using weak perturbing r.f. fields 9-40615
- benzaldehydes, monosubstituted, accurate values 9-30087
- benzenes, monosubstituted, ring P shifts, infinite dilution 9-23536
- 2,1,3-benzoselenadiazole, p.m.r. shifts 9-30088
- 2,1,3-benzothiadiazole, p.m.r. shifts 9-30088
- 2,1,3-benzoxadiazole, p.m.r. shifts 9-30088
- clathrates, p.m.r. of enclosed mols. 9-39924
- 2,4-dichlorophenyl methyl isopropylphosphoramidate, n.m.r. rel. to intermol. H-bonding, obs. 9-27879
- 3,5-dichlorosalicylaldehyde, protons in intramolecular H bond, temp. depend. 9-34665
- 1,1-difluoroethylene, isotropic-nematic shift 9-30105
- 1,4-dinitrosopiperazine, conformation rel. to NMR studies 9-32509
- 1, 4-dinitroso-2, 3, 5, 6-tetramethylpiperazines, α, β, ε, γ, δ isomers, predominant conformations, rel. to NMR studies 9-32509
- DL-threonine and DL-allothreonine, n.m.r. 9-23165
- DL-valine n.m.r. 9-23165
- ethyl halides, anisotropy in liq. cryst. solvents 9-38903
- ethyl fluoride dissolved in nematic liq. cry., anisotropies from NMR obs. 9-40613
- fluorobenzenes, trifluoromethyl- and methoxy-substituted, eff. of trifluoromethyl substitution on ring fluorine shielding 9-30118
- formamide-¹⁵N mol., from heteronuc. double reson. using weak perturbing r.f. fields 9-40615
- halide ions, hydrated, in aqueous soln. 9-32797
- N-heterocyclics, calc. of ¹³C shifts average-excitation-energy approx. 9-23127
- K-shell electron binding energies for first-row atoms in molecules 9-38821
- malate ion, internal shifts, ABX analysis 9-46400
- malic acid, internal shifts, ABX analysis 9-46400
- methyl halides in liq. cryst. solvents, anisotropy, theoretical calc. 9-44599
- methylquinolines, from p.m.r. spectra 9-38904
- monofluorides, aliphatic, effect of solvent 9-44549
- NH₃, NH p shift in protonation and Co(III) coordination rel. to neighbouring mag. anisotropy 9-28155
- nitrogen heterocyclics 9-44364
- n.m.r. powder patterns 9-43293
- non-polar molecules in liquids, proton resonance displacement, medium effects 9-40806
- pentafluorophenyl derivatives, correl. with coupling consts. and π-electronic interactions 9-42434
- perfluorovinyl derivatives, ¹⁹F n.m.r. 9-23148
- phenols, ortho-substituted, in dimethyl sulfoxide solns. 9-42444
- phenoxy radicals, fluorinated 9-34687
- rare earth metals, of K_{α1} X-ray lines during oxidation, role of f-electrons 9-37750
- resolution by simple phase alternated multiple pulse sequence, in solid 9-35729
- ring protons in alkylpyridines 9-36710
- selenols, proton shift of SeH group 9-34691
- trifluorochlorocyclobutanes, substituted, ¹⁹F n.m.r. spectra, complete assignment of resonances 9-30148
- vinyl ethers, and n.m.r. coupling consts., temp. depend., obs. 9-27919
- vinyl halides, and n.m.r. coupling consts., temp. depend., obs. 9-27919
- xenon fluorides and oxyfluorides, ¹³⁵Xe-¹⁹F coupling constant as function of ¹⁹F chemicals shift 9-34646
- BaFPO₃, ³¹P and ¹⁹F anisotropies 9-31169
- ⁸¹Br in KBrO₃ and NaBrO₃, in presence of strong nuc. quadrupole couplings 9-26670
- CdSe, Se K-absorpt. edges 9-39858
- ⁵¹Cl in NaClO₃, in presence of strong nuc. quadrupole couplings 9-26670
- Co complex, Co(II) of 1:3 bidentate Schiff's bases, spin density distrib. from isotropic proton resonance shifts 9-42411
- Co(III) complexes, anisotropic chem. shifts 9-45398
- Cu alloys, of Mossbauer spectra for ¹⁰⁹Sn impurity, electronic props. obs. 9-43222
- Eu cpds., divalent, isomer shift of Mossbauer absorpt. of ¹⁵¹Eu 9-45289
- F¹⁹, between gaseous F₂ and SiF₄ 9-42392
- ¹⁹F, rel. to nmr coupling constant ¹¹B-¹⁹F in various cpds. 9-32464
- ¹⁹F n.m.r. in AlF₃ modifications 9-48453
- ND₃, ND₂H, NDH₂ and NH₃, ¹⁵N n.m.r. 9-30430
- NH₃, ¹⁵N n.m.r. shifts in liq. and vapour 9-32798
- Ni complex, Ni(II) of 1:3 bidentate Schiff's bases, spin density distrib. from isotropic proton resonance shifts 9-42411
- ³¹P in methyl- and phenyl phosphorus compounds 9-25775
- Se in ZnSe and CdSe, K-absorpt. edges 9-39858
- Te, anisotropic 9-43272
- ZnP₂, solid, resolution by simple phase alternated multiple pulse sequence 9-35729
- Zn complex, 1:1 Zn (11)-malate, internal chem. shift, ABX analysis 9-46400
- ZnSe, Se K-absorpt. edges 9-39858

Chemical structure

- see also Bonds
- batrachotoxinin A, characterization using O-p-bromobenzoate derivative 9-26257
- covalent bond formation, softness of acceptors and donors, classification 9-38818
- cyclic molecules, superposition links 9-26255
- fluorenone ketyl, existence of paramagnetic and diamagnetic ion clusters 9-34923
- graphite, and graphitization, X-ray diffraction studies, samples from polynuclear aromatics 9-39257

Chemical structure continued

- polymers, cross-linked, thermostabilization during crystallization 9-46703
- polystyrene, from depolarization meas. by Raman spectra and dichroic meas. by i.r. 9-47380
- zeolites with faujasite-type framework, distribution of cations and molecules 9-28776
- $\text{Bi}_2\text{O}_3\text{-B}_2\text{O}_3\text{-(R}_2\text{O)}_2$ glass systems 9-46698
- Fe-Si alloys, microinhomogeneities in cast worked and annealed samples 9-48846
- NiFe_2O_4 , polarized neutron diff. exam. 9-48838
- $\text{Pb}_{0.81}\text{Sn}_{1-x}\text{Te}$ alloy system, stoichiometry relationship with lattice constant and alloy fraction 9-35065

Chemical technology

- boiling and simultaneous stirring of immiscible liquid layers, direct contact heat transfer 9-30461
- continuous chromatographic refining 9-31217
- internal reflection spectroscopy of electrochem. reaction 9-37840
- ^{243}Am separation from ^{244}Cm by precipitation of $\text{K}_3\text{AmO}_2(\text{CO}_3)_2$ 9-26802
- PuO_2 dense microspheres, prep. by sol-gel process, calcination and sintering 9-36631

Chemiluminescence *see* Chemical reactions; Luminescence**Chemisorption** *see* Chemical reactions; Sorption**Cherenkov radiation**

- see also* Counters/Cherenkov; Electrons/radiation
- by auroral electrons, rel. to radio noise generation 9-40076
- light, from N_2 gas, appl. in high energy electron beam monitor 9-29681
- plasma, warm uniaxial; formula for rad. 9-38978
- plasma excitation by modulated particle beam, nonlinear theory 9-46466
- point charge in motion in anisotropic plasma, spectrum 9-34759
- Vavilov-Cherenkov radiation due to magnetic monopole in transparent dielectric crystal 9-28648
- Vavilov-Cherenkov, from elongated charge bunch moving along axis of cylindrical channel in transparent medium 9-29340

Chirality *see* Elementary particles; Field theory, quantum**Chlorine**

- adsorbed atoms on silica gel, e.s.r. 9-39174
- adsorbed atoms on silica gel e.s.r. 9-30497
- atom, ($3^2\text{P}_{1/2}$) and ($3^2\text{P}_{3/2}$) states, kinetic spectroscopic studies in vac. u.v. 9-34534
- crystal, Raman spectrum and intermolec. forces 9-43245
- hot atom reaction with alkanes 9-43343
- neutral atoms, wavelengths, energy levels and analysis 9-29925
- photochemical recoil spectra 9-43333
- in seawater, of Red Sea bottom, 1795 to 2195 m depth 9-43372
- $\text{Cd}_2\text{Mg}_{1-x}\text{Te:Cl}$, double-acceptor defects and hole traps 9-41263
- Cl_2 , photodissoc. by translational spectroscopy 9-48513
- Cl_2 , press.-induced fundamental i.r. absorpt. band 9-30023
- Cl_2^- centres trapped in hydroxylammonium chloride X-irrad. single cryst., optical and thermal conversion 9-32995
- Cl^- concentration in Antarctic ice, obs. 9-33729
- Cl^+ and Cl^- , bombardment of Mo, secondary electron emission 9-31010
- Cl II, cascade-free transitions, radiative lifetimes 9-25691
- ^{35}Cl in NaClO_3 , chemical shift meas. in presence of strong nuc. quadrupole couplings 9-26670
- $\text{Cl} + \text{Br}_2 \rightarrow \text{ClBr} + \text{Br}$ reaction, energy disposal 9-39938
- Cl, cascade free transitions, radiative lifetimes 9-25691
- ZnS:Cl,Mn,Cu effect of activator conc. on electroluminescent props. 9-37781
- in ZnS phosphor, luminescence spectra, green II band contour obs., electric and photoexcitation 9-26786

Chlorine compounds

- absorption spectra in soln., transitions 9-30039
- chloride impurity diffusion in AgBr 9-40979
- chlorites, two-packet unit cell, systematic derivation of possible polytypes 9-39263
- ClO_2 , 4750 Å band syst., vib. analysis 9-32469
- ClO_2 , e.p.r. in KClO_3 , X-irrad. at low temp., ($\Delta M_S=1$, $\Delta M_I=\pm 1$ or ± 2) 9-49352
- ClO_2 , spectrophotometric determ. 9-31230
- ClO_2F , E-species force consts. 9-30050
- ClO_2 , spectrophotometric determ. 9-31230
- ClO radical, microwave spectrum, rot. transitions $J=7/2-1/2$ in $^2\Pi_{1/2}$ state 9-48514
- ClO radical, microwave spectrum 9-38836
- ClOO radical, absorpt. spectrum 2100-3000 Å 9-30152

Chondrites *see* Meteorites**Chromatic aberration** *see* Aberrations, optical**Chromatography**

- see also* Adsorption; Chemical analysis/adsorption
- continuous chromatographic refining 9-31217
- diglycerides analysis by coupled mass spectrometry-gas chromatography 9-31221
- ethyl alcohol, diethyl carbonate, diethyl oxalate determination in ternary mixture 9-39966
- gas, applic. to forensic science 9-27397
- gas, automatic chromatograph 9-49390
- gas, internal reflection spectrochem. anal. 9-37853
- gaseous inclusions in glass, gas chromatographic analysis 9-40966
- gel permeation and gradient elution methods compared for polyisobutenes 9-32548
- i.r. spectroscopy applic. 9-26844
- organic cpds., labelled, new anal. method using interrupted elution 9-24600
- polyisobutenes, mol. wt. determ. 9-32548
- thin-layer, reflectance spectrochem. analysis 9-37852
- water, detection using β^- ionization detectors 9-33689
- CdS, nonstoichiometry of crystals grown by different methods, gas chromatographic meas. 9-36978

Chromium

- alloying additions to Be, influence on microyield strength 9-35181
- antiferromagnet props., optical and pressure effects 9-45213
- antiferromagnetic critical exponents and electrical resistivity near Neel point 9-35582
- atom, with electronic configurations $3d^1$ and $3d^4p$, energy spectra, theoretical investig. 9-29940
- atomic spectrum, bibliography 9-38765

Chromium continued

- cleavage fracture, importance of crack nucleation and propagation 9-39438
- crack nucleation and propagation, importance in cleavage fracture 9-39438
- diffusion in Fe and low carbon steels, mechanism 9-46849
- diffusion in Nb, contribution of edge pits and sub-boundaries, optical microscope obs. 9-32985
- dislocation, Burgers vectors, two-beam diff. contrast meas. 9-32969
- ductile/brittle transition in pressurized polycryst., dislocation distrib. change 9-39427
- electrical resistivity anomaly in spin-flip transition region 9-35584
- electroplated coating on Cu, effect on stress-strain parameters 9-26328
- enthalpy and heat capacity at high temp. 9-39529
- film, electrical conductivity and Hall consts. 9-30848
- film, grown by molecular beam incidence, crystallite shape by light reflection 9-32909
- gettering effect, detection during evaporation and condensation in vacuum 9-30457
- magnetostriction and anomalous thermal expansion, orthorhombic structure $123\text{-}311^\circ\text{K}$ 9-39780
- n.m.r. of ^{52}Cr , Knight shift 9-24324
- optical isotope shift, nucl. vol. and mass eff. 9-29988
- oxidation 9-24556
- refractive index and absorption spectra rel. to mag. props., 293 and 400°K 9-24359
- resistance, temp. depend. minimum, mag. fields effect 9-39585
- resistivity, elec., anomaly near spin-flip temp. 9-26517
- resistivity temp. coeff. meas. near T_c 9-48969
- specific heat, anomalous, meas. near T_c 9-48969
- spin density wave, mag. field eff. 9-35580
- spin density wave calcs. 9-24325
- spin directions in single crystal, 122°K to 38.5°C, models 9-45214
- thermal conductivity, above and below Neel temp. 9-26444
- X-ray spectrum, $K\alpha$ doublet 9-27807
- e states energy band structure calc. by orthogonalized plane wave method 9-37405
- in Al_2O_3 far i.r. absorpt. spectrum in applied mag. field, Zeeman splitting of lines, single d electron obs. 9-31100
- in Al_2O_3 single cryst., low temp. thermal conductivity meas. 9-35086
- Cr^{2+} , in MgO , acoustic paramag. reson. interpret. taking account of Jahn-Teller effect 9-24346
- $\text{Cr}^{3+}\text{-Tb}^{3+}$ pair emission in $\text{TbAlO}_3\text{:Cr}^{3+}$ 9-39878
- Cr^{3+} , acoustic e.p.r. in LiNbO_3 , for internal fields of ferroelec. crystals 9-28748
- Cr^{3+} , anisotropic exchange interactions in Cr_2O_3 9-45212
- Cr^{3+} , e.p.r. in ruby, g-factor and fine structure lines up to 7 kbar 9-33655
- Cr^{3+} , e.s.r., in EuAlO_3 9-47435
- Cr^{3+} , e.s.r. and optical absorpt. in ZnGa_2O_4 and ZnAl_2O_4 , rel. to single-ion mag. interactions 9-45080
- Cr^{3+} , e.s.r. in TiO_2 , coupled with O vacancies 9-37801
- Cr^{3+} , optical spectra in LiNbO_3 and LiTaO_3 9-31104
- Cr^{3+} , relax. of excited states in Cr(III) complexes 9-39885
- Cr^{3+} coloration impurity in lanthanum glass, effect on light absorption 9-24372
- Cr^{3+} in Al with and without impurities, EPR 9-37796
- Cr^{3+} in Bils, e.s.r. of Cr^{3+} single ions and exchange-coupled Cr^{3+} pairs 9-24482
- Cr^{3+} in $\beta\text{-LiAlO}_3$, cathodoluminescence spectra and coordination with $\text{Fe}^{3+}\text{Mn}^{4+}$ 9-31150
- Cr^{3+} in MgAl_2O_4 spinel, theory of strong and weak trigonal field, optical spectrum and e.p.r. analysis 9-28644
- Cr^{3+} in $\text{MgO-Al}_2\text{O}_3$, absorption and fluorescence spectra 9-26778
- Cr^{3+} in paramagnetic ruby and $\text{K}_3\text{Co(CN)}_6$, ENDOR rel. to thermal mixing of nuclear spins 9-43310
- Cr^{3+} in ruby, population density in ^2E levels, measurement by excited state absorption 9-33534
- Cr^{3+} in SbI_3 , e.s.r. of Cr^{3+} single ions 9-24482
- Cr^{3+} in SrTiO_3 , as impurity-ion probe in spectroscopic exam. 9-26743
- Cr^{3+} in ZnWO_4 , absorption, i.r. emission and excitation spectra 9-33563
- Cr^{3+} in ZnWO_4 , anisotropic spin-orbit coupling obs. 9-33564
- Cr^{3+} ion in tetrahedral environment, Jahn-Teller eff. ground state analysis, e.s.r. spectra proposal 9-44259
- $\text{Cr}^{3+}\text{-Eu}^{3+}$ pair emission spectrum in $\text{EuAlO}_3\text{:Cr}^{3+}$ 9-39835
- Cr^{4+} absorpt. spectrum in Al-line glass, obs. 9-35655
- Cr(V) complex in ethylene glycol, proton dynamic polarizations 9-34926
- Cr I emission line shifts in compressed Ar, He, 3014-5328 Å 9-48390
- Cr III in $\text{NaMgAl(Cr(C}_2\text{O}_4)_2)_2\text{H}_2\text{O}$ single crystal, X and P band e.p.r. 9-49351
- Ni I emission line shifts in compressed Ar, He, 3050-3619 Å 9-48390
- RbMnF_3 , u.s. attenuation near mag. phase transitions freq., and temp. depend 9-48958
- on n-Si Schottky barrier, forward I-V characs. 9-43082

Chromium compounds

- alloys, antiferromagnetic props., optical and pressure effects 9-45213
- alloys, coexistence of mag. phases 9-39750
- chromel-alumel and chromel-capel microthermocouples, heat inertia in air jet, determ. 9-22300
- chromel-P/Au-Fe annealed temperature calibration extended 9-47841
- complex, hexaurea Cr(III) ion in crystals, spectra 9-33551
- Cr-Mn alloy, magnons and paramagnons, neutron scatt. study 9-45215
- halides, valence II and III, $K\alpha$ doublet, X-ray investigation 9-27807
- M.S.O. alloy, mag. shunt props., C addition effect 9-45050
- nickrome, dispersion hardened, strengthening mechanism 9-23909
- nickomic single crystals, strain-hardening rel. to structural state of quenched alloy 9-33100
- sandwich complexes, hyperfine coupling consts. and covalency 9-42420
- steel, carburized Cr-Mo, transform. features 9-41073
- steel, Cr-Ni-Mo high C low alloy, fatigue strength rel. to hardness, obs. 9-26345
- steel, shot-peening and Cr-plating effects 9-28365
- steel, X40MnCr22, mag. susceptibility at 5-1800°K 9-24330
- steels, embrittlement in temp. range of $\alpha\text{-}\gamma$ transformation 9-28369
- steels, hardened, struct. obs. from sound vel. meas. 9-23755
- Al-Cr dil. solid soln., mag. susceptibility and sp. ht. w.r.t. localized d-state props. 9-33269
- Al-Cu-Cr supersaturated solid solns., kinetics of decomp. 9-46937
- alloys with V, Nb and Ta, electrical resistivity as a function of temperature 9-39584
- Au-Cr alloys, short-range order 9-28257

Chromium compounds continued

- C/Cr/Ni/Si system, controlled solidification using monovariant eutectic reactions 9-36921
 CO-Cr binary alloys, α -phase, mag. props. 9-43158
 Co-(10 wt.%)Cr alloy, microstructure of oxide scales formed during high temp. oxidation 9-31194
 Co-(10 wt.%)Cr alloys, high temp. oxidation kinetics 9-31195
 Co-Cr alloys, non-collinear mag. structures with antiferromag. interaction between local mag. moments 9-45056
 20 wt.%Cr-35 wt.%Ni steel, creep-rate and grain boundary sliding 9-48901
 Cr-Al acetylacetonate mixed single crystals, spin-lattice relax. props. 9-49227
 Cr-Mn alloys, spin density wave calcs. 9-24325
 Cr-Mn alloys, X-ray K spectra 9-24439
 Cr-Mn steels, equilib. diag. for weld metals 9-23976
 Cr-(49wt.%)Ni-(1wt.%)Ti alloy, corrosion on exposure to pyrolysis conditions of sodium-base spent pulping liquors 9-28799
 Cr-(49wt.%)Ni-(1wt.%)Ti alloy, corrosion on exposure to pyrolysis conditions of sodium-base spent pulping liquors 9-28800
 Cr-Re alloys coexistence of mag. phases, neutron diff. obs. 9-39750
 Cr-(2 wt.%)Ta-(0.5 wt.%)Si alloy guide vane specimens, thermal fatigue testing 9-33075
 Cr-V, alloys spin density wave calcs. 9-24325
 (Cr,Fe)₃C₃ in alloy steels, X-ray and electron diff. obs. 9-48831
 Cr_{2-x}Fe_xAl, antiferromagnetic ordering, depend. on value of x 9-35579
 Cr₂BeO₄, spiral mag. structure, neutron diffraction investigation, 4.5°K 9-45211
 Cr₂O₃-MgO system, interdiffusion formation of MgCr₂O₄ single crystals 9-28319
 Cr₂O₃-NiO solid solution on Ni-Cr alloy, cation distrib. on alloy oxidation 9-23656
 Cr₂O₃-TiO₂ electric resistivity, freezing point, defects, mag. props. 9-49022
 Cr₂O₃, exchange interactions between Cr³⁺ ions 9-45212
 α -Cr₂O₃, inelastic magnon scattering, dispersion relns. including exchange integrals 9-35585
 Cr₂O₃, sintered, surface and fracture study rel. to metal content 9-37279
 Cr₂O₃, spin waves and exchange interactions, inelastic neutron scatt. obs. 9-47285
 Cr₂O₃ absorpt. spectrum of excitons, mag. Davydov splittings 9-33552
 Cr₃Ir, supercond. critical mag. field data 9-24163
 Cr₃Rh, supercond. critical mag. field data 9-24163
 Cr₃(CH₃COO)₆OC₅H₉O, low temp. specific heat 9-28426
 Cr alloys with Pt-series metals, structural and magnetic similarities 9-33438
 Cr complex, [Cr(OH)(en)₂]⁶⁺, mag. susceptibility meas. to 4.2°K, mol. and crystal struct. 9-47224
 Cr complex, K₃Cr(NCS)₆ in methanol-ethanol glass, 100°K, excited state absorption 9-38838
 Cr complex, tris (oxalatochromium) (III), zero-field splittings 9-24487
 CrAs and Mn-substituted CrAs, magnetic structure 9-45057
 CrB₂, antiferromagnetic behaviour, n.m.r. meas. 9-35583
 CrBr₃, ferromag., near critical temp., mag. eqn. of state 9-26649
 CrBr₃, ferromag., thermal conductivity 9-42976
 CrBr₃, ferromagnetic, Fresnel diffraction patterns, depend. on mag. field direction 9-31079
 CrBr₃, ferromagnetic domain structure, Lorentz microscopy at low temps. 9-26651
 CrBr₃ magnetic props near critical point, Faraday effect meas. 9-45139
 CrCl₃, anhydrous, specific heat below 4°K 9-30781
 CrCuO₂, magnetic properties, obs. 9-35530
 CrF₃, crystal growth from low melting flux 9-39207
 CrH, predissociation of upper electronic state of 3680 Å transition 9-42449
 CrH₂P₂O₇·2H₂O, i.r. spectra obs. of ionic dissoc. of constituent water 9-44324
 CrI₃, ferromagnetic domain structure, Lorentz microscopy at low temps. 9-26651
 Cr(III) chelate complexes with EDTA, luminescence 9-24446
 Cr(III) complexes, luminesc., relax. of excited states 9-39885
 CrO₂, Mossbauer effect of ⁵⁷Fe 9-45287
 CrO₂ single crystal, magnetic and magneto-optic props. 9-45141
 CrO₂-Cr₂O₃ system, elec. props. of non-stoichiometric oxides 100° to 450°C 9-28495
 CrSb₂, marcasite-type, mag. and elec. props. 9-35581
 CrTe, exchange striction, temp. depend. 9-33466
 Cu-Cr dilute alloy, magnetoresistance, 13° to 20°K, fields up to 200 kG 9-44910
 Cr (III) tris acetylacetonate, n. irr., ⁵¹Cr species and annealing, obs. 9-28817
 Fe-(18 at.%)Cr-(20 at.%)Ni alloy, dislocation damping and solute pinning 9-28292
 Fe-(49wt.%)Cr-(2wt.%)V, brittle fracture, slip mode effects 9-26356
 Fe-Cr-Ni alloy, extrinsic-intrinsic stacking-fault pairs 9-44711
 Fe-Cr-Ni alloys, dislocation damping 9-39363
 Fe-(50wt.%)Cr, oxidation 9-24556
 Fe-Cr alloy, oxidation, effect of Y and Gd 9-24559
 Fe-Cr alloy, pitting corrosion 9-31198
 Fe-Cr alloys, pitting and anodic dissolution surface prep. and deformation effects 9-24576
 Fe-Cr system, phase equilibria and transformation, pressure infl. 9-41059
 Fe-Ni-Cr-Be alloy, precip. processes, transmission electron microscopy obs. 9-39498
 Fe-Ni-Cr alloys dislocation mobility 9-39699
 (α -Fe₂O₃)(Cr₂O₃)_{1-x} solid solns., magnetochem. study of formative conditions 9-49189
 Fe-Ni-Cr alloys, eff. of Cr on martensitic transformation 9-23965
 Hf-Cr binary system, phase equilib. diag. 9-33149
 LiCl-CrCl₃, phase study on fusion, by n.m.r. 9-35259
 Nb₂O₅, supercond. critical mag. field data 9-24163
 Ni-10wt.% Cr alloys, thermal conductivity, description of apparatus 9-26451
 Ni-Cr-Fe alloys, atmospheric corrosion behaviour 9-37831
 Ni-Cr alloy, strain and fracture behaviour under cyclic loading 9-23915
 Ni-Cr alloy ball-milling, addition of inorganic salts for prod. of very fine powder 9-23932
 Ni-Cr alloys, non-collinear mag. structures with antiferromag. interaction between local mag. moments 9-45056

Chromium compounds continued

- Ni-Cr alloys, oxidation and cation distrib. in NiO-Cr₂O₃ solid soln. formed 9-23656
 Ni-Cr film, vacuum-deposited, resistivity increase on heat treatment 9-41043
 Ni-Cr films, Sn and solder whisker growth conditions and mechanism 9-48816
 Ni₃(Fe, Cr) alloys, atomic ordering effects 9-39297
 Ni₃(Fe, Cr) alloys, ferromag. ΔE -effect, Cr content depend. 9-47242
 Pd-Cr alloy, annealed at 510°C, weak ferromagnetism 9-49202
 Pd-Cr dilute mag. alloy, elec. resistivity below Kondo temp., eff. of coherence length 9-26508
 Pd-Cr dilute magnetic alloys, specific heat, temp. depend. below Kondo temp. 9-24050
 Ti-Cr binary alloys, martensite react., morphology and substruct. 9-26393
 V-Cr alloys, ⁵¹V resonance, Knight shift and Neel temp. 9-24324
 Zr-(1.2wt.%) Cr-(0.1wt.%) Fe alloy, quench hardening behaviour, cooling rate dependence 9-41034

Chromosphere *see Sun***Chronographs** *see Time measurement***Cinematography***see also Cameras*

- 3-D movies, computer generated, use of varifocal mirror 9-32073
 application to solar flare kinematics 9-38118
 cineradiography with field-emission tube 9-32097
 of elementary cavitation zones 9-23488
 holographic, continuous reconstruction 9-29444
 holographic, of rapid transient processes 9-31983
 international terminology 9-32075
 motion picture holography, Q-switched ruby laser applic. 9-25322
 spark, of shock wave damping by multiple refl. at slits 9-29315
 vocal cords, telecentric optical system 9-33964

Circuits*see also Amplifiers; Counting circuits; Oscillators*

- admittance, guarded three- and four-terminal meas., low freq. bridge 9-34134
 Boolean (logic) all-magnetic, using transfluxors, efficiency and optimum operating conditions determ. 9-40310
 boxcar, digital, solid state, of high linearity 9-29361
 braking, for geared subfractional motor 9-31895
 bridge, low freq., for guarded three- and four-terminal admittance meas. 9-34134
 capacitance bridge, three terminal, new design conductance network 9-29363
 Cockcroft-Walton voltage multiplier, modification 9-34138
 coincidence, subnanosecond, resolution stability of a tunnel diode 9-30945
 conductance network for three terminal capacitance bridge 9-29363
 continuous heating system, low temp. 9-22303
 control unit of automatically recording Mossbauer spectrometer, multi-channel analyser 9-36510
 converter, voltage-to-frequency based on continuous integration 9-31885
 damped oscillating circuit, approx-equiv. to lossless line with reactive load 9-43831
 d.c. controller, constant 9-45910
 discriminator, fast amplitude, nanosec. pulse ≤ 10 megapulse/sec 9-32270
 discriminator and filter, comparison of techniques for Ge(Li) detector signal time meas. 9-36519
 feedback frequency dividers, oscillating and phase-locked, stability criteria 9-22323
 frequency converter, harmonic rate of output voltage rel. to shape of control signal 9-41866
 generator with function $a_n x^n$, using multiplying prop. of Hall effect 9-43832
 heating, calorimetric, const. current, switch arrangement and power averaging 9-31894
 infinitely conducting network, interaction rad. with electron beam 9-41848
 integrated, uses in nuclear electronics 9-29671
 integrator and meter with low input impedance, 10^{-8} - 10^{-4} A, current meas. in accelerator 9-32284
 leading edge time pickoff from radiation detector pulses 9-22324
 lossless line feeding into capacitive load, exact response calc. using Laplace transform. 9-45909
 lossless line with reactive load, output pot. determ., equiv. to damped oscill. circuit 9-43831
 micro. thin metal film on curved substrate, etching technique 9-25162
 modules, fast d.c. coupled analogue fan-in and fan-out, 3 ns rise time 9-32268
 non-linear inductance receiver, fundamental freq. meas. of l.f. complex shape periodic signals 9-34129
 null-detector, employing electrometer tetrodes 9-31893
 parametron logic, applic. of variable permittivity ferroelec. ceramics 9-30969
 passive RC-analog, use for glass pressing study 9-34969
 potentiometer, light sensitive, appl. to fibres mechanical props. meas. 9-28328
 pseudo random freq. shift sequences, direct generation 9-34130
 pulse generator, fast, random, using photoelectrons from a weakly lit photomultiplier tube 9-29359
 pulse generator, of high precision with transistor as switch 9-29360
 for pulse like signals time integral, duration and time interval meas. 9-47888
 pulse shape discriminator, 0.3-10V, risetime 0.2-10 μ sec, design and applic. 9-32269
 radio receiver, a.m., sensitive, for ionospheric meas. 9-35869
 RC, electric simulation soln. of energy and mass transfer problems 9-27191
 RC combination for recording linear air track gliders 9-38187
 RC structures, distributed, time-domain analysis and meas. techniques, rel. to impulse meas. techniques 9-41868
 RC structures, distributed, time-domain analysis and meas. techniques, rel. to reciprocal time domain 9-41867
 RLC passive bandpass filter, with variable transmission gain 9-34132
 sampling, solid state, for low pulse repetition freqs. 9-25163
 servomechanical control for Helmholtz coils to compensate for field fluctuations 9-31906

Circuits continued

- spark timer, solid state 9-27157
- for spectrometer, scintillation, noise pulse elimination 9-40456
- static power supply with adjustable rectified voltage and low residual ripple 9-43826
- streamer chamber, 20 cm gap, meas. anal. and ang. resolution 9-25545
- superconducting, efficiency of flux pumping 9-39606
- synchronous machine, automatic control with static converter, soln. of theoretical eqns. 9-41869
- three-phase bridge of rectifiers, current decrease in load at const. firing angle 9-43830
- three-phase bridge of rectifiers, current in load for variable firing angle 9-43829
- transducers, piezomagnetic, dual forms of equivalent circuits 9-41828
- tunnel capacitor, for charge-quantization studies 9-37548
- voltage divider of composite C resistors for accelerator terminal volts. meas. 9-40306
- voltage multiplying circuit of Schenkel type, voltage efficiency calc. 9-29354
- neutron spectrometer with liq. organic scintillator, FERDoR unfolding method and code 9-34353

Clathrates *see* **Molecules; Organic compounds****Clay**

- bentonites, elec. resistivities 9-49017
- failure criterion, angle of internal friction 9-39433
- illite, Mossbauer effect obs. of Fe ion 9-37698
- illites, elec. resistivities 9-49017
- kaolins, elec. resistivities 9-49017
- Montmorillonite, Mossbauer effect obs. of Fe ion 9-37698
- montmorillonite aqueous gels, n.m.r. 9-23553
- and seawater, chemical equilibrium 9-45466
- suspensions, plastic flow behaviour surface prop. dependence 9-23548

Cleavage *see* **Crystals/faces; Fracture****Clebsch-Gordan coefficients** *see* **Field theory, quantum;****Nucleus/theory; Quantum theory****Climatology** *see* **Meteorology****Clock paradox** *see* **Relativity****Clocks** *see* **Time measurement****Cloud chambers**

- discharge, charged particles information determ. without films 9-22680
- Wilson, (n, α) reaction study, n generator pulsed source 9-29672

Clouds

- artificial ionized spherical, e.m. wave scatt. 9-31329
- atmosphere of cloudy sky, heat influx 9-31289
- atmospheric total cloudiness rel. to water vapour 9-49450
- clouds, noctilucent, exact identification w.r.t. auroral occurrences 9-31364
- condensation, numerical model of molecular diffusion causing mass transfer to and from cloud droplets 9-28881
- condensation kinetics and spectrum formation 9-37913
- convective, influence on large-scale stratification 9-33770
- cumulus, AgI seeding effect on width-height ratios 9-33769
- cumulus dynamics, thermodynamic equation 9-41508
- cumulus thermal structure rel. to droplet concentrations 9-24653
- detecting and ranging system, laser light, design and operation 9-48076
- development rel. props. nuclei 9-35820
- diffusion in Ekman layer 9-41509
- droplet coalescence, connection between Telford and kinetic-equation theory 9-24656
- droplet coalescence, effects of Davis-Sartor collision theory 9-26897
- electrical properties, manipulation for weather control 9-28862
- formation, lab. simulation 9-45492
- front system rel. to vertical movements distribution 9-35817
- gas, upper atmosphere, flowfields 9-28063
- glaciation of cumulus at approximately -4°C 9-24657
- ice, i.r. reflectivity compared with Venus obs. 9-38080
- ice, spectral scattering in near infrared, theory 9-47541
- ice crystal concentration, measurements 9-28876
- ice crystals, shape and riming properties 9-28877
- ionized, fluctuating mag. field mechanisms, applic. to quasi-stellar objects considered as radio-galaxies 9-29043
- liquid water attenuation of 33.5 GHz signal, and residual noise effect 9-33779
- microphysical processes leading to precipitation, review of present knowledge 9-31312
- model, mathematical framework for condensations, collection and advection 9-28874
- multiple scattered light, radiance and polarization 9-33768
- noctilucent, brightness contrast with sky 9-45513
- noctilucent, freq. rel. to mesospheric circulation 9-31355
- noctilucent, genesis and distribution 9-28879
- noctilucent, geographical spread 9-41558
- noctilucent, obs. in Germany 9-41559
- noctilucent, possible source of waves 9-24658
- noctilucent, seasonal frequency of occurrence 9-49473
- particle trapping coeff. determ., model 9-45493
- precipitating, properties meas. by weather radar, feasibility 9-33752
- radiation, longwave, flux rel. to cloud 9-35821
- radiation, total, at earth's surface, var. rel. to cloudiness 9-40027
- radio brightness vars. 9-35818
- Saharan dust, falling in Britain, July 1968 9-26900
- scattered radiation during formation, polarization and angular distribution changes 9-28887
- scattering, multiple, by cloudy planetary atmosphere 9-41527
- sky brightness (day) above water, rel. to cloudiness 9-40025
- above snow surfaces, charact. by solar radiation bidirectional reflectance, satellite study 9-35819
- space charge, artificial, effects 9-43399
- spherical cap approximation, validity in heterogeneous nucleation 9-28875
- supercooled, elec. field effects on ice formation 9-47538
- thunder, elec. field and conductivity obs. 9-31324
- total amount rel. to sunshine duration 9-47543
- Venus, effect on CO₂ bands and water vapour lines 9-41679
- Venus, infrared reflection spectra 9-47540
- Venus, rel. growth curve and phase effects 9-38077
- Venus, rel. phase curves 9-38079
- water content, radio-astronomical meas. 9-24655

Clusius-Dickel columns *see* **Isotope separation****Co-ordination complexes** *see* **For inorganic complexes see under appropriate metal compound heading****Coal**

- Karaganda dehydrated, elec. conductivity and dielec. loss rel. to petrographic ingredients, mineral impurities and metamorphism 9-44999
- optical const., i.r. region 9-24357
- spectral analysis in vacuum discharge, sensitivity improvement by NaCl, KCl addition 9-26845

Cobalt

- in alkali halides, absorption and i.r. emission 9-33548
- atom, electronic configuration 9-25697
- atom, energy spectra calc. for 3d⁷ and 3d⁴4p configs. 9-38767
- atom, K α line asymmetry indices in metal and cpds., chem. combination effect 9-25695
- atomic spectrum, bibliography 9-38765
- coercive force at high temp., effect of dispersoid parameters 9-45138
- content eff. on ageing induced changes in Fe-Ni alloys 9-23942
- corrosive surface reactions in field ion microscope 9-26827
- cosmic ray muon induced Fe³⁹ 9-48331
- defects, eff. of β - α transformation and plastic deformation 9-23804
- density-of-states functions, X-ray photoelec. spectroscopy study 9-44886
- diffusivity in Pr 9-44745
- electroless films on Si single crystal, internal stress 9-30654
- e.p.r. in Ni-Co and Zr-Co alloys, rel. to localized mag. moments 9-33634
- eutectic melting at contact with diamond and graphite 9-26358
- Fermi momentum determ. from annihilation spectra, valence electrons calc. 9-33229
- ferromagnetic, thickness-depend. of domain-width, critical thickness 9-39763
- ferromagnetic domain struct., e microscope obs. 9-33471
- film, high-coercivity, recorded magnetization patterns obs. by Lorentz microscopy 9-45165
- film, magnetic electrodes, structure from transmission electron microscopy 9-42718
- film, magnetization, neutron scattering studies 9-45167
- film magnetic temperature-sensitive for magneto-optic memory 9-45164
- films, domain wall width meas. by Lorentz microscopy 9-45166
- films, evaporated, rotatable initial susceptibility and magnetization reversal 9-33462
- films, ferromag. reson. absorpt. at r.f.'s 9-47423
- films, fine mag. struct. and coercive force 9-41321
- films, n.m.r. and ferromag. resonance, relaxation times, magnetic structure 9-33645
- Frenkel pair formation and mutual annihilation after electron irradi. 9-35084
- growth, hydrothermal 9-37027
- hexagonal, eff. of constraint on hysteresis cycle 9-28617
- hexagonal, noncollinear spin density, rel. to form factor 9-45121
- hexagonal crystal with internal stresses, magnetization and magnetostriction 9-37657
- hyperfine field at ¹¹⁹Su, anomalous temp. depend., 900° to 1300°K 9-47330
- hysteresis cycle, effect of constraint 9-28617
- interband optical transitions investigation, low temp. magneto-optic meas. 9-41136
- interstitials, di- and trivalent, incorporation 9-28282
- magnetic susceptibility of very thin ferromag. film, periodic variation 9-47257
- magnetostriction const. and shear const. meas. up to 26 kOe, -200 to 400 °C 9-41305
- in nitrate glass, absorpt. spectra rel. to Co coordination 9-26735
- optical absorpt. spectra in ZnWO₄ crystal 9-37731
- polymorphism, influence of atomic size factor 9-46954
- positron annihilation rel. to cryst. e struct., obs. 9-35325
- remanent domain structures, effect of crystal thickness, rectangular-prism-shaped single cryst. 9-24301
- remanent honeycomb domain structure, domain width depend. on crystal thickness 9-24300
- resistivity, temp. and mag. field depend. 9-24128
- self-diffusion in Ni-Co alloys, rel. to Co conc. 9-39386
- spin density, noncollinear 9-41304
- ⁵⁷Co n.m.r. in solns. rel. to Co-Cl complexes struct., obs. 9-40807
- Co-P films, coercive force and microstructure, effect of electroless Ni substrate 9-31041
- Co, magnetization and magnetothermal effect near Curie temp. 9-24271
- α -Co, magnon dispersion relation, anisotropy, neutron diff. obs. 9-41313
- Co²⁺, e.s.r. in K₂ZnF₄ and superhyperfine interaction const. 9-45257
- Co²⁺, e.s.r. in ZnO 9-28752
- Co²⁺, electrically induced e.p.r. transitions in CdTe 9-35711
- Co²⁺, red fluorescence in reduced germanate glass 9-31134
- Co²⁺, coloration impurity in lanthanum glass, effect on light absorption 9-24372
- Co²⁺ in α -Zn₃(VO₄)₂, crystal field studies 9-26668
- Co²⁺ in ag. soln., indirect determ. of short relax. time 9-30426
- Co²⁺ in K₂NiF₄, e.p.r. 9-41294
- Co²⁺ in MgF₂, exchange interactions obs. from far-i.r. spectra 9-41384
- Co²⁺ in Ni-Zn ferrites, Fe-rich, temp. spectra, mag. after-effects 9-28632
- Co²⁺ in P-O containing solvents, n.m.r. relax. and chem-exchange spin decoupling 9-23533
- Co²⁺, oxidation of some organic cpds. 9-24560
- Co II, electric dipole transition 3d⁴4p-d⁵, total line strengths and oscillator strengths 9-38768
- Co II, selection rules for forbidden d⁷p-d⁸ transitions, line strength calc. for 3d³4p-d⁸ 9-40542
- in Fe-Ni-Co alloys, complexometric determination 9-45430
- MnF₂:Co²⁺, localized magnetic mode, 1.2°K i.r. obs. 9-47291
- in MnF₂, localized mag. mode, temp. depend. 9-45227
- Mo-Nb-Co alloy, temp. depend. of hot composition from resistivity and susceptibility meas. 9-45067
- in Ni-Zn-Cr ferrites, small amounts effect on induced uniaxial mag. anisotropy 9-41326
- RbMgF₃-RbCoF₃, ferrimag., variation of mag. moments and Curie temp. with Co²⁺ conc. 9-47274
- in YFe garnet, magnetocryst. anisotropy and ferrimag. reson. 9-33480
- in YGa garnet, spin-reson. obs. 9-35575

Cobalt compounds

- alloy films, wall coercive force, strain sensitivity, 200 Å to 1500 Å thickness 9-45163
- alloys, high strength after ageing, patent 9-26377

Cobalt compounds continued

- CoO single cryst., transmission electron microscopy and etch pitting techniques. 9-42743
 $K\alpha$ line asymmetry indices, chem. combination effect 9-25695
 Ticonal 600 alloy, mag. props. and microstructure evolution rel. to comp. of α_1 and α_2 phases and saturation magnetiz. 9-44804
 Au-Co alloys, liquid ferromagnetic, thermodynamics near Curie and melting point 9-23531
 Au-Co alloys, precip., rel. to mag. hardness 9-41055
 Au-Cu-Co liquid alloy, susceptibility meas. 9-34921
 Co-Cr binary alloys, α -phase, mag. props. 9-43158
 CO-(10wt.%)Cr-(45wt.%)Fe alloy film, ferromagnetic domain struct., e microscope obs. 9-33471
 CO-Mn alloys, non-collinear mag. structures with antiferromag. interaction between local mag. moments 9-45056
 Co₂BaAl₂Fe₁₆O₇₂ ferroplax, magnetocryst. anisotropy const. determ. by magnetization curves 9-43170
 CO(III) complexes, residual paramag. obs. 9-35535
 COSO₄ aq., dielec. props. 9-46648
 CO-(10wt.%)Mn-(45wt.%)Fe alloy film, ferromagnetic domain struct., e microscope obs. 9-33471
 CdWO₄, local trapping levels, thermal activation energies and recomb. kinetics, thermoluminesc. props. rel. to X-ray luminesc. props. 9-39890
 Co-(42.54 at.%)Al alloys, electric and mag. props. 9-47069
 Co-Al alloys, local moment formation and resistivity minima 9-44908
 Co-(10 wt.%)Cr alloy, microstructure of oxide scales formed during high temp. oxidation 9-31194
 Co-(10 wt.%)Cr alloys, high temp. oxidation kinetics 9-31195
 Co-Cr alloys, non-collinear mag. structures with antiferromag. interaction between local mag. moments 9-45056
 Co-Cu solid solutions, magnetic hysteresis rel. to ageing time 9-26622
 Co-Fe-Be semi-hard mag. alloys, square hysteresis loop and low magnetotriation coercive force 9-45137
 Co-Fe-V alloys, high strength, high ductility, rel. to partially-recrystallized structure 9-44790
 Co-(8 wt. %)Fe, depolarization and secondary extinction, obs. 9-39267
 Co-(8 at. %)Fe alloy, large single cryst., low angle boundaries 9-37185
 Co-Ge alloys, liq., elec. resistivity 9-46652
 Co-Ni-Al-Cu-Nb-Fe alloys, magnetostruct. analysis 9-47251
 Co-Ni-Al-Cu-Ti-Fe alloys, magnetostruct. analysis 9-47251
 Co-Ni-Si alloys, ferromag., internally oxidized struct. obs. 9-48837
 Co-Ni alloy, martensitic transform. under tensile stress 9-26386
 Co-Ni alloys, internal friction during diffusionless phase transform. 9-37298
 Co-Ni alloys, internal friction meas. during $\alpha \rightarrow \beta$ transforms., -190° to 500°C 9-39400
 Co-Ni alloys, internal friction and elec. resistivity near Curie pt. 9-47074
 Co-(30.5wt.%)Ni alloy, allotropic transform., stress effects 9-23975
 Co-P alloys, amorphous layers, characterisation by very low coercive force 9-24311
 Co-Pt equiatomic alloy, magnetostriction, effect of tensile stress 9-45156
 Co-Sn dilute alloy, Mossbauer hyperfine field of ¹¹⁹Sn and resistivity study 9-47335
 Co-(7.45 wt.%)Ti solid soln., γ -phase, precip. during ageing, neutron diff. and chem. analysis 9-41065
 Co-V binary alloys, α -phase, mag. props. 9-43158
 Co-W alloy, stress rupture and superplasticity behavior, structural effects 9-26343
 Co-base superalloys, transmission electron microscopy study of microstructure 9-39298
 Co_{1-x}Cu_xRh₂S₄, mag. and elec. props. 9-41164
 Co_{1-x}Fe_xS₂, Mossbauer effect 9-45286
 Co₂BaIn₂Fe₁₆O₇₂, ferroplax, magnetocryst. anisotropy const. determ. by magnetization curves 9-43170
 Co₂Ta₂O₇-BaTiO₃ solid soln., s.h.f. dielec. props. 9-39689
 Co₂Ta₂O₇-BaTiO₃ solid soln., s.h.f. dielec. props. 9-47174
 Co₂W, magnetocryst. anisotropy const. determ. by magnetization curves 9-43170
 Co₃La₂(NO₃)₁₂·24H₂O, mag. phase transitions, obs. 9-39781
 Co₃O₄,⁵⁷Co, bulk material and ultra-fine particles, Mossbauer spectra 9-28666
 Co₃O₄, spinel, energy states from photoelec. emission meas. 9-41285
 Co₃O₄ single cryst. growth by chem. transport reaction using HCl gas 9-32871
 Co_{3-x}Cu_xR (R = rare earth permanent magnet material) 9-45120
 Co₂Mg_{0.8-x}Fe_{0.2}O₄, ferrite temp. depend. magnetic aftereffects, Co ion influence 9-35572
 Co₂Mn_{0.5-x}Fe_{0.5}O₄, ferrite, temp. depend. mag. after effects, Co ion influence 9-35572
 Co₂Ni_{0.5-x}Fe_{0.5}O₄, induced magnetic anisotropy mechanism 9-33474
 Co₂Ni_{0.8-x}Fe_{0.2}O₄, ferrite, temp. depend. mag. after effects, Co ion influence 9-35572
 Co complex, bis(selenourea)cobalt (II) thiocyanate, X-ray powder data, i.r. spectra and crystal structure 9-26227
 Co complex, bis(tricarballyc enecarbonyl) acetone, crystal and mol. structure 9-39264
 Co complex, Co(H(N₂))[P(C₆H₅)₃]₃, geometrical struct. 9-46361
 Co complex, Co(III) with α,α' -dipyridyl, proton magnetic resonance 9-32472
 Co complex, Co(II) of 1:3 bidentate Schiff's bases, spin density distrib. from isotropic proton resonance shifts 9-42411
 Co complex, cobalt (III) tris (N,N-diethylthiocarbamate, crystal and mol. structure 9-30559
 Co complex, cobalt (II) acetylacetonate, matrix-isolated spectrum, rel. to struct., 650-2200 cm⁻¹ 9-27870
 Co complex, trans-sulphiteisothiocyanate-bis (ethylenediamine)cobalt(III)dihydrate, stereochemistry and crystal structure 9-39265
 Co complex, tris(diethylthiocarbamate)cobalt (III), crystal and mol. structure 9-44661
 Co complex β -Co(II) phthalocyanine ground state from paramag. anisotropy obs. 9-32470
 Co complexes, quadrupole effects in e.p.r. 9-43278
 Co cyanide, magnetic susceptibility determ. by Faraday method, intermol. association 9-24276
 Co phthalocyanine, emission Mossbauer spectroscopy 9-27918
 CoBr₂·6H₂O, antiferromag., spin-flop states, low-temp. adiabatic studies 9-43191
 CoCO₃:⁵⁷Fe, antiferromag., Mossbauer obs. of Fe ion relax. 9-41364

Cobalt compounds continued

- CoCO₃, antiferromagnetic resonance spectrum splitting at low frequencies 9-28741
 CoCl₂·2H₂O magnon-phonon interaction, obs. in far i.r. 9-45077
 CoCl₂·6H₂O single cryst., mag. susceptibilities, low temp. 9-47284
 CoCl₂·2H₂O, antiferromag., far-i.r. mag. reson. absorpt., clustered multipole states obs. 9-33483
 CoCl₂·4CH₃OH, comparison with other divalent halogenides 9-23754
 CoCl₂·6D₂O single cryst., mag. susceptibilities, low temp. 9-47284
 CoCl₂·6H₂O, antiferromag., n.m.r. determ. of internal mag. fields at proton sites 9-47446
 CoCl₂·6H₂O, antiferromag., spin-flop states, low-temp. adiabatic studies 9-43191
 CoCr₂O₄, distant-neighbour B-B interactions, rel. to spin config. 9-45176
 CoCr₂O₄, ferrimagnet, high field susceptibility, temp. depend. 9-33473
 CoCr₂S₄ ferrimagnetic spinels, grown by vapour-liquid transport technique 9-39196
 p-CoCr₂S₄ ferromagnetic semiconductor magnetoresistance effect of exchange interaction 9-44956
 CoCs₂Cl₆, magnetic anisotropy 9-47230
 CoCs₂Cl₆, mag. struct., n. diff. obs. 9-39779
 CoF₃, crystal growth from low melting flux 9-39207
 CoF₃, inelastic scatt. of slow neutrons by two-magnon processes 9-43192
 CoF₃, phase transitions at pressures up to 160 kbar 9-44800
 CoF₃, magnetization of impurity Fe³⁺ ions, Mossbauer effect meas. 9-45298
 CoF₃, antiferromagnetic, magnon-optical phonon interaction, temp. depend. 9-47356
 CoFe₂O₄, uniaxial anisotropy induced at low temp. 9-43185
 CoGa intermetallic cpds., magnetic susceptibility 77°-1200°K 9-24281
 Co(H₂O)₆²⁺, electronic spectrum 9-48458
 Co(II) chloride solns. in water and alcohols, X-ray diff. 9-44548
 Co(II) cyanopyridine and chloropyridine complexes, far i.r. spectra 9-23038
 Co(III) complexes, anisotropic chem. shifts 9-45398
 Co(KSO₄)₂·2H₂O, probable struct. from X-ray powder data and similarity to krohnkite 9-35056
 Co(NH₃)₆³⁺, first band intensity, contrib. of odd vib. 9-23039
 CoNb₂S₄, synthesis and lattice constants on basis of hexagonal unit cell 9-39284
 CoO:Al(Li), self-diffusion of ¹⁸O 9-40982
 p-CoO:Li, drift mobility w.r.t. temp. from conductivity and Seebeck coeff. meas. 9-37518
 CoO:Li, monoxide to spin transition, role of cation vacancy density 9-48929
 CoO:Li single cry., dielec. props. 9-47157
 CoO/MnO solid solns., dielec. loss, const. and conductivity meas. w.r.t. freq. 9-35465
 CoO-Co₃O₄ films on Co, struct. and composition rel. to form above or below allotropic transf. temp. 9-32841
 CoO, complex defects 9-42806
 CoO, elec. conductivity, press. depend., saturation and phase separation obs. 9-35338
 CoO, self-diffusion of ¹⁸O 9-40982
 CoO, self-diffusion of O, mechanism 9-44731
 CoO, u.s. attenuation near antiferromag. critical pt. 9-44823
 CoO addition to discharge as aid to spectrochemical analysis of alkali elements 9-31229
 CoO coated glass sheets, optical and energy parameters 9-32038
 CoO energy states from photoelec. emission meas. 9-41285
 CoO magnetic excitations, theory 9-45063
 CoO magnetic semiconductor, band structure 9-47118
 CoO scales, plastic deform. behaviour, effect of stoichiometry 9-23882
 CoO single cry., dielec. props. 9-47157
 CoS₂, Curie pt. change under press., rel. to interatomic distance 9-33452
 CoS₂, mag. props. 9-33437
 Co(S₂Se_{1-x})₂, system, mag. props. 9-33437
 Co(S₂Se_{1-x})₂ system, ferromag. props. 9-33452
 Co(S₂Se_{1-x})₂ system, mag. and thermal props., thermostatical investigation 9-31029
 CoSO₄, u.s. absorption in ethylene glycol and water 9-30397
 CoSe₂, mag. props. 9-33437
 CoSe₂·x solid soln. single crystals and powder magnetiz. and susceptibility meas. 4.2° to 300°K 9-47245
 CoSeO₄, antiferromag. struct., Neel pt., neutron diff. powder obs. 9-49223
 CoSi, single crystal growth and characterization 9-37075
 CoSi₂ enthalpy changes at high temp. 9-39092
 CoTe_x, vapour transport growth of single crystals 9-23665
 Co-Pd alloys mag. fields on ⁶⁰Co and ¹¹⁵Sn nuclei, electron polarization 9-28620
 Cu-(12.6wt.%) Be-(0.2wt.%) Co-(0.1wt.%) Zn alloy, Mossbauer eff. 9-45288
 Cu-Be-Co, dil., constitution and behaviour 9-39274
 Cu-Co alloys containing coherent particles, critical resolved shear stress 9-44756
 Cu-Co alloys containing coherent precipitates, critical resolved shear stress 9-44755
 Cu-Co single crystal, w.r.t. precip. state 9-39428
 Cu-(2wt.%) Co alloy, structural transformations in precipitates on cold-rolling, Mossbauer obs. 9-30732
 Fe-Co-Ni alloy fine particles prep. by evaporation in inert gases, mag. props. 9-33459
 Fe-Co, alloy, f.c.c. precip. from Cu, mag. behaviour 9-26633
 Fe-(27 wt.%)Co alloy, coercive force at high temp., effect of dispersoid parameters 9-45138
 Fe-Co alloy, Fe-Rich nuclear transverse relaxation times of Fe, Suhl-Nakamura interaction 9-45240
 Fe-Co alloy, high-field susceptibility estimation at 0°K 9-47243
 Fe-Co alloy fine particles prep. by evaporation in inert gases, mag. props. 9-33459
 Fe-Co alloys, b.c.c., mean mag. moments 9-45142
 Fe-Ni-Al-Co-Ti alloys, thermomech. treatment effect on mag. props. 9-47259
 Fe-Ni-Co alloys, complexometric determination of elements 9-45430
 Gd-Co system, intermetallic cpds. over whole conc. range, lattice const. and mag. props. 9-48921
 HCoO₂ and DCoO₂, diffraction and spectra, O-H-O bond 9-32908
 Nb-Co liquid alloys, carbide grain during sintering 9-34952
 Ni-Co alloy, K-state existence 9-26507

Cobalt compounds continued

- Ni-Co alloy, magnetic moments, localized, of Co, e.p.r. investig. 9-33634
 Ni-Co alloys, positron annihilation spectra 9-39576
 Ni-Co alloys, self-diffusion of Co, rel. to Co conc. 9-39386
 Ni-Co films, electrolytically deposited, magnetocryst. anisotropy 9-41323
 Ni-Fe-Co films, anisotropy components separation by temp. depend study of anisotropy field 9-45170
 Ni-Fe-Co films, anisotropy components separation by temp. depend study of anisotropy field 9-45170
 Pd-Co-Sn alloys, ferromag., mag. props., Mossbauer obs. 9-43179
 Pd-Co alloy, local ordering and elec. resistance annealing effect 9-33255
 Pt-(0.07 at.%)Co alloy, low-temp. elec. resistivity 9-33257
 Pt-Co alloys, double ageing rel. to coercive force increase 9-26372
 Pt-Co dilute alloy, magnetoresistivity 9-44917
 Pt-(1 at.%)Co alloy with plastic strain, paramag. susceptibility, elec. resistivity and Mossbauer effect behaviour 9-43161
 Pt(23 wt.%) Co equi-atomic alloy single crystal having [111] orientation, mag. props. 9-45152
 Ti-(8 wt.%)Al-(4 wt.%)Co, mech. props. and structure 9-23956
 Ti-(8 wt.%)Al-(4 wt.%)Co alloy, heat treatment rel. to mech. props. 9-40994
 Ti-(8 wt.%)Al-(4 wt.%)Co alloy, microstruct. and heat treatment rel. to mech. props. 9-44747
 Ti-Al-Co alloy system, diagram for Ti-rich corner, struct. obs. 9-40919
 Zr-Co alloy, magnetic moments, localized of Co, e.p.r. investig. 9-33634

Cochlea *see Ear***Coherence** *see Electromagnetic waves; Lasers; Light/coherence; Masers***Cohesive energy** *see Bonds; Solids***Coincidence circuits** *see Counting circuits***Cold working**

- see also Plastic deformation; Slip; Work hardening*
 Fe prior to oxidation, increases rate at 200-600°C in 0.1-1 torr O₂ 9-41450
 metals, struct. changes and effect on yield and plastic flow 9-46925
 Ag-Mg solid soln. alloy, Ag-rich, stored energy, and elec. resistivity 9-48920
 Ag-Zn alloys, X-ray diff. study of cold-worked state, faults and dislocations 9-46935
 Al-(1 wt.%)Cd alloy rel. to pre-precipitation 9-23936
 Al-Si dilute alloys, recovery process 9-33104
 Al, Debye-Scherrer X-ray line broadening meas. 9-46776
 Al cold-rolled, yield strength determ. 9-28342
 Au-(0.1 wt.%)Cu alloy, fast neutron-irrad., effect on damage prod. and elec. resistivity recovery 9-43025
 Au, fast neutron-irrad., effect on damage prod. and elec. resistivity recovery 9-43025
 Cu-(2wt.%) Co alloy, structural transformations in precipitates on cold-rolling, Mossbauer obs. 9-30732
 Cu-Fe dilute alloys, martensite nucleation in Fe precipitation 9-37300
 Cu, fast neutron-irrad., effect on damage prod. and elec. resistivity recovery 9-43025
 Cu, prior to oxidation, increases rate at 200-600°C in 0.1-1 torr O₂ 9-41450
 Cu, recrystallization and recovery kinetics 9-39454
 Cu rolling at 20 and 290° K, effect on tensile props. 9-40993
 Fe magnetic permeability correlation with X-ray diffraction line broadening 9-45146
 InBi foil, effect of cold working on supercond. transition temp. 9-47078
 Mo, recovery 9-39463
 Mo single crystals, rolling texture exam. by X-ray diff. 9-41040
 Nb, cold-worked-peak obs. at 180°C 9-23870
 Ni, prior to oxidation, increases rate 200-600°C in 0.1-1 torr O₂ 9-41450
 Ta, cold-worked-peak obs. at 180°C 9-23870
 β -Ti alloy TS6, effect of initial state on dislocation struct. and mech. prop. changes on rolling 9-41031
 α -U, low-temp. phase transition depend. 9-26394
 Zn sheet, grain growth after deformation 9-26363

Collections of physical data

- Only comprehensive works of reference are listed here*
 astrophysics, collection and cataloging of data 9-28977
 coefficients of angular distrib. analysis of γ -rays emitted in nuc. reactions, tables in book 9-32300
 ionospheric obs. April (1968) 9-45521
 ionospheric obs. June (1968) 9-28939
 ionospheric observations March (1968) 9-31383
 neutron diffraction, coherent scatt. amplitudes, table 9-23724
 nuclear data library of UKAEA 9-22647
 physicochemical props. of elements, book 9-22026
 stars between declinations -35° and -40°, positions and proper motions, catalogue 9-28998
 super-strength alloys, high temp. effect on mechanical props. 9-33056
 thermal conductivity of 46 gases 9-36809
 vibrational frequencies of 54 mols. 9-23017
 X-ray crystallography, International Tables, phase relations of tetragonal space groups 9-23697
 γ - γ directional correl. coeffs., revised table 9-42125
 Yp collisions 9-29625
 Pu ceramic compounds, physical props. 9-22907

Collective model *see Nucleus/models***Collision processes**

- see also Atoms/electron scattering; Charge exchange; Elementary particles; Field theory, quantum/interactions; Ionization; Nuclear forces; Nuclear reactions and scattering; Scattering, particles; and under the individual particles*
 amorphous compounds, stopping of kilovolt ions 9-36678
 anisotropic probabilities in general cylindrical geometry 9-29862
 in asteroid belt, model 9-43622
 atmosphere, Davis-Sartor theory of droplet coalescence 9-26897
 atom-atom, in shock wave relaxation region, effect on precursor 9-46553
 atom-diatom molecule, anisotropy parameters from total cross-section meas. 9-34701
 Boltzmann collision integral approx. representation by Fock-Planck type operator 9-36148
 derivatives of classical deflection function 9-41742
 distribution function, radial, form rel. to collision operators 9-29210
 elastic, between sphere and wall of same material, gravitational perturbations 9-29181
 elastic and inelastic collisions using bouncing and non-bouncing balls 9-22030
 electron plasma oscillations, time damping evaluation 9-30267
 electron-atom, at low energies 9-46308
 electron-molecule, at low energies 9-46308
 electrons and molecules, for ionization gauge theory 9-40223
 excited state production cross-section in terms of imaginary part of integral involving wave function 9-36134
 rel. to flow through orifice, nearly free 9-46557
 gas, monatomic, ionizing shock structure 9-30294
 gas, single component, integral for elastic and inelastic collisions 9-48655
 gaseous mixtures, stopping of kilovolt ions 9-36678
 in gases, dipolar, thermal cond. and viscosity initial press. depend. 9-34835
 gases, rarefied; models 9-44518
 gases, rot. collision number and Eucken factor determ. 9-30335
 gases, transport props. and shock struct. rel. to inelastic collisions, 10⁴ °K 9-34841
 group II, between identical atoms, transitions between fine structure component, cross sections 9-48382
 hadrons, many body, high energy final state classification, new phase space plot 9-42027
 inert gas atoms, electron-atom collision parameters 9-42606
 integrals for components of dissociating air 9-23407
 ion-neutral particle, at low energies 9-46308
 ionized gas +ve column, Boltzmann electron eqn. soln. 9-23359
 ionosphere, D-region, high latitude obs. 9-33850
 ionosphere F region, electron collision freq., Delhi obs. 9-35886
 multilevel systems, transition rates 9-36644
 N₂ in arc discharge, collision with Cu atoms 9-46550
 neutral particles, ionizing at low energies 9-46308
 particle density matrix, rel. to kinetic eqn. 9-26018
 photons with relativistic electrons, ang. and energy distrib. of γ -quanta 9-29542
 in plasma with unequal electron and ion temp. effect on Thomson scattering 9-42515
 rearrangement, coupled channel method 9-22106
 relativistic Lorentz gas, elastic operator, Fokker Planck form 9-34051
 spectrometer, monoenergetic, electron impact, application 9-29897
 three-body rearrangement scatt., solvable quantum-mech. model 9-27174
 Townsend-Huxley expt. analysis; const. collisional cross section 9-39056
 Townsend-Huxley expt. analysis; const. collisional frequency 9-39055
 Voltzmann eqn. elastic collision integral, conversion into differential form 9-45773
 water droplets, rel. to coalescence and disruption 9-46604
 K⁻ with Ag and Br nuclei, hyperfragment and fragment prod. with Z \geq 4 9-40471
 CO₂ vibration-rotation transition in 00⁰1-10⁰ band, effect on saturation characteristics 9-22972
 Cs⁺-Ar rainbow scatt. rel. to interaction pot. between rare gas atom and alkali ions 9-25711
 He plasma, partially ionized, electron collision frequency 9-44417
 in He target, metastable H prod. by ϵ capture of p 9-40562
 Ne plasma, partially ionized, electron collision frequency 9-44417

Collision processes continued

- alkali at. beam with triat. halide mols. 9-25795
 alkali atom interactions with atoms and non-reactive diatomic mols., cross sections and van der Waals Constants 9-42342
 alkali atoms, excitation transfer in collisions between identical atoms 9-42339
 alkali atoms, thermal energy, from halogen atoms and mols.; curve crossing eff. on cross section 9-29969
 alkali excited atoms, scattering by merit gas atoms, theory 9-40556
 alkali metal, elastic collisions, effect of spin-orbit coupling 9-38793
 alkali metal vapours, fluorescence, collisions inducing transitions between sensitized doublet sublevels, obs. 9-29971
 alkali-alkali scatt. rel. to singlet potential of alkali diatoms 9-38866
 atom+mol. gas reaction in discharge flow syst., at. conc. meas. 9-26805
 atom-atom excitation cross-sections calc. by classical methods 9-44286
 atom-atom glory scatt., quantum effects 9-38787
 atom-atom ionization rates, semiempirical model 9-44273
 atom-ion, charge-overlap effects 9-38788
 balance eqn. for excited atoms corrected for diffusion and collisions of first and second kind 9-46309
 Born series, partial summation 9-48417
 charge-overlap effects, dispersion and induction forces 9-38788
 classical approx. in symmetrical resonance charge transfer 9-48428
 cross-sections, inverse bremsstrahlung, in screened potentials, classical calcs. 9-46271
 electron capture by positive ions, radiation damping in optical continuum, Weisskopf and Wigner theory 9-44248
 electron collisions with positive ions, asymptotic solns. of coupled eqns. 9-44283
 electron loss, free scatt. model 9-46310
 electron-atom ionization, threshold region, insight by exam. of doubly excited states of compound ion 9-34582
 electron-impact ionization cross-section for atoms Sc to Zn 9-27820
 electronic transitions in slow collision, theory 9-34568
 Fadeev eqns. used to determ. collision amplitudes 9-46311
 with film impurity layer on solid subst., atom props. influence on interaction singularities 9-42981
 final state interactions in atom-diatom collision 9-23199
 He, 4¹P-4¹F collisional transfer 9-32441
 inelastic, between excited and unexcited atoms, review 9-36679
 inert gas, ionized excited states formation through loss of metastable electron 9-34569
 inert gas, with N₂, excitation of rotational and vibrational motion of N₂⁺ ions 9-42470
 inert gas excitation cross-sections, absolute determ. by electron collision 9-46298
 inert gas ions and atoms with N₂, rel. to excitation of λ =4278 Å band of first negative system of N₂⁺ ion 9-30045
 inert gases, light scatt. and dielec. phenomena 9-32432
 interaction with electrons or ions in plasma 9-29970
 interatomic potential between alkali ions and rare-gas atoms using charge-transfer and Firsov's theory 9-25711
 inverse problem, WKB treatment 9-46312
 ion-atom, classical scattering, comprehensive approximation formula 9-34567
 ionization by ion bombardment near threshold energy, cross-section 9-25703

Collision processes continued
atoms continued

- ionization of hydrogen-like atom by proton impact, relativistic formula 9-40555
- level transitions rel. to electron energy distribution in low temp. plasma 9-40659
- long-range forces, nonadiabatic, general expression 9-32425
- many-state problem, scatt. matrix. formula and extension of BII approx. 9-32424
- metal, two atoms causing secondary ion emission 9-24258
- negative ions dissociation 9-32427
- Penning ionization cross-section calc. 9-32688
- perturbation effects in elastic differential cross-section meas. 9-38790
- photoionization cross section calc. 9-23339
- positive ions with electrons, asymptotic solns. of coupled eqns. 9-44283
- relaxation, anisotropic, of multipole moments, cross section in gas determ. 9-32426
- repulsive interaction between excited and ground state inert gas atoms 9-29968
- resonance theory of termolec. recomb. kinetics 9-48426
- scattering factor for heavy atoms 9-27824
- scattering theory, time-dependent semiclassical for relative motion 9-31773
- singlet states prod. by ion collisions relax. times of alignment 9-29983
- slow, asymptotic Coriolis interactions 9-29967
- spectral line shape theory from kinetic theory of gases 9-32406
- spectral pressure broadening in gases, theory 9-29906
- spin polarization of low-energy elastically scatt. electrons 9-34564
- superelastic collisions demonstrated using linear air track 9-43701
- X-ray emission spectra excited by α -bombardment, cross-section meas. for various atoms 9-46267
- p-H, energy loss rel. to proportional counters 9-46137
- p-H collisions, a new orbital to allow for intermediate molecular state 9-32436
- ¹³³Cs, self spin-exchange cross-sections meas. using microwave absorption between Zeeman sublevels 9-46314
- ¹¹⁴Cd resonance line, λ 3261 Å, broadening by pressure of inert gases, temp. effects 9-40557
- Ar-Ar⁺ energy spectrum of released electrons, investig. 9-22983
- Ar-H₂, total cross-section, for particular rotational j , m_j state of H₂ molecule 9-27945
- Ar, differential elastic scatt. of low-energy protons 9-44287
- Ar, excited state, repulsive interaction with He, Ne, Ar ground state atoms 9-29968
- Ar, incident beams of He, H, He⁺; electron and ion prod. cross section meas., 0.15-1.0 MeV 9-22982
- Ar, positron annihilation, models 9-38785
- Ar, positron annihilation rel. to applied elec-field and Ar density 9-38784
- Ar, O⁺; inelastic process energy transfer distrib. meas., 50-200 keV 9-46313
- Ar⁺-Ar, 0.5-6 MeV with large angle scatt., evidence for prod. of inner shell vacancies 9-32428
- Ar⁺-Ar charge-transfer cross-sections, oscillations 9-38791
- Ar⁺-Ar-Ar⁺, Ar; 3-body conversion rate coeff., ion sampling in discharge positive column 9-46317
- Ar⁺ ions, collisions with surface Cu atoms, charge exchange of scattered ions 9-48418
- Ar⁺-Ar, 100-400 keV, excitation and assoc. emission 9-44280
- Ar⁺+Ar excitation resonances for production of metastable atoms 9-34560
- Ar and H, -ve charge prod. cross section determ., 50-1000 eV 9-27826
- C+N atoms, interaction potentials 9-38792
- Cd, spin polarization transfer from optically pumped metastable helium atoms following Penning collisions 9-38803
- Cd at 5P₁ level, with rare gases and N, depolarization effective cross-sections 9-27822
- Cs-6³P_{3/2} states distrib. due to sat. hydrocarbon collisions, eff. cross sections 9-44279
- Cs, He⁺ and Ar⁺ total charge-transfer cross section meas., 10-1500 eV 9-46316
- Cs, hyperfine freq., effects of molec. buffer gases 9-22948
- Cs, quenching of reson. radiation by He 9-42343
- Cs⁺+He, threshold behaviour of the cross-section for excitation of Cs II reson. lines 9-48419
- Cs and alkali atoms, spin-exchange cross sections calc., partial wave anal. 9-22984
- Cs and Cu optically pumped spin exchange 9-40548
- Cu surface atoms, Ar⁺ bombard., charge exchange of scattered ions 9-48418
- D₂ transfer reactions with CO₂⁺, D₂O⁺ and H₂S⁺ 9-49374
- D⁺-D₂(H₂) charge-exchange collisions, search for isotope effect 9-44295
- H-H, excitation cross sections, impact parameter treatment, two-state approx. 9-42348
- H-H, ionization of excited atoms 9-22992
- H-H excitation cross sections, impact parameter treatment, four state approx. 9-44297
- H-He, H-N, H-Ar, electron loss, free scatt. model 9-46310
- H-Li, ionization of excited H atoms 9-22992
- H-N₂, low-energy, stripping and ionization obs. 9-34584
- H-Na ionization of excited H atoms 9-22992
- H-O₂, low-energy, stripping and ionization obs. 9-34584
- H-p, ionization cross-section calc. at low energy 9-32434
- H, electron loss of fast atoms passing through He, first Born approx. cross sections 9-48425
- H, excited, with protons, resonance charge transfer, classical approx. 9-48428
- H, excited, with protons, resonance charge transfer, quantal two-state approx. 9-48427
- H, p impact ionization 9-38797
- H, pair polarizability 9-32432
- H, photon scattering amplitude, exact expression, and Lamb shift in nonrelativistic approx. 9-36683
- H, proton collision, 0.5-50 KeV, parametric treatment 9-40563
- H, proton collision, parametric treatment, quantum considerations 9-40564
- H, proton impact, 0.5 to 50 keV, parametric treatment, theory 9-48430
- H₂-He fast beam, charge changing collision, He⁺ formation 9-29985
- H⁺, detachment by e impact 9-44293
- H⁺-H(1s) electron capture process, metastable H atom prod., cross section obs. 9-27827

Collision processes continued
atoms continued

- H⁺ on all elements in ground state 5-140 keV calc. of charge exchange ratio of excited to all captures 9-25717
- H⁺ polarized beam prod. from charge exchange reactions 9-34585
- H⁺ with molecular gas, charge exchange, products obs. 9-22995
- H⁺-N₂-HN₂⁺, Balmer- α , N₂⁺(0,0) 1st-ve band photon emission, cross sections meas. 9-22985
- H⁺-D₂(H₂) charge-exchange collisions, search for isotope effect 9-44295
- H⁺+He(1S)⁺-H(2S)+He⁺(1S) cross section normalization 9-22996
- H⁺+ (1s)-2H⁺(E)⁺+e⁻ cross-section calc. for e<500 Ev 9-32433
- H plasmas, effect on collisional-radiative ionization and recombination coeffs. 9-42495
- H target for precision scatt. cross-section meas. 9-44296
- H+H⁺, associative and collisional detachment, semi-classical calcs. 9-48429
- H(1s)+H(1s)->H(2lm)+H(2l'm'), 6.25 KeV-3.0 MeV, cross-section calc. using impact-parameter method 9-46331
- He-Ar, prod. and destruction of fast metastable He atoms, cross sections 9-38796
- He-H₂, prod. and destruction of fast metastable He atoms, cross sections 9-38796
- He-He, prod. and destruction of fast metastable He atoms, cross sections 9-38796
- He-Ne laser, multimode 0.63 μ , rel. to output power and spectrum 9-34164
- He-Ne laser, Ne atoms density nonlinear depend. on saturation, Ne exchange collisions explanation exchange collision, saturation parameter nonlinear depend. on density 9-25271
- He-Xe, prod. and destruction of fast metastable He atoms, cross sections 9-38796
- He-p, excitation of 7¹S state, changes in wave function representation 9-32439
- He, excitation by protons and electrons 9-27829
- He, fast, electron loss on passing through H and He, first Born approx. cross sections 9-48425
- He, high energy p ionization 9-38799
- He, incident beams of He, H, He⁺; electron and ion prod. cross section meas., 0.15-1.0 MeV 9-22982
- He, Li⁺ elastic differential scatt., cross section meas., 3-330 eV 9-46315
- He, p scatt., coupled-state calc., anomalies 9-32442
- He⁺-CO, excited C ions form. obs. 9-36724
- He⁺ prod. in afterglow plasma due to collisions between metastable ions 9-46336
- He⁺ with molecular gas, charge exchange, products obs. 9-22995
- He⁺+H(1s), resonance charge transfer 9-48435
- He and H, -ve charge prod. cross section determ., 50-1000 eV 9-27826
- He gas, cosine reflections induced by leaching Pyrex glass 9-36820
- He glow discharge, 2¹S state decay by e collisions, obs. 9-34808
- He metastable atoms, destruction in binary collisions 9-38802
- He with metastable He, elastic scatt., diffusion and excitation transfer 9-29984
- He⁺-He scatt., interac. potential meas. from extrema positions in interference patterns 9-40569
- He and ³He on clean W surface, thermal accommodation coeffs. 9-30501
- He⁺-He scatt., interac. potential meas. from extrema positions in interference patterns 9-40569
- He+p, polarization of Balmer- α radiation 9-22989
- Hg, effective section of inelastic collisions between atoms in 6³P₀ and 6³S₀ levels 9-22971
- Hg, excited, with unexcited Tl atoms 9-48421
- Hg, with electrons, polarization of electron beam, meas. by optical method 9-44284
- Hg⁺ in atomic Hg, charge-transfer cross sections 9-48420
- I⁺-Xe, 0.5-6 MeV with large angle scatt., evidence for prod. of inner shell vacancies 9-32428
- I(5²P_{1/2}), electr. excited, with Cl₂, Br₂, ICl and IBr, decay and rate const. 9-43319
- K-methyl iodide cross-sections, poor fit of Lennard Jones pot. 9-27823
- K-Ar, cross-sections, poor fit of Lennard-Jones pot. 9-27823
- K-Xe, cross-sections, poor fit of Lennard-Jones pot. 9-27823
- K, He⁺ and Ar⁺ total charge-transfer cross section meas., 10-1500 eV 9-46316
- K, in Rb vapour, causing sensitized fluoresc., energy transfer obs. 9-34573
- K⁺ in N₂, mobility, diffusion coeff. and reaction, determ. 9-23203
- K(2¹P_{1/2})+Rb(2¹S_{1/2})->K(2¹S_{1/2})+Rb(2¹P_{1/2})+ Δ E, fluorescence detected, cross-section meas. 9-32429
- K and alkali atoms, spin-exchange cross sections calc., partial wave anal. 9-22984
- K in Rb vapour, causing sensitized fluoresc. ⁴²P_{1/2}-⁴²P_{3/2} mixing in K 9-34574
- ³⁹K, self spin-exchange cross-sections meas. using microwave absorption between Zeeman sublevels 9-46314
- Li-HBr, optical pot. for molecule to reproduce obs. quenching of glory undulations 9-25798
- Li⁺ with H₂, vibr. excitation, mol. beam meas. 9-25796
- Li and alkali atoms, spin-exchange cross sections calc., partial wave anal. 9-22984
- Li target, proton charge exchange bombard., H atom formation cross section 9-27813
- Li(2²S and 2²P)-H₂, interac. energy surfaces, crossing of curves obs. 9-34570
- N, collision strengths and photoionization cross-sections 9-29972
- N, elastic scatt. by NO and CO molecules, characts. 9-25712
- N, recombination kinetics rel. to visible emission of mol. N₂ in yellow afterglow at low pressures 9-39029
- N₂-H-NH₂⁺ Balmer- α , N₂⁺(0,0) 1st-ve band photon emission, cross sections meas. 9-22985
- N⁺ in N₂, mobility, diffusion coeff. and reaction rates determ. 9-23347
- Na-Cs at beams, interaction 9-25713
- Na-He, Na in ²P state, cross-section behaviour obs. 9-29973
- Na-O₂, obs. of charge transfer, ionization and rearrangement 9-23204
- Na, 3²P_{1/2}-3²P_{3/2} mixing induced in collisions with CH₄, CD₄, C₂H₂, C₂H₄ and C₂H₆ 9-44288
- Na and alkali atoms, spin-exchange cross sections calc., partial wave anal. 9-22984
- Na target, proton charge exchange bombard., H atom formation cross section 9-27813

**Collision processes continued
atoms continued**

- Na with Ar buffer, obs. of dephasing collisions using Hertzian coherence in optical pumping 9-29966
²³Na, self spin-exchange cross-sections meas. using microwave absorption between Zeeman sublevels 9-46314
 Ne, collision strengths and photoionization cross-sections 9-29972
 Ne, excited state, repulsive interaction with He, Ne, Ar ground state atoms 9-29968
 Ne⁺, 2Ne → Ne⁺, Ne: 3-body conversion rate coeff., ion sampling in discharge positive column 9-46317
 Ne and H, -ve charge prod. cross section determ., 50-1000 eV 9-27826
 Ne optically pumped in ³P_{1/2} state, collisional depolarization with He and ground-state Ne 9-22973
 O, collision strengths and photoionization cross-sections 9-29972
 O, elastic scatt. by NO and CO molecules, characts. 9-25712
 O(¹D), electronic de-excitation by inert gases during vacuum u.v. photolysis of O₂ 9-35755
 Rb, He⁺ and Ar⁺ total charge-transfer cross section meas., 10-1500 eV 9-46316
 Rb and alkali atoms, spin-exchange cross sections calc., partial wave anal. 9-22984
 Rb vapour, sensitized fluoresc. by induced collisions with K atoms, energy transfer obs. 9-34573
 Rb vapour, sensitized fluoresc. by collisions with K atoms, ⁴²P_{1/2}-⁴²P_{3/2}=collisions with K atoms, ⁴²P_{1/2}-⁴²P_{3/2} mixing in K 9-34574
⁸⁵Rb, ⁸⁷Rb, self spin-exchange cross-sections meas. using microwave absorption between Zeeman sublevels 9-46314
 Sr, spin polarization transfer from optically pumped metastable helium atoms following Penning collisions 9-38803
 Tl, excited, with inert gases, depolarization, cross section meas. 9-22976
 U, scattering factor calc. by WKB method 9-27824
 Zn, spin polarization transfer from optically pumped metastable helium atoms following Penning collisions 9-38803

molecules

- acetylene, inelastic collisions with Na, total cross sections for ³P_{1/2}-³P_{3/2} mixing 9-44288
 alkali atom interactions with atoms and non-reactive diatomic mols., cross sections and van der Waals constants 9-42342
 alkali atoms, thermal energy, from halogen atoms and mols.; curve crossing eff. on cross section 9-29969
 anisotropy parameters determ. from M depend. of total cross-section 9-42468
 asymptotic evaluation of WKB matrix elements 9-38234
 atom + mol. gas reaction in discharge flow syst., at conc. meas. 9-26805
 atom scatt. by rigid rotor, reson. widths 9-23197
 atom-diatom, final state interactions 9-23199
 atom-diatom, inelastic transitions and quenching of glory extrema 9-38931
 atom-diatom mol., coupled eqns. and minimum principle 9-38932
 atom-diatom mol., molec. reorientation 9-27941
 atom-diatom mol., total cross-section, quenching of glory undulations 9-42467
 atom-triatomic mol., quantum transition probabilities 9-30160
 bimolecular reactions, mol. beam investigation 9-25792
 bimolecular reactions, theory 9-25793
 Born series, partial summation 9-48417
 crossed beams, effect of speed distrib. on nonreactive scatt. 9-44388
 decoupling approx., variational corrections 9-38930
 diatomic, h.f. effects on spin relax. in gases 9-34603
 diatomic beam, rotational transitions as result of scatt. at solid surface 9-42364
 diatomic mol. collision with atom, theory 9-36734
 dilute polar gases, averaged potentials and viscosity 9-42615
 electron impact excitation, polarization of molecular line radiation, theory 9-32449
 electron scatt. from real dipoles, diffusion cross-section, vel. depend. 9-34705
 electron scattering, improvement in the first Born theory 9-40572
 electron scattering by polar mos., rotational excitation 9-32448
 electron-molecule excitation and dissociative attachment, angular dependence of scattering products 9-34602
 energy transfer, Hamilton-Jacobi formalism 9-36735
 energy transfer of polyat. mols. 9-25794
 equilibrium producing, rel. to expansion of phase space, teaching paper 9-45777
 ethane, inelastic collisions with Na, total cross sections for ³P_{1/2}-³P_{3/2} mixing 9-44288
 ethylene, inelastic collisions with Na, total cross sections for ³P_{1/2}-³P_{3/2} mixing 9-44288
 fluorocarbons, dynamic nuclear polarization in soln. 9-44597
 gas, intermolecular collision processes and forces in dilute gases 9-36819
 halides, triat. and alkali at beam 9-25795
 integrals of modified Buckingham potential 9-40628
 ion-molecule, evidence of long-lived collisional complexes 9-47456
 ion-molecule collision complexes, long-lived, evidence from numerical studies 9-36732
 methane and methane-d₄, inelastic collisions with Na, total cross sections for ³P_{1/2}-³P_{3/2} mixing 9-44288
 microwave rotational lines of gases, width determ. using graphical method 9-44310
 molecular beam scatt. data anal. 9-38933
 negative ion-molecule reactions method of study 9-46430
 neutron scatt., in liquids, gases and solids, theory 9-48656
 nonpolar gases, press.-induced microwave absorpt. 9-30350
 nonreactive collisions, internal excitation 9-23197
 optical potentials 9-23198
 orbiting collisions, phase shift 9-34704
 polar mol. with electron, rot. transition cross-sections 9-42465
 polar molecules, rotational excitation by electrons 9-32448
 with power law potentials, collision operator spectrum 9-32558
 radiative transfer eqn. inversion for atm. ozone distrib. 9-28870
 rigid convex mols., collision integrals 9-42604
 rotational excitation, role of closed channels and resonances 9-34699
 rotational excitation and scatt., restricted distorted-wave approx. 9-30159
 second kind collision, velocity distrib. func. 9-27943
 semiclassical limit of inelastic scatt. amplitude 9-22095
 small-angle from anisotropic potentials 9-23200
 spin polarization of low-energy elastically scatt. electrons 9-34564
 subexcitation region, potential curve crossing 9-30161

**Collision processes continued
molecules continued**

- transition probabilities, distorted-wave approx. for reaction matrix 9-23202
 translational-vibrational energy transfer, steric factor 9-30162
 vibrational energy transfer in gases 9-23201
 vibrational transition probability calc. in high energy collision using time-independent Schrodinger eqn. 9-34698
 C₂H₄+C₂H₆→C₂H₄⁺+C₂H₆ intermediate-complex reaction obs. at ~1 eV 9-41443
 CD₄+CH₃OH⁺→CD₃+CH₃OHD⁺, stripping→complex transition 9-38936
 CD₄+X⁺→CD₃+XD⁺, deviations from stripping model 9-27944
 CN polar mols., rotational transition by electron collisions, differential cross sections 9-46360
 CN with electrons, rot. transition cross-sections 9-42465
 CO, e impact excitation structure obs. at 2.3 eV., electron affinity 9-34612
 CO, elastic scatt. of O and N atomic beams 9-25712
 CO, electron scatt., elastic at 500 eV, absolute differential cross sections 9-38800
 CO, ratio of cross-sections for self- and foreign-gas line broadening 9-25735
 CO₂, relax. time for rot. transitions calc. 9-44389
 CO₂, vibrational-rotational transitions, eff. of collisions on saturation nature 9-44323
 CO₂ dipole interaction with electrons, vibr. excitation obs. 9-36697
 CO₂(v₃) vibrationally excited, deactivation by collisions with CO₂ or N₂ 9-42387
 Cl₂, press.-induced fundamental i.r. absorpt. band 9-30023
 Cl+Br₂→ClBr+Br, crossed beams reaction, energy disposal 9-39938
 CsF, scatt. by Ar and He, cross sections and anisotropy parameters 9-44387
 CsF attractive interaction with rare gases, anisotropy factor and scattering cross section 9-44390
 D₂+CH₃OH⁺→D+CH₃OHD⁺, stripping→complex transition 9-38936
 D₂+X⁺→D₂XD⁺, deviations from stripping model 9-27944
 D⁺+D₂O→OD⁺+D₂, 0-3 eV obs. 9-46430
 H₂-Ar, total cross-section, for particular rotational j, m_J state of H₂ molecule 9-27945
 H₂-Li(²S and ²P) interac. energy surfaces, crossing of curves obs. 9-34570
 H₂, electron scatt., differential elastic and rotational excitations calc. 9-46363
 H₂, incident beams of He, H, He⁺; electron and ion prod. cross section meas., 0.15-1.0 MeV 9-22982
 p-H₂, rot. relax. in mixtures with He, Ne, Ar 9-42611
 H₂, target, low energy electron scatt., polarization and exchange effects 9-40591
 H₂⁺-H₂ inelastic collisions, 3-20 keV, dissociation obs. 9-44375
 H₂⁺, e scatt. 1sσ_g-2pσ_u transition, asymptotic closure cross section calc. 9-40573
 H₂⁺ collisional dissociation, ang. distrib. of protons, theory 9-40622
 H₂⁺ with molecular gas, charge exchange, products obs. 9-22995
 H₂ and H collision, -ve charge prod. cross section determ., 50-1000 eV 9-27826
 H₂ gas, n.m.r. relaxation time meas., 293-738°K, 7-135 atm., J depend. on collisions 9-34616
 H₂ with Li⁺, vibr. excitation, mol. beam meas. 9-25796
 H₂⁺ de-excitation by H₂, energy transfer 9-44494
 H⁺+H₂O→OH⁺+H₂, 0-3 eV obs. 9-46430
 H⁺-H₂ interac., change of charge states, elementary processes 9-30165
 HBr-HBr, vibrational transitions P_{1,0} probabilities 9-25797
 Li-NiBr scatt., optical pot. for molecule to reproduce obs. quenching of glory undulations 9-25798
 HCN, rot. energy transfer rates, by microwave double reson. 9-30028
 HCOO⁺+SF₆⁺→SF₅⁺+HCOOF, 0-3 eV obs. 9-46430
 HCl-HCl and H₂Cl-H₂Cl, vibrational transitions P_{1,0} probabilities 9-25797
 HCl polar mols., rotational transition by electron collisions, differential cross sections 9-46360
 HCl with electrons, rot. transition cross-sections 9-42465
 HF-H₂, He, Ar, vibrational transitions P_{1,0} probabilities 9-25797
 HI-Ar, HI; vibrational transitions P_{1,0} probabilities 9-25797
 H+H₂, optical potentials 9-23198
 He⁺+H₂, non-reactive, obs. at ~1 eV 9-41443
 (HeH)⁺, collision-induced dissociation 9-38921
 K+HBr(DBr)-KBr reactive, crossed mol. beam expts., angular and vel. distrib. of KBr 9-35741
 N₂, electron scatt., elastic at 500 eV, absolute differential cross sections 9-38800
 N₂, harmonic generation under alternating electric field 9-30300
 N₂, incident beams of He, H, He⁺; electron and ion prod. cross section meas., 0.15-1.0 MeV 9-22982
 N₂, Li⁺ elastic differential scatt. cross section meas., 3-330 eV 9-46315
 N₂ with inert gas atoms, excitation of rotational and vibrational motion of N₂⁺ ions 9-42470
 N₂, N₂⁺ 1st -ve system prod. by ion bombardment, rotational line intensities meas., 130°K 9-46429
 N₂⁺-e, excitation cross-section obs. 9-32479
 N₂⁺ reaction with CH₄ and CD₄, dynamics 9-39940
 N₂ and noble gas ions and atoms rel. to excitation of λ=4278 Å band of first negative system of N₂⁺ ion 9-30045
 N₂ with 0-200 eV, vac. u.v. light emission 9-32480
 N₂(A³Σ_u⁺), quenching in low vib. levels by N atoms 9-44340
 NH₃ inversion spectrum, press. broadening 9-42404
 NO, elastic scatt. of O and N atomic beams 9-25712
 Na-O₂ obs. of charge transfer, ionization and rearrangement 9-23204
 Ng₂, line mixing by collisions in far i.r. spectrum 9-38859
 O₂, Li⁺ elastic differential scatt. cross section meas., 3-330 eV 9-46315
 O₂⁺+D₂, evidence of long-lived DO₂⁺ 9-47456
 O₂(¹Δ_g) quenching by O₂, N₂ collisions, obs. 9-23206
 O₂(¹Δ_g) deactivation by O, N, benzene, obs. 9-34707
 O⁺+N₂O→NO⁺+NO, 0-3 eV obs. 9-46430
 O⁺+NO₂→NO₂⁺+O, 0-3 eV obs. 9-46430
 SF₆⁺+HCl-F₂Cl⁺+(SF₆Cl), 0-3 eV obs. 9-46430
 TIF attractive interaction with rare gases, anisotropy factor and scattering cross section 9-44390

Collision processes, plasma see *Plasma/collision processes*

Colloids

- see also *Electrophoresis; Emulsions; Gels; Sols; Thixotropy*
 capillary-porous, radiation distrib. for bilateral irradiation 9-23546
 casein sols., iso-electronic points rel. to ionic strengths, study with streaming current detector 9-23550
 charged plate-like parallel colloidal part. in 1-1 plus 2-1 electrolyte mixture, stability props., mutual antagonism 9-23545
 conference, 42nd National Symposium, Chicago, 1968 9-23542
 dilute suspensions of randomly oriented part., small-angle X-ray scatt., theory 9-26137
 in gas, detector using ionization chamber and a step-down amplifier, patent 9-34931
 gelatin sols., iso-electronic points rel. to ionic strengths, study with streaming current detector 9-23550
 globin sols., iso-electronic points rel. to ionic strengths, study with streaming current detector 9-23550
 light scatt. by colloidal spheres 9-36357
 light scatt. by spheroidal particles oriented by streaming 9-36903
 magnetic, magnetoviscosity 9-48722
 particle orientation by laser fields and effect on light scatt. 9-23543
 particle size distrib. from X-ray scatt. 9-36904
 in quartz, trapping of inclusions in cryst. growth 9-37043
 suspensions in liquids colloidal electrophoretic mobility meas. 9-46662
 suspensions with induced and permanent elec. particlemoments, electro-optical effects 9-42684
 Ag particles, electron m.f.p. limitation, refractive index meas., absorption coeff. determ. 9-41115
 C suspensions in insulating liq., electrophoretic development of electrostatic charge images 9-44604
 Cd centres in alkali halides 9-40970
 in KBr optical and thermal stability, elec. conducting obs. 9-46835
 NaCl:Cu, additively coloured with Na vapour, colloidal absorpt. bands 9-32998
 NaCl, coloured and annealed evolution, mechanism 9-26296

Colorimeters see *Colorimetry*

Colorimetry

- see also *Spectrochemical analysis; Spectrophotometry*
 (U^* , V^* , W^*) system, modification 9-40382
 chromaticity of colours from Fabry-Perot filter assoc. with standard white light 9-34213
 CIE tristimulus values, differences, perceptual significance 9-48098
 coordinates, colour, of various surface textures, rel. to illuminating and viewing geometries 9-41951
 in Europe, review 9-41950
 instrumentation, meas. concepts and computation methods in USA 9-41949
 instrumentation problems 9-27395
 instruments, 15 different kinds, comparative performance 9-41953
 neutral grays, shift induced by surrounding colour, estimation 9-48096
 spectrophotometer, Cary 14, accessories for colour meas. 9-41954
 using spectrophotometer, photometric accuracy 9-41952
 spectrophotometric meas., applic. to some Polish organic pigments 9-25371
 tristimulus instruments 9-34212
 white colours, comparison of blue tristimulus filters with standard observers 9-48097
 white reflectance standards, prep and calibration 9-34201

Colour

- see also *Photography/colour*
 cholesteric liq.-cryst. films, effect of mech. disturbance 9-39103
 chromaticity of colours from Fabry-Perot filter assoc. with standard white light 9-34213
 CIE tristimulus values, differences, perceptual significance 9-48098
 coordinates of various surface textures rel. to illuminating and viewing geometries 9-41951
 correction, optical system modulation transfer function 9-22445
 diamonds, effect of heat and pressure treatment 9-26366
 electrophotographic recording by 3 colour filter and thermoplastics, patent 9-22490
 interference, of thin layer, calc. 9-34202
 moon, (differential), time depend. and possible mechanisms 9-31586
 photochromic materials, photobleachable electron-beam-induced colouration 9-43201
 photochromic spiropyran layers, coloration by u.v. laser radiation 9-27916
 porcelain enamels, TiO₂ opacified, refraction by dispersed TiO₂ crystals 9-37687
 shift induced in neutral grays by surrounding colours, estimation 9-48096
 CaTiO₃:Fe-Mo, photobleachable electron-beam-induced colouration 9-43201

Colour centres

- absorption spectra due to impurity centres, shape obs. and Urbach's rule 9-33546
 alkali halide crystals, U bands, band shape and phonon broadening 9-46830
 alkali halide mixed cryst., F-centre prod. reduction due to disruption of replacement collision sequences 9-32991
 alkali halide-B₂O₃, p-irrad., e.s.r. of stable V centres 9-24480
 alkali halides, absorpt. spectra of small quasi-metallic particles, fine struct. and oscillatory effect 9-39370
 alkali halides, Cd doped and electrolytically coloured, band obs. 9-40970
 alkali halides, destruction due to radiation, domain subsystem behaviour 9-32989
 alkali halides, electron irradiation, saturation of F centre form 9-48867
 alkali halides, F₂⁺-model of R⁺ centre, electronic states obs. 9-39369
 alkali halides, F⁺ centre, polaron model applic. for calc. of electronic and ionic polarization effects 9-44716
 alkali halides, F-centre, Stark eff. of relaxed excited states 9-24392
 alkali halides, freqs. of localised modes due to U-centres 9-35265
 alkali halides, M-centre singlet-triplet splitting, calc. 9-35107
 alkali halides, V_K-centres, stability calc., model 9-42847
 alkali-halides, absorption of U₂-centres, effect of external stresses 9-49251
 alkaline earth fluorides, self-trapped hole and exciton obs. 9-46831
 alkaline earth fluorides, V_K centres, opt. and e.p.r. spectra, eff. of polarized bleaching light 9-23826
 alkaline earth oxides, F⁺-centres evidence 9-44689
 alkaline earth oxides and fluorides, F and F⁺ transitions Mollwo-Ivey plots 9-35108
 alkaline-earth fluorides, H and F bands 9-28302

Colour centres continued

- coronene in n-dodecane, phosphorescence temp. depend., centre formation, O sensitivity 9-23515
 coronene in n-octane, phosphorescence temp. depend., centre formation, O sensitivity 9-23515
 covalent solids, electronic states 9-28301
 e.p.r. investigation, techniques, book 9-38338
 F⁺ centres, model 9-40969
 F⁺ centre, polaron model applic. for calc. of electronic and ionic polarization effects 9-44716
 F⁺ mean square of modules of first dipole s-p transition 9-26291
 F centres creation by ionizing radiation above 77K, interpretation w.r.t. recomb. model of interstitials and vacancies 9-40968
 F colour centre formation, inhibited by Mn impurities, thermoluminescent investigation 9-31148
 glass, barium silicate containing Ti, effect of TiO₂ increase on gamma-induced centres 9-37693
 ice, irradiation, trapping of electrons 9-42980
 oxides, F⁺-centres evidence 9-44689
 phosphors, absorption causing wavelength depend. of loss in luminous efficiency after u.v. and X-irrad. 9-28721
 polar. molecules, cry., ESR studies of electrons trapped in dipole fields 9-40584
 quartz, brown synthetic, I centre 9-41426
 quartz, fused, transient 9-42854
 ruby, influence on lasing threshold 9-39372
 ruby, optical and p-ray colouring 9-39371
 ruby laser, influence on output energy 9-38377
 tetraphenylhydrazine, diphenylamino radical dimer as centre 9-42855
 titanate materials, due to ionic conductivity prod. by lattice defects 9-32942
 Ag halides, absorpt. spectra of small quasi-metallic particles, fine struct. and oscillatory effect 9-39370
 Ag halides, induced i.r. absorpt. due to bound polarons obs. 9-46829
 in Al₂O₃:Cr³⁺ laser, influence on output energy 9-38377
 BaF₂, h.f.s. consts. of V_K and V_F-centres, lattice vibr. influence 9-43274
 BaF₂, neutron-irrad., e.s.r., F- and V-centres thermal stability obs. 9-43275
 BaF₂, centre formation due to X-ray irradiation with and without H doping 9-26293
 BaF₂, M colour center, optical absorption 9-26292
 BaO, F-centre, e.s.r. obs. 9-35109
 Ca₁₀(PO₄)₆F₂, X-irrad., from OH and oxide ion impurities 9-40933
 CaF₂:H, X-ray prod. only with H doping and then 25 times larger than in SrF₂ and BaF₂ 9-26293
 CaF₂:Tr³⁺ (Tr³⁺=trivalent rare-earth), optical centres, thermodynamics 9-30614
 CaF₂:Y³⁺ p-irrad. cryst., Y²⁺ centre 9-39373
 CaF₂, α and β bands due to F and M centres, M centre structure and fluorescence lifetime obs. 9-26292
 CaF₂, h.f.s. consts. of V_K and V_F-centres, lattice vibr. influence 9-43274
 CaO, electron-lattice interaction in F centre 9-44717
 CaO, F⁺ and F centres obs. in absorpt. spectrum, paramag. reson. linewidth and hyperfine interactions obs. 9-45382
 CaO, luminesc. from F and F⁺ centres 9-49311
 CdS, activated recombination r-centre radiative capture of electrons, cross section determ., impurity photo-effect meas. 9-30798
 Cs halides, F-centre emission energies and lifetimes 9-32999
 CsBr, 380 keV e-irrad., absorpt. band obs. at 80°K 9-46832
 CsBr, U centre i.r. absorpt. 9-26294
 CsCe, U centre i.r. absorpt. 9-26294
 CsCl, 380 keV e-irrad., absorpt. band obs. at 80°K 9-46832
 CsF, F centre, optical absorpt. props. 9-39374
 CsI, 380 keV e-irrad., absorpt. band obs. at 80°K 9-46832
 CsI, U centre i.r. absorpt. 9-26294
 Fe, under u.v. irradiation, e.s.r. identification 9-40971
 K halides, F-centre emission energies and lifetimes 9-32999
 KBr:Ca(Cl), F-centre prod. rate due to electron irradiation 9-46834
 KBr:Cd, thermoluminesc. and optical absorpt., F centres formation 9-33606
 KBr:H⁺, lattice distortions and vibration local mode freq. calc. 9-28410
 KBr:KH, U₁- α pairs conversion into U₂-F pairs, bleaching with U₁ light, reverse reaction at 4.5°K, bleaching with F light 9-35112
 KBr:Na, production at 80°K 9-23827
 KBr:Na⁺, radiation-induced interstitial H⁻, H⁺ and V₁ centres from kinetics 9-42849
 KBr:Pb²⁺, electrolytically coloured, prod. and optical props. 9-32992
 KBr:Zn, thermoluminesc. and optical absorpt., F centres formation 9-33606
 KBr, colloidal and F-aggregate centres, optical and thermal stability, elec. conductivity obs. 9-46835
 KBr, F-centre, lattice expansion obs. 9-28304
 KBr, F-centre prod. by two-photon absorpt., quantum efficiency 9-44719
 KBr, F-centre prod. rate due to electron irradiation 9-46834
 KBr, F-centres, ENDOR spectroscopy, elec. field effects 9-35734
 KBr, F-centres, Stoke's shift, electronic absorption and emission bands, temp. depend. 9-24411
 KBr, F-centre, electronic structure calc. 9-40973
 KBr, F-centre, lattice dynamics rel. to electronic Raman spectra and lattice and electronic absorptions 9-35118
 KBr, F-centre spin-lattice relax., theory and optical meas., 0-50 kG 9-24342
 KBr, radiation-induced interstitial H-H⁺ and V₁ centre form. kinetics 9-42849
 KBr, thermoluminesc. F centres formation 9-33606
 KBr, U₂ centre Faraday rotation 9-33512
 KBr, vacuum u.v.-irrad., F-centre production, photostimulated electron emission obs. 9-30617
 KBr and KBr:KOH, O-centres as strong phonon scatterers, thermal conductivity obs. 9-42949
 KBr effect on elec. cond. of M centres 9-32988
 KCl:Ag(Ca, Cd, Co, Ti), F-centre prod. rate due to electron irradiation 9-46834
 KCl:Ca, F-centres, e.s.r. and optical absorpt. obs. 9-37191
 KCl:Cd, Raman scatt. by F-centres 9-33569
 KCl:Ca²⁺, F-centre mobilities, 540-700°C 9-40972
 KCl:Li F₂ centres, elec. field modulated absorpt., off-axis centre model 9-42851
 KCl:Mg, additively coloured, optical, elec. and e.s.r. obs. 9-48868
 KCl:Mn, F-centres growth rel. to time, room temp. 9-28303

Colour centres continued

- KCl:Pb, F centre prod. by impurities, α and V_K centre motion importance 9-44718
 KCl:Sr²⁺, F-centre mobilities, 540-700°C 9-40972
 KCl:Ag, X-irrad., photostimulated luminesc. due to hole release from V_K -centres 9-39897
 KCl, additive coloration, traps and trapping mechanism obs. from photostimulated thermoluminescence 9-47408
 KCl, effect on elec. cond. of M centres 9-32988
 KCl, electronic props. of F' centres 9-28296
 KCl, F-centre, electron wave function determ. from ENDOR 9-33237
 KCl, F-centre hyperfine interaction constants, temp. depend. 9-46836
 KCl, F-centre luminesc., decay time and quantum efficiency, temp. depend. 9-35685
 KCl, F-centre prod. rate due to electron irrad. 9-46834
 KCl, F-centre Stark eff. of relaxed excited states 9-24392
 KCl, F-centres, ENDOR spectroscopy, elec. field effects 9-35734
 KCl, F-colouring, first-stage, exptl. separation of two exponential components 9-30615
 KCl, F_K centres, a.c. photoconductivity meas. 9-39376
 KCl, F_K - and Z_1 -centres formation by anion vacancy migration 9-39375
 KCl, F-centers formation by pulsed electron beam at 80°K 9-35110
 KCl, F-centre, electronic structure calc. 9-40973
 KCl, F-centre, lattice dynamics rel. to electronic Raman spectra and lattice and electronic absorptions 9-35118
 KCl, F-centres, ENDOR line intensities 9-33653
 KCl, F-centres, e.s.r. and optical absorpt. obs. 9-37191
 KCl, F-centres, excited states, orbital Lande factor 9-47362
 KCl, M-centre singlet-triplet splitting, calc. 9-35107
 KCl, optical conversion of F to M centres with repetitive light pulses 9-46833
 KCl, paramag. reson. of O²⁻ centre, pulse saturation 9-47437
 KCl, production by 5keV electrons 9-23829
 KCl, radiation-induced interstitial H-, H⁻ and V_1 centres form. kinetics 9-42849
 KCl, U_2 centre Faraday rotation 9-33512
 KCl, V_K centre optically stimulated orientation 9-35113
 KCl, V and F, optical growth at 295°K, impurity eff. 9-23830
 KCl, vacuum u.v.-irrad., F-centre production, photostimulated electron emission obs. 9-30617
 KCl, wave function and isotropic h.f.s. of U_2 -centre 9-42850
 KCl, X-irrad., effect of Ca, Cd, Mn, Pb impurities on F- and M- band growth 9-28686
 KCl and KCl:KOH, O⁻ centres as strong phonon scatterers, thermal conductivity obs. 9-42949
 KCl deformed by indentation, strain bands decoration with F-centres 9-37242
 KCl F-center build-up under γ irradiation, vacancy source 9-32987
 KCl optical bleaching and X-irrad., simultaneous, e.s.r. obs. 9-42848
 KF, F-centre, Stark eff. of relaxed excited states 9-24392
 KI:(Ga³⁺), absorpt. bands and electr. struct. obs. 9-35111
 KI:(In³⁺), absorpt. bands and electr. struct. obs. 9-35111
 KI:TI, F-centre prod. by impurities, α and V_K centre motion importance 9-44718
 KI:(TI³⁺), absorpt. bands and electr. struct. obs. 9-35111
 KI, F-centre, electronic structure calc. 9-40973
 KI, F-centre, lattice dynamics rel. to electronic Raman spectra and lattice and electronic absorptions 9-35118
 KI, F-centre spin-lattice relax., theory and optical meas., 0-50 kG 9-24342
 KI, U_2 centre Faraday rotation 9-33512
 KI containing F-aggregate centres, α -band increase w.r.t. time, M-centres formation 9-32990
 KCl:Pb²⁺, electrolytically coloured, prod. and optical props. 9-32992
 Kd F₁ centres, accumulation due to proton irrad., 78°-380°K 9-30620
 Ki, F-centre prod. by two-photon absorpt., quantum efficiency 9-44719
 LiF:H⁻ (D⁻), U-centres, i.r. absorption due to localized vibrations 9-30619
 LiF:Mg²⁺m γ -ray coloration enhancement 9-39377
 LiF:Mn²⁺(Mg²⁺), F-centres, conversion from vacancies created by charge compensation, γ -ray coloration 9-28305
 LiF:U formation due to irradiation of various kinds obs. as a function of temp. 9-35115
 LiF, F-band formed by radiation with reactor neutrons and γ 9-35114
 LiF, F-centre hyperfine interaction constants temp. depend. 9-46836
 LiF, F-centres, thermal annealing, 25° to 400°C 9-32993
 LiF, F₁-centres, accumulation due to proton irrad., 78°-380°K 9-30620
 LiF, F-centres generated by X-ray irrad., 77-600K, interpretation w.r.t. recomb. model of interstitial-vacancies 9-40974
 LiF, N-region absorpt. spectrum obs. at 3°K 9-28688
 LiF, V_K -type centres, ENDOR hyperfine consts. and lattice distortion 9-46837
 LiF, X-ray irradiation formation of colour centres, eff. of impurities and heat treatment 9-32986
 MgF₂ single cryst., cluster, F- and M-centres due to electron- and neutron-irrad. 9-35117
 MgO, defect cluster centres in rel. to neutron-electron-irradiation or additive coloration 9-46838
 MgO, e.s.r. from F_K vacancy-pair centre 9-47438
 MgO, electron-phonon interaction in F-centre 9-44689
 MgO, F band, magneto-optical structure 9-35116
 MgO, n-irrad., R-like centre, Faraday rotation obs. 9-26295
 MgO, n-irrad., R-like centre, Faraday rotation obs. 9-28306
 NH₄OHCl, X-irrad., optical and thermal conversions of V_K centres 9-32995
 NH₄Cl:CO²⁺, Ni²⁺, VO²⁺, X-irrad., F-centres, e.p.r. obs. 9-32994
 NH₄ClO₄, u.v. photon induced centres 9-42853
 Na₂SO₄, SO₄²⁻, SO₃⁻ identified by ESR following X-irradiation 9-30616
 Na halides, F-centre emission energies and lifetimes 9-32999
 NaCl:Ag, X-irrad., photostimulated luminesc. due to hole release from V_K -centres 9-39897
 NaCl:Ca²⁺, V-centres rel. to X-ray irrad. temp., e.s.r. 9-30618
 NaCl:Ca(D⁺), thermoluminesc., F-centres formation 9-33606
 NaCl:Cu additively coloured with Na vapour, colloidal absorpt. bands obs., thermal stability 9-32998
 NaCl:Dy³⁺ luminescence spectra obs. to gauge changes taking place during electrolytic colouring 9-32996
 NaCl:Pb²⁺, electrolytically coloured, prod. and optical props. 9-32992

Colour centres continued

- NaCl, additive coloration 9-32997
 NaCl, charged F-aggregate centres, absorpt. and emission band obs. 9-35119
 NaCl, colouration depth produced by 25 keV electron bombardment 9-44720
 NaCl, coloured and annealed, rel. to colloid evolution 9-26296
 NaCl, F-centre, Stark eff. of relaxed excited states 9-24392
 NaCl, F-centres, ENDOR spectroscopy, elec. field effects 9-35734
 NaCl, F₁ centres, accumulation due to proton irrad., 78°-380°K 9-30620
 NaCl, F-centre, electronic structure calc. 9-40973
 NaCl, F-centre, lattice dynamics rel. to electronic Raman spectra and lattice and electronic absorption 9-35118
 NaCl, irrad., rel. to stored energy and release 9-46839
 NaCl, thermoluminesc., F and impurity centres formation 9-33606
 NaCl, vacuum u.v.-irrad., F-centre production, photostimulated electron emission obs. 9-30617
 NaCl, wave function and isotropic h.f.s. of U_2 -centre 9-42850
 NaCl F-centre build-up due to γ irradiation, source of vacancies 9-32987
 NaCl irrad. with ⁶⁰Co- γ -rays, effect of gas adsorpt. 9-48869
 NaCl point defects in crystals, square-shaped complexes of centres 9-44686
 NaF:H⁻ (D⁻), U-centres, i.r. absorption due to localized vibrations 9-30619
 NaF, F-centre, Stark eff. of relaxed excited states 9-24392
 NaF, γ -irrad., R=F₁⁺ centre conversion 9-40975
 NaF, M-centres reorientation by uniaxial plastic deformation of γ -irrad. crystals 9-26297
 NaF F-centre, electron wave function determ. from ENDOR 9-33237
 NaF single cryst., F-centre fluorescence, thermal quenching 9-33598
 Nd glass, formation during stimulated emission use 9-31109
 Rb halides, F-centre emission energies and lifetimes 9-32999
 RbCl:H, U₂-centres, ENDOR meas. 9-30621
 RbCl, F-centre, Stark eff. of relaxed excited states 9-24392
 RbCl, F₁-centres, accumulation due to proton irrad., 78°-380°K 9-30620
 Si:P, photoionization of A-centres, e.p.r. method 9-37636
 SrF₂, h.f.s. consts. of V_K and V_F -centres, lattice vibrs. influence 9-43274
 SrF₂, M-centre, optical absorption 9-26292
 SrF₂, with and without H doping, X-ray prod. of centers 9-26293
 SrO, additive coloration, absorpt. band and F' centres obs. 9-44721
 SrTiO₃, elec. field prod. at 20 V/mm, 100-165°C 9-40976
 Ti³⁺ in KCl:KBr-Tl crystal, symmetry of centres 9-42852
 ZnS:Cl phosphor luminescence spectra, green II band contour obs., electric and photoexcitation 9-26786
 ZnS:Cu phosphor luminescence spectra, green II band contour obs., electric and photoexcitation 9-26786
 ZnWO₄ single crystals, colouring 9-39378
 9-35114

Colour photography *see* **Photography/colour****Colour vision**

- CIF 1964 standard observer compared with blue tristimulus filters for whiteness 9-48097
 colour blindness, trichromatic-opponent colors theory 9-24982
 computer generated artificial images, comparison of perceived colours 9-33975
 deuteranomalous subjects, spectral sensitivity curves, visual process 9-24983
 flicker, in colour TV monitor 9-47703
 foveal achromatic interval and saturation 9-49612
 foveal acuity-luminance relns. for grating test object, effect of wavelength 9-27133
 foveal luminance thresholds for hue identification in small targets 9-27136
 individual differences, design of experiments and preliminary analysis 9-45707
 luminance non-additive at threshold 9-24982
 matching, large-field, and adaptation 9-31719
 mechanism and luminosity curves 9-33965
 perception considerations 9-38157
 perception rel. to chromatic background 9-33973
 response to sinusoidally modulated light, effect of spectral composition 9-33972
 retinal and occipital potentials due to wavelength changes 9-31710
 rods and long-wave cones, interaction 9-27137
 stereoscopy, colour 9-29133
 stimulus size, duration and retinal location, effect on colour appearance 9-33974
 underwater visibility with artificial illumination 9-31720
 velocity sensitive mechanisms for each colour 9-24981
 waveguide theory, applic. 9-38158

Columbium *see* **Niobium****Coma** *see* **Aberrations, optical****Combustion**

- see also* **Explosions; Flames; Heat of combustion; Reaction kinetics**
 acetylene production from natural gas, patent 9-47458
 atmospheric burners, charact. indices and interchange ability for air or other gas injection 9-41842
 cellulosic fuels, effect of organic impurities, chemical kinetics 9-35746
 Chamber, stability of burning process, including effect of elastic deform. of walls 9-39945
 dust-gas systems, preliminarily unprepared, behind reflected shock waves 9-47457
 electronic and ionic phenomena invest. 2 electrode probes 9-24545
 equilibrium, near, in nonpremixed systems, effect of chemical kinetics 9-26813
 flame, temperature meas. from α -part. energy loss 9-38320
 gas, normal burning, hydrodynamic stability to one-dimens. disturbances 9-22293
 gas dynamics of combustion 9-22292
 MHD, thermodynamic props. of combustion products of methane and oil with ionizing K seeds 9-36748
 obstacle in oxidising stream, with fuel exuded from leading edge 9-26812
 propane-air mixtures, constant volume, effect of containing wall linings 9-45881
 pulsating chambers as Helmholtz resonators 9-45838
 stability of burning process in elastic combustion chamber 9-39945
 C, vitreous, kinetics in low O₂ press. 9-26815

Combustion continued

- H₂, shock-initiated, chem. kinetics 9-39946
 NH₄ClO₄, limiting press. and solid temp. for deflagration 9-33660
 NH₄ClO₄, pressed-strands, burning vel. rel. to original particle size 9-26814
 NH₄ClO₄ alone and in fuel, eff. of ionizing, radiations 9-28787

Comets

- Arend-Roland, photographic obs. 5 May 1957, type-I tail development and kinematics 9-29073
 Barbon 1966 II, spectra obs. 9-36026
 Comet 1967 f, brightness, visual and photographic obs. 9-36025
 Encke, orbit, applic. of Hansen's method of general perturbations 9-38085
 Honda 1968c description 9-43631
 ice nucleus, size and mass evaluation 9-27087
 Kilsten (1966b), parabolic orbit 9-24881
 nongravitational forces in orbit calcs. 9-40179
 orbit calc., inclusion of nongravitational forces 9-40179
 orbits, method of general perturbations devised by Hansen, applic. to Encke 9-38085
 origin and nature, essay in book 9-41671
 P/Comet Encke, brightness, 1900-67 9-36025
 P/Comet Faye, brightness, 1900-67 9-36025
 P/Tempel 2, secular brightness decrease 1874-1967 9-36025
 planet-comet encounters, close 9-40180
 -solar wind interaction, ionization, ray formation, observational approach 9-29074
 solar wind interaction, model predicting size and shape of the contact discontinuity 9-47677
 surface brightness distrib. rel. to photodissociation of C₂ molecules 9-24882
 tails, composition discussed 9-29075
 tails, observations 9-47681
 tails, orientation determ., appl. to comet 1956 h 9-36024
 tails, review of physics 9-24883

Communications, optical *see Laser beams/applications***Compasses**

- No entries

Complementarity *see Physics fundamentals; Quantum theory***Composite particles**

- see also Alpha-particles; Deuterons; Helium-3; Tritons*
 diffraction scatt. of high energy particle 9-29627
 (O4) symmetry of bound state amplitude of two Dirac particles 9-48212
 photoproduction of composite particles, asymptotic behaviour in some models 9-46056
 with Regge mass spectrum 9-46083
 in S-matrix theory and in field theory 9-32229
 sakaton rearrangement, dual props. between s-, t- and u-channel amplitudes of 2-body processes 9-46069
 scattering amplitude, Weinbert's separation in K-matrix formalism 9-29626
 three- and two-nucleon systems, using n-d, p-d scatt. 9-27567
 urbarion model for hadrons, applied to vector meson decay into two pseudoscalar mesons 9-46109
 zitterbewegung for infinite component theories is analog of Bohr radius 9-38598
 α - α interaction effective potential, repulsive core and Pauli principle 9-34375

Compressibility

- see also High-pressure phenomena and effects*
 alkali metals, shock wave and static compression data 9-46882
 andalusite from synthetic aggregates, isothermal 9-44761
 buckling of long cylindrical shells with random axisymm. imperfections under axial compression 9-22214
 bulk modulus-density relationship 9-44760
 compressive deformation, effect of plastic buckling 9-37236
 cylinders and cones, sandwich, subjected to axial compression 9-23872
 derivatives at absolute zero 9-29159
 ductile porous materials, constitutive eqn. for dynamic compaction 9-35166
 earth, distribution calc., finite-strain theory 9-28852
 elastic materials, compressible-incompressible transition 9-22190
 elastic rectangle between two elastic half-spaces, adhesive or frictionless compression 9-31824
 explosive, organic polycrystalline, strain-rate sensitive, compressive wave propag. behaviour 9-39409
 glass ceramics, impact strength determ. device 9-33031
 glasses, impact strength determ. device 9-33031
 graphite, neutron irradi., 300°-1200°C, bulk expansion 9-46883
 kyanite from synthetic aggregates, isothermal 9-44761
 limestones and marbles, compressional velocity data representation near Lambda transition 9-46884
 metals paramag., rel. to e struct. 9-40996
 microline, shock data, 670 to 580 kb 9-44759
 modulus rel. to density of cohesive materials 9-35145
 nozzle, non-axially-symmetric annular, compression flow 9-40641
 oligoclase, shock data, 670 to 580 kb 9-44759
 polyisobutylene, contribs. from free-volume and molecular compression 9-46886
 polystyrene, contribs. from free-volume and molecular compression 9-46886
 porous materials, ductile, constitutive eqn. for dynamic compaction 9-35166
 relation with density and sonic vel., expt. verification 9-42647
 rotationally symmetric vessels symmetrically compressed by two constant and opposite pressures 9-26063
 shock-initiated flux compression, similitude 9-29313
 sillimanite from synthetic aggregates, isothermal 9-44761
 spinel phases, lattice parameters rel. to press. 9-30784
 tube, polygonal, buckling under combined compression and torsion 9-27195
 wustite, lattice parameters rel. to press. 9-30784
 BaTiO₃, isothermal, near ferroelec. transitions, Pippard scheme 9-30970
 Cd comparative with Cu and Pb at high press. 9-30655
 CdCr₂S₄(Se₄) up to 10 kbars pressure rel. to ferromag. phase transition 9-45119
 Ce, adiabatic, low-temp. phase transform effect 9-40997
 Cu-Ni alloy, rel. to para-ferromag. transition ordering, obs. 9-35167
 Cu comparative with Cd and Pb at high press. 9-30655

Compressibility continued

- Fe, porous, dynamic compaction props. 9-44762
 H₂ solid, ($\partial P/\partial T$), meas. and related props. 9-26424
 HgCr₂S₄(Se₄) spinels, up to 10 kbars pressure rel. to ferromag. phase transitions 9-45119
 InSb phases at high pressure and temps. 9-42922
 KH₂PO₄, isothermal, near ferroelec. transitions, Pippard scheme 9-30970
 LiH, data analysis 9-37235
 Na, b.c.c. phase 9-42737
 NaNO₃, isothermal, near ferroelec. transitions, Pippard scheme 9-30970
 NiS, lattice, pressure effects up to 8 kbar, T>T_N and T<T_N 9-44672
 Pb comparative with Cd and Cu at high press. 9-30655
 PbTiO₃, isothermal, near ferroelec. transitions, Pippard scheme 9-30970
 Pu-Al delta-stabilized alloys, adiabatic compressibilities temp. depend. 9-37224
 Pu-Ce delta-stabilized alloys, adiabatic compressibilities temp. depend. 9-37224
 β -SiC meas. by use of X-ray diffr. high pressure studies 9-48820
 Tb, rel. irreversible phase transition 9-39501
 triglycine sulphate, isothermal, near ferroelec. transitions, Pippard scheme 9-30970

gases

- monatomic, discontinuity structure 9-44518
 plasma, multicomponent collisionless, laminar structure of nonlinear waves 9-46515
 turbulent boundary layer on flat plate with air injection, experiment 9-42586

liquids

- alkanes, mol., temp. and press. depend. 9-42650
 alkanes, molecular compressibility, variation with temp. and press. 9-34904
 alloys, isothermal prediction from Percus-Yevick partial structure factors 9-40768
 calculation, to 40,000 atm. 9-44550
 cellulose acetate and triacetate in dilute solns, from density and acoustic vel. meas. 9-32769
 compression processes near elec. discharge, X-ray obs. 9-32767
 critical tension in column after reflection of compression pulse at surface 9-42618
 electrolyte solns., u.s. velocimeter determ. 9-48696
 headwaves formed by dielec. breakdown, X-ray photography 9-32768
 isothermal, and structure function of alkali metals, meas. 9-23465
 methane, mol., temp. and press. depend. 9-40789
 n-octane at const. density, mol. 9-40790
 organic, liquids and their mixtures, molecular compressibility and Rao's constant 9-30398
 n-pentane at const. density, mol. 9-40790
 shell-liquid impact anal., relative importance compared with viscosity, gravity and shell density 9-22186
 theory 9-48679
 toluene, at const. density, mol. 9-40790
 Ar, isothermal, up to 1000kg/cm² 9-46593
 Ar, shock compression, applic. of significant structure theory of liquids 9-28095
 B₂O₃, isothermal, 380° to 465°C, 1 to 300 b. 9-26084
³He, at zero temp. 9-34939
³He, calc. using ground-state energy quasiparticle energies and interaction function 9-34940
 Ne, isothermal, up to 1000 kg/cm² 9-46593

Compressive strength *see Mechanical strength/compressive***Compton effect**

- astronomical cause of γ -flux 9-29054
 double Compton cross section, meas. 9-29536
 electron gas, Maxwellian, relativistic Boltzmann eqn., for photon transport with noncoherent scatt. 9-31792
 electron spectrometer using Compton eff. to meas. photon spectra 9-46133
 electrons, 550 MeV relativistic, ang. and energy distrib. of γ -quanta 9-29542
 e.m. wave 'swinging' by generated Compton effect, source of radio emission 9-24717
 energy losses of energetic electrons, role in different cosmic objects 9-47610
 frequency shift, intensity-depend. 9-48131
 generalized Compton equation containing line broadening and defect term 9-46303
 induced, of plasma and electromag. waves under astrophysical conditions 9-43581
 inverse effect, determ. nature of cosmic isotropic X-radiation 9-49564
 line shape, quantum-mech. formulas 9-22533
 microwave Compton scatt. on cosmic ray electrons, cosmic γ prod. 9-27070
 nucleon scatt., invariant amplitudes and 3rd-order low-energy theorem 9-22522
 photons, polarization of Dirac output particle 9-22527
 photoproduction, Veneziano-like parameterizations 9-48175
 plasma, scatt. by electron, thermodynamic Green function technique, cross section calc. 9-32599
 polarization of scatt. radiation on relativistic electrons 9-48155
 Pomeranchuk trajectory, removal of nonsense factor 9-46058
 scattering, forward, contrib. of pole at $\alpha=0$ 9-32158
 scattering factors for aspherical free atoms 9-42340
 scattering from bound K-shell electron, matrix element calc. 9-38459
 spin-1 scatt., classical low energy theorems 9-42005
 sum rules and their saturation 9-48154
 summing semiconductor Compton spectrometer 9-46132
 X-ray scatt. by free electrons, increase by applic. of laser rad., no observable eff. 9-22529
 Z-dependence of pair cross-section 9-46063
 e, relativistic, scatt. of laser photons, γ polarization meas. 9-36430
 N, virtual, dominated by Pomeranchukon exchange 9-32128
 Ge(Li) detector meas. of Compton cross-section as college expt. 9-36522
 H, scattering on bound state, theory 9-32419
 LiH, profile analysis rel. to valence-electron wave functions 9-46789

Computation *see Calculation***Computer memories** *see Calculating apparatus/digital computers; Magnetic devices; Storage devices; Superconducting devices***Computers** *see Calculating apparatus*

- Concrete**
 barytes, as radiation attenuator 9-24945
 beam, composite with steel, partial interaction between elastically connected elements 9-26380
 bearing strength on loading through flexible plates 9-23904
 cement paste, drying under temp. gradient, role of moisture diffusion 9-34950
 failure criterion, angle of internal friction 9-39433
 reinforced bridges, fatigue behaviour of high strength deformed bars 9-23854
 shrinkage and thermal expansion, two-phase anal. 9-28392
- Condensation**
see also Drops; Fog
 adsorbed gases on homogeneous C surface 9-23592
 adsorbed mols., lateral force constant determ. expt. 9-23593
 atmospheric studies of interfacial water structure 9-31299
 Bose gas, ideal generalised scaling and critical eigenvector 9-31788
 n-butyl alcohol, laminar film, heat flux meas.- and Nusselt soln. 9-39141
 centres in expanding flow of supercooled vapour 9-28184
 cloud development rel. props. nuclei 9-35820
 cloud formation, lab. simulation 9-45492
 clouds, kinetics 9-37913
 clouds, mathematical model 9-28874
 cold plasma, thin film production 9-34995
 cryosurface, coefficient meas. at 4.2°K 9-40224
 droplet growth, solution effect, generalized eqn. 9-40826
 droplets, statistical model 9-39139
 of fluoride thin films on crystal surface, mechanism 9-28217
 in forced convection, heat transfer rel. to superheating 9-26162
 gas-condensate system, differential eqns. of filtration 9-48673
 gas-vapour mixture on vertical surface, in absence of forced convection, heat and mass transfer 9-28185
 heat and vapour propagation, analysis, Nolan, Pollak and Gardner type condensation nucleus counters 9-24634
 homogeneous nucleation, steady-state random walk theory 9-41776
 imperfect gases, cluster theory 9-32728
 of impurities in crystal, Fermi and Bose 9-47037
 effect on lens quality 9-36342
 many-body system condensing in periodic and homogeneous states 9-34040
 numerical model of molecular diffusion causing mass transfer to and from cloud droplets 9-28881
 popular article on change of state 9-48734
 refractory cathodes, effective heat of in Cs 9-44513
 steam, in forced convection flow, heat transfer rel. to superheating 9-26162
 surface free energy of embryonic droplets in liquid nucleation 9-39138
 transport of matter from vapour and noncondensable gas mixtures 9-23405
 vapour, saturated; laminar films on isothermal surfaces 9-30456
 in vapour gas mixtures behind shock waves in tube 9-39140
 water, dropwise, coeff. estimation from heat transfer meas. 9-23594
 water clusters in vapour phase H-bond energy determ. 9-44616
 water droplets, collision, coalescence and disruption 9-46604
 Ag, coeff., 600-900°C 9-39083
 Al mirror with MgF₂ coating, optical degradation 9-40111
 AlSb semiconducting films 9-28487
 Cr, in vacuum, gettering effect, detection 9-30457
 Na bubbles in cool liquid, sudden collapse 9-23595
 on AgI crystal nuclei 9-41510
 S, on a substrate at 77°K, prod. of unstable form. 9-30747
 S, unstable forms produced and studied by paramagnetic resonance 9-30746
- Condensation of gases** *see Liquefaction, gases*
- Conduction, electrical** *see Conductivity, electrical*
- Conduction, heat** *see Heat conduction*
- Conduction, ionic, solids** *see Ionic conduction, solids*
- Conduction bands** *see Crystal electron states/band structure*
- Conduction electron scattering** *see Crystal electron states/transport processes*
- Conductivity, electrical**
see also Ionic conduction, solids; Kondo effect; Semiconducting materials; Semiconductors; Skin effect; Superconducting materials; Superconductivity
 in antiferromagnetic systems, anomaly of the tensor near Neel point 9-45206
 compressible fluid, stead flow 9-23379
 cylinders, co-axial elliptic, enclosing linear isotropic homogeneous medium, analysis 9-43827
 dielectrics, literature digest, 1967 9-33368
 earth, deep layers, specific conductivity determ. 9-24622
 earth, distribution for spherical model 9-39988
 earth, resistivity vs. depth rel. to e.m. soundings 9-35793
 earth upper mantle 9-45557
 electron 1-dimens. motion through random ions, test-particle technique 9-22981
 electron gas in a magnetic field, expression for cond. 9-41141
 e.m. field scatt. by long imperfectly conducting wire, soln. 9-41858
 Fermi liquid, impure, charged and neutral 9-47785
 heterogeneous media 9-26502
 ionosphere, lower, conductivity determ. from v.l.f. sudden enhancements of strength 9-49497
 Kirchhoff's law generalization' proofs of Thevenins and Nortons' theorems and other consequences 9-47879
 metal film reactors, high ohmic value and field strength stability 9-25158
 metals, jump during melting 9-26156
 non-crystalline materials, localized states in pseudogap and near extremities of conduction and valence bands 9-33243
 nonequilibrium, large, in a closed cycle MPD channel with applied electric and magnetic fields 9-22331
 plasma, low-temp., temp. pulsations effect 9-38968
 plasma, nonrelativistic, and second order current response 9-23272
 plasma flow, stationary self-contracting, effect 9-23279
 pyrex and other radiolysis cell materials, effect of temp. 9-33683
 resistance between disc. electrodes applied to infinite plate conductor 9-40305
 rock, time variation criterion in earthquake prediction 9-26876
 in solar photosphere and sunspots, calc. 9-24916
- Conductivity, electrical continued**
 thermionic conduction stabilization against temperature change, effect of space charge cct. resistance 9-36263
 thunderclouds, obs. 9-31324
 of weakly interacting electron system in external elec. field, nonlinear tensor calc. 9-48984
 AgBr membranes, and diffuse double layer 9-31200
 Cs in liquid-gas transition, up to 2000°C and 100 to 320 atm. 9-40801
 Ge single crystals, resistivity, effects of heat treatments 9-37538
 Hg annular cylinder, current carrying, rel. stability 9-23250
 TiO₂-VO₂ sintered pseudobinary system, rel. to semiconductor-to-semiconductor transition 9-49088
- gases**
 air, weakly ionized, rel. to appl. mag. field, obs. 9-28080
 air ionization, effect on elec. conductivity 9-25966
 air plasma flow behind shock wave 9-40669
 arc, elec., wall-stabilized, static, temp. depend. 9-36793
 atmosphere, decrease due to pollution 9-41535
 inert, partially ionized 9-26037
 ion energies at cathode for conduction through rarefied gases 9-32698
 ionized externally, effect of electron adhesion to neutral atoms 9-44490
 ionized externally, space charge and diffusion effects 9-44489
 ionosphere, change rel. to energy loss factor 9-37976
 magnetoplasma, anomaly due to drift wave instability in shock 9-44427
 methane, electron drift vel., press. depend. 9-48616
 plasma, approximate calc. methods 9-42486
 plasma, high press. in capillary discharge 9-40714
 plasma, in steady mag. field 9-32611
 plasma, Lorentzian gas, average scalar conductivity calc. 9-25846
 plasma, many component, calc. 9-40661
 plasma, Ohm's law resulting from microinstability 9-44416
 plasma, partially ionized, calc. 9-38969
 plasma, time varying, and rel. to freq. 9-42498
 plasma, turbulent, decrease in d.c. conductivity during ion wave propag. 9-34753
 plasma in pinch discharge laser 9-47958
 scalar, in m.h.d. shock prod. devices, calc. rel. to current sheet growth 9-46494
 steam, high press. and temp., multiwire lead-in and meas. cell design 9-26038
 Ar plasma flow in presence of boundary layer, volt amp. characts. 9-44426
 He plasma, as function of time and space, spectroscopic meas. 9-42535
 Hg, at 2-6 g/cm³, 1200-2100 bar 9-23403
 N, compressed, electronegative impurities effect 9-34840
- liquids**
 bubbling column, resistance of bubbling layer rel. to local gas content 9-23440
 carbon tetrachloride, shock compressed, microwave technique 9-30419
 n-decane, negative-carrier mobility meas. 9-42672
 decane, using crossed-wire electrode system 9-40804
 dielectric; role of diffusion, theory 9-30415
 of dielectric liquids book 9-34917
 glasses, during heating and cooling, device 9-30420
 n-heptane, negative-carrier mobility meas. 9-42672
 hexane, liquid, charge carriers which are probably free electrons obs. 9-28151
 n-hexane, negative-carrier mobility meas. 9-42672
 hexane, using crossed-wire electrode system 9-40804
 metals, neutron diff. studies 9-48680
 n-octane, negative-carrier mobility meas. 9-42672
 organic, temp. depend. 9-26127
 particle current 9-34920
 polystyrene, electroconductivity, solvent and ionic conc. effects 9-23525
 rainwater, rel. to salinity meas., effects of temp., dust and elec. discharge 9-34879
 semiconductor, and Hall coeff., temp. depend. 9-40800
 shock compress liqs., microwave technique 9-30419
 statistical correlation in liquid solns. 9-39085
 Ag-Au alloys, form factors 9-39112
 Ag-Mn alloys, elec. resist. from partial interf. functions 9-30422
 AgTe, resistivity, Hall coeff. and thermoelec. power 9-37519
 AgCl aqueous solution, space charge limited ionic transport at solution interface 9-32833
 Au-Sn alloys, at. distrib. and elec. resist. 9-30423
 Ba in NH₃, conc. 2-7 MPM, 190-250°K 9-23521
 CS condensed, temp. up to 1200°K 9-26130
 Ca in NH₃, conc. 2-7 MPM, 190-250°K 9-23521
 Co-Ge alloys, resistivity, temp. coeffs. 9-46652
 Cs in NH₃, conc. >6 mole% metal, 200-300°K 9-23521
 Cu-Sn alloy from X-ray interference meas. 9-28098
 Cu resistivity from exploding wire expt., theory 9-44584
 Ga, resistance coeffs. for laminar flow through diffuser in crossed fields 9-27968
 GeS, and solid, activation energies, 20-750°C 9-30909
 *He, phonon-drag eff. in mobility of charged impurities, eff. on conductivity 9-30442
 Li₂SO₄-Na₂SO₄, molten, various concs. and temps. 9-30835
 Li condensed, temp. up to 1200°K 9-26130
 Sn-Au alloys, temp. depend., 235°-910°K 9-40803
 Sn, temp. depend., 235°-910°K 9-40803
 Sr in NH₃, conc. 2-7 MPM, 190-250°K 9-23521
 Yb in NH₃, conc. 2-7 MPM, 190-250°K 9-23521
- liquids, electrolytic**
see also Chemical analysis/electrochemical; Ion velocity/electrolytic
 conductance meas. with four-electrode a.c. potentiometer 9-35749
 mixed binary dissociable conductors, thermodynamic diagram of electrochemical equilibrium 9-39609
 mutual antagonism in 1-1 plus 2-1 electrolyte mixture and stability props. of colloidal part 9-23545
 quaternary ammonium salts in acetone, ion-pair formation 9-23524
 quaternary ammonium salts in acetone, transport mechanism 9-23523
 quaternary ammonium salts in acetone, pressure and temp. effects 9-23522
 AgNO₃-alkali nitrate molten mixtures, rel. to density 9-23520
 BN, in cryolite-Al melts 9-28798
 Ca(NO₃)₂:KNO₃ glass-forming melts, high-pressure 9-39113
 CsBr in H₂O-dioxane and H₂O-tetrahydrofuran mixtures 9-39114
 CsCl aqueous soln., 300-1000°C, up to 12 kbar 9-48717

Conductivity, electrical continued
liquids, electrolytic continued

H₂O, to 100 kbar and 1000°C 9-44585
KCl aqueous soln., 300-1000°C, up to 12 kbar 9-48717
LiCl aqueous soln., 300-1000°C, up to 12 kbar 9-48717
NaNO₃, molten, doped with monovalent nitrates, cationic mobilities 9-44586
TiNO₃-alkali nitrate molten mixtures, rel. to density 9-23520

measurement

of air plasma flow behind shock waves using cold electrodes 9-40669
alloys and metals, as function of temp., method 9-41157
anisotropic substs., modification of four aligned electrodes method 9-47886
dielectrics, surface resist., meas. apparatus 9-22322
diffusivity, apparatus for room temp., -900°C meas. 9-33191
ferrites, resist. temp. depend., 80-300°K 9-35327
four aligned electrodes method, modification for anisotropic substs. 9-47886
glasses, molten, during heating and cooling, device 9-30420
high temp., thermionic emission influence 9-44899
ionized flow, with high time resolution 9-38970
metals and alloys, as function of temp., method 9-41157
MHD combustion chamber reaction zone, electrodeless method 9-27271
microwave technique for shock compressed liqs. 9-30419
nuclear fuels, in-reactor, by Angstrom method 9-28431
probe method, combined, for shunt resistance and Q of delay systems meas. 9-43828
semiconductor, resistivity meas. 9-33280
semiconductors, resistivity meas. method, 80-375°K 9-24171
skin effect obs. at various frequencies of spatially inhomogeneous resistivity distrib. 9-27262
steam, high press. and temp., multiwire lead-in and meas cell design 9-26038
transistor, bipolar, with lightly doped collectors, series resistance meas. techniques 9-37565
Cs at supercritical temp. and press., device and method 9-40801

solids

alkali halides, obs. of Cd centres 9-40970
alkali halides, plastic deformation enhancement (Gyulai-Hartly effect), a.c. dielec. meas. 9-33373
alkali metal films and wires, effect of electron-electron scattering 9-37435
alkali metal nitrates, temp. depend. in stable state and during phase transition 9-24115
alkali metals, resistivities up to pressures of 600 kbar 9-30841
alkali metals and Cu, difference, explanation in terms of phonons 9-24060
alkali metals electrical and thermal resistivities calc. using Sharma-Joshi model for lattice dynamics 9-42995
alloy, dil., resistivities and Matthiessen's rule deviations 9-37432
alloy, dilute mag., resistivity below Kondo temp., eff. of coherence length 9-26508
alloys, resistivity meas. applic. to metallurgical processes analysis 9-46932
 α -brass, changes during cyclic straining, rel. to enhanced diffusion 9-44732
ceramics, meas. by a modulated electron beam technique 9-48973
chalcogenide semiconductor amorphous films, conduction and elec. switching 9-28491
clays and clay-sand mixtures from fresh and salt water areas 9-49017
coals, Karaganda dehydrated, and dielec. loss, rel. to petrographic ingredients, mineral impurities and metamorphism 9-44999
contact area, resistance applied stress dependence 9-28208
cylindrical sample in transverse mag. field, magnetomorph oscillations 9-37427
diamides, saturated and unsaturated, model 9-33249
diamond, resistance w.r.t. temp., substitutional N donor obs. 9-37401
differential, of hot electrons, Green's function approach, and noise 9-47028
diodes, tunnel effect, thin film, negative resistance 9-47142
duraluminium, plastically deformed at 77°K, recovery of resistivity 9-39581
earth's resistivity structure by inverse magnetotelluric analysis 9-37891
earth, anisotropy, magnetotelluric obs. 9-47507
earth layers, determ. by inverse magnetotelluric sounding 9-37890
electroacoustic surface waves in conducting solids 9-28425
electron plasma in metals 9-30824
electron spectra, low energy, established within and emitted from irradiated conducting materials 9-26466
Fermi ellipsoid with anisotropic relax. time, magnetoconductivity 9-44903
ferrites, activation energies from mag. relax. meas., and Koops inhomogeneities obs. 9-45000
ferrites, resist. temp. depend. meas., 80-300°K 9-35327
ferroelectric, hydrostatic-press. depend., in electron scatt. investigation 9-37591
film with surface defects, and electron scattering 9-49016
films, metal, ultra thin, by tunnelling through substrate 9-24122
films, size-quantized, anisotropy in h.f. conductivity 9-39577
formation resistivity factor of unconsolidated porous media, effect of particle shape 9-30831
Gantmakher effect, theory, rel. to electron mean free paths 9-37387
glass mixed alkali, resistivity non-linear variation due to alkali oxide replacement 9-39148
glasses, chalcogenide 9-30956
glasses, V₂O₅/P₂O₅, semicond., rel. to internal friction 9-35155
graphite-B, neutron irradi., function of B conc., rel. to defect clustering 9-30597
graphite, pyrolytic, electron-irrad., recovery of basal plane resistivity 9-28459
graphite irradi. by neutrons and electrons, resistivity var. during annealing 9-24070
high temp. meas., thermionic emission influence 9-44899
ice, rel. to dopant conc., meas. technique 9-37532
KMnO₄, temp. depend 9-33282
magnetic alloys, dilute, frequency depend., by impurity scatt. t-matrix 9-47064
magnetite, double-exchange, electron-hopping process and metal-nonmetal transition 9-41168
magnon drag contrib. 9-24332

Conductivity, electrical continued
solids continued

measurement apparatus, rel. to thermoelec. figure of merit 9-33191
metal, rel. to Fermi surface topology, derivation from h.f. wave dispersion curves 9-44904
metal, skin effect in mag. field, rel. to h.f. conductivity 9-49018
metal, temp. depend., carrier density and mobility obs. 9-39580
metal films, discontinuous, anomalous quantum-mechanical tunnelling 9-35331
metal monocrystalline film with lattice defects, and thermoelec. power 9-37434
metals, galvanomagnetic phenomena in quantum limit 9-30837
metals, high temp. refractory 9-39537
metals, localized moments, sub-Kondo temp. study 9-45041
metals, rel. phonon and thermal conduct. 9-24060
metals, temp. depend. at low temps. 9-44902
metals in mag. field, current distrib., resistance tensor, field depend. 9-30838
mica, surface conductivity, effects of annealing, temp. and mag. field 9-47153
muscovite mica, barrier action mechanism obs. 9-37587
naphthazarin metal complexes 9-43022
Ohm's law, original paper, Sir John Leslie, (1791) 9-47065
organic semiconductors 9-41193
organic semiconductors, mechanism in band and hopping models 9-28503
oxide films on base metal, conduction props. rel. to contacts 9-37572
photoconductor, field-dependent conductivity parameters determ. using high-field domains 9-39705
phthalocyanine, metal-free β -form single cryst., electron trapping and bulk conduction in vacuum 9-28462
polyethylene terephthalate film, induced by e. bombardment 9-26513
Polymerene terephthalate, films, induced by e. bombardment 9-26513
polymers, semiconducting, rel. to mol. struct. 9-47097
polystyrene films, induced by e. bombardment 9-26513
polystyrene sulfonic acid membrane, rel. to temp. and water absorption 9-28463
quantum theory 9-41126
quartz, cryst. and fused, pulsed-radiation-induced current obs. 9-44998
rare earth dialuminides, s.f. exchange interaction effects 9-24119
resistivity maximum during Guinier-Preston zone form. 9-37431
rock specimens containing disseminated sulphides, resistivity and induced polarization 9-37892
semi-insulator, thermally-activated ohmic and space-charge-limited conduction meas., localized levels obs. 9-43106
semiconductor, four-probe meas. methods, and Hall effect 9-44950
semiconductor, rel. to dopant conc., meas. technique 9-37532
semiconductor, resistivity meas. 9-33280
semiconductor multi-emitter struct., spreading resistance 9-37564
semiconductor P-type, negative resistance mechanism due to space charge injection 9-28493
semiconductor smoke, resistivity 9-44951
semiconductor thin films, dimensionless n-type negative resistance 9-35393
semiconductor with bipolar mechanism of conductance, negative differential resistance obs. 9-37517
semiconductors, isotropic, anisotropy in contact region 9-24170
semiconductors, phonon drag effect contrib. 9-33288
semiconductors, resistivity meas. method, 80-375°K 9-24171
semimetals, classical size effect theory in relax. time approx. 9-39579
solids with blocking contacts, resistance limited currents 9-26509
sorbitan tristearate ultrathin black films, resistivity 9-37580
steel, mild, resistance; effect of electron beam floating zone-melting 9-33109
superconductors in mixed state, flux flow resistance 9-30856
p-TiCN, principal axes 9-30914
thin films, vacuum-evaporated on flexible substrates, props. 9-35388
transistor, bipolar, with lightly doped collectors, series resistance meas. techniques 9-37565
transition metal cpds., metallic and non-metallic behaviour 9-41170
transition-metal cpds. with ordered vacancies, conductance 9-44920
transverse a.c. cond. due to electrons interact. with waves in strong d.c. field 9-24082
triphenylmethylarsonium 7-, -7, 8-, 8- tetracyanoquinodimethan single cryst., anisotropy 9-33314
zirconia, yttria-stabilized high-temp. electrodes 9-33248
Ag-Cd β -phase alloys, order-disorder transf., resistivity 9-35253
Ag-Mg solid soln. alloy, Ag-rich, and stored energy of cold working 9-48920
Ag-Pd alloys, residual resistivity conc. depend. 9-37436
Ag-Zn β -phase alloys, order-disorder transf., resistivity 9-35253
Ag, electron irradi., resistivity, stage I recovery mechanism 9-35083
Ag, resistivity isochronal and isothermal recovery after large plastic deformation 9-40947
Ag, resistivity rel. to temp., calc. using lattice dynamics model 9-35339
Ag₂O, at high oxygen pressure 9-24116
Ag₂Te, resistivity, Hall coeff. and thermoelec. power 9-37519
Ag₂Te, resistivity, phase diagram determ. 9-46956
Ag alloy Se based rectifier, asymmetry in impulse regime 9-41158
Ag thin film on glass 9-24121
p, β -AgI, change with time and temp. 9-33379
AgO powders, resistivity, effect of added impurities 9-28545
Al(0.06 at.%) Si, resist. rel. to Si atoms clustering in ageing, 300°C 9-30712
Al-Ag and Al-Au dilute alloys, impurity resistance, 1.2° to 300°K 9-30840
Al-Cu-Ag alloy, resistivity charges rel. to formation and dissolution of Ag-rich zones 9-46758
Al-I-Bi tunnel junctions, resistance versus bias meas., pressure effects up to 30 kbar, 77°K 9-37556
Al(0.13 at.%)Si, resist. rel. to Si atoms clustering in ageing, 300°C 9-30712
Al-(4.4 wt.%)Zn alloy, Be atoms influence on resistivity changes due to clustering 9-40932
Al-Zr alloys, quenched, resistivity meas. effect of superheating melt 9-39450
Al, grain boundary effects, 4.2° to 77°K 9-30849
Al, quadratic temp. depend. at low temps. 9-37437
Al, r.f. sputter-thinned resistivity 9-24123
Al₂O₃-Si, m.o.s., parallel conductance 9-49132

Conductivity, electrical continued
solids continued

- Al films, elec. field applied to substrate, effect on resistance-thickness relationship 9-32383
Al films, granular, microwave conductivity in supercond. transition region 9-26504
Al films, rel. to thickness 9-49023
Al films, single- and polycrystalline, thickness and temp. dependence 9-44905
Al single crystal, macrosound and n irrad. effects 9-46928
Al supercond. thin films, microwave conductivity 9-28481
alloys with V, Nb and Ta, electrical resistivity as a function of temperature 9-39584
Ar, e drift velocity saturation 9-26587
As₂S₃, effect of Ag and Cu impurities 9-33295
Au-(0.1 wt.%) Cu alloy, fast neutron irrad. at low temp., resistivity recovery 9-43025
Au-Pt, resistivity changes rel. to precipitation kinetics 9-28382
Au, fast neutron irrad. at low temp., resistivity recovery 9-43025
Au, Ohm's law verification up to 10⁹ A/cm² current densities 9-24126
Au, quenched resistivities of vacancies and Matthiessen's rule 9-35336
Au, resistivity rel. to temp., calc. using lattice dynamics model 9-35339
AuX ordered alloys, X=transition elements and mixtures, and electron and neutron diff. and sp. ht. studies 9-44659
Au resistivity, 325 to 1225°K 9-26440
Au thin film on glass 9-24121
Ba₂(x-y)Sr₂Na_{1-x}Nb₂O₁₅, resistivity for tetragonal series 9-35480
BaO, in vacuum and oxygen, electric field effect 9-30833
BaV₃S₃, resistivity rel. to temp., transition from metallic to semiconductor state 9-39255
Be, meas. for hot pressed block 9-37366
Bi, films, anomalies in resistivity 9-49020
Bi, molten, resistance meas. by rot. field method 9-39583
Bi, resistance changes obs. for III-V and IV-V equil. boundaries determ. 9-41071
Bi, resistance ratio in earth's mag. field, rel. to purity 9-33250
Bi_{1-x}Sb_x, resistivity rel. to electron states 9-30842
Bi₁₂GeO₂₀, permittivity, and growth and props. 9-42751
Bi₂O₃ layers, evaporated, temp. depend., band gaps, obs. 9-39162
Bi₂Te₃ (20 mol.%)Bi₂Se₃ solid solns., conc. inhomogeneities influence 9-41252
Bi₄(GeO₄)₃, and growth and props. 9-42751
Bi film, oscillations upon deform., 78° and 300°K 9-30845
Bi single cryst., size effect 9-33253
Bi thin films, 4.2-300K, quantification of electronic motion influence 9-39582
Bi thin films, thickness dependence, 4.2°-300°K 9-33251
C, dynamically compressed, metallic state existence 9-30847
C films, resistance decrease, rates of change, activation energies calc. 9-23937
CS₂ polymer, d.c. resistivity, conductivity and permittivity freq. depend. 9-34975
CaTiO₃, point defect formation study 9-28276
CaTiO₃, transient, data analysis for point defect diffusion coeffs. 9-28317
CaWO₄, thermally stimulated conductivity obs. of local trapping levels 9-39890
nCd_{1-x}Mg_xTe:(Al) mixed cryst., resistivity meas. 9-43054
Cd₃As₂-NiAs eutectic 9-41196
nCd-Cr₂Se₄:In, resistivity, normal Hall coeff. and Seebeck coeff. 9-45018
CdF₂:Y, semicond., resistivity 9-49077
CdS:I of hollow rods, 10⁸-10¹⁰ ohm. cm 9-39195
CdS, fast-neutron-irrad., change associated with radioactive decay 9-47104
CdS, influence of u.s. waves in 10-45 MHz freq. range 9-39619
CdS, photocond., conductivity variation of non-ohmic behaviours 9-43053
CdS elec. current rel. to temp. 9-37520
CdS films, longit. cathode conductivity under e. bombardment 9-41155
CdS photoconductive single cryst., electromech. coupling consts. correl. with resistivity inhomogeneities 9-35502
CdS resistivity inhomogeneities in single crystal 9-37507
CdS semicond. films, rel. to intercryst. barriers cond., >500 V cm⁻¹ 9-26542
CdS single cryst., photo- and e-conductance comparison 9-37617
CdS single crystal, d.c. and a.c. electroluminesc. props., negative resistance region 9-37777
CdS single crystal, double injected, transient processes 9-49074
p-CdSb, specific resistance temp. depend. in strong elec. field 9-24174
CdSe evaporated films 9-33299
CdSe films, simultaneous variation with space charge region, from depletion depth meas. 9-30905
p-CdSiAs₂ 9-44957
CdTe, increase after n irradiation, rel. to electronic props. of defect centres 9-49158
CdWO₄, thermally stimulated conductivity obs. of local trapping levels 9-39890
Ce-La alloys, nondil., resistance minima, Neel temp. and spin-compensated mag. state obs. 9-35337
Ce-Y alloys, nondil., resistance minima, Neel temp. and spin-compensated mag. state obs. 9-35337
Ce hydride nonstoichiometric crystals. 9-44907
CeO₂ and CeO₂:Gd³⁺ single crystals, 500° to 1500°K, thermoelec. power and O diffusion coeff. 9-33246
Ce(42:54 at.%)Al alloys, at room temp. 9-47069
Co-Al alloys, and thermoelec. power and magnetoresistance, 1.4° to 300°K 9-44908
Co-Ni alloys, resistivity near Curie pt. 9-47074
Co, temp. and mag. field depend. 9-24128
Co_{1-x}Cu_xRh₂S₄, resistivity, temp. independ. 9-41164
p-CoO:Li, temp. depend., drift mobility obs. 9-37518
CoO, press. depend., saturation and phase separation obs. 9-35338
CoO, rel. to defect struct. 9-42806
CoSi single crystals, liq. nitrogen to 400°C, Van der Pauw technique meas. 9-37075
Cr, resistance, temp. depend. minimum, mag. fields effect 9-39585
Cr, resistivity near Neel point, antiferromagnetic critical exponents 9-35582
Cr, resistivity temp. coeff. meas. near T_m 9-48969
Cr₂O₃:TiO₂, 293-1200°K 9-49022
Cr electrical resistivity anomaly in spin-flip transition region 9-35584

Conductivity, electrical continued
solids continued

- Cr film, and Hall consts. 9-30848
Cr metal, anomaly near spin-flip temp. 9-26517
CrO₃-Cr₂O₃ systems, non-stoichiometric oxides, 100° to 450°C 9-28495
CrSb₂, marcasite-type, resistivity, mag. props. obs. 9-35581
Cs, anomalous temp. dependence of resistivity at high pressure 9-24125
Cs, resistance, temp. depend. 1.65-5°K and 14-20.4°K 9-28465
CsI, effect of divalent impurities rel. to temp. 9-33380
Cu/Pb layers, proximity effect, induced excitation spectrum, density of states meas. 9-44944
α-Cu-Al alloys, meas., short-range ordered state and stable superlattice phase obs. 9-39275
Cu-Cu₂O eutectic alloys, resistivity 9-48907
Cu-Mn:Pt, Kondo divergence in conduction-electron scatt. amplitude 9-39558
Cu-Zn β phase alloys, order-disorder transf., resistivity 9-35253
Cu-(0.06-5.2 at.%)Mn, alloys, between 2 and 300°K, max. value 9-47068
Cu, cyclically deformed, resistivity change 9-33254
Cu, fast neutron irrad. at low temp., resistivity recovery 9-43025
Cu, grain boundary effects, 4.2° to 77°K 9-30849
Cu, low temp., deviations from Matthiessen's rule 9-41102
Cu, Ohm's law verification up to 10⁹ A/cm² current densities 9-24126
Cu, resistivity isochronal and isothermal recovery after large plastic deformation 9-40947
Cu, resistivity rel. to temp., calc. using lattice dynamics model 9-35339
Cu₂O, interdiffusion of O obs. 9-44733
Cu₂O, temp. depend. 9-28496
Cu₂S film, temp. depend. for acceptor level position 9-44949
Cu₂PSe films, and optical props., obs. 9-35398
Cu₂PSe₂ films, and optical props., obs. 9-35398
Cu₂PSe₂ films, and optical props., obs. 9-35398
Cu₂SbSe₄, resistivity temp. depend., energy gap calc. 9-26505
Cu deposition on backing, rel. temperature 9-26445
Cu films, rel. to thickness 9-49023
CuAlS₂(Se₂), single cryst. prepared by vapour transport with iodine 9-48797
Cu(9.5 wt.%)Be-(0.2 wt.%)Zn alloys, neutron irrad., rel. to ageing char. acts. 9-33115
EuO:Gd, dopant effect, temp. depend. indicating metallic conduction 9-33463
EuO:R³⁺ film, (R=rare earth oxide) resistivity meas. of transport props. rel. to mag. props. 9-47266
Fe-Al, Fe-Cr, and Fe oxides, chemisorption of O, eff. on surface elec. conductivity 9-37822
Fe-Al system intermetallics, resistivity 9-46890
Fe-N alloys, composition dependence rel. to martensite transform. start temp. 9-23982
Fe-Si solid solns., resistivity and Matthiessen's rule deviations 9-41167
Fe-Sn dilute alloys, and Mossbauer hyperfine field of -1.19Sn 9-47335
Fe, fast neutron-irrad. at low temp., resistivity recovery, isochronal annealing obs. 9-43027
Fe, high purity, resistivity 9-39448
Fe, shock-compression effects rel. to α- to ε-phase transition 9-26388
Fe, zone refined by deform. at -196°C, rel. to lattice defects study 9-26275
Fe_{1-x}Cu_xCr₂S₄ 9-28588
α-Fe₂O₃, influence of hydrostatic pressure, 20-100°C 9-33300
Fe₈₅(Ni₁₅-Mn₁₅) alloy, temp. depend. rel. to mag. ordering 9-41303
Fe₈₀P₁₀C₁₀ amorphous ferromag. alloy, resistivity minimum 9-37429
Fe alloys, binary Fe-rich, residual resistivities and Matthiessen's rule departures 9-39586
Fe carbides formed at tempering of quenched C steels 9-43020
Fe thin coatings, effect of Hg adsorption 9-37428
FeO_x (45 mol.%)P₂O₅ glass, mechanism from mechanical loss data 9-30640
Fe-Ni alloys, resistance, eff. of Co content on ageing induced changes 9-23942
n-, α- Ga₂O₃, O adsorp. dependence 9-49081
Ga single crystals, liq. He temp., in longit. mag. field, zero resist. 9-44900
GaAs:Cd, meas. rel. to diffusion process of Cd 9-46852
GaAs:Zn surface resistivity, post-implantation annealing depend. 9-33320
n-GaAs, electron bombardment damage, thermally stimulated meas. 9-35079
n-GaAs, meas. 9-33301
n-GaAs epitaxial layers, high-purity, resistivity 9-30907
GaAsiCd surface resistivity, post-implantation annealing depend. 9-33320
GaP:Zn, resistivity variation with dopant conc. 9-44954
GaP:Zn(O), indication of p-type conduction, photoluminescence 9-33604
n- and p-GaP, temp. depend. up to 400°C 9-39611
GaSb:Te, resistivity, rel. to temp. for conduction band structure 9-37530
GaSb, resistivity of crystals grown by floating zone technique 9-28229
Gd, resistivity anomalies 9-35340
Gd single cryst., resistivity meas., Lorenz functions 9-33195
Gd single crystals, rel. to Lorenz functions 9-47009
GdNi₂, anomalous behaviour near ferromag.-ordering temp., effect of molecular field 9-43021
GdPt₂, anomalous behaviour near ferromag.-ordering temp., effect of molecular field 9-43021
GdRh₂, anomalous behaviour near ferromag.-ordering temp., effect of molecular field 9-43021
Ge-Al₂O₃-In₂O₃ heterojunctions, switching effect 9-47141
Ge-In₂O₃ heterojunctions, switching effect 9-47141
Ge-Mg₂Sb₂ amorphous films, annealing study, rel. to reordering diffusion processes 9-34985
n-Ge, dislocation high-density saturation effects 9-43072
Ge, hot carriers, review 9-33329
n-p-Ge, non-ohmic conduction under strong mag. field 9-35420
n-Ge, relaxation 9-30925
Ge, resistivity calc. from reflection and transparency obs. 9-24190
Ge, surface, eff. of alcohol vapours 9-49101
Ge thin films, influence of surface states on temp. depend. 9-33326
GeS₂, and liquid, activation energies, 20-750°C 9-30909
GeTe, carrier energy spectrum changes due to solid solns. form. 9-47113
GeTe, carrier energy spectrum changes due to solid solns. form. obs. 9-47113
HfC rel. to C content 9-47114
Hg, resistivity of single cryst., size effect 9-39587

Conductivity, electrical continued
solids continued

- p-HgCr₂Se₄, ferromag., resistivity and mobility 9-44961
 n-HgTe, 4.2-200°K 9-33196
 n-HgTe, temp. depend. 9-35497
 HgTe epitaxial films, nonohmic conduction 9-28214
 Ho single cryst., resistivity meas., Lorenz functions 9-33195
 Ho single crystals, rel. to Lorenz functions 9-47009
 In, molten, resistance meas. by rot. field method 9-39583
 In, normal and supercond. states, 1.5 to 4.2°K 9-30871
 In, quadratic temp. depend. at low temp. 9-37437
 In, resistivity, 77 to 350°K 9-41104
 In films, temp. dependence rel. to longitudinal thermal magnetomorph effects 9-37430
 n-InAs, in fields up to 21 kOe at 90, 200 and 300°K 9-39622
 p-InP:Zn(Cd) impurity and intrinsic cond., 4-700°K 9-39623
 n-InSb, eff. of hydrostatic pressure up to 16 Katm. 9-28501
 n-InSb, hot-electron microwave incremental conductivity 9-49084
 p-InSb, in n-type surface inversion layer, low temp. 9-44963
 InSb, p- to n-type conductivity change due to donor action of β dislocations 9-33322
 n-p-InSb, X-ray induced changes 9-49086
 n-InSb, Z-pinch time evolution determ. 9-44964
 InSb_{1-x}Bi_x solid solns. 9-43058
 p-InSb nonlinear conductivity-potential relationship at 78°K 9-28510
 InSb polycryst. layers, resistivity meas., surface obs. 9-33325
 InSe, charge carrier mobility, temp. depend. 9-35404
 K, low temp. 9-37437
 K_{0.30}MoO₃, resistivity anisotropy from X-ray diff. and cryst. struct. obs. 9-37446
 K₂CsSb photocathode, energy band scheme 9-28584
 K₂O-SiO₂, vitreous, activation energy of conduction, and resistivity inflexions 9-41156
 KBr, additively coloured 9-46835
 KBr effect on elec. cond. of M centres 9-32988
 KBr pure and doped, anion contrib. at high temp. 9-35472
 KCl:Ca²⁺ 9-47154
 KCl effect on elec. cond. of M centres 9-32988
 KCl pure cryst. 9-47154
 Kr, e drift velocity saturation 9-26587
 La-Ce dilute alloys, resistivity meas. and Kondo temp. determ. 9-43152
 La-Ce dilute solid solns, resistivity data between 4° and 30°K rel. to Kondo phenomenon 9-44913
 La-Pr dilute solns., and effective mag. moment, rel. to Pr conc. 9-45066
 p-n-LaCoO₃, temp. coeff. due to carriers number and mobility variation 9-37527
 LaTe₂-LaSb₂ solid solns., Sb substitution effect on resistivity 9-39639
 Li/Ni/KCO₃, near eutectic mixture 9-30625
 Li₂O-SiO₂ glass, effect of metastable precipitate 9-24215
 Li₂SO₄-Na₂SO₄ various concs. and temps. 9-30835
 Li₂V₂O₇ 9-35328
 LiF, effect of thermal treatment, X- and γ -irradiation 9-28546
 LiF, pure and doped, X-ray excited, thermally stimulated conductivity obs. 9-45355
 LiF vacancies formed by reactor radiation, detect. by annealing and elec. cond. meas. 9-32949
 Mg-Bi alloys, amorphous, and thermoelec. power 9-30851
 Mg, n irradi., rel. to defect production and subsequent recovery 9-32940
 Mg_{0.4}Mn_{0.6}Fe_{0.4}O₄, influence of hydrostatic pressure, 20-100°K 9-33300
 MnO/CoO solid solns., dielec. conductivity meas. w.r.t. freq. 9-35465
 MnO/NiO solid solns., dielec. conductivity meas. w.r.t. freq. 9-35465
 MnO single cryst., dielec. conductivity meas. w.r.t. freq. 9-35465
 MnP single crystal, magnetic field effects in metamagnetic state 9-28460
 MnTe, magnon drag contrib. 9-24332
 Mo-Nb:Co alloy meas. rel. to Kondo temp. independ. of host composition 9-45067
 Mo-Nb alloys, theoretical and expt. values 9-24127
 Mo, neutron irradi., recovery, effect of hydrostatic pressure 9-35342
 α -MoTe₂ single cryst., photovoltage obs., dark conductivity meas. 9-33411
 NH₄Ag₂Si, high ionic conductivity, room temp., prep., patent 9-30965
 Na, in range 35-98°K, comparison with previous results 9-42978
 Na, low temp. 9-37437
 NaCl:BaCl₂ crystals, meas. rel. to dislocation density effect on ageing 9-46929
 NaCl:Ca, low temp. precip. influenced 9-37577
 NaCl, plastic deformation enhancement, a.c. dielec. meas. 9-33373
 NaCl whiskers, 150-600°K 9-28551
 Nb, resistivity, temp. depend. 9-49050
 NbC, 20°-2000°K, obs. 9-39588
 NbC 1200-3500°K, obs. on rod and tube samples 9-37374
 NbC hemispherical and monochromatic emissive power and specific resistivity, 1200-3500°K 9-39548
 NbO, temp. depend 9-37448
 NbO₂, 800°K region, phase transition obs. 9-33143
 n-NbO₂, temp. depend 9-37448
 Nd, due to exchange interaction and quadrupole scatt., temp. depend. 9-44901
 Ni-(49-51 at.%)Al alloys, at room temp. 9-47069
 Ni-C solid solns., Curie temps and residual resistivities 9-44914
 Ni-Co alloy, K-state existence 9-26507
 Ni-Cr film, vacuum-deposited, resistivity increase on heat treatment 9-41043
 Ni-Cu-H alloys, low-temp. resistance anomalies 9-37450
 Ni-Cu alloys, low-temp. resistance anomalies 9-37450
 Ni-Sn dilute alloy, and Mossbauer hyperfine field of ¹¹⁹Sn 9-47335
 Ni-W alloy, annealing effects, and local ordering 9-33255
 Ni, resistivity of quenched-in vacancies 9-23796
 Ni, temp. and mag. field depend. 9-24128
 Ni_{0.9}Fe_{0.1}O₄, influence of hydrostatic pressure, 20-100°K 9-33300
 Ni_{1-x}Zn_xFe₂O₄, temp. depend., 500°-1000°K, effect of magnetic structure 9-33310
 Ni₃Fe(Cr, Mo, W) ternary alloys, temp. variations, atomic ordering obs. 9-39297
 Ni thin films, conductance 9-39589
 β -NiAl, resistivity variation and conductivity spectra obs. 9-37449
 NiO, meas. rel. to stoichiometry of fluxed-melt grown crystals 9-37089
 NiO, press. depend., phase separation obs. 9-35338
 NiO, temp. and O partial press. depend. 9-44966
 NiO in O₂, meas. of diff. coeff. of cation vacancies, 750-1000°K 9-30588

Conductivity, electrical continued
solids continued

- Os, resistivity, 2 to 20°K 9-41169
 Pb, molten, resistance meas. by rot. field method 9-39583
 Pb_{0.92}Bi_{0.07}La_{0.01}(Fe_{0.405}Nb_{0.325}Zr_{0.27})O₃ ferroelec. thin films, resistivity 9-35487
 PbTe polycryst. layers, resistivity meas., surface obs. 9-33325
 Pd-Co alloy, annealing effects, and local ordering 9-33255
 Pd-Cr dilute mag. alloy, resistivity below Kondo temp., eff. of coherence length 9-26508
 Pd-Fe alloys, critical behaviour near mag. ordering temp. 9-44915
 Pd-Fe dilute alloys, low temp. resistivities 9-44916
 Pd-H system, resistance rel. to H content, temp. depend. 9-33256
 Pd-Si based alloy glasses, resistivity 9-42706
 Pd film, and Hall consts. 9-30848
 Pd thin films, conductance 9-39589
 PdP₃, resistivity D conc. dependence 9-24129
 Pr, due to exchange interaction and quadrupole scatt., temp. depend. 9-44901
 Pt-(0.07 at.%)Co, low-temp. resistivity 9-33257
 Pt-(1 at.%)Co alloy with plastic strain, resistivity behaviour 9-43161
 Pt-(1 at.%)Fe alloy with plastic strain, resistivity behaviour 9-43161
 Pt-SiO cermet thin films, resistances obs. 9-47155
 Pt, deformed, resistivity meas. for state I recovery 9-26277
 Pt, Ohm's law verification up to 10⁹ A/cm² current densities 9-24126
 Pt, quenched resistivities of vacancies and Matthiessen's rule 9-35336
 Pt film, and Hall consts. 9-30848
 Pt thin film on glass 9-24121
 Pt wires, size-depend. deviations from Matthiessen's rule, 1.2° to 4.2°K 9-49026
 RbAg₄Si, high ionic conductivity, room temp., prep., patent 9-30965
 RbNO₃ struct. transform. 160°K to melting pt. obs. 9-46962
 Rh-Ru-Fe alloys, resistivity and susceptibility as function of temp. 9-44918
 Sb, molten, resistance meas. by rot. field method 9-39583
 Sb, resistivity, reluctance, 300-750K 9-47076
 SbSI, eff. of O₂ adsorption 9-30496
 SbSI, paraelectric, nonlinear I-V characts. 9-28555
 Se currents, resistance limited, with blocking contacts 9-26509
 Si:Au, injection currents and negative resistance 9-28521
 Si:B, quenched-in defects obs. 9-39357
 Si:B(P), irradi. at 80°K, meas. rel. to carrier removal rates 9-44852
 n-Si:Li, resistivity obs. of electron-irrad. induced carrier-removal defects 9-49113
 Si:Na, resistivity temp. depend., ionization energy of impurity obs. 9-43077
 Si:Pt, resistivity 9-49110
 Si(Sb) film, epitaxial, on spinel substrate, resistivity and Hall effect meas. 9-36950
 Si, charges rel. to thermal defect investig. 9-32944
 Si, degenerate, d.c. meas. rel. to radiation damage on low temp. e-irrad. 9-28277
 Si, effect of dislocations 9-30932
 n-Si, epitaxial, resist. rel. to e. bombardment between 12-18 keV 9-37543
 Si, float-zone, doped, before and after γ -irradiation 9-28520
 n-Si, high purity, rel. to transient recombination lifetimes, 4.2°K to room temp. 9-35508
 Si, hot carriers, review 9-33329
 Si, implanted layers, post-annealing conductance behaviour 9-28519
 Si, polycryst., anisotropy due to differing vapour-depositions 9-35428
 Si, resistivity calc. from reflection and transparency obs. 9-24190
 Si, surface resistivity of base region, method and suitable struct. 9-33336
 Si diode, compensated, negative resistance and reversible switching phenomenon 9-49122
 Si thin films deposited by electron irradi. of tetramethylsilane resistivity obs. 9-44628
 SiO₂, vitreous, electronic and ionic (H⁺) contribs. 9-46856
 Sn, magnetoconductivity of 2-dimens, coherent network of coupled orbits, oscillations obs. 9-44919
 Sn, molten, resistance meas. by rot. field method 9-39583
 Sn supercond. thin films, microwave conductivity 9-28481
 SrO, in vacuum and oxygen, electric field effect 9-30833
 SrTiO₃ colour centres generation at 100-165°K in field of 20 V/mm resulting in cond. increases 9-40976
 SrTiO₃ single crystals, temp. depend. 9-39694
 Ta-N film, resistivity meas. rel. to N content and lattice structure 9-23625
 Ta, resistance meas. during supercond.-normal transition 9-37476
 Ta 1200 to 2800°K 9-43018
 TaC 1200-3500°K, obs. on rod and tube samples 9-37374
 Tb single cryst., resistivity meas., Lorenz functions 9-33195
 Tb single crystals, rel. to Lorenz functions 9-47009
 Te film, elec. resistance, effect of ferroelec. substrate on temp. depend 9-28502
 ThP₄, resistivity 9-35035
 ThC-UC solid solutions, 3,8 and 15 metal % U 9-26510
 ThP, resistivity 9-35035
 TiC, rel. to C content 9-47114
 TiC, resistivity 9-28468
 TiC 1200-3500°K, obs. on rod and tube samples 9-37374
 TiO₂:Cr₂O₃ 293-1200°K 9-49022
 TiO₂:VO₂ sintered pseudobinary system, rel. to semiconductor-to-semiconductant transition 9-49088
 TiO₂, non-stoichiometric defect struct. rationaliz. 9-26512
 TiO₂, elec. field enhanced, rel. donor impurities 9-26511
 TiO₂, plasma-grown crystals, const. value rel. to time 9-39198
 TiO₂, specially reduced single cryst., variation as function of d.c. field 9-47159
 Ti₃Ta₄Si, and optical props., lattice consts., obs. 9-35070
 TiTe₂ polycrystal, temp. dependence 9-26598
 TlInS₂(Se₂Te₂) single cryst. 9-44969
 p-TlSe: Pb, dopant conc. dependence rel. to valence-band structure 9-43059
 α -U, Matthiessen's Rule, deviations from, n irradi. defects 9-46805
 UC_{1-x}N_x, elec. resist. and Seebeck coeff., 80-1000°K obs. 9-35330
 UO₂-UN sintered mixtures 9-30730
 UO₂ cermet from UO₂-Mo system, Mo content depend. 9-35222
 UO₂, nearly stoichiometric single cryst., activation energies obs., 170-1250°K 9-33403
 V₂O₅, d.c., model, -165°K to +25°K 9-33247
 V₂V₃, metal-semiconductor transition, critical pressure 9-44921

Conductivity, electrical continued

- solids continued
- V films, temp. coeff. resistance thickness dependence (60-900 Å) 9-47077
- VO₂, semiconducting-metallic transition 9-28230
- VO₂ single cryst. grown by chem. transport reaction, semicond. to metallic transition obs. 9-32872
- VO₂ thin films, structure rel. to elec. props. 9-23629
- VO₂, composition dependence rel. to semicond. phase 9-28272
- W, e-irrad., resistivity rel. to Stage-I interstitial behaviour 9-26279
- W, Ohm's law verification up to 10⁷ A/cm² current densities 9-24126
- W film, and Hall consts. 9-30848
- Xe, e drift velocity saturation 9-26587
- Yb between 4.2-300°K, hysteresis effect 9-46953
- Yb metal-insulator transition, resistance meas. 9-41171
- Zn:Li single cryst., ohmic conduction and space charge limited currents between asymmetric contacts 9-33378
- Zn_{1-x}Hg_xTe solid solutions, 77°-400°K, 250-10000 Gs, additional, due to 'heavy carriers' 9-30913
- Zn whiskers, size effects 9-37454
- ZnO crystals, polar surfaces, and light reflectance meas. 9-42741
- ZnS films, longit. cathode conductivity under e. bombardment 9-41155
- ZnS single crystal grown from Ga and In melts 9-37095
- ZnSe epitaxial layers on Ge, obs. 9-35417
- ZnSe films, longit. cathode conductivity under e. bombardment 9-41155
- p-ZnSnSb₂, electro-physical props. obs. 9-35410
- ZnWO₄, thermally stimulated conductivity obs. of local trapping levels 9-39890
- ZrC, rel. to C content 9-47114
- ZrC 1200-3500°K, obs. on rod and tube samples 9-37374
- ZrC hemispherical and monochromatic emissive power and specific resistivity, 1200-3500°K 9-39548

Conductivity, thermal

- see also Heat conduction
- annulus with internal heat sources 9-40286
- binary mixtures near critical point, kinetic phen. 9-48735
- chromosphere and coronal gas, transport coefficient 9-29097
- of contact thermoreceivers, effect on transient responses 9-47831
- equation in presence of radiative energy transfer 9-27245
- Fermi liquid, impure, charged and neutral 9-47785
- insulator, glass fibre bonded with organic binder, patent 9-24061
- liquid metal cooling of ducts, thermal contact resistance, impurities effect 9-39093
- measurements on various substs, conference 9-26014
- mixture, binary, variational calc. 9-27192
- nonlinear equation, boundary conditions, theory 9-38319
- powder-vacuum insulation at high temp. 9-41096
- thin-layer elements of mech. strong insulating stacks, optimum apparent layer area 9-35460

Conductivity, thermal continued

- gases continued
- N₂-He, calc. using theory for relaxing non-polar gases 9-48661
- N plasma, calculation 9-36754
- NF₃, magnetic and electric fields effects 9-28076
- Ne, rel. to heat transfer between walls of vertical concentric cylinders, end effects 9-40749
- O₂-C₂H₂ meas. to investigate Lennard-Jones potential 9-36803
- O₂-He, calc. using theory for relaxing non-polar gases 9-48661
- O₂-N₂, calc. using theory for relaxing non-polar gases 9-48661
- SO₂ methyl chloride and dimethyl ether binary and ternary mixtures 9-36817
- liquids
- AgCl-AgI, molten eutectic mixture 9-39089
- alcohols, data considerations for standard reference materials 9-42703
- alkali hydroxides, aqueous solns. conc. depend., apparatus and results 9-44558
- alkali metal halides, varying conc. 9-36866
- alkali metals, atomic heat conduction 9-39111
- alkaline earth halides, varying conc. 9-36866
- behaviour near critical point 9-36852
- benzene-carbon tetrachloride, using semi-empirical relation for molecular interaction 9-36865
- benzene-toluene, using semi-empirical relation for molecular interaction 9-36865
- binary solns., general eqn. and obs. 9-28117
- cyclohexane-carbon tetrachloride, using semi-empirical relation for molecular interaction 9-36865
- dimethyl formamide, instrument for meas., 20-160°C 9-30388
- ethane derivatives, fluorine-chlorine, -125→+100° C, meas. by unsteady state relative method 9-36866
- formamide, instrument for meas., 20-160°C 9-30388
- n-heptyl alcohol, instrument for meas., 20-160°C 9-30388
- kinetic theory in local equilibrium model 9-23486
- methane derivatives, fluorine-chlorine, -125→+100° C, meas. by unsteady state relative method 9-36866
- organic binary mixtures, semi-empirical relationship 9-36865
- refrigerants and salt solns. 9-36866
- toluene, instrument for meas., 20-200°C 9-30388
- toluene-carbon tetrachloride using semi-empirical relation for molecular interaction 9-36865
- vibrational and rotational molecular contributions 9-36862
- water, diffusivity, -40° to +60°C 9-42965
- water, eqn. for coeff. 9-36853
- Bi₂Se₃ in stationary state, 700 to 1200°C 9-26094
- Ga₂Te, carrier mechanism, temp. depend. 9-33194
- HCL anhydrous, meas. 9-28118
- HCL liquid, anhydrous, meas. -75→+65°C, 40→100 bar press, relationship to density 9-36863
- He, by sound meas. 9-26141
- He, estimate, from G matrix 9-23559
- He, relaxation function expressions for thermal conductivity χ 9-32811
- He near A-point break-up of transport mode into several 9-26147
- ³He, coeff. calc. using ground-state energy and quasiparticle energies and interaction function 9-34940
- ³He thermal conductivity meas. to 1.5°-40°K, and up to 34 atm. press. 9-28163
- ⁴He, 2-50°K 9-46665
- ⁴He thermal conductivity meas. to 1.5-4.0°K, and up to 34 atm. press. 9-28163
- Rb in temp. range 87-788°C 9-40787
- Sb₂S₃, 830-1150°K, radiative mechanism 9-36864
- Sb₂Se₃-Sb(Te) alloy, mechanism electronic contribution due to carrier motion 9-34900
- Sb₂Se₃ mechanism, electronic contribution due to carrier motion 9-34900
- Sn-Bi system, component analysis 9-24065

Conductivity, thermal continued

- aerospace alloys, apparatus for meas. at cryogenic temps. 9-26454
- alkali metal vapours, dilatometric determ. 9-26029
- alloys and metals, as function of temp., method 9-41157
- apparatus, new list 9-25112
- contact method, simplified 9-43801
- cut-bar apparatus, heat losses 9-26441
- diffusivity, apparatus for room temp. -900°C meas. 9-33191
- disc surrounded by Pt of W ring which is heated by induction 9-37365
- of electrically conducting materials, temp. 500 to 3000°K, apparatus 9-39538
- electron beam technique, modulated, for ceramics 9-48973
- guarded hot plate apparatus, comparison of modes of operation 9-25125
- guarded hot plate apparatus for -80 to +100°C 9-26461
- heatproof sublimating materials, temp. dependence determ. 9-25122
- horizontal plate apparatus for gases, modification to find conduction/convection transition 9-36813
- hot wire cell for gases at high temp. 9-39096
- i.r. method for reinforced plastics up to 150°C 9-33187
- using linear dimension changes with temp. 9-41097
- longitudinal symmetrical heat flow apparatus for metals and alloys 9-26451
- metal, procedure 9-42975
- nuclear fuels, in-reactor, by Angstrom method 9-28431
- rod, high temp. technique 9-39534
- role of 2-dimens. temp. field 9-25121
- sediments, geothermal heat flow probe design 9-35771
- semiconductors, techniques 9-30791
- for solids, absolute nonstationary method using small plates 9-41098
- stationary waves method 9-26433
- steady-periodic heat flow method, evaluation for materials with temp. depend. props. 9-26435
- from time-dependent temp. distrib. 9-42963
- transient hot-wire cell for precision meas. on gases 9-36814
- tubes used for heat transfer meas. 9-36211
- BAO, method based on temperature function of emitting surfaces 9-30794
- BeO, heat losses in cut-bar apparatus 9-26441

Conductivity, thermal continued

- adhesives 9-37364
- aerospace alloys at cryogenic temps. 9-26454
- alkali halides, device for meas. between 60°K and 100°K 9-30790
- alkali metals, thermal resistance determ. using free electron approx. and Krebs model 9-24062

Conductivity, thermal

- air, meas. 39, and 95°C 9-36814
- alkali metal vapours, dilatometric determ. 9-26029
- arc, elec., wall-stabilized, static, temp. depend. 9-36793
- CO₂, convective heat transfer in tube at supercritical press. 9-26023
- rel. to collisions, inelastic, 10⁴°K 9-34841
- convective heat transfer in tube at supercritical press. 9-26023
- data on 46 substances at atmos. press. 9-36809
- dimethyl ether, ethyl chloride and SO₂, binary and ternary mixtures 9-36817
- dipolar, initial press. depend. 9-34835
- electron, of stars 9-43534
- horizontal plate apparatus, modification to find conduction/convection transition 9-36813
- hydrocarbons, at normal pressures 9-40751
- inert, multicomponent mixtures, comparison with theory 9-36811
- interaction with infrared, gaseous radiation 9-30341
- rel. to ionization instability 9-40711
- eff. of magnetic field 9-36808
- methane, 25°C-450°C and up to 1000 bars 9-46569
- methane, compressed, concentric cylinder meas. method 9-26027
- methyl chloride, SO₂ and dimethyl ether binary and ternary mixtures 9-36817
- mixtures, binary, approximate theory more nearly correct than rigorous theory 9-36812
- non-polar gas mixtures, thermal relaxation and heat transfer 9-48661
- non-polar polyatomic, role of rot. translational relax. 9-26020
- plasma, approximate calc. methods 9-42486
- plasma, many component, calc. 9-40661
- polar, in elec. field 9-42610
- polyatomic, conduction theory 9-34836
- quantum corrections in moderately dense gas 9-34834
- review of information of 46 gases at atmos. press. 9-26025
- rough, spherical particle gas in an external magnetic field 9-45798
- solar plasma props., role of electronic conduct 9-31643
- steam, at one atmos., and Prandtl number 9-28075
- Sutherland-Wassiljewa coeffs. calc. for inert gas mixtures 9-36810
- Van der Waals gas near critical pt., anomalous behaviour 9-26041
- Xe heat transfer rates in shock heated gas meas., 650-5000°K 9-26026
- Ar, at high temp., meas. with hot wire cell 9-39096
- Ar, compressed, concentric cylinder meas. method 9-26027
- Ar, rel. to heat transfer between walls of vertical concentric cylinders, end effects 9-40749
- Ar, heat transfer rates in shock heated gas meas., 650-5000°K 9-26026
- CO₂, compressed, concentric cylinder meas. method 9-26027
- CO₂ shock heated, effect of vibrational relaxation 9-36815
- p-H₂, rotational energy contribution, Eucken factor 9-26032
- He-Ar mixtures, heat transfer rates in shock heated gas meas., 650-5000°K 9-26026
- He, at high temp., meas. with hot wire cell 9-39096
- He, compressed, concentric cylinder meas. method 9-26027
- He, rel. to heat transfer between walls of vertical concentric cylinders, end effects 9-40749
- He, Lennard-Jones (6-9) potential calc. 9-26045
- He, meas. 39, and 95°C 9-36814
- N, compressed, concentric cylinder meas. method 9-26027
- N₂-C₂H₂ meas. to investigate Lennard-Jones potential 9-36803
- N₂-CO₂ mixture, from Prandtl number meas. 9-36816
- N₂-He mixtures, heat transfer from cylinders showing slip effects 9-46568
- N₂-Ne mixtures, heat transfer from cylinders showing slip effects 9-46568
- N₂ meas. 39, and 95°C 9-36814
- N₂, shock heated, effect of vibrational relaxation 9-36815

Conductivity, thermal continued
solids continued

alkali metals and Cu, difference, explanation in terms of phonons 9-24060
 alloys, by longitudinal symmetrical heat flow apparatus 9-26451
 alloys, phonon cond. determ. from expt. data 9-39535
 cast vitreous-crystalline materials in different compositions 9-39525
 cat brain, diffusivity 9-39542
 ceramics, BaTiO₃ base, influence of d.c. field in phase transition region 9-39545
 chalcogenides of group I, IV and IV, phonon conductivity depend. on mean mol. weight 9-48974
 compressed, concentric cylinder meas. method 9-26027
 contact area, resistance applied stress dependence 9-28208
 dielectric, analysis for large drift velocities of phonon gas 9-37363
 dielectrics with isotopic defects, Monte Carlo calc. 9-41095
 diffusivity meas. apparatus, room temp. to 900°C, using Angstrom method 9-33191
 ferroelectric cryst., KH₂PO₄-type, critical anomaly 9-39693
 films, electron microscopical specimen support 9-35289
 graphite, AGOT, 0.3-3°K 9-26442
 graphite, high temp. radial heat flow meas. 9-26443
 heatproof sublimating materials, temp. dependence determ. 9-25122
 heterogeneous mixture, 2 and 3 phases, theory 9-37362
 ice, diffusivity, -40° to +60°C 9-42965
 imperfect contacts, conductance 9-41099
 insulating materials, -80 to +100°C guarded hot plate apparatus 9-26461
 insulation, multilayer, thickness depend. 9-30788
 insulators, effect of magnon-phonon interactions 9-44847
 KH₂PO₄-type ferroelec. cryst., critical anomaly 9-39693
 lid over heated plane, good or bad cond. rel. to convective motions 9-34732
 low temp. measuring device for alkali halides 9-30790
 low temperature, heat pulse propagation expts. 9-26438
 magnetic lattice, high temp. limit 9-44843
 materials with temp. dependent props., steady-periodic-heat flow method, evaluation 9-26435
 metal, meas. procedure 9-42975
 metallic elements, state of knowledge 9-39539
 metals, absolute method, 38-345°C 9-39540
 metals, by longitudinal symmetrical heat flow apparatus 9-26451
 metals, heat resistant, review 9-33179
 metals, high temp. refractory 9-39537
 metals, rel. phonon and elec. conduct. 9-24060
 metals diffusivity meas., effect of pulse width 9-28432
 multilayer slabs, thermal attenuation 9-25123
 non-metallic elements, solid at normal temps. 9-26432
 oil shale, aboveground and in situ meas. 9-26436
 phenolic-nylon chars, thermal conductivity 9-26460
 phonon, mean mol. weight depend. 9-48974
 plastics, reinforced, and diffusivity, temp. dependence up to 150°C, meas. by i.r. method 9-33187
 polyethylene, from Gruneisen const. 9-46979
 polyethylene, thermal conductivity below 1°K, modification to theory 9-28433
 polymers, crystalline and glassy, from Gruneisen const. 9-46979
 polymers, high, linear amorphous, orientation anisotropy 9-35292
 polymethylmethacrylates, amorphous, orientation anisotropy 9-35292
 polystyrenes, amorphous, orientation anisotropy 9-35292
 polyurethane, guarded hot plate apparatus 9-26461
 porous beds of mixed beads, use of probe 9-39541
 quartz, fused 9-41098
 quartz, fused, precise meas., 0 to 650°C 9-37371
 rocket engine chamber insulation mats., thermal conductivity 9-38013
 rod, high temp. meas. technique 9-39534
 sand of Rajasthan desert, as function of moisture temp. and porosity 9-30789
 sapphire-sapphire contact, thermal resistance 9-39544
 sediments, ocean floor obs. 9-31282
 spin, effect on u.s. attenuation near critical pts. 9-44820
 stationary waves meas. method 9-26433
 steel 9-42975
 steel, stainless 9-41098
 superconductors, type II, irreversible, in mixed state 9-33266
 transition metal carbides, rel. to phonon scatt. by conduction electrons and lattice vacancies 9-47010
 triglycine sulphate, influence of d.c. field in phase transition region 9-39545
 umklapp processes during phonon decay, effect on resistivity 9-41074
 UO₂, density relationship 9-41110
 Ag₂S, anomalous temp. depend. of mechanism 9-30793
 Ag films on plastic substrate, thermal conductivity 9-33192
 Al, 78 to 373°K, apparatus descrip. 9-26439
 Al₂O₃:Cr(Fe, Mn, V) single cryst., low temp. meas. 9-35086
 Al₂O₃, meas. by disc method 9-37365
 Al₂O₃, self-supporting films 9-39543
 Al₂O₃(sapphire), low temp., heat pulse expts. 9-26438
 Al alloys, apparatus for meas. at cryogenic temps. 9-26454
 Au, 325 to 1225°K 9-26440
 B, β -rhombohedral, 80° to 1100°K, rel. to crystal structure 9-44845
 BaTiO₃ base ceramics, influence of d.c. field in phase transition region 9-39545
 Be, meas. for hot pressed block 9-37366
 BeO, meas., heat losses in cut-bar apparatus 9-26441
 Bi₂Te₃-Bi₂Se₃ alloys, rel. to lattice parameters 9-41100
 Bi₂Te₃ (20 mol.%)Bi₂Se₃ solid solns., conc. inhomogeneities influence 9-41252
 Bi₂Te₃, rel. to lattice parameters 9-41100
 CaF₂, rare-earth doped, in mag. fields 9-47008
 CaWO₄, meas. for Cp determ. 9-26427
 CdAs₂, 60° to 400°K 9-41101
 n-Cd₃As₂, electronic and lattice components at low temps. 9-33193
 CdGeAs₂, semicond. amorphous 9-37367
 CdS single crystals, doped and pure, 1.4 to 80°K 9-35290
 Ce-S solid solutions, transition metal doped, temp. depend. 9-37368
 Cr, above and below Neel temp. 9-26444
 CrB₄, ferromag. 9-42976
 Cu-(15 at.%)Al deformed alloy cryst., lattice component, low temp., phonon scatt. by dislocations obs. 9-35291

Conductivity, thermal continued
solids continued

Cu-Al alloys, meas. for dislocation phonon scattering values 9-41078
 Cu-Ni alloys, rel. to lattice parameters, temp. depend. at low temp. 9-26447
 Cu-Zn alloys, meas. for dislocation phonon scattering values 9-41078
 Cu, low temp., deviations from Matthiessen's rule 9-41102
 Cu, resistivity due to edge dislocation scattering of phonons 9-26446
 Cu₂S, anomalous temp. depend. of mechanism 9-30793
 Cu₃SbSe₄, lattice conductivity, temp. variation 9-26505
 Cu position on backing, rel. temperature 9-26445
 CuCl₂(CH₃NH₂Cl)₂ ferromagnet, by magnons 9-37369
 Fe 9-42975
 Fe, 78 to 373°K, apparatus descrip. 9-26439
 Fe, Armco, 50-800°C 9-39546
 Fe, intrinsic electronic resistivity 9-26448
 G chalcogenides, obs. 9-41103
 Ga, low temp., heat pulse expts. 9-26438
 Ga₂Te₃, phonon mechanism, temp. depend. 9-33194
 Ga single crystal, rel. to anisotropy of electron mean free path, 1.4° to 4.2°K 9-37370
 GaSb-InSb alloys, meas. rel. to phonon scattering by acceptor defects, 5° to 300°K 9-44870
 GaSb, meas. rel. to phonon scattering by acceptor defects 5° to 300°K 9-44870
 Gd, and Lorentz number, 0.4-4.2K 9-44846
 Gd single cryst., and Lorenz functions 9-33195
 Gd single crystals, 5° to 300°K, as function of temp 9-47009
 n-Ge, 0.3° to 4.2°K 9-42977
 Ge, variational calc. using anharmonic isotropic continuum model 9-26449
 GeS, up to 500°C, in Ar atmosphere 9-30795
 GeS obs. 9-41103
 GeSe, up to 500°C, in Ar atmosphere 9-30795
 GeSe obs. 9-41103
 GeTe obs. 9-41103
 HfB₂, and expansion, rel. to thermal stress resistance 9-35183
 HfSe, phonon-phonon resonant scatt. in obs. on thermal conductivity, 4-30°K 9-28409
 HgTe-CdTe crystal, composition depend. rel. to lattice dynamics 9-26450
 n-HgTe, electronic and lattice, 4.2-200°K 9-33196
 Ho 0.6-4.2°K; enhancement at 1°K, Lorenz no. inc., nuclear hyperfine contrib. 9-33197
 Ho single cryst., and Lorenz functions 9-33195
 Ho single crystals, 5° to 300°K, as function of temp. 9-47009
 In-(3.9 at.%)Pb alloy, type I-II supercond. transition obs. 9-47089
 In, 77 to 350°K 9-41104
 In, face electron Lorentz no. in high field limit 9-47195
 In, normal and supercond. states, 1.5 to 4.2°K 9-30871
 n-p-InSb, X-ray induced changes 9-49086
 KBr:CN, lattice contrib. rel. to phonon resonant scatt. 9-26408
 KBr:NO₂, lattice contrib. rel. to phonon resonant scatt. 9-28411
 KBr and KBr:KOH, change with OH⁻ dissoc., phonon scatt. by O⁻ centres obs. 9-42949
 KCl:CN, lattice contrib. rel. to phonon resonant scatt. 9-26408
 KCl:Li, phonon reson. scatt. obs., isotope and elec. field effects 9-42948
 KCl:NO₂, lattice contrib. rel. to phonon resonant scatt. 9-28411
 KCl and KCl:KOH, change with OH⁻ dissoc., phonon scatt. by O⁻ centres obs. 9-42949
 LiF, effect of thermal treatment, X- and γ -irradiation 9-28546
 LiF changes due to irradiation induced imperfections 9-33198
 Mg:Ge-Mg₂Sn solid solns., lattice component 9-33199
 Mg₂Si-Mg₂Sn(Ge) solid solns., lattice component 9-33199
 MgF₂, 25 to 900°K 9-48975
 MgF₂, anisotropy, correlation with phonon scattering 9-28412
 Mo films in BeO 9-24063
 Mo single crystal 9-41106
 Na, in range 35-98°C, comparison with previous results 9-42978
 NaNO₃, anisotropy at phase transition 9-30796
 Nb-Mo, solid solution alloys, lattice ratios in normal and superconducting state 9-30797
 Nb-Mo alloys, supercond. type-II, obs. in high mag. fields 9-47091
 Nb, supercond., near upper critical field 9-33200
 Ni-10wt% Cr alloys, description of apparatus 9-26451
 Ni, 2-100°K 9-48976
 Ni alloys, 2-100°K 9-48976
 Os, resistivity, 2 to 20°K 9-41169
 Pb films, quenched, meas. at 2-20°K 9-44848
 Pd, calculations from thermal diffusivity, at 675-1750°K 9-41107
 δ -Pu (10 at %) Ce, in temp. range 75-300°K 9-41108
 δ -Pu-Ga alloys, in temp. range 75-300°K 9-41108
 Sb₂S₃, 700-830°K 9-36864
 Si, polycryst., anisotropy due to differing vapour-depositions 9-35428
 SiO, evaporated films 9-39543
 SiO capacitor, calc. from thermal breakdown meas. 9-26463
 Sn-Cd, lattice contrib., dopant-conc. dependence, 1-4°K rel. to normal and superconducting states 9-26452
 Sn-Bi system, component analysis 9-24065
 SrO, Sr₂TiO₄ and SrTiO₃ radioactive heat source materials, obs. 9-26453
 TaNb: solid solution alloys, lattice ratios in normal and superconducting state 9-30797
 Tb single cryst., and Lorenz functions 9-33195
 Tb single crystals, 5° to 300°K, as function of temp 9-47009
 Ti alloys, apparatus for meas. at cryogenic temps. 9-26454
 Ti at high temperatures 9-41109
 UC₂O₇, depend. on O content, 100 to 1500°K 9-26458
 UC arc cast sintered, radiation eff., 150-1600°C 9-41111
 UO₂-SiO₂, with varying UO₂ concentrations over the range 100-800°C 9-26456
 UO₂-metal cermets, and preparation 9-26455
 UO₂, sintered, diffusivity 9-26457
 UO₂, sintered radiation eff., 150-1600°C 9-41111
 UO₂ cermet from UO₂-Mo system, Mo content depend. 9-35222
 ZrB₂, and expansion, rel. to thermal stress resistance 9-35183
 ZrH₂U fueled, SNAP reactor 9-26459

Confinement of plasma see *Plasma confinement***Constants**

astronomical and geophysical, in 1964 new I.A.U. system 9-41618
 Oort's A, determ. from Cepheids 9-31545

Contact angle *see* *Capillarity; Surface tension; Wetting*

Contacts, electrical

- blocking, solids with, resistance limited currents 9-26509
- elastic contact of two rough cylinders 9-36156
- electrification rel. to electrets 9-37601
- field ion microscopy, improved contact procedure 9-30832
- forces acting during separation 9-43017
- friction at wet contacts, depend. on interfacial potential 9-30702
- metal-CdS, work function at higher current densities 9-39733
- metal-glass, in high elec. fields 9-37584
- metal-semiconductor, perturbation, C-V charact. and equiv. cct. 9-47146
- metal-n-Si, minority carrier injection 9-26565
- molten metal bridge, microscopic, props. and rupture 9-40799
- noise, i.f. 9-47882
- oxide films on base metal, thermally grown, conduction props. 9-37572
- photoconductor-metal 9-47197
- to semiconductor, a.c. test method for separating contact influence from bulk props. 9-44978
- semiconductor multi-emitter struct., spreading resistance 9-37564
- semiconductor-dielectric, with potential trap for electrons in contact layer 9-26580
- superconducting point, Josephson effect 9-49061
- superconductor-normal metal junctions, dic. and microwave behaviour 9-35418
- thermodynamic optimum for connections at cryogenic temps. 9-22271
- wire bonds for semicond. devices, evaluation, NBS report 9-33280
- Au on CdSe polycryst. films, props. 9-41211
- CdS-metal, work function at higher current densities 9-39733
- on Ge, ohmic point contacts, study of I-V relation 9-37539
- Pb, pressure contacts in supercond. switches, device characteristics 9-30882
- Se with blocking contacts, resistance limited currents 9-26509
- Ta-Al point contacts, radiative emission at Ta energy gap freq. 9-25300

Continuous creation hypothesis *see* *Cosmology*

Convection

- air conditioning and building cooling systems, conference 9-34094
- air section having parallel faces, one- rotating about its axis 9-45877
- air-steam currents, u.s. anemometer design 9-36794
- atmosphere, spherical shell, rotating 9-26922
- in atmosphere, thermal, anelastic approximation 9-41482
- Benard problem for geophysical model with vertically varying exchange processes 9-41481
- boundary conditions for steady-state heat cond. problem, approx. soln. 9-22287
- boundary layer, effects of transverse press. grad. and streamwise second derivs., for low Prandtl numbers 9-23481
- boundary layer on plane vertical isothermal wall, stability criteria 9-25126
- buoyancy driven system, instabilities rel. to mechanical and buoyancy forces 9-48530
- in circular cylinder, induced by hot spot on floor, creeping flow to onset of laminar instability, numerical anal. 9-40747
- crystal growth, role of convection in vapour transport 9-36998
- in cumulus clouds, rel. to droplet concentrations 9-24653
- cylinder to fluid, heat transfer coeff. computation, empirical correl. of Prandtl, Grashof, Nusselt nos. 9-47836
- Earth's mantle, effect of low viscosity region 9-24613
- in earth's mantle, influence of boundary conditions and rotation 9-28851
- earth's mantle with variable phys. props. in ascending and horizontal flows 9-28839
- earth's upper mantle, two-component flow model 9-26855
- effect on turbulent viscosity variation 9-32574
- in enclosures of circular and rectangular floor plan, for localized heating from below 9-40746
- flow between rotating disks 9-32573
- fluid film, study method 9-47835
- fluid flow past non-isothermal vertical flat plate, general series soln. 9-32570
- fluid heat transfer, laminar natural convection, Ellis model 9-32559
- fluid in cubical cavity, flow equilb. stabilization by rotation 9-38946
- fluid in porous medium, convective flow stability 9-44535
- fluid layer, suddenly heated at high Rayleigh number, evolution of flow model 9-34728
- fluid layer with sinusoidal perturbation of wall temp., onset rel. to time modulation 9-34723
- fluid of variable viscosity heated from within 9-31256
- fluids, finite amplitude with changing mean temp., experimental 9-23231
- fluids, finite amplitude with changing mean temp., theory 9-23230
- forced, fluids at supercritical press. 9-26151
- forced boundary layer flow, superheating effect on condensation heat transfer 9-26162
- forced flow past flat plate with variable viscosity and thermal cond. 9-46586
- free, at low Prandtl numbers in laminar boundary layers 9-42625
- free, boundary layer flow, asymptotic soln. for large Prandtl nb. 9-30387
- free, from plane vertical surface with non-horizontal leading edge 9-34101
- in gap between core and cladding; cylindrical nuclear fuel element thermal stress analysis 9-25120
- gas solid suspensions, convective coeff. at Reynolds number 130,000 9-26136
- gravitational in earth's mantle 9-33723
- heat and mass transfer from rot. disc, surface suction/injection effects 9-27248
- heat transfer, bibliography 9-25130
- heat transfer, cylinder in rarefied gas 9-44524
- heat transfer from rot. disc with surface temp. step discontinuity in forced stream 9-27249
- heat transfer in tube at supercritical press. 9-26023
- heat transfer to ablation heat shield of entry vehicles 9-22304
- horizontal plate apparatus for gases, modification to find conduction/convection transition 9-36813
- interactive method of soln. to relevant eqn 9-38291
- internal, in insulated walls, heat leakage meas. 9-25119
- laminar, steady state, computation by Monte Carlo methods 9-25129
- laminar boundary layer equations governing transient free convection heat transfer from vertical semi-infinite plate 9-22291
- laminar boundary layer on heated surface, instability and disturbance amplification 9-34895
- laminar free, heat transfer from needle 9-22290

Convection continued

- laminar natural, boundary layer stability 9-25811
 - laminar natural convection flow about isothermally heated sphere at small Grashof number 9-23236
 - liquid layers, heated, flows induced by surface-tension gradients 9-23417
 - MHD, free, from horizontal plate 9-25837
 - MHD channel flow, effect of wall conductances 9-30197
 - natural, boiling crisis mechanism, role of gas phase 9-23600
 - natural, finite-difference computations comparison 9-22288
 - natural, from arc column, theory 9-32714
 - natural, at high Prandtl numbers, effects of viscous dissipation 9-25127
 - natural, in supercritical region 9-26150
 - natural, in vertical slot, stability of conduction and boundary layer regimes 9-40745
 - natural, of gas in closed region, loss of stability 9-45878
 - natural, water in turbulent flow at supercritical press., heat transfer studies 9-26090
 - on non-uniformly heated, rotating plane 9-22289
 - ocean thermohaline circulation for finite depth, applic. of one-parameter density model 9-35799
 - planetary interiors 9-27076
 - planetary interiors, dependence on the magnitude of the Rayleigh number 9-29065
 - planetary mantles, thermal and nonthermal convections 9-31602
 - plasma, two-stream instability, convective and absolute at equal temps. 9-28034
 - porous media, inhomogeneous, marginal stability 9-34102
 - in porous vertical slab, stability 9-34733
 - in rotating cylinder of fluid, thermally induced, influence of centrifugal accel. 9-34720
 - rotating fluid layer, laminar flow transition to thermal turbulence 9-34735
 - silicone oils, non-uniformly heated, rotating plane 9-22289
 - stars, massive, occurrence of semi-convection 9-43537
 - stars, normal and metal-deficient, depths at which convection starts, calc. 9-31527
 - thermal, at large Prandtl number, appl. statistical turbulence theories 9-27247
 - thermal, effect of stabilizing gradient of solute 9-39087
 - thermal and nonthermal in planetary mantles 9-31602
 - thermal- and rotation-induced convection movements of melt in Ge cryst. growth, impurity distrib. eff. 9-37079
 - tree, in vertical annular pipe with electrocond. fluid, rel. to mag. field, Rayleigh no. and Hartman parameter 9-27964
 - turbulent, movement and energy transfer analogy 9-46431
 - velocity, in viscous sublayer of fluid, U-component fluctuations 9-27956
 - water, forced, study of turbulent thermal boundary layer 9-23424
 - water, forced laminar flow in circular tube, uniform heat flux 9-25128
 - water, non-steady penetrative, simulating atm. inversion above heated ground 9-34896
 - water, thermal free convection from ice spheres, flow and heat transfer phen. obs. 9-23482
 - in water layer, continuously formed by melting ice, onset 9-32781
 - wavelength of motion on heated plane, effect of insulating or good heat cond. lid 9-34732
 - in wells, small diameter, and effect on temp. logging 9-35770
 - CO₂ heat transfer in tube at supercritical press. 9-26023
 - in N plasma jet, heat transfer 9-44460
 - in N plasma jet, heat transfer 9-44459
- Conversion electrons** *see* *Beta-ray spectral/conversion electrons; Gamma-rays/internal conversion*
- Cooling**
see also *Joule-Thomson effect; Low-temperature production; Magnetic cooling; Supercooling*
- adiabatic, ice crystal nucleation by lightning discharge 9-26908
 - air, flowing through heated porous mats, internal heat transfer 9-28074
 - air conditioning and building cooling systems, conference 9-34094
 - dissolution of soluble ice nuclei, laboratory study of local cooling 9-28863
 - double-sided, of tubular fuel element, boiling and superheating 9-22865
 - ducts, by liq. metal, thermal contact resistance, impurities effect 9-39093
 - dynamic technique of nuclear polarization enhancement 9-31061
 - film-cooling of a plasma generator anode 9-22336
 - gas dynamics and phase equilib. 9-30344
 - gas flow in rod clusters, transverse temp. diff., mixing rate determ. 9-34818
 - glass formation in alkali molybdate syst., critical cooling rate 9-30454
 - glasses, Na₂O-SiO₂, primary and secondary phase separation 9-30455
 - of laser, pulsed, open and closed cycle gas systems 9-38380
 - laser crystal and prevention of peripheral lasing, patent 9-36299
 - laser ruby rod by Cu conductor 9-38378
 - liquid, by gas bubble injection, heat and mass transfer 9-26074
 - local, ice nucleation model 9-28866
 - lunar cratered surface, infrared observations 9-31591
 - Newton's law, deviation factors 9-45876
 - Newtonian, in tidal theory at atmosphere 9-26896
 - nuclear power station, water flow meas. by ²⁴Na traces 9-28084
 - nuclear reactor, Na, K, B fluorides applic., patent 9-25678
 - nuclear reactor cores, gas coolant flow and temp. rise analysis 9-34491
 - plasma-jet generator, patent 9-48594
 - of protonosphere, night 9-40049
 - protonosphere night cooling 9-26918
 - reactor fuel element bundles, liquid metal cooled, temp. non-uniformities calc. 9-22888
 - refrigeration process using vapour compression, efficiency 9-40825
 - shock layer by radiative heat transfer 9-23383
 - surface self-oscillation temp. depend., heat transfer to turbulent liquid flow 9-24038
 - telescope, rocket-borne, by liquid He 9-38123
 - thermoelectric, effect on thermoelement operation in nonstationary conditions 9-49153
 - water in nuclear reactor container, meas. by thermocouple noise signal cross correl. 9-38740
 - CO gas, pulsed laser action 9-47979
 - H target used at Stanford Linear accelerator 9-29677
 - KCl:Li⁺(OH⁻), low temp. by electrocaloric effect 9-27143
 - Na, subcooled, at surfaces of high temp. spheres, rel. to motion and vapour formation 9-28116
 - Na₂O-SiO₂ glasses, primary and secondary phase separation 9-30455
 - RbCl:CN⁻, low temp. by electrocaloric effect 9-27143
 - S quenching from 160°C to -80°C, prod. of unstable form 9-30747

Cooling continued

- (Sb₂Te₃-Bi₂Te₃)-(Bi₂Te₃-Bi₂Se₃) thermocouple, transient response of thermoelec. cooling 9-28569
 U-(0.45 wt.%)Mo, rates rel. to phase transform. kinetics 9-41069
 Yb Fe garnet, ferrimagnetic, cooling by adiabatic magnetization 9-45194
 Zr-(1.2wt%) Cr-(0.1wt%) Fe alloy, rate effects on quench hardening behaviour 9-41034

Copper

- absorption line shape, theoretical, from cyclotron reson. expts. 9-35324
 addition (1%) to rolled Zn, eff. on atmospheric corrosion 9-37836
 in alkali halide crystals, theoretical anal. of hyperfine and superhyperfine interactions of stabilized atoms 9-37792
 amino-cupric ion, e.s.r. spectrum, -18°C-+72°C 9-42391
 atom form factor determ. by high voltage e. diff. 9-23722
 atom total γ cross-sections, 40-80 keV, mean values, analysis 9-22949
 atom vapour source, half-life after emission spectra, meas. by atomic absorpt. spectrometry 9-48391
 atomic spectrum, bibliography 9-38765
 atoms, excited and oriented by electron impact, in mag. field, polarization of spectral lines w.r.t. electron energies 9-29928
 atoms, surface, Ar⁺ bombard., charge exchange of scattered ions 9-48418
 band structure calc. using orthogonal-plane-wave modification 9-43004
 bond consts. of Be impurity atoms, variations 9-39181
 brass, Young's modulus and torsion modulus, calcs. by different methods 9-30629
 brittleness, post-irrad. hot, rel. to He-filled deform. defects 9-37260
 buckling, electroformed shell by axial compression, imperfections eff. 9-34070
 cathode growth at air-son. interface rel. to norvaline addition to sulphate electrolyte 9-28810
 Charpy V-notch, modified, impact vel. effect on deform. 9-48892
 composite with supercond. multifilament Ti-Nb filaments, coupling obs. 9-35369
 compressibility, comparative with Cd and Pb, at high press. 9-30655
 conductivity, thermal and elec., comparison with alkali metals 9-24060
 conductor, use in cooling ruby laser rod 9-38378
 contact, pot., stress induced shifts, obs. 9-43019
 corrosion, atmospheric exposure tests 9-24573
 crater formation by Fe microspheres at 0.5 to 10 km/sec. 9-30700
 creep stress, effect on angular distrib. of secondary cracks 9-46910
 cyclic hardening, strain bursts and coarse slip, interrelms. 9-28357
 cyclic hardening of single crystal. 9-30709
 cyclotron resonances linewidths submillimetric, and electron relaxation time 9-37419
 Debye-Waller factor of ⁵⁴Fe 9-41082
 defects produced during electron irradi., type determ. from microscope exam. 9-35082
 deformation of modified Charpy V-notch specimens, effect of impact vel. 9-48892
 deformed, monocrystalline struct. defects exam. by X-ray diffraction 9-40939
 deformed single crystals, mech. props., dislocation configs. and densities, effect of strain rate 9-41010
 density-of-states functions, X-ray photoelec. spectroscopy study 9-44886
 deposition on backing, elec. and thermal conductivity rel. temperature 9-26445
 diffusion, anharmonic-lattice-vibr. theory 9-44723
 diffusion in GaAs annealed cryst., effect of dislocations 9-44734
 diffusion in Li, interstitial-like 9-39384
 diffusion in Pb, Sn, In, and Ti, rapid, interstitial mechanism 9-28321
 diffusion of inert gases, influence on gas release of implanted ions, implantation energy and dose 9-35129
 diffusion of Zn in whiskers, coeff. depend. on diameter 9-26300
 dislocation density depend. on primary recrystallization after large plastic deformation 9-40947
 dislocation distrib. after fatigue at elevated temp. 9-30608
 dislocation etching of single cryst., pitting obs. 9-36988
 dislocations in single cryst., nonconservative motion, slip traces obs. on surfaces 9-39365
 dispersion curves, extended Bhatia model method 9-24012
 dynamic yield strength, mean, from strain meas. on 'mushroomed' ends of projectile 9-30662
 elastic behaviour of whiskers below yield pt. 9-39407
 elastic bulk eff., infl. of point defects 9-30631
 elastic consts., third-order, sensitivity to changes in electron-to-atom ratio and mag. eff. 9-37217
 electrical resistivity, effect of grain boundaries, 4.2° to 77°K 9-30849
 electrical resistivity recovery after fast neutron irrad. at low temp. 9-43025
 electrical resistivity rel. to temp., calc. using lattice dynamics model 9-35339
 electrode, electrodeposition and dissolution in standing wave sound field 9-47468
 electrode erosion in high current discharge and cathode spot temp., obs. 9-34798
 electrodeposited single crystals, structure and mech. props. 9-46786
 electrodeposition on to (100) plane of Cu in presence of chloride ions 9-24586
 electrodeposition parameters effect on growth habit and morphology 9-37034
 electron maximum range, 15 MeV, expl. determ. 9-26470
 electron states, bound, on current surface 9-47053
 electron-irradiated, dislocation pinning, temp. eff. 9-23812
 electronic structure, photoemission studies of optical densities of states 9-44891
 emittance at cryogenic temp., cyclic incident radiation technique 9-24064
 exploding wire phenomena, effect of nature and dims. 9-45419
 fatigue, bulk effects in [211] oriented single crystals, temp. effects 9-23914
 fatigue crack, propagating, dislocation substruct. 9-33077
 fatigue crack formation and propag. during cyclic deform., model 9-30682
 fatigue in single crystals, early stages, dislocation substructure and surface markings study 9-30637
 fatigue strength, effect of diffusion coatings 9-33058
 fatigue tested at 17.8 kc/sec, microhardness and microcracking 9-35190
 fatigued, elec. resistivity changes, defect struct. obs. 9-33254
 fatigued single crystal. dislocation distrib. in persistent slip bands 9-33076

Copper continued

- f.c.c. polycrystalline, flow stress and microstructure after shock-relief deformation 9-23879
 Fermi momentum determ. from annihilation spectra, valence electrons calc. 9-33229
 Fermi surface, effect of elastic deform., determ. using thermoelec. power 9-44884
 Fermi surface, hydrostatic press. effect, zero-press. de Haas-van Alphen freqs., n.m.r. obs. 9-47041
 film, density meas. compared with bulk Cu 9-30483
 film, evaporated, intrinsic tensile stress meas., temp. depend. 9-37233
 film, growth on alkali halides 9-23636
 film, internal friction for attenuation of mechanical oscillations 9-23856
 film, vacuum evaporated, structure defects 9-30488
 film on Zn (3 wt.%)Cu alloy, cracking rel. to grain boundary reaction type precip. in alloy 9-23957
 films, conductivity, rel. to thickness 9-49023
 films, thin, randomly and preferentially oriented, K absorpt. edge fine struct. 9-47383
 fire refining, W-Re thermocouple for melt temp. checking 9-38321
 flow, continuous epitaxial (001), on rocksalt, changes in twin structure during growth 9-39158
 flow-stress relation to strain and strain-rate, drop-hammer test 9-39406
 foil, insulating material for space flight, outgassing behaviour 100-1800°F obs. 9-38173
 foil, spatial distrib. of damage spots due to neutron irrad. 9-46806
 gamma ray scatt., 145 keV, differential elastic scatt. X-section 9-46263
 Gibbs free energy of self and impurity diffusion 9-33001
 grain boundary impurities, distrib. rel. to annealing, for tough-pitch and P-deoxidized samples 9-30600
 growth of deformed crystals, eff. of Ag impurity on initial stages 9-30525 in haemoglobin, e.p.r. 9-33641
 Hall coeff., depend. on crystal orientation, Fermi surface characteristics 9-26516
 Hall coeff., temp. depend., verification of phonon and dislocation contribution 9-28467
 Hall effect and phonon drag 9-43026
 heat transfer from cylindrical surfaces to liq. He I 9-36909
 heavily rolled sheet, electron transmission exam. 9-39272
 homogenization quenching, dislocation structure and grain growth 9-23938
 impedance oscillations rel. to transitions between surface quantum states 9-37411
 impurities in As₂S₃ on conductivity 9-33295
 impurity centres in GaAs, local vibrations and structures 9-33231
 impurity in calcite, infl. on cleavage surface energy 9-30479
 impurity in ZnS.CdS-Ag, effect on cathodoluminescence 9-24474
 internal friction, amplitude independent, -180 to 200°C, 9-17 kc/s 9-40998
 internal friction, effect of previous deform. in tension or torsion 9-41002
 internal friction of wire during plastic deform., study by torsional oscill. method 9-35154
 ionic spectra, new classifications and corrected wavelengths of selected lines 9-34549
 i.r. absorpt. and reflectivity meas., rel. to virtual bound state 9-45269
 K α X-radiation absorption by Pb in brass, depend. multiphase syst. 9-24440
 K α X-radiation absorption by Pb in brass, depend. on particle size in multiphase syst. 9-24440
 liquid, resistivity from exploding wire expt., theory 9-44584
 magnetoreflexion meas. and optical dielec. function change 9-49246
 magnetoresistance, 4.2°K 9-44912
 magnetoresistance, longit., effect of structural defects 9-49025
 magnetoresistance, transverse, 5 to 50°K, influence of lattice defects 9-47075
 magnetoresistance at 4.2°K in transverse fields up to 100 kG 9-41166
 magnetoresistance saturation ratio, 4° to 35°K 9-37444
 magnetoresistivity in single crystals with point defects 9-37443
 matrix-SiO₂ (Al₂O₃) particles interface, generation of dislocations local shear stresses 9-30611
 mech. props., dislocation configs. and densities in deformed single crystals, effect of strain rate 9-41010
 microyielding in polycrystals, dislocation arrangements after deform. 9-48897
 molten, wetting of sapphire, ruby and recrystallized alumina 9-34977
 neutron irrad. at low temp., elec. resistivity recovery 9-43025
 n.m.r. lines quadrupole broadening w.r.t. plastic deform., dislocations density obs. 9-35723
 n.m.r. of ⁶³Cu in elastically deformed foils 9-24507
 Ohm's law verification up to 10⁹ A/cm² current densities 9-24126
 open-orbit induced torque obs. 9-49024
 optical transitions, nature 9-24354
 oscillatory wire drawing, reduced stress and friction 9-37286
 oxidation and cracking, effect of prior cold working 9-41450
 oxidation kinetics in thin film range 9-43329
 oxygen ion bombardment effects on specific faces 9-44640
 phonon dispersion relations 9-37313
 photoelec. cross sections meas., E_y=280 keV 9-22945
 photoelectric yield meas. with Lallemand electronic camera 9-45028
 plasma due to exploding wire in vacuum, opt. and spectral props. 9-44440
 plastic behaviour of whiskers below yield pt. 9-39407
 plastic deform. in polycryst. preyield dislocation motion and multiplication obs. 9-35171
 plastic deformation, effects of electroplated Cr coatings 9-26328
 polycrystal, effect of orientation-dependent solidification 9-46931
 polycrystalline, effect of plastic deform. at about 77°K 9-37240
 polycrystalline, prestrain effect, unidirectional or cyclic twist, effect on stress-strain curve 9-46877
 positron annihilation in single crystal., temp. effect 9-33242
 positron annihilation rel. to cryst. e struct., obs. 9-35325
 proton energy losses 9-30807
 pseudomorphic growth of Ni monolayers and possibly thicker films 9-34989
 r-values and changes during tensile testing rel. to strain anisotropy and texture in sheet with cube orientation 9-39273
 recrystallisation and grain growth kinetics, intense u.s. energy influence 9-28380
 rolled, orientation distrib. of crystallites, electron microscopy determ. 9-48830

Copper continued

- rolled, tensile props. rel. to temp. at 4.2-290° K 9-40993
 secondary electron emission from (110) face, fine structure meas. in energy angular distribution, umklapp process 9-28585
 self-diffusion coeffs. meas. from annealing of spherical voids, 390° to 560°C 9-30624
 sheet, cold-rolled, Young's modulus, angular variation and texture depend. 9-30632
 shock wave hardened, softening and recrystallization during heating 9-33098
 shock-wave strengthened, final yield strength 9-35162
 slip, coarse, model of crack formation and propag., rel. to fatigue 9-48904
 slip bursts during cyclic deform. of single cryst. 9-33052
 slip traces on single cryst. surfaces w.r.t. non-conservative motion of dislocations 9-39365
 solid and liquid equations of state calc. from low temp. mechanical obs. 9-39090
 solubility in Si, effect of grain-boundaries 9-42797
 solubility of C 9-44788
 sound velocity, mag. field dependence, in ultrapure material 9-35274
 specific heat, pure single-crystal and polycrystalline, below 3°K 9-42968
 specific heat of Cu containing H₂, anomalous, 0.4° to 3.0°K 9-42969
 specific heats, extended Bhatia model method 9-24012
 spectra, 3d⁴s⁴p, g, and hyperfine structure calc. 9-44260
 staining of Ge crystals, method 9-24186
 strain centres with attendant prismatic dislocation loops, etch-pit and X-ray topograph obs. 9-32939
 strain hardening and softening by cycles of plastic deform. 9-23867
 strained single crystals, dislocations around SiO₂ particles, lattice rotations, electron microscope obs. 9-32911
 strengthening value with programmed loading depend. on preliminary deform. degrees 9-42890
 stress cracking by liq. metals 9-48941
 stress/strain diagram rel. to stress rate in elastic range 9-41008
 substitutional impurities in GaAs, electroabsorption study 9-35413
 substrate for epitaxial growth of Zn and Cd electrodeposits 9-30490
 surface deformation, preferential, existence by dislocation density 9-41016
 surface struct., low energy e diff. meas. 9-35044
 target for 12.3BeV/e p, cross-sections for prod of π, k, p, \bar{p} 9-38580
 thermal and elec. conductivity, low temp., deviations from Matthiessen's rule 9-41102
 thermal diffusivity meas., effect of pulse width 9-28432
 thermal expansion, Gruneisen parameters 9-26429
 thermal resistivity due to edge dislocation scattering of phonons 9-26446
 thin films, abnormal optical props. 9-31068
 torsional prestrain effects 9-46877
 trace impurities, spectrochemical analysis 9-35760
 unlubricated sliding with steel surface, high speed 9-41038
 u.s. hardening at 90°K, influence of pre-annealing at room temp. 9-28374
 u.s. three-phonon interactions 9-42942
 Wannier function localization 9-26482
 whisker growth in large quantity, role of Cu₂O globules 9-37110
 whiskers, as-grown, surface steps on pyramidal tips and longit. bounding surfaces 9-35031
 whiskers, diffusion of Zn, coeff. depend. on diameter 9-26300
 whiskers, elastic and plastic behaviour below yield pt. 9-39407
 whiskers, growth by halide reduction, electron-microscopic obs. 9-37111
 work-hardening under cycling of const. stress amp. of single cryst. 9-30709
 X-ray diff., extinction changes in lines during annealing 9-44662
 x-ray emission band, modulation due to alternating elastic strain 9-49303
 X-ray emission spectra, L_I and L_{III} bands, struct. of 3d band 9-45339
 Young's modulus orientation and temp. depend., -180 to 200°C, 9-17 kc/s 9-40998
 p , range and ionization energy losses, Bragg's cycle method meas., E_p =100-660 MeV 9-33213
 Cu²⁺ in soda-borate oxide glass, e.s.r. and optical spectra 9-37800
 and Cs, optically pumped, spin exchange 9-40548
 Cu-Xe, vacancy defect clusters 9-32947
 Cu/Au-Fe annealed temperature calibration extended 9-47841
 Cu/Pb layers, proximity effect, induced excitation spectrum, density of states meas. 9-44944
 Cu-Nb-S system, vapour growth of new single-crystalline phases 9-37007
 Cu-Pb normal metal-superconductor junctions, proximity effect by electron tunneling 9-24166
 Cu-W fibre-reinforced composite, stress-strain curve 9-42875
 Cu, core electrons, momentum distrib., anisotropy 9-30820
 Cu⁺ activator in alkali halide crystals, optical struct. of luminescence centres 9-47387
 Cu⁺ centres in alkali halides, u.v. absorpt. spectra 9-43237
 Cu⁺ centres in alkali halides, excitation and emission spectra, hydrostatic press. effect 9-41401
 Cu⁺ in NaCl, stress-induced dichroism in u.v. absorpt. bands, temp. depend. 9-45322
 Cu²⁺, e.p.r. in CdWO₄, linear elec. field effects 9-24486
 Cu²⁺, e.s.r. in ZnO 9-33637
 Cu²⁺ coloration impurity in lanthanum glass, effect on light absorption 9-24372
 Cu²⁺ diffusion in CuSO₄ aq. soln., e.p.r. obs. 9-34890
 Cu²⁺ e.s.r. in LiCl 9-43281
 Cu²⁺ a.s.n. spectra in ZnWO₄ 9-37802
 Cu²⁺ in CdS, e.p.r. of photoinduced centres 9-47433
 Cu²⁺ in Cu SO₄·5H₂O, spin-lattice relax. times, nucl. dynamic polarization obs. 9-47297
 Cu²⁺ in GaAs-Pb junctions doped at interface, zero bias anomalies 9-24197
 Cu²⁺ in KH₂PO₄, e.s.r. 9-26793
 Cu²⁺ in MgO, e.p.r. spectrum rel. to dynamic Jahn-Teller effect 9-24494
 Cu²⁺ in NH₃ soln., e.s.r. spectrum, -18°C→+72°C 9-42391
 Cu²⁺ in NH₄Cl, effect on A-type phase transition, e.s.r. and differential thermal analysis 9-33142
 Cu²⁺ in ZnS, absorption and excitation spectra, correlation with valence band structure 9-37732
 Cu²⁺ tetrahedrally coordinated in ZnO:Cu and ZnS:Cu; 3d-4p mixing importance w.r.t., i.r. emission decay 9-35599
 Cu²⁺ to Cu⁺, conversion due to γ -irrad. of copper acetate monohydrate 9-49386

Copper continued

- Cu²⁺·6H₂O in Jahn-Teller system, relax. behaviour, e.p.r. and electron-spin-echo obs. 9-31159
 Cu fatigued single cryst., dislocation struct. and persistent slip bands 9-30686
 Cu fatigued single cryst., dislocation struct. and persistent slip bands 9-30686
 Cu fatigued single cryst. dislocation distrib. in persistent slip bands 9-33076
 Cu I, 3d⁴s⁵ and 3d⁴s⁴p configurations 9-42331
 Cu I quadratic Stark shifts in some transitions 9-22950
 Cu II 3d⁴s¹D and ³D levels, isotope shift w.r.t. specific-mass effect, exchange polarization of 3d-shell 9-29927
⁶⁴Cu, diffusion in α - and γ -Fe rel. to defect interactions 9-46851
^{63,65}Cu associated centres in CdS, paramag. reson, 77°K 9-47432
 in Ge-Ga, anomalous distrib. in and near diffused layer, bipolar photoeffect obs. 9-45024
 in KCl, e.p.r. spectra of stabilized atoms, temp. depend. 9-35714
 in LiCl, e.p.r. spectra of stabilized atoms, temp. depend. 9-35714
 in N₂ arc discharge, spectral effects 9-46550
 in NaCl, additively coloured with Na vapour, colloidal absorpt. bands obs. 9-32998
 in NaCl e.p.r. spectra of stabilized atoms, temp. depend. 9-35714
 recrystallization and recovery kinetics 9-39454
 ZnO:Cu single cryst., e.p.r., ^{63,65}Cu hyperfine lines obs. 9-35718
 in ZnO and ZnS, ligand-field-band theory 9-37673
 ZnS:Cu,Mn,Cl effect of activator conc. on electroluminescent props. 9-37781
 in ZnS phosphor, luminescence spectra, green II band contour obs., electric and photoexcitation 9-26786
 in ZnSe as-grown cryst., luminesc. excitation spectra 9-43254
- Copper alloys**
 see also *Copper compounds*
 active slip volume of clusters 9-32983
 alloys polycryst., 10 and 15 at. %Zn, onset stress for deform. twins 9-32980
 bell metal, effective atomic number for photoelectric process of γ -rays 9-47213
 brass, 7/3, fatigue damage in combined torsion and bending, obs. 9-30687
 brass, annealed, propag. of large amplitude waves 9-42872
 brass, contact pot., stress induced shifts, obs. 9-43019
 brass, creep, temperature after effect 9-23896
 β -brass, dislocation pair, $a(110)+a(001)$ 9-28291
 α -brass, enhanced diffusion during cyclic straining 9-44732
 β_1 -brass, metastable, martensitic transformations, heat treatment, n. irrad. and deformation effects 9-23981
 β_1 -brass, neutron-irrad., thermal cycling, martensitic start temp. obs. 9-42928
 β -brass, ordered, energy bands using Green's function 9-48990
 α -brass, quenched, secondary defects exam. 9-40940
 α -brass, rolled, orientation distrib. of crystallites, electron microscopy determ. 9-48830
 α -brass, stress-corrosion cracking in CuSO₄/(NH₄)₂SO₄ soln. 9-26352
 brass, stress/strain diagram rel. to stress rate in elastic range 9-41008
 brass, Young's modulus and torsion modulus calcs. by different methods 9-30629
 brass foil as spectral indicator for discharge plasma exam. 9-25972
 brass plate, cross-shaped, yield surface after prestraining or cold rolling, expt., study 9-26327
 β -brass single cryst., creep behaviour near T_c 9-30668
 β -brass solid soln., X-ray diff., static atomic displacements influence on diffuse intensity 9-37132
 α -brass wire, internal friction during plastic deform., study by torsional oscill. method 9-35154
 α -brasses, shock deformation, stacking fault energy from dislocation distrib. 9-23879
 bronze, effective atomic number for photoelectric process of γ -rays 9-47213
 constantan, phonon emission spectra, thermal radiation obs. 9-42944
 corrosion, atmospheric 9-24572
 corrosion, atmospheric exposure tests 9-24573
 Cu-Al, dilute, impurity contribution to temp. depend. of Hall coefficient 9-28466
 Cu-Sn, liquid, X-ray interference function thermoelectric power and electrical resistivity determ. 9-28098
 Cu-Zn surface, rel. to fatigue strength of Cu 9-33058
 Dilute, de Haas-van Alphen studies of electron scattering 9-37423
 dilute, Hall coeff., room temp. to 1.5°K 9-44911
 dilute, Hall coeff. and transport props. 9-37442
 β -, long-range order influence on elastic consts. 9-39396
 manganin coil press. gauge, calibration to 60 kbar under hydrostatic press. 9-40215
 moments in ferromag. composition range determ. 9-43167
 Monel metal, for lecture demonstration of ferromag. curie point 9-22035
 Mossbauer effect in ¹¹⁹Sn impurity, electronic props. obs. 9-43222
 Ni-(20 wt.%)Cu, mag. moment distrib., mag. disorder neutron scatt. cross section meas. 9-35562
 nitridation, internal 9-28384
 stress cracking by liq. metals 9-48941
 stress-corrosion cracking, transgranular, interpret. 9-26349
 Pt alloys, of O₂, internal oxidation. 850-1000°C 9-24557
 (36wt.%) Zn, stress-corrosion cracking, electrochem. factors 9-23920
 Ag/Cu eutectic, rel. sputtering rates, temp. depend. 9-44851
 Ag(0.26 at.%)Cu, oxidized at 250 or 300°C, stress relaxations from internal friction spectra 9-48885
 Ag-Cu alloys, H₂S corrosion resistance enhanced by pressure deformation 9-30659
 Ag-Cu liq. and vapour quenched, metastable struct. obs. 9-40899
 Al-Cu-Ag, resistivity changes rel. to growth and dissolution of Ag-rich zones and vacancies 9-46758
 Al-Cu-Cr supersaturated solid solns., kinetics of decomp. 9-46937
 Al-Cu-Mg-Ag, S precip. obs. 9-48928
 Al-Cu-Mg, S precip. obs. 9-48928
 Al-(4 at.%)Cu, vacancies excess conc. during ageing and slow reaction mechanism obs. 9-48916
 Al-(4 at.%)Cu, grain-boundary precipitates, growth 9-35101
 Al-(4wt.%)Cu, transition precipitate structures formation, effect of cyclic straining 9-39490

Copper alloys continued

- Al-Cu, binding free energy bet. vacancies and second solute atom 9-23793
- Al-Cu, dilute, thermopower, temp. and size depend. 9-43123
- Al-Cu θ' precipitate, stacking faults, electron microscope exam. 9-35098
- Al(2.5 at.%)Cu(1.2 at.%)Mg, ageing, Si effect on initial stages 9-48915
- Al(4.3 wt.%)Cu, precip., effect of pressure 9-42917
- Al-CuAl₂ eutectic, directionally frozen, structure 9-39250
- Al-CuAl₂ eutectic, lattice rotations 9-39251
- Al-Zn-Mg-Cu, deformed, substructure and susceptibility to intergranular stress corrosion cracking 9-23811
- Al(0.3-0.4 wt.%) Cu bicrystal, grain boundary sliding rel. to deform. 9-46888
- Al-(2wt.%)Cu, solid-liquid interface, microstructure and composition variation 9-34961
- Au(46 at.%)Cu(4 at.%)Ni, order transform. of type $\alpha_{disorder} \rightarrow \alpha_{order}$, radiocrystallog. study 9-37304
- Au-Cu-Co, liquid, susceptibility meas. 9-34921
- Au-Cu-Zn β phase stability and elastic anisotropy 9-46957
- Au(25 at.%)Cu, elastic after-effect kinetics, resistance meas. 9-35161
- Au(0.1 wt.%)Cu, fast neutron irradiation at low temp., elec. resistivity recovery 9-43025
- Au-Cu, long- and short-range order w.r.t. thermoelec. power temp. depend. 9-37610
- Co-Ni-Al-Cu-Nb-Fe, magnetostruct. analysis 9-47251
- Co-Ni-Al-Cu-Ti-Fe, magnetostruct. analysis 9-47251
- Cu-(14.95 wt.%)Sn, b.c.c. to orthorhombic γ_1' martensite transformation, crystallography 9-30739
- Cu-(14.5 wt.%)Al(3.5 at.%)Ni with thermoelastic martensite, internal friction, amplitude depend. 9-42869
- Cu-Ag, oxidation and cation distrib. in Cu₂S-Ag₂S solid solution formed 9-23656
- Cu-Ag spectral lines, analytical, effect of additives 9-31228
- Cu-Ag surface, rel. to fatigue strength of Cu 9-33058
- Cu-Al:Fe dilute specific heat, 1.2° to 14°K 9-47001
- Cu-Al-Fe-Ni aluminium bronzes, ductility rel. to microstructure, 20-800°C 9-23894
- Cu(5 wt.%)Al, tensile deformation at room temperature 9-30680
- Cu(16 at.%)Al, short-range ordering kinetics 9-33120
- Cu-Al, Cu-based α -solid solutions dislocations, degree of splitting and anomalous after-effect 9-32968
- Cu-Al, dislocation phonon scattering values from thermal conductivity and dislocation density meas. 9-41078
- Cu-Al, latent hardening rel. to composition and prestrain 9-41015
- Cu-Al, martensitically transformed, Young's mod., yield stress and plastic deform. 9-35172
- Cu-Al, quenched, Frank dislocations dissociation, e diff. obs. 9-40959
- α -Cu-Al, short-range ordered state and stable superlattice phase obs. 9-39275
- Cu-(16 at.%)Al solid soln., high temp. creep behaviour 9-33043
- Cu-Al dislocation loops, complex Frank, stacking fault steps form. rel. to fault climb 9-40943
- Cu-Al martensite cryst. struct. stability, solute content effect 9-42929
- Cu-Al solid solns., stacking fault energy influence on high temp. creep 9-42887
- Cu-Al solid solns., stacking fault energy influence on high temp. creep 9-42886
- Cu-(0.2 wt.%)Al, internally oxidised, effect of Si additions on mech. props. 9-46903
- Cu-(15 at.%) Al, Shockley partial dislocations, unstable directions 9-35093
- Cu-Au(Al) films, effective surface diffusion coeffs., vol. diffusion effect in electron diff. obs. 9-39379
- Cu-B, irradiation, formation of He bubbles, influence of precipitates 9-41116
- Cu-(12.6wt.%)Be-(0.2wt.%)Co-(0.1wt.%)Zn, Mossbauer eff. 9-45288
- Cu-Be-Co, dil., constitution and behaviour 9-39274
- Cu-Be, ageing investigations from sp. ht. meas. by an adiabatic calorimeter 9-37285
- Cu-Be, precipitation hardening kinetics intense u.s. energy influence 9-28380
- Cu-Co, containing coherent precipitates, critical resolved shear stress 9-44755
- Cu-Co alloys, containing coherent particles, critical resolved shear stress 9-44756
- Cu-Co single crystal, w.r.t. precip. state 9-39428
- Cu-Cu₂O, eutectic, mech. props. and elec. resistivity 9-48907
- Cu-Fe, dilute, martensite nucleation in Fe precipitates 9-37300
- Cu-Fe dilute, magnetoresistance, 1.3° to 88°K, fields up to 200 kOe 9-44909
- Cu-Fe solid solns., homogeneous decomposition 9-48930
- Cu-Fe two-phase mats., internal microstresses rel. to plastic deform. 9-46881
- Cu-Ga, massive and martensitic transform., temp. 9-41066
- Cu-Ga solid solns., dislocation struct. and work hardening, electron microscopic exam. 9-41045
- Cu-Ga solid solns., width of split dislocations, effect of near order 9-42827
- Cu-Ge, dilute, impurity contribution to temp. depend. of Hall coefficient 9-28466
- α -Cu-Ge evaporated film, faulting meas. by X-ray diffraction 9-23820
- Cu-Ge solid solns., dislocation struct. and work hardening, electron microscopic exam. 9-41045
- α -Cu-Ge thin films, recrystallization 9-37278
- Cu-In, dilute, impurity contribution to temp. depend. of Hall coefficient 9-28466
- Cu-Mg solid solns., dilute, binding energy between dislocation and Mg atom 9-37175
- Cu-Mn-Al, structure study by X-ray and neutron diff. anal. and electron microscope exam. 9-37293
- Cu-Mn, dilute, electron spin resonance over 1.8°K to 300°K range 9-24489
- Cu-Mn, stress-corrosion cracking, electrochem. factors 9-23920
- Cu-Mn dilute, e.s.r., 1.8° to 300°K 9-26792
- Cu-Mn dilute, magnetoresistance, 1.3° to 88°K, fields up to 200 kOe 9-44909
- Cu-Mn(FeCr) dilute, magnetoresistance, 1.3° to 20°K, fields up to 200 kG 9-44910
- Cu-Ni-Fe, ⁵⁷Fe Mossbauer effect obs. of mag. ordering 9-39817
- Cu-Ni-Fe, hard-magnetic particle ensemble model, calc. 9-33453
- Cu-Ni-Fe, spinodal decomposition, electron microscope obs. 9-35242

Copper alloys continued

- Cu-Ni, compress. rel. to para-ferromag. transition ordering, obs. 9-35167
- Cu-Ni, damping behaviour and miscibility gap evidence 9-42870
- Cu-Ni, dilute ⁵⁷Fe Mossbauer studies 9-47331
- Cu-Ni, lattice thermal conductivity, temp. depend. at low temp. 9-26447
- Cu-Ni, rigid-band model and clustering eff. 9-26483
- Cu-Ni film, co-deposition by electron beam, struct., grain size and orientation 9-48763
- Cu-Ni i.r. absorpt. and reflectivity meas., rel. to virtual bound state 9-45269
- Cu-Ni photoemission and optical studies rel. to electronic structure models 9-45033
- Cu-Ni surface, rel. to fatigue strength of Cu 9-33058
- Cu-O liquid alloys, wetting of sapphire 9-26179
- Cu-Pd, interdiffusion, effect of coherency strains 9-35128
- Cu-Pd, internal oxidation by diffusion process, 850-1000°C 9-24557
- Cu-Sn, dilute, impurity contribution to temp. depend. of Hall coefficient 9-28466
- Cu-Sn, martensitically transformed, Young's mod., yield stress and plastic deform. 9-35172
- α -Cu-Sn, polycryst., twinning 9-39189
- α -Cu-Sn alloys polycryst., up to 5 at.%)Sn, onset stress for deform. twins 9-32980
- Cu-Sn liq. system, thermodynamics, Knudsen cell and mass spectrometric obs. 9-36860
- Cu-25wt.%)Sn effective atomic numbers for gamma interacts. 100-662 keV 9-24230
- Cu-75 wt.%)Sn, effective atomic number for pair prod. for γ energy 2.6-17.6 MeV 9-24232
- Cu-Ti system, phase equil. obs., thermodynamic props. 9-46679
- Cu-Ti-Al, decomp. nature, struct. changes on ageing electron microscopy 9-46938
- Cu-Ti-Al, dispersion-hardened, mechanical twinning 9-23926
- Cu-(2.3wt.%)Ti, aluminium additions, effect on decomp. kinetics 9-37292
- Cu-Ti, decomp. nature, struct. changes on ageing electron microscopy 9-46938
- Cu-Ti, dispersion-hardened, mechanical twinning 9-23926
- Cu-(39.8wt.%)Zn precipitation, effect of uniaxial tensile stress 9-46939
- Cu-(2.5 wt.%)Zr-(0.5 wt.%)Nb, radiation enhanced relaxation 9-41006
- Cu-(26 wt.%)Zn, ZnO films establishment and growth 9-26191
- α -Cu-Zn, activation vol. analysis at yield point w.r.t. dislocation intersection processes 9-39413
- Cu-Zn, Cu-based α -solid solns., dislocations degree of splitting and anomalous after-effect 9-32968
- Cu-Zn, dil., ⁶³Cu n.m.r. lines conc. depend., 1st order quadrupole effect obs. 9-35724
- Cu-Zn, dislocation phonon scattering values from thermal conductivity and dislocation density meas. 9-41078
- Cu-Zn, Ge-Ga solid soln. hardening 9-39472
- α -Cu-Zn, Hall effect meas. and phonon drag effects, 4.2° to 300°K 9-43026
- Cu-Zn, laser pulsed discharges, elimination of effects of tertiary elements 9-27297
- β_1 -Cu-Zn, martensitic transform., effect of neutron irradiation 9-37296
- Cu-Zn β -phase alloys, order-disorder transf., Hall coeffs., elec. resistivity 9-35253
- Cu-Zn dispersion relations for lattice vibrations from neutron scatt. 9-30766
- Cu-Zn single cryst., positron annihilation, Fermi surface change with increasing electrons per atom 9-33241
- Cu-Zn system phases, interdiffusion coeff., conc. depend. 9-46850
- Cu-(30 wt.%) Ni, substitutional Zener relaxation 9-26321
- (87wt.%)Cu-(13wt.%)Ni optical transitions, nature 9-24354
- Cu-(15 at.%)Al deformed crystal, lattice thermal conductivity 9-35291
- Cu-(0.06-5.2 at.%)Mn elec. resist. at 2-300°K, max. value 9-47068
- Cu-(7.5-25 at.%)Mn magnetic props. in pulsed fields up to 175 kOe, 77-300°K 9-43173
- Cu-Au solid soln., X-ray diff., static atomic displacements influence on diffuse intensity 9-37132
- Cu₂Pd, diffusion of H 9-23838
- Cu 2 at.%) Al, neutron irradiation, effects at elevated temps. 9-28330
- Cu 2 at.%) Mg, neutron irradiation, effects at elevated temps. 9-28330
- CuAu II, entropy of disorder, phase transition from CuAu I 9-30750
- Cu(9.5 at.%)Be-(0.2 at.%)Zn, neutron irradiation, ageing characts. from resistivity meas. 9-33115
- Cu(2wt.%) Co, structural transformations in precipitates on cold-rolling, Mossbauer obs. 9-30732
- Cu(1wt.%) Co, with Co precipitates, coherency loss by electron irradiation in microscope 9-28383
- CuMn, photoemission energy distrib. meas. rel. to impurity bound states 9-26613
- Cu(Mn), photoemission expts. rel. to virtual resonant bound states 9-45032
- CuPt, energy of ordering by tin soln. calorimetry 9-48934
- Cu(36wt.%)Zn, Fe and P influence on recrystn., grain growth inhibition 9-30718
- Cu(36wt.%)Zn, solubility of Fe and P, max. saturation and precipitation 9-30717
- Cu-Au, ordered, dislocation structure produced by plastic deformation 9-23813
- Cu-Ti, ageing kinetics, decomposition activation energies 9-23941
- GaP-Cu diodes, charge-carrier capture and effect on transition capacitance 9-35510
- Mn-(11 at.%)Cu, relax. peak obs. w.r.t. twinning surface disloc. 9-35156
- Mn-Cu, lattice distortion, elasticity and antiferromag. order 9-39783
- Mn-(11 at.%)Cu twinning surface dislocations, intrinsic resistive stress 9-35157
- (Mn_{0.95}Cu_{0.05}), antiferromag., Fe impurities obs. 9-41338
- Ni-Cu-H, low temp. elec. resistance anomalies 9-37450
- Ni-Cu, atmospheric corrosion behaviour 9-37831
- Ni-Cu, atmospheric corrosion behaviour 9-37831
- Ni-Cu, dilute, elastic consts., third-order, sensitivity to changes in electron-to-atom ratio and mag. eff. 9-37217
- Ni-Cu, ferro- and paramagnetic props., comparison 9-35539
- Ni-Cu, low temp. elec. resistance anomalies 9-37450
- Ni-Cu, minimum polarity models in mag. props. theory 9-45113
- Ni-Cu, near critical composition, magnetiz. polar. clouds of giant moments 9-26624
- Ni-Cu carburised, irradiation damage and the Portevin-le Chatelier eff. 9-28349

Copper alloys continued

- Ni-Cu giant moments near critical composition 4.2°K 9-45148
 Ni-Cu solid solutions, ferro- to paramag. transition, spht., Curie temp. and moment obs. 9-35554
 Ni-Fe-Cu films, anisotropy components separation by temp. depend. study of anisotropy field 9-45170
 Si brass, laser pulsed discharges, elimination of effects of tertiary elements 9-27297
 Si hardened, irradi., hot brittleness rel. to He-filled deform. defects 9-37260
 Sn-Cu, dil., internal friction anomalies near melting pt. 9-39399
 Sn-Cu spectrochem. analysis of e. evap. vacuum condensates, obs. 9-28832
 UO₂-Cu alloy, phase diagram and investigation of system 9-28395
 U-Zn-Cu, Hall coeffs. at -196-100°C 9-47071
 Zn-Cu, liquid, density meas. up to 700°C 9-30375
 Zn-(2 wt. %Cu) alloy, grain boundary reaction type precipitation from obs. of cracking in Cu films deposited on alloy surface 9-23957
 Zr-Cu reactor fuel claddings, oxidation and cracking in CO₂, obs. 9-37266

Copper compounds

see also *Copper alloys*

- acetate, p. relax. in H₂O, C₂H₅OH solns., obs. 9-48719
 acetate monohydrate, γ-irrad., conversion of Cu²⁺ to Cu⁺ 9-49386
 Alnico, Ti bearing, mag. props. rel. to structure 9-24310
 bornite, metastable phase, order study 9-26230
 chelates, in-plane chelates 9-31163
 complex, bis(N-n-propylsalicylaldiminato) copper(II), cryst. struct. 9-35058
 copper (II) salicylate adducts, e.p.r. and mag. susceptibility 9-37804
 Cu₂-xTe (x=0.25±0.04), cry. struct. e. diff. determ. 9-46785
 (CuMnZnO₄)_x(AFe₂O₄)_{(1-x)/2}, magnetic and electrical props. of solid solutions, where A=Cu²⁺, Ni²⁺, Zn²⁺, Co²⁺ or Ni²⁺ 9-30834
 formate tetrahydrate, antiferromag. reson., 1.4 to 15°K 9-45378
 formate tetrahydrate, two-dimensional antiferromagnet behaviour 9-26661
 phthalocyanine, atomic planes bordering a crack, config. 9-42904
 trichite whiskers, X-ray refraction effect on radiograph and topograph 9-40877
 bistropolionate and bisacetylacetionate, single cry. electronic spectra 9-24407
 Cu₄-xTe₂, tetragonal phase, γ¹ and γ¹¹ disordering modifications 9-42937
 CUSO₄ aq., dielec. props. 9-46648
 Ca-3wt. %Al-0.6wt. %Cu alloy, structural changes during precipitation of hard soln. 9-44789
 CaF₂:U⁴⁺, EPR and UPB spectra, superhyperfine interactions 9-39905
 CdS-Cu₂S heterojunctions in film photocells, charact. 9-46845
 Cu-Co solid solutions, magnetic hysteresis rel. to ageing time 9-26622
 Cu-Mn:Pt, Kondo divergence in conduction-electron scatt. amplitude 9-39558
 Cu-Pd alloys, photoemission studies for band structure 9-33423
 Cu_{0.8}Fe_{0.2}O₄ spinel formation from CuFe₂O₄ and α-Fe₂O₃ 9-30740
 Cu₂-sSe thin films, formation, struct. and props. 9-46721
 Cu₂CdGeS₄, cryst. struct., diff. obs. 9-39269
 Cu₂Cs₃Cl₇·2H₂O single cry., mag. ordering, NMR study 9-37643
 Cu₂O, 2s exciton excitation causing weak absorption line 9-33235
 Cu₂O, absorption spectrum contour, line broadening and asymmetry w.r.t. exciton-phonon inter. 9-35656
 Cu₂O, crucible-free method of single crystal growth from melt 9-37076
 Cu₂O, elec. conductivity and thermoelec. power, temp. depend. 9-28496
 Cu₂O, electro-optical absorpt. due to 1s exciton 9-49275
 Cu₂O, electroluminesc., temp. range expansion using M.O.S. system 9-37778
 Cu₂O, first order Raman spectrum, active mode determ. 9-39851
 Cu₂O, interdiffusion of O, obs. from elec. conductivity meas. 9-44733
 Cu₂O, photoconductivity, i.r.-induced, 110°K 9-24229
 Cu₂O, photoconductivity temp. dependence, 160-120°K, excitonic processes 9-24228
 Cu₂O, quenched, absorpt. spectra 9-28683
 Cu₂O, single cryst. growth in SiO₂ gel at near ambient temp. 9-46752
 Cu₂O, slow photoconductivity, assuming existence of three types of traps 9-30989
 Cu₂O, u.v. electroreflectance spectrum 9-35626
 Cu₂O globules, role in growth of Cu whiskers in large quantity 9-37110
 Cu₂S-Ag₂S solid solution on Cu-Ag alloy, cation distrib. on alloy oxidation 9-23656
 Cu₂S-CdS heterojunctions, heat-treated, photovoltaic effect mechanism 9-39650
 Cu₂S, thermal conductivity, anomalous temp. depend. 9-30793
 Cu₂S films, optical and electrical props. for band structure data 9-44949
 Cu₂S films, prep. and optical props. 9-46727
 Cu₃Au, tensile props. of single crystals 9-30710
 Cu₃La₂(NO₃)₁₂·24H₂O, mag. phase transitions, obs. 9-39781
 Cu₃PSe films, elec., electro-optical and optical props., obs. 9-35398
 Cu₃PSeL₂ films, elec., electro-optical and optical props., obs. 9-35398
 Cu₃PSeS₂ films, elec., electro-optical and optical props., obs. 9-35398
 Cu₃SbSe₄, elec. and thermal props., electr. struct. and transport props. obs. 9-26505
 β-Cu₂V₂O₇, semicond. props. evolution w.r.t. increasing x 9-41197
 Cu (II) benzoate, e.p.r. meas. at 9.1 and 12.0 GHz spin Hamiltonian parameters 9-49350
 Cu (II) glycyl-glycylglycine chloride sesquihydrate single cry. spectra, band obs. 9-24405
 Cu complex, bis(L-isoleucinato) copper (II), crystal structure rel. to L-isoleucine config. 9-26228
 Cu complex, bis(3-amino-1-phenyl-2-buten-1-ono) copper (II), crystal and mol. structure 9-30560
 Cu complex, bis(L-serinato)copper(II), crystal structure rel. to chelation effects on serine 9-26229
 Cu complex, bis(ethylenediamine) copper(II) nitrate, single crystal ESR spectrum, g value calc. 9-28744
 Cu complex, copper (II) acetylacetonate, matrix-isolated spectrum, rel. to struct., 650-2200 cm⁻¹ 9-27870
 Cu complex, CuAc acetate hexahydrate, mag. props. 9-33484
 Cu complex, Cu(II) adenine, mag. exchange and antiferromag. coupling 9-31048
 Cu complex, Cu(II) hydrogen o-phthalate dihydrate, cry. struct. and e.s.r. spectrum 9-48829
 Cu complex, Cu(II) tetramethylene diamine chloride, E.S.R. 9-33624

Copper compounds continued

- Cu complex, diphenyl sulphoxide perchlorate, ESR and opt. absorpt. studies 9-24488
 Cu complex, porphyrins, luminescence at liquid nitrogen temp. 9-47392
 Cu complexes, Cu-8-hydroxyquinolate substituted in organic crystals, ligand ENDOR 9-45408
 Cu complexes, quadrupole effects in e.p.r. 9-43278
 Cu complexes tetramine sulphate and selenate monohydrates, crystal structures 9-39268
 Cu II tetrahalo-anions, Raman spectra rel. to vibr. obs. 9-44327
 CuAlS₂(Se₂), preparation and properties of single crystal 9-48797
 CuBe cathode, photoelec. yield in vacuum u.v. 9-26616
 CuBr, luminescence, induced by giant ruby laser at 8°K 9-45345
 Cu(C₆H₅)₂(NH₂)₂Cl₄, transition temp. from a.c. susceptibility data 9-45107
 CuCO₃ soln. in acid, spectra resolution, 8000-13000 cm⁻¹ 9-27850
 CuCl, absorption spectrum, study of lines ν₄ (25571.5 cm⁻¹) and ν₅ (25501 cm⁻¹), 4.2°K 9-49274
 CuCl, gel growth 9-37033
 CuCl, gel growth by complex dilution method, comparison with new mats 9-30516
 CuCl, lattice vibr., rigid ion model applic. 9-46973
 CuCl, luminescence, induced by giant ruby laser at 8°K 9-45345
 CuCl, photoconductivity spectrum, exciton dissociation by localized elec. fields, vibr. struct. obs. 9-41138
 CuCl, transverse magneto refl. in near u.v. 9-35622
 CuCl, Zeeman effect of bound excitons 9-37721
 CuCl₂·2H₂O single crystal, antiferromag. reson. at low temp. 9-47425
 CuCl₂(CH₃NH₂)₂, ferromagnet, heat transport by magnons 9-37369
 CuCl₂·2H₂O, growth kinetics 9-37032
 CuCl₂·2H₂O, neutron inelastic scatt. obs. of librational freqs. 9-42955
 CuCl₂·2H₂O, vibrational analysis 9-38839
 CuCl₂·2H₂O antiferromagnetic spin flop transition, 1° to 4.2°K, adiabatic meas. study 9-45217
 CuCl crystals, refl. spectra, optical consts. determ. near excitonic absorpt. region 9-37710
 CuCl evaporated films, Faraday rotation due to excitons 9-24370
 CuCl kinetics of bixcicon formation 9-35318
 CuCr₂Se₄-xBr_x spinels, press. sintering 9-33126
 CuFe₆⁴⁺ octahedral ion, modified Wolfsberg-Helmholz molecular orbital calc. 9-37080
 CuFeS₂, ⁵⁷Fe, Mossbauer spectra, quadrupole splitting meas. 9-35634
 CuI, CuI₂ absorption of organic mols., stimulation and extinction of excitonic transitions 9-26194
 CuI absorption edge, donor-acceptor interactions and adsorption of organic mols. 9-25739
 Cu(II) complex bis (prolinato), polarized single cry. electronic spectra 9-24406
 Cu(II) complexes with tetradentate Schiff base ligands, anomalous sign reversal in circular dichroism spectra 9-36703
 Cu(II) cyanopyridine and chloropyridine complexes, far i.r. spectra 9-23038
 CuK₂(SO₄)₂·6H₂O, dynamic polarization of protons and their spin-lattice relaxation times 9-39786
 CuMn₂O₄ spinel, cation distrib. by neutron diff. meas. 9-40854
 Cu(NH₃)₄ soln., ⁶⁴Cu half-life, obs. 9-27683
 Cu(NH₃)₄SO₄·H₂O, antiferromag. ordering and spin arrangement, proton n.m.r. and susceptibility meas. 9-41334
 Cu(NH₃)₄(SCN)₂, principle g factors calc. from e.s.r. 9-33625
 Cu(NH₃)₄(SO₄)₂·6H₂O, structure parameter refinement from neutron diffraction data 9-39270
 Cu(NO₃)₂·HgO·3H₂O, crystal structure 9-39271
 Cu(NO₃)₂·2.5H₂O, paramag. relax. and adiabatic cooling 9-26662
 Cu(NO₃)₂·2.5H₂O, magnetization isotherms, 1.2° to 4.2°K 9-45218
 CuNb₂S₄, synthesis and lattice constants on basis of hexagonal unit cell 9-39284
 CuO-MoO₃, phase diagrams in O₂, air, and under O₂ press. 9-35256
 3CuO, P₂O₅, 24MoO₃, 58H₂O single cryst., e.s.r. spectra 9-35713
 CuRb(PO₃)₃, crystal data, existence in Cu(PO₃)₃-RbPO₃ system 9-30561
 CuRh₂O₄-NiRh₂O₄ system, deformed spinel structs. 9-30704
 CuRh₂S₄, supercond. 9-49034
 CuS, supercond. 9-49034
 CuSO₄, antiferromag., moment density distrib., polarized-neutron determ. 9-41335
 CuSO₄, Cu²⁺ diffusion in aq. soln., e.p.r. obs. 9-34890
 CuSO₄ solutions in glycol-water mixtures, u.s. absorpt. rel. to temp. 9-34903
 CuSO₄·5D₂O, deuteron, n.m.r. 9-39919
 CuSe₂, marcasite type superconductor, cry. struct. 9-28261
 CuSO₄ soln., ⁶⁴Cu half-life, obs. 9-27683
 CuSO₄·5H₂O, spin-lattice relax. times of Cu²⁺ by nucl. dynamic polarization 9-47297
 CuTe thin-film photocells, fabrication 9-33413
 CuTi(PO₃)₃, crystal data, existence in Cu(PO₃)₃-TiPO₃ system 9-30561
 ZnS/Cu, luminesc. decay times after proton-excitation 9-49318
 ZnS-Cu phosphor, electro and X-ray luminescence, nonadditivity changes 9-28727

Corbino effect see *Current, electrical*

Coriolis forces see *Dynamics*

Cornea see *Eye*

Corona, electric discharge

see also *Breakdown, electric*

streamers propag. in low field region of asymmetrical gap 9-34815

Corona, solar see *Sun/corona*

Coronagraphs see *Sun/corona*

Corpuscular streams see *Cosmic rays; Sun/radiation, corpuscular*

Correspondence principle see *Quantum theory*

Corrosion

- alloy, protection by anodic metal dispersion, patent 9-23946
 automation and computer techniques applied to research 9-24561
 α-brass, stress-corrosion cracking in CuSO₄/(NH₄)₂SO₄ soln. 9-26352
 cathode in spark discharge 9-43330
 electrodeposits on plastics 9-28797
 erosion rate at electrodes of an arc rotated by a transverse mag. field 9-42578
 fatigue crack propag. in mild steel, effect of corrosive environment 9-37262
 ferrous metals, tests after 7 years atmospheric exposure 9-24564
 graphite, radiolytic, by CO₂, effect of pore size variation on rate 9-41452

Corrosion continued

- kinetics, linear 9-24563
 metal, protection by anodic metal dispersion, patent 9-23946
 metal, rel. to limiting current using rotating disc method 9-24562
 metallic structure immersed in electrolyte solution, cathodic protection system, patent 9-45421
 metals, meas. of atmospheric factors 9-24565
 metals, structural, in sea-water, fresh-water and tropical atmos., 16 year exposure exam. 9-24566
 reactor corrosion of stainless steel, electron microprobe analysis of films <4 μ m 9-24607
 steel, austenitic stainless, fracture paths of stress corrosion cracks 9-39441
 steel, austenitic stainless, stress cracking susceptibility in chloride-containing high temp. water, effect of composition 9-26355
 steel, carbon and low alloy cast, atmospheric exposure 9-24580
 steel, Fe₃O₄ film growth characteristics in dil LiOH soln. at 300°C 9-39952
 steel, in NaOH soln. containing NaCl 9-24577
 steel, martensitic, low-C, precip.-hardened, anodic polarization meas., tempering effects 9-24578
 steel, mild, low temp. aqueous corrosion under reactor radiation 9-26826
 steel, mild, rates in various districts of Northern California 9-37830
 steel, passivity breakdown in borax soln. 9-24579
 steel, stainless, resistance increase by galvanic platinizing 9-24574
 steel, stainless, in MgCl₂ soln. transgranular stress-corrosion cracking, interpret. 9-26349
 steel, u.s. influence 9-37829
 stress-corrosion cracking, electrochemical parameters 9-23918
 stress-corrosion cracking, mechanical parameters 9-23917
 stress-corrosion cracking, transgranular, interpret. 9-26349
 tinplate, eff. of CS₂ and dithiocarbamates 9-28803
 Zircalloys, aqueous, at low temp. 9-26831
 Zircaloy, aqueous, pre-transition behaviour, comments 9-37826
 zircalloys, post-transition, by steam at 300°C and 340°C 9-28806
 (-36wt.%) Zn, stress-corrosion cracking, electrochem. factors 9-23920
 Ag-Cu alloys, by H₂S, resistance enhanced by pressure deformation 9-30659
 Al-(11 wt.%) Mg age-hardening alloy, stress-corrosion resistance, effect of deform, by hydrostatic extrusion 9-41051
 Al-Zn-Mg-Cu alloy, deformed, intergranular stress cracking, rel. to dislocation structure 9-23811
 Al-Zn-Mg alloy, weldable, stress-corrosion resistance, effect of quench rate, rel. to microstruct. changes 9-46919
 Al-base alloy, atmospheric test, tensile strength 9-37828
 Al, anaerobic, by sulphate-reducing bacteria 9-24567
 Al, atmospheric weathering tests, 7-year data 9-24569
 Al, literature review 9-26828
 Al alloys, atmospheric stress corrosion testing 9-37827
 Al alloys, cracking, stress conc. influence 9-44778
 Al alloys, hard-rolled, for architectural purposes 9-24570
 Al alloys, stress-corrosion induced prop. changes, nondestructive eval. 9-26829
 Al alloys, stress-corrosion crack detection using Rayleigh waves 9-42704
 Al and alloys, atmospheric, eff. of initial weather conditions 9-24568
 Al and alloys, atmospheric, results of 6 year exposure tests 9-24571
 Al mirror protection from Hg acetate 9-33672
 AlZnMg 1 alloy sheet, stress and layer corrosion susceptibility, effect of annealing as-cast alloy 9-46779
 BN, in cryolite-Al melts 9-28798
 Be, polycrystalline, anodic dissolution 9-24583
 Co. surface reactions due to chemisorbed layer in field ion microscope 9-26827
 Cr-(49wt.%)Ni-(1wt.%)Ti alloy, on exposure to pyrolysis conditions of sodium-base spent pulping liquors 9-28799
 Cr-(49wt.%)Ni-(1wt.%)Ti alloy, on exposure to pyrolysis conditions of sodium-base spent pulping liquors 9-28800
 Cu-Mn alloys, stress-corrosion cracking, electrochem. factors 9-23920
 Cu alloys, atmospheric 9-24572
 Cu alloys, transgranular stress-corrosion cracking, interpret. 9-26349
 Cu and alloys, atmospheric exposure tests 9-24573
 Fe-Cr alloy, pitting corrosion 9-31198
 Fe-Cr alloys, pitting and anodic dissolution, surface prep. and deformation effects 9-24576
 Fe, inhibition by amines, synergistic effects of anions 9-24575
 Fe, surface reactions due to chemisorbed layer in field ion microscope 9-26827
 Mg-base alloy, atmospheric test, tensile strength 9-37828
 Mg and alloys, book 9-39447
 Ni-Cr-Fe alloy, atmospheric behaviour 9-37831
 Ni-Cu alloy, atmospheric behaviour 9-37831
 Ni-Mo alloys, ferro- and paramag., electronic interact. between surface atoms and anionic complexes 9-28801
 Ni, atmospheric behaviour 9-37831
 Ni, surface reactions due to chemisorbed layer in field ion microscope 9-26827
 Pb-Ca battery grids, pressure cast 9-28802
 Pb-Sn alloy electrodes, electrochem. behaviour in different soln., corrosion resistance and passivation mechanism 9-33673
 Ti-(6 wt.%)Al-(4 wt.%)V, stress-corrosion cracking in anhydrous methanol 9-48894
 Ti-(8wt.%)Al-(1wt.%)Mo-(1wt.%)V alloy sheet, hog-salt-stress-corrosion cracking and effect on tensile props. 9-23923
 Ti-base alloys, atmospheric, resistance 9-37835
 Ti, aqueous-stress corrosion, infl. of comps. and ht. treatment 9-37833
 Ti, sea-water stress corrosion, metallurgical and mechanical aspects 9-37832
 Ti alloys, hot-salt stress corrosion cracking initiation 9-37265
 Ti alloys, stress-corrosion cracking in aq. NaCl at room temp. 9-23921
 Ti alloys, stress corrosion in methanolic soln. 9-23922
 Ti alloys stress-cracking resistance, eff. of ht. treatment 9-37264
 Ti and alloys, crevice corrosion 9-37834
 U₃Si nuclear reactor fuel, tests in 300°C water 9-28804
 U foils <2000 Å, preparation for electron microscopy rel. to stress corrosion cracking 9-23777
 Zn, literature review 9-26830
 Zn, rolled, atmospheric eff. 9-37837
 Zn in water, NaOH and other decinormal solns. 9-28805
 Zn rolled, atmospheric, eff. of 1% Cu addition 9-37836

Corrosion continued

- Zr-(1 at.%)Nb alloy, oxidation kinetics and corrosion behaviour in pressurized steam and air 9-35747
- Cosmic dust** see *Interplanetary matter; Interstellar matter; Meteorites*
- Cosmic noise** see *Cosmic radiations, radiofrequency*
- Cosmic radiations, radiofrequency**
 see also *Quasars; Radioastronomy; Sun/radiation, radiofrequency*
 3°K, earth's motion studied 9-40156
 3C 273 radio source, flux density variations, 5760 MHz 9-40160
 3C 279 radio source, flux density variations, 5760 MHz 9-40160
 3C 345 radio source, flux density variations, 5760 MHz 9-40160
 3C 84 radio source, flux density variations, 5760 MHz 9-40160
 absorption of 10 MHz rad. in local spiral arm 9-41662
 BL Lac, very rapid variation 9-45653
 brightness distrib. of extragalactic sources, general discussion 9-49566
 Compton effect, induced, of plasma and electromag. waves under astrophysical conditions 9-43581
 continuous survey at 1415MHz, between declinations 0° and 20° N 9-40159
 cosmic emission latitudinal depend. of galactic absorption 9-33894
 cp 1133 pulsar, search for high energy gamma rays, using atmos. Cherenkov tech. 9-29047
 Cygnus X-2 X-ray source, unsuccessful search for radio emission at 4.5 cm 9-41670
 emission and absorpt. in galactic disc, HI and HII regions 9-31520
 emission sources in decimeter band, spectral anomalies 9-27061
 extra-galactic, low frequency spectra 9-27059
 extragalactic background at 2.1 MHz 9-24739
 extragalactic sources, 32, linear and circular polarization at 3.12 cm 9-38056
 extragalactic sources, brightness distrib., general discussion 9-49566
 extragalactic sources, observed and intrinsic parameters, relationship 9-29040
 extragalactic radio sources in the i.r. 9-29051
 Faraday rotation and dispersion of pulsar signals, rel. to Galactic mag. field fluctuations 9-49531
 Faraday rotation meas. rel. to metagalactic mag. field 9-47624
 flux densities at 5009 MHz of 753 sources 9-41656
 flux densities of 103 sources 9-38056
 Galactic, at 610.5 MHz, contour map for region between longitude 55° and 64° 9-26995
 Galactic continuum at 4 GHz, survey between l^{II}=21° and l^{II}=31° 9-47627
 galactic sources, b^{II}<10° region, 178 MHz, obs. 9-41657
 galaxies, elliptical, E and SO noncluster, emission at 2640MHz 9-43579
 the Galaxy, low latitude survey, 1410 and 2650 MHz 9-24743
 H cloud optical depth determ. from absorpt. spectra of variable intensity sources 9-27049
 Haro's blue galaxies, search radioemission at 9.26 cm 9-24823
 HB 21, supernova remnant, contour map from obs. at 2695 MHz 9-47643
 intergalactic, emission at 21 cm 9-40119
 intergalactic radio absorption theory at low frequency 9-47651
 ionospheric noise absorption, sudden increases 9-45524
 ions, cosmic, fast 9-28985
 M31 and neighbourhood radio continuum survey 9-43518
 microwave background, ang. variations, macroscopic motion of metagalactic plasma explanation 9-38037
 microwave background, anisotropy, implications 9-36006
 microwave background radiation, discrete source explanation 9-26978
 model for source which exhibits breaking at 750 MHz 9-31571
 nebulae, 408 MHz emission, obs. 9-33900
 NGC 6857, 11 cm. obs., group of compact H II regions hypothesis 9-41627
 noise, sky brightness temp., 2-4.2 MHz 9-47608
 noise absorption, rel. to emission intensity at 3914 Å 9-43430
 noise ionospheric absorption 1959-65 obs. 9-40070
 non-thermal sources prod. by dissipation of mag. energy on collapse of interstellar cloud 9-41634
 nonthermal sources, acceleration of ultrarelativistic electrons and nuclei 9-49568
 NP 0532, pulsar, optical polarization meas. 9-45652
 occultation obs with sun, refraction and scatt. due to corona 9-31564
 occultation studies positions and structures of 10 sources 9-49567
 occulting disk of Sun at r.f. wavelengths, ang. size calc. 9-29039
 Orion A region, radiomap at 1.94 cm, 9-31515
 Parkes catalogue, 1780 sources, declination zone, +20° to -90° 9-31562
 polarization and flux densities of 156 sources at 21.2 cm, Galactic depolarization study 9-36007
 positions and optical identification of 255 sources between declinations +20° and -33° 9-31568
 positions of 75 sources, between declinations +20° and +27° 9-29045
 PSR 0833-45, pulsar, polarization structure and radiation emission from mag. poles 9-38058
 pulsars, mag. models and neutron stars, rel. to narrowness of rad. beam 9-41666
 pulsar, radio and optical emission, accounted for by rot. and oscill. mag. neutron stars 9-41659
 pulsar a rotating neutron star 9-33915
 pulsar CP 0328, dist. meas. 9-24824
 pulsar CP 0328, distance meas. by neutral H absorpt. 9-41663
 pulsar CP 0328, polarization of radio pulses 9-45640
 pulsar CP 1133, average pulse shape rel. to frequency 9-29048
 pulsar CP 1919, intensity distrib. rel. to origin of variations 9-29049
 pulsar CP 1919, proper motion of blue star 9-27065
 pulsar discoveries designated MP 0450, MP 1642 and MP 1818 9-45646
 pulsar discovery at suspected position of supernova, possible association 9-27064
 pulsar distances 9-27066
 pulsar distances, meas. from neutral H absorpt. 9-41663
 pulsar distances calcs. effect of H II regions and electron density 9-45605
 pulsar emission, 'dispersion measures' rel. to galactic H II 9-45604
 pulsar emission, mechanism rel. to oblique rotator model of neutron star 9-41660
 pulsar emission as mag. dipole rad. from rotating neutron star 9-43589
 pulsar flares, possibility of low-energy cosmic ray ejection 9-49571
 pulsar in Crab, generation of mag. flux and energy 9-45647
 pulsar in Crab Nebula, light curve shape rel. to colour and polarization 9-45644

Cosmic radiations, radiofrequency continued

- pulsar in Crab Nebula, optical pulse meas. rel. to wavelength indep. of velocity of light 9-41665
- pulsar in Crab Nebula, period change rel. to frequency of events producing pulsars 9-40165
- pulsar in Crab Nebula, television detection of optical pulses 9-43591
- pulsar NP0532, accurate meas. of pulse period 9-47656
- pulsar NP 0527, period and double-pulse struct. 9-41664
- pulsar NP 0532, discovery of strong light flashes 9-43590
- pulsar NP 0532, linear and circular polarization meas. 9-43596
- pulsar NP 0532, position, average pulse shape, dispersion and strong pulse characts. 9-43588
- pulsar NP 0532, search for nanosecond optical pulses 9-41668
- pulsar NP 0532, simultaneous optical and radio meas. showing simultaneous emission 9-47657
- pulsar NP 0532, strong light flashes, confirmation 9-41658
- pulsar NP 0532, strong pulsed X-ray signals, comparison with optical pulses 9-43605
- pulsar observations at Molonglo Radio Observatory using dispersion removal technique 9-36010
- pulsar PSR 0833-45, abrupt. decrease in periodicity 9-45642
- pulsar PSR 0833-45, abrupt. decrease in periodicity 9-45643
- pulsar PSR 0833-45, evidence supporting rotational model 9-47654
- pulsar PSR 0833-45, period decrease, rel. to mass increase 9-45650
- pulsar PSR 0833-45, polarization structure and radiation emission from mag. poles 9-38058
- pulsar PSR 0833-45, search for optical pulsations 9-43594
- pulsar PSR 0833-45, search for optical radiation 9-45645
- pulsar PSR 0833-45, sudden decrease in period explained in rotating neutron star hypothesis 9-43598
- pulsar PSR 0833-45, visible brightness obs. 9-43596
- pulsar PSR 0904+77, position and other parameters 9-40164
- pulsar PSR 2218+47, position and other parameters 9-40164
- pulsar radiation origin rel. to e.m. wave propagation theory 9-24827
- pulsar radiation from star with mag. field at angle to rotation axis 9-33917
- pulsar radio radiation from electrons with kinetic temp. $\sim 10^{10}$ K, criticism of theory 9-43597
- pulsar search at 1400 MHz, unsuccessful 9-43599
- pulsar search from Molonglo, distrib. in the Galaxy 9-31573
- pulsar signals, influence of solar corona, rel. to delay, fluctuations and 'smearing' 9-31576
- pulsar signals dispersion and Faraday rotation, rel. to Galactic mag. field fluctuations 9-49531
- pulsars, 37, catalogue 9-38057
- pulsars, absence of characts. in several X-ray sources 9-40168
- pulsars, amplitude variations, intrinsic and scintillation effects 9-33918
- pulsars, as neutron stars, popular article 9-49572
- pulsars, association with supernova explosions in ancient Chinese records 9-43592
- pulsars, clustering pattern along galactic plane 9-33919
- pulsars, CP 1919, CP 0950, CP 1133, spectral fine structure 9-27067
- pulsars, digital search methods in radio noise of telescopes, two types of anal. 9-43593
- pulsars, discovery reviewed 9-45654
- pulsars, distance estimates, comments on methods 9-45641
- pulsars, distance meas. by galactic HII absorption near 21 cm wavelength 9-31580
- pulsars, dynamic spectra 9-36009
- pulsars, Faraday rotation of radio waves, in plane of polarization 9-29050
- pulsars, frequency of events producing them from period change of Crab Nebula pulsar 9-40165
- pulsars, hypothesis of rotating neutron stars 9-31577
- pulsars, identification with ancient Chinese guest stars 9-47660
- pulsars, longterm fading of pulse intensities, frequency struct. 9-33920
- pulsars, magnetic models for radiation mechanisms 9-29046
- pulsars, mechanisms and magnetic models 9-49570
- pulsars, model of mag. dipole alignment with rotation axis, electrodynamics 9-43586
- pulsars, oblique rotator model, problem in pulse spacing 9-45651
- pulsars, obs. of very high energy gamma rays, implications 9-41661
- pulsars, period stability and slowing down 9-31578
- pulsars, periodicity changes 9-36012
- pulsars, periodicity rel. to nonradial gravity wave of degenerate neutron star 9-47658
- pulsars, periods, rel. to starquakes, on neutron stars 9-47642
- pulsars, possible formation from massive O stars 9-43595
- pulsars, props., explanation in stellar evolution theory including magnetoturbulence 9-27063
- pulsars, radiation mechanism and rotating neutron star model 9-31581
- pulsars, review of models 9-38059
- pulsars, search for ultra-short light pulses 9-47659
- pulsars, second periodic pulsation obs. 9-24826
- pulsars, seven, average energies at cm wavelengths 9-45649
- pulsars, survey 9-49563
- pulsars, theor. period distrib. deriv. 9-43587
- pulsars, theory 9-49569
- pulsars, white dwarf adiabatic atm. pulsation mechanism 9-31579
- pulsars and general relativity test 9-24825
- pulsars and white dwarfs, supercond. 9-24763
- pulsating radio sources, model 9-24828
- pulsating source PSR 1749-28, dispersion and pulse length 9-27062
- pulsating sources, model of H burning in white dwarf envelope 9-31575
- pulsating sources, obs. at 13 cm 9-31574
- pulsating sources, upper limits to gamma ray fluxes for three sources 9-33923
- pulsating sporadically, two near Crab Nebula 9-27052
- quasi-periodic v.l.f. emissions rel. to geomagnetic micropulsations 9-27068
- radio sources, 11-20 cm wavelength, linear polariz. props. and analysis 9-24831
- radio sources, 11-20 cm wavelength linear polariz. obs. 9-24830
- radio sources, rapidly pulsating, planetary model 9-31582
- radio sources, spectra at cm wavelengths 9-40163
- radiogalaxies, east-west linear polarization distrib. at 1418 MHz 9-36008
- radiogalaxies, plasma stability mechanism 9-41651
- scintillations near sun, rel. to solar wind 9-29091
- SCO XR-1, radio emitting region, mechanism and dimension 9-43600

Cosmic radiations, radiofrequency continued

- sky emission at decameter wavelengths, cosmic black body and galactic. obs. at 15, 20 and 30 cm 9-31563
- source counts, improvements and implications for cosmology 9-24819
- sources, interferometer meas. with trans-Pacific baseline 9-41667
- sources at 22.25 MHz, spectral flux densities 9-31570
- sources at 2.8 cm wavelength, 146, flux densities 9-47653
- sources at 4.3 mm wavelength, 23, obs. 9-47652
- sources in 3CR catalogue, relation between spectral index and flux density 9-43585
- southern radio sources, 123 obs. of brightness distribution by interferometric methods 9-43580
- spectra, continuum, of 387 sources, 178 MHz to 8000 MHz 9-36011
- spectra of 80 discrete sources at decametric wavelengths 9-40161
- spectra of 80 discrete sources at decametric wavelengths, analysis and classification 9-40162
- spectra of sources in revised 3C catalogue 9-40157
- spectrum and polarization of a source of synchrotron emission with components flying apart at relativistic velocities 9-33916
- supernova remnants, 16, emission between 408 and 2700 MHz, spectra derivation 9-31544
- synchrotron emission, polarised, generation and transfer 9-41650
- synchrotron rad., Scheuer luminosity meas. method queried for moving sources and quasars 9-27054
- synchrotron radiation from supernovae, galaxies and quasars 9-29042
- synchrotron radiation spectra below Razin cutoff, asymptotic form, extragalactic radio sources 9-27060
- troposphere, rain and snow effects on extraterrestrial mm. waves 9-31331
- variable radio sources, review 9-29052
- VRO 42 22.01 source, interferometric obs. for linear and circular polarizations 9-45648
- W49, obs. at 2800MHz with E-W resolution of $1/5''$ 9-40158
- W51, complex galactic source, obs. 9-31569
- W 43, distance determ. by coupling with neutral Hydrogen 9-31572
- Y2 Canis Minoris, red dwarf, prolonged radio emission obs. 9-45617
- H II minor southern galactic regions 9-24758
- H II region, radio recombination lines, eff. of thermal equilibrium 9-24761
- H II regions, 74 MHz obs., mean e temp. derivation 9-31521
- H II regions, radio-line data analysis and interpretation 9-43525
- H line oscillator strength wave mechanical exact expression 9-44291
- NH₃ microwave emission in Sagittarius region, rel. to dust cloud conditions 9-43574
- OH, galactic, pumping mechanisms for maser action 9-24740
- OH class II sources, anomalous emission in satellite lines 9-41655
- OH clouds, microwave line optical depths and excitation temps. 9-43567
- OH microwave emission, positions and spectra of fair new sources in Cygnus 9-47655
- from OH radicals, origin 9-24829
- OH reson. waves, polarization parameters and amplification and attenuation coeffs. 9-38053
- Cosmic rays**
- acceleration by pulsars, theory 9-24729
- alignment of interstellar grains by isotropic bombardment 9-43577
- angular distrib., use of matrices for describing 9-34339
- conference of 49 papers on various aspects 9-34337
- diffusion, composite model of, ejections from galaxy-core explosions 9-49525
- Dirac monopole flux, relativistic, at mountain heights, upper limit 9-40401
- electrodynamics, second approximation theory 9-33890
- electrons in galactic mag. field, anisotropy 9-40114
- energy below geomagnetic threshold, and heavy nuclei, Kosmos 19 and Kosmos 25 obs. after solar flare 9-38101
- energy flux near equator from ionizing component meas. at top of atmosphere 9-36505
- fireballs, existence and possible explanations 9-25495
- flux and energy spectrum, 42°N geomag. latitude balloon obs. (Oct. 1967) 9-28969
- galactic, admission to solar system 9-26987
- galactic, equilibrium spectra of secondary positrons and spectrum of γ -rays resulting from annihilation 9-31492
- galactic gas isotropy, resonant wave particle effects 9-33891
- galactic low energy, attempt to allow for sun's modulating eff. 9-35947
- geomagnetic cut-off rigidities in non-vertical directions 9-47596
- Harrison's cosmology shown to preclude universality of cosmic rays 9-26985
- intensity, response to solar wind turbulent fluctuations 9-35944
- interaction with light emission in expanding universe 9-41623
- interactions effects with wave-particles, propagation eff. 9-28984
- interplanetary obs. 9-47681
- in interplanetary space, discussion and review of obs. 9-35951
- in interplanetary space, motion when subject to regular mag. field and fluctuating solar wind 9-35948
- in interstellar gas, acceleration and isotropisation 9-24728
- in interstellar space, low energy, protons and heavy nuclei, upper limits 9-31494
- low-energy, possible ejectors from pulsar flares 9-49571
- mean free paths through far i.r. radiation field 9-35945
- metagalactic γ -ray spectrum from secondary particle prod. 9-47663
- modulation, 11-year, and solar activity 9-31647
- modulation, rel. to freq. depend. of interplanetary mag. field power spectra 9-43650
- noise absorption pulsations assoc. with geomag. Pc3 pulsation near local noon 9-45560
- nuclear component, particle telescope obs. from OSO-III (1967) satellite 9-24730
- observations in E. USSR (Aug.-Oct. 1966) 9-34338
- photoisintegration by universal radiation field, ultrahigh energy 9-43511
- propagation and anisotropy, theory for steady streaming 9-24725
- secondary and ionizing components intensity latitude depend. obs. (July-Oct. 1965) 9-35924
- solar, anisotropy behaviour during cosmic ray events, model 9-38110
- solar, effect on ionospheric electron production rate 9-45523
- solar, heavy nuclei, flux rises 9-22646
- solar, recording by lunar satellite Luna 11, (1966) 9-22644
- solar neutrino fluxes, sensitivity 9-29092
- universal in matter-antimatter universe 9-46123
- u.v., scattered, in earth's neighbourhood, observations by interplanetary stations Venera 2 and Venera 3 9-24847

Cosmic rays continued

X-ray bremsstrahlung associated with suprathermal protons 9-43603
e flux rel. to height, 42°N geomag. latitude balloon obs. (Oct. 1967) 9-28969

absorption

noise pulsations assoc. with geomag. Pc3 pulsations near local noon 9-45560

alpha-particles and helium nuclei

see also *Quasars; Radioastronomy; Sun/radiation r.f.*
fluxes, balloon obs. quiet solar period in Palestine, Texas (1964-65) 9-45563

path-length and interplanetary field calc. from d and ³He intensities 9-28983

solar low energy, use in interplanetary medium props. determ. 9-43647
spectra and modulations between 100 and 2000 MeV 9-32237

⁴He modulation new solar minimum, obs. 9-27573

⁴He energy spectrum, differential 9-29635

⁴He flux, Fort Churchill 1967 obs. 9-27574

apparatus

see also *Particle detectors*

detectors, Monte Carlo programme for simulating e.m. showers 9-44070
discharge counters, cylindrical, use for absolute intensity meas. 9-29631

identifier with f.e.t. analogue multiplier for IMP F and G spacecraft, design and calibration 9-38021

intensity monitoring recorder for satellites 9-29632

ionization chamber used aboard Kosmos 19 and Kosmos 25 satellites 9-38101

neutron counter for balloon and rocket expts., design and calibration 9-38602

particle telescope carried on OSO-III (1967) satellite 9-24730

primary electron detector system for OGO-E satellite experiments 9-38022

proportional counters, overfilled with cyclohexane 9-29630

scintillation counter telescope, design and testing 9-25490

solar proton energy spectrum, meas. method 9-45685

telescope, for equator points and vertical intensity measurements 9-46125
telescope, large area, high charge resolution using two scintillation detectors 9-27571

telescope, using Li drifted Si detectors having spherical segment shape 9-22645

telescope for obs. azimuthal asymm. and charge composition 9-36502

Vela 4 satellite, for energetic particle experiment 9-38020

water Cherenkov counter, directional but non-focusing, for muons 9-22643

e energy spectrum meas. system 9-35946

μ spectrometer, scattering correction, 6-316 GeV/c 9-22642

N energy meas. with n multiplicity monitor 9-29633

n flux up to 350 km, rocket meas. 9-43495

composition

charge composition obs. with telescope 9-36502

chemicals, Proton 1 and Proton 2 obs. 9-36501

comparison of element distrib. with that of the universe 9-34341

EAS, primary chemical constituents, 10¹⁵ eV 9-29636

equatorial obs. by Kosmos 53 satellite 9-36503

hadronic component in EAS, 3-dimens. Monte Carlo calc. 9-32232

heavy mass particles at sea level, a search 9-34344

heavy nuclei from sun not reflecting composition of solar atmosphere 9-38104

nuclei or Z>22, chem. comp. using meteoric minerals as detectors 9-34343

quarks, sea level search procedure and results 9-32137

quarks inducing nuc. fis., method to limit abund. in products 9-25491

of superheavy nuclei, Proton 1 and Proton 2 obs. 9-34342

⁷Be galactic, stability obs. 9-40116

deuterons

path-length and interplanetary field calc. from d and ³He intensities 9-28983

effects and interactions

see also *Nuclear reactions and scattering due to/cosmic rays*

accelerating mechanism in space 9-35949

atmosphere, neutrons production, flux as depth function 9-47551

charged component in stratosphere, coupling coeff. 9-45562

D-region, lower, e prod. by primary cosmic rays 9-26946

diffusion in interplanetary scatt. centres 9-24726

flares, small, eff. obs. 9-38105

galactic, solar activity modulation 9-43640

galactic, solar wind interaction 9-43664

ionization of heavy nucleus, intensity depend. on atmospheric height 9-42122

ionization of polar ionosphere 9-35867

ionosphere, lower ionization 9-40075

jets, secondary particles, azimuth angle distrib. 9-44072

modulation in interplanetary space by magnetic clouds, their relation to solar wind 9-35950

with solar wind 9-45683

wave-particle interaction effects on propagation 9-28984

μ , ultra-high energy, with nearly isotropic azimuthal distribution, mechanism of generation 9-25491

pp annihilation, metagalactic, study of γ spectra 9-43510

Co, muon-induced Fe59 9-48331

electrons

atmospheric meas. 9-40107

charge sign ratio and East-West asymmetry, 8.39V rigidity cut-off 9-32236

EAS, e space distrib. at primary energies 10⁷-10⁸ GeV, 2-300 m 9-34347

energy spectrum, differential 9-29635

energy spectrum and flux at high altitude in atmosphere 9-27575

energy spectrum meas. system 9-35946

- galactic non thermal radio emission relationship 9-43509

intensity of 2.7-21.5 MeV electrons in interplanetary space, obs. 9-49524

eff. of i.r. radiation 9-26989

microwave Compton scatt., cosmic γ prod. 9-27070

propagation, anisotropy due to synchrotron radiation 9-43508

propagation through far i.r. radiation field 9-35945

secondary, spectrum and fluoresc. efficiency in N₂; 3914 Å band 9-46127

spectrum, flux long-term time variation with solar activity, 500 MeV-5 GeV, 1966-8 9-40449

spectrum, interstellar, local, effect of solar modulation 9-43509

temporal distribution in EAS 9-44069

Cosmic rays continued**electrons continued**

e⁺, secondary, in the galaxy, equilibrium spectra and spectrum of γ -rays resulting from annihilation 9-31492

⁴He flux, Fort Churchill 1967 obs. 9-27574

jets see *Cosmic rays/showers and bursts***mesons**

diurnal anisotropy based on directional measurements 9-34340

diurnal var., theoretical calc. 9-47598

Forbush decrease, underground meson component (March 1966) obs. 9-41610

telescope detection, meteorological effects and their correction 9-42116
variation, diurnal, inclined telescope obs. 9-49511

π lifetime rel. to validity of special relativity tested in cosmic ray obs. 9-34022

muons

direct production, expt. survey 9-22641

diurnal intensity vars. near geomag. equator and primary anisotropy 9-43498

diurnal wave trains at 70 MWE during decreases 9-43497

EAS, multiple μ frequency, zenith angle depend. meas., interaction energy 200-3000 GeV 9-32234

EAS, muon-poor, origin 9-29637

EAS, μ component 9-34346

EAS, μ component at large zenith angle, depend. on energy and angle 9-32233

EAS central region, lateral distrib. meas. 9-32231

EAS muonic component density function determ., underground parallel penetrating particles analysis 9-42121

energy spectra, reln. to neutrino 9-42118

energy spectrum determ. from knock-on electron energy 9-42117

flux and energy spectrum, 42°N geomag. latitude balloon obs. (Oct. 1967) 9-28969

high-energy showers of penetrating part., analysis 9-25497
latitude knee, depend. on solar activity, particle energy, theoretical calc. 9-25492

lifetime rel. to validity of special relativity tested in cosmic ray obs. 9-34022

shower, radial extent, freq. and isotropy meas., 1500-6000 hg cm⁻² of rock penetration 9-32235

spectrometer, scattering correction, 6-316 GeV/c 9-22642

synchrotron shielding embankment effectiveness meas. using cosmic ray μ , obs. 9-22694

water Cherenkov counter for meas., directional but non-focusing 9-22643
zenith angle rel. meteorological parameters, 60 m.w.e. underground obs. 9-31467

e⁺e⁻, $\mu^+\mu^-$ pair production, energy spectra meas. 9-34348

$\mu^+\mu^-$, e⁺e⁻ pair production, energy spectra meas. 9-34348

neutrinos

energy spectra, reln. to muon 9-42118

recording of high energy events in India and S. Africa 9-38029

neutrons

in atmosphere at balloon altitudes, fast and slow, latitude var. obs. 9-27576

atmosphere, flux monitor design 9-36500

atmospheric distrib. in solar quiet years, ≤ 10 KeV, 57°N 9-25496

atmospheric distribution above 15 km, calc. for spherical scattering 9-31475

barometric coefficients, planetary distribution IQSY obs. 9-31468

counter for balloon and rocket expts., design and calibration 9-38602

diurnal var., theoretical calc. 9-47597

flare and hot condensation dependence 9-38106

flux up to 350 km altitude, rocket obs. 9-43495

height variation, 200-400 mb, 1-8 BV, latitude trend obs. 9-35936

latitude depend. of intensity obs. (July-Oct. 1965) 9-35924

latitude knee, depend. on solar activity, particle energy, theoretical calc. 9-25492

monitor, meas. energy by multiplicity of neutrons produced 9-29633

spectrum and flux determ. in solar quiet period, geomag. latitude 46°N 9-41608

spectrum from proton-microwave photon interaction, calc. 9-44073

nucleons

No entries

origin

chemical composition evidence 9-34341

Crab pulsar as cosmic ray source 9-33915

extragalactic, precluded by baryon inhomogeneity cosmology 9-46122

fluctuation origin 9-24727

fluctuation origin, source requirements, momentum-changing process 9-40117

galaxy-core explosions, ejection from 9-49525

liberation at galactic halo, rel. to relativistic fire-hose instability 9-48608

pulsar acceleration to high energy 9-24729

supernova explosion, experimental test 9-24805

two component model suggested by OGO-1 satellite model 9-27572

X-rays diffuse component 9-38603

photons

No entries

primary

5 $\times 10^{10}$ -10¹⁴ eV, Proton 1 and Proton 2 obs. 9-36504

10¹²-10¹³ eV energy spectrum calc. from Proton 1 and Proton 2 satellite obs. 9-34345

and albedo, intensities in near-earth space, obs. 9-25493

Crab nebula emission, detection by digitized spark chambers 9-35962

discrete gamma sources as origin of 100 MeV flux 9-45656

EAS, chemical composition, 10¹⁵ eV 9-29636

EAS, μ -poor, primary charged cosmic-rays as origin 9-29637

energy spectrum, differential 9-29635

energy spectrum of 11 year intensity vars., stratospheric obs. 9-31473

fluxes, balloon obs. quiet solar period in Palestine, Texas (1964-65) 9-45563

galactic, solar modulation in interplanetary spaces stratospheric obs. 9-31493

galactic γ -rays, origin rel. to interstellar gas 9-43608

in interplanetary mag. field, diffusion 9-26986

interplanetary streaming radial and azimuthal components rel. to diurnal vars. 9-47601

in interstellar space, low energy, upper limits 9-31494

metagalactic γ intensities, corrections and implications 9-45657

Cosmic rays continued**primary continued**

- metagalactic γ intensity from secondary π decay, upper limit calc. 9-29056
- microwave Compton scatt., cosmic γ prod. 9-27070
- modulation near solar minimum, obs. 9-27573
- nuclei, trans-iron, flux values, balloon obs. 9-46126
- path-length and interplanetary field calc. from d and ^3He intensities 9-28983
- primary shower spectrum cut-off condition 9-44073
- propagation through far i.r. radiation field 9-35945
- propagation through far i.r. radiation field 9-35945
- from pulsar CP 1133, search for high energy γ , using atmos. Cherenkov tech. 9-29047
- solar, 1-30 MeV, experiments 9-38112
- solar, 1-5 MeV, obs. of sharply increased counting rates, propag. along lines of force 9-38103
- solar, cut off diurnal vars. 1-30 MeV 9-47602
- solar, energetic, magnetotail penetration Vela 4 obs. (21 May-8 June 1967) 9-43665
- solar, from exponential source, energy spectrum at earth 9-25494
- solar, penetration to four Earth radi (1965-6) 9-41695
- solar, satellite obs. at 1100 km altitude (March 1966) 9-41696
- solar intensities and radiation dose rates from riometer obs. 9-46124
- solar low energy, magnetospheric entry (26 May 1967) 9-41551
- solar low energy, use in interplanetary medium props. determ. 9-43647
- solar over polar caps, nonuniformity (24 March 1966) 9-41609
- spectra and modulations between 100 and 2000 MeV 9-32237
- γ -ray distrib., energy >50 MeV, OSO-III (1967) satellite obs. 9-24731
- γ , high energy, from pulsars, implications and possible means of prod. 9-41661
- γ , primary flux meas. from balloon flights, high energy, enhanced in direction of galactic disc 9-45594
- γ atmospheric meas. 9-40107
- γ flux, enhanced in direction galactic disc. defect. on balloon flights 9-45594
- γ nuclear, rel. to solar 1-30 MeV γ cut off diurnal vars. 9-47602
- γ spectra, from metagalactic $\pi\pi$ annihilation 9-43510
- p, solar, cut off diurnal vars. 1-30 MeV 9-47602
- p, solar, intensities and radiation dose rates from riometer obs. 9-46124
- ^3He flux, Fort Churchill 1967 obs. 9-27574

protons

No entries

showers and bursts

- EAS, e space distrib. at primary energies 10^7 - 10^4 GeV, 2-300 m 9-34347
- EAS, exptl. data analysis, applic. of logarithmic normal distrib. 9-44071
- EAS, multiple μ frequency, zenith angle depend. meas., interaction energy 200-3000 GeV 9-32234
- EAS, muon component 9-34346
- EAS, muon-poor, origin 9-29637
- EAS, μ component at large zenith angle, depend. on energy and angle 9-32233
- EAS, μ component in central region, lateral distrib. meas. 9-32231
- EAS, primary, chemical composition, 10^{15} eV 9-29636
- EAS, radio pulses at 44, 105, 239 and 408 MHz 9-42120
- EAS, radio pulse prod., geomag. mechanism dominant at 32 and 44 MHz 9-44068
- EAS, temporal distribution of electrons 9-44069
- EAS hadronic component development, 3-dimens. Monte Carlo calc. 9-32232
- EAS muonic component density function determ., underground parallel penetrating particles analysis 9-42121
- e.m. showers, simulation using Monte Carlo programme 9-44070
- energy and ang. distrib., 100-400 GeV 9-29638
- Gaussian distrib. for anal. of extensive showers 9-44071
- jets, transverse momentum of particles, and determ. of fireball parameters in accelerators 9-42119
- showers poor in muons, ang. distrib. 9-48214
- stratosphere, subpolar bursts 9-40108
- SU(3) triplet particles responsible for cosmic-ray observations 9-44067
- e pulsating precip. events assoc. with geomag. Pc3 pulsations 9-45560
- μ , radial extent, freq. and isotropy meas., 1500-6000 hg cm^{-2} of rock penetration 9-32235
- μ component at large zenith angle, depend. on energy and angle 9-32233
- μ component in EAS central region, lateral distrib. meas. 9-32231
- μ frequency, zenith angle depend. meas., interaction energy 200-3000 GeV 9-32234

variations

- 27 day, obs. 9-38003
- 27-day, solar origin 9-36058
- 1959-66, survey of data from beyond the magnetosphere 9-38032
- anisotropy due to terrestrial atmosphere and mag. field, solar wind and mag. field, motion of earth and sun 9-35919
- asymptotic directions of vertical incidence for high latitudes 9-31471
- charge composition obs. with telescope 9-36502
- cosmic ray equator obs. (1963) 9-35923
- cyclic, sporadic variations obs. at various stations 9-35917
- cyclic correlation with sunspot detail 9-36057
- daily, rel. to Zurich sunspot number and cosmic ray amplitude 9-26967
- daily, second harmonic due to arrival along sun's polar or equatorial lines of force 9-28968
- diurnal, analysis of fluctuations 9-38004
- diurnal, annual modulation due to the inclination of Earth's axis, obs. analysis 9-35930
- diurnal, behaviour during mag. storms, analysis of obs. 9-35928
- diurnal, high-latitude atmospheric temp. effect, analysis of obs. at Tixie Bay 9-35931
- diurnal, meson component, theoretical calc. 9-47598
- diurnal, mesons, inclined telescope obs. 9-49511
- diurnal, nucleonic component, theoretical calc. 9-47597
- diurnal, obs. during 1964-5 solar minimum, analysis 9-35926
- diurnal, phase and amplitude during geomag. disturbance 9-49513
- diurnal, rel. to interplanetary streaming radial and azimuthal components 9-47601
- diurnal, solar co-ordinate depend. analysed using stations in N and S hemispheres 9-35929
- diurnal and sudden 2 hour intensity changes, seasonal relationship 9-35927
- diurnal variation of nuclear component during period of minimal solar activity 9-31470

Cosmic rays continued**variations continued**

- east-west asymmetry obs. by crossed telescope meas. (1965) 9-35921
- equatorial location expt. compared with theory 9-45564
- Forbush decrease, underground meson component (March 1966) obs. 9-41610
- Forbush decrease at solar maxima and minima compared, (1938-65) 9-35925
- Forbush decreases, short-lived world wide 9-49512
- galactic, solar modulation in interplanetary space stratospheric obs. 9-31493
- galactic, stratospheric, obs. data reviewed 9-38034
- galactic particle diffusion, magnetized plasma emitted by Sun 9-36059
- geomagnetic effects discussed 9-35922
- height, 200-400 mb, of neutron component, 1-8 BV, latitude trend obs. 9-35936
- intensity, 11 yr., stratospheric energy spectrum obs. 9-31473
- intensity, annual, rel. to position of active formations on Sun 9-35920
- intensity increases, stat. analysis 9-24708
- kinetic theory of cosmic particles in solar system 9-35919
- with latitude, at minimum solar activity, SPARMO balloon obs. 9-33872
- latitude depend. of intensity of secondary components obs. (July-Oct. 1965) 9-35924
- with lower atmospheric states 9-35935
- modulated spectrum near solar minimum, changes 9-27573
- modulation effects at solar minimum away from the Earth's field 9-38035
- muon, intensity, diurnal near geomag. equator and primary anisotropy 9-43498
- muonic component at 70 MWE during decreases, diurnal wave trains 9-43497
- nucleon and μ component, latitude knee theoretical calc. 9-25492
- polar regions, stratospheric obs. 9-43496
- radial gradient from simultaneous meas. on Zond 3 and Venera 2 9-38033
- review of various obs. anisotropies, diurnal and sidereal 9-35918
- secular, of intensity, 1953-56 obs. at Yakutsk 9-31472
- secular variations of intensity 9-43499
- sidereal-diurnal, possible spurious eff. discussed 9-35932
- sidereal-diurnal, use of equatorial co-ordinate system 9-35933
- sidereal-diurnal intensity anisotropy, obs. with large area telescope, temp. corrected 9-35934
- solar diurnal anisotropy, possible relation between diurnal modulation and particle rigidity 9-47599
- rel. to solar form. height in atm. 9-26964
- solar modulation of proton and alpha rigidities 9-45563
- solar wind effects, 'delay' caused by clash between solar and galactic magnetic fields 9-38102
- solar wind speed effect, mathematical model 9-45565
- e spectrum, flux long-term time variation with solar activity, 500 MeV-5 GeV, 1966-8 9-40449
- μ , zenith angle rel. meteorological parameters 60 m.w.e. underground 9-31467
- n, spatial distribution above 15 km, calc. for spherical scattering 9-31475
- n in atmosphere with latitude, fast and slow at balloon altitudes, latitude var. obs. 9-27576
- p, solar, cut off diurnal, vars. 1-30 MeV 9-47602

X-rays

- Cyg XR¹ source, upper limit on ang. diameter in energy range 25 to 100 keV 9-45655
- Cygnus X-2 source, search for radio emission at 4.5 cm, unsuccessful 9-41670
- diffuse, 1-13 kev, spectrum and Crab Nebula spectrum 9-24832
- diffuse background, cosmological implications of break in spectrum 9-43604
- discrete sources and diffuse background rad., rel. to new astronomical techs. 9-33921
- origin of diffuse component 9-38603
- SCO X-1 source, long term periodicity in optical intensity 9-43607
- Vir XR-1 point source, identification and emission mechanism 9-43606

Cosmogony see Cosmology**Cosmology**

- see also *Elements, origin*
- background rad. at 3°K, rel. to temp. of moving black body, and Earth's vel. through it 9-31489
- baryon inhomogeneity and the origin of extragalactic cosmic rays 9-46122
- Bianchi type V and type I cosmologies, nonrotating, evolution of anisotropy 9-49519
- big-bang model, implications of beta decay rate of neutron changed by mag. field 9-44058
- big-bang model, possible support from He abundance in population II stars, problems of soln. 9-43539
- black body radiation obs. at 15, 20 and 30 cm 9-31563
- Brans-Dicke, eff. on solar evolution and neutrino fluxes 9-29080
- characteristic cosmological length 9-26984
- closed time-like lines, paths in universes 9-43733
- continuous creation, search for H creation in Hg 9-45588
- contraststreaming self-gravitating streams, stability taking account of thermal conduction and radiative effects 9-48531
- cosmic 3°K background rad, anisotropy and velocity of Earth 9-45668
- cosmic emission latitudinal depend. of galactic absorption 9-33894
- cosmic rays propagation, effect of wave-particle interactions 9-28984
- cosmogonic fragmentation mechanism: gravitational instability in spheroidal masses 9-24733
- cosmological const. and deceleration parameter in closed radiation-type universe, numerical limitations 9-33885
- cosmological constant Λ , review 9-45593
- de Sitter model soln. generalized in 5-dimensional formalism 9-35942
- de Sitter soln., large mass values as recession progresses 9-33883
- Einstein gravitational-field eqns., Schwarzschild metric generalization 9-22075
- electrodynamics theory 9-24722
- electrodynamics, time symmetric, in Friedmann universe 9-43505
- electrons and relic emission interacting, calc. 9-31488
- expanding universe, props. of Fredman solns, to the Einstein equations 9-47613
- expanding universe, classical dynamics of test particle 9-24723
- expanding Universe, cosmic ray interaction with light emission 9-41623
- expanding universe, formation of condensation, general hydrodynamical eqns. 9-45592

Cosmology continued

- expanding Universe, models on basis of Brand-Dicke gravitational theory 9-38030
- extragalactic research, review 9-40194
- Friedman-Lemaître models, simplified treatment using observer's view 9-40113
- Friedmann models, homogeneous, luminosity- redshift relations, corrections 9-28978
- Friedmann universe, time symmetric electrodynamics 9-43505
- Friedmann universes, covariant e.m. potentials and fields 9-47731
- galactic clustering, second order, implications of its possible non-existence 9-45586
- galactic clusters, distribution in space, rel. to conditions when structure formed in Universe 9-35955
- galaxies, evolutionary requirements, Friedmann models with non-zero cosmological const. 9-31487
- galaxies formation, primeval fireball role in classical theory 9-26999
- galaxy form. in Lemaître model 9-47623
- gas spheres, masses 10^4 M. to 10^{20} M., hydrodynamical behaviour 9-49521
- relation to geophysics 9-49517
- globular clusters, primeval, mass computation 9-49518
- gravitating fluid, ideal, relativistic, magnetohydrodynamic behaviour 9-45589
- gravitational stability of infinite, perfectly- conducting cylinder, in aligned mag. field 9-35943
- gravitational wave emission and vibr. damping in relativistic starlike objects 9-28979
- gravitodynamics, generalized statistical mechanics of violent agitation 9-41622
- Harrison's cosmology shown to preclude universality of cosmic rays 9-26985
- hot-model, universe, residual radiation, deviation from Planck curve 9-47611
- Hubble constant and motion of sun w.r.t. galaxies 9-43653
- Hubble constant deriv. rel. to kinematics of local super cluster of galaxies 9-33896
- Hubble plot anomalies of quasars explained by gravit. lens image hypothesis 9-41654
- inertia and relatively, reln. 9-47741
- i.r. radiation, primeval fireball thermal rad., universe energy density 9-45590
- i.r. radiation, primeval fireball thermal rad., Universe energy density 9-43506
- isotropic homogeneous universe, extragalactic background rad. 9-26979
- kinematic model allowing for creation of matter, zero-point energy 9-33887
- Lemaître universe model, galaxy formation calc., perturbation theory and Newtonian cosmology 9-31509
- Lifshitz's relativistic theory for gravitational instability, Lagrangian coordinate condition adopted 9-33888
- massive high-velocity (rogue) stars, and trapezia 9-31490
- matter-antimatter separation at high temps., theory 9-42096
- matter-antimatter universe and cosmic ray origins 9-46123
- metagalactic magnetic field, meas. via Faraday rotation of extragalactic radio sources 9-47624
- metagalactic system, expansion in terms of bounce of gas sphere of mars 10^{20} M.? 9-49521
- microwave background radiation, discrete source explanation 9-26978
- Mixmaster universe (Bianchi type IX) and the homogeneity of the universe 9-33889
- model, open, containing rad. and matter, Friedmann solns., props. 9-28981
- neutral matter, eqn. of state and density fluctuations 9-41621
- neutron beta decay in uniform constant mag. field, rel. to early Universe and neutron stars 9-38583
- Newtonian universe, rotating, inevitability of point-singularity 9-40115
- observations and theory 9-26977
- particle creation by gravitational fields during first 10^{-20} sec. of big bang 9-38441
- perturbation of dust models applic. of tetrad formalism 9-31486
- popular survey for general reader 9-43504
- primordial gas clouds, gravitationally bound, formation 9-47616
- quasar red-shift anal., method using combination of gravit. and cosmological factors 9-43583
- radiation, 3°K , background, star light thermalization interpretation 9-28980
- radiative process without infinities, description 9-47614
- radio source counts, improvements and implications for cosmology 9-24819
- recent progress reviewed 9-38031
- red shift, large, in models of clusters of point masses 9-45584
- red shift, new hypothesis 9-26981
- red-shifts, emission and absorpt. of quasars and related objects 9-41653
- relativistic 9-26983
- residual radiation, deviation from Planck curve 9-47611
- Schwarzschild's incompressible sphere, relativistic, iterative scheme for soln. 9-45591
- self-gravitating gaseous mass, stability to non- adiabatic perturbation 9-47637
- self-gravitating system, one-dimensional, collective and collisional effects, theory and results 9-27000
- spatial variations of matter at time of He synthesis from primeval abundance variations 9-26980
- spontaneous emission theory in time-symmetric electrodynamics, consequences 9-41984
- steady state theory, red shift, stellar evolution 9-26982
- T-models, spherically-symmetric, in general relativity theory 9-41620
- T-models of 'sphere' in general relativity theory 9-43507
- transition rate of atomic electron and universe response, in direct particle theory 9-28982
- universe, expanding/inertial systems 9-33884
- universe, expanding, with negative curvature within Einstein-Friedman theory, mass 9-35941
- Universe, mean mass density, distrib. and contrib. of intergalactic H 9-40120
- Universe, quantum mechanical response of, electrodynamic of direction interparticle action 9-47612
- universe expansion, Hubble effect interpretation 9-49523
- universe rot., discussion 9-24721

Cosmology continued

- viscosity calcs., effect of various cross-section energy dependences 9-49520
- X radiation spectrum isotropic determ. by single mechanism 9-49564
- X-ray background, soft, recent meas. 9-47615
- the ν sea, briefly reviewed 9-38029
- H, intergalactic, distrib. and contrib. to mean mass density of Universe 9-40120

Cosmotron *see Particle accelerators*Costa Ribeiro effect *see Dielectric phenomena; Phase transformations*Cotton-Mouton effect *see Magneto-optical effects*Cottrell atmosphere *see Crystal imperfections/dislocations*Couette flow *see Flow; Hydrodynamics***Counters**

- see also Ionization chambers*
- correlation techniques, appl. to locating structure in expt. data 9-44075
- electrometer, wideband integrating, for weak fluxes 9-25528
- n. nuclear physics, review 9-36555
- photoelectron, techniques and applications 9-47921
- photon, vacuum u.v. region, penetration of water vapour 9-22368
- propane bubble chambers as low level counters for H^1 and C^{14} 9-36534
- soft X-ray, open mag. and channel multipliers 9-48225
- telescope, aperture junction and ang. distrib. determ. 9-25531
- γ detection efficiency, absolute calibration method 9-36506
- ^3He , wall effect for incident thermal neutrons 9-44091

accessories

- see also Counting circuits*
- circuit for proportional counter, cascade shaping with current amplifier 9-29630
- mixer circuit for improving performance of BF_3 counter bank for neutron time-of-flight meas. 9-29646

Cherenkov

- light rendered isotropic by use of POPOP 9-29656
- liquid H, improved to compare π^+ and π^- lifetimes 9-29655
- with water dielectric, directional but non-focusing, for relativistic muons 9-22643
- H liq. target, π^- interaction pt. localization 9-27591
- π^- interaction with H liquid target, interaction pt. localization 9-27591

crystal

- glass (mica) etch-pit method for neutrons 9-22914
- mica and glass detectors for neutron beam recording 9-34360

Geiger

- conversion with replaceable window 9-38613
- direct reading of flux and dose rate 9-22659
- easily heated, detecting α , β , γ radiation and suitable for meas. of exoelectron-glowcurves 9-29652
- self quenching, stabilization of working conditions 9-36513
- u.v. sensitive, with reverse quench voltage, patent 9-42132
- β flux recording inside β -emitting medium 9-25508
- Ar- alcohol, self-quenching, photon spectrum in discharge, obs. 9-25507

operation technique*see also Counting circuits*

No entries

proportional

- automatic gain control, for X-rays 9-25509
- cosmic ray neutron monitor for OGO-F, design 9-36500
- cyclohexane overfilled, circuit and characts. 9-29630
- flow type for wide temp. range, patent 9-34357
- gas, computer analysis of p recoil rel. to n spectra 9-22660
- gas-filled, ageing effects 9-48217
- proton recoil counters with multiple radiators, fast neutron dosimetry designs 9-27587
- proton recoil counting, spectrum distortion from amplifier overloads 9-42133
- pulse attenuataion computed 9-46136
- recoil-proton, graphical analysis of data to give neutron line spectra 9-48218
- wall-effect correction calc. for n spectrometry 9-29651
- waveform attenuation by amplifier with equal RC time const. 9-25510
- wire chambers using gas discharge 9-38614
- BF_3 n detection system, radial array, investigation of response 9-25506
- H, p energy loss through ionization 9-46137
- ^3He , in polyethylene moderated neutron detectors 9-48227

scintillation

- alkali halide crystals, impurity-centre distrib. laws, crystallochem. analysis 9-23798
- anthracene crystal scintillator, effect of zone refining on pulse height and shape 9-42136
- anthracene screens, prep. and props. 9-39860
- calibration using variable energy γ -rays 9-42006
- coincidence method, optical ionic feedback in photomultipliers 9-32254
- cylindrical, in axisymmetrical γ fields, calc. of efficiency and cross-section 9-48221
- cylindrical, in oblique γ field, calc. of efficiency and cross- section 9-46139
- Disperse scintillator system, efficiency for β -active substances 9-22670
- liquid, (NE 213), with neutron- gamma discrimination technique, description 9-22667
- liquid, calibration optimisation 9-22668
- liquid, computation of channels ratio, theory 9-48219
- liquid, deuterated-benzene based, for simultaneous capture and fusion cross section meas. 9-44224
- liquid, stabilization 9-25512
- organic, combined with Si photodiode for high energy charged particle detect. 9-42139
- overload error 9-25513
- p-quaterphenyl, crystal scintillator, effect of zone refining on pulse height and shape 9-42136
- phosphorescence transfer to bottle, solvent and additives in the presence of scintillator 9-38616
- plastic, detection eff. for 20-170 MeV n 9-25515
- plastic, in miniature neutron detector 9-36515
- plastic scintillators, light attenuation characts., use in large area particle detectors 9-22669
- plastic scintillators, light transit time compensator 9-40457
- plastic scintillators, NE102A, 'tail to peak' ratio for incident protons 9-42137

Counters continued**scintillation continued**

- quench correction and compensation for activity dependency on scintillator volume 9-38618
 radioactivity meas. on transparent liquids 9-34358
 small animal and infant, performance and calibration 9-38617
 solid state, for high energy charged particles 9-42138
 spectrometer, electronic elimination of noise pulses 9-40456
 telescope for cosmic ray studies, design and testing 9-25490
 trans-stilbene, crystal scintillator, effect of zone refining on pulse height and shape 9-42136
 α , specimen holder, design 9-44085
 β , 2π detector for low activities, using plastic scintillators 9-36514
 n detector with simultaneous meas. of time-of-flight and co-ordinates of interaction point 9-34359
 u inelastic scattering cross section meas., insensitive to γ -rays 9-22787
 CsI(Na) pulse shape, decay time, response function to charged particles 9-22666
 CsI(Tl) scintillator-Si photodiode, combination for γ -ray spectrometry, 180 keV to 1.5 MeV 9-27590
 He, mechanism and performance 9-48220
 Li glass detection bank for time-of-flight neutron meas. with reactor 9-25516
 NaI, cylindrical, in oblique γ fields, calc. of efficiency and cross-section 9-46139
 NaI, in Linac thick target bremsstrahlung spectra meas. 9-32276
 NaI cylindrical, in axisymmetrical γ fields, calc. of efficiency and cross-section 9-48221
 NaI(TL), internal energy standardization using 0.511 MeV annihilation and ^{40}K peaks, computer method 9-29649
 NaI(Tl), γ -ray pulse-height distrib., description using analyt. functions 9-22665
 NaI(Tl), γ ray emitting nuclides, whole body counting, techniques comparison 9-27119
 NaI(Tl), X-ray detection, ratio of 'escape-peak' to photo-peak 9-25514
 NaI(Tl) crystal calc. of No of photons emitted per scintillation 9-29654
 NaI(Tl) detectors, imbedded into or external to cylindrical gamma source, efficiency 9-42135
 NaI(Tl) efficiency calc, from liq β emitters activity obs. 9-22754
 NaI(Tl) total absorption detector, for γ and e in 4 to 14 GeV range 9-32255
 NaI(Tl) γ ray emitting nuclides, whole body counting, techniques comparison 9-27120
 for Pu extraction from irradi. fuel monitoring, in-line α -counters 9-32256

semiconductor

- applications 9-38619
 γ rays, avalanche-tunnel diode detector high temp. characts. 9-25524
 γ -ray, suitability of GaP-GaAs system 9-26539
 charge collection time and plasma eff., theory 9-25518
 contoured detectors, for i.r. and gamma 9-25527
 cryostat for, internal liquid circulation and swivelling cold finger 9-36520
 current pulse evaluation from Ramo theorem, energy balance eqn. 9-22672
 ΔE -E solid state, use of on-line computer 9-29657
 with diodes, 4-layer 9-48223
 energy and time resolution, efficiency 9-38619
 gamma ray detectors, material requirements 9-25522
 integrated E and dE/dx particle detectors made by ion implantation 9-48222
 ion implanted, window thickness, pulse height defect obs. 9-42142
 ion implanted contacts, conc. distrib. calcs. 9-42143
 noise, low frequency, analysis by correlation, at surface barriers 9-36521
 preamplifiers, charge sensitive, for use with solid state detectors 9-29658
 time delay effects for heavily ionizing particles due to plasma 9-44088
 for α -particle spectrometry design 9-34356
 e detection in high intensity γ background, counter width depend. 9-36526
 CdTe, γ detection props. 9-25523
 CsI(Tl) pulse shape discriminator for use with 9-25539
 GaAs γ detection props. 9-25523
 Ge, ion-implanted, preparation and performance 9-42144
 Ge, migration and precipitation of Li, control for detector production 9-26557
 Ge (Li), efficiency calibration, 8-98 keV, using X-ray machines 9-44086
 Ge (Li), testing, suitable γ source 9-29662
 Ge characterization 9-27592
 Ge(Li), appl. to reaction independent analysis of γ -ray ang. distrib. 9-42262
 Ge(Li), coaxial, charge trapping effects 9-36517
 Ge(Li), coaxial, well-type, for sum spectra of coincident gamma rays 9-36524
 Ge(Li), cryostat for, internal liquid circulation and swivelling cold finger 9-36520
 Ge(Li), cryostat. for detector 9-44089
 Ge(Li), determ. of Fano factor of Ge at 77°K 9-42145
 Ge(Li), efficiency and vol. rein. 9-25517
 Ge(Li), fast-timing data energy walk, pulse height compensation system 9-29659
 Ge(Li), γ -ray linear polarization sensitivity 9-38460
 Ge(Li), line shape anal. of γ -ray spectra 9-22711
 Ge(Li), p-i-n, reproducible method of chemically forming surface 9-46140
 Ge(Li), signal time meas., filter and discriminator techniques comparison 9-36519
 Ge(Li), ultra-high resolution, for low and high energy X-ray and γ -ray meas., characts. 9-36523
 Ge(Li), X-ray escape simultaneous with photopeak obs. 9-29661
 Ge(Li) 2 crystal Compton spectrometer, γ spectra meas. 9-27584
 Ge(Li) coaxial, undegated region eff. on Doppler-broadened line shape 9-32260
 Ge(Li) coincidence studies, β -decay of 18.6h decay of ^{159}Gd 9-38690
 Ge(Li) detector, γ -ray response characts., 0.1 to 2MeV. expt. determ. 9-42141
 Ge(Li) detector, resonance energy and yield meas. in $^{27}\text{Al}(\text{p},\text{p})^{28}\text{Si}$ 9-32258
 Ge(Li) detector, semi-empirical efficiency curve for 50 to 1400 keV γ -rays 9-42140
 Ge(Li) detector for high resolution γ -ray spectrometry, pulse pile-up problem 9-25521

Counters continued**semiconductor continued**

- Ge(Li) detector used in college expts. to meas. photoelectric, Compton, pair-production cross-sections 9-36522
 Ge(Li) diodes, applications 9-38619
 Ge(Li) rectangular detector drifted from 5 sides, collimated γ beam, pulse shape characteristics 9-32261
 Ge(Li) relative photopeak efficiency using ^{152}Eu source 9-22673
 Ge(Li) cylindrical, detection efficiencies calc. 9-32257
 γ -ray spectra computer analysis using photopeak method 9-48224
 Li drifted, charge collection variation with particle impact point, correction 9-44087
 NaI, γ - γ ang. correlation meas., 7 detector goniometer 9-32262
 NaI(Tl) crystal, dimensions, background and peak efficiency, 0.2-4 MeV 9-32259
 Si, 4 π geometry in β spectrometer 9-36511
 Si, surface barrier type, for low energy H^+ , He^+ , N^+ , Ne^+ and Ar^+ 9-36518
 Si amplifying, for portable gamma-ray survey meters 9-36525
 Si characterization 9-27592
 Si drifted, charge collection process with assumption of inhomogeneous elec. field 9-25519
 Si ΔE detector for π energy meas. 9-44090
 Si pn junction for high temp. operation 9-25525
 n-Si surface barrier detector mag. fields up to 60kOe, 4.2°K 9-41229
 Si surface barrier detector for charged particles at relativistic energies 9-42146
 Si(Li), Fano factor meas. 9-29660
 Si(Li) together with low noise preamplifier for meas. of low energy radiation 9-29660
- spark**
 pulse waveform generation 9-22663
 sensitivity in air meas. 9-22664
 γ cosmic ray detection from Crab nebula 9-35962
- statistical analysis**
 dead time in counters, soln. of 'inverse' problem 9-36507
 deadtime losses, automatic compensation 9-29645
 detectors, paralyzable and non-paralyzable and with dead time 9-29644
 discriminator thresholds, automated measurement and monitoring system for multiple channels 9-36533
 Lorentzian parameters, propag. of statistical counting errors 9-42127
 multichannel analyser in combination with on-line computer 9-27598
 nucleon flux intensities in atmosphere, calculated specific yield functions for neutron monitors 9-29634
 Poisson statistics analyzed for the student 9-46129
 resonance, oscillator distrib., calc. method 9-22652
 solid angle corrections, difficult geometry, Monte Carlo method 9-42126
 time-of-flight methods in n spectrometry, novel high-duty-cycle methods 9-29648
 γ astronomy expt., single set of variables 9-32241
 NaI slabs, γ -ray imaging props., detector scatt. effects, Monte Carlo calcs. 9-40458
- Counting circuits**
 amplifiers and discriminators, overload causing error in liquid scintillation counting 9-25513
 analogue-digital converter, fast, for pulse spectroscopy 9-29669
 avalanche-tunnel diode, γ detector, high temp. characts. 9-25524
 coincidence, double and triple, efficiency or resolution determ. method 9-25537
 coincidence, flexible system, 5 nsec to milliseconds resolving time 9-42151
 coincidence techniques for ^{198}Au foil absolute disintegrate rate meas. 9-32325
 coincidence techniques for meas. of level lifetimes in picosecond range 9-42150
 coincident pulses of β - γ , delay matching, gating analyzer 9-32267
 correlation unit, integrated, for n=4 variables 9-22679
 dead-time method, Rossi- α meas. 9-34349
 differential converter for nuclei lifetimes meas. 9-42148
 discriminator, fast amplitude, nanosec. pulse ≤ 10 megapulse/sec 9-32270
 electron-gamma ang. correl. arrangement 9-25499
 meter, logarithmic of wide dynamic range and having 8 decades 9-29667
 multichannel analyzer for separation of decay product background in α decay of ^{227}Th 9-22752
 pulse and freq. counter based on plastic integrated circuits 9-29362
 pulse attenuator with very low transit time variation 9-25536
 pulse converter, nanosecond, 7 bit A/D, sensitivity and circuit 9-25534
 pulse height analyser, multichannel, summing unit and visual readout 9-32266
 pulse height analyzer, multichannel, with memory, for space vehicles 9-38024
 pulse height analyzer, 150000 channel, 2 parameter, use of digital computer 9-44092
 pulse height analyzer, multi-channel, multi-parameter, design 9-36532
 pulse height analyzer and associated equipment for satellite appl. 9-42149
 pulse height compensator, non-linear, for time-to-amplitude converters 9-42147
 pulse height spectra, resolution using numerical least square method 9-22173
 pulse shape discriminator, 0.3-10V, risetime 0.2-10 μsec , design and applic. 9-32269
 pulse shape discriminator, high resolution of n, γ spectra simultaneously 9-29670
 pulse shape discriminator for use with CsI(Tl) detector 9-25539
 pulse shaping network, use in improving signal-to-noise ratios in β activity meas. 9-44170
 ratemeter, optimum value for duration of weighing function 9-25538
 ring counter, tunnel diode-transistor, improvements 9-44093
 secondary electron multipliers for soft X-radiation recording 9-38606
 time-to-amplitude converters, testing for linearity 9-29668
 time-to-pulse height converters, chance coincidence anal. 9-22678
 β - γ activity coincidence meas., automatic correction digital apparatus 9-22750

CPT (charge, parity, time) conservation see *Elementary particles/symmetry; Kaons/decay; Parity*

Cracks

- alloys sintered two-phase, formation 9-42902
 bearing metals, fatigue cracks by reciprocating rubbing 9-41032

Cracks continued

- α - brass, stress-corrosion $\text{CuSO}_4/(\text{NH}_4)_2\text{SO}_4$ soln., role of soln. variables 9-26352
- ceramic/glass mats., two-phase, crack formation due to applied stress around spheres 9-30677
- ceramics, interaction with microstructure, monitoring technique 9-33091
- circular external, thermal stress 9-45836
- continuum mechanics model 9-28371
- coplanar circular, stress distrib. for shear loading in infinite solid 9-47813
- copper phthalocyanine, config. of bordering atomic planes 9-42904
- detection, magnetic 9-39436
- dimension, rel. to fracture theory 9-48910
- disc-shaped, fatigue growth 9-33089
- edge perp. to half-plane, Wiener-Hopf technique, stress and displacements determ. 9-38281
- elastic solid, external elliptical crack, pot. functions and stress-intensity factors 9-33088
- electron fractography, two-stage replica technique using Bieden 9-39151
- erosive rupture due to friction and fluid flow around surface, mechanism 9-23912
- external, in infinite solid, steady state thermoelastic stress distrib. in vicinity 9-27211
- fatigue, in fuselage panel, vibration characts. 9-40273
- fatigue, propag. in mild steel, effects of stress history and corrosive environment 9-37262
- fatigue, propagation under dynamic stress 9-44777
- fatigue, tip deform. process, obs. using fatigue tester with micrographic apparatus 9-42896
- fatigue crack propag. and initiation in low cycle strain controlled fatigue 9-30683
- fatigue crack propag. nucleation theory elastic-plastic stress distrib. near crack tip effect 9-46909
- fatigue cracking during cyclic deform., model 9-30682
- fatigue cracks prod. by rolling, effect of surface-active subst. on origin 9-46907
- fatigue failure probability, rel. to heterogeneous dislocation assembly 9-23809
- fatigue growth of disc-shaped crack 9-33089
- formation, connection with slip lines 9-26335
- formation of microcrack at dislocation pile-up, activation energy 9-33086
- glass, cleavage crack propag. 9-30697
- glass, growth, effect of environment 9-48879
- glass/ceramic mats., two-phase, crack formation due to applied stress around spheres 9-30677
- Griffith, asymmetrically loaded surfaces, stress intensity factors 9-41792
- growth during cyclic loading 9-39437
- in heterogeneous media, anti-plane strain behaviour 9-33090
- ice, creep depend. of crack form. 9-44781
- low-stress failure, prediction from fracture toughness concept 9-28363
- metal carbides, refractory, surface layer fracture due to giant laser pulses 9-44774
- metal cylinders, thin-walled, explosively-loaded, fragmentation behaviour expansion velocity and material parameter dependence 9-42901
- microcrack linking, statistical model 9-30693
- monitoring techniques for propagation in polycrystalline ceramics 9-33091
- nucleation, thermally activated, rel. to dislocation pile-up structure 9-42817
- penny shaped, dynamic stress intensity factor for axisymmetric loading 9-22201
- penny shaped in elastic medium, response to plane harmonic shear wave 9-29228
- plastic energy dissipation due to penny-shaped crack 9-33033
- plastics, fiber reinforced, microcracking, elec. and luminescent effs. 9-26351
- polycapromide, stressed, submicroscopic, features of growth 9-33097
- polycapromide, submicroscopic, formation under load 9-33096
- polyethylene, nonorientated, 'silver' crack formation during creep 9-23925
- polyethylene film, zone structure near tip 9-28373
- polymers, nonoriented crystalline, 'silver' crack formation during creep 9-23925
- polymers, stressed, submicroscopic, charact. features of growth 9-33097
- polypropylene, submicroscopic, formation under load 9-33096
- polypropylene film, zone structure near tip 9-28373
- polyvinyl butyral, stressed microscopic, charact. features of growth 9-33097
- polyvinyl butyral, submicroscopic, formation under load 9-33096
- polyvinyl chloride, stressed, submicroscopic, charact. features of growth 9-33097
- polyvinyl chloride, submicroscopic, formation under load 9-33096
- propagating in quasi-brittle materials, quasi-state thermoelastic anal. 9-33087
- propagation in solids 9-45810
- rock, fracture dynamics 9-33062
- steel, 300M, propagation rel. to fracture toughness 9-33067
- steel, austenitic stainless, fracture paths of stress corrosion cracks 9-39441
- steel, austenitic stainless, stress corrosion, susceptibility in chloride-containing high temp. water, effect of composition 9-26355
- steel, brittle fracture with interaction between elastic crack and slip band, criterion 9-44779
- steel, C-Mn, quenched and tempered, critical crack opening displacement for fracture 9-30690
- steel, carbon, initiation and propag. under sinusoidal loading, obs. 9-30695
- steel, carbon, rel. to fatigue limit and branch point size effects, obs. 9-33078
- steel, cast, fatigue crack propag., microfractographic investig. 9-33080
- steel, fatigue crack propagation, effect of mean stress and material yield stress 9-30696
- steel, high-strength, plane of strain fracture toughness rel. to precracked Charpy W/A 9-35182
- steel, mild, surface-rolled, crack formation during fatigue, electron microscope obs. 9-35189
- steel, rail, fatigue, structure effect on rate of propag. 9-33092
- steel, stainless, in MgCl_2 soln., transgranular stress-corrosion cracking, interpret. 9-26349
- steel, stainless SUS 29, during thermal fatigue, 200-700°C 9-26353

Cracks continued

- steel, susceptibility to brittle cracking, effects of residual stresses and strain ageing 9-39439
 - strength calculation methods for sheet-metal parts with cracks 9-23919
 - stress distribution around holes drilled at ends 9-47801
 - stress-corrosion, electrochemical parameters 9-23918
 - stress-corrosion cracking, mechanical parameters 9-23917
 - stress-corrosion cracking, transgranular, interpretation 9-26349
 - stresses and displacement, elasticity theory 9-29231
 - tip, stress and strain intensification 9-37249
 - unstable elastic-plastic fracture brittle criterion rel. to energy balance considerations 9-44775
 - viscous fibres, propag. through layer between two elastic half-planes, tearing 9-33061
 - wedge, growth rel. to creep failure, model 9-48899
 - in wedge, mixed boundary value elasticity problems 9-31820
 - Zircaloy-2, irradi., rel. to fracture in BWR and PWR conditions, obs. 9-37258
 - Zircaloy-2 tubes, critical length for failure rel. to neutron irradi. and hydride precip. 9-39435
 - Al- Al_2O_3 , sintered two-phase, formation 9-42902
 - Al- Al_2O_3 alloys, formation, rel. to creep behaviour at 450°C 9-46898
 - Al-Zn-Mg-Cu alloy, deformed, intergranular stress corrosion cracking, rel. to dislocation structure 9-23811
 - Al, coarse slip model of formation and propag., rel. to fatigue 9-48904
 - Al, fatigue crack initiation and propag., correlation, effect of substructure, 9-30685
 - Al, growth during fatigue, effect of air pressure 9-46906
 - Al alloys, cracking, stress conc. influence 9-44778
 - Al alloys, fatigue crack propag., microfractographic investig. 9-33080
 - in Al alloys, stress corrosion, detection using Rayleigh waves 9-42704
 - Al in vacuum, cyclic fatigue, fatigue eff. on crack propag. 9-28364
 - B filament vapour deposited on W, rel. to chem. interaction 9-48866
 - Cd, fatigue crack nucleation 9-32981
 - Cr, polycrystalline, nucleation and propagation, importance in cleavage fracture 9-39438
 - Cu-Mn alloys, stress-corrosion cracking, electrochem. factors 9-23920
 - Cu-(36wt.%) Zn alloys, stress-corrosion cracking, electrochem. factors 9-23920
 - Cu, coarse slip model of formation and propag., rel. to fatigue 9-48904
 - Cu alloys, transgranular stress-corrosion cracking, interpret. 9-26349
 - Cu and alloys, stress cracking by liq. metals 9-48941
 - Cu cycled single cryst., fatigue crack formation and propag., model 9-30682
 - Cu films on Zn-(3 wt.%)Cu alloy, rel. to grain boundary reaction type precip. in alloy 9-23957
 - Cu single cryst., propagating fatigue crack, dislocation substructure. 9-33077
 - Fe-C alloy, microcrack formation, statistical analysis 9-30694
 - Fe-(3 wt.%)Si single crystals, nucleation, effect of stress concentrations 9-48911
 - Fe, H-charged, nucleation mechanism, fracture surfaces electron microscope obs. 9-39440
 - Fe ore, sintered, reduction cracking 9-33093
 - Ge, partial splits, chem. etching 9-44780
 - LiNbO_3 , crack nucleation obs. after plastic deform. due to mech. twinning 9-23887
 - Mg, coarse slip model of formation and propag., rel. to fatigue 9-48904
 - Mg, fatigue crack nucleation 9-32981
 - MgO , propag. in water, increased roughness of fracture surfaces obs. 9-42906
 - Mo, polycryst., crack nucleation at ductile-brittle transition 9-30742
 - Si, partial splits, chem. etching 9-44780
 - Ti-(6 wt.%)Al-(4wt.%)V alloy, stress-corrosion cracking in anhydrous methanol, mechanism 9-48894
 - Ti-(8wt.%)Al-(1wt.%)Mo-(1wt.%)V alloy sheet, hog-salt-stress-corrosion cracking and effect on tensile props. 9-23923
 - Ti, fatigue crack nucleation 9-32981
 - Ti alloys, hot-salt stress corrosion cracking initiation 9-37265
 - Ti alloys, stress-corrosion resistance, eff. of ht. treatment 9-37264
 - Ti alloys, stress-corrosion cracking in aq. NaCl at room temp. 9-23921
 - Ti alloys, stress corrosion in methanolic soln. 9-23922
 - Ti alloys, tolerance, influencing factors, review 9-37263
 - Ti alloys fatigue crack propagation, eff. of 3.5% NaCl aqueous saline environment 9-23924
 - U foils <2000 Å, preparation for electron microscopy rel. to stress corrosion cracking 9-32777
 - W, cleavage velocity determ. with u.s. fractography 9-33094
 - W single crystal, <100> cleavage, 77°K 9-33095
 - Zn, fatigue crack nucleation 9-32981
 - Zn bicryst., grain-boundary crack formation during deform. at high temp. 9-30698
 - Zr-Cu reactor fuel claddings in CO_2 , and oxidation, obs. 9-37266
- Cracking model** see *Nucleus/theory*
- Creation of electron pairs** see *Electron pairs*
- Creep**
- see also *Slip*
 - alumina, polycrystalline, compressive characts. 9-37244
 - brass, temperature after-effect 9-23896
 - β brass single cryst., behaviour near T_c 9-30668
 - buckling of viscoelastic beam column, isothermal conditions, soln. bounds, computer determ. 9-32887
 - creep-rupture expts., density meas. interpretation 9-39417
 - cyclic loading of tube, incremental calc. 9-23893
 - cylindrical shells, stress anal. under combined lateral and axial press. 9-31805
 - diffusion, under neutron irradiation 9-28308
 - dispersion struct., and relax. under humidity fluctuations 9-44601
 - ductility, effect of helium gas bubbles, on austenitic alloy 9-41021
 - failure from wedge crack growth, model 9-48899
 - rel. to fracture and mechanical strength, interdisciplinary approach, book 9-39431
 - ice, crack form depend. 9-44781
 - Inconel 625, n. irradi., creep strength reduction, 650°C 9-37250
 - life fraction hypothesis in creep testing, reaction-rate treatment 9-33041
 - magnetization, of cross-tie walls 9-49208
 - materials hardened by a second phase, recovery creep model 9-28354
 - metals, effect of superimposed vibrs. 9-39419
 - metals, fine grained, strength rel. to diffusion creep 9-46897
 - multiaxial damage eqn. modification and tangential rate 9-23892

Creep continued

- Nimonic 80A, under static and superimposed cyclic stresses 9-33048
polyacrylonitrile, and recovery meas. of rheo-optical behaviour 9-46900
polycarbonate craze, cyclic stress-strain behaviour, recovery 9-46879
polyethylene, nonoriented, 'silver' crack formation 9-23925
polymer relaxation, treatment including co-operation in molecular motion 9-23189
polymers, nonoriented crystalline, 'silver' crack formation 9-23925
polyurethane, nonlinear viscoelastic, stress relax., torsion creep 9-31838
primary creep model, from extension of Weertman's secondary model 9-44768
recovery creep model for mats, hardened by a second phase 9-28354
refractory materials, compressive characts. 9-37244
rupture, of 347 stainless steel at high temp. 9-33064
sapphire single crystal, high-temp., rel. to dislocation climb 9-30658
shells, stress anal. of creep buckling 9-31808
soil, rheological model considering structural transformations 9-26332
steel, austenitic, TiC particles plastic deform. and recrystn. 9-33045
steel, stainless, annealing of creep fracture damage 9-39457
steel, stainless, type 347, creep rupture at high temp. 9-33064
in steel at 550 and 565°C, obs. 9-35177
steel castings, 18-8 Mo stainless, creep-rupture test, high temp. strength obs. 9-44771
steels, 5Cr-0.5Mo, double notch creep rupture 9-33046
stochastic model, identification of flow units with dislocation segments 9-33040
stress redistribution time in creep in mechanical structures 9-22189
stress relaxation with inhomogeneous stress, const. determ. 9-35176
super-strength alloys, high temp. effect 9-33056
testing, reaction rate treatment of extrapolation methods 9-33042
testing, temp. meas. and control 9-39420
viscoelastic mat. as series of Kelvin models, running total of creep strain rel. to numerical method of stress analysis 9-27210
viscoelastic materials, linear, error functions 9-33019
Zircaloy, during neutron irradi., theory rel. to strain rates and defect form. 9-41023
Zircaloy during neutron irradi., in-pile behaviour and rad. enhanced climb mechanism obs. 9-28356
zircon, sintered, compressive characts. 9-37244
Ag, high-temp., contrib. to material transport in sintering 9-46916
Ag, stacking fault energy effect 9-39421
Al-Al₂O₃ alloys, behaviour at 450°C, rel. to crack formation 9-46898
Al, quenched and aged, rel. to plastic flow mechanism, 86°C 9-48900
Al, stacking fault energy effect 9-39421
Al axial stress variation eff. studied 9-39422
Al single crystals, dislocation motion in plastic flow during creep tests 9-30675
C, and dimensional changes, irradi. induced, rel. to struct. 9-41022
C, pyrolytic, deform. at high temp., from tensile stress in basal plane 9-39412
Cd single cryst., liq. He temp. 9-23895
CdS transient and steady, produced by bending at 200-400°C, influence of crystallographic orientation 9-42885
CoO scales, strength rel. to oxide stoichiometry 9-23882
20 wt.%Cr-35 wt.%Ni steel, rate at low stresses rel. to grain boundary sliding 9-48901
Cr-Ni-Nb stainless steel, annealing of creep fracture damage for irradi. and unirrad. samples 9-39457
Cu-(16 at.%)Al solid soln., high temp. 9-33043
Cu-Al solid solns., high temp., stacking fault energy influence 9-42887
Cu-Al solid solns., high temp., stacking fault energy influence 9-42886
Fe-(0.75 wt.%)Mn alloy, recovery processes 9-26334
Fe-Mo solid solns., stationary and transient creep, temp. and stress depend. 9-30669
 α -Fe, high temp. 9-30670
 α -Fe, tertiary, recovery meas. 9-39423
Hg single cryst., liq. He temp. 9-23895
Mg-Mn alloys, rel. to α -Mn precipitation, e. microscope exam. 9-28265
Mg-Zr alloy, in constant-load tests, curve anal. 9-30673
Ni-(1.18 at.%)Al alloy, effect of ultrasonic vibrations, 700°C 9-33047
Ni-Fe alloys, 550°-1000°C obs. 9-23897
Ni-Fe thin-films, 30 to 300Å thick, props. with creep observations 9-45068
Ni, behaviour after oxidation 9-39424
Ni, rel. to low-temp. hardening, electron microscope obs. 9-46913
Ni, stacking fault energy effect 9-39421
Ni alloys, cast or wrought, creep-rupture strength rel. to grain size and specimen size 9-37245
Ni alloys, re-heat-treatment eff. 9-23898
Ni base alloy, dispersion-hardening, grain size effect on resistance 9-33015
NiAl, stoichiometric, behaviour 9-28355
Pd, stacking fault energy effect 9-39421
Pt, stacking fault energy effect 9-39421
Pt annealed wire, transient rate 1270° to 1830°K 9-33024
Ti-(8 wt.%)Al-(4 wt.%)Co alloy, creep rupture props. rel. to heat treatment 9-40994
Ti-(8 wt.%)Al-(4 wt.%)Co alloy, creep rupture strength 9-23956
UC_{1.06}, compressive creep, 1200-1600°C, 3000-10,000 psi 9-23899
W-UO₂ cermet produced from coated particles, high temp. creep-rupture tests 9-23910
Zn single cryst., activation vol. determ. 9-39426
Zn single cryst., γ quanta irradi. effect anisotropy 9-39425

Critical constants, thermal

- alkali metals, parameters, and heat of vaporization 9-40828
alkane mixtures, Prigogine corresponding states theory and cell model prediction 9-42691
of Bose gas, dilute, hard sphere 9-47783
critical opalescence, nonlocal hydrodynamic eqns. 9-23576
fluids, thermodynamic and transport props. at critical point, singularities 9-26152
Freon 22, critical temp. meas. 9-36805
gas-liquid critical point, lattice gas model 9-36924
interface near crit. pt., struct. and free energy 9-42641
Ising model, three regular three- dimens. lattices, high-temp. critical props. 9-41775
light scatt. near critical point for fluids and non-fluids 9-36876
3-methylpentane-nitroethane coexistence curve near crit. pt. 9-23577
phase transition, second-order, impurity effects near critical point 9-46678

Critical constants, thermal continued

- temperature, acoustic method of determ. 9-39128
thermodynamic perturbation theory applied 9-34036
Ar, isothermal compressibilities and densities, theory and expt. 9-28174
Ar with admixed Ne and deuterium, meas. of self-diffusion in gas-liquid region 9-36828
CO₂, internal energy meas. near critical point, gravity effect 9-36916
Critical mixtures see *Solutions*
Critical opalescence see *Phase transformations; Solutions*
Crowdions see *Crystal imperfections/interstitials*
Cryogenics see *Cryostats; Low-temperature/phenomena; Low-temperature production; Low-temperature technique*
Cryopumping see *Vacuum pumps; Vacuum technique*
Cryoscopy see *Freezing; Low-temperature production; Low temperature technique*
Cryostats
for 1-300°K range 9-47707
continuous flow, for thermally stimulated currents in dielectric films meas. 9-45015
for crystal spectroscopy under uniaxial compression 9-38167
cylindrical, for luminescence tests at 55°K (solid N₂) 9-38168
for deformation (plastic) expts. down to 77°K 9-27144
for electron irradiation and subsequent photoconductivity studies of semiconductors 9-31724
glass and metal type for tests in 60°-300°K temp. range 9-33986
for low-temperature cables, patent 9-43692
Mossbauer absorber, in liquid He dewar 9-36091
precision automatic temp. regulator for 4.2-300°K range 9-27141
for semiconductor detector 9-44089
for Ge(Li)-detectors with internal liquid circulation and swivelling cold finger 9-36520
He liq., continuous transfer, field ion microscope appl. 9-38364
Cryotrons see *Superconducting devices*
Crystal chemistry
alkali halide scintillators, impurity-centre distrib. laws, crystallochem. analysis 9-23798
alkali-rare earth niobates with tungsten bronze structure, rel. to dielec. props. 9-24210
biotites, Fe ordering and ferrous-ferric ratio, Mossbauer obs. 9-41367
calcium chlorapatite, pure and Sb-activated, and luminescence 9-24444
calcium phosphates, pure and Sb-activated, and luminescence 9-24444
diethyldithiocarbamates of uranyl, two monoclinic polymorph phases 9-23787
electronegativity in covalent systems, quantum dielec. theory, electronic dielectric constant 9-46735
faujasite, dehydrated La-exchanged, position of mols. and cations at 420°C 9-32899
ferrites, spinel 9-45174
fluorides effective ionic radii 9-39182
group III-V compounds, habit and morphology, infl. of solvent and impurities 9-36981
group IV-VI cpds. and alloys, deviations from stoichiometry and lattice defects 9-39483
ilvaite, iron oxidation states and site symmetries determ. by Mossbauer spectrometry 9-24381
ion implanted crystals, investigation using directional effects in charged particle reaction yields 9-30598
ionicity, dielectric definition 9-38820
i.r. beam control, data for crystallochemical selection of materials 9-38394
isomorphic group construction, many-coloured, reln. with mag. group 9-28240
lanthanide metals and alloys, polymorphic struct., stacking sequence and influence of 4f electrons 9-30509
magnesium aluminate spinels, variable stoichiometry growth and characterization 9-37084
metal oxide solid solution formed on alloy oxidation, cation distrib. 9-23656
metal sulphide solid solution formed on alloy oxidation, cation distrib. 9-23656
oxide systems, effect of cationic field strengths in liquids 9-23579
oxides effective ionic radii 9-39182
Pa3 space group crystals, theoretical morphology 9-36976
perclase solid soln. containing Li⁺ and R³⁺ (Cr, Al, Fe) ions 9-23955
perovskites, complex ferroelectric, long- and short-range order of ions 9-46696
perovskites, conditions for existence, closer definition 9-46738
potassium trioxaloferrate, Fe(III) activity transfer process 9-39185
rare earth orthoferrites, analysis of Pb substitution in flux grown crystals 9-28237
rare-earth fluoride systems, nonstoichiometry 9-40915
Rochelle salt dielectric relaxation and crystal water stoichiometry, activation energy determ. 9-41234
semiconductors, admixtures with stoichiometric vacancies 9-47095
2,2,4,4-tetramethyl-3-oxoglutaric acid molec. and cryst. struct. 9-48788
transition metal chalcogenides and pnictides 9-26201
vanadium chalcogenides of NiAs-type structure 9-30575
zeolites, rare earth faujasite-type 9-24522
zeolites with faujasite-type framework, distribution of cations and molecules 9-28776
Ba in meteorites and terrestrial samples, isotopic analyses 9-45674
BaF₂, thermal ionization potentials of Nd²⁺, Dy²⁺, Ho²⁺ and Er²⁺ 9-46739
BaTiO₃, rare earths, conc. and diameter of ions, effect on elec. props. 9-39685
Ca-amphiboles, comp. changes and ferrous-ferric Fe ratio, Mossbauer obs. 9-41367
Ca₁₀(PO₄)₆Cl₂, Sb³⁺ solubility 9-42740
CaF₂, lattice distortion for cubic centres with impurity ions Ce³⁺ and Eu³⁺ 9-26198
CaF₂, thermal ionization potentials of Nd²⁺, Dy²⁺, Ho²⁺ and Er²⁺ 9-46739
CdS, nonstoichiometry of crystals grown by different methods 9-36978
CdTe thin film, co-evaporated, stoichiometric deviations, influence on nucleation and structure 9-36949
Cu-S-Ag₂S solid soln. on Cu-Ag alloys, cation distrib. on alloy oxidation 9-23656
CuMn₂O₄ spinel, cation distrib. by neutron diff. meas. 9-40854
Fe-(2 wt.%)Al alloy, Ge effect on internal oxidation 9-46740

Crystal chemistry continued

- Fe-(1 wt.%) Si alloy, be effect on internal oxidation 9-46740
 Fe, eff. of alloying elements on polymorphism 9-35009
 $\text{Fe}_3\text{O}_4\text{-Mn}_2\text{O}_3$ spinel system, chem. structure 9-32856
 Fe compounds, Mossbauer effect of ^{57}Fe , anomalous charge states of Fe, possible origin 9-35637
 FeLiO_2 , short range order, local displacement of ions and electrostatic energy 9-48935
 GaAs:Zn , Ge, Te, impurity segregation rel. to melt. comp., obs. 9-26210
 Ge, habit and morphology, infl. of solvent and impurities 9-36981
 In, coordinate correlation of valence electrons, rel. to structural changes and phase transform. 9-46741
 KCl, ion spherical symmetry determ. from structure factor meas. 9-23760
 LiNbO_3 , stoichiometry of single crystals 9-36977
 Mg_2SiO_4 , high press. modification 9-40908
 $\text{MgO:Al}_2\text{O}_3\text{:Cr}$, variable stoichiometry spinels, growth and characterization 9-37084
 MoS_2 , rhombohedral, geological conditions of formation 9-48782
 Ni-Mo alloy, effective charges and coeff. of diffusion of Ni 9-26202
 NiFe_2O_4 , disordered, Ni^{2+} migration to A-sites, X-band ferrimag. reson. obs. 9-35705
 $\text{NiO-Cr}_2\text{O}_3$ solid soln. on Ni-Cr alloys, cation distrib. on alloy oxidation 9-23656
 PbTe thin film, co-evaporated, stoichiometric deviations, influence on nucleation and structure 9-36949
 PRP, non-stoichiometry occurrence by lattice constant and density variation with composition 9-28268
 S-As mixtures, mol. complexity in cryst. and glassy phases, Raman obs. 9-35675
 S-Se mixtures, mol. complexity in cryst. and glassy phases, Raman obs. 9-35675
 S, mol. complexity in cryst. and glassy phases, Raman obs. 9-35675
 Sc_2O_3 , high-pressure transformations molar volume relationships 9-48779
 Si, habit and morphology, infl. of solvent and impurities 9-36981
 SmB_6 configuration of Sm, rel. to mag. ordering 9-45072
 SnI_4 structure type crystals, theoretical morphology 9-36976
 $\text{Sr}_2\text{CuSi}_2\text{O}_7$, akermanite analog, distorted tetrahedra of Cu^{2+} , X-ray obs. 9-35010
 SrF_2 , thermal ionization potentials of Nd^{3+} , Dy^{3+} , Ho^{3+} and Er^{3+} 9-46739
 $\text{Th}_2\text{Co}_{17}$, intermetallic 2-17 stoichiometry 9-26248
 $\text{Th}_2\text{Fe}_{17}$, intermetallic 2-17 stoichiometry 9-26248
 ThC, chemical bonding and mag. susceptibility at various temp. 9-28224
 $\text{TiO}_2\text{-SiO}_2$ glasses, cation distrib. 9-48781
 UO_2 , nonstoichiometry rel. to flow stress and strength 9-33049
 $\text{Y}_2\text{Al}_2\text{O}_7$, Cr^{3+} and Nd^{3+} impurity distribution, rel. to trivalent oxide solubility and cry. growth 9-36980
 $\text{Y}_2\text{Fe}_2\text{O}_7$, Cr^{3+} and Nd^{3+} impurity distribution, rel. to trivalent oxide solubility and cry. growth 9-36980
 YAl garnet single crystals, optical quality, incorporation of increased conc. of rare earth activator ions 9-37093
 YFe garnet, single crystal, homogeneous distribution of gallium, effect of pressure 9-36979
 ZnO, polarity, chem. etching behaviour obs. 9-32858
 ZnO, polarity, ion bombardment obs. 9-32857
- Crystal classes** see *Crystallography; Crystal structure, atomic*
Crystal counters see *Counters, crystal*
Crystal electron states
 see also *Colour centres*
 alkali halides: Eu^{2+} (Sm^{2+}), zero-phonon transitions 9-37716
 alkali metals, electron-ion interaction rel. to Fermi surfaces 9-26478
 alkaline earth oxides, irradi., electronic states of defects 9-44689
 alloy, binary, long-period superlattice, electron wave functions in periodic field 9-30818
 alloys, 1-dimens. general, Saxon-Hutner theorem proof 9-42989
 alloys, dilute magnetic, ground state energy calc. by Nagaoka-Suhl theory 9-45052
 alloys, electron effects w.r.t. exothermic binding energy 9-39180
 anthracene, two-photon absorpt. transition 9-39795
 anthracene crystals, hole injection from liquid redox electrodes 9-26475
 benzene, isotopically mixed crystals, singlet excited states 9-24097
 benzene isotopic mixed crystals, site effects in vibr. spectrum 9-43007
 conduction electron spin polarization correl. function and localized mag. moment 9-47240
 conduction-electron g shift, derivation 9-41423
 covalent solids, of colour centres 9-28301
 cyclotron and hydrogenic orbital, overlap integral 9-37381
 diamond, neutral isolated divacancy electronic structure 9-46810
 disordered state, Green functions for 'one-body' eqn. description 9-33219
 donor-acceptor pairs radiative recombination rate 9-49306
 duren, doped, energy transfer 9-24458
 effective mass equations, breakdown due to rapidly varying potentials 9-44878
 electron spin waves in nonmag. conductors 9-42990
 electronic structure calcs., point defects in ionic crystals 9-40928
 electrons, hot, in crossed elec. and quantizing mag. fields 9-47029
 electrons interacting with waves in strong d.c. field, calc. of transverse a.c. cond. 9-24082
 electrostatic potential, rel. to multipoles 9-48980
 e.m. oscillations, spontaneous excitation at freq. of several Hz 9-44862
 ferroelectric cryst., phonon states density in paraelec. phase 9-39681
 film with surface defects, decay, and conductivity 9-49016
 Friedel oscillations in screening charge about point impurity, modification by mag. field 9-48982
 GI method for electronic wave function applied to band structure of b.c.c. lithium 9-44887
 group theory applies. 9-46694
 helicon reson. obs. in strong pulsed mag. fields 9-24105
 helicon wave propag. in two-component plasma 9-43014
 helicon waves, giant quantum oscillation, rel. to electron mean free paths study 9-37388
 helicon waves, review 9-26489
 helicons in electron-hole plasma, weak turbulence 9-48550
 hydrogenic and cyclotron orbital, overlap integral 9-37381
 III-V compounds, matrix element of solely spin orbit coupling from second order optical susceptibility 9-35610
 inert-gas crystals, trapped-hole centres, theory 9-42991
 Kondo Hamiltonian, energy of basic state for particular J_z 9-47017

Crystal electron states continued

- lamellar struct., fluctuations of electron density 9-39747
 lanthanide metals and alloys, 4f electrons influence on families of polymorphic struct. 9-30509
 lattices, random, self-contained first-order approx. accounting for exclusion effect 9-24008
 magnetic, e. hopping mechanism from Mossbauer effect 9-26724
 many-electron systems, inhomogeneous, statistical exchange approximation 9-25043
 metal, electron relax. time from magnetoacoustic oscillations and tilt effect 9-47072
 metal, helicons, attenuation and polarization 9-39616
 metal, hot-electron relax., Boltzmann eqn. study 9-47020
 metal, magnetic ordering, coupled spin-plasma waves, interaction with charged particles 9-41297
 metal, screened uniform charge model 9-44864
 metal, slab-shaped, helicon propag., quantum oscillation, dispersion relations 9-43049
 metal, structure-dependent energy, cancellation of orthogonality charge 9-24088
 metal film, quantum oscillations of thermodynamic props. in weak mag. field 9-30812
 metal slab, c.m. wave transmission, effect of boundary scatt. on helicon transmission near cut-off 9-26491
 metals, core electron spectra, characts. structure due to electron-plasmon coupling 9-44861
 metals, nonferromagnetic, interaction of spin and cyclotron waves 9-33427
 metals, phonon frequency and electron-phonon interaction in strong mag. field 9-26471
 metals, pure, electronic props., theory 9-47023
 metals, quantum spin waves in non-ferromag. samples 9-47025
 3-methylpentane, viscosity depend. ionic processes 9-28720
 mixed molec. crystals. 9-24097
 mixed molec. crystals, triplet states 9-24098
 naphthalene, dark injection and radiative recomb. of electrons 9-41212
 naphthalene, isotopically mixed crystals, singlet excited states 9-24097
 operator group in presence of uniform mag. field 9-48983
 oxides, irradi., electronic states of defects 9-44689
 perturbation theory and alloying behaviour formalism 9-44859
 perturbations, spontaneous transverse, in parallel elec. and strong mag. fields 9-42986
 photoconducting materials, electron-hole plasma interactions with lattice vibrations 9-26415
 piezoelectric materials, electron-hole plasma interactions with lattice vibrations 9-26415
 plasmon-photon interaction in electron gas and coupled radiation field 9-22163
 poly(N-vinylcarbazole), carrier mobility 9-43133
 polynucleotides, homogeneous, structure from u.v. absorpt. spectra 9-26750
 positron annihilation in metals, lifetime, γ pairs distribution 9-24112
 pseudo potentials, local, leading to effective interioric pot., rel. to analytic behaviour of electron-ion form factor 9-35305
 pseudopotential, model 9-47026
 pseudopotential, muffin-tin, choosing criteria 9-33217
 pseudopotential theory, generalized, optimized pot. determ. 9-39555
 pseudopotentials, rapidly convergent, reformulation 9-44858
 pseudopotentials applic. to low energy electron diffraction, potential and inner potential calc. 9-44654
 pyrazine, fine struct. of Phosphores. at 4.2°K 9-24463
 quantum electronic spin acoustic waves 9-47027
 quasi particle properties in electron gas 9-26493
 relaxation time determ. from Alfvén waves absorpt in mag. field 9-37382
 RKKY interaction, (S_1, S_2)² form, contrib. 9-35304
 RKKY interaction, soluble model 9-37380
 semiconductor, heating of electrons and phonon bottleneck in crossed elec. and quantizing mag. fields 9-33278
 semiconductor, helicon interferometry and nonreson. cyclotron absorpt. method for props. determ. 9-47100
 semiconductor, helicons, attenuation and polarization 9-39616
 semiconductor, magnetic ordering, coupled spin-plasma waves, interaction with charged particles 9-41297
 semiconductor, slab-shaped, helicon propag., quantum oscillation, dispersion relations 9-43049
 semiconductors, low-resistivity, trap determination technique 9-49094
 semimetal, electron relax. time from magnetoacoustic oscillations and tilt effect 9-47072
 semimetal, helicon interferometry and nonreson. cyclotron absorpt. method for props. determ. 9-47100
 skin-effect acoustic generation in conductors, approx. theory 9-42962
 spin acoustic waves, quantum electronic 9-47027
 Stark ladder in solids 9-47021
 Stark ladder in solids 9-47022
 p-terphenyl crystals, hole injection from liquid redox electrodes 9-26475
 transition metal glasses, switching mechanism, high elec. field infl. 9-35476
 transition metals, resonant states 9-37379
 transition-metal pseudopotentials 9-47018
 Wannier representation, rigid-ion method 9-42988
 ZnS single crystals, thermoluminesc. after electron beam irradi., new trapping state 9-45356
 Ag-Zn alloy, concentration effect of free electrons on thermodynamic activity of Zn 9-26477
 AgBr:I electron-hole pair generation rel. to energy of incident photons 9-43251
 Ag(Mn) alloys, virtual resonant bound states, photoemission, expts. 9-45032
 Ag(pd) alloys, virtual resonant bound states, photoemission expts. 9-45032
 Al, i.f. helicon resonance obs., for Hall coeff. and magnetoresistance meas. 9-30839
 BaTiO₃, microwave absorpt. by free carriers 9-31101
 Bi:Te, helicon dispersion relations, depend. on mass density, effective mass determ. 9-35395
 Bi:Te, second-harmonic generation by damped Alfvén waves and helicons 9-41160
 Bi:Te layered structure, helicon propag. rel. to carrier drift effects 9-43015
 Bi, deformation potential for electrons and holes 9-37345

Crystal electron states continued

- Bi, electron relax. time from magnetoacoustic oscillations and tilt effect 9-47072
- Bi, second-harmonic generation by damped Alfvén waves and helicons 9-41160
- Bi_{1-x}Sb_x carrier numbers and mobilities from electronic props. 9-30842
- Bi₂Se₃, electrons effective mass depend. on carrier conc. 9-37390
- C films, spin destruct. proc. model, test by comparing activation energies 9-23377
- Cd, local pseudopotential, parameters 9-33221
- Cd, normal and supercond., deformation parameter rel. to anisotropy in u.s. attenuation 9-37338
- CdF₂, semiconducting, effective mass and scatt. mech. 9-41205
- CdS, wurtzite type, deform. potential consts. 9-26498
- CdSe film, charge density reduction by surface alloying of IN 9-33319
- Co, rel. to positron annihilation, obs. 9-35325
- Cr, itinerant spin-density excitation in light- scatt. obs. 9-47372
- Cu, core electrons, momentum distrib., anisotropy 9-30820
- Cu, rel. to positron annihilation, obs. 9-35325
- Cu(Mn) alloys, virtual resonant bound states, photoemission expts. 9-45032
- Fe(NH)(SO)₄·6H₂O: ⁵⁷Co²⁺, daughter Fe³⁺ stabilization rel. to H₂O radiolysis by Auger e, obs. 9-23801
- GaAs Raman scattering by cyclotron waves 9-33567
- GaP, shallow donors behaviour from diffusion of Se, S and Te in Ga₂(PO₄)₂ 9-35434
- GaSb-InSb alloys, phonon scattering by acceptor defects, thermal conductivity meas., 5° to 300°K 9-44870
- GaSb, phonon scattering by acceptor defects, thermal conductivity meas., 5° to 300°K 9-44870
- Ge, resistivity, photoconductive decay and Li drift props., heat treatment effects 9-37538
- GeS energy gap from elec. cond. activation energy, obs. 9-30909
- He, cavity form. following e trapping 9-23572
- Hg-Mg system, perturbation theory and alloying behaviour 9-44860
- HgSe, helicon resonance and quantum oscils. 9-24107
- HgTe, two helicon resonances obs. 9-43014
- InSb, helicon reson. obs. in strong pulsed mag. fields 9-24105
- n-InSb, helicon waves, dimensional resonances and waveguide effect 9-41201
- n-InSb, hot-electron relaxation times 9-30912
- InSb Raman scattering by cyclotron waves 9-33567
- K, helicon wave resonant damping 9-26494
- KBr, electronic structure of F centre 9-40973
- KCl, electron-hole recombination mechanism for defect production at 20°K 9-26276
- KCl, electronic structure of F centre 9-40973
- KI, electronic structure of F centre 9-40973
- LiH, pseudopotential approach, electron gas obs. 9-33222
- NaCl, electron-hole recombination mechanism for defect production at 20°K 9-26276
- NaCl, electronic structure of F centre 9-40973
- Nb, camer conc., normal state go into superconducting state at sufficiently low temps. 9-28478
- Ni, rel. to positron annihilation, obs. 9-35325
- Pb, energy wave-number charact. from exptl. phonon freqs. 9-44871
- PbS(Se)(Te), charge-density and spin-density fluctuations in single-particle Raman scatt. 9-47375
- Pd, density of states and electronic sp. ht. 9-37357
- Rd X-ray absorpt. spectra L series obs. 9-37748
- Rh X-ray absorpt. spectra L series obs. 9-37748
- Ru X-ray absorpt. spectra L series obs. 9-37748
- S, orthorhombic, energy distribution of electron and hole traps 9-37623
- Si, cooling of hot electrons in mag. field 9-49109
- Zn, normal and supercond. deformation parameter rel. to anisotropy in u.s. attenuation 9-37338

band structure

- 3d transition metals, appearance mechanism of Kβ₂ lines in X-ray spectrum 9-24433
- A^{IV}B^{VI}C^{VII} semiconducting cpds. peculiarities, investig. by group theory methods 9-37715
- alkali metals, Fermi sea to Brillouin zone boundaries transitions, Mayer-Naby peak in optical conductivity 9-28679
- alloys, binary, partially ordered, using Green's function 9-48990
- alloys, disordered substitutional, density of states analysis from simple model 9-26476
- alloys, valence effect as explanation of exothermic binding energy 9-39180
- anthracene, low-lying valence states 9-24239
- antiferromagnetism and Mott insulation in band model 9-44883
- APW method 9-48991
- augmented-plane-wave method, self-consistent 9-47036
- band, ferromagnetism, high-field studies by Mossbauer and mag. moment meas. 9-43166
- binary alloys, ferromagnetic, interband optical transitions investigation, low temp. magneto-optic meas. 9-41136
- BN X-ray determ 9-30811
- β-brass, ordered, using Green's function 9-48990
- Brillouin zone, direct interband transitions, elec. field effects 9-48993
- Brillouin-zone averages and energy-band interpolation, using crystalline interpolation technique 9-24090
- critical points, saddle-type, Coulomb interaction effect 9-44866
- degeneracy in non-conducting cryst. from optical absorpt. obs. 9-33547
- diamond, empirical pseudopot. approach 9-49000
- diamond, substitutional N donor obs. 9-37401
- diamond-type, effective carrier mass, contrib. of electron interaction with short-wavelength vibrations 9-44874
- diamond-type crystals, optical critical-point structure, strain effects 9-24395
- diametric crystals, determ. by Green's function method, rel. to potential strengths and separation of atoms 9-35309
- dielectric classification prediction 9-23654
- dimethyl terephthalate, ionization potential and electron affinity rel. to conducting and valence bands 9-37417
- disordered systems, problems 9-37396
- dispersion surfaces, low-energy electron-diffraction in 3-dimens. mixed Laue and Bragg reflections, review 9-37126
- effective mass, anisotropic, variational principle for arbitrary pots. 9-37394
- Crystal electron states continued**
- band structure continued**
- effective mass, phonon contribution to renormalization calc. in metals and alloys 9-28442
- electroabsorption below band gap 9-41356
- energy level connection with lattice parameters, electric field and periodic potential, Stark eff. 9-24092
- energy minima near Brillouin zone boundary location method 9-48988
- Ewald potential, generalized, for augmented-plane-wave method calc. 9-47035
- exchange and correl., local approx., for use in calc. 9-37393
- ferromagnetism in narrow energy band 9-24287
- ferromagnetism in nondegenerate narrow energy bands, variational principle 9-24288
- from field emission meas. 9-37628
- films, electronic structure, density of states and charge, 1-electron approx., simple model potential 9-41132
- by free-carrier and interband Faraday rotation 9-37395
- graphite, rel. to optical constants anisotropy 9-26697
- Green's function method 9-48991
- group II-VI compounds, empirical pseudopotential calcs. 9-37398
- group II-VI compounds, rel. to absorption and reflection spectra 9-37708
- group II-VI compounds, rel. to optical spectra 9-37399
- group IV-VI cpds., band edge structure 9-39627
- group IV-VI cpds., rel. to tunneling characts. 9-39655
- group theory applic., book 9-48989
- heterojunctions, degenerate, diagram analysis 9-33337
- homopolynucleotides, SCF LCAO cryst. orbital calc. 9-48521
- inorganic binary compounds, correlation between bond energies and forbidden bands 9-48780
- insulator-conductor interface, energy-band relationships from photo-injection obs. 9-39739
- interband transitions in Brillouin zone, elec. field effects 9-48993
- interface between metals, clean 9-36936
- ionic cryst., microscopic theory of band and local states 9-42999
- Kronig-Penney model, diatomic, generalized 9-47038
- lattice electrons in external mag. field, tight-binding and nearly-free-electron approach 9-41131
- Li₂Ni_{1-x}O solid solutions, donor levels caused by neutral Li interstitials 9-41134
- local and band character coexistence from model for calc. of Green's function of mixed cryst. 9-33216
- magnetic-Coulomb levels near saddle points 9-47039
- many-neighbour approx. rel. to band edges 9-48986
- metal, Brillouin zone construct. and influence on Fermi surface shape 9-39563
- metal, magnetic, time-reversal degeneracy 9-47034
- metal, two-band model, carrier density and mobility 9-39580
- metals, electron-interaction effects on soft X-ray emission spectrum, formalism and first-order theory 9-24434
- metals, groups IA and IIA, electronic transition model under high press. 9-44873
- metals, light, X-ray emission spectroscopic study 9-44877
- metals, magnetic, density-of-state X-ray photoelec., spectroscopy study 9-44886
- metals, pure, electronic props., theory 9-47023
- metals, pure, Fermi surface rel. to elementary bond theory 9-47024
- model potentials 9-48991
- Mott insulation and antiferromag. in band model 9-44883
- non-crystalline materials, conduction, localized states in pseudogap and near extremities of conduction and valence bands 9-33243
- one dimensional indefinite periodic models, analogue method 9-39561
- one-dimensional, in WKB approx. 9-44872
- one-dimensional aperiodic cryst., electron average momentum def. 9-44882
- optical densities of state photoemission studies 9-44876
- ordered and disordered systems, localization of electrons, bound bands 9-44879
- overlap integrals, tight-binding model applied to band structure of solids 9-35316
- photoemission, importance in determination 9-37397
- phthalocyanine, metal-free β-form single cryst., electron trapping and bulk conduction in vacuum 9-28462
- plane-wave tight-binding method, combined 9-42998
- polaron, piezoelectric, strong-coupled, effective mass calc. 9-39572
- polynucleotides, homogeneous, exciton 9-26488
- pseudo-atoms 9-48991
- quantizing curvature, surface electron mobility 9-44863
- rare earth-noble metal equiatomic cpds., rel. to mag. ordering 9-24334
- refractory metal oxides, forbidden gaps rel. to lattice energies and heat of atomization 9-30494
- s-band, strongly correlated magnetism 9-45045
- semiconducting amorphous alloys, model 9-33316
- semiconductor, deep levels in forbidden band by acceptor impurities 9-41207
- semiconductor, effective mass determ. from i.r. plasma refl., carriers degeneration depend. 9-44972
- semiconductor, free carrier transport props., study by magneto-plasma waves 9-28511
- semiconductor, heavily doped, energy scale of localized levels near surface 9-35416
- semiconductor, hexagonal, effect of bandgap on elasto-optic and electro-optic props. 9-35623
- semiconductor, induced light absorpt. by nonequil. holes, effect on two-photon photoconductivity 9-39708
- semiconductor, population inversion between free carrier zone and local centre levels by field effect 9-35394
- semiconductor, rel. to optical and transport props. 9-49091
- semiconductor, semimetal, helicon interferometry and nonreson. cyclotron absorpt. method for props. determ. 9-47100
- semiconductor A^{III}B^V cpds., optical effective mass of free carriers 9-47117
- semiconductor surface, electrorreflectance meas. 9-43215
- semiconductors, by photoemission studies 9-37397
- semiconductors, diamond-type 9-30915
- semiconductors, effect of dislocations, quantum mechanical treatment 9-33315
- semiconductors, electron redistrib. in photoconductivity at large light intensity 9-28574
- semiconductors, homogeneous and inhomogeneous mixed 9-37528

Crystal electron states continued
band structure continued

- semiconductors, interband magneto-optical oscillations of absorption coeff., splitting 9-33509
- semiconductors, magnetic, and elec., opt. and mag. props. 9-49064
- semiconductors, magnetic one-electron density-of-states 9-47118
- semiconductors, magnetoactive, rel. to localized magnons and indirect exchange 9-28607
- semiconductors, phonon-assisted optical absorption in crossed electric and mag. fields 9-28484
- semiconductors, photon absorpt. coeff. at low-temp., indirect two-photon transitions 9-37714
- semiconductors, superconducting energy-gap eqn. derivation by Green's function method 9-26521
- semiconductors, treated as disordered systems, problems 9-37396
- semimetal, helicon interferometry and nonreson. cyclotron absorpt. method for props. determ. 9-47100
- semimetals, superconducting energy-gap eqn. derivation by Green's function method 9-26521
- Slater exchange pot., reduction factor 9-48987
- superconducting alloys, electron interactions in 3d band 9-24151
- superconductor, two-band with nonmag. impurities, upper critical field 9-30857
- superconductor excitation spectrum, energy gaps obs. 9-43032
- superconductors, two-band, with paramag. impurities, interband scatt. of electrons, energy gap obs. 9-33264
- surface, LEED study, multiple scatt. and surface wave reson. effects 9-33228
- tetracene, low-lying valence states 9-24239
- thin film, model investigation and comparison with infinite cryst. 9-35310
- thiospinels, outer d-electrons description 9-28444
- tight-binding band calc., eff. of inclusion of overlap integrals 9-47033
- transition metal, energy-indep. model Hamiltonian 9-37392
- transition metal, systems, binary, IIIA-VIA groups, valence electrons and constitutional diagrams 9-39469
- transition metal borides, theory test from heat capacity meas., 1.5-18°K 9-28445
- transition metal dichalcogenides, from electron energy loss studies 9-30804
- transition metals 9-48991
- transition metals, approx. calc. 9-44892
- transition metals, b.c.c., rel. to generalized susceptibility calcs. and mag. props 9-26658
- 3d transition metals, b.c.c. and f.c.c., APW energy bands 9-28447
- transition metals, calc. method 9-33227
- transition metals, optical densities of states, photoemission studies 9-44891
- transition metals and alloys, b.c.c., approx. energy bands, spin-orbit interac. effect on paramag. susceptibility 9-35536
- transition-metal pseudopotentials 9-47018
- wurtzite type crystals, valence band structure calc. 9-48994
- X-ray determ. 9-30811
- X-ray emission spectroscopic study 9-44877
- zero-slope points in Brillouin zone 9-44875
- α -Ag-In dil. alloys, electronic transitions and band gaps from piezoreflectance 9-47325
- Ag-Mn alloy, models from photoemission and optical studies 9-45033
- Ag-Zn system, ϵ and η phase alloys, e. conc. and interactions from mag. susceptibility meas. 9-43150
- Ag, APW calc. 9-30819
- Ag orthogonalized plane wave method calc. 9-37400
- AgBr, brominated, acceptor ionization energy of neutral Ag vacancies obs. from optical absorpt. 9-41373
- Al, constant-energy surfaces, Korringa-Kohn-Rostoker calcs. 9-26479
- Al, relaxation times and temp. depend., from Hall effect's reversal 9-37438
- Al₂O₃ film, estimation from infl. of light on Al oxidation rate 9-31000
- Al₂O₃ X-ray determ. 9-30811
- AlN, calc. using orthogonalized plane wave method 9-26480
- p-AlSb, acceptor photoexcitation spectra, uniaxial stress eff. on lines 9-39832
- As, magneto-acoustic attenuation obs., giant quantum oscillations and spin splitting 9-35335
- As, parameters from i.r. magnetoreflection data for trigonal face 9-47320
- AuCu, order-disordered phases, peak in density of states assoc. with Brillouin zones 9-26395
- β -B, rhombic, effective mass of holes from absorpt. spectrum for lattice vibrs. 9-39834
- β -B, rhombic, effective mass of holes from absorpt. spectrum for lattice vibrs. 9-39834
- B from X-ray emission spectra 9-37742
- BN, from X-ray emission spectra 9-37742
- BN X-ray determ 9-30811
- BP, X-ray determ 9-30811
- Be, contribution to elastic shear constants, model potential theory validity 9-30630
- BeO, u.v. spectrum and reflectance calc. 9-28670
- Bi:Pb, determ. from magnetoresistance and Hall eff. meas. 9-30843
- Bi-Sb alloys, magnetoreflection obs. 9-41162
- Bi, deform. pot. for electrons and holes 9-33252
- BiO₂ layers, evaporated, band gaps obs. for optical and valence-conduction band transitions 9-39162
- Bi₂Te₃ pseudopotential approach 9-44885
- Bi-(0.3 at.%)Sn alloy, isoenergetic surfaces struct. at L-maximum 9-35312
- Cd, contribution to elastic shear constants, model potential theory validity 9-30630
- Cd, density of states, model-potential calc. 9-26131
- Cd, normal and supercond., effective energy gaps 9-37338
- Cd₂As₂, effective mass of electrons from thermoelectric power and Hall coeff. data 9-35313
- Cd₂As₂, non-parabolic model of conduction band and Fermi surface form from Shubnikov-de Haas effect obs. 9-41151
- Cd₂Hg_{1-x}Te, effective mass for composition range 0-30% 9-48995
- Cd₂Hg_{1-x}Te, energy difference between conduction and second valence band from Shubnikov-de Haas study 9-47061
- Cd₂Hg_{1-x}Te alloys, photovoltaic effect assoc. with effective mass gradient 9-39730
- Cd₂Hg_{1-x}Te solid solns., fund. reflectivity spectrum obs., 1.5-4 eV 9-45306
- CdS:Se mixed alloy system, pseudopotential calc. 9-37404

Crystal electron states continued
band structure continued

- CdS, Γ -point valence band, spin-orbit corrections 9-37403
- CdS, pseudopotential calc. 9-37404
- CdS, recombination kinetics at low temp. and high excitation intensities 9-49313
- CdS, valence band structure calc. 9-48994
- CdSi_{1-x}Se_x, g-factor of conduction band electrons 9-47040
- CdS_{1-x}Se_x, parameters determ. from refl. meas. in fund absorpt. region 9-47341
- CdS absorpt. edge, surface effects 9-45316
- CdS and CdSe, energy band models, self-consistent orthogonalized-plane-wave and empi refined refined orthogonalized-plane-wave calcs. 9-39567
- CdS(Se), from electroabsorption spectrum in exciton region 9-35625
- CdSb:Ag, effective mass of free holes from reflectivity meas. 9-39618
- CdSe, electron-bombarded and u.v. radiation illum., electron-hole pair form. energy 9-47133
- CdSe, Γ -point valence band, spin-orbit corrections 9-37403
- CdSe, pseudopotential calc. 9-37404
- CdSe, valence band structure calc. 9-48994
- CdTe, photoemission determination 9-37397
- α -p-Ce, self-consistent calc. 9-33230
- CeCl₃, electronic states of f' config. from Raman effect obs. 9-24424
- Co, ferromagnetic, interband optical transitions investigation, low temp. magneto-optic meas. 9-41136
- Co₃O₄, from photoelec. meas. 9-41285
- CoO, from photoelec. meas. 9-41285
- CoO, magnetic semiconductor 9-47118
- Cr-Mn alloys, rel. to spin density wave calcs. 9-24325
- Cr-V alloys, rel. to spin density wave calcs. 9-24325
- Cr, orthogonalized plane wave calc. method 9-37405
- Cr, rel. to spin density wave calcs. 9-24325
- Cr and alloys, itinerant antiferromag., optical and pressure effects, rel. to band structure 9-45213
- Cs, energy bands, wave functions, props. 9-48996
- CsI, Green's function method calc. 9-43003
- Cu/Pb layers, proximity effect, induced excitation spectrum, density of states meas. 9-44944
- Cu-Ni, rigid-band model and clustering eff. 9-26483
- Cu-Ni alloy, models from photoemission and optical studies 9-45033
- Cu-Ni alloys, reflectivity and i.r. absorpt. studies 9-45269
- Cu-Pd alloys, photoemission studies for resonant bound state model 9-33423
- Cu, 3d band from L_{II} and L_{III} X-ray emission spectra. 9-45339
- Cu, using orthogonalized-plane wave method modification 9-43004
- Cu₂S films, data from optical and electrical props. 9-44949
- Cu₃SbSe₄, effective mass of holes, from Seebeck coeff. obs. 9-26505
- Cu alloys, from Mossbauer effect obs. in ¹¹⁹Sn impurity 9-43222
- Cu optical densities of states, photoemission studies 9-44891
- Cu reflectivity and i.r. absorpt. studies 9-45269
- Dy structure, photoemission investigation in spectral range from 3.2 to 11.8 eV 9-39741
- Eu chalcogenides, deform. pot. calc. from absorpt. edge obs. 9-37722
- Eu chalcogenides, exchange interac. mechanism w.r.t. spin-polarized energy bands 9-39782
- EuO, reflectivity and band structure, energy range 1-9 eV 9-26702
- EuS, energy gap temp. depend. 9-37529
- EuS(Se), from optical reflection and absorption data 9-28505
- Fe-Be alloys, rel. to magnetization and sp. ht. 9-45143
- Fe-Co alloys, polycry., 3d-band shape study from high-field susceptibility obs. 9-37406
- Fe-Ni alloys, polycry., 3d-band shape study from high-field susceptibility obs. 9-37406
- Fe-7.4%Si single cry., 3d-band shape study from high-field susceptibility obs. 9-37406
- Fe, band ferromagnetism, high-field studies by Mossbauer and mag. moment meas. 9-43166
- Fe, ferromag. optical interband absorpt. freq. dispersion from curves of density states 9-39836
- Fe, ferromagnetic, interband optical transitions investigation, low temp. magneto-optic meas. 9-41136
- Fe, polycry., 3d-band shape study from high-field susceptibility obs. 9-37406
- Fe₂Te₃, d-band, in tight-binding approx. 9-39565
- (Ga, In) As alloys, Λ_1 - Λ_1 transition, electroreflectance interpretation 9-31084
- Ga₂In_{1-x}Sb, rel. to variation in electroreflectance with composition 9-45307
- Ga₂In_{1-x}Sb alloys, conduction band, rel. to Gunn effect 9-41199
- Ga superconducting energy gap, temp. depend., tunneling meas. 9-33271
- GaAs:Cd carrier conc., post-implantation annealing depend. 9-33320
- GaAs:Mn(Si), (Cd) impurities, electroreflectance 9-28661
- GaAs:Si, energy band tails and photoconductivity 9-39716
- GaAs:Zn, carrier conc., post-implantation annealing depend. 9-33320
- n-GaAs, deep level conc. from Hall eff. meas., 300-700°K 9-30916
- GaAs, energy gap temp. dependence, 300-973°K 9-43249
- GaAs, epitaxial, energy gap and effective-masses from oscillatory photoconductivity 9-26604
- GaAs, location of energy minima near Brillouin zone boundary 9-48988
- GaAs, Λ_3 - Λ_1 transition, electroreflectance interpretation 9-31084
- GaAs, using empirical pseudopot. method 9-49268
- GaAs_{1-x}P_x solid solutions, absorption from conduction bands or donor levels, temp. depend. 9-33554
- GaAs abrupt asymmetrical junctions, radiative tunneling 9-43253
- GaP, energy gap temp. dependence, 297-1273°K 9-43249
- GaP, using empirical pseudopot. method 9-49268
- GaP electrodes, charge transfer between energy states and redox systems, photoexcitation and electroluminesc. obs. 9-30990
- GaP forbidden band width from absorpt. spectrum, at 4.2-500°K 9-43239
- GaSb:Te, conduction, Hall coeff. and resistivity temp. depend. 9-37530
- GaSb, by empirical pseudopot. method 9-47119
- n-GaSb, energy gap between valleys in conduction band, magnetoresistance oscillations 9-39620
- GaSb, semi-empirical Kohn-Rostoker method 9-30923
- GaSe, energy structure, effect of Br impurity, absorpt. spectra 9-35412
- Ge, anisotropy of g-factor of free hole and conduction-band spin-orbit splitting 9-26484
- n-Ge, degenerate, density of states rel. to impurity conc. 9-41217

**Crystal electron states continued
band structure continued**

- Ge, density of states in amorphous form 9-31106
 p-Ge, forbidden band width from Hall effect meas. and resistivity, 600° to 800°K 9-28514
 Ge, heavily doped, critical points determination from u.v. refl. spectrum 9-35645
 Ge, magnetopiezotransmission obs. of effective masses 9-44982
 Ge, strain-split energy bands 9-24187
 Ge surface, atomically clean, model of spectrum of levels 9-47123
 Ge three-valley model for electrons in conduction band to explain obs. bulk negative differential conductivity 9-30924
 GeTe, calcs. 9-39794
 GeTe, carrier energy spectrum changes due to solid solns. form. 9-47113
 GeTe, k.p. band model 9-39628
 GeTe, relativistic, and electr. props. 9-43057
 GeTe, relativistic calcs. 9-39629
 Hg-CdTe alloy system, electron effective mass from magneto-optical obs. 9-39807
 Hg, effective mass, temp. effects, electron-phonon interaction effects 9-47032
 Hg_{1-x}Cd_xTe, effective masses determ. by helicon and nonreson. cyclotron absorpt. techniques 9-47101
 Hg_{1-x}Cd_xTe alloys, energy gap temp. and x depend. from photocond. obs. 9-41266
 HgS, synthetic single crystals, localized levels in energy gap by quenching of photoconductivity 9-28580
 α -HgS, valence band splitting, from absorpt. spectra meas. 9-28448
 HgSe, g-factor from de Haas-van Alphen effect 9-47062
 HgSe, inversion asymmetry splittings from oscillatory magnetoresistance 9-49013
 HgSe, nonparabolic conduction band parameters 9-48997
 HgSe, rel. to ionized-impurity-limited mobility 9-49092
 HgSe, spin-orbit splitting at Brillouin zone centre 9-35314
 HgTe-ZnTe, effective masses conc. depend. 9-35307
 HgTe, interband magneto-optical transitions, low temp. reflection and electroreflection study 9-47344
 HgTe, nonparabolic conduction band parameters 9-48997
 HgTe, parameters from magnetoresistance oscillations 9-49014
 HgTe, temp.-dependence from pressure meas. 9-48998
 HgTe, valence band, hole effective mass, rel. to temp. 9-30917
 In-Cd, effective mass meas. and applic. to electron-phonon interaction 9-47042
 In, density of states, model-potential calc. 9-26131
 In, electronic density of states, nonlinear pressure effect 9-37407
 In, and Fermi surface 9-35315
 In, Fermi surface model, de Haas-van Alphen meas. 9-30850
 In, relaxation times and temp. depend., from Hall field's reversal 9-37438
 In_{1-x}Ga_xP alloys, band structure and direct transition electroluminescence 9-24467
 InAs, λ_3 - λ_1 transition, electroreflection interpretation 9-31084
 InAs, third harmonic generation, mobile carrier nonlinearity, interband proc. 9-26547
 InAs_{1-x}P_x, rel. to variation in electroreflectance with composition 9-45307
 InAs_{1-x}Sb_x, rel. to variation in electroreflectance with composition 9-45307
 InP n-p junction region, recomb. radiation obs. 9-26767
 p-InSb, conductivity effective mass of holes 9-35407
 p-InSb, deep level compensation, influence on electrical props. 9-35406
 InSb, deformation potential constants 9-33307
 InSb, effective mass of electrons and scattering mechanisms 9-44973
 n-InSb, effective mass of electrons, infl. of hydrostatic pressure causing changes in elec. props. 9-28501
 InSb, effective masses determ. by helicon and nonreson. absorpt. techniques 9-47100
 InSb, energy levels and absorpt. spectrum of impurity centres 9-35408
 n-InSb, higher conduction band minima and assoc. impurity level props. 9-41202
 InSb, induced light absorpt. by nonequil. holes, effect on two-photon photoconductivity 9-39708
 InSb, Landau levels, effects on longit. magnetoacoustic absorpt. 9-26420
 n-p-InSb, X-ray irradi., bending of bands 9-49086
 InSb_{1-x}Bi_x alloys, optical gap obs. 9-43240
 InSb_{1-x}Bi_x solid solns., band gap obs. 9-43058
 p-InSb films, forbidden band width and effective mass thickness dependence at 90 and 300°K 9-41379
 K⁺, new model for potential 9-34518
 KCl, polaron theory, F-centre electron wave function determ. 9-33237
 KCl electronic spectra, 5-40 eV region, band parameters, determ. 9-37711
 Li, by self-consistent augmented-plane-wave method 9-47036
 Li, by self-consistent augmented-plane-wave method, lattice const. variation 9-47044
 Li, density of states, model-potential calc. 9-26131
 Li, using ab initio pseudopot. 9-43006
 Li_{1-x}Co_xO solid solutions, from photoelec. meas. 9-41285
 Li_{1-x}Ni_xO solid solutions, from photoelec. meas. 9-41284
 Li⁺, new model for potential 9-34518
 Li metal, b.c.c., determ. by GI method 9-44887
 LiT, using combined plane-wave tight-binding method 9-42998
 Mg, contribution to elastic shear constants, model potential theory validity 9-30630
 Mg₂Ge, and optical constants calcs. 9-24356
 Mg₂S, energy location, prominent structure shape and magnitude, calc. 9-41135
 Mg₂Si, and optical constants calcs. 9-24356
 Mg₂Sn, and optical constants calcs. 9-24356
 Mg₂Sn, from reflection spectra 9-35647
 MgSiP₂, semicond., energy gap meas. 9-44974
 γ -Mn, f.c.c., APW method 9-47045
 MnO, antiferromagnetic, spin-polarized APW method 9-44888
 MoS₂, eff. of pressure and temp. 9-28449
 Na, bcc, band structure parameters calc. from overlap integrals 9-35316
 Na⁺, new model for potential 9-34518
 NaF, polaron theory, F-centre electron wave function determ. 9-33237
 NaF, polaron theory, F-centre electron wave function determ. 9-33237
 NaF, valence band calc. by tight binding method 9-48999
 NaI, using combined plane-wave tight-binding method 9-42998

**Crystal electron states continued
band structure continued**

- Nb, superconducting energy gap anisotropy rel. to temp. depend. of Ginzburg-Landau parameters in upper critical field 9-28478
 Nd double h.c.p. rel. to generalized susceptibility 9-44889
 Ni-Cu alloys, minimum polarity models in mag. props. theory 9-45113
 Ni, ferromagnetic, interband optical transitions investigation, low temp. magneto-optic meas. 9-41136
 Ni, ferromagnetic, mag. breakdown effects 9-47249
 Ni²⁺-neutralization spectroscopy study 9-44890
 Ni reflectivity and i.r. absorpt. studies 9-45269
 Ni single cry., 3d-band shape study from high-field susceptibility obs. 9-37406
 β -NiAl, effective electron masses from conductivity spectra 9-37449
 β -NiAl, from optical props. obs. 9-47367
 NiO, magnetic semiconductor 9-47118
 NiO_{1-x}, from photoelec. meas. 9-41284
 Pb-SnTe alloy system, electron effective mass from magneto-optical obs. 9-39807
 Pb, effective mass, temp. effects, electron-phonon interaction effects 9-47032
 Pb, Landau-level widths, effective masses and magnetic-interaction effects obs. 9-26500
 Pb_{1-x}Sn_xSe semicond., laser emission rel. to cond. and valence band crossover, obs. 9-48045
 Pb_{1-x}Sn_xTe, from Hall effect and Seebeck coeff. hole conc. dependences 9-39632
 Pb_{1-x}Sn_xTe, reduced effective masses, g-factor magnitudes, from magnetoelectricity obs. 9-41406
 PbO-SnO mixed crysts. layers, photoconductive, energy gap determ. 9-41269
 PbO layers, vapour-deposited, band diagram and energy gap obs. from photoemission 9-39722
 PbS, relativistic calcs. 9-39629
 PbS and PbSe, relativistic augmented-plane-wave functions, rel. to direct-transition optical absorpt. 9-41387
 PbS and PbSe, spin-flip Raman scattering by carriers, cross-sections calc. 9-35674
 PbSe, interband transitions from characteristic electron energy losses 9-39553
 PbSe, relativistic calcs. 9-39629
 p-PbSe, two valence bands indicated by depend. of electrical props. on carrier density and temp. 9-35409
 PbSe, from transport props. meas. 9-39631
 n-PbS epitaxial films, layered distrib. of charge carriers from transverse magnetoresistance meas. 9-42996
 p-PbTe, effective mass of holes calc. from oscillatory magnetoresistance obs. 9-44967
 PbTe, fund. energy gap, press. coeffs. 9-33317
 p-PbTe, from helicon-nuclear-spin interaction 9-39910
 PbTe, interband transitions from characteristic electron energy losses 9-39553
 n- and p-PbTe, Landau level splitting rel. to carrier conc. from magnetoacoustic attenuation of quantum oscillations 9-28506
 PbTe, relativistic and electronic props. 9-43057
 PbTe, relativistic augmented-plane-wave functions, rel. to direct-transition optical absorpt. 9-41387
 PbTe, relativistic calcs. 9-39629
 PbTe, spin-flip Raman scattering by carriers, cross-sections calc. 9-35674
 PbTe, from transport props. meas. 9-39631
 PbTe, valence band structure 9-39633
 PbTe parameters from optical reflectivity, transmission and Faraday effect 9-39630
 Pbs, from transport props. meas. 9-39631
 Pd from obs. of L₁₁ white line of absorpt. X-ray spectra 9-37749
 Pr double h.c.p. rel. to generalized susceptibility 9-44889
 Pt-Co dilute alloy two-band model rel. to magnetoresistivity meas. 9-44917
 Re₃, calc. 9-47048
 ReO₃, calc. in tight-binding approximation 9-47047
 Se-Te solid solns., edge absorpt. and band gap obs. 9-43250
 Se single cryst., interband transitions rel. to fine struct. in reflectivity spectrum 9-43204
 Si, absorption edge modification by Radiation-induced defects 9-47132
 n-Si, degenerate, density of states rel. to impurity conc. 9-41217
 Si, effective mass equations, breakdown due to rapidly varying potentials 9-44878
 Si, electron inelastic scatt., interband transition excitation, E_g=30-200 eV 9-40887
 Si, empirical pseudopot. approach 9-49000
 p-Si, galvanomag. anisotropy and energy-depend. warping of valence bands 9-43075
 Si, heavily doped, critical points determination from u.v. refl. spectrum 9-35645
 SiC, empirical pseudopot. approach 9-49000
 n-SiC α (6H) crystals, cond. band struct., optical absorpt. at 0.6 μ 9-43243
 α (6H)-SiC valence band determ. from absorpt. spectra at 86°K 9-41389
 Sn, white, model from de Haas-van Alphen data 9-47049
 SnAs₃, supercond., carrier conc. and ionic model obs. 9-37474
 SnP₃, supercond., carrier conc. and ionic model obs. 9-37474
 SnS₂, pseudopotential calc. and optical constants 9-26485
 SnSe₂, pseudopotential calc. and optical constants 9-26485
 SnTe, APW calcs. with relativistic corrections 9-47050
 SnTe, calcs. 9-39794
 SnTe, fund. energy gap, press. coeffs. 9-33317
 SnTe, interband transitions from characteristic electron energy losses 9-39553
 SnTe, k.p. band model 9-39628
 SnTe, relativistic, and electr. props. 9-43057
 SnTe, relativistic calcs. 9-39629
 SrTiO₃, superconducting ceramic, Zr-doped, effective masses determ. 9-26532
 SrTiO₃, superconducting ceramic, Zr-doped, effective masses determ. 9-26532
 Tb, relativistic augmented-plane-wave calcs. 9-24095
 ThC, superconducting energy gap, anisotropy changes 9-30879
 TiC and related cpds., from X-ray spectra obs. 9-45340
 TiCl₃, photoconductive 9-41272

Crystal electron states continued
band structure continued

p-TiSe: Pb, rel. to conductivity and thermoelec. power meas. 9-43059
VO: films, from photoemission meas. 9-24255
Zn, contribution to elastic shear constants, model potential theory validity 9-30630
Zn, in magnetic fields, calc. using single band effective Hamiltonian 9-24096
Zn, normal and supercond., effective energy gaps 9-37338
ZnGeP₂, energy zone structure 9-30822
ZnO: Cu, ligand-field-band theory of Cu 9-37673
ZnS: Cu²⁺, valence band, correlation with absorption and excitation spectra 9-37732
ZnS, Γ -point valence band, spin-orbit corrections 9-37403
ZnS, using empirical pseudopot. method 9-49268
ZnS and ZnSe, energy band models, self-consistent orthogonalized-plane-wave and empirically refined orthogonalized-plane-wave calcs. 9-39567
ZnSe, Γ -point valence band, spin-orbit corrections 9-37403
ZnSe, using empirical pseudopot. method 9-49268
ZnSiAs₂, energy zone structure 9-30822
p-ZnSnSb₂, effective mass of holes, electro-physical props. obs. 9-35410

excitons

absorption in high mag. fields 9-43232
alkali halides, evidence for self-trapping of excitons 9-33589
alkali halides, two-photon spectroscopy 9-47349
ammonium halides, self-trapped, in recombination luminescence 9-33586
anisotropic crystals, interaction of optical excitons with phonons 9-33223
anthracene, anisotropy of triplet exciton diffusion 9-35137
Anthracene, charge transfer 9-33599
anthracene, dipole Davydov splittings 9-49006
anthracene, exciton-phonon (polariton) dispersion curve 9-39571
anthracene, fluoresc., singlet excitons diffusion coeff. obs. 9-41410
anthracene, transfer of excitation energy to new-type excitons 9-47055
anthracene, triplet excitons interaction with trapped electrons 9-39729
anthracene crystals, mechanism for photocurrent excitation spectrum 9-35509
in anthracene rel. to transient currents 9-28450
anthracene triplet exciton band-structure limits from n.m.r. 9-35667
benzene, doped crystals, triplet states 9-24098
benzene, Rydberg states in inert-gas matrices 9-46384
benzene crystals, doped, absorption spectra 9-31112
benzophenone, e.s.r. of triplet state 9-49358
binding energies of excitons bound to singly ionized donors 9-37412
centers near exciton zone, scatt. and absorption of e.m. waves 9-28708
collision with biexciton, inelastic 9-47054
9, 10-dichloroanthracene, Urbach rule and long-wave tail of exciton band 9-39849
dissociation by localized elec. fields, photoconductivity spectra and vibr. struct. obs. 9-41138
dragging eff. by interac. with electrons and holes 9-24100
electric and magnetic fields effects 9-24101
energy transfer by virtual excitons, Agranovich expression averaged for ensemble of mols. 9-49003
excitation band. rel. to excitation energy transfer between impurities, mechanism 9-43000
exciton-impurity complex, excitation by fast electrons 9-26487
excitonic insulator transition temp. in semicond. and semimetal region, depend. on sign of mathematical parameter 9-30884
group II-VI compounds, exciton electroreflectance spectra 9-37707
group II-VI compounds, rel. to absorption and reflection spectra interpretation 9-37708
lanthanide chelates of 1,10-phenanthroline, triplet exciton migration 9-31135
linear molec. crystals, absorpt. by charge-transfer excitons 9-24400
luminescence, exciton, 2-photon excitation, calc. of oscillator strengths 9-35677
magnetic crystals, nonlocalized, equilib. distrib. 9-49004
molecular complexes, oscillator forces of collective excitation due to electron transition 9-24099
molecular cryst., book 9-49005
molecular cryst., exciton-phonon interaction 9-42994
monomolecular crystals, biexciton theory, spectrum in form of energy bands 9-26486
Mott-Wannier, interaction in vibr. lattice, pot. energy operator 9-33234
naphthalene, doped crystals, triplet states 9-24098
naphthalene, triplet, spin relax. and optical spin polarization 9-39915
in optical and energy loss spectra of interacting system, relative positions of peaks 9-37385
perylene in N-isopropylcarbazole, electronic excitation energy transfer 9-31138
photodissociation by i.r. radiation, continuum model 9-28452
photoionization of large radius excitons, accompanied by carrier transfer to a different band 9-37410
phthalocyanines, origin of photocarriers 9-43131
plasma exciton reson. in plasma oscillations 9-37414
polarizability and magnetic field reversal in yellow series spectrum 9-26728
polarons and plasma-exciton waves 9-49008
polynucleotides, homogeneous, singlet band structures 9-26488
polyvinyl carbazole, transfer of electronic excitation energy 9-39882
radio-spectroscopic detection method 9-28451
semiconductor, dielec. screening of electron-hole interaction 9-49069
semiconductor, excitonic effects in electroabsorpt. 9-43051
semiconductor, excitonic effects in electroabsorpt. 9-43052
semiconductor, fieldless heating 9-39615
semiconductors, binding to ionized impurities 9-24184
semiconductors, diamagnetic excitons 9-30823
tetracene, fission of singlet excitons into pair of triplet excitons 9-49007
tetracene, fission of singlet excitons into triplet ones obs. 9-35320
tetracene single cry., singlet-triplet exciton fission as channel for radiationless decay 9-26779
tetracyanoquinodimethane ion-radical salts, exciton-controlled proton relax. 9-39926
transitions, dielec. const. tensor, polariton-phonon coupling effect on spatial dispersion 9-44893
triplet-triplet energy transfer in ordered and random media 9-28724
two-dimensional, deduced from absorption spectrum of GaSe 9-35319
Wannier, in mol. cryst., conc. change due to mag. field 9-39570
Ag halides, excitation-induced i.r. optical absorpt. obs. 9-39830
AgBr, piezo-optic study 9-39814

Crystal electron states continued
excitons continued

AgCl, exciton-phonon coupling effects in absorpt. spectrum 9-39831
AgCl rel. to u.v. excited luminesc. and photon multiplication, 80°K 9-26765
BaAs₂: Cu spectra, rel. to local vibrations and structure of impurity centres 9-33231
CdI₂ adsorption of organic mols., stimulation and extinction of excitonic transitions 9-26194
CdS, Auger recomb. involving free and bound excitons 9-43252
CdS, dissoc., and photocarrier recomb. 9-41261
CdS, exciton-phonon interaction 9-37709
CdS, intrinsic excitons, phonon-assisted emission 9-37765
CdS, line widths and phonon interaction 9-37766
CdS, oscillatory photoconductive and exciton spectra 9-39713
CdS, photocond., phonon-assisted exciton transitions in spectral response 9-43127
CdS, quenching of exciton-related photoluminesc. at elec. breakdown 9-35703
CdS, recombination kinetics 9-49313
CdS, two-photon excitation, rel. to stimulated exciton-photon luminescence 9-45343
CdS, Wannier exciton binding energy rel. to anisotropy 9-41137
CdS single cryst., internal photoeff. in exciton region of absorpt. spectrum 9-26603
CdS single cryst., intrinsic excitonic absorpt. and photoconductivity correl. from spectra obs. 9-35503
CdS single cryst. alloyed with In and Ga impurities, luminesc. 9-37756
CdS(Se) electroabsorption spectrum in exciton region, band structure 9-35625
CdSe, bound complexes, emission and absorpt. spectra, 4.2°K 9-37718
CdSe, Wannier exciton binding energy rel. to anisotropy 9-41137
Cd(SeS) platelets, laser emissions, excited with mode-locked He-Ne laser 9-31950
CsI, even-parity X-exciton two-photon spectrum obs. 9-26736
Cu₂O, in photoconductivity temp. dependence, 160-120°K 9-24228
Cu₂O, weak absorption line due to excitation of 2s exciton 9-33235
Cu₂O absorpt. spectrum contour w.r.t. exciton-phonon interac. 9-35656
CuCl, bound, Zeeman effect, absorpt. and emission spectra 9-37721
CuCl, dissoc. by localized elec. fields, photoconductivity spectra and vibr. struct. obs. 9-41138
CuCl, kinetics of biexciton formation 9-35318
CuCl, longitudinal and triplet state near first exciton bend, magnetoreflection meas. evidence 9-35622
CuCl evaporated films, in Faraday rotation anomaly 9-24370
CuCl optical consts. near excitonic absorpt. region, refl. spectra obs. 9-37710
GaAs, reflectance and photorefectance spectra obs. 9-41377
GaAs, stress-induced exchange splitting of optical structure, 77°K 9-28453
GaAs_xP_{1-x}, N isoelectronic trap, localization energy determ. 9-28488
GaP, excitonic mol. bound to isoelectronic trap N, photoluminesc. 9-39895
GaP, thermal and impact ionization for two-photon excitation case 9-47393
GaP fine struct. of absorpt. spectrum assoc. with exciton form. 9-43239
GaSe, Wannier exciton binding energy rel. to anisotropy 9-41137
GaSe layer semiconductor, existence of two dimensional exciton observed 9-35319
Ge, condensation of exciton gas 9-47127
Ge, diamag. excitons, detect of states 9-30823
Ge, excitonic condensation 9-41218
HgI₂ adsorptions of organic mols., stimulation and extinction of excitonic transitions 9-26194
KCl single cryst., conductivity and energy loss spectra, temp. depend. 9-33559
MoS₂, absorption, eff. of pressure and temp. 9-28449
MoS₂ absorpt. spectrum, illustrating the spectrophotometric derivative method 9-27409
PbI₂, electroabsorption in exciton region 9-33539
 α (6H)-SiC exciton-impurity complexes detect. from absorpt. spectra at 86°K 9-41389
V₂O₃ metal-semiconductor transitions on excitonic phase change, pressure depend. studies 9-30892
ZnO, spatial dispersion, refl. and transmission spectra 9-45309
ZnSe, oscillatory photoconductive and exciton spectra 9-39713
ZnTe, absorption spectra interpretation 9-37733

Fermi level
alkali ions, new model potential in solids 9-34518
dyes, photosensitive, rel. to redox reaction caused by photo-excited mols. 9-41973
oxide cathodes, work function reduction, electric field effect 9-30999
tetracene, quasi-Fermi-level energetic distance from space-charge-limited currents obs. 9-41204
Al, Fermi momentum determ. from annihilation spectra, valence electrons calc. 9-33229
CdS, photoconducting, thermal stabilization, non-equil. analogue 9-33409
Co Fermi momentum determ. from annihilation spectra, valence electrons calc. 9-33229
Cu, energy determination by piezo soft x-ray effect 9-49303
Cu Fermi momentum determ. from annihilation spectra, valence electrons calc. 9-33229
n-GaAs, position, Fermi energy calc. from thermoelectric power meas. 9-33301
Ni Fermi momentum determ. from annihilation spectra, valence electrons calc. 9-33229
NiO, of defect electrons near surface, rel. to catalytic activity effect of u.v. irradi. and metal supports 9-41446
PbO layers, vapour-deposited, photoemission obs. 9-39722
V meatline cpds, from X-ray absorpt. and emission spectra 9-37753

Fermi surface
alkali metals, rel. to electron-ion interactions 9-26478
alloy, dilute, topology determ. from supercond. transition temp. pressure dependence 9-47043
conductors, thin, electrons characs. along sound wave propag. direction 9-24029
cyclotron reson. in films with specularly reflecting surfaces, effect of Fermi surface 9-41149
ellipsoid with anisotropic relax. time, magnetoconductivity 9-44903

Crystal electron states continued**Fermi surface continued**

- integral identity rel. to inversion scheme for obtaining surface topology from de Haas-van Alphen effect 9-24091
 metal, free electron model study, Brillouin zone influence on shape 9-39563
 metal, topology rel. to conductivity derivation from h.f. wave dispersion curves 9-44904
 metal, two-band model, Fermi energies meas. 9-39580
 metal struct. rel. to field ionization, tunnelling probabilities obs. 9-47218
 metal struct. rel. to field ionization, tunnelling probabilities obs. 9-43146
 metals, monovalent, rel. of cohesive energy to kinetic energy of electrons in Fermi sea 9-39179
 metals, pure, rel. to electronic props. 9-47024
 metals, theory 9-48992
 nesting, imperfect effect on props. of itinerant electron antiferromagnet 9-47278
 noble metals, effect of elastic deform., determ. using thermoelec. power 9-44884
 topology effect on magnetoacoustic attenuation, deformation-potential theory 9-46995
 Ag-Cd β -phase alloys, order-disorder transf., Hall coeffs., w.r.t. change in Fermi surface 9-35253
 Ag-Zn β -phase alloys, order-disorder transf., Hall coeffs., w.r.t. change in Fermi surface 9-35253
 Ag, APW calc. 9-30819
 Ag, effect of elastic deform., determ. using thermoelec. power 9-44884
 As, de Haas-Shubnikov oscillations in magnetoresistance obs. 9-43024
 As, magnetoresistivity tensor, low field, carrier density and mobility determ., 77-305°K 9-35311
 AuAl₂, nearly-free-electron model rel. to high-field galvanomag. props. 9-47073
 AuGa₂, nearly-free-electron model rel. to high-field galvanomag. props. 9-47073
 AuIn₂, nearly-free-electron model rel. to high field galvanomag. props. 9-47073
 Be, de Haas-van Alphen effect obs., pseudopot. model, press. depend 9-43001
 Bi, model, rel. to magnetoplasma wave spectrum, effect of spatial dispersion 9-30826
 Bi, non-extremal sections, from magnetoresistance meas. on size-quantized films 9-49021
 Bi, singularities, magnetoacoustic effect studies 9-39564
 Bi DeHaas-van Alphen eff. studies, energy spectrum obs. 9-28446
 Cd-Zn, small-angle intersheet scatt. effects on galvanomag. props. 9-26515
 Cd, normal and supercond., effective zones rel. to anisotropy in u.s. attenuation 9-37338
 Cd, orbits, causing resonance oscillations of u.s. absorption, due to orbits on Fermi surface 9-30772
 Cd, rel. to u.s. absorpt., quantum oscillations 9-44822
 Cd, small-angle intersheet scatt. effects on galvanomag. props. 9-26515
 CdAs₂, form, from Shubnikov-de Haas effect obs., rel. to non-parabolic model of conduction band. 9-41151
 Cd single crystal rel. to Sondheimer oscillations in Hall resistivity 9-37441
 Cu-Zn alloy single cryst., change with increasing electrons per atom, positron annihilation obs. 9-33241
 Cu-Zn β -phase alloys, order-disorder transf., Hall coeffs. w.r.t. change in Fermi surface 9-35253
 Cu, characteristics from Hall coeff. depend. on crystal orientation 9-26516
 Cu, effect of elastic deform., determ. using thermoelec. power 9-44884
 Cu, hydrostatic press. effect, zero-press. de Haas-van Alphen freqs., n.m.r. obs. 9-47041
 Fe, model accounting for magnetoresist. and Hall eff. meas. 9-24093
 In-Cd, 3rd-band principal cross-sectional area rate of change meas., band struct. effective mass determ. 9-47042
 In-Cd dil. alloy, topology determ. from supercond. transition temp. pressure dependence 9-47043
 In, and electronic structure 9-35315
 In, model calc. of β tube cross section 9-43005
 In, pseudopotential model, de Haas-van Alphen meas. 9-30850
 K, electron wave functions, hyperfine interaction depend. on cellular potential 9-39566
 Mo, de Haas-van Alphen meas. 9-26499
 Mo, r.f. size effect investig., 1.7° to 4.2°K 9-37408
 Na, electron wave functions, hyperfine interaction depend. on cellular potential 9-39566
 Nd double h.c.p. rel. to generalized susceptibility 9-44889
 Ni, de Haas-van Alphen data, band structure including mag. breakdown effects 9-47249
 Ni (110), rel. to polarized positron annihilation 9-24114
 β -NiAl, overlapping into higher Brillouin zones from thermoelec. power obs. 9-37449
 β -NiAl, topology, rel. to free electron absorpt. behaviour 9-47367
 Pb, third-zone sheet model for high field magneto-resistance 9-28458
 n- and p- PbTe, shape rel. to carrier conc. from magneto-acoustic attenuation of quantum oscillations 9-28506
 Pd Fermi radius velocity and orbital g factor exptl. determ. 9-47046
 Pr double h.c.p. rel. to generalized susceptibility 9-44889
 Pt, Fermi radius, velocity and orbital g factor exptl. determ. 9-47046
 Re₃, calc. 9-47048
 Sb, hydrostatic press. depend. 9-37409
 Sb, pressure-depend., de Haas-van Alphen eff. meas. 9-30821
 Sn, white, model from de Haas-van Alphen data 9-47049
 Tb, relativistic augmented-plane-wave calcs. 9-24095
 Te, behaviour in high and low magnetic fields 9-30827
 Te, hole Fermi surface, shape, Shubnikov-de Haas eff. meas. 9-26552
 Th theor. model, relativistic augmented-plane-wave calc. 9-24108
 Zn-Ag dilute alloys, relax. time meas. from de Haas-van Alphen studies 9-37424
 η -Zn-Cu, contrib. to coeff. between -196-100°C 9-47071
 Zn-Mn dilute alloys, relax. time meas. from de Haas-van Alphen studies 9-37424
 Zn, normal and supercond., effective zones rel. to anisotropy in u.s. attenuation 9-37338
 Zn, rel. to u.s. absorpt., quantum oscillations 9-44822

Crystal electron states continued**impurity states and effects**

- alkali halides: Eu²⁴ (Sm²⁶), electron-phonon coupling for centres rel. to zero-phonon transitions 9-37716
 alloys, dil. mag., Kondo resistivity of interacting impurity pair 9-24270
 alloys, dil. mag., orbital degeneracy effects 9-24269
 alloys, dilute, effect of localized states on impurity X-ray spectrum 9-49301
 alloys, dilute, electronic contrib. to specific heat 9-26426
 alloys, dilute, screening, nonlinear Thomas-Fermi eqn. soln. 9-47019
 alloys, dilute magnetic, electron-electron interaction and supercond. above Kondo temp. 9-44925
 alloys with paramagnetic impurities, gapless superconductivity region 9-43033
 Anderson model, self-consistent sols. 9-41130
 anisotropic materials, effect on thermoelec. props. 9-26595
 anthracene, low-temp. hole injection and hole trap distrib. 9-44970
 anthracene, trap charact. and optical de-trapping obs. from photo-electron emission from alkali metal contacts obs. 9-33232
 anthracene, triplet excitons interaction with trapped electrons 9-39729
 antiferromagnetism, split-band model, gaplessness for range of conc. 9-31045
 atoms, two-electron, eigenstates of (sp)³P multiplet and phonon-induced optical transitions 9-41372
 bands in mag. field, model form. and conduction 9-42997
 benzene, doped crystals, triplet states 9-24098
 benzene, isotopic impurities, singlet excited states 9-24097
 binary alloys, Green function and energy spectrum evaluation 9-37163
 carriers trapped by dislocation, anomalous Zeeman effect 9-33533
 corundum, paramagnetic ion impurities, group theoretical classification 9-28443
 Coulomb interaction effect at saddle-type critical pts. 9-44866
 diamond, semicond., oscillatory photoconductivity spectrum assoc. with acceptor centre, role of phonons 9-41258
 diamond, substitutional N donor obs. 9-37401
 dirty two-band superconductors, current density in limiting case of large non-mag. impurity conc. 9-26522
 disordered lattice, localization of electron states 9-44895
 donor, shallow, dipole-dipole hyperfine const. for lattice nuclei 9-37674
 electron interaction with randomly distrib. impurity, inclusion of cryst. lattice field in treatment 9-24083
 electron liquid, screening of fixed charge 9-41124
 electron transition rates, non-radiative, in lattice-localized-electron system 9-24089
 electron trap parameters determ. from thermoluminescent or conductivity glow curves 9-44880
 electron trap transitions, eqns. for thermolum. and thermally stimulated currents for simple models 9-44881
 electron-impurity system, dynamic magnetoconductivity for strong coupling case 9-30813
 electronic excitation energy transfer between impurity molecules 9-33220
 excitation energy transfer between impurities, mechanism 9-43000
 exciton dissoci. by localized elec. fields, photoconductivity spectra and vibr. struct. obs. 9-41138
 Fermi liquid in random scatt. centres, transport eqn., quasiparticle description in macroscopic and low-temp. limit 9-25055
 Friedel oscillations in screening charge about point impurity, modification by mag. field 9-48982
 Gd³⁺ in LaF₃, energy levels from optical absorption spectra 9-33556
 glasses containing transition metal ions, conduction 9-30964
 Hall eff. in hopping transport 9-30898
 hot-electron transport problems 9-24084
 ice, dopant conc. and conductivity relation, meas. technique 9-37532
 insulator with multiple trapping, injected current time-depend. flow, thermal release and transit time 9-39668
 ionic cry., elec. fields and polariz. prod. by defect charge density, lattice summations 9-33215
 ionic cry., electrostatic pots. and spatial deriv. about pt. defects 9-33214
 ionized centres, scattering rel. to negative longit. magnetoresistance 9-28457
 Kerner model of impure lattice, validity of Saxon-Hutner theorem 9-47038
 Li₂Ni₂O solid solutions, donor levels caused by neutral Li interstitials 9-41134
 light absorpt. centres, electron-vib. spectrum, band broadening mechanisms 9-26730
 local and band character coexistence from model for calc. of Green's function of mixed cryst. 9-33216
 magnetic alloys, dilute, frequency depend. elec. cond. effect of t-matrix impurity scatt. 9-47064
 metal, electron spin polarization around mag. impurity, calc. using Kondo effect 9-41287
 metal, paramag. impurity, inelastic scatt. of electrons 9-37383
 metal, screening of charged impurity, mag. field effect 9-33218
 metal-GaAs contacts, variation of contact resistance with impurity conc. and implications 9-30953
 metals, dilute, screening, nonlinear Thomas-Fermi eqn. soln. 9-47019
 metals, ferromagnetic, hyperfine fields 9-45255
 metals with paramagnetic impurities, spin density fluctuation spectrum 9-43149
 metals with paramagnetic impurities, spin density fluctuation spectrum 9-43149
 mixed molec. crystals, energy levels 9-41129
 molecular, with defect levels, light absorpt. intensity and polarization ratio 9-33541
 naphthalene, doped crystals, triplet states 9-24098
 naphthalene, isotopic impurities, singlet excited states 9-24097
 non-orthogonal states, second quantized formalism 9-45250
 optical electronic transitions between local and zone states in impurity centres 9-43227
 p-n diodes, conc. of shallow and deep impurities, infl. on C-V relns. 9-35448
 paramagnetic, effect on superconductivity 9-49031
 paramagnetic scatt. in tunneling between superconductors 9-44929
 perturbation, strongly localized, symmetrized charge density calc. for s and p bands 9-42992
 photo-c.m.f. in p-n junctions due to ionization of impurity centres 9-37626
 photoconductivity, conf. 9-39702

Crystal electron states continued**impurity states and effects continued**

- phthalocyanine, metal-free β -form single cryst., electron trapping and bulk conduction in vacuum 9-28462
- phthalocyanines, trapping levels obs. 9-49166
- polar molecules, trapped electrons in dipole fields, ESR studies 9-40584
- polareons, polarization mechanism of e.m. wave absorption 9-31096
- pseudolocal resonances and optical manifestations due to strongly localized perturbation 9-42992
- Schottky diodes, conc. of shallow and deep impurities, infl. on C-V relns. 9-35448
- semi-insulator, localized levels obs. from meas. of ohmic and space-charge-limited conduction 9-43106
- semiconductor, carrier emission rates and cross-sections impurity photocurrent and photocapacitive methods 9-39636
- semiconductor, carrier self-oscills. 9-37512
- semiconductor, carriers mixed scatt. on ionized impurities, parameter determ. 9-37509
- semiconductor, deep impurity centres, theory and i.r. props. 9-39635
- semiconductor, deep level acceptors in forbidden band, theoretical model 9-41207
- semiconductor, discharging method for trapping level calcs. 9-39613
- semiconductor, doped, percolation obs. of semicond.-to-metal transition rel. to impurity conc. 9-49095
- semiconductor, extrinsic, mag. freeze-out of electrons 9-43060
- semiconductor, extrinsic, magneto-optical effects theory 9-43061
- semiconductor, heavily-doped, electron shielding 9-24183
- semiconductor, illuminated, occupation ratio of dislocation acceptor levels 9-26556
- semiconductor, impurity diffusion via vacancy mechanism, theory 9-44975
- semiconductor, photoconductivity, conf. 9-39702
- semiconductor, photoionization spectrum of deep impurities 9-39634
- semiconductor, resonant phonon interactions effect on absorpt. line shapes 9-26741
- semiconductor organic p-n junctions, diffusion doped 9-35436
- semiconductor single cryst. growth from melt, homogeneous impurity incorporation 9-30520
- semiconductors, compensated, carrier scattering by ionized impurities 9-39557
- semiconductors, dopant conc. and conductivity relation, meas. technique 9-37532
- semiconductors, e. scatt. by neutral acceptors 9-28490
- semiconductors, exciton binding to ionized impurities 9-24184
- semiconductors, impurity bombardment produced ionization under arbitrary elec. fields 9-30900
- semiconductors, magnetoactive, localized magnons, electrons and indirect exchange 9-28607
- semiconductors, photomagnetic effect in impurity absorption region 9-33412
- semiconductors, screened ionized impurities, contribution to magnetoresistance 9-30919
- spin-orbit coupling of transition element impurity in noble metal 9-47303
- superconducting binary alloys, transition temp. increase, mechanism 9-24139
- superconducting film with mag. impurities, far-i.r. study of energy-gap props. 9-41185
- superconductor, two-band with nonmag. impurities, upper critical field 9-30857
- superconductors, s-d interband impurity scatt., d-band transition temp. decrease 9-33261
- superconductors, single-zone, isotropic, with paramag. impurities, conduction state 9-37455
- superconductors, spin fluctuations assoc. with form. of localized mag. moments 9-47082
- superconductors, two-band, with paramag. impurities, thermodynamic props. 9-33264
- tetracene, trapping levels obs. from space-charge-limited currents 9-41204
- transistor, double- diffused with Gaussian impurity distrib., intrinsic transport parameters 9-33350
- transition element in noble metal, effective spin-orbit coupling 9-47303
- transition metal oxides impurity conduction rel. to polaron theory 9-49009
- transition metals, dielec. sweeping of impurity pot. 9-43100
- trapping level non- exponential distrib. determ. by space-charge-limited currents using differential method 9-41125
- tunneling and band struct. at low temp. 9-47037
- Urbach's rule confirmed for impurity absorption 9-45310
- valence electron model of atoms 9-33545
- vibrational spectrum of lattice with isolated interstitial impurity atom 9-40930
- Ag halides, induced i.r. absorpt. due to bound polarons 9-46829
- AgBr, brominated, acceptor ionization energy of neutral Ag vacancies obs. from optical absorpt. 9-41373
- AgCd dil. alloys, electronic contrib. to specific heat 9-26426
- AgCl: Cd, relax. of vacancy-dipoles 9-33372
- AgCl transition-metal doped single cryst., relax. of vacancy-dipoles 9-33372
- AgMn alloy, from photoemission meas. 9-26613
- AgPd dil. alloys, electronic contrib. to specific heat 9-26426
- Al₂O₃: Si, m.o.s., trap distrib. from interface characts. 9-49132
- p-AlSb, acceptor photoexcitation spectra, uniaxial stress eff. on lines 9-39832
- B, trapping processes, thermally stimulated current obs. 9-43062
- Bi:Sn, distrib. coeff. and acceptor valency determ. 9-43002
- Bi-(0.3 at.%)Sn alloy, isoenergetic surface struct. at L-maximum obs. 9-35312
- CaF₂, elec. fields and polariz. prod. by defect charge density, lattice summations 9-33215
- CaF₂, electrostatic pots. and spatial deriv. about pt. defects 9-33214
- CaS:Cu, trap levels from phosphores. and thermal glow curves 9-35693
- CaS:Cu,Zn, trap level distrib. 9-35694
- CaWO₄, local trapping levels, thermal activation energies and recomb. kinetics, thermoluminesc. props. rel. to ray luminesc. props. 9-39890
- n-Cd_{1-x}Mg_xTe:Al mixed cryst., donor ionization energy x-depend. w.r.t. Hall coeff. and resistivity meas. 9-43054
- n-Cd₃P₂, impurity-band edge transitions w.r.t. photoconductive response and photoluminesc. 9-39712
- Cd_{0.9}Mg_{0.1}Te:Cl, double-acceptor defects and hole traps 9-41263

Crystal electron states continued**impurity states and effects continued**

- CD₂:Y, semicond., resistivity and Hall coeff. obs. rel. to Y conc. 9-49077
- CD₂:Y, trapped electron theories rel. to i.r. absorpt. and transport props. 9-47354
- CD₃:Pt, photo e.m.f. association with r-centres in i.r. region, stimulation mechanism 9-30997
- CD₃, carrier trapping effects resolving by use of supercond. cavities 9-41209
- CD₃, hole-trap depletion layer form. 9-41210
- CD₃, injection and field-induced excitation of charge carriers 9-43108
- CD₃, thermally-stimulated-current curves determ. of electron traps 9-41259
- CD₃, trap conc. determ. by space charge currents 9-37402
- CD₃, trapping obs. via acoustoelec. eff. using pulsed u.s. meas. 9-24031
- CD₃ single cryst. alloyed with In and Ga, luminesc. 9-37756
- CD₃, carrier trapping rel. to photocurrent I-V characts. 9-26602
- n-CdTe:Br, donor level in conduction band, i.r. spectrum obs. 9-26734
- n- CdTe:In (Al, Cd), heat treated, multiply charged acceptors, photo-Hall effect obs. 9-49075
- CDWO₄, local trapping levels, thermal activation energies and recomb. kinetics, thermoluminesc. props. rel. to ray luminesc. props. 9-39890
- p-CoO:Li, elec. conduction obs. 9-37518
- Cs halides, F-centre emission energies and lifetimes 9-32999
- Cu-Al, dilute alloy, impurity contribution to Hall coeff., 77°-300°K 9-28466
- Cu-Ge, dilute alloy, impurity contribution to Hall coeff. 77°-300°K 9-28466
- Cu-In dilute alloy, impurity contribution to Hall coeff. 77°-300°K 9-28466
- Cu-Sn dilute alloy, impurity contribution to Hall coeff. 77°-300°K 9-28466
- Cu, Wannier function localization 9-26482
- Cu₂S-CdS heterojunctions, heat-treated, hole trapping and photovoltaic effect mechanism 9-39650
- CuCl, exciton dissoci. by localized elec. fields, photoconductivity spectra and vibr. struct. obs. 9-41138
- CuMn alloy, from photoemission meas. 9-26613
- EuSe, mag. polaron effects in photoconductivity 9-39714
- p-GaAs: Cd, epitaxial, photoluminesc. w.r.t. conduction band-acceptor recombination theory 9-37783
- GaAs: Cd ion implanted layers, surface resistivity, annealing depend. 9-33320
- GaAs: Cu, vibrational structure rel. to nature of centres 9-33231
- p- GaAs: Fe, radiative transitions between deep acceptors and valence band 9-47395
- GaAs: Mn(Si), (Cd), electroluminescence 9-28661
- GaAs: Si, compensated, localized vibrational modes contrib. to i.r. absorpt. band 9-47357
- GaAs: Si, energy band tails and photoconductivity 9-39716
- n-GaAs: Si, epitaxial, photoluminesc. w.r.t. conduction band-acceptor recombination theory 9-37783
- GaAs: Si epitaxial p-n junctions, radiative recomb. mechanism 9-47138
- GaAs: Zn, noise spectra in thermal equil. and under optical excitation, electron fluctuations obs. 9-41198
- GaAs: Zn ion implanted layers, surface resistivity, annealing depend. 9-33320
- GaAs, diffused junction laser, annealing effects, optimum temp. rel. to impurity conc. 9-45958
- GaAs, diode based laser, spectral characteristics rel. to impurity energy states near conduction band 9-34178
- n-GaAs, dopant conc. effects on radiative efficiency and deep-level luminescence in crystals grown by liq.-phase epitaxy 9-47396
- n-GaAs, electron-donor recomb. and h.f. phonon generation 9-39520
- n-GaAs, epitaxial, far-i.r. photocond., mag. field effects on hydrogenic donor states 9-45022
- GaAs, i.r. photocond. spectra of shallow donors in mag. fields 9-41265
- GaAs, ion implantation profiles of ⁸⁵Kr, rel. to incident energy, orientation and dose 9-47120
- GaAs, ionized impurity scatt. influence on Gunn-effect charact. 9-39637
- p- GaAs, luminesc. involving As vacancy-acceptor centres 9-45346
- n-GaAs, slightly doped, Hall effect at low temp. 9-33303
- n-GaAs, space charge layer capacitance 9-35400
- GaAs, substitutional Cu impurities, electroabsorption study 9-35413
- GaAs, trap-controlled bunching of electrons in acoustoelec. domains 9-44976
- GaAs electron capture cross section by Cu ion centres 9-49106
- GaAs epitaxial layers, donor extrinsic photoconductivity spectral meas. in mag. fields 9-39717
- GaP:⁶⁵Zn(75Se), vapour-grown, substrate orientation effect on dopant incorporation 9-30920
- GaP: Bi, Zeeman splitting of recomb. radiation 9-45347
- GaP: Bi, Zeeman splitting of recomb. radiation of excitons bound to impurities 9-45347
- GaP: Zn, resistivity and Hall coeff. variation with dopant conc. 9-44954
- GaP: Zn conc., room- temp. hole conc. variation with Zn partial press. of growth ambient 9-30529
- GaP: Zn soln.-grown, O solubility 9-33321
- p-GaP: Zn(O), red emission, config. coordinates applic. 9-37761
- GaP-Cu diodes, induced photovoltaic effect, charge-carrier capture, effect on transition capacitance 9-35510
- GaP, donor and acceptor multiple fields and effects 9-43063
- n-GaP, electron mobility and impurity conc., 77° to 400°K 9-26544
- GaP, interimpurity recombinations involving isoelectronic trap Bi 9-39866
- GaP, pair spectra involving Si donors 9-45358
- GaP, photoluminesc. of isoelectronic trap N, bound excitonic mol. obs. 9-39895
- GaP, vibrational modes, localized, i.r. absorpt. obs. 9-35657
- GaP electrodes, charge transfer between energy states and redox systems, photoexcitation and electroluminesc. obs. 9-30990
- GaSb-InSb alloys, phonon scattering by acceptor defects, thermal conductivity meas., 5° to 300°K 9-44870
- GaSb, phonon scattering by acceptor defects, thermal conductivity meas., 5° to 300°K 9-44870
- GaSe: Br, energy structure, absorpt. spectra 9-35412
- Gd³⁺ in 5 hexagonal crystals, energy levels 9-33555
- Ge: Au, i.r. absorpt. rel. to hole transitions from impurity levels to valence band 9-44981

Crystal electron states continued**impurity states and effects continued**

- n-Ge:Au(Sb), injecting contacts influence on impurity photocond. kinetics 9-47203
 Ge:B, i.r. absorpt. rel. to hole transitions from impurity levels to valence band 9-44981
 p-Ge:Be, photoconductivity spectra 9-37619
 Ge:Ga, bipolar photoeffect due to anomalous Cu distrib. in and near diffused layer 9-45024
 p-Ge:GaAs, radiative recomb., influence of local pot. fluctuations, low-temp. 9-39867
 Ge:Sb, far i.r. absorpt. spectra, excitation lines shift, conc. depend. 9-35659
 Ge:Sb, percolation obs. of semicond.-to-metal transition rel. to impurity conc. 9-49095
 Ge, adsorption of CO, effect on donor and acceptor character of surface states 9-43074
 p-Ge, centres, photo-Hall effect and generation-recombination noise 9-28513
 n-Ge, degenerate, density of states rel. to impurity conc. 9-41217
 Ge, dislocation acceptor levels, occupation ratio rel. to temp. 9-26556
 Ge, electron capture cross section by Cu ion centres 9-49106
 Ge, energy and conc. determ. by highly sensitive photoresponse technique 9-39644
 Ge, heavily doped, u.v. refl. spectrum 9-35645
 n-Ge, hole traps. prod. due to 50 keV ion irradi. 9-47124
 p-Ge, impurity photocond. spectra in field of 0.5-100 V/cm at temp. 8-15°K 9-37620
 Ge, intervalley electron scattering under uniaxial compression 9-35421
 Ge, magnetoconcentration effect due to carriers redistrib. at impurity centres, Hall const. temp. depend. obs. 9-39645
 n-Ge, phonon scatt. by neutral donors 9-44983
 Ge, Zeeman splittings of shallow acceptor states 9-41378
 Ge, Fe as recombination centre, study by transient p-n junction technique 9-33330
 Ge alloyed, strongly, donor complexes form. mechanisms 9-49096
 n-p-Ge non-ohmic conduction under strong mag. field, rel. of donors 9-35420
 p-Ge plastically bent, photocond. obs., trapping effect due to dislocations 9-35507
 Ge, quenched, thermal acceptors and vacancy behaviour 9-49107
 I, trapping states 9-41133
 n-InAs, elec. props. influenced by impurity scatt. 9-39622
 InAs, pot. barrier interaction of depletion regions 9-39720
 InAs_{1-x}P_x, vapour-deposited epitaxial layers, n-, p-doping during growth obs. 9-30910
 p-InP:Zn(Cd) Hall coefficient, max. at 30°K due to impurity band conc. 9-39623
 n-InSb:Ge, amplitude-depend. u.s. attenuation at liq.-He temp. 9-44825
 p-InSb:Zn(Ge), electronic transitions and band structure of acceptors 9-37727
 InSb, bulk quantum efficiency, rel. to doping conc. and temp. 9-35414
 InSb, deep-level, props., NBS report 9-33280
 InSb, donor-impurity excitation spectra in high mag. fields 9-45320
 p-InSb, donor action of β dislocations, p- to n-type conductivity change 9-33322
 InSb, donor and acceptor centres, energy levels and absorpt. spectrum 9-35408
 InSb, heat-treated Hall effect obs. of deep acceptor level 9-39638
 n-InSb, negative photocond. in impurity absorpt. region 9-47205
 n- and p-InSb, photoconductivity spectra 9-30992
 InSb₂, deep donor levels 9-26551
 K halides, F-centre emission energies and lifetimes 9-32999
 KCl:Ag⁺, stress-induced dichroism in u.v. absorpt. bands, temp. depend. 9-45322
 KCl:Au, absorpt. bands, mechanism of form. 9-49277
 KCl:Li⁺(OH⁻), tunnel splitting of impurity motional ground states rel. to elec. cooling 9-27143
 KCl:Li⁺(OH⁻)(CN⁻), splitting in impurity motional spectrum rel. to low temp. anomalies in dielectric behaviour 9-26583
 KCl:OH, tunnelling states from specific heat obs. at 0.3°K 9-44834
 KCl, F⁺ colour centre, electronic props. 9-28296
 KMgF₂(CoF₃), paramagnetic ion impurities, group theoretical classification 9-28443
 LaTe₂-LaSb₂ solid soln., Sb substitution effect on resistivity and thermoelec. power 9-39639
 Li, spin-flip scatt. cross-section for conduction electrons of impurity atoms 9-41346
 Li, spin-flip scatt. cross-section for conduction electrons of impurity atoms 9-41345
 LiF, O effect on low temp. ionic conductivity 9-39671
 Na, spin-flip scatt. cross-section for conduction electrons of impurity atoms 9-41346
 Na, spin-flip scatt. cross-section for conduction electrons of impurity atoms 9-41345
 Na halides, F-centre emission energies and lifetimes 9-32999
 NaCl:Cu⁺, stress-induced dichroism in u.v. absorpt. bands, temp. depend. 9-45322
 NaCl, elec. fields and polariz. prod. by defect charge density, lattice summations 9-33215
 NiO, high temp. defect struct. rel. to elec. props. 9-44966
 Pb:Gd(Mn), supercond., far-i.r. study of energy-gap props. 9-41185
 PbTe polycryst. layers, intrinsic behaviour due to impurity compensation by surface states 9-33325
 Pd-Ag alloys, rel. to anisotropic scattering, effect on Hall coeff. 9-37451
 Pb-Rh dil. alloys, exchange enhanced, density of states at E_F from field-dependent mag. susceptibility 9-26625
 Pt(0.07 at %Co) alloy, low-temp. elec. resistivity 9-33257
 Rb halides, F-centre emission energies and lifetimes 9-32999
 Rb halides, F-centre emission energies and lifetimes 9-32999
 RbCl:CN⁻, tunnel splitting of impurity motional ground states rel. to elec. cooling 9-27143
 Se, trapping and capture levels rel. to space charge and surface voltage on exposure to light 9-39727
 Se, vitreous, hole Hall mobility and trap parameters determ. in multiple trapping case 9-39668
 Si:Al(B), electron-irrad., defects effect on photoconductivity spectra 9-44985
 n-Si:As, photomagneto- and photoconductive effects, low temp. 9-39723

Crystal electron states continued**impurity states and effects continued**

- Si:Au, electron and hole emission rates at centres from photocurrent and photocapacitive meas. 9-39636
 Si:B i.r. absorpt. rel. to hole transitions from impurity levels to valence band 9-44981
 Si:Bi, resonant phonon interactions effect on absorpt. line shapes 9-26741
 Si:Li-diffused, P donor and Li-O complex levels, and behaviour on irradi., e.s.r. obs. 9-26794
 n-Si:Li, electron-irrad. induced carrier-removal defects 9-49113
 Si:Li, thermal ionization energy of Li and Li-O complexes from Hall effect meas. 9-47131
 Si:Na, ionization energy obs. from resistivity and Hall coeff. temp. depend. meas. 9-43077
 Si:P, ESR, absorpt. intensity 9-35717
 Si:P, percolation obs. of semicond.-to-metal transition rel. to impurity conc. 9-49095
 Si:Zn photoconductors, noise and changing recomb. traffic obs. 9-41270
 Si-Si₃N₄ films, trapping levels obs. 9-33359
 Si-SiO₂-Al system, C-V hysteresis curve due to presence of donors and acceptors in SiO₂ layer 9-35432
 Si, absorption edge modification by radiation-induced defects 9-47132
 Si, As isoelectron diffusion studies 9-37208
 n-Si, degenerate, density of states rel. to impurity conc. 9-41217
 Si, dopant effects of Li, Na, Be, Cl, Al and O on carrier lifetime 9-24234
 Si, electron capture coeffs. of group III acceptors 9-39647
 Si, epitaxial, doping and solid soln. prop. and behaviour 9-44984
 n-Si, heavily doped, enhanced Au solubility effect 9-30929
 Si, heavily doped, u.v. refl. spectrum 9-35645
 p-Si, interaction between radiation defects and impurities during high-temp. annealing 9-37547
 Si, intervalley electron scattering under uniaxial compression 9-35421
 n-Si, trap filling mechanism 9-26577
 Si alloyed, strongly, donor complexes form. mechanisms 9-49096
 SiB, intervalley electron scatt. 9-43076
 n-SiC, deep donor level obs. 9-49097
 p-SiC, radiative recombination at deep levels 9-28711
 n-SiC α (6H) crystals, Ni impurity levels contributing to transitions of bound electrons 9-43243
 α (6H)-SiC exciton-impurity complexes detect. from absorpt. spectra at 86°K 9-41389
 SiO₂-Si m.o.s. struct., diffused Zn effects on C-V characts. 9-33362
 SrS:Cu, trap levels from phosphoresc. and thermal glow curves 9-35693
 SrS:Cu,Zr, trap level distrib. 9-35694
 SrTiO₃:Eu³⁺, electronic coupling to optical phonons 9-33166
 SrTiO₃, O deficient, paramag. centres effect on supercond. transition temp. 9-37475
 SrTiO₃, struct. obs. in photoconductivity excitation spectra 9-45025
 SrTiO₃, trapping phenomena, photoconductivity meas. 9-39725
 Sm³⁺ in CaF₂ type I, trigonal crystal field energy levels 9-33244
 Ti₂O₃:V³⁺, inelastic scatt. mechanisms involving mag. impurities in negative magnetoresistance at 4.2°K 9-47070
 YGa garnet: Yb³⁺, F_{7/2} levels, Raman-Zeeman obs. 9-49300
 Zn:Li single cryst., space charge limited currents between asymmetric contacts 9-33378
 ZnO:Ni, emission process mechanisms w.r.t. activator excitation energy transfer to electrons in traps 9-39874
 ZnO, surface states assoc. with chemisorbed species 9-43008
 ZnO, trapping and capture levels rel. to space charge and surface voltage on exposure to light 9-39727
 ZnS, self-activated, trap level optical depths from i.r. induced photoconductivity and luminesc. obs. 9-41273
 ZnSb:Te, effect of doping of crystn. process and elec. props. 9-42757
 ZnSe:Ge(Pb) as hole traps, EPR meas. 9-35706
 ZnTe:Li(P), shallow acceptor centres, luminescence 2-300°K 9-26769
 ZnWO₄, local trapping levels, thermal activation energies and recomb. kinetics, thermoluminesc. props. rel. to ray luminesc. props. 9-39890
- plasma**
- Alfven waves absorpt., rel. to electron relaxation-time determ. 9-37382
 bubble form. by laser irradi., rel. to conduction band definition 9-26490
 in counters, semiconductor, time delay effects for heavily ionizing particles 9-44088
 electron-hole, slightly noncompensated, wave propagation cutoff 9-26492
 electron-hole, weak turbulency of helicons 9-48550
 exciton polarons and plasma-exciton waves 9-49008
 graphite, principle oscillatory freqs. 9-47060
 helicon wave propag. in two-component plasma 9-43014
 Josephson plasma resonance, deriv. using quantum phase operators 9-44927
 I.f. oscillations of inhomogeneous solid-state plasma 9-43013
 magnetoplasma resonance, scattering theory of small-particle absorption, ellipsoidal sample in e.m. cavity excitation 9-41150
 metal, surface plasmons 9-39574
 metal film, self-supporting, covered by oxide layers, eff. on opt. props. 9-26672
 metal surfaces, rough, plasmons coherent contrib. to reflectivity 9-35317
 metal-semiconductor sandwich, magneto-plasma wave propagation 9-30952
 metals, positron excitation in an electron plasma 9-30824
 oscillations, localized plasmons and plasma-exciton reson. obs. 9-37414
 oscillations in crystals bombarded with 20 keV electrons 9-41140
 oscillations in semiconductor with non-standard dispersion law in presence of elec. and mag. fields 9-37504
 plasmons, surface, on optically excited metal grating, coherent and incoherent radiation emission 9-24371
 quantum, in high mag. fields, dielec. function and magnetization waves 9-41143
 semiconducting, Raman scatt. by coupled plasmon-cyclotron-harmonic modes, nonlocal effects 9-33238
 semiconductor, coupled plasmon-optical-phonon system, sum rules 9-43048
 semiconductor, degenerate, electron-plasmon interaction and tunneling meas. 9-41195
 semiconductor, effective mass determ. from i.r. plasma refl., carriers degeneration depend. 9-44972
 semiconductor, electron-hole, instability of pinch effect 9-39575
 semiconductor, ferromag., spin-plasma surface wave interac. 9-33323
 semiconductor, finite-amplitude helical mode 9-47102

Crystal electron states continued
plasma continued

- semiconductor, Gunn-instability, two-valley model, soft modes and associated critical fluctuations 9-30895
semiconductor metal junction excess tunneling current due to electron-plasmon interac. calc. 9-37553
semiconductors, electric drift instability criterion 9-35322
Ag-Pd alloys, freq. conc. depend. 9-37436
Ag, resonance in photoemission 9-33422
Ag film resonance emission, temp. depend., 90-770°K 9-23641
Ag films, rough, optical stimulation of non-radiative surface plasmons 9-37415
Ag surface waves, nonradiative, excitation; scatt. radiation 9-41145
Ag thin films, plasma reson. radiation, correl. with surface roughness 9-44621
Al, helicon waves for Hall coeff. accurate determ. 9-24124
Al 50 keV electron irradiation, surface plasmons radiation, 10.1 eV peak 9-41146
Al film in vac., light irradiation, photoelectric yield, plasma resonance obs. 9-41282
Bi, Alfvén-wave propag. and mass density calcs. 9-24106
Bi, magnetoplasma waves, spatial dispersion effect on spectrum 9-30826
CdTe, Gunn effect 9-49090
Cs on W, decay rate of surface plasmons 9-32849
Ga foils, plasma oscillations 9-41148
n-Ge, thermal pinch effect 9-43073
Ge slice, carrier density wave instability rel. to enhanced carrier diffusion 9-26555
HgTe, two helicon resonances obs. 9-43014
In, helicon waves for Hall coeff. accurate determ. 9-24124
InSb, electron-hole, radial Hall voltage 9-37416
n-InSb, Z-pinch, time evolution determ. from conductivity meas. 9-44964
n-InSb pinch effect, theory and expt. 9-41147
K, correlation-prod. magnetoplasma mode, expt. evidence 9-26495
K, helicon waves for Hall coeff. accurate determ. 9-24124
Na, helicon waves for Hall coeff. accurate determ. 9-24124
NaCl, instability during electrical breakdown, formation of gas bubbles 9-41235
PbSe, valence plasmon excitation energies from charact. electron energy losses 9-39553
n-PbTe, magnetoplasma effects, local and non-local 9-47059
PbTe, valence plasmon excitation charges from charact. electron energy losses 9-39553
Si diodes, in anode-cathode space, light emission during second breakdown 9-39652
Sn foils, plasma oscillations 9-41148
SnTe, valence plasmon excitation energies from characteristic electron energy losses 9-39553
ZnSe, Gunn effect 9-49090

polarons

- alkali halides, effective mass, translational energy depend., cyclotron reson. obs. 9-39573
anthracene, polaron dispersion relations 9-39571
biaxial and uniaxial crystals, polaron dispersion 9-37413
centrosymmetric crystals, polaron obs. by small-angle light scatt. 9-24429
crystalline and noncrystalline materials, theory including impurity conduction 9-49009
effective-mass wave functions for polaron in external fields 9-43011
electron-excess colour centres model, applic. to calc. of electronic and ionic polarization effects on F^+ centre 9-44716
exciton, and plasma-exciton waves 9-49008
Hall and drift mobility, temp. depend., large coupling constants 9-35321
Hall effect and small polaron motor, adiabatic approx. 9-43009
impurity-centre-localized, e.m. wave absorption, polarization mechanism 9-31096
mobility calc. Kohn-Luttinger diagram method 9-33236
piezoelectric, effective mass and energy calcs. by Feynman method 9-41139
piezoelectric, strong-coupled, effective mass calc. 9-39572
polaron inelastic scattering by longitudinal optical phonons as luminescence mechanism 9-37757
polaron modes at ideal surfaces 9-49010
polaron resonant scatt., composite particle treatment 9-45334
polaron scattering by phonons in radiation emission 9-24443
polaron-phonon coupling effect on spatial dispersion rel. to dielec. const. in exciton transition 9-44893
polaritons, interacting, in dielectric, excitation spectrum 9-47057
rutile, in Hall mobility temp. dependence, 300-1250°K 9-24181
small, non-adiabatic, Hall eff. in hopping transport 9-30898
small, transition probability for low coupling between carrier and lattice and small phonon dispersion 9-43010
transition metal oxides, theory including impurity conduction 9-49009
in transition-metal oxides, present status review 9-28454
transitions from large to nearly-small polarons, theory 9-47056
Ag halides, induced i.r. absorpt. due to bound polarons 9-46829
AgBr, drift mobility, high temp. 9-43012
AgBr, piezo-optic study 9-39814
Ag halides, effective mass, translational energy depend., cyclotron reson. obs. 9-39573
BaTiO₃, tetragonal, polaritons in Raman scatt. 9-35671
CdO, effects on i.r. absorpt spectrum 9-24404
CdS, luminescence from polaron inelastic scattering by longitudinal optical phonons 9-37757
EuSe, mag. polaron effects in photoconductivity 9-39714
GaP, parametric luminescence, involving polaron excitation 9-49317
KCl, band structure and theory, F-centre electron wave function determ. 9-33237
KTiO₃, polaron obs. by small-angle light scatt. 9-24429
NaF band structure and theory, F-centre electron wave function determ. 9-33237
SrTiO₃:Zr, supercond., transitions from large to nearly-small polarons 9-47056
SrTiO₃, polaron obs. by small-angle light scatt. 9-24429
TiBr, mass and relax. time of photocarriers from cyclotron reson. obs. 9-39726
TiCl, mass and relax. time of photocarriers from cyclotron reson. obs. 9-39726
TiCl, photoconductive, transport props. 9-41272
- Crystal electron states continued**
polarons continued
ZnO, parametric luminescence, involving polariton excitation 9-49317
- surface**
adatom interactions, indirect, through AB-type crystals 9-34998
band structure calcs. from LEED meas. 9-33228
bound states on curved surface 9-47053
cubic lattice model 9-39568
electron mobility, for linear quantizing band curvature 9-44863
electron relaxation times and specularity of scattering from surface state reson. 9-37411
Green's function method for three-dimens. cryst. 9-39569
metal, electron distrib., self-consistent props. 9-47052
metal, e.m. wave absorpt. rel. to surface roughness 9-45268
metal, field ionization rel. to Fermi-surface struct., tunnelling probabilities obs. 9-47218
metal, field ionization rel. to Fermi-surface struct., tunnelling probabilities obs. 9-43146
metal, magnetic levels 9-49001
metal, rough, plasmons coherent contrib. to reflectivity 9-35317
metal, static-field penetration and atomic polarization effects 9-43137
metal, surface pot, charact. in free-electron model 9-41276
metals, impedance and boundary scattering anomalous skin depth conditions 9-37426
metals, u.s. wave attenuation by magnetic surface states 9-28418
m.o.s. struct., surface states densities evaluation 9-49131
of one-dimensional bands in WKB approx. 9-44872
semiconductor, degeneracy effects 9-43066
semiconductor, ferromag., spin-plasma surface wave interac. 9-33323
semiconductor, heavily doped, energy scale of localized levels near surface 9-35416
semiconductor, internal reflection spectra 9-43229
semiconductor, non-equilib. phenomena 9-43065
semiconductor, optical absorpt. due to bands in energy gap 9-39827
semiconductor, theory 9-49100
semiconductor electroreflectance meas. rel. to band structure 9-43215
semiconductor multi-emitter struct., spreading resistance 9-37564
semiconductor photoelec. emission determ. 9-43142
semiconductors, bands of electronic surface states, calc. 9-30899
semiconductors, quasi-continuous spectrum of levels in forbidden band 9-35415
semiconductors with low surface recombination of current carriers, elastic wave instability 9-30897
theory, evaluation 9-47051
thin film, model investigation and comparison with infinite cryst. 9-35310
three-dimensional cryst., energy bands calc. 9-33233
transition metals, surface tension calc. using method of moments 9-49002
Al-Al₂O₃-ZnTe, I-V characts. of tunnelling junction 9-33357
Al, mode loss for Hall coeff. accurate determ. 9-24124
Al₂O₃-Si, m.o.s., interface characts. reactive sputtered 9-49132
Bi-(0.3 at.%)Sn alloy, isoenergetic surfaces struct. at L-maximum 9-35312
CdS, photoconducting, non-equil. contact pot. difference 9-33409
CdS absorpt. edge obs. 9-45316
Cu, bound states on curved surface 9-47053
Cu, quantum state transitions rel. to impedance oscillations 9-37411
Ga state resonances, effect of relax time, from amplitude and linewidth temp. depend. 9-37411
n-GaAs, density obs. from field-emitted electrons energy distrib. meas. 9-35517
n-GaAs with impurity band, temp. depend. of trapped charge 9-35400
Ge, atomically clean, model of spectrum of levels 9-47123
Ge, carrier mobility and scattering 9-35419
Ge, donor and acceptor character, of states, effect of CO adsorption 9-43074
n-Ge, ion irradiat., props. change 9-47124
Ge, SiO₂-passivated, dominant electronic props. rel. to annealing treatment 9-49104
Ge, rel. to thermal desorption of water in ultra high vac. 9-35425
n-Ge 'fast' surface states temperature and frequency dependence 9-47126
Ge electrode polarization state from electroreflectance meas. at semiconductor-electrolyte interface 9-49102
Ge films, elec. instabilities and ionization of surface centres 9-47122
Ge thin films, influence on temp. depend. of Hall coeff. and conductivity 9-33326
In, mode loss for Hall coeff. accurate determ. 9-24124
p-InSb, conductivity in n-type surface inversion layer, low temp. 9-44963
InSb, field effect and surface photocond. obs. 9-43130
InSb polycryst. layers, elec. surface props. 9-33325
K, mode loss for Hall coeff. accurate determ. 9-24124
Na, mode loss for Hall coeff. accurate determ. 9-24124
Ni-neutralization spectroscopy study 9-44890
PbSe epitaxial films, models from field-effect meas. 9-41190
PbTe epitaxial films, two models from field-effect meas. 9-41190
PbTe polycryst. layer elec. surface props. 9-33325
Si-SiO₂ structures, density rel. to thermal oxidation conds. of Si 9-26560
Si, mag. field effects on transport props., anomalous magnetoconductance obs. 9-28523
p-Si, minority carrier mobility meas., recombination, analytical treatment 9-37544
Si inversion layers, quasiparticle g factor for spin splittings 9-24103
SiO₂ film on Si, and interface, charge density and electron donor sites 9-43099
Sn, electron reflection, specularity 9-37411
ZnO, states assoc. with chemisorbed species 9-43008
- transport processes**
acoustoelectric phonon generation observed in X-ray diffraction microscopy 9-46997
alkali halides, electron-phonon interaction, transmission secondary emission 9-44868
alkali halides, electron-phonon interaction second. electron transport 0.25-7.5 eV 9-44867
alkali metal films and wires, electron-electron scattering effect on resistivity 9-37435
alkali metals, electron-phonon interaction in optical conductivity, Mayer-Naby peak 9-28679
alkali metals, electron-phonon interactions, anisotropy 9-37389
alkali metals, electron-phonon interaction, modification for correlation effects 9-35308

Crystal electron states continued
transport processes continued

alkali metals electrical and thermal resistivities calc. using Sharma-Joshi model for lattice dynamics 9-42995
 alloys, dilute, magnetic; thermopower, electrical and thermal resistivity calc. by Suhl-Nagaoka theory 9-45051
 anisotropic crystals, interaction of optical excitons with phonons 9-33223
 anthracene, current carriers mobilities, temp. depend. 9-33312
 anthracene, electron and hole mobilities, high-temp. depend. 9-24087
 anthracene, electron- bombarded, carrier generation process obs. 9-33226
 anthracene, low-temp. hole injection and hole trap distrib. 9-44970
 anthracene, tight binding calc. of current carrier mobilities 9-33313
 antiferromagnetic metals, electron scatt. on thermally fluctuating spins near Neel point 9-45206
 Bloch electron in mag. field, wave functions and energy levels, perturbation approach 9-44865
 carrier conc. field depend. in high elec. field 9-39559
 carrier lifetimes in the presence of trapping 9-47096
 chalcogenide glasses, photo-excited carriers transport and generation 9-39709
 p-chloranil, electron injection in single cryst. by aqueous electrolyte contact 9-41203
 conductivity tensor, nonlinear, of weakly interacting electron system in external elec. field 9-48984
 conductors, thin, electron scatt., magnetoacoustic eff. sensitivity 9-24029
 Coulomb interaction effect at saddle-type crit. pts. 9-44866
 cylindrical sample in transverse mag. field, Boltzmann, eqn. applic. to magnetomorphic oscillations in isothermal elec. conductivity 9-37427
 diamond-type, electron interaction with short-wavelength vibrations, rel. to effective carrier mass 9-44874
 diamond-type cryst., interac. of electrons with phonons, effective mass of carriers 9-26473
 diamond-type cryst., interac. of electrons with phonons, effective mass of carriers 9-26473
 differential conductivity and current fluctuations of hot electrons, Green's function approach 9-47028
 drift mobility techniques for study of elec. transport props. 9-39660
 dye-photosemiconds., org., flash investigation 9-24182
 dynamic magnetoconductivity for strong coupling case in electron-impurity system 9-30813
 electron mean free paths, anisotropy, from resonances 9-37388
 electron mean free paths from Gantmakher effect theory 9-37387
 electron-phonon interactions, u.s. attenuation obs. 9-37330
 electron-phonon interaction, strong, effect on umklapp processes during phonon decay 9-41074
 electron-phonon interaction, translational invariance in uniform fields and density matrix eqn. in Wigner representation 9-48985
 electron-phonon interaction in high elec. fields, Wannier-Stark levels 9-42993
 electronic crystals, electrodynamics 9-47030
 Esaki tunnelling probability of tunnel diode 9-33348
 exciton dragging eff. by interac. with electrons and holes 9-24100
 exciton-bicxicon inelastic collision 9-47054
 Fermi liquid in random scatt. centres, quasiparticle description in macroscopic and low-temp. limit 9-25055
 ferroelectric, electron scatt. obs. 9-37591
 ferromagnet, quasicalssical theory of galvanomag. effects 9-47255
 ferromagnetic tunnel junction, electron-magnon effects 9-47238
 glasses containing transition metal ions, conduction 9-30964
 group IV-VI cpds., rel. to band edge structure 9-39627
 group IV-VI cpds., rel. to tunneling characts. 9-39655
 haematite, effect of weak ferromag.-antiferromag. transition 9-44869
 hopping transport for non-adiabatic small polarons and impurity conduction, Hall eff. 9-30898
 impurities in hot-electron transport problems 9-24084
 impurity band conduction in mag. field 9-42997
 insulating films, Fowler-Nordheim tunneling, eff. of nonparabolic momentum 9-39661
 insulator, carrier transport from photo-injection obs. 9-39739
 insulator with multiple trapping, injected current time-depend. flow, thermal release and transit time 9-39668
 insulators, magnon-phonon interactions rel. to thermal conductivity 9-44847
 interacting system of cryst. electrons, optical and energy loss spectra, dynamical theory 9-37385
 ionic cryst., strong phonon interactions in photo-Hall mobility 9-39701
 Kondo model describing interaction of conduction electrons with localized mag. impurity 9-39560
 localized carriers, trapping and release 9-33224
 magnetite, double-exchange, electron-hopping process and metal-nonmetal transition 9-41168
 magnetite, stoichiometric and non-stoichiometric, fast electron-hopping process, Mossbauer obs. 9-39818
 magnon drag 9-24332
 metal, Fermi surface existence and shape depend. 9-39563
 metal, two-band model, carrier density and mobility 9-39580
 metal-Si Schottky barrier diodes 9-47143
 metals, anisotropic mean free path, from galvanomag. meas. 9-37386
 metals, boundary scattering and surface impedance, anomalous skin depth conditions 9-37426
 metals, galvanomagnetic tensor from Boltzman eqn., approx. expression 9-37433
 metals, normal and supercond., microwave phonon-electron interac. 9-37384
 metals; pure, Fermi surface considerations 9-47024
 m.i.m. struct., carrier transport 9-41228
 m.i.m. tunnel junctions, effect of deep traps on barrier heights 9-44994
 molecular cryst., exciton-phonon interaction 9-42994
 molecular cryst. thin layers with intermol. H-bonds, charge carrier generation mechanism 9-33366
 molecular crystals, effects explained in terms of energy gap 9-28450
 molecular crystals, exciton-phonon interaction influence on light absorpt. bands 9-43234
 m.o.s.t., enhancement n-channel, with high electron mobility 9-37563
 Mott-Wannier excitons interaction in vibr. lattice, pol. energy operator 9-33234
 noble metals, phonon drag and Hall coeff. 9-43026
 noise, 1/f, rel. to mobile charge carriers number 9-39614
 non-crystalline materials, conduction and switching 9-28485

Crystal electron states continued
transport processes continued

oligonanilinic donor-acceptor complexes, carrier conductivity 9-33225
 one-dimensional aperiodic cryst., electron average momentum def. 9-44882
 oxides, mixed valency-type, phase transition due to electronic ordering 9-41127
 phonon enhancement of density of states, solid alkali metal 9-30814
 phonon instability in phonon-electron system in mag. field 9-26472
 photoconductor, charge carriers recomb. kinetics 9-41255
 phthalocyanine, metal-free β -form single cryst., electron trapping and bulk conduction in vacuum 9-28462
 polarons, Hall and drift mobility, temp. depend., large coupling constants 9-35321
 polyethylene, electron mobility determ. by injection through cathode method 9-47156
 polymers, semicond. condensation type, rel. to mol. struct. 9-47097
 potential scatt. effect on effective J values in Kondo problem 9-39556
 quantum crystals, transport theory of phonon gas 9-30758
 resistance, elec., quantum theory 9-41126
 rubber, charge transport, mechanism from elec. props. meas. 9-41128
 rutile, Hall mobility temp. dependence, 300-1250°K 9-24181
 Schottky barrier diodes, metal-Si 9-47143
 semiconductor, carrier emission rates and cross-sections impurity photocurrent and photocapacitive methods 9-39636
 semiconductor, carriers, fieldless heating 9-39615
 semiconductor, carriers energy distrib. influence on effective mass determ. from i.r. plasma refl. 9-44972
 semiconductor, coupled plasmon-optical-phonon system, sum rules 9-43048
 semiconductor, degenerate, electron-plasmon interaction and tunneling meas. 9-41195
 semiconductor, discharging method for trapping level calcs. 9-39613
 semiconductor, electron scattering under effect of e.m. field 9-30901
 semiconductor, electron-hole interaction, dielec. screening 9-49069
 semiconductor, ferro- and antiferromag., current carrier mobility, spin-electron interac. effect 9-37516
 semiconductor, free carrier distrib. functions determ. by Raman scatt. 9-49071
 semiconductor, helicon interferometry and nonreson. cyclotron absorpt. method for props. determ. 9-47100
 semiconductor, many-valley, with anisotropic scattering time, h.f. props. 9-47099
 semiconductor, nonlinear galvanomagnetic phenomena in crossed elec. and mag. fields 9-37511
 semiconductor, nonpolar, long-wavelength phonon scatt. of carriers 9-49070
 semiconductor, optical mixing by mobile carriers 9-44952
 semiconductor, population inversion between free carrier zone and local centre levels by field effect 9-35394
 semiconductor, rel. to band struct. 9-49091
 semiconductor, screened Coulomb interaction rel. to photoconductivity and photoreflectance 9-39703
 semiconductor, Sondheimer oscillations of magnetoresistance tensor components, transverse elec. field effect 9-39617
 semiconductor, unipolar, self-oscillation of carriers 9-37512
 semiconductor carrier lifetime meas. 9-33280
 semiconductor carrier lifetime meas., bibliography 9-33293
 semiconductor electron-phonon interaction, expt. investigation, using acoustic propag. 9-33294
 semiconductor free carrier sweep-out in space charge field after pulse injection 9-30896
 semiconductor nonequilibrium carrier density, current instability study 9-41194
 semiconductor thin films, inelastic carrier scattering, influence on thermogalvanomagnetic effect 9-35494
 semiconductors, carrier lifetime and mobility meas. by microwave techniques 9-33292
 semiconductors, carriers mixed scatt. on acoustic lattice vibrs. and ionized impurities, parameters determ. 9-37509
 semiconductors, compensated, carrier scattering by ionized impurities 9-39557
 semiconductors, current saturation, theory of electron-phonon interaction 9-44953
 semiconductors, electron redistrib. in photoconductivity at large light intensity 9-28574
 semiconductors, electron-hole interac., screened 9-26541
 semiconductors, ferro- and antiferromagnetic electron-magnon interac., conduction band shift 9-28504
 semiconductors, impurity bombardment produced ionization under arbitrary elec. fields 9-30900
 semiconductors, interac. of electrons with phonons, effective mass of carriers 9-26473
 semiconductors, interac. of electrons with phonons, effective mass of carriers 9-26473
 semiconductors, magnetic, and elec., opt. and mag. props. 9-49064
 semiconductors, magnetoactive, electrons, localized magnons and indirect exchange 9-28607
 semiconductors, non-polar, electronic mobility at intermediate and high elec. fields 9-37515
 semiconductors, phonon drag effect contrib. to elec. conductivity 9-33288
 semiconductors, polar, phonon-cyclotron broadening of Stokes scattering 9-28701
 semiconductors, screening, effect of carrier-wavelength 9-30886
 semiconductors, superconductivity, theory 9-26521
 semiconductors, three-dimensional systems of solns., phase-space analysis in subspaces 9-35392
 semiconductors with complex band structure, electron-phonon interaction screening 9-37510
 semiconductors with high carrier mobility, u.s. absorption coeff. oscills. in h.f. electric field 9-41086
 semimetal, helicon interferometry and nonreson. cyclotron absorpt. method for props. determ. 9-47100
 semimetals, superconductivity, theory 9-26521
 small-angle, effect on magnetoresistance scattering 9-37425
 superconducting metals, microwave phonon-electron interac. 9-37384
 superconducting order parameter, fluctuations, effect on tunneling density of states 9-49036

Crystal electron states continued
transport processes continued

- superconducting thin films, critical current for diffuse refl. of electrons from walls 9-39594
- superconductors, electron-phonon coupling press. depend. in electronic thermal expansion calcs. 9-44838
- superconductors, two-band, with paramag. impurities, interband scatt. of electrons, energy gap obs. 9-33264
- surface mobility, for linear quantizing band curvature 9-44863
- tetracene, charge carrier mobility meas. 9-30817
- in thermal expansion phonon-enhancement contrib. calcs. 9-44838
- transistor, double-diffused with Gaussian impurity distrib., intrinsic transport parameters 9-33350
- transition metal carbides, phonon scatt. by electrons rel. to thermal conductivity 9-47010
- trapping level non-exponential distrib. determ. by space-charge-limited currents using differential method 9-41125
- tunneling between superconductors through paramagnetic impurity barrier, Kondo eff. influence 9-44929
- tunneling of field emitted electrons from W through Zr and χ -N adsorbed layers 9-30960
- tunnelling, introductory article 9-49058
- Ag dilute alloys, and Hall coeff., 1.5° to 50°K and room temp. 9-37442
- AgBr, brominated, hole mobility temp. depend. from optical absorpt. and conductivity 9-41373
- Al-Al₂O₃ triodes, hot-electron transport 9-49128
- Al-GaSe-Au struct., carrier transport 9-41228
- Al-Ga_{1-x}As solid solns. with forbidden band width gradient, minority carriers penetration depth 9-47389
- Ar, e drift velocity saturation 9-26587
- As-Se alloy system, photo-excited carriers transport and generation 9-39709
- As₂Se₃ amorphous films, drift mobility of carriers, hopping conduction 9-26474
- β -B, rhombic, free carrier absorpt., band edge and lattice vibr. spectrum 9-39834
- B carrier mobility, trapping levels and temp. depend. 9-28494
- Bi-Te, carrier density from helicon dispersion relations 9-35395
- Bi-Te layered structure, carrier drift effects on helicon propag. 9-43015
- Bi-Sn alloys, carrier influence on magnetoresistance anisotropy 9-41161
- Bi, carrier influence on magnetoresistance anisotropy 9-41161
- Bi, electron-hole recombination temp. dependence, 2-50°K 9-35306
- Bi₂Se₃, carrier conc., electrons effective mass depend. 9-37390
- Bi single cryst., size effects in elec. conduction due to phonon boundary scatt. and electron mean-free path 9-33253
- Bi whisker, electron mean free path meas. from resistance changes during elastic bending 9-37453
- C diffuse scatt. at crystallite boundaries, negative magnetoresistance obs. 9-24277
- CaO, electron-lattice interaction in F centre 9-44717
- Cd:Zn, small-angle intersheet scatt. effects on galvanomag. props. 9-26515
- Cd-Zn alloys, rel. to Hall resistivity meas. below 77°K 9-37440
- Cd, small-angle intersheet scatt. effects on galvanomag. props. 9-26515
- n-Cd_{1-x}Mg_xTe:(Al) mixed cryst., optical mode scatt. mobility 9-43054
- Cd:Hg_{1-x}Te, intrinsic carrier concs. and mobilities, rel. to semimetal-semiconductor transition 9-49078
- CdF₂:Y, and optical props. rel. to trapped electron theories 9-47354
- CdS, acoustoelectric phonon generation observed in X-ray diffraction microscopy 9-46997
- CdS, behaviour of holes and electrons revealed by laser excitation 9-49157
- CdS, carrier trapping effects resolving by use of supercond. cavities 9-41209
- CdS, current saturation and oscillation, nonlinear theory 9-47105
- CdS, electron-phonon packets, observation by microwave transmission and Brillouin scattering meas. 9-47106
- CdS, high-field domains, transition between stationary and moving 9-33324
- CdS, lattice scattering of electrons 9-47031
- CdS, semicond., beta-excitation, carrier mobilities and lifetimes obs., electron-hole prod. energy 9-33298
- CdS, two channel capture mechanism of holes at sensitizing recomb. centres 9-41262
- CdS single cryst., carrier dragging due to laser rad. 9-28578
- CdS single cryst., photo- and e-conductance comparison 9-37617
- CdS single crystal, d.c. and a.c. electroluminesc. props., electron and hole injection 9-37777
- CdS sintered layers, photoelectronic behaviour ambient-dependence 9-47200
- CdSb, magnetic susceptibility carrier conc. dependence, inequivalent valley model 9-26621
- CdSe, current saturation and oscillation, mechanism rel. to acoustoelec. eff. in piezoelec. mats. 9-26543
- Co_{1-x}Cu_xRhS₄, conduction due to holes in valence band 9-41164
- p-CoO:Li, drift mobility w.r.t. temp. from conductivity and Seebeck coeff. meas. 9-37518
- α -Cu-Zn alloy, phonon drag and Hall effect meas., 4.2° to 300°K 9-43026
- Cu-Zn dilute alloys, virtual p-electron scatt. obs. from 1st order quadrupole effect obs. of ⁶³Cu n.m.r. spectrum 9-35724
- Cu, electron relaxation time and submillimetric cyclotron reson. linewidth 9-37419
- Cu₂O, electron and hole mobility, temp. depend. 9-28496
- Cu₂SbSe₄, electron-hole mobility ratio, energy gap, from Hall eff. obs. 9-26505
- Cu dilute alloys, and Hall coeff., 1.5° to 50°K and room temp. 9-37442
- Fe₃O₄ electron hopping in octahedral sites, Mossbauer linewidth study of ⁵⁷Fe 9-45294
- Ga, single crystal, electron mean free path anisotropy in thermal conductivity, 1.4° to 4.2°K 9-37370
- GaAs:Cd, average mobility, post-implantation annealing depend. 9-33320
- GaAs:Zn, average mobility, post-implantation annealing depend. 9-33320
- n-GaAs, conc. and mobility of electrons in conduction band 9-33301
- p-GaAs, Cs coated, photoemission obs. 9-49082
- n-GaAs, displaced Maxwellian calcs. 9-24176
- n-GaAs, generation and detection of 10¹² Hz phonons 9-49083
- GaAs, hot electron diffusion rate 9-47112

Crystal electron states continued
transport processes continued

- p-GaAs, majority carrier lifetime 9-37618
- GaAs abrupt asymmetrical junctions, radiative tunneling 9-43253
- GaAs electron drift velocity for different temperatures, analytical approach 9-49079
- GaAs electron population inversion induced by high elec. fields 9-26545
- GaAs hot electron effects at microwave frequencies 9-24177
- GaAs single cry., electrolum. by tunnel injection of minority carriers 9-24178
- GaP:S, electron-phonon interaction in extrinsic photoconductivity 9-41264
- GaP:Zn, carrier conc., room-temp. hole conc. variation with Zn partial press. of growth ambient 9-30529
- GaP-Cu diodes, induced photovoltaic effect, charge-carrier capture, effect on transition capacitance 9-35510
- n-GaP, electron mobility and impurity conc., 77° to 400°K 9-26544
- GaP electrodes, charge transfer between energy states and redox systems, photoexcitation and electroluminesc. obs. 9-30990
- GaSb-InSb, e. scatt. mode 9-24085
- GaSb, e. scatt. mode 9-24085
- p-Ge:Au, diode, radial carrier currents, influence on I-V characts. 9-35444
- n-Ge:Mn, spontaneous current oscillations due to excitation of recomb. waves 9-41216
- Ge:Sb, electron-phonon scatt. donor conc. dependence 9-24086
- p-Ge, carrier conc. decrease after deform. w.r.t. donor action of dislocations 9-35424
- Ge, carrier scattering and surface mobility 9-35419
- Ge, conductivity of hot carriers, review 9-33329
- n-Ge, dislocation acceptor level position obs., effect of non-dislocation defects generated during deform. on mobility 9-37540
- n-Ge, dislocation high-density saturation effects 9-43072
- n-Ge, effect of elastic deform. on thermoelec. power in drag effect region 9-37611
- Ge, exclusion of nonequil. hot carriers 9-47125
- n-Ge, Hall coeff. depend. on carrier conc. in low mag. fields 9-24180
- p-Ge, high-field energy distrib. and heavy hole diffusion coeffs. 9-24179
- Ge, hot current carrier surface recombination velocity and diffusion constant dependence on high elec. field 9-41213
- p-Ge, minority carrier mobility strain depend. 9-49105
- Ge, phonon mean free path from transmitted phonon drag data 9-35423
- n-Ge, phonon scatt. by neutral donors 9-44983
- Ge, scattering mechanisms, hot-electron studies 9-37541
- Ge impurity-assisted intervalley electron scatt. under uniaxial compression 9-35421
- Ge slice, carrier diffusion, enhanced, rel. to carrier density wave instability 9-26555
- GeTe, carrier mobility, obs. of energy spectrum changes due to solid solns. form 9-47113
- Hg, electron-phonon interaction rel. to conduction electron props. 9-47032
- Hg_{0.8}Cd_{0.2}Te, sweep-out of minority carriers 9-39719
- Hg_{1-x}Cd_xTe, carrier densities and mobilities determ. by helicon and nonreson. cyclotron absorpt. techniques 9-47101
- HgSe, rel. to dominant scattering mechanism 9-48997
- HgSe, ionized-impurity-limited mobility and band struct. 9-49092
- HgTe-ZnTe, electron scatt. mechanism 9-35307
- HgTe, rel. to dominant scattering mechanism 9-48997
- HgTe, e. scatt. mechanisms in intrinsic and impurity states at high and low temps. 9-30815
- HgTe epitaxial films, nonohmic conductions, electron mobility 9-28214
- In:Cd, electron-phonon interaction mass-enhancement factor estimate 9-47042
- In alloys, dislocation and boundary scattering, effect on low field Hall effect 9-37445
- In superconductor, flow stress increase and electron dislocation interaction 9-44939
- In whisker, electron mean free path meas. from resistance changes during elastic bending 9-37453
- n-InAs, carrier density, mobility and effective mass from elec. meas. 9-39622
- InAs, third harmonic generation, mobile carrier nonlinearity, interband proc. 9-26547
- InAs_{1-x}P_x vapour-deposited epitaxial layers, electron mobilities obs. 9-30910
- InP, current carrier lifetimes, 78°-300°K 9-37621
- InSb, carrier mobilities and densities determ. by helicon and nonreson. absorpt. techniques 9-47100
- n-InSb, carrier recombination and trapping effects 9-35401
- n-InSb, electron-hole prod. and Gunn effect 9-41202
- n-InSb, films, energy scattering of conduction electrons, piezoelectric contributions 9-26549
- InSb, free carriers causing scattering of light, assoc. with band nonparabolicity 9-33306
- InSb, hole scattering mechanism, deformation potential constants 9-33307
- n-InSb, hot electron temp. w.r.t. elec. field 9-33308
- n-InSb, microwave emission and acoustoelec. domain, decay 9-35402
- InSb, microwave third harmonic generation at low temp. 9-35403
- n-InSb, scattering mechanism, infl. of hydrostatic pressure causing changes in elec. props. 9-28501
- p-InSb effective electron mass determ. from cyclotron reson. 9-37420
- n-InSb minority carrier lifetime, temp. depend. 80°-210°K 9-39621
- InSb thin films 9-33309
- InSe, mobility of charge carriers from conductivity and Hall coeff. meas., temp. depend. 9-35404
- InTe layers, tetragonal phase, hole conc. and mobility 9-41200
- K, electron-electron interaction effects on optical absorpt. 9-49279
- K, electron-phonon interaction, modification for correlation effects 9-35308
- K, electron mean free path, meas. by r.f. size effect 9-30816
- KCl single cryst., conductivity and energy loss spectra, temp. depend. 9-33559
- Kr, e drift velocity saturation 9-26587
- p-n-LaCoO₃, mobility activation energy due to spin-state trapping 9-37527
- Li, electron-phonon interaction, modification for correlation effects 9-35308
- Li, phonon lifetime, electronic contrib. 9-37391

Crystal electron states continued
transport processes continued

- MgO, electron-phonon interaction in F-centre 9-44689
 MnO, highly mobile electrons obs., high temp. 9-44965
 MnTe, magnon drag contrib. 9-24332
 χ -N, adsorbed layer on W, tunneling of field emitted W, tunneling of field emitted electrons 9-30960
 Na, electron-electron interaction effects on optical absorpt. 9-49279
 Ni_{1-x}Zn_xFe₂O₄, generation energy and mobility of carriers, influence of magnetic structure 9-33310
 Ni thin films, current carriers mean free path 9-39589
 NiO, highly mobile electrons obs., high temp. 9-44965
 Pb-In alloys, electron-phonon coupling correction for normal state electronic specific heat 9-33182
 Pb, electron-phonon coupling pressure dependence from tunneling meas. 9-33165
 Pb, electron-phonon interaction rel. to conduction electron props. 9-47032
 Pb superconductor, flow stress increase and electron dislocation interaction 9-44939
 PbS, scattering mechanism from transport props. meas. 9-39631
 PbSe, scattering mechanism from transport props. meas. 9-39631
 n-PbS epitaxial films, layered distrib. of charge carriers from transverse magnetoresistance meas. 9-42996
 p-PbTe-CdTe alloy, scattering of light-mass from magnetoresist. meas. 9-41206
 PbTe, scattering mechanism from transport props. meas. 9-39631
 Pd-Ag alloys, anisotropic impurity scattering, rel. to Hall coeff. 9-37451
 Pd, thin films, current carriers mean free path 9-39589
 Rb, electron-phonon interaction, modification for correlation effects 9-35308
 Se, amorphous, photo-excited carriers transport and generation 9-39709
 Se, hole conc. and carrier mobility, infl. of crystallization method, 250°-360°C 9-30986
 Se, vitreous, hole Hall mobility and trap parameters determ. in multiple trapping case 9-39668
 n-Si:As(P,Sb), electron-phonon interaction in extrinsic photoconductivity 9-41264
 Si:Au, electron and hole emission rates at centres from photocurrent and photopacitive meas. 9-39636
 Si:B, impurity-assisted intervalley electron scatt. 9-43076
 Si-Ge layers, minority carrier lifetime from transient response 9-35431
 p-Si-on-sapphire films, oxidation effect 9-35405
 Si, carrier lifetime, effect of dislocations 9-30931
 p-Si, carrier lifetimes, effect of neutron irradiation 9-47130
 Si, conductivity of hot carriers, review 9-33329
 n-Si, electron mobility field depend., 77K 9-35429
 Si, exclusion of nonequil. hot carriers 9-47125
 n-Si, field depend., 77K 9-35429
 Si, ν irradiated, annealed, minority carrier lifetimes 9-46807
 p-Si, minority carrier lifetime decrease during high-temp. annealing 9-37547
 n-Si, minority carrier lifetime rel. to dislocation 9-35430
 p-Si, rel. to n irradi. induced defect clusters and annealing, elec. meas. 9-47129
 n-Si, transverse magnetoresistance of hot carriers rel. to scattering 9-30930
 n-Si, trap filling mechanism 9-26577
 n-Si epitaxial films on sapphire, vacuum evaporated, Hall mobilities and carrier concs. 9-49111
 Si impurity-assisted intervalley electron scatt. under uniaxial compression 9-35421
 Si minority carrier lifetime, effect of dislocations 9-24191
 Si photoconductivity, effect of electron-hole scatt. 9-37624
 Si single cryst., l.f. noise, influence of opt. rad. and carrier conc. depend. 9-26561
 Si transmitted phonon drag in diffused N-P-N and P-N-P structures 9-37546
 Si(Li), electric field profile and electron drift velocity in $\langle 111 \rangle$ direction, room temp., 2-48 kV/cm 9-33335
 SiO₂, thermally grown, in m.i.m. structure, Fowler-Nordheim tunneling 9-43098
 SiO₂ amorphous films, carrier transport 9-45006
 Sn whisker, electron mean free path meas. from resistance changes during elastic bending 9-37453
 SnTe, intervalley deform. pot. for electron-phonon scatt. 9-43057
 Te, electron-hole pair recombination in internal friction 9-23871
 p-Te, warm hole energy relax. time 9-49087
 TiO₂:V³⁺, inelastic scatt. mechanisms involving mag. impurities in negative magnetoresistance at 4.2°K 9-47070
 TiO₂, electron mobility calc. from defect controlled elec. props. data 9-26512
 TiCl₃, photoconductive, polaron transport props. 9-41272
 U₂O₃, phase transition due to electronic ordering 9-41127
 Xe, e drift velocity saturation 9-26587
 Zn_{1-x}Hg_x-Te solid solutions, heavy carrier effects on galvanomagnetic props. 9-30913
 Zn whisker, electron mean free path meas. from resistance changes during elastic bending 9-37453
 Zr adsorbed layer on W, tunneling of field emitted electrons 9-30960

Crystal energy see Bonds; Crystals; Solids/structure**Crystal field theory**

- alkali halide crystals, electronic polarizability of ions 9-31058
 p_2 quartet e.p.r. under uniaxial stress 9-39906
 CaF₂:U⁴⁺, spin-phonon interaction from u.s. paramag. resonance 9-33623
 calcium formate, field splittings, raman spectra 9-47378
 complexes with T_{2g} cubic field ground term, paramag. anisotropy and axial ligand field 9-49229
 cubic fields with tetragonal and trigonal distortions in transition metal ions 9-47304
 electric field tensors, fifth-order, rel. to tertiary electro-optical effect 9-24369
 electronic configurations in strong crystal fields, determ. of possible states 9-41349
 energy levels in distorted octahedral ligand environments 9-24347
 ferritin-hemoglobin azide, low-spin, anisotropy in g-values due to Jahn-Teller interac. and rhombic field of azide and imidazole 9-35600
 garnets: rare earth ions, selection rules in absorpt. spectra 9-24416
 Jahn-Teller impurities, dynamic, Zeeman eff. 9-31057
Crystal field theory continued
 ligand field spectra, characterization by diffuse reflectance spectroscopy 9-37672
 lithium formate monohydrate, field splittings, Raman spectra 9-47378
 magnetic dipole transitions in octahedral complexes of transition metal ions 9-49230
 magnetic insulators, and exchange effects, book 9-47223
 magnetic sublattice monocryst., parameters depend. of susceptibility anisotropy above ordering temp. 9-39746
 non-Kramers doublet, effective spin-1 formalism for transitions 9-33616
 non-orthogonal states, second quantized formalism 9-45250
 pair interaction Hamiltonian in fictitious angular momentum space 9-45249
 paramagnetic salts, from optical props. 9-33498
 phosphors, structure effects on field-splitting and luminescence 9-24442
 quasi-spin formalism 9-26666
 rare earth ions, ligands electric field grad. and nuclear moments 9-22955
 rare earth metal salts, rel. to anomalous paramag. susceptibility 9-45089
 rare earths f'd configs., electrostatic interaction 9-49231
 rare-earth complexes, limitations in electronic spectra calcs., use of overlap and Coulomb integral calcs. 9-45248
 rare-earth ions, 4f¹⁵d configurations in fluorite type crystal, strong-field approx. 9-41350
 ruby 9-28642
 singlet ground state systems, collective excitations and mag. props. 9-45253
 spin-orbit coupling of transition metal impurity in noble metal 9-47303
 strontium formate dihydrate, field splittings, Raman spectra 9-47378
 transition metal complexes, limitations in electronic spectra calcs., use of overlap and Coulomb integral calcs. 9-45248
 transition metal impurity in noble metal, effective spin-orbit coupling 9-47303
 transition metal ion octahedral complexes, magnetic dipole transitions 9-49230
 transition metal ions, cubic fields with tetragonal and trigonal distortions 9-47304
 Al₂O₃ field modified by dynamic Jahn-Teller effect, energy levels of single d electron from i.r. spectra of doped cryst. in mag. field 9-31100
 BaWO₄:Er³⁺ e.p.r. obs. rel. unified descrip. of scheelites 9-41424
 CaF₂:Dy³⁺ f₈ quartet e.p.r. under uniaxial stress 9-39906
 CaF₂:Gd³⁺, spin-lattice coeffs. determ. from uniaxial stress studies on e.p.r. 9-45380
 CaF₂:Gd³⁺, splitting of ⁶P_{7/2} and ⁶I_{7/2} terms of Gd³⁺ 9-31056
 CaF₂:Nd³⁺, ion level splitting in visible absorption spectra at liquid oxygen temp. 9-47352
 Ca(NbO₃):Nd³⁺, ⁴F_{3/2}→⁴I_{11/2} transition, splitting scheme rel. to stimulated emission 9-27332
 CaWO₄:Eu²⁺ crystal field splittings and hyperfine structure consts., 4.2 and 78°K 9-43200
 CaWO₄:Nd³⁺, ion level splitting in visible absorption spectra at liquid oxygen temp. 9-47352
 CaWO₄:Tb³⁺, parameters from absorpt. and fluorescence spectral analysis, 4.2-77°K 9-33550
 CaWO₄, scheelite, calc. 9-43199
 3Ca₃(PO₄)₂.Ca(F_{1-x}Cl_x):Mn²⁺ synthetic, effect of incorp. of Cl on Mn²⁺ positions from e.p.r. meas. 9-47431
 Dy, parameters determ. from magnetocryst. anisotropy study using spin-wave theory 9-37655
 ErAl garnet, energy levels and g-factor 9-45319
 ErGa garnet, energy levels and g-factor 9-45319
 Eu₂O₃, magnetic susceptibility, effect of field and anisotropic exchange 9-45062
 EuFe garnets, elec. field gradients on Eu³⁺ nuclei 9-35603
 Fe₂(MoO₄)₃, garnet-type, parameters for octahedral Fe³⁺ from Mossbauer effect 9-49261
 FeB₂O₇.X(X=Cl,Br,I), splitting of Fe²⁺ ion in cubic phase, Mossbauer investigation 9-35638
 FeF₃, Fe²⁺ quadrupole splitting obs. in paramag. state, by Mossbauer effect 9-24383
 Hf complex, Hf (IV) benzoyl-phenyl-hydroxylamine, (n, ν) recoil, effect on ν - γ ang. correl. 9-35597
 Hf complex, Hf(IV) acetyl-acetonate, polycrystalline, after-effect in (n, ν) reaction 9-35598
 KH₂PO₄, linear electro-optic effect, theory 9-33517
 LaCl₃:Pr³⁺, parameter variations 9-28643
 LiYF₄:Er³⁺, parameters, tetragonally distorted cube consideration of rare earth site 9-31107
 MgAl₂O₄:Cr³⁺ spinel, weak and strong trigonal field 9-28644
 MgO:Cr³⁺, stressed 9-28642
 MnF₂, Mn²⁺ ion axial field splitting, ⁵S ion spin Hamiltonian explanation 9-45247
 MnO, parameters from transition energies of five lowest-energy crystal-field absorpt. bands 9-39840
 MnO, transition intensities rel. to antiferromag. 9-45252
 α -MnS, transition intensities rel. to antiferromag. 9-45252
 NdCl₃, paramagnetic susceptibility calc. 9-33440
 NdP, NdAs, NdSb, mag. props. 9-35590
 Ni_{1-x}Zn_xFe₂O₄, interpretation of semiconductor props. rel. to temp., influence of magnetic structure 9-33310
 Ni₃B₂O₇.X (X=Cl,Br,I), ferroelec., and optical absorpt. characts. 9-45259
 Ni₃B₂O₇.X(X=Cl,Br,I), splitting of Fe²⁺ ion in cubic phase, Mossbauer investigation 9-35638
 Ni²⁺ crystal field eff. on paramagnetic behaviour 9-28645
 Ni complex hexakis (imidazole) nickel (II) nitrate, single cry. spectrum, spin-allowed and -forbidden band assignments 9-35663
 NiF₆, field splitting, SCF-MO calc. 9-33495
 Pu₂, from Mossbauer obs. of Pu₂Fe 9-39821
 SmAl garnet levels of Sm³⁺ calc. from absorption and emission spectra 9-43244
 SmGa garnet, levels of Sm³⁺ calc. from absorption and emission spectra 9-43244
 SrMoO₄ e.p.r. obs. rel. unified descrip. of scheelites 9-41424
 Tb, parameters determ. from magnetocryst. anisotropy study using spin-wave theory 9-37655
 ThO₂:Np³⁺, splitting of J levels, absorpt. spectrum analysis 9-35665
 TiO₂, dynamic spin Hamiltonian for Fe³⁺ impurity, eigenvalues 9-26667
 YGa garnet: Tm³⁺, selection rules in absorpt. spectrum 9-24416
 YAl garnet: Sm³⁺(Dy³⁺), energy levels of ⁶H and ⁶F multiplets 9-45254
 Yga garnet: Sm³⁺(Dy³⁺), energy levels of ⁶H and ⁶F multiplets 9-45254

Crystal field theory continued

- α -Zn₂(VO₄)₂:Co²⁺, rel. to absorpt. spectra 9-26668
 ZnF₂, Mn²⁺ ion axial field splitting, ⁵S ion spin Hamiltonian explanation 9-45247
 ZnO:Cu, ligand-field-band theory of Cu 9-37673
 ZnO:Cu, tetrahedrally coordinated Cu²⁺ obs., 3d-4p mixing importance w.r.t. i.r. emission decay 9-35599
 ZnS:Cu, ligand-field-band theory of Cu 9-37673
 ZnS:Cu, paramagnetic centres, e.p.r. 9-28751
 ZnS:Cu, tetrahedrally coordinated Cu²⁺ obs., 3d-4p mixing importance w.r.t. i.r. emission decay 9-35599

Crystal fields *see Crystals/internal fields***Crystal imperfections***see also Colour centres*

- alkali halide whiskers, shape depend. of radiation induced defects 9-32941
 alkali halides, f.c.c., contrib. to ionic conductivity and tracer diffusion 9-44729
 alkali halides, glide band broadening at yield point 9-32938
 alkali halides, lattice defects influence on dislocation mobility 9-39362
 alkali halides, rel. to low energy electrons degradation 9-33211
 alkaline earth oxides, irradi., electronic states of defects 9-44689
 alkaline-earth chalcogenides, point defect form, energy calc. 9-44688
 alloys, B2 type, fault energy created by slip 9-42841
 alloys, disordered, pair effects and self-consistent corrections 9-46816
 alloys, quenched dilute, non-equilib. segregation of impurities, model rel. to grain boundary hardening 9-48919
 alloys, stacking fault energies, precise determination 9-32976
 alloys, twin boundaries, coherent, free energy and surface free energy 9-44714
 anthracene, pure and doped single cryst., line defects distrib. 9-37182
 atoms displaced by implanted ions or energetic recoil atoms 9-33201
 α -brass, quenched, secondary defects exam. 9-40940
 cavities, internal necking rel. to ductile fracture 9-30676
 ceramic systems, very high press. effect 9-30553
 ceramics, defect structures, review 9-30727
 corundum, light scatt. effects 9-33522
 cubic polycrystals, effect of stacking-fault distortions on X-ray diff. lines 9-39227
 defect containing crystals, superconducting critical temp. variation using ion density correlation functions 9-49033
 defects, method of formation into ion microscope specimens 9-40936
 defects, reconstruct. of displacement fields from electron micrographs 9-23790
 d.h.c.p. cryst. with deform. stacking faults, X-ray diff. pattern 9-30612
 diamond, platelets, rel. to u.v. absorpt. and luminesc., obs. 9-26732
 diatomic cubic lattice, line defects localized vibrations 9-30755
 dielectric, transparent solid, filamentary damage formation by laser beam 9-48847
 dielectrics, radiation damage, ellipsometric analysis 9-35295
 dislocations with jogs, distribution functions 9-32961
 dolomite, X-ray topographic obs. 9-32958
 electron diff. exam., discontinuous displacement fields reconstruction from many-beam micrographs 9-40882
 electron scattering diagram, modification in transmission electron microscopy 9-48845
 epitaxial films grown on high-alloyed GaAs substrates 9-36944
 f.c.c. cryst., X-ray diff. by stacking faults 9-42842
 f.c.c. cryst. with intrinsic and extrinsic stacking faults, X-ray diff., model 9-32887
 f.c.c. metals, Gibbs free energy 9-33001
 ferrites, polycryst., grain boundary barrier layers rel. to elec. props. 9-46828
 ferromagnetic thin films, point defects eff. on spontaneous magnetization 9-31040
 Ferrovac E iron, effect on thermal component of flow stress 9-41011
 film with surface defects, electron scattering and conductivity 9-49016
 fissionable materials, impurity-doped, growth of gas-filled pores, effect of impurity atoms 9-32955
 garnet inclusion in natural diamond, X-ray study 9-42804
 garnets, flux-grown, internal growth defects, etching and X-ray topographic obs. 9-32937
 glass, filamentary damage formation by laser beam 9-48847
 glass, gaseous inclusions in glass, gas chromatographic analysis 9-40966
 grain boundaries, large-angle, complete conjugation model 9-37116
 grain boundary analysis by appl. of theory of continuous distribution of dislocations 9-37170
 grain boundary migration mechanism 9-23823
 grain boundary migration rate 9-37186
 grain boundary nucleation kinetics 9-42752
 grain-boundary precipitates, growth 9-35101
 graphite-B, neutron irradi., defect clustering, effect of B, physical prop. meas. 9-30597
 graphite, neutron irradiation, internal friction coeff. temp. depend., -180 to 500°C, 1 Hz 9-35153
 graphite, pyrolytic stress-annealed, rel. to graphitization electron microscope obs. 9-35054
 graphite irradi. at high temp., defect nucleation, cry. perfection influence 9-23794
 group II-VI compounds, defect characterization, diffusivity and elec. meas. 9-37156
 group II-VI compounds, e.p.r. of defect centres 9-37803
 group IV-VI cpds. and alloys, lattice defects and deviations from stoichiometry 9-39483
 h.c.p. cryst., X-ray diff. by stacking faults 9-42842
 hexamethylenetetramine grown from soln. and vapour, var. in quality 9-39202
 ice, diffusion and relax. phenom. 9-28318
 ice, point defects and their effect on elec. and mech. props. 9-48832
 inclusion, spherical, in elastic or viscoelastic matrix 9-31819
 inclusions and pores, moving, growth theory 9-44684
 inclusions in ferromag. materials, coercive force increase, exptl. test of Neel's theory 9-47244
 inclusions in solids, effect on stress distrib. 9-42877
 inert gases, defect structure of condensed solid, electron microscope obs. 9-37159
 insulators, e.p.r. defect study 9-46350
 interaction with conduction electrons, u.s. attenuation obs. 9-37330
 ion microscope specimens, method of introducing structural defects 9-40936

Crystal imperfections continued

- ion-induced defects in single crystals 9-26177
 ionic cry., lattice distortion due to pt. defects, electrostatic pots. and spatial deriv. 9-33214
 isotopic defect, lattice dynamics, response func., photon scatt. cross section eqn. determ. 9-24007
 L1₂ lattice, stacking fault pairs, intrinsic-extrinsic 9-30613
 laser radiation damage generated by self-focusing in active materials and nonlinear crystals 9-44680
 lattice defect field-ion micrographs, computer interpretation 9-23808
 lattice defects, diffusion in stream field 9-46842
 lattice disordering by ion bombard. rel. to focusing and channelling 9-35294
 macrodefects, radiation produced, electron microscope investigation 9-32984
 magnesite, X-ray topographic obs. 9-32958
 martensite, C-bearing, assoc. with ageing 9-39462
 in mechanical behaviour of solids, crystallographic aspects, book 9-39431
 metal, expt. and theory, book 9-48792
 metal, fine particles prep. by gas evaporation method with plasma jet flame, lattice imperfection 9-33128
 metal monocrystalline film with lattice defects elec., conductivity and thermoelec. power 9-37434
 metals, b.c.c., glide band broadening at yield point 9-32938
 metals, stacking fault energies, precise determination 9-32976
 metals, twin boundaries, coherent, free energy and surface free energy 9-44714
 nonstoichiometric cpds. interac. between point defects, thermodynamic activity variation 9-37160
 opal, SiO₂.nH₂O, packing imperf. rel. to stacking faults and polytypism 9-42843
 opals, stacking faults, electron microscopy study 9-40917
 oxides, irradi., electronic states of defects 9-44689
 oxides, mass transfer conf. 9-44726
 oxides, point defect form, energy calc. 9-44688
 oxides, point defects characterization 9-44687
 p-n step junction structural irregularities rel. to avalanche breakdown 9-43078
 photoannealing of chemical radiation damage, effect on. 9-23933
 point defect, vibr. self-entropy, pseudol. model 9-48944
 pits of arbitrary shape, two-magnon scattering amplitude 9-45101
 planar defects, defects obs. by fluorescence 9-28450
 point defects in ionic cryst., electronic structure calc. 9-40928
 point defect conc. as aid in thermodynamic activities calc. 9-30714
 point defect hardening, effect of lattice friction 9-41033
 point defect moving on set of equivalent sites, permissible jumps 9-48848
 point defects, elec. props., Boltzmann eqn. soln., utilization of symmetry 9-32943
 point defects in ionic cryst., electronic structure of F centre 9-40973
 polycrystals, defect interactions, two-dimens. model 9-37155
 polymers, defect effects on i.r. spectra 9-47379
 pore diffusion kinetics, review 9-37188
 pore growth under internal press. effect 9-42803
 pores and inclusions, moving, growth theory 9-44684
 quantum theory of defects, flow of defections and impurities 9-40927
 quartz, Brazil twin boundaries, X-ray topographic obs., diff. contrast effects 9-42845
 quartz, p-irrad., glow curves rel. to dose, defect synthesis 9-26273
 radiation damage, model involving thermal vibr. of atoms 9-41114
 radiation defect formation by channeling particles 9-33203
 random distribution of defects, scattering of x-rays 9-28244
 review of defect assessment in synthetic single crystals 9-36971
 rolling of body centred metals, patent 9-28285
 ruby, filamentary damage formation by laser beam 9-48847
 sapphire, cavitation in veiled region of melt-grown cryst. 9-35092
 sapphire, filamentary damage formation by laser beam 9-48847
 segregation, non-equilib., effect on near-surface diffusion 9-48871
 semiconducting cpds., antiphase boundaries 9-40937
 semiconductor, degenerate, recombinations via defects, rate expressions 9-30888
 semiconductors, binary, atomic displacement threshold energy, calc. and expt. 9-35297
 semiconductors, e.p.r. defect study 9-46350
 silicon iron, twin and grain boundary effects on plastic deform., 185 and 300°K 9-41018
 specific heat, eff. on singularity nature near second kind phase transition points 9-44832
 stacking faults, deformation, in h.c.p. crystals, X-ray diff. rel. to solute segregation effects in alloys 9-23818
 stacking faults, distinction between intrinsic and extrinsic in field-ion micrographs 9-32977
 stacking faults, double-fault in h.c.p. crystals, diff. theory 9-23819
 stacking faults, electron diffraction obs., contrib. to fine structure of spots 9-30536
 stacking faults, overlapping, three parallel, e diff. contrast 9-32978
 stacking faults in h.c.p. and f.c.c. polycrystals, diff. line profile, general theory 9-23817
 steel, cast, size effect in fatigue fracture 9-35188
 steel, low C, impurity redistribution, eff. of ht. treatment 9-23939
 steel, microcracks initiated by 17.8 kc/sec oscillations 9-35190
 steel, nonmetallic inclusions, effect on strength 9-48905
 steel, stainless, stacking fault energies intrinsic: extrinsic ratio 9-23821
 steel, transformer, annealed, dispersed inclusions, eff. on core losses 9-23802
 subgrains, misalignment determ. by Schulz method 9-32886
 superconductors, type-II, defects in flux-line lattices 9-28286
 superconductors type-II, interaction between fluxoid and lattice defect 9-47086
 tetracyanoquinodimethan complexes, effect on mag. susceptibility, between 2-5°K and room temp. 9-47233
 thermodynamic props. 9-44681
 titanate materials, lattice defects, origin 9-32942
 transition metals, b.c.c., point defects, review 9-26274
 transition fault in bicryst., X-ray diff. theory 9-32982
 twin band-grain boundary junctions, relative interfacial free energy meas. 9-44712
 twin/grain boundary relative free energy ratio meas., role of misorientations 9-44713
 two-dimensional defect, effect on lattice vibrations 9-42943

Crystal imperfections continued

- wüstite, nonstoichiometric, defect complexes and microdomains, stat. thermodynamic analysis 9-44685
 Zircaloy, formation during neutron irradiation, rel. to creep 9-41023
 Ag-Ge alloys quenched from melt., formation of faulted close-packed structures 9-40938
 Ag-Pd alloys, stacking fault densities from X-ray diffraction line profiles 9-40961
 Ag-Sn h.c.p. alloys, stacking fault energies 9-40960
 Ag, stacking fault energy effect on creep 9-39421
 β -Ag₂S defective order of cations 9-40929
 Ag films on mica, inclined fault concs. rel. to presence of various gases during deposition 9-35097
 Ag halides, f.c.c., contrib. to ionic conductivity and tracer diffusion 9-44729
 AgCl:Mn, potential difference during plastic deformation 9-23877
 AgCl, zone refining indicating that blue lum. band is due to defects 9-35679
 Al-(4 at.%) Cu alloy, grain-boundary precipitates, growth 9-35101
 Al-Cu alloy θ' precipitate, stacking faults, electron microscope exam. 9-35098
 Al-(3-15 wt.%) Mg, alloys, stacking faults, effect of small alloying additions of Ti, Zr, Be, Mn 9-40946
 Al-Si dilute alloys, cold-worked, role of Si atoms in defects creation during deform. and recovery 9-33104
 Al-Zn-Mg alloys, grain boundary precipitate distribution rel. to boundary misorientation 9-39489
 Al-(10 wt.%) Zn alloy, irradiated at 78°K, Guinier-Preston zone formation 9-30715
 Al-(40 at.%) Zn alloy, stacking fault formation rel. to ageing 9-32979
 Al-Zn eutectoid, grain boundary sliding and grain rotation rel. to superplastic behaviour 9-23900
 Al, defect substructure, due to fatigue stressing in vacuum 9-28364
 Al, grain boundary effect on elec. resistivity, 4.2° to 77°K 9-30849
 Al, stacking fault energy effect on creep 9-39421
 Al₂-Cr₂BeO₄, alexandrite, anti-phase boundaries electron microscopy obs. 9-35104
 Al₂O₃ bicrystals, [1100] tilt boundaries, relative grain boundary energy and surface diffusion coeff. 9-26290
 Al alloys, Be-vacancy interactions 9-44692
 Al single crystal, pit formation during heat treatment 9-32946
 Au-(0.1 wt.%) Au alloy, fast neutron irradiation, cold work effect on damage prod. and elec. resistivity recovery 9-43025
 Au films, Au-ion irradiation, substage III annealing, activation energies 9-33106
 Au foils, Kr-ion irradiation, damage transmission electron microscopy, energy depend. obs. 9-32957
 β' AuZn, defect structure from lattice parameter meas. 9-23881
 B filament vapour deposited on W, cracks rel. to chem. interaction 9-48866
 Ba₂NaNb₂O₁₂ striations in polished samples grown from melts of high thermal gradients 9-39208
 Ba₂NaNb₂O₁₂:Fe³⁺, Ir⁴⁺, whisker-like inclusions rel. to optical absorpt. at 5300 Å 9-28651
 BaTiO₃, annealed in hydrogen, defect structure identification from i.r. spectra bands 9-35105
 C stacking faults, 001 reflections, analysis 9-37183
 Ca₁₀(PO₄)₆F₂ X-irradiation, paramag. centres form. from OH and oxide ion impurities 9-40933
 CaCO₃, defect distribution across fission fragment tracks rel. to healing 9-26467
 CaF₂, lattice distortion due to pt. defects, electrostatic pots. and spatial deriv. 9-33214
 CaO, e.s.r. of N centre due to neutron irradiation 9-37794
 CaSO₄·2H₂O crystal, i.r. absorption, H bond vib., electronic spectra meas. 9-23799
 CaTiO₃, point defects diffusion coeffs. by analysis of transient elec. conductivity data 9-28317
 CaTiO₃, point defects formation, elec. conductivity and Seebeck coeff. study 9-28276
 CaWO₄:Nd, assessment and control in crystals used for laser devices 9-37157
 Cd, cyclically stressed, slip band extrusions and twin boundary filamentary growths 9-32981
 Cd whiskers, lattice imperf., X-ray diffraction, obs. 9-37109
 CdS, shown by dark cond. meas. during heat treatment, 500 to 700°C 9-49076
 CdS, vapour grown, stacking faults 9-37174
 CdS hollow conical single crystal, grown from vapour 9-35017
 CdSe, high-temp. defect equilibria, investigation by self-diffusion and electrical transport props. meas. 9-37200
 CdTe, electronic props. of defect centres 9-49158
 Co-(8 at.%) Fe alloy, large single crystal, low angle boundaries 9-37185
 Co-base superalloys, stacking fault energy effect on dislocation substructure 9-39298
 Co, structure and conc. of defects, eff. of $\beta \rightarrow \alpha$ transformation and plastic deformation 9-23804
 CoO, complex defects 9-42806
 Cr, distortion due to antiferromag. ordering, orthorhombic structure 123-311°K 9-39780
 CsI, ¹³³Xe trapping by natural and irradiation defects, obs. 9-37202
 Cu-Al solid solns., stacking fault energy influence on high temp. creep 9-42887
 Cu-Al solid solns., stacking fault energy influence on high temp. creep 9-42886
 α -Cu-Ge evaporated film, faulting meas. by X-ray diffraction 9-23820
 Cu, cyclically deformed, point defects contrib. to elec. resistivity 9-33254
 Cu, effect on longit. magnetoresistance 9-49025
 Cu, fast neutron irradiation, cold work effect on damage prod. and elec. resistivity recovery 9-43025
 Cu, fast neutron irradiation, cold work effect on damage prod. and elec. resistivity recovery 9-43025
 Cu, grain boundary effect on elec. resistivity, 4.2° to 77°K 9-30849
 Cu, grain growth during homogenization quenching 9-23938
 Cu, influence on transfer magnetoresistance at 10°K 9-47075
 Cu, point defects infl. on elastic bulk effect. 9-30631
 Cu, spherical voids, annealing kinetics rel. to self-diffusion coeffs. meas., 390° to 560°C 9-30624
 Cu, strain centres with attendant prismatic dislocation loops, etch-pit and X-ray topograph obs. 9-32939

Crystal imperfections continued

- Cu alloys, clusters, active slip volume 9-32983
 Cu electroformed shell buckling by axial compression, imperfections eff. 9-34070
 Cu foil, damage spots due to neutron irradiation, spatial distrib. 9-46806
 Cu single crystals with point defects, magnetoresistivity 9-37443
 Fe-(0.75 at.%) Mn alloy, annealed, grain boundary fine struct. obs. 9-35102
 Fe-(40 at.%) Al, alloy, ordering and struct. distortions, X-ray diffraction obs. 9-42784
 Fe-Cr-Ni alloy, extrinsic-intrinsic stacking-fault pairs 9-44711
 Fe-Mo alloy precipitates, 2-dimens. fine faults, electron microscope obs. 9-42787
 Fe-Si alloys, microinhomogeneities in cast, worked and annealed samples 9-48846
 Fe-W alloy precipitates, 2-dimens. fine faults, electron microscope obs. 9-42787
 α , γ -Fe, grain-boundary diffusion and trapping of Cu by inclusions or impurities in Cu diffusion mechanism 9-46851
 Fe, strain annealed crystals, subgrain boundaries in {011} {112} occluded grains 9-23824
 Fe, zone refined by deform. at -196°C, lattice defects study by elec. resistivity meas. 9-26275
 Fe microcracks initiated by 17.8 kc/sec oscillations 9-35190
 Fe single crystal plates produced by strain-anneal method, effect of stretching on imperfect structures 9-32913
 Fe stacking fault, field-ion microscopic obs. 9-40962
 Fe(NH)₄(SO)₄·6H₂O: ⁵⁷Co²⁺, daughter Fe³⁺ stabilization rel. to H₂O radiolysis by Auger e. obs. 9-23801
 FeO, nonstoichiometric, defect complexes and microdomains 9-44685
 GaAs:Te, stacking faults, electron microscope exam. 9-23822
 GaAs, striations, dislocation-induced defects and doping behaviour, cathodoluminescent studies 9-43267
 GaAs, surface inhomogeneities from contact potential meas. on etched faces 9-26554
 n-GaAs, thermally stimulated conductivity meas. 9-35079
 GaAs_{1-x}P_x solid soln. crystal grown from Ga-rich soln., lattice distortions 9-35206
 GaP, defect structure, depend. on growth, method, dislocations and stacking fault density 9-30602
 GdFe garnet, line, interaction with domains, optical obs. 9-45179
 Ge: Au(Au, Sb) single crystals, nature of inclusions and structural features 9-42807
 n-Ge:Sb, electron irradiated, 80° to 200°K 9-35080
 Ge-As solid soln., during precip., nature of defects 9-44682
 n-Ge, e. irradiation, induced defects at 30°K, annealing process 9-35081
 Ge, grain boundary interband optical props. 9-26737
 Ge, internal recontacted splits, elec. props., gas adsorption and X-ray studies 9-42846
 Ge, neutron-irradiated, struct. effects 9-44695
 Ge, point defects, review 9-37209
 Ge layer, epitaxially-grown, distribution of imperfection centres 9-37158
 HgSe, homogeneity range and concentration-pressure isotherms 9-37508
 In, thin films, supercond., ang. depend. of critical field rel. to defect conc. 9-47088
 In alloys, boundary scattering, effect on low field Hall effect 9-37445
 p-InSb, radiation defects formation by illumination 9-28283
 Ir, point defect clusters caused by proton irradiation, field ion microscope exam. 9-35085
 KBr, n and ν induced defects, low temp. annealing 9-40967
 KCl-NaCl, anomalies in struct. from enthalpies of crystallization 9-37161
 KCl, aggregate centre formation under ionizing irradiation, rel. to fracture surface energy changes 9-28372
 KCl, defect production by X-irradiation, at 20°K, electron-hole recombination mechanism 9-26276
 KCl, He filled pores temp. induced migration, obs. 9-37189
 KCl, ion irradiation, prod., stabilization by trapped Xe, obs. 9-37205
 KCl, X-ray K emission spectra of potassium obs., lattice defects determ. 9-36693
 KCl thin films, point defect-coagulates due to electron irradiation, during microscope exam. 9-42808
 LiCl, reactor-irradiated, defects in X-ray- and thermoluminescence 9-28729
 LiF, defect distribution across fission fragment tracks rel. to healing 9-26467
 LiI, single crystalline, pure and Mg doped, free energy of defect form. and activation energy for motion 9-47161
 Mg, cyclically stressed, slip band extrusions and twin boundary filamentary growths 9-32981
 Mg, n irradiation, production and recovery, low temp. 9-32940
 MgAl₂O₄, stacking fault density rel. to flux growth 9-37086
 MgAl₂O₄, vertically pulled crystals, strain defects 9-46743
 MgO, cavity form. by annealing 9-44693
 MgO, defect cluster centres in rel. to neutron-electron-irradiation or additive coloration 9-46838
 MgO, point defect form. energy calc. 9-44688
 Mo, deformed struct., X-ray diffraction topography 9-42815
 MoO₃, heated, crystallographic shear planes and non-stoichiometry, obs. 9-35106
 N₂, defect structure of condensed solid, electron microscope obs. 9-37159
 NH₄Cl, paramagnetic centre, radiation induced e.p.r. spectrum 9-33631
 NH₄H₂PO₄, mother-liquor inclusions in solution-grown crystals 9-40862
 NaBr:Ca²⁺ single crystal, paramag. centres, e.s.r. obs. 9-33633
 NaCl:Ca²⁺ single crystal, paramag. centres, e.s.r. obs. 9-33633
 NaCl: CdCl₂, dipole aggregation, kinetics 9-39356
 NaCl, defect production by X-irradiation, at 20°K, electron-hole recombination mechanism 9-26276
 NaCl, lattice distortion due to pt. defects, electrostatic pots. and spatial deriv. 9-33214
 NaCl, point defects in crystals producing cellular substructure 9-44686
 NaCl, thin films, point defect-coagulates due to electron irradiation, during microscope exam. 9-42808
 NaCl as-grown crystal, line defects, X-ray diffraction obs. 9-37144
 NaCl cleavage surface, role of surface imperfections on selective nucleation of gold 9-37004
 NaCl single crystal surface, polygonization by electron bombardment 9-30513
 NaClO₃, mother-liquor inclusions in solution-grown crystals 9-40862
 Nb-Zr, flux pinning by grain boundaries 9-28474

Crystal imperfections continued

- Nb, etch pits and sub-boundaries obs. by optical microscopy, defect contribution to diffusion 9-32985
- Ni-C eutectic alloy, stacking faults involving rots. about flake graphite, microscopy obs. 9-44671
- Ni-Fe alloy, large single cryst., low angle boundaries 9-37185
- Ni-base superalloys, stacking fault energy effect on dislocation substructure 9-39298
- Ni, critical magnetic neutron scattering, temp. and intensity shift 9-26636
- Ni, secondary defects formation after neutron-irrad. 9-32959
- Ni, stacking fault energy effect on creep 9-39421
- Ni explosion-shocked, thermal recovery processes, electron microscope obs. of microstruct. 9-44696
- Ni large single cryst., low angle boundaries 9-37185
- NiAl, nonstoichiometric, lattice defects 9-40941
- O₂, defect structure of condensed solid, electron microscope obs. 9-37159
- Pb_{1-x}Sn_xTe single crystals, metallic inclusions by electrolytic etching 9-30569
- Pb superconducting thin films, eff. on resistivity and crit. temp. 9-26531
- Pd, stacking fault energy effect on creep 9-39421
- Pt, quenched, polyhedral void obs., e. microscope and field ion microscope exam. 9-23815
- Pt, stacking fault energy effect on creep 9-39421
- Pt, state I recovery by residual elec. resistivity meas. 9-26277
- RbBr, point defects, effects on n.m.r. spin echo line shapes 9-30610
- Se single cryst., small-angle boundaries, X-ray topographic obs. 9-44709
- Si:Li, O, dopant interaction with electron-irrad. produced defects 9-42813
- Si-SiO₂, defect production by 1 MeV electrons 9-49357
- Si, bulk and surface defects, X-ray detection, applic. in integrated circuit fabrication 9-30604
- Si, defects induced by P deep diffusion 9-32975
- Si, degenerate, radiation-induced defects on low temp. e-irrad. 9-28277
- Si, grain-boundary effect on solubility of Cu 9-42797
- Si, internal recontacted splits, elec. props., gas adsorption and X-ray studies 9-42846
- Si, γ irradiated, annealed, interactions of point defects with impurities 9-46807
- Si, lattice deform. due to high-energy ion implantation, X-ray exam. 9-35103
- p-Si, neutron irrad. induced defect clusters and annealing, elec. meas. rel. to transport props. 9-47129
- Si, point defects, review 9-37209
- n-Si, pulsed 10 MeV electron irrad., rapid annealing of damage 9-35446
- Si, rad. induced atomic displacements, and interaction with Li impurities 9-48844
- p-Si, radiation defects interac. with impurities during high-temp annealing 9-37547
- Si, thermal point defects, density, lattice parameter and elec. props. investigation. 9-32944
- Si foils, ion irrad., defect prod. 9-44683
- Si foils, ion irrad. e. diff. diagrams 9-44697
- Si n-p-n structures, stacking faults as sites for diffusion pipes 9-30603
- Si on sapphire film, electrically and optically active defects 9-37545
- Si single crystal, ion-implanted Au layer, structure 9-39307
- Si surfaces, stacking fault nucleation, growth and annihilation mechanisms 9-42844
- SiC, defect structure, review 9-26245
- SiO₂-nH₂O, opal, packing imperf. rel. to stacking faults and polytypism 9-42843
- Sn-Cd lamellar eutectic, fault structure 9-28299
- Sn, grain growth in presence of surface active and inactive impurities 9-48865
- SrF₂:Er³⁺, conc. depend. of site symmetry 9-24490
- Ta, diffusion of interstitial He 9-23843
- Te single cryst., small-angle boundaries, X-ray topographic obs. 9-44709
- ThO₂, point defect form. energy calc. 9-44688
- Ti, cyclically stressed, slip band extrusions and twin boundary filamentary growths 9-32981
- TiO, nonstoichiometric, defect complexes and microdomains 9-44685
- TiO_{2-x}, reduced rutile, ionic defects rel. to mech. and dielec. relax. of hopping electrons 9-44690
- α -U, radiation defects and Matthiessen's rule 9-46805
- UO₂, bubble mobility rel. to fission gas release, obs. 9-37190
- UO₂, fission gas bubbles and sintering pores irrad. stability, obs. 9-37187
- UO₂, nonstoichiometric defect complexes and microdomains 9-44685
- UO₂, point defect form. energy calc. 9-44688
- V, neutron-irrad., cylindrical damage cells, transmission electron microscopy 9-44698
- V, rad. induced clusters and loops, stabilized by annealing 9-39367
- V domain boundaries, lattice distortion formation 9-32960
- W, chemically vapour-deposited, bubble growth at grain boundaries 9-28300
- W, defects due to bombardment of deuterons of 0.1 MeV 9-37162
- W, deformed struct., X-ray diff. topography 9-42815
- W, point defects infl. on elastic bulk effect 9-30631
- W, single cryst., deuteron irrad. damage, ion microscope exam. 9-39358
- W b.c.c. single crystal, effect on thermal component of flow stress 9-41011
- YAl garnet:Nd, assessment and control in crystals used for laser devices 9-37157
- YAl garnet, point defects rel. to etch figures 9-44641
- Zn, cyclically stressed, twin boundary filamentary growths 9-32981
- Zn, pure, grain boundary relax. 9-44715
- Zn bicryst. grown from melt, grain boundary sliding anisotropy 9-40964
- Zn bicryst. grown from melt, grain boundary sliding anisotropy 9-40965
- Zn single cryst., X-ray diff. topography 9-35096
- Zn stacking fault formation in {1012} twins, from slip dislocation-deform. twin interactions 9-26289
- ZnS/ZnSe mixed crystal, e.p.r. of defect centres 9-37803
- ZnS, e.p.r. of defect centres 9-37803
- ZnS, stacking fault periodicity and polytypism rel. to growth in vac. or inert atm. 9-35099
- ZnS epitaxial layers on Si electron microscopy obs. 9-34994
- ZnS grown from vapour, stacking faults distrib., rel. of polytypism 9-37184
- ZnS polytypism and a.c. electroluminescence 9-24468
- ZnS powders, point defects effect on lattice dimensions and phase transitions 9-40923
- ZnSe, e.p.r. of defect centres 9-37803

Crystal imperfections continued**dislocations**

- alkali halide crystals, relaxation rate, effect rel. to temp. 9-33026
- alkali halides, dislocation mobility, influence of lattice defects 9-39362
- alkali halides, edge dislocation interaction with Burgess vectors 9-23618
- alkali halides, etch figures, effect of neutron irrad. on dimensions 9-40945
- alkali halides, in plastic deformation enhanced conductivity (Gyulai-Hartly effect) mechanism 9-33373
- alloy, elastically inhomogeneous, dislocation model of strength 9-39430
- alloys, bi-metallic, pile-up of dislocations 9-42823
- anisotropic bicrystals and half-spaces, forces rel. to elastic anisotropy and boundary misorientation 9-32966
- anisotropic displacement fields 9-37169
- anthracene, doped single crystal, impurities eff. and annealing props. of disloc. 9-37182
- array, planar, in displacement depend. stress field, stress intensification at tip 9-32962
- b.c.c. crystals, and interstitial atoms, interaction energy 9-28289
- b.c.c. crystals, quasi-dipoles, field-ion image contrast 9-48857
- bituminal interface, partially bonded, forces of interaction with stationary screw dislocation 9-35089
- β -brass, $a(110)+a(001)$ pair 9-28291
- α -brasses, distrib. rel. to stacking fault energy in shock-deformation 9-23879
- breakaway, thermal, from row of equally spaced pinning points 9-42819
- Burgers vectors, two-beam diff. contrast meas. 9-32969
- carriers trapped by dislocation, anomalous Zeeman effect 9-33533
- charged, effect on dielec., piezoelec. and elastic props. 9-48856
- climb, rel. to change of shape in single- and poly-crystals 9-30658
- climb mechanism, review 9-28287
- continuous distribution, fatigue applic., review of expt. results rel. to theory 9-23807
- creep, stochastic model, identification of flow units 9-33040
- cubic crystals, quadrupole broadening, (111)/(110) slip system 9-32965
- cylindrical body, restricted random distrib., mean square stress 9-48854
- damping and solute pinning, discussion 9-28293
- diamonds, synthetic, in left- and right-screw growth spirals 9-23671
- diffraction contrast for groups of edge or screw dislocations 9-42824
- diffused transistors, detection by Sirtl etch technique, effect on transistor properties 9-35451
- diffusion 'climb' mechanism causing unbending of cryst. 9-26324
- in dispersed barrier hardening temp. dependence analytical model 9-46818
- dissociated prismatic loops, model 9-35091
- distribution, continuous, theory and applic. to grain boundary analysis 9-37170
- dolomite, X-ray topographic obs. 9-32958
- double loop unpinning, thermally assisted 9-46817
- edge, and edge dipoles, close to free surface, contrasts 9-30605
- edge, near surface layer, exact analysis 9-26283
- edge groups, diff. contrast 9-42824
- edge pair in perpendicular slip planes, influence on work-hardening and strain-ageing 9-44786
- elastically anisotropic materials, and plane boundaries 9-38282
- elastic interactions in finite body 9-48855
- electron and X-ray scatt., derivation of dynamic theory 9-39224
- electron diffraction obs., contrib. to fine structure of spots 9-30536
- electron microscope examination of foils, shadowing technique to reveal struct. 9-28246
- energy factor, orientational derivative formula 9-40942
- f.c.c. alloys and related superlattices, passing 9-39360
- f.c.c. metals, degree of confinement for slip character, eff. on cyclic deformation and fatigue 9-30674
- field-ion micrographs, computer interpretation 9-23808
- fluorapatite, arrangements 9-42826
- forest-cut processes, force-distance diagrams, critique of methods 9-30653
- Frank, e. diff. contrast rel. to dissoci., calc. 9-40958
- generation at particle-matrix interface for SiO₂ and Al₂O₃ particles in Cu matrix, local shear stresses 9-30611
- glide and climb motion superposition at high temps. 9-37180
- guanidinium aluminium sulphate hexahydrate, ferroelec., sites rel. to dehydration nuclei 9-37115
- h.c.p. metal, twinning elastic energy factor 9-35090
- heterogeneity in assembly, effect on fatigue failure probability 9-23809
- in heterogeneous media, anti-plane strain behaviour 9-33090
- ice single cryst. growth from melt, disloc. struct. 9-37080
- interaction energy with interstitial atoms 9-44705
- interaction force between parallel dislocation with vortex line 9-44704
- interaction with antiphase domain boundaries 9-44700
- interaction with boundaries, stress field changes 9-42816
- interaction with interstitials, energy considerations 9-46812
- internal friction, amplitude dependent, caused by thermal kinks in dislocations 9-41001
- internal friction, effect of dislocation interactions on the Bordoni peak 9-42868
- with jogs, distribution functions 9-32961
- kinetic singularities during rolling 9-23805
- L1₂ lattice, rel. to formation of intrinsic/extrinsic stacking fault pairs 9-30613
- loops in anisotropic mats., interaction energy, line integral expressions 9-42818
- magnetite, X-ray topographic obs. 9-32958
- magnons scattering, ferromagnetic relaxation time for infl. resonance line-width 9-33620
- in martensitic phase transitions mechanism, movement under stress 9-33134
- in mechanical behaviour of solids, atomistic viewpoint, book 9-39431
- metal, b.c.c., locking produced by interstitial solutes, rel. to yield point 9-41028
- metal, expt. and theory, book 9-48792
- metal crystals, irrad. or quenched, sweeping-up of loops by glide dislocations during deform. 9-32963
- metal whiskers, axial screw-dislocation search 9-48853
- metals, b.c.c., screw, rel. to slip controlled by Peierls mechanism, geometry 9-44710
- metals, f.c.c., elastic interaction between Frank loops and glide dislocations, activation energy 9-39359
- metals, hexagonal, damping assoc. with elastic wave vibr. modes 9-48890
- metals, melt-grown, microsegregation and cryst. perfection 9-37060

Crystal imperfections continued
dislocations continued

- metals, polycryst., motion w.r.t. rate depend. plastic flow constitutive relation 9-37257
- mobile, linear continuum theory 9-42820
- mobile screw dislocation, continuum theory investigation 9-42821
- mobility, effect of core structure 9-26284
- mobility, effect of localized lattice defects 9-41033
- movement as basic process in slip 9-41025
- muscovite, dislocation planes, electron microscopy 9-23748
- Peierls mechanism, strain-rate sensitivity of flow stress 9-39404
- Peierls-Nabarro model, treated from line or planar singularity in anisotropic medium, Fourier transform. 9-45816
- phonon scattering by Cottrell atmospheres surrounding dislocations 9-46966
- pile-up, distance between leading dislocations determ. 9-44703
- pile-up, rel. to microcrack formation, activation energy 9-33086
- pile-up formation, dynamics 9-48858
- pile-up structure rel. to thermally activated crack nucleation 9-42817
- pinned, thermal breakdown 9-37167
- pinning points, statistical study of distance distrib. 9-44701
- plastic deformation in α -single crystals 9-46889
- plasticity theory, small-strain, Ni-base alloy, planar slip material 9-31834
- polyethylene, screw dislocation mobility, Peierls stress 9-46825
- polyethylene, yield mechanism based on motion of dislocation loops 9-30734
- polyethylene-stainless-steel lap joints yield mechanism based on motion of dislocation loops 9-30734
- quartz, lattice displacement meas-by X-ray moire topography 9-26287
- quartz, struct. of centres on 0001 surface 9-42839
- quartz, synthetic, assoc. with plastic deform. and recovery, transmission electron microscope obs. 9-40955
- random distrib., restricted, in cylindrical body, mean square stress 9-48854
- randomly distrib., root mean square internal stress determ. 9-42822
- rock-salt type cryst., latent hardening due to interac. of dislocations 9-35191
- sapphire, veiled region, reaction obs. by X-ray topography 9-35092
- screw, interaction with boundaries, stress field changes 9-42816
- screw, mobile, continuum theory investigation 9-42821
- screw, rel. to slip controlled by Peierls mechanism, geometry 9-44710
- screw groups, diff. contrast 9-42824
- semiconductor junction delineation and dislocation revealing by $\text{HIO}_4\text{-HF-H}_2\text{O}$ system 9-33339
- semiconductors, effect on electronic spectrum, quantum mechanical treatment 9-33315
- in solid-solution hardening due to size effects mechanism 9-46927
- solute atom-dislocation interactions, limitations of binding energy theory 9-28288
- sound radiation produced when passing through elastic modulus discontinuity plane 9-37353
- splitting effect on Bordoni peak width in internal friction 9-44753
- stable struct. obs. in NaCl-type cryst. 9-42825
- statistical derivation of eqns. for continuous distrib. in linear elastic medium 9-23806
- steel, martensite, internally twinned, slip dislocations movement 9-42828
- steels, medium carbon St.40, tempering effects at 250-700°C on density 9-40948
- stress distributions and forces acting, graphical representation 9-32967
- stressed solid involving finite stream, thermodynamic theory 9-49408
- structure, connection with slip lines 9-26335
- superdislocation in ordered alloys, line tension rel. to antiphase boundary energy 9-46819
- superdislocations in L_1_2 superstructure blocking stress 9-44699
- superlattice B_2 , starting stress of glissile superdislocation 9-26282
- surface layer, rich, form. during plastic deform. 9-46895
- surface layer, rich, form. during plastic deform. 9-46896
- twinning surface dislocations, intrinsic resistive stress 9-35157
- unpinning, equilib. configs. and activation energies 9-37168
- velocities, stress depend. 9-44702
- velocity, internal stress fields influence 9-39361
- velocity-stress exponent, temp. depend., discrepancy due to activation entropy 9-26285
- wurtzite lattice, perfect dislocations 9-32964
- Ag-Sn h.c.p. alloys, configs. obs. and stacking fault energy determ. 9-40960
- Ag, complex Frank loops, stacking fault steps form. rel. to fault climb 9-40943
- Ag, density depend. on primary recrystallization after large plastic deformation 9-40947
- Ag, motion rel. to material transport in sintering 9-46916
- Ag, quenched, Frank dislocations dissociate, e diff. obs. 9-40959
- Ag single cryst., charact. motion, etch pit obs. 9-40944
- AgCl, latent hardening due to interac. of dislocations 9-35191
- AgCl single crystals, etch pits, rel. to structure 9-46748
- Al(1 at %) Ag alloys, dissociated prismatic loops, model verification 9-35091
- Al-Ag alloys, surrounding precipitate, diffusion controlled relaxation causing internal friction peaks 9-35152
- Al-CuAl₂ eutectic alloy, directionally frozen, structure 9-39250
- Al-Mg-Zn alloy, distrib. influence on recryst. 9-37276
- Al-Mg-Zn alloy, distrib. variation with plastic deform. w.r.t. ageing time 9-37280
- Al-Mg alloy, stress-induced knitting of networks with four-fold nodes 9-44706
- Al(3-15wt.%)Mg, alloys, struct. by X-ray diff. and electron microscopy 9-40946
- Al(0.5 at.%)Mg alloy, rel. to hardening mechanism at 86°K 9-30699
- Al-Ta dil. alloys, effect on ²⁷Al n.m.r. 9-24504
- Al-Zn-Mg-Cu alloy, deformed, structure rel. to intergranular stress corrosion cracking 9-23811
- Al-Zn alloys, structs. formed by Zn precip. breakdown of spinodal structs. 9-37291
- Al-Zn eutectoid, generation and motion rel. to grain boundary sliding and grain rotation, superplastic conditions 9-23900
- Al-Zn solid soln. and precip. hardened alloy cryst., plastically deformed, dislocation distrib. 9-39364
- Al, configurations at 350°C, X-ray topographical investig. 9-46820
- Al, deformed, density obs. from quadrupole broadening of n.m.r. lines 9-35723

Crystal imperfections continued
dislocations continued

- Al, disloc. substructural distrib. correl. with fatigue props. in vacuum 9-28364
- Al, influence on damping in plastic deform., amplitude dependence 9-30661
- Al, u.s. wave attenuation as function of strain and temp. 9-37332
- Al₂O₃, corundum, impurity-doped, decorated disloc. movements during annealing 9-37172
- α -Al₂O₃, loop formation after neutron irradi. and high temp. annealing 9-23810
- Al₂O₃ bicrystals, core model for grain boundaries from relative energy of tilt boundaries 9-26290
- Al₂O₃ particles-Cu matrix interface, generation, local shear stresses 9-30611
- Al foils, cold-worked obs. during annealing, h.v. electron microscopy 9-42909
- Al foils, fatigued, structures, direct correlation of surface deform. features 9-23878
- Al single cryst., disloc. configurations produced by annealing in air and vacuum, comparison 9-37171
- Al single crystals, motion during tensile or creep tests 9-30675
- As (111) cleavage face vaporization, pit growth at spiral dislocation site 9-30467
- α -As single crystals, in plastic deformation 9-46889
- Au(46.1 at.%)Cd alloy, pseudo-elastic flow due to twinning surface dislocations 9-35156
- B₂C, cry. growth and two-dimens. nucleation at screw dislocations, obs. 9-28290
- BaF₂, stepped lines and half-loops, rel. to discrepancies in etch patterns on matched pairs 9-37173
- Ca₂F(PO₄)₃, fluorapatite, arrangements 9-42826
- CdI, evidence for disloc. dislocations 9-48859
- CdI₂, tilt boundaries of dislocations in single cryst. growth, arcs formation on X-ray photographs 9-30606
- CdI₂, tilt boundaries of dislocations in single cryst. growth, closed rings formation on X-ray photographs 9-30607
- CdS, effects on emission spectra under X-ray excitation, 77°K 9-37771
- CdS, vapour-grown, correlation with disloc. models 9-37174
- CdS creep, transient and steady, due to motion of dislocations 9-42885
- CdS growth from vapour, whisker behaviour 9-46759
- CdS plastically deformed single cryst., density depend. of optical spectra 9-35644
- Co-base superalloys, substructure role in precipitate nucleation 9-39298
- Cr, pressurized at 10-25 kbars, ductile/brittle transition, dislocation distrib. change 9-39427
- Cr Burgers vectors, two-beam diff. contrast meas. 9-32969
- Cu:SiO₂ strained single crystals, lattice rotations assoc. with structure, electron microscope obs. 9-32911
- Cu-Al, complex Frank loops, stacking fault steps form. rel. to fault climb 9-40943
- Cu-Al, quenched, Frank dislocations dissociate, e diff. obs. 9-40959
- Cu(15 at.%)Al alloy, Shockley partial dislocations, unstable directions 9-35093
- Cu(15 at.%)Al deformed alloy cryst., phonon scatt. by dislocations, thermal conductivity meas., low temp. 9-35291
- Cu(16 at.%)Al solid soln., dislocation mechanisms in high temp. creep obs. 9-33043
- Cu-Al alloys, phonon scattering values from thermal conductivity and dislocation density meas. 9-41078
- Cu-Ga solid solns., split, effect of near order on width 9-42827
- Cu-Ga solid solns., struct. determ. by electron microscopy 9-41045
- Cu-Ge solid solns., struct. determ. by electron microscopy 9-41045
- Cu-Mg solid solns., dilute, binding energy with Mg atom 9-37175
- α -Cu-Zn alloys, activation vol. analysis at yield point w.r.t. dislocation intersection processes 9-39413
- Cu-Zn alloys, phonon scattering values from thermal conductivity and dislocation density meas. 9-41078
- Cu-base α -solid solns., degree of splitting and anomalous after-effect 9-32968
- Cu, cross-slip of screw components in fatigue-cell formation 9-23914
- Cu, deformed, density obs. from quadrupole broadening of n.m.r. lines 9-35723
- Cu, density near surface, preferential deformation 9-41016
- Cu, distrib. after fatigue at elevated temp. 9-30608
- Cu, edge, scattering of phonons, thermal resistivity 9-26446
- Cu, electron-irrad., temp. eff. on pinning 9-23812
- Cu, microyielding, arrangements after deform. 9-48897
- Cu, relaxation time rel. to contribution to temp. depend. of Hall coeff. 9-28467
- Cu, structure during homogenization quenching 9-23938
- Cu cyclically deformed rel. to elec. resistivity 9-33254
- Cu deformed single crystals, configs. and densities, effect of strain rate 9-41010
- Cu density depend. on primary recrystallization after large plastic deformation 9-40947
- Cu fatigued single cryst., dislocation struct. and persistent slip bands 9-30686
- Cu fatigued single cryst. dislocation distrib. in persistent slip bands 9-33076
- Cu polycryst., motion and multiplication obs. in preyield plastic deform. 9-35171
- Cu single cryst., disloc. substruct. assoc. with propagating fatigue crack 9-33077
- Cu single cryst., dislocation etching, pitting obs. 9-36988
- Cu single cryst., non-conservative motion, slip traces obs. on surfaces 9-39365
- Cu single crystals, substructure, during early stages of fatigue 9-30637
- Cu whiskers grown by halide reduction, screw-disloc. mechanism, electron-microscopic obs. 9-37111
- Cu(1wt.%)Co, loop formation on electron irradi. and loss of coherency of Co precipitates 9-28383
- Cu-Au ordered alloy, structure produced by plastic deformation 9-23813
- Fe(0.05 wt.%)C alloy, dislocation-interstitial interactions 9-30594
- Fe(18 at.%)Cr-(20 at.%)Ni alloy, damping, and solute pinning 9-28292
- Fe-Cr-Ni alloys, dislocation damping 9-39363
- Fe(11 at.%)Mo alloys, diffusion-controlled motion past precipitate barriers, deformation mechanism, 700°-950°K 9-35173

Crystal imperfections continued
dislocations continued

- Fe-Ni-Cr-Be alloy, influence on semicoherent intermediate b.c. tetragonal phase formed during precip. 9-39498
 Fe-Ni-Cr alloys, mobility 9-39699
 Fe-(3 wt.%)Si, configs. at stages of yielding 9-44766
 Fe-Si alloys, distrib. in cast, worked and annealed samples 9-48846
 Fe-(3 wt.%)Si alloy, edge and screw mobilities, h.v. electron transmission microscopy meas. 9-42829
 Fe, (100) edge dislocation, structure 9-46822
 Fe, $a < 110^\circ$, field-ion microscope evidence for existence 9-30609
 Fe, Burgers vectors, two-beam diff. contrast meas. 9-32969
 Fe, Ferovac-E, shock-loaded, twinning mechanism of dynamic yielding 9-41017
 Fe, neutron irradiat., channelling 9-48860
 Fe, pinning and mobility, interstitials distrib. effect 9-46821
 Fe, prestrained interactions between shock-induced dislocations 9-32915
 Fe single cryst., cutting of screw disloc. rel. to work hardening rate 9-35197
 Fe single crystal dislocation density in 0-0.05 strain range 9-33028
 Fe single crystals, mechanism of plastic deformation 9-23884
 GaAs:Te, triple loops, image contrast 9-44707
 GaAs, annealed, effect on Ca diffusion behaviour 9-44734
 GaAs_{1-x}P_x heterojunction, misfits, formation, propag., interaction and densities 9-47140
 GaAs luminescent diodes, due to lattice mismatch, optical obs. 9-24448
 GaP, density, depend. on growth method 9-30602
 GaSb, densities of crystals grown by floating zone technique 9-28229
 n-Ge, acceptor level position 9-37540
 Ge, behaviour during thermocyclic treatment 9-37176
 p-Ge, carrier conc. decrease after deform. w.r.t. donor action of dislocations 9-35424
 Ge, extrinsic photocond. from edge dislocations 9-45023
 n-Ge, high-density saturation effects 9-43072
 p-Ge, plastically bent, photocond. obs., trapping effect due to dislocations 9-35507
 Ge, prismatic loops, electron microscope obs. 9-42831
 Ge, prod. by bending about (211) axis at 730°C 9-40953
 Ge, production by As diffusion at 830°C, orientation of dislocation lines 9-42830
 Ge, rel. to intensity jumps near K-abs. edge 9-33572
 Ge single cryst., distrib. during plastic deform., etch pit obs. 9-42832
 Ge surface (III), thermooxidized dislocation loops, prod. by scratches, loop vel. temp. depend. 9-32970
 In alloys, scattering, effect on low field Hall effect 9-37445
 In superconductor, motion through electron gas, plastic flow obs. 9-44939
 p-InSb, donor action of β dislocations, p- to n-type conductivity change 9-33322
 InSb, mobility, temp. and stress depend. 9-42833
 KBr, edge dislocation interaction with Burgess vectors 9-23618
 KBr, etch figures, effect of neutron irradiation on dimensions 9-40945
 KBr, interactions with pinning centres, from Young's modulus investig. 9-32971
 KBr, visualization by condensation method 9-44708
 KCl, etch figures, effect of neutron irradiation on dimensions 9-40945
 KCl, melt-grown, thermal etching obs. 9-37178
 KCl, screw dislocations revealed by etching on (100) cleavage faces 9-48861
 KCl, study by etch patterns on cleavage planes 9-37177
 KCl bent crystal treated at 550-750°C, straightening caused by dislocation diffusion 9-42884
 KI, edge dislocation interaction with Burgess vectors 9-23618
 KI, visualization by condensation method 9-44708
 LiF, edge dislocation interaction with Burgess vectors 9-23618
 LiF, initial dislocation density eff. on radiation induced changes in thermal conductivity 9-33198
 LiF, latent hardening due to interac. of dislocations 9-35191
 LiF, viscous drag and dislocation densities, u.s. obs. 9-37179
 LiF etch figures, effect of neutron irradiation on dimensions 9-40945
 LiF movement of charged in fields of 10 KV/cm 9-42834
 LiF single cryst., struct. under sharp thermal change conditions 9-42835
 LiF single crystals, multiplication under periodic and increasing stress 9-40949
 MgAl₂O₄, disloc. density rel. to flux growth 9-37086
 Mn-(11 at.%)Cu alloy, relax. peak obs. w.r.t. twinning surface dislocations 9-35156
 Mn-(11 at.%)Cu alloy, twinning surface dislocations, intrinsic resistive stress 9-35157
 Mo-(0.5-0.20 wt.%)Ti,Zr alloys, deformed, effect of annealing at 1100-2000°C on struct. 9-40951
 Mo, as-group, grinding and abrasion effect on struct., electron microscopy obs. 9-42836
 Mo, density and structure of grain boundaries, revealed by etching in hot Ar stream 9-32972
 Mo, electron irradiated, pinning and depinning, 45° to 330K 9-28294
 Mo, large helical dislocations, X-ray obs., derivation of equilibrium vacancy conc. 9-35094
 Mo, mobility mechanism 9-46823
 Mo crystal irradiat. with u.s. of 150 W/cm², prod. of dislocations 9-40952
 Mo deformed by hydrostatic extrusion, structure determ. by electron microscopy 9-40950
 MoS₂, contact boundary with Mg films 9-32973
 NH₄H₂PO₄, reactions, and glide elements 9-42838
 NaCl: BaCl₂, density effect on ageing, elec. conductivity meas. at 550°C 9-46929
 NaCl, deformed single cryst., density obs. by etch pits and X-ray diff. 9-32974
 NaCl, edge dislocation interaction with Burgess vectors 9-23618
 NaCl, etch figures, effect of neutron irradiation on dimensions 9-40945
 NaCl, glide and climb motion superposition at high temps. 9-37180
 NaCl, in plastic deformation conductivity enhancement, (Gyulai-Hartly effect) mechanism 9-33373
 NaCl as-grown cryst., X-ray diff. obs. 9-37144
 NaCl bent crystal treated at 660-750°C, straightening caused by dislocation diffusion 9-42884
 NaCl crystals, origin of dislocation from etch pit obs. 9-39212
 NaCl single crystal, formation during bending, optical polarization investig. 300° to 1.4°K 9-33036
 NaCl viscous drag and dislocation densities, u.s. obs. 9-37179

Crystal imperfections continued
dislocations continued

- NaF, edge dislocation interaction with Burgess vectors 9-23618
 NaF, identification by electrolytic coloration and chem. etching 9-23814
 NaF, obs. from thermal etch patterns 9-48787
 NaNO₃ single cryst. grown by Kyropoulos method 9-35027
 Nb-N system, precip. of N on dislocations, kinetics 9-30744
 Nb-(25 at.%)Ti-(10 at.%)Zr alloy, solution-treated, density increase on ageing, rel. to recrystallization 9-33122
 Nb, deformed type II superconductor, eff. of distribution on specific heat rel. to fluxoid pinning 9-30875
 Nb, dislocation atmosphere formation rel. to strain-ageing 9-28381
 Nb, n-irradiat., channelling 9-42837
 Nb, pinning of dislocations by impurity interstitials during strain ageing 9-35198
 Nb alloys, superconducting, pinning temp. and field dependence from hysteresis meas. 9-24153
 Nb single cryst., dislocation interaction, temp. depend. of flow and function stress 9-39366
 Nb single cryst., pinning of fluxoids w.r.t. temp. and mag. field 9-39601
 Nb single crystals deformed at high strain rates, sub-structure, and mech. props. and density 9-48898
 Ni-base superalloys, substructure role in precipitate nucleation 9-39298
 Ni, density reduction in initial stages of plastic deformation 9-23888
 Ni, electrochemically polarized single crystals, near surface sources as model basis 9-41019
 Ni, mag. aftereffect due to dislocation displacement inside domain walls, effect of dissolved O 9-39766
 NiAl, nonstoichiometric, rel. to lattice defects 9-40941
 NiAl, stoichiometric, rel. to creep 9-28355
 NiO, epitaxial, density, and bulk imperfections 9-35034
 Ni₄ (4.61 at.%)Cd alloy, twinning surface dislocations, intrinsic resistive stress 9-35157
 Pb, injected dislocation density determ. from work hardening rate 9-41046
 Pb single cryst., u.s. absorpt. damping, temp. and freq. depend. 9-41089
 Pb superconductor, motion through electron gas, plastic flow obs. 9-44939
 PbTe, appearance during epitaxial growth on rocksalt 9-37113
 Pt, quenched, prismatic loop obs., e. microscope and field ion microscope exam. 9-23815
 RbBr deformed, effect on n.m.r. spin echo line shapes 9-30610
 RbFeF₃, ferromagnet, pinning sites for domain walls and nucleation sites for reversal mag. domains. 9-45126
 Sb (111) cleavage face vaporization, pit growth at spiral dislocation site 9-30467
 Se single cryst., X-ray topography 9-44709
 Si:P single cryst., distrib. obs. during plastic deform. 1st. stage 9-30665
 Si-Fe, theory of susceptibility and coercive force 9-33457
 n-Si, dislocation density eff. on minority carrier lifetime 9-35430
 Si, dislocations, effect on conductivity 9-30932
 Si, effect on carrier lifetime 9-30931
 Si, effect on lifetime of minority carriers 9-24191
 Si, formation mechanism due to e bombardment 9-26286
 Si, induced by P deep diffusion 9-32975
 Si, misfit dislocation associated with precipitates of boron 9-37164
 Si, one-to-one correspondence obs. on 14 mm slice, chem. etching and X-ray topography 9-40954
 Si, plastically deformed, struct. obs. 9-42840
 Si, strain compensation by diffused impurities 9-46824
 Si crystal grown in (100) direction, dislocation reaction 9-48863
 Si grown in (100) direction, single edge dislocation obs. by chemical etching and microscopy 9-48862
 Si n-p-n structures, sites for diffusion pipes 9-30603
 Si semiconductor devices, eff. on performance 9-37551
 Si surfaces, in stacking fault nucleation, growth and annihilation mechanisms 9-42844
 SiC surface, etching by improved techniques 9-46749
 SiO₂ particles-Cu matrix interface, generation, local shear stresses 9-30611
 Sn epitaxial film, rel. to residual strains 9-39160
 Ta, relaxation at low temp., Peierls' stress and Bordoni peak 9-23816
 Te single cryst., X-ray topography 9-44709
 β -Ti alloy TS6, work-hardened, struct. rel. to initial state 9-41031
 α -U, energy rel. to temp. and depend. 9-37181
 UO₂, cubic, behaviour in {100}, {110} and {111}-glide planes 9-40956
 UO₂ single crystal substructure, strain rate 10⁻³-10⁻¹ min, 750-1400°C 9-35095
 UO₂ single crystal substructure, strain rate 10⁻³-10⁻¹ min, 750-1400°C 9-40957
 W, interactions, rel. to micro-strain to macro-strain transition 9-23890
 W, parallel array, impurity segregation obs. in neutron irradiated sample 9-28295
 W, quantum-mechanical tunneling 9-26288
 YAl garnet, rel. to etch figures 9-44641
 YFe garnet, effect on magnetiz. process, direct investigation 9-47276
 Zn, dislocation contrib. to u.s. attenuation 9-39521
 Zn, forest density depend. of critical shear stress 9-46878
 Zn, selective etching, mechanism 9-40856
 Zn, slip, interaction with deform. twin boundaries, rel. to stacking fault formation 9-26289
 Zn, vapour-grown, thermal etching obs. 9-48864
 Zn single cryst., X-ray diff. topography 9-35096
- impurities**
 A¹¹⁰B⁺ semiconductors, behaviour, thermodynamic predictions 9-49093
 absorption spectra due to impurity centres, shape obs. and Urbach's law 9-33546
 alkali halide scintillators, distrib. laws, crystallochem. analysis 9-23798
 alkali halides, Cd doped and electrolytically coloured, band obs. 9-40970
 alkali halides, Cu⁺ and Ag⁺ centres excitation and emission spectra, hydrostatic press. effect 9-41401
 alkali halides, in plastic deformation enhanced conductivity (Gyulai-Hartly effect) mechanism 9-33373
 alkaline earth tungstates, Bi doped, u.v.-induced colouration, fading and darkening processes obs. 9-45282
 alloys quenched dilute, non-equilib segregation, model rel. to grain boundary hardening 9-48919
 anthracene, doped single cryst., residual impurities as line defect sources 9-37182
 binary alloys, Green function and energy spectrum evaluation 9-37163

Crystal imperfections continued
impurities continued

- β - brass solid, static atomic displacements influence on diffuse intensity of scatt. X-rays 9-37132
- calcite, effect of trace impurities on Cleavage surface energy 9-30479
- calcite, e.s.r. of AsO_4^{2-} in γ -irrad. cryst. 9-39903
- center vibrational mixing of two close-lying levels, effect on wide vibration band 9-28677
- contaminations affecting surface decoration patterns 9-32954
- distribution during directed crystallization process 9-40931
- distribution during directional crystalln., anal. of influences 9-48852
- distribution meas., differential capacitance technique 9-28508
- doping struct. determ. by backscatter of He^+ 9-35411
- F colour center formation, inhibited by Mn impurities, thermoluminescent investigation 9-31148
- f.c.c. cryst., force-const. changes effect on coherent neutron scatt. rel. to vibr. props. 9-42953
- fissionable materials, impurity-doped, effect of impurity atoms on growth of gas-filled pores 9-32955
- graphite, Br intercalation and dimensional deform. 9-26223
- group III-V semiconductors, freqs. of localised modes due to substitutional impurities 9-35265
- harmonic 1D cry., isotopically disordered, transmission props. 9-26280
- ice, doping with He and Ne 9-46814
- impurity-vacancy complexes, equilibrium concn. eqn. 9-46813
- interaction with lattice vibrations 9-30757
- ions, implanted, investigation using directional effects in charged particle reaction yields 9-30598
- ions, lattice destruction during implantation and post-irrad. annealing 9-30599
- ions with spin 1, 3/2 and 5/2, e.s.r. spectra, angular variation 9-31156
- orthoferrites, flux grown crystals, Pb substitution 9-28237
- paramagnetic, effect on superconductivity 9-49031
- polar impurities motion in alkali halides, effect of localized lattice vibr. 9-33159
- quartz, trapping of colloidal inclusions in growth 9-37043
- semiconductor doping by ion implantation 9-41208
- semiconductors, amount of dissolved impurities rel. to stoichiometric vacancies 9-47095
- semiconductors, concentration deduction from Schottky-barrier (C,V) characteristics, possible errors 9-30918
- solute atom position, by X-ray fluoresc. scatt. 9-23797
- statistical mechanics at low temp. 9-47037
- steel, inclusion anal. by colour X-ray images 9-48851
- steel, Si, infl. of H on mechanical and magnetic relaxation effects 9-30644
- superconductor, dirty type II, effect of small superparamag. grains on transition temp. 9-44932
- surface equilib. concn. 9-23616
- surface-active, effect on epitaxial processes 9-42721
- Ag-Au layered struct., static atomic displacements influence on diffuse intensity of scatt. X-rays 9-37132
- Ag, grown by electrodeposition, eff. of impurity on large step-height spiral growth on surface 9-23825
- AgBr, impurity halide diffusion 9-40979
- AgCl, impurity halide diffusion 9-40979
- AgO powders, effect of added impurities on elec. resistivity 9-28545
- Al-Cu alloys, binding free energy bet. vacancies and second solute atom 9-23793
- Al-Ta dil. alloys, effect on ^{27}Al n.m.r. 9-24504
- Al-(4.4 wt.%)Zn alloy, Be atoms influence on elec. resistivity changes due to clustering 9-40932
- Al, thermal diff. controlled pinning of dislocations by substitutional atoms 9-37332
- $\text{Al}_2\text{O}_3\text{:Cr(Fe,Mn,V)}$ single cryst. low temp. thermal conductivity meas. 9-35086
- Al_2O_3 , corundum, doped, decorated dislocations movements during annealing 9-37172
- Al_2O_3 , gaseous impurities, effect on hot-pressing 9-35202
- Al alloys, Be-vacancy interactions 9-44692
- Al alloys, Be-vacancy interactions 9-44691
- Al force-const. changes effect on coherent neutron scatt. rel. to vibr. props. 9-42953
- $\text{Ba}_2\text{NaNb}_2\text{O}_{15}\text{:Pt}^{4+}, \text{Ir}^{4+}$, defect-induced absorpt. at 5300 Å 9-28651
- C, co-deposition of B, effect on dynamic elastic mod. and internal friction 9-26320
- C, turbostratic, Na and B doping and e.s.r., effect of heat treatment 9-26791
- $\text{Ca}_{10}(\text{PO}_4)_6\text{F}_2$, OH and oxide ion giving rise to specific absorpt., fluoresc., and colour and paramag. centres form 9-40933
- $\text{CaF}_2\text{:Ce}^{3+}$, presence of permanent dipoles 9-37166
- CaF_2 , fluoride, synthetic, inhomogeneities, optical investig. 9-37165
- CaF_2 , rare-earth doped, thermal conductivity in mag. fields 9-47008
- CaO , e.s.r. spectrum obs. of paramag. lines due ion impurities 9-45381
- CaO , gaseous impurities, effect on hot-pressing 9-35202
- CaWO_4 , synthetic inhomogeneities, optical investig. 9-37165
- $\text{CdCl}_2\text{:Ag}$, irrad., optical absorpt. and e.p.r. obs. 9-49272
- CdS , paramag. reson. of $\text{Fe}^{3+}\text{-Cu}$ associated centres, 77°K 9-47432
- CoF_2 , magnetization of Fe^{2+} ions, Mossbauer effect meas. 9-45298
- Cr^{3+} , optical spectra in LiNbO_3 and LiTaO_3 9-31104
- CsCl structures, i.r. localized modes, shell models 9-23800
- CSl , divalent impurities, effect on electrical conductivity rel. to temp. 9-33380
- Cu -(0.2 wt.%)Al alloy, internally oxidised, effect of Si additions on mech. props. 9-46903
- Cu, bond constns. of Be atoms, variations 9-39181
- Cu, tough-pitch and P-deoxidized, grain boundary distrib. for as-cast and annealed conditions 9-30600
- Cu_3Au , solid soln., static atomic displacements influence on diffuse intensity of scatt. X-rays 9-37132
- Cu alloys, Mossbauer effect in ^{119}Sn , electronic props. obs. 9-43222
- $\text{Cu(36wt\%Zn, Fe and P)}$ influence on recrystn. 9-30718
- Fe, ^{133}Cs mag. hyperfine field, Mossbauer spectra 9-37699
- Fe, ion implanted, investigation using directional effects in charged particle reaction yields 9-30598
- Ga_2Te_3 , solubility in crystal with stoichiometric vacancies rel. to local elastic stresses 9-40934
- GaAs:Cu, local vibrations and structure of centres 9-33231
- GaAs:Zn,Ge,Te, segregation rel. to melt. comp., obs. 9-26210
- GaAs, doped regions, i.r. absorpt. after neutron irrad., rel. to defect production 9-37725

Crystal imperfections continued
impurities continued

- GaAs, ion implantation profiles of ^{85}Kr 9-47120
- Ge:Ga with anomalous Cu distrib. in and near diffused layer, bipolar photoeffect obs. 9-45024
- Ge single cryst. growth from melt, convection-induced impurity distrib. 9-37079
- In_2Te_3 , solubility in crystal with stoichiometric vacancies rel. to local elastic stresses 9-40934
- K, Na diffusion mechanism, computer calc. 9-44736
- K halides, e.s.r. of trapped N_2^- 9-31166
- KBr:Ca(Cl) , F-centre prod. rate due to electron irrad. 9-46834
- KBr:Cd(Zn) , thermoluminesc. and optical absorpt. obs. of F centres formation 9-33606
- KBr:H^- , lattice distortions and vibration local mode freq. calc. 9-28410
- KBr:Li^+ , off-centre behaviour lattice parameter dependence 9-35087
- KBr:OH^- , rot. barrier height 9-40935
- KBr, i.r. absorpt. of Li^+ , particle in curved box model 9-47364
- $\text{KCl:Ag(Ca, Cd, Co, Ti)}$, F-centre prod. rate due to electron irrad. 9-46834
- KCl:CO_3^{2-} , i.r. absorpt. spectra of ion vibrs. 9-41382
- $\text{KCl:Ca(Cd, Mn, Pb)}$, infl. on growth of F and M optical absorption bands 9-28686
- KCl:NO_3^- , i.r. absorpt. spectra of ion vibrs. 9-41382
- KCl:OH^- , rot. barrier height 9-40935
- KCl:Pb F centre prod. by electron irrad., α and V_k centre motion importance 9-44718
- KCl:SO_4^{2-} , i.r. absorpt. spectra of ion vibrs. 9-41382
- KCl:Ti , F centre prod. by electron irrad., α and V_k centre motion importance 9-44718
- KCl:TiCl , lattice defects, X-ray diff. study 9-46815
- KCl, eff. on optical growth of V and F colour centres at 295°K 9-23830
- KCl, lattice defects, X-ray diff. study 9-46815
- KCl:Li^+ , off-centre behaviour lattice parameter dependence 9-35087
- KI, Raman spectrum of S_2^- and Se_2^- mols. 9-49294
- Li, Cu interstitial-like diffusion 9-39384
- $\text{LiNbO}_3\text{:MgO}$ single cryst., doping eff. on acoustic wave attenuation 9-37334
- $\text{LiTaO}_3\text{:MgO}$ single cryst., doping eff. on acoustic wave attenuation 9-37334
- Mg, distribution of Sn, Pb, and Zn during directed crystallization process 9-40931
- MgAl_2O_3 stoichiometric spinel, trace detection by neutron activation analysis 9-35088
- MgO , diffusion of Ca^{2+} 9-44739
- MgO , F-containing trapped-hole centre, structure from ENDOR meas. 9-39355
- MgO , gaseous impurities, effect on hot-pressing 9-35202
- $(\text{Mn}_{0.95}\text{Cu}_{0.05})$ alloy, Fe obs., elec. and mag. props. 9-41338
- MnF_2 , magnetization of Fe^{2+} ions, Mossbauer effect meas. 9-45298
- NH_4Cl , Cu^{2+} impurity effects on λ -type phase transition, e.s.r. and differential thermal analysis 9-33142
- Na, K diffusion mechanisms, computer calc. 9-44736
- $\text{NaBa}_2\text{Nb}_2\text{O}_{15}$, H content, absorpt. spectra obs. 9-41374
- NaCl:Ca(Cd) , thermoluminesc. and optical absorpt. obs. of F centres formation 9-33606
- NaCl:OH^- , rot. barrier height 9-40935
- NaCl:BaCl_2 single cryst. pulled from melt, oriented impurity precipitates 9-30601
- NaCl, in plastic deformation enhanced conductivity (Gyulai-Hartly effect) mechanism 9-33373
- NaCl, surface active MnCl_2 and PbCl_2 impurities, effect on microstruct. of growth surfaces 9-23765
- NaCl colour centre complexes around impurity clusters 9-44686
- NaCl structures, i.r. localized modes, shell models 9-23800
- NaI:Tl,NaI:In centres due to O-containing impurities which reduce activator luminescence 9-33613
- Nb, O additions in single crystals, eff. on elastic. constants and u.s. attenuation, 4.2° to 313°K 9-30634
- Nb, superconducting, effect on magnetization curve shape 9-44943
- Nb_3Sn , correlation with critical current density, and microstructure 9-41180
- Nb ferroelasticity due to H as lattice gas, obs. 9-23868
- Nd glass, occlusions extraction and microanalysis 9-32956
- Ni, dissolved O effect on mag. aftereffect due to displacement of dislocations inside domain walls 9-39766
- Ni in NaCl, influence on dielectric loss 9-35467
- O_2^- centres in alkali halide crystals, thermal quenching 9-39861
- Pb-Na solid solns., effect of Ag on discontinuous precip. 9-39500
- $\text{PbTe:}^{27}\text{Fe}$, Mossbauer obs. of Fe ions 9-39819
- PbZrO_3 , eff. on enthalpy changes during dielectric phase transitions 9-26584
- quartz, synthetic, inhomogeneities, optical investig. 9-37165
- RbCl:OH^- , rot. barrier height 9-40935
- S_2^- centres in alkali halide crystals, thermal quenching 9-39861
- Si:Li, thermal ionization energy of Li impurity 9-47131
- Si:P, photoionization of impurity atoms, e.p.r. method 9-37636
- p-Si, deuterium-irradiated, energy spectra of defects 9-30589
- Si, interaction of Li with rad. induced atomic displacements 9-48844
- Si, ion implanted, investigation using directional effects in charged particle reaction yields 9-30598
- Si, γ irradiated, annealed, interactions of point defects with impurities 9-46807
- Si, precipitation of boron 9-37164
- Si containing C isotopes, vibr. absorpt. of C and C-O complexes 9-41390
- Si epitaxial layers, C conc. obs. 9-46725
- in SiO_2 film on Si, combined m.o.s. and radiochemical analysis 9-42814
- Sn, surface active and inactive, effect on grain growth 9-48865
- Ta, refining by electron beam melting 9-33101
- $\text{Te:}^{57}\text{Fe}$, Mossbauer obs. of Fe ions 9-39819
- α -U low-temp. phase transition depend. 9-26394
- W, neutron irradiated, segregation within dislocation array 9-28295
- $\text{Y}_2\text{Al}_2\text{O}_7$, Cr^{3+} and Nd^{3+} impurity distribution, rel. to trivalent oxide solubility and cry. growth 9-36980
- $\text{Y}_2\text{Fe}_2\text{O}_7$, Cr^{3+} and Nd^{3+} impurity distribution, rel. to trivalent oxide solubility and cry. growth 9-36980
- YAl garnets, synthetic, inhomogeneities, optical investig. 9-37165
- $\text{YVO}_4\text{:Eu}$, effects on luminesc. processes 9-47409
- ZnS, Raman scatt. by Mn impurities, vibr. resonant modes obs. 9-43247
- ZnS structures, i.r. localized modes, shell models 9-23800

Crystal imperfections continued
interstitials

- alloys, f.c.c. ferromag., rel. to mag. lag and anisotropy 9-45130
atoms, interaction energy with dislocations 9-44705
b.c.c. crystals, atoms, and dislocations, interaction energy 9-28289
diffusion, noble and transition metals in metallic systems 9-42812
F centres creation by ionizing radiation interpretation by recomb. model 9-40968
Frenkel pairs prod. at low temp. electron irradi., influence of subthreshold events 9-32952
graphite-B, neutron irradi., loop clustering, effect of B, electron microscope obs. 9-30595
graphite-B, neutron irradi., loop nucleation, effect of B 9-30596
graphite, loops on irradi. 300 to 1350°C, rel. to lattice parameter changes 9-28280
graphite irradi. at high temp., nucleation, cry. perfection influence 9-23794
interaction with dislocations, energy consideration 9-46812
ions, implantation by nuclear reactions, techniques 9-33210
metals, electron radiation damage 9-30592
Nb hydrides and deuterides, ordering transformations in solid solutions 9-23990
noble metals, rapid diffusion in Pb, Sn, In and Tl, mechanism 9-28321
quartz, incorporation of di- and trivalent cobalt 9-28282
rutile single crystals, formation during chemical reduction 9-32945
self-diffusion in interstitial phases 9-23832
simulation method appl. to recomb. of vacancies and interstitials 9-30591
Snoek relax. with internal stresses 9-44754
solutions, noble and transition metals in metallic systems 9-42812
transition metal carbides, self-diffusion in interstitial phases 9-23832
wurtzite type crystals, eff. on absorption and emission band polarization 9-33544
Zircaloy-4, rel. to non-linear irradi. growth 9-37375
Ag, electron irradi., stage I recovery of elec. resistivity 9-35083
AgBr, motion in diffusion 9-28312
AgCl, motion in diffusion 9-28312
Al, α -irradi., internal friction peaks ascribed to reorientation of interstitial clusters 9-39398
Al, in correlated recovery of Stage I, behaviour from energy dependence obs. 9-28379
Au, electron irradiated, clusters below stage III annealing 9-30593
CaF₂, ENDOR obs. of H- and F- compensated tetragonal Nd³⁺ centres 9-47449
Co, Frenkel Pair formation and mutual annihilation after electron irradi. 9-35084
Cu, electron irradi., clusters 9-35082
Fe-(0.05 wt.%)C alloy, dislocation-interstitial interactions 9-30594
Fe, distrib. effect on dislocation behaviour 9-46821
Fe ternary alloys, reorientation causing magnetic disaccommodation 9-26635
p-InSb, Frenkel defects. formation by illumination 9-28283
Ir, proton irradi., conc. decrease during annealing 9-35085
KB₄, radiation-induced H⁺, H⁻ and V_i centres form. kinetics 9-42849
KBr:Na⁺, radiation-induced H⁺, and H⁻ and V_i centres form. kinetics 9-42849
KBr, ionizing rad. induced, prod. rate at low temp. 9-32948
KCl, radiation-induced H⁺, H⁻ and V_i centres form. kinetics 9-42849
K, as Na diffusion mechanism, computer calc. 9-44736
Li, Cu interstitial-like diffusion 9-39384
Li₂Ni_{1-x}O solid solutions, donor levels caused by neutral Li interstitials 9-41134
LiF, recomb. model of interstitial-vacancies in interpretation of F centres due to X-ray irradi. 9-40974
Na, as K diffusion mechanism, computer calc. 9-44736
Nb, migration of impurity interstitials during strain ageing 9-35198
O atoms in Ta, diffusion coeff. and activation energy, relax. obs. 9-28284
RbCl:H, U₂-centres, ENDOR meas. 9-30621
n-Si:P, γ -irradiated, rel. to thermal donor formation 9-32951
Si, boron implanted and annealed, condensed defect structure distrib. 9-32953
Ta hydrides and deuterides, ordering transformations in solid solutions 9-23990
UC single cryst., Rn 220 recoil atoms interstitial diffusion 9-28325
V hydrides and deuterides, ordering transformations in solid solutions 9-23990
W, e-irradi., Stage-I defect behaviour 9-26279
W, vacancies, due to deuteron bombardment at 0.1 MeV 9-37162

VACANCIES

- alkali halides, in plastic deformation enhanced conductivity (Gyulai-Hartly effect) mechanism 9-33373
alkali halides, Schottky defect formation energy 9-48849
alkali metals, relax. and migration energy, lattice-dynamical calc. 9-23792
diamond, neutral isolated divacancy electronic structure 9-46810
diffusion, thermal 9-28278
excess conc. effect on precip. nucleation rate 9-42926
F centres creation by ionizing radiation interpretation by recomb. model 9-40968
graphite, lines and loops on irradi. 300 to 1350°C, rel. to lattice parameter changes 9-28280
graphite, oxidation rel. to etch pit ion formation 9-28281
graphite irradi. at high temp., nucleation, cry. perfection influence 9-23794
ice, irradi., rel. to electron trapping 9-42980
impurity-vacancy complexes, equilibrium conc. eqn. 9-46813
inert-gas crystals, Monte Carlo simulation 9-23795
jump number, mean in annealing expts., depend. on sink size and shape 9-46808
metals, concentration effect rel. to surface energy 9-32830
metals, influence on oxidation kinetics 9-28794
molybdenite, oxidation rel. to etch pit ion formation 9-28281
rutile single crystals, formation during chemical reduction 9-32945
simulation method appl. to annealing of vacancies 9-30590
simulation method appl. to recomb. of vacancies and interstitials 9-30591
solid solns., ordered, equilib. conc. 9-42809
solute segregation in vacancy gradients generated by sintering and temp. changes 9-23791
transition metal carbides, phonon scatt. by lattice vacancies rel. to thermal conductivity 9-47010

Crystal imperfections continued
vacancies continued

- vacancy-flow term in diffusion, rel. to conc. distortion by impurities, deviations from thermodynamic equilib. 9-23831
wustite, ordered struct. obs. 9-26232
AgBr, mechanism for impurity halide diffusion 9-40979
AgCl: Cd single cryst., relax. of vacancy-dipoles 9-33372
AgCl, diffusion correlation factor 9-28313
AgCl, mechanism for impurity halide diffusion 9-40979
AgCl, Sr²⁺ diffusion in AgCl, vacancy mechanism, ions with no outer d-shell 9-46857
AgCl transition-metal doped single cryst., relax. of vacancy-dipoles 9-33372
Al-(2.5 at.%) Cu-(1.2 at.%) Mg alloy, ageing, Si effect on vacancy form. 9-48915
Al-Cu-Ag alloys, conc. rel. to form. and dissolution of Ag-rich zones 9-46758
Al-Cu alloys, binding free energy bet. vacancies and second solute atom 9-23793
Al-(4 at.%) Cu alloy, excess conc. during ageing and slow reaction mechanism obs. 9-48916
Al-Zn-Mg alloys, role of Mg as reversible-vacancy trap 9-23979
Al, in correlated recovery of Stage I, behaviour from energy dependence obs. 9-28379
Al, ion irradiated, clusters 9-28279
Al, thermal diff. controlled pinning of dislocations by deform. prod. vacancies 9-37332
Al, vacancy migration as explanation of quenching eff. on internal friction 9-46809
Al alloys, Be-vacancy interactions 9-44691
Ar, formation and self-diffusion activation energies, many-body effects 9-46693
Au, cluster formations due to dechanneling of channeled keV Au ions 9-47016
Au, ion and neutron irradiated, clusters 9-28279
Au, ion bombarded, depth distrib. of clusters 9-30586
Au, quenched resistivities of vacancies and Matthiessen's rule 9-35336
Co₂Ni_{0.5-3}Fe_{2.5}O₄, in induced magnetic anisotropy mechanism 9-33474
CoO: Al(Li) mechanism for ¹⁸O self-diffusion 9-40982
CoO: Li system, cation vacancy density, role in monoxide to spinel transition 9-48929
CoO, mechanism for ¹⁸O self-diffusion 9-40982
CsBr, Schottky disorders w.r.t. ionic conductivity obs. 9-33398
CsCl-type ordered alloys, distrib. 9-30585
Cu: Xe, clusters 9-32947
Cu, in correlated recovery of Stage I, behaviour from energy dependence obs. 9-28379
Cu, electron irradi., clusters 9-35082
Cu monocrystalline, deformed, clusters along {111} planes from X-ray diffraction study 9-40939
GaAs, neutron irradi., i.r. absorpt. of doped regions rel. to vacancy prod. 9-37725
Ge, quenched, association with thermal acceptors 9-49107
He cavity formation following electron trapping 9-23572
³He, b.c.c., nonlocalized vacancy formation 9-32812
 β -In₂S₃ ordering, associated antiphase boundaries and twins 9-30587
Ir, fission-fragment damage and formation mechanism 9-42810
KBr, ionizing rad. induced, prod. rate at low temp. 9-32948
KCl: Pb²⁺, vacancy pairs aggregation, effect on optical absorption and emission spectra 9-31108
KCl: TlCl, vacancy conc. inc. with impurity conc. 9-46815
KCl, anion migration for formation of F_a- and Z_i-colour centres 9-39375
KCl, effect of surface density on Au nucleation sites 9-40848
KCl, possible trivacancy mechanism contribution to ionic conductivity 9-28552
KCl, vacancy conc. inc. with impurity conc. 9-46815
KCl F-center build-up under γ irradiation, vacancy source 9-32987
K, as Na diffusion mechanism, computer calc. 9-44736
LiF: Mn²⁺(Mg²⁺), γ -ray colouration, charge compensation vacancies conversion into F-centres 9-28305
LiF, formation energy of individual cation vacancies 9-42811
LiF, recomb. model of interstitial-vacancies in interpretation of F centres due to X-ray irradi. 9-40974
LiF, separate form. energies of positive and negative ion vacancies 9-48850
LiF formed by reactor radiation, detect. by annealing and elec. cond. meas. 9-32949
MO, equilibrium conc. derivation from X-ray obs. of large helical dislocations 9-35094
MgO, cavity form. by annealing 9-44693
Na, as K, diffusion mechanism, computer calc. 9-44736
NaCl: Pb²⁺, vacancy pairs aggregation, effect on optical absorption and emission spectra 9-31108
NaCl, formation energy of individual cation vacancies 9-42811
NaCl, in plastic deformation enhanced conductivity (Gyulai-Hartly effect) mechanism 9-33373
NaCl, possible trivacancy mechanism contribution to ionic conductivity 9-28552
NaCl F-center build-up due to γ irradiation, source of vacancies 9-32987
NaCl single cryst., thermal expansion meas., Schottky defects conc. rel. to temp. depend. 9-37360
NaCl void formation and migration in a single crystal subject to a temperature gradient 9-32950
NbCo_{0.75}, ordering, neutron diff. obs. 9-40913
Ni, ion bombarded, depth distrib. of clusters 9-30586
Ni, ion irradiated, clusters 9-28279
Ni, quenched-in, elec. resistivity 9-23796
NiO in O₂, diff. coeff. of cation vacancies, 750-1000°C 9-30588
Pb²⁺ vacancy pairs, diffusion in NaCl and KCl, dielectric absorption meas. 9-31108
Pd thermal, formation energy from diffusivity meas. 9-41107
Pt-Fe dilute solid, interac. of quenched-in vacancies with Fe atoms 9-26278
Pt, quenched resistivities of vacancies and Matthiessen's rule 9-35336
RbCl, possible trivacancy mechanism contribution to ionic conductivity 9-28552
n-Si:P, γ -irradiated, rel. to thermal donor formation 9-32951
Si-B, quenched-in defects, elec. and photo-conductivity obs. 9-39357

Crystal imperfections continued
vacancies continued

- p-Si, deuterium-irradiated, energy spectra of defects 9-30589
 Si surface in stacking fault nucleation, growth and annihilation mechanism 9-42844
 TaC_{0.76}, ordering neutron diff. obs. 9-40913
 U void effect on neutron spectral indices and fast fission ratio 9-38737
 UC void effect on neutron spectral indices and fast fission ratio 9-38737
 V₂Te₈ 9-37151
 W, interstitial, due to deuterium bombardment at 0.1 MeV 9-37162
 W, n irradi., annealing rel. to vacancy clustering obs. 9-44694
 Zn, formation parameters from thermal expansion meas. on single crystals 9-46811
 ZrO₂(Ti), rel. to trapping centres in thermoluminescence 9-39891

Crystal properties

- anisotropic, biaxial and uniaxial, principal optical constants 9-47312
 distribution coefficient, depend. on temp. fluctuations in melt 9-39204
 f.c.c., absolute stability limit eqn. derived from free energy configurational component 9-42693
 glide and rotation during sedimentation in graphite 9-39368
 magnetic triclinic, isogyre eqn. 9-24362
 metals, structural anisotropy, stereology 9-46914
 non-enantiomorphous class 4 crystal, optical activity 9-49242
 physical, independent constants derivation by Galin's method 9-24264
 piezo-optical rotation and rel. to symmetry 9-47318
 polarized crystals, symm. and props. using group intersection theory 9-46737
 quartz vibrator, singly rotated, force-freq. coeff. chart 9-37596
 rare-earth ethylsulphates, covalency eff. 9-35008
 Cs adsorbed on tungsten evidence for its non-metallic character 9-32849
 Hg single cryst., size effect on elec. resistivity 9-39587
 KBr lattice expansion following F-center formation 9-28304
 MeF₂:Ce³⁺, lowest Stark sublevels of 4f¹, 5d¹ configurations determ. 9-22947

Crystal structure

- see also Polymorphism*
 alkali halide films, grown from melt, cell and platelet structure 9-23627
 Alnico, Ti bearing, eff. on coercive force 9-24310
 B filament vapour deposited on W, cracks rel. to chem. interaction 9-48866
 ballases, natural and synthesized, growth conditions 9-26197
 blocking pattern method, scanning device 9-25529
 chlorites, two-packet unit cell, systematic derivation of possible polytypes 9-39263
 cubic polycrystals, X-ray diff. line breadth analysis 9-39227
 cyclohexanol, phase transformation, morphology 9-35251
 diamond, lattice vibrations symmetry, theory 9-23999
 dielectric classification, structure, ionization pot., band structure prediction appl. 9-23654
 diffraction techniques demonstrated using laser light and polymer spheres 9-47712
 double crystal X-ray diff. method for microstrain analysis of BeO single crystals 9-42765
 graphite artificially densified by natural gas decomposition, pore size distrib. changes, new porosimeter obs. 9-23753
 rel. to growth, conference, 1968 9-32867
 hexaferrites, numerical shorthand description 9-40900
 ice cylinders, unstable, growth of perturbations in shape of single cryst. growing in water 9-35019
 Lang X-ray topography, use of pendellosung fringes 9-46765
 lanthanide metals and alloys, polymorphic families, influence of 4f electrons 9-30509
 magnetite, stoichiometric and non-stoichiometric, Mossbauer obs. 9-39818
 metal, fine particles prep. by gas evaporation method with plasma jet flame 9-33128
 metals, changes due to cold working and annealing, effect on plastic flow and yield 9-46925
 metals, f.c.c., evaporated, nuclei shapes, stability obs. 9-32895
 microstrain analysis of BeO single crystals, double-crystal X-ray diff. method 9-42765
 molybdenum permalloy tape effect on stress sensitivity and mag. squareness ratio 9-49205
 mounanaite, PbFe₂(VO₄)₂(OH)₂, X-ray powder obs. 9-32925
 mimonic single crystals, strain-hardening rel. to state of quenched alloy 9-33100
 plasma oscils. exam. by 20 keV electrons, effect of h.c.p., f.c.c., b.c.c. structs. 9-41140
 polycrystals, defect interactions, two-dimens. model 9-37155
 polyethylene annular spherulites, fine structure and deform. mech., direct electron microscopic investig. 9-26254
 polyethylene extended chain cryst. growth and morphology 9-26213
 polyethylene terephthalate, crystallinity rel. to mech. props. 9-42863
 striated solute distrib. prod. by temp. oscillations during growth from melt 9-37059
 tetrahedrally coordinated, dielectric theory of cohesive energies 9-23698
 zincblende, lattice vibrations symmetry, theory 9-23999
 Al-(11 wt.%Mg) age-hardening alloy, deform. by hydrostatic extrusion effect 9-41051
 Al-(40 wt.%Zn), alloys, structural changes during ageing 9-23943
 β' AuZn, defect structure from lattice parameter meas. 9-23881
 Ba₂Fe₂Zn₂O₇, numerical shorthand description 9-40900
 Be-(1.3 wt.%Ni) alloy, changes due to low-temp. and mixed ageing 9-39464
 BeO single crystals, analysis of microstrains using double-crystal X-ray diff. 9-42765
 C, rel. to dimensional changes and creep, irradi. induced 9-41022
 C deposits, effect of deposition surface topography 9-26226
 CdIn₂S₄/In₂S₃ mixed cryst., photoluminesc. w.r.t. struct. props. 9-33614
 CdIn₂S₄, photoluminesc. w.r.t. struct. props. 9-33614
 CdS hollow conical single cryst. grown from vapour 9-35017
 Cu single crystals, electrodeposited, structure and mech. props. 9-46786
 Fe, effect of H₂ atmos. on perfection 9-44666
 Fe complex, thio-p-toluoyldisulfidobis (dithio-p-toluato) iron (III), crystal and mol. structure 9-42785
 Hf complex, Hf(IV) acetyl-acetonate, polycrystalline, after-effect in (n_p) reaction 9-35598
 InSb phases at high pressure and temps. 9-42922
 K_{0.38}MoO₃, and elec. resistivity considerations, X-ray diff. obs. 9-37446
 K₂NbO₇, orthorhombic, from X-ray meas. 9-26238

Crystal structure continued

- (KPO₃)_x, rel. to valence angles and dihedral angles in PO₄ tetrahedra 9-40906
 Mg₂P₂O₇, rel. to valence angles and dihedral angles in PO₄ tetrahedra 9-40906
 Mg pyroxenes, before and after phase inversion 9-42934
 MgAl₂O₄, vertically pulled from melt, morphology and defects 9-46743
 Mn-In alloys 9-31017
 Na₃P₂O₇, rel. to valence angles and dihedral angles in PO₄ tetrahedra 9-40906
 Nb₂O₅, modifications, influence on emission spectra intensity 9-33560
 Nb-(75 at %)Ti quenched alloy, e. microscope and X-ray diffraction study 9-23767
 Ni-Zn-Si system, of β and ternary phases in equilib. at 800°C 9-35209
 Ni₂Zn₃Si, cubic Ti₂Ni type struct. and close packing theory 9-32924
 Pr(ReO₃)₂.H₂O, crystallographic constants, computation from observed interfacial angles 9-39302
 SiC filament vapour deposited on W 9-48866
 SiO₂ thermally oxidised, symmetry of surface state density 9-23773
 Ta₂O₅ modifications influence on emission spectra intensity 9-33560
 TiFeS₂, ragunite 9-30574
 UO₂, nonstoichiometry rel. to flow stress and strength 9-33049
 V₂C₃, superlattice structures, disordering by electron microscope beam bombardment 9-26468
 VO₂, composition dependence 9-28272
 WO₃, symmetry in structures stable at room temp. 9-23655
 ZnS epitaxial films, electron microscope and diff. obs. 9-37684
 ZnSe epitaxial films, electron microscope and diff. obs. 9-37684
 Zr, (1017) hydride habit plane 9-35013
- microstructure**
see also X-ray examination of materials/microstructure
 alloy El1437B, kinetics of precip. phase rel. to ageing and temp. in range 700-850°C 9-41047
 alloys, two-phase, development during liquid-phase sintering 9-42919
 alnico alloy single crystals precipitation dendritic structure and mag. props. 9-44792
 alumina whiskers/Ni composites, electron microscope obs. 9-33169
 anthracene solidified vitreous solns., absorpt. spectra, aggregates existence obs. 9-46701
 austenitic alloy foils, irradi., void size determ. 9-48755
 b.c.c. structure, grain boundaries with periodic patterns 9-40872
 binary eutectic microstructures controlled solidification technique 9-23676
 α-brass, rolled, orientation distrib. of crystallites, electron microscopy determ. 9-48830
 cement, Portland, solidified by hydration, constitutional supersaturation 9-37137
 ceramic systems, very high press. effect 9-30553
 ceramics, carbide-boride-graphite, fusion-cast 9-30729
 ceramics, polycrystalline, interaction with cracks, monitoring technique 9-33091
 connective tissues, eutectic struct. from electron micrographs 9-48839
 contrast developed by vapour-deposited multi-layer system 9-46764
 crystallite size distrib. in coarse-grained samples, X-ray method 9-26218
 cyano-(19) anthracene solns., absorpt. spectra, aggregates struct. obs. 9-46702
 domains, size, determ. from tails of X-ray diff. profiles 9-40879
 eutectics between compounds, preferred orientation 9-39245
 ferrites, spinel 9-45174
 fluor-phlogopite crystallites, grown from vapour, polytypism obs. 9-37010
 glass, i.r. spectroscopy 9-30469
 glass, stereo obs. using secondary electron emission mode of scanning microscope 9-32825
 grain boundaries, large-angle, complete conjugation model 9-37116
 grain growth during secondary recrystallization, effect of volume energy 9-32881
 grain size effect in low energy p and X-ray scattering 9-49399
 graphite, pyrolytic stress-annealed, imperfections rel. to graphitization, electron microscope obs. 9-35054
 graphite whiskers, anomalous, electron microscope exam. 9-46783
 graphitized C fibres, fine struct., X-ray diff. and electron microscopy obs. 9-30557
 Guinier-Preston zone form., resistivity maximum 9-37431
 iron-base recipitation hardening alloy, rel. to hardness 9-39468
 martensite fine structure in transmission electron micrographs rel. to crystallography of phase transformations 9-28397
 metals, melt-grown, microsegregation and cryst. perfection 9-37060
 metals and ceramics, book 9-23961
 muscular tissues, eutectic struct. from electron micrographs 9-48839
 nickel ferrous ferrite 9-48836
 particle size distrib. analysis from field-ion microscope data 9-33117
 polychloroprene, crystallite orientation in stretched networks 9-48746
 polyethylene, crystallites mol. and textural orientation, applied stress eff. 9-30584
 polyethylene, crystallites mol. and textural orientation, applied stress eff. 9-30584
 polyethylene-polyisobutene mixtures, X-ray obs. 9-30474
 polymethylmetacrylate, block 9-42802
 polypropylene, lamella orientation effect on mechanical relax. 9-48745
 polytetrafluoroethylene films, morphology rel. to light-scatt. patterns 9-46709
 pore-grain boundary interaction rel. pore and grain sizes 9-32897
 quartz glass, i.r. refl. spectroscopy obs., 1000-1300°C 9-26175
 rare-earth silicates, di- and trivalent 9-30752
 refractories, periclase-spinelide, porous 9-42781
 steel, (Cr,Fe) C₂ identification and transform. obs. 9-48831
 steel, austenitic containing Al and Ti, soln.-treated, equil. precip. formed on ageing obs. 9-46949
 steel, C-Mn, effect on cleavage strength in various compositions after different heat treatments 9-39432
 steel, Fe-(2.0 wt.%V)-(0.2 wt.%C) alloy, carbide particle coarsening, field-ion study 9-33118
 steel, ferrite-pearlite, correl. with ductile fracture resistance 9-46899
 steel, high-pressure effects 9-23967
 steel, induction hardened, fatigue strength rel. to retained ferrite microstruct., obs. 9-26348
 steel, mild, surface-rolled, electron microscope obs. during fatigue 9-35189

Crystal structure continued
microstructure continued

- steel, nucleation of metallic and sulphide phases on high m.p. oxide precipitates within silicate inclusions 9-23954
- steel, rel. to n irrad. embrittlement, theory 9-37261
- steel castings, continuous, effect on mech. props. 9-39467
- steels, grain boundary precip. of boron-rich phase causing brittleness 9-41042
- subgrains, misalignment determ. by Schulz method 9-32886
- texture determination, quantitative, automatic conversion of X-ray data to pole figures 9-30550
- Ticonal 600 alloy, evolution rel. to comp. of α_1 and α_2 phases and saturation magnetiz. 9-44804
- topological approach 9-23962
- trioxane, polymerized regions produced by narrow electron beam 9-37824
- welded clad metal diffusion layer structure 9-40983
- Zircaloy tubes, texture rel. to orientation of hydride precip. 9-39188
- Ag-Bi eutectic 9-37131
- Ag-Cu alloys, liq. and vapour quenched, metastable struct. obs. 9-40899
- Ag, sintered electrode, changes after repeated low current cycling 9-31205
- AgBr, bubble orientation in epitaxial growth from melt 9-48817
- Al-Cu-Ag alloys, formation and dissolution of Ag-rich zones 9-46758
- Al-CuAl₂ eutectic alloy, directionally frozen 9-39250
- Al-CuAl₂ eutectic alloy, lattice rotations 9-39251
- Al-Mg-Zn alloy, Guinier-Preston zones formation during ageing 9-37280
- Al-Zn-Mg alloy, weldable, quench rate effect 9-46919
- Al-Zn alloys, after Zn precip., along grain boundaries and within grains 9-37291
- Al-(0.3-0.4 wt.%) Cu bicrystal, grain boundary sliding rel. to deform. 9-46888
- Al, f.c.c. polycrystalline, after shock-relief deformation 9-23879
- Al, substructure effect on fatigue crack propag. 9-30685
- Al₂-xCr₃BeO₄, alexandrite, anti-phase boundaries, electron microscopy obs. 9-35104
- Al and alloys, cell struct. rel. to hydrostatic extrusion 9-41029
- Al bicrystal, grain boundary sliding rel. to deform. 9-46888
- Al extrusions 9-39252
- Al single cryst., cyclically strained surface microrelief obs. by X-ray diff. method 9-46777
- Al thin films, surface hillocks prod. by annealing, thermal cycling effect, electron micrographs 9-30705
- Al thin films evaporated on air-cleaved NaCl, electron microscope obs. 9-26185
- AlZnMg 1 alloy, influence of high temp. annealing 9-46779
- Au-X ordered alloys, X-transition elements and mixtures, electron and neutron diff. studies 9-44659
- B, β -rhombohedral, modifications prod. by transit of induction coupled Ar plasma 9-37133
- B filaments, vapour-deposited, X-ray diff. and e. microscope exam. 9-46780
- BN, pyrolytic, effect of compression annealing or hot working 9-41041
- BaTiO₃, domain boundaries transmission electron microscopy 9-35477
- BaTiO₃, domain struct. and tilt. angles of twins, Berg-Barrett X-ray determ. 9-37145
- Be, effect of improper sample preparation 9-39446
- C, diffuse scat. at crystallite boundaries, negative magnetoresistance obs. 9-24277
- C, non-graphitizable micropore system from X-ray small angle scattering 9-37136
- C, pyrolytic, deposited in fluidized beds from hydrocarbons, microstruct. trends with deposition rate 9-24536
- C, thermal black, closed porosity and cry. domain sizes study by oxidation 9-28258
- C hard, partially graphitized above 2000°C, layer stacks and spheres 9-28396
- CO-base superalloys, transmission electron microscopy 9-39298
- CdS grown on {111} faces of GaAs, effect of substrate temp. on struct. 9-48758
- CdTe layers growth, struct. depend. on underlying temp., electron microscopic obs. 9-40846
- Co-(10 wt.%)Cr, oxide scales formed during high temp. oxidation 9-31194
- Co-Ni-Si alloys, ferromag., internally oxidised 9-48837
- Co-P films, effect of electroless Ni substrate 9-31041
- 20 wt.%Cr-35 wt.%Ni steel, grain boundary sliding and creep-rate 9-48901
- Cr film, grown by molecular beam incidence, crystallite shape by light reflection 9-32909
- Cu-Al-Fe-Ni aluminium bronzes, rel. to ductility, 20-800°C 9-23894
- Cu-B alloy, precipitate influence on He bubble form. during irrad. 9-41116
- Cu-Be-Co dil. alloys 9-39274
- Cu-Ni films, co-deposited by electron beam, grain size and orientation 9-48763
- Cu, extinction changes in X-ray diff. lines during annealing 9-44662
- Cu, f.c.c. polycrystalline, after shock-relief deformation 9-23879
- Cu, rolled, orientation distrib. of crystallites, electron microscopy determ. 9-48830
- Cu₃Au, domain size effect on work hardening rel. to tensile props. of single crystals 9-30710
- Cu films, vacuum evaporated, structure defects 9-30488
- Cu heavily rolled sheet, electron transmission exam. 9-39272
- Cu sheet with cube orientation, r-values and changes during tensile testing rel. to strain anisotropy and texture 9-39273
- Er₂O₃ film, grain growth kinetics on pulse annealing 9-40842
- Er₂O₃ film, grain growth kinetics on pulse annealing 9-40841
- Fe-(25 at.%)Al alloys, one- and two-phase struct., e. microscope obs., rel. to magnetization and magnetocrystalline anisotropy 9-26648
- Fe-Al alloys, domain struct. and short range order, depend on Al conc. 9-23757
- Fe-Mo alloy precipitates, electron microscope obs. 9-42787
- Fe-Ni-C martensites, twinning during phase transf. in fine struct. obs. from electron micrograph 9-26233
- Fe(40 at.%)Ni alloy oxidized at high temp., scale struct. and chem. composition 9-33669
- Fe-Ni films, ferromag., differential susceptibility obs. 9-43182
- Fe-(32 at.%)Pt alloy, quenched, X-ray diff. obs. 9-46787

Crystal structure continued
microstructure continued

- Fe-Si alloys, antiphase boundaries, charact., electron microscopy study 9-37142
- Fe-(3 wt.%)Si alloys of different impurities, secondary recrystn. textures 9-39474
- Fe-W alloy precipitates, electron microscope obs. 9-42787
- Fe, electrolytically deposited under different electrolysis conditions 9-44663
- Fe, grain size, effect on pressurization effects on yield behaviour 9-28346
- Fe, grain size, effect on pressurization effects on yield behaviour 9-28347
- Fe, prestrained, shock-induced substructural changes, electron microscope obs. 9-32915
- Fe, rel. to n irrad. embrittlement, theory 9-37261
- Fe alloys, growth morphology and solute segregation during solidification 9-23952
- Fe electrodeposited, data on fine struct. obs. in electron microscope 9-36942
- Fe rod, under surface, after electron beam bombardment melting and quick cooling 9-33110
- Fe single crystal plates produced by strain-anneal method, effect of stretching on imperfect structures 9-32913
- Fe- $\leq(0.04 \text{ wt.}\%)C$ quench aged alloy, changes due to cyclic straining 9-33079
- Ga₂In_{1.5}Sb solid soln. growth, electron microprobe scans 9-30719
- GdFe garnet epitaxial films, prep. by r.f. sputtering structural and mag. props. 9-49210
- Ge:Au(Au,Sb) single crystals, and nature of inclusions 9-42807
- In, changes and phase transform., use of coordinate correlation of valence electrons 9-46741
- β -In-Sn, antiphase boundaries and twins associated with ordering of In vacancies 9-30587
- Mg-Mn alloys, creep specimens and thermally aged, α -Mn precipitate, e. microscope exam. 9-28265
- MgAl₂O₄ hot-pressed spinel 9-30706
- MgO wedge crystals, thickness fringes in electron micrograph profiles 9-26240
- Mn-Ni constitutional diagram 9-39502
- Mn_{1.88}Fe_{1.12}O₄, tetragonal and cubic struct. obs., 300K 9-44668
- Mn fine particles prep. by evaporated in Ar, electron microscope and diff. obs. 9-42790
- Mo, deformed and annealed, X-ray diff. topography 9-42815
- Mo cellular struct. form. by hydrostatic extrusion 9-40950
- Mo single crystal, rolling texture, X-ray diff. exam. 9-41040
- MoO₃, with small amounts MoO₂, dendritic and platelet structs. 9-30526
- NaCl, infl. of crystal orientation on grain boundaries 9-26340
- NaCl cellular substruct. prod. by point defects 9-44686
- NaCl grown from H₂O soln. with Mn⁺⁺, X-ray diff. topographs 9-37144
- NaCl growth surfaces, effect of surface-active impurities 9-23765
- Nb₃Sn, impurity content and critical current density 9-41180
- NbC-Co system, development during liquid-phase sintering 9-42919
- Ni-C eutectic alloy, flake graphite struct. and defects obs., microscopy 9-44671
- Ni-Si-Ti alloys, rel. to tensile props. 9-48902
- Ni-Si alloys, ferromag., internally oxidised 9-48837
- Ni-Si alloys, rel. to tensile props. 9-48902
- Ni-base superalloys, transmission electron microscopy 9-39298
- Ni, explosion-shocked, thermal recovery processes, electron microscope obs. 9-44696
- Ni, f.c.c. polycrystalline, after shock-relief deformation 9-23879
- Ni, polycrystalline after plastic deformation, X-ray diff. 9-23768
- Ni, shock hardening effect in pressure range 820 to 1500 kbar 9-30701
- Ni₃Fe, annealed samples, antiphase boundary study 9-46791
- Ni alloy B-1900 high-temp., effects on exposure at 980°C 9-48913
- Ni alloys with Cu substructure, phase structure 9-35064
- Ni aluminates, and ferrites w.r.t. deviation from stoichiometry 9-30707
- Ni electrodeposits, effect of metallic contamination 9-37146
- Ni micro-indentation hardness profile 9-28348
- NiO, domain struct. and tilt angles of twins, Berg-Barrett X-ray determ. 9-37145
- NiO scales, rel. to mech. props., factorial expt. 9-23852
- Pb-base alloys, optical metallography 9-39301
- Pb, migration of large angle grain boundaries and form. of annealing twins 9-30570
- Pb_{1-x}Sn_xTe single crystals, cellular substructure by electrolytic etching 9-30569
- PbS epitaxial film growth on rocksalt, structure during vac. condensation 9-40844
- PbSe as-grown single cryst., transmission electron microscope obs. 9-46792
- Pb(UO₂)₂(VO₄)₂·5H₂O, curienite, new mineral species, anal. to francevillite 9-37147
- Pb-(0-56.5at.%)Bi superconducting alloys, type I and II, rel. to mag. behaviour 9-43041
- Pd alloys with Cu substructure, phase structure 9-35064
- Pt alloys with Cu substructure, phase structure 9-35064
- α -Pu, revealed by new electrolytic polishing and etching technique 9-39304
- Si, defects detection by X-rays, applic. in integrated circuit fabrication 9-30604
- Si, grain-boundary effect on solubility of Cu 9-42797
- Si primary spherulite growth and morphology in Al-(20wt.%)Si alloys 9-23775
- SiC, vapour-deposited, rel. to deposition condition 9-23774
- SiC, vapour-deposited, rel. to deposition condition 9-39306
- Sn-Cd eutectic, plane to cell transition on solidification 9-23585
- Sn-Cd lamellar eutectic, fault occurrence 9-28299
- Sn, texture studies by galvanomag. anisotropy at low temp. 9-32929
- Ta, imperfect structure in single crystal rods 9-32930
- TaSe₂, X-ray diffraction of new polymorph 9-35011
- ThC, substructure existence around 830°C 9-28070
- Ti-(8 wt.%)Al-(4 wt.%)Co alloy, rel. to heat treatments 9-23956
- Ti-(8 wt.%)Al-(4 wt.%)Co alloy, rel. to mech. props. 9-44747
- Ti-Al-Co alloy system, Ti-rich, optical microscope and X-ray diff. obs. 9-40919
- Ti-Cr binary alloys, martensite react., morphology and substruct. 9-26393
- Ti-(5 at.%) Mn alloy martensites, electron microscope obs. 9-39311
- Ti-(8 wt.%) Mn alloy heat-treated transmission electron microscope obs. 9-35214

Crystal structure continued
microstructure continued

- U, cavitation swelling and anisotropic grain growth, effect of alloying additions 9-33206
 U alloys, dilute, cavitation swelling, temp./exposure thresholds 9-41117
 UC, fission gas swelling, bubble nucleation time and temp. depend. 9-38736
 V, effects of neutron irradiation 9-39367
 W-(1wt.%)Gd₂O₃ alloy, ion microscope exam. of matrix 9-41057
 W-(1wt.%)Gd₂O₃ alloy, ion microscope exam. of matrix 9-41057
 W, deformed and annealed, X-ray diff. topography 9-42815
 W, vapour deposited, texture 9-37152
 W polycrystalline, cold worked and annealed, preferred grain orientation from ion microscope exam. 9-40889
 W powder, substructure, and block size distrib., X-ray diff. obs. 9-46796
 Zn bicrystals, grain-boundary slide-hardening 9-42889
 Zn electrodeposited from aqueous KOH soln. with zincate ions, electrolyte flow effect on morphology 9-33679
 Zn polycryst., grain size and texture during thermal cycling 9-32879
 ZnO-B₂O₃ syst., lamellar glass-cryst. structures from eutectic solidification 9-36930

Crystal structure, atomic

- see also *Crystal electron states; Crystals/lattice mechanics; Electron diffraction crystallography; Neutron diffraction crystallography; X-ray crystallography*
 absolute configuration, determ. from anomalous scatt. by O 9-30538
 anharmonic 2D cry. model, pair correlation function and long range order 9-37118
 base-centered or body-centered monoclinic lattice distinction 9-46762
 charge and momentum density, theory and expt. 9-23693
 chloropropene, NMR, light scatt. studies, heterogeneous character of vulcanization 9-23789
 Coding and generating system for layered tetrahedrally close-packed struct. 9-35036
 complex anions, octahedral, space dispositions 9-40871
 constrained refinements and program system 9-40870
 covalent cpds., structure factors from X-ray powder intensity meas. 9-23715
 dielectric single crystal substrates, real structure rel. to selective nucleation at surface local long range active centres 9-36990
 electron optical phase contrast calcs. for ats. and at. groups 9-32893
 Euclidean invariant states, strongly transitive 9-43721
 f.c.c. film, diffraction line broadening rel. to particle size and strain 9-44657
 groups in space and time, 4-d Euclidean crystal classes corresponding to mag. point groups 9-28251
 groups in space and time, central extensions 9-28241
 H-bond length, isotope effect 9-42370
 hexagonal systems, X-ray powder pattern interpretation by a BECM-4 computer 9-39241
 ion implantation by nuclear reactions, techniques 9-33210
 ionic and metallic bonded crystals, strength as function of time and temp. 9-41026
 ionic compounds, Madelung consts. and lattice self-potentials calc. 9-36973
 ionic crystals, survey of results of powder meas. rel. to electron states and charge distrib. 9-23692
 ionic radii, multivalent self-consistent set deriv. 9-32854
 lamellar struct., fluctuations of ordering parameter phase 9-39747
 lattice deformation detection technique based on shadow effect 9-28242
 lattice parameters connection with energy levels, Stark eff., Green's function 9-24092
 lattice plane geometry 9-23695
 layered tetrahedrally close-packed struct., coding and generating system 9-35036
 least-squares refinement, accidentally absent reflexions treatment 9-30535
 magnetic ad nuclear struct. by profile refinement method, neutron diff. powder technique 9-40891
 magnetic symmetry and limiting groups 9-24263
 magnetic symmetry groups 9-24261
 rel. to mechanical behaviour of solids, book 9-39431
 Miller indices demonstration model 9-22034
 molecular cry., 'oriented gas model' applic. to i.r. spect. 9-24389
 molecular position in lattice, calc. method 9-30534
 molecular wave functions from ab initio wave functions and applic. to X-ray diff. struct. analysis 9-32884
 ordering arrangements from satellite reflections in X-ray diff. patterns 9-39225
 orthorhombic systems, X-ray powder pattern interpretation by a BECM-4 computer 9-39242
 P₃,²¹₁¹ crystals, second harmonic generation 9-26680
 paramagnetic species, point symmetry and expt. Hamiltonian 9-39222
 Patterson function projections, arbitrary, interpret. using superposition method 9-40896
 perovskite cell, parameter representing deform. 9-33032
 phosphors, effects on luminescence 9-24442
 point groups, character of irreducible non-equivalent loaded co-representations 9-28239
 pseudo-symmetric centrosymmetric cryst., phase determ. 9-42761
 Q-functions compared to translational functions 9-23696
 refinement by filtering in least squares method 9-39237
 refinements, constrained, program system 9-40870
 rhombohedral systems, X-ray powder pattern interpretation by a BECM-4 computer 9-39241
 scattering factor asphericity, effect on temp. factor 9-39221
 semiconducting properties prediction from atomic disposition and interactions 9-30894
 semiconductor, impurity atom distributions meas., differential capacitance technique 9-28508
 semiconductor single crystal substrates, real structure rel. to selective nucleation at surface local long range active centres 9-36990
 short-range-disordered chains, electron state density curves, perturbation treatment 9-37117
 Shubnikov groups, non-crystallographic 9-30533
 sign factors, direct determ. by maximum determinant method 9-48818
 rel. to slip systems 9-42888
 space dispositions of octahedral complex anions 9-40871
 space group C_{4v} (wurtzite, selection rules 9-35038
 space group selection rules 9-35037

Crystal structure, atomic continued

- space groups of colour symmetry 9-42762
 space groups within Abelian finite group rel. to construction of space groups and mag. groups 9-23694
 stereographic projection computer plotting 9-48828
 structural phase factors, determ. using conditional probability laws 9-48819
 structure factor determ. by elastic scatt. of X-rays and neutrons, lattice vibrations correction 9-24014
 structure factors, significance 9-23691
 tetragonal systems, X-ray powder pattern interpretation by a BECM-4 computer 9-39241
 thermal motion in harmonic approx., representational surfaces 9-40869
 unit cell determ. from powder data, fully automatic program 9-48826
 weighted periodic vector set extractions from Patterson function 9-23742
 X-ray scatt. by heavily distorted crystals, theoretical study 9-37119
 Al co-ordination no. in titanobarium glass and ceramic, from X-ray emission spectra 9-41398
 Ar/Kr solidified mixtures, rel. to Ar conc., e diff. study 9-28255
 Mn in Mn cpds., effective co-ordination charges from X-ray absorption spectra K lines 9-37745
 Nd in Nd cpds., effective co-ordination charges from X-ray absorption spectra K lines 9-37745
- alloys**
 ageing, X-ray diff. eff. rel. to elastic lattice distortion 9-23746
 b.c.c., short-range order, equilibria and kinetics 9-41054
 β -brass, long-range order parameter influence on lattice parameter and phonon spectrum 9-39396
 β -brass X-ray diff., static atomic displacements influence on diffuse intensity 9-37132
 brass-like close-packed, stacking-sequences, energetic significance 9-28249
 h.c.p., with deformation stacking faults, X-ray diff. rel. to solute segregation effects 9-23818
 noble metal, long period structs. 9-23745
 ordering, early stages, applic. of model for diffusion on cubic lattices 9-30622
 semiconducting cpds., antiphase boundaries 9-40937
 solid solns., substitutional, relax. time model for short-range order changes and Zener relax. 9-46870
 steel, Fe-Mn-C, martensite struct., X-ray diff. obs. 9-46948
 steel, γ -martensite rel. to carbon content 9-37294
 structure factors from X-ray powder intensity meas. 9-23715
 Thomas-Fermi model 9-40898
 Ag-Au solid solns., lattice parameters 9-39247
 Ag-Cu liq. and vapour quenched, metastable struct. obs. 9-40899
 Al (<0.22at.%)Ti solid solution, lattice parameter comp. dependences 9-42918
 Al-Mg-Zn, lattice parameters rel. to ageing during pre-precipitation 9-41049
 Al-Zr, quenched, superheating melt effect 9-39450
 Au-Cr, short-range order 9-28257
 Au-Mn, short-range order 9-28257
 Au₃Cu, long- and short-range order w.r.t. thermoelec. power temp. depend. 9-37610
 β' -Au-Zn, long-range order, X-ray diff. meas. 9-28256
 Bi-Sn, structure and parameters of superconducting phase 9-23752
 Co-(7.45 at.%)Fe solid soln., γ -phase precip. during ageing, neutron diff. and chem. analysis 9-41065
 Cr alloys with Pt-series metals, similar ordering rel. to similar mag. characts. 9-33438
 Cu-(16 at.%)Al alloy, short-range ordering kinetics 9-33120
 α -Cu-Al alloys, short-range ordered state and stable superlattice phase obs. 9-39275
 Cu-Al martensite cryst. struct. stability, solute content effect 9-42929
 Cu-Be-Co, dil. constitution and lattice const. meas. 9-39274
 Cu-Mn Al phase formation on heat treatment and ageing 9-37293
 Cu₃Au X-ray diff., static atomic displacements influence on diffuse intensity 9-37132
 Fe-(40 at.%)Al, ordering and struct. distortions, X-ray diff. obs. 9-42784
 Fe-Al, phase relations, X-ray diff. obs. 9-44664
 Fe-Al, short-range order, X-ray diffuse scatt. obs. 9-44665
 Fe-C martensite, short-range order, rel. to diffuse electron scattering 9-32912
 Fe-Mn-C, stress-induced ordering of C from internal friction temp. dependence meas. 9-23862
 Fe-(32 at.%)Pt, quenched, ordering, X-ray diff. obs. 9-46787
 Fe-Si single cryst., antiphase boundaries, props. 9-26231
 GaAs_{1-x}Fe_x solid soln. cryst. grown from Ga-rich soln., X-ray diff. obs. 9-35206
 Gd-Co system, of intermetallic cpds. over whole conc. range 9-48921
 Li-Ag(Cd,Al), lattice parameters 9-42789
 Li-Mg, lattice parameters 9-42789
 Mn-Cu, lattice distortion on cooling through Neel temp., rel. to long-range mag. order 9-39783
 Mn-Pd system near MnPd₃, and mag. struct. 9-35588
 MnAlGe, ternary, and ferromagnetic structure by neutron and X-ray diffraction 9-35660
 Nb₃Sn alloy, supercond., lattice parameters and grain size, correl. with hysteresis charact. 9-39769
 Ni₃(Fe, Cr), ordering effects 9-39297
 Ni₃(Fe, Mo), ordering effects 9-39297
 Ni₃(Fe, W), ordering effects 9-39297
 Pb₃Sn_{1-x}Te_x lattice constant relationship with alloy fraction and stoichiometry 9-35065
 PbZr_{1-x}Ti_xO₃, perovskitic ferroelec., for x=0.9, 0.58, x-ray and neutron diff. obs. 9-44673
 Pd-(14 at.%)Fe, low-temp. sp. ht. changes due to short-range order changes 9-33183
 Pd-In, room temp. lattice spacing 9-30571
 (50at.%)Pd-Pt alloy, diffusive dispersion at high temps. short range order 9-44674
 Pt-In, room temp. lattice spacing 9-30571
 Pt-Sn, room temp. lattice spacing 9-30571
 Pt₃Mn, ordering effect on spontaneous magnetization 9-39770
 Rh₂Cu₂Ni₂O₄ solid soln., of spinel type phases 9-30704
 Sn alloys, simple hexagonal, axial ratio rel. to total energy 9-40918
 Ti-(50 wt.%)Nb, X-ray diff. and electron microscope obs. 9-42792
 Ti, fine structure, rel. to mechanical strength and toughness 9-37252
 U-Nb system, monoclinization of α -U lattice 9-40920

Crystal structure, atomic continued elements

- atoms displaced by implanted ions or energetic recoil atoms 9-33201
electron diff., second order reflection vanishing voltages calc. 9-32896
graphite, dimensional variations during Br intercalation 9-26223
graphite, lattice parameter and dimensional changes on irradi. 300 to 1350°C 9-28280
metals, structure factors from X-ray powder intensity meas. 9-23715
Ag single crystal, surface atoms in (100) and (110) faces, mean displacement studies at low temp. 9-39248
Al, absolute X-ray scatt. factors from transmission meas. on powder sample 9-28254
Al, atom form factor determ. by high voltage e. diff. 9-23722
Al atomic scatt. factors from thermal diffuse intensities meas. 9-32900
As high purity, single crystal, at 4.2, 78 and 299°K 9-39254
B, β -rhombohedral, rel. to thermal conductivity, 80° to 1100°K 9-44845
Be, 77° to 300°K 9-32902
C, no-graphitizing, random layer size and disorder effects, profile anal. 9-28260
Cl, Raman data 9-43245
Cm metal 9-48742
Cs adsorbed on tungsten evidence for its non-metallic character 9-32849
Cu:SiO₂ strained single crystals, lattice rotations, electron microscope obs. 9-32911
Cu, atom form factor determ. by high voltage e. diff. 9-23722
Fe filings and whiskers, effect of H atoms. 9-44666
 β -Ga, X-ray powder data 9-39277
Ge, scattering factor, from X-ray reflection integral intensities 9-40902
Ge, X-ray absorpt. coeff., oscillator strength for K-electrons 9-32916
In, lattice parameters, temp. variation 9-30785
Li quantum mechanical construction 9-26239
 α -Mn and mag. structure 9-44645
Mn fine particles prep. by evaporated in Ar, electron microscope and diff. obs. 9-42790
Mo, neutron irradi., hydrostatic press. induced recovery of lattice parameter increases 9-40909
Mo surface layers, work hardened, changes prod. by vacuum annealing 9-32932
Nb surface layers, work-hardened, changes prod. by vacuum annealing 9-32932
Ni, atom form factor determ. by high voltage e. diff. 9-23722
Pb film deposition on (110) face of W, at. diameter of 3.50 Å 9-42720
S unstable form prod. by quenching or radiation 9-30747
S unstable forms prod. by condensation, studied by paramagnetic resonance 9-30746
Se and Se:Pd films, electron diff. meas. 9-42796
Si, (111) 7 \times 7, cleaving at 850°K 9-35068
Si, absolute scatt. factor determ. 9-23771
Si, boron implanted and annealed, condensed defect structure distrib. 9-32953
Si, lattice parameter charges rel. to thermal defect investig. 9-32944
Si Laue reflected and refracted beams, rocking curve oscillations 9-32928
V, lattice distortion, formation of domain boundaries 9-32960
W, Debye-Waller f factor determ. from 46.5 keV γ Mossbauer absorpt. 9-46795
W surface layers, work-hardened, changes prod. by vacuum annealing 9-32932

inorganic compounds

- alkali halide cryst., diatomic, interatomic forces and cohesive energies 9-28250
alkali halides, temp. parameters of ions 9-30507
alkali metal intermetallic cpds., D₁₃ struct. type 9-39243
alkali metal ion fluorides, MFeF₃, rel. to mag. props. 9-35063
aluminium methylammonium alum., elementary cell parameters in phases I and II, temp. depend. 9-42927
bornite, metastable phase, order study 9-26230
ClFCF cry. growth by hydrolysis of ClF₃, X-ray diffraction, structure determ. 9-26205
clinopyroxenes, parameter b, rel. to Al content and ionic substitution 9-30554
faujasite, hydrated Ca-exchanged, positions of cation and molecules 9-30556
ferritin macromol., X-ray diff. study of inorg. core, comparison with Fe hydroxides 9-37139
fluorides, effective ionic radii 9-39182
grandierite, (Mg, Fe)Al₃Si₃BO₆ 9-30564
haematite, Morin transition and lattice spacing w.r.t. particle size 9-32914
henritermierite, Ca₃(Mn_{1.5}Al_{0.5})[(SiO₄)₂/(OH)₄], tetragonal hydrogarnet 9-32905
ice, effect on mech. and elec. props. 9-48832
inert gases, dynamical surface props. by molecular dynamics method 9-39191
inert gases, dynamical surface props. in quasiharmonic approximation 9-39190
intermetallic cpds., D₁₃ struct. type 9-39243
kimrite (hydrated Ba feldspar), satellite occurrence in inverse lattice 9-46782
korninkite, symmetry, powder diag., X-ray obs. 9-37140
lanthanide compounds, lattice parameters, interrelationship with melting point and heat of formation 9-34956
leucophanite, confirmation 9-39244
metal oxides, carbides, nitrides, survey of results of powder meas. rel. to electron states and charge distrib. 9-23692
mounanaite, PbFe₂(VO₄)₂(OH)₂, X-ray powder obs. 9-32925
muscovite, dislocation planes, electron microscopy 9-23748
oxides effective ionic radii 9-39182
Perovskite-type crystals, orthorhombic deformation of cubic lattice, dipole field connection 9-28558
phosphates of type MNH₄PO₄.H₂O (M=Cd, Co, Mg, Mn, Fe, Ni) and MK₂PO₄.H₂O (M=Cd, Co, Mg, Mn and Ni) 9-37138
pyrrhotite, Fe₇S₈ 9-39281
quaternary normal tetrahedral struct. cpds. diff. obs. 9-39269
rare earth, RCrTeO₆ cpds., rel. to PbSb₂O₆ structure 9-32919
rare earth aluminates, perovskite type structure and rhombohedral lattice distortion 9-42795
rare earth iron borates, RFe₂BO₁₂, X-ray powder diffraction patterns and cell parameters 9-37149
rare earth-indium intermetallic cpds., R₂In and R₃In 9-28252
rare-earth cobaltides, T₂Co₂ (T=Gd, Tb, Dy, Ho, Er and Tm) 9-39313

Crystal structure, atomic continued inorganic compounds continued

- rare-earth fluoride systems, nonstoichiometry 9-40915
rare-earth molybdates, lattice parameters rel. to temp. 9-35067
rare-earth-In cpds.: RIn₃ 9-39751
rare-earth-transition metal Laves phase, lattice parameters 9-35066
Rhabdite meteoritic minerals 9-30552
samsonite 9-39246
sodium faujasites, synthetic, lattice parameter Al content dependence, framework ion ordering 9-44669
 β -spodumene, stereographic projection 9-48828
titanium oxides, family of ordered phases and nature of slightly-reduced rutile 9-44675
transition metal compound thin films with rocksalt struct. supercond. props. 9-36959
transition metal molybdates, anion coordination changes in phase transformations. 9-35244
transition metal phosphides, solid solns., and mag. props. 9-44676
transition metal spinel manganites, n. diff. obs. 9-28253
transition metal thionibates, lattice constants on basis of hexagonal unit cell 9-39284
transition-metal complexes 9-23744
vermiculites, dehydration, i.r. spectroscopy 9-44658
Welinite (Mn²⁺Mn³⁺SiO₃), lattice parameters 9-23764
yugawaralite, Ca₂Al₂Si₂O₁₂.8H₂O, X-ray obs. 9-39258
zeolite, La-exchanged type X, cations and mol. positions at 25, 425 and 735°C 9-39249
ZrB₂, lattice parameters, transmission e. microscope exam. 9-37096
[Cr₄(OH)₆(en)₆]¹⁴⁺ salts, from X-ray exam. 9-47224
AgBiSe₂-AgBiS₂ system, high-temp. β -phase, X-ray and neutron diff. studies 9-42782
AgCl, deform. of ions, X-ray obs. 9-30507
 γ -AgI, X-ray diff. obs. 9-33379
AgSbS₂, miargyrite, artificial n.q.r. meas. for low temp. α form 9-47451
 β -Al-Mg, electron diffraction, transmission and reflection study 9-26222
AmO₂F₂, lattice constants 9-23749
Ba₄(_{1/2})Na₂(_{2/3})Nb₁₀O₃₀, ferroelec. 9-46781
Ba₄(_{1/2})Na₂(_{2/3})Nb₁₀O₃₀, lattice parameters, density and thermal expansion coeffs. 9-37134
BaF₂, structure factor determ. by elastic scatt. of neutrons lattice vibrations correction 9-24014
BaGe₄O₉, verification of contained Ge₂O₉ 9-23751
BaMnO₃, perovskite-like, struct. relations at high press. 9-35241
BaOF₂O₃, X-ray diff. obs. 9-47283
BaSO₄-SrSO₄-PbSO₄, lattice constants and subsolidus phase relations 9-23949
BaTiO₃, chain structure rel. to phase transition 9-32901
BaTiO₃, lattice deformations of (100) free surface 9-28210
BaTiO₃ tilt angles of twins in various lattice planes, Berg-Barrett X-ray determ. 9-37145
BaVS₃, prep., refinement 9-39255
Be SO₄.4H₂O, Raman and i.r. vib. spectra obs. 9-24423
Bi₂GeO₁₀, lattice parameters, and growth and props. 9-42751
 δ -Bi₂O₃, cubic, structure electron diff. study 9-42783
Bi₄(GeO₄)₃, lattice parameters, and growth and props. 9-42751
BiCrO₃, distortion and mag. props. 9-28608
BiFeO₃, X-ray and neutron diff. obs. 9-37135
BiMnO₃, distortions, and mag. props. 9-28608
Br₂, high-press. form 9-32903
CS₂, high-press. form 9-32903
(Ca, Cd)₁₀(PO₄)₆FeCl structural and optical props., Pb and Mn activated 9-47382
Ca₂Al₂Si₂O₁₂.8H₂O, yugawaralite, X-ray obs. 9-39258
Ca complex 1,3-diphosphorylimidazole 9-30580
CaAl₂O₄, high pressure transformations 9-44799
CaB₂O₄(III), high pressure phase 9-39259
CaB₂O₄(IV) high pressure phase single crystal 9-39260
CaF₂, lattice and interstitial sites, similarity 9-36974
CaF₂, lattice distortion for cubic centers with impurity ions Ce³⁺ and Eu³⁺ 9-26198
CaK₃H(PO₄)₃, lattice parameters and space group determ. 9-30558
CaNH₄P₂O₇, monoclinic form, struct. obs. 9-37143
CaO, lattice data, 12 to 300°K, rel. to thermal expansion coeff. 9-28429
CaP₂O₁₁, unit cell, space group and other data 9-35055
CaSiO₃ high pressure polymorph 9-39261
CaTiSiO₅ grown by Czochralski method, monoclinic cell dimensions, space group 9-39209
Cd-Zr system, structure of intermetallic compounds 9-39266
 α -Cd₃As₂, refinement 9-39262
Cd complex, bis(selenourea)cadmium (II) thiocyanate, X-ray powder data and i.r. spectra 9-26227
CdFe₂O₄, oxygen parameter and degree of inversion, X-ray meas. 9-44660
CdSnAs₂ supercond. polymorph, high-press., B1(NaCl) type struct., lattice const. 9-41178
CdTe thin film, co-evaporated, influence of stoichiometric deviations 9-36949
CeF₃, confirmation by ¹³⁹F n.m.r. 9-24506
CeSi 9-39207
Co_{1-x}Fe_xS₂ 9-45286
Co complex, bis(selenourea)cobalt (II) thiocyanate, X-ray powder data and i.r. spectra 9-26227
Co complex, bis(tricobalt enneacarbonyl)acetone, and mol. structure 9-39264
Co complex, cobalt (III) tris (N,N-diethyldithiocarbamate, and mol. structure 9-30559
Co complex, trans-sulphiteisothiocyanate-bis (ethylenediamine)cobalt(III)dihydrate 9-39265
Co complex, tris(diethyldithiocarbamate)cobalt (III), and mol. structure 9-44661
CoCl₂.4CH₃OH, comparison with other divalent halogenides 9-23754
Co(KSO₄)₂.2H₂O, probable, from X-ray powder data and similarity to kohnkite 9-35056
CoNb₂S₄, lattice constants on basis of hexagonal unit cell 9-39284
Cs_{0.14}NiO₂, electron diffraction investigation 9-40905
CsBr₃, X-ray diff. obs., Br₂ and I₂ systems comparison 9-35057
CsMnF₃, perovskite-like, struct. relations at high press. 9-35241
CsNO₃, trigonal form space group from pyroelectric props. 9-30977
Cu_{2-x}Se thin films 9-46721

Crystal structure, atomic continued

inorganic compounds continued

- Cu_{2-x}Te ($x=0.25\pm0.04$), hexagonal phase β^{II} in Cu-Te system, e. diff. determ. 9-46785
- Cu₂CdGeS₄, superstruct. of wurtzite, diff. obs. 9-39269
- Cu_{4-x}Te₂ tetragonal phase, γ^I and γ^{II} disordering modifications 9-42937
- Cu complex, bis-(L-isoleucinato) copper (II), rel. to L-isoleucine config. 9-26228
- Cu complex, bis-(3-amino-1-phenyl-2-buten-1-ono) copper (II), and mol. structure 9-30560
- Cu complex, bis(L-serinato)copper (II), rel. to chelation effects on serine 9-26229
- Cu complex, Cu(II) hydrogen o-phthalate dihydrate 9-48829
- Cu complexes tetramine sulphate and selenate monohydrates 9-39268
- Cu complex, CuCl₂CH₃CN 9-32910
- Cu complex, bis(N-n-propylsalicylaldiminato)copper(II) 9-35058
- CuMn₂O₄ spinel, degree of inversion 0.84, and cation distrib., determined from neutron diff. meas. 9-40854
- Cu(NH₄)₂(SO₄)₂·6H₂O, structure parameter refinement from neutron diffraction data 9-39270
- Cu(NO₃)₂·H₂O·3H₂O, 3-d X-ray analysis 9-39271
- CuNb₂S₄, lattice constants on basis of hexagonal unit cell 9-39284
- CuRb(PO₃)₃ 9-30561
- CuSe₂, marcasite type superconductor 9-28261
- CuTi(PO₃)₃ 9-30561
- Eul₂, monoclinic form 9-35059
- EuO:Gd, lattice constant, dopant effect 9-33463
- Fe-Ni oxide spinel, grown by arc image technique 9-48804
- Fe₂(CO)₁₁P(C₆H₅)₃ 9-37141
- FeS₈, pyrrhotite 9-39281
- Fe complex, (Fe bis-salicylidene-ethylenediamine)₂O pyridine₂ oxo-bridge five-co-ord struct. 9-33486
- Fe complex, iron (III)-benzhydroxamate trihydrate 9-39276
- FeLiO₂, disordered phase, from X-ray diff. meas. 9-48935
- FeNb₂S₄, lattice constants on basis of hexagonal unit cell 9-39284
- Ga₂Mg 9-26234
- Ga₃Mg₂ 9-26235
- GaAsO₄·2H₂O, (4000-200 cm⁻¹), X-ray diffraction examination 9-30024
- Gd₂O₃·SiO₂, cell parameters, atomic coords., temp. factors and interatomic distances determ. 9-40901
- GdBr₃, and canted antiferromagnetism 9-45226
- H₂B₂O₃, bond lengths molecular-orbital treatment 9-39279
- H₃Fe(CN)₆, X-ray and neutron diff. study 9-23756
- H₃PO₄·1/2H₂O, refinement 9-39278
- H₄Fe(CN)₆, X-ray and neutron diff. study 9-23756
- HCl and DCl Raman data 9-43246
- HCO₂ and DCO₂ 9-32908
- Hbr and DBr, Raman data 9-43246
- HF₂, e. density in H atom, theory and expt. 9-23759
- HgCu(OH)(NO₃)₂·2H₂O, e-d X-ray analysis 9-39271
- In₂O₃, anion coordination and vol. changes in high press. phase trans-forms. 9-35244
- In complex, tetraethylammonium tetrachloroindate (III) 9-26236
- K_{0.4}(NiO₂), electron diffraction investigation, and effect of replacing K by Rb and Cs 9-40905
- K₂Cr₂O₇ single crystal, symmetry class from Raman spectra meas. 9-47374
- K₂SO₄, space groups and study by Hartman method 9-46745
- K₂MoCl₆ crystal structure 9-40904
- K₂Y(Si₂O₇(OH))₂, crystal structure 9-23762
- K₂Nb₂O₇, mica-like single cryst. 9-30522
- KBr:Li⁺, lattice parameter effects on off-centre behaviour 9-35087
- β -K₂CeF₆ 9-26237
- KCl:Li⁺, lattice parameter effects on off-centre behaviour 9-35087
- KCl-KI mixed crystal phosphor, luminescence obs. 9-33588
- KCl-KI mixed crystal phosphors, luminescence behaviour obs. 9-33588
- KCl, ion spherical symmetry determ. from structure factor meas. 9-23760
- KCl, structure factor determ. by elastic scatt. of X-rays, lattice vibrations correction 9-24014
- KCuF₃ single cryst., polytype struct., X-ray diff. exam. 9-32917
- KHgBr₃·H₂O 9-39280
- KNO₃, high-press. forms 9-32903
- KNaPt(CN)₄·3H₂O 9-23761
- KNb₂OP₈ mica-like single cryst. 9-30522
- KNbO₃, chain structure rel. to phase transition 9-32901
- KNbO₃, ferroelec., X-ray and micro-electron diffraction investig. 9-46788
- KZnF₃ single crystal perovskite structure, hydrothermally synthesized 9-42746
- La-Co system, of intermediate phases 9-28262
- La-exchanged faujasite, dehydrated, positions of mols. and cations at 420°C 9-32899
- [(1-x)La, x Ca]MnO₃ 9-33127
- La₂O₃, B-type monoclinic, lattice parameters and cell volumes 9-30562
- LaNbO₄ single crystals, prep. and props. 9-44644
- LaOOH, synthetic 9-30563
- Li, lattice const. variation in augmented-plane-wave energy-band calc. 9-47044
- Li₂Ge₂O₇, rel. to growth by Czochralski method 9-37082
- Li₂TiO₃, refinement 9-48833
- Li₂RhH₂, ($x=4.5$), X-ray, neutron diff. meas. 9-48834
- Li₂V₂O₇, lattice const. discontinuity 9-35328
- LiH, Compton profile analysis rel. to valence-electron wave functions 9-46789
- LiH, lattice data, 12 to 300°K, rel. to thermal expansion coeff. 9-28429
- LiO₂, absolute struct. 9-32918
- LiYF₄, of cry. grown from melt. 9-23683
- (Mg, Fe)Al₂SiBO₃, grandierite 9-30564
- Mg₂PtO₄, unit cell const. 9-32868
- Mg₂Si, electron density distrib. in single crystals. effect of multiple diffraction on meas. 9-28263
- Mg₂SiO₄, high press. modification 9-40908
- Mg₂NF₂ 9-39282
- MgNH₄P₃O₇, orthorhombic form, exptl. intensities and struct. obs. 9-37143
- MgO, cell dimens. rel. to transition metal ion addition from chromite mixture 9-32921
- MgO, lattice data, 12 to 300°K, rel. to thermal expansion coeffs 9-28429
- MgSiP₂, lattice parameters and unit cell 9-44974

Crystal structure, atomic continued

inorganic compounds continued

- Mn_{1-x}Cr_xAs, 4.2-900°K 9-47226
- Mn₂GeS₄, orthorhombic, neutron diff. obs. 9-35589
- Mn₂O₄, high pressure transformations 9-44799
- Mn⁴⁺Mn³⁺₂·2SiO₂ (wielinite), lattice parameters 9-23764
- Mn₂Fe_{1-x}·xHoO₃, unit cell parameters and mag. props. 9-35060
- Mn₂Fe_{2-x}O₄ ferrites, cubic and tetragonal, i.r. absorpt. spectra obs. 9-39841
- MnNb₂S₄, lattice constants on basis of hexagonal unit cell 9-39284
- MnSb, lattice parameters, pressure depend. 9-28264
- MnSnO₃, disordered ilmenite 9-39285
- MnTe, lattice parameters, pressure depend. 9-28264
- MnTiO₃, II high press. phase, X-ray analysis 9-44667
- Mo₂Br₂, positions of light atoms 9-39286
- N₂D₄, from Raman spectra obs., -70 to -195°C 9-39853
- N₂H₄, from Raman spectra obs., -70 to -195°C 9-39853
- (NH₄)₂MnF₃ 9-30566
- (NH₄)₂F(S₂)/2H₂O, refinement 9-39288
- (NH₄)₂ClS₂O₆ 9-39293
- (NH₄)₂UO₂F₂, and twinning 9-30565
- NH₄F, molecular form factors of NH₄⁺, X-ray diff. 9-32884
- NH₄F, wurtzite type struct., space group P6₃/mc, h.c.p. sublattices displacement, neutron and X-ray diff. obs. 9-39293
- NH₄FeF₃, rel. to mag. props. 9-35063
- NPCl₂(NSOCl)₂ 9-39287
- Na₂Mn₂Si₂O₇, superposition method determ. 9-40911
- Na₂Pd(CN)₄·3H₂O stacking of heavy atoms in crystals structure 9-35062
- Na₃P₂O₆·14H₂O 9-35061
- Na₂Nd₂Ge₂O₈, lattice dimensions, interplanar dists. and diffraction line intensities, X-ray studies 9-40866
- NaCN, neutron diffraction investig. rel. to arrangement of (CN)⁻ group, model 9-28266
- NaCeGeO₄, lattice dimensions, X-ray diff. studies 9-40866
- NaCl, deform. of ions, X-ray obs. 9-30507
- NaCl grown from H₂O soln. with Mn²⁺, X-ray diff. obs., lattice spacing 9-37144
- NaLa(MoO₄)₂ and NaLa(MoO₄)₂·H₂O, interatomic dists. and lattice dimensions, determ. by X-ray diffraction, and prep. 9-40912
- NaNbO₂F₂, refinement 9-39289
- NaNbO₃·CdTiO₃ solid solns., rel. to dielec. props. 9-39695
- NaNbO₃, comparison with ferroelec. phase 9-39290
- NaNiF₃, two forms obs. 9-44670
- NaPrGeO₄, interplanar dists. and diffraction line intensities, X-ray studies 9-40866
- NaSmGeO₄, lattice dimensions, interplanar dists. and diffraction line intensities, X-ray studies 9-40866
- Nb₂Cr₂Si₃, θ -phase in Nb-Cr-Si system 9-46790
- Nb₂O₃·WO₃ system, non-periodic shear struct., electron microscope obs. and evaluation 9-39291
- NbC_{0.75}, ordering, neutron diff. obs. 9-40913
- NbH_x ($x<0.9$), lattice const. of phases rel. to temp. 9-31185
- NbO₂, collapse of long-range ordering of Nb-Nb w.r.t. phase transition 9-33143
- Nd-Co system, of intermediate phases 9-28262
- Nd₂(MoO₄)₃·Nd₂(WO₄)₃ system, phase struct., differential thermal analysis and X-ray diff. obs. 9-37305
- Nd₂Fe_{3-x}Sc_xP₂ garnets, ($9<x<1.5$) 9-47247
- Ni-Zn ferrite thin film, prep. and electron diff. obs. 9-45184
- Ni-rare earth cpds., RNi₂, cell struct. role in struct. determ. of other cpds. 9-30567
- Ni₂ZnSi₂, interatomic distances and packing density for cubic Ti₂Ni type struct. 9-39294
- Ni complex, bis(dimethyldithiophosphato)nickel(II) 9-39296
- Ni complex, bis(selenoureia)nickel(II) thiocyanate, X-ray powder data and i.r. spectra 9-26227
- Ni complex, diaquobis(L-serinato)nickel(II), rel. to chelation effects on serine 9-26241
- Ni complex, dibrometetrapirozolenickel(II), and mol. structure 9-26243
- Ni complex, hexakis(imidazole)nickel(II) nitrate 9-39295
- Ni complex, N,N'-dimethyl-4,4'-dipyridinium tetracyanonickelate (II) 9-26242
- Ni faujasite zeolite, Ni(II) distrib., obs. 9-30568
- Ni ferrite, film, prep. and electron diff. obs. 9-45184
- α -NiAs₂ 9-23770
- NiCl₂·6H₂O, room temp. and 4.2°K, by neutron diff. 9-42793
- NiCrO₃ corundum structure obs. from X-ray powder diff. exam. 9-43160
- NiFe₂O₄, polarized neutron diff. exam. 9-48838
- NiNb₂S₄, lattice constants on basis of hexagonal unit cell 9-39284
- NiO, tilt angles of twins in various lattice planes, Berg-Barrett X-ray determ 9-37145
- NiS, pressure effect rel. to lattice compressibility, T>T_M and T<T_M, 9-44672
- NiSO₃·6H₂O 9-39294
- 3(NH₄)₂·0.7MoO₃·4H₂O, thermal decomposition intermediate phases, from X-ray diff. 9-30745
- α -Nd₂(MoO₄)₃, paramag. 9-39292
- OsSe₂ 9-23770
- β -Pb_{0.193}V₂O₅, monoclinic, lattice parameters and space group determ. 9-28267
- Pb apatites, mineral 9-37148
- Pb complex, lead(II)O,O-disopropylphosphorodithioate 9-42794
- PbBr₂, determ. from Weissenberg data 9-39299
- PbClBr(I), determ. from Weissenberg data 9-39299
- α -Pb(N₃)₂, neutron diffraction study 9-39300
- PbTe thin film, co-evaporated, influence of stoichiometric deviations 9-36949
- Pb(UO₂)₂(VO₄)₂·5H₂O, curienite, new mineral species, anal. to francevillite 9-37147
- Pb[La_{0.5}(M³⁺)_{0.5}]₂Ti_{1-x}O₃, (M=Nb or V), rel. to dielec. and piezoelectric props. 9-24220
- Pd complex, bis(N-t-butylsalicylaldiminato)palladium(II), and molecular conformation 9-23769
- Pr₂O₃, B-type monoclinic, lattice parameters and cell volumes 9-30562
- Pr₂La_{1-x}Al₂, lattice parameters rel. to magnetic data 9-28597
- Pr₂La_{1-x}Al₂, lattice parameters rel. to magnetic data 9-28597
- PrP, lattice constants variation with composition for nonstoichiometry occurrence 9-28268
- Pr(ReO₄)₃·3H₂O, unit cell parameters 9-39302

Crystal structure, atomic continued
inorganic compounds continued

- Pt complex, potassium aminotrichloroplatinate monohydrate, interatomic dist., bond lengths 9-26244
Pt complex, trans-bisglycinatoplatinum(II) 9-39303
PtAs₂ 9-23770
Rb_{0.14}NiO₃, electron diffraction investigation 9-40905
RbNO₃, trigonal form space group from pyroelectric props. 9-30977
RbNiF₃, perovskite-like, struct. relations at high press. 9-35241
RuO₂, lattice constant X-ray determ., 30-702°C rel. to thermal expansion 9-24056
RuSe₂ 9-23770
S₆(NH)₂, three isomers 9-39305
Si-O, lattice periodicity, X-ray transmission 9-32926
SiC, review 9-26245
SiC phase in SiC-B₄C system, from 2200-2550°C 9-48939
SiC polytypes 6H, 4H and 15R, and pure polytype preparation 9-40916
β-SiC whiskers, from X-ray diffraction, comments 9-32927
(Sr_{0.8}Ba_{0.2})₂Zn₂F₁₂O₂₂ hexagonal ferrite, localization of Zn²⁺ ions, neutron scat. meas. 9-42798
Sr₂Fe₂O₇, neutron diff. obs. of cryst. and mag. struct. 9-41341
α-Sr₂P₂O₇, in centrosymmetric group Pnam 9-30573
Sr₂VO₄Cl:Mn, site symmetry, Mn²⁺ at V position, from absorpt. spectra 9-35664
SrB₂O₄, III and IV high pressure phases 9-39308
SrMnO₃, perovskite-like, struct. relations at high press. 9-35241
SrTiO₃ lattice parameters change near phase transform, at 108°K, meas. and obs. 9-30748
β-Ta₂O₅, unit cell meas. 9-39309
TaCa_{0.76}, ordering, neutron diff. obs. 9-40913
TaH_x (x<0.8), lattice const. of phases rel. to temp. 9-31185
Ta-N system, ordering phases and intrusion superstructures 9-46794
Ta-O system, ordering phases and intrusion superstructures 9-46794
TbCo₁₁, rel. to intermetallic 2-17 stoichiometry 9-26248
TbFe₁₁, rel. to intermetallic 2-17 stoichiometry 9-26248
ThP₄ 9-35035
ThP-UP solid soln. 9-33123
ThP 9-35035
Ti₂ZrO₃, suboxide in Ti-Zr-O system 9-26249
Ti-Ni-II, complex, existence 9-35069
TiO₂, polymorphism under dynamic loading 9-39482
Ti(Pt_{0.84}Ni_{0.16})₃ 9-39310
TiTa₂S₄, lattice const., elec. and optical props., obs. 9-35070
TiFeF₃, rel. to mag. props. 9-35063
TiInS₂(Se₂Te₂), parameters, X-ray obs. 9-44969
TiNO₃, trigonal form from pyroelectric props. 9-30977
TiNiF₃, perovskite-like, struct. relations at high press. 9-35241
S-U₃O₈, existence of δ phase 9-28271
β-U₃O₈ monocystals 9-28233
U₃Si, no change on irradi. shown by X-ray diff. 9-40921
V₃Au, and n.m.r., obs. 9-39223
V₄C₃, coherence with α-Fe matrix, critical magnitude meas. 9-32931
V₅Te₈, quenched samples and cpds. obtained after slow cooling 9-37151
VSe₂ system, NiAs-like struct. cpds. obs. 9-30575
VTe₂ system, NiAs-like struct. cpds. obs. 9-30575
W₂C rhombic modification, neutron diff. obs. 9-32933
Y-Ni cpds., role of YNi₃ cell in struct. determ. of other cpds. 9-30567
Y_{2.8}-Bi_{0.1}Ca_{0.9}Fe_{1.9}Si_{0.1}O (x=0.6-1.3), unit cell dimensions 9-37047
Y₂C₃, lattice parameter meas. showing homogeneity range after high pressure synthesis 9-35372
Y₂SiBeO₄, refinement 9-39314
Y₄Co₃, unit cell parameters, space group 9-39313
YAl garnet: Nd³⁺(Er³⁺) obs. 9-35954
YAsO₄ rare-earth doped, lattice parameters rel. to doping ratios 9-39215
YB₆ 9-26251
YFe garnet, X-ray multiple diffraction study 9-37153
YPO₄ rare-earth doped, lattice parameters rel. to doping ratios 9-39215
YVO₄ rare-earth doped, lattice parameters rel. to doping ratios 9-39215
Yb₃Fe_{2.5}Co_{0.5}O₁₂ (x=0.5-4.0), unit cell dimensions 9-37047
Zn₂PtO₄ 9-32868
Zn₂N_{1-x}Fe_{2-x}O₄ ferrite system, cation distrib. from neutron diff. obs. 9-41329
Zn (II) complex, n-butylphenylphosphinate polymer, monoclinic and orthorhombic forms, X-ray diff. obs. 9-39315
ZnFe₂O₄, oxygen parameter by neutron diffraction 9-30576
ZnS powders, lattice dimensions and phase transitions, effect of point defects 9-40923
Zr-C system, phase and lattice parameter ranges 9-30754
(Zr_{1-x}Ti)₂Zn₂, lattice parameter, rel. to magnetization and Curie temp. 9-26650
Zr₄Co₄Ge₄, V-phase 9-26253
Zr(HPO₄)₂·H₂O, rel. to ion exchange mechanism 9-23779
ZrSiO₄, high pressure transformations 9-44799

organic compounds

- 1,2,5,6-dibenzanthraquinone, cell parameters and space group 9-39320
1-(2,6-dichlorobenzyl)-6-hydroxy-1,4,5,6-tetrahydro-nicotinamide dihydrate 9-39330
meso-3,3'-di-(p-chlorophenyl)bi-3-phthalidyl, refinement 9-39331
9-dicyanomethylene-2,7-dinitrofluorene 9-30578
2-(2,4'-dinitrobenzyl) 9-30579
dodecadimethylaminocyclohexaphosphazhexane, (N-P)₆ ring cpd., and mol. structure 9-30583
1,5-endomethylenquinolizidinium p-toluenesulfonate 9-35076
1,2,3,7,8,9-hexachlorodibenzo-p-dioxin, and identification as hydropericardium-producing factor 9-39335
3,5,8,10-tetramethylcycloheptazulene, monoclinic form 9-39350
trimethylenediammonium dihydrochloride 9-32936
acetonitrile and acetonitrile-d₃ 9-28696
1-acetyl-2-ethoxy naphthalene 9-32934
N-acetyl-N'-phenylselenourea 9-26256
β-adenosine-2'-β-undine-5'-phosphoric acid 9-39316
3-amino-1,4-naphthoquinone 9-26267
5-anilino-3-oxo-2-phenyl-2,3-dihydro-1H-pyrazole [3,4-a] thiazole 9-39317
batrachotoxinin A, characterization using O-p-bromobenzoate derivative 9-26257
benzene, high-pressure 9-32903
benzocyclopentapyran 9-39321
1,2-benzodithiol-3-one oxime, and mol. structure 9-26258
benzophenone, and mol. structure 9-46797

Crystal structure, atomic continued
organic compounds continued

- 3,4'-bisoxazole, refinement from 3-d X-ray data 9-39338
bis(diphenylphosphino) acetylene, and mol. structure 9-26261
bis(diphenylmethyl) diselenide, X-ray analysis 9-39322
α-bromine-anthraquinone, and molecular structure 9-42799
2α-bromo-5β-bromomethyl-5α-methyl-2β-oxo-1,3,2-dioxaphosphorinane 9-26259
p-bromobenzoyl derivative of ε'-caesalpin, heavy-atom method 9-39324
6-bromoisofenchone, and mol. structure 9-23784
6β-bromoprogesterone 9-39323
t-butyl N, N-dimethyltrithioperacbamate 9-39325
calcium 1,3-diphosphorylimidazole 9-30580
carbazole, N-heterocyclic, space group determ. 9-30581
carbon tetrachloride, high-pressure forms 9-32903
carboxylic acids, dimeric, mol. config., i.r. obs. 9-30093
catalase, hexagonal 9-23780
2-chlorobiphenyl-4-carboxylic acid, X-ray diff. obs. 9-35073
2-chloroquinoline, refinement at -140°C 9-46798
2-chlorotropone-cycloheptatriene adduct, and molecular structure 9-39327
citric acid, anhydrous, X-ray diff. obs. 9-35074
citric acid, anhydrous, X-ray diff. obs. 9-44677
copper phthalocyanine, atomic planes bordering a crack, config. 9-42904
cyclic molecules, superposition links 9-26255
cyclic phosphazene, N₆P₆ (NMe)₆, and mol. structure 9-30583
cyclohexanoxime, substituted 9-39336
3-deoxy-2-c-hydroxymethyl-D-erythro-pentate 9-39345
dibenzodimethoxy compound, polycyclic prod. by anti-[2,2] paracyclonaphthane photolysis, obs. 9-30577
dibenzoequinene, polycyclic, prod. by anti-[2,2] paracyclonaphthane photolysis, obs. 9-30577
11β,12α-dibromo-3α,9-oxidocholanic acid methyl ester 9-39329
3,5-dichloroanthranilic acid 9-35075
diethyldithiocarbamates of uranyl, two monoclinic polymorph phases, and chemical study 9-23787
digitoxigenin 9-26260
dimethoxytrimethylantimony, X-ray diff. determ. 9-30582
anti-2,6-dimethyl-4-chloro-N-methylbenzaloxime 9-39341
dimethylglyoxime, space group symmetries and H bond calcs. 9-40853
2,9-dimethyl-1,10-phenanthroline 9-39342
3,5-dinitro-4-methylbenzoic acid 9-23781
4,5-dioxo-2-thioxo-1,3-dithiolan, β form 9-39328
estriol, and molecular structure 9-39333
estriol, phase determ., computer program for least squares method 9-39332
fulvenes, heterosubstituted 9-39334
galvinoxyl radical, mol. struct. and packing 9-40625
glycylglycine hydrochloride 9-26263
β-gorgonene-Ag NO₃ 9-23782
gramicidin C bromohydrate, synthesis and X-ray study 9-42800
heptamethylbenzene tetrachloroaluminate 9-23783
hexaiodobenzene, X-ray investigation, and mol. struct. 9-46799
hexameric phosphonitric dimethylamide, (N-P)₆ ring cpd., and mol. structure 9-30583
hexamethylenetetramine-borine 9-26264
α-(2-hydroxy-3,5-dibromobenzylidene)-p-butyrolactone, diff. obs. 9-39337
lead stearate, multilayer assemblies, determ. by electron microscopy and X-ray diff. 9-39349
metal phthalocyanine thin films, mol. orientations obs. 9-23786
methane, lattice constants, 4.2-75°K 9-40926
methoxytetraphenylantimony, X-ray diff. determ. 9-30582
methyl cephalonate bromoacetate, X-ray exam. 9-39340
methyl diphenyl-thio (seleno-) phosphinite 9-39339
N-methyl-3-phenyl-4-bromoisoxazolin-5-one 9-40925
N-methyl-4-phenylisoxazolin-5-one 9-26266
4-methyl-3-(p-bromophenyl)-1,2,5-oxadiazole, 5-oxide, X-ray diff. obs. 9-40924
4-methyl-3-(p-bromophenyl)-1,2,5-oxadiazole, 2-oxide, X-ray diff. obs. 9-44678
N-methyl-ethylenethiourea 9-48840
N-methyl-trimethylenethiourea 9-48840
monomethylammonium trichloromercurate, space group and unit cell dims. 9-46800
4-nitroaniline, partly deuterated, two-dimensional neutron diff. exam. 9-46801
nylon-6, surface and bulk crystallinity, i.r. spectroscopy 9-48843
pentachloroethoxyoxycodide 9-39346
pentathietrithiol, proton mag. reson. investig. 9-25777
pentaphenylantimony 9-23785
3-phenylisoxazolin-5-one, X-ray obs. 9-42801
-3-phenylisoxazolin-5-one, X-ray obs. 9-35077
polyethylene, thermal expansion of unit cell 9-48842
polyethylene, unit cell dimensions, variations rel. to crystallization, annealing and deformation conditions 9-46803
polyethylenes, dielectric loss factor depend. 9-28550
potassium caprate, refinement 9-39326
potassium hydrogen malonate, ambiguity in least-squares analysis 9-39347
potassium oxalate monohydrate, and mol. structure, refinement 9-26265
pyridoxal phosphate oxime, X-ray analysis and least squares refinements 9-39344
2-(2-pyridylmethylthio)benzoic acid 9-39348
quinclidinyl benzilate hydrobromide 9-35078
Rochelle salt, orientations of H₂O mols., p.m.r. determ. 9-45405
secondary ammonium halides, long-chain, X-ray study 9-37154
sodium 2-oxovalerate, and mol. structure 9-26268
spermidine phosphate trihydrate 9-26269
steroids, oxide, 11β,12α-dibromo-3α,9-oxidocholanic acid methyl ester 9-39329
terpenoids, C₂₅, X-ray exam. of methyl cephalonate bromoacetate 9-39340
p-terphenyl 9-32935
tetraacyclohexylcycloocta-phospine, unit cell parameters and space group 9-39351
2,2,4,4-tetramethyl-3-oxoglutaric acid 9-48788
tetraphenylcyclobutadiene molybdenum dicarbonyl bromide, from X-ray diff. meas. 9-48841
1,4-thallous benzoate-thiourea complex, crystal structure 9-39319

Crystal structure, atomic continued
organic compounds continued

- L-threonine-L-phenylalanine-pnitrobenzyl ester hydrobromide 9-26270
 thymine anhydrate 9-39352
 2,4,6-tribromoaniline 9-39318
 tricycloquinazoline, and refinement 9-39353
 trioxane, low-temp., X-ray obs. 9-44679
 trisethylsulphonylmethane 9-26271
 L-tryptophane, from powder patterns 9-39354
 L-tyrosine from powder patterns 9-39354
 urea nitrate 9-23788
 uronium nitrate, n. diff. exam. 9-26272
 xanthone, 3-D synthesis 9-46802
 $\text{Fe}_2(\text{CO})_9$ ($\text{CH}_3\text{-C}_6\text{H}_4\text{-SO}_2\text{-N}=\text{C}(\text{OCH}_3)\text{-CH}=\text{CH-C}(\text{OCH}_3)$) 9-26262
 Hf complex, Hf (IV) benzoyl-phenyl-hydroxylamine, (n, η) recoil, effect on ν - γ ang. correl. 9-35597
 (N-P), ring compounds,
 dodecadimethylaminocyclohexaphosphazehexaene and mol. struct. 9-30583
 SbCl_3 : naphthalene, 2, 1 complex, molecular stacking 9-39343
 ThP 9-33123

Crystal symmetry see *Crystallography; Crystal structure, atomic***Crystallites** see *Crystal structure/microstructure***Crystallization**see also *Crystals/growth*

- effect on absorption and fluorescence spectra of n-paraffin solutions of aromatic compounds 9-26771
 alkali halides, transient nucleation from aqueous supersaturated solns. 9-48810
 alloy, binary, solidification in presence of heat flow, interface distrib. coeff. 9-37100
 Aurami's eqn., significance of exponent n questioned 9-32874
 binary condensed system, nucleation and coarsening, diffusion eqn. use 9-32875
 binary condensed system, nucleation and coarsening, diffusion eqn. use 9-35029
 binary system forming eutectic mixture, dynamics 9-23963
 borolanthanum glasses by additions of various oxides 9-34971
 calcium tartrate, nucleation and growth in gels 9-37029
 chalcogenides $\text{A}^{\text{I}}\text{B}^{\text{IV}}\text{C}^{\text{VI}}$ with perovskite structure, synthesis 9-42755
 cluster formation free energy in nucleation theory, rot. and translation contrib. 9-37101
 conference, 1968 9-32867
 copolymers of butene with α -olefins, phase changes, lattice expansion, helix modification obs. 9-32880
 cylinder, solid, in supercooled liq., stability of shape 9-35023
 diamond, from metal solutions, review 9-37017
 p-dihalobenzenes, heterogeneous nucleation on cleaned alkali halide cryst., molecular config. obs. 9-37105
 glass, activation energy; Johnson-Mehl-Avrami eqn. correction 9-42754
 glasses, dense Ba flints and crown 9-39206
 graphite, from metal solutions, review 9-37017
 group II-VI compounds, hydrothermal 9-37023
 growth velocity of small particles, heat of crystn. and particle size effects 9-48791
 heterogeneous nucleation, electrostatic contribution to total interfacial energy 9-30523
 ice, heterogeneous primary nucleation in water and aqueous solns. 9-37035
 ice cylinders in supercooled water, stability of shape 9-35023
 impurity distrib. during directed process 9-40931
 kinetics of growth from solution 9-37018
 lead titanates, hydrothermal conditions 9-37044
 lead zirconates, hydrothermal conditions 9-37044
 mechanism rel. to quasi-line luminescence spectra 9-23098
 from metal solutions, review 9-37017
 metal systems, kinetics, rel. to normal growth mechanism 9-36992
 metals, f.c.c., evaporated, nuclei shapes, stability obs. 9-32895
 methyl siloxane polymers NMR studies 9-30471
 nucleation, cluster formation free energy, rot. and translation contrib. 9-37101
 nucleation, non-steady state, role in form. of isotropic and anisotropic phases 9-48809
 nucleation, selective, at surface local long range active centres, rel. to real structure of substrate 9-36990
 nucleation, transient, in solns., relax. time importance 9-48810
 nucleation during cryst. growth, 2- and 3-dimens. 9-42753
 nucleation kinetics in solutions 9-37019
 nucleation on grain boundaries, incubation times and freqs. 9-42752
 nucleation on liquid surface of small area 9-37099
 polyamides, in alcohol suspensions of mineral particles, heterogeneous nucleation 9-35030
 polycaprolactam without thermal history, time lag temp. depend. 9-32874
 polycarbonate films, under acetone vapour, e. microscope exam. 9-26183
 polycarbonates 9-32873
 polyethylene, crystallinity determ. by density meas. 9-46706
 polyethylene, effect on unit cell dimensions 9-46803
 polyethylene, linear, in 1-chloronaphthalene, optical investigation by light scatt. 9-28238
 polyethylene, linear, in p-xylene, optical investigation by light scatt. 9-28238
 polyethylene, surface structure different when crystallized in contact with Au or Teflon 9-23614
 polymers, cross-linked, rel. to chem. structure thermostabilization 9-46703
 polymers, drawn, crystallinity determ. by density meas. 9-46706
 polymers, linear high, chain-folding and molecular-species segregation 9-46705
 polyolefins from dil. soln., optical investigation by light scatt. 9-28238
 polypropylene, effect of melting on nucleation 9-32878
 polypropylene, low-molecular-weight fractions, rel. to morphology and phase transformations 9-46714
 polypropylene, under pressure, structure and thermal behaviour of phases formed 9-46711
 polystyrene, isotactic, spherulitic growth rate, obs. 9-28202
 polytetrafluoroethylene room temp. crystallization NMR studies, molecular rotation 9-30472
 polyurethanes linear, crystallization from melt 9-26212

Crystallization continued

- porcelain enamels, TiO_2 opacified, rate control for adjustment of parameters controlling optical props. 9-37687
 Portland cement raw mixture, growth rate of alite on rapid heating 9-48922
 Portland cement raw mixture, growth rate of alite on rapid heating 9-46942
 proustite, good optical quality crystals 9-37064
 pyrrargyrite, good optical quality crystals 9-37064
 quartz glass, struct., i.r. refl. spectroscopy obs., 1000-1300°C 9-26175
 rare earth oxides, solid solns. in binary systems, Verneuil method 9-37062
 rare earth vanadates, in Na_3VO_4 , Li_3VO_4 and V_2O_5 , conditions from solubility data 9-40777
 recrystallization, low temperature tube 9-23686
 recrystallization kinetics, intense u.s. energy influence 9-28380
 rubber, natural stress-induced crystn. in rapid stretching, obs. 9-28201
 secondary recrystallization, rel. to grain growth, effect of volume energy 9-32881
 solid solutions, review 9-37017
 steel, austenite nucleation sites 9-26387
 steel, mechanism, struct. form. 9-48794
 steel, nucleation of metallic and sulphide phases on high m.p. oxide precipitates within silicate inclusions 9-23954
 steel, structural recrystallization, effect of phenomena in α -phase 9-33136
 water droplets, nucleation rel. to shock waves, pre-heating, aeration and elec. field, obs. 9-39134
 zeolite A, kinetics 9-23685
 Ag_3AsS_3 (proustite), good optical quality crystals 9-37064
 Ag_3SbS_3 (pyrrargyrite), good optical quality crystals 9-37064
 Ag heterogeneous nucleation on W field emitter tip, electron microscopic obs. 9-48812
 Ag on NaCl, rel. to epitaxy 9-23689
 AgI nucleation and growth in gels 9-37029
 $\text{Al}_2\text{O}_3\text{-SiO}_2$ glasses, nucleation mechanism 9-32826
 Al single cryst., preferred nucleation mechanism obs. during recrystn. after pt. deform. 9-42908
 Au, nucleation and nucleus growth on defined silver faces 9-37003
 Au crystallites on (100) KCl surface, mobility 9-37204
 Au on NaCl cleavage surface, role of surface imperfections on selective nucleation 9-37004
 BN, from metal solutions 9-37017
 CdS films, vacuum deposited, oriented 9-42724
 CdTe films, stimulated recrystn. rel. to cond. and hole mobility 9-39163
 CdTe thin film, co-evaporated, nucleation and structure, influence of stoichiometric deviations 9-36949
 Cu, deformed, initial stages of growth, eff. of Ag impurity 9-30525
 Cu, shock wave hardened, recrystallization and softening during heating 9-33098
 $\text{Cu}(36\text{wt}\%)\text{Zn}$, Fe and P influence on recrystn., grain growth inhibition 9-30718
 Dy_2O_3 films, recrystn. behaviour on pulse annealing 9-30489
 Er_2O_3 films, recrystn. behaviour on pulse annealing 9-30489
 Fe epitaxial films 9-42723
 GaP, from stoichiometric melt and from Ga-rich solution, comparison 9-23672
 Ge films, heterogeneous nucleation 9-48813
 Ge molten drops 9-40865
 HfO_2 , hydrothermal conditions 9-37044
 Hg, transient nucleation in electrodeposition 9-37036
 Hg, vapour, on Pyrex glass, heterogeneous nucleation impurity effects, 225-263°K 9-39216
 HgTe, temp. effect on resistivity and Hall effect 9-44960
 Ho_2O_3 films, recrystn. behaviour on pulse annealing 9-30489
 KCl-NaCl solid soln., enthalpies of crystn., anomalies in struct. obs. 9-37161
 KCl supersaturated soln., effect of various substrates on nucleation 9-32876
 LaB_6 , gas-phase and seed pulling from molten drop 9-37081
 $\text{Li}_2\text{O-Ga}_2\text{O}_3\text{-SiO}_2$ system, of glass 9-44619
 $\text{Li}_2\text{O-2SiO}_2$ glass, rate rel. to neutron irradiat. 9-40833
 Li borate glass, quantitative thermal differential analysis 9-42756
 Mg, impurities (Sn, Pb, and Zn) distrib. during directed process 9-40931
 NH_4I , nucleation and growth on muscovite mica 9-37037
 $\text{Na}_2\text{O-Al}_2\text{O}_3\text{-SiO}_2\text{-H}_2\text{O}$, hydrothermal, 250°, 350°, 450°, 550°C, pressures between 200 and 2000 9-40867
 NaCl-KCl, differential thermal microanal. 9-28391
 NaCl, electron transparent, nucleation in (100) orientation 9-37103
 $\text{Na}(\text{SiO}_3)_2$ glass, spectral obs. 9-28674
 Nb (25 at.%)Ti (10 at.%)Zr alloy, solution-treated, recrystallization on ageing 9-33122
 Nb₃Sn, Sn-rich phase boundary 9-44648
 Ni, shock wave hardened, recrystallization and softening during heating 9-33098
 PbI₂, nucleation and growth in gels 9-37029
 PbO-SiO₂ system, sequences in silica phase 9-26390
 PbTe thin film, co-evaporated, nucleation and structure, influence of stoichiometric deviations 9-36949
 PbTiO₃, homogeneously to form glass ceramics 9-46941
 Pd-Si based alloy glasses 9-42706
 Sb₂S₃ films, formation process, X-ray study 9-42726
 Se, infl. of method on thermoelectric props., 250°-360°C 9-30986
 Se amorphous films, effect of condensation velocity 9-44649
 Se amorphous films, electron bombardment-induced 9-32842
 TeO₂ based glass crystallizability 9-41352
 TiO_2 , hydrothermal conditions 9-37044
 $\text{Y}_2\text{O}_3\text{-Bi}_2\text{O}_3\text{-Ca}_2\text{Fe}_2\text{-Si}_2\text{O}_{12}$ ($x=0.6-1.3$), from PbO/B₂O₃ solvent 9-37047
 YVO_4 in $\text{Na}_3\text{VO}_4\text{-Li}_3\text{VO}_4$ and V_2O_5 , conditions from solubility data 9-40777
 $\text{Yb}_3\text{Fe}_2\text{-Ga}_2\text{O}_{12}$ ($x=0.5-4.0$), from PbO/PbF₂ solvent 9-37047
 Zn polycryst., recrystallization during thermal cycling 9-32879
 ZnS:Ag, thermal recrystallization effects on particle size and morphology 9-30555
 ZnSb:Te, effect of doping on process, and elec. props. 9-42757
 ZrO₂, hydrothermal conditions 9-37044

Crystallographysee also *Electron diffraction crystallography; Isomorphism; Neutron diffraction crystallography; X-ray crystallography*
 alkali feldspars in granite of Plan de la Tour, symmetry, and presence of microcline 9-28226

Crystallography continued

- alkali halides, ionic radii deriv. using repulsive energy method 9-35006
 crystal, magnetic and many-coloured classes, interrel., and determ. 9-28240
 dimethylglyoxime, H bond calcs. and van der Waals forces 9-40853
 elements, collection of data, book 9-22026
 films, thin, anisotropy of kinetic phenomena w.r.t. cryst. symmetry 9-33289
 goniometer for ultra high vacuum 9-23643
 group theory applies. 9-46694
 ionic, lattice self-potentials and Madelung consts. calc. 9-36973
 magnetic lattices derived from crystal lattices 9-31013
 optical, using polarizing microscope, book 9-48777
 point groups, character of irreducible non-equivalent loaded co-representations 9-28239
 polarized crystals, symm. and props. using group intersection theory 9-46737
 refractory metal oxides, lattice energies, rel. to fundamental props. 9-30494
 semiconductors, anisotropy of kinetic phenomena in surface channels w.r.t. cryst. symmetry 9-33289
 Shubnikov groups, non-crystallographic 9-30533
 stereographic projections of struct. complete plotting 9-48828
 stress-strain relations for all cryst. systems, rel. to orientation vector and scalar moduli 9-39403
 Wulff-Bragg law for cm. e.m. waves, demonstration apparatus 9-46763
 BaTiO₃, incorporation of Sb into lattice sites 9-36972
 Bi, electroerosion technique for cutting single crystals 9-23660
 Cu- (14.95 wt.%) Sn alloys, habit plane and shape strain assoc. with formation of orthorhombic γ' martensite plates 9-30739
 Sb incorporation into BaTiO₃ lattice sites 9-36972

Crystals

see also Liquid crystals

- blocking, α -particle track recording using cellulose nitrate plastic 9-42763
 bulk modulus-density relationship 9-44760
 t-butyl chloride, lattice energies 9-39670
 cast vitreous-crystalline materials in different compositions, thermophysical properties 9-39525
 cleaving and cutting instruments 9-32864
 dispersion, rotatory, quantum-mechanical evaluation 9-35616
 elastic wave normal mode phase vels. in cubic crystal plate 9-46869
 guanidium aluminium sulphate hexahydrate, ferroelec., dehydration nuclei rel. to dislocation sites 9-37115
 internal motions, n.m.r., use of relax. function 9-31168
 light wave and u.s. wave propag., analogies 9-37325
 metal, laws at high cooling rates, book 9-48792
 metal azides, thermal decomp. prod. by fracture 9-30531
 metal carbonates, thermal decomp. prod. by fracture 9-30531
 non-ideal, superconducting critical temp. variation using ion density correlation functions 9-49033
 optics taking into account magnetoelectric effect 9-24350
 organic evidence non-hydrogen-bonded hydroxyl groups 9-42739
 pentaerythritol tetranitrate, thermal decomp. prod. by fracture 9-30531
 review, crystals for research and technological applications 9-36971
 single, for targets, surface prep. 9-32882
 stress-strain relations for all systems, rel. to orientation vector and scalar moduli 9-39403
 stressed, elastic wave propag. and acoustical birefringence 9-30642
 sucrose, growth mechanism from aqueous soln. at 0°C 9-39203
 surfaces, anisotropic, pseudo-surface waves, characts. 9-27222
 uniaxial, optical const. determination with concave grating monochromator 9-25385
 α -particle scatt., track pattern recording using cellulose nitrate plastic 9-42763
 Ag, grown by electrodeposition, large step-height spirals on surface, origin 9-23825
 Al, (p, α) reaction, α -particle track recording using cellulose nitrate plastic 9-42763
 Eu₂(WO₄)₃ single cryst., nucl. reson. fluoresc. of 3 eV ¹⁵²Sm recoil atoms, anisotropic pot. obs. 9-35596
 He liq., continuous transfer, for u.h. vacuum field ion microscope 9-34148
 Na₂O-R₂O₃-GeP₂-H₂O system (R=rare earth element), hydrothermal, and crystal structure studies 9-40866

electron states *see Crystal electron states*

etching

- garnets, flux-grown, obs. of internal growth defects 9-32937
 glass, tensile strength increase 9-35184
 glass (mica) etch-pit counter for neutrons 9-22914
 graphite, hexagonal, pit ion formations rel. to vacancy oxidation 9-28281
 guanidium aluminium sulphate hexahydrate, pattern correl. with dehydration figures 9-37115
 metals, cubic, dodecahedral pits rel. to orientation determ. of faces 9-48784
 natrolite, of cleavage faces 9-42745
 poison and solvent undersaturation interdependence 9-28227
 polycarbonate film, charged-particle irradi., etching rate accel. by u.v. irradi. in O₂ atmos 9-32271
 r.f. sputter 9-46747
 sapphire, by fluorinated hydrocarbons in gas phase 9-36987
 sapphire, for obtaining surfaces suitable for Si film deposition 9-23658
 semiconductor II-VI cpds., chem. polishing 9-44977
 semiconductor junction delineation and dislocation revealing by HIO₄-HF-H₂O system 9-33339
 solid-liquid-vapour etching process 9-36986
 AgCl single crystals, pits, rel. to dislocation structure 9-46748
 BaF₂, on matched pairs, discrepancies in patterns rel. to stepped dislocations 9-37173
 Cu, etch-pit obs. of strain centres, correl. with X-ray topographs 9-32939
 CoO single cryst., selected etch. pitting technique 9-42743
 Cu single cryst., dislocation etching, pitting obs. 9-36988
 GaAs, development of etchant to reveal dislocations on {100} and {111} faces 9-26200
 Ge, with I vapour, 200° to 800°C, characts. 9-42744
 Ge partial splits 9-44780
 Ge single cryst., etch pit obs. of dislocation distrib. during plastic deform. 9-42832
 K₄NbO₁₇, etchants at 25 and 50°C 9-26238
 KBr, dislocation figures, effect of neutron irradi. on dimensions 9-40945

Crystals continued**etching continued**

- KCl, dislocation figures, effect of neutron irradi. on dimensions 9-40945
 KCl, melt-grown, thermal etching obs. of dislocations 9-37178
 KCl (100) cleavage faces, evidence for screw dislocations 9-48861
 KCl cleavage planes with different etchants, rotation of etch pits rel. to study of dislocation 9-37177
 KCl vacuum heating at 150-500°C, etch figures obs. by decoration with Au 9-40855
 LiF, dislocation figures, effect of neutron irradi. on dimensions 9-40945
 Mg-Al-Zr-Be alloy, correlation of polarized facets and orientation 9-39186
 Mo, in hot Ar stream, rel. to showing dislocation structure 9-32972
 Na₂Al₂Si₃O₁₀·2H₂O, natrolite, of cleavage faces 9-42745
 NaCl, deformed, single cryst., etc. pits obs. of dislocation density 9-32974
 NaCl, dislocation figures, effect of neutron irradi. on dimensions 9-40945
 NaCl, interdependence of poison and undersaturation of solvent 9-28227
 NaCl, on (110) fractured faces 9-48785
 NaF, technique for dislocation identification 9-23814
 NaF, thermal, of cleaved surfaces, at 860-930°C 9-48787
 Nb, etch pits and sub-boundaries obs. by optical microscopy, defect contribution to diffusion 9-32985
 Ni, thermal etch structures for surface energy anisotropy determ. 9-46716
 Pb_{1-x}Sn_xTe single crystals, electrolytic etching revealing metallic inclusions and cellular substructure 9-30569
 Pu, electrode in inorganic acid, a.c., patent 9-23803
 α -Pu, new electrolytic technique for revealing microstructure 9-39304
 Se single crystal, trigonal, etch pit observations 9-28228
 Si, by H₂S gas, surface exam. 9-32837
 Si, dislocations quantitative relation determ. in 14 mm slice 9-40954
 Si, instability of SiO₂ and Si₃N₄ nuclei in H₂-H₂O and H₂-HCl mixtures 9-32866
 n-Si, photoengraving and effect of illumination 9-33334
 Si films, epitaxial growth on Si substrate and oxide layers, etch pits obs. 9-30491
 Si partial splits 9-44780
 SiC, improved technique 9-46749
 α -SiC in H at high temp., variation with susceptor mat. and inert gas atmospheres 9-30514
 SiC with H₂, etch rate 9-26204
 Sn-Pb dilute alloys, electropolishing procedure to produce etched or polished surfaces 9-39959
 Sn, electropolishing procedure to produce etched or polished surfaces 9-39959
 YAl garnet, figures, rel. to point defects, dislocations and orientation 9-44641
 Zn, selective, at dislocations, mechanism 9-40856
 Zn, vapour-grown, thermal etching of dislocations 9-48864
 ZnO, polarity obs. 9-32858
 ZnSe, using bromine/methanol and hot HCl etchants 9-46750
- excitons** *see Crystal electron states/excitons*
- faces**
- alnico-type cast hard magnets, b.c.c. 9-35014
 crystal growth, morphological stability at interface separating solid and liq., review 9-37016
 cyclohexanol, phase transformation, morphology 9-35251
 diphenyl, appearance and growth of non-singular crystal surfaces 9-37014
 growth and appearance of non-singular crystal surfaces 9-37014
 habit of solution grown crystals, macroscopic model 9-23669
 ice cylinders, unstable, growth of perturbations in shape of single cryst. growing in water 9-35019
 inert gases, dynamical props. by molecular dynamics method 9-39191
 inert gases, dynamical props. in quasiharmonic approximation 9-39190
 interface stability of large facets on soln. grown cryst. 9-36984
 morphological stability of lamellar eutectics 9-36935
 muscovite, cleavage study by spectrometry by Auger electrons 9-42742
 orthoclase, cloven in vacuum, electrostatic distrib. obs. on faces 9-37571
 polyethylene extended chain cryst. growth and morphology 9-26213
 Rochell salt, nonisothermicity investig. during growing and dissolving from solns. 9-26203
 solution grown, large faceted surfaces, interface stability 9-36984
 splitting along cleavage planes, apparatus 9-32865
 surface tension in ionic cryst. in presence of dipole moments 9-32831
 Ag single crystal, (100) and (110) faces, mean displacement of surface atoms, low temp. studies 9-39248
 Cu, oxygen ion bombardment effects 9-44640
 Fe-(3wt.%)Si alloy, (110) and (100) planes, infl. of annealing 9-34979
 GaAs, epitaxial growth, effect of facet development on ¹²⁵Te distribution 9-36985
 GaAs, surface inhomogeneities from contact potential meas. on etched faces 9-26554
 Ge, epitaxial grown by GeCl₄-H₂ reaction, surface morphology obs. 9-46761
 Ge decoration of cleavage surfaces 9-48749
 K₂SO₄, study by Hartman method 9-46745
 LiNO₃, surface distortion, i.r. data 9-48750
 MgAl₂O₄, vertically pulled, morphology and defects 9-46743
 NaCl, microstructure of growth surfaces, eff. of surface active impurities 9-23765
 NaCl single crystal, polygonization by electron bombardment 9-30513
 NaNO₃, surface distortion, i.r. data 9-48750
 NiO, epitaxially grown on MgO, morphology rel. to reaction temp. and H₂O/Br vapour ratio 9-35034
 Pt, (100), electron scattering obs. 9-46746
 W, thermal faceting rel. to O₂ adsorpt., effect on work function 9-35012
 Y₂Al₂O₇ habit changes of single crystals, grown from a PbO-PbF₂ flux 9-40922
 Y₂Ga₂O₇ habit changes of single crystals, grown from a PbO-PbF₂ flux 9-40922
 Zn, cleavage planes 9-48786
 ZnO, polar surfaces, elec. conductivity and light reflectance meas. 9-42741
 ZnO single-cryst. basal faces, nonequilib. vaporization rates 9-46690
 ZnS:Ag, morphology, thermal recrystallization effects 9-30555
 ZnS, blende, cleaved, diffuse patterns in slow electron diffraction 9-28274
 Zr single crystal, (1017) hydride habit plane 9-35013

growth

see also Crystallization; Epitaxy; Zone melting and refining

Crystals continued

growth see *Crystallization; Epitaxy; Zone melting and refining*
 alite, on rapid heating of Portland cement raw mixture 9-46942
 alite, on rapid heating of Portland cement raw mixture 9-48922
 alloys with wide solidification ranges, single-cryst. growth technique 9-32877
 alumina trichites, prod. and props. 9-35016
 anthracene, oriented growth in electric field 9-37097
 arc transfer process 9-36994
 ballases, natural and synthesized, conditions from structure study 9-26197
 binary eutectic microstructures, controlled solidification technique 9-23676
 borosilicate glass, dendritic growth obs. during Ag^+ diffusion in elec. field 9-48872
 calcium tartrate, nucleation and growth in gels 9-37029
 in capillary tubes, apparatus 9-48789
 centrifugation method for single cryst. growth from soln. 9-37022
 chemical transport, simplified models, review 9-37816
 chemical transport reactions, theory 9-37817
 chemical vapour deposition, transmission e microscopy 9-37002
 conference, 1968 9-32867
 cyclohexanol, phase transformation rates 9-35251
 Czochralski, nonmixing cells due to crucible rotation 9-46753
 Czochralski, rot. reversal effect 9-40863
 dendrites, composition of axial parts in solid solns., effect of cooling rate 9-48814
 dendritic, in pure systems, analysis extension 9-23687
 dendritic, of pure mats. 9-37107
 dendritic steady-state of platelet, shape soln., branching 9-37108
 dendritic, theoretical investigations 9-26214
 diamond, from Co-C and Mn-C systems 9-37028
 diamond, growth from metal solution, review 9-37017
 diamond on seed crystal, process 9-30528
 diamond whiskers, expt. technique 9-40868
 diamonds, artificial, prep. method. C phase diagram 9-33135
 diamonds, synthetic, from metal-carbon systems 9-23670
 diamonds, synthetic, left- and right-screw growth spirals 9-23671
 dielectric surface, nuclei formation around point charges 9-42747
 diffusion along substrate surface during growth from vapour 9-48796
 diffusion method 9-48790
 diffusion-controlled interpart. interference eff., influence on morphological stability 9-37058
 diffusionless, of new phase during transformation in binary system 9-35015
 diphenyl, and formation, from vapour phase 9-40861
 diphenyl, appearance and growth of non-singular crystal surfaces 9-37014
 diphenyl, from vapour, diffusion along substrate surface 9-48796
 electric field effect on rate 9-23663
 electrodeposition parameters effect on growth habit and morphology 9-37034
 encapsulation of polycrystalline wires 9-37000
 epitaxial, from mol. beams, model 9-26216
 epitaxial, of layers from vapour phase through liq. alloy, low temp. deposition, patent 9-30530
 epitaxial growth on collodion, rock salt and mica obs. by electron diffraction 9-30492
 equipment for growth at very high gas pressures 9-37001
 eutectics, lamellar and rod-like, review 9-37049
 ferrite single cryst. by chem. transport reactions 9-44643
 film, surface network growth morphology 9-23632
 fluor-phlogopite, nucleation and growth from vapour polytypism obs. 9-37010
 fluorapatite, Czochralski-growth 9-37069
 flux-reaction technique for synthesizing ion. cpds. 9-28234
 furnace, high-pressure multi-purpose, design and construction 9-37053
 garnet film, growth on non-garnet single crystal, patent 9-46723
 garnets, flux-grown, internal growth defects, etching and X-ray topographic obs. 9-32937
 garnets, seeded growth from molten salts 9-37045
 gel growth by complex dilution method, prediction of results 9-30516
 in gels, cusps struct. obs. 9-44605
 graphite, from solution 9-48800
 graphite, growth from metal solution, review 9-37017
 graphite, single cry. film and flaky dendritic crystals, from C-Fe melt 9-26209
 graphite, single crystal films and dendritic crystals from carbon-iron melt 9-37067
 graphite, spherulitic 9-37068
 graphite single crystal, by pyrolysis of acetylene over metals 9-39192
 group II-IV-V₂ semiconducting compounds, solution and vapour-growth 9-37063
 group II-VI compounds, from solution using tin as solvent 9-37073
 group II-VI compounds, general aspects 9-36995
 group II-VI compounds, hydrothermal crystallization 9-37023
 group III-V compounds, from metal solns., infl. of solvent and impurities on habit and morphology 9-36981
 heteroepitaxial films, rotation and translation of islands 9-46722
 hexamethylenetetramine from soln. and vapour phase 9-39202
 high temperature and high pressure solution growth, review 9-37015
 ice, after method by Helmholtz 9-23681
 ice, deposition rate, numerical modelling 9-40821
 ice, falling, rate obs. for 1 min. after nucleation 9-41511
 ice, heterogeneous primary nucleation in water aqueous solns. 9-37035
 ice, in supercooled water and supercooled metal fluoride solns. 9-39217
 ice, pulling ribbons from melt, new method 9-23680
 ice agglomeration into T formation, lab. expt. 9-41512
 ice dendrites in supercooled water, growth rates 9-39200
 ice in supercooled water, morphological stability and ice-water interfacial free energy 9-37102
 ice single cryst. cylinders in water, morphological instability 9-35019
 ice single cryst. from melt, dislocation struct. obs., X-ray diffr. topographs 9-37080
 ice single crystals, segregation of NH_4F 9-30518
 inductor-crucible, developments 9-37061
 interface, melt-solid, morphology obs. by technique using inert gas bubbles 9-39205
 interface, solid-liquid, temp. and vel. meas. by thermolec. probe 9-39210
 interface stability during growth from stirred melts 9-37056

Crystals continued

interface stability of large facets on soln. grown cryst. 9-36984
 irradiation influence, equil. surface struct. changes 9-37021
 kinetic coefficient and activation energy at small supersaturations 9-42748
 kinetics of growth from aqueous solutions 9-37020
 lead titanates, hydrothermal conditions 9-37044
 lead zirconates, hydrothermal conditions 9-37044
 liquid encapsulation crystal pulling at high pressures 9-37052
 magnesium aluminate spinels, variable stoichiometry and characterization 9-37084
 magnetite single cryst. by chem. transport reactions 9-44643
 from melt, impurity enrichment at crystal-melt interface 9-48802
 melt, striated solute distrib. prod. by temp. oscillations 9-37059
 melt grown by effective seed radius, characterization of shape and heat flow 9-37050
 melt-grown oxide crystals, developments review 9-37048
 metal films, activation energy calc. rel. to three stages 9-23631
 metal from melt and in solid phase, theory and expt., book 9-48792
 metal oxides, ternary, by chemical transport 9-36999
 metal single crystals from melt 9-23675
 from metal solutions, review 9-37017
 metal systems mechanism and crystallization kinetics 9-36992
 metals, hexagonal, monocrystals 9-30515
 metals, melt-grown, microsegregation and cryst. perfection 9-37060
 metastable thin film epitaxial struct., review 9-34987
 β -methyl naphthalene, anisotropic growth velocity from morphological-kinetic data 9-40860
 morphological stability at interface separating solid and liq., review 9-37016
 new-phase nucleus, kinetics, theory 9-48811
 noble metals, films, on alkali halides 9-23636
 normal, thermodynamical theory 9-48793
 nucleation, 2- and 3-dimens. 9-42753
 nucleation, selective, at surface local long range active centres, rel. to real structure of substrate 9-36990
 nucleation kinetics in solutions 9-37019
 nucleus, two dimen., growth on substrate, morphological stability 9-30524
 nucleus formation, theory 9-40858
 oxide crystals, melt-grown, developments, review 9-37048
 oxide crystals, mixed, vertical float zone technique 9-37051
 plates, thin, from gas phase 9-48761
 polyethylene extended chain cryst., morphology 9-26213
 polymers, simplified treatment including chain folding, review 9-36989
 polystyrene, isotactic, spherulitic growth rate, obs. 9-28202
 potash alum., kinetic coefficient and activation energy at small supersaturations 9-42748
 proustite, Czochralski method 9-37065
 proustite, good optical quality, crystallization from melt 9-37064
 pulling, capillary seed technique applic. 9-46754
 pyrrargyrite, Czochralski method 9-37065
 pyrrargyrite, good optical quality, crystallization from melt 9-37064
 quartz, spires and terraces occurring on hydrothermally grown crystals 9-44642
 quartz, synthetic inhomogeneities, optical investig. 9-37165
 quartz, trapping of colloidal inclusions 9-37043
 quartz, synthetic, hydrothermal method, and resonator properties 9-39201
 rare earth orthoferrites, flux grown crystals, Pb substitution 9-28237
 rare earth oxides, solid solns. in binary systems, Verneuil method 9-37062
 rare earth vanadate, RVO_4 -type, flux-growth 9-26211
 rare-earth metals and binary alloys, single crystals 9-37078
 refractory cry., by vapour transport react., thermodynamic analysis 9-28231
 review of research 9-36971
 ribbon pulling from melt, new method 9-23680
 Rochelle salt, nonisothermicity investig. during growing and dissolving from solns. 9-26203
 ruby, 0° boules with hexagonal maphology, Verneuil method 9-37066
 ruby, single cryst., by thermal imaging tech. 9-36993
 ruby, synthetic, flame fusion method, inf. of molten film thickness on crystal perfection 9-23677
 salol, from melt in capillary tubes, retardation of growth rate 9-37273
 sapphire, from melt, dislocations and cavitation in veiled region 9-35092
 sapphire whiskers, effect on tensile strength 9-35180
 semi-transparent mats., solid-liq. interface stability 9-37057
 semiconductor single cryst., from melt, homogeneous impurity incorporation 9-30520
 semiconductors, homogeneous single crystals, synthesis and growth from solution 9-37054
 semiconductors, pulling, capillary seed technique applic. 9-46754
 single crystals in systems involving phase transformation 9-23661
 small crystals, theory, using periodic boundary conditions 9-37055
 solid soln. single crystal, method, patent 9-46751
 solid solutions, review 9-37017
 solution growth, large faceted surfaces, interface stability 9-36984
 solution growth, high-temp. and high pressure, review 9-37015
 solution growth, kinetics 9-37018
 solution growth, macroscopic model for habit 9-23669
 Soret effect rel. to solidification of single- and two-phase systems 9-23673
 $\text{Sr}(\text{AsO}_4)\text{Cl}$ isomorphism with Cr spodosite 9-35664
 step motion on crystal surfaces 9-36991
 stirred melts, stability of solid-liq. interface during growth 9-37056
 sucrose, rate curves rel. to surface diffusion model 9-37098
 sucrose from aqueous soln. at 0°C, growth rates 9-39203
 surface, displacement of nonmolecular stop, structure and kinetics 9-42749
 surface diffusion during growth from vapour on substrate 9-48796
 surfaces, non-singular, appearance and growth 9-37014
 temperature determ. for axially symmetric bodies, theory 9-48801
 temperature fluctuation effects in melt, effective distrib. coeff. 9-39204
 thermal imaging technique for single cryst. growth 9-36993
 thin film prod. by cold plasma condensation 9-34995
 triglycerides, recrystallization at low supercooling 9-37106
 vacuum apparatus for deposition and in-situ Galvanomag. meas. 9-39193
 vapour growth, diffusion-limited, dynamics 9-36998
 vapour phase, molecular processes involved 9-37009

Crystals continued

- velocity of small particles, heat of crystn. and particle size effects 9-48791
- Verneuil crystals, uncommon, characterization 9-37066
- Ag, electrodeposition parameters effect on growth habit and morphology 9-37034
- Ag, films, on alkali halides 9-23636
- Ag, hydrothermal 9-37027
- Ag₂S formation, influence of AgBr surface structure on mechanism 9-37024
- Ag₃AsS₃, (proustite), Czochralski method 9-37065
- Ag₃AsS₃, (proustite), good optical quality, crystallization from melt 9-37064
- Ag₃SbS₃, (pyrargyrite), Czochralski method 9-37065
- Ag₃SbS₃, (pyrargyrite), good optical quality, crystallization from melt 9-37064
- Ag film, in ultra high vac., influence of air, N₂, O₂ and H₂O vapour on growth 9-34993
- Ag film, nucleation on MoS₂ single crystal 9-34992
- Ag film on mica, presence of H₂, O₂ or H₂O rel. to conc. of inclined faults 9-35097
- Ag on NaCl, epitaxy and nucleation 9-23689
- AgBr, epitaxial from melt, formation of oriented bubbles 9-48817
- AgI, nucleation and growth in gels 9-37029
- AgTe monocrystals, by chemical transport reaction 9-42759
- Al₂O₃, corundum Verneuil method, decorated dislocations movements during annealing 9-37172
- Al₂N₄, anisotropic growth, neutron irradiation 9-40857
- Al films, elec. field effect on form. and substruct. 9-48762
- Al supercond. granular thin films 9-28481
- AlF₃, from low melting flux 9-39207
- AlP, from Al solution, solubility rel. to temp. 9-37025
- Ar big single cryst., mosaic spread, thermal etching and preferential orientation obs. 9-40859
- As, hydrothermal 9-37027
- As₂Se₃ single crystal 9-23678
- Au-Ag alloy, nucleation on amorphous substrate 9-26187
- Au, films, on alkali halides 9-23636
- Au, hydrothermal 9-37027
- Au, nucleation and nucleus growth on defined silver faces 9-37003
- Au, nucleation on amorphous substrate 9-26187
- Au evaporated on Ag substrates, epitaxy, effect of surface imperfections 9-37112
- Au evaporated on NaCl and KCl, effects of forced high nucleation densities 9-32843
- Au film, in ultra high vac., influence of air, N₂, O₂ and H₂O vapour on growth 9-34993
- Au films on NaCl, epitaxial and polycryst. rel. to H₂O, CO₂ contamination 9-46724
- Au on NaCl cleavage surface, role of surface imperfections on selective nucleation 9-37004
- Au single crystals, in gels 9-37026
- B₄C and nucleation, two-dimens., at screw dislocations, obs. 9-28290
- BA₃, cubic and orthorhombic, B contact with As vapour 9-23664
- BN, from metal solutions 9-37017
- Ba₂NaNb₂O₇, transparent, striation-free by low-thermal-gradient Czochralski technique 9-39208
- Ba₂NaNb₂O₇, P⁴⁺, Ir⁴⁺ rel. to optical defects 9-28651
- BaFe₂O₉ single cryst. in polycrystalline aggregate, solid state growth, eff. of aggregate parameters 9-36996
- Bi₂GeO₉, by Czochralski method, and props. 9-42751
- Bi₂GeO₉, Czochralski method, and optical transmission 9-40864
- Bi₂O₃ layers, by evaporation, props. 9-39162
- Bi₄(GeO₃)₃ Czochralski method 9-23679
- Bi₄(GeO₃)₃, by Czochralski method, and props. 9-42751
- BiSb, orthorhombic needles from gaseous phase 9-32870
- C, and structure, vaporization, mech. props., growth and gasification studies, book 9-46695
- C film deposited on Ag, coherence 9-37112
- Ca₁₀(PO₄)₆F₂, Czochralski-growth 9-37069
- CaF₂, fluorite, synthetic, inhomogeneities, optical investig. 9-37165
- CaTiSiO₅, by Czochralski method 9-39209
- CaWO₄:Nd, imperfection assessment and control in crystals used for laser devices 9-37157
- CaWO₄, synthetic, inhomogeneities, optical investig. 9-37165
- Cd₂Hg_{1-x}Te 9-37070
- Cd₂Hg_{1-x}Te, by vertical-zone melting method 9-46755
- Cd₂Hg_{1-x}Te, from melt, stoichiometry control rel. to props. 9-46756
- Cd chalcogenides, from solution using tin as solvent 9-37073
- Cd electrodeposits on Cu single crystals 9-30490
- CdCr₂S₄(Se₄) single crystals 9-44646
- CdCr₂Se₄, by topochemical reactions 9-23662
- CdGa₂S₄ single cryst., Stockbarger technique 9-35024
- CdGeAs₂, zone-melting method 9-37071
- CdIn₂S₄ single cryst. Stockbarger technique 9-35024
- CO single crystal, from vapour, optimum growth conditions derivation from sublimation studies 9-34967
- CdS:I hollow rods by iodine vapour transport 9-39195
- CdS, from metallic solution 9-37031
- CdS, from reacting solutions 9-37030
- CdS, vapour growth from controlled atmospheres of constituent elements 9-37006
- CdS, vapour phase growth, eff. of different methods on nonstoichiometry 9-36978
- CdS epitaxial films, prod. by gas transport reactions 9-42722
- CdS epitaxial single cryst. layers on ZnS platelets 9-34988
- CdS from vapour, whisker disloc. behaviour 9-46759
- CdS from vapour phase, model for existence of various crystal forms 9-39194
- CdS hollow conical single crystal, from vapour, struct. and defect obs. 9-35017
- CdS on {111} faces of GaAs by evaporation, star-like growth hillocks 9-48758
- CdS single crystals, controlled composition, from vapour phase 9-37005
- CdSe, rapid non-detonative synthesis 9-37074
- CdSe, vapour phase deposits growth on single crystal substrates 9-46726
- CdTe, simultaneous, with Te whiskers by vapour phase reaction 9-28232
- CdTe, single crystals by liquid encapsulation 9-37072
- CdTe, vapour phase deposits growth on single crystal substrates 9-46726
- CdTe layers, struct. depend. on underlying temp. 9-40846

Crystals continued

- CeFeO₃ orthoferrite, polycryst. 9-45055
- Co₂ single cryst. from PbF₂ flux melts 9-35025
- CfOF, hydrolysis of CfF₃, X-ray diffraction, structure determ. 9-26205
- Co, hydrothermal 9-37027
- Co₃O₄ single cryst. by chem. transport reaction using HCl gas 9-32871
- CoCr₂S₄ ferrimagnetic spinel, by vapour-liquid transport technique 9-39196
- CoF₂, from low melting flux 9-39207
- CoSi, single crystals by Czochralski technique 9-37075
- CoTe_x, vapour transport for single crystals 9-23665
- CrF₃, from low melting flux 9-39207
- CsPbCl₃, rel. to phase transitions 9-39211
- Cu-Nb-S system, vapour growth of new single-crystalline phases 9-37007
- Cu, electrodeposition parameters effect on growth habit and morphology 9-37034
- Cu, films, on alkali halides 9-23636
- Cu₂O, single cryst., in SiO₂ gel at near ambient temp. 9-46752
- Cu₂O, single crystals from melt, crucible-free method 9-37076
- Cu whiskers, in large quantity, role of Cu₂O globules 9-37110
- CuAlS₂(Se₂), by vapour transport with iodine 9-48797
- CuCl, gel growth 9-37033
- CuCl, gel growth by complex dilution method, comparison with new mats. 9-30516
- CuCl₂·2H₂O, kinetics 9-37032
- Dy single crystals, by three methods 9-37078
- Er_xBi_{1-x}FeO₃, Bi substitution effect on mag.-reorientation temp. 9-32869
- Er single crystals, by three methods 9-37078
- EuS, vapour phase, high-temp. 9-37008
- EuSe, vapour phase, high-temp. 9-37008
- EuTe, vapour phase, high-temp. 9-37008
- Fe-Ni oxide spinel, by arc image technique 9-48804
- Fe-Si ordered alloys, antiphase boundaries formed during growth and cooling, props. 9-26231
- Fe, strain annealed, subgrain boundaries in {011} {112} occluded grains 9-23824
- Fe epitaxial layers on oriented Au support, electron microscope exam. 9-48759
- Fe whiskers, reduction, initial stage 9-26215
- α-Fe whiskers by chem. vapour deposition, in situ electron microscope obs. 9-44650
- FeCr₂S₄ ferrimagnetic spinel, by vapour-liquid transport technique 9-39196
- Ga_xIn_{1-x}Sb solid soln. using temp.-gradient zone melting 9-30719
- GaAs:Cr, epitaxial, from solution 9-48760
- GaAs:Zn,Ge,Te, impurity segregation rel. to melt. comp., obs. 9-26210
- GaAs, epitaxial, effect of facet development on ¹²⁵Ie distribution 9-36985
- GaAs, vapour-grown, facet effect 9-30921
- GaAs_{1-x}P_x solid solns. from Ga-rich solns., lattice distortion and atomic struct. obs. 9-35206
- GaAs epitaxial layers, chemically-deposited, growth and perfection 9-36951
- n-GaAs epitaxial layers, high purity, by vapour deposition 9-30907
- GaP:Zn epitaxial growth on GaAs and GaP substrates by water vapour transport method 9-30529
- GaP, from Ga solutions, vapour phase and liquid epitaxial deposition, defect structure depend. on method 9-30602
- GaP, by liquid encapsulation crystal pulling at high pressures 9-37052
- GaP, pulling by liquid encapsulation 9-37077
- GaP, from stoichiometric melt and from Ga-rich solution, comparison 9-23672
- GaS polycrystalline and single crystals, mechanism 9-39611
- GaSb, floating zone techniques 9-28229
- Gd₂Fe₂O₇ films, parameters effect on mag. struct. and props. 9-42722
- Gd single cryst., using distillation chamber, purification 9-35026
- Gd single crystals, by three methods 9-37078
- Ge, epitaxial, by GeCl₄-H₂ reaction, growth rate and surface morphology obs. 9-46761
- Ge, interface stability during growth from stirred melts 9-37056
- Ge, from metal solns., infl. of solvent and impurities on habit and morphology 9-36981
- Ge, pulling ribbons from melt, new method 9-23680
- Ge films, on sapphire by chemical vapour transport 9-36961
- Ge layers, non-dislocational, from vapour, conditions 9-42750
- Ge single cryst. from melt, convection-induced impurity 9-37079
- HfO₂, hydrothermal conditions 9-37044
- Hg-Zn alloy single cryst. by stationary mould solidification technique 9-32877
- Hg, transient nucleation in electrodeposition 9-37036
- HgCr₂Se₄ single cryst., ferromag., by chem. transport 9-44961
- HgS Cinnabar monocryst., by hydrothermal method 9-44647
- α-HgS single cryst. from Hg-rich solns. 9-35020
- HgTe films, epitaxial 9-28214
- Ho single crystals, by three methods 9-37078
- InAs-InP alloy system for injection lasers, charact. 9-41921
- InAs_{1-x}P_x vapour-deposited epitaxial layers 9-30910
- InP, by liquid encapsulation crystal pulling at high pressures 9-37052
- K₂Al₂(SO₄)₂·24H₂O, potash alum., kinetic coefficient and activation energy at small supersaturations 9-42748
- K₂Nb₆O₁₇, melt-grown 9-26238
- K₂Nb₆O₁₇ mica-like single-cryst. from melt 9-30522
- K₂Pb₂La₂Nb₁₀O₃₆, from ternary systems and dielec. constants 9-23682
- K₂Sr₂La₂Nb₁₀O₃₆, from ternary systems, and dielec. constants 9-23682
- KCl, from melt, dislocations obs. using thermal etching 9-37178
- KCoF₃, from low melting flux 9-39207
- KNb₂O₇ mica-like single-cryst. from melt 9-30522
- KNiF₃, from low melting flux 9-39207
- KTa₂Nb_{1-x}O₇, from melt, patent 9-48805
- KZnF₃ single crystal with perovskite structure, hydrothermal synthesis 9-42746
- La₂O₃:S:Eu, for luminesc. studies 9-43257
- LaNbO₄ single crystals, prep. and structural props. 9-44644
- Li₂GeO₁₅, Czochralski method 9-37082
- LiYF₄, pure and rare-earth doped, Czochralski method 9-37083
- LiYF₄, Stockbarger technique, from melt 9-23683
- Mg₂PtO₄ 9-32868
- MgAl₂O₄, spinel, vert. pulling technique 9-28235
- MgAl₂O₄, vertically pulled from melt, morphology and defects 9-46743
- MgAl₂O₄ spinel crystals, stoichiometric, by flux evaporation 9-37085
- MgAl₂O₄ spinel single crystals, stoichiometric, flux method 9-37086

Crystals continued

- MgF₂, hih melting point, from vapour phase 9-23666
 MgO:Al₂O₃:Cr, variable stoichiometry spinels, and characterization 9-37084
 MgO, single crystals, from solution 9-35021
 MgO:Al₂O₃ system, spinel growth by flame fusion method 9-23684
 MgSiP₂, growth and energy gap meas. 9-44974
 MgTe-CdTe single crystals, new material for visible light-emitting diodes 9-47418
 α -Mn single crystals, and physical r. props. 9-44645
 MnFe₂O₄ single crystals. 9-37087
 MnO single crystals, by heating in closed chamber of pressed powder 9-39840
 MoO₃, with small amounts MoO₂, dendritic and needle-type crystals., spiral-type growth mechanism 9-30526
 NH₄FeF₆ from soln., X-ray diffraction powder study 9-26207
 NH₄H₂PO₄, solution grown, mother-liquor inclusions formation at saturation 9-40862
 NH₄I, on muscovite mica 9-37037
 Na₂P₂O₇·6H₂O, from aqueous soln., influence of surface-active agents 9-37038
 NaCl, evaporation fronts in (100) surfaces, movements 9-30517
 NaCl, vapour phase, molecular processes involved 9-37009
 NaCl from H₂O soln. with Mn²⁺, X-ray diff. topographs 9-37144
 NaCl from melt, by Czochralski method, form. of two-dimensional nuclei on {001} faces 9-39212
 NaCl surfaces, microstructure, effect of surface-active impurities 9-23765
 NaCl whiskers, regrowth from pure and poisoned solutions 9-37039
 NaClO₃, solution grown, mother-liquor inclusions formation at saturation 9-40862
 NaN₃ single cryst. by Kyropolus method 9-35027
 Nb₃Sn, from solid Nb-lq. Sn reaction, diffusion and soln./deposition mechanisms 9-48764
 NbC-Fe(Ni,Co) liquid alloys, carbide grain growth during sintering 9-34952
 Ni-Ge alloy single crystals, prep. by Czochralski method 9-42758
 Ni, electrodeposition parameters effect on growth habit and morphology 9-37034
 Ni, hydrothermal 9-37027
 Ni, pseudomorphic on Cu, for monolayer and possibly thicker films 9-34989
 Ni bicryst., oriented, by electron beam floating-zone technique 9-46757
 Ni platelets and whiskers by thermal and chem. decomp. of NiI₂ and NiBr₂ 9-35018
 NiF₂, from low melting flux 9-39207
 NiFe₂O₄, by pulling method 9-37088
 NiFe₂O₄, from fluxed melts under pressure 9-35028
 NiO, epitaxial, by vapour hydrolysis of NiBr₂ on MgO 9-35034
 NiO, fluxed-melt growth 9-37089
 P, black, using equipment for growth at very high gas pressures 9-37001
 Pb films on (110) face of W, during u.h. vac. deposition 9-42720
 PbI₂, nucleation and growth in gels 9-37029
 Pb(N₃)₂, spontaneous explosion during growth 9-37040
 PbO single crystals, hydrothermal growth and phase width 9-37041
 PbTe, epitaxial, substructural transitions in early stages 9-26186
 PbTe, n- and p-types, prep. of low conc. high mobility mats. 9-39624
 PbTe on rocksalt, epitaxial deposits 9-37113
 Pb(ZrTi)O₃, single crystals, using KF-PbF₂-Pb(PO₃)₂ as a flux 9-48806
 Pd alloys, method for single crystals 9-39213
 Pd method for single crystals 9-39213
 PrP, transport reaction for growth 9-39197
 Pt, hydrothermal 9-37027
 α -Pu single cryst. from β to α solid-state phase transform. at high press. 9-35247
 RbFeF₆ from soln., X-ray diffraction powder study 9-26207
 Re pyrolytic deposition from ReCl₅ 9-39199
 Rh, single, by electron-beam zone melting 9-48807
 Rh method for single crystals 9-39213
 SbSI, of orientated fibriform cryst. 9-48808
 Se-Te system, single cryst. growth phenomena 9-36997
 Se amorphous films, effect of condensation velocity on crystn. 9-44649
 Se single crystals in gels at ambient temp. 9-37042
 Si, by reduction of SiCl₄ by hydrogen, mechanism 9-48794
 Si, from metal solns., infl. of solvent and impurities on habit and morphology 9-36981
 Si₃N₄ layers, deposition using photochem. reaction 9-46728
 Si deposition from SiCl₄ reduction, on graphite 9-37011
 Si epitaxial layers, chemically-deposited, growth and perfection 9-36951
 Si films, epitaxial, on Si substrate and oxide layer, role of surface migration 9-30491
 Si layer on Al₂O₃ substrate, method, patent 9-23667
 Si layers, epitaxially, from vapour phase through liq. alloy, low temp. deposition, patent 9-30530
 Si p-n junction, epitaxial, for photoelec. converters 9-31904
 Si primary spherulite growth and morphology in Al-(20wt.%)Si alloys 9-23775
 Si single epitaxy on sapphire 9-34990
 SiC, by vapour transport react. 9-28231
 SiC, mechanisms, review 9-26245
 SiC deposition from vapour and microstructure 9-39306
 SiC deposition from vapour and microstructure 9-23774
 SiO₂ thermal growth, use of Si₃N₄ as alkali barrier liner 9-33358
 SiP₂ orthorhombic single cryst., from Sn soln., p-type semicond. obs. 9-35022
 Sm_{1-x}Bi_xFeO₃, Bi substitution effect on mag.-reorientation temp. 9-32869
 Sn-(0.5-8.0)Bi alloys, Sn dendrite growth as function of supercooling 9-48815
 Sn-(1.0-6.0wt.%)Sb alloys, Sn dendrite growth as function of supercooling 9-48815
 Sn dendrites, as function of supercooling 9-48815
 Sn supercond. thin films 9-28481
 Sn whiskers by vapour deposition, electrooptical investigations 9-39218
 Sr₂CuSi₂O₇, and other analogs of akermanite, technique and crystal structure 9-35010
 Sr₂(VO₄)Cl, isomorphism with Cr spodiosite 9-35664
 Ta₂Si₃, by vapour transport react. 9-28231
 Tb single crystals, by three methods 9-37078
 Te, blade-like, from vapour 9-23668
 Te, Czochralski method 9-39214

Crystals continued

- Te, hydrothermal 9-37027
 Te whiskers, simultaneous, with CdTe crystals by vapour phase reaction 9-28232
 Th₃P₄, by Th powder and P vapour direct reaction, struct. obs. 9-35035
 Th oxychalcogenides 9-30519
 ThP, by Th₃P₄ decomposition, struct., obs. 9-35035
 TiO₂, hydrothermal conditions 9-37044
 TiO₂ using an induction plasma torch, in absence of H₂ 9-39198
 TiFeF₄ from soln., X-ray diffraction powder study 9-26207
 β -U₃O₈ monocystals 9-28233
 U oxychalcogenides 9-30519
 UB_x, by vapour transport react. 9-28231
 V oxy-carbonate, new 9-28236
 VC single cryst., floating zone technique 9-37090
 VO₂, thermal decomposition technique 9-28230
 VO₂ single-cryst. by isothermal flux evap. 9-28236
 VO₂ single-cryst. growth by isothermal flux evap. 9-28236
 VO₂ single-cryst. by chem. transport reaction using TeCl₄ 9-32872
 W, grain growth, e emission microscope obs. 9-37127
 W, from vapour rel. to texture 9-37152
 W pyrolytic deposition from WF₆ 9-39199
 W single, on glowing tips in N₂-H₂ mixture 9-26206
 Y₂-xBi_x(Ca₂Fe₂-xSi₂O₁₂ (x=0.6-1.3), crystallization from PbO/B₂O₃ solvent 9-37047
 Y₃Al₅O₁₂, Cr³⁺ and Nd³⁺ impurity distribution, rel. to trivalent oxide solubility and cry. growth 9-36980
 Y₃Al₅O₁₂, free from strained central core 9-28235
 Y₃Al₅O₁₂ using PbO-PbF₂ flux, melt composition effect on crystal habit 9-40922
 Y₃Fe₅O₁₂, Cr³⁺ and Nd³⁺ impurity distribution, rel. to trivalent oxide solubility and cry. growth 9-36980
 Y₃Ga₅O₁₂, using PbO-PbF₂ flux, melt composition effect on crystal habit 9-40922
 YAl garnet:Nd, imperfection assessment and control in crystals used for laser devices 9-37157
 YAl garnet, hollow cathode floating-zone method 9-37091
 YAl garnet single crystals, optical quality, incorporation of increased conc. of rare earth activator ions 9-37093
 YAl garnets, synthetic, inhomogeneities, optical investig. 9-37165
 YAlO₃, hollow cathode floating-zone method 9-37091
 YAsO₄, rare-earth doped, by oscillating temp. flux technique 9-39215
 YFe, preparation, improvement in yield 9-37092
 YFe garnet, seeded growth from molten salts 9-37045
 YFe garnet films, with narrow ferrimagnetic resonance linewidth, epitaxial 9-36952
 YFe garnet single crystals, from flux 9-37046
 YFe garnet single crystals, flux method, rel. to distribution of gallium 9-36979
 YPO₄, rare-earth doped, by oscillating temp. flux technique 9-39215
 YVO₄, rare-earth doped, by oscillating temp. flux technique 9-39215
 Yb₃Fe₅-xGa_xO₁₂ (x=0.5-4.0), crystallization from PbO/PbF₂ solvent 9-37047
 Zn-Cd alloy single cryst., orientation depend. of solute partition coeff. 9-37104
 Zn₂PtO₄ 9-32868
 Zn bicryst., from melt, grain boundary sliding anisotropy 9-40964
 Zn bicryst., from melt, grain boundary sliding anisotropy 9-40965
 Zn chalcogenides, from solution using tin as solvent 9-37073
 Zn electrodeposits on Cu single crystals 9-30490
 Zn growth form, alteration as result of diffusion non-homogeneity of super-saturation 9-37013
 Zn single cryst. from vapour in H atmosphere, cavities form. obs. 9-48799
 Zn spherical single cryst. from supersaturated vapour just below melting pt. 9-48798
 Zn whiskers, X-ray diff. topography of imperfections 9-35096
 ZnCr₂S₄(Se₄) single crystals 9-44646
 ZnIn₂S₄ single cryst., Stockbarger technique 9-35024
 ZnO films on 74-26 brass, early and thick scales stage obs. 9-26191
 ZnO single crystals by vapour phase reaction method 9-37012
 ZnO-B₂O₃ system, lamellar glass-cryst. structures grown from eutectic solidification 9-36930
 ZnS, from vapour, in vac. or inert atm., rel. to cryst. shape, stacking faults and polytypism 9-35099
 ZnS, from vapour, stacking faults distrib., rel. of polytypism 9-37184
 ZnS, from Ga and In melts 9-37095
 ZnS cubic, molten flux growth 9-37094
 ZnS epitaxial layers on Si, defects obs. by transmission electron microscopy 9-34994
 ZnS films evaporated on to NaCl, epitaxial growth 9-32844
 ZnS phosphors, prep. method effects on luminescence spectra 9-24470
 ZnS single large and needlelike 9-48795
 ZnSe, rapid non-detonative synthesis 9-37074
 ZnTe, rapid non-detonative synthesis 9-37074
 Zr, d crystals on W and Nb, temp. depend. for binding energy determ. 9-23652
 ZrB₃, r.f. induction heated floating zone method 9-37096
 Zr(HPO₄)₂, characts. and ion-exchange props. 9-26208
 Zr(HPO₄)₂·2H₂O, characts. and ion-exchange props. 9-26208
 ZrO₂, hydrothermal conditions 9-37044

hyperfine field interactions

- alloys, dilute, nearly ferromagnetic, Korringa relation breakdown 9-24503
 benzene in perdeuterobenzene cry., ESR of phosphorescent state, hyperfine and fine struct. obs. 9-35719
 electric field gradient at nuclear site including Sternheimer effect 9-47306
 ferromagnetic alloy, anisotropy of γ -radiation effect by oriented nuclei, orientation meas. by hyperfine interaction 9-37654
 ferromagnetic hosts containing dilute impurities 9-33493
 glass, soda-silica, Tm³⁺-doped, parameters determ. by Mossbauer effect 9-37702
 haemoglobin, e.p.r. of Fe and Cu, superhyperfine struct. rel. to Cu-N interaction 9-33641
 ion implantation, range and energy loss 9-30803
 ion implantation and mag. dipole hyperfine interaction meas. 9-31059
 ions, slowing down, appl. to hyperfine interactions meas. 9-30802
 isotope separators, various types and use for ion implantation expts. 9-29993

Crystals continued

hyperfine field interactions continued

- Jahn-Teller impurities dynamic, anisotropic part of hyperfine splitting, Zeeman eff. obs. 9-31057
- lattice nuclei near shallow donor, dipole-dipole hyperfine const. 9-37674
- matrix elements for d_{xy} config. in weak octahedral field 9-24348
- mesitylene in B-trimethylborazole cry., EPR of phosphorescent state, fine and hyperfine struct. obs. 9-24500
- metals, ferromagnetic, impurity fields 9-45255
- nitrosyliron bis(N,N-diethyldithiocarbamate) 9-39823
- nonmagnetic hosts containing dilute magnetic impurities 9-33493
- nuclear mag. energy levels in rotating frame, acoustic excitation 9-35601
- potassium aminedisulphate, quadrupole coupling in $N(SO_3)_2^-$ from e.s.r. meas. 9-39916
- potassium thiocyanate, gamma-irrad., pattern obs. in e.p.r. spectrum of radical species 9-45392
- rare-earth S-state ions hyperfine coupling const. in cubic cryst., temp. depend., theory 9-33496
- recoilless nuclear resonance spectra, pseudoquadrupole shift and asymmetric line broadening 9-24509
- relaxation effect on ang. correl. and distrib. of radiation from oriented nuclei 9-41351
- RKKY interaction between two mag. moments, soluble model 9-37380
- spin systems, strongly polarized, population transfer obs. 9-39901
- zeolites, effect of sorbed mol. on quadrupole coupling constants of ^{23}Na and ^{27}Al 9-43300
- Ag atoms stabilized in alkali halide crystals, theoretical anal. 9-37792
- Am, lowtemp. 9-47334
- Au-Fe alloys, in ^{57}Fe Mossbauer effect spectra, rel. to mag. ordering obs. 9-39817
- Au-Fe alloys at ^{197}Au 9-49259
- Au, 6s hyperfine-structure coupling constant pressure dependence, relativistic calc. in Wigner-Seitz model 9-26481
- BaF $_2$: $^{151}Eu^{2+}$ hyperfine coupling const., temp. depend. 9-33496
- BaF $_2$, of H atoms, temp. depend. 9-31060
- BaF $_2$, of V_K and V_L -centres, lattice vibrs. influence 9-43274
- BaO, isotropic and anisotropic hyperfine const. for F-centre 9-35109
- BaOF $_2$ O $_3$ h.f.s., Mossbauer obs., antiferromag. order 9-47283
- Ca $_2$ Fe $_2$ Ge $_2$ O $_8$ paramag. garnet, elec. quadrupole interac. of octohedral Fe $^{3+}$ 9-43221
- Ca $_2$ FeSi $_2$ O $_8$ paramag. garnet, elec. quadrupole interac. of octohedral Fe $^{3+}$ 9-43221
- CaCO $_3$:Pb $^{2+}$, e.p.r. obs. 9-41425
- CaF $_2$: $^{151}Eu^{2+}$ hyperfine coupling const., temp. depend. 9-33496
- CaF $_2$:U $^{4+}$, superhyperfine, in EPR and UPR spectra 9-39905
- CaF $_2$, ENDOR obs. of Gd $^{3+}$, transferred hyperfine interaction 9-49363
- CaF $_2$, H- and D- compensated tetragonal Ce $^{3+}$ centres, ENDOR 9-39927
- CaF $_2$, of H atoms, temp. depend. 9-31060
- CaF $_2$, of V_K and V_L -centres, lattice vibrs. influence 9-43274
- CaO, F $^+$ and F centres obs. 9-45382
- CaO, in e.s.r. spectrum obs. of paramag. lines due to ion impurities 9-45381
- CaWO $_4$:Eu $^{2+}$, crystal field splittings and hyperfine structure consts., 4.2, and 78°K 9-43200
- Cd $_2$ Fe $_2$ Ge $_2$ O $_8$ paramag. garnet, elec. quadrupole interac. of octohedral Fe $^{3+}$ 9-43221
- CdCr $_2$ S $_4$, $^{111,113}Cd$ n.m.r., isotropic fields and transferred spin polarization obs. 9-43297
- CdCr $_2$ S $_4$ (Se $_4$) chalcogenide spinels, hyperfine interac. of nuclei w.r.t. exchange interac., n.m.r. 9-31170
- CdCr $_2$ Se $_4$, $^{111,113}Cd$ n.m.r., isotropic fields and transferred spin polarization obs. 9-43297
- CeO $_2$:Gd $^{3+}$, hyperfine struct. anomaly for Gd 9-35733
- Co-Pd alloys, mag. fields on ^{60}Co and ^{119}Sn nuclei, e polarization 9-28620
- Co at ^{119}Sn , anomalous temp., dependence 900-1300°K 9-47330
- CoCO $_3$: ^{57}Fe , antiferromag., mag. field obs. and Fe ion relax. in Mossbauer spectra 9-41364
- Cs, relativistic analysis 9-24349
- CsFeF $_3$ structure from Mossbauer studies of ^{57}Fe , and magnetiz. meas. 9-45058
- Cu-Ni-Fe alloys, in ^{57}Fe Mossbauer effect spectra, rel. to mag. ordering obs. 9-39817
- Cu atoms stabilized in alkali halide crystals, theoretical anal. 9-37792
- Cu complex, diphenyl sulphoxide perchlorate, ESR obs. 9-24488
- Dy, calorimetric investigation 9-47305
- DyCrO $_3$ and paramagnetic relax. from ^{161}Dy Mossbauer effect 9-24379
- ErCrO $_3$, magnetic hyperfine structure from ^{166}Er Mossbauer meas., 4-40°K 9-24380
- Eu, Mossbauer effect meas. rel. to sublattice magnetiz. behaviour 9-45219
- EuFe garnets, elec. field gradients on Eu $^{3+}$ nuclei 9-35603
- Fe(48.2 at.%) Ni alloy, hyperfine mag. splitting on ^{57}Fe from Mossbauer spectrum 9-35636
- Fe(48.5 at.%) Rh alloy, anomalous hyperfine field at recoiled ^{103}Rh nuclei 9-35564
- Fe, ^{131}Cs Mossbauer spectra, positive mag. field 9-37699
- Fe, at ^{180}Hf nuclei, IMPACT study 9-45256
- Fe, containing implanted Pr, hyperfine field obs. using nuclear orientation 9-35604
- Fe, implantation perturbed ang. correl. expts. after inelastic proton scatt. 9-33494
- Fe, internal mag. field at Os after Coulomb recoil implantation 9-39765
- Fe, Mossbauer effect and obs. of band ferromag. 9-43166
- Fe $_3$ O $_4$ magnetite, ^{57}Fe Mossbauer spectrum 9-45295
- Fe containing Hf, hyperfine field obs. and g factors of ^{177}Hf 321 keV level 9-35606
- Fe containing Hf, hyperfine field determ. using Mossbauer expts. 9-35605
- Fe foil containing radioactive nuclei, perturbed ang. correls. meas. 9-35602
- Fe hyperfine mag. splitting on ^{57}Fe from Mossbauer spectrum 9-35636
- ^{57}Fe Mossbauer spectroscopy, hyperfine params. analytical calc. 9-24382
- FeCO $_3$, paramag. Fe $^{2+}$ interac., Mossbauer spectra 9-26723
- FeF $_3$, ^{57}Fe hfs, critical temp. depend. Mossbauer spect. meas. 9-24384
- Fe-Pd alloys, mag. fields on ^{60}Co and ^{119}Sn nuclei, e polarization 9-28620
- Fe. nucl. orientation/mag. reson. of $^{198,199}Au$, hyperfine anomaly, non-contact contrib. to effective field obs. 9-37805
- Gd, at ^{180}Hf nuclei, IMPACT study 9-45256

Crystals continued

hyperfine field interactions continued

- o-H $_2$ triangular cluster, energy levels due to quadrupole interactions in crystal 9-28646
- Hf compounds, of ^{181}Hf , quadrupole interaction, time differential ang. correl. studies 9-33497
- HgCr $_2$ S $_4$ (Se $_4$) chalcogenide spinels, hyperfine interac. of nuclei w.r.t. exchange interac., n.m.r. 9-31170
- K $_2$ CoF $_4$, antiferromag., transferred, n.m.r. meas. 9-45257
- K $_2$ NiF $_4$, paramag., ^{19}F NMR, hyperfine coupling obs. 9-37806
- K $_2$ PtCl $_6$, between quad-rupolar relaxation of ^{35}Cl and molecular rotation of PtCl $_6$ 9-31174
- K $_2$ ZnF $_4$:Co $^{2+}$, superhyperfine, e.s.r. meas. 9-45257
- K $_2$ ZnF $_4$:Mn single crystal, transferred, e.s.r. meas. 9-45387
- K $_3$ Fe(CN) $_6$, Mossbauer effect obs. 9-26725
- KCl, e.p.r. of stabilized Cu and Ag atoms, hyperfine and superhyperfine struct. consts., temp. depend. 9-35714
- KCl, F-centre hyperfine interaction constants, temp. depend. 9-46836
- KCl, superhyperfine, of H and D centres, zero-pt. vibr. influence, ENDOR obs. 9-45409
- KCl, wave function and isotropic h.f.s. of U $_2$ -centre 9-42850
- KClO $_3$ elec. quadrupole interaction of ^{40}K found by new resonance technique 9-29752
- KH $_2$ PO $_4$, quadrupole and Zeeman interactions, rotary saturation and spin calorimetry 9-28757
- LiCl, e.p.r. of stabilized Cu and Ag atoms, hyperfine and superhyperfine struct. consts., temp. depend. 9-35714
- LiCl, e.s.r. of Cu $^{2+}$ centres 9-43281
- LiF:Mn $^{2+}$, phonon-induced corrections to transferred hyperfine coupling 9-33628
- LiF:Mn $^{2+}$, from e.p.r. at 9.5 GHz 9-37798
- LiF, ENDOR hyperfine consts. and lattice distortion of V_K -type centres 9-46837
- LiF, F-centre hyperfine interaction constants, temp. depend. 9-46836
- LiF Mn $^{0+}$ coupling parameter temp. depend. 9-43282
- LiFe $_2$ Mn $_2$ PO $_4$ antiferromagnet, from Mossbauer spectrum 9-26726
- MgO: ^{57}Co , Mossbauer spectra, ^{57}Fe hyperfine interac. for multiple charge states 9-33530
- MgO:Mn $^{4+}$, rel. to tetragonal and octahedral sites of Mn $^{4+}$, e.s.r. obs. 9-24496
- MgO, e.s.r. from vacancy-pair centre, ^{25}Mg interaction obs. 9-47438
- Mn $_2$ Fe $_2$ PO $_4$ single cryst., anisotropic field due to local Jahn-Teller distortion in ^{55}Mn n.m.r. of ^{51}Mn at β -site 9-43299
- MnTe $_2$, antiferromag. and paramag., ^{125}Te Mossbauer obs. 9-43225
- MoD $_3$:V, e.s.r. 9-39907
- N(SO $_3$) $_2^-$ in potassium aminedisulphonate, quadrupole coupling for ^{14}N from e.s.r. meas. 9-39916
- Na $_2$ Fe(CN) $_5$ NO $_2$ H $_2$ O, nuclear effective-field-gradient and mean square displacement of Fe sites 9-24385
- Na $_2$ SO $_3$ 5H $_2$ O γ -irrad. single cryst., g- and ^{35}S hf-tensor parameters for trapped radicals 9-35716
- NaCl, e.p.r. of stabilized Cu and Ag atoms, hyperfine and superhyperfine struct. consts., temp. depend. 9-35714
- NaCl, Na nuclear mag. energy levels in rotating frame, acoustic excitation 9-35601
- NaCl, wave function and isotropic h.f.s. of U $_2$ -centre 9-42850
- NaF, ENDOR hyperfine consts. and lattice distortion of V_K -type centres 9-46837
- Nd, calorimetric investigation 9-47305
- Ni, Mossbauer effect and obs. of band ferromag. 9-43166
- NiFe, Ni hyperfine field and its application to the detection of long-range order 9-26637
- Ni $^{2+}$, e.s.r. ratio of cubic field and spin-orbit interac. parameters 9-28645
- NiFe $_2$ and cryst. field splitting, SCF-MO calc. 9-33495
- NiFe $_2$ O $_4$, substituted, Mossbauer study of mag. fields on Sn nuclei 9-26727
- Np, low temp. 9-47334
- NpAl $_2$, of ^{237}Np , and susceptibility meas. 9-47334
- NpC, of ^{237}Np , and susceptibility meas. 9-47334
- PrAl $_2$ cubic Laves cpd. from heat capacity meas. 0.1° to 1.0°K, rel. to mag. moment quenching 9-45071
- PrBi, paramag., as nuclear ordering mechanism 9-26669
- PrCo $_2$, cubic Laves cpd. from heat capacity meas., 0.1° to 1.0°K, rel. to mag. moment quenching 9-45071
- PrNi $_2$ cubic Laves cpd., from heat capacity meas. 0.1° to 1.0°K, rel. to mag. moment quenching 9-45071
- Pt-Fe system near Pt $_3$ Fe composition, temp. dependence from Mossbauer eff. 9-24275
- Rb, relativistic analysis 9-24349
- RbFeF $_3$, constants calc. and spin density determ. n.m.r. meas. 9-41435
- RbFeF $_3$, from n.m.r. of ^{19}F , ^{87}Rb and ^{85}Rb 9-28760
- Sc single cryst., orbital interaction, n.m.r. 9-49192
- Sm, calorimetric investigation 9-47305
- SrF $_2$: $^{151}Eu^{2+}$ hyperfine coupling const., temp. depend. 9-33496
- SrF $_2$, of H atoms, temp. depend. 9-31060
- SrF $_2$, of V_K and V_L -centres, lattice vibrs. influence 9-43274
- Ta cpds., (A=181), nuclear quadrupole constants interpretation 9-45258
- TmCl $_3$ 6H $_2$ O, recoilless nuclear resonance spectra, pseudoquadrupole shift and asymmetric line broadening 9-24509
- UF $_4$, n.m.r. of ^{19}F , dipolar broadening due to anisotropic interac. 9-33651
- YbFe garnet: Lu, supertransferred, temp. depend. 9-35607
- ZnO:Cu single cryst., e.p.r. $^{63,65}Cu$ obs. 9-35718
- ZnO:Gd $^{3+}$, e.p.r., interactions with odd Gd isotopes 9-33636
- ZnSe:Ge(Pb) impurities as hole traps, EPR meas. 9-35706
- ZnTe:Pb, e.p.r. of Pb $^{3+}$, hyperfine and superhyperfine structure from ^{207}Pb and ^{125}Te 9-47439

imperfections see Crystal imperfections

internal fields

see also Crystal field theory

- alkali dithioferates (III), mg. fields 9-43220
- Au-(10 at.%)In, Au-10%Zn alloys, electric field grad. shown to be not simply prop. to valence diff. of components 9-30780
- electric, determ. of electric field gradient at nuclear site and static quadrupole moment 9-47306
- electric field grad. shown to be not simply prop. to valence diff. of components 9-30780
- electron-wave interaction, transverse a.c. cond. calc. 9-24082
- ferromagnetic alloy, effective mag. field determ. by low-temp. nuclear orientation meas. 9-37654

Crystals continued**internal fields continued**

- ionic cry., elec. fields and polariz. prod. by defect charge density, lattice summations 9-33215
 ionic cry., electrostatic pots. and spatial deriv. about pt. defects 9-33214
 LaF₃:Gd³⁺ energy levels of Gd³⁺ from optical absorption spectra 9-33556
 magnetic field diffusion in ferromag. body 9-41734
 semiconductor, impure, effect on optical absorption 9-24402
 spinel, Ni²⁺ doped 9-43242
 CaF₂, ENDOR meas., comparison between Ce³⁺-H⁻ and Ce³⁺-F⁻ 9-37808
 CaF₂, elec. fields and polariz. prod. by defect charge density, lattice summations 9-33215
 CaF₂, electrostatic pots. and spatial deriv. about pt. defects 9-33214
 CaWO₃:Nd³⁺, cryst. field parameters 9-49232
 CdFe₂O₄, electric field gradient sign at octahedral site from Mossbauer spectrum 9-35633
 Co-Pd alloys, mag. fields on ⁶⁰Co and ¹¹⁹Sn nuclei, e polarization 9-28620
 electric field gradient sign at octahedral site from Mossbauer spectrum 9-35633
 EuFe garnets, electric field gradients, on Eu³⁺ nuclei 9-35603
 Fe, internal mag. field at Os after Coulomb recoil implantation 9-39765
 Fe(III) fluoro and bromo complexes 9-24409
 Fe-Pd alloys, mag. fields on ⁶⁰Co and ¹¹⁹Sn nuclei, e polarization 9-28620
 Gd³⁺ in 5 hexagonal crystals, energy levels 9-33555
 LaF₃:Ce³⁺ crystal field parameters based on hexagonal b//c// 9-28647
 LaF₃:Nd³⁺ crystal field parameters based on hexagonal symm. 9-28647
 LiNbO₃:Cr³⁺ 9-31104
 LiTaO₃:Cr³⁺ 9-31104
 MgF₂:Ce³⁺, lowest Stark sublevels of 4f¹, 5d¹ configurations determ. 9-22947
 NaCl, elec. fields and polariz. prod. by defect charge density, lattice summations 9-33215
 NaCl, electrostatic pots. and spatial deriv. about pt. defects 9-33214
 NaCl, electrostatic pots. and spatial deriv. about pt. defects 9-33214
 NaCl, in Na vacancy, appl. of lattice potential and energy calcs. 9-36974
 NiO, depend. of 10Dq on metal-ligand distance 9-39789
 PbMoO₄:Np³⁺ 9-31110
 Sm³⁺ in CaF₂ type I, trigonal crystal field energy levels 9-33244
 V₂As, normal, elec. field gradient from n.m.r. obs. 9-39923
 W, mean inner pot. from electron diffraction 9-28273
 YGa garnet:Yb³⁺, Raman-Zeeman obs. 9-49300
 ZnS:Ni²⁺, spin-orbit coupling and cryst. field parameters 9-33435

lattice mechanics

see also Mossbauer effect

- adenosine, i.r. absorption spectra, 230-30 cm⁻¹, 20 to -175°C, crystal lattice vib. anal. 9-25783
 adsorbed surface layer on model cryst. vibr. props. 9-37311
 alkali halide, phonon broadening in U bands 9-46830
 alkali halide mixed crystal of LiCl-RbCl type, optical vibrations 9-39512
 alkali halides, anharmonicity rel. to i.r. absorpt. 9-47348
 alkali halides, Debye-Waller coeffs. of ions 9-30507
 alkali halides, dynamical matrix and three-body overlap forces, coupling coeffs. 9-39506
 alkali halides, freqs. of localised modes due to U-centres 9-35265
 alkali halides, influence of heavy impurities on optical vibrations 9-39512
 alkali metals, vacancy, relax and migration energy, lattice-dynamical calc. 9-23792
 alkali metals, volume depend. electron-lattice interaction rel. to thermoelectric power parameter 9-33402
 alloys, disordered, phonon freq. spectra, interpolation formula 9-44807
 amorphous substance, vibration spectrum, calc. by variational method 9-42941
 anharmonic, theory of interatomic pot. 9-30759
 anharmonic cryst., linear chain props. 9-35264
 anharmonic cryst., theory 9-31356
 anharmonic terms in elastic energy of ideal crystals 9-26414
 anharmonic-vibration theory of diffusion 9-44723
 anharmonicity and thermal diffusion scatt. in structure factor determ. by elastic scatt. of X-rays and neutrons 9-24014
 anisotropic cubic crystals, polarization vectors of lattice vibrations 9-26406
 benzene isotopic mixed crystals, site effects in vibr. spectrum 9-43007
 β-brass, phonon spectrum, long-range order parameter influence 9-39396
 c LiF(001) surface modes, correl. with preferential scatt. of Ar 9-42714
 caesium halides, three-body interaction rel. to stability 9-24005
 CaF₄:U⁴⁺, spin-phonon interaction from u.s. paramag. resonance 9-33623
 chemisorption energy, influence of lattice vibrations calc. 9-47460
 constant, phonon emission spectra, thermal radiation obs. 9-42944
 crystal, anharmonic, stability conditions determ. using two-time Green function 9-42940
 cubic crystals, behaviour of constant freq. surfaces near (111) direction 9-24004
 cubic crystals, localised modes, molecular model 9-35265
 cubic lattices with long-range interactions, dispersion relations and freq. spectra 9-39505
 cytidine, i.r. absorption spectra, 230-30 cm⁻¹, 20 to 175°C, crystal lattice vib. anal. 9-25783
 Debye-Waller factors, anharmonic contribs. 9-26404
 diamond, Debye temp. at low temps., X-ray meas. 9-24043
 diamond, phonon contribution to surface entropy 9-23617
 diamond, semicond., role of phonons in oscillatory photoconductivity spectrum 9-41258
 diamond structures, lattice vibrs. symm., theory 9-23999
 diamond-like structures, heat capacity and quasi-chaotic dynamics 9-33180
 diamond-type, electron interaction with short-wavelength vibrations, rel. to effective carrier mass 9-44874
 diatomic cubic lattice, localized vibrations of line defects 9-30755
 2,3-dibromobutane, vibrational assignments and force consts. 9-34663
 2,3-dibromopentane, vibrational assignments and force consts. 9-34663
 dielectric, second sound and heat transfer for large drift velocities of phonon gas 9-37363
 dielectric crystals, second sound and phonon Poiseuille flow, effect of Umklapp-processes 9-46968
 diethyltin oxide, dynamic anisotropy and line asymmetry from Mossbauer eff. 9-39822
 disordered diatomic chain, vibrs. 9-44808
 disordered state, Green functions for 'one-body' eqn. description 9-33219
 dynamics, condensed systems total electronic energy as function of nuclear displacements 9-24003
 dynamics, electron total energy expansion 9-24001
 dynamics, electronic contrib. to dynamical tensor 9-24002
 dynamics, quantum theory 9-24000
 dynamics, shell model derivation and relation to dielectric constant theory 9-35262
 elastic vibrations interac. with spin-waves 9-28599
 electronic excitation energy, role of lattice vibrations in transfer process 9-33220
 ethylene and ethylene-d₄ cryst., far i.r. vibr. 9-45333
 Euclidean, invariant states, props. and symmetry 9-23992
 f.c.c. cryst., surface atoms mean square displacements and vels., temp. depend. 9-44806
 f.c.c. cryst. with point defects, force-const. changes effect on coherent neutron scatt. 9-42953
 ferroelectric, KH₂PO₄-type, acoustical phonons and sound attenuation 9-39693
 ferroelectric, rel. to critical scattering and dielec. props. 9-49141
 ferroelectric crystal, one phonon differential neutron scatt. cross section, calc. 9-48943
 ferroelectrics with tungsten-bronze struct., vibrs., Raman meas. 9-41079
 ferromagnets, semi-infinite, volume and surface phonon and magnon states, annihilation probabilities 9-26630
 force consts. relationship with quadrupole coupling consts. 9-42363
 frequency spectrum and momentum autocorrelation function 9-37310
 graphite quasisarmonic freq. shifts of adsorbed He and Ne atoms 9-48769
 group II-VI compounds 9-46969
 group II-VI compounds, semicond., optical studies 9-46982
 group III-V semiconductors, freqs. of localised modes due to substitutional impurities 9-35265
 group IV-VI cpds, cubic, semiconductors rel. to dielec. props. 9-39666
 group IV-VI cpds, n scatt. obs. rel. to ferroelectricity 9-39680
 guanosine, i.r. absorption spectra, 230-30 cm⁻¹, 20 to -175°C, crystal lattice vib. anal. 9-25783
 h.c.p., freq. distrib. functions calc., FORTRAN computer program 9-33158
 helical polymer mols., hyperpolarizability and i.r. phonon dispersion 9-32541
 hydrates, neutron inelastic scatt. obs. of librational freqs. 9-42955
 ice, dynamic model of l.f. vibration 9-24013
 ice, far-i.r. spectra of orientationally-ordered and -disordered phases 9-33557
 impurity atoms, two-electron-eigenstates of (sp)³P multiplet and phonon-induced optical transitions 9-41372
 impurity interaction with lattice vibrations 9-30757
 impurity magnons, spin-wave theory 9-28598
 impurity resonance mode localization 9-24006
 inert gas solids, h.c.p., phonon spectrum and zero point energy 9-23998
 inert gases, dynamical surface props. by molecular dynamics method 9-39191
 inert gases, dynamical surface props. in quasisarmonic approximation 9-39190
 insulating cryst., use of models of forces between atoms 9-44635
 interstitial impurities in crystals, lattice vib. spectrum, theory of substitutional solid soln. 9-40930
 iodurene, vibr. study by Raman and i.r. spectra 9-44813
 ionic, with homopolar bonding, vibration spectrum and thermodynamic functions 9-24009
 ionic cryst., semi-infinite, normal modes 9-44809
 ionic cryst., strong phonon interactions in photo-Hall mobility 9-39701
 ionic crystals, Reststrahlen frequency 9-30756
 isopropyl bromide, vibrational assignments and force consts. 9-34663
 isotopic defect, response func., photon scatt. cross section eqn. determ. 9-24007
 lattice with two-dim. defect, natural vibrations 9-42943
 localised modes in cubic crystals, molecular model 9-35265
 localized modes, fundamental lattice vib. absorpt., temp. depend., calc. 9-33153
 localized vibn. mode during adsorption, modification of energy and preexponential factor 9-48768
 magnetic materials, parametric excitation of phonons by parallel pumping 9-37308
 magnetic materials, phonons parametric excitation by parallel pumping 9-37640
 metal, Debye-Waller factors, temp. depend. 9-35261
 metals, normal and supercond., microwave phonon-electron interac. 9-37384
 methylchloroform, cryst. and plastic, rel. to far i.r. absorpt., obs. 9-24419
 mixed linear chains, vibration spectrum, at displacements and i.r. absorpt. 9-24401
 molecular crystals, group-theoretical anal. 9-41075
 molecular torsional vibrations, dynamics 9-26402
 monatomic, thermal vibrs. obs. 9-46965
 monatomic cubic cryst., accidental degeneracies of phonons 9-28408
 naphthalene, low freq. phonons near Brillouin zone boundaries 9-24020
 neodymium ethylsulphate, paramag. relaxation, phonon re-absorption and spectral spin diffusion 9-33491
 neutron dispersion in system of one-dimensional anharmonic oscillator, exact results 9-30765
 neutron scatt. by mols., theory 9-48656
 non-cubic, quasilocal phonon vibrational states, special form 9-33154
 nonlinear effects, theoret. treatment in second-quantization representation 9-23997
 nonpiezoelectric, transverse microwave phonons, magnetostriuctive generation 9-45272
 one-dimensional crystals, vibrations and surface modes 9-28407
 one-phonon reson. in coherent inelastic neutron scatt., position and widths assignment, data analysis method 9-30764
 optical phonons, exciton-enhanced Raman scatt., theory 9-35670
 oscillations, long-wave, in ionic crystals 9-26407
 paramagnetic crystal, ion-phonon interaction, effect on resonance absorpt. of γ quanta 9-33524

Crystals continued**lattice mechanics continued**

Crystals continued

lattice mechanics continued

- paramagnets, coupled spin-phonon modes, interpret. of excitation energies 9-49193
- particle near lattice point, distribution function 9-26401
- phonon bottleneck, temp. depend. on spin resonance line shape determ. 9-23996
- phonon breakdown 9-23994
- phonon conductivity rel. to thermal and elec. 9-24060
- phonon decay, spontaneous, umklapp processes, contrib. to thermal resistivity 9-41074
- phonon effects and photoconductivity, conf. 9-39702
- phonon emission spectra, thermal radiation obs. 9-42944
- phonon energy spectrum including magnon contrib. 9-46967
- phonon instability in phonon-electron system in mag. field 9-26472
- phonon scattering by Cottrell atmospheres surrounding dislocations 9-46966
- phonon spectra of partially cryst. materials, microwave and far i.r. absorpt. 9-35263
- phonon-electron interaction in pseudo-potential theory 9-28442
- phonon-enhancement in electronic thermal expansion 9-44838
- phonons, interaction with surface acoustic waves 9-28416
- phonons, low-q, peak broadening in low energy electron diff. 9-32889
- phonons, transverse, microwave, magnetostrictive generation in nonpiezoelec. crystals 9-45272
- photoconducting materials, vibrations interaction with electron hole plasma 9-26415
- piezoelectric materials, vibrations interaction with electron hole plasma 9-26415
- polar impurities motion in alkali halides, effect of localized lattice vibr. 9-33159
- polarization vectors of vibrations in anisotropic cubic crystal 9-26406
- poly 1,4-bis(β hydroxyethoxy) phenylene adipat, vib. forms from i.r. spectrum 9-37734
- polyethylene, lattice freq. analysis of crystalline and fold structure 9-46710
- polyethylene, multiphonon contribs. to directional phonon freq. functions 9-46981
- polymers, crystalline and glassy, Gruneisen const. and thermal props. 9-46979
- powdered inorg. crystals, i.r. freqs., interpretation 9-31111
- pyridinium H-bonded halides, i.r. and Raman lattice modes 9-49290
- quantum crystals, transport theory of phonon gas 9-30758
- quantum crystals with large amplitude anharmonic vibrations, theory 9-46963
- α -quartz, anharmonic props. rel. to Raman linewidth and shift temp. dependence 9-24428
- quartz, phonon interactions at degeneracies of acoustic phonon branches 9-48947
- quartz thermal emission of phonons obs. 9-30761
- radiation damage model including thermal vib. of atoms 9-41114
- random, self-contained first-order approx. accounting for exclusion effect 9-24008
- Reststrahlen frequency in ionic crystals 9-30756
- sapphire, thermal emission of phonons obs. 9-30761
- second sound, microscopic theory and damping 9-39504
- semiconductor, carriers mixed scatt. on acoustic lattice vibrs., parameter determ. 9-37509
- semiconductor, III-V, localised modes obs. 9-44810
- semiconductor, resonant phonon interactions effect on absorpt. line shapes 9-26741
- semiconductors, current saturation, theory of electron-phonon interaction 9-44953
- semipolar crystals 9-46969
- spin-phonon system, thermal noise analysis 9-30760
- spin-phonon systems, thermal noise 9-37309
- superconducting metals, microwave phonon-electron interac. 9-37384
- superconductors, phonon microwave excitation 9-26405
- thermal diffuse scatt. contrib. to integrated Bragg scatt. intensities 9-23716
- thin films, surface vibration modes 9-48945
- thin films quantum theory of atomic vibrations 9-23995
- three-body interaction in ionic crystals 9-24005
- thymidine, i.r. absorption spectra, 230-30 cm^{-1} , 20 to -175°C , crystal lattice vib. anal. 9-25783
- Umklapp processes w.r.t. resistivity maximum during Guinier-Preston zone form. 9-37431
- urea, vibrations, i.r. Raman meas. 9-48948
- uridine, i.r. absorption spectra, 230-30 cm^{-1} , 20 to -175°C , crystal lattice vib. anal. 9-25783
- u.s. three-phonon interactions in single-crystals, theory 9-42942
- u.s. waves at microwave freqs. interactions with lattice vibrations 9-33170
- Van Hove singularities, effect on specific heat 9-41091
- vibrating lattice, interaction of Mott-Wannier excitons through phonon modes, pot. energy operator 9-33234
- vibration absorpt., fundamental, by localized modes, temp. depend., calc. 9-33153
- vibrational modes, i.r. absorpt. lines, temp. depend. 9-33157
- vibrational self-entropy of point defect, pseudomol. model 9-48944
- v.s. vibrational modes in resonating crystal by X-ray diff. topography 9-39226
- Watson integrals evaluation, effect of defects on vib. and spin wave spectrum 9-34039
- zincblende structures, lattice vibrs. symm., theory 9-23999
- ^{119}Sn monomeric and polymeric cpds., anisotropic Lamb-Mossbauer factor, influence of bonding 9-27915
- Ag-Au solid soln., vibrational entropy and thermal vibrations, correlation 9-33151
- Ag, phonon dispersion relation for symmetry directions 9-46970
- Ag, Kreb's lattice dynamics model for electrical resistivity calc. 9-35339
- AgCl, vibration spectrum and thermodynamic functions 9-24009
- Al-Ag dilute solid solution alloys, vibrational entropy, electronic influence 9-39508
- Al-Zn dilute solid solution alloys, vibrational entropy, electronic influence 9-39508
- Al, anharmonic phonon widths, shifts and dispersion curves, wave number depend. 9-35266
- $\alpha\text{-Al}_2\text{O}_3$ symmetry props. of normal modes of vib., group theory anal. 9-39507

Crystals continued

lattice mechanics continued

- Al_2O_3 , non-collinear phonon interac. mechanism applic. to u.s. absorpt. of transverse waves 9-39519
- Al granular films, phonon spectrum rel. to superconductivity enhancement mechanism 9-24150
- Al with point defects, force-const. changes on coherent neutron scatt. 9-42953
- AlN, microcryst., surface modes and finite size effects, i.r. absorpt. meas. 9-37717
- AlN, phonon structure of Mn^{4+} activator centres 9-24010
- Au, Kreb's lattice dynamics model for electrical resistivity calc. 9-35339
- $\beta\text{-B}$, rhombic, lattice vibr. spectrum, band edge and free carrier absorpt. 9-39834
- BaF_2 , anharmonicity and thermal diffuse scatt. in neutron analysis of structure factors 9-24014
- BaF_2 , vibr. atom, Edgeworth map. rel. to smearing function 9-42954
- BaF_2 , vibrs. influence on h.f.s. const. of V_L and V_T -centres 9-43274
- $\text{Ba}(\text{OD})_2\cdot\text{D}_2\text{O}$, lattice vibration spectrum 9-33167
- BaTiO_3 , critical fluctuations from n scatt. obs. 9-33386
- BaTiO_3 , dynamical model for displacement correlation of Ti-ions and anomalies of X-ray scattering 9-35267
- BaTiO_3 , Mossbauer γ -rays scatt. by opt. phonons assoc. with paraelec. ferroelec. phase transition 9-39691
- BaTiO_3 , rel. to critical scattering and dielec. props. 9-49141
- BaTiO_3 , tetragonal, polaritons and TO phonons in Raman scatt. 9-35671
- Be, hexagonal, vibrational spectrum 9-42946
- Be, phonon dispersion relations, pseudopotential calcs. 9-24011
- BeO , normal vibr. modes, expt. and theory 9-42945
- Bi, supercond. amorphous, phonon spectrum by electron tunneling, transition temp. obs. 9-41076
- C fibres, longit. vibrations along c-axis, neutron spectrometry 9-28414
- CO , vibrs., freq. distrib., low temp. 9-41077
- $\text{Ca}_{10}(\text{PO}_4)_6\text{F}_2$, coupled PO_4^{3-} vib. 9-37317
- CaCO_3 , symmetry props. of normal modes of vib., group theory anal. 9-39507
- $\text{CaF}_2\text{:Tm}^{2+}$ acoustical phonon tunable detector 9-26403
- CaF_2 , vibrs. influence on h.f.s. const. of V_L and V_T -centres 9-43274
- CaO , phonon dispersion curves 9-39509
- $\text{Cd}_{1-x}\text{Zn}_x\text{S}$, i.r. active lattice modes from reflectivity spectra 9-47343
- $\text{Cd}_2\text{Zn}_{1-x}\text{S}$ mixed semicond., phonon vibr. spectrum 9-42947
- CdGeAs_2 , semicond. amorphous, Debye model calc. of phonons mean free path 9-37367
- CdO , phonon effects on i.r. absorpt. spectrum 9-24404
- CdO , vibrations effect on optical props. 9-35613
- CdS , acousto-electric phonon generation, X-ray diff. microscopy obs. 9-46997
- CdS , carrier scattering by acoustic mode of lattice 9-33297
- CdS , phonon spectra of acoustic domains 9-37312
- CdS , properties using phonon dispersion model 9-46972
- $\text{CdS}_{1-x}\text{Se}_x$, photon-phonon interactions in Raman spectra 9-26752
- $\text{CdS}_{1-x}\text{Se}_x$ mixed-crystal system, phonon freqs. from i.r. reflectance and transmittance spectra 9-46971
- CdS multiple-phonon-resonance Raman eff., reln. with fluorescent-emission spectrum 9-26754
- CdS multiple-phonon resonant Raman scatt., frequency spectra of higher orders 9-26753
- CdTe , local vibrational mode of Br, i.r. absorpt. 9-45317
- CdTe , vibration modes of Be, i.r. absorpt. 9-45318
- CeF_3 , optical phonons in polarized i.r. reflectance 9-47345
- Cl, Raman frequencies 9-43245
- $\alpha\text{-Cr}_2\text{O}_3$, inelastic magnon scattering dispersion relns. including exchange integrals 9-35585
- CsBr , localized vibrational modes of U centres in i.r. absorpt. 9-26294
- CsBr , vibrations group theory analysis, wave vector group and phonon dispersion reln. 9-35268
- CsCl , localized vibrational modes of U centres in i.r. absorpt. 9-26294
- $\text{CsI:Li}^+(\text{Na}^+, \text{K}^+, \text{Rb}^+, \text{TI}^+)$ impurity induced far i.r. absorpt., rel. to phonon density 9-37720
- CsI , localized vibrational modes of U centres in i.r. absorpt. 9-26294
- $\text{Cu}(15 \text{ at.}\%)\text{Al}$ deformed alloy cryst., phonon scatt. by dislocations, thermal conductivity meas., low temp. 9-35291
- Cu-Al alloys, dislocation phonon scattering values from thermal conductivity and dislocation density meas. 9-41078
- Cu-Zn alloys, dislocation phonon scattering values from thermal conductivity and dislocation density meas. 9-41078
- Cu-Zn alloys, dispersion relations for lattice vibrations from neutron scattering 9-30766
- Cu , anharmonic-vibration theory of diffusion 9-44723
- Cu , Debye-Waller factor of ^{57}Fe 9-41082
- Cu , dispersion curves, extended Bhatia model method 9-24012
- Cu , Kreb's lattice dynamics model for electrical resistivity calc. 9-35339
- Cu , phonon dispersion relations 9-37313
- Cu , phonon relaxation time rel. to contribution to temp. depend. of Hall coeff. 9-28467
- Cu , phonon scattering by edge dislocations, thermal resistivity 9-26446
- CuCl , lattice vibrs., rigid ion model applic. 9-46973
- Dy, spin-phonon coupling mechanism in critical sound scatt. near Neel temp. 9-24027
- Fe-Si alloys, magnon dispersion relationships 9-24297
- $\alpha\text{-Fe}$, phonon dispersion relations calc. from Sharma-Joshi theory, specific heat calc. 9-48946
- Fe_2O_4 , atomic vibration, mean square amplitude determ. 9-41081
- FeS_2 , i.r. active modes from reflectivity spectra 9-46974
- Ga, lattice vibrations, group-theoretical analysis 9-35269
- Ga, phonon dispersion relation, neutron inelastic scatt. obs. 9-33160
- Ga, supercond. amorphous, phonon spectrum by electron tunneling, transition temp. obs. 9-41076
- GaTe , phonon mechanism of heat transport, temp. depend. 9-33194
- GaAs:Cu , vibrations, local and structure of impurity centres 9-33231
- GaAs:Si , compensated, local mode absorpt. and defects 9-47357
- n-GaAs, generation and detection of 10^{12} Hz phonons 9-49083
- n-GaAs, h.f. phonon generation and detection 9-39520
- GaAs, n-type, non-degenerate, epitaxial, thermal displacement of longit. magnetophonons 9-26546
- GAP, acoustical and optical phonons, energy determ. from absorpt. spectrum 9-43239
- GAP, localized vibrational modes of impurities, i.r. absorpt. obs. 9-35657
- GAP, quasi-chain dynamics for heat capacity calc. 9-33180

Crystals continued

Lattice mechanics continued

- Ge, anharmonic isotropic continuum model calcs. for thermal conductivity 9-26449
- Ge, Debye-Waller factor and anomalous X-ray absorpt., 293-5°K 9-23758
- GeTe, phonon temp. dependence calc. rel. to ferroelectricity 9-39692
- group IV-VI cpds., phonon temp. dependence calcs. rel. to ferroelectricity 9-39692
- H₂-D₂ solid solution, fundamental bands at 4°K 9-28684
- o-H₂, solid, spin-lattice coupling, low-temp. thermodynamic effects 9-44811
- HBr and DBr, Raman vibr. 9-43246
- HCl and DCl, Raman vibr. 9-43246
- He, vibrational props., harmonic coupling parameters 9-23573
- HgSe, phonon-phonon and phonon-Hg interstitial scatt., ratio determ. from meas. of thermal conductivity 9-28409
- HgTe-CdTe crystal, thermal cond., thermopower and sp. ht. rel. to composition and lattice dynamics 9-26450
- Ho, paramag., phonon dispersion relations, neutron spectrometry 9-28415
- Ho, spin-phonon coupling mechanism in critical sound scatt. near Neel temp. 9-24027
- n-InSb, three-phonon process between amplified and thermal phonons w.r.t. decay of acoustoelec. domain 9-35402
- K, Mossbauer obs., recoilless fraction and thermal shift for 29.4 keV transition in ⁴⁰K 9-42952
- K, phonon frequencies from electron-phonon interaction modification with correlation effects 9-35308
- K, vibr. normal modes freqs. and lifetimes, anharmonic effects 9-46975
- K, vibrational spectrum, computation 9-39510
- KBr:CN, phonon resonant scatt. 9-26408
- KBr:H⁻, local mode frequency computation, relaxed and unrelaxed lattice 9-28410
- KBr:Li⁺, lattice resonant modes, stress-induced shifts 9-24015
- KBr:Li⁺, off-centre behaviour lattice parameter dependence 9-35087
- KBr:NO₂⁻, phonon resonant scatt. 9-28411
- KBr:Ti³⁺, electron-lattice interaction, absorption spectra meas. 9-41386
- KBr, F centre, rel. to electronic Raman spectra and lattice and electronic absorptions 9-35118
- KBr and KBr:KOH, O⁻ centres as strong phonon scatterers, thermal conductivity obs. 9-42949
- KCl:CN, phonon resonant scatt. 9-26408
- KCl:Li, microwave freq. phonon generation 9-26409
- KCl:Li, phonon reson. scatt. obs. from thermal conductivity meas., isotope and elec. field effects 9-42948
- KCl:Li⁺, off-centre behaviour lattice parameter dependence 9-35087
- KCl:NO₂⁻, phonon resonant scatt. 9-28411
- KCl, anharmonic thermal vibrations, X-ray meas., 300° to 800°K 9-44812
- KCl, anharmonicity and thermal diffuse scatt. in X-ray determ. of structure factors 9-24014
- KCl, F centre, rel. to electronic Raman spectra and lattice and electronic absorptions 9-35118
- KCl, phonon dispersion curves at 115°K 9-46976
- KCl, phonon dispersion relations at 80 and 300 K 9-33161
- KCl and KCl:KOH, O⁻ centres as strong phonon scatterers, thermal conductivity obs. 9-42949
- KCl:Ti³⁺, electron-lattice interaction, absorption spectra meas. 9-41386
- KH₂PO₄-type ferroelec. cryst., acoustical phonons and sound attenuation 9-39693
- KH₂PO₄, rel. to critical scattering and dielec. props. 9-49141
- KI:Ag⁺, lattice resonant modes, stress-induced shifts 9-24015
- KI, dispersion relations 9-30762
- KI, F centre, rel. to electronic Raman spectra and lattice and electronic absorptions 9-35118
- KI:Ti³⁺, electron-lattice interaction, absorption spectra meas. 9-41386
- KMnF₃, soft phonon modes, neutron scatt. obs. 9-33155
- KTaO₃, soft optic mode interaction in u.s. attenuation 9-24025
- LaF₃, optical phonons in polarized i.r. reflectance 9-47345
- LaMg(NO₃)₃:Ce, phonon avalanche, lifetime and acoustic spectrum meas. 9-39511
- Li, phonon freq. and Gruneisen parameters, pseudopotential calcs. 9-26410
- Li, phonon frequencies from electron-phonon interaction modification with correlation effects 9-35308
- Li, vibrations and nonlocal model potential 9-26411
- LiF:H⁻(D⁻), i.r. absorption due to localized vibrations of ions 9-30619
- LiF:Mn²⁺, phonon-induced corrections to transferred hyperfine coupling 9-33628
- LiF dislocation-phonon interaction, damping const., u.s. obs. 9-37179
- LiF dislocation-phonon interaction, damping const., u.s. obs. 9-37179
- Mg, hexagonal, vibrational spectrum 9-42946
- Mg, phonon dispersion relations calc. from model pot. 9-37316
- MgF₂, phonon scattering, correlation of anisotropic features with thermal conductivity 9-28412
- MgF₂ single cryst., phonon propag., anisotropic phonon-phonon scatt. 9-37314
- MgO:Cr, phonon scatt. by paramag. ions, from thermal magnetoresist., 0.4-4.0°K 9-33162
- MgO:Fe²⁺, microwave phonon detection by phonon-photon double-quantum transitions 9-37315
- MgO:Ni²⁺, spin-phonon interactions, molecular orbital theory 9-39787
- MgO, acoustic paramag. reson. interpret. including anharmonic forces and random lattice strains 9-24346
- MgO, phonon dispersion curves 9-39509
- MgO, phonon scatt. by paramag. ions, from thermal magnetoresist., 0.4-4.0°K 9-33162
- Mn_{0.5}Zn_{0.5}Fe₂O₄, atomic vibration, mean square amplitude determ. 9-41081
- Mn₃-Fe₂O₄, Debye-Waller factor meas. from Mossbauer spectra 9-37701
- Mn₂Fe₂O₄ ferrites, cubic and tetragonal, vibr. classification from i.r. absorpt. spectra analysis 9-39841
- MnO, phonon frequencies from reststrahlen spectrum analysis 9-24398
- Mo, phonon dispersion relations calc. from Sharma-Joshi theory 9-48946
- Mo, vibration modes 9-35270
- NH₄Cl, below -30.5°K, force const., dispersion curves, freq. spectra 9-28413

Crystals continued

Lattice mechanics continued

- NH₄Cl, vibr. normal modes, coherent inelastic neutron scatt. meas. 9-46980
- NH₄ClO₄, molec. freedom of NH₄ ion 9-48970
- NaK_{1-x}TaO₃, optical phonons rel. to dielec. phase transitions, 4-600°K 9-47366
- Na bond energy and lattice const., construction of crystal using quantum mechanics 9-42950
- NaBa₂Nb₂O₁₃ and related ferroelectrics, vibr., Raman meas. 9-41079
- NaCl:Cu²⁺, i.r. obs., resonant mode broadening 9-33164
- NaCl-type, model 9-46964
- NaCl, anharmonic thermal vibrations, X-ray meas., 300° to 800°K 9-44812
- NaCl, F centre, rel. to electronic Raman spectra and lattice and electronic absorptions 9-35118
- NaCl, phonon dispersion relations from n scatt. meas. at 80 and 300°K 9-24021
- NaCl:Ti³⁺, electron-lattice interaction, absorption spectra meas. 9-41386
- NaF:H⁻(D⁻), i.r. absorption due to localized vibrations of ions 9-30619
- NaF, and second-order Raman spectrum 9-35673
- NaF, normal modes of vibr. obs., freq. spectra 9-46977
- NaI:NaCl, gap and resonant modes assoc. with Cl⁻ impurity from far i.r. absorpt. spectrom. 9-24413
- NaNO₂, ferroelec., rel. to temp. depend. of far i.r. absorption 9-33163
- NaNO₂, rel. to critical scattering and dielec. props. 9-49141
- Nb, Kohn anomalies 9-24017
- Nb, phonon freq. meas. 9-24016
- NdF₃, optical phonons in polarized i.r. reflectance 9-47345
- Ne, Buckingham potential, anharmonic parameters 9-33152
- Ne, phonon dispersion relations for cryst. at 2 densities, coherent inelastic neutron scatt. obs. 9-46978
- Ne, phonon spectra theor. temp. depend., phonon Green function calc. 9-26413
- Ni-Fe alloys, dispersion relations for lattice vibrations from neutron scattering 9-30766
- Ni, atomic vibr. and relax. at (110) surface, calc. 9-35271
- Ni, Debye-Waller factor 9-28427
- Ni, dispersion curves, extended Bhatia model method 9-24012
- NiFe₂O₄, atomic vibration, mean square amplitude determ. 9-41081
- Pb-Tl dilute solid solution alloys, vibrational entropy, electronic influence 9-39508
- Pb, energy wave-number charact. from exptl. phonon freqs. 9-44871
- Pb, phonon emission spectra, thermal radiation obs. 9-42944
- Pb, phonon spectrum by tunneling and n. scatt. meas. 9-26413
- Pb, phonon spectrum pressure depend. from tunneling meas. 9-24018
- Pb, phonon spectrum pressure dependence from tunneling meas. 9-33165
- Pb₄₀Tl₆, phonon spectrum by tunneling and n. scatt. meas. 9-26413
- Pd, Debye-Waller factor of ⁵⁷Fe 9-41082
- PrF₃, optical phonons in polarized i.r. reflectance 9-47345
- Pt, Debye-Waller factor of ⁵⁷Fe 9-41082
- Rh, phonon frequencies from electron-phonon interaction modification with correlation effects 9-35308
- Se-Te mixed cryst., long wavelength optical lattice vibr., i.r. reflectivity obs. 9-39826
- Si:Bi, resonant phonon interactions effect on absorpt. line shapes 9-26741
- SiC, cubic, phonon-dispersion curve calcs. 9-24019
- SiO₂, glassy state, vibrational analysis 9-28198
- SnS, dynamic anisotropy and line asymmetry from Mossbauer eff. 9-39822
- SnTe, phonon temp. dependence calc. rel. to ferroelectricity 9-39692
- SnTe soft phonon k=0 TO mode, low temp. region 9-37318
- SrF₂:Tm³⁺ acoustical phonon tunable detector 9-26403
- SrF₂, vibr. influence on h.f.s. consts. of V_L and V_T centres 9-43274
- SrO, phonon dispersion curves 9-39509
- SrO, phonon dispersion curves configs. from elastic props. obs. 9-48883
- Sr(OD)₂.D₂O, lattice vibration spectrum 9-33167
- SrTiO₃:Eu³⁺, impurity-lattice coupling to optical phonons 9-33166
- SrTiO₃, normal vib. modes. rel. to antiferroelec. phase transition at 110°K 9-24223
- SrTiO₃, soft-mode instability at [111] zone boundary in 110°K phase transition 9-23986
- SrTiO₃, soft optical phonon, neutron scatt. obs. 9-35272
- Ta, vibrational spectrum, computation 9-33168
- Tb, spin-phonon coupling mechanism in critical sound scatt. near Neel temp. 9-24027
- Ti hydrides, H and D vibr. and thermal n cross-sections 9-30767
- TiCl₃, elastic const. and Debye temp. calc. from force field 9-35142
- TiCl₃, vibr. spectrum, phonon freq. calc. using shell model, sp. ht. temp. depend. 9-30763
- W phonon dispersion relations calc. from Sharma-Joshi theory specific heat calc. 9-48946
- YF₃, vibr. rel. to symmetry props. at pts. in Brillouin zone 9-42951
- YFe garnet rods, transversally magnetised, resonance absorption of longitudinal phonons 9-28421
- YFeO₃, h.f. lattice vibr. deduced from absorpt. and refl. spectra 9-41080
- Zn, hexagonal, vibrational spectrum 9-42946
- ZnFe₂O₄, atomic vibration, mean square amplitude determ. 9-41081
- ZnS, cubic, rel. to Raman spectrum 9-47376
- ZnS, Raman scatt. by Mn impurities, vibr. resonant modes obs. 9-43247
- ZnSe:Al, i.r. absorption of localized vibration 9-47369
- ZnSnP₂, vibrational frequencies from i.r. reflection spectra 9-35614
- Zr hydrides, H and D vibr. and thermal n cross-sections 9-30767

orientation

- eutectics between compounds, preferred orientation in microstructures 9-39245
- f.c.c. metal film, diff. line broadening rel. to particle size and strain 9-44657
- ferrimagnetics, grain orientation influence on domain wall continuity and initial susceptibility 9-31042
- film, magnetic, easy-axis orientation, 'magnetic masking' method 9-24314
- goniometer head for diffractometers used at -170 to 700°K 9-48783
- ice, columnar, origin of preferred orientation 9-36983
- metals, cubic, determ. from dodecahedral etch pits 9-48784
- metals, hexagonal, elastic wave vib. modes orientation depend. 9-48890
- m.o.s.f.e.t., effect on electron mobility 9-33351
- m.o.s.f.e.t., p-channel, effect on mobility, surface state density and noise 9-33361

Crystals continued
orientation continued

- n.m.r. structural investigation, rel. to second moment parameters 9-41433
olivine, in upper mantle beneath ocean, rel. to seismic anisotropy 9-33718
polyethylene films, rel. to substrate surface energy i.r. obs. 9-34986
polystyrene, isotactic, crystallite orientation rel. to crystallinity, obs. 9-30475
precision setting on goniometer head in diffractometer 9-23657
sapphire, selection for deposition of Si films 9-23658
sapphire whiskers, effect on tensile strength 9-35180
steel, Cr-Ni-Mo, γ -phase rel. to austenite matrix 9-23951
thin films, vacuum-evaporated on flexible substrates, props. 9-35388
twin/grain boundary relative free energy ratio meas., role of misorientations 9-44713
X-ray determ. applic. of visual method 9-23719
Zircaloy tubes, of hydride precip., rel. to texture and stresses 9-39188
AgBr, bubble orientation in epitaxial growth from melt 9-48817
Al, Hall coeff. depend 9-35334
Al wires, changes in crystallite orientation during 1% plastic deformation 9-35170
Be sheet, rel. to ductility behaviour around transition temp. 9-26333
Bi₂Te₃-Bi₂Se₃ pressed powder compacts, preferred orientation meas. by pulsed neutron diff. 9-32862
C fibres, preferred, effect on (h,k) interferences in electron diffraction 9-28259
C fibres, preferred, rel. to e.s.r. g values 9-32904
CdTe, simultaneous growth with Te whiskers 9-28232
Cu-(14.95 wt.%)Sn alloys, relationships assoc. with formation of orthorhombic γ' martensite plates 9-30739
Cu, Hall coeff. depend., Fermi surface characts. 9-26516
Fe-Ni-Al alloys, elastic stresses effect during decomp. of saturated solid solns. on precipitated phase particles orientation 9-39475
Fe-Si dil. alloy, depend. of grain growth rate during secondary recrystn. 9-39456
Fe single crystals, produced by strain-anneal method, relation between stretching amount and preferred orientation 9-35163
Fe single crystals, rel. to work hardening 9-26370
Fe single crystals, whiskers and alloy wires, infl. on Mattencci effects 9-33454
Fe single crystals deformed at -75°C, yield drop orientation dependence 9-33028
Ge, effect on dislocation distrib. on As diffusion 9-42830
Mg-Al-Zr-Be alloy, correlation with polarized etching facets 9-39186
Mo faces, revealed by etching in hot Ar stream 9-32972
NaCl, infl. on mechanical strength and grain boundary structure 9-26340
Ni, rel. to internal frictions studies, 77° to 298°K 9-26317
 α -Pu rel. to self-irradiation effs. 9-24072
Si-SiO₂ m.o.s.f.e.t., effect on electron mobility 9-33351
Sn, films vac. deposited on glass, preferred orientation rel. to deposition parameters 9-39164
Sn, rel. to u.s. absorpt. in supercond. transition 9-37336
Ta single crystal rods produced by melting and by strain-anneal method, imperfect structures 9-32930
YAl garnet, rel. to etch figures 9-44641
Zn-Cd alloy, single cryst. growth, orientation depend. of solute partition coeff. 9-37104
ZnO film deposition by triode sputtering, crystallographic orientation 9-39187

polarons *see* *Crystal electron states/polarons***twinning**

- alloys, coherent boundaries, free energy and surface free energy 9-44714
alloys, in relief of ordering strains 9-35252
b.c.c. twin intersections 9-44639
camphor, fcc, mobility of non-coherent twin boundaries 9-40963
ferroelectric, orientation of domain walls 9-43112
in martensitic phase transformations under stress mechanism 9-33134
metals, coherent boundaries, free energy and surface free energy 9-44714
metals, f.c., accommodation of constrained deformation by slip and twinning 9-26281
1-p-nitrobenzeneazo-2-naphthol (Para Red), X-ray diff. obs. 9-32863
opals, electron microscopy study 9-40917
pseudo-merohedral, treatment of overlapped data 9-30510
pseudo-merohedral, Weissenberg photographs, chart for use in interpretation 9-30511
quartz, Dauphine twin boundaries, electron and X-ray diffraction contrasts 9-30572
silicon iron, effect on plastic deform. at 185 and 300°K 9-41018
steel, martensite, internally twinned, slip dislocations movement 9-42828
steel, martensite, microtwins, electron microscope obs. 9-46744
surface dislocations, intrinsic resistive stress 9-35157
 α -Ti, coarsened grained, twin formation during fatigue 9-33083
Ag, rolled, constrained deformation accommodation by slip and twinning, discussion 9-26281
Au-(46.1 at.%)Cd alloy, pseudo-elastic flow due to twinning surface dislocations 9-35156
Au-(46.1 at.%)Cd alloy, twinning surface dislocations, intrinsic resistive stress 9-35157
Bi, rel. to Bauschinger effect 9-42880
Cd, cyclic twinning, slip band extrusions and twin boundary filamentary growths obs. 9-32981
(92wt.%)Co-(8wt.%)Fe constrained deformation accommodation by slip and twinning 9-26281
 α -Cu-Sn alloys, polycryst. 9-39189
 α -Cu-Sn alloys polycryst., up to 5 at.% Sn, onset stress for deform. twins 9-32980
Cu-Ti-Al dispersion-hardened alloys, mechanical 9-23926
Cu-Ti dispersion-hardened alloys, mechanical 9-23926
 α -Cu-Zn alloys polycryst., 10 and 15 at.% Zn, onset stress for deform. twins 9-32980
Cu continuous epitaxial (001) film on rocksalt, structure changes during growth 9-39158
Fe-Ni-C martensites, twinning during phase transf. in fine struct. obs. from electron micrograph 9-26233
Fe-Ni alloy, mag. domain wall distribution rel. to coherent boundaries of twin crystal 9-37651
Fe-(3 wt.%)Si, alloy, polycryst., pressurization effect 9-33053
Fe-(3 at.%)Si, polycrystalline, nucleation of mechanical twins 9-46826
Gd film, electron irradi., nucleation mechanism due to thermal stresses, electron microscope exam. 9-35100

Crystals continued
twinning continued

- LiNbO₃, plastic deform. due to mech. twinning, crack nucleation obs. 9-23887
Mg-(5.1 wt.%) Zn alloy, deform., inhibition by precipitates 9-46827
Mg, cyclic twinning, slip band extrusions and twin boundary filamentary growths obs. 9-32981
Mn-(11 at.%)Cu alloy, relax. peak obs. w.r.t. twinning surface dislocations 9-35156
Mn-(11 at.%) Cu alloy, twinning surface dislocations, intrinsic resistive stress 9-35157
(NH₄)₂UO₂F₆, and crystal structure 9-30565
Pb, annealing twins formed in bicrystals, 200-300°C 9-30570
Si in Al-(20wt.%)Si alloy, rel. to primary spherulite growth and morphology 9-23775
Sn high-speed photography obs. 9-23659
Ti-Cr binary alloys, martensite transf. obs. 9-26393
Ti, cyclic twinning, slip band extrusions and twin boundary filamentary growths obs. 9-32981
U alloys, type II in martensitic transformations 9-30512
Zn, high-speed photography obs. 9-23659
Zn, rel. to Bauschinger effect 9-42880
Zn, slip dislocation-deform. twin interactions, rel. to stacking fault formation 9-26289
Zn cyclic twinning, twin boundary filamentary growths obs. 9-32981

whiskers

- alkali halide whiskers, shape depend. of radiation induced defects 9-32941
alumina, in Ni, electron microscope obs. 9-33169
copper tritrite, X-ray refraction, effect on radiograph and topograph 9-40877
diamond, growth technique 9-40868
ferromagnetic micron-sized, free pole and magnetization distrib. 9-45134
graphite, anomalous structure, electron microscope exam. 9-46783
metal, axial screw-dislocation search 9-48853
reinforcement fibres for composite materials 9-23971
sapphire tensile strength, temp. depend. 9-35180
solder, on Ni-Cr thin films, growth conditions and mechanism 9-48816
ureas, di-substituted symmetric, growth at different temp. and conc. 9-39219
Bi, electron mean free path meas., from resistance changes during bending 9-37453
Cd, lattice imperf., X-ray diff. obs. 9-37109
CdS growth from vapour, disloc. behaviour 9-46759
Cu, as-grown, surface steps on pyramidal tips and longit. bounding surfaces 9-35031
Cu, diffusion of Zn, coeff. depend. on diameter 9-26300
Cu, elastic and plastic behaviour below yield pt. 9-39407
Cu, growth by halide reduction, transmission electron-microscopic investigation 9-37111
Cu, growth in large quantity, role of Cu₂O globules 9-37110
 α -Fe, growth, by chem. vapour deposition, in situ electron microscope obs. 9-44650
Fe, reduction growth, initial stage 9-26215
In, electron mean free path meas., from resistance changes during bending 9-37453
NaCl, elec. conductivity, 150-600°C 9-28551
NaCl, regrowth from pure and poisoned solutions 9-37039
Ni, growth by thermal and chem. decomp. of NiI₂ and NiBr₂ 9-35018
2H-SiC, growth rel. to presence of O₂ in reacting system 9-35032
 β -SiC, structure identification by X-ray diffraction, comments 9-32927
SiC whisker reinforced composite materials 9-35236
 α -SiN, vapour deposition production method, patent 9-23688
Sn-(1.0-5.0wt.%)Pb alloys, Sn dendrite growth as function of supercooling 9-48815
Sn, electron mean free path meas., from resistance changes during bending 9-37453
Sn, formation by vapour deposition, electronoptical investigations 9-39218
Sn, on Ni-Cr thin films, growth conditions and mechanism 9-48816
Te simultaneous growth with CdTe crystals by vapour phase reaction 9-28232
Zn, electron mean free path meas., from resistance changes during bending 9-37453
Zn, growth, X-ray diff. topography of imperfections 9-35096
Zn, size effect on resistivity 9-37454
Zn galvanomagnetic props., size effects 9-30853

Curie temperature *see* *Ferroelectric materials; Ferroelectric phenomena; Magnetic properties of substances***Curie-Weiss law** *see* *Magnetic properties of substances/paramagnetic; Paramagnetism***Curium**

- vapour pressure and cryst. struct. 9-48742
²⁴⁴Cm, separation of ²⁴³Am by precipitation of K₃AmO₂(CO₃)₂ 9-26802
Cm³⁺, ground-state splitting in ZrSiO₄, HfSiO₄ and ThSiO₄ 9-33626

Curium compounds

No entries

Current, electrical

- air sparks, impulse testing in nanosecond range 9-42577
air-earth current density, global diurnal vars. 9-28891
alternating, small effect on Weston cell e.m.f. 9-27266
pre-breakdown in high vacuum, voltage dependence 9-44509
charge current satisfying homogeneous wave eqn., induced e.m. field 9-29334
in composite superconductors, stabilized density 9-49027
in conducting medium, appearance during e.m. wave propag. 9-25144
d.c., constant, controller 9-45910
density meas. near cathode 9-34799
earth current indices, estimation 9-33725
earth model covered by uniformly deep ocean, intensity variation 9-49422
electrodes, porous, of Pb accumulators, distrib. 9-33677
generators, high-energy, explosively driven 9-47880
hydrocarbon liquid, flowing through tube, electric current generation 9-26129
impulse with small growth time, method of formation 9-41863
liquids, organic steady-state and transient space-charge-limited currents by injection from tunnel cathode 9-34919

Current, electrical continued

- in polyethylene films, biaxially oriented and cast, rel. to appl. field, obs. 9-35463
- runaway intensity in toroidal discharge 9-28043
- saturation, in radiolysis cells, effect of temp. 9-33683
- semiconductor with inelastic electron scattering, oscillations in mag. field 9-33287
- static power supply with adjustable rectified voltage and low residual ripple 9-43826
- superconducting surface sheath, induced persistent 9-49035
- superconductor, current stability conditions 9-30863
- supercurrent, idealized model 9-24133
- thermally stimulated, glow curves, eqns. for simple models of electron trap transitions 9-44881
- three-phase bridge of rectifiers, current decrease in load at const. firing angle 9-43830
- three-phase bridge of rectifiers, current in load for variable firing angle 9-43829
- Al layer, anodized, output during shock-wave loading 9-24117
- GaAs, oscillations connected with acoustoelectric domain motion 9-35399
- n-Ge, oscillations due to gradient instability, freq. and amplitude 9-33328
- He liq. after injection of hot electrons, attenuation and lifetime 9-39121
- W controlled fracture switching 9-33068

Current algebra

- (SU(6) \times SU(6)) to one-particle state, spin algebra extension 9-43959
- axial interaction, induced pseudo-scalar and parity non-conservation 9-36424
- axial-vector current, anomalies 9-48138
- Cabibbo-Radicati sum rule, applic. in nuclear physics 9-34428
- commutation relations abstracted from quark-model commutators 9-22543
- commutation relations for currents defined by Lagrangians derived from Riemannian metrics, geometric formula 9-27436
- conformal group, finite-component field representations 9-34011
- conserved current linear in one of the canonical variables, use of Goldstone theorem 9-41980
- current-current commutation relations used in quantum hydrodynamics 9-46436
- current-current models, η_{00}/η_{ij} -ratio 9-22578
- current-current theories, consistent dynamical formulation, current algebra validity 9-32114
- dispersion relations approach 9-29526
- dynamical basis investigated at low energy limit for π photoproduction 9-48188
- elementary particle graduate level text book emphasizing the pole of currents 9-40397
- e.m. current and partial conservation of tensor current 9-48204
- and e.m. interactions 9-25427
- rel. to Fubini sum rules satisfied by Born- approx. amplitudes in class of infinite component field theories 9-48130
- G $_2$ -Lie group, properties 9-27452
- gauge-invariant analysis of ρ , ω , $\phi \rightarrow 2\pi\gamma$ decays 9-44042
- Hadrons, metastable, weak decays, review of current algebra results 9-42024
- hard meson, use in calculating $K \rightarrow \pi\mu(e)\nu$ decay parameters 9-44012
- hard-meson analysis of K_{12} decay 9-29567
- impression of present situation in particle physics 9-22513
- infinite-component field model 9-27433
- infinite-component field model of local vector and axial vector current algebra 9-27434
- interactions, weak, applications 9-34248
- isovector current-density representation, alternative formulation 9-46051
- Kawarabayashi-Suzuki-Riazuddin-Fayyazuddin reln. and crossing symmetry 9-38446
- in Lagrangian field theories, breakdown 9-32113
- and Lagrangian field theory, relation, algebraic formalism 9-27436
- local vector and axial vector, infinite-component field model 9-27434
- low-energy pion physics by equal-time commutators 9-44017
- mass condition operator adjoined 9-40409
- minimal algebra, criteria 9-27449
- moments, electric dipole and mag. quadrupole based current algebra, agreement with experiment 9-48144
- nonfactorizing saturation, charge-current commutation rules 9-38445
- on-mass-shell, in ρ^0 - ρ^{\pm} mass difference calc. 9-27539
- PCAC propagator, sum rule connecting spin zero and spin one parts 9-43942
- photo- and electroprod. at threshold by equal-time commutators 9-43968
- photoproduction, Veneziano-like parameterizations 9-48175
- and Regge-pole theory 9-22561
- review, commutation relations used by sandwiching between states of infinite momentum 9-22541
- review of discussions at Vienna conference, Aug-Sep 1968 9-36422
- review of methods, applications to semileptonic and nonleptonic decay 9-40396
- S-matrix theory of currents 9-32149
- spectral function sum rules in quantum field-theory model describing spin one and zero part. 9-38481
- SU(3) \times SU(3) algebra, current divergences 9-42021
- Sugawara model for leptons, fermion avatars 9-38463
- and sum rule methods, review 9-36423
- sum rules, high energy contribs., evaluation method 9-32139
- sum rules, Veneziano model for π - π scatt., higher resonances contrib. 9-22599
- T-products and spectral-function sum rules in a theory of currents 9-46049
- transformation rule, for actual beams 9-25408
- unitarity corrections 9-48139
- unitarizing procedure, applic. to s-wave $K^+\pi$ scatt. amp. 9-27509
- validity, and consistent dynamical formulation of current-current theories 9-32114
- vector and axial vector currents, time-ordered, high-momentum props., matrix elements obs. 9-25426
- and weak hadron decay 9-36438
- weak interacting particles, theory based on SU $_2$ 9-41997
- A $_{1\rho}$ systems, comparison of calc. methods 9-42089
- $K^0 \rightarrow \pi^+\pi^-\pi^0(\mu^+\mu^-)$, axial form axial form factors determ. 9-38517
- $K \rightarrow \pi\mu(e)\nu$ form factors, predictions of current algebra using integral representations of current correlation functions 9-42067
- $\nu n \rightarrow l^+\pi^0$ prediction for differential cross-section 9-46060

Current algebra continued

- π , double electro- and photoproduction 9-27515
- π Compton scatt., use of current algebra combined with Lovelace-Veneziano amplitude 9-48184
- $\pi\pi$ scatt., S wave phase shifts, one parameter fit using current algebra 9-44035
- $\pi\pi$ scattering lengths, current algebra and the Veneziano model 9-22598
- $\pi\pi$ scattering lengths calc. 9-25469
- $\pi\pi \rightarrow \pi\pi$ scatt length calc. 9-48199
- X $_0$ meson and branching ratios, PCAC theory 9-38544

Curvature measurement *see Mechanical measurement***Cutting** *see Forming processes***Cyanogen (C $_2$ N $_2$)** *see Carbon compounds***Cyclotron resonance**

- acoustic, in n-InSb, microwave emission 9-48967
- alkali halides, polaron effective mass obs., translational energy depend. 9-39573
- amplification of whistlers in magnetosphere 9-41554
- beam loss due to the $\nu_{-} \approx 1$ and $3\nu_{-} \approx 3$ resonances 9-46149
- cut-off of cyclotron harmonics and plasma instability 9-30287
- in discharge, rel. to elec. field freq. 9-44499
- electron, in plasma, rel. to circ. polarized microwave damping 9-44434
- electron, microwave heating of plasma, stochastic model 9-25851
- electron mean free paths study 9-37388
- in films with specularly reflecting surfaces in absence of mag. field 9-41149
- graphite natural cry., interpretation 9-26497
- ion-molecule reaction rates meas. by ion cyclotron reson. 9-45415
- metal slab, helicon wave damping by Doppler-shifted cyclotron resonance 9-26491
- particle acceleration at resonance, effect of electrostatic field 9-38347
- plasma, cyclotron harmonic waves, resonant mode coupling 9-44471
- plasma acceleration by local reson. 9-42492
- in plasma electron velocity at sum and difference freq. due to elec. field w.r.t. static mag. field direction 9-32648
- plasma heating by modulated beam in mirror machine 9-44458
- scattering theory of small-particle absorption, ellipsoidal sample in e.m. cavity excitation 9-41150
- semiconductors, many-valley, phonon-assisted 9-28492
- semimetals, h.f. field effects 9-37418
- Ag, thin slab, mass of neck orbits and orbital diameters 9-26496
- Ag halides, polaron effective mass obs., translational energy depend. 9-39573
- Bi, measured and calculated wave spectrum 9-49012
- Cu, expts. rel. to absorpt. line shape and relax. time 9-35324
- Cu, submillimetric linewidths, and electron relaxation time 9-37419
- Ga, expts. rel. to absorpt. line shape and relax. time 9-35324
- Ge, impurity-assisted intervalley electron scatt. under uniaxial compression, reson. linewidth broadening 9-35421
- p-Ge, resonance absorpt. at 36 Gc/s, 100-1500 Oe, 2-50°K 9-43071
- H $_2$, D $_2$ and HD, ion-mol. reactions 9-43313
- Hg-CdTe alloy system, magneto-optical obs. 9-39807
- Hg, absorpt. spectrum obs. 9-35323
- n-InSb, electron, quantum effects 9-26540
- InSb deformation potential shift const. calc. 9-43046
- N $_2$ +H $_2$ ion-mol. reaction kinetics 9-31184
- Pb-SnTe alloy system, magneto-optical obs. 9-39807
- n-PbTe, rel. to non-local magnetoplasma effects 9-47059
- Si:B, stress-associated, intervalley electron scatt. rate obs. 9-43076
- p-Si, resonance absorpt. at 36 Gc/s, 100-1500 Oe, 2-50°K 9-43071
- Si impurity-assisted intervalley electron scatt. under uniaxial compression, reson. linewidth broadening 9-35421
- Te, expts. rel. to mass const. of valence band and secondary lines at high freq. 9-35324
- Te, isoenergetic surfaces ellipsoids at low mag. field, obs. 9-30827
- Te, p-type, quantum effects 9-44896
- TlBr, photocarriers polaron mass and relax. time obs. 9-39726
- TlCl, photocarriers polaron mass and relax. time obs. 9-39726
- Xe-methane charge exchange, obs. by double reson 9-44495

Cyclotrons *see Particle accelerators/cyclotrons***Czocharalski method** *see Crystals, growth***D-layer** *see Ionosphere/D-region***Damping***see also Internal friction*

- asymptotic, of disturbances in supersonic viscous heat-conducting gas, second approximation 9-23384
- beam-plasma interaction, h.f. instability collisional damping 9-44480
- circular elastic cylinder under axisymmetric end loads, exponential decay of stresses 9-31826
- collisional of electron waves in plasma, small amplitude relativistic calc. 9-44469
- Duffing eqn., soln. with large damping 9-22179
- e.m., circuit in seismometer, design 9-41468
- glass fibre torsional oscillations, meas. apparatus 9-37223
- ion cyclotron waves in mirror confined plasma 9-44467
- Landau, of electrostatic ion waves in uniform mag. field due to He contamination in Xe plasma 9-30279
- Landau, of ion acoustic wave in collision-free plasma with gravity field 9-46525
- Landau, of ion acoustic waves in plasma 9-25920
- Landau, of longitudinal plasma oscils. 9-40700
- liquid surface waves, ripple damping coeff. 9-36837
- of longitudinally excited displacements in two material cable 9-45843
- of microwave circ. polarized in plasma with collisional losses, electron cyclotron process 9-44434
- mumetal, magnetomech. damping, temp. effect 9-31036
- optical resonator, introduction and calibration, method 9-22376
- plasma oscillation, perturbed electron distribution function, linearized kinetic equation 9-32660
- plasma resonance oscillations, formula for Landau damping 9-44465
- of plasma waves, longitudinal, by collision 9-44468
- seismic waves, distortion by random interferences 9-26873
- shock waves, by multiple refl. at slits, spark cinematography 9-29315
- solids, phenomenological description of behaviour by a nonlinear viscoelastic law 9-47819
- transverse plasma waves, calc. using Landau equation 9-32661
- transverse vibrs. in meas. of internal friction, strain depend. calc. method 9-31810
- Water surface waves, ripple damping coeff. 9-36837

Damping continued

- Cu-Ni alloys, behaviour and miscibility gap evidence 9-42870
 Fe, magnetomech. damping, temp. effect 9-31036
 Fe-Ne single-mode laser, damping parameters of 0.63 μm line, nonlinear press. depend. 9-34165
 LiF, recovery of amplitude independ. damping 9-42882
 Ni, magnetomech. damping, temp. effect 9-31036
 Zn. pure, grain boundary relax. 9-44715

Dark space *see Discharges, electric***Data tables** *see Collections of physical data; Tables, mathematical***Dating** *see Earth/age; Radioactive dating***Daughter** *see Nucleus; Radioactivity***Dawn chorus** *see Atmospherics; Ionosphere***Dayglow** *see Airglow***de Haas-van Alphen effect**

- see also Diamagnetism; Magnetic properties/diamagnetic*
 amplitude, rel. to Dingle temp. and relax. time 9-37421
 electron-gas model, size effects on oscils. 9-24102
 experimental system, description 9-28456
 g factor, quasiparticle, for spin-splittings 9-24103
 integral identity rel. to inversion scheme for obtaining Fermi surface from effect 9-24091
 metals, domain structure 9-30828
 Ag-Au dilute alloys, rel. to scattering temp. 9-37422
 Ag single crystal rel. to mag., domains, pulsed n.m.r. studies of ^{109}Ag 9-45393
 Be, Fermi surface obs. and press. depend., pseudopot. model construct. 9-43001
 Be, magnetic breakdown 9-39749
 Bi Fermi surfaces 9-28446
 Cu-based alloys, electron scattering studies 9-37423
 Cu, zero-press. freqs. rel. to Fermi surface, in situ n.m.r. obs. 9-47041
 Fe, model accounting for magnetoresist. and Hall eff. meas. 9-24093
 HgSe, 1.6-4.2°K, for electronic g-factor evaluation 9-47062
 HgSe, spin-orbit splitting at Brillouin zone centre 9-35314
 In, v.l.f. oscillations, carrier effective mass 9-30850
 Mo, meas. 9-26499
 Ni, ferromagnetic, band structure calcs. including mag. breakdown effects 9-47249
 Pb, Landau-level widths, effective masses and magnetic-interaction effects obs. 9-26500
 Pd, Fermi surface props. including Fermi radius velocity and orbital g factor, exptl. determ. 9-47046
 Pt Fermi surface props. including Fermi radius velocity and orbital g factor, exptl. determ. 9-47046
 Sb Fermi surface, pressure- depend. meas. 9-30821
 Sb in He, Fermi surface, hydrostatic press. depend. 9-37409
 SiP₂, oscillations obs. 9-49015
 Sn, white, in band structure and Fermi surface model derivation 9-47049
 Zn-Ag dilute alloys, rel. to relax. time meas. 9-37424
 Zn (0.005at.%)Mn alloy, Kondo scatt. anisotropy obs. 9-24109
 Zn-Mn dilute alloys, rel. to relax. time meas. 9-37424

Debye temperature *see Specific heat***Debye-Huckel theory** *see Conductivity, electrical/liquids, electrolytic; Electrochemistry; Solutions***Debye-Scherrer cameras** *see Cameras; X-ray**crystallography/apparatus***Debye-Waller factors** *see Crystals/lattices mechanics; Electron diffraction crystallography; X-ray crystallography***Decay periods** *see Hyperons/decay; Kaons/decay;**Mesons/decay; Pions/decay; Radioactivity/decay periods***Decay schemes** *see Hyperons/decay; Kaons/decay;**Mesons/decay; Pions/decay; Radioactivity/decay schemes***Decomposition** *see Dissociation***Decomposition, thermal** *see Chemical reactions***Decoration techniques** *see Crystal imperfections/dislocations; Crystals/etching***Defects** *see Crystal imperfections***Deformation**

- see also Bending; Elastic deformation; Plastic deformation*
 adhesive contact of cylindrical punch with elastic half-space, soln of rocking and translation parallel to plane 9-38279
 alkali halides, potential determ. from piezobirefringence meas. 9-24364
 alloy, ordered, line tension of a superdislocation 9-46819
 Bauschinger effect in quench-hardened spring steel, effect of tempering temperature 9-23885
 bubble, ellipsoidal, in slightly viscous fluid 9-38941
 bubble, moving in inviscid liq, under sudden press. change 9-34865
 buckling, axisymmetric, of thin-walled imperfect spherical shells 9-45807
 buckling, modes of odd degree, of a spherical shell under uniform pressure 9-43780
 buckling, nonlinear, of a spherical shell, under uniform pressure 9-45825
 buckling of long cylindrical shells with random axisymm. imperfections under axial compression 9-22214
 calorimeter, liq.-vapour, calibration technique 9-29331
 constrained, accommodation in f.c.c. metals by slip and twinning 9-26281
 crystal lattice, e.p.r. line widening obs. 9-35708
 cylinders and cones, sandwich, subjected to axial compression 9-23872
 cylindrical shell of varying wall thickness, radial deform. under edge loading, influence coeffs. 9-25070
 cylindrical shells, strain displacement relationships 9-22192
 elastic plastic, strain components finite, thermomechanical coupling 9-34069
 elastically anisotropic half-space, field, and stress 9-38282
 electron microscope examination of foils by shadowing technique surface markings 9-28246
 eye, effects of hard and soft contact lenses 9-36084
 fatigue crack tip deform. process, obs. using fatigue tester with micro-graphic apparatus 9-42896
 finite, theory of plane stress 9-22206
 flexible shell, concept of finite elements rotations and small strains in anal. 9-31807
 forest-cut processes, force-distance diagrams, critique of methods 9-30653
 glass powders, shrinkage, sintering by viscous deformation 9-35227
 grain boundary migration mechanism 9-23823

Deformation continued

- holographic meas., use of short laser pulses 9-29445
 interplanetary plasma flow, large-scale mag. field variations 9-43643
 metal crystals, irradi. or quenched, rel. to sweeping-up of loops by glide dislocations 9-32963
 metal single cryst. during microscope exam. 9-39235
 metals, f.c.c., accommodation of constrained deformation by slip and twinning 9-26281
 metals, high-speed mechanism 9-23875
 metals, Na⁺ and K⁺ ions thermionic emission, gases effect 9-45036
 metals, sandblasting rel. to glow-curve characs. of exo-electrons 9-47212
 perovskite cell, parameter representation 9-33032
 plates, tapered, analysis of post buckling 9-38273
 polybutene-1, high-speed, exam. by photographic light-scatt. technique 9-46901
 polyethylene, effect on unit cell dimensions 9-46803
 polyethylene, high-speed, exam. by photographic light-scatt. technique 9-46901
 polyethylene, low-density, study by stress, strain, i.r. absorpt. meas. 9-27933
 polyethylene, oriented, lamellae out-of-plane deform. mechanism, shear resist. obs. 9-28358
 polyethylene annular spherulites, mechanism, direct electron microscopic investig. 9-26254
 polymer film, electromechanical, rel. to dielectric breakdown 9-43110
 polymer films, polycrystalline, characterization rel. to molecular orientation 9-30666
 polymers, amorphous, reversible, singularities in development curve 9-26331
 polypropylene, oriented, lamellae out-of-plane deform. mechanism, shear resist. obs. 9-28358
 polypropylene fibre; spinning, drawing and heat setting 9-39416
 pressure vessel, elliptical cross section, by internal press. 9-31803
 rate sensitivity rel. to elongation 9-23874
 rod, microwave meas. method 9-30636
 semiconductor crystals of cubic symmetry, illuminated, effect 9-44764
 shallow circular arch, large deflection behaviour using Rayleigh-Ritz finite element method 9-31806
 shape change due to dislocation climb, single- and poly-crystals 9-30658
 shells, creep buckling stress anal. 9-31808
 shells, intersecting, effect of yield surfaces on the limit pressure 9-45809
 shells, multisandwich, of arbitrary shape, large deflections 9-43779
 silica glass, hardness meas., low-temp., indentation and densification obs. 9-28375
 spherical shell, buckling modes, instability and eff. of geometric imperfections 9-22213
 spherical shell, buckling modes, review 9-22212
 spherical shells, thin-walled, imperfect, axisymmetric buckling 9-45807
 stability of heterogeneous orthotropic axially compressed cylindrical shells 9-38270
 steel, Bauschinger effect, effect of tempering temperature 9-23885
 steel, spring, quench-hardened, Bauschinger effect, tempering temp. influence 9-39391
 steel, stainless, annealing of creep fracture damage 9-39457
 steel castings, continuous, for sufficient strength props. 9-39467
 strain displacement relationships, in cylindrical shells 9-22192
 surface layer, cyclic nature of accumulation of distortions of second kind rel. to fatigue nature of wear 9-23929
 by thermal gradient in perfect crystals, effect on X-ray propag. 9-23772
 tube, polygonal, buckling under combined compression and torsion 9-27195
 viscoelastic media, non-stationary temp. stresses anal. 9-28334
 viscous solids, finite quasi-static 9-42879
 of water drop in electric field 9-28146
 ^{235}U enriched tubes, buckling in light water 9-23913
 Ag, electron irradi., stage I recovery mechanism, elec. resistivity meas. 9-35083
 AgCl, ions deform., X-ray obs. 9-30507
 Al (11 wt.%)Mg age-hardening alloy, by hydrostatic extrusion, effect on struct. and props. 9-41051
 Al-Si dilute alloys, cold-worked, recovery process 9-33104
 Al-Zn-Mg-Cu alloy, dislocation structure and susceptibility to intergranular stress corrosion cracking 9-23811
 Al (0.3-0.4 wt.%) Cu bicrystal, effect on grain boundary sliding 9-46888
 Al, bicrystal, effect on grain boundary sliding 9-46888
 Al foils, fatigued, surface markings, direct correlation of dislocation structures 9-23878
 Al polycrystal, effect of orientation-dependent solidification 9-46931
 Al single cryst., recrystn. after pt. deform. 9-42908
 Bi films, rel. to resistivity oscillations, 78° and 300°K 9-30845
 Cu, glassy, induced anisotropy 9-39147
 CdS, wurtzite type, potential constns. 9-26498
 (92wt.%)Co (8wt.%)Fe constrained deformation accommodation by slip and twinning 9-26281
 Cr-Ni-Nb stainless steel, creep fracture damage, annealing 9-39457
 Cu-Al, latent hardening rel. to composition and prestrain 9-41015
 Cu (5 wt.%) Al alloy, tensile, at room temperature 9-30680
 Cu, internal friction, effect of previous deform. in tension or torsion 9-41002
 Cu, modified Charpy V-notch, effect of impact vel. 9-48892
 Cu, preferential surface deformation existence by dislocation density 9-41016
 Cu polycrystal, effect of orientation-dependent solidification 9-46931
 Cu single cryst. strengthening value with programmed loading depend. on preliminary deform. degrees 9-42890
 Fe-C alloy, shape strain for (225)_r martensitic transformation 9-28344
 Fe-Cr alloys, effect on pitting and anodic dissolution 9-24576
 Fe-Mn-C alloy, shape strain for (225)_r martensitic transformation 9-28344
 Fe-Ni-C alloy, shape strain for (259)_r martensitic transformation 9-28344
 Fe-Si single cryst., lattice distortion and X-ray topographic contrast due to 90° domain wall 9-33460
 Fe, zone refined at -196°C, lattice defects study by elec. resistivity meas. 9-26275
 Fe single crystal plates produced by strain-anneal method, effect of stretching on imperfect structures 9-32913
 Fe single crystals deformed at -75°C, yield drop orientation dependence 9-33028
 Fe single crystals hardness tests 9-35192
 p-Ge, carrier conc. decrease w.r.t. donor action of dislocations 9-35424

Deformation continued

- n-Ge, dislocation acceptor level position obs., effect of non-dislocation defects generated 9-37540
- Ge, influence on anisotropy of thermoelectric power 9-35496
- Ge junctions, anisotropic, effect on characteristics 9-35440
- InSb, potential constants, hole scattering mechanisms 9-33307
- K, commercial and high purity, mechanism at low temp. 9-46893
- KBr laser windows, damage obs. 9-31943
- Mo, internal friction, effect of previous deform. in tension or torsion 9-41002
- NaCl, deformed, single cryst. dislocation density obs. 9-32974
- NaCl, ions deform., X-ray obs. 9-30507
- Ni-Ti alloy, grain boundary deform. rel. temp. under constant strain 9-23889
- Ni polycrystal, effect of orientation-dependent solidification 9-46931
- Pt, stage I recovery by residual elec. resistivity meas. 9-26277
- Si, by thermal gradient, effect on X-ray propag. 9-23772
- Si crystal in uniaxial compression, deform. const. determ. from absorpt. spectra 9-41012
- Si single crystals, percussion marks on surface, divergent X-ray diffr. pattern 9-33037
- SiO₂, vitreous pile-exposed, ionization expansion 9-35175
- α -Ti, mechanism below 0.4 T_m, comments 9-28351
- Ti, thermally activated parameters from stress relaxation 9-28350
- U, fission gas induced swelling, as function of external hydrostatic press., 0-1000 bar 9-38735
- UC, fission gas swelling, bubble nucleation time and temp. depend. 9-38736
- W (5 at %)Re single cryst., during ion microscope exam. 9-39235
- Zn crystals, at high strain rates 9-23891
- Zn sheet, causing grain growth 9-26363

Delay lines, ultrasonic *see Acoustics; Ultrasonics***Delbruck scattering** *see Photons/scattering***Demagnetization** *see Magnetization process***Dember effect** *see Photoelectromagnetic effects***Demonstrations** *see Teaching/demonstrations***Dendrites** *see Crystallization; Crystals/growth***Densitometry**

- photographic film transmittance fluctuations rel. to r.m.s. density 9-34235
- scanning system, digital, appl. to X-ray crystallography 9-32080

Density

- methane, orthobaric density in critical region 9-48739
- plasma, electron-beam generated, distribution theory 9-32602
- UO₂, effect on thermal conductivity 9-41110
- KZnF₃ single crystal perovskite structure, hydrothermally synthesized 9-42746

Effect on

- effect on transport coeffs. 9-23404
- in flows, high-speed 9-23834
- measurement, accurate method 9-45728
- Ar, isotherms to 10 kbar and 400°C 9-32732
- Ar plasma in Knudsen arc 9-42585
- Ba vapour 9-42702
- N₂, to 400°C and 10000 bar 9-44520
- Ne over range 28°K-70°K pressures up to 240 at. 9-30325
- TiNO₃ fused, vapour press. and density meas., 250-450°C, b.p. and transpiration method 9-34966

liquids

- alloy, excess vol. analysis 9-39471
- dilatometer for meas. liq. expansion at elevated temp. 9-46582
- n-hexane, superheated 9-23466
- hydrocarbons, saturated; b.p. mol. wt. cf. with Ar 9-32758
- immiscibility phase boundaries determ. 9-40778
- measurement, accurate method 9-45728
- nonconductivity binary mixture, height distribution 9-28092
- random packing density of hard sphere models 9-30366
- relation with compression and sonic vel., expt. verification 9-42647
- relation with refractive index 9-23496
- simple, change in transmission zone 9-46621
- stratified, internal wave generation with mixed region collapse, modelling expt. 9-34862
- thallous formate aqueous soln. saturated 20-28°C 9-28329
- water, structurally modified, hydrostatic weighing method for meas. 9-23464
- AgNO₃-alkali nitrate molten mixtures, rel. to elec. cond. 9-23520
- Al, polytherms 9-40781
- Ar, up to 1000 kg/cm² 9-46593
- BeF₂-LiF molten solns. 9-42639
- Cd(NO₃)₂-glycine-water system, cpd. existence from viscometric and densimetric obs. 9-23461
- HCl anhydrous, depend. of thermal conductivity 9-28118
- HCl anhydrous, relationship with thermal conductivity 9-36863
- Hg-In alloys, volume change on formation 9-28115
- Li-Na system, immiscibility phase boundaries determ. from density meas. 9-40779
- Ne, up to 1000 kg/cm² 9-46593
- Sn-Tl alloys, rel. to atomic and ionic volume calcs 9-30370
- Tl-Se system, immiscibility phase boundaries determ. from density meas. 9-40779
- TiNO₃-alkali nitrate molten mixtures, rel. to elec. cond. 9-23520
- Zn and alloys, meas. up to 700°C 9-30375

solids

- alloy, excess vol. analysis 9-39471
- aluminium methylammonium alum., volumetric meas., 78° to 291°K 9-42927
- cohesive, rel. to compressibility modulus 9-35145
- films, thin, data using scanning electron microscope 9-30544
- glasses, V₂O₅-P₂O₅, semicond., 100° to 400°K 9-35155
- ice, mean grain size determ. with meas. of light attenuation coeff. 9-45464
- lunar soil, determ. by automatic stations 9-27071
- microgram samples, flotation tech. determ. using thallous formate soln. 9-28329
- nylon 66 yarns, drawn, shrinkage on annealing 9-46707
- phosphates of type MNH₂PO₄·H₂O (M=Cd, Co, Mg, Mn, Fe, Ni) and MKPO₄·H₂O (M=Cd, Co, Mg, Mn and Ni) 9-37138
- polyethylene, drawn, crystallinity determ. 9-46706
- polymers, drawn, crystallinity determ. 9-46706

Density continued**solids continued**

- rare-earth fluoride systems, nonstoichiometry obs. 9-40915
- rosin films, light sensitive volume changes, spectral characts. 9-28698
- rutile single crystals, change during reduction, nature of defects formed 9-32945
- shell cap, relative importance in liq. impact anal. compared with gravity and liq. viscosity and compressibility 9-22186
- snow, mean grain size determ. with meas. of light attenuation coeff. 9-45464
- steel, cold-rolled transformer, specific vol. rel. to annealing temp. 9-39455
- transition metal molybdenates, changes in high press. phase transforms. rel. to anion coordination 9-35244
- Ba_{4/3}(_{1/2})Na_{2/3}Nb₁₀O₃₀, and lattice parameters and thermal expansion coeffs. 9-37134
- C, densification and expansion, irradi. induced 9-41022
- C, pyrolytic, effect of high neutron exposure 9-40992
- Cd comparative with Cu and Pb at high press. 9-30655
- Cu comparative with Cd and Pb at high press. 9-30655
- Cu film, vapour deposited, rel. to bulk Cu 9-30483
- Ge, 'amorphous', vapour deposited, X-ray diff. absorpt. obs. 9-33012
- HfB₂, consolidation mechanisms in high-B₂ densification mechanisms in high-pressure, hot-pressing 9-35223
- In₂O₃, changes in high press. phase transforms rel. to anion coordination 9-35244
- K₄Nb₆O₁₇, and volume expansion in water 9-26238
- NaCl powder, densification in air during sintering by plastic flow or volume diffusion 9-35232
- Nb single crystals deformed at high strain rates, and mech. props. and dislocation sub-structure 9-48898
- Pb comparative with Cd and Cu at high press. 9-30655
- PrP variation with composition for nonstoichiometry occurrence 9-28268
- Pr(ReO₄)₃·3H₂O, calc. from crystal structure data 9-39302
- Pu(C,P,S) powders, densification 9-35238
- Si, charges rel. to thermal defect investig. 9-32944
- UC(P,S) powders, densification 9-35238
- YFe garnet, dense ferrimagnetic perovskite allotropic form, existence 9-26252

Density measurement

- atmosphere, ρ scatt. gauge design by multivariable search method 9-24636
- bone, from X-ray film image by computer 9-47700
- in creep-rupture expts., interpretation 9-39417
- gas, accurate determ. method 9-45728
- gradient meas. in transparent media, Schlieren technique 9-32006
- liquid, accurate determ. method 9-45728
- microgram solid samples flotation tech. using thallous formate soln. 9-28329
- plasma, ionospheric, from phase-freq. obs. 9-31414
- plasma cloud, charge concentration meas. 9-30258
- upper atmosphere, kinetic theory and gas-surface interactions 9-26919
- water, structurally modified, hydrostatic weighing method 9-23464
- Ar afterglow, electron density and temp. 9-28048

Desorption *see Sorption***Detonation**

- see also Explosions; Shock waves*
- effect of turbulence 9-36203
- front thickness in non-steady wave motion 9-31888
- gas, appl. to shock wave generation in liqs. 9-46627
- in has, ideal, undergoing reversible reaction, shock flow 9-48645
- liquid explosive, instability of front 9-36204
- liquid explosives, excitation by a light impulse 9-31855
- spherical waves in gas mixtures, flash photography 9-31856
- spinning, three-dimens. polar appl. and wave confluences 9-34093
- wave propagation in spray medium theory and experiment 9-29317
- waves, instability criteria 9-25108
- waves of arbitrary profile, gasdynamic stability 9-25111
- AgN₃, by collapsing air bubble 9-28788
- Al powder-oxygen mixtures, investigation 9-27234
- CO-O₂ mixtures, spinning, three-dimens. polar, and wave confluence shown in hodograph space 9-34093
- O₂-Ar-acetylene mixtures, spinning, three-dimens. polar and wave confluence representation 9-34093
- β -PbN₆, bycollapsing air bubble 9-28788

Deuterium

- absorption in zircalloys, rel. to post-transition corrosion by steam at 300°C and 340°C 9-28806
- desorption from Ti-sponge 9-30499
- ion beams, negative, polarized, prod. from 2S^{1/2} metastable deuterium 9-40565
- isotope exchange on Ni-Al₂O₃ catalyst between H and H₂O vapour, obs. 9-28790
- liquid, ortho-, refr. index, 3200Å Cherenkov radiation, 24.2°K 9-40791
- neutron, thermal, absorpt. cross section, obs. 9-25617
- permeation, diffusion and solubility in Pyrex glass 9-40987
- plasma prod. by subnanosec. laser pulses 9-34775
- plasma production by giant pulse-laser irradi. of solid, characts. 9-28021
- sticking coeff. and desorption rate variations during condensed gas layer growth on liq. He cooled surfaces 9-48770
- target, ionization by impact of high-energy triatomic molecular H beam 9-46328
- track sensitive target within Ne-H bubble chamber 9-25542
- u.v. absolute spectral energy distrib. 9-36666
- viscosity at constant density, 20.4-300°K 9-36824
- γ bombard., \sim 1 GeV, π backward photoprod., pion nucleon final state interaction effect 9-44025
- D/H ratio in Venus atmosphere, deductions from Lyman α Mariner 5 obs. 9-43628
- D₂-H₂ mixed solid solutions, i.r. spectra induced into vibrational first harmonics, 4°K 9-33558
- D₂, autoioniz. and predissoc., eff. of isotopic substitution 9-28039
- D₂, emission in extreme u.v. from autoionizing levels 9-28042
- D₂ optical pumping of alkali atoms, depolarization cross sections significance 9-34558
- D₂ transfer reactions with CO₂⁺, D₂O⁺ and H₂S⁺ 9-49374
- D₂+CH₃OH⁺→CH₃OHD⁺, stripping-complex transition 9-38936
- D₂+X⁺→D+XD⁺, deviations from stripping model 9-27944
- D⁻ in alkali fluorides, i.r. absorption due to localized vibrations of ions 9-30619

Deuterium continuedD⁺+D₂O→OD⁺+D₂ 9-46430in KCl, superhyperfine interactions of D₂⁰ centres, zero-pt. vibr. influence, ENDOR obs. 9-45409

Pd, diffusion and solubility 9-37206

in Pd, effect on elec. resistivity 9-24129

Deuterium compounds *see Hydrogen compounds***Deuterons***see also Cosmic rays/deuterons; Nuclear reactions and scattering due to/ deuterons*

disintegration in a pulse approximation 9-27568

elements Z₁=20 to Z₂=30, stopping-power meas., excitation pot. and shell corrections calc. 9-33208

energy loss in evaporated metal film 9-28439

form factor, electrical, func. of physical S-matrix and n-p scatt. phase shift 9-22637

magnetic dipole moment, calc. with baryons resons. in ground state 9-34394

minimum percent D state calc. 9-34395

moments, mag. and elec. quadrupole, Dashen- Frautschi type calc. method 9-32230

plasma, laser produced, electron temperature 9-44409

production, aligned high energy beam, from scatt. off p 9-29628

production in pp→pn⁺(π^+), diff. cross section. ang. distrib., d momentum spectra meas., M_p=21.1 GeV/c 9-29612

singlet, (S=0, T=1) production in p-induced nuclear reactions obs. 9-38698

two-nucleon potential, non-relativistic 9-42166

two-nucleon potential, non-relativistic 9-38634

vibrational analysis with trial wave function that is a linear combination of oscillator states 9-40472

wave function meas. using π photoproduction interaction 9-42074Ar⁺+D₂→ArD⁺+D reaction, crossed-beam appl. 9-41442D+H₂→DH+H 9-41439N₂⁺+D₂→N₂D⁺+D reaction, crossed-beam appl. 9-41442**effects**Nb₃Sn, 3 MeV, on critical current density of superconducting layers 9-41184

W, defect production at 0.1 MeV 9-37162

W single cryst., irradi. damage, ion microscope exam. 9-39358

interactions Γ d binding energy, eff. of $\Gamma N=\Sigma N$ transitions on the binding energy of Faddeev theory applic. 9-44061 π d→ π pn cross section, ang. distrib. meas., E_p=850 MeV 9-36462K⁺d at low energy; possibility of I=0, Y=0 baryons 9-42097K⁺d→K⁺ π^+ π^+ d at 2.24 BeV/c 9-32178K⁺d→K⁺ π^+ π^+ pn, N⁺* and N⁺⁺ prod., E_K=2.24 BeV/c 9-32178K⁺d→ Σ^+ π^+ π^+ , breakdown of impulse approx. in deuteron, evidence 9-25448 $\bar{\nu}_e$ dissociation, neutral weak-interc. search 9-27569pd→pp π^+ π^+ , N*(1470) prod. at 7.0 GeV/c 9-25486

pd→ppn, 6.5-13.0 MeV, obs. of quasifree and sequential decay mechanisms 9-48338

 π^+ d→(p)n π^+ π^+ , evidence against prod. of I=5/2 baryon reson. of mass 1640 MeV/c² 9-42114 π^+ d→pn π^+ π^+ , I=1/2 baryon resonance obs., 1640 MeV/c², M π =2.26 GeV/c 9-27562 π^+ d E_p=2.7 GeV/c, four-charged- particle final states 9-32186 π^+ d neutral π p enhancements at 8 GeV/c 9-46095 π^+ d→ppD⁰ 2.7 GeV/c, D⁰→ π^+ δ^+ and δ^+ → π^+ η study 9-38543 π^+ d→pp π^+ π^+ , 3.65 BeV/c, π^+ π^+ π^+ in ω^0 and η^0 regions obs. 9-34299 π photoproduction on d, impulse approximation tested, d wave-function meas. 9-42074**photodisintegration**

angular distrib., 240-320 MeV, spark chamber obs. 9-25489

differential cross-section 9-38599

momentum-dependent potentials influence, off-energy-shell effects study 9-34387

threshold theorems from kinematic singularities and helicity amplitude constraints 9-22638

polarization

elastic scattering, influence of polarizability 9-44210

source using Stern-Gerlach separation and resonant charge transfer 9-27555

sources and targets 9-38579

N-d elastic scatt., impulse approx. framework 9-32210

²H(d,p)³H 100-500 KeV analysis 9-22818**scattering***see also Protons and antiprotons/scattering, proton-deuteron*

back-scattering from Ti and Nb, energy distribution 9-39549

quadrupole deformation effect at high energies 9-29629

shadow term, Glauber form, upper energy limit to validity 9-27570

 α d, elastic, distortion effects 9-44066

d,p, aligned high energy d beam production 9-29628

dd, diffraction scatt. depend. on quasifree scatt. amplitude of d constituents 9-29627

dp, small-angle, elastic, 1.69 GeV/c, differential cross-sections, analysis 9-22639

ed, elastic high momentum transfers, X-sections, form factors 9-27465

ed, recoil-d vector polarization, depend. on e.m. form factor, S and D phase diff. 9-25419

Ad, using Fadeev eqns with nonlocal separable potentials and medium energy 9-44062

N-d, d polarization, in impulse approx. framework 9-32210

nd polarization expt., rel. to 3N three-nucleon systems 9-27567

nd spin-dependence obs. 9-27560

pd, cross section meas., d contains N*(1688), E_p=1 GeV 9-42103

pd, polarization expt., rel. to 3N three-nucleon systems 9-27567

 π^+ d, differential cross section meas., M_p=2-5.5 GeV/c 9-38524 π d, 895 MeV/c, cross section obs. 9-25459 π d, Glauber shadow, inelastic contrib. estimated with Regge-pole theory 9-34307 π d→pn π^+ , at high energies with large momentum transfer to neutron 9-42077**Development, photographic** *see Photographic process/development***Diamagnetic resonance** *see Cyclotron resonance***Diamagnetism***see also Cyclotron resonance; de Haas-van Alphen effect; Magnetic properties/diamagnetic*

atoms, Thomas-Fermi and Thomas-Fermi-Dirac eqns. calc. 9-42324

electron-gas, size effects on susceptibility 9-24102

molecules, susceptibility, approx. calc., perturbed Hartree-Fock theory 9-30010

molecules mag. props., induced current density susceptibility and shielding 9-29999

superconductor, type II, assoc. of flux mobility props. 9-41175

susceptibility for breakdown model 9-28592

Diamonds

adhesive interaction with metals 9-23930

artificial, prep. method, C phase diagram 9-33135

ballases, natural and synthesized, structure rel. to growth conditions 9-26197

band struct., empirical pseudopot. approach 9-49000

channeling charact. of protons and the ions 9-47012

diamond, Debye temp. at low temps., X-ray meas. 9-24043

electronic structure of neutral isolated divacancy 9-46810

eutectic melting at contacts with metals of iron triad 9-26358

formation from graphite in presence of metals, mechanism 9-41064

garnet inclusion, X-ray study 9-42804

growth from Co-C and Mn-C systems 9-37028

growth on seed crystal, process 9-30528

heat and pressure treatment effect on colour, e.p.r., i.r. absorption, u.v. and visible spectra 9-26366

interaction with silicon at high pressures and temps. 9-26807

in interstellar dust, to explain absorpt. and other phenom. 9-31561

ion-implanted, annealing, characteristic X-rays 9-35194

luminescence and u.v. absorpt. rel. to platelet defects, obs. 9-26732

oxidation to form surface oxides, props. and struct. 9-24555

particles in interstellar dust, optical consts. and extinction curves hypothesis 9-43575

positron annihilation 9-30830

semiconducting, oscillatory photoconductivity spectrum, role of phonons 9-41258

stimulated Raman gain meas. 9-25734

surface, epitaxy of C 9-35033

surface entropy, phonon contributions 9-23617

synthetic, growth from metal-carbon systems 9-23670

synthetic, growth spirals, left- and right-screw, dislocation obs. 9-23671

whisker growth technique 9-40868

X-ray luminescence spectra, electron vibratory series 9-43263

N donor, substitutional, obs. 9-37401

TiC, X-ray emission K α band of C 9-26762**Dichroism** *see Pleochroism***Dielectric devices**

capacitor, high-stability film, performance data 9-49149

charge image detector for extended spatial distrib., applic to spectrometry 9-27263

discharging, thermally-stimulated, system for semiconductor trap level exam. 9-39613

frequency converters, travelling wave, derivation of Hamiltonian 9-31891

heterocontact, semiconductor-dielectric, with potential trap for electron in contact layer 9-26580

insulators, working life when subjected to partial surface discharges 9-49147

literature digest, 1967 9-33368

mirror, high-reflectivity, light scattering 9-32020

moisture probe, h.f., response to soluble salts 9-49389

resonator, radiation Q factor, theory 9-25138

trigatron spark gap in liq. dielectrics, characts. 9-32789

triglycine sulphate, pyroelec. detector, h.f. response 9-45014

triglycine sulphate pyroelec. detector, h.f. response 9-45014

u.s. delay-line crystals, photoelastic constants 9-49148

Al-Al₂O₃ triodes, hot-electron transport 9-49128

Al metallized polycarbonate and polyethylene terephthalate capacitors 9-39698

BaTiO₃ capacitor, mat. purity rel. to device charact. 9-49150Nb₂O₅, thin films, potential use as capacitor from dielectric props. 9-30981Si₃N₄ films, in capacitors, props. 9-24212

SiO capacitor, thermal conductivity calc. from breakdown meas. 9-26463

Ta capacitor, improvement in elec. characts. 9-49151

Ta capacitor, preparation from low-density film and device characts. 9-49152

Zn metallized polycarbonate and polyethylene terephthalate capacitors 9-39698

Dielectric loss *see Dielectric phenomena; Dielectric properties of substances***Dielectric measurement**

capacitance changes, small, technique 9-29358

capacitance of high cond. materials, transformer ratio bridge 9-34135

charge and discharge current waveform recording 9-29357

chemistry, uses 9-24214

complex, reflectometer with normal incidence scanning 9-36370

dielectrometer based on heterodyne beat method, for mols, dipole moments 9-45907

drift mobility techniques for study of elec. transport props. 9-39660

insulators, h.v., electrically stressed surface temp. and pot. distrib., simultaneous meas. 9-47887

internal discharge resistance in samples with artificial cavities 9-29356

liquids, complex permittivity to 9455MHz, rel. to scale of calibration for relative meas. 9-44578

liquids, high complex permittivities by cavity compensation, graphical soln. 9-44579

liquids, permittivity meas. at cm. wavelengths improvements to apparatus 9-48709

literature digest, 1967 9-33368

permittivity, to 1200°C, polarimetric method for refractories 9-38342

polar liqs., conductance network for three terminal capacitance bridge 9-29363

porous dielectrics, permittivity, accuracy 9-24213

probe, capacitative for meas. of surface charge distribution 9-31892

time domain measurement of h.f. and l.f. constant, relax. time and loss 9-47885

KI, dielectric constant at high temperature using K-band SWR technique 9-39665

TiO₂, rutile, flux grown, without contacting electrodes 9-45002

Dielectric phenomena*see also Electric strength*

- anisotropic, bounds for associated two-dimensional quantities 9-22321
 antiferroelectric transition, phenomenological theory of second-order transition 9-47184
 capacitor and inductor energy storage demonstrated 9-43702
 in chemistry, uses 9-24214
 Clausius Mossotti formula, corrections 9-33365
 cohesive energies, theory, of tetrahedrally coordinated crystals 9-23698
 Cole-Cole eqns. for relaxing systems 9-36245
 dielectrics and insulation, conference 9-33676
 dielectrophoresis in lossy media, theory and biological appls. 9-28145
 diffusion in direction of increasing dielec. const., under action of elec. field 9-42670
 electric field in dielectric with statistically homogeneous random permittivity 9-22111
 electron gas, free, susceptibility on interaction with e.m. wave field 9-25884
 electron gas, Lindhard functions with finite-electron-lifetime 9-41142
 electron gas, screening function, self-consistent higher-order corrections 9-31793
 electron microscope specimen charging model 9-39230
 exciton transitions, dielec. const. tensor, polariton-phonon coupling effect on spatial dispersion 9-44893
 Fermi-Thomas response of metal surface to external point charge 9-44620
 ferroelectric cryst., Curie temp. elec. field depend. in paraelec. phase 9-39681
 frequency conversion, parametric, derivation of the Hamiltonian 9-31891
 in gamma-electric cell, radiation effects in high-voltage operation geometrical nonlinearities of elastic dielectric, Murnaghans' reln. 9-31897
 insulator, wave-number and freq.-depend. function 9-35461
 internal discharge resistance in samples with artificial cavities 9-29356
 Kronig-Kramers relations under saturation conditions 9-26796
 Kronig-Kramers transforms, practical props. 9-24501
 Lindhard functions with finite-electron-lifetime for free-electron gas 9-41142
 melting in h.f. elec. field, analytical investig. by one-dim. thermal conductivity eqn. 9-44614
 membrane, low dielec., energy of ion crossing rel. to 'pores' and 'carriers' 9-39954
 microwave cavity perturbation by lossy dielectrics 9-41859
 molecular cryst. thin layers with intermol. H-bonds, charge carrier generation mechanism 9-33366
 Mott insulation and antiferromag. in band model 9-44883
 nonlinear, self-focusing of large-amplitude waves 9-36247
 phase shift for total reflection of e.m. waves 9-34118
 plasma, quiescent or turbulent, longit. dielec. permeability 9-34754
 plasma, two-temperature, dielectric constant, analysis and applic. 9-27990
 polycrystalline random medium subjected to const. average elec. field, two-point elec. field correlation tensor determ. 9-43102
 polymers, crystalline heterochain, relaxation 9-24216
 reflection coefficient, thin rod, 9300MHz 9-38341
 relaxation rel. to mol. dipolar autocorrelation function 9-34599
 relaxation times distribution, calc. from experimental data 9-35464
 resonator cavity, TE_{012} , design curves, quality factor, e.s.r. spectrometer input 9-38332
 second-harmonic generation by picosecond optical pulses 9-47938
 surface charge distribution on dielectric, capacitive probe for meas. 9-31892
 thermodielectric eff. and pyroelec. cryst. 9-28568
 transient radiation originating at electron transience from vacuum to dielectric, photographic registration 9-24208
 tunneling of W field emitted electrons through Zr and χ -N absorbed layers 9-30960
 two layers between metal plates with charge at interface, soln. of electrostatic pot. 9-36246
 virtual work principle, confusion on specialization of field eqns. from elastic to rigid dielectrics 9-27199
 GaAs lattice, microwave permittivity temperatures between 100°K and 600°K 9-24169
 KCl, relax. effects due to air-gaps in specimen-electrode contacts 9-37581
 KI, dielectric constant at high temp. 9-39665
 Mn^{2+} in $(NH_4)_2SO_4$ single cry. EPR investig. in paraelec. phase 9-31165
 NaCl, relax. effects due to air-gaps in specimen-electrode contacts 9-37581

ferroelectric *see Ferroelectric phenomena***Dielectric properties of substances***see also Electric strength*

- alcohols, props. over wide temp. range, time domain meas. 9-47885
 benzene on silica gel, isotherm. 1 Mc/sec, 25°C 9-42735
 breakdown in organic liquids produced by laser radiation 9-48710
 constant meas., dielectrometer for mols. dipole moments 9-45907
 cylinder in stream of incompressible conducting liquid, non-viscous magnetic boundary layer 9-30189
 insulators, inorganic binary compound, correlation between bond energies and forbidden bands 9-48780
 literature digest, 1967 9-33368
 macromolecules with one short dipole, relaxation 9-46426
 molecular systems, relax. rel. to mol. dipolar autocorrelation function 9-34599
 molecules with inversion or internal rot. modes, relaxation, correl. function treatment 9-42365
 organic, conductivity temp. depend. 9-26127
 permittivity of double-layer ellipsoid 9-31889
 phosphosilicate glass films in m.g.o.s. structures, polarization process 9-33363
 plasma, quiescent or turbulent, longit. dielec. permeability 9-34754
 plasma inhomogeneous, with almost monoenergetic component, const. 9-48559
 poly(4-methylstyrene), effective dipole moment 9-32550
 refractory, permittivity meas. to 1200°C by microwave polarimetry 9-38342
 relaxation times, distributions, Argand diagrams 9-33370
 resistance, surface, meas. apparatus 9-22322
 rocksalt, thin films, breakdown 9-33381
 solid/liquid transfer of ionization processes between states, kinetics 9-28553

Dielectric properties of substances continued

- solute molecules, partially oriented, orientation parameters from anisotropy of const. 9-42371
 transition metal glasses, switching mechanism, high elec. field infl. 9-35476
 As_2S_3 , constant, space charge eff. involving ionic conduction 9-39662
 AlN films grown by reactive sputtering, dielectric props. 9-37575
 GeO_2 thin films, a.c. and d.c. behaviour 9-39664
 Ge surface, slow potential change mechanism 9-30927
 $NH_4PF_6 \cdot NH_4F$, phase transitions from n.m.r. relaxation times anomalies 9-35727
 Nb_2O_5 thin films, growth and potential use as capacitor 9-30981
 NbO vapour deposited films, evaluation rel. to m.o.s. behaviour 9-30958
 $Pb(La_{0.5}(M^{2+})_{0.5}Ti_{1-x}O_3$, ($M=Nb$ or V), const., and spontaneous polarization 9-24220
 RbH_2AsO_4 , normal and deuterated, constant, relative loss tangent 9-39697
 SbSI, orientated fibroform cryst., dielec. and piezoelec. consts. 9-48808
 Si surface, slow potential change mechanism 9-30927
 SiO_2 thin films, chemical vapour deposition apparatus 9-26189
 $SnTiO_3$, dielectric constant obs. of normal and reduced crystal at various temp. and various fields 9-30961
 $ZnO:Li$, u.s. wave attenuation, temp. and freq. depend. 9-37339

- air, weakly ionized, permittivity rel. to appl. mag. field, obs. 9-28080
 fluctuations affecting optical mode conversion in gas lens 9-43912
 inert, afterglow plasmas, pulsed discharge excitation 9-34805
 inert gases, collision-induced second virial coeff. 9-32432
 plasma with collisions, permittivity tensor, calc. 9-48603
 relaxation and molecular behaviour 9-26126
 He breakdown by a laser beam 9-48725

liquids and solutions

- air, dielectric const. at microwave frequencies in X-band 9-46647
 albumin, bovine serum, aq. solns., r.f. and microwave obs. 9-28147
 alkyl ethers, microwave, relax. mechanism 9-42671
 amides, relax. rel. to intermol. association 9-26128
 aminoethylethanamine, rel. to mol. struct., -70 to 60°C 9-30417
 aniline dil., solns., at microwave freq. relaxation data and dipole moments 9-48711
 anisidines, o-, m- and p-, dielectric constants and dipole moments 9-36898
 anisole-benzene mixtures, internal field effects 9-46649
 aromatic amines, disubstituted, at microwave freq., relaxation data and dipole moments 9-48711
 boiling heat transfer, hydrodynamic theory, effect of elec. field 9-23596
 1- and 2-butanol, relaxation at high pressures 9-32791
 butyl alcohol, dielec. const. freq.-temp. meas. by helical resonator method 9-36895
 t-butyl chloride, microwave absorpt. 9-39670
 carbon disulphide, press., vol., and temp. effects 9-39109
 carbon tetrachloride, press., vol., and temp. effects 9-39109
 carbon tetrachloride, shock compressed, elec. cond. and permitt., microwave technique 9-30419
 charge collection from moving stream 9-42669
 Chloroform-triethylamine system, role of mol. anisotropy 9-48712
 chloroform in electron-donor solns. 9-23518
 column supported by elec. field, diam. rel. to voltage 9-23517
 complex permittivities, meas., by cavity compensation at 9455MHz, graphical method 9-44579
 complex permittivity meas. rel. to scale of calibration for relative meas. 9-44578
 conduction enhancement by insulating particles 9-36894
 conductivity and breakdown of dielectric liquids, book 9-34917
 constant, theory rel. to shell model of lattice dynamics 9-35262
 -decane, negative-carrier mobility meas. 9-42672
 didodecyl sulphide, microwave, relax. mechanism 9-42671
 dielectrophoresis in lossy dielec. media, theory and biological appls. 9-28145
 diethanolamine, rel. to mol. struct., -70 to 60°C 9-30417
 diffusion in direction of increasing dielec. const. under action of elec. field 9-42670
 dimethyl formamide, in mixture of benzene and liq. paraffin, internal field at microwave freqs. 9-46650
 p-dioxane-water, dilute solns. 9-34928
 ethyl alcohol, dielec. const. freq.-temp. meas. by helical resonator method 9-36895
 field-induced polarization, obs. in microelectrophoresis cell 9-35750
 n-heptane, negative-carrier mobility meas. 9-42672
 hexane, charge collection from moving stream 9-42669
 n-hexane, negative-carrier mobility meas. 9-42672
 isopentane, press., vol., and temp. effects 9-39109
 local fields and correl. functions 9-47152
 methyl alcohol, dielec. const. freq.-temp. meas. by helical resonator method 9-36895
 methylpolysiloxanic oils, electrohydrodynamical behaviour at -20-80°C 9-36896
 mixtures, internal field effects 9-46649
 monoethanolamine, rel. to mol. struct., -70 to 60°C 9-30417
 nitroanisoles, o-, m- and p-, dielectric constants and dipole moments 9-36897
 nitrobenzene, saturation in dipolar and nondipolar organic solvents 9-32792
 n-octane, negative-carrier mobility meas. 9-42672
 octanol isomers, press. effect on relax. 9-30418
 organic steady-state and transient space-charge-limited currents by injection from tunnel cathode 9-34919
 pentanol, primary, secondary and tertiary, polarization and saturation 9-46651
 permittivity meas. at cm. wavelengths improvements to apparatus 9-48709
 phthalic esters, electrohydrodynamical behaviour at -20-80°C 9-36896
 polar molecules in nonpolar solvents, dielectric absorpt., meas. of molecular relaxation 9-23088
 polar solvents in electron transfer reactions 9-31182
 polar-non-polar solvent mixtures, rel. to shift of absorption bands of polar molecules 9-30410
 pressure depend. of dielec. polarization 9-32788
 propyl alcohol, dielec. const. freq.-temp. meas. by helical resonator method 9-36895
 pure polar liquid dipole moment computation, empirical eqn. 9-46646

Dielectric properties of substances continued
liquids and solutions continued

- relaxation and molecular behaviour 9-26126
- toluene, press., vol., and temp. effects 9-39109
- trigatron spark gap, characts. 9-32789
- CoSO₄ aq., dielec. consts. and loss factors, relax. time 9-46648
- CuSO₄ aq., dielec. consts. and loss factors, relax. time 9-46648
- H₂O, changes during adsorption by solids 9-48716
- H₂O, industrial, permittivity and loss angle meas. 9-44580
- He breakdown by a laser beam 9-48725
- O₂, dielectric const. at microwave frequencies in X-band 9-46647
- MNDO₄ aq., dielec. consts. and loss factors, relax. time 9-46648
- N₂, d.c. pre-breakdown phenom., study by electron field emission from metal electrode 9-44581
- N₂, dielectric const. at microwave frequencies in X-band 9-46647
- NH₃, complex dielec. const. at 3 GHz, as function of temp. 9-34918
- Na-K alloys, electromigration 9-30416
- Na-NH₃, complex const. meas. and relax. obs. 9-44582
- Na-NH₃ solutions, complex dielec. constants as function of molar conc. 9-34918
- SiO₂ aq., dielec. consts. and loss factors, relax time 9-46648

solids

- alkali halide crystals, electronic polarizability of ions 9-31058
- alkali halide crystals, interaction of Pt electrodes, capacitance enhancement 9-49134
- alkali halide crystals, loss, dislocations and Maxwell-Wagner polarization 9-33371
- alkali halides, a.c. dielec. meas. of enhanced conductivity following plastic deformation (Gyulai-Hartly effect) 9-33373
- alkali metal niobates based highly dense piezoelectric material 9-39676
- alkali-rare earth niobates with tungsten bronze structure, rel. to crystal chemistry 9-24210
- alloy, dilute magnetic, const. calc. 9-39667
- anharmonic crystal, interatomic pot. theory 9-30759
- antiferroelectric transition model, exact solution 9-45011
- backward-travelling-wave parametric interactions, steady-state theory 9-34188
- breakdown, research trends, review 9-30968
- t-butyl chloride, microwave absorpt. 9-39670
- calcium stearate Langmuir film, electric conduction 9-37583
- cannphor (d and d'), as function of temp., at 1, 10 and 100 kHz 9-49135
- capacitance, temp. coeffs. 9-47151
- capacitor capacity, static-field penetration and atomic polarization effects 9-43137
- caruba wax, eff. of ionic additives on heterocharge 9-37573
- ceramic, ferroelectric, var. with elec. field, applic. to parametron 9-30969
- ceramics, piezoelectric, props. rel. to orientational dielec. polarization 9-47187
- charge density on surface, meas. 9-37574
- coals, Karaganda dehydrated, loss, and elec. conductivity, rel. to petrographic ingredients, mineral impurities and metamorphism 9-44999
- covalent crystals, electronic constant from quantum theory of electronegativity 9-46735
- cupric formate tetrahydrate, paraelec.-antiferro. transition, DMR obs. of struct. and water mol. motion changes 9-35730
- diamond-type crystals, optical critical-point structure, strain effects 9-24395
- effect of dislocations, charged 9-48856
- dispersion in inhomogeneous dielectrics, three-layer description 9-24209
- dispersion in semiconductors, variation in laser beam field 9-35390
- drift mobility techniques for study of elec. transport props. 9-39660
- electrets, surface charge, eff. of atmospheric pressure 9-37602
- electroacoustic surface wave propag. 9-28425
- electrophotographic layers, photoinduced discharge, effect of capture 9-30967
- ferrites, microwave props. 9-45172
- ferroelectrics, dielec. const. in infralow-freq. range, method and calc. rels. 9-37589
- film, characterization by internal photoemission 9-39659
- films, size-quantized, anisotropy in h.f. conductivity 9-39577
- films in semiconductor devices 9-37550
- gas-filled space in dielectric, no. of discharges per period alternating applied voltage 9-30966
- glass slip, loss angles at low temp., calorimetric meas. 9-33375
- glasses containing transition-metal ions, conduction 9-30964
- group IV-VI cpds, cubic, semiconductors 9-39666
- hydroxyapatite monocrystals, polarization anisotropy 9-30978
- ice, effect of structure and point defects 9-48832
- ice, NaOH-doped 9-39669
- ice, relax. mechanism, diffusion theory 9-28318
- inert gas crystals, constant theory in individual-ion model 9-35468
- insulating films, Fowler-Nordheim tunneling, eff. of nonparabolic momentum 9-39661
- insulating stacks of thin-layer elements, mechanically-strong, optimum apparent layer area 9-35460
- insulator, image force dielec. const. from photo-injected carriers obs. 9-39739
- insulator paramagnetic salts, elec. dipole transition strength calc. 9-33498
- insulator with multiple trapping, injected current time-depend. flow, thermal release and transit time 9-39668
- insulators, working life when subjected to partial surface discharges 9-49147
- ionic crystals, Reststrahlen frequency 9-30756
- ionic crystals, shock polarization, rel. to lattice characts. 9-30957
- local fields and correl. functions 9-47152
- loss tangent and permittivity, incomplete data, analysis 9-47158
- magnetite, double-exchange, electron-hopping process and metal-nonmetal transition 9-41168
- Maxwell-Wagner-Sillars effect, linear model 9-37570
- metal film, rel. to optical props. non-local theory 9-26703
- metal interfaces, effective const. determ. 9-41230
- metals, freq. derivatives of dielec. functions, apparatus for direct meas. 9-33367
- metals, improved high reflectivity ellipsometry method for dielec. const. determ. 9-35462
- molecular cryst. thin layers with intermol. H-bonds, charge carrier generation mechanism 9-33366
- molecular crystals, dielectric constant formalation of long wave-length binding energy 9-35005
- mylar films high conduction 9-37585
- nonpolar molecules randomly distrib. correction to Clausius Mossotti formula 9-33365
- oxide films on base metal, conduction props. rel. to contacts 9-37572
- oxides, ionic conductivity, survey and expl. problems 9-45003
- paraelectric, losses in microwave range, effect of domains 9-43101
- Pb₂MgNb₂O₆-Pb₂NiNb₂O₆ system, loss and relaxation 9-28564
- perovskites, complex, solid solns., s.h.f. dielec. props. 9-39678
- polycaprolactam, dispersion, methyl substitution effect 9-32544
- polycrystalline random medium subjected to const. average elec. field, two-point elec. field correlation tensor determ. 9-43102
- polyethylene, electron mobility determ. by injection through cathode method 9-47156
- polyethylene, film, decay processes of surface electric charges 9-49136
- polyethylene, loss angles at low temp., calorimetric meas. 9-33375
- polyethylene terephthalate, loss angles at low temp., calorimetric meas. 9-33375
- polyethylenes, loss factor depend. on crystalline structure 9-28550
- polymer film, prep. and characts. 9-33399
- polymer laminate materials, multiparameter control of props. 9-33364
- polymethacrylic acid esters below glass transition point, secondary β loss max, temp. depend. 9-32549
- polypropylene, loss angles at low temp., calorimetric meas. 9-33375
- polyvinylfluoride, rel. to d.c. cond. and glass-rubber transition, 10-150°C 9-30962
- porous dielectrics, permittivity meas., accuracy 9-24213
- PTFE, loss angles at low temp., calorimetric meas. 9-33375
- pyroelectric crystals, thermoelectric effect 9-28568
- quartz, cryst. and fused, pulsed-radiation-induced current obs. 9-44998
- radiation damage, ellipsometric analysis 9-35295
- rare-earth borides, const., relax. and N/m² ratio determ. from plasma refl. edge obs. 9-39802
- refractory metal oxides, dielec. const. rel. to lattice energies and heat of atomization 9-30494
- relaxation and molecular behaviour 9-26126
- review, crystals for research and technological applications 9-36971
- Rochelle salt, props. of nonferroelec. cuts over wide freq. range 9-47181
- Rochelle salt dielectric relaxation and crystal water stoichiometry, activation energy determ. 9-41234
- rubber-sulphur systems, comparison of viscoelastic and dielectric props. 9-33376
- rutile group minerals, second-rank tensor anion polarizabilities 9-37576
- semi-insulator, thermally-activated ohmic and space-charge-limited conduction meas., localized levels obs. 9-43106
- semiconductor, Gunn-instability, two-valley model, freq. and field-depend. dielec. const. 9-30895
- semiconductor, helicon interferometry and nonreson. cyclotron absorpt. method 9-47100
- semiconductor model, microscopic function 9-26582
- semiconductors, three-layer description of dispersion 9-24209
- semimetal, helicon interferometry and nonreson. cyclotron absorpt. method 9-47100
- Si₃N₄:P films, surface potential drifting 9-37579
- silicone resin films on Si 9-30959
- sorbitan tristearate ultrathin black films, resistivity 9-37580
- surface conductivity, effects of annealing, temp. and mag. field 9-47153
- teflon films, high conduction 9-37585
- tetrafluoroethylene-hexafluoropropylene copolymers, γ -irrad., low-temp. relax. obs. 9-26586
- thiourea, ferroelec. phase transitions, effect of hydrostatic pressure on const. 9-28567
- transition metals, dielec. sweeping of impurity pot. 9-43100
- tryglycine sulphate, 0.5 to 4.5 kMc/s 9-30975
- tryglycine sulphate, pressure depend. of ferro-paraelectric transition, 0-23 kbar 9-41248
- tryglycine sulphate, props. of nonferroelec. cuts over wide freq. range 9-47181
- tryglycine sulphate group ferroelectrics in polar and nonpolar cuts, pyroelec. coeff. and dielec. const. deriv. 9-43122
- tryglycine sulphate, dielec. const. by thermal noise method 9-49145
- zeolite, synthetic Linde type-A, with adsorbed vapours 9-41233
- AgCl:Mn, potential difference at defects during plastic deformation 9-23877
- AgO powders, resistivity, effect of added impurities 9-28545
- Al₂O₃, microwave dielectric constant, 375 kb 9-28547
- Al₂O₃ sprayed coating, elec. insulation. rel. gas-flame deposition process in Ar with Cs admixture 9-24211
- As₂S₃ films, bombardment conductivity, columnar ionization 9-33369
- Ba₂(x-y)Sr₂(y-x)Nb₂O₁₀, constants, spontaneous polarization and Curie temp. 9-35480
- BaTi_{1-x}Ni_xO₃ single crystal, constant, -192° to 300°C at 1 KHz, and optical props. 9-41362
- BaTiO₃-Co₂Ta₂O₇ solid soln., s.h.f. props. 9-47174
- BaTiO₃-CdTiO₃ solid soln. single crystals 9-47172
- BaTiO₃-Co₂Ta₂O₇ solid soln., s.h.f. props. 9-39689
- BaTiO₃-Ni₂Nb₂O₇ solid soln., s.h.f. props. 9-47174
- BaTiO₃-Ni₂Nb₂O₇ solid soln., s.h.f. props. 9-39689
- BaTiO₃-SrTiO₃ solid soln. dielectric constant, reversible, depend. on field strength above Curie point 9-41239
- BaTiO₃, microwave-absorption fluctuations at Curie temp. 9-28559
- BaTiO₃, polycrystalline, dielectric constant, reversible depend. on field strength above Curie point 9-41239
- BaTiO₃, static dielec. const., hydrostatic-press. depend., in electron scatt. investigation 9-37591
- BaTiO₃ dielectric constant dispersion in wide range of freqs. and temps. 9-39688
- BaTiO₃ dielectric constant in s.h.f. region, contrib. to theory of dispersion 9-47173
- BaTiO₃ s.h.f. dispersion of dielectric const. 9-39686
- BaTiO ceramics and single crystals, s.h.f. dispersion of dielec. constant in low-temp. phases 9-39687
- Bi_{1-x}GeO_{2x}, permittivity, and growth and props. 9-42751
- Bi₂(GeO₄)₃, permittivity, and growth and props. 9-42751
- CS₂ polymer, d.c. resistivity, conductivity and permittivity freq. depend. 9-34975
- CaF₂:NaF, relaxation by dielec. loss 9-28548
- CaTiO₃-based binary solid solns., conc. depend. and temp. coeff. of dielec. const. 9-39663
- CdO, conduction, and optical props., effect of lattice vibrations 9-35613

Dielectric properties of substances continued
solids continued

- CdS, calculation of constant using phonon dispersion model 9-46972
 CdS, injection and field-induced excitation of charge carriers 9-43108
 CoO:Li single cry., dielec. const. and loss variations, relax. mechanism 9-47157
 CoO single cry., dielec. const. and loss variations, relax. mechanism 9-47157
 Eu chalcogenides, Dispersion, i.r. reflectivity obs. 9-39799
 GaSb, const. calc. 9-47119
 Ge, extrinsic photoconductor, relax. effects on speed of response 9-43129
 GeTe, imaginary part of freq. dependent dielec. function calc. 9-39794
 InP, optical freqs. and dielec. const. meas. 9-47314
 InSb, lattice dielec. const. determ. by helicon and nonreson. absorpt. techniques 9-47100
 K₂NiF₆, static const. at various d.c. field strengths 9-37582
 K₂Nb₂O₇, constant meas. and temp. dependence up to 700°C 9-26238
 K₂Nb₂O₇, mica-like single cryst. 9-30522
 K₂Pb₂Lap₂Nb₁₀O₃₀, dielec. constant temp. and composition dependence 9-23682
 K₂Sr₂La₂Nb₁₀O₃₀, dielec. constant temp. and composition dependence 9-23682
 KBr, constant and loss function deduction from extreme u.v. reflection spectrum 9-28673
 KCl:KOH, as-grown and annealed, paraelec. reson., tunneling behaviour obs. 9-39673
 KCl:Li⁺(OH⁻)(CN⁻), low temp. anomalies rel. to splitting in impurity motional spectrum 9-26583
 KCl:Pb²⁺, absorption meas. for activation energies of vacancy pair diffusion 9-31108
 KCl single crystals, electronic spectra, 5-40 eV region, complex dielec. const. determ. 9-37711
 KD₂PO₄, ferroelec. anomalies in dielec. and piezoelec. props. 9-41244
 KD₂(SeO₃)₂ ferroelec. single cryst., dielec. const. temp. depend. 9-32855
 KI, dispersion relations 9-30762
 KNb₂O₆, mica-like single cryst. 9-30522
 KTa_{1-x}Nb_xO₃, static dielec. const., hydrostatic press. depend., in electron scatt. investigation 9-37591
 KTa_{1-x}Nb_xO₃ under d.c. biasing fields 9-35473
 KTaO₃, static dielec. const., hydrostatic press. depend., in electron scatt. investigation 9-37591
 KCl:OH, electrocaloric phenomena, thermodynamics, paraelec. cooling obs. 9-37588
 Kd₂PO₄ crystal, permittivity, effect of strong elec. field 9-41241
 Li₂O-SiO₂ glass, effect of metastable precipitate on conductivity and formation of loss peaks 9-24215
 Li₂O-2SiO₂ glass, effect of neutron irradiation 9-40833
 LiBr films, losses at low temp., mechanisms 9-49137
 LiF, power factor, effect of thermal treatment, X- and γ-irradiation 9-28546
 LiIO₃, electric and piezoelectric behaviour 9-37595
 Mg₂Ge, constants from reflectance meas., 0.6-11.0 eV at 77°K 9-24355
 Mg₂S, imag. part of freq. depend. function, calc. 9-41135
 Mg₂Si, constants from reflectance meas., 0.6-11.0 eV at 77°K 9-24355
 Mg₂Sn, constants from reflectance meas., 0.6-11.0 eV at 77°K 9-24355
 MnO:Li, loss and dipole relaxation 9-35466
 MnO/CoO solid solns., dielec. const., loss and conductivity meas. w.r.t. freq. 9-35465
 MnO/NiO solid solns., dielec. const., loss and conductivity meas. w.r.t. freq. 9-35465
 MnO, static const. determ. from reflectivity obs. 9-45308
 MnO single cryst., dielec. const., loss and conductivity meas. w.r.t. freq. 9-35465
 (Na_{1-x}Li_x)NbO₃ solid solution ceramics, dielectric constant rel. to temp. 9-26389
 Na₂K_{1-x}TaO₃, transitions rel. to phonon modes from i.r. and Raman spectra, 4-600°K 9-47366
 NaCl:Ni, loss, influence of impurity 9-35467
 NaCl:Pb²⁺, absorption meas. for activation energies of vacancy pair diffusion 9-31108
 NaCl, a.c. dielec. meas. of enhanced conductivity following plastic deformation (Gyulai-Hartley) effect 9-33373
 NaNO₂, ferroelec. phase transition, low freq. dielec. const. obs. 9-35486
 NaNO₂, permittivity anisotropy at phase transition 9-30796
 NaNbO₃:CdTiO₃ solid solns. 9-39695
 NiO:Li single cryst., dielec. const., interfacial polarization effect 9-35469
 NiO, conductivity, permittivity and loss tangent, 10⁻⁵ Hz, dispersion effects 9-45001
 NiO, freq. depend. of permittivity, meas. rel. to stoichiometry of fluxed-melt grown crystals 9-37089
 NiO single cryst., dielec. const., interfacial polarization effect 9-35469
 Pb_{0.92}Bi_{0.07}La_{0.01}(Fe_{0.405}Nb_{0.325}Zr_{0.27})O₃ ferroelec. thin films, const. meas. 9-35487
 PbFe_{0.3}Nb_{0.5}O₃ ferroelectric. props. over wide temp. and freq. range 9-41243
 PbMg_{0.33}Nb_{0.67} props. over wide temp. and freq. range 9-41243
 PbTiO₃-PbMg_{0.33}Nb_{0.67} ferroelectric and paraelectric compositions near morphotropic boundary, tetragonal and rhombohedral phase mixture 9-43103
 Pb(Zr,Ti)O₃ piezoelectric ceramic, adulterated, high-field losses 9-26585
 PbZrO₃, antiferroelec., props. over wide temp. and freq. range 9-41243
 PbZrO₃, antiferroelec. → paraelec. transform., effect of hydrostatic press. 9-47190
 PbZrO₃, phase transitions, impurity eff. on enthalpy changes 9-26584
 Pr-SiO₂ cermet thin films, resistances obs. 9-47155
 RbD₂PO₄, permittivity, anomalous behaviour below Curie point 9-47177
 RbH₂PO₄, ferroelec. anomalies in dielec. and piezoelec. props. 9-41244
 RbH₂PO₄ single cryst., relative dielec. and piezoelec. const. meas. 9-44749
 SbSI, dielectric constant, dynamical nonlinearity 9-35488
 SbSI, paraelectric, nonlinear I-V chars. 9-28555
 SbSI, paraelectric region, damping of u.s. waves as function of illumination, near phase transition temp. 9-46992
 SbSI, permittivity, loss tangent and coercive force, temp. and hydrostatic pressure depend., 30 to -60°C 9-43104
 SbSI, temp. and hydrostatic press. depend. 9-28565
 SbSI ferro-paraelectric transition, effect on u.s. absorpt. coefficient and velocity 9-42960
 SbSI splitting into ferro- and paraelec. layers, elec. field effect 9-41250
 Se, charge accumulation 9-33377

Dielectric properties of substances continued
solids continued

- Se, vitreous, hole Hall mobility and trap parameters determ. in multiple trapping case 9-39668
 Si₃N₄ films, constant and breakdown voltage 9-24212
 Si₃N₄, impurity-doped films, electrical and physicochemical props. 9-37578
 SiO₂ amorphous films, anodic growth, dielec. breakdown and carrier transport 9-45006
 SiO₂ films, constant and loss, freq. depend. 9-28549
 SiO₂ films incomplete loss functions, analysis 9-47158
 SiO₂ fused, γ irradi., current-voltage depend. 9-49138
 SiO₂ in Si-SiO₂-Al structure, elec. strength rel. to thickness 9-35475
 SiO_x films, annealed a.c. and d.c. cond. processes at high and low fields 9-47160
 SiO films, elec. pulse breakdown 9-45005
 SiO thin film, breakdown mechanism, surface irregularities 9-41236
 SnTe, imaginary part of freq. dependent dielec. function calc. 9-39794
 Sr, Bi₂/3 TiO₃-CaTiO₃ system solid solns., tan δ, ε and temp. coeff. of ε 9-41231
 SrTiO₃, single crystals, dielec. const., loss tangent and conductivity, temp. depend. 9-39694
 SrTiO₃, static dielec. const., hydrostatic press. depend., in electron scatt. investigation 9-37591
 TiO₂, rutile, flux-grown, from meas. without contacting electrodes 9-45002
 TiO_{2-x}, reduced rutile, relax. of hopping electrons rel. to ionic defects 9-44690
 TiO₂ specially reduced single cry., dielec. const. and loss, variation 9-47159
 U₂O₃, temp. depend. 9-41232
 UO₂, temp. depend. 9-41232
 YFe garnets:Ca²⁺(Si⁴⁺), microwave loss and permittivity 9-33374
 Yb metal-insulator transition, resistance meas. 9-41171
 ZnO, conductivity, permittivity and loss tangent, 10⁻¹⁰ Hz, dispersion effects 9-45001
 ZnO electrophotographic layers, space charge density, effect of elec. field 9-30963
 ZnS:Cl, photodielectric 9-24237
 solids, ferroelectric see *Ferroelectric materials*
Dielectric relaxation see *Dielectric phenomena; Dielectric properties of substances*
Dielectric strength see *Electric strength*
Differential analysers see *Calculating apparatus*
Differential equations
 (δ²/δxδx+axδ/δx+byδ/δy)/P(x,y,t=0)=φ(x,y) 9-22048
 asymptotic evaluation for solution 9-36112
 boundary layer applic., numerical method soln. 9-22049
 diffusion eqn., edge diffraction soln. 9-38195
 fluid dynamics, almost incompressible flow equations, numerical solution 9-40640
 fluid dynamics, numerical transport of turbulence 9-38939
 gas flow, inviscid, stabilisation of difference schemes by artificial diffusion 9-36798
 global numerical ocean model 9-35804
 gravity and acoustic waves, linearised, numerical model 9-37931
 hyperbolic, 2D, of second order, analysis by substitution method, spreading 9-25028
 hypersonic gas flow, finite-difference technique for numerical computation 9-36796
 L(F)+Qδ²F/δT²=0 iterative method of soln 9-38291
 linear, Lie algebra 9-22054
 MHD, axially symmetric flow past fixed bodies, numerical approach 9-34746
 of motion, Lie groups determ. 9-22053
 nonlinear, soln. by convolution on complex plane 9-41734
 nonlinear Boltzmann, accuracy of Monte Carlo solutions 9-34829
 nonlinear partial, computation of compressible ideal flow patterns 9-40734
 operators, second order ordinary, eigenvalues distrib. 9-31743
 star structure, PL expansion for coordinate stretching and interface location 9-35974
 Thomas-Fermi, mathematical aspects 9-47726
 Thomas-Fermi-Dirac and TFD-Gombas eqns., analytical solns. 9-38754
 wavefunctions for bound states and scattering, soln. 9-47754
 WKB approximation method of soln. sufficiency condition for validity 9-38235
Diffraction
 diffusion eqn., edge diffraction soln. 9-38195
 fluid wave diff. of two-fluid system due to step in bottom topography 9-40763
 Kelvin waves, by sharp bend on rotating earth 9-28858
 plane wave by impedance wedge 9-38205
 sea waves, basic theory and engineering aspects 9-49431
 seismic P, SV and SH waves and shadow boundary shifts 9-28844
 seismic P waves by core, long period amplitudes near shadow edge 9-28845
 shock wave obliquely impinging on obtuse wedge, accompanying regular refl. 9-34092
 by slot in plane screen, eigenvalue problem 9-47853
 surface and internal waves in heavy incompressible fluid 9-38948
 wave equation, reduced, subject to mixed boundary value conditions, uniqueness of soln. 9-22068
acoustic waves
 Bragg cell applic. to optical signal processing 9-27365
 corrections to absorption coeffs and sound velocity meas. 9-22250
 cylinders, aluminium, in water, pulsed circumferential waves generation 9-29277
 interface, periodic, especially sinusoidal 9-45858
 plane, by rounded edge of semiinfinite plates, numerical soln. 9-22259
 shock diffraction by sharp wedge, blast trace analysis 9-46561
 by two spheres in infinite isotropic medium 9-36181
 of variable amplitude and phase, by finite plane object 9-41827
acoustic waves, ultrasonic
 in absorption meas. 9-47822
 evanescent u.s. waves, detect. by Bragg diff. of laser light 9-29278
 plane monochromatic wave, by small number of elastic or semi-rigid cylinders, theory and expt. 9-43787
 review 9-25099

Diffraction continued**acoustic waves, ultrasonic continued**

in velocity meas. 9-47822
velocity meas. in liquids, interferometric method, diffraction effects 9-46631

electromagnetic waves

aerial, integral eqn. for polar diagram, when diffraction takes place on aerial surface 9-36242
algebraic formulation in Hilbert space derivation, finite energy source 9-22312
by array of rectangular transverse section bars, for oblique incidence 9-38331
boundary conditions and relation of incident wave 9-47850
by cascaded apertures 9-29345
circular aperture in a plane screen between different media 9-22311
classical theory, basic duality in algebraic formulation 9-47852
by conducting half plane, cylindrical wave diff., soln. 9-43811
by conducting network, energy distrib. determ. 9-43809
coordinate transformation application 9-34122
diffracted rays at open-ended waveguide edge 9-47863
energy distribution in different orders 9-27258
image formation processes, exceeding normal limit of resolution 9-34197
interface, periodic, especially sinusoidal 9-45858
by ionospheric disturbances, travelling 9-31412
in lattice of plane rectangular elements, infinite, approx., calc. 9-47855
obstacles, perfectly conducting effect on accuracy of direction-finding 9-29343
plane wave diff. by cylinder, transient response of penumbral currents 9-41856
resonator, plane mirror, coupled, diff. losses 9-45892
screen with rectangular slots, transmission coefficient at oblique incidence 9-29344
spherical segment, ideally conducting, calc. 9-36227
threshold phenomena, theory contrib. 9-47854
by transmission network, numerical study 9-45896
Wiener-Hopf simultaneous eqns., boundary value problems 9-34121

electrons *see* **Electron diffraction****light***see also* **Holography**

by acoustic waves in anisotropic media, modified Bragg formalism 9-27387
acousto-optic, applic. to tunable optical filter 9-36378
a.m., by u.s. plane wave, theory and expt. 9-32021
in amplitude diffraction grating imaging 9-32017
aperture, annular, aberration-free, theory 9-29466
aperture, small, in black screen, extension of Kirchhoff theory 9-25363
Bragg, detection of evanescent u.s. waves 9-36175
Bragg, of laser beam by sound beam, relative efficiency as function of interaction geometry 9-34211
Bragg, study of elastic second-harmonic generation by longit. u.s. beams 9-37225
Bragg applic. to optical imaging of multiple microwave u.s. beams in solids 9-36189
character recognition by incoherent Fourier transformation 9-25365
Czerny-Turner spectrometer, multiply diffracted light, experimental confirmation of theory 9-32055
in dielectric medium traversed by u.s. wave, orientation and deterioration 9-36353
disk, incoherently irradi., calc. 9-41944
edge, coherently illuminated, defocused image, energy distribution 9-36355
filters, spectral adaptation by light bundling 9-48108
Fraunhofer, demonstration 9-41729
Fresnel images, optical correlation 9-36352
Fresnel single slit patterns, theory and obs. 9-40378
Fresnel transform, simplification of theory 9-27389
Fresnel zone, single, field calc. 9-46000
Fresnel zone plate, image formation in visible and soft X-ray region 9-27385
Fresnel zone plate, variable pattern, moire synthesis 9-27386
Fresnel zone plate problem; soln. 9-43916
holographic imaging with coherent fields, theory 9-27355
image of general periodic bar pattern through aberration-free annular aperture 9-43909
images of coherently illuminated objects in presence of aberrations 9-34207
inverse, using Bjorkas identity on e.m. far field backscattered 9-47851
inverse diff. problem, soln. and representation of field as ang. spectrum of plane waves 9-22456
laser light from monolayer of polymer spheres, for demonstrating crystal structure techniques 9-47712
lens for pupil correction, apodization problem 9-46001
microscope, phase contrast, effects of varying conjugate area of phase plate 9-27400
microscope exit pupil enlargement, holographic, using partially coherent light 9-22466
moire aspect of holography 9-27351
proving screens obtained by superposition of recordings from some aperture onto photographic plate 9-25360
Rayleigh criterion analogy approach to modulation transfer function estimation 9-38399
resolution limit for line objects and circular aperture 9-43918
slit aperture pattern with exponentially correl. illumination, corrected expression 9-27384
spectrometer with circular aperture, line breadth theory 9-25384
by supersonic waves, Raman-Nath eqns., exact soln. 9-22457
by supersonic waves, Raman-Nath eqns., soln. 9-27390
theory of Schlieren methods 9-32005
by u.s. standing wave, spectrum analysis by holographic method 9-36320
u.s. technique rel. to photoelastic coeffs. determ. 9-26308
vertical polarization, two parallel strips in a plane 9-32019
wave fields, angular-spectrum representation 9-36354
waves, self-action in non-linear medium e.m. theory 9-25351
zone plates, Fresnel and 1st order 9-46002
CrBr₃, ferromagnetic, Fresnel patterns, depend. on mag. field direction 9-31079

neutrons *see* **Neutron diffraction****X-rays** *see* **X-ray diffraction****Diffraction by acoustic waves** *see* **Acoustic waves/effects; Diffraction/light****Diffraction gratings**

amplitude imaging, effect of diffraction and interference 9-32017
concave, corrections to Beutler's theory 9-29467
concave vacuum, monochromator with 1 m variable range and translational scanning 9-41964
in Czerny-Turner, spectrograph 9-46023
echelettes and laminar, effectiveness rel. λ/c 9-27258
electron, transparent line, written with fine electron probe 9-26219
holographic, with arbitrary loss, theory and experiment 9-45999
holographically made, spectrographic performance 9-34214
intra-cavity laser, for single wavelength operation 9-27296
use in laser interferometer 9-41941
metal, optically excited, surface plasmons incoherent and coherent radiation emission 9-24371
Michelson interferometer adjustment for white light fringes using transmission grating 9-25354
photographic, production using triangular interferometer 9-27380
plane, false spectra, laser illumination 9-32018
plastic, with restricted thermal expansion, production method 9-25364
pulse compression theory 9-43917
reflectivity in ultrashort X-ray region 9-36351
resolving power 9-22464
sine wave, testing of eye transfer function 9-49611
sine-wave, generated by convolution of line grating with gaussian blur, explicit eqn. 9-25362
sine-wave, stabilized and non-stabilized, contrast threshold meas. 9-36086
sinusoidal, modulation visibility thresholds rel. to spatial freq. 9-34206
square-wave, convoluted with gaussian spread function, modulation of produced sine-wave grating 9-25361
u.v., affect of simulated space environment 9-27383
Nd: glass laser cavity reflector appln. for spectral band narrowing 9-25296

Diffraction/scopy *see* **Diffraction/light; Optical images****Diffusion**

see also **Neutrons and antineutrons/diffusion; for diffusion of matter, see Diffusion in gases; Diffusion in liquids; Diffusion in solids**
binary mixtures near critical point, kinetic phen. 9-48735
cement paste, drying under temp. gradients, role of moisture diffusion 9-34950
chemically reactive fluids, effect on light scatt. 9-31181
coefficient dependence on solute conc., effect on longit. dispersion 9-36743
concentration-dependent problem, mathematical similarity to flow in free boundary layer 9-38945
convective, liq.-solid interface, accel. by u.s. sound field 9-23615
creep under neutron irradiation 9-28308
dielectric, in direction of increasing dielec. const., under action of elec. field 9-42670
drift-tube expts., collector props. effects 9-44530
in earth's rad. belts, rel. to precipitation losses 9-37950
Earth's radiation belt, electrons, radial coeff. (1.76 < L < 5) 9-24682
effect on turbulent viscosity variation 9-32574
Ehrenfests' wind-tree model, normal and abnormal diffusion of particles 9-36138
electrons in outer rad. belt, energy > 100 keV, radial 9-40064
flows, time-depend., and first-order reaction 9-23226
fluid, self-diffusion and time depend. of pair correlation 9-23208
fluids, dense supercritical, mutual diffusion 9-31796
of gas into cavitation void, effect on sound radiation 9-28087
ion beams in Poiseuille flow 9-22358
ionic, an electrostatic deposition 9-23409
in Lorentzian field, of light particles, time dependent 9-44393
magnetic, lift given to a current wire moving over the field 9-22343
of magnetic field in ferromagnetic body 9-41734
magnetoplasmas, r.f.-excited, theory 9-32596
magnetospheric electrons, pitch angle diffusion, review 9-37948
in magnetospheric plasma, pitch-angle 9-37950
of magnetospheric trapped radiation, inward, effect of convection electric fields 9-43435
methylbenzyl cyanides, consts. for mole. and internal rot. from n.m.r. study 9-46657
mixed dense fluids 9-30167
mixture, binary, variational calc. 9-27192
nonlinear, in heterogeneous media, transient phen., coupled analogue simulation 9-25044
plane source diff., non-ideal conditions 9-29220
plasma collisional diff. in toroidal stellarator 9-25905
plasma electrons in velocity space 9-44414
plasma in toroidal stellarator 9-40678
plasma turbulent diffusion and ion heating during current instability 9-30289
radial, of charge carriers in cathode dark space region of a d.c. glow discharge 9-30311
rel. to radiating power of cylindrical cavity 9-41838
radiation, high-density, in unidimens. medium 9-41788
in radiation belt, outer, of equatorial particles 9-45517
random coil, translational diffusion const. 9-48518
solar protons, low energy, entry into magnetosphere 9-41551
ternary critical states, in multicomponent metallic systems 9-24518
thermal, cast vitreous-crystalline materials in different compositions 9-39525
time lag treatment of non-Fickian axial distance-dependent anomalies 9-40261
tracer diffusion coeff., kinetic theory 9-43769
CO₂ lasers, effect on gain saturation 9-47969
Na³⁵Cl, in NaCl-H₂O 9-23476
 δ -Pu, stabilized, Al obs. 9-28323

acoustic waves*see also* **Scattering/acoustic waves**

auditoria sound discrimination 9-34089
cylindrical, at grating of perfectly compliant cylinders 9-25100

electromagnetic waves*see also* **Scattering/electromagnetic waves**

in luminescent diffusive medium, pulse characts., calc. 9-25149

light*see also* **Reflectivity; Scattering/light**

boundary wave, reformulation of Kirchhoff theory, and implications 9-27388

Diffusion continued
light continued

- coherent, intensities and angular distributions calc. 9-46005
- diffusion discs, optical characteristics 9-22460
- disperse scintillator system, efficacy of a disperse system composed of scintillation granules and a solution for β -active substances 9-22670
- in luminescent diffusive medium, pulse characts., calc. 9-25149
- in self-focusing liquids, spectral composition, Q-switched ruby laser beams 9-26116
- self-focusing of intense beams in nonlinear dielects. 9-48092

Diffusion columns *see Diffusion in gases/thermal; Isotope separation***Diffusion in gases***see also Flow/gases*

- air, aeration meas. by $^{10}\text{B}(\text{n},\alpha)^7\text{Li}$ reaction on methylboric acid label 9-24609
- air, of organic and other vapours coeff. meas. 9-30326
- alkali metals diff. coeff. meas. using buffer gas 9-29942
- ambipolar coefficient, effective, rel. to electron loss in air afterglow 9-44505
- artificial, stabilisation of difference schemes for inviscid flow eqn. 9-36798
- atmospheric, from linear source in surface layer 9-35815
- atmospheric, lateral, rel. to finite time of admixture injection 9-40020
- atmospheric Ekman layer, of large cloud 9-41509
- balance eqn. for excited atoms corrected for diffusion and collisions of first and second kind 9-46309
- binary mixture, slip velocity calc. 9-23408
- calculation techniques in dilute gases 9-36819
- coefficient and spin relax. cross section for alkalis 9-42332
- rel. to collisions, inelastic, 10^4 K 9-34841
- crystal growth, role of diffusion in vapour transport 9-36998
- electron drift motion and resonance scatt. 9-46578
- electron plasma, injected beam velocity diffusion 9-44479
- electrons in electrostatic field, longitudinal diffusion 9-39057
- electrons in weakly ionized gas, book 9-25841
- equations of mixtures 9-26047
- inert, of slow electrons, cross section microwave obs. 9-23273
- inert gas atoms, metastable, in same gas 9-30356
- ionized, multicomponent, Monoat, gas in mag. field 9-44488
- ionized externally, effect on elec. conductivity 9-44489
- of ions, coefficient meas. by amplitude-frequency methods 9-30299
- Knudsen cells, attainment of equilib 9-33658
- Knudsen cells, attainment of equilib. 9-28774
- of light particles, eqn. boundary conditions 9-40755
- from line source in turbulent boundary layer 9-34842
- longitudinal, electrons in electrostatic field 9-39057
- in Ne discharge positive column, of plasma 9-44506
- plasma, diffusion modes across uniform magnetic field, pressure dependence 9-42493
- plasma, high electron temp., transverse coeff. in mag. field, meas. 9-46468
- plasma, in velocity space, variational study 9-25929
- in plasma, magnetoactive weakly ionized, of strong electron conc. inhomogeneities 9-38960
- plasma, nonthermal (in rel. to ions.) 9-31403
- in plasma, stationary toroidal 9-25849
- plasma, two-dimens., test particle diffusion and friction coeffs. 9-38961
- plasma in mag. field, transverse coeff. rel. to electron temp. 9-46469
- plasma in stationary deionizing flux, diff. accumulation 9-40660
- plasma in uniform magnetic field 9-40658
- polar (mixed) gases, coeffs. determ. from viscosity data 9-36827
- shock aerodynamic tube for diffusor study 9-42599
- shock waves precursor electrons and ions 9-25872
- Townsend-Huxley expt. analysis; const. collisional cross section 9-39056
- Townsend-Huxley expt. analysis; const. collisional coefficient 9-39055
- turbulent, electron loss, at low pressure, microwave breakdown 9-32707
- turbulent, nonadiabatic, of suspensions in atm. boundary layers 9-31304
- turbulent flow in low speed wind tunnel 9-36826
- waves in plasma, effect of collisions 9-48603
- Ar, dense with Ne and deuterium, self-diffusion in critical gas-liquid region 9-36828
- Ar, of Cs and K vapours 9-39059
- H₂-Kr, intermolecular forces 9-46580
- H₂, electron drift and resonance scatt. in terms of H₂⁺ temporary states 9-46578
- H atoms in H₂, and in H₂-He, H₂-Ar mixtures 9-39060
- He-Kr, intermolecular forces 9-46580
- He, of Cs and K vapours 9-39059
- He in discharge positive column, medium press. 9-25980
- He metastable atoms in He 9-29984
- He plasma, partially ionized, electron collision frequency 9-44417
- Hg⁺ in parent gas, mobility as function of temp. 9-48420
- K⁺ in N₂, coeff. determ., transport eqn. soln. 9-23203
- N₂, of K ions, and drift velocity 9-40756
- N₂, electron drift and resonance scatt. in terms of H₂⁺ temporary states 9-46578
- N⁺ in N₂, mobility, diffusion coeff. and reaction rates determ. 9-23347
- Ne-Xe system 9-42616
- Ne-inert-gas systems 9-42617
- Ne plasma, partially ionized, electron coefficient 9-44417
- Rn decay products, transport proc. in air 9-32327
- Rn decay products transport proc. in air 9-22762
- SO₂, dimethyl ether and ethyl chloride binary and ternary mixtures 9-36817

thermal

- atmospheric, in westerly wind field 9-41498
- for binary mixtures, tube connecting two reservoirs 9-46579
- column operation rel. to intermol. pot. calcs. 9-34843
- column theory, expt. verification 9-46581
- column theory for multicomponent systems, expt. verification 9-39061
- eff. of dimers 9-36686
- ethylene-N₂ mixtures, influence of dimers 9-36686
- intermolecular potential function determ. 9-42466
- ionized, multicomponent, Monoat, gas in mag. field 9-44488
- ionosphere, topside, for multi-charged ion mixtures 9-45519
- nonisothermal, nonstationary, in 2 bulb geometry 9-26046
- sequential analysis applic. 9-47527
- transpiration, rot. collision number and Eucken factor determ. 9-30335
- Ar-CO₂, He mixtures, influence of dimers 9-36686
- Ar, column operation rel. to intermol. pot. calcs. 9-34843

Diffusion in gases continued
thermal continued

- CO-chloromethane system, composition dependence of thermal diffusion factor 9-39058
- CO₂-Ar, Kr mixtures, influence of dimers 9-36686
- CO₂-chloromethane system, composition dependence of thermal diffusion factor 9-39058
- H₂-Kr, intermolecular forces 9-46580
- He-Ar mixtures, influence of dimers 9-36686
- He-Kr, intermolecular forces 9-46580
- He-methyl chloride mixture 9-32740
- Kr-CO₂ mixtures, influence of dimers 9-36686
- Kr, column operation rel. to intermol. pot. calcs. 9-34843
- Kr isotope mixtures in column, verification of theory 9-39061
- N₂-ethylene mixtures, influence of dimers 9-36686
- Ne, column operation rel. to intermol. pot. calcs. 9-34843
- Xe, column operation rel. to intermol. pot. calcs. 9-34843

Diffusion in liquids*see also Flow-liquids*

- ¹³C, and ¹⁴C substituted mols, isotope eff. 9-32777
- aniline, deuterated doped with cyclohexane, molecular diffusion effect on NMR 9-28157
- aniline, deuterated doped with cyclohexane, molecular diffusion effect on NMR 9-44596
- benzene, carbon tetrachloride, of N₂ and Ar, open-tube obs. 9-30383
- benzene-toluene mixture, self-diffusion obs. 9-36856
- binary mixture, Bearnman theory, Rice-Allnatt extension of Rice-Kirkwood theory checked 9-34888
- carbon tetrachloride, of N₂ and Ar, open-tube obs. 9-30383
- classical, Stokes-Einstein expression deriv. molecular model 9-34869
- coefficients meas. by means of laser interferometric technique 9-44553
- cyclohexane, diffusion in benzene, meas. by laser interferometric technique 9-44553
- dialysis, effect of ultrasound on diffusion rate 9-34893
- dielectric, effect on conduction process theory 9-30415
- N, N-dimethylformamide, anisotropic molec. rot., n.m.r. 9-30433
- electrolyte diffusion meas. by diaphragm cell 9-35751
- entrainment across density interface, turbulent, molecular diffusivity effects 9-23473
- gas from ascending bubbles, behaviour of vol. and gas press. 9-46606
- laminar flow over defined shapes, diffusion from free surface into liquid film 9-48690
- lattice structure not supported 9-36845
- macromolecules in soln., rotary diffusion broadening of Rayleigh lines 9-39104
- membrane oxygenator, patent 9-23479
- metal, vol. diffusion coeffs. of melts rel. to equil. charact. 9-39131
- metals, at melting point, isotopic mass dependence 9-30376
- Na, self-diffusion coeff. 9-42643
- polar liqs., self-diffusion coeffs. and rotational correl. 9-28111
- poly- α -amino acid solns., from light scatt. 9-42657
- poly-N-isobutylmaleinimide, rel. to mol. props. 9-23193
- polyisobutylene in very dilute solns., obs. 9-32545
- polymer soln., hydrodynamic interaction, variational calc. 9-42460
- pulsation diff. method 9-44554
- pulsation method, diff. coeff. determ. 9-44555
- rotary, of macromols. in soln., detect. by broadening of Rayleigh lines 9-39104
- rotational, meas. by light scatt. 9-28128
- salt solutions, molecular diffusivity rel. to instability of salt fingers 9-33748
- self-diffusion, theory 9-48679
- statistical correlation in liquid solns. 9-39085
- styrene-butyl methacrylate graft copolymer 9-32553
- styrene-methyl methacrylate graft copolymer 9-32553
- sucrose in water, theory and meas. 9-23476
- surface heterodiffusion coeff. determination by mass transfer method 9-37193
- ternary system with 2 isotope forms of same subst. in soln. 9-23475
- ternary systems, diffusion coeffs. calc. from diaphragm cell expts. 9-34889
- o-terphenyl, self-diffusion rel. to mol. motion, 9-39925
- tetrachloroethylene doped with nitromethane, molecular diffusion eff. on NMR 9-44596
- tetrachloroethylene doped with nitromethane, molecular diffusion eff. on NMR 9-28157
- toluene-cyclohexane mixture, self-diffusion obs. 9-36856
- turbulent, effective coefficient magnitude 9-39064
- urea in water, theory and meas. 9-23476
- water, diffusion coeffs. of inert gases 9-28112
- water, neutron diffusion meas., 18-280°C 9-30380
- water, self-diffusion, temp. depend. 9-32778
- CaCl₂ soln., diff. coeff. determ. by pulsation method 9-44555
- CuSO₄ aq. soln., of Cu²⁺, e.p.r. obs. 9-34890
- Fe, of S and O at 1560°C 9-48691
- H₂O, of Ne, Kr, Xe, CO and NO, 10¹⁰ to 60°C 9-26086
- H₂O in aq. solns. 9-44547
- Hg, self-diffusion coeff. 9-42643
- Hg electrodiffusion of Bi, effect of Tl, In and Sn additions 9-46623
- K, self-diffusion coeff. 9-42643
- KCl soln., diff. coeff. determ. by pulsation method 9-44555
- Li, self-diffusion coeff. 9-42643
- LiNO₃ of ²³Na, ¹³⁷Cs, temp. depend. obs. 9-34891
- Na, of Cd and In, rel. to temp., and electromigration 9-31201
- NaCl soln., diff. coeff. determ. by pulsation method 9-44555
- NaNO₃ of ²³Na, ¹³⁷Cs, temp. depend. obs. 9-34891
- Pb, self-diffusion coeff. 9-42643
- RbNO₃ molten, self-diff. coeff., 318-499°C 9-30381
- RbNO₃ of ²³Na, ¹³⁷Cs, temp. depend. obs. 9-34891
- Sn-Zn alloys, liquid, self-diffusion coeffs. meas. 9-28113
- Sn, electrodiffusion of Bi, effect of Tl additions 9-46623
- UO₂, irradiated, of Xe and Kr, from fission bubble growth kinetics 9-28152

thermal

- n-alkanes + cyclic hydrocarbons, Soret coeffs. 9-30382
- crystal melt, mechanism during directional crystalln. 9-48852
- isotopes in liquid mixtures 9-23472
- phenol-water mixture, temp. depend. of diffusion coeff. from light scatt. analysis 9-40794

Diffusion in liquids continued
thermal continued

- radiation pressure theory, orientation depend. on speed of sound and conductivity 9-46622
- Soret coeffs. meas. apparatus 9-30382
- statistical correlation in liquid solns. 9-39085
- and structural order 9-23458
- weightlessness conditions, transport processes, influence of oscillations 9-23474

Diffusion in solids

see also *Permeability, mechanical*

- alkali halides, by divalent ions 9-28314
- alkali halides, chemical interdiffusion coeff. 9-28311
- alkali halides, f.c.c. defects contrib. to tracer diffusion 9-44729
- alkali metals, vacancy relax. and migration energy, lattice-dynamical calc. 9-23792
- alloy, binary, thin films, effective surface diffusion coeffs., vol. diffusion effect in electron diff. obs. 9-39379
- alloys, eff. of radiation 9-24068
- anion vacancy migration for F_2 - and Zr -colour centre formation 9-39375
- anthracene, exciton triplet anisotropy 9-35137
- apophyllite ($KFCa_2Si_6O_{20} \cdot 8H_2O$), of H_2O , p.m.r. study 9-47447
- Ar, diffusion coeff. determ. 9-44722
- binary systems, interdiffusion coeffs. determ., Matano-Boltzmann method improvement 9-40977
- borosilicate glass, of Ag^+ under elec. field, dendritic growth obs. 9-48872
- α -brass, enhanced during cyclic straining 9-44732
- chemical, surface effs. 9-35120
- coefficient D calc. for diffusion from vapour phase, anal. of conc. curves 9-28207
- coefficient from sorption data at variable external conc. 9-46840
- coefficients determ., volume, grain-boundary and surface, from sintering data 9-42857
- concentration depend. of coeffs., from measured conc. profiles 9-33000
- constants, effect of surface roughness, theory 9-42858
- on cubic lattices model and applic. to early stages of ordering 9-30622
- Darken equation in the determination of interdiffusion coefficients 9-37192
- diphenyl, along substrate surface during growth from vapour 9-48796
- doped oxide as source 9-37195
- enhancement by ionizing radiation, mechanisms 9-42856
- excitons, singlet, in anthracene crystals, tetracene doped, evidence for long-range exciton-impurity interaction 9-24457
- f.c.c. metals, of H_2 , activation energy 9-23841
- f.c.c. metals, self and impurity, Gibbs free energy 9-33001
- α -Fe, u.s. determ. of diffusion coeff. of carbon at 408° and 430°C 9-37196
- ferrite, dissolution kinetics of Fe_3C 9-48874
- films, vacuum-deposited, effect on thickness of deposited metal 9-40838
- gas atoms, capture by moving gas bubble 9-35121
- graphite, mechanism, and rel. to irradiated sample 9-40981
- graphite, neutron irradiated in CO_2 , uptake of Br 9-28316
- graphite, of non-gaseous fission products, rel. to escape 9-26299
- graphite channel, air radial diffusion rel. to oxidation kinetics 9-26824
- group II-VI compounds, defect characterization rel. to self-diffusion meas. 9-37156
- in growth of cryst. from vapour, along substrate surface 9-48796
- rel. to growth of single crystals 9-48790
- high vapour press. solids at cryogenic temps., diffusion rates, meas. method 9-44722
- ice, rel. to relax. phenom. 9-28318
- inert gas bombarded, mechanisms 9-37194
- interstitial, noble and transition metals in metallic systems 9-42812
- ion-electron pairs in shock tube walls, shock wave upstream photoionization 9-43797
- ionic defects across activation barrier, elec. field depend. 9-28307
- Kirkendall effect, low pressure effect 9-40978
- of lattice defects in stress field 9-46842
- lattice-vibration theory, anharmonic 9-44723
- measurement of transistor parameters 9-43088
- metal, near-surface, effect of non-equilib. segregation 9-48871
- metal, of diffusion-coating element during high-temp. oxidation 9-48870
- metal oxides, nonstoichiometric, chem. diffusion coeffs. 9-44727
- metal oxides, surface diffusion, review 9-37198
- metal surfaces, tracer diffusion studies, use of microtome 9-46843
- metallizing 9-46915
- metals, electrochem. methods for meas. at high temp. 9-46841
- Mo, of P, interstitial mechanism 2000-2220°C 9-35132
- of Mossbauer nuclei, stochastic model treatment 9-41363
- multicomponent, effective binary diffusion coeff., use and limitations 9-44728
- near-surface, effect of non-equilib. segregation 9-48871
- noble metals, of Pb, Sn, In, and Tl, rapid, interstitial mechanism 9-28321
- oxides, ideal conditions for direct meas. 9-44743
- oxides, mass transfer conf. 9-44726
- pentaerythritol, water mol. diff. as impurity, proton mag. reson. investig. 9-25777
- polymers, crystalline 9-23846
- polymers, of low mol. wt. penetrants, models, mechanisms and laws, review 9-39389
- of pores, kinetics, review 9-37188
- in pressure gradient, kinetic treatment 9-44725
- Pyrex glass, of deuterium 9-40987
- pyrocarbons, self-diffusion meas. 9-44730
- quartz, paths of ions during electrolysis, rel. to conductivity 9-39387
- rare-earth metals, Zener parameter rel. to atomic number 9-33008
- rare-earth oxides, of O 9-26304
- self, in interstitial phases 9-23832
- self-diffusion model for filamentary-crystal growth from vapour, formula-tion 9-36991
- semiconductor, field-dependent, space-charge wave instability 9-43047
- semiconductor organic p-n junctions, diffusion doped 9-35436
- semiconductors, binary compound, review of data 9-26298
- semiconductors, multivalley, effect of transverse e.m.f. of diffusion lengths 9-49073
- soda-lime glass of H_2O , near and within transform. range 9-46854
- steel, high-speed cutting, W vol. and grain-boundary diffusion, role in carbide precip. kinetics 9-39383
- steel, low C, of Cr. mechanism 9-46849

Diffusion in solids continued

- sucrose, surface diffusion model rel. to growth rate curves 9-37098
- surface, role in crystal growth from vapour phase 9-37009
- surface heterodiffusion coeff. determination by mass transfer method 9-37193
- tracer, isotope effect obs. 9-44724
- tracer diffusion studies in metal surfaces, use of microtome 9-46843
- transition metal carbides, self-diffusion in interstitial phases 9-23832
- unbending of cryst. 'climb' mechanism 9-26324
- vacancies in crystals, thermal diff. 9-28278
- vacancy-flow term, rel. to conc. distortion by impurities, and deviation from thermodynamic equilib. 9-23831
- volume diffusion-controlled Ostwald ripening, particle size distribution 9-39460
- welded clad metal diffusion layer structure, diffusion activation energy and coeff. of reactive diffusion 9-40983
- wires, sintering by surface diffusion 9-44783
- wires, sintering by surface diffusion 9-44782
- Ag-Au alloys, Kirkendall shift, press. and vacancy-flow effects 9-46848
- Ag-Au alloys, of Ag, by high temp. electrochem. method 9-46841
- Ag, of Sb, intercryst., temp. depend. 9-46846
- Ag,S evaporated layer, diffusion processes obs. with photoemission electron microscope 9-40980
- Ag from linear dimens. changes 9-41097
- Ag halides, by divalent ions 9-28314
- Ag halides, f.c.c., defects contrib. to tracer diffusion 9-44729
- Ag thermal diffusivity from linear dimens. changes 9-41097
- AgBr, interstitial motion 9-28312
- AgBr, of chloride and iodide tracers 9-40979
- α -AgCd, rel. to activation energies of Zener relaxation 9-33025
- AgCl, interstitial motion 9-28312
- AgCl, of Au^+ , low temp. suppression by chlorine 9-46847
- AgCl, of bromide and iodide tracers 9-40979
- AgCl, of Sr^{2+} , activation energy 9-46857
- AgCl, vacancy correlation factor 9-28313
- α -Ag-Cd alloys, self-diffusion 9-33002
- Al-Au thin films, anomalies 9-35123
- α -Al₂O₃, of β -active fission products, obs. 9-30623
- Al₂O₃, surface diffusion, obs. review 9-37198
- Al₂O₃ bicrystals, surface coeff., from relative energies of $[1100]$ tilt boundaries 9-26290
- Al dil. alloys of solute atoms, rel. to ^{27}Al n.m.r. relax. meas. 9-47443
- Al thermal diffusivity from linear dimens. changes 9-41097
- AlSb, of Zn, chemical and isoconcentration, Longini's interstitial/substitutional model 9-35125
- AlSb, of Zn, chemical and isoconcentration, conc. depend. 9-35124
- Ar, self-diffusion vacancy mechanism, many-body effects 9-46693
- Ar (100) surface, Ar ad-atom barriers on three structs. 9-35000
- Au-Ag alloys, interdiffusion, effect of gradient energy 9-37199
- Au, self-diffusion, 335-390°C, conc. profiles and coeffs. 9-23835
- Au, self-diffusion meas. in single cryst. 9-39381
- Au, thermomigration of ^{197}Au and ^{125}Sb 9-35126
- Ba, of H₂, 200 to 620°C, and solubility limit of BaH₂ 9-28315
- BaF₂:U of Kr and Xe, for neutron-irrad. single cryst. 9-35127
- BaF₂, of ^{89}Sr , cation defects study 9-39382
- BaF₂, of Kr and Xe, for neutron-irrad. single cryst. 9-35127
- Bi-Cd, partial coeffs., from zone of contact liq. layer conc. meas., 180°C 9-33003
- Bi-Sn, partial coeffs., from zone of contact liq. layer conc. meas., 160°C 9-33003
- Bi, electrotransfer of small Sb and Zn impurities 9-48873
- Bi₂O₃-B₂O₃(-R₂O) glass systems, Co tracer exam. rel. to chem. struct. 9-46698
- C self-diff., role in C-CO₂ interac., temp. >2000°K 9-28779
- Ca, self, and of low solubility impurities 9-23836
- CaCO₃, self-diffusion of by isotope exchange with CO₂ 9-46844
- CaCO₃, self-diffusion of O by isotope-exchange with CO₂ 9-46844
- CaD₂, of ^{89}Sr , cation defects study 9-39382
- CaTiO₃, of point defects, coeffs. by analysis of transient elec. conductivity data 9-28317
- CdS, of Ag, in prep. of shear-mode-evaporated u.s. transducers 9-42957
- CdSe, self-diffusion of Cd, rel. to high temp. defect equilibria 9-37200
- CdTe, self-diffusion of Cd, 700-1000°C 9-37201
- CEFs, of ^{129}Te , from n.m.r. meas. 9-24506
- CoO₂ and CeO₂:Gd³⁺ single crystals, of O, 1040° to 1535°K, and elec. conductivity and thermoelec. power 9-33246
- CoO:Al(Li), of ^{60}Co , coeff. meas. and vacancy mechanism obs. 9-40982
- CoO, of ^{60}Co , coeff. meas. and vacancy mechanism obs. 9-40982
- CoO, self-diffusion of O, mechanism 9-44731
- CsCl, neutron-irrad., of rare gases, effect of α to β phase transform. 9-33004
- CsI, neutron-irrad., of rare gases, effect of α to β phase transform 9-33004
- CsI, of ^{133}Xe , trapping by natural and irrad. defects, obs. 9-37202
- CsI, of ^{133}Xe , use of fission recoil doping techniques 9-23837
- Cu-Ag alloy, effect of Be additive on Ag diff. along crystallite boundary 9-31228
- Cu-Au(Al) alloy films, effective surface coeffs., vol. diffusion effect in electron diff. obs. 9-39379
- Cu-Pd alloys, interdiffusion, effect of coherency strains 9-35128
- Cu-Pd alloys, of O₂, internal oxidation, 850-1000°C 9-24557
- Cu-Pt alloys, of O₂, internal oxidation, 850-1000°C 9-24557
- Cu-Zn system phases, interdiffusion coeff., conc. depend. 9-46850
- Cu, lattice-vibration theory, anharmonic 9-44723
- Cu, self, coeffs. meas. from annealing of spherical voids, 390° to 560°C 9-30624
- Cu₂O, interdiffusion of O, obs. from elec. conductivity meas. 9-44733
- Cu₃Pd, of H 9-23838
- Cu alloy coatings, effect on fatigue strength of Cu 9-33058
- Cu of inert gases, influence on gas release of implanted ions, implantation energy and dose 9-35129
- Cu whiskers, of Zn, coeff. depend. on diameter 9-26300
- E₂O₃, self-diffusion coeffs. of O, by isotope exchange method 9-44741
- Er₂O₃ polycryst., cation self-diffusion coeffs. 9-42860
- Fe-Al system intermetallics, of Fe, coeffs. 9-46890
- Fe-C, of ^{59}Fe , rel. to effect of C on ^{59}Fe mobility in grain boundaries 9-37203
- Fe-Ni alloys, electrotransport of components, tracer technique 9-28320
- Fe, malleable cast, of S, rel. to microdistribution of sulphur during annealing 9-23950

Diffusion in solids continued

- α -Fe, of ^{64}Cu rel. to defect interactions 9-46851
 α -Fe, of N_2 rel. to Fe-N solubility, Ni effects 9-23840
 Fe, self-diffusion in δ , γ and α -phases, isotope effect meas. using ^{52}Fe - ^{59}Fe 9-26301
 Fe, self-diffusion isotope effect, mass depend. 9-35130
 Fe b.c.c. phase, of Be, temp. depend. 9-23839
 Fe of Cr, mechanism 9-46849
 GaAs: Si-p junctions, minority carrier diffusion length from photo-e.m.f. spectra 9-37614
 GaAs, annealed, of Cu, dislocations effect 9-44734
 GaAs, of S, and variation of diffusion coeff. with As pressure 9-35434
 GaAs, of Zn, 1000°C 9-28327
 GaAs, of Zn, chemical and isoconcentration, Longini's interstitial/substitutional model 9-35125
 GaSb, Zn, chemical and isoconcentration, Longini's interstitial/substitutional model 9-35125
 Ge-MgSb₂ amorphous films, reordering process under annealing 9-34985
 Ge, Li-ion drift mobility, 23.8° and 61.2°C 9-35131
 Ge, mechanism, review 9-37209
 Ge, migration of Li, control for radiation detector production 9-26557
 Ge, of As at 830°C, dislocation generation 9-42830
 H, interstitially dissolved in metals, solubility meas. for phase transitions 9-35122
 of H up thermal gradient in Zircaloy-2 9-28310
 n-InP, of Au 9-46853
 InSb, self-diffusion 9-44735
 K, of Rb 9-40984
 KCl: Pb²⁺, of vacancy pairs, activation energies from dielectric absorption meas. 9-31108
 KCl, of Au crystallites on surface 9-37204
 KCl, Xe trapping rel. to ion irradi. damage stabilization, obs. 9-37205
 KCl bent crystal treated at 550-750°C, straightening by dislocation diffusion 9-42884
 KFCa₂Si₂O₇·H₂O (apophyllite), of H₂O, p.m.r. study 9-47447
 K, of Na, vacancy and interstitial mechanism, computer obs. 9-44736
 La, f.c.c., self- and of Au 9-33005
 Li/Na/KCO₃ of ^{23}Na and ^{24}Na , near eutectic mixture 9-30625
 Li, of Cu, interstitial-like 9-39384
 Li₂SO₄, f.c.c., diff. of ^{23}Na and ^{24}Na 9-33006
 Mg, of low solubility impurities 9-23836
 MgO-Cr₂O₃ system, interdiffusion formation of MgCr₂O₄ single crystals 9-28319
 MgO, of Ca²⁺ impurity 9-44739
 MgO, of divalent impurity cations 9-44737
 MgO, of Fe and Ni 9-44738
 MgO, of Ga³⁺ 9-26302
 MgO, surface diffusion, obs. review 9-37198
 Mn, self-diffusion in b.c.c. δ - and f.c.c. γ -phase 9-39385
 Mo-W alloys, electrotransport of components, tracer technique 9-28320
 Mo, N diffusivity 9-40985
 N₂, diffusion and flow in natural rocks 9-30332
 NH₄Cl, bubble migration in temp. gradient, sublimation mechanism 9-35134
 NH₄NO₃, of NH₄⁺, nuc. mag. relax. time meas. 9-30628
 Na, of Au, and solubility, 0° to 77°C 9-42861
 Na, of K, vacancy and interstitial mechanism, computer obs. 9-44736
 NaCl:Ca(Cd), Na⁺ and ionic conductivity, conc. depend., heats of assoc. 9-39672
 NaCl: Pb²⁺, of vacancy pairs, activation energies from dielectric absorption meas. 9-31108
 NaCl, of Cd²⁺, ionic conductivity meas. 9-30626
 NaCl, of Kr, Xe and Rn, after irradi. by 10¹⁷ to 2 x 10¹⁶ ions/cm² 9-48875
 NaCl, of Mn²⁺, coeff. determ. by e.p.r. 9-30627
 NaCl, of Na in applied elec. field, vacancy pair obs. 9-44740
 NaCl, surface diffusion, role in crystal growth from vapour phase 9-37009
 NaCl bent crystal treated at 550-750°C, straightening by dislocation diffusion 9-42884
 NaCl powder, densification in air during sintering by volume diffusion 9-35232
 Nb, of ^{51}Cr , contribution of etch pits and sub-boundaries, optical microscope obs. 9-32985
 Nb, of C, coeff. determ. 9-35133
 Nb, of P, interstitial mechanism, 1300-1800°C 9-35132
 Nd₂O₃, self-diffusion coeffs. of O, by isotope exchange method 9-44741
 Ni-Co alloys, self-diffusion of Co, rel. to Co conc. 9-39386
 Ni-Fe alloys, radiation enhancement, rel. to directional ordering 9-44742
 Ni-Mo alloys, of Ni, coeff. and eff. charge 9-26202
 Ni-rich binary alloys, effect of small alloying additions on vol. diffusion at 900-1200°C 9-40986
 NiO, self-diffusion of O, mechanism 9-44731
 O, interstitial atoms in Ta, diffusion coeff. from elastic energy dissipation obs. 9-28284
 Pb, of Cd, diffusivity obs., mechanism 9-46855
 PbO evaporated thin films, of Bi, autoradiographic exam. 9-26303
 PbTe, of Pb and Te 9-44744
 Pd-Ag alloy films, effective surface coeffs. vol. diffusion effect in electron diff. obs. 9-39379
 Pd, α -phase, of H₂ and D₂ meas. 9-37206
 Pd alloys, H diff. coeff. and variation with H conc. 9-28322
 Pr, b.c.c., self- and of La, Ho and In 9-33007
 Pr, of Co, Ag and Au, solute diffusivities 9-44745
 Pt, of O₂, on oriented field emitters 9-23648
 RbCl, of ^{23}Na , 377-707°C 9-23842
 Re, C diffusion into, u.s. meas. at high temp. 9-42966
 Se films, of Ag, lateral diffusion rel. to thin-film couple behaviour 9-42859
 Si:As(P), of Li 9-24234
 n-p-n-Si: B, P h.f. transistors, dopant diffusion anomalies 9-39653
 in Si: P, γ -irradiated, of O, rel. to thermal donor formation 9-32951
 Si/SiO₂/Si₃N₄ double layer films, of Na 9-26305
 Si, B- or P-diffused layers, strain compensation by impurities 9-46824
 Si, mechanism, review 9-37209
 Si, Na solubility 9-40988
 Si, of As, isoconcentration diffusion studies 9-37208
 Si, of As using AsH₃ 9-28324
 Si, of B, rel. to formation of crystallographic precipitates 9-37164
 Si, of B and P, theory and expt. 9-48877
 Si, of B and P, through SiO layers 9-48876

Diffusion in solids continued

- Si₃N₄, of Na 9-26305
 Si n-p-n structures, defects as sites for diffusion pipes 9-30603
 Si of P, induced defects obs. 9-32975
 n-SiC: N of B and Al in prep. of electroluminesc. diodes, anomalous nature 9-37776
 SiC, of Al, by heating to 1800-2400°C for 2-30 hours 9-33009
 SiC, semiconducting, review of data 9-26298
 SiO₂, vitreous, of H₂, H⁺ transport contrib. 9-46856
 SiO layers on Si, of B and P 9-44876
 Sm₂O₃, self-diffusion coeffs. of O, by isotope exchange method 9-44741
 SrF₂: U of Kr and Xe, for neutron-irrad. single cryst. 9-35127
 SrF₂, of ^{89}Sr , cation defects study 9-39382
 SrF₂ of Kr and Xe, for neutron-irrad. single cryst. 9-35127
 Ta, of C, coeff. determ. 9-35133
 Ta, of He, interstitial 9-23843
 Te, of Ag, lateral diffusion along thin film in Ag-Te couple 9-35135
 TiC_{0.67}, of ^{46}Cr , anomalous 9-46858
 TiO₂, of Fe, anisotropy of diffusion front depend. on relative orientation of crystals 9-46859
 U-(1.5 wt.%)Mo alloy, of C, UC gamma phase precipitation structure refinement depend. 9-35260
 UC, of Rn and fission Xe, obs. 9-37214
 UC single cryst., Rn 220 recoil atoms interstitial diffusion 9-28325
 UO₂, bubble migration in temp. gradient, sublimation mechanism 9-35134
 UO₂, of fission gas atoms from bubbles, re-solution process into irradi. material 9-28326
 UO₂, of Rn and fission Xe, obs. 9-37214
 UO₂, of U in sintering rel. to O/U ratio, obs. 9-37287
 UO₂, surface diffusion, obs. review 9-37198
 UO₂, U self-diffusion, 1200-1600°C 9-37211
 UO₂, O and U self-diffusion rel. to comp., obs. review 9-37210
 UO₂, U self-diffusion, 1200-1600°C 9-37211
 UO₂ (x.0.005 < x < 0.217), U and O self-diffusion, 780-1650°C 9-37215
 V, of C, coeff. determ. 9-35133
 W, of metal adsorbates, cluster form. in adsorpt. layer 9-40851
 W, of N₂, high temp. solubility 9-35136
 W, of Nb, Ta and W isotopes, lattice coeffs. meas. 9-40989
 W, surface diffusion of adsorbed CO 9-39176
 W, surface self-diffusion, 2,560-3,150°K, by adatom process 9-44622
 Y₂O₃ polycryst., cation self-diffusion coeffs. 9-42860
 Zn: Ag, of ^{65}Zn and ^{110}Ag , effect of dopant 9-40990
 Zn: Ag, solute and solvent diffusion enhancement 9-23845
 Zn, electromigration 9-23844
 Zr-Al alloy, of N, pumping speed meas. 10⁻⁶-1 torr, 300 and 500°C 9-37197
 α -Zr, O₂ diffusivity and parabolic oxidation kinetics 9-26306
 β -Zr, thermomigration and electromigration 9-39388
- Thermal**
 alloy, diffusivity meas. w.r.t. temp. method 9-41157
 disk, diffusivity meas., stepwise heating method 9-23833
 metal, diffusivity meas. w.r.t. temp., method 9-41157
 metals, thermomigration 9-28309
 metals near melting point, meas. method employing i.r. laser 9-37354
 porous media, dusty-gas theory for thermal transpiration 9-39380
 soil, model applic. to temp. and heat flux profile calc. 9-31254
 vinyl acetate- methyl acrylate copolymer, solubility and diffusion of benzene 9-33010
 GaAs, of Cd, profiles as a function of temp. and As vapour pressure 9-46852
 KCl, of He filled pores, obs. 9-37189
 Mo single crystal, thermal diffusivity 9-41106
 Pu_{0.2}U_{0.8}O_{2-x}, of O rel. to stoichiometry, 1200-2000°C 9-37207
 Ti at high temperatures 9-41109
 (U,Pu)O₂ fuel, mechanisms rel. to stoichiometry 9-37213
 UO₂, of O, and comp. gradient form. 1300-2500°C 9-37212
 UO₂ fuel, mechanisms rel. to stoichiometry 9-37213
- Diffusion pumps** see *Vacuum pumps*
Digital computers see *Calculating apparatus/digital computers*
Dilatometers see *Length measurement; Volume measurement*
Dimensions
 see also *Units*
 C, pyrolytic, effect of high neutron exposure 9-40992
- Dimers** see *Molecules; Polymers*
Dineutrons see *Neutrons*
Diodes see *Electron tubes; Plasma devices; Rectifiers; Semiconducting devices/diodes and tunnel and interface devices*
Dipole moments see *Molecules/moments; Nucleus/electric moment; Nucleus/magnetic moment*
Diquarks see *Quarks*
Dirac electron theory see *Electron theory*
Dirac equation see *Quantum theory/wave equations*
Discharge tubes see *Electron tubes; Gas-discharge tubes; Ion sources; Particle accelerators; X-ray tubes*
Discharges, electric
 see also *Arcs, electric; Breakdown, electric; Corona, electric discharge; Plasma; Sparks, electric*
 a.c., between metal-dielectric electrodes 9-34807
 air, at 7.5-20 cm. gap distances, aftercurrent obs. 9-48623
 air, d.c. and a.c., variation of striking and extinction voltages 9-23358
 arc column and discharge chamber wall of vortex linear plasma generator, heat transfer 9-29322
 arc form. under pulsating voltage between positive peak and plane in surrounding air 9-46548
 axisymmetric pulse discharge channel, temp. profile 9-38958
 balance eqn. for excited atoms corrected for diffusion and collisions of first and second kind 9-46309
 brass foil spectral indicators use for near-electrode plasma layer exam. 9-25972
 breakdown, in uniform-field gap, initiation by an electron, calcs. 9-39031
 capillary, with evaporating wall, energy balances 9-40714
 capillary, with vaporizing wall, temp. and press. rel. geometry and current 9-25978
 cathode, hollow, rel. to feeding cct. parameter changes 9-48618
 cathode arc tracks, current density meas. 9-32711
 circuit for magneto-optical 100ns shutter 9-29500
 coaxial, soft X-rays dominant source determ. 9-25010

Discharges, electric continued

- conducting zone radius, effect of thickness and material of wall 9-38959
 current density meas. near cathode 9-34799
 d.c. plasma, self excited and forced i.f. waves 9-44472
 dielectric, current waveform meas. and recording 9-29357
 dielectric with artificial cavities, resistance meas. 9-29356
 duoplasmatron-type, emitted particles energy spectra 9-38990
 electrode products emitted by d.c. arcs in vacuum ambient, analysis 9-34816
 electrophotographic layers, photoinduced, effect of capture 9-30967
 exploding wire, obs., book 9-29138
 flow systs., gas reactions meas. 9-26805
 gap length rel. to sensitivity spectral of analysis 9-49395
 gas, one-dimensional, with lateral heat transfer, volt-ampere charact. theory 9-39023
 gas, oscillation props. due to metallic walled tubes 9-25971
 gas, polymerization prod. of thin films 9-40845
 rel. to gas flow vel. meas. 9-32718
 in gas-filled space in solid dielectric, no. per period of alternating applied voltage 9-30966
 gaseous, initiation by negative ions desorption from cathode surface 9-42576
 gaseous, resonance-sustained, review 9-36783
 gases, electronegative, constricted and unstable positive columns 9-34804
 growth in rot. homopolar plasma device, obs. 9-25857
 hollow cathode, concentric spherical 9-44498
 hollow-cathode, current oscillations 9-44422
 hollow-cathode, eigenvalues of cylindrical microwave cavity 9-36219
 hollow-cathode, electron emission, photoeffect 9-33421
 I-V characteristics, arbitrary electrode geometry 9-46538
 impulse in vacuum, electrode thermoelastic destruction 9-48620
 impulsive in axial rot. air flow 9-25976
 independent in moving gas, onset, elec. field rel. to transfer vels. of neutral flows 9-48628
 inert gases, discharge voltage, minimum, in static fields 9-23350
 insulators, partial surface discharges, effect on working life 9-49147
 interelectrode gap, charged- particle density and electric field variation, charact. 9-32701
 ion charge transfer in gaseous discharges, review 9-32699
 laser, pinch, plasma electron temp. and conductivity 9-47958
 laser spark, two-wavelength holography investigation 9-31981
 laser sparks, discharge through two separate 9-46547
 lightning characteristics determined from e.l.f. atmospherics 9-28893
 liquid, cavity collapse 9-48675
 liquid, compression processes, X-ray obs. 9-32767
 liquid, electrocapillary discharge 9-23516
 low pressure, i.f. oscillations 9-44497
 magnetron diode, ion current rel. to mag. induction, calc. 9-27287
 medium pressure column, inhomogeneous electron temperature 9-23349
 rel. to MHD linear generator, auxiliary d.c. discharges effect on performance 9-48558
 Monte Carlo simulation of discharges in gases 9-42570
 in non-uniform electric and transverse mag. fields, characteristics 9-28046
 nonstationary arc, V-I charact. 9-42580
 Osaka cold cathode discharge tube used as an oscillation prod. e.m. waves 9-36785
 parameter modulation, acoustic wave propagation in partially ionized plasma 9-36765
 in particle detection 9-38614
 Penning, mechanism, rel. to getter-ion pumps 9-24994
 Penning cell, axial ion current, press. depend. 9-23351
 Penning discharge at low magnetic field, electrical characteristics 9-48619
 Penning low press., hollow cathode effect 9-48627
 Penning tube, local mag. field deformation eff. 9-32642
 penning with heated cathode, plasma outflow into vacuum region free of mag. field 9-46540
 PIG, in various field configs. 9-25839
 plane air-gap, elec. field strength, distortions due to additional space charges 9-23361
 plasma, by exploding wire, expansion vel. 9-25852
 plasma, charged arc, in Cs vapour, spectral line intensity and complexity 9-38971
 in plasma, effect on confinement and heating 9-28003
 plasma, enhanced oscillations, scatt. laser light obs. 9-39004
 plasma, magnetized positive column in turbulence 9-42554
 in plasma, microwave frequency excited, electron energy distribution 9-30232
 plasma, straight turbulent, dynamic characteristics 9-27975
 plasma, weakly ionized, helical instability onset 9-25959
 plasma absorption coefficient meas. using laser pulses 9-28000
 plasma focus, meas. anisotropies, neutron emission method 9-25866
 plasma generation when pressed out to wall by mag. field 9-40715
 plasma heating in electrodeless discharges 9-34748
 plasma ion oscillations in discharges produced by back diffusion plasma sources 9-28022
 plasma positive column, Tonks-Dattner resonances, nonlinear behaviour due to r.f. generation 9-44424
 plasma-beam, wall potential effs., stability obs. 9-23310
 plasma-beam interaction, time behaviour of electron temp., meas. 9-42489
 point-to-plane gap, mapping field 9-34797
 polythene cavity under high direct electric stresses at elevated temperatures, discharge-repetition rate 9-28054
 positive column, i.f., asymmetric modes 9-25933
 positive column, low current medium press., dynamics 9-48624
 positive column const. current, cathaphoresis 9-25754
 positive column i.f. waves axisymmetric modes 9-25932
 positive column low press., impedance for small currents 9-44500
 positive column plasma, cathode characteristics 9-39028
 positive column plasma, equivalent dielectric tensor 9-32594
 positive column Tonks-Dattner resonances, kinetic model 9-25931
 pulsed, dynamics of spectral lines of electrode in region close to electrode 9-36791
 pulsed in N₂, O₂ and ether or methane mixtures, simultaneous HCN and H₂O laser emissions 9-22404
 pulsed light source, efficiency optimization 9-32042
 reflex, instabilities rel. to anomalous diffusion 9-46526
 r.f., ion extraction from plasma 9-39022

Discharges, electric continued

- r.f. in C containing gases, C deposition, ionic species involved obs., mass spectr. 9-23353
 semiconductor thermally-stimulated discharging, method for trap level exam. 9-39613
 shock waves from spark discharges 9-30317
 silent, production of atm. ozone 9-41544
 in spark chambers, electronic elimination of subsequent radiation pick-up 9-42152
 spectral indicators use for near- electrode plasma layer exam. 9-25972
 spectrochemical analysis of alkali elements by introducing oxides of Co, Ti and V 9-31229
 spectrum preexcitation plasma structure control of laser light source 9-25241
 sputtering r.f. gas, conductance and capacitance, mag. field depend. meas. 9-36784
 streamer propag. and props., qualitative theory 9-36786
 striations in plasma, moving, large amplitude 9-34749
 surface discharge channel, gas density distrib., interferometer meas. 9-30308
 surface-discharge, inductive ignition by vaporize of exploding wires 9-25970
 temperature determ. from spectrum in case of hyperfine structure 9-28044
 thetatron, plasma wave excitation and dissipation 9-25936
 toroidal, runaway current intensity 9-28043
 transient, charge carriers current fraction, transference numbers 9-46535
 vacuum, prod. of very short X-ray pulses 9-33997
 water drop in electric field 9-28146
 Z-pinch discharge, form. and accel. of current layer 9-23284
 Ar- alcohol Geiger counter, photon spectrum 9-25507
 Ar-Cs, r.f., mass spectra obs. of ionic species 9-36787
 Ar-Cs positive column contraction 9-48632
 Ar-Hg medium press, axial cathaphoresis 9-48630
 Ar, decaying, e conc. by laser interferometry, 10⁻²-3 mm Hg 9-28050
 Ar, electron temp. rel. to dissociative recombination of Ar₂⁺ 9-34795
 Ar, excitation source for solns. spectrochem. analysis, 2450 MHz 9-28822
 Ar, medium press., effect of Hg vapour 9-23352
 Ar, pulsed, e vel. distrib. and conc., 0.02 torr 9-28049
 Ar, r.f., mass spectra obs. of ionic species 9-36787
 Ar, r.f. discharge in non-resonant mag. field, breakdown characts. 9-25986
 Ar, use in spectral examination of S, P and C in steel 9-47480
 Ar flow plasma, electron temp. meas. 9-27978
 Ar in plasma, spectral absorptivity calc. from radiance spectral density 9-23301
 Ar ion laser, electron temp. and density, calc. 9-47960
 Ar plasma column, axial current density meas. 9-34768
 Ar positive column contraction 9-48632
 Ba II lines emitted by discharge along surface of liquid jet, Stark width 9-40716
 Bi-buffer gas, pulsed, spectra, obs. 9-25692
 CF₂ capillary, ion-oscillations, intensity determination, first, second, third and fourth stages of ionization 9-25973
 CO₂-N₂-He-H₂O flowing laser, effect on mol. comp. 9-40352
 CO₂-N₂ mixture, current depend. decay of CO₂ 00¹ level 9-34159
 CO₂-air-He mixtures rel. to CO₂ 00¹-10⁰ and 00¹-02⁰ transition amplification coeffs., obs. 9-25255
 CO₂ laser, dissociation 9-41899
 CO₂ lasers, gas temp. and electron density in discharge 9-25256
 Co₂-N₂-He, electron energy distrib., influence of lasing action 9-34800
 Cs-Ar, low press., Cs depletion in positive column 9-34802
 Cs-Ar, low press., radial and axial Cs-atom distrib., absorpt. spectra obs. 9-34801
 Cs, e drift vel. and energy distrib. function 9-39024
 Cs atomic level populations, electron temp., energy distribution determined 9-34536
 Cs I lines electronic excitation cross sections meas. in plasma 9-27816
 Cs plasma thermionic discharge, electron energy distrib. 9-34756
 Cs positive column, electron density and drift vels. 9-46541
 Cs vapour, ionic composition of arc-discharge plasma 9-36759
 Cs vapour, ionic composition of arc-discharge plasma 9-36759
 Cu electrode erosion in high current discharge and cathode spot temp., obs. 9-34798
 H₂ pre-ionized, fast pulsed, plasma properties 9-39025
 H conical Z pinch, obs. 9-40680
 H spark at small pd values, plasma discharge development 9-39032
 He-Ar electron energy distrib. functions electron mobilities and collision rates calc. 9-48621
 He-Ne, depolarizing and velocity- changing collision correl. 9-39026
 He-Ne dispersive phase shift at 6328 and 6401 Å due to Ne 1s₂ metastables 9-47991
 He-Ne mixture, conc. depend. on level meas. by absorption method 9-23354
 He-Ne mixture, He level population depend. on Ne atom conc. 9-25974
 He, 12-13 torr pressure, voltage-current characteristics, hot hollow cathode 9-25994
 He, electron energy distrib. functions electron mobilities and collision rates calc. 9-48621
 He, medium-pressure, positive column theory 9-44502
 He, optically pumped, production of intense polarized e. beams 9-28045
 He, population of highly excited states, effect of stepwise ionization 9-46539
 He, r.f. discharge in non-resonant mag. field, breakdown characts. 9-25986
 He as vacuum u.v. spectroscopy light source, radiative power, calc. 9-27410
 He excitation in +ve column discharge 9-25721
 He I population in hollow cathode 9-48635
 He plasma, acoustic i.f. oscillations and kinetics of heating obs. at low temp. 9-39010
 He positive column medium press. 9-25980
³He, decaying, e conc. by laser interferometry 10⁻²-3 mm Hg 9-28050
⁴He, decaying, e conc. by laser interferometry, 10⁻²-3 mm Hg 9-28050
 Hg-vapour plasma, current rise slow rates, correlation with pinch 9-42523
 Hg positive column, two-stage processes 9-30312
 Kr, decaying, e conc. by laser interferometry, 10⁻²-3 mm Hg 9-28050
 N₂-O₂, investigation of ionic charge exchange 9-30303

Discharges, electric continued

- N₂, decaying, c conc. by laser interferometry, 10⁻²-3 mm Hg 9-28050
 N₂, pink afterglow in mag. field 9-30315
 N₂⁺, matrix elements of electronic transition in first negative band system meas. by discharge in air flow 9-27865
 N₂⁺ rotational bands excited in hollow cathode discharge, Boltzmann distrib. 9-23055
 N₂ spectral line expansion and shift with Cu present 9-46550
 Ne, atom temp. meas., plasma inhomogeneity effects 9-34803
 Ne, conditions for generation at $\lambda = 1.15\mu$ 9-25975
 Ne, energy loss of primary electrons 9-48622
 Ne, excitation mechanism in hollow cathode 9-22961
 Ne, r.f. discharge in non-resonant mag. field, breakdown characts. 9-25986
 Ne flash tube, digitisation method for potential changes 9-27588
 Ne in plasma, spectral absorptivity calc. from radiance spectral density 9-23301
 Ne ion acoustic waves rel. to moving striations 9-48636
 Ne ionization waves of type p 9-42603
 Ne plasma column parameters 9-44507
 Ne positive column, electron energy distribution and plasma diffusion 9-44506
 Ni electrode erosion in high current discharge and cathode spot temp. obs. 9-34798
 O₂ pulse discharge loss rel. to applied voltage 9-30309
 O pulse, with confined channel, electron concentration and temperature 9-41968
 SO₂-He laser excitation 9-27327
 W electrode erosion in high current discharge and cathode spot temp., obs. 9-34798
 Xe, column resistance as function of tube dimensions 9-32613
 Xe pulse, discharge pressure and spatial radiation dist. meas. 9-30307
 Xe pulsed lamp, radiation rel. energy supplied 9-41969
 Zn-Hg-Kr, excitation energy transfer from Hg to Zn in afterglow, process 9-48422
 ZnSe, hollow cathode, spectral anal. of excess Zn, comparison with d.c. arc 9-37859

glows

- a.c. at audio frequencies, electron temp. obs. 9-28047
 air afterglows, electron loss mechanisms 9-44505
 anomalous, diffusion eqn. soln. computation, volume recombination mechanism determ. 9-40720
 boundary between luminescence of basic gas and impurity, movement rate 9-42574
 cathode dark space, radial diffusion of charge carriers 9-30311
 cold-cathode device, patent 9-40722
 d.c., periodic phenomena 9-40721
 emission current rel. to cathode space and positive column lengths 9-42571
 Garton flash tube 9-30313
 in hollows cathode optical investigation 9-40719
 inert gas afterglow plasmas, dielec. props. 9-34805
 inert gas afterglows, spectral line shapes 9-44503
 inertial effect 9-32703
 ionized gas +ve column, Boltzmann electron eqn. soln. 9-23359
 Joshi effect, cent percent negative in gas phototube beyond threshold photoemission 9-42573
 Joshi effect, spectral sensitivity under visible radiations 9-30310
 low pressure, positive column, electric equivalent circuit, impedance behaviour 9-23357
 modulated, positive column nonlinear effects 9-48626
 nonsteady, neutral gas pressure transient behaviour 9-48625
 positive column, ion and drift waves 9-48629
 positive column, moving striations, electron-energy distribution variation 9-32704
 positive column oscillations in external e.m. field 9-36789
 pulse, high current with separated flames at 1 atm., near-electrode plasma obs. 9-40718
 radial diffusion of charge carriers, cathode dark space 9-30311
 steady-state, striation formation 9-42572
 voltage changes, nanosecond, damped plasma oscillation effects 9-44501
 Ar-Hg, positive column plasma, effect of cathode p. ops. 9-48631
 Ar, electron temp., density and gas-temp. meas. 9-28048
 Ar afterglow plasma, electron temp. gradient, spatially nonuniform parameters effect on transport processes 9-34755
 Ar h.p. 20 ns spark channel, radiance saturation and afterglow emission 9-30314
 Ar positive column, light fluctuations correlation 9-34806
 CO, electron-ion recombination, diffusion coeff., 775°K 9-48617
 CO₂-N₂-He-H₂O, spectra, 2800-6500 Å, 3-7 torr 9-25979
 CO₂-N₂-He, spectra 2800-6500 Å, 3-7 torr 9-25979
 CO₂, dissociation, in positive column 9-38919
 CO₂, mass spectrometric sampling, constricted ion-getter pump, 50-1000 μ , 50-200 mA 9-36790
 CO₂, spectra 2800-6500 Å, 3-7 torr 9-25979
 H₂-ve glow, electron temp. and density determ. by diffusion and recombination, 0.06-0.6 torr 9-40723
 H₂ positive column plasma, low press., distribution of ionization states 9-46542
³H thin sources prod. 9-42238
 He, 2³S state decay by e collisions, obs. 9-34808
 He, afterglow, formation of mol. He 9-23263
 He 0.5-4.0 mm positive column m longitudinal magnetic field comparison with binary collision theory 9-34809
 He afterglow plasma, electron temp. gradient, spatially nonuniform parameters effect on transport processes 9-34755
 He h.p. 20 ns spark channel, radiance saturation and afterglow emission 9-30314
 He negative glow, secondary and ultimate electron groups 9-48634
 He plasma, afterglow, decay, props. 9-23286
 He(2³S) chemiluminesc. reactions with N₂, O₂, CO and CO₂ 9-43318
 Hg-Kr mixture, positive column, moving striations, electron-energy distribution variation 9-32704
 Hg-Kr positive column afterglow, 2nd kind collisions cross section estimation 9-25981
 Hg-Ne mixture, positive column, moving striations, electron-energy distribution variation 9-32704
 Hg plasma, early afterglow, free-fall decay 9-34810
 N₂, pink afterglow, electrostatic probe obs. 9-44504

Discharges, electric continued**glows** continued

- N₂, yellow afterglow at low pressures, visible emission rel. to atomic recombination kinetics 9-39029
 Ne, metastable atom densities rel. to press. and current, electronic collision terms 9-44508
 Ne 0.5-4.0, positive column m longitudinal magnetic field, comparison with binary collision theory 9-34809
 Ne hollow cathode, with appl. mag. field, ionization waves, obs. 9-25982
 Ne negative glow, secondary and ultimate electron groups 9-48634
 SO₂, chemiluminesc. afterglow, temp. depend. 9-43323
 SiBr₄ vapour spectrum 9-48483
 TI, 6³P_{3/2} state, lifetime and effective cross section obs. 9-29949
 Xe pulsed large dia. tube, spectral intensity and waveform obs. 9-32705
- high frequency**
 air in coaxial cavity, cyclotron resonance rel. to elec. field freq. 9-44499
 butyrophenone, mol. plasma, dissociation 9-46545
 cylindrical and spherical geometries, calorimetric meas. 9-32640
 electron-excitation capacitive discharge, e velocity distrib. function, high-energy component existence 9-46536
 electrodeless electric-excitation capacitive discharge, resonance effects, existence of two regimes 9-46537
 frequency range, optimum for high press. 9-23356
 gas, fourth harmonic power at 55 GHz, charact. 9-36221
 O₂, lower than atm. press. 9-36788
 plasma, evolved power and temperature 9-25977
 plasma resonances, non-linear effects 9-32588
 potential difference, (const.) between electrodes and plasma, obs. 9-44425
 resonant, 10 cm range, electron energy distribution 9-32700
 Ar, 1s and 2p level population, electronic temp., conc. meas., 9500 MHz 9-32702
 Ar in coaxial cavity, cyclotron resonance rel. to elec. field freq. 9-44499
 Ar ion laser, vacuum u.v., spectroscopic studies 9-25242
 CO₂, lower than atm. press. 9-36788
 He in microwave resonant cavity, 2.7 GHz, electron conductivity ratio meas. 9-23288
 Kr, 1s and 2p level population, electronic temp., conc. meas., 9500 MHz 9-32702
 Kr in microwave resonant cavity, 2.7 GHz, electron conductivity ratio meas. 9-23288
 N₂, lower than atm. press. 9-36788
 NO, β , γ systems, transition dipole moment determ. 9-48472
 Ne, electron conc., temp. radial distrib., spectra emission intensity determ. 9-23355
 Ne in microwave resonant cavity, 2.7 GHz, electron conductivity ratio meas. 9-23288
 Xe, 1s and 2p level population, electronic temp., conc. meas., 9500 MHz 9-32702
 Xe, electrodeless, relationships between radiation power and thermal loss at high pressures 9-39027
 Xe electrodeless, characts. 9-40717
 Xe in microwave resonant cavity, 2.7 GHz, electron conductivity ratio meas. 9-23288
- Disintegration** *see Beta-decay theory; Nuclear decay theory; Radioactivity*
Disintegration energies *see Radioactivity*
Dislocations *see Crystal imperfections/dislocations*
Dispersions relations
see also Field theory, quantum; S-matrix theory
 No entries
- Disperse systems**
see also Aerosols; Colloids; Emulsions; Foams; Powders; Sols; Suspensions
 aerosols, monodisperse, generation using disintegrated liquid jet 9-34933
 cellulose, microcrystalline, flow birefringence study 9-34930
 creep and relax. under humidity fluctuations 9-44601
 e.m. wave scatt. on spherical polydispersions, book 9-40293
 gas suspension, counterflow decelerated, solid distrib. in chamber determ. by beta-raying 9-28160
 gas-solids, convective heat-transfer coeff. at Reynolds number 130,000 9-26136
 latex particles, sulfonated, secondary electroviscous effect calc. from zeta pot. 9-32801
 light attenuation by particles with small real refr. index 9-34200
 liquids, stimulated Brillouin scatt., phonon-freq. depend. of steady-state gain 9-44568
 mist evaporation by intense light beam 9-42699
 particulate, heat (mass) transfer, particle size and residence time distrib. effects 9-23539
 polydisperse layer, fluidization rate calc. and criteria 9-27946
 polyisobutylene, polydispersity from diffusion meas. 9-32545
 quartz, trapping of colloidal inclusions in growth 9-37043
 rheological props. of structured systems when translated by vibr. 9-42683
 scintillator granules, theory of light scatt. rel. to efficiency as β -dosimeter 9-22670
 sodium caprylate-water-ethylene glycol (glycerol) (tetraethylene glycol), phase equilibrium 9-23547
 spray cooler analysis of two-phase flow 9-23541
- Dispersion, acoustic**
 in gas, effect of molecular dissociation and radiative heat transfer 9-48663
 quartz, Rayleigh waves dispersive properties 9-48959
- ultrasonic**
 bitumens in rubber transition zone 9-30450
 1,1,1-trichloroethane vapour, obs. at 30°C, relaxation constants calc. 9-32737
 p-H₂, and mixtures with He, Ne, Ar, rot. relax. 9-42611
- Dispersion, optical**
see also Optical constants; Refractive index/light
 Chance Pilkington glasses, F and C dispersion, mean reference index 9-22471
 crystals, rotatory power, quantum-mechanical evaluation 9-35616
 dielectrics, isotropic, dispersion in absorption bands 9-35617
 F and C, for typical Chance Pilkington glasses, mean reference index 9-22471
 glass, mean reference index and wavelength 9-43205
 in holography of transparent objects 9-48069
 liquids, organic, temp. depend. cell for meas. 9-28130

Dispersion, optical continued

- poly-N-isobutylmaleinimide, polydispersivity obs. 9-23193
 for scattering by seawater particles and turbulence 9-44564
 tertiary alcohols, specific rotation and mag. rotary dispersion 9-48697
 water vapour, atmospheric, anomalous dispersion calculations 9-33774
 Eu chalcogenides, i.r. dielec. dispersion 9-39799
 He-Ne, discharge, dispersive phase shift at 6328 and 640Å due to Ne I s₁ metastables 9-47991
 NaClO₃ single crystals near critical temp., combination dispersion in Raman spectra 9-28703
 NbO vapour deposited films 9-30958
 Nd³⁺, curves w.r.t. La³⁺ in aqueous chloride solutions 9-26111
 Sm³⁺, curves w.r.t. La³⁺ in aqueous chloride solutions 9-26111
 Te single crystal, rotatory power, interpret. 9-37686
 ZnO, excitons spatial dispersion, refl. and transmission spectra 9-45309
 ZnTe, semicond., Pockels' coeff. meas. and dispersion in rel. to refr. index and absorpt. coeff. 9-39811

Dispersion relations

- see also *Field theory, quantum; S-matrix theory*
 acoustic waves in dissociated radiating gas 9-48663
 beam-plasma system, bounded with finite temperature, dispersive properties 9-39006
 biaxial and uniaxial crystals, polaritons 9-37413
 broad area, subtraction, for forward pp scatt. 9-32218
 collinear, in calc. of π - π scatt. lengths 9-40430
 covariant, in current algebra formulation 9-29526
 and current algebra and Regge pole theory, relationship 9-32187
 drift waves in partially ionized plasma 9-28038
 electron plasma oscils., dispersion eqn. soln. 9-42540
 electrodynamics partial-wave amplitudes 9-25416
 helicons propagating in slab-shaped semicond. and metals 9-43049
 kaon-nucleon, in $g_{\pi\pi}$ and $g_{\pi K}$ coupling consts. calc. 9-32181
 of lattices, simple cubic with long range interactions 9-39505
 magnetic, in transport props. of dil. polyatomic gases 9-23406
 magnetospheric transverse waves, rel. to plasma isotropy 9-49469
 oceanic Rayleigh waves 9-45446
 for phase velocities, in rel. to velocity meas. by seismic logging 9-35789
 plasma, collisionless in uniform field, covariant theory 9-32590
 plasma, ion-ion velocity space instability 9-32676
 plasma, spatially inhomogeneous, upper hybrid mode 9-25861
 plasma bound finite-length instabilities 9-23331
 plasma e.m. waves 9-48561
 in plasma rot. cylinder, for electrostatic i.f. waves 9-25950
 in plasma waveguide, magnetized 9-42508
 plasma waves, group velocity and index determ. from implicit function 9-40695
 for Rossby wave, average, in presence of random currents 9-43377
 seismic longitudinal waves, phase velocity in thinly layered media 9-33715
 sideways, calc. of nucleon mag. moments and g_A/g_V , rel. bet. calcs. using $J=1/2$ baryon reson. model 9-22622
 superconvergence relations for inelastic mes.-mes. scatt. 9-25457
 superconvergent sum rules for broken-symmetry case, deriv. 9-27495
 whistler amplitude in cold plasma in mag. field 9-44433
 KN give different value for AKN coupling constant from SU(3) symmetry 9-34294
 pp scatt., expanding unphysical part in Chebyshev polynomials 9-34323
 π -p scatt. data, CERN group fit fails to represent data 9-36481
 π photoproduction in γ N interact., evaluation of multipoles 9-22592
 in π N low energy theorems derivation 9-32194
 π N scatt., for inverse of crossing-even forward amplitude 9-32196
 π -S-wave scatt. model 9-29595
 π - π scatt., forward dispersion relations for phase shifts analysis 9-38535
 in ρ^+ - ρ^0 mass difference calc. 9-27539
 in Z^+ - γ decay rate determ. 9-32226
 Ag, phonon relation for symmetry directions 9-46970
 Al, anharmonic phonon curves, wave number depend. 9-35266
 CaO, phonon dispersion curves 9-39509
 Cu, phonon 9-37313
 Ga, phonon from neutron inelastic scatt. obs. 9-33160
 Ho, phonon 9-28415
 KCl, phonon at 80 and 300 K 9-33161
 KI, rel. to modified shell model 9-30762
 Mg, phonon, from model pot. 9-37316
 MgO, phonon dispersion curves 9-39509
 MnF₂, antiferromag., magnon, and exchange interac. 9-45228
 Ne single cryst. at 2 densities, phonon relations, inelastic neutron scatt. meas. 9-46978
 SrO, phonon dispersion curves 9-39509

Dispersions see *Disperse systems***Displacement measurement** see *Length measurement; Strain gauges***Dissociation**

- see also *Heat of dissociation; Ionization; Molecules/dissociation*
 air, behind hypersonic shock, energy transfer mechanisms 9-46564
 air, collision integrals for components 9-23407
 carboxylic acids, dilute, aqueous consts. rel. to u.s. absorpt. 9-48695
 electron formation in slightly dissociated gaseous media, equilibrium diagram 9-39013
 exciton photodissoc. by i.r. radiation, continuum model 9-28452
 molecular complexes, adsorbed, equil., refl. meas. 9-39166
 steam, 1000-5000°K, 0.001-100b, thermodynamic functions 9-30458
 water solns., acid-based, pressure eff. on ioniz. equilibria 9-42676
 Al-Cu-Cr supersaturated solid solns., kinetics of decomp. 9-46937
 Bi-Th system, Bi dissoci. press. 9-39937
 CO₂ in laser discharge 9-41899
 Cu-Fe solid solns., homogeneous decomposition 9-48930
 Cu-Ti-Al alloys, decomp., struct. changes on ageing, electron microscope obs. 9-46938
 Cu-Ti alloys, decomp., struct. changes on ageing, electron microscope obs. 9-46938
 FeS₂, in neutral or reducing gases, mechanism 550°-700°C 9-33670
 IBr reversible photodissoc. laser system 9-34166
 n-KMnO₄, thermal decomposition in solid phase 9-37818
 NiBr₂ chem. decomp., Ni platelets and whiskers growth obs. 9-35018
 NiI₂, chem. decomp., Ni platelets and whiskers growth obs. 9-35018
 PbS-PbTe system, spinodal decomposition 9-39941

electrolytic

- see also *Ions; Electrolytic*
 phenols, excited, determ. from fluoresc. quenching 9-39108

Dissociation continued**electrolytic continued**

- thermodynamic diagram of electrochemical equilibrium of mixed binary dissociable conductors 9-39609
 Wien dissoci. as a rate process 9-41453
 CsCl aqueous soln., from elec. conductivity meas. 300-1000°C, up to 12 kbar 9-48717
 H₂O, to 100 kbar and 1000°C 9-44585
 KCl aqueous soln. from elec. conductivity meas. 300-1000°C up to 12 kbar 9-48717
 LiCl aqueous soln. from elec. conductivity meas. 300-1000°C, up to 12 kbar 9-48717

Dissolution see *Solubility; Solutions***Distillation**

- see also *Isotope separation*
 CO₂ gaseous and condensed, isotropic fractionation, 220-303°K 9-23588
 Gd, single cryst. purification and growth 9-35026

DNA see *Macromolecules***Domains** see *Ferroelectric phenomena; Magnetization state; Superconductivity***Domains, antiphase** see *Alloys; Crystal structure/microstructure; Solids/structure***Doping** see *Semiconducting materials; Semiconductors***Doppler effect**

- activation coeff. in nuclear reactors, inhomogeneous material effect 9-32376
 atom system, radiative process with excessive broadening, noise spectral contour determ. 9-38764
 Burnout-V turbulently heated plasma, Doppler broadened spectra emission 9-44443
 demonstration apparatus, X-band, single antenna 9-43709
 differential velocity meas. using optical radiation 9-47722
 ionosphere, decametric radiowave produced by powerful explosion on ground 9-38831
 ionosphere, decametric waves, due to acoustic wave 9-41574
 ionosphere, first-order effect, electron content determ. 9-41575
 ionosphere, h.f. radio ground backscatter, shifts 9-31390
 on ionospheric and tropospheric propagation in satellite communication, computer program 9-45575
 ionospheric ground backscatter, h.f., shift 9-41577
 use in laser determ. turbulence and \approx velocity vector 9-43714
 laser system, possible meas. of turbine blade vibrs. 9-41811
 line-narrowing, laser-induced, in coupled Doppler-broadened transitions 9-22934
 nuclear energy level transitions, lifetime meas. of various nuclei with A=10 to A=21 9-36568
 nuclear mean lifetimes, Doppler shift, meas. method 9-29706
 plasma, warm uniaxial; rad. emitted by uniformly moving radiator 9-38978
 plasma oscils. excitation by modulated electron beam 9-46521
 plasma oscils. excitation by modulated ion beam 9-48602
 use in plasma velocity determ. with photoelec. recording 9-40692
 in radio astronomy 9-33914
 reactivity coeff. in nuclear reactors, calc., allowance for inhomogeneity 9-29872
 on reactor spectrum, meas. at cryogenic temp. 9-29886
 on reactor spectrum, theory and meas. on ZPR-6 assembly 9-29877
 relativistic, in spectral lines ambiguity 9-22436
 relativistic Mossbauer emission by rotating source 9-45750
 in satellite r.f. transmission, as test of validity of relativity 9-41615
 spectral line broadening of ions in stochastic varying fields in plasma 9-40663
 spectral line structure from noise spectrum of coherently amplified radiation 9-25689
 temperature coeff. use to terminate prompt critical pulse of fast reactor 9-25670
 velocity measurement when combined with Schlieren system 9-38191
 wind and precipitation velocity, radar determ. 9-41507
 O I λ 6300 line in nightglow, shifts in wavelength 9-45514
 SF₆, narrow reson. in Doppler line of rot.-vibr. transitions of ν_3 band by CO₂-laser emission method 9-46375

Dosimetry

- see also *Radiation monitoring; Radioactivity measurement; X-ray measurement*
 of β -emitting liquids, theory of disperse system of scintillation granules 9-22670
 biological specimens, in high energy neutron beam, absorbed dose meas. 9-36082
 p-ray detection instruments calibration 9-38622
 calorimeters, isothermal, CO₂/graphite rigs radiation meas. 9-22915
 constant-rate irradiation device, patent 9-36530
 cylindric shell-shaped iron shield with air-gap, containing ⁶⁰Co, dose build-up 9-34506
 dosimeter, solid state digital, integrating for X-rays 9-25533
 fast neutron and gamma radiation, dosimeter, patent 9-32264
 fluorescent-coated phototransistor dosimeter 9-36528
 gaseous O₂, yield of O₃ at v. high dose rate 9-39963
 Geiger-Muller detector, direct reading of flux and dose rate 9-22659
 human body, rotational technique, patent 9-41715
 ionizing radiation, 10-25Mrad, using thermoluminescence of LiF 9-38621
 LET dependence of thermally stimulated exoelectron emission 9-37634
 multimegarad p, use of oxalic acid soln. 9-24950
 of neutron beam, high energy 9-36082
 organic halide conductivity cell model 9-29665
 phosphor, thermoluminescent, detector, 10⁻³-10¹⁰R, patent 9-29666
 phosphor-terfenol dosimeter for radioactive jewellery 9-34363
 phosphors, thermoluminescent, relative sensitivities obs. 9-24466
 photoluminescent dosimeter, readout using pulsed u.v. laser, patent 9-32265
 polyvinyl chloride film, high press. luminescence depend. on photon intensity, patent 9-22677
 proton, solar event dose rates from riometer obs. 9-46124
 radiation meas., thermoluminescent device of CaSO₄:Mn+impurity ions, preparation, patent 9-27596
 radionuclides absorbed dose, formalism for calculation 9-27124
 rate from radioactive fallout, and ionization 9-24669
 scintillation counter, small animal and infant, performance and calibration 9-38617
 space flight permissible doses, substantiation 9-31687

Dosimetry continued

- spherical, capsule type glass dosimeter, improvements 9-27595
- surface radioactive contamination, detection, patent 9-48229
- thermoluminescence of feldspar separated by sands rel. to accident dosimetry 9-49609
- thermoluminescent dosimeter reader with autoranging facilities 9-36081
- thermoluminescent dosimeters, limitations 9-22675
- thermoluminescent dosimeters, limitations in low radiation meas. 9-22676
- thermoluminescent personnel monitors 9-24948
- water phantom, dose distrib. from high energy neutron beam 9-36082
- γ in presence of n, using hexafluorobenzene scintillator 9-36531
- γ using i.r. stimuable ZnS with time lapse indication 9-27597
- X-rays, high energy, use of Farimer-Baldwin and Victrometer ionization chambers 9-25511
- ^{252}Cf spontaneous fission, fast n dosimetry meas. 9-38135
- $\text{CaSO}_4(\text{Mn})$ film phosphors for use in thermoluminescent dosimeters 9-27594
- Co isotopes, retention in rat 9-24949
- FeSO_4 , for meas. of low energy X-rays 9-25011
- LiF, thermoluminescent heat stable, patent 9-36529
- LiF detectors performance, lattice defect structures effect 9-49610
- LiF dosimeters, energy depend. at electron energies from 10 to 35 MeV 9-34364
- LiF thermoluminescent, efficiency depend. on grain size 9-22674
- LiF;Eu,Mg thermoluminescent, radiation meas., patent 9-28730
- P-Au neutron activation detector applic. in reactors 9-46141
- S-Au neutron activation detector applic. in reactors 9-46141

Double refraction

- see also *Electromagnetic wave propagation; Optical constants; Optical rotation; Polarised light*
- alkali halides, piezobirefringence in deformation potentials determ. 9-24364
- birefringence, acoustical, in stressed crystals 9-30642
- birefringence effect on light scatt., using classical theory, appl. to thin polymer films 9-49244
- birefringence for polarized light passing through randomly oriented particles 9-41528
- birefringence method for cryst. piezo- and elasto-optical coeffs. temp. depend. determ. 9-39813
- birefringent filter, passband, tuning and design 9-34220
- birefringent materials, e.m. propag. obs. 9-45262
- castor oil, acoustically induced birefringence study 9-23495
- colloidal suspensions with induced and permanent elec. particlemoments, birefringence 9-42684
- cotton fibres, obs. 9-28656
- crystal plates, cascade sets, path difference and polarization directions effect on wave fronts 9-45270
- crystal plates, thickness interferometry 9-41354
- gas mols., birefringence effect on light scatt., by classical theory 9-49244
- Kerr cell, linearity improved with four electrodes 9-34907
- magnetic cubic crystals, linear mag. birefringence 9-45185
- molecules, diamagnetic, elec. birefringence, quantum theory 9-46347
- polymer film, birefringence effect on light scatt., classical treatment 9-49244
- polymer films, oriented, birefringence effect on low-angle light scatt. 9-49243
- polymer solns., optical activity, model for depend on mol. wt. and stereoregularity 9-28132
- quartz birefringence and appl. $\lambda/2$ and $\lambda/4$ plates 9-28655
- ramie fibres, obs. 9-28656
- rare earth iron garnets, linear mag. birefringence 9-45185
- stress induced, use in circular dichroism meas. 9-46007
- trirefringence, non-occurrence 9-27392
- Au sol, u.s. wave induced birefringence 9-36908
- CsPbCl_3 , birefringence temp. dependence 9-39211
- $\text{CuAlS}_2(\text{Se}_2)$, and refractive indices 9-48797
- KH_2PO_4 , of second harmonic, in thin crystals 9-31076
- MnCO_3 , antiferromag., acoustic birefringence 9-46985
- Se single crystal, ordinary and extraordinary 9-26699
- Yb orthoferrite, birefringent, e.m. propag. obs. 9-45262

electric see *Electro-optical effects***flow**

- cellulose tricarbanilates in benzophenone, 55-110°C 9-39102
- polar diagrams, sensitivity to deformability of particles 9-32783
- poly-N-isobutylmaleinimide, segmental anisotropy independent of mol. wt. 9-23193
- styrene-butyl methacrylate graft copolymer 9-32553
- styrene-methyl methacrylate graft copolymer 9-32553

magnetic see *Magneto-optical effects***mechanical**see also *Photoelasticity*

- polyacrylonitrile, rheo-optical behaviour from creep, creep recovery and birefringence meas. 9-46900
- polymer networks, semicryst., stretched, rel. to crystallinity 9-31077
- polyurethane, birefringence obs. 9-35159
- polyvinyl chloride, stress-optical behaviour, effects of temp., and plasticizer content 9-47319

Double resonance see *Nuclear magnetic resonance and relaxation; Paramagnetic resonance and relaxation***DPPH (Diphenylpicrylhydrazyl)** see *Free radicals; Organic compounds***Drawing** see *Forming processes***Drops**

- charged, suspended, equilib. and coalescence 9-44544
- circulating and oscillating liquid, terminal velocity 9-23439
- cloud formation, lab. simulation 9-45492
- coalescence, and interfacial films profile and flow 9-30365
- coalescence, connection between Telford and kinetic- equation theory 9-24656
- coalescence, effects of Davis-Sartor collision theory 9-26897
- coalescence at liq.-liq. interface, effect of surface active agent 9-36838
- conducting deformed sphere, dynamic behaviour in elec. field 9-47884
- cumulus clouds, concentrations rel. to thermal structure 9-24653
- disintegration under intense elec. forces dynamics and validity of spheroidal assumption 9-28091
- droplet condensation, statistical model 9-39139
- ethanol formed by jet injection into N_2 or He gas streams, max. size. 9-34864

Drops continued

- evaporating stationary sphere, force in presence of similar sphere 9-40827
- film boiling, evaporation rate, electrostatic force effects 9-34964
- flow patterns inside separating droplet 9-46605
- fluctuations of centre of mass and homogeneous nucleation theory, embryo equil. distrib. 9-46683
- fluctuations of centre of mass and homogeneous nucleating theory, embryo equil. distrib. 9-36923
- in gas stream, heat and mass transfer 9-34866
- growth, solution effect, generalized eqn. 9-40826
- heat transfer, moving relative to gas stream 9-34866
- impact, high-speed photographic obs. 9-32754
- liquid, resting on flat surface, shape 9-23444
- mass transfer, moving relative to gas stream 9-34866
- rain, intensity and radar reflectivity standard deviations of values calc. from size distribution 9-41515
- rain on mountain slope melting lauer, size distribution 9-41514
- raindrops, large, internal circulation and shape 9-28880
- in reaction zone of spray detonations, history 9-29317
- separation, flow patterns inside droplet obs. 9-46605
- sessile, surface tension and contact angle calc. from shape using non-linear regression method 9-34867
- surface free energy of embryonic droplets in liquid nucleation from vapour 9-39138
- surface shape on horizontal plane 9-30363
- surface tension calc. from pendent drops shape 9-32775
- water, 100%, charged in nonuniform a.c. field, temp. estimation 9-40822
- water, collisional charging, wind tunnel expt. 9-31325
- water, deform. and discharge in elec. field 9-28146
- water, formed by jet injection into N_2 or He gas streams, max. size. 9-34864
- water, freezing, fragmentation in free fall 9-26898
- water, freezing in hydrophobic liquid 9-34963
- water, nucleation at deep supercooling in He, H_2 , O_2 , Ar and CO_2 9-26075
- water, on water surface, supported by air layer 9-30364
- water, production apparatus giving uniform size drops at controlled intervals 9-47704
- water, restructured, density meas. by hydrostatic weighing 9-23464
- water, supercooled, of AgI nuclei de-activation 9-42696
- water containing crystals, freezing temp. 9-42697
- water droplets, collision, coalescence and disruption 9-46604
- water injection into compressed air, temp. levelling rel. to droplet size 9-23435
- N_2 , droplet breakup in dispersed flow film boiling 9-26166
- Sn, liquid inert sessile, rel. to surface energy of Fe determ. 9-32836

Drying

- cement paste, under temp. gradients, role of moisture diffusion 9-34950
- convection in mechanism 9-30460
- jet, aerodynamics and heat mass transfer 9-25116
- moist sheet in contact with hot plate, calc. of temp. and moisture distrib. 9-23586
- sublimation dehydration, heat and mass transfer mechanisms 9-28183
- $\text{BaCl}_2 \cdot \text{H}_2\text{O}$ and $\text{BaCl}_2 \cdot \text{D}_2\text{O}$ systems, dehydration and polymorphic phase boundaries to 40 kbar 9-28171

Ductility see *Plastic flow; Plasticity***Dusts** see *Aerosols; Powders***Dynamics**see also *Ballistics; Kinematics; Rotating bodies; Vibrations*

- air track gliders, recording 9-30487
 - analytic, 2nd order relativistic eqns. deriv. methods 9-40236
 - classical, differential and S matrix transformation operators 9-29169
 - classical, in homogeneous closed expanding universe 9-24723
 - cross correl. in structural systems, dispersion and nondispersion waves 9-29222
 - Depler problem, using classical and quantum group dynamics 9-43750
 - energy balance rel. to projective extensions of Poincare and Galilei groups 9-31753
 - estimating behaviour of linear and nonlinear systems 9-33892
 - falling cat motion, model 9-45804
 - gas, perfect, relativistic theory of growth of second order discontinuities 9-32715
 - Hamilton's least action principle, computer programme to produce graph to illustrate 9-36099
 - Hamiltonian finite matrix, recormalization 9-38197
 - harmonic oscillator, rotating, two-dimen., demonstration of coupling and Coriolis force for students 9-45719
 - helicopter rotor blade airloads, bending moments and motions 9-25063
 - integrals of motion, canonical perturbation for complete set 9-22184
 - laws of, and optimization 9-25062
 - libration, soln. of ideal reson. problem 9-31495
 - Liouville equation eigenvalues, one dimens. system 9-22153
 - liquid drop disintegration in high elec. field, and validity of spheroidal assumption 9-28091
 - non-invariance groups of dynamical systems, construction 9-41739
 - non-linear systems with parametric excitation 9-22178
 - nuclear reactor, steam cooled, fast power, linear analytical model 9-34488
 - one dimens. system, Liouville equation, eigenvalues 9-22153
 - oscillating spring and weight, spring forces analysed 9-36100
 - particle trajectories in gas-particle flow in nozzles 9-34819
 - point with variable mass 9-22182
 - protostar, spherically symm., collapsing 9-29008
 - relativistic systems with variable mass 9-43771
 - rotating body, linearized eqns. with matrix formalisms 9-47799
 - slip between rolling ball and track, factors affecting contact conditions 9-31801
 - spinning particle, classical treatment, book 9-41766
 - spinning particle with structure relativistic treatment 9-34019
 - structural systems, energy propag., cross correl. analysis 9-29222
- Dynamometers** see *Force measurement*
- Dynamos** see *Electrical machines*
- Dysprosium**
- electronic structure, photoemission investigation in spectral range from 3.2 to 11.8 eV 9-39741
 - ferromagnetic metal, nucl. spin-lattice relax. for ^{163}Dy 9-33490
 - ferromagnetic resonance in for i.r. 9-49341
 - growth of single crystals by three methods 9-37078

Dysprosium continued

- Hall effect and mag. susceptibility, 90° to 400°K, fields up to 15 kOe 9-33258
 helical spin structure, representation theory 9-45108
 hyperfine interactions, calorimetric investigation 9-47305
 hysteresis loop displacement due to mag. viscosity 9-41291
 magnetic ordering, microscopic theory 9-24313
 magnetocrystalline anisotropy, spin-wave theory 9-37655
 u.s. attenuation near mag. phase transitions freq. and temp. depend 9-48958
 u.s. scatt., critical, in paramag. region near Neel temp. 9-24027
 Dy³⁺, in CaF₂, luminescence spectra, 4.2° and 77°K 9-33578
 Dy²⁺, e.p.r. in CaF₂ at T=4.2°K in wavelength range 1.7-2.35 mm 9-33622
 Dy²⁺ in CaF₂, SrF₂ and BaF₂, thermal ionization potentials 9-46739
 Dy³⁺ in CaF₂, p₈ quartet e.p.r. under uniaxial stress 9-39906
 Dy³⁺ in CaF₂, thermal conductivity in mag. fields 9-47008
 Dy³⁺ in DyAl garnet, electronic Raman effect 9-24425
 Dy³⁺ ions in disordered systems, e.p.r. line shapes 9-28742
 Dy³⁺ trional centre in CeO₂, ENDOR studies of charge compensation mechanisms 9-33652
 Dy³⁺ in CaF₂:Ce³⁺, Ce³⁺ codopant eff. on luminescence 9-35682
⁶⁵Dy, L-spectrum s-line, 2023.4 XU 9-48392
⁶⁵Dy, L emission spectrum forbidden transitions, obs. 9-38766
 YVO₄:Dy, luminesc. 9-47398

Dysprosium compounds

- germanides, Mossbauer spectra obs. of chem. bond charact. 9-37696
 silicides, Mossbauer spectra obs. of chem. bond charact. 9-37696
 Dy-Y paramag. susceptibility and Hall eff. meas. 9-37644
 Dy-Y alloy, Hall effect and mag. susceptibility, 90° to 400°K, fields up to 15 kOe 9-33258
 Dy₂O₃ films, recrystallization behaviour on pulse annealing 9-30489
 Dy₃Al₂, mag. props., 4.2 to 700°K 9-26632
 Dy₂Ge₃, mag. susceptibilities rel. to D_{8h} structure 9-43157
 Dy₂Si₃, mag. susceptibilities rel. to D_{8h} structure 9-43157
 Dy₂Ho_{1-x}Sb_x, Neel and paramag. Curie temp., mag. exchange mechanisms 9-28595
 DyAl garnet, electronic Raman effect of Dy³⁺ 9-24425
 DyAl garnet, Faraday effect, Verdet const. freq. depend., obs. 9-28657
 DyAl garnet, magneto-optical effects and Monte Carlo calc. 9-24408
 DyAl garnet, thermal expansion, 1° to 4°K 9-44840
 DyAlO₃, absorpt. spectra, mag. structure and metag. transitions investigation 9-31105
 Dy(ClO₄)₃ in ice, Mossbauer study 9-33532
 DyCrO₃, hyperfine interactions and paramagnetic relax. 9-24379
 DyFe₂Cr_{1-x}O₃ system, mag. props. 9-43156
 Er-Dy alloys, single crystals mag. props. rel. to Dy concentrations 9-45060
 Gd-Dy dil. alloy, exchange interactions 9-43171
 SmFeO₃-DyFeO₃ solid soln. single crystal, spin reorientation, 2° to 500°K 9-45235

E-layer see *Ionosphere/E-region***Ear**

- see also *Hearing*
 cat, auditory nerve, single fibres, spike discharge obs., two-tone stimuli 9-29124
 cochlear partition, Brownian motion-press. fluctuations, estimates 9-31693
 differential electrode technique for cochlear microphonics recording, theory 9-29123
 external, acoustic models with simple geometry 9-31695
 inner, mechanical model and musical perception 9-40199
 musical combination tones and oscills. of ear mechanism 9-43708
 replica and real human ears, sound press. generated by nearby source 9-31694

Earphones see *Transducers***Earth**

- see also *Geodesy; Geophysics*
 anisotropic spherical model, stress discontinuities propagation, ray paths and travel times 9-47490
 asymmetric active regions, seismicity and gravity anomalies 9-39986
 basalt layer thickness rel. to upper mantle physical parameters 9-33722
 brightness, Cosmos 149 equipment for obs. 9-45577
 brightness, Cosmos 149 obs. 9-40029
 compression distribution calc. finite-strain theory 9-28852
 continent locations rel. to initial positions of tension rifts in expanding Earth 9-41470
 continental drift, gravitational sliding mechanism 9-45434
 continental drift described, popular article 9-49403
 core, mag. waves rel. to secular geomag. field vars. 9-26956
 cosmic dust accretion rate, estimation from cosmogenic ²⁶Al 9-31279
 crust, rift and fracture zones of mid-oceanic ridges rel. to seismicity 9-33716
 crust and upper mantle, dynamic evolution rel. to seismic anomalies 9-31263
 crust and upper mantle heterogeneity from refracted seismic wave amplitudes 9-31272
 crust evolution rel. to lunar highland composition 9-31593
 crustal models from oceanic seismic obs. 9-31266
 crustal structure models, selection using surface wave velocities 9-37889
 crustal structure rel. to particle motion ellipticity in Rayleigh waves 9-35790
 crystal thickness, ren. to relief, demonstrated by Alpine folding ridges 9-26881
 density inhomogeneities redistribution rel. to angular displacement of rot. axis 9-49405
 density inhomogeneities redistribution rel. to angular displacement of rot. axis 9-49404
 eigenvector expansions of Green's dyads for theoretical earth models 9-24626
 emissivity, 8-14 microns spectral region 9-31278
 expansion, effect on sea level rel. to the continents 9-41471
 fault rupture in Iran earthquake, Aug. 1968 9-28848
 faults dip angle calc. from surface deformation 9-45452
 geopotential, odd zonal harmonics of degree <33, satellite orbits analysis 9-31240
 gravitation field determ. from surface measurements 9-31606
 hydrodynamical interaction between liquid core motions and level inclinations of core mantle interface 9-47506

Earth continued

- incompressibility at mantle-core boundary 9-45458
 insolation fluctuations due to secular variations in elements of orbit 9-24738
 interior, essay in book 9-41671
 isostatic adjustment as soln of free boundary problem in slab with viscosity depend. on depth 9-47504
 layer thicknesses by inverse magnetotelluric sounding 9-37890
 liquid core, interactions with solid mantle 9-47506
 lithodynamics of sea 9-43361
 lithographic plate rotation, paleomag. reconstruction 9-40109
 lithosphere, sea floor spreading rel. to heat flow and gravity 9-31274
 lithosphere discontinuities and upper mantle attenuation, lateral vars. 9-45449
 longitude variations 9-33739
 mantle, gravitational convection 9-33723
 mantle-core boundary, incompressibility 9-45458
 Mohorovicic discontinuity, gravimetric investigations 9-33721
 motion in elec. conducting fluid core, rel. to kinematics of geomagnetic secular variation 9-31469
 motion through ether, detection, null result, relativistic explanation 9-29179
 night side limb darkening, 1-3 μ and 3-7.5 μ 9-41520
 obliquity, secular change, friction between mantle and core theory 9-29067
 occultation of stars, photometrical observation from the moon 9-31674
 orbit, determ. by meas. radial velocity of radio-wavelength spectral-line source 9-29100
 oscillations, free-perturbation theory 9-37870
 oscillations spectra 9-31286
 pole, free motions, ellipticity of trajectory 9-26885
 quadrupole moment, effect on precession of a gyroscope 9-37992
 radiowaves, e.l.f., propag. in seawater or below ground surface, zonal harmonic calc. 9-45459
 satellite system, early history, rel. to obs. of lunar surface 9-31590
 satellites, natural, direct and indirect evidence 9-27079
 sea-floor spreading, gravitational mechanism 9-49421
 seismic wave propagation in self-gravitating anisotropic Earth, mathematical theory 9-26877
 solar-terrestrial environment, conference 9-29096
 solar-terrestrial relations, historical survey 9-38107
 solid-firmoviscous boundary, SH wave refl. and transmission 9-35791
 spherical oscillations excited by finite dislocations 9-47514
 thermal interaction with atmosphere and diurnal temp. wave propagation 9-24640
 upper mantle structure, study using seismic wave reflection from discontinuities 9-49416
 upper mantle structure, thin low velocity layers for body and surface waves 9-43360
 velocity of flow in material, calc. via viscosity as function of radial co-ord., rel. to isostasy 9-49419
 velocity w.r.t. cosmic 3°K background radiation anisotropy 9-45668
 viscosity function of radial co-ord., calc. of components of vel. of flow in mantle 9-49419
- EEG**
 see also *Radioactive dating*
 No entries
- composition**
 calculations based on mathematical model 9-43621
 crust, rare-earth content and distrib. in rocks 9-37896
 crust and upper mantle, combined geological, geophysical and geochemical methods 9-43359
 crustal structure seismic refraction method, Missouri 9-26879
 and density distrib., testing of models 9-33724
 mantle, lateral heterogeneities, data analysis 9-45457
 mantle, phase transformation at 200 to 1200km depths 9-45455
 mantle kinematics, non-waveguide model 9-31273
 mantle reconnaissance tool, P and S waves relative amplitudes 9-47494
 mantle-core boundary, change in incompressibility, model 9-33720
 upper mantle, ultramafic rock relationship, elemental abundances 9-47505
 K in rocks, gamma spectrometer surface obs. 9-37893
 Mg₂SiO₄, implications of high press. phase 9-40908
 Si in core, abundance from upper limit in iron meteorites 9-41683
 Th in rocks, gamma spectrometer surface obs. 9-37893
 U in rocks, gamma spectrometer surface obs. 9-37893
- electricity**
 conductivity distribution for spherical model 9-39988
 conductivity of sea bed in shallow waters, determ. 9-35792
 crust's effective complex dielectric const., radio-electromagnetic profiling method 9-24621
 crust, upper layers, elec. props. of rock rel. to e.m. field equations 9-33727
 current in AB line of freq. soundings with nonsinusoidal generator 9-39989
 current indices, estimation 9-33725
 current induction by equatorial electrojet 9-45460
 current rel. mag. field vars. period 10-200 secs., obs. 9-26961
 deep layers, specific conductivity determ. 9-24622
 electric fields induced by deep sea tides 9-31275
 e.m. field in presence of a thin conducting layer 9-35794
 e.m. fields, unsteady, props. rel. to electrical prospecting 9-35795
 induced current density, depth of maximum 9-49423
 induction, e.m. for spherical model 9-39988
 inhomogeneities affecting polarization of geomag. micropulsations 9-33869
 layered geoelectric structures, dynamic freq. characts. 9-33726
 magnetotelluric soundings, effective penetration depth of e.m. field 9-33728
 model covered by ocean of uniform depth, current intensity variation 9-49422
 prospecting by elec. methods, book 9-31270
 resistivities of layers, determ. by inverse magnetotelluric sounding 9-37890
 resistivity anisotropy, magnetotelluric obs. 9-47507
 resistivity structure by inverse magnetotelluric analysis 9-37891
 resistivity vs. depth rel. to e.m. soundings 9-35793
 ring current, self consistent in Earths dipole field 9-37995
 rocks, igneous and metamorphic, conductivity in r.f. field, obs. 9-26503
 rocks in upper crust, boundary equations 9-26882

Earth continued**electricity continued**

- sounding, d.c. geoelectric, book 9-39990
- sounding of crust using industrial current flow 9-28853
- upper mantle conductivity 9-45557

heat

- aftershock sequence, heat liberation calc. 9-26857
- convection, fluid model of variable viscosity heated from within 9-31256
- estimation of radioactive content 9-31253
- flow rel. to sea floor spreading mechanism 9-31274
- geyser, Old Faithful, mechanics of action 9-31255
- low radioactivity rocks of W. Australia, flow meas. 9-28838
- magmatic processes rel. to Sr isotopes in porphyritic alkali basalt 9-31276
- mantle, convections, effect of low viscosity region 9-24613
- mantle convection with variable phys. props. in ascending and horizontal flows 9-28839
- soil, temp. and flux profiles, applic. of thermal diffusion model 9-31254
- surface, bulk transfer coefficient 9-47489
- temperature gradient and thermal cond. in sediments, heat flow probe meas. 9-35771
- temperature vs. depth 9-35793
- thermal field near surface, effect of past climate charges 9-47488
- topographic disturbance, superficial thermal gradients, rapid estimation 9-26856
- upper mantle, convection, two-component flow model 9-26855
- wells, small diameter, convective flow and effect on temp. logging 9-35770

magnetic field

- activity forecasting using solar corona features, method 9-24704
- activity rel. to auroral absorption 9-31374
- activity rel. to ionospheric v.l.f. bursts 9-40071
- activity rel. to vertically moving ionized formations 9-40078
- aeromagnetic profiles, nonlinear filtering 9-47588
- anomalies, depths of sources, statist. determ. 9-31453
- anomalous, energy spectrum 9-43479
- anomalous in ocean, statistical characts. 9-31451
- axis, coincidence with rotation axis, paleomag. investigation 9-40098
- axis inclination rel. to foF2 N-S asymmetry 9-45542
- cavity boundaries, Explorer 10 obs. 9-38094
- closed lines, high-latitude limit 9-35873
- co-ordinate L system based on actual config. of quiet geomag. field 9-31445
- component relation with induced Earth currents in equatorial region 9-45460
- components meas. from moving body using celestial orientation 9-45552
- configuration above auroral zones 9-47600
- conjugacy, auroral and magnetic, hypotheses 9-40106
- core-mantle coupling effect on rotation perturbations 9-37994
- cosmic ray equator obs. (1963) 9-35923
- cosmic ray variations due to geomagnetic field 9-35922
- cosmic rays cut-off rigidities in non-vertical directions 9-47596
- Cosmos 49 obs., spherical harmonic analysis 9-26957
- declination meas. from moving object using vertical and solar components 9-43473
- of dipole, l.f. in conducting medium, influence of mag. sphere 9-33854
- dipole field, non-linear symmetric inflation due to radiation belts 9-45518
- drift, westward, rel. to earth's core rotation 9-43474
- earth-ionosphere cavity, effect on super l.f. noise 9-31395
- east-west component recording, importance for s.s.c. morphology 9-33862
- equatorial ionospheric anomaly, theories 9-35885
- field dependence of nuclear spin relaxation, observation of free precession of nuclear magnetization in earth's magnetic field 9-33855
- from and behaviour, from direction and strength meas. and rock magnetism 9-45547
- geomagnetic observations 9-40096
- geomagnetic tail, current sheet waves damping by radiation 9-47560
- geomagnetic tail, e.m. noise in current sheet 9-47559
- geomagnetospheric wake, at 500 and 1000 Earth radii, plasma obs. 9-38109
- gravimetric and magnetic inverse problem, joint solution 9-49506
- H and Z components, proton magnetometer meas. 9-45553
- inclination, archeological obs. errors 9-26968
- induction by deep sea tides 9-31275
- intensity map, global, for 1965 epoch 9-31446
- interaction with solar wind 9-33953
- interaction with solar wind 9-31644
- ion clouds motion and ambipolar diffusion 9-37977
- ionization in F-region, geomag. control of vertical drift 9-31429
- ionosphere conductivity variations near dip equator during solar eclipse (Nov., 1966) 9-24690
- magnetometric data transformation into tectonic maps by digital template analysis 9-45555
- magnetosphere, anomalous resistivity along lines of force 9-40050
- magnetosphere, outer, average mag. field config. 9-28967
- magnetosphere, quantitative mag. field models, review 9-37945
- magnetosphere boundary distance rel. to geomag. field non-dipole component, IMP-1 obs. 9-26924
- magnetospheric tail, calc. from auroral oval obs. 9-35845
- magnetotelluric problems, conductor network presentation 9-45548
- measurement, rocket-released attitude stabilized magnetometer 9-41592
- measurement at site having collocated array of various types of sensors 9-33849
- microstructures and disturbances spectral analysis (Feb 1965 and March 1966) 9-41598
- model 9-24702
- model, rel. to asymptotic directions of vertical incidence for high latitudes 9-31471
- model, with 1 horizontal and 30 radial dipoles 9-31444
- model constructed from Cosmos 49 obs. 9-45554
- model midnight meridian magnetospheric field 9-31350
- models based on five different coefficients for spherical harmonics expansion, comparison with meas. 9-43475
- new coordinate system calc. 9-41594
- normal component, separation by moving average method 9-43476
- oscillations near earth's bow shock front 9-35894
- paleomag. pole migration rel. to change in nondipole field component 9-31450
- potential, calc. from multipole series 9-41595

Earth continued**magnetic field continued**

- potential field data treatment, bicubic spline interpolation 9-45549
 - precession as cause of geomagnetism 9-24703
 - preliminary obs. in tail of geomag. cavity 9-38093
 - response, asymmetrical, to interplanetary field 9-26963
 - ring current, self consistent in Earth's dipole field 9-37995
 - structure at large distances 9-45550
 - at surface and in outer space, representation by dipole model 9-45551
 - surface phenomena rel. to magnetospheric processes 9-47595
 - tail, review 9-37946
 - tail, simultaneous meas. on three satellites at 1000 earth radii 9-40047
 - Tunguska meteorite effects 9-26916
 - Van Allen belt, axisymmetric 9-28935
 - Z_{acc} residual, spatial structure 9-40099
- magnetic field, variations**
see also Magnetic storms
- activity and spread F, delays between, latitude vars. 9-37985
 - activity rel. ionosphere total electron content night midlatitude behaviour 9-24689
 - activity rel. to auroral absorpt. near S. Geomag. Pole 9-35856
 - activity rel. to mid latitude v.l.f. emissions at conjugate points 9-40102
 - Arctic Ocean sediments, stratigraphy and faunal patterns 9-45566
 - auroras, polar, k_p index rel. to energy of injected particles 9-31465
 - automatic evaluation of ionospheric current systems 9-38000
 - bays, disturbance vectors distrib., N. Hemisphere obs. 9-28961
 - conjugate point phenomena, review 9-35901
 - correlation with troposphere disturbances 9-45487
 - data, at Dourbes (Belgium), during April (1968) 9-49509
 - day classification for statistical work 9-33859
 - declination influence on F2 ionospheric layer summit 9-47579
 - deep-sea sedimentary cores, short period polarity events 9-45567
 - disturbance field, low latitude, axial symmetry 9-35908
 - disturbance field asymmetry rel. to solar wind incidence 9-35914
 - disturbance index 27 day var., semiannual modulation 9-43480
 - disturbances, rel. to quiet component of 9.1 cm solar emission 9-38100
 - disturbances rel. to auroral absorption, diurnal pattern 9-31466
 - disturbed period auroral conjugacy March 1968 obs. 9-41565
 - diurnal, and their meas., review 9-49508
 - diurnal, declination, horizontal and vertical intensities, Nurmijarvi Geo-physical Observatory (1967) 9-31474
 - diurnal, Ulan Bator 1966 obs. 9-31447
 - diurnal and associated upper atmosphere phenomena, review 9-47591
 - Dourbes (Belgium), 1967, survey 9-43481
 - drift rate estimation, equivalence of two methods 9-37996
 - effects on ionization irregularities in ionosphere, obs. 9-49500
 - electron concentration variations in topside ionosphere, between 60°N and 60°S, rel. to 9-40090
 - e.m. field from oscillating magnetic dipole over anisotropic earth, propag. 9-37993
 - e.m. solar-terrestrial events (Feb 1965) 9-41605
 - geomagnetic activity rel. to quiet solar wind energy flux 9-26965
 - horizontal and vertical intensity and declination elements, data 9-49510
 - horizontal near 8° dip latitude, increase 9-35897
 - hydromagnetic emissions, full-Moon enhancement 9-41603
 - rel. to interplanetary mag. field 9-47594
 - intervals of pulsations of decreasing periods, influence of exospheric resonance cavity 9-35907
 - ionosphere, F-region, dynamical behaviour during bays 9-35889
 - ionosphere, lower, turbulence-conditioned, estimation 9-33826
 - rel. to ionospheric irregularities distribution 9-41586
 - K_p of polar auroras rel. to energy of injected particles 9-31465
 - K_p and interplanetary transverse field fluctuations, correl. 9-43648
 - K_p rel. radiation belt (outer) intensity spike 9-40067
 - K_p rel. to auroral absorption occurrence patterns 9-43494
 - K_p rel. to sporadic E at Hong Kong 9-35882
 - local gradient fluctuations, activity index 9-33860
 - long-period, energy density during mag. storms 9-33863
 - lunar daily, sunspot dependence obs. 9-33871
 - lunar daily periodicities study by spectral analysis 9-24706
 - lunar-diurnal, rel. to ionospheric lunar tides, obs. 9-26958
 - in magnetic storms, short-period pulsations rel. to solar corpuscular streams and magnetosphere interactions, obs. 9-28964
 - magnetograms, scanning installation, semiautomatic 9-31449
 - magnetospheric, during storm recovery 9-43483
 - micropulsations rel. to quasi periodic v.l.f. emissions 9-27068
 - micropulsation, possible modes 9-33866
 - micropulsation periods, depend. on size of magnetosphere 9-47557
 - micropulsation polarization rel. to geoelec. inhomogeneities 9-33869
 - micropulsation wave packets, ssc, freq.-time dispersion and polarization effects 9-33870
 - micropulsations, 0.2 to 5 Hz, rel. to magnetospheric wave amplification 9-47558
 - micropulsations, Doppler obs. of associated ionospheric fluctuations 9-47575
 - micropulsations, high-latitude, polarization obs. 9-33867
 - micropulsations, magnetospheric elec. field estimation from freq. drift 9-31354
 - micropulsations, Pc1, polarization and amplitude history, graphic method 9-43490
 - micropulsations at Arctic and Antarctic conjugate points, obs. 9-41602
 - micropulsations rel. to magnetospheric tail perturbations 9-33868
 - micropulsations rel. to proton flare (7 July 1966) 9-40105
 - in ocean, surface and bottom 9-40097
 - ocean edge, geomagnetic effects 9-28959
 - Pc1 and Pi1 events, source and propagation 9-26962
 - Pc1 micropulsation freq. changes during sudden magnetospheric deformation 9-45559
 - Pc1 pearl pulsations rel. to 11 year solar cycle 9-45561
 - Pc1 pulsations rel. to mag. storms 9-31462
 - pc3, pc4 and pi2, latitude variations, obs. 9-33865
 - pc3 and pc4 microstructure 9-33864
 - Pc3 at conjugate points, obs. 9-31460
 - Pc3 pulsations simultaneous with pulsating electron precip. events near local noon 9-45560
 - Pc5 pulsations, spatial localization 9-40103
 - Pc 1 micropulsations, 0.2 to 5.0 Hz and rel. to hydromag. wave amplification 9-28966
 - Pc 1 pulsations, obs. in equatorial Africa 9-41612
 - Pc-1 pulsation obs. 9-31463

Earth continued

- magnetic field, variations continued**
 period 10-200 secs., rel. earth currents, obs. 9-26961
 perturbations rel. to heating of upper atm. 9-41601
 pi2 micropulsations at low latits., obs. 9-38002
 Pi 2 micropulsations, night equatorial 9-31464
 polar daily disturbances correl. with E_s blanketing 9-33856
 pulsations, irregular, rel. to auroral and v.l.f. emission pulsations 9-43487
 pulsations, mid-latitude, correlation affected by ionospheric absorption 9-35900
 pulsations of decreasing period, 12 Feb. 1964, interval correlations 9-31461
 pulsations of decreasing period, rel. to ionosphere reson. characts., obs. 9-28965
 recording equipment freq. characts. standardization 9-31454
 reversals, 1967 Bakerian lecture 9-24709
 reversals, true rate 9-45556
 reversals in polarity 9-47590
 ring currents, Vlasov- equation study 9-47567
 ring-current field in combination with D_{st} variations, analysis 9-33861
 S_d variation ascribed to polar electrojets 9-35904
 S_d cyclic changes 9-31456
 S_d, rate of change, planetary distribution 9-31459
 S_d, reference level in calc. 9-43489
 S_d(h) rel. to relative sunspot number 9-43491
 Scotland, and seismic absorption 9-47587
 secular, anomaly 9-35896
 secular, calc. from marine, aerial and satellite obs. 9-43478
 secular, drift velocity 9-35898
 secular, in a perfectly conducting core, Kinematics 9-31469
 secular, marine mag. survey obs. 9-31448
 secular, rel. to crustal movements 9-31271
 secular, rel. to mag. waves in earth's core 9-26956
 secular, rel. to sub-Alfven eqn. hydromag. instability 9-43482
 secular charge prediction for 1965-67, confirmation 9-49507
 solar activity, July-Sept. 1966 obs. 9-31641
 solar eclipse effect, near dip equator, (Nov., 1966) 9-35916
 solar flare association, clarifying dynamo wind structure 9-35915
 solar wind interaction at various dipole axis inclinations, magnetopause surfaces and fields 9-43493
 sounding methods 9-31452
 space and time, separation by moving averages 9-43477
 space around earth, search coil magnetometer, design and experiments 9-35895
 spherical harmonic analysis of disturbances 9-31458
 Sq, anomalous, and bay cause determ. 9-24705
 Sq, latitudinal and longitudinal patterns of parameters, effect of global anomalies 9-40101
 Sq, variability 9-43488
 Sq(H) day to day variability, solar control 9-37997
 Sq currents in 3 dimen. ionosphere 9-37998
 Sq local variability in N. Germany 9-33858
 sudden commencement propag. along magnetotail (8 Jul 1966) 9-26960
 sudden commencements and impulses, causes 9-41607
 upper mantle, and electrical conductivity 9-45557
 vertical component lunar variations, effect of sea tides 9-37999
 v.l.f. in auroral zone, sounding rocket obs. (25 May 1968) 9-49476
 westward drift estimation, equation 9-35899
 world charts, statistical analysis 9-33857
 OH emission in upper atmosphere, effect of geomag. disturbances 9-45508

rotation

- astronomical concurrent obs. 9-33734
 axis, angular displacements rel. to mantle 9-49404
 axis, angular displacements rel. to mantle 9-49405
 boundary value problem, free air geoid as solution 9-28837
 core rotation rel. to geomag. westward drift 9-43474
 deceleration, satellite determ. 9-28854
 effect of earthquakes on Chandler wobble 9-31265
 eigenvibrations, finite dislocation excitation, toroidal oscillations 9-33731
 fluctuation and polar movement, comparison with tropospheric wind vector 9-31306
 fluctuations, progressive and librational motions of pole 9-33745
 influence on convection in mantle 9-28851
 installations pole position, determination by graphical method 9-37898
 motion of mean pole 9-33735
 motion of triaxial rigid body orbiting oblate primary, first-order theory 9-31496
 normal mode eigenfrequencies of a slowly rotating, slightly aspherical and anisotropic pole 9-24625
 perturbations for spheroidal oscillations and freq. change formula deriv. 9-37897
 perturbations rel. to core-mantle e.m. coupling 9-37994
 polar motion derived from time and latitude obs. 9-33742
 polar secular motion and continental drift, symposium, Stresa (1967) 9-33702
 polar wandering, estimation of lithospheric drift 9-31479
 polar wandering and continental drift 9-33743
 pole, Chandler's motion, parameters determ. from obs. over 119 years 9-43350
 pole motions and continental drift, accuracy of determination 9-33746
 pole movement, azimuthal variations obs. (1963-1965) 9-26886
 pole movement and latitude variations 9-33738
 precession as cause of geomagnetism 9-24703
 tides contribution to rotation study 9-33741
 two-week nutation and tidal deformations 9-43349
 variation of longitude 9-33737
 variations in latitude, relations with polar motion 9-33736

Earth satellites *see* **Satellites, artificial**

Earthquakes *see* **Seismology**

Eberhard effect *see* **Photographic materials**

Ebullition *see* **Boiling**

Echelons *see* **Diffraction gratings**

Echo

- see also* **Architectural acoustics; Reverberation; Sound ranging**
 anechoic termination for small acoustic filters, design and evaluation 9-43794
 e.m., in collisionless plasma, generation process 9-32662
 ferrimagnetic pulse, amplification 9-45239

Echo continued

- ion-wave, spatial, in plasma, theory and experiment 9-34785
 plasma wave, Coulomb collisions and microturbulence effect 9-30217
 radio, ionospheric irregularities observed by topside sounders 9-35878
 sonar, automatic distinction between hard and soft objects, fish detect. appl. 9-41831
 sounders, radio echo, for polar ice sheet depth 9-26883
 time delay, u.s. between successive echoes, meas. technique 9-29261
- Eclipses** *see* **Moon; Sun/eclipses**
- Eddy-currents**
 devices, coupled-circuit method of force calc. 9-31896
 ferromagnet, after Barkhausen jump, negative jumps origin obs. 9-39767
 losses rel. to thickness of sample, meas. method 9-26506
 Fe79Si3 alloy, depend. of losses on sample thickness 9-26506
 Tb, micro-, internal friction damping 9-26319

Edge emission *see* **Luminescence/solids, inorganic; Luminescence/solids, organic**

Education *see* **Teaching**

Effusion *see* **Flow/gases**

Eightfold way *see* **Elementary particles/symmetry; Field theory, quantum**

Einstein-de Haas effect *see* **Gyromagnetic effect**

Einsteinium

No entries

Einsteinium compounds

No entries

Elastic constants

- see also* **Compressibility; Stress/strain relations**
 anthracene, u.s. meas. 9-35143
 b.c. tetragonal cryst., elastic and force consts. for 1-2-3 neighbours non-central interactions 9-40995
 β -brass, long-range order influence 9-39396
 brass, Young's modulus and torsion modulus, calcs. by different methods 9-30629
 chalcogenide glasses, vitreous, rel. to struct. and softening temp. 9-48744
 coefficients of quadratic form for elastic energy density in terms of lattice force constants 9-23847
 composites, filamentary, with hexagonal symm., calc. 9-37216
 compressibility, rel. to density of cohesive materials 9-35145
 crystal with paraelastic defects, dynamic behaviour 9-48889
 crystals, bulk modulus-density relationship 9-44760
 cubic crystals near λ -transition, Garland's relation validity 9-44750
 fluid of hard spheres 9-36741
 fluxoid lattice near upper critical field 9-35139
 glass, T-40, 3rd order const., acoustoelastic effect obs. 9-35141
 glasses, V₂O₅.P₂O₅, semicond., and densities, 100° to 400°K 9-35155
 graphite, polycrystalline, microporosity eff. on elastic modulus and yield curve 9-28343
 graphite, pyrolytic, Young's modulus, by flexural vibration technique 9-46864
 group III-V cpds., gradient-elastic nuclear acoustic resonance 9-23851
 Gruneisen parameters relation in low symmetry cryst. 9-39392
 h.c.p. metals, elastic energy factors for twinning dislocations 9-35090
 insulating cryst., use of models of forces between atoms 9-44635
 isotropic solid, number of nth order coeffs. 9-48880
 metals, simple, pseudopotential calc. 9-46862
 metals paramag., rel. to e. struct. 9-40996
 minerals, data on 10 compounds 9-44748
 mirrors of foamed material 9-32029
 perlite, rel. to porosity 9-30635
 polyamides, modulus obs. 9-32544
 1,4- polybutadiene rubber, dynamic modulus rel. to trapped and untrapped entanglements 9-30651
 polycarbonate craze, from cyclic stress-strain behaviour 9-46879
 polycrystalline aggregate, quasi- isotropic, numerical comparison 9-30629
 polymethylmethacrylate, from acoustic velocities press. and temp. depend. meas. 9-35276
 Pyrex, 3rd order const., acoustoelastic effect obs. 9-35141
 rubbers, cross-linked, dynamic modulus rel. to trapped and untrapped entanglements 9-30651
 rubbers, vulcanised natural, dynamic modulus rel. to trapped and untrapped entanglements 9-30651
 rutile polycrystalline, pressure derivatives of elastic props. 9-39394
 shear and bulk moduli apparent, geometrical depend. 9-22199
 silica, vitreous, 3rd order const., acoustoelastic effect obs. 9-35141
 single cryst., pressure depend. 9-26310
 solid, effect of charged dislocations 9-48856
 steel, carbon, polycryst. 9-35275
 steel, cold-rolled transformer, Young modulus rel. to annealing temp. 9-39455
 steel, spring, quench-hardened, Young's modulus depend. on tempering temp. 9-39391
 styrene-butadiene rubber, dynamic modulus rel. to trapped and untrapped entanglements 9-30651
 two-phase materials, bulk modulus 9-42864
 type-II superconductors, from magnetostriiction meas. 9-26620
 viscoelastic composite systems, bounds for real and imaginary parts 9-31836
 Al-Li alloys, Young's modulus increase with Li conc. 9-39395
 Al, high temp. 9-37219
 Al₂O₃, sapphire Young's modulus at high temp., u.s. meas. 9-42966
 Al₂O₃ polycrystals, pressure and temp. derivatives of isotropic moduli 9-46863
 AlSiB, gradient-elastic tensor determ. by nucl. acoustic resonance 9-23851
 α -As single crystals, for slip systems observed in plastic deform. 9-46889
 Au-Cu-Zn alloys, anisotropy, rel. to β phase stability 9-46957
 BaF₂, pressure and temp. derivs. 9-33016
 Be, shear constants, band structure contribution, model potential theory validity test 9-30630
 C, dynamic, effect of B-doping or stress-graphitization 9-26320
 CaF₂, pressure and temp. derivs. 9-33016
 Cd, shear constants, band structure contribution, model potential theory validity test 9-30630
 CdS, calculation using phonon dispersion model 9-46972
 CdS in constant elec. field, compliance consts. from freq. of longitudinal and contour modes 9-33395
 Ce, low-temp. phase transform. effect 9-40997
 γ -Ce alloys, Young's modulus anomalous decrease, low temp. 9-44751

Elastic constants continued

- Cr steels, hardened, from sound vel. meas. 9-23755
 Cu-Al alloys, martensitically transformed, Young's mod. 9-35172
 Cu-Sn alloys, martensitically transformed, Young's mod. 9-35172
 Cu, bulk eff., infl. of point defects 9-30631
 Cu, cold-rolled sheet, Young's modulus, angular variation and texture depend. 9-30632
 Cu, third-order const., sensitivity to changes in electron-to-atom ratio and mag. effs. 9-37217
 Cu, Young's modulus and torsion modulus, calcs. by different methods 9-30629
 Cu, Young's modulus orientation and temp. depend., -180 to 200°C, 9-17 kc/s 9-40998
 Cu whiskers, Young's modulus increase with strain 9-39407
 Fe, grey cast, 4.295°K 9-48893
 Fe-Ni alloys, Young's modulus, eff. of Co content on ageing induced changes 9-23942
 GaAs, gradient-elastic tensor determ. by nucl. acoustic resonance 9-23851
 GaSb, gradient-elastic tensor determ. by nucl. acoustic resonance 9-23851
 Gd, magneto-elastic interactions 9-24312
 He, rot., vortex lattices, shear modulus 9-39126
 HfCo₂, 4.2-300°K 9-42866
 Ho, from phonon dispersion relations 9-28415
 In-Th alloys, meas. during martensitic transformation rel. to elastic and anelastic behaviour 9-42865
 InAs, gradient-elastic tensor determ. by nucl. acoustic resonance 9-23851
 InSb, gradient-elastic tensor determ. by nucl. acoustic resonance 9-23851
 KBr, Young's modulus investig., rel. to interaction of dislocations with pinning centres 9-32971
 Li single cryst., temp. depend. 9-37220
 LiBr, single crystal, adiabatic const., from 300 to 4.2°K 9-48881
 LiF, thermal-neutron irradi. effect 9-46865
 Mg, shear constants, band structure contribution, model potential theory validity test 9-30630
 MgF₂ single cryst. 9-33017
 MgF₂ single cryst., from phonon propag. obs. 9-37314
 MgO polycrystalline periclae, rel. to press. 9-42867
 MgZn₂ single crystals 9-28331
 Ni₄Br, high press. u.s. determ., phase phase transitions 9-30633
 Na, temp. and pressure dependence 9-28332
 Nb, supercond., vortex lattice, compressional and shear const. 9-30873
 Nb single crystals, eff. of O additions, 4.2° to 313°K 9-30634
 Nd, u.s. attenuation meas., 4.2-300°K, correl. of anomalies with antiferromag. transitions 9-35146
 Ni-Cu dilute alloys, third-order const., sensitivity to changes in electron-to-atom ratio and mag. effs. 9-37217
 Ni, third-order const., sensitivity to changes in electron-to-atom ratio and mag. effs. 9-37217
 Ni₃Al single-cryst. 9-35140
 Ni₃Fe(Cr, Mo, W) ternary alloys, Young's modulus temp. depend., atomic ordering obs. 9-39297
 NiO scales, factorial expt. rel. to Ni oxidation process 9-23852
 Pd-(50 wt.%)Au alloy, Young's modulus temp. depend. 9-44752
 Pr, u.s. attenuation meas., 4.2-300°K, correl. of anomalies with antiferromag. transitions 9-35146
 Pt annealed wire, shear modulus, amplitude and temp. depend. 9-33024
 Pu-Al delta-stabilized alloys, temp. depend., elastic and anelastic behaviour obs. 9-37224
 Pu-Ce delta-stabilized alloys, temp. depend., elastic and anelastic behaviour obs. 9-37224
 Rb, pressure derivatives 9-23853
 RbH₂AsO₄, normal and deuterated 9-39696
 RbH₂PO₄ single cryst. 9-44749
 Re wire, Young's modulus at high temp., u.s. meas. 9-42966
 α-S meas. 9-48882
 SiO₂-C fibre reinforced, Young's modulus 9-44773
 SiO₂ quartz polycrystalline, pressure derivatives of elastic props. 9-39394
 Sm, u.s. attenuation meas., 4.2-300°K, correl. of anomalies with antiferromag. transitions 9-35146
 SrO, from u.s. elastic wave speeds obs. 9-48883
 SrTiO₃ single cryst., compliance temp. depend. by reson.-antireson. method 9-41000
 SrTiO₃ single cryst., compliance temp. depend. by reson.-antireson. method 9-40999
 Ti b.c.c., anisotropy 9-46867
 Ti b.c.c., anisotropy determ. 9-46866
 TiO₂, and Debye temp., calc. from force field 9-35142
 UO₂-UN sintered mixtures, Young's modulus 9-30730
 W, bulk eff., infl. of point defects 9-30631
 W, e-irrad., dynamic Young's modulus rel. to Stage-I interstitial behaviour 9-26279
 YFe garnet, anisotropy, investigation by magnetoelastic interac. 9-37221
 Zn, shear constants, band structure contribution, model potential theory validity test 9-30630
 ZrCo₂, 4.2-300°K 9-42866

mechanisms

- anisotropic media, using static homogeneous deform. field 9-35138
 anisotropy of polycryst. materials, u.s. technique 9-37218
 polymers, change, acoustical investigation 9-36835
 rock salt, seismic pulse method 9-26311
 storage and loss moduli of high polymers, by glueing to steel 9-33020
 u.s. at high temp. 9-42966
 u.s. three-phonon interactions in determ. third-order constants 9-42942

Elastic deformation

- see also *Bending; Stress/strain relations; Torsion*
 β₁-brass, metastable, effect on martensitic transformations 9-23981
 buckling behaviour, models for various cases 9-38274
 circular cylinder under axisymmetric end loads, exponential decay of stresses 9-31826
 combustion chamber walls, rel. to stability of burning process 9-39945
 Cosserat surface, static and dynamic solns. for finite deform 9-38280
 cylindrical shell under edge loading, influence coeffs. for varying wall thickness 9-25070
 displacement due to shear of pitot tubes with rectangular mouths 9-38942
 elasto-plastic deform. of bar by long. torsion, variational methods for calc. 9-45830
 linear continuum subjected to follower-type surface load, adjoint systems for stability problems 9-45818

Elastic deformation continued

- noble metals, effect on Fermi surface, determ. using thermoelec. power 9-44884
 nonlinear viscoelastic bodies with hidden parameters, props., uniqueness 9-27209
 planes with uniform transverse stretch, soln. of deform. fields 9-31825
 polar elastic materials, general soln. for torsion 9-41794
 postbuckling behaviour and imperfection sensitivity, effect of nonlinear prebuckling state 9-25071
 radial, of cylindrical shells with variable wall thickness 9-27194
 rectangle between two elastic half-spaces, adhesive or frictionless compression 9-31824
 rods, slender, spatial deflection problems 9-47810
 shell, cylindrical finitely deformed thin, stability 9-22202
 shells, cylindrical, with variable wall thickness, along axis 9-27194
 stability of thin shells, expt. study of effect of general imperfections 9-38276
 steel plate with circular hole, under cyclic loading 9-23886
 Ag, effect on Fermi surface, determ. using thermoelec. power 9-44884
 Cu, effect on Fermi surface, determ. using thermoelec. power 9-44884
 Cu foils, effect on ⁶³Cu n.m.r. 9-24507
 n-Ge, influence on thermoelec. power 9-37611
 Ta, dislocation relax. at low temp., max. in dissipation vs temp. curve, and Reieris stress 9-23816
- Elastic fatigue**
 accelerated, under progressive loading, Prot testing, modification 9-26344
 bearing metals, fatigue cracks by reciprocating rubbing 9-41032
 brass, 7:3, in combined torsion and bending, obs. 9-30687
 concrete bridges, reinforced, behaviour of high strength deformed bars 9-23854
 crack, disc-shaped, fatigue growth 9-33089
 crack formation and propag. during cyclic deform., model 9-30682
 crack propag. and initiation in low cycle strain controlled fatigue 9-30683
 crack propag. nucleation theory, elastic-plastic stress distrib. near crack tip effect 9-46909
 crack tip deform. process, obs. using fatigue tester with micrographic apparatus 9-42896
 cracks prod. by rolling, effect of surface-active subst. on origin 9-46907
 damage, linear cumulative theory for low-cycle fatigue region 9-33073
 damage accumulation, general linear theory 9-33072
 dislocations, continuous distribution, review of expt. results rel. to theory 9-23807
 failure probability, rel. to heterogeneous dislocation assembly 9-23809
 f.c.c. metals, cyclic, eff. of slip character 9-30674
 rel. to fracture and mechanical strength, interdisciplinary approach, book 9-39431
 low-cycle behaviour under biaxial strain distrib. 9-33073
 metal, new interpretation 9-42897
 metals, fatigue strength, combined effects of macro- and microstructures and residual stresses on deposition 9-39434
 metals, strength in welded joints, effects of reactive stresses 9-23902
 plastic solids, failure criteria in space of stress invariants 9-39433
 slip bands, persistent, nucleation 9-33071
 soda-lime-silica glass, dynamic fatigue 9-42899
 steel, 0.3% C, fatigue strength rel. to stress waveform, obs. 9-26346
 steel, carbon, branch point and fatigue limit, size effects, obs. 9-33078
 steel, carbon, cracking under sinusoidal loading, obs. 9-30695
 steel, carbonitrided, retained austenite effect on fatigue strength 9-30688
 steel, cast, crack propag., microfractographic investig. 9-33080
 steel, cast, fatigue fracture, effect of size distrib. of internal defects 9-35188
 steel, Cr-Ni-Mo high C low alloy, fatigue strength rel. to hardness, obs. 9-26345
 steel, crack propagation, effect of mean stress and material yield stress 9-30696
 steel, high-strength, max. fatigue limit, optimal suitable tensile strength level 9-33082
 steel, induction hardened, fatigue strength rel. to retained ferrite microstruct., obs. 9-26348
 steel, low-endurance behaviour, uniaxial and biaxial, comparison 9-23858
 steel, low-endurance studies under cyclic torsion 9-23860
 steel, mean C and low-alloyed, hardening and softening during fatigue fracture 9-30689
 steel, mild, crack propag., effect of corrosive environment and stress history 9-37262
 steel, mild, surface-rolled, electron microscope obs. of slip line and crack formation 9-35189
 steel, Ni maraging, props., effect of shot peening 9-26315
 steel, push-pull low endurance, 20°C and 450°C 9-23859
 steel, rail, cracks, structure effect on rate of propag. 9-33092
 steel, stainless, neutron irradiated, behaviour, review 9-23861
 steel, stainless SUS 29, thermal fatigue cracks, 200-700°C 9-26353
 steel high strength, fatigue failure, fractographic investig. 9-33081
 steel(45 wt.%)Cr, heat treated, shot-peening and Cr-plating effects 9-28365
 steel(18 wt.%)Ni, maraging-steel, heat-treated 9-30691
 strength at stress concentration 9-30684
 in wear mechanism, physical confirmation from cyclic nature of accumulation of distortions of second kind in surface layer 9-23929
 Al-Zn-Mg alloy, props., effect of shot peening 9-26315
 Al, alloys, prevention of fretting fatigue 9-42898
 Al, crack growth, effect of air pressure 9-46906
 Al, cyclic freq. and tensile fatigue eff. in vacuum, defect substruct. distrib. and crack propag. obs. 9-28364
 Al alloy, low-endurance studies under cyclic torsion 9-23860
 Al alloy, property variations with batches 9-23855
 Al alloys, crack propag., microfractographic investig. 9-33080
 Al alloys unnotched, effect of depth of machining cut 9-33074
 Al crack initiation and propag., correlation effects of substruct. 9-30685
 Al foils, surface deform. markings, direct correlation of dislocation structures 9-23878
 Al single cryst., cyclically strained surface microrelief obs. by X-ray diff. method 9-46777
 Al single crystals, coarse slip model of crack formation and propag. 9-48904
 Al surface layer stress effect 9-23880
 Cd, damage under cyclic stresses 9-32981
 Cr(2 wt.%)Ta(0.5 wt.%)Si alloy guide vane specimens, thermal fatigue testing 9-33075

Elastic fatigue continued

- Cu, bulk effects in [211] oriented single crystals, temp. effects 9-23914
 Cu, single cryst., crack formation and propag. during cyclic deform., 9-30682
 Cu, strength, effect of diffusion coatings 9-33058
 Cu cyclically deformed in torsion, elec. Resistivity change w.r.t. defects 9-33254
 Cu dislocation distrib. after fatigue at elevated temp. 9-30608
 Cu single cryst., dislocation struct. and persistent slip bands 9-30686
 Cu single cryst., propagating fatigue crack, dislocation substruct. 9-33077
 Cu single cryst. dislocation distrib. in persistent slip bands 9-33076
 Cu single crystals, coarse slip model of crack formation and propag. 9-48904
 Cu single crystals, early stages, dislocation substructure and surface markings study 9-30637
 Fe, cast, globular, hardening and softening during fatigue fracture 9-30689
 Fe-(0.04 wt.%)C quench aged alloy, hardening and softening obs. under cyclic straining 9-33079
 LiF single cryst., 350-650°C 9-30692
 Mg, damage under cyclic stresses 9-32981
 Mg and alloys, bkn. 9-39447
 Mg (0.7 at%) Mn, at 400°C, for extruded, annealed and aged samples 9-30638
 Mg single crystals, coarse slip model of crack formation and propag. 9-48904
 Ni, rel. space charge at high temp. 9-26318
 Ti-(8 wt.%)Al-(4 wt.%)Co alloy, rel. to heat treatment 9-40994
 Ti-(8 wt.%)Al-(4 wt.%)Co alloy, fatigue strength 9-23956
 Ti-(6 wt.%)Al-(4 wt.%)V Wear alloy, impact fatigue surface treatment 9-37259
 α -Ti, coarse-grained, twin formation 9-33083
 Ti, damage under cyclic stresses 9-32981
 Ti alloys, crack propagation, eff. of 3.5% NaCl aqueous saline environment 9-23924
 Zn, damage under cyclic stresses 9-32981

Elastic limit

- see also *Slip*
 alloys, substitutional, serrated yielding 9-39411
 circular plates, yield-point loading 9-34065
 graphite, polycrystalline, microporosity eff. on elastic modulus and yield curve 9-28343
 yielding, serrated, initiation at high temp. 9-42874
 Al-Zn alloys, yield strength rel. to spinodal decomp. 9-37289
 Co-Fe-V alloys, yield-strength rel. to partially-recrystallized structure 9-44790
 Cu, microyielding, dislocation arrangement after deform. 9-48897
 Cu whiskers, elastic and plastic behaviour below yield pt. 9-39407
 Ni₃(TiAl) alloy hardened by coherent and ordered precip., yielding 9-39408
 Ni base alloy, dispersion-hardening, grain size effect on yield point 9-33015

Elastic losses see *Internal friction***Elastic relaxation**

- see also *Creep*
 graphite, stress relax. at high temps. 9-46874
 graphite, stress relax. at high temps. 9-46873
 ice, diffusion mechanism 9-28318
 paraelastic, Green's function approach 9-48889
 polycaprolactam, water content effect 9-33027
 polychloroprene films, and i.r. dichroism rel. to crystallinity and orientation, obs. 9-30650
 polyvinyl chloride, unplasticized rel. to crystallinity 9-30652
 protein adsorbed layers, hysteresis and stress-relax. 9-23450
 Snoek, internal stresses effect 9-44754
 solid solns., substitutional, relax. time model for short-range order changes and Zener relax. 9-46870
 stress, in wide range of strain repetition frequency for liquid polymers, acoustic meas. 9-36835
 Ag-(31 at.%)Zn alloy, kinetics of elastic after-effect from resistance changes meas. 9-35161
 α -AgCd, Zener relaxation, activation energies 9-33025
 Au-(25 at.%)Cu alloy, kinetics of elastic after-effect from resistance changes meas. 9-35161
 Cu-(30 wt.%)Ni, substitutional Zener relaxation 9-26321

Elastic waves

- see also *Acoustic waves; Magnetoelastic waves; Seismic waves*
 bar, rectangular infinite, stress propag. 9-43783
 bending vibrations in bars, propag. 9-34079
 conical internal refraction condition in tetragonal and hexagonal cry. 9-30641
 crystal (cubic), plate, normal mode phase vels. 9-46869
 in crystals, stressed, propag. and acoustical birefringence 9-30642
 on crystals (anisotropic) surfaces 9-27222
 cylinder, transradially isotropic, SH waves 9-27220
 cylindrical shell, circumferentially travelling wave flutter, limiting amplitudes, nonlinear anal. 9-22243
 in cylindrical shell-core syst., stress wave propag. and refl., transient response formulae 9-22191
 diffraction by cylindrical discontinuities, effect of couple-stresses 9-41818
 elastic rod, large amplitude longit. wave propag., solns. rel. to end velocity 9-27221
 elastic-plastic wave generation by absorpt. of e.m. radiation in thin surface layer 9-45846
 emission during discontinuity of medium 9-22244
 extensional, in thin cylindrical shell, end response 9-29244
 flexural, transmission across elastic spacers at plate junctions 9-22242
 impact on elastic quarter space, analysis 9-29257
 infinite isotropic plate, transient non-axisymmetric wave propag. solns. 9-31845
 inverse digital filtering, stability theory 9-25094
 inverse scatt. problem in stratified region, soln. and computational procedure 9-29256
 isotropic medium, transverse, SH waves 9-27219
 laminated random media, mean wave propag. 9-47821
 layer-half space systems, surface wave structure and dispersion 9-45844
 Love, propagation at 285 MHz 9-25093
 medium with random inhomogeneity distrib., distortion theory 9-26874

Elastic waves continued

- metals, hexagonal, vibr. modes orientation depend. and assoc. dislocation damping 9-48890
 in micropolar elastic solid, effect of microstructure 9-29258
 microwave noise power, conversion from thermal spin fluctuations by pulsed mag. field 9-37226
 monochromatic, propagation in infinite micropolar elastic plate 9-47820
 in non-simple solids of grade n, plane wave propag. 9-31847
 nonlinear media, two-dimensional wave propagation problem, development of computer program 9-41819
 in oceanic wave-guides, diagnostic diagrams and transfer functions 9-26866
 plane, normal incidence to stratified medium, inverse scatt. problem 9-29256
 plane harmonic shear wave, effect on penny shaped crack in elastic medium 9-29228
 plate, elastic, response to cyclic longit. force 9-29254
 plates, flexural wave insulation by arbitrary obstacle 9-25091
 plates, two, semi-infinite, joined at various angles, flexural wave refl. 9-25092
 propagation in layered media, finite difference methods, seismograms 9-26863
 pulse, plane compressional, diffraction by circular cavity, shadow zone response 9-41817
 pulse grouping during destruction of heterogeneous specimens 9-22245
 pulse propag. in sphere, finite-difference calc. 9-40276
 α -quartz, light scatt. by surface waves 9-47307
 radiation from propagating phase boundary, earthquake source model 9-24619
 random medium, general method for velocity and attenuation determ. 9-36119
 Rayleigh, secondary wave propag., finite deformation theory 9-29253
 Rayleigh waves, subsurface characts. 9-31844
 rods, elastic, nonhomogeneous, longit. wave propag. 9-27223
 scattering in heterogeneous media, ultrasonic testing of inhomogeneities 9-29279
 schlieven meas. in transparent solids 9-38296
 second-harmonic generation by longit. u.s. beams, Bragg diff. obs. 9-37225
 seismic, in quarter plane, propag. eqn. finite difference soln. 9-35778
 seismic, scattering by random field of surface scatterers 9-39983
 in semi-infinite stratified medium 9-45845
 semiconductors, surface instability, current carriers with low recombination rate 9-30897
 shear, polarized, harmonic, diff. by finite crack, integral transforms appl. 9-29255
 stress in uniaxially prestressed plastic viscoplastic unbounded media, harmonic dispersion analysis 9-31846
 stress wave propag. and refl. in cyl. shell-core systems, transient response formulae 9-22191
 surface of piezoelectric crystals, excitation and detection 9-43784
 surface waves, charact. and props. 9-36171
 surface waves, light scatt. obs. 9-47307
 thinly layered random medium, transmission and reflection 9-22246
 vibrations, random, of thin elastic plates 9-29252
 in Al alloys, Rayleigh use in detecting stress corrosion cracks 9-42704
 Bi_{1-x}GeO_{2-x}, piezoelec., elasto-optic matrix elements for longit. waves 9-33394
 Bi_{1-x}SiO_{2-x}, piezoelec., elasto-optic matrix elements for longit. waves 9-33394
 CdS bending oscillations excited by elec. current 9-44763
 CdS film-fused quartz system, surface wave structure and dispersion 9-45844
 CdS thin layers, current fluctuations 9-35396
 Fe, Armo, attenuation calc. using rate-depend. plastic flow constitutive relation w.r.t. dislocation motion 9-37257
 InSb substrate film system, surface wave, attenuation 9-47121
 LiNbO₃, vel. and energy propag. direction for plane longit. wave with vector along Y-axis of rod 9-37228
 LiNbO₃, attenuation of microwaves rel. to temp., 80-950°K 9-41007
 Se, amorphous, propagation velocity rel. to Ge content 9-30646
 Sr_{1-x}Ba_xNb₂O₆, ferroelec., elasto-optic matrix elements for longit. waves 9-33394
 SrO, longit. and transverse u.s. wave speeds, elastic consts. determ. 9-48883
 YFe garnet single crystal, resonant absorpt., in absence of external mag. field 9-30649

Elasticity

- see also *Compressibility; Mechanical strength; Stresses, internal; Thermoelasticity; Viscoelasticity*
 adhesive contact of cylindrical punch with elastic half-space, soln of rocking and translation parallel to plane 9-38279
 alloy, elastically inhomogeneous, dislocation model of strength 9-39430
 alloys, inhomogeneous, effect of constraints on electron energy loss meas. 9-48978
 anharmonic crystal, interatomic pot. theory 9-30759
 anisotropic half-space, stress and deform. fields 9-38282
 anisotropic materials in Hertzian contact stress field effects 9-41793
 anisotropic mats. with coupled stresses, energy functions for cubic and hexagonal systems 9-22200
 anisotropic of polycryst. materials, u.s. technique 9-37218
 bar, circular, elasto-plastic props. under axial load and torque 9-36167
 bar, infinite cylindrical, embedded in elastic medium, diffusion of axial load 9-41800
 bar-mass system subjected to rectangular force pulse, approx. using spring mass 9-45819
 beam, thin-walled elastic, dynamic stability of flexural vibrations 9-40274
 beam deflection eqns. when values of the modulus of rigidity for right and left spans are different 9-34068
 beams, natural frequency analysis, with random imperfections 9-43782
 beams, uniform, transverse vibrational freq., effect of non-homogeneity 9-22234
 beams response under concentrated moving masses 9-31828
 bending instability of orthotropic shallow-stiffened cylinders 9-36161
 boundary values of homogeneous, isotropic half-plane 9-27200
 buckling, local, of thin flat-walled structures combined shear and stress: stability function 9-36158
 cantilever stability under eccentric follower force, effect of warping rigidity 9-43778

Elasticity continued

- circular cylinder, exponential decay of stresses from axisymmetric end loads 9-31826
- circular rod in plane strain and with suddenly removed radial pressure 9-22216
- compliance, effect of charged dislocations 9-48856
- compressible materials, transition to incompressible 9-22190
- concentrated load and Green's functions in elastostatics, displacements and stress singularities determ. 9-38283
- cones, solid truncated, yielding under quasistatic and dynamic loading 9-22219
- continuous isotropic medium, stress in diagonal 9-43775
- continuous media with local solid friction, model 9-45806
- continuum, doubly periodic array of material discontinuities, uniaxial loading, stress, displacement fields 9-34073
- Cosserat continuum, intrinsic theory 9-22204
- Cosserat surface, elastic-plastic theory 9-22209
- Cosserat surface, static and dynamic solns. for finite deform 9-38280
- crack in wedge, mixed boundary value problems 9-31820
- crack problem, stresses and displacement, two-dimensional theory 9-29231
- cracks, penny shaped, in isotropic medium, dynamic stress intensity factor for axisymmetric loading 9-22201
- crystal systems, stress-strain relations rel. to orientation vector and scalar moduli 9-39403
- crystals, simultaneously ferroelec. and ferroelastic, exam. of possible species 9-47166
- crystals, theories of elastic props. and elastic waves of equal phase vel. 9-43777
- cylinders, hollow finite, under axially symmetric deform. 9-31816
- cylindrical bore in infinite medium, travelling loads, response 9-34072
- cylindrical shell, circumferentially travelling wave flutter, limiting amplitudes, nonlinear anal. 9-22243
- cylindrical shells, axisymmetrical motions, anal. inc. rotary inertia and shear correction factor 9-22227
- defective solid, thermodynamic props. 9-44681
- deflection of disk spring with frictional effect 9-27206
- deformations, finite, theory of plane stress 9-22206
- dielectric, virtual work principle, confusion on specialization to rigid dielectrics 9-27199
- disc with stress couples, equil. problem, soln. in linear theory 9-25073
- ductile porous materials, constitutive eqn. for dynamic compaction 9-35166
- eigenvector expansions of Green's dyads for theoretical earth models 9-24626
- elastic fields, multipolar, layered half space 9-22193
- elastic-plastic and rigid-plastic plates of arbitrary thickness and flat bars of arbitrary width, stability 9-47809
- elastic-plastic continua with simple force dipole 9-25082
- elastic-plastic cylindrical shell under axial compression, instability 9-34071
- elastic-plastic deformation, strain components finite, thermomechanical coupling 9-34069
- elastic-plastic flow eqns formulated and applied 9-22198
- elastic-plastic plates, impulsively loaded, bending waves 9-41796
- elastic-plastic stress distrib. near crack tip effect on fatigue crack propag. nucleation theory 9-46909
- elastic-plastic structures, iterative soln. of incremental problem 9-31827
- elasto-viscoplastic solid, effect of time rate of change of temp. on behaviour 9-25066
- elastodynamic source fields dynamical theory, basic rupture parameters 9-26878
- elastoplasticity, linear, complementary plastic work theorems 9-41807
- elastostatic two-dimensional problems, equilibrium stress field model for finite elements 9-22207
- elastostatics, 3-dim. solution by a set of three stress functions 9-36162
- energy density, quadratic coeffs., rel. to crystal lattice force consts. 9-23847
- extensions of flat plate, electrical analogue 9-27205
- ferroelectric ceramic, microwave field modulation 9-43111
- finite element method of analysis, theoret. foundations 9-22203
- flexure of prismatic beams with longitudinal cavities, membrane analogy 9-34064
- flexure of triangular sections subject to terminal loads 9-38284
- flow, two-dimensional elastic, difference equations 9-34067
- Fourier transform methods 9-34066
- glass, T-40, acoustoelastic effect 9-35141
- graphite, EGCR-type AGOT, props. at room temp., 1000, 2000 and 4500°F 9-41009
- half-plane with edge crack, Wiener-Hopf technique, stress and displacements determ. 9-38281
- half-space torsional oscillations 9-27214
- h.c.p. metals, elastic energy factors for twinning dislocations 9-35090
- hexagonal anisotropic medium, Green function of theory 9-43776
- inclusion problem, general non-homogeneous, formulation and soln. procedure 9-27202
- incompressible and near-incompressible material, assumed stress hybrid finite element method 9-41797
- inelastic inclusion in elastic or viscoelastic matrix 9-31819
- infinite solid, stress, distribts. for shear loading over two coplanar circular regions with cracking 9-47813
- inhomogeneous materials, elastic pot. theory 9-31815
- inhomogeneous thin shells, equil. existence and uniqueness of solns. in linear theory 9-25074
- isotropic spherical bodies in Hertzian contact, stress field effects 9-41793
- Kantorovich method, extended, for soln. of eigenvalue problems 9-41798
- Lame problems in gradient theory 9-22195
- large deflection bending behaviour of beam subjected to point loads 9-36159
- layer, indentations by moving punches 9-45821
- linear, basic eqns. reduced to generalization of Hamilton's canonical formalism 9-27198
- linear, stability conditions 9-27203
- liquid film, correction of eqn. for Gibb's elasticity 9-23452
- load-penetration relationship for rigid, flat-ended punch of arbitrary cross section 9-38277
- loaded shells of revolution, asymptotic props. of Reissner eqns. 9-22197
- lower bounds on structural performances under cyclic loading and temp., use of elastic solns. 9-22210
- media with stress couples, equil. problem, soln. in linear theory 9-25073

Elasticity continued

- membrane stresses invariant function in tensorial notation 9-22187
- metals, f.c.c., elastic interaction between Frank dislocation loops and glide dislocations, activation energy 9-39359
- micropolar, basic solns. to wave eqns. in unlimited medium 9-47802
- micropolar continuum, structural model 9-27197
- micropolar fluids, eqns. of motion, constitutive eqns. and boundary conditions 9-31822
- microstructural materials, constitutive eqns. and uniqueness theorems using specific free energy function 9-38278
- mixture of two solids, constitutive coeffs. determ. 9-27201
- moving boundary conditions in elastic medium 9-29233
- neoprene film, constitutive relation 9-39393
- non-simple of grade n, plane wave propag. 9-31847
- notch effects interference, approx. calc. 9-25072
- nylon 6.6 fibres, oriented, anisotropy, expt. values compared with aggregate theory 9-35147
- optimal structural design for given dynamic deflection 9-40267
- oriented materials, elastic network model in kinetic theory of fracture 9-46908
- orthotropic, incompressible and nearly-incompressible, variational theory 9-22208
- Parallelepiped, compressed neo-Hookean rectangular, stability 9-25080
- piezoelectric rectangular plate, bending, theory 9-36160
- plane, with constraining couples, fund. problems leading to fixed limit integral eqns. 9-40265
- plane shear-pressure wave in elastic-plastic half-space, closed form solution 9-22218
- plane theory, infinite strip problem, analytic continuation method 9-31814
- plastic-elastic matrix, elastic-fibre reinforced, continuum model 9-31823
- plastic-elastic tube, instabilities under internal pressure and axial pressure 9-45808
- plate, infinite, isotropic, elastic, with vertical harmonic load, vibrations analysis 9-45842
- plate, transient plane bending wave propag., three-dimensional analysis methods applicability 9-45815
- plate containing rigid rectangular inclusion, complex variable method of stress analysis, parametric study 9-25077
- plate theory, generalized two-dim. 9-41802
- plate theory, generalized two-dimensional 9-40268
- plate with two equal reinforced circular openings, stresses 9-25079
- plates, anisotropic, deflections, asymptotic theory 9-45824
- plates, solid, optimal design 9-45820
- plates, with relaxed continuity requirements, variational principles 9-22205
- pointwise bounds 9-47806
- pointwise bounds, hypercircle method improvement 9-47804
- polyethylene fibres, oriented, anisotropy, expt. values compared with aggregate theory 9-35147
- polyethyleneterephthalate fibres, oriented, anisotropy, expt. values compared with aggregate theory 9-35147
- polymers, dynamic prop. meas. using support 9-23864
- polypropylene fibers, oriented, anisotropy, expt. values compared with aggregate theory 9-35147
- porous materials, ductile, constitutive eqn. for dynamic compaction 9-35166
- postbuckling behaviour and imperfection sensitivity, effect of nonlinear prebuckling state 9-25071
- Pyrex, acoustoelastic effect 9-35141
- ramp unloading of radial pressure on long cylindrical bar 9-29230
- reciprocity theorem for material with microstructure, applics. 9-47816
- reciprocity theorems for materials with microstructure 9-47815
- rectangle between two elastic half-spaces, adhesive or frictionless compression 9-31824
- rectangular plates, dynamics within 3-dim. theory 9-31821
- rectangular strips, end problem when narrow side under fractions and shearing forces 9-34063
- rock elastic velocity anisotropy rel. to stress 9-31257
- rubber, energy contribs. to elastic stress 9-46860
- rubber, free retraction obs. 9-39390
- rubber, general random network bead-spring model 9-35144
- rubber-like materials, constitutive relation 9-39393
- sandwich panels in supersonic gas flow, dynamic stability and vibration 9-22231
- sandwich plates, supersonic flutter 9-47807
- second-order elasticity theory for deriving changes in seismic travel times with stress variations 9-26869
- semi-infinite body under step-wide conc. surface impact load 9-29227
- semi-infinite strip, exact solns. of biharmonic problem, new class 9-25075
- semiconductor, hexagonal, elasto-optic and electro-optic props., effect of bandgap 9-35623
- shell, circular cylindrical simply supported, subjected to uniform line load along a generator, bending 9-25078
- shell, cylindrical finitely deformed thin, stability 9-22202
- shell, perforated ribbed cylindrical, stresses under internal pressure 9-41799
- shells, circular cylindrical, of varying thickness multiple scale soln. 9-45823
- shells, conical, orthotropic and isotropic, bending and buckling 9-47812
- shells, cylindrical, limit analysis by dynamic programming 9-41795
- shells, cylindrical, stress diffusion from axially loaded stiffeners 9-29229
- shells, cylindrical infinite, strengthened with ring ribs, dynamic behaviour 9-45822
- shells, multisandwich, of arbitrary shape, large deflections 9-43779
- shells, thin, inhomogeneous, equil., existence and uniqueness of solns. in linear theory 9-25074
- shells, two cylindrical, of equal diameter, stresses at intersection 9-47808
- shells and plates, three-dim. and two-dim. analysis of transient stress waves, effective applic. regions 9-41801
- silica, vitreous, acoustoelastic effect 9-35141
- singularity, line or planar, in an anisotropic medium, Fourier transform. 9-45816
- solid pellets, tightly fitting, press. forcing along fluid-filled elastic tubes, model, soln. 9-22168
- solid soln., free energy, microscopic theory 9-37288
- solids, I.F. magnetoacoustic effect, stiffness and attenuation, mag. field depend. 9-35283
- solids with differing props. in compression, tension and torsion theory 9-26307

Elasticity continued

- spherical shells, closed, Green's functions, exact, and approx. solns. 9-22211
- spherical slit in elastic half-space 9-22196
- stability of 3-D elastic bodies 9-36165
- stability of thin shells, expt. study of effect of general imperfections 9-38276
- stability of undistorted states of loaded body 9-22199
- steel and concrete composite beam, partial interaction between elements 9-26380
- stress pulse damping in thin elastic rod 9-27204
- structural systems, discrete, general theory for branching analysis 9-43774
- symmetric, three-layered, elastic plates with light rigid filler, bending theory 9-25076
- thin rod, large amplitude longit. wave propag., soln. rel. to end velocity 9-27221
- three-dimensional eqns. applied to calc. of axially symmetric vibrations of fluid-filled shell 9-27213
- torsion, elastic-plastic, of hollow bars, stress analysis by quadratic programming 9-36166
- two-dimensional, mixed boundary value problem, Green's function soln. 9-45814
- unstable elastic-plastic fracture brittle criterion rel. to energy balance considerations 9-44775
- variational principle and convergence of finite-element method based on assumed stress distribution 9-40266
- vibration, torsional, of rigid circular body on infinite elastic stratum 9-41812
- vibrations, free and forced in elastic layer, displacement and freq. expansion, asymptotic analysis method 9-34077
- wedge, stress distrib. with mixed boundary conditions 9-47805
- windows, response to sonic bangs, acoustic-elastic effects 9-41835
- wires under axial tension, torsional stiffness 9-34059
- Al notched columns with fixed ends, failure under load 9-48906
- Au-Cu-Zn alloys, anisotropy, rel. to β phase stability 9-46957
- Cu whiskers below yield pt. 9-39407
- Fe, grey cast, 4-295°K 9-48893
- He, rot., vortex lattices 9-39126
- In-Th alloys, elastic and anelastic behaviour during martensitic transform. 9-42865
- Mn-Cu alloys, anomalies below Neel temp. 9-39783
- Nb ferroelasticity due to H as lattice gas, obs. 9-23868
- Pu-Al delta-stabilized alloys, behaviour at low temp. 9-37224
- Pu-Ce delta-stabilized alloys, behaviour at low temp. 9-37224
- Ti alloys, sheet 9-23849

liquids

- see also Compressibility/liquids*
- convected, behaviour 9-44539
- critical tension in column after reflection of compression pulse at surface 9-42618
- elastico-viscous fluid, fluctuating flow past porous wall with variable suction 9-34734
- flow reversal in rotating-plate expt. rel. to elasticity and edge effects 9-39063
- polymers, liquid, properties, acoustic meas. 9-36835

Elastometers *see Rubber***Elastoplasticity** *see Plasticity***Elastoresistance** *see Piezoresistance***Electrets**

- see also Electrostatics*
- contact electrification 9-37601
- decay of net surface charge, electrets with non-isothermal history 9-49146
- films, production and charge decay 9-37600
- hydroxyapatite monocrystals, strongly anisotropic electret behaviour 9-30978
- ice, effect 9-37603
- ice thermoelectrets, h.f. doped 9-37604
- ionic membranes 9-37599
- linear systems formalism of phenomenological theory 9-37597
- naphthalene, magnetoelectret state 9-30979
- naphthalene thermoelectret, pure and doped glow-peak analysis 9-37606
- non-isothermal, charge decay theory 9-49146
- polarization and decay, review of theories 9-37569
- polymer, in aqueous solutions, interfacial phenom. 9-37608
- shellac wax, thermo- or magneto-electret depend. on conditions 9-37607
- surface charge, eff. of atmospheric pressure 9-37602
- thermo-electret, magnetic anisotropy var. with time 9-35528
- time-temperature superposition theory 9-37598
- waxes, magnetoelectret state 9-30979
- KCl, behaviour, ionic thermal currents 9-37605

Electric breakdown *see Breakdown, electric***Electric charge**

- see also Space charge*
- calcium silicates, surface charge on contact with NaOH electrolytic solution 9-24581
- conservation law based on arbitrary level of zero potential 9-32822
- electret, non-isothermal decay theory 9-49146
- electron microscope specimen charging model 9-39230
- ice, on evaporation in vac. 9-39129
- image detector for extended spatial distrib., applic. to spectrometry 9-27263
- at interface of two dielec. layers between metal plates, soln. of electrostatic pot. 9-36246
- localized clusters, eqns. for e.m. field distrib. and density of subst. 9-25191
- orthoclase, cloven in vacuum, electrostatic distrib. obs. on faces 9-37571
- point, 'relativistic' blurring 9-22346
- polyethylene film, decay processes of surface charges 9-49136
- polyethylene films, biaxially oriented and cast, surface charge decay obs. 9-35463
- polystyrene latex particles suspended in air 9-46661
- radiation under influence of constant external force 9-25178
- water droplets, effects on collision, coalescence and disruption 9-46604
- NaCl surface relief by AgCl evaporation on C replica 9-32848
- Si, p-n junction, electrical structure by AgCl evaporation on Crepica 9-32847

Electric discharges *see Discharges, electric***Electric fields***see also Electromagnetic fields*

- in atmosphere, stationary distribution in near-ground layer 9-49454
 - atmospheric, role in weather modification 9-28862
 - atmospheric ground layer 9-35825
 - near conductor, gravity induced, qualitative model 9-34111
 - of conductors carrying steady currents 9-45724
 - discharge inception stresses in dielectric with air-filled cavity 9-35474
 - during discharge onset in moving gas, rel. to transfer vels. of neutral flows 9-48628
 - earth, induced by deep sea tides 9-31275
 - gravitation induced, near a metal 9-22320
 - homogeneous and heterogeneous media, two-dimensional behaviour using analytic functions 9-45906
 - interplanetary v.l.f., Pioneer 8 obs. 9-24891
 - ionized, equipot. determ. using double cylindrical probe 9-45908
 - along laser beam axis, distribution from gas breakdown exam. 9-28055
 - in magnetosphere, estimation from micropulsation freq. drift 9-31354
 - mapping field in a point-to-plane gap 9-34797
 - in MHD rectangular channel with semi-infinite electrodes 9-25825
 - near ground, effect of atmospheric aerosol 9-43398
 - penetration of fractionally accommodating plasma boundary 9-36770
 - in plasma, meas. using surface charge induction method 9-42537
 - plasma, turbulent, spectrum 9-48546
 - radial, for electron orbiting device, patent 9-49617
 - at sharp edge, eqns. for blade above plate and above rod 9-29900
 - in shield, metallic, cylindrical, for ionospheric precipitation current meas. 9-31417
 - undergraduate text 9-38188
 - in uniform waveguide, computer program for computation 9-34125
- effects**
- a.c., electrostatic oscillations in plasma 9-25927
 - alkali halide scintillators, rel. to thermoluminescence 9-45354
 - anthracene molecules in cyclohexane, rel. to radiation-induced fluorescence 9-44351
 - antiferromagnets, rutile, rel. to Stark effect 9-45197
 - atomic energy levels, exact propagator for electron 9-29911
 - atoms, rel. to resonance radiative processes 9-48385
 - attapulgite, orientated, suspension in aqueous soln., light scattering studies 9-34929
 - auroral electrojet, heating of ions and electrons 9-33823
 - p-azoxyanisole liquid crystals in alternating fields, X-ray structure study 9-42634
 - ceramics, BaTiO₃ base, d.c. field effect on thermal conductivity in phase transition region 9-39545
 - conducting sphere, deformed, electrostatic energy change 9-47884
 - conductivity tensor, nonlinear, of weakly interacting electron system in external elec. field 9-48984
 - cosmic ray accelerating mechanism in space 9-35949
 - crystal, vibrating, direction of exciting field rel. to spectral characts. 9-41251
 - crystal growth, effect on rate 9-23663
 - dielectric liquids, on boiling heat transfer, hydrodynamic theory 9-23596
 - dielectrics, melting in h.f. field, analytical investig. by one-dim. thermal conductivity eqn. 9-44614
 - electroluminescence excitation in indirect gap semiconductors 9-30887
 - electron diffusion in various gases parallel to elec. fields obs. 9-31909
 - electrons, hot, in crossed elec. and quantizing mag. fields 9-47029
 - electrostatic focusing, periodic, theory and experiment 9-31914
 - electrostriction of deformable conductors in uniform elec. field, calc. 9-45012
 - exciton dissociation, by localized fields, photoconductivity spectra and vibr. struct. obs. 9-41138
 - exciton states 9-24101
 - exoelectron emission, photostimulated, effect of light intensity and electric field 9-37630
 - ferroelectric ceramic, permittivity var., applic. to parametron 9-30969
 - films, magnetic anisotropy induction 9-24315
 - flame propagation obs. 9-31861
 - fluid interface, perturbations with transverse electrostatic field 9-32569
 - fluid interface stressed by perpendicular field, small-amplitude motions and charge relaxation 9-32790
 - fluid surface, parametric instability in alternating field 9-23207
 - galvanomagnetic effects in high elec. fields, theory 9-30829
 - growth of crystals of highly anisotropic dielec. polarizability 9-37097
 - ice formation in supercooled mists 9-47538
 - ion production by liquid atomization in vacua 9-23526
 - liquid, effect on cavitating vortex street in wake of cylinder 9-48676
 - liquid column support, diam. rel. to voltage 9-23517
 - liquid drop disintegration, dynamics and validity of spheroidal assumption 9-28091
 - liquids, molecular alignment induced, effect on n.m.r. spectrum 9-30435
 - liquids, nonconducting binary mixtures, critical phenom. 9-28092
 - magnetization creep of cross-tie walls 9-49208
 - magnetostatic surface waves, amplification by interaction with drifting charge carriers in crossed elec. and mag. fields 9-43816
 - mechanical response of solid cylindrical conductors to axial elec. currents 9-45837
 - medium of inhomogeneous dielec. const., flow of matter in direction of increasing dielec. const. 9-42670
 - methylpolysiloxanic oils, surface deformation in fields 10 keV max. 9-36896
 - microdroplet deposition from sprayed suspensions for e. microscopy 9-42686
 - nitrobenzene, n.m.r. of ¹⁴N, molecular alignment induced by elec. field, eff. on spectrum 9-30435
 - nitromethane, n.m.r. of ¹⁴N, molecular alignment induced by elec. field, eff. on spectrum 9-30435
 - in NMR, obs. in ¹⁴N spectrum of nitrobenzene 9-34683
 - non-uniform microwave fields in plasmas, sum and difference freq. generation, analysis 9-46514
 - organic liquids, induced flash-like heterophase radiation 9-26124
 - photography, slowing up in latent image formation 9-48126
 - phthalic esters, surface deformation in fields 10 keV max. 9-36896
 - piezoelectric materials in strong fields, under high press., electromechanical characts. 9-47185
 - plasma, inhomogeneous, parametric eff. of alternating field 9-34782
 - plasma, slightly ionized, induced anisotropy in a.c. conductivity 9-46482
 - plasma, sum and freq. generation by two nonuniform r.f. fields in static mag. field 9-32648

Electric fields continued**effects continued**

- on plasma drift temperature instability in time modulated mag. field 9-23335
- plasma electron beam, h.f. modulation, energy and temp. eff. 9-30286
- polythene cavity under high direct electric stresses at elevated temperatures, discharge-repetition rate 9-28054
- protein sprayed suspensions, deposition of microdroplets for e. microscopy 9-42686
- pyrene molecules in cyclohexane, rel. to radiation-induced fluorescence 9-44351
- Rochelle salt, on ferroelec. props., ^{23}Na n.m.r. obs. 9-26593
- rodlike macromols., orientation by a.c. fields, light scatt. 9-23502
- semiconductor, current fluctuations 9-33286
- semiconductor, galvanomagnetic phenomena in crossed elec. and mag. fields 9-37511
- semiconductor, heating of electrons and phonon bottleneck in crossed elec. and quantising mag. fields 9-33278
- semiconductor, nonpiezoelectric, with ambipolar conduction, rel. to sound amplification 9-33175
- semiconductor, Sondheimer oscillations of magnetoresistance tensor components 9-39617
- semiconductor diode, rel. to thermionic emission current, filamentation 9-33342
- semiconductor with non-standard dispersion law, rel. to plasma oscillations 9-37504
- semiconductors, rel. to galvanomagnetic effects, theory 9-28486
- solutions, effect on thermodynamic props. and surface tension 9-48692
- superconducting alloys in strong alternating field, dynamic props. of parameter Δ in T_c region 9-30864
- superconductor, conductivity above transition temp. 9-30860
- superconductor, type-I thick slab, field penetration, intermediate-state config. 9-30866
- superimposed, displacement of spiralling electrons 9-27278
- transition metal glasses, switching mechanism 9-35476
- triglycine sulphate, d.c. field effect on thermal conductivity in phase transition region 9-39545
- viscosity, shear, of linear polar molecule gas 9-48644
- water, field ionization 9-32691
- water drop, deformation and discharge 9-28146
- water droplets nucleation and supercooling, obs. 9-39134
- work function reduction of oxide cathodes 9-30999
- Al, electron emission, secondary, produced by relativistic primary electrons in high field 9-31009
- Al film, on critical thickness during deposition by vacuum evaporation 9-32838
- Al film growth 9-48762
- Ar luminescence, α -particle induced, effect on continuum centred at 1250 Å 9-42328
- BaO, electrical conductivity 9-30833
- BaTiO₃ base ceramics, d.c. field effect on thermal conductivity in phase transition region 9-39545
- BiSb alloys, emission of microwave radiation in weak electric field 9-31102
- CdS-SiO₂ film system, extinction of frozen-in conductivity 9-28577
- CdS film, extinction of frozen-in conductivity 9-28577
- CdS single crystal, photo Hall mobility, temperature dependence 9-28582
- p-CdSb, on current density, mobility and magnetoresistance 9-24174
- CdTe:Co²⁺, electrically induced e.p.r. transitions 9-35711
- CdWO₄:Cu²⁺, e.p.r. spectra 9-24486
- CdWO₄:Mn²⁺, e.p.r. spectrum, effect on hyperfine structure 9-31162
- GaAs electron population inversion induced by high elec. fields 9-26545
- n-Ge:Sb Hall effect distortion in strong fields 9-37537
- n-Ge, magnetoresistance, transverse, current density depend. in strong fields and strong mag. fields, 16.6°K 9-33327
- p-Ge, with deep impurities, recombination and scattering of carriers 9-28516
- ⁴He, optically oriented metastable, spectra of absorpt. and 1st harmonics signals for magnetiz. component, modulation effects 9-32813
- p-InSb nonlinear conductivity-potential relationship at 78°K 9-28510
- KBr ENDOR spectroscopy of F-centres 9-35734
- KBr photoluminescence, room-temperature, electric-field-enhanced 9-45359
- KCl:Li thermal conductivity meas. and phonon reson. scatt. obs. 9-42948
- KCl ENDOR spectroscopy of F-centres 9-35734
- KD₂PO₄ crystal, rel. to dielec. permittivity 9-41241
- KI:TL, intercentre luminescence 9-39871
- LiF charged dislocation movement, in fields of 10 KV/cm 9-42834
- NF₃, thermal conductivity, rel. to mag. fields effects 9-28076
- NaCl, ground-state splitting of Mn²⁺, e.p.r. obs. 9-43284
- NaCl ENDOR spectroscopy of F-centres 9-35734
- PbI₂, electroabsorption in exciton region 9-33539
- PbTiO₃-PbMgWO₃-PbZrO₃ solid solns., depend. of permittivity, 20 kV/cm max. 9-43103
- SbSI ferroelectric, mobile and stationary phase boundaries rel. to elec. field 9-41250
- Se, amorphous, refractive index and absorption edge 9-35618
- Si p-n junction, space charge layer on photoresponse edge 9-37558
- SrO, electrical conductivity 9-30833
- SrTiO₃ colour centre prod. at 20 V/mm and 100-165°C 9-40976
- TiO₂ elec. conductivity, field enhanced, rel. donor impurities 9-26511
- Tl I spectra, influence of field on level crossings 9-48404
- W, desorption of Y, 300° to 630°K 9-46733
- ZnO electrophotographic layers, effect on space charge density 9-30963
- ZnS:Cu, modulation and excitation of i.r. luminescence 9-35702
- ZnS films, electroluminescent, low temp. elec. props. in strong fields 9-28461
- ZnSe electrically conducting photoluminescent films, prep. 9-31127

Electric strength

see also Breakdown, electric

- solid/liquid dielectric complex impulse strength rel. to ionization processes 9-28553
- N₂, at elevated pressures and small gap spaces 9-42575

Electrical conduction *see Conductivity, electrical***Electrical current** *see Current, electrical***Electrical machines**

- acoustic power radiated, calc. method 9-36172
- Cockcroft-Walton voltage multiplier, modification 9-34138

Electrical machines continued

- converter, static commutator, using 3-phase synchronous machine 9-45911
- d.c. conduction pump, charact. dynamic conductance determ. 9-27269
- d.c. with electronic commutating, from static converter on synchronous machine, eqn. soln. 9-41869
- flux displacers for power pulse generation, use of supercond. multipole magnets 9-36249
- generators Hall, null voltage compensation methods 9-39648
- homopolar generator as energy store for large lasers 9-29428
- motor, d.c., with armature under const. voltage, speed control 9-47889
- motor, geared, subfractional, braking circuits 9-31895
- synchronous, automatically controlled 3-phase, operation as static commutation converter 9-45911
- thermally accelerated life testing of electronic components 9-40307
- voltage pulse generator, subnanosecond risetime and adjustable duration 9-34137
- Electrical measurement**
see also Entries describing measurement methods for specific electrical quantities and effects may also be found listed under the various headings for the subjects concerned
- admittance, guarded three- and fourterminal meas., low freq. bridge 9-34134
- breakdown voltage between 2-cm brass spheres with gaps <0.005 cm, effect of irradiation 9-34813
- correlation technique, broad band, using x-y oscilloscope 9-34133
- current density near cathode 9-34799
- cylindrical samples, non-contact determ. of props. theory 9-25161
- electrical technology, conference, New York, USA (1968) 9-29353
- electrolyte conductance meas. with four-electrode a.c. potentiometer 9-35749
- electrometer, vacuum tube for teaching lab. 9-29150
- fibre potentials, scanning electron microscope meas. 9-38344
- geophysical prospecting applications 9-31269
- glavanometer, long-period, for seismic recording 9-31259
- insulators, h.v., electrically stressed surface temp. and pot. distrib., simultaneous meas. 9-47887
- m.i.s. structure surface state meas. device 9-43096
- moisture probe, h.f., capacitance response to soluble salts as function of conductance 9-49389
- parameter fluctuation spectrum meas. 9-38343
- probe, four-point, for Hall effect and conductivity meas. in semiconductors 9-44950
- probe method, combined, for shunt resistance and Q of delay systems meas. 9-43828
- resistance, precise automatic a.c. potentiometer for low temp. resist. thermometry 9-47840
- solid-liquid interface impedance meas. 9-47467
- voltmeter, applic. of quantum supercond. 9-41189
- voltmeter based on Josephson effect, operating characts. 9-49059
- voltmeter with 10⁻¹²V resolution, design, use of supercond. modulator 9-40214
- SiO₂ film on Si, m.o.s. analysis of impurities 9-42814

Electrical properties of substances

see also individual properties, e.g. Conductivity, electrical; Dielectric properties of substances, etc.

- brass contact pot., stress induced shifts 9-43019
- cylindrical samples, non-contact determ. of props. theory 9-25161
- electroacoustic surface waves in conducting solids 9-28425
- elements, collection of data, book 9-22026
- ferrites, polycryst., rel. to gain boundary layer barriers 9-46828
- field distrib., obs. from electron micrograph 9-46773
- gas, charged, electrohydrodynamic flow over wavy wall 9-40731
- gas, charged, electrohydrodynamic supersonic flow, over wavy wall, oscillating piston problem model 9-40732
- gas, optical meas. applic. of Schlieren prism 9-34199
- gas, weakly ionized, two-temp., Joule-heating effect in parallel flow 9-40730
- gases, electrohydrodynamic Rayleigh and oscillating plate problems 9-46552
- gases, ionized, elec. susceptibility meas. with cavity resonator 9-34136
- glass, high pressure effects 9-28193
- glass, metal-glass contacts, electric field effects 9-37584
- hexane, liquid, charge carriers which are probably free electrons obs. 9-28151
- hydrocarbon liquid, flowing through tube, electric current generation 9-26129
- ionic cry., elec. fields and polariz. prod. by defect charge density, lattice summations 9-33215
- ionic cry., electrostatic pots. and spatial deriv. about pt. defects 9-33214
- liquid chains, non-exponential range of localized electron states 9-48715
- liquid drop, cond., dynamic behaviour in elec. field 9-47884
- liquid metal cylinder, radially osc., volume electrodynamic force 9-25828
- liquids, Kerr constant determ. and Kerr cell filling apparatus 9-30421
- liquids, organic steady-state and transient space-charge-limited currents by injection from tunnel cathode 9-34919
- membranes of 100 Å thickness elec. phenom. anal. by changes in absorpt. 9-47695
- metal, surface impedance in weak mag. field, field strength and electron surface reflection depend. 9-26514
- metallic systems transport props. 9-45910
- multifilid systems, generalized Ohm's law 9-23209
- nematic liquid crystal, polarization and curvature strain reln., piezoelectric theory 9-28148
- plastics, conducting, elec. uniformity evaluation technique 9-43023
- plastics, fiber reinforced, elec. eff. of fracture 9-26351
- poly-3-vinyl-9-ethylcarbazole, elec. behaviour on γ -irradiation 9-24120
- rock in upper layers of Earth's crust 9-33727
- rocks, igneous and metamorphic, in r.f. field, obs. 9-26503
- rocks in upper crust, boundary equations 9-26882
- rubber, meas. rel. to charge transport mechanism 9-41128
- seeded diatomic gases, electrical characteristics of gasdynamic boundary layers 9-26036
- steel contact pot., stress induced shift 9-43019
- Al contact pot., stress induced shifts 9-43019
- Au contact pot., stress induced shifts 9-43019
- Bi, electron mean free path, temp. depend. 9-30846
- CaF₂, elec. fields and polariz. prod. by defect charge density, lattice summations 9-33215
- CaF₂, electrostatic pots. and spatial deriv. about pt. defects 9-33214

Electrical properties of substances continued

CdS, current saturation, two kinds 9-24118
Cu, liq., resistivity from exploding wire expt., theory 9-44584
Cu contact pot., stress induced shifts 9-43019
(CuMn:O₂),(AF₂O₂)_(1-x) solid solutions, where A=Cu²⁺, Ni²⁺, Zn²⁺, Co²⁺ or Ni²⁺ 9-30834
Cu-Ti alloys, character and time depend. indication of two stages of decomposition 9-23941
Ga single crystals, liq. He temp., in longit. mag. field., zero resistance 9-44900
n-Ge, Hz absorpt. effects 9-39642
Ge, studies of internal recontacted splits 9-42846
n-Ge field distrib., obs. from electron micrograph 9-46773
Ge surface, variation, when modified by alkylchlorosilane 9-48924
In-Te system, thin films, depend. on conc. 9-30485
K, size effect, r.f., in cylindrically shaped samples 9-43028
Li_{1-x}V_xO₂, anomaly in props. 9-35328
Na, molten, spin-flip scatt. of conduction electron 9-32793
NaCl, elec. fields and polariz. prod. by defect charge density, lattice summations 9-33215
NaCl, electrostatic pots. and spatial deriv. about pt. defects 9-33214
Si, studies of internal recontacted splits 9-42846
Si₃N₄ impurity-doped films, and physicochemical props. 9-37578
Sn, voltage peaks rel. to electron focusing by longit. mag. field 9-26519
SnO₂, semiconducting properties 9-35329
TiO₂, defect controlled props. 9-26512
Zn, electromigration 9-23844
ZnS films, electroluminescent, in strong elec. fields, low temp. props. 9-28461
ZnS single crystal grown from Ga and In melts 9-37095

Electrical units see Units

Electricity unit systems, book 9-47718

Electricity, direct conversion

electrofluid dynamic generators, application of electrohydrodynamic spraying for production of charged aerosols 9-27265
electrostatic generator 9-22335
gamma-electric cell, with epoxy or polystyrene dielectric, high voltage operation 9-31897
steady state, sinusoidal thermodynamics 9-27264
thermoelectric generator, solar air-cooled, weight and energy characts. optimization 9-31902
thermoelectric generator for superconducting solenoids 9-31900
KNO₃, solid state battery, form. 9-47890
Si photocell for thermophotolec. converter 9-39731
Zn/O electrochemical system, use of fluidized bed Zn anode to overcome dendrite form. 9-37839

fuel cells

design, developments and applications 9-29364
electrode, carbonaceous, production, patent 9-22326
electrode, catalyst, containing microporous silver, fabrication technique, patent 9-31898
electrodes, hydrophobic, in aqueous perfluorocarboxylic acid, patent 9-22327
electrolytes, gas solubilities and transport props. 9-22328
glucose/oxygen for artificial heart 9-36250
molten-carbonate, use of ceramics as insulators, electrodes and electrolyte diaphragms 9-31899
permeable gas diaphragm formation, patent 9-30334
power output improvement, using anode voltage-time curve, patent 9-43833
H₂/CO fuel mixtures oxidation, use of Pt-Ni catalysts as anodes 9-29365
K/Hg amalgams, e.m.f. meas for 6 compositions and up to 500°C 9-36926
WO₃:Pt activated electrodes, mechanism and performance 9-47891

magnetohydrodynamic

acceleration rel. to efficiency, limited circles of channel flows 9-25164
channel, boundary layer at cold electrode, interact. with basic flow, and effects 9-25167
channel generators, efficiency rel. to boundary layers at electrodes 9-29366
conduction machines with flow branching, pot. distrib. and e.m. head 9-27268
d.c. conduction pump, charact. dynamic conductance determ. 9-27269
dissociated real gas in thermal equilb., channel flow 9-25165
electrodeless conductivity meas. in reaction zone of combustion chamber 9-27271
energy losses, calc. from blow- in effects through porous walls of MHD channel 9-27963
flat channel with non-cond. partition, integral resistance rel. to partition length 9-25166
generator, electrodes, for high temp. fluid, using refractory material patent 9-45914
generator, flowing plasma, energy storage and transfer, experiment and theory 9-41174
generator, linear, effect of auxiliary d.c. discharge on performance 9-48558
generator, potential drop of cooled electrode 9-22333
generator, transport processes 9-27982
generator and compressor closed cycle, thermodynamic analysis 9-25168
generator plant, high temp. air heater arrangement, patent 9-43834
generator plasmas, diagnostic techniques 9-28012
generator with Hall effect, two-dimens. analysis 9-45912
generators, with cathode and anode duct of refractory material, for plasma stability, patent 9-45913
generators electrode and boundary-layer temperatures effects 9-22330
generators with external chain of nonlinear inductances, transition process in channel 9-41870
induction machine model, calc. of e.m. effects rel. to secondary circuits 9-27267
introductory paper 9-25018
ionized gas in generator channel, Ohm's law 9-22329
MGD, Rankine and Brayton cycle comparison 9-25169
MGD plant, open cycle, temp. reduction due to injected additives 9-22334
MPD closed-cycle channel, large nonequilibrium conductivity, with applied electric and magnetic fields 9-22331
plasma power generators 9-27270
power generation, Japanese review 9-22332

Electricity, direct conversion continued

solar cells

energy concentration by parabolotoroidal mirrors 9-31993
heterojunction, max energy conversion efficiencies calc. 9-29367
reflecting surfaces and transparent insulation exam., applic. of optical instruments 9-32010
school heating, economic comparison with conventional method 9-22325
thermoelectric generator with cylindrical collector 9-31901
CdS ceramic photovoltaic cell, props. and model 9-25171
CdTe, film photoconverters props. 9-31903
GaAs, photoelec., construct., fabrication and props. 9-45021
Si, impurity-doped, effects of Li, Na, Be, Cl, Al and O on carrier lifetime 9-24234
Si p-n junctions, epitaxial growth for photoelec. converters 9-31904
thermionic
converter with cylindrical electrodes, dismountable 9-22337
generator, radiation coupling between heat source and collector plates, patent 9-22338
generator, without liquid pools, gas temp. sensitivity reduction, patent 9-43835
interelectrode gap, potential distribution, transverse mag. field effect 9-41871
plasma diodes, electron instabilities 9-47892
plasma ionization equilibrium in low volt arc 9-47893
volt ampere characts., calc. 9-47893
Cs absorption by W electrode rel. surface defects 9-24254
Pt and Th group metals in Cs vapour, report on various aspects 9-25170
W electrode surface, polycrystalline, work function obs. 9-24254

Electro-deposition see Electrolytic deposition

Electro-optical effects

see also Electroluminescence; Optical constants
acetaldehyde, parameter characterizing electric field in ground electronic state 9-25756
acetone, and acetone-d₆ mol., calc. from Raman line intensity 9-27883
alkali halides, Kerr eff., dynamic meas. 9-33514
arsenates, parameters in 400-700 nm range at room temperature 9-31086
p-azoxyanisole liq. cry., sematic mesophase obs. 9-26112
p- azoxyanisole nematic liq. crystals. 9-30405
charge image detector for extended spatial distrib., applic. to spectrometry 9-27263
colloidal suspensions with induced and permanent elec. particlemoments 9-42684
crystal, ADP-type, optical beam discrete deviation meas. 9-26708
crystal, tertiary effect rel. to fifth order elec. field tensor 9-24369
crystals, centrosymmetric, model modification 9-24368
in cubic crystals, phase and polarization of light waves 9-41357
dimethyl aniline-chloranil film, quadratic 9-45281
dimethyl aniline-tetracyanoquinodimethane complexes, quadratic 9-45281
electroabsorption below band gap 9-41356
electroabsorption oscillations magnitude, elec. field strength depend. 9-49248
w.r.t. e.m. wave refl.-refr. at interface bet. isotropic mats. under applied static elec. field 9-25145
Faraday, differential, meas. of ionospheric electron content, errors 9-33843
ferroelectric crystals, rel. to pyroelectric coeff. 9-24225
glass-ceramic system, properties 9-35484
group II-VI compounds, exciton electroreflectance spectra 9-37707
group IV-VI cpds. electroreflectance 9-39809
Kerr cell, linearity improved with four electrodes 9-34907
Kerr eff., interaction between anisotropic mols., field-induced phase transition 9-23498
Kerr effect for subpicosecond pulse generation 9-27394
Kerr effect meas. in aq. solns. of inorg. salts 9-30402
in liquid crystals, obs. 9-28127
liquids, Kerr constant determ. and Kerr cell filling apparatus 9-30421
liquids, Kerr effect meas., laser technique 9-26106
materials, literature digest, 1967 9-33368
methane and fluorinated derivatives, Kerr const., hyperpolarizability determ., 632.8 nm 9-42613
molecules, diamagnetic, elec. birefringence, quantum theory 9-46347
multicrystal modulator, patent 9-40374
niobates, tungsten-bronze-type ferroelectric crystals, experimental study 9-28658
organogermanium mols., vibrational bonds, spectra 9-46397
phosphates, tetragonal, parameters in 400-700 nm range at room temperature 9-31086
quartz Q modulator in laser 9-40347
refractive-index anisotropy in nonpolar fluids 9-38938
review of results 9-31078
Rochelle salt crystals, rel. to light modulator use 9-43216
semiconductor, electroabsorption coeff., excitonic effects 9-43051
semiconductor, electroabsorption coeffs., excitonic effects 9-43052
semiconductor, hexagonal, and elasto-optic props., effect of bandgap 9-35623
semiconductor surface, electroreflectance meas. rel. to band structure 9-43215
single crystal properties reviewed 9-28659
stratified media, electroreflectance 9-35624
tetramethyl ammonium tri-iodomercurate, props. 9-43217
trenchloride, primary effect 9-35629
water Kerr cell, enhanced scatt. Bramanly effect 9-40792
 α - Ag-In dil. alloys, piezoreflectance 9-47325
Ag₃AsS₃, l.f. unclamped coefficients meas. 9-31082
Ba_{1-x}Sr_xNa_{1-2x}NbO₃, voltage for half-wave retardation of 0.6328 μ radiation 9-35480
BaTiO₃, wavelength dependence, 0.4 to 1.1 μ 9-47323
Bi₂GeO₂₀, and growth and props. 9-42751
Bi₂SiO₂₀, photoactivity and field-induced changes in optical rot. 9-35621
Bi₂(GeO₄)₃, and growth and props. 9-42751
CS₂ Kerr cells, laser internal microwave modulation 9-36285
CaF₂, rare-earth-doped, photo-reversible charge transfer 9-33406
CdS plate, d.c. driven, focusing effect 9-26707
CdS(Se), electroabsorption spectrum in exciton region, band structure 9-35625
CdTe, rel. to modulation appls., 3.39 and 10.6 μ 9-49249
CdTe, study by using radiation in 20 to 120 micron range 9-28660
CdTe films, electroabsorption oscillations magnitude, elec. field strength depend. 9-49248
CdTe films, high elec. fields effects on absorpt. spectra 9-41376

Electro-optical effects continued

- Cu₂O, elec. field effects on direct transition to 1s exciton 9-49275
 Cu₂O, u.v. electroreflectance spectrum 9-35626
 Cu₃PSe films, obs. 9-35398
 Cu₃PSe₂ films, obs. 9-35398
 Cu₃PSe₂ films, obs. 9-35398
 CuCl evaporated films, Faraday rotation due to excitons 9-24370
 GE electroreflectance spectra, satellite structure 9-31093
 (Ga, In), As alloys, electroreflectance interpretation of Λ_3 - Λ_1 transition 9-31084
 Ga_{0.9}In_{0.1}Sb, electroreflectance, variation with composition 9-45307
 GaAs:Mn(Si), (Cd) impurities, electroreflectance 9-28661
 n-GaAs, electroabsorpt. spectra at 300 and 77.3°K 9-39837
 GaAs, electroreflectance interpretation of Λ_3 - Λ_1 transition 9-31084
 n-GaAs, electroreflection characts. in electroabsorpt. spectra rel. to low free carrier density 9-37723
 GaAs, Franz-Keldysh, light modulation 9-39810
 GaAs, study by using radiation in 20 to 120 micron range 9-28660
 GaAs modulation of CO₂ laser at 10.6 μ 9-37691
 GaAs nonlinear coefficient, 2nd order, at mm. wave difference freqs. 9-31083
 GaP, p-n junction, reverse-biased mechanism 9-24196
 Ge, low-temp. electr-reflectance spectra, 0.7-2.6 eV 9-35627
 Ge, magneto-electro-reflectance in crossed and parallel-field config. 9-39806
 Ge electrode polarization state determ from electroreflectance meas. at semicond-electrolyte interface 9-49102
 Ge review of results 9-31078
 InAs, electroreflectance interpretation of Λ_3 - Λ_1 transition 9-31084
 InAs_{1-x}P_x, electroreflectance, variation with composition 9-45307
 InAsSb_{1-x}, electroreflectance, variation with composition 9-45307
 n-InSb films, Faraday rotation at 23.4 GHz, room temp. 9-49250
 KCl:Li F₂ centres, elec. field modulated absorpt., off-axis centre model 9-42851
 KD₂PO₄, detection of photon- photon scattering, interaction of microwave and laser beams 9-24358
 KD₂PO₄, transverse effect and light modulation by crossed rods, obs. 9-33516
 KD₂PO₄ crystal, fourth-order 9-41358
 KH₂AsO₄, and isomorphs, 42 m symmetry, half-wave retardation voltage 9-35628
 KH₂PO₄, electro- and piezooptical coeffs., dispersion and temp. depend. 9-33515
 KH₂PO₄, linear effect, theory 9-33517
 KH₂PO₄, transverse effect and light modulation by crossed rods, obs. 9-33516
 KH₂PO₄ crystal, freq. doubling, effect of lasers radiation parameters 9-45280
 KH₂PO₄ crystal, optical rectification effect 9-47326
 LaB₆, single crystals. 9-37081
 LiNbO₃, coeffs., signs 9-33396
 LiNbO₃, linear, melt composition depend. 9-26709
 LiNbO₃ oblique-cut plates, longitudinal halfwave voltages, optimum calc. 9-31062
 NH₄H₂PO₄, electro- and piezooptical coeffs., dispersion and temp. depend. 9-33515
 NH₄H₂PO₄, induced in antiferroelec. phase, temp. depend. 9-31085
 NH₄H₂PO₄, transverse effect and light modulation by crossed rods, obs. 9-33516
 Nb₂O₅ films, electroreflectance interferometry rel. to thickness determ. 9-30486
 Pb zirconate-titanate ceramics, optical and electrooptical properties, improvements 9-35485
 PbI₂, electro-reflection meas. 9-47324
 PbTe, Faraday effect in band structure parameter determ. 9-39630
 RbH₂AsO₄, normal and deuterated 9-39697
 RbH₂PO₄, transverse effect and light modulation by crossed rods, obs. 9-33516
 RbH₂PO₄ crystal, fourth-order 9-41358
 Si, electroreflectance rel. to photoreference spectrum 9-43231
 Sr₂Ba_{1-x}Nb₂O₆, temp. dependence 9-26710
 SrTiO₃, electroreflectance spectra investigation 9-45025
 Ta₂O₅ films, electroreflectance interferometry rel. to thickness determ. 9-30486
 ZnO, i.r. electroabsorption in multi-phonon region 9-33565
 ZnO, i.r. electroreflectance, elec. Gruneisen const. calc. 9-33540
 ZnS, absorption shift and high-field domain development 9-26711
 ZnS, cubic, linear effect rel. to first-order Raman scatt. 9-47376
 ZnS single cryst., electro-absorpt. 9-39812
 ZnTe, semicond., Pockels' coeff. meas. and dispersion, absorpt. band role in nonlinear coeff. derivation 9-39811

Electroacoustic transducers *see Transducers***Electrocathoporesis** *see Electrophoresis***Electrochemistry**

- see also Chemical analysis/electrochemical; Electrolysis; Electrolitic deposition*
 casein colloids, iso-electronic points, study with streaming current detector 9-23550
 charged insoluble monolayers, influence of monovalent counterions 9-23447
 concentration cells for atmospheric gas analysis 9-41457
 for diffusion meas. in metals 9-46841
 electroanalysis in laminar flow, boundary-layer and d polarization 9-47464
 electrolyte melts, several components, activity coeff. expression 9-33674
 electrolyte solns., extension of Debye-Huckel theory 9-37838
 electrolytes, aqueous 1-1, at 25°C, integral eqn. computations, error analysis 9-35748
 electrolytes in aqueous solutions, activity coefficients, 0 to 100°C 9-31199
 electrolytes in system of capillaries, viscosity meas. 9-26832
 electrophoretic mobility in insulating liquids, apparatus for meas. 9-46662
 film, plasma anodized, voltage drop meas. model 9-26188
 friction at wet contacts, depend. on interfacial potential 9-30702
 fuel cell electrolytes, gas solubilities and transport properties 9-22328
 gelatin colloids, iso-electronic points, study with streaming current detector 9-23550
 globin colloids, iso-electronic points, study with streaming current detector 9-23550

Electrochemistry continued

- heterocyclic amine N-oxides, anion radicals, polarography rel. to e.s.r. 9-36715
 hydrated electrons, thermodynamic props. kinetic relations 9-39955
 ion exchange control, mechanism 9-31177
 ion exchange control, transport processes 9-31178
 laboratory electronic instrumentation 9-49613
 principles and applications, book 9-33675
 pyritinol/5'-thiopyridoxine, redox pot. 9-28809
 reaction, spectroscopic obs. by internal reflection 9-37840
 saturation currents in system: anthracene- liq. redox electrode, temp. depend 9-24585
 semiconductor-electrolyte interface, impedance meas. 9-43067
 solvated electrons and p.d. between two immiscible media, thermodynamic explanation 9-39958
 steel, passivity breakdown in borax soln. 9-24579
 steel, stainless, passivity in H₂SO₄, galvanic platinizing effects 9-24574
 thermo-chains, electrolyte melts 9-30386
 thermodynamics of electrons in solutions diluted into liq. ammonia at -35°C 9-39956
 Walden, product rule for electrolytes, generalized 9-28808
 Weston cells, e.m.f. increase on passing small a.c. 9-27266
 AgBr membranes, elec. cond. and diffuse double layer 9-31200
 Be, polycrystalline, anodic dissolution 9-24583
 CoSO₄ dissociation and recombination rate using u.s. absorption 9-30397
 Cu-Mn alloys, of stress-corrosion cracking 9-23920
 Cu-(36wt.%)Zn alloy, of stress-corrosion cracking 9-23920
 Hg zero-potential determ. by dropping electrode 9-24582
 In amalgams, powder, electrochemical props. 9-49380
 NaF, electrolytic colouration technique for dislocation identification 9-23814
 NaNO₃:AgNO₃ melt, thermo-chains 9-30386
 NiSO₄ dissociation and recombination rate using u.s. absorption 9-30397
 Pb-Sn alloys, behaviour in different solns., corrosion resistance and passivation mechanism 9-33673
 ZrO₂:CeO₂ binary system, solvated electron study 9-39957
- electrodes**
 anthracene-liquid redox, temp. depend of saturation currents 9-24585
 batteries, electrodeposition, conference 9-33676
 current distribution on plane electrode below limiting current 9-31204
 free radicals near surface, synchronous detection by e.s.r. 9-25788
 fuel cell catalyst electrode, containing microporous silver, fabrication technique, patent 9-31898
 metal, anodic behaviour in 1M sulphamic acid-formamide solns., polarization curves 9-31202
 molten metal reversible electrodes for thermoelec. power meas. of molten salts 9-28149
 Poisson's eqn., uniform bounding functions for certain one-dimens. form 9-35752
 porous systems, effect of finite-contact-angle meniscus 9-31203
 porous two-phase, anomalous distrib. of current conversion 9-49381
 redox, liquid, hole injection into organic crystals 9-26475
 rotating-anode cell, cathode ionic mass transfer obs. 9-47466
 solid-liquid interface impedance meas. 9-47467
 vibration, ionic mass transfer obs. 9-47465
 Ag, anodic oxidation 9-49382
 Ag, anodic oxidation 9-49383
 Ag, sintered, microstructure changes after repeated low current cycling 9-31205
 Ag differences during charging after five full charge-discharge cycles 9-26833
 Cu, cathode growth at air-soln. interface rel. to norvaline addition to sulphate electrolyte 9-28810
 Fe-Cd couple, galvanic behaviour in NaHCO₃, NaNO₃ and NaCl solns. 9-28811
 GaP, charge transfer between energy states of electrons and redox systems, photoexcitation and electroluminesc. obs. 9-30990
 Ge polarization state from electroreflectance meas. at semicond-electrolyte interface 9-49102
 Hg electrocapillary curves, automatic recording 9-49384
 Mo, anodic and cathodic polarization behaviour 9-31206
 Pb, anodic passivation mechanism in various media 9-33678
 Pb accumulators, current distrib. in porous electrodes 9-33677
 Pd alloy, H diff. coeff. and variation with H conc. 9-28322
 Pt-Ni electrocatalysts for H₂/CO fuel cell anodes 9-29365
 Pt, on alkali halide crystals, interaction rel. to capacitance enhancement 9-49134
 WO₃:Pt activated, for fuel cells, mechanism and performance 9-47891
 Zn fluidized bed anode in Zn/O secondary battery, to overcome dendrite form. 9-37839

Electrodes *see Cathodes; Electrochemistry/electrodes***Electrodynamics**

- see also Eddy currents; Quantum electrodynamics*
 accelerated charge, at rest or freely falling rel. to gravitational field, radiation 9-38214
 beam dynamics in proton linacs 9-46157
 bunching in ALS linac 9-46148
 charge clusters localized by intrinsic e.m. field 9-25191
 charged particle beams transit thro' non-adiabatic mag. field 9-25175
 charged particle in constant magnetic field and alternating electric field 9-40311
 charged particle in oscillating e.m. field, dynamic variables 9-41873
 charged particle in random inhomogeneous medium, radiation calc. 9-29371
 charged particle motion in nonlinear plasma, energy losses 9-30215
 charged particle moving in a medium with ionization losses and in a non-uniform magnetic field 9-44094
 charged particles in crossed homogeneous elec. and mag. dipole fields 9-43484
 classical, soln. of Maxwell's equations in Friedmann universes 9-22347
 classical spinning point charge in arbitrary motion, asymptotic properties of radiated field 9-43846
 Compton scatt., intensity-depend. freq. shift 9-48131
 cosmic, second approximation theory 9-33890
 cyclotron loss due to ν_4 - $\nu_2=1$ and $3\nu_4$ - $\nu_2=3$ resonances 9-46149
 Dirac particle with mag. dipole moment, covariant eqns. of motion 9-34145
 earth's motion through ether detection, null result relativistic explanation 9-29179

Electrodynamics continued

electron (quantized Dirac field) in classified time-dependent e.m. field, theory 9-38346
electron flow from pulsed high current field emission cathodes, dynamics 9-45923
electron interacting with e.m. field, Rayleigh-Ritz method used to derive field eqns. 9-46043
electron rectilinear motion near speed of light in any field 9-36255
electron ring accelerator using 25 MeV beam injected into static magnetic field 9-46171
of electron trap on slowly moving charged spacecraft 9-43454
electron velocity meas. in annular beams 9-31913
electronic crystals, transverse oscils. 9-47030
electrons, spiralling, displacement by superimposed electric fields 9-27278
electrons moving in const. elec. field, radiation spectrum 9-43848
elementary measurement electrodynamics, classical 9-34143
e.m. momentum in matter, relativistic aspects, 'try simplest cases' resolution 9-29374
empirical law, action between two current elements; review 9-29373
energy theory paradox in Lorentz-Dirac-Wheeler-Feynman-Rohrlich theory 9-29377
escape solutions in theory of Prigogine 9-29376
f.e.m. mass of spheroidal bodies moving || to the axis of a conductor 9-36253
flying objects 9-22345
gases, multicomponent, partly ionized, with space charge, equations 9-44487
gravitational force on falling electrons and positrons, exptl. determ. 9-25421
gyroresonant acceleration in a magnetostatic field 9-25847
injection and containment of charged particles in cusp mag. field 9-48578
interplanetary charged particle acceleration 9-43644
ion motion in electrostatic dipole fields 9-31921
Lorentz's work on electrodynamics of moving bodies traced 9-43697
Lorentz force equation for orbital motion, numerical solution 9-31923
Lorentz-Dirac-Wheeler-Feynman-Rohrlich theory, energy conservation paradox 9-29377
Lorentzian invariant, energy paradox 9-29375
Maxwell's equations solution in approximation to geometrical optics 9-29333
metal particles in vacuum, motion reversal and energy increase on field emission 9-31003
motion in superposed constant and exponentially decaying fields 9-45919
motion under a periodic cubic force 9-40312
nonlinear, wave theory close to exact soln. 9-36256
nonlinear, wave theory close to exact soln. 9-47844
oscillations for particles passing through a resonance, vertical damping eff. 9-46146
particle in dipole mag. field, var. of first adiabatic invariant 9-25176
particle in spiral mag. field 9-24892
particle motion in force-free mag. field 9-45918
particle motion in multiple-cusp magnetic fields 9-25177
perturbation theory, charge distribution function 9-34144
phase space dynamics, book 9-40313
plasma, boundary value problems 9-25878
in pulsars 9-43586
radiation of charge under influence of constant external force 9-25178
relativistic blurring of point charge 9-22346
relativistic charged particle, lifetime, with autointeraction, in constant homogeneous mag. field 9-36254
spin-one particle in external e.m. field, equations of motion 9-38451
time symmetric, in Friedmann universe 9-43505
two oppositely charged particles, separation of Hamiltonian 9-38233
two-body problem, history and future trajectories of particles determ. 9-31907
e diffusion parallel to electric field, theory 9-31908

Electroendosmosis see Electrophoresis

Electrojet see Atmosphere/upper; Atmospheric electricity; Ionosphere

Electrokinetic effects

see also Electrophoresis
apatite in aqueous soln., zeta potential, changes on addition of Ca and F 9-24584
calcium silicates, surface charge on contact with NaOH electrolytic solution 9-24581
clay suspensions, effect on plastic flow behaviour 9-23548
electrodialysis in laminar flow, boundary-layer and d polarization 9-47464
e.m. compression of metallic foil for prod. of transient MOe mag. fields 9-47894
latex particles, sulfonated, zeta pot., secondary electroviscous effect calc. 9-32801
polystyrene sol., electroviscous effects in dispersions of monodisperse latices 9-23551
Na, electromigration of Cd and In rel. to temp. 9-31201
Pd, proton and deuteron migration 9-37206

Electroluminescence

anthracene, recomb. radiation temp. depend. 9-39894
cathodoluminescent pulse light sources, sulphide applications 9-33609
cell construction and characteristics for brightness, variation with frequency and voltage 9-47417
devices, utilization of II-VI compounds 9-41413
diode, non-coherent, frequency response at low injection levels, derivation 9-31151
diodes on anthracene, double injection, charact. 9-49336
direct electron beam fluoro-radiography 9-32098
field-excited in indirect-gap semiconductors 9-30887
groups II-VI compounds, review 9-49331
injection, behaviour in semicond. devices 9-28734
liquid, electrochemilum. pulse delay w.r.t. elec. excitation 9-44575
low temperature, phosphors, used as display portion of infrared image converters 9-28733
m.i.m. structures 9-47411
quantum efficiency meas. using 2 π -geometry elliptic mirror 9-28735
semiconductor with narrow forbidden band, polarization electroluminesc. props. 9-47412
triplet state of mol. inactivated by paramag. positive ion 9-44574
Al_xGa_{1-x}As:Si diodes, props. and efficiency 9-37775
Al_xGa_{1-x}P diodes prep. by liq. phase epitaxy, green band obs. 9-47413

Electroluminescence continued

Cd_{1-x}Mg_xTe p-n junction, props., and prep. 9-26569
CdS:Ag cell, d.c., efficiency of i.r. emitting phosphors 9-41415
CdS-(40 wt.%) ZnS:Cu cell, d.c., efficiency of i.r. emitting phosphor 9-41415
CdS single crystal, static current-voltage charac. and at 120 c/s 9-37777
CdS thin films, polycrystalline, vacuum evaporated 9-31152
Cu₂O, temp. range expansion using M.O.S. system 9-37778
GaAs:Ge, p-n junction, reverse-biased, light emission charact. 9-49332
GaAs:Si(Ge) p-n junction, photoresponses and emission spectra 9-26570
GaAs-AlAs diffused diodes, injection electroluminesc. 9-37780
GaAs_{1-x}P_x, vapour grown diodes, efficiency optimization 9-31153
GaAs_{1-x}P_x diffused diodes 9-37779
GaAs single cry. by tunnel injection of minority carriers 9-24178
GaP:Zn-O diodes, output charact. 9-41403
GaP diode, negative resistance 9-26574
GaP diodes, green-light-emitting, grown by liq. phase epitaxy, spectral props. 9-49121
GaP diodes, injection electroluminesc. reduction by reverse operation, obs. 9-26784
GaP diodes, peak quantum efficiency and current relationship 9-28736
GaP diodes, prod., characts. and appls. 9-49333
GaP electrodes, redox processes 9-30990
GaP p-n diodes 9-33610
n-GaP vapour grown epitaxial diodes with green emission at room temp. 9-41224
In_xZn, oxygen implanted, cathodoluminescence spectra 9-39892
In_xGa_{1-x}P alloys, band structure and direct transitions 9-24467
n-SiC:N diodes, props. and anomalous nature of B and Al diffusion during prep. 9-37776
SiC, p-n junctions, brightness rel. to temp. 9-26785
SiC diffusional p-n junctions, injectational, temp. depend. 9-45357
SiC diodes, brightness determined by reverse bias 9-37561
SiC p-n junctions, tunnelling and avalanche processes 9-43081
ZnO-CdSe alloy systems 9-47415
ZnS:Cu, frequency study rel. to trap analysis 9-49334
ZnS:Cu, Gudden-Pohl effect, flash intensity and temp. depend. 9-39893
ZnS:Cu, shallow trap participation in decays, variable temp. above liquid nitrogen temp. 9-33611
ZnS:Cu(Mn, I) evaporated thin films, d.c. electroluminescence and photoluminescence 9-33612
ZnS:Mn, Cu cell, d.c., efficiency of i.r. emitting phosphors 9-41415
ZnS:Mn,Cu,Cl powder phosphors, d.c. props. 9-37781
ZnS:Mn films, polarization effects in non-stationary processes 9-24469
ZnS:Pb, Gudden-Pohl effect, flash intensity and temp. depend. 9-39893
ZnS-Mn sublimated during pulsed excitation 9-49335
ZnS, layer formation and activation, patent 9-49308
Zn(S_{100-n}Se_n):Cu,I Gudden-Pohl effect and phosphoresc. spectra rel. to emission centres, obs. 9-35696
ZnS crystal, comparison with photoluminesc. spectra 9-26787
ZnS films, low temp. elec. props. in strong fields 9-28461
ZnS Lumocen devices, rare-earth and transition-metal fluoride doped 9-35700
ZnS phosphors, and simultaneous photo-excitation 9-47414
ZnS polytypism and a.c. electroluminescence 9-24468
ZnS role of impact ionization and tunnel effect 9-43265
ZnS type devices 9-41413
ZnSe:Cu,I, and photoluminesc., temp. depend. rel. to centres, obs. 9-35701

Electrolysis

see also Conductivity, electrical/liquids, electrolytic; Dissociation/electrolytic; Electrochemistry; Electrolytic deposition; Ion velocity/electrolytic
cell, for gas production from electrolyte, patent 9-47470
cells, review, non-technical 9-35753
electrolyte diffusion meas. by diaphragm cell 9-35751
metallic structure corrosion, cathodic protection system, patent 9-45421
metallizing 9-46915
quartz, ion diffusion paths 9-39387
review, non-technical 9-35753
water in electrolytic cell with porous electrodes, patent 9-31207
water in electrolytic cell with permeable electrodes, patent 9-28813
Fe, electrolytically deposited under different conditions, rel. to fine crystal structure 9-44663
GaAs crystal in KOH, current density-anodic potential curves at low currents 9-24587
H and O liberation together on electrode, electrode glow 9-41454
NaCl:Dy³⁺ luminescence spectra obs. to gauge changes taking place during electrolytic colouring 9-32996
Sn-Pb dilute alloys, electropolishing procedure to produce etched or polished surfaces 9-39959
Sn electropolishing procedure to produce etched or polished surfaces 9-39959
ZrO₂, stabilized, in Cu solutions, oxygen ion conductivity 9-35754

Electrolytes, theory see Electrochemistry; Solutions

Electrolytic conductivity see Conductivity, electrical/liquids, electrolytic

Electrolytic deposition

anodic oxide films form., Tafel slopes field depend. 9-47471
arc transfer process of cryst. growth 9-36994
corrosion of electrodeposits on plastics 9-28797
electroplating, spark-source mass spectroscopy impurity determination 9-26837
growth habit and morphology, effect of electrodeposition parameters 9-37034
impurity analysis by spark-source mass spectroscopy 9-26837
metal, in standing wave sound field, localization of deposit 9-47469
oxide films, anodic, form., Tafel slopes field depend. 9-47471
plating small engineering parts and sputter cleaning 9-28812
steel, stainless, galvanic platinizing and passivity in H₂SO₄ 9-24574
Ag, growth habit and morphology, effect of electrodeposition parameters 9-37034
Am, by mol. plating method 9-43331
Cu, growth habit and morphology, effect of electrodeposition parameters 9-37034
Cu cathode growth at air-soln. interface rel. to norvaline addition to sulphate electrolyte 9-28810
Cu electrode, current and pot. behaviour in standing wave sound field 9-47468

Electrolytic deposition continued

- Cu on to (100) plane of Cu in presence of chloride ions 9-24586
- Cu single crystal, electrodeposited, mech. props. and structure, rel. to deposition conditions 9-46786
- Fe from sulphate bath, data on fine struct. obs. in electron microscope 9-36942
- Hg, transient nucleation 9-37036
- Ni, growth habit and morphology, effect of electrodeposition parameters 9-37034
- Ni, metallic contamination effect on struct. and ductility 9-37146
- Re, deposit charact. and cathode efficiency obs. 9-37841
- Sn, surface texture 9-36933
- Zn from aqueous KOH soln. with zincate ions, electrolyte flow effect on morphology 9-33679

Electrolytic tanks *see* *Calculating apparatus/analogous apparatus***Electromagnetic fields**

- acetone, boiling, heat transfer depend. 9-23597
- quantum theory in gyrotropic medium 9-41849
- beam-column, effect on small mech. oscils. 9-27215
- benzol, boiling, heat transfer depend. 9-23597
- charge current induced, where charge current satisfies homogeneous wave eqn. 9-29334
- compression of metallic foil for transient MOe mag. field prod. 9-47894
- conducting gas, rel. to acceleration 9-42479
- continuum electromechanical dynamics, one dimensional analysis, book 9-29337
- diffracted by transmission network, numerical study 9-45896
- distribution in model of localized charge clusters 9-25191
- earth's motion through ether detection 9-29179
- in earth, rel. to elec. props. of upper crust rock 9-33727
- on edge of conductor, variation with curvature 9-27254
- effect on decay probabilities for μ , π and neutrino-emitting electrons 9-27469
- Einstein-Maxwell fields, non-zero charge-current distrib., space-times studied 9-36217
- Einstein-Maxwell null fields with non-zero current distrib., conditions on Ricci Tensor 9-34110
- electron interacting with e.m. field, Rayleigh-Ritz method used to derive field eqns. 9-46043
- energy-density $> 1 \text{ kJ/cm}^2$, in vacuo and in material media 9-29335
- energy-momentum tensor for anisotropic dispersive media, relativistic formulation 9-22306
- equations, matrix formulation in measurable quantities 9-27253
- equations in space-time, stationary action principle 9-22307
- ethanol, boiling, heat transfer depend. 9-23597
- explosions of condensed detonators, investigation in near zone 9-38306
- in Friedmann universes, soln. 9-22347
- and gravitational field, unified geometric description 9-27167
- helical sheath, by current distribution on surface 9-36238
- intensity, visible images, $\lambda = 1.7$ - 2.5 mm . 9-29339
- intensity fluctuations in weakly inhomogeneous medium 9-47849
- laser radiation, effect on five-photon ionization of Na atom 9-48412
- lumped parameter electromechanical dynamics, transducer and rotating machine applic., book 9-29336
- Maxwell rels. and Riemann space characts. 9-22077
- in metals, acoustic wave generation 9-26422
- molecule subjected to external fields, force and torque on nuclei 9-34600
- in moving media, a relation between field quantities 9-47842
- non-interference of elec. and mag. fields 9-38322
- in nonlinear media, soln. by convolution on complex plane 9-41734
- optical, temperature functions 9-27358
- oscillating, effect on movement of charged particle 9-41873
- positive column oscillations in external e.m. field 9-36789
- quantum theory, in absence of charges, text book 9-41756
- quasi-flat, production by array of ideally cond. waveguides, problems and limitations 9-36235
- relativistic correl. in presence of random sources 9-25137
- semiconductor, effect on electron elastic scattering 9-30901
- shielding effect of thin-walled flat rotational ellipsoid 9-34108
- shock wave prod. in gas by sudden applic. of crossed mag. and elec. fields 9-28071
- source-excited, in wave guide of 2 parallel plate dielectrics, theor. analysis 9-34109
- spherical conducting shell, e.m. transient response, quasistatic soln. 9-34107
- statistical theory using functional methods 9-38203
- three-dimensional geometries, computer solutions 9-45889
- time-invariant conservative fields, three-dimens., boundary problems soln. with computer 9-31751
- undergraduate text 9-38188
- vector potential of source-free vector field 9-29332
- water, boiling, heat transfer depend. 9-23597

Electromagnetic oscillations

- see also Magnetohydrodynamics; Masers; Plasma/oscillations*
- 0.34mm. wave generation by beating ruby laser R_1 and R_2 lines 9-25283
- cavities, supercond. microwave, tuning 9-37482
- cavity, Alvarez, radially displaced drift-tube, reson. freqs. variation 9-43806
- discharge at 55 GHz, fourth harmonic power generation, charact. 9-36221
- earth-ionosphere cavity, super l.f. noise, geomagnetic field effect 9-31395
- Fabry-Perot resonator, spherical, excitation by small aperture 9-31867
- metal, in h.f. wave dispersion curves 9-44904
- microwave frequency doubling, quantum mechanical, in ruby 9-25139
- resonator, dielectric, radiation Q factor, theory 9-25138
- Nb r.f. cavities, fabrication 9-39605

Electromagnetic radiation *see* *Electromagnetic waves; Gamma-rays; Light; Radiation; X-rays***Electromagnetic wave propagation**

- see also Absorption; Diffraction, etc.; Plasma/electromagnetic waves*
- absorbing media, group velocity and energy transport 9-25143
- in anisotropic inhomogeneous medium with spherical symmetry 9-47846
- in bounded media, parametrically modulated 9-47848
- coherence function, 4th order, in random medium 9-45988
- in conducting medium, appearance of direct current or e.m.f. 9-25144
- delay and distortion in moving plasma 9-40297
- dielectric, nonlinear self-focusing of large amplitude waves 9-36247
- from dipole, oscillating magnetic over anisotropic earth 9-37993

Electromagnetic wave propagation continued

- in elastic and fluid media, electromechanical dynamics, three dimensional analysis, book 9-29338
 - gravitational interaction changing freq., test with laser two-beam interferometer 9-41743
 - ground backscatter, h.f., Doppler shift 9-41577
 - impulse, penetration into cavity of conducting cylinder 9-43807
 - interaction with medium with non-linear mag. susceptibility, Landau-Lifshitz and Maxwell eqns. 9-45375
 - interface of nonlinear media, surface waves study 9-29342
 - isotropic media, spherically stratified, refractive-index profiles giving transcendental solutions 9-25140
 - light beam, intense, through mist, evaporation effect 9-42699
 - light pulse in semi-infinite isotropically diffusing medium 9-22447
 - luminescent diffusive medium, pulse characts., calc. 9-25149
 - Maxwell's eqns. matrix formulation, for plasma 9-40671
 - Maxwell eqn. soln. for anisotropic electrooptic medium 9-41357
 - medium with resonant emission or absorption, transient response, maser experiment 9-25141
 - metal, dispersion of ordinary and extraordinary h.f. waves 9-44904
 - metal slab, effect of boundary scatt. on helicon transmission near cut-off 9-26491
 - methyl bromide, double irradi. by i.r. and r.f. beams 9-46402
 - moving media, radially, first order vector wave equation solution 9-38335
 - nonpiezoelectric crystal, magnetostrictive generation of microwave phonons 9-45272
 - Osaka cold cathode discharge tube used as an oscillation prod. e.m. waves 9-36785
 - in plasma layer, TE wave, large amplitude 9-47869
 - plasmons, surface, on optically excited metal grating, coherent and incoherent radiation emission 9-24371
 - polar cap absorpt., riometer obs., correl. with satellite obs. of solar proton fluxes 9-31394
 - pulse dispersion, simple expt. 9-47711
 - radio pulses from cosmic ray air showers at 44, 105, 239 and 408 MHz 9-42120
 - in radnom medium, general method for velocity and attenuation determ. 9-36119
 - solids possessing Faraday rot. and birefringence 9-45262
 - Sommerfeld and Brillouin precursors in microwave domain, exptl. obs. 9-34116
 - superconducting film across rectangular guide 9-30881
 - surface wave, effect of gap between slow-down array and dielectric 9-47847
 - swinging, by generated Compton effect, producing powerful cosmic radio source 9-24717
 - theory and expt. of long waves, textbook 9-40228
 - theory rel. to origin of pulsar radiation 9-24827
 - at transition between isotropic media 9-41855
 - transmission, lossless line with reactive load, output voltage expression 9-31870
 - transmission by moving uniaxially anisotropic slab 9-34119
 - transverse wave packet momentum, energy and power density 9-38330
 - Vavilov-Cerenkov radiation due to magnetic monopole in transparent dielectric crystal 9-28648
 - v.l.f. band for communications between two subterranean stations 9-47867
 - v.l.f. finite amplitude packet, growth, with reference to magnetosphere 9-22318
 - CDs, magnetomicrowave effects at 38 GHz, charge carrier density control by photogeneration 9-30922
 - Ge, magnetomicrowave effects at 38 GHz, charge carrier density control by photogeneration 9-30922
 - InSb, m.o.s., surface charge wave propag. in mag. field 9-47150
 - InSb, microwave third harmonic generation at low temp. 9-35403
 - Yb orthoferrite 9-45262
- atmosphere**
- 112-118 MHz range, field strength and terrain roughness relationship 9-35827
 - absorption, normal and abnormal, high latitudes 9-33788
 - absorption meas. at 31.9 cm wavelength 9-31330
 - Arctic communications, physical problems 9-33789
 - attenuation in 183-325 GHz band obs. 9-45893
 - cloud attenuation at 33.5 GHz, rel. to liq. water content, residual noise effect 9-33779
 - focused beam, use of wave fluctuations in remote turbulence probing, theory 9-33757
 - h.f. waves across auroral zone, Winnipeg-Resolute Bay oblique sounder circuit 9-33793
 - laser beam, 1.54 micron, transmission charact. 9-34117
 - long-wave radiative transfer, computer calculations 9-31332
 - magnetosphere, Chetayev's solutions 9-24672
 - meteor burst communications absorption and multipath propagation, Arctic 9-33791
 - micron wavelength propagation effects 9-37915
 - microwave and i.r., remote sensing of an inhomogeneities 9-33781
 - microwaves, remote sensing using radiometric techniques review 9-33780
 - millimeter wavelength, earth-space communications 9-37928
 - millimeter wavelength, rain attenuation effects 9-33795
 - polar cap absorption, characteristics 9-33787
 - propagation, transauroral, induced phase perturbation, observed fine structure 9-40058
 - radar probing of structure 9-33783
 - radiation measurements used in indirect sensing statistical information content 9-24660
 - radio noise on 28 Mc/s, from aurora 9-47563
 - radio refractive index, gradient, 1965, India 9-28895
 - radio refractive index, upper troposphere over India 9-28894
 - radio sensing using satellites, density obs. 9-33782
 - rainfall attenuation, mm wavelengths radiometry for earth-space radio links 9-37927
 - Rake tropospheric scatter channel-sounding technique for remote sensing of atmospheres refractive structure 9-33784
 - Rake tropospheric scatter channel-sounding technique for remote sensing of atmospheres refractive structure 9-33785
 - scattering and attenuation by rain 9-40040
 - scattering by artificial ionized spherical cloud 9-31329
 - scintillation boundary for satellite radio signals 9-31391
 - starlight path, remote probing of optical strength of turbulence and of wind velocity 9-33758

Electromagnetic wave propagation continued
atmosphere continued

statistical characterisations of perturbations produced weak scattering approximation 9-31872
stepped frequency oblique soundings at high latitudes 9-33794
troposphere, inversion layer study by simultaneous lidar and refractometer soundings 9-43380
troposphere, rain and snow effects on extraterrestrial mm. waves 9-31331
tropospheric diffraction phenomena 9-37926
two-layered, diffuse refl. and transmission from scatt. and transmission functions 9-24662
Venus, cm and deci-cm waves 9-45670
v.h.f. bistatic auroral backscatter communication 9-33792
v.l.f., periodic fading over polar path during sunset and sunrise 9-33790
v.l.f. emissions, day and night differences, applic. to storm periods 9-49468
v.l.f. radio signals, phase behaviour 9-24663
v.l.f. records obtained during polar cap absorption and auroral disturbances 9-33840
wind turbulence meas. using Doppler radar system, feasibility study 9-31308

guided waves

anisotropic media, resolution of thermodynamic paradox 9-29348
antennae of night-flying moths, h.f. dielectric waveguide 9-33962
cavity resonances in accelerating frames of reference 9-34113
in circular waveguide, H-wave with finite amplitude 9-47861
circular waveguides with inhomogeneous focusing media, vector theory 9-22310
cylindrical system with inhomogeneous focusing media, asymptotic solution of vector fields and propagation constants 9-31874
dielectric rod in plasma, analysis with diagnostic applic. 9-45899
dielectric thin rod, reflection coeff. at 9.3GHz 9-38341
diffracted rays at open-ended waveguide edge 9-47863
dioptr. cylindrical, behaviour in oversized waveguide 9-45897
dipole-surface oscillations on a dielectric-vacuum boundary 9-36237
earth-ionosphere guide v.l.f. 9-38337
earth-ionosphere v.l.f. spherical and plane models 9-31385
ferrites waveguide resonator quick evaluation of characts. rel. to analog phase shifters 9-43815
fibre optical bundles, propag. 9-36375
Goubau surface wave lines, mode coupling, eigen. value equation using point matching method 9-31875
inductive iris double discontinuity 9-29347
inhomogeneous focusing media, wall effects, losses and fast to slow transition 9-34124
interaction with nonmagnetic dielectric particles immersed in infinite homogeneous isotropic nonmagnetic medium 9-27260
ionospheric satellite communication channel, averaged field 9-43436
ionospheric waveguide upper boundary, equivalent diurnal height var. 9-49496
magnetolectric media, comments 9-47864
magnetolectric media, solution of field problem in circular waveguide 9-31879
magnetostatic, along ferrite-semiconductor film interface, amplification 9-43816
microwave cavity perturbations by lossy dielectrics and plasmas 9-41859
microwaves in rectangular guide with superconducting film across 9-30881
optical communication, beam guidance by Schlieren prism 9-34199
optical in gaseous lens like medium, mode conversion due to fluctuations 9-43912
overdimensional, study of symmetrical scatter irises 9-47859
in periodic structures with glide symmetry 9-45898
phase velocities and inclinations of wave in groove with inclined comb 9-22315
plasma, magnetized dispersion props. 9-42508
plasma slab in waveguide, nonlinear interaction of microwave field 9-36767
plasma waveguide, phase vels. of symmetric modes 9-25883
plasma waveguide for whistler freq. range, theory 9-34126
plasma waveguide props. 9-48561
plasma waveguides, confined, e.m. modes 9-42504
rectangular waveguide, scattering by cylindrical post parallel to electric field vector of dominant mode 9-25147
rectangular waveguides, partially filled with inhomogeneous dielectric, closed form solution for TE mode 9-31878
resonators, open, with spherical mirrors, Q-factor determ. 9-34115
resonators, used to extend band and reduce noise in parametric amplifier 9-36248
semiconductor filled rectangular guide with uniform transverse magnetic field 9-31877
super l.f. noise in earth-ionosphere cavity, geomagnetic field effect 9-31395
surface wave G-line, dielectric shield for environmental protection 9-31876
surface waves, equality of group speed and energy speed 9-45900
TE wave non-linear focussing in two-level system 9-22316
terrestrial e.l.f. in seawater or below ground surface, zonal harmonic calc. 9-45459
transmission cables, supercond., geometric arrangement for maximizing power transmission capability 9-35382
transmission lines, supercond. thin film, slow-wave propag. obs. 9-37481
transverse, interaction with electron beam in magnetostatic field, theory 9-47862
transverse, interaction with electron beam in magnetostatic field, theory 9-47862
in uniform waveguide, computer program for computation of fields 9-34125
waveguide, rectangular, warm-plasma filled, strong transverse mag. field 9-25153
waveguide array for prod. of quasi-flat e.m. field, problems, limitations 9-36235
waveguide component, dielectric $\Lambda/4$ -transformer, transformation parameters determ. 9-40294
waveguide filled with stratified dispersion material, dispersion characts. of TE and TM waves 9-42506
waveguide filled with warm uniaxial plasma, characteristics 9-25152
waveguides, double dielec. tube, low loss 9-47865
Ag-glass-Cu optical waveguide, coaxial 9-34218
n-InSb waveguide, dimensional resonances of helicon waves 9-41201

Electromagnetic wave propagation continued
guided waves continued

Y Fe garnet slab, transversely magnetised, surface magnetostatic waves, boundary conditions 9-47860

ionosphere
absorption, auroral type in mag. conjugated regions 9-35861
absorption effect on mid-latitude geom. pulsation correlations 9-35900
anisotropic, wave trajectories from satellites, computation 9-41573
antipode focussing, idealized model 9-45522
antipode focussing, idealized model 9-45522
auroral absorption electron density observation, radio communication problems 9-33839
conductivity and radiowave propag. probes, design 9-43456
cosmic r.f. noise absorption 1959-65 obs. 9-40070
D layer transmission, reflection coeff. and elec. field distribution 9-41861
D region l.f. continuous wave expt. 9-26945
D-layer freq., variation obs., rel. to electron conc. profile 9-40086
D-region profiles rel. to A3 l.f. absorption obs. 9-35880
Doppler effect, first-order, electron content determ. 9-41575
Doppler effect on decametric radiowave produced by powerful explosion on ground 9-33831
Doppler effect on decametric waves by acoustic wave 9-41574
ducts, multipath effects in topside sounding 9-43440
E_z continuous reflections, duration 9-45539
E_z limiting and blanketing freqs. relationship, obs. 9-28951
E-layer, radiowave triple splitting mid-latitude IQSY obs. 9-31423
earth-ionosphere cavity, super l.f. noise, geomagnetic field effect 9-31395
electron density local and integral values, rel. to coherent radio waves from satellites 9-37971
e.l.f. and v.l.f., effects of ions in lower region, differential eqns. 9-40074
e.l.f. emission, l.f. cutoff 9-28944
e.l.f. pulse distortion after propag. through antipode 9-43437
e.l.f. waves, reflection coeffs. calc. under effect of ions. 9-24686
F1 layer junction frequencies for latitudes higher than 35°N 9-33852
F2 critical freq., space-time forecasting expt. 9-26951
F2 critical freq. rel. to sunspot no., hysteresis 9-49502
F2 decrease in tropical forenoon, obs. 9-33853
F₂ signal location on oblique sounding oscillograms 9-26955
F region backscatter irregularities, long range 9-40094
F-region loss coefficient estimation from concentration profiles 9-40091
Faraday rotation, time lag in occurrence of Q-T point 9-37974
Faraday rotation obs. of Explorer 22 signals at 2 stations, comparative evaluation 9-49485
ground backscatter elevation angles rel. to sunset ionospheric tilting, 16 MHz 9-41581
h.f. communications systems, survey of effects 9-33834
for incidence at 30° and 80°, 10 to 30 kHz, heavy ion effects 9-40074
for inhomogeneous medium with dielectric const. varying as square distance 9-41861
lower, conductivity determ. from v.l.f. sudden enhancements of strength 9-49497
lower, phase of partially reflected waves, recording method 9-49482
lunar artificial ionosphere for radiocommunication purposes 9-36017
magnetoplasma, compressible lossy, fields and propag., unified approach 9-47870
meteor scatter communications, survey 9-33832
noise band generation by Cherenkov rad. from auroral electrons 9-40076
nonvertical, effect on topside sounder data reduction 9-31416
outer v.l.f. bursts rel. to mag. activity 9-40071
penetration frequencies predictions, comparison with topside-sounder data 9-35884
phase path variation and emergence angle calc. 9-40296
plasma waveguide for whistler freq. range, theory 9-34126
polarization analysis 9-31880
probability density calc., computer program 9-43770
pulse dispersion for vertical incidence and applic. Alouette topside sounder 9-41576
radio, h.f., Doppler shifts on ground backscatter 9-31390
radio absorption, anomalous, characts. in auroral zone 9-43428
radio waves, quasi-transverse propag., correction to first order Faraday rot. theory 9-49483
radio waves absorption at different frequencies, lunar variation 9-37970
radio waves traversing auroral ionosphere, fading morphology 9-33836
radiowave, fluctuations, correl. with sunspot number 9-31382
radiowave absorption in broken terrain, meas., 9-45525
radiowave field strength slow changes, effect of vertical movement 9-45526
radiowave scattering by moving body trail 9-31388
radiowaves scattered by small scale inhomogeneities, polarization 9-41860
reflected pulses, freq. correl. obs. with spectral analyser 9-40084
reflected signal, envelope correl. coefficient and spectrum width 9-31384
reflected waves, electron collisions effect on polarisation 9-49481
reflections, from lightning, rel. to stroke height 9-37924
reflections from large horizontal gradients in topside ionosphere, satellite sounder observations 9-33838
refraction and attenuation, l.f., 60 to 6000 km 9-31387
r.f. absorpt. freq. depend. rel. to latit., season and solar activity 9-28941
satellite radio signals, severe amplitude scintillations during sunrise 9-24713
scatter by mag. field aligned ionization 9-31392
scattering, induced and mixed, properties 9-31389
scintillation of satellite 40 MHz signals, variation with observers latit. 9-31393
scintillation of satellite signals, Nakagami m-distrib. description 9-47573
scintillation of satellite signals, scintillation index determ. methods 9-45528
scintillation of satellite signals, statistical analysis 9-47572
scintillations, proposed index for meas. 9-45520
sporadic E propagation, significance in determining MUF 9-33851
sudden freq. deviations rel. to solar microwave bursts 9-49591
temporal and spatial characteristics of h.f. signals 9-33835
Thomson scattering with unequal electron and ion temp. effect of collisions 9-42515
topside resonance, explanation in terms of oblique echoes 9-31415
u.l.f. radio waves, validity of $f_{\text{cos i}}$ theorem of absorpt. 9-43447
v.h.f. riometer and forward-scatter observations 9-33833
v.l.f., effect of polar cap event as means of early low latitude detection 9-28942
v.l.f., influence of electron density irregularities 9-33829

Electromagnetic wave propagation continued
ionosphere continued

- v.l.f. between conjugate points, evaluation 9-35862
- v.l.f. emissions, triggered, mechanism 9-24687
- v.l.f. long path transmission, effect of total solar eclipse (1968) 9-37975
- v.l.f. observations, ion composition determination 9-35872
- v.l.f. records obtained during polar cap absorption and auroral disturbances 9-33840
- v.l.f. signals from ground, latitudinal cutoff OGO 2 obs. 9-43441
- v.l.f. whistler cutoff 9-24688
- v.l.p. transmission effects of PCA, obs., between March (1966) and June (1967) 9-49484
- waveguide, v.l.f. 9-38337
- waveguide, v.l.f. spherical and plane models 9-31385
- waveguide satellite communication channel, averaged field 9-43436
- whistler-mode waves in 10 Hz to 540 kHz range, experiment design and operation 9-35863
- whistlers, 1-10 kHz, transmission calc. and obs. 9-31386

Electromagnetic waves

- see also Diffraction; Reflection, etc.; Light/electromagnetic theory*
- amplification of pulses using system of weakly anharmonic oscillators 9-34114
- Antarctic snow and ice cover study, method 9-33730
- backward-travelling-wave parametric interactions, steady-state theory 9-34188
- γ -radiation field perturbation at barrier due to hole-type inhomogeneity 9-26599
- coherence, classical and quantum theory 9-22305
- Compton effect, induced, of waves under astrophysical conditions 9-43581
- corrugated surface wave line, E_0 mode, spaced metallic discs, field distrib. depend. 9-31871
- generator for millimeter and submillimeter diffraction radiation 9-29341
- gravitational effect on pulse equal in magnitude but opposite in direction to that in red shift 9-34018
- impulsive radiation, rel. to generation of plastic yield and reverse yield waves 9-45829
- incident on semicond. slab., microwave second harmonic generation 9-35387
- incident wave relation with diffracting object, boundary condition anal. 9-47850
- interaction with electron, in quantized field, wave function determ. 9-38469
- Kapitza-Dirac eff., multiple scatt. approach 9-25142
- in moving lossy media, time- depend. and-harmonic Green's functions 9-22309
- negative energy waves, non-linear interaction 9-22308
- nonlinear electrodynamics and optics, theory close to exact solns. 9-47844
- parametric generation, pulsed in distributed systems 9-47845
- radiation absorpt. and press. force of wave on object with varying polarizability changes 9-45891
- radiation jets, extended source construct. 9-22067
- radio emission, visible images, $\lambda=1.7-2.5$ mm. 9-29339
- resurgent wave field assoc. with total refl. of limited wave by dioptric plane 9-43808
- self-focusing, computer studies 9-34112
- two, moving towards each other, radiation of scalar particle in field 9-41851
- undergraduate text 9-38188
- v.l.f. band for communications between two subterranean stations 9-47867
- $\text{Cd}_x\text{Ca}_{1-x}\text{O}$ Reststrahlenbands and intrinsic absorption edge 9-47342
- in YFe garnet and ferrite rods, magnetized, dynamic mode and surface waves 9-33478

radiators

- aerial, integral eqn. for polar diagram, when diffraction takes place on aerial surface 9-36242
- aerial amplification losses, depend. on phase and amplitude fluctuations 9-36243
- antenna; cylindrical, finite, dielectric-coated, input conductance theor. study 9-36240
- antenna, infinite cylindrical, in uniaxial compressible plasma, admittance, susceptance and conductance behaviour 9-25154
- antenna, supercond. 9-37480
- antenna, thin cylindrical, in plasma 9-48571
- antennae, paraboloid, optimum setting rel. to gravit. deform., wind and temp. 9-36239
- circularly polarized, rad. through Mars-entry capsule ionized wake, effects 9-47868
- electric dipole in two-layer earth, ground-wave excitation, optimisation 9-40295
- impedance system, plane semi-infinite, with vertical dipole on boundary 9-43817
- lightning, ball, from thunderstorms 9-43402
- lightning, linear, emission in decimeter range 9-43403
- linear antenna synthesis, optimal soln. of problem 9-22317
- parabolic mirrors, radiation pattern 9-36241
- sources distributed over conical surface, analysis using Green's function 9-41853
- triangular lattice array, properties 9-25155
- waveguide, round, field excitation by stationary source, Fourier series representation 9-36222

Electromagnetism

- see also Electrodynamics; Quantum electrodynamics*
- background radiation and quantum theory, a relationship 9-22100
- charge current satisfying homogeneous wave eqn., induced e.m. field 9-29334
- college-level textbook on electricity and magnetism 9-31866
- conservation of six components of angular momentum 9-27252
- Einstein-Maxwell equations, solution for a cylindrical, electric current 9-22078
- electromagnetic theory, book 9-47843
- electromechanical continuum balance eqn., role of source function 9-41850
- Faraday's law, demonstration of teaser 9-45887
- Friedmann universes, covariant e.m. potentials and fields 9-47731
- Helmholtz eqn. with spheroidally symmetric boundaries, weak-separable soln. 9-31865

Electromagnetism continued

- induction in thin strip, for understanding geomagnetic effects at ocean edge 9-28959
- induction various teaching approaches 9-45722
- infinite cylinder of finite conductivity and variable density in the presence of a magnetic field, radial pulsations 9-43805
- interaction radiation of electron beam with infinitely cond. network 9-41848
- levitation in hollow conductors, analysis 9-38324
- levitation of conducting planar tape, analysis 9-38323
- magnetic fields in rotating frames of reference 9-47873
- magnetic monopoles, multiply charged Dirac., search 9-27448
- Maxwell's eqns., multipole solns. in nonspeading class 9-25028
- monopoles in elec. field, quantization model 9-45888
- plasma erosion source, e.m. acceleration of coagulation 9-30262
- point charge, relativistic blurring 9-22346
- reciprocity theorem, time reversibility in optical proof 9-27255
- S-matrix theory incorporation, analytical props. of scatt. amplitude for long-range forces 9-38240
- skin effect studies in ferromagnetic conductors 9-38325

Electromagnets *see* Magnets**Electromechanical effects *see* Electrostriction; Piezoelectricity****Electrometers *see* Electrical measurement****Electromotive force**

- photo-Hall e.m.f., polarity inversions 9-33290
- plasma, inertial, magnitude 9-30231
- teaching the concept 9-22037
- voltage multiplying circuit of Schenkel type, voltage efficiency calc. 9-29354
- of Weston cells, increase on passing small a.c. 9-27266
- CdTe film, d.c., caused by microwave field, investig. 9-30885
- Na, liquid, along external mag. field, induced by flow, expl. discovery 9-36899

Electron affinity *see* Atoms; Ionization; Molecules; Solids**Electron annihilation *see* Electron pairs/annihilation****Electron avalanches *see* Breakdown, electric****Electron beams***see also Electron optics; Particle accelerators*

- 3.4 MeV, 250A, 300 ns, emittance measurement and optimisation 9-45924
- 25 MeV, injected into static magnetic field to form ring accelerator 9-46171
- absorption in air and plastic, 20 to 50000 eV 9-37376
- alkali halides, low energy electrons, stopping power, extrapolated range and degradation 9-33211
- annular, from magnetron gun, axial velocity meas. 9-31913
- apparatus using crossed beam techniques with cylindrical velocity selector for study of atomic ionization 9-25963
- brightness and directional beam intensity w.r.t. tangential vel. of emission at cathode for Schottky and field emission 9-31912
- Brillouin flow, transition region, design and calc. 9-38355
- bunching in ALS linac 9-46148
- collisionless thermalization in plasma rel. to wave modes, collision m.f.p. and effective thickness 9-48599
- deflection, air core coils 9-47902
- delineation and penetration 9-29380
- direct beam fluoro-radiography 9-32098
- drift-beam instability damping by feedback 9-45926
- electrostatic focusing, periodic, theory and experiment 9-31914
- electrostatic focusing system, periodic, design 9-36260
- energy and angular distribution after passing through barriers of varying thickness 9-24075
- energy dissipation by normally incident monoenergetic beams, algorithm 9-41121
- energy distrib., single-cryst. spherical cathode 9-22350
- energy distribution after passing through barriers 9-24074
- energy spread in electron-optical instrum. 9-40317
- extraction from plasma in vacuum 9-30208
- flow field visualisation, low density, excitation technique 9-46563
- flow from pulsed high current field emission cathodes, dynamics 9-45923
- fluorescence probe for hypersonic He flow visualisation 9-46559
- gas discharge guns, e energy distribution 9-25181
- gun, multipactoring principle used as basis of electron source 9-29381
- gun, ring-shaped, for floating zone refining apparatus, emission and focusing characts. 9-38350
- gun, three-electrode, beam current stream coeff. 9-22349
- gun heated by electron bombardment, cathode temp. stabilization 9-40316
- guns, caustic curves 9-40315
- high-current density, Brillouin-focused, axially symmetric using magnetic compression 9-22348
- interaction in plasma, rel. to whistler mode excitation of e.m. waves 9-25885
- ion source, electrostatically focused electron beam, efficiency 9-29388
- in ion source, thickness calc. for optimal focusing 9-38351
- klystron quasiperiodic focusing by permanent magnets 9-31869
- in linac, 300 MeV, transport 9-46156
- in linear accelerator, 2 GeV, bunching of output 9-44098
- in linear accelerator, formation of electron jet, calculations of transverse oscillations 9-29382
- lucite, energy-loss spectra for high-energy electrons as function of depth 9-37377
- magnetic focusing, two aspects 9-31916
- Metal oxides, e.s.r. obs. rel. to catalytic behaviour 9-35709
- monitor for high energy beams, detects Cerenkov light from N_2 gas 9-29681
- monochromatisation and improvement of emission images by means of mirror 9-22351
- Penning structure, axial flow with excess energy 9-25189
- in plasma, radial self-focussing under beam instability conditions 9-30214
- plasma beam instability, h.f. modulation effect on energy and temp. of accelerated electrons 9-30286
- in plasma betatron, axial field, runaway beam obs. 9-32280
- plasma-beam discharge, wall potential effects, stability obs. 9-23310
- polarization of low-energy beams, meas. by optical method 9-44284
- polarized prod. by cross-fire of atomic beam and unpolarized electron beams 9-27281
- polarized, prod. by ionization of K beam with u.v. light 9-27282
- polarized, production from optically pumped He discharges 9-28045

Electron beams continued

- polarized, slow, prod. by scatt. 6.75eV electrons at Hg atomic beam 9-40318
- positron, production, applic. in scatt. and annihilation expts., popular review 9-43847
- probe analyzer, technique for taking colour photographs 9-31234
- quantum fluctuations of radiation and electron dynamics in 1.5 GeV synchrotron 9-47067
- range, mean projected, calc. at high energies 9-47014
- regulator, for use in e-impact ion source 9-43860
- retarded potential difference technique for achieving fine energy resolution 9-45925
- ribbon type, approximate equations for density, potential and velocity perturbations 9-41877
- scattering, highly focused kV beams, by thin film-substrate system 9-35047
- short life packets for injection into linear accelerator, use of deflecting maze-struct. 9-44097
- in solids, transmission and backscatt. of 4-12 MeV e 9-44849
- source of polarized electrons obtained from intense K atomic beam 9-40459
- space-charge neutralized, stability rel. to finite ion mass effect 9-41876
- spreading, thermal and space-charge, analysis 9-25183
- transit-time tube, magnetic focusing system, patent 9-45931
- transition metal chalcogenides, energy loss rel. to band struct. determ. 9-30804
- velocity distribution, directional analyser, electrostatic 9-29372
- gun with highly stable tip and needle cathodes 9-25182
- A g colloidal particles, electron m.f.p. limitation, refractive index meas., absorption coeff. determ. 9-41115
- Ag, energy loss spectra in i.r. region 9-28441
- Al, energy loss spectra in i.r. region 9-28441
- inAl, factors affecting energy-range relation 9-35302
- Al, high energy, measured energy loss 9-39551
- Al films, energy-loss spectra, convolution effects by electron transmission 9-47015
- Be, energy loss spectra in i.r. region 9-28441
- CdS, radiative capture by activated recombination r-centres, cross section determ., impurity photo-effect meas. 9-30798
- Ga, solid and liq. foils, energy loss spectra of 50 keV electrons 9-41148
- KAl(SiO₃)₂, energy-loss spectra for high-energy electrons as function of depth 9-37377
- NiO, antiferromagnetic, coherent exchange scattering with lattice electrons, rel. to mag. structure 9-45230
- PbSe, characteristic energy losses 9-39553
- PbTe, characteristic energy losses 9-39553
- RbBr single cryst., positron anisotropic penetration, X-ray spectrum obs. 9-35300
- Si(Li), energy-loss and straggling, spectrum 9-30810
- Sn, focusing by longit. mag. field 9-26519
- Sn, solid and liq. foils, energy loss spectra of 50 keV electrons 9-41148
- SnTe, characteristic energy losses 9-39553

absorption *see* **Electrons/absorption****effects***see also* **Beta-rays/effects**

- acetonitrile, pulse radiolysis, formation of solvated electron, obs. 9-27880
- alkali halides, F-centre prod. rate, impurity conc. effect 9-46834
- alkali halides, irradi., saturation of F centre form 9-48867
- anthracene molecules in cyclohexane, induced fluorescence, effect of elec. field 9-44351
- aragonite, transformation to calcite, to lime in electron microscope 9-26385
- aromatic monomers and dimers, luminesc., 1MeV beam 9-43259
- bombardment by mono-energetic electrons, back-scattering coeff. determ. 9-47011
- chloral hydrate, e.p.r. rel. to conc. of produced paramag. centres 9-33638
- crystals bombarded with 20 keV electrons, exam. of plasma oscills. 9-41140
- diffraction study with v. fine beams 9-40319
- epitaxy modifications of f.c.c. metals evaporated on to alkali halide substrate 9-46760
- exciton-impurity complex, excitation by fast electrons 9-26487
- Frenkel pairs prod. at low temp. irradi., influence of subthreshold events 9-32952
- n-Ge, scanning electron micrograph using beta conductive signal, elec. field distrib. 9-46773
- glasses, alkali-ion movements in electron-probe microanalysis 9-34968
- graphite, irradi., low temp., stored energy and elec. resistivity var. 9-24070
- graphite, pyrolytic, irradiated, recovery of basal plane elec. resistivity 9-28459
- hydrocarbons, dissociative excitation by fast electrons 9-23174
- inert gases, neutral mols. prod. by pulsed-beam 9-44345
- injection into electron plasma, time var. of energy loss and velocity diffusion 9-44479
- interaction radiation with infinitely cond. network 9-41848
- interaction with (helicon) whistler wave in semiconductor plasma 9-24104
- interaction with transverse e.m. wave in magnetostatic field 9-47862
- interaction with transverse e.m. wave in magnetostatic field 9-47862
- ionization chambers irradi. with pulsed e beams, recombination effects 9-38615
- liquid ionization, free ion yield determ. by charge scavenging 9-23528
- mesitylene, e.s.r. study of radical formed on e. irradiation 9-42439
- metal, interaction with coupled spin-plasma waves 9-41297
- metallic targets in vacuo, automatic heating and temp. control 9-29329
- metals, radiation damage 9-30592
- metals, X-ray emission, 100-1000 eV electron bombard. obs. 9-25013
- metastable N₂, H₂, N₂O and CO₂ mols. 9-32478
- 3-methylpentane, ion mobility 9-28720
- microwave scatt. from magnetoplasma, enhancement 9-23318
- modulated, plasma oscills. excitation 9-46521
- m.o.s. struct., irradi., continuous polarizing voltage effect on props. 9-47149
- photochromic materials, photobleachable colouration obs. 9-43201
- plasma, evolution and waves spectrum, adiabatic formulation 9-25925
- in plasma, inhomogeneous, Vlasov eqn. solved 9-46473
- plasma, unstable oscillations at surface obs. 9-36773
- plasma instabilities 9-34788
- plasma interaction, h.f. vibration stimulation 9-44474
- plasma interaction, linear instability in mag. field 9-25951

Electron beams continued
effects continued

- on plasma longitudinal waves, energy transfer 9-44470
- plasma oscillations, v.h.f., excitation 9-46522
- polyethylene terephthalate film, conduction by e. bombardment 9-26513
- polymers, luminesc., 1MeV beam 9-43259
- polymethylmethacrylate, transient radiation, spatial distribution 9-37764
- polystyrene film, conduction induced by e. bombardment 9-26513
- polytetrafluoroethylene, oriented, pulse irradi., e.s.r. 9-43291
- pyrene molecules in cyclohexane, induced fluorescence, effect of elec. field 9-44351
- quartz, cryst. and fused, pulsed-radiation-induced current obs. 9-44998
- radiolysis with electron pulses, effect of temp. on yields 9-33685
- semiconductor, atomic displacement threshold energy, calc. and expt. 9-35297
- semiconductor, interaction with coupled spin-plasma waves 9-41297
- semiconductors, irradiation and subsequent photocond. studies, low-temp. set up 9-31724
- Si, degenerate, irradi. at low temps., damage obs. 9-28277
- steel, mild, floating zone melting 9-33109
- surface pulsed heating by bombardment 9-41122
- tetramethylsilane, adsorbed, dissoc., thin Si films deposition obs. 9-44628
- thermoluminescence of single crystals before and after electron beam irradi. 9-45356
- transient radiation originating at electron transience from vacuum to dielectric, photographic registration 9-24208
- trioxane to polyoxymethylene by electron beam, struct. obs. 9-37824
- water radiolysis, nanosecond pulse expts., nonhomogeneous kinetics rel. to e(H₂O) behaviour 9-35756
- Ag, maximum range, 15 MeV, exptl. determ. 9-26470
- Ag, stage I recovery, elec. resistivity meas., annealing 9-35083
- Al, bombarded in high elec. field, rel. to secondary electron emission 9-31009
- Al, damage in <100> direction 9-42805
- Al, maximum range, 15, 4.1 and 9.8 MeV, exptl. determ. 9-26470
- As₂S₃ films, e. bombardment conductivity, columnar ionization 9-33369
- Au, irradiated interstitial clusters below stage III annealing temp. 9-30593
- Au, maximum range, 15 MeV, exptl. determ. 9-26470
- BaTiO₃ crystals and ceramics, fast e. effect on electrophysical props. 9-41238
- BaTiO₃ eff. of fast electric bombardment 9-39686
- Be, maximum range, 15 MeV, exptl. determ. 9-26470
- Be evaporation, controlling method 9-39145
- CaTiO₃:Fe-Mo, photobleachable colouration obs. 9-43201
- CdS, bombarded, i.r. attenuation of induced photocond. current 9-47198
- CdS, bombarded, rel. to microwave elec. conductivity and luminescence, 300°K 9-30903
- CdS, laser effect on e. bombardment, radiative recombination mechanism 9-24445
- CdS films, longit. cathode conductivity 9-41155
- CdSe, electron-hole pair form. energy determ. 9-47133
- CdTe laser, excitation by bombardment, characts. 9-34176
- Co, energy depend. of atomic displacement, low temp. 9-35084
- Cs atom, impact ionization, cross section obs. 9-34556
- Co-Ni film co-deposition from two pure sources 9-48763
- Cu, e-irrad., dislocation pinning, temp. eff. 9-23812
- Cu, maximum range, 15 MeV, exptl. determ. 9-26470
- Cu, nature of defects produced 9-35082
- Cu(1wt%) Co, coherency loss of Co precipitates in electron microscope 9-28383
- Dy₂O₃ films, pulse annealing, effect on recrystallization behaviour 9-30489
- Er₂O₃ films, pulse annealing, effect on recrystallization behaviour 9-30489
- Fe, crystal structure after bombardment melting 9-33110
- GaAs:Cd, irradi., luminesc. changes 9-49316
- GaAs, bombarded, rel. to microwave elec. conductivity and luminescence, 300°K 9-30903
- n-GaAs, bombardment damage, thermally stimulated conductivity meas. 9-35079
- Gd film, thermal stresses causing nucleation of twins, electron microscope exam. 9-35100
- n-Ge:Sb, electron irradiated, defects study, 80° to 200°K 9-35080
- n-Ge, defects production on irradi. at 30°K, annealing process 9-35081
- Ge, irradiated, fast recovery 9-33331
- H₂ and D₂, excited atom prod. by fast electron impact 9-23168
- H₂O vapour, excited H atoms prod. 9-30151
- H⁺ ionization, computation 9-34577
- H ionization, exchange cross sections 9-34578
- He atoms excitation, polarization of emitted light 9-29958
- Hg vapour, electron-impact spectrum 9-44263
- Ho₂O₃ films, pulse annealing, effect on recrystallization behaviour 9-30489
- K atom, impact ionization, cross section obs. 9-34556
- KCl:Pb, F centre prod. by impurities, α and V_K centre motion importance 9-44718
- KCl, colour centre production, 5keV electrons 9-23829
- KCl, F centre formation 9-35110
- KCl thin films, point defect coagulates due to irradi. during microscope exam. 9-42808
- KI:TI, F centre prod. by impurities, α and V_K centre motion importance 9-44718
- LiF cathode photoelec. yield in vacuum u.v. 9-26616
- LiF irradi., Y-absorpt. band obs. 9-37726
- LiH, absorption and luminescence spectra, radiation eff. 9-33585
- MgF₂ single cryst., rad. damage, comparison with neutron damage, optical absorpt. obs. 9-35117
- MgO, irradi., zero-phonon line study 9-45325
- MgO single crystals, irradi., hardening 9-33099
- Mo, irradiated, dislocation pinning and depinning, 45° to 330°K 9-28294
- N₂, energy-loss spectrum, perturbations due to config. interactions 9-38858
- N₂⁺ first negative system, excited by low-energy electrons, rot. temp. 9-30040
- Na atom, impact ionization, cross section obs. 9-34556
- NaCl, colour centre form. depth, due to 25 keV bombardment 9-44720
- NaCl single crystal surfaces, polygonization on bombardment 9-30513
- NaCl thin films, point defect coagulates due to irradi. during microscope exam. 9-42808

Electron beams continued
effects continued

- Ni, low temp. irradi., resistivity and magnetization damage rates 9-33205
 Ni₃Mn, low temp. irradi., resistivity and magnetization damage rates 9-33205
 O₂, dissociative attachment of electrons, crossed beam expts., effect of O₂ source temp. 9-40623
 O₂ yield of O₂ at v. high dose rates 9-39963
 PbS, bombarded, rel. to microwave elec. conductivity and luminescence, 300°K 9-30903
 Rb atom, impact ionization, cross section obs. 9-34556
 Se amorphous films, bombardment-induced crystallization 9-32842
 Si:Al(B), irradi., defects effect on photoconductivity spectra 9-44985
 Si:B(P), irradi., at 80°K, conductivity and Hall effect meas. rel. to carrier removal rates 9-44852
 n-Si:Li, irradi., defects obs. using Hall coeff. and resistivity meas. 9-49113
 Si:Li, O₂ radiation-produced defects interaction with impurity atoms 9-42813
 Si:SiO₂, defect prod. at 1 MeV 9-49357
 Si, dislocations formation, possible mechanism 9-26286
 n-Si, epitaxial, resist. rel. to e. bombardment between 12-18 keV 9-37543
 n-Si, high purity, irradi., rel. to transient recombination lifetimes 9-35508
 n-Si, pulsed 10 MeV irradi., rapid annealing of damage 9-35446
 Si, rad. induced atomic displacements 9-48844
 Si p-n junctions, ≤ 30 keV, irradiated rel. to instability in reverse I-V char. 9-28531
 Si single cryst. wafers, thermal stresses investigation by source image distortion 9-35164
 SiO₂, natural, irradi., 'A' band and absorpt. in near i.r. correl. 9-41391
 Ta, refining by electron beam melting 9-33101
 U₃O₈, transmission microscopy, O sublattice stability obs. 9-39312
 UO₂, transmission microscopy, O sublattice stability obs. 9-39312
 V₆C₈, ordered, microscope beam bombardment, radiation damage 9-26468
 W, interstitial Stage-I behaviour after e-irradi. 9-26279
 ZnS films, longit. cathode conductivity 9-41155
 ZnSe films, longit. cathode conductivity 9-41155

ionization *see* Electrons/ionizationionization *see* Electrons/ionization**Electron capture** *see* Ions/recombination; Radioactivity/electron capture**Electron diffraction**

- by crystals, soln. of electron states in terms of Bloch waves 9-30543
 fine beam, use of transmission electron microscope 9-40319
 intensity profile record of diffractometer, improvement by optical means 9-27283
 Kapitza-Dirac effect, review 9-45927
 LEED, inelastic effects, systematic inclusion 9-35045
 low energy, in thermionic emission energy conversion study 9-25170
 pseudopotentials applic. to potential and inner potential calc. 9-44654
 by standing e.m. waves, Kapitza-Dirac eff; quantum mechanical, Born approx. scatt. theory 9-45927
 N₂⁺ structure determ. 9-27867

Electron diffraction crystallography

- see also* Crystal structure, atomic
 atom form factor determ. by high voltage diff. 9-23722
 Bloch's theorem consequences on dynamical theory of diff. contrast 9-35046
 clean surface, LEED intensities using Weiner-Hopf technique 9-39228
 Debye ring, second order, intensity variation with accelerating voltage 9-28245
 defects, discontinuous displacement fields reconstruction from many-beam micrographs 9-40882
 diffuse scatt. by weakly distorted cryst., intensity, dynamic theory 9-46770
 dislocations, Frank, diff. contrast rel. to disloc., calc. 9-40958
 dislocations, scatt. dynamic theory, derivation 9-39224
 dispersion surfaces and band structure in 3-dimens. mixed Laue and Bragg reflections, review 9-37126
 display and simultaneous intensity meas. of pattern, apparatus 9-30542
 distorted cryst., dynamical theory 9-42767
 error sources, electronic and mechanical 9-23699
 fine structure of spots due to presence of stacking faults and dislocations 9-30536
 high energy diffraction, reflection technique, for examining surface struct. 9-48752
 in inhomogeneous primary ray field, phase meas. obs. from diff. patterns 9-42772
 in inhomogeneous primary ray wave field, amplitude and phase meas. for nonperiodic struct. 9-42774
 in inhomogeneous primary ray wave field, phase meas. from grating patterns, optical analogue expts. 9-42773
 integrated intensity meas., geometrical aspects and errors due to non-monochromatic radiation 9-23727
 intensities variation with energy loss 9-35053
 Kossel and Kikuchi lines, intensity evaluation 9-40886
 lattice parameter and electron wavelength ratio determ. from Kikuchi line intersections 9-42775
 LEED, inelastic effects, systematic inclusion 9-35045
 LEED beams, non-specular, scattering by (100) face of f.c.c. metal single crystals, props. 9-46778
 LEED intensities, multiple diffraction origin 9-23778
 line profiles rel. to stacking faults in h.c.p. and f.c.c. polycrystals, general theory 9-3817
 low-energy intensities, dynamical origin 9-37125
 n-beam dynamical diff. effect on diff. intensities from polycryst. materials 9-30541
 non-parallel beam, pattern formation 9-44653
 orientation contrast from inclusions 9-32890
 phonons, low-q, peak broadening in low energy diff. 9-32889
 powder specimen accurate relative intensity meas. techniques and apparatus 9-23700
 pseudopotentials applic. to potential and inner potential calc. 9-44654
 scalar wave dynamical diff. theory, matrix formalism 9-23701
 scanning-electron-beam anomalous transmission patterns 9-42776
 structure factor determ. from dynamical effects 9-23732
 surface, LEED, band struct. calcs. 9-33228
 surface structure determ. by LEED and energy analysis of scattered electrons determ. methods 9-42708

Electron diffraction crystallography continued

- symmetry of diff. patterns of slow electrons rel. to crystal symmetry 9-23723
 thermal diffuse scatt., dynamical calc. 9-40883
 transmission by plate-shaped foil, systematic refls. w.r.t. multiple beam theory 9-40885
 transparent line grating written with fine electron probe 9-26219
 RbBr, orientations in thin films 9-39229
 RbCl, orientations in thin films 9-39229
 RbI, orientation in thin films 9-39229
 W crystal, determ. mean inner potential 9-28273
- Electron diffraction examination of materials**
 alloy, binary, thin films, effective surface diffusion coeffs., effect of vol. diffusion 9-39379
 alumina particles dispersed in Al matrix, orientation contrast, obs. 9-32890
 contrast of three parallel overlapping stacking faults 9-32978
 crystal defects, rel. to diagram, modification in transmission electron microscopy 9-48845
 Cu_{2-x}Te (x=0.25±0.04), cry. struct. 9-46785
 cumene, molecular structure 9-23111
 cyclohexadienes, in gas phase, struct. and conformations study 9-46389
 diagrams, use of Ewald plane 9-44697
 excitation of single atomic electrons 9-40884
 films, thin, growth obs. using high energy scanning electron diff. system 9-39161
 foil, plate-shaped, transmission, systematic refls. w.r.t. multiple beam theory 9-40885
 gases, relativistic scatt. factors 9-30017
 gases, temp. effect 9-32457
 Kikuchi line doubling in strong bands 9-23763
 liquid metals and alloys, review 9-36846
 low-energy intensities, dynamical origin 9-37125
 molecular struct., comparison with optical spectroscopy 9-36713
 n-beam dynamical diff. effect on diff. intensities from polycryst. materials 9-30541
 orientation contrast from inclusions 9-32890
 oxidation of Cu single crystals in water 9-31196
 phenylcyclobutane, molecular structure 9-23111
 polyethylene, surface structure different when crystallized in contact with Au or Teflon 9-23614
 polypropylene, low-molecular-weight fractions, morphology and phase transformations on crystallization 9-46714
 quartz, diffraction contrast of Dauphine twin boundaries 9-30572
 scanning-electron-beam anomalous transmission patterns 9-42776
 second order reflection vanishing voltages calc. 9-32896
 steel, (Cr,Fe) C₃ identification and transform. obs. 9-48831
 steel, plastic deform., ferrite recryst. 9-37295
 steel, stainless, 304, interfacial free energies 9-28297
 steel, stainless, 304, interfacial free energies 9-28298
 surface struct. by low energy e diff. 9-35044
 tetracyclohexylcyclotetraphosphine, molecular and crystal structure 9-39351
 Ag-Cu alloys, liq. and vapour quenched, metastable struct. obs. 9-40899
 Ag, quenched, Frank dislocations disloc., obs. 9-40959
 Ag evap. films, variation of intensities with energy loss 9-35053
 Ag single crystal, surface atoms in (100) and (110) faces, mean displacement studies at low temp. 9-39248
 β -Al-Mg, structure by transmission and reflection methods 9-26222
 Al-(6wt.%)Zn(2wt.%)Mg, precipitate distrib., constituent phases from complex pattern analysis 9-28390
 Al, atom form factor determ. by high voltage e. diff. 9-23722
 Al (100) surface, props. of non-specular LEED scattered beams 9-46778
 Al epitaxial films on NaCl substrates, nucleation and growth struct. 9-36945
 Al evap. films, variation of intensities with energy loss 9-35053
 Al films on W(110) face, structure from LEED obs. 9-26184
 Ar/Kr solidified mixtures, lattice parameters rel. to Ar conc. 9-28255
 Ar/Ne solidified mixtures, crystallized phases 9-28255
 Au-Cr alloys, short-range order 9-28257
 Au-Mn alloys, short-range order 9-28257
 Au₄X ordered alloys, X=transition elements and mixtures, and resistivity and specific heat studies 9-44659
 Au evap. films, variation of intensities with energy loss 9-35053
 B₂Cl₄, molec. struct. 9-44319
 Bi₂O₃₋₇₋₈ films, orientation rel. to substrate 9-44624
 δ -Bi₂O₃, cubic structure 9-42783
 Bi films, orientation rel. to substrate 9-44624
 C fibres, preferred orientation effects on (h,k) interferences 9-28259
 CdO films prepared by d.c. reactive sputtering 9-48756
 CdS, {0001} surfaces, LEED obs. 9-28211
 Cu-Al, quenched, Frank dislocations disloc., obs. 9-40959
 Cu-Au(Al) alloy films, effective surface diffusion coeffs., vol. diffusion effect 9-39379
 Cu, atom form factor determ. by high voltage diff. 9-23722
 Cu_{2-x}Se thin films, at. struct. 9-46721
 Cu single crystals in water oxidizing 9-31196
 Fe-C martensite, diffuse scattering due to short-range order 9-32912
 Fe-Si, interference method for domain wall width meas. in thin sections 9-41310
 Fe, interference method for domain wall width meas. in thin sections 9-41310
 Fe(CO)₅, gas phase, molecular structure refinement 9-38841
 GaP films, vacuum-deposited, structural props. 9-42719
 HF gaseous polymers 9-42395
 β -In₂S₃, ordering of In vacancies, associated antiphase boundaries and twins 9-30587
 KNbO₃, ferroelec., cry. struct. 9-46788
 Mg films on W(110) face, structure from LEED obs. 9-26184
 MgAl₂O₄, Kikuchi line doubling in strong bands 9-23763
 MgAl₂O₄, Kikuchi patterns, multiple-beam dynamic effects 9-48835
 MgO, Kikuchi line doubling in strong bands 9-23763
 Mn fine particles prep. by evaporated in Ar, electron microscope and diff. obs. 9-42790
 MoO₃, Moire pattern due to electron bombardment in microscope 9-42791
 Mo(100) surface, interaction with O₂, LEED 9-42732
 NaAlF₄, molecule 9-48473
 NaAlF₄, molecule 9-44342
 Ni-Zn ferrite thin film, prep. and cryst. struct. obs. 9-45184

Electron diffraction examination of materials continued

- Ni, atom form factor determ. by high voltage e. diff. 9-23722
 Ni ferrite thin film, prep. and cryst. struct. obs. 9-45184
 Pb film formation on (110) face of W by u.h. vac. deposition 9-42720
 Pd-Ag alloy films, effective surface diffusion coeffs., vol. diffusion effect 9-39379
 Pd (100) surface, props. of non-specular LEED scattered beams 9-46778
 Pt, (100) face, scattering obs. 9-46746
 Pt, atomic scatter factor for electrons, 50-2.5 keV 9-46793
 Pt, chemisorption of gases 9-26818
 Se and Se-Pd film, crystal structure 9-42796
 Si (111) and (100) surfaces, by reflection high energy electron diff. 9-48752
 Si foils, ion irradi., e. diff. diagrams 9-44697
 Si thin films deposited by electron irradi. of tetramethylsilane 9-44628
 SiCl₄, molec. struct. 9-44319
 Sn films on glass, surface struct. exam. 9-39164
 Sn films on W (110) face, structure from LEED obs. 9-26184
 Ta-N film, lattice struct. rel. to N content 9-23625
 Ta-N system, ordering phases and intrusion superstructures 9-46794
 Ta-O system, ordering phases and intrusion superstructures 9-46794
 TiO₂, reactive vacuum evaporated, struct. determ. 9-42729
 V(100), gas adsorpt., LEED 9-30500
 W, LEED intensities, multiple diffraction origin 9-23778
 W crystal, determ. mean inner potential 9-28273
 W surfaces, C contamination, FEM-LEED studies 9-35071
 WSi₂-n-Si interface, surface structure rel. to barrier height reaction-process dependence 9-42715
 ZnO, (0001) surfaces, LEED obs. 9-28211
 ZnS, blende, cleaved faces, diffuse patterns 9-28274
 ZnS epitaxial films, struct. 9-37684
 ZnSe epitaxial films, struct. 9-37684
 Zr(25 at.%) Ti alloy ω phase, as-quenched form 9-37307

Electron emission

- see also Noise/electrical; Photoelectricity*
 atom-atom collisions, free scatt. model 9-46310
 exo-emission, charged particles discrimination 9-39735
 exoelectron glow curves, temp. position and influence of work function 9-33415
 exoemission, Geiger counter meas. 9-29652
 functions $\psi(r)$, $\psi(y)$, and $\Theta(y)$; for $\gamma \geq 1$; evaluation 9-45027
 hollow-cathode discharge, photoeffect 9-33421
 m.i.m. structure, injected electron currents through insulator 9-35457
 oxide cathodes, eff. of dispersed Ni in coating 9-24245
 positron emission from polyethylene absorber 9-24244
 pyrites, exoemission during the phase transformations, 300°-650°K 9-24248
 sandblasted metals, glow-curve characts. of exo-electrons 9-47212
 Schottky, brightness and directional beam intensity w.r.t. tangential vel. of emission at cathode 9-31912
 surface layers during sliding friction 9-24247
 into vacuum from GaAs p-n junction 9-28529
 Ag-PrO_x-M structure, I-V characts. 9-45029
 Al-PrO_x-M structure, I-V characts. 9-45029
 Al atom, L shell electron and photon emit d simultaneously 9-40553
 Au-PrO_x-M structure, and I-V characts. 9-45029
 Au films, dispersed, emission centres, rad. spectra 9-26606
 BeO, exoelectron emission, self-excitation, diffusion controlled 9-26607
 CaSO₄, e irradiated, exoelectronic emission 9-41402
 GaP, work function, giant temp. depend 9-35514
 LiF, thermally stimulated, effect of surface treatment, ageing and meas. method 9-43138
 Mg atom, L shell electron and photon emitted simultaneously 9-40553
 Ni, ion-neutralization spectroscopy rel. to electronic structure 9-44890
 S atom, L shell electron and photon emit d simultaneously 9-40553
 Si atom, L shell electron and photon emit d simultaneously 9-40553
 Sn-PrO_x-M structure, I-V characts. 9-45029
 W, by metastable inert-gas atoms, adsorbate effects 9-31002
 W, Ge coated, with oxygen adsorption, emission charact. stability 9-45030
 W gas-covered single cryst., ion-induced electron ejection 9-41275
 W(111) and (110), by metastable He and Ar atoms 9-31001

field emission

- band structure of metals determ. 9-37628
 brightness and directional beam intensity w.r.t. tangential vel. of emission at cathode 9-31912
 cineradiographic X-ray tube applic. 9-32097
 cold-cathode systems 9-39736
 dynamics of electron flow from pulsed high current cathodes 9-45923
 electron-molecule interactions, field emitted energy distribution derivative rel. to molecular spectra 9-25725
 examination technique for adsorption 9-41277
 metal in liquid N₂, study of d.c. pre-breakdown phenom. of liq. 9-44581
 metal particles in vacuum, motion reversal and energy increase 9-31003
 metal protrusions, validity of Fowler-Nordheim eqn. 9-49170
 p-type semiconductors, theory 9-31004
 semiconductor, space-charge-limited currents depend. 9-33416
 work function determ. of crystal 9-37628
 Ag-Cs-O photocathodes, external field enhanced photoemission 9-37631
 Cd₃P₂, anomalous temp. depend. of current 9-43139
 CdP₃ 9-24249
 n-GaAs, energy distrib. 9-35517
 n-ge, microwave field, effect of Cs-coating 9-39737
 InSb, field effect and surface photocond. obs. 9-43130
 Mo, Cs and Ba coated, field emitted electrons, total energy distribution measurement 9-45031
 Mo-Re alloys, eff. of ht. treatment 9-24250
 p-Si, nonlinear, depend. on temp. and light intensity 9-26608
 Sr atoms adsorbed on W surface 9-24251
 TiO₂, concept for final photocurrent calc. 9-24236
 W, Cs and Ba coated, field emitted electrons, total energy distribution measurement 9-45031
 W, from single planes with adsorbed CO 9-39176
 W, tunneling of electrons through Zr and χ -N absorbed layers 9-30960
 W, rel. to U adsorption, and preferred growth regions 9-32850
 W single crystal planes, temp. depend. 9-24252
 W tip, shape obs. by electron microscope, comparison with F-N curve, and radii of curvature 9-39738

photoelectric

- Al thin film, extreme u.v., rel. polarization and angle of incidence 9-31072

Electron emission continued**photoelectric continued**

- alkali metal contacts into anthracene, dark- and photo-current meas., trap charact. and optical de-trapping obs. 9-33232
 alkali-antimonide cathodes, thermosensitive discontinuities and hystereses at high light intensities 9-39740
 angular distribution 9-40552
 anthracene, of alkaline metal and alkaline earth electrons, conducting levels obs. 9-47215
 anthracene crystals. 9-49176
 atomic binding energy determ. 9-29961
 from Au cathode u.v. irradi., use in an accelerator 9-46172
 Auger e spectrometer for analysis of contaminants on the surface in ultrahigh vacuum work 9-39150
 band structure determination using photoemission studies 9-37397
 Bell metal, uniqueness of effective atomic number 9-47213
 1,2-benz-anthracene cryst., photoioniz. threshold meas. 9-33424
 bronze, uniqueness of effective atomic number 9-47213
 counting from photon statistics for quantum-mech. photodetector-laser system 9-29395
 electronic structure of solids, optical density of states 9-44876
 exit depth of photoelectron 9-37629
 exoelectron emission, photostimulated, effect of light intensity and electric field 9-37630
 insulator, photo-injection, carriers transport 9-39739
 Joshi effect, cent percent negative in gas phototube beyond threshold photoemission 9-42573
 materials, prep. props. and uses, book 9-49173
 metal cathodes, yield in vacuum u.v., reproducibility and stability 9-26616
 from metal contact into KBr 9-26611
 metals magnetic, density of-state X-ray photoelec. spectroscopy study 9-44886
 metals with dielectric coatings, near u.v. region, reduction of emission 9-26612
 m.i.s. systems, transient photocurrents and internal photoemission 9-39656
 perylene cryst., photoioniz. threshold meas. 9-33424
 photocathodes, emitted electron kinetic energy theory 9-41281
 photocathodes, prep. props. and uses, book 9-49173
 polarization of emitted electrons, effects of electron-magnon inelastic scatt. 9-47214
 pyrene cryst., photoioniz. threshold meas. 9-33424
 rhodamin-B cryst., photoioniz. threshold meas. 9-33424
 Sb-Cs photoelement, spectral sensitivity rel. to voltage changes 9-31006
 semiconductor surface props. determ. 9-43142
 semiconductors, band structure determination 9-37397
 solder, uniqueness of effective atomic number 9-47213
 spin orientation of electrons emitted by circularly polarized light 9-46304
 Transition metals, optical densities of states 9-44891
 into vacuum, escape probability 9-33420
 white gold, uniqueness of effective atomic number 9-47213
 work function computation by Fowler analysis 9-26610
 Ag-Cs-O photocathodes, external field enhanced photoemission 9-37631
 Ag-Mn alloy, studies rel. to electronic structure models 9-45033
 Ag, epitaxial, yield meas. with Lallemand electronic camera 9-45028
 Ag, with u.v. irradi. 9-43143
 Ag plasma resonance 9-33422
 AgMn alloy, energy distrib. meas. rel. to impurity bound states 9-26613
 Ag(Mn) alloys, rel. to virtual resonant bound states 9-45032
 Ag(pd) alloys, rel. to virtual resonant bound states 9-45032
 Al-Al₂O₃ films in vacuum u.v. 9-37632
 Al film in vac., light irradiation, plasma resonance obs. 9-41282
 Au, epitaxial; yield meas. with Lallemand electronic camera 9-45028
 Au, with u.v. irradi. 9-43143
 Au thin film, Extreme u.v. rel. polarization and angle of incidence 9-31072
 AuCu₃ order-disorder eff. obs. 9-26395
 Bi-Ag-Cs sensitivity rel. voltage changes 9-31006
 CdTe, band structure determination 9-37397
 Co₃O₄ energy and yield of photoelectrons in photon range 6.6-11.2 eV 9-41285
 CoO energy and yield of photoelectrons in photon range 6.6-11.2 eV 9-41285
 Cs₃Sb cathodes, thermosensitive discontinuities and hystereses at high light intensities 9-39740
 Cs₃Sb depth, of emission, spectral dependence 9-43144
 Cu-Ni alloy, studies rel. to electronic structure models 9-45033
 Cu-Pd alloys, for band structure 9-33423
 Cu, epitaxial, yield meas. with Lallemand electronic camera 9-45028
 Cu optical densities of states 9-44891
 CuBe cathode, yield in vacuum u.v. 9-26616
 CuMn alloy, energy distrib. meas. rel. to impurity bound states 9-26613
 Cu(Mn) alloys, rel. to virtual resonant bound states 9-45032
 Dy, investigation of electronic structure in spectral range from 3.2 to 11.8 eV 9-39741
 GaAs-Cs-O, low work function, heterojunction model 9-35520
 GaAs-Cs-Sb, heterojunction, mechanism of emission 9-49175
 GaAs-poly-N-vinyl carbazole-Au systems transient photocurrents and internal photoemission 9-39656
 GaAs, activated by Cs and BaO adsorbed layers, spectral response charact. 9-26614
 p-GaAs, Cs coated, transport props. obs. 9-49082
 GaAs_{1-x}P_x covered with low work function layers 9-39742
 GaAs_{1-x}P_x photocathode, p-type, Cs activated, with high quantum yield for visible spectrum 9-49174
 n-GaAs single cryst., external, C-V charact. and work function meas. 9-41283
 n-GaAs single cryst., external, C-V charact. and work function meas. 9-41283
 GaAs surface, effects of heat cleaning 9-35519
 p-GaSb, caesiating and oxidation effects 9-43145
 Gd, ferromag., electron polariz. obs. 9-26615
 Gd, polarization of emitted electrons, effects of electron-magnon inelastic scatt. 9-47214
 Hg-solution interface of electrolytes, mechanism 9-30424
 InGaAs-Cs-O, low work functions, heat treated 9-35518
 K₂CsSb photocathode, energy band scheme 9-28584
 KBr, vacuum u.v.-irradi., F-centre production, photostimulated e. emission obs. 9-30617

Electron emission continued
photoelectric continued

- KCl, vacuum u.v. irradi., F-centre production, photostimulated electron emission obs. 9-30617
 Li₂Co₂O solid solutions, energy and yield of photoelectrons in photon range 6.6-11.2 eV 9-41285
 Li₂Ni₂O solid solution, energy and yield of photoelectrons in photon range 6.6-11.2 eV 9-41284
 LiF cathode, yield in vacuum u.v., eff. of irradi. 9-26616
 NaCl, vacuum u.v. irradi., F-centre production, photostimulated electron emission obs. 9-30617
 Ni(111) surfaces, clean and Cs-covered 9-26617
 Ni films, props. obs., correl with optical props., vacuum u.v. 9-45260
 NiO_{1-x}, energy and yield of photoelectrons in photon range 6.6-11.2 eV 9-41284
 Pb cross-section obs. 84 and 100 KeV 9-44282
 PbO layers, vapour-deposited, Fermi level obs. 9-39722
 Pd, cross-section obs. for 662 keV γ 9-29962
 Pt cross-section obs. 84 and 100 KeV 9-44282
 SrF₂ cathode, yield in vacuum u.v. 9-26616
 Ta, cross-section obs. 84 and 100 KeV 9-44282
 Ta, cross-section obs. for 662 keV γ 9-29962
 VO₂ films, electronic structure obs. 9-24255
 W, with adsorbed methanol, spectra rel. to orbitals involved in surface bonding 9-44634
 ZnSe epitaxial layers on Ge, obs. 9-35417

secondary

- anisotropic from single cryst. temp. depend. determ. from thermal scatt. effect on incident electron mean free path 9-39743
 anthracene, charact. losses, carrier generation process obs. 9-33226
 Auger, electron-excited, efficiencies of prod. and detection 9-33425
 charging of α -active aerosols 9-26139
 exoelectron emission, thermally stimulated, LET dependence 9-37634
 metal surfaces, gas covered, He, O₂, N₂, CO, Ar beams, mechanism 9-31007
 metals, total yield and charact. energy losses 9-31008
 multipliers, for soft X-radiation recording 9-38606
 multiplying action as basis for electron gun design 9-29381
 plasma-metal contact, electron energy spectrum 9-37633
 Al, produced by relativistic primary electrons in high elec. fields 9-31009
 Al film, energy spectrum, prod. by α particles and fission fragments 9-49177
 Cu, from (110) face, fine structure meas. in energy angular distribution, umklapp process 9-28585
 GaP(Cs) dynodes with 20-40 gain 9-24256
 Mo target, bombarded by positive and negative ions of Cl, O and H 9-31010
 Na, core electrons collision with fast primary electrons, energy and angular distribution of excitation 9-31011
 W single cryst., temp. depend. of anisotropic emission 9-39743
 W single crystal, origin of angular depend. 9-37635

thermionic

- see also Cathodes*
 current rel. to cathode space and positive column lengths 9-42571
 currents in the presence of positive ion injection into cylinders and spheres 9-33417
 rel. to electrical conductivity meas. at high temp. 9-44899
 electron density distributions, axially symmetric equilibrium, exact soln. 9-31005
 energy distrib. meas. 9-33418
 high energy, alloy-evaporation processes on hot metal filaments 9-35204
 metal surface, laser-heated, time resolved 9-32835
 oxide cathode, surface distrib., obs. 9-49172
 plasma-metal function, surface ionization, thermodynamic study 9-24260
 rare-earth metal cpds., preparation, coating techniques and properties 9-41279
 refractory materials in vacuo, Ar and Cs vapour 9-43140
 semiconductor diode, current due to strong elec. field, filamentation 9-33342
 B-S-C solid soln. cathode for MHD 9-24253
 BaSrO cathode in nonreactive atmosphere for gas laser use, properties 9-49171
 BaZrO₃ cathode in reactive atmosphere for gas laser use, properties 9-49171
 Cs₂O, CsOH and Cs₂O₃, oxidation products studied by differential thermal analysis 9-26609
 InGaAs-CsO, low work function, heat treated 9-35518
 Mo-(27 at.%)Re alloy single crystal, (100) face 9-47211
 Ta-(20 at.%)Mo alloy single crystal, (100) face 9-47211
 W-(5 at.%)Re alloy single crystal, (100) face 9-47211
 W oxides, properties 9-33419
 W converter electrode, polycrystalline surface, work function investigation 9-24254

Electron energy states *see Crystal electron states***Electron gas**

- see also Metals/theory; Plasma; Solids/theory; Superconductivity*
 Coulomb gas in intermediate coupling region 9-34047
 degenerate, single-particle spectrum, ground state energy 9-47058
 density distributions, axially symmetric equilibrium, exact soln. 9-31005
 diamagnetic susceptibility, size effects 9-24102
 dielectric functions, Lindhard, with finite-electron- lifetime for free-electron gas 9-41142
 dielectric permittivity tensor in field of plane e.m. wave propag. along mag. field 9-41786
 dielectric screening function, self-consistent higher-order corrections 9-31793
 dielectric susceptibility on interaction with e.m. wave field 9-25884
 disordered lattice, localization 9-44895
 entropy of relativistic e gas 9-47787
 fluctuation correlation functions in nonequilib. gas 9-25058
 g factor of two-dimens. interacting e gas 9-24103
 hot, degenerate; Coulomb scatt. on nuclei, ν pair bremsstrahlung calc. 9-42009
 kinetic energy calc., Fermi and Weizsacker contributions non-additive 9-25057
 long-range forces, and vibrational behaviour 9-27190
 in magnetic field, nonuniform, potential difference quantum oscillations 9-30825

Electron gas continued

- magnetic field effects, Vlasov descriptions 9-28035
 magnetism of conduction electron in alternating elec. field 9-28455
 Maxwellian, Compton scatt., relativistic Boltzmann eqn, for photon transport 9-31792
 Maxwellian, photon scatt. rel. to radiant heat transfer calcs. 9-22109
 metal, screening functions, approx. integral eqn. 9-41144
 metal surface, semi-infinite model, self-consistent calc. of electron distrib. 9-47052
 metals, shear viscosity, correl.-function calc. 9-49011
 nonlinear size effects in a mag. field 9-41141
 orbital paramagnetic control, to magnetiz. 9-44894
 photon-plasmon interaction, coupled radiation field 9-22163
 positronium formation by passage of positrons 9-44898
 potential of average force, new coeffs. in expansion in terms of plasma parameter ϵ 9-45797
 quantum electronic spin acoustic waves 9-47027
 quantum theory, anomalous mag. moment in intense field 9-38264
 quasi particle properties 9-26493
 relativistic Lorentz, elastic collision operator, Fokker-Planck form 9-34051
 ring diagram approx. pair distrib. function corrections 9-22151
 in semiconductors, degenerate, recombination radiation during pinch effect 9-49307
 semimetals, potential difference quantum oscillations in nonuniform mag. field 9-30825
 transverse a.c. cond. due to electron interact. with waves in strong d.c. field 9-24082
 white dwarf's envelope behaviour in strong magnetic field 9-31525
 Wigner lattice vibr., anharmonic effects 9-31791
 with anomalous magnetic moments in intense magnetic fields, quantum theory 9-29217
 in LiH, charge-density fluctuations calc. 9-33222
 in O₂, swarm expts. anal., Boltzmann transport equation appl. 9-23344

Electron guns *see Electron beams***Electron lenses**

- see also Electron microscopes; Electron optics*
 axisymmetric, single, spherical aberration meas. 9-36259
 electric-magnetic, non-circular corrected, design 9-25186
 electromagnetic, round with space charge, spherical aberration 9-22354
 quadrupole, spherical aberration considering pole-piece and electrode shape effect 9-43850
 unipotential, using four-electrode gun with apertured accelerating electrode earthed, patent 9-47912

electrostatic

- axial pot., approx. calc. 9-41878
 einzel lenses of three apertures, props. 9-43849
 image formation, trigonometric relationships 9-38352
 periodic focusing system, design 9-36260
 quadrupole, aberrations due to field asymmetries 9-31915
 systems with minimum 3rd order aberrations, design 9-38353

magnetic

- astigmatism-corrected deflection systems 9-36261
 axisymmetric, 5th order spherical aberration 9-41857
 Brillouin focusing, transition region, design and calc. 9-38355
 deflection errors, third- and fifth-order, analysis 9-38354
 focal props. and aberrations, recent data survey 9-34146
 focusing, two aspects 9-31916
 focusing system for t.w.l., patent 9-40323
 for high energy beams design 9-45930
 iron-less, flat helical 9-40322
 klystron quasiperiodic focusing 9-31869
 microscope axisymmetric probe system, 3rd and 5th order aberration correction 9-43851
 objectives with unsaturated pole pieces, design 9-25187
 octopole, cardinal points 9-47901
 octopoles, chromatic aberration 9-47900
 optical charact., influence of hollow supercond. cylinders 9-45929
 quadrupoles, cardinal points 9-47901
 quadrupoles, chromatic aberration 9-47900

Electron microscope examination of materials*see also Ion microscopes*

- Ag sols, prepared on nitrate melts 9-36907
 AgI sols prepared in nitrate melts 9-36907
 albite, artificially produced alpha-recoil tracks for dating 9-47511
 alumina whiskers/Ni composites, roll-bonded and hot-pressed 9-33169
 aragonite, transformation to calcite, to lime 9-26385
 Au sols, prepared in nitrate melts 9-36907
 austenitic alloy, foil, thickness and void size determ. 9-48755
 α -brass, orientation distrib. of crystallites 9-48830
 ceramics, three-dimens. obs. using secondary electron emission mode of scanning microscope 9-32825
 crystal defects, reconstruct. of displacement fields from micrographs 9-23790
 crystal growth by chemical vapour deposition 9-37002
 dislocations, edge, and edge dipoles, close to free surface, contrasts 9-30605
 ferrites, sintered, residual pores behaviour obs. 9-42921
 fibre potentials, scanning electron microscope meas. 9-38344
 fibre strain obs. with electron microscope stage modification 9-32891
 foils from regions near cracks in massive bodies, preparation technique 9-44656
 foils shadowing technique to reveal deformation marking 9-28246
 fractography, two-stage replica technique using Bioten 9-39151
 gelatin gels, vacuum freeze-dried, struct. rel. to cryst. nucleation 9-34936
 glass, three-dimens. obs. using secondary electron emission mode of scanning microscope 9-32825
 glasses, Na₂O-SiO₂, primary and secondary phase separation obs. 9-30455
 graphite-B, neutron irradi., effect of B on interstitial loop clustering 9-30595
 graphite, pyrolytic stress-annealed, imperfections, rel. to graphitization obs. 9-35054
 graphite whiskers, anomalous structures 9-46783
 graphitized C fibres, fine struct. 9-30557
 Gunn effect domains, probing 9-24185
 ice, evaporating, fine surface struct. < 1 μ m thick 9-39129
 image contrast preservation after inelastic scattering 9-42777
 inert gases, defect structure of condensed solid 9-37159

Electron microscope examination of materials continued

- ion-eroded surfaces, topography 9-35048
 lead stearate, multilayer films, struct. determ. 9-39349
 martensite fine structure in transmission electron micrographs rel. to crystallography of phase transformations 9-28397
 nylon 66 fibres, fractographic analyses and prelim. obs. 9-42895
 opal, $\text{SiO}_2 \cdot n\text{H}_2\text{O}$, packing imperf. rel. to stacking faults and polytypism 9-42843
 opals, 3-dimens. packing of spheres, stereopictures determ. 9-40917
 oxide films on glasses and insulators, electrically conducting 9-26182
 oxide powders, calcination process 9-35221
 Permalloy film, rel. to mag. anisotropy 9-26646
 permalloy films obtained by cathode plasma sputtering, struct. exam. 9-40843
 Permalloy layers with non-mag. layer composite, struct. obs. 9-43183
 polycarbonate films, crystallization under acetone vapour 9-26183
 polyethylene annular spherulites, fine structure and deform. mechanism 9-26254
 polypropylene, structure of phases formed on pressure-crystallization 9-46711
 precipitate coherency loss on electron irradiation in h.v. electron microscope 9-28383
 proteins in microdroplets electronically deposited from sprayed suspension 9-42686
 quartz, synthetic, dislocations assoc. with plastic deform. and recovery, transmission microscopy 9-40955
 ribosomes, e microscope exam., statistical anal. to determ. length 9-29110
 scanning, selected area channelling considerations 9-26220
 semiconductor, scanning obs. of monochromatic cathodoluminesc. rel. to microanal. 9-43266
 semiconductor oxides, devices and integrated circuit connections, review 9-32892
 silica gels, vacuum freeze-dried, struct. rel. to cryst. nucleation 9-34936
 steel, austenitic, irradiation, and annealing, He bubbles obs. 9-33108
 steel, austenitic containing Al and Ti, soln.-treated, equil. precip. formed on ageing obs. 9-46949
 steel, Cr-Ni-Mo, orientation relationship between χ -phase and austenite 9-23951
 steel, martensite, low-C internally twinned, tempering charact. 9-41052
 steel, martensite, microtwins 9-46744
 steel, mild, surface-rolled, slip line and crack formation during fatigue 9-35189
 steel, plastic deform., ferrite recryst. 9-37295
 steel, stainless, 304, interfacial free energies 9-28297
 steel, stainless, 304, interfacial free energies 9-28298
 steels, medium carbon St.40, tempering at 250-700°C on dislocation distrib. 9-40948
 thin films transmission sections on solid substrates, ion etching preparation 9-40888
 topography, composition, elec. behaviour 9-30544
 triglycine sulphate, ferroelectric, visualization of domain structure 9-41249
 Ag-Bi eutectic, struct. of Ag-rich phase 9-37131
 Ag-Cu alloys, liq. and vapour quenched, metastable struct. obs. 9-40899
 Ag-S evaporated layer, diffusion processes obs. with photoemission electron microscope 9-40980
 Ag heterogeneous nucleation on W field emitter tip 9-48812
 Al-(15wt.%)Ag alloys, h.c.p. γ plates formation mechanism 9-30738
 Al-Cu alloy θ' precipitate, stacking faults 9-35098
 Al-Fe alloys, Fe-rich, applic. of dark ground microscope to transf. diagram construct. 9-33131
 Al-Mg-Si alloy, images, quality deterioration with specimen thickness, 50-100 KeV 9-23747
 Al-Mg-Si alloys, precipitates influence on recryst. behaviour 9-39452
 Al-(3-15wt.%)Mg alloys, dislocation struct. determ. 9-40946
 Al-Zn-Mg 1 type alloy, blue tint of glossy anodized extruded profiles 9-39833
 Al-(40 wt.%)Zn, alloys, structural changes during ageing 9-23943
 Al-Zn alloys, of dislocation structs. formed from spinodal breakdown by Zn precip. 9-37291
 $\text{Al}_2\text{-xCr}_x\text{BeO}_4$, alexandrite, anti-phase boundaries 9-35104
 Al epitaxial films on NaCl substrates, nucleation and growth struct. 9-36945
 Al foils, cold-worked, annealing processes 9-42909
 Al thin films, surface hillocks prod. by annealing, thermal cycling effect, micrographs 9-30705
 Al thin films evaporated on air-cleaved NaCl, struct. obs. 9-26185
 Au foils, Kr irradiation, damage, energy depend. 9-32957
 Au particles, sintering behaviour 9-26365
 B_2O_3 -PbO-Al $_2\text{O}_3$ system glasses, spinodal decomposition 9-39492
 B filaments, vapour-deposited, crystal structure 9-46780
 Be(OH)_2 powders, calcination process 9-35221
 Ca-3wt.%Al-0.6wt.%Cu alloy, structural changes during precipitation of hard soln. 9-44789
 $\text{CaSO}_4 \cdot 2\text{H}_2\text{O}$, glass-reinforced plaster, fracture studies 9-42894
 CdS photoconductive single crystal, electroacoustic props. correl. with resistivity homogeneities, mirror obs. 9-35502
 CdTe layers growth, struct. depend. on underlying film. 9-40846
 Co-Ni-Si alloys, ferromag., internally oxidised struct. obs. 9-48837
 Co-base superalloys, microstructure, interaction between imperfections and precipitates 9-39298
 Co electroless film, crystallite structure 9-42718
 Co film, high-coercivity, Lorentz microscopy obs. of recorded magnetization patterns 9-45165
 Co films, domain wall width meas. by Lorentz microscopy 9-45166
 CoO single crystal, thin foils prep. method for transmission microscopy 9-42743
 CoO-Co $_3\text{O}_4$ films on Co. struct. and comp. rel. to form above or below allotropic transform. temp. 9-32841
 Cr, pressurized at 10-25 kbars, dislocation distrib. change w.r.t. ductile/brittle transition 9-39427
 Cu-SiO $_2$, strained single crystals, lattice rotations assoc. with structure 9-32911
 α -Cu-Al alloys, short-range ordered state and stable superlattice phase obs. 9-39275
 Cu-(0.2 wt.%)Al alloy, internally oxidised, effect of Si additions on mech. props. 9-46903
 Cu-Ga solid solns., dislocation struct. determ. 9-41045
 Cu-Ge solid solns., dislocation struct. determ. 9-41045

Electron microscope examination of materials continued

- α -Cu-Ge thin films, recrystallization 9-37278
 Cu-Mn-Al phase formation on heat treatment and ageing 9-37293
 Cu-Ni-Fe alloys, spinodal decomposition 9-35242
 Cu-Ti-Al alloys, decomp. nature, struct. change on ageing, electron microscopy 9-46938
 Cu-Ti-Al alloys, decomp. nature, struct. changes on ageing, electron microscopy 9-46938
 Cu, nature of defects produced during electron irradiation 9-35082
 Cu, rolled, orientation distrib. of crystallites 9-48830
 Cu, slip traces on single crystal surfaces w.r.t. non-conservative motion of dislocations 9-39365
 Cu fatigued single crystal, dislocation struct. and persistent slip bands 9-30686
 Cu heavily rolled sheet, struct. obs. 9-39272
 Cu single crystal, propagating fatigue crack, dislocation substruct. 9-33077
 Cu whiskers, growth by halide reduction 9-37111
 $\text{Cu}_{10}\text{W}_{90}\text{CO}$, loss of coherency of Co precipitates due to electron irradiation 9-28383
 Cu-Au ordered alloys, dislocation structure produced by plastic deformation 9-23813
 Dy $_2\text{O}_3$ film, recrystallization under electron beam heating 9-30489
 Er $_2\text{O}_3$ film, recrystallization under electron beam heating 9-30489
 Fe-(0.75 at.%) Mn alloy, annealed, grain boundary fine struct. obs. 9-35102
 Fe-(25 at.%)Al alloys, one- and two-phase struct. obs., magnetiz. and magnetocrystalline anisotropy 9-26648
 Fe-Al alloys, domain struct. and short range order, depend on Al conc. 9-23757
 Fe-Al alloys, Fe-rich, applic. of dark ground microscope to transf. diagram construct. 9-33131
 Fe-Cr-Ni alloy, extrinsic-intrinsic stacking-fault pairs 9-44711
 Fe-Mo alloy precipitates, fine faults and crystal struct. obs. 9-42787
 Fe-Ni-C martensites, twinning during phase transf. in fine struct. obs. from electron micrograph 9-26233
 Fe-Ni-Cr-Be alloy, precip. processes, transmission microscopy obs. 9-39498
 Fe-Si alloys, antiphase boundaries, crystallographic charact. 9-37142
 Fe-Si ordered alloys, antiphase boundaries obs., props. 9-26231
 Fe-(3 wt.%)Si alloy, edge and screw dislocation mobilities, h.v. transmission meas. 9-42829
 Fe-W alloy precipitates, fine faults and crystal struct. obs. 9-42787
 Fe, Bloch wall and stripe domain struct., direct obs. 9-26641
 Fe, electrodeposited, fine structure data 9-36942
 Fe, H-charged, fracture surfaces, crack nucleation mechanism obs. 9-39440
 Fe, prestrained, shock-induced substructural changes, electron microscope obs. 9-32915
 Fe epitaxial layers on oriented Au support, growth modes 9-48759
 Fe film, high-coercivity, Lorentz microscopy obs. of recorded magnetization 9-45165
 α -Fe whiskers growth by deposition, in situ obs. 9-44650
 GaAs:Te, stacking faults 9-23822
 GaSb, cathodoluminescence, investig. 9-24471
 Gd film, nucleation mechanism of twinning due to thermal stresses set up by electron irradiation 9-35100
 Ge, dislocation loops, nature 9-42831
 n-Ge scanning electron micrograph using beta conductive signal, elec. field distrib. 9-46773
 grain growth and surface layer formation obs. by emission microscopy 9-37127
 Ho_2O_3 film, recrystallization under electron beam heating 9-30489
 β -In $_2\text{S}_3$, ordering of In vacancies, associated antiphase boundaries and twins 9-30587
 K $_2\text{O}$ -SiO $_2$ vitreous solids, phase separation obs. 9-41156
 KCl thin films, point defect coagulates due to irradiation during microscope exam. 9-42808
 Li $_2\text{O}$ -SiO $_2$ glass, metastable precipitate formation on heat treatment 9-24215
 Mg-Mn alloys, creep specimens and thermally aged, α -Mn precipitate, obs. 9-28265
 MgO single crystal, mean and anomalous absorpt. coeffs. of electrons 9-32920
 MgO wedge crystals, thickness fringes in micrograph profiles 9-26240
 Mn-Ni constitutional diagram 9-39502
 Mn fine particles prep. by evaporation in Ar, electron microscope and diffraction obs. 9-42790
 Mo as-grown single crystal, grinding and abrasion effect on dislocation struct. 9-42836
 Mo deformed by hydrostatic extrusion, dislocation struct. exam. 9-40950
 Mo foil, secondary recryst. mechanism obs. 9-46923
 MoO $_3$, Moiré pattern due to electron bombardment 9-42791
 N $_2$, defect structure of condensed solid 9-37159
 Na, liquid, interactions with 304 stainless steel 9-28209
 Na $_2\text{O}$ -SiO $_2$ glasses, primary and secondary phase separation obs. 9-30455
 NaCl:Ni, precipitated particles obs. with electron microscope 9-40910
 NaCl thin films, point defect coagulates due to irradiation during microscope exam. 9-42808
 Nb-N system, N precipitates on Nb dislocations 9-30744
 Nb-(75 at.%)Ti quenched alloy, phases and crystal struct. 9-23767
 Nb $_2\text{O}_5$ -WO $_3$ system, non-periodic shear struct. obs. 9-39291
 Ni-C eutectic alloy, flake graphite struct. and defects obs. 9-44671
 Ni-Si alloys, ferromag., internally oxidised, struct. obs. 9-48837
 Ni-base superalloys, microstructure, interaction between imperfections and precipitates 9-39298
 Ni, explosion-shocked, thermal recovery processes obs. 9-44696
 Ni, low-temp. hardening nature and effect on creep at high temp. 9-46913
 Ni electrodeposits, struct. and ductility, effect of metallic contamination 9-37146
 O $_2$, defect structure of condensed solid 9-37159
 Pb-Na solid solns., effect of Ag on discontinuous precip. 9-39500
 PbS-PbTe system, spinodal decomposition 9-39941
 PbSe as-grown single crystal, transmission microscopy obs. 9-46792
 Pd-Si based alloy glasses, amorphous, phase separation and struct., transmission obs. 9-42706
 Pt, quenched, secondary defect obs. 9-23815
 Se-Te system, single crystal growth phenomena 9-36997
 Si, precipitation of boron 9-37164

Electron microscope examination of materials continued

- Si foils, ion irradiat., defect prod. 9-44683
 Si thin films deposited by electron irradiat. of tetramethylsilane 9-44628
 $\text{SiO}_2 \cdot n\text{H}_2\text{O}$, opal, packing imperf. rel. to stacking faults and polytypism 9-42843
 β -Ti foils, preparation for transmission electron microscopy 9-46772
 Te, lateral diffusion of Ag along thin films in Ag-Te couple 9-35135
 ThO_2 gels, calcination process 9-35221
 ThO_2 powders, calcination process 9-35221
 Ti-Cr binary alloys, martensite react., morphology and substruct. 9-26393
 Ti-(8 wt.%) Mn alloy, heat-treated, microstruct. 9-35214
 Ti-(50 wt.%) Nb alloy, struct. 9-42792
 Ti (5 at.%) Mn alloy martensites 9-39311
 U_3O_8 , transmission, O sublattice stability obs. 9-39312
 U foils <2000 Å, prep. 9-23777
 UO_2 , transmission, obs. of electron absorpt. and O sublattice stability 9-39312
 V, neutron-irrad., cylindrical damage cells, transmission obs. 9-44698
 W field-emission tip, shape change and radii of curvature 9-39738
 W surfaces, C contamination, FEM-LEED studies 9-35071
 W tip, reshaping by surface diffusion at 2500°K, form. of solid drops 9-48753
 ZnS epitaxial films, struct. 9-37684
 ZnS epitaxial layers on Si, defects obs. 9-34994
 ZnS oxidation obs. 9-49379
 ZnS polytypes, contrast effs. at 2H-4H interface 9-28275
 ZnSe epitaxial films, struct. 9-37684
 ZrB₂, structure of precipitates, lattice parameters and crystallographic orientations 9-37096
 Zr(25 at.%) Ti alloy ω phase, as-quenched form 9-37307
 Zr-(1 at.%) Nb alloy, corrosion behaviour in pressurized steam and air 9-35747

Electron microscopes

see also *Ion microscopes*

- 3MeV instrument, characts. and features 9-40331
 characteristic image centres, coincidence 9-31918
 contrast due to pot. variations, isolation 9-43855
 emission, surface material determ. from electron energy distribution 9-22357
 emission, with ultrahigh vacuum object chamber 9-47905
 emulsion on glass or mylar film base, sensitivity, edge sharpness and halation for 1000kV beam 9-38357
 filter system, mag., fast 9-40321
 h.-v. (1.5 mv) Toulouse, design and operation 9-31917
 ion-induced emission microscope, design, improved image contrast due to specimen contamination 9-28247
 lenses, superconducting, for 500-kV microscope column 9-36258
 microchamber for obs. at high temp. and controlled press. 9-44655
 million-volt, techniques 9-41879
 Philips EM300, with better resolving power and charact. 9-22356
 REMN mass-produced, with optical grating 9-36262
 scanning, resolving power 9-43854
 scanning, selected area channelling patterns 9-46775
 sensitivity of emulsion and brightness of fluoresc. screen, energy depend. for 100kV to 600kV electrons 9-38356
 specimen heating, rotation and tilt, patent 9-38358
 specimen transfer device, high vacuum, low temp., design 9-36088
 spherical and chromatic aberration correction using mirror with superimposed mag. field 9-25188
 state of the art, survey 9-43853
 Stereoscan Mk II, operation as scanning transmission e microscope 9-43856
 transmission scanning, image contrast 9-47904

Electron microscopy

see also *Crystal structure, atomic*

- aberration, chromatic, and energy loss 9-40320
 aberration, spherical, circumvention rel. holography development 9-22432
 airtight cover for hygroscopic and easily oxidizable substances 9-27284
 beam scattering, highly focused kV by thin film-substrate system 9-35047
 contrast phenomena in emission microscopy 9-40330
 density curves, photographic checking 9-43857
 electrolytic polishing of transmission samples with automatic switching 9-39231
 electronic deposition of sprayed suspensions rel. to sample preparation 9-42686
 foils, preparation for transmission electron microscopy 9-46772
 foils from regions near cracks in massive bodies, preparation technique 9-44656
 image contrast preservation after inelastic scattering 9-42777
 image contrast rel. to beam coherence, in Mollenstedt-type instrum. 9-40326
 irradiated materials, plastic/carbon two-stage replication 9-39445
 linear and nonlinear transfer systems, problems of image interpretation 9-40325
 Lorentz, small-angle scatt. use 9-40327
 Lorentz, stroboscopic microscopy 9-40329
 Lorentz, transmission, for mag. domain structure obs., Foucault technique improvement 9-39233
 Lorentz images, ripple contrast of mag. thin films 9-40328
 Lorentz microscopy at low temps. 9-41880
 in magnetic domains and boundaries visualiz. of ferromag. sample 9-28612
 magnetic domains and walls, diff. contrast study 9-26641
 many-beam images, sensitivity to form of absorption and extinction parameters 9-35049
 mirror, for thermionic converter electrode surface study 9-24254
 phase contrast calcs. for single ats. and at. groups 9-32893
 polymeric samples, preparation method 9-23190
 precipitate coherency loss on electron irradiat. in h.v. electron microscope 9-28383
 probe system, axisymmetric, 3rd and 5th order aberration correction 9-43851
 quality deterioration of images with specimen thickness, 50-100 KeV 9-23747
 resolving power, testing 9-40324
 scanning, selected area channelling patterns 9-46775
 scanning electron micrographs, feature dimensions determ. using stereographic technique 9-39232

Electron microscopy continued

- scattering, small angle, in Lorentz microscopy 9-40327
 scattering by charged spherical particles 9-40332
 spatial filtering of micrographs by laser 9-48053
 specimen charging model 9-39230
 stage modification for straining fibers 9-32891
 transmission, absorpt. effects 9-39312
 transmission, electron scatt. diagram modification due to cryst. defects 9-48845
 unsharp masking technique used in printing micrographs 9-46771
 Be foil preparation using chemical saw 9-39256
 Si thin sample preparation 9-26190

Electron mobility, solids see *Crystal electron states/transport processes*

Electron multiplier phototubes see *Photomultipliers*

Electron multipliers see *Electron tubes; Photomultipliers*

Electron nuclear double resonance (ENDOR) see *Nuclear magnetic resonance and relaxation; Paramagnetic resonance and relaxation*

Electron optics

see also *Beta-ray spectrometers; Electron lenses; Ion optics; Particle optics*

- aberration, chromatic, and energy losses of beams in electron microscopy 9-40320
 aberration, spherical, for round e.m. lens with space charge 9-22354
 aberration rel. Eikonal coefficients 9-25185
 aberrations due to perturbations of rot. symmetry, correction 9-25184
 astigmatism-corrected deflection systems, magnetic line scheme 9-36261
 back-scatter coeff. for oblique incidence of mono-kinetic electrons 9-45928
 beam in accelerator, linear induction, in longitudinal magnetic field 9-48240
 beams deflection, micron-size, air core coils 9-47902
 display LEED, in retarding field analyzer for Auger electron spectroscopy 9-32246
 electrostatic focusing, periodic, theory and experiment 9-31914
 energy spread in instruments 9-40317
 filter system, magnetic, fast, in electron microscope 9-40321
 guns, caustic curves 9-40315
 image contrast rel. to beam coherence, in electron microscopes 9-40326
 image error calcs. for systems with straight axis 9-22355
 imaging system for microminiaturization of stencils 9-22353
 interferometric meas. mag. flux trapped in supercond. hollow cylinder 9-25172
 klystron quasiperiodic focusing by permanent magnets 9-31869
 Lallemand camera with electron multiplier for use in photoelec. studies 9-47903
 in linac, 300 MeV, deflecting syst. 9-46156
 magnetic compression of axially symmetric Brillouin-focused high-current-density electron beams 9-22348
 micro-recorder, TV controlled 9-43852
 mirror, elliptical, focusing and dispersion 9-45932
 mirror, image of potential distributions at object surface 9-22352
 phase contrast calcs. for single ats. and at. groups 9-32893
 quadrupole system for ionization gauge 9-38180
 for shadow images, using adjustable stigmator, patent 9-47911
 systems with minimum 3rd order aberrations, design 9-38353
 textbook 9-29165

Electron pairs

see also *Positronium*

- in nuclear emulsions, energy estimation 9-46142
 $e^+e^- \rightarrow \omega \rightarrow \pi^+\pi^-$, field-current identity and vacuum polarization eff. of hadrons 9-40408
 in He, e-nucleus and e-e coalescence, cusp values and e densities, error cor. 9-40566

annihilation

- bound states and ladder approx. 9-41152
 C-invariance for hadronic processes induced 9-42010
 carbon tetrachloride, positron lifetimes 9-44583
 cosmic-ray positrons in galaxy, spectrum of resulting γ -rays 9-31492
 cross section total, high energy behaviour 9-48159
 cyclohexane, discontinuity obs. for polymorphic transition at -86°C 9-32859
 ladder approx. and bound states 9-41152
 metals, positron thermalization, effect of superconducting transition 9-24111
 in organic media and alkali halides 9-33239
 photon production, double logarithmic asymptotics, cross section formula 9-29547
 polymers, positron lifetimes, correl. with intermol. forces 9-33240
 positron, finite slit-length correction 9-44897
 superconductive metals, positron annihilation 9-26501
 $e^+e^- \rightarrow \mu^+\mu^-$, rel. to causality and e.m. for factors 9-48145
 $e^+e^- \rightarrow \mu^+\mu^-$, backward annihilation amplitude, s-antisymmetrical part double logarithmic asymptotics 9-34256
 $e^+e^- \rightarrow \gamma\gamma$, differential cross section calc., double-logarithm asymptotics corrections 9-34255
 $e^+e^- \rightarrow \omega \rightarrow \pi^+\pi^-\pi^0$, ω^0 partial decay width meas. 9-29545
 $e^+e^- \rightarrow \pi^+\pi^-$, rel. to determ. of ρ parameters 9-36474
 $e^+e^- \rightarrow \pi^+\pi^-$ in ρ^0 resonance region, π e.m. form factor determ., cross section meas. 9-29544
 $e^+e^- \rightarrow \pi^+\pi^-$, γ circular polarization and π form factor calc. 9-29548
 $e^+e^- \rightarrow \rho^0$ meas. by K^0K^0 , 3π decay modes 9-29599
 K^0 prod. from $0 \rightarrow K^0K^0$ used to meas. CP violation 9-46089
 Al, Fermi momentum determ. from annihilation spectra, valence electrons calc. 9-33229
 Ar, positron annihilation, models 9-38785
 Ar, positron annihilation rel. to applied elec-field and Ar density 9-38784
 Ce, γ - α phase transition meas. 9-46946
 Ce, Fermi momentum determ. from annihilation spectra, valence electrons calc. 9-33229
 Co, rel. to cryst. e struct., obs. 9-35325
 Cu-Zn alloy single cryst., Fermi surface change with increasing electrons per atom 9-33241
 Cu, Fermi momentum determ. from annihilation spectra, valence electrons calc. 9-33229
 Cu, rel. to cryst. e struct., obs. 9-35325
 Cu single cryst., temp. effect 9-33242
 GeCl₄, positron lifetimes in liquid 9-44583
 Nb-Al alloys, superconducting critical temp. eqn. parameters calc. 9-39598

Electron pairs continued
annihilation continued

- Ni-Co alloys, spectrum obs. 9-39576
 Ni, Fermi momentum determ. from annihilation spectra, valence electrons calc. 9-33229
 Ni, rel. to cryst. e struct., obs. 9-35325
 Ni (110) crystal, polarized positron annihilation 9-24114
 SiCl₄, positron lifetimes in liquid 9-44583
 SnCl₄, positron lifetimes in liquid 9-44583
 V₂O₅, positron lifetime spectra rel. to semiconductors to metal transition 9-47063

production

- cosmic ray μ , e and μ pair production, energy spectra meas. 9-34348
 cross section, by 1.25-4 GeV electrons 9-27468
 in nuclear emulsions, energy estimation 9-46142
 one-photon prod. in mag. field, probability calc. 9-43974
 quantum theory of creation due to e anomalous mag. moment in intense field 9-38264
 spontaneous formation during mutual approach of heavy nuclei and vacuum polarization 9-48158
 Z-dependence of cross section 9-46063
 by ν , high energy, in field of strong e.m. wave 9-29546
 $\pi^0 \rightarrow e^+e^-$, analysis, rate comp. to 2 photon mode 9-22590
 Ge(Li) detector, meas. of pair-production cross-section as college expt. 9-36522

Electron paramagnetic resonance *see Paramagnetic resonance and relaxation*

Electron probe analysis *see Chemical analysis/X-ray*

Electron resonance *see Cyclotron resonance; Paramagnetic resonance and relaxation*

Electron spin resonance *see Paramagnetic resonance and relaxation*

Electron states in solids *see Crystal electron states*

Electron structure of solids (crystallography) *see Crystal structure, atomic*

Electron structure of solids (energy structure) *see Crystal electron states*

Electron theory

- see also Quantum electrodynamics*
 classical spinning point charge in arbitrary motion, asymptotic properties of radiated field 9-43846
 Dirac, rel. to hidden momentum forces 9-22531
 Dirac eqn. bound state soln. for spherically symmetric pot. 9-48157
 Dirac eqn. for rectilinear periodic motion 9-32134
 Dirac eqn. with equivalent oscillator potential, SU(3) symmetry, exact soln. 9-38468
 Dirac equation, transformation generalization 9-29538
 Dirac monopole flux, relativistic, at mountain heights, upper limit 9-40401
 Dirac particle, one-particle operators 9-29539
 heavy electron 9-48133
 quantum theory of e behaviour at low levels in mag. field 9-22530
 radiative corrections to μ , β decay quantum electrodynamics 9-25403

Electron theory of metals *see Crystal electron states; Metals/theory*

Electron traps *see Crystal electron states/impurity states and effects*

Electron tubes

- see also X-ray tubes*
 alkali plasma diode, d.c. props. 9-38359
 bipolar space charge limited current between coaxial cylinders and concentric spheres 9-47907
 channel multiplier, operation at -78.5°C 9-40333
 image orthicon for low intensity light pulses 9-25378
 klystron, reflex space charge effect on starting current and reflector voltage 9-41852
 magnetron diode, ion current rel. to mag. induction, calc. 9-27287
 meshless shutter with capacity of 9 images 9-29385
 multiplier, Channeltron, pulse saturated, pulse pair resolution 9-47906
 multiplier, high current, beam perturbations improvement on last dynode, patent 9-47909
 multipliers, continuous channel, degradation of gain 9-29384
 multipliers used in pulse-counting mode, detection efficiency variation 9-29383
 physical basis of modern electronics, book 9-47908
 shutter tube for high-speed photography 9-31919
 storage tubes, electron optical current modulation 9-40334
 thermionic conduction stabilization against temperature change, effect of space charge cct. resistance 9-36263
 transit time, magnetic focusing system, for long focussed electron beam along axis, patent 9-45931
 TV camera tube, for high sensitivity image pick-up, patent 9-33405
 vacuum probe, explanation of phenomena based on law of temperature change 9-31726

Electron-phonon interactions *see Crystal electron states/transport processes; Crystals/lattice mechanics*

Electrons

- see also Beta-rays; Cosmic rays/electrons; Crystal electron states; Noise/electrical; Nuclear reactions and scattering due to electrons; Photoelectricity; Plasma; Positronium; Positrons; Space charge*
 This heading includes both negative and positive electrons when the differences between them are of no special significance
 acceleration by electrodynamic space-charge effect 9-32278
 aurora, low-energy spectra and pitch angle distrib., rocket obs. 9-40055
 aurora, primary energy spectra, rocket obs. 9-35851
 auroral, calc. of parameter m by Stormer method 9-45516
 auroral, obs. (1964-7) 9-35848
 auroral precip., presence of mono-energetic beams 9-49475
 auroral temp. and secondary electron distrib., rocket obs. 9-35850
 compression, static, of relativistic rings 9-25547
 density distribution in D-region, comparison of Russian and British data based on same v.l.f. and l.f. propagation 9-37982
 density ionosphere D-region, collision frequencies during quiet sun period, radiowave interaction meas. 9-26947
 diffusion in various gases parallel to elec. fields obs. 9-31909
 diffusion parallel to electric field, theory 9-31908
 Dirac quantized field interacting with classical time-dependent e.m. field, theory 9-38346
 energy distribution in current extraction systems from oxide cathode 9-41278
 energy spectrum, from collision of Ar⁺ ions with Ar atoms 9-22983
 falling, gravitational force, exptl. determ. 9-25421
 fluence from and in conducting mats. due to γ irradi. 9-24066

Electrons continued

- free, trapped, energy levels, transition probabilities determ. using Na atomic beam 9-29540
 hydrated, behaviour during nanosecond pulse radiolysis 9-35756
 ionosphere, low density regions, diurnal, seasonal and spatial variations 9-35876
 ionosphere, production rate variations 9-45529
 ionosphere content, latitude dependence obs. (March 1966) 9-41579
 low-altitude space, back scattered, spatial distributions and time histories 9-38026
 low-energy velocity meas. apparatus, patent 9-38611
 magnetic moment, anomalous, eff. on e.m. field nonlinear Lagrangian 9-38470
 magnetic moment, anomalous, meas. for free electrons 9-29540
 magnetosphere, day side, low energyOGO 3 obs. 9-28916
 membranes, anal. of elec. phenom. by change in absorption for activated samples 9-47695
 near metal in gravitational field, force 9-40405
 metal surface reflection, rel. to surface impedance in weak mag. field 9-26514
 motion, rectilinear, near speed of light in any field 9-36255
 plasma, microwave heating, method 9-30211
 production, Callan-Gross sum rule failure in perturbation theory 9-27463
 relativistic rings, static compression 9-25547
 relativity, general, spherically charged particle model 9-22087
 solvated, yield in polar. liqs. 9-42674
 spin, anomalous torque eff. on g-2 expt. 9-38586
 spin and orbital motion in homogeneous mag. field, g-factor anomaly determ. 9-40404
 system, interaction with external radiation 9-32402
 trapped dielectron, theory 9-46613
 $e^-e\nu$, decay probabilities, effect of e.m. field 9-27469
 in Bi, mean free path, temp. depend. 9-30846

absorption

see also Beta-rays/absorption

in transmission microscopy 9-39312

UO₂ transmission microscopy 9-39312

interactions

- conductivity tensor, nonlinear, of weakly interacting electron system in external elec. field 9-48984
 electroproduction, partial-wave amplitudes, fixed- t dispersion reln. 9-25416
 electroproduction at threshold by current-algebra sum rules 9-43968
 electroproduction of π , kinematic discussion and dynamical model. 9-25460
 e.m. wave, monochromatic, quantized field system, wave function determ. 9-38469
 oscillator well, electric dipole and quantized e.m. field, creation-annihilation operators determ. 9-32133
 π photoproduction, impulse approx. calc. in elastic channel, $E_p=200-500$ MeV 9-25453
 relativistic, collisions with photons, ang. and energy distrib. of γ -quanta 9-29542
 resonant processes in colliding beam expt., i.r. radiative corrections 9-27464
 transition effect for electron-photon shower, calc. 9-43973
 $e^- \rightarrow \mu^- \mu^+$, search, upper limit 9-29541
 $e^- \rightarrow \mu^- \mu^+$, effect of β -interaction 9-43972
 $e^- \rightarrow \lambda \bar{\lambda}$ (λ =part. of arbitrary spin), obs. of timelike form factors and spectral function of photon 9-29534
 $eN \rightarrow eNI$, and $ITN \rightarrow VN$, p - ν analogy model 9-34297
 $eN \rightarrow e\pi N$, pNN^* vertex momentum-transfer depend., dispersion theor. model 9-29604
 $ep \rightarrow e\pi^+ (1236) \pi^0$ prod. meas., f_e , f_{π} , F_1 determ. from excitation curve 9-36471
 CdS, radiative capture by activated recombination r-centres, cross section determ., impurity photo-effect meas. 9-30798

ionization

- H⁺-H, associative and collisional detachment, semi-classical calcs. 9-48429

radiation

- see also Bremsstrahlung; Cherenkov radiation; Electrodynamics; Synchrotron radiation*
 spectrum, moving in const. elec. field 9-43848
 β decay of ³²P, bremsstrahlung spectra obs. 9-22532

scattering

see also Atoms/electron scattering Beta-rays/scattering

- acute angle inelastic, and polarisability of scattering systems 9-44232
 auroral-zone, bounce resonant scatt. 9-28927
 back-scatter coeff. for oblique incidence of mono-kinetic electrons 9-45928
 back-scattering coeff. for bombardment by mono-energetic electrons 9-47011
 benzanthracene, excitation by electron impact 9-30083
 benzene, cross section and spin polarization meas., $E_e=60-1600$ eV 9-23167
 benzene, inelastic, rel. to excitation cross-sections 9-30082
 bismuth triphenyl, cross section and spin polarization meas., $E_e=60-1600$ eV 9-23167
 Boltzmann operator, semigroups 9-34054
 carbon tetrachloride, cross section and spin polarization meas., $E_e=60-1600$ eV 9-23167
 by charged spherical particles, obs. by electron shadow microscopy 9-40332
 Compton scatt. of laser photons, γ polarization meas. 9-36430
 by crystals, single atomic electron excitations 9-40884
 electron-nucleon, inelastic, study using canonical field theory 9-22534
 by e.m. wave, Kapitza-Dirac eff., multiple scatt. approach 9-25142
 ethyl iodide, cross section and spin polarization meas., $E_e=200-600$ eV 9-23166
 fast inelastic, quantum-mech. formulas 9-22533
 film, thin crystalline, scattering origin determ. 9-48757
 film with surface defects, and conductivity 9-49016
 impression of present situation in particle physics 9-22513
 Kapitza-Dirac eff. 9-34242
 metallic surfaces, charact. energy loss spectra, method for clean surface maintenance in vacuum 9-32832
 molecular targets, improvement in the first Born theory 9-40572
 from molecules, real dipoles, diffusion cross-section, vel. depend. 9-34705

Electrons continued**scattering** continued

- molecules, relativistic scatt. factors 9-30017
 - by molecules, resonant scatt., ang. distrib. 9-27855
 - by paramagnetic impurity in metal 9-37383
 - in polar gases, by rotating dipole 9-38819
 - in semiconductor, elastic, effect of e.m. field 9-30901
 - semiconductors, by neutral acceptors 9-28490
 - by solids, backscatt. of 4-12 MeV e 9-44849
 - spectrum distortion by radiative effects, correction method 9-40503
 - in stellar atmospheres, effect on curves of growth 9-47636
 - thickness meas. of coatings and foils 9-29166
 - water, cross section and spin polarization meas., $E_e=60-1600$ eV 9-23167
 - e-N for scatt. on light nuclei 9-25614
 - ed, elastic, high momentum transfers, X-sections, form factors 9-27465
 - ed, recoil-d vector polarization, depend. on e.m. form factor, S and D phase diff. 9-25419
 - ee, elastic, amplitude in quantum electrodynamics at infinite energy 9-40403
 - ep, elastic, amplitude in quantum electrodynamics at infinite energy 9-40403
 - eN, rel. to virtual nucleon compton scatt. 9-32128
 - ev, elastic, detection possibility 9-22536
 - Co, elastic and inelastic channel obs. in reson. scatt. 9-23057
 - Fe-C martensite crystal, diffuse, due to short-range order 9-32912
 - H₂, rot. excitation by electron impact, exchange and polarization effects 9-40591
 - H₂⁺ target, $1s\sigma_g 2p\sigma_u$ transition, asymptotic closure cross section calc. 9-40573
 - by Hg atomic beam, prod. of slow polarized beams 9-40318
 - I₂, cross section and spin polarization meas. $\theta_e=200-600$ eV 9-23166
 - N₂ elastic and inelastic channel obs. in reson. scatt. 9-23057
 - No elastic and inelastic channel obs. in reson. scatt. 9-23057
 - O₂, elastic and inelastic channel obs. in reson. scatt. 9-23057
 - Si solid, interband transition excitation, $E_e=30-200$ eV 9-40887
- scattering, electron-proton**
- 3.963 and 5.159 GeV obs. 9-25420
 - elastic at large momentum transfers 9-34325
 - elastic at large momentum transfers 9-34327
 - high momentum transfer, sum rules and current commutators 9-27466
 - inelastic, field-theory calcs. rel. to scaling laws, cross-sections and momentum of the virtual photon 9-38472
 - initial and final p states spin correlation 9-44052
 - photon, virtual, longitudinal, search for contribution 9-38471
 - polarization phenomena, in high-energy region 9-25417
 - polarization-odd effects, $E_e \approx 10$ GeV 9-25418
 - radiative corrections 9-46061
 - radiative corrections, $N^*(1236)$ resonance contrib. calc. 9-40402
 - target, polarized p designed for 4 GeV expts. 9-27556
 - vector-meson dominance model, longitudinal and transverse cross section calc. 9-29543
 - ep-ep γ , differential cross section meas., wide-angle bremsstrahlung, $E_e=1$ GeV 9-36432
 - p e.m. form factors determ., 15-50 fm⁻² 9-40445

Electrophoresis

- alumina, fabrication with good surface finish 9-35219
- cell, microelectrophoresis, for liq. of low dielec. coeff., construct., field-induced polarization obs. 9-35750
- ceramics, fabrication with good surface finish 9-35219
- dielectric diffusion in direction of increasing dielec. const. for elec. field interact. with subst. 9-42670
- dielectric sphere, transient electrophoresis 9-47463
- dielectrophoresis in lossy dielec. media, theory and biological applcs. 9-28145
- latex particles, sulfonated, zeta pot. meas. and secondary electroviscous effect calc. 9-32801
- liquids of low dielec. const., microelectrophoresis cell construct., field-induced polarization obs. 9-35750
- microelectrophoresis cell for liq. of low dielec. coeff., construct., field-induced polarization obs. 9-35750
- photoelectrophoresis, colour imaging method 9-40389
- spherical dielec. particle, transient electrophoresis 9-47463
- zone, universal separation chamber 9-47883
- C colloidal suspensions, in insulating liq., development of electrostatic charge images 9-44604
- He-Ne mixtures, ionic analysis of cataphoresis 9-42569

Electrophotography see *Photography***Electrophotoluminescence** see *Electroluminescence***Electropolishing** see *Surface structure***Electroproduction** see *Beta-rays/effects; Electrons; Nuclear reactions and scattering/due to electrons***Electrostatic generator** see *High voltage techniques; Particle accelerators/linear***Electrostatic lenses** see *Electron lenses/electrostatic; Ion optics***Electrostatics**see also *Electrets; Electric charge; Electric fields*

- conducting sphere, deformed, pot. energy in elec. field 9-47884
- crystals, potential, rel. to multipoles 9-48980
- cyclotron resonances, effect of field on particle acceleration 9-38347
- deposition in ionic diffusion experiments 9-23409
- droplets evaporation, applied voltage effects 9-34964
- equipotential and field line plots of 2-charge system for the student 9-47716
- fields, homogeneous and heterogeneous media, two-dimensional behaviour using analytic functions 9-45906
- generator, principles demonstration 9-45904
- h.f. waves in non-uniform plasma in mag. field 9-30278
- ionospheric plasma, resonances obs. 9-24684
- Laplace's eqn. solution, validity of representation 9-27159
- orthoclase, cloven in vacuum, electrostatic distrib. obs. on faces 9-37571
- plasma, Poisson and Vlasov eqn. shock-like solns. 9-25868
- point charge between two infinite parallel conducting plates, soln. by imaging 9-45905
- potential of two dielectric layers between metal plates, for any one-dimens. surface charge 9-36246
- potential well for electron flow in spherical geometry, experimental studies 9-30243
- sphere in dielectric medium, dipole moment estimation 9-25160

Electrostrictionsee also *Piezoelectricity*

- of deformable conductors in uniform elec. field, calc. 9-45012
- ionic crystals, finite non-piezoelectric, temp. independent coeffs., equations 9-47186
- in light field, refractive index change, e.m. theory 9-25351
- mixing of light beams, acoustic generation 9-34083
- purification of MHD plasma, patent 9-40668
- CdS photoconductive single cryst., electromech. coupling consts. correl. with resistivity inhomogeneities 9-35502
- KBr, coeff. calc. using theory for finite non-piezoelec. ionic crystal composed of point charges 9-47186
- KCl, coeff. calc. using theory for finite non-piezoelec. ionic crystal composed of point charges 9-47186
- NaCl, coeff. calc. using theory for finite non-piezoelec. ionic crystal composed of point charges 9-47186
- Pb(Zr_{0.5}Sn_{0.5}Ti_{0.5})O₃ ternary system, constants during antiferro-ferroelectric phase change 9-24222

Electroviscous effect see *Colloids; Viscosity***Elementary particles**

- see also *Baryons; Energy loss of particles; Field theory, quantum; Hadrons; Leptons; Nucleons and antinucleons; Nucleus; Particle detectors; Quantum theory; Quarks; Strange particles; and individual particles, e.g. Electrons, Mesons*
- acausal distance existence at high energies 9-41992
- axial interaction, induced pseudo-scalar and parity non-conservation 9-36424
- conference report (1967) 9-46045
- decay of type $s \rightarrow l + 0 + 0$, with parity conservation, test for spin determ. 9-29530
- decaying pairs, interference phenomena in recording 9-48143
- diffraction peak for particles with arbitrary spins 9-48146
- Dirac, bound state of two O(4) composite model 9-48212
- Dirac Coulomb problem bound state soln., Hilbert space for de Sitter group O(4,1) irreducible rep. 9-38444
- discrete quantized states of baryons and bosons rel. to spectroscopy 9-43980
- electric dipole moments, meas. reviewed 9-43960
- elementary text book 9-41993
- experimental methods, conference, 1968 9-38604
- Faddeev eqns. angular-momentum reduction, symmetrical and unsymmetrical coupling schemes rein. 9-41991
- form factor, lower bound, and radius, upper bound 9-25409
- four-particle states configuration-space of arbitrary symmetry, translationally invariant 9-48213
- graduate level text book emphasizing the pole of currents 9-40397
- impulse and momentum metrics, fluctuation 9-43963
- magnetically charged 9-22503
- mass formula using logarithmic function of integral 9-32120
- mass unit, new, derived from flat gravitation theory 9-47733
- massless, multiplet general structure analysis, irreducible corepresentation 9-27447
- one-particle zero-mass helicity state, relativistic invariant decomposition 9-34245
- origin in gravitational interactions during first 10⁻²⁰ sec. of big bang 9-38441
- polarized target technology 9-27445
- radius, upper bound, and form factor, lower bound 9-25409
- recent advances, book on current topics 9-40395
- spin half-odd-integral, first order wave equations 9-32122
- spinning particle, classical treatment, book 9-41766
- spins and parity of resonant states investigated using polarization data 9-27443
- tachyons and their interactions, quantum mechanical description 9-43735
- wave equations for half-odd-integral spin particles 9-32122
- Nd:LaMg (NO₃)₃ p relaxation time of several hundred hours at 0.3-0.4°K rel. to prod. of polarized samples 9-29524

interaction, strong

- in comprehensive textbook on the theory of elementary particles 9-32116
- Regge trajectory residue functions for scalar and vector currents 9-22553
- relationship between strong, weak, e.m. interactions and gravitation 9-41752
- SU(3), involving quark model and Lagrangian theory 9-22552
- theories with too much symmetry 9-25411
- U(3) symmetry 9-32117
- U(6,6) theory 9-22552
- vector dominance model anomaly found in π^+ prod. by polarized photons 9-29581

 μ -e, search for in process $e^+e^- \rightarrow \mu^+\mu^-$ 9-29541**interactions**

- see also *Field-theory, quantum/interactions; Nuclear reactions and scattering. Entries on interactions involving named particles are listed under the particles concerned, e.g. Mesons/interactions; Cosmic rays/effects and interactions*
- Bethe-Salpeter eqn., soln. with square-well potential 9-38449
- classical description and S-matrix theory 9-48152
- cross sections calc. with arbitrary spin, canonical method 9-36425
- cut-off, general class, boson fields 9-22518
- e.m., in the atom 9-44240
- e.m., review of recent developments 9-36426
- e.m., U(3) symmetry 9-32117
- and e.m. interactions 9-25427
- high energy, phase-shift analysis, modification 9-27455
- of a massless part., kinematic factors, discontinuities 9-27454
- multiple formation, asymptotic equalities of cross-sections 9-22519
- non-invariance groups of dynamical systems, construction 9-41739
- One pion-exchange $K^+\pi^-K\pi^+\Delta^{++}$ 7.3 GeV/c, pole extrapolation analysis of 9-25444
- with photons, S-matrix theory study 9-25413
- production processes by U_s, peripheral absorpt. model 9-41996
- Schrodinger two-particle operators, assoc. eigenfunction expansions 9-41995
- spin effect in inelastic processes at high energies 9-43961
- spin-one particle in external e.m. field, equations of motion 9-38451
- strong, e.m. and weak, present status 9-32123
- two-particle and three-particle thresholds, second-type singularities relationship 9-25410
- unstable system, use of a single field operator 9-41994

Elementary particles continued
interactions, weak

in comprehensive textbook on the theory of elementary particles 9-32116
conservation laws formulation for isolation law, isochirality 9-34249
CP violation, quark model and phenomenological weak Hamiltonian 9-38448
CP-nonconserving theories, universal of current-current form 9-48141
current algebra applic. 9-34248
 $\Delta \neq 0$ violation in weak interactions, avoidance 9-34260
decays, leptonic and semileptonic 9-40396
divergences that arise in perturbative treatment of weak-interaction models 9-36428
e.m. corrections, 2nd order, to G_M/G_V for β decay, 9-38582
experimental progress 9-36427
Nagoya modified model 9-34250
neutral neutrino current existence serach for $K^+ \rightarrow \pi^+ \bar{\nu} \nu$ decay mode 9-44011
nonleptonic, leading divergences extended to all orders of perturbation theory 9-41998
nonleptonic decay, selection rules, current x current interactions, review 9-40398
relationship between strong, weak, e.m. interactions and gravitation 9-41752
renormalizable, model; μ and n decay vector coupling constants equality 9-32124
singularity and divergence amelioration, selection rules violation 9-38453
spurion exchange in decay, Heisenberg field theory 9-32106
 $SU(3)$ symmetry breaking model with two angles 9-27480
symmetry of weak and e.m. interactions in a unified model 9-43970
theory based on SU_2 current algebra, $\Delta T = 1/2$ rule and the Cabibbo angle 9-41997
time-reversal invariance of semileptonic weak Hamiltonian 9-38447
 $U(3)$ symmetry 9-32117
V-A theory, analysis of deviations 9-41999
 π production kinematic discussion and dynamical model. 9-25460

scattering

absorptive parts in amplit, relation found to Feynman integral of tetrahedron graph 9-43957
amplitude, physical-region discontinuity eqn., S -matrix macroscopic causality condition 9-36429
amplitude, stable and convergent extrapolation procedure 9-42003
amplitude phase in t -plane, analytic props. 9-46055
asymptotic theorems from analyticity and $SU(2)$ 9-27456
convergent, stable expansions for amplitude, for least squares and interpolation in roots of unity 9-43962
cross sections calc. with arbitrary spin, canonical method 9-36425
data representation by analytic functions, theory 9-48148
Faddeev eqns. used in Ad scatt, AN amplitudes 9-44062
Feynman amplitude for 4 spinless particles, spin J particle exchange, daughters and Weinberg field theory 9-38454
Feynman amplitudes differential props. and independent analytic continuations 9-42001
Feynman amplitudes differential props. for all single-loop diagrams 9-42002
forward, elastic, relation between asymptotic phase and modulus 9-46054
forward scatt. amplitude reln. to backward scatt. cross section 9-34251
Froissart bounds with any spin 9-40400
Froissart-Martin bound, asymptotic expansions 9-42000
helicity amplitudes rel. to polarization meas., high energies 9-48140
high-energy large-angle differential cross section, exponential decrease 9-46053
invariant functions and discrete symmetries for 2×2 processes 9-43964
Jost function poles, physical interpretation 9-25412
Mandelstam representation, asymptotic behaviour 9-46076
non-relativistic time-dependent theory 9-22520
partial wave expansion, convergence problem 9-43958
partial-wave expansion in crossed channel for amplitudes invariant under Galilei group 9-48149
phase-shift analysis, use of τ -criterion 9-46046
polarized targets and spin-0-spin- $1/2$ scatt. 9-27443
potential scatt. amplitude, 2-particle, Gilbert-Schmidt expansion 9-34252
quadrupole irrad. of elementary particles 9-43963
quantum electrodynamical treatment from with vanishing cross-section of finite energy 9-38440
radiative corrections, multiple Coulomb scatt. effect and removal of i.r. divergences 9-38450
relativistic theories and antiparticle concept 9-48147
scattering lengths, complementary bounds calc. 9-32125
Schrodinger two-particle operators, assoc. eigenfunction expansions for time-dependent scatt. 9-41995
soluble model with indefinite metric, s -matrix unitarity in $N\theta\theta$ sector 9-22521
spin 0-spin $1/2$, polarization eff. 9-27446
spin flip and polarization 9-42004
spin zero particles, 2, off shell amplitudes continued to imaginary axis 9-32126
spin- $1/2$ particles, non-Fredholm Bethe-Salpeter equations 9-38455
spin-dependence at very high energy 9-27458
three-body calc. with local potentials 9-48151
three-body off-the-energy-shell amplitudes, analytic continuation 9-43965
three-particle systems, connection betw. resonances or bound states 9-27457
two-body, large angle differential cross-section 9-40399
two-particle systems, connection betw. resonances or bound states 9-27457
vertex functions at large momentum transfer exponential decrease of Wu-Yang type 9-46052
vertex functions of fields belonging to arbitrary representations of Lorentz group, invariant amplitude expansion 9-48150

symmetry
C.e.m. invariance, $X^0 \rightarrow \eta^0 \pi^+ \pi^-$, μ, e branching ratio determ. 9-40416
C.e.m. noninvariance, $\eta^0 \rightarrow \pi^+ \pi^-$, μ, e branching ratio determ. 9-40416
C-invariance for hadronic processes induced by e^+e^- collisions 9-42010
charge, violation in AN interaction, π -photon exchange 9-34332
chiral, results deduced from 9-43979
chiral symmetry, algebraic realization, rel. to Veneziano model 9-42036
chiral symmetry and nonlinear Lagrangians 9-42014
chiral symmetry groups, generalized, rel. to classification of hadrons 9-42015
CP, rel. to $K_{1,2} \rightarrow \pi^0 \pi^0$ interference 9-38512

Elementary particles continued
symmetry continued

CP invariance, hypothesis of long-lived K state with $CP = +1$ disproved 9-22576
CP invariance, $K, \rho \rightarrow pp$ 9-27500
CP invariance and K^0 decay 9-22575
CP invariance in K and Σ decays 9-36427
CP invariance validity, investigation of K^0 decay expts. 9-32119
CP violating parameter determ. from $K_S^0 K_L^0$ regeneration amplitude in Cu at 2.5 GeV/c 9-42065
CP violation, charge asymmetry, violation of T -reversal invariance, $\delta = \delta Q$ rule 9-22581
CP violation, impression of present situation in particle physics 9-22513
CP violation, maximal, in weak interaction model 9-42028
CP violation, possible models for strong weak interac. 9-22516
CP violation, superweak model supported 9-38509
CP violation and $\Delta S = \Delta Q$ 9-29529
CP violation and $K_L \rightarrow \pi^0 \pi^0$ 9-22577
CP violation in the neutral K system, possible origin 9-32169
CP violation in weak hadronic decay 9-36438
CP violation in weak interactions, quark model and phenomenological weak Hamiltonian 9-38448
CP violation model of decays with conservation and violation in second and third orders of primary interaction 9-32118
CP violation parameters in current-current model 9-34246
CP violation superweak model test, $K_L \rightarrow \pi^+ \pi^-$, phase difference in decay amplitudes meas. 9-27501
CP-nonconserving theories, universal 9-48141
CP-violation, hyperweak theory, hadronic and leptonic interactions analysis 9-29528
CPT and locality for self-conjugate multiplets 9-29552
CPT and T invariance test in K^0 decay 9-34285
CPT invariance, Cherenkov counter for comparing lifetimes of π^+ and π^- 9-29655
CPT invariance test of $K^0 \rightarrow \pi^+ \pi^-$ η charge asymmetry determ. 9-38510
CPT theorem, test using comparison of lifetimes of charged pions 9-27513
CPT theorem and odd-dimensional space-time 9-34247
C.P.T violation surveyed 9-22542
current-current models, η_{500}/η_{1370} ratio 9-22578
 $\Delta \neq 0$ violation in weak interactions, avoidance 9-34260
 $\Delta I = 1/2$, $m K \rightarrow \pi \pi$, derivation by method of Nishijima, and its violation 9-32168
 $\delta I = 1/2$ rule, breaking in K decay empirical angle treatment 9-48179
 $\Delta S = -\Delta Q$ in K and Σ decays 9-36427
 $\Delta S = \Delta Q$ and CP violation 9-29529
dynamics 9-36434
electric dipole moments, meas. reviewed 9-43960
e.m. current in unitary symmetry 9-27453
e.m. interactions 9-25427
 $G \rightarrow SO(6,1) \times U(1)$ global dynamical unification group, $SU(3)$ multiplets and baryon wave eqns. rel. to mass formula 9-46070
gemel symmetry and superconvergence relations, for $O(4)$ amplitudes 9-43988
geometrical, rel. to unstable particle spectrum 9-25424
hyperon decay, nonleptonic, new pole model 9-32225
in interactions, strong, weak and e.m. of leptons and hadrons 9-22551
 K -parity for systems with $SU(3)$ and charge-conjugation symmetry 9-42013
Lie algebras, semi-simple, dynamical symmetries as function groups, $s=2r$ realizations 9-25423
Lorentz invariance breakdown, field operators nonvanishing vacuum expectation values determ. 9-41975
minami symmetry and baryon trajectories 9-32208
non-conserved hadronic currents and CP violation 9-43981
 $O(4)$ symmetry of bound state amplitude of two Dirac particles 9-48212
polarization measurement rel. to helicity amplitudes for two-body scatt. at high energies 9-48140
PT violations in p reson. scatt. by nuclei in mag. field 9-29779
 $SI(2,C)$, unitary representations in basis of subgroup $E(2) @ D$ 9-29551
 $SO(4)$ symmetry and Regge trajectories 9-25438
strong-interaction theories with too much symmetry 9-25411
 $SU_2 @ SU_2$ or SU_3 , K_{13} form factors as symmetry probe 9-42017
 SU_3 or $SU_2 @ SU_2$, K_{13} form factors as symmetry probe 9-42017
 $SU(2) \times SU(2)$ chiral current, construction of canonical field theory 9-46041
 $SU(2) @ SU(2)$, non-linear realizations describing π vector meson 9-38434
 $SU(3) \times SU(3)$ breaking and form factors of $K \rightarrow \pi \mu(e) \nu$ 9-44009
 $SU(3)$, prediction, of AKN coupling constant differs from that of KN dispersion relations 9-34294
 $SU(3)$ breaking and PCVC 9-48160
 $SU(3)$ breaking in weak and e.m. interac., model 9-27480
 $SU(3)$ canonical metric for classification of meson-meson low energy processes 9-32162
 $SU(3)$ currents, possibility of universal interaction coupling to 2γ 9-22545
 $SU(3)$ group representation, Fermion operator realization 9-27451
sum rules on basis of asymptotic SU_3 symmetry breaking and strong superconvergence 9-42018
 T violation in Λ , Σ^- decay, search 9-29615
 T -odd and CP-noninvariant correlation in $K_L^0 \rightarrow \pi^+ \pi^- \pi^- \gamma$; $\eta^0 \rightarrow \pi^+ \pi^- \pi^- \gamma$ 9-34278
time reversal invariance and the decay $\pi^+ \rightarrow e^+ \nu_e e^- e^-$ 9-32183
time reversal invariance in e.m. interaction 9-27443
time reversal invariance tests 9-27446
time-reversal invariance of semileptonic weak Hamiltonian 9-38447
 $U(3)$, of strong, e.m. and weak interactions 9-32117
 $U(6,6)$ theory of strong interactions 9-22552
unitary symmetry, e.m. current 9-27453
unitary symmetry and $SU(3)$, introduction 9-25425
CP, CPT, invariance tested in $K_L \rightarrow \pi \pi$ 9-46088
 $\Delta S = \Delta Q$ violation in $\Sigma^+ \rightarrow n \alpha \mu \nu$ decays, branching ratios determ. 9-22632
 η asymm. without C nonconservation? 9-32165
 $K^0 \rightarrow \pi \pi \pi$, CP violation in weak $\Delta T = 1/2$ interactions 9-27505
 $\mu \rightarrow e^+ e^-$ asymm. and spectrum of low energy positrons 9-42011
CP nonconservation parameter determ. from $K_L^0 \rightarrow \pi^0 \pi^0 / K_L^0 \rightarrow \pi^0 \pi^0 \pi^0$ branching ratio 9-34280
 $K \rightarrow \pi e^+ e^- (\mu^+ \mu^-)$, probability and branching ratios estimation 9-27506
 $SU(3)$, V-symmetry props. 9-38478

Elementary particles continued
theory

- causal and time sequence of events reln. 9-38443
- cosmological constant Λ , review 9-45593
- decay, nonleptonic, $\Delta I = 1/2$ rel. to duality and absence of resonances in exotic channels 9-48142
- Dirac theory and existence of magnetic monopoles 9-22503
- dispersion theory sum rules, review 9-48135
- $\Delta S = \Delta Q$, test of rule in $K^0 \rightarrow \pi^0 \nu \bar{\nu}$ 9-27503
- eight-point function, Veneziano model 9-46077
- form factors, e.m. and causality 9-48145
- G_2 -Lie group, properties 9-27452
- Goldberger-Treiman relation, alternative derivation 9-46048
- Goldstone particles, development of corresponding model in solid-state physics with antiferromagnetic props. 9-25405
- Green-Volkov algebra in configuration space 9-32112
- helicity states within hyperplane formalism 9-48137
- impression of present situation in particle physics 9-22513
- magnetic monopoles, multiply charged Dirac, search 9-27448
- mass-splitting parameters, phenomenological, and current-current theory 9-48162
- massless particles, canonical wave eqn. derived from symmetric spinor formulation multipole solns. 9-48136
- massless particles, description 9-38442
- massless particles, localizability in relativistic quantum mechanics 9-29525
- moments electric dipole and mag. quadrupole based on algebra of fields, experimental contradiction 9-48144
- partial differential relativistic wave eqns. with solns. and Poincare invariant 9-25407
- partial wave expansion, convergence problem 9-43958
- Poincare group, representation in $E(2)$ basis 9-43722
- Poincare group, zero-mass representation and conformal invariance 9-41737
- proton, internal structure hypothesis 9-22623
- relativistic eqn. for particles with spin j in the $2[2j+1]$ -component formalism 9-22512
- self-consistency conditions for coupling constants from applying gauge conditions to production 9-46096
- $SO_{6,1}$, external and internal motion unification, $SU(3)$ multiplet mass splitting, no symmetry breaking 9-29527
- space-time variables, removal from description of interior 9-22074
- Spectral function sum rules, T-products in a theory of currents 9-46049
- spin $1/2$ particles, relativistic wave eqns. in Pauli algebra 9-25406
- spin values rel. to rot. vel. and deform. 9-22517
- Sugawara's theory of currents proposed tests 9-46050
- transformation rule, for actual beams 9-25408
- unstable, covariant, creation and annihilation operators 9-29507
- unstable particles, mass distribution, admissibility conditions 9-22602

Elements

- excitation pot. for elements $Z_1=20$ to $Z_2=30$ from stopping-power obs. 9-33208
- physicochemical data, book 9-22026
- shell corrections for elements $Z_1=20$ to $Z_2=30$ from stopping-power obs. 9-33208
- solids and liquids, vapour-pressure, melting point and boiling point data 9-46689
- synthesis of new elements, review 9-44105
- transuranic, production 9-25608
- transuranium, synthesis, popular articles 9-44148
- C-Cu, theoretical wavelengths for K α -type X-ray emission in stars 9-24432
- He, abundance in population II stars, rel. to cosmological big-bang model, problems in soln. 9-43539
- He primeval abundance, variations, rel. to early galaxy formation 9-26980

origin

- see also *Cosmology; Thermonuclear reactions*
- model for their synthesis within objects exploding at very high temperature 9-45585
- popular article on their synthesis in the universe 9-49522
- in stars, synthesis during C thermonuclear burning 9-40142
- $^{208}\text{Pb}(n,\gamma)^{209}\text{Pb}$, activation cross sections, range relevant to stellar nucleosynthesis 9-42292
- B, from nuclear reaction in sun, α induction inclusion 9-36015
- ^{10}B , ^{11}B , production in p nuclear spallation of ^{12}C 9-36601
- Be, from nuclear reaction in sun, α induction inclusion 9-36015
- Ca $^+$ in upper atmosphere, obs. and theory 9-35832
- H, search for mass proportional creation in Hg 9-45588
- He prod. in 'big-band' expansion, rel. to effect of beta decay rate of a neutron 9-44058
- K 9-35832
- Li 9-35832
- Li, from nuclear reaction in sun, α induction inclusion 9-36015
- Na 9-35832

relative abundances

- in A field stars, mood atmosphere abund. analysis 9-43527
- A stars, peculiar, heavy- element abundances 9-31526
- in cosmic rays and universe, comparison 9-34341
- in γ Gem star, model-atmosphere abund. analysis 9-43527
- in HD 2421 star, model-atmosphere abund. analysis 9-43527
- heavy-elements in peculiar A stars 9-31526
- HR 5317, close binary, from curve of growth analysis 9-35995
- interstellar abundance anomalies 9-24724
- K giants, of C, O, and N 9-43528
- metal-to-H ratio in G8-K2 giants determ. with BVR photometry 9-27012
- metals, effect on K-line absolute magnitudes 9-31542
- metals, richness of stars in nuclei of galaxies, CN absorpt. obs. 9-31501
- NGC 7662, planetary nebula, and ionization stratification 9-35959
- in o Peg star, model-atmosphere abund. analysis 9-43527
- rare earths in CaF $_2$, spectrochem. determination 9-33695
- rare earths in sun 9-41687
- rare-earths in GaAs, ultra-trace determination 9-33696
- α Serpents, metal abundance ratios from curves of growth 9-35982
- stars, late type, evolved, technique for obtaining differential abundances 9-49543
- in stars, synthesis and distrib. theories 9-35969
- stellar abundances of light elements 9-35968
- trace, in iron meteorites, analytical methods 9-28835
- in ultramafic rock, rel. to upper mantle 9-47505

Elements continued**relative abundances continued**

- in θ Vir star, model-atmosphere abund. analysis 9-43527
- WZ Cassiopeiae, twenty-seven elements from spectral anal. 9-49554
- Be in Ib supergiants and Cepheids 9-24796
- Ca $^+$ in upper atmosphere, obs. and theory 9-35832
- Ce, in sun, from equivalent widths and central intensities of Ce II lines 9-40187
- H/He ratio in stars, effect on atm. structure 9-24767
- H, intergalactic, distrib. and contrib. to mean mass density of Universe 9-40120
- H $_2$, interstellar 9-43565
- H in gaseous nebulae, high-level populations 9-28992
- He, of stars in globular cluster M15 9-27044
- He, solar, rel. to ν detection by $^{37}\text{Cl}(\nu, e)^{37}\text{Ar}$ 9-45682
- He in H II regions, radio recombination lines obs. 9-35964
- K 9-35832
- Li 9-35832
- Li depletion in main sequence stars, observational time-scales 9-35973
- Li in Ib supergiants and Cepheids 9-24796
- Na 9-35832
- Si burning in stars and sun, equilibrium distrib. of elements 9-49549

Emission spectra see *Luminescence; Spectra; X-ray spectra/emission***Emissivity**

- air, radiating power in range 0.2 to 3μ at 10^4K , 1 atm. 9-40753
- air plasma, meas. in vacuum u.v. region 9-48590
- angular radiation coeff. for elements of cylindrical arch on rectangular base 9-40281
- black body cylindrical cavity with temp. gradient, radiating power 9-41837
- cavities, by measuring reflection factor 9-27237
- of cavity radiator, meas. methods for pyrometry applic. 9-27251
- of cylindrical cavity with diffusion 9-41838
- furnace, radiative transfer between gas and wall including emissivity of wall 9-34832
- materials, up to 100°C , meas. 9-28678
- metals, high m.p.t., effect of oxide films 9-28435
- of metals, high temp., refractory 9-39537
- of metals, rel. to surface roughness 9-43233
- methane, spectral in 3.3μ band at 297, 673 and 923°K 9-46401
- natural surfaces, 8-14 microns spectral region 9-31278
- non-diffuse cavity surfaces, calc. 9-31859
- opaque substance, surface porosity effect on emittance 9-49269
- plane surface, total hemispheric emissivity meas. with conventional thermal cond. apparatus 9-26462
- silicates, i.r., obs. and cloudy atmosphere model of spectral emission from condensed powder 9-28693
- spectral reflection factor meas. equipment for use in $15\text{-}2100^\circ\text{C}$ and $4000\text{-}12000 \text{ \AA}$ range 9-38311
- steel, 304 stainless, cryogenic temp., cyclic incident radiation technique 9-24064
- surface radiation, rel. to macroscopic roughness 9-41359
- thermal radiation, e.m. tunneling between highly absorbing media 9-37372
- Al, cryogenic temp., cyclic incident radiation technique 9-24064
- Al, SiO $_2$ -coated, determ. 9-37373
- Ar temp. range $6000\text{-}12000$ for 1,10 and 100 cm layers 9-26035
- BiSb alloys, emission of microwave radiation in weak electric field 9-31102
- CO $_2$ -H $_2$ O mixtures, analytical calc. 9-26028
- CO $_2$ radiating power in range 0.2 to 3μ at 10^4K , 1 atm. 9-40753
- CaF $_2$, and thermal radiation, obs. 9-35651
- Cu, cryogenic temp., cyclic incident radiation technique 9-24064
- H $_2$ O temp. range $6000\text{-}12000$ for 1,10 and 100 cm layers 9-26035
- H plasma 9-48554
- H temp range $6000\text{-}12000$ for 1,10 and 100 cm layers 9-26035
- He temp. range $6000\text{-}12000$ for 1,10 and 100 cm layers 9-26035
- MO, relationship with specific electrical resistivity above 400°K 9-39547
- Mo, effect of oxide film 9-28435
- Mo spectral emittance, i.r. 9-45327
- N $_2$ plasma, meas. in vacuum u.v. region 9-48590
- N $_2$ radiating power in range 0.2 to 3μ at 10^4K , 1 atm. 9-40753
- NH $_3$ temp. range $6000\text{-}12000$ for 1,10 and 100 cm layers 9-26035
- Nb, relationship with specific electrical resistivity above 400°K 9-39547
- Nb spectral emittance, i.r. 9-45327
- NbC, hemispherical and monochromatic power and specific resistivity, $1200\text{-}3500^\circ\text{K}$ 9-39548
- NbC $1200\text{-}3500^\circ\text{K}$, 0.65μ obs. 9-37374
- O $_2$ plasma, meas. in vacuum u.v. region 9-48590
- Sn $_2$ vapour 9-42612
- Ta-Nb alloys, spectral coeff. 1300 to 2000°K at 0.65μ 9-40795
- Ta integral hemispherical radiating power, 1200 to 2800°K 9-43018
- Ta spectral emittance, i.r. 9-45327
- TaC $1200\text{-}3500^\circ\text{K}$, 0.65μ obs. 9-37374
- Ta+10%W, relationship with specific electrical resistivity above 400°K 9-39547
- Ti, relationship with specific electrical resistivity above 400°K 9-39547
- TiC $1200\text{-}350^\circ\text{K}$, 0.65μ obs. 9-37374
- W, spectral, discrepancies in measured data 9-26744
- Zr spectral emittance, i.r. 9-45327
- ZrC, $1200\text{-}3500^\circ\text{K}$, 0.65μ obs. 9-37374
- ZrC, hemispherical and monochromatic power and specific resistivity, $1200\text{-}3500^\circ\text{K}$ 9-39548

Emulsions
see also *Colloids*

- aqueous, film curvature at oil/water interface 9-34935
- film curvature at oil/water interface 9-34935
- particle size by light scatt. 9-36906
- photographic, density and exposure relationship, linearity conditions 9-29494
- photographic, linear multiple image storage 9-36409
- polymers with polar groups, orienting effect of aqueous phase on structure 9-32803

Emulsions, nuclear see *Nuclear track emulsions***Emulsions, photographic** see *Nuclear track emulsions; Photographic materials***ENDOR (electron nuclear double resonance)** see *Nuclear magnetic resonance and relaxation; Paramagnetic resonance and relaxation*

Energy bands *see* *Crystal electron states/band structure;*

Metals/theory; Semiconducting materials; Semiconductors

Energy gaps *see* *Crystal electron states/band structure; Semiconducting materials; Semiconductors; Superconducting materials; Superconductivity*

Energy levels *see* *Atoms/structure; Molecules; Nucleus/energy levels; Spectra*

Energy loss of particles

α -particle energy struggling through gases 9-29818
alloys, inhomogeneous, electron loss meas., effect of elastic constraints 9-48978

amorphous compounds, stopping of kV ions by elastic collisions 9-36678
charged particle moving in a medium with ionization losses and in a non-uniform magnetic field 9-44094

by crystal, spatial and energy distrib. of scatt. ions 9-48979

crystals, rad. damage, anisotropic effects 9-33202

cylindrical targets, attenuation factor for scattered radiation 9-44850

electron beams, 20 eV to 50000 eV, absorpt. in air and plastic 9-37376

electron energy and angular distribution after passing through barriers of varying thickness 9-24075

electron energy distribution after passing through barriers 9-24074

electronic stopping, structure effects 9-33209

electrons, mean projected range calc. at high energies 9-47014

electrons energy dissipation by normally incident monoenergetic beams, algorithm 9-41121

elements $Z_1=20$ to $Z_2=30$, excitation pot. and shell corrections calc. from stopping-power meas. 9-33208

gaseous mixtures, stopping of kV ions by elastic collisions 9-36678

ion penetration in amorphous target 9-42983

ions in semiconductors 9-35411

ions range in cryst. rel. to focusing and channelling 9-35294

linac beam, detection system using self-powered γ -ray detectors 9-36546

luce, energy-loss spectra for high-energy electrons as function of depth 9-37377

metal films, evaporated, low energy protons and deuterons 9-28439

in motion in nonlinear plasma 9-30215

in random inhomogeneous medium, two methods 9-29371

stopping power of heavy ions in few MeV range, meas. 9-42985

stopping power of matter for protons and muons, contribs. of spin, mag. moment and factors 9-44855

Ta, stopping power, 5-13.5 MeV protons, deuterons, 8-20 MeV ^3He , ^4He 9-22780

track visualization in plastics, charged particle registration 9-25540

transition metal dichalcogenides, of electrons, rel. to band structure 9-30804

transition radiation prod. by 20-50 MeV electrons in opt. freq. range, meas. of fast particle energy 9-40504

α in air, particle path length determ. 9-45716

α in flames, temp. meas. 9-38320

p in Al single crystal, channeled along [110] direction 9-30801

p in H, in proportional counter 9-46137

^{252}Cf heavy ion source, attenuation in Al, Ag and Au foils 9-28440

Ag, electron loss spectra in i.r. region 9-28441

Ag, electron maximum range, 15 MeV, exptl. determ. 9-26470

Ag colloidal particles, electron m.f.p. limitation, refractive index meas. 9-41115

Ag foil target, ^{252}Cf heavy ion source 9-28440

Al, 0.5-30 keV protons 9-30807

Al, by protons, range and energy loss meas., $E_p=100$ -660 MeV 9-33213

Al, electron loss spectra in i.r. region 9-28441

Al, electron maximum range, 15, 4.1 and 9.8 MeV, exptl. determ. 9-26470

Al, electrons, fast, factors affecting range meas. 9-35302

Al, high energy electrons, measured loss 9-39551

Al, low-energy depth distributions obtained by sputtering 9-47013

Al, stopping power for 0.6-2.4 MeV protons 9-33212

Al films, electron spectra, convolution effects by electron transmission 9-47015

Al foil target, ^{252}Cf heavy ion source 9-28440

Al stopping power, 5-13.5 MeV protons, deuterons, 8-20 MeV ^3He , ^4He 9-22780

Ar stopping power for ions ($Z=3$ -13) 9-39014

Au, electron maximum range, 15 MeV, exptl. determ. 9-26470

Au, fast ions channeled in single cryst., pot. energy and stopping power 9-30805

Au, fast ions channeled in single cryst., pot. energy and stopping power 9-30806

Au, of Pb in collision cascades, 3-169 eV 9-39552

Au foil target, ^{252}Cf heavy ion source 9-28440

Be, electron loss spectra in i.r. region 9-28441

Be, electron maximum range 15 MeV, exptl. determ. 9-26470

Bi, 0.5-30 keV protons 9-30807

C, 0.5-30 keV protons 9-30807

C, by protons, range and energy loss meas., $E_p=100$ -660 MeV 9-33213

Cu, $^2\text{H}(d, n)^3\text{He}$ reaction, channelling of deuterons parallel to 110 lattice rows 9-40518

Cu, 0.5-30 keV protons 9-30807

Cu, by protons, range and energy loss meas., $E_p=100$ -660 MeV 9-33213

Cu, electron maximum range, 15 MeV, exptl. determ. 9-26470

Fe, 0.5-30 keV protons 9-30807

Ga, solid and liq. foils, energy loss spectra of 50 keV electrons 9-41148

Ge, 0.5-30 keV protons 9-30807

Ge, stopping power for p of 0.35-5.50 MeV 9-30808

In, stopping power for 0.6-2.4 MeV protons 9-33212

KAl(SiO₃), energy-loss spectra for high-energy electrons as function of depth 9-37377

KCl, low-energy depth distribts. obtained by sputtering 9-47013

Nb, back-scattering of keV hydrogen ions 9-39549

Ne discharge, of primary electrons 9-48622

Ni, 0.5-30 keV protons 9-30807

Pb, by protons, range and energy loss meas., $E_p=100$ -660 MeV 9-33213

PbSe, characteristic electron energy losses 9-39553

PbTe, characteristic electron energy losses 9-39553

Pt, low-energy depth distributions obtained by sputtering 9-47013

Sb, 0.5-30 keV protons 9-30807

Si, 0.5-30 keV protons 9-30807

Si, range of implanted B, P and As 9-44856

Si cryst., proton planar channelling, energy spectrum temp. effects 9-37378

Si(Li), energy-loss and straggling by high energy electrons, π^+ , and protons 9-30810

Energy loss of particles continued

Sn, by protons, range and energy loss meas., $E_p=100$ -660 MeV 9-33213

Sn, solid and liq. foils, energy loss spectra of 50 keV electrons 9-41148

SnTe, characteristic electron energy losses 9-39553

Ti, 0.5-30 keV protons 9-30807

Ti, back-scattering of keV hydrogen ions 9-39549

UC, 'channeling'-effect, applic. to fission gas release studies 9-37214

UO₂, 'channeling'-effect, applic. to fission gas release studies 9-37214

W, desorption spectrum of trapped rare gas ions obs. 9-36970

Zn, stopping power for 0.6-2.4 MeV protons 9-33212

Enthalpy *see* *Thermodynamic properties*

Enthalpy measurement *see* *Calorimetry*

Entropy

see also *Thermodynamics*

compound system, extremum principle 9-43799

crystallized solid of long chain molcs. 9-22139

definition in non-equilibrium states 9-43762

derivatives at absolute zero 9-29159

of electron gas, relativistic 9-47787

in ergodic theory, book. 9-47793

Gibb's law validity in strongly coupled systems 9-38251

ideal and non-ideal systems, entropy differences, classical and quantum fluid cases 9-41780

kinetic eqn. of strongly coupled system, microscopic interpretation 9-22143

linkage significance in theory of measurements 9-25020

liquids, square well with infinite walls calc. 9-30385

nonlinear optical effects 9-47308

production in two-phase mixture, nonequilibrium relations 9-46677

reactions, var., determination from exptl. equil. curves, method 9-37814

vaporization, inorganic gas, b.p. molecular weight and volume meas. 9-34965

properties of substances

adsorbed surface layer on model cryst., change due to layer 9-37311

9,10-anthraquinone, calc. for ideal gas 9-46418

1,4-naphthoquinone, calc. for ideal gas 9-46418

semiconductors and semimetals, excess entropy of fusion due to configuration of bonding electrons 9-28175

steam, 0-800°C, 0-1000 bar, using a new eqn. of state 9-34831

Ag-Au solid soln., vibrational entropy and thermal vibrations, correlation 9-33151

Al-Ag dilute solid solution alloys, vibrational entropy, electronic influence 9-39508

Al-Bi system, excess entropies from phase equil. obs. 9-46679

Al-In system, excess entropies from phase equil. obs. 9-46679

Al-Zn dilute solution alloys, vibrational entropy, electronic influence 9-39508

BiF₃, of fusion and sublimation 9-30021

Cd-Hg alloys, entropies of mixing, rel. to phase equil. and transform. 9-48878

Cd, rel. to enthalpy of sublimation 9-39146

CeMg(NO₃)₆ pure dipole-dipole system, and susceptibility 9-45054

Cu-Th system, excess entropies from phase equil. obs. 9-46679

CuAu II alloy, of disorder, phase transition from CuAu I 9-30750

He superfluid component 9-23567

Hg-Ga liq. alloys, excess entropies 9-30369

Hg-Pb alloys, liq., excess, from anal. of enthalpies of mixing 9-39091

Hg-Sn liq. alloys, excess entropies 9-30369

Hg-Ti alloys, liq., excess, from anal. of enthalpies of mixing 9-39091

KBr, exptl. data analysis, rel. to anharmonic contrib. 9-24048

KCl, exptl. data analysis, rel. to anharmonic contrib. 9-24048

MnCl₂·4H₂O, 0.4°-4.2° in mag. fields 9-44835

NaCl-H₂O system, phase entropy diagrams for different compositions 9-26161

NaCl, exptl. data analysis, rel. to anharmonic contrib. 9-24048

Ni-Mo alloy, H solubility, conc. depend. of entropy of soln. 9-39478

Ni-W alloy, H solubility, conc. depend. of entropy of soln. 9-39478

Pb-Ti dilute solid alloys, vibrational entropy, electronic influence 9-39508

TiNO₃ fused, m.p. heat and standard entropy of vaporization meas. 9-34966

Zn, rel. to enthalpy of sublimation 9-39146

Epitaxy

see also *Crystals/growth*

deposition chamber, patent 9-30527

p- dihalobenzenes, heterogeneous nucleation on cleansed alkali halide cryst. 9-37105

epitaxial growth on collodion, rock salt and mica obs. by electron diffraction 9-30492

films, grown on high-alloyed GaAs substrates, defects 9-36944

garnet film, growth on non-garnet single crystal, patent 9-46723

group IV-VI alloy films, growth techniques and surface research 9-39157

growth from mol. beams, model 9-26216

islands in growth of heteroepitaxial films, rotation and translation 9-46722

layer growth from vapour phase through liq. alloy, low temp. deposition, patent 9-30530

layer thickness meas. by i.r. interference method 9-30482

of metals, f.c.c. evaporated on to alkali halide substrates, effect of electron bombardment 9-46760

metastable thin film epitaxial struct., growth, review 9-34987

polytypism model 9-44638

surface-active impurities effect 9-42721

Ag on MgO, in electron microscope, (100) cleaved surface mechanism determ. 9-39220

Ag on NaCl, rel. to nucleation 9-23689

Al on NaCl, nucleation and growth structure 9-36945

Al thin films evaporated on air-cleaved NaCl, structure, electron microscope obs. 9-26185

Au evaporated on Ag substrates, effect of surface imperfections 9-37112

Au films on NaCl, rel. to H₂O contamination 9-46724

Au on MgO, in electron microscope, (100) cleaved surface mechanism determ. 9-39220

Au on NaCl and KCl, effects of forced high nucleation densities 9-32843

C on diamond 9-35033

Cd electrodeposits, growth on Cu single crystals 9-30490

CdS films, prod. by gas transport reactions 9-42722

CdS on GaAs, heteroepitaxial growth hillocks and crystal structs. 9-48758

CdS single cryst. layers growth on ZnS platelets 9-34988

Epitaxy continued

- CdTe thin film, co-evaporated, nucleation and structure, influence of stoichiometric deviations 9-36949
 Cu continuous (001) film on rocksalt, changes in twin structure during growth 9-39158
 Fe₂O₃ films on steel, in growth characteristics in dil LiOH soln. at 300°C 9-39952
 Fe films, recrystallization 9-42723
 Fe layers on oriented Au support, electron microscope exam. 9-48759
 GaAs, chemically-deposited layers, growth and perfection 9-36951
 GaAs, growth, effect of facet development on ¹²⁵Te distribution 9-36985
 GaAs:P_{1-x} liq. layers growth in Ga-GaAs-GaP system 9-36917
 n-GaAs high-purity layers prep. and props. 9-39097
 GaAs layers, donor extrinsic photoconductivity meas. in mag. fields 9-39717
 GaAs p-n junction and Schottky barrier diodes, guard rings growth 9-30943
 GaP:Zn growth on GaAs and GaP substrates by water vapour transport method 9-30529
 GdFe garnet epitaxial film, prep. by r.f. sputtering mag. and structural props. 9-49210
 Ge:P layer production by spark doping 9-39159
 Ge, films from GeCl₄-H₂ system, smooth surface conditions 9-36948
 Ge films, growth on GaAs by GeI₂ disproportionation reaction 9-36947
 Ge films, heteroepitaxy on GaAs 9-36946
 Ge films on GaAs 9-36946
 Ge growth by GeCl₄-H₂ reaction, rate obs. surface morphology 9-46761
 Ge layer, epitaxially-grown, distribution of imperfection centres 9-37158
 Ge layers on GaAs, plastic deformation 9-37241
 HgTe films, growth and transport props. 9-28214
 InAs_{1-x}P_x single cryst. layers prep. by vapour-deposition 9-30910
 InP growth on GaAs substrates in open flow system 9-23630
 Ni film on Cu, pseudomorphic growth 9-34989
 NiO single crystals, growth by vapour hydrolysis of NiBr₂ on MgO 9-35034
 PbS on rocksalt, film growth mechanism 9-40844
 PbTe, growth on NaCl, substructural transitions in early stages 9-26186
 PbTe on rocksalt, growth and morphology 9-37113
 PbTe thin film, co-evaporated, nucleation and structure, influence of stoichiometric deviations 9-36949
 Si(-Sb) film, on spinel substrate, Hall effect and resistivity meas. 9-36950
 Si, chemically-deposited layers, growth and perfection 9-36951
 Si deposition by H₂ reduction of chlorosilanes, gas press. and velocity effects 9-28215
 Si films, growth on Si substrate and oxide layer, role of surface migration 9-30491
 Si layer growth from vapour phase through liq. alloy, low temp. deposition, patent 9-30530
 Si layers, C conc. obs. 9-46725
 Si p-n junction, epitaxial, for photoelec. converters 9-31904
 Si single crystal film on sapphire, charact. 9-34990
 SiC p-n junctions, avalanche breakdown 9-35442
 Sn film, residual strains rel. to mismatch at interface 9-39160
 YFe garnet films, ferromag. reson. 9-45372
 YFe garnet films on YAl garnet and GdGa garnet, microwave phonon generation 9-44816
 YFe garnet films with narrow ferrimagnetic resonance linewidth, growth 9-36952
 Zn electrodeposits, growth on Cu single crystals 9-30490
 ZnO thin film of CdS, sapphire, by sputtering 9-36953
 ZnS films, optical props. and struct. 9-37684
 ZnS films evaporated on to NaCl, epitaxial growth 9-32844
 ZnS layers on Si, defects obs. by transmission electron microscopy 9-34994
 ZnS on W or Mo substrates 9-28216
 ZnSe, epitaxial, high purity preparation 9-36954
 ZnSe films, optical props. and struct. 9-37684
 ZnSe layers on Ge, preparation process 9-34991
 ZnSe on Ge, close-spaced HCl process 9-37114
 ZnSe on Ge, elec. and photoelec. props. 9-35417

Equations

see also *Differential equations; Integral equations*

- Bargmann-Wigner, satisfying classical fields on space-like mass shells 9-38204
 Bergman-Wigner eqn. theory of confluence 9-34239
 Bethe-Salpeter non-Fredholm, for scatt. of spin-1/2 particles 9-38455
 Boltzmann chem.-kinetic eqn., variational soln. 9-39934
 Boltzmann eqn., 2-time doublet including delayed neutrons 9-27774
 boundary-value, problems nonlinear, existence of solutions 9-47725
 difference, f(n+1)+f(n-1)=[E- π (n)]f(n); spectral theory 9-36113
 difference, for two-dimensional elastic flow 9-34067
 Diophantine, soln. by ALGOL 60 algorithm and program 9-29170
 Duffing, generalized with large damping 9-22179
 electron-hydrogen atom scattering, multiple solutions of Hartree-Fock equations 9-36682
 Eulerian, of precession and nutation of self-gravitating bodies, soln. 9-47618
 Hartree-Fock and Hartree-Bogoliubov eqns. with exact symmetries 9-27189
 hydrodynamic, in tensorial form valid for any curvilinear coordinate systems 9-40635
 ionospheric continuity, inclusion of particle source of ionization in continuity equation 9-31400
 Kråmers, exact time-depend. analysis 9-43768
 laminar boundary layer, governing transient free convection heat transfer from vertical semi-infinite plate 9-22291
 Landau, solns. and curves for envelope diagram 9-22170
 Laplace's eqn. solution, validity of representation 9-27159
 Logunov-Tavkhelidze, use in $\pi\pi$ scatt. dynamics 9-38533
 of motion in internal centrally symmetric field in general relativity 9-22083
 one-dimensional hyperbolic difference schemes for variable pseudoviscosity 9-34708
 Orr-Sommerfeld, for 2D flow, asymptotic soln. by multiple-scales method 9-23235
 Raman-Nath difference-differential eqn. for diff. of light by supersonic waves, soln. 9-27390
 Raman-Nath difference-differential eqn. for diff. of light by supersonic waves, exact soln. 9-22457

Equations continued

- stochastic applic. of method of moments giving linear algebraic eqns. 9-22111
 symmetry and local group structure of eqns. of physics 9-25029
 transfer, direct line solution, for nonstationary radiation field 9-25060
 transport, neutron, time depend., analysis by matched asymptotic expansions 9-34480
 Vlasov-Boltzmann for classical liquids, solution and existence of zero sound 9-32761
 wave; weakly nonlinear, periodic soln. in E₃, with spherical symmetry 9-34015
 for H plasma jets when chemical reactions resulting from methane decomposition take place, dissipation terms calc. 9-38994
- Equations of state**
 see also *Thermodynamics*
 arbitrary shape particles, scale particle theory 9-41783
 condensed media, model for shock Hugoniot 9-23455
 near critical point, parametric representation 9-26154
 near critical point, representation 9-44612
 critical states of binary mixtures 9-34949
 Gaussian molecules 9-29218
 hard sphere gas at high temp., expression for quantum-mechanical free energy 9-45790
 hard-disk fluid 9-30168
 Hartree-Fock atoms, virial theorem and pressure calc. 9-39554
 incomplete, relationships between and props. of, from thermodynamic identities 9-43759
 linear parametrization, near critical point 9-40815
 measurement, weighting technique at high press. 9-42690
 metals, formulation from low temp. mechanical obs. 9-39090
 molecular fluid with square-well potential Monte Carlo calc. of face energy. 9-36738
 neutral matter, and density fluctuations 9-41621
 particles mixture, canonical ensemble theory 9-39046
 Thomas-Fermi, modification to include effect of shell structure 9-34041
 water, 350-650°C, 165.37-1000 bar 9-30448
 Ar, compressed fluid, 9-42690
 Ar, critical region, predictions compared with expt. 9-28174
 Sn, P-T diagram interpretation 9-36914
- gases**
 coefficients of virial series, recurrent relationship 9-39048
 dense, derivation from binary correlation function 9-42607
 dissociating, 2nd virial coeff. uncoupled atoms 9-23391
 dissociating nonideal, 3rd virial coeff. from interaction of 3 atoms 9-40743
 ethylene, isotopic, meas. of 2nd virial coeffs. at 236.04°K. 9-48660
 excited gas, virial eqn. and coeffs. 9-30340
 Feon-21 vapour, P-T relations, exptl. investigation, 293° to 473°K, 1.5 to 68.5 bar 9-40816
 Fermi, magnetized, thermodynamic approach 9-25056
 Fermi gas, magnetized, thermodynamic approach 9-25054
 Fermi-Dirac relativistic gas at high temp., calc. methods 9-34050
 Freon 22, meas. 9-36805
 hard-sphere, high-temp. quantum mechanics 9-22128
 interaction second virial coeffs. from -125° to 50°C, meas. and correl. 9-44522
 law of corresponding states, graphical method of testing 9-36804
 Lennard-Jones gas, two-dimensional third virial coefficient 9-42605
 methane, second virial coeff. 9-34833
 methanes, halogen-substituted, second virial coeffs. 9-36807
 mixtures of nonspherical mols., third virial coeffs. 9-42608
 PVT meas. up to 10 kilobars, apparatus 9-30333
 real gases, second virial coeffs. evaluation using corresponding states principle 9-48659
 second virial coeff., Regge representation 9-39047
 second virial coeff., Regge representation and low temp. resons. 9-34830
 second virial coeffs. for real gases, evaluation using corresponding states principle 9-48659
 third-constant of 3-constant system, ratio of Boyle volume and unit compressibility law volume 9-32729
 virial coeff., 2nd, calc. for free atom system 9-40744
 virial coeff., second of pure gases and mixtures, two methods of determination 9-46567
 virial coeff., third, for intermolec. potentials with hard-sphere cores 9-44521
 virial coeff. from PVT data 9-36806
 virial coefficient 9-40743
 virial expansion of Maxwell-Boltzmann distribution of real gas 9-23369
 virial theorem for polyatomic mols. 9-48658
 water new equation of state for 0-800°C and 0-1000 bar 9-34831
 Ar, free energy from perturbation theory 9-46610
 Ar, isotherms to 10 kbar and 400°C 9-32732
 Ar, pair potential 9-48657
 Ar, second virial coeff. 9-34833
 CO₂, second virial coeff. 9-34833
 He, Lennard-Jones gas, quantum mechanical second virial coeff. 9-39049
 Kr, potential parameters from viscosity and second virial data 9-34838
 N₂, isotherms to 400°C and 10000 bar 9-44520
 N₂, second virial coeff. 9-34833
 N atomic, 2nd virial coeffs. 9-26019
 O atomic, 2nd virial coeffs. 9-26019
 Xe, extrapolation of Ar eqn. state of higher temp. and press., use in fuel swelling calcs. 9-40742
 Xe, free energy from perturbation theory 9-46610
- liquids**
 charged monolayer at liq. interface, kT-coeff. of ideal eqn. 9-34873
 Freon 22, determ. 9-36805
 under high pressure, exploding wave prod. of shock waves for determ. 9-36843
 at high pressure, self-consistent u.s. meas. method 9-34872
 Lennard-Jones liq., with repulsive forces, perturbation theory. 9-46610
 non-uniform, molecular distributions 9-30367
 seawater 9-35802
 shock Hugoniot model 9-23455
 u.s. method for meas. at high press. 9-34872
 water, isothermal data fits to analytical and expt. eqn., review 9-36844
 Al formulation from low temp. mechanical obs. 9-39090
 Ar, expt. determ. 9-39071
 Ar, interatomic potential and equations of state 9-28093
 Cu formulation from low temp. mechanical obs. 9-39090

Equations of state continued
liquids continued

- Hg, isothermal data fits to analytical and expt. eqn., review 9-36844
 Ne, interatomic potential and equations of state 9-28093
 Pb formulation from low temp. mechanical obs. 9-39090
 Sn formulation from low temp. mechanical obs. 9-39090
 W formulation from low temp. mechanical obs. 9-39090

solids

- construction from u.s. and shock wave data 9-23873
 determination by shock wave flow anal. in system of plates and spaces 9-48972
 f.c.c. crystals, quasi-harmonic approx. by self-consistent field method 9-44611
 ferromagnet near critical pt., parametric representation 9-26154
 Hartree-Fock, virial theorem and peessure calc. 9-39554
 high temp., suitability for geophys. applic. 9-30777
 metals, monovalent, virial theorem applic. to cohesive energy calc. 9-39179
 Murnaghan Tait and Birch eqns. applied to organic high polymers 9-37361
 periclase, and geophysical implications 9-28843
 polymers applic. of Murnaghan, Tait and Birch eqns. 9-37361
 shock and isothermal rel. to Gruneisen's parameter 9-28430
 shock wave, reduction to isothermal eqns. of state 9-28335
 Al formulation from low temp. mechanical obs. 9-39090
 BaF₂, u.s., calc. from pulse-echo meas. 9-33016
 CaF₂, u.s., calc. from pulse-echo meas. 9-33016
 CrBr₃, ferromag., near critical temp., mag. eqn. of state 9-26649
 Cs, to 23 kbar, 20-280K 9-40831
 Cu formulation from low temp. mechanical obs. 9-39090
 Fe, u.s. eqn. 9-26310
 Li, 0 °K 9-33222
 LiH, 0 °K 9-33222
 Pb formulation from low temp. mechanical obs. 9-39090
 Sn formulation from low temp. mechanical obs. 9-39090
 W, shock-loaded at 950°C Hugoniot meas. 9-44829
 W formulation from low temp. mechanical obs. 9-39090

Erbium

- ductility and plastic deform., 77 to 750°K 9-30663
 in group II-VI cpds. containing alkali metal compensators luminesc. 9-31128
 growth of single crystals by three methods 9-37078
 magnetic ordering, microscopic theory 9-24313
 magnetic susceptibility, effect of hydrostatic pressures 9-28594
¹⁶⁹Er, nuc. hyperfine splitting, temp. depend., Mossbauer eff. obs. 9-24272
 Er²⁺ in CaF₂, SrF₂ and BaF₂, thermal ionization potentials 9-46739
 Er³⁺, energy transfer with Tm³⁺, and with Ho³⁺, in Y₃Al₅O₁₂ 9-31126
 Er³⁺, fluoresc. in SrF₂, quantum efficiencies and lifetimes 9-24453
 Er³⁺ e.p.r. in BaWO₄, SrMoO₄ and scheelite-type crystals 9-41424
 Er³⁺ in LiYF₄, energy levels from absorption and luminescence spectra 9-31107
 Er³⁺ in MgAl₂O₃ stoichiometric spinel, trace detection by neutron activation analysis 9-35088
 Er³⁺ in SrF₂, e.s.r., conc. depend. of site symmetry 9-24490
 Er³⁺ in ZnS, thermoluminescence and photoluminescence 9-37774
 Er³⁺ in ZnTe, acceptor-doped, e.p.r. and photoluminesc. obs. 9-41431
 Er³⁺ trigonal centre in CeO₂, ENDOR studies of charge compensation mechanisms 9-33652
 Er³⁺(4f¹¹), spin-spin interactions determ. from matrix element expression 9-38774
 Er I, Zeeman effect obs. 9-46277

Erbium compounds

- ethylsulphate, spin-lattice relaxation anisotropy 9-26665
 ferrite garnets, Faraday effect, mag. field effect 9-49216
 E₂O₃, self-diffusion coeffs. of O, by isotope exchange method 9-44741
 Er-Dy alloys, single crystals mag. props. rel. to Dy concentrations 9-45060
 Er_{1-x}Bi_xFeO₃, spin reorientation and optical absorpt., substitution effect 9-45061
 Er_{1-x}Bi_xFeO₃, synthesis, mag. reorientation temp. rel. to Bi substitution 9-32869
 Er_{1-x}Y_xFeO₃, spin reorientation and optical absorpt., substitution effect 9-45061
 Er₂O₃, thin films, grain growth kinetics on pulse annealing 9-40842
 Er₂O₃, thin films, grain growth kinetics on pulse annealing 9-40841
 Er₂O₃ films, recrystallization behaviour on pulse annealing 9-30489
 Er₂O₃ polycryst., cation self-diffusion coeffs. 9-42860
 ErAg, mag. phases invest. 9-24272
 ErAl garnet, crystal-field energy levels and g-factors 9-45319
 ErAl garnet, Faraday effect, Verdet const. freq. depend. obs. 9-28657
 ErCO₃Ni_{0.5} mag. phases invest. 9-24272
 ErCONi, mag. phases invest. 9-24272
 ErCl₃ single cryst., mag. susceptibilities 9-33432
 ErCo₃, mag. phases invest. 9-24272
 ErCo₃, ferrimag., press variation of curie point 9-45154
 ErCrO₃, ¹⁶⁶Er Mossbauer effect 9-24380
 ErFe garnet, optical absorpt. spectra at 4.2°, 20° and 62°K, mag. moment and G-factor determ. 9-45319
 ErGa garnet, ⁴I_{15/2}→⁴S_{3/2} transition, Er³⁺ g-tensor anisotropy determ., Zeeman eff. obs. 9-23040
 ErGa garnet, crystal-field energy levels and g-factors 9-45319
 ErNi₂, mag. phases invest. 9-24272

Ergodic theorem see *Statistical mechanics***Errors** see *Measurement errors; Random processes***Esaki diodes** see *Semiconducting devices/tunnel and interface devices***Esaki effect** see *Semiconducting devices/junctions***Etalons** see *Interferometers***Etching** see *Crystals/etching***Ether drift** see *Relativity/special; Velocity/light***Ettingshausen effect** see *Magnetothermal effects***Europium**

- critical-point behaviour, anomalous, Mossbauer effect meas. 9-45219
 muonic atom isotopes, K and L x-rays meas. 9-29997
 valence states in compounds 9-32853
^{151,152}Eu, hyperfine struct. and nucl. quadrupole moment, spark spectrum obs. 9-29929
 Cr²⁺-Eu³⁺ pair emission spectrum in EuAlO₃:Cr²⁺ 9-39835

Europium continued

- Eu⁺, formation and luminescence in NaCl and KCl 9-26768
 Eu²⁺, fluorescence in binary alkaline earth orthosilicate systems, depend. on composition 9-28717
 Eu²⁺, hyperfine coupling const. in CaF₂, SrF₂ and BaF₂, temp. depend. 9-33496
 Eu²⁺, luminescence in BaO-MgO-P₂O₅ system 9-31131
 Eu²⁺ activated aluminosilicate phosphors 9-47390
 Eu²⁺ in alkaline-earth borate-phosphates, luminescence 9-35678
 Eu²⁺ in CaF₂, e.p.r., effect of nearby Jahn-Teller tunneling level 9-45383
 Eu²⁺ in CaF₂, spin-lattice coeff. determ. from uniaxial stress effects on e.p.r. spectra 9-33492
 Eu²⁺ in CaWO₄, crystal field splittings and hyperfine structure consts., 4.2 and 78°K 9-43200
 Eu²⁺ in CdF₂, e.p.r. at 300, 77 and 1.5°K 9-28745
 Eu³⁺, afterglow lifetime and radiationless transitions in aqueous solns., deuterated and undeuterated 9-28141
 Eu³⁺, electric field gradients in EuFe garnets 9-35603
 Eu³⁺ impurity ions in cubic centres in CaF₂, lattice distortion 9-26198
 Eu³⁺ in CaF₂, emission and excitation spectra, Eu-O complexes identification 9-47391
 Eu³⁺ in La₂O₃S, fluorescence characts. 9-43257
 Eu³⁺ in rare earth-Fe garnets, anisotropic props. due to exchange interac. 9-33475
 Eu³⁺ in rare earth oxysulphates (Ln₂ SO₆), fluoresc., phosphors obs. 9-43258
 Eu³⁺ in solids, fluoresc. and absorpt. spectra intensities 9-39876
 Eu³⁺ in Y₂O₃, luminescence spectra, satellite lines due to ion-pairs 9-24449
 Eu I oscillator strength, f-values determ. by hook method 9-34537
 SrTiO₃:Eu³⁺, impurity-lattice coupling to optical phonons 9-33166
 in Y₂O₃, emission from two symmetry sites 9-33562
 YVO₄:Dy, Eu, luminesc. 9-47398
 YVO₄:Eu, photo-, cathodo- and thermo- luminesc., impurity effects 9-47409

Europium compounds

- chalcogenides, absorpt. edge press. depend. 9-37722
 chalcogenides, antiferromag-exchange mechanism w.r.t. spin-polarized energy bands 9-39782
 chalcogenides, dielec. dispersion and optical phonon freqs. from reflectivity meas. 9-39799
 chalcogenides, reflectivity 9-49238
 divalent, isomer shifts of Mossbauer absorpt. of ¹⁵¹Eu 9-45289
 germanides Mossbauer spectra obs. of oxidation states and chem. bond charact. 9-37696
 silicides Mossbauer spectra obs. of oxidation states and chem. bond charact. 9-37696
 Eu-Ti-O system, phase relations in portion of 1400°C isotherm 9-35257
 Eu₂O₃, magnetic susceptibility, effect of anisotropic exchange and crystal-line field 9-45062
 Eu(WO₄)₃ single cryst., nucl. reson. fluoresc. of 3 eV ¹⁵²Sm recoil atoms, anisotropic pot. obs. 9-35596
 Eu benzoylacetate solutions at -150°C energy of threshold rel. spectral compos. stimulating light 9-28134
 Eu complex, europium (III)-bis-phenanthroline-tris-carboxylate, fluorescence spectra, analysis 9-31132
 EuAlO₃:Cr³⁺, Cr³⁺-Eu³⁺ pair emission 9-39835
 EuAlO₃:Cr³⁺, e.s.r. 9-47435
 EuCl₃:Gd³⁺ pair and Gd³⁺-Eu³⁺ interac. consts., e.p.r. 9-33439
 EuCl₃ aq. soln., Cotton-Mouton effect through absorpt. band 9-39100
 EuCrO₃, antiferromagnet, weak-ferromagnetic moment obs. 9-24302
 EuF₃.2H₂O, Mossbauer spectrum of ¹⁵¹Eu;O₂, shift obs. 9-35635
 EuFe garnet, anisotropy in exchange interac., Mossbauer obs. 9-33475
 EuFe garnets, electric field gradients on Eu³⁺ nuclei, crystalline fields 9-35603
 EuI₃, monoclinic form, cryst. struct. 9-35059
 Eu(III) solns. in H₂O, D₂O and CH₃CN, new fluorescence emission band 9-36891
 EuO:Gd, dopant effect on magnetic and electrical props. 9-33463
 EuO:R³⁺ film, (R=rare earth oxide), mag., magneto-optical, optical and transport props. 9-47266
 EuO, i.r. transmission, mag. birefringence and Faraday rotation 9-45273
 EuO, magnetic birefringence, infrared transmission and Faraday rotations 9-24365
 EuO, magnetic phase transitions, effect of press. to 10 kbar, compressibility and vol. depend. 9-24327
 EuO, magnetic phase transitions, effect of press. to 10 kbar, compressibility and vol. depend. 9-33485
 EuO, near mag. phase transition, vel. change with const. attenuation 9-24030
 EuO, reflectance 69K-1.5K, spin-polarized splitting of peaks 9-37690
 EuO, reflectivity and band structure, energy range 1-9 eV 9-26702
 EuO, refractive index and photoconductivity effect of mag. order 9-45266
 EuO, u.s. propagation, attenuation, temp. and mag. field depend. 9-44824
 EuO ferromagnetic, ¹⁵¹Eu spin lattice relax., field and temp. depend 9-45244
 EuO film, hologram, thermomagnetic writing and reconstruction of hologram 9-48060
 EuS, energy gap temp. depend., mag. sp. ht. and Curie const. calc. 9-37529
 EuS, magnetic phase transitions, effect of press. to 10 kbar, compressibility and vol. depend. 9-33485
 EuS, magnetic phase transitions, effect of press. to 10 kbar, compressibility and vol. depend. 9-24327
 EuS, specific heat, comparison with classical Heisenberg model 9-30782
 EuS, vapour phase growth, high-temp. 9-37008
 EuS ferromagnetic films at low temp., mag. struct. by use of Lorentz microscopy 9-41880
 EuS refractive index and photoconductivity effect of mag. order 9-45266
 EuS(Se), band structure from optical reflection and absorption data 9-28505
 EuSe, magnetic phase transitions, effect of press. to 10 kbar, compressibility and vol. depend. 9-24327
 EuSe, magnetic phase transitions, effect of press. to 10 kbar, compressibility and vol. depend. 9-33485
 EuSe, optical consts. 9-49238
 EuSe, photoconductivity, mag. polaron effects 9-39714
 EuSe, vapour phase growth, high-temp. 9-37008
 EuSe mag. props. under hydrostatic pressure 9-47287

Europium compounds continued

- EuSe single crystal, magnetic phase transition, neutron diff. study 9-47288
 EuTe, antiferromagnetic resonance linewidth, temp. depend. 9-45376
 EuTe, mag. props. under hydrostatic pressure 9-47287
 EuTe, vapour phase growth, high-temp. 9-37008
 Mg-Eu system, phase diagram 9-33150
 PbTe-EuTe system, investigation by thin film techniques 9-39486
 Sm₂Eu₂Fe mixed garnet, anisotropy in exchange interac., Mossbauer obs. 9-33475

Evaporation

see also Vaporization

- alloys, on hot metal filaments, emission of high-energy electrons 9-35204
 atoms or molecules from solid surface, spatial var. meas. with molecular scanner 9-42709
 energy exchange at earth's surface heat budget equation 9-26892
 gas evaporation method with plasma jet flame for prep. of the fine metal particles 9-33128
 isotope exchange meas., condensation coeff. elimination 9-39083
 and isotope thermo-diffusion in non-polar liq. mixtures 9-23472
 lake surface retarding monolayer, layer, effect on temp. 9-47515
 liquid, flow rate density of non-equilib. adiabatic stream, theory 9-30463
 metal, light absorbing, kinetics 9-23605
 mist, by intense light beam 9-42699
 organic liq. retardation, partial ester of polyhydric ether alcohol addition, patent 9-23589
 quantum fluids, rate temp. depend. 9-26144
 refractory cathodes, effective heat of, in Cs 9-44513
 retardation, monolayer role 9-30464
 sphere, stationary, force in presence of similar sphere 9-40827
 vacuum, ionization-gauge rate monitor and push-pull Miller op. amp. 9-43694
 water, from capillaries, flow in surface layers 9-44533
 water, from soil, vertical flow eqn. and flow meas. 9-34854
 water, retardation by hexadecanol monolayers 9-23591
 Be, by controlled electron beam 9-39145
 Cr, in vacuum, gettering effect, detection 9-30457
⁴He from superfluid He, rate temp. depend. 9-26144
 Pb and In particles in vacuum, velocity distribution 9-32818
 PbTe in inert gas, lowering of rate 9-32817
 PuO_{2-x}, hypostoichiometric, 2070° to 2380°K 9-26169
 US-UO₂ mixtures 9-28774
 US-UO₂ mixtures, evaporation mixtures 9-33658

Evershed effect *see Sunspots*

Examination of materials *see Electron diffraction examination of materials; Electron microscope examination of materials; Neutron diffraction examination of materials; X-ray examination of materials*

Exchange interactions

- alloys, dil. mag., Kondo resistivity of interacting impurity pair 9-24270
 alloys, dil. mag., orbital degeneracy effects 9-24269
 alloys, dil. magnetic, dynamic susceptibility calcs. 9-35525
 antiferromagnet, in spin-forbidden resonance energy transfer mechanism 9-24323
 antiferromagnet, Ising model super-exchange, transition props. 9-49220
 antiferromagnet, metal, rel. to spin wave spectrum 9-28638
 CdCr₂S₄(Se₄) spinels, rel. to pressure depend of ferromag. phase transitions 9-45119
 direct, theory 9-24265
 ferromagnets, ratio of 1st. to 2nd neighbour exchange 9-49197
 g factor, quasiparticle 9-24103
 garnets, germanate, mag. ordering obs. 9-47231
 Heisenberg model, isotropic, with long-range interactions, absence of ferromag. and antiferromag. 9-49194
 Heisenberg spin system, theory 9-24296
 Heisenberg two-spin model exact soln by Green's junction methods 9-29148
 insulators 9-49186
 insulators, and e.s.r. and applic., book 9-47222
 integrals momentum dependence, eff. on Kondo temp. 9-31044
 isotropic exchange, anomalous level shifts and splittings, Lande rule deviations 9-33428
 Kondo model describing interaction of conduction electrons with localized mag. impurity 9-39560
 liquids, chemical exchange rel. to rotational relax. 9-39117
 in magnetic ion pairs optical spectrum, effect 9-39824
 metal, anomalous correl. changes in antiferromag. and ferromag. exchange due to connections in paramag.-impurity ground-state 9-33436
 metal, electron spin polarization around mag. impurity, calc. using Kondo effect 9-41287
 metal with localized impurity s-d model mag. field effects 9-47220
 metals, antiferromag., s-d, rel. to paramag. and antiferromag. reson. freqs. 9-37669
 metals, ferromagnetic, contact model rel. to spin wave theory corrections 9-45092
 metals, pure, rel. to electronic structure 9-47024
 metals, second-order effects in localized moments 9-35527
 metals and mag. insulators, and cry. field, book 9-47223
 pair interaction Hamiltonian in fictitious angular momentum space 9-45249
 perovskites antiferromag., magnon-exciton and localized magnons, theory 9-45198
 rare earth compounds, and electrostatic high degree 9-47227
 rare earth dialuminides, s-f effects on elec. conductivity 9-24119
 rare earth-Zn cpds., depend. on interatomic spacing, comparison with rare earth-Cd cpds. 9-35556
 ruby, energy transport mechanisms 9-45305
 s-d theory of zero-bias tunneling anomalies, g-shifts 9-37642
 s-f coupling, spin screw structure, temp. depend. 9-45204
 semiconductors, magnetoactive, indirect, rel. to spin polarons 9-28607
 transition metal salts, and electrostatic high degree 9-47227
 two-centre, anisotropy 9-26619
 BiI₃:Cr³⁺, e.s.r. of coupled Cr³⁺ pairs 9-24482
 n-CdCr₂S₄, ferromagnetic semiconductor, effect on magnetoresistance 9-44956
 CdCr₂S₄(Se₄) chalco-genide spinels, rel. to isotropic hyperfine interac., n.m.r. 9-31170
 CdCr₂S₄(Se₄) exchange striction rel. to absorb. edge 9-45155
 CeBr, magnetic tensors from adiabatic susceptibility meas. 9-47229
 CoCr₂O₄, distant-neighbour B-B interactions, rel. to spin config. 9-45176

Exchange interactions continued

- p-CoCr₂S₄, ferromagnetic semiconductor, effect on magnetoresistance 9-44956
 CoS₂ ferromagnet 9-33437
 Co(S₂Se_{1-x}) system 9-33452
 Cr₂O₃, anisotropic, between Cr³⁺ ions 9-45212
 Cr₂O₃, inelastic neutron scatt. obs. 9-47285
 Cr³⁺-Eu³⁺ pair coupling mechanism, emission spectrum in EuAlO₃:Cr³⁺ obs. 9-39835
 CrTe, exchange striction, temp. depend. 9-33466
 CsMnF₃ antiferromagnetic, exchange consts. from magnetoelastic wave vels. 9-47286
 Cu(NO₃)₂.2.5H₂O, antiferromag., rel. to magnetization isotherms, 1.2° to 4.2°K 9-45218
 CuSO₄, antiferromag., strong superexchange interactions obs. from mag. moment density determ. 9-41335
 Dy₂Hol_{1-x}Sb, overlap eff. in exchange mechanisms from mag. props. obs. 9-28595
 Eu₂O₃, anisotropic, effect on mag. susceptibility 9-45062
 Eu chalcogenides, antiferromag. exchange mechanism w.r.t. spin-polarized energy bands 9-39782
 EuCl₃:Gd³⁺ pair and Gd³⁺-Eu³⁺ interac. consts., e.p.r. 9-33439
 EuFe garnet, anisotropic props., ¹⁵¹Eu and ⁵⁷Fe Mossbauer obs. 9-33475
 EuO:Gd, dopant effect on Curie point attributed to additional interaction via conduction electrons 9-33463
 EuO:R³⁺ film, (R=rare earth oxide), rel. to transport, mag., magneto-optical and optical props. 9-47266
 α-Fe₂O₃, of magnetic ions, effect on shift of Mossbauer spectrum 9-26720
 p-FeCr₂S₄, ferromagnetic semiconductor effect on magnetoresistance 9-44956
 α-Ga₂O₃, of magnetic ions, effect on shift of Mossbauer spectrum 9-26720
 Gd-Dy dil. alloy 9-43171
 Gd₂CoMnO₆, perovskite, rel. to metamagnetism 9-35587
 Gd³⁺ superexchange parameters in anhydrous chlorides, interpretation 9-27852
 Gd compounds cubic, rel. to mag. structure and susceptibility meas. 9-45225
 GdFe garnet, Sn-substituted, rel. to critical mag. isotherm 9-43188
 H formation by charge exchange proton bombard. of Li and Na 9-27813
 H ionization, exchange cross sections 9-34578
 He-Ne laser, Ne atoms density nonlinear depend. on saturation, Ne exchange collisions explanation exchange collision, saturation parameter nonlinear depend. on density 9-25271
³He solid with ⁴He impurities, effect on heat capacity, n.m.r. 9-28168
 HgCr₂S₄(Se₄) chalco-genide spinels, rel. to isotropic hyperfine interac., n.m.r. 9-31170
 HgCr₂S₄(Se₄) spinels, rel. to pressure depend of ferromag. phase transitions 9-45119
 InSb, acoustic nuclear mag. reson. of ¹¹⁵In, ¹²¹, ¹²³Sb, rel. to line broadening 9-45401
 KZnF₃:Mn²⁺, nearest-neighbour const., e.p.r. determ. 9-45386
 Li target, proton bombard., H atom formation by charge exchange, cross section 9-27813
 LuCrO₃, magnon sideband emission in fluorescence spectrum, average nearest-neighbour interac. obs. 9-31136
 LuFeO₃ orthoferrite 9-45182
 MgF₂:Co²⁺ far-i.r. absorpt. spectra obs. 9-41384
 Mn_{0.6}Zn_{0.4}Fe₂O₄, superexchange in Mn²⁺-O²⁻-Fe³⁺ linkages, from sublattice magnetizations temp. depend. obs. 9-39777
 Mn₂Cr₂S₄ solid solutions, sign and size of integral, evaluation from neutron diff. and magnetic structure study 9-28615
 MnF₂, antiferromag., and magnon dispersion relation 9-45228
 MnSe₂S₄, from mag. susceptibility meas. 15° to 295°K 9-47292
 MnWO₄, heubermite, antiferromag., struct. obs. 9-43194
¹⁴N and ¹³C, optically pumped spin exchange 9-32418
 (NH₄)₂PtCl₆, of Ir⁴⁺ ions, ENDOR investig., 4°K 9-49364
 Na target, proton bombard., H atom formation by charge exchange, cross section 9-27813
 Nd₂Dy_{1-x}Sb, overlap eff. in exchange mechanisms from mag. props. obs. 9-28595
 Ni_{1-x}Zn_xFe₂O₄, participation of 3d carrier electrons 9-33310
 Ni₃Ga, enhanced mag. susceptibility decreasing with nonmagnetic impurity addition 9-26639
 NiFe₂O₄, substituted, rel. to mag. fields on Sn nuclei 9-26727
 NiO, antiferromagnetic, coherent scattering of low energy 9-45230
 O₂ molecules in O₂-Ar solid mixtures, from mag. susceptibility meas. 9-45231
 Pd-Cr alloy, annealed at 510°C, ferromag. and antiferromag., at low temp. 9-49202
 Pd-Fe dilute alloys, effective exchange integral obs. 9-44916
 Pd-Rh, enhancement from mag. susceptibility field-dependence meas. 9-26625
 PrBi, paramag., bet. ions, as nuclear ordering mechanism 9-26669
 Pt-Co dilute alloy s-d model rel. to magnetoresistivity meas. 9-44917
 RbMgF₃-RbCoF₃, ferrimag. range, B-B interac. calcs. 9-47274
 RbMnF₃, antiferromag. magnon-exciton, and localized magnons, theory 9-45198
 Sc, enhanced mag. susceptibility decreasing with nonmagnetic impurity addition 9-26639
 Sm₂Eu₂Fe mixed garnet, anisotropic props., ¹⁵¹Eu and ⁵⁷Fe Mossbauer obs. 9-33475
 SmFe garnet, anisotropic props., ¹⁵¹Eu and ⁵⁷Fe Mossbauer obs. 9-33475
 SrO[(Sr_{1-x}La_xMn²⁺)(Mn²⁺-O²⁻)₂] layered structure, ferromag. Mn²⁺-O-Mn²⁺ interaction, from magnetization meas. 9-45153
 TbFe garnet, Sn-substituted, rel. to critical mag. isotherm 9-43188
 YCrO₃, magnon sideband emission in fluorescence spectrum, average nearest-neighbour interac. obs. 9-31136
 YFe garnet, Sn-substituted, rel. to critical mag. isotherm 9-43188
 YFeO₃ orthoferrite 9-45182
 Yb³⁺-O²⁻-Fe³⁺ system, superexchange integrals 9-45076

Exchanges, chemical

see also Isotope exchanges

- α-ω-diphenylpolyene ketone charge transfer complexes with tetracyanethylene and chloranil, spectra 9-42443
 anion exchange, determination of Pu in blood 9-29113
 deuterization of non-volatile compounds using heavy water in inert solvent 9-26804
 electron-transfer rates in soln., errors in e.s.r. meas. 9-45412

Exchanges, chemical continued
 faujasite, dehydrated La-exchanged, position of mols. and cations at 420°C 9-32899
 faujasite, hydrated Ca-exchanged, positions of cations and molecules 9-30556
 feldspars, alkaline, Na-K exchange, microscopic obs. 9-37810
 glass, tensile strength increase by ion-exchange 9-35184
 interhalogen exchange reactions, molec. beam kinetics 9-49367
 ion exchange, liquid-side mass transfer coefficients 9-31176
 ion exchange, liquid-side mass-transfer coeff., Nernst-Planck model 9-24525
 ion exchange mechanism, electrochemically controlled 9-31177
 ion exchange transport processes, electrochemically controlled 9-31178
 ion exchanger kinetics 9-45414
 ion-atom slow interchange reactions, temp. depend 9-43312
 ion-exchange equilib. diagrams involving weakly dissociated electrolytes, estimations 9-26803
 liquids, equations of motion of nuclear magnetism, in presence of chemical exchange 9-44592
 liquids, rel. to rotational relax. 9-39117
 quantum mech., coupled-channels approach 9-45413
 rare earth ion exchange of synthetic faujasites 9-24527
 rate determ. by n.m.r. 9-24526
 σ -bonded four-centre exchange reaction complexes 9-48463
 zeolites, anhydrous, heat of exchange between gaseous ion and ion in zeolite 9-49368
 Ar with adsorbed H on stainless steel 9-39170
 Co³⁺ in P-O containing solvents, n.m.r. relax. and spin decoupling 9-23533
 Fe²⁺ ions in Y zeolite and Dowex 50 resin, Mossbauer effect 9-43226
 H₂+D₂ and H₂+I₂, mechanism 9-48463
 H⁺/Cu²⁺-Cl⁻ ion exchange, liquid-side mass transfer coefficients 9-31176
 In³⁺ in In³⁺-HClO₄-HNO₃ and In³⁺-NClO₄-NaNO₃ behaviour, ion exchange exp. 9-37812
 K/H and K/Li ion exchange in synthetic resin, kinetics 9-41438
 Pu, determination in blood by anion exchange 9-29113
 TiPO₄ ion exchanger for recovery of Cs from nuclear wastes 9-24593
 Zr(HPO₄)₂·H₂O, ion exchange mechanism rel. to crystal structure 9-23779
 Zr(HPO₄)₂, ion-exchange props. 9-26208
 Zr(HPO₄)₂·2H₂O, ion-exchange props. 9-26208
 Zr(PO₄)₂ gels, ion exchange and sorption rel. to comp., obs. 9-28789

Excimers *see* *Molecules/excitation*

Excitation *see* *Atoms/excitation; Molecules/excitation; Nuclear excitation; Vibrations/excitation*

Excitons *see* *Crystal electron states/excitons*

Excitons, molecular *see* *Molecules; Polymers*

Exoelectron emission *see* *Electron emission*

Exosphere *see* *Atmosphere/upper*

exp-6 potential *see* *Kinetic theory; Molecules/intermolecular mechanics*

Expanding universe *see* *Cosmology*

Expansion, thermal *see* *Thermal expansion*

Explosions
 see also *Detonation; shock waves*
 in circular disc, shock wave radiation 9-35160
 condensed detonators, e.m. field, in near zone, investigation 9-38306
 cumulative, rel. to acceleration of solid particles 9-25064
 current generator, high-energy, explosively driven 9-47880
 energy propag. through atmosphere and lower ionosphere 9-31409
 galaxy-core, ejection of cosmic rays, composite model 9-49525
 hot-spot initiation in explosives, theoret. calc. 9-25110
 liquid explosive, detonation front instability 9-36204
 magnetic field generation in flux-compression, flux loss and energy balance 9-45916
 metal cylinders, thin-walled explosively-loaded, fragmentation behaviour
 expansion velocity and material parameter dependence 9-42901
 point energy source, shock wave propag. into cold atm. with density varying exponentially with altitude 9-34091
 spherical charge in air, shock wave parameters calc. 9-45870
 steel shells, closed, response to blast of internal charges 9-40279
 thermal, degenerated processes 9-47459
 thermal, under high hydrostatic pressure 9-36205
 underground, identification by teleseismic data 9-45451
 underwater, gravitational effect on shape of bubble formed 9-46602
 underwater, high intensity impulse generation by exploding wire 9-29283
 underwater, hydroacoustic signals from CHASE V explosion of Cape Mendocino 9-29268
 underwater, seismic signals power spectrum and covariance function, model 9-49409
 underwater, seismic signals power spectrum and covariance function, model 9-45436
 wire, elec., light emission, time depend. obs. 9-46029
 wire, fast-explosion striations, mechanical mechanism 9-47337
 wire, high intensity underwater sound impulse propagation 9-29283
 wires, causing inductive ignition of surface-discharge 9-25970
 wires, dwell time gas dynamics 9-27235
 wires, electrical, plasma light emission at low pressure 9-30241
 wires, expansion vel. of discharge plasma 9-25852
 wires, for pulsed charging of capacitors for high voltage prod. in plasma accelerators 9-42519
 wires, with dark pause, voltage peak calc. 9-41836
 Ag wires, nature and dimens. effect on exploding phenomena 9-45419
 AgN₃, initiation by collapsing air bubble 9-28788
 Al powder-oxygen mixtures, detonation investigation 9-27234
 Au wires, nature and dimens. effect on exploding phenomena 9-45419
 Cu wires, nature and dimens. effect on exploding phenomena 9-45419
 Pb(N₃)₂, spontaneous, during growth 9-37040
 β -PbN₆ initiation by collapsing air bubble 9-28788

nuclear
 in atmosphere, ground-press. waves rel. to winds, models 9-24645
 in atmosphere, subsequent sudden enhancement of atmospherics 9-47550
 Chinese (Dec 1966 and June 1967), effect on ⁸⁹Sr/⁹⁰Sr ratio in rain 9-43406
 Chinese sixth test, debris tested in Sweden for activity and particle characts. 9-49458
 discrimination from earthquakes 9-24614
 ionospheric effects 9-31404
 Nevada, S wave travel times and amplitudes 9-35780

Explosions continued
 nuclear continued
 resultant microbarographic oscillations 9-33761
 Starfish, resulting inner radiation zone electron flux, obs. (1965) 9-26934
 underground, cavity radius, prediction 9-49425
 underground, constructive use 9-26887
 underground, earthquakes study 9-49415
 γ spectra computed from published data 9-24665
 γ spectra computed from published data 9-33796

Extensive air showers *see* *Cosmic rays/showers and bursts*

Extensometers *see* *Strain gauges; Thermal expansion*

Extra-terrestrial radiation *see* *Cosmic radiations, radiofrequency; Sun/radiation*

Extrusion *see* *Forming processes*

Eye
 see also *Vision*
 astigmatism, statistical data and interpretation 9-31711
 blue arcs phenomenon, obs. 9-24963
 cat, electrophysiological retinal changes following retinal deprivation 9-24985
 cone orientations distribution, Stiles-Crawford effect explanation 9-38153
 conjunctival photography of blood flow 9-49605
 cornea, light scattering theory 9-38155
 corneal damage thresholds for CO₂ laser radiation 9-43690
 corneal irradiation by CO₂ laser, anterior chamber meas. 9-47697
 damage due to laser radiation, probability analysis 9-38151
 deformation effects of hard and soft contact lenses 9-36084
 electroretinograph response, 90-120 minute fluctuations 9-31712
 electroretinographic response to light stimulus 9-31713
 electroretinographical variability rel. to b wave duration 9-29127
 frog's retina, responses of class-2 movement-detecting neurons 9-24989
 human, structure and operation, summary 9-36083
 human laser beam effects, damage threshold theory 9-45704
 human pupil contraction, latency var. due to stimulus and/or adaptation level 9-27131
 image formation, review 9-29125
 laser hazards 9-45702
 laser radar hazards, analysis and reduction methods 9-38152
 lens, refr. index distrib. 9-47702
 methionine shown incorporated in rhodopsin of frog by ¹⁴C labelling 9-24988
 ocular tissue, u.s. energy trans. problems 9-38134
 optic tract fibre, recordings of cat for two spots of varying light on different parts of retina 9-24984
 parietal, of iguana, obs. 9-24987
 pathology rel. to pictorial art 9-31714
 rabbit cornea, damage thresholds for CO₂ laser radiation 9-38159
 resolving power, dependence on various combinations of aberrations 9-27129
 retina, structure and functions 9-33965
 retinal and occipital potentials due to wavelength changes 9-31710
 rods and long-wave cones, interaction to produce colour sensation 9-27137
 transfer function, sine wave gratings tests 9-49611

F-centres *see* *Colour centres*

F-layer *see* *Ionosphere/F-region*

Faculae *see* *Sun*

Fallout
 see also *Atmosphere/radioactivity; Nuclear reactions and scattering; Radioactivity*
 aerosol interaction with ground surface 9-35828
 air and rain obs. (Jan.-June 1967) 9-31335
 from Chinese sixth nuclear test, debris tested in Sweden for activity and particle characts. 9-49458
 in ground, attenuation of γ radiation by snow-cover 9-33797
 in ground attenuation of γ radiation by snow-cover 9-24666
 population exposure risk from re-entering isotopic power devices 9-28901
 radioactive, dose rate and ionization 9-24669
 radioactive pollution, global, meas. by airborne ¹³⁷Cs γ spectrometry 9-37894
 radionuclide fractionation of particles from land surface burst 9-28897
 vertical distrib. of fission products in Kesselwandferner glacier 9-47513
 worldwide, contamination of biological and environmental samples, detection using gamma-ray spectrometer 9-44081
 ¹³¹I in milk, Midwest USA obs. and explanation 9-26913
 Sr⁹⁰, stratospheric residence time and interhemispheric mixing in rain 9-40041
 ⁸⁹Sr/⁹⁰Sr in rain, effect of Chinese nuclear explosions (Dec 1966 and June 1967) 9-43406
 ⁹⁰Sr yield, Chinese thermonuclear explosion (1967) 9-28898
 ⁶⁵Zn, origin after 1967 Chinese nuclear tests 9-24668

Faraday effect *see* *Magneto-optical effects*

Fatigue *see* *Elastic fatigue*

Fermi gas *see* *Quantum fluids/fermion systems*

Fermi level *see* *Crystal electron states/Fermi level*

Fermi surface *see* *Crystal electron states/Fermi surface*

Fermion systems *see* *Quantum fluids/fermion systems*

Fermions
 see also *Elementary particles; Quantum fluids/Fermion systems; Statistical mechanics/quantum*
 antiparticle concept rel. to relativistic scatt. 9-48147
 conservation of number, parafield theory 9-22514
 Fermi and Yukawa theories equivalence, examples of second degree programs 9-43939
 Fermi atoms adsorbed on substrate at low temp., specific heat 9-46730
 lattice statistical problems, many-fermion techniques applications 9-34035
 polarization in nuclear reactions, conditions 9-40498
 quarks of spin 1/2, quark model new predictions 9-38477
 Regge trajectories, Barger and Clines rule rel. to bound states of Dirac particle 9-48157
 spin 1/2 fermion-antifermion system of zero total mass, solm. of Bethe-Salpeter eqn. 9-38449
 spinless, interacting, nonrelativistic quantum mech. in terms of currents 9-29532
 SU(3) group representation, operator realization 9-27451
 Sugawara model for leptonic currents 9-38463

Fermions continued

- systems, natural orbitals, divergences, and variational principles 9-48369
trajectories, curvature 9-22569

Fermium

No entries

Fermium compounds

No entries

Ferrimagnetic resonance

see also *Ferromagnetic resonance*

- ferrites, linewidth from magnetization meas. in approach to saturation of hysteresis loop 9-37662
ferrites, mag. anisotropy effect 9-39898
linewidth, independent grain and dipole narrowing theories comparison 9-45373
pulse echo amplification 9-45239
rare-earth ferrites, mag. anisotropy effect 9-39898
uniaxial and cubic cryst., mag. anisotropy effect 9-39898
Mn_{1.26}Fe_{1.74}O₄, linewidth, independent grain and dipole narrowing theories comparison 9-45373
NiFe₂O₄, disordered, X-band obs., Ni²⁺ migration to A-sites 9-35705
RbNiF₃, uniaxial ferrimagnet, 77-200°K 9-28740
Y₂Fe₂O₁₂ linewidth, independent grain and dipole narrowing theories comparison 9-45373
YFe garnet: Cu²⁺ 9-45374
YFe garnet: Co single cryst. 9-33480
YFe garnet: Ho, linewidth and fine structure 9-26790
YFe garnet films, linewidths <1 Oe, epitaxial growth 9-36952
YFe garnet single crystals, line width meas. rel. to distribution of gallium 9-36979

Ferrimagnetism

see also *Ferromagnetism*

- Heisenberg, classical, ferrimagnets, critical-point behaviour 9-26654
magnon effects on thermal transport in insulators 9-44847
screw spin structure with orthorhombic anisotropy energy, magnetization process 9-28627
FeCl₂.H₂O magnon-phonon interaction rel. to ordering obs. in far i.r. 9-45077

Ferrites

see also *Magnetic properties of substances*

- anisotropy and porosity, approach to saturation of hysteresis loop 9-37662
conductivity, activation energies from mag. relax and Koops inhomogeneity obs. 9-45000
(CuMn₂O₄)_x(AFe₂O₄)_(1-x), magnetic and electrical props., where A=Cu²⁺, Ni²⁺, Zn²⁺, Co²⁺ or Ni²⁺ 9-30834
devices applic. to microwave integrated circuits 9-43840
disk, ferromagnetic resonance shift shape effect 9-33617
dissolution kinetics of Fe₃C 9-48874
ellipticity of $\pi/2$ -spin waves 9-31027
exchange integrals for ferrites with two different ions in different domains 9-45181
ferrimagnetic reson., mag. anisotropy effect 9-39898
ferrite core memory using single major remanent state of one polarity for both digital information states 9-43844
ferromagnetic precession relax. by spin-wave excitation in polycrystalline ferrites 9-24337
grain boundary barrier layers in polycryst. rel. to elec. props. 9-46828
hexa-, ferromag. reson. bandwidth, nature 9-45362
interface with current-carrying semiconductor film, amplification of magnetostatic surface waves 9-43816
internal friction and ΔE effect, depend. on magnetizing field 9-26655
initial permeability, freq. depend. due to spins and wall resonances 9-35569
Lexa-ferrites, numerical symbols for describing structure 9-40900
magnetic moments, magnetization directions interpretation w.r.t. cryst. fields and bonds 9-28628
magnetic permeability tensor, dispersion eqn. freq. branches 9-47268
magnetic relax. and Koops inhomogeneities 9-45000
magnetic reversals by uniform rot. of magnetization vector 9-47269
magnetoelastic macroscopic coeff., connection with spin-phonon Hamiltonian microscopic coeffs. 9-26656
magnetoelastic modes in saturated ferrimagnets, models composed of two coupled transmission lines 9-28626
microwave, used in analog phase shifters, quick evaluation of characts. 9-43815
microwave props. 9-45172
nickel ferrous ferrite, microstruct. control 9-48836
nonlinear effects at high f.r. fields 9-47270
permeability, microwave, in weak mag. fields, effect of domain structure 9-33472
permeability tensor in various coordinate systems 9-39775
planar anisotropy, magnetostatic mode meas. of 4nM_s 9-45173
polycrystalline, grain boundary barrier layers rel. to elec. props. 9-46828
polycrystalline, initial microwave tensor susceptibility, statistical analysis 9-49215
polycrystalline uniaxial, mag. stiffness obs. by torsion pendulum method 9-35570
pore size effect on remanence ratios 9-43172
rare-earth, ferrimagnetic reson., mag. anisotropy effect 9-39898
rare-earth garnets, magnetization near curie point 9-45175
relaxation times from dynamic h.f. absorpt. rel. to mag. aftereffect 9-41325
resistivity temp. depend. meas., 80-300°K 9-35327
resonances, subharmonic, and magnetization precession 9-35704
single cryst. growth by chem. transport reactions 9-44643
sintered, residual pores behaviour obs. 9-42921
sphere, electromagnetics resonances, axial-symmetric modes 9-27256
spinel, ferrimagnetic single crystal, u.v. complex polar-Kerr effect 9-45275
spinel, mag., microstruct., cryst. chem 9-45174
spinel and garnet type, X-ray absorpt. spectra, composition and different states 9-37743
in steel, Widmanstätten ferrite form. 9-46947
thermal spin fluctuations conversion to elastic microwave power by pulsed field 9-37226
threshold microwave-field amplitude for unstable growth of spin waves under oblique pumping 9-43186
wave (e.m., magnetostatic and spin) propag., dispersion equation and soln. 9-45171

Ferrites continued

- Ba₂Zn₂Fe₁₀O₂₂ hexagonal, absorpt. and Faraday rotation, 300°K, 1 to 8 μ 9-45277
BaZn₂Fe₁₀O₂₂ and Mn substituted single crystals, ferromag. reson. 9-45365
Ba₂Fe₂Zn₂O₁₀, numerical symbols for describing structure 9-40900
BaFe₂O₁₉, polycryst., mag. stiffness meas. 9-35571
BaFe₂O₁₉ hexagonal, absorpt. and Faraday rotation, 300°K, 1 to 8 μ 9-45277
BaFe₂O₁₉, magnetocryst. anisotropy consts. determ. by magnetization curves 9-43170
BaOFe₂O₃, struct. and mag. props., X-ray and neutron diff., Mossbauer effect 9-47283
BaSc₂Fe_{12-x}O₁₉ hexagonal single cryst., anomalous intensity distrib. in satellites in neutron diff. obs. 9-31043
BaSc₂Fe_{12-x}O₁₉(M), helicoidal antiphase spin ordering, neutron diffraction 9-37663
CdFe₂O₄, oxygen parameter and degree of inversion, X-ray meas. 9-44660
CeFeO₃ orthoferrite, prop., mag. props., Mossbauer spectra 9-45055
Co₂W, magnetocryst. anisotropy consts. determ. by magnetization curves 9-43170
Co₂Mg_{0.8-x}Fe_{2-x}O₄ ferrite temp. depend. magnetic aftereffects, Co ion influence 9-35572
Co₂Mn_{0.5-x}Fe_{2-x}O₄ ferrite, temp. depend. mag. after effects, Co ion influence 9-35572
Co₂Ni_{0.5-x}Fe_{2-x}O₄ induced anisotropy mechanism 9-33474
Co₂Ni_{0.5-x}Fe_{2-x}O₄ ferrite, temp. depend. mag. after effects, Co ion influence 9-35572
CoFe₂O₄, uniaxial anisotropy induced at low temp. 9-43185
FeFe₂O₄ synthetic magnetite, chemical and thermal remanence, relative stability 9-39776
Li_{0.5}Fe_{2.5}O₄, switching props., effects of grain size 9-45180
Li_{0.5}Fe_{2.5}O₄ spinel, absorpt. and Faraday rotation, 300°K, 1 to 8 μ 9-45277
Li ferrites, magnetoelastic macroscopic coeff. connection with spin-phonon Hamiltonian microscopic coeffs. 9-26656
Li ferrites, thermal transport, effect of magnons 9-44847
LiGa, magnetostriction consts., temp. depend. 9-28629
LuFeO₃, exchange interaction and g factor determ. 9-45182
Mg-Fe, magnetocrystalline anisotropy and magnetization, depend. on O content 9-28633
Mg_{0.53}Mn_{0.47}Fe₂O₄ single crystal, ferromag. reson. props., 77°K to room temp., 9100 MHz 9-49342
MgFe₂O₄ spinel, absorpt. and Faraday rotation, 300°K, 1 to 8 μ 9-45277
MgMnZn memory cores, origin of threshold-response delay 9-49217
Mn-Zn, coarse-grained, permeability and harmonic distortion increase with induction 9-35573
Mn_{0.6}Zn_{0.4}Fe₂O₄, sublattices magnetizations and superexchange interactions, neutron diff. and Mossbauer obs. 9-39777
Mn_{0.03}Fe_{0.97}O₄ spinel single cryst., ⁵⁵Mn n.m.r. of Mn³⁺ at B-site, anisotropic hyperfine field due to local Jahn-Teller distortion 9-43299
Mn_{1.26}Fe_{1.74}, ferrimag. reson. linewidth, independent grain and dipole narrowing theories comparison 9-45373
Mn_{1.88}Fe_{1.12}O₄, tetragonal and cubic struct. obs., 300K 9-44668
Mn₂Fe_{3-x}O₄, cubic and tetragonal, i.r. absorpt. spectra, lattice vibr. classification 9-39841
MnFe₂O₄, growth of single crystals 9-37087
Ni-Fe, magnetocrystalline anisotropy and magnetization, depend. on O content 9-28633
Ni-Zn:Co²⁺, Fe-rich, temp. spectra, mag. after-effects 9-28632
Ni-Zn-Cr, Co admixtures effect on uniaxial mag. anisotropy 9-41326
Ni-Zn film, prep. and mag. props. 9-45184
Ni_{0.36}Zn_{0.64}Fe₂O₄, ferromagnetic resonance linewidth and shift from tensor susceptibility meas. 9-37666
Ni_{1-x}Zn_xFe₂O₄, ferrimagnetically ordered, semiconductor props. 9-33310
Ni film, prep. and mag. props. 9-45184
NiCo, dense, anisotropy broadening of ferromag. reson. 9-45368
NiCo, mag. annealing, effect of Co ion conc. 9-47273
NiCo mag. annealing effect on magnetomechanical coupling coeff. 9-47273
NiFe₂O₄, polarized neutron diff. exam. 9-48838
NiFe₂O₄, substituted, mag. fields on Sn nuclei 9-26727
NiFe₂O₄ spinel, absorpt. and Faraday rotation, 300°K, 1 to 8 μ 9-45277
NiFe₂O₄ synthetic, chemical and thermal remanence, relative stability 9-39776
NiFe₂O₄ with [111] texture, anisotropy and ferromag. reson. 9-45367
NiMn_{0.05}Fe_{1.95}O₄, ferromagnetic resonance linewidth and shift from tensor susceptibility meas. 9-37666
NiZn, ferromag. reson. linewidth, temp. depend. 9-33618
(Sr_{0.8}Ba_{0.2})₂Zn₂Fe₂O₄, hexagonal, magnetization curves rel. to critical fields 9-26657
(Sr_{0.8}Ba_{0.2})₂Zn₂Fe₁₀O₂₂ hexagonal, localization of Zn²⁺ ions, neutron scatt. meas. 9-42798
TmFeO₃, domain structure and wall energy temp. dependence 9-47275
Y_{1-2x}Ca_{2x}Fe_{3-2x}O₁₂ garnets, Mossbauer effect using Fe⁵⁷, role of Fe³⁺ ions 9-41365
Y₂Fe₂O₁₂, ferrimag. reson., linewidth, independent grain and dipole narrowing theories comparison 9-45373
YFe Garnet, InSb hybrid structure, interaction between spin waves and electrons 9-24320
YFe garnet, spontaneous magnetization temp. depend., 4.2-290°K 9-41328
YFe garnet and ferrite rods, dynamic mode surface waves 9-33478
YFe garnets:Ca²⁺(Si⁴⁺), microwave dielec. loss and permittivity 9-33374
YFeO₃, exchange interaction and g factor determ. 9-45182
YFeO₃ weak ferromagnet, susceptibility tensor, temp. depend. 9-43187
Yb orthoferrite, e.m. propag. 9-45262
Zn_{0.87}Mn_{0.13}Fe₂O₄, mag. struct., neutron diff. obs. 9-43189
Zn_{0.11}-xFe₂O₄ system, Yafet-Kittel mag. ordering 9-41329

Ferroacoustic resonance see *Crystals/lattice mechanics*; *Ferromagnetic resonance*

Ferroelectric devices see *Dielectric devices*

Ferroelectric materials

- alkali metal niobates based highly dense piezoelec. material 9-39676
antiferroelectric transition model, exact solution 9-45011
antiferroelectrics, two-dimens. hydrogen-banded, critical behaviour 9-35491

Ferroelectric materials continued

- antiferromagnet, spontaneous polarization depend. on sublattice magnetization 9-30971
- capacitance, temp. coeffs. 9-47151
- ceramic, losses in strong microwave field, parametric interaction mechanism 9-43111
- ceramic, permittivity var. with elec. field, applic. to parametron 9-30969
- ceramics, pyroelectric effect 9-39684
- ceramics, VK-2, VK-4 and VK-6, film Varikonds nonlinear and switching props. 9-39675
- ceramics with different types of crystal struct., orientational dielec. polarization calcs. 9-47163
- crystals, one phonon differential neutron scatt. cross section, calc. 9-48943
- crystals, simultaneously ferroelec. and ferroelastic, exam. of possible species 9-47166
- cupric formate tetrahydrate, paraelec.-antiferro. transition, DMR obs. of struct. and water mol. motion changes 9-35730
- dicalcium strontium propionate-acetate mixed cryst., $\text{Ca}_2\text{Sr}(\text{C}_2\text{H}_3\text{CO}_2)_{6(1-x)}$, $(\text{CH}_3\text{CO}_2)_x$, hysteresis loops 9-35481
- dielectric const. in infrared-freq. range, method and calc. rels. 9-37589
- dynamic susceptibility, influence of electrocaloric effect 9-39674
- films, possible proximity eff. 9-33385
- glass-ceramic systems, electrooptic properties 9-35484
- guanidinium aluminium sulphate hexahydrate, dehydration nuclei rel. to dislocation sites 9-37115
- hydrogen-bonded antiferroelectrics, Rys F model, generalization to include all ionized vertices 9-35491
- ice, effect of structure and point defects on phase 9-48832
- lattice vibr. spectra of tungsten-bronze type mats., Raman meas. 9-41079
- light and spin wave interaction 9-26588
- literature digest, 1967 9-33368
- MnTO_3 ($\text{T}=\text{Y}, \text{Nb}, \text{Er}, \text{Tm}, \text{Yb}, \text{Lu}$), hysteresis cycles and direct obs. of domains 9-26590
- niobates, tungsten-bronze type crystals, electrooptic properties, experimental study 9-28658
- non-polar crystals, scattering, dynamical and dielec. props. 9-49141
- nonlinearity at s.h.f. investig. 9-47165
- order-disorder, average dipole moment, formula 9-43113
- perovskite, cell deformation parameter behaviour near transition pt. rel. to elec. ordering 9-33032
- perovskite structure mats., dispersion of dielec. constant at h.f. and s.h.f. 9-39677
- perovskites, complex, long- and short-range order of ions 9-46696
- perovskites, complex, solid solns., s.h.f. dielec. props. 9-39678
- polarization, depend. on temp. and field, effective Hamiltonian 9-35479
- polarization, spontaneous, in potassium ferrocyanide type, microscopic mechanism 9-47168
- polarized state formation in polycrystalline materials 9-39679
- polycrystalline, formation of polarized state 9-39679
- pyroelectric and electrooptic coeffs., relationship 9-24225
- pyroelectric coeff. in infrared-freq. range, method and calc. rels. 9-37589
- relaxation process near Curie temp. 9-35483
- rochelle salt, ^{23}Na and ^2D spin-lattice relax. rel. to ferroelec. mode contrib. 9-24345
- rochelle salt, electro-optical effect, rel. to light modulator use 9-43216
- rochelle salt, ferroelec. phase transitions, e.s.r. 9-30972
- rochelle salt, freq. characters, 9-47181
- rochelle salt, influence of ^{60}Co γ rays on properties 9-47179
- rochelle salt, lab. expt. to demonstrate ferroelec. props. 9-37590
- rochelle salt, polarization obs. by ^{23}Na N.M.R., elec. field and γ -irrad. effects 9-26593
- rochelle salt, water molecule dynamics from n.m.r. exam. 9-28765
- rochelle salt, X and γ irradiated, Barkhausen effect 9-47180
- rochelle salt dielectric relaxation and crystal water stoichiometry, activation energy determ. 9-41234
- s.h.f. properties of oxygen octahedron ferroelec. and antiferroelec. mats. 9-47164
- sound attenuation and thermal conduction in KH_2PO_4 -type 9-39693
- tetramethyl ammonium tri-iodomercurate, electro-optical props. 9-43217
- thiourea, phase transitions, effect of hydrostatic pressure 9-28567
- triglycine sulphate, dielec. behaviour 0.5 to 4.5 kMc/s 9-30975
- triglycine sulphate, ferro-paraelec. transitions, 0-23 kbar 9-41248
- triglycine sulphate, film, eff. of electrode material on props. 9-33387
- triglycine sulphate, freq. characters, 9-47181
- triglycine sulphate, influence of ^{60}Co γ rays on properties 9-47179
- triglycine sulphate, i.r. spectra, transition obs. 9-35615
- triglycine sulphate, polarization switching processes, effect of u.s. vibrations 9-47183
- triglycine sulphate, pyroelectric effect under γ -irradiation 9-47182
- triglycine sulphate, second harmonic generation and scatt. by domains 9-45010
- triglycine sulphate, visualization of domain structure at electron microscope level 9-41249
- triglycine sulphate, X and γ irradiated, Barkhausen effect 9-47180
- triglycine sulphate crystals, pyroelectric effect 9-39684
- triglycine sulphate group ferroelectrics in polar and nonpolar cuts, pyroelec. coeff. and dielec. const. deriv. 9-43122
- triglycine sulphate substrate, effect on conduction of Te films 9-28502
- triglycine sulphate-isomorphous ferroelec. solid soln., optical investig. 9-47371
- tryglycine sulphate, dielec. const. by thermal noise method 9-49145
- tryglycine sulphate lab. expt. to demonstrate ferroelec. props. 9-37590
- tungsten-bronze, properties and improvements 9-35490
- twin crystals, orientation of domain walls 9-43112
- uniaxial, phase transition, singularity of thermodynamic quantities 9-43114
- $\text{Ba}_1(\text{Sr}_{0.5}\text{NaNb}_2\text{O}_{15})$, spontaneous polarization, room-temp., pulsed-field method 9-35478
- $\text{Ba}_{2(1-x-y)}\text{Sr}_{1-2x}\text{Nb}_2\text{O}_{15}$, Curie temp., spontaneous polarization and dielec. constants 9-35480
- $\text{Ba}_2\text{NaNb}_2\text{O}_{15}$, single crystal and single domain, nonlinear optical props. study 9-26687
- $\text{Ba}_2\text{NaNb}_2\text{O}_{15}$ 0.53 μm source continuous, in 1.06 μm YAlG:Nd laser cavity 9-40362
- $\text{Ba}_2\text{NaNb}_2\text{O}_{15}$ spontaneous polarization, room-temp., pulsed-field method 9-35478
- $\text{Ba}_{4(1-x)}\text{Na}_{2-2x}\text{Nb}_{10}\text{O}_{38}$, cryst. struct. 9-46781
- BaM^{2+}F ($\text{M}=\text{Mg}, \text{Co}, \text{Ni}, \text{Zn}$) spontaneous polarizations 9-45009

Ferroelectric materials continued

- BaTiC_3 -CdS boundary, photoeffects 9-43128
- BiFeO_3 , atomic struct. obs., X-ray and neutron diffr. 9-37135
- BiMn_2O_5 9-45208
- CaMn_2O_4 induced by antiferromag. transitions and mag. symmetry 9-45208
- $\text{Fe}_3\text{B}_2\text{O}_{13}\text{X}$ ($\text{X}=\text{Cl}, \text{Br}, \text{I}$), Mossbauer, spectra of ^{57}Fe , 80°-1100°K 9-35638
- $\text{Gd}(\text{MoO}_4)_3$, phenomenon analogous to Barkhausen effect 9-30976
- $\text{K}_4\text{Fe}(\text{CN})_6$, phase changes rel. to polarization, dielec. props and stability criteria, theoretical analysis 9-41240
- $\text{K}(\text{D}_{0.55}\text{H}_{0.45})\text{PO}_4$, pressure depend. of transition temp. from neutron diffr., up to 10 kbar 9-49143
- KD_2PO_4 , ferroelec. anomalies in dielec. and piezoelec. props. 9-41244
- KD_2PO_4 , H atom potentials rel. to phase transition mechanism, i.r. spectra obs. 9-26589
- KD_2PO_4 , Ising spin system, relaxation process near Curie temp. 9-35483
- KD_2PO_4 , phase transition obs. from calorimetric meas., KH_2PO_4 comparison 9-41242
- KD_2PO_4 , pressure depend. of transition temp. from neutron diffr., up to 10 kbar 9-49143
- KD_2PO_4 crystal, dielectric permittivity, effect of strong elec. field 9-41241
- KD_2PO_4 crystal, fourth-order electro-optical effect 9-41358
- $\text{KD}_3(\text{SeO}_3)_2$ single cryst., dielec. const. temp. depend., H-bond role in phase transition 9-32855
- $\text{KH}_2\text{PO}_4:\text{Cu}^{2+}$, e.s.r. 9-26793
- KH_2PO_4 -type, proton dynamics and ultrasonic attenuation 9-49140
- KH_2PO_4 -type, sound attenuation and thermal conduction, critical anomaly 9-39693
- KH_2PO_4 , Curie pt. obs. with and without tunnel effect 9-33388
- KH_2PO_4 , domain struct. by Fraunhofer diffraction and Toepler shadow methods 9-47175
- KH_2PO_4 , domains boundaries, X-ray topography obs. 9-28556
- KH_2PO_4 , electrocaloric effect 9-35482
- KH_2PO_4 , H atom potentials rel. to phase transition mechanism, i.r. spectra obs. 9-26589
- KH_2PO_4 , incoherent inelastic scattering cross section 9-28560
- KH_2PO_4 , neutron diffr. intensity anomalies near phase transition pt. 9-40903
- KH_2PO_4 , phase transition obs. from calorimetric, dielectric and electrocaloric meas., KD_2PO_4 comparison 9-41242
- KH_2PO_4 , proton tunneling, n. scatt. obs. 9-24219
- KH_2PO_4 , Slater model, first order phase transition 9-45008
- KH_2PO_4 , transition, dilatometric invest. 9-28561
- KH_2PO_4 , u.s. wave propag. near transition temp. 9-48949
- KH_2PO_4 crystals, dynamical scattering and dielec. props. 9-49141
- KH_2PO_4 , heat capacity anomaly near T. 9-43117
- KNO_3 , solid state battery, form. 9-47890
- KNO_3 film, dielec. characters. 9-49144
- KNbO_3 , cry. struct., X-ray and micro-electron diffraction investig. 9-46788
- KNbO_3 , phase transition rel. to chain structure 9-32901
- $\text{KTa}_{1-x}\text{Nb}_x\text{O}_3$, electron scatt. obs. 9-37591
- KTaO_3 , electron scatt. obs. 9-37591
- $\text{LiD}_3(\text{SeO}_3)_2$ single cryst., H-bond network, deuteron mag. reson. obs. 9-33389
- LiNbO_3 , internal fields by acoustic e.p.r. of Cr^{3+} and Nd^{3+} 9-28748
- LiNbO_3 , spontaneous polarization, room-temp., pulsed-field method 9-35478
- LiTaO_3 , spontaneous polarization, room-temp., pulsed-field method 9-35478
- $\text{ND}_4\text{D}_2\text{PO}_4$, pressure dependence of transition temp. from neutron diffr. 9-49143
- $\text{NH}_4\text{H}_2\text{PO}_4$, pressure dependence of transition temp. from neutron diffr. 9-49143
- $\text{NH}_4\text{PF}_6\cdot\text{NH}_4\text{F}$, phase transitions from n.m.r. relaxation times anomalies 9-35727
- $(\text{NH}_4)_2\text{BeF}_4$, transition, n.m.r. study, mag. screening of ^{19}F 9-43118
- $(\text{NH}_4)_2\text{SO}_4$, order-disorder transition 9-33391
- $(\text{NH}_4)_2\text{SO}_4$, order-disorder transition 9-33390
- $(\text{Na}_{1-x}\text{Li}_x)\text{NbO}_3$ solid solutions ceramics, new stable phase, transition to anti-ferroelectric state 9-26389
- $\text{Na}_2\text{K}_{1-x}\text{TaO}_3$, dielectric behaviour rel. to phonon modes from i.r. and Raman spectra, 4-600°K 9-47366
- $\text{NaBa}_2\text{Nb}_2\text{O}_{15}$, O_{15} transition temp. variations on quenching 9-28562
- $\text{NaBa}_2\text{Nb}_2\text{O}_{15}$ and related mats., lattice vibr. spectra, Raman meas. 9-41079
- $\text{NaD}_3(\text{SeO}_3)_2$ single cryst., H-bond network and phase transition obs. from deuteron and ^{23}Na mag. reson. 9-33392
- $\text{Na}(\text{D}_{0.5}\text{H}_{0.5})_2(\text{SeO}_3)_2$ system, phase diagram 9-30973
- $\text{NaNH}_2\text{SO}_4\cdot 2\text{H}_2\text{O}$ leuconite, n.m.r. and phase transitions 9-43301
- NaNO_2 , far i.r. reflectivity spectra, temp. depend. 9-41370
- NaNO_2 , far i.r. absorption, temp. depend. 9-33163
- NaNO_2 , phase transition at -95°C, thermal expansion and dielec. const. obs. 9-35486
- NaNO_2 , u.s. attenuation near critical pts. 9-44827
- NaNO_2 crystals, dynamical, scattering and dielec. props. 9-49141
- NaNbO_3 , structure, comparison with normal room temp. structure 9-39290
- $\text{Ni}_3\text{B}_2\text{O}_{13}\text{X}$ ($\text{X}=\text{Cl}, \text{Br}, \text{I}$), crystal field and optical absorpt. characters. 9-45259
- $\text{Ni}_3\text{B}_2\text{O}_{13}\text{X}$ ($\text{X}=\text{Cl}, \text{Br}, \text{I}$), Mossbauer, spectra of ^{57}Fe , 80°-1100°K 9-35638
- $\text{Pb}_{0.92}\text{Bi}_{0.07}\text{La}_{0.01}(\text{Fe}_{0.405}\text{Nb}_{0.325}\text{Zr}_{0.27})\text{O}_3$ thin films, polarization, hysteresis, coercivity, Curie temp., resistivity, dielec. const. 9-35487
- Pb zirconate-titanate ceramics, optical and electrooptical properties, improvements 9-35485
- $\text{PbFe}_{0.5}\text{Nb}_{0.5}\text{O}_3$ props. over wide temp. and freq. range and reversible characters. 9-41243
- $\text{PbMg}_{0.33}\text{Nb}_{0.67}\text{O}_3$ props. over wide temp. and freq. range and reversible characters. 9-41243
- $\text{Pb}(\text{Sc}_{1/2}\text{Nb}_{1/2})_{1-x}\text{Ti}_x\text{O}_3$ system, phase transitions, and structural props. 9-28563
- PbTiO_3 , low temp. phase transitions 9-43119
- PbTiO_3 - PbMgWO_3 - PbZrO_3 solid solns., permittivity in static fields, 20 kV/cm max. 9-43103
- $\text{Pb}(\text{Zr}_{0.5}\text{Sn}_{0.5})\text{O}_3$ ternary system, electrostriction constants during antiferro-ferroelectric phase change 9-24222

Ferroelectric materials continued

- PbZrO₃, antiferroelec. → paraelec. transform., effect. of hydrostatic press. 9-47190
 PbZrO₃, antiferroelectric domain structures 9-35492
 PbZrO₃ antiferroelectric, props over wide temp. and freq. range 9-41243
 Pb(ZrTi)O₃, single crystals, growth and hysteresis loops 9-48806
 Pb(La_{0.5}(M³⁺+0.5x)_{0.5}Ti_{1-x}O₃, (M=V or Nb), props. rel. to composition 9-24220
 RbD₂PO₄, permittivity, anomalous behaviour below Curie point 9-47177
 RbH₂AsO₄, ⁸⁷Rb n.m.r. quadrupole coupling, elec.-field-gradient tensors, transition obs. 9-33393
 RbH₂PO₄, ferroelec. anomalies in dielec. and piezoelec. props. 9-41244
 RbH₂PO₄, high temp. phase transition 9-47176
 RbH₂PO₄ crystal, fourth-order electro-optical effect 9-41358
 RbHSO₄, transition mechanism from p.m.r. obs. 9-26800
 Sb₂S₃, pyrocurrents due to spontaneous polarization 9-41246
 Sb₂S₃ single crystals, optical props. in phase transition temp. range 9-45261
 SbSI, Curie temp. lowering, permittivity, temp. and hydrostatic pressure depend. 9-28565
 SbSI, damping of u.s. waves as function of illumination, near phase transition temp. 9-46992
 SbSI, dielectric constant, dynamical nonlinearity 9-35488
 SbSI, Kern-Harbeck effect, effect of hydrostatic pressure 9-26591
 SbSI, phase transition near critical Curie pt., optical obs. 9-24221
 SbSI, phase transition point from thermal expansion coeff. 9-30974
 SbSI elec. field effect on phase boundaries, splitting mechanism 9-41250
 SbSI properties 9-41245
 SbSI u.s. absorpt. coefficient and velocity up to Curie point (20°C) 9-42960
 SbSI photopyro-effect 9-24243
 SnTe-GeTe, phase transition from Mossbauer effect obs. 9-26592
 SnTe, phase transition from Mossbauer effect obs. 9-26592
 (Sr,Bi,Lu)MnO₃ solid solns., new ferroelec.-ferromag. material 9-47178
 (Sr,Bi)MnO₃ solid solns., new ferroelec.-ferromag. material 9-47178
 Sr_{0.5}Ba_{0.5}Nb₂O₆, spontaneous polarization, room-temp., pulsed-field method 9-35478
 Sr_{1-x}KNb₂O₁₅, spontaneous polarization, room-temp., pulsed-field method 9-35478
 Sr₂Ba_{1-x}Nb₂O₆, elasto-optic matrix elements 9-33394
 Sr₂Ba_{1-x}Nb₂O₆, electro-optical effect, temp. dependence 9-26710
 SrTiO₃:Cr³⁺, dielec. constant temp. and elec. field dependence rel. to optical line shifts 9-24415
 SrTiO₃:Fe:Mo and Ni:Mo, photochromic, optical and EPR studies 9-26742
 SrTiO₃, antiferroelectric phase transition at 110°K rel. to normal vib. modes 9-24223
 SrTiO₃, dispersive-type, acoustic anomalous behaviour near Curie point 9-35277
 SrTiO₃, dispersive-type, dynamics of soft mode 9-41247
 SrTiO₃, electron scatt. obs. 9-37591
 SrTiO₃, in one para., and two ferroelectric states simultaneously at 0°K 9-28566
 SrTiO₃, single crystals, dielec. const., loss tangent and conductivity, temp. depend. 9-39694
 TbCrO₃, induced by antiferromag. transitions and mag. symmetry 9-45208
 triglycine sulphate, domains boundaries, X-ray topography obs. 9-28556

barium titanate

- acoustic anomalous behaviour near Curie point 9-35277
 birefringence calc. from dipole field correction due to lattice deformation 9-28558
 capacitor, mat. purity rel. to device charact. 9-49150
 ceramic, s.h.f. dispersion of dielec. constant in low-temp. phases 9-39687
 critical fluctuations from n scatt. obs. 9-33386
 cubic-tetragonal transitions in high resistivity single cryst. 9-43115
 dielectric constant, reversible depend. on field strength above Curie point 9-41239
 dielectric constant dispersion in wide range of freqs. and temps. 9-39688
 dielectric constant in s.h.f. region, contrib. to theory of dispersion 9-47173
 dipolar fields and energy of 180° domains 9-28557
 dispersive-type, dynamics of soft mode 9-41247
 domain boundaries, transmission electron microscopy 9-35477
 c-domain single crystals, dielec. props. in decimeter wave region 9-47170
 domain walls, visibility on X-ray diffr. topographs and comparison with Fe-Si ferromag. walls 9-39682
 electro-optic effect, wavelength dependence, 0.4 to 1.1 μm 9-47323
 electron scatt. obs. 9-37591
 ferroelec. transition, Pippard scheme for sp. ht., thermal expansion and isothermal compressibility 9-30970
 film, eff. of electrode material on props. 9-33387
 films, thin, prep. by vacuum deposition 9-46729
 irradiation effects on electrophysical props. of crystals and ceramics 9-41238
 microwave-absorption fluctuations at Curie temp. 9-28559
 Mossbauer γ-rays scatt. by opt. phonons assoc. with paraelec.-ferroelec. phase transition 9-39691
 Nettleton's work and the position of Ti atom rel. to polariz. inversion reviewed 9-33384
 nonlinear properties of single crystals under linear compression 9-39690
 nucleation models for 1st.-order transition from 9-42924
 phase transition rel. to chain structure 9-32901
 phase transitions in single crystals, influence of uniaxial compression 9-47169
 polarization, depend. on temp. and field, effective Hamiltonian 9-35479
 polarization reversal, press. effect 9-43116
 polarization reversal in sinusoidally varying fields 9-24218
 pyroelectric effect in single crystals and Co, Fe or Ni doped crystals 9-39684
 Raman scattering by polaritons in tetragonal crystals rel. to dielec. constant calc. 9-35671
 rare-earth doping effects on elec. props. 9-39685
 scattering, dynamical and dielec. props. of crystals 9-49141
 s.h.f. dispersion of dielec. constant in low-temp. phases 9-39687
 s.h.f. dispersion of dielectric constant 9-39686
 surface state of single crystals, X-ray diffr. study 9-39683
 tetragonal, domain reactions in ageing 9-49142
 BaTi_{1-x}Ni_xO₃ dielectric constant, -192° to +300°C at 1 KHz, single crystals and optical props. 9-41362

Ferroelectric materials continued

- barium titanate continued**
 BaTiO₃:Co, electromechanical props. 9-47171
 BaTiO₃:CdTiO₃ solid soln. single crystals, elec. props. 9-47172
 BaTiO₃:Co₂Ta₂O₇ solid soln., s.h.f. dielec. props. 9-39689
 BaTiO₃:Co₂Ta₂O₇ solid soln., s.h.f. dielec. props. 9-47174
 BaTiO₃:Ni₂Nb₂O₇ solid solns., s.h.f. dielec. props. 9-47174
 BaTiO₃:Ni₂Nb₂O₇ solid solns., s.h.f. dielec. props. 9-39689
 BaTiO₃:SrTiO₃ solid soln. dielectric constant, reversible, depend. on field strength above Curie point 9-41239
 triglycine sulphate, domains boundaries, X-ray topography obs. 9-28556
- Ferroelectric phenomena**
 antiferroelectric transition, phenomenological theory of second-order transition 9-47184
 antiferroelectrics, two-dimens. hydrogen-banded, critical behaviour 9-35491
 Barkhausen effect in X and y irradiated crystals 9-47180
 Cochran's theory, extensions reviewed 9-33384
 Curie temp. elec. field depend. in paraelec. phase 9-39681
 demonstration in laboratory using Rochelle salt, triglycine sulphate 9-37590
 dicalcium strontium propionate-acetate mixed cryst., Ca₂Sr(C₂H₃O₂)₆(n₂). (CH₃CO₂)₆, hysteresis loops 9-35481
 domain structures, theory 9-41309
 domain-orientation current charact., anomalies 9-45007
 in group IV-VI cpds., from a scatt. obs. of lattice dynamics 9-39680
 hydrogen-bonded antiferroelectrics, Rys F model, generalization to include all ionized vertices 9-35491
 losses in ceramic subjected to strong microwave field, parametric interaction mechanism 9-43111
 order-disorder ferroelectrics, average dipole moment, formula 9-43113
 paraelectric large signal susceptibility with Gaussian distrib. of relax. times 9-24217
 Perovskite-type crystals, accompanying orthorhombic deformation of cubic lattice 9-28558
 phase transitions, diffused, thermal expansion coeff. anomalies calc. 9-33383
 phase transitions, sp. ht., thermal expansion, isothermal compress., Pippard scheme 9-30970
 piezoelectrics, mag. ordered, induced ferroelec. mag. obs. 9-39748
 recording of signal by polarizing ferroelectrics 9-47167
 relaxation process near Curie temp. 9-35483
 semiconductors instability phenomena, nonlinear eqn. for electric induction 9-41237
 thermal expansion coeff., anomalous component near broad phase transition point 9-42972
 in GeTe, from phonon temp. dependence calc. 9-39692
 in group IV-VI cpds., from phonon temp. dependence calcs. 9-39692
 KD₂PO₄, Ising spin system, relaxation process near Curie temp. 9-35483
 KD₂(SeO₄) single cryst., dielec. const. temp. depend., H-bond role in phase transition 9-32855
 KH₂PO₄, partially deuterated, ferroelectric mode obs. 9-26756
 KH₂PO₄, transition, dilatometric invest. 9-28561
 Mn²⁺ in (NH₄)₂SO₄ single cryt., EPR investig. in ferroelec. phase 9-31165
 Sn oxide-ceramic devices, field effect studies 9-35489
 in SnTe, from phonon temp. dependence calc. 9-39692
- Ferromagnetic relaxation**
 ferrites, h.f. mag. absorpt., relax. time spectra, theory and expt. 9-41325
 Mn₂Fe_{3-x}O_{41/2}(x<1), and resonance linewidth 9-28739
 YFe garnet, Ca-V-substituted, effective linewidth due to anisotropy near reson. 9-31055
 YFe garnet, effective linewidth due to porosity near reson. 9-31055
 YFe garnet, processes, investigation with propagating magnetostatic spin waves 9-45241
- Ferromagnetic resonance**
see also Ferrimagnetic resonance
 antiferromagnetic spiral, spin wave resonance 9-37786
 dislocations effects on line-width from relax. time of scattered magnons 9-33620
 ferrite, polycrystalline, precession relax. by spin-wave excitation 9-24337
 ferrite disk, shape effect from shift meas. 9-33617
 ferrites, subharmonic reson. and magnetization precession 9-35704
 ferromagnetic thin film, influence of subdomain struct. 9-43180
 films, thin, polycryst. mag., eqns. for Fourier transforms of magnetization components, general case soln. 9-47422
 haematite, thermally processed 9-43270
 hexaferrites, nature of bandwidth 9-45362
 invariant form, phenomenological theory 9-24475
 line-width, infl. of dislocations from relaxation time of scattered magnons 9-33620
 lines, inhomogeneous broadening 9-45363
 liquid ferromagnet, isotropy considerations 9-23529
 metal plates, field and linewidth, ang. depend. 9-45364
 mode calcs., hyperbolic and trigonometric 9-41417
 nonlinear instability at 9.3 Gc/s 9-41418
 nonlinear theory 9-37787
 Permalloy films, reson. absorpt. at r.f.'s 9-47423
 permalloy films irradiated reson. patterns in parallel and perp. orientations 9-45370
 Permalloy layers with non-mag. layer composite 9-43183
 spherical sample, theory and meas. method 9-45360
 uniaxial ferromagnet, uniform reson., oscill. behaviour of mag. moment 9-26789
 Ba_{1-x}Fe_xO₆₀ and Mn substituted single crystals, 9-45365
 Ca_{2-x}Bi_{2-x}Fe_{x-2}V_xO₁₂, garnet, rel. to magneto-elastic coupling coeff. 9-37664
 Co films, relaxation times 9-33645
 Co films, reson. absorpt. at r.f.'s 9-47423
 Dy, in for i.r. 9-49341
 FeBO₃ linewidth, anisotropy fields and g factor, obs. 9-47424
 Ga_{0.85}Fe_{0.15}O₃, angular depend. of line width 9-37788
 K₂CuCl₄·2H₂O, anomalous, nature 9-45366
 Mg_{0.53}Mn_{0.47}Fe₂O₄ single crystal, props., 77°K to room temp., 9100 MHz 9-49342
 Mn-FeNi film with ferro-antiferromagnetic interaction 9-37789
 Mn₂Fe_{3-x}O_{41/2}(x<1), linewidth 9-28739
 Ni-Fe thin layers, effect of O on spin wave excitation 9-45369
 Ni-V alloys, absorption, g-value temp. depend. 9-24477
 Ni-Zn ferrite thin film 9-45184
 Ni, 20-380°C 9-24476

Ferromagnetic resonance continued

Ni, resonant field, line width and temp. depend. determ., 9.2 – 26.2 Gc/s, –160 to 20°C 9-41419
Ni_{0.36}Fe_{0.64}O₄ 9-37666
Ni ferrite thin film 9-45184
NiCo ferrites, dense, anisotropy broadening 9-45368
NiFe₂O₄ with [111] texture, and anisotropy 9-45367
NiMn_{0.05}Fe_{0.95}O₄, linewidth and shift from tensor susceptibility meas. 9-37666
NiZn, ferrite, linewidth temp. depend. 9-33618
PbTiO₃-LaFeO₃ solid solns., 9 GHz absorption 9-39784
Pd(–5at.%)Ni alloy, anisotropy determ. 9-24478
Tb, in for. i. 9-49341
Tb single crystal, 2.5-3 mm. rel. to magnetoelastic effects 20° to 240°K 9-45158
Y_{3-x}Tb_xFe_{5-x}Ga₂O₁₂, with Tb³⁺ and Ga³⁺, anisotropy of reson. field and line width 9-33619
YFe garnet, and Ca-V-substituted, effective linewidth due to porosity and anisotropy, field depend., microwave freqs. 9-45371
YFe garnet, no 2-magnon scatt., ferromag. resonance linewidth, 9.3 GHz. 4.2-300 K 9-41420
YFe garnet epitaxial films 9-45372
YGa garnet, double, obs. 9-49343

Ferromagnetics see *Magnetic properties of substances*/ferromagnetic Ferromagnetism

see also *Antiferromagnetism*; *Exchange interactions*; *Ferrimagnetism*; *Ferromagnetic relaxation*; *Ferromagnetic resonance*; *Magnetic properties*/ferromagnetic; *Magnetization process*; *Magnetization state*
amorphous, model, non-requirement of crystal structure 9-35550
b.c.c. lattices, symmetric Bloch walls, effect of domain width on thickness and energy 9-24298
Bloch walls in thin films, transient gyromagnetic behaviour 9-26640
coercive force due to inclusions exptl. test of Neel's theory 9-47244
combination scattering of sound 9-48961
correlation theory in narrow energy band 9-24287
critical indices for system of spins of arbitrary dimensionality on lattice of arbitrary dimensionality 9-45095
critical phenomena, generalized molecular field calc. 9-35545
critical point spin correlation functions, exponent inequalities 9-45097
Curie point, ferromagnetism demonstration using Monel metal 9-22035
dilute, critical behaviour 9-28600
Dzyaloshinsky-Moriya ferromagnet, stat. model w.r.t single cryst. 9-33448
film, saturation magnetism, review 9-49209
Heisenberg ferromagnet, Green's function methods 9-28606
Heisenberg ferromagnet, spontaneous magnetization, upper bound 9-49196
Heisenberg ferromagnet, two-dimensional, with S=1/2, transition temp. 9-45107
Heisenberg ferromagnet with arbitrary anisotropy energy, role of monionic correl. functions 9-39755
Heisenberg magnets, spin pair correlation studied using thermal Green function method 9-33449
Heisenberg magnet, u.s. attenuation, heuristic improvement 9-41087
Heisenberg model, anisotropic, mag. order impossibility 9-41289
Heisenberg model, classical anisotropic, high temp., critical indices 9-45096
Heisenberg model, general spin anisotropic, high temp. series expansion 9-47770
Heisenberg model, Griffiths' theorems 9-35549
Heisenberg model, isotropic, with long-range interactions absence 9-49194
Heisenberg model, spin correl. functions, high temp. expansions 9-33450
Heisenberg quasi-two-dimensional, rel. to 3-dim. mag. systems 9-45098
induced anisotropy meas., systematic errors 9-37652
Ising, one-dimensional, non-existence of spontaneous magnetization 9-24286
Ising chain model of spin interactions in rare-earth chlorides 9-33456
Ising ferromag., dilute, of simple cubic lattice, critical behaviour 9-28600
Ising ferromagnets, randomly diluted, nonanalytic behaviour of magnetization 9-43163
Ising lattice system, pair correls. influence on phase transition 9-41300
ising lattices with random arrangements of ferromag. and antiferromag. bonds 9-49200
Ising model, Bogoliubov inequality applic. 9-25047
Ising model, correlations at critical point 9-24294
Ising model, critical point behaviour with higher-neighbour interactions 9-47769
Ising model, field-theoretic and functional- integral aspects 9-31776
Ising model, Green's function approach 9-35540
Ising model, high-temp. sp. ht. 9-35542
Ising model, isothermal susceptibility by Kubo formula 9-39756
Ising model, magnetization in nonzero mag. field 9-39757
Ising model, mobile-electron 9-47236
Ising model, spin correl. functions, high temp. expansions 9-33450
Ising model, time-depend. one-dimens., extension to spin S=1 9-35541
Ising model, uncoupling of correlation functions 9-33443
Ising model sp. ht. above Curie temp., Pade approximant analysis 9-37645
Ising model with general spin and phase transition, theorems 9-22114
Ising model with long-range interac., expansion of free energy per spin 9-25045
Ising model with long-range interaction, critical behaviour 9-41301
Ising model with second-neighbour interac., exact results and approx. soln. 9-33445
Ising system, dynamic behaviour near critical point 9-45099
Ising type model, exact solution 9-33444
itinerant d-electron model 9-45094
linear spin chain, two-magnon absorpt. intensity and magnetoelc. effect 9 39760
liquid, isotropy considerations 9-23529
liquid, model, non-requirement of crystal structure 9-35550
localized-moment behaviour above Curie temp., by the theory of itinerant ferromagnets 9-43164
Lorentz field and dipole coupling, excess exchange energy, const. calc. 9-41302
magnetic domain structure in crystals 9-31032
magnon coherent states 9-26627
magnon-drag thermoelectric power analysis, mag. field eff., low temp. 9-33400

Ferromagnetism continued

magnons, effective g factor rel. to excitation energy 9-45106
magnons, g factor renormalization 9-28603
magnons, localized, around impurity spin, energies 9-26626
magnons scattered on dislocations, ferromagnetic relaxation time for infl. of dislocations on resonance line-width 9-33620
metals, localized magnons rel. to reduced susceptibility function 9-47235
movement theorem for resonance line shapes arising from decoupled Green's function eqns. 9-34034
in nondegenerate narrow energy bands, variational principle 9-24288
paramagnetic metals, anomalous Hall eff. through ferroparamagnetism transition 9-28593
parametric amplification of non-uniform spin wave modes, Green's function theory of system 9-45043
phonon energy spectrum including magnon controls 9-46967
s-band, strongly correlated magnetism 9-45045
second order phase transitions, Landau theory modified near critical point 9-31782
sound velocity renormalisation at Curie point 9-39514
spherical model, generalised 9-24292
spin-orbit coupling effects on transition metal ions in crystalline environments 9-24285
stars, neutron, ferromag. transition conditions for dense nuclear matter 9-41642
superparamagnetic relax. time, magnetic field effects 9-24317
susceptibility increase by action of additional pulsating field 9-45132
thin films, statistical approach, reduced matrix procedure 9-31038
transition to paramagnetic state, thermo. props. 9-31031
transport theory 9-47255
two-magnon scattering amplitudes for pits of arbitrary shape 9-45101
U.S. attenuation at low temp. 9-49198
wavenumber-dependent susceptibility, connection proportional to system entropy 9-26629
XY model, isothermal susceptibility by Kubo formula 9-39756
XY model with impurity spin, transform. of spin to Fermi operators 9-41298
FeCl₂.H₂O, magnon-phonon interaction rel. to ordering obs. in far i.r. 9-45077
YFe garnet, i.r. radiation scattering by two magnon processes 9-45337

spin wave theory
correlation function approximation, self-consistent, for Ising ferromagnet. 9-28602
cubic crystals, ellipticity of $\pi/2$ -spin waves 9-31027
dynamic characteristics at low temp. 9-31033
ferrites, dispersion equation and soln. for plane spin waves 9-45171
films, thin, band model for mag. props. 9-31037
Heisenberg, linear-chain, magnetically-coupled impurities, analysis 9-45093
heisenberg, self-energy calcs. 9-45103
Heisenberg, spin wave interactions theory using time-depend. Green function technique 9-24289
Heisenberg cubic model, expression for critical index of spin diffusion coeff. 9-41296
Heisenberg ferromagnet, a spin-wave theory 9-49199
Heisenberg ferromagnet, long wavelength spin fluctuation near critical point, freq. estimation 9-43162
Heisenberg ferromagnet, optical surface spin-waves 9-26628
Heisenberg ferromagnet, spin motions, energy and magnetization equil. values w.r.t. temp. 9-41299
Heisenberg ferromagnet, with magnetic impurity, perturbed states 9-39761
Heisenberg model, critical props. 9-24291
Heisenberg model, f.c.c.<1 alloys, transformation props. of states under crystal symmetry operations 9-45104
Heisenberg model, spin correl. functions, high temp. expansions 9-33450
Heisenberg spin system, one-dimens., freq.-dependent self-correlation function 9-24293
Heisenberg spin system, two-dimensional, phase transition 9-24295
Heisenberg system, including polar excitations and exchange interactions 9-24296
Heisenberg, finite linear chains spin operators time dependence 9-24290
impurity magnons, mode modification 9-28598
insulators of ellipsoidal shape, 1st-order instability threshold for arbitrary pumping config. 9-45102
interaction of beam of paramagnetic molecules with ferromagnet, spin wave amplification 9-31028
Ising, 3-dimens. ferromagnet, spin-spin correlation function above Curie temp. 9-28604
Ising, interaction, with integral spin, monotonicity of correlation 9-47237
Ising ferromagnet, critical-point correl. exponents, rigorous inequalities 9-35543
Ising ferromagnet, self-consistent correlation function approximation 9-28602
Ising ferromagnet. S=1/2. scaling form of spin-spin correlation function above Curie temp. 9-37648
Ising model, recurrence formulas for graphs for compact form of partition function 9-34037
Ising model, spin correl. functions, high temp. expansions 9-33450
Ising system dynamic behaviour 9-47234
isothermal susceptibility of ferromagnet 9-39756
isotropically interacting classical spins of arbitrary dimensionality, linear chain, exact soln. 9-33446
magnetization, temp. depend. correction to Bloch formula rel. to anharmonic effs. in magnon system 9-31033
magnetoelastic interaction with lattice vibrations 9-28599
magnon assembly, zero sound oscillation 9-49195
magnon effects on thermal transport in insulators 9-44847
magnon interactions in hematite 9-35552
magnon states, volume and surface, probabilities for existence 9-26630
magnon states coherent excitation by transverse r.f. mag. field 9-47239
magnon states propagation, effect of sudden change in external mag. field 9-35548
matnetization curves and spin correlation functions, numerical calc. 9-26631
metals, corrections 9-45092
metals, impurity excitations rel. to reduced-susceptibility function 9 47235
metals, multiband theory of inelastic neutron scatt. at low temp. 9-33447
neutron scatt. by spin waves near Curie pt. 9-49201
non-linear interaction terms 9-35544

Ferromagnetism continued**spin wave theory continued**

- Permalloy layers with non-mag. layer composite, reson. obs. 9-43183
 phenomenological theory, book 9-47223
 resonance in thin films, excitation of uniform precession mode 9-43165
 spin-1/2 Heisenberg ferromagnet, critical temp. and indices, decoupling scheme calc. 9-35546
 spin-1/2 Heisenberg ferromagnet, thermodynamic behaviour 9-31026
 spin-1/2 Heisenberg ferromagnet, Wick's theorem, diagrammatic representation 9-31025
 spin-1/2 XY model on f.c.c. lattice, partition function and specific heat, high temp. series expansion 9-39759
 stability at finite temp. 9-39754
 three-dimensional model with classical spins of high-dimensionality 9-45105
 transient evolution of power adsorbed under e.m. excitation influence of mag. dipole rad. 9-37646
 transient growth of uniform and parametric states with dipole radiation 9-28601
 Al-I-N film tunnel junctions (M=Ni,Pd alloys, Fe, Gd), excitation rel. to electron tunnelling 9-44995
 $\text{CuCl}_2(\text{CH}_3\text{NH}_2\text{Cl})_2$, heat transport by magnons 9-37369
 Dy magnetocryst. anisotropy 9-37655
 Fe, critical and spin-wave scatt. of neutrons 9-31030
 Fe, dynamics, neutron scattering study 9-45110
 Fe, high-field studies of band ferromag. 9-43166
 Fe, spin diffusion const., theoretical estimate 9-41306
 Fe:B spin-wave gap, n.m.r. detection 9-45109
 Ho, excitations in conical and spiral mag. phases 9-45111
 Ho, spin wave dispersion relation in spiral mag. phase 9-45112
 Ni-Fe alloys, press. depend. of wave energies 9-33455
 Ni-Fe thin layers, excitation depend on O 9-45369
 Ni, high-field studies of band ferromag. 9-43166
 Ni, neutron scatt. by spin waves near Curie pt. 9-49201
 Ni spectrum, neutron scatt. meas. 9-45115
 Tb magnetocryst. anisotropy 9-37655
 YFe garnet, magnetostatic, propag. rel. to relaxation processes investigation 9-45241

Ferromagnets *see* **Magnetic properties of substances/ferromagnetic****Feynman diagrams** *see* **Field theory, quantum/interactions****Fibre optics** *see* **Fibres/optical****Fibres**

- collagen, broad-line n.m.r. of H_2O and D_2O 9-43304
 composites, filamentary, with hexagonal symm., elastic const. 9-37216
 cotton, birefringence, obs. 9-28656
 elastic, reinforcing plastic-elastic matrix, continuum model 9-31823
 electrical rot., meas., using scanning electron microscope 9-38344
 and filament and films, form., patent 9-46961
 glass, anelasticity, apparatus for damping of torsional oscillations 9-37223
 glass, effect of cloth covers on absorpt. acoustic waves 9-39516
 glass, Mossbauer obs. of struct. 9-45302
 glass, strength and struct. 9-30468
 glass, thermal insulator, bond with organic binder, patent 9-24061
 glass-fiber paper, insulating material in space, outgassing behaviour obs., 100-1800°F 9-38173
 graphitized C, fine struct. 9-30557
 inorganic, refractory, reinforced composite materials 9-35236
 light scatt. at normal incidence 9-33518
 light scatt. by fibres immersed in liquid rel. to birefringence meas. 9-28656
 mechanical props., meas. using light sensitive potentiometer 9-28328
 nylon 6,6, oriented, elastic anisotropy, expt. values compared with aggregate theory 9-35147
 nylon 66, spectral study of structural change due to heat treatment 9-27938
 nylon-6, surface and bulk crystallinity, i.r. spectroscopy 9-48843
 optical, scattering at oblique incidence 9-26713
 polycapromide, sound velocity temp. depend., infl. of processing method 9-24024
 polyethylene, oriented, elastic anisotropy, expt. values compared with aggregate theory 9-35147
 polyethylene terephthalate, oriented, elastic anisotropy, expt. values compared with aggregate theory 9-35147
 polypropylene, oriented, elastic anisotropy, expt. values compared with aggregate theory 9-35147
 polypropylene deformation, during prep., spinning, drawing and heat setting 9-39416
 ramie, birefringence, obs. 9-28656
 reinforcement for composite materials 9-23971
 strain obs. with electron microscope stage modification 9-32891
 threads, synthetic complex, struct. 9-44795
 viscous, crack propag. through layer between two elastic half-planes, tearing 9-33061
 X-ray diffraction, pole figure integrator 9-44652
 B, tensile strength at high temp. after exposure to air, effect of SiC coating 9-30679
 B, vapour deposited on W, cracks rel. to chem. interaction 9-48866
 B filaments, vapour-deposited, crystal structure 9-46780
 C, lattice vibrations along c-axis, neutron spectrometry 9-28414
 C, polyacrylonitrile based, stress graphitization 9-39493
 C, preferred orientation effect on (hk) interferences in electron diffraction 9-28259
 C, reinforcing SiO_2 , mech. props. of composite material 9-44773
 C, structure determ. by e.s.r., g values rel. to preferred orientation 9-32904
 C monofilaments, glassy, prep., struct. isotropy 9-28195
 C to reinforce alloys, popular article 9-46944
 SiC, critical surface tension of wetting, rel. to interact. with resins and coupling agents 9-23620
 SiC, vapour deposited on W, macrostruct. 9-48866

optical

- beam waveguide, astigmatic, 3-dimensional, ray theory 9-27401
 bundles, filling factor, photometric determ. 9-38413
 bundles, rad. propag. 9-36375
 coaxial waveguide, radiation pattern 9-32036
 glass, opalescent, from $\text{SiO}_2\text{-B}_2\text{O}_3$ melt with metallic oxide, patent 9-23613

Fibres continued**optical continued**

- glass composition for use in device core material, development and properties 9-41957
 glass composition study for high ultra-violet transmission, properties 9-22472
 glasses chemical compatibility, definition and meas. 9-38412
 light transmissivity, effect of interdiffusion of glass 9-34219
 medical field applic., review 9-46014
 minimal coupling between neighbouring fibres 9-32035
 pile of fibre-optic components, photo-optical charact. 9-48106
 plastic, loss measurements and loss mechanisms 9-32034
 plastic, off-axis transmission charact. 9-36374
 principles and practical developments, review 9-29474
 quartz, fused, for u.v. transmission 9-48104
 system, grazing total internal reflection ray obs. 9-38400
 urine velocity meas. applic. 9-46015

Field emission *see* **Electron emission/field emission****Field emission microscopes** *see* **Electron microscopes; Ion microscopes****Field theory, classical**

- see also* **Electromagnetism; Gravitation; Relativity**
 arbitrary Green's function formulation of arbitrary fields 9-22064
 conformal group, finite-component field representation 9-34011
 conservation laws, geometrical theorem on asymptotic space-time props. 9-43723
 field clots, variation of width with time 9-34014
 five dimensional, particle self-energy concept, analysis 9-27163
 gauge fields, non-Abelian, long-range self-interaction 9-43724
 geodesic Killing orbits and bifurcate Killing horizons 9-34007
 geomagnetic potential, calc. from multipole series 9-41595
 Hamiltonian structure canonical formalism, higher time and/or spatial derivatives 9-31752
 Huygens model, $\Gamma_{\mu\nu}$ interpretation 9-22063
 particle in central field, perturbative forces 9-22183
 radiation from a point source, mass zero limit compared with mass zero theory 9-41740
 resistance of linear isotropic homogeneous medium, analysis 9-43827
 self-coupling classical field theories, an example 9-45741
 separation of potential fields for Laplace eqn. 9-36117
 on spacelike mass shells 9-38204
 statistical, using functional methods 9-38203
 time-invariant conservative fields, boundary problems soln. by computer using integral eqns. 9-31751

Field theory, quantum

- see also* **Dispersion relations; Elementary particles; Physics fundamentals; Quantum theory**
 abelian fields, special type 9-22492
 algebraic, spectrum of internal symmetries 9-22493
 analytic representation 9-22494
 asymptotic limits on annihilation-creation operators 9-38424
 for atomic electron shells calc. 9-48380
 Bergman-Wigner eqn. theory of confluence 9-34239
 Bethe-Salpeter bound-state wave function, normalization condition derivation 9-25399
 Bethe-Salpeter eqn. in momentum space, bound-state soln. 9-41979
 Bose field canonical commutation rel. representation form, connection with finitely many degrees of freedom 9-29508
 Bose field Lagrangian functions relativistic theory in scalar representation 9-32100
 boson fields with cut-off interactions 9-22518
 bound states props., poles and branch points 9-36414
 c-number generating functionals, formalism 9-43938
 canonical commutation relations to theories involving local currents 9-41987
 causality and locality in S-matrix framework 9-36419
 Chew-Low type equations, new solutions 9-43945
 chiral transformations for hadrons, chiral invariant Lagrangian, current equal-time commutator and conservation law 9-34257
 commutation relations, non-equivalent representations, aspects of theory of meas. 9-29513
 of composite particles, rel. to S-matrix theory 9-32229
 composite systems, e.m. interactions 9-34237
 compositeness conditions 9-22501
 in comprehensive textbook on the theory of elementary particles 9-32116
 conformal group, finite-component field representations 9-34011
 coupling const. continuation for total K and T matrices 9-36415
 creation and annihilation operators of covariant, unstable particle 9-29507
 of currents, realization, and solvable model 9-32136
 De Sitter symm. one particle theory 9-22506
 with degenerate Lagrangians, algebraic approach 9-29511
 dimensionality minimality principle, space topology and SU symmetries for fundamental eqn. 9-40393
 Dirac eqn. spin operator, covariant generalization 9-27426
 Dirac equation, five classes of transformations 9-32107
 Dirac field, interpretation of energy momentum tensor 9-22510
 Dirac field, nonlocal expressions for energy and particle-density 9-43946
 Dirac theory and existence of magnetic monopoles 9-22503
 dispersion theory sum rules, review 9-48135
 eikonal expansion, relativistic, rel. to elastic scatt. 9-41983
 electrodynamics, scalar, gauge invariance and mass 9-32111
 electromagnetic, background radiation and quantum theory, a relationship? 9-22100
 electron-nucleon inelastic scatt., field theoretical model 9-22534
 Feynman graphs asymptotics in spinor theory, integer t-channel ang. mom. 9-29522
 Feynman propagator in imaginary time, Monte Carlo integration 9-36421
 Feynman-parameter representations for momentum- and configuration-space diagrams 9-40394
 Feynman-parameter representations of old-fashioned perturbation diagrams, rules 9-29523
 Feynman-parameter representations of perturbation diagrams, renormalization procedure 9-22511
 four-point function, holomorphy envelope, comments on Wu's upper bound 9-46039
 G-SL(2,k), irreducible unitary representations, square integrable, explicit formulae for characters 9-27431
 gA^3 theory, related functional derivative eqn. 9-48129

Field theory, quantum continued

gauge fields and algebra of polarizations, c-number soln. of source-free field eqn. 9-38425
gauge-fields algebra, current-algebra relations recovering for current mixing model 9-29515
Goldstone particles in de Sitter space of -ve curvature, degenerate vacuum assumption 9-41977
Goldstone theorem and its application to various theories, review 9-41980
Green's method for ^{88}Sr 2^+ and 3^+ states 9-36590
Haag's theorem, generalization 9-43956
hadrons scatt., quasipotential relativistic model, amplitude for small, large momentum transfer, high energy 9-29556
Hamiltonian uniqueness in field theories 9-43936
Hankel-transformed perturbation theory functions 9-29520
harmonic oscillator representation by motion of charged particle in elec. field, extension to excited state 9-22495
infinite momentum frame transition, Hilbert space of states 9-38430
infinite-component field model of current algebra 9-27433
infinite-component field model of local vector and axial vector current algebra 9-27434
invariant quasi-free states, eff. of Bogoliubov transformations on fermion field 9-28769
Ising model, functional-integral aspects 9-31776
Jost-Schroer theorem generalization 9-29506
Klein-Gordon field, new energy-momentum tensor 9-29514
Klein-Gordon Field, square integrable, with interaction, probability density 9-32109
Klein-Gordon multiparticle states, measure-theoretical description 9-41982
Lagrangian, breakdown of current algebra 9-32113
Lagrangian, canonical; field quantization, current algebras and sum rules 9-38431
Lagrangian, degenerate, algebraic approach 9-29511
Lagrangian, phenomenological, invariant, construct. 9-27429
Lagrangian systems, quadratic eigenvalue and assoc. time-depend. problems, existence and completeness theorems, soln. 9-22496
Lagrangian theory and current algebras, relation, algebraic formalism 9-27436
lagrangians, phenomenological, general struct. 9-27428
Lee model, standard and extended with inelasticity, self-energy and scatt. phase shifts 9-27440
Lee model with symmetry breaking, application of Goldstone theorem 9-41980
Lee point-coupling relativistic model, Haag theorem 9-27435
Lie algebras, semi-simple, nonexistence theorem for realizations 9-41978
Lie model generalization, appl. to K-meson singular scatterings 9-43944
local, without divergences 9-22504
local fields, invariance props. w.r.t. transformation groups involving arbitrary functions 9-29512
logic structure, quantum, field definition 9-22091
Lorentz group, Majorana representations, in infinite-component field theory 9-22507
Lorentz invariance breakdown, field operators nonvanishing vacuum expectation values determ. 9-41975
Low equations, stability of solns. 9-41976
massless particles, free field covariant transformation under Poincare group 9-38432
mechanism diagrams to express singularities of unitarity integrals 9-38422
momentum- and configuration-space diagrams, Feynman-parameter representatives, general rules 9-40394
 $\lambda\phi^4$ ladder approx. soln. of Bethe-Salpeter eqn., daughter Regge trajectory eqn. 9-36418
Noether theorem on quasi-stochastic semigroup of relativistic endomorphisms 9-41974
nonlocal field, 2-dimens. space-time, source of isospin freedom 9-34238
nonlocalized, Wightman formulation, Jost pts., quasilocalizability and theorem proofs 9-38435
observable algebra and gauge transforms 9-43948
oscillator, anharmonic, functional calculus in low approx. 9-27432
parafield theory in conservation of number of fermions 9-22514
PCAC propagator, sum rule connecting spin zero and spin one parts 9-43942
perturbation diagrams, Feynman-parameter representations, renormalization procedure 9-22511
perturbation diagrams, old-fashioned, Feynman-parameter representation 9-29523
perturbation series, renormalized regularized, convergence 9-36417
phase factors in discrete symmetry operations 9-40391
Poincare commutators for generators of inhomogeneous Lorentz transformation 9-43949
propagators of massive and massless high spin particles 9-43941
quark and antiquark composite systems, bilocal field theory appl. 9-43977
radiative corrections, i.r., electron colliding beam expt. 9-27464
Regge behaviour of production amplitudes 9-25396
relativistic, commutator expectation value weakening, local field theorem 9-22505
relativistic, localizability of massless particles 9-29525
renormalization theory 9-34244
scalar field, conserved vector currents induced symmetries 9-25394
scalar field operator, behaviour of vacuum expectation value 9-27425
spectral function sum rules in field-theory model describing spin one and zero part. 9-38481
spectral function sum rules of Lee-Weinberg-Zumino theory applic. of Stuckelberg formalism 9-43951
spectral-function sum rules, vector dominance eff. 9-25398
spinor amplitudes in invariant space; analyticity, unitarity, crossing and constraints 9-38433
spinor filds $2(2s+1)$ component free, theory 9-27424
spinor sign change observation under 2π rotations 9-32101
spinor theory in which primary field is transformed according to SU(3) representation 9-43943
state vector spaces with indefinite metric 9-32108
SU(3) \times SU(3) field-algebra Lagrangians, Violation of Weinberg's second sum rule 9-27430
textbook including quantization covariant perturbation, Bethe-Salpeter eqn. 9-48132

Field theory, quantum continued

textbook showing relation between Feynman, canonical and dispersion theory 9-43947
of two-particle subsystems, general formalism 9-25400
unitarity of renormalized matrix in axiomatic field theory, problems of 'dressing' of the operators 9-27439
of unstable particles, and nonunitary representations of Poincare group 9-22500
vector spaces with indefinite metric and pole-type ghosts 9-32104
vertex functions at large momentum transfer exponential decrease of Wu-Yang type 9-46052
Weinberg, and daughters, recurrence reln. for Feynman amplitude for 4 spinless particles scatt. 9-38454
wick's theorem used in the transformation of system quantities 9-43760
Wick theorem for boson system, allowing evaluation of time-ordered products of Heisenberg operators 9-46038
Wightman functions, representation in terms of two-point singular functions 9-32103
Yang-Mills fields, generalized, self-coupled, gauge invariance of S-matrix 9-25401
zero-mass π theories invariant under c-number translations of π field, general framework study 9-48185
N field multiplet, chiral transformation 9-22508
 $N^{3/2}$ from πN , mass and width calc., model Hamiltonian determ. 9-27565
 $N^{3/2}$ from πN , mass and width calc., model Hamiltonian determ. 9-34336
pp interac., fireball production, parameters calc., E=30-250 GeV 9-32215

electromagnetic field see *Quantum electrodynamics*

interactions

see also *Elementary particles/interactions; Nuclear reactions and scattering. Entries on interactions involving named particles are listed under the particles concerned*
Bethe-Salpeter equation in unequal mass Wick-Cutkosky model, moving system, solns. 9-43940
bilocal fields 9-43977
charged spin- $1/2$ field, canonical quantiz. in presence of e.m. interac. 9-29510
current commutation reln., field depend., Lagrangian gauge invariance 9-25395
Fermi and Yukawa theories equivalence, examples of second degree programs 9-43939
Feynman amplitudes, renormalized, parametric integral representation 9-41988
Feynman diagrams, high energy behaviour via electric circuit analogy 9-41990
Feynman integrals, divergent, origin shifts 9-41989
gravitation, particle production during first 10^{-20} sec. of big bang 9-38441
Mandelstam representation, compatibility with crossing symmetry and unitarity 9-36413
many-particle states, creation, annihilation, Heisenberg fields 9-25397
non-linear, non-local, convergent theory 9-22502
nonlocal interac., asymptotic limits of annihilation-creation operators 9-22497
particles with elec., mag. charges, chiral equivalence and mag. charge quantization 9-38429
unstable elementary system, the use of a single field operator 9-41994
Wick-Cutkosky model in moving system, soln. of Bethe-Salpeter eqn. 9-43940

interactions, strong

see also *Elementary particles/interactions, strong*
Bethe-Salpeter amplitudes in static model 9-43955
SU(2) \times SU(2) chiral current, construction of canonical field theory 9-46041

interactions, weak

see also *Elementary particles/interactions, weak*
Heisenberg's non-linear theory, weak interactions introduced 9-32106

meson field

see also *Mesons; Nuclear forces*
asymmetries of space and time in particle physics 9-22515
chiral transformations, group theoretic approach 9-22508
current operator, observed, identification with meson field 9-22547
meson-nucleon Lagrangians, chiral SU(2) \times SU(2) symmetric, construct. 9-27493
pseudoscalar, massive gauge fields 9-41981
scalar theory with inclusion of symmetry breaking 9-41980
strong-coupling solns. with hard core for elastic N-N interac. 9-27548
SU(2) \otimes SU(2), non-linear realization describing π and vector meson fields 9-38434
sum rules for spectral functions 9-29516
in textbook of quantum mechanics 9-41756
vector meson interacting with gravitational field 9-38222
 π field, SU(2) \otimes SU(2), 3D nonlinear realization 9-38434

quantization

see also *Quantum theory/quantization*
bilocal fields 9-43977
charged spin- $1/2$ field, canonical quantiz. in presence of e.m. interac. 9-29510
from classical symplectic structure, and variational theory 9-46037
correlation theory of quantized e.m. field, dynamical eqns. 9-46036
Fermi field, local, infinite-component, transforming under representation of SL(2,C), construct. 9-22507
impossibility of quantizing Maxwell's eqns by means of a potential $A_\mu(x)$ 9-46044
infinite-component fields transforming under Majorana representations of Lorentz group 9-22507
magnetically charged particles, quantization condition connecting electric and mag. charges 9-22503
Majorana fields, Fourier components with spacelike momenta 9-22507
of photomixing 9-25355
Ranita-Schwinger eqn., generalization to resolve gauge invariance inconsistency 9-32105

scattering

see also *Elementary particles/scattering*
amplitude phase in t-plane, analytic props. 9-46055
Bethe-Salpeter eqn., calc. of phase-shifts, least squares method 9-34265
Bethe-Salpeter eqn., correction 9-27442

Field theory, quantum continued
scattering continued

- Bethe-Salpeter formalism, scattering Green's function, synthesis of multiple poles 9-46074
bound states in potential- scatt. theory, Hilbert space of n -particle system 9-43937
Compton, intensity-depend. freq. shift 9-48131
Feynman integral associated with tetrahedron graph, and absorptive parts of scatt. amplitudes 9-43957
Fubini sum rules satisfied by Born-approx. amplitudes in class of infinite-component field theories 9-48130
Haag-Ruelle scattering theory, Wightman field with non-trivial S -matrix, asymptotic completeness 9-29509
interactions, separable non-local, Schwinger variational principle 9-32102
Levinson's theorem in Lee model with ghosts 9-46040
luminescence, parametric, statistics of field and photocounts 9-28738
Nambu-Salpeter-Bethe eqn. numerically solved for N - N scatt. 9-44049
non-relativistic time-dependent theory 9-22520
nonrelativistic, causality condition formulation and applic. 9-27427
Pade approximant to partial-wave scatt. amplitude, denominator convergence to Jost function 9-38428
phase-shifts and mass shift relation in standard and extended Lee models 9-27440
Pomeranchuk theorem, asymptotic amplitudes, equivalence and relations 9-29521
Reggeon-graph technique 9-27441
vertex functions of fields belonging to arbitrary representations of Lorentz group, invariant amplitude expansion 9-48150
ep inelastic, field-theory calcs. rel. to scaling laws, cross-sections and momentum of the virtual photon 9-38472

Films

- absorbance at surface opposite surface of incidence 9-49237
adsorbed, with slowly rotating disc, viscosity and velocity field determ. 9-34714
anti-reflecting coatings, thickness control in vacuum deposition 9-38402
Bose, thin, demonstration of 'Further Generalized Bose Concentration' and ODLRO 9-25053
coatings, three layer anti-reflection, design 9-27377
concentrator, aberration 9-31996
Cu, abnormal opt. props. 9-31068
epoxy resin adhesive, transparency changes due to u.v. irradiation 9-47328
fluid, convection, study method 9-47835
of fluid, viscous, adjacent to gas stream, waves 9-42631
individual layer thickness interferometric control. errors 9-38404
interference colour, calc. 9-34202
metal, constants calc. from complex refl. and transmitted amplitudes, series expansion 9-32013
metallic, min. optical thickness and max. absorption in standing wave 9-41360
metallic, thickness and complex index determ. 9-27378
nonabsorbing on nonabsorbing substrate, ellipsometric thickness meas. 9-28212
periodic assemblies, pass and stop intervals, discrimination between 9-25353
photographic, linear multiple image storage 9-36409
photographic, resolution determination with resolvometer 9-34236
photographic, transmittance fluctuations rel. to r.m.s. density 9-34235
polymers, film-forming, melt rheology 9-26048
quality evaluation using optical particle detector 9-23623
radiant power flow and absorbance 9-36377
reflectivity rel. to transmission 9-41940
rubber adhesive, transparency changes due to u.v. irradiation 9-47328
thickness meas. by optical method 9-36941
thickness rel. to beam coherence and wavelength 9-41940
Ag, thin, preparation method 9-22449
CdTe film photoconverters, props. 9-31903

liquid

- see also Adsorbed layers; Contact angle; Helium/liquid; Superfluidity; Surface tension*
 n -alkoxy ethanol monomolecular films, surface viscosity at various temp. and pressures 9-23448
boiling, nucleate, heating surface effects 9-36925
boiling in boundary layer flows, heat transfer, phase flow and friction determ. 9-32816
charged monolayers, influence of monovalent counterions in subsolution 9-23447
cholesteric liq.-cryst., optical props. 9-39103
contact angle, meas. technique 9-36839
contact angle and depth of free-energy minimum 9-48689
detergent, interface properties 9-23446
diffusion from free surface into film in laminar flow over defined shapes 9-48690
emulsion, curvature at oil/water interface 9-34935
flow down inclined plane, nonlinear development of long surface wave instabilities 9-40767
Gibb's elasticity eqn., correction 9-23452
heat transfer to falling films 9-23445
interface monolayer thickness calc. from van der Waals gas constant a 9-23449
interfacial, flow and profile rel. to drops coalescence 9-30365
interference holography 9-34185
kerosene, rheology near solid boundary 9-39069
lake evaporation retarding monolayer, effect on temp. 9-47515
lubricant ultra-thin, obs. by multiple gas laser beam 9-36842
mass transfer, gas-liquid and solid-liquid, on inclined plane 9-34868
monolayer, in evaporation retardation 9-30464
oil thickness between rolling discs meas., variable-magnetic-reluctance technique 9-36841
profile, elastohydrodynamic, time-depend. meas., optical-interference method 9-36840
rheology near solid boundary 9-39069
soap, peristaltic mode rel. to frequency analysis of scattered light 9-46634
tension, rel. to disjoining press. and contact angles betw. film and bulk liq. 9-44543
water, vertical flow, temp. profile meas. 9-30384
GaAs_xP_{1-x} epitaxial layer growth in ga -GaAs-GaP system 9-36917
He II, vorticity associated with flow 9-48733
He unsaturated films, model describing onset of superfluidity and third sound 9-40813

Films continued**liquid continued**

- He vortex surface effects 9-26142
N₂, dispersed flow film boiling, expt and anal. 9-26166

Films, solid

- see also Thickness measurement*
acoustic props. of thin films, meas. tech. 9-37323
alkali halides, grown from melt, cell and platelet structures 9-23627
alloy, binary, effective surface diffusion coeffs. vol. diffusion effect in electron diff. obs. 9-39379
alloy evaporation processes on hot metal filaments, emission of high-energy electrons 9-35204
anodic oxide films form., Tafel slopes field depend. 9-47471
anthracene scintillator screens, prep. and props. 9-39860
atom collision with hard impurity layer, atom props. influence on interaction singularities 9-42981
austenitic alloys, irradi., thickness and void size determ. 9-48755
boiling from elec. conducting wire to boiling water, heat transfer obs. at different pressures 9-30462
c PbI₂, photosensitive, holographic recording 9-38390
crystalline, electron scattering origin determ. 9-48757
density data using scanning electron microscope 9-30544
deposition, substrate temp., laser meas. 9-25132
dielectric, etch rates meas. technique 9-23633
dielectric, evaporated, optical coating, stress meas. 9-37231
electron beam scattering, highly focussed kV, by thin film-substrate system 9-35047
electron microscopical specimen support, thermal conduction 9-35289
electron microscopy investigation of transverse sections on solid substrates, ion etching preparation 9-40888
electron probe micro-analysis method for films $<4\mu m$ 9-24607
electroplating prep. of mag. thin film structures for data storage 9-28621
epitaxial, grown on high-alloyed GaAs substrates, defects 9-36944
epitaxial layer thickness meas. by i.r. interference method 9-30482
f.c.c. metal, orientated, anal. of diffraction line broadening 9-44657
ferromagnetic, thermal recording of optical images on thin films 9-47265
and fibres and filaments, form., patent 9-46961
filter deposition, multilayer, in high current vacuum system 9-36958
flexible, strength meas. 9-26336
fluoride, condensation mechanism 9-28217
foils, electron microscope to reveal deformation markings and dislocation structure 9-28246
garnet, growth on non-garnet single crystal, patent 9-46723
glass, chemical vapour deposition apparatus 9-26189
glass, chemical vapour deposition apparatus 9-26189
graphite, growth from carbon-iron melt 9-37067
graphite glide and rotation during sedimentation 9-39368
group IV-VI alloy epitaxial films, growth techniques and surface research 9-39157
growth, obs. using high energy scanning electron diff. system 9-39161
growth of thin plates from gas phase 9-48761
heteroepitaxial, rotation and translation of islands in growth 9-46722
Hoffmann ripple theory, reinterpretation 9-49206
insulating, shock tube meas. of thermal parameters 9-39524
interfacial amorphous type, polarization struct. and struct. information transmission 9-32840
interference microscopy of thickness, replication method 9-23622
lead stearate, multilayer, structure 9-39349
metal, energy loss of low energy protons and deuterons 9-28439
metal, evaporated, optical coating, stress meas. 9-37231
metal, quantum oscillations of thermodynamic props. in weak mag. field 9-30812
metal, thickness during deposition, continuous ellipsometric determination 9-32845
metal, thin; ω_s surface plasma waves prod. by light excitation 9-25941
metal, thin, activation energy calc. rel. to three stages of growth 9-23631
metal, thin, oxidation problems 9-39950
metal, vacuum deposition prep. process on plastic, patent 9-28218
metal oxide, parabolic law for growth kinetics 9-39951
metal phthalocyanine, thin, cry. struct. and mol. orientation 9-23786
metallic, thickness meas., hill-climbing technique 9-39804
metallic, thin, on curved substrates, etching technique for microcircuit prod. 9-25162
metals, d.c. sputtering with r.f.-induced substrate bias 9-23634
metals, macro- and microstructures and residual stress after deposition, combined effects on fatigue strength 9-39434
metastable thin film epitaxial struct., growth, review 9-34987
molecular layers on bulk substrate, m.p. lowering, n.m.r. meas. 9-40817
networks growth morphology of electron-beam deposited films 9-23632
noble metals, growth on alkali halides 9-23636
nucleation, growth and sputtering techniques, conference 9-33990
oligatomic, preparation, and mag. props. 9-45162
optical thin, deposition control by quartz crystal monitor 9-36957
oxide, anodic, form., Tafel slopes field depend. 9-47471
oxide, on glasses and insulating materials, investigation of structure with electron microscope 9-26182
oxidized stressed surface layer on thin metal foils, bending 9-31189
permalloy, by cathode plasma sputtering, struct. determ. by electron microscopy 9-40843
Permalloy layers with non-mag. layer composite, struct., electron microscope obs. 9-43183
phonons, quantum theory of atomic vibrations 9-23995
polycarbonate, charged-particle irradi., etching rate accel. by photo-oxidation effect 9-32271
polycarbonate, crystallization under acetone vapour, e. microscope exam. 9-26183
polychloroprene, i.r. dichroism and stress rel. to crystallinity and orientation, obs. 9-30650
polycrystalline, stress relief mechanism 9-28339
polyethylene, crack, zone structure near tip 9-28373
polyethylene, surface crystallinity rel. to substrate surface energy, i.r. obs. 9-34986
polyethylene terephthalate, oriented drawn films, tensile and shear yield stress 9-30667
polymer, polycrystalline, deformation characterization rel. to molecular orientation 9-30666
polymer photoresist, scattering effects in ion beam exposure, comments 9-32846
polymers, film-forming, molecular constitution 9-25791
polymers, friction and lubrication 9-26360

Films, solid continued

- polypropylene, crack, zone structure near tip 9-28373
 polytetrafluoroethylene, morphology rel. to light-scatt. patterns 9-46709
 polyvinyl chloride-acetate copolymer very thin films, prep. and meas. 9-34981
 polyvinylchloride, stretched, dioctyl-, diethyl phthalate plasticizers i.r. dichroism rel. to orientation, obs. 9-28654
 preservation during specimen preparation by epoxy-sandwich technique 9-35193
 production by low press. sputtering system of magnetron type, new design 9-31728
 protective, single and double, thickness meas. using radioactive isotopes 9-39154
 rare-earth alloy of Co-Sm system, high-coercive- force, prep. by getter sputtering 9-44627
 refractory metal oxides, lattice energies, heat of atomization, bond energy and dissociation energies, rel. to fund. props. 9-30494
 residual stresses 9-37232
 semiconductor, thermomagneto-magnetic effect, influence of inelastic carrier scattering 9-35494
 size effects on diagram, susceptibility of free-electron gas 9-24102
 sputtered multicomponent thin, composition model 9-44623
 sputtering, r.f., of thin multilayers, deposition rate and uniformity 9-36955
 sputtering apparatus, r.f., patent 9-46551
 stress in optical thin films, production during deposition, mechanism and control 9-28341
 stresses, internal, thin films on Si substrates, Twyman-Green interferometry meas. 9-35165
 superconducting, ultra-thin, high T_c obs. and enhanced electron-phonon coupling 9-37459
 superconducting thin films, strain effect on T_c 9-41177
 surface coating, r.f. inductive plasma sputtering process 9-46720
 surface coating on strained substrate, fracture 9-42900
 thermal conduction of electron microscopical specimen support 9-35289
 thickness meas. of coatings and foils 9-29166
 thin, anisotropy of kinetic phenomena w.r.t. cryst. symmetry and thermodynamics 9-33289
 thin, on reflecting surface, thickness meas. by ellipsometry 9-36939
 thin, piezoelec. transducer applications 9-30980
 thin, prod. by cold plasma condensation 9-34995
 thin, prod. by gas discharge polymerization 9-40845
 thin, superconductors, type I, varying thickness, flux distribution observations 9-28472
 thin, vacuum evaporated, particulate contamination 9-44626
 thin foils, ^4He charge state fractions 9-39550
 vacuum-deposited, effect of diffusion on thickness 9-40838
 vibration modes, surface 9-48945
 welded clad metal diffusion layer structure 9-40983
 Ag-Ge, structure anal. by X-ray diffraction 9-28213
 Ag-Se couple, lateral diffusion 9-42859
 Ag, deposited in ultra high vac., influence of air, O_2 , N_2 and H_2O vapour on growth 9-34993
 Ag, evap., electron diff. intensities variation with energy loss 9-35053
 Ag, growth on alkali halides 9-23636
 Ag, hypersonic attenuation, 8.4-10.0GHz 9-44821
 Ag, nucleation on MoS_2 single crystal 9-34992
 Ag, on mica, inclined fault concs. rel. to presence of H_2 , O_2 or H_2O during deposition 9-35097
 Ag, on plastic substrate, thermal conductivity 9-33192
 Ag, thickness during deposition, continuous ellipsometric determination 9-32845
 Ag $_2$ S, struct. transform., compared with bulk state 9-48927
 Ag $_2$ Se, struct. transform., compared with bulk state 9-48927
 Ag $_2$ Te, struct. transform., compared with bulk state 9-48927
 Ag films, evap., electron diff. intensities variation with energy loss 9-35053
 Ag thin optical, prep. method 9-22449
 AgCl, evaporation on C replica of Si p-n junctions 9-32847
 AgCl, evaporation on C replica of NaCl surface 9-32848
 Al-Au, diffusion anomalies 9-35123
 Al, alloying into Ge, obs. 9-33116
 Al, deposition by vacuum evaporation, effect of electric field on critical thickness 9-32838
 Al, electron energy-loss spectra, convolution effects by electron transmission 9-47015
 Al, evap., electron diff. intensities variation with energy loss 9-35053
 Al, evaporated, intrinsic tensile stress meas., temp. depend. 9-37233
 Al, fatigued, surface deform. markings, direct correlation of dislocation structures 9-23878
 Al, granular, microwave resistivity in supercond. transition region 9-26504
 Al, growth, elec. field effect on form. and substruct. 9-48762
 Al, internal friction studies for attenuation of mechanical oscillations 9-23856
 Al, photoelectric yield, plasma resonance in vac. due to light irradiation 9-41282
 Al, secondary electrons, energy spectrum, prod. by α particles and fission fragments 9-49177
 Al, supercond., strain effect on T_c 9-41177
 Al, thermal cycling effect on surface hillocks prod. by annealing 9-30705
 Al $_2$ O $_3$, 500 to 6000Å, traps, study using thermoluminescence glow curves in range 30 to 300°C 9-33245
 Al $_2$ O $_3$, band structure parameters estimation from infl. of light on Al oxidation rate 9-31000
 Al $_2$ O $_3$, growth kinetics on Cu-Al alloys 9-23635
 Al $_2$ O $_3$, O K-shell X-ray prod. by 20-100keV protons 9-24073
 Al $_2$ O $_3$, self-supporting, thermal conductivity 9-39543
 Al $_2$ O $_3$, small-angle scatt. of ^{32}S and ^{16}O beams 9-35298
 Al alloys, X-ray transmission thickness gauging, composition effects 9-39156
 Al chemically vapour deposited, adhesion to steel 9-28376
 Al epitaxial films on NaCl substrates, nucleation and growth struct. 9-36945
 Al foils cold-worked, annealing processes, h.v. electron microscope obs. 9-42909
 Al on W(110) face, structure from LEED obs. 9-26184
 Al oxide anodic films growth on fine wires, mech. effects, oxide plasticity enhancement 9-31192

Films, solid continued

- Al thin films evaporated on air-cleaved NaCl, structure, electron microscope obs. 9-26185
 AlSb, semiconducting, condensation 9-28487
 Au/Pb supercond. layered films, evap. and co-evap. prep., transition obs. 9-26528
 Au-Ag, alloys, nucleation on amorphous substrate 9-26187
 Au, Au-ion irradi., substages III annealing, activation energies 9-33106
 Au, deposited in ultra high vac., influence of air, O_2 , N_2 and H_2O vapour on growth 9-34993
 Au, evap., electron diff. intensities variation with energy loss 9-35053
 Au, growth on alkali halides 9-23636
 Au, nucleation on amorphous substrate 9-26187
 Au, sputtered, hillock growth and stress relief 9-42717
 Au evaporated on NaCl and KCl, effects of forced high nucleation densities 9-32843
 Au field ion microscopy 9-23626
 Au films, evap., electron diff. intensities variation with energy loss 9-35053
 Au on NaCl, epitaxial and polycryst. rel. to H_2O , CO_2 contamination 9-46724
 Au on W, props. observed by field-ion and field emission microscopy 9-23624
 Ba, desorption of Ar, temp. dependence 9-40849
 BaO-SiO $_2$ glass, two-phase structure development 9-26174
 BaTiO $_3$ ferroelec. thin films, prep. by vacuum deposition 9-46729
 Be, adsorption of N, H, O, CO on thick film obs. 9-36964
 Be, preparation for transmission electron microscopy using chemical saw 9-39256
 BeO, small-angle scatt. of ^{32}S and ^{16}O beams 9-35298
 Bi, orientation rel. to substrate 9-44624
 BiO $_{2.7-2.8}$, orientation rel. to substrate 9-44624
 Bi $_2$ O $_3$ layers, prep. by evaporation and props. 9-39162
 C, deposited on Ag, coherence 9-37112
 C, evaporated, e.s.r., effect of water vapour 9-39904
 C, evaporated, graphitization under heat treatment, 1000° to 2200°C 9-39453
 C, pyrolytic, deposited in fluidized beds from hydrocarbons, comparison, 1200-1400°C 9-24536
 C, small-angle scatt. of ^{32}S and ^{16}O beams 9-35298
 C annealing, activation energies 9-23937
 C deposition, effect of substrate structure 9-44625
 C deposition on Fe and Ni surfaces from methane, ethane and ethylene 9-24535
 C deposits, surface topography, effect on structure and mech. strength 9-26226
 C foils, thin, ^4He charge state fractions 9-39550
 Cd electrodeposits, growth on Cu single crystals 9-30490
 CdS-fused quartz system, elastic surface wave structure and dispersion 9-45844
 CdS, deposited on cleavage surfaces of NaCl, KCl, KBr, and on amorphous cellulose nitrate, structure 9-40840
 CdS, epitaxial growth of single cryst. layers on ZnS platelets 9-34988
 CdS, heteroepitaxial, on GaAs, growth hillocks and cryst. structs. 9-48758
 CdS, vacuum deposited, oriented crystallization 9-42724
 CdS epitaxial, prod. by gas transport reactions 9-42722
 CdS-CdTe heterojunctions, photoelec. effects 9-30988
 CdSe, transistor 9-49125
 CdSe, vapour phase deposits growth on single crystal substrates 9-46726
 CdTe, co-evaporated, nucleation and structure, influence of stoichiometric deviations 9-36949
 CdTe, of anomalously high photovoltage, number of microphotoelements determ. 9-37613
 CdTe, stimulated recrystn., effect on visible and cryst. struct. and cond. 9-39163
 CdTe, vapour phase deposits growth on single crystal substrates 9-46726
 CdTe layers, growth, struct. depend. on underlying temp. 9-40846
 Co-(10 wt.%)Cr, oxide scales formed during high temp. oxidation, microstructure 9-31194
 Co, electroless, crystallite structure from transmission electron microscopy 9-42718
 Co, electroless, on Si single crystal, interfacial stress 9-30654
 CoO-Co $_3$ O $_4$ on Co, struct. and composition rel. to prod. above or below allotropic transform. temp. 9-32841
 CoO, plastic deform. behaviour, effect of stoichiometry 9-23882
 CoO thin foils prep. method for transmission electron microscopy 9-42743
 Cr, electroplated, on Cu single crystal, effect on stress-strain parameters 9-26328
 Cr, grown by molecular beam incidence, crystallite shape by light reflection 9-32909
 Cu-Au(Al) alloy, effective surface diffusion coeffs., vol. diffusion effect in electron diff. obs. 9-39379
 α -Cu-Ge alloys, recrystallization 9-37278
 α -Cu-Ge evaporated, faulting meas. by X-ray diffraction 9-23820
 Cu-Ni, controlled deposition using electron beam and two pure sources 9-48763
 Cu, continuous epitaxial (001), on rocksalt, changes in twin structure during growth 9-39158
 Cu, elastically deformed, ^{63}Cu n.m.r. 9-24507
 Cu, evaporated, intrinsic tensile stress meas., temp. depend. 9-37233
 Cu, growth on alkali halides 9-23636
 Cu, internal friction studies for attenuation of mechanical oscillations 9-23856
 Cu, thin, randomly and preferentially oriented, X-ray K absorpt. edge fine structure 9-47383
 Cu, vacuum evaporated, structure defects 9-30488
 Cu, vapour deposited, density meas. by X-ray absorpt. 9-30483
 Cu $_2$ -Se, epitaxial layers, formation, struct. and props. 9-46721
 Cu $_2$ S, prep. and optical props. 9-46727
 Cu $_2$ Se, struct. transform., compared with bulk state 9-48927
 Cu $_2$ Te, struct. transform., compared with bulk state 9-48927
 Cu alloy coatings, effect on fatigue strength of Cu 9-33058
 Cu deposition on backing, thermal conductivity rel. temperature 9-26445
 Cu heavily rolled sheet, electron transmission exam. 9-39272
 Cu on Zn-(3 wt.%)Cu alloy, cracking rel. to grain boundary reaction type precip. in alloy 9-23957
 Cu oxidation kinetics in thin film range 9-43329
 Dy $_2$ O $_3$, recrystallization behaviour on pulse annealing 9-30489

Films, solid continued

- Er₂O₃, grain growth kinetics on pulse annealing 9-40842
 Er₂O₃, grain growth kinetics on pulse annealing 9-40841
 Er₂O₃, recrystallization behaviour on pulse annealing 9-30489
 EuO, hologram thermomagnetic writing and reconstruction of hologram 9-48060
 Fe-(40 at.%)Ni alloy oxidized at high temp., scale struct. and chem. composition 9-33669
 Fe, electrodeposited, electron microscope fine structure data 9-36942
 Fe₂O₃, growth characteristics on steel in dil LiOH soln. at 300°C 9-39952
 Fe epitaxial, recrystallization 9-42723
 Fe epitaxial layers on oriented Au support, electron microscope exam. 9-48759
 Fe on Ir, props. observed by field-ion and field emission microscopy 9-23624
 GaAs:Cr epitaxial layers, growth from solution 9-48760
 GaAs, epitaxial layers, chemically-deposited, growth and perfection 9-36951
 GaAs, formation by flash evaporation 9-36960
 GaAs, semi-insulating, formation, Cr diffusion through SiO₂, patent 9-28219
 n-GaAs epitaxial layers, high-purity, prep. and props. 9-30907
 GaP, vacuum-deposited, structural and optical evaluation 9-42719
 garnet epitaxial, prep. by r.f. sputtering structural props. 9-49210
 Gd, nucleation mechanism of twinning due to thermal stresses set up by electron irradi., electron microscope exam. 9-35100
 GdFe garnet, rel. to magneto-optical recording 9-45271
 Ge-Mg₂Sb₂ amorphous, reordering diffusion process under annealing 9-34985
 Ge, epitaxial, from GeCl₄-H₂ system, smooth surface conditions 9-36948
 Ge, epitaxial deposition on GaAs 9-36946
 Ge, growth and perfection, on sapphire by chemical vapour transport 9-36961
 Ge, heteroepitaxy on GaAs 9-36946
 Ge, heterogeneous nucleation 9-48813
 on Ge, X-ray stress topography 9-32839
 Ge, X-ray stress topography 9-34983
 Ge epitaxial growth on GaAs by GeI₂ disproportionation reaction 9-36947
 Ge layers, non-dislocational, growth from vapour, conditions 9-42750
 Ge on GaAs, plastic deformation 9-37241
 Ho₂O₃, recrystallization behaviour on pulse annealing 9-30489
 In-Te system, phase composition rel. to conc. 9-30484
 In, supercond., strain effect on T_c 9-41177
 InP epitaxial growth on GaAs substrates in open flow system 9-23630
 InSb substrate system, attenuation of elastic surface waves 9-47121
 KCl point defect coagulates due to electron irradi. during microscope exam. 9-42808
 LiNbO₄, sputtered, deposition and piezoelectric characts. 9-42725
 Mg on W(110) face, structure from LEED obs. 9-26184
 Mo on BeO, thermal conductivity 9-24063
 Mo vacuum deposited, struct. and props. in rel. to deposition rate and temp. 9-36943
 NaCl, point defect coagulates due to electron irradi. during microscope exam. 9-42808
 Nb-NbO-Pb Josephson junctions, fabrication by use of getter-sputtering 9-35377
 Nb-Ti-N, supercond. critical current-field meas. in continuous mag. fields 9-35362
 Nb, preparation for nuclear studies 9-48766
 Nb, tunnel junctions fabrication 9-37494
 Nb₂O₅, thickness meas. by electroreflectance interferometry 9-30486
 Nb₃Sn layers, growth from solid Nb-liq. Sn reaction, formation kinetics 9-48764
 Nb superconducting, a.c. losses 9-30878
 NbN, high-field supercond. props. 9-35363
 NbN film prepared by reactive sputtering, upper critical field H_{c2} 9-35359
 Ni-Cr, Sn and solder whisker growth conditions and mechanism 9-35359
 Ni-Fe, annealing in mag. field, effect of elastic stresses 9-33029
 Ni-Re alloy, electro-deposited, phase and chemical composition 9-44791
 Ni-Zn ferrite, prep. 9-45184
 Ni, chemisorption of H on films, static capacitor examination of surface potential 9-24547
 Ni, electroless, on Si single crystal, internal stress 9-30654
 Ni, evaporated, intrinsic tensile stress meas., temp. depend. 9-37233
 Ni, on Cu, pseudomorphic growth for monolayers 9-34989
 Ni, struct. and conductance 9-39589
 Ni, thin, ultraclean, release of compressive intrinsic stress by gas adsorption 9-44758
 Ni ferrite, prep. 9-45184
 NiFe, electrodeposited, stress meas. 9-37234
 NiFe, scales, mech. props. factorial expt. 9-23852
 Pb-PbO-Pb Josephson junctions, barrier-thickness depend. on d.c. quantum interference effect 9-35378
 Pb, quenched after vacuum evaporation, thermal cond. meas. at 2-20°K 9-44848
 Pb vacuum deposited on (110) face of W 9-42720
 PbO, evaporated, diffusion of Bi, autoradiographic obs. 9-26303
 PbS epitaxial film growth on rocksalt by condensation in vac., formation mechanism 9-40844
 PbTe-EuTe system, solid solution investigations 9-39486
 PbTe, co-evaporated, nucleation and structure, influence of stoichiometric deviations 9-36949
 PbTe, epitaxial growth on NaCl, substructural transitions in early stages 9-26186
 Pd-Ag alloy, effective surface diffusion coeffs., vol. diffusion effect in electron diff. 9-39379
 Pd, struct. and conductance 9-39589
 RbBr, electron diffraction study and orientations of halide 9-39229
 RbCl, electron diffraction study and orientations of halide 9-39229
 RbI, electron diffraction study and orientations of halide 9-39229
 Sb₂S₃, crystallization process, X-ray study 9-42726
 Se, lateral diffusion of Ag, rel. to thin-film couple behaviour 9-42859
 Se amorphous, crystallization, electron bombardment-induced 9-32842
 Se amorphous, effect of condensation velocity on crystn. 9-44649
 Se and Se-Pd, crystal structure 9-42796
 Si/SiO₂/Si₃N₄ double-layer, diffusion and distrib. of Na 9-26305
 Si/SiO₂/Si₃N₄ double-layer films, Na diffusion and distrib. 9-26305

Films, solid continued

- Si, epitaxial growth on Si substrate and oxide layer, role of surface migration 9-30491
 Si, epitaxial layers, chemically-deposited, growth and perfection 9-36951
 Si, preparation for observation with electron microscope 9-26190
 Si, with diffusion mask of SiO₂, X-ray topography of strains 9-26246
 Si₃N₄ layers, deposition using photochem. reaction 9-46728
 Si₃N₄ single-layer, diffusion and distrib. of Na 9-26305
 Si₃N₄ single-layer, Na diffusion and distrib. 9-26305
 Si crystalline layer growth on Al₂O₃ substrate, method 9-23667
 Si deposition by electron irradi. of tetramethylsilane, electron diff. and microscopy obs. 9-44628
 Si epitaxial deposition by H₂ reduction of chlorosilanes, gas press. and velocity effects 9-28215
 Si epitaxial layers, C conc. obs. 9-46725
 Si foils, ion irradi., defect prod. 9-44683
 Si foils, ion irradi., e diff. diagrams 9-44697
 Si on sapphire, substrate orientation selection 9-23658
 Si single epitaxy on sapphire 9-34990
 SiC, cubic, reactive deposition, procedure 9-42727
 SiC, formation by reactive deposition and chem. conversion, chem. processes 9-42728
 SiO, evaporated, thermal conductivity 9-39543
 SiO₂, 500 to 6000 Å, traps, study using thermoluminescence glow curves in range 30 to 300°C 9-33245
 SiO₂, chemical vapour deposition apparatus 9-26189
 SiO₂, chemical vapour deposition apparatus 9-26189
 SiO₂, doped, deposited from SiH₄ and B₂H₆ or PH₃, diffusion sources for Si device fabrication 9-23638
 SiO₂, doped, deposited from SiH₄, diffusion characts. and applns. 9-23637
 SiO₂, electron-gun deposited, effects of heating in air 9-48765
 SiO₂, on Si, combined m.o.s. and radiochemical analysis of impurities 9-42814
 SiO₂, SiH₄-O₂ reaction system study 9-23639
 SiO₂ amorphous films, anodic growth rel. to dielec. breakdown 9-45006
 SiO₂ on Si, characterization by electron microprobe and ellipsometry 9-23628
 SiO₂ on Si, surface and interface elec. props. 9-43099
 SiO₂ thermal growth, use of Si₃N₄ as alkali barrier liner 9-33358
 Sn, supercond., as high-speed radiation detectors 9-35367
 Sn, supercond., strain effect on T_c 9-41177
 Sn, supercond., upper critical field meas. 9-35368
 Sn electrodeposited coatings, surface texture 9-36933
 Sn epitaxial, residual strains rel. to mismatch at interface 9-39160
 Sn on W(110) face, structure from LEED obs. 9-26184
 Sn vac. deposited, crystal orientation rel. to pressure deposition rate and thickness 9-39164
 SnTe epitaxial growth on collodion, rock salt and mica obs. by electron diffraction 9-30492
 β-Ti foils, preparation for transmission electron microscopy 9-46772
 Ta-N, parametric study 9-23625
 Ta, preparation by reactive sputtering in mixed Ar/O atmospheres, mechanism 9-42716
 Ta, preparation for nuclear studies 9-48766
 Ta₂O₅, thickness meas. by electroreflectance interferometry 9-30486
 TaO capacitor films, Mo additive, mass spectrometry 9-39968
 Te, lateral diffusion of Ag in Ag-Te couple 9-35135
 Ti-Zr film in getter-ion pump, residual gas analysis 9-38176
 TiO₂, preparation and optical applics. 9-36962
 U foils <2000 Å, preparation for electron microscopy rel. to stress corrosion cracking 9-23777
 V, preparation for nuclear studies 9-48766
 VO₂, structure rel. to elec. props. 9-23629
 WSi₂ on n-Si, reaction-process effects on barrier heights 9-42715
 YFe garnet, epitaxial, on YAl garnet and GdGa garnet, microwave phonon generation 9-44816
 YFe garnet, with narrow ferrimagnetic resonance linewidth, epitaxial growth 9-36952
 Zn, preparation by high-vac. evaporation 9-36963
 Zn:SiO₂:Mn phosphors, deposition by vapour phase reaction and vacuum evaporation 9-30493
 Zn electrodeposits, growth on Cu single crystals 9-30490
 ZnO, epitaxial, on CdS, sapphire; sputtering, perfection depend. on substrate polish, temp. 9-36953
 ZnO, growth on 74-26 brass, early and thick scales stage obs. 9-26191
 ZnO thin-film transducer prep. using vapour transport technique 9-48767
 ZnS, epitaxial, struct., electron microscope and diff. obs. 9-37684
 ZnS, epitaxial growth on films evaporated on to NaCl 9-32844
 ZnS epitaxial layers on Si, defects obs. by transmission electron microscopy 9-34994
 ZnS on W or Mo substrates, epitaxy 9-28216
 ZnSe, epitaxial, struct., electron microscope and diff. obs. 9-37684
 Zr alloys, breakdown of oxide 9-40839
- electrical properties**
 alkali metal, effect of electron-electron scattering 9-37435
 calcium stearate Langmuir, conduction 9-37583
 capacitor, high-stability, performance data 9-49149
 ceramics, ferroelectric VK-2, VK-4 and VK-6, film Varikond, nonlinear and switching props. 9-39675
 chalcogenide glass based diodes, dynamic V-I characts. 9-24201
 chalcogenide glasses, bulk and thin film switching and memory effects 9-49062
 chalcogenide semiconductor amorphous, conduction and elec. switching 9-28491
 chalcogenide thin films, amorphous semiconducting, negative capacitance 9-33283
 conduction in ultrathin metal films by tunnelling through substrates 9-24122
 conductivity, h.f., of size-quantized films, anisotropy obs. 9-39577
 cyclotron reson. films with specularly reflecting surfaces 9-41149
 dielectric, crystal for thermally stimulated currents 9-45015
 dielectric, in semiconductor devices 9-37550
 dielectric film characterization by internal photoemission 9-39659
 discontinuous, metal, conductivity explained by anomalous quantum-mechanical tunnelling 9-35331
 electrets, production and charge decay 9-37600
 electronic structure, density of states and charge, 1-electron approx., simple model potential 9-41132

Films, solid continued**electrical properties continued**

- electrophotographic layers, photoinduced discharge, effect of capture 9-30967
- insulating, literature digest, 1967 9-33368
- metal monocrystalline, with lattice defects conductivity and thermoelec. power 9-37434
- m.i.m. struct., carrier transport 9-41228
- mylar, high field conduction 9-37585
- mylar, non destructive breakdown 9-47162
- mylar, non-destructive breakdown 9-49139
- oxide on base metal, conduction props. rel. to contacts 9-37572
- PbS polycrystalline, photocond. rel. to chemisorption of O 9-37622
- phosphosilicate glass in m.g.o.s. structures, polarization processes 9-33363
- photocells with Cds-Cu₂S heterojunctions, charact. 9-46845
- piezoresistive isotropy of thin oriented films 9-35326
- polyethylene, biaxially oriented and cast, elec. transport, obs. 9-35463
- polyethylene, decay processes of surface charges 9-49136
- polymer, dielectric breakdown rel. to electromechanic deformation 9-43110
- polymer, photovoltaic effect in vacuum u.v. 9-43136
- polymer dielectric, prep. and characts. 9-33399
- Polymerene terephthalate, conduction induced by e bombardment 9-26513
- polystyrene, conduction induced by e. bombardment 9-26513
- Pt on glass substrate 9-24121
- r.f. size effect in determ. skin depth 9-24110
- rocksalt, breakdown 9-33381
- Se, amorphous, anomalous photocond., role of Hg vapour 9-47206
- semiconductor, dimensionless n-type negative resistance 9-35393
- semiconductor, thin, non-homogeneity controlling 9-35389
- semiconductors, III-V and II-VI, photoconduction mechanism 9-33404
- silicone resin films on Si 9-30959
- size quantized, h.f. conductivity, anisotropy 9-39577
- sorbitan tristearate ultrathin black films, resistivity 9-37580
- superconducting, critical current in mixed state 9-49032
- superconducting, effect of thickness on d.c. Josephson current 9-37462
- superconducting, nonlinear h.f. props. 9-49030
- superconducting, weakly coupled, resistive transition 9-35345
- superconducting critical current for diffuse refl. of electrons from walls 9-39594
- superconducting narrow thin-films, quantum phase correlations and fluctuations 9-24159
- superconducting temp. enhancement for very thin films 9-30869
- superconducting thin-film bridges, vortex fluctuations 9-24164
- superconductivity in quantizing semiconducting films with metallic coating 9-49038
- superconductor containing mag. impurities, far-i.r. study of energy-gap props. 9-41185
- superconductors, Josephson eff. at r.f., props. and applic. 9-28471
- with surface defects, conductivity and electron scattering 9-49016
- teflon, high field conduction 9-37585
- teflon capacitor breakdown studies 9-37586
- tetracene, temperature-independent conducting state 9-33284
- thin electronic energy bands and surface states, model investigation and comparison with infinite cryst. 9-35310
- thin films, vacuum-evaporated on flexible substrates, props. 9-35388
- thin-layer elements of mech. strong insulating stacks, optimum apparent layer area 9-35460
- Ti as a function of temp. (300-13°K), thickness and substrate 9-37452
- transition metal compound thin films with rocksalt struct. supercond. props. 9-36959
- triglycine sulphate, ferroelec. props., eff. of electrode material 9-33387
- Zr as a function of temp. (300-13°K), thickness and substrate supercond. obs. 9-37452
- Ag on glass substrate 9-24121
- Al-Al₂O₃, photoemission in vacuum u.v. 9-37632
- Al-Al₂O₃-Bi_{1-x} Sb_x junctions, oscillatory effects on electron tunnelling 9-39657
- Al-GaSe-Au struct., carrier transport 9-41228
- Al, conductivity, rel. to thickness 9-49023
- Al, conductivity of single- and polycrystals, thickness and temp. dependence 9-44905
- Al, photoelec. emission rel. u.v. polarization and angle of incidence 9-31072
- Al, r.f. sputter-thinned, resistivity 9-24123
- Al, supercond., dirty, Knight shift, BCS-Yosida depend. 9-45394
- Al, supercond., strain effect on T_c 9-41177
- Al₂O₃ sprayed, insulation rel. gas-flame deposition process in Ar with Cs admixture 9-24211
- Al anodized, output during shock-wave loading 9-24117
- Al fine particles prepared by evaporation in He gas, enhanced superconductivity 9-33270
- Al granular, superconducting fluctuations in 3-d regime causing excess conductivity 9-26527
- Al granular, superconductivity enhancement 9-24149
- Al granular, superconductivity enhancement mechanism, expt. evidence 9-24150
- Al supercond. granular, microwave conductivity 9-37466
- Al supercond. thin films, microwave conductivity 9-28481
- Al superconducting transition enhanced in films of 35-80 Å 9-30869
- AlN films grown by reactive sputtering, dielectric props. 9-37575
- Al-Al₂O₃-Al noise meas. to verify tunnelling 9-33356
- As₂S₃, e bombardment conductivity, columnar ionization 9-33369
- As₂Se₃ amorphous films, drift mobility of carriers, hopping conduction 9-26474
- As₂Se₃Te semiconductor diode, switching, filamentary conduction 9-35449
- Au/Pb layered films, supercond. props. 9-26528
- Au-Ni thermocouples, vacuum-evaporated, thermoelec. power and Seebeck coeff. thickness depend. 9-45017
- Au, current noise 9-28464
- Au, dispersed, electron emission centres, rad. spectra 9-26606
- Au, electromigration role of thermal gradients 9-34984
- Au on glass substrate 9-24121
- Au photoelec. emission rel. u.v. polarization and angle of incidence 9-31072
- B, photoconductivity 9-35500
- BaTiO₃, ferroelec. props., eff. of electrode material 9-33387

Films, solid continued**electrical properties continued**

- BaTiO₃ ferroelec. thin films, prep. by vacuum deposition 9-46729
- Bi, anomalies in resistivity 9-49020
- Bi, complex impedance characteristics, 2-15 μ , equivalent circuit tested 9-37439
- Bi, conductivity and Hall effect, 4.2-300K 9-39582
- Bi, elec. conductivity and Hall effect, thickness dependence, 4.2°-300°K 9-33251
- Bi, photoelectromag. effect meas. 9-47209
- Bi, resistivity oscillations upon deform., 78° and 300°K 9-30845
- Bi, size-quantized, magnetoresistance meas. rel. to non-external sections of Fermi surface 9-49021
- Bi, superconducting, transition curves in perpendicular field, superconducting fluctuations 9-44931
- Bi, superconducting transition temp. size dependence 9-30870
- Bi₂O₃ evaporated layers, conductivity temp. depend. and band gaps obs. 9-39162
- Bi₂Se₃ semiconducting properties 9-30889
- Bi₂Te₃ semiconducting properties 9-30889
- Bi plates, r.f. size effect in determ. skin depth 9-24110
- CaF₂ capacitor breakdown studies 9-37586
- CdO, d.c. reactive sputtered, Hall mobilities and electron densities 9-48756
- CdS:Ag shear-mode-evaporated u.s. transducers, preparation 9-42957
- CdS-SiO₂, frozen-in conductivity extinction by elec. field 9-28577
- CdS, frozen-in conductivity extinction by elec. field 9-28577
- CdS, longit. cathode conductivity under e. bombardment 9-41155
- CdS, on Ge plates, switching effect 9-43079
- CdS, semicond., cond. rel. to intercryst. barriers, >500 V cm⁻¹ 9-26542
- CdS thin layers, current fluctuations due to elastic waves 9-35396
- CdSe-SiO₂ C-U characts. at semiconductor-insulator boundary 9-30951
- CdSe, charge density reduction by surface alloying of IN 9-33319
- CdSe, conductivity and space charge region variation, from depletion depth meas. 9-30905
- CdSe, evaporated, conductivity and Hall effect 9-33299
- CdSe, props. of Au contacts 9-41211
- CdTe, conductivity, investig. at microwave freq. 9-30904
- CdTe, conductivity and hole mobility rel. to stimulated recrystn. 9-39163
- CdTe, d.c. electromotive force caused by microwave field, investig. 9-30885
- CdTe, electroabsorption oscillations magnitude, elec. field strength depend. 9-49248
- CdTe, photovoltaic effect, anomalously high, nature 9-26605
- CdTe APN, photocurrent kinetics and relax. time 9-26601
- CdTe photoconverter element 9-31903
- CeF₃, CeO₂ capacitor breakdown studies 9-37586
- Co₂, a.c. and d.c. behaviour 9-39664
- Cr, conductivity and Hall const. 9-30848
- Cu/Pb layers, proximity effect, induced excitation spectrum, density of states meas. 9-44944
- Cu, conductivity, rel. to thickness 9-49023
- Cu₂S, thermoelec. power and temp. depend. of conductivity acceptor level position 9-44949
- Cu₃PSe₄, cond. and thermo e.m.f., obs. 9-35398
- Cu₃PSe₄, cond. and thermo e.m.f., obs. 9-35398
- Cu₃PSe₄, cond. and thermo e.m.f., obs. 9-35398
- Cu deposition on backing, specific resistance rel. temp. 9-26445
- Fe thin coatings, conductivity, effect of Hg adsorption 9-37428
- Ga, superconducting transition temp. size dependence 9-30870
- GaAs epitaxial layers, donor extrinsic photoconductivity spectral meas. in mag. fields 9-39717
- n-GaAs epitaxial layers, high-purity, resistivity and Hall coeff. obs. 9-30907
- Ge-Si-As-Te, glassy, breakdown mechanism 9-33305
- Ge, instabilities and ionization of surface centres 9-47122
- Ge, plasma anodized, voltage drop meas. model 9-26188
- Ge, resistance changes at high elec. fields, space-charge region surface conductivity effects 9-41214
- Ge Hall coeff. and conductivity, influence of surface states on temp. depend. 9-33326
- Hf as a function of temp. (300-13°K), thickness and substrate 9-37452
- HgTe, epitaxial, magnet resistance, nonohmic conduction and electron mobility 9-28214
- In-(2 at.%)Pb superconducting type-I, flux flow noise determ. 9-24152
- In-Te system, photoelectric and elec. props. rel. to conc. 9-30485
- In, thermal magnetomorphoric effects, longitudinal 9-37430
- In, thin, quenched, effect of preferred growth on ang. depend. of critical field 9-47088
- n-InSb, energy scattering of conduction electrons, piezoelectric contributions 9-26549
- n-InSb, Faraday rotation at 23.4 GHz at room temp. 9-49250
- InSb, transport props. 9-33309
- InSb Hall transducers, props. 9-24195
- KNO₃ film, ferroelec. phenomena 9-49144
- LiBr, dielectric losses at low temp., mechanisms 9-49137
- LiNbO₃, sputtered, piezoelec. characts. 9-42725
- MgF₂ capacitor breakdown studies 9-37586
- Mo, Fermi surfaces, r.f. size effect investig. 1.7° to 4.2°K 9-37408
- MoO₃ in capacitance depend. on geometry, a.c. meas. 9-37566
- Nb-Nb₂O₃-Nb superconducting tunneling junction, theoretical and exptl. investig., and applic to e.h.f. 9-26536
- Nb-Pb thin films, method for fabricating good superconducting tunnel junctions 9-28471
- Nb, supercond., flux flow and Nernst effect obs. 9-41182
- Nb, superconductivity 9-35365
- Nb₂O₅, growth and dielectric props. rel. to use as capacitor 9-30981
- NbO, vapour deposited 9-30958
- Ni-Cr vacuum-deposited, resistivity increase on heat treatment 9-41043
- Ni, conductance, current carriers mean free path 9-39589
- Ni, photoemissive props. and correl. with optical props., vacuum u.v. 9-45260
- Pb-Gd(Mn), supercond., far-i.r. study of energy-gap props. 9-41185
- Pb, supercond., fluctuation rounding of resistive transition 9-41186
- Pb, supercond., Nernst effect and flux flow obs. 9-41183
- Pb, superconducting transition temp. determ. from tunneling and resistive meas. 9-43040
- Pb, superconducting upper critical field rel. to deposition on substrates held at low temps. 9-28480

Films, solid continued**electrical properties continued**

- Pb₉₂Bi₈0.01La_{0.01}(Fe_{0.405}Nb_{0.325}Zr_{0.27})O₃, ferroelec. 9-35487
 Pb supercond., resistivity and crit. temp., eff. of imperfections 9-26531
 PbO-SnO mixed cryst. layers, photoconductivity 9-41269
 PbO layers, vapour-deposited, photoconductivity, photoemission and band struct. obs. 9-39722
 PbS, epitaxial, photosensitivity mechanism 9-49161
 n-PbS epitaxial, charge carrier distrib., layered, from transverse magnetoresistance meas. 9-42996
 PbS film, absolute quantum yield due to internal photoelec. effect 9-33410
 PbS photosensitization from photocond. props. rel. to oxide formation 9-37615
 PbTe polycryst. layers, surface props. 9-33325
 PbTe thick layers, transport props., heat treatment effects 9-39625
 Pd, conductance, current carriers mean free path 9-39589
 Pd, conductivity and Hall consts. 9-30848
 Pt-SiO cermet, resistances obs. 9-47155
 Pt, conductivity and Hall consts. 9-30848
 Si:(Sb) epitaxial, on spinel substrate, resistivity and Hall effect meas. 9-36950
 Si-Si₃N₄, trapping levels obs. 9-33359
 p-Si-on-sapphire, oxidation effect 9-35405
 Si, deposited by electron irradi. of tetramethylsilane, resistivity obs. 9-44628
 n-Si, epitaxial, on sapphire, vacuum evaporated 9-49111
 Si, high voltage photovoltaic eff. 9-24241
 Si, resistance changes at high elec. fields, space-charge region surface conductivity effects 9-41214
 Si, thin, minority carrier lifetime meas., three methods, comparison 9-39646
 Si₃N₄:P, surface potential drifting 9-37579
 Si₃N₄, dielectric props and applics. 9-24212
 Si₃N₄, impurity-doped, and physicochemical props. 9-37578
 Si on sapphire, rel. to film thickness and doping density 9-37545
 SiO, pulse breakdown 9-45005
 SiO₂, amorphous, anodic growth, dielec. breakdown and carrier transport 9-45006
 SiO₂, dielectric loss functions, incomplete, analysis 9-47158
 SiO₂, I-V characts. rel. to temp., dielectric constant and loss, freq. depend. 9-28549
 SiO₂, in semiconductor devices 9-37550
 SiO₂, pyrolytic, breakdown, nature, 77° to 223°K 9-33382
 SiO_x, annealed, a.c. and d.c. cond. processes at high and low fields 9-47160
 SiO capacitor breakdown studies 9-37586
 Sn, narrow thin-films, superconducting, quantum phase correlations and fluctuations 9-24159
 Sn, supercond., strain effect on Tc 9-41177
 Sn, superconducting, conductivity temp. dependence at 20 GHz 9-43042
 Sn, superconducting upper critical field rel. to deposition on substrates held at low temps. 9-28480
 Sn supercond. thin films, microwave conductivity 9-28481
 Sn granular, superconducting fluctuations in 3-d regime causing excess conductivity 9-26527
 Ta-N, resistivity meas. rel. to N content and lattice struct. 9-23625
 Ta-Ta₂O₅-Nb superconducting tunneling junction, theoretical and exptl. investig., and applic. to e.h.f. 9-26536
 Ta₂O₅ films, negative photocond. 9-24235
 Ta capacitor, preparation from low-density film and device characts. 9-49152
 Te-Ag photovoltaic eff. obs. on contact 9-35511
 Te-Bi photovoltaic eff. obs. on contact 9-35511
 Te, conduction, effect of ferroelec. substrate 9-28502
 V, temp. coeff. resistance thickness dependence (60-900 Å) 9-47077
 VO₂, photoemission rel. to electronic structure 9-24255
 VO₂, rel. to structure 9-23629
 W, conductivity and Hall consts. 9-30848
 Zn_{1-x}Cd_x-Te ternary system, photovoltaic effect 9-24242
 ZnO, epitaxial, on CdS, Sapphire; resistivity and Hall mobility determ. 9-36953
 ZnO electrophotographic layers, space charge density, effect of elec. field 9-30963
 ZnS, electroluminescent, in strong elec. fields, low temp. props. 9-28461
 ZnS, longit. cathode conductivity under e. bombardment 9-41155
 ZnSe, longit. cathode conductivity under e. bombardment 9-41155

magnetic properties

- anisotropy induced by elec.-field 9-24315
 cylindrical, plated on nonferromag. wires, anisotropy field and easy axis orientation meas. 9-24306
 cylindrical electrodeposited, prep., characterization domain, wall creep and thermal stabilization 9-45161
 domain wall energy, combined Bloch and Neel type 9-28625
 domain wall profiles, determ. using inversion procedures 9-49207
 domain walls, 180°, 360° and multiple system, energies 9-33468
 domain-wall energy density meas. method for thin films 9-43168
 easy-axis orientation, 'magnetic masking' method 9-24314
 electroplating prep. of structures for data storage 9-28621
 ferromagnetic, differential susceptibility w.r.t. effective field 9-33470
 ferromagnetic, residual magnetization creep in demagnetizing self-fields 9-39772
 ferromagnetic, saturation magnetism 9-49209
 ferromagnetic, spontaneous magnetization, eff. of point defects 9-31040
 ferromagnetic, statistical approach, reduced matrix procedure 9-31038
 ferromagnetic, stripe domain nucleation 9-31039
 ferromagnetic, thin, domain obs. in pulse periodical fields by stroboscopic Lorentz microscopy 9-40329
 ferromagnetic, thin film, spin-wave resonance calcs. 9-41417
 ferromagnetic, two-dimens. Bloch-type domain walls 9-35567
 ferromagnetic props. in band model 9-31037
 ferromagnetic resonance in thin polycryst. films, Fourier transforms eqn. soln. for general case 9-47422
 ferromagnetic thin film, mag. spectrum and ferromag. reson., subdomain struct. 9-43180
 Kerr effect applications 9-33510
 laser beam recording of digital information and readout presentation 9-45159
 magnetization config. during high speed flux reversal, Kerr magneto-optic camera meas. 9-32082

Films, solid continued**magnetic properties continued**

- magnetization creep of cross-tie walls 9-49208
 magnetization spread, dynamic analysis using Landau-lifshitz eqn. for distrib. systems 9-45160
 magneto-optic readout system, heat problem 9-41872
 magnon theory carried over to phonon theory 9-23995
 memory element closed-flux, development 9-43841
 memory stores, photon- and electron-beam-accessed, improvement of signal-to-noise ratio 9-43843
 multilayer vacuum-deposited, rel. to thickness, substrate temp. and conductor metals 9-33469
 oligatomics, thickness depend. magnetization and Curie temp., and prep. 9-45162
 Permalloy, anisotropy, rotatable, in electron-microscope specimens 9-26646
 permalloy, annealing behaviour of induced anisotropy, ageing and stabilization effects 9-37660
 permalloy, Bloch wall motion excited by fast-rising hard-axis pulses 9-45168
 permalloy, electrodeposited, magnetism reduction 9-49191
 permalloy, ferromag. reson. absorpt. at r.f.'s 9-47423
 permalloy, ferromagnetic, coercive force and fine mag. struct. 9-41321
 Permalloy, high-speed flux reversal and relax. processes, dynamic Kerr obs. 9-37661
 Permalloy, hysteresis magnetising angle, mag. anisometer meas. 9-43184
 Permalloy, irradiated, spin wave resonance 9-45370
 permalloy, reactor irradi. and subsequent annealing effect on anisotropy field 9-47253
 Permalloy, susceptibility, effect of surface roughness 9-49211
 permalloy film, high speed flux reversal and relaxation processes, dynamic Kerr obs. 9-45169
 permalloy film with ternary paramagnetic additions as memory dev. 9-36252
 Permalloy layers with non-mag. layer composite 9-43183
 permealloy, thin, effect of mag. annealing and elastic stress 9-41322
 recording medium, patent 9-47899
 remagnetization, energy conversion and dynamic hysteresis loops 9-24266
 ripple obs. with Lorentz microscopy 9-40328
 spin wave reson., excitation of uniform precession mode 9-43165
 stray-field-free micromag. config. applic. to Bloch- and Neel-walls, stripe domains and ripple struct. 9-35559
 superconducting (type II) films, equilib. config. of flux lines 9-43034
 thin, ferromag., soft mag. materials review 9-39753
 thin film theory, Curie pt., magnetization and moment fluctuations 9-49181
 vacuum apparatus for deposition and in-situ Galvanomag. meas. 9-39193
 wall coercive force, strain sensitivity, 200 Å to 1500 Å thickness 9-45163
 Al-I-M (M=Ni, Pd, NiPd alloys, FeGd), electron tunnelling, rel. to spin wave excitation 9-44995
 Al, supercond., dirty, Knight shift, BCS-Yosida depend. 9-45394
 CO-(10wt.%)Mn-(45wt.%)Fe, ferromagnetic domain struct., e microscope obs. 9-33471
 CO-(10wt.%)Cr-(45wt.%)Fe, ferromagnetic domain struct., e microscope obs. 9-33471
 Co-P, coercive force, effect of electroless Ni substrate 9-31041
 Co-p, temperature-sensitive, for magneto-optic memory 9-45164
 Co, domain wall width meas. by Lorentz microscopy 9-45166
 Co, ferromag. reson. absorpt. at r.f.'s 9-47423
 Co, ferromagnetic domain struct., e microscope obs. 9-33471
 Co, high-coercivity, recorded magnetization pattern obs. by Lorentz microscopy 9-45165
 Co, magnetization, neutron scattering studies 9-45167
 Co, n.m.r. and ferromag. resonance, relaxation times, magnetic structure 9-33645
 Co, rotatable initial susceptibility and magnetization reversal 9-33462
 Co electroless, structure rel. to coercivity 9-42718
 Co ferromagnetic, coercive force and fine mag. struct. 9-41321
 Co thin films electrolytically deposited on Cu, periodic variation of susceptibility maximum 9-47257
 CrBr₃, ferromagnetic domain structure, Lorentz microscopy obs., at low temps. 9-26651
 CrI₃, ferromagnetic domain structure, Lorentz microscopy obs., at low temps. 9-26651
 EuO:R³⁺, (R=rare earth oxide), and magneto-optical props. 9-47266
 EuS, 200Å thick, at low temp., struct. determ. by Lorentz microscopy 9-41880
 Fe-Ni, Faraday effect field depend., perpendicular anisotropy obs. 9-47322
 Fe-Ni, ferromag., differential susceptibility obs. of struct. 9-43182
 Fe-Ni alloy, variation in susceptibility with thickness 9-39773
 Fe-Pd alloys, coercive force rel. to grain size 9-28622
 Fe, ferromagnetic domain struct., e microscope obs. 9-33471
 Fe, high-coercivity, recorded magnetization pattern obs. by Lorentz microscopy 9-45165
 Fe, magnetiz. meas. as thickness inc. atomic layer by layer 9-28619
 Fe, magnetization, neutron scattering studies 9-45167
 Fe, magnetization distrib. about single mag. particle 9-43181
 Fe ferromagnetic, coercive force and fine mag. struct. 9-41321
 Fe platelets, charged 90° Bloch walls obs. 9-43169
 Fe single crystal, Hall effect, rel. to thickness 9-47267
 FeRh first-order antiferromag. transition role of O₂ 9-45223
 Gd₃Fe₅O₁₂, struct. and props. rel. to growth parameters 9-47272
 GdFe garnet epitaxial, prep. by r.f. sputtering, and structural props. 9-49210
 Mn-FeNi with ferro-antiferromagnetic interaction, ferromag. reson. 9-37789
 Nb, supercond., flux flow and Nernst effect obs. 9-41182
 Ni-Co, electrolytically deposited, magnetocryst. anisotropy 9-41323
 Ni-Co, electrolytically deposited, magnetocryst. anisotropy 9-41323
 Ni-Fe-Cu(Co) anisotropy compounds separation by temp. depend study of anisotropy field 9-45170
 Ni-(19 wt.%)Fe, energy of combined Bloch and Neel type domain wall 9-28625
 Ni-Fe, 30 to 300Å thick, props. with creep observations 9-45068
 Ni-Fe, 30 to 300Å thick, props. with creep observations 9-45068
 Ni-Fe, electrodeposited, magnetization ripple wavelength meas., Lorentz microscopy 9-28624

Films, solid continued**magnetic properties continued**

- Ni-Fe tapes, surface domain patterns, Kerr magneto-optic studies 9-26653
 Ni-Fe thin films electrodeposited on scratched surfaces, uniaxial mag. anisotropy 9-28623
 Ni-Zn ferrite 9-45184
 Ni, amorphous, ferromagnetic props. 9-26652
 Ni, eff. of columnar domain struct. on mag. props. of Fe-Si alloys 9-26647
 Ni, electrodeposited, magnetocryst. anisotropy, lattice distortion effect 9-39774
 Ni, Faraday effect field depend., perpendicular anisotropy obs. 9-47322
 Ni ferrite 9-45184
 Ni ferromagnetic, coercive force and fine mag. struct. 9-41321
 Ni-(22 wt.%)Fe, infl. of mech. stress on coercive force 9-24316
 Pb, supercond., Nernst effect and flux flow obs. 9-41183
 SnO₂ films, negative magnetoresistance 9-33311
 YFe garnet epitaxial, ferromag. reson. 9-45372

optical properties

- absorbance at surface opposite surface of incidence 9-49237
 by absorption in semiconducting backing 9-24351
 alkali chloride solid solns., fund. absorpt. in extreme u.v. 9-35662
 anthracene thin film, crystalline phase, fluorescence spectra and X-ray diffraction 9-35689
 constants determ. from reflectance or transmittance data 9-26695
 Cu thin films, abnormal props. 9-31068
 dyes, opaque, in electronic band region, const. determ. by spectrointerference method 9-31067
 image recording on ferromagnetic thin films, resolving power of thermal method 9-28662
 lossless material, Magneto-optical effects rel. to propag. impedance and polarization perturbations 9-25369
 metal, calc. from complex refl. and transmitted amplitudes, series expansion 9-32013
 metal, non-local theory 9-26703
 metal, optical const. during deposition, continuous ellipsometric determination 9-32845
 metal, self-supporting, covered by oxide layers, eff. of plasma oscill. 9-26672
 metal oxides, reactively sputtered 9-30487
 metallic, constants, hill-climbing technique 9-39804
 metallic, min. optical thickness and max. absorption in standing wave 9-41360
 nonabsorbing on isotropic absorbing substrate, ellipsometric refraction meas. 9-33504
 optical consts. determination using polarization measurements 9-47311
 oxide on high M.Pt. metals, effect on emissivity 9-28435
 paint on black substrate, 0.8-2.0 μ range, reflection and scattering 9-43206
 paint-like coatings computer calc. incorporating Fresnel's law, Snell's law, Bier's law and kinetic theory 9-37689
 periodic assemblies, pass and stop intervals, discrimination between 9-25533
 polyimide:Ag, i.r. absorpt. spectra, obs. 9-26749
 polymer with partially ordered structure, scatt. theory 9-37694
 polymers, birefringence effect on light scatt. 9-49244
 polymers, oriented birefringence effect on low-angle light-scatt. patterns 9-49243
 polymers, synthesized, vacuum u.v. absorpt. spectra, electr. struct. obs. 9-31116
 polynucleotides, homogeneous, vacuum u.v. absorpt. spectra rel. to electronic struct. 9-26750
 polytetrafluoroethylene, morphology and light-scattering patterns 9-42707
 polyvinyl alcohol, ultraviolet absorption spectra 9-35669
 refractive index meas. method 9-31071
 rosin, spectral characts. of light sensitive volume changes 9-28698
 thickness selection for given spectral transmission characts. 9-46016
 thin, discontinuous and absorbing, ellipsometric equations for thickness prediction, validity 9-36940
 thin, in vacuum u.v., review 9-26696
 thin, semiconductor, modes of propagating light waves 9-35386
 thin, slightly absorbing, optical constants and thickness, ellipsometric meas. 9-37678
 thin layer on metal surface, reflection determ. of i.r. spectrum 9-35648
 Ag, foil thickness determ. by curves of constant transmission 9-23640
 Ag, optical const. during deposition, continuous ellipsometric determination 9-32845
 Ag, plasma resonance emission, temp. depend., 90-770°K 9-23641
 Ag, surface roughness correl. with plasma reson. radiation 9-44621
 Ag, thin, abnormal absorpt. in vacuum and gas atmosphere 9-47347
 Ag rough films, optical stimulation of non-radiative plasmons 9-37415
 Ag thin evaporated films, opt. consts., transmittance 9-47313
 Ag thin films, opt. consts. near plasma freq., influence of struct. 9-37680
 Au, dispersed, light emission centres, rad. spectra 9-26606
 Au thin evaporated films, opt. consts., transmittance 9-47313
 Bi, hologram storage with > 6% efficiency and 1000 lines/mm resolution 9-45970
 Bi₂O₃-TeO₂, absorption 9-35649
 Bi₂O₃ evaporated layers, transmission and refl. meas., band gap obs. for optical transitions 9-39162
 CaSO₄(Mn) phosphors for use in thermoluminescent dosimeters 9-27594
 CdO, c.d. reactive sputtered, absorpt. edge obs. 9-48756
 CdO, effect of lattice vibrations, 300° and 85°K 9-35613
 CdS, absorpt. spectrum, intense ruby laser radiation effect 9-35652
 CdS, electroluminescence in vac. evaporated films 9-31152
 CdS, thin films on Al, i.r. reflectivity spectra showing absorption peaks 9-26733
 CdSe textured, recombination processes 9-31123
 CdTe, absorpt. spectra in high elec. fields 9-41376
 CdTe, electroabsorption oscillations magnitude, elec. field strength depend. 9-49248
 CdTe semiconductor, photosensitivity spectrum, influence of temp. 9-33535
 CsI thin film, far u.v. absorption spectrum obs. and interpreted 9-37730
 Cu₂-Se, epitaxial layers, transparency and opt. homogeneity 9-46721
 Cu₂S, absorption const. variation, refractive index and photo sensitivity data for forbidden band width 9-44949
 Cu₂S, and prep. 9-46727

Films, solid continued**optical properties continued**

- Cu₂PSe, electro-optical props., refl. and transmission, 0.4-15 μ 9-35398
 Cu₂PSeI, electro-optical props., refl. and transmission, 0.4-15 μ 9-35398
 Cu₂PSeS₂, electro-optical props., refl. and transmission, 0.4-15 μ 9-35398
 CuCl, Faraday rotation due to excitons 9-24370
 Ga light absorpt. in different gaseous media 9-45265
 GaP, vacuum-deposited, rel. to structural props. 9-42719
 GdFe garnet, absorpt. spectra, 2000-5000 Å 9-35658
 Ge, indices independent of thickness, construction method 9-39793
 In, light absorpt. in different gaseous media 9-45265
 In, optical consts., far u.v. 9-37681
 n-InSb, Faraday rotation at 23.4 GHz at room temp. 9-49250
 p-InSb, fundamental absorpt. edge thickness depend. in forbidden band-width determ. 9-41379
 KBr-KCl solid soln., fundamental absorpt. spectra 9-28685
 KBr-NaBr solid soln., fundamental absorpt. spectra 9-28685
 KBr-RbBr solid soln., fundamental absorpt. spectra 9-28685
 KI thin film, far u.v. absorption spectrum obs. and interpreted 9-37730
 Na, anomalous absorpt., rel. to bulk metal and effect of temp. 9-35631
 Na₃AlF₆, evaporated, influence of various parameters on refractive index 9-33503
 NaI thin film, far u.v. absorption spectrum obs. and interpreted 9-37730
 NbO, vapour deposited 9-30958
 Ni, in vacuum u.v., correl. with photoemission obs. 9-45260
 PbTe thick layers, optical transparency, heat treatment 9-39625
 Si film on isotropic absorbing substrate, refl. index obs. 9-33504
 Si on sapphire, rel. to film thickness and doping density 9-37545
 SiO₂, transmission and reflection spectra, thickness depend., 7-11 μ 9-24374
 SiO₂ interference influence on reflection spectrum in SiO₂-Si system, 9 μ region 9-35619
 SiO₂ on Si, thickness meas. by variable angle monochromatic fringe obs., reflectivity corrections 9-34982
 SnO₂ semiconducting layers on glass, i.r. reflection depend. on surface resistivity 9-26729
 Ta-N, absorption meas. rel. to N content and lattice struct. 9-23625
 Ta₂O₅ films, negative photocond. 9-24235
 TiF₄, evaporated, influence of various parameters on refractive index 9-33503
 TiO₂/MgF₂ double anti-reflective system for optical glass surface 9-36962
 TiI, strain-reduced, absorpt. 9-43219
 Xe, photoabsorpt. near N_{IV},v edge, comparison with gaseous Xe 9-26745
 ZnO, epitaxial, on CdS, sapphire; optical absorption edge and refractive index determ. 9-36953
 ZnS:Cu(Mn, I) evaporated thin films, d.c. electroluminescence and photoluminescence 9-33612
 ZnS:Mn, electroluminescence processes, non-stationary, polarization effects 9-24469
 ZnS, epitaxial, optical consts., absorpt. 9-37684
 ZnS coating on ferromagnetic materials to enhance domain study by Kerr reflection 9-35558
 ZnS Lumocen devices, rare-earth and transition-metal fluoride doped, electroluminesc. 9-35700
 ZnSe, epitaxial, optical consts., absorpt. 9-37684
 ZnSe electrically conducting photoluminescent films, prep. 9-31127
 ZnSe on NaCl, reflectivity 9-48099
- Filters**
 dialysis and ultrafiltration technique 9-24940
 inverse digital, wave processes, stability theory 9-25094
 piezoelectric, nonhomogeneous, acoustic response w.r.t. piezoelec. stress 9-37348
 porous and fractured beds, nonstationary filtering analysis 9-42645
 seismic, time varying deconvolution 9-37880
 signal enhancing technique for auditory detect. in noise 9-29122
 soil, stratified, nonhomogeneous, water filtering 9-43364
 soil parameters, role in horizontal drainage 9-42644
 superconducting, multiresonator band-pass and band-reject 9-37483
 X-ray spectra analysis equip. description 9-36337
 in Ge(Li) detector signal time meas., comparison and of discriminator techniques 9-36519
- Filters, electrical** *see Circuits*
- Filters, optical**
see also Absorption/light; Films, solid/optical properties
 absorption, sharp band resonance 9-32037
 birefringent, in Fabry-Perot interferometer, passband, tuning and design 9-34220
 blue tristimulus type, superiority for white colours 9-48097
 Christiansen, for investigation of multi-component systems 9-22473
 coated glass sheets, optical and energy parameters 9-32038
 crystal, double refracting, for photometric calibration of photographic plates 9-40390
 diffraction filters, spectral adaptation by ray bundling 9-48108
 electronically tunable, utilizing acousto-optic diffraction 9-36378
 Fabry-Perot, assoc. with standard white light Chromaticity calc. 9-34213
 Fabry-Perot interferometers in series as narrow solar filter 9-36037
 frequency nonsaturating filter in semicond. laser feedback cct., effect on emission spectrum 9-29431
 glass, flatness required for astrometric accuracy, quantitative meas. 9-27114
 induced transmission, design and layer thickness monitoring 9-48107
 interferometers, Fabry-Perot, aberrations 9-48105
 interferometric, use in attenuating Rayleigh component in Brillouin spectroscopy 9-40385
 i.r., far region, grids preparation 9-36376
 laser wavelength selector, intracavity interference 9-36273
 narrow-band light absorption, design from coloured glasses with a given spectral characteristic 9-25376
 neutral density, production techniques 9-27402
 with percussion response represented by dot network, photographic prod. and applic. 9-40387
 polychromator, direct reading photomultiplier tube, for laser microprobe emission spectroscopy 9-46021
 quadratic theory rel. to partially coherent opt. systems 9-45983
 reflection type, multilayer 9-41958
 spatial, realization with polarized light 9-36379
 spatial, with least mean square error 9-32039
 spatial filtering experiments for the undergraduate laboratory 9-43699

Filters, optical continued

- spatial filtering system alignment 9-34221
- spatial hologram applications 9-36328
- spectral and luminesc. props., effect on ruby laser pulse parameters 9-36305
- thickness selection for given spectral transmission charact. 9-46016
- thin film periodic assemblies, pass and stop intervals of discrimination between 9-25353
- thin films, radiant power flow and absorptance 9-36377
- wedge filters with variable absorpt. for emission spectral anal., preparation and use 9-46028
- Wiener spatial filter, realization 9-48109
- Ag glass-Cu waveguide, coaxial 9-34218
- Rb cell, efficiency for ^{87}Rb doublet hyperfine components, rel. to temp. and press. of Ar content 9-29945
- $^{85}\text{Rb}/^{87}\text{Rb}$ mixture, for hyperfine components of ^{87}Rb main doublet 9-38770

Finlay-Freundlich red-shift hypothesis see *Astronomical spectra; Cosmology; Gravitation; Relativity*

Fireball model see *Cosmic rays; Elementary particles; Field theory, quantum/ Interactions; Nuclear reactions and scattering*

Fission see *Nuclear fission*

Flames

- acetylene, oxidation mechanism 9-33661
- air-acetylene low press., ionization and recombination processes 9-42563
- atmospheric burners, charact. indices rel. to air or gas injection 9-41842
- electronic and ionic phenomena invest. 2 electrode probes 9-24545
- ethylene oxide-oxygen, mass spectrometric study 9-28785
- furnace, radiative heat transfer between gas and wall, Monte Carlo 3D analysis 9-34832
- luminous, radiant heat transfer and soot formation 9-36213
- photometer for spectrochemical analysis 9-41459
- plasma, electron temp., probe meas. 9-30252
- propagation in electric field 9-31861
- propagation normal velocity, analytical calc. 9-47837
- propane-air, electrically augmented, temp. and heat transfer meas. in discharge zone 9-25131
- radiative charact., layer-wise obs. 9-22294
- temp. meas. apparatus 9-45882
- temperature meas. by spectral absorpt method 9-45879
- temperature meas. by spectral emission method 9-45880
- temperature meas. from α -part. energy loss 9-38320
- thermoelectric effect at thermodynamic equilibrium 9-36763
- turbulent, vel. in homogeneous gas media, theory and expt. comparison 9-27250
- H_2 -Ar-air, turbulent, atoms fluoresc. power efficiencies, obs. 9-24601
- N_2O - H_2 properties for atomic absorption and emission spectroscopy 9-31224
- N_2O -acetylene, stabilization technique 9-35745
- O_2 - H_2 , turbulent, atoms fluoresc. power efficiencies, obs. 9-24601
- O_2 -acetylene, turbulent, atoms fluoresc. power efficiencies, obs. 9-24601
- OH absorpt. line profile, atm. and reduced press., Zeeman scanning 9-28786
- Oz-acetylene, atomic absorpt. and emission enhancement rel. to free-atom form., obs. 9-22936
- Zn absorpt. line profile, atm. and reduced press., Zeeman scanning 9-28786

Flare stars see *Stars*

Flares, solar see *Sun/flares*

Flash photolysis see *Photochemistry*

Flicker noise see *Electron tubes; Noise/electrical*

Floating zone refining see *Zone melting and refining*

Flocculation see *Sedimentation*

Flow

see also *Boundary layers; Diffusion; Jets; Plastic flow; Turbulence; Viscosity*

- aerospace simulation, conference, Farmingdale, NY, USA (1969) 9-48652
- almost incompressible flow equations, numerical solutions 9-40640
- axially symmetric, of stratified rot. fluid in spherical annulus of narrow gap 9-46449
- boundary layer, laminar natural convection, stability 9-25811
- boundary layer, non-stationary, near rotating disc 9-23220
- boundary layer, reverse transition, special cases of general criterion 9-34727
- boundary layer, turbulent, reverse transition criteria 9-34824
- boundary layer over heated vertical plate, effect of buoyancy forces 9-34729
- boundary layers, laminar compressible, soln. by quasilinearization 9-23371
- boundary-layer, asymptotic non-Newtonian, with suction 9-23219
- boundary-layer flows, injection effects in high Prandtl number 9-27951
- broadside motion of thin disc along axis of fluid-filled circular duct 9-23469
- bubbles, gas, flowing into fluid, speed 9-40766
- buoyancy driven system, instabilities rel. to mechanical and buoyancy forces 9-48530
- centred unsteady, integral of motion 9-44399
- channel, incompressible turbulent boundary layers, study 9-25820
- channel, interaction with intense transverse resonant acoustic field 9-32578
- channel, two-dimensional, generation by transverse waves in walls 9-40638
- compressible boundary layer, anal. of similar solns. rel. to velocity overshoot 9-25809
- compressible laminar boundary-layer eqns., reverse flow solns. 9-32575
- of conducting liquid near nonconducting sphere, crossed electric and magnetic fields 9-23254
- convection boundary layer, transverse press. grad. effects and streamline second derivs. 9-23481
- convection velocities in a viscous sublayer 9-27956
- convective, about vertical surface, instability and disturbance amplification 9-34895
- convective, at high Rayleigh number, temporal development of model 9-34728
- convective, of fluid in cubical cavity, equilb. stabilization by rotation 9-38946

Flow continued

- convective in circular cylinder with localized heating, numerical anal. of creeping flow to onset of laminar instability 9-40747
- convective motion on heated plane, wavelength rel. to conductivity of lid 9-34732
- convective onset rel. to time modulation of wall temp. when also heated from below 9-34723
- Couette, applic. approx. kinetic theory method 9-30180
- Couette, between parallel plates, laminar heat transfer rel. to boundary conds. 9-28090
- Couette, near critical point, wall heat transfer and skin friction 9-23374
- couette, rotating, wave-number selection for Taylor vortices 9-34724
- Couette, rotating, wavelength var. and changes in wave-form and mean flow 9-34726
- Couette for elastoviscous liquids, superposed, stability 9-32747
- critical speed and torque meas. for eccentric rotating cylinders rel. to Taylor vortices 9-30177
- in curved pipe, laminar dispersion 9-25807
- cylinder, circular, in cross-flow up to $\text{Re}=5 \times 10^4$, local pressure distrib. and skin friction 9-25805
- cylindrical Couette, torque upper bounds 9-34741
- diffusion coefficient dependence on solute conc., effect on longit. dispersion 9-36743
- downstream of grid of parallel rods, isotropy in turbulence 9-46591
- in droplet, separating 9-46605
- duct, sub-Alfvénic, with nonuniform mag. field 9-25832
- duct entrance region, eigenvalue soln. 9-25819
- eddy viscosity, concept and constraints 9-34717
- elastico-viscous fluid, fluctuating flow past porous wall with variable suction 9-34734
- of elastico-viscous fluid in wavy cyl. tube, heat transfer obs. in slow steady flow 9-27953
- entrainment, solid-phase, during fluidization 9-25808
- entry-length, in vertical cooled pipe 9-25810
- expansion, shock wave structure, numerical calc. 9-31852
- expansion shock wave structure expt. investigation 9-31853
- films, interfacial, and profile rel. to drops coalescence 9-30365
- finite, amplitude convection with changing mean temp., experimental 9-23231
- finite amplitude convection with changing mean temp., theory 9-23230
- flat plate unsteady boundary layer, incompress. laminar 9-30174
- fluctuating, of an elastico-viscous fluid near stagnation point 9-23431
- fluid, boundary layer over impulsively started flat plate 9-34739
- fluid, convective in porous medium, stability 9-44535
- fluid, finite irrot. compressible frictionless, due to motion of solid, virtual mass tensor, first invariant obs. 9-32571
- fluid, inviscid incompressible past 2-dimens. sails, interaction determ. 9-34827
- fluid, turbulent inviscid incompressible, decaying turbulence spectrum at large Reynold's number 9-48674
- fluid, viscous, incompressible and electrically conducting, hydromag. forced flow against porous rot. dish 9-23255
- fluid convection past non-isothermal vertical flat plate, general series soln. 9-32570
- fluid dynamics, numerical, transport of turbulence 9-38939
- fluid filtration through porous media, chem. reaction, simulation problems 9-38947
- fluid in rotating system, spin-up problem, demonstration 9-29152
- fluid in square duct, turbulent, intensity of temps. fluctuation 9-25823
- fluid mechanics of magnetically balanced arcs in cross flows 9-25990
- fluid with variable conductivity, Joule dissipation in nonuniform mag. field 9-39088
- fluids, laminar in curved pipe, heat transfer series expansion soln. 9-23246
- fluids, laminar natural convection flow about isothermally heated sphere at small Grashof number 9-23236
- fluids, three, cross flow heat exchangers, performance depend. on 2 fluids temp. effectiveness 9-27955
- fluids generation by mechanochemical means in continuous materials 9-29318
- fluids in cavity, axisymmetric, numerical solution 9-42477
- gas solid suspension, at Reynolds number 130,000, convective heat-transfer coeff. 9-26136
- geostrophic in rot. cylinder, non-linear interaction of inertial modes obs. 9-46435
- glass, alkali borate and B_2O_3 , Newtonian viscous, deviations 9-28197
- glasses, viscous 9-28194
- gravity wave train phenom. in cylindrical canal 9-23221
- grid turbulence, energy spectra of longit. and lateral vels. rel. to eddy form 9-46556
- grid turbulence, longit. vel. fluctuations, correl. meas. using digital harmonic anal. 9-28066
- half-jet, incompressible, low Reynold's number instability 9-26071
- heat conducting, viscous; variational methods 9-23228
- heterogeneous systems, second law of thermodynamics 9-23225
- hydromagnetic forced against porous rot. dish, of viscous incompressible and elec. cond. fluid 9-23255
- incompressible, induced by infinite rotating disc in rarefied gas, heat and momentum transfer 9-25117
- incompressible conducting fluid, during injection of laminar jet into channel, numerical soln. 9-40642
- incompressible fluid flow problems, conducting paper analogue 9-30176
- incompressible fluid over sphere, numerical soln. (for Reynolds no. 1-1000) 9-44531
- incompressible laminar jet contained between walls, linearized anal. 9-38943
- incompressible plane rotational, elec. analogue study of jets 9-25803
- induced by coax disks in relative rotation, composite Ekman boundary layer problem 9-46451
- interface of relative motion, reflection and refraction of plane sound waves 9-45856
- interfacial, near two-phase boundary, critical wave length from linear theory 9-40633
- irrotational hydrodynamic field round sphere in incompressible fluid 9-25800
- jet, axisymmetric with parabolic vel. profile, stability, critical Reynolds' number 9-34719
- laminar, incompressible viscous fluid, Navier-Stokes eqn. 9-23222
- laminar, near the entrance and exit of a pipe 9-34715
- laminar, Newtonian fluids, vertical tubes, heat transfer studies 9-28114

Flow continued

- laminar, non-Newtonian fluids, heat transfer studies 9-26088
 laminar boundary layer, anal. of second-order effects 9-34722
 laminar boundary layer, heat and mass transfer rel. to variable suction or injection velocity 9-25998
 laminar boundary layer for Mach nos. to 15 9-46433
 in laminar boundary layers, free convection at low Prandtl numbers 9-42625
 laminar boundary layers, multicomponent, behaviour prediction by integral-matrix method 9-23216
 laminar boundary layers, tune depend., 2-dimen., anal. 9-25821
 laminar flow of pseudoplastic fluids 9-40786
 laminar in duct, Fourier-Kirchhoff eqn. soln. 9-30173
 laminar radial flow between 2 disks, compressibility influence, computer applic. to soln. improvement 9-48533
 laminar steady, for dilute suspension of viscoelastic spheres 9-44603
 laminar stream over reactive surface, with periodic fluctuation of chemical species mass fraction 9-25815
 limiting laminar layer separation 9-46442
 Mach 3.4 Reynolds no $0.6 \times 10^5 \text{ cm}^{-1}$, expt. study 9-46440
 Maxwell fluid, visco-elastic, flow bet. torsionally oscillating discs 9-25814
 Maxwell fluid, visco-elastic, flow due to torsional oscillations of plane 9-23239
 MHD, calc. for determining optimum conditions of power generation 9-38954
 MHD, convective channel, effect of wall conductances 9-30197
 MHD, free surface study 9-46452
 m.h.d., linearized in plane, integral rep., convex bodies 9-30200
 MHD, two-dimensional aligned-field 9-23257
 MHD, variational principle for stationary equilibria 9-32584
 MHD collisionless, past slender bodies, effect of tensor conductivity 9-25865
 m.h.d. Couette, in slip-flow regime 9-38949
 MHD flow in transverse magnetic field in tube of square cross-section with conducting walls 9-30198
 MHD in container, effect of rotational mag. force 9-25833
 MHD laminar, of electrically conducting incompressible fluid between wavy walls 9-27966
 m.h.d. of weakly conducting fluid in rotating straight pipe 9-23251
 mixing of two parallel streams, laminar, displacement effects 9-36742
 mixing zone between 2-dimen. free stream and fluid at rest 9-32577
 non-isothermal, between rotating disks 9-32573
 non-Newtonian, in stratified porous media and in axisymmetric geometries 9-23223
 non-Newtonian fluid about an unsteady rotating disk 9-23215
 nonpolar shear, stability and two neutrally stable solutions 9-30179
 nozzle, non-axially-symmetric annular, compression 9-40641
 one-dimensional, with turbulence augmentation and press. grad., vel. and temp. distrib. 9-34718
 optical visualization 9-46450
 orifice, coeff. variations with changes in plate eccentricity 9-32580
 Orr-Sommerfeld eqn., asymptotic soln. by multiple-scales method 9-23235
 oscillating foil in plunging or pitching modes, lifting problem, second-order theory 9-23410
 oscillatory, 3 dimens., in supercritical nozzles 9-34742
 parietal temp. eff. in laminar layer limited in 3-D 9-46440
 particle sizing technique in moving streams 9-47719
 pipe, transition, turbulent slug velocity 9-25817
 pitot tubes with rectangular mouths, displacement effects under turbulence 9-38942
 plane, of continuous medium with dry friction, defining equations formulation 9-36747
 plane asymmetric, in turbulent region, stress, distrib. 9-40637
 plasma, velocity determination by measurement of induced potential 9-25854
 plasma vortex, double, axially traversing multiple mag. fields 9-32607
 over plate, semi-infinite, time depend. laminar boundary layers anal. 9-25821
 Poiseuille, diffusion of ion sheet 9-23258
 Poiseuille, in pipes, annuli and channels, stability 9-23240
 poiseuille, plane, steady and time-depend., linear stability 9-23237
 Poiseuille, stability in incompressible fluids 9-23253
 Poiseuille pipe, stability 9-25816
 porous media, inhomogeneous, marginal stability 9-34102
 potential vortex flow near stationary surface, soln. 9-23243
 powders, viscometer for meas. 9-23610
 Prandtl number, high, injection effects in boundary layer flows 9-27951
 pseudoplastic fluids, heat transfer to laminar flow 9-40786
 pulsatile, in elastic tubing systems, containing wave ref. tubes 9-32579
 Rayleigh's problem, effect of Coriolis forces 9-48536
 Rayleigh flow, 2-dim, viscous, incompressible, past infinite porous flat plate 9-23422
 rectilinear, turbulent distribution function soln. 9-32568
 reversion of turbulent to laminar flow, in presence of severe favourable press. grad. 9-39036
 Reynolds similarity, exactness investigation 9-25996
 rotating fluid, laminar convection transition to thermal turbulence 9-34735
 rotational at rest at infinity, unsteady, sound generation 9-27949
 second order, steady radial flow between infinite parallel discs, one rotating and other at rest 9-27952
 secondary, in vertical slot, rel. to instability of regimes of natural convection 9-40745
 secondary, steady, between rotating cylinders 9-36745
 separated, dividing streamline and momentum integral analysis, semi-empirical parameters 9-38944
 shear, of stratified fluids, reflection and stability of internal gravity waves 9-27958
 shear, turbulent vorticity in, direction of maximum 9-25818
 shear instabilities in rotating systems 9-23233
 shear layers, free, compressible, turbulent, initial development 9-32577
 in shock tubes, laser beam diagnosis 9-45867
 skin friction near trailing edge of flat plate 9-46444
 solute, across membranes, hydrodynamic, irreversible thermodynamic approaches, comparison 9-36857
 sphere and viscous fluid in cylindrical tube, theoretical study of slow motion 9-25812
 spiral, hydromag. stability 9-40648
 stability exchange principle, perturbation theorem 9-34738

Flow continued

- starting vel. determ. in circular tube 9-46446
 steady, of finitely conducting, compressible fluid 9-23379
 steady plane Poiseuille flow, linear stability 9-23237
 steady rotation of sphere in viscous conducting fluid 9-42480
 steady in variable-area duct with mass transfer at walls, conservation eqns. 9-26050
 stratified fluid, 3-dim., applic. of asymptotic evaluation of Fourier integrals 9-36112
 stratified fluids, wakes produced by two-dimensional body 9-23229
 stratified over obstacle, two-dimens., test of validity of Long's model, effect of wake turbulence 9-40758
 stratified over obstacle in half space, perturbation approx. for lee wave generation 9-34731
 stratified rotating fluid, time-depend. motion 9-46447
 stratified rotating fluid in spherical annulus of narrow gap, steady axially symmetric motion 9-46449
 stratified shear flow over semi-elliptical obstacle, lee-wave functions and field 9-34730
 stream intermixing, isobaric 9-40643
 streamline, in perfect incompressible fluid, const. velocity, section movement anal. 9-46439
 superfluid, dense; vortex waves and rungs eqn., soln. at zero temp. 9-30446
 supersonic, effect of plane plate, vel. fluctuations 9-40636
 surface of infinitely deep heavy fluid, pressure distrib. rel. to stationary waves of finite amplitude 9-23245
 surface-velocity grad. in 3D boundary layers, meas. tech. 9-30359
 suspension, orientation distrib. function of rigid particles 9-46660
 three dimensional separation on inclined ellipsoid 9-46441
 three-dimensional boundary layers, surface vel. grad., meas. tech. 9-30359
 three-dimensional flow-field velocity components, holographic meas. 9-48538
 time-dependent, diffusion and first-order reaction 9-23226
 time-dependent plane Poiseuille flow, linear stability 9-23237
 transient heat transfer near stagnation-pt. 9-48535
 turbulent, amplification of weak magnetic fields, calc. 9-48541
 turbulent, asymmetrical effects 9-45806
 turbulent, boundary layer, compressible with pressure gradient 9-23218
 turbulent, compressible boundary layers, preliminary study on the local skin friction coefficient 9-30181
 turbulent, fully developed, in circular tube and parallel plate channel 9-34740
 turbulent, high-temp., photoelec. meas. 9-36744
 turbulent, homogeneous, one dimensional representation, pseudo-random function algebra 9-44391
 turbulent, mean vel. meas., non-directional probe design 9-46437
 turbulent, pipe flow, outline of second-order theory 9-23423
 turbulent boundary layer on smooth wall, effect of press. gradient on law of wall 9-34725
 turbulent compressible boundary layers in 3-dimensional flow, approximate solutions 9-27950
 turbulent pipe flow through mired right-angle bend, prod. of downstream secondary circulation 9-27954
 turbulent shear, accelerations defining mean turbulent trajectories 9-40639
 turbulent shear, nonstratified, spectral eqn. elementary soln. 9-32576
 turbulent shear, phenomenological theory 9-32574
 turbulent wakes behind circular cylinders, one-dimens. spectra for large range Reynolds number 9-46589
 two-dimensional, shear layer between two parallel streams 9-23234
 two-dimensional, through non-uniform gauzes, computational method 9-46448
 on two-dimensional networks, theory 9-44398
 two-dimensional sink in density-stratified porous medium 9-23232
 unsteady, viscous, past a semi-infinite flat plate, using Stokes approximation 9-46445
 velocimetry, holographic, data processing methods 9-48539
 velocity distribution in randomly packed spheres, conference 9-34094
 velocity distributions of fluid for randomly packed beds of spheres 9-34716
 velocity vector, 3D, laser Doppler meas. 9-43714
 viscoelastic fluids, validity of Squire's theorem for stability of parallel flow 9-40757
 viscous, about sphere in contact with plane wall in slow linear shear flow 9-30175
 viscous, interaction with intense acoustic field, exam. method 9-32578
 viscous, near trailing edge of a flat plate, local skin friction 9-46444
 viscous, in rotating pipe, spiral wave instabilities 9-34721
 viscous fluid, between coaxial rotating cylinders 9-34849
 viscous fluid, sonic flow, stream function 9-46438
 viscous incompressible fluid, Navier-Stokes equations 9-48534
 wall-similarity in three-dimensional turbulent boundary layers 9-23217
 water, forced laminar, free convection influence in circular tube, uniform heat flux 9-25128
 zonal, interaction with quasi-stationary long wave 9-34844
- gases**
 see also *Acoustic streaming; Aerodynamics; Anemometers; Supersonic flow*
 air, and water, Reynolds similarity, exactness investigation 9-25996
 air, axial rotational with impulsive discharge, temp. profile 9-25976
 air, subsonic in contraction section, flow field and heat transfer meas. 9-28065
 air, through collection of tubes, heat transfer 9-30327
 air flow over ridge, lee waves, numerical calc. 9-43389
 air flow over ridge, lee waves, numerical calc. 9-37912
 atmospheric, baroclinic zonal, effect of horizontal shear on wave structure 9-41499
 atmospheric shear with friction, vortices and circulating cylinder motions 9-41500
 axisymmetric hypersonic, over slender body, with strong viscous interaction and shock wave 9-25999
 boundary layer at sea-air interface 9-31307
 boundary layer on plate, shock-induced, transition to turbulence and heat transfer 9-40739
 in canals, narrow, viscous flow with heat transfer, integral correlation method 9-32721
 circulation control by slot-blowing, rel. to circular cylinder 9-23375
 collisionless into vacuum, approximate calc. 9-46555

Flow continued

gases continued
 compressible ideal flow patterns; shock waves 9-40734
 conducting, quasi-one dimensional, longitudinal short wave oscills. stability 9-40650
 in constrictor, interaction with electric arc, theory and experiment 9-40726
 control circuits, thermoresisting 9-36799
 convective, in enclosures with localized heating from below, soln. for circular and rectangular floor plans 9-40746
 coolant in rod clusters, transverse temp. diff., mixing rate determ. 9-34818
 in electric arc or plane, Schlieren study, use of Ar laser 9-22384
 electrohydrodynamic, over wavy wall, supersonic case, oscillating piston problem model 9-40732
 electrohydrodynamic Rayleigh and oscillating plate problems 9-46552
 electrohydrodynamics, over wavy wall 9-40731
 electron beam excitation technique for low density flow field visualisation 9-46563
 flowfields around upper atmosphere clouds 9-28063
 nearly free molecular, asymptotic theory 9-23377
 high-speed, density and velocity meas. 9-23834
 hot gas, subsonic flow in cooled channel, profile meas. via heat transfer and stagnation press. 9-23372
 hypersonic, finite difference technique for numerical computation 9-36796
 hypersonic, He, electron beam visualisation 9-46559
 integral correlation for viscous gas flow with heat transfer in narrow canals 9-32721
 inviscid, stabilisation of difference schemes for eqn. by artificial diffusion 9-36798
 ionized, elec. conductivity meas. 9-38970
 ionized, from interstellar globule 9-29036
 ionized weakly, past discontinuous wall potential 9-32637
 jet, real turbulent, propag. calc. 9-42593
 jet, turbulent high temp., parameter calc. 9-42592
 jets, emitting gas, boundary layer approximation 9-42588
 Knudsen effusion, Monte Carlo analyses of thin-edged and channel orifices 9-30466
 m.h.d. theory in hypersonic approx., general solns. 9-23247
 mixture expansion, autorefriegeration causing heavier components to liquefy; separation at supersonic velocities 9-26163
 molecular slit flow, nearly-free, local and average mass flow rates 9-34820
 neutral, transfer vels. rel. to elec. field during independent discharge onset in moving gas 9-48628
 non-equilibrium, mol. vel. distrib. function for weak shock, asymptotic solns. 9-30329
 nozzle, convergent-divergent 9-28062
 nuclear reactor coolants, and temp. rise, analysis 9-34491
 one dimensional, high temp. with heat exchange 9-23378
 through orifice, nearly free 9-46557
 parallel, of weakly ionized two-temp. gas, Joule heating effect 9-40730
 perfect gas, through nozzle, simulation, difference method for Cauchy problem solution 9-25997
 planetary boundary layer, with neutral thermal stability, wind spiral model 9-41501
 plasma, steady, shock structure 9-40670
 plasma in homopolar, three-dimens. distrib., secondary flaws effects 9-48582
 plasma in Penning discharge with heated cathode 9-46540
 plasma in shock tube, parameters rel. working channel construction 9-27976
 porous layer, non-stationary filtration, for nonlinear resistance layer, numerical solns. 9-40736
 potential, three dimensional, in a curved duct, using a perturbation method 9-48647
 pulsating systems, small acoustic filters evaluation 9-43794
 rarefied, applic. of Luke's weight coeffs. for evaluating linearised Rayleigh problem 9-36797
 rarefied, motion of circular cylinder due to surface temp. distrib. 9-25995
 rarefied, uniform flow for small Knudsen numbers 9-42587
 shear, turbulent, streamline curvature and buoyancy analogy with meteorological parameters 9-41477
 shock detachment distance for flow around cylinders and spheres 9-32601
 shock initiated one dimens., for ideal gas undergoing reversible reaction 9-48645
 near shock tube diaphragm, shock waves motion and stream parameters 9-41833
 slip flow, soln. for general specular-diffuse boundary cond. in kinetic theory 9-40733
 sonic flow of viscous heat-conducting gas around bodies of revolution 9-48646
 spectral components growth in wind-generated wave train 9-23433
 steady plane supersonic, containing arbitrarily large number of shocks, calculation 9-36795
 stream, oxidising, rel. to combustion of fuel exuded from obstacle's leading edge 9-26812
 subsonic, thermal choking by radiation absorption 9-32720
 superimposed on d.c. electric arc, effect on arc-flow-electrode interacts 9-23365
 supersonic, around segmented bodies, gas quality effect 9-42591
 supersonic, around two parting bodies 9-44514
 supersonic jet, flow around infinite wedge 9-44515
 supersonic rotational inviscid, round convex corner, solns. using coord. system 9-26000
 supersonic trail behind blunt bodies 9-42590
 over surface causing erosive rupture 9-23912
 thermally radiating, boundary-layer limiting soln. 9-26002
 thermodynamically perfect, about fixed obstacle reduction of similarity parameters 9-46554
 transient expansion from a storage reservoir 9-23380
 turbulent, intensity and freq. spectrum of longit. component, optical investigation 9-28064
 turbulent, low Reynolds number flow in circular tubes, thermal entry problem 9-34821
 velocity meas. by elec. discharge 9-32718
 velocity variation in normal ionizing shock wave 9-36801
 viscosity variation through porous media 9-26042

Flow continued

gases continued
 visualization by chemical reaction 9-32719
 wedge of polytropic gas, expansion into vacuum, frontal shape rel. to adiabatic index 9-23376
 Ar, in converging nozzle, continuum, slip and free mol. regimes 9-32722
 Ar stream with Cs, arc in mag. field 9-23367
 H real, transient expansion from a storage reservoir 9-23380
 He, mixing of trace gas, rel. to in-pile release rate of radioactive gases 9-25679
 He, thermal transpiration at low pressures, use of leached Pyrex tube 9-36820
 N₂, diffusion and flow in natural rocks 9-30332
 S, turbulent, heat content of plane layer 9-40750

liquids
see also Acoustic streaming; Double refraction/flow; Hydrodynamics; Superfluidity
 annular system, heat transfer from short heated section 9-23412
 blood, determ. by conjunctival photography 9-49605
 boundary-layer flow equation 9-36836
 capillary, threshold pressure gradients 9-23436
 capillary flow of smectic and cholesteric liq. crystals 9-48671
 carboxy methyl cellulose, aqueous soln., laminar flow, heat transfer studies 9-26088
 Cellofasc solns., dil., through tubes and granular beds, relax. effects 9-32748
 in channel with step, numerical method for nonlinear problem 9-34852
 conducting inviscid, past symmetric airfoil with stream-parallel mag. field 9-40649
 conducting liquid under actions of rotating magnetic field in infinitely long cylinder 9-30190
 with convected elasticity, behaviour 9-44539
 convection, forced, past a flat plate with variable viscosity and thermal cond. 9-46586
 convection induced by surface-tension gradients: expts. with heated point source 9-23417
 convective, effect of stabilizing gradient of solute 9-39087
 coolant in nuclear reactor, heat flow and Nusselt no. determ. 9-22898
 detergent films, bulk and surface viscosity 9-23446
 dielectric cylinder in stream of incompressible conducting liquid, non-viscous magnetic boundary layer 9-30189
 diffusive in porous medium with isopycnic boundaries, equiv. with Yih's soln. for non diffusive flow 9-40761
 dusty viscous liq. unsteady flow through circular cylinder 9-48669
 elastico-viscous, due to rotating plate, flow reversal due to edge effects 9-39063
 evaporating, flow rate density of non-equilib. adiabatic stream, theory 9-30463
 film down inclined plane, stability rel. to finite-amplitude disturbance 9-40767
 finite cavity flow of axial symmetry, inclusion of effect of flow models at cavity termination 9-46587
 forced, heat transfer influence on melting and solidification 9-23578
 free flow at large Reynold's numbers, hydromag. stability of two dimensional jet 9-46599
 Glycerol solns., Couette flow between rot. cylinders, relax. effects 9-32749
 human aortic valve model, fluid mechanics and closure mechanism 9-49601
 hydrocarbon liquid, flowing through tube, electric current generation 9-26129
 hydromagnetic, near accelerated plate in presence of mag. field 9-34744
 kerosene, rheology near solid boundary 9-39069
 laminar, between rotating parallel discs 9-23421
 laminar, frag coefficients and transfer factors for spheres 9-28083
 laminar, over defined shapes, diffusion from free surface into liquid film 9-48690
 laminar, polarization anal. of electrodiagnosis 9-47464
 laminar, surface tension effects on rate of dissolution of solid surface 9-48668
 laminar, uniformly porous channel, applied mag. field, heat transfer calcs. 9-34851
 laminar in annulus, heat transfer and temp. distrib. 9-23480
 laminar incompressible at circular tube entrance, rel. of flow and temp. profile 9-23419
 laminar jet mixing from rectangular nozzle into uniform stream, theory 9-30362
 liquid crystals, smectic and cholesteric, capillary flow 9-48671
 in magnetohydrodynamic duct, free surface 9-30187
 magnetohydrodynamic generator, optimisation, restriction of angle of mouth of duct. 9-30192
 metal, velocity profile in circular pipe, comparison with mag. field addition 9-25827
 MHD Hg current in ducts with sudden widening 9-30201
 mutually soluble, filtered mixing in porous medium with one-sided miscible displacement 9-39079
 non-Newtonian, velocity profiles by photomicroscopy 9-46588
 non-Newtonian fluid, generalised plane Couette flow 9-40759
 ocean circulation, wind-driven, three-dimensional model 9-26889
 oriented, degrees of equilib. destruction of structure 9-23418
 patterns and velocities prod. by helical ribbon impellers in cylindrical tanks 9-44534
 in pipe, turbulent, average vel. distrib. rel. to viscous sublayer 9-46590
 plane-parallel stream, stability, Rayleigh method 9-42622
 polyacrylamide solns., Couette flow between rot. cylinders, relax. effects 9-32749
 polyacrylamide solns., dil., through tubes and granular beds, relax. effects 9-32748
 polyethylene oxide dilute solns., behaviour of critical Taylor number rel. to conc. 9-44538
 polymer solns., dil., through tubes and granular beds, relax. effects 9-32748
 polymer solution in tube, rel. to lowering of turbulent heat exchange 9-40785
 potential uniform non-viscous flow disturbed by an oval of Cassini 9-23414
 radial filtering currents, non-stationary, plane, when sources and sinks continuously distributed within bounded regions 9-39062
 reattaching of jet flows, analysis 9-32757
 rheology near solid boundary 9-39069

Flow continued**liquids continued**

- rotating, unsteady, in partially filled right circular cylinder 9-26049
- rotating motion past sphere at middle of circular pipe 9-48670
- rotationally symmetric vortex, breakdown 9-32752
- salt water, stably stratified, laminar, past flat plate 9-26055
- shear, interaction with internal gravity waves 9-26053
- shear, second-order gravity wave interactions 9-28089
- silicone gum viscous sphere on flat surface, due to gravity 9-32745
- steady, round cylinder, numerical soln. at Reynolds numbers 40 200 and 500 9-34848
- Stokes, non-axisymmetrical of viscous liq. in space between eccentric spheres 9-32746
- stratified flows, steady, soln. using eqn. with horiz. co-ords. as space variables 9-40760
- sugar, aqueous soln., laminar flow, vertical tubes, heat transfer studies 9-28114
- over surface causing erosive rupture 9-23912
- surface-velocity grad. in 3D boundary layers, meas. tech. 9-30359
- swirling flow in converging funnel, vel. profiles in boundary layer at wall 9-34846
- tar solution in tube, rel. to lowering of turbulent heat exchanges 9-40785
- three-dimensional boundary layers, surface vel. grad., meas. tech. 9-30359
- transverse perturbation velocities in rectangular duct, two-dimensional flow of compressible fluid 9-30204
- transverse turbulent velocity fluctuations close to wall, limiting behaviour 9-42626
- in tube, asymm. and short, deviations from laminar flow when $R \sim 10^3$ 9-36830
- in tube, horizontal displacement by other liquid 9-42623
- turbulent, cooled surface, self-oscillation temp. depend. 9-24038
- turbulent, temperature and velocity fluctuations, and power spectra 9-35805
- turbulent in pipe, time characts. and temp. pulsation spectrum 9-26056
- turbulent in square channel, space-time temp. pulsations 9-39095
- turbulent track, friction and heat exchange, transverse magnetic field 9-30203
- turbulent with elec. conduction, in tube with longit. mag. field, heat transfer 9-39094
- two immiscible liq. of different heights betwn. parallel plates, vel. distrib. and press. gradient obs. 9-30357
- two layers, down an incline, role of viscosity stratification 9-23420
- unstable motion of electrically conducting liquid, slow rotating disc, presence of strong axial magnetic field 9-30207
- unstable motion of electrically conducting liquid slow rotating disc, presence of strong axial magnetic field 9-30206
- unsteady, due to small motions of cylinders, calc. 9-34853
- unsteady, of dusty viscous liq. through circular cylinder 9-48669
- unsteady, of viscous liq. between oscillating plates 9-46585
- urine velocity meas., fiber optic method 9-46015
- variable viscosity, turbulent, heat transfer 9-40783
- velocities and patterns prod. by helical ribbon impellers in cylindrical tanks 9-44534
- velocity gradients at surface for flow round cylinder at Reynolds numbers 5×10^3 to 10^5 9-34847
- velocity profile, with temp-depend. viscosity and heat transfer 9-26083
- viscoelastic fluids and reduction of turbulent drag. 9-42621
- with viscosity stratification, stability of free-surface inclined flow under gravity 9-26051
- viscous, around circular cylinders, numerical soln. 9-26061
- viscous, down inclined plane, long surface users generation; theory 9-46595
- viscous, with solid particle suspension, laminar motion 9-42624
- viscous flow in canal bounded by two porous concentric circular arcs 9-26082
- viscous fluid nonstationary jet motion theory 9-44397
- viscous past body, with mag. field in dirn of flow, boundary layer eqns 9-28082
- vortex shedding and wake form. behind inclined flat plate, low R obs. 9-34845
- wall pressure fluctuations in flow past rough wall 9-46584
- water, in 60° wedge, path of particle on collapse 9-23376
- water, cavity, collapsing, field flow behind 9-23429
- water, cooling of power station pump, ^{24}Na tracer meas. method 9-28084
- water, flow pattern from free convection obs. 9-23482
- water, forced, supercritical, through curvilinear channels, heat transfer obs. 9-26089
- water, in surface layers when evaporating from capillaries 9-44533
- water, laminar flow, vertical tubes, heat transfer studies 9-28114
- water, past Pt resistance type thermometer, dynamic response 9-34104
- water, past smooth wall with single projection, wall press. fluctuations, spectral characts. 9-46583
- water, polymer additive effect on grid turbulence 9-44536
- water, temp. profile meas. along film 9-30384
- water, turbulent at supercritical press., natural convection, heat transfer study 9-26090
- water, turbulent flow in smooth walled pipe, wall press. field obs. 9-42627
- water in nuclear reactor container, meas. by thermocouple noise signal cross correl. 9-38740
- water jet, turbulent, in still gas, core length rel. to nozzle config., obs. 9-42632
- water movement in porous mats, evap. during second stage of drying 9-34854
- H_2O , and air, Reynolds similarity, exactness investigation 9-25996
- H_2O , turbulent, velocity and eddy viscosity distrib. in pipe wall region 9-26054
- He II, counterflow in rot. channel 9-48731
- He II, heat induced counterflow, local boiling and cavitation 9-44609
- He II, under low press. heads, influence of dissipation in superfluid component 9-48730
- Na, rel. to induced e.m.f. along external mag. field, (α -effect) 9-36899
- Na suspensions with high solid concentration 9-23544
- NaK, turbulent temp. fluctuations, meas. 9-23426

two-phase

- air-water mixtures, concurrently down vertical pipes, expt. 9-26001
- annular, disturbance waves coalescence 9-23227
- annular dispersed, mechanism and meas. technique 9-39035
- boundary layer problem, mathematical similarity to conc.-dependent diffusion problem 9-38945

Flow continued**two-phase continued**

- ceramic bodies, aqueous conductivity, method 9-28387
- critical flow, compress., dynamics and thermodyn. 9-32572
- drops moving relative to gas stream, heat and mass transfer 9-34866
- energy loss due to friction, gas and solid phase mechanical interaction 9-30328
- filtration in a porous medium, equations and boundary-value problems 9-48672
- fluid-particle suspension, induced by infinite rotating disk 9-26135
- Freon-22, critical heat flux modeling, comparison with water 9-34736
- gas bubbles in liquid, eqns. of motion 9-23442
- gas-condensate system, differential eqns. of filtration 9-48673
- gas-particle; trajectories of particles in nozzles rel. to erosion by impact 9-34819
- liquids, gravity waves in plane horizontal flow 9-46594
- MHD, steady, of two conducting incompressible immiscible fluids between conducting plates under closed cct. conditions 9-27967
- momentum conservation eqns. with phase conversions 9-25822
- non-Newtonian, heat transfer 9-23242
- non-Newtonian, pressure drop and hold-up 9-23241
- pressure wave in gas-liquid system with large void fraction 9-28122
- slow viscous, Vivo-dimensional bubbles 9-23443
- in spray cooler 9-23541
- stability, single heated channel, self-sustained hydrodynamic oscills., integrated analytical model 9-34737
- in tube at supercritical press., convective heat transfer 9-26023
- water, oscillations in boundary layer, meas. by obs. tension in fibre suspended at right angles 9-32750
- water/air, exchange processes in bubble column 9-23224
- Ar-ethyl alcohol adiabatic annular dispersed flow, phase and vel. distrib., obs. 9-46558
- Ar-water adiabatic annular dispersed flow, phase and vel. distrib., obs. 9-46558
- CO_2 in tube at supercritical press., convective heat transfer 9-26023
- He, pressure drop and heat transfer meas. device 9-46664

Flow birefringence *see Double refraction/flow***Flowmeters***see also Anemometers*

- eddy current, for high-temp. liquid metal systems, performance tests 9-36831
- e.m., magnetic pole pieces, optimum size rel. to sensitivity 9-26057
- fibre at right angle to flow, tension meas. 9-32750
- for reactor liquid metal coolant 9-36634
- for vacuum systems, meas. of small gas inflow 9-38181

Fluctuations *see Brownian motion; Random processes**see also Brownian motion; Random processes*

- in Bose-Einstein syst. 9-36145
- cosmic rays, origin 9-24727
- critical opalescence, nonlocal hydrodynamic eqns. 9-23576
- drop centre of mass, and homogeneous nucleation theory, embryo equil. distrib. 9-36923
- drop centre of mass, and homogeneous nucleation theory, embryo equil. distrib. 9-46683
- earth rotation, polar progressive and librational motions 9-33745
- in Fermi-Dirac syst. 9-36145
- flow of an elastico-viscous fluid near stagnation point 9-23431
- in fractional and multiple occupancy syst. 9-36145
- geomagnetic storms, mid- and high-latitude, statistical analysis 9-35905
- intensity fluctuations of two random signals, two correlated random walk processes in 2TW-dimens. space as model 9-31886
- intensity fluctuations of two random signals, two correlation random walk processes in 2TW-dimens. space as model 9-31887
- laser pulse, giant, variation on passing through nonlinear absorber 9-45968
- light scattering by fluids, theory 9-23497
- liquids, theory 9-48679
- local geomagnetic gradients, activity index 9-33860
- log-amplitude, of laser beam in turbulent atmosphere 9-31320
- and magnetic susceptibility 9-31905
- in plasma, turbulent, e.m. and kinetic energy 9-27973
- quantum mechanical, far from equilib. theory 9-22135
- superconducting junction, athermal fluctuations effect on radiation line broadening in Josephson effect 9-41188
- superconductors, spin fluctuations assoc. with form. of localized mag. moments 9-47082
- thermal, effect on microcrack formation in crystals at dislocation pile-up 9-33086
- thermal, of magnetic moments in single domain rock grains 9-33874
- thermionic conduction stabilization against temperature change, effect of space charge cct. resistance 9-36263
- turbulent, in viscous sublayer 9-23212
- Pb films, effect on resistive transition to supercond. 9-41186

Fluid flow *see Flow***Fluid mechanics** *see Hydrodynamics***Fluidized powders** *see Flow; Fluids; Powders***Fluids***see also Gases; Liquids*

- anisotropic incompressible conducting, radial-vortex motion in mag. field 9-38952
- axisymmetric, with parabolic vel. profile, stability 9-34719
- Boussinesq, spin-down in circular cylinder 9-32566
- buoyancy driven system, instabilities rel. to mechanical and buoyancy forces 9-48530
- Burger's eqn. for dealing with Navier-Stokes eqn. 9-25806
- cavity flow, axisymmetric, numerical solution 9-42477
- charged particle equil. system, thermodynamics 9-36737
- classical, hydrodynamic limit of Enskog eqn., soln. 9-44395
- classical fluid, single-particle distrib. function derived from relaxation-fluctuation theory 9-31778
- Classical integral equation for pair distribution function which is an interpolation of HNC and PY eqns. 9-32562
- compressible, conducting, steady flow 9-23379
- compressible, steady isotropic motion, press. fluctuations obs. 9-23238
- conducting inviscid, in coaxial channel with helical field, degeneration and stability of m.h.d. modes 9-32581
- contraststreaming self-gravitating streams, stability taking account of thermal conduction and radiative effects 9-48531
- convection, evolution of flow model at high Rayleigh number 9-34728

Fluids continued

- convection onset rel. to time modulation of wall temp. when also heated from below 9-34723
 convection past non-isothermal vertical flat plate, general series soln. 9-32570
 convection with changing mean temp., experimental 9-23231
 convection with changing mean temp., theory 9-23230
 critical, scatt. function in simple model 9-34709
 at critical point, thermodynamic and transport props., singularities 9-26152
 in cubical cavity, convective equilb. stabilization by rotation 9-38946
 cylindrical tube obeying Stokes' law, hydrodynamic field of ellipsoid of revolution 9-32565
 dense, in stat. mech. book 9-40252
 dense, molec. dynamics of microscopic props. 9-38937
 diffusion, mutual, in dense supercritical fluids 9-31796
 diffusion in mixed dense fluids 9-30167
 elastico-viscous, heat transfer in slow steady flow in wavy cyl. tube 9-27953
 electrically induced refractive-index anisotropy in nonpolar fluids 9-38938
 e.m. scattering study of critical props. 9-36233
 entropy differences between ideal and non-ideal systems 9-41780
 equilibrium theory, Born-Green-Yvon and Kirkwood hierarchies 9-40631
 ferrofluids, use in acoustic transducers 9-27229
 film, convection, study method 9-47835
 filtering, porous and fractured beds, nonstationary analysis 9-42645
 flow, boundary layer over impulsively started flat plate 9-34739
 flow, inviscid incompressible past 2-dimens. sails, interaction determ. 9-34827
 flow, isentropic; eqn. of motion nonmetric formulation and restriction 9-38221
 flow, laminar in curved pipe, heat transfer series expansion soln. 9-23246
 flow, one-dimensional, with turbulence augmentation and press. grad., vel. and temp. distrib. 9-34718
 flow, stability exchange principle, perturbation theorem 9-34738
 flow around circular cone, non-linear equations soln., integral relations method 9-46562
 flows on two-dimensional networks theory 9-44398
 fluidization rate of polydisperse layer 9-27946
 Freon-22, critical heat flux modeling, comparison with water 9-34736
 Gaussian mols., eqn. of state 9-29218
 guiding centre theory 9-40655
 hard spheres, elastic moduli 9-36741
 hard-disk, radial distrib. functions and eqn. of state 9-30168
 hard-sphere distrib. functions and augmented van der Waals theory 9-31794
 heat assist devices, fluid mechanical problems 9-38131
 heat conduction exam. by sinusoidal heat pulse technique 9-29324
 heat transfer, forced convection, at supercritical press., review 9-26151
 heat transfer, laminar natural convection, Ellis model 9-32559
 heat transfer in tube with high heat flux 9-27241
 heat transfer to agitated non-Newtonian fluids 9-44556
 heat-generating, flowing in circular tube with flat velocity profile, heat transfer 9-22284
 heavy, infinitely deep, pressure distrib. on flow surface rel. to stationary waves of finite amplitude 9-23245
 hypernetted-chain approx. appl. to Lennard-Jones fluid 9-29209
 hypersonic near wake flow, FORTRAN program for calculation of solutions 9-40632
 incompressible, in coaxial channel with helical field, degeneration and stability of m.h.d. modes 9-32581
 incompressible, irrotational hydrodynamic field round sphere 9-25800
 incompressible sphere, relativistic, iterative scheme for soln. 9-45591
 interface, pulse shapes of refl. and refr. spherical waves 9-30183
 interface stressed by perpendicular electric field, small-amplitude motions and charge relaxation 9-32790
 inviscid heterogeneous incompressible, Rayleigh-Taylor instability with Hall currents 9-34710
 Kirkwood instability for hard rods 9-29219
 Kirkwood-Salsburg integral eqn. and virial coeff. of Lennard-Jones mols. 9-32557
 laminar natural convection flow about isothermally heated sphere at small Grashof number 9-23236
 light scatt. ley multicomponent fluids 9-39099
 light scattering, correlation and fluctuation props., single-mode laser input 9-32561
 light scattering, fluctuation theory 9-23497
 long-range pair-correl. function, theory 9-30166
 Lorentzian, light particle diffusion, time dependent 9-44393
 magnetic, viscosity in mag. field 9-48532
 Maxwell, visco-elastic, flow bet. torsionally oscillating discs 9-25814
 Maxwell, visco-elastic, flow due to torsional oscillations of plane 9-23239
 mechanics of magnetically balanced arcs in cross flows 9-25990
 methane and methane-d₄, phys. props., theory 9-39143
 methane and methane-d₄, phys. props., theory 9-44617
 micropolar, with stretch eqns. of motion, constitutive eqns. and boundary conditions 9-31822
 molecular with square-well potential, equation of state, Monte Carlo calc. of Free energy 9-36738
 monatomic, second order constitutive eqns. 9-46128
 oscillations in viscous incompressible sphere, own gravitation and surface stress, viscosity eqn. 9-23214
 pair correlation, time depend. in terms of self diffusion and static structure 9-23208
 paramagnetic conducting, coupled magnetosonic waves 9-42677
 Percus-Yevick approx. for truncated Lennard-Jones (12-6) potential appl. to Ar 9-23210
 polar, dynamical Langevin eqn. 9-42472
 porous media, inhomogeneous, marginal stability 9-34102
 potential vortex flow near stationary surface, soln. 9-23243
 radiation scatt., statistical props. 9-42474
 Rayleigh-Taylor's instability, eff. of mag. field and Coriolis forces 9-46434
 Rayleigh-Taylor instability with Hall currents 9-34710
 relativistic, thermodynamically, accelerated wave, no shock, ray velocity, covariant formulation 9-36118
 Rivlin-Ericksen type validity of Squire's theorem, conditions necessary 9-40757

Fluids continued

- rotating, differentially heated, amplitude vacillation characteristics determined by multi-probe technique 9-27947
 rotating, inertia oscillations, instability, effects of radial law of depth 9-25801
 rotating cylinder, centrifugally driven thermal convection, soln. by boundary layer methods 9-34720
 rotational flow at rest at infinity, unsteady, sound generation 9-27949
 shells, spherical fluid-filled; frequency spectra 9-45841
 silicone, positron lifetimes 9-27467
 square-well potential, radial distrib. function 9-42473
 stratified, wakes produced by flow of two-dimensional body 9-23229
 stratified with shear, reflection and stability of internal gravity waves 9-27958
 supercritical, dense, mutual diffusion. coeff. 9-31796
 supercritical, turbulent heat transfer 9-39050
 superposed, in cylindrical tube, bubble prod. by Taylor instability, motion 9-23441
 surface, parametric instability in alternating elec. field 9-23207
 systems, dissipationalless, exchange invariance 9-42475
 temperature variability, effect on heat transmitted in heat regenerator 9-47834
 thermal instability in layers, horizontal and vertical temp. gradients 9-32563
 thermal instability of a fluid heated from below 9-25799
 thermodynamic props. of two-component fluids, Monte Carlo calc. in isothermal-isobaric ensemble 9-32560
 three-fluid cross flow heat exchangers, performance depend. on 2 fluids temp effectiveness 9-27955
 turbulence, functional integration theory, velocity-correlation tensor determ. 9-36739
 turbulence structure meas. using c.w. lasers, S/N ratio ratio and spectral broadening 9-46443
 turbulent, decay of proton spin echoes, rel. to Kolmogorov scaling laws 9-30178
 turbulent fluctuations in viscous sublayer 9-23212
 turbulent mixing, passive scalar properties, zero-gradient points and minimal gradient surfaces 9-30169
 turbulent mixing, scalar fields fine structure, spectral theory 9-30170
 van de Waals, and fluid mixtures, transport processes near critical points, models 9-44392
 viscoelastic, boundary-layer flow equation 9-36836
 viscoelastic, network model 9-27948
 viscoelasticity, macromol. fluid, network model 9-38940
 viscous, ellipsoidal bubble dissolution 9-38941
 viscous, finite elec. cond., incompressible, magnetohydrodynamic disturbances due to oscillating dipole introduction 9-34747
 viscous, hydrodynamics of pairs of spheres falling along line of centres 9-25802
 viscous, incompressible and elec. cond., hydromag. forced flow against porous rot. dish 9-23255
 viscous, natural convection in vertical slot, stability of conduction and boundary layer regimes 9-40745
 viscous, waves, harmonic components 9-25813
 viscous flow near entrance and exit of a pipe 9-34715
 viscous fluid-filled elastic tubes, press.-forcing of tightly fitting pellets 9-22168
 viscous incompressible rotating, source and sink on axis 9-44532
 waves, spherical, refl. and refr. from fluid interface, pulse shape determ. 9-30183
 Wiener-Hermite expansion used for exact soln. for incompressible inviscid fluid 9-32567
 Yvon-Born-Green heirarchy and its truncations, consistency 9-46432
 Ar, Percus-Yevick approx. for truncated Lennard-Jones (12-6) potential 9-23210
 CO₂, chemical pot. equation, function of density and temp., critical region 9-26155
⁴He chemical pot. equation, function of density and temp., critical region 9-26155
 Xe, chemical pot. equation, function of density and temp., critical region 9-26155
- Fluorescence** *see Luminescence*
Fluorescent screens *see Luminescent devices*
Fluorimetry *see Chemical analysis*
Fluorine
 atom, core polarization and hyperfine structure calc. 9-46273
 atom, hyperfine structure calc., g.s. first-order wave function 9-32408
 atom, polarization wave functions for ground state 9-34532
 colour centre formed on u.v. irradi., e.s.r. identification of y impurity 9-40971
 dissociation energy 9-44374
 forbidden transitions in isoelectronic sequence, relative line strengths 9-36653
 molecule, oscillator strengths, corrections to recent results 9-30037
 molecule, rotation spectrum 9-29484
 muonic, 2p-1s X-rays obs., 2p pionic levels population determ. 9-44301
 in organic solvents, Overhauser effect study of multiple interactions 9-48718
 plasma, line radiation energy, 10⁴ to 10⁵K 9-40676
 Zeeman eff. in ²P_{1/2} level, (1,0)-(1,-1) transition, g factor calc. 9-32411
 F, n.m.r. in CeF₃, showing ionic diffusion 9-24506
 F₂, nuclear mag. shielding 9-42392
 F₂, valence-bond and atoms-in-mols. calc. 9-38857
 F₂, valence-bond and atom-in-mols. calc. 9-38857
 F-Ce³⁺ ENDOR obs. in CaF₂ 9-37808
 F⁻ in K₂CoF₄, n.m.r. of transferred hyperfine interactions 9-41294
 F²⁺ collision strengths for electron impact transitions 9-34563
 F VI, 2p² ¹D level, mean life 9-25708
¹⁹F-¹¹B nmr coupling constant in various compounds, rel. to ¹⁹F chemical shift 9-32464
 H-F branched chain reaction based chem. laser 9-47984
- Fluorine compounds**
 fluorides, crystal growth from low melting flux, (AlF₃, CrF₃, NiF₂, KNiF₃, CoF₂ and KCoF₃) 9-39207
 fluorides, effective ionic radii 9-39182
 fluorides, melting points 9-23581
 fluorides, mixed, Nd³⁺-doped, radiative lifetime of metastable ion, anomalous temp. dependence 9-41405
 F₂, compressed, rot. and translational induced spectra 9-36700

Fluorine compounds continued

- FSO₂ radical, CNDO-MO calc. 9-44326
Hf₂⁺, e. density in H atom, theory and expt. 9-23759

Foams

- see also Bubbles
No entries

Focasons see *Crystals/lattice mechanics; Sputtering***Focussed collision sequences** see *Sputtering***Fog**

- artificial, 0.63 μ laser beam propag. 9-28886
dispersal techniques for static and dynamic environments 9-45483
dissipation by irradiation 9-31313
polarization of laser light after scattering 9-35824

Fokker-Planck equation see *Transport processes***Foldy-Wouthuysen transformation** see *Field theory, quantum***Forbush decreases** see *Cosmic rays/variations***Force** see *Dynamics***Force constants** see *Molecules/vibration***Force measurement**

- Atwood's machine, a simple frictionless rotation-free one 9-36101
eddy-current devices, coupled-circuit method of calc. 9-31896

Form factors see *Elementary particles/theory***Forming processes**

- alloy formation between low and high melting pt. metals by reduction of volatile halides 9-39466
alumina powders, hot-pressing technique 9-35201
alumina whiskers/Ni composites, roll-bonded, electron microscope obs. 9-33169
 α -brass, rolled, orientation distrib. of crystallites, electron microscopy determ. 9-48830
brass plate, cross-shaped, yield surface after prestraining or cold rolling, expt., study 9-26327
ceramic powders, vibration pressing 9-35217
ceramics, extrusion, press-forging 9-35216
extrusion, drawing and rolling, introductory book 9-38286
fabrication problems, shaping and densification limitations 9-35215
fibres, filaments and films, patent 9-46961
hot rolling of strip, slip-line fields and deformation 9-23944
metals, welded joints, fatigue strength, effects of reactive stresses 9-23902
orbital grinder-polisher for preparation of irradiated specimens 9-39465
plaster moulds, capillary action 9-30703
powders, isostatic hot pressing technique 9-35228
quartz comminution, net energy input rel. to fineness 9-26374
quartz comminution, net energy input rel. to fineness 9-26375
rolling, singularities of dislocation kinetics 9-23805
sheet metal, planar directionality and re-formability rel. to prestrain 9-35200
spheres of controlled size from powders by planetary rolling 9-35199
steel, 12% Cr-Co-Mo, tempering, precip. obs. 9-42932
steel, martensite, low-C internally twinned, tempering charact. 9-41052
steel, oscillatory wire drawing, presence of reduced stress and friction 9-37286
steel castings, continuous, microstruct. and effect on mech. props. 9-39467
steel strip compacting from powder, popular article 9-48918
surface preparation by cutting, lapping, polishing and etching 9-42711
trichite-reinforced composite materials 9-35235
two-phase composite, shrinkage anal. in terms of component props. 9-28392
welding of very thin foil, electron beam method 9-36089
Al-(11 wt.%)Mg alloys age-hardening deform. by hydrostatic extrusion, effect on struct. and props. 9-41051
Al-10wt.%Pu fuel elements, injection casting in Pyrex molds 9-22897
Al, and alloys, hydrostatic extrusion rel. to tensile strength and struct. 9-41029
Al, oscillatory wire drawing, presence of reduced stress and friction 9-37286
Al₂O₃, hot pressing, effect of gaseous impurities 9-35202
Al alloys, unnotched, machining cut depth effect on fatigue 9-33074
Al extrusions, microstruct. 9-39252
Al thin film alloying into Ge, obs. 9-33116
CaO, hot-pressing, effects of gaseous impurities 9-35202
Cu, oscillatory wire drawing, presence of reduced stress and friction 9-37286
Cu, rolled, orientation distrib. of crystallites, electron microscopy determ. 9-48830
Fe-(19 at.%)Ni alloy, rolling, fracture obs. 9-33066
Fe alloys, low-C, martensite, aus- and bar-forming, strength increase obs. 9-42912
Ge alloying of thin Al film, obs. 9-33116
HfB₂, consolidation mechanisms in high- P_2 , densification mechanisms in high-pressure, hot-pressing 9-35223
Mg-(5 at.%)Li-(1.5 at.%)Al alloy, rolling, rel. to plastic deform. 9-33035
Mg-Ni system, contact fusion 9-26373
Mg and alloys, book 9-39447
MgO, hot-pressing, effects of gaseous impurities 9-35202
Mo-Zn alloys by reduction of volatile halides 9-39466
Mo as-grown single crystal, grinding and abrasion effect on dislocation struct. 9-42836
Pb layers, bright, for supercond. resonating cavities 9-39607
Ti-(8 wt.%)Al-(4 wt.%)Co alloy, fabrication and forgeability 9-23956
U-(3.96 at.%)Si alloy, fabrication effects on structure 9-33124
Zn and Zn base alloy ingots, rolling, patent 9-35203

Fortran see *Calculating apparatus/digital computer programmes***Fountain effect** see *Helium-liquid; Superfluidity***Fourier analysis**

- see also *X-ray crystallography/calculation methods*
character recognition by incoherent Fourier transformation 9-25365
elasticity problems, Fourier transform methods 9-34066
fast Fourier transform applic. to response calc. of linear distributed system to homogeneous random acoustic field 9-45847
fast neutron attenuation in uniform media, transform soln. for plane source 9-22846
multiple integrals, asymptotic evaluation 9-36112
optical transfer function, interpret, theory rel. to its moments 9-25346
oscillatory problems, demonstration of Fourier solns. using combination tones 9-43708
spectroscopy, real-time, operation and performance 9-36384

Fourier analysis continued

- in spectroscopy, transform technique, review 9-32051
transformation, fast, of large arrays of data 9-25379

Fourier series see *Series; Transformations, mathematical***Fourier-transform spectroscopy** see *Fourier analysis; Spectroscopy***Fractionation** see *Distillation***Fracture**

see also *Mechanical strength*

- in alnico-type cast hard magnets, b.c.c. 9-35014
bending, torsion and radial fluid pressure, interpret. 9-26350
ceramic materials, oxides 9-33011
ceramics, toughness meas., rel. to work of fracture 9-37247
crack, penny-shaped, fracture criterion and plastic energy dissipation 9-33033
ductile, mechanics by internal necking between adjacent cavities 9-30676
dynamic, time-depend. criterion 9-33063
elastic solid containing external elliptical crack, stress-intensity factors and pot. functions 9-33088
electron fractography, two-stage replica technique using Bioden 9-39151
fibres, viscous, tearing 9-33061
glass, by impact 9-28370
glass, chemically strengthened, behaviour, rel. to stress profile 9-28336
glass, cleavage crack propag. 9-30697
glass, fracture surface energy 9-42903
glass, reinforced, strength and fracture behaviour 9-30678
glass plate, toughened, shape of front, spark photography 9-30681
Hastelloy N, irradi., rel. to temp. and strain rate 9-41030
ionic crystals cleavage rel. to surface tension in presence of dipole moments 9-32831
linear elastic to gross strain transition temp., dynamic tear test definition 9-35185
and mechanical strength, interdisciplinary approach, book 9-39431
metal azides, initiation of thermal decomp. direct obs. 9-30531
metal carbides, refractory, surface layer fracture due to giant laser pulses 9-44774
metal carbonates, initiation of thermal decomp., direct. obs. 9-30531
metal single crystal, criterion 9-44776
Nimonic 80A under static creep stresses with superimposed cyclic stresses 9-33048
nylon 66 fibres, fractographic analyses and prelim. obs. 9-42895
oriented materials, kinetic theory using elastic network model 9-46908
orthoclase, cloven in vacuum, electrostatic distrib. obs. on faces 9-37571
pentaerythritol tetranitrate, initiation of thermal decomp. direct obs. 9-30531
Perspex, non-crystalline 9-26357
plastics, fiber reinforced, elec. and luminescent eff. 9-26351
polycapromide, mechanical damage, accumulation under static load 9-33039
polystyrene, mechanical damage accumulation under static load 9-33039
rock, stability of propag., terminal vel., dynamic stresses due to propag. crack 9-33062
rubber, SBR, fracture obs., -57°C and at different strain rates 9-35187
steel, 300M, fracture toughness and crack propagation 9-33067
steel, austenitic stainless, fracture paths of stress corrosion cracks 9-39441
steel, brittle fracture, statistical model 9-35186
steel, brittle fracture with interaction between elastic crack and slip band, criterion 9-44779
steel, C-Mn, cleavage strength, microstructure effects in various compositions after different heat treatments 9-39432
steel, C-Mn, quenched and tempered, Charpy-V notch tests, critical crack opening displacement 9-30690
steel, cast, fatigue fracture, effect of size distrib. of internal defects 9-35188
steel, cast, fatigue fracture surfaces, microfractographic investig. of crack propag. 9-33080
steel, dynamic strain aging and notch brittle fracture 9-33114
steel, ferrite-pearlite, ductile fracture resistance 9-46899
steel, high strength, fatigue failure, fractographic investig. 9-33081
steel, high-strength, fracture toughness and uniaxial tensile props. relationship 9-33060
steel, high-strength, plane of strain fracture toughness rel. to precracked Charpy W/A 9-35182
steel, low C, explosively produced spall fractures, metallographic features 9-26354
steel, martensitic Cr, behaviour under cyclic loading 9-23915
steel, mean C and low-alloyed, fatigue fracture, hardening and softening abs. 9-30689
steel, plate, anisotropic, neck-and-split tensile fracture 9-33065
steel cylinder, strain at fracture under explosive loading conds. 9-30660
steel-(0.36 wt.%)C, toughness, instrumented Charpy impact test 9-28366
surface coating on strained substrate 9-42900
time and plasticity effects 9-48910
toughness concept and prediction of low-stress failure in materials 9-28363
toughness source rel. to tensile parameters 9-37249
unstable elastic-plastic, brittle criterion rel. to energy balance considerations 9-44775
water droplets in free fall, freezing and shattering phenom. 9-28181
Zircaloy-2, irradi., in BWR and PWR conditions, obs. 9-37258
Zircaloy-2 tubes, critical crack length rel. to neutron irradi. and hydride precip. 9-39435
Al, spall layer thickness from fracture criterion 9-33063
Al, surface layer stress effect 9-23880
Al₂O₃, brittle, below 1000°C 9-33084
Al alloy cylinder, strain at fracture, and ductility under explosive loading conds. 9-30660
Al alloys, fatigue fracture surfaces, microfractographic investig. of crack propag. 9-33080
Al fibres, mechanical damage, accumulation under static load 9-33039
Al notched columns with fixed ends, failure under load 9-48906
 α -As single crystals, rel. to dislocations 9-46889
CaSO₄·2H₂O, glass-reinforced plaster, studies using scanning electron microscope 9-42894
Co-W alloy, stress rupture and ductility, structural effects 9-26343
Cr, polycrystalline, by cleavage, importance of crack nucleation and propagation 9-39438
Cr₂O₃, sintered, surface anal. for metal content 9-37279
Fe-(49wt.%)Cr-(2wt.%)V, brittle fracture, slip mode effects 9-26356

Fracture continued

- Fe-(19 at.%)Ni alloy during rolling 9-33066
 Fe-(3 wt.%)Si, alloy, polycryst., pressurization effect 9-33053
 Fe, H-charged, electron microscope obs. of surfaces, crack nucleation mechanism 9-39440
 Fe₂O₃, sintered, surface anal. for metal content 9-37279
 Fe cast, globular, fatigue fracture, hardening and softening obs. 9-30689
 HfB₂, modes 9-35183
 KBr laser windows, damage obs. 9-31943
 KCl surface energy, ionizing irradiation effects 9-28372
 MgO, fully dense polycryst., and strength 9-42893
 MgO, increased roughness of fracture surfaces when crack propagates in water 9-42906
 Mo, polycryst., fracture stress at ductile-brittle transition temp., crack nucleation obs. 9-30742
 NaCl, of (110) faces, exam. by multiple beam interferometry 9-48785
 Ni-Cr alloy, behaviour under cyclic loading 9-23915
 SiO₂-C fibre reinforced composite, toughness rel. to bonding 9-44773
 Ti-(5 wt.%)Al-(2.5 wt.%)Sn alloy, toughness at cryogenic temps. 9-37253
 Ti alloy sheet, toughness at room and cryogenic temps. 9-37255
 Ti alloys, commercial grade, toughness at cryogenic temps. 9-37253
 W, cleavage velocity determ. with u.s. fractography 9-33094
 W, controlled, applic. to high-speed elec. current switching 9-33068
 W, polycryst. cast, brittle fracture stress, effect of temp. and pressurization 9-44757
 W, rel. to Rh additions and lowering of ductile-brittle transition temp. 9-39415
 W single crystal, $\langle 100 \rangle$ axis, cleavage cracks, 77°K 9-33095
 Zn, cleavage planes 9-48786
 Zn, cleavage surface energy by tensile technique 9-30481
 Zn in liquid Hg, brittle, effects of alloying 9-23916
 ZrB₂, modes 9-35183

Francium

No entries

Francium compounds

No entries

Frank-Condon factors *see Spectra***Frank-Read sources** *see Crystal imperfections/dislocations***Fraunhofer lines** *see Astronomical spectra; Spectra; Sun/spectra***Free field rooms** *see Acoustical laboratories***Free radicals**

- L-alanine-1-¹³C irradiated at low temp. 9-33686
 alkyl, e.s.r. evidence for planar shape 9-44377
 alkyl bromides, solid-phase radiolysis, e.p.r. 9-39912
 in anthracene single cryst., recomb. kinetics, rel. to mol. motion 9-32535
 aromatic, fluorinated, ¹⁹F hyperfine splittings in e.s.r. spectra 9-46396
 aromatic stable intermediates in pyrolysis, e.s.r. 9-40604
 benzene anion, e.s.r. relax. 9-46424
 benzyl, delocalization of unpaired electron density 9-36728
 benzyl, from gas-phase pulse radiolysis of benzyl chloride in cyclohexane 9-43339
 benzyl, from toluene and ethyl benzene, emission spectrum in vapour state 9-34694
 benzyl, spin density distrib. 9-42427
 bicyclo(2,2,1) heptane radical, E.S.R. 9-46398
 bis (perfluoromethyl) nitroxide, gas-phase e.s.r. relax. 9-32739
 1, 3- butadiene, aq. soln., propagating type, e.s.r. spectra obs., spin density determ. 9-2925
 from butanes, methyl-substituted, γ -irrad., e.s.r. spectra 9-48499
 chemical reaction intermediates, high temp., rate eqns., consecutive-parallel and Rice-Herzfeld mechanisms 9-35739
 crystals, dipolar ineshifts, theory 9-43287
 cycloheptatrienyl, photoionization 9-23345
 cyclooctatetraene anion, e.s.r. temp. dependence 9-44589
 cytosine, γ -irrad., structure, theoretical study 9-44354
 cytosine monohydrate, γ -irrad. cryst. 9-45390
 diaryl N oxides, methoxy-substituted, e.s.r. obs. 9-27912
 dibenzocyclohexadienyl in anthracene single crystal, radiation induced, ENDOR studies 9-39913
 dibromomethyl, matrix i.r. spectrum and bonding 9-44378
 dichloromethyl, matrix i.r. spectrum and bonding 9-46425
 difluoromethyl, i.r. spectrum in solid Ar 9-48517
 3,4-dihydro-2,4,6-triphenyl-s-tetrazin-1(2H)-yl, struct. by crystal packing analysis and X-ray diff. 9-48516
 N,N'-dimethylpyrazine cation, e.s.r. relax. 9-23117
 2,2-diphenyl-1-picryl-hydrazyl, diluted, ground-state g factor, mag. field depend. 9-43276
 diphenylamine derivatives, methoxy-substituted e.s.r. obs. 9-27912
 diphenylamino dimer as colour centre in molec. cryst. 9-42855
 diphenylmethyl, e.s.r. 9-48495
 DPPH, MO-LCAO calc. 9-42453
 durene, doped cryst., electronic energy transfer 9-24458
 near electrode surfaces, synchronous detection by e.s.r. 9-25788
 electrolytes in aq. soln., glass-like, γ -irrad., electron trapping at -196°C 9-24399
 electron-transfer rates in soln., errors in e.s.r. meas. 9-45412
 electronic structure, self consistent field calcs. 9-34601
 ethyl radical, spin polar, and delocalization, unrestricted Hartree-Fock method 9-27923
 ethyltoluene photodissociation products, fluorescence spectra on trapping in crystalline matrices 9-47402
 ferrocene, γ -irrad., e.s.r. 9-43288
 fluorenyl, e.s.r. 9-48495
 fluorinated anions, spin density distributions 9-38872
 galvinoxyl, cry., mol. struct. and packing 9-40625
 gas phase, detection by e.s.r. spin trapping techniques 9-42451
 gas reactions in discharge flow systs., conc. meas. methods 9-26805
 D- glucose, frozen aqueous solns., irradiation, e.s.r. study 9-42454
 glycine hydrochloride, X-irrad. 9-43340
 glycine irradiation, anisotropic hyperfine splitting of e.s.r. 9-23178
 heterocycles, N and S containing, radical anions, spin density distributions 9-32518
 heterocyclic amine N-oxides, anion, e.s.r. rel. to polarography 9-36715
 n-hydrocarbons, pairwise trapping of e.s.r. 9-45427
 hydrogen bridge formation in soln., study by dynamic nuclear polarization 9-42450
 hydroxyurea, X-irrad., e.s.r. of radical pairs 9-45426
 iminoxyl series, as chains of spins with antiferromag. interaction, from susceptibility meas. 9-31023

Free radicals continued

- isopropyl, chem. activated, competitive unimolec. decomp. 9-24546
 malonamide, X-irrad., e.s.r. of σ -electron radical 9-38924
 mesitylene, e. irradiation, e.s.r. study of radical formed 9-42439
 methyl, MO theory of hyperfine interactions 9-38874
 methyl, proton hyperfine splitting temp. depend. 9-36729
 methyl, thermal, source of pure beams 9-34606
 methyl and methyl-d₃, e.s.r. in aq. soln. 9-42455
 methyl radical, spin polar, and delocalization, unrestricted Hartree-Fock method 9-27923
 1-methylphenalenyl, e.s.r. meas. of spin densities, hyperconjugation eff. calc. 9-34677
 monocarboxylic acid radical anions, e.s.r. obs., 77°K 9-42452
 monochloroethyl, chemically activated, decomposition 9-39947
 monodeterotrophenyl, e.s.r. spectra obs., empirical energy estimation 9-23177
 1-nitro-2,4,6-triphenylbenzene, anomalous N h.f.s. 9-27924
 organic cyanide crystals, γ -irrad., e.s.r. of trapped electrons 9-47440
 organic solids, formed by H-atom bombard. 9-43324
 in oxidation of polymers 9-26825
 oxydiethanoic acid, free radical formed on e. irradiation, in e.s.r. in zero field 9-42442
 perchlorodiphenylmethyl, e.s.r. 9-38908
 perchlorotriphenylmethyl, e.s.r. 9-38908
 perinaphthenyl, e.s.r. 9-48495
 phenoxyl, fluorinated, spin densities from n.m.r. linewidths 9-34687
 1-phenylphenalenyl, spin densities, hyperconjugation eff. calc., e.s.r. study 9-34677
 piperidine iminoxyls, substituted, interconversion 9-38912
 in polyethylene, irradiation, decay rel. to steric config. and matrix mol. motion, obs. 9-27936
 polymerization, dynamics in continuous stirred tank reactor 9-33664
 polymers, irradiation, pairwise trapping, e.s.r. 9-33687
 in proteins, irradiation-induced, e.s.r. study 9-24941
 pyridinyl, excitation splitting of u.v. absorpt. bands by formation of charge transfer type dimers 9-40626
 π radicals, delocalization of unpaired electron density 9-36728
 π -electron radicals, Cl hyperfine interactions 9-48515
 π -electron radicals, MO theory of isotropic hyperfine interactions 9-38874
 structural information from e.p.r. hyperfine splitting technique 9-46350
 in sucrose frozen aqueous solns., gamma-irrad., e.s.r. study 9-42454
 synchronous detection by e.s.r., near electrode surface 9-25788
 σ , containing C, H, N and O atoms, H and n e.p.r. coupling consts., extended Huckel calcs. 9-23025
 2,2,6,6-tetramethyl-4-hydroxypiperidine-1-oxyl, mag. props. and e.s.r. 9-45091
 tetraphenylcyclopentadienone radical anion, e.s.r. and molecular orbital study 9-30143
 2- and 3-phenyl, e.p.r., inequivalence of CH₂ protons 9-36722
 toluene ion radicals, spin delocalization and vibr. electronic interaction 9-38917
 trichloromethyl in soln., ESR spectrum 9-40624
 2,4,5-triphenylimidazolyl, e.s.r. spectrum interpretation 9-27913
 triphenylmethyl, methyl and fluorine substituted, ENDOR spectra 9-48721
 triphenylmethyl, spin density distrib. 9-42427
 triphenylmethyl, substituted, e.s.r. 9-36723
 tropenyl, e.s.r. relax. 9-46424
 tropenyl, e.s.r. spectra obs., empirical resonance energy estimation 9-23177
 vinyl acetate, aq. soln., propagating type, e.s.r. spectra obs., spin density determ. 9-27925
 vinyl propionate, aq. soln., propagating type, e.s.r. spectra obs., spin density determ. 9-27925
 vinyl radical, spin polar, and delocalization, unrestricted Hartree-Fock method 9-27923
 BrO, microwave spectrum 9-44376
 CF, i.r. spectra, matrix isolated 9-45424
 CHO⁺, heat of formation 9-24542
 CN, electron affinity and ht. of formation 9-30296
 ClO, microwave spectrum 9-38836
 ClO, microwave spectrum, rot. transitions $J=3/2 \rightarrow 1/2$ in ² $\Pi_{1/2}$ state 9-48514
 ClO₂, absorption spectra in soln., transitions 9-30039
 ClOO, absorpt. spectrum, 2100-3000 Å 9-30152
 H-atom radicals formed in aromatic rings of phenylalanine, tyrosine and tryptophan 9-46423
 H₂CF, i.r. spectra, matrix isolated 9-45424
 HCF, i.r. spectra, matrix isolated 9-45424
 HCO, CH stretching, anharmonic potential constants 9-38852
 N₃, spectroscopic obs. in soln. 9-38860
 NCS, electronic absorpt. spectrum, rot. and vib. anal. 9-23175
 NO₂, absorption spectra in soln., transitions 9-30039
 NS, molecular structure by gas phase e.p.r. 9-46369
 OH, galactic, radio emission 9-24829
 OH, in X-irrad. ice crystals. 9-47436
 OH band contamination of nightglow obs. 9-41560
 OH π -centroid calc. by Hulbert-Hirschfeld method 9-30018
 OH (² Σ^+) from photodecomp. of H₂O, initial rot. distrib. 9-38867
 PF₄, isotropic hyperfine splittings and molec. struct. 9-23065
 PH₂, emission bands, rot. anal. 9-23176
 S radicals in ultramarines, e.p.r. investigation 9-36727
 SF, gas-phase electron reson. spectra 9-42416
 SO₂ in aq. soln., e.p.r. linewidth depend on temp. viscosity 9-30054
 SeF, gas-phase electron reson. spectra 9-42416
 SiF₃, i.r. spectrum 9-31211

Freezing

see also Melting; Supercooling

- alloy, binary, solidification in presence of heat flow, interface distrib. coeff. 9-37100
 alloy dilute binary, nonlinear stability investig. of solid-liq. interface 9-36920
 alloy melt, binary, interface stability 9-34958
 alloys, stationary model solidification technique for single-cryst. growth 9-32877
 aromatic solns. in n-paraffin, rate eff. on luminescence 9-28142
 binary single and two-phase systems, influence of Soret eff. 9-23673
 cluster formation free energy in nucleation theory, rot. and translation contrib. 9-37101

Freezing continued

p-dihalobenzenes, heterogeneous nucleation on cleaned alkali halide cryst., molecular config. obs. 9-37105
dilute binary alloy, interface stability 9-23582
drop, fluctuations of centre of mass and homogeneous nucleation theory, embryo equil. distrib. 9-36923
drop, fluctuations of centre of mass and homogeneous nucleation theory, embryo equil. distrib. 9-46683
elastomers, gas bubbles nucleation and growth 9-34972
eutectic, controlled, for microstructures growth 9-23676
eutectics, solidification, theory 9-46684
eutectics, solidification, theory comments 9-46685
forced pipe flow, influence of heat transfer 9-23578
gelatin gels, vacuum freeze-dried, cryst. nucleation rel. to struct. 9-34936
glaciation of cumulus at approximately -4°C 9-24657
ice crystal walls, forming activity 9-34962
ice nucleation in supercooled water, time lag, activation energy, formation probability 9-32814
metal matrix composites, controlled solidification using monovariant eutectic reactions 9-36921
metals and alloys, nucleation phenomena in liq. to solid transform. 9-48736
nucleation, cluster formation free energy, rot. and translation contrib. 9-37101
nucleation, supersaturated vapour, equil. thermodynamics applic. 9-34959
nucleation during cryst. growth, 2- and 3-dimens. 9-42753
ocean, maximum wind-generated lead 9-49424
from plane chill, analytical solutions, exact and approx., comparison 9-39135
raindrop, fragmentation in free fall 9-26898
silica gels, vacuum freeze-dried, cryst. nucleation rel. to struct. 9-34936
silica sol., for microporous silica prep. 9-46732
Steel, from plane chill, analytical solutions, exact and approx., comparison 9-39135
trinitrotoluene, glass transition from undercooled melt at 258°K 9-39137
water, effect of dimethylsulphoxide and dimethylsulphone in soln. 9-32763
of water, hot and cold compared 9-42695
water, supercooled, dynamically induced nucleation, physical stimuli obs. 9-34957
water containing AgI, rel. to droplet temp. determ. 9-40822
water droplets, nucleation and supercooling rel. to shock waves, pre-heating, aeration and elec. field, obs. 9-39134
water droplets in free fall, shattering rel. to possible rotation 9-28181
water drops containing AgI crystals 9-42697
water drops submerged in hydrophobic liquid 9-34963
water-dimethylsulphoxide system, phase diagram 9-32815
Ag/Au/Si system, controlled solidification using monovariant eutectic reactions 9-36921
AgI particles, de-activation of ice forming 9-42696
Al, from plane chill, analytical solutions, exact and approx., comparison 9-39135
Al₂O₃/Y₃Al₅O₁₂ system, eutectic solidification 9-34960
Al₂O₃, volume change obs. 9-40820
Al polycrystal, orientation-dependent, effect on lattice deform. 9-46931
Al-(2wt.%Cu), microstructure and composition variation rel. to freezing rate 9-34961
Bi-Te alloys, nucleation, NMR obs. 9-23583
Bi alloys, nucleation, NMR obs. 9-23583
Bi nucleation, eff. of small addition of solute 9-28180
Bi nucleation, supercooling depend. on liq. drop size 9-28179
C/Cr/Ni/Si system, controlled solidification using monovariant eutectic reactions 9-36921
Cr₂O₃-TiO₂ freezing point determ. 9-49022
Cu polycrystal, orientation-dependent, effect on lattice deform. 9-46931
Fe alloys, effect of alloying element on freezing pt. 9-33148
Fe alloys, solidification, growth morphology and solute segregation 9-23952
³He-⁴He mixtures, liquid-solid transition obs., freezing curve drawn 9-32804
Li aluminosilicate glass system, changes during pyroceramic formation 9-36922
Ni-Ga-B dil. alloys, phase equil. during solidification 9-39136
Ni polycrystal, orientation-dependent, effect on lattice deform. 9-46931
Pb nucleation, eff. of small addition of solute 9-28180
Pb nucleation, supercooling depend. on liq. drop size 9-28179
Sn-Cd eutectic, plane to cell transition on solidification 9-23585
Sn-Cd lamellar eutectic, fault structure on solidification 9-28299
Sn-Zn eutectic, undercooling at the solid-liquid interface 9-46686
Sn nucleation, eff. of small addition of solute 9-28180
Sn nucleation, supercooling depend. on liq. drop size 9-28179
TiO₂-Cr₂O₃ freezing point determ. 9-49022
Zn-Cd alloy, single cryst. growth, orientation depend. of solute partition coeff. 9-37104
Zn-Cd alloys, solute trapping by rapid solidification 9-26160
ZnO-B₂O₃ eutectic solidification, lamellar glass-cryst. structures 9-36930

Frenkel defects see *Crystal imperfections/interstitials*
Frequency see *Time measurement*
Friction
see also *Internal friction*
air currents over inhomogeneous soils 9-31301
atmospheric, effect on barometric field numerical forecasting 9-49446
cohesive plastic mats., angle of internal friction 9-39433
cones, solid truncated, from yielding meas. under quasistatic and dynamic loading 9-22219
cylinder, circular, in cross-flow up to Re=5×10⁴, skin, and local pressure distrib. 9-25805
deflections of disk spring 9-27206
dry, for continuous medium plane flow 9-36747
dry, testing, basic principles, review 9-36157
between Earth's core and mantle, cause of secular change in obliquity 9-29067
elastic contact of two rough cylinders 9-36156
energy balance assoc. with boundary friction in presence of surface-active substances 9-23931
erosive rupture cause, mechanism 9-23912
fluctuation model 9-37269
in Gauss-Argand diagram, rel. to wind 9-49452

Friction continued

Hertzian contacts, viscoelastic behaviour under ramp-type loads 9-41003
internal variable, in fluid sphere, impulse sound propagation 9-38298
metal and rocks, coeff., comparative estimate in air and u.h. vacuum 9-26359
Nylon-6, and wear props., γ irradi. effects obs. 9-39444
plasma, two-dimens., test particle dynamical coeff. 9-38961
polyethylene, and wear props., γ irradi. effects, obs. 9-39444
polymer films 9-26360
polymers, glasslike, high elastic states, depend. on temp. 9-27931
skin, balance design 9-28069
skin, local, coefficient, preliminary study, in compressible turbulent boundary layers 9-30181
skin friction, derivation of Karman-Schoenherr formula 9-28072
skin friction in supersonic flow, thin film gauge for meas. 9-23244
sliding, rel. to exoelectronic emission of surface layers 9-24247
slip between rolling ball and track, factors affecting contact conditions 9-31801
steel, behaviour up to 500°C 9-41039
steel, unlubricated surfaces, variation 9-41037
steel and ground basalt, coeff. obs. at ultrahigh vacuum 9-37271
wear of surfaces, probabilistic model 9-37270
wet contacts, depend. on interfacial potential 9-30702
Cu and steel surfaces, unlubricated sliding at high speeds 9-41038
Fe, chemisorbed film effects 9-37272

Frictional electricity see *Electric charge; Electrostatics*
Fuel cells see *Electricity, direct conversion/fuel cells*
Fugacity see *Diffusion in gases; Kinetic theory/gases*
Functions
approximation theory, review 9-22046
Chebyshev polynomial expansion of 'well-behaved' function, coeffs. evaluation 9-36114
D functions, powers of distributions 9-38193
delta functions in eval. of integration const. of Einstein-Maxwell eqns. 9-45764
distribution, in classical stat. mech. representation by functional integrals 9-38249
Galerkin, for asymmetric thermoelasticity, generalization 9-45835
Hankel-transformed perturbation theory functions 9-29520
integral identity rel. to inversion scheme for obtaining Fermi surface from de Haas-van Alphen effect 9-24091
Lagrange, in general theory of displacement 9-31804
partition function for coupled molecular motion in a liquid 9-48678
schrauben functions and mag. operators 9-31748
special, book for physicists and chemists 9-31742
spherical harmonic development of distribution function in neutron slowing down 9-38731
Sturm-Liouville, use of expansions in nuclear physics 9-44104
time correlation used to derive the eqns. of hydrodynamics 9-34055
two-point, with noncanonical light-cone singularities, analytic representations 9-43716
Wiener-Hermite expansion with time-dependent ideal random function 9-32567
Wightman functions, representation in terms of two-point singular functions 9-32103

Fundamental concepts see *Physics fundamentals*
Fundamental constants see *Constants*
Fundamental particles see *Elementary particles*
Furnaces see *Heating*
Furry theorem see *Quantum electrodynamics*
Fusion see *Heat of fusion; Melting; Nuclear fusion*
g-factor see *Elementary particles; Gyromagnetic ratio; Nucleus; Spectra*
G-matrix see *Molecules/internal mechanics*
Gadolinium
¹⁵³Gd, ¹⁵⁷Gd, hyperfine struct. meas. by atomic beam mag. reson., nuc. moments calc. 9-22952
atom, x-ray L emission spectra, new forbidden lines 9-22953
configuration identification using Zeeman effect 9-44262
Curie temp., from heat capacity obs. 9-30779
emission bands, M_{IV} and M_V absorption spectra 9-28707
ferromagnetic, photoemission, electron polariz. obs. 9-26615
growth and purification of single cryst. 9-35026
growth of single crystals by three methods 9-37078
hyperfine field interaction on ¹⁸⁰Hf, IMPACT study 9-45256
L-spectrum, new quadrupole transitions 9-22951
Lorentz number and thermal conductivity, 0.4-4.2K 9-44846
Lorenz functions, elec. resistivity and thermal conductivity 9-33195
magnetic ordering, microscopic theory 9-24313
magneto-elastic interactions 9-24312
microquantities determ. using luminescence of SiO₂-Na₂SO₄-Gd phosphor 9-49323
photoelectric cross-sections of gamma-rays 30-100keV 9-24231
photoemission of electrons, polarization, effects of electron-magnon inelastic scatt. 9-47214
purification and growth of single cryst. 9-35026
resistivity anomalies 9-35340
thermal conductivity, elec. resistivity and Lorenz functions 9-33195
thermal conductivity and Lorenz number, 0.4-4.2K 9-44846
thermal conductivity of single crystal as function of temp 5° to 300°K 9-47009
thermo e.m.f. and thermomag. effect, mag. field strength depend., low temp. 9-39700
Fe-Cr alloy, effect on oxidation 9-24559
Gd³⁺, e.p.r. in ZnO, hyperfine interaction with odd Gd isotopes 9-33636
Gd³⁺, energy levels in CaF₂ 9-43238
Gd³⁺, ground-state splitting in ZrSiO₄, HfSiO₄ and ThSiO₄ 9-33626
Gd³⁺, in CdF₂, e.p.r. 9-37795
Gd³⁺ absorpt. and fluoresc. spectra in LaF₃, GdF₃ and CaF₂:GdF₃ 9-35660
Gd³⁺ e.s.r. in lanthanum ethyl sulphate, zero-field splitting anomaly 9-39914
Gd³⁺ in 5 hexagonal crystals, energy levels 9-33555
Gd³⁺ in aq. soln., electronic energy levels 9-26118
Gd³⁺ in CaF₂, crystal field splitting of ⁶P_J and ⁶I_J terms 9-31056
Gd³⁺ in CaF₂, ENDOR obs. 9-49363
Gd³⁺ in CaF₂, spin-lattice coeffs. determ. 9-45380

Gadolinium continued

- Gd³⁺ in CaF₂, spin-lattice coeff. determ. from uniaxial stress effects on e.p.r. spectra 9-33492
 Gd³⁺ in CaO, spin-lattice coeff. determ. from uniaxial stress effects on e.p.r. spectra 9-33492
 Gd³⁺ in CeO₂, ENDOR obs. of nucl. mag. moments and hyperfine struct. anomaly for Gd 9-35733
 Gd³⁺ in LaF₃, optical absorption spectra 9-33556
 Gd³⁺ in YCl₃·6H₂O, e.s.r. 9-28747
 Gd³⁺ in YPO₄, YVO₄, YAsO₄, e.p.r. spectra obs. 9-43286
 Gd³⁺ pair and Gd³⁺-Eu³⁺ interac. const. in EuCl₃, e.p.r. 9-33439
 Gd³⁺ superexchange parameters in anhydrous chlorides, interpretation 9-27852
 MnF₂, u.s. attenuation near mag. phase transitions freq., and temp. depend 9-48958
 Pb:Gd film, supercond., far-i.r. study of energy-gap props. 9-41185

Gadolinium compounds

- cubic, magnetic structure and exchange interactions 9-45225
 ferrite garnets, coercive force, temp. depend. near compensation temp. 9-49214
 Y-Gd dil alloy, at 1000 ppm., mag. saturation moment 9-49190
 Gd-Co system, intermetallic cpds. over whole conc. range, lattice const. and mag. props. 9-48921
 Gd-Dy dil. alloy, exchange interactions 9-43171
 Gd-69wt.%La alloy, nuclear component of specific heat for effective mag. field at impurity nuclei 9-33461
 Gd-Sc alloys, magnetic structure props. 4° to 300°K 9-45125
 Gd-Y alloys, magnetic structure props. 4° to 300°K 9-45125
 Gd₂CoMnO₆, perovskite, metamagnetism 9-35587
 Gd₂O₃:Bi³⁺, luminescence 9-31125
 Gd₂O₃, emission bands, M_{IV} and M_V absorption spectra of Gd 9-28707
 Gd₂O₃:SiO₂, crystal structure determ. 9-40901
 Gd(MoO₄), phenomenon analogous to Barkhausen effect 9-30976
 Gd₂(SO₄)₃·8H₂O, Faraday eff. in e. p. r. 9-28746
 Gd₂Fe₂O₇, film, ferrimag. domain struct. and props. rel. to growth parameters 9-47272
 Gd₂Ge₃, mag. susceptibilities rel. to D_{8h} structure 9-43157
 Gd₂Si₃, mag. susceptibilities rel. to D_{8h} structure 9-43157
 Gd₂Pb, phase diagram determination 9-41060
 GdAlO₃, antiferromagnetic ordering, symmetry considerations and magneto-electric eff. meas. 9-31050
 GdBr₃, canted antiferromagnetism 9-45226
 GdCl₃, thermal transport, effect of magnons 9-44847
 Gd(Co_{1-x}Ni_x), transition metal moment collapse 9-45084
 GdCrO₃, absorption and fluorescence spectrum of Cr³⁺ magnon-assisted 9-49321
 GdF₃:CaF₂ mixed cryst., Gd³⁺ absorpt. and fluoresc. spectra, energy levels obs. 9-35660
 GdF₃, Gd³⁺ absorpt. and fluoresc. spectra, energy levels obs. 9-35660
 GdFe₂, transverse Kerr magneto-optical effect and optical props. 9-45274
 GdFe garnet, circular domains, density and size 9-47271
 GdFe garnet, domain interaction with atomic scale imperfections, optical obs. 9-45179
 GdFe garnet, Faraday rot. 9-43214
 GdFe garnet, Faraday rotation at 1.15μ, 100° to 450°K 9-49218
 GdFe garnet, Sn-substituted, critical mag. isotherm 9-43188
 GdFe garnet, thermal expansion at 296-1400°K 9-41093
 GdFe garnet epitaxial film, prep. by r.f. sputtering mag. and structural props. 9-49210
 GdFe garnet film, rel. to magneto-optical recording 9-45271
 GdGa garnet, thermal expansion at 296-1400°K 9-41093
 Gd(10wt.%Lu) alloy, nuclear component of specific heat for effective mag. field at impurity nuclei 9-33461
 GdNi₂, electrical resistivity temp. depend. near mag. transition 9-43021
 GdPt₂, electrical resistivity temp. depend. near mag. transition 9-43021
 GdRh₂, electrical resistivity temp. depend. near mag. transition 9-43021
 La_{1-x}Gd_xAl₂ alloys, supercond. transition temp., eff. of press. 9-28477
 Sc:Gd dil. alloy, at 1000 ppm, mag. saturation moment 9-49190
 W(1wt.%Gd)O₃ alloy, ion microscope exam. of matrix 9-41057

Galaxies*see also Nebulae*

- arms, spiral, explosive origin 9-35957
 classification by photographic image rectification, pitch and inclination angle determ. 9-33899
 classification of farms and stellar content 9-38038
 clustering, second order, cosmological implications of its non-existence 9-45586
 clusters, distribution in space, rel. to conditions when structure formed in Universe 9-35955
 clusters and groups of southern galaxies, descriptions 9-47628
 cold thin disk models, WKBJ analysis of free oscils. 9-40127
 compact, spectroscopic and photographic obs. 9-49534
 disk, spiral structures as non-axisymm. perturbations 9-40130
 dwarf elliptical, structure and mechanisms loading to well-mixed star distrib. 9-40128
 dynamics of self-gravitating systems, structure of galaxies 9-47622
 elliptical, E and SO noncluster, radio emission at 2640 MHz 9-43579
 evolution from H₂ gas, mechanism 9-43519
 evolution from H₂ gas in hot universe 9-43520
 evolution in Friedmann models with non-zero cosmological const. 9-31487
 explosive origin of spiral arms 9-35957
 extragalactic objects in the local group, high-velocity cloud complexes 9-43513
 formation, primaeval fireball role in classical cosmology theory 9-26999
 formation in Lemaitre universe model, perturbation theory and Newtonian cosmology 9-31509
 H II regions, observation with high angular resolution and high positional accuracy 9-24756
 Haro's blue galaxies, search radioemission at 9.26 cm 9-24823
 interaction with metagalactic u.v. background radiation and limit on density of intergalactic gas 9-26990
 intergalactic matter, gaseous, photon and cosmic-ray components, review 9-26993
 i.r. radiation obs., evolution theory formulation 9-43506
 i.r. radiation obs., evolution theory formulation 9-45590
 Irr, superassociations statistics determ. 9-24749
 irregular, distrib. of H II regions 9-35963
 isophotal wavelength of U, B, V, R systems for photometry meas. 9-35987

Galaxies continued

- Lemaitre model, possibility of galaxy form. 9-47623
 local group, review 9-38039
 Local Group intergalactic space, physical conds. study with virial theorem. 9-24751
 local supercluster kinematics and solar motion w.r.t. galaxies 9-33896
 Lyman α emissions, anisotropic 9-43516
 M101, asymmetry in neutral H distrib. rel. to tidal effects 9-41626
 M31, model distribution of mass 9-26998
 M31, nuclear region, UBVRHKI photometry 9-40123
 M31 and M33, neutral-atomic-hydrogen link, search 9-45596
 M31 and neighbourhood radio continuum survey 9-43518
 M33, ellipsoidal distrib. of H II regions 9-47632
 M82, exploding galaxy, colours, linear polarization and mag. field mapping of outer filaments 9-49533
 M82, Seyfert-like, seen edge on 9-28989
 M87, optical extent, luminosity and mass 9-43517
 M87, photometry of the outer corona 9-45598
 M 31, mass distribution model 9-45597
 Magellanic Cloud, photometry of clusters, comparison with those in the Galaxy 9-27043
 Magellanic Cloud, planetary nebulae nuclei early evolution, photoelectric study 9-31513
 Magellanic cloud, small, young stars and neutral H distrib., correl. 9-31500
 Magellanic clouds, high-energy X-ray sources search 9-29053
 Magellanic clouds, large and small, two-colour composite photographs 9-31499
 Magellanic Clouds, planetary nebulae radial vel. meas. 9-31512
 Magellanic clouds, southern planetary nebulae masses and galactic distrib., photoelectric study 9-31511
 magnetic field, viscous and thermal generator propositions 9-33898
 magnetic field model, turbulent generation 9-43515
 Markarian's, with u.v. continuum, spectral observations 9-26997
 mass and velocity distributions normal to plane, one-dimensional computer model 9-27000
 mass determ., radio observations preferred to optical 9-31505
 masses and ang. momenta from radio spectral data 9-35954
 metagalactic gamma intensity and isotropic background flux 9-29056
 metagalactic magnetic field, meas. via Faraday rotation of extragalactic radio sources 9-47624
 metagalactic plasma, macroscopic motion, cause of microwave background ang. variations 9-38037
 metagalactic system, expansion in terms of bounce of gas sphere of mars 10²⁶ M.? 9-49521
 metagalaxy, thermal balance and energy loss of intergalactic gas 9-24742
 microwave background, ang. variations, macroscopic motion of metagalactic plasma explanation 9-38037
 model, two-dimensional, consisting of 2000 rods of mass 9-28991
 nebular and interstellar matter, book 9-24741
 negative viscosity phenomena book 9-32564
 NGC 1052, spectrophotometric study of core, 3400 to 6300 Å 9-47630
 NGC 1275 Seyfert galaxy, evidence of light variation 9-35953
 NGC 3077, Irr-II galaxy with large amount of dust, vel. field 9-40126
 NGC 3593, SO galaxy with large amount of gas, rot. and mass 9-40125
 NGC 4151, Seyfert, optical variation of nucleus obs. 9-31503
 NGC 4631, edge on spiral galaxy, search for radio halo 9-47631
 NGC 5253, emission spectra obs., radial velocity determ. 9-35958
 NGC 6574, rotation and mass 9-28990
 NGC 7625, SO galaxy with large amount of dust, rot. and mass 9-40124
 nonlinear waves in disc-like galaxy 9-25053
 nucleosynthesis theory, rel. to abundances of ²⁴⁴Pu and ¹²⁹I in early solar system 9-45658
 nucleus, explosions, cosmic-ray generation, composite model 9-49525
 oscillations, free, of cold thin disk model, WKBJ analysis 9-40127
 photoelectric data, four-colour, on 64 galaxies mainly in Virgo Cluster region 9-31502
 positions for 62 sources between declinations +20° and -33° 9-31568
 radio, 11-20 cm wavelength, linear polariz. obs. 9-24830
 radio, 11-20 cm wavelength, linear polariz. props. and analysis 9-24831
 radio, 14 identifications and positions between declinations +20° and +27° 9-29045
 radio, distinguishability from quasars 9-29040
 radio, east-west linear polarization distrib. at 1418 MHz 9-36008
 radio, normal, and radio quiet, south of +20° declination, UVB system data 9-31565
 radio, spectra of revised 3C catalogue sources 9-40157
 radio type, Hubble plot anomaly explained by gravit. lens image model 9-41654
 radiogalaxies, plasma stability mechanism 9-41651
 radiogalaxies, some properties 9-27116
 rotation and mass of NGC 6574 9-28990
 SBc, superassociations statistics determ. 9-24749
 Sc, superassociations statistics determ. 9-24749
 Schrodinger operator criterion for stability of galaxies and gas spheres 9-35956
 Seyfert, efficiency of Bowen fluoresc. mechanism, comparison with that of planetary nebulae 9-49535
 Seyfert, light and colour variations along the radii of 8 obs. 9-31504
 Seyfert, model, Fe X and Fe XIV line strengths calc. 9-45599
 Seyfert, NGC 1275, evidence of light variation 9-35953
 Small Magellanic Cloud, high-excitation Wolf-Rayet star spectrum 9-24791
 spectra, red shift, new hypothesis 9-26981
 spectral studies, progress review 9-40129
 spectrophotometric gradients 9-24750
 spiral structure 9-41624
 spiral structure, density wave model 9-31508
 spiral structure, origin hypothesis 9-47629
 stability, Schrodinger operator criterion 9-35956
 stability and the Hartree-Fock exchange operator 9-45600
 stability of galactic arm, Lagrange and Jacobi identities 9-31498
 stellar distrib. function, Chapman-Enskog treatment, eff. of recession of high vel. stars 9-31507
 stellar evaporation from outer parts of a galaxy, effects on dynamics 9-31506
 variable, discovery, observation techniques, some light curves and interpretations of periodicity 9-24752
 Virgo cluster, distance and Hubble const. obs. 9-47669
 Virgo cluster, intergalactic H, Gaussian absorpt. profile 9-26991

Galaxies continued

W49 and W75, OH emission sources, time variations 9-35952
W51, complex radio source obs. 9-31569
CN absorption in nucleus 9-31501
Fe X line strength in Seyfert model 9-45599
Fe XIV line strength in Seyfert model 9-45599
H, intergalactic, density and ionization by quasi-stellar objects 9-36004
H, intergalactic, distrib. and contrib. to mean mass density of Universe 9-40120
H, neutral atoms, between the galaxies M31 and M33, surface density 9-45596
H α , r.f. spectral line search, brightness temp. <0.24°K 9-41625
H I, intergalactic, emission at 21 cm 9-40119
H II regions, analysis of radial distrib. on twenty-five galaxies 9-28996
H II regions, chemical sputtering of ice grains and mantles 9-24759
H II regions in twenty nearby galaxies, atlas 9-35965
O VII and V III lines, explaining soft X-ray sky background 9-27069
OH, pumping mechanisms for maser action 9-24740
OH emission sources, time variations 9-35952

the Galaxy

anticyclonic distrib. of giant M stars 9-47625
anticentre region, H ion conc. determ., interferometric meas., 13.1 MHz 9-31497
book, formed from collection of recent non-technical articles 9-33897
brightness distrib. and structure 9-26996
central region, comparison with Galaxies showing nuclear structure 9-24747
classification in 'Combination' category 9-38038
clusters, comparison with those in Magellanic Cloud 9-27043
continuum radiation at 4. GHz, survey between $l^{\text{II}}=21^\circ$ and $l^{\text{II}}=31^\circ$ 9-47627
cosmic emission, absorption, latitudinal depend. 9-33894
cosmic ray gas isotropy, resonant wave particle effects 9-33891
cosmic-ray positrons, secondary, equilibrium spectra and γ -spectrum resulting from annihilation 9-31492
depolarization of radiation from extragalactic sources 9-36007
force law K_{sc} , calc using obs. of the A0-A2 NGC stars 9-28987
galactic light, diffuse, λ 2100-2800 Å, unsuccessful search 9-40121
Galactic plane, between longit. 32° and 49° radio survey 9-40122
Gould's Belt and structure of local magnetic field 9-24746
Gould belt kinematics, an expanding group? 9-24744
hard radiation from Galactic centre, balloon obs. 9-49573
heavy element enrichment, rel. to explosive nucleosynthesis in stars 9-49546
high latitudes, presence of horizontal branch stars 9-47626
horizontal branch, stars at high Galactic latits., positrons magnitudes and spectra 9-47626
instability 9-24748
local spiral arm, 10 MHz absorpt. rel. to physical conditions of medium 9-41662
low latitude survey, 1410 and 2650 MHz, source list 9-24743
M stars, grant, space density in Galactic anticentre 9-47625
magnetic field, origin 9-49530
magnetic field fluctuations, from pulsar signals dispersion and Faraday rotation 9-49531
mass, and gravit. const. vars. rel. to globular clusters age 9-33895
mass, relativistic distribution in spherically symmetric model 9-49532
mass and velocity distributions normal to plane, one-dimensional computer model 9-27000
Milky Way diffuse light, interpret. 9-24745
nebulae, planetary, southern; masses and galactic distrib., photoelectric study 9-31511
Norma region in S. Milky Way, space densities of stars rel. to spectral type and distance from Sun 9-26994
Onion arm, length from position and distance of Ros 4 9-47647
planetary nebulae nuclei early evolution, photoelectric study 9-31513
pulsar distribution from data of Molongio 9-31573
radiation scatt. by interstellar matter, interpretation 9-28988
radio emission, nonthermal, relationship to cosmic ray electrons 9-43509
radio emission at 610.5 MHz, contour map for region between Galactic longits. 55° and 64° 9-26995
radioemission, distributed, obs. at 15, 20 and 30 cm 9-31563
radiowave emission and absorpt. in galactic disk 9-31520
Southern H II regions, minor, obs. 9-24758
space densities of stars in Norma region of Milky Way, rel. to spectral type and distance from Sun 9-26994
stellar orbits in galactic plane, evaluation in generalized Kepler motion 9-24760
G I, H II, comparative motions in Galaxy 9-35967
H I cold cloud, from line spectra meas. 9-43514
NH $_3$ microwave emission in Sagittarius region, rel. to dust cloud conditions 9-43574

Gallium

absorption line shape, theoretical, from cyclotron reson. expts. 9-35324
acoustic resonances in plates, e.m. excitation 9-48957
atom A=67 and 72, hyperfine structure in $^2P_{3/2}$ and $^2P_{1/2}$ states 9-36661
atomic spectrum, bibliography 9-38765
conductivity, thermal, in single crystal, anisotropy of electron mean free path, 1.4° to 4.2°K 9-37370
crystals, single, zero resistance obs. 9-44900
film, light absorpt. rel. to different gas environments 9-45265
fluorescence direct line type, excitation mechanism 9-48409
heat pulse expts. for low temp. thermal transport 9-26438
liquid, nuclear spin-lattice relax. of $^{69,71}\text{Ga}$ 9-26134
liquid, resistance coeffs. for laminar flow through diffuser in crossed fields 9-27968
liquid, X-ray scatt. obs. over wide temp. range 9-30371
melting process, viscometric investigation 9-40818
optical constants, meas. along principal axes 9-33502
phonon dispersion relation, neutron inelastic scatt. 9-33160
plasma oscillations in liquid and solid foils 9-41148
spectral determ. in samples below reliable separation threshold, by plotting intensities of spectrogram lines 9-37854
superconducting, isotope effect 9-28475
superconducting amorphous, phonon spectrum by electron tunneling 9-41076
superconducting energy gap, temp. depend., tunneling meas. 9-33271
superconducting film, transition temp. size dependence 9-30870
surface state resonances, effect of relax. time from amplitude and linewidth temp. depend. 9-37411

Gallium continued

thermal expansion meas. by liq. Ga immersion dilatometer rel. to anharmonic effects 9-47007
in CdS single cryst., luminesc., exciton obs. 9-37756
in CdTe, spectrographic determination use of alumina-cup electrode 9-35761
Ga-in-Hg solution, X-ray diffraction study, radial distrib. functions, co-ord. numbers and scatt. functions 9-28100
 β -Ga, crystal structure from X-ray powder data 9-39277
Ga, lattice vibrations, group-theoretical analysis 9-35269
 δ -Ga, superconducting props. 9-44937
Ga $^{3+}$ diff. in MgO 9-26302
(Ga $^{3+}$) $_2$ in KI, absorpt. bands of ion centres obs., electr. struct. 9-35111
Ga $^{3+}$, ferromagnetic resonance in Y-Fe-Ga garnet with Tb impurity 9-33619
Ga V, elec. dipole transition configs. obs. 9-48398
Ge:Ga, bipolar photoeffect due to anomalous Cd distrib. in and near diffused layer 9-45024
p-Ge:GaAs, radiative recomb., influence of local pot. fluctuations, low-temp. 9-39867

Gallium compounds

Ga $_2$ In $_2$ -Sb, electroreflectance, variation with composition 9-45307
garnets, rare earth, i.r. lattice spectra 9-47338
Al-GaSe-Au struct., carrier transport 9-41228
Al-Ga $_2$ -xSb injection lasers, charact. 9-27335
Al-Ga $_2$ -xSb:Si electroluminesc. diodes, props. and efficiency 9-37775
Cu-Ga alloys, massive and martensitic transform. temp. 9-41066
Cu-Ga solid solns., dislocation struct. and work hardening, electron microscopic exam. 9-41045
Cu-Ga solid solns., width of split dislocations, effect of near order 9-42827
ErGa garnet, $^4I_{15/2} \rightarrow ^3F_4$ transition, Er $^{3+}$ g-tensor anisotropy determ., Zeeman eff. obs. 9-23040
G $_2$ Te $_2$, thermal conductivity, temp. depend., phonon and carrier mechanism 9-33194
GaP: ^{63}Zn (^{75}Se), vapour-grown, substrate orientation effect on dopant incorporation 9-30920
Ga-GaAs-GaP system, liquidus-solidus isotherms, GaAs $_x$ P $_{1-x}$ soln, growth obs. 9-36917
Ga-In liquid alloy, Knight shift calc. from pseudopotential formalism 9-23532
Ga-Sb system, liquidus curve 9-30449
Ga $_{0.85}\text{Fe}_{0.15}\text{O}_3$, ferromag. reson. 9-37788
Ga $_2$ Mg, crystal structure 9-26234
 β -Ga $_2$ O: Fe^{3+} e.p.r. spectrum, theoretical and expt. obs. of low-symmetry effects 9-41427
n-, α -Ga $_2$ O $_3$, elec. cond., O adsorpt. dependence 9-49081
 α -Ga $_2$ O $_3$, Mossbauer spectrum, effect on shift of exchange interaction of mag. ions 9-26720
 β -Ga $_2$ O $_3$, X-ray spectral investigation of chemical bonding 9-49304
Ga $_2$ Te $_2$, stoichiometric vacancies, meas. of impurity solubilities 9-40934
Ga $_3$ Nb $_3$, superconductivity rel. to Si $_2$ U $_3$ type structure 9-39596
Ga $_3$ Mg $_2$, crystal structure 9-26235
Ga $_2$ In $_2$ -xSb alloys, Gunn effect and conduction band struct. 9-41199
Ga $_2$ In $_2$ -xSb solid soln., growth and characterization using temp.-gradient zone melting 9-30719
GaAs-Ga $_2$ Al $_3$ -xAs laser diodes, low-threshold room-temperature, preparation 9-25307
GaAs-Ga $_2$ Al $_3$ -xAs laser diode structures, low-threshold room-temperature, characteristics 9-25308
GaAs, energy gap temp. dependence, 300-973°K 9-43249
GaAs, Franz-Keldysh effect light modulation 9-39810
GaAs $_x$ -xP $_x$ covered with low work function layers, photoemission 9-39742
GaAs $_x$ -xP $_x$ solid solns. cryst. growth from Ga-rich soln., lattice distortions and atomic struct. 9-35206
GaAs $_x$ P $_{1-x}$, low-level interband optical absorpt. 9-47358
GaAs $_x$ P $_{1-x}$, epitaxial layer growth in ga-gaAs-GaP system 9-36917
GaAs $_x$ -x, absorpt. spectra and Hall coeff. temp. depend. 9-33554
GaAsP diodes, yellow emission 9-41225
GaAs $_x$ -xP $_x$ solid solns., absorpt. spectra and Hall coeff. temp. depend. 9-33554
GaP:Bi, Zeeman splitting of recomb. radiation from excitons 9-45347
GaP:Mn, Li diffused, Li tripple ion e.p.r. detection 9-24493
GaP:S, electron-phonon interaction in extrinsic photoconductivity 9-41264
GaP:Zn-O electroluminescent diodes, output charact. 9-41403
GaP:Zn, resistivity and Hall coeff. variation with dopant conc. 9-44954
GaP:Zn epitaxial growth, carrier and Zn conc. obs. 9-30529
GaP:Zn soln.-grown, O solubility 9-33321
p-GaP:Zn(O), red emission, config. coordinates applic. 9-37761
GaP:Zn(O), photoluminescence, Hall effect and conductivity 9-33604
GaP-Cu diodes, induced photovoltaic effect, charge-carrier capture, effect on transition capacitance 9-35510
GaP-GaAs system, suitability for room temp. gamma ray counters 9-26539
Ga(P,As) injection laser, memory effects, obs. 9-48043
GaP, absorption spectrum between 4.2-500°K, fine struct. assoc. with exciton form. 9-43239
GaP, band struct. and reflectivity 9-49268
GaP, chemical and isoconcentration diffusion of Zn, Longini's interstitial/substitutional model 9-35125
GaP, crystal growth by liquid encapsulation crystal pulling at high pressures 9-37052
GaP, crystal growth from stoichiometric melt and from Ga-rich solution, comparison 9-23672
GaP, crystal pulling by liquid encapsulation 9-37077
GaP, defect structure, depend. on growth method 9-30602
GaP, donor and acceptor multipole fields and effects 9-43063
GaP, electrolum. diode, peak quantum efficiency rel. to current 9-28736
n-GaP, electron mobility and impurity conc., crystals grown by cooling of Ga soln. 9-26544
GaP, energy gap temp. dependence, 297-1273°K 9-43249
GaP, heat capacity 55°K-300°K 9-33180
GaP, indirect gap semicond., resonant Raman scatt. 9-41395
GaP, interimpurity recombinations involving isoelectronic trap Bi 9-39866
GaP, luminescence, parametric, involving polariton excitation 9-49317
GaP, pair spectra involving Si donors 9-45358

Gallium compounds continued

- GaP, photoluminesc. of isoelectronic trap N, bound excitonic mol. obs. 9-39895
 GaP, photoluminescence, i.r. radiation effect 9-24472
 GaP, two-photon excitation, intensity behaviour of recomb. radiation of excitons 9-47393
 GaP, vibrational modes, localized, of impurities, i.r. absorpt. obs. 9-35657
 GaP, work function, giant temp. depend 9-35514
 GaP and GaAs⁺ P1-x junctions, prep. and characterization, cryst. struct. rel. to elec. props. 9-35434
 GaP crystal, reflection and photolum. spectra obs., 77.3°K 9-24397
 GaP diode, pulsed, radiation props. 9-38387
 GaP diodes, green-light-emitting, grown by liq. phase epitaxy, spectral props. 9-49121
 GaP diodes, injection electroluminesc. reduction by reverse operation, obs. 9-26784
 GaP diodes, prod., characts. and appls. 9-49333
 GaP electrodes, redox processes, charge transfer reactions, photoexcitation and electroluminesc. obs. 9-30990
 GaP electroluminescent diode, negative resistance 9-26574
 GaP films, vacuum-deposited, structural and optical evaluation 9-42719
 GaP parametric gain near lattice resonance 9-25197
 GaP Schottky barrier diodes, props at 25-500°C 9-33345
 n-GaP vapour grown epitaxial electroluminesc. diodes with green emission at room temp. 9-41224
 GaP(Cs) dynodes with 20-40 gain 9-24256
 GaP(Sb) channeling charact. of protons and the ions 9-47012
 GaS, reflection spectra meas. rel. to interband transitions 9-28671
 GaS, spectral distribution of photoconductivity, eff. of hydrostatic pressure 9-28579
 GaS preparation, purity and elec. conductivity 9-39611
 GaSb:Te, conduction band structure, Hall coeff. and resistivity, temp. depen. 9-37530
 GaSb-InSb, e. scatt. mode 9-24085
 GaSb-InSb alloys, thermal conductivity meas. rel. to phonon scattering by acceptor defects, 5° to 300°K 9-44870
 GaSb-ZnTe heterojunction, fabrication and props. 9-49067
 GaSb, band struct. calc. by empirical pseudopot. method, and optical props. 9-47119
 GaSb, cathodoluminescence, investig. by scanning electron microscope with modulated beam 9-24471
 GaSb, e. scatt. mode 9-24085
 GaSb, energy band structure, semi-empirical Kohn-Rostoker method 9-30923
 GaSb, gradient-elastic tensor determ. by nuclear acoustic resonance 9-23851
 GaSb, growth by floating zone techniques, elec. props., dislocated density 9-28229
 n-GaSb, magnetoresistance oscillations, energy gaps between valleys in conduction band 9-39620
 p-GaSb, photoemission caesiating and oxidation effects 9-43145
 GaSb, thermal conductivity meas. rel. to phonon scattering by acceptor defects, 5° to 300°K 9-44870
 GaSb enthalpy of fusion 9-30449
 GaSb single crystal rocking curves, anomalous absorpt. effects on shape 9-35043
 GaSe, energy structure, effect of Br impurity, absorpt. spectra 9-35412
 GaSe, reflection spectra meas. rel. to interband transitions 9-28671
 GaSe, spectral distribution of photoconductivity, eff. of hydrostatic pressure 9-28579
 GaSe, Wannier exciton binding energy rel. to anisotropy 9-41137
 GaSe layer semiconductor, existence of two dimensional exciton observed 9-35319
 GaTe-GeTe system, u.s. propagation velocity, conc. depend. 9-28417
 GaTe, spectral distribution of photoconductivity, eff. of hydrostatic pressure 9-28579
 Gap:Zn, oxygen implanted, cathodoluminescence spectra 9-39892
 Gap photodiodes for optical modulation 9-39651
 Hg-Ga liq. alloys, thermodynamic activities 9-30369
 In-Ga phase diagram, quasi-chem. equi. model 9-44610
 (In-Ga)Fe garnet, Mossbauer effect 9-49263
 In_xGa_{1-x}P alloys, band structure and direct transition electroluminescence 9-24467
 InGaSn alloy activation in generator elements of rad. loop in water reflector of IRT reactor 9-32384
 InGaSn alloy in activity generator elements of rad. loop of IRT reactor, influence on active section of water reflector 9-32385
 InSb-GaSb alloy, press-induced transform, behaviour 9-37301
 Ni-Ga-B dil. alloys, phase equi. during solidification 9-39136
 Pu-Ga alloy, delta-stabilized, % of α -Pu by X-ray meas. 9-39479
 δ -Pu-Ga alloys, thermal cond. in temp. range 75-300°K 9-41108

gallium arsenide

see also *Semiconducting materials/gallium arsenide*

- acoustic domain, subsonic 9-24032
 acoustic wave generation, subharmonic 9-30908
 acoustoelec. domains, Brillouin scatt. studies 9-37352
 acoustoelectric interaction, piezoelec. and elastic anisotropy 9-41090
 anodic dissolution in KOH, current density-anodic potential curves at low currents 9-24587
 diffusion of Cu in annealed cryst., effect of dislocations 9-44734
 diffusion of Zn, chemical and isoconcentration, Longini's interstitial/substitutional model 9-35125
 diffusion of Zn, 1000°C 9-28327
 electro-optic nonlinear coeff., 2nd order, at mm. wave difference freqs. 9-31083
 electroabsorption spectra of n-type crystals at 300 and 77.3°K 9-39837
 electroabsorption spectra of plane-parallel, n-type crystals at low free-carrier density 9-37723
 electroluminescence in single cryst. by tunnel injection of minority carriers 9-24178
 electrooptical effects between 20 to 120 micron range 9-28660
 epitaxial, oscillatory photoconductivity 9-26604
 epitaxial growth, effect of facet development on ¹²⁵Te distribution 9-36985
 epitaxial growth of Ge films by GeI; disproportionation reaction 9-36947
 epitaxial layers, chemically-deposited, growth and perfection 9-36951
 epitaxial layers, extrinsic photoconductivity spectral meas. in mag. fields, donor obs. 9-39717
 epitaxial layers, photoemission efficiency 9-33615

Gallium compounds continued**gallium arsenide continued**

- epitaxial layers of Ge, plastic deformation 9-37241
 e.s.r., g-factor shift of Fe³⁺ and Mn²⁺, covalency influence 9-43280
 e.s.r. line width of transition metal impurities 9-45384
 etchant development, to reveal dislocations on {100} and {111} faces 9-26200
 exciton reflectance and photorefectance 9-41377
 heteroepitaxy of Ge films 9-36946
 high resistivity, far i.r. absorption at 82°K 9-49276
 injection lasers, life studies 9-27338
 laser, injection, Hermite-Gauss intensity patterns by optical feedback 9-45965
 laser, optically coupled injection-type, quenching effect 9-38388
 luminescence, injection, in p-type, Ge-doped 9-49337
 luminescent diodes, mismatch dislocation obs. 9-24448
 magnetophonon displacement and negative longit. magnetoresistance 9-26546
 microwave emission study of acoustic freqs. in acoustoelec. domains 9-48966
 n-type, edge photoluminesc. band profiles 9-47394
 n-type, external photoemission in single cryst., work function 9-41283
 n-type, field-emitted electrons, energy distrib. band and surface obs. 9-35517
 optical consts. determ., non-ideal surface 9-49239
 optical mixing of laser radiation, third-order 9-26688
 p-n junctions, avalanche breakdown 9-47139
 p-type, temp. dependence of photocond. lifetime in single crystals 9-37618
 photoconductivity spectral meas. of epitaxial layers in mag. fields, donor obs. 9-39717
 photoelectronic emission, eff. of activation of Cs and BaO adsorbed layers 9-26614
 photoemission, effects of heat cleaning 9-35519
 photorefectance and reflectance spectra, intense exciton struct. obs. 9-41377
 radiative efficiency and deep-level luminescence in n-type crystals grown by liquid-phase epitaxy, dopant conc. effects 9-47396
 radiative tunneling in abrupt, asymmetrical junctions 9-43253
 rare-earths determination by ultra-trace method 9-33696
 reflectance modulation by optical carrier injection 9-28672
 reflectivity and band struct. 9-49268
 Si doped p-n junctions, photo-e.m.f. spectra at 300 and 77°K 9-37614
 surface inhomogeneities from contact potential meas. on etched faces 9-26554
 thick film formation by flash evaporation 9-36960
 u.s. wave propagation at high temp. 9-46999
 Ag-GaAs Schottky-barrier u.v. detector 9-43125
 GaAs:Cr, epitaxial growth from solution 9-48760
 GaAs:Cu, vibrational structure rel. to nature of impurity centres 9-33231
 GaAs:Te, photoluminescence, influence of heat treatment 9-37782
 GaAs:Te, stacking faults, electron micro. exam. 9-23822
 GaAs:Te, triple dislocation loops, image contrast 9-44707
 GaAs:Zn, Ge, Te, impurity segregation rel. to melt. comp., obs. 9-26210
 GaAs:Zn luminescence, broad-band emission near 1.38 eV, temp., excitation-intensity and stress dependences 9-24447
 GaAs_{1-x}P_x heterojunction, dislocation misfits, formation, propag., interaction and densities 9-47140
 GaP(Sb) channeling charact. of protons and the ions 9-47012
 gradient-elastic tensor determ. by nuclear acoustic resonance 9-23851
 laser, injection, gradual degradation rel. to optical flux and current density 9-31962

Galvanomagnetic effects see *Magnetoelectric effects***Galvanothermomagnetic effects** see *Magnetoelectric effects; Magnetothermal effects***Gamma-ray astronomy** see *X- and gamma-ray astronomy***Gamma-ray sources** see *Gamma-rays***Gamma-ray spectra**

see also *Nuclear decay theory*

- absorption peaks in non-destructive activation analysis, effect of shift on determ. accuracy 9-24608
 analysis, computer spectrum shifting and dead time correction 9-27140
 anisotropy from oriented nuclei in mag. resonance 9-42192
 correlation of γ from energy level transitions summing effect correction 9-29639
 cosmic, metagalactic, from secondary particle prod. 9-47663
 E2 transitions in doubly even sd shell, 2⁺ state excitation 9-27618
 heavy ion bombardment of light nuclei, from compound nuclei 9-27760
 infinite medium of a uniform mixture of elements 9-22840
 line shape anal. of spectra obtained with Ge(Li) detector 9-22711
 Mossbauer spectroscopy, characts., equipment and appls. 9-47329
 Mossbauer spectroscopy, source of non-zero radius, cosine effect 9-44076
 neutron capture, facility using electron linear accelerator for study 9-44206
 nuclear explosions, computed from published data 9-24665
 nuclear explosions, computed from published data 9-33796
 polarized, circular, due to (n, γ) reactions rel. to energy levels of several nuclei 9-27725
 probability distrib. function of counts in various channels, study 9-22651
 pulse-height distrib. in NaI(Tl) scintillators, description using analyt. functions 9-22665
 reaction γ in alpha emitters, rel. to anal. of ligh element impurities 9-25603
 rock outcrop surface, spectrometer obs. 9-37893
 from semicond. detectors, computer analysis using photopeak method 9-48224
 variance-covariance matrix calc. 9-22651
 (n, γ), spectrometer, diffraction 9-36509
 (n, γ) spectra, various metals subject to high n flux 9-27726
 Y-N π γ , mag. mom. spectra contrib.; matrix element power series expansion 9-34331
 in ¹²⁴Sb-¹²⁴Te, reduced probability and intensity 9-48292
¹⁴⁰Ce(p, γ)¹⁴¹Pr, E1 transition and β matrix elements determ., E _{β} =9-11 MeV 9-29735
²⁰⁰Hg, low-lying excited levels 9-34404
¹⁷⁰Lu-¹⁷⁰Yb decay 9-42252
¹¹⁰Pd(α , γ) Coulomb excitation, levels dererm., E _{α} ~10 MeV 9-22722

Gamma-ray spectra continued

¹³⁰Tb Ge (Li) detector and 1024 channel pulse height analyser investig. 9-44180
¹¹⁶Pd→¹¹¹Ag, levels, spin and parity determ. 9-34419
^{116m}Pd→¹¹¹Ag, levels, spin and parity determ. 9-34419
¹⁷¹Er→¹⁷¹Tm, energy levels determ. 9-32310
¹⁵¹Gd decay, transition energies 9-48313
¹⁵¹Gd→¹⁵¹Eu, decay 9-42251
¹⁴¹Pr(γ, γ), levels determ., E_γ=4.8-7.7 MeV 9-27634
¹⁴¹Pr(n, γ), ¹⁴²Pr neutron resonance capture 9-46237
¹⁸Ta, 133-482 keV cascade, angular correlation meas. by differential method 9-38675
¹²¹Xe→¹²¹I, transitions meas. 9-29766
¹⁵²Eu energy transitions 9-44157
¹⁵²Eu used to calibrate Ge(Li) detectors 9-22673
¹⁹²Ir, β-γ angular correl. studies on two cascades 9-34423
¹⁹²Pt, E2:M1 multipole mixing ratio from γ-γ meas. 9-25585
²⁴²Pu(n, γ)²⁴²Am, levels spin and parity determ. 9-27651
²¹⁷Th, reactor-neutron fission yields 9-22837
¹⁵²W, multipole orders of low-energy γ transitions 9-44159
^{123m}Te isomeric transitions, γ-γ angular correlations 9-46205
²⁴³Am γ emission by αγ coincidences 9-46226
¹³⁷Cs resonance n capture, transition obs. 9-25577
¹¹⁵In^m isomeric state half-life determ. 9-27630
¹⁵³Sm→¹⁵³Eu, using Ge-Li detector, higher precision meas. 9-40494
¹³⁷Xe→¹³⁷I, transitions meas. 9-29766
^{184m}Re→¹⁸⁴W decay γ-ray and conversion-electron spectra 9-40495
¹³⁷Cs→¹³⁷Ba, energy levels determ. 9-32310
¹⁰⁵Ag→¹⁰⁵Pd electron capture decay, γ radiation 9-46224
¹³⁷Ba(n, γ)¹³⁶Ba, in singles and in coincidence, using Ge(Li) detector 9-42224
¹³⁷Ba(n, γ)¹³⁶Ba neutron resonance capture 9-46237
¹⁵⁹Dy→¹⁵⁹Tb, energy level scheme determ. 9-44158
¹⁶Er, rel. to props. of excited states 9-38672
¹⁴⁷Gd from ¹⁴⁷Sm(He, Zn); isomeric transition, M4 prob. determ. 9-29736
¹⁷⁵Lu from ¹⁷⁵Hf decay, M1+E2 transitions, probabilities and mixing parameters determ. 9-22733
¹⁴³Pm and prep. by ¹⁴⁴Sm(n, γ)¹⁴³Sm→¹⁴³Pm, obs. 9-33688
¹²⁵Sb decay 9-22757
¹⁵²Tb decay, γ-γ coincidence, ¹⁵²Gd levels obs., applic. of data processing method 9-25563
^{106g}Rh→¹⁰⁶Pd, decay scheme determ. 9-22755
^{106m}Ag→¹⁰⁶Pd decay 9-42248
¹⁴⁶Eu→¹⁴⁶Sm, internal conversion coeffs. determ., levels, deduced, spin and parity assignment 9-48312
¹⁸⁶Ir→¹⁸⁶Os conversion coeffs., using Ge(Li) detector 9-42253
¹⁴⁶Nd from ¹⁴⁶Pm decay, γ spectra meas., energy levels determ. 9-34420
¹⁶⁰Pd(¹⁶O, ¹⁶O) Coulomb excitation, levels determ., E₀=42-49 MeV 9-22722
¹⁶⁰Pd(α, α'), Coulomb excitation, levels determ., E₀≈10 MeV 9-22722
¹⁴⁶Pm→¹⁴⁶Nd, γ spectra meas., energy levels determ. 9-34420
¹⁴⁶Pm→¹⁴⁶Sm, γ spectra meas., energy levels determ. 9-34420
¹⁴⁶Sm from ¹⁴⁶Pm decay, γ spectra meas., energy levels determ. 9-34420
^{127m}Te, isomeric transitions, γ-γ angular correlations 9-46205
¹⁹⁷Au, resonance, pressure depend. of energy 9-39816
¹⁰⁷Cd, γ radiation 9-44149
¹⁶⁷Er, intensity variation on resonant neutron capture 9-22796
¹⁴⁷Gd→¹⁴⁷Eu, decay, e-γ coincidence spectra 9-40492
¹⁹⁷Hg decay, 50→1000keV 9-42254
¹⁹⁷Hg decay, 50→1000keV 9-42254
¹⁴⁷Nd γ spectra dis. 9-27682
¹⁴⁷Nd→¹⁴⁷Pm, γ-γ ang. correlation determ. 9-40496
¹⁸⁷Re, on absorpt. of thermal neutrons and 4.41 eV neutrons 9-22798
¹⁷⁷W, Ge scintillation spectrometer meas. 9-38674
^{138m}Pr→¹³⁸Ce, energies and relative intensities 9-42250
¹³⁷Ba(n, γ)¹³⁶Ba, transitions and levels determ. 9-38705
¹⁵⁸Ho decay, E_γ>1000 KeV 9-48314
¹⁶⁰Pd(¹⁶O, ¹⁶O), Coulomb excitation, level determ., E₀=42-49 MeV 9-22722
¹⁶⁰Pd(α, α') Coulomb excitation, levels determ., E₀≈10 MeV 9-22722
²³⁸Pu in waste drum, assay using intensity of 765 keV line 9-37864
¹⁶⁸Tm→¹⁶⁸Er decay, e-γ coincidence spectra 9-40492
¹⁶⁸Yb from ¹⁶⁸Lu decay, level, spin and parity determ. 9-27676
^{109g}Pd→¹⁰⁹Ag, levels, spin and parity determ. 9-34419
^{199m}Hg, conversion coefficients and fluorescence yields obs. 9-42255
¹³⁹Ba→¹³⁹La, levels and decay scheme determ. 9-27674
¹⁴⁹Eu Ge(Li) detector and 1024 channel pulse height analyser investig. 9-44180
¹⁴⁹Gd, Ge(Li) detector and 1024 channel pulse height analyser investig. 9-44180
¹⁵⁹Ho decay obs. 9-48315
²³⁹Np, γ transitions studied by α-γ coincidences 9-42256
¹⁴⁹Tb, Ge (Li) detector and 1024 channel pulse height analyser investig. 9-44180
¹⁵⁷Tb in ¹⁵⁹Gd beta decay using Ge(Li)-Ge(Li) γ-ray coincidence 9-38690
²⁷Al from ²⁷Mg(α, p), pγ spectra 4.58 MeV level obs., E₀=9-13 MeV 9-25656
²⁷Al from ²⁷Al (n, γ), Q-value, excitation energy, decay scheme determ. 9-22801
²⁷Al in ²⁷Al(n, γ)²⁸Al using Ge(Li) spectrometer 9-38706
⁷As, decay, γ-ray energies and relative intensities 9-46223
⁷As decay, γ-ray energies and relative intensities 9-46223
⁷As decay, γ-ray energies and relative intensities 9-46223
¹⁰B-¹⁰Be isobaric analogue state from ⁹Be(d, p), E₀=2.8 MeV, ¹⁰Be levels determ. 9-29712
¹⁰B, from ⁹Be(d, n), γ-ray branching of 3.59 MeV state 9-29711
¹³⁵Ba isotopes (A=131, 133, 135 and 139), from (n, p) reactions 9-42249
¹⁰B(n, γ)¹¹B thermal n capture, Doppler broadening 9-42201
⁷⁴Br from (¹²C, ⁸²Cu); decay scheme determ. 9-38686
⁷⁴Br→⁷⁴Se decay 9-38685
⁴⁰Ca, decay with Ge(Li) detector 9-42213
¹⁰⁸Cd isomer, p excited, and half-life, obs. 9-27631
¹⁰⁸Ce(n, γ), γ spectra meas. 9-34452
⁵⁷Co, excited through ⁵⁷Fe(α, p), between levels up to 1.90 MeV 9-29754
⁶⁰Co γ spectrum, Monte Carlo calc. 9-25597
⁶⁰Co→⁶⁰Ni 9-34416
⁶⁰Co→⁶³Ni, β spectrum endpoint determ. 9-34416
⁶⁰Co→⁶²Zn 9-42246
¹⁴C(p, γ)¹⁵N, γ transition mixing ratio determ., E_γ=352-634 keV 9-29713

Gamma-ray spectra continued

⁴⁸Cr positron decay; energy and intensity obs., ⁴⁸V levels determ. 9-48320
⁶⁰Cu, by Ge(Li) and NaI(Tl) detectors 9-42245
⁶⁰Cu→⁶⁰Ni, decay scheme, levels, spin and parity determ. 9-27681
⁶⁶Cu→⁶⁶Zn, 2.37 MeV O⁺ level population obs. 9-27684
Er isomer, p excited, and half-life, obs. 9-27631
Eu₂(WO₄)₃ single cryst., nucl. reson. fluoresc. of 3 eV ¹⁵²Sm recoil atoms, anisotropic pot. obs. 9-35596
⁵⁷Fe, 14 KeV radiation, Bragg scattering by Fe:Si ideal crystal 9-37700
⁶¹Fe→⁶¹Co decay 9-44174
Fe(n, n')^γ, γ spectra meas. 9-34452
⁶⁶Ga decay 9-42247
⁶⁷Ga decay 9-42247
⁷²Ga decay 9-42247
⁶⁶Ge→⁶⁶Ga, transitions, levels, spin and parity determ. 9-38662
γ-γ coincidence spectra, data-processing method 9-25563
⁴¹K decay 9-40490
La(n, n')^γ, γ spectra meas. 9-34452
^{80m}Br decay, transitions rel. intensities and energies 9-42216
²⁵Mg(α, n)²⁸Si, 8.543 MeV ²⁸Si level lifetime meas., E₀ ~ threshold energy 9-38655
⁵³Mn, decay of 1290 keV level, cascades 9-44146
⁹⁸Mo from ⁹⁸Nb, decay scheme determ., γ, β spectra and coincidence meas. 9-34414
²⁴Na, rel. to spin values of doublet at 1.34 MeV 9-27650
²⁴Na in ²³Na(n, γ)²⁴Na using Ge(Li) spectrometer 9-38706
²²Na(α, p)²⁷Al, spectra from 16 resonances 9-46242
⁹⁰Nb→⁹⁰Mo decays 9-44176
⁹⁷Nb→⁹⁷Mo, γ spectra meas., levels determ. 9-32330
²⁴Ne→²⁴Na, delayed γ-ray spectrum study of β decay 9-42243
⁶²Ni→⁶²Co, levels and spin determ. 9-38660
⁶²Ni(p, p), p ang. distrib. meas., energy levels determ., E₀=12 MeV 9-32322
⁶²Ni(p, p), p ang. distrib. meas., energy levels determ., E₀=12 MeV 9-32322
¹⁴N(n, p)¹⁵N thermal n capture, Doppler broadening 9-42201
¹⁴O(¹⁶He, n)¹⁵Ne levels, lifetimes, spin, decay modes determ. 9-25567
Os isotopes, (A=178→181), Ge scintillation spectrometer meas. 9-38674
¹³P(p, p)¹³S resonances 9-42283
Rb isotopes (A=81, 82, 83, 84 and 86) 9-38687
⁸²Rb decay to ⁸²Kr, obs. 9-22747
⁸⁷Rb from ⁸⁷Kr decay, levels determ. 9-27685
Re isotopes, (A=177→179) Ge scintillation spectrometer meas. 9-38674
⁹⁷Ru→⁹⁷Tc, level structure determ. 9-27686
⁴⁰Sc decay, β-γ circular polarization correlation in decay Fermi/Gamow-Teller matrix element ratio determ. 9-32328
⁷⁵Se decay, energy and rel. intensities meas. 9-48321
²⁶Si, levels, spins, γ-branching and mixing ratios determ. 9-32314
³⁰Si(p, p)³¹P, p levels, spin and parity determ., E₀=3-4 MeV 9-27658
Sn isomer, p excited, and half-life, obs. 9-27631
⁹³Tc and ⁹³Tc, half-life obs. 9-48290
⁹⁴Tc and ^{94m}Tc half-life obs. 9-48290
⁹⁴Tc^m decay to ⁹⁴Mo, energy levels 9-38680
⁹⁶Tc→⁹⁶Mo, energies and relative intensities 9-44175
Tm(n, n')^γ, γ spectra meas. 9-34452
⁴⁸V high-energy obs. 9-36591
V(n, n')^γ, γ spectra meas. 9-34452
⁶²Zn, nuclear resonant scatt. of capture γ ground-state transition width determ. of 7368 keV level 9-46217
⁹²Zr→⁹²Nb, 724 and 756 keV transition intensities determ. for ⁹²Zr decay 9-27671

Gamma-ray spectrometers

see also Beta-ray spectrometers; X-ray spectrometers
airborne, use in global radioactivity pollution meas. 9-37894
angular correlation meas., new method 9-40453
combination n-γ detection 9-32249
combination n-γ detection, below 4 MeV, PuBe new spectrum structure 9-32248
Mossbauer, automatically recording, control unit, multichannel analyser 9-36510
Mossbauer, detection, simple method dispensing with multi-channel analyzer 9-29650
Mossbauer constant acceleration, determ. of zero velocity 9-46134
Mossbauer eff., variable temp. absorber in longitudinal external mag. field 1.5-300°K 9-27585
Mossbauer spectrometer for graduate laboratories 9-43712
Mossbauer spectroscopy, characts., equipment and applics. 9-47329
photopeak efficiency of NaI(Tl) expt. meas. 9-29663
radioactivity growth-decay data, least squares analysis by computer programme 9-38682
rotating-disc, for Mossbauer effect meas. 9-40454
satellite data processing system 9-38018
scintillation, photoefficiency 9-32245
scintillation, rocket borne, for cosmic ray obs. 9-31584
for space appl. 9-25505
space satellites, on-board calibration system using Co⁶⁰ and Am²⁴¹ sources 9-38017
spectra determined by meas. Compton e spectrum 9-46133
summing semiconductor Compton spectrometer 9-46132
(n, γ), automated spectra recording 9-36509
¹⁷⁰Lu radioact. decay, transitions and ¹⁷⁰Yb obs. 9-25601
CsI(Tl) scintillator-Si photodiode, combination for γ-ray spectrometry, 180 keV to 1.5 MeV 9-27590
Ge:Li, neutron fast/thermal ratio determ. 9-25526
Ge, Walford-Doust rapid calibration method, some corrections 9-22657
n-Ge crystals, bombarded with thermal and fast neutrons 9-46131
Ge(Li), coaxial, as well-type detector for sum spectra of coincident gamma rays 9-36524
Ge(Li), ultra-high resolution, for low and high energy meas., characts. 9-36523
Ge(Li) detector, NaI(Tl) small split annulus Compton continuum meas. 9-32247
Ge(Li) detector for high resolution γ-ray spectrometry, pulse pile-up problem 9-25521
Ge(Li) type, for detection of radionuclides in biological and environmental counting 9-44081
NaI(Tl), internal energy standardization using 0.511 MeV annihilation and ⁴⁰K peaks, computer method 9-29649

Gamma-rays

- see also Cosmic rays/photons*
 cascades, unresolved, angular correlation and linear polarization 9-34253
 from Compton scattering of laser photons from relativistic electrons 9-48155
 cosmic γ due to microwave Compton scatt. on cosmic ray electrons 9-27070
 diffraction on crystals containing Mossbauer nuclei at lattice sites with nonuniform elec. field 9-31087
 energy distribution from $^{157}\text{Tb}(n,n'\gamma)$ reaction 9-29810
 exponential decay from excited states, anomaly, field model soln. 9-22704
 fallout on ground attenuation of γ radiation by snow-cover 9-24666
 fallout on ground attenuation of γ radiation by snow-cover 9-33797
 galactic, flux, explanation w.r.t. far-i.r. background rad. 9-26989
 reflection from two-layer barrier 9-25414
 shielding studies at 10 MeV with γ from positron annihilation 9-22528
 source 3.85. MeV γ , without Doppler broadening consisting of PuO_2 - ^{10}B mixture 9-29662
 source for excitation of atoms using $^{10}\text{B}(n,\alpha)^7\text{Li}$ 9-29953
 sources, quasi-monochromatic, for nuclear research, 5 MeV < E 9-48246
 SU(3) currents, possibility of universal interaction coupling to 2γ 9-22545
 variable energy, generation and uses, especially scintillation detector calibration 9-42006
 Cu, mean total γ cross-sections, 40-80 keV, analysis 9-22949
 Pb, mean total γ cross-sections, 40-80 keV, analysis 9-22949
 from Pu isotopes, ration with α particles 9-25604
 Sn, mean total γ cross-sections, 40-80 keV, analysis 9-22949
 W, mean total γ cross-sections, 40-80 keV, analysis 9-22949

absorption

- see also Mossbauer effect*
 chemical analysis using γ transmission spectra 9-37845
 cylindrical source, slit collimator, penetration factor calc. 9-29537
 in paramagnetic crystal, resonance absorpt. of quanta, effect of ion-phonon interaction 9-33524
 in porosimeter, Hg, new, design 9-23753
 radionuclides in man, whole body counting with NaI(Tl) detectors, techniques comparison 9-27119
 radionuclides in man, whole body counting with NaI(Tl) detectors, techniques comparison 9-27120
 ^9Be , in giant dipole resonance region, cross section meas., $E_\gamma=250$ MeV 9-34435
 Fe, cross section energy depend. determ., $E_\gamma=10$ -26.5 MeV 9-29782
 ^{57}Fe E2-M1 absorption in Mossbauer spectra, transition probabilities calc. 9-22742

angular distribution

- anomalous conversion, $e\text{-}\gamma$ angular correl. meas. 9-32299
 $\gamma\text{-}\gamma$ ang. correlations following Coulomb excitation, E2/M1 admixtures obs. 9-36612
 coefficients of angular distrib. analysis of γ -rays emitted in nuc. reactions, tables in book 9-32300
 Compton effect on 550 MeV relativistic electrons, and energy distrib. 9-29542
 correlation meas., new method 9-40453
 correlations, following multiple Coulomb excitation, quantum mechanical effects 9-44126
 nuclear explosions, computed from published data 9-24665
 nuclear explosions, computed from published data 9-33796
 from nuclei, aligned, reaction independent analysis from Ge(Li) detector obs. 9-42262
 $\gamma\text{-}\gamma$ correlation meas. π^- stopping in hydrogen 9-27520
 ^{137}Xe , $\gamma\text{-}\gamma$ ang. correls. 9-22728
 Bi single crystal, from positron annihilation, effect of temp. 9-24113
 ^{60}Co γ spectrum, Monte Carlo calc. 9-25597
 Hf complex, n irradi., effect of (n, γ) recoil on ($\gamma\text{-}\gamma$) ang. correl. 9-35597
 Hf complex, synthetic and n irradi., perturbed differential ang. correl. obs. of γ cascade 9-35598
 (NH_4) $_2\text{HfF}_7$, relaxation determ. by $\gamma\text{-}\gamma$ angular correlation 9-37675
 $^{31}\text{P}(\text{p},\gamma)^{32}\text{S}$, for 1.248 and 1.438 MeV resonances 9-42283

detection, measurement

- see also Dosimetry; Gamma-ray spectrometers; Particle detectors; Radioactivity measurement*
 40-2400 MeV, energy determ. in X chamber 9-22681
 angular correlation, new method 9-40453
 atmosphere, surface layer, gamma field variation 9-31333
 background analysis for NASA 600MeV proton synchrocyclotron of short- and long-lived gamma rays 9-46159
 cameras, aperture indexed collimators 9-22650
 coincidence meas., detection efficiency absolute calibration method 9-36506
 detector, semiconductor, material requirements 9-25522
 dose from internal emitters, assessment of Monte Carlo calculations 9-27118
 energy spectra at two-layer barrier 9-25415
 Geiger counter 9-29652
 hexafluorobenzene scintillator dosimeter, for use in mixed γ and n fields 9-36531
 instrument calibration 9-38622
 intensity measurement, pulses of ns. duration and 10^{10} to 10^{11} roentgens/s range 9-46130
 LET dependence of thermally stimulated exoelectron emission 9-37634
 oxalic acid, use in multienergy γ dosimetry 9-24950
 particle telescope carried on OSO-III (1967) satellite 9-24730
 particle-gamma angular correl. apparatus 9-44074
 radiation monitor, environmental, low level, with high sensitivity, stability and dynamic range 9-36512
 reactor external detectors for in-core power meas. 9-22912
 reactor intensity distrib. rel. to shield composition 9-31688
 scintillators, cylindrical, in axisymmetrical γ fields, calc. of efficiency and cross-section 9-48221
 showers, simulation using Monte Carlo programme 9-44070
 sky-skan for discrete sources 9-24834
 survey meter, portable, using Si amplifying radiation detectors 9-36525
 in thermal reactor power meas. 9-36639
 $\beta\text{-}\gamma$ emitter activity, coincidence method, automatic correction digital app. 9-22750
 $\gamma\text{-}\gamma$ directional correl. coeffs., revised table 9-42125
 from $^{10}\text{B}(\alpha,\text{p})^{11}\text{C}$ and $^{10}\text{B}(\alpha,\alpha')^{10}\text{B}$, cross sections 9-27741
 CdTe, improved, between -100°C and +100°C 9-22671

Gamma-rays continued**detection, measurement continued**

- GaAs, CdTe use in detection 9-25523
 Ge(Li) detector, determ. of Fano factor of Ge at 77°K 9-42145
 Ge(Li) detector, response characts., 0.1 to 2MeV, expt. determ. 9-42141
 Ge(Li) detector, semi-empirical efficiency curve, 50 to 1400 keV 9-42140
 $^{41}\text{K}(\text{He},\text{d})^{42}\text{Ca}$ obs. 9-48284
 NaI slabs, γ -ray imaging props., detector scatt. effects, Monte Carlo calcs. 9-40458
 NaI(Tl) crystal, antineutrino shielding at 0.661 MeV meas. 9-32243
 NaI(Tl) detectors, imbedded into or external to cylindrical gamma source, efficiency 9-42135
 NaI(Tl) scintillation crystal, calc. of no. of photons emitted per scintillation 9-29654
 Si(Li) and Ge(Li) detectors, energy linearity and resolution, comparison of theory and experiment 9-36516
 ZnS i.r. stimuable use in dosimeter with time lapse indication 9-27597

effects

- see also Nuclear reactions and scattering due to/photons*
 β -alanine, low temp. photoconversion 9-31208
 alkali halide- Br_2O_3 glasses, e.s.r. of stable V centres 9-24480
 alloys, effective atomic numbers calc. 9-24230
 anthracene and deuterated anthracene, rad. induced paramag. centres, EPR obs. 9-24499
 binary liquid solutions, irradiated, stratification effects 9-30368
 γ -photoelectric cross-sections 9-24231
 chloral hydrate, e.p.r. rel. to conc. of produced paramag. centres 9-33638
 conducting materials, fluence of low-energy electrons, established and emitted 9-24066
 copper acetate monohydrate, irradi., conversion of Cu^{2+} to Cu^+ 9-49386
 crystal growth, equil. surface struct. changes 9-37021
 cytosine, γ -irrad., free radical produced, structure study 9-44354
 cytosine monohydrate, cryst., e.s.r. 9-45390
 Dictyostelium discoideum, slime mold, gamma ray resistance 9-24938
 durene, gamma irradi. comparison d.e.p.r. signals with u.v. irradi. 9-47421
 ethylene, γ -induced polymerization obs. 9-33665
 exciton luminescence, 2-photon excitation, calc. of oscillator strengths 9-35677
 ferrocene, e.s.r., free radicals 9-43288
 fission delayed, effect on average number of prompt neutrons emitted in fission 9-25664
 glass, barium silicate containing Ti, γ -induced optical absorpt. 9-37693
 D-glucose aqueous ice, e.s.r. study of free radicals formed 9-42454
 hexafluoropropene-tetrafluoroethylene copolymer, rupture, tensile strength hardness following γ -irradiation 9-33069
 hexafluoropropene-vinylidene fluoride copolymer, rupture, tensile strength hardness following γ -irradiation 9-33069
 IMPATT, diodes, performance 9-49118
 on magnetite, magnetic props. change 9-37665
 metal oxides, e.s.r. obs. rel. to catalytic behaviour 9-35709
 3-methylpentane, ion mobility 9-28720
 Mossbauer conversion electrons used to investigate props. of a surface 9-30476
 nuclear reson. expts., analysis of pure quadrupole spectra, method 9-43825
 Nylon-6 friction and wear props., obs. 9-39444
 organic cyanide crystals, e.s.r. of trapped electrons 9-47440
 photoeffect and conversion processes upon Mossbauer radiation absorpt., interference 9-48270
 polyethylene friction and wear props., obs. 9-39444
 polytetrafluoroethylene, irradi. atmos. effects, n.m.r. obs. 9-24511
 poly-3-vinyl-9-ethylcarbazole, elec. behaviour 9-24120
 potassium thiocyanate, irradi., e.p.r. spectrum of radical species 9-45392
 on pyrrhotite, magnetic props. changes 9-37665
 quartz, γ -irrad., glow curves rel. to dose, defect synthesis 9-26273
 resonant radiation interaction with single crystal nuclei and electrons, inelastic channel suppression 9-24377
 RNA, ribosomal soln. irradi. resistance 9-26132
 Rochelle salt, Barkhausen effect in irradiated crystal 9-47180
 Rochelle salt, effect of ^{60}Co γ rays on ferroelec. props. 9-47179
 Rochelle salt, on ferroelec. props., ^{23}Na n.m.r. obs. 9-26593
 Schottky-Barrier diodes, γ -irrad., stress eff. 9-24202
 styrene, polymerization and post-polymerization 9-24554
 sucrose aqueous ice, e.s.r. study of free radicals formed 9-42454
 triglycine sulphate, Barkhausen effect in irradiated crystal 9-47180
 triglycine sulphate, effect of ^{60}Co γ rays on ferroelec. props. 9-47179
 triglycine sulphate, effect on elec. and spectral props. 9-47182
 triglycine sulphate, irradi., hindered motion of CH_2 in CH_2COO^- , e.s.r. obs. 9-35720
 X-ray fluorescence, conversion yield 9-24464
 X-ray fluorescence, target backing enhancement effects 9-24465
 γ -electric cell, high voltage operation with epoxy or polystyrene dielectric 9-31897
 Ag $_2\text{CO}_3$, e.s.r. of irradi. crystals 9-37791
 Al $_2\text{O}_3$ films, 500 to 6000Å, traps, study using thermoluminescence glow curves in range 30 to 300°C 9-33245
 BaTiO $_3$ crystals and ceramics, ^{60}Co γ rays effect on electrophysical props. 9-41238
 CaCO $_3$:AsO $_4^{2-}$, e.s.r. 9-39903
 CaF $_2$:Y $^{3+}$, Y $^{2+}$ colour centre 9-39373
 CdCl $_2$:Ag, irradi., optical absorpt. and e.p.r. obs. 9-49272
 Gd, γ -photoelectric cross-sections 9-24231
 n-Ge:Sb, Hall effect distortion 9-37537
 Ge(Li), X-ray escape simultaneous with photopeak obs. 9-29661
 H atoms, stability in irradiated aqueous solutions, e.s.r. study 9-39962
 Hf γ -photoelectric cross-sections 9-24231
 KBr, low temp. annealing of induced defects 9-40967
 KCl fracture surface energy changes 9-28372
 La γ -photoelectric cross-sections 9-24231
 LiF:Mg $^{2+}$, irradi., coloration, enhancement 9-39377
 LiF:Mn $^{2+}$ (Mg $^{2+}$), coloration, charge compensation creation of vacancies, conversion into F-centres 9-28305
 LiF:U colour centres, formation obs. 9-35115
 LiF, effect on i.r. absorption 9-39839
 LiF, irradiated, effect on physical props. 9-28546
 LiF irradi., Y-absorpt. band obs. 9-37726
 LiF vacancies formed by reactor radiation, detect. by annealing and elec. cond. meas. 9-32949
 Na $_2\text{S}_2\text{O}_5$:H $_2\text{O}$ irradi. single cryst., e.s.r. obs. of trapped radicals 9-35716
 NaCl, colour centres due to ^{60}Co - γ irradi. effect of gas adsorpt. 9-48869

Gamma-rays continued
effects continued

Ni-Fe alloys, ordering transformations 9-23973
n-Si:P, irradiated, thermal donor formation 9-32951
Si, float-zone, doped, electrical conductivity before and after irradiation 9-28520
p-Si, radiation defects,interac. with impurities 9-37547
SiO₂ films, 500 to 6000Å, traps, study using thermoluminescence glow curves in range 30 to 300°C 9-33245
SiO₂ fused, γ irradi., current-voltage depend. 9-49138
Th γ -photoelectric cross-sections 9-24231
Zn single cryst., irradi. effect on creep 9-39425

internal conversion

see also Beta-ray spectral/conversion electrons
anomalous conversion, e- γ angular correl. meas. 9-32299
K, L, M-shell conversion coeffs. for 30<Z<103, tables 9-46216
¹⁸⁰Hf nuclear structure effect on N- and O- shell electrons internal conversion 9-34384
¹⁵⁸Sm, coeff. for E1, E2, M1, M2 transitions on K shell, E_p=1.9 MeV 9-29765
¹⁵⁸Sm, K-conversion coeff., E1, E2, M1, γ transitions 1-17 MeV multipolarities calc. 9-25576
¹⁷⁰Yb, 84.3 keV transition, α_K meas. 9-29739
¹⁵²Sm, K conversion coeff. of 444.1 KeV transition, rel. to β -vibrational band transitions in ¹⁵²Sm 9-46211
¹⁹³Ir coeffs. calc. 9-48298
¹⁰³Rh, 53 keV γ -ray K-shell internal conversion coeff. 9-46202
¹¹⁴Cd, coeff. for E1, E2, M1, M2 transitions on K shell, E_p=1.9 MeV 9-29765
¹¹⁴Cd, K-conversion coeff., E1, E2, M1, γ transitions 1-17 MeV multipolarities calc. 9-25576
¹¹⁹In, 35.6 keV transition, K-conversion coefficient meas. 9-42221
¹⁷¹Lu, 114 MeV, M1+E2 transition obs. 9-25584
¹⁶⁶Er, 80.6 keV transition, α_K meas. 9-29739
¹⁴⁶Eu-¹⁴⁶Gd, Sm, coeffs. determ. 9-48312
^{199m}Hg, conversion coefficients and fluorescence yields obs. 9-42255
¹⁹⁸Hg 158 keV E2 transition, N-subshell IC coeff. meas. 9-40486
⁶⁶Ge-⁶⁶Ga, γ spectra meas., levels determ. 9-38662

scattering

see also Compton effect
Compton sum rules and their saturation 9-48154
grain size effect on low energy rad. 9-49399
perturbation by cylindrical hole 9-27461
by plasma, dense opaque, as means of temp. determ. 9-40689
polarized on reflection from crystal, polarization determ. from Mossbauer spectrum 9-30532
resonant interaction with nuclei and electrons in crystal, disappearance of inelastic channel of nuclear reaction 9-26465
scintillators, cylindrical, in axisymmetrical γ fields, calc. of efficiency and cross-section 9-48221
spin-1 Compton scatt., classical low energy theorems 9-42005
Z-dependence of pair cross-section 9-46063
 $\gamma\pi\pi\pi$ Compton scattering, threshold behaviour 9-29582
 $\gamma\pi\pi\pi$ photoproduction amplitudes 9-29582
¹⁸¹Ta 480 keV transition parity mixing, γ circular polarization meas. 9-27640
from Cu, differential elastic scatt. X-section of 145 keV γ 9-46263
from Ag, differential elastic scatt. X-section of 145 keV γ 9-46263
from Al, differential elastic scatt. X-section of 145 keV γ 9-46263
Al single crystal, Bragg reflected, polarization from Mossbauer spectrum 9-30532
from Fe, differential elastic scatt. X-section of 145 keV γ 9-46263
pb, 145-662 keV, diff. cross section meas., Rayleigh scatt, formula determ. 9-46318
from Pb, differential elastic scatt. X-section of 145 keV γ 9-46263
from Sn, differential elastic scatt. X-section of 145 keV γ 9-46263

Gamow-Teller transitions see Beta-decay theory; Nucleus/energy levels

Garnets

see also Ferrites
ferromagnetic randomly substituted systems, moment substitution depend., comment 9-41324
ferrite, rare-earth monocrystals, magnetization near Curie points 9-45175
gallate, paramag., containing rare-earth ions, mag. props. 9-47231
garnet, elastic anisotropy, investigation by magnetoelastic interac. 9-37221
germanate, paramag., containing rare-earth ions, mag. props. 9-47231
growth on non-garnet single crystal, patent 9-46723
henritermierite, Ca₃(Mn_{1.5}Al_{0.5})(SiO₄)₂(OH)₄, tetragonal hydrogarnet, cryst. struct. 9-32905
internal growth defects of flux-grown cryst., etching and X-ray topographic obs. 9-32937
olivine-garnet in meteorite 9-27089
rare earth, single crystals, Raman and far i.r. spectra comparison 9-39850
rare earth gallium, sp. ht. rel. to magnetic transitions 9-24051
rare earth ion doped, selection rules in absorpt. spectra 9-24416
rare earth ion, exchange resonance and optical Faraday effect 9-45278
rare earth iron, linear mag. birefringence 9-45185
rare earth iron, pure and Ga-doped, ferromagnetic single crystal, u.v. complex polar-Kerr effect 9-45275
rare-earth iron, Sc substituted, Fe ions canted spin struct., Mossbauer effect obs. 9-37667
seeded growth from molten salts 9-37045
spectrochemical determinations using laser microprobe 9-37848
Al rare earth, i.r. lattice spectra 9-47338
Bi_{0.32}Ca_{2.68}Fe_{2.66}V_{1.34}O₁₂ ferrogarnet, mag. anisotropy, -183° to 100°C 9-45131
BiCaV ferrogarnet single crystal, rotatory mag. hysteresis losses 9-45136
Ca₂₃Bi₂-xFe_{23-x}V₂O₁₂, magneto-elastic coupling coeff. from ferromag. reson. method 9-37664
Ca₃Fe₂Ge₂O₁₂ paramagnetic Mossbauer spectra of ⁵⁷Fe, at room temp. 9-43221
Ca₃Fe₂Si₂O₁₂ paramagnetic Mossbauer spectra ⁵⁷Fe, at room temp. 9-43221
Cd₃Fe₂Ge₂O₁₂ paramagnetic Mossbauer spectra of ⁵⁷Fe, at room temp. 9-43221
Ce activated, fluorescence 9-26777
DyAl, antiferromag., optical absorpt. spectrum, Monte Carlo calc. rel. to interpret. 9-24408

Garnets continued

DyAl, electronic Raman effect of Dy³⁺ 9-24425
DyAl thermal expansion, 1° to 4°K 9-44840
Er ferrite, Faraday effect, mag. field effect 9-49216
ErAl, crystal-field energy levels and g-factors 9-45319
ErFe, optical absorpt. spectra at 4.2°, 20° and 62°K, mag. moment and G-factor determ. 9-45319
ErGa, ¹⁵¹Er-¹⁵²Er ³S₂ transition, Er³⁺ G-tensor anisotropy determ., Zeeman eff. obs. 9-23040
ErGa, crystal-field energy levels and g-factors 9-45319
EuFe, anisotropy in exchange interac., Mossbauer obs. 9-33475
Fe, single crystal, resonant absorpt. of elastic waves in absence of external mag. field 9-30649
Fe₂(MoO₄)₃, Mossbauer spectra, parameters for octahedral Fe³⁺ 9-49261
Fe rare earth, i.r. lattice spectra 9-47338
Ga rare earth, i.r. lattice spectra 9-47338
Gd₃Fe₂O₁₂ film, ferrimag. domain struct. and props. rel. to growth parameters 9-47272
Gd ferrite, coercive force, temp. depend. near compensation temp. 9-49214
GdFe, epitaxial film, prep. by r.f. sputtering mag. and structural props. 9-49210
GdFe, Faraday rot. 9-43214
GdFe, Faraday rotation at 1.15 μ , 100° to 450°K 9-49218
GdFe, optical absorption spectra, 2000-5000 Å 9-35658
GdFe, Sn-substituted, critical mag. isotherm 9-43188
GdFe circular domains density and size 9-47271
GdFe domain interaction with atomic scale imperfections optical obs. 9-45179
GdFe film, rel. to magneto-optical recording 9-45271
GdFe thermal expansion at 296-1400°K from lattice const. 9-41093
GdGa substrate, YFe garnet epitaxial films, microwave phonon generation 9-44816
GdGa thermal expansion at 296-1400°K from lattice const. 9-41093
Ho ferrite, Faraday effect, mag. field effect 9-49216
(In-Ga)Fe, Mossbauer effect 9-49263
Nd:YAl garnet rods, index of refraction and thermal expansion coeff. 9-22412
Nd₃Fe₂-xSc_xO₁₂, (9<x<1.5), existence, crystallography and mag. props. 9-47247
Sm₂Eu_{1-x}Fe, mixed, anisotropy in exchange interac., Mossbauer obs. 9-33475
SmAl, absorption and emission spectra used to calculate field of Sm³⁺ ion 9-43244
SmFe, anisotropy in exchange interac., Mossbauer obs. 9-33475
SmGa, absorption and emission spectra used to calculate field of Sm³⁺ ion 9-43244
Tb₃Fe₂O₁₂ Faraday effect, anisotropy in i.r. region 9-31081
Tb ferrite, Faraday effect, mag. field effect 9-49216
TbFe, exchange magnetostriction 9-24319
TbFe, Faraday rot. 9-43214
TbFe, Faraday rotation at 1.15 μ , 100° to 450°K 9-49218
TbFe, Sn-substituted, critical mag. isotherm 9-43188
TbFe, substituted, volume magnetostriction 9-43155
TmAl single crystal, n.m.r. of ¹⁶⁹Tm and ²⁷Al 9-45407
Y_{3-x}Bi_xO₁₂Ca₂Fe₂-xSi_xO₁₂ (x=0.6-1.3), crystallization from PbO/B₂O₃ solvent 9-37047
Y_{3-x}Tb_xFe₂-xGa_xO₁₂, ferromag. resonance of Tb³⁺ and Ga³⁺, anisotropy of rreson. field and line width 9-33619
Y₃Al₅O₁₂, Cr³⁺ and Nd³⁺ impurity distribution, rel. to trivalent oxide solubility and cry. growth 9-36980
Y₃Al₅O₁₂, free from strained central core 9-28235
Y₃Al₅O₁₂, optical absorpt., 10- to 55000 cm⁻¹ wave no. 9-35666
Y₃Al₅O₁₂ habit changes of single crystals, grown from a PbO-PbF₂ flux 9-40922
Y₃Fe₂O₁₂, Cr³⁺ and Nd³⁺ impurity distribution, rel. to trivalent oxide solubility and cry. growth 9-36980
Y₃Ga₂O₁₂:Tm³⁺, photoluminesc., optical transitions obs. 9-49338
Y₃Ga₂O₁₂ habit changes of single crystals, grown from a PbO-PbF₂ flux 9-40922
Y₃Mn_{0.1}Fe_{4.9}O₁₂, mag. anisotropy and magnetostriction at 300°K 9-49219
Y₃Gd_{3-x}Al_{3x}(In/Sc)₂Fe_{8-11-2x}O₁₂, isomagnetization lines 9-39778
YAL, E.P.R. and relax. processes of Nd³⁺ 9-24498
YAL garnet: Sm³⁺ (Dy³⁺), crystal-field energy levels of ⁶H and ⁶F multiplets 9-45254
YAL, etch figures, rel. to point defects, dislocations and orientation 9-44641
YAL, growth by hollow cathode floating-zone method 9-37091
YAL, laser-excited Raman spectra, 100-800 cm⁻¹ 9-49298
YAL, Nd doped, imperfection assessment and control in crystals used for laser devices 9-37157
YAL garnet:Nd, optical pumping using K-Hg discharge lamp 9-25201
YAL garnet:Nd³⁺, optical transition props. using Jarrell-Ash 1m Ebert scanning spectrometer 9-26751
YAL garnet:Nd laser, 100 W output, 3% efficiency 9-48031
YAL garnet:Nd laser, feedback-controlled, dynamics 9-48030
YAL garnet:Nd laser, Kr lamp pumping, 105 W output 9-48033
YAL garnet:Nd laser, Q-switched, coherence length corresp. to pulse length 9-48035
YAL garnet:Nd laser, repetitively Q-switched, pulse-to-pulse stability 9-48032
YAL garnet:Nd lasers, diode pumped, c.w. operation, 46 mW output at 1.0614 μ m with 1% efficiency 9-48034
YAL garnet : Nd³⁺ laser, self-Q-switching at 77°K 9-36309
YAL garnet : Nd laser, continuous operation by injection luminescent pumping 9-25301
YAL single crystals, optical quality, incorporation of increased conc. of rare earth activator ions 9-37093
YAL substrate, YFe garnet epitaxial films, microwave phonon generation 9-44816
YAL synthetic cryst., inhomogeneities, optical investig. 9-37165
YAL thermal expansion at 296-1400°K from lattice const. 9-41093
YFe:Co, single cryst., magnetocrystalline anisotropy and ferrimag. reson. 9-33480
YFe:Ho, ferrimagnetic resonance linewidth and fine structure 9-26790
YFe:Si, photoinduced mag. anisotropy 9-24307
YFe, and Ca-V substituted, effective linewidth due to porosity and anisotropy, field depend., microwave freqs. 9-45371

Garnets continued

- YFe, axially magnetized rod, magnetoelastic wave instability threshold 9-37668
 YFe, Ca-V-substituted, effective linewidth due to porosity, relax. obs. 9-31055
 YFe, Ca^{2+} - and Si^{4+} -doped, microwave dielec. loss and permittivity 9-33374
 YFe, chem. polishing 9-40835
 YFe, dense ferrimagnetic perovskite allotropic form, existence 9-26252
 YFe, effective linewidth due to porosity, relax. obs. 9-31055
 YFe, Faraday rot. 9-43214
 YFe, films, epitaxial, on YAl garnet and GdGa garnet, microwave phonon generation 9-44816
 YFe, i.r. radiation scattering by two magnon processes 9-45337
 YFe, longit. magnon-phonon interaction in obliquely magnetized rods 9-35574
 YFe, magnetoelastic pulse prod. by Schlomann method, pulse sequences 9-43178
 YFe, magnetostatic, surface waves excitation and propagation charact. 9-28586
 YFe, no 2-magnon scatt., ferromag. resonance linewidth, 9.3GHz, 4.2-300 K 9-41420
 YFe, optical absorpt. and emission studies of Ho^{3+} ions 9-45331
 YFe, partially magnetized bar, generation and propagation of magnetoelastic waves 9-33479
 YFe, preparation, improvement in yield 9-37092
 YFe, relaxation processes investigation with propagating magnetostatic spin waves 9-45241
 YFe, rod, axially magnetized, magnetostatic mode instabilities 9-45189
 YFe, rod, axially magnetized, magnetoelastic wave instability threshold 9-45190
 YFe, rods, transversally magnetised, resonance absorption of longitudinal phonons 9-28421
 YFe, rods (110) oriented, magnetoelastic wave propag. 9-45187
 YFe, rods containing turning point, magnetostatic mode excitation 9-45188
 YFe, seeded growth from molten salts 9-37045
 YFe, single crystals, effect of pressure on homogeneous distribution of gallium 9-36979
 YFe, Sn-substituted, critical mag. isotherm 9-43188
 YFe, spontaneous magnetization temp. depend., 4.2-290°K 9-41328
 YFe, spontaneous magnetization temp. depend., 4.2-290°K 9-41328
 YFe, thermal transport, effect of magnons 9-44847
 YFe, with Tb admixture, meas. of domain wall mobility 9-41327
 YFe, X-ray multiple diffraction study of struct. 9-37153
 YFe dislocation effects on magnetiz. process, direct investigation 9-47276
 YFe epitaxial films, ferromag. reson. 9-45372
 YFe films with narrow ferrimagnetic resonance linewidth, epitaxial growth 9-36952
 YFe Ga-substituted, cation distrib., by Mossbauer effect spectroscopy 9-45303
 YFe garnet: Cu^{2+} , ferrimag. reson. 9-45374
 YFe garnet: Si, i.r. sensitive ferrimag., relax. and mag. anneal of anisotropy 9-45191
 YFe garnet, (Ca, V, In)-substituted, anisotropy and magnetostriction meas. 9-45192
 YFe Garnet, InSb hybrid structure, interaction between spin waves and electrons 9-24320
 YFe magneto-optical modulation 9-36335
 YFe Nd laser, passive locking 9-34174
 YFe single crystals, flux growth 9-37046
 YFe slab, transversely magnetised, surface magnetostatic waves, boundary conditions 9-47860
 YFe thermal expansion at 296-1400°K from lattice const. 9-41093
 YFe two-magnon scatt. of i.r. radiation 9-24421
 YGa:Co single cryst., spin reson. obs. 9-35575
 YGa, double ferromag. reson. obs. 9-49343
 YGa, optical absorpt. and emission studies of Ho^{3+} ions 9-45331
 YGa, Tm^{3+} -doped, selection rules in absorpt. spectrum 9-24416
 YGa, Yb doped, $^2F_{7/2}$ levels, Raman-Zeeman obs. 9-49300
 YGa garnet: Sm^{3+} (Dy^{3+}), crystal-field energy levels of ^6H and ^6F multiplets 9-45254
 YGa laser-excited Raman spectra, 100-800 cm^{-1} 9-49298
 YGa thermal expansion at 296-1400°K from lattice const. 9-41093
 Yb₂Fe_{3-x}Ga_xO₁₂ (x=0.5-4.0), crystallization from PbO/PbF₂ solvent 9-37047
 Yb Fe garnet, ferrimagnetic, cooling by adiabatic magnetization 9-45194
 YbAl laser-excited Raman spectra, 100-800 cm^{-1} 9-49298
 YbFe, angled spin configs., spectroscopic study 9-45193
 YbFe, canted spin config. 9-47277
 YbFe, ferrimagnet, magnetic torques consistent with canted sublattice configuration 9-35576
 YbFe, magnetization rel. to supertransferred hyperfine field of Lu 9-35607
 YFe, Faraday rotation at 1.15 μ , 100° to 450°K 9-49218

Gas analysis *see* Chemical analysis**Gas flow** *see* Flow/gases**Gas-discharge tubes**

- see also* Counters; Ion sources
 air, a.c. and d.c., variation in striking and extinction voltages at low press. 9-23358
 arc, rotation for plasma stabilization, patent 9-34790
 cold-cathode device, patent 9-40722
 electron flow in diodes, mobility-limited flow for collision freq. proportional to electron speed 9-41882
 electron flow in diodes, transition from inertia-limited to mobility-limited flow 9-41881
 electron gun, e energy distribution 9-25181
 Garton flash tube 9-30313
 interelectrode gap, charged-particle density and electric field variation, charact. 9-32701
 ion energy at cathode derived from collisional ionization cross-sections 9-32698
 i.r. emitters for spectroscopy 9-32072
 laser, Q-switched, spinning-prism, flash tube firing time control 9-27294
 laser, supported within housing by means of membrane that also acts as partition, patent 9-34160
 magnetron, cold cathode cylindrical, anomalous electron current 9-47910
 metallic walled, oscillation props. of discharge prod. 9-25971

Gas-discharge tubes continued

- multiple-electrode (vacuum) gap characts., influence of low pressure hydrogen 9-41883
 vacuum u.v. region, penetration of water vapour 9-22368
 Ne, for He-Ne laser mode-locking 9-25263
 Ne flash tube, digitisation method for potential changes 9-27588
 Xe flash tubes, performance analysis 9-32043
 Xe lamp, low voltage, spectral investigation 9-41970
 Xe pulsed large dia. tube, spectral intensity and waveform obs. 9-32705
- Gases**
see also Kinetic theory/gases
 acousto-optical radiation, sensitivity of detectors in analysers 9-37851
 adsorption of mixtures, thermodynamic approach 9-34996
 in aqueous soln., behaviour 9-39080
 binary mixture, reaction rate effect on temp. and conc. distrib. in near-wall region 9-28777
 binary mixtures, components of diff. mol. wt., two-temp. hydrodynamics 9-26012
 binary mixtures transport props. 9-46576
 Brownian motion anisotropy rel. temp. gradient, oil drop and smoke particle obs. 9-26022
 bubbles ascending in liq., diffusion of gas and behaviour of vol. and gas press. 9-46606
 combustion, gas dynamics 9-22292
 confined, acoustic vel. meas., const. geometry amplitude detect. method 9-30347
 dense, equation of state 9-42607
 density-stratified, internal wave generation with mixed region collapse 9-34862
 desorption of H following Ar⁺ bombardment 9-39172
 diatomic, acoustic plane wave propag., kinetic description 9-26033
 diatomic, seeded, electrical characteristics of gasdynamic boundary layers 9-26036
 dipolar, thermal cond. and viscosity, initial press. depend. 9-34835
 discharge at 55 GHz, fourth harmonic power generation, charact. 9-36221
 dissociating and diffusing, acoustic wave propagation, theory with particular cases 9-23398
 electrohydrodynamic Rayleigh and oscillating plate problems 9-46552
 electron diffusion in various gases parallel to elec. fields obs. 9-31909
 enthalpy distribution for hot-core and cold-region of arc heater 9-23393
 e.s.r. investigation, techniques, book 9-38338
 e.s.r. relaxation 9-32739
 Fermi-Dirac relativistic gas at high temp., equation of state, calc. methods 9-34050
 gasdynamics, possibilities of optical methods 9-29458
 high temp. meas. by live-reversal method. 9-26021
 high temperature, bibliography 9-41718
 hydromagnetic shocks, oblique, two in succession, effect 9-46575
 ideal, with internal dissipation, h.f. sound waves 9-26031
 imperfect, cluster theory 9-32728
 ionized partially, transport coefficient calc. 9-25059
 i.r. absorption analyser, developments 9-28825
 isothermal, spectral line emission study rel. to irreversibility of radiative transfer 9-46272
 light resonance absorpt. saturation, spatial effects 9-39054
 local gas content in bubbling column, meas. via elec. resistance of bubbling layer 9-23440
 mixing apparatus for producing atmospheres with low concentrations of some gases 9-32716
 mixture, transport equations, 13-moment solutions 9-42606
 mixtures, composition determ. using float balance 9-34003
 mixtures, shock wave struts and separation of component vels and temps. 9-34826
 mixtures, stopping of kV ions by elastic collisions 9-36678
 molecular, stimulated Raman scattering and gain pressure dependence 9-27835
 monatomic, dilute, light scattering theory using Burnett equations 9-30352
 monatomic, distribution-function autocorrelation calc. 9-34045
 nonpolar, press.-induced microwave absorpt. 9-30350
 nonpolar linear mol., depolarized Rayleigh light scatt. and tensor polariz. reson. 9-39053
 normal burning, hydrodynamic stability to one-dimens. disturbances 9-22293
 perfect, relativistic theory of growth of second-order discontinuities 9-32715
 permeable diaphragm in fuel cell, formation patent 9-30334
 phase equilibrium and dynamics during volume heating and cooling 9-30344
 polar, thermal conductivity in elec. field 9-42610
 polyatomic, Chapman-Enskog theory applic. for rough sphere, loaded sphere and spherocylinder models 9-46566
 polyatomic, thermal conduction theory 9-34836
 pressure fluctuations of gas inside acoustical black box, spatial correl. 9-30346
 pressure waves propagation in infinite uniform media 9-42596
 PVT meas. up to 10 kilobars, apparatus 9-30333
 radiative transfer in optically thick, hot gas outer layer 9-48664
 Raman spectra intensities and depolarization ratios for Hg arc irradi. 9-46340
 rarefied, motion of circular cylinder due to surface temp. distrib. 9-25995
 rarefied, sound propagation kinetic theory 9-30348
 rarefied gases, kinetic theory, gas-solid interaction, book 9-44519
 rarefied stream, pressure measuring systems time delay 9-43715
 Rayleigh scatt. cross section and normal depolarization meas. 9-48665
 relaxation rates, nonlinear shift by admixtures 9-30345
 sampling at high press., large conductance mol. leak construction 9-40216
 spectral pressure broadening in gases, theory 9-29906
 statistical mechanics, book 9-40252
 temperature meas., microasuction pyrometer 9-44523
 thermally excited, Fourier emission spectroscopy, background suppression 9-40576
 transport coeffs., density depend. 9-23404
 transport props. and shock struct. rel. to inelastic collisions, 10⁴ °K 9-34841
 turbulent, spherical wave propag. 9-40752
 two-dimensional, of long thin rods, statistics 9-34828
 Van der Waals gas near critical pt., transport props. 9-26041

Gases continued

- vibrational energy transfer 9-23201
 virial coeff. second of pure gases and gas mixtures, 288-323°K 9-46428
 Ar, 'effective' intermolec. pair potential 9-30339
 Li₂ in ideal state, 100 to 1000°K, thermodynamic props. 9-42609

Gegenschein *see* **Zodiacal light****Geiger counters** *see* **Counters/Geiger****Gelatin**

- gels, sedimentation studies 9-23552
 gels, vacuum freeze-dried, struct. rel. to cryst. nucleation 9-34936

Gels

- blending fractions effect on viscoelastic props. of crosslinked polymers 9-46708
 crystal growth, cusps struct. obs. 9-44605
 crystal growth by complex dilution method, prediction of results 9-30516
 gelatin, sedimentation studies 9-23552
 gelatin, vacuum freeze-dried, struct. rel. to cryst. nucleation 9-34936
 medium for crystal growth 9-37029
 medium for CuCl crystal growth 9-37033
 medium for growth of Au single crystals 9-37026
 medium for Se single crystal growth at ambient temp. 9-37042
 microgels, presence on flowing liquid detect. from optical birefringence 9-32783
 montmorillonite, aqueous, n.m.r. 9-23553
 poly-p-chlorostyrene, chain struct. stability, i.r. obs. 9-28140
 polymer mol. size distrib. change due to crosslinking, math. theory 9-41447
 polypropylene, chain struct. stability, i.r. obs. 9-28140
 polystyrene, isotactic, chain struct. stability, i.r. obs. 9-28140
 polyvinylalcohol, light scatt. obs. 9-37695
 silica, 'adsorbate, adsorbent' interactions, role of surface hydroxyls 9-48723
 silica, benzene sorption and dielectric isotherm, 1 Mc/sec, 25°C 9-42735
 silica, mag. susceptibility of adsorbed NO mols. 9-44631
 silica, monolayer adsorption of aliphatic normal alcohols 9-23649
 silica, vacuum freeze-dried, struct. rel. to cryst. nucleation 9-34936
 zirconia, sol-gel process for prep. of stabilized particles 9-30731
 Fe(oh), nuclear gamma resonance 9-31088
 PuO₂, sol-gel process and calcination to produce dense microspheres 9-36631
 SiO₂, desorption rates of CO₂-Ar mixtures at various temps. 9-46663
 SiO₂, use in Cu₂O single cryst. growth 9-46752
 SiO₂, aerogels, adsorpt. of Ar and N₂ 9-30498
 ThO₂, calcination process, electron microscope exam. 9-35221
 Zr(PO₄)₂, ion exchange and sorption rel. to comp., obs. 9-28789

Generators *see* **Electrical machines****GEOCHEMISTRY** *see* **Earth/composition****GEOCHRONOLOGY** *see* **Earth/age; Radioactive dating****Geodesy***see also* **Gravity**

- boundary value problem, solvability of integral equations and convergence of numerical solutions 9-31247
 conformal transformations in three dimensions 9-31243
 continental drift, gravitational sliding mechanism 9-45434
 correlations within geodetic computations 9-31250
 differential and integral aspects 9-31245
 ellipsoidal Earth generalization of Chapman's theory of radiation absorption 9-41522
 geodetic control by means of astronomic and Torsion balance obs. 9-31242
 geoid, conformal projection on international ellipsoid 9-31252
 global systems from mixed data 9-31248
 gravimetric meas. of earth, mass, vol. and density, applic. of new mathematical model 9-43352
 mathematical model of observations 9-49407
 minor axis direction geodetic reference spheroids 9-33704
 Molodenski investigation method 9-35767
 oblateness, geometric interpretation and direct determ. 9-31237
 radar altimetry from spacecraft, theory and procedures 9-39976
 reference ellipsoid boundary value solution 9-47487
 triangulation by satellites, Polish experiments 9-31249
 triply orthogonal coordinate systems 9-31244

Geoelectricity *see* **Earth/electricity****Geomagnetism** *see* **Earth/magnetic field****Geometrical optics** *see* **Optics/geometrical****Geometry**

- geodesic Killing orbits and bifurcate Killing horizons 9-34007
 rectangular surfaces intersecting, angular coeff. calc. 9-25025
 triply orthogonal coordinate systems, geodesy 9-31244

Geons *see* **Gravitation****Geophysical prospecting**

- electrical, using unsteady e.m. fields in earth 9-35795
 electrical evaluation of deposit 9-31269
 electrical methods, book 9-31270
 c.m., deep, using D_{st} mag. soundings 9-43358
 geoelectric sounding, d.c., book 9-39990
 magnetotelluric sounding curves with allowance for sphericity, characts. 9-45456
 seismic depth computation, 3 dimensional, using space sampled velocity logs 9-37881
 X-ray fluorescence analyser using avalanche detector, planetary geochemical exploration 9-37863

Geophysics*see also* **Atmosphere; Earth; Oceanography; Siemology**

- activity, solar and geophysical (Feb. 1965 and March 1966) 9-41703
 asthenospheric layer waveguide simulation, internal inhomogeneities 9-26871
 atmospheric ²¹²Bi and ²¹²Pb meas., applications 9-24670
 computations methods for Bureau International de L'Heure, continental drifts meas. 9-33740
 conducting base depth determined by magnetotelluric sounding, effect of first layer 9-26880
 constants in 1964 new I.A.U. system 9-41618
 continental drift, polar motion and earth's rotation, concurrent astronomical obs. 9-33734
 continental drift, popular article 9-47486
 continental drift, relative rates 9-33733
 continental drift described, popular article 9-49403

Geophysics continued

- continental drift fit of Australia and Antarctica 9-43368
 cosmic dust accretion rate, estimation from cosmogenic ²⁶Al 9-31279
 relation to cosmology 9-49517
 crust's effective complex dielectric const., radio-electromagnetic profiling method 9-24621
 crustal movement investigation, precise declination meas. method 9-43363
 data, at Dourbes (Belgium), during April (1968) 9-49509
 deformation of viscous solid, finite quasi-static 9-42879
 earth rotation study, contribution from tides 9-33741
 electrical sounding of earth crust using industrial current flow 9-28853
 equations of state, high temp., examination of suitability 9-30777
 expanding Earth hypothesis and oceanic rises 9-41470
 expanding Earth hypothesis and oceanic rises, rel. to sea level control 9-41471
 extraterrestrial dust, airborne collections at remote sites 9-37869
 geyser, Old Faithful, mechanics of action 9-31255
 installations pole position, determination by graphical method 9-37898
 internal gravity waves, progressive shape in fluids 9-25824
 interpretation efficiency, estimation 9-33701
 inverse theory, generalized, applics. 9-43351
 Irish Sea, sea bed survey in north-east, description of rocks found 9-43369
 Italian Geophys. Assoc. 16th annual meeting, Naples (1967) 9-41462
 L vector from noisy data, amplitude error 9-37868
 longitude variations 9-33739
 longitudinal differences determined from radio tracking data 9-33744
 mantle, boundary conditions and rotation, influence on convection 9-28851
 mean pole and earth rotation fluctuations 9-33745
 motion of mean pole 9-33735
 multilayered medium under inclined surface loads, static response 9-49420
 Newfoundland and Labrador areas, shelf and continental slope, morphology 9-43365
 nuclear explosions, underground, constructive use 9-26887
 overdetermined systems of linear eqns., soln. 9-31458
 polar motion derived from time and latitude obs. 9-33742
 polar secular motion and continental drift, symposium, Stresa (1967) 9-33702
 polar wandering and continental drift 9-33743
 pole coordinates, definitive values from 1941 to 1948 taken from ILS obs. 9-33747
 pole motions and continental drift, accuracy of determination 9-33746
 pole movement and latitude variations 9-33738
 potential field due to randomly distributed sources, spectrum 9-37867
 power spectra, coherence and bispectra of geophysical data, discrete Fourier Transform, application 9-26853
 Rajasthan desert meas. of thermal conductivity of sand 9-30789
 spherical earth model, static deformation by internal dislocations 9-39975
 spherical harmonics transformation under change of reference frame 9-45733
 stressed solid involving finite stream, thermodynamic theory 9-49408
 tectonic evolution in Chile, factor of sea floor spreading 9-45474
 temperature gradient and thermal cond. in sediments, heat flow probe meas. 9-35771
 thermal field near surface, effect of past climate charges 9-47488
 topographic disturbance, superficial thermal gradients, rapid estimation 9-26856
 variation of longitude 9-33737
 variations in latitude, relations with polar motion 9-33736

Germanium*see also* **Semiconducting devices; Semiconducting materials/germanium**

- : 9-47012
 amorphous, conduction, localized states in pseudogap and near extremities of conduction and valence bands 9-33243
 amorphous, sharp absorption edge at 0.5eV 9-31106
 amorphous, vapour deposited, density from X-ray diffr. absorpt. obs. 9-33012
 annealing of defects produced by e. irradi. at 30°K 9-35081
 atomic spectrum, bibliography 9-3765
 blooming patterns detection in solids, scanning 9-25529
 cleavage surfaces, decoration 9-48749
 cracks, partial, chem. etching 9-44780
 Debye-Waller factor and anomalous X-ray absorpt., 293-5°K 9-23758
 density of vapour deposited, 'amorphous' Ge from X-ray diffr. absorpt. obs. 9-33012
 diffusion mechanism and point defects, review 9-37209
 dislocation behaviour during thermocyclic treatment 9-37176
 dislocation distrib. during plastic deform., etch pit obs. 9-42832
 dislocation loops, naute, electron microscope obs. 9-42831
 dislocation loops prod. by scratches on surface (III), loop vel. temp. depend. 9-32970
 dislocations generated by diffusion of As at 830°C 9-42830
 dislocations prod. by bending about <211> axis at 730°C 9-40953
 electro- and magneto-optical props. 9-31078
 electron irradiated, defects study, 80° to 200°K, n-type Sb-doped sample 9-35080
 electroluminescence spectra, satellite structure 9-31093
 epitaxial films from GeCl₄-H₂ system, smooth surface conditions 9-36948
 epitaxial growth by GeCl₄-H₂ reaction, rate obs. surface morphology 9-46761
 epitaxial layers on GaAs, plastic deformation 9-37241
 epitaxially grown layers, distribution of imperfection centres 9-37158
 e.p.r. of trapped holes in ZnSe 9-35706
 etching with I vapour, 200° to 800°C, characts. 9-42744
 Faraday rot., interband 9-33511
 films, epitaxial growth on GaAs by GeI₂ disproportionation reaction 9-36947
 films, heteroepitaxy on GaAs 9-36946
 films, heterogeneous nucleation 9-48813
 films, on sapphire by chemical vapour transport, growth and perfection 9-36961
 g-factor of free hole, anisotropy, and conduction-band spin-orbit splitting 9-26484
 grain boundary interband optical props. 9-26737
 growth from metal soln., habit and morphology, infl. of solvent and impurities 9-36981

Germanium continued

- growth from stirred melts, interface stability 9-37056
 growth of non-dislocation layers from vapour, conditions 9-42750
 growth of ribbons by pulling from melt, new method 9-23680
 growth of single cryst. from melt, convection-induced impurity distrib. 9-37079
 heat capacity, 30° to 500°C, anharmonic effects in thermodynamic props. 9-47002
 imperfection centres, distribution in epitaxially grown layers 9-37158
 impurity and defect energies and conc. determ. by highly sensitive photo-sensitive technique 9-39644
 K-shell fluorescence yield 9-24454
 magneto-electro-reflectance in crossed and parallel-field config. 9-39806
 melting curve to 65 kbar 9-39132
 molten drops, crystallization 9-40865
 Mossbauer effect of ⁷⁶Ge, Coulomb excited after recoil implantation 9-33531
 muonium depolarization processes in single cryst. 9-29994
 n-type, dislocation high-density saturation effects 9-43072
 n-type, thermoelectric power, influence of elastic deform. 9-37611
 neutron-irradiated, struct. effects 9-44695
 optical mixing of laser radiation, third-order 9-26688
 p-type, photocond. spectra in fields of 0.5-100 V/cm at temp. 8-15°K 9-37620
 piezorefective spectra 9-35646
 photoconductivity, magneto-, oscillatory 9-39718
 photoconductor, extrinsic, response characts. 9-43129
 proton energy distribution and channelling in lattice 9-30809
 proton energy losses 9-30807
 proton stopping power for protons of 0.35-5.50 MeV 9-30808
 reflectance modulation by optical carrier injection 9-28672
 reflection spectra, u.v., effect of heavy doping 9-35645
 resistance thermometer, calibration to 0.4°K 9-25133
 scattering factor, atomic, from X-ray reflection integral intensities 9-40902
 spectroscopy, atomic absorpt. characts., obs. 9-28829
 splits, internal recontacted, elec. props. gas adsorption and X-ray studies 9-42846
 sputtered ejection pattern of atoms for [100] surfaces, temp. depend. 9-35301
 substrate for thin films, X-ray stress topography 9-34983
 substrate for thin films X-ray stress topography 9-32839
 surface, physisorption at low temps., ellipsometric investigation 9-42730
 surface layer struct., thermodesorption and mass spectra obs. 9-36967
 surface modified by alkylchlorosilane, adhesion and elec. charact. variation 9-48924
 surface with Na, K and Cs submonolayers, low energy diffraction obs. 9-30480
 thermal conductivity variational calc. using anharmonic isotropic continuum model 9-26449
 thin film construction with optical indices independent of thickness 9-39793
 Voigt effect, oscillatory 9-45276
 X-ray absorpt. coeff., oscillator strength for K-electrons 9-32916
 X-ray absorption spectra, dislocations effect on intensity jumps near K-edge 9-33572
 Zeeman splittings of shallow acceptor states 9-41378
 in Fe-(2 wt.%)Al alloy, effect on internal oxidation 9-46740
 in Fe-(1 wt.%)Si alloy, effect on internal oxidation 9-46740
 Ge: Au, hopping photoconductivity mechanism, depend. on temp. and Au conc. 9-35506
 Ge: Au(Au,Sb) single crystals, nature of inclusions and structural features 9-42807
 p-Ge: GaAs, radiative recomb., influence of local pot. fluctuations, low-temp. 9-39867
 Ge: Sb, n-type electron irradiated, defects study, 80° to 200°K 9-35080
 n-Ge: Sb Hall effect distortion by Nernst-Ettingshausen and Righi-Leduc effects 9-37537
 Ge: Sn, radiative recomb. 9-37762
 Ge-As solid solution, new phase precipitation mechanism 9-35243
 n-Ge atomically clean surface, interaction with O 9-46718
 Ge VI, elec. dipole transition configs. obs. 9-48398
 Ge(Li), detector, efficiency and vol. reln. 9-25517
 n-InSb: Ge, amplitude-depend. u.s. attenuation at liq.-He temp. 9-44825
 Li-ion drift mobility, 23.8° and 61.2°K 9-35131
 NaCl windows for CO₂ laser 10.6 μ m radiation, power transmission 9-26675
 in Se, content depend. of mechanical wave propagation velocity 9-30646
 thermal conductivity, 0.3° to 4.2°K, n-type 9-42977
 ZnSe: Ge, EPR of trapped holes 9-35706

Germanium compounds

- B₈ compounds, Mossbauer resonant absorption 9-33528
 chalcogenides, thermal conductivities 9-41103
 Mossbauer resonant absorption in cpds. with B₈ structure 9-33528
 Ag-Ge alloys quenched from melt., formation of faulted close-packed structures 9-40938
 Ag-Ge films, vapour-quenched on vitreous SiO₂, struct. anal by X-ray scattering 9-28213
 (1-x)AlLiO₃-xGeAlLiO₄ solid soln., spinel phase, stability domain boundaries 9-33119
 Al thin film alloying, obs. 9-33116
 CeF₃, n.m.r. of ¹⁵F, showing ionic diffusion 9-24506
 Co-Ge alloys, liq., elec. resistivity 9-46652
 α -Cu-Ge evaporated film, faulting meas. by X-ray diffraction 9-23820
 Cu-Ge solid solns., dislocation struct. and work hardening, electron microscopic exam. 9-41045
 α -Cu-Ge thin films, recrystallization 9-37278
 Fe-Ge alloys, Fe-rich, mass spontaneous magnetization, 298 K 9-39768
 (1-x)FeLiO₃-x(GeFeLiO₄) solid soln., spinel phase, stability domain boundaries 9-33119
 Ge-Al₂O₃-In₂O₃ heterojunctions, switching effect 9-47141
 Ge-As solid soln., defects during precip., nature 9-44682
 Ge-In₂O₃ heterojunctions, switching effect 9-47141
 Ge-Mg-Sb₂ amorphous films, reordering diffusion process under annealing 9-34985
 Ge-Mn alloys, mag. props. in liq. and solid state rel. to Mn conc. 9-47232
 x(GeLiO₃)-y(GeZnO₄) solid soln., spinel phase, stability domain boundaries 9-33119
 GeCl₄, positron lifetimes in liquid 9-44583
 GeCl₄, spectral analysis of contamination by ampoules, obs. 9-31231

Germanium compounds continued

- GeCl₄, vibr. freqs. and stretching force consts., i.r. obs. 9-27874
 GeCl₄, fundamentals, Cl isotopic splitting, using low temp. Raman cell 9-32068
 GeD₃AsD₃, i.r. spectra in gas and solid phase, Raman spectra in liq. phase, vib. analysis 9-30026
 GeD₃AsH₃, i.r. spectra in gas and solid phase, Raman spectra in liq. phase, vib. analysis 9-30026
 GeD₃CN force constants of mol. calc. by Urey-Bradley force field 9-30027
 GeD₃PD₂, i.r. spectra in gas and solid, Raman spectra in liq. phase, vib. analysis 9-30025
 GeD₃PH₂, i.r. spectra in gas and solid, Raman spectra in liq. phase, vib. analysis 9-30025
 GeF₂ i.r. vibr. spectra in gas and solid Ar, Ne, obs. 9-27853
 GeH₃AsD₃, i.r. spectra in gas and solid phase, Raman spectra in liq. phase, vib. analysis 9-30026
 GeH₃AsH₃, i.r. spectra in gas and solid phase, Raman spectra in liq. phase, vib. analysis 9-30026
 GeH₃CN, force constants of mol. calc. by Urey-Bradley force field 9-30027
 GeH₃PD₂, i.r. spectra in gas and solid, Raman spectra in liq. phase, vib. analysis 9-30025
 GeH₃PH₂, i.r. spectra in gas and solid, Raman spectra in liq. phase, vib. analysis 9-30025
 Ge(Li) detector, relative photopeak efficiency using ¹⁵²Eu source 9-22673
 GeO₂-K₂O system, phase equilibria and thermal expansion data 9-26398
 GeO₂, bond type, cryst. energy calc. 9-30504
 GeO₂, rutile-type, thermal expansion meas. by X-ray method 9-24055
 GeO₂, vitreous, n diff. patterns 9-28269
 GeO₂ glass with 0 to 55 mol.% PbO, Raman and reflection spectra 9-28675
 GeO₂ vitreous state, vibrational analysis using i.r. absorpt. and reflection spectra 9-28196
 GeS, elec. card. activation energy in solid and liquid, 20-750°C 9-30909
 GeS, thermal conductivity, up to 500°C, in Ar atmosphere 9-30795
 GeS thermal conductivity 9-41103
 GeSe, thermal conductivity, up to 500°C, in Ar atmosphere 9-30795
 GeSe thermal conductivity 9-41103
 GeTe-GaTe system, u.s. propagation velocity, conc. depend. 9-28417
 GeTe, carrier energy spectrum changes due to solid solns. form. 9-47113
 GeTe, k.p. band model 9-39628
 GeTe, optical props., band structure and supercond. props. 9-39794
 GeTe, relativistic band structure 9-39629
 GeTe, relativistic band struct. and electr. props. 9-43057
 GeTe degenerate semiconductor, review of exptl. data on superconductivity 9-41179
 GeTe ferroelectricity, evidence from phonon temp. dependence calcs. 9-39692
 GeTe thermal conductivity 9-41103
 Mn-Ge alloys, phase equilb. diagram 9-48938
 MnAlGe, ternary alloy, magnetic structure by neutron and X-ray diffraction 9-35560
 Ni-Ge alloy single crystals, mag. props. 9-47261
 Ni-Ge alloy single crystals, prep. by Czochralski method 9-42758
 Ni-Ge single crystals, remagnetization hysteresis energy losses, field depend. 9-43175
 Pb-Ge chalcogenide alloys, solid solution range, and optical props. 9-30721
 SiO₂: GeO₂ glass, i.r. spectra 9-49267
- Getters** see Adsorption; Electron tubes; Vacuum technique
Giant pulsations see Earth/magnetic field; Magnetic storms
Gibbs function see Thermodynamic properties
Ginzberg-Landau theory see Superconductivity
Glaciers
 Antarctic ice media, rad. diffusion, extinction coeff. rel. to grain size 9-39992
 dating of small sample, ²¹⁰Pb method 9-47512
 depth sounders, radio echo, for polar ice sheets 9-26883
 drift topographies, differentiation by statistical analysis of slope data 9-37895
 glaciation activity rel. to solar activity and solar cycle of 2,600 years 9-26884
 ice dynamics 9-35796
 Kesselwandferner, vert. distrib. of fission prod. fallout 9-47513
 relatively rapid motion of ice sheets 9-24624
 seismic determ. of internal friction near melting point, Athabasca obs. 9-31277
- Glass**
 see also Optical materials; Vitreous state
 adhesion to Au underlayer by intermediate adherent layer, mechanism determ. 9-39480
 adsorption of benzoic acid, rate and magnitude meas. 9-30502
 alkali, effect of composition on susceptibility to hygroscopic clouding 9-34970
 alkali, mixed, non-linear variations of props. due to replacement of alkali oxides 9-39148
 alkali borate, Newtonian rheological behaviour, deviations 9-28197
 alkali silicate, internal friction meas. by torsional pendulum 9-26314
 alkali silicate, internal friction peaks, effect of second alkali addition 9-48886
 alkali-borosilicate, relaxation time spectrum and fluctuation theory 9-26096
 alkali-halide B₂O₃, γ -irrad., e.s.r. of stable V centres 9-24480
 aluminoboro-phosphate, absorpt. and fluoresc. spectra of Mo³⁺ 9-47350
 anelasticity, apparatus for damping of torsional oscillations 9-37223
 australites, fission track etch pits studies, sample age correction and thermal history by annealing 9-45463
 barium silicate, containing Ti, gamma-induced optical absorpt. 9-37693
 borate, n.m.r., water content 9-26797
 borolanthanum, immiscibility and catalytic crystallization, additions of various oxides 9-34971
 borosilicate, diffusion of Ag⁺ in elec. field, dendritic growth obs. 9-48872
 borosilicate, wetting by hydrophobic liqs., effect of adsorbed water 9-34978
 ceramic/glass mats., two-phase, strengths, crack formation and stresses around part. obs. 9-30677
 ceramics, transparent 9-49234
 chalcogenide, base for thin film diodes, dynamic V-I characts. 9-24201

Glass continued

- chalcogenide, bulk and min-film switching and memory effects 9-49062
 chalcogenide, conduction, localized states in pseudogap and near extremities of conduction and valence bands 9-33243
 chalcogenide, elec. conductivity and opt. absorpt. 9-30956
 chalcogenide, element with fused-in electrodes, dynamic and static I-V characts. 9-26563
 chalcogenide, vitreous, elastic const., softening temp. and struct. 9-48744
 chalcogenide systems, chemical composition and formation 9-26172
 chalcogenide, transient photoconductivity 9-39709
 Chance Pilkington glasses, F and C dispersion, mean reference index 9-22471
 chemically strengthened, strength and fracture behaviour, rel. to stress profile 9-28336
 cleavage crack propag. 9-30697
 coloured, given spectral characteristic, filter design 9-25376
 colourless, transmission 300 to 400 n.m. range 9-39792
 composition development for fibre optic devices, properties 9-41957
 coordination of Fe^{2+} 9-26199
 crack growth, effect of environment 9-48879
 crown, very dense, crystallizability 9-39206
 crystallization from $\text{Li}_2\text{O}-\text{Ga}_2\text{O}_3-\text{SiO}_2$ system 9-44619
 crystallization kinetics, activation energy; Johnson Mehl-Avrami eqn. correction 9-42754
 cylinders, long thin, scattering angular distribution at oblique incidence 9-26713
 desorption of conically pumped noble gases, pre-exponential factor 9-39171
 desorption of ionically pumped Ar from clean and metallized surfaces 9-30495
 dielectric loss angle at low temp., calorimetric meas. 9-33375
 e.p.r. of Fe 9-37797
 etch-pit counter for neutrons 9-22914
 fibre optics, composition study for high ultra-violet transmission, properties 9-22472
 fibre, Mossbauer obs. of struct. 9-45302
 fibre, opalescent, from $\text{SiO}_2-\text{B}_2\text{O}_3$ melt with metallic oxide, patent 9-23613
 fibre optical materials, chem. compatibility definition and meas. 9-38412
 fibre thermal insulator, bond with organic binder, patent 9-24061
 fibres, strength and struct. 9-30468
 filamentary damage formation by laser beam 9-48847
 films, chemical vapour deposition apparatus 9-26189
 filters, flatness required for astrometric accuracy, quantitative meas. 9-27114
 flint, nonlinear polarization by intense $0.53\mu\text{m}$ light 9-40832
 fluoroberyllate glass energy transfer from Nd to Yb in hosts with nonuniformly broadened activator lines 9-33584
 fluoroberyllate, e.s.r. of divalent Mn 9-45385
 formation in alkali molybdate syst., critical cooling rate 9-30454
 fracture by impact 9-28370
 fracture surface energy 9-42903
 gaseous inclusions in glass, gas chromatographic analysis 9-40966
 germanate, reduced, red fluorescence of Fe^{2+} , Ni^{2+} and Co^{2+} 9-31134
 glass-crystal system, shape of dispersed particles rel. to strength 9-48884
 high pressure effects at diff. temps., review 9-28193
 hole-burning effect on effective stimulated emission cross-section 9-48010
 impact compressive strength determ. device 9-33031
 interdiffusion, effect on light transmissivity of fiber elements 9-34219
 internal friction studies of stabilisation of glass sheet 9-26312
 ionic conducting, metal-glass contacts, electric fields effect 9-37584
 i.r., Schlieren exam. by evaporographic converter 9-38408
 i.r. spectroscopy for structure examination 9-30469
 laser, high power 9-48012
 laser, silica, $\text{Cr}^{3+} \rightarrow \text{Yb}^{3+}$ energy transfer mechanism, obs. 9-29430
 laser beam, monopulse focusing, induced Mandelstam-Brillouin scatt. 9-25317
 laser damage 9-33520
 lasers, recent advances 9-36301
 lasers, specific gain coefficient, direct measuring device 9-48016
 for lasers, spectroscopic data 9-41912
 light back scatter rel. to surface roughness and spatial scatter 9-37692
 low loss, ellipsometric determ. of surface reflectances 9-39801
 melts, vibr. spectra meas., with i.r. reflectance spectrometer 9-46020
 metastable oxide phases obtained by rapid quenching, expt. and theory 9-23612
 and mica detectors for neutron beam recording 9-34360
 microheterogeneous, phase connectivity origin 9-26173
 mirrors of foamed material 9-32029
 molten, cooling on metal surface, u.s. vibration effect on adherence 9-28388
 molten, elec. cond. meas. during heating and cooling, device 9-30420
 molten, molecular-kinetic processes, theory 9-28192
 Mossbauer obs. of struct. 9-45302
 $\text{Na}_2\text{O}-\text{SiO}_2$ alkali-ion movement, electron-probe microanalysis 9-34968
 nitrate, Co(II)-doped, absorpt. spectra rel. to Co coordination 9-26735
 non-oxide chalcogenide structure, i.r. reflectance spectroscopy 9-36928
 nonoxide, thermal expansion at low temp., obs. 9-42970
 opal, scatt. and absorption of light 9-36363
 optical, mechanical strength 9-37248
 optical, properties and applications 9-33500
 optical, silicate and sulphur selenide, mechanical strength 9-26341
 optical, transmission props., effect of false flashes 9-35630
 optical dispersion, mean reference index and wavelength 9-43205
 organic, trapped e.s.r. and optical absorpt. rel. to matrix polarity, 77°K 9-28695
 phosphate, absorpt. spectra of first row transition metal ions 9-33543
 phosphate glasses, Nd^{3+} -doped, radiative lifetime of metastable ion anomalous temp. dependence 9-41405
 phosphorescence, weak with long afterglow, spectral characts. 9-38360
 phosphosilicate glass films in m.g.o.s. structures, polarization process 9-33363
 phosphosilicate glass films in m.g.o.s. structures, polarization processes 9-33363
 photochromatic, reversible photochemical reactions 9-26714
 photosensitive, e.s.r. spectra of neutral Au atom 9-39911
 plate, toughened, shape of fracture front 9-30681
 porous, containing supercond. metals as granular superconductors 9-47083

Glass continued

- porous, sorption of pyridine, i.r. spectra 9-26196
 potassium germanate, structure 9-26398
 powder compacts, shrinkage isotherms rel. to water vapour partial press. 9-33129
 powders, shrinkage, sintering by viscous deformation 9-35227
 pressing study using passive RC-analog 9-34969
 Pyrex, acoustoelastic effect 9-35141
 Pyrex, adsorption of N at very low pressure, obs. 9-36969
 pyrex, Hg vapour, heterogeneous nucleation, impurity effects, 225-263°K 9-39216
 Pyrex, permeation, diffusion and solubility of deuterium 9-40987
 quartz, crystn. and struct., i.r. refl. spectroscopy obs., 1000-1300°K 9-26175
 quartz, fused, and $\text{BeF}_2\text{-XF}$ system, comparison of i.r. spectra 9-41375
 refractive index, changes production by Na-Li ion-exchange technique 9-49241
 refractive index and expansion coefficient, temperature dependence 9-26698
 refractive index as function of wavelength and temperature, meas. on various types 9-37685
 reinforced, strength and fracture behaviour 9-30678
 scintillators for neutron radiography 9-42134
 selection of type for cemented doublet lens 9-25348
 semiconductor, props. rel. to use as switches 9-30934
 sheet, internal friction, under high stress 9-46868
 silica, densified, energy spectrum 9-46700
 silica, hardness and low-temp. deform. 9-28375
 silica, vitreous, n diff. patterns 9-28269
 silica, water vapour adsorption 9-42736
 silicate glass with Nd^{3+} ions, structure of stimulated emission bands 9-35650
 soda-boric oxide, e.s.r. and optical spectra of Cu^{2+} 9-37800
 soda-lime, diffusion of water near and within transform range 9-46854
 soda-lime compacts, sintering during constant rates of heating 9-33130
 soda-lime-silica glass, dynamic fatigue 9-42899
 soda-silica, Tm doped, Mossbauer effect obs. of Tm^{3+} crystalline elec. field parameters 9-37702
 sodium borosilicate, internal friction of high-viscosity phase 9-26313
 spherical surfaces, polished, curvature radius meas. by autocollimating device 9-36340
 strength, tensile, increase by etching and ion-exchange 9-35184
 substrate for CdSe and CdTe vapour phase deposits growth on cleavage face 9-46726
 surface tension by capillary flow technique 9-36854
 T-40, acoustoelastic effect 9-35141
 target for ($^4\text{He},^3\text{H}$) stripping reaction at 120MeV, cross sections 9-42310
 tektites and other natural varieties, bubbles gas content 9-46697
 thin films, chemical vapour deposition apparatus 9-26189
 three-dimensional and stereo obs., using secondary electron emission mode of scanning microscope 9-32825
 titanobarium, Ti valence and Al co-ordination no. determ. from X-ray emission spectra 9-41398
 transition metal, electrical switching mechanism, high elec. field infl. 9-35476
 transition metal ion containing, conduction and thermopower 9-30964
 with transition metal ions, conduction, rel. to polaron theory 9-49009
 trinitrotoluene, from undercooled melt at 258°K 9-39137
 vinyl acetate methyl acrylate copolymer possible glass transition at 21°C 9-33010
 viscous flow 9-28194
 AgCl photochromic, properties 9-33521
 Al-lime: Cr^{3+} , absorption spectrum 9-35655
 $\text{Al}_2\text{O}_3-\text{SiO}_2$ system, metastable glass-in-glass separation and crystn. nucleation 9-32826
 As-S/Al composite system, bonding mechanism 9-32852
 As_2Se_3 semiconductor diode, switching, filamentary conduction 9-35449
 of $\text{B}_2\text{O}_3-\text{PbO}-\text{Al}_2\text{O}_3$ system, spinodal decomposition 9-39492
 B_2O_3 Newtonian rheological behaviour, deviations 9-28197
 Ba flints, dense, crystallizability 9-39206
 Ba silicate: U(IV), paramag. susceptibility 9-33442
 $\text{BaO}-\text{SiO}_2$ films, two-phase structure development 9-26174
 $\text{BaO}-\text{TiO}_2$ system, sputter-coded, four fold co-ordination of Ti ions 9-32827
 $\text{BeF}_2\text{-XF}$ system with X-alkali ion, structure, i.r. spectra obs. 9-41375
 $\text{Bi}_2\text{O}_3-\text{B}_2\text{O}_3(\text{-R}_2\text{O})$ systems, structure and props. 9-46698
 Co coated sheets, optical and energy parameters 9-32038
 $\text{FeO}_x(45 \text{ mol.}\%) \text{P}_2\text{O}_5$, mechanical loss data rel. to electrical conduction mechanism 9-30640
 H adsorption, 300-500°K 9-40850
 $\text{K}_2\text{O}-\text{PbO}-\text{SiO}_2$, luminescence centres 9-31129
 $\text{K}_2\text{O}-\text{SiO}_2$, luminescence spectra 9-39872
 $\text{K}_2\text{O}-\text{SiO}_2$ alkali-ion movement, electron-probe microanalysis 9-34968
 $\text{K}_2\text{O}-\text{SiO}_2$ system, elec. conduction and phase separation by electron microscopy 9-41156
 La, light absorption, effect of coloration impurities Nd^{3+} , Pr^{3+} , Cr^{3+} , Cu^{2+} , Fe^{3+} , Ni^{2+} , Co^{2+} , Mn^{2+} and Ce^{4+} 9-24372
 $\text{Li}_2\text{O}-\text{SiO}_2$ metastable precipitate formation and effect on elec. props 9-24215
 $\text{Li}_2\text{O}-\text{SiO}_2$ luminescence spectra 9-39872
 $\text{Li}_2\text{O}-2\text{SiO}_2$ type, struct. after neutron irradiat., effect on crystn. 9-40833
 $(\text{Li}_2\text{O}, \text{MgO}), \text{Al}_2\text{O}_3-\text{nSiO}_2$, thermally crystallized, high-quartz solid soln. phases 9-28398
 Li aluminosilicate system, changes during pyroceramic formation 9-36922
 Li borate, crystallization, thermal differential analysis 9-42756
 Na-B-Si, spectra, Raman, e.p.r., i.r. and electronic 9-26757
 $\text{Na}_2\text{O}-\text{SiO}_2$, luminescence spectra 9-39872
 $\text{Na}_2\text{O}-\text{SiO}_2$ primary and secondary phase separation 9-30455
 Na borosilicate, phase-separated, viscosity and transform. temp. 9-46680
 Na germanate, Nd activated, e.p.r. spectra 9-39909
 $\text{NaHSO}_4\text{-KHSO}_4$, Mo V spectrum 9-37729
 $\text{Nd}(\text{SiO}_3)_2$ vibration spectra changes over range 548-850°K 9-28674
 Nd, laser, picosecond pulses, evidence for self-focusing in gas breakdown 9-25983
 Nd, occlusions extraction and microanalysis 9-32956
 Nd^{3+} doped, high repetition rate operation 9-48017
 Nd^{3+} doped, laser application, patent 9-48046
 Nd (trivalent) activated, photochemical stability 9-41455
 Nd doped, surface damage threshold improvement by chemical polishing 9-26171

Glass continued

- Nd glass laser with plane-polarized emission 9-36308
 Nd laser, monomode giant pulse, coherent pumping 9-34172
 Nd laser, picosecond pulse width meas. by GaAs surface harmonic generation 9-34173
 Nd laser eff. obs. 9-48028
 Nd laser rod oscillation patterns, streak camera obs. 9-45959
 Nd stimulated emission parameter deterioration during use 9-31109
 Nd type, absorbed pumping energy rel. to activator content 9-48029
 (61.3 wt.%)P₂O₅, (14.7 wt.%)ZnO, (8.4 wt.%) Al₂O₃, (0.2 wt.%) Nd₂O₃, (14.9 wt.%) Yb₂O₃ and (0.5 wt.%) Er₂O₃ for Er³⁺ laser 9-25290
 PbO-GeO₂ system, with 0 to 55 mol % PbO, reflection and Raman spectra 9-28675
 Pd-Si based alloy, form., stability and struct. 9-42706
 Rb₂O-SiO₂, luminescence spectra 9-39872
 Se, based preparation, i.r. transmission 8-15 microns, patent 9-24352
 SiO₂, effect of ⁴He and ³He on low-temp. ht. capacity 9-42733
 SiO₂, glassy state, vibrational analysis 9-28198
 SiO₂ attenuation coeff. using double beam spectrophotometer 9-25383
 SiO₂-GeO₂, i.r. spectra 9-49267
 Sm activated quartz, luminescence and absorption 9-41407
 TeO₂-V₂O₅-BaO spectral transmittance and microhardness 9-39847
 TeO₂ based, high refraction, opt. props. and crystallizability 9-41352
 Ti₂O-SiO₂, cation distrib. 9-48781
 V₂O₅-P₂O₅, semicond., internal friction, elastic moduli and densities, and elec. conductivity, 100° to 400°K 9-35155
 Vycor, porous, containing superfluid fraction of liquid helium 9-34943
 Yb³⁺, doped, laser application, patent 9-48046

Glass-metal seals *see* **Seals****Glow discharges** *see* **Discharges, electric/glow****Gols** *see* **Hypernuclei****Gold**

- adsorption lifetimes and binding energies on W surfaces 9-39177
 adsorption of Co and H₂, spectroscopic obs. 9-35001
 atom, hyperfine structure of 6p²P_{3/2} state reson. scatt. investigation 9-44255
 blocking contacts on CdS, reduction of work function with increasing photocurrent 9-39732
 bremsstrahlung cross-section for electrons of 50-500 keV 9-22977
 contact. pot., stress induced shifts, obs. 9-43019
 contacts on CdSe polycryst. films, props. 9-41211
 crystallites on (100) KCl surface, mobility 9-37204
 crystals, Xe ions bombard., threshold of damage obs. 9-30800
 Debye-Waller factors, temp. depend. 9-35261
 deposits on satellites, sputtering by atmos. N₂ beams, rel. to surface binding energy 9-24076
 diffusion and solubility in Na, 0° to 77°K 9-42861
 diffusion in f.c.c. La 9-33005
 diffusion in n-InP 9-46853
 diffusion in Pb, Sn, In, and Tl, rapid, interstitial mechanism 9-28321
 diffusivity in Pr 9-44745
 doping of Si, eff. on surface characts. 9-37535
 electrical resistivity recovery after fast neutron irradi. at low temp. 9-43025
 electrical resistivity rel. to temp., calc. using lattice dynamics model 9-35339
 electron irradiated, interstitial clusters below stage III annealing temp. 9-30593
 electron maximum range, 15 MeV, exptl. determ. 9-26470
 electronic props. and hyperfine interactions, pressure dependences, relativistic calcs. in Wigner-Seitz model 9-26481
 energy-loss spectra of fast ions channeled in single cryst., pot. energy and differential-stopping-power functions 9-30805
 epitaxy on MgO, in electron microscope, (100) cleaved surface mechanism determ. 9-39220
 evaporated on Ag substrates, epitaxy, effect of surface imperfections 9-37112
 evaporated on C replica of Ag substrate epitaxy, effect of surface imperfections 9-37112
 evaporated on NaCl and KCl effects of forced high nucleation densities. 9-32843
 exploding wire phenomena, effect of nature and dims. 9-45419
 field ion microscopy 9-23626
 film, growth in ultra high vac. on mica, influence of air, O₂, N₂ and H₂O vapour 9-34993
 film, growth on alkali halides 9-23636
 film, thin, photoelec. emission rel. u.v. polarization and angle of incidence 9-31072
 film conductors, electromigration, role of thermal gradients 9-34984
 film on NaCl, epitaxial and polycryst. rel. to H₂O, CO₂ contamination 9-46724
 film on W, props. observed by field-ion and field emission microscopy 9-23624
 films, current noise 9-28464
 films, sputtered, hillock growth and stress relief 9-42717
 films, thin evaporated, optical props. 9-47313
 foil bremsstrahlung, spectrometer for meas. using Compton eff. 9-46133
 foil target, attenuation of heavy ions, obs. 9-28440
 Gibbs free energy of self and impurity diffusion 9-33001
 in glass, photosensitive, e.s.r. spectra obs. 9-39911
 growth, hydrothermal 9-37027
 growth of single crystals in gels 9-37026
 Hall effect and phonon drag 9-43026
 ion and neutron irradiated, vacancy clusters 9-28279
 ion bombarded, depth distrib. of vacancy clusters, 295°K and 80°K 9-30586
 ion bombardment of Au and Ni, 80-150 keV at 295°K and 80°K, depth distrib. of vacancy clusters 9-30586
 ion-implanted layer in Si single crystal, structure 9-39307
 ions, channeled keV, in Au, dechanneling, vacancy clusters formation, 9-47016
 irradiation by Pb ions, collision cascades, 3-169 eV 9-39552
 magnetoreflection meas. and optical dielec. function change 9-49246
 molten, wetting of sapphire, ruby and recrystallized alumina 9-34977
 neutron irradi. at low temp., elec. resistivity recovery 9-43025
 nucleation and nucleus growth on defined silver faces 9-37003
 nucleation density of gold trapped by imperfections on cleavage surface of NaCl 9-37004
 nucleation on amorphous substrate 9-26187

Gold continued

- Ohm's law verification up to 10⁹ A/cm² current densities 9-24126
 particles, sintering behaviour by electron microscopy 9-26365
 photoelectric emission in fair u.v. 9-43143
 photoelectric yield meas. with Lallemand electronic camera 9-45028
 proton transmission through thin crystals, 400keV 9-42979
 self-diffusion meas. in single cryst. 9-39381
 self-diffusion in single crystals., 335-390°C, conc. profiles and coeffs. 9-23835
 shock velocity, u_s, and particle velocity, u_p, in hydrostatic compression, applic. of interpolation formula for relationship between u_p and u_s 9-42871
 sols, prepared in nitrate melts, electron micrographs 9-36907
 solubility of C 9-44788
 surface diffusion on KCl crystals, 130-500°C 9-40848
 surface obs. by large-angle Ar⁺ scatt. on single crystal 9-48748
 thermal diffusivity, 325 to 1225°K 9-26440
 thermionic work function changes following 100-600 eV inert gas ion bombardment 9-24257
 thermomigration of ¹⁹⁵Au and ¹²⁵Sb 9-35126
 thin film on glass, elec. conductivity 9-24121
 vacancies, quenched resistivities and Matthiessen's rule 9-35336
¹⁹⁵Au, thermomigration in Au 9-35126
 Al-GaSe-Au struct., carrier transport 9-41228
 Au/Au contacts, adhesion w.r.t. contact resistance 9-33132
 Au/Pb supercond. layered films, phase composition and transition obs. 9-26528
 Au/Pt group metal contacts, adhesion w.r.t. contact resistance 9-33132
 Au-poly-N-vinyl carbazole-GaAs systems, transient photocurrents and internal photoemission 9-39656
 Au, energy-loss spectra of channeled-ions in monocryst., model 9-30806
 Au⁺ diffusion in AgCl, low temp. suppression by chlorine 9-46847
 Au films, Au-ion irradi., substages III annealing, activation energies 9-33106
 Au films, dispersed, light and electron emission centres 9-26606
 Au-Fe thermocouples, reproducibility tests 9-22299
 Ge:Au, i.r. absorpt. rel. to hole transitions from impurity levels to valence band 9-44981
 in Ge, conc. and temp. depend. of hopping photoconductivity mechanism 9-35506
 Si:Au, electron and hole emission rates at centres from photocurrent and photopacative meas. 9-39636
 in n-Si, enhanced solubility effect 9-30929
 on n-Si Schottky barrier, forward I-V characts. 9-43082
- Gold compounds**
 liq. alloys, at. distrib. and elec. resist. 9-30423
 nucleation on amorphous substrate 9-26187
 solid-sols., solute Knight shift and spin-lattice relax. 9-43295
 white gold, effective atomic number for photoelectric process of γ-ray 9-47213
 Ag/Au/Si system, controlled solidification using monovariant eutectic reactions 9-36921
 Ag-Au alloy, liq., elec. resistivity, form factors 9-39112
 Ag-Au alloys, diffusion of Ag, high temp. electrochem. method meas. 9-46841
 Ag-Au alloys, Kirkendall shift, press. and vacancy-flow effects 9-46848
 Ag-Au dilute alloys, de Haas-van Alphen effect studies, rel. to scattering temp. 9-37422
 Ag-Au layered struct. solid soln., X-ray diff. static atomic displacements influence on diffuse intensity 9-37132
 Ag-Au solid soln., vibrational entropy and thermal vibrations, correlation 9-33151
 Ag-Au solid solns., lattice parameters 9-39247
 Al-Au dilute alloy, impurity resistance, 1.2° to 300°K 9-30840
 Au-Ag alloys, interdiffusion, effect of gradient energy 9-37199
 Au-(46.1 at.%)Cd alloy, pseudo-elastic flow due to twinning surface dislocations 9-35156
 Au-(46.1 at.%)Cd alloy, twinning surface dislocations, intrinsic resistive stress 9-35157
 Au-(50 at.%)Cd alloy, plastic deformation influence on martensite transformation 9-39491
 Au-Co alloys, liquid ferromagnetic, thermodynamics near Curie and melting point 9-23531
 Au-Co alloys, precip., rel. to mag. hardness 9-41055
 Au-(46 at.%)Cu-(4 at.%)Ni alloy, order transform. of type α disorder=1 order, radio-crystallog. study 9-37304
 Au-Cu-Co liquid alloy, susceptibility meas. 9-34921
 Au-Cu-Zn alloys, β phase stability and elastic anisotropy 9-46957
 Au-(25 at.%)Cu alloy, elastic after-effect kinetics, resistance meas. 9-35161
 Au-(0.1 wt.%)Cu alloy, fast neutron irradi. at low temp., elec. resistivity recovery 9-43025
 Au-Fe alloys, ⁵⁷Fe Mossbauer effect obs. of mag. ordering 9-39817
 Au-Fe alloys, hyperfine fields of ¹⁹⁹Au 9-49259
 Au-Fe dilute alloys, Mossbauer absorpt. spectra of ⁵⁷Fe 9-45285
 Au-In alloy as bonding material for u.s. props. meas. in solids at high temp. 9-46983
 Au-(10at. %)In, specific heat meas. at 3°K, nuclear term obs., crystal electric field studied 9-30780
 Au-Mn alloys, martensitic transformations near equiatomic composition 9-26379
 Au-Mn alloys, short-range order 9-28257
 Au-Ni thin film thermocouples, vacuum- evaporated, thermoelec. power and Seebeck coeff. thickness depend. 9-45017
 Au-Pt, precipitation kinetics, coherent and incoherent, study by resistivity changes 9-28382
 Au-Si solid soln., Precipitation effect on i.r. vibration spectrum of O 9-45315
 Au-Sn system, metastable γ-brass and non-equilib. Hume-Rothery phases 9-35255
 Au-V dilute alloys, n.m.r. low-temp. mag. props. obs. 9-45395
 Au-V dilute magnetic alloys, specific heat, temp. depend. below Kondo temp. 9-24050
 β⁺-Au-Zn alloy, order, long-range, X-ray diff. meas. 9-28256
 Au-10at.%Zn, specific heat meas. at 3°K, nuclear term obs., crystal electric field studied 9-30780
 Au...Pd,Ca₂, supercond., thermal and mag. susceptibility behaviour 9-49047
 Au-Su alloy long- and short-range order w.r.t. thermoelec. power temp. depend. 9-37610

Gold compounds continued

- Au₄X ordered alloys, X=transition elements and mixtures, electron and neutron diff., resistivity and specific heat studies 9-44659
 AuAl₂, high-field galvanomag. props. 9-47073
 AuB mass spectrometric determ. of dissoc. energy 9-24528
 AuCu₃, diffuse scatterings and superlattice reflections, new type 9-23750
 AuCu₃, order-disorder eff., reflectivity and photoemission 9-26395
 AuCu₃, order transform. of type α -disorder=1 order, radiocrystallog. study 9-37304
 AuGa₂, high-field galvanomag. props. 9-47073
 AuIn₂, high-field galvanomag. props. 9-47073
 AuSb₂, low-field galvanomag. coeffs. 9-41159
 AuSi, dissociation energy of molecule 9-46421
 β' AuZn, plastic deformation, comp., temp., strain-rate and grain size dependence 9-23881
 Cu-Au alloy films, effective surface coeffs., vol. diffusion effect in electron diff. obs. 9-39379
 CuAu II alloy, entropy of disorder, phase transition from CuAu I 9-30750
 Cu-Au ordered alloy, dislocation structure produced by plastic deformation 9-23813
 Fe-Au, thermoelectric power at low temps. and field dependence 9-35495
 Nb₂Au₃Pt_{1-x} system, supercond. transition temp., annealing conditions influence 9-44942
 Pd (50 wt.%) Au alloy, Young's modulus temp. depend. 9-44752

Grain boundaries see *Crystal imperfections; Crystal structure/microstructure*

Gramophones see *Sound reproduction*

Granato-Lücke theory see *Crystal imperfections/dislocations*

Granular structure

- aggregates, polycrystalline, topological approach 9-23962
 carbide grain growth during liquid phase sintering of NbC-Fe(Co,Ni) alloys 9-34952
 displacements in granular medium 9-35224
 grain growth and pore-grain boundary interactions 9-32897
 grain growth during secondary recrystallization, effect of volume energy 9-32881
 grain size distribution analysis 9-35225
 grains and voids, volume distribution 9-39481
 superconductors in porous glass, critical fields obs. 9-47083
 X-ray fluoresc. analysis grain-size effect, nomograms 9-28833
 Fe strain induced grain growth 9-42788
 Ag thin films, grain size influence on opt. consts, near plasma freq. 9-37680
 Al films, superconducting fluctuations in 3-d regime causing excess conductivity 9-26527
 Al films, superconductivity enhancement 9-24149
 Al films, superconductivity enhancement mechanism, expt. evidence 9-24150
 Al supercond. films, microwave conductivity 9-37466
 Cu heavily rolled sheet, electron transmission exam. 9-39272
 Fe-49 wt.%) Ni alloys commercial effect of grain size on initial permeability 9-49204
 Fe, strain annealed crystals, subgrain boundaries in {011} {112} occluded grains 9-23824
 Li_{0.5}Fe_{2.5}O₄, grain size effect on switching speed and coercive force 9-45180
 Mg-Zn-Zr alloy, strain-rate hardening, grain-size depend. 9-39443
 MgO, grain diameter distribution, influence of purity 9-39283
 Ni-Ti alloys, boundary deformation rel. to temp. under constant strain 9-23889
 Ni alloys, cast or wrought, grain size effect on creep-rupture strength 9-37245
 Ni base alloy, dispersion-hardening size effect on yield point, strain hardening and creep resistance 9-33015
 Pb-base alloys, grain size and growth, optical metallography 9-39301
 Sn-Cd eutectic, plane to cell transition on solidification 9-23585
 Sn-Cd lamellar eutectic, fault occurrence 9-28299
 Sn films, superconducting fluctuations in 3-d regime causing excess conductivity 9-26527
 steel, Si {111} {211} texture, rel. to secondary recrystallization 9-46922
 U, anisotropic grain growth, effect of alloying additions 9-33206
 UO₂, porosity effect on kinetics of grain growth 9-26250
 W grain growth, e emission microscope obs. 9-37127

Graphite

- absorption of light, Rosseland and Planck mean coeffs. 9-49548
 adsorption of Ar, fourth-order interaction using third virial coeff. of 2-dimens. Lennard-Jones gas 9-42605
 adsorption of He and Ne atoms, quasiharmonic freq. shifts 9-48769
 adsorption of I and desorp. in vacuum and Ar, 27-1100°C 9-28221
 AGOT grade, thermal conductivity 0.3-3°K 9-26442
 air-graphite suspensions, heat transfer agent, hydrodynamics, expt. 9-30437
 artificial polycryst., dimensional deform. during Br intercalation 9-26223
 boronated, oxidation 9-28795
 from carbazole and fluorene, enhanced prod. by copyrolysis with aryne precursors 9-26811
 carbide-boride-graphite ceramics, fusion-cast, phase assemblages, microstruct. props. 9-30729
 channel, air oxidation studies, radial diffusional effects 9-26824
 chemical structure and graphitization, X-ray diffraction studies, samples from polynuclear aromatics 9-39257
 composites, well oriented, prep. and props. 9-23972
 constitutive eqns., nuclear grade for space applics. 9-33057
 corrosion, radiolytic, by CO₂, effect of pore size variation on rate 9-41452
 cyclotron resonance in natural cry., interpretation 9-26497
 diffusion mechanism, and rel. to irradiated sample 9-40981
 EGCR-type AGOT, mechanical props. at room temp., 1000, 2000 and 4500°F 9-41009
 elastic modulus and yield curve, eff. of microporosity 9-28343
 electrode temp. meas. for arcs in room air 9-30321
 eutectic melting at contacts with metals of iron triad 9-26358
 fibres, C, fine struct. 9-30557
 fission products, non-gaseous, escape behaviour of products recoiled into graphite 9-26299
 formation of diamond in presence of metals, mechanism 9-41064
 g-factor and diamagnetic anisotropies, relationship 9-47228
 glide and rotation during sedimentation 9-39368

Graphite continued

- grains, in malleable cast irons, microtopography during annealing 9-23950
 graphite:B, neutron irradi., defect clustering, effect of B, physical prop. meas. 9-30597
 graphite:B, neutron irradi., interstitial loop clustering, effect of B, electron microscope obs. 9-30595
 graphite:B, neutron irradi., nucleation of interstitial loops, effect of B 9-30596
 graphite, microporosity changes during thermal and radiolytic oxidation 9-26224
 graphite-pyrocabon composite mats. obtained by natural gas decomposition, n. irradi. eff. 9-28436
 growth, spherulitic 9-37068
 growth from solution 9-48800
 growth of single crystal by pyrolysis of acetylene over metals 9-39192
 growth of single crystal films and dendritic crystals from carbon-iron melt 9-37067
 Hall coefficient and magnetoresistance, 1.5° to 300°K 9-41153
 hexagonal lattice, etch pit conformations via vacancy oxidation 9-28281
 integral X-ray refl. coeff., comparison with LiF, 0.7 to 2.1 Å 9-47384
 internal friction studies 9-48887
 internal friction coeff. temp. depend., defects due to neutron irradiation, -180 to 500°C, 1 Hz 9-35153
 interstellar particles, hydrogen coated, formation and optical props. 9-43572
 irradiation by neutrons and electrons, low temp. 9-24070
 lattice parameter and dimensional changes on irradi., 300 to 1350°C 9-28280
 Madagascar, withrhombohedral phase, g-factor anisotropy, method and results 9-24484
 natural cry., cyclotron reson., interpretation 9-26497
 neutron irradiated, 300°-1200°C, bulk expansion 9-46883
 neutron thermalization params., 2.99≤B^{1/2}≤25.30, 14 MeV 9-25666
 Neutron thermalization studied by time-step and Monte Carlo methods 9-22851
 neutron wave, modulated, asymptotic params. calc. 9-25665
 neutron wave propagation 9-34478
 neutron wave propagation analysis 9-32373
 neutron-bombarded, uptake of Br and formation of lamellar cpds. with K obs. 9-28316
 optical constants anisotropy rel. to band structure 9-26697
 oxidation kinetics in CO₂, 10⁻³ to 40 atm., 700 to 1300°C 9-41449
 particle shell round NML cygnus, as model for i.r. rad. origin 9-33902
 plasma in single cryst., principle oscillatory freqs. 9-47060
 polycrystalline, microporosity eff. on elastic modulus and yield curve 9-28343
 pore size distrib. changes after artificial densification by natural gas decomposition 9-23753
 porosity determ. by Hg porosimetry and He intrusion, limitations of Hg method 9-26225
 potential and inner potential calc. from pseudopotentials applic. to low-energy electron diffraction 9-44654
 pyrographite, opt. const., i.r. region 9-24357
 pyrographite, surface energy 9-42712
 pyrolytic, electron-irrad., recovery of basal plane resistivity 9-28459
 pyrolytic, flexural strength, post deposition high temp. treatment eff. 9-23906
 pyrolytic, irradi. at high temp., defect nucleation, cry. perfection influence 9-23794
 pyrolytic, negative magnetoresistance 9-41163
 pyrolytic, Young's modulus, by flexural vibration technique 9-46864
 pyrolytic stress-annealed, struct., imperfections and graphitization, electron microscope obs. 9-35054
 quasiharmonic freq. shifts of adsorbed He and Ne atoms 9-48769
 reaction of single cry. with H₂O vapour in He e. microscope investig. 9-24537
 reaction with H₂ at 1900°-2400°K 9-43315
 reactivity to O, eff. of neutron bombardment 9-35743
 shear, direct basal-plane, in single crystals 9-46875
 single cry., irradi. at high temp., defect nucleation, cry. perfection influence 9-23794
 single crystal films, and flaky dendritic crystals, growth from C-Fe melt 9-26209
 sliding against stainless steel, interface geometry rel. to wear 9-41036
 sorption of atomic and mol. H, temp. depend. obs. 9-39169
 sorption of Cs, characts. at high temp. and low Cs pressures 9-39168
 stress relaxation at high temps. 9-46874
 stress relaxation at high temps. 9-46873
 stress-graphitized pyrolytic C, dynamic elastic mod. and internal friction 9-26320
 thermal conductivity, high temp. radial heat flow meas. 9-26443
 thermal conductivity of AGOT grade, 0.3-3°K 9-26442
 thermal degassing after radiolytic oxidation in CO₂ or CO₂ + methane, comparison with thermal oxidation 9-28220
 thermoelectric power, 300° to 7°K 9-26597
 tube, oxidation kinetics, effect of non-uniform burn off, theor. anal. 9-26823
 ultrapurification by preburning, for emissions and mass spectrography 9-34227
 whiskers, anomalous structure, electron microscope exam. 9-46783
 X-ray diffraction studies 9-48822
 Young's modulus in pyrolytic sample, by flexural vibration technique 9-46864
 neutron spectra from spherical shell obs. 9-27783
 C film, evaporated graphitization under heat treatment, 1000° to 2200°C 9-39453
¹⁴C labelled, oxidation in reactors, equipment for meas. by chemical and radiochemical methods 9-38734
 in Ni-C eutectic alloy, flakes struct. 9-44671
 TiC, X-ray emission K α band of C 9-26762

Graphs

- see also *Nomograms*
 Cotton-Mouton resonance effect representation 9-43922
 data, smoothed, graphical reconstruction 9-25019
 envelope diagrams, analyticity, solns. to Landau eqns. 9-22170
 Ising model, recurrence formulas 9-34037
 least-squares adjustment of weighted data to general linear eqn. 9-45802
 neutron, line spectrum, graphical analysis from recoil proton proportional counter data 9-48218

Graphs continued

- optical constant of mixtures, computation by graphical method 9-35612
- paper, square root, nuclear spectra plot 9-25061
- stress distribution representation, and forces acting on dislocations 9-32967
- vapour-liq. equilib., binary and ternary mixtures, vapour composition graphical determ. 9-23587

Gratings *see* *Diffraction gratings; X-ray diffraction***Gravimeters** *see* *Gravity***Gravitation**

see also *Gravitons; Relativity*

- accelerated charge, at rest or freely falling rel. to gravitational field, radiation 9-38214
- atomic beam deflection obs. 9-43725
- axial-symmetrical fields, stationary, internal solution 9-25035
- binary mixtures, thermodynamic theory 9-23454
- Birkhoff's theory, four-vector force 9-29187
- Birkhoff's theory and potential of point mass 9-22088
- Bondi-Sachs analysis of empty space fields, pure radiation news function 9-38220
- Brans-Dicke scalar field geometrization 9-38208
- Brans-Dicke theory, eff. on solar evolution and neutrino fluxes 9-29080
- Brans-Dicke theory, rel. to model of expanding Universe 9-38030
- clusters of point masses, models with large red shift 9-45584
- collapse, appl. of spherically symmetric metric with perturbations 9-31491
- collapse, coupling of angular momentum with grav. field 9-31532
- collapse in Treder-theory 9-45756
- contraststreaming self-gravitating streams, stability taking account of thermal conduction and radiative effects 9-48531
- cosmic microwave background anisotropy, induced by large scale density inhomogeneity 9-36006
- critical point of pure subst., asymmetry of gravity deflections 9-36915
- Earth's gravitational pot., odd zonal harmonics, evaluation from satellite orbits analysis 9-31240
- Earth's field determined from surface meas. 9-31606
- effect on frequency, Taurus A phenom. and geometrical field theory 9-33906
- Einstein's eqn. of motion of test part in 'weak gravitational field' modification 9-34016
- Einstein's eqns., approx. radiative solns., construction 9-45763
- Einstein's equations in mixed initial and boundary value problems 9-25037
- Einstein's field eqns. soln. in spherically symmetric matter distrib. 9-27165
- Einstein empty space field eqns. soln., Newman-Penrose method for twisting degenerate metrics 9-45760
- Einstein eqns., approximate radiative soln. construction 9-22071
- Einstein field eqns., Reissner-Nordstrom soln. generalization 9-45762
- Einstein vacuum field eqns. in Weyl co-ordinates, exact soln. 9-41751
- e.m. cavity resonances in accelerating frames of reference 9-34113
- and e.m. field, unified geometric description 9-27167
- e.m. radiation, effect on a pulse equal in magnitude but opposite in direction to that in red shift 9-34018
- e.m. wave interaction, test using beats in laser two-beam interferometer 9-41743
- energy density, calc. by natural gauge of tetrad field 9-26854
- energy positive-definite, proof from covariant decomposition of symmetric tensor 9-29185
- equations, general solns., singularities 9-38209
- exit trajectories, optimum, with specified transfer angle 9-29223
- expanding universe, density inhomogeneity growth from small perturbation 9-24737
- external field, response to variation, and implications for equal-time commutators 9-47745
- field, axisymmetric stationary vacuum, equiv. to 3-dimens. relativity theory 9-29180
- field, influence on light propagation 9-22080
- field, variational principle 9-31755
- field equations in Birkhoff's theory, from potential of point mass 9-36126
- field in static spherical shell of matter, exact soln. 9-34017
- field quantization from modified theory of general relativity 9-29184
- finite-range model 9-41748
- flat gravitation applied to relativistic quantum mechanics 9-47733
- flat gravitation as a useful model theory 9-47732
- G, Mach's principle and a relationship between e.m. strong and weak interactions 9-41752
- galactic structure; dynamics of self-gravitating systems 9-47622
- Galaxy, G and mass vars. rel. to globular clusters age 9-33895
- gauge conditions in gravitational interactions 9-47742
- geometrization of the Brans-Dicke scalar field 9-38208
- gravitational to magnetic energy conversion, obs. in Crab Nebula pulsar 9-45647
- gravitodynamics, generalized statistical mechanics of violent agitation 9-41622
- gravito-inertial field, neutral particle gravitational and inertial mass difference 9-31754
- graviton bremsstrahlung and i.r. divergence 9-47743
- hydrodynamical eqns. for ideal, relativistic, charged gravitating fluid 9-45589
- induced electric field near a metal 9-22320
- induction field communications expt., 1660 Hz 9-38210
- instability, non-Jeans type, for system of stars and interstellar matter 9-41648
- instability of infinite isothermal stratified medium under uniform rot. using principle of exchange of stabilities 9-26992
- Lagrangian field density and singularity, quadratic corrections 9-47734
- Lifshitz's relativistic theory for gravitational instability, Lagrangian coordinate condition adopted 9-33888
- light deflection and Snell's law, corpuscular theory 9-29155
- linear spin-two field without self-interaction 9-22069
- lorentz-invariant theories, anal. of one-body problem 9-27166
- minkowski metric, asymmetric non-static deviation 9-47746
- Newton's const. variation with grav. potential, assumption and possible test 9-47620
- nonrelativistic, generalized, polytropic gas spheres 9-27008
- non-saturation of gravitational forces in boson and Fermion quantum mechanical systems 9-43734
- particle affected by gravitational and e.m. actions, quantum relativistic energy 9-47748

Gravitation continued

- particle origin, quantum field theory 9-38441
- perturbations due to elastic collisions 9-29181
- perturbations produced by suddenly accelerated bodies 9-29188
- Petrov type D metrics all derived 9-47730
- primordial gas clouds, gravitationally bound, formation 9-47616
- radiation, coincidences over 1000 km base line 9-40235
- rarefaction wave and medium fly-off in variable field 9-26976
- relativistic generalized theory 9-25036
- Riemannian spaces, embedding in Euclidean or Minkowskian spaces 9-43726
- rotating Newtonian universe, inevitability of point-singularity 9-40115
- Schwarzschild field, deflection of light 9-27169
- Schwarzschild field, precision of a moving gyroscope 9-27168
- Schwarzschild problem, quaternion soln. allowing for zero neutrino mass 9-31758
- self-gravitating, collisionless system, approach to Lynden-Bell quasi-equilib. distrib. 9-27016
- spheroidal expansions of rot. gas masses, gravitational instability, cosmogonic fragmentation mechanism 9-24733
- spinning body without gravitational waves 9-22180
- stability, local, of non-rot. system of particles in gravitational Einstein field 9-24734
- stability of infinite, perfectly-conducting cylinder, in aligned mag. field 9-35943
- stellar self-gravitating system in uniform motion, gravitohydrodynamic instability criterion 9-24732
- stress Tensors, non-conserved in presence of gravitation, commutator 9-40237
- three-body problem, unrestricted, Hill stability 9-24736
- Treder's theory, spherically symmetric vacuum solns., collapse 9-45756
- unified theory of gravitation and symmetry violation of U(3) 9-38219
- Weyl and zero-rest-mass scalar fields coupled 9-43736
- p gravitational moment 9-22624
- K atomic beams, deflection obs. 9-43725

Gravitational collapse *see* *Gravitation***Gravitational red shift** *see* *Relativity/general***Gravitational waves**

- angular-momentum flux for gravitational radiation to octupole order 9-45755
- in Einstein space, exact soln. 9-45746
- Einstein vacuum field equations, complete set of normal hyperbolic solutions 9-41749
- Einstein-Maxwell field, asymptotic expansions 9-29186
- emission of gravitational radiation, a useful news function 9-38220
- fluid surface, parametric, excitation in alternating elec. field 9-23207
- generation, continuous 9-29182
- gravitational radiation theory, invariant formulation 9-22084
- internal, in liquid, interaction with shear flow 9-26053
- internal gravity waves, progressive shape in fluids 9-25824
- ionosphere, wave obs. from separate sites, cross spectra, effect of bandwidth on interpretation 9-28947
- ionosphere F region, fine structure obs. 9-31440
- Kundt solution of Einstein equations 9-22085
- plane, analysis rel. to field energy density 9-26854
- propagation, gravitational rotation field hypothesis 9-45744
- propagation across decreasing mag. field in conducting fluid 9-24691
- radiation, investigation by successive approximations 9-45749
- radiation jets, extended source construct. 9-22067
- spinning body without gravitational waves 9-22180
- starlike relativistic objects emission, and vibr. damping 9-28979
- vector theory, two-field hypothesis 9-45745
- water basins, proper gravitational and planetary vibrations, numerical determ. 9-37903
- H₂O, scattering by circular dock 9-26069

Gravitons

No entries

Gravity

see also *Geophysical prospecting*

- anomalies due to disturbing mass in Nordling Ries 9-49406
- asymmetric active regions, positive and negative anomalies and seismicity 9-39986
- at Atlantic ridge, calc. and obs. 9-31274
- atomic beam deflection obs. 9-43725
- boundary value problem, stability of solution 9-31246
- diethyl ether, effect on light scatt. near crit. pt. 9-30406
- earth, energy integral for satellites, application 9-33878
- field approximation by equivalent source technique 9-37883
- force on falling electrons and positrons, exptl. determ. 9-25421
- g measurement by free fall, apparatus 9-22032
- geoides in English Channel, deviations from mean level 9-24611
- gravimeter, marine, linear smoothing of obs. 9-37873
- gravimeters, vibrating string, scale division calc. 9-37871
- gravimeters, vibrating string, tilt calibration 9-37872
- gravimetric meas. of earth, mass, vol. and density, applic. of new mathematical model 9-43352
- gravimetry at sea in towed gondola 9-31238
- horizontal gradient deflections, interpolation, torsion balance measurements 9-35769
- horizontal gradients in S.W. Ohio, torsion balance obs. 9-31241
- importance in shell-liquid impact anal., compared with liq. and shell mat. parameters 9-22186
- induction of electric field near conductor, qualitative model 9-34111
- inhomogeneous mass distribution, symmetric matrix method for rapid interpretation 9-45435
- internal gravity waves, progressive shape in fluids 9-25824
- invariable pendulum meas., humidity effect 9-45803
- linearised waves, in atmosphere, numerical model 9-37931
- liquid columns, effect on light scatt. near crit. pt. 9-30406
- low degree longitude harmonics, observations from 12 and 24 hour satellites 9-31239
- magnetic and gravimetric inverse problem, joint soln. 9-49506
- measurement, absolute: interferometric method; portable device 9-40231
- model for non-rotating field 9-31251
- modification of ion-acoustic waves 9-31336
- Mohorovicic discontinuity, gravimetric investigations 9-33721
- Moldenskii investigation method 9-35767
- Moon, field, acceleration residues over ringed Maria, rel. to 'mascons' 9-33924

Gravity continued

- ocean bottom surveys by deep submersibles 9-37874
- satellite orbital perturbations as function of gravity anomalies 9-24716
- sea-floor spreading, gravitational mechanism 9-49421
- specific heat, liquids, effect on meas. and position of phase interface near critical point 9-36859
- torsion balances on moving bases, theory 9-33703
- vertical gradient, determination while in motion, use of two damped gravimeters 9-24612
- waves, internal, in fluid with spatially varying mean flows, ray tracing 9-42478
- waves, multiple, due to shallow water interaction with submerged bars 9-45470
- waves in an upper half-space, modelling by an induced current 9-35768
- waves in ocean, seismic generation 9-35803
- waves in plane horizontal flow of two immiscible liqs. 9-46594
- waves in thermosphere, 10^{-3} to 10^{-2} Hz, calc. 9-41585
- CO₂, internal energy meas. near critical point, gravity effect 9-36916

Green's function methods

- alloys, dil. mag., eqns. for orbital degeneracy effects 9-24269
- alloys, dil. magnetic, dynamic susceptibility calcs. 9-35525
- Bethe-Salpeter formalism, scattering Green's function, synthesis of multiple poles 9-46074
- Bose superfluid, and relns. between kinetical coeffs. 9-22155
- crystal, anharmonic, for the determ. of stability conditions 9-42940
- differential conductivity and current fluctuations, hot electrons 9-47028
- disordered systems, applic. to amorphous solid vibrational props. 9-33219
- elastostatics, displacements and stress singularities determ. 9-38283
- electron gas, nonequib., rel. to correlation functions of occupation numbers and current density 9-25058
- electronic absorption and emission bands moments calc. 9-24411
- ferromagnet, uniaxial anisotropic, magnetization and elem. excitations spectrum 9-24308
- Heisenberg ferromagnet, rel. to spin-wave self-energy calcs. 9-45103
- Heisenberg spin system, two-dimensional, phase transition prediction 9-24295
- Heisenberg two-spin model exact soln. 9-29148
- in many-body problems, linearizing double-time functions by moment-conserving decoupling procedure 9-31784
- metal with localized impurity rel. to s-d exchange model mag. field effects 9-47220
- metals, conduction electron distrib. function and non-local conductivity 9-37426
- metals, local mag. moments rel. to correlation effect on occurrence 9-45042
- monomolecular crystals, biexciton spectrum in form of energy bands 9-26486
- one-particle, for completely disordered system 9-44857
- perovskites, antiferromag. rel. to localized magnon and magnon-exciton interactions 9-45198
- plasma, Compton scatt. by electrons, thermodynamic Green function technique, cross section calc. 9-32599
- superpotentials, rapidly convergent, rel. to reformulation 9-44858
- relativity, general, appl. of generalized Greens theorem 9-22086
- scattering, coinciding simple poles 9-32141
- semiconductors, superconducting energy-gap eqn. derivation 9-26521
- semimetals, superconducting energy-gap eqn. derivation 9-26521
- solids, Stark eff., new approach 9-24092
- superconducting upper critical field, function derivation rel. to symmetry considerations 9-24138
- zero-frequency anomalies, and relation with correlation functions 9-42987
- Hg, electron-phonon interaction rel. to conduction electron props. 9-47032
- KBr, F-centre, electronic absorption and emission bands moments calc., temp. depend. 9-24411
- Pb, electron-phonon interaction rel. to conduction electron props. 9-47032
- RbMnF₃ antiferromag. rel. to localized magnon and magnon-exciton interactions 9-45198
- ⁸⁷Sr, 2⁺ and 3⁺ states, behaviour 9-36590

Grey atmosphere see *Radiative transfer; Stars/radiation***Grinding** see *Forming processes***Group theory**

- (SU(6)) \times (SU(6)) to one-particle state, spin algebra extension 9-43959
- applications to physics, book 9-45739
- in atomic physics, review 9-46266
- broken-symmetry sum rules for PP \rightarrow PV type react., deriv. from superconvergent dispersion relations 9-27495
- compact inhomogeneous groups and algebras, classification and complete reducibility 9-22056
- conformal group, finite-component field representations 9-34011
- contraction procedure generalization 9-38202
- de Sitter group rel. to Foldy-Wouthuysen transforms. 9-41736
- duality diagrams classification in three-triplet model of hadron scatt. 9-43992
- E(2) \otimes D subgroup, unitary irreducible representations of SL(2,C) 9-29551
- electron in crystal, in presence of uniform mag. field 9-48983
- in electronic energy band calc. and classification in solids 9-48989
- electronic-vibronic interaction, investig. using symmetry theory 9-30005
- energy operators reduction by use of symmetry in molecular vibrations theory 9-23014
- Euclidean invariant states, strongly transitive 9-43721
- F₄ and its generators 9-43720
- finite groups, representations, Lie-like approach to theory 9-41738
- G₂-Lie group, properties 9-27452
- Galilei group, possible non-singular metric 9-31753
- GL(2) representation theory, involutorial matrices 9-45734
- IO(n) algebra, class of representations 9-22059
- IU(n) algebra, class of representations 9-22059
- Lagrangian gauge problem of classical mechanics, single, free particle 9-22175
- in lattice vibrations analysis 9-35269
- Lie algebra, finite-dimens., Poincare partially integrable local representations and mass-spectrum 9-27160
- lie algebra, semisimple, Clebsch-Gordon series, multiplicity, reduction to soln. of linear eqn. syst. 9-22058

Group theory continued

- Lie algebras, semi-simple, dynamical symmetries as function groups, s=2r realizations 9-25423
- Lie and symmetric spaces, book 9-34010
- Lie classical compact groups, inner and restriction multiplicity 9-22055
- Lie group and phenomenological Lagrangians 9-27428
- Lie groups, compact, global theory, Book 9-31745
- Lie groups expansion and representations of S(3,C) 9-43718
- Lie groups of equations of motion 9-22053
- Lie groups of linear equations 9-22054
- local structure of Klein-Gordon, Dirac and Schrodinger eqns. 9-25029
- lorentz, restricted, geometrical symmetry in unstable model, spectrum applic. 9-25424
- Lorentz and other groups, comparative study 9-47728
- Lorentz group, homogeneous, intrinsic spinor tech. applic. 9-25040
- Lorentz group, Majorana representations, in infinite-component field theory 9-22507
- Lorentz group over finite field, Dirac spinors related props. 9-22062
- molecular symmetry models for undergraduate chemistry course 9-48447
- molecular vibrations, spectral analysis and structure, group theory applic., book 9-42368
- non-invariance groups of dynamical systems, construction 9-41739
- nonunitary symmetry groups, Eckart-Wigner theorem, matrix elements and connections 9-22061
- nuclear shell model, M-scheme approach 9-22703
- O(2,1), reduction w.r.t. noncompact O(1,1) basis, master analytic representations method 9-22060
- O(2,1) semisimple Lie group, appl. of Kirillov construction 9-43717
- O(3,1), dynamical model, dispersion sum rules for baryon spectrum 9-36499
- O(3,1) partial-wave analysis of off-forward nucleon-nucleon scatt., qualitative aspects 9-22621
- O(3,1) representations in bispinor space and geometrized Clifford algebras 9-43719
- O(3,1) symmetry; $\pi^+\pi^0$ associated production reaction 9-32189
- O(3,1) symmetry formalism in high-energy behaviour analysis of KN charge exchange react. 9-22585
- O(3) \otimes SU(2) \otimes SU(3) symmetry, baryon mass spectrum in strong-coupling model 9-38553
- O(4,1) de Sitter group irreducible rep. Hilbert space, Dirac Coulomb problem bound state soln. 9-38444
- O(4) symmetry, broken, consequences for Regge trajectories 9-46082
- O(4) symmetry, Regge trajectories of Bethe-Salpeter eqn., weak-coupling limit 9-32150
- O(5) irreducible representations, polynomial bases 9-45736
- O(n,1) algebra, class of representations 9-22059
- O-simple semigroups, theory, book 9-31749
- orthogonal group, polynomial bases for the irreducible representations 9-38200
- Poincare, harmonic analysis, unitary rep. matrix element calc. 9-27161
- Poincare, superselection rules and diagonalization 9-31746
- Poincare and Galilei groups, projective extensions rel. to 5-dim. space 9-31753
- Poincare group, nonunitary irreducible representation 9-22500
- Poincare group, reducible representations, reduction to standard helicity representations 9-22057
- Poincare group, representation in E(2) basis 9-43722
- Poincare group, unitary representations in a class of representations of the conformal group 9-38199
- Poincare group, zero-mass representation and conformal invariance 9-41737
- Poincare group constructed as semiproduct of full Lorentz group and translation group 9-25407
- Poincare invariance and manifestly covariant equations 9-45738
- point groups, key to classification 9-45737
- polarization process, reversed upper central series 9-36116
- of quantum mechanical system, non-maximally degenerate 9-43746
- r₄ Lie group applied to 2s²2pⁿ and 3s²3pⁿ3dⁿ atomic configurations 9-27801
- ray representations, algebraic theory 9-34012
- relativistic scattering 9-42030
- representation on a continuous basis, example 9-38201
- seniority and quasispin, relation, generalization to arbitrary groups 9-44118
- short book introducing the subject to physicists 9-31750
- simplectic groups, contractions 9-40233
- SL(2, C)/SU(2) harmonic functions, partial wave analysis of scattering amplitudes 9-36120
- SL(2,C), unitary representations in basis of subgroup E(2) \otimes D 9-29551
- SL(2C), Majorana representations, in infinite-component field theory 9-22507
- SL(3,C) representations, and expansion of Lie groups 9-43718
- SO_{6,1} elementary particles external and internal motion unification, SU(3) multiplet mass splitting, no symmetry breaking 9-29527
- SO(5,2) representation, boson mass spectrum and pion form factor obs., generaliz. to SO(m,2) 9-27473
- SO(p,q) group representations derived by means of canonical realization of SO(p,q) Lie algebra 9-29172
- in solid state 9-46694
- Sp₄, algebra, irreducible representations construction by para-boson operator 9-41781
- SU₆(6), broken, in meson-baryon scatt., E-meson prod. obs. 9-32167
- SU(2) \times SU(2) chiral groups and phenomenological Lagrangians 9-27428
- SU(2) \times SU(2) chiral symmetric meson-nucleon Lagrangians 9-27493
- SU(2) broken symmetry of isospin, sum rules for π -N coupling const. 9-36475
- SU(2) harmonic functions, scalar product 9-27162
- SU(3) \times SU(3), chiral, meson-meson scatt. length determ. 9-25441
- SU(3) \times SU(3) algebra, current divergences 9-42021
- SU(3) \times SU(3) chiral, symmetry, nonlinear realizations 9-27472
- SU(3) \times SU(3) chiral charge algebra, kaons mixing angle with $J^P=1^+$ determ. 9-36465
- SU(3) \times SU(3) chiral groups and phenomenological Lagrangians 9-27428
- SU(3) \times SU(3) field-algebra Lagrangians, Violation of Weinberg's second sum rule 9-27430
- SU(3) \times SU(3) invariant Lagrangian constructs., non-linear realisations 9-36437
- SU(3) \times SU(3) of invariant strong interactions, effective Lagrangian 9-36442
- SU(3) \times R₃, polynomial bases and Wigner coefficients 9-29682

Group theory continued

- SU(3), Fermion operator realization 9-27451
 SU(3), of 3-dimens. classical harmonic oscillator, Hilbert space generators 9-31770
 SU(3), Wigner D-functions 9-29173
 SU(3) calcs., introduction 9-25425
 SU(3) canonical metric for classification of meson low energy processes 9-32162
 SU(3) finite transformation props. on 3-dimens. complex space 9-36115
 SU(3) in mixed-shell space (Op, Od, Is) 9-38638
 SU(3) multiplets and baryon wave eqns. from $G=SO(6,1) \times U(1)$ global dynamic unification group, mass formula 9-46070
 SU(3) representation on 6-dimens. sphere, 3-body problem coordinates and observables 9-29685
 SU(3) structure of ν -e parity states mass spectrum, decay sum rules studied 9-46113
 SU(3) \otimes SU(3), e.m. mass spectrum of vector mesons, quark model 9-44040
 SU(3) symmetry, octet breaking in $3/2$ -baryon decays, sum rules 9-29623
 SU(3) symmetry, sensitivity of total X-section relations to small deviations 9-27484
 SU(3) symmetry breaking for scalar mesons 9-32164
 SU(3) symmetry breaking in semileptonic decays 9-22548
 SU(3)/Z(3), description and rel. to subgroup of R(8) 9-22052
 SU(3) \otimes SU(3) symm. breaking theorem 9-22572
 SU(4) scheme, matrix element equality in μ capture 9-29788
 SU(6), relativistic, and non-linear Lagrangians 9-42016
 SU(6) Clebsch-Gordan coefficients for product $35 \otimes 70$ 9-47729
 SU(6)-symmetry and decays of 2^+ meson 9-36486
 SU(1, 1) hadrons scatt. amplitude for 4 equal mass particles, anal. 9-25431
 topology concepts, applic. to physics 9-31747
 U(3,1), non-compact, representation; nuclear collision scatt. amplitude analysis 9-29777
 U(3) \times U(3) chiral symmetry, invariant Lagrangian construction 9-34013
 U(3) \otimes (3), chiral lagrangian breaking 9-46071
 U(3) symmetry model, octet-broken, for vector-mes. decays 9-27536
 U(n,1) algebra, class of representations 9-22059
 G_n complete linear group, admittance calc. during transition to G_{n-1} subgroup, Young's method 9-40232
 SU(3), V-symmetry props. 9-38478

Gruneisen coefficient see *Specific heat; Thermal expansion*

Gudden-Pohl effect see *Electroluminescence*

Guiner-Preston zones see *Crystal structures/microstructure*

Gunn devices see *Gunn effect; Microwave techniques and devices; Semiconductor devices*

Gunn effect

- bibliography supplement 9-35454
 diode, vibrs. and low-freq. oscillations, mag. field influence 9-39654
 domain dynamics, intervalley scattering model 9-30893
 domain dynamics in two-dimensional form, theory 9-49127
 n-GaAs bulk element, current instabilities, dielectric surface loading effect 9-28540
 oscillations, coherence 9-33291
 semiconductor, Gunn-instability, two-valley model, soft plasma modes, critical fluctuations and optical props. 9-30895
 voltage modulation across travelling domain, patent 9-44993
 FaAs, optical modulation device 9-33352
 Ga_{0.5}In_{0.5}Sb alloys, rel. to conduction band struct. 9-41199
 GaAs, interaction of Gunn domains with ⁷¹Ga nuclei 9-35391
 GaAs, ionized impurity scatt. influence on Gunn-effect charact. 9-39637
 GaAs, photoexcited current oscillations by two bulk negative resistance effects 9-28489
 GaAs, threshold field and electron distrib. func. Boltzmann eqn. calc. 9-33304
 GaAs Gunn diode small-signal cond. freq. independence, obs. 9-49129
 n-InSb, higher conduction band minima and assoc. impurity levels obs. 9-41202

Gyromagnetic effect

- magnetomechanical ratio g' rel. to g factor, Kittel-Van Vleck relation 9-41293
 non-insulated paramagnetic subst., g -factor determ. by rapid modulation method 9-43271
 transient, in mag. thin film Bloch walls 9-26640

Gyromagnetic ratio

- conduction-electron g shift, derivation 9-41423
 deformed odd-odd nuclei, rotational levels 9-48266
 2,2-diphenyl-1-picryl-hydrazyl free radical, diluted, ground-state g factor, mag. field depend. 9-43276
 ethylene sulfide, mol. g values meas. 9-40612
 Fe(III) complexes, g -factors and shifts 9-28225
 ferrihaemoglobin azide, low-spin, anisotropy 9-35600
 ferromagnet, effective g factor of magnons and rel. to excitation energy 9-45106
 g factor of two-dimens. interacting electron gas 9-24103
 g factor rel. to magnetomech. ratio g' for paramag. centres, Kittel-van Vleck relation validity for negative factors 9-41293
 graphite, withrhombohedral phase, g -factor anisotropy determ. 9-24484
 graphite and pyrocarbons, g -factor anisotropy, rel. to diamag. anisotropy 9-47228
 group II-VI compounds, relation between D and anisotropic g tensor 9-47429
 magnons in ferro- and antiferromagnetism, g factor renormalization 9-28603
 O₂ (¹P_{1/2}) precision calcs. 9-36656
 pyrocarbons and graphite, g -factor anisotropy, rel. to diamag. anisotropy 9-47228
 ruby:Cr³⁺, e.p.r. g -factor and fine structure lines up to 7 kbar 9-33655
 shifts in s-d exchange theory of zero-bias tunneling anomalies 9-37642
 p Larmor freq. gravity shift meas. 9-38567
¹²⁵Te, nuclear g -factor of 322 keV intruder state 9-44153
¹⁷¹Hf in Fe, hyperfine field obs. and g factors of 321 keV level 9-35606
²⁰⁸Pb, 3- octopole vibr. state, g factor obs. 9-34408
²⁰⁸Pb collective 3- state, g -factor calc. 9-42233
¹⁴⁹Pm, 114 keV state 9-46209
 B, g (¹P_{1/2 3/2}) factors, calc. 9-36658
 BaWO₄:Er³⁺, g -factor from e.p.r. meas. 9-41424
 C black, e.s.r. g -shift, eff. of heat treatment 9-24485
 CdS_{1-x}Se_x, g -factor of conduction band electrons 9-47040

Gyromagnetic ratio continued

- CeMg(NO₃)₃, ground-state g factor, mag. field depend. 9-43276
 Co³⁺ in Co(III) complexes 9-45398
 Cu, A=63.63, ⁴F_{3/2} and ⁴P_{3/2} levels h.f.s. and g values meas., atomic-beam mag.-resonance method 9-32410
 Cu complex, bis(ethylenediamine) copper(II) nitrate, single crystal ESR spectrum, g value calc. 9-28744
 Cu(NH₃)₄(SCN)₂, principle g factors calc. from e.s.r. 9-33625
 D₂O, molecular g value determ. 9-34618
 F, Zeeman eff. in ²P_{1/2} level, (1,0)→(1,-1) transition, g factor calc. 9-32411
 Ge, anisotropy of g -factor of free hole and conduction-band spin-orbit splitting 9-26484
 H₂O, molecular g value determ. 9-34618
 HgSe, g -factor from de Haas-van Alphen effect 9-47062
⁴¹K, g -factor of $7/2^-$ state at 1.29 MeV, spin precession method 9-36586
⁸³Kr, g -s. and 1st excited state mag. mom., g -determ., Mossbauer eff. 9-27667
 N, g (³S_{3/2}), calc. to i ppm 9-36657
¹⁵NH₃, from molecular Zeeman effect 9-42408
 NS, electronic g value from e.s.r. spectrum 9-46369
 Ni-V alloys, g -value rel. to temp. from ferromag. resonance 9-24477
 RbI, II, excited levels spectral determ. 9-29944
 Si:Li-diffused, for Li-O complex, e.s.r. obs. 9-26794
 SrMoO₄:Er³⁺, g -factor from e.p.r. meas. 9-41424
 ZnO:Fe³⁺, g tensor anisotropy 9-26795

Gyroscopes

- precession, effect of Earth's quadrupole moment 9-37992
 precession in a Schwarzschild field 9-27168
 rotation axis readout, Fresnel-drag ring-laser method 9-45992

Hadrons

- algebra of observables and tribes of Regge poles 9-29558
 arbitrary spin, conformal invariance of wavefunctions 9-32140
 Cabibbo angle determ., comment on divergence cancellation 9-36436
 chiral dynamics, Lagrangian construction without A₁ by Weinberg non-linear realization method 9-38475
 chiral symmetry and nonlinear Lagrangians 9-42014
 chiral transformations for fields, chiral invariant Lagrangian, current equal-time commutator and conservation law 9-34257
 composite relativistic models, form factors asymptotic behaviour 9-38473
 conference, hadron spectroscopy 9-42012
 conformal invariance of wavefunctions for arbitrary spin particles 9-32140
 CP-violation invariance in weak e.m. and miniweak parity conserving interactions 9-43985
 current algebra with a mass addition 9-40409
 current divergences in the SU₃ \times SU₃ algebra 9-42021
 $\Delta S \neq 0$, violation in semileptonic weak interactions, avoidance 9-34260
 dualities, types which exist, in quark model 9-46067
 duality, graphical form 9-22546
 dynamics of symmetry 9-36434
 e.m. mass difference and SU(3) bootstrap model 9-48163
 e.m. mass differences, equal-time commutators, and oscillating spectral functions 9-42022
 e.m. mass differences, equal-time commutators and oscillating spectral functions 9-29553
 e.m. mass differences and sum rules in Lagrangian model 9-29554
 form factors, isovector, electromag., calc. by dispersion theoretic methods 9-38479
 Gamow-Teller resonances, variational treatment 9-48161
 gemel families in Bethe-Salpeter eqn., π decoupling theory 9-36435
 geometrical model of free quantum particle, mass, spin and parity spectra prediction 9-34258
 Guggenheimer mass formula confirmed 9-43982
 isobaric analogue resonances, variational treatment 9-48161
 K-parity for systems with SU(3) and charge-conjugation symmetry 9-42013
 Lagrangian invariant under U₃ \times U₃, method of construction 9-43979
 Lagrangian models, generalized chiral symmetry groups 9-42015
 Lie algebras, semi-simple, dynamical symmetries as function groups, $s=2r$ realizations 9-25423
 matrices, internal symm. crossing, props. 9-22550
 multichannel unitary and crossing equations in static limit 9-22556
 multiplets, self-conjugate, classification for local and nonlocal symmetries 9-29552
 multipole theory, mass formula in SU(6) theory 9-32138
 N-point function, Veneziano model construction 9-42020
 non-linear Lagrangians and relativistic SU(6) 9-42016
 O(4, 2), O(6) representation, wave eqn. algebras 9-27474
 pair production rates, statistical thermodynamics model 9-42026
 production by e^-e^+ annihilation, cross section 9-48159
 production higher ang. momentum case, Khuri-Trieman-type eqns. 9-27475
 resonances, overlapping, in 3-particle final state, cross section 9-38474
 resonances, spin, information from decay angles 9-44039
 SO(5, 2) representation, boson mass spectrum and pion form factor obs., generaliz. to SO(m, 2) 9-27473
 SO(ν), SU(ν) and SU(ν) \otimes SU(ν) representation functions and their reduction 9-38480
 SU(3) \times SU(3) chiral, symmetry, nonlinear realizations 9-27472
 SU(3) \times SU(3) invariant Lagrangian constructs., non-linear realisations 9-36437
 SU(3) calcs., introduction 9-25425
 SU(3) currents, possibility of universal interaction coupling to 2γ 9-22545
 SU(3) multiplet mass splitting, no symmetry breaking, SO_{6,1} external and internal motion unification 9-29527
 SU(3) multiplets and baryon wave eqns. from $G=SO(6,1) \times U(1)$ global dynamic unification group, mass formula 9-46070
 substructure search 9-22544
 sum rules, asymptotic, breakdown in perturbation theory 9-29549
 sum rules and covariance 9-42023
 sum rules on basis of asymptotic SU₃ symmetry breaking and strong superconvergence 9-42018
 taejectories, baryon and Minami symmetry 9-32208
 third spectroscopy impression of present situation in particle physics 9-22513
 U(3) \otimes U(3), chiral, symm. breaking 9-46071

Hadrons continued

- unstable particle spectrum using model satisfying geometrical symmetry 9-25424
- urbaryon model for hadrons, applied to vector meson decay into two pseudoscalar mesons 9-46109
- vacuum polarization eff. and field-current identity 9-40408
- width, calc. as function of mass 9-25428

current

- axial-vector current, anomalies 9-48138
- Cabbibo model, 1st and 2nd class strangeness changing, CP violating current 9-25450
- Cabbibo theory, one-angle theory and new measurements of baryon leptonic decay 9-40410
- current-current theory rel. to phenomenological, mass-splitting parameters 9-48162
- e.m. current and partial conservation of tensor current 9-48204
- e.m. current possibility of unitary singlet component 9-46068
- equal-time behaviour of current commutators in perturbation theory 9-42019
- field theory, realization, and solvable model 9-32136
- iso-vector, applic. to Lagrangian ρ and photon propagators 9-22547
- leading weak divergences in self-masses, renormalization 9-46072
- matrix elements 9-32142
- non-conserved, interaction with zero-mass ghost poles of nonet field 9-43981
- non-Lagrangian models 9-38486
- PCVC and SU(3) breaking 9-48160
- S-matrix theory of current, integral representations of third and fourth order current elements obtained 9-34261
- scalar and vector currents identified in residue functions associated with Regge trajectories 9-22553
- spectral density sum rules, current algebra and zero-mass extrapolation 9-38547
- spectral function sum rules in quantum field-theory model 9-38481
- SU(2) \times SU(2) chiral current, construction of canonical field theory 9-46041
- Sugawara's theory and nonstrong interactions 9-38489
- sum rules, high energy contribs., evaluation method 9-32139
- symmetry of interactions 9-22551
- vector and axial vector currents, time-ordered, high-momentum props., matrix elements obs. 9-25426
- Veneziano-type model for $A_1 \rho \pi$ system 9-38550
- weak magnetic form factor determ. 9-38587

decay

- assuming first-class Hadronic weak current 9-38587
- current algebra review for weak, metastable case 9-42024
- form factors in broken $SU_6 \times O_3$ 9-42025
- nonleptonic, leading divergences, expression in terms of σ commutator products 9-38488
- semileptonic, SU(3) symmetry breaking 9-22548
- three-body proc., higher ang. momentum case, Khuri-Treiman-type eqns. 9-27475
- weak, review 9-36438
- weak decays of metastable hadrons, review of current algebra results 9-42024

interactions

- Bethe-Salpeter eqn., formulas for the expansion coefficients of the eigenvalues and residues 9-32141
- Bethe-Salpeter eqn., soln. with square-well potential 9-38449
- Bethe-Salpeter equation in unequal mass Wick-Cutkosky model, moving system, solns. 9-43940
- bootstrap eqn. and cabbibo angle 9-38487
- chiral dynamics, new formulation 9-27478
- collisions, many-body, high-energy, final state classifications, new phase space plot 9-42027
- d'Espagnat theory of nonleptonic weak interactions, contrary nuclear evidence 9-32143
- decays, nonleptonic, leading divergences, expression in terms of σ commutator products 9-38488
- dual resonance models factorization in, general treatment 9-48164
- and e.m. interactions 9-25427
- e.m. mass differences calc. 9-46073
- e.m. weak, CP-violation invariance 9-43985
- equipment potential approach, Bethe-Salpeter and invarity eqn. 9-38485
- Glauber multiple-scatt. series for nucleus, cross sections determ., high energy 9-38482
- Glauber theory, applic. to photoprod. reaction 9-38483
- high energy, with nuclei, and Glauber corrections 9-27477
- high-energy collisions, semi-statistical model 9-36440
- intermediate and high energy, brief review 9-36441
- Lagrangian, phenomenological, determ. by nonlinear realization of chiral group 9-34263
- leading weak divergences in self-masses, renormalization 9-46072
- Lee model, nonrelativistic, approx. soln. in all sectors 9-32144
- Lorentz-pole modified anal. of amplitude, single pole, j_0 diff. cross section contrib. 9-34262
- Lorentz-pole modified anal. of amplitude, single pole, j_0 diff. cross section contrib. 9-27476
- meson exchange, 2.dimens. Bethe-Salpeter eqn., computer soln., ladder approx. P_{π^0} 9-34276
- momentum transfers amplitude depend., product emission in Orear angle region 9-38484
- multiparticle, high-energy, longitudinal phase plots 9-36439
- nonstrong, general, perturbations about Sugawara's theory of currents 9-38489
- parity conserving miniweak, CP-violation invariance 9-43985
- resonance in high energy physics, review 9-36443
- single-meson-exchange forbidden reactions, forward peaks obs. 9-43984
- strong, impression of present situation in particle physics 9-22513
- strong, invariant w.r.t. broadened calibrating $Su(3) \times SU(3)$, effective lagrangian 9-36442
- strong, model going beyond SU(3) 9-22552
- strong, survey of baryon and boson resonances 9-22554
- sum rules, low energy, for $t \neq 0$ 9-27479
- symmetry of interactions 9-22551
- three-hadron collision, double peripheral model, phenomenological calc. 9-22549
- two body reactions at high energy model corrections to one-particle exchange model 9-43983

Hadrons continued**interactions continued**

- two-body, with part. of arbitrary spin, restrictions on spin-density matrices due to internal symmetry 9-22555
- vector dominance model anomaly found in π^+ prod. by polarized photons 9-29581
- Veneziano model, generalized, incorporation of isospin 9-29555
- weak, maximal CP violation model 9-42028
- weak, problems of theory 9-42029
- weak and e.m., SU(3) breaking 9-27480
- scattering**
- amplitude, SU(1,1) group anal. for 4 particles of equal mass 9-25431
- amplitude calc. and exchange diagrams unitarization, algebraic method 9-25430
- amplitude unitary transformation, invariant expansion on cone 9-34264
- amplitudes, Eikonal and Mandelstam representations, relationship 9-32145
- amplitudes, high-energy behaviour, investig. using branch pts. in complex ang. momentum plane 9-27490
- amplitudes, infinite class of solns., implications for bootstraps based on sum rules 9-32160
- amplitudes, low-energy limit, theorem deriv. and applic. 9-27481
- amplitudes, off-mass-shell extension, determ. using S-matrix theory 9-32149
- analyticity, factorization and Lorentz symmetry for amplitude near $t=0$ 9-42041
- Argand loops, not a means of locating resonances 9-29560
- backward, superconvergent sum rules 9-46075
- balazs method, appl. to p -bootstrap problem in the 2π system 9-32161
- Bardakci-Regge amplitude five-point function, single-particle prod., Regge exchange model 9-27486
- baryon-Regge trajectories at $W=0$, derivatives in πN scatt. 9-48194
- baryonic isomultiplets, Regge sequences 9-40437
- Bethe-Salpeter eqn., calc. of phase shifts, least squares method 9-34265
- Bethe-Salpeter eqn. for ρ scatt., O(4) expansion 9-38520
- Bethe-Salpeter formalism synthesis of multiple poles out of simple coinciding poles 9-46074
- bootstrap, ρ , and generalized potential in N/D framework 9-38491
- bootstrap, superconvergent; exchange degeneracy and fixed singularities in complex j -plane 9-25439
- bootstrap models, principle of complementarity, small hadronic parameters 9-34274
- branch points in angular momentum plane, information from phase of certain scatt. amplitudes 9-43995
- broken symmetries, closed expression for energy levels 9-32157
- charge-exchange react., high-energy polarizations, theory 9-27491
- composite particles with Regge mass spectrum 9-46083
- conspiracy, unequal-mass for arbitrary spin 9-48173
- continuous moment sum rules reformulation 9-36451
- crossing-symmetric amplitudes with Regge behaviour, alternative construct. 9-29562
- Dalitz plot, avoidance of 'double counting' and asymmetry 9-46080
- degeneracy exchange and Regg dips. 9-34271
- differential scatt. cross section sum rules, sakaton rearrangement, unchanged spin state 9-42040
- diffraction scatt., large angle, amplitude calc. 9-43989
- diffraction scatt., large-momentum-transfer, polarization and production determ. 9-42032
- duality, strong, unambiguous definition for unitary amplitudes 9-43987
- duality, unitarity and Pomeranchuk singularity 9-42053
- duality and secondary trajectories 9-48170
- dynamical method satisfying unitarity and using Veneziano model 9-34266
- eikonal expansion, relativistic, rel. to elastic scatt. 9-41983
- elastic, crossing equations and kinematic constraints 9-32146
- elastic, interpretation using self-consistent multiple-quark-scatt. analysis 9-27482
- exchange degeneracy, test by processes related by $s \leftrightarrow u$ crossing 9-48174
- exchange degeneracy from FESR and Y^* resonances 9-43999
- exchange models, high-energy, direct-channel amplitudes, description by fermion Regge poles 9-36449
- extremal f/f' mixing 9-34272
- Faddeev eqns. with sum of separable and nonseparable potentials 9-27483
- Faddeev relativistic eqns., anomalous singularities, simple approx. 9-32147
- fireball model, particle ang. distrib. at high energy 9-36444
- gemel symmetry and superconvergence relations, for O(4) amplitudes 9-43988
- half-off-shell matrix elements, differential eqns. 9-22557
- helicity amplitudes investigated within formalism of covariant spin operators 9-34275
- high energy, correlation between polarizations and the complex zeros of elastic amplitudes 9-44000
- high energy, phenomenological representation using k -matrix and OPE mechanism 9-43990
- high-energy, Regge-pole exchanges, applic. of absorption correct 9-29563
- high-energy, statistical model 9-42039
- high-energy behaviour of amplitudes, investig. using branch pts. in complex ang. momentum plane 9-27490
- inelastic, Regge cuts, absorption model and diffractive effects 9-48171
- infinite-resonance model, high-energy forward elastic amplitudes saturation 9-36445
- interference models, generalised, validity proof 9-40414
- isospin crossing matrix props. 9-38490
- kinematic reflections in multiple-production processes, amplitude Regge asymptotic terms 9-38499
- kinematical constraints at $t=0$ for regularized helicity amplitudes 9-42050
- lepton-hadron, lepton-pair amp., minimal current algebra applic. 9-27449
- Levinson's relation extension and extinct bound states 9-25429
- Lorentz-pole modified anal. of amplitude, single pole, j_0 diff. cross section contrib. 9-27476
- Lorentz-pole modified anal. of amplitude, single pole, j_0 diff. cross section contrib. 9-34262
- Mandelstam denominators in complex s -plane, zero points, for relativistic two-body processes 9-36447
- Mandelstam representation for logarithmically singular potentials, proof 9-38426

Hadrons continued**scattering continued**

- Mandelstam representation positive spectral functions, amplitude restrictions 9-42033
- Mandelstam representation, asymptotic behaviour 9-46076
- multi-particle amplitude as a function of group theoretical variables, multi-Regge model 9-43996
- multi-Regge baryon exchange and central interactions 9-34324
- multi-Reggeon behaviour of production complitudes 9-42038
- multiperipheral dynamics at zero momentum transfer, Lorentz symmetry 9-38498
- multiperipheral Regge model 9-42046
- multiple, structure and high energy phenomena, from phenomenological formula 9-42031
- O(4,2) model of strong interactions, for Regge trajectories and high energy phenomenology 9-42044
- P¹ Regge trajectory, ansatz for residue 9-22566
- partial-wave amplitude, correct asymptotic λ behaviour 9-42034
- phase contours, including reaction amplitudes having Regge behaviour at high energies 9-48176
- polarizations, high-energy, theory using Regge poles with SU(3) and exchange degeneracy 9-27491
- poles, fixed, in many-channel, 2-body scatt. amplitudes 9-32151
- poles in impact parameter plane 9-43986
- Pomeranchuk exchange in multiperipheral model, distrib. in the Toller azimuthal angle 9-40415
- Pomeranchuk pole, bootstrap multi-Regge eqn. vacuum pole soln. nonexistence 9-36456
- Pomeranchuk pole props., rel. to branch pts., small momentum transfer 9-27488
- Pomeranchuk singularity, genesis investigated in a model where enhancement can be observed as a phase-space effect 9-46078
- Pomeranchuk term, model 9-25437
- Pomeranchuk trajectory slope, determ. from phenomenological 'multi-Veneziano' model 9-46079
- production amplitudes signature, 2-Reggeon exchange model 9-36455
- pseudoscalar-baryon, high-energy polarizations, theory 9-27491
- quark model, large angle, high energies 9-22559
- quasipotential relativistic model, amplitude for small, large momentum transfer, high energy 9-29556
- Regge amp. partial waves, 'top positions' of loops 9-40411
- Regge behaviour, Veneziano-type model for $\pi\pi$ scatt. 9-38532
- Regge cuts, absorption model and diffractive effects in elastic scatt. 9-48171
- Regge cuts, duality and exotic resonances 9-22564
- Regge cuts, effects on high energy forward elastic-scatt. amplitudes 9-29557
- Regge cuts, finite-energy sum rules based on multiple scatt. model 9-43998
- regge cuts coupled, signature determ. 9-38493
- Regge daughter sequences, M=0, constraints due to broken O(4) symmetry 9-38494
- Regge daughter trajectories, general form in broken symm. problems 9-32157
- Regge families and Lorentz symmetry 9-42045
- Regge finite energy sum rules, infinite set of daughter trajectories required for saturation 9-36454
- Regge model, crossing symm., in complex t plane, fixed s , behaviour 9-32159
- Regge model, double, for multiparticle prod. processes, cross sections calc. 9-22563
- Regge pole, model for $\pi^+\pi^-$ charge exchange scatt. 1-2.5 GeV/c 9-27529
- Regge pole amplitudes, unitary corrections as introduced by Baker-Blankenbecker formalism 9-32152
- Regge pole exchanges, resonance interpretation of Argand diagram loops 9-32153
- Regge pole generalized interference model for πN scatt. 9-29589
- Regge pole model, $\rho+B$, for $\pi N \rightarrow \omega N$ 9-32188
- Regge pole model for large angle 9-32155
- Regge pole model for strange vector and tensor meson exchange processes 9-32207
- Regge pole s -channel partial-wave projections Argand diagram loops, resonance identification 9-38497
- Regge pole theory, systematic review of recent developments 9-48168
- regge pole theory, systematic review of recent developments 9-48167
- Regge pole theory and impact factor representation, differentiation 9-44057
- Regge pole theory rel. to spin-dependence of high energy scatt. 9-27458
- Regge poles, curvature of fermion trajectories, background integral, bootstraps 9-22569
- Regge poles, fermion, domination of process, high energy asymptotics 9-34273
- Regge poles, Freedman-Wang cancellation and daughter trajectory 9-32156
- Regge poles, higher symmetries, and amplitudes, introduction 9-43993
- Regge poles, review 9-22568
- Regge poles in Coulomb field 9-27489
- Regge poles in πN and KN charge exchange scatt. at high energy 9-44027
- Regge recurrences, narrow-width, trajectory rise 9-27487
- Regge representation for forward scatt. of unequal-mass particles, helicity amplitude determ. 9-42048
- Regge singularities, self-consistent 9-29559
- Regge singularities, t -channel, self-consistent with s -channel unitarity eqn. 9-25436
- Regge theory, backward unequal-mass scattering processes, branch cut contributions 9-48172
- Regge trajectories, constraints imposed by broken O(4) symmetry 9-46082
- regge trajectories, exchange degeneracy, conditions requiring flat total X-sections and absence of exotic reson. 9-36453
- Regge trajectories, group theoretical approach to conspiracy for arbitrary masses 9-48169
- Regge trajectories, infinitely rising, crossing-symmetric model and asymptotic behaviour 9-29564
- Regge trajectories, linearly rising, rep. of dynamical O(3,1)-SL(2C) group 9-36457
- Regge trajectories, non linear increases if consistent finite energy sum rules 9-22565

Hadrons continued**scattering continued**

- Regge trajectories, rising indefinitely, performing dynamical calc. 9-36452
- Regge trajectories $\alpha(t)$, left hand cuts 9-42052
- Regge trajectories and SO(4) symmetry 9-25438
- Regge trajectories, Barger and Clines rule rel. to bound states of Dirac particle 9-48157
- Regge trajectories in s and t channels, Veneziano modification to CLA model 9-43994
- Regge trajectories of Bethe-Salpeter eqn., weak-coupling limit, O(4) symmetry 9-32150
- Regge trajectories rise and fall in potential scatt. 9-40413
- Regge trajectory, polynomially bounded, crossing symmetric amplitude 9-34268
- Regge trajectory, self-consistent, in multiperipheral model, Pomeranchuk trajectory slope determ. 9-38496
- Regge trajectory mixing, form of vertex πR scatt. 9-38520
- Regge trajectory residue functions as basis for treatment of strong interactions 9-22553
- Regge-behaved, crossing-symmetric amplitude 9-40412
- Regge-cut model for π^0 photoproduction 9-46097
- Regge-pole exchanges, applic. of absorptive correct 9-29563
- Regge-pole families and Toller poles: $t \neq 0$ 9-42049
- Regge-pole families and Toller poles, equivalence 9-32154
- Regge-pole families contrib. to helicity amplitudes; daughters, conspiracies and Lorentz symmetry 9-38495
- Regge-pole inelasticity, partial waves, and model for S -matrix 9-46107
- Regge-pole parameter dispersion sum rules applic. 9-22562
- Regge-pole theory, links with current algebra 9-22561
- Regge-pole theory review of recent developments 9-22560
- Reggeization of kinematically free amplitudes 9-27519
- Reggeized Σ_{α} , Σ_{β} exchange model for $\pi^+\pi^-K^0\Lambda$ 9-29585
- relativistic, group theoretical description near zero momentum transfer 9-42030
- resonances, interfering, spin-density matrix and momentum anal. 9-36448
- rising Regge trajectories and crossing-symmetric asymptotic behaviour 9-25435
- ρ Regge parameters and modified finite-energy sum rules 9-34270
- sakaton rearrangement, dual props. between s -, t - and u -channel amplitudes of 2-body processes 9-46069
- spectral functions, ν -double, inconsistency with unitarity, diffraction peaks 9-36450
- strong-interaction, duality diagrams for s - and t -channel descriptions and nonexotic reson. assumption 9-25432
- SU(3) bootstrap model rel. to e.m. mass differences 9-48163
- sum rules, finite energy and nonlinearly rising Regge trajectories 9-22565
- superconvergent sumrules construction and testing for linear combination of products of amplitudes 9-42037
- three particle, asymptotic form of the wave function 9-32148
- three-body, lower bounds on phase shifts, method using Fadeev eqns. 9-27485
- three-particle unitarity eqns. in static S -matrix theory, class of exact solns. 9-25434
- three-triplet model, duality diagrams Regg and Pomeranchon exchanges 9-43992
- toller poles M value rel. to validity of O(3,1) expansion of two-body scatt. 9-48165
- total cross-section relations, sensitivity to small deviations from SU(3) symmetry and vector mes. universality 9-27484
- transverse-momentum Gaussian cross sections, asymptotic exponentials, distrib. 9-42035
- two-body, relativistic, Mandelstam denominators in complex s -plane, zero points 9-36447
- two-body scatt. amplitude, multiparticle terms, phenomenological model 9-22558
- two-Reggeon-one-particle vertex is independent of associated Toller angle ω if the trajectory of one is zero 9-34267
- unitarity and non-Regge singularities 9-42042
- unitarity structure of amplitudes 9-42043
- Venezian model, parameter constraint by N/D method 9-38492
- Veneziano's amplitude and current algebra 9-44034
- Veneziano amplitude, interference models and Argand loops 9-42051
- Veneziano amplitude, Lorentz expansion to infinite sequence of Toller poles 9-22567
- Veneziano amplitude, S^0 behaviour and Lorentz poles 9-43997
- Veneziano form 9-42047
- Veneziano formula averaging procedure, unitarity enforcement methods 9-36446
- Veneziano formulae, positivity conditions 9-43991
- Veneziano model, algebraic realization of chiral symmetry 9-42036
- Veneziano model, continued partial-wave projection and complex- t -plane singularities 9-46081
- Veneziano model, duality 9-34269
- Veneziano model, generalized, incorporation of isospin 9-29555
- Veneziano model, nonunitary without strong duality 9-43987
- Veneziano model, unitarized, appl. to expt. data 9-36477
- Veneziano model analysis of $pp \rightarrow \pi^+\pi^-\pi^0$ 9-46119
- Veneziano model applied to $\pi\pi$ scatt. 9-29588
- Veneziano model for 8-point function 9-46077
- Veneziano model for large angle pp scatt. 9-44055
- Veneziano model parity constraints, 2 particles with spin 9-25433
- Veneziano-like parametrizations for photoproduction, Compton scatt., and current algebra 9-48175
- Veneziano-type model for $A_1 \pi\pi$ system 9-38550
- Veneziano-type model for $\pi\omega$ scatt. 9-46101
- Wick-Cutkosky model, Regge families 9-48166
- Δ Regge trajectory residue at $\alpha = 1/2$, possible zero at wrong-signature sense-point 9-38594
- π -hadron, π scatt. length expression derivation 9-38523

Haemoglobins see Proteins**Halium**

- film on various substrates, elec. props. 9-37452
- photoelectric cross-sections of gamma-rays 30-100keV 9-24231

Hafnium compounds

- hafnia with rare-earth oxides additions, effects and phase relationship of solid soln. formed 9-30723
- oxide (carbide, chloride) mixture with Zr oxide (carbide, chloride), X-ray fluorescence analysis 9-41461

Hafnium compounds continued

¹⁸¹Ta quadrupole interaction studies using time differential ang. correl. 9-33497
Hf-Cr binary system, phase equilib. diag. 9-33149
Hf-Si binary system, phase equilib. diag. 9-33258
Hf-V binary system, phase equilib. diag. 9-33149
Hf complex, Hf (IV) benzoyl-phenyl-hydroxylamine, (n,p) recoil, effect on γ -ang. correl. 9-33597
Hf complex, Hf(IV) acetyl-acetonate, polycrystalline, after-effect in (n,p) reaction 9-35598
HfB₂, densification in high-pressure pressing, mechanisms 9-35223
HfB₂, hot-pressed, bending strength, fracture mode and thermal stress resistance 9-35183
HfC-IaC solid soln., thermal expansion 9-26430
HfC, elec. conductivity, thermoelec. power, Hall coeff., rel. to C content 9-47114
HfCO₂, elastic constants, 4.2-300°K 9-42866
HfO₂-Sc₂O₃ system, phase diagram and equilibria, solubility 9-39476
HfO₂, crystallization under hydrothermal conditions 9-37044
HfO₂, lattice energies, heat of atomization, bond energy and dissociation energies, rel. to fund props. 9-30494
HfO₂, monoclinic, e.p.r. of Fe³⁺ 9-33627
HfO₂, phase diagram determination 9-23991
HfSiO₄:Cr³⁺, e.s.r. ground-state splitting 9-33626
HfSiO₄:Gd³⁺, e.s.r. ground-state splitting 9-33626
HFx²⁻ anions (X=Cl or Br), electronic absorption spectra 9-30060
Nb-Ti-Zr-Hf alloy system, constitution and supercond. props. 9-39597

Half-lives see Radioactivity/decay periods

Hall effect

see also Semiconducting materials; Semiconductors
n-CdCr₂Se₄:In, normal coeff., and Seebeck coeff. and elec resistivity 9-45018
coaxial Hall accelerator, analysis 9-22684
ferroelectric, temp. depend. of Hall mobility, electron scatt. obs. 9-37591
ferromagnet, transport theory 9-47255
ferromagnetic single cryst., anisotropy, spin-orbit interaction influence 9-37653
fluids, Rayleigh-Taylor instability with Hall currents 9-34710
graphite:B, neutron irradi., function of B conc., rel. to defect clustering 9-30597
graphite, coeff., and magnetoresistance, 1.5° to 300°K 9-41153
Hall generators, null voltage compensation methods 9-39648
in hopping transport, non-adiabatic small polarons and impurity conduction 9-30898
ionic cryst., photo-Hall mobility, strong phonon interactions obs. 9-39701
magnetic materials with large para-process, anomalous coeff. 9-49185
metal, temp. depend., carrier density and mobility obs. 9-39580
in MHD channel flow heat transfer 9-25831
and MHD eqns. evolution 9-38950
MHD generator, two-dimens. analysis 9-45912
m.o.s. structure, Hall mobility of inversion layer carriers 9-37567
multiplying property, applic. to generator with $\alpha_n x^2$ function 9-43832
noble metals, max. at low temp., rel. to phonon drag 9-43026
paramagnetic metals, anomalous eff. through ferroparamagnetism transition 9-28593
plasma, acceleration in polytron machine 9-28011
in plasma, time varying, rel. to freq. 9-42498
and polaron, small-motion, adiabatic approx. 9-43009
polarons, Hall and drift mobility, temp. depend., large coupling constants 9-35321
resistivity maximum during Guinier-Preston zone form. 9-37431
rutile, mobility temp. dependence, 300-1250°K 9-24181
semiconductor, bounded, Lorentz-field amplification, computer solutions 9-37502
semiconductor, four-probe meas. methods, and elec. conductivity 9-44950
semiconductor, liq., coeff., and conductivity, temp. depend. 9-40800
semiconductors, coeff. determ. method, 80-375°K 9-24171
in semiconductors, impurity 9-49072
in semiconductors, meas. using an extension of Goldsmid's bridge 9-44979
semiconductors, NBS report 9-33280
semiconductors, photo-Hall e.m.f., polarity inversions 9-33290
semiconductors, strongly compensated, Hall coeff., anomalous temp. depend. 9-33285
solutions, d.c. transport coeffs. 9-23519
superconductors, type II, Hall angle calc. 9-49043
thin films, vacuum-evaporated on flexible substrates, props. 9-35388
turbulent MHD 9-23260
voltage induced in plasma by mag. field, nonlinearity 9-36762
Ag-Cd β -phase alloys, order-disorder transf. 9-35253
Ag-Zn β -phase alloys, order-disorder transf. 9-35253
Ag₂Te, solid and liq. 9-37519
Ag dilute alloys, coeff., 1.5° to 50°K and room temp. 9-37442
Ag dilute alloys, coeff., room temp. to 1.5°K 9-44911
AgSb_{0.8}Fe_{0.2}:Te, coeff. determ. 9-24171
Al, coeff. accurate determ. from helicon waves and surface mode loss 9-24124
Al, cryst. orientation depend. 9-35334
Al, field reversal, rel. to band relax. times and temp. depends. 9-37438
Al, high field coeff., l.f. helicon resonance obs. 9-30839
AuAl₂, high-field mas. rel. to nearly-free-electron model of Fermi surface 9-47073
AuGa₂, high-field meas. rel. to nearly-free-electron model of Fermi surface 9-47073
AuIn₂, high-field meas. rel. to nearly-free-electron model of Fermi surface 9-47073
Bi-Pb, band structure determ. 9-30843
Bi:Sn, coeff. meas., Sn distrib. coeff. and acceptor valency determ. 9-43002
Bi_{1-x}Sb_x, rel. to energy gap and Fermi level position 9-30842
Bi thin films, 4.2-300°K, const. variations 9-39582
Bi thin films, thickness dependence, 4.2-300°K 9-33251
C, coeff., and magnetoresistance, 1.5° to 300°K 9-41153
C, soft, doped with acceptors, coeff. and magnetoresistance, 2° to 300°K 9-41154
Cd:Zn, resistivity meas. 9-41165
Cd:Zn, resistivity meas. rel. to small-angle intersheet scatt. 9-26515

Hall effect continued

Cd-Zn alloys, resistivity meas. below 77°K, scattering phenomenon 9-37440
Cd, resistivity meas. 9-41165
Cd, resistivity meas. rel. to small-angle intersheet scatt. 9-26515
n-Cd_{1-x}Mg_xTe:(Al) mixed cryst., coeff. meas. 9-43054
Cd₃As₂-NiAs eutectic 9-41196
Cd₃As₂, coeff. depend. on mag. field and temp. for effective mass of electrons 9-35313
Cd single crystal, Sondheimer oscillations in coeff. 9-37441
CdF₂:Y, semicond., coeff. meas. 9-49077
CdS, coeff. and mobility, elec. and mag. field depend. 9-33297
CdS single crystal, mobility at high electric field, temperature dependence 9-28582
p-CdSb, coeff. temp. depend. in strong elec. field 9-24174
CdSe evaporated films 9-33299
p-CdSiAs₂, mobility obs. 9-44957
n-CdTe:In (Al, Cd), heat treated, photo-Hall effect obs. of multiply charged acceptors 9-49075
Cr film, consts., and elec. conductivity 9-30848
Cu-Al dilute alloy, impurity contribution to temp. depend., 77-300°K 9-28466
Cu-Ge dilute alloy, impurity contribution to temp. depend., 77-300°K 9-28466
Cu-In dilute alloy, impurity contribution to temp. depend., 77-300°K 9-28466
Cu-Sn dilute alloy, impurity contribution to temp. depend., 77-300°K 9-28466
 α -Cu-Zn alloy, and phonon drag effects, 4.2° to 300°K 9-43026
Cu-Zn β -phase alloys, order-disorder transf. 9-35253
Cu, coeff. rel. to cry. orientation, Fermi surface characts. 9-26516
Cu, temp. depend. rel. to phonon and dislocation contribution 9-28467
Cu₃SbSe₄, temp. depend., electron-hole mobility ratio 9-26505
Cu dilute alloys, coeff., 1.5° to 50°K and room temp. 9-37442
Cu dilute alloys, coeff., room temp. to 1.5°K 9-44911
Cu single crystals with point defects, and magnetoresistivity 9-37443
Dy-Y alloy, magnetic field and temp. depend. in ferromag., helicoidal antiferromag. and paramag. states 9-33258
Dy-Y alloys in the paramag. temp. interval 9-37644
Dy, magnetic field and temp. depend. in ferromag., helicoidal antiferromag. and paramag. states 9-33258
EuO:Gd, coefficient and mobility dopant effect 9-33463
Fe, Fermi surface and de Haas-van-Alphen eff. model 9-24093
Fe₉₀Pt₁₀C amorphous ferromag. alloy 9-39578
Fe single crystal film, rel. to thickness 9-47267
n-GaAs, meas. 9-33301
n-GaAs, slightly doped, at low temp. 9-33303
GaAs_{1-x}P_x solid solutions, coeff., temp. depend. 9-33554
n-GaAs epitaxial layers, high-purity, max. electron Hall mobilities 9-30907
GaP:Zn, coeff. variation with dopant conc. 9-44954
GaP:Zn(O), indication of p-type conduction, photoluminescence 9-33604
GaSb:Te, coeff. rel. to temp., for conduction band structure 9-37530
GaSb, coefficient of crystals grown by floating zone technique 9-28229
n-GaAs, deep level conc., 3000-700°K 9-30916
Ge:Sb, obs. of semicond.-to-metal transition rel. to impurity conc. 9-49095
n-Ge:Sb distortion by Nernst-Ettingshausen and Righi-Leduc effects 9-37537
n-Ge, carrier conc. depend. in low mag. fields 9-24180
n-Ge, coeff. anisotropy in strong non-quantizing mag. fields 9-39643
Ge, const. temp. depend. magnetoconc. effect due to carriers redistrib. at impurity centres 9-39645
n-Ge, dislocation high-density saturation effects 9-43072
p-Ge, heavily doped, meas. rel. to forbidden band width, 600° to 800°K 9-28514
p-Ge, impurity centres, and generation-recombination noise 9-28513
n-p-Ge non-ohmic conduction under strong mag. field, Hall angle anomalous elec. field depend. 9-35420
n-Ge obs. 4.2° to 7.9°K 9-28512
Ge thin films, influence of surface states on temp. depend. 9-33326
HfC, coeff. obs. rel. to C content 9-47114
Hg_{1-x}Cd_xTe alloys, 1 eV band gap, photo-Hall effect 9-41267
HgTe, at 300° and 77°K, rel. to crystn. temp. 9-44960
n-HgTe, temp. depend. 9-35497
In, coeff. accurate determ. from helicon waves and surface mode loss 9-24124
In, coeffs. meas. for high field 9-47195
In, field reversal, rel. to band relax. times and temp. depends. 9-37438
In, thermal effect, temp. depend. 9-35341
In alloys, relaxation time anisotropy, effect of scattering 9-37445
InAs-ZnSe solid solns., and elec. props. 9-44962
p-InP:Zn(Cd), mobility, 20-700°K 9-39623
p-InP, doped into n-type, temp. depend. 9-28500
n-InSb, anomalies rel. to absence of inversion centre 9-26550
InSb, heat treated, deep acceptor level obs. 9-39638
n-InSb, hot electron temp. w.r.t. elec. field meas. 9-33308
InSb, radial Hall voltage in electron-hole plasma 9-37416
InSb_{1-x}Bi_x solid solns. 9-43058
InSb polycryst. layers, Hall-voltage meas., surface obs. 9-33325
InSb thin film transducers, props. in strong mag. field at liq. He temps. 9-24195
InSb thin films, transport props. obs. 9-33309
InSe, coefficient meas., temp. depend. of charge carrier mobility 9-35404
K, coeff. accurate determ. from helicon waves and surface mode loss 9-24124
Mg single crystals, room temp. 9-26518
Na, coeff. accurate determ. from helicon waves and surface mode loss 9-24124
NbO₂, 800°C region, phase transition obs. 9-33143
Ni, hydrostatic press. effects, 77 and 290°K, \leq 7kbar 9-30852
 β -NiAl, coeff. proportionality to conductivity 9-37449
Pb_{1-x}Sn_xTe, hole conc. dependence rel. to band structure determ. 9-39632
p-PbSe, coeff. meas., depend. on carrier density and temp., indication of two valence bands 9-35409
PbTe polycryst. layers, Hall-voltage meas., surface obs. 9-33325
Pd-Ag alloys, coeff., effect of anisotropic impurity scattering 9-37451
Pd film, consts., and elec. conductivity 9-30848
Pt film, consts., and elec. conductivity 9-30848

Hall effect continued

- Sb, const. determ., 300-750K 9-47076
 Se trigonal single cryst., d.c. meas. 9-44968
 Si:B(P), irradi. at 80°K, meas. rel. to carrier removal rates 9-44852
 n-Si:Li, coeff., electron-irrad. induced carrier-removal defects obs. 9-49113
 Si:Li, pulled-crucible and float-zone samples, thermal ionization energies 9-47131
 Si:Na, coeff. temp. depend., ionization energy of impurity obs. 9-43077
 Si:P, obs. of semicond.-to-metal transition rel. to impurity conc. 9-49095
 Si:(Sb) film, epitaxial, on spinel substrate, and resistivity meas. 9-36950
 p-Si-on-sapphire films, oxidation effect 9-35405
 n-Si, Al implanted, temp. dependence of R_{H} 9-35426
 Si, degenerate, coeff. meas. rel. to radiation damage on low temp e-irrad. 9-28277
 n-Si epitaxial films on sapphire, vacuum evaporated, mobilities 9-49111
 Si on sapphire film, Hall mobility rel. to thickness and doping density 9-37545
 Sn, rolling and recrystallization texture study by rotation diagrams 9-32929
 SnAs_3 , const. meas., conduction obs. 9-37474
 SnP_3 , const. meas., conduction obs. 9-37474
 Tb-Y alloy, magnetic field and temp. depend. in ferromag., helicoidal antiferromag. and paramag. states 9-33258
 Tb-Y alloys in the paramag. temp. interval 9-37644
 Tb, magnetic field and temp. depend. in ferromag., helicoidal antiferromag. and paramag. states 9-33258
 Tb single crystal, anomalous and ordinary 9-45090
 ThC-UC solid solutions, 3.8 and 15 metal % U 9-26510
 TiC, coeff. obs. rel. to C content 9-47114
 TiCl₃, photoconductive, band struct. and polaron transport props. obs. 9-41272
 TiInS₂(Se₂,Te₂) single cryst. 9-44969
 V₂O₅ and related oxides, const., and thermopower, rel. to nature of metallic state, up to 800°K 9-30836
 V₂O₅, meas., and elec. conduction model 9-33247
 VO_x, composition dependence rel. to semicond. phase 9-28272
 W film, const., and elec. conductivity 9-30848
 Y, magnetic field and temp. depend. in ferromag., helicoidal antiferromag. and paramag. states 9-33258
 η Zn-Cu, alloys, coeff. at -196-100°C 9-47071
 Zn, coeff. at -196-100°C 9-47071
 Zn₂Hg_{1-x}Te solid solutions, 77°-400°K, 250-10000 Gs 9-30913
 ZnSb:Te, increase due to effect of doping 9-42757
 p-ZnSnSb₂, obs., coeff. meas., electro-physical props. 9-35410
 ZrC, coeff. obs. rel. to C content 9-47114

Hall generators see *Electricity/direct conversion; Semiconducting devices*

Hall mobility see *Semiconducting materials; Semiconductors*

Halogens

- in arc, effect on cathode spot damage 9-30322
 atoms, radiative electron capture dis., photodetachment calcs. 9-27817
 compounds, effect on molecular spectra of air 9-34629
 halides, force constants, mean-square quantities and bond energies, universal parameter 9-38840
 hydrides, reduced potential curves 9-38835
 interhalogen exchange reactions, molec. beam kinetics 9-49367
 ions, hydrated, in aqueous soln., nuclear magnetic shielding 9-32797
 scattering by atoms, molec., of thermal energy alkali atoms cross section curve crossing eff. 9-29969
 HY+X \rightarrow HX+Y (X, Y=F, Cl, Br, I), product energy distrib. from i.r. chemiluminescence methods 9-41444
 H+X \rightarrow HX+X (X=F, Cl, Br, I), product energy distrib. from i.r. chemiluminescence, methods 9-41444

Hamidashi effect see *Ferroelectric materials; Ferroelectric phenomena*

Hard-sphere gases see *Quantum fluids; Statistical mechanics*

Hardness

- see also *Abrasion; Work hardening*
 b.c.c. metals, solution hardening, comments 9-46912
 b.c.c. metals, solution hardening, comments 9-46911
 hardening of mats. by a second phase, recovery creep model 9-28354
 hexafluoropropene-tetrafluoroethylene copolymer, γ -irradiation eff. 9-33069
 hexafluoropropene-vinylidene fluoride copolymer, γ -irradiation effects 9-33069
 iron-base precipitation hardening alloy, rel. to microstructure 9-39468
 metals, b.c.c., f.c.c. and h.c.p., strain-hardening effects 9-37239
 metals, true stress/true strain curve deriv. 9-23865
 nichrome, hardening processes in strengthening mechanism 9-23909
 nimonin single crystals, strain-hardening rel. to structural state of quenched alloy 9-33100
 point defect hardening, effect of lattice friction 9-41033
 precipitation-hardening of mats. by a second phase, recovery creep model 9-28354
 rock-salt type cryst., latent hardening w.r.t. prestrain, role of dislocations interac. 9-35191
 Rockwell, of brittle materials, meas. 9-42905
 silica glass, Vickers diamond pyramid meas., low-temp., indentation and densification obs. 9-28375
 solid-solution hardening due to size effect 9-46927
 steel, 0.095%V, changes during heat treatment 9-33138
 steel, on ageing rel. to weldability 9-30713
 steel, austenitic, effect of previous deform. 9-33059
 steel, austenitic stainless and EN25, strain hardening and softening prod. by plastic deform. cycling 9-23867
 steel, Cr-Ni-Mo high C low alloy, rel. to fatigue strength, obs. 9-26345
 steel, high-pressure effects 9-23967
 steel, mean C and low-alloyed, hardening and softening during fatigue fracture 9-30689
 steel, nitrided, nature of hardness 9-23927
 steel, surface-hardened, effective case depth, error probability 9-39442
 Zircaloy, in-pile hardening and softening behaviour during neutron irradi. 9-28356
 Ag-Cu alloys, H₂S corrosion resistance enhanced by pressure deformation 9-30659
 AgCl, latent hardening w.r.t. prestrain, role of dislocations interac. 9-35191
 Al-Mg-Zn alloy, ageing kinetics obs. 9-37280
 Al-(11 wt.%)Mg age-hardening alloy, deform. by hydrostatic extrusions effect 9-41051

Hardness continued

- Al-(0.5 at.%)Mg alloy, quenches, hardening mechanism at 86°K 9-30699
 Al-Zn-Mg alloys, preprecip. obs. 9-23979
 Al-Zn alloys, effect of spinodal decomp. 9-37289
 Al-Zr alloys, quenched, microhardness meas. effect of superheating melt 9-39450
 Al, strain hardening and softening prod. by plastic deform. cycling 9-23867
 α -Al₂O₃, increase due to neutrons, decrease after annealing 9-23810
 AlN, infl. of high static and dynamic pressures 9-26361
 Be-(1.3 wt.%)Ni alloy, changes due to low-temp. and mixed ageing 9-39464
 Bi₁₂GeO₂₀, microhardness, and growth and props. 9-42751
 Bi₄(GeO₄)₃, microhardness, and growth and props. 9-42751
 Cu-Al, latent hardening rel. to composition and prestrain 9-41015
 Cu-Zn, Ge, Ga solid soln. hardening 9-39472
 Cu, cyclic hardening, strain bursts and coarse slip 9-28357
 Cu, fatigue-hardening at elevated temp., dislocation distrib. 9-30608
 Cu, shock wave hardened, softening and recrystallization during heating 9-33098
 Cu, u.s. hardening at 90°K, influence of pre-annealing at room temp. 9-28374
 Cu strain hardening and softening prod. by plastic deform. cycling 9-23867
 Fe-Al system intermetallics micro hardness 9-46890
 Fe-(30 at.%)Ni-(5 at.%)Nb austenitic alloys, structure and hardening, comments 9-46934
 Fe-(30 at.%)Ni-(5 at.%)Nb austenitic alloys, structure and hardening, comments 9-46933
 Fe-Ni-Mn-Ti martensitic alloys, ageing 9-37283
 Fe, cast, globular, hardening and softening during fatigue fracture 9-30689
 Fe μ -spheres at 0.5 to 10km/sec on Pb, Cd, Ag, Cu and Al, crater investigation 9-30700
 Fe single crystals hardness anisotropy 9-35192
 Fe-Ni alloys, eff. of Co content on ageing induced changes 9-23942
 Fe- \leq (0.04 wt.%)C quench aged alloy, hardening and softening obs. under cyclic straining 9-33079
 K₄Nb₆O₁₇ 9-26238
 K₂NF₃ single crystal perovskite structure, hydrothermally synthesized 9-42746
 LiF, latent hardening w.r.t. prestrain, role of dislocations interac. 9-35191
 Mg-Sn alloys, solution hardening, room temp. 9-23984
 Mg-Zn-Mn alloy, age hardening, patent 9-48942
 Mg-Zn-Zr alloy, strain-rate hardening, grain-size depend. 9-39443
 MgO, water-induced toughening 9-42906
 MgO single crystal, electron and neutron irradi., hardening 9-33099
 Nb, solid solution hardening by Ta, V and W, theory and expt. 9-28385
 Nb single cryst., neutron-irrad. hardening, eff. on temp. depend. of yielding 9-26371
 Ni, low-temp. hardening, rel. to creep at high temp. 9-46913
 Ni, shock hardening in pressure range 820 to 1500 kbar, rel. to microstructure 9-30701
 Ni, shock wave hardened, softening and recrystallization during heating 9-33098
 Ni₃ (TiAl) alloy, w.r.t. hardened by coherent and ordered precip., yielding 9-39408
 Ni base alloy, dispersion-hardening, grain size effect on strain hardening 9-33015
 Ni strain-hardened by impulse loading, recovery behaviour 9-28348
 Pd and alloys, dispersion hardening, patent 9-26391
 Pt and alloys, dispersion hardening, patent 9-26391
 Rh and alloys, dispersion hardening, patent 9-26391
 Rh single crystal grown by electron-beam zone melting, microhardness 9-48807
 steel, carburized Cr-Mo, C content effect 9-41073
 Ta, effect of electron beam melting 9-33101
 TeO₂-V₂O₅-BaO glass, microhardness 9-39847
 Th₃P₄ 9-35035
 ThP₃ 9-35035
 Zn bicrystals, grain-boundary slide-hardening 9-42889
 Zr-(1.2wt%) Cr-(0.1wt%) Fe alloy, quench hardening behaviour, cooling rate dependence 9-41034

Hardness, magnetic see *Magnetic properties of substances/ferromagnetic*

Harmonic analysis see *Acoustic analysis; Calculating apparatus; Fourier analysis*

Harmonic generation, optical see *Lasers; Optics*

Harmonic oscillators see *Quantum theory*

Hartree-Fock method see *Atoms/structure; Solid/structure*

Heating

- see also *Ear; Speech*
 amplitude discrimination in noise, effect of duration 9-31705
 audiometers, international standard reference zero 9-31702
 auditory system models, mathematical and electrical 9-31698
 Bekesy thresholds meas. by continuous and pulsed tones, comparison 9-40209
 binaural loudness summation, pressure level independ. of interaural correlation coeff. 9-24957
 cochlear microphonic, stability over time, anaesthetised cats obs. 9-38150
 cochlear of Guinea pig, props. of summing pot. 9-38149
 cochlear responses to binaural stimuli and function of efferents 9-24962
 consonance of static complex tones and its calc. method 9-40206
 consonance sensation of various two component dyad tones 9-40205
 detectability, effects of temporal and lateral uncertainty 9-40207
 detection-recognition task, simultaneous, recognition performance as function of detect. criterion 9-31699
 dichotic tone and noise signal fusion, microstructure and effect of imposed envelope 9-40210
 directional tests using dummy head 9-38141
 engine sounds, identification, training techniques 9-31696
 fatigue, auditory, during articulation, obs. 9-24955
 f.m. and the difference limen for freq. 9-40203
 f.m. sinusoids, pitch determ. 9-40208
 frequency selectivity during amplitude discrimination of signals in noise 9-40204
 frequency transitions at different rates, discrimination 9-38145
 gas and jitter discrimination tests 9-31709
 harmonic, second, aurally generated, strength estimation 9-40202

Hearing continued

human, evolution 9-31703
identification of diesel engine sounds 9-24960
intensity discrimination at 2000 Hz, effect of contralateral noise 9-38147
jitter detection thresholds, masking noise and pulse level effects 9-29117
lateralization and detect. of tonal signal in white noise 9-38144
limen, difference, for freq., tracking system 9-40203
loudness, dichotic summation obs. 9-29120
loudness, spectral distrib. and temporal structure depend. 9-38140
loudness function, monaural, for 1000 Hz tone 9-29119
loudness functions, monaural, under masking 9-38148
loudness level, calc., improvements to Niesse method 9-29116
Mach bands, an analogy of edge effects in masking 9-31704
masking, edge effects analogous to Mach bands in vision 9-31704
masking, perceptual, in multiple sound backgrounds 9-27127
masking, sine and cosine, ear's filter investigation 9-31697
masking, temporal, and perception of order 9-40201
masking level differences with and without interaural disparities in masker intensity, obs. 9-31700
music, rock-and-roll, damage risk, sound and spectrum obs. 9-24958
musical combination tones and oscills. of ear mechanism 9-43708
musical perception and a mechanical model of the inner ear 9-40199
neurons of cochlear nucleus (cat), alterations of afferent, tone-evoked activity 9-24961
noise acceptability, criteria levels, two surveys aboard ship 9-22267
noise from roller bearings, subjective response, establishment of objective criteria 9-29298
noise thresholds for l.f. octave bands of noise 9-43691
noisiness, judged, of moderated and multiple tones in broad-band noise 9-27128
peristimulatory loudness adaption meas. 9-31701
pitch, subjective, of pure tones, sound level, masking noise and duration tune effects 9-40200
pitch of f.m. sinusoids 9-40208
pitch perception in white-noise mask 9-29118
ratings, multiple, of sixteen sound stimuli, psychoacoustic appls. 9-31706
receiver operating characts. and psychometric functions, simple and pedestal detect. conditions 9-38143
residue pitch, nonlinear distortion hypothesis, incompatibility with obs. 9-38146
residue pitch change, noise masking 9-38146
signal enhancing technique for auditory detect. in noise 9-29122
sinusoids detection, signal duration effect on performance 9-24959
stereophony, head orientated, efficiency 9-41820
suprathreshold adaption, peristimulatory, obs. in 38 normal adults, 250 to 6000 Hz 9-31707
temporal integration and periodicity pitch, obs. and explanation 9-27126
threshold meas., low pass and high pass filtered noise, pure-tone masking effects 9-29121
thresholds during stroboscopic visual stimulation 9-38142
tone masking before, during and after brief silent periods in noise 9-31708

Heat

see also *Radiation/heat; Thermodynamics*
age of heat distribution estimates, backward solution of heat equation 9-41843
definitions, review 9-45721
flow concept, basic thermodynamic factors 9-45875
in polyethylene terephthalate, generation during plastic deformation, model 9-33034
rotating thermal field 9-25118
transformation in relativistic thermodynamics 9-22270

Heat capacity see *Specific heat*

Heat conduction

see also *Conductivity, thermal*
'thermal inertia', aptness of term 9-27243
atmosphere, upper, response to transient heating 9-41541
conduction eqn. solution, n diffusion theory techniques 9-26434
cylinder, hollow, axisymmetric problem, solution 9-38318
cylinder, non-stationary problems, approximate method for solution 9-38317
determining temperature, inc. intergeometry of heat transfer surfaces 9-27244
eigenfunction soln. 9-29154
in film type detector, time const. 9-25136
in fluids, sinusoidal heat pulse technique 9-29324
flux distribution in rod fuel elements rel. to geometrical tolerances and fissile mat. segregation 9-36232
generalized boundaries, Green's function construction using integral eqn. method 9-43802
guarded hot plate apparatus, comparison of modes of operation 9-25125
heat, in thermally radiated 1-dimens. solid, transient surface temp. soln. 9-22286
heat transfer simultaneous with radiation, 2 absorbing media, intimate contact 9-36210
in liquid crystals, linear theory 9-39077
low radioactivity rocks of W. Australia, flow meas. 9-28838
low temperature, heat pulse propagation expts. 9-26438
molecular, into medium from radiating sphere 9-36212
from moving heat source, self-burial conditions determ. 9-25124
multilayer slabs, thermal attenuation 9-25123
non-simple, note 9-27246
nonlinear boundary problem, use of Lagrangian techs. 9-25115
nonlinear problems, applic. perturbation method 9-40287
planetary atmospheres, radiative terms arising from O and CO net emission 9-26894
in radioisotope thermal source, internal, and effects 9-26437
resistance to flow, 2 thick solid bodies in contact in vacuum 9-34099
slab, non-stationary problems, approximate method for solution 9-38317
in solid, transport mechanism 9-39536
solid/liquid, bounded by 2 concentric spherical surfaces, temp. gradient 9-29325
solids, boundary layer approximations 9-41094
sphere, non-stationary problems, approximate method for solution 9-38317
steady, with mixed boundary conditions, variational principles 9-34100
steady-state, approx. soln. with convective boundary conds. 9-22287
temperature dependent characteristics of materials, determination methods theory 9-38319
temperature field in samples, 2 dimens., role in cond. coeff. determ. 9-25121

Heat conduction continued

theory for non-simple, solid, 2 non-coincident temps. 9-30792
transient, in multiregion systems with non-linear boundary conditions 9-25120
unsteady conditions in finite hollow circular cylinders 9-22285
variational methods applic. to viscous heat conducting flows 9-23228
Cu, for cooling of laser ruby rod 9-38378

Heat exchange see *Heat transfer*

Heat flow see *Convection; Heat conduction; Heat transfer*

Heat losses see *Heat transfer*

Heat measurement see *Calorimeters; Calorimetry*

Heat of adsorption

patchwise heterogeneous surface, calc. from condensation approx. 9-34999
Ar on silica aerogels 9-30498
Kr, on graphitized C black, expt. compared with condensation theory 9-34999
N₂ on silica aerogels 9-30498

Heat of combustion

No entries

Heat of crystallization see *Crystallization*

Heat of dissociation

AuB, mass spectrometric determ. 9-24528
Te₂, calc. from emission spectra meas. 9-34644
UOS 9-28774
UOS 9-33658

Heat of formation

carboxylic acids, in vapour phase, heat of dimerization, spect. obs. 9-23107
hydrocarbons, MINDO calc. 9-30122
lanthanide compounds, interrelationship with melting point and lattice parameters 9-34956
organic cpds. containing N or O, MINDO calc. 9-27899
refractory metal oxides, rel. to lattice energies and heat of atomization 9-30494
Al carbides, determination 9-49369
AlP 9-36927
Be carbides, determination 9-49369
BiF₃, enthalpy determ. by solution calorimetry 9-30021
CHO⁺ 9-24542
CN, from study of photoionization of HCN 9-30296
CeC₂ system 9-32821
H₃O⁺, by electron impact 9-32692
H₃S⁺, by electron impact 9-32692
Hg-Pb alloys, liquid, enthalpies of mixing, anal. rel. to excess entropies 9-39091
Hg-Tl alloys, liquid, enthalpies of mixing, anal. rel. to excess entropies 9-39091
LaB₆ expt. and calc. 9-40830
NH₄⁺, by electron impact 9-32692
PuN, and thermal functions, 700 to 3040°K 9-26809
UC_{1-x}O_x, from thermochem. study 9-28783

Heat of fusion

semiconductors and semimetals, excess entropy of fusion due to configuration of bonding electrons 9-28175
Ar-N mixtures, enthalpies 9-39528
BiF₃, from heat capacity meas. 9-30021
GaSb, enthalpy 9-30449
Sb, enthalpy 9-30449

Heat of mixing see *Heat of solution*

Heat of reaction

proton solvation, expt. determ. 9-28807
Be(g)+AlCl(g) 9-48511

Heat of solution

alcohols, normal, thermodynamics 9-23484
benzene-o,o'-ditolyl (or diphenyl or diphenyl methane) mixing effects 9-48683
diphenyl methane-o,o'-ditolyl, mixing effects 9-48683
mixing heats continuous determ., isothermal enthalpy titration 9-40784
refractory metal oxides, rel. to bond energy values and dissociation energies 9-30494
Mo of N 9-40985
ThC-ThN pseudo-binary systems, excess free energies of mixing at 2820°C 9-40819
UC-UN, pseudo-binary systems, excess free energies of mixing at 2820°C 9-40819

Heat of sublimation

BeCl₂ 9-48511
C, and vaporization 9-48740
Cd, ΔH° vs ΔS° correlation and torsional and Knudsen vapour pressure techniques 9-39146
Fe, from vapour pressure meas., 1813-1973°K 9-23604
Ti, from vapour pressure meas., 1953-2193°K 9-23604
Zn, ΔH° vs ΔS° correlation and torsional and Knudsen vapour pressure techniques 9-39146

Heat of transformation

metal, liq. melts, vol. diffusion coeffs. rel. to heat of melting 9-39131
plasma erosion source, e.m. acceleration of coagulation 9-30262
CuPt alloys, energy of ordering, tin soln. calorimetry 9-48934
PbZrO₃, dielectric phase transition, impurity eff. 9-26584

Heat of vaporization

alkali metals, and critical parameters 9-40828
graphites, by laser evap., mass spectr. anal. 9-23601
refractory metal oxides, heat of atomization, rel. to fundamental props. 9-30494
Cm metal 9-48742
K/Hg amalgam at 20 compositions and up to 10 atm. pressure 9-36926
NaCl weak aqueous solns. 9-26161

Heat of wetting see *Wetting*

Heat pumps see *Heat transfer*

Heat radiation see *Radiation/heat*

Heat transfer

see also *Convection; Heat conduction; Radiation/heat; Radiative transfer*
to ablation heat shield of entry vehicles, convective and radiative, anal. 9-22304
acetone, boiling, depend. on e.m. field 9-23597
air, cooling heated porous mats, internal 9-28074

Heat transfer continued

- air, end-wall radiative transfer, shock-tube meas. 9-23395
- air, in subsonic flow through contraction section 9-28065
- air flow in collection of tubes 9-30327
- air-graphite suspension, expt. 9-30437
- air-ocean interface, heat flux and temp. variation 9-47528
- annular 2-phase flow, non-equilib., phase distrib., burnout prediction 9-34096
- annular flow system, from short heated section 9-23412
- Ar, shock heated gas meas., thermal conductivity calc., 650-5000 °K 9-26026
- atmosphere, between air and water surface 9-24643
- benzole, boiling, depend. on e.m. field 9-23597
- bibliography 9-34097
- bibliography, Japanese works 9-22283
- blunt body critical point, heat exchange in presence of radiation 9-42597
- boiling, effect of temp.-induced surface tension gradient 9-32776
- in boundary layer, shock-induced on flat plate 9-40739
- in n-butyl alcohol film condensation, meas. and Nusselt soln. 9-39141
- in capillary discharge channel with evaporating wall 9-40714
- chlorotrifluoromethane, natural convective, comparison with N₂O and CO₂ 9-28170
- in condensation from forced convection flow, effect of superheating 9-26162
- conduction and radiation, simultaneous, 2 absorbing media, intimate contact 9-36210
- convection, cylinder to fluid, empirical correl. of Prandtl, Grashof, Nusselt nos. 9-47836
- convection, forced, fluids at supercritical press., review 9-26151
- convection, natural, in supercritical region 9-26150
- convection boundary layer, transverse press. grad. effects and streamwise second derivs. 9-23481
- convection free, boundary layer flow, asymptotic soln. for large Prandtl nb. 9-30387
- convective, bibliography 9-25130
- convective, from arc column, theory 9-32714
- convective, from rot. disc, surface suction/injection effects 9-27248
- convective, from rot. disc with surface temp. step discontinuity in forced stream 9-27249
- convective, in gray and transparent media free flow, boundary layer eqn. soln. 9-29326
- convective at supercritical press. in tube, CO₂ expt. 9-26023
- convective heating of slab, Biot's variational method 9-34098
- dielectric liquids, in boiling, effect of elec. field 9-23596
- disc, rotating, isothermal, infinite in fluid, induced incompressible flow 9-25117
- droplet condensation mechanism, model 9-39139
- in drying by jets 9-25116
- dynamics of packed beds with intraphase transfer 9-22281
- Earth's surface, bulk transfer coefficient 9-47489
- in elastico-viscous fluid slow steady flow in wavy cyl. tube 9-27953
- electric arc column and discharge chamber wall of vortex linear plasma generator 9-29322
- emissivity of cavities by meas. reflection factor 9-27237
- entry-length of vertical cooled pipe 9-25810
- equation for contact thermoreceiver 9-47831
- ethanol, boiling, depend. on e.m. field 9-23597
- exchange coeff. for near-water atm. layer 9-40010
- exchanger incorporation in nuclear reactor, patent 9-29873
- exchangers with threaded pipes, efficiency 9-38315
- film, laminar, boiling in boundary layer flows 9-32816
- in film boiling from elec. conducting wire to boiling water, film thickness meas. for various press. 9-30462
- in flow, laminar, through porous channel with applied mag. field, calcs. 9-34851
- fluid, heat-generating, flowing in circular tube with flat velocity profile 9-22284
- fluid, laminar natural convection, Ellis model 9-32559
- fluid, non-Newtonian, agitated 9-44556
- fluid, supercritical, turbulent conditions 9-39050
- fluid in tube with high heat flux 9-27241
- fluid with variable conductivity in nonuniform field, Joule dissipation determ. during flow 9-39088
- fluids, at supercritical press., forced convection, review 9-26151
- flux, turbulent, meas. errors 9-44400
- flux from thermally thick wall, single thermocouple meas. 9-25114
- flux transducer, low temp. high sensitivity 9-45874
- during forced convection, from Ta sphere to Na liquid 9-26092
- in forced pipe flow, influence on melting and solidification 9-23578
- free convection, laminar, from vertical plate, simultaneous mass transfer 9-26085
- free convective, cylinder in rarefied gas 9-44524
- Freon 114, natural convection in supercritical region 9-26150
- Freon-12 boiling in region of centrifugal forces, coeffs. rel. to inertia over-loadings 9-23603
- gas, rarefied, from spheres and cylinders, kinetic theory expressions 9-30342
- gas, rarefied, in plane Couette flow, use of BGK model 9-32733
- gas, viscous, flowing in narrow canals. integral correlation method 9-32721
- gas, weakly ionized, two-temp., Joule heating effect in parallel flow 9-40730
- gas-solid suspensions at Reynolds number 130,000, convective coeff. 9-26136
- gas-vapour mixture condensation in absence of forced convection 9-28185
- glycol, non-Newtonian, in non-circular tubes, theory and expt. 9-44559
- in heterogeneous flow systems simultaneous with mass transfer 9-23225
- hot gas flow in cooled channel, subsonic, rel. to flow profile 9-23372
- hypersonic, laminar; and boundary layer transition on blunted cones 9-36800
- between immiscible liquid layers with simultaneous boiling and stirring 9-30461
- i.r. radiative equilibrium under large path length conditions 9-23392
- in jet flows, turbulent, interferometric study 9-33373
- laminar, in Couette flow between parallel plates, rel. to boundary conds. 9-28090
- laminar Couette flow near critical point, wall heat transfer 9-23374
- by laminar flow in radial mag. field between coaxial cylinders 9-32585
- in laminar flow of liquids with temp. depend. viscosity 9-26083

Heat transfer continued

- to laminar flow of pseudoplastic fluids 9-40786
- laminar fluid flow in curved pipe, series expansion soln. 9-23246
- laminar free-convection, from needle 9-22290
- laminar incompressible flow at circular tube entrance, temp. profiles 9-23419
- in laminar separated supersonic flow, integral calc. 9-40729
- laminar thermal-entry-region; with axial conduction and third kind boundary condition, exact soln. 9-22280
- in laser, pulsed active hollow rod 9-40358
- lateral, in one-dimensional gas discharge, volt-ampere charact. theory 9-39023
- leakage of insulated walls with internal convection 9-25119
- liquid, non-Newtonian, in non-circular tubes, theory and expt. 9-44559
- liquid alkali metals, atomic heat conduction 9-39111
- in liquid crystals, conduction and dissipation, linear theory 9-39077
- to liquid films, falling 9-23445
- liquid flow in annulus, and temp. distrib. 9-23480
- liquid metal cooling of ducts, thermal contact resistance, impurities effect 9-39093
- liquid turbulent flow, cooled surface, seri-oscillation temp. depend. 9-24038
- in liquid turbulent flow in tube with elec. conduction and longitud. mag. field 9-39094
- liquids with variable viscosity in turbulent flow 9-40783
- local surface heating of plates and calc. of 'critical thicknesses' 9-27236
- loop at Harwell, description 9-27242
- between metallic surfaces (dissimilar) in contact, effect of thickness 9-24035
- between metallic surfaces (similar) in contact, theor. model 9-24034
- between metallic surfaces in contact, effect of surface oxidation 9-24036
- between metallic surfaces in contact, surface roughness and waviness effect 9-24037
- in MHD channel flow, thermal entrance regions 9-25831
- mixture of liquids with widely different b.p. 9-23599
- non-conductive liquid in homogeneous electrostatic field 9-32780
- non-Newtonian, two-phase flow 9-23242
- non-Newtonian fluid about an unsteady rotating disk 9-23215
- non-polar gas mixtures 9-48661
- nonlinear boundary problem, applic. of Lagrangian techs. 9-25115
- nuclear reactors liquid coolant laminar stream, Nusselt no. determ. 9-22898
- ocean, wind generated open lead, heat exchange 9-49424
- oil layer, stationary and mobile, in homogeneous electrostatic field 9-32780
- packed beds or systems with turbulence promoters, effect of viscous forces 9-25804
- to particles, spherical, with source under countercurrent conditions 9-40285
- in particulate systems, particle size and residence time distrib. effects 9-23539
- peak heating for control surfaces, turbulent, at Mach 6 9-26006
- phenolic-nylon chars, low-density, mechanism 9-26460
- polymer solution in tube, lowering of turbulent exchange during flow 9-40785
- polystyrene foams, eff. of thickness and temp. 9-41113
- over porous flat plate, with variable suction or injection velocity 9-25998
- propane-air flame, electrically augmented in discharge zone 9-25131
- radiant, from luminous flame 9-36213
- radiation, equation, for scattering medium, numerical solution 9-22279
- radiation, nongray, nonisothermal, in optically thin region 9-22274
- radiative, regular thermal conditions in solid bodies 9-44844
- radiative in closed system of bodies separated by light transmitting medium 9-25113
- radiative in gas, effect on acoustic waves 9-48663
- reactor fuel element bundles, liquid metal cooled, temp. non-uniformities calc. 9-22888
- regenerator, effect of variability of fluid temp. 9-47834
- responsible for energy fluxes to Ar MPD arc anode 9-32610
- in rotating sphere sublimating in rarefied air 9-23607
- rotating thermal field 9-25118
- and roughness drag at Mach 3 9-23386
- shock wave formation 9-22282
- in solar hothouse foundations, quasi-stable 9-31860
- in solid, transport mechanism 9-39536
- sphere, rotating, under free convection, thermal boundary layer schlieren method study 9-29327
- insublimation dehydration, analytical study 9-28183
- superconducting magnets, cooled, stability principles 9-35384
- surface, meas. by transient technique 9-34095
- surface and self-fluidised layer, exchange mechanism 9-38316
- systems and surface meas. transient techniques, conference 9-34094
- systems design; fluid velocity distributions in randomly packed beds 9-34716
- tar solution in tube, lowering of turbulent exchange during flow 9-40785
- temperature dependent characteristics of materials, determination methods theory 9-38319
- thermal entry for low Reynolds number turbulent flow 9-34821
- to thermometer towed in water, dynamic frequency response 9-34104
- three-fluid cross flow heat exchangers, performance depend. on 2 fluids temp effectiveness 9-27955
- time dependent coeff., quenching of spherical nuclear fuel element 9-25677
- time-dependent withdrawal from slab fuel elements in nuc. reactor, model 9-22868
- transient, near stagnation-pt. in steady flow of viscous incompressible fluid 9-48535
- tubes used in meas., method of calc. thermal conductivity 9-36211
- turbulent boundary layer on plate, effect of boundary conds. 9-27240
- unsteady flow problems, applic. of variational methods 9-22278
- variable, static thermoelastic problems inversion transformation soln. 9-25085
- wall to gas, for high wall-temp., meas. 9-40748
- water, boiling, depend. on e.m. field 9-23597
- water, during dropwise condensation, estimation of coeff. 9-23594
- water, during turbulent flow at supercritical press., natural convection effect 9-26090
- water, natural circulation, supercritical press. system 9-26091
- in water flowing through rock fractures 9-43353
- water in supercritical forced flow through curvilinear channels 9-26089

Heat transfer continued

water injection into compressed air, temp-levelling rel. to droplet size 9-23435
water layer with variable coeff. of heat exchange absorbing solar radiation 9-45478
water surface with air flow, heat transfer coefficient surface instability, temp. and vel. depend 9-34837
Ar, between vertical concentric cylinders at different temps., end effects 9-40749
Bi bonding betw. ceramic nuclear fuel and cladding 9-22892
CO₂, natural convective, comparison with N₂O and chlorotrifluoromethane 9-28170
CO₂ in tube, convective, at supercritical press. 9-26023
D₂O moderator to coolant channels, study of local boiling risk 9-25673
H liq. whirling layer under high heat flux obs. 9-26052
He-Ar mixture, shock heated, meas., thermal conductivity calc., 650-5000 °K 9-26026
He, liquid, inflow compensation 9-48724
to He, superfluid and supercritical 9-36910
He, between vertical concentric cylinders at different temps., end effects 9-40749
He I, from cylindrical Cu surfaces 9-36909
He superfluid, in wide tubes 9-36911
He two-phase flow, meas. device 9-46664
to HeI, review 9-46667
in Hg boiling, with thermal load 2×10⁶ Wm⁻² 9-44557
K boiling in tubes, coeffs., mean and local 9-23487
N₂-He mixtures, from cylinders, showing slip effects 9-46568
N₂-Ne mixtures, from cylinders, showing slip effects 9-46568
N₂ nucleate pool boiling, rel. to surface roughness and material 9-28189
N₂O, natural convective, comparison with CO₂ and chlorotrifluoromethane 9-28170
in N plasma jet, convective 9-44459
in N plasma jet, convective 9-44460
Na, subcooled, from hot spheres, rel. to vaporization at surfaces 9-28116
NaK, liquid, turbulent thermal characts. meas. 9-23426
NaOH dilute solns., from thin Pt wire, variation 9-46625
Ne, between vertical concentric cylinders at different temps., end effects 9-40749
from Pt wire in dil. NaOH solns., variation 9-46625
S gas, plane layer, radiant convective exchange with solid substrate 9-40750
Xe shock heated gas meas., thermal conductivity calc., 650-5000 °K 9-26026
Zr-(1.2wt%) Cr-(0.1wt%) Fe alloy parameters in cooling rate calcs. rel. to quench hardening behaviour 9-41034

Heat treatment

alkali halide cryst. with O₂⁻ and S₂⁻ impurity centres, thermal quenching of luminesc. 9-39861
alkali halide cryst. with O₂⁻ impurity centres, thermal quenching of luminesc. 9-39863
alloys, quenched dilute, non-equilibrium segregation, of impurities, model rel. to grain boundary hardening 9-48919
alumina glazes, quenching effect on strength 9-23935
alumina powders, hot-pressing technique 9-35201
alumina whiskers/Ni composites, hot-pressed, electron microscope obs. 9-33169
anthracene single cryst., radical recomb. kinetics rel. to mol. motion from e.p.r. annealing obs. 9-32535
brass, annealed, propag. of large amplitude waves 9-42872
diamond, ion-implanted, annealing, X-ray monitoring 9-35194
diamonds, effect on colour, e.p.r., i.r. absorption, u.v. and visible spectra 9-26366
disordered solids after ion-bombardment, annealing 9-48912
element, 1 dimens., elastic plastic, ratcheting growth induced by thermal cycling 9-25086
glass powder compacts, sintering at constant rates of heating 9-33130
glassy metastable oxide phases, quenching rel. to structure 9-23612
graphite, graphitization and chem. structure, X-ray diffraction studies, samples from polynuclear aromatics 9-39257
graphite, pyrolytic, post deposition heat treatment effect on flexural strength 9-23906
magnetite, annealing, effect on remanent magnetization and coercive force 9-45570
martensite, tempering, rel. to VC precip. 9-33121
metal crystals, quenched, sweeping-up of loops by glide dislocations during deform. 9-32963
metal quenching expt techniques and results 9-42907
metallic materials, annealing effect on struct., yield and plastic flow 9-46925
metals, hot workability and plastic deform. props. 9-35174
mica, annealing effect on surface conductivity 9-47153
molybdenum permalloy tape effect on stress sensitivity and mag. squareness ratio 9-49205
m.o.s. capacitors, effect on low current d.c. gain, with various ambient atmospheres and contamination 9-28539
nylon 66 yarns, drawn, effect of annealing in silicon oil and in air 9-46707
photoannealing of chemical radiation damage, effect of crystal defects 9-23933
polybutene-1 single crystal, annealing, 70-90°C, stability 9-39458
polyethylene, effect on unit cell dimensions 9-46803
polyethylene, fold structure changes on annealing 9-46712
of polymers, heat coefficients during thermal destruction 9-41112
quenching of spherical nuclear fuel element, with time dependent heat transfer coeff. 9-25677
quenching rate meas. methods. comparison 9-26364
recrystallization, secondary, role of surface energy 9-46917
recrystallization, secondary, role of vol. energy in 'nuclei' form. 9-46918
refractories, dense porous, mech. deterioration due to thermal cycling 9-33014
silica, glass, annealing of indentations due to hardness meas., densification obs. 9-28375
silica glass, densified, annealing rel. to energy spectrum 9-46700
steel, 0.095%V, precip. reactions and hardness changes 9-33138
steel, quenched, carbide phase formation during low-temp. tempering, mechanism 9-33137
steels, effect of austenite superheating and cooling in oil 9-41042
steels, hot workability and plastic deform., props. 9-35174
thermal recrystallization effects on particle size and morphology 9-30555

Heat treatment continued

transistors, effect on low current d.c. gain, with various ambient atmospheres and contamination 9-28539
transition metal spinel manganites, eff. on inversion degree from neutron diff. and on magnetic props. 9-28253
vacancies, effect on mean jump number 9-46808
Ag, dislocation density depend. on primary recrystallization after large plastic deformation 9-40947
Ag, electron irradi., annealing, stage I recovery, elec. resistivity meas. 9-35083
Ag, work hardening between 77 and 1200°K, three stage curve 9-46926
AgCl diffusion anneal in external chlorine atm., effect on Au⁺ diffusion 9-46847
Al-(1 wt.%)Cd, alloy, quenched rel. to pre-precipitation 9-23936
Al-(0.5 at. %)Mg alloy, quenches, hardening mechanism at 86°K 9-30699
Al-(0.5wt.%)Zr, recrystallization, infl. of precipitated particles 9-44794
Al, 1100, isothermal recrystallization kinetics after deform. under u.s. vib. 9-37238
Al, correlated recovery of Stage I, energy dependence 9-28379
Al, quenched, faulted dislocation loops, annealing behaviour 9-39451
Al, quenched and aged, plastic flow mechanism, 86°K 9-48900
α-Al₂O₃, annealing after neutron irradi., hardness decrease, dislocations formation 9-23810
Al₂O₃, corundum, impurity-doped, decorated disloc. movements during annealing 9-37172
Al₂O₃, hot pressing, effect of gaseous impurities 9-35202
Al foils, cold-worked annealing processes, h.v. electron microscope obs. 9-42909
Al single cryst., disloc. configurations produced by annealing in air and vacuum, comparison 9-37171
Al single cryst., recrystn. after pt. deform. 9-42908
Al single crystal, rel. to pit formation 9-32946
Al thin films, thermal cycling, effect on surface hillocks prod. by annealing 9-30705
Au, electron irradiated, interstitial clusters below stage III annealing 9-30593
Au, quenched resistivities of vacancies and Matthiessen's rule 9-35336
Au films, Au-ion irradi., substages III annealing, activation energies 9-33106
BN, pyrolytic, effect of compression annealing on microstruct. 9-41041
Be, irradiated, release of gas 9-37282
Be, isostatically hot-pressed, influence of microyield strength depend. on grain size 9-35181
C, hard, over 2000°C, partial graphitization, study of structures present 9-28396
C, turbostratic, with B and Na doping, temp. effect on e.s.r. 9-26791
C black, e.s.r., eff. on g-shift 9-24485
C film, evaporated, graphitization, 1000° to 2200°C 9-39453
C films, annealing, activation energies 9-23937
C saccharose, (hard coke), effects 9-37277
CaO, hot pressing, effect of gaseous impurities 9-35202
n-CdTe:In (Al, Cd), photo-Hall effect obs. of multiply charged acceptors 9-49075
Cu, annealing at room temp., influence on u.s. hardening at 90°K 9-28374
Cu, annealing of spherical voids, rel. to self-diffusion coeffs. meas., 390° to 560°C 9-30624
Cu, correlated recovery of Stage I, energy dependence 9-28379
Cu, dislocation density depend. on primary recrystallization after large plastic deformation 9-40947
Cu, extinction changes in X-ray diff. lines during annealing 9-44662
Cu, homogenization quenching, dislocation structure and grain growth 9-23938
Cu, recrystallization and recovery kinetics 9-39454
Cu, shock wave hardened, rel. to softening and recrystallization 9-33098
Cu, tough-pitch and P-deoxidized, annealing eff. on distrib. of grain boundary impurities 9-30600
Cu₂O, quenched, absorpt. spectra 9-28683
Dy₂O₃ films, pulse annealing, effect on recrystallization behaviour 9-30489
Er₂O₃ films, pulse annealing, effect on recrystallization behaviour 9-30489
Er₂O₃ thin films, grain growth kinetics on pulse annealing, bulk-like growth 9-40842
Er₂O₃ thin films, grain growth kinetics on pulse annealing, bulk-like growth 9-40841
Fe-Co alloys, b.c.c., quenched, rel. to saturation magnetization 9-45142
Fe-(3 wt.%)Si alloy under annealing atmosphere, surface energy relative variation for (110) and (100) planes 9-26180
Fe, fast neutron-irrad., isochronal annealing obs. of elec. resistivity recovery 9-43027
Fe, malleable cast, microtopography of graphite grains and microdistribution of sulphur during annealing 9-23950
Fe rod, crystalline structure under surface electron beam bombardment melting and quick cooling 9-33110
Fe single crystal plates produced by strain-anneal method, effect of stretching on imperfect structures 9-32913
Fe single crystals, produced by strain-anneal method, relation between stretching amount and preferred orientation 9-35163
GaAs: Cd, annealed, luminesc. changes 9-49316
GaAs:Te, influence on photoluminescence 9-37782
GaAs:Zn(Cd), post-implantation annealing, elec. props. depend. 9-33320
GaAs, annealed, dislocations effect on Cu diffusion behaviour 9-44734
n-GaAs, annealing under excess As vapour 9-33281
GaAs, diffused junction laser, annealing effects 9-45958
Ge-Mg₂Sb₂ amorphous films, conductance meas., rel. to reordering diffusion processes 9-34985
n-Ge, annealing of defects produced by e. irradi. at 30°K 9-35081
n-Ge, effect of non-dislocation defects generated on mobility and magnetoresistance 9-37540
Ge, quench-induced thermal acceptors and associated vacancy behaviour 9-49107
Ge, quenching rel. to diffusion mechanism and point defects, review 9-37209
Ge single crystals, effects on resistivity, photoconductive decay and Li drift props. 9-37538
Ge surfaces, SiO₂-passivated, annealing effects on dominant electronic props. 9-49104
He II, thermal quenching of superfluidity in long channels, critical state condition 9-44608

Heat treatment continued

- HfB₂, consolidation mechanisms in high-pressure hot-pressing 9-35223
 Ho₂O₃ films, pulse annealing, effect on recrystallization behaviour 9-30489
 In, thin films, effect of annealing on supercond. critical field behaviour 9-47088
 InSb, Hall effect obs. of deep acceptor level 9-39638
 Ir, proton irradi., interstitial, conc. decrease during annealing 9-35085
 KBr:S₂⁻ cryst., thermal quenching of luminesc. 9-39869
 KBr, low temp. annealing of n and p induced defects 9-40967
 KCl, diffusion annealing in straightening of bent crystals 9-42884
 KCl vacuum heating at 150-500°C, prod. of etch pits 9-40855
 Li₂O-SiO₂ glass, metastable precipitate formation and effect on conductivity 9-24215
 of Li aluminosilicate glass during formation 9-36922
 LiF, effect on physical props. 9-28546
 LiF, thermoluminescence changes 9-33607
 LiF annealing of F-centres, 25° to 400°C 9-32993
 MgAl₂O₄ spinel, hot pressing behaviour 9-30706
 MgCo₃, hot pressing, behaviour 9-33111
 MgO, cavity form. by annealing 9-44693
 MgO, hot pressing, effect of gaseous impurities 9-35202
 Mg(OH)₂, hot pressing, behaviour 9-33111
 MnCO₃-ZnO-Fe₂O₃ system, calcination 950-1100°C, Mn-Zn ferrite production 9-35742
 Mo, annealing under high vacuum, use of cryogenic vacuum pumps 9-26367
 Mo foil, secondary recrystn. mechanism, electron microscopy obs. 9-46923
 Mo surface layers, work-hardened, vacuum annealing rel. to crystal struct. changes 9-32932
 NH₄OHCl, X-irrad., thermal conversion of V_K centres 9-32995
 NaBa₂ Nb₂ O₁₅ quenching effects on ferroelectric transition temp. 9-28562
 NaCl:Cu, additively coloured with Na vapour, colloidal absorpt. bands obs., thermal stability 9-32998
 NaCl, diffusion annealing in straightening of bent crystals 9-42884
 Na(SiO₃)₂ glass, 548-850°C, spectral obs. 9-28674
 Nb, quenching and annealing eff. on relax. peaks in internal friction meas. 9-30639
 Nb₃Ga-Nb₃Al system, low-temp. annealing effect on supercond. transition temp. 9-37469
 Nb₃Ge-Nb₃Al system, low-temp. annealing effect on supercond. transition temp. 9-37469
 Nb₃Sn-Nb₃Al system, low-temp. annealing effect on supercond. transition temp. 9-37469
 Nb surface layers, work-hardened, vacuum annealing rel. to crystal struct. changes 9-32932
 Ni-Fe films, annealing in mag. field, effect of elastic stresses 9-33029
 Ni, annealing to internal friction studies, 77° to 298°K 9-26317
 Ni, dynamic recrystn. during high temp. deform. 9-41020
 Ni, explosion-shocked, thermal recovery processes, electron microscope obs. 9-44696
 Ni, shock wave hardened, rel. to softening and recrystallization 9-33098
 Ni, stabilizing annealing treatment after plastic deform., creep strength increase obs. 9-46913
 Pb, migration of large angle grain boundaries and form. of annealing twins 9-30570
 Pb, recrystn. process, nucleation and boundary migration obs. 9-48914
 PbTe, n- and p-types, annealing in prep. of low conc. high mobility mats. 9-39624
 PbTe thick layers, effects on transport props. and optical transparency 9-39625
 Pd-Cr alloy, annealed at 510°C, weak ferromagnetism 9-49202
 Pd annealing process for single crystals 9-39213
 Pt, deformed, stage I recovery by residual elec. resistivity meas. 9-26277
 Pt, quenched, secondary defect obs., e. microscope and field ion microscope exam. 9-23815
 Pt annealed wire, internal friction, shear modulus and transient creep rate 9-33024
 Pt., quenched resistivities of vacancies and Matthiessen's rule 9-35336
 Pu, exothermic $\gamma \rightarrow \alpha$ phase transform. just prior to $\alpha \rightarrow \beta$ transform. temp. 9-42935
 PuC(P,S) powders, densification 9-35238
 Rh annealing process for single crystals 9-39213
 Si:As(P), Li-diffused, γ -irrad., annealing rate dose dependence 9-24234
 Si-B, quenched in defects, elec. and photo-conductivity obs. 9-39357
 Si-SiO₂ interface, e.p.r. rel. to p-Si post-oxidation treatment in H₂ or He 9-49357
 p-Si, annealing at high temp., interac. between radiation defects and impurities, reverse annealing obs. 9-37547
 p-Si, annealing of n irradi. induced defect clusters, elec. meas. rel. to transport props. 9-47129
 p-Si, annealing of neutron irradiated samples 9-47130
 Si, boron implanted and annealed, condensed defect structure distrib. 9-32953
 Si, degenerate, annealing of radiation-induced defects on low temp. e-irrad. 9-28277
 Si, implanted layers, post-annealing conductance behaviour 9-28519
 Si, γ irradiated, two stage process between 100-280°C 9-46807
 Si, point defects generated by quenching, density, lattice parameter and elec. props. investig. 9-32944
 Si, quenching rel. to diffusion mechanism and point defects, review 9-37209
 n-Si epitaxial films on sapphire, vacuum evaporated, post-oxidation annealing effects on elec. props. 9-49111
 Si p-n junction, annealing of radiation-induced defects, isochronal temp. 9-24199
 SiO₂ films, electron-gun deposited, effects of heating in air 9-48765
 SrTiO₃ at 1000°C in vac., prod. colour centres 9-40976
 Ta, refining by electron beam melting 9-33101
 Ta single crystal rods produced by melting and by strain-anneal method, imperfect structures 9-32930
 Ti, annealing effect on oxidation kinetics 9-33671
 Ti, infl. on aqueous-stress corrosion 9-37833
 Ti, n. irrad. commercially pure, low temp. annealing effects on tensile props. 9-33112
 TiC particles recrystn. in austenitic steel during creep 9-33045
 α -U, low-temp. phase transition depend. on annealing 9-26394
 UC(P,S) powders, densification 9-35238

Heat treatment continued

- V, degassing of wires by heating 9-35195
 V, stabilization of rad. induced defects by annealing 9-39367
 W, n irrad., rel. to vacancy clustering obs. 9-44694
 W, with U multilayer adsorpt., work function in transition region 9-32850
 W surface layers, work-hardened, vacuum annealing rel. to crystal struct. changes 9-32932
 Zn, ingots, rolling, patent 9-35203
 Zn polycryst., recrystallization during thermal cycling 9-32879
 ZrB₂, hot pressing, densification 9-30708
- alloys**
 austenite, deformed, recrystallization kinetics 9-33107
 β_1 -brass, metastable, thermal cycling effects on martensitic transformations 9-23981
 β_1 -brass, neutron-irrad., thermal cycling, martensitic start temp. obs. 9-42928
 brass, temperature after-effect 9-23896
 El437B, fine structural changes rel. to ageing and temp. in range 700-850°C 9-41047
 Fe-(3wt.%)Si alloy, infl. of annealing on surface energy of (110) and (100) planes 9-34979
 Nimonic type, recrystn. 9-41044
 permalloy films, annealing behaviour of induced anisotropy, ageing and stabilization effects 9-37660
 permalloy films, reactor irrad. and subsequent annealing effect on anisotropy field 9-47253
 permalloy thin film, effect of mag. annealing on mag. props. 20-200° C 9-41322
 steel, 12% Cr-Co-mo, tempering, precip. obs. 9-42932
 steel, austenitic, annealed, He bubbles obs. 9-33108
 steel, austenitic, TiC particles recrystallization 9-33045
 steel, C-Mn, rel. to microstructure effect on cleavage strength obs. 9-39432
 steel, cold-rolled transformer, annealing temp. rel. to props. 9-39455
 steel, high-pressure effects on microstructure and hardness after different cooling rates 9-23967
 steel, low C, eff. on impurity redistribution 9-23939
 steel, martensite, low-C internally twinned, tempering charact. 9-41052
 steel, martensitic, low-C, precip.-hardened, tempering effects on corrosion (anodic polarization meas.) 9-24578
 steel, mild, electron beam floating zone-melting 9-33109
 steel, plastic deform., ferrite recrystn. between 450-700°C 9-37295
 steel, rel. to sound velocity 9-42911
 steel, spring, quench-hardened, tempering temp. influence on Bauschinger effect 9-39391
 steel, stainless, annealing of creep fracture damage 9-39457
 steel, thermomech. treated and quench-hardened, inherited strength charact. obs. 9-46920
 steel, transformer grade with S coated surface, secondary recrystn., role of surface energy 9-46917
 steel, weldability rel. to ageing 9-30713
 steel-(18 wt.%)Ni maraging steel, fatigue tests 9-30691
 steels, medium carbon Si40, effect of tempering at 250-700°C 9-40948
 steels, Mo, quenched and tempered, B influence on carbide precip. 9-48931
 super-strength, high temp. effect on mechanical props. 9-33056
 zircalloys, effect on post-transition corrosion by steam at 300°C and 340°C 9-28806
 zirconia-rare-earth oxide solid soln., preheating products obs. 9-30724
 Ag-Cu, liq. and vapour quenched, metastable struct. obs. 9-40899
 Al-Cu-Mg-Ag, quenching, effect on S precip. 9-48928
 Al-Cu-Mg, quenching, effect on S precip. 9-48928
 Al-Cu θ' precipitate, as-aged, stacking faults 9-35098
 Al-Mg-Si, recrystn. behaviour, influence of precipitates 9-39452
 Al-Mg-Zn, recrystn., dislocation arrangement influence 9-37276
 Al-Si, dilute, cold-worked, isochronal annealing obs., recovery process 9-33104
 Al-Zn-Mg, weldable, quench rate effect on stress-corrosion resistance and microstruct. 9-46919
 Al(30 at. %)Zn, quenching, rel. to side-bands in Debye-Scherrer patterns 9-46936
 Al(6wt.%)Zn(2wt.%)Mg, rel. to precipitate, nature and morphology 9-28390
 Al-Zr-Si, recrystn. and age hardening, influence of Si 9-42910
 Al-Zr, quenched, superheating melt effect on struct. and props. 9-39450
 AlZnMg 1, annealing effect on microstruct., and sheer susceptibility to layer and stress corrosion 9-46779
 Al-Fe, enhanced Fe solubility by rapid quenching 9-42916
 Co-Fe-V alloys, partially-recrystallized structure rel. to high ductility and yield strength 9-44790
 Cr-Ni-Nb stainless steel, annealing of creep fracture damage 9-39457
 Cr-(2 wt.%)Ta-(0.5 wt.%)Si guide vane specimens, thermal fatigue testing 9-33075
 α -Cu-Ge thin films, recrystallization 9-37278
 Cu-Mn-Al struct. study by X-ray and neutron diff. anal. and electron microscope exam. 9-37293
 Fe-C, surface contamination during H₂ annealing, effect on oxidation 9-36938
 Fe-C, tempering, phase transform. singularities 9-39496
 Fe-Ni-Al-Co-Ti, thermomech. treated, effect on mag. props. 9-47259
 Fe-Ni-Al-Ti, thermomech. treated, effect on mag. props. 9-47259
 Fe-(40 wt.%) Ni-(6 wt.%) Nb precipitation behaviour, ageing at 775°C 9-46951
 Fe-(32 at.%)Pt, quenched, ordering changes during annealing, X-ray diff. obs. 9-46787
 Fe-Si, primary recryst., ageing effect on texture form. 9-46921
 Fe-Si dil. alloy, secondary recrystn., grain growth rate orientation depend. 9-39456
 Fe-Si secondary recrystallization by solute-induced boundary restraint 9-44785
 Fe-(3 wt.%)Si alloys of different impurities, recrystn. during high-temp. annealing 9-39474
 Fe-(3 wt.%)Si cold-rolled-(110)[001]-oriented single crystals, primary recrystallization textures, effect of AlN 9-44784
 Fe, low-C, martensite, aus- and mar-forming, strength increase obs. 9-42912
 Mg-Zn-Mn, patent 9-46960
 MgCd, phase recrystallization rel. to grain size 9-23969

Heat treatment continued
alloys continued

- Mo-(0.05-0.20wt.%)Ti,Zr deformed, effect of annealing at 1100-2000°C on dislocation and mechanical props. 9-40951
 Mo-(10wt.%)Fe solid solutions, precipitation after rapid cooling, rel. to annealing time 9-35207
 Mo-Re, eff. on field emission and surface struct. 9-24250
 Nb-(40wt.%)Zr-(10wt.%)Ti superconducting hollow cylinders. rel. to mag. shielding capacity at 4.2°K 9-43174
 Nb-Zr, supercond., cellular decomp. and precipitation 9-39499
 Nb₃Al-Nb₃Ge, annealing effect on supercond. T_c 9-30877
 Nb₃Au_{1-x}Pt_x system, annealing conditions influence on supercond. transition temp. 9-44942
 Nb(25 wt.%)Zr, supercond., fluxoid pinning by second phases obs. 9-49049
 Ni-Cr film, vacuum-deposited, resistivity increase 9-41043
 Ni-Fe, dynamic recrystn. during high temp. deform. 9-41020
 Ni-base, B-1900 high-temp., microstruct. effects on exposure at 980°C 9-48913
 Ni, recovery of mech. props. by re-heat-treatment 9-23898
 Pd-Co, annealing effects, rel. to elec. resistance and local ordering 9-33255
 Pd-Fe quenching from the range 820-950°C, effect on Mossbauer spectrum 9-41369
 Pd annealing process for single crystals 9-39213
 Pt-Fe dilute solid soln., interac. of quenched-in vacancies with Fe atoms 9-26278
 steel-(5 wt.%)Cr, rel. to shot-peening and Cr-plating effects on fatigue 9-28365
 steel, Si {111} texture, secondary recrystallization 9-46922
 Ti-(8 wt.%)Al-(4 wt.%)Co, effect on structure and mechanical props. 9-23956
 Ti-(8 wt.%)Al-(4 wt.%)Co, rel. to mech. props. 9-40994
 Ti-(8 wt.%)Al-(4 wt.%)Co, rel. to mech. props. 9-44747
 Ti-(8 wt.%)Mn, microstruct., electron microscope obs. 9-35214
 Ti-(20 at.%)Nb, effect on superconducting props., study by magnetiz., critical current density and transition temp. meas. 9-39603
 Ti eff. on stress-corrosion cracking resistance 9-37264
 U-(3.96 at.%)Si, effect on structure 9-33124
 Zn base, ingots, rolling, patent 9-35203
 Zr-(1.2wt.%)Cr-(0.1wt.%)Fe quench hardening behaviour, cooling rate dependence 9-41034

Heating

- Antarctic stratosphere, effect of solar corpuscular rad. (Spring 1963) 9-41484
 atmosphere, upper, transient response 9-41541
 auroral electrojet fields, effect on ions and electrons 9-33823
 calibration heater for liquid-vapour deformation calorimeter 9-29331
 calorimetric, const. current, switch arrangement and power averaging 9-31894
 continuous heating system, low temp. 9-22303
 electric furnace, linear controlled temp. rise technique 9-36216
 finite sized bodies, by radiation, calc. of inside temp. via surface temp. 9-22297
 fluid layer, with sinusoidal perturbation of wall temp., convection onset rel. to time modulation 9-34723
 fluid with variable conductivity in nonuniform field, Joule dissipation determ. during flow 9-39088
 furnaces, resistance heated, low thermal gradients, for molten salt spectrophotometry 9-36090
 gas dynamics and phase equilb. 9-30344
 hypersonic flow around blunt body, heating theory 9-26007
 during hypersonic flow over slender cone, circumferential nonuniform 9-44517
 induction heating power-lead coupling, demountable, for uhv 9-31725
 ionosphere, F-region, during magnetic storms 9-45546
 of ionosphere, rel. to hydromagnetic waves 9-47577
 of ionosphere E region, tidal, radar scatter temp. obs. 9-43462
 localized, of hollow cylinder, numerical anal. of creeping flow to onset of laminar instability 9-40747
 magnetospheric plasma by e.m. waves generated in magnetosheath 9-41552
 metal surface, by laser beam, time-resolved temp. meas. 9-32835
 plasma, in h.p. electrodeless discharges 9-34748
 plasma, laser induced breakdown, enhanced heating at shock front of blast wave 9-30233
 plasma, turbulent, by current, energy loss and efficiency investig. 9-36752
 plasma electrons, at cyclotron freq. in nonuniform mag. field 9-27974
 plasma electrons, microwave method 9-30211
 plasma in mirror machine, modulated beam cyclotron resonance 9-44458
 plate, bilyaer; monotonically, thermal props. temp. depend. 9-29323
 plate with local surface heating, calc. of 'critical thicknesses' 9-27236
 of protons in magnetosphere, stochastic, by fast hydromag. wave 9-43412
 school, conventional and solar methods, economic comparison 9-22325
 solar corona, as result of Landau damping of ion-acoustic waves 9-36073
 solar wind, due to long wavelength turbulence 9-36055
 of solar wind ions, electrostatic, beyond 0.1 AU 9-43667
 structural materials, laser beam effects and applications 9-33178
 superheating effect on condensation heat transfer in forced convection 9-26162
 surface effects on nucleate film boiling 9-36925
 surfaces, by electron bombardment 9-41122
 turbulent, in toroidal system with current 9-36751
 turbulent, of plasma ions during electron-sonic instability 9-30288
 upper atm., rel. to geomag. perturbations 9-41601
 vertical flat plate, buoyancy forces effect on boundary layer flow 9-34729
 wall, near compressible boundary layer, effect on velocity overshoot 9-25809

Heaviside layer see *Ionosphere***Heavy water** see *Water***Height measurement** see *Length measurement***Heisenberg model** see *Ferromagnetism; Statistical mechanics***Helicity** see *Elementary particles; Field theory, quantum***Helicons** see *Crystal electron states***Helions** see *Alpha-particles; Helium-3***Heliotron** see *Plasma devices***Helium**

abundance in H II regions, radio recombination lines obs. 9-35964

Helium continued

- abundance in population II stars, determ. problems, rel. to cosmological big-bang model 9-43539
 alignment relax. times of singlet states prod. by ion collisions 9-29983
 arc discharge, nature of continuous spectrum, determ. using relax. method 9-44512
 atom, 3^{1,2}D, 4^{1,1}F levels excited by electron impact, obs. 9-32441
 atom, 7¹S state, changes in wave function representation 9-32439
 atom, (2s²sp)³P cpd. state decay by 2-electron emission 9-40568
 atom, and isotropic series, non-exponential orbitals 9-48372
 atom, appl. of two new formulae for expectation values lower bounds 9-40241
 atom, dipole transition probabilities, corrections, struct. of perturbation series 9-48381
 atom, electron scatt., low energy, reson. structure 9-42353
 atom, electron scatt., resonant differential ≈ 19.3 eV 9-42352
 atom, excitation by low energy electrons, cross section calc. 9-38853
 atom, excitation by protons and electrons 9-27829
 atom, Hartree-Fock energies of 1¹S and 2¹S states 9-36684
 atom, ionization by high energy p 9-38799
 atom, laser transitions, lifetimes of upper and lower excited-state levels as fn. of press. 9-48431
 atom, mean excitation energies upper and lower bounds calc. 9-38779
 atom, metastable, destruction in binary collisions 9-38802
 atom, metastable state transitions, computation of oscillator strengths 9-32440
 atom, natural orbitals, direct calc. 9-38742
 atom, oscillator strength for 1¹S-2¹P transition 9-29980
 atom, p scatt., coupled-state calc., anomalies 9-32442
 atom, Schrödinger eqn. soln., new coord. system 9-40567
 atom, self-consistent field equation, deviation from spherical symmetry and calc. of expectation values 9-29914
 atom, spatial wave func. from symmetry reln. 9-25718
 atom, transitions between doubly excited states and 2¹S state, line strengths calc. 9-42350
 atom, transitions from ground to 3¹D, 4¹P states, generalized oscillator strengths 9-46333
 atom, variational calc. of correlation eff. on g.s. 9-22958
 atom electron impact excitation at low energy, detection with SF₆ 9-29982
 atom excitation ³P-⁴D by optical pumping, prob. calc. 9-23000
 atom oscillator strength of 1¹S-2¹P transition, calc. using Hanle method 9-38776
 atom singlet-triplet transition prob. variational calc. 9-29981
 atomic beam, fast, charge changing collision with H₂, He⁻ formation 9-29985
 atomic beam, scattering by CF₄, CHF₃ and CH₂F₂ determ. of atom-molecule potential-energy functions 9-38794
 atomic beam in H₂, N₂, Ne and Ar gases, charge equilb. fractions obs. 9-40559
 atomic spectra, using Van de Graaff accelerator 9-22998
 atoms, charge state change for proton interaction, 5-50 keV 9-44483
 atoms, electrons elastic scatt., ang. distrib. 9-34587
 atoms, excitation by H₂⁺ and H₃⁺ ions, 1-150 keV, cross sections 9-48410
 atoms, fast, electron loss on passing through H and He, first Born approx. cross sections 9-48425
 atoms, interaction of two metastable triplets 9-48434
 atoms, metastable, prod. and destruction in He charge changing collisions 9-38796
 atoms, polarization of electron impact light 9-29958
 atoms 2¹S state decay by e collisions in glow discharge, obs. 9-34808
 atoms adsorbed on graphite, quasiharmonic freq. shifts. 9-48769
 auto-ionization, P states calc. 9-46329
 beam, average cross section for ionization by electron plasma 9-44486
 bubble formation in irradi. Cu-B alloy, influence of precipitates 9-41116
 bubbles in irradi. and annealed austenitic steel 9-33108
 burning phase in massive star, pulsational props. 9-24798
 charge state fractions in C thin foils 9-39550
 coalescence, cusp values and electron densities, correl. bet. errors 9-40566
 collision with H, -ve charge prod. cross section determ., 50-1000 eV 9-27826
 collision with incident beams of H, He, He⁺⁺; electron and ion prod. cross section meas., 0.15-1.0 MeV 9-22982
 compressed gas, thermal conductivity, concentric cylinder meas. method 9-26027
 diffusion, interstitial, in Ta 9-23843
 discharge, 12-13 torr pressure, voltage-current characteristics, hot hollow cathode 9-25994
 discharge electron energy distrib. functions electron mobilities and collision rates calc. 9-48621
 discharge positive column, medium press. 9-25980
 earth's exosphere, planetary, lateral transport 9-29059
 electron, elastic scattering from ³Si, metastable state, calc. 9-46307
 electron elastic scatt., phase shifts, isoelectronic sequence extrapolation techniques 9-29964
 electron scatt., elastic and inelastic, from ground state, first Born approx. calc. 9-32422
 electron scatt., elastic at 500 eV, absolute differential cross sections 9-38800
 embrittlement of Incoloy 800 9-35179
 emissivity, temp. range 6000-12000°K for 1,10 and 100 cm layers 9-26035
 excitation mechanism in discharge plasma +ve column 9-25721
 flowing, mixing of trace gas rel. to in-pile meas. on radioactive gases 9-25679
 gas, diffusion of Cs and K vapours 9-39059
 gas viscosity meas. pot. fitted 9-36823
 globular cluster M15, abundance, and age, of stars 9-27044
 Hanle effect on 2¹P He 9-38776
 Hartree-Fock eqn. perturbation treatment for 2p²1D state 9-32438
 θ -pinch, excitation, electron density and temp., possible population inversion 9-36771
 interatomic potentials 9-38801
 ionization of Al, cross section and K-shell X-ray yield meas., E=25-200 keV 9-22940
 ionized partially, elec. conductivity 9-26037
 in ionosphere, night over Arecibo 9-24685
 ions, channeling charact. in diamond-type lattices 9-47012

Helium continued

- ions, earth's polar wind 9-26925
 ions channeled in Au monocryst., energy-loss spectra 9-30806
 isotope shift of $2^1S_0-2^1P_1$ line meas. 9-25719
 isotopes, polar wind escape mechanism 9-28913
 laser, He-Ne, lasing frequency shifts due to discharge tube parameters 9-27323
 light source for vacuum u.v. spectroscopy, radiative power, calc. 9-27410
 metastable atoms, elastic scatt. in He 9-29984
 metastable atoms, electron ejection from W surfaces 9-31001
 methyl chloride mixture, thermal diffusion 9-32740
 molecule scatt. by LiF cryst. surface 9-48751
 neutral number densities in thermosphere, lower, day-night vars. 9-26920
 optically pumped, metastable, ion polarization via Penning collisions 9-38803
 photoionization, resonant line shapes, dispersion calc. 9-46334
 in planetary nebulae, n^3D-2^3P series, strengths 9-27002
 plasma, afterglow, decay, props. 9-23286
 plasma, cryogenic, sound oscillations, excitation and damping 9-48606
 plasma, high-freq., elec. fields, spect. meas. 9-23287
 plasma afterglow, formation of mol. He 9-23263
 plasma highly ionized, magnetically confined column 9-25891
 plasma in homopolar rot. device, 10^{-2} mm Hg, electron collision freq. and current growth 9-25857
 plasma in linear Z-pinch tube, spectroscopic studies 9-23306
 positron double-electron capture in atoms, cross section calc., $E_{pos} \leq 250$ eV 9-46335
 primeval abundance variations, rel. to spatial variations at time of synthesis, and galaxy formation 9-26980
 projector, IV characteristic calc. 9-27285
 quenching rate in He-Ne discharge He level population depend. on Ne atom conc. 9-25974
 scattering of CsF molecules, cross sections and anisotropy parameters 9-44387
 semiconducting spectrometer for Am-Be neutron source 9-44084
 separation from Ne-He mixture 9-23590
 solar abundance, rel. to ν detection by $^{37}\text{Cl}(\nu, e^-)^{37}\text{Ar}$ 9-45682
 solar prominences, ratio of $H\alpha/D3$, variation in outer regions 9-36066
 spectral line absorpt. coeffs. from Fabry-Perot profiles 9-34586
 in steel, austenitic, irradiated, and annealed, bubbles formation 9-33108
 stellar abundance, in M3, M13, M15 and M92 globular clusters 9-43548
 streamer chamber, ionization meas. 9-46144
 thermosphere, lower, conc. from mass spectrometer obs. 9-28906
 twilight 10830 Å emission, identification and photometric obs. 9-31363
 K- ^4He , validity of DGBT formula 9-46338
 electron scatt., 100-400 eV, inclusion of adiabatic and nonadiabatic distortion eff. 9-23003
 $\text{Co}_2\text{-N}_2$ -He discharge, lasing action influence on electron energy distrib. 9-34800
 $\text{Cs}^+ + \text{He}$ collision, threshold behaviour of the cross-section for excitation of Cs II reson. lines 9-48419
 H-He atomic collision, electron loss, free scatt. model 9-46310
 H_2^+ electron density variational calc. 9-27841
 He-Ar collisions, prod. and destruction of fast metastable He atoms 9-38796
 He-Ar discharge electron energy distrib. functions electron mobilities and collision rates calc. 9-48621
 He- CO_2 gas mixture, absolute viscosity determ. using 200 foot stainless steel capillary 9-36825
 He- H_2 anisotropic intermolec. potential and spin-lattice relax. 9-30354
 He- H_2 arc discharge, nature of continuous spectrum, determ. using relax. method 9-44512
 He- H_2 collisions, prod. and destruction of fast metastable He atoms 9-38796
 He-He collisions, prod. and destruction of fast metastable He atoms 9-38796
 He-Na atomic collision, Na in 2^1P state, cross-section behaviour 9-29973
 He-Ne cw laser, temporal correlations in radiation at threshold 9-22400
 He-Ne laser, generation intensity and inversion density rel. to hollow cathode diameter 9-25266
 He-Ne laser, h.f. pulse excited, characts., obs. 9-25267
 He-Ne laser, interference application for obtaining nonpolarized, single frequency radiation 9-25269
 He-Ne laser, Ne atoms density nonlinear depend. on saturation, Ne exchange collisions explanation exchange collision, saturation parameter nonlinear depend. on density 9-25271
 He-Ne laser, new cascade transition, induced emission at 2.3956μ , mechanism 9-22402
 He-Ne laser, radiation output and polarization, infl. of transverse mag. field 9-22395
 He-Ne laser, self-locked, pulse velocity meas. 9-41903
 He-Ne laser radiation within hollow cathode 9-47994
 He-Ne laser resonator, $3s_2-3p_4$ Ne transition line spectral width meas. 9-22960
 He-Ne laser with small discharge space, max. amplification depend. on tube axis position 9-29406
 He-Ne mixture, He quenching rate calc. from He level population depend. on Ne atom conc. 9-25974
 He-Ne mixtures, ionic analysis of cataphoresis 9-42569
 He-Xe collisions, prod. and destruction of fast metastable He atoms 9-38796
 He- e^+ bound state search, 3-body variational wave func. converging expansion 9-46322
 He-like systems, double perturbation theory 9-38756
 He, Li^+ elastic differential scatt. cross section meas., 3-330 eV 9-46315
 He $_2$, 510-611 Å absorpt. spectrum 9-44332
 He $_2$, $F^1\Pi_u$ and $F^3\Pi_u$ states, quantum-mechanical exam. 9-34626
 He $_2$, potential energy curve, empirical form 9-32461
 He $_2$ isotopic mols. interatomic potentials 9-38801
 He $_2$ molecule, $^1\Sigma_g^+$ state, quantum mechanical study 9-27860
 He $_2$ molecule, $F^1\Pi_u$ and $F^3\Pi_u$ states, quantum mechanical study 9-27861
 He $_2^+$ existence, mass spectra obs. in plasmas 9-36760
 He $_2^+$ existence, mass spectra obs. in plasmas 9-36760
 He $^+e^-$ S and S. elastic scatt., Rydberg state quantum defects calc. 9-32397
 He $^+$ backscattered beam used to determ. crystal dope structure 9-35411
 He $^+$ channeling in W cryst., Rutherford scatt. and L and M X-ray yields obs. 9-41120
 He $^+$ charge-exchange collision with molecular gas, products obs. 9-22995
 He $^+$ conc. in ionosphere 200 to 630 km, obs. 9-43464

Helium continued

- He $^+$ ions, 5-45 keV, passage through molecular gases causing ionization and fragmentation 9-42558
 He $^+$ prod. in afterglow plasma due to collisions between metastable ions 9-46336
 He $^+$ producing autoionization levels of Ne 9-23343
 He ^+CO collisions, excited ions form. obs. 9-36724
 He $^{2+} + \text{H}(1s)$ collisions, resonance charge transfer 9-48435
 He I, 10830 Å line in star β Lyr, investigation 9-24785
 He I, Stark broadening of allowed and forbidden transitions, calcs. 9-42349
 He I (1.083μ) in sunlit aurora, and OI(5577Å) brightnesses, obs. 9-47566
 He I twilight emission, 1.083 μ resonance line obs., Feb. 1968-Feb. 1969 9-40052
 He II boson system excitation spectrum derivation, repulsive core and attractive well 9-28165
 He II solar line intensity meas., utilization 9-24901
 ^3He , ultrafine struct. meas. in 1D levels 9-46269
 $^3\text{He}^+$ polarized ion source 9-40335
 He atom in ^4He liquid at T=0, theory 9-23555
 ^3He on W, small energy accommodation coeffs., classical theory 9-35004
 ^4He , optically oriented metastable, spectra of absorpt. and 1st harmonics signals for magnetiz. component, modulation effects 9-32813
 He $^+$ - ^4He , scatt., interac. potential meas. from extrema positions in interference patterns 9-40569
 He $^+$, modulated fluorescent light, $4^2S_{1/2}$ and $4^2P_{1/2}$ levels, observation of resonance effect 9-25720
 He and ^3He , thermal accommodation coeffs. on clean W surface 9-30501
 He atoms optical rot. in 2^3S_1 state in plasma, effect on electron density and radiation 9-38984
 He fluid, critical region chemical pot. function of density and temp. 9-26155
 He on W, small energy accommodation coeffs., classical theory 9-35004
 He ions, channeled in the Au single cryst., energy loss spectra 9-30805
 He- ^3He separation by sorption sieve 9-42733
 He- ^4He , scatt., interac. potential meas. from extrema positions in interference patterns 9-40569
 HeI, local thermodynamic equilib., validity criteria 9-23277
 HeI in hot stars, departure from LTE 9-45615
 He+p charge-transfer collisions, polarization of Balmer- α radiation 9-22989
- III**
 a.c. discharges between metal-dielectric electrodes 9-34807
 afterglow plasma, electron temp. gradient, spatially nonuniform parameters effect on transport processes 9-34755
 arc in superimposed gas flow, arc-flow-electrode interacts and mode behavior 9-23365
 arc-tube heater with elec. field, enthalpy distrib. 9-23393
 atmospheric, nonthermal escape 9-45504
 breakdown, laser induced, time and space development of space parameters 9-28053
 breakdown by a laser beam 9-48725
 breakdown pot. obs., secondary ionization coeffs. calc., mild steel electrodes 9-34811
 breakdown waves, radiation-driven, laser light scatt. mechanism 9-23362
 bubbles in austenitic alloy, effect on creep ductility 9-41021
 discharge, hollow cathode, He I population 9-48635
 discharge, optically pumped, production of continuous beam of polarized electrons 9-28045
 discharge in microwave resonant cavity, 2.7 GHz, electron conductivity ratio meas. 9-23288
 discharge negative glow, secondary and ultimate electron groups 9-48634
 discharges, positive column theory 9-44502
 electron density and radiation of atoms, effect of optical orientation of ^4He atoms 9-38984
 electron impact spectra, retarding field energy analyzer meas., instrumental effects 9-34351
 flow, hypersonic, visualisation by electron beam fluorescence probe 9-46559
 flux in lower thermosphere 9-31345
 in ice, selective doping 9-46814
 inverse pinch, m.h.d. prod. of collisional shocks, characts. 9-46495
 ionization, primary specific, meas. 9-30297
 ionization by e, ang. correlation distrib. and energy of 2e meas. $E_e=50,114$ eV 9-23004
 ionization by electron impact, total ioniz. and ioniz. fluctuations 9-25964
 ionization currents, pre-breakdown, spatial growth 9-48433
 laser, c.w. oscill. in pure He, 95.8 and 216.3μ 9-45953
 laser action, excitation and relaxation effects 9-48431
 laser oscillation, visible, 7065 Å 9-47993
 Lennard-Jones gas, quantum mechanical second virial coeff. 9-39049
 magnetic splitting determ. 9-29936
 metals, f.c.c. irradiated, hot brittleness rel. to He-filled deform. defects 9-37260
 photoexcitation and photoionization, simultaneous, 186 Å obs. 9-23001
 plasma, acoustic l.f. oscillations and kinetics of heating at low temp. 9-39010
 plasma, afterglow, decay of e temp. investigated 9-32592
 plasma, afterglow, electron temp. gradient, spatially nonuniform parameters effect on transport processes 9-34755
 plasma, afterglow in mag. field, microwave scattering and noise emission 9-48568
 plasma, decaying, neutral particle collisions 9-46475
 plasma, diff. and mass flow effect on ioniz. degree 9-32597
 plasma, electron conc. from He I 4922 and 4472 Å line widths 9-30261
 plasma, inductive, electric conductivity as function of time and space, spectroscopic measurements 9-42535
 plasma, laser-produced, spectroscopic studies 9-34776
 plasma, partially ionized, transport and balance coefficients 9-44417
 plasma, thermodynamic functions, approximate calc. 9-46464
 plasma discharge, population of highly excited states, effect of stepwise ionization 9-46539
 positive column in longitudinal mag. field, 0.5-4.0 mm pressure, comparison with binary collision theory 9-34809
 r.f. discharge in non-resonant mag. field, breakdown characts. 9-25986
 shock refl. in T-tube, obs. 9-30324
 spark discharge channel, h.p. radiance saturation and afterglow emission 9-30314

Helium continued
gas continued

streams, concurrent injection of ethanol or water jets, max. drop diam. 9-34864
supercooled, water drop nucleation 9-26075
supercritical, two phase flow, pressure drop and heat transfer meas. device 9-46664
in T-tube, obs. of refl. shock 9-30324
thermal conductivity at high temp., meas. with hot wire cell 9-39096
thermal conductivity meas. at 35 and 90°C 9-36814
thermal transpiration at low pressures, use of leached Pyrex tube 9-36820
Townsend coeff. by taking indirect ionization into account 9-48613
between vertical concentric cylinders, heat transfer and end effects for various temp. differences 9-40749
virial coefficient, second, quantum mechanical, Lennard-Jones gas 9-39049
viscosity and thermal cond., calc. using Lennard-Jones (6-9) potential 9-26045
Ar-He mixtures, influence of dimers on thermal diff. factor 9-36686
CO₂-N₂-He laser power enhancement by noncontracted discharge 9-22390
CO₂-N₂-He-H₂O glow discharge, spectra, 2800-6500 Å, 3-7 torr 9-25979
CO₂-N₂-He glow discharge, spectra, 2800-6500 Å, 3-7 torr 9-25979
Cr I emission line shifts in compressed He, 3017-4651 Å 9-48390
He-Cd ion laser, stable operation, d.c. cataphoresis technique 9-47989
He-Kr intermolecular forces and (thermal) diffusion 9-46580
He-Ne, discharge, depolarizing and velocity-changing collision correl. 9-39026
He-Ne, laser, localizer-beam flying application 9-31947
He-Ne 6328 Å laser, external polarization technique using permanent magnet 9-29418
He-Ne laser, 0.6 ns pulses duration meas., beat-frequency detection method 9-48074
He-Ne laser, amplification and oscillation mechanism 9-29416
He-Ne laser, freq. stabilization by external Ne absorpt. tube in mag. alternating field 9-25261
He-Ne laser, gain coeff. temp. dependence calc. 9-41905
He-Ne laser, Lamb dip minimum, discharge tube parameter effects on frequency shifts 9-22397
He-Ne laser, line width and amplitude fluctuations, theory contrib. 9-29408
He-Ne laser, mode-locked, pulse compression to 1.85 factor 9-47988
He-Ne laser, multimode 0.63 μ output power and spectrum rel. to collisions 9-34164
He-Ne laser, operating in TEM_{nm} modes, radiation divergence meas. 9-47992
He-Ne laser, positive column calc. for dispersive effects eval. 9-43884
He-Ne laser, pumping intensity, effect on relationship between gain and temperature 9-25268
He-Ne laser, radiative power rel. to discharge gap geometry 9-47995
He-Ne laser, short transient, effect of inserted liquid cells 9-25276
He-Ne laser Brewster angle attenuator within laser cavity, eqns. of polarization and attenuation 9-31969
He-Ne laser construction for operation at 6328 Å 9-29415
He-Ne laser for space 9-47990
He-Ne laser in transverse mag. field, energy characts. 9-40354
He-Ne laser interferometric technique 9-46478
He-Ne laser plasma parameters characterization 9-34163
He-Ne lasers, collisional line broadening, gas pressure effects 9-22396
He-Ne lasers, higher order phase-locking phenomena, mode quenching and forced locking methods for obtaining high bit-rate pulses 9-31945
He-Ne lasers, self-locked, enhancement of second-harmonic power generation 9-22437
He-Ne lasers for science and technology, operation 9-41906
He-Ne mixture, ionization currents, prebreakdown, spatial growth 9-48433
He-Ne mixture, plasma production, N²⁺ ion production and loss during decay period, density time depend. 9-40666
He-Ne single-mode laser, damping parameters of 0.63 μm line, nonlinear press. depend. 9-34165
He₂, absorption spectrum 600-620 Å 9-34625
He⁺ concentration in daytime F2-region between 200 km and peak altitude, direct measurement 9-24701
He⁺ concentration in daytime F2-region between 200 km and peak altitude, direct measurement 9-31436
He⁺ electron beam ionization, obs. near threshold 9-25963
He⁺ ionosphere concentration 300 to 600 km 9-31397
He⁺+H₂ non-reactive collision at ~1 eV, obs. 9-41443
He⁺ concentration and temp. at 1000-1200 km, cosmos 5 obs. 9-45505
He I auroral emission obs. 9-33819
He II line spectrum, 303.8 to 230.7 Å and 206.2 to 120 Å, production 9-44298
He, nuclear spin-lattice relax., surface-induced, nature and interpret. 9-26039
He and ³He, props. reviewed, book 9-32806
He and ³He, proton bombardment, charge exchange and ioniz. cross sections 9-48614
³He in atmosphere, loss and production 9-43410
³He discharge, decaying, e conc. by laser interferometry, 10⁻²-3 mm Hg 9-28050
³He optically pumped, nuclear polarization meas., sensitive low-field magnetometer 9-23002
³He discharge, decaying, e conc. by laser interferometry, 10⁻²-3 mm Hg 9-28050
³He-⁴He plasma, He⁺ and He⁺ existence, mass spectra obs. 9-36760
He-N₂ mixture, thermal relaxation and heat transfer 9-48661
He-Ne laser, detection technique at 3.39 μ 9-47987
He-Ne laser cathode temp. effect on illuminating power 9-29417
He-O₂ mixture, thermal relaxation and heat transfer 9-48661
He(2³S) chemiluminesc. reactions with N₂, O₂, CO and CO₂ 9-43318
in thermosphere, midlatitude 150 to 450 km, concentration and temp. 9-28905
in KCl, pores, He filled, temp. induced migration, obs. 9-37189
N₂-He mixtures, heat transfer cylinders showing slip effects 9-46568
Ne-He laser interferometer for improvements of detections of fringe shifts in plasma density meas. 9-25910
Ni I emission line shifts in compressed He, 3369-3619 Å 9-48390
Xe-He mixture, laser stimulated conc. scatt. of light 9-46286

Helium continued
liquid

see also *Quantum fluids; Statistical mechanics/quantum; Superfluidity*
³He-⁴He mixture, heat of mixing dis. at 0.05°K 9-32810
absorption of u.v. radiation 9-44565
breakdown by a laser beam, stimulated Mandel'shtam Brillouin scatt. 9-48725
bubble chamber, u.s. expansion techs 9-34365
bubbles, two electron, formation and instability 9-40811
con. size increase near gas-liquid critical point 9-46672
cooling of rocket-borne telescope 9-38123
cryostat, continuous transfer, for u.h. vacuum field ion microscope 9-34148
current attenuation and lifetime on injection of hot electrons 9-39121
depth meas., gauge design using carbon resistor sensing elements 9-31760
depth meas., superconducting depth gauge 9-44606
effective mass, rearrangement energy mag. susceptibility and transport coeffs. 9-23559
electron trapped in bubble, optical props. 9-23560
electronic bubble state, optical properties 9-34938
film on crystalline quartz substrate, ellipsometric thickness meas. 9-28212
films, unsaturated, model describing onset of superfluidity and third sound 9-40813
films, vortex surface effects 9-26142
heat influx compensation 9-48724
heat transfer of supercond. composites 9-49041
impurity ions, mobility calcs. 9-46666
impurity mobility theory, 'helium-drag' effect 9-34937
lambda temp. depression, rotating 9-48726
Mossbauer absorber cryostat 9-36091
phase transitions in the pair-Hamiltonian model 9-40258
quantum theory, three problems 9-23554
Raman scatt., from photon-roton excitations, amplitude calc. 9-32808
Raman scatt. of light from rotons, spectrum intensity and polarization 9-32805
rotons, Raman scatt. of light, spectrum, intensity and polarization 9-32805
specific heat of He³/He⁴ mixture near junction of lambda and phase-separation curve 9-40812
structure factor, wavelength depend. and free boson excitation structure 9-46669
superfluid, evaporation rate of ⁴He atoms, temp. depend. 9-26144
superfluid, heat transport in wide tubes 9-36911
superfluid, positive ion mobility, scatt. by elementary excitations 9-40814
superfluid, scaling behaviour in microscopic approach to theory 9-34945
superfluid and supercritical, heat transfer 9-36910
superfluid component entropy 9-23567
superfluid flow, pressure-driven; press.-vel. depend. determ. 9-36912
superfluid fraction contained in porous Vycor glass 9-34943
surface thickness, theoretical determination of ³He and ⁴He 9-39124
surface wave vel. freq. depend. near λ point 9-23556
thermal conductivity, sound meas. 9-26141
transport coeffs. near λ-point, analysis into modes 9-26147
two-phase flow, pressure drop and heat transfer meas. device 9-46664
viscosity coeffs., sound meas. 9-26141
vortex rings, meas. of an impulse of a beam of rings 9-28164
wave functions, Bose-Einstein condensation 9-39122
³He-He II system, Brillouin light spectrum, line shape 9-34941
He/³He specific heat of mixture near junction of lambda and phase-separation curve 9-40812
He I, heat transfer from cylindrical Cu surfaces 9-36909
He I, mobility of charges up to solidification 9-30443
He II, core radius of quantum vortices using boson gas model 9-26145
He II, counterflow in rot. channel 9-48731
He II, excitations energy spectrum calc. including phonon-phonon interactions 9-48732
He II, rotating, quantized vortex lines, detection 9-28166
He II, rotating, vortex lines obs. 9-23568
He II, superfluid, temp. depend. of critical heat current 9-39125
He II, thermal quenching of superfluidity in long channels, critical state condition 9-44608
He II, thermodynamic functions, analytic expressions and macroscopic props. 9-23564
He II, viscosity, roton-roton contribution calc. 9-44607
in He II counterflow, heat induced, local boiling and cavitation 9-44609
He II flow under low press. heads, dissipation in superfluid component influence 9-48730
He II in random phase approx., persistent mass currents 9-46673
He II thermal quasiparticle radiation, pulsed carbon film heater obs. 9-23569
³He, atom in ⁴He at T=0, theory 9-23555
³He, binding energy and other properties at zero temp. 9-34939
³He, Fermi-liquid parameters in Brueckner theory 9-46671
³He, impurity mobility theory, 'helium-drag' effect 9-34937
³He, low excited states and statistical and transport properties 9-34940
³He, spin-lattice relaxation times, 1.4° to 2.1°K 9-30441
³He, surface thickness, theoretical determination 9-39124
³He and ⁴He, props. reviewed, book 9-32806
³He dilute soln. in ⁴He, osmotic pressure 9-23565
³He impurity quasipart. in superfluid ⁴He, excitation spectrum, effective interact. energy 9-23563
³He in ⁴He, dilute solutions, viscosity, 0.1-1.2°K 9-26143
³He props. and solns. in ⁴He, review 9-23562
³He thermal conductivity meas., to 1.5-4.0°K, and up to 34 atm. press. 9-28163
³He, decay threshold of quasiparticles under pressure, variation in nature 9-48729
³He, Fermi versus Bose condensation, superconductivity 9-24140
³He, ion motion and vortex-ring formation 0.05-0.5 K 9-46668
³He, phonon-drag eff. in mobility of charge impurities 9-30442
³He, structure factor, apparent discrepancy between theory and expt. 9-48727
³He, superfluid, containing ³He impurity quasipart., excitation spectrum, effective interact. energy 9-23563
³He, surface thickness, theoretical determination 9-39124
³He, thermal pulses, Schlieren photography 9-48728
³He, viscosity and thermal conductivity, 2-50°K 9-46665
³He, vortex ring creation in presence of ³He impurities 9-23558

Helium continued**liquid continued**

- ⁴He film flow suppressing evaporator for dilution refrigerator 9-33987
- ⁴He ground state, three-phonon vertex in BDJ description 9-42688
- ⁴He monolayer, quantum theory 9-23557
- ⁴He pair distrib. function, calc. 9-41784
- ⁴He superfluid, containing ³He, dilute soln., phonon-quasiparticle interactions, microscopic theory 9-34942
- ⁴He thermal conductivity meas., 1.5-4.0 °K and up to 34 atm press. 9-28163
- ³He-⁴He dilute soln., surface tension 9-30444
- ³He-⁴He dilution refrigerators 9-29139
- ³He-⁴He mixture, equilibrium, transport props. and 2 quasiparticle scatt. amplitude determ. 9-46670
- ³He-⁴He mixture, ground-state energy 9-32810
- ³He-⁴He mixture, impurity mobility theory, 'helium-drag' effect 9-34937
- ³He-⁴He mixtures, degenerate, osmotic press. down to 0.027°K 9-42687
- ³He-⁴He mixtures, liquid-solid transition obs., freezing curve drawn 9-32804
- ³He-⁴He soln. ion motion and vortex-ring formation, 0.05-0.5 K 9-46668
- ³He-⁴He solution, spin-lattice relaxation times, 1.4° to 2.1°K 9-30441
- ³He-⁴He solutions, conc. dependent polarization 9-32807
- ³He-⁴He weak solns., e.m. waves Rayleigh scatt. 9-39123
- HeI, heat transfer, review 9-46667
- HeII, electron extraction from quantized vortex lines 9-34944
- impurities, dilute solns., mobility at low temps. 9-26140

liquid, sound propagation

- attenuation at 1 GHz, obs. 9-23561
- detection of thermomagnetic effect modulation 9-39523
- films, unsaturated, model giving accurate expression for third sound 9-40813
- first and second divergence of damping, near λ -point 9-26147
- first sound attenuation near λ -point, coupling with second sound 9-28167
- second sound in superfluid helium, relaxation function expressions for thermal conductivity χ 9-32811
- second sound vel. near T_λ 9-34947
- superfluid transition, thermodynamics of isentropic sound velocity 9-46674
- surface waves in presence of second sound 9-27186
- third-sound obs. in superflow 9-34946
- wave modes props., second viscosity coeffs. and thermal conductivity evaluation 9-26141
- ³He-He II system, Brillouin light spectrum, line width due to 1st sound, 2nd and central diffusion peaks 9-34941
- He II, attenuation of second sound due to flow of film from beaker into resonant cavity 9-48733
- He II, steady-state counterflowing normal and superfluid, second sound-entrainment 9-23566
- ³He, absorpt. coeffs. and relax. times 9-30445
- ³He, first and zeroth sound velocity, calc. using ground-state energy and quasiparticle energies and interaction function 9-34940
- ³He zero sound, transverse, attenuation 9-23570
- ⁴He, sound attenuation and velocity meas. down to 0.1°K 9-32809
- ⁴He, structure changes, Schlieren photography 9-48728
- ⁴He, velocity of sound at 1MHz near critical point 9-36913
- ³He-⁴He superfluid solns., fourth sound, λ point to 0.5°K 9-26146

solid

- electron trapping cavity formation, optical and transport props. of trapping center 9-23572
- lattice dynamics at high pressure 9-23573
- nuclear magnetic susceptibility of ³He spin system in isotopic mixture, 0.3-1.2°K 9-46675
- second sound obs. reviewed 9-42689
- vortex lattices, elasticity 9-39126
- ³He, ⁴He impurities, increase of exchange interac., effect on heat capacity, n.m.r. 9-28168
- ³He, b.c.c., nonlocalized vacancy formation 9-32812
- ³He, bcc, anomalous specific heat 9-46676
- ³He, crystalline transformation 9-34948
- ³He, g.s. energy, cluster expansion computation 9-23571
- ³He and ⁴He, props. reviewed, book 9-32806
- ³He b.c.c. cry., temp. pulse propag., second sound below 0.58°K 9-26148
- ⁴He, e.m. waves Rayleigh scatt. 9-39123
- ⁴He, second sound rel. to thermal pulse behaviour 9-28169
- ³He-⁴He mixtures, liquid-solid transition obs., freezing curve drawn 9-32804

Helium compounds

- CO-N₂-He lasers, high power, high efficiency 9-22391
- CO₂-N₂-He-H₂O flowing laser, elec. discharge effect on mol. comp. 9-40352
- He-Ne laser 3-mirror resonator, mirror motion influence on generation power 9-22399
- He-Ne laser in mag. field, nonlinear effects in output intensity 9-45954
- He-Ne mixture, conc. depend. on level meas. by absorption method in hollow cathode discharge 9-23354
- HeH⁺, existence in room-temp. plasmas, mass spectrometric obs. 9-25969
- HeAr and HeNe, interatomic potentials 9-38854
- HeH⁺, bond-stretching-energy curves calc. 9-30012
- HeH⁺, one-centre calc. with unlimited radial basis 9-38846
- (HeH)⁺ mol. ion, collision-induced dissociation 9-38921
- HgSe, helicon resonance and quantum oscills. 9-24107

Helium-3

- counters, wall effect for incident thermal neutrons 9-44091
- ion beam, polarized, attempt to produce 9-27583
- polarized beam prod. 9-27739
- seawater, deep, terrestrial primordial evidence 9-45468
- target, gaseous for nuclear scatt. expt., prod. using optical pumping and electron exchange 9-27583
- target, polarized, for high energy scatt. expt. 9-27582
- μ^- capture probability calc. 9-32340

interactions

- π photoproduction, impulse approx. calc. in elastic channel, $E_\gamma=200-500$ MeV 9-25453
- μ capture and pseudoscalar coupling constant 9-27704

scattering

- ³He(α , α')³He rel. to 7 MeV resonance 9-27739

Hellmann-Feynman theorem see *Quantum theory***High voltage techniques**

- Cockcroft-Walton voltage multiplier, modification 9-34138
- corona tube stabilizer for h.v. prod., design 9-22663

High-pressure phenomena and effects

- alkali halides, Cu⁺ and Ag⁺ centres excitation and emission spectra 9-41401
- alkali halides, luminesc. of O₂ impurity centres 9-39864
- alkali metals, electrical resistivities up to 600 kbar 9-30841
- alkali metals, shock wave and static compression data 9-46882
- ammonium halides, melting curves and phase transitions 9-30452
- benzene, cryst. struct. 9-32903
- bromine, cryst. struct. 9-32903
- 1- and 2-butanol, dielec. relaxation 9-32791
- carbon tetrachloride, cryst. struct. 9-32903
- ceramic systems, structure, defects and reactivity 9-30553
- ceramics, densification, isostatic pressing technique 9-30726
- diamond-silicon interaction 9-26807
- diaphragm, circular, plastic bulging 9-31833
- dielectric polarization of liqs. 9-32788
- Fe(III) reduction to Fe(II) in solids, reversible 9-37825
- ferromagnetic minerals, demagnetization of remanent magnetization by pressure application 9-24710
- galvanic cell for determ. of thermodynamic props. in Fe-O system 9-44828
- girdle type high press. unit for range 20-70 kb 9-33988
- glass, at diff. temps. 9-28193
- heptane, frozen, fluoresc. spectra of coronene and 1,12-benzoperylene 9-32517
- isostatic pressing technique for prod. of dense ceramics 9-30726
- Laves phase alloys, ferromag. pressure depend of Curie temp. 9-45129
- magnetic props. meas. using vibrating coil magnetometer 9-45047
- manganin coil press. gauge, calibration to 60 kbar under hydrostatic press. 9-40215
- material state at up to 10¹⁷ atm. and 10⁸ °K 9-25052
- melting curves of volatile materials 9-48737
- melting law 9-36919
- octanol isomers, dielec. relax. 9-30418
- organic polar liqs., dielec. props. 9-39109
- phase transf., h.p.-induced, visual obs. 9-30735
- piezoelectric materials in strong elec. fields, under high press., electromechanical characs. 9-47185
- polypropylene, crystallization rel. to structure and thermal behaviour of phases formed 9-46711
- α -quartz, Raman spectrum 9-31118
- quartz-crystal viscometer, resonant freq. changes with pressure to 8000 atm. 9-41809
- ruby: Cr³⁺, hydrostatic pressure up to 7 kbar, e.p.r. 9-33655
- steel, effects on microstructure and hardness 9-23967
- thermal explosions 9-36205
- thiourea, ferroelec. phase transitions 9-28567
- three-stage apparatus, modified Bridgman anvil, operational details 9-49616
- transducer for i.r. meas. to 10000 atm. 9-34005
- transition metal difluorides, phase transform. and stability 9-37299
- triphenylene phosphoresc., matrix site effects 9-49326
- urea, aq. solns., u.s. absorpt. and velocity 9-30400
- u.s. method for eqn. of state of liq. 9-34872
- viscometer, low-shear-rate, for 120000 lb/in² 9-36740
- ZrB₂ densification during hot pressing 9-30708
- Ag halides, B1-type, phase transform., X-ray diff. obs. 9-41063
- Ag halides, melting curves 9-44615
- AgCl, up to 100 kbar, eff. on velocity of ultrasound 9-24023
- AgCl(Br), optical absorpt. edge press. shift 9-45312
- Al-(4.3 wt.%)Cu alloy, effect on precip. 9-42917
- Al-I Bi tunnel junctions, resistance versus bias meas., effects up to 30 kbar, 77°K 9-37556
- Al₂O₃, microwave dielectric constant, 375 kb 9-28547
- Al supercond. critical temp. 9-37467
- AlN, static and dynamic, influ. on hardness 9-26361
- Ar, eqn. of state 9-42690
- Ar, isotherms to 10 kbar and 400°C 9-32732
- Ar, liq., eqn. of state 9-39071
- Ar, liq., thermodynamic props. 9-39070
- Ar h.p. 20 ns spark channel, radiance saturation and afterglow emission 9-30314
- Au, electronic props. and hyperfine interactions, relativistic calcs. in Wigner-Seitz model 9-26481
- BaMnO₃ perovskite-like struct., phase transf. and stability relations 9-35241
- BaTiO₃ polarization reversal 9-43116
- C, dynamically compressed, metallic state existence 9-30847
- CS₂, cryst. struct. 9-32903
- CaAl₂O₄, high pressure transformations 9-44799
- Ca(NO₃)₂:KNO₃ glass-forming melts, elec. cond. 9-39113
- CdO-Cr₂O₃-O₂ system, 2 to 3500 atm. O pressure 9-28404
- CdSnAs₂ supercond. polymorph prep. 9-41178
- CoF₂, phase transitions, up to 160 kbar 9-44800
- CoS: Curie pt change 9-33452
- Cr and alloys, rel. to itinerant antiferromag. optical and pressure effects 9-45213
- CsMnF₃ perovskite-like struct., phase transf. and stability relations 9-35241
- CsNiF₃ structure and mag. props. 9-45059
- Er, effect on magnetic susceptibility, up to 6 kbar 9-28594
- EuSe, mag. props. 9-47287
- EuTe mag. props. 9-47287
- Fe-3 wt.%)Si alloy, polycryst., effect on slip, twinning and fracture 9-33053
- Fe, yield behaviour changes, effect of grain size 9-28347
- Fe, yield behaviour changes, effect of grain size 9-28346
- α -Fe₂O₃, hydrostatic pressure influence on electrical conductivity and thermoelectric power 9-33300
- FeCl₃.6H₂O, oxidation state, pressure causes charge transfer 9-27851
- FeCl₃.6NH₃, oxidation state, pressure causes charge transfer 9-27851
- FeF₃.3H₂O, oxidation state, pressure causes charge transfer 9-27851
- GaS(Se, Te), pressure eff. on spectral distribution of photoconductivity 9-28579
- H₂O, cond. and ionic dissoc., 100 kbar and 1000°C 9-44585
- H₂O, modification, change in physical and chem. props. 9-26076

High-pressure phenomena and effects continued

- He h.p. 20 ns spark channel, radiance saturation and afterglow emission 9-30314
⁴He, liquid, decay threshold of quasiparticles variation in nature 9-48729
 HgCr₂S₄(Se₄) spinels, ferromag. phase transitions, pressure depend. up to 10 kbar 9-45119
 HgCr₂S₄(Se₄) spinels ferromag. phase transitions, pressure depend up to 10 kbar 9-45119
 Ho, effect on magnetic susceptibility, up to 6 kbar 9-28594
 In, electronic density of states, nonlinear pressure effect, H₂ change 9-37407
 n-InSb thermolec. power and conductivity up to 16 Katm. 9-28501
 Ir supercond. transition temp. 9-44940
 KBr window for i.r. spectroscopy under high pressure 9-32065
 KNO₃, cryst. struct. 9-32903
 Mg_{0.8}Mn_{0.2}Fe₂O₄, hydrostatic pressure influence on electrical conductivity and thermoelectric power 9-33300
 MgCO₃, hot pressing, behaviour 9-33111
 MgO-Cr₂O₃-O₂ system, phase equilibrium, 2 to 3500 atm. O pressure 9-28404
 Mg(OH)₂, hot pressing, behaviour 9-33111
 Mn₂O₄, high pressure transformations 9-44799
 MnAs, magnetic props. 9-24303
 MnF₂, phase transitions, up to 160 kbar 9-44800
 MnF₂, polymorphism, X-ray diff. obs., phase diagram and transforms. 9-39184
 Mo, neutron irradi., effect of hydrostatic pressure on elec. resistance recovery 9-35342
 Mo, neutron irradi., recovery of lattice parameter increases 9-40909
 Mo, polycryst., pressurization depend. of ductile-brittle transition temp. 9-30742
 N₂, isotherms to 400°C and 10000bar 9-44520
 NH₄Br, phase transitions 9-30633
 NaBrO₃, n.q.r., press. and temp. depend. of ²³Na freq. 9-39928
 NaCl, transition pressure for NaCl-CsCl struct., quantum mech. calc. 9-23985
 NaF, transition pressure for NaCl-CsCl struct., quantum mech. calc. 9-23985
 Ni, shock hardening in range 820 to 1500 kbar, rel. to microstructure 9-30701
 Ni_{0.9}Fe_{2.1}O₄, hydrostatic pressure influence on electrical conductivity and thermoelectric power 9-33300
 NiF₂, phase transitions up to 160 kbar 9-44800
 NiFe₂O₄, furnace for single crystal growth from fluxed melts 9-35028
 NiO-Cr₂O₃-O₂ system, phase equilibrium, 2 to 3500 atm. O pressure 9-28404
 NiS, compressibility of lattice, T>T_a and T<T_a 9-44672
 Pb-Bi alloys, d.h.c.p. phase form 9-44802
 Pb supercond. critical temp. 9-37467
 Pd-Ni alloy, effect on Curie temp. up to 6 kbar 9-28611
 RbNiF₂ perovskite-like struct., phase transf. and stability relations 9-35241
 Sb, superconductivity 9-39602
 Sb₂S₃ and Sb₂Se₃, photoelec. props. 9-28571
 SbSI, dielectric props., and temp. depend., 30 to -60°C 9-43104
 SbSI, ferroelec., anomalous shift of absorpt. edge, Kern-Harbeck effect 9-26591
 Se rectifiers, critical breakdown voltage from I-V characs. 9-26564
 SrMnO₃ perovskite-like struct., phase transf. and stability relations 9-35241
 TiCl(Br), optical absorpt. edge press. shift 9-45312
 TiNiNiF₂ perovskite-like struct. phase transf. and stability relations 9-35241
 UC_{1.08}, compressive creep, 1200-1600°C, 3000-10,000 psi 9-23899
 V₂V₃, metal-semiconductor transition, critical pressure 9-44921
 Y-C₃, synthesis and superconducting props. 9-35372
 Y-C₃, synthesis and superconducting props. 9-35372
 ZnF₂, phase transitions, up to 160 kbar 9-44800
 ZrSiO₄, high pressure transformations 9-44799

High-speed photography *see Cinematography; Photography/high-speed***High-temperature phenomena and effects**

- air microwave breakdown temp. depend. 9-32708
 diamond-silicon interaction 9-26807
 electrical conductivity meas. of solids, thermionic emission influence 9-44899
 emissivity of high M.Pt. metals, effect of oxide films 9-28435
 exploding wire process as source for studies 9-29138
 Ising model, sp. ht. 9-35542
 material state at up to 10¹⁷ atm. and 10⁸ °K 9-25052
 materials, physics and chemistry, bibliography 9-41718
 mechanical behaviour of solids, interdisciplinary approach, book 9-39431
 MGD plant, open cycle, temp. reduction due to injected additives 9-22334
 plasma, physics of, book 9-23262
 refractory materials, compressive creep characs. 9-37244
 refractory materials, permittivity, microwave polarimetric meas. to 1200°C 9-38342
 research instruments 9-40213
 sapphire whiskers, tensile strength 9-35180
 solids, u.s. props., Au-In alloy use as bonding material 9-46983
 solids, vaporization, matrix isolation techniques 9-28190
 Ar microwave breakdown temp. depend. 9-32708
 Cs-graphite system, sorption characs., low Cs pressures 9-39168
 Cu-(16 at.%)Al solid soln., creep behaviour 9-33043
 α-Fe, creep 9-30670
 H₂O, cond. and ionic dissoc., 100 kbar and 1000°C 9-44585
 MnF₂, polymorphism, X-ray diff. obs., phase diagram and transforms. 9-39184
 N₂ microwave breakdown temp. depend. 9-32708
 Ni-Fe alloy creep, 550°-1000°C., obs. 9-23897
 W, solubility of N₂ 9-35136
 Zn bicryst., grain-boundary crack formation during deform. at high temp. 9-30698

History

- aurora, work of Birkeland and his successors 9-33999
 eclipses, reliability of ancient records 9-29081
 electrical conduction in solids, Sir John Leslie, (1791) 9-47065
 geomagnetic field 9-45547
 the great experiments of physics, book 9-22029

History continued

- Lorentz's electron theory of relativity development reviewed 9-43697
 lunar auxiliary tables and related texts from late Babylonian period 9-41673
 nebulae, astronomical obs. 9-22027
 nebulae observations by four 16th-17th century astronomers 9-34000
 pulsars, identification with ancient Chinese guest stars 9-47660
 Quantum theory, compilation of 17 famous articles, book 9-27172
 solar granulation, review of early observations 9-27101
 X-ray crystallographic intensities meas. 9-23703

Hodoscopes *see Cosmic rays/apparatus; Particle detectors***Hole theory of liquids** *see Liquids/theory***Holes** *see Crystal electron states; Semiconducting materials; Semiconductor***Hollow cathode** *see Discharges, electric***Holmium**

- diffusion in b.c.c. Pr 9-33007
 growth of single crystals by three methods 9-37078
 Lorenz functions, elec. resistivity and thermal conductivity 9-33195
 magnetic susceptibility, effect of hydrostatic pressures 9-28594
 magnetic transition, cone-to-spiral, near 20°K, by soft spin-wave modes 9-43151
 Mossbauer effect study of single crystal mag. structure 9-47333
 phonon dispersion relations, neutron spectrometry 9-28415
 spin-wave dispersion relation in spiral mag. phase 9-45112
 spin-wave excitations in conical and spiral mag. phases 9-45111
 thermal conductivity, 0.6-4.2°K: enhancement at 1°K, Lorenz no inc., nuclear hyperfine contrib. 9-33197
 thermal conductivity, elec. resistivity and Lorenz functions 9-33195
 thermal conductivity of single crystal as function of temp 5° to 300°K 9-47009
 u.s. attenuation near mag. phase transitions freq. and temp. depend 9-48958
 u.s. scatt., critical, in paramag. region near Neel temp. 9-24027
 X-ray satellite reflections due to aspherical 4f charge density, theory and expt. 9-24441
 Ho²⁺, (f-f) absorption spectrum obs. in CaF₂ 9-28682
 Ho²⁺ in CaF₂, SrF₂ and BaF₂, thermal ionization potentials 9-46739
 Ho³⁺, coherent emission from electro-optic crystals, obs. 9-26738
 Ho³⁺, energy transfer with Er³⁺ in Y₃Al₅O₁₂ 9-31126
 Ho³⁺ in CaF₂, luminescence absorption and relaxation spectra 9-35681
 Ho³⁺ in CaF₂, thermal conductivity in mag. fields 9-47008
 Ho³⁺ in LiNbO₃ electro-optic crystals, second-harmonic radiation at 77°K 9-43203
 Ho³⁺ in YGA garnet and YFE garnet optical absorpt. and emission studies 9-45331
 Ho³⁺ optical centres in CaF₂ luminesc. 9-33579
 in YFe garnet, ferrimagnetic resonance linewidth and fine structure 9-26790

Holmium compounds

- ferrite films, Faraday effect, mag. field effect 9-49216
 Ho₂O₃ garnets, recrystallization behaviour on pulse annealing 9-30489
 HoCo₃, ferrimag., compensation temp. press. variation 9-45154

Holography

- acoustic, laser flying spot hologram recording technique 9-29293
 acoustic, non-time-averaged instantaneous 9-36193
 acoustic, phase-only 9-29440
 acoustic, underwater, practical aspects 9-43793
 acoustic and microwave, temporal reference 9-25146
 acoustic applications 9-22432
 acoustic holograms by electronic means 9-27230
 acoustic image reconstruct. from sampled sound-wave hologram 9-34086
 acoustic imaging 9-48058
 acoustic principles and applic. 9-48067
 acoustical, image distortion in reconstructions from phase-only diagrams 9-36192
 acoustical imaging of sources of radiated acoustic energy 9-43791
 acoustics, laser light reconstruction 9-22433
 alternative techniques not employing holograms 9-40371
 ofanimate objects, toleration of dark reconstructions rel. to more movement 9-41928
 application to supersonic aerodynamics 9-31985
 and its applications, introduction 9-34179
 ballistic, applic. of laser beams 9-31986
 biomedical applications of holography, popular article 9-49598
 camera, for recording interferograms 9-46032
 camera, wide view-angle 9-1925
 capabilities and applications, review 9-34182
 cine-interferometry, submicrosecond, of transmission objects 9-48055
 circular, of 3D objects, using a cone 9-27347
 coherent imaging and holography, review for undergraduates 9-25321
 complex spatial filtering by holographic Fourier subtraction 9-22427
 contouring using single, multifreq. ruby laser pulse 9-48056
 dark reconstruction toleration rel. to more movement of object 9-41928
 deconvolution method of object reconstruction 9-48062
 deformation meas., use of short laser pulses 9-29445
 development and applications 9-22432
 diffraction gratings, holographically made, spectrographic performance 9-34214
 diffraction of light by u.s. standing wave, spectrum analysis by holographic method 9-36320
 diffraction pattern, moire phenomena with unaided eye 9-27351
 double image elimination using single sideband waves 9-40367
 dual-beam prod. scheme with prism, Q-switched ruby laser 9-29442
 dynamic event observation 9-36329
 film-grain noise, small-signal analysis 9-27353
 Fourier, useful object space calc. 9-22431
 Fourier-transform grams obtained using Fresnel zone plate achromatic fringe interferometer 9-40365
 Fourier-transform system, lensless, field of view enlargement, multiple-reference source technique 9-34184
 Fraunhofer, reliability for bubble chamber photography 9-27600
 Fresnel, partial coherence 9-45975
 general theory, reformulated 9-36331
 generation and reconstruction by computer 9-27357
 gratings, reconstructing response and efficiency 9-27354
 gratings of arbitrary loss, theory and experiment 9-45999
 heterodyne technique for phase and amplitude sampling, laser beam probe 9-48073

Holography continued

- hologram, microwave, photoetching technique 9-34183
- hologram imaging by ray tracing, evaluation 9-36323
- holograms, incoherent, bias level reduction 9-36321
- holograms, quaternary phase-only, computer generated 9-36325
- holographic image brightness, function which characterizes photographic film 9-27346
- image degradation, atmospheric 9-40366
- image degradation in undersampled holograms 9-27349
- image digital reconstruction 9-36330
- image enhancement technique, linear and nonlinear operations with hardware, review 9-29443
- image formation using laser brightening, charact. 9-36326
- image formation with arbitrary holographic type surfaces 9-34198
- image sharpness restoration 9-40370
- imaging with coherent fields, diffraction theory 9-27355
- information processing applic. 9-48064
- inhomogeneous medium, penetration 9-45974
- intensity pattern mapping process, using integral transform 9-27352
- interference, of liquid films 9-34185
- interference fringes 9-43873
- interferograms, multiple beam, production 9-45972
- interferometric fringe display contrast, optimizations 9-31977
- interferometry, 'time average' multiple exposure and 'real time', theory 9-29441
- interferometry, appl. to meas. of combination mode vibr. patterns 9-38292
- interferometry, double-exposure dark-field, fringe. multiplication applic. 9-45995
- interferometry, multiple-beam, for object phase variation meas. 9-36324
- interferometry, principles and applic. 9-45994
- interferometry with phase-modulated illumination 9-48089
- introductory tutorial paper 9-36327
- kinematic, continuous reconstruction 9-29444
- large hologram prod. by using diffuser as a beam splitter 9-43904
- with laser (Jena ZGL 300) 9-43905
- laser beam interactions with ionised gases 9-34793
- laser source, repetitive Q-switching 9-29476
- laser spark, two-wavelength investigation 9-31981
- liquid surface, refinements and variations 9-36190
- mathematical analysis 9-27345
- medical appls. 9-49600
- microscope exit pupil enlargement using partially coherent light 9-22466
- microscopic, review 9-48061
- modulated laser beams, amplitude and/or phase, spectral analysis method 9-25330
- motion picture, Q-switched ruby laser applic. 9-25322
- multiple exposure, 360° view 9-31976
- multiple exposure, time varying three-dimensional fields 9-31975
- nondestructive testing 9-42862
- nonlinear, 5 point analysis 9-40369
- nonlinear effects due to photographic mat., polynomial reln. between exposure and amp. transmittance 9-25327
- object flux transmittance, power spectrum determ. 9-40368
- with partially coherent radiation 9-31980
- phase holograms, quaternary, computer generated 9-36325
- phase recording by interference between reconstructed wavefronts from separate holograms 9-22430
- photochromic film use 9-22428
- photoelastic model, sum of principal stresses 9-31818
- photographic recording, compensation of motion blur by shutter modulation 9-45973
- plasma density meas., methods 9-44461
- for plasma diagnostics, survey of investigations (1966-1967) 9-30257
- point, multiple imaging 9-31978
- polarization recording with an encoded reference beam 9-22426
- presentation in undergraduate course 9-38389
- principles and applications, book 9-48070
- pseudoscopic image, appearance and location rel. to diff. operator 9-47852
- pulsed laser reflected light, with stop action 9-27339
- radiation wavefield scatt. by object during photography, 3-dimens holgram reconstruction 9-27348
- of randomly moving objects 9-48057
- of rapid transient processes 9-31983
- rapidly moving object position and velocity meas. 9-31984
- reciprocity theorem appl. 9-41929
- reconstruction using time varying elec. signals 9-41926
- recording on photopolymer materials 9-25324
- recording using temporal modulation 9-25325
- reflection holograms, pushed ruby laser, single-mode 9-22425
- review for undergraduates 9-25321
- rotation-stroke, for vibr. surface phase meas. 9-43792
- scanned u.s., refinements and variations 9-36190
- scanning of source, object and receiver 9-31979
- Schlieren and phase-contrast methods 9-34181
- Shock waves caused by hypervelocity projectiles 9-22435
- signal-to-noise ratios for holograms, subjects in strong incoherent light 9-31974
- spatial filter applications 9-36328
- spatial filtering experiments for the undergraduate laboratory 9-43699
- spatial filtering for image deblurring and aperture synthesis 9-48063
- speckle noise elimination, multiple beam technique 9-25326
- in spectrography, Fourier, high luminosity and low noise 9-46018
- state of the art (1969), review book 9-40372
- storage of three-dimens. meas. information, applics. 9-45971
- in strain detection 9-42873
- stroboscope method for vibrations study 9-31843
- stroboscopic, using mode-locked laser 9-48059
- table, inexpensive 9-36319
- theory and applications 9-29439
- three-dimensional diffuse objects, high-quality hologram prod. using single-mode ruby laser 9-48065
- total internal reflection, applic. to microscopy 9-41927
- transient event recording, reconstruction and evaluation 9-31982
- transmission of holograms on facsimile channels 9-48068
- of transparent objects, using dispersion 9-48069
- for ultrasonic images, 3-dimensional 9-27350
- u.s., limitations 9-36191
- U.S., liq. surface and scanned, refinements and variations 9-36197

Holography continued

- u.s., review mainly covering Gabor hologram 9-48066
- u.s. imaging techniques for optically opaque structures 9-29295
- velocimetry, data processing methods 9-48539
- velocimetry, three dimensional flow-fields 9-48538
- vibration amplitude meas. using Powell and Stetson fringes 9-22434
- volume, image storage and reconstruction process 9-27356
- work at USSR State Optical Institute 9-38392
- X-ray Fraunhofer, hologram, image reconstruction with visible light 9-46003
- X-ray hologram, plane-grating, construction with electron microprobe 9-38391
- X-ray images, three-dimensional, prod. 9-22429
- Bi films, holograms with > 6% efficiencies and resolutions close to 1000 lines/mm 9-45970
- EuO film, thermomagnetic writing and reconstruction of hologram 9-48060
- MnBi magnetic, Curie-point writing 9-25323
- PbI₂, photosensitive films, holographic recording 9-38390

Hot-atom chemistry *see* *Chemical analysis/radioactive; Nuclear reactions and scattering/chemical effects; Radiochemistry*

Hubble model *see* *Cosmology*

Hugoniot diagrams *see* *Equations of state*

Humidity

- see also* *Atmosphere/humidity; Hygrometers; Moisture*
- atmosphere, strong and weak absorption spectra 9-24638
- pendulum length, effect 9-45803
- of soil, psychrometer for meas., 50-thermocouple with digital recorder 9-33732

Hydrodynamics

- see also* *Flow/liquids; Jets; Liquid oscillations; Liquid waves; Magneto-hydrodynamics; Viscosity/liquids*
- air-graphite suspension as heat transfer agent 9-30437
- almost incompressible flow equations, numerical solutions 9-40640
- atmospheric, instability for quasi-geostrophic model, numerical solns. 9-41497
- Boussinesq fluid in circular cylinder, spin down 9-32566
- bubble, ellipsoidal, in slightly viscous fluid 9-38941
- buoyancy driven system, instabilities rel. to mechanical and buoyancy forces 9-48530
- buoyancy forces effect on boundary layer flow over heated vertical plate 9-34729
- cavity containing fluid, nonlinear oscillations 9-41790
- classical fluid, Enskog eqn. soln. 9-44395
- couette flow, rotating, wave-number selection for Taylor vortices 9-34724
- Couette flow, rotating, wavelength var. and changes in wave-form and mean flow 9-34726
- critical fluid, eqns. and scatt. function 9-34709
- critical opalescence, nonlocal eqns. 9-23576
- cylinder, circular, in cross-flow up to $Re=5 \times 10^6$, local pressure distrib. and skin friction 9-25805
- cylindrical tube obeying Stokes' law, hydrodynamic field of ellipsoid of revolution 9-32565
- density-stratified medium, internal wave generation with mixed region collapse 9-34862
- diffusive flow in porous medium, soln. equiv. with Yih's for non-diffusive flow 9-40761
- disc moving in two superposed liqs., gravity wave drag at interface 9-26066
- DNA, properties 9-23415
- drops, charged suspended, equilb. and coalescence 9-44544
- elastico-viscous fluid, fluctuating flow past porous wall with variable suction 9-34734
- elastohydrodynamic, time-depend. film profile meas., optical-interference method 9-36840
- equations in tensorial form valid for any curvilinear coordinate systems 9-40635
- flexible cylinder, submerged, towed, lateral motions rel. to end shapes and tow-rope length 9-26596
- flow of finite irrot. incompressible frictionless fluid 9-32571
- fluid, viscous incompressible rotation, source and sink on axis 9-44532
- fluid interface, perturbations with transverse electrostatic field 9-32569
- fluids, Rayleigh-Taylor instability with Hall currents 9-34710
- gravity waves, internal, in fluid with spatially varying mean flows, ray tracings 9-42478
- gravity waves attenuation, turbulent conditions 9-30182
- gravity waves in rot. homogeneous ideal fluid 9-27957
- interfacial flow near two-phase boundary, critical wave length from linear theory 9-40633
- irrotational field round sphere in incompressible fluid 9-25800
- Laplace's tidal eqns. over sphere, eigenvalue calcs. 9-49428
- liquid compression processes near elec. discharge, X-ray obs. 9-32767
- liquid-vapour interface in accel. container, large-amplitude irrotational motion 9-34711
- mutually soluble liquids, filtered mixing in porous medium with one-sided miscible displacement 9-39079
- in Newtonian mechanics textbook 9-36155
- non-linear interaction of inertial modes rel. to steady geostrophic circulation 9-46435
- non-Newtonian eqns. influence on rheological model 9-36829
- nonlinear waves propag. along rotation axis in fluid 9-44540
- numerical, transport of turbulence 9-38939
- oscillating foil in plunging or pitching modes, lifting problem, second-order theory 9-23410
- oscillations retarding falling spheres 9-32742
- plane plate in supersonic flow field, vel. fluctuations 9-40636
- power law flow in the wake of a flat plate 9-44394
- quantum, commutators for interacting Bose system 9-45794
- quantum, using current-current commutation relations 9-46436
- radial filtering currents, non-stationary, plane, when sources and sinks continuously distributed within bounded regions 9-39062
- Rayleigh-Taylor's instability, eff. of mag. field and Coriolis forces 9-46434
- Rayleigh-Taylor instability, effect of surface tension 9-46598
- Reiner-Rivlin fluid, permanent rectilinear flow theory 9-23411
- rotating cylinder of fluids, boundary layer soln. of centrifugally driven thermal convection 9-34720
- rotating fluid, turbulent jets and plumes, similarity solutions 9-23213

Hydrodynamics continued

- rotating fluid bounded by concentric spheres, free periods of oscill. 9-46596
- rotating fluids, instability of inertia oscillations, effects of radial law of depth 9-25801
- rotating plate in elastico-viscous liq., flow reversal due to edge effects 9-39063
- rotations, non-stationary, linearized of a viscous liquid 9-32744
- similarity solns., props. 9-23211
- slow steady rotation of sphere in second-order fluids 9-34850
- sphere and viscous fluid in cylindrical tube, theoretical study of slow motion 9-25812
- sphere in viscous medium, resistance and vel. determ. 9-30172
- sphere oscillation in compressible viscous fluid in slip regime 9-40634
- sphere in viscous liq., drag experienced with vel. depend. on single time scale 9-26080
- spheres falling in viscous fluid, along line of centres 9-25802
- spheres in laminar flow, drag coeffs. and transfer factors 9-28083
- spin-up, delay times meas., liq. He II contrast 9-23413
- spinwave theory in antiferromagnets 9-45203
- stability of axisymmetric jet with parabolic vel. profile 9-34719
- stability of fluid motions, energy method for determination of sufficient conditions 9-42620
- statistical dynamics of a turbulent incompressible fluid 9-48534
- steady flow around cylinder, numerical soln. at Reynolds numbers 40, 200 and 500 9-34848
- stratified flow over obstacle, wake turbulence and validity of Long's model 9-40758
- stratified flows, steady, soln. using eqn. with horiz. co-ords. as space variables 9-40760
- stream, conducting, coupled via mag. or elec. field to elastic medium 9-25829
- tangled vortex lines, degree of knottedness 9-34712
- Taylor instability, nonlinear osc., soln. near cutoff wave number 9-46597
- time-correlation functions characterizing hydrodynamic systems 9-34055
- turbulence, incompressible fluid, physical model 9-44537
- turbulent drag reduction by viscoelastic fluids, mechanism 9-42621
- turbulent wakes behind circular cylinders, one-dimens. spectra for large range Reynolds number 9-46589
- velocity gradients at surface, for flow round cylinder at Reynolds numbers 5×10^3 to 10^5 9-34847
- viscous flow near entrance and exit of a pipe 9-34715
- viscous flow in rotating pipe, spiral wave instabilities 9-34721
- viscous fluid, steady-state motion caused by ellipsoid of rotation and round disc 9-42619
- viscous fluid flow between coaxial rotating cylinders 9-34849
- wall reattachment theory, developments 9-23416
- zonal flow and quasi-stationary long wave, interaction 9-34844
- H liq. whirling layer under high heat flux 9-26052
- Hg surface waves, influence of axial magnetic field 9-30358

Hydrogen

- see also Deuterium; Protons and antiprotons; Tritium*
- absorption by Ar, influence of temp. history, 9°K 9-36966
- adsorption on Au, spectroscopic obs. 9-35001
- adsorption on Si surfaces, differently oriented, atom recombination kinetics 9-36968
- annealing of Fe-C alloy, surface contamination effects 9-36938
- atom, 5-70 keV, Mg vapour, electron transfer cross-section meas. 9-22997
- auroral emission, location midnight reversal 9-33816
- bond strengths, significance of i.r. freq. shifts 9-25726
- burning in envelope of white dwarf, as model for pulsating radio source 9-31575
- charge exchange with I ion beam, equilibrium charge state 9-46319
- chemisorption on transition metals, self-consistent model 9-24548
- combustion, shock-initiated, chem. kinetics 9-39946
- desorption from 100 nickel surface, study of binding states 9-23646
- diffusion in Ba, 200 to 620°C 9-28315
- diffusion in Cu-Pd 9-23838
- diffusion in f.c.c. metals, activation energy 9-23841
- diffusion in Pd alloys, coeff. variation with H conc. 9-28322
- diffusion of H atoms in H₂ 9-39060
- diffusion up thermal gradient in Zircaloy-2 9-28310
- disturbance effects on Kr 1236 Å and Xe 1295 Å resonance beams 9-44265
- electrolysis, liberation with O on electrode, electrode glow 9-41454
- emissivity, temp. range 6000-12000°K for 1,10 and 100 cm layers 9-26035
- e.p.r. coupling consts. for α radicals containing C, H, N and O atoms, extended Huckel calcs. 9-23025
- formative time lags in breakdown 9-34814
- galaxy evolution from gas, mechanism 9-43519
- galaxy evolution from gas in hot universe 9-43520
- in galaxy M101, asymmetry of distrib. rel. to tidal effects 9-41626
- hydrogenation of Ni crystals, effect on deformation 9-46892
- intergalactic, in Virgo cluster of galaxies 9-26991
- interstellar, neutral absorpt., rel. to meas. of pulsar distances 9-41663
- interstitial, diffusion in metals, phase diagrams and solubility meas. for gas to liquid transition 9-31522
- ionized, partially, structure of shock waves 9-48653
- ionosphere F region equilibrium distributions, atoms and ions 9-24700
- isotope exchange between liquid ammonia and H, separation factor 9-31180
- liquid, specific heat deriv. from molecular model 9-34869
- liquid, stability of electronic bubbles 9-46608
- liquid, use in Saturn V, problems 9-45572
- liquid whirling layer under high heat flux, thermal, and hydrodynamic obs. 9-26052
- Lyman α , Venus, Mariner 5 obs. 9-31614
- Lyman α from Venus, Mariner 5 obs. interpretation 9-24870
- maser, atomic jet populations meas. 9-45943
- metallic from mol. bond transition 9-42738
- in metals, content, n.m.r. determ. 9-43345
- molecular beam, high-energy triatomic, ionization on impact with D target 9-46328
- in nebulae, gaseous, high-level populations 9-28992
- NGC 5253 galaxy, H α emission spectra obs. 9-35958
- penetration in solids, mechanism for cavitation damage? 9-44746
- plasma, collisional-radiative ionization coeffs. rel. to atomic collisions 9-42495

Hydrogen continued

- plasma, eqn. of state and ionization degree, calc. 9-38957
- plasma, finite partition functions 9-46461
- plasma, highly ionized, relaxation theory applies. 9-40651
- plasma, nonthermal, ions and atoms density ratios 9-32605
- plasma current instability in strong alternating elec. field 9-25960
- plasma in homopolar rot. device, 10^{-4}mm Hg , electron collision freq. and current growth 9-25857
- plasma in impulse tube, electron density and temp. meas. by rapid scan spectrometer 9-44419
- plasma jet, methane decomposition reactions, dissipative terms calc. 9-38994
- radiation from $3^3\text{D} \rightarrow 2^3\text{P}$ transition, polarization 9-32430
- reaction with graphite at 1900°C 2400°K 9-43315
- solar Lyman α profile rel. to geocorona, rocket obs. 9-29084
- solar spectrum, Jefferies-Thomas computation and obs. rel. to photosphere and chromosphere models 9-31637
- solid, coating interstellar graphite particles, formation and optical props. 9-43572
- solid, thin foil, prod. for targets in high vacuum 9-27147
- solid pellets, launching device for laser irradi. expts. 9-45709
- solubility in Ni-Mo and Ni-W alloys 9-39478
- sparks at small pd values, plasma discharge development 9-39032
- in steel, austenitic, internal friction and embrittlement obs. 9-33085
- superconducting solid to liq. transition under influence of zero pt. energy 9-42738
- target with cooling system for use with high power e and γ beams at SLAC 9-29677
- thermometer, vapour press., comparison with Pt resistance thermometer 9-45885
- transient expansion from a storage reservoir of real H 9-23380
- in tungstates, n.m.r. obs. in metal heteropolytungstates 9-43303
- Venus, content in upper atmosphere 9-40172
- Z pinch discharge, conical, obs. 9-40680
- in Fe filings and whiskers, effect of cry. struct. and thermal expansion 9-44666
- H-F branched chain reaction based chem. laser 9-47984
- H-N mixtures, diffusive separation using isotope solvents 9-28824
- H₂-Ar-air flames, turbulent, atoms fluoresc. power efficiencies, obs. 9-24601
- H₂-D₂ mixed solid solutions, i.r. spectra induced into vibrational first harmonics, 4°K 9-33558
- H₂-D₂ solid solution, fundamental bands at 4°K 9-28684
- H₂-XeF₄, SbF₅ mixtures photolysis, HF chem. laser emission, obs. 9-31944
- H₂, electron drift and resonance scatt. in terms of H₂⁺ temporary states 9-46578
- o-H₂, solid, order of phase transition 9-46955
- p-H₂, thermal conductivity, rotational energy contribution, Eucken factor 9-26032
- H₂ and H collision, -ve charge prod. cross section determ., 50-1000 eV 9-27826
- H₂ collision with incident beams of H, He, He⁺⁺; electron and ion prod. cross section meas., 0.15-1.0 MeV 9-22982
- H₂ gas, n.m.r. relaxation time meas., 293-738°K, 7-135 atm., J depend. on collisions 9-34616
- H₂ liq., thin-walled target, p scatt., uniform solid angle available 9-32244
- H₂ transport and reactivity applic. to control of nuclear reactor 9-22883
- H α line contours in emission nebulae 9-41630
- H β auroral emission obs. 9-31372
- H γ auroral emission obs. 9-33819
- H⁺ in CaF₂:R³⁺, (R=rare earth), spectra 9-47353
- H II regions, electron temp. distrib., opt. and radio meas. 9-24757
- H(2s) metastable atom prod. in H⁺-H(ls) electron capture process, cross section obs. 9-27827
- He⁺ on Rb. K. Cs; total charge-transfer cross section meas., 10-1500 eV 9-46316
- in NaBa₂Nb₂O₅, absorpt. spectra obs. 9-41374
- in Ni, electrolytic, influence on magnetomech. damping 9-39401
- o-H₂, solid, spin-lattice coupling, low-temp. thermodynamic effects 9-44811
- O₂-H₂ flames, turbulent atoms fluoresc. power efficiencies, obs. 9-24601
- osptopic effect in NaH₂(SeO₃); crystals 9-30973
- p-H₂, rot. relax., and in mixtures with He, Ne, Ar 9-42611
- Pd/H₂ syst., susceptibility meas., 50°C - 100°C 9-41295
- in SmCO₃, influence on mag. props. 9-45073
- in α -Ti, effect on relaxation spectrum 9-30648
- in α -Ti, effect on relaxation spectrum 9-30647

ions

- back-scattering of high energy ions in Nb and Ti 9-39549
- Balmer line, emission and absorption coefficient in arc plasma 9-34576
- charge exchange and electron loss with H₂O vapour, energies 1 to 60 keV 9-44493
- collision with ground state of all elements, 5-140 keV calc. of charge exchange exchange ratio of excited to all captures 9-25717
- earth's polar wind 9-26925
- electron transfer cross-sections, 5-70 keV, in Mg vapour 9-22997
- excited ionization by neutralizing accel. protons in gaseous targets 9-46327
- θ -pinch, density, temp. and mag. field structs of plasma shock fronts 9-46497
- inverse pinch, m.h.d. prod. of collisional shocks, characts. 9-46495
- ionization model, ohmically heated electrons 9-23342
- ionization of Al, cross section and K-shell X-ray yield meas., E=25-200 keV 9-22940
- plasma, expansions in Laval nozzles, approximate calc. 9-46471
- plasma, highly ionized, decay, spectral and microwave obs. 9-40665
- plasma, normal ionizing shock waves, electrode config. effects 9-44429
- plasma, radiative energy transfer, Planck and Rosseland coeffs., line and continuum rad. 9-48554
- plasma, thermodynamic functions, approximate calc. 9-46464
- plasma, transient, prod. by normal ionizing shock wave 9-23276
- plasma discharge column, low press., distribution of ionization states 9-46542
- plasma production by giant pulse-laser irradi. of solid, characts. 9-28021
- plasma temp. from intensity ratio H β to background 9-30261
- positive ions, drift vel. and lateral diffusion in hydrogen 9-44491
- production by impact of triatomic high-energy molecular H beam on D target 9-46328
- from pulsed sources, increased yields 9-43861

Hydrogen continued
ions continued

- Stark effect, asymmetry in Balmer lines in transverse elec. field 9-48423
stars, G. K. and M., i.r. region photometric study of emission spectra 9-31539
Sturm-Liouville matrix eigenvalue problem, oscillation theory and computational procedure, $3s\sigma$ state 9-32475
D⁺-polarized beam from charge exchange in Cs 9-25192
D⁺-D₂(H₂) charge-exchange collisions, search for isotope effect 9-44295
H₂-ve glow, electron temp. and density determ. by diffusion and recombination, 0.06-0.6 torr 9-40723
H₂, pre-ionized, fast pulsed discharge, plasma props. 9-39025
H₂, D₂ and HD, ion-mol. reactions, ion cyclotron reson. 9-43313
H₂⁺, $\Sigma_u^+(2p\sigma_u)$ state 9-44328
H₂⁺, discrete vib. states due only to long-range forces 9-44328
H₂⁺, excitation, collision-induced, angular depend. of dissoc. cross-section and rel. to internuclear distances 9-23169
H₂⁺, geometric-mean variation function 9-42397
H₂⁺, ns- σ Rydberg series, one-centre calc. 9-36698
H₂⁺, r.f. spectral line search, in galaxy, brightness temp. $\leq 0.25^\circ\text{K}$ 9-41625
H₂⁺, r.f. spectrum 9-27854
H₂⁺, relativistic theory 9-23047
H₂⁺, three parameter wave function, investigation 9-23048
H₂⁺ charge-exchange collision with molecular gas, products obs. 9-22995
H₂⁺ collisional dissociation, ang. distrib. of protons, theory 9-40622
H₂⁺ dissociation by inelastic collisions between H₂ and H₂⁺, 3-20 keV 9-44375
H₂⁺ electron density variational calc. 9-27841
H₂⁺ electron scatt., $1s\sigma_g 2p\sigma_u$ transition, asymptotic closure cross section calc. 9-40573
H₂⁺ probe for meas. plasma density 9-32638
H₂⁺-H₂ collisions, charge transfer and vibrational excitations 9-23051
H₂⁺ de-excitation by H₂, energy transfer 9-44494
H₂²⁺ evidence for existence in some new Aston bands 9-36680
H₂²⁺ and H₄²⁺, square and rectangular states, electronic wavefunctions 9-48462
H-, auto-ionization, P states calc. 9-46329
H-Ce³⁺ ENDOR obs. in CaF₂ 9-37808
H⁻, detachment by e impact 9-44293
H⁻, doubly excited states of high principle quantum number, implications for e-atom ionization 9-34582
H⁻, nonexistence of 1 sns autoionization states 9-44292
H⁻ in alkali fluorides, i.r. absorption due to localized vibrations of ions 9-30619
H⁻ in KBr, lattice distortions and vibration local mode freq. calc. 9-28410
H⁻ ionization by e impact, computation 9-34577
H⁻ polarized beam from charge exchange in Cs 9-25192
H + H₂, associative and collisional detachment, semi-classical calcs. 9-48429
H + H₂O → OH⁺ + H₂, 0-3 eV obs. 9-46430
H⁺-H(1s) electron capture process, metastable H atom prod., cross section obs. 9-27827
H⁺ and H⁻, bombardment of Mo, secondary electron emission 9-31010
H⁺ charge-exchange collision with molecular gas, products obs. 9-22995
H⁺ conc. in ionosphere 200 to 630 km, obs. 9-43464
H⁺ concentration in daytime F2-region between 200 km and peak altitude, direct measurement 9-31436
H⁺ concentration in daytime F2-region between 200 km and peak altitude, direct measurement 9-24701
H⁺ ionosphere concentration 300 to 600 km 9-31397
H⁺ polarized beam prod. from charge exchange reactions 9-34585
H⁺ producing autoionization levels of Ne 9-23343
H⁺ transport in vitreous silica during H₂ permeation 9-46856
H⁺-D₂(H₂) charge-exchange collisions, search for isotope effect 9-44295
H⁺+H(1s)→2H⁺(E⁺+e⁻) cross-section calc. for E<500 eV 9-32433
H⁺+He(1S²)→H(2S)+He⁺(1S) cross section normalization 9-22996
H II and H I regions, emission and absorpt. of radiowaves 9-31520
H II region, formation round interstellar globule, ionized gas flow 9-29036
H II regions, 74 MHz radio obs., mean e temp. derivation 9-31521
H II regions, α - and β -radio recombination lines for $40 \leq n \leq 225$, prediction 9-35966
H II regions, distrib. in irregular galaxies 9-35963
H II regions, electron temps. 9-49540
H II regions, He abundance from radio recombination lines obs. 9-35964
H II regions, radial vels. of the gas and associated stars 9-40133
H II regions in twenty nearby galaxies, atlas 9-35965
HD⁺+HD→HD₂⁺+H collision mechanism at ~1 eV, obs. 9-41443
HD⁺+Hd→H₂D⁺+D collision mechanism at ~1 eV, obs. 9-41443
H α line in solar spectrum rel. to non-uniform model of chromosphere 9-36070
H β emission in pulsating aurora 9-35853
K/H ion exchange in synthetic resin, kinetics 9-41438
N-H→HN₂⁺ Balmer- α , N₂⁺(0,0) 1st-ve band photon emission, cross sections meas. 9-22985

neutral atoms

- adsorption and Ar exchange on stainless steel 9-39170
adsorption on glass surfaces, 300-500°K 9-40850
adsorption on ZnO polar surface, effect on props. 9-42741
beam, average cross section for ionization by electron plasma 9-44486
beam, magnetic separation and Focalization, phase-space calc. method 9-27828
beam emerging from C foil, periodic intensity fluctuations in Balmer spectrum 9-46332
Born-Oppenheimer treatment, appl. to treatment of the molecular problem 9-46323
chemisorption on Ni films, static capacitor examination of surface potential 9-24547
collision of excited atoms with protons, resonance charge transfer, quantal two-state approx. 9-48427
collision of excited atoms with protons, resonance charge transfer, classical approx. 9-48428
Compton scattering on bound state, theory 9-32419
diffusion in H₂, and in H₂-He, H₂-Ar mixtures 9-39060
dynamic polarizability bounds, complementary variational principles 9-32431
electron capture into n=6 level, by 5-70 keV protons in Mg vapour and Ne 9-46330

Hydrogen continued
neutral atoms continued

- electron elastic-scatt. channel above 10 eV, calc. and obs. resonances, comparison 9-34581
electron loss of fast atoms passing through He, first Born approx. cross sections 9-48425
electron scatt., ang. distrib. meas., cf. Glauber theory prediction 9-38798
electron scatt., Fadeev eqns. used to determ. collision amplitudes 9-46311
electron scatt., low and high energy, elastic, channel coupling effects 9-34565
electron scatt., variational calcs. for resonance widths by Bransden and Dalgarno method 9-44294
electron-impact ionization of 2s and 2p states, cross-sections 9-34583
energy level nuclear corrections calc. by effective potential model, review 9-36681
excitation by fast protons, asymptotic expressions for cross sections 9-34579
excited atom prod. by electron impact on H₂ and D₂ 9-23168
excited atoms prod. by electron impact on hydrocarbons 9-23174
in exosphere and thermosphere, vertical distrib., airglow H α obs. 9-26923
formation in proton charge exchange collisions with Na and Li 9-27813
g-factor of e and p, relativistic treatment of shielding 9-46324
galactic, r.f. spectral line source radial vel. meas., astronomical unit determ. 9-29100
Green's function, reduced for ground state 9-46325
hot-atom reactions with cyclohexane 9-43344
hyperfine state selection by longitudinal periodic field mag. lens 9-29979
interaction with light wave field in second order perturbation theory 9-42347
intergalactic, emission at 21 cm 9-40119
intergalactic density and ionization by quasi-stellar objects 9-36004
interstellar, 21 cm spectra towards high latit. early type stars 9-49561
interstellar, correl. with dust, 21 cm. data in RR Lyrae stars direction 9-31560
interstellar, effect on atm. density 9-49463
interstellar cloud, cooling after cloud collision, and abundance ratio to H₂ 9-24816
interstellar clouds, mag. fields determ., from Zeeman effect obs. 9-36001
interstellar clouds, optical depth determ., new method 9-27049
in interstellar grains, rel. to absorpt. of stellar u.v. rad. below 1215 Å 9-43576
interstellar regions of anomalous by low polarization, caused by B2 star 9-40155
interstellar solid grains, isothermal clouds, masses of stars formation and freq. distrib. 9-35976
interstellar solid grains, role in stellar formation 9-35977
ionization, by proton impact 9-38797
ionization, exchange cross sections 9-34578
ionization, impact by protons transport factor for attached electron 9-32435
ionization, two-photon 9-29975
ionization, two-photon, in ground state 9-34580
ionization by collisions with H, Li, Na 9-22992
ionization by low energy p, cross-section calc. 9-32434
ionization by p of <500 eV, cross-section calc. 9-32433
in Jovian atmosphere, production 9-41676
Lamb shift, time dependence of frequency in semiclassical theory 9-38437
Lamb shifts obs. using spatially periodic potentials 9-42346
as lattice gas in Nb, causing ferroelasticity, obs. 9-23868
level separation, $2^2S_{1/2}$ - $2^2P_{1/2}$ meas. by atomic beam r.f. method 9-40561
Ly α solar emission line profile, 1206.52 Å, rocket obs. 9-41689
in Magellanic cloud, (small), correl. with young stars distrib. 9-31500
maser, beam preparation for operation with unpolarized atoms 9-40338
maser, electronic circuit analogue, oscill. depend on atomic beam flux 9-36268
maser, single-hyperfine-state selector efficiency 9-45942
maser triplet splitting of $\Delta m=0$ transition 9-47925
mean excitation energies upper and lower bounds calc. 9-38779
metastable, prod. in He target by e capture of p 9-40562
in nebulae, gaseous, general soln. of b₀ problem 9-35960
oscillator strengths for electric dipole transitions 9-29976
pair polarizability 9-32432
photon scattering, using infinite component wave equations 9-41757
photon scattering amplitude, exact expression, and Lamb shift in nonrelativistic approx. 9-36683
in planetary nebulae, Balmer emission lines strengths 9-27002
positronium formation in e⁺ scatt., cross-section calc. 9-46064
proton collision, 0.5-50 keV, parametric treatment 9-40563
proton collision, parametric treatment, quantum considerations 9-40564
protons impact, 0.5 to 50 keV, parametric treatment, theory 9-48430
radio emission, line oscillator or strength wave mechanical exact expression 9-44291
in RbCl, interstitial, ENDOR meas. 9-30621
reaction rates with Cl₂ and F₂ 9-43316
reaction rates with olefins 9-43334
reaction rates with olefins 9-43335
reaction with formaldehyde, gas-phase, kinetic isotope effects 9-28781
reaction with methane, kinetics, e.s.r. determ. 9-47454
recombination reaction, H ats. as third bodies 9-25786
recombination with H, Ar, H₂, 2500-7000°K, rate consts., shock wave obs. 9-29978
refractivity in far u.v., Pade summation of Cauchy dispersion eqn. 9-48666
scattering of electron and positron, phase shift, target atom distortion meas. 9-22993
shock front in stellar atmospheres, stability, dissipation and propag. 9-24762
solar prominences, ration of H α /D β , variation in outer regions 9-36066
sorption on graphite obs. 9-39169
spark discharges development, streak photography obs. 9-30319
stability in irradiated aqueous solutions, e.s.r. study 9-39962
symmetry, discrepancy in recent treatments 9-22990
target for precision scatt. cross-section meas. 9-44296
in thermosphere and exosphere, vertical profiles giving more consistent results 9-33803
wave functions describing levels with width 9-29977
X-ray scatt., with transitions between arbitrary atomic shells 9-46326
electron scatt., threshold to 50 eV, excitation to 2p state, resonance obs. 9-22994

Hydrogen continued**neutral atoms continued**

- p-H collisions, a new orbital to allow for intermediate molecular state 9-32436
- beam preparation for maser operation with unpolarized atoms 9-40338
- in CaF_2 , SrF_2 and BaF_2 , hyperfine interactions, temp. depend. 9-31060
- D/H ratio in Venus atmosphere, deductions from Lyman α Mariner 5 obs. 9-43628
- Ge surface, effect on elec. props. 9-28515
- H-E⁺ scatt. resonance below positronium threshold, 3-body variational wave func. converging expansion 9-46322
- H-H collisions, excitation cross sections, impact parameter treatment, four state approx. 9-44297
- H-H collisions, excitation cross sections, impact parameter treatment, two-state approx. 9-42348
- H-H spin exchange cross section using H maser 9-25716
- H-He, H-N, H-Ar, collision proc. electron loss, free scatt. model 9-46310
- H-N₂ collisions, low-energy, stripping and ionization obs. 9-34584
- H-O₂ collisions, low-energy, stripping and ionization obs. 9-34584
- H, $2^2S_{1/2}$ - $2^2P_{3/2}$ interval, meas. 9-25715
- H, Gaussian-orbital approach, by minimization of variance 9-29974
- H, thin-film detector using MoO_3 9-22987
- H _{α} , H _{β} Balmer line profiles emission in vortex-cooled arc, broadening meas. 9-27825
- H _{β} Balmer line broadening in plasma, particle conc. meas. 9-25859
- H, e⁻ S-wave elastic scatt. zero-energy length determ. 9-32397
- H _{β} , Stark broadening of line profile in plasma column 9-42345
- H- ground state calc., 3-body variational wave func. converging expansion 9-46322
- H⁺-H(1s) electron capture process, metastable H atom prod., cross section obs. 9-27827
- H I cold cloud in the Galaxy, from line spectra meas. 9-43514
- H I regions, ionization by cosmic rays and subsequent radiowave absorpt. 9-31520
- H II region structure and props. in nebulae, arbitrary density distrib. model 9-24755
- H wave mechanical, heuristic model, solns. 9-22991
- H+C₂D₁₀→HD+C₂D₈, translational-energy depend. 9-39944
- H+D₂→HD+D reaction kinetics 9-41439
- H+H⁺, associative and collisional detachment semi-classical calcs. 9-48429
- H+H+M→H₂+M, resonance theory of recombination kinetics 9-48426
- H(1s)+H(1s)→H(2lm)+H(2l'm'), 6.25 KeV-3.0 MeV, cross-section calc. using impact-parameter method 9-46331
- H(1s)+He²⁺ collisions, resonance charge transfer 9-48435
- H(2S) from H⁺+He(1S²) collision, cross section normalization 9-22996
- H α , line intensity in aurora from spectrograms 9-43425
- H α line profile in M8 nebula 9-41629
- H β emission, absence in westward travelling surge of electrojet on March 3, 1968 9-47569
- in KCl, superhyperfine interactions of H⁺ centres, zero-pt. vibr. influence, ENDOR obs. 9-45409
- S₂, relativistic corrections 9-44290

neutral molecules

- abundance variation in interstellar H clouds during cooling after collision 9-24816
- adsorption on Be thick films obs. 9-36964
- arc, cascade, radial temp. distributions, meas. up to 27,000°K 9-40728
- arc in superimposed gas flow, arc-flow-electrode interacts and mode behaviour 9-23365
- beam, average cross section for ionization by electron plasma 9-44486
- collision of beam with Li⁺, vibr. excitation meas. 9-25796
- in dark interstellar clouds, prod. mechanism criticism 9-36003
- dipole props. 9-38849
- dissoc. energy and vibr. terms calc. 9-36725
- dissociation above 1000°K, kinetic props. 9-38920
- dissociation zone in star, rel. to Hayashi effect 9-29021
- driver gas in shock tube, study of reflected shock interacts 9-23382
- electron scatt., low energy, polarization and exchange effects 9-40591
- electron scattering, new resonance 9-46364
- electronic states, X¹ Σ_g^+ and E¹ Σ_g^+ , scaled atoms-in-molecules theory 9-34619
- excitation by low energy electrons, cross section calc. 9-38853
- excitation by slow e, rot. transitions with vibr. quantum excitation, calc. 9-38843
- Franck-Condon factors for band systems 9-44330
- Franck-Condon factors for three band systems 9-32476
- Franck-Condon factors for three band systems 9-30032
- fundamental state, study of one-centre expansion 9-23041
- gas target, traversed by He beam, charge equilb. fractions obs. 9-40559
- gaseous, μ - nuclear capture rate obs. 9-27705
- p-H₂ enrichment of first transition series metal oxides 9-24524
- interstellar, localized, critical grain temp. for formation and deposition in dense clouds 9-24814
- interstellar clouds, development of Stromgren sphere 9-24811
- interstellar clouds, evidence 9-43565
- interstellar dust clouds, content 9-43566
- ionization by N⁺ and N²⁺ ions, 0.2 to 1.8 and 0.5 to 1.8 MeV, resp. 9-28040
- ionization by p, rel. to use in proportional counter 9-46137
- ionization coeffs, meas. 9-32690
- linear chain of ortho-hydrogen mols. in ground rotational state, quadrupole interaction 9-25790
- liquid, nuclear bombard. target, thin parallel walled 9-40452
- lowest double-minimum state E, F¹ Σ_g^+ , theoretical calc. 9-42394
- mass proportional creation, search in freezing and distillation of Hg 9-45588
- metastable species prod. by electron excitation 9-32478
- N₂, simultaneous adsorpt. and W at 300°K, obs. 9-23651
- permeation in vitreous silica, H⁺ transport 9-46856
- photodissociation 9-25785
- photoionization, angular distribution of electrons, calc. 9-34591
- quasi-bound states calc. 9-48461
- Raman scatt., laser excited, width of Q(1) line 9-30031
- Raman scattering freq. shift, focused laser beam induced 9-25740
- refractivity in far u.v., Pade summation of Cauchy dispersion eqn. 9-48666
- resonant scatt. of electrons, ang. distrib. 9-27855
- scattering by He, reorientation of molec. rot. 9-27941

Hydrogen continued**neutral molecules continued**

- scattering of beam at solid surface using Jackson and Howarth theory 9-42364
- solid, i.r. absorption associated with orientational excitation 9-24410
- sorption on graphite obs. 9-39169
- in stars, late type, press. induced opacity 9-35978
- sticking coeff. and desorption rate variations during condensed gas layer growth on liq. He cooled surfaces 9-48770
- supercooled, water drop nucleation 9-26075
- wavefunctions in infinite internuclear separation limit, Hartree-Fock eqn. 9-38816
- CO₂ adsorption on W(100) surface rel. to work function change 9-42734
- CO adsorption on W single crystal faces, surface potentials determ. 9-48775
- D₂ singlet states pot. function calc. 9-23042
- D₂+O₂⁺, evidence of long-lived DO₂⁺ 9-47456
- D+H₂=DH+H 9-41439
- H₂-Ar collision, total cross-section, for particular rotational j , m_j state of H₂ molecule 9-27945
- H₂-D₂ gas mixture, π -meson capture 9-36473
- H₂-He anisotropic intermolec. potential 9-30354
- H₂-Kr intermolecular forces and (thermal) diffusion 9-46580
- H₂-Li(2²S and 2²P) interac. energy surfaces 9-34570
- H₂, autoioniz. and predissoc. rates, eff. of isotopic substitution 9-28039
- H₂, bond-stretching-energy curves calc. 9-30012
- H₂, electron scatt., differential elastic and rotational excitations calc. 9-46363
- H₂, emission in extreme u.v. from autoionizing levels 9-28042
- H₂, Heitler-London model, associated rotational props. 9-38848
- H₂, mag. props. 9-27859
- H₂, one-centre calc. with unlimited radial basis 9-38846
- ²S-H₂, polarizability and internuclear distance 9-32432
- H₂, primary specific ionization of relativistic particles 9-39015
- H₂, projected Hartree product wavefunctions and CI calc. 9-29894
- H₂, solid, n.m.r. line shapes 9-41434
- H₂, transition moments for Lyman band 9-24810
- H₂, Venus, photodissociation 9-49583
- H₂, D₂ and HD, ion-mol reactions, ion cyclotron reson. 9-43313
- H₂⁺-H₂ inelastic collisions, 3-20 keV, dissociation obs. 9-44375
- H₂⁺-H₂ collisions, charge transfer and vibrational excitations 9-23051
- H₂ and D₂, dissoci. by electron impact, excited atom prod. 9-23168
- H₂ Lyman-band oscillator strengths 9-27856
- H₂ Lyman and Fulcher bands, vibr.-rot. interaction effects in Franck-Condon factors 9-30029
- H₂ reactivity to atomic N and O 9-43317
- H₂ singlet states, pot. function calc. 9-23042
- H₂ solid, ($\partial^2 P/\partial T^2$) meas. and related props. 9-26424
- O-H₂ triangular cluster, energy levels due to quadrupole interactions in crystal 9-28646
- H₄, configuration interaction in VB wavefunction for potential energy surfaces 9-48463
- H₄, square and rectangular states, electronic wavefunctions 9-48462
- H⁺-H₂ interac., change of charge states, elementary processes 9-30165
- HD, n.m.r. spin coupling const. calc. 9-27857
- HD singlet states pot. function calc. 9-23042
- H-H collisions, optical potentials 9-23198
- Hd, autoioniz. and predissoc., eff. of isotopic substitution 9-28039
- He⁺+H₂ non-reactive collision at ~1 eV, obs. 9-41443
- He fast beam charge changing collision, He⁺ formation 9-29985
- N₂O-H₂ flame properties for atomic absorption and emission spectroscopy 9-31224
- Na-H₂, radiation generation depend. on Na and electron conc. 9-27324
- Na-H₂ laser, Na 4²S_{1/2} population inversion and gain, calc. 9-36293
- o-H₂, very dil. soln. in p-H₂, nuclear spin-lattice relaxation 9-34924
- Oh₂, reaction rate coeffs. 9-39939
- Pd, diffusion and solubility 9-37206

Hydrogen compounds

see also Ice; Steam; Water

- H₂Cl collisions with H₂Cl, vibrational transitions P_{1,0} probabilities 9-25797
- halides, reduced potential curves 9-38835
- HBr collisions, with HBr, vibrational transitions P_{1,0} probabilities 9-25797
- HCl collisions with HCl, vibrational transitions P_{1,0} probabilities 9-25797
- α -HIO₃ crystal, relative nonlinear optical coefficient, corrected value 9-33499
- hydrate melts, viscosity and spin-lattice relax. time, temp. depend. 9-28105
- hydrides, diatomic, first-row config.-interaction studies 9-38828
- hydrides, second-row diatomic, molec. charge distrib. and binding 9-48464
- hydronium ion-water system, isotopic abundances 9-48437
- D₂O, thermal n. absorpt. and diffusion params., obs. 9-25617
- D₂O laser, absolute freq. meas. 9-36282
- D₂O laser transitions, self-correlations 9-42393
- D₂S, absorption spectra, far i.r. 9-27858
- D₂S, centrifugal distortion constants and inertia defects, calc. introducing anharmonicity influence 9-38851
- D₂Se, centrifugal distortion constants and inertia defects, calc. introducing anharmonicity influence 9-38851
- D₂Se, Stark effect and electric dipole moment 9-38850
- DBr+K→KBr reactive collisions, crossed mol. beam expts., angular and vel. distbs. of KBr 9-35741
- DCN i.r. vibrational spectra depend. on intermolecular interactions, gas-soln. transition in solvent 9-30033
- DCI cry., i.r. absorpt. spectrum and struct. 9-47360
- DF-CO₂ chem. pumped laser 9-29412
- DNO₃, vapour and liquid, molecules physically true force constants, normal co-ord. treatment 9-46362
- DO₂⁺, evidence of in O₂⁺+D₂ collisions 9-47456
- H-C plasma at 40 000°K and 70 atm., coeff. of continuous absorpt. calc. 9-44444
- H, Cl, Br, I, product energy distrib. from i.r. chemiluminescence, methods 9-41444
- H₂/CO fuel cell mixtures, use of Pt-Ni catalysts as anodes 9-29365
- H₂-D₂ mixtures, solid phase separation 9-23983
- H₂B₂O₃, molecular structure, molecular-orbital treatment 9-39279
- H₂CO, vibrational band envelopes 9-34622
- H₂O₂, vac. u.v. photolysis, mechanism 9-31210

Hydrogen compounds continued

- $\text{H}_2\text{O}(\omega) + \text{HD}(\omega) \rightarrow \text{H}_2\text{O}(\omega)$, spectroscopic and statistical mechanics constants compared 9-28773
 H_2O laser transitions, self-correlations 9-42393
 H_2S , absorption spectra, far i.r. 9-27858
 H_2S , centrifugal distortion constants and inertia defects, calc. introducing anharmonicity influence 9-38851
 H_2S , mol. wave-functions and d orbitals rel. to bonding 9-34617
 H_2S , photodissociation 9-43336
 H_2S , SCF calcs. 9-23075
 H_2S^+ , c.p.r. hyperfine coupling consts., d orbitals effect 9-32458
 H_2S^+ , c.p.r. hyperfine coupling consts., d orbitals effect 9-32458
 H_2S as etchant for Si 9-32837
 H_2S crystals, pulsed-NMR line shapes, computation and analysis 9-43294
 H_2S liquid, refractive index 9-44562
 H_2S photolysis, H-atom prod. and addition to olefins 9-43334
 H_2Se , centrifugal distortion constants and inertia defects, calc. introducing anharmonicity influence 9-38851
 $\text{H}_3\text{Fe}(\text{U})$ ϵ -cryst. struct. 9-23756
 H_3O^+ , heat of formation by electron impact 9-32692
 $\text{H}_3\text{PO}_4 \cdot 1/2\text{H}_2\text{O}$ crystal structure and refinement 9-39278
 H_3S^+ , heat of formation by electron impact 9-32692
 $\text{H}_4\text{Fe}(\text{CN})_6$ cryst. struct., H-bonds and isotope eff. obs. 9-23756
 $\text{HBr}:\text{Pb}^{2+}$, Ti^+ chem. analysis by luminesc., 77°K 9-33697
 HBr , dipole moment from far i.r. dispersion obs. 9-48460
 HBr , vibr. relax. in shock waves 9-42396
 HBr_2 , i.r. spectra at 20°K 9-44320
 HBr and DBr , Raman spectra of crystals 9-43246
 HBr dissociation kinetics in shock waves 9-47455
 HCl^{15}N , coupling consts., n.m.r. obs. 9-34621
 HCN , dipole moment variation with vibrational state 9-30047
 HCN , laser line width meas. technique 9-41900
 HCN , lattice energies, high and low temp. forms, calc. as sum of long- and short-range interactions 9-30505
 HCN , microwave double reson., rot. energy transfer rates 9-30028
 HCN , photoionization 9-30296
 $(\text{HCN})_2$ gas phase H-bonded complexes, i.r. spectra 9-25742
 HCN gas maser, repetitive Q modulation 9-34154
 HCN gas phase H-bonded complexes, i.r. spectra 9-25742
 HCN i.r. vibrational spectra depend on intermolecular interactions gas-soln. transition in solvent 9-30033
 HCN laser, 890 GHz line, c.w. gain charact. 9-47985
 HCN laser, frequency locking at 890 GHz to microwave frequency standard 9-41901
 HCO radical, CH stretching, anharmonic potential constants 9-38852
 $\text{HCOO}^+ + \text{SF}_6 \rightarrow \text{SF}_5^+ + (\text{HCOOF})$ 9-46430
 HCP spectroscopic study 9-23043
 $\text{HCl}:\text{Pb}^{2+}$, Ti^+ chem. analysis by luminesc., 77°K 9-33697
 HCl , hot solution for etching ZnSe 9-46750
 HCl , spectral emission lines from hot vapour, conc. dependences 9-25696
 HCl , vibr. relax. 9-32474
 HCl , vibr. relax. behind shock waves 9-30030
 HCl and DCl , Raman spectra of crystals 9-43246
 HCl and DCl in shock waves, vibr. relax. 9-38847
 HCl effect of inter-molecular interactions on vibrational spectra in i.r. region 9-23050
 HCl formed by H atom reaction with Cl_2O , chemiluminesc. obs. 9-47453
 HCl liquid anhydrous, meas. of thermal conductivity 9-28118
 HCl liquid anhydrous, thermal conductivity meas. -75 to +65°C, 40-100 bar press, relationship to density 9-36863
 HCl mol., rot. transition by electron collisions 9-42465
 HCl polar molts., rotational transitions by electron collisions, differential cross-sections 9-46360
 HCl sources in atmosphere of Venus 9-24880
 HCl vibr. states in $\text{H} + \text{SCl}_2$, S_2Cl_2 , SOCl_2 , SO_2Cl_2 reactions, i.r. chemiluminesc. obs. 9-32473
 $\text{HClO}_4 \cdot \text{H}_2\text{O}$, reorientation of H_3O^+ ion, study by n.m.r. 9-24508
 $\text{HCl} + \text{SF}_6 \rightarrow \text{F}_2\text{Cl} + (\text{SF}_6\text{H})$, 0.3 eV obs. 9-46430
 HCoO_2 and DCoO_2 , diffraction and spectra, O-H-O bond 9-32908
 HF , chem. laser emission in XeF_4 , $\text{SbF}_5\text{-H}_2$, methane mixtures photolysis, obs. 9-31944
 HF absorption spectrum in 600-1100 Å region 9-34625
 HF chem. laser using $\text{UF}_6\text{-H}_2$ 9-36292
 HF collisions with H_2 , He, Ar, vibrational transitions $\text{P}_{1,0}$ probabilities 9-25797
 HF gaseous polymers, struct. determ. by electron diff. 9-42395
 HF mol., perturbation of rot. lines by F_2 , at 200 bar 9-36700
 HF sources in atmosphere of Venus 9-24880
 HI , vibr. relax. in shock waves 9-42396
 HI collisions with Ar and HI , vibrational transitions $\text{P}_{1,0}$ probabilities 9-25797
 $\alpha\text{-HIO}_3$ nonlinear optical coeff. meas. relative to KH_2PO_4 , $\text{NH}_4\text{H}_2\text{PO}_4$ and LiNbO_3 9-26690
 $\alpha\text{-HIO}_3$ soln. grown cryst., acousto-optic device applic. 9-37326
 $\text{HIO}_4\text{-HF-H}_2\text{O}$ system in semicond. junction delineation and dislocation revealing 9-33339
 HNO , mol. pot. energy curves, unrestricted Hartree-Fock calc. 9-23044
 HNO_3 , vapour and liquid, molecules physically true force constants, normal co-ord. treatment 9-46362
 HNO_3 , in atmosphere, upper, solar i.r. absorption balloon obs. 9-47530
 $\text{H} + \text{X}_2 \rightarrow \text{HX} + \text{X}$ ($\text{X} = \text{F}, \text{Cl}, \text{Br}, \text{I}$), product energy distrib. from i.r. chemiluminescence, methods 9-41444
 $\text{hbr} + \text{K} \rightarrow \text{KBr}$ reactive collisions, crossed mol. beam expts., angular and vel. distrib. of KBr 9-35741
 Hf_2 , ϵ density in H atom, theory and expt. 9-23759
 Ni-Cu-H alloys, low temp. elec. resistance anomalies 9-37450

Hydrogen ion concentration *see Electrochemistry*

Hydromagnetics *see Magnetohydrodynamics*

Hydrometry *see Flowmeters*

Hydrophones *see Oceanography; Transducers*

Hydrostatics

- Archimedes' principle by kinetic theory 9-28060
 floatation of ellipsoid of revolution on ideal fluid, its virtual mass 9-32741
 weighing method for meas. density of restructured water 9-23464

Hygiene *see Medical science*

Hygrometers

- i.r., for direct method of determ. turbulent transport of physical quantities 9-24644

Hyperfine structure *see Crystals/hyperfine field interactions; Paramagnetic resonance and relaxation; Spectra*

Hyperfragments *see Hypernuclei*

Hypernuclei

- $\Lambda\Lambda^0\text{He}$ binding energies by Hartree-Fock model 9-42209
 fragment, non-mesic and π -mesic decay rate determ. 9-38644
 hyperfragment prod. with $Z \geq 4$ in 7.5 GeV/c K^- interact. with Ag and Br nuclei 9-40471
 hypertriton, realistic local n-p potential, structure determ. 9-42208
 nonmesonic decay with a direct transition of Λ hyperon into neutron 9-44128
 production from 10.1 GeV/c K^- interaction with emulsion nuclei 9-40470
 $\Lambda^0\text{HC}$, $\pi^+\pi^-$ mesonic decays ratio determ. 9-25572
 Λ binding energy of 103 mesonic hyperfragments obs. 9-22721
 $\Lambda^0\text{H}^+$ mesonic decay, lifetime meas. 9-38651
 $\Lambda^0\text{He}$, π^+ decay obs. and branching ratio rel to π decay 9-38652
 $\Lambda^0\text{He}^4$ mesonic decay, lifetime meas. 9-38651
 $\Lambda^0\text{He}^3$ mesonic decay, lifetime meas. 9-38651
 $\Lambda^0\text{H}^+$ mesonic decay, lifetime meas. 9-38651
 $\Lambda^0\text{Be}$ Λ binding energy 4.93 ± 0.55 MeV 9-22721
 $^3\text{H}_\Lambda$, decay rates and branching ratios by separable-potential model wave functions 9-44136
 $\Lambda^0\text{H}$ binding energy depend. on 3π exchange ΛNN force 9-25573
 $\Lambda^0\text{H}$, decay rates and branching ratios by separable-potential model wave functions 9-44136
 $\Lambda^0\text{H}$ binding energies by Hartree-Fock model 9-42209
 $\Lambda^0\text{H}$, photoproduction 9-29721
 $\Lambda^0\text{He}$, binding energy determ. from ΛN potential 9-42111
 $\Lambda^0\text{He}$, bound energies, for parameters of ΛN and $\Lambda\Lambda$ interactions 9-27628
 $\Lambda^0\text{He}$, photoproduction 9-29721
 $\Lambda^0\text{He}$, $\Lambda^0\text{He}$, $\Lambda^0\text{He}$ bringing energies for ΛN and $\Lambda\Lambda$ interaction parameters 9-44137
 $\Lambda^0\text{He}$, binding energy determ. from ΛN potential 9-42111
 $\Lambda^0\text{He}$ binding energies by Hartree-Fock model 9-42209
 $\Lambda^0\text{He}$, bound energies, for parameters of ΛN and $\Lambda\Lambda$ interactions 9-27628
 $\Lambda^0\text{He}$, bound parameters of ΛN and $\Lambda\Lambda$ interactions 9-27628
 $\Lambda^0\text{He}$ binding energy depend. on 3π exchange ΛNN force 9-25573

Hyperons

see also Mesons; Nuclear reactions and scattering due to/hyperons

- in hyperfragments, binding energy of 103, obs. 9-22721
 Λ , binding energy in nuclear matter 9-42180
 Λ polarization in $\text{K}^- \text{n} \rightarrow \Lambda \pi^-$ at 3 GeV/c 9-32177
 ΛKN coupling constant $g_{\Lambda\text{KN}}$ from KN dispersion relations disagrees with $\text{SU}(3)$ symmetry 9-34294
 ω^- prod. in 10 GeV/c $\text{K}^- \text{p}$ interaction 9-34334
 $\Sigma_{\pi\pi}$, $\Sigma_{\pi\pi}$ exchange in $\pi^- \text{p} \rightarrow \text{K}^0 \Lambda$ 9-29585
 Σ^- polarization in $\pi^- \text{p} \rightarrow \Sigma^- \text{K}^+$, 1130 MeV/c 9-29621
 Σ decay, CP invariance and $\Delta S = -\Delta Q$ 9-36427

absorption

No entries

capture

No entries

decay

- four-body semileptonic, rates obs. 9-22630
 leptonic, Cabibbo angle determ. without assuming $\text{SU}(3)$ symm. 9-32224
 P -wave, singlet-octet condition 9-42109
 p -wave amplitudes of nonleptonic decay, selection rule derivation from duality principle 9-34330
 spurion+baryon $\rightarrow \pi$ +baryon, model for P -wave decay of hyperons 9-46121
 symmetry breaking in nonleptonic decay, new pole, model 9-32225
 weak magnetism term in sdecay assuming first-class adronic weak currents 9-38587
 weak radiative decays, $\alpha \rightarrow \beta \gamma$, $\alpha \rightarrow \beta \pi$, amplitudes related 9-42108
 weak radiative decays $\alpha \rightarrow \beta \gamma$, $\alpha \rightarrow \beta \pi$, low energy theorem relating, all two-body decay rates calc. 9-42108
 $\Lambda \rightarrow \text{p}$ Cabibbo angle determ. without assuming $\text{SU}(3)$ symm. 9-32224
 $\Lambda \rightarrow \text{peve}$ branching ratio for 204 β decays 9-48211
 $\Lambda \rightarrow \text{pev}$, T-odd correlation between Λ polarization and e^- momenta, coeff. determ. 9-29615
 $\text{n} \rightarrow \text{p}$ Cabibbo angle determ. without assuming $\text{SU}(3)$ symm. 9-32224
 $\Omega^- \rightarrow \Xi^- \text{p}$, p -wave decay, forbidden by selection rule derived from duality principle 9-34330
 $\Sigma^- \rightarrow \Lambda \text{e}^- \nu$, branching ratios, vector and axial-vector coupling consts. ratio 9-25484
 $\Sigma^- \rightarrow \text{ne}^- \text{p}$, axial-vector to vector coupling constant 9-34333
 $\sigma^- \rightarrow \text{ne}^- \text{p}$, branching ratios 9-29617
 $\Sigma^- \rightarrow \text{nev}$ T-odd correlation between Σ^- polarization e^- momenta, coeff. determ. 9-29615
 $\Sigma^- \rightarrow \text{nu}^- \text{p}$, branching ratios 9-29617
 $\Sigma^+ \rightarrow \Lambda \text{e}^+ \nu$, branching ratios, vector and axial-vector coupling consts. ratio 9-25484
 $\Sigma^+ \rightarrow \text{pp}$, rate obs., pole model theory 9-38589
 $\Sigma^+ \rightarrow \text{pp}$ decay rate from unsubtracted dispersion relations 9-32226
 $\Sigma^+ \rightarrow \Lambda \text{e}^+ \nu$ obs., branching ratio, ratio of vector to axial vector constant 9-25485
 $\Sigma^+ \rightarrow \text{ne}(\mu) \text{p}$ search, $\Delta S = \Delta Q$ violation, branching ratios determ. 9-22632
 $\Sigma \rightarrow \Lambda$ Cabibbo angle determ. without assuming $\text{SU}(3)$ symm. 9-32224
 $\Sigma \rightarrow \Lambda \pi$ $\text{O}(4)$ symm. and particle mixing treatment 9-25472
 $\Sigma \rightarrow \text{np}$, p -wave decay, forbidden by selection rule derived from duality principle 9-34330
 Ξ^- and Ξ^0 lifetime meas. 9-38590
 $\Xi^- \rightarrow \Lambda \text{e}^- \nu$ obs. 9-38590
 $\Xi^- \rightarrow \Lambda \text{pev}$, S-wave $\pi\Lambda$ phase shift information 9-32192
 $\text{Y} \rightarrow \text{N}\pi$, γ spectra calc., mag. mom. contrib., matrix element power series expansion 9-34331

detection, measurement

No entries

effects

No entries

interactions

see also Hypernuclei

- f'd binding energy, eff. of $\text{f'N} \rightarrow \Xi\text{N}$ transitions on the binding energy of Faddeev theory applic. 9-44061
 $\Lambda\Lambda$, from bound energies of ΛHe^4 , ΛHe^3 and $\Lambda\Lambda\text{He}^6$ 9-27628
 ΛN , from data on bound energies of Λe^4 , ΛHe^3 and $\Lambda\Lambda\text{He}^6$ 9-27628

Hyperons continued
interactions continued

ΛN , π -photon exchange, charge symmetry violating eff. 9-34332
 ΛN and $\Lambda\Lambda$ interactions parameters from binding energies of hypernuclei 9-44137
 ΛN reviewed, forces, models 9-36497
 $\Lambda N=\Sigma N$, virtual transition eff. on Λd binding energy, Faddeev theory applic. 9-44061
 Λp , potential model analysis, effective range parameter determ. 9-38588
 $\Lambda\Lambda$, soluble model, $Y_1^*(1385)$ resonance amplitude domination 9-22595
 Σ^+ p , potential model analysis, 3S_1 resonance, effective range parameter determ. 9-38588
Yp, review of data 9-29625

magnetic moment

Λ^0 determ. from 151 events selected from 874 decays 9-27561

mass

No entries

production

$(\Sigma^- n)$ bound states, search in K^- capture in 4He 9-29618
 $(\Sigma^- nn)$ bound states, search in K^- capture in 4He 9-29618
 $K^0\Lambda^0$ by π^- meson interactions with light nuclei 9-25447
 Λ^0 from $K^- p$, cross section meas., $M_K=7.7$ GeV/c 9-38513
 Λ^0 prod. by 925 MeV π^- interact. in nuclei, cross-sections 9-29814
 λ and two charged part. final states obs. in $K^- p$ interact., 4.1 and 5.5 GeV/c 9-29573
 λ from $K^- n$, polarization, diff. cross section meas., $M_K=4.5$ GeV/c 9-27499
 $\Lambda^0\Sigma^0$ pairs from lepton-antilepton annihilation 9-29616
 $\Lambda^0\Sigma^+$ pairs from lepton-antilepton annihilation 9-29616
 ΛK in $\pi p \rightarrow \Lambda K + n\pi$, $n=0, 1, 2, 3, 4$, 5.95 BeV/c obs. 9-27518
 $\pi^+ p \rightarrow \Lambda \bar{\Lambda} n$ phenomenological treatment of props. of $\Lambda \bar{\Lambda}$ system 9-42110
 Σ^- in $\pi^- p \rightarrow \Sigma^- K^+$, polariz. meas., 1130 MeV/c 9-29621
 σK in πp reacts., two particle exchange model 9-29619
 Ξ^0 in $K^- p \rightarrow \Xi^0 K^0$, 1.7-2.7 GeV/c polarization and cross-section obs. 9-38590
 Ξ in $K^- p$ interact. 1.7, 2.1, 2.4-2.7 GeV/c, cross-section and polarization 9-38590
 σ^2 multibody final states in $K^- p$ interact., 5.5. GeV 9-29620

resonances

spin, information from decay angles 9-44039
 $(\Sigma^- n)$ bound states, search in K^- capture in 4He 9-29618
 $(\Sigma^- nn)$ bound states, search in K^- capture in 4He 9-29618
 Ξ (2500 MeV) and its decay scheme 9-44014
 Ξ^0 (1930) prod. in $K^- p \rightarrow \Xi^- K^+ \pi^0$ and $K^- p \rightarrow \Xi^0 K^+ \pi^-$ 1.7-2.7 GeV/c 9-38590
Yp collisions, review of data 9-29625

scattering

ΛN , potentials and Λ^1He , Λ^1He binding energies determ. 9-42111
 Λd , using Faddeev eqns with nonlocal separable potentials and medium energy 9-44062
 $\pi\Lambda$, Veneziano model, S-wave scatt. length found 9-42080
 $\pi\Lambda$ and $\pi\Sigma$ σ term evaluation, consistency with current divergence algebra 9-22597
 $\pi\Sigma$ sum rules and p -hadron coupling const. determ. 9-29600
 $\pi\Sigma$ sum rules and p -hadron coupling const. determ. 9-22611
 $\pi\Sigma$ sum rules and p -hadron coupling const. determ. 9-22611
 $\pi\Sigma$ sum rules and p -hadron coupling const. determ. 9-29600
YN, Regge poles and their properties in zero-energy limit 9-22631

spin and parity

Σ parity rel. to K in $\pi p \rightarrow K\Sigma$ 9-27523

Hyperonics see Ultrasonics

Hypertritons see Hypernuclei; Tritons

Hypervirial theorem see Quantum theory

Hypochromism see Absorption/light; Polymers

Hysteresis

see also Dielectric phenomena; Dielectric properties of substances; Ferroelectric phenomena; Magnetization process
dicalcium strontium propionate-acetate mixed cryst., 6(1-x)(CH₃CO₂)_{0.5x}, ferroelec. hysteresis loops 9-35481
domain wall-pinning model 9-45048
ferrites, approach to saturation, anisotropy and porosity from magnetization meas. 9-37662
ferromagnet at Curie temp., loop degeneration, demonstration 9-43704
haematite, Kerr eff. oscillograph 9-26644
ionosphere, F2 critical freq. var. with sunspot no. 9-49502
magnetic films, dynamic losses and energy conversion during remagnetization 9-24266
in microstrain region, anelastic strains 9-23866
minor loops, calc. for anisotropic permanent magnet 9-28605
molybdenum permalloy tape mag. squareness ratio and stress sensitivity, effect of comp. and heat treatment 9-49205
Permalloy films, magnetising angle, mag. anisometer meas. 9-43184
Permalloy films, rotational, effect of surface roughness 9-49211
Permalloy layers with non-mag. layer composite 9-43183
protein adsorbed layers, and stress-relax. 9-23450
superconductors, type-II, quantitative understanding from props. of flux-line lattice defects 9-28286
BiCaV ferromagnet single crystal, rotatory mag. losses 9-45136
Co-Fe-B semi-hard mag. alloys, square loop, and low magnetization, coercive force 9-45137
Co, hexagonal, eff. of constraint on cycle 9-28617
Cu-Co solid solutions, ageing time depend. 9-26622
Dy, loop displacement due to mag. viscosity 9-41291
Fe-Si alloy, infl. of Ni films columnar domain struct. on susceptibility peaks 9-26647
KNO₃ ferroelectric film, square loop 9-49144
MnAlGe ferromag., uniaxial of domain struct. appearance 9-41311
MnTO₃ ($t=y$, Ho, Er, Tm, Yb, Lu), hysteresis cycles by X-ray intensity meas. 9-26590
Nb-Sn superconducting alloys, effect of alloy constitution 9-37659
Nb₃Sn alloy, supercond., correl. with struct. charact. 9-39769
Nb₃Sn supercond. alloy, loss, magnetization meas. 9-35364
Nb alloys, superconducting, rel. to dislocation pinning temp. and field dependence 9-24153
Ni-Fe alloy single crystals, remagnetization loss 9-47261
Ni-Ge single crystals, remagnetization energy losses, field depend. 9-43175

Hysteresis continued

Ni, magneto-elastic hysteresis and internal friction 9-23863
Ni single crystal rod, plastic deformation depend. meas., room temp. 9-41315
Pb_{0.92}Bi_{0.07}La_{0.01} (Fe_{0.405}Nb_{0.325}Zr_{0.27})O₃ ferroelec. thin films 9-35487
PbO₆Fe₂O₃ ferromag., uniaxial, of domain struct appearance 9-41311
Pb(ZrTi)O₃ single crystals, elec. loops at various temps. 9-48806
SbSI phase transition, nonequilibrium carrier effects 9-24233
Si-SiO₂-Al system, C-V curve 9-35432
Tb, loop displacement due to mag. viscosity 9-41291
Ti-Nb supercond. alloy, loss, magnetization meas. 9-35364
U₃As₄ single cryst., zero-field magnetization obs. 9-37656
U₃P₄ single cryst., zero-field magnetization obs. 9-37656
Yb in electrical resistivity curve, between 4.2-300°K 9-46953

Ice

see also Glaciers; Snow
absorption of light, Rosseland and Planck mean coeffs. 9-49548
Antarctic, radiation diffusion, extinction coeff. rel. to grain size 9-39992
Antarctic, structure and composition with fissure detection, e.m. methods 9-33730
atmospheric particles, charge separation in melting 9-31326
charge transfer meas. during evaporation in vac. 9-39129
charging of spheres rotated through cloud or precipitation particles 9-41534
clouds, i.r. reflectivity comparison with Venus obs. 9-38080
clouds, spectral scattering in near infrared, theory 9-47541
columnar, preferred orientation, origin 9-36983
concentrations in clouds, measurements 9-28876
crack form. depend on creep 9-44781
crystal agglomeration into T formation, lab. expt. 9-41512
crystal deposition, growth rate, numerical modeling 9-40821
crystal walls, forming activity 9-34962
crystallization of cylinders in supercooled water, stability of shape 9-35023
crystals, airborne, sun's image 9-33775
crystals growth, after method by Helmholtz 9-23681
current motion in glacier sheet 9-24624
dendrite growth rates in supercooled water 9-39200
diffusion and relax. phenom. 9-28318
doping with in He and Ne 9-46814
dynamics, numerical characts., and rels. 9-35796
electret effect 9-37603
falling crystals, velocity and growth rate for 1 min. after nucleation in fog 9-41511
far-i.r. spectra of orientationally-ordered and -disordered phases 9-33557
formation in supercooled mists, elec. fields effects 9-47538
frost, infrared reflection spectra 9-47540
glacier near melting point, internal friction from seismic obs. 9-31277
grain size determ. from density and one of light attenuation coeffs. 9-45464
growth in supercooled water and supercooled metal fluoride solns., at 0.1-2.5°C 9-39217
growth of ribbons by pulling from melt, new method 9-23680
growth of single cryst. cylinders in water, morphological instability 9-35019
growth of single cryst. from melt, dislocation struct. 9-37080
hailstones, brake-up induced by u.s. waves 9-45491
hailstones, natural tracer distribution 9-28878
h.f. doped thermoelectrets 9-37604
ice I, absorptivity 4000-30 cm⁻¹ 9-45264
ice-water interfacial free energy and morphological stability theory 9-37102
irradiated, electron trapping 9-42980
irradiated, H atom yields, effect of O on determ. e.s.r. study 9-31164
l.f. vibration, dynamic model 9-24013
local cooling, nucleation model 9-28866
local cooling resulting from dissolution of soluble ice nuclei, laboratory study 9-28863
melting, convection in continuously formed water layer 9-32781
in natural clouds, shape and riming properties 9-28877
neutron scatt., slow inelastic 9-48681
n.m.r., pulsed-, line shapes of crystals, computation and analysis 9-43294
normal and tangential forces on moving strip, stress analysis 9-29226
nucleation, heterogeneous primary, in water and aqueous solns. 9-37035
nucleation by lightning discharge, shock waves and adiabatic cooling 9-26908
nucleation in supercooled water, time lag, activation energy, formation probability 9-32814
nuclei rel. to rainfall onset 9-41517
phase transform. in ice: Fe²⁺, Sn⁴⁺, Eu³⁺, conc. depend., Mossbauer obs. 9-33140
in sea, effect on surface temp. 9-43371
semiconductor, conductivity rel. to dopant conc., meas. technique 9-37532
sheets, polar, radio echo equipment for depth sounding 9-26883
solid solutions containing SnCl₂ and Dy(CIO₄)₃, Mossbauer spectra 9-33532
sputtering in H II regions, chemical 9-24759
structure and point defects, effect on elec. and mech. props. 9-48832
surface energies of ice-water vapour, ice-water, ice-ice boundaries, expld. determ. 9-39153
thermal diffusivity, -40° to +60°C 9-42965
vitreous, short ordering range and transform. to diamond cubic struct. 9-46699
volume free energy associated with soluble nuclei 9-28868
X-irradiated single crystals, OH radicals 9-47436
Ca²⁺ concentration in Antarctic, obs. 9-33729
Cl⁻ concentration in Antarctic, obs. 9-33729
Fe²⁺ and Eu³⁺ doped, pseudo-melting at -65°C 9-28178
K⁺ concentration in Antarctic, obs. 9-33729
NH₄F segregation in single crystals 9-30518
Na⁺ concentration in Antarctic, obs. 9-33729
NaOH-doped, dielec. props. 9-39669
nucleation on AgI crystals 9-41510
SO₄²⁻ concentration in Antarctic, obs. 9-33729

Ignition see Combustion

Illumination

see also Brightness
phase-modulated, for hologram interferometry 9-48089
n-Si, effect on photoengraving 9-33334

Image converters and amplifiers

- astronomical observation systems 9-24937
- camera, functional influences on design 9-32047
- camera for over-wide time intervals 9-32048
- camera system for single photoelectron recording 9-34224
- channel plate, use in field ion microscopes 9-43862
- charge image detector, for extended spatial distrib., applic. to spectrometry 9-27263
- electron-beam-scanned acoustic image transceiver 9-36194
- enhancement technique, linear and nonlinear operations with hardware, review 9-29443
- framing camera tubes and recording systems 9-29480
- Fresnel correlation technique, patent 9-34223
- holographic image sharpness restoration 9-40370
- Imacon camera system 9-32046
- image tube, Lenard-window, for astronomical use 9-45695
- image-intensifier framing camera, development 9-29478
- infrared, low-temp. phosphor application 9-28733
- intensifier, statistical brightness gain 9-32045
- intensifier for high-speed spectroscopy 9-32049
- intensifier tubes with multiple integral images 9-29387
- multiframe, registration of ruby laser giant pulse formation 9-31956
- nonlinear-optical, image-contrast 9-48111
- orthicon for low intensity light pulses 9-25378
- pattern storage, insulating layer, patent 9-41885
- sensors, low light-level imaging, limiting resolution 9-29477
- spectra, optical, methods of recording 9-27405
- storage devices, book 9-38414
- storage tubes, electron optical current modulation 9-40334
- Telford camera, development 9-29479
- ultrashort light pulse recording by timebase tube 9-34225
- u.s., solid state, design 9-34087
- u.s. imaging system using diode switching 9-29294
- u.s. imaging system using liq. surface levitation effect, materials inspection appl. 9-29292
- u.s. imaging systems, appl. to nondestructive testing 9-27232
- BaLuF₃, Yb³⁺-Er³⁺ and Yb³⁺-Ho³⁺ ions, i.r. to visible conversion 9-49266
- BaYF₃, Yb³⁺-Er³⁺ and Yb³⁺-Ho³⁺ ions, i.r.-pumped visible and u.v. emission, mechanisms 9-48110
- BaYF₃, Yb³⁺-Er³⁺ and Yb³⁺-Ho³⁺ ions, i.r. to visible conversion 9-49266
- Y₂OCl₂:Yb³⁺, Er³⁺ phosphors for i.r. to visible conversions 9-49324
- Y₂OCl₂, Yb³⁺-Er³⁺ and Yb³⁺-Ho³⁺ ions, i.r.-pumped visible and u.v. emission, mechanisms 9-48110

Image intensifiers see *Image converters and amplifiers*

Image orthicons see *Electron tubes*

Impact

see also *Ballistics*

- ceramics, impact resistivity dynamic characts. rel. to brittleness 9-46905
- Charpy machine, instrumented, for fracture toughness meas. in steel 9-28366
- collision exchange interferometry on steel and glass models 9-29457
- dampers, multiple unit, analytical and expt. studies 9-27193
- on elastic quarter space, analysis 9-29257
- elastic-plastic axisymmetric impact of circular plates 9-38271
- equations of analytical dynamics 9-22181
- glass, in fracture processes 9-28370
- glass ceramic compressive strength, determ. device 9-33031
- glass compressive strength, determ. device 9-33031
- liquid drops, high-speed photographic obs. 9-32754
- missiles, metal cylindrical flat ended, longitud., rel. to plastic deform. 9-41808
- shell-liq., permanent deform., study of liq. and shell parameter significance 9-22186
- steel, mild, projectile, strain meas. on 'mushroomed' ends rel. to mean dynamic yield strength 9-30662
- U.S. waves, excited in plane solid sheets, visualization techniques 9-34057
- water droplets, effects on collision, coalescence and disruption 9-46604
- Al shell-liquid impact, permanent cap deform. rel. to liq. props., shell mat. and acceleration 9-22186
- Be, n irradi., impact resist., obs. 9-28368
- Cu projectile, strain meas. on 'mushroomed' ends rel. to mean dynamic yield strength 9-30662
- Fe μ -spheres at 0.5 to 10 km/sec on Pb, Cd, Ag, Cu and Al, crater investigation 9-30700
- Ti-(6 wt.%)Al-(4 wt.%)V Wear alloy, impact fatigue surface treatment 9-37259
- UO₂ cermet from UO₂-Mo system, strength depend. on porosity and Mo content 9-35222

Impedance, acoustic see *Acoustic impedance*

Imperfections in solids see *Alloys; Crystal imperfections; Solids/structure*

Impurities see *Crystal imperfections/impurities; Crystals/growth; Semiconducting materials*

Impurity electron states and effects see *Crystal electron states/impurity states and effects*

Independent particle model see *Nucleus/models*

Indeterminacy

- denied in quantum physics 9-43738
- Heisenberg's uncertainty principle experimental violation envisagement 9-38223
- idealized expts. and the light they shed on meas., popular article 9-47752
- measurement in quantum mechanics, review 9-43743
- measurement process, axioms in quantum mechanics 9-34027
- quantum theory and limits on the meas. of length 9-43741

Indium

- alloying to surface of CdSe film for charge density reduction 9-33319
- atoms, hyperfine struct. of 5s²5d³D_{3/2} and 5s²6d²D_{3/2} states in In I-spectrum 9-44264
- band structure, de Haas-van Alphen meas. 9-30850
- n-CdCr₂Se₄:In seebeck coeff. normal Hall coeff. and elec resistivity, effect of In conc. 9-45018
- diamagnetism enhancement above T_c due to thermal fluctuations 9-41292
- diffusion and electromigration in liq. Na 9-31201
- diffusion in b.c.c. Pr 9-33007
- diffusion in noble metals, rapid, interstitial mechanism 9-28321

Indium continued

- electrical conductivity, in normal and supercond. states, 1.5 to 4.2°K 9-30871
- electronic density of states, nonlinear pressure effect 9-37407
- electronic density of states for liquid and solid, model-potential calcs. 9-26131
- Fermi electron surface, model calc. 9-43005
- Fermi surface and electronic structure 9-35315
- film, light absorpt. rel. to different gas environments 9-45265
- film, thin, supercond., quenched, effect of preferred growth on ang. depend. of critical field 9-47088
- films, thin, optical props. in far, u.v. 9-37681
- fluorescence direct line type, excitation mechanism 9-48409
- Hall and Righi-Leduc coeffs. for high field 9-47195
- Hall coeff., accurate determ. from helicon waves and surface mode loss 9-24124
- Hall field reversal, rel. to band relax. times and temp. depends. 9-37438
- internal friction anomalies near melting pt. 9-39399
- lattice parameters, temp. variation 9-30785
- liquid, ¹¹⁵In n.m.r. obs. 9-23534
- liquid, nuclear spin-lattice relax. of ¹¹⁵In 9-26134
- molten, electrical resistance meas. by rot. field method 9-39583
- molten, velocity distribution of evaporated particles in vacuum 9-32818
- optical props. of thin films in far u.v. 9-37681
- resistivity, low temp., quadratic temp. depend. 9-37437
- Righi-Leduc and Hall coeffs. for high field 9-47195
- stopping power for 0.6-2.4 MeV protons 9-33212
- structural changes and phase transform., use of coordinate correlation of valence electrons 9-46741
- sunspot abundance from sunspot spectra 9-31657
- superconducting, enclosed, coalescence 9-28476
- superconducting, u.s. shear-wave attenuation amplitude dependence near T_c 9-26418
- supercurrent decrease in gapless region 9-43038
- thermal conductivity, elec. resistivity, Seebeck coeff., 77 to 350°K 9-41104
- thermal conductivity in normal and supercond. states, 1.5 to 4.2°K 9-30871
- thermal expansion, anisotropic 9-30785
- thermal fractional expansion 9-42971
- thermal Hall effect, temp. depend. 9-35341
- thermal magnetomorph effect, longitudinal 9-37430
- u.s. attenuation in normal and superconducting states, non-free-electron behaviour 9-26417
- whisker, elastically bent, resistance increase below 8°K, rel. to electron mean free path meas. 9-37453
- X-ray L_{III} absorpt. spectra obs., uni- and trivalent in halides 9-37746
- Bi whisker, elastically bent, changes, rel. to electron mean free path meas. 9-37453
- in CdS single crystal, luminesc., exciton obs. 9-37756
- n-CdTe:In, heat treated, multiply charged acceptors, photo-Hall effect obs. 9-49075
- in CdTe, spectrographic determination use of alumina-cup electrode 9-35761
- in Hg, effect on electrodiffusion of Bi 9-46623
- In:Cd, band struct. effective mass meas. and applic. To electron-phonon interaction 9-47042
- in In³⁺-HClO₄-HNO₃ and In³⁺-HClO₄-NaNO₃ systems, ion exchange expt. 9-37812
- In⁺ energy parameters in KCl 9-31052
- (In⁺)₂ in KI, absorpt. bands of ion centres obs., electr. struct. 9-35111
- In I, hyperfine struct. of 5s²5d³D_{3/2} and 5s²6d²D_{3/2} states, Stark eff. invest. 9-29938
- In whisker, elastically bent, changes, rel. to electron mean free path meas. 9-37453
- PbTe:In, Mossbauer effect of ¹²⁵Te, depend. of probability on degree of doping 9-39820
- Sn whisker, elastically bent, changes, rel. to electron mean free path meas. 9-37453
- YVO₄:In, photo- and cathodo-luminesc. 9-47397

Indium compounds

- alloys, Hall effect, low field, effect of scattering 9-37445
- amalgams, powder, electrochemical props. 9-49380
- halides, X-ray Ln uni- and trivalent In absorpt. spectra 9-37746
- rare earth-indium intermetallic cpds., R₂In and R₃In, crystal structure and lattice constants 9-28252
- α -Ag-In dil. alloys piezoreflectance 9-47325
- Ag-In liq. alloy system, thermodynamics, Knudsen cell and mass spectrometric obs. 9-36860
- Al-In system, phase equil. obs., thermodynamic props. 9-46679
- Au-In alloy as bonding material for u.s. props. meas. in solids at high temp. 9-46983
- Au-(10at. %)In, specific heat meas. at 3°K, nuclear term obs., crystal electric field studied 9-30780
- Ga-In liquid alloy, Knight shift calc. from pseudopotential formalism 9-23532
- Ga₂In₃-Sb solid soln., growth and characterization using temp.-gradient zone melting 9-30719
- Ge-Al₂O₃-In₂O₃ heterojunctions, switching effect 9-47141
- Ge-In₂O₃ heterojunctions, switching effect 9-47141
- Hg-In alloys, liquid, vol. change on formation and thermal expansion coeff. 9-28115
- Hg-In liquid alloy, Knight shift calc. from pseudopotential formalism 9-23532
- In-AgSe solid soln. forming junction with Se, photocell for i.r. 9-41274
- In-Sb phase diagrams, quasi-chem. equil. model 9-44610
- In-Bi alloys, supercond., metastable states obs. 9-44938
- In-(3at.%)Bi magnetization curves, demagnetization coeff. dependence 9-26529
- In-Cd dil. alloy, Fermi surface topology from supercond. transition temp. dependence 9-47043
- In-Ga-Sb phase diagram, quasi-chem. equil. model 9-44610
- (In-Ga)Fe garnet, Mossbauer effect 9-49263
- In-Pb system, surface tension, temp. and conc. depend. 9-23471
- In-(3.9 at.%)Pb alloy, type I-II supercond. transition obs. 9-47089
- In-(2 at.%)Pb superconducting, type-I, films, flux-flow noise determ. 9-24152
- In-Sn thermal fractional expansion 9-42971
- In-SrTiO₃ junctions, surface pot. barrier and supercurrent flow obs. 9-49056

Indium compounds continued

In-Te system, thin films, elec. and photoelec. props. rel. to conc. 9-30485
In-Te system, thin films, phase composition rel. to conc. 9-30484
In-Th alloys, elastic and anelastic behaviour during martensitic transform. 9-42865
In-Tl alloys, thermal expansion in vicinity f.c.c.-f.c.t. transition 9-28434
In-Tl liquid alloy, Knight shift calc. from pseudopotential formalism 9-23532
In-rare-earth cpds.: RIn₃, mag. props. 9-39751
In_{1/3}Cu_{2/3}Cr₂X₄ (X=S or Se), ionic ordering on A-sites by X-ray diffraction 9-28588
In_{1-x}Ga_xP alloys, band structure and direct transition electroluminescence 9-24467
In₂O₃, anion co-ordination and volume changes in high press. phase transforms. 9-35244
In₂O₃, X-ray spectral investigation of chemical bonding 9-49304
In₂S₃/CdIn₂S₄ mixed cryst., photoluminesc. w.r.t. struct. props. 9-33614
β-In₂S₃, ordering of In vacancies, associated antiphase boundaries and twins 9-30587
In₂Te₃, stoichiometric vacancies, meas. of impurity solubilities 9-40934
In complex, tetraethylammonium tetrachloroindate (III), crystal structure 9-26236
InAs-InP system for injection lasers, growth and charact. 9-41921
InAs-ZnSe solid solns., conductivity, carrier mobility and conc. and thermo-e.m.f. 9-44962
n-InAs, meas. of elec. cond. thermolec. power, magnetothermo-e.m.f. and Nerwst-Ettingshausen coeff. 9-39622
InAs, pot. barrier interaction of depletion regions 9-39720
InAs, powdered, propagation and dimensional resonances of helicon-like waves 9-30891
InAs, third-order mixing of laser radiation 9-26688
InAs, third harmonic generation, mobile carrier nonlinearity, interband proc. 9-26547
InAs_{1-x}P_x, electroreflectance, variation with composition 9-45307
InAs_{1-x}P_x epitaxial layers prep. by vapour-deposition, electron mobilities and n-, p-doping obs. 9-30910
InAs_{1-x}Sb_x, electroreflectance, variation with composition 9-45307
InAs single crystal rocking curves, anomalous absorpt. effects on shape 9-35043
InBO₄ (where B=P, V, Nb) as phosphor host lattices 9-45352
InBi, ¹¹⁵In n.m.r. spectrum, temp. depend. 9-45402
InBi foil, effect of cold working on supercond. transition temp. 9-47078
InCl₃ alkali-metal chloride molten mixtures, Raman spectra 9-44570
InGaSn alloy activation in generator elements of rad. loop in water reflector of IRT reactor 9-32384
InGaSn alloy in activity generator elements of rad. loop of IRT reactor, influence on active section of water reactor 9-32385
In(NCS)₃⁺ complexes, electronic spectra 9-40593
p-InP:Zn(Cd), Hall coefficient and elec. cond. meas. at 4-700°K 9-39623
InP, crystal growth by liquid encapsulation crystal pulling at high pressures 9-37052
n-InP, diffusion of Au 9-46853
p-InP, doped into n-type, Hall coeff., elec. conductivity and hole mobility, temp. depend. 9-28500
InP, optical freqs. and dielec. consts. meas. 9-47314
InP, recomb. radiation from n-p junction, hydrostatic press. effects, obs. 9-26767
InP bulk ionized, recombination radiation rel. to elec. field 9-49315
InP epitaxial growth on GaAs substrates in open flow system 9-23630
InSb-GaSb alloy, press-induced transform, behaviour 9-37301
InSb-InAs alloy, press-induced transform, behaviour 9-37301
InSb, gradient-elastic tensor determ. by nuclear acoustic resonance 9-23851
InSb, YFe Garnet hybrid structure, interaction between spin waves and electrons 9-24320
InSb_{1-x}Bi_x alloys, optical absorpt. and gap obs. 9-43240
InSb_{1-x}Bi_x solid solns., Hall effect, elec. conductivity, band gap obs. 9-43058
InSe, mobility of charge carriers from conductivity and Hall coeff. meas., temp. depend. 9-35404
InSe, reflection spectra meas. rel. to interband transitions 9-28671
InTe, layers, tetragonal phase, electronic and optical props 9-41200
InTe, polymorphs, stability of high-pressure phases, effect of neutron irradiation 9-35250
La_{1-x}Ce_xIn alloys, supercond., transition temp. rel. to pressure, 0-23kbar 9-47090
Mn-In alloys, solid and liq., structure and mag. props. 9-31017
Pb-In alloys, specific heat in normal and superconducting state 9-33182
Pb-In superconducting alloys, second generalized Ginzburg-Landau parameter, temp. dependence 9-24157
Pb-In superconducting alloys, critical field and generalized Ginzburg-Landau parameter κ₂ determ. 9-24156
Pd-In alloys, lattice spacings and mag. susceptibilities, solid solubility of In 9-30571
Pt-In alloys, lattice spacings and solid solubility of In 9-30571

indium antimonide

see also Semiconductor materials/indium antimonide
absorpt. spectra between 50-1400 μ at 1.5°K 9-37727
acoustic nuclear mag. reson. of ¹¹⁵In, ^{121,123}Sb, exchange line broadening 9-45401
difference-freq. generation, far i.r., temp.-depend. phase matching, CO₂ laser input 9-31066
dislocation mobility, temp. and stress depend. 9-42833
donor-impurity excitation spectra in high mag. fields 9-45320
film, p-type, 120-370 Å thick, fundamental absorpt. edge, at 90 and 300°K 9-41379
gradient-elastic tensor determ. by nuclear acoustic resonance 9-23851
liquid, n.m.r. of ¹¹⁵In, and ^{121,123}Sb 9-23534
magnetoacoustic absorpt., longit., Landau levels effects 9-26420
microwave emission, low-field, from n-type 9-26763
p-type, radiation defects, formation by illumination 9-28283
phase diagram, P-T, at high pressures and temps. 9-42922
photoconductivity, two-photon, effect of induced light absorpt. by nonequil. holes 9-39708
radiation defects, formation by illumination, p-type 9-28283
self-diffusion 9-44735
thermal conductivity and elec. transport changes due to X-ray irradi. 9-49086
u.s. generation using ¹¹⁵In spin system 9-46984
InSb, helicon reson. obs. in strong pulsed mag. fields 9-24105

INDOR (internuclear double resonance) *see Nuclear magnetic resonance and relaxation*

Inductance

e.m. induction, various teaching approaches 9-45722
non-linear receiver circuit, fundamental freq. meas. of i.f. complex share periodic signals 9-34129
superconducting linear struct., kinetic inductance meas. 9-35349
superconductor, resistive, inductive behaviour 9-35353
tunnel diode, effect on capacitive loading 9-37562

Inert gases

see also the individual gases
afterglows, spectral line shapes 9-44503
atom, ionized excited states formation through loss of metastable electron 9-34569
atom, van der Waals const. with excited alkali atoms 9-36677
atom-atom ionization rates, semiempirical model 9-44273
atomic beam, refl. from high temp. W ribbon in low press. O or ethylene atm. 9-40558
atoms, collisions with N₂, excitation of rotational and vibrational motion of N₂⁺ ions 9-42470
atoms, ion induced re-emission from polycryst. W 9-33207
atoms, scattering of excited alkali atoms, collision induced transitions, calcs. 9-40556
broadening of resonance lines in Ba, Ca and Sr, effective cross-sections 9-48388
bubble, hot, thermal stability in cool reactive liq. 9-28073
bubble in solids, growth with constant rate of gas generation 9-32823
collision broadening of resonance line of ¹¹⁴Cd ¹³²61 Å, temp. effects 9-40557
collision-induced light scatt. and dielec. phenomena 9-32432
condensed, refr. indices 9-47316
crystals, dynamical surface props., by molecular dynamics 9-39191
crystals, dynamical surface props. in quasiharmonic approximation 9-39190
crystals, individual-ion model, dielectric const. theory 9-35468
crystals, vacancies, Monte Carlo simulation 9-23795
desorption, thermal, from W (110) and (211) surfaces 9-44633
desorption curves, successive approx. calc. 9-23642
desorption from glass, pre-exponential factor 9-39171
diffusion coeffs. in water 9-28112
diffusion in Cu, influence on gas release of implanted ions, implantation energy and dose 9-35129
diffusion in inert gas bombarded solids, mechanisms 9-37194
diffusion in Ne-inert-gas systems 9-42617
diffusion in neutron-irrad. CsCl and CsI, effect of phase transform. 9-33004
discharge excitation, pulsed, dielec. props. of afterglow plasma 9-34805
discharge voltage, minimum, in static fields 9-23350
disturbance effects on Xe 1295 Å and Kr 1236 Å resonance beams 9-44265
electrons in, slow diffusion cross section microwave obs. 9-23273
excitation cross-sections, absolute determ. by electron collision 9-46298
interatomic potential between alkali ions and rare-gas atoms using charge-transfer and Firsov's theory 9-25711
intermolecular potential parameters from sound vel. data 9-36733
ion bombardment of W and Au, effect on work function 9-24257
ion laser, multiwatt output, maximum inversion density and output power conditions 9-47963
ion laser, tube design for 2.3 W c.w. output in u.v. 9-47964
ionization, primary specific, meas. 9-30297
ionization, primary specific, of relativistic particles 9-39015
ionization by N⁺ and N²⁺ ions, 0.2 to 1.8 and 0.5 to 1.8 MeV, resp. 9-28040
ionization coeff., max., analytical representation 9-30306
ionized partially, elec. conductivity 9-26037
ionizing particle track, electron-ion recomb. and scintillation mechanism 9-30304
ions and atoms, rel. to excitation of λ=4278 Å band of first negative system of N₂⁺ ion 9-30045
metastable atoms, diffusion in same gas 9-30356
metastable atoms, electron ejection from W surfaces 9-31002
in meteorites, stony, age determ. 9-24889
molecules, neutral, prod. by electron-beam pulses 9-44345
optical pumping of ^{85,87}Rb, excited state mixing obs. 9-34561
plasma, alkali seeded, electron temp. meas. by line reversal 9-25917
plasma ionization wave propag., microwave-induced 9-32616
plasmas, collisional-radiative electron-ion recomb., rate 9-30219
pumping enhancement in sputter ion pump, depend. on enhancement geometry 9-38177
quenching of alkali metal fluorescence 9-38780
reflection of beam on surface of W ribbon 9-48754
refractivity in far n.v., Pade summation of Cauchy dispersion eqn. 9-48666
in seawater, conc. variations obs. 9-47517
solid, defect structure, electron microscope obs. 9-37159
solid, h.c.p., phonon spectrum and zero point energy 9-23998
solid, theory of large amplitude anharmonic crystal vibrations 9-46963
solid, trapped-hole centres, theory 9-42991
solid matrices, Rydberg states of benzene impurity 9-46384
solids, Debye temp., eff. of triple-dipole forces 9-39530
Sutherland-Wassiljewa coeffs. calc. for inert gas mixtures 9-36810
thermal conductivity of multicomponent mixtures, comparison with theory 9-36811
Verdet coeff. meas. 9-23399
Cs absorpt. lines shift due to inert gas presence, obs. and model 9-29926
effect on N₂ radiation generated during B³ΠgA³Σ⁺u transition 9-38864
Rb-rare gas mol. formation, Rb polarized atom relaxation in rare gas, theory 9-32534
scattering of CsF and TlF, anisotropy factor 9-44390

Inflammability *see Combustion*

Information theory
see also Entropy; Random processes; Statistical analysis/applications
application to lasers 9-40346
electro-optical, 100 phase-coherent channels, high data rates, for pulse signals 9-27421
image restoration uncertainty 9-27374
Markov noise, photographic 9-40388
modulation transfer function of radiologic system 9-27423
of photon beams 9-43865

Information theory continued

sampling theorem, generalized, functions series-expansion 9-29174

Infrared detectors *see* **Bolometers**; **Radiation detectors****Infrared sources** *see* **Light sources**; **Radiation/heat****Infrared spectra** *see* **Spectra****Instruments**

see also **Laboratory apparatus and technique**; **Measurements**; **Recording**; and **under specific subjects**, e.g. **Astronomical instruments**. Some specific instruments are listed separately, e.g. **Spectrometers**; **Thermometers**. Where no separate headings exist, entries describing instruments may be found included under the headings of the appropriate quantities or subjects

basic instrumentation for engineers and physicists, book 9-40230

dielectrometer based on heterodyne beat method, for mols, dipole moments 9-45907

diffraction apparatus, Welch-Bragg, improved mounting 9-23702

for high-temperature research 9-40213

meter to measure velocity on an air track 9-22043

spark timer, solid state 9-27157

Insulating materials, acoustic *see* **Noise abatement****Insulating materials, electrical** *see* **Dielectric properties of substances****Insulating materials, thermal** *see* **Conductivity, thermal****Integral equations**

acoustic radiation problems, improved integral formulation 9-29264

in acoustic radiation problems, nonexistence and nonquickness failures 9-29263

class of infinite sets, soln. by modified residue-calculus technique 9-25027

computer solution of boundary problems in time-invariant conservative fields 9-31751

for electrolytes, aqueous 1-1, primitive-model, error analysis 9-35748

exponential, for radiative transfer problems, accurate and efficient soln. 9-47792

geodetic boundary value problem, convergence of numerical solutions 9-31247

hot reactions, special solns. 9-43342

identity rel. to inversion scheme for obtaining Fermi surface from de Haas-van Alphen effect 9-24091

initial-value methods, arising in theories of the solar atmosphere 9-27106

nonlinear Boltzmann, accuracy of Monte Carlo solutions 9-34829

for pair distribution function of classical fluids, interpolation of HNC and PY eqns. 9-32562

Percus-Yevick type, polymer excluded vol. 9-32540

from sea noise vertical directivity investigation 9-28855

thermoelasticity, plane coupled micropolar, steady vibrations 9-45834

waves, shear, diff. by finite crack, integral transforms appl. 9-29255

Wiener-Hopf, simultaneous, finite set, applic. to diff. in e.m. theory, boundary-value problems 9-34121

Integrals*see also* **Calculus**; **Green's function methods**

asymptotic evaluation of WKB matrix elements 9-38234

atomic, containing $r\rho^2$ correl. factors with unlinked indices 9-44246

atomic correlation, recursive and analytical evaluation 9-34031

cluster, calc. for quantum plasma 9-48544

collision integrals of gas or rigid convex mols. 9-42604

contour for currents and coil forces in 2-dimens. mag. field 9-34141

Feynman integrals, divergent, origin shifts 9-41989

functional, representation of distribution functions in statistical mechanics 9-38249

 $G(3d4s)$, in Ca I, distortion 9-29924

Helmholtz, radiation from vibr. surfaces appl., vanishing of surface-press. contrib. 9-29243

Kirchoff, computation using integral representation of Macdonald function 9-25095

Kondo, evaluation 9-38194

molecular electronic struct. calc. 9-44312

molecular multicentre; three- and four- centre, calc. 9-29998

molecular multicentre, bipolar expansion 9-36646

molecular three-body nuclear attraction 9-30009

motion, complete set, canonical perturbation 9-22184

multicentre, evaluation by polished brute-force techniques 9-44233

multicentre electron repulsion integrals, convergence props. 9-44235

multicentre electron repulsion integrals convergence props. 9-44234

multidimensional, new method for evaluation 9-38196

multiple, props., S -matrix singularity structure over real contours 9-36108

phase-space, and distributions, methods of calculation 9-25660

renormalization, an illustration from classical physics 9-41732

transport, evaluation 9-41787

two-centre Coulomb, analytic expression 9-44236

two-centre exchange, atomic orbitals 9-38741

unitarity in S -matrix theory singularities and discontinuities expressed in terms of M diagrams 9-38422

Volkswagen eqn. elastic collision integral, conversion into differential form 9-45773

Watson, evaluation approx. method, Chebyshev type approx. 9-34039

Wiener, application to quantum statistics 9-25051

Intensity measurement

electron diff. patterns, and simultaneous display, apparatus 9-30542

electron diffractometer, profile recording, optical improvement 9-27283

fluctuations of two random signals, two correlated random walk processes in 2TW-dimens. space as model 9-31886

fluctuations of two random signals, two correlation random walk processes in 2TW-dimens. space as model 9-31887

light, errors rel. to standard W lamps 9-25388

X-ray and gamma radiation 9-46130

acoustics

flow noise, nearfield, from vehicle/water boundary layers 9-45865

frequency response of multimode transmission media 9-45864

loudness level, calc., improvements to Niesse method 9-29116

near-field cross-power of partially coherent sound fields, and prediction of far field intensity 9-41823

pings reflected from ocean surface, fluctuations 9-47520

Interatomic forces, between bound atoms *see* **Bonds**; **Molecules/internal mechanics**; **Solids****Interatomic forces, between free atoms** *see* **Collision processes/atoms****Interface tension** *see* **Surface tension****Interference**

generalized law, derivation from e.m. field eqns. 9-27253

Interference continued

nonlinear effects in spontaneous emission by atoms, with allowance for collisions 9-29919

photons, low-intensity, through Fabry-Perot interferometer 9-41943

seismic waves, damping law distortion 9-26873

of seismic waves, in cased wells logging 9-35788

X-rays, single quanta, reflection at Bragg angle 9-30540

acoustic waves

h.f., large amplitude, nonlinear interaction, creation of difference-frequency wave 9-45859

electromagnetic waves

No entries

light*see also* **Films, solid/optical properties**

in amplitude diffraction grating imaging 9-32017

colour of thin layer, calc. 9-34202

contour lines on opaque objects, interferometric generation 9-36932

demonstration 9-41729

diode laser emerging rays, prevention, patent 9-48047

film, elastohydrodynamic, time-depend. profile meas., optical-interference method 9-36840

fringes, conic sections 9-22452

fringes, evanescent 9-43914

fringes on phase objects, rel. to photography using spatial filtering 9-43932

gas spontaneous emission, nonlinear effects 9-27804

grating use to centralize interferometer white light fringes 9-25354

Hermite-Gauss intensity patterns prod. by optical feedback of GaAs laser 9-45965

holographic fringes 9-43873

interferogram, automated, analysis technique 9-32015

intracavity laser wavelength selector 9-36273

i.r., in epitaxial layer thickness meas. 9-30482

laser beam refl. from plane parallel plates, equally inclined interference fringes effect 9-36316

layer thickness selection for given spectral transmission characts. 9-46016

Lloyd's mirror fringes, degree of coherence 9-45996

moire patterns from multiple sources 9-27382

Moire patterns from surface, topography applic. 9-39149

multiple beam, monochromatic light modulation theor. anal. 9-29464

patterns at large path differences, with gas laser source 9-38403

photomixing, quantum theory 9-25355

Raman-Brillouin 9-25367

of surface waves, equal and opposite 9-43914

Al-Zn-Mg 1 type alloy, blue tint of glossy anodized extruded profiles 9-39833

GaAs laser parallellepipied, 5-cm., 10.6 μ coherent radiation obs. 9-43896K₂D₂PO₄, detection of photon- photon scattering, interaction of microwave and laser beams 9-24358SiO₂ film, reflection spectra meas. in SiO₂-Si system, 9 μ region 9-35619**Interference spectroscopy** *see* **Spectroscopy****Interferometers**

Fabry-Perot, interference effects produced by single photons 9-41943

acoustic waves

composite, u.s. for velocity and temp. coeff. meas. in liquids 9-23494

double cry. u.s., use in sound vel. meas. in liqs. 9-26095

u.s., for rarefied gases, up to 20000 MHz/atm. 9-46572

electromagnetic waves

with autonomous heterodynes, investigation of radio brightness distribution over source 9-45691

Canadian long-baseline radioastronomical instrument 9-38124

long-baseline, 'absolute' direction, possible determination 9-38126

maser, 337 μ m c.w. for determ. plasma electron conc. and collision freq. 9-25909

multielement, autonomous reception for radiation source image 9-43810

three-branch X-band, design and construction 9-38332

X-ray, transmission 9-44651

light

angle measuring interferometer, modified design 9-32016

axial twist and planar inversion 9-32014

differential, photographs and their evaluation 9-32022

diffuse light direct obs. 9-45991

Fabry-Perot, appl. to small absorption coeffs. of gases 9-29465

Fabry-Perot, as filters, aberrations 9-48105

Fabry-Perot, with birefringent filter, passband, tuning and design 9-34220

Fabry-Perot, double passed with pressure scanning 9-22453

Fabry-Perot, series as narrow solar filter 9-36037

Fabry-Perot, using unbaked thin film 9-41942

Fabry-Perot resonators, review and literature survey 9-25225

Fresnel zone plate achromatic fringe, use in obtaining Fourier transform holograms 9-40365

grating use to centralize interferometer white light fringes 9-25354

intensity, applic. in physics and astronomy 9-45998

laser, applic. to deep spherical surface and microscope objective meas. 9-26176

laser, for determining acceleration due to gravity 9-45730

laser, heterodyne, plasma atomic phenomena studies 9-36349

laser, spherical, off-axis excitation of coupled cavity 9-31965

laser, using diffraction grating 9-41941

laser two-beam, test of proposed gravitational interaction with e.m. waves 9-41743

laterally spaced, surfaces of constant order 9-25358

lummer-Gehrcke, plate surface errors, tolerance limits 9-34205

Mach-Zehnder type, for measurement of cross-sectional electron distribution in the theta-pinch D plasma 9-42483

Michelson, adjustment for white light fringes using transmission grating 9-25354

Michelson, use for laser wavelength meas. in i.r. and far i.r. 9-36281

Michelson, use in spectroscopy 9-46025

Michelson, with laser source, for vibrational displacement phase meas. 9-43781

microprofilometer with single objectives 9-36350

multi-ray interference bands, distributions of light intensity 9-22455

Perot-Fabry, attributed to Boulouch and Fabry 9-36348

refractometer, automatic, for liquids and gases 9-22465

stellar, non-monochromaticity effect on visibility of fringes 9-48090

for testing steeply curved surfaces, non-contacting method 9-34203

Interferometers continued**light continued**

- thermometric, for air temp. 25-30 km 9-37910
- triangular, use in making photographic grating 9-27380
- two-beam, interference pattern, depth of modulation with laser illumination 9-34204
- variable shear prism, design 9-22450
- wavefront shearing, for testing large aperture opt. systs., design 9-27379
- CO₂ laser, applic. to plasma electron density meas. 9-23315
- CO₂ laser interferometer, transient low-density plasma meas. 9-40353
- Ne-He laser, calibration system for extensometers 9-25356
- Ne-He laser source causing improvements of detections of fringe shifts for plasma density meas. 9-25910

Interferometry

- astronomical observation of southern radio sources, 123 obs. of brightness distribution 9-43580
- electron optical meas. mag. flux in supercond. hollow cylinder 9-25172
- holographic, 'time average' multiple exposure and 'real time', theory 9-29441
- holographic, principles and applic. 9-45994
- Length meas. of parallel end standards to 1m 9-41731
- plasma diagnostics by focused interferometers 9-30254
- Twyman-Green, for meas. of stresses in thin films on Si substrates 9-35165
- X-ray two-beam, rel. to crystal phase determ. 9-26217

acoustic waves

- u.s. velocity in liquids, meas., effect of diffraction 9-46631

electromagnetic waves

- electron concentration in hypersonic flows, two-wavelength laser method 9-48588
- long-baseline, time and freq. standards 9-36107
- long-baseline interferometer, bandwidth extension for radioastronomy 9-38125
- plasma electron conc. distrib. meas., effect of refraction 9-48587
- OH interstellar clouds, 1665 MHz long-baseline obs. 9-38052

light

- alternatives to holography 9-40371
- collision exchange interferometry on steel and glass models 9-29457
- crystal plates, birefringent, thickness meas. 9-41354
- Fabry-Perot appl. to water spray droplet vl. determ. 9-42685
- films, metallic, thickness and complex index determ. 9-27378
- filtering, use in attenuating Rayleigh component in Brillouin spectroscopy 9-40385
- Fresnel-drag ring-laser method for rotation axis readout of spinning gyroscope 9-45992
- fringe counting and interpolation with electro-optic modulation 9-22454
- fringe shift meas. using matched photoresistor pairs 9-25372
- gas absorption coeffs., small, Fabry-Perot meas. 9-29465
- gas-laser diagnostics of plasma 9-46510
- grating 9-45997
- hologram, with phase-modulated illumination 9-48089
- holographic, double-exposure dark-field, fringe multiplication applic. 9-45995
- holographic, for analysing optical path changes in solid laser rods by optical pumping 9-48088
- holographic cine-interferometry, submicrosecond, of transmission objects 9-48055
- holographic fringe display contrast, optimization 9-31977
- holographic multiple-beam, for object phase variation meas. 9-36324
- holography, of liquid films 9-34185
- homogeneity meas. of refr. index, two angle method 9-48091
- interferograms, multiple beam, holographic production 9-45972
- laser, with heterodyne detection, vibration meas. instrument 9-31970
- laser, industrial meas. applications 9-45967
- laser, velocity of light, JILA/NASA/NBS experiment 9-25357
- laser applications 9-27381
- laser source, repetitive Q-switching 9-29476
- laser wavelength meas. in i.r. and far i.r. using Michelson interferometer 9-36281
- long path, a frequency controlled laser 9-43900
- measurement, suppression of phase-difference fluctuations 9-43915
- microscopy of thin films, replication method 9-23622
- Moire fringes used to meas. plastic deformation in particular extrusion 9-35168
- moire patterns, random, integral-geometric analysis 9-25359
- optically rough surface, meas. using CO₂ laser source 9-45993
- photoelastic model, holographic determ. of sum of principal stresses 9-31818
- photographic 3 dimens. recording, diff. efficiency improvement 9-27411
- photographic grating production using triangular interferometer 9-27380
- shearing by wavefront reconstruction using a single exposure 9-22451
- statistical analysis of transonic currents 9-29468
- thermal stress fields determination 9-29469
- thickness control of coatings, individual layers, errors 9-38404
- wavefront shearing interferometer design for testing large aperture opt. systs. 9-27379
- NaCl, (110) fractured faces exam. by multiple beam method 9-48785
- NaF, topography of thermal etch patterns by multiple beam method 9-48787
- Nb₂O₅ films, electroreflectance interferometry rel. to thickness determ. 9-30486
- Ne-He laser interferometer for improvements of detections of fringe shifts in plasma density meas. 9-25910
- SiO₂ film on Si, thickness meas. by variable angle monochromatic fringe obs., reflectivity corrections 9-34982
- Ta₂O₅ films, electroreflectance interferometry rel. to thickness determ. 9-30486

Intergalactic matter *see Galaxies***Intermetallic compounds** *see Alloys; Semiconducting materials and under the compounds and alloys of the individual metals***Intermolecular forces** *see Molecules/intermolecular mechanics***Internal conversion** *see Beta-ray spectral/conversion electrons; Gamma-rays/internal conversion***Internal friction**

- alkali silicate glass, effect of second alkali addition on peaks 9-48886
- alkali silicate glass, torsional pendulum meas. 9-26314
- amplitude dependent, associated motion of thermal kinks in dislocations 9-41001

Internal friction continued

- amplitude-dependent, of materials under inhomogeneous strain, evaluation 9-35150
- anelasticity in metal specimens, improved meas. apparatus 9-35151
- angle of, for coarse materials 9-35149
- Bordoni peak theory, allowance for dislocation interactions 9-42868
- Bordoni peak width, internal stresses and dislocation splitting effect 9-44753
- ceramic ferroelectric, of formula Pb_{0.95} Sr_{0.05}(Zr_{0.53}Ti_{0.47})O₃+3%PbO 9-41004
- ferrites, FXC 3E1, FXC 7A2, depend. on magnetizing field 9-26655
- ferromagnetic metals, mag. field effect 9-23848
- ferromagnetic metals, mag. field effect 9-33013
- glass, sheet, under high stress 9-46868
- glass, sodium borosilicate, high-viscosity phase 9-26313
- glass fibre, anelasticity, apparatus for damping of torsional oscillations 9-37223
- glass sheet, stabilisation study 9-26312
- glasses, V₂O₅.P₂O₅, semicond., 100° to 400°K, rel. to elec. conductivity 9-35155
- graphite, coeff. temp. depend. determ., defect due to neutron irradiation, -180 to 500°C, 1 Hz 9-35153
- graphite, studies 9-48887
- ice near melting point, internal friction from seismic glacier obs. 9-31277
- lattice, effect on point defect hardening 9-41033
- Marx three components oscillator for meas. at low and high temp. in vacuum 9-33022
- metal specimens, anelasticity meas., improved apparatus 9-35151
- due to precipitation 9-33021
- solid solns., substitutional, relax. time model for short-range order changes and Zener relax. 9-46870
- steel, austenitic, H-charged 9-33085
- strain depend. in transverse vibrs., calc. method 9-31810
- two-phase system, theory, rel. to phase transform. 9-33018
- Ag-(0.26 at.%)Cu alloy, oxidized at 250 or 300°C, stress relaxations from internal friction meas. 9-48885
- Ag-(0.2-0.4 at.%)Al alloys, oxidized 9-48885
- Ag, oxidized 9-48885
- Al-Ag alloys, peak due to γ' phase precipitation 9-35152
- Al, α -irrad., relax. peaks ascribed to reorientation of interstitial clusters 9-39398
- Al, damping in plastic deform., amplitude depend. 9-30661
- Al, films, for attenuation of mechanical oscillations 9-23856
- Al, quenching eff., rel. to vacancy migration 9-46809
- α - brass wire, during plastic deform., study by torsional oscill. method 9-35154
- C, effect of B-doping or stress-graphitization 9-26320
- CaF₂:NaF, mechanical relaxation study 9-28548
- Cd, anomalies near melting point 9-39399
- Co-Ni alloys, during diffusionless phase transform. 9-37298
- Co-Ni alloys, meas. during $\alpha \rightarrow \beta$ transforms., -190° to 500°C 9-39400
- Co-Ni alloys near Curie pt. 9-47074
- Cu-(14.5 wt.%)Al-(3.5 at.%)Ni alloy with thermoelastic martensite, amplitude depend. 9-42869
- Cu-Ni alloys, damping behaviour and miscibility gap evidence 9-42870
- Cu, amplitude dependency on previous deform. in tension or torsion 9-41002
- Cu, amplitude independent, -180 to 200°C, 9-17 kc/s 9-40998
- Cu films, for attenuation of mechanical oscillations 9-23856
- Cu wire, during plastic deform., study by torsional oscill. method 9-35154
- Fe-Mn-C alloys, temp. dependence rel. to stress-induced ordering of C 9-23862
- Fe-Mn alloys, temp. dependence and effect of adding C 9-23862
- Fe-(3 at.%)Si, magnetoelastic, anisotropy 9-33023
- Fe, singularities during $\alpha \rightarrow \gamma$ transformation 9-23857
- In-Th alloys, meas. during martensitic transformation rel. to elastic and anelastic behaviour 9-42865
- In, anomalies near melting point 9-39399
- Mg, n irrad., rel. to defect production and subsequent recovery 9-32940
- Mn-(11 at.%)Cu alloy, relax. peak obs. w.r.t. twinning surface disloc. 9-35156
- Mo, amplitude dependency on previous deform. in tension or torsion 9-41002
- Mo, electron irradiated, rel. to dislocation pinning and depinning, 45° to 330°K 9-28294
- Nb, cold-worked, peak obs. at 27°K 9-23870
- Nb, quenched, 100-280°K, relax. peaks obs., eff. of quenching and annealing 9-30639
- Nb, strain-ageing meas. rel. to dislocation atmosphere formation 9-28381
- Nb strain amplitude dependence rel. mag. state 9-26316
- Ni, electrolytic, ferromag. component and magnetomech. damping H influence obs. 9-39401
- Ni, magneto-elastic hysteresis and internal friction 9-23863
- Ni, studies, 77° to 298°K 9-26317
- Np, in l.f. inverted-torsion pendulum, 20-595°C 9-35158
- Pb, anomalies near melting point 9-39399
- Pb_{0.95}Sr_{0.05}(Zr_{0.53}Ti_{0.47})O₃+3%PbO ferroelectric ceramic 9-41004
- Pb₂MgNb₂O₅-Pb₂NiNb₂O₅ system, temp. and conc. depend. 9-28564
- Pt annealed wire, 500° to 1980°K 9-33024
- Pu-Al delta-stabilized alloys, anelastic behaviour at low temp. 9-37224
- Pu-Ce delta-stabilized alloys, anelastic behaviour at low temp. 9-37224
- Sn-Sb(Cu,Ni) dil. alloys, anomalies near melting pt. 9-39399
- Sn, anomalies near melting point 9-39399
- Ta, cold-worked, peak obs. at 27°K 9-23870
- Ta, dislocation relax. at low temp., max. in dissipation vs temp. curve, and Reierls stress 9-23816
- Tb micro-eddy current damping 9-26319
- Te, by electron-hole pair recombination 9-23871
- α -Ti, relaxation spectrum, effect of H content, comment 9-30648
- α -Ti, relaxation spectrum, effect of H content 9-30647
- V-O solid soln., resistance-heated, degassing process obs. 9-39942
- V wires, meas. after heating, rel. to degassing 9-35195
- W, e-irrad., rel. to Stage-I interstitial behaviour 9-26279
- Zn, anomalies near melting point 9-39399
- in Zr-H alloys at low temps. 9-41005

Liquids *see Liquids; Viscosity/liquids***Internal stresses** *see Stresses, internal***Internuclear double resonance (INDOR)** *see Nuclear magnetic resonance and relaxation*

Interplanetary magnetic fields

- clouds, motion rel. to solar wind 9-35950
- constancy of structure (1957-65) 9-36059
- cosmic ray diffusion 9-26986
- directional discontinuities, Dec. 16, 1965-Jan. 4, 1966, Pioneer 6 obs. 9-31624
- energy density and pressure, Mariner 2 obs. (Sep-Oct 1962) 9-43641
- fluctuations, IMP 2 obs. 9-29078
- fluctuations, transverse and Kp index, correl. 9-43648
- geomag. response, asymmetrical 9-26963
- rel. to geomagnetic vars. and mag. storms 9-47594
- inhomogeneities, from solar and galactic cosmic ray obs. 9-43640
- kinetic theory of cosmic particles in solar system 9-35919
- in lunar wake, perturbed, Explorer 33 and 35, obs. 9-27090
- modulation, residual from cosmic ray d and ³He spectra 9-28983
- motion rel. to theoretical models 9-38091
- and plasma, Explorer 10 obs. 9-38094
- plasma flow mag. field large scale vars. rel. to deformation 9-43643
- polarity, rel. to photospheric mag. field polarity 9-38113
- power spectra freq. depend. 9-43650
- preliminary obs. in tail of geomag. cavity 9-38093
- radial dependence at 1.0 to 1.5 AU, Mariner 4 obs. 9-41684
- regular, effect on motion of cosmic rays 9-35948
- shock waves and other discontinuities, IMP 3 obs. (1965, 1966, 1967) 9-24893
- solar plasma, thermal and e.m. flux in sectors 9-27099
- stochastic, role in galactic particle admission to solar system 9-26987
- structure rel. to distrib. of sunspots, flares and floculi on the Sun 9-35920
- varying, response of moon 9-31594

Interplanetary matter

- Alfven waves, large amplitude, inference from Mariner 5 obs. 9-45676
- charged particle energy changes due to turbulent plasma fluctuations 9-43644
- charged particle in spiral mag. field, dynamics 9-24892
- cosmic dust, terrestrial, accretion rate, estimation from cosmogenic ²⁶Al 9-31279
- cosmic ray streaming radial and azimuthal components 9-47601
- disturbances, magneto-acoustic, Alfven and acoustic velocities, calc. from Mariner 2 obs. 9-43642
- dust, evidence from absorpt. effects in photoelec. photometry of bright stars 9-27091
- dust, orbital parameters rel. to Doppler shifts in zodiacal light spectrum 9-31362
- dust clouds, model, thermal emission calcs. 9-27092
- electric field, v.l.f., Pioneer 8 obs. 9-24891
- energy density rates of motion and magnetic field Mariner 2 obs. (Sep-Oct 1962) 9-43641
- inhomogeneities, small scale, velocities 9-31623
- irregularities studied using scintillations of the quasar 3C273 9-43582
- lunar libration clouds, detectability at small phase angles 9-33926
- at lunar libration point 14, unsuccessful search 9-45665
- lunar surface interaction 9-38067
- lunar wake dependence on solar wind characts. 9-49588
- meteoric, piezoelec. detector obs. 10³ to 10⁸ km 9-47679
- meteoroid flux, analysis of Explorer 16 and Lunar Orbiter obs. 9-29076
- micrometeorite flux on earth estimated from density of interplanetary particles 9-43645
- penetration of magnetosphere 9-37952
- photoelectric screening of bodies in interplanetary space 9-43646
- plasma, charged particle acceleration obs. rel. to fast proton peak 9-43651
- plasma, current density at null points 9-38092
- plasma, irregularities, radioastronomical investigations of motions and dimensions 9-24890
- plasma, magnetized and ionized gas and its relation to the sun and earth 9-24894
- plasma, observations 9-47681
- plasma and mag. fields, motion rel. to theoretical models 9-38091
- plasma densities, determ. from radar obs. of Venus 9-33946
- plasma electrons during flare and quiet periods, Pioneer 6 obs. 9-29079
- plasma flows, velocity and width calcs. from probe obs. 9-33945
- properties determ. using low energy solar protons and alphas (28 May 1967) 9-43647
- radial components and solar wind velocity, correl. Mariner 5 obs. 9-45676
- radiation gradient, radial, Mariner 4 and 5 obs. 9-49589
- satellite obs. simultaneous with geomagnetic tail obs. 9-40047
- scattering centres, cosmic ray diffusion 9-24726
- sector structure during sunspot increase (1966, 1967) 9-43649
- small masses attracted to planet-embryo, gravitational accretion rel. to planetary rotation 9-49587
- solar corpuscular radiation, geophysical effects 9-38111
- solar plasma, geomag. tail region, at 500 and 1000 Earth radii, characts. 9-38109
- solar plasma, radio scintillation obs. 9-38108
- solar plasma props. 9-31643
- solar protons, electrostatic heating beyond 0.1 AU 9-43667
- solar wind direction, IMP 1 obs. (27 Nov 1963 to 24 Feb 1964) 9-45684
- solar wind plasma, Mariner 2 obs. 9-38090

Interstellar matter

- absorption band, (4430Å), asymm. profiles meas., electronographic method 9-29035
- albedo at λ 2100-2800 Å, from search for diffuse galactic light 9-40121
- anomalies in relative abundances of elements 9-24724
- as A, Zeeman effect meas. of interstellar mag. field in Perseus arm 9-36002
- Bok globules in the Orion nebula 9-45633
- collapse into cluster of photostars, i.r. radiation of residual gas 9-29020
- cosmic ray protons and heavy nuclei, low energy, upper limits 9-31494
- critical density ratio, rel. to matter concentration in expanding universe 9-24737
- density, correl. with density of X-ray sources 9-38064
- diamond particles, optical const. and extinction curves opposing hypothesis 9-43575
- diamonds in dust grains, to explain observed phenom. 9-31561
- diffuse galactic radiation interpretation 9-28988
- dissociation of molecules by absorption of line radiation 9-27921
- dust, correl. with atomic H, 21 cm. data in RR Lyrae stars direction 9-31560

Interstellar matter continued

- dust, in NGC 3593, an SO galaxy, rot. and mass 9-40125
- dust, in NGC 7625, an SO galaxy, rot. and mass 9-40124
- dust alignment, Monte Carlo model investigation of two mechanisms 9-29034
- dust clouds, circumstellar, conversion of optical to infrared radiation, intermediate case 9-43569
- dust clouds, circumstellar, transfer of radiation, extreme cases 9-43568
- dust clouds, dark, 48, neutral H content 9-43566
- dust from supanova, as possible source of interstellar absorpt. bands 9-43578
- dust grains, review of models 9-27051
- electrons and relict emission interacting, calc. 9-31488
- extinction curve in Cepheus, use of binodal size distrib. 9-43570
- formaldehyde, microwave detection 9-29037
- gas, dynamics and phase equilib. during volume heating and cooling 9-30344
- gas, heating and ionizing by cosmic ray protons 9-24728
- gas, low energy cosmic ray acceleration and isotropisation 9-24728
- gas in galactic disc, density rel. to collisional prod. mechanism of gamma rays 9-43608
- globule, flow of ionized gas 9-29036
- grain alignment due to rad. press., gas collisions and cosmic ray bombardment 9-43577
- grain nucleation and growth, review 9-24817
- grains, defective, prod. and optical effect 9-43573
- graphite, hydrogen coated, formation and optical props. 9-43572
- gravitational instability, non-Jeans type 9-41648
- hydromagnetic waves, resonant interaction with charged particles 9-41619
- hydromagnetic waves, resonant interaction with charged particles 9-45587
- IC 1805 region, absorpt. spectrophotometric obs. 9-47650
- intergalactic gas and interaction of metagalactic radiation with galaxies 9-26990
- ionized gas, distribution 9-45632
- Local Group, physical const. study with virial theorem. 9-24751
- models, polarization-to-extinction ratio criterion 9-29033
- neutral part. and solar wind protons, charge-transfer interac. in solar syst. 9-24812
- opacity and temp. of interstellar grains, upper limit using balloon-born instrument 9-29102
- particle spin orientation in space 9-27047
- plasma, relativistic, growth rate of fire hose instability, rel. to cosmic ray liberation 9-48608
- plasma gravitational instability, finite Larmor radius and conductivity effects 9-24815
- plasma inhomogeneities, discrete source scintillation investigation 9-43571
- protostar, spherically symm., collapsing, dynamics 9-29008
- random splitting model for protostar formation 9-24779
- reddening, function of heliocentric distance and galactic latitude and longitude 9-47649
- shock front in atomic H, stability, dissipation and propag. 9-24762
- in solar system, neutral part. and solar wind protons, charge-transfer interac. 9-24812
- spectra and radio emission of the solid particles and dark nebulae of space 9-24741
- intergalactic absorption, book 9-24741
- structure and dynamics of interstellar medium 9-29038
- near sun, galactic Lyman α emission obs. 9-43516
- variable λ 4430 absorption 9-27050
- water molecules, detection by microwave rad. 9-41649
- H, atomic, correl. with dust, 21 cm. data in RR Lyrae stars direction 9-31560
- H, intergalactic, in Virgo cluster of galaxies, Gaussian absorpt. profile 9-26991
- H, neutral, absorpt. rel. to pulsar distances 9-41663
- H, neutral, in dark dust clouds 9-43566
- H, neutral, in galaxy M101, distrib. asymmetry rel. to tidal effects 9-41626
- H, oscillator strengths for electric dipole transitions 9-29976
- H₂, dense clouds, existence 9-43565
- H₂, localized, critical grain temp. for formation and deposition in dense clouds 9-24814
- H₂, transition moments for Lyman band 9-24810
- H₂ (solid) coated graphite particles, formation and optical props. 9-43572
- H₂ formation in dark clouds, criticism of production mechanism 9-36003
- H₂ mol. clouds, D-type fronts and associated shock fronts 9-24811
- H₂ mol. clouds, development of Stromgren sphere 9-24811
- H atoms, incoming, effect on atmospheric H density 9-49463
- H atoms in interstellar grains, rel. to absorpt. of stellar u.v. rad. below 1215 Å 9-43576
- H clouds, cooling after cloud collisions, variation in abundance of H₂ 9-24816
- H clouds, optical depth determ., new method 9-27049
- H condensation onto interstellar grains, role in stellar formation 9-35977
- H grains, isothermal clouds, formation and freq. distrib. of masses of stars 9-35976
- H I cold cloud in the Galaxy, from line spectra meas. 9-43514
- H I regions, motion in Galaxy, comparison with H II regions 9-35967
- H I regions, photodestruction rate of H mols. 9-45634
- H II region, formation round interstellar globule, ionized gas flow 9-29036
- H II regions, electron temp. distrib., opt. and radio meas. 9-24757
- H II regions in twenty nearby galaxies, atlas 9-35965
- H line, 21 cm spectra towards high latit. early type stars 9-49561
- H neutral, clouds, mag. fields determ. from Zeeman effect obs. 9-36001
- HI, radiation absorpt. near 21 cm wavelength rel. to pulsar distances 9-31580
- HI anomalous by low polarization regions, caused by B2 star 9-40155
- HI clouds Zeeman effect splitting of 21 cm line rel. to interstellar mag. field meas. 9-36002
- NH₃ microwave emission in Sagittarius region, rel. to dust cloud conditions 9-43574
- Na, D lines in spectra of 75 stars 9-43547
- Na, profiles of D lines in 77 stars 9-40154
- OH, i.r. pumping 9-27048
- OH, microwave emission, spectra and position of fair new sources in Cygnus 9-47655
- OH clouds, 1665 MHz long-baseline interferometric obs. 9-38052

Interstellar matter continued

- OH clouds, microwave line optical depths and excitation temps. 9-43567
OH clouds, radioastronomy obs., popular review 9-45635
OH emission near HII regions, nebular filaments 9-27006
SH, search for 111-MHz lines 9-49562

Interstitials *see Crystal imperfections/interstitials***Invariance (CP, CPT)** *see Elementary particles/symmetry***Iodine**

- adsorption on graphite and desorpt. in vacuum and Ar, 27-1100°C 9-28221
in alkali halide mixed crystals, p-irrad., recoil radio-I species, obs. 9-28818
ion, Zeeman effect for forbidden line and emission spectrum 1.31-2.24 μ obs. 9-29935
bond hybridization in iodomethanes 9-32519
electron scattering cross section and spin polarization meas., $E_e=200-600$ eV 9-23166
 I_2 beam resonance line reference for Ar laser frequency stabilization 9-25245
ion beam in H, 4.5 MeV, equilibrium charge state 9-46319
ions channeled in Au monocryst., energy-loss spectra 9-30806
molecule 11-5 band R(127) line hyperfine components, saturated absorpt., 633nm 9-48465
positron annihilation 9-30830
radioiodine recoils from p-irradiated Cs-compound targets 9-49388
trapping states 9-41133
inultrabasic rocks and carbonates neutron activation analysis 9-45461
vapour, etching of Ge, 200° to 800°C, characts. 9-42744
 ^{127}I , nuclear decay effects on electronic structure of decaying atom and its bonding in cpds. from Mossbauer meas. 9-38769
 ^{127}I ions, channeled in the Au single cryst., energy loss spectra 9-30805
 ^{129}I frozen solns., Mossbauer determ. effect 9-31089
 ^{129}I abundance in early solar system 9-45658
 I , $5^2P_{1/2} \rightarrow 5^2P_{3/2}$ transition, generation termination mechanism 9-46295
 I_2 , Morse oscillator, temp. depend. 9-32457
 I_2^+ , resonance Raman spectrum 9-38856
 I_2 fluoresc. excited by Kr⁺ laser 9-38855
 I_2 in gas mixture, nonlinear thermal Rayleigh scatt. of light 9-32738
 I_2 liquid, i.r. absorption spectra temp. depend., induced dipole moment and correlation function determ. 9-42660
 I^- prod. when I^+ passes through various gases, 1-4.5 MeV 9-30302
 I^+ -Xe 0.5-6 MeV with large angle scatt., evidence for prod. of inner shell vacancies 9-32428
 $I(5^2P_{1/2})$, electr. excited, react. with Cl₂, Br₂, ICl and IBr, study 9-43319

Iodine compounds

- iodide impurity diffusion in AgCl and AgBr 9-40979
bonding of decaying ^{127}I atom from Mossbauer meas. of nuclear decay effects 9-38769
HIO₄-HF-H₂O system in semicond. junction delineation and dislocation revealing 9-33339
IBr reversible photodissoc. laser system 9-34166
 IF_6^+ , vibrational assignments 9-25743

Ion beams

- see also Energy loss of particles; Ion optics; Mass spectrometers; Particle accelerators; Sputtering*
accelerator, heavy ion, 'double tube' version suggested 9-46155
 $Ar^{+}+D_2$ (or CD_4) $\rightarrow ArD^{+}+D$ (or CD), deviations from stripping model 9-27944
on crystal, spatial and energy distrib. of scatt. ions 9-48979
detection, non-destructive, using residual gas ionization 9-46152
diffusion in Poiseuille flow 9-22358
electrostatic sweep system for performing uniform ion bombardment 9-29992
energy loss in Al, Ag and Au foils 9-28440
energy loss spectra, 20-250 keV, high resolution spectrometer 9-34149
focussing by plasma lens 9-27288
focussing in transverse magnetic fields 9-47915
gun apparatus, design 9-26177
heavy, -ve, production and focussing 9-25193
heavy, problems of beam dynamics in synchrotrons 9-46168
high energy acceleration, use of static magnetic field 9-46170
implantation experiments, use of various types of separators 9-29993
implantation into lattices using nuclear reactions, techniques 9-33210
injector of negative polarized ions 9-38362
for ion implantation in semiconductors 9-35411
ion-molecule reaction, crossed beam techniques 9-41442
magnetron diode discharge current, rel. to mag. induction, calc. 9-27287
metal low-energy, sputtering yields on polycryst. films 9-44854
microparticle charging apparatus, patent 9-38363
of operating neutron tubes, studying technique 9-22360
optical properties, effect of emission surface 9-36267
positioning system, automatic, for low energy beams 9-48235
pulse system which produces 4 MeV pulses of 0.5 ns duration 9-25194
range and energy loss during implantation, hyperfine interactions meas. appl. 9-30803
scattering of atomic beams from plasmas, collective effects 9-25856
slowing down, mechanisms, appl. to implantation and hyperfine interactions meas. 9-30802
spectrometer, heavy-ion energy loss, 20-250 keV 9-34149
stopping, electronic, structure effects 9-33209
stopping in gaseous mixtures and amorphous compounds, by elastic collisions 9-36678
velocity distribution, directional analyser, electrostatic 9-29372
As, implanted in Si, range, $E=1.0$ to 1.7 MeV 9-44856
Au, channeled keV, in Au, dechanneling, vacancy clusters formation 9-47016
Au, energy-loss spectra of channeled-ions in monocryst., model 9-30806
Au, energy-loss spectra of fast ions channeled in single cryst., pot. energy and differential-stopping-power functions 9-30805
Au, Pb ion collision cascades, 3-169 eV 9-39552
Bi, implanted in Si, range, $E=0.15$ to 1.8 MeV 9-44856
 $CH_3OH^{+}+D_2$ (or CD_4) $\rightarrow CH_3OHD^{+}+D$ (or CD_3), stripping-complex transition 9-38936
 $CO^{+}+D_2$ (or CD_4) $\rightarrow COD^{+}+D$ (or CD_3), deviations from stripping model 9-27944
 D^- polarized beams prod. from 2S $^{1/2}$ metastable deuterium 9-40565
 H^+ , charge exchange and electron loss on impact with H₂O mols. 9-44493
 H^+ , low-energy differential elastic scatt. by Ar atoms 9-44287
 H^+ , polarized beam prod. from charge exchange reactors 9-34585

Ion beams continued

- He^+ backscattered beam used to determ. crystal dope structure 9-35411
 He channeling charact. in diamond-type lattices 9-47012
 3He , polarized, prod. 9-27739
 3He polarized, attempt to produce 9-27583
 I in H, 4.5 MeV, equilibrium charge state 9-46319
Li, multicharged, acceleration in the Kurchatov cyclotron (USSR) 9-42162
 $N_2^{+}+D_2$ (or CD_4) $\rightarrow N_2D^{+}+D$ (or CD_3), deviations from stripping model 9-27944
 $(NO^+)^*$, de-excitation cross-section in NO 9-34792
 ^{16}O small-angle scatt. in C, BeO, Al₂O₃ thin foils 9-35298
P, implanted in Si, range, $E=0.5$ to 1.7 MeV 9-44856
 ^{32}S small-angle scatt. in C, BeO, Al₂O₃ thin foils 9-35298
in W channeling, critical angle variations for low-energy, light and heavy ions 9-24078
in W cryst., channeling of MeV He^+ , Rutherford scatt. and L and M X-ray yields obs. 9-41120

effects

- atoms ioniz., near threshold energy, cross-section 9-25703
defect prod. in single cryst. 9-26177
dielectrics, radiation damage, ellipsometric analysis 9-35295
disorder, annealing 9-48912
implantation, lattice destruction and post-irrad. annealing 9-30599
incident on target at grazing angles, rel. to angular and energy distrib. of secondary ions 9-37638
inert gas diffusion in Cu, influence on gas release of implanted ions, implantation energy and dose 9-35129
ion implantation and hyperfine interaction meas. 9-31059
ion-induced emission electron microscope, design 9-28247
ion-neutralization spectroscopy of O, S, Se adsorbed on Ni 9-32484
metals, f.c.c., bombarded, faceting influence on ejection patterns 9-44853
modulated, plasma oscills. excitation 9-48602
plasma, cold, isotopic; interaction during recharging, no mag. field 9-36266
plasma, nonisothermal, excitation of slightly turbulent oblique ion waves 9-36774
polymer films, photoresist, scattering effects, comments 9-32846
semiconductor doping, ion bombardment by exploding wire technique 9-28509
surface erosion, electron microtopography obs. 9-35048
transient fields following implantation, theory 9-30802
(Ag_n) clusters emerging from surface on bombard. with Kr ions 9-26618
Ag crystals, Xe ions bombard., threshold of damage obs. 9-30800
Al, irradiated, vacancy clusters 9-28279
Au, Hg⁺ or Au⁺ bombarded, 80-150 keV at 295°K and 80°K, depth distrib. of vacancy clusters 9-30586
Au, irradiated, vacancy clusters 9-28279
Au crystals, Xe ions bombard., threshold of damage obs. 9-30800
Au films, Au-irrad., annealing of defects, activation energies 9-33106
Au foils, Kr irrad. damage, energy depend. 9-32957
Au thermionic work function change 9-24257
Cl⁺ and Cl⁻, bombardment of Mo, secondary electron emission 9-31010
Cu faces, effect of oxygen ion bombardment 9-44640
GaAs, implantation profiles of ^{85}Kr , rel. to incident energy, cryst. orientation and dose 9-47120
n-Ge, surface props. obs. after 50 keV irrad. 9-47124
 $H_2^{+}-H_2$ collisions, charge transfer and vibrational excitations 9-23051
 H^+ and H^- , bombardment of Mo, secondary electron emission 9-31010
 H^+ producing autoionization levels of Ne 9-23343
 He^+ producing autoionization levels of Ne 9-23343
Kr bombarding Ag target, multiatomic clusters of (Ag_n)— emergence 9-26618
Li implantation technique rel. to prod. of Si p-n junction detectors 9-28532
Mo target, bombardment by positive and negative ions of Cl, H and O, secondary electron emission 9-31010
 N_2^{+} reactions with CH₄ and CD₄, dynamics 9-39940
Ne⁺ producing autoionization levels of Ne 9-23343
Ni, Hg⁺ or Au⁺ bombarded, 80-150 keV at 295°K and 80°K, depth distrib. of vacancy clusters 9-30586
Ni, irradiated, vacancy clusters 9-28279
Ni ion-neutralization spectroscopy rel. to electronic structure 9-44890
O₂—electron detachment by ions with energies 3 to 100 eV 9-34572
O—electron detachment by ions with energies 3 to 100 eV 9-34572
O⁺ and O⁻, bombardment of Mo, secondary electron emission 9-31010
Si, lattice deform. due to high-energy implantation, X-ray exam. 9-35103
Si foils, e diff. diagrams 9-44697
Si foils, e microscope defect investigation 9-44683
Si single crystal, Au implanted layer, structure 9-39307
Si surface contamination, determination by large angle ion scattering 9-33333
SiO₂, vitreous pile-exposed, expansion 9-35175
W-Mo alloy, slow, rel. to secondary ion emission 9-24259
W, desorption spectrum of trapped rare gas ions obs. 9-36970
W, induced re-emission of inert gas atoms 9-33207
W, induced re-emission of noble gas atoms 9-30799
W (110) and (211) surfaces, thermal desorption spectra obs. 9-44633
W gas-covered single cryst., ion-induced electron ejection 9-41275
W oxide secondary ions, sputtering probability with Ar⁺ 9-42982
W thermionic work function change 9-24257
ZnO, bombardment behaviour, polarity obs. 9-32857
ZnS:Cu luminesc. damage 9-45349

Ion counters *see Counters***Ion emission**

- cathode dispersion of metals dielectrics and semiconductors, anisotropy 9-45035
desorption from electrode of ion source 9-39744
surface effects, effect on optical props. of ion beams 9-36267
CF₂ capillary, ion oscillations, intensity determination, first, second, third and fourth stages of ionization 9-25973
Cs, field emission from positive electrode 9-28583
 $Yb^{3+}-Er^{+}$ and $Yb^{3+}-Ho^{+}$ from BaYF₃ and BaLuF₃, for i.r. to visible conversion 9-49266
 $Yb^{3+}-Er^{+}$ and $Yb^{3+}-Ho^{+}$ from BaYF₃ and Y₂OCl₃, i.r.-pumped visible and u.v. emission, mechanisms 9-48110
secondary
angular and energy distrib., from ions incident on target at grazing angle 9-37638

Ion emission continued**secondary continued**

- from compounds with complex anions, anions, Ar bombardment 9-49178
 kinetic emission, theory 9-35521
 metal, due to collision of two atoms 9-24258
 metal, origin of multicharged ions prod. by ionic bombardment 9-47216
 negative heavy ion source 9-45935
 Ag surface on bombard. with Kr ions, (Ag_x) clusters prod. 9-26618
 Mo single crystal, angular relationships in energy spectra of scatt. ions 9-47217
 W-Mo alloy, effect of slow ions 9-24259
 W oxides secondary ions, sputtering probability with Ar⁺ 9-42982

thermionic

- from alkali metal iodides on Pt wire, 1080°C, time var. positive ion emission 9-39745
 glass-fiber paper for insulation in space, outgassing behaviour obs., 100-1800°F 9-38173
 metal surface, laser-heated, time resolved 9-32835
 quartz paper, for insulation in space, outgassing behaviour obs., 100-1800°F 9-38173
 Al foil used for insulation in space flight 9-38173
 Au work function changes following 100-600 eV inert gas ion bombardment 9-24257
 Cu foil used for insulation in space flight 9-38173
 K⁺ from metals subject to deformation, gases effect 9-45036
 Na⁺ from metals subject to deformation, gases effect 9-45036
 Ni foil used for insulation in space flight 9-38173
 Sr from SrO surfaces on W and Re 9-37637
 Ta foil used for insulation in space flight 9-38173
 TiO₂ thermal emission obs., 10⁻⁸-10⁻⁹ torr. 9-41280
 W work function changes following 100-600 eV inert gas ion bombardment 9-24257

Ion exchange *see Exchanges, chemical; Ions, electrolytic***Ion microscopes**

- b.c.c. crystals, dislocation quasi-dipoles, field-ion image contrast 9-48857
 field, appl. to Au 9-23626
 field, u.h. vacuum, continuous transfer liq. He cryostat. 9-34148
 field, use of channelled image intensifier 9-43862
 field ion, W tip, meas. of surface free energy anisotropy 9-34980
 field-, data rel. to particle size distrib. analysis 9-33117
 field-ion micrographs, distinction of intrinsic from extrinsic stacking faults 9-32977
 metal single cryst. exam., deform. prod. 9-39235
 sample with structural defects, method of formation 9-40936
 steel, Fe-(2.0 wt.%)V-(0.2 wt.%)C alloy, field-ion study of carbide particle coarsening 9-33118
 Field, takeable and demountable, with continuous flow liq. He cryostat 9-38364
 He projector, IV characteristic calc. 9-27285
 Ir, field ion microscope exam. of point defect clusters caused by proton irradi. 9-35085
 W, field-ion exam. of defects produced by deuteron bombardment at 0.1 MeV 9-37162
 W single cryst., deuteron irradi. damage obs. 9-39358

Ion mobility *see Ion velocity***Ion optics**

- see also Alpha-particle spectrometers; Ion microscopes; Mass Spectrometers; Particle optics.*
 beam properties, effect of emission surface 9-36267
 drift type, cylindrically symmetric, behaviour of ion swarm 9-25683
 focusing by plasma lens 9-27288
 focussing, vacuum gauge 9-25003
 focussing of ion beams in transverse magnetic fields 9-47915
 Hortig accelerator, induced betatron oscils. and mag. deflectors 9-46164
 magnetic analyzers, improved quantum treatment 9-22361
 for mass spectrometer, quadrupole lens system for ribbon beam form. 9-34517
 mass spectrometer scheme with energy focusing for micro-impurity analysis 9-47914
 for mass spectrometry, quasi-parallel beams prod. 9-34516
 quadrupole mass filter, resolving power rel. to no. of ion oscillations 9-22362
 spectrograph, mag., wide range 9-46261

Ion pumps *see Vacuum pumps***Ion sources**

- see also Ion emission/thermionic*
 arc, vibrating contact, props. 9-27286
 cyclotron, variable energy, Orsay, operation and heavy ion injection obs. 9-38629
 design, oscillating e beam type 9-38361
 using duoplasmatron plasma jet, ions from solid and gaseous elements 9-43859
 electron bombardment, beam thickness calc. for optimal focusing 9-38351
 electron-impact, regulation of electrons 9-43860
 electrostatically focused electron bombardment, efficiency 9-29388
 heavy, outline 9-46167
 heavy ions, r.f. source not requiring an extraction electrode 9-41887
 magnetron-type, low-press. residual gas analysis apparatus 9-38182
 monoplasmatron, slit source, parameters affecting emission characts. 9-41886
 negative heavy ions using secondary emission 9-45935
 polarized, principle and development 9-47913
 pulsed, negative hydrogen ions and atoms, increased yield 9-43861
 r.f. discharge, ion extraction 9-39022
 RPD source for time-of-flight mass spectrometer 9-22359
 D⁺ polarized beam from charge exchange in Cs 9-25192
 D⁺ bursts, short duration, apparatus and use for neutron bursts prod. 9-27604
 H⁺ and atoms, pulsed, increased yield 9-43861
 H⁺ polarized beam from charge exchange in Cs 9-25192
³He⁺, polarized, design 9-40335

Ion velocity

- directional analyser, electrostatic and ions 9-29372
 distribution in low-density plasma beams 9-28013
 energies at cathode for conduction through rarefied gases 9-32698
 mobility as interacting Fermi liqs., temp. depend. 9-40259

Ion velocity continued

- in partially ionized gas, in constant elec. field 9-40713
 swarm experiments, maximum likelihood methods applic. 9-31922
¹³⁷Cs mobility in alkali nitrate molten salts obs. 9-34891
 Ge, Li-ion drift mobility, 23.8° and 61.2°C 9-35131
 H positive ions, drift vel. and lateral diffusion 9-44491
 He I, mobility of charges up to solidification 9-30443
 He liq., due to ion size increase near gas-liquid critical point 9-46672
 K⁺ on N₂, mobility, diffusion coeff. and reaction, determ. 9-23203
 N⁺ in N₂, mobility, diffusion coeff. and reaction rates determ. 9-23347
²²Na mobility in alkali nitrate molten salts obs. 9-34891
 O₂⁺ and O₄⁺ in oxygen, drift vel. obs. 9-23348
 SF₆, drift velocity of ions, time-of-flight meas. 9-42564
 Xe⁺ in very pure Xe, mobility meas. 9-44492

electrolytic

- see also Conductivity, electrical/liquids, electrolytic; Electrophoresis*
 mobility of free electrons in dielec. liqs. 9-42673
 nitrate ions in liquid NaNO₃, eff. on elec. conductivity 9-44586
 LiNO₃ molten, electromigration mobilities of ⁶Li and ⁷Li, 313°-488°C 9-45422

ionic conduction, solids

- γ , β -AgI, activation energies 9-33379
 alkali halides, f.c.c., defects contrib. 9-44729
 contribution trivacancy 9-28552
 glasses containing transition-metal ions 9-30964
 ice, NaOH-doped 9-39669
 kinetic theory 9-43769
 migration of ionic defects across activation barrier, elec. field depend. 9-28307
 oxides, mass transfer conf. 9-44726
 oxides, survey and exptl. problems 9-45003
 quartz, diffusion paths during electrolysis 9-39387
 Ag halides, f.c.c. defects contrib. 9-44729
 CaF₂ obs. with differing conc. of DyF₃, HoF₃ and TmF₃ 9-35470
 CsBr, w.r.t. Schottky disorders 9-33398
 CsI, effect of divalent impurities rel. to temp. 9-33380
 Fe-Ni alloys, ion electrotransport, tracer technique 9-28320
 K₂CoF₄ single cry., currents 9-35471
 K₂CoF₄, rel. to static dielec. const. 9-37582
 KBr, additively coloured 9-46835
 KBr, pure and doped, anion contrib. at high temp. 9-35472
 KCl:Mg, additively coloured, props. 9-48868
 KCl, possible trivacancy mechanism 9-28552
 KCl, thermal currents and electret behaviour 9-37605
 KI: Cd single cryst., w.r.t. temp. 9-41253
 KI single cryst., w.r.t. temp. 9-41253
 LiF, low temp., effect of O 9-39671
 LiI, single crystalline, pure and Mg doped 9-47161
 Mo-W alloys, ion electrotransport, tracer technique 9-28320
 NiHAgAl₃, high ionic conductivity, room temp., prep., patent 9-30965
 NaCl:Ca(Cd), and Na⁺ diffusion, conc. depend., heats of assoc. 9-39672
 NaCl, possible trivacancy mechanism 9-28552
 NaCl, solubility of free Cd²⁺ 9-30626
 NaCl in applied elec. field, vacancy pair diffusion obs. 9-44740
 NaCl whiskers, 150-600°C 9-28551
 PbCl₂ single cryst. 9-43107
 RbAg₄Al₃, high ionic conductivity, room temp., prep., patent 9-30965
 RbCl, possible trivacancy mechanism 9-28552
 SiO₂, vitreous, H⁺ transport mechanism at high temps. and in low pressure H₂ atmos. 9-46856
 SiO₂, amorphous films, rel. to avalanche multiplication of electrons 9-45006
 SiO₂, fused, γ irradi., current-voltage depend. 9-49138
 ZrO₂, stabilized, oxygen ion conductivity by electrolysis in Cu solutions 9-35754
- ionization**
see also Dissociation; Electrons/ionization; Photoionization
 air-acetylene flame, low press. 9-42563
 atom, cross-section for Penning ionization 9-32688
 atom autoionization states, variational-bound method, configurations superposition 9-22924
 atomic, quantum treatment in book on approximation methods 9-40242
 atoms, by ion bombardment near threshold energy, cross-section 9-25703
 atoms, L- and M-shell, by heavy charged particles 9-34557
 atoms, maximum cross-sections 9-42335
 autoionization, vibrationally induced, discussed 9-34591
 benzene ion-mol. reactions 9-24541
 p-benzoquinone, by nondissoc. e attachment in ground and excited state fields 9-32694
 charged particle moving in a medium with ionization losses and in a non-uniform magnetic field 9-44094
 cometary matter, by interaction with solar wind, and ray formation, observational approach 9-29074
 cosmic ray heavy nucleus enders, intensity depend. on atmospheric height 9-42122
 crps-section, apparatus to produce monenergetic beam computer technique to determ. near threshold behaviour 9-25963
 density of ions in ionizing beams 9-23340
 electron affinities of heavy elements 9-44274
 electron-atom, threshold region, insight by exam. of doubly excited states of compound ion 9-34582
 electron-impact ionization cross-section for atoms Sc to Zn 9-27820
 field mass spectroscopy, high resolution, molecular ions formation 9-29904
 hydrogen-like atom, proton impact, relativistic formula 9-40555
 inert gas, ionized excited states formation through loss of metastable electron 9-34569
 ion-molecule reactions, electron density rearrangement theory 9-28778
 ionosphere, F-region, energetic particle contrib., critical freq. obs. 9-31435
 of ions by electron impact, evaluation of cross section by modified classical binary encounter model 9-25962
 of ions by electron impact obs. on various substs. 9-46296
 K-shell, by e impact, recal. of Burhops' results 9-46289
 meteor radio ionization trail meas. 9-47678
 multiphoton, perturbed propagation kernel, theory 9-25202
 nuclear emulsions, latent image form. rel. to recomb. of positive holes and electrons 9-34366
 Penning processes, theory 9-42557

Ionization continued

plasma, low-temp., electron diffusion concept 9-40708
plasma, non-equilibrium, relaxation 9-46456
plasma jet, effect of additions of elements on electrical field 9-48122
from radioactive fallout, artificial and natural 9-24669
by u.v. radiation from target in laser beam focus 9-36780
work function of two contacting spherical particles of different size 9-39019
Al, autoionization state, ²D absorption oscillator strength 9-22939
Al, by H, He ions, cross section and K-shell X-ray yield meas., E=25-200 keV 9-22940
Al, K ionization by e⁻ impact, cross section anomalies obs., 3-20 keV 9-46291
Al ²⁺, isoelectronic series, theoretical ionization energies and oscillator strengths 9-22927
Ar atoms and ions, long-lived autoionization states, mass spectra 9-38782
ArHg⁺ associative ioniz., formation 9-40709
Bi ionization multiplication M-shell vacancies arising from L-subshell vacancies 9-48407
CN, electron affinity 9-30296
Ca autoionizing lines, oscillator strength obs. m shock tube 9-22944
Cs plasma, and simultaneous free-electron Maxwellization 9-34750
Cs plasma, nonequilib., and population of excited atomic states, low pres-sures 9-42484
H, 2s and 2p states, cross-sections for electron- impact ionization 9-34583
H, by p impact 9-38797
H, fast atoms passing through He, first Born approx. cross sections for electron loss 9-48425
of H₂ average cross section of beam for ionization by electron plasma 9-44486
H-, P auto-ionization states calc. 9-46329
H⁺+H(1s)→2H⁺(E)+e⁻ cross-section calc. for E<500 Ev 9-32433
H atom, by p collision, transport factor for attached electron 9-32435
H atom, two-photon 9-29975
of H atoms, average cross section of beam for ionization by electron plasma 9-44486
H by p, rel. to use in proportional counter 9-46137
of H excited atom by collisions with H, Li, Na 9-22992
H highly ionized plasma, relaxation theory applics. 9-40651
H ions prod. by high-energy triatomic molecular H beam on D target 9-46328
He, by high energy p 9-38799
He, fast atoms passing through H and He, first Born approx. cross section for electron loss 9-48425
He, P auto-ionization states calc. 9-46329
He, plasma, diff. and mass flow effect on ioniz. degree 9-32597
He, population of highly excited states, effect of stepwise ionization 9-46539
He resonant photo-ionization line shapes, dispersion calc. 9-46334
inHe streamer chamber, meas. 9-46144
HeHg⁺ associative ioniz., formation 9-40709
Hg, Penning ioniz., E energy distrib. population of Hg⁺ states 9-40709
of He average cross section of beam for ionization by electron plasma 9-44486
I⁻ prod. when I⁺ passes through various gases, 1-4.5 MeV 9-30302
Kr atoms, long-lived autoionization states, mass spectra 9-38782
Li, electron affinity 9-44281
Mg⁺, isoelectronic series, theoretical ionization energies and oscillator strengths 9-22927
N₂ photoionization cross section, electron phase shift calc., simple model potential construction 9-46258
Na, isoelectronic series, theoretical ionization energies and oscillator strengths 9-22927
Na atom, five-photon, role of structure and radiation field 9-48412
O₂, dissociative attachment of electrons, crossed beam expts., effect of O₂ source temp. 9-40623
Xe atoms, long-lived autoionization states, mass spectra 9-38782

ionization

gases
see also Charge exchange; Plasma
air, behind hypersonic shock, rate const. and energy transfer mechanisms 9-46564
air, by alpha particles 9-25966
air, relaxation behind shock waves 9-42560
air, relaxation zone length behind strong shock front 9-25961
air, water vapour influence 9-46534
in air afterglow, rel. to electron loss 9-44505
alkali metal, cross section calc. from atomic shell structure 9-23341
alkali metal atoms, by slow electrons, role of incident wave distortion due static and polarization pot. 9-32689
atom-atom ionization rates, semiempirical model 9-44273
Boltzmann eqn., inelastic scatt. prob. and collision freq. determ. 9-22150
cascade, by powerful ultrashort light pulses 9-30295
cascade, during optical breakdown in broad range of radiation fluxes 9-48612
cavity resonator for studying elec. susceptibility of ionized gases 9-34136
collision dominated +ve column, Boltzmann electron eqn. 9-23359
diatomic, secondary coeffs., breakdown pot., mild steel electrodes 9-34812
diffusion in multicomponent, monoat. ionized gas in mag. field 9-44488
electron energy distribution in moving slightly ionized gas 9-48615
electron adhesion to neutral atoms of externally ionized gas, effect on elec. conductivity 9-44490
electron formation in slightly dissociated media, equilibrium diagram 9-39013
electron temperature stability for arbitrary collision cross section 9-25965
exothermic waves in magnetic field, calculations 9-30225
He, photoexcitation and photoionization, simultaneous, 186 Å obs. 9-23001
hydrocarbons C₃-C₈ double charged ions decomp., kinetic energy release 9-40712
hydrogenic ion plasma, coeffs. calc. by collisional-radiative model 9-42494
inert, partially ionized, elec. conductivity 9-26037
inert, primary specific, meas. 9-30297
inert gases, by N⁺ and N²⁺ ions, 0.2 to 1.8 and 0.5 to 1.8 MeV, resp. 9-28040

ionization continued

gases continued
inert gases, max. coeff., analytical representation 9-30306
inert gases, primary specific ionization of relativistic particles 9-39015
instability development rel. to radiation and heat conductivity 9-40711
interstellar distribution 9-45632
in interstellar globule, flow investigation 9-29036
ion diffusion coefficient meas. by amplitude-frequency method 9-30299
ion energies at cathode for conduction through rarefied gases 9-32698
ion-atom slow interchange reactions, temp. depend 9-43312
ion-molecule reaction rates meas. by ion cyclotron reson. 9-45415
ion-molecule reactions, anomalous low- energy behaviour 9-33659
ion-molecule reactions in methane, Kr, and O₂, using pulsed mass spec-trometer 9-24544
in ionosphere interaction inter- and underlayers, allowance for in conc. profile calc. 9-45535
jet, microwave plasma production 9-30263
laser-induced, elec. field distrib. along beam axis 9-28055
methane, α-irrad., ion-mol. reactions 9-45428
methane, electron drift vel., press. depend. 9-48616
MHD generator channel, Ohm's law 9-22329
MHD generator combustion chamber, possible utilization of ionization 9-27271
molecular gases, ionization and fragmentation by 5-45 keV He⁺ ions 9-42558
monatomic, ionizing shock structure 9-30294
monatomic, thermodynamic props. 9-23346
motion of front, effect of outflow of ionized gas, analysis 9-40707
multifluid systems, generalized Ohm's law 9-23209
noble gases, electron-ion recomb. in ionizing particle track, scintillation mechanism 9-30304
optically then surrounding X-ray source, electron temp. and ionization equilb. obs. 9-36013
optically thick, surrounding X-ray source, physical conditions 9-36014
plasma shock wave, switch-on, structure calc. 9-25874
polyatomic, secondary coeffs., breakdown pot., mild steel electrodes 9-34812
radiation front behind window, props. of radiation-induced waves 9-44482
radiation-driven breakdown wave propagation, hydrodynamic model, ionization effects 9-42614
secondary electrons, spectrum and fluoresc. efficiency in N⁺ 3914 Å band 9-46127
shock heated, ionization rate, measurements, investigation for use of Lecher wire method 9-25919
supersonic flow around cylinder with oscillating surface 9-30265
in thermionic convertor plasma, equilibrium 9-47893
velocity variation in normal ionizing shock wave 9-36801
Ar, by microwaves, strongly ionised low press. plasma 9-48592
Ar, secondary coeffs. and breakdown pot., mild steel electrodes 9-34811
Ar⁺ results near threshold using new techniques 9-25963
Ar⁺+Ar excitation resonances for production of metastable atoms 9-34560
Ar plasma, K seeded, by auxiliary d.c. discharges 9-48558
CO, electron-ion recombination, diffusion coeff., 775°K 9-48617
D₂, autoionization rel. to emission in extreme u.v. 9-28042
D₂ vibronic autoioniz. and predissoc., eff. of isotopic substitution 9-28039
H, by low energy p, cross-section calc. 9-32434
H, excited atoms, by neutralization of accel. protons 9-46327
H, formative time lags in breakdown 9-34814
H, homogeneous plasma, coeffs. calc. by collisional-radiative model 9-42494
H₂, autoionization rel. to emission in extreme u.v. 9-28042
H₂, ionization coeffs. meas. 9-32690
H₂, model, ohmically heated electrons 9-23342
H₂, primary specific ionization of relativistic particles 9-39015
H₂,D₂ and HD, ion-mol. reactions, ion cyclotron reson. 9-43313
H₂⁺, incident on rare gas mols., dissoci. ang. depend. 9-23169
H₂ by N⁺ and N²⁺ ions, 0.2 to 1.8 and 0.5 to 1.8 MeV, resp. 9-28040
H₂ vibronic autoioniz. and predissoc., eff. of isotopic substitution 9-28039
H₂O, field ionization 9-32691
H₂O vapour, α-irrad., ion-mol. reactions 9-45428
H₂O⁺, heat of formation from electron impact 9-32692
H₂S⁺, heat of formation from electron impact 9-32692
H plasma, collisional-radiative ionization coeffs. rel. to atomic collisions 9-42495
H plasma, normal ionizing shock waves, electrode config. effects 9-44429
HD vibronic autoioniz. and predissoc., eff. of isotopic substitution 9-28039
He-Ne mixture, spatial growth of pre-breakdown ionization currents 9-48433
He-Ne mixtures, ionic analysis of cataphoresis 9-42569
He, primary specific, meas. 9-30297
He, secondary coeffs. and breakdown pot., mild steel electrodes 9-34811
He, spatial growth of pre-breakdown ionization currents 9-48433
He, Townsend coeff. by taking indirect ionization into account 9-48613
He⁺ results near threshold using new techniques 9-25963
He atoms, by 5-50 keV protons 9-44483
He by e, ang. correlation distrib. and energy of 2e meas. Ee=50,114 eV 9-23004
He by electron impact, total ioniz. and ioniz. fluctuations 9-25964
He II plasma, displacement due to particle currents in temp. gradient direction 9-48552
He positive column, medium press. 9-25980
³He and ⁴He, proton bombardment, eff. cross sections 9-48614
Hel, local thermodynamic equilb., validity criteria 9-23277
Hg autoionizing states obs. in 4-15 eV e bombardment 9-32421
Kr, secondary coeffs., and breakdown pot., mild steel electrodes 9-34811
Kr atoms, by 5-50 keV protons 9-44483
N, electron-ion recombination 9-34796
N₂:O₂ mixture, electron radiation, 1.5 MeV, thermal electron prod. and removal, 1-10 torr 9-40710
N₂, harmonic generation under alternating electric field 9-30300
N₂, ionization coeffs. meas. 9-32690
N₂, primary specific ionization of relativistic particles 9-39015
N₂ reactions with CH₄ and CD₄, dynamics 9-39940
N₂ by N⁺ and N²⁺ ions, 0.2 to 1.8 and 0.5 to 1.8 MeV, resp. 9-28040
N₂ in H-N₂ low energy collisions 9-34584

ionization continued**gases continued**

- N_2+H_2 ion-mol. reactions, using ion cyclotron reson. 9-31184
 N Townsend coeffs., in gas containing radioactive impurities 9-39017
 NH_3 and ND_3 , dissociative attachment of electrons 9-46422
 NH_4^+ , heat of formation from electron impact 9-32692
 NO_2 , dissociative attachment of electrons 9-32693
 NO_2^+ in air, production 9-43387
 $(NO)^+$ *, de-excitation cross-section in NO 9-34792
 Ne, secondary coeffs. and breakdown pt., mild steel electrodes 9-34811
 Ne, spatial growth of pre-breakdown ionization currents 9-48433
 Ne, total excitation cross section, determ. using Townsend's primary ionization coeff. 9-42561
 Ne atoms, by 5-50 keV protons 9-44483
 Ne autoionizing levels, prod. by H^+ , He^+ and Ne^+ beams 9-23343
 O_2 , ionization and attachment coeffs. 9-39018
 O_2 , electron radiation, 1.5 MeV, thermal electron prod. and removal, 1-10 torr 9-40710
 O_2 , electron swarm expts. anal., Boltzmann transport equation appl. 9-23344
 O_2 , primary specific ionization of relativistic particles 9-39015
 O_2^+ + D_2 , evidence of long-lived DO_2^+ 9-47456
 O_2 in H_2O , low-energy collisions 9-34584
 Xe, secondary coeffs. and breakdown pot., mild steel electrodes 9-34811
 Xe atoms, by 5-50 keV protons 9-44483
 Xe laser, c.w. operation 9-48000

Ionization**liquids**

- dielectric, book 9-34917
 by electrohydrodynamic spraying techs. 9-23526
 by electrons, free ion yield determ. by charge scavenging 9-23528
 hydrocarbon radiolysis, rate const. for scavenging of electrons 9-43341
 indigo pigments in dioxane and acid solns. by v.v., obs. 9-28153
 ion-pair recomb. rates in liqs. of low dielec. const. 9-30425
 mobility of free electrons in dielec. liqs. 9-42673
 neutralization of isolated ion pair in polar liqs. 9-42674
 neutralization of isolated ion pair in polar liqs. 9-42675
 organic liqs., electron and γ -irrad., viscosity-depend. recomb. luminesc. 9-28720
 polymethacrylic acid, viscosimetric investigation of conformation transition on ionisation 9-23196
 water solns., acid-base, pressure eff. on ioniz. equilibria, 25°C, extensions 9-42676
 by X-rays, free ion yield determ. by clearing field 9-23527

solids

- anthracene cation trapped in boric acid glass, spectra 9-42423
 1,2-benz-anthracene cryst., photoioniz. threshold meas. 9-33424
 impact, far i.r. modulation 9-36334
 metal surface, field ionization rel. to Fermi-surface struct., tunnelling probabilities obs. 9-43146
 metal surface, field ionization rel. to Fermi-surface struct., tunnelling probabilities obs. 9-47218
 Millikan apparatus modified, photoioniz. threshold meas. 9-33424
 organic, electron and γ -irrad., viscosity-depend. recomb. luminesc. 9-28720
 perylene cryst., photoioniz. threshold meas. 9-33424
 photoionization of large radius excitons, accompanied by carrier transfer to a different band 9-37410
 pyrene cryst., photoioniz. threshold meas. 9-33424
 rhodamin-B cryst., photoioniz. threshold meas. 9-33424
 Ca^+ in Antarctic ice, concentration obs. 9-33729
 Cl^- in Antarctic ice, concentration obs. 9-33729
 $n-InSb$ pinch effect in impact ionization 9-41147
 K^+ in Antarctic ice, concentration obs. 9-33729
 Na^+ in Antarctic ice, concentration obs. 9-33729
 SO_4^- in Antarctic ice, concentration obs. 9-33729
 $Si-p$, photoionization of impurity atoms and colour centres using e.p.r. 9-37636
 ZnS by impact, role in electroluminescence 9-43265

Ionization, atmosphere

- see also Atmosphere/radioactivity: Ionosphere*
 by cosmic rays, lower ionosphere 9-40075
 E_2 layer ionization index 9-40087
 F layer, effects of fast neutral particles 9-45541
 F-region, during magnetic storms 9-45546
 H_2O vapour, charge transfer cross sections, lab. expt. 9-25967
 ionosphere, F-region, electron production and loss rates 9-47584
 magnetic-field-aligned, e.m. wave scatt. 9-31392
 minimum height, calc. in spherical-Earth approximation 9-41583
 polar ionosphere, by solar cosmic rays 9-35867
 solar ionizing radiation, increase during two flares, May (1967) 9-43677
 tropical night-time F-layer, large ionization source needed for maintenance 9-28952
 upper, by satellite 9-31353
 upper atmosphere 9-35859
 velocity, effect of polarization field due to acoustic wave 9-41578
 Ca^+ in upper atmosphere, abundance and theory of origin 9-35832

Ionization, surface

- see also Electron emission/thermionic; Ion emission/thermionic; Work function*
 aniline molecules, thermal ionization proof 9-33426
 Cs atoms on W and Pt surfaces, ionization coeffs. determ. 9-45034
 metal, field ionization rel. to Fermi-surface struct., tunnelling probabilities obs. 9-47218
 metal, field ionization rel. to Fermi-surface struct., tunnelling probabilities obs. 9-43146
 plasma-metal function, thermodynamic study 9-24260
 semiconductor surface, photoelec. emission determ. 9-43142
 Ge films, surface centres, and elec. instabilities 9-47122
 $LiCl$ on Re and oxygenated Re surfaces, efficiency increase 9-35522
 Mo , of Br, on (100) face 9-49179
 Mo , of Li atoms, electron affinity determ. 9-44281
 Na , $NaCl$, $NaBr$, NaI on Re and oxygenated Re surface, efficiency increase 9-35522

Ionization chambers

- background reduced by self-coincident gating arrangement 9-29653
 current fluctuation meas. of neutron flux, patent 9-32253
 detector of colloid suspension in gas, patent 9-34931

Ionization chambers continued

- Farmer-Baldwin and Victrometer, for dosimetry of high energy X radiation 9-25511
 fibre electroscop, test jig 9-46138
 fission for rapid calc. of $^{238}U/^{235}U$ ratio in fission fragments 9-22661
 for Kosmos 19 and Kosmos 25 cosmic ray obs. 9-38101
 photometer, appl. to solar X-rays, 8-12 Å, obs. 9-24907
 plane parallel plate, pulsed electron beam irradi., recombination effects 9-38615
 POGO, for total ionization meas. outer radiation zone 9-40067
 R.C.13, for reactor control and thermal neutron flux meas., description 9-22662
 γ , well type, for determ. of radionuclide activities 9-44169
 γ calibration of 4 π well chamber, calc., 0.1-4 MeV 9-27589
 X-ray meas. with inflated balloon ionization chamber 9-27152

Ionization gauges *see Vacuum gauges***Ionization potential**

- atoms, $Z=31-92$, higher stages 9-44275
 benzenes, methyl substituted, SCF-MO semiempirical calcs. 9-30092
 borazines, methyl substituted, SCF-MO semiempirical calcs. 9-30092
 crystals, determ. using proposed dielec. classification 9-23654
 cycloheptatrienyl radical 9-23345
 N,N -dimethylformamide, SCF calc., rel. to accidental near-degeneracies of n_o and π_2 MO's 9-38898
 ethylene, halogen substituted, intra-molecular electric fields effects 9-42559
 formamide, SCF calc., rel. to accidental near-degeneracies of n_o and π_2 MO's 9-38898
 formic acid, SCF calc., rel. to accidental near-degeneracies of n_o and π_2 MO's 9-38898
 isoelectronic atoms and ions, C-like to F-like, excitation and ionization energies calc. 9-44277
 N -methylformamide, SCF calc., rel. to accidental near-degeneracies of n_o and π_2 MO's 9-38898
 molecules, intra-molecular electric fields effects 9-42559
 molecules, prediction using new method for estimating energies of electronic transitions 9-30015
 nitrogen heterocyclics, lowest potential 9-39016
 trioxymethylene 9-22359
 BH_3 , appearance potential from BH_3CO decomp. 9-43314
 BaF_2 , thermal, of Nd^{2+} , Dy^{2+} , Ho^{2+} and Er^{2+} 9-46739
 CO_2 , e affinity, upper limit established 9-34612
 CaF_2 , thermal, of Nd^{2+} , Dy^{2+} , Ho^{2+} and Er^{2+} 9-46739
 Cs atomic cluster, technique and obs. 9-29956
 Hg 9-48411
 Hg Penning ioniz. 9-40709
 K atomic cluster, technique and obs. 9-29956
 Li double mol., atomic cluster obs. 9-29956
 N_2 in plasma 9-23302
 NO^- 9-32693
 Na atomic cluster, technique and obs. 9-29956
 Na-K mixture, atomic cluster obs. 9-29956
 O_2^- 9-32693
 S_2 9-44484
 Se_2 9-44484
 SrF_2 , thermal, of Nd^{2+} , Dy^{2+} , Ho^{2+} and Er^{2+} 9-46739
 Te_2 9-44484

Ionized gases *see Ionization/gases; Plasma***Ionosondes** *see Ionosphere measuring apparatus***Ionosphere**

- see also Electromagnetic wave propagation/ionosphere*
 below 3000 km, electrons low density regions, diurnal, seasonal and spatial variations 9-35876
 absorption meas. characteristics, obs. by beacon satellite 9-26936
 acoustic waves, Faraday rot. obs. from satellite 9-33827
 associative detachment reactions, maintaining high electron densities, riometer and satellite obs. 9-31394
 auroral, ion-acoustic instabilities, effects of ion-neutral collisions 9-40057
 auroral, latitudinal movements, scintillation meas. 9-41584
 characteristics from altitude variations of positive ion densities at night 9-26939
 composition and temp., night over Arecibo 9-24685
 composition measurements using r.f. probe 9-26943
 conductivity change rel. to energy loss factor 9-37976
 conductivity enhancement, auroral 9-40056
 conductivity variations near dip equator during solar eclipse (Nov., 1966) 9-24690
 conjugate region, presunrise effects, electron temperature 9-31401
 constants related to variations of solar wind velocities 9-28859
 constants related to variations of solar wind velocities 9-45480
 continuity equation, inclusion of particle source of ionization 9-31400
 cosmic noise absorption, sudden increases 9-45524
 current system, Sq, contribs. of various tidal winds 9-47574
 current system, two called due to magnetotail flux increase 9-24674
 current systems, computer analysis, program 9-38000
 currents, models 9-35858
 deionization processes 9-40044
 density and temp., effect of solar flux, theoretical study 9-45538
 diffusion in nonthermal plasma 9-31403
 disturbances, travelling, obs. using geostationary satellites 9-31412
 DP-current system dynamics for geomag. storms 9-47593
 drift, north-south, near mag. equator 9-26941
 dynamo action, magnetospheric current calc. 9-31376
 electrojet, equatorial night, electron drift vel. v.h.f. radar obs. 9-31377
 electrojet equatorial with meridional current system, model 9-49479
 electron conc. profiler, calc. allowing for inter- and underlayer ionization 9-45535
 electron conc. profiles, calc. from oblique ionograms 9-31398
 electron conc. vars. across duct rel. to ionogram traces 9-43440
 electron content, Doppler shift determ. by Diadem satellites 9-41580
 electron content, latitude dependence obs. (March 1966) 9-41579
 electron content, slab thickness and scintillations, meas. from low-latitude stations 9-35877
 electron content, total, correction for layer height changes 9-28949
 electron content by synchronous orbit beacon experiment 9-49490
 electron content determ. from first-order Doppler effect 9-41575
 electron content meas., Explorer 22, evaluation method 9-35865
 electron content meas. by differential Faraday effect, errors 9-33843
 electron content observations at different stations, comparison 9-40073

Ionosphere continued

electron content over Khartoum, satellite obs. (1964-65) 9-28945
 electron densities, differential absorption meas., seasonal variations, below 100 km in mid-latitude 9-37972
 electron densities and atmospheric circulation, seasonal variations, below 100 km at mid-latitude 9-37973
 electron density, electron and ion temp. ionic composition, meas. methods review 9-33848
 electron density, local and integral values, meas. by coherent radio waves from satellites 9-37971
 electron density, sensitive a.m. radio receiver design 9-35869
 electron density and collision freq. changes during stratospheric warming (Dec. 1967-Jan. 1968) 9-49489
 electron density distrib. rel. to radio wave echoes 9-33838
 electron density distribution, above winter Pole 9-31418
 electron density meas. with high power incoherent scatter radar app. 9-33845
 electron density measurements, local and propagation methods 9-43448
 electron density vars., vertical distrib. polar ionosphere 9-26938
 electron precipitations in and near auroral zone IQSY obs. 9-26931
 electron production rate, variations 9-45529
 electron total content, midlatitude night behaviour during mag. disturbances 9-24689
 electron total number, Faraday effect ATS-3 obs. 9-43443
 electron-density irregularities observed by topside sounders 9-35878
 electrostatic field prod. by dynamo effect 9-26935
 electrostatic resonances, obs. 9-24684
 energetic electrons at synchronous altitude, general features and diurnal variations 9-45531
 equatorial electrojet, electron density irregularity, observation and interpretation 9-26932
 equatorial electrojet region, Dst values 9-24707
 f_{min} obs. rel. to determ. auroral absorption zone position variations 9-40060
 fluctuations associated with mag. micropulsations, Doppler obs. 9-47575
 formations, ionized, vertically moving, dimensions and directions 9-31407
 gas dynamics of satellites and diagnostic probes 9-49495
 geomagnetic field lines, closed, high-latitude limit 9-35873
 gravity waves following SC mag-storm, propag. effects 9-43453
 gravity waves propagation, conducting fluid in magnetic fields 9-49486
 gravity waves propagation, interaction with magnetic field 9-24691
 hydromagnetic propagation in ionospheric waveguide, theory 9-28940
 hydromagnetic waves, non-uniform, 2-dimen., transmission and refl., theory 9-37969
 hydromagnetic waves, spectrum and rel. to heating 9-47577
 inhomogeneities, radioastronom. spaced receiver obs. 9-45533
 inhomogeneities, small scale portion of spectrum, radio astronomical obs. at 13.54 MHz 9-33844
 intermediate E-F region thickness vars., daytime IGY and IQSY obs. 9-45534
 ion clouds motion and ambipolar diffusion in Earth's mag. field 9-37977
 ion composition, 150 to 1500 km, for minimum solar activity 9-49488
 ion composition deduced from v.l.f. observations 9-35872
 ion temperature in 250-475 km range, diurnal variation 9-35864
 ionic composition, Thomson scatter and topside sounder meas., comparison 9-35875
 ionization velocity, effect of polarization field due to acoustic wave 9-41578
 ionized formations, vertical displacement 9-31406
 ionized formations, vertically moving, rel. to solar and mag. activity 9-40078
 ionized layer motion, wind and electrostatic field prod., in inclined mag. field 9-26940
 irregularities, Antarctic distribution, diurnal mag. and solar cycle effects 9-41586
 irregularities, comparison of scintillation depths of radio star and satellite scintillations 9-24692
 irregularities caused by atmospheric waves, theory and experimental evidence 9-33842
 irregularities rel. to radio scintillation obs. 9-49494
 low, electron production rate rel. to solar cosmic ray parameters and earth environment 9-45523
 lower, conductivity determ. from v.l.f. sudden enhancements of strength 9-49497
 lower, drift meas., correlation vs. similar-fade analysis 9-49498
 lower, electron conc. meas. by rocket, winter days of normal and anomalous absorption 9-40072
 lower, electron concentration vs. height during auroral absorption 9-31402
 lower, ion pair annihilation by aerosols 9-43439
 lower, ionization by cosmic rays 9-40075
 lower, propag. energy from explosions 9-31409
 lower, semi-diurnal tidal wind, seasonal phase changes 9-49491
 lower, storm events at medium latitudes 9-33841
 lower, theory, equipment and investigation 9-43456
 lower, vertical movement effect on radiowave field strength slow changes 9-45526
 lower, vertical wind 9-49492
 magnetic storm sudden commencement effects at solar activity extremes 9-31408
 magnetic storms, polar region, long-period wave generation 9-40100
 magnetoionic wave components in oblique incidence, statistical characts. 9-43442
 movements, vertical of ionized formations, spatial distribution 9-40079
 neutral, wave propag., Explorer 32 obs. 9-28912
 nighttime, influence of corpuscular fluxes in magnetosphere 9-35868
 nuclear explosion effects 9-31404
 observations, April (1968) 9-45521
 observations June (1968) 9-28939
 observations March (1968) 9-31383
 outer, v.l.f. bursts, rel. to mag. activity 9-40071
 parameters, planetary distribution spherical Harmonic analysis 9-40069
 phase investigation problems 9-45537
 plasma density profiles from phase-freq. obs. 9-31414
 plasma resonances, periodicities in amplitude 9-31410
 plasma temperature and ion abundance profiles deduced from Explorer XXXI and Alouette II data 9-35874
 plasma wave instabilities over aurora 9-43451
 plasmopause and reln. to ion composition 9-26937

Ionosphere continued

polar, electron concentration meas. 9-31396
 polar, electron precipitation heating 9-43466
 polar, H⁺ and He⁺ wind 9-26925
 polar, horizontal gradients 9-43452
 polar, ionization by solar cosmic rays 9-35867
 polar, suprathermal electrons, Explorer 31 obs. 9-43446
 polar electron flux, energy spectra from photometric and riometric obs. 9-43430
 polar wind, He isotopes escape mechanism 9-28913
 predawn photoelectron conjugate effects calc. 9-35866
 proton gyrofrequency harmonics obs. 9-47571
 radio noise bands explained by incoherent gyroresonance radiation of superthermal electrons 9-33837
 radio scintillation, star and satellite, power spectrum obs. 9-49494
 recombination, night, study using height model 9-31399
 recombination coefficient, effective, at 65 km altitude 9-45530
 research from space vehicles 9-37979
 resonance phenomena, lower hybrid, OGO 2 obs. 9-28943
 resonances, subsidiary 9-40082
 ring current rel. to auroral oval position 9-43431
 satellite scintillations, latitudinal vars., obs. 9-31405
 seismic continuous travelling coupling, May 1968 Japan earthquake obs. 9-43355
 solar activity, July-Sept. 1966 obs. 9-31641
 solar flare effects data 9-49593
 solar flare effects rel. to form. height in atm. 9-26964
 Sq currents in 3 dimen. ionosphere 9-37998
 structure, remote sensing system 9-33847
 structure and motion radio sounding system development 9-33846
 sudden phase anomaly, interpretation 9-40083
 temperature, electron density and ionic composition meas. by Thomson scatt. 9-31413
 temperature and density, effect of solar flux, theoretical study 9-45538
 temperature shape parameter, probe obs. 9-49493
 temperatures, ion electron and neutral from ion composition distribution 9-43445
 thermal structure, partial theory and temperature profile calculation 9-26942
 thermosphere, lower, composition from mass spectrometric obs. (Summer 1967) 9-28906
 thermosphere, midlatitude 150 to 450 km N₂, O₂ and He concentration and temp. 9-28905
 thermosphere, O line near 63 μ , thermal effect of radiative transfer 9-40081
 thermosphere, temp. and density 150-300 km, 1964-5 satellite obs. 9-31342
 thermosphere lower, O₂ dissociation 9-49487
 thermospheric gravity waves, 10^{-3} to 10^{-2} Hz, calc. 9-41585
 thermospheric structure and vars. 9-49460
 Thomson scatt. meas., influence of non-Maxwellian electron distrib. 9-41587
 tides, luni-solar 9-31411
 tides rel. to geomag. field lunar-diurnal vars., obs. 9-26958
 tilting, sunset, rel. to ground backscatter elevation angles, 16 MHz 9-41581
 topside, charged particle vertical transport velocity 9-43450
 topside, e density and temp., Ariel III obs. 9-45527
 topside, global electron density distributions 9-35870
 topside, ion composition and charged particle temperature, sounding rocket measurements 9-28946
 topside, thermal diffusion for mixtures including multiply-charged ions 9-45519
 topside, variations during geomagnetic storms, review 9-35871
 topside Alouette sounder, applic. pulse dispersion theory 9-41576
 topside charged particle temperature 9-31397
 topside electron density in summer after ground sunset rel. to altitude 9-45536
 topside ion and electron temp. rel. to concentration profiles 9-43449
 topside latitudinal temperature structure 9-26944
 topside polar, electron conc. vars. during mag. storm, Alouette 1 obs. 9-45532
 topside resonance, explanation in terms of oblique echoes 9-31415
 topside sounder data reduction, effect of nonvertical propag. 9-31416
 topside structure in summer after ground sunset rel. to altitude 9-45536
 topside suprathermal photoelectron flux, retard. potential obs. 9-41582
 turbulence-conditioned mag. fluctuations, estimation 9-33826
 vertical-incidence measurements and magnetograms, Bangkok and Thailand, annular solar eclipse, November (1965) 9-31419
 v.l.f. radio noise obs. during auroral absorption event 9-33830
 wave motions assoc. with plasma instabilities during particle precip. 9-47576
 waveguide hydromagnetic propag. 9-28950
 waveguide upper boundary, equivalent diurnal eight var. 9-49496
 waves, vertical energy flux due to ground disturbance 9-35816
 winds, dynamics 9-40077
 H⁺ concentration, 300 to 600 km 9-31397
 He, night over Arceibo 9-24685
 He⁺ concentration, 300 to 600 km 9-31397
 He escape, nonthermal in polar regions 9-45504
 He flux, lower thermosphere 9-31345
 O₂, night over Arceibo 9-24685
 O₂⁺ recombination with ionospheric electrons 9-37958
 O₂ at 100 to 150 km, u.v. absorption rocket obs., Woomera 9-37932
 O₂ dissociation, lower thermosphere 9-49487
 O₂ lower thermosphere 9-49487
 O⁺+N⁺ concentration, 300 to 600 km 9-31397

D-region

auroral electrons, positive ions and particles >40 keV, rocket obs. 9-35881
 collision frequency, high latitude 9-33850
 electron concentration profile, radio obs. 9-40086
 electron concentration profiles from l.f. continuous wave obs. 9-26945
 electron densities and collision frequencies during quiet sun period, radio-wave interactions meas. 9-26947
 electron density, rocket obs. during solar eclipse (May 20 1966) 9-31421
 electron density, simultaneous meas. by two ground based techniques, comparison 9-41589
 electron density distributions, comparison of Russian and British data based on same v.l.f. and l.f. propagation 9-37982

Ionosphere continued**D-region continued**

- electron density profile 65-95 km 9-41590
- electron prod. by primary cosmic rays in lower D-region 9-26946
- gravity wave motions 9-28947
- ion chemistry, survey 9-37981
- ionic mobilities use for measurements 9-24694
- lunar tides study by absorption analysis 9-37980
- profiles rel. to A3 Lf. absorption obs. 9-35880
- transmission, reflection coeff. and elec. field distribution 9-41861
- water cluster ions, origin due to vapour reactions, lab. obs. 9-43457

E-region

- auroral, night time, ionization changes rel. to local mag. disturbances 9-31424
- auroral, night time, rocket obs. of electron densities 9-31424
- auroral Es, midday 13 Dec 1967, airborne obs. 9-40059
- E2 ionization index, electron production and effective recombination 9-40087
- E2 continuous reflections, duration 9-45539
- E_{reg} disappearance rel. to pulsations of decreasing period, obs. 9-28965
- E_s, effect of meteor currents 9-37983
- E_s, stability, rel. to wind shear theory stratifications 9-26949
- E_s form., spatial redistrib. of E-region ionization 9-26948
- E_s freq. characts. and fine struct. rel. to transparency, obs. 9-28951
- E_s ionization rel. to wind shear, rocket obs. 9-47580
- E_s stratifications, critical freq., lifetime and spatial distrib., obs. 9-26950
- elec. field rel. to F region drift velocity 9-35883
- electron and ion temp., height variations, depend. on neutral gas temp. variations 9-31425
- electron conc., rate of variation 9-43460
- electron cooling by O₂ vibrational excitation 9-43444
- foE_s variations (1943 to 1965) 9-43458
- foE variation during solar eclipse, explained by quasi-equilibrium between electron density and soft X-rays emission on sun 9-24898
- foE_s vars. during solar cycle 9-43491
- frequency deviations, sudden, effect of X-ray and extreme u.v. solar flare bursts 9-43438
- ion chemistry, survey 9-37981
- ion compos. after mag. storm, 30 May 1967 night obs. 9-43459
- ionization irregularities, drifts and anisotropy, rel. to geomag. activity, obs. 9-49500
- irregularities, gravity wave prod., photochemical and dynamical effects 9-31427
- microstructure and vertical motion, kitesonde obs. interpretation 9-37984
- midlatitude charge density irregularities 9-43461
- neutral gas temp. variations, rel. to electron and ion temps. height variations 9-31425
- phase height oscills., short period, pulsed radio wave obs. 9-31420
- Polarcap sporadic E, backscatter obs. 9-24695
- radiowave triple splitting, mid-latitude, IQSY obs. 9-31423
- solar eclipse obs. rel. to theory 9-47570
- sporadic, blanketing, of different intensities, time and latitude vars. 9-31426
- sporadic, mid latitude 9-40085
- sporadic, propagation, significance in determining MUF 9-33851
- sporadic, thin layers 9-40089
- sporadic at Hong Kong rel. to mag. Kp 9-35882
- sporadic clouds, midlatitude Explorer 20 obs. 9-45540
- sporadic formation due to vertically inhomogeneous wind, instability 9-31422
- temperature and ion-neutral collision frequency, radar Thomson scatter obs. 9-40088
- temperatures, radar scatter obs. rel. to possible tidal heating 9-43462
- wind driven instability in lower part 9-49501
- O atom excitation rel. to e, ion and neutral gas cooling 9-47581

F-region

- acoustic gravity waves propag., ion drag effect 9-43471
- auroral emission of OI (6300Å), mechanism 9-26952
- backscatter irregularities, long range 9-40094
- circulation and neutral winds from Thomson scatter obs. 9-31442
- drift, molecular ions, allowance for in determ. kinetic parameters of ionization-recombination 9-31430
- drift, vertical, of ionization, geomag. control 9-31429
- drift velocity rel. to E region elec. field 9-35883
- dynamical behaviour during geomag. bay disturbances 9-35889
- effect on transverse conductance of magnetic force tubes 9-35897
- electric field excitation due to upward moving acoustic wave 9-43468
- electron collision freq., Delhi obs. 9-35886
- electron conc. vars. during mag. storm, s. hemisphere 9-31433
- electron concentration, seasonal and day-to-day variations 9-45579
- electron concentration at solar min., scatter obs. 9-31432
- electron concentration variations between 60°N and 60°S, rel. geomagnetic disturbances 9-40090
- electron density distribution during eclipse of 12 Nov, 1966; temporal variation 9-35891
- electron density distribution in South Atlantic geomagnetic anomaly, effects of temperature change 9-45545
- electron plasma resonance wave induction from earth 9-31441
- electron production and loss rates, geostationary satellite transmission obs. 9-47584
- electron production and loss rates from v.h.f. Faraday rotat. 9-24697
- electron temp. and density profiles, 120 to 630 km (2 March 1966, Wallops Island) 9-45544
- electrons, effective temp. and vertical drift vel. from conc. profiles 9-24698
- equatorial, neutral and charged particle temperatures, diurnal variation 9-28958
- equatorial, structure, review 9-35892
- equatorial geomagnetic anomaly, theories review 9-35885
- F1, formation rel. to ion conc. height profiles 9-31439
- F1 layer junction frequencies for latitudes higher than 35°N 9-33852
- F1 structure vars. and temp., IGY and IQSY 9-43469
- F1-F2 transition, analysis using 'overlay' technique 9-31434
- F2, asymmetric diurnal variations 9-37990
- F2, dynamic coupling with protonosphere 9-24696
- F2, e temp. and thermal imbalance, diurnal and seasonal vars., calc. 9-28955
- F2, electron conc. rel. to lunar tidal phenomena, at low latitudes 9-47583
- F2, H⁺ concentration 200 to 630 km, obs. 9-43464

Ionosphere continued**F-region continued**

- F2, He⁺ conc. 200 to 630 km obs. 9-43464
- F2, horizontal drifts and anisotropy of irregularities, correl. analysis 9-41591
- F2, mid-latitude, coupled ion and neutral air equations, solution 9-24699
- F2, N⁺ and N₂⁺ concentration 200 to 630 km, obs. 9-43464
- F2, NO⁺ conc. 200 to 630 km obs. 9-43464
- F2, O⁺ and O₂⁺ concentration 200 to 630 km, obs. 9-43464
- F2, polar, Universal Time control, rel. to vertical drifts caused by atm. winds 9-43472
- F2, prolate irregularities formation 9-40093
- F2 asymmetries rel. to world-wide neutral air winds and electrodynamic drift 9-47582
- F2 critical freq., diurnal vars. rel. to mag. declination 9-37986
- F2 critical freq., space-time forecasting expt. 9-26951
- F2 critical freq. rel. to maximum freq. E_s layer 9-43463
- F2 critical freq. rel. to pulsations of decreasing period, obs. 9-28965
- F2 critical freq. rel. to sunspot no., hysteresis 9-49502
- F2 decrease in tropical forenoon, obs. 9-33853
- F2 disturbances in polar mag. storms rel. to ionization drifts 9-26953
- F2 electron concentration enhancements from inner radiation belt particles 9-40092
- F2 heating during geomag. disturbance due to electron precipitation 9-43466
- F2 height variations enhancing 6300Å nightglow emission 9-41557
- F2 inhomogeneities, small scale, drift velocity vectors 9-31438
- F2 ion compos. obs. rel. to chemistry and dynamics 9-43464
- F2 ionization state, mean annual characteristic 9-31431
- F2 layer, ionization troughs below max. 9-47585
- F2 layer heights at low latitudes, night decreases at near conjugate points 9-37991
- F2 layer summit, mag. declination influence 9-47579
- F2 max. seasonal anomaly rel. to O, N₂ concs. 9-28956
- F2 maximum, ionization-recombination kinetic parameters determ. allowing for molecular ion drift 9-31430
- foF2, N-S asymmetry rel. to geomag. axis inclination 9-45542
- foF2, rel. to 11 year solar cycle 9-45543
- foF2 data rel. to total electron content determ. 9-37987
- foF2 N-S asymmetry, increase with solar activity 9-45542
- foF2 vars., predawn effect due to sunrise at mag. conjugate points 9-43467
- F₂ disturbances in mag. storms, 0-60°N 9-28957
- F₂ layer characteristics, Gram-Charlier series distribution 9-26954
- F₂ signal location on oblique sounding oscillograms 9-26955
- foF2 space-time vars. 9-43470
- gravity waves, fine structure temperature obs. 9-31440
- gravity waves, Thomson scatter obs. 9-35890
- gravity waves during magnetic storm (13 Sept., 1967) 9-49505
- heating and ionization during mag. storms 9-45546
- high-latitude, behaviour and structure 9-35887
- ionization, energetic particle contrib., critical freq. obs. 9-31435
- ionization from fast neutral particles 9-45541
- ionization heating during mag. storms 9-45546
- loss coefficient estimation from concentration profiles 9-40091
- mid-latitude, electron density profile during severe ionospheric storms 9-35888
- motions, plasma and neutral 9-31437
- night, nonlinear charge exchange and dissociative recombination, effect on decay 9-31443
- night cooling reduction due to conduction from protonosphere 9-40049
- night ion-molecule reactions, rate calc. from loss coefficient obs. 9-40091
- nighttime recomb. and variable drift effects 9-49503
- penetration frequencies predictions, comparison with topside-sounder data 9-35884
- polar, electron content enhancement at 78°N, 0900 local mean time Norway 9-37989
- polar, electron density diurnal vars. 9-37988
- solar eclipse obs. rel. to theory 9-47570
- spread and mag. activity, delays between, latitude vars. 9-37985
- stratification associated with travelling disturbances 9-43465
- stratification during solar minimum 9-40095
- thermosphere, midlatitude and auroral zone, electron cooling obs. 9-31428
- tropical night-time layer, maintenance by large source of ionization 9-28952
- upper, electron temp. obs. 9-28954
- Venus, F1 type region, Mariner 5 and Venera 4 interpretation 9-38074
- vertically moving ionized fprmsations, dimensions 9-28953
- winds, diurnal and seasonal vars. from Thomson scatt. obs. 9-49504
- winds, neutral-air, for asymmetric global press. system 9-47586
- O⁺ reaction with O₂ and N₂ night rate calc. from loss coefficient obs. 9-40091
- H and H⁺ equilibrium distributions 9-24700
- O⁺, N⁺, H⁺, He⁺, NO⁺, O₂⁺ and N₂⁺, concentrations between 200 km and peak altitude, direct measurement 9-24701
- O⁺, N⁺, H⁺, He⁺, NO⁺, O⁺ and N₂⁺, concentrations between 200 km and peak altitude, direct measurement 9-31436
- O⁺ ions production 9-24697
- O and O⁺ equilibrium distributions 9-24700
- O atom excitation rel. to e, ion and neutral gas cooling 9-47581

Ionosphere measuring apparatus

- automatic atmospheric waveform recorder for routine ionos. study 9-47578
- conductivity and radiowave propag. probes, design 9-43456
- D-region electron density, comparison of two ground based methods 9-41589
- digital radio pulse vertical sounding systems called dynasonde and kitesonde 9-33846
- drift measuring receivers, closely spaced, data analysis 9-28948
- electron trap on slowly moving charged spacecraft, behaviour 9-43454
- field mill application for electric field meas. 9-42537
- image intensifier and camera for auroral H_α emission 9-31372
- incoherent scatter radar app. for meas. electron densities 9-33845
- ion spectrometer design 9-37978
- irregularity direct detection, satellite instrument 9-49499
- Langmuir probes, for particle densities and temperatures, theory and development 9-41588
- Langmuir probes (orbital) in collisionless plasma with mag. field, current volt characts. 9-43455

Ionosphere measuring apparatus continued

- mass spectrometer on Explorer XXXI satellite, in-flight calibration and performance 9-35879
 multisensor array for ionospheric phenomena obs. 9-33849
 phase-freq. characts. determination, installation 9-31414
 for precipitation currents, metallic cylindrical shield, exposure factor 9-31417
 probes, gas dynamics 9-49495
 radio technique using steerable h.f. antenna arrays for scanning azimuth and elevation angles, one- and two-way propagation 9-33847
 research from space vehicles 9-37979
 r.f. probe, composition measurement 9-26943
 spectral analyser, h.f. multichannel, for reflected pulses 9-40084
 Thomson scatter radar technique review of theory, facilities and applications 9-33848

Ions

- see also Atoms; Ion emission/thermionic; Molecules; Plasma*
 alkali halides, interionic separation correl. with interparticle distance at m.p. 9-35007
 alkali halides, radii deriv. using repulsive energy method 9-35006
 alkali halides, temp. parameters of ions 9-30507
 atmospheric, light, abundance obs. by OGO, interpretation 9-41546
 atomic, frozen core approx. for systems with one valence electron in addition to filled shells, prop. 9-22926
 benzol [cd] pyrene-6-one, doubly charged negative ion 9-30305
 boron-like, perturbation treatment of Hartree-Fock equations for ground states 9-34520
 cosmic, fast, radio emission of 9-28985
 D-region, Physical and chemical processes 9-37981
 desorption, electron-induced, from Pt-Ir, Mb; u.h.v. gauge, mass spectrometric investigation 9-38178
 diffusion during electrostatic deposition 9-23409
 diffusion in quartz during electrolysis, rel. to conductivity 9-39387
 e-region, physical and chemical processes 9-37981
 in electrostatic dipole fields 9-31921
 exchanger kinetics film diffusion 9-45414
 formulation and calculations for $2p^6$ ions in gaseous nebulae, excitation of forbidden lines 9-27004
 ion-molecule reactions, energy depend. of intermediate complex formation 9-49371
 ionization of various ions, mass-sections obs. 9-46296
 metals, interionic separation correl. with interparticle distance at m.p. 9-35007
 mobilities, lower ionosphere use for measurements 9-24694
 multivalent, derivation of set of self-consistent ionic radii 9-32854
 negative, collision with atom, electron detachment 9-32427
 negative ion-molecule reactions method of study 9-46430
 non-hydrogen-like, width and shifts of spectral lines 9-44250
 O II lines in M8 nebula, brightness 9-31517
 one-electron ion in uniform elec. field, high-order perturbation theory 9-34528
 oxygen-tetrahedra cpds., geometric contrib. to non-linear polarizability 9-35611
 pairs in lower ionosphere, annihilation by aerosols 9-43439
 penetration range in amorphous target 9-42983
 polar latitudes, ionization maximum 9-33828
 positive, excitation by electrons, effective Gaunt factors 9-38778
 production by electrical atomization of liqs. in vacua 9-23526
 radii, multivalent, self-consistent set derivation 9-32854
 semiconductor doping by ion implantation 9-41208
 spectra, persistent line intensities in d.c. arc, calc. 9-24602
 Thomas-Fermi eqn. for positive ions, analytical solns. 9-29905
 transport across membrane, noise spectra and relax. times obs. 9-34892
 traversal of liquid solns., physical conditions for continuous sensitivity 9-30373
 vertical-incidence measurements and magnetograms, Bangkok and Thailand, annular solar eclipse, November (1965) 9-24693
 water cluster in ionospheric D region, origin due to vapour reactions, lab. obs. 9-34547
 water molecules, discrete in the vicinity of two oppositely charged ions 9-23462
 Ag^+ analytical self-consistent-field wave function, cusp conditions 9-22938
 $AgCl$, deform. of ions, X-ray obs. 9-30507
 Ar, population inversion, excitation mech. for transitions of Ar III and Ar IV 9-28041
 Ar plasma, density and current distributions 9-32604
 Ar II, excited level lifetime 9-34559
 AsO_4^{3-} , geometric contrib. to non-linear polarizability 9-35611
 C energy levels, radiative lifetimes 9-36659
 CH_3^+ and CH_3^- , potential energy surfaces 9-27903
 Cr^{4+} absorpt. spectrum in Al-line glass, obs. 9-35655
 Cu^{2+} diffusion in $CuSO_4$ aq. soln., e.p.r. obs. 9-34890
 Cu II tetrahalo-anions, Raman spectra rel. to vibrs. obs. 9-44327
 in D plasma, heating in very fast theta pinch 9-30212
 F^{2+} , collision strengths for electron impact transitions 9-34563
 Fe, relax. times, determ. from Mossbauer data 9-25710
 Fe^+ , Mg^+ , Ca^+ , Na^+ and K^+ , earth's atmosphere, measurements of reaction with ozone 9-40044
 Fe^{3+} in $Fe(NH_4)(SO_4)_6 \cdot H_2O$, $^{57}Co^{2+}$, daughter ions stabilization rel. to H_2O radiolysis by Auger e. obs. 9-23801
 Fe II solar lines, theoretical equivalent widths calc. 9-36036
 Fe II tetrahalo-anions, Raman spectra rel. to vibrs., obs. 9-44327
 Fe II tetrahalo-anions, Raman spectra rel. to vibrs., obs. 9-44327
 Fe IV lines in spectrum of the star MH α 328116 9-35979
 H_2^+ , discrete vib. states due only to long-range forces 9-44328
 H_2^+ , geometric-mean variation function 9-42397
 H_2^+ and H_2^+ , exciting He atoms, 1-150 keV, cross sections 9-48410
 H^- , detachment by e impact 9-44293
 H^- , from pulsed sources, increased yield 9-43861
 H^- , nonexistence of 1 sns autoionization states 9-44292
 He^+H^+ , existence in room-temp. plasmas, mass spectrometric obs. 9-25969
 He^+ existence, mass spectra obs. in plasmas 9-36760
 He^+ existence, mass spectra obs. in plasmas 9-36760
 He^+ formation in H_2 -He fast beam collision 9-29985
 He^+ prod. in afterglow plasma due to collisions between metastable ions 9-46336
 He like, from He I to Ne IX, intercombination oscillator strengths 9-36662

Ions continued

- Hel, local thermodynamic equilib., validity criteria 9-23277
 Hg^{2+} , nuclear quadrupole anti-shielding factor, calc. using three different wave-functions 9-34540
 I⁻ prod. when I^+ passes through various gases, 1-4.5 MeV 9-30302
 In⁺ energy parameters in KCl 9-31052
 LiH⁺, electronic struct. 9-44335
 $LiNbO_3:Nd^{3+}$, absorpt. and luminesc. spectra, 4,2-295°K 9-28689
 Mn II tetrahalo-anions, Raman spectra rel. to vibrs. obs. 9-44327
 N, radiative-lifetime meas. 9-36663
 N_2^+ structure determ. using gas phase electron diff. 9-27867
 N_2^+ geometries by approx. SCF-MO theory which considers intermol. differential overlap 9-34637
 N^+ atm., night time distrib. with incidence of aurora 9-28931
 NO_2^+ , charge distrib. and orbital energies of ground state, CNDO calc. 9-44339
 NO_2^+ , N^{14} quadrupole coupling const. calc. 9-42401
 NO_2^+ and NO_2^+ , electronic struct. and geometry 9-48467
 NO_3^+ , solvation of nitrate ion, i.r. spectroscopic evidence 9-42661
 NO_3^+ symmetry in solns., metal cations effects, obs. 9-36887
 $NO(SO_3)^{2-}$ in potassium aminedisulphonate, quadrupole coupling for ^{14}N from e.s.r. meas. 9-39916
 Na^+ , collision strengths for electron impact transitions 9-34563
 NaCl, deform. of ions, X-ray obs. 9-30507
 Nd^{3+} , energy-level scheme in $CaWO_4$ 9-49232
 Nd^{3+} in $SeOCl_2$ laser liquid, spectroscopic props. rel. to conc., acidity and temp. 9-26120
 Ne^{1+} collision strengths for electron impact transitions 9-34563
 Ni^{2+} , absorpt. spectra in spinel 9-43242
 O_2^+ electron detachment using ion beams with energies 3 to 100 eV 9-34572
 O_4^{2+} , O_4^{2+} , geometries by approx. SCF-MO theory which considers intermol. differential overlap 9-34637
 O^- electron detachment using ion beams with energies 3 to 100 eV 9-34572
 O^+ , collision strengths for electron impact transitions 9-34563
 O^{2+} forbidden lines excitation, resons. in cross sections 9-22974
 O energy levels, radiative lifetimes 9-36659
 OH, liberation in alkali halides, direct absorpt. band obs. 9-43236
 PO_4^{3-} , geometric contrib. to non-linear polarizability 9-35611
 S I transition probabilities, near vacuum u.v., obs. 9-23366
 SO_4^{2-} , geometric contrib. to non-linear polarizability 9-35611
 Se I transition probabilities, near vacuum u.v., obs. 9-23366
 Si I transition probabilities, near vacuum u.v., obs. 9-23366
 Th, ionic solvation and growth of ThO_2 sols. 9-23549
 Ti II, line strengths for the transition array $(3d^3+3d^4s)-3d^24p$, calc. 9-34522
 Tl^+ energy parameters in KCl 9-31052
 Zn II tetrahalo-anions, Raman spectra rel. to vibrs. obs. 9-44327
- recombination**
 in air ionized by alpha particles 9-25966
 air-acetylene flame, low press. 9-42563
 dielectronic 9-44496
 dielectronic recombination, effects of electron and radiation density 9-42567
 F2 maximum, ionization-recombination kinetic parameters determ. allowing for molecular ion drift 9-31430
 hydrogenic ion plasma, coeffs. calc. by collisional-radiative model 9-42494
 inert-gas plasmas, collisional-radiative recomb. rate 9-30219
 ion-pair recomb. rates in liqs. of low dielec. const. 9-30425
 ionic crystals, recombination luminescence investigated by EPR relaxation 9-33576
 in ionization chambers irradiated with pulsed electrons 9-38615
 in ionosphere, at 65 km altitude, effective coefficient 9-45530
 ionosphere, F-region, nighttime recomb. and variable drift effects 9-49503
 Natanson formula generalization 9-34794
 in night-time F region, nonlinear loss and decay 9-31443
 noble gases, electron-ion recomb. in ionizing particle track, scintillation mechanism 9-30304
 in plasma, dense low temp. with ternary collisions 9-46474
 plasma, low-temp., electron diffusion concept 9-40708
 rate constant calc. using Monte Carlo trajectory calc. of e impact excitations 9-32420
 three-body, at moderate and high gas densities 9-34794
 three-body process 9-39020
 Ag halide crystals, flash and afterglow kinetics, ionic processes 9-33577
 Ar_2^+ , dissociative recombination, electron-temp. dependence 9-34795
 CO , electron-ion recombination, diffusion coeff., 775°K 9-48617
 $CoSO_4$ in soln. rate determ. using u.s. absorption 9-30397
 H, homogeneous plasma, coeffs. calc. by collisional-radiative model 9-42494
 H plasmas, collisional-radiative recombination coeffs. rel. to atomic collisions 9-42495
 KCl:Ag phosphors, types I and II luminescence, two competing recombination processes 9-33581
 LiH laser irradi., plasma electron-ion recombination 9-44464
 N, electron-ion recombination 9-34796
 N_2 , electron temp. depend. 9-32697
 N^+ and O^+ , recombination radiation in vacuum ultraviolet, shock tube studies 9-25968
 N plasma continuum radiation, 975-37000 Å 9000-13500°K, 1, 2 atm. press. obs. 9-23302
 NaCl:Cu, NaCl:Cu:Ag recombination luminescence, trapping of electrons and holes determ. by EPR meas. 9-33587
 Ne_2^+ , electron temp. dependence obs. 9-32696
 $NiSO_4$ in soln. rate determ. using u.s. absorption 9-30397
 O_2^+ , electron temp. depend. 9-32697
 O_2^+ recombination with ionospheric electrons 9-37958
- scattering**
 Au surface obs. by large-angle Ar^+ scatt. on single crystal 9-48748
- Ions, electrolytic**
see also Conductivity, electrical/liquids, electrolytic; Dissociation/electrolytic
 alkyl ammonia anions-nonyl alcohol H-bonds, i.r. obs. 9-27885
 aromatic cpds. in halogenated liqs., molec. cations obs. by pulse radiolysis 9-31215
 association of counterions to polyelectrolytes in soln. 9-44552
 association of counterions to polyelectrolytes in soln. 9-42642

Ions, electrolytic continued

- benzene anion solns., ion pairing and temp. depend. of linewidth 9-42680
correlation functions in non-homogeneous charged region 9-22140
N,N'-dimethylpyrazine cation, e.s.r. relax. 9-23117
electrodialysis in laminar flow, boundary-layer and d polarization 9-47464
energy on crossing low dielec. membrane, effect of 'pores', 'carriers', thickness and ion-pair form. 9-39954
formate ions, counter current electromigration ^{14}C isotope effect 9-48439
hydration in gas phase 9-24530
methylammonium ions, counter current electromigration ^{14}C isotope effect 9-48439
monovalent counterions in subsolution, influence on charged monolayers 9-23447
neutralization of isolated ion pair in polar liqs. 9-42674
neutralization of isolated ion pair in polar liqs. 9-42675
oxalate ions, counter current electromigration ^{14}C isotope effect 9-48439
polyelectrolyte soln. with mono- and divalent counter ions, rodlike model 9-42636
rare earths, trivalent, spectral intensities in soln. 9-36885
solvated electrons and p.d. between two immiscible media, thermodynamic explanation 9-39958
toluene ion radicals, spin delocalization and vibr.-electronic interaction 9-38917
triphenylene triplet dianion, zero-field-splitting calc. 9-42446
Co(II) in water and alcohols, X-ray diff. 9-44548
Fe $^{2+}$, Mossbauer effect in Y zeolite and Dowex 50 resin 9-43226
Gd $^{3+}$ in aq. soln., electronic energy levels 9-26118
In $^{3+}$ in In $^{3+}$ -HClO $_4$ -HNO $_3$ and In $^{3+}$ -NClO $_4$ -NaNO $_3$ behaviour, ion exchange expt. 9-37812
LiCl in alcohol soln. association and dissoc. from relax curves u.s. absorpt. 9-23493
Sc(III), solvation in H $_2$ O-acetone, p.m.r. 9-42682
Tb $^{3+}$ in aq. soln., electronic energy levels 9-36886
Th(IV), solvation in H $_2$ O-acetone, p.m.r. 9-42682
Y(III), solvation in H $_2$ O-ace tone, p.m.r. 9-42682

Isasers see Lasers**Iridium**

- chemisorption of CO, i.r. spectra, temp. effect 9-43325
fission-fragment damage and formation mechanism 9-42810
point defect clusters caused by proton irradi., interstitial conc. decrease during annealing 9-35085
superconducting transition temp., press. effect 9-44940
Ir $^{4+}$ in Ba $_2$ NbNb $_2$ O $_{15}$, optical defect 9-28651
Ir $^{4+}$ ions, exchange-coupled and single, cross-relaxation in (NH $_4$) $_2$ PtCl $_6$, e.p.r. meas. 9-49356
Ir $^{4+}$ ions, exchange-coupled and single, hyperfine interactions in (NH $_4$) $_2$ PtCl $_6$ 9-49364
in MgAl $_2$ O $_3$ stoichiometric spinel, trace detection by neutron activation analysis 9-35088

Iridium compounds

- Fe-(30-50wt.%)Ir $\gamma \rightarrow \alpha$ and $\gamma \rightarrow \epsilon$ transform. rel. to Ir content, dilatometric meas. 9-41067
IrCl $_6^{2-}$, mag. circular dichroism in cryst. (CH $_3$ NH $_2$) $_2$ SnCl $_6$ 9-41353
IrO $_2$, ht. capacity 0.54 $^\circ$ -10 $^\circ$ K 9-48971

Iron

- 3d-band shape from high-field susceptibility obs. 9-37406
abundance in terrestrial planets, total mass fraction calc. 9-43621
abundance in Mercury's core and mantle, models 9-45669
adhesion, effect of chemisorbed film 9-37272
Armco, elastic wave attenuation 9-37257
Armco, thermal conductivity, 50-800 $^\circ$ C 9-39546
atom, electric dipole transition 3d 4 p-d 8 , total line strengths and oscillator strengths 9-38768
atom, electronic configuration 9-25697
atom, energy spectra calc. for 3d 7 and 3d 4 p configs. 9-38767
atom, relative oscillator strength, obs. 9-45678
atom, selection rules for forbidden d-p-d 8 transitions, line strength calc. for 3d 7 p-d 7 9-40542
atomic spectrum, bibliography 9-38765
attenuation of shear waves, effect of Fe $^{2+}$ 9-37335
band, ferromagnetism, high-field studies by Mossbauer and mag. moment meas. 9-43166
b.c.c. phase, diffusion of Be, temp. depend. 9-23839
Bloch wall and stripe domain struct., e microscopy 9-26641
Bloch walls, charged 90 $^\circ$ in thin platelets 9-43169
brittleness, n irradi. induced, rel. to microstruct., theory 9-37261
cast, globular, fatigue fracture, hardening and softening obs. 9-30689
cast, malleable, microtopography of graphite grains and microdistribution of sulphur 9-23950
cast, resistivity and mech. props., review 9-33179
with chemisorbed film, effect on friction and adhesion props. 9-37272
cold-worked mag. permeability and X-ray diffraction line broadening correlation 9-45146
corrosion inhibition by amines, synergistic effect of anions 9-24575
corrosive surface reactions in field ion microscope 9-26827
crystal structure underrod after electron beam bombardment melting and quick cooling 9-33110
de Haas-van Alphen eff. and Fermi surface 9-24093
density-of-states functions, X-ray photoelec. spectroscopy study 9-44886
diffusion in MgO 9-44738
diffusion in TiO $_2$, anisotropy of front depend. on relative orientation of crystals 9-46859
diffusion of ^{64}Cu in α - and γ -iron rel. to defect interactions 9-46851
diffusion of Be in b.c.c. phase, temp. depend. 9-23839
diffusion of Cr, mechanism 9-46849
diffusion of S and O at 1560 $^\circ$ C 9-48691
dilute solutions in Cu-Al alloys, specific heat 1.2 $^\circ$ to 14 $^\circ$ K 9-47001
dislocation, Burgers vectors, two-beam diff. contrast meas. 9-32969
dislocation, $\{100\}$ edge dislocation, structure 9-46822
dislocation and slip mechanism of plastic deformation in single crystals 9-23884
dislocation behaviour, interstitials distrib. effect 9-46821
dislocations, a $\langle 110 \rangle$, field-ion microscope evidence for existence 9-30609
domain wall width meas. in thin sections by electron interference method 9-41310
dynamic yield behaviour of shock-loaded Ferovac-E 9-41017

Iron continued

- electrical resistivity recovery after fast neutron-irrad. at low temp., isochronal annealing obs. 9-43027
electrodeposited, data on fine struct. obs. in electron microscope 9-36942
electrolytically deposited, fine crystal structure under different electrolysis conditions 9-44663
epitaxial films, recrystallization 9-42723
epitaxial layers on oriented Au support, electron microscope exam. 9-48759
e.p.r. in glass 9-37797
eutectic melting at contact with diamond and graphite 9-26358
 α -Fe, u.s. determ. of diffusion coeff. of carbon at 408 $^\circ$ and 430 $^\circ$ C 9-37196
Fe(III) reduction to Fe(II) in solids at high press., reversible 9-37825
Ferovac-E, shock-loaded, dislocation twinning mechanism of dynamic yielding 9-41017
in ferredoxin of Euglena, atomic state from Mossbauer spectroscopy 9-32537
ferromagnetic, optical interband absorpt. 9-39836
ferromagnetic anisotropy energy calc. by perturbation theory 9-47254
ferromagnetic domain struct., e microscope obs. 9-33471
Ferovac E, strain ageing behaviour rel. to applied ageing stress and interstitial conc. in soln. 9-41050
Ferrovac E, temp. depend. of flow stress 9-41011
film, Hall effect, rel. to thickness 9-47267
film, high-coercivity, recorded magnetization patterns obs. by Lorentz microscopy 9-45165
film, magnetization, neutron scattering studies 9-45167
film, magnetization distrib. about single mag. particle 9-43181
film on Ir, props. observed by field-ion and field emission microscopy 9-23624
films, fine mag. struct. and coercive force 9-41321
films, magnetiz. meas. as thickness inc. atomic layer by layer 9-28619
foil, containing radioactive nuclei, perturbed ang. correl. meas. 9-35602
friction effect of chemisorbed film 9-37272
gamma ray scatt., 145 keV, differential elastic scatt. X-section 9-46263
grain growth, strain induced 9-42788
in haemoglobin, e.p.r. 9-33641
hardness anisotropy of single crystals 9-35192
hyperfine field interaction on ^{181}Hf , IMPACT study 9-45256
in Illite, Mossbauer effect obs. of oxidation state, coordination symmetry and site distortion 9-37698
implantation perturbed ang. correl. expts. after inelastic proton scatt. 9-33494
impurity in calcite, infl on cleavage surface energy 9-30479
interband optical transitions investigation, low temp. magneto-optic meas. 9-41136
internal friction singularities during $\alpha \rightarrow \gamma$ transformation 9-23857
internal mag. field at Os after Coulomb recoil implantation 9-39765
interstitial distrib. effect on dislocation behaviour 9-46821
intrinsic electronic thermal resistivity 9-26448
ion implanted crystals, investigation using directional effects in charged particle reaction yields 9-30598
ion relax. in CoCO $_3$: ^{57}Fe , Mossbauer obs. 9-41364
ions, relax. times determ. from Mossbauer data 9-25710
isotope effect, self-diffusion, mass depend. 9-35130
lattice constants and thermal expansion, effect of H atmos. 9-44666
liquid, absorpt. of N from a plasma 9-46455
liquid, vapour pressure, 1813-1973 $^\circ$ K 9-23604
magnetic saturation and magnetic moments of nuclei 9-26634
magnetization, temp. variation, and high-field susceptibility at 0 $^\circ$ K 9-47243
magnetization by twisting in weak field, Matteucci effects 9-35566
magnetomechanical damping, 78 $^\circ$ to 300 $^\circ$ K 9-45157
magnetomechanical damping effects 9-31036
Mattenczi effect in single crystals, whiskers and alloy wires 9-33454
meteorites, shocked, unshocked, Mossbauer spectra using reson. scatt. technique 9-24887
microcracks initiated by 17.8 kc/sec oscillations 9-35190
microprojectiles at 0.5 to 10 km/sec., crater formation 9-30700
microtopography of graphite grains and microdistribution of sulphur in malleable cast irons 9-23950
in Montmorillonite, Mossbauer effect obs. of oxidation state, coordination symmetry and site distortion 9-37698
Mossbauer absorpt. in ^{57}Fe from Curie pt. to γ - δ transition 9-41366
Mossbauer effect obs. of spins in Sc substituted rare-earth iron garnets, canted struct. 9-37667
Mossbauer effect of ^{57}Fe , hyperfine mag. splitting, effect of texture 9-35636
Mossbauer spectra near triple pt., comparison bet. α , ϵ and γ Fe, isomer shifts 9-26722
Mossbauer spectra of ^{133}Cs , positive mag. hyperfine field 9-37699
Mossbauer spectra r.f. sidebands, magnetically induced in spectrum 9-47332
neutron diff. by cryst. excited by magnetostructure resonator 9-48823
neutron irradiated, dislocation channelling 9-48860
neutron-irradiated at low temp., elec. resistivity recovery, isochronal annealing obs. 9-43027
n.m.r./nucl. orientation of 198 , ^{199}Au , non-contact contrib. to effective field obs. 9-37805
nodular, Ce determ. by X-ray analysis 9-35763
nuclear transverse relaxation times, rel. to emission or absorpt. of magnon 9-45240
optical interband absorpt. in ferromag. Fe 9-39836
optical isotope shift, nucl. vol. and mass eff. 9-29988
ore, sintered, reduction cracking 9-33093
oxidation and cracking, effect of prior cold working 9-41450
oxidation in O $_2$ /H $_2$ O vapour mixtures at 950 $^\circ$ C 9-33668
Peierls mechanism, strain-rate sensitivity of flow stress 9-39404
phase stability, review 9-48936
polymorphism, eff. of alloying elements 9-35009
polymorphism, influence of atomic size factor 9-46954
porous, dynamic compaction props. 9-44762
precipitates in Cu-Fe dilute alloys, martensite nucleation 9-37300
pressurization effects on yield behaviour, effect of grain size 9-28347
pressurization effects on yield behaviour, effect of grain size 9-28346
proton energy losses 9-30807
pure, grain size and strain rate effect on lower yield stress 9-42881
recombination centre in Ge, study by transient p-n junction technique 9-33330

Iron continued

- self-diffusion in δ , γ and α -phases, isotope effect meas. using ^{57}Fe - ^{59}Fe 9-26301
- self-diffusion isotope effect, mass depend. 9-35130
- shock-compressed, α -to ϵ -phase transition, conductivity and demagnetization obs. 9-26388
- shock-induced substructural changes in prestrained samples 9-32915
- single crystal plates produced by strain-anneal method, effect of stretching on imperfect structures 9-32913
- solid, surface energy determ. by inert sessile drop method 9-32836
- solid solns., sintering procedure contrib. 9-39449
- solubility, with P in Cu(36wt.%Zn) 9-30717
- solubility in Al, enhanced value obtained by rapid quenching 9-42916
- spark source mass spectroscopic analysis of high purity sample 9-31219
- spin, diffusion const., theoretical estimate 9-41306
- spin dynamics, neutron scattering study 9-45110
- spin-wave and critical scatt. of neutrons 9-31030
- stacking fault, field-ion microscopic obs. 9-40962
- strain annealed crystals, subgrain boundaries in $\langle 011 \rangle \{112\}$ occluded grains 9-23824
- strain rate behaviour in pure shear 9-42876
- stretching amount and preferred orientation of single crystal plates produced by strain-anneal method 9-35163
- in the Sun, highly ionized oscillator strengths and wavelengths of some X-ray and extreme u.v. spectrum lines 9-24903
- surface struct., low energy ϵ diff. meas. 9-35044
- tensile properties, 4-295°C, grey cast 9-48893
- thermal conductivity, 50-800°C, Armo iron 9-39546
- thermal conductivity, 78 to 373°C, apparatus descrip. 9-26439
- thin coatings, Hg adsorption, effect on elec. cond. 9-37428
- transverse Kerr magneto-optic effect and optical props. 9-45274
- u.s. eqn. of state 9-26310
- vibrating cryst., neutron diff. obs. 9-48823
- whiskers, reduction growth, initial stage 9-26215
- work hardening in single cryst., orientation depend. 9-26370
- work-hardening rate of single cryst., temp. depend. 9-35197
- yield drop in single crystals, deformed at -75°C, orientation dependence 9-33028
- yield stress, lower, grain size and strain rate effect 9-42881
- zone refined by deform. at -196°C, elec. resistivity study of lattice defects 9-26275
- ^{133}Xe implanted, Mossbauer, spectra of subsequently excited ^{133}Cs 9-35632
- $\text{Al}_2\text{O}_3\text{:Fe}^{3+}$ single crystal, paramagnetic relax. absorpt. of hypersound 9-33172
- in Al_2O_3 single cryst., low temp. thermal conductivity meas. 9-35086
- Au-Fe thermocouples, reproducibility tests 9-22299
- $\text{CaTiO}_3\text{:Fe-Mo}$, photobleachable electron-beam-induced colouration obs. 9-43201
- Cu-Al:Fe dilute alloy, specific heat 1.2° to 14°K 9-47001
- in Cu(36wt.%Zn), influence on recrystallization 9-30718
- Fe:Si, Bragg scattering of 14keV Mossbauer radiation of ^{57}Fe nuclei 9-37700
- in Fe-Al and Fe-Mo alloys, X-ray K-absorpt. edges, position investig. 9-33571
- Fe-Cd couple, galvanic behaviour in NaHCO_3 , NaNO_3 and NaCl solns. 9-28811
- in Fe-Ni-Co alloys, complexometric determination 9-45430
- Fe-O system, phase boundaries and thermodynamic props. by e.m.f. meas. 9-30741
- Fe-Si frame single crystal, negative Barkhausen jumps, existence, character and rate during magnetization 9-37658
- Fe, critical and spin-wave scatt. of neutrons 9-31030
- α -Fe, flow stress, strain-rate sensitivity, 0° to 900°C 9-30671
- α -Fe, high temp. creep 9-30670
- α -Fe, kamacite, shock-induced preferred disorder 9-42938
- α -Fe, phonon dispersion relations calc. from Sharma-Joshi theory, specific heat calc. 9-48946
- α -Fe, stress relaxation and use of Johnston-Gilman eqn. in analysis of thermally activated flow 9-30672
- α -Fe, tertiary creep, recovery meas. 9-39423
- α -Fe, thermally activated flow, analysis, 78°-320°K 9-23883
- Fe^+ , 3d 6 config., energy spectrum 9-48397
- Fe^+ , earth's atmosphere, measurements of reaction with ozone 9-40044
- Fe^{2+} , electronic struct. and quadrupole splittings in hemoglobin 9-42459
- Fe^{2+} , Mossbauer effect in Y zeolite and Dowex 50 resin 9-43226
- Fe^{2+} , red fluorescence in reduced germanate glass 9-31134
- Fe^{2+} impurity ions in MnF $_2$ and CoF $_2$ magnetization Mossbauer effect meas. 9-45298
- Fe^{2+} in FeF $_3$, crystal-field splitting in paramag. state, Mossbauer eff. obs. 9-24383
- Fe^{2+} in MnF $_2$, near i.r. absorpt. 9-49280
- Fe^{3+} :Cu associated centres in CdS, paramag. reson, 77°K 9-47432
- Fe^{3+} , e.s.r. and optical absorpt. in ZnGa_2O_4 and ZnAl_2O_4 , rel. to single-ion mag. interactions 9-45080
- Fe^{3+} , e.s.r. in PbTiO $_3$ and SrTiO $_3$ at Q band and 70GHz 9-45389
- Fe^{3+} , spin-lattice relaxation in rutile for X- and F-band transitions 9-47300
- Fe^{3+} coloration impurity in lanthanum glass, effect on light absorption 9-24372
- Fe^{3+} e.p.r. in α -AlOOH and β -Ga $_2$ O $_3$, theoretical and expt. obs. of low symmetry effects 9-41427
- Fe^{3+} e.p.r. in corundum, angular dependence obs. 9-47428
- Fe^{3+} e.p.r. in HfO $_2$ and ZrO $_2$ 9-33627
- Fe^{3+} impurity in TiO $_2$, dynamic spin Hamiltonian, eigenvalues 9-26667
- Fe^{3+} in β -LiAl $_2$ SO $_4$, cathodoluminescence spectra and coordination with Mn $^{2+}$ 9-31150
- Fe^{3+} in $\text{Fe}(\text{NH}_4)(\text{SO}_4)_2 \cdot 6\text{H}_2\text{O}$: $^{57}\text{Co}^{2+}$, daughter ions stabilization rel. to H $_2$ O radiolysis by Auger e. obs. 9-23801
- Fe^{3+} in GaAs, g-factor shift, covalency influence 9-43280
- Fe^{3+} in garnets, elec. quadrupole interac. at octahedral sites 9-43221
- Fe^{3+} in glass, coordination 9-26199
- Fe^{3+} in group II-VI compounds, e.p.r., theory 9-47429
- Fe^{3+} in Linde L-zeolite, Mossbauer obs. 9-49258
- Fe^{3+} in quartz, zero-field e.p.r. 9-43279
- Fe^{3+} in synthetic brown quartz, e.p.r. 9-41426
- Fe^{3+} in ZnO, e.s.r. meas. rel. to g tensor anisotropy 9-26795
- Fe^{3+} Mossbauer spectra in paramagnets with nonaxially symmetric crystal field, mag. field effect on hyperfine struct. 9-49257
- α -Fe Debye-Waller factors, temp. depend. 9-35261

Iron continued

- Fe I-III atom and ions up to 15000°K, statistical sums and distribution, over electron states 9-38751
- Fe I, oscillator strengths and transition probabilities, 2100-9900Å 9-29930
- Fe I and Fe II lines, 3190 to 3315 Å, absolute gf-values 9-34538
- Fe II lines in η Carinae, relative intensities rel. to intrinsic reddening 9-40148
- Fe II solar lines, theoretical equivalent widths calc. 9-36036
- Fe III in tetrahedral and octahedral environments using Mossbauer spectra of iron orthoclase 9-45291
- Fe IV lines in spectrum of the star MH α 328116 9-35979
- α -Fe whiskers growth by chem. vapour deposition, in situ electron microscope obs. 9-44650
- ^{54}Fe Mossbauer effect following n capture by ^{56}Fe , recoil effects in metallic iron and alloys obs. 9-43224
- ^{57}Fe radioisotope source for X-ray diffraction analysis 9-26847
- ^{57}Fe , u.s. meas. using Mossbauer eff. 9-37697
- Fe(III) activity transfer process in potassium trioxalatoferrate 9-39185
- FeXII solar emission lines, relative intensity as function of temp. and electron density 9-43683
- p-GaAs:Fe, radiative transitions between deep acceptors and valence band 9-47395
- H-charged, crack form, mechanism 9-39440
- high purity, prod. and resistivity 9-39448
- in (Mn $_{0.95}$ Cu $_{0.05}$) alloy, antiferromag., mag. and elec. props. obs. 9-41338
- MnF $_2$:Fe $^{3+}$, localized magnetic mode 1.2°K 9-47291
- NaCl:Fe from melt, X-ray luminesc. 9-37772
- Pr implanted, hyperfine, field obs., using nuclear orientation 9-35604
- in U alloys, determ. by atomic absorption spectroscopy 9-26839
- Yb $^{3+}$ - α -Fe $^{2+}$ system, superexchange integrals 9-45076
- ZnSiF $_6$:6H $_2$ O:Fe $^{2+}$, Mn $^{2+}$, single cryst., spin-lattice relax. of ^1H and ^{19}F 9-35594
- Iron alloys**
- see also Iron compounds; Steel*
- alnico, decomposition of solid soln. from X-ray diff. anal. 9-39473
- alnico-type cast hard magnets, b.c.c., brittle fracture 9-35014
- armco, ductile-brittle transition temp., eff. of previous deformation 9-28345
- armco iron, plastic flow stress, temp. and strain rate depend., 150° to 250°K 9-33044
- austenite, deformed, recrystallization kinetics 9-33107
- austenitic, foils, irradi., determ. of thickness and void size 9-48755
- binary, residual resistivities and Matthiessens's rule departures 9-39586
- Fe-Ni-Mn-Ti, martensitic, pre-precip. stage during ageing 9-37283
- films, wall coercive force, strain sensitivity, 200 Å to 1500 Å thickness 9-45163
- Incoloy-800, irradi., void vol. fractions and bulk density changes 9-48755
- Invar, forced magnetostriction, absolute saturation magnetization press. coeffs., 4.2K 9-41320
- Invar, mag. anomaly in thermal expansion and spontaneous vol. magnetostriction 9-43177
- invar, sound vel. at low temp. 9-44817
- martensite, low-C, thermomech. treatment rel. to strength increase 9-42912
- (225) γ martensite transf., role of plastic accommodation 9-26383
- M.S.O., mag. shunt props., C addition effect 9-45050
- mumetal, magnetomechanical damping effects 9-31036
- permalloy, Barkhausen and ΔE effects, rel. to applied stress 9-45147
- Permalloy, magnetic anisotropy, rotatable, in electron-microscope specimens 9-26646
- permalloy, ternary paramagnetic additions for production of magnetic film for memories 9-36252
- permalloy film, high speed flux reversal and relaxation processes, dynamic Kerr obs. 9-45169
- permalloy films, anisotropy field, neutron irradi. and isothermic annealing effect 9-47253
- permalloy films, annealing behaviour of induced anisotropy, ageing and stabilization effects 9-37660
- Permalloy films, Bloch wall motion excited by fast-rising hard-axis pulses 9-45168
- Permalloy films, dynamic Kerr obs. of high-speed flux reversal and relax. processes 9-37661
- permalloy films, ferromag. reson. absorpt. at r.f.'s 9-47423
- Permalloy films, susceptibility, effect of surface roughness 9-49211
- Permalloy layers with non-mag. layer composite, mag. props. and struct. 9-43183
- permalloy single-crystal platelet, helical and other stripe structures 9-47248
- permalloy transducer, in magnetometer 9-34140
- Permalloy wires, magnetic domain nucleation and wall propagation, influence of structure and composition 9-35561
- phase equil., effect of alloying element 9-33148
- precipitation hardening alloy, composition, structure and hardness 9-39468
- shock load obs., applic. to Arizona meteorite fragments 9-43636
- silicon, plastic deform. at 185 and 300°K effect of twin and grain boundaries 9-41018
- solidification, growth morphology and solute segregation 9-23952
- ternary, magnetic disaccommodations due to interstitials reorientation 9-26635
- Ticonal 600, mag. props. and microstructure evolution rel. to comp. of α_1 and α_2 phases and saturation magnetiz. 9-44804
- Ticonal X, magnetic microstruct. by neutron diff. 9-49203
- Al-(68.9 at.%Fe), galvanomagnetic effect, longitudinal 9-24278
- Al-Fe, dilute, thermopower, temp. and size depend. 9-43123
- Al-Fe, Fe-rich, transf. diagram construct., electron microscope applic. 9-33131
- Au-Fe, ^{57}Fe Mossbauer effect obs. of mag. ordering 9-39817
- Au-Fe dilute alloys, Mossbauer absorpt. spectra of ^{57}Fe 9-45285
- Au-Fe hyperfine field of ^{197}Au 9-49259
- Co-Fe-V high strength, high ductility, rel. to partially recrystallized structure 9-44790
- Co-(8 wt.%Fe), depolarization and secondary extinction, obs. 9-39267
- Co-(8 at.%Fe) large single cryst., low angle boundaries 9-37185
- Co-FeBe semi-hard mag. square hysteresis loop and low magnetostriction coercive force 9-45137
- Co-Ni-Al-Cu-Nb-Fe, magnetostruct. analysis 9-47251
- Co-Ni-Al-Cu-Ti-Fe, magnetostruct. analysis 9-47251

Iron alloys continued

- Cu-Al-Fe-Ni aluminum bronzes, ductility rel. to microstructure, 20-800°C 9-23894
- Cu-Fe, dilute, martensite nucleation in Fe precipitates 9-37300
- Cu-Fe dilute, magnetoresistance 1.3° to 88°K , fields up to 200 kOe 9-44909
- Cu-Fe dilute alloy, magnetoresistance, 1.3° to 20°K fields up to 200 kG 9-44910
- Cu-Fe solid solns., homogeneous decomposition 9-48930
- Cu-Ni-Fe, ^{57}Fe Mossbauer effect obs. of mag. ordering 9-39817
- Cu-Ni-Fe, hard-magnetic particle ensemble model, calc. 9-33453
- Cu-Ni-Fe, spinodal decomposition, electron microscope obs. 9-35242
- Fe-(3 wt.%)Si transformer sheet, domain wall motion, freq. depend. and wall bowing 9-39764
- Fe-(0.75 at.%)Mn, annealed, grain boundary fine struct. obs. 9-35102
- Fe-(25 at.%)Al, electron microscopy investig., one- and two-phase struct. obs., magnetiz. and magnetocrystalline anisotropy 9-26648
- Fe-(40 at.%)Al, ordering and struct. distortions, X-ray diff. obs. 9-42784
- Fe-Al, domain structure and short range order, depend. on Al conc. 9-23757
- Fe-Al, Mossbauer effect following n capture, recoil effects obs. 9-43224
- Fe-Al, phase relations, X-ray diff. obs. 9-44664
- Fe-Al, short-range order, X-ray diffuse scatt. obs. 9-44665
- α -Fe-Al, superlattice phases, equilibria and transforms 9-46952
- Fe-Al, X-ray K-absorpt. edges of Fe, position investig. 9-33571
- Fe-Al ageing, precip. of (FeMn)₂AlC 9-33139
- Fe-Al single cryst., mag. anisotropy and order 9-47252
- Fe-Al single cryst., mag. susceptibility superimposed on saturation magnetization 9-47258
- Fe-Al system intermetallics, microhardness, strength, elec. resistivity, thermal expansion, Fe diffusion coeffs. 9-46890
- Fe-Al(Co) Fe-rich, nuclear transverse relaxation times of ^{57}Fe , Suhl-Nakamura interaction 9-45240
- Fe-Au, thermoelectric power at low temps. and field dependence 9-35495
- Fe-Be, magnetization and sp. ht. 9-45143
- Fe-C, diffusion of ^{35}S , rel. to effect of C on ^{35}S mobility in grain boundaries 9-37203
- Fe-C, microcrack formation, statistical analysis 9-30694
- Fe-C, oxidation at 500°C 9-31197
- Fe-C, phase transform. singularities during tempering and cold plastic deform. 9-39496
- Fe-C, shape strain for (225)₂ martensitic transformation 9-28344
- Fe-C, surface contamination during H₂ annealing 9-36938
- Fe-C martensite crystal, diffuse electron scattering due to short-range order 9-32912
- Fe-(0.05 wt.%)C, dislocation-interstitial interactions 9-30594
- Fe-Co-Ni, fine particle preparation by gas evaporation with plasma jet flame 9-33128
- Fe-Co-Ni fine particles prep. by evaporation in inert gases, mag. props. 9-33459
- Fe-Co, 3d-band shape from high field susceptibility obs. 9-37406
- Fe-Co, b.c.c., mean mag. moments 9-45142
- Fe-Co, f.c.c., precip. from Cu, mag. behaviour 9-26633
- Fe-Co, high-field susceptibility estimation at 0°K 9-47243
- Fe-(27 wt.%)Co coercive force at high temp., effect of dispersoid parameters 9-45138
- Fe-Co fine particles prep. by evaporation in inert gases, mag. props. 9-33459
- Fe-(18 at.%)Cr-(20 at.%)Ni, dislocation damping and solute pinning 9-28292
- Fe-(49wt.%)Cr-(2wt.%)V, brittle fracture, slip mode effects 9-26356
- Fe-Cr-Ni, dislocation damping 9-39363
- Fe-Cr-Ni, extrinsic-intrinsic stacking-fault pairs 9-44711
- Fe-(50wt.%)Cr, oxidation 9-24556
- Fe-Cr, oxidation, effect of Y and Gd 9-24559
- Fe-Cr, pitting corrosion 9-31198
- Fe-Cr, Ti oxide inclusions, predominating cpds. from fine structure microanalysis of emission X-ray spectra 9-37752
- Fe-Cr pitting and anodic dissolution, surface prep., and deformation effects 9-24576
- Fe-Cr system, phase equilibria and transformation, pressure infl. 9-41059
- Fe-Cu two-phase mats, internal microstresses rel. to plastic deform. 9-46881
- Fe-Ge, Fe-rich, mass spontaneous magnetization, 298 K 9-39768
- Fe-(30-50wt.%)Ir $p \rightarrow \alpha$ and $p \rightarrow \epsilon$ transform. rel. to Ir content, dilatometric meas. 9-41067
- Fe-(0.75 wt.%)Mn, recovery processes during creep 9-26334
- Fe-Mn-C, shape strain for (225)₂ martensitic transformation 9-28344
- Fe-Mn-C alloys, internal friction temp. dependence rel. to stress-induced ordering of C 9-23862
- Fe-Mn-Ni with Ti added, ageing 9-48917
- Fe-Mn, internal friction temp. dependence, and C addition effect 9-23862
- Fe-(11 at.%)Mo, precipitation eff. on mechanical behaviour 9-35173
- Fe-Mo, X-ray K-absorpt. edges of Fe, position investig. 9-33571
- Fe-Mo precipitates, fine faults and cryst. struct., electron microscope obs. 9-42787
- Fe-Mo solid solns., creep behaviour, temp. and stress depend. 9-30669
- Fe-N, martensite transform. start temp. composition dependence 9-23982
- Fe-(30 at.%)Ni-(5 at.%)Nb austenitic, structure and hardening, comments 9-46934
- Fe-(30 at.%)Ni-(5 at.%)Nb austenitic, structure and hardening, comments 9-46933
- Fe-Ni-Al-Co-Ti alloys, thermomech. treatment effect on mag. props. 9-47259
- Fe-Ni-Al-Ti, thermomech. treatment effect on mag. props. 9-47259
- Fe-Ni-Al, b.c.c., mag. moment behaviour rel. to composition changes 9-24274
- Fe-Ni-Al, decomp. of supersaturated solid solns., elastic stresses effect 9-39475
- Fe-Ni-C, shape strain for (259)₂ martensitic transformation 9-28344
- Fe-Ni-Co alloys, complexometric determination of elements 9-45430
- Fe-Ni-Cr-Be, precip. processes, transmission electron microscopy obs. 9-39498
- Fe-Ni-Cr, dislocation mobility 9-39699
- Fe-Ni-Mn, f.c.c., intrinsic magnetization, 77°K to Curie temp. 9-45144
- Fe-(30 wt.%)Ni, b.c.c. and f.c.c., electron energy spectra, sensitivity to $\alpha \rightarrow \gamma$ transform. 9-39856
- Fe-(19 at.%)Ni, fracture during rolling 9-33066
- Fe-(40 at.%)Ni, invar, magnetostriction, effect of tensile stress 9-45156

Iron alloys continued

- Fe-(30wt.%)Ni, martensite, isothermal transform. rates, Kaufman and Cohen's model 9-46950
- Fe-Ni, 3d-band shape from high-field susceptibility obs. 9-37406
- Fe-Ni, electrotransport and diffusion, tracer technique 9-28320
- Fe-Ni, high field susceptibility estimation at 0°K 9-47243
- Fe-Ni, in liq. Hg, ductility and toughness 9-42891
- Fe-Ni, invar, model, contrib. 9-37649
- Fe-Ni, magnetic domain wall distribution rel. to coherent boundaries of twin crystal 9-37651
- Fe-Ni, treatment for low temp. use, patent 9-26362
- Fe-(49 wt.%)Ni commercial, effect of S on initial permeability 9-49204
- Fe-(40 at.%)Ni oxidised at high temp., scale struct. and chem. composition 9-33669
- Fe-Ni films, ferromag., differential susceptibility obs. of struct. 9-43182
- Fe-Ni fine particles prep. by evaporation in inert gases, mag. props. 9-33459
- Fe-Ni r.f. magnetic susceptibility, effect of added electrons 9-28587
- Fe-Ni thin film, variation in mag. susceptibility with thickness 9-39773
- Fe-Ni thin films, Faraday effect field depend., perpendicular anisotropy obs. 9-47322
- Fe-(40 wt.%)Ni-(6 wt.%)Nb precipitation behaviour, ageing at 775°C 9-46951
- Fe-(48.2 at.%)Ni, Mossbauer effect of ^{57}Fe , hyperfine mag. splitting, effect of texture 9-35636
- Fe-(27wt.%)Ni austenitic alloys, effect of Al, Si, Mn, and Cr on martensite form. during plastic deform. 9-41068
- Fe-P, amorphous layers, characterisation by very low coercive force 9-24311
- Fe-Pd, thin films, coercive force rel. to grain size 9-28622
- Fe-(32 at.%)Pt, quenched, fine struct., X-ray diff. obs. 9-46787
- Fe-(48.5 at.%)Rh, anomalous hyperfine field at recoiled ^{103}Rh nuclei 9-35564
- Fe-Ru, h.c.p., ϵ -phase, mag. props. 9-43159
- Fe-(3.25 wt.%)Si, domain width, thickness depend., critical thickness 9-39763
- Fe-(1 wt.%)Si, Ge effect on internal oxidation 9-46740
- Fe-(3 wt.%)Si, edge and screw dislocation mobilities h.v. electron transmission microscopy meas. 9-42829
- Fe-(3 wt.%)Si, ferromag. domains, X-ray topographic obs., diff. contrast on walls 9-26643
- Fe-(3 at.%)Si, magnetoelastic internal friction, anisotropy 9-33023
- Fe-(3 at.%)Si, polycrystalline, nucleation of mechanical twins 9-46826
- Fe-(3 wt.%)Si, polycrystalline, slip, twinning and fracture, effect of presurization 9-33053
- Fe-(3 wt.%)Si, yielding dislocation configs. obs., delay-time model 9-44766
- Fe-(0.6wt.%)Si, Barkhausen and ΔE effects, rel. to applied stress 9-45147
- Fe-(3 wt.%)Si, domain shape, comparison between calc. and obs. 9-41307
- Fe-Si, antiphase boundaries, crystallographic charact., electron microscopy study 9-37142
- Fe-Si, dil., secondary recrystn., grain growth rate orientation depend. 9-39456
- Fe-Si, domain wall width meas. in thin sections by electron interference method 9-41310
- Fe-Si, Fe-rich, mass spontaneous magnetizations, 298 K 9-39768
- Fe-Si, ferromag. domain walls, image contrast, origin, X-ray topography obs. 9-28614
- Fe-Si, grain-oriented, with high permeability, mag. props. characts. 9-45145
- Fe-Si, magnetic props., infl. of galvanically deposited Ni films 9-26647
- Fe-Si, ordered, antiphase boundaries, props. 9-26231
- Fe-Si, primary recryst., ageing effect on texture form. 9-46921
- Fe-Si, spin-wave dispersion relationship 9-24297
- Fe-Si 3% lamination, grain-oriented, magnetization energy depend. on direction 9-24273
- Fe-Si ferromag. domain walls, visibility on diff. topographs and comparison with BaTiO₃ ferroelec. walls 9-39682
- Fe-Si grain-oriented, soft mag. materials review 9-39753
- Fe-Si microinhomogeneities in cast, worked and annealed samples 9-48846
- Fe-Si secondary recrystallization by solute-induced boundary restraint 9-44785
- Fe-Si single cryst., lattice distortion and X-ray topographic contrast due to 90° ferromag. domain wall 9-33460
- Fe-Si solid solns., resistivity and Matthiessen's rule deviations 9-41167
- Fe-Si textured, mag. props. for Si > 3.25% 9-45124
- Fe-7.4%Si, 3d-band shape from high-field susceptibility obs. 9-37406
- Fe-(3.7 wt.%)Si magnetomechanical damping 78° to 300°K 9-45157
- Fe-(3 wt.%)Si alloy, of (110) and (100) planes infl. of annealing 9-34979
- Fe-(3 wt.%)Si alloys of different impurities, recrystn. during high-temp. annealing 9-39474
- Fe-(3 wt.%)Si cold-rolled-(110)[001]-oriented single crystals, primary recrystallization textures, effects of AlN 9-44784
- Fe-(3 wt.%)Si single crystal, surface energy relative variation for (110) and (100) planes, under annealing atmosphere 9-26180
- Fe-(3 wt.%)Si single crystals, crack nucleation, effect of stress concentrations 9-48911
- Fe-Sn dilute, Mossbauer hyperfine field of ^{119}Sn and resistivity study 9-47335
- Fe-V, binary, α -phase, mag. props. 9-43158
- Fe-W precipitates, fine faults and cryst. struct., electron microscope obs. 9-42787
- Fe-(2 wt.%)Si, Ge effect on internal oxidation 9-46740
- Fe₂Ge₃-Mn₂Ge₃ solid solns., saturation magnetiz. meas. and Curie temp. 9-45065
- (1-x)Fe₂LiO₃-x(FeGeLiO₄) solid soln., spinel phase, stability domain boundaries 9-33119
- Fe₃(Ni_{1-x}Mn_x)₂ moment-induced mag. scattering and magnetovolume effect 9-41303
- Fe₃P₁₃C₇, amorphous ferromag., Hall effect 9-39578
- Fe₃P₁₃C₇, amorphous ferromag., resistivity minimum 9-37429
- Fe(Pl₂Pd₁₋₂)₃ ordered alloys, spontaneous magnetization depend. on composition 9-24309
- Fe-(9.3 at.%)Mo, ϵ -phase precip., superimposed deform. effect 9-39497
- Fe-Ni, eff. of Co on hardening, martensite ageing at high temp. 9-23942
- Fe-(31.4at.%)Ni, magnetization, hydrostatic and shock-wave compression effects 9-43176
- Fe-Ni-Cr, eff. of Cr on martensitic transformation 9-23965

Iron alloys continued

- Fe-Pd, mag. fields on ^{60}Co and ^{119}Sn nuclei, electron polarization 9-28620
 Fe- $\leq(0.04 \text{ wt.}\%)$ C, quench aged, under cyclic straining, mech and microstruct. changes 9-33079
 Fe97Si3, eddy current losses rel. to thickness 9-26506
 Mo(10wt%)Fe solid solutions, precipitation behaviour after rapid cooling 9-35207
 NbC-Fe, liquid, carbide grain growth during sintering 9-34952
 Ni-Cr-Fe, atmospheric corrosion behaviour 9-37831
 Ni-Fe-Cu(Co) films, anisotropy components separation by temp. depend study of anisotropy field 9-45170
 Ni-Fe, creep, 550°-1000°C obs. 9-23897
 Ni-Fe, dynamic recrystn. during high temp. deform. 9-41020
 Ni-Fe, γ -radiation eff. on ordering transformations 9-23973
 Ni-Fe, radiation enhancement of diffusion from directional ordering expts. 9-44742
 Ni-Fe, spin wave energies, press. depend. 9-33455
 Ni-(19 wt.%)Fe magnetic films, mech. of combined Bloch and Neel type domain wall 9-28625
 Ni-(22 wt.%)Fe thin films, infl. of mech. stress on coercive force 9-24316
 Ni-Fe dispersion relations for lattice vibrations from neutron scatt. 9-30766
 Ni-Fe film, electrodeposited, magnetization ripple wavelength meas., Lorentz microscopy 9-28624
 Ni-Fe films, magnetic annealing, effect of elastic stresses 9-33029
 Ni-Fe hyperfine fields meas. by ^{61}Ni Mossbauer effect 9-45300
 Ni-Fe large single cryst., low angle boundaries 9-37185
 Ni-Fe tapes, surface domain patterns, Kerr magneto-optic studies 9-26653
 Ni-Fe thin films electrodeposited on scratched surfaces, uniaxial mag. anisotropy 9-28623
 Ni-Fe thin layers, effect of O on spin wave excitation 9-45369
 Ni-(17 wt.%)Fe, coercive force, previous loading rate effect 9-47241
 Ni3Fe, annealed thin samples, antiphase boundary study 9-46791
 Ni3Fe, Cr), atomic ordering effects 9-39297
 Ni3(Fe, Mo), atomic ordering effects 9-39297
 Ni3(Fe, W), atomic ordering effects 9-39297
 Ni3(Fe,Cr), ferromag. ΔE -effect, Cr content depend. 9-47242
 Ni3(Fe,Mo), ferromag. ΔE -effect, Mo content depend. 9-47242
 Pd-(14 at.%)Fe, low-temp. sp. ht. changes due to short-range order changes 9-33183
 Pd-Fe, dilute, low temp. elec. resistivities 9-44916
 Pd-Fe, elec. resistivity, critical behaviour near mag. ordering temp. 9-44915
 Pd-Fe dilute, ferromagnetic, $\partial m/\partial T$ meas. temp. and mag. field depend., rel. to spin-wave exchange stiffness coeff. 9-47263
 Pd-Fe dilute, spin polarization range, conc. depend 9-45116
 Pd-Fe ferromag., conc. depend. magnetization 9-45151
 Pd-Fe Mossbauer spectrum rel. to quenching temp. in the range 820-950°C 9-41369
 Pt-Fe dilute solid soln., interac. of quenched- in vacancies with Fe atoms 9-26278
 Pt-Fe system near Pt3Fe composition, magnetic behaviour from Mossbauer effect meas. 9-24275
 Pt-(1 at.%)Fe with plastic strain paramag. susceptibility, elec. resistivity and Mossbauer effect behaviour 9-43161
 Rh-Fe dilute alloy, magnetoresistance 1.3° to 20°K, up to 200 kG 9-44910
 Rh-Ru-Fe resistivity and susceptibility as function of temp. 9-44918
 Si-Fe, susceptibility and coercive force, dislocation theory 9-33457
 Zr-(1.2wt%) Cr-(0.1wt%) Fe, quench hardening behaviour, cooling rate dependence 9-41034

Iron compounds

- see also Ferrites; Iron alloys; Steel
 biotites, Mossbauer obs. of Fe ordering and ferrous-feric ratio 9-41367
 carbides formed at tempering of quenched C steels, elec. conductivity props. 9-43020
 cementite, thermal stability under α irradiation 9-47000
 complexes, low-spin (d^7) mols., Mossbauer effect 9-45296
 Fayalite, shocked, unshocked, Mossbauer spectra using reson. scatt. technique 9-24887
 ferric oxide cpds., ferrimagnetic single crystal, u.v. complex polar-Kerr effect 9-45275
 ferric salts, spin-spin and spin-lattice relaxation times, meas. by Mossbauer effect 9-31053
 ferritin macromol., X-ray diff. study of inorg. core, comparison with Fe hydroxides 9-37139
 garnets, rare earth, i.r. lattice spectra 9-47338
 haematite, antiferromag., nuclear diff. of resonant γ radiation, rel. to mag. structure 9-49262
 haematite, electron transport props., effect of weak ferromag.-antiferromag. transition 9-44869
 haematite, magnetic props. by Kerr eff. 9-26644
 haematite, Morin transition and lattice spacing w.r.t. particle size 9-32914
 haematite, spin axis rotation 9-45064
 haematite, thermally processed, ferromag. reson. 9-43270
 haematite, weakly ferromag., antiferromag. reson. 9-39899
 hematite single cryst., magnetoelect. props. 9-31049
 magnetically-ordered, ^{57}Fe Mossbauer spectra near disordering temp. 9-26721
 magnetite, double-exchange, electron-hopping process and metal-nonmetal transition 9-41168
 magnetite, single cryst. growth by chem. transport reactions 9-44643
 magnetite, stoichiometric and non-stoichiometric, Mossbauer spectra, struct. and fast electron-hopping process obs. 9-39818
 magnetite content of type I carbonaceous meteorite, by X-ray diffractometry 9-31622
 martensite, crystallography of phase transformations rel. to fine structure in transmission electron micrographs 9-28397
 Mossbauer effect of ^{57}Fe , anomalous charge states of Fe, possible origin 9-35637
 Mossbauer line, contrib. to theory of quadrupole splitting 9-49260
 Mossbauer line, contrib. to theory of quadrupole splitting 9-45290
 orthoclase, Mossbauer spectra for in tetrahedra and octahedral environments 9-45291
 oxide phase in Fe-Mn nodules, Mossbauer determ. of particle size 9-42786
 pyrites, exoelectron emission during phase transformations 9-24248

Iron compounds continued

- trivalent, Mossbauer line, contrib. to theory of quadrupole splitting 9-45290
 trivalent, Mossbauer line, contrib. to theory of quadrupole splitting 9-49260
 wustite, nonstoichiometric, defect complexes and microdomains, stat. thermodynamic analysis 9-44685
 wustite, ordered struct. obs. 9-26232
 wustite, thermodynamic props. determ. by coulometric titration in high temp. galvanic 9-44828
 Ca-amphiboles, Mossbauer obs. of comp. changes and ferrous-feric Fe ratio 9-41367
 (Cr,Fe) γ -C γ in alloy steels, X-ray and electron diff. obs. 9-48831
 Fe-Al, Fe-Cr, and Fe oxides, chemisorption of O, eff. on surface elec. conductivity 9-78222
 α -Fe-C-N solid solution, permeability disaccommodation, -40°-+180°C 9-26322
 Fe-Mn nodules, particle size determ. of Fe oxide phase by Mossbauer effect 9-42786
 Fe-Ni oxide spinels, cryst. growth by arc image technique 9-48804
 Fe-Pd, γ solid solutions, thermodynamic props. 9-30753
 Fe-Pt, γ solid solutions, thermodynamic props. 9-30753
 Fe $_{1-x}$ Cu $_x$ Cr $_x$ Si $_x$, magnetic props., conductivity and ionic ordering 9-28588
 Fe $_{1-x}$ O $_x$ transitions in single phase region, thermodynamic props. 9-28402
 Fe γ B, spin-wave gap, n.m.r. detection 9-45109
 Fe γ O $_3$ -SiO $_2$ -CaO-Al $_2$ O $_3$ system, hydraulic strength 9-23907
 α -Fe γ O $_3$, mag. peaks obs. using linear electron accelerator 9-42779
 α -Fe γ O $_3$, mag. phase transitions 9-35531
 α -Fe γ O $_3$, magnon interaction effects 9-35552
 α -Fe γ O $_3$, Mossbauer spectrum, effect on shift of exchange interaction of mag. ions 9-26720
 Fe γ O $_3$, sintered, surface and fracture study rel. to metal content 9-37279
 (α -Fe γ O $_3$) $_x$ (Cr γ O $_3$) $_{1-x}$ solid solns., magneto-chem. study of formative conditions 9-49189
 Fe γ O $_4$ mossbauer linewidth study of ^{57}Fe rel. to electron hopping in octahedral sites 9-45294
 Fe γ P, ferromag., Mossbauer effect 9-33527
 Fe γ Te, d-band struct. in tight-binding approx. 9-39565
 Fe γ (MoO $_4$) $_3$, Mossbauer spectroscopy, parameters for octahedral Fe $^{3+}$ 9-49261
 Fe γ Al, critical scatt. of X-rays stat. analysis 9-26715
 Fe γ Al, long-range order variation near transition temp. 9-26397
 Fe γ B γ O $_3$ (X-Cl,Br,I), Mossbauer spectra of ^{57}Fe , 80°-1100°K 9-35638
 Fe γ BO $_3$, magnetization and Mossbauer effect, spin orientations 9-41314
 Fe γ C, cohenite, shock induced preferred disorder 9-42938
 Fe γ C dissolution kinetics in ferrite 9-48874
 Fe γ (CO) $_3$ (P(C γ H $_3$)) $_3$, crystal structure 9-37141
 Fe γ O $_4$ /Mg γ Fe γ O $_4$ - α - γ spinel system, ferrimag., cation distrib. and temp. depend. in magnesioferrite 9-35737
 Fe γ O $_4$ -Mn γ O $_4$ spinel system, chem. structure 9-32856
 Fe γ O $_4$, atomic vibration, mean square amplitude determ. 9-41081
 α -Fe γ O $_4$, electrical conductivity, thermoelectric power, 20-100°C, effect of hydrostatic pressure 9-33300
 Fe γ O $_4$, low temp. phase transition, Mossbauer spectra changes, 85°-298°K 9-28668
 Fe γ O $_4$, magnetite, ^{57}Fe Mossbauer spectrum hyperfine fields 9-45295
 Fe γ P, schreibersite, shock induced preferred disorder 9-42938
 Fe γ Si $_3$, ferromagnetic props. by Mossbauer spectroscopy 9-33467
 Fe γ Se $_4$, neutron diffraction study of magnetic structure 9-33477
 Fe γ N in α -Fe, Ni effects 9-23840
 Fe γ Si $_3$, magnetiz. curves under high field 9-35565
 Fe γ Si $_3$, pyrrhotite, crystal structure 9-39281
 Fe γ Se $_4$, magnetiz. curves under high field 9-35565
 Fe γ -xMn γ As $_3$, 2.00 $\leq x \leq 2.35$, first order ferrimag. to antiferromag. transitions 9-45178
 Fe γ Ga γ -xO $_3$, anisotropy energy and anisotropic magnetization 9-33476
 (Fe γ Mg γ -x)SiO $_3$ 0.269 $\leq x \leq 1.0$, mag. behavior from n.g.r. of ^{57}Fe , 300° to 1.7°K 9-45292
 (Fe γ Mg γ -x)SiO $_3$ 0.269 $\leq x \leq 1.0$ n.g.r. of ^{57}Fe , 300° to 1.7°K 9-45292
 Fe (III) complexes, g-factors and covalency 9-28225
 Fe complex, (Fe bis-silyliden- ethylenediamine);O pyridine; oxo-bridge five-coord struct. 9-33486
 Fe complex, bis-dithioacetoylacetone tetrachloro ferrate(II), Fe II bonding, Mossbauer obs. 9-38842
 Fe complex, Fe(II) with α,α' -dipyridyl, proton magnetic resonance 9-32472
 Fe complex, iron (III)-benzhydroxamate trihydrate, crystal and molecular structure 9-39276
 Fe complex, tetramethyl ammonium tetrachloro ferrate(II), Fe II bonding, Mossbauer obs. 9-38842
 Fe complex, thio-p-toluyldisulfidobis (dithio-p-toluoato) iron (III), crystal and mol. structure 9-42785
 Fe II tetrahalo-anions, Raman spectra rel. to vibr. obs. 9-44327
 Fe III tetrahalo-anions, Raman spectra rel. to vibr. obs. 9-44327
 FeAs $_2$, Mossbauer resonance studies 9-45297
 FeBO $_3$ ferromag. reson. obs. 9-47424
 FeBr $_3$, metamagnetic transition from Mossbauer obs. 9-24328
 FeCO $_3$, paramag. Fe $^{2+}$ hyperfine interac., Mossbauer spectra 9-26723
 FeCO $_3$, metamagnetic single-crystal, Mossbauer meas. 2.5°K to above Neel temp. 9-45293
 Fe(CO) $_5$, gas phase, molecular structure, electron diff. data 9-38841
 FeCl $_3$, mag. dipole absorpt. in far i.r. 9-35586
 FeCl $_3$, metamagnetic transition from Mossbauer obs. 9-24328
 FeCl $_3$ frozen aqueous solns., p.m.r. studies 9-33646
 FeCl $_3$ hydrates, covalency eff. from Mossbauer studies 9-28667
 FeCl $_3$ magnetic excitations, theory 9-45063
 FeCl $_3$ perpendicular magnetization in high mag. fields. nonlinear behaviour at low-temp. 9-45220
 FeCl $_3$ ·2H $_2$ O magnon-phonon interaction, obs. in far i.r. 9-45077
 FeCl $_3$ ·4H $_2$ O, antiferromag., spin-flop states, low-temp. adiabatic studies 9-43191
 FeCl $_3$, low-temp. mag. susceptibility 9-45224
 FeCl $_3$ in Linde L-zeolite, Mossbauer obs. 9-49258
 FeCl $_3$ ·6H $_2$ O, oxidation state. pressure causes charge transfer 9-27851
 FeCl $_3$ ·6NH $_3$, oxidation state, pressure causes charge transfer 9-27851
 FeCl $_4$ (CH $_3$) $_3$ N $_3$, Mossbauer effect 9-33526
 FeCr $_2$ S $_4$ ferromagnetic spinels, grown by vapour-liquid transport technique 9-39196

Iron compounds continued

- p-FeCr₂S₄ ferromagnetic semiconductor, magnetoresistance effect of exchange interaction 9-44956
 FeCuO₂ magnetic properties, obs. 9-35530
 FeF₃, critical fluctuations near Neel point n.m.r. line width anomaly 9-45399
 FeF₃, Fe²⁺ crystal-field splitting in paramag state, Mossbauer eff. obs. 9-24383
 FeF₃ antiferromagnet, ¹⁹F n.m.r. obs. from 4.2 K to critical region 9-35725
 FeF₃, ⁵⁷Fe hyperfine struct., critical temp. depend. 9-24384
 FeF₃·3H₂O, oxidation state, pressure causes charge transfer 9-27851
 (FeFe)²⁺ in aq. solns., e.s.r. spectra 9-36901
 FeFe₂O₄ synthetic magnetite, chemical and thermal remanence, relative stability 9-39776
 Fe(III)Cl₃ in methanol, solute structure obs. 9-34878
 Fe(III) fluoro and bromo complexes, d-d spectra 9-24409
 FeLiO₂, α, Q_{II} and β phases, order-disorder transf., differential thermal analysis 9-26396
 FeLiO₂, short range order, local displacement of ions and electrostatic energy 9-48935
 FeMn₂O₄, magnetic structure, neutron diffraction investigation 9-45177
 (FeMn)₂AlCl precip. in Fe-Al alloy 9-33139
 Fe(NH₄)₂(SO₄)₆·6H₂O·⁵⁷Co²⁺, daughter Fe³⁺ stabilization rel. to H₂O radiolysis by Auger e, obs. 9-23801
 FeNb₂S₄, synthesis and lattice constants on basis of hexagonal unit cell 9-39284
 FeO, nonstoichiometric, defect complexes and microdomains 9-44685
 Fe(OH)₃ gels, nuclear gamma resonance 9-31088
 α-, β-, γ-, FeOOH, synthetic, mag. props. 9-47289
 α-FeOOH fine particles, Neel temp. particle size depend. 9-47290
 FeP₂, Mossbauer resonance studies 9-45297
 Fe(Pd,Pt), ferromag. to canted-ferri-mag. transition 9-45123
 FeRh films, first-order antiferromag. to ferromag. transition, role of O₂ 9-45223
 FeRh system, first-order antiferromag. to ferromag. transition, mechanism 9-45222
 FeRh, magnetic and magneto-optic props. 9-45141
 FeS, Mossbauer resonance studies 9-45297
 FeS₂, lattice vibrations, i.r.-active modes from reflectivity spectra 9-46974
 FeS₂, oxidation mechanism, in O₂ and in neutral or reducing gases 9-33670
 FeSO₄, for meas. of low energy X-rays 9-25011
 FeSb₂, Mossbauer resonance studies 9-45297
 FeSb₂O₄, antiferromagnetic structure using Mossbauer eff. 9-41336
 FeSe, Mossbauer resonance studies 9-45297
 FeSi₃, i.r. reflectivity 9-33505
 FeTiS₄, magnetic props. low-temp. depend on mag. field during cooling 9-45221
 H₂Fe(CN)₆ cryst. struct. 9-23756
 H₂Fe(CN)₆ cryst. struct., H-bonds and isotope eff. obs. 9-23756
 Mn-FeNi film with ferro-antiferromagnetic interaction, ferromag. reson. 9-37789
 MnCO₃·ZnO·Fe₂O₃, calcination, Mn-Zn ferrite production 9-35742
 Ni-Zn-Cr ferrites, effect of Co on induced uniaxial mag. anisotropy 9-41326
 NiO-Fe₂O₃ system, solid-state reactions 1100 to 1300°C, kinetics rel. to reaction layer thickness 9-37820
 YFe Garnet, InSb hybrid structure, interaction between spin waves and electrons 9-24320

Irradiation effects see *Biological effects of radiations; Chemical effects of radiations; Physical effects of radiations*

Ising lattice see *Lattices, theory and statistics*

Ising model see *Alloys; Ferromagnetism*

Isomerism

see also *Nuclear isomerism*

- (R-O)₂P(=S)(S-H), rot. isomers rel. to P-S-H vibrs., obs. 9-30066
 p-azophenyldiphenylcarbamyl chloride, interconversion of cis and trans isomers under effect of light 9-24589
 acetaldoxime, cis- and trans-, microwave spectra, molec. consts. 9-40605
 acrolein, variable temp. and variable solvent n.m.r. study 9-30431
 1,2-bis(dihaloboryl)ethanes, conformers 9-38882
 butadiene, cis- and trans-, SCF MO and CI calc. 9-27890
 butene-2, Cd-photosensitized isomerization, energy transfer by benzene 9-31212
 chloroacetyl halides, rotational 9-30094
 1,1-dichloro-2-methyl propane, rotational isomerism, NMR investig. 9-23162
 ethyl alcohol, microwave rot. spectrum 9-34668
 ethylene-d₂, Cd-photosensitized cis-trans-geminal interconversion 9-31213
 1-fluoro-1, 1, 2, 2-tetrachloroethane, rotational, acoustic and i.r. determ. 9-27896
 m-halobenzaldehydes, rotational 9-42436
 α-(2-hydroxy-3,5-dibromobenzylidene)-γ-butyrolactone, diff. obs. 9-39337
 isoprene, identification of trans form. 9-30125
 isopropenyl groups rel. to =CH₂ stretching vibr. bands splitting, obs. 9-44370
 methylstyrene, electronic u.v. vapour absorpt. spectra study 9-23142
 nitrobenzene, molecular isomers calc. by orbital method 9-44365
 nitrochlorobenzene, molecular isomers calc. by orbital method 9-44365
 nitroethane Na salts, geometrical isomers, i.r. and Raman obs. 9-27905
 nitromethane Na salts, geometrical isomers, i.r. and Raman obs. 9-27905
 1-nitropropane Na salts, geometrical isomers, i.r. and Raman obs. 9-27905
 2-nitropropane Na salts, geometrical isomers, i.r. and Raman obs. 9-27905
 phenylcyclobutane, rotational isomerism from e. diff. exam 9-23111
 photisomerism, molec. rearrangements theory 9-44337
 polyenes, photo and thermal isomerization mechanisms 9-35738
 polyoxyethylenes, mol. optical anisotropy calc. from rot. isomers 9-48526
 propionyl fluoride, rotational 9-48505
 propylene imine, cis and trans. 9-44369
 propylene 1-d₁, thermal and NO catalyzed cis-trans isomerization 9-43328
 stilbene, photoisomerism, theory 9-43337
 stilbene in dil. toluene soln., γ-ray-induced trans-cis isomerization, temp. depend. 9-40560

Isomerism continued

- 1,1,2,2-tetrabromo and tetrachloroethane, rotational isomerism, NMR investig. 9-23162
 1,1,2,2-tribromo and trichloroethane, rotational isomerism, NMR investig. 9-23162
 1,1,2-trichloroethane, u.s. relax. and vol. change during internal rot. 9-42652
 trideuteronitromethane Na salts, geometrical isomers, i.r. and Raman obs. 9-27905
 Fe, isomer shifts from α to ε and γ, Mossbauer spectra near triple pt. obs. 9-26722
 Mn₂-xFe_xO₄, isomer shift in Mossbauer spectra 9-37701
 N₂F₄, trans and gauche 9-23505
 S₈(NH)₂, crystal and molecular structure obs. 9-39305
- Isomerization** see *Isomerism*
- Isomorphism**
 group construction, many-coloured, reln. with mag. group 9-28240
 methyl diphenyl-thio-(seleno-) phosphinite, crystal structure 9-39339
 KH₂AsO₄ isomorphs 42 m symmetry, linear electro-optical effects 9-35628
- Isotope effects**
 alcohols, free and self-associated OH stretching, freqs. and anharmonicity consts., depend. on deuterium substitution 9-30070
 benzene, effect of deuteration on fluoresc. lifetime of liq. 9-48706
 benzene cryst., isotopic impurities, singlet excited states 9-24097
 benzene isotopic mixed crystals, site effects in vibr. spectrum 9-43007
 n-butane, photoionization yields and absorpt. cross-sections 9-30298
 charge exchange cross-sections at high energies, isotopic effect using H and D 9-30301
 classical liquids, mass depend. of viscosity and diffusion 9-30376
 collagen fibres, broad-line n.m.r. of H₂O and D₂O 9-43304
 crystal lattice dynamics of defect response func., photon scatt. cross section eqn. determ. 9-24007
 in diffusion in crystals 9-44724
 diffusion in liquids, of ¹²C, ¹⁴C substituted mols. 9-32777
 electronic states of mixed molec. crystals 9-41129
 ethanol, i.r. spectra of isotopic monomers 9-38891
 ethylene, photoionization yields and absorpt. cross-sections 9-30298
 gas-phase reactions, kinetic effects, temp. depend. 9-28780
 H₂ autoioniz. and predissoc. rates, eff. of isotopic substitution 9-28039
 H-bond length 9-42370
 hydrazinium hydrogen oxalate, cryst., D-substitution effects rel. to H-bond symmetry, 3600-200 cm⁻¹ 9-24393
 isotope shift due to neutron number, n charge distrib. effect first-order perturbation approach 9-44242
 methane and methane-d₄, phys. props., theory 9-39143
 methane and methane-d₄, phys. props., theory 9-44617
 naphthalene cryst., isotopic impurities, singlet excited states 9-24097
 naphthalenes, partially deuterated, triplet lifetime, isotope effect calc. 9-40617
 phenanthrene oriented in biphenyl, D isotope effect in zero-field splittings 9-43289
 phenol, free and self-associated OH stretching, freqs. and anharmonicity const., depend. on deuterium substitution 9-30070
 shifts' anomalies of elements with N=28, 50, 82, correl. between nucl. beams and liaison energy variations 9-46337
 shifts in atoms, simple and complex spectra, electronic quantities 9-29986
 thermomodification in liquid mixtures 9-23472
 N-trimethylborazines, isotopically substituted, i.r. spectra, band obs. 9-27906
 tryptophan, fluoresc. quenching and solvent isotope effect 9-32787
¹³¹,¹³²Cs, isotope shifts w.r.t. ¹³³Cs, by scanning level crossing signal 9-29990
²⁰⁶Pb, ²⁰⁷Pb, 7229 Å transition, isotope shifts 9-22963
 Ag I spectrum, isotope shift meas., error sources and soln. 9-29987
 AgCl, e.s.r. of Ni²⁺, ³⁵Cl and ³⁷Cl variant distrib. 9-43273
 B, on supercond. transition temp. of ZrB₂ 9-24132
 Ba II spectrum, isotope shift meas., error sources and soln. 9-29987
¹⁴C enrichment by counter current electromigration 9-48439
 Ca, optical isotope shift, nucl. vol. and mass depend. shift 9-29988
 Cd, supercond., intermediate effect coeff. from transition temp. meas. 9-44936
 Cd vapour laser, isotope shifts and c.w. operation 9-29410
 Ce I, infrared lines, isotope shifts 9-29989
 Ce IV spectrum, shifts between ¹⁴⁰Ce and ¹⁴²Ce 9-34533
 Cr, optical isotope shift, nucl. vol. and mass depend. shift 9-29988
 Cs I spectrum, isotope shift meas., error sources and soln. 9-29987
 Cu II 3d⁹4s¹D and ³D levels, isotope shift w.r.t. specific-mass effect, exchange polarization of 3d-shell 9-29927
 D₂ autoioniz. and predissoc., eff. of isotopic substitution 9-28039
 D⁺-D₂(H₂) charge-exchange collisions, search for isotope effect 9-44295
 Fe, optical isotope shift, nucl. vol. and mass depend. shift 9-29988
 Fe, self-diffusion, mass depend. 9-35130
 Fe, self-diffusion in δ, γ and α-phases, isotope effect meas. using ⁵⁷Fe-⁵⁹Fe 9-26301
 Ga, superconducting transitions 9-28475
 H/D in charge exchange mass spectra of hydrocarbons 9-25722
 H-atom-formaldehyde gas-phase reaction, kinetic effects 9-28781
 H₂ and D₂, dissoci. by electron impact, excited atom prod. 9-23168
 H₂Fe(CN)₆ and DaFe(CN)₆ 9-23756
 H⁺-D₂(H₂) charge-exchange collisions, search for isotope effect 9-44295
 H molec. beams, scatt. from Ag(111) surface 9-42713
 HCO₂ and DCO₂, bonding in crystals 9-32908
 Hd autoioniz. and predissoc. rates, eff. of isotopic substitution 9-28039
 He, 2¹S-2³P₁ line isotope shift meas. 9-25719
 He beams, scatt. from Ag(111) surface 9-42713
 Hg, 1.5295 μm laser line, isotopic struct., obs. 9-34541
 KCl:Li thermal conductivity meas. and phonon reson. scatt. obs. 9-42948
 KH₂(D₂)(SeO₃), dielec. anomaly in deuterated cpd. rel. to H-bonding in KH₂(SeO₃) 9-32855
⁶Li and ⁷Li electromigration mobilities in molten LiNO₃, 313°-488°C 9-45422
 Mo, optical isotope shift, nucl. vol. and mass depend. shift 9-29988
 Mo:B supercond. transition temp. 9-30872
 NH₃ and ND₃, dissociative attachment of electrons 9-46422
 NS emission spectra, isotope shift studies 9-34635
 Na uranyl acetate, eff. of deuteration of acetate group 9-23005
 NaH₃(SeO₃) crystals, unusual H effect 9-30973
 Nd spectrum, interpretation of shifts 9-34548

Isotope effects continued

Ne, solid, many-body corrections to volume differences 9-48778
Ni, optical isotope shift, nucl. vol. and mass depend. shift 9-29988
in O₂⁺ second negative bands, revised rot. and vib. consts. 9-23063
PS emission spectra, isotope shift studies 9-34635
SO₂ isotopes in solid Kr matrices i.r. spectra 9-42417
SO B³Σ-XΣ- bands, shift studies 9-23071
SbO, B-X, C-X and D-X systems investigation 9-23072
Sn atomic spectrum, odd-even isotope shifts 9-34542
Sr, optical isotope shift, nucl. vol. and mass depend. shift 9-29988
Ti, optical isotope shift, nucl. vol. and mass depend. shift 9-29988
W₂B supercond. transition temp. 9-30872
Xe isotopes, i.r. laser lines, shift meas., specific mass effect, nucl. deform. consts. 9-29991
Zr, optical isotope shift, nucl. vol. and mass depend. shift 9-29988

Isotope exchanges

ammonia-hydrogen isotope exchange reaction, separation factor meas. 9-31180
deuterization of non-volatile compounds using heavy water in inert solvent 9-26804
evaporation rate meas., condensation coeff. elimination 9-39083
CaCO₃, calcite, C and O self diffusion 9-46844
D between H and H₂O vapour on Ni-Al₂O₃ catalyst, obs. 9-28790
D+H₂=DH+H reaction kinetics obs. and calc. 9-41439
H₂O(*g*)+HD(*g*)=H₂O+HDO(*g*), spectroscopic and statistical mechanics constants compared 9-28773
H₂O+D₂O=2HDO equil., zero-point energy 9-31179
H+D₂=HD+D reaction kinetics obs. and calc. 9-41439
LiH-H system with isotopic impurities, thermodynamic equil. 9-37813
NO₂⁺+NO₂⁻ 9-41440
NO+NO₂⁻ 9-41440
¹⁸O₂ with CO in shock waves 9-49370
²³O with rare earth sesquioxides, O self-diffusion coeffs. meas. 9-44741

Isotope separation

see also Radiochemistry
ammonia-hydrogen isotope exchange reaction, separation factor meas. 9-31180
gas mixtures for spectrochem. analysis, diffusive separation 9-28824
metals, Tohoku University 9-23006
separator, electrostatic sweep system for performing uniform ion bombardment 9-29992
separators, various types and use for ion implantation expts. 9-29993
Tohoku University separator 9-23006
¹⁷¹Tm, preparation by irradiating ¹⁶⁹Tm, then leaving to allow ¹⁷⁰Tm to decay and separating Yb, patent 9-22905
⁴⁸Ca/⁴⁶Ca ratios from precipitation of CaCO₃ 9-42356
H-N mixtures for spectrochem. analysis, diffusive separation using Pd capillary 9-28824
⁴He-³He, sorption sieve 9-42733
Kr, in thermal-diffusion column 9-39061
LiH-H system with isotopic impurities, coeff. deviation and cryst. contrib. 9-37813
¹⁴N and ¹⁵N in thermal diffusion column 9-46581
¹⁶O and ¹⁸O in thermal diffusion column 9-46581

Isotope shifts see Isotope effects; Spectra

Isotopes

production, particle accelerator proposals 9-36542
radioactive, applic. to protective film thickness meas. 9-39154
rare earth, cross sections for (n,2n), (n,α), and (n, p) reactions at 14.2 MeV 9-22793
synthesis of new isotopes, review 9-44105
transfer system, 6 second, for short-lived isotopes from production to study facilities 9-44300
¹¹³Cd resonance line, λ 3261 Å, temp. depend. of broadening effects 9-29934
¹¹⁴Cd and ¹¹³Cd, spectral line resonance broadening temp. dependence 9-40541
²³⁴Th/²³⁸U ratios and distribution in the ocean 9-47519
²³⁷U production from neutron irradi. of ²³⁵U and accumulation in Pu 9-44209
³⁹Ar atmospheric activity, detection using proportional gas counter 9-45498
B mass spectrometry study of isotope production by high energy proton bombardment of targets of C and O, applications to nucleosynthesis and cosmic rays 9-22784
Be, mass spectrometry study of isotope production by high energy proton bombardment of targets of C and O, applications to nucleosynthesis and cosmic rays 9-22784
Be II lines in solar spectrum, isotropic wavelength shifts 9-27095
CO₂, partition functions calc. 9-32468
CO₂ gaseous and condensed, isotopic fractionation, 220-303°K 9-23588
⁶³Cu, ⁴F_{7/2} and ⁴P_{3/2} levels h.f.s. and g_J values meas., atomic-beam mag.-resonance method 9-32410
⁶⁵Cu, ⁴F_{7/2} and ⁴P_{3/2} levels h.f.s. and g_J values meas., atomic-beam mag.-resonance method 9-32410
⁵⁵Er, new isotope. prod. by α bombard of ¹⁵⁶Dy, radioact. decay obs. 9-48436
Li, mass spectrometry study of isotope production by high energy proton bombardment of targets of C and O, applications to nucleosynthesis and cosmic rays 9-22784
Mo, odd-mass, low energy props. using intermediate coupling approach 9-22749
Sb, mag. moment calc. using moving triton model 9-46204
U isotopic analysis using X-ray fluorescence combined with A-activity meas. 9-33690
U isotopic analysis using X-ray fluorescence combined with α-activity meas. 9-24598

detection

see also Mass spectra; Radioactivity
A=104, isotope production from ²⁴⁹Cf, ^{12,13}C; α emission, isotope identification 9-42219
²⁴⁰Pu in Pu by optical emission spectroscopy 9-32443
³⁴S by band spectroscopy 9-46283

relative abundances

see also Elements/relative abundances
in heavy water, photometric determ. 9-49392
in water-hydronium ion system 9-48437
²⁴⁰Pu in Pu by optical emission spectroscopy 9-32443

Isotopes continued

relative abundances continued

²⁴⁴Pu, in early solar system, rel. to continuous galactic nucleosynthesis theory 9-45658
¹¹⁵In and ¹¹³In mixture, conc. of ¹¹⁵In, thermal neutron absorpt. method 9-45431
²³⁵U/²³⁸U by Ge (Li) detector 9-27830
¹⁷⁶Lu and ¹⁷⁵Lu mixture, conc. of ¹⁷⁶Lu, thermal neutron absorpt. method 9-45431
¹²⁹I, in early solar system, rel. to continuous galactic nucleosynthesis theory 9-45658
Ba in meteorites and terrestrial samples 9-45674
¹³C/¹²C ratio of enriched ethyl acetate, burning in CO₂ stream method, meas. with gas density meter 9-34588
Ca search for natural variations 9-44299
³He excess in seawater, evidence for primordial abundance 9-45468
Kr in meteorites 9-49393
³⁴S, by band spectroscopy 9-46283
⁵⁹V/⁵¹V in chondrites and terrestrial matter 9-41681
Xe, variation (132, 130) of thirteen i.r. laser lines, relative displacement 9-48438
Xe extracted from Te minerals, anomalies 9-42354
Xe in meteorites 9-49393

Jahn-Teller effect

alloys, with localized electrons, as explanation of exothermic binding energy 9-39180
electronic impurity states interac. with Jahn-Teller coupling, Zeeman eff. 9-31057
ferrihaemoglobin azide, low-spin, anisotropy in g-values w.r.t. dynamic interac. 9-35600
instability with accidental degeneracy 9-45251
relaxation in system containing Cu²⁺.6H₂O 9-31159
relaxation in system containing Cu²⁺.6H₂O, model 9-31160
stability of configurations with almost degenerate electronic state 9-39788
Al₂O₃:Ti(V, Cr) far-i.r. absorpt. spectrum in applied mag. field, energy levels of single d electron obs. 9-31100
CaF₂:Eu²⁺ identification tunneling level using e.s.r. 9-45383
CdF₂:V³⁺, V²⁺ optical spectra, EPR and ENDOR 9-47385
Cr³⁺ ion in tetrahedral environment, ground state analysis, e.s.r. spectra proposal 9-44259
He liq., static effect in excited state of electronic bubble 9-34938
He liquid, electron trapped in bubble, light scatt. 9-23560
La₂Mg₃(NO₃)₁₂.24H₂O:Cu²⁺.6H₂O, relaxation behaviour, e.p.r. and electron-spin-echo obs. 9-31159
Li₄, instability, diatomics-in-mols. calc. 9-30034
LiCl, e.s.r. of Cu²⁺ centres 9-43281
MgO:Cu²⁺, dynamic effect at 4.2°K 9-24494
MgO, of octahedrally coordinated Cr³⁺ 3d³ ion 9-24346
Mn₁₀(Fe₁₉O₄₉)₁₀ single cryst., local distortion of ⁵⁵Mn at B-site in ⁵⁵Mn n.m.r., anisotropic hyperfine field obs. 9-43299
Mn₁₂-xFe_xO₄ Mossbauer spectra, quadrupole splitting obs. 9-37701
Mn₂Fe_x-xO₄ ferrites, cubic and tetragonal, of octahedral Mn²⁺, local tetragonal distortions obs. from absorpt. band splitting 9-39841
in OsF₆ i.r. spectrum 9-34647
in ReF₆ i.r. spectrum 9-34647
in RuF₆ i.r. spectrum 9-34647
in TeF₆ i.r. spectrum 9-34647
Ti complex, hexaurea Ti(III) triiodide, crystal spectra 9-39848
VCl₄, static distortion of ground state 9-30059
Zn(BrO₃)₂.6H₂O:Cu²⁺, relaxation behaviour, e.p.r. and electron-spin-echo obs. 9-31159

Jet stream see Atmosphere/movements

Jets

see also Sprays
air, impinging on water and wet cement, shapes of cavities formed 9-40762
axisymmetric, with parabolic vel. profile, stability 9-34719
circular cross-section, under surface tension, finite amplitude effect on stability 9-39067
discharge along surface of liquid jet, emitted Ba II lines, Stark width 9-40716
in drying processes, aerodynamics, heat and mass transfer 9-25116
ethanol, concurrent injection into N₂ or He gas streams, max. drop dia. 9-34864
gas, energy emitting, flow analysis 9-42588
gas, plasma prod. by microwave ionization 9-30263
gas, real, turbulent, propag. calc. 9-42593
gas, turbulent high temp., parameter calc. 9-42592
half-jet, incompressible, low Reynolds number instability 9-26071
impingement of flat surfaces, analytical soln. and occurrence of dry zone 9-46600
incompressible laminar, contained between walls, linearized anal. 9-38943
incompressible plane rotational flows, elec. analogue study 9-25803
laminar, injected into channel, numerical soln. of flow of incompressible conducting fluid 9-40642
laminar mixing of viscous fluid from rectangular nozzle into uniform stream, theory 9-30362
liquid, disintegrated, generation of monodisperse aerosols 9-34933
liquid, perfectly conducting, stability in magnetic field 9-30195
non-Newtonian, expansion-contraction behaviour 9-26070
plasma, elec. field exam., effect of easily ionizable elements 9-48122
plasma, in toroidal magnetic field, motion 9-30250
plasma generator, patent 9-48594
and plumes in turbulent rot. fluid, similarity solutions 9-23213
propane, Joule-Thomson coeff. meas. 9-36818
radiation, scalar, e.m. or gravitational, extended source construct. 9-22067
reattaching of flows, analysis 9-32757
in stratified atmosphere, buoyant, phase space solution 9-24650
supersonic, flow around infinite wedge 9-44515
supersonic, outflow into channels, calc. of min. press. in channel and press. in front of flow 9-28067
supersonic turbulent from axisymmetric nozzle with underexpansion 9-42594
turbulent, in cylindrical chamber with infinite opposing stream 9-40644
turbulent, of air, plasma and real gases, book 9-40737
turbulent flow, heat transfer and temp. distrib., interferometric study 9-23373

Jets continued

- two-dimensional, hydromag. stability of free flows at large Reynold's numbers 9-46599
 viscous, cylindrical, electrohydrodynamic instability under const. potential 9-40764
 viscous fluid, nonstationary flow analysis 9-44397
 wall reattachment theory, developments 9-23416
 water, concurrent injection into N_2 or He gas streams max. drop dia. 9-34864
 water, turbulent, in still gas, core length rel. to nozzle config., obs. 9-42632
 water injection into compressed air, temp. levelling rel. to droplet size 9-23435
 Ar, supersonic, intermolecular binding 9-23035
 Ar and Ar-He plasma, electron conc. v.h.f. Fabry-Perot and opt. Stark obs. 9-42522
 CO_2 , supersonic, intermolecular binding 9-23035
 H plasma, equations when chemical reactions resulting from methane decomposition take place, dissipation terms calc. 9-38994
 N_2 , axisymmetric, liquid at supercritical press. 9-40765
 Xe, supersonic, intermolecular binding 9-23035

Jets, cosmic-ray see *Cosmic rays/showers and bursts*

Jogs see *Crystal imperfections/dislocations*

Johnsen-Rahbek effect see *Adhesion; Electrostatics*

Johnson noise see *Noise/electrical*

Jordan-Thiry field see *Cosmology; Relativity/general*

Josephson junction see *Superconducting devices*

Josephson tunnelling effect see *Superconductivity; Superconducting devices*

Joshi effect see *Discharges, electric/glow*

Joule-Thomson effect

No entries

Jupiter see *Planets*

K-capture see *Radioactivity/electron capture*

Kaons

- excited states prod., search in K^+p collisions 9-36467
 mixing angle with $J^P=1^+$ from chiral $SU(3)\times SU(3)$ charge algebra 9-36465
 $K_1^-K_s^+$ regeneration in Cu, optical model calc. 9-34290
 K^- capture on complex nuclei 9-42293
 K^0K^0 mass differences, high and low energy contribs. 9-42061
 K^0K^0 evidence for $I=0, J=0$ state 9-34291
 K^+-K^0 e.m. mass diff. due to tadpole, $\pi\pi\rightarrow\gamma\gamma$ 9-27498
 K^+-K^0 on-shell e.m. mass difference, calc. using four-point function identities 9-29572
 $K^+-\pi^+=K^{*+}$ predicted sum rule for masses of octet bosons. 9-38540
 K^0 , phenomenological theory and decay 9-22575
 K^0 , tests for T and TCP invariance in decay rates 9-34285
 $K\pi\pi$ enhancement at 1780 MeV in K^+p at 12 GeV/c 9-34284
 ΛKN coupling constant g_{Λ^2} from KN dispersion relations disagrees with $SU(3)$ symmetry 9-34294
 $\pi\pi\rightarrow K\bar{K}$ $K-\Sigma$ relative parity determ. 9-27523

decay

- branching ratios, charged-to-neutral 9-27504
 Cherenkov counter using POPOP for rendering light homogeneous 9-29656
 CP invariance, hypothesis of long-lived K state with $CP=+1$ disproved 9-22576
 CP invariance and $\Delta S=\Delta Q$ 9-36427
 CP violation 9-22516
 CP violation, superweak model supported 9-38509
 CP violation in the neutral K system, possible origin 9-32169
 CP violation model of decays with conservation and violation in second and third orders of primary interaction 9-32118
 empirical angle treatment, breaking of $\Delta I=1/2$ rule 9-48179
 $J^P=1^+$ kaons, mixing angle and decay coupling const. calc. 9-32175
 noneleptonic, meson-pole models 9-32173
 Ree determ. from long lived neutral kaon leptonic decays 9-32176
 weak radiative decays, sum rules, F_0/F_π eval. 9-32171
 $(K^+\rightarrow\mu^+\pi^0\nu)/(K^+\rightarrow e^+\pi^0\nu)$ branching ratio 9-34288
 $K_s\rightarrow\gamma$ decay widths 9-32171
 K_0 and K_1 ($J^P=1^+$ mesons) mixing angle and decay coupling const. calc. 9-32175
 K_1K_0 new unitary sum rule obtained using S-matrix 9-29570
 K^0K^0 decay, partial width formulation of unitarity sum rules 9-42069
 K_1^0 and K_2^0 decays, S-matrix description 9-42070
 $K^0\rightarrow K^*\pi^0$ prediction in new two-angle theory for $SU(3)$ breaking 9-27480
 $K^0\rightarrow\pi^0\pi^0/K_1^0\rightarrow\pi^0\pi^0$, branching ratio meas. 9-34280
 $K^0\rightarrow\pi^+\pi^-\gamma$ T-odd and CP-noninvariant correlation 9-34278
 $K^0\rightarrow\pi\pi$, CP nonviolation theory 9-27500
 K_1 CP violating overlap with K_2 , Ree, determ. 9-32176
 K_1-K_2 amplitude proportional to scattering amplitudes differences 9-48181
 K_1-K_2 , test of CP and CPT 9-46088
 $K_1\rightarrow\pi^+\pi^0$ meas. of strange interaction form factor and charge asymmetry 9-42071
 K_2^0 , anomalous, applic. of Goldstone theorem 9-34289
 $K_2\rightarrow\pi^+\pi^0$, charge asymmetry determ., CPT invariance test 9-38510
 K_2 appl. of algebraic model describing symm. breaking 9-32174
 $K_2^0\rightarrow\mu^+\mu^-$, search 9-27512
 $K^-\rightarrow\pi^0e^- \nu/K_1^-\rightarrow\pi^0e^- \nu$ ratio from Cabibbo model of hadron currents 9-25450
 $K^-\rightarrow\pi^0\eta$, radiative correction calc. 9-44010
 $K^0\rightarrow\pi^0\pi^0$, $\pi\pi$ scatt. length and low energy phase shift determ. 9-27531
 $K^0\rightarrow\pi\pi$, axial-vector form factor determ. πK scatt. amplitude 9-38504
 $K^0\rightarrow\pi\pi$, CP violating parameters meas. using $0\rightarrow K^0\bar{K}^0$ prod. in colliding e beams 9-46089
 $K^0\rightarrow\pi\pi$, time-reversal symmetry breaking 9-25445
 $K^0\rightarrow\pi\pi$, interference term, depend. on ϵ and τ decay amp. 9-27505
 $K^+\rightarrow\pi^+\pi^0$, decay rate upper limit, ang. distrib. and dipion invariant-mass plot, form factor fits 9-38505
 $K^+\rightarrow\pi^+\pi^0$ rates 9-34288
 $K^+\rightarrow\mu^+$, weak interactions of urabryons, pseudoscalar coupling magnitude determ. 9-27471
 $K^+\rightarrow\pi^0\pi^+$, rate w.r.t. $K^+\rightarrow\mu^+\pi^+$ 9-29571
 $K^+\rightarrow\pi^+\pi^0$, search possibilities 9-25446
 $K^+\rightarrow\pi^+\pi^0e^+\nu$, rates and branching ratio determ., axial form factors determ. from current algebra 9-38517

Kaons continued**decay continued**

- $K^+\rightarrow\pi^+\pi^0\pi^0$, π^+ energy spectrum meas., fit to σ -resonance model 9-38506
 $K^+\rightarrow\pi^+\pi^0$, decay parameters estimated 9-46071
 $K^+\rightarrow\pi^0e^+\nu/K_1^+\rightarrow\pi^0e^+\nu$ width calc. in new two-angle theory for $SU(3)$ breaking 9-27480
 $K^0\rightarrow\pi^+\pi^-\pi^0$, possible charge asymmetry 9-34281
 K^0 , non-exponential character, theory 9-22575
 K^0 , CP violation, charge asymmetry, violation of T-reversal invariance, $\Delta S=\Delta Q$ rule 9-22581
 $K^0\rightarrow\pi^+\pi^-$ and symmetry violation 9-22542
 $K^0\rightarrow\pi\pi$, η_{00}/η_{11} [ratio in current-current models 9-22578
 $K^+\rightarrow\pi^+\pi^0$ rate w.r.t. $K^+\rightarrow\mu^+\pi^+$ 9-29571
 $K^+\rightarrow\mu^+\pi^0$ rate w.r.t. $K^+\rightarrow\mu^+\pi^+$ 9-29571
 $K_2^0\rightarrow\pi^0\pi^0/K_1^0\rightarrow\pi^0\pi^0$ ratio determ., comparison with regeneration data 9-22580
 $K\rightarrow X\pi$ and $K\rightarrow X$, zero energy theorems relating decays 9-22594
 $K\rightarrow\mu\nu$, low-energy theorem for struct.-depend. axial-vector form factor in soft-K and pole dominance approx. 9-29569
 $K\rightarrow\lambda\pi\nu$, form factor theorem and matrix element formula, $SU(3)\otimes SU(3)$ symmetry broken 9-40419
 $K\rightarrow\pi\mu(e)\nu$, form factors using dynamical groups $f(4,2)$ 9-42068
 $K\rightarrow\pi\mu(e)\nu$ form factors, inequalities 9-29568
 $K\rightarrow\pi\mu(e)\nu$, decay parameters calc. using hard-meson current algebra 9-44012
 $K\rightarrow\pi\mu(e)\nu$, form factor information using $SU(3)\times SU(3)$ symmetry breaking assumption 9-44009
 $K\rightarrow\pi\mu(e)\nu$, form factor resolution 9-44013
 $K\rightarrow\pi\mu(e)\nu$, possible contrib. of $\Delta S=\Delta Q$ amplitudes 9-42072
 $K\rightarrow\pi\mu(e)\nu$, appl. of algebraic model describing symm. breaking 9-32174
 $K\rightarrow\pi\mu(e)\nu$ form factors, current algebra and double integral representations 9-42067
 $K\rightarrow\pi\mu(e)\nu$ form factors assuming $SU_3\otimes SU_3$ current commutation relations 9-42017
 $K\rightarrow\pi\mu(e)\nu$ form factors in a strong interaction model 9-32170
 $K\rightarrow\pi\mu(e)\nu$ hard-meson current algebra analysis 9-29567
 $K\rightarrow\pi\mu(e)\nu$ parameters, second order symm. breaking 9-32172
 $K\rightarrow\pi\mu(e)\nu$, CP violation, use in distinguishing bet. forms of $e-\mu$ universality 9-38465
 $K\rightarrow\pi\pi$, $\Delta I=1/2$ derived by method of Nishijima, and its violation 9-32168
 $K\rightarrow\pi\pi\pi$, absolute rates calc. using associative algebraic model 9-46090
 $K\rightarrow\pi\pi\pi$, consequences of $\Delta T=1/2$ rule, verification 9-27507
 $K\rightarrow\pi\pi\pi$, using model for $\pi\pi$ with p dominance in $I=J=1$ channel and ϵ dominance in $I=J=0$ channel 9-38511
 $K\rightarrow\pi\pi\pi$, $\pi\pi$ scatt. lengths from veneziano formula 9-44038
 $K\rightarrow\pi\pi\pi(e)\nu$, axial vector form factors, momentum dependent, subtracted dispersion relations and current algebra 9-34287
 $K^0\rightarrow\pi^+\pi^-K^0$, $\pi^+\pi^-$ phase difference in decay amplitudes 9-27501
 K_1^0 and π_1^0 decay const. f_0 and f_π equality 9-22548
 K^0 , exclusion of one type of nonexponentiality 9-46091
 $K^0\rightarrow\pi\pi$ rates, test for T and TCP invariance 9-34285
 $K^0\rightarrow\mu^+\mu^-$, upper limit on branching ratio 9-48180
 $K^0\rightarrow 2\pi$, investigation of CP invariance validity 9-32119
 $K^0\rightarrow\pi\pi$, test of the $\Delta=0$ rule 9-27503
 $K^0\rightarrow\pi\mu(e)\nu$, CP violating parameters meas. using $0\rightarrow K^0\bar{K}^0$ prod. in colliding e beams 9-46089
 $K^0\rightarrow\pi\pi$, rates, test for T and TCP invariance 9-34285
 KK_s , $O(4)$ symmetry and particle mixing treatm. 9-25472
 $K^*\rightarrow K^0\pi^+$, rate determ. using effective Lagrangian 9-48203
 $K_1^0\rightarrow\pi^+\pi^0$, rate meas. and analysis 9-22579
 $K_1^0\rightarrow\pi^+\pi^0$ existence, rel. to CP violation 9-22577
 $K_1^0\rightarrow\pi^+\pi^0$ and $K_2^0\rightarrow\pi^+\pi^0$, interference 9-38512
 $K_2^0\rightarrow\pi^+\pi^0$ and $K_1^0\rightarrow\pi^+\pi^0$ interference 9-38512
 $K^+\rightarrow\pi^+\pi^0$, search rel. to existence of neutrino neutral currents 9-44011
 $K\rightarrow\mu\nu$, V-A theory deviations 9-41999
 $K\rightarrow\pi e^+\pi^0$ ($\mu^+\pi^0$), probability and branching ratios estimation 9-27506
 $K\rightarrow\pi\pi\pi$, CP-nonconserving, Glasgow model applic. using current algebra tech. 9-27502

interactions

- $K^+p\rightarrow K^+\pi^+\pi^+$ at 12.6 GeV/c, $\bar{K}^*(890)\pi^-$ and $\Delta^{++}(1238)\pi^-$ systems, study 9-22615
 $K^0K_2^0$ regeneration amplitude in Cu at 2.5 GeV/c, η_{11} -phase determ. 9-42065
 $K^+p\rightarrow K^*(890)\pi^+$, 7.3 GeV/c, double-Regge-pole analysis 9-48183
 $K^+p\rightarrow e^+\pi^+$, rescattering model, applic. to ang. distrib. 9-29574
 K^- , hyperfragments produced in 1.5, 3.0, 5.0 and 10.1 GeV/c interac. comparative study 9-48182
 K^- capture in diamond loaded emulsions 9-44007
 $K^-n\rightarrow\lambda\pi^-$ neutrals, $\eta(550)\pi^-$ enhancement obs. 9-40433
 K^-p at 10 GeV/c, ω^- prod. 9-34334
 $K^-p\rightarrow e^+K^0$ cross-section, polarization, 1.7, 2.1, 2.4-2.7 GeV/c 9-38590
 K^- (1.5 GeV/c with Ag and Br nuclei, hyperfragment and fragment prod. with $Z\geq 4$ 9-40471
 $K^-\rightarrow\Lambda\pi^-\eta$, $\pi^-\eta$ reson. prod. at 4.5 GeV/c 9-34313
 K^- d at low energy; possibility of $I=0, Y=0$ baryons 9-42097
 $K^-d\rightarrow K^-\pi^+n$ at 2.24 BeV/c 9-32178
 $K^-d\rightarrow K^-\pi^+pn$, N^{*+} and N^{*++} prod., $E_k=2.24$ BeV/c 9-32178
 $K^-d\rightarrow\Sigma^+\eta$, breakdown of impulse approx. in deuteron, evidence 9-25448
 $K^-n\rightarrow K^-\pi^+\pi^-n$ dominance of $N^*K^-\pi^+(71\pm 7)\%$, $E_k=2.24$ BeV/c 9-32178
 $K^-n\rightarrow\Lambda(1405)\pi^-$ 9-25448
 $K^-n\rightarrow\Lambda(1520)\pi^-$ 9-25448
 $K^-n\rightarrow\Lambda\pi^-\pi^-$, cross-sections, Λ polar., 3 GeV/c 9-32177
 $K^-n\rightarrow\Lambda\rho^-\pi^-$, $\rho^-\pi^-$ resonance in $\Lambda(1300)$ mass region, 40 MeV width, spin and parity analysis 9-42064
 $K^-n\rightarrow\Sigma^-\pi^0$, cross-sections, 3 GeV/c 9-32177
 $K^-n\rightarrow\Sigma^-\pi^0$ in $K^-d\rightarrow\Sigma^-\pi^0$, 1600-1800 MeV, formation of $Y^*(1665)$ 9-38596
 $K^-n\rightarrow\Sigma^-\pi^0$ in $K^-d\rightarrow p\Sigma^-\pi^-$, 1600-1800 MeV, formation of $Y^*(1665)$ 9-38596
 $K^-n\rightarrow\Sigma^-\pi^0$, cross section meas., $M_k=4.5$ GeV/c 9-27499
 $K^-n\rightarrow Y_0^*(1520)\pi^-$ at 3 GeV/c, y_0^* decay branching ratios and study of prod. proc. 9-38597
 $K^-n\rightarrow\lambda\pi^-$, Λ polarization, diff. cross section meas., $M_k=4.5$ GeV/c 9-27499
 K^-p , 1.33 GeV/c, resonance prod. in $Y\pi\pi$ final states 9-40447
 K^-p , 3-body final state, double peripheral production mechanism, 6 GeV/c 9-34283

Kaons continued

interactions continued
K⁺p, 4.1 and 5.5 GeV/c, obs. of final states with two charged part. and visible λ 9-29573
K⁺p, 594-820 MeV/c, elastic-scatt. and zero-prong-plus-V⁰ events' results 9-27508
K⁺p, 6 GeV/c, prod. of 3 strange particles with strangeness -1 9-36466
K⁺p, Ξ reson. at 2500 MeV, and its decay schemes, and other Ξ states 9-44014
K⁺p-K⁺ ω p, modified double-Regge analysis, momentum and particle distrib. determ. 9-42063
K⁺p-K⁺p, K⁰n partial and differential cross sections meas., M_K=0.6-1.2 MeV/c 9-46092
K⁺p-K⁺p π^+ π^+ , reson. cross-sections, $\bar{K}N\pi\pi$ final states analysis, 6 GeV/c 9-25449
K⁺p-K⁺ $\pi^+\pi^+$ p at 2.24 BeV/c 9-32178
K⁺p-K⁺ π^+ neutrals, production cross section meas., M_K=7.7 GeV/c 9-38513
K⁺p-K⁺ π^+ p, Deck virtual-diffraction background calc., E_K=6, 10 GeV/c 9-42062
K⁺p-K⁺n high energy charge-exchange reaction using Regge poles 9-44027
K⁺p-K⁺ π^+ (890)p, diff. cross section, spin density matrix element energy transfer depend., Reggeized helicity amplitude 9-34282
K⁺p-K⁺ π^+ (890)n, diff. cross section, spin density matrix element energy transfer depend., Reggeized helicity amplitude 9-34282
K⁺p-K⁺ π^+ (1320) spin-parity assignment, Pomeron exchange at 10 GeV/c 9-46112
K⁺p-L spin-parity assignment, Pomeron exchange at 10 GeV/c 9-46112
K⁺p-L⁺ neutrals, production cross section meas., M_K=7.7 GeV/c 9-38513
K⁺p- $\Sigma\pi$ partial-wave analysis, resonance formation in mass region, 1.6-1.8 GeV/c 9-46093
K⁺p- Ξ -K⁺ π^+ , 1.7-2.7 GeV/c, cross-section and polarization obs., I=0 baryon exchange and Y₀^{*}(2100) prod. 9-38590
K⁺p- Ξ -K⁺ π^+ , Ξ + (1930) enhancement obs. 9-38590
K⁺p- Ξ^0 K⁺ π^- , 1.7, 2.1, 2.4-2.7 GeV/c cross-section and polarization obs. 9-38590
K⁺p- $\pi^-\Sigma^+$, K⁺ exchange particle and trajectory determ., O(3,1) symmetry analysis 9-32189
K⁰p- $\Lambda\pi^+$, observation of Y⁺ π^+ (1616) 9-44065
K⁰p- $\Lambda\pi^+\pi^0$, observation of Y⁺ π^+ (1700) 9-44065
K⁺p-K⁰ π^0 (890) π^+ -K⁺ $\pi^+\pi^+$ π^+ , 12.7 GeV/c comparison of data with diffractive prod. model 9-36468
K⁺d-K⁺pp charge exchange, at 3 GeV/c 9-34293
K⁺n-K⁺p charge exchange, at 3 GeV/c 9-34293
K⁺n-K⁺p high energy charge-exchange reaction using Regge poles 9-44027
K⁺p, 12 GeV/c, K $\pi\pi$ enhancement at 1780 MeV 9-34284
K⁺p, 12.7 GeV/c, A₁⁺ π^0 production 9-42092
K⁺p, 3.5 GeV/c, K⁰(1300) and (1400) prod. 9-36489
K⁺p, 5 GeV/c, double reson. prod. of K⁰(892) and N⁰ π^+ 1236 9-42094
K⁺p, multiple π prod., K and K⁰ obs., 3.5 GeV/c 9-36467
K⁺p in H₂, E_K=3.0 GeV/c, reson. prod. obs. 9-27534
K⁺p-K⁺p $\pi^+\pi^+$ π^+ , K and K⁰ obs., 3.5 GeV/c 9-36467
K⁺p-K⁺p $\pi^+\pi^+\pi^0$, K and K⁰ obs., 3.5 GeV/c 9-36467
K⁺p-K⁺ π^0 p, 4.6 and 9.0 GeV/c 9-29598
K⁺p-K⁺ ω p, double Regge description of ω prod., 4.6 and 9.0 GeV/c 9-29598
K⁺p-K⁰ π^+ π^+ , Regge pole exchange analysis, M_K=7.3 GeV/c 9-40420
K⁺p-K⁺ π^+ (890)p, diff. cross section, spin density matrix element energy transfer depend., Reggeized helicity amplitude 9-34282
K⁺p-K $\pi\Delta^+$, 7.3 GeV/c, evidence for K π resonance near 1.1 GeV 9-25444
K⁺n-K⁺p high-energy behaviour analysis using O(3,1) symmetry formalism 9-22585
KK- $\pi\pi\pi$, 5-pt. Veneziano model, meson resonance couplings 9-36464
KN- $\Delta\pi$, vertex function, nature rel. to Deck effect 9-48202
KN-KN, spin and parity of reson. formed by spin-rot. parameter meas. 9-22570
KN-K Ξ , superconvergence and Y₁⁺ π^+ (1385)BP coupling 9-22636
KN-K π (890)n Regge pole anal., M_K=2-13 GeV/c 9-22583
KN-K $\pi\Delta^+$ (32), spin and parity of reson. formed by spin-rot. parameter meas. 9-22570
Kn production mechanisms 9-29583
Kn- ω - π^0 , cross-sections, 3 GeV/c 9-32177
K⁺p-K⁰ π^0 total and differential cross sections meas., resonance formation, 1.26-1.84 GeV/c 9-22584
K⁺p-K⁺n high-energy behaviour analysis using O(3,1) symmetry formalism 9-22585
K⁺p-K⁺ π^+ π^+ , 1.26 and differential cross sections meas., resonance formation, 1.26-1.84 GeV/c 9-22584
K⁺p-K⁺ π^+ (890)p, $\pi\omega$ class determ., O(3,1) symmetry 9-22582
Kp-K $\Omega\pi\pi^+$, reson. cross-sections, K $\pi\pi$ final states analysis, 6 GeV/c 9-25449
Kp-K⁺ $\pi^+\pi^+$, reson. cross-sections, $\bar{K}N\pi\pi$ final states analysis, 6 GeV/c 9-25449
 π K-K ρ K, Veneziano amplitude determ., A₂-KK decay mode suppression determ. 9-42091
C and Fe targets, at 12 GeV/c, muon pair prod. 9-32135
Fe and C targets, at 12 GeV/c, muon pair prod. 9-32135
K⁺p, 5.5 GeV/c, prod. of Σ^+ multibody final states 9-29620
KK-K $\bar{K}\pi$ 5-pt. Veneziano model, meson resonance couplings 9-36464

production

photoproduction process, Regge parametrization of formulas 9-27516
0⁺-K⁰K⁰ in e colliding beams, used to investigate CP violation in k²- $\pi\pi$ 9-46089
K⁰K⁰, enhancements in slow anti-proton annihilation in hydrogen 9-34292
K⁰ from e-Be collision, yield meas., E_e=10,16 GeV 9-29566
K⁺ yields at small angles, by 70 GeV proton- aluminium interactions 9-44019
K⁰ from K⁺p, cross section meas., M_K=7.7 GeV/c 9-38513
K⁰A⁰, by π^- meson interactions with light nuclei 9-25447
K⁺, prediction by scaling law, 20-70 GeV and 300 GeV p 9-48187
K⁺ from pp, cross section determ. from soft-kaon approx., P_{lab}=2.4 GeV/c 9-38570
K⁺ high-energy forward photoproduction in Regge-pole model, cross section determ. 9-38507

Kaons continued

production continued
K⁰, from $\gamma\gamma$ -K⁰ Σ^+ , E(γ) up to 5 GeV 9-44008
pp- Λ K⁺p, 6BeV cross-section obs. 9-27553
pp- Σ K⁺p, 6 BeV, cross-section obs. 9-27553
Be target bombarded by 12.3BeV/c p. 9-38580
Ga target bombarded by 12.3BeV/c p. 9-38580
resonances see Mesons/resonances
scattering
Lie's quantum field theory generalized model appl. 9-43944
Pade approx. to s-matrix, resonances and Regge trajectories calc. 9-25458
K⁺p backward scatt., double Regge pole exchange 9-34295
K⁺ on ⁷He, scatt. lengths, multiple scatt. calc. 9-32180
K⁺ on ⁴He, scatt. lengths, multiple scatt. calc. 9-32180
K⁺d, scatt. lengths, multiple scatt. calc. 9-32180
K⁺p, hybrid model explanation 9-36469
K⁺p, parameterizations reviewed 9-34294
K⁺p, scatt. length and K-matrix parametrization, Λ KN coupling const. prediction 9-42066
K⁺ π scatt. lengths, multiple scatt. calc. 9-32180
K⁺N, s-wave scatt. lengths in effective chiral Lagrangian model 9-27510
K⁺p, backward, elastic, exchange degenerate Λ -trajectory interpretation 9-38514
K⁺p, backward, Regge trajectories, exchange degenerate pairs, interference, dip cancellation 9-38508
K⁺p, cross section meas., diffractive peak obs., M_K=7.3 GeV/c 9-25452
K⁺p, polarization ang. distrib. meas., M_K=1.2-2.5 GeV/c 9-25451
K⁺p, s-wave, applic. of unitarized current-algebra to amplitude 9-27509
K⁺p elastic scattering at 864, 969 and 1207 MeV/c 9-44015
 $\sigma(K^+\pi^-\Delta^+)=3\sigma(K^+\pi^-\Sigma^+)=3\sigma(K^+\pi^-\Delta^+)$ 9-29575
K⁺p-K⁰ Δ^+ 3⁺/2-isobar prod. reaction, M1 dominance hypothesis 9-32200
K⁺p, ang. distrib. meas., 5.2 and 6.9 GeV/c 9-40421
K⁺p, on-mass shell evaluation of scatt. amplitude 9-38515
K⁺p, u-channel Regge pole exchanges, structure energy and total cross section depend. 9-40429
K⁺p elastic differential cross section meas., E_K>8 GeV 9-36480
K⁺p elastic scatt., momentum depend. of diff. slopes 9-38530
KK⁺K⁺, absence of backward peaks, rel. to existence of meson towers 9-48200
KK Veneziano-type amplitudes construction nonet scheme 9-42058
KK Veneziano-type amplitudes construction nonet scheme 9-42058
KN, data for possible determ. $\pi\Lambda\sigma$ couplings 9-46104
KN, high-energy, new Regge-pole models 9-22587
KN, small angle, Regge-pole eikonal theory 9-38516
KN low energy, finite-energy sum rule check of Kim's analysis 9-32179
KN sum rules based on Khuri amplitudes, degeneracy of Regge trajectories 9-48178
KN-KN, s-wave scatt. length calc. taking into account symmetry breaking of chiral SU(3) \otimes SU(3) 9-27511
Kp, baryon compressibility coeff., calc. from cross section 9-44047
K π , coupling consts. g_{AK π ²} and g_{BK π ²} calc. using kaon-nucleon dispersion relations 9-32181
K⁰p-K⁰p regenerative cross-section, predictions from Regge-pole models 9-22587
K⁺p, s-wave scatt. length and effective range determ. 9-22586
K⁺p, elastic, cross section and ang. distrib. meas. M_K=3.55 GeV/c 9-22588
K⁺p polarization, predictions from Regge-pole models 9-22587
K π sum rules, Adler-Weisberger type, high energy contrib. evaluation 9-32139
 π^+ K⁺, absence of backward peaks, rel. to existence of meson towers 9-48200
 π K, amplitude by chiral Lagrangian calc. K₄ decay axial-vector form-factor determ. 9-38504
 π K, sum rules and ρ -hadron coupling const. determ. 9-22611
 π K, sum rules and ρ -hadron coupling const. determ. 9-29600
 π K, Veneziano type amplitude calc. 9-42076

KDP see Potassium compounds

Keratin see Proteins

Kerr effect see Electrico-optical effects; Magneto-optical effects

Kicksorters see Counting circuits

Kikuchi lines see Electrons/scattering

Kinematics

centrifetal force magnitude, elementary derivation 9-43710
Coriolis force, matrix proof 9-43772
hodograph, velocity, of inverse-square central force motion 9-29158
magnetic fields in rotating frames of reference 9-47873
optimum transfers between nearly near-circular non-coplanar orbits, powered phases eff. 9-22176
particle in central field, perturbative forces 9-22183
pumping on a swing, demonstration apparatus 9-45726
relativistic motion in straight line, comments 9-47735
of solar flares, from high time-resolution cinematography 9-38118
stability of motion, Lyapunov method 9-22185
three body problem, elliptically restricted, equation of motion general soln. 9-43773

Kinetic theory

application to Couette flow 9-30180
aqueous metal nitrates, types of interaction 9-44569
Chapman-Enskog method generalized to derive the eqns. of hydrodynamics by the time-correlation function method 9-34055
classical fluid, equilibrium correlation functions 9-31778
diffusion 9-43769
entropy definition for non-equilibrium states 9-43762
hard sphere gas, virial coeffs. calc. with new integral equation 9-32562
inhomogeneous systems, coupled equations 9-32730
ionic conductivity 9-43769
Lennard-Jones liquids lumary mixture, Monte Carlo calc. of thermodynamic props. 9-34894
linear-response theory and irreversibility in strong mag. field, transport phenomena 9-36135
liquid thermal transport coeffs., local equilibrium model 9-23486
liquids, classical, collective modes 9-32761
liquids and dense gases, model eqn. 9-26017
London-Van der Waals force, between solid surfaces, temp. depend. 9-45934
moon-solar wind interaction 9-27100

Kinetic theory continued

- plasma, BBGKY eqns., mathematical basis 9-23266
 plasma, collisional, in curved mag. field, stability 9-32671
 plasma, stable and weakly unstable 9-25947
 plasma, stable and weakly unstable 9-46532
 pressure of ideal gas on moving piston, calc. 9-43757
 role in upper atmosphere density measurements 9-26919
 semiconductors with narrow conductivity band, eqn. soln. 9-26537
 Senftleben-Beenakker effects for rough sphere gas in a magnetic field 9-45798
 sound propagation in rarefied gas 9-30348
 text book, undergraduate, introducing the various kinetic equations 9-43753
 van der Waals potential between particle and conducting wall, and between two polarizable particles 9-23205
 water, Monte Carlo calc. using Rowlinson's intermolecular pair pot 9-34874
 wave propag. and linear Boltzmann equation spectrum 9-22107

gases

see also *Association/gases; Brownian motion; Collision processes; Diffusion in gases; Equations of state/gases; Joule-Thomson effect; Molecules/intermolecular mechanics*

- Archimedes' principle derivation 9-28060
 Boltzmann eqn. asymptotic soln. for Maxwellian molecules 9-32731
 Boltzmann gas, coupled equations 9-32730
 Chapman-Enskog-Burnett treatment for diffusion in an ionized gas 9-44488
 constant, ratio of Boyle volume and unit compressibility law volume 9-32729
 dense, model eqn. 9-26017
 density matrix eqn. 9-26018
 distribution function, light and heavy molecules 9-48615
 distribution function Lorentz-invariance in phase space 9-38254
 distribution within a vacuum system 9-38174
 energy exchange, nonequilibrium statistical operator 9-23390
 evaporating particle in pure vapour, force on it due to motion and temp. gradients 9-26015
 H-function at local Maxwellian state 9-39042
 intermolecular force estimation using method of determining diffusion in polar gases 9-36827
 Krook's relaxational eqn. generalization 9-46565
 Lennard-Jones gas, two-dimensional third virial coefficient 9-42605
 Lennard-Jones potential, unlike pair interaction investigated by obs. of thermal conductivity 9-36803
 many-body T matrix, application 9-40256
 many-body T matrix, application 9-40257
 many-particle-T-matrix application 9-29214
 Maxwell-Boltzmann distribution, virial expansion 9-23369
 moderately dense, normalization of reduced distribution function 9-30337
 multicomponent, partly ionized, with space change, in electric field, equations 9-44487
 non-relativistic limit and its range of validity 9-39041
 nonlinear Boltzmann equations, accuracy of Monte Carlo solutions 9-34829
 physical and chemical kinetics, Monte-Carlo method 9-39044
 plasma, review 9-40657
 plasma, weakly ionized, electron temp. near surfaces, calc. using Boltzmann equation 9-44408
 plasma Boltzmann eqn. with isotropic distribution function and reflecting boundary conditions 9-46462
 and plasmas, book 9-30338
 potentials for air and content gases from viscosity meas. 9-36823
 rarefied, book 9-44519
 reacting mixtures, transport coefficients 9-26016
 relative velocity, average values calc. 9-39045
 rigid convex mols., collision integrals 9-42604
 rotational collision number and Eucken factors 9-30335
 slip flow soln. for general specular-diffuse boundary cond. 9-40733
 space, time symmetries role 9-39043
 spectral line shape as a special case of kinetic theory 9-32406
 spherocylindrical molecules, trimodal shock structure solutions 9-30336
 supersonic flow, sharp leading edge problem 9-26009
 Townsend-Huxley expt. analysis; const. collisional cross section 9-39056
 Townsend-Huxley expt. analysis; const. collisional frequency 9-39055
 transport coeffs., theory for moderately dense state, review 9-36802
 transport coeffs. from molecular dynamics for very small system 9-23394
 Van der Waals gas, critical anomalies of transport coeffs. 9-26041
 van der Waals gas constant a in interface monolayer thickness calc. 9-23449
 virial coeff. from PVT data 9-36806
 CO₂ thermal disturbances, radiative decay 9-30343
 C+N atoms, collision integrals for 2×10^4 to 1×10^6 K 9-38792
 N molecule A²Σ⁺, gas phase energy pooling 9-44338
 OCS, line broadening of various rotational transitions due to dipole-dipole, dipole-quadrupole interac., obs. 9-34639
 Pb and In evaporated particles in vacuum, velocity distribution 9-32818

liquids see *Liquids/theory*

Kink bands see *Crystal imperfections/dislocations; Plastic deformation*

Kirkendall effect see *Diffusion in solids; Precipitation*

Klystrons see *Electron tubes; Microwave techniques and devices*

Knight shift see *Nuclear magnetic resonance and relaxation*

Knudsen number see *Flow; Hydrodynamics*

Kohn effect see *Crystal electron states; Crystals/lattice mechanics*

Kondo effect

- alloy, dil. mag., Kondo spin-compensated state, range and spatial variation 9-33429
 alloy, dilute mag., resistivity below Kondo temp., eff. of coherence length 9-26508
 fluctuation theory, Anderson's dilute alloy model 9-41288
 frequency depend. elec. cond. in terms of impurity scatt. t-matrix 9-47064
 impurity spin system, static susceptibility calc. from pseudofermion fn. 9-45053
 integral evaluation 9-38194
 metal, electron spin polarization around mag. impurity obs. 9-41287
 metals, localized moments sub-Kondo temp. props. 9-45041
 orbital degeneracy effects on mag. impurity in nonmagnetic metal 9-24269

Kondo effect continued

- particle number and density of states, theorem 9-39560
 potential scatt. effect on effective J values 9-39556
 resistivity of interacting impurity pair 9-24270
 s-d model, correct ground state energy, decoupling procedure 9-35547
 spin correlation between mag. impurity and conduction electrons in dilute mag. alloy 9-31021
 superconducting tunneling through barrier with paramagnetic impurities 9-44929
 in superconductors, investigation by Nagaoka method 9-44930
 temperature and resonance, conduction electron scatt. from mag. impurity 9-31020
 Cu-Al:Fe dil. alloy assoc. excess specific heat 9-47001
 Cu-Mn:Pt, electrical resistivity, conduction-electron scatt. amplitude, suppression determ. 9-39558
 Cu-(0.06-5.2 at%)Mn alloys, effect of Kondo log T term on elec. resist. at 2-300°K 9-47068
 Fe₈₀P₁₀C alloy, amorphous ferromag., resistivity minimum 9-37429
 La:Ce Kondo superconductor, quasibound states obs. 9-33268
 La-Ce dilute alloys, supercond. quasibound states 9-44941
 La-Ce dilute alloys, temp. determ. from thermoelec. power and resistivity meas. 9-43152
 La-Ce dilute solid solns, elec. resistivity data between 4° and 30°K 9-44913
 Mo-Nb:Co alloy, temp. of hot composition from resistivity and susceptibility meas. 9-45067
 Pd-Cr dilute mag. alloy, resistivity below Kondo temp., eff. of coherence length 9-26508
 Pt-(0.07 at.%)Co alloy, low-temp. elec. resistivity 9-33257
 Pt-Co dilute alloy, rel. to magnetoresistivity meas. 9-44917
 Rh-Ru-Fe alloys, susceptibility and resistivity as function of temp. rel. to Kondo temp. 9-44918
 Ti₂O₃:V, Fe, low-field magnetoresistance anomaly, condensation obs. 9-31018
 Zn-(0.005 at.%)Mn alloy, anisotropy of Kondo scatt., obs by de Haas-van Alphen effect 9-24109

Kramers-Kronig relations see *Dielectric phenomena; Optical properties of substances*

Krypton

- adsorption on cleaved faces of absorbents with lamellar struct., formation of first condensed layer 9-48776
 atom, mean excitation energies upper and lower bounds calc. 9-38779
 atom 5871 Å line shape determ. by correlation method 9-43926
 atomic spectrum, bibliography 9-38765
 atoms, charge state change for proton interaction, 5-50 keV 9-44483
 atoms, long-lived autoionization states, mass spectra 9-38782
 breakdown pot. obs., secondary ionization coeffs. calc., mild steel electrodes 9-34811
 conductivity ratio of electrons meas. in microwave resonant cavity discharge, 2.7 GHz 9-23288
 diffusion in Cu, influence on gas release of implanted ions, implantation energy and dose 9-35129
 diffusion in H₂O, coeffs., 10° to 60°C 9-26086
 diffusion in irradiated UO₂, from fission bubble growth kinetics 9-28152
 diffusion in NaCl, after irradi. by 10⁸ to 2 × 10¹⁶ ions/cm² 9-48875
 diffusion in SrF₂ and BaF₂ neutron-irrad. single cryst. 9-35127
 discharge, 1s and 2p level population, electronic temp., conc. meas., 9500 MHz 9-32702
 discharge, decaying, e conc. by laser interferometry, 10⁻²-3 mm Hg 9-28050
 electron elastic scattering from ³p metastable state, calc. 9-46307
 fission, search for n prod. 9-40527
 gas, viscosity calc. by eqn. 9-30355
 gas viscosity meas. pot. fitted 9-36823
 heat of adsorption on graphitized C black, expt. compared with condensation theory 9-34999
 intermolecular potential calcs. rel. to thermal-diffusion column operation 9-34843
 ion damage in Au foils, energy depend. 9-32957
 ion implantation profiles in GaAs, rel. to incident energy, orientation and dose 9-47120
 ion laser, transitions, interaction mechanisms 9-29411
 ion-mol. reactions with methane 9-24544
 ionized partially, elec. conductivity 9-26037
 ions bombarding Ag target, multiatomic clusters of (Ag_n)⁺ emergence 9-26618
 lamp, pumping of YAl garnet:Nd laser for 105 W output 9-48033
 laser, ionized, spectral transitions competition 9-45955
 laser oscillator, ion-type, signal freq. spectrum when operating at 5682 Å 9-25248
 liquid, sound vel. isotherms and effective at. radii, obs. 9-30396
 in meteorites, anomalous isotopic composition 9-41682
 meteorites (chondrites), isotopic composition 9-49393
 resonance beam at 1236 Å, disturbances by inert gases and H₂ 9-44265
 shock waves, spectral distrib. of u.v. and visible radiation 9-48654
 solid, electron drift velocity saturation 9-26587
 solid, wetting, critical surface tension and contact angle meas. 9-23451
 solids, specific heat meas., 0.4-12°K and extrapolation to 0°K 9-24041
 thermal-diffusion column operation rel. to intermol. pot. calcs. 9-34843
 vapour press. between 72° and 91°K 9-39144
²³²Cf, fission yield obs., by examination of Al foils 9-40526
 Ar/Kr, solidified mixtures, lattice parameters rel. to Ar conc., e diff. study 9-28255
 Ar-Kr liq. mixtures, thermodynamic props., Monte Carlo calc. in isothermal-isobaric ensemble 9-32560
 Ar-Kr simple liquid mixtures, shear viscosity 9-36851
 on Ar (100) surface, equilib. conc. 9-23616
 H₂-Kr intermolecular forces and (thermal) diffusion 9-46580
 He-Kr intermolecular forces and (thermal) diffusion 9-46580
 Hg-Kr discharge positive column afterglow, 2nd kind collisions cross section estimation 9-25981
 Hg-Kr laser, visible and ultraviolet frequency range, patent 9-22403
 Kr, potential parameters from viscosity and second virial data 9-34838
 Kr⁺, symmetric charge transfer, (²P_{3/2} → ²P_{1/2}) 9-44261
 KrII excitation and population inversion 9-29921
 KrIII in quasi c.w. ion laser, o/p at 3507, 4067 and 4131 Å 9-25233
 O(¹D)-Kr interaction, electronic de-excitation of O(¹D) during vacuum u.v. photolysis of O₂ 9-35755
 photoionization continua, 40-60 Å region, discrete structure 9-34531

Krypton compoundsKrF₂, structure from i.r. spectrum 9-25744**Kuhn-Thomas sum rule** *see* *Molecules/electronic structure***Kurie plots** *see* *Beta-decay theory; Beta-ray spectra***Kyropoulos method** *see* *Crystals/growth***Laboratories***see also* *Acoustical laboratories*

general physics, in science faculty of U.N.A.M. (Universidad Nacional

Autonoma de Mexico) 9-36098

Institut d'Optique (Orsay), research projects (1964-7) 9-31991

teaching laboratory as place of research 9-36097

University of Flinders, Australia, 2nd year lab. course 9-25015

Laboratory apparatus and technique

apertures, circular, 'knife-edge', prod. method 9-45708

camera, fixed focus, applications 9-46030

ceramic tube fabrication, varying props. 9-35218

chemical saw for Be foil preparation for transmission electron microscopy

9-39256

continuous chromatographic refining 9-31217

contour lines on opaque objects, interferometric generation 9-36932

crystal cleaving and cutting instruments 9-32864

crystal splitting along cleavage planes 9-32865

curve resolver for damped sine wave mixtures 9-36087

cuvette with He-Ne laser for Raman spectroscopy of small specimens

9-49293

dispenser of fixed volumes of liquids 9-24990

drift of structure with internal rearrangement, cross-correl. and cross-spec-

tra methods of velocity meas. 9-22044

drop producer (water), uniform size, controlled time intervals 9-47704

electrometer vacuum tube 9-29150

electron micrographic images, radial symm. testing and recording device

9-33982

electron microscope specimen transfer device, high vacuum, low temp.,

design 9-36088

electron probe microanalysis, small sample mounting method 9-39970

electron velocity meas., low-energy, patent 9-38611

electronic lab. techniques and instrumentation, book 9-49613

electronics experiments, teaching manual 9-29143

electrostatic generator, principles demonstration 9-45904

field-emission examination of surface adsorption 9-41277

film quality evaluation using optical particle detector 9-23623

flash photolysis, nanosec., and absorpt. spectra of excited singlet states

9-39964

furnace, radiative heat transfer between gas and wall, Monte Carlo 3D

analysis 9-34832

furnace for single crystal growth from fluxed melts 9-35028

g measurement by free fall 9-22032

gas mixing apparatus for producing atmospheres with low concentrations of

some gases 9-32716

the great experiments of physics, book 9-22029

hodograph, velocity, of inverse-square central force motion 9-29158

instruments for high-temp. research 9-40213

Kerr cell filling apparatus 9-30421

Langmuir probe automatic second derivative plotters, audio signal injection

9-32639

linear motion achievement using optical flats 9-33977

magnetic field lines display 9-29157

magnetic probes, versatile epoxy casting technique 9-34139

meteorological field data analysis, automation 9-41480

microchamber for electron microscope obs. at high temp. and controlled

press. 9-44655

microelectrodes, glass capillary, piezoelec. driving device 9-33978

micromanipulator, remotely controlled 9-47706

micropump, high precision, delivering 0.01-0.65 ml. fluid per beat

9-33976

microsampling by laser-microscope system 9-24594

molecular scanner for surface features, by spatial variations in emission of

atoms or mols. 9-42709

molecular-beam generator 9-23028

neutron diffractometer at Bucharest Institute of Atomic Physics 9-37130

N.M.R. adiabatic magnetization expts sample moving system 9-40303

nuclear physics lab. digital monitoring and control system 9-38165

optical particle detector for film quality evaluation 9-23623

optics lab. for undergraduates arts college 9-27155

particle size determ. by composite method 9-23611

pellets of solid hydrogen, launching device for laser irradi. expts. 9-45709

platform, adjustable, for laboratory 9-36103

plating thickness on small balls, meas. technique 9-31738

plugging meter, exptl. continuous- indication, for impurity monitoring in liq.

alkali metals 9-24991

polyethylene pellets, laboratory preparation 9-38415

practical physics, text book of methods 9-40226

practical physics teaching, new techniques 9-22033

recrystallization, low temperature tube 9-23686

refractory metal microsampling by laser-microscope system 9-24594

rheogoniometer design, molten polyethylene stress meas. 9-39065

sample (deformed and under tensile stress) holder for low temp. neutron

irrad. 9-29137

school microscope 9-27399

seal, Conax, using cold setting rubber 9-33985

seismograph, interferometric, with high magnification, strain recording

9-31268

semiconductor diodes, advanced laboratory tunnelling experiment

9-28535

spark timer, solid state 9-27157

spark timer for undergraduate laboratory 9-41728

statistical analysis for the laboratory experi- mentalist, book 9-33979

strobe photos with 'Big Swinger' camera 9-46031

superconductivity and flux quantization, undergraduate experiment

9-27156

teaching laboratory as place of research 9-36097

thermal-diffusion column operation rel. to intermol. pot. calcs. 9-34843

U.N.A.M. (Universidad Nacional Autonoma de Mexico) general physics

course, lab. work importance 9-36098

Van de Graff accelerator, expt. suggestions 9-29153

vertical sensors, especially dual pendulum type 9-31721

zone electrophoresis, universal separation chamber 9-47883

CdS i.f. transducers, vapour deposition method 9-33984

He-Ne laser construction for operation at 6328 Å 9-29415

Laboratory apparatus and technique continued

Hg porosimetry, limitations in use with graphite 9-26225

Ne-Hc mixture, separation in liquefier 9-23590

Lamb shift *see* *Spectral/atoms***Lambda (λ) point** *see* *Helium/liquid; Phase transformations***Lamps** *see* *Light sources***Lande splitting factor** *see* *Spectra; Zeeman effect***Langmuir probes** *see* *Discharges, electric; Plasma/diagnostics; Space**vehicles/ instrumentation***Lanthanides** *see* *Rare earth metals***Lanthanons** *see* *Rare earth metals***Lanthanum**

diffusion in b.c.c. Pr 9-33007

f.c.c., self-diffusion and solute diffusion of Au 9-33005

glass, effect of coloration impurities Nd³⁺, Pr³⁺, Cr³⁺, Cu²⁺, Fe³⁺, Ni²⁺Co²⁺ Mn³⁺, and Ce⁴⁺ 9-24372

lanthanide metals and alloys, families of polymorphic struct., influence of 4f

electrons 9-30509

magnetic susceptibility between 0.36-300°K 9-49190

n.m.r. in hexagonal metals, Knight shifts, spin relax. rates and quadrupole

coupling consts. 9-31171

photoelectric cross-sections of gamma-rays 30-100keV 9-24231

vapour, over LaB₆, partial press. 9-40830

La-Ce Kondo superconductor, quasibound states obs. 9-33268

La₂ mol., visible spectrum 9-46366La³⁺, dispersion curves in aqueous chloride solutions rel. to Nd³⁺ andSm³⁺ 9-26111PbTe:La, Mossbauer effect of ¹²⁵Te, depend. of probability on degree of

doping 9-39820

Lanthanum compounds

borolanthanum glass, immiscibility and catalytic crystallization, additions

of various oxides 9-34971

ethyl sulphate, e.s.r. spectra, Gd³⁺ zero-field splitting anomaly 9-39914LaF₃:Gd³⁺ energy levels of Gd³⁺ from optical absorption spectra

9-33556

melting point, heat of formation, lattice parameters, interrelationship

9-34956

perovskite cpds. prep., struct., phase transf. behaviour, props. 9-33127

Gd-69wt.%La alloy, nuclear component of specific heat for effective mag.

field at impurity nuclei 9-33461

La-Ce dilute alloy, Kondo superconductor, quasiband states 9-44941

La-Ce dilute alloys, Kondo temp. determ. from thermoelec. power and

resistivity meas. 9-43152

La-Ce dilute solid solns. Kondo phenomena 9-44913

La-Co system, crystal structures of intermediate phases 9-28262

La-Pr dilute solns., elec. resistivity and effective mag. moment rel. to Pr

conc. 9-45066

La_{1-x}Ce_xAl₃ alloys, supercond. transition temp., eff. of press. 9-28477La_{1-x}Gd_xAl₃ alloys, supercond. transition temp., eff. of press. 9-28477La₂Mg₃ (NO₃)₁₂:T³⁺, (T=Ce, Nd, Sm), e.s.r. temp. dependence, T₁/T₂

ratios 9-24483

La₂Mg₃ (NO₃)₁₂:T³⁺, (T=Ce, Nd, Sm), Orbach relax. processes, T₁ and T₂

9-24492

La₂Mg₃(NO₃)₁₂:24H₂O:Nd³⁺ enhancement of proton polarization due to

'solid effect' 9-24512

La₂Mg₃(NO₃)₁₂:24H₂O:Cu²⁺.6H₂O, relaxation behaviour, e.p.r. and elec-

tron-spin-echo obs. 9-31159

La₂Mg₃(NO₃)₁₂:24H₂O, Ni²⁺ electron spin-lattice relaxation rate by direct

process 9-45245

La₂Mg₃(NO₃)₁₂:24H₂O, Nd doped, proton spin relaxation time dependence

on Nd concentration 9-47299

La₂O₃:Eu, preparation and fluoresc. characts. of Eu³⁺ 9-43257La₂O₃, B-type monoclinic, lattice parameters and cell volumes 9-30562La₂O₃ enthalpy and specific heat 298.15 to 1600°K 9-41105La_{1-x}Ce_xIn alloys, supercond., transition temp. rel. to pressure, 0-23kbar

9-47090

LaB₆, crystallization gas-phase and seed pulling from molten drop

9-37081

LaB₆, sp. ht., low temp. 9-47003LaB₆ cathode poisoning 9-42731LaB₆ enthalpy and heat capacity, 1100-2200°K 9-26428LaB₆ thermodynamic props., 1340 to 2300°K 9-40830LaBr₃, e.p.r. of coupled Ce³⁺ and Nd³⁺ rel. to high degree electrostatic and

exchange interactions 9-47227

LaCl₃:Pr³⁺, cryst. field 9-28643LaCl₃:Tb³⁺, emission yields and lifetimes of D levels of Tb³⁺ rel. to temp.

and conc. 9-35690

LaCl₃ e.p.r. of coupled Ce³⁺ and Nd³⁺ rel. to high degree electrostatic and

exchange interactions 9-47227

p-n-LaCoO₃, semicond. props. 9-37527LaF₃:Ce³⁺ crystal field parameters based on hexagonal symm. 9-28647LaF₃:Nd³⁺ crystal field parameters based on hexagonal symm. 9-28647LaF₃:Nd³⁺ crystals, double freq. generation 9-40360LaF₃:Nd³⁺ oriented single cryst., far i.r. electr. and vibronic transitions

9-39843

LaF₃:Nd³⁺ single cryst., far i.r. electronic and vibronic transitions obs.

9-35653

LaF₃:Tr³⁺, (Tr=transition metal), photo- and X-ray luminescence

9-31145

LaF₃, Gd³⁺ absorpt. and fluoresc. spectra, energy levels obs. 9-35660LaF₃, luminescence of Nd³⁺, conc. quenching 9-31126LaF₃, polarized i.r. reflectance, optical phonons and mag. symmetry

9-47345

LaF₃, trivalent rare-earth ion doped phosphorescence 9-43260LaFeO₃:PbTiO₃ solid solns. magnetic props. 9-39784LaMg (NO₃), radiation damage eff. 9-28438LaMg (NO₃), radiation eff. on NMR proton relaxation time 9-28767LaMg (NO₃) in Nd matrix, p relaxation times at 0.3-0.4°K for prod. of

polarized samples 9-29524

LaMg(NO₃):Ce, phonon avalanche, lifetime and acoustic spectrum meas.

9-39511

LaNa(MoO₄):Nd³⁺ crystals, use in c.w. laser 9-40359LaNa(MoO₄): energy transfer from Nd to Yb in hosts with nonuniformly

broadened activator lines 9-33584

LaNbO₄ single crystals, prep. and structural props. 9-44644

LaO mol., emission spectrum, rot. analysis of indigo system 9-46365

LaOOH, synthetic, crystal structure 9-30563

LaTe₂:LaSb₂ solid soln., Sb substitution effect on resistivity and thermoelec.

power 9-39639

Lanthanum compounds continued

LuFeO₃ orthoferrite, exchange interaction and g factor determ. 9-45182

Laser beams

1.54 micron, atmospheric propagation charact. 9-34117
 atmospheric turbulence effects, meas. 9-28890
 backscatter along oblique atmospheric paths, calc. 9-33777
 backscatter imagery, polarization effects 9-36364
 backscattered power, effect of atm. hygroscopic particles 9-41529
 Brewster angle attenuator within laser cavity, eqns. of polarization and attenuation 9-31969
 Brillouin scatt., large angle, heterodyne spectroscopy obs. 9-38393
 chlorophyll solns., monomeric and associated, optical transmission coeff. 9-28131
 coherence characts. of radiation with known spectral characts. 9-48054
 concentration with aspheric lenses 9-25313
 deflection by mag. field 9-29435
 deflection using holographic scanning techniques 9-36322
 detector using photoelectric effect in cooled semiconductors 9-34186
 divergence of radiation of gas lasers operating in TEM_{nm} modes, meas. 9-47992
 electric field distribution along axis from gas breakdown exam. 9-28055
 elimination of unwanted emission lines 9-29484
 ellipsometric quantities, determ. 9-40379
 fluctuation struct. of giant pulse, variation on passing through nonlinear absorber 9-45968
 focussed, intensity distrib. numerical solns. 9-38132
 frequency controlled, for long path interferometry 9-43900
 frequency transforming by stimulated four-field parametric scatt. 9-29436
 gas laser TEM₀₀ mode far-field patterns, calc. 9-47951
 Gaussian, second harmonic and parametric generations 9-25331
 Gaussian in turbulent atmosphere, log-amplitude mean 9-47546
 images formed by matrix control, patent 9-34180
 intensity fluctuations, single-mode gas lasers, statistical analysis 9-25235
 interferometry, precision long-path, for velocity of light 9-25357
 i.r., transparency at of atm. surface layer 9-40036
 light scatt. at 90° by dense plasma focus 9-25886
 line breadth and intensity correlation, quantum mechanical estimate 9-48051
 liquids, small-scale filaments, tracks of moving foci explanation 9-32784
 in liquids, thermal blooming and instability due to absorption 9-26099
 in liquids, thermal defocusing, time dependence experiment 9-26100
 meter for output meas. 9-31989
 Mie total and differential backscattering cross-sections for Junge aerosol models 9-22459
 modulated, amplitude and/or phase, spectral analysis, holographic method 9-25330
 modulation and demodulation 9-40373
 modulation by differential detector with solid state devices 9-29446
 multiply reflected, maximum vel. process photography 9-31972
 output angle dependence on resonator adjustment and beam transforming system 9-29403
 p.c.m., increase of information capacity 9-36317
 photon, correl. between independ. beams, stimulated refl. expt. 9-43901
 picosecond pulses generation, progress 9-47931
 in plasma, dense, penetration and self-focusing 9-48574
 in plasmas, theory of scatt. and exptl. considerations 9-42516
 propagation in atmosphere, log-amplitude variance meas. 9-31321
 propagation theory 9-40340
 pulsed and c.w. in near-earth propag., scintillation magnitude saturation 9-31968
 quantum phase noise observations, laser oscillator 9-25207
 radiation in atmospheric ground layer, fluctuations of angle of arrival 9-43899
 radiation propag., scattered background, spotted structure 9-44602
 Rayleigh thermal scatt., stimulated, time and freq. depend. 9-29434
 reflection from plane parallel plates, equally inclined interference fringes effect 9-36316
 ruby, monopulse synchronisation with Nd laser pulse using luminous liquid shutter 9-29421
 ruby second harmonic and cryptocyanine laser emission mixing 9-25318
 scattering, stimulated thermal, in isotropic media 9-43814
 scattering, stimulated thermal, in isotropic media 9-43813
 self-bending of non-uniform intense beam in NaCl cryst. 9-47327
 self-focusing of beams in a plasma, by ponderomotive forces 9-43902
 semiconductor, resonance mixing of freqs. 9-41931
 spectral charact. meas. method 9-31971
 spectroscopy, Raman 9-48117
 statistical properties, meas. techniques 9-25312
 switched, time evolution 9-45966
 thermal self-defocusing effect, time-constant 9-47927
 transmission through atmosphere 9-31322
 transverse-mode selection effects on wavefront of ruby laser 9-48052
 in turbulent atmosphere, log-amplitude fluctuations 9-31320
 ultrashort pulse recording 9-27359
 u.v., c.w. second harmonic generation by ADP and KDP in argon-ion laser cavity 9-27363
 CO₂, beam splitter, ZnSe coated NaCl 9-48099
 CO₂, thermal defocusing, wind effects 9-22424
 CdS, electron-pumped, 10 MW peak power 9-48038
 He-Ne, 0.6 ns pulses duration meas., beat-frequency detection method 9-48074
 He-Ne, modulation by ADP crystal, manufacture 9-31988
 He-Ne, with Brewster windows, elliptical polarization of output 9-25314
 KH₂PO₄ crystal, freq. doubling, effect of lasers radiation parameters 9-45280
 in NaCl, self-bending of non-uniform intense beam 9-47327
 Nd: glass Q-switched laser, static and dynamic investigation of beam 9-25294
 Nd:YAlG, mode-locked, stability by feed-back loop method 9-48027
 Nd, monopulse synchronisation with ruby laser pulse using luminous liquid shutter 9-29421
 Nd³⁺: glass and ruby, ps. pulses with GW power generation, meas. and applcs. 9-31964
 Nd emission, temporal struct. in mode self-locking regime 9-45969

applications

Aluman, spectrochem. analysis, impurity emission rel. to matrix effects, obs. 9-24604
 atmospheric, optical visibility meas. 9-28885

Laser beams continued**applications continued**

atmospheric abundance and distrib. of Na, meas. by tuned laser radar at night 9-49466
 atmospheric backscatter expt., fluorescence as noise source 9-37920
 atmospheric optical characts. determ. 9-40034
 ballistic photography and holography 9-31986
 bathymetric sensor, airborne for near-shore beach meas. 9-35807
 biological particles, counting and sizing 9-47692
 biology and medicine 9-49599
 blast wave production in low pressure gases, density and time depend., image converter photographs and probe data 9-34757
 chemical analysis, Q-switched ruby laser for emission microspectroscopic elemental analysis 9-22411
 depolarization properties of surfaces illuminated by coherent light 9-32023
 detecting and ranging system, range equations, parameters, design and operation 9-48076
 diffusion coeffs. in liquids, meas. by interferometric technique 9-44553
 discharge plasma absorption coefficient meas. 9-28000
 distance photography with regulated pulses 9-29438
 Doppler determ. turbulence and 3D velocity vector 9-43714
 Doppler system for vibr. meas. of turbine blades 9-41811
 earth satellites position meas. 9-35939
 electron concentration meas. in hypersonic flows, interferometry method 9-48588
 engineering and applications, conference, Washington (1969) 9-47928
 evanescent u.s. waves, detect. by Bragg diff. of laser light 9-29278
 excitation sources in Raman spectroscopy 9-40384
 films, lubricant ultra-thin, obs. by multiple beam 9-36842
 filter production with dot networks representation of percussion response, for multiple picture prod. 9-40387
 flash photolysis, nanosec., using Q-switched laser, excited singlet states 9-39964
 flow diagnostics in shock tubes 9-45867
 fluorescence, radiative lifetime meas. in sub-nanosecond range using mode locked lasers 9-28716
 helical polymer molcs, hyperpolarizability 9-32541
 heterodyne detection, randomly distorted signal beam 9-31987
 heterodyne detection, randomly distorted signal beam 9-31987
 heterodyning coherent light field for phase and amplitude sampling 9-48073
 high-speed framing photography 9-32095
 high-speed photography 9-29505
 hologram, acoustic, recording technique using flying spot 9-29293
 holography (Jena ZGL 300) 9-43905
 interference patterns at large path differences, with gas laser source 9-38403
 interferometer, for study of plasma diagnostics 9-46510
 interferometer, heterodyne, plasma atomic phenomena studies 9-36349
 interferometer, using diffraction grating 9-41941
 interferometry 9-27381
 ion temperature measurement in theta pinch ISAR 3 by laser forward scattering 9-25897
 Kerr effect meas., liquids 9-26106
 Kerr effect meas. in aq. solns. of inorg. salts 9-30402
 length meas. industrial interferometry 9-45967
 light source for Schlieren photography 9-48125
 liquid spectroscopy 9-36882
 magnetic field in plasma, meas. by Faraday effect on resonant laser rad. 9-38998
 manometer, using change in refractive index of liquid 9-32717
 metals near melting point for thermal diffusion and specific heat meas. 9-37354
 meteorology remote sensing of vector wind velocity by optical heterodyne measurement of Doppler shifts 9-33766
 microprobe emission spectroscopy, elec. spark cross-excitation for samples 10-25 μm diam 9-47476
 microsampling by laser-microscope system 9-24594
 nodal patterns of surface vib. obs. by laser speckle 9-42710
 nonlinear optical coefficients of KH₂PO₄, NH₄H₂PO₄, LiNbO₃ and α-HIO₃, measurement, corrected values 9-33499
 nonlinear optics, multiple scatt. processes 9-27344
 nonlinear optical of semiconductors at 10.6 μ, obs. 9-28650
 optical tracking, photon counting by multi-coincidence method 9-45574
 photoelasticity, dynamic, ultra high speed recording system 9-29232
 photographic source; giant pulse ruby laser, for high-speed aeroballistic range photography 9-46035
 photography, high-speed, with pulsed beam and smear camera 9-46034
 photoneutron prod. by heavy metal target bombardment 9-34329
 plasma, Ba⁺, diagnosis using tunable dye lasers 9-44463
 plasma absorption coefficient determ. 9-42530
 plasma density meas., methods 9-44461
 plasma density meas. by dispersion-corrected, three-wavelength laser heterodyne 9-42528
 plasma diagnostics by scattering 9-32636
 plasma diagnostics from collective light scatt. at 90° 9-46488
 plasma diagnostics from cooperative scatt. at 90° from cold, dense plasma 9-32687
 plasma heating, neutron generation 9-46120
 plasma mag. field to electron conc. ratio meas. by Voigt effect 9-40687
 plasma prod. and heating model and expt. data 9-46511
 plasma production by Q-switched laser 9-42539
 plasma production for thermonuclear research 9-46512
 plasma production from single solidified gas particle 9-39000
 plasma production on solid irradiation, optical absorption and expansion 9-38983
 plasma temp. meas. by absorption 9-38997
 plasma turbulence, scattering experiment for charact. meas. 9-46533
 practical, incentives to research 9-36272
 radiation therapy, depth focusing 9-47699
 Raman spectra determ. using He-Ne laser as excitation source 9-49293
 Raman spectra prod. in liquids and solids, obs. using Br-dioxane complex 9-36883
 Raman spectroscopic apparatus 9-29484
 range finder, stabilization system, patent 9-41924
 range finding, design and application 9-36106
 range measurements to lunar corner reflector 9-33927
 rare earth ion, trivalent, spectra, analysis of Stark structure 9-31092

Laser beams continued

applications continued

- recorder, electro-optical, multichannel, high data rates, for pulse signals 9-27421
- recording of digital information on thin mag. film 9-45159
- refractory metal microsampling by laser-microscope system 9-24594
- resonator length shifts meas. down to 10^{-3} Å with two-mode laser 9-47941
- ruby, Q-switched, in motion picture holography 9-25322
- satellite tracking 9-28972
- satellite tracking, multi-coincidence method of photon counting, sampling technique 9-38014
- scattering of picosecond pulses for second sound detection 9-24022
- Schlieren photography, mode-locked laser light source, synchronization with spark-producing lasers 9-27403
- second harmonic generator using organic molecular crystal, patent 9 41934
- source for Raman spectrometer 9-22478
- spark gap triggering for kilovolt pulses 9-29390
- spatial filtering of electron micrographs 9-48053
- spectrochemical analysis, impurity emission rel. to matrix effects, obs. 9-24604
- spectrochemical determinations in garnets 9-37848
- spectroscopy, selective excitation 9-46019
- Steel, stainless, spectrochem. analysis, impurity emission rel. to matrix effects, obs. 9-24604
- streak camera, time resolution meas. 9-32088
- structural material heating 9-33178
- superregenerative amplifiers 9-36318
- surface and microscope objective interferometric meas. 9-26176
- thin film substrate, temp. meas. 9-25132
- troposphere, inversion layer study by simultaneous lidar and refractometer soundings 9-43380
- u.v. pulsed, use in photoluminescent dosimeter readout, patent 9-32265
- vacuum reduction by sputtering of absorbent titanium oxide-magnesium oxide film at u.h.f. 9-43693
- velocity measurement, by combined Schlieren system and Doppler effect 9-38191
- vibration meas. interferometry with heterodyne detection 9-31970
- vibration of surfaces meas. using speckle pattern effect 9-38293
- vibrational displacement phase meas. by Michelson interferometer 9-43781
- vibrational relax. meas. of HCl in shock waves 9-38847
- vibrations meas. 9-45839
- Zircaloy-2, spectrochem. analysis, impurity emission rel. to matrix effects, obs. 9-24604
- Al plasma excitation using ruby laser 9-38781
- CO₂ interferometer, plasma electron density meas. 9-23315
- CO₂ laser interferometry of rough surfaces 9-45993
- Kr⁺ laser, I₂ fluoresc. 9-38855
- Nd:glass, second-harmonic generation in crystals in systems with diffraction-limitation and high-spectral-radiance 9-41917
- Nd³⁺: glass and ruby, ps. pulses with GW power, review 9-31964
- Nd glass laser, picosecond pulse substructure, measurement using compression techniques 9-31951
- Ne-He laser interferometer for improvements of detections of fringe shifts in plasma density meas. 9-25910
- U spectrochem. analysis, impurity emission rel. to matrix effects, obs. 9-24604
- UO₂ spectrochem. analysis, impurity emission rel. to matrix effects, obs. 9-24604

effects

- anthracene, fluorescence spectra, excited by giant-pulse ruby laser 9-35691
- atmospheric, 1.2 km path, scintillation at 0.632 and 10.6μ 9-31973
- atmospheric absorption 9-47549
- atmospheric attenuation and backscatter 9-28885
- attenuation at 0.63 μ in artificial fogs, wood smokes and model media 9-28886
- biological cells, model 9-49602
- Bragg diffraction by sound beam, relative efficiency as function of interaction geometry 9-34211
- breakdown, optical, in air by laser operating in mode-synchronization regime 9-25984
- Brillouin spectra, stimulated 9-41394
- coherent effect of pulsed radiation 9-41923
- colloid particle orientation 9-23543
- corneal damage thresholds for CO₂ laser radiation 9-43690
- corneal irradiation by CO₂ laser, anterior chamber meas. 9-47697
- crystal, non-linear, induced quasi-continuum, sum frequency power variation with crystal length 9-31064
- crystal, plasma bubble form. rel. to conduction band definition 9-26490
- damage in glasses 9-33520
- depolarization at 6328 Å due to atmospheric transmission 9-37916
- dielectric; nonlinear, second-harmonic generation by picosecond pulses 9-47938
- dielectric, transparent solid, filamentary damage formation 9-48847
- Doppler-broadened transitions, coupled, line-narrowing effects 9-22934
- ethers, methyl and ethyl, decomposition 9-31187
- evaporation from ¹⁰⁹Tl target, ang. distrib. 9-41930
- eye hazards from laser radar, analysis and reduction methods 9-38152
- false spectra from plane grating 9-32018
- ferroelectric cryst., second harmonics generation 9-39791
- frequency conversion, experiments using continuously pumped repetitivity Q-switched ruby laser 9-25320
- gas breakdown, bibliographical review 9-25985
- gas breakdown, enhanced heating at shock front of blast wave 9-30233
- gas ionization, cascade, by powerful ultrashort light pulses 9-30295
- glass, filamentary damage formation 9-48847
- glass, flint, nonlinear solarization by intense 0.53μm light 9-40832
- glass, induced Mandelstam-Brillouin scatt., ruby laser monopulse focus-ing 9-25317
- graphite vaporization, mass spect. analysis 9-23601
- human vision, damage threshold theory 9-45704
- interaction with plasma, nonlinear confining forces 9-25887
- in ionised gases, interactions and applic. 9-34793
- ionizing effect of u.v. radiation from target in focus 9-36780
- liquid, molecular, laser-induced secondary beam absorpt. obs. 9-32506
- liquid, Raman lines with laser excitation, intensities and depolarization ratios 9-46640

Laser beams continued

effects continued

- in liquid, self focusing and stimulated Mandelstam-Brillouin and Raman scattering 9-42654
- liquids, organic, stimulated Brillouin scattering, Stokes light and hyper-sound generation at room temp. 9-39107
- liquids in external resonator, stimulated scatt. of light of Rayleigh light wing 9-46637
- melanoma cells in vitro, ruby laser radiation effect 9-49603
- metal carbides, refractory, surface layer fracture due to giant pulses 9-44774
- metal surface, heated, time-resolved temp. meas. 9-32835
- metal surface, microcrater prod., shape and ordering rel. to purity 9-46715
- metal surface disintegration debris rel. to screening of incident radiation 9-29437
- metals, pure, fracture patterns, rel. to irradiation conditions and thermo-physical props. of target 9-48909
- metals, time-dependent interaction, liquid-vapour ratio 9-48738
- naphthalene, fluorescence spectra, excited by giant-pulse ruby laser 9-35691
- ocular damage, probability analysis based on optical and atmospheric parameters 9-38151
- ocular hazards 9-45702
- organic liquid, dielectric breakdown produced 9-48710
- phase modulation of liquid trapped filaments 9-25329
- photochromic spiropyran layers, coloration by u.v. laser radiation 9-27916
- photographic materials long-wave blackening rel. to two-photon process, obs. 9-27413
- photon echoes and combination tones in gases, effects of level degeneracy on polarization dependence, analogy 9-31967
- pigment solution generation during ruby laser 2nd harmonic radiation 9-43332
- plasma, confinement, radiation pressure eff. 9-46490
- plasma, radiation absorpt., transparency effect 9-25888
- plasma blast wave production, microwave meas. 9-42499
- plasma prod. and heating, temp. meas. 9-48586
- plasma prod. by irradiation of solid surfaces 9-23323
- plasma production 9-28020
- pulse compression by electro-optical Doppler shifter 9-25310
- quartz, second harmonic generation 9-39791
- quartz, stimulated Brillouin scattering, Stokes light and hypersound generation at room temp. 9-39107
- radar, eye hazards, analysis and reduction 9-38152
- radiation damage generated by self-focusing in active materials and non-linear crystals 9-44680
- Raman scatt., spontaneous and stimulated 9-41394
- Rayleigh scatt. off molecules, stray light elimination 9-36359
- ruby, filamentary damage formation 9-48847
- ruby, forced Raman scatt. of frozen liquids 9-37737
- ruby, two-photon decay enhancement 9-26766
- ruby laser, Q-switched, picosecond pulse generation rel. to cavity geometry 9-25292
- sapphire, filamentary damage formation 9-48847
- scattering by plasma, effect of charged particle neutral collisions 9-46485
- second harmonic generation in crystals of space group P3₁,21₁³ 9-26680
- self-insulation of materials in a medium against intense light 9-27343
- self-trapped filaments in liquids, obs. 9-26102
- semiconductor in a strong mag. field light absorption 9-39828
- semiconductors, frequency depend. of dispersion 9-35390
- semiconductors, nonlinear absorpt. and restriction of light intensity 9-26685
- solid surfaces, reflection coeff. dependence on radiation parameters 9-43208
- sparks, discharge through two separate 9-46547
- spectral broadening and self-steepening in dispersive medium with non-linear μ 9-25315
- Stark splitting of light waves, dynamic: interaction 9-43903
- steel in water, self-insulation against intense light 9-27343
- stimulated Raman scattering, analysis of threshold condition 9-27342
- stimulated thermal Rayleigh scattering in fluids 9-25309
- stress waves in carbonaceous materials, homogenization and dispersion 9-48888
- structural material heating 9-33178
- on tissue, normal and turnover 9-49604
- triglycine sulphate, second harmonic generation and scatt. by domains ferroelec. domains 9-45010
- γ, polarized, prod by Compton scattering of laser photons from relativistic electrons 9-48155
- AgCl, u.v. excitation of luminescence, spectral distrib. and decay, low temp. meas. 9-47388
- Al target, plasma prod., u.v. spectrum obs. 9-36769
- CO₂, corneal damage thresholds 9-38159
- CO₂ laser, i.r. beam, self-defocusing effect, thermally induced 9-26108
- CO₂ lasers, variable attenuator for 10.6-μ wavelength region 9-25316
- CdS film absorpt. spectrum 9-35652
- CdS single cryst., carrier dragging due to laser rad. 9-28578
- Co-N₂-He discharge, influence on electron energy distrib. 9-34800
- Cu-Zn alloys and Si brass, elimination of effects when using pulsed discharges 9-27297
- D₂ solid, giant pulse prod. of plasma, props and conds for isotropic plasma 9-28021
- D plasma prod. by subnanosec. pulses 9-34775
- GaP, two-photon excitation, intensity behaviour of recomb. radiation of excitons 9-47393
- H, solid irradiation, solid pellet launching device 9-45709
- H₂, solid, giant pulse prod. of plasma, props and conds for isotropic plasma 9-28021
- H₂, stimulated Raman scattering, induced freq. shift obs. 9-25740
- He-Ne, interact. with excited Ne atoms, study of transition probabilities 9-25699
- He, induced breakdown, plasma development analysis 9-25844
- He, liquid and gas elec. breakdown 9-48725
- He breakdown, incident light scatt. at breakdown front, mechanism 9-23362
- Hg atom, line shift by high power laser pulse 9-25709
- K, atomic absorpt. spectrum, shift and splitting in radiation field 9-29937
- KH₂PO₄ crystals, optical rectification of mode-locked pulses 9-26712

Laser beams continued**effects continued**

- KH₂PH crystal, optical rectification effect dispersion 9-47326
 Li, solid, giant pulse prod. of plasma, props and conds for isotropic plasma 9-28021
 LiF luminescence, 230-540 nm spectral obs. 9-28710
 LiH pellet irradi., plasma electron-ion recombination 9-44464
 LiO₂, ruby laser irradi., causing strong second harmonic generation of 3470 Å 9-26692
 LiO₂, second harmonic production 9-26691
 LiNbO₃ crystals, optical rectification of mode-locked pulses 9-26712
 N, compressed gas, depolarization of Brillouin scattered light as function of gas density and laser power 9-28079
 N₂, breakdown under picosec. ruby-laser pulse 9-46544
 NaClO₃, second-harmonic generation of light, total refl. phenomena 9-47310
 Nd:glass laser, Q-switched, picosecond pulse generation rel. to cavity geometry 9-25292
 Nd:glass laser spikes, picosecond time structure 9-25311
 radiative splitting of K levels in ruby-laser rad. field 9-27809
 on SF₆, continuous parametric amplification of 10.6 μ signals from CO₂ laser 9-27340
 SF₆, saturation of vibr. energy levels by i.r. absorpt., rel. to press. and buffer gases 9-48480
 on SF₆ 10.6 μ signals, cross saturation 9-28081
 in V phthalocyanide, ruby pulse length reduction in forced Mandel'shtam-Brillouin scatt. 9-28129
 Xe ²P_{3/2} and ²P_{1/2} levels under laser irradi., mag. depolarization expts. 9-46288
 YFe garnet, i.r. radiation scattering by two magnon processes 9-45337
 ZnSe, mixing of CO₂ and He:Ne laser radiation 9-26694
 TiTe, ruby laser lines mixing for submillimeter-wave generation 9-24353

Lasers*see also Light/coherence*

- a.m. and f.m. mode locked pulses, analytic expressions 9-25218
 amplifier, in homogeneously broadened, transient behaviour of ultrashort e.m. pulses 9-29399
 analysis combining Schrodinger and Maxwell equations 9-25211
 angular distribution reduction by open resonator with ang. distrib. selector 9-36279
 array for use in noncoherent space-to-ground communications 9-31966
 associated atomic and molecular theory, review 9-40344
 atomic motion effect on spectrum and quantum statistics, theory 9-25213
 auto-collimator for adjustment of laser tube mirrors, patent 9-25319
 bibliography, 4000 refs. 9-45944
 bleach-out effect, nonlinear wave equations description 9-38365
 book, theory, expt. and applics. 9-40339
 cavity reflectors alignment 9-36271
 cavity resonators, u.s. beam transmission, patent 9-47947
 cavity with nonlinear crystal, 2nd harmonic generation, coherence and saturation props. 9-22374
 characteristics, ideal, for space communication, comparison with presently available 9-31930
 coherence effect on light amplification, semiclassical theory comparison with expt. 9-43874
 composite, two rods in series, axial mode freqs. and losses 9-25231
 continuous, power output calorimeter 9-43804
 correlations in light at threshold 9-22400
 coupled, resonators relative detuning, operating conditions 9-41891
 eigenmodes of spatially inhomogeneous lasers, determ. 9-40342
 with electro-opt. quartz Q modulator 9-40347
 e.m. and quantum mechanical theory 9-40345
 engineering and applications, conference, Washington (1969) 9-47928
 Fabry-Perot cavities, two, coupled, types of oscils. 9-43877
 field and population fluctuations, calcs. 9-25212
 fields, time depend. soln. of master equation 9-29397
 f.m., frequency stabilization, patent 9-41889
 frequency stability, ultrahigh, using nonlinearly absorbing gas cell 9-45946
 frequency stabilization 9-47939
 giant pulse production by coherent pumping 9-31934
 giant pulse system, optical cavity incorporation with active and passive Q-switching, patent 9-36280
 high speed frequency selector, patent 9-40341
 intensity oscillations, population inversion, phenomenological theory 9-22373
 introductory review 9-22370
 large, homopolar generator as energy store 9-29428
 lines, frequency and stability meas. in far infrared 9-31929
 low-noise internal modulation type, patent 9-36270
 materials, physical and chemical properties 9-25209
 medium polarization and population difference in amplitude modulated e.m. field 9-40343
 mirror supporting structure, patent 9-47948
 mode calc., numerical and kernal expansion procedures 9-27304
 mode competition for case of homogeneous line broadening 9-22375
 mode coupling in lengths-modulated laser, theory 9-38368
 mode locked signals, spectral criterion 9-25217
 mode locking, applications and prospects 9-36274
 mode selection apparatus, patent 9-40348
 mode-locking and ultrashort pulse formation, mechanism 9-22379
 mode-locking rel. to Lamb theory 9-25220
 model 9-29396
 modulation and control by means of intra-cavity time varying perturbation 9-27298
 modulation transfer function, polychromatic light 9-48082
 molecular amplifier electronics, review 9-47908
 multi-line, single wavelength operation using intra-cavity diffraction gratings 9-27296
 multi-mode generation, freq. and intensity, calc. 9-27310
 multimode action, Fokker-Planck eqn. exact stationary soln. including phase locking 9-25216
 noise props. 9-40346
 nuclear, pulsed homogeneous, feasibility 9-25274
 operation in quasi-stationary mode, induced radiation profile meas. 9-29400
 optical harmonics, stimulated Mandelstam-Brillouin scatt. obs. 9-25208
 oscillating modes, coupled, interaction 9-27312
 oscillators, for inverted state pumping, patent 9-47949
- Lasers continued**
 output, active medium separation for reference oscillator and remainder for power amplifier 9-27301
 output power meas. and optical properties 9-25209
 parameters determination, fluorescence method 9-31931
 parametric amplifier and freq. converter, P-representation 9-34150
 phase-modulated single-mode, slow mirror motion effects analysis rel. to freq. stabilization 9-25215
 phenomenon and equipment 9-41892
 photodetector-laser system, quantum-mech., photoelectron counting statistics 9-29395
 phthalocyanine soln. phototropic shutters, transmission, obs. 9-36277
 pi-pulse propagation through two-level inverted medium, exact solution 9-25210
 population inversion between sublevels of ground state 9-43870
 power output rel. to resonator geometry, calc. 9-25221
 powerful nsec., pulse generation using Mandel'shtam-Brillouin and stimulated Raman scatt. 9-27302
 pulse, energy output, calorimeter 9-43804
 under pulsed and continuous regimes, powerful phonon-photon signal generation 9-29402
 pumping, efficiency enhanced by enclosing ionisable gas within transparent enclosure surrounding laser crystals, patent 9-31925
 Q-switched, rod and lamp alignment within spherical reflector 9-27295
 Q-switched, intensity recovery from correl. data 9-43871
 Q-switched, spinning-prism, flash tube firing time control 9-27294
 Q-switches from pyrylium salts 9-47933
 Q-switching by a semicond. mirror, change in plasma freq. by carrier heating 9-36275
 Q-switching by telescope and rotatable mirror, patent 9-31932
 quantum electronics, vol.1. of book 9-47918
 quantum electronics, vol.2 of book 9-47919
 quantum electronics conference, 1968, Miami, USA 9-25196
 quantum fluctuations, six variable description 9-25214
 quantum mechanical multi-time-correlation functions 9-43868
 quantum system under oscillation, resonant emission of difference frequency due to optical mixing, theory and expt. 9-31933
 quantum theory 9-43875
 radiation coupled, interaction effects 9-47937
 radiation generation competition, 2 transitions, same upper state 9-22371
 Raman, high brightness studies, fundamental requirements 9-27299
 Raman scatt., stimulated, excitation in dispersing cavity 9-22410
 regenerative amplifier with oscillator of short resonator length, use as power amplifier 9-25230
 repetitive Q-switched, light sources for interferometry and holography 9-29476
 resonator, temp. dependent incidence of optical radiation; patent 9-47946
 with resonator mirrors with variable transmission over cross-section, spatial and energy charact. 9-29401
 resonator optimization rel. to minimal pulse-width generation by Q-switching 9-34156
 ring, running waves pulsation freq. stabilization rel. to amplitude of fluctuations 9-43869
 ring mode, status and performance limitations 9-27311
 ruby, Q-switched, excitation of LiNbO₃ crystal, stimulated tunable Raman emission 9-35672
 self-focusing of radiation in active materials and nonlinear crystals 9-44680
 self-locked, eff. of dispersion on phase modulation 9-22378
 semi-classical theory, equations and solutions 9-22372
 single mode, comparison of semi-classical and quantum theories 9-43872
 single mode, stabilised, with optical resonant cavity and reflective end members, patent 9-47950
 spark image structure 9-43867
 spectral and energy characts. of laser with plane mirrors, effect of stationary waves 9-47934
 spherical, interferometer, off-axis excitation of coupled cavity 9-31965
 steady-state generation and stability of laser with additional mirror 9-47935
 Steady excitation of c.w. radiation mode in spike region, stable pumping conditions 9-29420
 stimulated emission rel. to radiation laws 9-45872
 stochastic processes, quantum and classical 9-45945
 surface interactions, mechanisms 9-27300
 tactical systems, sensor protection with saturable interferometric devices 9-47930
 three-mirror cavities, types of oscils. 9-43877
 with transparent filter, monopause rise time and spectral width 9-47936
 transverse mode locking using intracavity modulators 9-25222
 transverse modes, competition and stimulated switching effects 9-25223
 tunable pulsed coherent light generator, selective up-conversion of broad-band i.r. source 9-27341
 tunable pulsed coherent light generators, selective up-conversion of broad-band IR source 9-27341
 tuning, acousto-optic, of optical parametric oscillators 9-25232
 ultrahigh freq. stability using nonlinearly absorbing gas cell 9-45946
 u.v., using organic-scintillator mols. 9-27303
 variable frequency, high Q electro-optic interferometer positioned in low Q resonator, patent 9-34155
 wavelength selector, intracavity interference filter 9-36273
 wavelength selector and output coupler 9-47929
 Nd³⁺ glass, high-coherence high power system at 1.0621 μ 9-47932
 O²⁺, prod. of population inversion by optical pumping from He⁺ 9-34167
- gaseous**
 absolute freq. meas., extension to 84 μ range 9-36282
 amplification and self excitation 9-40345
 amplifiers, polarization effects 9-25237
 cavity diaphragm for tuning, patent 9-31941
 circular, interac. of two field oscillators, quantum investigation without perturbation theory 9-29407
 construction for operation at 6328 Å 9-29415
 coupling, strong mode, induced by intracavity saturable absorbing medium 9-22380
 CW ion stabilization of transverse mode spectra 9-43879
 developments and uses, review 9-36284
 discharge tube supported within housing by means of membrane that also acts as partition, patent 9-34160
 discharge vessels, patent 9-48049
 double resonance, saturation parameters 9-47955
 double resonance theory 9-38370

Lasers continued

gaseous continued

dual-polarization, frequency and polarization charact., non-linear interactions effects 9-31936
electron emitters, properties 9-49171
emission modes, with circular resonator 9-25234
engineering and application, review 9-47956
frequency selector 9-45948
frequency stabilization 9-27315
gain coeff. meas., suitable attenuator 9-25240
generation, effect of reabsorption 9-38369
with grating for highly polarized output in far infrared 9-47957
high press. performance, m.f.p. active centers \ll emitted radiation wavelength 9-29405
high-intensity, semiclassical theory for single-mode operation case 9-41890
inert, ion, quasi c.w. ultra violet high power 9-25233
inert gas ion, multiwatt output, maximum inversion density and output power conditions 9-47963
inert gases ions, tube design for 2.3 W c.w. u.v. output power 9-47964
infrared, polyatomic, patent 9-22381
ion, quenching depend. on press., current, mag. field theory 9-31938
ion, r.f. inductively excited, with aperture-magnetic confinement 9-25236
line broadening parameters, determ. with hole-burning technique 9-25238
with magnetic field applied to gas discharge path between resonator mirrors at right angles to resonator axis, patent 9-30854
microwave modulation by CS₂ Kerr cells 9-36285
with mirrors, dielectric coated plane parallel intensity vs mirror swing 9-47959
molecular ion type, mechanism and conditions of operation 9-47953
operated with Brewster angle windows, characteristics 9-25257
optical pumping of mol. gases by own radiation 9-34157
photon echoes and combination tones in gases, effects of level degeneracy on polarization dependence, analogy 9-31967
pinch discharge, plasma electron temp. and conductivity 9-47958
plasma structure control, spectrum preexcitation by an electric discharge 9-25241
with plasma tube having variable cross-section and discharge current, patent 9-48009
population densities of vibrational levels, meas. 9-45951
population inversion, adiabatic, obs. from transmission of chirped pulses 9-44341
radiation emission build-up, fluctuations and statistical phenomena 9-29409
relaxation, anisotropic, collision-induced, in mag. field 9-31940
ring, c.w., mode coupling, model 9-40356
ring, c.w., theory w.r.t. mode-coupling effects 9-40355
ring, on vibrating support, frequency charact. 9-29404
for science and technology, operation 9-41906
simultaneous amplification and refocusing, patent 9-38371
single mode laser signal, stat. model 9-43878
single-frequency, with wavelength 3.39 μ , intensity fluctuations, exptl. invest. 9-36283
single-frequency operation with thin metal film mode selection filters 9-47940
single-mode, radiation intensity fluctuations, statistical analysis 9-25235
spectral line breadth and two-mode beating, calc. 9-41893
submillimetre-wave, theory and construction 9-31937
TEM₀₀ mode far-field patterns, calc. 9-47951
temperature, molecular, meas. 9-45951
theory, simultaneous action of r.f. perturbations and induced optical transitions in Zeeman laser 9-47954
transverse mode distortion with volume increase of active medium 9-40349
water-vapor, mechanism of population inversion in discharges, explanation of laser action, laser line data 9-22394
wavelength meas., i.r. and far i.r., using Michelson interferometer 9-36281
Zeeman, linear phase anisotropy influence 9-31939
Zeeman, polarization time behaviour approx. solns. 9-34158
Ar, CW, fundamental TEM₀₀ mode intensity distrib. amplification saturation depend. 9-22385
Ar, construction and operational characts., plasma jet as cathode 9-40351
Ar, continuous-mode, threshold for line excitation rel. to press., unsaturated gain characts. 9-25247
Ar, frequency stabilization using I₂ beam reference 9-25245
Ar, ion oscillator operating at 4880 Å, signal freq. spectrum 9-25248
Ar, longitudinal alternating mag. field effect on emission 9-41894
Ar, properties for Schlieren obs. of gas flow in arc or plasma 9-22384
Ar, second-harmonic generation, c.w., 2572 Å 9-27318
Ar, self-focusing, thermal, transient and steady-state 9-22383
Ar, single-frequency, gain saturation of 4880 Å line 9-25246
Ar, source for l.f. heterodyne anemometry experiments 9-47721
Ar, super-mode f.m., monochromatic generation at 5145 Å 9-27317
Ar, thermal properties improvement by using pyrolytic graphite 9-31946
Ar, toroidal, inductively coupled r.f.-excited, with aperture-magnetic confinement 9-47961
Ar⁺, 4880 Å, single pass gain as function of discharge current 9-45949
Ar⁺ interactions between 4881 Å and 5147 Å lines 9-27316
Ar⁺ transitions, interaction mechanisms 9-29411
Ar capillary discharge, radial distrib. of excited atoms and ions 9-36289
Ar II, amplification coeff. and rad. intensity rel. to saturation phenom. 9-36287
Ar II, d.c., perturbation spectroscopy, 3p¹ 4p14p level transition 9-25244
Ar in Schlieren study of gas flow in elec. arc or plasma 9-22384
Ar ion, c.w., excitation mechanism 9-25243
Ar ion, discharge electron temp. and density, calc. 9-47960
Ar ion, introductory paper 9-36288
Ar ion, miniature, for hologram reconstruction; design and charact. 9-47962
Ar ion, single-frequency operation, output spectrum charact. 9-47965
Ar ion, transverse modes properties 9-36286
Ar ion, vacuum u.v. discharge, spectroscopic studies 9-25242
Ar ion, vacuum ultraviolet perturbation spectroscopy 9-22382
Ar simplified 9-22386
C I, laser lines, obs. 9-46280
CO₂-N₂-He high power, high efficiency 9-22391
CO₂-N₂-He power enhancement by noncontracted discharge 9-22390

Lasers continued

gaseous continued

CO-air-He, Q switched, 1 to 7.7 kW peak powers 9-47952
CO, vibration-rotation transitions for 00⁰1-10⁰0 band, collision effects on saturation characteristics, experimental results 9-22972
CO₂-DF chemically pumped 9-29412
CO₂-He, high peak power generation dependent on CO₂ partial pressure 9-41896
CO₂-N₂-He-H₂O, flowing, elec. discharge effect on mol. comp. 9-40352
CO₂-N₂-He, discharge plasma excited by radial r.f. field , 250W output power 9-36290
CO₂-N₂-He, electron energy distribution and vibrational excitation rates 9-27320
CO₂-N₂-He, with confocal unstable resonator, properties 9-47973
CO₂-N₂-He amplifier, time-dependent processes 9-38372
CO₂-N₂-He discharge current charges due to generation 9-47980
CO₂-N₂-He with flow, 10-120 Torr, continuous wave operation 9-47966
CO₂-N₂-He with flow, kilowatt continuous wave 9-47967
CO₂-N₂, central tuning dip on individual transitions 9-47999
CO₂-N₂, high peak power generation dependent on CO₂ partial pressure 9-41896
CO₂-air-He mixtures, CO₂ 00⁰1-10⁰0 and 00⁰1-02⁰0 transitions amplification coeffs., obs. 9-25255
CO₂, 00⁰1 level decay in pulsed CO₂-N₂ gas discharges 9-34159
CO₂, amplifier tube, photon-induced current changes 9-47976
CO₂, damage to KBr windows by fracture and deform. 9-31943
CO₂, deactivation of vibr. excited ν_3 by collisions with CO₂ or N₂ 9-42387
CO₂, development for space applications, survey 9-47982
CO₂, gain saturation, relaxation and molecular diffusion effect 9-47969
CO₂, high peak power generation 9-41896
CO₂, inversion dependence on pump pulse repetition frequency 9-45952
CO₂, modulation by GaAs at 10.6 μ 9-37691
CO₂, molecular, thermodynamic approach for design 9-41898
CO₂, passive Q-switching using mixture of SF₆ and C₂FCl 9-27319
CO₂, plasma properties 9-47972
CO₂, population inversion by direct electron excitation 9-25250
CO₂, populations of 00⁰1, 10⁰0 and 02⁰0 levels 9-45951
CO₂, pulsed, excitation mechanisms 9-43880
CO₂, pulsed pumping, inversion as time function, theory and experiment 9-36291
CO₂, Q-switched pulsed discharge, properties dependent on different gas mixtures 9-41897
CO₂, Q-switched pulses, frequency-swept, charact. 9-47968
CO₂, rad. absorpt. by SF₆ and mol. vibr. induced 9-25750
CO₂, radiation, atmospheric absorpt. of P(20) line 9-33772
CO₂, rapid assembly method for laser tubes 9-34162
CO₂, rotating-mirror Q-switched, peak power 120 kW with 200 ns pulse-width 9-47970
CO₂, sealed, power increase by gas rotation 9-31942
CO₂, self pulsing and cavity dumping 9-34161
CO₂, single-mode operation 9-29413
CO₂, single frequency, short-term stability 9-25254
CO₂, small bore, characts. at 10.6 μ m from optical gain and microwave radiometer meas. 9-25252
CO₂, spontaneous emission between 6000 and 9000 Å, spectra 9-47971
CO₂, transverse discharge configuration, gain charact. 9-47974
CO₂, variable attenuator for 10.6- μ wavelength region 9-25316
CO₂, vibr. temps. from visible sidelight emission, obs. 9-47977
CO₂, vibrational energy transfer under laser conditions with and without water vapor 9-47975
CO₂, window materials investigation 9-26675
CO₂, 00⁰1 population level meas. and obs. 9-43882
CO₂ amplifiers, rot. relax. and gain saturation 9-41895
CO₂ cavity, Q switching 9-29414
using CO₂ chemically derived in electric discharge 9-43883
CO₂ folded laser, optimum transmission coeff. and power output 9-47978
CO₂ freq. stabilization by absorpt. saturation of SF₆ obs. 9-46375
CO₂ gas temp. and electron density in discharge 9-25256
CO₂ input, InSb difference-freq. generation, far i.r., temp.-depend. phase matching 9-31066
CO₂ interferometer, transient low-density plasma meas. 9-40353
CO₂ levels relaxation times by collisions with foreign gases 9-27321
CO₂ plasma dissociation 9-41899
CO₂ population and gas temp. vs discharge current 9-47981
CO₂ pulse, with double modulation and bleachable filters 9-25251
CO₂ pulsed, power increase from vibrational relax. and population inversion of molecule 9-48457
CO₂ pulsed repetitively and wavelength selective 9-25249
CO₂ rot. transition by collisions, relax. time calc. 9-44389
CO₂-N₂-He, continuous, with high power density 9-45950
CO electronic transitions, pulsed action at cooling of gas 9-47979
CO₂, gain measurements in fluid mixing laser systems 9-22392
CO₂, inversion kinetics, use of pulse pumping combined with Q-switching 9-22389
CO₂, mode competition for case of homogeneous, line broadening 9-22375
CO₂, radiation, effects of wind on thermal defocusing 9-22424
CO₂, rotational relaxation rate 9-22387
CO₂, spontaneous emission from discharges, spectroscopic investigation 9-22388
Cd II-He, c.w. transition, 3250 Å 9-47983
Cd vapour, isotope shifts and c.w. operation 9-29410
Co₂, amplifier, 1kW average power, with optical a.m. 9-25253
Co₂, lifetime of 00⁰V levels rel. to discharge current and power dissipation 9-43881
Cu vapour, pulsed, design 9-25258
D₂O, 84 μ absolute freq. meas. 9-36282
D₂O transitions, self-correlations 9-42393
D₂O vapour, far i.r. oscillations, correlation 9-27322
H-F branched chain reaction based 9-47984
H₂, high brightness Stokes source, operating characts. 9-25259
H₂, new oscillations at 7525 Å 9-47986
H₂-vapor, hydrogen as buffer gas, effect on output power 9-41902
H₂O, pulsed undulation in output waveforms 9-25260
H₂O transitions, self-correlations 9-42393
HCN, 890 GHz line, c.w. gain charact. 9-47985
HCN, frequency locking at 890 GHz to microwave frequency standard 9-41901
HCN, spectral linewidth meas. technique 9-41900

Lasers continued**gaseous continued**

- HF emission in XeF₄, SbF₅-H₂, methane mixtures photolysis, obs. 9-31944
- H₂S, far i.r., comparison with H₂O 9-22393
- He-Cd ion, stable operation, d.c. cataphoresis technique 9-47989
- He-Ne, 3-mirror resonator, mirror motion influence on generation power 9-22399
- He-Ne, 5 mW output power, design for use in space 9-47990
- He-Ne, amplification and oscillation mechanism 9-29416
- He-Ne, Brewster angle attenuator within laser cavity, eqns. of polarization and attenuation 9-31969
- He-Ne, collisional line broadening, gas pressure effects 9-22396
- He-Ne, combined with Nd³⁺ glass laser for high-powered highly coherent source 9-47932
- He-Ne, construction for operation at 6328 Å 9-29415
- He-Ne, density nonlinear depend. on saturation, Ne exchange collisions explanation 9-25271
- He-Ne, discharge, dispersive phase shift at 6328 and 6401 Å due to Ne 1s_s metastables 9-47991
- He-Ne, dispersion phenomena at 3.39 μm 9-25265
- He-Ne, freq. stabilization by external Ne absorpt. tube in mag. alternating field 9-25261
- He-Ne, gain coeff. temp. dependence calc. 9-41905
- He-Ne, generation intensity and inversion density rel. to hollow cathode diameter 9-25266
- He-Ne, h.f. pulse excited, generation intensity and pumping threshold, obs. 9-25267
- He-Ne, higher order phase-locking phenomena, mode quenching and forced locking methods for obtaining high bit-rate pulses 9-31945
- He-Ne, im mag. field nonlinear effects in output intensity 9-45954
- He-Ne, interference application for obtaining nonpolarized, single frequency radiation 9-25269
- He-Ne, Lamb dip minimum, discharge tube parameter effects on frequency shifts 9-22397
- He-Ne, Lamb dip minimum, freq. shifts 9-25262
- He-Ne, lasing frequency shifts due to discharge tube parameters 9-27323
- He-Ne, line width and amplitude fluctuations, theory contrib. 9-29408
- He-Ne, localizer-beam flying application 9-31947
- He-Ne, long life and charact. improvement 9-31946
- He-Ne, mode-locked, pulse compression to 1.85 factor 9-47988
- He-Ne, mode-locking using auxiliary Ne discharge tube 9-25263
- He-Ne, operating in TEM_{nm} modes, radiation divergence meas. 9-47992
- He-Ne, positive column calc. for dispersive effects eval. 9-43884
- He-Ne, pumping intensity, effect on relationship between gain and temperature 9-25268
- He-Ne, radiation output and polarization, infl. of transverse mag. field 9-22395
- He-Ne, radiation within hollow cathode 9-47994
- He-Ne, radiative power rel. to discharge gap geometry 9-47995
- He-Ne, resonator containing GaAs diode laser, non equilibrium carrier 9-38383
- He-Ne, ring, optimum composition ratio 9-41904
- He-Ne, self-locked, enhancement of second-harmonic power generation 9-22437
- He-Ne, self-locked, pulse velocity meas. 9-41903
- He-Ne, short-transient effect of inserted liquid cells 9-25276
- He-Ne, single-mode, damping parameters of 0.63 μm line, nonlinear press. depend. 9-34165
- He-Ne, single mode, comparison of semi-classical and quantum theories 9-43872
- He-Ne, with Brewster windows, elliptical polarization of output 9-25314
- He-Ne, with four-mirror T-shaped resonator, longitudinal mode selection 9-43885
- He-Ne, with pure Ne isotope or Ne²⁰, Ne²² 50-50 mixture, mode locking study 9-25264
- He-Ne, with self-locked transverse modes 9-22401
- He-Ne 6328 Å, external polarization technique using permanent magnet 9-29418
- He-Ne cascade transition, induced emission at 2.3956 μ, mechanism 9-22402
- He-Ne charact. using interferometric technique 9-46478
- He-Ne cw, temporal correlations in radiation at threshold 9-22400
- He-Ne high-gain strongly saturated 3.39 μ amplifier, experimental study of polarization-dependent gain saturation and nonlinearity-induced anisotropy 9-22398
- He-Ne multi-mode 0.63 μ, output power and spectrum rel. to collisions 9-34164
- He-Ne plasma parameters characterisation 9-34163
- He-Ne radiation, 0.63 μ, intensity fluctuations 9-38373
- He-Ne for science and technology, operation 9-41906
- He-Ne in transverse mag. field, energy characts. 9-40354
- He-Ne with 3.39 μ line, travelling wave generation 9-47996
- He-Ne with small discharge space, max. amplification depend. on tube axis position 9-29406
- He, excitation and relaxation effects on laser action 9-48431
- He, pure, c.w. oscill., 95.8 and 216.3 μ 9-45953
- He, visible laser oscillation at 7065 Å, population inversion 9-47993
- He-Ne, effect of cathode temperature on illuminating power 9-29417
- He-Ne, oscillation-detection technique at 3.39 μ 9-47987
- Hg-He, near-infrared operating charact. 9-47997
- Hg-Kr, visible and ultraviolet frequency range, patent 9-22403
- Hg, 1.5295 mμ line isotopic struct., obs. 9-34541
- I, ⁵⁷P_{1/2}-⁵⁷P_{3/2} transition, generation termination mechanism 9-46295
- I, atomic, output pulse durations with Q-switching and mode locking 9-25272
- IBr reversible photodissoc. system 9-34166
- K vapour, induced versus parametric scattering processes 9-47998
- Kr, ion oscillator operating at 5682 Å, signal freq. spectrum 9-25248
- Kr⁺ transitions, interaction mechanisms 9-29411
- Kr ionized, spectral transitions competition 9-45955
- N₂, interaction between first and second positive systems 9-25239
- N₂O-N₂ molecular central tuning dip on individual transitions 9-47999
- N atoms in N₂-He mixture 9-41907
- N I, laser lines, obs. 9-46280
- N₂, O₂ and ether or methane mixtures, pulsed discharge, simultaneous HCN and H₂O emissions 9-22404
- Na-H₂, Na 4S_{1/2} population inversion and gain, calc. 9-36293
- Na-H₂, radiation generation depend. on Na and electron conc. 9-27324
- Ne-He, calibration system for extensometers 9-25356

Lasers continued**gaseous continued**

- Ne, 3.39 μm line width from Lamb-dip 9-27325
- Ne, 5401 Å, pulsed, developments, review 9-25270
- Ne I 2s_{1/2} laser level transition probabilities and mean lives 9-48413
- Ne ion, u.v., c.w., 10 mW 9-27326
- O oscillographic and interferometric obs. 9-41908
- O population inversion process obs. 9-41908
- O₂, simplified 9-22386
- OCS, far i.r. obs. 9-22393
- SO₂-He mixture, pulsed discharge excitation 9-27327
- Sn II-He, c.w. transitions, 6453 and 6844 Å 9-47983
- So₂, far i.r. obs. 9-22393
- UF₆-H₂, HF chem. laser, operation and chem. 9-36292
- Xe, high ionization states, c.w. operation 9-48000
- Xe discharge tube at 30 cm Hg press., powered by homopolar generator 9-29428
- Xe highly saturated laser field, zero- field level-crossing effects in cascade process. 9-32415
- Xe²⁺, pulsed mode, high-power output at 5353 Å 9-22405
- Zn II-He, c.w. transitions, 7479 and 7588 Å 9-47983
- Zn ion, role of charge exchange 9-25273

liquid

- amplification coeff. and geometrical optics, calc. 9-22406
- cyanine dye in methanol soln. laser 9-36296
- cyanine dyes, conditions for and characts. of lasing action 9-41909
- diethylthiaticarbocyanin dye, stimulated Raman scatt. 9-28137
- dye 9-48003
- dye, cw operation 9-25278
- dye, flashlamp excitation, measurement of critical population inversion 9-27328
- dye, fluorescing excitation and properties 9-36294
- dye, frequency- and time-dependent gain characteristics 9-25275
- dye, picosecond impulses, line profiles 9-48008
- dye, tunable, use in diagnosis of Ba plasma 9-44463
- dye, ultrashort pulses, generation and applic. 9-48004
- dye solns., 4-photon resonant parametric interaction 9-48001
- organic dye, flashlamp for pumping 9-48005
- organic dye, flashlamp pumped, time dependent spectroscopy 9-22408
- organic dye, flashlamp-excited, gain analysis 9-48007
- organic dye, optical generation, excited with impulse lamps 9-29419
- organic dye, short-cavity, charact. 9-48006
- organic dye, source of losses 9-25277
- organic dye, spectra dependent on concentration and dye length 9-36295
- organic dye lasers, review 9-43887
- organic luminophore solns., characts. of stimulated radiation 9-43886
- pulsed, high-energy, alternating flow system properties 9-27329
- rhodamine 6G, methanolic, cw operation 9-25278
- Rhodamine 6G dye, threshold inversion and triplet state conc., wavelength depend. 9-43888
- rhodamine dye laser, flashlamp pumped, spectral output 9-22408
- scintillator dyes, near 4000 Å wavelength, pumping with second harmonic of Q-switched ruby laser 9-31949
- CS₂, with large optical Kerr effect, subpicosecond pulse generation 9-48002
- Eu benzoyleacetate solutions at -150°C energy of threshold rel. spectral comp. stimulating light 9-28134
- Nd³⁺: SeOCl₂ liquid spectroscopic props. rel. to Nd ion conc., acidity and temp. 9-26120
- POCl₃, SnCl₄, Nd₂O₃ soln., emission charact. 9-45956
- SeOCl₂:Nd³⁺, connected to glass laser, amplifier system 9-31948
- SeOCl₂ solns., aprotic, luminesc. and energy transfer of rare earth ions 9-22407

semiconductor

- CdS, 5 MW flash sources, for stop-motion photography, using field emission devices 9-36311
- compound material having two p.n. junctions, patent 9-41918
- diode, interference prevention in emerging rays, patent 9-48047
- diode, peak emission shift with cavity Q, temp. and doping depend. 9-27334
- diode, radiative recomb. quantum efficiency, temp. depend. 9-25302
- diode, strong device, junction beam modulation, patent 9-43895
- emission spectrum, effect of freq. nonsaturating filter in feedback cct. 9-29431
- Ga(P,As), injection, memory effects, obs. 9-48043
- heterojunctions, laser action possibility 9-35453
- injection, with compound resonator 9-48037
- junction, time delays and Q-switching theory 9-43893
- junction, time delays and Q-switching, computer calc. and comparison with experiments 9-43894
- p-n junction, emission in near-infrared and visible portion, review 9-48036
- principles and props. 9-40363
- transverse, on laser diodes, dielectric-waveguide modes 9-34175
- tunable Raman radiation, patent 9-40364
- Al_xGa_{1-x}As, injection, charact. 9-27335
- CdS, electron-pumped, 10 MW, light emission 9-48038
- CdS, electron beam pumped, high power and efficiency 9-34177
- CdS, lasing transitions 9-36312
- CdS, mechanism of laser emission rel. to recombination processes under high excitation 9-37758
- CdS, stimulated emission on e. bombardment, radiative recombination mechanism 9-24445
- CdSe, electron beam pumped, high power and efficiency 9-34177
- CdTe, excited by electron bombardment, characts. 9-34176
- GaAs:Ge, transition to band edge or impurity states 9-25303
- GaAs:Ge,Si,Sn,Zn diffused, semiplanar geometry, construction and performance 9-25305
- GaAs-Ga_xAl_{1-x}As diode structures, low-threshold room-temperature, preparation 9-25307
- GaAs-Ga_xAl_{1-x}As diode structures, low-threshold room-temperature, characteristics 9-25308
- GaAs, diffused junction, annealing effects, optimum temp. rel. to impurity conc. 9-45958
- GaAs, dislocation-free, electron-beam-pumped, nonuniform emission charact. 9-41920
- GaAs, under e. beam excitation 9-22421
- GaAs, injection-type, radiation power hysteresis 9-27337
- GaAs, injection, dynamics of emission in continuous and pulsed region 9-48044

Lasers continued

semiconductor continued
GaAs, injection, efficiency and characts. at 300°K 9-36310
GaAs, injection, life studies 9-27338
GaAs, injection, noncatastrophic degradation of power output 9-31963
GaAs, p-n junction diode, superradiance spectra and inhomogeneity distribution 9-36315
GaAs, photon loss in active and passive regions 9-29433
GaAs diode, coherence 9-43897
GaAs diode, damped relaxation oscillations, regular pulse train 9-31961
GaAs diode, spontaneous emission line breadth, doping depend. 9-27336
GaAs diode based, spectral characteristics rel. to impurity energy states near conduction band 9-34178
GaAs diode in gas laser resonator, absorption by non equilibrium carriers 9-38383
GaAs diodes, dependence of differential external quantum efficiency and gain on reflectivity 9-45963
GaAs diodes, differential quantum efficiency and gain dependent on resonator length 9-45964
GaAs diodes, space radiation effects 9-22422
GaAs diodes, topography of absorptivity and emissivity 9-25306
GaAs injection, continuous wave, optical pulsations 9-48039
GaAs injection, end-surface mirror production 9-29432
GaAs injection, Hermite-Gauss intensity patterns by optical feedback 9-45965
GaAs injection, modulation at 1 GHz 9-38385
GaAs junction, dependence of total stimulated light power and gain factor on laser length 9-48041
GaAs junction, Q-switched, pulse spiking 9-41919
GaAs junction, resonant mode spectra at currents 1.5 to 3 times threshold level 9-48042
GaAs junction, stripe geometry 9-25304
GaAs junction, total stimulated light power, temperature dependence 9-48040
GaAs junction laser, optimum stripe width for continuous operation 9-36313
GaAs optically coupled injection-type, quenching effect 9-38388
GaAs parallelepiped, 5-cm., interference of 10.6 μ coherent radiation 9-43896
GaAs platelets, time behaviour of modes 9-36314
GaAs pn junction, with reduced optical loss, room temp. close-confinement improvement 9-38384
GaP pulsed diodes, radiation props. 9-38387
GaSb stimulated emission beam, displacement in mag. field 9-45961
InAs-InP alloy system for injection-lasers, 1.06 μ emission, crystal growth and charact. 9-41921
Pb_{0.88}Sn_{0.12}Te diode lasers, quantum-phase-noise limited Lorentzian power spectral densities 9-43898
Pb_{1-x}Sn_xSe, x<0.28, emission temp., comp. depend. rel. to energy band crossover, 1.5-100°K 9-48045
Pb_{1-x}Sn_xSe diodes, mag. field depend. of i.r. laser emission 9-41922
Pb_{1-x}Sn_xTe(Si), emission characts. temp. and composition dependence 9-38386
SiC pulsed diodes, radiation props. 9-38387

solid
amplification and self excitation 9-40345
with combined active medium, props. 9-25280
continuous, temperature field calc. of active medium 9-22409
crystal cooling and prevention of preferential lasing, patent 9-36299
disc-shaped pumping through large end face, patent 9-36300
Er³⁺: glass, improvement using phosphate glass 9-25290
excitation, pulse, effective technique for cylindrical laser 9-34169
excitation, pulse, effective technique for cylindrical laser 9-27330
filaments, single and braided, forced radiation 9-36298
frequency conversion, experiments using continuously pumped repetitivity Q-switched ruby laser 9-25320
glass: Nd₂O₃, operation in quasi-stationary mode, induced radiation profile meas. 9-29400
glass: trivalent Yb and Nd ions, with minimum heating and improved absorption, patent 9-48046
glass, behaviour of Nd, Yb and Er ions, review 9-25293
glass, behaviour of Nd, Yb and Er ions, review 9-25293
glass, connected to SeOCl₂ liquid laser, amplifier system 9-31948
glass, delivering 500 joules in 30 ns and 250 joules in 5 ns 9-25281
glass, high power 9-48012
glass, Nd doped, monomode giant pulse, coherent pumping 9-34172
glass, recent advances 9-36301
glass, silica, Cr³⁺→Yb³⁺ energy transfer mechanism, obs. 9-29430
glass, specific gain coefficient, direct measuring device 9-48016
glass slab, Nd³⁺-doped, high repetition rate operation 9-48017
internal losses, fluorescence method 9-48013
mode locking and ultrashort pulse generation with nonlinear refractive index 9-48014
mode-locked, partially, oscillating modes effect on two-photon fluoresc. 9-43890
multimode, locking 9-41911
operation and Q switching techniques 9-41912
optical path change holographic interferometry 9-48088
organic dyes, xanthene and coumarin groups, lasing action, flashlamp-pumped 9-45960
parameters determ., fluorescence method 9-29429
pulsed, review 9-48011
pulsed active rod, hollow, heat transfer problem 9-40358
pumping chambers, elliptic-cylindrical, optimum design 9-22415
Q modulated, electrooptically, operation with misalignment and its correction 9-40357
Q switching based on triplet-triplet transitions of organic mols. 9-25279
Q Switched, synchronisation of two lasers 9-31953
Q-switching techniques for room-temp. operation 9-22414
rods, soft crystal, differential erosion rate polishing 9-43889
ruby, 0.34m.m. wave generation by beating R₁ and R₂ lines 9-25283
ruby, ²E metastable population kinetics and Q-switched reson. losses, obs. 9-36302
ruby, applic. to high-speed framing photography 9-32095
ruby, Ar ion laser pumped, operation at room temp. and 77°K 9-25288
ruby, coherence effect on light amplification 9-43874
ruby, composite, spectral and phase characts. 9-48023
ruby, conversion of focused radiation to X-rays in hot dense plasma 9-42517
ruby, for pumping LiNbO₃, parametric oscillation 9-28663

Lasers continued

solid continued
ruby, freq. conversion by polymethyn dyes 9-34171
ruby, generation spectrum rel. to resonator active crystal orientation 9-38379
ruby, giant pulse form. registration by multiframe image converter 9-31956
ruby, improved high-coherent output using optical t.w. amplifier 9-25286
ruby, influence of colour centres on lasing threshold 9-39372
ruby, intensely excited, emission power and time constant obs. 9-45941
ruby, inversion coefficient, theoretical and expl. investig. 9-31928
ruby, kinetics of free generation spectrum in travelling-wave regime with mode discrimination excluded 9-27333
ruby, mode-locked, pulse duration 9-25285
ruby, mode-locked, with rooftop prism cavity, picosecond pulses with transverse-mode operation 9-43891
ruby, modification of pulsed refl. mode for high-power-pulse transmission mode operation 9-48071
ruby, off-resonance frequency doubling meas. 9-31952
ruby, organic dye bleachable absorbers, fluorescence decay times, recovery times and nonlinearities 9-26113
ruby, oscillator-amplifier, pulse transmission mode technique, design and charact. 9-48019
ruby, output energy degradation due to colour centre formation 9-38377
ruby, partial giant pulse prod. for stroboscopy 9-29425
ruby, passive Q-switching based on stimulated Mandel'shtam-Brillouin scattering of light 9-36306
ruby, pulse parameters rel. to spectral and luminesc. props. of passive filters 9-36305
ruby, pumped by Ar ion laser, spiking behaviour 9-27331
ruby, Q-switched, emission charact. and pulse stretching 9-48018
ruby, Q-switched, for emission microspectroscopic elemental analysis 9-22411
ruby, Q-switched, picosecond pulse generation rel. to cavity geometry 9-25292
ruby, Q-switched, spectral composition of diffused light in self-focusing liquids 9-26116
ruby, Q-switched, travelling-wave oscillations, method 9-48020
ruby, Q-switched for dynamic event holography 9-36329
ruby, Q-switching by natural chlorophyll and derivatives 9-36303
ruby, Q-switching by organic solvents 9-29423
ruby, radiation field in active rod, effect of nonuniformity on dynamics 9-36304
ruby, reflection holograms, pulsed single-mode 9-22425
ruby, regular spiking, spectral output and far-field pattern as influenced by resonator mirror vibrations 9-41913
ruby, relevant props. 9-31954
ruby, repetitively Q-switched, continuously pumped, and harmonic generation 9-25284
ruby, repetitively Q-switched, continuously pumped, applications to second-harmonic generation and stimulated Raman scattering 9-25320
ruby, resonator ended by a rectangular prism 9-22416
ruby, self-Q-switching, saturable absorber, at 77°K 9-38376
ruby, self-Q-switching at 77°K and 300°K 9-36309
ruby, sequentially modulated system, for recording dynamic photoelasticity 9-29232
ruby, single-mode, giant pulse, high spectral brightness, production and diagnosis 9-38375
ruby, single-mode, passive Q-switched, dynamic behaviour 9-25287
ruby, single-mode high-power, using multi-elements 9-36307
ruby, space field structure, h.f. modulation 9-43892
ruby, space radiation effects 9-22422
ruby, stable freq. monochromatic mode 9-45957
ruby, transverse-mode selection effects on wavefront 9-48052
ruby, tunable far-i.r. rad. generated from difference freq. between two lasers 9-31955
ruby, u.s. modulation 9-48072
ruby, with external mirrors for discrimination mode exclusion, kinetic spectrum 9-48022
ruby, with population inversion in whole crystal 9-48025
ruby, with resonator having Q-factor modulation 9-29422
ruby crystals, optical homogeneity rel. to laser emission characts. 9-26674
ruby film deposited on metal plate, patent 9-48048
ruby pulse power amplification during induced Mandelstam-Brillouin back-scatt. 9-22417
ruby Q switched, single pulse with opto-mechanical shutter 9-41914
ruby refr. index change during pumping 9-29424
ruby ring single-direction, construction method 9-48021
ruby rod, distribution of temperature during pumping 9-22418
ruby rod, heat removed by Cu conductor 9-38378
ruby single freq., with variable radiation freq., spectral characts. under giant pulse operation conditions 9-41915
ruby single-frequency, with active Q-switch 9-48024
shock wave generation by giant laser interaction with solid target 9-41910
single-frequency operation with thin metal film mode selection filters 9-47940
three level, with extremely long lifetime at room temperature, patent 9-25282
tunable, beam-pumped, patent 9-48050
two-component medium, ultrashort pulse propag. 9-38374
YAl garnet: Nd³⁺ self-Q-switching at 77°K 9-36309
Ba₂NaNb₃O₁₅ 9-25198
Ba₂NaNb₃O₁₅, tunable, 13 W threshold power 9-25289
Ba₂NaNb₃O₁₅ parametric oscillation and freq. doubling 9-37677
CaF₂:Sm²⁺ basic characts. 9-38380
CaF₂:Sm²⁺ crystal, electron-vibrational transitions, rel. to laser spectrum 9-37704
CaO.2Al₂O₃, single cryst., good room temp. transmittance, 0.6-4/ μ , patent 9-31957
CaO.2Al₂O₃, single cryst., good room temp. transmittance, 0.6-4/ μ , patent 9-31957
CaWO₄:Nd³⁺, stimulated emission cross-section meas. 9-41916
Cd(SeS) platelets, laser emissions, excited with mode-locked He-Ne laser 9-31950
GaAs, i.r. emitter diodes 9-22423
GaAs, injection gradual degradation, role of optical flux and current density 9-31962

Lasers continued
solid continued

- GaAs injection laser, features and operation, applic. in communication syst. 9-45962
GaP parametric gain near lattice resonance 9-25197
LaNa (MoO₄)₂:Nd³⁺ crystals, c.w. 9-40359
LiNbO₃ surface harmonic generation from non-linear polarisation 9-29427
LiNbO₃ parametric emission, spontaneous, power and bandwidth 9-25198
LiNbO₃ stimulated optical emission, tunable, without resonator 9-48026
LiYF₄:Er³⁺, Ho³⁺, pulsed laser action at 77°K 9-25291
Nd: glass, Q-switched, static and dynamic investigation of beam 9-25294
Nd: glass, Q-switching by organic solvents 9-29423
Nd: glass, spectral band narrowing using diffraction grating as one cavity reflector 9-25296
Nd: glass doped, surface damage threshold improvement by chemical polishing 9-26171
Nd:CaWO₄, imperfection assessment and control in crystals used for laser devices 9-37157
Nd³⁺:CaWO₄ fundamental longitudinal modes exam. 9-22419
Nd:glass, comparative pumping efficiency of Xe, Ar and Kr flashlamps 9-31958
Nd:glass, mode-locked, pulse duration 9-25285
Nd:glass, Q-switched, picosecond pulse generation rel. to cavity geometry 9-25292
Nd:glass, for second-harmonic generation in crystals in systems with diffraction-limitation and high-spectral-radiance 9-41917
Nd:glass, spikes, picosecond time structure 9-25311
Nd:glass discs, tilted and face pumped, for large aperture system 9-25299
Nd:YAl garnet, c.w., pumping efficiency using alkali additive lamps 9-31959
Nd:YAl garnet, imperfection assessment and control in crystals used for laser devices 9-37157
Nd:YAl garnet, mode-locked with intracavity LiNbO₃ phase modulator 9-25297
Nd:YAl garnet, static and dynamic behaviour 9-25298
Nd:YAl garnet rods, index of refraction and thermal expansion coeff. 9-22412
Nd³⁺:YAl garnet, quasicontinuous giant pulse emission of ⁴F_{3/2}-⁴I_{3/2} transitions at 1.32 μm 9-22420
Nd-glass, conversion of focused radiation to X-rays in hot dense plasma 9-42517
Nd-glass, kinetics of free generation spectrum in travelling-wave regime with mode discrimination excluded 9-27333
Nd³⁺-glass slab pulse amplifier chain with successive beam sweeping 9-22413
Nd-glass, pumped by energy from homopolar generator 9-29428
Nd, stimulated combinational scattering of radiation in liq. N₂ 9-36879
Nd, Yb and Er ions behaviour in various glass hosts review 9-25293
Nd, Yb and Er ions behaviour in various glass hosts, review 9-25293
Nd³⁺ glass, combined with He-Ne laser for high-powered highly coherent source 9-47932
Nd³⁺: glass and ruby, ps. pulses with GW power generation, meas. and applics. 9-31964
Nd³⁺: glass, flint glass nonlinear solarization by second harmonic 9-40832
Nd³⁺:CaF₂-SrF₂, stimulated emission, 300°K 9-29426
Nd³⁺:Ca(NbO₃)₃, stimulated transitions, crystal field splitting terms 9-27332
Nd³⁺:LaF₃, double freq. generation 9-40360
Nd³⁺:YAl garnet, comparative pumping efficiencies of Xe, Ar and Kr flashlamps 9-31958
Nd³⁺:fluoride crystals, radiative lifetime of metastable ion, anomalous temp. dependence 9-41405
Nd³⁺:glass, high repetition rate operation 9-38381
Nd³⁺, structure of stimulated emission bands in CaWO₃ and silicate glass 9-35650
Nd³⁺ in silicate glasses, hole burning effect on effective stimulated emission cross-section 9-48010
Nd doped glass, pulsed with selected 2nd harmonic radiation 9-38382
Nd glass, generation of i.r. radiation in polymethine dye 9-34168
Nd glass, laser eff. obs. 9-48028
Nd glass, picosecond pulse substructure, measurement using compression techniques 9-31951
Nd glass, picosecond pulse width meas. by GaAs surface harmonic generation 9-34173
Nd glass, stimulated emission parameter deterioration during use 9-31109
Nd glass, with plane-polarized emission 9-36308
Nd glass and ruby, picosecond pulses, evidence for self-focusing in gas breakdown 9-25983
Nd glass rod oscillation patterns, streak camera obs. 9-45959
Nd glass system, diffraction-limited high radiance 9-25295
Nd second harmonic radiation, conversion coeff. rel. to space-time distribution 9-40361
Nd; temporal struct. of emission in mode self-locking regime 9-45969
Rb quantum generator, short-term frequency stability of frequency standard 9-36297
SrF₂, photoreduction Nd³⁺→Nd²⁺ under stimulated emission conditions 9-31960
Ta-Al point contacts, radiative emission at Ta energy gap freq. 9-25300
YAl garnet:Nd, 100 W output, 3% efficiency 9-48031
YAl garnet:Nd, continuous 0.53 μm source using Ba₂NaNb₅O₁₅ 9-40362
YAl garnet:Nd, diode pumped, c.w. operation, 48 mW output at 1.0614 μm with 1% efficiency 9-48034
YAl garnet:Nd, feedback-controlled, dynamics 9-48030
YAl garnet:Nd, Kr lamp pumping, 105 W output 9-48033
YAl garnet:Nd, Q-switched, coherence length corresp. to pulse length 9-48035
YAl garnet:Nd, repetitively Q-switched, pulse-to-pulse stability 9-48032
YAl garnet : Nd, continuous operation by injection luminescent pumping 9-25301
YAlO₃:TR³⁺, as active laser medium 9-48015
YFe garnet:Nd, passive mode locking 9-34174

Latent heat

see also *Heat of adsorption, etc.; Thermodynamic properties*
propane, of vaporization meas. 9-36818

Latent image see *Photographic process***Lattice constants** see *Crystal structure, atomic***Lattice dynamics** see *Crystals/lattice mechanics***Lattice energy** see *Bonds; Crystals; Solids***Lattice gas** see *Statistical mechanics***Lattices theory and statistics**

- adsorbed monomer cluster distrib. on one-dimens. lattice, matrix method calcs. 9-34997
anharmonic oscillators, coupled, 2D, approach to thermal equilib., computer studies 9-31777
approximation method for lattice statistics 9-31775
cohesive energies, dielectric theory of tetrahedrally coordinated crystals 9-23698
crystal, transport eqns. of correlation function for quasi-momentum density 9-30778
crystal nonlinear effects, theoret. treatment in second-quantization representation 9-23997
cubic lattices with long-range interactions, dispersion relations and freq. spectra 9-39505
dimer, 3-dimens problem, incidence matrix non-existence 9-36137
dimer problem, partition function rederivation using S-matrix method 9-43755
electronic struct. of random lattice, Green's function, coexistence of local and band character 9-33216
frequency spectrum and momentum autocorrelation function 9-37310
gas, cluster prop. of correlation function above critical temp. 9-29205
gas-liquid critical point, lattice gas model 9-36924
infinite quantum lattice systems, ground state investigation 9-22119
Ising, 3-dimens., inhomogeneous, critical behaviour 9-36136
Ising, antiferromag. decorated, magnetic field effect 9-24322
Ising, two-dimensional-square, applic. of thermodynamic perturbation theory 9-34036
Ising, with impurities, phase transition 9-29207
Ising ferromag., dilute, of simple cubic lattice, critical behaviour 9-28600
Ising model, 3-dimens, free energy, specific heat depend. on temp. 9-25048
Ising model, Bogoliubov inequality applic. 9-25047
Ising model, critical point behaviour with higher-neighbour interactions 9-47769
Ising model, generating functional and Green's function hierarchy 9-41774
Ising model, Green's function approach 9-35540
Ising model, next-nearest-neighbour 9-38245
Ising model, recurrence formulas for graphs 9-34037
Ising model, thermodynamic quantities, self-consistent field near critical pt. 9-39758
Ising model, three regular three-dimens. lattices, high-temp. critical props. 9-41775
Ising model, three-dimensional finite, partition function calc. for 27 point array 9-36142
Ising model near transition point, honeycomb and triangular lattices 9-47772
Ising spin partly decorated honeycomb and dice lattices, conditions for 3 transition temp. 9-31799
Ising spin syst., thermodynamic and distrib. functions, analytic and clustering props. 9-22112
lattice gas, continuum analogue 9-22113
linear chain, antiferromagnetic, Fermi liquid theory 9-49221
linear chain with next-nearest-neighbour interactions, two spin deviations 9-29206
magnetic, derivation 9-31013
magnetic, inhomogeneous, critical behaviour 9-36136
magnetic lattice gas with Ising interaction, one dimen., soln. 9-40245
many-fermion techniques applications 9-34035
molecules, interacting linear systems, decay of pair correlation function 9-34700
monomer-dimer problem, exact series-expansion study 9-25046
movement theorem for resonance line shapes arising from decoupled Green's function eqns. 9-34034
next-nearest-neighbour Ising model 9-38245
point defects, simulation of random walks and reacts. 9-30590
point defects, simulation of random walks and reacts. 9-30591
polymer chains, lattice-model, Brownian motion 9-34696
random, self-contained first-order approx. accounting for exclusion effect 9-24008
random walk problem for excitons in photosynthesis 9-38244
random-walk model for hydrocarbon-type chains with short-range correlations 9-44379
self-avoiding walks on tetrahedral lattice 9-45776
self-avoiding lattice polygons, number estimation 9-41777
shock waves, finite amplitude in mass points chain 9-36201
spin-1/2 XY model on f.c.c. lattice, partition function and specific heat, high temp. series expansion 9-39759
three-dimensional lattices, two self-avoiding walks 9-47771
triangular lattice, Rys F model 9-47768
Watson integrals evaluation, approx. method, Chebyshev type approx. 9-34039
Wigner e lattice vibrs., anharmonic effects 9-31791
zeros of great canonical distrib. functions 9-40246
NaCl, transition pressure for NaCl→CsCl struct., quantum mech. calc. 9-23985
NaF, transition pressure for NaCl→CsCl struct., quantum mech. calc. 9-23985

Laves phases see *Alloys; Phase transformations/solid-state***Lawrencium**

No entries

Lawrencium compounds

No entries

LCAO calculations see *Molecules/electronic structure; Orbital calculation methods***Lead**

- see also *Superconducting materials/lead*
absolute viscosity as function of temp., liquidus to 500°C 9-30378
anodic passivation mechanism in various media 9-33678
atom total ν cross-sections, 40-80 keV, mean values, analysis 9-22949
compressibility, comparative with Cu and Cd, at high press. 9-30655
crater formation by Fe microspores at 0.5 to 10 km/sec. 9-30700
diffusion in noble metals, rapid, interstitial mechanism 9-28321
diffusivity of Cd, mechanism 9-46855
dislocation damping of u.s. absorpt. in single cryst., temp. and freq. depend. 9-41089

Lead continued

- electron-phonon interaction rel. to conduction electron props. 9-47032
energy wave-number charact. from exptl. phonon freqs. 9-44871
e.p.r. of trapped holes in ZnSe 9-35706
eqns. of state, specific heat and thermal expansion 9-39090
films, quenched, thermal cond. meas. at 2-20°K 9-44848
films grown on (110) face of W, by u.h. vac. deposition 9-42720
gamma ray scatt., 145 keV, differential elastic scatt. X-section 9-46263
Gibbs free energy of self and impurity diffusion 9-33001
grain boundary migration and form. of annealing twins, 200-300°C 9-30570
impurities in Ni alloys and steels, determ. 9-28830
internal friction anomalies near melting pt. 9-39399
ion collision cascades in Au, 3-169 eV 9-39552
isotopes, single-stage growth by triple filament method 9-47475
isotopes, triple-filament analysis for calibration of mass spectrometer 9-47475
Landau-level widths effective masses and magnetic-interaction effects 9-26500
liquid, self-diffusion coeff. 9-42643
liquid, stress cracking of Cu and alloys 9-48941
luminescence of complexes in NaCl 9-33593
magnetoresistance, high-field, Fermi surface third-zone sheet model 9-28458
molten, electrical resistance meas. by rot. field method 9-39583
molten, velocity distribution of evaporated particles in vacuum 9-32818
nucleation, eff. of small addition of solute 9-28180
nucleation, supercooling depend. on liq. drop size 9-28179
phonon emission spectra, thermal radiation obs. 9-42944
phonon spectrum pressure dependence from tunneling meas. 9-33165
photoelectric cross-section of atom obs. at 84, 100 KeV 9-44282
recrystallization process, nucleation and boundary migration obs. 9-48914
scattering of γ -rays 145-662 keV diff. cross section meas. Rayleigh scatt. formula determ. 9-46318
superconducting, intermediate state, effect of transport current 9-49054
superconducting, r.f. absorption in cavity resonators, measurements for TE and TM modes 9-47092
superconducting film, transition temp. determ. from tunneling and resistive meas. 9-43040
superconducting resonating cavities, technology of prod. 9-39607
superconducting r.f. absorption in cavity resonators, measurements for TE and TM modes 9-47092
superconducting transition temp. pressure dependence in electronic thermal expansion phonon enhancement calcs. 9-44838
surface tension, 1300-2200°K 9-28110
u.s. absorpt., in single cryst. dislocation damping, temp. and freq. depend. 9-41089
u.s. shear-wave attenuation in superconducting state 9-24026
work hardening and injected dislocation density determ. 9-41046
n single crystal monochromator, efficiency and optimization 9-32251
neutron dose in critical assembly 9-37284
p, range and ionization energy losses, Bragg's curve method meas., $E_p=100-660$ MeV 9-33213
 ^{210}Pb radioactive dating of glacier 9-47512
 ^{206}Pb , ^{207}Pb , ^{208}Pb , ^{7229}A isotope shifts in ^{7229}A transition 9-22963
Au/Pb supercond, layered films, phase composition and transition obs. 9-26528
KCl:Pb, F centre prod. by impurities, α and V_K centre motion importance 9-44718
K α Cu and Mo X-radiation absorption, depend. on particle size in multi-phase syst. 9-24440
Pb-plexiglass layers, shock wave energy cumulation 9-37229
Pb-Ca battery grids, pressure cast, abnormal corrosion 9-28802
Pb $_{40}\text{Tl}_6$ phonon spectrum by tunneling and n. scatt. meas. 9-26413
Pb $^{2+}$ conc. in HCl, LiCl, HBr, LiBr, luminesc. meas., 77°K 9-33697
Pb $^{2+}$ impurity in CaWO $_4$, phosphoresc. enhancement 9-39884
Pb $^{2+}$ in NaCl, KCl and KBr, prod. and optical props. of colour centres formed by electrolysis 9-32992
Pb $^{2+}$ e.p.r. in CaCO $_3$ at 77°K and 9.3 G/c/s, hyperfine interaction 9-41425
Pb $^{3+}$ in ZnTe, photo-induced paramagnetic resonance of Pb $^{3+}$ 9-47439
Pb- polyethylene shields, fast-neutron attenuation, S_a calc. 9-33963
phonon spectrum pressure depend. from tunneling meas. 9-24018
ZnSe:Pb, EPR of trapped holes 9-35706

Lead compounds

- $_{90.95}\text{Sr}_{0.05}(\text{Zr}_{0.5}\text{Ti}_{0.47})\text{O}_3+3\%\text{PbO}$ ferroelectric ceramic, internal friction 9-41004
alloys, binary, equi. partition coeff. rel. to strength 9-44772
alloys, liquid, ^{207}Pb Knight shift, electronic struct. of impurities obs. 9-32800
alloys, metallographic microstructure 9-39301
apatites, mineral, struct. and spectra study 9-37148
binary alloys, partition coefficient relation with strength 9-26399
PbCrO $_4$ -C, BaSO $_4$, powder mixtures, diffuse reflectance 9-24360
Pbm $_{0.33}\text{Nb}_{0.67}\text{O}_3$ ferroelectric, dielec. props. over wide temp. and freq. range 9-41243
PbTe thin film, co-evaporated, influence of stoichiometric deviations on nucleation and structure 9-36949
salt photoconducting detectors, development reviewed 9-45026
silicate glasses, K $_2$ O-PbO-SiO $_2$, luminescence centres 9-31129
solder effective atomic number for photoelectric process of γ -rays 9-47213
searate, multilayer films, struct. determ. by electron microscopy and X-ray diff. 9-39349
titanates, crystallization under hydrothermal conditions 9-37044
zirconates, crystallization under hydrothermal conditions 9-37044
BiFeO $_3$ -Pb(Fe $_x$ Nb $_{1-x}$) $_3$ solid solution, spontaneous magnetic moment by neutron diffraction 9-33482
In (3.9 at.%)Pb alloy, type I-II supercond. transition obs. 9-47089
In (2 at.%)Pb superconducting, type-I, films, flux-flow noise determ. 9-24152
Pb $_{1-x}\text{Zr}_x\text{TiO}_3$ transducer ceramic, mechanical loss, large amplitude static and dynamic stress effects. 9-39397
Pb-(0/25 wt.%)Bi, superconducting, surface-sheath nucleation field, temp. depend. 9-35366
Pb-Bi alloys, d.h.c.p. phase form under h.p. 9-44802
Pb-Bi eutectic, drop on stainless steel, surface tension and contact angle calc. from shape 9-34867

Lead compounds continued

- Pb-Ge chalcogenide alloys, solid solution range, and optical props. 9-30721
Pb-(10wt.%) In alloy, powder, type II supercond., flux pinning by oxide film coating 9-49045
Pb-In alloys, specific heat in normal and superconducting state 9-33182
Pb-In superconducting alloys, critical field and generalized Ginzburg-Landau parameter κ_2 determ. 9-24156
Pb-In superconducting alloys, second generalized Ginzburg-Landau parameter, temp. dependence 9-24157
Pb-In system, surface tension, temp. and conc. depend. 9-23471
Pb-Na solid solns., discontinuous precip., Ag effect 9-39500
Pb-(8.2 wt.%)Na solid solns., precip., three mechanisms 9-35210
Pb-Sn-Te system, phase diagram 9-36918
Pb-Sn alloy electrodes, electrochem. behaviour in different solns., corrosion resistance and passivation mechanism 9-33673
Pb-Sn alloys, absolute viscosity as function of temp. and composition 9-30378
Pb-Sn alloys, liq., stress cracking of Cu and alloys 9-48941
Pb-Sn liquid alloy, Knight shift calc. from pseudopotential formalism 9-23532
Pb-33wt%Sn, solder, effective atomic numbers for gamma interacts. 100-662 keV 9-24230
Pb-33 wt% Sn, effective atomic number for pair prod, for γ energy 2.6-17.6 MeV 9-24232
Pb-SnTe alloy system, magneto-optical effects, band struct. and cyclotron reson. obs. 9-39807
Pb-(1.6wt.%)Ti superconductor, type II, rectangular flux line lattice 9-28479
Pb-Tl alloy, superconducting, fluxons, nucleation and propagation in thin cylindrical specimens 9-44933
Pb-Tl dilute solid solutions, vibrational entropy, electronic influences 9-39508
 β -Pb $_{0.193}\text{V}_{0.807}\text{O}_8$, monoclinic, crystal struct. and space group determ. 9-28267
Pb $_{0.7}\text{In}_{0.3}$ -GaAs:Zn junction, supercond. tunneling effects, ang. depend. in mag. field 9-43044
Pb $_{0.88}\text{Sn}_{0.12}$ Te diode lasers, quantum-phase-noise limited Lorentzian power spectral densities 9-43898
Pb $_{0.92}\text{Bi}_{0.08}$ or $\text{La}_{0.01}(\text{Fe}_{0.405}\text{Nb}_{0.325}\text{Zr}_{0.27})\text{O}_3$, ferroelec., props. 9-35487
Pb $_{1-x}\text{Sn}_x\text{Se}$, semicond., laser emission rel. to energy band crossover, obs. 9-48045
Pb $_{1-x}\text{Sn}_x\text{Se}$ diodes, mag. field depend. of i.r. laser emission 9-41922
Pb $_{1-x}\text{Sn}_x\text{Te}$, band structure from Hall effect and Seebeck coeff. hole conc. dependences 9-39632
Pb $_{1-x}\text{Sn}_x\text{Te}$, emission in mag. fields, band struct. obs. 9-41406
Pb $_{1-x}\text{Sn}_x\text{Te}$ single crystals, metallic inclusions and cellular substructure by electrolytic etching 9-30569
Pb $_{1-x}\text{Sn}_x\text{Te(Se)}$, laser action and photoelec. 9-38386
Pb $_2\text{Ti}_2\text{O}_7\text{F}_2$ pyrochlore, X-ray diff. pattern 9-40914
Pb $_2\text{MgNb}_2\text{O}_9$ -Pb $_2\text{NiNb}_2\text{O}_9$ system, dielectric loss and internal friction 9-28564
Pb $_{40}\text{Ti}_6$ phonon spectrum by tunneling and n. scatt. meas. 9-26413
Pb $_{55}\text{Ni}_{45}\text{Te}$ alloy system, relationship between lattice constant, alloy fraction and stoichiometry 9-35065
Pb alloys, superconducting, preparation, patent 9-24158
Pb complex, lead (II) O,O-diisopropylphosphorodithioate, cryst. struct and bonding 9-42794
Pb (Sc $_{1/2}\text{Nb}_{1/2}$) $_2$ -TiO $_3$ system, ferroelec. and structural props. 9-28563
Pb zirconate-titanate ceramics, optical and electrooptical properties, improvements 9-35485
PbBr $_2$ photoconductivity at liq. N $_2$ temp. 9-39721
PbBr $_2$ crystal structure 9-39299
PbCl $_2$, adsorption in NaCl pellets 9-48771
PbCl $_2$ photoconductivity at liq. N $_2$ temp. 9-39721
PbClBr(I), crystal structure 9-39299
PbF $_2$ -AlF $_3$ system, phase diagram, DTA and X-ray powder obs. 9-44805
PbFe $_{0.5}\text{Nb}_{0.5}\text{O}_3$, spontaneous magnetoelec. eff. 9-28596
PbFe $_{0.5}\text{Nb}_{0.5}\text{O}_3$ props. over wide temp. and freq. range 9-41243
PbFe $_2(\text{VO}_4)_2(\text{OH})_2$, mounanaite, X-ray powder obs. 9-32925
PbI $_2$, electro-reflection meas. 9-47324
PbI $_2$, electroabsorption in exciton region 9-33539
PbI $_2$, nucleation and growth in gels 9-37029
PbI $_2$, polytypism 9-46742
PbI $_2$ photosensitive films, holographic recording 9-38390
PbMn $_{0.3}\text{Nb}_{0.7}\text{O}_3$ 9-28596
PbMoO $_4$:Np $^{4+}$, energy-level scheme for Np $^{4+}$ 9-31110
PbMoO $_4$ crystalline, melt grown, acousto-optic device applic. 9-49254
Pb(N $_3$) $_2$, spontaneous explosion during growth 9-37040
 α -Pb(N $_3$) $_2$ crystal structure by neutron diffraction 9-39300
 β -PbN $_6$, explosion initiation by collapsing air bubble 9-28788
PbO-B $_2\text{O}_3$ system glasses, spinodal decomposition 9-39492
PbO-Cr $_2\text{O}_3$ -O $_2$ ternary system, phase relations and reactions at high temps. 9-28405
PbO-GeO $_2$ glass system with 0 to 55 mol % PbO, reflection and Raman spectra 9-28675
PbO-SnO mixed cryst. layers, photoconductivity 9-41269
PbO, yellow, optical absorpt. and photocond., in polarized light 9-49284
PbO $_2$, polymorphs, stability of high-pressure phases, effect of neutron irradiation 9-35250
PbO evaporated thin films, diffusion of Bi, autoradiographic obs. 9-26303
PbO layers, vapour-deposited, photoconductivity, photoemission and band struct. obs. 9-39722
PbO single crystals, hydrothermal growth and phase width 9-37041
PbO $_2$ -6Fe $_2\text{O}_3$ ferromagnet, uniaxial, domain struct. hysteresis 9-41311
PbP-SiO $_2$ system, crystallization sequences in silica phase 9-26390
PbRe, bandstructure, parameters from optical reflectivity, transmission and Faraday effect 9-39630
PbS-PbTe system, spinodal decomposition 9-39941
PbS, band structure and scattering mechanism from transport props. meas. 9-39631
PbS, conductivity and luminescence induced by intensive electron bombardment, 300°K 9-39093
PbS, dipole moment from Stark components of microwave rotational transitions 9-30051
PbS, optical absorption, direct-transition, from relativistic augmented-plane-wave functions 9-41387
PbS, Raman scatt. from single-particle excitations of carriers, charge-density and spin-density fluctuations contribs. 9-47375

Lead compounds continued

PbS, spin-flip Raman scattering by carriers 9-35674
 PbS (100) surface, O₂ chemisorption 9-39949
 PbS diode, stimulated recombination radiation 9-33595
 PbS epitaxial film growth on rocksalt by condensation in vac., formation mechanism 9-40844
 PbS epitaxial films, photosensitivity mechanism 9-49161
 PbS film, absolute quantum yield due to internal photoelec. effect 9-33410
 PbS polycrystalline film, prod. of photosensitive centres, photocond. props. meas. 9-37615
 PbS polycrystalline film, photocond. rel. to chemisorption of O 9-37622
 PbSO₄:Sm(Ce) luminescence centres investigated 9-33594
 PbSO₄-BaSO₄-SrSO₄ 9-23949
 PbSe, band structure and scattering mechanism from transport props. meas. 9-39631
 PbSe, characteristic electron energy losses 9-39553
 p-PbSe, electrical props., depend. on carrier density and temp., indication of two valence bands 9-35409
 PbSe, optical absorption, direct-transition, from relativistic augmented-plane-wave functions 9-41387
 PbSe, Raman scatt. from single-particle excitations of carriers, charge-density and spin-density fluctuations contribs. 9-47375
 PbSe, relativistic band structure 9-39629
 PbSe, spin-flip Raman scattering by carriers 9-35674
 PbSe as-grown single cryst., transmission electron microscope obs. 9-46792
 PbSe epitaxial films, field effect meas. at 30 Hz-70 kHz small and large signal meas. 9-41190
 n-PbSe epitaxial films, layered distrib. of charge carriers from transverse magnetoresistance meas. 9-42996
 PbTe:⁵⁷Fe, Mossbauer obs. of Fe ions 9-39819
 PbTe:(In,La), Mossbauer effect of ¹²⁵Te, depend. of probability on degree of doping 9-39820
 p-PbTe-CdTe alloy, scattering of light-mass holes from magnetoresist. meas. 9-41206
 PbTe-CdTe alloys, phase equilibria 9-42923
 PbTe-EuTe system, investigation by thin film techniques 9-39486
 PbTe, ¹²⁵Te Mossbauer emission spectra following thermal neutron capture in ¹²⁴Te 9-37703
 PbTe, absorption of polar mols. rel. to surface charge distrib. exam. 9-39173
 PbTe, band structure and scattering mechanism from transport props. meas. 9-39631
 PbTe, characteristic electron energy losses 9-39553
 PbTe, diffusion coeffs. of Pb and Te 9-44744
 PbTe, epitaxial growth on NaCl, substructural transitions in early stages 9-26186
 n- and p-PbTe, Fermi surface shape and Landau level splitting rel. to carrier conc. 9-28506
 PbTe, fund. energy gap, press. coeffs. 9-33317
 p-PbTe, Knight shifts and band structure by helicon-nuclear-spin interaction 9-39910
 n-PbTe, magnetoplasma effects, local and non-local 9-47059
 PbTe, n- and p-types, prep. of low conc. high mobility mats. 9-39624
 PbTe, optical absorption, direct-transition, from relativistic augmented-plane-wave functions 9-41387
 p-PbTe, oscillatory magnetoresistance, effective mass of holes calc. 9-44967
 PbTe, Raman scatt. from single-particle excitations of carriers, charge-density and spin-density fluctuations contribs. 9-47375
 PbTe, relativistic band structure 9-39629
 PbTe, relativistic band struct. and electr. props. 9-43057
 PbTe, rot. spectrum, 11-15 GHz 9-48478
 PbTe, thermoelec. material, chemical compatibility with alloys 9-26808
 PbTe, valence band structure 9-39633
 PbTe epitaxial deposits on rocksalt, growth and morphology 9-37113
 PbTe epitaxial films, field effect meas. at 30 Hz-70 kHz small and large signal meas. 9-41190
 PbTe in inert gas, lowering of evaporation rate 9-32817
 PbTe polycryst. layers, elec. surface props. 9-33325
 PbTe spin-flip Raman scattering by carriers 9-35674
 PbTe thick layers, transport props. and optical transparency, heat treatment effects 9-39625
 Pb(Ti_{1-x}Zr_x)O₃, PbO vapour pressure meas. 9-23609
 PbTiO₃-LaFeO₃ solid solns, magnetic props. 9-39784
 PbTiO₃-PbZrO₃-PbMgO₃-W₂O₃ solid solns., piezoelec. props. 9-47188
 PbTiO₃, c.s.r. studies of Fe³⁺ at Q band and 70GHz 9-45389
 PbTiO₃, low temp. phase transitions 9-43119
 PbTiO₃ ferroelec. transition, Pippard scheme for sp. ht., thermal expansion and isothermal compressibility 9-30970
 PbTiO₃ glass-ceramics, composites for homogeneous crystn. 9-46941
 PbTiO₃-PbMgWO₃-PbZrO₃ solid solns., permittivity in static fields, 20 kV/cm max. 9-43103
 Pb(UO₂)₂(VO₄)₂·5H₂O, curienite, analysis rel. to francevillite, cry. struct., props. 9-37147
 Pb(Zr,Ti)O₃ piezoelectric ceramic, adulterated, high-field losses 9-26585
 Pb(Zr_{1-x}Sn_x)TiO₃ ternary system, electrostriction constants during antiferro-ferroelectric phase change 9-24222
 PbZr_{1-x}Ti_xO₃, perovskite ferroelec., atomic struct. for x=0.9, 0.58, X-ray and neutron diff. obs. 9-44673
 PbZrO₃, antiferroelec.-paraelec. transform., effect of hydrostatic press. 9-44790
 PbZrO₃, antiferroelectric, dielec. props. over wide temp. and freq. range 9-41243
 PbZrO₃, antiferroelectric domain structures 9-35492
 PbZrO₃, enthalpy changes in dielectric transitions, impurity eff. 9-26584
 Pb-(0.56.Sat.%)Bi superconducting alloys, type I and II, rel. to mag. behaviour 9-43041
 Pb(La_{0.8}(Nb⁵⁺)_{0.2})_{1-x}Ti_xO₃ ceramics Ferroelec., dielec., piezoelec. and struct. props. 9-24220
 Pb(La_{0.8}(V⁵⁺)_{0.2})_{1-x}Ti_xO₃ ceramics, ferroelec., dielec., piezoelec., and struct. props. 9-24220
 Sn-Pb, dilute alloys, electropolishing procedure to produce etched or polished surfaces 9-39959
 Sn-(1.0-5.0wt.%)Pb alloys, Sn dendrite growth as function of supercooling 9-48815
 Ti-Pb-Bi alloys, superconductivity from tunneling meas. 9-24161
 Zn-Pb alloys, liquid, density meas. up to 700°C 9-30375

Leak detection

No entries

Leather *see* **Materials****Lee model** *see* **Field theory, quantum**

LEED *see* **Electron diffraction**; **Electron diffraction crystallography**; **Electron diffraction examination of materials**

Length measurement

see also **Micrometry**; **Strain gauges**; **Thickness measurement**
 astrometric study of BD+20°2465 flare star, comparison of two measuring machines 9-31522
 on comparator principle 9-25023
 dilatometer, capacitance type for low temp. thermal expansion meas. 9-42970
 dilatometer, optical lever, for low temp. use 9-26429
 films of bubble chambers, equipment with image plane digitizers 9-48230
 interferometry of parallel end standards to 1m 9-41731
 laser interferometry, industrial applications 9-45967
 laser range finder, stabilization system, patent 9-41924
 laser rangefinder design and application 9-36106
 lunar range, laser meas. to corner reflector 9-33927
 measuring base, 12m, length stabilized 9-34002
 nylon 66 yarns, drawn, shrinkage on annealing 9-46707
 particle size, analysis and analyzers 9-26378
 position sensing, digital, using photoelec. linear meas. system 9-25022
 proximity gauge, capacitive 9-25021
 Venus, radar time-of-flight obs. 9-27082
 Co-Ni alloys, transform. kinetics, dilatometric meas. 9-37298
 He liq. depth, gauge design using carbon resistor sensing elements 9-31760

Length standards *see* **Standards**

Lennard-Jones and Devonshire theory *see* **Liquids/theory**

Lennard-Jones potential *see* **Kinetic theory**; **Molecules/intermolecular mechanics**

Lenses

see also **Electron lenses**

56mm bifocal with crescent-shaped reading portion 9-48081
 aberration balancing merit function in automatic design, use of modulation transfer function 9-45980
 aberrations, primary, single, positive systems 9-29450
 acoustic, fluid, Luneberg-Gutman, wave analysis 9-29297
 acoustic, imaging charact. 9-36196
 acoustic, underwater, nearly spherical, low aberration 9-27233
 cemented with epoxy resins, spots 9-36343
 ceramic, for control of u.s. energy 9-36195
 diffraction apertures, cascaded, focusing of e.m. waves 9-29345
 doublet, cemented, glass type selection 9-25348
 eye, refr. index distrib. 9-47702
 eye contact, hard and soft, ocular deformation effects 9-36084
 eyepieces, symmetric with improved aberration correction 9-36339
 flat-field microscope objectives 9-36341
 focometer, circular ray paths 9-27372
 focons, hollow, illumination characteristics 9-34191
 fogging, effect 9-36342
 Fresnel, astigmatism, expression 9-27371
 gaseous, optical mode conversion due to fluctuations of dielec. constant 9-43912
 ideal, in coherent optical systems, Fourier transform representation and approximations 9-45981
 magnetic, optical props., H hyperfine state selection 9-29979
 magnetic, quadrupole, appl. to beam matching 9-41875
 microobjectives, lathe for parafocality setting 9-34192
 microscope objectives, image performance testing and optical transfer function meas. 9-46013
 for pupil, correction apodization problem 9-46001
 relay f/3, 245 mm, high resolution design 9-41938
 rotationally symmetric, maximum modulation transfer function 9-29453
 single, positive systems, primary aberrations 9-29450
 spherical surfaces, polished, curvature radius meas. by autocollimating device 9-36340
 superconducting, for 500-kV electron microscope column 9-36258
 surface deformation due to temp. image quality variation theoretical soln. 9-29451
 surface testing, non-contacting interferometer 9-34203
 testing, optical transfer functions meas., digital computer applic. 9-31997
 testing, spot diagram generator 9-22467
 thermal focussing of light beams, steady-state solutions 9-41937

aspherical
 laser beam concentration system 9-25313

photographic
 evaluation, use of crossed cylinder lens 9-32079
 focal length and flange focal distance, electronic meas. 9-46033
 objectives, flare 9-38420
 triplet objectives, spherical aberration calc. 9-31999

Leptons

see also **Electrons**; **Mesons**; **Muons**; **Neutrinos** and **antineutrinos**
 annihilation nonperturbative sum rule, e.m. current constituents and anomalous commutators 9-27463
 Clifford algebra eqn., reduction to Dirac-type form 9-48156
 Dirac eqn. in de Sitter space, group theory derivation 9-32129
 e.m. props., eff. of weak interactions on anomalous mag. mom. and H Lamb shift 9-38464
 fermions, massless, neutrino exchange scatt., coupled channel case 9-32131
 heavy, existence; theor. and expt. evidence 9-27462
 interactions, weak and electromagnetic, symmetry 9-43970
 invariance of weak and e.m. interac. under U(2)×U(2) 9-22551
 lepton-antilepton annihilation, production of $\Lambda^0\Sigma^0$ and $\Lambda^0\Sigma^0$ hyperon pairs 9-29616
 lepton-lepton weak interactions, effects 9-43969
 lepton-nucleon scatt., asymptotic sum rules at infinite momentum 9-38566
 lepton-pair scatt. amp. from hadrons, minimal current algebra applic. 9-27449
 magnetic moments, contrib. from leptonic boson by Yukawa-type interaction 9-34254
 neutrino (massless) exchange in high energy scatt. 9-32130
 pair production by high energy neutrinos in field of strong e.m. wave 9-29546

Leptons continued

- polarization in K_{β} decay, radiative corrections calc. 9-44010
 strange leptons assumed to avoid violation strangeness conservation 9-34260
 Sugawara model, fermion avatars 9-38463
 symmetry and self mass 9-43970
 $e-\mu$ universality, alternative form applic., of CP violation in $K \rightarrow \pi\mu(e)\nu$ in distinguishing bet. forms 9-38465
 $\Lambda^0 \Sigma^0$ pair production from lepton-antilepton annihilation 9-29616
 $\Lambda^0 \Sigma^0$ pair production from lepton-antilepton annihilation 9-29616

Lie groups see *Group theory. For applications see Elementary particles; Field theory, quantum*

Ligands see *Bonds; Molecules*

Light

- see also *Diffraction; Interference, etc.; Doppler effect; Radiation*
 beam focussing by thermal lenses, steady-state solutions 9-41937
 beams, self-focusing in nonlinear medium 9-25335
 crystal, propag., irreversibility rel. to magnetoelec. effect 9-43218
 deflection in Schwarzschild field 9-27169
 disturbing signals in rapid flash kinetic meas., suppression 9-26834
 ferroelectric, interaction with spin waves 9-26588
 filaments, self-trapping interpretation, liquids 9-28125
 forerunner formation during traversal of vacuum-medium interface by pulse front 9-29462
 Gaussian, clipped photon-counting fluctuations, spectrum 9-31990
 gravitational deflection and Snell's law, corpuscular theory 9-29155
 impulse, excitation of detonation of liq. explosives 9-31855
 nuclear properties, discovery 9-27459
 propagation, Born and Rytov approx., accuracy and validity 9-43913
 propagation, distortionless, through optical medium 9-25334
 propagation, influence of gravitational field 9-22080
 propagation in medium with random refractive index inhomogeneities in Markov random process approx. 9-41939
 propagation of narrow beam in scattering medium adjoining reflecting surface 9-29460
 pulse, propagation in semi-infinite isotropically diffusing medium 9-22447
 pulses, energy measurement, use of black body type calorimeters 9-34106
 ultrashort pulse recording 9-27359

coherence

- see also *Lasers*
 of beam passing through nonabsorbing layer, rel. to thickness and wavelength 9-41940
 cavity with nonlinear crystal, 2nd harmonic generation, coherence and saturation props. 9-22374
 degradation in random media 9-22366
 degrees of freedom of image effect of coherent illum. 9-48083
 detection of incoherent objects by a quantum limited opt. system 9-45982
 diffraction images of coherently illuminated objects 9-34207
 equivalence theorem, reformulation in terms of Laguerre polynomials 9-47920
 field in random medium, effective refr. index 9-27257
 fields, weakly and strongly coherent, rel. to monochromatism 9-27291
 fourth-order function, propag. in homogeneous isotropic random medium 9-25199
 function, 4th order, propag. in random medium 9-45988
 generation by lasers under pulsed and continuous regimes 9-29402
 heterodyne technique for phase and amplitude sampling, laser beam probe 9-48073
 high-resolution spectral analysis 9-29392
 information processing applic. 9-48064
 rel. to laser amplification, semiclassical theory comparison with expt. 9-43874
 laser radiation with known spectral characts., coherence characts. 9-48054
 lossy media, higher order coherence function propag. 9-35608
 mixed thermal and coherent radiation, twofold joint photocount statistics 9-45940
 optical system design for quasi-monochromatic partially coherent illumination 9-25343
 partial, effect on modulation transfer function meas. for small slit 9-48084
 partial, Fresnel holography 9-45975
 partial defocus correction of optical system 9-29455
 partially coherent-radiation scatt. by discrete scatterers, Heisenberg operator determ. of intensity 9-34152
 photon beam, experimental meas. 9-27290
 pulsed coherent radiation, self-induced transparency obs. 9-43863
 pulsed laser radiation, effects 9-41923
 in semiconductors, self-transparency effect caused by ultra short pulse 9-49252
 spatial filtering and freq. modulation in photography of phase objects 9-43932
 Stokes parameters and coherence matrix, unified treatment of algebra 9-40336
 surface harmonic generation from non-linear polarisation 9-29427
 theory, classical and quantum 9-22305
 theory and research in Italy 9-25200
 ultrashort pulse propag. in medium with two-photon reson. absorpt. 9-29391
 ^{199}Hg source, photon time-of-arrival distrib. obs. 9-27292
 GaAs injection laser rel. to intensity distrib. of radiation emitted by resonator 9-45965
 GaAs laser diode emission, spatial coherence 9-43897
 GaAs laser parallelepiped, 5-cm., interference of 10.6 μ coherent radiation 9-43896
 SF₆ gas, transmission of coherent optical pulses 9-46574

electromagnetic theory

- beam, strong, slowly diverging in optically laminated nonuniform medium 9-43911
 diffraction, self-focussing, self-action in nonlinear medium 9-25351
 Gaussian beam fluctuations in random medium, correls. 9-45987
 reflection, total, role of lateral wave 9-45989
 TE-wave in nonlinear media, steady-state self-channeling 9-37676
 wave theory and its applications, textbook 9-40227

modulation

- a.m., by u.s. plane wave, theory and expt. 9-32021
 birefringence, piezo-optical effect application 9-46007
 Debye-Sears fused-silica wideband spatial modulator 9-27366

Light continued**modulation continued**

- electro-optic, multicrystal structure, patent 9-40374
 far i.r., ionization 9-36334
 h.f., by u.s. progressive waves 9-34187
 i.r. beam control, data for crystallochemical selection of materials 9-38394
 laser, ruby, u.s. modulation 9-48072
 laser beam, amplitude and/or phase, spectral analysis, holographic method 9-25330
 laser beam, differential detector with solid state devices 9-29446
 laser beams, modulation and demodulation 9-40373
 laser modulation and control by means of intra-cavity time varying perturbation 9-27298
 lens, rotationally symmetric, maximum modulation transfer function 9-29453
 light modulators, linear spatial filtering 9-48075
 optical heterodyne detection, randomly distorted signal beam 9-31987
 optical pulse generator, patent 9-41935
 optimum modulation shape for specific pulse characts. of a photoresistor 9-41933
 p.c.m. laser, increase of information capacity 9-36317
 phase, for hologram interferometry 9-48089
 phase, of liquid trapped laser beam filaments 9-25329
 propagation of modulated light in semi-infinite scattering medium 9-38395
 pulse generator using electrooptic switch, variable width in subnanosecond range 9-36333
 radiation chopper, operation analysis, calculation of amplitudes 9-25336
 Rochelle salt, application from electro-optical effect 9-43216
 second order, of transversal beam by mag. reson. in Na orientated vapour 9-22438
 sinusoidal, visual response rel. to spectral composition 9-33972
 submarine viewing situation, modulation transfer function dependent on range and seawater properties 9-30404
 transfer function for opt. wave in turbulent medium 9-44527
 transfer function of optical system, colour correction 9-22445
 variable frequency modulator for u.s. stroboscopes 9-46012
 Ar laser, super-mode f.m., monochromatic generation at 5145 Å 9-27317
 CO₂ laser modulation by GaAs at 10.6 μ 9-37691
 CS₂ Kerr cell application to lasers 9-36285
 CO₂ laser amplifier, a.m., 1 kW average power 9-25253
 GaAs Gunn-effect modulator 9-33552
 GaP photodiode characts. 9-39651
 KD₂PO₄, using transverse electro-optical effect in crossed rods, obs. 9-33516
 KH₂PO₄, 45° Z cut, and isomorphs 9-35620
 KH₂PO₄, using transverse electro-optical effect in crossed rods, obs. 9-33516
 LiNbO₃, modulator of i.r., quality factor 9-34190
 NH₄H₂PO₄, using transverse electro-optical effect in crossed rods, obs. 9-33516
 NH₄H₂PO₄ crystal for modulating beam of He-Ne laser, design of production model 9-31988
 RbH₂PO₄, using transverse electro-optical effect in crossed rods, obs. 9-33516
 YFe garnet magneto-optical effect 9-36335
 ZnS, travelling wave, improved efficiency, 40 MHz to 15 GHz 9-27362
- quantum theory** see *Photons; Quantum electrodynamics; Quantum theory*
- velocity** see *Velocity/light*
- Light guides** see *Optical instruments*
- Light modulation** see *Light/modulation*
- Light sources**
 see also *Lasers; Monochromators; Photometry/light sources; Spectroscopy/light sources*
 5MW 2ns super radiant, for use with electron accelerator, photography 9-48124
 1500-2700 Å spectral range, calibration with synchrotron radiation 9-36380
 arc. lamp cathodes l.p. high-current energy balance 9-48640
 cathodoluminescent tube, sulphide applications 9-33609
 differential light fluxes, automatic polar recording photogoniometer 9-22474
 flashlamp for laser pumping, time-resolved spectroscopy 9-29483
 flashlamp for organic dye lasers pumping 9-48005
 Garton flash tube 9-30313
 gas lasers with grating for highly polarized output in far infrared 9-47957
 intensity control for u.v. spectroscopy 9-43931
 laser, giant-pulse ruby, for high-speed aeroballistic range photography 9-46035
 laser, mode-locked, for Schlieren photography 9-48125
 laser, pulsed, for high-speed photography 9-46034
 laser, repetitive Q-switched, for interferometry and holography 9-29476
 laser beam, second harmonic and parametric generations 9-25331
 for long-distance i.r. flash photography 9-32074
 noise field, photo-bunching effects, enhancement 9-34153
 oceanographic strobe with pressure-equalized electronics 9-36381
 parametric generators, freq. tuning in green range 9-27361
 pulsed discharge, efficiency optimization 9-32042
 self-absorbing, spatial resolution of volume emission coeff. 9-32040
 spectrophotometry with tilting-filter photometer 9-36367
 stimulated, total power from GaAs junction lasers, temperature dependence 9-48040
 vacuum monochromator, scattered light, measurement and elimination 9-34230
 Ar h.p. 20 ns spark channel, radiance saturation and afterglow emission 9-30314
 Ba₂NaNb₃O₁₅, 0.53 μ m source, continuous, in 1.06 μ m YACG:Nd laser cavity 9-40362
 GaAs:Ge, p-n junction, reverse-biased, emission charact. 9-49332
 He h.p. 20 ns spark channel, radiance saturation and afterglow emission 9-30314
 Hg lamp, red spectrum improved by addition of various substs., patent 9-22475
 Hg PRK-4, brightness, 300-1000 μ 9-27404
 K-Hg discharge lamp for optical pumping YAl garnet:Nd 9-25201
 Kr lamp, pumping of YAl garnet:Nd laser for 105 W output 9-48033

Light sources continued

- Si diodes, anode-cathode space plasma, emission during second breakdown 9-39652
- Ti getter for u.v., Hinteregger-lamp improvement 9-32041
- W filament lifetime under constant-current heating 2000° to 2950°K 9-34222
- W strip lamp spectral radiance standard 9-25377
- Xe flash tubes, performance analysis 9-32043

Lighting *see Illumination***Lightning**

- ball, microwaves generation 9-43402
- ball, motion in electrostatic field 9-35826
- characteristics determined from e.l.f. atmospheres 9-28893
- discharge, nucleation of ice crystals, shock waves and adiabatic cooling 9-26908
- discharges, audio frequency pressure variations 9-37921
- e.m. radiation, review of Japanese developments since 1963 9-37925
- erratic paths, l.f., radiation 9-45497
- linear, radio emission in decimeter range 9-43403
- multiple stroke, v.l.f. radiation from subsequent return strokes 9-37922
- point discharge, pulse tech. for meas. using electrodes capacitively coupled with spruce tree 9-45496
- return stroke, spectroscopic study, high speed, time resolved, qualitative analysis 9-26909
- return stroke, spectroscopic study, high speed, time resolved, time-dependent model 9-26911
- return stroke, spectroscopic study, high speed, time resolved, quantitative analysis 9-26910
- r.f. noise, and sources distrib., Ariel III obs. 9-49457
- spectra, split, stroke and space resolved 9-41537
- stroke height from ionospheric reflections 9-37924
- temperature calculation 9-31328
- undergraduate reference book 9-41536

Linear accelerators *see Particle accelerators/linear***Linewidths** *see Spectral line breadth***Liouville equation** *see Statistical mechanics***Liquefaction, gases**

- see also Low-temperature production*
- mixture expansion, causing heavier components to liquefy, permeating through wall, at supersonic veloc. 9-26163
- Ne-He mixture, separation 9-23590
- O₂, apparatus 9-24993

Liquid crystals

- p-azoxyanisole, nematic, thermal fluctuations identified by Rayleigh laser scatt. 9-40793
- p-azoxyanisole, nematic mesophase, perturbation of order by second component, e.s.r. study 9-42633
- p-azoxyanisole, optical rot. and electro-optic effect 9-30405
- p-azoxyanisole, trans. light temp. depend. and electro opt. eff., nematic mesophase obs. 9-26112
- p-azoxyanisole, X-ray structure study in alternating elec. fields 9-42634
- p-azoxyphenetole, 100 cm⁻¹ absorption band 9-34913
- benzene, n.m.r. shift and quasicryst 9-30432
- Brillouin scattering 9-46644
- capillary flow of smectic and cholesteric liq. crystals 9-48671
- cholesteric, anisotropic, energy of disclination line, orientation depend. 9-39078
- cholesteric, capillary flow 9-48671
- cholesteric films, optical props. 9-39103
- cholesterol, texture, rel. to domain occurrence 9-40774
- cholesterol benzoate, pyrene fluoresc. decay time rel. to cryst. phases, obs. 9-32786
- cholesterol derivatives, elec. field induced orientation and solute mols. optical absorpt. 9-34876
- cholestry-2-(2-ethoxyethoxy) ethyl carbonate, Brillouin scatt. 9-46644
- 4,4'-dihexyloxybenzene as solvent in i.r. spectroscopy 9-48682
- electro-optical effect obs. 9-28127
- fluorinated Schiff base, molec. config. and order from n.m.r. 9-28159
- fluoromethanes, partially oriented, proton and ¹⁹F n.m.r. 9-30434
- 4,4'-di-n-heptyloxyazobenzene smectic mesophase, solute e.p.r., obs. 9-32796
- i.r. absorption spectrum effect 9-34913
- mesophase transition obs., depolarized light intensity and optical microscopy 9-32764
- methyl halides, n.m.r. chem.-shift anisotropy in liq. cryst. solvents 9-38903
- methyl halides in liq.-cryst. solvents, chem. shift anisotropy 9-44599
- for molecule orientation in polarized i.r. spectroscopy 9-44336
- molecules oriented, polarized electronic spectroscopy 9-46349
- nematic, distortion of cholesteric structure by magnetic field 9-32794
- nematic, e.s.r. of spin-labelled nematogenic probes 9-44588
- nematic, heat conduction and dissipation, linear theory 9-39077
- nematic, NMR of dissolved ethyl fluoride obs. 9-40613
- nematic electric polarization, and curvature strain, reln., piezoelectric theory 9-28148
- nematic mesophase, perturbation of order by second component, e.s.r. study 9-42633
- partially oriented, twisting theory 9-36847
- polymer diluent, role in anisotropic plastic material production 9-26078
- potassium oleate in D₂O soln., n.m.r. meas. on smectic phase 9-40775
- smectic, capillary flow 9-48671
- surface waves, struct. and dispersion 9-39076
- terephthalbis(aminofluorobenzene), molec. config. and order from n.m.r. 9-28159
- for thermographic mapping of semiconductor junctions, techniques 9-37555
- vinyl oleate, mesophases, n.m.r. obs. 9-46659

Liquid flow *see Flow/liquids***Liquid helium** *see Helium/liquid***Liquid lasers** *see Lasers/liquid***Liquid metals**

- alkali, isothermal compressibility and structure function determ. 9-23465
- alkali, plugging meter, exptl. continuous- indication, for impurity monitoring 9-24991
- alkali, thermoelectric powers, changes at melting point 9-40802
- boiling, transient analysis rel. to fast reactor safety 9-39142
- in conduction MHD machine with flow branching, potential distrib. and e.m. head 9-27268

Liquid metals continued

- cylinder, radial oscillations induced by const. and alternating mag. fields 9-25828
- duct cooling, thermal contact resistance, impurities effect 9-39093
- electrical conductivity, neutron diff. studies 9-48680
- electron transport, Boltzmann eqn. 9-48713
- electron transport, wave function model 9-48714
- flow in circular pipe, velocity profile with and without mag. field 9-25827
- impurity states, localized, magnetic susceptibilities 9-28150
- isotope thermodiffusion constants 9-23472
- MHD channel flow, resistance rel. to laminar/turbulent transition 9-27962
- neutron diff. studies, connection with elec. conductivity 9-48680
- statistical correlation on transfer phenomena 9-39085
- structural similarities deduced from classification system 9-44545
- structure and props., theoret. exam 9-46611
- structure studies by means of X-ray, n and e diffraction 9-36846
- thermopower, temp. depend. 9-39110
- transition metals, electron transport, wave function model 9-48714
- ultrasound excitation by electrodynamic excitation 9-23492
- u.s. attenuation, dense-gas formulation 9-34902
- u.s. velocity and obs. 900-1000°C 9-30395
- volume diffusion coeffs. rel. to equilib. charact. 9-39131
- v.p. determ., encapsulation technique 9-32820
- Ag, surface tension, 1300-2200°K 9-28110
- Al, solubility of AlP, 900-1200°C 9-30372
- Bi, nuclear spin-lattice relax. of ²⁰⁹Bi 9-26134
- Bi, surface tension, 1300-2200°K 9-28110
- Bi and Cd, partial diffusion coeffs. from conc. meas. in zone of contact liq. layer, rel. to Darken formula 9-33003
- Bi and Sn, partial diffusion coeffs. from conc. meas. in zone of contact liq. layer, rel. to Darken formula 9-33003
- Cd, density of states, model-potential calc. 9-26131
- Cs condensed phase, temp. up to 1200°K, elec. conductivity 9-26130
- Fe, absorpt. of N from a plasma 9-46455
- Fe, diffusion of S and O at 1560°C 9-48691
- Fe, vapour pressure 9-23604
- Ga, nuclear spin-lattice relax. of ^{69,71}Ga 9-26134
- Ga, resistance coeffs. for laminar flow through diffuser in crossed fields 9-27968
- Ga, thermal expansion meas. by liq. Ga immersion dilatometer, rel. to anharmonic effects 9-47007
- Ga, X-ray scatt. obs. over wide temp. range 9-30371
- Ga foils, plasma oscillations 9-41148
- Hg-Ga system, (0.96 and 0.02 mole fraction Hg) radial distrib. and scatt. functions, co-ord. numbers, by X-ray scatt. 9-28100
- Hg-In alloys, volume change on formation, and thermal expansion coeff. 9-28115
- Hg, self-diffusion coeff. 9-42643
- Hg, structure, X-ray diff. obs. 9-32762
- Hg, thermal expansion, 50-700°C, liq. Ga immersion dilatometer meas., rel. to anharmonic effects 9-47007
- Hg, u.s. attenuation, dense-gas formulation 9-34902
- Hg surface waves, influence of axial magnetic field 9-30358
- In, density of states, model-potential calc. 9-26131
- In, n.m.r. of ¹¹⁵In, Knight shift and spin-lattice relax. rate temp. dependence 9-23534
- In, nuclear spin-lattice relax. of ¹¹⁵In 9-26134
- K-Cs binary alloys, electron spin susceptibilities, Knight shift 9-39116
- K-Rb binary alloys, electron susceptibilities, Knight Shift 9-39116
- K, incipient boiling superheat meas. 9-26165
- K, self-diffusion coeff. 9-42643
- Li, density of states, model-potential calc. 9-26131
- Li, self-diffusion coeff. 9-42643
- Li, shear viscosity meas. rel. to classical theory, and isotope mass effects 9-30376
- Li condensed phase, temp. up to 1200°K, elec. conductivity 9-26130
- Na-Cs binary alloys, electron spin susceptibilities, Knight shift 9-39116
- Na, conduction-e.p.r., -200°C to +300°C 9-26133
- Na, diffusion and electromigration of Cd and In 9-31201
- Na, electron microscope observations of interactions with 304 stainless steel 9-28209
- Na, flow rel. to induced e.m.f. along external mag. field (α -effect) 9-36899
- Na, nuclear spin-lattice relax. of ²³Na 9-26134
- Na, optical absorpt., plasmon effect 9-44572
- Na, self-diffusion coeff. 9-42643
- Na, subcooled, heat transfer from hot spheres, and vapour formation at surfaces 9-28116
- NaK, turbulent temp. fluctuations in flow field 9-23426
- Pb-Sn alloys, stress cracking of Cu and alloys 9-48941
- Pb, electronic structure of impurities, Knight shift obs. 9-32800
- Pb, self-diffusion coeff. 9-42643
- Pb, stress cracking of Cu and alloys 9-48941
- Pb, surface tension, 1300-2200°K 9-28110
- Rb-Cs binary alloys, electron spin susceptibilities, Knight shift 9-39116
- Rb, nuclear spin-lattice relax. of ^{85,87}Rb 9-26134
- Sb, n.m.r. of ^{121,123}Sb, Knight shift and spin-lattice relax. rate temp. dependence 9-23534
- Sb, nuclear spin-lattice relax. of ^{121,123}Sb 9-26134
- Sn-Tl alloys, density determ. rel. to atomic and ionic volumes 9-30370
- Sn, elec. resistivity, 235°-910°C 9-40803
- Sn foils, plasma oscillations 9-41148
- Ti, vapour pressure 9-23604
- Tl, surface tension, 1300-2200°K 9-28110
- Zn, density meas. up to 700°C 9-30375

Liquid oscillations

- in boundary layers, use of tension in fibre suspended at right angles to flow to meas. 9-32750
- in communicating vessels for vertical variable loadings 9-42678
- critical modes in m.h.d. flow between rotating cylinders, rel. to onset of instability 9-38953
- in cylindrical cavity, nonlinear equations 9-41790
- in falling sphere retardation 9-32742
- metal cylinder, radial oscs. induced by mag. fields, hydrodynamic press. 9-25828
- non-tidal seas, free water surfaces oscillations, probability distribution of random variables 9-49432
- Rayleigh-Taylor instability, effect of surface tension 9-46598
- rotating fluid bounded by concentric spheres, free periods of oscill. 9-46596

Liquid oscillations continued

- in sea, deep, inertial period 9-49441
- sea, surface oscillations caused by wind 9-49434
- surface, mean level 9-26065
- surface swells, existence conditions 9-42630
- Taylor instability, soln for nonlinear oscill. near cutoff wavenumber 9-46597

Liquid waves

see also Acoustic waves

- density-stratified medium, internal generation with mixed region collapse 9-34862
- double Kelvin, with continuous profiles in rot. shallow ocean, trapping modes 9-23434
- explosives, detonation front instability 9-36204
- gravity, deep water long crested random, mass transport 9-28857
- gravity, in plane horizontal flow of two immiscible liqs. 9-46594
- gravity, ocean longwaves, amplification by circular islands, model 9-35798
- gravity wave drag at interface, due to disc moving in two superposed inviscid liqs. 9-26066
- gravity waves in shear flow, second-order resonant interactions 9-28089
- internal, diffraction 9-38948
- internal gravity waves, interact. trapping by periodic variations in density grad. 9-26888
- internal short period waves, statistical anal. of assoc. currents 9-45465
- inviscid Taylor instability near cutoff wave number, nonlinear theory 9-46597
- Kelvin waves, diffraction by sharp bend on rotating earth 9-28858
- kinematic, in Gulf Stream 9-31284
- lee wave generation in stratified flow over semi-elliptical obstacle 9-34730
- lee-wave modes in stratified flow over obstacle, test of Long's model 9-40758
- ocean, gravity internal, temp. oscills. on shelf and open sea 9-39998
- oceanic, internal, wave numbers and group vels., freq. depend., model 9-47516
- propagation along rotation axis 9-44540
- in rotating shallow ocean, double Kelvin waves with continuous profiles, trapping modes 9-23434
- salt solution, stratified, axisymmetric internal waves generated by moving oscillating sphere 9-34861
- two-fluid system, diffraction due to step on bottom with surface above interface 9-40763
- Ω , schlieren optical investigation 9-39066
- H₂O, long standing, in curved canal, dynamics 9-26068

surface

see also Oceanography

- capillary waves, longitudinal, experimental evidence 9-44542
- Cauchy-Poisson problem 9-26067
- confused seas, wavelength and period 9-28856
- diffraction 9-38948
- diffraction of sea waves 9-49431
- in film flow down inclined plane, nonlinear development and stability 9-40767
- generated by single pressure impulse 9-49438
- generation by pressure air flow, effect of viscosity stratification 9-26051
- in incompressible gas flow presence, narrow band theory 9-42631
- long waves, non-linear, viscosity effect 9-34859
- non-tidal seas, free water surfaces oscillations, probability distribution of random variables 9-49432
- ocean, generated by turbulent wind, freq. power spectra 9-39994
- ocean, unusually high, Poisson's law applic. 9-49427
- ocean wind waves, length modification in narrow coastal zone, calc. 9-35801
- oscillating perfect liq., mean level of face surface, expression 9-26065
- under point impulse, asymptotic response as damped gravity wave, creep wave and diffusive motion 9-26067
- Rayleigh, and microseisms, lateral refraction, North Atlantic 9-28840
- ripple damping coeff. 9-36837
- sea, for continuously changing density, 3D problem 9-37901
- sea, surface oscillations caused by wind 9-49434
- sea waters, turbulence 9-49435
- sea wave measurements using wave recorders 9-49440
- short-period water waves, hydrodynamic theories and their applcs. 9-49429
- short-period waves causing hydrodynamic pressure forces 9-49437
- solitary waves in trapezoidal channels, variation of height across crests 9-34860
- Stokes waves, non-linear dispersion 9-34863
- swells, existence conditions 9-42630
- thermally excited capillary waves, scattering spectrum 9-28088
- transmission and reflection by movable strip, theory 9-30360
- tsunamis, model for multiple mountain ring structures on moon 9-31597
- on viscous liquid with small Reynolds number, generation theory 9-46595
- water, displacement in wind-generated wave train 9-23433
- water, ripple damping coeff. 9-36837
- water, shallow, directional variation due to arbitrary periodic surface press. 9-34858
- water, variable tangential stress effect 9-32756
- water, wind-wave interactions investigation of shear stresses 9-44541
- water wave transformation with change in coastal conditions 9-49430
- water waves in channels and around islands, spectra calc. 9-30361
- water waves mechanics, tests under laboratory conditions 9-49439
- wind generated, breaking and equilib. spectrum 9-31285
- wind wave development, initial, lab. expt. 9-40000
- Hc, velocity-freq. relation near λ point 9-23556

Liquid-drop model *see Nucleus/models***Liquids**

see also Association/liquids; Diffusion in liquids; Solutions

- acoustic pulse distortion in thermally relaxing liqs. 9-30392
- atomization, acoustic, mechanism 9-46626
- bubble growth kinetics in acoustic field, effect of surface active substances 9-46601
- classical, coherent neutron scatt., effective field approxs. 9-39072
- critical tension under dynamic stress conditions 9-42618
- density fluctuations correlation length, bulk modulus relaxation time depend. 9-46617
- dielectric; conduction process role of diffusion, theory 9-30415

Liquids continued

- electroacoustic waves, dynamics 9-40788
 - e.p.r. investigation, techniques, book 9-38338
 - fountain effect, u.s., influence of static press. on height 9-23490
 - heat transfer, non-Newtonian, in non-circular tubes, theory and expt. 9-44559
 - high temperature, bibliography 9-41718
 - hypersonic relax., temp. depend. 9-30393
 - impurity analysis by spark-source mass spectroscopy 9-26837
 - laser and u.s. spectroscopy 9-36882
 - liquids, electroacoustic wave, solitary, stability 9-42648
 - mixing, rapid, energetic model 9-33656
 - molecular, nonlinear effects induced by laser light 9-26103
 - n.m.r., adiabatic fast passage alteration by mag. field modulation 9-44591
 - nonconducting binary mixtures, critical phenom. 9-28092
 - nonlinear, molecular orientation by strong light field, c.m. theory 9-25351
 - organic, cohesion energy-vol.-temp. relations, obs. 9-28094
 - orientational correlations and depolarization of scattered light 9-23499
 - Raman scattering, forced, comparison with frozen state 9-37737
 - reactive, cool, thermal stability of hot inert gas bubble 9-28073
 - self-focusing, spectral composition of diffused light, Q-switched ruby laser 9-26116
 - shock wave generation by gas detonation 9-46627
 - submillimetre wave refraction 9-28133
 - surface cavity form, by impinging air jet, shape, expt. and anal. 9-40762
 - surface levitation effect, u.s. imaging appl. for materials inspection 9-29292
 - transparent, radioactivity meas. by scintillation counter 9-34358
 - U.S. velocity and absorption, pulse-echo measurements and computer program 9-42649
 - u.s. wave vel. meas. at 0.7-30 MHz by elec. interference 9-46628
 - viscous, stimulated light scattering at surface 9-42655
 - S-As mixtures, mol. complexity, Raman obs. 9-35675
 - S-Se mixtures, mol. complexity, Raman obs. 9-35675
 - S, mol. complexity, Raman obs. 9-35675
- structure**
- alloys, Percus-Yevick partial structure factors 9-40768
 - amides, intermol. assoc. rel. to dielec. relax. 9-26128
 - benzene, n.m.r. shift and quasicryst 9-30432
 - binary solutions, stratification effects, γ radiation induced 9-30368
 - t-butyl alcohol-water mixtures, molecule clusters and small angle X-ray scatt. 9-28101
 - characterization 9-23457
 - citric acid, supersaturated aqueous solns., molecular cluster formation 9-30374
 - classification of monoat, liqs. 9-44545
 - collective motion, theory 9-23456
 - critical binary mixture, diffuse interface, optical reflectivity obs. 9-39084
 - critical binary mixture, interfacial tension 9-34886
 - Cs, molten, neutron beam exam. 9-39075
 - cyclohexane-methanol mixtures, near-critical, interfacial tension 9-34886
 - distinguishability from dense gas 9-36845
 - electron states, localized, in chains, non-exponential range 9-48715
 - equilibrium destruction during flow of oriented liquids 9-23418
 - glycerine, normal and deuterated, OH hindered rot., cold n scatt. obs. 9-28097
 - hexane, liquid, charge carriers which are probably free electrons obs. 9-28151
 - immiscibility phase boundaries determ. from density meas. 9-40778
 - interpretation by computing coordination number 9-40769
 - metals, u.s. wave investigations 9-30395
 - metals, X-ray, neutron and electron diff. 9-36846
 - methyl-d₃-acetylene, anisotropic molec. reorientation 9-40809
 - neutron diffraction examination, applications 9-37785
 - neutron diffraction examination, applications 9-47419
 - neutron elastic diff. studies 9-48680
 - nitrites, molten, molec. vibr. 9-39105
 - optical correl. functions from neutron scatt. data 9-40773
 - phenylchlorobiphenyl, detect. of vitrons at 40 MHz 9-39098
 - phenol-water mixture, light scatt. meas. of conc. fluctuations near critical point 9-40794
 - phenylacetylene, rotational motion, from spin-lattice relax. 9-39120
 - polar liqs., rotational correl. times 9-28111
 - poly-p-chlorostyrene, isotactic, chain struct. stability in solns., i.r. obs. 9-28140
 - polypropylene, isotactic, chain struct. stability in solns., i.r. obs. 9-28140
 - polystyrene, isotactic, chain struct. stability in solns., i.r. obs. 9-28140
 - theory 9-48679
 - and thermal diffusion 9-23458
 - 1,1,2-trichloroethane, u.s. relax. and vol. change during internal rot. 9-42652
 - urea solns. in water 9-30400
 - water, anomalous in capillaries, similarity with normal water 9-40771
 - water, at 25°C, X-ray diff. and radial distrib. function 9-28099
 - water, continuum model, interpretation 9-39074
 - water, effect of dimethylsulphoxide and dimethylsulphone in soln. 9-32763
 - water, McMurry-Russell model and neutron scatt. law at 0.05 eV 9-27559
 - water, Monte Carlo calc. using Rowlinson's intermolecular pair pot 9-34874
 - water, slow inelastic neutron scatt. 9-48681
 - water, transition obs. using sound velocity meas. 9-40772
 - water, two-state versus continuum model 9-39073
 - water, X-ray forward scatt. coeff. 9-40770
 - Al pair correlation fn. and pair potential 9-44546
 - Ar, shock compression, applic. of significant structure theory of liquids 9-28095
 - D₂O from neutron scatt. at ~ 0.65 eV and energy-transfer cross-sections 9-28096
 - Ga, X-ray scatt. obs. over wide temp. range 9-30371
 - H₂O modification at high pressure and temp. 9-26076
 - ⁴He, structure factor, apparent discrepancy between theory and expt, 9-48727
 - ³He-⁴He mixture, calc. of binding energy 9-32810
 - He-Ga system (0.96 and 0.02 mole fraction Hg), X-ray study of radial distrib. functions and co-ord. numbers 9-28100
 - Hg, X-ray diff. obs. 9-32762
 - ionic solns., i.f. motions of H₂O mols. 9-44547

Liquids continued**structure continued**

- Li-Na system, immiscibility phase boundaries determ. from density meas. 9-40779
 Na, molten, neutron beam exam. 9-39075
 NbF₅, Raman spectra rel. to possible polymerization state 9-26119
 TaF₅, Raman spectra, rel. to possible polymerization state 9-26119
 Tl-Se system, immiscibility phase boundaries determ. from density meas. 9-40779

theory

- see also *Dielectric phenomena; Equations of state/liquids*
 approximate theories 9-48679
 binary mixtures, thermodynamic theory of gravitational eff. 9-23454
 binary mixtures of water and organic liquids, molecular motion from n.m.r. meas. 9-46654
 Bose liq., response props., symmetry breakdown rel. to superfluid density 9-38258
 chemical exchange and rotational relaxation 9-39117
 classical, isotope mass effects on viscosity and diffusion 9-30376
 classical, mols. all vibrating, some having translatory motion, appl. to transport props. 9-34869
 classical, zero sound dispersion law 9-28121
 condensed matter, conference 9-48981
 distribution function theory 9-48679
 dynamics and time-depend. correl. functions 9-48679
 energy migration in two-dimens. liq., dynamical theory 9-34870
 exciton dynamics in simple liquid 9-32760
 fluctuations 9-48679
 fused salts, effect of internal Coulomb field on viscosity 9-32770
 kinetic theory of collective modes in classical liquids 9-32761
 light scatt., treatment of field fluctuations 9-48699
 magnetic reson. spectra moments rel. to slow mol. motions correl. time 9-23453
 mixture of Lennard-Jones liquids, Monte Carlo calc. of thermo props. 9-34894
 neutron scatt. and molecular dynamics 9-26077
 non-uniform, molecular distributions 9-30367
 partition function for coupled molecular motion 9-48678
 polar, electron transfer reactions, radiationless transition probability 9-31182
 potential for alkali ions, new model 9-34518
 random packing density of hard sphere models 9-30366
 refractive index-density relation 9-23496
 Reiner-Rivlin, permanent rectilinear flow 9-23411
 rotational relaxation and chemical exchange 9-39117
 rough spheres, Rice-Allnatt theory of transport props. 9-36147
 shock Hugoniot 9-23455
 simple liquid, exciton dynamics 9-32760
 solutions, semigrand isobaric-isothermal ensemble distrib. functions 9-40247
 transport proc., stat. mech. approximate theories and models 9-26079
 trapped dielectron 9-46613
 two-dimensional, pair distrib. functions and scaling functions 9-32759
 u.s. relaxation, theory with vib. point as group of mols. 9-30389
 velocity autocorrelation function and structure function of simple liquid, unified approximation 9-34871
 zero-sound in classical liquids 9-32761
 Al pair correlation fn. and pair potential 9-44546
 Ar, 12-6 potential, Monte Carlo calc. 9-39070
 Ar, atomic overlap, neutron diff. obs. 9-34875
 Ar, interatomic potential and equations of state 9-28093
 Ar, velocity autocorrelation function and neutron scatt. cross sections, calc. 9-34871
 He, photon-roton excitation, Raman scatt., calc. of amplitude 9-32808
 He, single particle energy evaluation 9-23559
 *He ground state, three-phonon vertex in BDJ description 9-42688
 Ne, interatomic potential and equations of state 9-28093
 Rb, atomic overlap, neutron diff. obs. 9-34875
 Zn, neutron diff. anal. for ion-ion pot. determ. 9-23459

Lithium

- abundance in Ib supergiants and Cepheids 9-24796
 abundance in main sequence stars, depletion, observational time-scales 9-35973
 atom, ²S and ²P, spin-optimized, self-consistent field wave function determ. 9-40544
 atom, e scatt., 2s, 2p close-coupling eqns., soln. from threshold to 54.4 eV 9-48416
 atom, mag. hyperfine struct. and core polarization in excited states 9-34545
 atom, photoionization cross-section, many-body calc. 9-34571
 atom, proton charge exchange bombard., H atom formation cross section 9-27813
 atom, variational calc. of correlation eff. on g.s. 9-22958
 atom, variational calc. of ground state energy 9-46279
 atom energy levels splitting calc., transition from quadratic to linear stark eff. for spectral lines 9-22957
 atom g.s. anal., spin orbitals and Fermi contact term 9-22959
 atom h.f.s. 1s²2p¹P calc., Brueckner-Goldstone theory 9-27810
 atomic beams, glory scatt. liq. fluorocarbons and hydrocarbons 9-42471
 atoms, hyperfine splittings and press. shifts of ⁷Li and ⁶Li, optical pumping expt. 9-40550
 atoms collision ionization of H excited atoms 9-22992
 band struct. calc. by self-consistent augmented-plane-wave method 9-47036
 band struct. calc. by self-consistent augmented-plane-wave method, lattice const. variation 9-47044
 band struct. calc. using ab initio pseudopot. 9-43006
 catalysis of carbonyl compound condensation reactions 9-47461
 concentration in various materials, neutron activation analysis 9-26850
 condensed, elec. conduct. for temp. up to 1200°K 9-26130
 conduction-electron spin reson., pulsed-microwave studies 9-33629
 crystals, atomic construction using quantum mechanics 9-26239
 diffusion in Si:As(P) 9-24234
 diffusion of Cu, interstitial-like 9-39384
 elastic const. of single cryst., temp. depend. 9-37220
 electron affinity 9-44281
 electronic density of states for liquid and solid, model-potential calcs. 9-26131
 energy levels calc. using step-like model potential function and perturbation theory 9-44243

Lithium continued

- equation of state at 0°K 9-33222
 e.s.r., spin-flip scatt. cross-section for conduction electrons of impurity atoms 9-41345
 in Ge, migration and precipitation control for radiation detector production 9-26557
 ion drift mobility in Ge, 23.8° and 61.2°C 9-35131
 ion implantation technique rel. to prod. of Si p-n junction detectors 9-28532
 ions, multicharged, acceleration in the Kurchatov cyclotron (USSR) 9-42162
 isotopes formation cross section for proton spallation of ¹⁶O 9-44203
 lattice const. variation in augmented-plane-wave energy-band calc. 9-47044
 lattice vibrations and nonlocal model potential 9-26411
 liquid, isotope mass effects on shear viscosity 9-30376
 liquid, self-diffusion coeff. 9-42643
 liquid, viscosity up to 1500°C 9-40780
 metal, b.c.c., energy band calcs. by GI method 9-44887
 origin in solar system 9-36015
 particles in LiF, e.s.r. linewidth of conduction electrons 9-33630
 phonon frequencies from electron-phonon interaction modification with correlation effects 9-35308
 phonon lifetime, electronic contrib. 9-37391
 photoionization, ground and four excited levels as function of expelled electron's energy 9-36674
 photoionization cross section 9-42338
 photoionization cross-section, many-body calc. 9-34571
 plasma, emission lines, 5000 to 10000°K 9-40675
 plasma, expansions in Laval nozzles, approximate calc. 9-46471
 plasma, high-density, linear Stark broadening 9-34765
 plasma production by giant pulse-laser irradi. of solid, characts. 9-28021
 scattering by alkali atom, spin-exchange cross section calc., partial-wave anal. 9-22984
 on solar surface, depletion turbulent diffusion explanation 9-36029
 target, thin, sealed in Ni for low; contamination, technique 9-29647
 targets, metal, transference from evaporator to target can, technique 9-48215
 in upper atmosphere, abundance and theory of origin 9-35832
 vapour, optical pumping, Dehmelt-type transients for ⁷Li, obs. 9-36669
 vapour pressure, saturated, 1200-2160°K 9-26170
 in CdTe:Yb, Er, effect of charge compensation on rare-earth doping, e.p.r. study 9-47434
 CoO:Li, self-diffusion of ¹⁸O 9-40982
 in p-CoO, elec. conduction obs. 9-37518
 e.s.r., spin-flip scatt. cross-section for conduction electrons of impurity atoms 9-41346
 in GaP:Mn, Li diffused, Li tripple e.p.r. detection 9-24493
 K/Li ion exchange in synthetic resin, kinetics 9-41438
 KCl:Li, phonon reson. scatt. obs. from thermal conductivity meas., isotope and elec. field effects 9-42948
 KCl:Li F_a centres, elec. field modulated absorpt., off axis centre model 9-42851
 Li-NBr scatt., optical pot. for molecule to reproduce * obs quenching of glory undulations 9-25798
 Li, phonon freq. and Grueneisen parameters, pseudopotential calcs. 9-26410
 Li₂ in ideal gas state, 100 to 10000°K, thermodynamic props. 9-42609
 Li₂ mols., state functions rel. to nucl. separation 9-48466
 Li₄, diatomic-in-mols. theory 9-30034
 Li⁺ photodetachment cross-section calc. 9-46297
 Li⁺ collision with H₂ mol. beam, vibr. excitation meas. 9-25796
 Li⁺ i.r. absorpt. in KBr, particle in curved box model 9-47364
 Li⁺ in KBr, KCl, off-centre behaviour lattice parameter dependence 9-35087
 Li⁺ in KCl, splitting in impurity motional spectrum rel. to dielectric behaviour at low temps. 9-26583
 Li⁺ in KCl, tunnel splitting of impurity motional ground states rel. to elec. cooling 9-27143
 Li⁺ ions differential scatt. by He, N₂ and O₂, elastic cross sections meas., 3-330 eV 9-46315
 Li⁺ new model potential, suitable for liquids and solids 9-34518
 Li I, mean lives of 2p²P^o levels, oscillator strengths 9-44256
 Li I^o transitions assigned for 2934, 3714 Å lines 9-25698
⁷Li, K⁺ mesic X-ray yields 9-36685
 Li(2² and 2²p)-H₂ interact, energy surfaces 9-34570
 molecule, double, ionization pot. of atomic cluster, obs. 9-29956
 in N₂O₃, flame photometry determ., quenching effects of different acids 9-37857
 in NiO, dielec. const., interfacial polarization effect 9-35469
 n-Si:Li, electron-irrad., defects obs. using Hall coeff. and resistivity meas. 9-49113
 Si:Li, O₂, dopant interaction with electron-irrad. produced defects 9-42813
 in Si, e.s.r. 9-26794
 in Si, interaction with rad. induced defects 9-48844
 in Xe solid, absorption spectrum, multiplet struct. 9-22956
 in ZnTe, luminescence rel. to shallow acceptor centres 9-26769

Lithium compounds

- additions to acetone and ethyl methyl ketone effect on u.v. absorpt. spectra 9-36888
 diff. of ²²Na and ²⁴Na 9-33006
 ferrites, magnetoelastic macroscopic coeff., connection with spin-phonon Hamiltonian microscopic coeffs. 9-26656
 ferrites, thermal transport, effect of magnons 9-44847
 formate monohydrate, crystalline, Raman spectra 9-47378
 glass, Li aluminosilicate, changes during pyroceramic formation 9-36922
 hydrides mol. const., by molec. beam elec. reson. 9-30061
 LiCl:Pb²⁺, Ti⁴⁺ chem. analysis by luminesc., 77°K 9-33697
 LiTaO₃:MgO single cryst., doping eff. on acoustic wave attenuation 9-37334
 lithium acetate dihydrate monocrystal, optical const., temp. depend 9-47315
 periclase solid soln. containing Li⁺ and R³⁺ (Cr, Al, Fe) ions 9-23955
 β-spodumene, cryst. struct., stereographic projection 9-48828
 β-spodumene, thermal expansion 9-26431
 surface (001), preferential scatt. of Ar, correl. with lattice props. 9-42714
 sylvine crystals, effect of surface preparation 9-41027
 vacancy form. energies, for positive and negative ions 9-48850

Lithium compounds continued

- Al-Li alloys, charact. temp., Young's modulus, linear expansion coeff., variation with Li conc. 9-39395
 $\text{Ba}_{0.75}\text{Ca}_{0.25}\text{Nb}_2\text{O}_6\text{Nd}^{3+}$ coherent emission obs. 9-26738
 Li/Na/K CO_3 diffusion of ^{23}Na and ^{14}C near eutectic mixture 9-30625
 Li-Ag(Cd,Al) alloys, lattice parameters 9-42789
 Li-Mg alloys, lattice parameters 9-42789
 Li-NH $_3$ systems, low-temp. ht. capacities 9-39531
 Li-Na system, immiscibility phase boundaries determ. from density meas. 9-40779
 $\text{Li}_{0.5}\text{Fe}_{0.5}(\text{Gr}_{0.2}\text{O}_4)$ ferrite with Fe^{3+} in tetrahedral and Gr^{3+} in octahedral domains, exchange integrals 9-45181
 $\text{Li}_{0.5}\text{Fe}_{2.5}\text{O}_4$ switching props., effects of grain size 9-45180
 $\text{Li}_{0.5}\text{Fe}_{2.5}\text{O}_4$ spinel ferrite, absorpt. and Faraday rotation, 300°K, 1 to 8 μ 9-45277
 $\text{Li}_2\text{Ge}_2\text{O}_5$, growth by Czochralski method and properties 9-37082
 $\text{Li}_2\text{O}-\text{Ga}_2\text{O}_3-\text{SiO}_2$ system, glass crystallization 9-44619
 $\text{Li}_2\text{O}-\text{SiO}_2$ glass, luminescence spectra 9-39872
 $\text{Li}_2\text{O}-\text{SiO}_2$ glass, metastable precipitate formation and effect on elec. props 9-24215
 $\text{Li}_2\text{O}-2\text{SiO}_2$ glass, struct. after neutron irradi., Dielec. and X-ray meas. 9-40833
 $(\text{Li}_2\text{O},\text{MgO})_x(\text{Al}_2\text{O}_3)_y\text{nSiO}_2$ glasses, thermally crystallized, high-quartz solid soln. phases 9-28398
 $\text{Li}_2\text{SO}_4-\text{K}_2\text{SO}_4$ phase diagram from differential thermal anal. 9-48923
 $\text{Li}_2\text{SO}_4\text{-Na}_2\text{SO}_4$ solid and molten, elec. cond. 9-30835
 $\text{Li}_2\text{SO}_4\text{-H}_2\text{O}$, neutron inelastic scatt. obs. of librational freqs. 9-42955
 Li_2TiO_3 , cryst. struct. refinement 9-48833
 Li_2VO_4 , solubility of YVO_4 and rare earth vanadates, crystn. conditions and structure 9-40777
 Li_4RhF_x , ($x=4,5$), structure and bonding obs. 9-48834
 $\text{Li}_x\text{Co}_{1-x}\text{O}$ solid solutions, energy states from photoelec. emission meas. 9-41285
 $\text{Li}_x\text{Co}_{1-x}\text{O}$ solid solution, prepared at 1500°K 9-41134
 $\text{Li}_x\text{Ni}_{1-x}\text{O}$ solid solutions, donor levels caused by neutral Li interstitials 9-41134
 $\text{Li}_x\text{Ni}_{1-x}\text{O}$ solid solutions, energy states from photoelec. emission meas. 9-41284
 $\text{Li}_2\text{V}_2-\text{O}_2$, phase relation, elec. and mag. props. 9-35328
 Li^+H and Li^+D , polarization in shock waves, rel. to role of ion mass 9-30957
 Li borate glass crystallization, thermal differential analysis 9-42756
 β - LiAlO_2 , cathodoluminescence spectra and coordination of Mn^{2+} , Fe^{3+} , and Cr^{3+} 9-31150
 LiBO_2 mol. config., electron diff. obs. 9-23029
 LiBi supercond. 9-49034
 $\text{LiBr}:\text{Pb}^{2+}$, Ti^+ chem. analysis by luminesc., 77°K 9-33697
 LiBr , $^{79}\text{Br}/^{81}\text{Br}$ nuclear quadrupole ratio determ. 9-23054
 LiBr , single crystal, adiabatic elastic consts. from 300 to 4.2°K 9-48881
 LiBr in aqueous solution, ^{81}Br n.m.r. relaxation times 9-32799
 LiBr films, dielectric losses at low temp., mechanisms 9-49137
 $\text{LiCl}-\text{CrCl}_3$, phase study on fusing between 500 and 700°C, by n.m.r. 9-35259
 $\text{LiCl}-\text{KCl}$ eutectic: MnCl_2 , e mag. reson. and K_4MnCl_6 form., obs. 9-28749
 LiCl , e.s.r. of Cu^{2+} centres 9-43281
 LiCl , n.m.r. irradi. time and chemical shift meas. in aq.-methanol mixture 9-30035
 LiCl , reactor-irrad., X-ray- and thermoluminescence 9-28729
 LiCl in alcohol soln, us absorpt. props at 25°C relax. curves rel. to ion assoc. and dissoc. 9-23493
 LiCl e.p.r. of stabilized Cu and Ag atoms, hyperfine and superhyperfine struct. consts., temp. depend. 9-35714
 LiCl surface ionization on Re and oxygenated Re surface 9-35522
 LiD , core model for single-centre calc. of elec. field gradients 9-42398
 $\text{LiD}_3(\text{SeO}_3)_2$ ferroelec. single cryst., H-bond network, deuteron mag. reson. obs. 9-33389
 $\text{LiF}:\text{Eu}$, Mg thermoluminescent material, radiation dosimetry meas., patent 9-28730
 $\text{LiF}:\text{Mn}^{2+}$, phonon-induced corrections to transferred hyperfine coupling 9-33628
 LiF , surface phenomena and dislocations 9-23618
 LiF , valence-bond and atoms-in-mols. calc. 9-38857
 LiF aqueous soln., elec. conductivity 300-1000°C, up to 12 kbar 9-48717
 LiF coated Al mirrors, highest reflectance in vacuum ultraviolet 9-32011
 LiF crystals, tensile strength rel. to surface preparation 9-41027
 LiF dislocations, viscous drag and densities 9-37179
 LiF dosimeters, energy depend. at electron energies from 10 to 35 MeV 9-34364
 LiF films, u.v. spectra of adsorbed Xe and CO 9-44630
 LiF target, incident p , α ; cross section meas. for calibration 9-32242
 $\text{LiF}-\text{NaF}$ mixed cryst., ^{23}Na first-order quadrupole splittings, nucl. double reson. obs. 9-35735
 $\text{LiFe}_{0.8}\text{Mn}_{0.2}\text{PO}_4$ antiferromagnet. Mossbauer effect 9-26726
 LiGa ferrites, magnetostriction consts., temp. depend. 9-28629
 $\text{LiH}-\text{H}$ system with isotopic impurities, thermodynamic equilib. 9-37813
 LiH , absorption and luminescence spectra, radiation eff. 9-33585
 LiH , compressibility data analysis 9-37235
 LiH , Compton profile analysis rel. to valence-electron wave functions 9-46789
 LiH , electronic struct., valence-bond calc. 9-44334
 LiH , mol. transcorrelated wave eqn. numerical soln. 9-34628
 LiH , mol. wavefunctions in infinite internuclear separation limit, Hartree-Fock eqn. 9-38816
 LiH , one-centre calc. with unlimited radial basis 9-38846
 LiH , pseudopotential approach, electron gas obs. 9-33222
 LiH , thermal expansion 12-300°K, deriv. from lattice parameter data 9-28429
 LiH^+ , electronic struct. 9-44335
 LiH laser irrad., plasma electron-ion recombination 9-44464
 LiH molecules, self-consistent field eqn. in multicong. approx. 9-40592
 LiH particle irrad. by laser beam for thermonuclear plasma prod. 9-46512
 LiI , single crystalline, pure and Mg doped, ionic cond. 9-47161
 LiIO_3 , electric and piezoelectric behaviour 9-37595
 LiIO_3 , production of second harmonic of Nd laser 9-26691
 LiIO_3 , strong second harmonic generation of 3470 Å after ruby laser irrad. 9-26692
 LiIO_3 cryst., absolute struct. 9-32918
 LiMnPO_4 , antiferromag. reson. in single cryst. 9-39900

Lithium compounds continued

- LiMnPO_4 , magnetoelectric effect interpretation 9-24331
 LiNO_3 , cryst. surface distortion, i.r. data 9-48750
 LiNO_3 , molten, diffusion and ionic mobility of ^{23}Na , ^{137}Cs obs., temp. depend. 9-34891
 LiNO_3 molten electromigration mobilities of ^6Li and ^7Li , 313°-488°C 9-45422
 $\text{LiNbO}_3:\text{Cr}^{3+}$, optical spectra 9-31104
 $\text{LiNbO}_3:\text{Cr}^{3+}$ single crystals, dichroism 9-39803
 $\text{LiNbO}_3:\text{Ho}^{3+}$, electro-optic crystals, second harmonic radiation of Ho^{3+} at 77°K 9-43203
 $\text{LiNbO}_3:\text{MgO}$ single cryst., doping eff. on acoustic wave attenuation 9-37334
 $\text{LiNbO}_3:\text{Nd}^{3+}$, absorpt. and luminesc. spectra, 4.2-295°K 9-28689
 $\text{LiNbO}_3:\text{Nd}^{3+}$, electro-optic crystals, second harmonic radiation and parametric oscils. of Nd^{3+} at room temp. 9-43203
 $\text{LiNbO}_3:\text{Nd}^{3+}$, Tm^{3+} , Ho^{3+} coherent emission obs. 9-26738
 $\text{LiNbO}_3:\text{Tm}^{3+}$, electro-optic crystals, second harmonic radiation of Tm^{3+} at 77°K 9-43203
 LiNbO_3 , absorption spectra of clear, yellow and bleached crystals 9-28687
 LiNbO_3 , acoustic e.p.r. of Cr^{3+} and Nd^{3+} , for internal fields of ferroelec. crystals 9-28748
 LiNbO_3 , electro-optic coeffs., signs 9-33396
 LiNbO_3 , electro-optic effect, linear depend. on melt composition 9-26709
 LiNbO_3 , ferroelec., spontaneous polarization, room-temp., pulsed-field method 9-35478
 LiNbO_3 , microwave frequency acoustic surface wave propagation losses 9-33173
 LiNbO_3 , mixing of two longit. u.s. waves along (001) direction 9-42959
 LiNbO_3 , modulator of i.r., quality factor 9-34190
 LiNbO_3 , optical parametric oscillations, pumped with ruby laser 9-28663
 LiNbO_3 , plane longit, elastic wave with vector along Y-axis of rod, vel and energy propag. direction 9-37228
 LiNbO_3 , plastic deform due to mech. twinning, crack nucleation obs. 9-23887
 LiNbO_3 , second-harmonic generation with mode-selection and high-spectral-radiance Nd:glass laser system 9-41917
 LiNbO_3 , stoichiometry of single crystals 9-36977
 LiNbO_3 , surface radiation from nonlinear optical polarization, obs. 9-26682
 LiNbO_3 , tunable stimulated Raman oscillator Q-switched ruby laser excitation 9-35672
 LiNbO_3 attenuation of microwaves rel. to temp., 80-950°K 9-41007
 LiNbO_3 crystal, relative nonlinear optical coefficient, corrected value 9-33499
 LiNbO_3 crystals, optical rectification of mode-locked pulses 9-26712
 LiNbO_3 nonlinear optical coeff. meas. relative to KH_2PO_4 , $\text{NH}_4\text{H}_2\text{PO}_4$ and $\alpha\text{-HIO}_3$ 9-26690
 LiNbO_3 oblique-cut plates, longitudinal halfwave voltages, optimum calc. 9-31062
 LiNbO_3 on quartz substrate, acoustic-surface-wave transducer 9-48951
 LiNbO_3 parametric emission, spontaneous, power and bandwidth 9-25198
 LiNbO_3 stimulated optical emission, tunable, without resonator 9-48026
 LiNbO_3 surface wave piezoelec. coupling across air gap 9-26594
 LiNbO_3 u.s. microwave pulses, Brillouin scatt. obs. 9-35278
 LiNbO_4 sputtered films, deposition and piezoelectric characts. 9-42725
 LiO_2 , i.r. spectrum, molec. struct. 9-44333
 LiT energy-band calc. using combined plane-wave tight-binding, method 9-42998
 $\text{LiTaO}_3:\text{Cr}^{3+}$, optical spectra 9-31104
 LiTaO_3 , ferroelec., spontaneous polarization, room-temp., pulsed-field method 9-35478
 LiTaO_3 , microwave u.s. attenuation 9-44826
 $\text{LiYF}_4:\text{Er}^{3+}$, absorption and fluorescence spectra for Er^{3+} energy levels 9-31107
 $\text{LiYF}_4:\text{Er}^{3+}$, Ho^{3+} , pulsed laser action at 77°K 9-25291
 $\text{LiYF}_4:\text{Nd}^{3+}$, polarized fluoresc. and absorpt., excitation spectra, lifetime decay and linewidths 9-39877
 LiYF_4 , crystal growth, Stockbarger technique, lattice params. and opt. props. 9-23683
 LiYF_4 , pure and rare-earth doped growth by Czochralski method 9-37083
 LiBr , n.m.r. relax. time and chemical shift meas. in aq.-methanol mixture 9-30035
 $\text{Mg}(5 \text{ at.}\%)\text{Li}(1.5 \text{ at.}\%)\text{Al}$ alloy, plastic deform. during rolling, mechanism 9-33035
 NaCl rock salt, crystals, effect of surface preparation 9-41027
 SiC phase in $\text{SiC}-\text{B}_4\text{C}-\text{C}$ system, struct. from 2200-2550°C 9-48939
 $\text{SiO}_2-\text{Al}_2\text{O}_3$ system, immiscibility, metastable glass-in-glass separation and crystn. nucleation 9-32826

lithium fluoride

- absorption spectrum in N-region at 3°K 9-28688
 cathode, photoelec. yield in vacuum u.v., effect of irrad. 9-26616
 colorability due to X-irradiation, eff. of impurities and preliminary heat treatment 9-32986
 colour centre formation due to irradiation of various kinds obs. as a function of temp. 9-35115
 colour centres, F-band formed by radiation with reactor neutrons and γ 9-35114
 damping, amplitude independ., recovery 9-42882
 dislocation, charged movement prod. by elec. field 10 KV/cm max. 9-42834
 dislocation etch figures, effect of neutron irrad. on dimensions 9-40945
 dislocation multiplication in single crystals under periodic and increasing stress 9-40949
 dislocation struct. under sharp thermal change conditions 9-42835
 dosimeter, thermoluminescent heat stable, patent 9-36529
 ductility at low temp. 9-33038
 elastic moduli, thermal-neutron irrad. effect 9-46865
 elasto-optical and piezo-optical coeffs., temp. depend. 9-39813
 electron emission, thermally stimulated, effect of surface treatment, ageing and meas. method 9-43138
 e.p.r. linewidths of conduction electrons in Li particles 9-33630
 e.p.r. of Si , rel. to paramag. fault 9-49353
 F-centres generated by X-ray irrad., 77-600K, interpretation w.r.t. recomb. model of interstitial-vacancies 9-40974
 F-centre hyperfine interaction constants, temp. depend. 9-46836
 F-centres, thermal annealing, 25° to 400°C 9-32993

Lithium compounds continued**lithium fluoride** continued

- fatigue in single cryst., 350-650°C 9-30692
integral X-ray refl. coeff., 0.7 to 2.1 Å, obs., and comparison with graphite 9-47384
ionic conductivity, low temp., effect of O 9-39671
i.r. absorption, subsequent to n- and p-irradiation 9-39839
i.r. matrix spectra, linear dimer Li₂F₂ obs. 9-23053
irradiated, Y-absorpt. band obs. 9-37726
latent hardening due to dislocations interact. 9-35191
luminescence, laser induced, 230-540 nm spectral obs. 9-28710
piezo-optical and elasto-optical coeffs., temp. depend. 9-39813
powder, X-ray diff. patterns obtained using ⁵⁵Fe sources 9-40907
radiation effect on physical props. 9-28546
stress relaxation, dislocations mechanism, -196°-150°C 9-33026
surface scatt. of He mols. 9-48751
thermal conductivity changes following irradiation induced imperfections 9-33198
thermal expansion coeffs., explt. method applic. and accuracy 9-24053
thermoluminescence, in ionizing radiation meas., 10-250Mrad. 9-38621
thermoluminescence, effect of thermotreatment 9-33607
thermoluminescence and thermally stimulated conductivity after X-ray excitation 9-45355
thermoluminescence, depend. on particle size 9-41412
thermoluminescent dosimeter efficiency rel. to grain size 9-22674
TLD, optical absorpt. correl. with thermoluminesc. 9-45323
triboluminescence 9-43268
u.v. transparency reduced in air by formation of surface film 9-33523
V_K-centres, ENDOR hyperfine consts. and lattice distortion 9-46837
vacancies, cationic, formation energies 9-42811
vacancies formed by reactor radiation, detect. by annealing and elec. cond. meas. 9-32949
with MgF₂ and MgO impurities, absorption spectra 9-41383
X-ray index of refraction of single crystal 9-39798
CaCO₃, fission fragment tracks, structure and healing 9-26467
crystal, absorption determ., 2-25 μ 9-24373
Li₂F₂ lin. dimer species, obs. in i.r. matrix spectra of LiF 9-23053
LiF:H⁺ (D⁺), i.r. absorption due to localized vibrations of ions 9-30619
LiF:Mg²⁺, p-ray coloration enhancement 9-39377
LiF:Mn²⁺, e.p.r. at 9.5 GHz 9-37798
LiF:Mn²⁺(Mg²⁺), p-ray colouration, conversion into F-centres of vacancies created by charge compensation 9-28305
LiF:U, luminesc. decay and fundamental series emission 9-35695
LiF:BeF₂ molten solns., viscosity and density 9-42639
Mn²⁺ hyperfine coupling parameter, temp. depend. 9-43282
RbCl, F₁-centre accumulation due to proton irradi., 78°-380°K 9-30620

Lithosphere *see Earth***Localized states** *see Crystal electron states***Loges (molecular bonds)** *see Bonds; Molecules/electronic structure***Lorentz transformation** *see Relativity/special***Lorentz-Lorenz relation** *see Dielectric phenomena***Lorenz number** *see Conductivity, electrical/solids; Conductivity, thermal/solids***Loschmidt number (= Avogadro number)** *see Constants***Loudness** *see Hearing; Intensity measurement, acoustics***Loudspeakers** *see Acoustic radiators***Love waves** *see Elastic waves; Seismic waves***Low-temperature phenomena**

- see also Helium/liquid; Helium/solid; Joule-Thomson effect; Superconducting materials; Superconductivity; Superfluidity*
conductivity, elec. of metals, temp. depend. 9-44902
density matrix, low temp. expansion for systems described by a potential 9-31779
Freon-12, boiling in region of centrifugal forces, heat transfer rel. to inertia overloads 9-23603
i.r. spectroscopy improved resolution 9-32446
magnetite-containing rocks, low temp. treatment rel. to transitional thermoremanent magnetization 9-33877
metal, b.c.c., flow stress 9-33051
metals, ferromag., multiband theory of inelastic neutron scatt. 9-33447
plasma, resonant power absorption from externally driven elec. field 9-30271
polyethylene, thermal conductivity below 1°K, modification to theory 9-28433
tensile properties of grey cast iron, 4-295°K 9-48893
Ag, thermal expansion 9-33188
Ce, phase transform. effect on elastic behaviour 9-40997
Cu (15 at.%)Al deformed alloy cryst., lattice thermal conductivity 9-35291
Cu(NO₃)₂ · 2.5H₂O, adiabatic cooling 9-26662
Ga single crystals, liq. He temp., in longit. mag. field, zero resist. 9-44900
n-Ge, free electron density, mobility and Hall coeff., 4.2° to 7.9°K 9-28512
InSb, microwave third harmonic generation 9-35403
IrO₂, ht. capacity 0.54-10°K 9-48971
KBr, ionizing rad. induced vacancies and interstitials, prod. rate 9-32948
KCl:Li⁺(OH⁻)(CN⁻), dielectric behaviour rel. to splitting in impurity motional spectrum 9-26583
MnCl₂·4H₂O, ht. capacity, mag. moment, 0.4-4.2°K in mag. fields 9-44835
Ni-Cu-H alloys, elec. resistance anomalies 9-37450
Ni-Cu, alloys, elec. resistance anomalies 9-37450
Pd-Ag alloys, thermal expansion 9-33188
Pd (14 at.%)Fe alloy, sp. ht. changes due to short-range order changes 9-33183
Pd-Fe dilute alloys, elec. resistivities 9-44916
Pd, thermal expansion 9-33188
Pu-Al delta-stabilized alloys, elastic and anelastic behaviour 9-37224
Pu-Ce delta-stabilized alloys, elastic and anelastic behaviour 9-37224
RuO₃, ht. capacity 0.54°-10°K 9-48971
SiO₂ glass, effect of ³He and ⁴He on ht. capacity 9-42733
Zn, u.s. attenuation in single cryst. 9-33174

Low-temperature production

- see also Joule-Thomson effect; Liquefaction/gases; Magnetic cooling*
refrigerator, dilution, ⁴He film flow suppressing evaporator 9-33987
technique 9-24992
ytterbium yttrium ethyl sulphate crystal for nuclear spin refrigerator 9-27579

Low-temperature production continued

- He refrigerator, closed cycle, for Mossbauer studies 20°K-300°K 9-27619
³He solutions in ⁴He, advantages of applic. 9-23562
³He-⁴He dilution refrigerators 9-29139
KCl:Li⁺(OH⁻), electric cooling rel. to tunnel splitting of impurity motional ground states 9-27143
RbCl:CN⁻, electric cooling rel. to tunnel splitting of impurity motional ground states 9-27143

Low-temperature technique

- ceramic material preparation, cryochemical method 9-33125
continuous heating system, circuitry 9-22303
cryogenic system for optical spectroscopy 9-34226
cryogenic systems, automatic temp. controller design 9-31864
diffusion rates in high vapour press. solids at cryogenic temps., meas. method 9-44722
dilatometer, optical lever 9-26429
Doppler coeff. meas. on nuclear reactors 9-29886
Peltier meas. below 4°K 9-30983
recrystallization, low temperature tube 9-23686
resistance thermometer self-balancing Wheatstone bridge 9-41847
specific heat apparatus for meas. down to 0.015°K 9-24040
specific heat meas., adiabatic 9-25135
superconducting coil, forced-cooled, hydrodynamics and current stability 9-26535
surface cryopumping, condensation coeff. meas. 9-40224
temperature regulating system for 4-300°K 9-27142
thermodynamic optimum for refrigeration electrical connections 9-22271
thermometer, semiconductor diode, for low temp. 9-26572
vibrator, piezoelec., remotely controlled, for low temp. region of cryostat, 9-34080
voltmeter with 10⁻¹²V resolution, design, use of supercond. modulator 9-40214
Fe-Ni alloys, treatment for use at low temp., patent 9-26362
Ge resistance thermometer, calibration to 0.4°K 9-25133
H₂ solid, thin foil prod. for targets 9-27147
He liq. depth meas., gauge design using carbon resistor sensing elements 9-31760
⁴He film flow suppressing evaporator for dilution refrigerator 9-33987

LS coupling *see Atoms; Spectra/atoms***Lubrication**

- see also Friction*
conference, Plymouth, May (1967) 9-40991
contacts, rolling/sliding, temp. calcs. 9-31862
oil, viscosity index improvement by copolymers, patent 9-23192
polymer films 9-26360
surface-active oils, effect on origin of contact fatigue cracks 9-46907
surface-active substances introduction, boundary friction energy balance 9-23931
ultra-thin film obs., multiple gas laser beam technique 9-36842
Ti, lubricants and wear coatings 9-37268

Ludwig-Soret effect *see Diffusion in solids***Luminescence**

- see also Electroluminescence; Luminescent devices; Thermoluminescence*
amino acids, aromatic, rel. to u.v. induced photochem. transforms. 9-28816
anthracene adsorbed on NaY zeolite rel. to e state, 77 and 290°K 9-28222
anthracene molecules in cyclohexane, radiation-induced fluorescence, effect of elec. field 9-44351
N-arylcabazoles, and u.v. absorpt. 9-25759
ON-aryl carbazoles, intramol. triplet energy transitions 9-23108
atom resonance fluorescence and Hanle eff. for excitation times of interfering levels 9-25702
atom system, radiative process with excessive Doppler broadening, noise spectral contour determ. 9-38764
atoms, interacting, resonance radiation 9-38789
atoms, resonance radiative processes in strong field 9-48385
azapyridocyanines, fluorescence and phosphorescence transitions 9-23093
benzene derivatives, phosphoresc. lifetime rel. to σ, π-mixing and C-H vibr. 9-23095
Bowen fluoresc. mechanism in planetary nebulae and Seyfert galaxies, efficiency comparison 9-49535
n-butyl alcohol, as means of determ. phase transitions 9-42692
chemisorptive 9-43326
chloronaphthalene, 1,4-, 1,5-, 2,6- rel. to e spectra, obs. 9-27891
crystals, stimulated resonance fluorescence of impurity ions 9-43256
crystals, X-ray fluoresc. scatt., location of solute atom position 9-23797
DNA-orange acridine complexes rel. to phage DNA struct., obs. 9-27926
energy transfer between electronic states interacting with boson field 9-39562
estrone, intrinsic fluoresc. spectrum interpretation 9-34667
exciton luminescence, 2-photon excitation, calc. of oscillator strengths 9-35677
fluorescence, radiative lifetime meas. in sub-nanosecond range using mode locked lasers 9-28716
fluorescence as noise source in laser backscatter expt. 9-37920
fluorescence energy transfer between monomol. layers, separation law 9-24452
fluorescence spectra of cpd. emitting from monomer and excimer states, isobestic pts. 9-40574
heavy elements, L₂- and L₃-subshell fluorescence yields 9-34525
impurity spectra, connection with electronic excitation transfer processes 9-33220
intensity decay determ. by correl. analysis 9-41400
intersystem crossing processes to individual zero-field levels of lowest triplet state, rate constant 9-42359
i.r. activated visible fluorescence mechanisms 9-26774
laser, partially mode-locked, two-photon fluoresc., oscillating modes effect 9-43890
Lunar, correl. with K_p index, irrelevance of magnetospheric effects 9-47666
methyl alcohol, as means of determ. phase transitions 9-42692
methyl-pyridinium salts, anomalous Stokes shifts and fluorescence decay times 9-34679
methylbenzene derivatives, phosphoresc. lifetime rel. to σ, π-mixing and C-H vibr. 9-23095
molecular cryst., fluorescence and exciton phenomena, book 9-49005

Luminescence continued

- molecule, complex, in viscous soln., spectral depend. of fluorescence rotational depolarization 9-23012
- molecules, phosphorescing, effect on spectrum of saturating zero-field transitions with microwave radiation 9-38804
- molecules, phosphorescing, most probable intersystem crossing route, spectroscopic determ. 9-40575
- 2-naphthaldehyde, vibronic spin-orbit interaction effect on phosphorescence 9-34681
- 2-naphthyl methyl betone, vibronic spin-orbit interaction effect on phosphorescence 9-34681
- organic cpds., fluoresc. band widths rel. to inter-, intra-mol. H-bonding, obs. 9-23081
- parametric, statistics of field and photocounts 9-28738
- phenanthrene 3400-Å spectrum rel. to totally symmetric vibronic perturbations 9-38911
- phenylalanine fluorescence spectrum excited by vacuum U.V. obs. 9-30149
- phosphor, layer formation and activation, patent 9-49308
- phosphorescing molecules, effect on spectrum of saturating zero-field transitions with microwave radiation 9-38804
- phosphorescing molecules, most probable intersystem crossing route, spectroscopic determ. 9-40575
- photo- and electro-, quantum efficiency meas. using 2 π -geometry elliptic mirror 9-28735
- photochemistry, vibronic effects 9-39960
- photoluminescent materials, quantum efficiency spectra 9-31154
- porphyrin molecules, eff. of heavy atoms on intercombination transitions 9-25779
- propiphenone, time-resolved phosphoresc., spectra identification 9-44368
- n-propyl alcohol, as means of determ. phase transitions 9-42692
- pyrazine in acid medium, nature and symmetry of phosphorescent state, c.p.r. and luminescent meas. 9-46417
- pyrene in frozen solns. rel. to excimer form., obs. 9-48507
- pyrene in methylcyclopentane at low temp., fundamental vib. freqs. from quasilinear fluorescence spectrum 9-38913
- pyrene molecules in cyclohexane, radiation-induced fluorescence, effect of elec. field 9-44351
- quantum electronics conference, 1968, Miami, USA 9-25196
- radiation pulse characts. in luminesc. diffusive medium, calc. 9-25149
- resonance capture theory, role of Langmuir oscillations 9-22918
- resonance fluorescence, radiation freq. variation 9-31130
- rhodamine 6Zh, reson. excitation energy transfer from 3-methoxybenzantron 9-25780
- rhodamine C, reson. excitation energy transfer from 3-methoxybenzantron and rhodamine 6Zh 9-25780
- semiconductor, obs. of monochromatic cathodoluminesc. in scanning electron microscope, rel. to microanal. 9-43266
- semiconductors, wide band gap, intrinsic and shallow intrinsic 9-49309
- semiconductors at high pumping densities, universal relation between absorpt. and luminesc. 9-47346
- solids, emission spectrum bandwidth variation at mid-height rel. to temp. 9-47386
- solids, spatial study of ionoluminesc., applic. to microanal. 9-49329
- spectropolarimetric studies, elimination of instrument polarization 9-32054
- temperature quenching of local paramagnetic centers in ionic crystals 9-33575
- tetrachloro-p-xylene, excimer emission in rigid organic glass, 280nm excitation, 77°K 9-32530
- triphenylmethyl trapped in methylcyclopentane, fluorescence spectrum at very low temp. 9-46413
- triplet triplet energy transfer, relative orientation of involved molecules 9-42360
- tryptophan fluorescence spectrum excited by vacuum U.V. obs. 9-30149
- two-photon fluorescence pattern determ. of ultrashort pulse width 9-25195
- tyrosine fluorescence spectrum excited by vacuum U.V. obs. 9-30149
- X-ray fluorescence, γ -excited, conversion yield determ. 9-24464
- X-ray fluorescence, γ -excited, target backing enhancement effects 9-24465
- X-ray fluorescence, selective excitation compensation 9-33605
- X-ray fluorescence spectrometry, improved calc. methods 9-47482
- X-ray fluorescence technique in pathology 9-29112
- Al₂O₃ anode films, photoluminescence 9-49330
- Ar, α -particle induced, in elec. field 9-42328
- Cd atoms excited at 5 $\frac{1}{2}$ p level, Hertzian coherence conservation in sensitized fluoresc. 9-46275
- Ga, direct line fluorescence, excitation mechanism 9-48409
- GaSb, cathodoluminescence, investig. by scanning electron microscope with modulated beam 9-24471
- HCl formed by H atom reaction with Cl₂O, chemiluminesc. obs. 9-47453
- HCl in H+SCl₂, S₂Cl₂, SOCl₂, SO₂Cl₂ reactions, i.r. chemiluminesc. rel. to vibr. states 9-32473
- ⁴He*, 4³S_{1/2} and 4²P_{1/2} levels, observation of resonance effect 9-25720
- In direct line fluorescence, excitation mechanism 9-48409
- KBr:TL, rel. to activator incorporation 9-39870
- N-O chemiluminescence, investigation of features 9-28737
- Ne 2p₂ level, population relax. times, obs. using laser 9-46300
- TL, direct line fluorescence, excitation mechanism 9-48409
- Xe ²P_{3/2} and ²P_{1/2} levels under laser irradi., mag. depolarization expts. 9-46288
- gases**
- alkali metal vapours, fluorescence, collisions inducing transitions between sensitized doublet sublevels, obs. 9-29971
- alkali metals, fluorescence quenching by inert gases 9-38780
- anthracene vapour, triplet-triplet annihilation 9-38905
- benzene, low-pressure vapour 9-30079
- electron beam excitation technique for low density flow field visualisation 9-46563
- i.r. chemiluminesc. meas. of at. and free radical conc., discharge flow systs. 9-26805
- metal states in flames, fluoresc. yield rel. to underpopulation of doublet excited states 9-48379
- 9-methylanthracene, discrete fluorescence spectrum 9-46407
- naphthalene vapour, triplet-triplet annihilation 9-38905
- noble gases, scintillation mechanism based on rad. emission and de-excitation of mol. in ionizing particle track 9-30304
- OCS in bulk, steady state transient 'wiggles' phenomenon, relax. times meas. 9-44528

Luminescence continued**gases continued**

- phenanthrene vapour, triplet-triplet annihilation 9-38905
- radiative decay of polyatomic mols. quantum mech. 9-42358
- O₂ (¹ δ_g) quenching by O₂, N₂ collisions and air, obs. 9-23206
- CO₂, imprisoned 4.35 μ spontaneous emission, pressure depend. of decay rate 9-38833
- HY+X \rightarrow HX+Y (X, Y=F, Cl, Br, I), product energy distrib. from i.r. chemiluminescence, methods 9-41444
- H+X₂ \rightarrow HX+X (X=F, Cl, Br, I), product energy distrib. from i.r. chemiluminescence, methods 9-41444
- He, hypersonic flow visualisation by electron beam probe 9-46559
- He(2³S) chemiluminesc. reactions with N₂, O₂, CO and CO₂ 9-43318
- Hg vapour fluoresc. in double reson. expt. correlated intensity fluctuations 9-36670
- I₂, excited by Kr⁺ laser 9-38855
- K(²P_{1/2}) + Rb(³S_{1/2}) \rightarrow K(²S_{1/2}) + Rb(²P_{1/2}) + ΔE , fluorescence detected, cross-section meas. 9-32429
- N₂ in metastable E² Σ_g^+ state, emission spectrum and radiative lifetime, mol.-beam meas. 9-38863
- N₂O vac. u.v. photolysis, deactivation of N(²D) 9-49385
- NH₃ in bulk, steady state transient 'wiggles' phenomenon, relax. times meas. 9-44528
- NO₂ excited by Ar⁺ and Kr⁺ lasers 9-40596
- NO titration method chemiluminesc., reacts. 9-41445
- Na 3p²P atoms, cross section for de-excitation by Ar 9-38780
- Na mixtures with CH₄, CD₄, C₂H₂, C₂H₄ and C₂H₆, sensitized fluorescence 9-44288
- Rb vapour, sensitized fluoresc. by induced collisions with K atoms, energy transfer obs. 9-34573
- Rb vapour, sensitized fluoresc. by collisions with K atoms, ⁴²P_{1/2}-⁴²P_{3/2} mixing in K 9-34574
- SO₂, chemiluminesc. afterglow, temp. depend. 9-43323
- liquids and solutions**
- 3,4-benzpyrene in aq. lauryl sulphonate solns., excimer fluoresc. 9-40798
- acetylanthracene and glycerine, rotational depolarization of fluorescence 9-26125
- acridine dye absorption, luminescence and polarized luminescence spectra, 77°K 9-23113
- anthracene in glycerol solns., fluorescence, emission anisotropy 9-23513
- aromatic aldehydes, perturbing vibrations 9-42426
- aromatic compounds, n-paraffin solutions, effect of rate of freezing and concentration 9-28142
- azulenes, protonated 1-substituted, fluoresc., 20°C 9-28143
- benzene, effect of deuteration on fluoresc. lifetime of liq. 9-48706
- benzene, substituted; charge-transfer state eff. 9-30084
- 3,4-benzopyrene conc. quenching and quasi-line luminescence spectra temp. depend. obs. 9-23098
- α -chloronaphthalene in n-paraffin, quasiline phosphoresc. spectra 9-46409
- chlorophyll, a and b, energy transfer by meas. of quantum output, polarization and decay time 9-36892
- cholesterol benzoate liq. crystals, pyrene fluoresc. decay time, obs. 9-32786
- coronene in n-dodecane, phosphorescence temp. depend., centre formation, O sensitivity 9-23515
- coronene in n-octane, phosphorescence temp. depend., centre formation, O sensitivity 9-23515
- cyanine dye absorption, luminescence and polarized luminescence spectra, 77°K 9-23113
- cyanine dyes, conditions for and characts. of lasing action 9-41909
- diphenyl derivatives, phosphoresc., fluoresc. in of one-, multi-component solvents 9-34915
- 2,5-diphenyl-1,3,4-oxadiazole dioxo derivatives of scintillator activators, rel. to intermol. H-bonds, obs. 9-30414
- dye laser fluorescing, excitation and properties 9-36294
- electrochemiluminescence, pulse delay w.r.t. elec. excitation 9-44575
- fluorescein in glycerine soln., effect of concentration 9-42668
- fluorescence decay time from Neporent's modified relation 9-48704
- fluorescence of thin liq. layers, meas. device 9-34914
- β -fluoronaphthalene-D₇ in n-paraffin, quasiline phosphoresc. spectra 9-46409
- α -fluoronaphthalene-D₇ in n-paraffin, quasiline phosphoresc. spectra 9-46409
- glycerine in water, low level excitation of sonolum. 9-36871
- Halfer's hydrocarbons, protonated, fluoresc., 20°C 9-28143
- helixenes in 1,4-dioxan soln., fluorescence spectra, quantum efficiencies and lifetimes 9-40616
- ion recomb., organic liqs. from electron and γ -irrad. 9-28720
- measurement, phosphorescence transfer to bottle, solvent and additives in the presence of scintillator 9-38616
- naphthalene, fluoresc. and phosphoresc., added ethyl bromide effects, obs. 9-28138
- naphthalene in n-paraffin, quasiline phosphoresc. spectra 9-46409
- naphthalenes, α -phenylated, fluoresc. and phosphoresc. spectra 9-42441
- organic, flash-like heterophase radiation induced by strong elec. fields 9-26124
- organic compounds, phosphorescence, non-exponential decay 9-23512
- organic dye absorbers, ruby laser, fluorescence decay times and recovery times 9-26113
- organic luminescent analysis without spectral decomposition of fluorescence 9-33698
- organic luminophor solns., characts. of stimulated radiation 9-43886
- organic solns., vac.-u.v.-excited, inter- and intramole. processes 9-42667
- 3-oxy, 4-phenyl, 1,2-benzfluorenone, spectra 9-32785
- phenols, quenching, dissc. const. determ. 9-39108
- 2-phenyl-5-(4 biphenyl)-1,3,4-oxadiazole derivatives, excimer emission 9-44577
- ²-phenylindole, self-quenching through H-bonding 9-44576
- photoluminescence, theory and expt., book 9-31209
- photoluminescence quenching 9-48705
- phthalimide, fluorescence decay and depolarization 9-23514
- phthalimide in alcohol and glycerine, fluoresc. polarization, temp. depend. 9-36893
- phthalimide derivatives, fluorometric characteristics depend. on oxygen 9-23149
- phthalimide solutions, anisotropy in fluorescent emission obs. 9-23509
- phthalocyanine dyes, ruby laser absorbers, fluorescence decay times and recovery times 9-26113
- poly(β -naphthyl methacrylate) in 4 solvents, critical opalescence 9-28144

Luminescence continued**liquids and solutions continued**

- poly(β -vinyl naphthalene) in 3 solvents, critical opalescence 9-28144
 poly(butyl methacrylate) in isopropanol, critical opalescence 9-28144
 poly(dimethyl siloxane) in tetralin, critical opalescence 9-28144
 polycyclic azines perturbing vibrations 9-42426
 polymethine dyes, ruby laser absorbers, fluorescence decay times and recovery times 9-26113
 pseudo-isocyanine, fluoresc. meas. with 200 MHz modulated fluorometer 9-48707
 pulse decay, kinetics rel. to triplet state inactivation by paramag. positive ion 9-44574
 pyrene in ethanol, delayed fluoresc. rel. to solute re-encounter probability 9-34916
 pyrene in ethanol, fluorescence spectra, isobestic pts. 9-40574
 pyrene in propylene glycol, phosphoresc., normal, M^* and D^* fluoresc. 9-48708
 rare earth complexes with tetrakis(trifluoro- acetone) and rhodamine-C, benzene solns., fluoresc. 9-42664
 self-quenching through H-bonding 9-44576
 sololuminescence in liq. of high viscosity containing air bubbles, low level excitation 9-36871
 thiocarbocyanine dye absorption, luminescence and polarized luminescence spectra, 77°K 9-23113
 triphenylmethane dye absorption, luminescence and polarized luminescence, 77°K 9-23113
 triplet state of luminesc. mol. inactivated by paramag. positive ion 9-44574
 tryptophan, fluoresc. quenching and solvent isotope effect 9-32787
 xanthene dye absorption, luminescence and polarized luminescence spectra, 77°K 9-23113
 CeCl₃ in aqueous soln., fluoresc. quenching by org. ligands 9-42665
 Eu²⁺ afterglow lifetime and radiationless transitions in aqueous solns., deuterated and undeuterated 9-28141
 Eu(III) solns. in H₂O, D₂O and CH₃CN, new fluorescence emission band 9-36891
 H₂O, boiling, emission bands, phase transition luminescence 9-40797
 Mn(II), fluoresc. in molten salts 9-42666
 Ru complex, tris(2,2'-bipyridine)ruthenium(II) dichloride, luminesc. 9-42414
 SeOCl₂, energy transfer from Nd³⁺ to Yb³⁺, and through to Er³⁺ 9-22407
 Tb³⁺ afterglow lifetime and radiationless transitions in aqueous solns., deuterated and undeuterated 9-28141

solids, inorganic

- ABO₄ (A=Sc, In; B=P, V, Nb) cpds. as phosphor host lattices 9-45352
 alkali hadides doped with homologous anions and cations, nature of vibronic transitions 9-33580
 alkali halide phosphors, fluoresc. spectra, band obs. 9-24455
 alkali halide phosphors, metal-ion activated, absorption spectra 9-31098
 alkali halides, Cu⁺ and Ag⁺ centres excitation and emission spectra, hydrostatic press. effect 9-41401
 alkali halides, evidence for self-trapping of excitons 9-33589
 alkali halides, luminescence of O₂⁻ and S₂⁻ centres investigated 9-33591
 alkali halides, noble metal ion activated, optical struct. of luminescence centres 9-47387
 alkali halides, O₂⁻ and S₂⁻ impurity centres, spectra obs. 9-39861
 alkali halides, O₂⁻ impurity centres, effect of hydrostatic press. 9-39864
 alkali halides, O₂⁻ impurity centres, spectra obs. 9-39862
 alkali halides, O₂⁻ impurity centres, thermal quenching 9-39863
 alkali halides, of rare earth ions 9-33592
 alkali halides, P-activated 9-33583
 alkali halides, temp. quenching of activator centres, domain behaviour 9-32989
 alkali halides, triboluminesc. 9-43268
 alkaline earth metal halophosphate-zinc silicate-manganese mixture, responsive to u.v., patent 9-33597
 alkaline-earth borate-phosphates:Eu²⁺ 9-35678
 aluminoboro-phosphate glasses, fluoresc. spectra of Mo³⁺ 9-47350
 ammonium halides, recombination lum. from self-trapped excitons 9-33586
 anthracene, delayed fluorescence 9-33599
 calcium chlorapatite, Sb-activated 9-24444
 calcium halophosphate, activated by Sb, temperature quenching 9-26780
 calcium phosphates, Sb-activated 9-24444
 diamond, rel. to platelet defects, obs. 9-26732
 diamond, X-ray electron vibratory series 9-43263
 emission band polarization due to donor-acceptor associates, wurtzite type cry. 9-33544
 energy transfer from Nd to Yb in hosts with nonuniformly broadened activator lines 9-33584
 fluorapatite, activated by rare earth, Mg lamp excitation, spectra obs. 9-31133
 fluorberyllate glass energy transfer from Nd to Yb in hosts with nonuniformly broadened activator lines 9-33584
 fluorescence determ. of laser parameters 9-29429
 garnet, Ce activated, fluorescence 9-26777
 germanate glass, reduced, red fluorescence of Fe²⁺, Ni²⁺ and Co²⁺ 9-31134
 glass, weak phosphorescence with long afterglow, spectral characts. 9-38360
 glasses, K₂O-PbO-SiO₂, lum. centres 9-31129
 group II-VI cpds., Er-activated and containing alkali metal compensators, emission spectra and transitions 9-31128
 impurity atoms, two-electron-eigenstates of (sp)³P multiplet and phonon-induced optical transitions 9-41372
 ionic crystals, recombination luminescence investigated by EPR relaxation 9-33576
 lanthanide chelates of 1,10-phenanthroline, triplet exciton migration 9-31135
 laser internal losses, fluorescence method 9-48013
 phosphor, thermoluminescent, radiation dosimeter, 10⁻³-10³R, patent 9-29666
 phosphor particles in systems, emission spectra under 2537 Å excitation 9-31139
 phosphors, crystal structure effects 9-24442
 phosphors, effect of long term u.v. and X-irrad. on luminous efficiency, reflectance and glow curves 9-28721
 plastic scintillators, light attenuation characts., use in large area particle detectors 9-22669

Luminescence continued**solids, inorganic continued**

- polariton inelastic scattering by longitudinal optical phonons as mechanism 9-37757
 polariton scattering by phonons in radiation emission 9-24443
 quartz glass, Sm activated 9-41407
 radiative recombination rate of donor-acceptor pairs 9-49306
 rare earth oxysulphates (Ln₂SO₄), fluoresc., phosphors obs. 9-43258
 ruby, energy transport mechanisms 9-45305
 ruby, fluorescence excitation process 9-47400
 ruby, laser-enhanced two-photon decay 9-26766
 ruby, macroscopic fluorescence 9-31954
 ruby, nonradiative transition between ⁴T_{1,2} and ²E states, relaxation time constant 9-26776
 ruby, pink, resonance fluorescence, sharp line excitation 9-26775
 semiconductors, recombination radiation during pinch effect for strong degeneracy of electron gas 9-49307
 silver halide phosphors, temp. quenching of luminescence, mechanism 9-33601
 tetracene, mag. field depend., indicator of decay of singlet exciton into two triplets 9-35320
 Ag halides, flash and afterglow kinetics, ionic processes 9-33577
 AgBr:Ir excitation spectra of single cryst. and of nucl. emulsion type Ya-2 9-43251
 AgBr edge emission spectrum temp. depend., 4.2-50°K 9-35680
 AgBr phosphors, temp. quenching of luminescence Schon-Klasens and Lambe-Klick mechanisms 9-33602
 AgBr:Ag₂S phosphors, temp. quenching of luminescence Schon-Klasens and Lambe-Klick mechanisms 9-33602
 AgCl, neutralization of localized electrons by interstitial ions 9-33603
 AgCl, spectral distrib. and decay, low temp. meas., u.v. laser excitation 9-47388
 AgCl, temp. quenching mechanism 9-28709
 AgCl, u.v. excited, photon multiplication, 80°K 9-26765
 AgCl, zone refining indicating that blue lum. band is due to defects 9-35679
 AgI, sensitization by adsorbed pigments, obs. 9-26764
 AgNO₃, spin polarization in triplet state 9-37769
 Al₂O₃:Cr³⁺ duration and width of R-line rel. to Cr³⁺ concentration 9-31122
 α-Al₂O₃, phosphoresc., activation energies obs. 9-39889
 Al₂O₃, sintered alumina, effects of Mn and Na additions on glow curve 9-28728
 Al₂Ga_{1-x}As solid solns. with forbidden band width gradient, recomb. radiation 9-47389
 Al cpds., fluoresc. spectra, K_α satellites 9-49327
 Au films, dispersed, light emission centres 9-26606
 Ba:SiO₄-Sr:SiO₄ system, composition depend. of Eu²⁺ fluorescence 9-28717
 BaClF:Sm²⁺, thermal effects 9-41409
 BaO-MgO-P₂O₅ system, of Eu²⁺ 9-31131
 BaO cathodoluminescence investigated 9-28731
 BaSO₄:Pb, emission efficiency and quantum yield for X-ray excitation 9-49322
 (BaSrO) cathodoluminescence investigated 9-28731
 Ca₁₀(PO₄)₆F₂, specific fluoresc., from OH and oxide ion impurities 9-40933
 Ca₂SiO₄-Ba₂SiO₄ system, composition depend. of Eu²⁺ fluorescence 9-28717
 Ca₂SiO₄-Sr₂SiO₄ system, composition depend. of Eu²⁺ fluorescence 9-28717
 CaCO₃ calcite, tunable four-photon optical parametric noise, 4300-5860 Å 9-49253
 CaF₂:Dy³⁺, Ce³⁺ Ce³⁺ codopant eff. 9-35682
 CaF₂:Dy³⁺(Na⁺), luminescence spectra, 4.2° and 77°K 9-33578
 CaF₂:Eu²⁺ emission and excitation spectra, Eu-O complexes identification 9-47391
 CaF₂:Gd³⁺, Pr³⁺, intensity rel. to interaction of Pr³⁺ with Gd³⁺ 9-45341
 CaF₂:Gd³⁺, 76³⁺, cumulative luminesc., obs. 9-35683
 CaF₂:Gd³⁺ decay of 1° and P° levels 9-28681
 CaF₂:GdF₃ mixed cryst., Gd³⁺ fluoresc. spectra, energy levels obs. 9-35660
 CaF₂:Ho³⁺ luminescence absorption and relaxation spectra 9-35681
 CaF₂:Sm²⁺, thermal effects 9-41409
 CaF₂:Sm²⁺ crystal, spectrum, temp. depend. 9-37704
 CaF₂:Tb³⁺, Yb³⁺, quanta summation processes 9-45342
 CaF₂, optical centres of Ho³⁺ 9-33579
 CaF₂, M color centre structure, fluorescence lifetime and thermal orientation 9-26292
 Ca(NbO₃):Nd³⁺ crystal laser, spectrum of 4F_{3/2}→⁴I_{11/2} transition, 77 and 300°K 9-27332
 CaO, assoc. with F and F⁺ centres 9-49311
 CaS:Cu, phosphoresc. decay and thermal glow curves rel. to trap levels 9-35693
 CaS:Cu,Zr, phosphoresc. decay rel. to Cu activation and trap level distrib. 9-35694
 CaS phosphors, rare earth activated, decay characteristics and thermoluminescence 9-31146
 CaSiO₃:Mn(Pb), excited by u.v., induction phenomena 9-49310
 CaWO₄:Tb³⁺, fluorescence spectra, 4.2-77°K, rel. to crystal field parameters 9-33550
 CaWO₄-CdWO₄:Tb³⁺ 9-39865
 CaWO₄, emission efficiency and quantum yield for X-ray excitation 9-49322
 CaWO₄, phosphoresc. enhancement by (AsO₄)³⁻, (SbO₄)³⁻ and Pb²⁺ impurities 9-39884
 CaWO₄, X-ray, local trapping level obs., rel. to thermoluminesc. props. 9-39890
 CaWO₄ phosphors sintered in HCl stream, props. 9-28722
 n-Cd₃P₂, photoluminesc. and photoconductivity obs. 9-39712
 n-Cd₃P₂, recomb. radiation, optically excited, and stimulated emission, obs. 9-49312
 CdIn₂S₄/In₂S₃ mixed cryst., photoluminesc. w.r.t. struct. props. 9-33614
 CdIn₂S₄, photoluminesc. w.r.t. struct. props. 9-33614
 CdS, 'edge emission', time decay results supporting donor-acceptor pair model 9-49314
 CdS, Auger recomb. involving free and bound excitons 9-43252
 CdS, dislocation effects on emission spectra under X-ray excitation, 77°K 9-37771
 CdS, exciton line widths and phonon interaction 9-37766

Luminescence continued**solids, inorganic continued**

- CdS, fluorescence of crystals grown from metallic solution 9-37031
 CdS, induced by intensive electron bombardment, 300°K 9-30903
 CdS, from inelastic scattering of polaritons by longitudinal optical phonons 9-37757
 CdS, laser emission, radiative recombination mechanism 9-24445
 CdS, phonon-assisted emission of free excitons 9-37765
 CdS, photoluminesc. field quenching at elec. breakdown 9-35703
 CdS, recombination and luminescence processes in single crystals 9-37759
 CdS, recombination kinetics at low temp. and high excitation intensities 9-49313
 CdS, recombination processes under high excitation 9-37758
 CdS, semicond., emissions from acoustoelec. domain 9-45344
 CdS, stimulated exciton-photon, excitation by two- and three-photon absorpt. of giant laser pulse 9-45343
 CdS plastically deformed single cryst., fluoresc. spectra depend. on dislocation density 9-35644
 CdS single cryst. alloyed with In and Ga impurities 9-37756
 CdS single crystals grown from controlled atmospheres of constituent elements 9-37006
 CdSe, recombination and luminescence processes in single crystals 9-37759
 CdSe textured films, recombination processes 9-31123
 CdTe, photo- and cathode-luminescence 9-35699
 CdTe, photoluminescence, 20-80°K, fine structure of spectra 9-37760
 CdWO₄, X-ray, local trapping level obs., rel. to thermoluminesc. props. 9-39890
 CeO₂:Sm luminescence centres investigated 9-33594
 Cr complex, hexaurea Cr(III) ion in crystals 9-33551
 Cr(III) chelate complexes (four) with EDTA 9-24446
 Cr(III) complexes, relax. of excited states 9-39885
 CsI-Tl electroluminescence intensity depend. on exciting voltage parameter 9-26783
 CsMnCl₃, broadband fluoresc., temp. depend. 9-49319
 Cu complex, porphyrins at liquid nitrogen temp. 9-47392
 CuBr induced by giant ruby laser at 8°K 9-45345
 CuCl, induced by giant ruby laser at 8°K 9-45345
 CuCl, Zeeman effect of bound excitons 9-37721
 Eu(WO₄) single cryst., nucl. reson. fluoresc. of 3 eV ¹⁵²Sm recoil atoms, anisotropic pot. obs. 9-35596
 Eu²⁺, fluorescence in binary alkaline earth orthosilicate systems, dependence on composition 9-28717
 Eu²⁺ activated aluminosilicate phosphors 9-47390
 Eu³⁺ fluoresc. intensities 9-39876
 Eu complex, europium (III)-bis-phenanthroline-tris-carboxylate, fluorescence spectra, analysis 9-31132
 GaAs: Cd, electron-irrad., intrinsic and annealed, changes 9-49316
 p-GaAs: Cd, epitaxial, photoluminesc. w.r.t. conduction band-acceptor recombination theory 9-37783
 p-GaAs: Fe, radiative transitions between deep acceptors and valence band 9-47395
 GaAs: Ge, p-type, injection luminescence 9-49337
 n-GaAs: Si, epitaxial, photoluminesc. w.r.t. conduction band-acceptor recombination theory 9-37783
 GaAs: Si epitaxial p-n junctions, radiative recomb. mechanism 9-47138
 GaAs: Si(Ge) p-n junction, photoresponses and emission spectra 9-26570
 GaAs: Te, photoluminescence, influence of heat treatment 9-37782
 GaAs: Zn, broad-band emission near 1.38 eV, temp., excitation-intensity and stress dependences 9-24447
 n-GaAs, Edge photoluminesc. band profiles 9-47394
 n-GaAs, heavily doped, grown by liquid-phase epitaxy, radiative efficiency and deep-level luminescence 9-47396
 GaAs, induced by intensive electron bombardment, 300°K 9-30903
 p-GaAs, involving As vacancy-acceptor centers 9-45346
 GaAs, laser quality, cathodoluminescent studies 9-43267
 GaAs, radiative recombination from photoexcited hot carriers, effective temp. Maxwellian distrib. 9-41404
 GaAs bulk ionized, recombination radiation rel. to elec. field 9-49315
 GaAs diodes, rel. to mismatch dislocation obs. 9-24448
 GaAs epitaxial layers, efficiency 9-33615
 GaAs junctions, abrupt, asymmetrical, radiative tunneling 9-43253
 GaAsP diodes, yellow emission 9-41225
 GaP: Bi, Zeeman splitting of recomb. radiation from excitons 9-45347
 p-GaP: Zn(O), red emission, config. coordinates applic. 9-37761
 GaP: Zn(o), photoluminescence 9-33604
 GaP, interimpurity recombinations involving isoelectronic trap Bi 9-39866
 GaP, pair spectra involving Si donors 9-45358
 GaP, parametric, involving polariton excitation 9-49317
 GaP, photo-induced i.r. radiation 9-24472
 GaP, photoluminesc. of isoelectronic trap N, bound excitonic mol. obs. 9-39895
 GaP, red luminesc. generation, role of Zn and O doping 9-33321
 GaP, two-photon excitation, intensity behaviour of recomb. radiation of excitons 9-47393
 GaP crystal, reflection and photolum. spectra obs., 77.3°K 9-24397
 GaP diodes, green-light-emitting, grown by liq. phase epitaxy, spectral props. 9-49121
 GaP electrodes, redox processes, photoluminesc. obs. of charge transfer 9-30990
 GaP p-n diodes, photoluminescent spectra, rel. to electroluminescence 9-33610
 GaSb, cathodoluminescence, investig. by scanning electron microscope with modulated beam 9-24471
 Gd₂O₃: Bi³⁺ 9-31125
 GdCrO₃ fluorescence and absorption spectrum of Cr³⁺ magnon-assisted 9-49321
 GdF₃, Gd³⁺ fluoresc. spectra, energy levels obs. 9-35660
 p-Ge: GaAs, radiative recomb., influence of local pot. fluctuations, low-temp. 9-39867
 Ge: Sn, radiative recomb. 9-37762
 Ge, K-shell fluoresc. yield 9-24454
 n-Ge, recombination radiation spectrum 9-35684
 HBr: Pb²⁺, Tl⁺ rel. to chem. analysis, 77°K 9-33697
 HCl: Pb²⁺, Tl⁺ rel. to chem. analysis, 77°K 9-33697
 Hg halides, fluoresc., excitation-induced i.r. absorpt. obs. 9-39830
 HgI₂, electro-photoluminescence 9-39896

Luminescence continued**solids, inorganic continued**

- InP, recomb. radiation from n-p junction, hydrostatic press. effects, obs. 9-26767
 InP bulk ionized, recombination radiation rel. to elec. field 9-49315
 InSb, low-field microwave emission, contacts effects 9-49068
 K₂O-PbO-SiO₂ glasses, lum. centres 9-31129
 K₂O-SiO₂ glass, spectra 9-39872
 K halides, P-activated, obs. 9-33583
 KBr: O₂⁻, config. coordinate curves of local vibr. of centre 9-39868
 KBr: S₂⁻, spectra obs., config. coordinate curves, thermal quenching 9-39869
 KBr: Ti, In, X-ray luminesc. build-up, obs. 9-35698
 KBr, yield of NO₂⁻ centres, exciting light freq. depend. 9-31124
 KBr photoluminescence, room-temperature, electric-field-enhanced 9-45359
 KCl: Ag, X-irrad., photostimulated luminesc., due to hole release from V_K-centres 9-39897
 KCl: Ag, Tl, X-ray luminesc., build-up, obs. 9-35698
 KCl: Ag phosphors, types I and II luminescence, two competing recombination processes 9-33581
 KCl-KI mixed crystal phosphors obs. 9-33588
 KCl, F-centre, decay time and quantum efficiency, temp. depend. 9-35685
 KCl, of Eu⁺ 9-26768
 KCl, yield of NO₂⁻ centres, exciting light freq. depend. 9-31124
 KF: U, decay, model for fundamental series emission 9-35695
 KI: In, X-ray luminesc. build-up, obs. 9-35698
 KI: Tl, intercentre luminescence, elec. field effs. 9-39871
 KI: Tl phosphors, kinetics of thermal decomposition of activator hole centres 9-33582
 KI- AgI 9-47404
 KI, yield of NO₂⁻ centres, exciting light freq. depend. 9-31124
 KI and KI(In) self-luminesc. decay, additional traps 9-37784
 KI containing F-aggregate centres, excited spectra, α -band increase w.r.t. time 9-32990
 KMnCl₃, broadband fluoresc., temp. depend. 9-49319
 La₂O₃: Eu, fluoresc. characts. of Eu³⁺ 9-43257
 LaCl₃: Tb³⁺, emission yields and lifetimes of D levels of Tb³⁺ rel. to temp. and conc. 9-35690
 LaF₃: Tr³⁺ (Tr=transition metal), photo- and X-ray luminescence 9-31145
 LaF₃, concentration quenching of Nd³⁺ 9-31126
 LaF₃, Gd³⁺ fluoresc. spectra, energy levels obs. 9-35660
 LaF₃, trivalent rare-earth ion doped phosphorescence 9-43260
 LaNa(MoO₄)₂ energy transfer from Nd to Yb in hosts with nonuniformly broadened activator lines 9-33584
 Li₂GeO₅, props. rel. to growth by Czochralski method 9-37082
 LiO-SiO₂ glass, spectra 9-39872
 β -LiAlO₂, cathodoluminescence spectra and coordination of Mn²⁺, Fe³⁺, and Cr³⁺ 9-31150
 LiBr: Pb²⁺, Tl⁺ rel. to chem. analysis, 77°K 9-33697
 LiCl: Pb²⁺, Tl⁺ rel. to chem. analysis, 77°K 9-33697
 LiCl, reactor-irrad., X-ray- and thermoluminescence 9-28729
 LiF: U, decay, model for fundamental series emission 9-35695
 LiF, triboluminesc. 9-43268
 LiF laser induced, 230-540 nm spectral obs. 9-28710
 LiH, absorption and luminescence spectra, radiation eff. 9-33585
 LiNbO₃: Cr³⁺ 9-31104
 LiNbO₃: Nd³⁺, and absorpt., 4.2-295°K 9-28689
 LiNbO₃, surface radiation from nonlinear optical polarization, obs. 9-26682
 LiTaO₃: Cr³⁺ 9-31104
 LiYF₄: Er³⁺, fluorescence spectra, Er³⁺ energy levels 9-31107
 LiYF₄: Nd³⁺, polarized fluoresc. and absorpt., excitation spectra, lifetime decay and linewidths 9-39877
 LuCrO₃, Cr³⁺ fluorescence spectrum, magnon sideband emission 9-31136
 LuCrO₃ fluorescence and absorption spectrum of Cr³⁺ magnon-assisted 9-49321
 Mg₂(VO₄)₂ in sintered oxides and salts, thermal stabilization, obs. 9-35687
 Mg cpds., fluoresc. spectra, K₂ satellites 9-49327
 MgO-Al₂O₃: Cr³⁺ absorption and fluorescence spectra 9-26778
 Mn in ZnS phosphors, Gudden-Pohl effect, sensitizing of Mn 9-45348
 Na₂O-SiO₂ glass, spectra 9-39872
 Na germanate glass, Nd activated 9-39909
 Na salicylate, fluorescence radiation, angular distribution 9-45350
 Na salicylate, fluorescent flux, magnetic field dependent 9-37767
 NaCl: Ag, characts. associated with fine substructure 9-39873
 NaCl: Ag, X-irrad., photostimulated luminesc. due to hole release from V_K-centres 9-39897
 NaCl: Ag, X-ray luminesc. build-up, obs. 9-35698
 NaCl: Cu, characts. associated with fine substructure 9-39873
 NaCl: Cu, NaCl: Cu: Ag recombination luminescence, trapping of electrons and holes detect. by EPR meas. 9-33587
 NaCl: Dy³⁺ luminescence spectra obs. to gauge changes taking place during electrolytic colouring 9-32996
 NaCl: Fe from melt, X-ray luminesc. 9-37772
 NaCl: Pb phosphor, luminescence obs. 9-33593
 NaCl-KCl mixed crystal phosphors obs. 9-33588
 NaCl, of Eu⁺ 9-26768
 NaF: U, decay, model for fundamental series emission 9-35695
 NaF single cryst., F center fluorescence, thermal quenching 9-33598
 NaF(u) phosphor, fluoresc. spectra, band obs. 9-24455
 NaI: Ga(In, Sn, Pb), intracenter processes investigated 9-33590
 NaI: In centres due to O-containing impurities which reduce activator luminescence 9-33613
 NaI: Tl, characts. associated with fine substructure 9-39873
 NaI: Tl centres due to O-containing impurities which reduce activator luminescence 9-33613
 NaI(Tl) crystal, gamma photofraction functions 9-26782
 Nd³⁺: fluoride crystals, radiative lifetime of metastable ion, anomalous temp. dependence 9-41405
 Pb_{1-x}Sn_xTe, emission in mag. fields, band struct. obs. 9-41406
 PbMoO₄: Np⁴⁺, energy-level scheme for Np⁴⁺ 9-31110
 PbS induced by intensive electron bombardment 300°K 9-30903
 PbSO₄: Sm(Ce) luminescence centres investigated 9-33594
 Rb₂O-SiO₂ glass, spectra 9-39872
 RbMnCl₃, broadband fluoresc., temp. depend. 9-49319

Luminescence continued**solids, inorganic continued**

- RbMnF₃:Na²⁺, fluorescence temp. dependence of Mn²⁺ and Na⁺ rel. to Mn²⁺→Na⁺ energy transfer 9-24456
- RbMnF₃:Nd³⁺ fluorescence characts., temp. effects, 5 to 300°K 9-28718
- Sc₂O₃:Bi³⁺ 9-31125
- Se, trigonal single cryst., photoluminescence 9-41414
- p-SiC:B, N, interimpurity recombination radiation 9-28712
- SiC:Be, spectra rel. to Be conc., 77 to 500°K 9-28713
- α-SiC, radiative recombination at deep impurity states 9-28711
- SiO₂-Na₂SO₄-Gd, use in Gd microquantities determ. 9-49323
- xSiO₂-(1-x)Al₂O₃:Eu²⁺ phosphors 9-47390
- Sm²⁺, thermal effects 9-41409
- SnO in Ar, Kr, Xe matrices, fluoresc. in D-X system, matrix-induced intersystem crossing 9-49286
- SnS in Ar, Kr, Xe matrices, fluoresc. in D-X system, matrix-induced intersystem crossing 9-49286
- SrF₂:Er³⁺, quantum efficiencies and lifetimes 9-24453
- SrF₂:Sm²⁺, thermal effects 9-41409
- SrF₂:Tb³⁺, Yb³⁺, quanta summation processes 9-45342
- SrO, cathodoluminescence investigated 9-28731
- SrO.4B₂O₃:Sm₂O₃, photoluminescence and absorption, synthesized at diff. temp. 9-31155
- SrS:Cu,Zr, phosphoresc. decay rel. to Cu activation and trap level distrib. 9-35694
- SrS:Cu phosphoresc. decay and thermal glow curves rel. to trap levels 9-35693
- SrTiO₃:Cr³⁺(Mn⁴⁺), fluorescence spectra 9-26743
- SrTiO₃, photoluminesc. excitation spectra investigation 9-45025
- Tb³⁺, 4f-5d excitation energy 9-49320
- TbAlO₃:Cr³⁺, emission of Cr³⁺:Tb³⁺ pairs 9-39878
- Tb(OH)₃ ferromagnetic, fluorescence spectrum rel. to low temp. mag. and thermal props. 9-47401
- U fluorescence, X-ray, as a method of isotopic analysis 9-24598
- U fluorescence, X-ray, as a method of isotopic analysis 9-33690
- W, chemisorptive 9-43326
- Y_{1-x}Eu_xVO₄:Tb brightness and instability control by doping, patent 9-24450
- Y₂O₃:Eu³⁺, spectra satellite lines due to ion-pairs 9-24449
- Y₂O₃:Bi³⁺ 9-31125
- Y₃Al₅O₁₂, concentration quenching of Nd³⁺ 9-31126
- Y₃Al₅O₁₂, energy transfer between Er³⁺ and Tm³⁺, and Er³⁺ and Ho³⁺ 9-31126
- Y₃Ga₅O₁₂:Tm³⁺, photoluminesc., optical transitions obs. 9-49338
- Y₃Ga₅O₁₂, concentration quenching of Nd³⁺ 9-31126
- Y₃OCl₇:Yb³⁺, Er³⁺ phosphors for i.r. to visible conversions 9-49324
- YAl garnet: Nd³⁺(Er³⁺) obs. 9-33596
- YAl garnet:Nd³⁺, fluorescence rel. to effect of lutetium on optical props. 9-37093
- YCrO₃, Cr³⁺ fluorescence spectrum, magnon sideband emission 9-31136
- YCrO₃, fluorescence and absorption spectrum of Cr³⁺ magnon-assisted 9-49321
- YOCl:lanthanides, cathodo- and photo-luminesc., obs. 9-28732
- YOCl, rare earth activated, fluoresc. with u.v. irradi., photo- and cathode luminesc. 9-37768
- YPO₄:Ce, u.v. phosphor, sensitized by Th ions 9-31140
- YVO₄:Dy, effect of Eu and Tb impurities 9-47398
- YVO₄:Eu, phosphor, method of preparation, patent 9-28715
- YVO₄:Eu, photo-, cathodo- and thermo-luminesc., impurity effects 9-47409
- YVO₄:In, photo- and cathodo-luminesc. 9-47397
- YVO₄:Nd³⁺, and absorpt. and stimulated emission spectra 9-26746
- YVO₄:lanthanides, 0.7-1.1 μ, and Y₂O₃ analysis appls. 9-28714
- ZnSiO₄:Mn phosphors, film deposition by vapour phase reaction and vacuum evaporation 9-30493
- Zn₂(VO₄)₂ in sintered oxides and salts, thermal stabilization obs. 9-35687
- ZnO(BO)₂, pure cubic, electron trap distrib. obs. 9-45353
- ZnO:Ni, emission process mechanisms w.r.t. activator excitation energy transfer to electrons in traps 9-39874
- ZnO, parametric, involving polariton excitation 9-49317
- ZnO, ruby laser irradiated, obs. 9-35686
- ZnO phosphor, radical recombination characts. 9-31141
- ZnS:Ag scintillation decay due to α particles and fission fragments 9-47410
- ZnS:Bi, electronic struct. of luminesc. centre 9-24462
- ZnS:Cl phosphor spectra, green II band contour obs., electric and photoexcitation 9-26786
- ZnS:Cu, i.r., modulation and excitation by a.c. fields 9-35702
- ZnS:Cu, ruby laser irradiated, obs. 9-35686
- ZnS:Cu²⁺, excitation band of i.r. emission, correlation with valence band structure 9-37732
- ZnS:Cu phosphor spectra, green II band contour obs., electric and photoexcitation 9-26786
- ZnS:Cu rad. damage due to incident ions 9-45349
- ZnS:Cu(Mn, I) evaporated thin films, d.c. electroluminescence and photo luminescence 9-33612
- ZnS:Er³⁺, photoluminescence, with additional alkali, Cu and halogen doping 9-37774
- ZnS:Mn phosphor photoluminescence, effect of Te on quantum efficiency 9-43261
- ZnS:Zn, ruby laser irradiated, obs. 9-35686
- ZnS/Cu, decay time meas. decay after proton-excitation 9-49318
- ZnS:CdS:Mn, u.v. and visible photoluminesc., i.r. reinforcement 9-47416
- ZnS-CdS-Cu phosphors excited with 365 nm line, i.r. quenching 9-41408
- ZnS-Cu, phosphors excited with 365 nm line, i.r. quenching 9-41408
- ZnS-Cu, photoluminescence, eff. of coactivator conc. 9-24473
- ZnS-Cu phosphor, electro and X-ray excitation, nonadditivity changes 9-28727
- ZnS, afterglow due to tunneling 9-37763
- ZnS, correl. with polytypism tendency 9-35099
- ZnS, self-activated, i.r. induced luminesc., correl. with photoconductivity obs. 9-41273
- ZnS, ZnS-Sm, ZnS-Tu and ZnS-Eu phosphors, radical recombination characts. 9-31141
- Zn(Si₁₀₀-Se₄):Cu,I phosphoresc. and Gudden-Pohl effect spectra rel. to emission centres, obs. 9-35696
- ZnS electro- and photo-luminescence spectra, comparison 9-26787
- ZnS phosphors, prep. method effects on spectra 9-24470
- ZnS phosphors, sensitizing of Mn in the Gudden-Pohl effect 9-45348

Luminescence continued**solids, inorganic continued**

- ZnS phosphors, simultaneous electro- and photo-excitation investig. 9-47414
- ZnS powder, triboluminesc., jet powder technique 9-26788
- ZnS single crystals grown from Ga and In melts 9-37095
- ZnS.CdS-Ag cathodoluminescence depend. on Cu impurity 9-24474
- p-ZnSe:Cu, red and green, investig. of imperfections responsible 9-49164
- ZnSe:Cu,I, photo-, electroluminesc. temp. depend. rel. to centres, obs. 9-35701
- ZnSe, as-grown, with Cu impurity, excitation spectra 9-43254
- ZnSe, pair spectra and edge emission 9-24451
- ZnSiP₂, recombination radiation spectrum, eff. of different impurities and preparation techniques 9-26770
- ZnTe:Li(P), shallow acceptor centre obs., 2-300°K 9-26769
- ZnTe, Er³⁺ and acceptor co-doped, photoluminesc. emission and e.p.r. obs. 9-41431
- ZnWO₄ X-ray trapping level obs., rel. to thermoluminesc. 9-39890
- ZrO₂-CaO:Bi, luminescence following exposure to Hg illumination, depend. on CaO conc. 9-39875
- solids, organic**
- β-diketone salts, triplet-state energy and zero-field splitting 9-23116
- anthracene, crystalline, radiating-centres inhomogeneity, fluorometric phase spectra, -196°C 9-39879
- anthracene, excited state mean lifetime and photolum. yield depend. on impurity conc. 9-26772
- anthracene, fluoresc., singlet excitons diffusion coeff. obs. 9-41410
- anthracene, fluorescence spectra, excited by giant pulse ruby laser 9-35691
- anthracene, radiative recomb. role in carrier generation process 9-33226
- anthracene crystals, tetracene doped, evidence for long-range exciton-impurity interactions 9-24457
- anthracene crystals, fluoresc. spectrum 9-45351
- anthracene scintillator screens, prep. and props. 9-39860
- anthracene thin film scintillation, α and electron produced, new crystalline phase 9-35689
- aromatic aldehydes, perturbing vibrations 9-42426
- aromatic hydrocarbons, polarization of electronic transitions 9-31137
- aromatic hydrocarbons in polymethylmethacrylate, temp. effects 9-28723
- aromatic monomers and dimers, high-energy electron excitation 9-43259
- arylpyrazolones, spectra depend. on structure, mol. different portions contrib. 9-30074
- benzene, ³B_{1u}-¹A_{1g} transition, factor-group splitting in vibrationless zero-zero absorption band 9-35692
- benzene, molec. distortions and phosphoresc. 9-30081
- benzene, relative phosphoresc. radiative rates in two cyclohexane sites 9-28725
- benzene, vibronic intensity distrib. 9-30080
- benzil in stilbene cryst., polarization characts. rel. to trans-planar config. of benzil 9-34660
- benzo-[g,h,i]-perylene, benzene soln. and solid film, fluoresc. spectra 9-34661
- benzophenone, phosphoresc. spectrum 9-39886
- benzophenone-naphthalene, triplet energy transfer in cryst. and glassy state 9-28724
- p-benzoquinone, triplet-singlet-π* emission in cryst. and e-donor-acceptor complexes, -180°C 9-31142
- Copper porphyrins, quartet luminescence 9-26773
- coronene in hexyl alcohol frozen soln., infl. of soln. struct. and oxygen 9-49325
- coumarin and related cpds., triplet state 9-30096
- 2,5-diphenyl-1,3,4-oxadiazol dioxo derivatives of scintillator activators, rel. to intermol. H-bonds, obs. 9-30414
- α,α-dipyridyl, at 55°K using cylindrical cryostat 9-38168
- durene, doped cryst., electronic energy transfer 9-24458
- ethyltoluene photodissociation products, fluorescence spectra of trapped radicals in crystalline matrices 9-47402
- fluorescent layers for photographic plates, formation method, patent 9-27414
- formaldehyde in low-temp. solns., fluoresc. and induced phosphoresc. 9-39880
- heptane, frozen, fluoresc. spectra of coronene and 1,12-benzoperylene at high press. 9-32517
- hydrocarbons, aromatic, in solid matrix, flash excited luminescence, triplet lifetime meas., 77°K 9-43255
- ion recomb., from electron and p-irrad. 9-28720
- mesitylene, temp. depend. of phosphoresc. lifetime 9-31143
- n-paraffin frozen solutions of aromatic compounds, absorption and fluorescence spectra, effect of crystallization conditions 9-26771
- naphthalene, dark injection and radiative recomb. of electrons 9-41212
- naphthalene, delayed fluoresc. and triplet exciton life 9-24459
- naphthalene, fluoresc. quantum yield 9-33600
- naphthalene, fluorescence spectra, excited by giant pulse ruby laser 9-35691
- naphthalene, molecular admixture, relation between emission spectrum and solubility 9-28719
- naphthalene, triplet states, optical detect. of e.s.r. 9-37770
- naphthalene phosphoresc. in mixed crystals also containing anthracene guest mols. 9-43262
- naphthalene solns., phosphoresc. decay time conc. depend. 770°K 9-35697
- naphthalenes-d₂, phosphoresc. lifetimes 9-46609
- Naphthalene frozen soln. in hexane, phosphorescence spectra depend. on conc. 9-26781
- perylene in N-isopropylcarbazole, electronic excitation energy transfer 9-31138
- phenanthrene, solns. phosphoresc. decay time conc. depend. 770°K 9-35697
- phenanthrene frozen soln. in hexane phosphorescence spectra depend. on conc. 9-26781
- phenanthrene frozen soln. in octane, phosphorescence spectra depend. on conc. 9-26781
- phenanthrene oriented in biphenyl, deuterium isotope effect in zero-field splittings 9-43289
- phenothiazine, phosphoresc. triplet state 9-39888
- phenothiazine, phosphoresc. triplet state, e.s.r. 9-39887
- phenoxazine, phosphoresc. triplet state 9-39888
- phenoxazine, phosphoresc. triplet state, e.s.r. 9-39887
- phthalates, zinc and cadmium 9-47399

Luminescence continued

- solids, organic** continued
 phthalocyanine, free base, matrix isolated, fluoresc. spectra 9-49289
 plastics, fiber reinforced, visible light emission due to fracture 9-26351
 polariton scattering by phonons in radiation emission 9-24443
 poly (1-vinylnaphthalene), intramolec. triplet energy transfer 9-24461
 polycyclic azines, perturbing vibrations 9-42426
 polymers, high-energy electron excitation 9-43259
 polymethylmethacrylate, transient radiation, spatial distribution 9-37764
 polynyl carbazole, transfer of electronic excitation energy 9-39882
 proflavin in rigid org. medium, delayed fluorescence, one- or two-photon mechanisms 9-47403
 pyrazine, phosphoresc. $^3B_{2u}(n-\pi^*)$ - $^1A_{1g}$ excitonic struct. 9-47405
 pyrazine, fine struct. of Phosphoresc. at 4.2°K 9-24463
 pyrazine in durene and 1:4 dichlorobenzene, phosphorescence decay obs. 9-31144
 quinoline-heptane solns., phosphoresc. rel. to heptane phase transform., 55-123°K 9-28726
 quinoline-hexane solns., phosphoresc. rel. to hexane phase transform., 55-123°K 9-28726
 quinoxaline, radiative and radiationless decay consts. 9-39883
 quinoxaline, triplet states, optical detect. of e.s.r. 9-37770
 radiative and radiationless decay of triplet subcomponents, meas. 9-39883
 all-trans-retinal 9-24460
 rubber, uniaxially oriented, fluorescent light polarization meas. 9-39881
 scintillators based on styrene copolymers with vinyl derivatives of 2, 5-diaryloxazoles and 2, 5-diphenyl-1, 3, 4-oxadiazole 9-31149
 solid solns., e. excitation energy transfer 9-35688
 tetracene single cry., fluorescence efficiency, mag. field eff. 9-26779
 tetrakis-(dimethylamino)-ethylene, chemiluminesc. 9-23159
 triphenylamine-irrad. 3-methylpentane recomb. detect. of ion mobility 9-28720
 triphenylene, matrix site effects, to 30 kbar 9-49326
 triplet-triplet energy transfer in ordered and random media 9-28724
 tryptophan, fluoresc. quenching and solvent isotope effect 9-32787
 of uranylpropionate crystals, 3500-10000 Å, circular dichroism and polarization 9-43213
 zinc phthalocyanine, matrix isolated, fluoresc. spectra 9-49289
 4-Br-stilbene, fluoresc., vibr. analysis, 77°K 9-28699
 4-Br-stilbene, fluoresc., vibr. analysis, 77°K 9-28699
 4,4'-di-Cl-stilbene, fluoresc., vibr. analysis, 77°K 9-28699
 4-Cl-stilbene, fluoresc., vibr. analysis, 77°K 9-28699
 4-F-stilbene, fluoresc., vibr. analysis, 77°K 9-28699
 4-I-stilbene, fluoresc., vibr. analysis, 77°K 9-28699

Luminescence chambers

No entries

Luminescent devices

- see also Counters/scintillation*
 cathodoluminescent pulse light sources, sulphide applications 9-33609
 diode, electrolum., on anthracene, double injection, charact. 9-49336
 electroluminescent cell construction and characteristics for brightness, variation with frequency and voltage 9-47417
 electroluminescent comb cells utilizing elec. conducting photoluminesc. ZnSe films, fabrication 9-31127
 electroluminescent diode, non-coherent frequency response at low injection levels, derivation 9-31151
 fluorescence microscope, NUS research instrument 9-48100
 fluorescent screen brightness, energy depend. for 100 to 600kV electrons 9-38356
 fluorescent-coated phototransistor dosimeter 9-36528
 phosphors, thermoluminescent, relative sensitivities obs. 9-24466
 thermoluminescent dosimeter of CaSO₄:Mn+impurity ions, preparation, patent 9-27596
 thermoluminescent dosimeters as personnel monitors 9-24948
 tracer stability on sand grains 9-41399
 X-ray fluoresc. spectrometer using spherically curved cryst., sensitivity 9-33993
 AL_{0.5}Ga_{0.5}As:Si electroluminesc. diodes, props. and efficiency 9-37775
 CdS:Ag electroluminescent cell, d.c., efficiency of i.r. emitting phosphors 9-41415
 CdS-40 wt.% ZnS:Cu electroluminescent cell, d.c., efficiency of i.r. emitting phosphors 9-41415
 GaAs AlAs diffused diodes, injection electroluminesc. 9-37780
 GaAsP diodes, yellow emission 9-41225
 GaP-ZnO electroluminescent diodes, output charact. 9-41403
 GaP diodes, peak quantum efficiency and current relationship 9-28736
 GaP electroluminescent diode, negative resistance 9-26574
 n-GaP vapour grown epitaxial electroluminesc. diodes with green emission at room temp. 9-41224
 MgTe-CdTe visible light-emitting diodes, new material 9-47418
 Ne lamp as light transformer 9-40386
 PbS diode, stimulated recombination radiation 9-33595
 n-SiC:N electroluminesc. diodes, props. and anomalous nature of B and Al diffusion during prep. 9-37776
 SiC p-n junctions, tunnelling and avalanche processes at electroluminescence 9-43081
 Y₂OCl:Yb³⁺, Er³⁺ phosphors for i.r. to visible conversions 9-49324
 YVO₄:Eu, phosphor, method of preparation, patent 9-28715
 ZnS:Mn, Cu electroluminescent cell, d.c., efficiency of i.r. emitting phosphors 9-41415
 ZnS:Mn,Cu,Cl copper coated, high brightness panels, preparation and d.c. electroluminescent props. 9-37781
 ZnS Lumocen films, rare-earth and transition-metal fluoride doped, electroluminesc. 9-35700
 ZnSe electrically conducting photoluminescent films, prep. 9-31127

Lumino(pho)rs *see Luminescences/solids, inorganic; Luminescence/solids, organic; Luminescent devices*

Lutetium

- magnetic ordering, microscopic theory 9-24313
 muonic atom isotopes, K and L x-rays meas. 9-29997
 Lu-Dy activation in reactor, meas. of hyperfine struct. of thermal spectrum 9-22876
 in YbFe garnet, supertransferred hyperfine field, temp. depend. 9-35607

Lutetium compounds

- Gd(10wt.%)Lu alloy, nuclear component of specific heat for effective mag. field at impurity nuclei 9-33461
 Lu₂O₃ enthalpy and specific heat 298.15 to 1600°K 9-41105

Lutetium compounds continued

- LuCrO₃, Cr³⁺ fluorescence spectrum, magnon sideband emission 9-31136
 LuCrO₃ absorption and fluorescence spectrum of Cr³⁺, magnon-assisted 9-49321

Luxemburg effect *see Electromagnetic wave propagation/ionosphere*

M-centres *see Colour centres*

M-regions *see Sun*

Mach's principal *see Relativity*

Mach number *see Aerodynamics; Shock waves; Supersonic flow*

Machines, electrical *see Electrical machines*

Macromolecules

- see also Molecules/configuration and dimensions, macromolecules; Polymers; Proteins*
 β -adenosine-2'- β -uridine-5'-phosphoric acid, structure 9-39316
 biological, in solution, conformation effects on ang. correl. pattern of gamma rays 9-32536
 biomolecules in soln., rotn. and translation meas. using laser beat freq. spectroscopy 9-48113
 catalase, hexagonal crystalline and molecular structure 9-23780
 chain, distrib. functions 9-44382
 chain molecules, Monte Carlo computer simulation 9-42462
 dextran, u.s. absorpt. in aq. solns. 9-42653
 dielectric props. of long chains with one short dipole 9-46426
 DNA, double-stranded, room-temp. supercond. 9-49057
 DNA, π -electronic structs. 9-48520
 ferritin, X-ray diff. study of inorg. core, comparison with Fe hydroxides 9-37139
 graft copolymers, hydrodynamic and optical props. of solns. 9-32553
 helix-coil transition in triple-stranded macromol. 9-48519
 light scatt., comb. cascade and star models 9-42456
 linear chain of ortho-hydrogen mols. in ground rotational state, quadrupole interaction 9-25790
 long chain, entropy of crystallized solid 9-22139
 multistranded, first-order phase transitions 9-23181
 network model for viscoelastic macromolecular fluid 9-27948
 photosensibilization of biomolecules, e.s.r. study of solvent effect 9-47472
 polynucleotides, homogeneous, exciton band structures 9-26488
 polynucleotides, homogeneous, vacuum u.v. absorpt. spectra, rel. to electronic struct. 9-26750
 polyvibroadynic acid, higher-order phase transitions 9-23180
 random coil, translational diffusion const. 9-48518
 RNA, ribosomal soln. γ irradi. effects 9-26132
 rodlike, oriented in a.c. fields, light scatt. 9-23502
 rotary-diffusion broadening of Rayleigh lines scatt. from solns. 9-39104
 secondary and tertiary struct., problem of seeing in atomic dimensions 9-38925
 semirigid, light scattering theory, statistical zigzag model 9-23179
 two-stranded, higher-order phase transitions 9-23180

Madelung constant *see Solids/structure*

Maggi-Righi-Leduc effect *see Magnetothermal effects*

Magnesium

- atom, binding energy with dissolution in Cu-Mg dilute solid solns. 9-37175
 atom, dipole polarizabilities, elec., and dipole shielding factors from Hartree-Fock wave eqns. 9-44241
 atom vapour source, half-life after emission spectra, meas. by atomic absorpt. spectrometry 9-48391
 diffusion of low solubility impurities 9-23836
 dynamic stress-strain release paths up to 200kb 9-39405
 elastic shear constants, band structure contribution, model potential theory validity 9-30630
 fatigue damage under cyclic stress, slip band extrusions and twin boundary filamentary growths 9-32981
 films, dislocations at contact boundary with MoS₂ 9-32973
 films on W(110) face, (structure from LEED obs. 9-26184
 forbidden transitions in isoelectronic sequence, relative line strengths 9-36653
 Hall effect in single crystals, room temp. 9-26518
 hexagonal, vibrational spectrum 9-42946
 impurity distribution during directed crystallization process 9-40931
 metallurgy, book 9-39447
 neutron irradi. damage and recovery, low temp. 9-32940
 n.m.r., single crystal, quadrupole interaction and Knight shift 9-39920
 oxidized surface, work function, contact potential difference method 9-31000
 phonon dispersion relations calc. from model pot. 9-37316
 radiative Auger effect, simultaneous emission of X-ray photon and L-shell electron 9-40553
 slip, coarse, model of crack formation and propag., rel. to fatigue 9-48904
 superconductivity predictions 9-35358
 surface free energy anisotropy, from equilib. shapes of Ar bubbles 9-46717
 target in 3 MeV Van de Graaff accelerator, vacuum evaporation prep., thickness determ. 9-29680
 u.v. spectrum, 2000-500 Å, auto-ionized line series 9-42330
 vapour, electron transfer cross-sections for 5-70 keV H atoms and ions 9-22997
 work function, correlation energy contribution using pseudopotential model 9-35515
 KCl:Mg, additively coloured, optical, elec. and e.s.r. obs. 9-48868
 Mg-Ni system, contact fusion 9-26373
 Mg⁺, earth's atmosphere, measurements of reaction with ozone 9-40044
 Mg⁺, isoelectronic series, theoretical ionization energies and oscillator strengths 9-22927
 Mg²⁺ in LiF, γ -ray coloration enhancement 9-39377
 Mg II, H and K line profiles, comparison of models for chromosphere 9-31636
 Mg II doublet lines in solar spectrum, balloon obs. 9-24900
 spectral lines, Stark broadening and displacement rel. plasma high temp. meas. 9-25913

Magnesium compounds

- alloys, effect of decomposition of the supersaturated soln. on u.s. attenuation 9-46990
 alloys, mechanical properties, effect of low temps. 9-23905
 alloys, metallurgy, book 9-39447

Magnesium compounds continued

- aluminate spinels, variable stoichiometry, growth and characterization 9-37084
attenuation of shear waves 9-37335
fluorescence spectra, K_{β} satellites 9-49327
magnesia, cryochem. method for prep. 9-33125
magnetite, cryst. defects, X-ray topographic obs. 9-32958
Mg-Al eutectic alloy, superplastic deform. mechanism 9-42883
olivine-garnet in meteorite 9-27089
periclase solid soln. containing Li^{+} and R^{+3} (Cr, Al, Fe) ions 9-23955
pyroxenes, phase relations study via inversion of clinoenstatite at high temp. 9-24934
spinel, Ni^{2+} doped, absorpt. spectra 9-43242
Ag-Mg solid solution alloys, Ag-rich, stored energy of cold work and elec. resistivity 9-48920
Al-Cu-Mg-Ag alloys, S precip. obs. 9-48928
Al-Cu-Mg alloys, S precip. obs. 9-48928
Al-(2.5 at.%)Cu-(1.2 at.%)Mg alloy, Si effect on initial stages 9-48915
Al-Mg-Si alloy, electron microscope images, quality deterioration with specimen thickness, 50-100 KeV 9-23747
Al-Mg-Si alloys, recryst. behaviour, influence of precipitates 9-39452
Al-Mg-Si alloys containing Mg₂Si, 2-stage ageing effect 9-39461
Al-Mg-Zn alloy, recryst., dislocation arrangement influences 9-37276
Al-Mg-Zn alloys, ageing and plastic deform. 9-37280
Al-Mg-Zn pre-precipitation, lattice parameters rel. to ageing 9-41049
Al-(11 wt.%)Mg alloys age-hardening deform. by hydrostatic extrusion, effect on struct. and props. 9-41051
Al-Mg alloy, Stress-induced knitting of dislocation networks with four-fold nodes 9-44706
Al-(0.5 at.%)Mg, quenched, hardening mechanism at 86°K 9-30699
Al-(3-15 wt.%)Mg alloys, dislocation struct. by X-ray diff. and electron microscopy 9-40946
Al-Zn-Mg-Cu alloys, deformed, substructure and susceptibility to intergranular stress corrosion cracking 9-23811
Al-Zn-Mg, alloys precipitation near grain boundaries 9-39489
Al-Zn-Mg 1 type alloy, blue tint of glossy anodized extruded profiles 9-39833
Al-Zn-Mg alloy, fatigue props., effect of shot peening 9-26315
Al-Zn-Mg alloy, weldable, stress-corrosion resistance, effect of quench rate, rel. to microstruct. changes 9-46919
Al-Zn-Mg alloys, preprecip., hardness and small-angle X-ray scatt. me. 9-23979
Al-Zn-Mg properties rel. to natural ageing and ageing between 100-340°C 9-37281
Al-(6wt.%)Zn(2wt.%)Mg alloy, precipitate nature and morphology 9-28390
AlZnMg 1 alloy, annealing effect on microstruct., susceptibility to stress and layer corrosion 9-46779
Al-2at%Mg-2at%Mg; reversion and reaging 9-41048
CaNH₄P₃O₈, cry. struct. 9-37143
n-Cd_{1-x}Mg_xTe:(Al) mixed cryst., Hall coeff. and resistivity w.r.t. electron mobility, carrier conc. and donor ioniz. energy 9-43054
Cu-Mg solid solns., dilute, binding energy between dislocation and Mg atom 9-37175
Hg-Mg system, perturbation theory and alloying behaviour 9-44860
Li-Mg alloys, lattice parameters 9-42789
Mg-Al-Zr-Be alloy, correlation of orientation and polarized etching facets 9-39186
Mg-Bi alloys, amorphous, prep. elec. conductivity and thermoelec. power 9-30851
Mg-Eu system, phase diagram 9-33150
Mg-Fe ferrites, magnetization and magnetocrystalline anisotropy, infl. of O content 9-28633
Mg-(5 at.%)Li-(1.5 at.%)Al alloy, plastic deform. during rolling, mechanism 9-33035
Mg-Mn alloys, creep specimens and thermally aged, α -Mn precipitate, e. microscope exam. 9-28265
Mg-Mn monocrytals, change of anisotropy of mag. viscosity, -196°C to Curie point 9-45183
Mg-Sn alloys, solution hardening, room temp. 9-23984
Mg-Zn-Mn alloy, age hardening, patent 9-48942
Mg-Zn-Mn alloy, heat treated, patent 9-46960
Mg-Zn-Zr alloy, strain-rate hardening, grain-size depend. 9-39443
Mg-Zn-Zr cast alloy system, dendritic growth forms, non-equilib., of phase ZnZr, conversion 9-41056
Mg-(5.1 wt.%)Zn alloy, deform. twinning inhibition by precipitates 9-46827
Mg-Zr alloy, creep curve anal. in const. load tests 9-30673
Mg-base alloys, tensile strength during atmospheric corrosion test 9-37828
(Mg,Fe)₂SiO₄, olivine, optical absorpt. spectra, 1.7° to 290°K 9-45324
(Mg,Fe)Al₂Si₂O₈, grandierite, crystal structure 9-30564
(Mg_{0.4}Mn_{0.6})Fe₂O₄, electronic conductivity, thermoelectric power 20-100°C, effect of hydrostatic pressure 9-33300
Mg_{0.53}Mn_{0.47}Fe₂O₄ single crystal, ferromag. reson. props., 77°K to room temp., 9100 MHz 9-49342
Mg₂Ge-Mg₂Sn solid solutions, lattice thermal conductivity 9-33199
Mg₂Ge, optical constants and electronic band structure calcs. 9-24356
Mg₂Ge, optical constants from reflectance meas., 0.6-11.0 eV at 77°K 9-24355
Mg₂P₂O₇, glassy and crystalline, valence angles and dihedral angles rel. to structure 9-40906
Mg₂PtO₄, synthesis and unit cell consts. 9-32868
Mg₂Si-Mg₂Sn(Ge) solid solutions, lattice thermal conductivity 9-33199
Mg₂Si, band structure and dielec. function 9-41135
Mg₂Si, electron density distrib. in single crysts. effect of multiple diffraction on meas. 9-28263
Mg₂Si, optical constants and electronic band structure calcs. 9-24356
Mg₂Si, optical constants from reflectance meas., 0.6-11.0 eV at 77°K 9-24355
Mg₂SiO₄, crystal struct. of high press. modification, geophys. implications 9-40908
Mg₂Sn, optical constants and electronic band structure 9-24356
Mg₂Sn, optical constants from reflectance meas., 0.6-11.0 eV at 77°K 9-24355
Mg₂SnO₄, thermal neutron capture, chem. and Mossbauer study 9-26852
Mg₂Su, energy band structure from reflection spectra 9-35647
Mg₂Cd, ordered and disordered, soft X-ray L₂₃ emission edge-breadth 9-43248

Magnesium compounds continued

- Mg₂Cd single crystal, basal slip, 77° to 500°K, critical resolved shear stress 9-33054
Mg₂NF₃, crystal structure 9-39282
Mg₂Sb₂-Ge amorphous films, reordering diffusion process under annealing 9-34985
Mg₂(VO₄)₂, luminesc. in sintered oxides and salts, obs. 9-35687
Mg (0.7 at.%) Mn, fatigue at 400°C, for annealed and/or aged samples 9-30638
MgAl₂O₃ stoichiometric spinel, trace detection by neutron activation analysis 9-35088
MgAl₂O₄:Cr³⁺ spinel, theory of strong and weak trigonal field, optical spectrum and e.p.r. analysis 9-28644
MgAl₂O₄, Kikuchi line doubling in strong bands 9-23763
MgAl₂O₄, Kikuchi patterns, multiple-beam dynamic effects 9-48835
MgAl₂O₄, spinel, crystal growth by vert. pulling 9-28235
MgAl₂O₄, vertically pulled crysts., morphology and defect characts. 9-46743
MgAl₂O₄ spinel, hot pressing behaviour 9-30706
MgAl₂O₄ spinel ceramics, sintered, kinetics of formation 9-28389
MgAl₂O₄ spinel crystals, stoichiometric, growth by flux evaporation 9-37085
MgAl₂O₄ spinel single crystals, stoichiometric, growth by flux method 9-37086
MgAl₂O₄ substrate, epitaxial Si films, Hall effect and resistivity meas. 9-36950
MgBr₂:A²⁺-X²⁺-X²⁺ system (0,0) bands rotational analysis 9-42399
MgBr spectra, A²⁺I²⁺-X²⁺ system, rot. analysis of (0,0) bands 9-30036
MgCO₃, hot pressing, behaviour 9-33111
MgCaSiO₄, monticellite, e.s.r. of Mn²⁺ 9-24497
MgCd, phase recrystallization rel. to grain size 9-23969
MgCr₂O₄, antiferromag.-paramag. transform. of first order 9-49224
MgCr₂O₄, magnetic structure, neutron diff. study 9-28630
MgCr₂O₄ single crystal formation by interdiffusion in MgO-Cr₂O₃ system 9-28319
MgF, vibr. transition probabilities and r-centroids for A-X system 9-46367
MgF₂:Co²⁺, exchange interactions obs. from far-i.r. spectra 9-41384
MgF₂, high melting point crystals, growth from vapour phase 9-23666
MgF₂, phonon scattering, correlation of anisotropic features with thermal conductivity 9-28412
MgF₂, thermal cond., 25 to 900°C 9-48975
MgF₂ ceramic, hot-pressed, u.s. shear wave propag. meas. 9-46983
MgF₂ overcoated Al mirrors for space flight optical degradation due to u.v. radiation and condensation obs. 9-40111
MgF₂ single cryst., elastic consts. 9-33017
MgF₂ single cryst., electron- and neutron-rad. damage comparison, optical absorpt. obs. 9-35117
MgF₂ single cryst., phonon propag., anisotropic phonon-phonon scatt. 9-37314
MgF₂ thin film capacitor, break-down studies 9-37586
MgF₂ vapour, absorption spectra bands obs., ν_2 bending vib. assignment 9-23037
MgFe₂O₄ spinel ferrite, absorpt. and Faraday rotation, 300°K, 1 to 8 μ 9-45277
MgH line spectrum solar center-to-limb behavior 9-31633
MgMnZn ferrite memory cores, origin of threshold response delay 9-49217
MgMoO₄-MoO₃ system, thermo-optical determ. of equilibrium diagram for new phase 9-23978
MgNH₄P₃O₈, crys. struct. 9-37143
MgNO₃-water solns., i.r. and Raman spectra rel. to NO₃⁻ symmetry, obs. 9-36887
MgO:⁵⁷Co Mossbauer spectra, Fe multiple charge states, hyperfine interac. and relax. processes 9-33530
MgO:Al₂O₃:Cr, variable stoichiometry spinels, growth and characterization 9-37084
MgO:Cr, phonon scatt. by paramag. ions, from thermal magnetoresist., 0.4-4.0°K 9-33162
MgO:Cr³⁺, stress-induced crystal. field 9-28642
MgO:Cu²⁺, dynamic Jahn-Teller effect at 4.2°K 9-24494
MgO:Fe²⁺ microwave phonon detection by phonon-photon double-quantum transitions 9-37315
MgO:Mn²⁺, e.s.r. rel. to tetragonal and octahedral sites of Mn²⁺ 9-24496
MgO:Ni²⁺, e.p.r. line shape 9-24495
MgO:Ni²⁺ spin-phonon interactions, molecular orbital theory 9-39787
MgO-Al₂O₃:Cr³⁺ absorption and fluorescence spectra 9-26778
MgO-Cr₂O₃-O₂ system, phase equilibrium at high O pressures 9-28404
MgO-Cr₂O₃ system, interdiffusion formation of MgCr₂O₄ single crystals 9-28319
MgO-P₂O₅-BaO system, luminescence of Eu²⁺ 9-31131
MgO, chromite solid solution, effect of transition metal ions on MgO cell dims. 9-32921
MgO, Ag and Au epitaxy mechanism of (100) cleaved surface in electron microscope 9-39220
MgO, cation solid solns., Mg_{1-x}(R⁺, R²⁺)O type 9-39477
MgO, cavity form. by annealing 9-44693
MgO, defect cluster centres in rel. to neutron-electron-irradiation or additive coloration 9-46838
MgO, diffusion of Ca²⁺ impurity 9-44739
MgO, diffusion of divalent impurity cations 9-44737
MgO, diffusion of Fe and Ni 9-44738
MgO, e.s.r. from Fe²⁺ vacancy-pair centre 9-47438
MgO, electron-phonon interaction in F-centre 9-44689
MgO, electron irradi., neutron irradi. and additively coloured crystals, zero-phonon line study 9-45325
MgO, electron microscope images of single cryst., mean and anomalous absorpt. coeffs. 9-32920
MgO, F-containing trapped-hole centre, structure from ENDOR meas. 9-39355
MgO, F band, magneto-optical structure 9-35116
MgO, fully dense polycryst., strength and fracture 9-42893
MgO, Ga³⁺ diff. 9-26302
MgO, grain diameter distribution, influence of purity 9-39283
MgO, hot-pressing, effects of gaseous impurities 9-35202
MgO, Jahn-Teller effect of octahedrally coordinated Cr²⁺ 3d⁴ ion, in acoustic paramag. reson. interpret. 9-24346
MgO, Kikuchi line doubling in strong bands 9-23763
MgO, n-irrad., R-like centre, Faraday rotation obs. 9-28306
MgO, n-irrad., R-like centre, Faraday rotation obs. 9-26295

Magnesium compounds continued

- MgO, phonon dispersion curves 9-39509
 MgO, phonon scatt. by paramag. ions, from thermal magnetoresist. 0.4-4.0°K 9-33162
 MgO, point defect form. energy calc. 9-44688
 MgO, positron annihilation 9-30830
 MgO, recrystallization kinetics during sintering 9-33105
 MgO, solution growth of single crystals 9-35021
 MgO, surface diffusion, obs. review 9-37198
 MgO, thermal expansion wgt., 12 to 300°K, deriv. from lattice parameter data. 9-28429
 MgO, water-induced toughening 9-42906
 MgO added to borolanthanum glasses, immiscibility and catalytic crystallization 9-34971
 MgO irregular crystall., sintering under high press. 9-30728
 MgO molecule, oscillator strengths, corrections to recent results 9-30037
 MgO polycrystalline periclase, elastic parameters rel. to press. 9-42867
 MgO powder in contact with high refr. index glass, reflection props. 9-43209
 MgO single crystals, electron and neutron irradi., hardening 9-33099
 MgO wedge crystals, thickness fringes in electron micrograph profiles 9-26240
 Mg(OH)₂, hot pressing, behaviour 9-33111
 MgO.Al₂O₃ system, spinel crystal growth by flame fusion method 9-23684
 MgSiP₂, semicond., growth, lattice parameter and energy gap 9-44974
 MgTe-CdTe solid solution, new material for visible light-emitting diodes 9-47418
 MgZn₂, single crystalline elastic constants 9-28331

Magnetic amplifiers *see Amplifiers; Magnetic devices*

Magnetic anisotropy *see Magnetic properties of substances; Magnetization state*

Magnetic bays *see Earth/magnetic field, variations; Magnetic storms*

Magnetic bottles *see Magnetic fields; Plasma confinement*

Magnetic cooling

- Cu(NO₃)₂ · 2.5H₂O, adiabatic cooling 9-26662

Magnetic devices

- Boolean (logic) all-magnetic circuits using transfluxors, efficiency and optimum operating conditions determ. 9-40310
 coil systems, square, for highly uniform field prod. 9-25173
 cores, flake, high permeability, improved Q-factor, permeability flux stability and temp. variation, patent 9-45917
 crack detection 9-39436
 demagnetizer, for solid specimens, construction and theory 9-22344
 Ferrites core memory using single major remanent state of one polarity for both digital information states 9-43844
 Helmholtz coils, servomechanical control systems to compensate for field fluctuations 9-31906
 history-effect memory using single major remanent state of one polarity for both the digital information states 9-43844
 magneto-optic readout system, heat problem 9-41872
 medical applications 9-45697
 memory, permalloy film with ternary paramagnetic additions 9-36252
 memory, plated-wire, mag.-field computation using integral/matrix-eqn. technique 9-43845
 memory cells 9-43839
 memory element, closed-flux, development 9-43841
 memory stores, film, photon- and electron-beam- accessed, improvement of signal-to-noise ratio 9-43843
 microwave ferrite, development 9-43840
 recording media preparation by gas plating method, patent 9-29370
 recording medium, patent 9-47899
 rotating probe for field strength meas. of electromagnets 9-22342
 solenoid producing field up to 30kOe and consuming 500 kW 9-43838
 substrate coating orientation, magnetic applicator blade, patent 9-22341
 wire memories, DRO-plated, life expectancy from accelerated ageing process 9-43842
 MgMnZn ferrite memory cores, origin of threshold response delay 9-49217
 Mn_x-(M,Fe)₂B₄, (M=Co,Ni), ferromagnetic, composition rel. to applic. in thermal switches, patent 9-33451

Magnetic domains *see Magnetization state/domains*

Magnetic field measurement

- CRO and rotating coil used to measure 9-22340
 earth's components meas. from moving body using celestial orientation 9-45552
 earth's H and Z components using proton magnetometer 9-45553
 electromagnet, rotating probe for strength meas. 9-22342
 geomagnetic variations, sounding methods 9-31452
 geomagnetic vars., recording equipment freq. characts. standardization 9-31454
 magnetograms, scanning installation, semiautomatic 9-31449
 magnetometer, differential and digital, applic. of quantum supercond. 9-41189
 magnetometer, for Earth's field, rocket released construction and preliminary results 9-41593
 magnetometer, for Earth's field, rocket- released attitude stabilized. 9-41592
 magnetometer, persistent current, using vibr. supercond. plane to shuttle 9-35374
 magnetometer, torque, for use in superconducting magnets 9-49060
 magnetometer, vibrating-coil, rel. to pressure effects on mag. props. 9-45047
 magnetometer based on Josephson effect, operating characts. 9-49059
 magnetometer with permalloy transducer 9-34140
 nuclear magnetometers, remote- controlled 9-36251
 plasma, by Faraday effect on resonant laser radiation 9-38998
 in plasma, using laser resonant radiation 9-40687
 probes, versatile epoxy casting technique 9-34139
 proton-resonance field stabilizer 9-34142
 semiconductor diode V-I characteristics, utilization of change on applic. of mag. field 9-29368
 simulation through electrolytic flow of field near superconductor surface 9-24130
 space earth, search coil magnetometer experiments 9-35895
 spectrometer, β , double focussing $\pi\sqrt{2}$, saturated Fe core transformer 9-46135
 superconducting magnets, torque magnetometer 9-49060
 near superconducting surface, simulation by electrolytic flow 9-24130

Magnetic field measurement continued

- two-dimensional, currents and coil forces as contour integrals 9-34141
 vectormagnetograph, simultaneous astronomical field direction meas., calibration technique 9-31684
³He gas optically pumped, nuclear polarization meas., sensitive low-field magnetometer 9-23002

Magnetic fields

- see also Earth/magnetic field; Electromagnetic fields; Interplanetary magnetic fields; Sun/magnetism*
 amplification of weak fields in turbulent flow 9-48541
 applied to axially symmetric stream with clamp, magnetohydrodynamic laminar boundary layer 9-30191
 constant, produced by semi-ellipsoidal air-cored coils 9-27275
 cylindrical annular sectors, uniformly magnetized 9-25174
 diffusion in ferromagnetic body 9-41734
 display of lines by ordering of particles 9-29157
 earth, induced by deep sea tides 9-31275
 in e.m. system, scalar and vector potential numerical determ., rel. to non-linearity of ferromag. mats. 9-27274
 exothermic waves of ionised gases in magnetic field, calculations 9-30225
 in ferromagnetic nonlinear medium, diffusion 9-47895
 Galactic, fluctuations, calc. from pulsar signals dispersion and Faraday rotation 9-49531
 galactic, viscous and thermal generator propositions 9-33898
 Galactic field, origin 9-49530
 generation in turbulent fluid, infinitely cond., applic. to galactic mag. field 9-43515
 generation in flux-compression, flux loss and energy balance 9-45916
 helical, calculation of symmetry 9-28010
 Helmholtz coils, servomechanical control systems to compensate for field fluctuations 9-31906
 h.f., threshold energy absorpt. by uniaxial antiferromagnet 9-49222
 homogeneous, magnet assemblies for production, patent 9-27277
 induced inside rot. spherical conductor by external sources, calc., Moon appl. 9-31599
 in interstellar clouds of neutral H, Zeeman effect obs. 9-36001
 local structure in the Galaxy and Gould's Belt 9-24746
 magnetic, lift given to a current wire moving over the field, magnetic field diffusion problem 9-22343
 magnetohydraulic track behind circular cylinder 9-30188
 medical applications 9-45697
 megagauss, flux-compression production 9-29369
 megaersted, liner implosion prod. 9-45915
 metal film, quantum oscillations of thermodynamic props. 9-30812
 negative V" way toroidal field with helical multipole 9-32631
 non-adiabatic, transit of charged part. beams, transverse energies and mag. moments 9-25175
 for non-destructive detection of abnormal portion in steel plate 9-28589
 non-linear media, finite difference eqns. 9-27276
 across plasma current between conducting deflectors, longitudinal stability 9-30282
 plasma electrons, strength rel. to plasma lifetime, absorpt. conditions and u.h.f. energy attenuation 9-27974
 plasma jet in toroidal magnetic field, motion 9-30250
 plasma shock wave interactions 9-27992
 production by bioelec. currents in humans, detection and analysis 9-45701
 in rotating frames of reference 9-47873
 in solenoid, cooled, dependence on battery parameters 9-47896
 solenoid producing field up to 30kOe and consuming 500 kW 9-43838
 spectrometer, uniform field with screens, fringing field distrib. 9-34352
 insuperconducting cylinder, electron interferometric meas. 9-25172
 superconducting solenoids, inside-notch- corrected for high homogeneity, design 9-35557
 superconductor, type-I, current-carrying intermediate state and coupled motion of flux 9-30867
 transient above MOe region, prod. by e.m. compression of metallic foil 9-47894
 turbulent flooding of stream of electrically conducting liquid 9-30205
 uniform, prod. by square coil systems, study 9-25173
 in uniform waveguide, computer program for computation 9-34125
 whiskers ferromagnetic micron-sized rel. to magnetization distrib. and free poles 9-45134
 Ar plasma, impulse drivers, interactions 9-30229
 Gd-(9wt.%)La alloy, effective field at impurity nuclei from nuclear component of specific heat 9-33461
 Na, liquid, e.m.f. along external field, induced by flow, (α -effect) 9-36899
 Nb wire, superconducting, effect of tension on critical fields 9-35532
 NbTe, supercond., critical mag. fields rel. to varying carrier conc. 9-33274
 (Sr_{0.8}Ba_{0.2})₂ZnFe₂O₄, hexagonal ferrites, critical, from magnetization curves 9-26657
- effects**
 antiferromagnet, uniaxial phase transitions 9-45199
 antiferromagnetic decorated Ising lattice, eff. on magnetization, susceptibility and heat capacity 9-24322
 arc rotation rel. to erosion rate at electrodes 9-42578
 on Brownian motion of particles with mag. mom. 9-27177
 charged particle moving in a medium with ionization losses and in a non-uniform magnetic field 9-44094
 charged particles in superposed Heliotron and biconical cusp fields, equation of motion 9-32629
 current grid, reflection of shock waves, theoretical analysis 9-38305
 cylindrical domain Bloch wall flattening 9-24299
 cylindrical sample in transverse field isothermal elec. conductivity, magnetomorphic oscillations 9-37427
 distortion of cholesteric structure of liquid 9-32794
 disturbance measurements in theta pinch coil, h.f. analogue model 9-25896
 disturbances in Maxwell viscoelastic solid 9-29236
 Ekman boundary layer, analysis 9-30194
 elastic solids, l.f. magnetoacoustic effect, rel. to stiffness and attenuation 9-35283
 electron beam compression, high-current density, Brillouin-focused, axially symmetric 9-22348
 electron gas in mag. field, Vlasov description 9-28035
 electron in crystal, using group theory 9-48983
 electrons, hot, in crossed elec. and quantizing mag. fields 9-47029
 e.m. radiation, polarized, reson. scatt. in weak fields 9-38333
 e.m. waves, amplitude modulation by modulated fields, modified theory and applic. to communications during blackout 9-32617

Magnetic fields continued**effects continued**

- e.m. waves, amplitude modulation by modulated fields, modified theory and applic. to communications during blackout 9-32617
 exciton polarizability and magnetic field reversal in yellow series spectrum 9-26728
 exciton states 9-24101
 ferrites rel. to microwave permeability, effect of domain structure 9-33472
 ferromagnet in finite applied field, heat capacity singularity 9-44831
 on ferromagnetic bodies, susceptibility increase by additional alternating field 9-45132
 ferromagnetic films, residual magnetization creep in demagnetizing self-fields 9-39772
 ferromagnetic magnon states propagation, effect of sudden change in external field 9-35548
 ferromagnetic metals, on energy dissipation mechanism 9-33013
 ferromagnetic metals, on energy dissipation mechanism 9-23848
 ferromagnets, impure, specific heat 9-44830
 FeTi₂S₂ during cooling rel. to low-temp. mag. props. 9-45221
 fluid with variable conductivity in nonuniform field, Joule dissipation determ. during flow 9-39088
 gas of rough spherical molecules, change in thermal conductivity 9-45798
 geomagnetic field effect on super l.f. noise in earth-ionosphere cavity 9-31395
 geomagnetic field effect on super l.f. noise in earth-ionosphere cavity 9-31395
 Gunn diode, vibrs. and low-freq. oscillations 9-39654
 He-Ne 6328 Å laser, external polarization technique using permanent magnet 9-29418
 hot electron gas, nonlinear size effects 9-41141
 on interstellar dust cloud grain orientation 9-29033
 jet, perfectly conducting liquid, stability 9-30195
 jet, two-dimensional, hydromag. stability of free flows at large Reynold's numbers 9-46599
 Josephson junctions, zero-voltage current 9-35373
 laser beam deflection 9-29435
 linear-response theory and irreversibility transport phenomena 9-36135
 magnetic colloids, magnetoviscosity 9-48722
 magnetoplasma; collisionless, Maxwellian, nonrelativistic boundless, Landau damping of longitudinal electron oscillations 9-39009
 magnetostatic surface waves, amplification by interaction with drifting charge carriers in crossed elec. and mag. fields 9-43816
 magnon-drag thermoelectric power analysis, low temp. 9-33400
 metal, antiferromag., rel. to mag. spectrum 9-28638
 metal, diamag. resonance in field normal to surface 9-31019
 metal, screening of charged impurity 9-33218
 metal, surface impedance, field strength depend. 9-26514
 metal sharing by alternating magn. fields 9-41013
 metal with localized impurity, s-d exchange model 9-47220
 metals, antiferromag. magnetoresistance 9-26659
 metals, elec. conductivity 9-30838
 metals, phonon freq. and electron-phonon interaction 9-26471
 metals, surface levels 9-49001
 mica, on surface conductivity 9-47153
 modulation, influence on paramagnetic absorption line width in ESR spectrometers 9-38825
 molecular crystal, Wannier excitons conc. change 9-39570
 on muonium, modulated μ^+ -spin precession (beats) prod. 9-36433
 on neutron beta decay rate, astrophys. implications 9-44058
 paramagnet with nonaxially symmetric crystal field, rel. to hyperfine struct. of Fe³⁺ Mossbauer spectra 9-49257
 particle momentum in inhomog. mag. field calc. 9-31910
 Penning discharge charact. 9-32642
 permalloy film, high speed flux reversal and relax. processes, dynamic Kerr obs. 9-45169
 permalloy thin film, effect of mag. annealing on mag. props. 9-41322
 in plane MHD channel flow, own field eff. on power curves 9-27983
 plasma, collisional, in curved fields, kinetic theory of stability 9-32671
 plasma, collisionless, magnetic curvature effect on density gradient drift instabilities 9-32686
 plasma, relativistic oscillations, covariant treatment 9-30264
 plasma cylinder, magnetized; ion thermal resonances induction 9-36775
 plasma density gradient drift instabilities, mag. curvature effect 9-30281
 on plasma drift temperature instability in time modulated mag. field 9-23335
 plasma in static field, sum and difference freq. generation due to two nonuniform elec. fields 9-32648
 plasma jet cutoff 9-34771
 plasma periodic quadrupole min. B field, optimum config. 9-32668
 plasma string with a.c., stabilisation with quadrupole field 9-40667
 plasma waves excitation and damping, Thomson scatter meas. 9-32663
 pulsed field conversion of thermal spin fluctuations to elastic microwave power 9-37226
 Rayleigh-Taylor's instability, eff. of mag. field and Coriolis forces 9-46434
 rockets in evacuated tubes, mag. suspension and guidance by supercond. magnets 9-37499
 semiconductor, absorption of light in a laser beam field 9-39828
 semiconductor, antiferromag., transform. into metal 9-37505
 semiconductor, antiferromag., transform. into metal 9-24168
 semiconductor, galvanomagnetic phenomena in crossed elec. and mag. fields 9-37511
 semiconductor, heating of electrons and phonon bottleneck in crossed elec. and quantising mag. fields 9-33278
 semiconductor with inelastic electron scattering, current oscillations 9-33287
 semiconductor with non-standard dispersion law, rel. to plasma oscillations 9-37504
 semimetals, giant sound absorption oscillations, rel. to ang. depend. of amplitude 9-48955
 solutions, effect on thermodynamic props. and surface tension 9-48692
 spherical multipole, hot plasma confinement 9-25900
 spherical multipole, hot plasma confinement and production, experimental results 9-25901
 steel, C, martensitic pt location 9-46959
 superconducting alloys, rapidly alternating field of large amplitude, behavior of rparameter Δ 9-37463
 superconductor type II in alternating field, effect on current flow 9-28473

Magnetic fields continued**effects continued**

- tetracene, variation in fluorescence intensity, indicator of decay of singlet exciton into two triplets 9-35320
 on thermal conductivity of gases 9-36808
 thermal spin fluctuations conversion to elastic microwave power by pulsed field 9-37226
 thermionic converter gap, potential distribution 9-41871
 train mag. suspension and guidance by supercond. magnets 9-37500
 transverse, on laser diodes, dielectric-waveguide modes 9-34175
 two oppositely charged particles, partial separation of Schrodinger eqn. 9-38233
 u.s. waves, oscillations, rotation angle of plane of polarization and ellipticity 9-44814
 vehicles mag. suspension and guidance by supercond. magnets 9-37500
 viscosity of mag. fluid 9-48532
 Ar discharge emission 9-41894
 Bi-Sb semiconducting alloys, magnetoresistance anomalies, 4.2° to 10°K 9-30890
 Cd, diamag. resonance in field normal to surface 9-31019
 Cd, ultrapure, sound velocity 9-35274
 CdS, magnetomicrowave effects at 38 GHz, charge carrier density control by photogeneration 9-30922
 CeMg(NO₃)₃, ground-state g factor reduction 9-43276
 Co, resistivity, depend. and temp. depend. 9-24128
 Cr, resistance temp. depend. minimum 9-39585
 Cr spin density wave 9-35580
 Cu, ultrapure, sound velocity 9-35274
 Er ferrite garnet, Faraday effect 9-49216
 EuO, ferromagnetic, ¹⁵³Eu spin-lattice relax., and temp. depend. 9-45244
 EuO, u.s. propagation, attenuation, and temp. depend. 9-44824
 Fe-Au, thermoelectric power at low temps. and field dependence 9-35495
 FeCl₂ magnetization in perpendicular field, nonlinear behaviour at low temp. 9-45220
 n-GaAs, degenerate, giant peak in magnetoresistance 9-44959
 n-GaAs, epitaxial, effect on hydrogenic donor states, far-i.r. photocond. obs. 9-45022
 GaAs, semi-insulating, photoconductivity 9-39715
 GdFe garnet, circular domain formation by pulsed field. 9-47271
 n-Ge:Sb Hall effect distortion in strong fields 9-37537
 Ge, magnetomicrowave effects at 38 GHz, charge carrier density control by photogeneration 9-30922
 n-Ge, magnetoresistance, transverse, current density depend. in strong fields and strong mag. fields, 16.6°K 9-33327
 Ge diodes with semi-infinite base, I-V characs. and transient processes 9-43083
 n-p-Ge field non-ohmic conduction under strong field 9-35420
 H, hyperfine state selection by longitudinal periodic field mag. lens 9-29979
 H atom beam separation and focalization, phase-space calc. method 9-27828
 He-Ne laser, transverse field eff. on radiation output and polarization 9-22395
 Hg surface waves, influence of axial magnetic field 9-30358
 Ho ferrite garnet, Faraday effect 9-49216
 n-InSb, rel. to sound amplification 9-24028
 InSb continuous coherent oscillation, freq. depend. on applied transverse field 9-26548
 KTa_{1-x}Nb_xO₃, dielectric properties 9-35473
 MnAlGe uniaxial single crystal, external field prod. domain struct. hysteresis 9-41311
 MnP metamag. single crystal, eff. on thermoelec. power 9-35498
 MnP single crystal, elec. resistivity in metamagnetic state 9-28460
 N₂, pink afterglow 9-30315
 NF₃, thermal conductivity, rel. to elec. field effects 9-28076
 Na salicylate, on fluorescent flux 9-37767
 Nb-Ti-N thin films, supercond. critical current-field meas. in continuous fields 9-35362
 Nb-Ti supercond. tubes, steady-state flux jumping in superimposed a.c. and d.c. fields 9-37471
 Nb-(40wt.%)Zr-(10wt.%)TiNb-(40wt.%)Zr-(10wt.%)Ti superconducting hollow cylinders, mag. shielding in applied mag. fields at 4.2°K 9-43174
 Ni-Fe films, annealing, effect of elastic stresses 9-33029
 Ni-Zn-Cr ferrites, mag. annealing at 3 kOe, at 250°C, prod. uniaxial anisotropy on Co containing samples 9-41326
 Ni, phase transition, neutron scattering investig. 9-24305
 Ni, rel. to internal friction studies, 77° to 298°K 9-26317
 Ni, resistivity, depend. and temp. depend. 9-24128
 Pb_{1-x}Sn_xS₂ diode i.r. laser emission 9-41922
 PbO₆Fe₂O₃ uniaxial single crystal, external field prod. domain struct. hysteresis 9-41311
 Pd-Fe dilute alloy, ferromag., σ σ M/ σ T meas., and temp. depend 9-47263
 Pd-Ni alloys, Stoner enhancement, field depend at high mag field 9-45087
 Pd-Rh dilute alloys, mag. susceptibility, field-depend at high mag. fields. 9-45070
 Si, cooling of hot electrons 9-49109
 Sn, electron focusing 9-26519
 Tb ferrite garnet, Faraday effect 9-49216
 Zn, band structure, calc. using single band effective Hamiltonian 9-24096
 Zn, supercond., microwave absorpt. 9-47094
- Magnetic films** see *Films, solid/magnetic properties*
Magnetic flux see *Magnetic field measurement; Magnetic fields*
Magnetic hysteresis see *Magnetization process*
Magnetic lenses see *Electron lenses/magnetic; Ion optics*
Magnetic measurement
 see also *Magnetic field measurement. Entries describing measurement methods for specific magnetic quantities and effects may also be found listed under the various headings for the subjects concerned*
 anisotropy field of cylindrical films plated on nonferromag. wires 9-24306
 cylindrical samples, non-contact determ. of props. theory 9-25161
 demagnetization curve of magnetically-hard material, errors in functional relationship B(H) 9-40309
 liquids, susceptibility and mag. moment, viscometer meas. 9-28154
 magnetization, of low-volume superconductors, by electronic integrator 9-39591
 magnetometer, digital vacuum torque, for use 300-1000°K 9-27272
 magnetometer, torque, for meas. of small mag. anisotropies 9-27273

Magnetic measurement continued

- magnetometer, torque, for meas. of small mag. anisotropies 9-40308
- susceptibility of superparamag. substs., recording instrum. 9-38345
- time variations of magnetization, sensitive automatic method 9-22339

Magnetic memories *see Calculating apparatus; Magnetic devices***Magnetic mirrors** *see Magnetic fields; Plasma confinement***Magnetic properties of dissolved atoms in dilute alloys**

- conduction electron spin polarization correl. function 9-47240
- dynamic susceptibility calcs. 9-35525
- electrical cond., frequency depend., in terms of impurity scatt. t-matrix 9-47064
- electron spin polarization around impurity, calc. using Kondo effect 9-41287
- ferromagnet, impure, rel. to specific heat mag. field dependence 9-44830
- ground state energy calc. by Nagaoka-Suhl theory 9-45052
- Heisenberg ferromagnet, linear-chain, spin-wave analysis of magnetically-coupled impurities 9-45093
- hyperfine fields at impurities in metals 9-33493
- Kondo effect rel. to fluctuations on impurity sites 9-41288
- Kondo model describing interaction of conduction electrons with localized mag. impurity 9-39560
- Kondo resistivity of interacting impurity pair 9-24270
- Korringa relation breakdown in nearly ferromagnetic materials 9-24503
- localized moments, susceptibility study at sub-Kondo temp. 9-45041
- metal s-d exchange model, mag. fields effects 9-47220
- metals with paramag. impurities, spin density fluctuation spectrum 9-43149
- nuclear mag. reson. saturation in diamag. materials with paramag. impurities 9-41432
- nuclear spin relax. mechanism 9-24338
- orbital degeneracy effects 9-24269
- paramagnetic impurities, gapless superconductivity region 9-43033
- paramagnetic impurities in single-zone superconductors, conduction state 9-37455
- Ruderman Kittel-Kasuya-Yosida indirect-exchange interaction, temp. depend. 9-37639
- s-d model, decoupling treatment of Kondo effect for correct ground state energy 9-35547
- self-consistency conditions for localized mag. moment in free-electron gas 9-37641
- spin impurity effect on energy spectrum of X-Y model 9-43148
- spin propagator and static susceptibility calc., above Kondo temp. 9-45053
- spin-wave impurity excitations rel. to reduced susceptibility function 9-47235
- Suhl-Nagaoka theory, calc. of thermopower, electrical and thermal resistivity 9-45051
- superconductivity and electron-atom interaction above Kondo temp. 9-44925
- Au-V, n.m.r. obs. of low-temp. props. 9-45395
- Cu-(1wt.%)Mn, spin splitting contrib. to Mn mag. moment 9-24282
- Cu-Al:Fe, rel. to excess specific heat 9-47001
- Cu-(1wt.%)Mn, spin splitting contrib. to Mn mag. moment 9-24282
- Cu-Mn(Fe,Cr), magnetoresistivity in high-fields 9-44910
- Cu-Ni: ⁵⁷Fe from Mossbauer exam. 9-47331
- CuPd-(1wt.%)Mn, spin splitting contrib. to Mn mag. moment 9-24282
- Fe, hyperfine interaction in ¹⁸⁰Hf, IMPACT study 9-45256
- Fe, internal mag. field at Os after Coulomb recoil implantation 9-39765
- Fe film, magnetization distrib. about single mag. particle 9-43181
- Gd, hyperfine interaction in ¹⁸⁰Hf, IMPACT study 9-45256
- Mo-Nb:Co Kondo temp. independ. of host composition from resistivity and susceptibility meas. 9-45067
- Ni₃Ga, decrease of magnetization of itinerant electrons by spin-orbit scatt. on impurities 9-26639
- Pd-Ag, susceptibility meas 9-45069
- Pd-Co alloys, ferromag. with paramag. Sn nuclei 9-43179
- Pd-Fe spin polarization range, conc. depend 9-45116
- Pd-Rh, exchange enhanced, field-dependent susceptibility 9-26625
- Pd-Rh susceptibility meas. 9-45069
- Pt-Co magnetoresistivity 9-44917
- Pt-Fe solid soln., inc. in susceptibility due to interac. of Fe with quenched-in vacancies 9-26278
- Rh-Fe magnetoresistivity in high-fields 9-44910
- Rh-Ru:Fe susceptibility and resistivity temp. dependence rel. to Kondo temp. 9-44918
- Sc, decrease of magnetization of itinerant electrons by spin-orbit scatt. on impurities 9-26639
- Sc alloyed with nonmagnetic metals, susceptibility between 0.36 and 300°K 9-49190
- (SnTe)_{1-x}(MnTe)_x 9-39771
- Ti₂O₃:V³⁺, inelastic scatt. mechanisms involving mag. impurities in negative magnetoresistance at 4.2°K 9-47070

Magnetic properties of substances

see also Films, solid/magnetic properties

see also Films, solid/magnetic properties

No entries

- alkali dithioferates (III), molar susceptibilities 9-43220
- alloy, dil. mag., Kondo spin-compensated state, range and spatial variation 9-33429
- alloy, dilute, spin correlation function perturbation calc. 9-28591
- anisotropic bodies, polarizability 9-45038
- binary pnictides with marcasite type struct. 9-31016
- book, materials and their properties 9-49187
- copper (II) salicylate adducts, susceptibility and e.p.r. 9-37804
- couplings, macroscopic theory extension and representations 9-41286
- crystals, Raman effect scattering, matrices determ. from mag. point groups irreducible corepresentations 9-24422
- cubic crystals, linear mag. birefringence 9-45185
- cylindrical samples, non-contact determ. of props. theory 9-25161
- dipole pair interacting anisotropic of arbitrary bond angle theoretical coercive field 9-45046
- elements, collection of data, book 9-22026
- ethylene oxide, molec. anisotropy 9-42431
- ethylene sulfide, susceptibility anisotropies 9-40612
- ferrites, permeability tensor in various coordinate systems 9-39775
- ferrites, spinel 9-45174
- ferrites, susceptibility and magnetization, microwave meas. 9-45172
- ferrites core memory using single major remanent state of one polarity for both digital information states 9-43844

Magnetic properties of substances continued

- films, thin, theory, Curie pt., magnetization and moment fluctuations 9-49181
- fluoroacetylene, mag. susceptibility anisotropy 9-25764
- fluorobenzene, molec. anisotropy 9-44359
- flux quantization of superconducting rings, and Bose condensation 9-28483
- galvanomagn. using polarized neutron diff., error anal. 9-24268
- ferromagnetic crystal, John's method determ. 9-24264
- graphite and pyrocarbons, g-factor anisotropy, rel. to diamag. anisotropy 9-47228
- Hall coeff., anomalous, in materials with large para-process 9-49185
- Heisenberg spin system, self-consistent eqn. for dynamical critical phenomena 9-33430
- helical spin structures, representation theory 9-45108
- helicoidal structures, couplings 9-43147
- induction density fluctuations, interaction with nonlocalized excitons, rel. to equilib. distrib. 9-49004
- ketene, molec. susceptibilities anisotropy 9-30126
- lamellar struct., critical field obs. 9-39747
- liquid crystals, nematic, distortion of cholesteric structure by magnetic field 9-32794
- liquids, susceptibility and mag. moment, viscometer meas. 9-28154
- maghemite, Curie temp. estimation 9-35537
- magnetic group, reln. with isomorphic many-coloured crystal group 9-28240
- magnetic lattices derived from crystal lattices 9-31013
- magnetite dispersed powder susceptibility for low field, intensity, freq. independence obs. 9-43502
- materials and applications 9-45039
- materials and applications 9-45039
- metal, local moments, correlation effect on occurrence 9-45042
- metal, paramag.-impurity ground state, corrections 9-33436
- metal coupled spin-plasma waves, interaction with charged particles 9-41297
- metal cyanides, magnetic susceptibilities meas. 9-24276
- metals, itinerant spin-density excitation in light-scatt. obs. 9-47372
- metals, nonferromagnetic, interaction of spin and cyclotron waves 9-33427
- metals, transverse susceptibility, rel. to Kubo formalism and relaxation of localized moments 9-35526
- metals, transverse susceptibility rel. to second-order exchange effects in localized moments 9-35527
- micromagnetics, domain pattern from soln. of fundamental eqn. 9-45118
- minerals, thermodynamic props. 9-30776
- M.S.O. alloy shunt props., C addition effect 9-45050
- neutron scatt. exam., theory of electrostatic interactions 9-37129
- neutron scatt. investigations 9-49188
- neutron scattering by ions, differential cross section 9-24267
- neutron scattering obs., forward scatt. amplitudes 9-31014
- one and two-dimensional systems, ordering 9-41289
- ordering, theory using Green's functions 9-45037
- parametric amplification of non-uniform spin wave modes, Green's function theory of system 9-45043
- Permalloy films, Bloch wall motion excited by fast-rising hard-axis pulses 9-45168
- permalloy thinfilms, electrodeposited, magnetism reduction 9-49191
- permeability, anomalous, induced by stress var. after weak-field demagnetization 9-31012
- phonons parametric excitation by parallel pumping 9-37640
- piezocalvanomagnetic crystal, John's method determ. 9-24264
- piezomagnetic coefficients 9-24262
- pyrocarbons and graphite, g-factor anisotropy, rel. to diamag. anisotropy 9-47228
- quartz, 30 to 60% magnetite, galvanomag. effect 9-43500
- rare earth diselenides, susceptibility temp. depend. 9-43154
- rare earth orthoferrites, Bi-substituted, (R₁-Bi₂FeO₃), rel. to composition 9-32869
- rare-earth metals, book 9-47223
- rare-earth orthoferrites, ordering and orientation from specific heat meas., 1.5-20°K 9-33184
- rare-earth-In cpds: RIn₃, susceptibilities 9-39751
- research review 9-43837
- rocks, susceptibility for low field intensity, freq. independence obs. 9-43502
- Ruderman-Kittel-Kasuya-Yosida indirect-exchange interaction, temp. depend. 9-37639
- semiconductor, coupled spin-plasma waves, interaction with charged particles 9-41297
- semiconductors, magnetic, and elec. and opt. props. 9-49064
- semimetals, magnetic impurities, dynamical effect on excitonic phase in temp. region T > T_K 9-49183
- singlet crystal-field ground state systems, and collective excitations 9-45253
- SrFe_{1-x}Cr_xO_{3-y} perovskites, and Mossbauer study 9-47336
- stagnation flow against rotating magnetized disc 9-42482
- steel, Si, relaxation effects, infl. of H impurity 9-30644
- superconducting (type II) thin films, equilib. config. of flux lines 9-43034
- superconductor, Amperian mag. systems, shape and orientation effects 9-30859
- superconductor, low-volume, magnetization meas. by electronic integrator 9-39591
- susceptibility and fluctuation 9-31905
- susceptibility anisotropy above ordering temp. of monocry., cryst. field parameters depend 9-39746
- symmetry and limiting groups 9-24263
- symmetry groups 9-24261
- symmetry-restrictions, space-time, rel. to thermogalvanomagnetic coeffs. 9-47192
- thermo-electret., anisotropy var. with time 9-35528
- thermomagnetic crystal, John's method determ. 9-24264
- transition metal phosphides, solid solns., and crystal structure 9-44676
- transition metal spinel manganites, single phase stability domains, eff. of heat treatment 9-28253
- transition metals, b.c.c., from generalized susceptibilities calcs. using electronic structure 9-26658
- 3d transition metals in liquid Sn, susceptibilities 9-28150
- transition temp. and anisotropy effect of pressure, meas. using vibrating-coil magnetometer 9-45047
- tunneling anomalies, zero-bias, s-d exchange theory, g-shifts 9-37642

Magnetic properties of substances continued

- two-spin system coupled Gydipolar interaction, hyperfreq. electronic susceptibility 9-41416
- Y:Gd at 1000 ppm, saturation moment 9-49190
- [Cr(OH)₆(en)]³⁺ salts, susceptibility meas. down to 4.2°K 9-47224
- Ag-Zn system, susceptibility of ϵ and η phase alloys 9-43150
- Au-Co alloys, hardness rel. to precip. 9-41055
- AuX ordered alloys, X=transition elements and mixtures, structure, electron and neutron diff. studies 9-44659
- Be breakdown and de Haas van Alphen effect 9-39749
- Be intermetallic cpds., behaviour at 4.2°K, n.m.r. investigation 9-45396
- Bi_{1-x}Sb_x, susceptibility rel. to carriers, energy gap and Fermi level 9-30842
- Bi_{0.5}Sb_{0.5}:Sn,Te alloy, thermomag. and galvanomag. props. 9-49154
- Bi_{0.5}Sb_{0.5}:Sn,Te alloy, thermomag. and galvanomag. props. 9-49154
- BiMn₂O₇ symmetry and ferroelec. induced by antiferromag. transitions 9-45208
- CaFe₂O₄ neutron diff. obs. of mag. peaks using a linear electron accelerator 9-42779
- CaMn₂O₄ symmetry and ferroelec. induced by antiferromag. transitions 9-45208
- CdSb, susceptibility temp. and carrier conc. dependence, inequivalent valley model 9-26621
- CeF₃, symmetry rel. to polarized i.r. reflectance obs. 9-47345
- CeFeO₃ orthoferrite, ordering 9-45055
- CeMg(NO₃)₃ pure dipole-dipole system, susceptibility and entropy 9-45054
- Co-(42-54 at.%)Al alloys, at room temp. 9-47069
- Co-Cr alloys, non-collinear structures with antiferromag. interaction between local moments 9-45056
- Co-Fe-Ba semi-hard mag. alloys. square hysteresis loop and low magnetostriiction coercive force 9-45137
- Co-Mn alloys, non-collinear structures with antiferromag. interaction between local moments 9-45056
- Co, magnetization and magnetothermal effect near Curie temp. 9-24271
- CoCl₂·2H₂O, magnon-phonon interaction, obs. in far, i.r. 9-45077
- CoO excitations theory 9-45063
- Cr-Re alloys, coexistence of commensurable and oscillatory phase, neutron diff. obs. 9-39750
- Cr alloys, coexistence of commensurable and oscillatory phase 9-39750
- Cr alloys with the Pt-series metals, similar characts. rel. to structural similarity 9-34348
- CrAs and Mn-substituted CrAs, structure 9-45057
- CrCuO₂, obs. 9-35530
- CsFeF₃ magnetization rel. to ⁵⁷Fe h.f.s. 9-45058
- CsMnCl₃·2H₂O, phase diagram 9-35534
- CsNiF₃, high pressure forms 9-45059
- Cu-Co solid solutions, hysteresis rel. to ageing time 9-26622
- Ko-(7.5-25 at.%)Mn magnetisation curve in pulsed mag. fields up to 175 kOe between 77-300°K 9-43173
- (CuMn₂O₄)_{1-x}(AF₂O₄)_x solid solutions, where A=Cu²⁺, Ni²⁺, Zn²⁺, Co²⁺ or Ni²⁺ 9-30834
- Dy-Y alloy, susceptibility, in ferromag., helicoidal antiferromag. and paramag. states 9-33258
- Dy, hysteresis loop displacement due to mag. viscosity 9-41291
- Dy, susceptibility, in ferromag., helicoidal antiferromag. and paramag. states 9-33258
- Dy helical spin structures representation theory 9-45108
- DyAl garnet, rel. to thermal expansion, 1° to 4°K 9-44840
- DyFe₂Cr_{1-x}O₇ system 9-43156
- Er-Dy alloys, single crystals rel. to Dy concentration 9-45060
- ErAg, mag. phases investig. 9-24272
- ErCo_{1.5}Ni_{0.5} mag. phases investig. 9-24272
- ErCO₂ mag. phases investig. 9-24272
- ErCl₃ single cryst., susceptibilities meas. and anisotropy variation with temp. 9-33432
- ErCoNi, mag. phases investig. 9-24272
- ErFe garnet, moment and G-factor determ., optical absorpt. spectra at 4.2°, 20° and 62°K 9-45319
- ErNi₂ mag. phases investig. 9-24272
- EurO₃, susceptibility, effect of anisotropic exchange and crystalline field 9-45062
- EuSe, mag. polaron effects in photoconductivity, temp. depend. rel. to ordering 9-39714
- Fe-Ni-Al alloys, b.c.c., mag. moment behaviour rel. to composition changes 9-24274
- Fe-Ni r.f. susceptibility, effect of added electrons 9-28587
- Fe_{1-x}Cu_xCr₂S₄, behaviour interpretation from sulphospinel model 9-28588
- α -Fe₂O₃ neutron diff. obs. of mag. peaks using linear electron accelerator 9-42779
- (α -Fe₂O₃)_{1-x}(Cr₂O₃)_x solid solns., rel. to formative conditions 9-49189
- Fe₂Ge_{1-x}Mn_xGe_{1-x} solid solns., saturation magnetiz. and Curie temp. 9-45065
- (Fe_{0.5}Mg_{0.5})SiO₃, 0.269< x ≤1.0, ordering, from n.g.r. of ⁵⁷Fe, 300° to 1.7°K 9-45292
- FeCO₃ metamagnetic single crystal, antiferromag. Mossbauer meas., 2.5°K to above Neel temp. 9-45293
- FeCl₃ excitations theory 9-45063
- FeCl₂·H₂O, magnon-phonon interaction rel. to ordering obs. in far i.r. 9-45077
- FeCuO₂, obs. 9-35530
- FeTiS₄ low-temp., depend on mag. field during cooling 9-45221
- Gd-Co system, saturation and coercive force study of intermetallic cpds. 9-48921
- He liquid, susceptibility 9-23559
- He solid isotopic mixture nuclear magnetic susceptibility of ³He spin system, 0.3-1.2°K 9-46675
- ³He, liq., susceptibility at zero temp. 9-34939
- ³He, liq., susceptibility calc. using ground-state energy and quasiparticle energies and interaction function 9-34940
- K complex, tris-oxalato-chromate trihydrate, anisotropy and susceptibility meas., ligand field theory, 300-90°K 9-26623
- La-Pr dilute solns., effective mag. moment and elec. resistivity, rel. to Pr conc. 9-45066
- La, susceptibility between 0.36-300°K 9-49190
- LaF₃, symmetry rel. to polarized i.r. reflectance obs. 9-47345
- Li_{0.5}Fe_{2.5}O₄, squareness, switching coeff., coercive force and switching time, effect of grain size 9-45180
- Li₂V₂O₇, anomaly in props., susceptibility reduction 9-35328

Magnetic properties of substances continued

- MgMnZn ferrite memory cores, origin of threshold response delay 9-49217
- Mn-In alloys, solid and liquid 9-31017
- Mn_{1-x}Cr_xAs, between 4.2 and 900°K 9-47226
- α -Mn₂O₃·Fe₂O₃, system structures 9-45078
- Mn₂Fe_{1-x}Ho_xO₄, rel. to unit cell parameters 9-35060
- MnP single crystal spin structures transform to fan structures 9-47246
- Mnp helical spin structures representation theory 9-45108
- N¹⁵N¹⁵O₂, molec. g value and mag. anisotropy 9-38862
- NO molecules adsorbed on silica gel. 9-44631
- Nb₃Al, supercond., susceptibility meas. 9-39599
- NbC_x, susceptibility, temp. and comp. depend., 20-300°K, $x=0.70-0.98$ 9-43153
- NbO₂, susceptibility in 800°C region, phase transition obs. 9-33143
- Nd, exchange interaction and quadrupole scatt., effect on elec. resistivity, temp. depend. 9-44901
- NdF₃, symmetry rel. to polarized i.r. reflectance obs. 9-47345
- NdP, NdAs, NdSb, metamag. behaviour 9-35590
- Ni-(49-51 at.%)Al alloys, at room temp. 9-47069
- Ni-Cr alloys, non-collinear structures with antiferromag. interaction between local moments 9-45056
- Ni-Fe-Cu(Co) films, anisotropy components separation by temp. depend. study of anisotropy field 9-45170
- Ni-Fe thin-films, 30 to 300Å thick, props. with creep observations 9-45068
- Ni-Fe thinfilms, 30 to 300Å thick, props. with creep observations 9-45068
- NiS₂, no mag. ordering 9-33437
- α -O₂, solid far i.r. absorption and antiferromagnetic resonance mode at 4.2°K 9-28691
- OCS, molec. susceptibility anisotropy 9-30046
- Pd-Ag dilute alloys, susceptibility meas., 4.2° to 300°K, fields up to 55 kG 9-45069
- Pd-Fe dilute alloy, spin polarization range, conc. depend. 9-45116
- Pd-In alloys, room temp. susceptibilities 9-30571
- Pd-Rh dilute alloys, susceptibility, field-depend., at high mag. fields 9-45070
- Pd-Rh dilute alloys, susceptibility meas., 4.2° to 300°K, fields up to 55 KG 9-45069
- Pr, exchange interaction and quadrupole scatt., effect on elec. resistivity, temp. depend. 9-44901
- PrAl₂, cubic Laves cpds. Pr³⁺ moment partial quenching 9-45071
- PrCo₂ cubic Laves cpds., Pr³⁺ moment partial quenching 9-45071
- PrF₃, symmetry rel. to polarized i.r. reflectance obs. 9-47345
- PrNi₂, cubic laves cpd., Pr³⁺ moment partial quenching 9-45071
- Pr, depend. on nonstoichiometry, 4.2°-500°K 9-28268
- Pr-Fe system near PtFe composition, ordering from Mossbauer effect meas. 9-24275
- Rh-Ru-Fe alloys, susceptibility and resistivity as function of temp. 9-44918
- Sc:Gd at 1000 ppm, saturation moment 9-49190
- Sc, susceptibility between 0.36-300°K 9-49190
- Sc single cryst., susceptibility and anisotropy 9-49192
- SmB₆, susceptibility rel. to electronic config. of Sm. 1° to 800°K 9-45072
- SmCo₅, influence of absorbed H 9-45073
- TaC_x susceptibility, temp. and comp. depend., 20-300°K, $x=0.73-0.97$ 9-43153
- Tb-Y alloy, susceptibility, in ferromag., helicoidal antiferromag. and paramag. states 9-33258
- Tb, hysteresis loop displacement due to mag. viscosity 9-41291
- Tb, susceptibility, in ferromag., helicoidal antiferromag. and paramag. states 9-33258
- TbCrO₃ symmetry and ferroelec. induced by antiferromag. transitions 9-45208
- Th₃P₄, susceptibility 9-35035
- ThC, chemical bonding and mag. susceptibility at various temp. 9-28224
- ThP susceptibility 9-35035
- Ti-O alloys, susceptibility, var. with temp. and alloying rel. to electronic struct. 9-35533
- Ti, susceptibility, var. with temp. rel. to electronic struct. 9-35533
- UBi, structure and ordering, neutron diff. investigation 9-47294
- UPo_{0.7}Se_{0.3} powder, metamag. state obs. 9-33434
- V complex, hexaurea V(III) ion in crystals 9-35654
- VF₂ single crystal and powdered samples, structure, neutron diff. study 9-45074
- Y, susceptibility, in ferromag., helicoidal antiferromag. and paramag. states 9-33258
- Y, susceptibility between 0.36-300°K 9-49190
- Y₂Cr₃, high pressure synthesis, susceptibility meas. showing superconductivity over entire homogeneity range, and high pressure synthesis 9-35372
- Yb₂O₃, struct. obs. 9-45075
- Zn_{1-x}Mn_xS crystals, 0.004< x <0.4, photo-induced susceptibility changes, 77° to 400°K 9-45279
- ZnS:Ni²⁺, susceptibilities and spin-orbit coupling 9-33435

antiferromagnetic

see also Antiferromagnetism

- copper formate tetrahydrate, two-dimensional behaviour from paramag. susceptibility meas. 9-26661
- corundum structure and α -Fe₂O₃ and Cr₂O₃ spin structure antiferromagnets, spin waves 9-41332
- Cr-Mn alloy, magnons and paramagnons, neutron scatt. study 9-45215
- Dzyaloshinskii interaction, exptl. determ. of 'sign' 9-31047
- e.m.wave propag. in material showing resonance in submillimeter region 9-45375
- ferroelectric, sublattice magnetization rel. to spontaneous polarization 9-30971
- GdCrO₃ magnon-assisted absorption and fluorescence spectrum of Cr³⁺ 9-49321
- haematite, electron transport props., effect of weak ferromag.-antiferromag. transition 9-44869
- haematite, structure from nuclear diff. of resonant γ radiation 9-49262
- Heisenberg antiferromag., neutron mag. scattering 9-45202
- Heisenberg quantum-mechanical, staggered susceptibility 9-45100
- hematite single cryst., magnetoelastic props. 9-31049
- LuCrO₃, magnon-assisted absorption and fluorescence spectrum of Cr³⁺ 9-49321
- magneto-optic effect, quadratic Cotton-Mouton effect 9-49245
- magneto-optical effect, origin and magnitude 9-24366
- magnetoelastic oscillations in mag. fields close to critical value 9-45196

Magnetic properties of substances continued
antiferromagnetic continued

- magnon energies, time-depend., theory 9-35578
manganese formate dihydrate, deuterated, n. diff. obs. 9-24336
manganese formate dihydrate, with weak canting interaction, phase transition 9-33489
metal, paramag.-impurity ground state, corrections 9-33436
metal, spin waves in mag. field 9-28638
metals, excitation spectrum in long wave limit 9-37669
metals, magnetoresistance in mag. field 9-26659
metamagnetism, crystal field effect, in NdP, NdAs, NdSb 9-35590
nuclear spin-lattice relax., exchange enhancement 9-47296
paramagnetic impurities, 3-d, in itinerant metal, Neel temp., energy density var. 9-28634
radicals in iminoxyl series, susceptibility meas., rel. to Heisenberg one-dimensional model 9-31023
rare earth diselenides, ordering probability 9-43154
rare earth double oxides, heat capacities, mag. ordering and susceptibilities, obs. 9-47004
rare earth orthoferrites, and spectroscopic props. 9-45232
rare earth orthoferrites, domain wall mobility stroboscope obs. 9-45233
rare earth-noble metal equiatomic cpds, ordering rel. to band structure 9-24334
rare earth-Zn cpds, with CsCl struct. 9-35556
rare earth niobates in strong pulsed fields 9-35592
rare-earth trihalides, hexagonal, susceptibility meas., long-range order obs. from Cl n.q.r. 9-41340
resistivity (electrical) tensor, anomaly near Neel point 9-45206
rutile, Stark effect in d.c. elec. field, rel. to Loudon Hamiltonian 9-45197
scattering, critical, of unpolarized neutrons, cross sections 9-24321
semiconductor, rel. to transform into metal in strong mag. field 9-37505
semiconductor, rel. to transform into metal in strong mag. field 9-24168
semiconductor, spin-electron interac. effect on current carrier mobility 9-37516
semiconductors, current carriers, indirect exchange and localized magnons 9-28607
spin configurations in two sublattice slab 9-45205
spin structures, temp. depend under s-f interaction 9-45204
spin waves in antiferromagnets with corundum structure and α -Fe₂O₃ and Cr₂O₃ spin structure 9-41332
spin-flipping, dynamical behaviour 9-47279
spin-flipping, numerical integration of phenomenological eqns. for orthorhombic and uniaxial systems 9-47280
spin-flop states, low-temp. adiabatic studies 9-43191
steel, X40 Mn-Cr 22, susceptibility at 5°-1800°K 9-24330
sublattice magnetization vector, dynamical behaviour 9-47280
sublattice magnetization vector, dynamical behaviour near spin-field critical field 9-47279
symmetry, book 9-47223
transition metal chalcogenides with Cr₂S₄ structure, susceptibility meas. 9-24329
two-sub lattice antiferromagnet, spin wave Green's function, reciprocal lattice sum evaluation for 10 points 9-28635
uniaxial, magnetiz. props. near field causing sublattice magnetiz. reversal 9-45195
uniaxial, threshold absorpt. of h.f. mag. field 9-49222
uniaxial sample, phase transitions, mag. field induced 9-45199
alkali metal iron fluorides, MFeF₃, (M = Na, K Rb), rel. to crystal structure 9-35063
BaMnF₄, spin-flop transition 9-43193
BaOFe₂O₃, ordering, neutron diff. and Mossbauer effect obs. 9-47283
BaSc₂Fe_{12-x}O₁₉ hexagonal ferrite single crystal, intensity anomalies due to superposition of reflex satellites 9-31043
BiCrO₃, below 123°K and crystal distortions 9-28608
BiFeO₃-Pb(Fe_{0.5}Nb_{0.5})O₃ solid solution spontaneous magnetic moment by neutron diffraction 9-33482
CaF₂, nucl. state prod. and obs. 9-45207
Ce-La alloys, nondil., resistively-determined Neel temp., spin-compensated mag. state obs. 9-35337
Ce-Y alloys, nondil., spin-compensated mag. state from resistance minima obs. 9-35337
Ce₂Mg₃(NO₃)₁₂·24H₂O, obs. antiferromagnetic in millikelvin range 9-45210
CeB₆, inverse susceptibility at high temp., theory 9-45209
Co_{1-x}Cu_xRh_{0.5}S₄, for 0 ≤ x ≤ 0.4 9-41164
Co₂La₂(NO₃)₁₂·24H₂O, phase transitions, obs. 9-39781
Co₂O₄, bulk material and ultra-fine particles, ordering from Mossbauer obs. 9-28666
CoBr₂·6H₂O, spin-flop states, low-temp. adiabatic studies 9-43191
CoCo₂·7Fe, ordering rel. to Fe ion relax., Mossbauer obs. 9-41364
CoCl₂·2H₂O, far-i.r. mag. reson. absorpt., clustered multiple spin excitations, flipped spin states propag. 9-33483
CoCl₂·6D₂O single cryst., susceptibilities, low temp. 9-47284
CoCl₂·6H₂O, spin-flop states, low-temp. adiabatic studies 9-43191
CoCl₂·6H₂O single cryst., susceptibilities, low temp. 9-47284
CoCs₂Cl₃, mag. struct., n. diff. obs. 9-39779
CoF₂, inelastic scatt. of slow neutrons by two-magnon processes 9-43192
CoF₂, magnon-phonon interaction, temp. dependence 9-47356
CoO, critical pt., u.s. attenuation obs. 9-44823
Co(S_{0.5}Se_{1-x})₂, system, thermostatical investigation 9-31029
Co(S_{0.5}Se_{1-x})₂, system 9-33437
CoSe₂, spin ordering with MnSe₂ type 9-33437
CoSeO₄, struct. and Neel pt., neutron diff. powder obs. 9-49223
Cr-Mn alloys, spin density wave calcs. from band structure 9-24325
Cr-V alloys, spin density wave calcs. from band structure 9-24325
Cr, critical exponents and electrical resistivity near Neel point 9-35582
Cr, spin-flip transition region, electric resistivity anomaly 9-35584
Cr, spin density wave calcs. from band structure 9-24325
Cr_{0.7}Mn_{0.3}As, structure, Neel temp. at 263°K 9-45057
Cr_{2-x}Fe_xAl, ordering, depend. on value of x 9-35579
Cr₂BeO₄, spiral structure, neutron diffraction investigation, 4.5°K 9-45211
 α -Cr₂O₃, dispersion relns. including exchange integrals 9-35585
Cr₂O₃, spin waves and exchange interactions, inelastic neutron scatt. obs. 9-47285
Cr₂O₃ absorpt. spectrum of excitons, mag. Davydov splittings 9-33552
Cr₂O₃TiO₂ antiferro at room temp. with high Cr₂O₃ content 9-49022
Cr alloys with V, Nb, Ta, elec. resistivity, temp. dependence 9-39584
Cr and alloys, optical and pressure effects, rel. to band structure 9-45213
Cr single crystal, spin directions, 122°K to 38.5°C, models 9-45214

Magnetic properties of substances continued
antiferromagnetic continued

- Cr spin density wave, mag. field eff. 9-35580
CrAs, structure, Neel temp. at 280°K 9-45057
CrB₂, ordering, Neel temp., n.m.r. meas. 9-35583
CrO₂ single crystal, and magneto-optic props. 9-45141
CrSb₂, marcasite-type 9-35581
Cs₂MnCl₂·2H₂O, anisotropy temp. dependence, 0.35-20°K 9-24326
Cs₂MnCl₂·2H₂O, ordering, n.m.r. obs. 9-41333
CsMnF₃, magnon-phonon interaction and exchange consts. determ. 9-47286
CsMnF₃, n.m.r. linewidth of ⁵⁵Mn, field depend., 1.8 and 4.2°K 9-33649
CsMnF₃ hexagons nuclear and electronic spin-wave relax rate 9-45216
Cu(7.5-25 at.%)Mn alloys, subsystem, from mag. curves 9-43173
Cu₂Cl₂·2H₂O single cry., mag. ordering 9-37643
Cu₂La₂(NO₃)₁₂·24H₂O, phase transitions, obs. 9-39781
Cu complex, adenine Cu(II), coupling and mag. exchange 9-31048
Cu complex, CuCa acetate hexahydrate 9-33484
Cu(NH₃)₄SO₄·H₂O ordering and spin arrangement, proton n.m.r. and susceptibility meas. 9-41334
Cu(NO₃)₂·2.5H₂O, magnetization isotherms, 1.2-4.2°K, rel. to exchange interactions 9-45218
CuSO₄, moment density distrib., polarized-neutron determ. 9-41335
Dy₂Ge₃, susceptibilities rel. to D_{8h} structure 9-43157
Dy₂Si₃, susceptibilities rel. to D_{8h} structure 9-43157
Dy₂Ho_{1-x}Sb_x, Neel and param. Curie temp. 9-28595
DyAlO₃, mag. structure and metamag. transitions, absorpt. spectra investigation 9-31105
ErCrO₃, hyperfine structure from ¹⁶⁶Er Mossbauer meas., 4-40°K 9-24380
EuCrO₃, weak-ferromagnetic moment obs. 9-24302
EuSe effect of hydrostatic pressure 9-47287
EuSe single crystal, 4.2°K, neutron diff. study 9-47288
EuTe effect of hydrostatic pressure 9-47287
Fe-Co alloy, f.c.c., precip. from Cu, behaviour 9-26633
Fe-Ru h.c.p. alloys, ϵ -phase, ordering obs. at low temp. 9-43159
Fe₂BO₄, magnetization and Mossbauer effect, spin orientations 9-41314
Fe₃(Ni_{1-x}Mn_x)₃, alloy, moment-induced scattering and magnetovolume effect 9-41303
Fe_{3-x}Mn_xAs₂, 2.00 ≤ a ≤ 2.35, first order ferrimag. to antiferromag. transitions 9-45178
Fe complex, (Fe bis-salicylidene-ethylenediamine)O pyridine, oxo-bridge five-co-ord struct. 9-33486
FeBr₂, metamagnetic transition for Mossbauer obs. 9-24328
FeCl₂, metamagnetic transition for Mossbauer obs. 9-24328
FeCl₂ magnetization in perpendicular field, nonlinear behaviour at low temp. 9-45220
FeCl₂·4H₂O, spin-flop states, low-temp. adiabatic studies 9-43191
FeCl₃, low-temp. susceptibility 9-45224
FeF₂, ¹⁹F n.m.r. obs. from 4.2 K to critical region 9-35725
FeF critical fluctuations near Neel point n.m.r. line width anomaly 9-45399
 α -FeOOH, fine particles, Neel temp. particle size depend. 9-47290
 α -, β -, γ -FeOOH, synthetic 9-47289
Fe(Pt_{1-x}Pd_x)₃ ordered alloys, spontaneous magnetization depend. on composition 9-24309
FeRh films, first-order antiferromag. to ferromag. transition role of O₂ 9-45223
FeRh system, first-order antiferromag. to ferromag. transition, mechanism 9-45222
FeSb₂O₄, structure, using Mossbauer eff. 9-41336
Gd-Sc alloys rel. to Gd concentration structure 9-45125
Gd-Y alloys, rel. to Gd concentration, structure 9-45125
Gd₂CoMnO₆, perovskite, metamagnetism 9-35587
Gd₂Ge₃, susceptibilities rel. to D_{8h} structure 9-43157
Gd₂Si₃, susceptibilities rel. to D_{8h} structure 9-43157
GdAlO₃, ordering structure, symmetry considerations and magnetoelectric eff. meas. 9-31050
GdBr₃, canted antiferromagnetism 9-45226
Gd compounds cubic, structure and susceptibility meas. rel. to exchange interactions 9-45225
HgCr₂S₄ spinel, mag. structure depend. of n.m.r. of ^{199,201}Hg and ⁵¹Cr nuclei at 1.4°K 9-45400
K₂CoF₄, n.m.r. and transferred hyperfine interactions 9-45257
K₂CoF₄, two-dimensional, optical absorpt. 4.2° to 300°K 9-45321
LiFe_{0.8}Mn_{0.2}PO₄, Mossbauer effect obs. 9-26726
MgCr₂O₄, antiferromag.-paramag. transform. of first order 9-49224
Mn-Cu alloys, long range order rel. to lattice distortion and vol. expansion on cooling through Neel temp. 9-39783
Mn-Pd alloy system near MnPd₃, struct. 9-35588
 γ -Mn, structure confirmation by neutron diffraction 9-31051
Mn, susceptibility, He temp. to 2000°K 9-24333
(Mn_{0.95}Cu_{0.05}) alloy, Fe impurities obs. 9-41338
Mn₂Ge₂Sb_{1-x}, transition from helical to antiferromag. 9-24318
Mn₂GeS₄, orthorhombic, neutron diff. obs. 9-35589
Mn₃La₂(NO₃)₁₂·24H₂O, phase transitions, obs. 9-39781
Mn₃ prep. and structure 9-44645
Mn Te magnon drag contrib. to transport props. 9-24332
MnCl₂·4H₂O, sp. ht. high-resolution meas. near Neel temp. 9-24046
MnCl₂·4H₂O, spin-flop states, low-temp. adiabatic studies 9-43191
MnCl₂·4H₂O mag. moment, 0.4°-4.2°K in mag. fields 9-44835
MnF₂:Co, localized mode, temp. depend. 9-45227
MnF₂:Fe²⁺(Co²⁺) localized mode, 1.2°K, i.r. obs. 9-47291
MnF₂, critical Zeeman effect anisotropy 9-35642
MnF₂, magnetic-phase boundary from u.s. and differential magnetization meas. 9-41339
MnF₂, magnon dispersion relation and exchange interac. 9-45228
MnF₂, magnon sideband theory 9-45229
MnF₂, magnon sidebands in absorpt. spectrum 9-35661
MnF₂, Raman effect scattering, matrices determ. from mag. point groups irreducible corepresentations 9-24422
MnF₂, Suhl-Nakamura interaction from ⁵⁵Mn n.m.r. obs. 9-26798
MnO, magnon energies 9-35591
MnO, rel. to crystal field transition intensities 9-45252
MnO, spin-polarized energy-band structure 9-44888
MnP, metamag. struct. 9-41337
 α -MnS, magnon energies 9-35591
 α -MnS, rel. to crystal field transition intensities 9-45252
MnSeS₄ susceptibility meas. rel. to exchange interactions 15° to 295°K 9-47292

Magnetic properties of substances continued
antiferromagnetic continued

- MnSeO₄, Neel pt. 9-49223
 MnSnO₃, disordered ilmenite, susceptibility 9-39285
 MnTe₂, ordering rel. to ¹²⁵Te Mossbauer obs. 9-43225
 MnTiO₃ II high press. phase, ordering, Mossbauer effect and e.s.r. obs. 9-44667
 MnWO₄, huebnerite, struct. 9-43194
 NiHFeF₃, rel. to crystal structure 9-35063
 NaNiF₃, orthorhombic canted, mag. resonance and anisotropic g factors 9-45361
 Nd, transitions, correl. with anomalies in elastic and anelastic props. 9-35146
 Nd₂Ge₃, susceptibilities rel. to D_{8h} structure 9-43157
 Nd₂Si₃, susceptibilities rel. to D_{8h} structure 9-43157
 Nd₂Dy_{1-x}Sb, Neel and paramag Curie temp. 9-28595
 Nd double h.c.p. generalized susceptibility and Fermi surface 9-44889
 Nd monochalcogenides, transition due to critical field, moments 9-49225
 NdP,NdAs,NdSb, w.r.t. cryst. field effect 9-35590
 Ni, spin-wave spectrum, neutron scatt. meas. 9-45115
 NiCrO₃, low temp. structure 9-43160
 NiF₂, one- and two-magnon excitations, temp. depend., spin correl. functions 9-33441
 NiO, coherent exchange scattering of low-energy electrons 9-45230
 NiO, magnon energies 9-35591
 NiS, ordering rel. to lattice compressibility 9-44672
 NiSeO₄, struct. and Neel pt., neutron diff. powder obs. 9-49223
 O₂ molecules in O₂-Ar solid mixtures, susceptibility meas. rel. to exchange interactions 9-45231
 PbTiO₃-LaFeO₃ solid solns., static mag. props. 77-900°K 9-39784
 Pr, transitions, correl. with anomalies in elastic and anelastic props. 9-35146
 Pr double h.c.p. generalized susceptibility and Fermi surface 9-44889
 Rb₂MnCl₄·2H₂O, ordering, n.m.r. obs. 9-41333
 RbFeF₃, magneto-optical effects, origin and magnitude 9-24366
 RbFeF₃, tetragonal to orthorhombic ferromag. 87°K, and optical props. 9-47293
 RbMnF₃, critical scattering of neutrons and sublattice magnetiz. 9-45234
 RbMnF₃, flopped, excitation of electronic and nuclear spin waves 9-47282
 RbMnF₃, Heisenberg antiferromag., neutron mag. scattering 9-45202
 RbMnF₃, n.m.r. linewidth of ⁵⁵Mn, field depend., 1.8 and 4.2°K 9-33649
 RbMnF₃, spin-waves in absorpt. spectra 9-39845
 RbMnF₃, spin-waves in absorpt. spectra 9-39844
 RbMnF₃ nuclear acoustic resonance, temp. depend. 4.3-38°K 9-46993
 Sm, transitions, correl. with anomalies in elastic and inelastic props. 9-35146
 SmFeO₃-DyFeO₃ solid soln. single crystal, spin reorientation, 2° to 500°K 9-45235
 Sr₂Fe₂O₇, neutron diff. obs. of cryst. and mag. struct. 9-41341
 SrFeO_{3.75(0.5)}Cr_{0.25(0.5)}O₃-perovskites and Mossbauer study 9-47336
 Ti₂O₃, existence, neutron-polarization analysis 9-45236
 Ti_{1-x}Cr₂O_{3-x}, ESR determ. of weak antiferromagnetism 9-49022
 Tm magnetoelasticity, transverse, in fields up to 22 kOe temp. depend. between 22 and 53°K 9-41318
 α-U, low temp. obs. 9-26394
 UAs, ordering 9-33488
 UBi, neutron diff. obs. 9-39785
 UFeO₄, and structure 9-45238
 UOSe, moment, structure and Weiss const. 9-33487
 UP-US solid solns. 9-45117
 UP_{1-x}S₂ system, (0<x<0.33), phase diag., neutron diff. investigation 9-45237
 USb, antiferromagnetic ordering 9-33488
 USb, neutron diff. obs. 9-39785
 USb and U₃Sb₄, structure and ordering, neutron diff. investigation 9-47294
 UX₂ type cpds., symmetry 9-37670
 UP_{1-x}S₂ (x=0.05) m structure 9-41342
 V-Cr alloys, ⁵¹V Knight shift and Neel temp. 9-24324
 YCrO₃, Davydov splitting, direct obs. 9-24335
 YCrO₃ magnon-assisted absorption and fluorescence spectrum of Cr³⁺ 9-49321
 Zn_{0.87}Mn_{0.13}Fe₂O₄, ordering, neutron diff. obs. 9-43189
 Zn_{1-x}Cd_xCr₂Se₄ susceptibilities and moments 9-31035
 ZnCr₂O₄, antiferromag.→paramag. transform. of first order 9-49224

diamagnetic

see also Haas-van Alphen effect; Diamagnetism

- aromatic molecules, diamagnetic susceptibility and anisotropy 9-30065
 benzene, anisotropy, antisymmetrical MO calc. 9-23097
 bi(anthracene 9,10-dimethylene) photo-isomer, susceptibilities and anisotropies 9-45081
 conjugated hydrocarbon mols., ring-current contrib. 9-36709
 10,10'-dianthronyl, susceptibilities and anisotropies 9-45081
 graphite and pyrocarbons, anisotropy, rel. to g-factor anisotropy 9-47228
 meta-, magnetization density waves and thermodynamic pot. for 2-dimens., case 9-45079
 metal, diamag. resonance in mag. field normal to surface 9-31019
 potassium acid phthalate, susceptibilities and anisotropies 9-45081
 pyrocarbons and graphite, anisotropy, rel. to g-factor anisotropy 9-47228
 spinels, single-ion mag. interactions 9-45080
 superconductor, susceptibility at transition, fluctuating Cooper pairs contrib. 9-33260
 superconductors, transition temp. region, large anomaly in susceptibility 9-39592
 susceptibility for breakdown model 9-28592
 susceptibility value from Zeeman effect 9-42408
 tetracyanoquinodimethan complexes, susceptibility from 2.5°K to room temp. 9-47233
 Au_{1-x}Pd_xGa₂, susceptibility as function of Pd content 9-49047
 Cd, diamag. resonance in mag. field normal to surface 9-31019
 H₂ mol., nucl. shielding and susceptibility 9-27859
 In, enhancement above T_c due to thermal fluctuations 9-41292
 MgF₂·Co²⁺, exchange interactions obs. from far-i.r. spectra 9-41384
 Nb, superconducting, surface magnetization 9-30876
 Pd/H₂ syst., susceptibility meas., 50°-100°K 9-41295
 ThP, rel. to nuclear magnetic relax. of ³¹P 9-24343
 ZnAl₂O₄, single-ion mag. interactions, e.s.r. and optical absorpt. meas. of Cr³⁺ and Fe³⁺ 9-45080

Magnetic properties of substances continued
diamagnetic continued

- ZnGa₂O₄, single-ion mag. interactions, e.s.r. and optical absorpt. meas. of Cr³⁺ and Fe³⁺ 9-45080

ferrimagnetic

see also Ferrimagnetism

- coercive force, temp. depend. near compensation temp. 9-49214
 ferrites, activation energies from mag. relax. meas., and Koops inhomogeneities obs. 9-45000
 ferrites, anisotropy and porosity, approach to saturation of hysteresis loop 9-37662
 ferrites, anisotropy effect on ferrimag. reson. 9-39898
 ferrites, FXC 3E1, FXC 7A2 internal friction and AE effect, magnetizing field depend. 9-26655
 ferrites, initial permeability, freq. depend. due to spins and wall resonances 9-35569
 ferrites, mag. moments, magnetization directions interpretation 9-28628
 ferrites, microwave permeability, in weak mag. fields, effect of domain structure 9-33472
 ferrites permeability tensor, dispersion eqn. freq. branches 9-47268
 garnets, randomly substituted systems, moment substitution depend., comments 9-41324
 garnets rare-earth monocystals magnetization near Curie points 9-45175
 lanthanide-nickel cpds., Ln₂Ni₁₇, characts. 9-47260
 magnetite, remanent magnetization and coercive force, effect 9-45570
 magnetite, stoichiometric and non-stoichiometric, meas., mag. field at nuclei, electron-hopping process obs. 9-39818
 magneto-optical effect, origin and magnitude 9-24366
 magnetoelastic modes in saturated ferrimagnets, models composed of two coupled transmission lines 9-28626
 minerals, remanent magnetization rel. to γ-radiation 9-37665
 pulse echoes, amplification 9-45239
 rare earth iron garnets, linear mag. birefringence 9-45185
 rare-earth ferrites, anisotropy effect on ferrimag. reson. 9-39898
 rare-earth iron garnets, Sc substituted, Fe ions canted spin struct., Mossbauer effect obs. 9-37667
 rare-earth niobates in strong pulsed fields 9-35592
 screw spin structure with orthorhombic anisotropy energy, magnetization process 9-28627
 susceptibility, domain wall continuity rel. to grain orientation 9-31042
 uniaxial and cubic cryst., anisotropy effect on ferrimag. reson. 9-39898
 Co_{0.8}Mg_{0.8-x}Fe_{2.2}O₄, ferrite temp. depend. magnetic aftereffects, Co ion influence 9-35572
 Co_{0.8}Mn_{0.8-x}Fe_{2.2}O₄, ferrite, temp. depend. mag. after effects, Co ion influence 9-35572
 Co₂Ni_{0.8-x}Fe_{2.2}O₄, induced anisotropy mechanism 9-33474
 Co₂Ni_{0.8-x}Fe_{2.2}O₄, ferrite, temp. depend. mag. after effects, Co ion influence 9-35572
 CoCr₂O₄, distant-neighbour B-B interactions, rel. to spin config. 9-45176
 CoCr₂O₄ powder, high field susceptibility, temp. depend. 9-33473
 CoCr₂S₄ spinel, Curie temp. and mag. moment meas. 9-39196
 CoFe₂O₄, uniaxial anisotropy induced at low temp. 9-43185
 CsFeF₃, rel. to crystal structure 9-35063
 EbMgF₃-RbCoF₃ system and opt. props. 9-45186
 ErCo₃, Curie point variation with press-to 6kbar 9-45154
 EuFe garnet, anisotropy in exchange interac., Mossbauer obs. 9-33475
 Fe₂Se₄ structure, neutron diffraction study 9-33477
 Fe_{0.8}Mn_{0.2}As₂, 200≤a≤2.35, first order ferrimag. to antiferromag. transitions 9-45178
 Fe₂Ga_{2-x}O₃, anisotropy energy and anisotropic magnetization 9-33476
 FeCr₂S₄ spinel, Curie temp. and mag. moment meas. 9-39196
 FeMn₂O₄, structure at low temps., neutron diffraction investigation 9-45177
 Fe(Pd,Pt), ferromag. to canted-ferrimag. transition 9-45123
 Gd₂FeO₁₂ film, domain struct. and props. rel. to growth parameters 9-47272
 GdFe garnet, circular domains density and size 9-47271
 GdFe garnet, Sn-substituted, critical mag. isotherm 9-43188
 GdFe garnets, domain interaction with atomic scale imperfections, optical obs. 9-45179
 HoCo₃, compensation point variation with press-to 6kbar 9-45154
 Li_{0.5}Fe_{0.5}(Gd_{0.5})O₄, with Fe³⁺ in tetrahedral and Gd³⁺ in octahedral domains, exchange integrals 9-45181
 Mg-Fe ferrites, magnetocrystalline anisotropy and magnetization, depend. on O content 9-28633
 Mg-Mn monocystals, change of anisotropy of mag. viscosity, -196°C to Curie point 9-45183
 MgCr₂O₄, structure, neutron diff. study 9-28630
 Mn-Zn ferrite, coarse-grained, permeability and harmonic distortion increase with induction 9-35573
 Mn_{0.6}Zn_{0.4}Fe₂O₄, sublattice magnetization temp. depend. and superexchange interactions 9-39777
 Mn₂Co₂C, crystal structure 9-28631
 Mn₂GeSb_{1-x}, ferrimag. to helical transition 9-24318
 Ni-Fe ferrites, magnetocrystalline anisotropy and magnetization, depend. on O content 9-28633
 Ni₂Zn:Co²⁺ ferrites, Fe-rich, temp. spectra, mag. after-effects 9-28632
 Ni_{1-x}Zn_xFe₂O₄, structure effect on semiconducting props. 9-33310
 NiFe₂O₄, mag. moments at room temp. from polarized neutron diff. exam. 9-48838
 NiFe₂O₄, substituted, local fields on Sn nuclei 9-26727
 RbMgF₃-RbCoF₃ system, variation of mag. moments and Curie temp. with Co²⁺ conc. 9-47274
 RbNiF₃, hexagonal, mag. resonance and anisotropic g factors 9-45361
 RbNiF₃, magneto-optical effects, origin and magnitude 9-24366
 RbNiF₃, Raman scatt. by mag. excitations 9-45336
 Sm₂Eu_{1-x}Fe mixed garnet, anisotropy in exchange interac., Mossbauer obs. 9-33475
 SmFe garnet, anisotropy in exchange interac., Mossbauer obs. 9-33475
 (Sr_{0.8}Ba_{0.2})₂Zn₂Fe₂O₄, hexagonal ferrites, magnetization curves and anisotropy const. temp. depend. 9-26657
 TbFe garnet, Sn-substituted, critical mag. isotherm 9-43188
 TmFeO₃, domain structure and wall energy temp. dependence 9-47275
 Y_{2-x}Bi_xCa₂Fe₂Si₂O₁₂ (x=0.6-1.3) ferrimag. Curie temp. 9-37047
 Y_{2-x}Ca_{2x}Fe_{2-x}V₂O₁₂ garnets, Mossbauer effect using Fe⁵⁷, role of Fe³⁺ ions 9-41365
 Y₂Mn_{0.1}Fe_{4.9}O₁₂, anisotropy, first order const. 9-49219
 Y₂Gd_{0.3}Al_{0.7}(In/Sc)₂Fe_{11-n}O₁₂, garnet, isomagnetization lines 9-39778

Magnetic properties of substances continued ferromagnetic continued

- YFe garnet: Si, i.r. sensitive, relax. and mag. anneal of anisotropy 9-45191
- YFe garnet:Co, magnetocrystalline anisotropy and ferrimag. reson. 9-33480
- YFe garnet, (Ca, V, In)-substituted, anisotropy and magnetostriction meas. 9-45192
- YFe garnet, dense perovskite allotropic form, Curie temp. and moment 9-26252
- YFe garnet, i.r. radiation scattering by two magnon processes 9-45337
- YFe garnet, longit. magnon-phonon interaction in obliquely magnetized rods 9-35574
- YFe garnet, Sn-substituted, critical mag isotherm 9-43188
- YFe garnet, spontaneous magnetisation rel. to temp. in range 4.2-290°K 9-41328
- YFe garnet, two magnon scatt. of i.r. radiation 9-24421
- YGa garnet:Co, spin reson. in single cryst. 9-35575
- Yb_{1-x}Fe_xGa_{1-x}O₁₂ (x=0.5-4.0) ferrimagnetic Curie temp. 9-37047
- Yb Fe garnet, cooling by adiabatic magnetization 9-45194
- YbFe garnet: Lu, magnetization rel. to supertransferred hyperfine field of Lu 9-35607
- YbFe garnet, angled spin configs., spectroscopic study 9-45193
- YbFe garnet, canted spin config. 9-47277
- YbFe garnet, magnetic torques consistent with canted sublattice configuration, 4.2°K 9-35576
- Zn_{0.87}Mn_{0.13}Fe₂O₄, struct., neutron diff. obs. 9-43189
- Zn_{1-x}Ni_x-Fe₂O₄ ferrite system, mag. struct., Yafet-Kittel ordering and angles 9-41329
- ferromagnetic**
see also *Ferromagnetic relaxation; Ferromagnetic resonance; Ferromagnetism; Magnetization process; Magnetization state*
- Al-V dil. solid soln., susceptibility w.r.t. localized d-state props. 9-33269
- alloys, f.c.c., lag and anisotropy due to interstitials 9-45130
- alloys, f.c.c. <1>2 struct., transformation props. of spin-wave states under crystal symmetry operations 9-45104
- Alnico, Ti bearing eff. on coercive force 9-24310
- alnico alloy, α and α' phases, saturation magnetization, temp. instability of permanent magnets 9-45149
- alnico alloy single crystals, and precip. 9-44792
- amorphous, model, non-requirement of crystal structure 9-35550
- Barkhausen jumps, negative, as consequence of eddy currents, origin and props. 9-39767
- Bloch walls in thin films, transient gyromag. behaviour 9-26640
- Co_{2-x}Cu_xR (R= rare earth, permanent magnetic material 9-45120
- coercive force due to inclusions expl. test of Neel's theory 9-47244
- domain structures, single-axis, of materials with uniaxial symmetry 9-28613
- domain study using Kerr effect, enhancement through ZnS coating 9-35558
- domain wall-inclusion interaction, theories and examples 9-26642
- dynamic characteristics at low temps. 9-31033
- exchange, 1st and 2nd neighbour, ratio 9-49197
- ferrofluids, use in acoustic transducers 9-27229
- film, mag. spectrum and ferromag. reson. rel. to subdomain struct. 9-43180
- film, saturation magnetism, review 9-49209
- film, spin wave reson., excitation of uniform precession mode 9-43165
- film, spin-wave resonance calcs. 9-41417
- film, wall coercive force, strain sensitivity, 200 Å to 1500 Å thickness 9-45163
- films, differential susceptibility w.r.t. effective field 9-33470
- films, domain obs. in pulse periodical fields by stroboscopic Lorentz microsc. 9-40329
- films, residual magnetization creep in demagnetizing self-fields 9-39772
- films, spontaneous, magnetization, eff. of point defects 9-31040
- films, thin, band model 9-31037
- films, thin, soft mag. materials review 9-39753
- films, thin, stripe domain nucleation 9-31039
- films, two-dimens. Bloch-type domain walls 9-35567
- films ripple obs. with Lorentz microscopy 9-40328
- fluid, with 10% Fe in fine Weiss domain size suspension, eqn. of state 9-31857
- forced magnetostriction, in band model 9-33465
- galvanomagnetic effects, transport theory 9-47255
- haematite, electron transport props., effect of weak ferromag.-antiferromag. transition 9-44869
- haematite, moment orientation rel. to internal stresses, Kerr eff. 9-26644
- haematite, weakly ferromag., antiferromag. reson. 9-39899
- Hall effect, extraordinary, in single cryst., spin-orbit interaction influence on anisotropy 9-37653
- h.c.p. crystals, structure determ. 9-24279
- heat capacity singularity in finite applied field 9-44831
- Heisenberg, eqns. for second-order Green's functions 9-45037
- Heisenberg ferromagnet, two-dimensional, with S=1/2, transition temp. 9-45107
- Heisenberg ferromagnet with arbitrary anisotropy energy, role of monionic correl. functions 9-39755
- Heisenberg quantum-mechanical, staggered susceptibility 9-45100
- hysteresis loop degeneration at Curie temp., demonstration 9-43704
- with inclusions, spherical magnetic, magnetization distrib. 9-45133
- induced anisotropy meas., systematic errors 9-37652
- insulators of ellipsoidal shape, 1st-order spin-wave instability threshold for arbitrary pumping config. 9-45102
- internal effective mag. field determ. by low-temp. nuclear orientation meas. 9-37654
- invar alloy, press. effect on Curie temp. for collective electron ferromagnet 9-28610
- Invar alloy, spontaneous volume magnetostriction theory, thermal expansion anomaly 9-43177
- junction, tunnel, electron-magnon effects 9-47238
- lanthanide-nickel cpds., Ln₂Ni₁₇, characts. 9-47260
- liquid, isotropy considerations 9-23529
- liquid, model, non-requirement of crystal structure 9-35550
- magnetic colloids, magnetoviscosity 9-48722
- magneto-optic effect, quadratic Cotton-Mouton effect 9-49245
- metal, paramag.-impurity ground state, corrections 9-33436
- metal oxide powders partially reduced, high coercivity 9-49212
- metallic polycrystalline, negative Barkhausen jumps, existence, character and rate during magnetization 9-37658

Magnetic properties of substances continued ferromagnetic continued

- metals, book 9-47223
- metals, multiband theory of inelastic neutron scatt. at low temp. 9-33447
- metals, stressed, energy dissipation mechanism 9-33013
- metals, stressed, energy dissipation mechanism 9-23848
- metamagnetism, crystal field effect, in NdP, NdAs, NdSb 9-35590
- minerals, demagnetization of remanent magnetization by pressure application 9-24710
- mumetal, magnetomech. damping, temp. effect and rel. to magnetocryst. anisotropy and easy direction magnetostriction 9-31036
- neutron extinction by polycrystals 9-41308
- neutron scattering obs., anomalous capture of thermal polarized n by nuclei 9-26464
- Ni-(20 wt.%)Cu, mag. moment distrib., mag. disorder neutron scatt. cross section meas. 9-35562
- n.m.r. signals amplification, charact. features 9-43292
- oligatomic films, magnetization and Curie temp., thickness depend. 9-45162
- Permalloy, anisotropy, rotatable, in electron-microscope specimens 9-26646
- permally, film, coercive force and fine mag. struct. 9-41321
- permally films, anisotropy field, neutron irradi. and isothermic annealing effect 9-47253
- permally films, annealing behaviour of induced anisotropy, ageing and stabilization effects 9-37660
- Permalloy films, dynamic Kerr obs. of high-speed flux reversal and relax. processes 9-37661
- Permalloy layers with non-mag. layer composite 9-43183
- permally single-crystal platelet, helical and other stripe structures 9-47248
- permally thin film, effect of mag. annealing and elastic stress 9-41322
- Permalloy wires, domain nucleation and wall propagation influence of structure and composition 9-35561
- pore size effect on remanence ratios 9-43172
- pore size effect on remanence ratios 9-43172
- Pt-(23 wt.%)Co coercive force and B-H meas. 9-45152
- rare earth iron garnets, exchange resonance and Faraday effect 9-45278
- rare earth-Zn cpds. with CsCl struct. 9-35556
- rare-earth chlorides, coupled Ising chains and magnetic ordering 9-33456
- RbFeF₃ domain wall-dislocation interactions 9-45126
- saturation and magnetic moments of nuclei 9-26634
- semiconductors, current carriers, weak interac. case 9-28504
- semiconductors, current carriers, weak interac. case 9-28504
- semiconductor, spin-electron interac. effect on current carrier mobility 9-37516
- semiconductors, current carriers, indirect exchange and localized magnons 9-28607
- (SnTe)_{1-x}(MnTe)_x alloys 9-39771
- spin structures, temp. depend under s-f interaction 9-45204
- spin-1/2 Heisenberg ferromagnet, critical temp. and indices, decoupling scheme calc. 9-35546
- spin-orbit coupling effects on transition metal ions in crystalline environments 9-24285
- spin-wave systems, transient evolution of power adsorbed under e.m. excitation influence of mag. dipole ras. 9-37646
- steel, austenitic, magnetization variation rel. to mag. field 9-23966
- steel, cold-rolled transformer, coercive force rel. to annealing temp. 9-39455
- steel, transformer, covered with Ni film, initial permeability, infl. of tensile stress 9-28618
- steel, transformer, deformed, coercive force and magnetostriction, strain effects 9-45140
- Ticonal 600 alloy, rel. to comp. of α_1 and α_2 phases and saturation magnetization 9-44804
- Ticonal X, magnetic microstruct. by neutron diff. 9-49203
- transition metals, atomic susceptibility and moment 9-45083
- uniaxial anisotropic, magnetization and elem. excitations spectrum Green's functions method 9-24308
- uniaxial ferromagnets, switching threshold of applied field for magnetization reversal or domain form. 9-35557
- wave number-dependent susceptibility, connection proportional to system entropy 9-26629
- whiskers micron-sized free pole and magnetization distrib. 9-45134
- yttrium ferrite, extinction of neutrons 9-41308
- Ag-Ni solid solns., superparamag. meas. of Ni precipitation 9-35212
- Al-Cr dil. solid soln., susceptibility w.r.t. localized d-state props. 9-33269
- Al-Mn dil. solid soln., susceptibility w.r.t. localized d-state props. 9-33269
- Al₂V, susceptibility temp. dependence 9-28616
- Au-Co alloys, liquid, thermodynamics near Curie and melting point 9-23531
- Au-Cu-Co liquid alloy, susceptibility meas. 9-34921
- Au-Fe alloys, ordering from ⁵⁷Fe Mossbauer effect meas. 9-39817
- BaFe₁₂O₁₉, magnetocryst. anisotropy consts. determ. by magnetization curves 9-43170
- BaFe₁₂O₁₉ single crystal M₂ and K₁ as functions of temp form mag. meas. 9-47256
- BaSc₂Fe₁₂O₁₉ hexagonal ferrite single cryst., intensity anomalies due to superposition of reflex satellites 9-31043
- Ba₁₂Ca_{2.68}Fe_{2.66}V_{1.34} O₁₂ ferrogarnet, anisotropy, -183° to 100°C 9-45131
- BiCaV ferrogarnet single crystal, rotatory hysteresis losses 9-45136
- BiMnO₃, below 103°K, and crystal distortions 9-28608
- CO₂BaAl₂Fe₁₆O₂₇ ferroplax, magnetocryst. anisotropy consts. determ. by magnetization curves 9-43170
- CO-(10wt.%)Cr-(45wt.%)Fe alloy films, domain struct., e microscope obs. 9-33471
- (1-x)CdCr₂S₄xCdCr₂Se₄, mixed system, Curie temp., model 9-28609
- CdCr₂Se₄, from n.m.r. obs. of ¹¹¹Cd and transferred spin polarization 9-43297
- CdCr₂Se₄ 3d transition metal ion substituted spinels, moments 9-35551
- CdCr₂Se₄(Se₄) exchange striction rel. to absorb. edge 9-45155
- CdCr₂Se₄(Se₄) transferred spin polarization rel. to n.m.r. of Cd 9-47444
- CdCr₂Se₄, from n.m.r. obs. of ¹¹¹Cd and transferred spin polarization 9-43297
- Co-Al alloys, composition dependence 9-47069
- Co-Ni-Al-Cu-Nb-Fe alloys, induced anisotropy consts., saturation magnetization, coercive force, temp. depend. 9-47251
- Co-Ni-Al-Cu-Ti-Fe alloys, induced anisotropy consts., saturation magnetization, coercive force, temp. depend. 9-47251

Magnetic properties of substances continued
ferromagnetic continued

- Co-P films, coercive force, effect of electroless Ni substrate 9-31041
Co-p alloys, amorphous layers, low coercive force characterisation 9-24311
Co, hexagonal, form factor and noncollinear spin density 9-41304
Co, hexagonal, noncollinear spin density, rel. to form factor 9-45121
 α -Co, magnon dispersion relation, anisotropy, neutron diff. obs. 9-41313
Co, thickness-depend. of domain width, critical thickness 9-39763
Co_{1-x}Fe_xS₂ 9-45286
Co₂BaIn₂Fe_{16-x}O₂₇, ferroplax, magnetocryst. anisotropy const. determ. by magnetization curves 9-43170
Co₂W, magnetocryst. anisotropy const. determ. by magnetization curves 9-43170
Co₃O₄, bulk material and ultra-fine particles, ordering and superparamagnetism from Mossbauer obs. 9-28666
Co coercive force at high temp., effect of dispersoid parameters 9-45138
Co domain struct., e microscope obs. 9-33471
Co film, coercive force and fine mag. struct. 9-41321
Co film, initial susceptibility, rotatable, Kerr effect studies 9-33462
Co films, uniaxial structure, n.m.r. and ferromag. resonance, relaxation times 9-33645
Co hexagonal, eff. of constraint on hysteresis cycle 9-28617
Co thin films electrolytically deposited on Cu, periodic variation of susceptibility maximum 9-47257
Co (10wt.%)Mn-(45wt.%)Fe alloy film, domain struct., e microscope obs. 9-33471
CoS₂, Curie pt. change under press., rel. to interatomic distance 9-33452
CoS₂, exchange interaction 9-33437
Co(S₂Se_{1-x})₂, system, thermostatical investigation 9-31029
Co(S₂Se_{1-x})₂ system 9-33437
Co(S₂Se_{1-x})₂ system, exchange interaction, iso-volume mag. phase diagram 9-33452
CoSe_{2-x} solid, soln. single crystals and powder, magnetiz. and susceptibility meas. 4.2° to 300°K 9-47245
Co-Pd alloys, mag. fields on ⁶⁰Co and ¹¹⁹Sn nuclei 9-28620
Cr, itinerant spin-density excitation in light-scatt. obs. 9-47372
Cr_{0.4}Mn_{0.6}As, structure, Curie temp. at 160°K 9-45057
CrBr₃, diffraction pattern photographs rel. to magnetization 9-31079
CrBr₃, domain structure, Lorentz microscopy at low temps. 9-26651
CrBr₃ near critical point Fraday effect meas. 9-45139
CrBr₃ near critical temp., mag. eqn. of state 9-26649
CrI₃, domain structure, Lorentz microscopy obs., at low temps. 9-26651
CrTe, exchange striction, temp. depend. 9-33466
Cu-Ni-Fe alloys, hard-magnetic particle ensemble mode, calc. 9-33453
Cu-Ni-Fe alloys, ordering from ⁵⁷Fe Mossbauer effect meas. 9-39817
Cu-Ni alloy, para-ferromag. transition ordering rel. to compress., obs. 9-35167
Cu-Ni alloys, near critical composition, magnetiz. polar, clouds of giant moments 9-26624
Cu-(7.5-25 at.%)Mn alloys superparamagnetic subsystem, mag. moments and sizes of mag. clusters 9-43173
Cu(C₆H₁₁NH₃)₂Cl₄, transition temp. for Heisenberg ferromag. with S=1/2 9-45107
CuCl₂(CH₃NH₂Cl), heat transport by magnons 9-37369
Dy, magnetocryst. anisotropy, spin-wave theory 9-37655
Dy, ordering, microscopic theory 9-24313
Dy₂Al₃, 4.2 to 700°K 9-26632
Dy₂Ge₃, susceptibilities rel. to D_{8h} structure 9-43157
Dy₂Si₃, susceptibilities rel. to D_{8h} structure 9-43157
DyAlO₃, mag. structure and metamag. transitions, absorpt. spectra investigation 9-31105
Er, ordering, microscopic theory 9-24313
EuCrO₃, antiferromagnet, weak-ferromagnetic moment obs. 9-24302
EuDSe hydrostatic pressure effects 9-47287
EuO-Gd, Curie point, dopant effect, increase due to exchange interaction via conduction electrons 9-34363
EuO:R³⁺ film, (R=rare earth oxide), and magneto-optical props. 9-47266
EuO order, effect on refractive index and photocond. 9-45266
EuS, mag. sp. ht., susceptibility and Curie const. calc. from energy gap temp. depend. obs. 9-37529
EuS order, effect on refractive index and photocond. 9-45266
EuS thick films at low temp., mag. struct. by use of Lorentz microscopy 9-41880
EuSe single crystal, 1.9°K, neutron diff. study 9-47288
Fe-(25 at.%)Al alloys, one- and two-phase struct. obs., magnetiz. and magnetocrystalline anisotropy 9-26648
Fe-Al alloy single cryst., susceptibility superimposed on saturation magnetization 9-47258
Fe-Al alloy single cryst., anisotropic const., order obs. 9-47252
Fe-Co-Ni alloy fine particles prep. by evaporation in inert gases 9-33459
Fe-(27 wt.%)Co alloys, coercive force at high temp., effect of dispersoid parameters 9-45138
Fe-Co alloy, f.c.c. precip. from Cu, behaviour 9-26633
Fe-Co alloy, high-field susceptibility, estimation at 0°K 9-47243
Fe-Co alloy fine particles prep. by evaporation in inert gases 9-33459
Fe-Ni-Al-Co-Ti alloys, effect of thermomech. treatment 9-47259
Fe-Ni-Al-Ti alloys, effect of thermomech. treatment 9-47259
Fe-Ni-Mn alloys, f.c.c., intrinsic magnetization, 77°K to Curie temp. 9-45144
Fe-49 wt.%)Ni alloys, commercial effect of S on initial permeability 9-49204
Fe-Ni alloy, high-field susceptibility, estimation at 0°K 9-47243
Fe-Ni alloy, invar. model, contrib. 9-37649
Fe-Ni alloys, domain wall distribution rel. to coherent boundaries of twin crystal 9-37651
Fe-Ni films, differential susceptibility obs. of struct. 9-43182
Fe-Ni thin film, variation in mag. susceptibility with thickness 9-39773
Fe-Ni thin films, Faraday effect field depend., perpendicular anisotropy obs. 9-47322
Fe-Ni alloy fine particles prep. by evaporation in inert gases 9-33459
Fe-P alloys, amorphous layers, low coercive force characterisation 9-24311
Fe-Pd alloys, thin films, coercive force rel. to grain size 9-28622
Fe-(48.5 at.%)Rh alloy, anomalous hyperfine field at recoiled ¹⁰³Rh nuclei 9-35564
Fe-(3.25 wt.%)Si thickness-depend. of domain width, critical thickness 9-39763
Fe-Si, grain-oriented, with high permeability, characts. 9-45145

Magnetic properties of substances continued
ferromagnetic continued

- Fe-Si alloys, coercive force, infl. of galvanically deposited Ni films 9-26647
Fe-Si alloys, domain obs. by X-ray topography 9-28614
Fe-Si alloys, spin-wave dispersion relationships determ. 9-24297
Fe-Si alloys, textured, for Si>3.25% 9-45124
Fe-Si frame single crystals, negative Barkhausen jumps, existence, character and rate during magnetization 9-37658
Fe-Si grain-oriented, soft mag. materials review 9-39753
Fe-Si single cryst., lattice distortion and X-ray topographic contrast due to 90° domain wall 9-33460
Fe-(3.7 wt.%)Si magnetomechanical damping, 78-300°K 9-45157
Fe-(3.7 wt.%)Si magnetomechanical damping 78-300°K 9-45157
Fe-V binary alloys, α -phase susceptibility meas., Curie temp., paramag. moment conc. depend. 9-43158
Fe, critical and spin-wave scatt. of neutrons 9-31030
Fe, demagnetization under shock-compression rel. to α - to ϵ -phase transition 9-26388
Fe, high-field susceptibility and mag. moment obs. of band ferromag. 9-43166
Fe, internal mag. field at Os after Coulomb recoil implantation 9-39765
Fe, magnetomech. damping, temp. effect and rel. to easy direction magnetostriiction 9-31036
Fe, saturation and magnetic moments of nuclei 9-26634
Fe, spin diffusion const., theoretical estimate 9-41306
Fe, spin dynamics, neutron scatt. study 9-45110
Fe, spin ordering for band calc. of optical absorpt. 9-39836
Fe, temp. variation of magnetization and high-field susceptibility at 0°K 9-47243
Fe₂B spin-wave gap, n.m.r. detection 9-45109
 α -Fe₂O₃, magnon interaction effects 9-35552
Fe₂P, ferromag. coupling of spins, moment obs., Mossbauer effect meas. 9-33527
Fe₂BO₆, magnetization and Mossbauer effect, spin orientations 9-41314
Fe₂Si₄, mag. field at Fe nuclei, Mossbauer spectroscopy 9-33467
Fe₆₅(Ni₃₅Mn₂₅)₃₅, alloy, moment-induced scattering and magnetovolume effect 9-41303
Fe₇S₈, magnetiz. curves under high field 9-35565
Fe₇Se₈, magnetiz. curves under high field 9-35565
Fe₈₀P₁₅Co₅ amorphous alloy, Hall effect 9-39578
Fe anisotropy energy calc. by perturbation theory 9-47254
Fe cold-worked, permeability and X-ray diffraction line broadening correlation 9-45146
Fe domain struct., e microscope obs. 9-33471
Fe film, coercive force and fine mag. struct. 9-41321
Fe film, magnetization distrib. about single mag. particle 9-43181
Fe platelets, charged 90° Bloch walls obs. 9-43169
Fe single crystal film, rel. to Hall effect 9-47267
Fe ternary alloys, disaccommodation due to interstitials reorientation 9-26635
⁵⁷Fe cpds. Mossbauer spectra near disordering temp. 9-26721
Fe films, magnetiz. meas. as thickness increases atomic layer by layer 9-28619
FeCO₃ magnetometric single crystal, antiferromag. Mossbauer meas., 2.5°K to above Neel temp. 9-45293
FeCl₂, dipole absorpt. in far i.r. 9-35586
Fe(PdPt), ferromag. to canted-ferri-mag. transition 9-45123
Fe(Pt,Pd,_x) ordered alloys, spontaneous magnetization depend. on composition 9-24309
FeRh films, first order antiferromag. transition role of O, 9-45223
FeRh system, first-order antiferromag. to ferromag. transition, mechanism 9-45222
FeRh and magneto-optic props. 9-45141
Fe₃(wt.%)Si alloy, domain obs. by X-ray topography 9-26643
Fe-(31.4at.%)Ni alloy, magnetization, hydrostatic and shock-wave compressions effects 9-43176
Fe-Pd alloys, mag. fields on ⁶⁰Co and ¹¹⁹Sn nuclei 9-28620
Gd-Dy dil. alloy, exchange interactions 9-43171
Gd-(92.5%)La alloy, effective mag. field at impurity nuclei from nuclear component of specific heat 9-33461
Gd-(10wt.%)Lu alloy, effective mag. field at impurity nuclei from nuclear component of specific heat 9-33461
Gd-Y alloys, rel. to Gd concentration, structure 9-45125
Gd, magneto-elastic interactions 9-24312
Gd, magnon-electron inelastic scatt. effect on polarization of photoemitted electrons 9-47214
Gd, ordering, microscopic theory 9-24313
Gd₂CoMnO₆, perovskite, metamagnetism 9-35587
Gd₂Ge₃, susceptibilities rel. to D_{8h} structure 9-43157
Gd₂Si₃, susceptibilities rel. to D_{8h} structure 9-43157
GdN cubic structure and susceptibility meas. rel. to exchange interactions 9-45225
GdNi₂, electrical resistivity temp. depend. near mag. transition 9-43021
GdPt₂, electrical resistivity temp. depend. near mag. transition 9-43021
GdRh₂, electrical resistivity temp. depend. near mag. transition 9-43021
Ho, spin-wave excitations in conical and spiral mag. phases 9-45111
Ho, spin wave dispersion relation in spiral mag. phase 9-45112
Ho single crystal, structure from Mossbauer effect study 9-47333
Lu, ordering, microscopic theory 9-24313
LuCrO₃, Cr³⁺ fluorescence spectrum, magnon sideband emission 9-31136
Mn_x-x(M,Fe)₂B₄, (M=Co,Ni), temp. and comp. dependence, applics., patent 9-33451
Mn₂Cr_{1-x}S solid solutions, sign and size of exchange integrals, evaluation from neutron diff. and magnetic structure study 9-28615
Mn₂Fe_{1-x}Ho_xO₄, at 4.2°K, max. moment for x=0.7 9-35060
MnAlGe, ternary alloy, structure by neutron and X-ray diffraction 9-35560
MnAlGe uniaxial single crystal, domain struct. hysteresis 9-41311
MnAs, density distrib. of electrons with non-compensated spins, form factors calc. 9-35553
MnAs, pressure effects 9-24303
MnBi, density distrib. of electrons with non-compensated spins, form factors calc. 9-35553
MnP, metamag. struct. 9-41337
MnP, transformation to fan structure 9-26645
MnP metamag. single cryst., mag. field effs. on thermoelec. power 9-35498

Magnetic properties of substances continued
ferromagnetic continued

- MnP single crystal, in metamagnetic state, mag. field effects on elec. resistivity 9-28460
- MnSb, density distrib. of electrons with non-compensated spins, form factors calc. 9-35553
- β_1 -MnZn, high-field susceptibility 9-33464
- NaNiF₃ single crystal, antiferromag. reson. in wavelength range 1.2-10 μ m, fields up to 150 kOe, temp. 77-150°K 9-41421
- Nb-Sn superconducting alloys, mag. hysteresis and alloy constitution 9-37659
- Nb-(40wt.%)Zr-(10wt.%)Ti superconducting hollow cylinders, mag. shielding in applied mag. fields at 4.2°K 9-43174
- Nb₃Sn alloy, supercond., hysteresis and correl. with struct. charact. 9-39769
- Nd, f.c.c. phase, room temp. and liq. He temp. stabilization, electronic props. 9-35555
- Nd₃Fe₅₋₆Sc₁₋₂P₂ garnets, ($9 < x < 1.5$) 9-47247
- Nd₂Ge₃, susceptibilities rel. to D_{8h} structure 9-43157
- Nd₂Si₃, susceptibilities rel. to D_{8h} structure 9-43157
- NdCl₃, coupled Ising chains and magnetic ordering 9-33456
- NdCo₅, Curie point variation with press-to 6 kbar 9-45154
- NdP, NdAs, NbSb, w.r.t. crystal field effect 9-35590
- Ni-C solid solns., Cr₂ and Cr₃ types and residual resistivities 9-44914
- Ni-Co films, electrolytically deposited, magnetocryst. anisotropy 9-41323
- Ni-Co films, electrolytically deposited, magnetocryst. anisotropy 9-41323
- Ni-Cu alloy, giant moments near critical composition, 4.2°K 9-45148
- Ni-Cu alloy, minimum polarity models 9-45113
- Ni-Cu alloy, moments in ferromag. composition range determ. 9-43167
- Ni-Cu solid solns., ferro- to paramag. transition, sp.h.t., Curie temp. and moment obs. 9-35554
- Ni-Cu alloys near critical composition, magnetiz. polar. clouds of giant moments 9-26624
- Ni-Cu(Zn) alloys, comparison with paramag. props. 9-35539
- Ni-(19 wt.%)Fe films, energy of combined Bloch and Neel type domain wall 9-28625
- Ni-(17 wt.%)Fe alloy, coercive force, previous loading rate effect 9-47241
- Ni-Fe alloy single crystals, saturation, coercive force, hysteresis loss and Curie temp. 9-47261
- Ni-Fe alloys, directional ordering obs. rel. to radiation enhancement of diffusion 9-44742
- Ni-Fe alloys, spin wave energies, press. depend. 9-33455
- Ni-Fe film, electrodeposited, magnetization ripple wavelength meas., Lorentz microscopy 9-28624
- Ni-Fe thin films electrodeposited on scratched surfaces, uniaxial mag. anisotropy 9-28623
- Ni-Zn-Cr ferrites, Co conc. depend. of induced anisotropy between 20-270°C from reson. meas. 9-41326
- Ni, amorphous film, Curie points, spontaneous magnetization 9-26652
- Ni, anisotropy energy calc. by perturbation theory 9-47254
- Ni, breakdown effect, rel. to band structure 9-47249
- Ni, critical neutron scattering, temp. and intensity shift due to imperfections 9-26636
- Ni, electrolytic, magnetomech. damping, H influence 9-39401
- Ni, high-field susceptibility and mag. moment obs. of band ferromag. 9-43166
- Ni, Jordan type after-effect, domain wall configuration during magnetization reversal 9-31034
- Ni, magneto-elastic hysteresis and internal friction 9-23863
- Ni, magnetomech. damping, temp. effect and rel. to magnetocryst. anisotropy and easy direction magnetostriction 9-31036
- Ni, moment fluctuations rel. to diffuse X-ray scattering, anomalously high intensities near Curie point 9-24304
- Ni, neutron scatt. by spin waves near Curie point 9-49201
- Ni, phase transition region near Curie pt., investig. with polarized neutrons 9-37650
- Ni, saturation and magnetic moments of nuclei 9-26634
- Ni, susceptibility 9-45114
- Ni, temp. variation of magnetization 9-47243
- Ni, thin films, Faraday effect field depend., perpendicular anisotropy obs. 9-47322
- Ni_{0.36}Ni_{0.64}Fe₂O₄, resonance linewidth and shift from tensor susceptibility meas. 9-37666
- Ni₃Al-Fe phase alloys, giant moment inducement 9-45085
- Ni₃Al phase alloys, transition from exchange-enhanced paramag. to weak ferromag. 9-45085
- Ni₃Fe, Ni hyperfine field and its application to the detection of long-range order 9-26637
- Ni₃Ga-Fe phase alloys, giant moment inducement 9-45085
- Ni₃Ga, decrease of magnetization of itinerant electrons by spin-orbit scatt. on impurities 9-26639
- Ni₃Ga phase alloys, transition from exchange-enhanced paramag. to weak ferromag. 9-45085
- Ni₃La₂(NO₃)₁₂·24H₂O phase transitions, obs. and pair-exchange model 9-39781
- Ni₃(Fe, Cr) alloys, ΔE -effect, Cr content depend. 9-47242
- Ni₃(Fe, Mo) alloys, ΔE -effect, Mo content depend. 9-47242
- Ni (110) crystal, polarized positron annihilation 9-24114
- Ni film, coercive force and fine mag. struct. 9-41321
- Ni films, electrodeposited, magnetocryst. anisotropy, lattice distortion effect 9-39774
- Ni magnetochemical damping 78-300°K 9-45157
- Ni polycrystalline wires, Barkhausen discontinuities size distrib., sample shape depend. 9-41316
- Ni response function calculation 9-26638
- Ni single cryst. mag. aftereffect due to displacement of dislocations inside domain walls, dissolved O atoms effect 9-39766
- Ni single cryst. moment and hyperfine constant, 4.2°K to 300°K 9-45150
- β -Ni(10₂)₂·2H₂O, ferromagnetism, remanence and spontaneous magnetization 9-47262
- NiMn_{0.05}Fe_{0.95}O₄, resonance linewidth and shift from tensor susceptibility meas. 9-37666
- Ni-(22 wt.%)Fe, thin films, coercive force, infl. of mech. stress 9-24316
- PbO₆Fe₂O₃ uniaxial single crystal, domain struct. hysteresis 9-41311
- Pd-Co-Sn alloys, effective fields meas. at paramag. Sn nuclei and effect on Curie temp. 9-43179
- Pd-Cr alloy, annealed at 510°C, weak 9-49202
- Pd-Fe alloys, conc. depend. of static and dynamic magnetization 9-45151
- Pd-Fe dilute, alloy, $\partial M/\partial T$ meas. temp. and mag. field depend., rel. to spin-wave exchange stiffness coeff. 9-47263

Magnetic properties of substances continued
ferromagnetic continued

- Pd-(~5at.%)Ni alloy, anisotropy from ferromag. resonance 9-24478
- Pd-Ni alloy, Curie temp., effect of hydrostatic pressure 9-28611
- Pr, f.c.c. phase, room temp. and liq. He temp. stabilization, electronic props. 9-35555
- PrCl₃, coupled Ising chains and magnetic ordering 9-33456
- PrCo₅, Curie point variation with press-to 6 kbar 9-45154
- Pt-Co alloys, coercive force increase after double ageing 9-26372
- Pt-Fe dilute solid soln., inc. in susceptibility due to interac. of Fe with quenched in vacancies 9-26278
- Pt-Mn alloys, mag. structure, n diff. analysis 9-35563
- Pt/Mn alloy average moments, atomic ordering effects on spontaneous magnetization 9-39770
- Rb₃CoCl₆, heat capacity meas. comparison with Ising model, transition obs. 9-39532
- RbFeF₃ orthorhombic from tetragonal antiferromag. 87°K, and optical props. 9-47293
- RbNi(CO)F₃, mag. circular dichroism and Faraday rotat 9-33513
- Ru-Ni solid solns., superparamag. meas. of Ni precipitation 9-35212
- Sc, decrease of magnetization of itinerant electrons by spin-orbit scatt. on impurities 9-26639
- Si-Fe, susceptibility and coercive force, disloc. theory 9-33457
- SnO₂, cassiterite, natural crystals, origin 9-47264
- (Sr,Bi,La)MnO₃ solid solns., new ferroelec.-ferromag. material 9-47178
- (Sr,Bi)MnO₃ solid solns., new ferroelec.-ferromag. material 9-47178
- SrFe₂O₁₉ single crystal, M_r and K₁ as function of temp. from mag. meas. 9-47256
- SrO[(Sr_{1-x}La_xMn_{0.3}³⁺Mn_{0.7}⁴⁺)O₃] layered structures, 1.4° to 300°K 9-45153
- Tb, magnetocryst. anisotropy, spin-wave theory 9-37655
- Tm magneto-resistance, transverse, in fields up to 22 kOe, temp. depend. between 4.2 and 22°K 9-41318
- U₃As₄ single cryst., magnetocrystalline anisotropy, hysteresis and magnetization obs. 9-37656
- UP₃ single cryst., magnetocrystalline anisotropy, hysteresis and magnetization obs. 9-37656
- UF₆, structure and spin density distrib. 9-45127
- UF₆O₄, and structure 9-45238
- UGa₃ (x=1,2,3), susceptibility 9-33458
- UP-US solid solns. 9-45117
- VAl₃ and related cpds., magnetiz. and susceptibility meas. 9-45128
- YCo₅, Curie point variation with press-to 6 kbar 9-45154
- YCo₃, YCo₅ and Y₂Co₇ single crystals, moments, polarized-neutron diff. study 9-47250
- YCrO₃, Cr³⁺ fluorescence spectrum, magnon sideband emission 9-31136
- YFe garnet, Ca-V-substituted, effective linewidth due to anisotropy near reson. 9-31055
- YFe garnet, effective linewidth due to porosity, relax. obs. 9-31055
- YFe garnet, Si doped, photoinduced magnetic anisotropy 9-24307
- YFe garnet slab, magnetostatic, surface waves excitation and propagation charact. 9-28586
- YFeO₃, susceptibility tensor, temp. depend. 9-43187
- Zn_{1-x}Cd_xCr₂Se₄ susceptibilities and moments 9-31035
- (Zr_{1-x}Nb_x)Fe₂ with cubic Laves structure, Curie temp., pressure depend 9-45129
- (Zr_{1-x}Ti_x)Fe₂ with cubic Laves structure, Curie temp., pressure depend 9-45129
- (Zr_{1-x}Ti_x)Fe₂ with cubic Laves structure, Curie temp., pressure depend 9-45129
- (Zr_{1-x}Ti_x)Zn₂ Curie temp. and magnetization rel. to lattice parameter 9-26650

paramagnetic*see also Paramagnetic resonance and relaxation; Paramagnetism*

- anisotropic, spin diffusion and propag. modes 9-45082
- antiferromagnet, Uniaxial phase transition from spin-flop phase mag. field induced 9-45199
- association factor of mag. ions in diamag. matrix, applic. to ruby 9-49340
- crystal, resonance absorpt. of γ quanta, effect of ion-phonon interaction 9-33524
- g factor rel. to magnetomech. ratio g' for centres, Kittel-Van Vleck relation 9-41293
- garnets, germanate and gallate containing rare-earth ions, susceptibility, moment 9-47231
- h.c.p. crystals, structure determ. 9-24279
- ions in soln., deuteron mag. reson. 9-46653
- liquids and electrolyte solutions, nonresonant absorption 9-23530
- metal, interaction with antiferromag. excitation branches, rel. to spin wave spectrum 9-28638
- metal, paramag.-impurity ground state, corrections 9-33436
- metals, susceptibility elasticity rel. to e struct. 9-40996
- neutron scattering rel. to short-range-order 9-24283
- non-insulated, g-factor determ. by rapid modulation method 9-43271
- paramagnet with nonaxially symmetric crystal field, hyperfine struct. of Fe³⁺ Mossbauer spectra, mag. field effect 9-49257
- radicals in iminoxyl series, susceptibility meas., rel. to Heisenberg one-dimensional model with antiferromag. interaction 9-31023
- rare earth metal salts, anomalous susceptibility caused by crystal field 9-45089
- rare earth-Zn cpds. with CsCl struct. 9-35556
- ruby, distrib. of ions in matrix, and mag. reson. line intensities 9-49340
- ruby, nuclear spin thermal mixing rel. to ENDOR saturation transfer mechanism 9-43310
- susceptibility, meas. using vibrating-coil magnetometer 9-45047
- susceptibility value from Zeeman effect 9-42408
- tetracyanoquinodimethan complexes, susceptibility from 2.5°K to room temp. 9-47233
- 2,2,6,6-tetramethyl-4-hydroxypiperidine-1-oxyl radical, susceptibility and e.s.r. spectra 9-45091
- thermodynamic and h.f. props. of paramagnet with negative anisotropy const. at low temp. 9-31022
- transition metal chalcogenides with CrS₄ structure, susceptibility meas. 9-24329
- transition metal ion complexes, octahedral, susceptibility rel. to excited configs. 9-39752
- transition metals, atomic susceptibility 9-45083
- transition metals and alloys, b.c.c., susceptibility, effect of spin-orbit interaction 9-35536
- Al₃V, susceptibility temp. dependence 9-28616
- alloy, para-ferromag. transition ordering rel. to compress., obs. 9-35167

Magnetic properties of substances continued paramagnetic continued

- Au-Cu-Co liquid alloy, susceptibility meas. 9-34921
 CO complex β -CO(II) phthalocyanine, anisotropy rel. to ground state, obs. 9-32470
 CeBr₃, adiabatic susceptibility meas., rel. to interaction tensors 9-47229
 Co-Al alloys, Pauli paramagnetism composition dependence 9-47069
 Co-Cr binary alloys, α -phase, susceptibility meas., Curie temp., moment 9-43158
 Co-V binary alloys, α -phase, susceptibility meas., Curie temp., moment 9-43158
 Co_{1-x}Cu_xRh₂S₄, for $\sim 0.7 \leq x \leq 1$ 9-41164
 Co(III) complexes, residual paramag. obs. 9-35535
 CoGa intermetallic cpd., susceptibility, 77-1200°K 9-24281
 Cr₂O₃TiO₂, paramagnetic props. obs. 9-49022
 CrSb₂, marcasite-type 9-35581
 CsCuCl₃, rel. to bonding 9-24044
 Cu₂Cs₃Cl₂·2H₂O single cry., mag. ordering 9-37643
 β -Cu₂V₂O₇, Langevin to temp. independ. paramag. change w.r.t. increasing x 9-41197
 Dy-Y alloys, susceptibility and Hall eff. meas. 9-37644
 Dy, critical sound scatt. near Neel temp., spin-phonon coupling mechanism 9-24027
 Dy₂Ge₃, susceptibilities rel. to D_{8h} structure 9-43157
 Dy₂Si₃, susceptibilities rel. to D_{8h} structure 9-43157
 Dy₂Ho_{1-x}Sb_x, Neel and paramag. Curie temp. 9-28595
 Er, susceptibility, effect of hydrostatic pressure 9-28594
 EuCl₃:Gd³⁺ pair and Gd³⁺-Eu³⁺ interac. const., e.p.r. 9-33439
 Fe-Ru h.c.p. alloys, ϵ -phase, magnetization, susceptibility X-ray diff. obs., Pauli-paramag. temp. depend. 9-43159
 Fe-V binary alloys, α -phase susceptibility meas., Curie temp., paramag. moment conc. depend. 9-43158
 Fe₂Te₃, Pauli susceptibility in tight-binding approx., d-band struct. obs. 9-39565
 Gd₂Ge₃, susceptibilities rel. to D_{8h} structure 9-43157
 Gd₂Si₃, susceptibilities rel. to D_{8h} structure 9-43157
 Gd(Co_{1-x}Ni_x), transition metal moment collapse 9-45084
 Ge-Mn alloys, liq. and solid, movement decrement rel. to Mn conc. 9-47232
 Ho, critical sound scatt. near Neel temp., spin-phonon coupling mechanism 9-24027
 Ho, susceptibility, effect of hydrostatic pressure 9-28594
 K₂CoF₄, susceptibility by n.m.r. of F⁻ transferred hyperfine interaction 9-41294
 K₃Co(CN)₆:Cr³⁺, nuclear spin thermal mixing rel. to ENDOR saturation transfer mechanism 9-43310
 Li₂RhH₂ (x=4.5), susceptibility meas. rel. to structure and bonding 9-48834
 LuFeO₃ othoferrite, susceptibility, exchange const. determ. 9-45182
 MgCr₂O₄, antiferromag.-paramag. transform. of first order 9-49224
 MnAs, pressure effects 9-24303
 MnO, n. scatt. rel. to short-range order 9-24283
 MnTe₂, ordering rel. to ¹²⁵Te Mossbauer obs. 9-43225
 MnTiO₃, II high press. phase, susceptibility rel. to Curie Weiss low 9-44667
 Na, spin susceptibility, phase transform. effect 9-35538
 Nb, superconducting, surface magnetization 9-30876
 Nd₂Ge₃, susceptibilities rel. to D_{8h} structure 9-43157
 Nd₂Dy_{1-x}Sb_x, Neel and paramag. Curie temp. 9-28595
 NdCl₃, susceptibility, crystal field calc. 9-33440
 Ni-Al alloys, Pauli paramagnetism composition dependence 9-47069
 Ni-Cu alloy, giant moments near critical composition, 4.2°K 9-45148
 Ni-Cu solid solns., ferro- to paramag. transition, sp.ht., Curie temp. and moment obs. 9-35554
 Ni-Cu(Zn) alloys, comparison with ferromag. props. 9-35539
 Ni-Rh alloy, spin fluctuations from sp. ht. and thermal expansion anomalies 9-45086
 Ni-V binary alloys, α -phase, susceptibility meas., Curie temp., moment 9-43158
 Ni, susceptibility 9-45114
 Ni₃Al:Fe phase alloys, giant moment inducement 9-45085
 Ni₃Al phase alloys, transition from exchange-enhanced paramag. to weak ferromag. 9-45085
 Ni₃Ga:Fe phase alloys, giant moment inducement 9-45085
 Ni₃Ga phase alloys, transition from exchange-enhanced paramag. to weak ferromag. 9-45085
 NiCrO₃, room temp. props. 9-43160
 NiF₂, one- and two-magnon excitations, temp. depend., spin correl. functions 9-33441
 NiS, ordering rel. to lattice compressibility 9-44672
 NiSe₂, weak const. paramag. with metallic conductivity 9-33437
 NpAl₂ susceptibility meas. and Mossbauer hyperfine interaction 9-47334
 NpC susceptibility meas. and Mossbauer hyperfine interaction 9-47334
 O₂ molecules in O₂-Ar solid mixtures, susceptibility meas. rel. to exchange interactions 9-45231
 PbFe_{0.5}Nb_{0.5}O₃, spontaneous magnetoelec. eff. 9-28596
 PbMn_{0.5}Nb_{0.5}O₃, spontaneous magnetoelec. eff. 9-28596
 Pd/H₂ syst., susceptibility meas., 50°-100°K 9-41295
 Pd-Ni alloy, Curie temp., effect of hydrostatic pressure 9-28611
 Pd-Ni alloy, spin fluctuations from sp. ht. and thermal expansion anomalies 9-45086
 Pd-Ni alloys, susceptibility meas. rel. to Stoner enhancement 9-45087
 Pd-Rh exchange enhanced alloys, field-depend. mag. susceptibility, 200 kG 9-26625
 Pd susceptibility, unenhanced 9-45088
 Pr₂La_{1-x}Al₂, magnetization data 9-28597
 Pr₂La_{1-x}Al₂, magnetization data 9-28597
 Pt-(1 at.%)Co alloy with plastic strain, susceptibility behaviour 9-43161
 Pt-(1 at.%)Fe alloy with plastic strain, susceptibility behaviour 9-43161
 Pt-Ni alloys, electron spin fluctuation interaction effects from sp. ht. enhancement 1.15° to 4.2°K 9-44837
 Pu₂S₄, susceptibility, 4° to 1000°K 9-24284
 PuO_{1.52}, susceptibility, 4° to 1000°K 9-24284
 PuS, susceptibility, 4° to 1000°K 9-24284
 PuS₂, susceptibility, 4° to 1000°K 9-24284
 RbFeF₃, spin densities and hyperfine interacs. at ¹⁷F, ⁸⁷Rb and ⁸⁵Rb from n.m.r. 9-32760
 Re, susceptibility, 20.4° to 293°K 9-31024
 Tb-Y alloys, susceptibility and Hall eff. meas. 9-37644

Magnetic properties of substances continued paramagnetic continued

- Tb, critical sound scatt. near Neel temp., spin-phonon coupling mechanism 9-24027
 Th_{1-x}Er_x, spin correlations rel. to superconducting transition temp. comp. dependence 9-24160
 TiC, susceptibility 9-28468
 UGa_x (x=1,2,3), susceptibility 9-33458
 U(IV) in Na silicate glass, susceptibility 9-33442
 UN, ¹⁴N n.m.r. obs. 9-37807
 UP, rel. to nuclear magnetic relax. of ³¹P 9-24343
 V₂Ga, supercond., critical fields temp. depend. from magnetiz. obs. 9-44945
 Y, susceptibility, 20.4° to 293°K 9-31024
 YFeO₃ orthoferrite, susceptibility, exchange const. determ. 9-45182
 ZnCr₂O₄, antiferromag.-paramag. transform. of first order 9-49224
 Zr₂Co-Zr₂Ni mixed cryst., susceptibility 9-33276
- ## transitions
- antiferromagnet, uniaxial antiferromag. spin phase cap. and paramag. phases mag. field induced 9-45199
 antiferromagnetic, critical concs. for several lattice types 9-49200
 biquadratic exchange and quadrupolar ordering 9-45044
 double-shock method for pressure limit detection 9-35524
 ferromagnetic, critical concs. for several lattice types 9-49200
 first-order, structure changes in ordered phase 9-31015
 haematite, effect of weak ferromag.-antiferromag. transition on electron transport props. 9-44869
 haematite, Morin transition and lattice spacing w.r.t. particle size 9-32914
 haematite, spin axis rotation 9-45064
 h.c.p. crystals, paramag.-ferromag. transition 9-24279
 Heisenberg ferromagnet, two-dimensional, with S=1/2, temp. 9-45107
 Heisenberg spin system, two-dimensional, Green-function theory 9-24295
 invar alloy, press. effect on Curie temp. for collective electron ferromagnet 9-28610
 manganese formate dihydrate, with weak canting interaction, critical phenomena 9-33489
 metals, anomalous Hall eff. through ferroparamagnetism transition 9-28593
 Ni-Cu solid solns., ferro- to paramagnetism, sp.ht., Curie temp. and moment obs. 9-35554
 piezoelectrics, mag. ordered, induced ferroelec. mag. obs. 9-39748
 Pu₂S₄, para- to antiferromagnetic at 15°K 9-24284
 pyrites, exoelectron emission during phase transformation, 300°-650°K 9-24248
 rare earth gallium garnets, rel. to sp. ht. 9-24051
 rare earths, rel. to u.s. attenuation freq. and temp. depend 9-48958
 rare-earth metals, critical scatt. of sound 9-37333
 rare-earth-In cpds.: RIn₂ 9-39751
 titanomagnetites, Curie temp. estimation 9-35537
 transport properties near critical points 9-45040
 BaMnF₄, antiferromag., spin flop transition 9-43193
 BiMn₂O₄, antiferromag., rel. to mag. symmetry and ferroelec. 9-45208
 CaMn₂Op₄ antiferromag., rel. to mag. symmetry and ferroelec. 9-45208
 CdCr₂S₄(Se₄) spinels, ferromag. phase transitions pressure depend 9-45119
 CdCr₂S₄(Se₄) spinels, ferromag. phase transitions, pressure depend 9-45119
 Co(S,Se_{1-x})₂ system, metamag. transition 9-31029
 Cr, critical exponents and electrical resistivity near Neel point 9-35582
 Cr, thermal conductivity above and below Neel temp. 9-26444
 Cr rel. to u.s. attenuation, freq., and temp., depend 9-48958
 Cu(C₆H₁₁NH₃)₂Cl₂, temp., for Heisenberg ferromag. with S=1/2 9-45107
 CuCl₂·H₂O antiferromagnetic spin flop transition. 1° to 2.5°K antiferromagnetic spin flop transition, 1° to 4.2°K adiabatic meas. study 9-45217
 Cu(NH₃)₄SO₄·H₂O, short range to long-range ordered state, from proton n.m.r. and susceptibility meas. 9-41334
 Dy₂Ho_{1-x}Sb_x, Neel and paramag. Curie temp. 9-28595
 Er-(90 at.%)Dy ferromagnetic at 65°K 9-45060
 ErCo₂, mag. phase transition of first order 9-24272
 ErFeO₃, Y and Bi substituted, effect on spin reorientation 9-45061
 Eu, anomalous critical-point behaviour, Mossbauer effect meas. study 9-45219
 EuO:Gd, dopant effect on Curie point attributed to additional interaction via conduction electrons 9-33463
 EuO:R³⁺ film, (R=rare earth oxide), Curie temp. 9-47266
 EuO, magnetic phase transitions, effect of press. to 10 kbar, compressibility and vol. depend. 9-33485
 EuO, pressure effects to 10 kbar, vol. depend. of exchange interact. 9-24327
 EuSe, pressure effects to 10 kbar, vol. depend. of exchange interact. 9-24327
 EuSe single crystal, ferromag. to antiferromag., neutron diff. study 9-47288
 Eus, pressure effects to 10 kbar, vol. depend. of exchange interact. 9-24327
 Fe, critical and spin-wave scatt. of neutrons 9-31030
 α -Fe₂O₃, critical field meas., nature of transitions obs. 9-35531
 Fe_{2-x}Mn_xAs₂, 2.00 $\leq x \leq$ 2.35, first order ferrimag. to antiferromag. transitions 9-45178
 FeCl₃, low-temp. antiferromag. 9-45224
 Fe(Pd,Pt), ferromag. to canted-ferrimag. 9-45123
 FeRh films, first-order antiferromag. to ferromag. transition role of O₂ 9-45223
 FeRh system, first-order antiferromag. to ferromag., mechanism 9-45222
 Gd-Sc alloys, rel. to Gd concentration structure 9-45125
 Gd-Y alloys, ferro to antiferromag. rel. to Gd concentration 9-45125
 Gd₂CoMnO₆, perovskite, antiferromag.-ferromag., rel. to metamagnetism 9-35587
 GdNi₂, ferromagnetic-ordering temp., effect of molecular field 9-43021
 GdPt₂, ferromagnetic-ordering temp., effect of molecular field 9-43021
 GdRh₂, ferromagnetic-ordering temp., effect of molecular field 9-43021
 Ho, cone-to-spiral transition near 20°K by soft spin-wave modes 9-43151
 MgCr₂O₄, antiferromag.-paramag. transform. of first order 9-49224
 Mn₂Ge₂Sb_{1-x}, ferrimag. to helical and helical to antiferromag. 9-24318
 MnBi, Curie-point magnetic holography 9-25323
 MnCr₂S₄ thiospinel, low temp., neutron diff. obs. 9-47225
 MnF₂, antiferro-paramagnetic phase boundary from u.s. and differential magnetization meas. 9-41339
 MnF₂ rel. to u.s. attenuation, freq. and temp., depend 9-48958

Magnetic properties of substances continued
transitions continued

- MnP, ferromagnetic state to fan structure 9-26645
 MnP single crystal, screw and ferromagnetic spin structures to fan structure 9-47246
 Nd, antiferromag., correl. with anomalies in elastic and anelastic props. 9-35146
 Nd₂Dy_{1-x}Sb, Neel and paramag. Curie temp. 9-28595
 Nd monochalcogenides, antiferromag.-ferromag. due to critical field 9-49225
 Ni, phase, effect of mag. field, neutron scattering investig. 9-24305
 Ni₃Al phase alloys, exchange-enhanced paramag. to weak ferromag. 9-45085
 Ni₃Ga phase alloys, exchange-enhanced paramag. to weak ferromag. 9-45085
 Pr, antiferromag., correl. with anomalies in elastic and anelastic props. 9-35146
 Pt-Fe system near Pt₃Fe composition, from Mossbauer effect meas. 9-24275
 PuO_{1.52}, para- to antiferromagnetic at 15°K 9-24284
 PuS, para- to antiferromagnetic at 15°K 9-24284
 PuS₂, para- to antiferromagnetic at 15°K 9-24284
 Rb₃CoCl₆, from heat capacity meas. 9-39532
 RbFeF₃, tetragonal antiferromag. to orthorhombic ferromag. and optical props. 9-47293
 Sm, antiferromag., correl. with anomalies in elastic and anelastic props. 9-35146
 SmFeO₃-DyFeO₃ solid soln. single crystal, spin reorientation, 2° to 500°K 9-45235
 TbCrO₃ antiferromag. rel. to mag. symmetry and ferroelec. 9-45208
 UP, low temp., neutron diff. study 9-28590
 YGa garnet:Co, strong mag.-dipole transitions from spin reson. obs. 9-35575
 Zn_{1-x}Cd_xCr₂Se₄ mixed phase syst., susceptibilities and moments 9-31035
 ZnCr₂O₄, antiferromag.-paramag. transform. of first order 9-49224

Magnetic resonance and relaxation

- see also *Antiferromagnetic resonance; Ferrimagnetic resonance; Ferromagnetic relaxation; Ferromagnetic resonance; Nuclear magnetic resonance and relaxation; Paramagnetic resonance and relaxation*
 association factor of mag. ions in diamag. matrix, applic. to ruby 9-49340
 atomic beam mag. reson. for hyperfine struct. meas. of ¹⁵³Gd, nuc. moments calc. 9-22952
 cerium ethyl sulphate:Nd, optical detection of spin lattice relax. and cross-relax. between Nd and Ce 9-35595
 dipolar molecules, solvent depend., using microwave absorption 9-36900
 double irradiation in multilevel spin systems 9-25157
 ferrimagnetic echo amplification 9-45239
 ferrites, planar-anisotropic, magnetostatic mode meas. of 4nM_s 9-45173
 ferromagnetic spherical sample, theory and meas. method 9-45360
 forbidden lines and 'solid effect,' correl. function formulation 9-49339
 forced oscillations and magnetic resonance in the introductory laboratory 9-41727
 Heisenberg chain, linear, spin-lattice relax. 9-41347
 ions, paramag., spin-lattice relax., magneto-optical meas. 9-40299
 lanthanum ethyl sulphate:Nd, optical detection of spin lattice relax. 9-35595
 liquids, spectra moments rel. to slow mol. motions correl. time 9-23453
 magnetically dilute solids, spectral diffusion and phase relaxation, spin echo formula 9-41344
 methyl bromide, double irr. by i.r. and r.f. beams 9-46402
 multiple quanta transitions, Jules Haag synchronisation theory applic. 9-47420
 non-Kramers doublet, effective spin-1 formalism for transitions 9-33616
 nuclear spin-lattice relaxation, tone-burst meas. 9-43823
 Overhauser effect, double resonance spectrometer for obs. 9-31883
 phase modulation in experiments 9-27261
 proton-resonance field stabilizer 9-34142
 rare earth ethylsulphates, sm³⁺ spin-lattice relaxation time calc. 9-43197
 ruby, line intensities, and distrib. of paramag. ions in matrix 9-49340
 spin relaxation through modulating the orientation 9-47295
 spin ticking effect, new form of equation 9-42374
 spin-lattice relax., semidiagonal Raman process 9-35593
 spin-lattice relax. effect on u.s. attenuation near critical pts. 9-44820
 spin-relaxation, for arbitrary magnitude of stochastic perturbation 9-28639
 spin-spin and spin-lattice relaxation times, meas. by Mossbauer effect 9-31053
 stochastic disturbance induction of relaxation in a spin system 9-28639
 superconducting powders, type II, echo formation 9-24147
 superconductors, type II, spin diffusion 9-24339
 TMPD-TCNQ, spin-lattice relax., temp. depend. 9-41347
 two-spin system coupled Gydipolar interaction, hyperfreq. electronic susceptibility 9-41416
 water, spin-lattice relax., temp. depend. 9-32778
 CaF₂:V³⁺, spin-lattice coupling consts. 9-31054
 CaF₂, spin-lattice relax. times of Yb³⁺ by nucl. dynamic polarization 9-47297
 CoCl₂·2H₂O, antiferromag. far-i.r. absorpt., clustered multiple states, flipped spin states propag. 9-33483
 Cr-Al acetylacetonate mixed single crystals, spin-lattice relax. props. 9-49227
 CsMnF₃ hexagonal antiferromag. nuclear and electronic spin -wave relax rate 9-45216
 CuSO₄·5H₂O, spin-lattice relax. times of Cu²⁺ by nucl. dynamic polarization 9-47297
 He-H₂ gaseous mixtures, spin-lattice relax. 9-30354
 KCl, energy parameters of In⁺ and Tl⁺ 9-31052
 MgO:⁵⁷Co, ⁵⁷Fe relax. processes, Mossbauer spectra 9-33530
 Na oriented vapour, second order modulation of transversal light beam 9-22438
 NaNiF₃, orthorhombic canted antiferromag., and anisotropic g factors 9-45361
 RbNiF₃, hexagonal ferrimag., and anisotropic g factors 9-45361
 Xe, decays and Lande factors of 7p_{1/2} and 7p_{3/2} levels, meas. 9-46285

Magnetic storms

- 1964, April 1-2, magnetosphere tail and polar cap obs. rel. to neutral sheet instability 9-26959
 auroral ozone decrease, X-ray ionization effect 9-41570
 bays, simultaneous outer rad. belt energetic electron obs. 9-31381

Magnetic storms continued

- cosmic ray diurnal variation enhanced 9-35928
 cosmic ray vars., diurnal phase and amplitude 9-49513
 D_{st} field for storm 18-19 June, 1936, new analysis 9-43486
 D_{st} midnight intensification rel. to auroral oval position 9-43431
 D_{st} variations, use in deep e.m. soundings 9-43358
 data by incidence sounding techniques 9-49593
 Doppler temperature, 6300 Å, interferometric obs. (30 Oct.-2 Nov. 1968) 9-49459
 DP-current system dynamics, July 8, 1966 and August 29, 1966 as examples 9-47593
 associated electron intensities in outer radiation zone 9-43434
 energy characts., instantaneous, interpretation 9-31455
 energy density of long-period fluctuations 9-33863
 equatorial electrojet region, Dst values 9-24707
 F₂ layer disturbances in polar storms rel. to ionization drifts 9-26953
 F₂ layer disturbances, 0-60°N 9-28957
 F-region ionization and heating during storms 9-45546
 features related to solar wind structure 9-35911
 fluctuations, mid- and high-latitude, statistical analysis 9-35905
 geomagnetic rel. to flare-induced interplanetary storms 9-47594
 hydromagnetic emissions associated with storm sudden commencements 9-35912
 ionosphere, topside polar, storm time electron conc. vars. 9-45532
 rel. ionosphere topside electron conc. vars., s. hemisphere 9-31433
 magnetosphere inflation, OGO-2 obs. (March 1966) 9-41597
 magnetospheric, causing non uniform growth of ring current belt 9-31378
 magnetospheric, day and night differences of v.l.f. emissions 9-49468
 rel. to magnetospheric convection 9-37951
 magnetospheric substorm, various manifestations 9-35902
 magnetospheric substorms, effect on neutral sheet 9-24674
 micropulsation wave packets, ssc, freq.-time dispersion and polarization effects 9-33870
 microstructures and disturbances spectral analysis (Feb 1965 and March 1966) 9-41598
 neutral sheet during storm, 1963 Explorer 14 obs. 9-28918
 relation to Pc1 pulsations 9-31462
 plasma obs. from Explorer 34 (30 May, 5 Jun and 25 Jun 1967) 9-24673
 polar, in auroral zone, development 9-31457
 polar, intensity rel. to DR vars. 9-45558
 polar, magnetospheric and auroral mechanisms 9-43484
 polar disturbances, minor, development and decay, (May, 1964) 9-35910
 in polar ionosphere, long-period wave generation 9-40100
 polar magnetic disturbances, constitution 9-35909
 polar substorm, 16 Dec. 1964, interpretation of N hemisphere obs. 9-28963
 polar substorms, theory 9-41599
 polar substorms rel. to aurora's, expt. and theory review 9-37957
 pulsations, short-period, rel. to solar corpuscular streams and magnetosphere interaction, obs. 9-28964
 recovery phase, magnetosphere field structure 9-43483
 related events in ring current and aurora 9-38001
 ring current particle distribution of disturbance (17 Apr 1965) 9-26933
 SC, ionospheric aeronomic parameters response 9-43453
 SCs and SLs, bays in magnetic field at equatorial electrojet stations in India 9-28962
 solar activity, effect of coronal formation 9-47592
 rel. to solar corpuscular streams active periods diurnal distrib., obs. 9-26966
 rel. to solar flare 21-28 May(1967) 9-43492
 solar flare effects rel. to form. height in atm. 9-26964
 rel. to solar wind, quiet, plasma and e.m. fluxes 9-26965
 substorm, auroral, related micropulsations and electron precipitation 9-35913
 substorms, magnetosphere, synchronous orbit obs. (Dec 1966 and Jan 1967) 9-43485
 substorms, successive v.l.f. and optical emissions 9-41533
 substorms, magnetospheric, rel. to assoc. current system 9-41600
 sudden commencement, electron precipitation, balloon obs. 9-35903
 sudden commencement, ionospheric effect at solar activity extremes 9-31408
 sudden commencement, outer zone electron flux rel. to solar proton events (5 Feb 1965) 9-41606
 sudden commencement, recurrence rel. to solar revolution 9-28960
 sudden commencement morphology, importance of recording east-west component 9-33862
 sudden commencements and impulses in American equatorial zone, IGY obs. 9-41596
 associated telluric ocean current effect on GEK meter obs. 9-43373
 topside ionosphere variations, review 9-35871
 v.l.f. emissions, medium latit., storm-time evolution, satellite obs. (May 25/26 1967) 9-37939
 work of Birkeland and successors, historical review 9-33999
 world-substorm, definition 9-35906

Magnetic traps see *Plasma confinement***Magnetic wells** see *Plasma confinement***Magnetism**

- see also *Antiferromagnetism; Diamagnetism; Earth/magnetic field; Exchange interactions; Ferrimagnetism; Ferromagnetism; Gyromagnetic effect; Magnetohydrodynamics; Paramagnetism; Rock magnetism; Stars/magnetism; Sun/magnetism*
 coercive force of set of non-interacting particles with spontaneous magnetization 9-35523
 college-level textbook on electricity and magnetism 9-31866
 couplings in helical mag. structures 9-43147
 ellipsoid, permeability tensor equations 9-33431
 films, thin, theory 9-49181
 and magnetic materials 9-45039
 magnetic monopoles Feynman-Dyson perturbation theory 9-38438
 material properties research review 9-43837
 materials and their props., book 9-49187
 metals, Kubo formalism and relaxation of localized moments 9-35526
 metals, second-order exchange effects, in localized moments 9-35527
 monopole, existence, prod. of Vavilov-Cerenkov radiation in transparent dielectric crystal 9-28648
 rare earth compounds, high-degree electrostatic and exchange interactions 9-47227
 rare-earth ferrite garnet monocrystals near Curie point 9-45175
 role in technology 9-43836
 s-band, strongly correlated 9-45045

Magnetism continued

- scaling laws for interacting systems, critical behaviour of thermodynamic quantities 9-41290
 spontaneous, set of non-interacting particles, coercive force 9-35523
 theoretical, elements of, book 9-47223
 transition-metal salts high-degree electrostatic and exchange interactions 9-47227
 two-phase random medium, variational bounds on bulk props. 9-43754
 undergraduate text 9-38188
 unit systems, book 9-47718
 In-(3.9 at.%)Pb alloy, type I-II supercond. transition obs. 9-47089
 Ni-Co films, electrolytically deposited, magnetocryst. anisotropy 9-41323
 YFe garnet, spontaneous, temp. dependence, 4.2-290°K 9-41328

Magnetization process

- see also *Ferromagnetic relaxation*
 antiferromagnet, uniaxial, props. near field causing sublattice reversal 9-45195
 antiferromagnetic sublattice magnetization vector, dynamical behaviour 9-47280
 antiferromagnetic sublattice magnetization vector, dynamical behaviour 9-47279
 chemical, of rocks, laboratory studies 9-24711
 curves and minor loops calc., contrib. 9-28605
 demagnetization curve of magnetically- hard material, errors in functional relationship B(H) 9-40309
 demagnetizer, for solid specimens, construction and theory 9-22344
 diorite, hornblende biotite quartz, nonreproducible self reversal 9-43501
 effective magnetic viscosity field, physical meaning 9-33875
 ferrites, directions, interpretations w.r.t. cryst. fields and bonds 9-28628
 ferrites, polycrystalline, initial microwave tensor susceptibility, statistical analysis 9-49215
 ferrites, uniform precession and subharmonic reson. existence 9-35704
 ferromagnet, conducting, negative Barkhausen jumps as consequence of eddy currents, origin 9-39767
 ferromagnet, near T_c , generalized molecular field calc. 9-35545
 ferromagnet, near T_c , generalized molecular field calc. 9-35545
 ferromagnet, uniaxial anisotropic, temp. and ext. mag. field depend., Green's functions method 9-24308
 ferromagnet with domain structure, thermo props. of transition to paramagnetic state 9-31031
 ferromagnetic bodies, susceptibility increase by superimposing alternating field 9-45132
 ferromagnetic films, residual magnetization creep in demagnetizing self-fields 9-39772
 ferromagnetic minerals, demagnetization of remanent magnetization by pressure application 9-24710
 ferromagnetic thin films, spontaneous, eff. of point defects 9-31040
 ferromagnets, polycrystalline metallic, existence, character and rate of negative Barkhausen jumps 9-37658
 films, elec. field-induced anisotropy 9-24315
 films, remagnetization, energy conversion and dynamic hysteresis loops 9-24266
 Heisenberg ferromagnet, spontaneous magnetization, upper bound 9-49196
 magnetite, remanent magnetization and coercive force, effect of annealing 9-45570
 magnetite magnetic viscosity rel. to demagnetizing field 9-38011
 magnetostrictive excitation of magnetic moments by u.s. 9-41319
 natural remanent orientation and intensity, geological shock effects 9-45569
 Ni, in weak field by twisting, Matteucci effects 9-35566
 paramagnet with negative anisotropy const., temp. correction to magnetiz. 9-31022
 permalloy, Barkhausen and ΔE effects, rel. to applied stress 9-45147
 Permalloy films, high-speed flux reversal and relax. processes, dynamic Kerr obs. 9-37661
 screw spin structure with orthorhombic anisotropy energy 9-28627
 second order phase transitions, Landau theory modified near critical point 9-31782
 spontaneous, generalized molecular field calc. 9-35545
 superconductor, type II, irreversible magnetization evanescent decay obs. of flux creep mechanisms 9-43036
 superconductors, applic. of model of transiently stabilized Nb₃Sn magnets 9-37484
 susceptibility of linear antiferromagnetic chain 9-49221
 CeMg(NO₃)₃, high-field, calibration error correct. 9-43277
 Co_{1-x}Cu_xRh₂S₄, spontaneous, for $0.4 \leq x \leq 0.7$ 9-41164
 Co hexagonal crystal with internal stresses, and magnetostriction 9-37657
 CoCr₂O₄, powder, high field susceptibility, temp. depend. 9-33473
 CsFeF₃, spontaneous, and Mossbauer studies of ⁵⁷Fe 9-45058
 Er_{1-x}Bi_xFeO₃, reorientation temp. rel. to Bi substitution compared with Y 9-32869
 EuO:Gd, spontaneous, dopant effect 9-33463
 Fe-Ge alloys, Fe-rich, mass spontaneous magnetization, 298 K 9-39768
 Fe-Ru h.c.p. alloys, ϵ -phase, Pauli-paramag. temp. depend. obs. 9-43159
 Fe-Si 3% lamination, grain-oriented, energy depend. on direction 9-24273
 Fe-Si alloys, Fe-rich, mass spontaneous magnetization, 298 K 9-39768
 Fe-Si frame single crystal, existence, character and rate of negative Barkhausen jumps 9-37658
 Fe-(0.6 wt.%)Si alloy, Barkhausen and ΔE effects, rel. to applied stress 9-45147
 Fe, in weak field by twisting, Matteucci effects 9-35566
 α -Fe₂O₃, critical fields meas. and transitions obs. 9-35531
 Fe₂S₃, magnetiz. curves under high field 9-35565
 Fe₂S₃, magnetiz. curves under high field 9-35565
 Fe₂Ga_{2-x}O₃, anisotropic 9-33476
 FeCl₃, nonlinear behaviour in perpendicular mag. field. at low temp 9-45220
 FeFe₂O₄, synthetic magnetite, chemical and thermal remanance, relative stability 9-39776
 Fe(Pt_{1-x}Pd_x)₂ ordered alloys, spontaneous magnetization depend. on composition 9-24309
 Fe-(31.4at.%)Ni alloy, hydrostatic and shock-wave compressions effects 9-43176
 Mg-Fe ferrites, spontaneous, depend. on degree of oxidation 9-28633
 Mg-Mn monocystals, change of anisotropy of mag. viscosity, -196°C to Curie point 9-45183

Magnetization process continued

- Mn_{0.6}Zn_{0.4}Fe₂O₄, sublattice, temp. depend., superexchange interactions obs., neutron diff. and Mossbauer study 9-39777
 β 1-MnZn, high-field susceptibility 9-33464
 Nb-Ti supercond. sheets as stabilizing walls for levitated rings, flux penetration obs. 9-37493
 Nb₃Sn supercond. alloy, hysteretic loss and flux-jump stability obs. 9-35364
 Ni-Fe ferrites, spontaneous, depend. on degree of oxidation 9-28633
 Ni, Barkhausen and ΔE effects, rel. to applied stress 9-45147
 Ni, reversal, domain wall configuration, Jordan type after-effect 9-31034
 Ni polycrystalline wires, Barkhausen discontinuities size distrib., sample shape depend. 9-41316
 Ni single crystal rod, reversal due to plastic deformation, room temp. 9-41315
 NiFe₂O₄ synthetic, chemical and thermal remanance, relative stability 9-39776
 β Ni(IO₃)₂ · 2H₂O, spontaneous magnetization and remanent magnetism obs. 2.2-20.5°K 9-47262
 Pd-Fe dilute alloy, ferromag., $\partial M / \partial T$ meas., temp. and mag. field depend., rel. to spin-wave exchange stiffness coeff. 9-47263
 Pd-Fe ferromag. alloys, conc. depend. of static and dynamic props. 9-45151
 Pd-(~5at.%)Ni alloy, ferromag. resonance determ. 9-24478
 PtMn alloy, spontaneous magnetization, atomic ordering effect 9-39770
 Sm_{1-x}Bi_xFeO₃, reorientation temp. rel. to Bi substitution compared with Y 9-32869
 Ti-Nb, multifilament, and Cu composites, coupling obs. 9-35369
 Ti-Nb supercond. alloy, hysteretic loss and flux-jump stability obs. 9-35364
 V₂Ga, supercond., critical fields temp. depend. obs. 9-44945
 YFe garnet, dislocation effects, direct investigation 9-47276
 YFe garnet, spontaneous, temp. dependence, 4.2-290°K 9-41328

Magnetization state

- alnico alloy, α and α' phases, saturation, temp. instability of permanent magnets 9-45149
 anhyseretic, assembly of single-domain particles 9-45135
 antiferromagnet, uniaxial, props. near field causing sublattice magnetiz. reversal 9-45195
 couplings, macroscopic theory extension and representations 9-41286
 critical phenomena, dynamical, self-consistent approach 9-33430
 cross-tie walls, creep 9-49208
 electron gas, orbital paramagnetic contrib. 9-44894
 Fe-Ni-Al-Ti alloys, remanance, effect of thermomech. treatment 9-47259
 ferrites, anisotropy and porosity from meas. in approach to saturation of hysteresis loop 9-37662
 ferrites, planar-anisotropic, magnetostatic mode meas. of 4nM_s 9-45173
 ferrites, polycryst. uniaxial, mag. stiffness obs. by torsion pendulum method 9-35570
 ferrites, pulse reversals by uniform rot. of magnetization vector 9-47269
 ferromagnet with spherical magnetic inclusions, magnetization distrib. 9-45133
 ferromagnetic, temp. depend. correction to Bloch formula rel. to anharmonic effs. in magnon system 9-31033
 ferromagnetic thin film saturation magnetism 9-49209
 films, Hoffmann's ripple theory, reinterpretation 9-49206
 films, magnetic, dynamic spread analysis using Landau-Lifshitz eqn. for distrib. systems 9-45160
 films, magnetization config. during flux reversal, Kerr magneto-optic camera meas. 9-32082
 haematite, spin axis rotation 9-45064
 Invar, absolute saturation magnetization press. coeffs. from forced magnetostriiction obs., 4.2K 9-41320
 liquid ferromagnet, isotropy considerations 9-23529
 local magnetization in s-d model 9-49182
 magnetite, gamma ray induced changes 9-37665
 of magnetite, inverse thermoremanent 9-35937
 of magnetite containing rocks, transitional thermoremanent, and rel. to low temp. treatment 9-33877
 metal, density waves and thermodynamic pot for Z- dimens. case 9-45079
 molecular field calculation, computation of magnetization of a molecular field ferromagnet, Fortran IV program 9-30013
 M.S.O. alloy shutt props., C addition effect 9-45050
 non-existence of spontaneous state in one-dimensional Ising ferromagnet. 9-24286
 oligatonic films, thickness depend. 9-45162
 permalloy single-crystal platelet, helical and other stripe structures 9-47248
 polycrystalline, anisotropy from magnetization curve 9-41312
 pyrrhotine, gamma ray induced changes 9-37665
 rare-earth niobates in strong pulsed fields 9-35592
 rock, pressure-induced variations, variations, pressure-induced, complex interpretation 9-33873
 of rocks, baked contact 9-33876
 rocks, remanent magnetization stability 9-47603
 rocks of tertiary age, secondary natural state 9-38010
 saturation and magnetic moments of nuclei 9-26634
 sedimentary rocks, post-depositioned remanent magnetization 9-38005
 semimantary rocks, natural remanent 9-35938
 spin-1/2 Heisenberg ferromagnet, low-temp. expansion 9-31026
 structure, transmission Lorentz microscopy obs., Foucault technique improvement 9-39233
 superconductor, low-volume, meas. by electronic integrator 9-39591
 Ticonal 600 alloy, saturation, from mag. props. and microstructure evolution 9-44804
 time variations meas., sensitive automatic method 9-22339
 whiskers, ferromagnetic micron-sized distrib. and free poles 9-45134
 BaFe₂O₁₉, magnetocryst. anisotropy const. determ. by magnetization curves 9-43170
 BaFe₂O₁₉, polycryst., mag. stiffness meas. 9-35571
 CO₂BaAl₂Fe₁₆O₂₇ ferroplax, magnetocryst. anisotropy const. determ. by magnetization curves 9-43170
 Co-Ni-Al-Cu-Nb-Fe alloys, saturation, temp. depend. 9-47251
 Co-Ni-Al-Cu-Ti-Fe alloys, saturation, temp. depend. 9-47251
 Co, near Curie temp. 9-24271
 Co₂Ba₂Fe₁₆O₂₇ ferroplax, magnetocryst. anisotropy const. determ. by magnetization curves 9-43170
 Co₂W, magnetocryst. anisotropy const. determ. by magnetization curves 9-43170

Magnetization state continued

- Co film, high-coercivity, recorded pattern obs. by Lorentz microscopy 9-45165
 Co film, neutron scattering studies 9-45167
 Co films, reversal, Kerr effect studies 9-33462
 Co thin films electrolytically deposited on Cu, periodic variation of susceptibility maximum 9-47257
 CoF₂ of impurity Fe²⁺ ions, Mossbauer effect meas. 9-45298
 CoSe₂S₂ and susceptibility meas. 4.2° to 300°K 9-47245
 CrBr₃, ferromagnetic, magnetization direction eff. on Fresnel diffraction patterns 9-31079
 CrBr₃ near critical temp., mag. eqn. of state 9-26649
 Cu-Ni alloys, near critical composition, distrib. in polar. clouds of giant moments 9-26624
 Cu(NO₃)₂·2.5H₂O, magnetization isotherms, 1.2° to 4.2°K 9-45218
 Dy, magnetocryst. anisotropy, spin-wave theory 9-37655
 ErFeO₃, Y and Bi substituted, effect on spin reorientation 9-45061
 Eu, sublattice behaviour, Mossbauer effect meas. of hyperfine interaction 9-45219
 Fe-(25 at.%)Al alloys, one and two-phase struct. obs., magnetiz. and magnetocrystalline anisotropy 9-26648
 Fe-Al alloy single cryst., susceptibility superimposed on saturation magnetization 9-47258
 Fe-Be alloys, and sp. ht. 9-45143
 Fe-Co-Ni alloy fine particles prep. by evaporation in inert gases 9-33459
 Fe-Co alloy fine particles prep. by evaporation in inert gases 9-33459
 Fe-Co alloys, b.c.c., saturation, rel. to quenching and composition 9-45142
 Fe-Co alloys, high-field susceptibility, 3d-band shape study 9-37406
 Fe-Ni-Al-Co-Ti alloys, remanance, effect of thermomech. treatment 9-47259
 Fe-Ni-Mn alloys, f.c.c., saturation, 77°K to Curie temp. 9-45144
 Fe-Ni alloy fine particles prep. by evaporation in inert gases 9-33459
 Fe-Ni alloys, high-field susceptibility, 3d-band shape study 9-37406
 Fe-7.4%Si single cry., high-field susceptibility 3d-band shape study 9-37406
 Fe, polycry., high-field susceptibility, 3d-band shape study 9-37406
 Fe, saturation and magnetic moments of nuclei 9-26634
 Fe₃PO₈, spin orientation obs. 9-41314
 Fe₃Ge₂-Mn₂Ge₂ solid solns., saturation, and Curie temp. 9-45065
 Fe film, high-coercivity, recorded pattern obs. by Lorentz microscopy 9-45165
 Fe film, magnetization distrib. about single mag. particle 9-43181
 Fe film, neutron scattering studies 9-45167
 Fe films, meas. as thickness increases atomic layer by layer 9-28619
 Ho, conical and spiral phases, spin-wave excitations 9-45111
 Ho, spiral phase, spin wave dispersion relation 9-45112
 Mn_{1-x}Cr_xAs, spin states between 4.2-900°K 9-47226
 MnF₂ of impurity Fe²⁺ ions, Mossbauer effect meas. 9-45298
 MnP single crystal spin structure as function of mag. field and temp. 9-47246
 Nb-Ta alloys, superconducting transition temp. and electronic sp. heat temp. depend., conc. depend. 9-28478
 Nb-Ti superconducting wire, single core and twisted multi-strand 9-26526
 Nb, superconducting energy gap anisotropy rel. to temp. depend. of Ginzburg-Landau parameters 9-28478
 Nb, superconductivity, effect of purity on curve shape 9-44943
 Nb rel. internal friction strain amplitude dependence 9-26316
 Nb wire, superconducting, curve, effect of tension 9-35532
 NdP, NdAs, NdSb, saturation magnetiz. and large anisotropy w.r.t. crystal field eff. 9-35590
 Ni-Co films, electrolytically deposited, magnetocryst. anisotropy 9-41323
 Ni-Cu alloys, near critical composition, distrib. in polar. clouds of giant moments 9-26624
 Ni-Fe film, electrodeposited, magnetization ripple wavelength meas., Lorentz microscopy 9-28624
 Ni-Fe thin films electrodeposited on scratched surfaces, uniaxial mag. anisotropy 9-28623
 Ni-Ge single crystals, remagnetization hysteresis energy losses, field depend. 9-43175
 Ni, plastic deform. and thermoremanence destruction 9-35568
 Ni, saturation and magnetic moments of nuclei 9-26634
 Ni₃Fe(Cr, Me, W) ternary alloys, saturation magnetization temp. depend., atomic ordering obs. 9-39297
 Ni₃Mn, damage rates during low temp. e irradi. 9-33205
 Ni films, electrodeposited, magnetocryst. anisotropy, lattice distortion effect 9-39774
 Ni single cry., high-field susceptibility, 3d-band shape study 9-37406
 RbMnF₃ sublattice, and critical mag. scattering of neutrons 9-45234
 Sc single cryst., susceptibility and anisotropy 9-49192
 SmCo₅, influence of absorbed H 9-45073
 SmCo₅ pressed-powder magnets, saturation, and high energy product 9-49213
 (Sr_{0.8}Ba_{0.2})₂Zn₂Fe₂O₄, hexagonal ferrites, curves rel. to critical fields 9-26657
 Tb, changes rel. to micro-eddy currents, internal friction damping 9-26319
 Tb, magnetocryst. anisotropy, spin-wave theory 9-37655
 U₃As₄ single cryst., magnetocrystalline anisotropy 9-37656
 U₃P₄ single cryst., magnetocrystalline anisotropy 9-37656
 UPa_{1.75}Sn_{0.25} powder, metamag. obs. 9-33434
 Y_{0.5}Gd_{0.5}(Al_{0.5}In_{0.5})₂Fe₁₅(In₁₂O₁₂)₂, garnet, isomagnetization lines 9-39778
 YFe garnet-Co, magnetocryst. anisotropy 9-33480
 YFe garnet, longit. magnon-phonon interaction in obliquely magnetized rods 9-35574
 YFe garnet rod, magnetoelastic wave instability threshold 9-37668
 YFeO₃ weak ferromagnet, susceptibility tensor, temp. depend. 9-43187
 YbFe garnet, canted spin config. 9-47277
 (Zr_{1-x}Ti_x)Zn₂ and Curie temp., rel. to lattice parameter 9-26650

domains

- assembly of single-domain particles anhyseretic magnetization 9-45135
 Bloch wall interaction with spherical cavity, energy 9-39762
 Bloch-walls in thin films, stray-field-free micromag. config. 9-35559
 crystalline thin foil, e microscopy, diff. contrast 9-26641
 cylindrical, flattening of Bloch wall under infl. of mag. field 9-24299
 ferrimagnet, topography rel. to susceptibility 9-31042
 ferrites, structure effect on microwave permeability in weak mag. fields 9-33472

Magnetization state continued**domains continued**

- ferromagnetic crystals, diagonal structure analysis 9-31032
 ferromagnetic film, stripe domain nucleation 9-31039
 ferromagnetic films, two-dimens. Bloch-type domain walls 9-35567
 ferromagnetic lattices, b.c.c., effect of width on thickness and energy of symmetric Bloch walls 9-24298
 ferromagnetic material, study using Kerr effect, enhancement through ZnS coating 9-35558
 ferromagnetic materials of uniaxial symmetry 9-28613
 ferromagnetic sample, domains and boundaries, visualiz. methods 9-28612
 ferromagnetic thin film, mag. spectrum and ferromag. reson. rel. to subdomain struct. 9-43180
 ferromagnetic thin films, obs. in pulse periodical fields by stroboscopic Lorentz microscopy 9-40329
 ferromagnets, alignment producing changes in Mossbauer spectral area 9-28664
 ferromagnets, uniaxial, switching threshold of applied field for magnetization reversal or domain form. 9-35557
 film, energy of combined Bloch and Neel type domain wall 9-28625
 film wall profiles, determ. using inversion procedure 9-49207
 films, thin, stray-field-free micromag. config. applic. to Bloch- and Neel-walls, stripe domains and ripple struct. 9-35559
 films, walls, 180°, 360° and multiple system, energies 9-33468
 films magnetic cylindrical electrodeposited, wall creep, and prep., characterization thermal stabilization 9-45161
 hematite, Kerr eff. photographs of domain structure on remagnetization 9-26644
 Lorentz microscopy determ. of wall thickness using small-angle scatt., 9-40327
 magnetostrictive stimulation of walls by u.s. 9-41319
 micromagnetics, solution of fundamental eqn. 9-45118
 mumetal, magnetomech. damping w.r.t. domain jumps 9-31036
 Neel-walls in thin films, stray-field-free micromag. config. 9-35559
 Permalloy films, Bloch wall motion excited by fast-rising hard-axis pulses 9-45168
 Permalloy wires, nucleation and wall propagation, influence of structure and composition 9-35561
 rare earth of thoferrites, wall mobility by direct stroboscopic obs. of moving walls 9-45233
 ripple struct. in thin films, stray-field-free micromag. config. 9-35559
 in rock grains, thermal fluctuations of magnetic moments 9-33874
 spherical cavity interaction with Bloch wall, energy 9-39762
 spike-like, shape theory 9-41307
 stripe, in thin films, stray-field-free micromag. config. 9-35559
 structure props., theory 9-41309
 Ticonal X, magnetic correlation in magnetized and demagnetized state 9-49203
 wall energy density meas. method for thin films 9-43168
 wall thickness by small angle electron scatt. in Lorentz microscopy 9-40327
 wall-inclusion interaction, theories and examples 9-26642
 wall-pinning model of hysteresis 9-45048
¹⁰⁹Ag single crystal, due to de Haas-van Alphen effect, pulsed n.m.r. studies of 9-45393
 Co, remanent honeycomb structure, width depend. on crystal thickness 9-24300
 Co, remanent structures effect of crystal thickness; rectangular-prism-shaped single cryst. 9-24301
 Co, thickness-depend. of domain width, critical thickness 9-39763
 Co films, wall width meas. by Lorentz microscopy 9-45166
 CrBr₃, Lorentz microscopy obs. at low temps. 9-26651
 CrI₃, Lorentz microscopy obs. at low temps. 9-26651
 EuS thick films, at low temp., size and orientation by Lorentz microscopy 9-41880
 Fe-Ni alloys, domain wall distribution rel. to coherent boundaries of twin crystal 9-37651
 Fe(3.25 wt.%)Si, thickness-depend. of domain width, critical thickness 9-39763
 Fe(3 wt.%)Si, X-ray topographic obs., diff. contrast on walls 9-26643
 Fe-Si, ferromag. domain walls, image contrast, origin, X-ray topography obs. 9-28614
 Fe-Si, wall width meas. in thin sections by electron interference method 9-41310
 Fe-Si, walls visibility on X-ray diff. topographs and comparison with BaTiO₃ ferroelec. walls 9-39682
 Fe(3 wt.%) Si alloy, domain shape, comparison between calc. and obs. 9-41307
 Fe-Si single cryst., lattice distortion and X-ray topographic contrast due to 90° domain wall 9-33460
 Fe-3.7 wt.% Si 9-45157
 Fe(3 wt.%)Si transformer sheet, 180° wall motion, freq. depend. and wall bowing 9-39764
 Fe, Bloch wall and stripe domain struct. obs., e microscopy 9-26641
 Fe, magnetomech. damping w.r.t. domain jumps 9-31036
 Fe, wall width meas. in thin sections by electron interference method 9-41310
 Fe boundary movements, stress-induced damping of assoc. mech. vibrations, 78° to 300°K 9-45157
 Fe platelets, charged 90° Bloch walls obs. 9-43169
 GdFe garnet, circular, density and size 9-47271
 GdFe garnet, interaction with atomic scale imperfections, optical obs. 9-45179
 Li_{0.5}Fe_{0.5}(Gr_{0.5})_{0.5}O₄ ferrite with Fe²⁺ in tetrahedral and Gr³⁺ in octahedral domains, exchange integrals 9-45181
 Ni(19 wt.%)Fe films, energy of combined Bloch and Neel type domain wall 9-28625
 Ni-Fe tapes, Kerr magneto-optic studies of surface patterns 9-26653
 Ni, domain wall configuration during magnetization reversal, Jordan type after-effect 9-31034
 Ni, magnetomech. damping w.r.t. domain jumps 9-31036
 Ni single cryst., mag. aftereffect due to displacement of dislocations inside walls, dissolved O atoms effect 9-39766
 Ni single crystals, structure temp. depend. determ. by magneto optical Kerr technique 9-41317
 Ni. boundary movements, stress-induced damping of assoc. mech. vibrations 78° to 300°K 9-45157
 RbFeF₃, ferromagnet, wall interaction with dislocations direct obs. 9-45126

Magnetization state continued
domains continued

- Steel, Si, grain-oriented, static and 60 Hz structures, effect of longit. tensile stress 9-45122
 TmFeO₃, structure and wall energy temp. dependence 9-47275
 YFe garnet with Tb admixture, meas. of domain wall mobility 9-41327

Magneto-optical effects

see also *Optical constants; Zeeman effect*

- binary alloys, ferromagnetic interband transitions investigation, low temp. 9-41136
 capacitor discharge circuit for 100ns shutter 9-29500
 Co, ferromagnetic, interband transitions investigation, low temp. 9-41136
 Cotton-Mouton effect, r.t., graphic representation in Gaussian case rel. to Lorentzian case 9-47872
 Cotton-Mouton effect through absorpt. band 9-39100
 Cotton-Mouton resonance, for Lorentzian absorpt., graphic representation 9-43922
 cubic crystals, linear mag. birefringence 9-45185
 electron gas, dielectric permittivity tensor determ. 9-41786
 EPR meas. of ion relaxation, method 9-40299
 Faraday, use in meas. mag. field of plasma 9-38998
 Faraday, use in visualiz. of domains and boundaries of ferromag. sample 9-28612
 Faraday effect, meas. in visible and u.v. by automatic spectropolarimeter 9-48118
 Faraday rot. materials, e.m. propag. obs. 9-45262
 Faraday rot. spectroscopy, contour distortion rel. to non-monochromaticity 9-34228
 Faraday rotation, a.c., phase and amplitude rel. to spin-lattice relaxation time 9-49228
 Faraday rotation in high magnetic fields using high speed integrators 9-31080
 Faraday rotation meas. for band parameters 9-37395
 Faraday rotator, low mag. field, using glass rectangular parallelepiped 9-25345
 Fe, ferromagnetic, interband transitions investigation, low temp. 9-41136
 ferric oxide epds., ferrimagnetic single crystal, u.v. complex polar-Kerr effect 9-45275
 ferrimagnet, origin and magnitude 9-24366
 ferro- and antiferromagnets, quadratic Cotton-Mouton effect 9-49245
 ferromagnetic domain study using Kerr effect, enhancement through ZnS coating 9-35558
 Galactic mag. field fluctuations, from pulsar signals dispersion and Faraday rotation 9-49531
 haematite, Kerr eff. for magnetic props. 9-26644
 hologram, thermomagnetic writing and reconstruction on EuO film 9-48060
 inert gases, Verdet coeff. meas. 9-23399
 ionosphere, Faraday rotation in radiowave propag. 9-49483
 Jupiter, decametric radio bursts, orientation of polarization ellipse, Faraday effect obs. 9-43624
 Kerr, for thin film magnetic properties 9-33510
 Kerr, use in visualiz. of domains and boundaries of ferromag. sample 9-28612
 Kerr camera, nanosecond, for thin film magnetization config. on flux reversal 9-32082
 laser beam deflection by mag. field 9-29435
 magnetoplumbite, ferrimagnetic single crystal, u.v. complex polar-Kerr effect 9-45275
 memory systems, magnetic film, photon- and electron-beam-accessed, rel. to shot noise reduction 9-43843
 neodymium ethylsulphate, transient mag. behaviour, Faraday effect study 9-33491
 noble metals, magnetoref. meas., optical dielec. function change 9-49246
 permalloy film, dynamic Kerr obs. of high speed flux reversal and relax. processes 9-45169
 Permalloy films, dynamic Kerr obs. of high-speed flux reversal and relax. processes 9-37661
 in planar lossless mat., contrib. of propag. impedance and polarization perturbations 9-25369
 plasma, θ -pinch, Faraday rotation meas. 9-38995
 rare earth iron garnets, exchange resonance and Faraday effect 9-45278
 rare earth iron garnets, linear mag. birefringence 9-45185
 rare earth iron garnets, pure and Ga-doped, ferrimagnetic single crystal, u.v. complex polar-Kerr effect 9-45275
 recording 9-45271
 review of results 9-31078
 semiconductor, extrinsic, theory 9-43061
 semiconductors, splitting of interband oscillations of absorption coeff. 9-33509
 spinel ferrites, ferrimagnetic single crystal, u.v. complex polar-Kerr effect 9-45275
 steel, Si grain oriented, Kerr effect obs. of domain structures, effect of longit. tensile stress. 9-45122
 systems with plane symmetry, particle optics 9-45920
 tertiary alcohols, specific rotation and mag. rotary dispersion 9-48697
 Ag, magnetoref. meas., optical dielec. function change 9-49246
 antiferromagnet, origin and magnitude 9-24366
 As, i.r. magnetoreflexion data for trigonal face rel. to band parameters 9-47320
 Au, magnetoref. meas., optical dielec. function change 9-49246
 Ba₂Zn₂Fe₁₂O₂₂ hexagonal ferrite, Faraday rotation and absorpt., 300°K, 1 to 8 μ 9-45277
 BaFe₁₂O₁₉ hexagonal ferrite, Faraday rotation and absorpt., 300°K, 1 to 8 μ 9-45277
 Bi-Sb alloys, magnetoreflexion obs. of band struct. 9-41162
 Bi, Kerr polar effect, resonance obs. 9-47321
 CO:P film magnetic temperature-sensitive for memory store 9-45164
 CaF₂:Dy²⁺ crystals, magneto-optical rotation in f-d-transitions 9-49247
 CaF₂:Eu²⁺ spin-lattice relaxation rel. to phase and amplitude of Faraday rotation 9-49228
 CaWO₄:Nd³⁺, Faraday effect obs. of ¹I_{9/2}-²P_{1/2} transition, assignments of ground-state sub-levels 9-39805
 Co films, Kerr effect studies rel. to magnetization reversal process 9-33462
 CrBr₃, Faraday effect meas. of mag. props. near critical point 9-45139
 CrO₂ single crystal, and magnetic props. 9-45141
 Cu, magnetoref. meas., optical dielec. function change 9-49246
 CuCl, transverse magneto ref. in near u.v. 9-35622

Magneto-optical effects continued

- DyAl garnet, antiferromag., absorpt. spectrum, mag. interaction interpret. and Monte Carlo calc. 9-24408
 DyAl garnet, Faraday effect, Verdet const. freq. depend., obs. 9-28657
 Er ferrite garnets, Faraday effect, mag. field effect 9-49216
 ErAl garnet, Faraday effect, Verdet const. freq. depend., obs. 9-28657
 EuCl₃ aq. soln., Cotton-Mouton effect through absorpt. band 9-39100
 EuO:R³⁺ film, (R=rare earth oxide), Faraday and Kerr rotations 9-47266
 EuO, Faraday rotation, mag. birefringence and i.r. transmission 9-45273
 EuO, magnetic birefringence, infrared transmission and Faraday rotations 9-24365
 Fe-Ni thin films, Faraday effect field depend., perpendicular anisotropy obs. 9-47322
 Fe(3 wt.%)Si transformer sheet, longit. Kerr effect obs. of domain wall motion freq. depend. and wall bowing 9-39764
 Fe, transverse Kerr, and optical props., 0.35 to 1.0 μ 9-45274
 FeRh, and magnetic props. 9-45141
 Gd₂(SO₄)₃.8H₂O, Faraday eff. in e.p.r. 9-28746
 GdFe₃, transverse Kerr, and optical props., 0.35 to 1.0 μ 9-45274
 GdFe garnet, Faraday rot. 9-43214
 GdFe garnet, Faraday rotation at 1.15 μ , 100° to 450°K 9-49218
 GdFe garnet film, recording 9-45271
 n-Ge:Sb, microwave Faraday rot. 9-41355
 Ge, interband Faraday rot. 9-33511
 Ge, magneto-electro-reflectance in crossed and parallel-field config. 9-39806
 Ge, oscillatory Voigt effect 9-45276
 Ge magnetoabsorpt. oscillation spectra 9-30823
 Ge magnetopiezotransmission obs. of effective masses 9-44982
 Ge review of results 9-31078
 Hg-CdTe alloy system, i.r. cyclotron reson. and band struct. obs. 9-39807
 HgTe, interband transitions, low temp. reflection and electroreflection study 9-47344
 Ho ferrite garnets, Faraday effect, mag. field effect 9-49216
 InSb, optical mixing, third order, mag. field dependence 9-26689
 IrCl₆²⁻, mag. circular dichroism in cryst. (CH₃NH₃).SnCl₆ 9-41353
 KBr-KI mixed crystals, Faraday rotation in high mag. fields 9-26706
 KBr, Faraday rotation in high magnetic fields using high speed integrators 9-31080
 KBr, Faraday rotation of U₂ centres 9-33512
 KCl-KBr mixed crystals, Faraday rotation in high mag. fields 9-26706
 KCl, Faraday rotation in high magnetic field using high speed integrators 9-31080
 KCl, Faraday rotation of U₂ centres 9-33512
 KI, Faraday rotation of U₂ centres 9-33512
 Li_{0.5}Fe_{2.5}O₄ spinel ferrite, Faraday rotation and absorpt., 300°K, 1 to 8 μ 9-45277
 MgFe₂O₄ spinel ferrite, Faraday rotation and absorpt., 300°K, 1 to 8 μ 9-45277
 MgO, F band, paramagnetic Faraday-rotation pattern, 1.8°K 9-35116
 MgO, n-irrad., Faraday rotation obs. of R-like centre 9-26295
 MgO, n-irrad., Faraday rotation obs. of R-like centre 9-28306
 NO, mag. rot. spectrum of $\Lambda^2\Sigma^+ \rightarrow {}^2\Pi$ transition 9-44337
 Ni-Fe tapes, Kerr eff. studies of surface domain patterns 9-26653
 Ni, ferromagnetic, interband transitions investigations, low temp. 9-41136
 Ni films, properties in visible and near infrared regions 9-39808
 Ni single crystals domain structure temp. depend. by Kerr technique 9-41317
 Ni thin films, Faraday effect field depend., perpendicular anisotropy obs. 9-47322
 NiFe₂O₄ spinel ferrite, Faraday rotation and absorpt., 300°K, 1 to 8 μ 9-45277
 Pb-SnTe alloy system, i.r. cyclotron reson. and band struct. obs. 9-39807
 Pb_{1-x}Sn_xTe, emission in mag. fields, band struct. obs. 9-41406
 RbFeF₃, origin and magnitudes of Faraday and Cotton-Mouton effects 9-24366
 RbNi(CoF₃, Faraday rotation and mag. circular dichroism 9-33513
 RbNiF₃, origin and magnitudes of Faraday and Cotton-Mouton effects 9-24366
 Si oriented doped single cry., microwave Faraday rot. at room temp., Verdet const. 9-24367
 TbFe₂O₁₂ garnets, Faraday effect, anisotropy in i.r. region 9-31081
 Tb ferrite garnets, Faraday effect, mag. field effect 9-49216
 TbAl garnet, Faraday effect, Verdet const. freq. depend., obs. 9-28657
 TbFe garnet, Faraday rot. 9-43214
 YFe garnet: Si, i.r. sensitive ferrimag., relax. and mag. anneal of anisotropy 9-45191
 YFe garnet, Faraday rot. 9-43214
 YFe garnet, modulation applic. 9-36335
 Yb orthoferrite possessing Faraday rot., e.m. propag. obs. 9-45262
 Yfe barnet, Faraday rotation at 1.15 μ , 100° to 450°K 9-49218
 Zn_{1-x}Mn_xS crystals, 0.004< x <0.4, photo-induced mag. susceptibility changes, 77° to 400°K 9-45279

Magnetoacoustic effects

- conducting porous medium, refl. of waves on free boundary 9-42961
 conductors, thin, in mag. field, electron scatt. obs. 9-24029
 deformation-potential theory of attenuation 9-46995
 elastic solids, i.f., stiffness and attenuation, mag. field depend. 9-35283
 ferromagnets, combination scattering of sound 9-48961
 geometrical optics of acoustic waves in mag. media 9-27227
 magnetostrictors, high power, sound output and efficiency, nonlinear design technique 9-29281
 metal, oscillations and tilt effect, electron relax. time determ. 9-47072
 periodic wave in hot plasma, instability 9-30275
 plasma, turbulent magnetosonic wave attenuation 9-48553
 semimetal, oscillations and tilt effect, electron relax. time determ. 9-47072
 As, giant quantum oscillations in attenuation, spin splitting obs. 9-35335
 Bi, acoustomagnetoec. effect meas. rel. to electron-hole recombination temp. dependence, 2-50°K 9-35306
 Bi, anisotropy of giant quantum oscill. in magnetoacoustic attenuation 9-37345
 Bi, Fermi surface study, singularities 9-39564
 Bi, oscillations and tilt effect, electron relax. time determ. 9-47072
 Ca-Bi-v-ferrite, decrement of increasing mag.-acoustic oscillations 9-37346
 EuO, near mag. phase transition, vel. change with const. attenuation 9-24030

Magnetoacoustic effects continued

- InSb, longit. absorpt., Landau levels effects 9-26420
 n- and p- PbTe, attenuation of quantum oscillations for Fermi surface shape and Landau level splitting rel. to carrier conc. 9-28506
 RbMnF₃, antiferromagnetic, frequency- dependent v.s. absorption 9-46993

Magnetocaloric effects *see* **Magnetothermal effects****Magnetocrystalline anisotropy** *see* **Magnetic properties of substances; Magnetization state****Magnetoelastic effects** *see* **Magnetochemical effects; Magnetoelastic waves****Magnetoelastic waves**

- antiferromagnet, oscillations in mag. fields close to critical value 9-45196
 in crystal, induced by interac. of lattice vibrations with spin waves 9-28599
 delay time analysis by field pulsing spin and elastic contributions 9-49180
 ferromagnet, interaction rel. to phonon-two-magnon processes, phonon energy spectrum 9-46967
 hematite single cryst., magnetoelastic interaction obs. 9-31049
 magneto-thermo-elastic plane waves, phase velocity and energy loss 9-25084
 parametric excitation by parallel pumping 9-37640
 phonon pumping of nuclear magnon pairs, with acoustic waves 9-33481
 phonons parametric excitation in mag. materials 9-37308
 p-Ge, light holes effect on galvanomagnetic effects 9-44980
 YFe, partially magnetized bar, generation and propagation 9-33479
 YFe garnet, pulse prod. by Schlomann method and sequences 9-43178
 YFe garnet films, epitaxial, on YAl garnet and GdGa garnet, contrib. to microwave phonon generation 9-44816
 YFe garnet rod, axially magnetized, instability threshold 9-45190
 YFe garnet rod, axially magnetized, magnetoelastic mode instabilities 9-45189
 YFe garnet rods, $\langle 110 \rangle$ oriented, propag. 9-45187
 YFe garnet rods containing turning point, magnetoelastic mode excitation 9-45188
 9-44716

Magnetolectric effects

see also **Hall effect; Magnetoresistance**

- antiferromagnet, ferroelectric, spontaneous polarization depend. on sublattice magnetization 9-30971
 crystal, rel. to light propag. 9-43218
 in crystal optics 9-24350
 electron-impurity system, dynamic magnetoconductivity for strong coupling case 9-30813
 existence and occurrence in materials 9-47221
 Fermi ellipsoid with anisotropic relax. time, magnetoconductivity 9-44903
 ferromagnet, transport theory 9-47255
 galvanomagnetic effects in high elec. fields, theory 9-30829
 galvanomagnetic tensor, approximate expression 9-37433
 linear spin chain, spontaneous polarization, and two-magnon absorpt. 9-39760
 metals, galvanomagnetic phenomena in quantum limit 9-30837
 metals, meas. rel. to anisotropic mean free path 9-37386
 metals with mag. breakdown, magnetoconductivity, quantum mech. calc. 9-35333
 naphthalene, magnetoelctret state 9-30979
 piezoelectrics, mag. ordered, induced ferroelec. mag. obs. 9-39748
 semiconductor, galvanomagnetic effects in strong elec. fields 9-47098
 semiconductor, galvanomagnetic phenomena in crossed elec. and mag. fields 9-37511
 semiconductor thin films, thermogalvanomagnetic effect, influence of inelastic carrier scatt. 9-35494
 semiconductors, in strong elec. fields, theory 9-28486
 susceptibility, upper bounds 9-35529
 thermogalvanomagnetic coeffs. rel. to space-time symmetry restrictions 9-47192
 waxes, magnetoelctret state 9-30979
 Al-(68.9 at.%)Fe alloy, longitudinal galvanomag. eff. 9-24278
 Al, Hall coeff. and magnetoresistance, l.f. helicon resonance obs. 9-30839
 AuSb₃, low-field galvanomag. coeffs. 9-41159
 Bi, low-field galvanomag. coeffs. temp. depend. 9-49019
 CdS, magnetomicrowave effects at 38 GHz, charge carrier density control by photogeneration 9-30922
 Cu, open-orbit induced torque obs. 9-49024
 Fe, single crystals, whiskers and alloy wires, Mattencci effect 9-33454
 GdAlO₃, meas. and symmetry considerations for antiferromagnetic ordering 9-31050
 n-Ge:Sb, Nernst-Ettingshausen and Righi-Leduc effects, distorted Hall effect 9-37537
 Ge, magnetoconcentration effect due to carriers redistrib. at impurity centres, Hall const. temp. depend. obs. 9-39645
 Ge, magnetomicrowave effects at 38 GHz, charge carrier density control by photogeneration 9-30922
 In, longitudinal thermal magnetomorph effect 9-37430
 LiMnPO₄, interpretation 9-24331
 Mn-(78.5 at.%)Ni alloy, longitudinal galvanomag. eff. 9-24278
 PbFe_{0.5}Nb_{0.5}O₃, spontaneous 9-28596
 PbMn_{0.5}Nb_{0.5}O₃, spontaneous 9-28596
 p-Si, galvanomag. anisotropy and energy-depend. warping of valence bands 9-43075
 p-Si inversion layer, obs. 9-37542
 Sn, galvanomag. anisotropy rel. to texture investigations 9-32929
 Sn, magnetoconductivity of 2-dimens, coherent network of coupled orbits, oscillations obs. 9-44919
 TiCl₃, photoconductive, band struct. and polaron transport props. from magnetoconductive effect obs. 9-41272
 Zn_{0.5}Hg_{0.5}Te solid solutions, 'heavy carrier' eff., 77°-400°K, 250-10000 Gs 9-30913
 Zn whiskers, props., size effects 9-30853
- Magnetogasdynamics** *see* **Magnetohydrodynamics**
- Magnetohydrodynamic generators** *see* **Electricity, direct conversion/magnetohydrodynamic**
- Magnetohydrodynamic waves** *see* **Magnetohydrodynamics; Plasma/magnetohydrodynamics; Plasma/oscillations**
- Magnetohydrodynamics**
see also **Plasma/magnetohydrodynamics**
 atmosphere, upper, wave excitation by finite source 9-49470
 axially symmetric flow past fixed bodies, numerical approach 9-34746
 boundary layer theory, similarity transformations applic. 9-25838

Magnetohydrodynamics continued

- boundary layers with pressure gradient and heat transfer, numerical results 9-32583
 channel flow, heat transfer in thermal entrance regions 9-25831
 channel flows, acceleration regions rel. to efficiency and limiting circles 9-25164
 coaxial Hall accelerator, analysis 9-22684
 compressible fluid, group analysis of system of eqns. and invariant solns. 9-40646
 conducting gas in strong nonstationary e.m. field, acceleration 9-42479
 conducting liquid flow near nonconducting sphere, crossed electric and magnetic fields 9-23254
 conducting liquid under actions of rotating magnetic field in infinitely long cylinder 9-30190
 convection, free, from horizontal plate 9-25837
 convective channel flow, effect of wall conductances 9-30197
 Couette flow in slip-flow regime 9-38949
 dielectric cylinder in stream of incompressible conducting liquid, non-viscous magnetic boundary layer 9-30189
 dissociated real gas in thermal equilb., channel flow in m.h.d. generator 9-25165
 duct, various states of operation 9-30193
 duct flow, sub-Alfvenic with nonuniform mag. field 9-25832
 earth's core, mag. waves rel. to secular geomag. field vars. 9-26956
 earth's radiation belt proton dynamics 9-31380
 earth's radiation belt protons, interactions with hydromag. waves 9-31379
 effect on hydrodynamic turbulence and motion of particle suspensions in viscous fluids, singular-perturbation methods 9-27986
 Ekman boundary layer, axial magnetic field effect 9-30194
 electric field in rectangular channel with semi-infinite electrodes 9-25825
 electroconducting fluid in vertical pipe, stationary thermal convection rel. to mag. field prod. by current 9-27964
 e.m. flowmeters, for viscous fluid, optimum size of mag. pole pieces 9-26057
 entrance flow in plane channel, with cross flow, ion slip, Hall currents and wall injection 9-46454
 equations evolution: Hall effect 9-38950
 flat plate at zero incidence 9-23252
 flow, free surface study 9-46452
 flow, linearized in plane, integral rep., convex bodies 9-30200
 flow, steady compressive, structure of waves and wakes rel. to dissipative effects 9-25836
 flow in container, effect of rotational mag. force 9-25833
 flow in magnetohydraulic duct, electrically conducting liquid with free surface 9-30187
 flow in linear rectangular channels, effect of blow-in through porous walls 9-27963
 flow near accelerated plate in presence of mag. field 9-34744
 flow of conducting gas, quasi-one dimensional, longitudinal short wave osills. stability 9-40650
 flow of electrically conducting incompressible fluid between wavy walls 9-27966
 flow of Hg current in ducts with sudden widening 9-30201
 flow of two conducting incompressible immiscible fluids between conducting plates under closed cct. conditions 9-27967
 flow over sphere with cylindrical afterbody, press. distrib. over front hemisphere 9-34743
 flow theory in hypersonic approx., general solns. 9-23247
 flows, two-dimensional aligned-field 9-23257
 flows, variational principle for stationary equilibria 9-32584
 fluid, weakly conducting, flow in rotating straight pipe 9-23251
 fluid flow between rotating cylinders, oscillatory critical modes and instability onset 9-38953
 fluid motion and disturbances due to sudden introduction of oscillating dipole 9-34747
 fluid stream, highly conducting, coupled via parallel mag. field to elastic medium 9-25829
 generator optimisation, restriction of angle of mouth of duct. 9-30192
 gravitating fluid, ideal, relativistic, system of hydrodynamical eqns. governing behaviour 9-45589
 gravity wave propagation across decreasing mag. field in conducting fluid 9-24691
 gravity-coupled waves in solar atmosphere 9-27107
 Hall effect in fluid flow in presence of thin profiles 9-27960
 Hartmann-Poiseuille flows, asymptotic approach 9-34745
 heat transfer by laminar flow in radial mag. field between coaxial cylinders 9-32585
 hydromagnet theory 9-40645
 hydromagnetic emissions associated with storm sudden commencements 9-35912
 hydromagnetic forced flow of viscous incompressible and elec. cond. fluid against porous rot. dish 9-23255
 hydromagnetic model of sunspot cycle 9-38114
 hydromagnetic propagation in ionospheric waveguide, theory 9-28940
 hydromagnetic spiral flows, stability 9-40648
 hydromagnetic waves, resonant interaction with charged particles 9-41619
 hydromagnetic waves, resonant interaction with charged particles 9-45587
 infinite cylinder, hydromagnetic pulsations 9-48540
 insulating cylinder in cond. fluid, with transverse mag. field, steady longit. motion 9-23249
 insulator with same mag. permeability as medium 9-23252
 interplanetary Alfven waves in the interplanetary inference from Mariner 5 obs. 9-45676
 interplanetary mag. field fluctuations, IMP 2 obs. 9-29078
 ionosphere, waveguide propag. 9-28950
 irreversible processes, variational description 9-30185
 jet, perfectly conducting, stability in mag. field 9-30195
 laminar boundary layer, axially symmetric stream with clamp 9-30191
 liquid, inviscid, steady flow past symmetric airfoil with stream-parallel mag. field 9-40649
 liquid metal cylinder, radial oscs. induced by const. and alternating mag. fields 9-25828
 magnetic boundary layer, non-viscous, in flow round dielectric body 9-25826
 magnetic field generation in infinitely cond., turbulent fluid 9-43515
 magnetic line, curvature behind pseudo-stationary shock 9-25834
 magnetopolitropes, gaseous, equilb. and stability 9-47635

Magnetohydrodynamics continued

- magnetospheric proton heating, stochastic, by fast hydromag.-wave 9-43412
 mean velocity between parallel plates, in transverse field, turbulence effects 9-27969
 metal, liquid, flow in circular pipe, velocity profile, compared with data with no field 9-25827
 metals, liquid, channel flow, resistance rel. to laminar/turbulent transition 9-27962
 in microscale 9-23248
 modes in coaxial channel with helical field, degeneration and stability 9-32581
 non-equilibrium gas, steady flow past sharp cornered wall 9-40647
 nonequilibrium, theory of thin airfoils, aligned magnetic field 9-27965
 oscillatory flow along plane porous wall with variable suction 9-30202
 plane one-dimensional flow, effect of own mag. field on channel 9-27983
 plasma current between conducting deflectors in magnetic field, longitudinal stability 9-30282
 Poiseuille flow with finite conductivity in aligned mag. field, stability 9-23253
 powdery fuel for generators, work function of two contacting spherical particles 9-39019
 quasilinear flow calc. for determining optimum conditions of power generation 9-38954
 radial-vortex motion of anisotropic incompressible conducting fluid 9-38952
 Rayleigh-Taylor's instability, eff. of mag. field and Coriolis forces 9-46434
 rectangular pipes in transverse fields, velocity distrib. 9-27961
 relativistic, Alfvén shock waves, discontinuities of velocity four-vector col-linear with those of mag. field 9-30184
 relativistic, circulation and related topics 9-30196
 relativistic, shock waves, existence and uniqueness theorems 9-46453
 rotating fluid, weakly conducting, plane turbulent motion, asymptotic analysis 9-44401
 rough body in flow 9-23252
 shock wave decay 9-23258
 shock wave oblique propag in the solar corona 9-32723
 shock waves, existence and uniqueness theorems in relativistic case 9-46453
 simple wave in conductive medium in stationary gravitational field 9-36749
 solar activity, corpuscular radiations, electrotechnical problems 9-31658
 solar activity mechanism 9-49592
 solutions of eqns., exact 9-23256
 stagnation flow against rotating magnetized disc 9-42482
 star toroidal oscillations, decay time 9-31524
 steady rotation of sphere, non-conducting, in current-carrying fluid 9-42481
 steady rotation of sphere in viscous conducting fluid 9-42480
 stress tensor has non-dissipative components 9-25830
 sub-Alfvén eqns., instability and rel. to geomag. secular vats. 9-43482
 systems of equations and boundary conditions 9-30186
 thermodynamic props. of combustion products of methane and oil with ionizing K seeds 9-36748
 track behind circular cylinder, effect of transverse magnetic field 9-30188
 transverse perturbation velocities in rectangular duct, two-dimensional flow of compressible fluid 9-30204
 turbulence, effect on Lorentz field strength and Hall coeff. 9-23260
 turbulent flooding of stream of electrically conducting liquid in longitudinal magnetic field 9-30205
 turbulent track, friction and heat exchange transverse magnetic field 9-30203
 unstable motion of electrically conducting liquid, slow rotating disc, presence of strong axial magnetic field 9-30207
 unstable motion of electrically conducting liquid slow rotating disc, presence of strong axial magnetic field 9-30206
 validity for magnetosphere 9-35839
 viscous incompressible flow over oscillating conducting plate 9-25835
 viscous liquid flow past body with mag. field in dirn of flow, boundary layer eqns. 9-28082
 wave, large amplitude intermediate, behaviour in presence of reflected particles 9-23259
 waves in a finitely conducting fluid-mass immersed in a nonuniform magnetic field 9-38951
 waves in magnetosphere, amplification 9-47558
 waves produced by uniform magnetic field plus field of volume current unidirectional with field 9-32582
 weak magnetic fields amplifications in turbulent flow, calc. 9-48541
 BaO-Ar suspensions as closed-cycle working fluids, coagulation 9-30436
 Ga, liquid, laminar flow through diffusion in crossed fields, resistance coeffs. 9-27968
 Hg, velocity distrib. in rectangular pipes, effect of transverse field 9-27961
 Hg annular cylinder, current carrying, stability rel. elec. conduct. and viscosity 9-23250

Magnetomechanical effects

- see also Gyromagnetic effect; Magnetoelastic waves; Magnetostriction*
 cylinder, viscoelastic, magnetoelastic torsional vibration 9-29235
 disturbances in Maxwell viscoelastic solid 9-29236
 ferrites, macroscopic coeff., connection with spin-phonon Hamiltonian Microscopic coeffs. 9-26656
 metallic foil, e.m. compression for transient MOe mag. field prod. 9-47894
 mumetal, damping behaviour, temp. effect 9-31036
 $\text{Ca}_{2-x}\text{Bi}_{1-x}\text{Fe}_{1-x}\text{O}_{12}$, garnet, magneto-elastic coupling coeff. from ferro-mag. reson. method 9-37664
 Cu-Ni alloy, compress rel. to para-ferromag. transition ordering, obs. 9-35167
 Fe-(3.7 wt.%)Si alloy, damping, 78° to 300° 9-45157
 Fe, damping, 78° to 300°K 9-45157
 Fe, damping behaviour, temp. effect 9-31036
 Fe, single crystals, whiskers and alloy wires, Mattencci effect 9-33454
 Fe magnetization by twisting in weak field, Matteucci effects 9-35566
 Ni, damping behaviour, temp. effect 9-31036
 Li ferrite, macroscopic coeff., connection with spin-phonon Hamiltonian microscopic coeffs. 9-26656
 Ni, electrolytic, H influence on damping 9-39401
 Ni, magneto-elastic hysteresis and internal friction 9-23863
 Ni magnetization by twisting in weak field, Matteucci effects 9-35566

Magnetomechanical effects continued

- Ni, damping, 78° to 300°K 9-45157
 Tb single crystal magnetoelastic effects ferromag. reson. at 25-3mm, 20° to 240°K 9-45158
 YFe garnet, axially magnetized rod, instability threshold 9-37668
 YFe garnet, elastic anisotropy, investigation by magnetoelastic interac. 9-37221
Magnetometers *see Magnetic field measurement*
Magnetoreflexion *see Magneto-optical effects*
Magnetoresistance
see also Magnetolectric effects
 conducting solid, microwave meas. 9-35332
 g factor, quasiparticle, for spin splittings in magnetoconductivity oscils. 9-24103
 graphite:B, neutron irradi., function of B conc., rel. to defect clustering 9-30597
 graphite, and Hall coeff., 1.5° to 300°K 9-41153
 graphite, pyrolytic, negative magnetoresistance 9-41163
 metals, antiferromag. in mag. field, temp. and field depend. 9-26659
 model, effect of small-angle scattering 9-37425
 negative longit., behaviour due to scattering on ionized impurity centres 9-28457
 semiconductor, Sondheimer oscillations of tensor components, transverse elec. field effect 9-39617
 semiconductors, contribution of screened ionized impurities 9-30919
 Ag, 4.2°K single cryst. 9-44912
 Al, neutron-irradi., Kohler rule validity at 4.2K 9-44906
 Al, transverse, i.f. helicon resonance obs. 9-30839
 As, de Haas-Shubnikov oscillations, Fermi surface obs. 9-43024
 As, low field tensor, Fermi surface carrier density and mobility determ., 77-305°K 9-35311
 AuAl₃, high-field meas. rel. to nearly-free-electron model of Fermi surface 9-47073
 AuGa₂, high-field meas. rel. to nearly-free-electron model of Fermi surface 9-47073
 AuIn₃, high-field meas. rel. to nearly-free-electron model of Fermi surface 9-47073
 Bi:Pb, band structure determ. 9-30843
 Bi-Sb semiconducting alloys, anomalies in strong mag. fields, 4.2° to 10°K 9-30890
 Bi-Sn alloys, anisotropy, carrier influence 9-41161
 Bi, anisotropy, carrier influence 9-41161
 Bi, surface effect 9-30844
 Bi_{1-x}Sb_x, rel. to energy gap and Fermi level position 9-30842
 Bi films, size-quantized, meas. rel. to non-extremal sections of Fermi surface 9-49021
 Bi resistance ratio in earth's mag. field, rel. to purity 9-33250
 C, and Hall coeff., 1.5° to 300°K 9-41153
 C, negative magnetoresistance, due to diffuse scatt. at crystallite boundaries 9-24277
 C, soft, doped with acceptors, and Hall coeff., 2° to 300°K 9-41154
 Cd:Zn, and Hall resistivity meas. 9-41165
 Cd:Zn, rel. to small-angle intersheet scatt. 9-26515
 Cd, and Hall resistivity meas. 9-41165
 Cd, rel. to small-angle intersheet scatt. 9-26515
 Cd₃As₂-NiAs eutectic 9-41196
 Cd₃As₂, Shubnikov-de Haas effect, Fermi surface form and non-parabolic model of conduction band obs. 9-41151
 Cd₃Hg_{1-x}Te, Shubnikov-de Haas effect 9-47061
 n-CdCr₂S₄, near Curie temp., effects of exchange interaction between carriers and mag. moments 9-44956
 CdS, coeff., elec. and mag. field depend. 9-33297
 p-CdSb, eff. of field strength 9-24174
 Co-Al alloys, and elec. resistivity and thermoelec. power 1.4° to 300°K 9-44908
 Co whiskers, 4.2, 77 and 294°K 9-24128
 Cu-Fe dilute alloys, 1.3° to 88°K, fields up to 200 kOe 9-44909
 Cu-Mn-(Fe,Cr) dilute alloys, 1.3° to 20°K, fields up to 200 kG 9-44910
 Cu-Mn dilute alloys, 1.3° to 88°K, fields up to 200 kOe 9-44909
 Cu, 4.2°K single cryst. 9-44912
 Cu, at 4.2°K in transverse fields up to 100 kG 9-41166
 Cu, longit., effect of structural defects 9-49025
 Cu, transverse, 5 to 50°K, influence of lattice defects at 10°K 9-47075
 Cu saturation ratio, 4° to 35°K 9-37444
 Cu, single crystals with point defects 9-37443
 EuO:Gd, dopant effect 9-33463
 Fe, Fermi surface and de Haas-van Alphen eff. model 9-24093
 p-FeCr₂S₄, near Curie temp., effect of exchange interaction between carriers and mag. moments 9-44956
 Ga single crystals, liq. He temp., in longit. mag. field, zero resist. 9-44900
 n-GaAs, degenerate, giant peak obs. 9-44959
 n-GaAs, magnetophonon oscillations, 77 to 340°K 9-28497
 GaAs, n-type, non-degenerate, epitaxial, negative longit. magnetoresist. and displacement of longit. magnetophonons 9-26546
 n-GaSb, oscillations, energy gaps between valleys in conduction band 9-39620
 n-Ge, effect of non-dislocation defects generated during heating and deform. 9-37540
 n-Ge, intermediate mag. field region 9-24189
 n-Ge, transverse, current density depend. in strong elec. and mag. fields, 16.6°K 9-33327
 n-Ge, transverse, elec. field strength depend. 9-49103
 HgSe, Shubnikov-de Haas effect, inversion asymmetry splittings 9-49013
 HgSe, Shubnikov-de Haas obs., spin-orbit splitting at Brillouin zone centre 9-35314
 HgTe, Shubnikov-de Haas, magnetophonon and spin-magnetophonon oscillations 9-49014
 HgTe epitaxial films 9-28214
 n-InSb, anomalies rel. to absence of inversion centre 9-26550
 K, longit., strain depend. 9-35343
 K, saturating and linear effects 9-37447
 Na, longit. strain depend. 9-35343
 Ni whiskers, 4.2°, 77° and 294°K 9-24128
 Pb, high-field, Fermi surface three-zone sheet model 9-28458
 n-PbS epitaxial, transverse magnetoresistance meas. 9-42996
 p-PbTe-CdTe alloy, meas. rel. to scattering of light-mass holes 9-41206
 p-PbTe, oscillatory, effective mass of holes calc. 9-44967
 Pt-Co dilute alloy 9-44917
 Rh-Fe dilute alloys, 1.3° to 20°K, fields up to 200 kG 9-44910
 n-Si, 77°K 9-28522

Magnetoresistance continued

- n-Si, room temp. at high elec. field 9-41219
- n-Si, transverse, of hot carriers rel. to scattering 9-30930
- Si surfaces, anomalous magnetoresistance 9-28523
- SnO₂ films, negative magnetoresistance 9-33311
- Te, Shubnikov-de Haas eff., Fermi surface of holes shape obs. 9-26552
- Ti₂O₃:V, Fe, low-field magnetoresistance anomaly, Kondo condensation obs. 9-31018
- Ti₂O₃:V³⁺, negative phenomena at 4.2°K 9-47070
- Tm, transverse, 4.2-60°K, in fields up to 22 kOe 9-41318

Magnetosphere

- Alfven waves, standing, ATS 1 obs. 9-31357
- aurora's rel. to polar substorms, review 9-37957
- auroral arcs, azimuth diurnal pattern and charged particle motion along arc 9-43484
- auroral phenomena, universal instability role 9-41566
- banded chorus, v.l.f., OGO 1 and 3 obs. 9-41550
- bimodal diffusion, trapped particle energy spectra 9-41572
- bounce resonant interaction between trapped particles and pulsations 9-37938
- boundary shape at large distances 9-45550
- bow shock, transmission of Alfven waves 9-45507
- charged particle phenomena, synchronous geostationary satellite obs. 9-33801
- charged particles eqns. of motion 9-43484
- collisional multicomponent cold, cyclotron whistlers rel. to mag. field latitude vars. 9-40051
- configuration of mag. field lines above auroral zone 9-47600
- convection and rel. to storms, aurora and rad. belts, review 9-37951
- corpuscular flux, influence on nighttime ionosphere 9-35868
- currents, Birkeland field aligned at auroral latitudes 9-28934
- currents, models 9-35858
- currents due to ionos. dynamo action 9-31376
- cyclotron radiation, Doppler shifted, calc. 9-49471
- day side, low energy electrons, OGO 3 obs. 9-28916
- electric currents, along mag. field lines 9-31375
- electric field estimation from micropulsation freq. drift 9-31354
- electron boundary, high latitude, rel. geomag. axis orientation 9-28914
- electron concentration determ. from whistler obs. 9-43400
- electron precipitation, balloon obs. (Jan-Feb 1968) 9-41553
- electrons, energetic terrestrial, behind bow shock and upstream of solar wind 9-28917
- electrons, in magnetotail 2000 and 100000 km simultaneous obs. (Mar-Apr 1965) 9-35840
- electrons, trapped, pitch angle diffusion review 9-37948
- e.l.f. noise, spatial extent and occurrence freq., OGO 3 obs. 9-31356
- e.m. field propagation, Chetayev's solutions 9-24672
- expansions and contributions rel. to equatorial trapped particle diffusion 9-45517
- geomagnetic disturbance propag. in unevenly magnetized cold plasma 9-31352
- geomagnetic tail, review 9-37946
- geomagnetic tail, weakly connected model 9-35841
- hydromagnetic emission, directional, and currents along geomag. field lines 9-40061
- hydromagnetic oscillations, electron motion effects along mag. field lines 9-37935
- hydromagnetic wave amplification 9-47558
- hydromagnetic wave amplification, 0.2. to 5.0 Hz and rel. to Pc 1 micropulsations 9-28966
- ionization spikes, high latitude, POGO ion chamber obs. 9-43420
- l.f. waves, 100 to 10³ Hz, review 9-37947
- low shock, electrical cond. from macroscopic eqn. 9-47556
- magnetic field structure during storm recovery 9-43483
- magnetopause, polar, influx of charged particles at the mag. cusps. 9-37937
- magnetopause, structure, transverse vel. component effect 9-37936
- magnetopause, tail and bow shock, book 9-24683
- magnetosheath oscillations frequency calc. 9-43421
- magnetosonic wave propag. across mag. field in warm collisionless plasma 9-24675
- magnetosonic wave rays 9-37934
- magnetotail, neutral sheet, two-dimen. model 9-31358
- magnetotail, solar energetic proton penetration Vela 4 obs. (21 May-8 June 1967) 9-43665
- MHD validity 9-35839
- micropulsation periods, depend. on size 9-47557
- model midnight meridian magnetospheric field 9-31350
- neutral sheet, structure, 1963 Explorer 14 obs. 9-28918
- neutral sheet boundary, 2 dimens. Chapman-Ferraro problem 9-24674
- neutral sheet in the magnetotail, two-dimen. model 9-31358
- neutral sheet of tail, relativistic electron flux and directional distribution, Pioneer 7 obs. 9-43416
- outer, average mag. field config. 9-28967
- outer, energetic particle anisotropic flux 9-43413
- outer geomag. field, particle flux obs., review 9-37965
- outer radiation zone, particle dynamics, review 9-37964
- outer zone electron flux, drift periodic echoes 9-28937
- parameters from structured micropulsation obs. 9-26962
- Pc1 micropulsation freq. changes during sudden deformation 9-45559
- penetration by interplanetary plasma 9-37952
- physics of, conference (Washington D.C., Sep. 1968) 9-35842
- plasma, low energy, review 9-37949
- plasma, pitch angle diffusion 9-37950
- plasma during mag. storms (mid-1967), Explorer 34 obs. 9-24673
- plasma heating by e.m. waves generated in magnetosheath 9-41552
- plasma instabilities rel. to dissipation 9-37950
- plasma sheet as electron source during auroral breakup 9-28928
- plasma structure, waves and energetic particles 9-28919
- plasmopause, plasma sheet and energetic trapped electrons, satellite obs. 9-37941
- plasmopause, recent research 9-31359
- plasmopause and reln. to ion composition in topside ionosphere 9-26937
- plasmopause detection from OGO and antarctic ground stations, methods comparison 9-43423
- polar latt. electron concentration enhancement at 1000 km, 1962-64 obs. 9-43418
- polar magnetic disturbances, constitution 9-35909
- polar wind, H⁺ and He⁺ 9-26925
- polar wind, He isotopes escape mechanism 9-28913

Magnetosphere continued

- processes during mag. storm 9-31457
- processes rel. to geomag. surface phenomena 9-47595
- proton belt, bimodal diffusion 9-41571
- proton cyclotron harmonic waves, electrostatic, from e.l.f. data, Alouette 2 obs. 9-49478
- proton flux and field pulsation, resonant with 300 sec. period, Explorer 26 obs. 9-43419
- proton heating, stochastic, by fast hydromag.- wave 9-43412
- quantitative magnetic field models, review 9-37945
- resistivity, anomalous, along lines of force 9-40050
- resonance processes rel. to Pc3,4 pulsations 9-40104
- ring current particle distributions from mag. obs. 9-26933
- ring currents measurable at low latitude stations 9-47589
- sheath, magnetic emissions near 100 Hz 9-41604
- sheath, plasma flow pattern, Vela 3 obs. 9-41549
- solar plasma flow around 9-37943
- solar proton entry, low energy (26 May 1967) 9-41551
- solar protons, 5-21 and 21-70 Mev, penetration to synchronous altitude 9-43417
- solar protons over polar caps, nonuniformity (24 March 1966) 9-41609
- solar wind interaction, lab. experiments, review 9-37944
- solar wind interaction magnetosheath Explorer 34 obs. 9-40190
- solar wind interaction with mag. field 9-37942
- storm asymmetric inflation, OGO-2 obs. (March 1966) 9-41597
- streams, oblique incidence, space-time relationships 9-31351
- subsolar, dimens. determ. from terrestrial obs. of geomag. micropulsations 9-47555
- substorm, various manifestations 9-35902
- substorm study, review, book 9-24676
- substorms, major features rel. to assoc. current system 9-41600
- substorms, Synchronous orbit obs. (Dec 1966 and Jan 1967) 9-43485
- sudden commencement propag. along tail (8 Jul 1966) 9-26960
- supersonic plasma flow around 2 dimens. mag. dipole 9-38966
- surface dynamics, instability mechanisms 9-24677
- tail, electron bursts rel. auroral precipitation 9-40048
- tail, mag. storm April 1-2 1964 rel. to neutral sheet instability, obs. 9-26959
- tail, model for origin of daytime aurora 9-33808
- tail field calc. from auroral oval obs. 9-35845
- tail meas. at 1000 earth radii, obs. with 3 satellites 9-40047
- tail perturbations rel. to irregular geomag. micropulsations 9-33868
- transpolar exospheric plasma, plasmosphere termination 9-28915
- transverse waves and instabilities 9-49469
- trapped particle, drift shells, topology 9-43429
- trapped particles, bounce resonant scattering 9-28936
- trapped radiation diffusion inward, effect of convection electric fields 9-43435
- viscous boundary-layer, analysis 9-33802
- v.l.f. emissions, medium latit., storm-time evolution, satellite obs. (May 25/26 1967) 9-37939
- v.l.f. emissions, morning and night differences, applic. to storm periods 9-49468
- v.l.f. emissions, properties 9-31360
- v.l.f. finite amplitude wave packet growth, theory 9-22318
- v.l.f. noise triggering during whistler duct drift across mag. shell, triggering 9-43414
- v.l.f. propagation between conjugate points, evaluation 9-35862
- v.l.f. triggering by Morse dots at 14.7 kHz 9-43415
- wave particle interaction experiments 9-28920
- waves, hydromag. 3 dimens., emission characts. calc. 9-30223
- whistler characts. change in disturbed mag. field 9-45506
- whistler mode v.l.f. signals, amplification 9-26926
- whistler propag. 9-40046
- whistlers, cyclotron resonance amplification 9-41554

Magnetostriction

- crystals, nonpiezoelectric, magnetostrictive generation of transverse micro-wave phonons 9-45272
- ferrites, FxC 3E1, FxC 7A2, internal friction and ΔE effect, magnetizing field depend. 9-26655
- ferromagnetic perfect cryst., distortions introd. 9-28612
- forced, in band model of magnetism 9-33465
- hematite single cryst., magnetoelastic interac. obs. 9-31049
- Invar alloy, spontaneous volume magnetostriction theory, thermal expansion anomaly 9-43177
- Invar alloys, forced magnetostriction, absolute saturation magnetization press. coeffs., 4.2K 9-41320
- magnetite in weak fields at liquid nitrogen temps. 9-31476
- magnetostrictors, high power, sound output and efficiency, nonlinear design technique 9-29281
- mumetal, easy direction magnetostriction rel. to magnetomech. damping temp. effect 9-31036
- non-uniform config. effect 9-47219
- in rocks, from liquid nitrogen temp. to Curie point, meas. 9-31476
- steel, transformer, deformed, strain effects 9-45140
- steel, transformer, effect of tensile stress 9-45156
- type-II superconductors, due to surface currents 9-26620
- CdCr₂S₄/Se₄ ferromagnetic semiconductor, exchangestriction rel. to absorpt. edge shift 9-45155
- Co-Fe-B semi-hard mag. alloys, and square hysteresis loop, coercive force 9-45137
- Co-Pt equiatomic alloy, effect of tensile stress 9-45156
- Co hexagonal crystal with internal stresses and magnetization 9-37657
- Co single crystal, const. and shear const. meas. up to 26 kOe, -200 to 400 °C 9-41305
- Cr, antiferromag. ordering cry. distortions, electrical-resistance strain gauges 9-39780
- Fe (40 at.%)Ni Invar alloy, effect of tensile stress 9-45156
- Fe (3 wt.%)Si, ferromag. domains, X-ray diff. contrast on walls due to magnetostriction 9-26643
- Fe-Si alloys, infl. of galvanically deposited Ni films 9-26647
- Fe, easy direction magnetostriction rel. to magnetomech. damping temp. effect 9-31036
- LiGa ferrites, temp. depend. 9-28629
- Ni, easy direction magnetostriction rel. to magnetomech. damping temp. effect 9-31036
- Ni, effect of tensile stress 9-45156
- Ni single crystal rod, plastic deformation depend. meas., room temp. 9-41315

Magnetostriiction continued

- NiCo ferrite, mag. annealing effect on magnetomechanical coupling coeff. 9-47273
 TbFe garnets, exchange 9-24319
 TbFe garnets, substituted, volume component 9-43155
 $\text{Y}_3\text{MnO}_7\text{Fe}_4\text{O}_{12}$ 9-49219
 YFe garnet, (Ca, V, In)-substituted, and anisotropy meas. 9-45192

Magnetothermal effects

- Ettingshausen coefficient of type II superconductors 9-49043
 machine, ideal, magnetocaloric conversion 9-31857
 metal, Ettingshausen-Nernst. coeff. temp. depend., carrier density and mobility obs. 9-39580
 modulation and detection by second sound in He 9-39523
 semiconductor thin films, thermogalvanomagnetic effect, influence of inelastic carrier scatt. 9-35494
 semiconductor with inelastic electron scattering, in strong elec. and mag. fields 9-33287
 superconductor, type-I, Ettingshausen effect, current-carrying intermediate state obs. 9-30867
 in superconductors, existence 9-37456
 thermogalvanomagnetic coeffs. rel. to space-time symmetry restrictions 9-47192
 Bi-(0.3 at.%)Sn alloy, rot. curves of e.m.f., valence band struct. obs. 9-35312
 Bi, and thermo-e.m.f. props., 3° to 80°K 9-30984
 Bi, anomalous behaviour at low temps. and high mag. field, theoretical 9-47193
 Bi, Nerst-Ettingshausen effect, anomalous, theoretical 9-47194
 Co, near Curie temp. 9-24271
 Cu_3SbSe_4 , transverse Nerst-Ettingshausen eff. 9-26505
 $\text{CuCl}_2\cdot 2\text{H}_2\text{O}$, antiferromagnetic spin flop transition studies 1° to 4.2°K 9-45217
 Gd, mag. field strength depend. of thermo e.m.f. and thermomag. effect, saturation effect values, low temp. 9-39700
 n-HgTe, Nerst-Ettingshausen effect, longitudinal and transverse 9-35497
 n-HgTe, Nerst-Ettingshausen galvanothermagnetic effect, 20-300°K rel. to e. scatt. mechanisms 9-30815
 In, longitudinal thermal magnetomorphous effect 9-37430
 In, Rigbi-Leduc coeffs. for high field 9-47195
 n-InAs, e.m.f. and Nerst-Ettingshausen eff. 9-39622
 MgO:Cr, thermal magnetoresist. rel. to phonon scatt. by paramag. ions, 0.4-0.4°K 9-33162
 MgO, thermal magnetoresist. rel. to phonon scatt. by paramag. ions, 0.4-0.4°K 9-33162
 $\text{MnCl}_2\cdot 4\text{H}_2\text{O}$, ht. capacity, 0.4°-4.2°K in mag. fields 9-44835
 Nb-Mo alloys, Nerst-Ettingshausen coeffs., obs. in high mag. fields 9-47091
 Nb, Nerst effect obs. of flux flow 9-41182
 Ni, internal stress effect on thermoremanence 9-45016
 Pb films, Nerst effect obs. of flux flow 9-41183
 Yb Fe garnet, cooling by adiabatic magnetization 9-45194

Magnetrons *see Electron tubes; Microwave techniques and devices***Magnets***see also Superconducting magnets*

- alnico alloy, α and α' phases, temp. effects on induction 9-45149
 alnico-type cast b.c.c. hard, brittle fracture 9-35014
 assemblies for high homogeneity fields, patent 9-27277
 electromagnets, rotating probe for field strength meas. 9-22342
 for ions, heavy, Hortig accelerator, mag. deflectors 9-46164
 for nuclear magnetic resonance apparatus, patent 9-47878
 permanent, for quasiperiodic focusing of klystron 9-31869
 permanent, temp. effects on induction 9-45149
 pole pieces in e.m. flowmeter, optimum size 9-26057
 pot, thermally sensitive, with ferro-magnetic housing, patent 9-47898
 Pt-(23 wt.% Co coercive force and B-H meas. 9-43152
 round, ideal, beam analyzers quantum behaviour 9-22361
 for seismometer transducer, optimum size determ. 9-41468
 solenoid, pure Cu cooled to 80-20°K, impulsive field dependence on battery parameters 9-47896
 solenoid design, book 9-47897
 vertical symmetry plane, use in ring accelerators 9-48245
 $\text{Co}_5\text{-xRu}_x$ (R=rare earth), permanent, material props. 9-45120
 Nb₃Sn, superconducting, a.c. power loss meas. 9-37498
 SmCo₅, Co-rich part permanent magnets, energy products $20\times 10^6\text{G.Oe}$ 9-33433
 SmCo₅ pressed powder, high energy product 9-49213

Magnons *see Ferromagnetism***Magnus effect** *see Aerodynamics***Majorana effect** *see Magneto-optical effects***Majorana forces** *see Nuclear forces***Makler effect** *see Electron emission/secondary; Photomultipliers***Mandelstam representation** *see Elementary particles/scattering***Manganese**

- ^{55}Mn in meteoritic iron, neutron activation analysis 9-39974
 atomic spectrum, bibliography 9-38765
 magnetic susceptibility, He temp. to 2000°K 9-24333
 particles prepared by evap. in Ar, electron microscope and diff. obs. 9-42790
 polymorphism, influence of atomic size factor 9-46954
 self-diffusion in b.c.c. δ - and f.c.c. γ -phase 9-39385
 X-ray absorption spectra K lines obs., effective co-ordination charges determ. 9-37745
 Al-Ag alloy addition, eff. on strain-induced solute disposition stability control of mech. strength 9-28360
 in Al_2O_3 , sintered alumina, effect on glow curve 9-28728
 in Al_2O_3 single crystal, low temp. thermal conductivity meas. 9-35086
 Fe-Mn nodules, particle size determ. of Fe oxide phase by Mossbauer effect 9-42786
 n-Ge:Mn, spontaneous current oscillations due to excitation of recomb. waves 9-41216
 in KCl, impurity eff. on growth of F and M optical absorption bands 9-28686
 luminescence in ZnS phosphors, sensitizing, Gudden-Pohl effect 9-45348
 in Mg, worked, annealed and aged samples, effect on elastic fatigue 9-30638
 Mn-FeNi film with ferro-antiferromagnetic interaction, ferromag. reson. 9-37789
 Mn-Zn ferrite production from $\text{MnCO}_3\text{-ZnO-Fe}_2\text{O}_3$ calcination 9-35742

Manganese continued

- γ -Mn, antiferromagnetic structure confirmation neutron diffraction 9-31051
 γ -Mn, f.c.c., electron band structure by APW method 9-47045
 Mn^0 hyperfine coupling in LiF, parameter temp. depend. 9-43282
 Mn^{2+} , diffusion in NaCl, coeff. determ. by e.p.r. 9-30627
 Mn^{2+} , ESR, in monticellite (MgCaSiO_4) 9-24497
 Mn^{2+} , e.p.r. in CdWO_4 , effect of external elec. field on hyperfine structure 9-31162
 Mn^{2+} , e.p.r. in irr. NaCl 9-35715
 Mn^{2+} , e.p.r. in KZnF_3 , determ. of nearest-neighbour exchange const. 9-45386
 Mn^{2+} , e.p.r. in NaF, 4 spectra obs., spin-Hamiltonian method analysis, 93-573K 9-39908
 Mn^{2+} , e.s.r. in fluoroborate glass 9-45385
 Mn^{2+} , e.s.r. in K_2ZnF_4 , and transferred hyperfine interactions 9-45387
 Mn^{2+} , spin-lattice relaxation time in ZnS:Mn, Li 9-47301
 Mn^{2+} , e.p.r. exchange-narrowed in MnF_2 , KMnF_3 and RbMnF_3 , discrepancies between theory and expt. 9-45388
 Mn^{2+} , e.p.r. in aq. soln., 3.2 cm and 10 cm spectra, comparison 9-34922
 Mn^{2+} , e.p.r. in ZnSO_4 , fine struct. and cryst.-field interac. obs. 9-33635
 Mn^{2+} in $3\text{Ca}(\text{PO}_3)_2\cdot\text{Ca}(\text{F}_{1-x}\text{Cl}_x)_2$, synthetic, e.p.r. rel. to effect of incorp. of Cl on Mn^{2+} positions 9-47431
 Mn^{2+} in $(\text{NH}_4)_2\text{SO}_4$ single cry., EPR study in paraelec. and ferroelec. phases 9-31165
 Mn^{2+} in $\beta\text{-LiAlO}_3$, cathodoluminescence spectra and coordination with Fe^{3+} 9-31150
 Mn^{2+} in GaAs, g-factor shift, covalency influence 9-43280
 Mn^{2+} in LiF, phonon-induced corrections to transferred hyperfine coupling 9-33628
 Mn^{2+} in MnF_2 and ZnF_2 , axial field splitting, ^5S ion spin Hamiltonian explanation 9-45247
 Mn^{2+} in NaCl, ground state splitting, elec. field effect, e.p.r. obs. 9-43284
 Mn^{2+} in $\text{RbMnF}_2\text{:Nd}^{3+}$, fluorescence temp. dependence rel. to $\text{Mn}^{2+}\rightarrow\text{Nd}^{3+}$ energy transfer 9-24456
 Mn^{2+} ion, in organic solvents, e.p.r. spectra in 10 cm band 9-42679
 Mn^{2+} ion spectrum analysis, 600-9300 Å 9-38771
 Mn^{2+} in LiF, e.p.r. at 9.5 GHz 9-37798
 Mn^{3+} coloration impurity in lanthanum glass, effect on light absorption 9-24372
 Mn^{3+} in $\text{Mn}_{0.03}\text{Fe}_{1.97}\text{O}_{4.97}$, ^{55}Mn n.m.r. at B-site, anisotropic hyperfine field due to local Jahn-Teller distortion 9-43299
 Mn^{4+} , e.s.r. of $[\text{Mn}(\text{IV})\text{O}_6\text{Mo}_2\text{O}_{26}]^{6-}$ in dil. $(\text{NH}_4)_6\text{h}_2\text{O}$ 9-43283
 Mn^{4+} activator centres in AlN, phonon structure 9-24010
 Mn^{4+} in $[(1-x)\text{La}, x\text{Ca}]\text{MnO}_3$ perovskite cpds 9-33127
 Mn^{4+} in $\beta\text{-LiAlO}_3$, cathodoluminescence spectra and coordination with Cr^{3+} 9-31150
 Mn^{4+} in MgO at tetragonal and octahedral sites of Mn^{4+} 9-24496
 Mn^{4+} in SrTiO_3 , as impurity-ion probe in spectroscopic exam. 9-26743
 α -Mn single crystals, prep. and physical props. 9-44645
 $\text{Mn}(\text{II})$, fluoresc. in molten salts 9-42666
 Pb:Mn film, supercond., far-i.r. study of energy-gap props. 9-41185
 ZnS:Mn,Cu,Cl effect of activator conc. on electroluminescent props. 9-37781
 ZnS-CdS:Mn, u.v. and visible photoluminesc., i.r. reinforcement 9-47416
 $\text{ZnSiF}_6\cdot 6\text{H}_2\text{O}:\text{Fe}^{2+}, \text{Mn}^{2+}$, single cryst., spin-lattice relax. of ^1H and ^{19}F 9-35594

Manganese compounds

- $\text{Mn}^{4+}\text{Mn}_3^{2+}\text{SiO}_7$ (welinite), crystal structure 9-23764
 Cr-Mn alloy, magnons and paramagnons, neutron scatt. study 9-45215
 formate dihydrate, deuterated, antiferromagnetic structure from n. diff. obs. 9-24336
 formate dihydrate antiferromagnet with weak canting interaction, mag. phase transition 9-33489
 manganin coil press. gauge, calibration to 60 kbar under hydrostatic press. 9-40215
 minerals, i.r. spectra obs. on 10 minerals 9-28690
 permanganates, i.r. spectra 9-24412
 rancieite, chem. analysis, X-ray powder diff. and dehydration studies 9-32922
 steel, X40MnCr22, mag. susceptibility at 5-1800°K 9-24330
 Ag-Mn alloys, photoemission and optical studies rel. to electronic structure models 9-45033
 AgMn alloys, photoemission meas. rel. to impurity bound states 9-26613
 Ag(Mn) alloys, photoemission expts., rel. to virtual resonant bound states 9-45032
 Al-Mn dil. solid soln. mag. susceptibility and s.p.h. w.r.t. localized d-state props. 9-33269
 Al-Mn dilute alloys, n.m.r., low temp. phen., impurity obs. 9-28754
 Au-Mn alloys, martensitic transformations near equiatomic composition 9-26379
 Au-Mn alloys, short-range order 9-28257
 $\text{CaO-Mn}_2\text{O}_3\text{-ZnO-Fe}_2\text{O}_4$ system, phase diagram 9-46958
 Co-Mn alloys, non-collinear mag. structures with antiferromag. interaction between local mag. moments 9-45056
 Cr-Mn alloys, X-ray K spectra 9-24439
 Cr-Mn steels, equilib. diag. for weld metals 9-23976
 Cu-Mn:Pt, Kondo divergence in conduction-electron scatt. amplitude 9-39558
 Cu-Mn-Al, structure study by X-ray and neutron diff. anal. and electron microscope exam. 9-37293
 Cu-Mn, dilute, electron spin resonance over 1.8°K to 300°K range 9-24489
 Cu-Mn alloys, stress-corrosion cracking, electrochem. factors 9-23920
 Cu-Mn dilute alloy magnetoresistance, 1.3° to 20°K, fields up to 200 kG 9-44910
 Cu-Mn dilute alloys, e.s.r., 1.8° to 300°K 9-26792
 Cu-Mn dilute alloys, magnetoresistance, 1.3° to 88°K, fields up to 200 kOe 9-44909
 Cu-(1wt.%)Mn alloy, spin splitting contrib. to Mn mag. moment 9-24282
 Cu-(7.5-25 at.%)Mn alloys magnetic props. in pulsed fields up to 175 kOe, 77-300°K 9-43173
 CuMn alloys, photoemission meas. rel. to impurity bound states 9-26613
 Cu(Mn) alloys, photoemission expts. rel. to virtual resonant bound states 9-45032
 CuPd-(1wt.%)Mn alloy, spin splitting contrib. to Mn mag. moment 9-24282
 Fe-(0.75 at.%) Mn alloy, annealed, grain boundary fine struct. obs. 9-35102

Manganese compounds continued

- Fe-Mn-C alloys, internal friction temp. dependence rel. to stress-induced ordering of C 9-23862
- Fe-Mn-C alloys, shape strain for (225) γ martensitic transformation 9-28344
- Fe-Mn-Ni with Ti added, ageing 9-48917
- Fe-Mn alloys, internal friction temp. dependence, and C addition effect 9-23862
- Fe-Ni-Mn-Ti martensitic alloys, pre-precip. stage during ageing 9-37283
- Fe-Ni-Mn alloys, f.c.c., intrinsic magnetization, 77°K to Curie temp. 9-45144
- Fe₂Ge₂Mn₂Ge₂ solid solns., saturation magnetiz. meas. and Curie temp. 9-45065
- Fe-(0.75 wt.%)Mn alloy, recovery processes during creep 9-26334
- Ge-Mn alloys, mag. props. in liq. and solid state rel. to Mn conc. 9-47232
- MnSO₄ aq., dielec. props. 9-46648
- Mg-Mn alloys, creep specimens and thermally aged, α -Mn precipitate, e. microscope exam. 9-28265
- Mg-Zn-Mn alloy, age hardening, patent 9-48942
- Mg-Zn-Mn alloy, heat treated, patent 9-46960
- Mn-Ag molten alloys, elec. resist. from partial interf. functions 9-30422
- Mn-(11 at.%)Cu alloy, relax. peak obs. w.r.t. twinning surface disloc. 9-35156
- Mn-(11 at.%)Cu alloy, twinning surface dislocations, intrinsic resistive stress 9-35157
- Mn-Cu alloys, lattice distortion, elasticity and antiferromag. order 9-39783
- Mn-Ge alloys, phase equil. diagram 9-48938
- Mn-In alloys, solid and liq., structure and mag. props. 9-31017
- Mn-(78.5 at.%)Ni alloy, galvanomagnetic effect, longitudinal 9-24278
- Mn-Ni constitutional diagram 9-39502
- Mn-Pd alloy system near MnPd₃, cryst. and mag. struct. 9-35588
- Mn-Zn ferrite, coarse-grained, permeability and harmonic distortion increase with induction 9-35573
- Mn_{0.5}Zn_{0.5}Fe₂O₄, atomic vibration, mean square amplitude determ. 9-41081
- (Mn_{0.95}Cu_{0.05}) alloy, antiferromag., Fe impurities obs. 9-41338
- Mn_{1-x}Cr_xAs mag. and crystallographic study at 4.2-900°K 9-47226
- Mn_{0.03}Fe_{1.97}O₄ single cryst., ⁵⁵Mn n.m.r. of Mn²⁺ at B-site, anisotropic hyperfine field due to local Jahn-Teller distortion 9-43299
- Mn_{1.26}Fe_{1.74}, ferrimag. reson. linewidth, independent grain and dipole narrowing theories comparison 9-45373
- Mn_{1.88}Fe_{1.12}O₄, tetragonal and cubic struct. obs., 300K 9-44668
- Mn_{2-x}Cr_{2x} n.m.r. freqs. and nuclear relax. times, 4° to 300°K, using nuclear spin echoes 9-45403
- Mn₂Co₂C, ferrimagnetic structure 9-28631
- Mn₂Ge₂Sb₂, new magnetic transformation, ferrimag. to helical and helical to antiferromag. 9-24318
- Mn₂GeS₄, orthorhombic, nucl. and mag. struct., neutron diff. obs. 9-35589
- α -Mn₂O₃-Fe₂O₃ system, magnetic structures 9-45078
- Mn₂P₇O₇, n.m.r., ³¹P, paramagnetic shift of resonance from pH₀ 9-47448
- Mn₂(CO)₁₀ nematic soln., polarization of absorpt. bands in i.r. region 9-44336
- Mn_{2-x}Fe_xO₄, Mossbauer spectra 9-37701
- Mn₂-(M,Fe)₂B₄ (M=Co,Ni), ferromagnetic, composition rel. to applic. in thermal switches, patent 9-33451
- Mn₂La₂(NO₃)₁₂·24H₂O, mag. phase transitions, obs. 9-39781
- Mn₂O₄-Fe₂O₃ spinel system, chem. structure 9-32856
- Mn₂O₄, high pressure transformations 9-44799
- Mn₂Cr_{1-x}S solid solutions, sign and size of exchange integrals 9-28615
- Mn₂Fe_{1-x}O₄ perovskites, unit cell parameters and mag. props. 9-35060
- Mn₂Fe_{2-x}O₄ ($x < 1$), ferromagnetic resonance linewidth and relaxation 9-28739
- Mn₂Fe_{2-x}O₄ ferrites, cubic and tetragonal, i.r. absorpt. spectra, lattice vibr. classification 9-39841
- Mn complex ⁵S state of Mn²⁺ in soln., e.s.r. X-band spectra obs. 9-30038
- Mn II tetrahalo anions, Raman spectra rel. to vibr. obs. 9-44327
- Mn Se₂S₄ exchange interactions from mag. susceptibility meas. 15° to 295°K 9-47292
- MnAlGe ferromagnet, uniaxial, domain struct. hysteresis 9-41311
- MnAlGe ternary alloy, magnetic structure by neutron and X-ray diffraction 9-35560
- MnAs, ferromag., electron density distrib. 9-35553
- MnAs, magnetic props. pressure dependence 9-24303
- MnBi, Curie-point magnetic holography 9-25323
- MnBi, ferromag., electron density distrib. 9-35553
- MnCO₃-ZnO-Fe₂O₃, calcination, Mn-Zn ferrite production 9-35742
- MnCO₃, antiferromag., acoustic birefringence 9-46985
- MnCl₂·H₂O in organic solvents, e.p.r. spectra in 10 cm band 9-42679
- MnCl₂·4H₂O, antiferromag., spin flop states, low-temp. adiabatic studies 9-43191
- MnCl₂·4H₂O, ht. capacity, mag. moment, 0.4°-4.2°K in mag. fields 9-44835
- MnCl₂·4H₂O, sp. ht. high-resolution meas. near Neel temp. 9-24046
- MnCl₂·4H₂O, thermal transport, effect of magnons 9-44847
- MnCl₂⁴⁻ tetrahedral complexes, covalent bonding 9-37799
- MnCl₂⁶⁻ octahedral complexes, covalent bonding 9-37799
- MnCr₂S₄ thiospinel, low temp. mag. transition, neutron obs. 9-47225
- MnF₂·Co, localized mag. mode, temp. depend. 9-45227
- MnF₂·Fe²⁺, near i.r. absorpt. 9-49280
- MnF₂·Fe²⁺(Co²⁺) magnetic mode, localized 1.2°K, i.r. obs. 9-47291
- MnF₂, antiferromag., magnon dispersion relation and exchange interac. 9-45228
- MnF₂, antiferromag., Raman effect scattering, matrices determ. from mag. point groups irreducible corepresentations 9-24422
- MnF₂, antiferromag. critical Zeeman effect anisotropy 9-35642
- MnF₂, e.p.r. of Mn²⁺ and ¹⁹F n.m.r. exchange narrowed discrepancies between theory and expt. 9-45388
- MnF₂, magnetic-phase boundary from u.s. and differential magnetization meas. 9-41339
- MnF₂, magnon sideband theory 9-45229
- MnF₂, magnon sidebands in absorpt. spectrum 9-35661
- MnF₂, Mn²⁺ ion axial field splitting, ⁵⁵S ion spin Hamiltonian explanation 9-45247
- MnF₂, n.m.r. of ⁵⁵Mn, rel. to Suhl-Nakamura interaction 9-26798
- MnF₂, phase transitions at pressures up to 160 kbar 9-44800
- MnF₂, polymorphism at high press. and temp., phase diagram and transforms. obs. 9-39184

Manganese compounds continued

- MnF₂, sound vel. near Neel pt. 9-44818
- MnF₂ magnetization of impurity Fe²⁺ ions Mossbauer effect meas. 9-45298
- MnF₂ single crystal slab, absorption spectra in far i.r. and visible, multiple magnons 9-45326
- MnF₂ u.s. attenuation near mag. phase transitions freq., and temp. depend 9-48958
- MnFe₂O₄, growth of single crystals 9-37087
- Mn(II), fluoresce. in molten salts 9-42666
- Mn(II) complexes of spin-1/2 with large ligand field splittings, e.p.r. 9-41428
- Mn(NCS)₂²⁻, Mn(NCS)₆⁴⁻, Mn(NCSe)₆²⁻, Mn(NCSe)₆⁴⁻, Mn(N₃)₄²⁻ complexes, electronic spectra 9-40593
- MnNb₂S₄, synthesis and lattice constants on basis of hexagonal unit cell 9-39284
- MnO:Li dipole relaxation 9-35466
- MnO/CoO solid solns., dielec. const., loss and conductivity meas. w.r.t. freq. 9-35465
- MnO/NiO solid solns., dielec. loss, const. and conductivity meas. w.r.t. freq. 9-35465
- MnO, absorpt. spectrum, 300-1.7°K 9-47365
- MnO, antiferromag., magnon energies 9-35591
- MnO, antiferromagnetic, spin-polarized energy-band structure 9-44888
- MnO, crystal-field transitions, absorpt. spectra obs. 9-39840
- MnO, crystal field transition intensities rel. to antiferromag. 9-45252
- MnO, dielec. and Reststrahlen parameters determ. from reflectivity obs. 9-45308
- MnO, highly mobile electrons obs., high temp. 9-44965
- MnO, paramagnetic, n. scatt. rel. to short-range-order 9-24283
- MnO, photoconductivity 9-28581
- MnO, reststrahlen spectrum analysis 9-24398
- MnO single cryst., dielec. const., loss and conductivity meas. w.r.t. freq. 9-35465
- MnP, metamag. struct. 9-41337
- MnP, transformation from ferromag. state to fan structure 9-26645
- MnP helical spin structures, representation theory 9-45108
- MnP single crystal, elec. resistivity in metamagnetic state, mag. field effects 9-28460
- MnP single crystal, spin structure as function of mag. field and temp. 9-47246
- MnP metamag. single cryst., mag. field effs. on thermoelec. power 9-35498
- α -MnS, antiferromag., magnon energies 9-35591
- α -MnS, crystal field transition intensities rel. to antiferromag. 9-45252
- α -MnS single cryst., absorpt. spectra, fine struct. 9-43241
- MnSO₄ mixture in H₂O-ethylene glycol, u.s. absorpt. obs. 9-39097
- MnSb, ferromag., electron density distrib. 9-35533
- MnSb, lattice parameters, pressure depend. 9-28264
- MnSeO₄, antiferromag. Neel pt. 9-49223
- MnSn₂, antiferromag., Mossbauer effect 9-41368
- MnSnO₃, disordered imenite, struct. and mag. prop. 9-39285
- MnTO₃ (x=y, No, Er, Tm, Yb, Lu), hysteresis cycles and ferroelec. domains, X-ray method 9-26590
- MnTe, antiferromag. and paramag., ¹²⁵Te Mossbauer effect 9-43225
- MnTe, antiferromag. semiconductor, magnon drag contrib. to transport props. 9-24332
- MnTe, lattice parameters, pressure depend. 9-28264
- MnTiO₃ II high press. phase, struct. and mag. prop. 9-44667
- MnWO₄, huebnerite, mag. struct. 9-43194
- β -MnZn ferromagnet, high-field susceptibility 9-33464
- Pt-Mn alloys, ordered, magnetic structure, n. diff. analysis 9-35563
- Pt₂Mn alloy, spontaneous magnetization, atomic ordering effect 9-39770
- (SnTe)_x-(MnTe)_{1-x} alloys, mag. props. 9-39771
- Ti(5 at.%) Mn alloy martensites, electron microscope obs. 9-39311
- Ti(8 wt.%) Mn alloy, heat-treated, electron microscope obs. 9-35214
- Zn(0.005 at.%) Mn alloy, anisotropy of Kondo scatt., obs by de Haas-van Alphen effect 9-24109
- Zn-Mn dilute alloys, relax. time meas. from de Haas-van Alphen studies 9-37424

Manometers

- see also *Vacuum gauges*
- liquid optical refraction change used to meas. press. 9-32177
- multitube, inclined, design 9-38192
- thermocouple manometric transducers, error evaluation 9-31741

Many-body problems

- arbitrary shape particles, scale particle theory 9-41783
- Bogoliubov condition for surface layers at large distance 9-27185
- Bogoliubov inequality used to determ. depend. of free energy 9-31786
- Boltzmann eqn., inelastic scatt. prob. and collision freq. determ., slightly ionized gas 9-22150
- broken symm. and decay of order in restricted dimensionality 9-43764
- classical mechanics of N-body system, algorithm for soln. 9-47776
- common approximations 9-22146
- complex system whose Hamiltonian contains small interaction odd under time-reversed 9-45787
- coordinate systems, relative, description of n particles 9-46255
- Coulomb gas in intermediate coupling region 9-34047
- coupled oscillatory system, temp. depend. cooperative phenomena 9-45786
- crystal, impure; electronic states determ. 9-40255
- crystalline order in two dimensions 9-34044
- decoupling procedure, moment-conserving, for linearizing double-time Green's functions 9-31784
- distribution function Lorentz-invariance in phase space 9-38254
- electron systems, inhomogeneous, statistical exchange approximation 9-25043
- gases, many-body T matrix, application 9-40256
- gases, many-body T matrix, application 9-40257
- ground-state wave function symmetry 9-34046
- hadron collisions, high energy, final state classification, new phase space plot 9-42027
- hard sphere gas at high temp., expression for quantum-mechanical free energy 9-45790
- hard sphere gas, virial coeffs. calc. with new integral equation 9-32562
- hard sphere infinite system, variational principle for equilibrium 9-29213
- Hartree-Bogoliubov theory validity in exactly soluble n-body problem model 9-25558
- Hartree-Fock approximated systems near equil., dynamics 9-38252

Many-body problems continued

- Hermite reciprocity law and ang. mom. states, equivalent particle ionifications, boson and fermion state reln. 9-36143
 integral transform correlated trial functions, systematic construction 9-44237
 interacting systems, equilib. disturb. function integral representation 9-45788
 interactions, relatively compact, Schrodinger Hamiltonian spectrum, spin-orbit coupling 9-27183
 Ising model, field-theoretic and functional-integral aspects 9-31776
 Liouville equation eigenvalues, one dimens. system 9-22153
 mass operator connection with 6, 10, 14, -point Green function 9-31785
 micropolar continuum, structural model 9-27197
 monatomic fluids, second order transport relations in fluid 9-46128
 monatomic gases, distribution-function autocorrelations calc. 9-34045
 muonic molecules, S-state matrix elements 9-38928
 N-body problem, quantum mechanical 9-40253
 N-bug problem, path traversed 9-45717
 n-particle phase space in terms of invariant momentum transfers 9-22149
 N-representability problem, conditions on geminals 9-40248
 neutron scatt. by harmonic oscillator, quasiclassical method validity 9-40254
 nonconserved mutual exchange systems, kinetic eqn. soln. 9-38257
 nonconserved mutual exchange systems kinetic eqn. 9-38256
 nuclear three-body, discrete least squares method for Schrodinger eqn. solution 9-36129
 Omne's trees, their number 9-47781
 one dimen., infinitely many particle systems, classical statistical mechanics 9-22147
 ordering of one and two dimen. systems with continuous symm., without symm. breaking field 9-43764
 particle assembly, rotund rigid, cohesionless, behaviour 9-22152
 phase transition of homogeneous and periodic systems 9-34040
 phase-space integrals computation method 9-27180
 plasma, quasi-particle concept development and applic. 9-40656
 plasma simulation, clouds-in-clouds, clouds-in-cells physics 9-36757
 quantum mechanical, with strong forces, extension of Jastrow's method 9-43763
 quantum or classical nonrelativistic syst., inequalities for free energy 9-25050
 quasi linear canonical transformation method 9-47779
 response to quasistatic changes in vol., correl.-function expressions for viscosity coeff. and shear and bulk moduli 9-22148
 ring diagram approx. pair distrib. function corrections 9-22151
 scattering amplitude in non-relativistic quantum mechanics 9-27173
 Schrodinger eqn., in spherical coord. systems 9-47753
 screening const. evaluation for charged particle systems interacting with Coulomb forces 9-38253
 solution by quantum mechanical methods for repulsive potentials 9-38456
 spin system with non-magnetic atoms impurity, electronic states determ. 9-40255
 stochastic types of motion in system of coupled harmonic oscillators 9-45789
 superconductor with paramag. impurities, oscillation spectrum of vortex filaments 9-38261
 superradiant system of N atoms, time depend. energy loss 9-38255
 transport equations for the electron-impurity model, deriv. methods 9-47777
 velocity field definition 9-47778
 vortex filaments oscillation spectrum for charged Bose gas and superconductor models 9-38261
 Ar, solid self-diffusion 9-46693
 Ar liquid, velocity autocorrelation function, hindered-translation model 9-22154

Many-particle systems *see Statistical mechanics/quantum***Markov processes** *see Statistical analysis***Mars** *see Planets***Masers**

- atomic, tuning by magnetic quenching, patent 9-40337
 atomic clocks 9-43866
 composite, two rods in series, axial mode freqs. and losses 9-25231
 H₂ triplet splitting of $\Delta m=0$ transition, experiment 9-47925
 for hydrogen-hydrogen spin exchange cross section obs. 9-25716
 interferometer, $337 \mu\text{m c.w.}$, for plasma diagnostics 9-25909
 model, simple dynamics 9-29163
 molecular amplifier electronics, review 9-47908
 optical, polishing the ends at Brewster's angle 9-25203
 paramagnetic, with different working substances, comparative properties 9-36269
 polishing the ends of an optical plasma tube at Brewster's angle 9-25203
 quantum electronics, vol. 1 of book 9-47918
 quantum electronics, vol. 2 of book 9-47919
 quantum fluctuations of parametric oscillator, theory 9-25204
 ruby, inversion coefficient, theoretical and exptl. investig. 9-31928
 semiclassical approx., validity 9-41888
 travelling wave, generation competition, 2 transitions, same upper state 9-25205
 BiSb alloys, emission of microwave radiation in weak electric field 9-31102
 H, atomic beam prep. for operation with unpolarized atoms 9-40338
 H, atomic jet populations meas. 9-45943
 H, electronic circuit analogue, oscill. depend. on atomic beam flux 9-36268
 H, single-hyperfine-state selector efficiency 9-45942
 HCN gas, repetitive Q modulation 9-34154
 La₂Mg₃(NO₃)₁₂·24H₂O: Ni²⁺, possible maser material 9-45245
 OH, galactic, pumping mechanisms for action 9-24740
 TiO₂:Cr³⁺, travelling wave, frequency transformation 9-31927
 V³⁺:Al₂O₃, optically pumped mm wave, rate equation analysis 9-31926
optical *see Lasers; Optical pumping*

Mass spectra

- see also Chemical analysis/by mass spectrometry*
 s-aryltetrazoles, properties, and n.m.r. 9-34658
 of baryons in quark model, eigenfunctions 9-27546
 benzol [cd] pyrene-6-one, negative ion 9-30305
 of π -cyclopentadienyl derivatives of organometallic compounds, no carbonyl groups 9-34515
 ethane, C₂D₆, C₂D₅H, by charge exchange, H/D isotope effect 9-25722

Mass spectra continued

- ethylene oxide-oxygen flame in heated vertical flow reactor 9-28785
 field ionization and electron impact, rule concerning comparative interpretation 9-29902
 fluoroaromatic cpds., metastable transitions obs. 9-24532
 graphite vaporization by laser evap. 9-23601
 hydrocarbons C₃-C₈ double charged ions decomp. kinetic energy release 9-40712
 methane, CD₄, CD₃H, by charge exchange, H/D isotope effect 9-25722
 methanol 9-31220
 of mononuclear fluorocarbon derivatives of transition metals 9-34514
 on photoplates, quantitative interpretation, computer program 9-26838
 in pulse counting mode, obtained using continuous channel electron multiplier 9-42320
 A₁(1300) meson reson., double pole explanation 9-25476
 Ag-In liq. alloy system, thermodynamics 9-36860
 Ar-Cs r.f. discharge, ionic species obs. 9-36787
 Ar atoms and singly charged ions, long-lived autoionization states 9-38782
 Ar r.f. discharge, ionic species obs. 9-36787
 As-Se system, laser-induced vaporization 9-28187
 CeC, stability 9-32490
 Cu-Sn liq. alloy system, thermodynamics 9-36860
 Ge surface layer, desorbing particles obs. 9-36967
 H₂⁺, evidence for existence in some new Aston bands 9-36680
 He₂H⁺ existence in room-temp. plasmas 9-25969
³He-⁴He plasmas, He₂⁺ and He₃⁺ existence obs. 9-36760
 KCl, vaporization of single cryst. 9-48741
 Kr atoms, long-lived autoionization states 9-38782
 N₂, metastable peaks 9-42568
 NO, metastable peaks 9-42568
 U isotopes, dispersion power and line form 9-47914
 UC, stability 9-32490
 US-UO₂ vapour system 9-28774
 US-UO₂ vapour system 9-33658
 Xe atoms, long-lived autoionization states 9-38782

Mass spectrometers

- see also Ion optics*
 analyzer, r.f., for use as different types of non-magnetic mass spectrometer 9-25682
 atmospheric neutral and positive ion concentration meas., design 9-35835
 calibration, absolute, by triple-filament analysis of lead samples 9-47475
 calibration by general mass center method 9-42319
 diverging-elec. field type 9-22923
 double focusing spark source spectrograph, charact. curve for Ilford Q-2 plate 9-42355
 double focussing machine 9-38745
 drift type, cylindrically symmetric, behaviour of ion swarm 9-25683
 electrical deflection type, resolving power 9-38746
 electron impact, monoenergetic for inelastic electron collision proc. 9-29897
 field ionization, high resolution, molecular ions formation 9-29904
 field ionization calc. of elec. field at sharp edge 9-29900
 high vacuum, disturbance by hot filament ionization gauge 9-27146
 ion optic scheme with energy focusing for micro-impurity analysis 9-47914
 for ions mass range 1 to 100 analysis in single sweep, patent 9-40533
 isotopic portable automatically operated, providing onstream ²³⁵U analyses for control of UF₆ withdrawal stream 9-44238
 isotope analysis of solid samples improved by reducing background 9-29899
 magnetic, uniform field with screens, fringing field distrib. 9-34352
 magnetic sector field, for ionospheric composition meas. on Explorer XXXI satellite, in-flight calibration and performance 9-35879
 magnetic spectrograph, wide range, ion optics 9-46261
 monopole, ion trajectories calc. 9-36648
 monopole, non-magnetic, flight-type, operation and maintenance manual 9-42321
 non-magnetic, flight type suitable for space vehicles 9-43688
 omegatron, instrumentation, electronic and high-vacuum 9-29903
 omegatron, sensitivity increase by using time separation process 9-27797
 for organic compounds analysis, high resolution, design and performance 9-37847
 patent 9-22921
 pulse counting method 9-42320
 quadrupole field mass analyzer, poor peak shape, field and electrode structure imperfection 9-38744
 for residual gas analysis at high vacuum 9-24597
 residual gases in k-Ar geochemistry 9-43362
 respiratory, specifications and design requirements 9-36649
 r.f., improvement using square-wave voltage 9-42318
 r.f. electrostatic field analysis of grid 9-25681
 separator, on-line, for fast burst reactor 9-40530
 spark chamber, wire, on-line for high-energy secondary beam momentum spectrum 9-27601
 triple-axis, one working configuration, for phonon problems 9-39236
 PbS photosensitized film, anal. of outgassing products indicating presence of oxides 9-37615
accessories
see also Ion sources
 all-glass heated inlet to extend upper operating temp. 9-29901
 for ion beams, quasi-parallel, prod 9-34516
 ion lens system, quadrupole, for ribbon beam form. 9-34517
 laser coupling technique for solid materials vaporization 9-22922
 time-of-flight, charact. of RPD ion source 9-22359
applications
see also Chemical analysis/by mass spectrometry
 chemical reaction in crossed molecular beams, product detection 9-39938
 extension of particle biprism exptl. 9-38349
 gas pressure monitoring in medicine and biology 9-47696
 ion desorption, electron induced, from Pt, Pt-Ir, Mb in u.h.v. gauge 9-38178
 ion-molecule reactions, pulsed spectrometer 9-24544
 lunar atmospheric constituents, feasibility 9-47668
 omegatron, gas analysis in u.h.v., no memory eff. max. 500°C, design 9-36647
 photochemical recoil spectroscopy 9-43333
 photoionization study, apparatus and techniques 9-39021
 B, isotope production by high energy proton bombardment of targets of C and O, applications to nucleosynthesis and cosmic rays 9-22784

Mass spectrometers continued
applications continued

- Be, isotope production by high energy proton bombardment of targets of C and O, applications to nucleosynthesis and cosmic rays 9-22784
 CO₂ glow discharge sampling, constricted ion-getter pump, 50-1000 μ , 50-200 mA 9-36790
 Cl₂, photodissoc. by translational spectroscopy 9-48513
 Cs plasma, analysis of dominant ionic species 9-42485
 H₂, reaction with graphite at 1900°-2400°K 9-43315
 H atom reactions with Cl₂ and F₂ 9-43316
 H plasma discharge column, low press., determ. ionization state distribution 9-46542
⁴⁰K and Ca stable nuclides in iron meteorites, meas. using surface ionization technique 9-40182
 Li isotope production by high energy bombardment of targets of C and O, applications to nucleosynthesis and cosmic rays 9-22784
 Sn stable isotopes from fast n ²³⁵U fission, relative yields, tandem mass spectrometer 9-38725
 Ti and V stable nuclides in iron meteorites, meas. using surface ionization technique 9-38089
 Xe-methane ionic reactions, using tandem spectrometer 9-42566

Mass standards *see Standards***Mass transfer** *see Transport processes***Master equation** *see Transport processes***Materials**

- see also Individual materials (if separately named) e.g. Ruby*
 anisotropic, magnetic polarizability 9-45038
 bone, absorbed dose of nucleons ≤ 400 MeV, calc. 9-24942
 brick, reflectivity, diffuse near i.r. 9-39800
 cement, wet, cavity form. by impinging air jet, shape 9-40762
 composite, photomicrographic analysis 9-46943
 composite, reinforced by SiC whiskers and inorganic refractory fibres 9-35236
 epoxy resin, as adhesive at low temp. props. 9-26382
 heterogeneous, elastic pulse grouping during destruction 9-22245
 high temperature physics and chemistry, bibliography 9-41718
 metal carbides, refractory, surface layer fracture due to giant laser pulses 9-44774
 nondestructive proof testing, applic. of u.s. emission obs. under stress 9-37324
 nondestructive testing, u.s. transducer charact. 9-36183
 paints, reflectivity, diffuse near i.r. 9-39800
 plastic deformation, effect of mode of unloading on residual lattice strains 9-39410
 plastics, filament wound reinforced, technology 9-35237
 Portland cement raw mixture, heated rapidly, rel. to growth rate of alite crystals 9-48922
 Portland cement raw mixture, heated rapidly, rel. to growth rate of alite crystals 9-46942
 refractories, periclase-spinelide, porous, microstruct. 9-42781
 refractory, permittivity meas. to 1200°C by microwave polarimetry 9-38342
 refractory (AlN) melting technique 9-34955
 refractory oxides, struct. transform., high temp. 9-30736
 rock, elec. props. in upper layers of Earth's crust 9-33727
 rock salt, seismic pulse meas. of elastic props. 9-26311
 slate, reflectivity, diffuse near i.r. 9-39800
 space environmental effects 9-48977
 thermal props. determ., methods 9-36209
 trichite-reinforced composites 9-35235
 tubular, bulge method of determ. stress-strain charact. 9-28338
 two-phase, bulk modulus, shrinkage and thermal expansion 9-42864
 two-phase composite, shrinkage and thermal expansion, simple anal. 9-28392
 u.s. emission under stress, meas. and recording tech. 9-37324
 varnish, as adhesive at low temp. props. 9-26382
 X-ray microscopy, materials science applic., bibliography 9-23721

Materials testing *see Mechanical strength***Mathematical methods** *see Calculation; Statistical analysis***Mathematics**

- Appell hypergeometric series, F₂, analytic continuation to vicinity of singular point, $x=y=1$ 9-36109
 boundary-value, problems nonlinear, existence of solutions 9-47725
 calculus of delta functions used in eval. of integration consts. in general relativity 9-45764
 convection, natural, finite-difference computations comparison 9-22288
 cross correl. in structural systems, dispersion and nondispersion waves 9-29222
 direct line solution of transfer equations for nonstationary radiation field 9-25060
 ergodic problems of classical mechanics, book 9-22177
 farfield radiation from plane boundaries, operational method for integral equations soln. 9-27224
 finite element method theoret. foundations 9-22203
 Hilbert space, tensors 9-45732
 interpolation theory, intermediate spaces 9-22047
 invariant function of membrane stresses 9-22187
 inverse theory, generalized, applics. to geophysics 9-43351
 iteration method for bound states 9-22171
 Laplace's eqn. solution, validity of representation 9-27159
 linear operators for quantum mechanics, book 9-31763
 modified residue-calculus technique 9-25027
 orbits, periodic, Trojan, for the reson. $1/2$ 9-29069
 orbits asymptotic to periodic orbit, construction 9-28986
 perturbations, nonlinear, generalization of Bogoliubov and Mitropolsky's theory 9-38266
 pulse height spectra, resolution using numerical least square method 9-22173
 renormalization of finite matrix Hamiltonian 9-38197
 Schwarzschild and Tolman coordinate systems, reln. 9-25026
 seismic wave propagation in self-gravitating anisotropic Earth, mathematical theory 9-26877
 similarity solns. to problems in hydrodynamics 9-23211
 spectral analysis by least squares fit, approximate method 9-47794
 topography representation, validity of truncated series of surface harmonics 9-27073
 variational methods applic. to viscous heat conducting flows 9-23228

Matrices

- algebraic, for (d+s)^p configs., construction 9-38749

Matrices continued

- application to cosmic-ray ang. distrib. 9-34339
 crossing, internal symm., props. for arbitrary compact symm. group 9-22550
 crystal field interactions for d₅ config. 9-24348
 density matrices, linear inequalities 9-34008
 Euler angles, a generalization 9-45735
 involutorial, based on GL(2) representation theory 9-45734
 matrix elements in systems with nonunitary symmetry 9-22061
 Mueller, applic. to polarizing system characterization 9-32024
 plates, laminated, vibr. charact. calc. using transform. matrix 9-25089
 random, with random bias, eigenvalue distrib. calc. 9-27184
 renormalization of finite matrix Hamiltonian 9-38197
 S-state elements for muonic molecules 9-38928
 Schrodinger coupled equations, resolution of system 9-38231
 symmetry-projected single-determinant wavefunctions, density matrices 9-47755
 von Neumann density matrix for macrocanonical ensemble, low temp. expansion 9-31779

Matrix-isolation methods *see Free radicals; Molecules***Matteucci effect** *see Magnetoelectric effects; Magnetomechanical effects***Maxwell effect** *see Double refraction/flow***Maxwell equations** *see Electromagnetism***Maxwell-Boltzmann distribution** *see Kinetic theory; Statistical mechanics***Measurement**

- see also Instruments; Recording; Standards; Units; Acoustical measurement; Dielectric measurement; Electrical measurement; Magnetic measurement; Mechanical measurement; Radioactivity measurement; Thermal measurement; X-ray measurement. Some specific quantities are listed separately, e.g. Calorimetry; Density measurement. Where no separate heading exists, measurement methods and instruments are included among the other entries under the heading of the appropriate quantity or subject*
 emittance, 3.4 MeV electron beam of 250A and 300 ns 9-45924
 fluid flow, transverse turbulent velocity fluctuations close to wall, limiting behaviour 9-42626
 particle beam profile, using visible synchrotron radiation 9-46154
 quantum theory 9-31737
 single meas. sequences, empirical acceptability conditions 9-40229

errors

- see also Statistical analysis*
 graphical reconstruction of smoothed data 9-25019
 ionosphere electron content by differential Faraday effect 9-33843
 magnetic form factor determ. using polarized neutron diff., error anal. 9-24268
 meteorology, observational errors, growth rate investigation methods 9-49444
 neutron importance in reactors 9-32392
 seismology, optimization 9-35772
 spectroscopy, rel. to spectrometer params. 9-25381
 theory, significance of entropic linkage 9-25020

Mechanical measurement

- Individual quantities and instruments are listed separately e.g. Length measurement*

- extensometer, laser calibration system 9-25356

- mass, metrological progress 9-31739

Mechanical properties of substances

- see also Individual properties, e.g., Abrasion; Elastic deformation; Mechanical strength; Plastic deformation; Slip; Wear; etc.*
 anelastic strain and hysteresis observed in microstrain region 9-23866
 ceramic materials, oxides 9-33011
 chlorinated biphenyls, h.f. 9-39098
 constitutive coeffs. determ. for mixture of two elastic solids 9-27201
 ferromagnetic metals, stressed, energy dissipation mechanism 9-33013
 ferromagnetic metals, stressed, energy dissipation mechanism 9-23848
 fibres, meas. using light sensitive potentiometer 9-28328
 graphite, nuclear grade for space applics., constitutive eqns. 9-33057
 ice, effect of structure and point defects 9-48832
 metals, heat resistant, review 9-33179
 mixtures, constitutive eqns. 9-23370
 plastic plate, reinforced, input impedance determ. 9-37227
 poly(ethylene terephthalate) oriented drawn films, mech. anisotropy in yield stress 9-30667
 polyethylene terephthalate, rel. to molecular wt., temp. and crystallinity 9-42863
 polymeric solids, forced flexural resonance spectrometer for meas. in the acoustic range 9-46871
 polymers, dynamic mechanical characteristics evaluation method. 9-26309
 polymers, semicrystalline, anisotropy rel. to mol. orientation 9-36929
 polypropylene, isotactic, relax. rel. to polymorphism and lamella orientation 9-48745
 recovery of cold-worked Mo 9-39463
 refractories, dense porous, mech. deterioration due to thermal cycling 9-33014
 solid bodies in non-corrosive liquids (adsorption effect) 9-44629
 steel, mild; effect of electron beam floating zone melting 9-33109
 steel, Si, relaxation effects, infl. of H impurity 9-30644
 steel castings, continuous, microstruct. effect 9-39467
 viscoelastic, of heterogeneous media 9-31837
 viscoelastic materials, linear, relax. tests, error functions 9-33019
 Al oxide anodic films, mech. effects during growth on fine wires 9-31192
 C, structure, vaporization, growth and gasification studies, book 9-46695
 CaF₂:NaF, relaxation by internal friction 9-28548
 Cu (0.2 wt.%) Al alloy, internally oxidized, effect of Si additions 9-46903
 Cu (30 wt.%) Ni, substitutional Zener relaxation 9-26321
 Cu deformed single crystals, and dislocation configs. and densities, effect of strain rate 9-41010
 Cu sheet with cube orientation, r-values and changes during tensile testing rel. to strain anisotropy and texture 9-39273
 Cu-Ti alloys, character and time depend. indication of two stages of decomposition 9-23941
 Fe, armo, ductile-brittle transition temp., eff. of previous deformation 9-28345
 Fe, grey cast, 4.295°K 9-48893
 FeOx (45 mol.%) P₂O₅ glass, loss data rel. to electrical conduction mechanism 9-30640
 K₂Nb₆O₁₇ mica-like single cryst. 9-30522
 KNb₃O₈ mica-like single cryst. 9-30522

Mechanical properties of substances continued

- Mo-(0.05-0.20wt.%)Ti,Zr alloys, deformed, effect of annealing at 1100-2000°C 9-40951
 Mo, annealed under high-vacuum 9-26367
 Mo cold worked, recovery 9-39463
 Nb single crystals deformed at high strain rates, and dislocation sub-structure and density 9-48898
 Ni, oxidation effect 9-39424
 Ni alloys, recovery by re-heat-treatment 9-23898
 Pb_{1-x} Zr_x TiO₃ transducer ceramic, mechanical loss, large amplitude static and dynamic stress effects. 9-39397
 Pb₃MgNb₂O₇-Pb₃NiNb₂O₇ system, correlated dispersion accompanying dielectric relaxation 9-28564
 Ti-(6 at.%)Al-(4 at.%)V alloy, plane-strain cyclic and sustained load flow growth charact. 9-30722
 Ti-(8 wt.%)Al-(4 wt.%)Co alloy microstruct. and heat treatment effects 9-44747
 β-Ti alloy TS6, work- hardened, rel. to initial state 9-41031
 TiO_{2-x}, reduced rutile, relax. of hopping electrons rel. to ionic defects 9-44690

Mechanical strength

- see also Elasticity; Hardness*
 alloy, elastically inhomogeneous, dislocation model 9-39430
 brittle failure, overstressing effects 9-33070
 of cements for chemical bonding of alumina powders 9-35229
 ceramic materials, oxides 9-33011
 ceramic/glass mats., two-phase, stresses around spheres and crack formation, obs. 9-30677
 ceramics, toughness meas., rel. to work of fracture 9-37247
 concrete bearing strength on loading through flexible plates 9-23904
 crack strength calculation methods for sheet-metal parts 9-23919
 flexible films 9-26336
 and fracture, interdisciplinary approach, book 9-39431
 fracture theory, as function of crack dimension 9-48910
 fracture toughness concept and prediction of low-stress failure in materials 9-28363
 glass, chemically strengthened, rel. to stress profile 9-28336
 glass fibres 9-30468
 glass-crystal composites, effect of shape of dispersed particles 9-48884
 glass/ceramic mats., two-phase, stresses around spheres and crack formation, obs. 9-30677
 of glasses, optical 9-37248
 graphite, nuclear grade for space applics., constitutive eqns. 9-33057
 graphite, pyrolytic, flexural strength, post deposition high temp. treatment eff. 9-23906
 grossly deformed solids, simple empirical formula 9-46902
 insulating stacks of thin-layer elements, optimum apparent layer area 9-35460
 lunar soil, determ. by automatic stations 9-27071
 metal/alumina interfaces, room-temp., corrols. with phys. props. 9-23903
 metals, effect on fragmentation behaviour of explosively-loaded thin-walled cylinders 9-42901
 metals, fatigue, in welded joints, effects of reactive stresses 9-23902
 metals, fatigue strength, combined effects of macro- and microstructures and residual stresses on deposition 9-39434
 metals, fine grained, effect of diffusion creep 9-46897
 nichrome, dispersion hardened, strengthening mechanism 9-23909
 optical glass, silicate and sulphur selenide 9-26341
 plastics, filament wound reinforced, technology 9-35237
 pressure vessel, elliptical cross section, by internal press. 9-31803
 quartz ceramics, as influenced by caking and crystn. 9-48908
 soda-lime-silica glass, strain rate effects 9-42899
 solids, strong, and whisker reinforced metals 9-39429
 steel, 0.3%C, fatigue strength rel. to stress waveform, obs. 9-26346
 steel, 300M, fracture toughness and crack propagation 9-33067
 steel, austenitic, effect of previous deform. 9-33059
 steel, case hardened, for repeated bending stress 9-42892
 steel, Cr-Ni-Mo high C low alloy, fatigue strength rel. to hardness, obs. 9-26345
 steel, H-11, vacuum-melted, yield strength, effect of prestraining and ageing 9-46904
 steel, high-strength, fracture toughness rel. to precracked Charpy W/A 9-35182
 steel, induction hardened, fatigue strength rel. to retained ferrite microstruct., obs. 9-26348
 steel, low temp. effect on props. 9-23905
 steel, mild, dynamic yield strength, mean, from strain meas. on "mushroomed" projectiles 9-30662
 steel, stainless type 304L, fuel element cladding, burst tests after irradi. 9-26339
 steel, susceptibility to brittle cracking, effects of residual stresses and strain ageing 9-39439
 steel, thermomech. treated and quench- hardened, inherited strength charact. obs. 9-46920
 steel castings, 18.8 Mo stainless, high temp. tests 9-44771
 steel castings, continuous, deform. necessary obs. 9-39467
 steel-(0.36 wt.%)C, fracture toughness, instrumented Charpy impact test 9-28366
 Al-Ag alloys, increase by strain-induced solute disposition stability control, eff. of addition 9-28360
 Al, f.c.c. polycrystalline, after shock-relief deformation 9-23879
 Al, SiO₂ fibre reinforced, effect of irradiation 9-26338
 Al alloys, low temp. effect on props. 9-23905
 Al alloys, treatment for high strength, patent 9-26376
 Al containing 3D network of Al₂O₃ particles, strengthening 9-26337
 Al notched columns with fixed ends, failure under load 9-48906
 Be, isostatically hot-pressed, microyield strength rel. to grain size 9-35181
 C deposits, effect of deposition surface topography 9-26226
 C fibre, increasing with Young's modulus, if stress graphitized 9-39493
 Co-Fe-V alloys, high strength, high ductility rel. to partially recrystallized structure 9-44790
 Co alloys, high strength after ageing, patent 9-26377
 Cu-Al alloys, martensitically transformed, yield stress 9-35172
 Cu-(0.2 wt.%)Al alloy, internally oxidised, effect of Si additions 9-46903
 Cu-Cu₂O eutectic alloys 9-48907
 Cu-Sn alloys, martensitically transformed, yield stress 9-35172
 Cu, dynamic yield strength, mean, from strain meas. on "mushroomed" projectiles 9-30662
 Cu, f.c.c. polycrystalline, after shock-relief deformation 9-23879

Mechanical strength continued

- Cu, fatigue, effect of diffusion coatings 9-33058
 Cu, shock-wave strengthened, final yield strength 9-35162
 Cu single cryst. strengthening value with programmed loading depend. on preliminary deform. degrees 9-42890
 Fe alloys, low-C martensite, rel. to thermomech. treatment 9-42912
 HfB₃, hot pressed, bending and fracture modes 9-35183
 Mg alloys, low temp. effect on props. 9-23905
 MgO, fully dense polycryst., and fracture 9-42893
 Mo-(0.05-0.20wt.%)Ti,Zr alloys, deformed, effect of annealing at 1100-2000°C 9-40951
 NaCl, infl. of crystal orientation 9-26340
 Ni, f.c.c. polycrystalline, after shock-relief deformation 9-23879
 Ni, shock-wave strengthened, final yield strength 9-35162
 Ni alloys, cast or wrought, grain and specimen size eff. on creep-rupture characts 9-37245
 Ni alloys, low temp. effect on props. 9-23905
 Pb binary alloys, rel. to equil. partition coeff. 9-44772
 Pb binary alloys, relation with partition coefficient 9-26399
 SiO₂-C fibre reinforced, fracture toughness and rupture modulus 9-44773
 Ti-(6 at.%)Al-(4 at.%)V alloy, plane-strain cyclic and sustained load flow growth charact. 9-30722
 Ti-(6 wt.%)Al-(4 wt.%)V alloy, toughness of two-phase microstructures 9-37251
 Ti alloy sheet, texture strengthening at room and cryogenic temps. 9-37255
 Ti alloys, commercial grade, toughness at cryogenic temps. 9-37253
 Ti alloys, low temp. effect on props. 9-23905
 Ti alloys, relation to fine structures 9-37252
 Ti alloys, texture strengthening, cryogenic temps. 9-37254
 W-UO₂ cermet produced from coated particles, high temp. creep-rupture tests 9-23910
 Zn, loss due to adsorption, anisotropy 9-23911
 ZrB₂, hot-pressed, bending, and fracture modes 9-35183
- compressive**
 alumina strengthening by glazing and quenching 9-23935
 buckling of cylindrical shells, imperfections eff., axial compression 9-34070
 glass, reinforced, strength and fracture behaviour 9-30678
 glass ceramics, impact strength determ. device 9-33031
 glasses, impact strength determ. device 9-33031
 Inconel 625, n irradi., stress rupture props. and creep strength, 650°C 9-37250
 Al cold-rolled, yield strength determ. 9-28342
 Be, n irradi., impact resist., obs. 9-28368
 CaO-Al₂O₃-Fe₂O₃-SiO₂ system, hydraulic strength of compounds 9-23907
 Cu electroformed shell buckling by axial compression, imperfections eff. 9-34070
 Fe-Al system intermetallics 9-46890
 UO_{2-x}, depend on nonstoichiometry and temp. 9-33049
- shear**
 modulus, oxides, negative pressure dependence 9-28359
 polyethylene, oriented, rel. to lamellae out-of-plane deform. mechanism, obs. 9-28358
 polyoxypropylene, rupture and change in supermolecular structure 9-28362
 polypropylene, oriented, rel. to lamellae out-of-plane deform. mechanism, obs. 9-28358
 Ni-Al alloys, critical shear stress temperature dependence 9-23908
- tensile**
 crystals with ionic and metallic bonds, time-to-rupture as function of tensile stress and temp. 9-41026
 glass, increase by etching and ion-exchange 9-35184
 hexafluoropropene-tetrafluoroethylene copolymer, γ -irradiation eff. 9-33069
 hexafluoropropene-tetrafluoroethylene copolymer, rupture, tensile strength hardness following γ -irradiation 9-33069
 Incoloy 800, He embrittlement, eff. 9-35179
 Inconel 625, n irradi., creep strength reduction, 650°C 9-37250
 metal, b.c.c., low temp., effect of interstitial solutes 9-41028
 polycarbonate, cyclic tensile testing 9-46879
 polyvinyl chloride, unplasticized, 100-180°C 9-30652
 rubber SBR, tensile stress at break obs., temp. and strain rate depend 9-35187
 rubbers, rel. crosslinkage lability and relax., obs. 9-28361
 sapphire whiskers, temp. depend. 9-35180
 steel, C-Mn, cleavage strength, microstructure effects in various compositions after different heat treatments 9-39432
 steel, H-11, vacuum-melted, effect of prestraining and ageing 9-46904
 steel, high-strength, fracture toughness and uniaxial tensile props. relationship 9-33060
 steel, mild: effect of electron beam floating zone melting 9-33109
 steel castings, 18.8 Mo stainless, high temp. tests 9-44771
 steel-(5 wt.%)Cr, heat treated, fatigue tests 9-28365
 steel-(18 wt.%)Ni, maraging steel, heat-treated 9-30691
 super-strength alloys, high temp. effect 9-33056
 yarn, for suspension of atm. studying instruments, hazard of wind shears 9-31305
 Zircaloy-4, at low strain rates, in-pile, un- and post-irrad. obs. 9-37256
 Al-Zn alloys, effect of spinodal decomp. 9-37289
 Al-base alloys, during atmospheric corrosion test 9-37828
 Al, and alloys, rel. to hydrostatic extrusion and struct. 9-41029
 Al alloy, fatigue investigation, prop. variations with batch 9-23855
 B fibres, at elevated temp. after exposure to air, effect of SiC coating 9-30679
 CaF₂ crystals, effect of surface preparation 9-41027
 Cu, rolled temp. depend. 4.2-290°K 9-40993
 Cu sheet with cube orientation, r-values and changes during tensile testing rel. to strain anisotropy and texture 9-39273
 Fe-Al system intermetallics 9-46890
 Fe-Ni alloys in liq. Hg, toughness and ductility 9-42891
 Fe, grey cast, 4-295°K 9-48893
 LiF crystals, effect of surface preparation 9-41027
 Ni-Si-Ta alloys, rel. to heat treatment and mech. props. 9-48902
 Ni-Si alloys, rel. to heat treatment and microstruct. 9-48902
 Ni, behaviour after oxidation 9-39424
 Ti-(8wt.%)Al-(1wt.%)Mo-(1wt.%)V alloy sheet, hot-salt-stress-corrosion cracking effects 9-23923
 Ti-(8 wt.%)Al-(4 wt.%)Co alloy, rel. to heat treatment 9-40994

Mechanical strength continued**tensile** continued

- Ti-(8 wt.%)Al-(4 wt.%)Co alloy, and creep rupture and fatigue strengths 9-23956
 Ti, n. irradi. commercially pure, effect of low temp. annealing 9-33112
 β -Ti alloy TS6, work-hardened, rel. to initial state 9-41031
 UO₂-UN sintered mixtures 9-30730

Mechanics*see also Dynamics*

- action principle, general, using Lie algebra, interaction picture appl. 9-38267
 analogy of Lane-Robson model of isobaric analogue states 9-29703
 analytical, new equations and some higher order differential operators 9-22181
 Atwood's machine, a simple frictionless rotation-free one 9-36101
 classical, group theoretical foundations of Lagrangian gauge problem, single, free particle 9-22175
 classical, rel. to quantum mechanics, spin concept 9-47757
 classical of N-body system, algorithm for soln. 9-47776
 classical system, description with two distinct canonical formalisms 9-43745
 continuum, approach mechanical behaviour of solids, book 9-39431
 ergodic problems of classical mechanics, book 9-22177
 Euler angles, a generalization 9-45735
 flexible thread ejection from container due to internal pressure 9-36153
 Lagrangian, 2p-pole linear syst., irreducible representations 9-36154
 Lagrangian minimization method for vibration of a cylindrical shell 9-34076
 Newton's third law, need for clarification 9-41789
 non-local variational, imbedding, adjoint theorems and existence 9-47798
 non-local variational, linear operators and variational imbedding with one unknown 9-47796
 non-local variational, stationarity conditions with one unknown 9-40234
 non-local variational, stationarization with several depend. variables 9-47797
 non-local variational Euler-Langrange operator properties 9-40262
 optimum transfers between nearly near-circular non-coplanar orbits, powered phases eff. 9-22176
 random force and its time derivative, numerical tables 9-47621
 slip between rolling ball and track, factors affecting contact conditions 9-31801
 stability of motion within a finite interval of time 9-47795
 text book for undergraduate, with simultaneous vector and tensor usage and full treatment of relativity 9-31800
 textbook on Newtonian mechanics, French 9-36155

Mechanics of gases *see Aerodynamics***Mechanics of liquids** *see Hydrodynamics***Medical science***see also Physiology; Radiation protection*

- aerospace, health physics support program 9-27121
 aneurysms, intracranial occlusion by ferromag. thrombi 9-45699
 aortic valve, closure mechanism fluid mechanics 9-49601
 bio-fluid flow, velocity profiles by photomicroscopy 9-46588
 bioelectric currents in humans, mag. field prod., detection and analysis 9-45701
 blind u.s. pulse refl. method as mobility aid 9-22265
 bone density meas. by computer analysis of X-ray film image 9-47700
 cat brain, thermal diffusivity 9-39542
 cystic fibrosis diagnosis, neutron activation analysis appl. 9-49608
 dialysis technique, novel 9-24940
 DNA in phages, filament struct. from lum. with orange acridine, obs. 9-27926
 fiber optics appl., review 9-46014
 glucose/oxygen fuel cell for artificial heart 9-36250
 heart assist devices, fluid mechanical problems 9-38131
 holography appl. 9-49600
 hydropericardium-producing factor, identification as 1,2,3,7,8,9-hexachloro-dibenzop-p-dioxin 9-39335
 intravascular navigation of catheter, supercond. magnet system 9-35380
 laser beam applications 9-49599
 laser beams, focussed, intensity distrib., numerical solns. 9-38132
 lenses, ceramic, for control of u.s. energy 9-36195
 magnetic field and mag. device appl. 9-45697
 mass spectrographic gas pressures monitoring 9-47696
 neutron radiography appl. 9-49607
 ocular tissue, u.s. energy transmission problems 9-38134
 pathology, optical, X-ray and electron microscopic 9-29112
 piezoelectric converter for cardiac assistance device 9-38130
 POD catheter, for small vessel exploration 9-45700
 radiation therapy, laser beams depth focusing 9-47699
 radiotherapy, use of betatron as radiation generator 9-46173
 technology, chemical analysis methods, book 9-41714
 urine velocity meas., fiber optic method 9-46015
 γ dose from internal emitters, assessment of Monte Carlo calculations 9-27118
 γ ray emitting nuclides in man, whole body counting with NaI(Tl) detectors, techniques comparison 9-27120
 γ ray emitting nuclides in man, whole body counting with NaI(Tl) detectors, techniques comparison 9-27119
 Pu in blood, determ. by anion exchange 9-29113

Meissner effect *see Superconductivity***Melting***see also Zone melting and refining*

- arc melter, construction 9-33103
 atmospheric ice particles, charge separation 9-31326
 diagram determ., selection of spectroscopic buffer 9-28176
 diamond-metal contact eutectic melting 9-26358
 dielectrics, in h.f. elec. field, analytical investig. by one-dim. thermal conductivity eqn. 9-44614
 in forced pipe flow, influence of heat transfer 9-23578
 graphite-metal contact eutectic melting 9-26358
 ice, convection in continuously formed water layer 9-32781
 ice, Fe²⁺ and Eu³⁺ doped, pseudo-melting at -65°C 9-28178
 law at high press. relating changes in molar vol. to entropy 9-36919
 Lindemann's law, calculations along melting line 9-28177
 Lindemann's law reformulated in terms of stat. mech. partition function 9-46682
 metal, liq., vol. diffusion coeffs. rel. to charact. temp., melting pt. and heat of melting 9-39131

Melting continued

- metals, 'electrical explosion' investigation 9-26156
 nylon 66, double melting rel. to phases, obs. 9-34954
 polyethylene dissolution in xylene and octadecane 9-44616
 polyethyleneglycoladipate, thermooptic obs. 9-23195
 polypropylene, effect of melting on nucleation 9-32878
 solid/liquid, bounded by 2 concentric spherical surfaces, temp. gradient, heat conduction 9-29325
 statistical thermodynamics 9-30451
 Ag, fusing wires surrounded by air, energy balance 9-42694
 Ag halides, curves, h.p. 9-44615
 AlN refractory, technique 9-34955
 Ar, at high press. 9-42690
 Ar Lindemann's law, calculations along melting line 9-28177
 Ga, viscometric investigation 9-40818
 Ge, curve to 65 kbar 9-39132
 Hg-T₂ viscometric investigation 9-40818
 Mg-Ni system, contact fusion 9-26373
 Mo-Rh alloy, metal-metal carbide eutectic temp. determ. 9-34951
 Mo elec. cond. jump 9-26156
 Mo enthalpy and specific heat near melting point. 9-37356
 NaCl-KCl, differential thermal microanal. 9-28391
 Ni elec. cond. jump 9-26156
 Pt elec. cond. jump 9-26156
 U-Al₂-Al₃Mo₅Mo system, equilibria 9-39133
 W-Mo alloy, metal-metal carbide eutectic temp. determ. 9-34951
 W-Rh alloy, metal-metal carbide eutectic temp. determ. 9-34951
 W elec. cond. jump 9-26156
 ZrTe₂O₈, fusion and vaporization characts. 9-26159

Melting point

- alkali halides, interparticle distance correl. with interionic separation 9-35007
 ammonium halides, curves to 40 kbar 9-30452
 copolymers of butene with α -olefins, obs. 9-32880
 f.c.c. crystals, theoretical derivation from free energy 9-42693
 fluorides, inorganic 9-23581
 ice, Fe²⁺ and Eu³⁺, pseudo-melting pt. at -65°C 9-28178
 lanthanide compounds, interrelationship with heat of formation and lattice parameters 9-34956
 liquid alkali metals, thermoelectric power changes 9-40802
 lowering of bulk m.p. by molecular layers, n.m.r. obs. 9-40817
 metal, rel. to vol. diffusion coeffs. of melts 9-39131
 metals, internal friction anomalies 9-39399
 metals, interparticle distance correl. with interionic separation 9-35007
 N-methyl-ethylenethiourea 9-48840
 N-methyl-trimethylenethiourea 9-48840
 polymers, prediction 9-37361
 refractory metal oxides, rel. to lattice energies and heat of atomization 9-30494
 solid and liquid elements, data 9-46689
 volatile materials, curves to 15 kbar 9-48737
 BiF₃ 9-30021
 CaO-Ta₂O₅ system, of different phases 9-39494
 CoSi single crystals, optical and DTA meas. 9-37075
 CuO-MoO₃ system, of equilib. cpds, in air, O₂ press. 9-35256
 Sn-Sb(Cu,Ni) dil. alloys, internal friction anomalies 9-39399
 ThC-ThN mixtures, in N₂ atmos., maximum rel. to composition 9-40819
 ThP-UP solid solutions 9-33123
 ThP 9-33123
 UC-UN mixtures, in N₂ atmos., maximum rel. to composition 9-40819

Membranes

- as analogy for flexure of beams with longitudinal cavities 9-34064
 circular, response to simultaneous const. spin and precessional motion 9-29246
 cylindrical shell, circumferentially travelling wave flutter, limiting amplitudes, nonlinear anal. 9-22243
 electro-osmotic meas. of average radius 9-23477
 lipid-cholesterol, spherical, normal mode vibrs. 9-41816
 low dielectric, ion energy in crossing, effect of 'pores', 'carriers', thickness and ion-pair form. 9-39954
 Onsager's reciprocal relation not always true in bulk flow theory 9-32779
 oxygenator, diffusion device, patent 9-23479
 permeability, transport parameters 9-26087
 permeable gas diaphragm in fuel cell. formation, patent 9-30334
 precipitate-membrane, development and structure 9-24517
 skew, natural freqs. and modes 9-29249
 solute flow across membranes, hydrodynamic irreversible thermodynamic approaches, comparison 9-36857
 stresses, invariant function in tensorial notation 9-22187
 thickness 100Å activated, anal. of elec. phenom. by changes in absorbpt, 9-47695
 AgBr, elec. cond. and diffuse double layer 9-31200

Memory devices *see Calculating apparatus; Magnetic devices; Storage devices; Superconducting devices***Mendelevium**

No entries

Mendelevium compounds

- Mg-Zn alloy, single-cryst. growth by stationary mould solidification technique 9-32877

Mercury

- acoustic bond, low temp. 9-31722
 adsorption on Fe thin coatings, effect on elec. cond. 9-37428
 annular cylinder, current carrying, stability rel. viscosity and elec. conduct. 9-23250
 arc plasma tube electron density and temp., Langmuir probe analysis 9-42538
 arc Raman spectra of gases, review 9-46340
 arcs, high pressure, stable, radiation portion, indirect determination 9-30323
 atom, electron scatt., large angle, low energy, elastic, channel coupling effects 9-34565
 atom, energy transfer from 7S₁ level to 4D₂ level of Zn in discharge, process 9-48422
 atom, excitation by electron impact, rel. to meas. of polarization of incident electron beam 9-44284
 atom, excitation of metastable state, 6³P₂ by electrons of 4-15 eV, obs. by secondary emission 9-32421
 atom, excited, collisions with unexcited Tl atoms 9-48421
 atom, line shift by high power laser pulse 9-25709

Mercury continued

- atom, spectral line resonance broadening temp. dependence 9-40541
 boiling, with thermal load up to $2 \times 10^8 \text{ W m}^{-2}$ 9-44557
 creep deform. of single cryst. at liq. He temp. 9-23895
 cyclotron reson., absorpt. spectrum obs. 9-35323
 electrode, electrocapillary curves, automatic recording 9-49384
 electrodeposition, transient nucleation 9-37036
 electron-impact spectrum of vapour 9-44263
 electron-phonon interaction rel. to conduction electron props. 9-47032
 equations of state, analytical and experimental, isothermal data fit, review 9-36844
 excitation and deactivation of metastable atoms in 6^3P_1 level 9-22971
 flow in square channel, turbulent, space-time temp. pulsations 9-39095
 freezing and distilling, search for mass proportional creation of H 9-45588
 gas, electrical conductivity, at 2.6 g/cm^3 , 1200-2100 bar 9-23403
 ion bombardment of Au and Ni, 80-150 keV at 295°K and 80°K , depth distrib. of vacancy clusters 9-30586
 ionization, Penning, population of Hg^+ states 9-40709
 ionization potentials 9-48411
 lamp, red spectrum improved by addition of various substs., patent 9-22475
 lamp PRK-4, brightness, 300-1000 μ 9-27404
 laser line, $1.5295 \text{ m}\mu$, isotopic struct., obs. 9-34541
 liquid, effect on ductility and toughness of Fe-Ni alloys 9-42891
 liquid, interfacial energy of Zn (0001) plane, 298°K 9-40837
 liquid, reflectivity, normal and at 45° 9-46638
 liquid, rel. to brittle fracture of Zn 9-23916
 liquid, self-diffusion coeff. 9-42643
 liquid, structure, viscosity coeff. 9-32762
 liquid, u.s. attenuation, dense gas formulation 9-34902
 MHD current in ducts with sudden widening 9-30201
 photoelectric emission at Hg-solution interface, mechanism 9-30424
 plasma, dynamic sheath growth 9-40679
 plasma, free-fall decay in early afterglow 9-34810
 plasma, thermal, 1000 to 15000°K and 10 torr to 50 atm, conc. of ionization states 9-44420
 plasma oscillations, frequency in terms of discharge conditions 9-39003
 porosimetry, limitations in use with graphite 9-26225
 positive column, two-stage processes 9-30312
 radioisotopes, enrichment by neutron irradiation of diphenylmercury solns. 9-37843
 resistivity of single cryst., size effect 9-39587
 spectra relative brightness and optical excitation functions meas. 9-29933
 spectral line absorpt.-conc. relationships 9-25696
 Stark effect, shifts in $^3\text{P}_1$ and $^3\text{P}_2$ excited states 9-36660
 surface pressure prediction, fatty acids on surface, test of two-dimensional scaled-particle theory 9-40782
 surface waves, effect of axial magnetic field 9-30358
 thermal expansion meas. by liq. Ga immersion dilatometer rel. to anharmonic effects 9-47007
 thermodynamic props., u.s. pulse-repetition technique 9-23483
 turbulent flow in pipe, time characts. and temp. pulsation spectrum 9-26056
 vapour, double reson. expt., correlated intensity fluctuations 9-36670
 vapour, effect on medium press. Ar discharge 9-23352
 vapour, heterogeneous nucleation on Pyrex glass, impurity effects, $225-263^\circ\text{K}$ 9-39216
 vapour, plasma oscillations, frequency in terms of discharge conditions 9-39003
 vapour, two-photon stimulated processes, study 9-26731
 vapour absorpt. and condensation on Se films, inducement of anomalous photocond. 9-47206
 velocity distribution of flow in rectangular pipes in transverse mag. field 9-27961
 ^{201}Hg , 6^3P_1 level, hyperfine struct. and Lande factor 9-29931
 ^{201}Hg atoms disturbed by imaginary elec. field, Zeeman diagram 9-46278
 ^{199}Hg green line profile from photometric meas. of Fabry-Perot rings 9-27808
 ^{199}Hg source, photon time-of-arrival distrib. obs. 9-27292
 $^{199,201}\text{Hg}$, 6^3P_1 - $6^3\text{D}_{1,2}$ and 6^3P_1 - 6^3D_2 transitions, hyperfine struct. 9-29932
 ^{199}Hg , 6^3P_1 level, hyperfine struct. and Lande factor 9-29931
 Ar-Hg discharge, medium press., axial cathaphoresis 9-48630
 Hg-Cs arc plasma, probe obs. 9-38972
 Hg-in-Ga solution, X-ray diffraction study, radial distrib. functions, coord. numbers and scatt. functions 9-28100
 Hg-He ion laser, near-infrared operating charact. 9-47997
 Hg-Kr discharge positive column afterglow, 2nd kind collisions cross section estimation 9-25981
 Hg-Kr laser, visible and ultraviolet frequency range, patent 9-22403
 Hg $^+$ in atomic Hg, charge-transfer cross sections 9-48420
 Hg $^{2+}$, nuclear quadrupole anti-shielding factor, calc. using three different wave-functions 9-34540
 Hg electrodiffusion of Bi, effect of Tl, In and Sn additions 9-46623
 Hg zero-potential determ. by dropping electrode 9-24582
 Hgl absorption spectrum, 600-950 \AA new resonance window obs. 9-27798
 K/Hg, amalgam, fuel cell potential and thermo-dynamic props. 9-36926
 in Xe solid, absorption spectrum, multiplet struct. 9-22956

Mercury (planet) see *Planets***Mercury compounds**

- chalcogenides, band structure and transport parameters 9-48997
 halides, vibr. spectra 9-40589
 (Hg,Cd)Te photodetectors for 1.5μ 9-49160
 HgCu(OH)(NO $_3$) $_2$ ·2H $_2$ O, crystal structure 9-39271
 Ag-rich binary and ternary alloys, work function rel. to surface tension 9-24246
 Cd-Hg alloys, phase equil. and transform., thermodynamic investigations 9-48878
 Cd, Hg- $_x$ Te alloys, photovoltaic effect assoc. with effective mass gradient 9-39730
 Cd, Hg- $_x$ Te solid solns., fund. reflectivity spectrum, 1.5-4 eV, band struct. obs. 9-45306
 Hg-CdTe alloy system, magneto-optical effects, band struct. and cyclotron reson. obs. 9-39807
 Hg-Ga liq. alloys, thermodynamic activities 9-30369
 Hg-In alloys, liquid, vol. change on formation and thermal expansion coeff. 9-28115

Mercury compounds continued

- Hg-In liquid alloy, Knight shift calc. from pseudopotential formalism 9-23532
 Hg-Mg system, perturbation theory and alloying behaviour 9-44860
 Hg-Pb alloys, liquid, thermodynamic anal. of entropies and enthalpies 9-39091
 Hg-Sn liq. alloys, thermodynamic activities 9-30369
 Hg-Tl alloys, liquid, thermodynamic anal. of entropies and enthalpies 9-39091
 (Hg,Cd)Te as i.r. detector material 9-47204
 Hg $_x$ Cd $_{1-x}$ Te, sweep-out of minority carriers 9-39719
 Hg $_x$ Cd $_{1-x}$ Te, helicons and nonreson. cyclotron absorpt. method of props. determ. 9-47101
 Hg $_x$ Cd $_{1-x}$ Te alloys, 1 eV band gap, photoconductivity 9-41267
 Hg $_x$ Cd $_{1-x}$ Te alloys, photoconductivity and material parameters 9-41266
 Hg $_x$ Tl $_{1-x}$, melting process, viscometric investigation 9-40818
 Hg (II) complex, o-phenanthroline, Raman and i.r. spectra, vib. freq. determ. 9-23052
 Hg complexes with o-phenylenebisdimethylarsine, i.r. spectra 9-23078
 HgBr, band spectrum in u.v. region, analysis and new vib. const. of systems 9-46184
 HgBr, vibr. spectra 9-34627
 HgCl, vibr. spectra 9-34627
 HgCl $_2$, ^{35}Cl Zeeman quadrupole reson. 9-43269
 HgCr $_2$ S $_4$ spinel, n.m.r. of ^{199}Hg , ^{201}Hg and ^{53}Cr nuclei at 1.4°K , depend on mag. structure 9-45400
 HgCr $_2$ S $_4$ (Se $_4$) chalcogenide spinels, hyperfine and exchange interac. systematics, n.m.r. 9-31170
 HgCr $_2$ S $_4$ (Se $_4$) spinels ferromagnetic phase transitions, pressure depend 9-45119
 HgCr $_2$ Se $_4$, ferromag., cryst. growth, semicond. and optical props. 9-44961
 Hgl, vibr. spectra 9-34627
 Hgl $_2$, electro-photoluminescence 9-39896
 Hgl $_2$ adsorption of organic mols., stimulation and extinction of excitonic transitions 9-26194
 Hgl $_2$ vapour, optical absorpt. 9-42612
 HgS, fundamental absorption edge 9-47361
 α -HgS, growth of single cryst. from Hg-rich solns. 9-35020
 HgS, hydrothermal growth of Cinnabar monocryst. 9-44647
 HgS, Raman spectra 9-31117
 HgS, synthetic single crystals, photoelectric props. 9-28580
 α -HgS, valence band splitting, from absorpt. spectra meas. 9-28448
 HgSe, band structure and transport parameters 9-48997
 HgSe, electron and hole effective mass 9-24094
 HgSe, g-factor from de Haas-van Alphen effect 9-47062
 HgSe, homogeneity range and concentration-pressure isotherms 9-37508
 HgSe, ionized-impurity-limited mobility and band struct. 9-49092
 HgSe, phonon-phonon resonant scatt. in obs. on thermal conductivity, $4-30^\circ\text{K}$ 9-28409
 HgSe, powdered, propagation and dimensional resonances of helicon-like waves 9-30891
 HgSe, Shubnikov-de Haas effect, inversion asymmetry splittings 9-49013
 HgSe, spin-orbit splitting at Brillouin zone centre 9-35314
 HgTe-CdTe crystal, thermal cond., thermopower and sp. ht. rel. to composition and lattice dynamics 9-26450
 HgTe-ZnTe, conduction band struct. and electron scatt. mechanism 9-35307
 HgTe, band structure, temp. dependence from pressure meas. 9-48998
 HgTe, band structure and transport parameters 9-48997
 HgTe, e. scatt. mechanisms in intrinsic and impurity states at high and low temps. 9-30815
 HgTe, e. electron and hole effective mass 9-24094
 n-HgTe, electronic and lattice thermal conductivity, elec. conductivity, thermoelectric power $4.2-200^\circ\text{K}$ 9-33196
 n-HgTe, galvanothermoelectric effects 9-35497
 HgTe, Hall effect and resistivity rel. to crystn. temp. 9-44960
 HgTe, interband magneto-optical transitions, low temp. reflection and electroreflection study 9-47344
 HgTe, magnetoresistance oscillations 9-49014
 HgTe, powdered, propagation and dimensional resonances of helicon-like waves 9-30891
 HgTe, two helicon resonances obs. 9-43014
 HgTe, valence band, hole effective mass. rel. to temp. 9-30917
 HgTe films, epitaxial growth and electrical props. 9-28214
 HgTe single crystals, u.s. absorpt., 10-300 MHz, 1.2° to 380°K 9-42958
 In amalgams, powder, electrochemical props. 9-49380

Mesic atoms see *Atoms, mesic and muonic***Mesic molecules** see *Molecules, mesic and muonic***Mesomorphic state** see *Liquid crystals***Meson field theory** see *Field theory, quantum/meson field***Mesons**

- see also *Atoms, mesic and muonic; Cosmic rays/mesons; Hyperons; Kaons; Molecules, mesic and muonic; Pions*
 of abnormal charge parity, spin 0 and 1, props. and decay obs. 9-46087
 chiral transformations, linear and nonlinear equivalence in Euclidean space 9-42054
 exchange, 2-dimens. Bethe-Salpeter eqn., computer soln., ladder approx. $P_\pi=0$ 9-34276
 heavy pseudoscalar, coupling const., from N-N scatt., analysis 9-42055
 mass spectra in quark model, mass depend. on quark-meson coupling const. 9-36458
 meson-baryon coupling constants, sum rules 9-48135
 meson-baryon couplings, rescattering eff. in quark model 9-38500
 meson-nucleon Lagrangians, chiral SU(2) \times SU(2) symmetric, construct. 9-27493
 pseudoscalar dynamical calc. of parameters using Lipmann-Schwinger eqn. 9-38542
 pseudoscalar soft, weak mass splittings, SU(3) \times SU(3) algebra calc. 9-27492
 pseudoscalar-meson, neutral, theory; equal-time anticommutator of baryon current, structure 9-44001
 quark model, relativistic formulation 9-44002
 scalar, breaking of SU(3) symmetry 9-32164
 scalar, contrib. to N-N scatt., eliminated 9-44051
 SU(3) canonical metric for classification of meson low energy processes 9-32162
 urbaryon model 9-46109
 η - χ^0 SU(3) singlet-octet mixing angle, expression w.r.t. κ mass 9-25443

Mesons continued

h predicted with $J=1$, $P=-1$, $I=0$, $C=+1$, $G=+1$ 9-22542
 $K^1-\pi^2=K^1+\pi^2$ predicted sum rule for masses of octet bosons. 9-38540
 O^- , rel. to anomalous K_s^0 decay 9-34289
 ρ and f partial widths in $\pi\pi$ scatt., calc. 9-44034
 ρ bootstrap soln. and narrow-width approx., equivalent-potential approach 9-27543

absorption

process, successive stages, expt. results analysis and large mesic mol. model 9-40571

capture

see also *Nuclear reactions and scattering due to mesons*
 No entries

decay

of abnormal charge parity, spin 0 and 1, props. and decay obs. 9-46087
 $\eta \rightarrow \pi^0 \gamma$, radiative decay and relevant spectra 9-38503
 isotopic spin, the 2- and 3- π channels, review 9-40398
 leptonic pair in new two-angle theory of weak and e.m. interactions with $SU(3)$ symm. breaking 9-27480
 O^- , Hamiltonian, current algebra, radiative correction and CP violation 9-36438
 quark-antiquark model with L excitation for 2^+ , 1^+ and 0^+ mesons 9-36485
 semileptonic, new two-angle theory for $SU(3)$ breaking 9-27480
 two-body, strong, in $U_6 \times U_6 \times O_3$ symmetry scheme 9-44003
 vector \rightarrow pseudoscalar + pseudoscalar, in urbaryon model of hadrons 9-46109
 vector-mesons, continuum contribs. using octet-broken $U(3)$ symmetry model 9-27536
 weak, algebraic symm. breaking model rel. to strangeness-changing suppression 9-25440
 $0 \rightarrow K^0 K^0$ in e colliding beams, used to investigate CP violation in $K^0 \rightarrow \pi\pi$ 9-46089
 $0 \rightarrow \rho\pi$ $O(4)$ symm. and particle mixing treatment 9-25472
 1^- selection rule on G^+ parity 9-25472
 2^+ selection rule on G^+ parity 9-25472
 $A_1 \rightarrow \rho^0$ 9-25454
 $A_1 \rightarrow \rho\pi$, partial width, s- to d-wave coupling ratio 9-25457
 A_2 , study using Veneziano model 9-38546
 $A_2 \rightarrow \pi\eta$, crossing-symmetric Regge model applic. 9-38551
 $A_2 \rightarrow KK$ decay mode suppression from $\pi K \rightarrow \rho K$ veneziano amplitude determ. 9-42091
 $A \rightarrow \pi^+ \pi^- \pi^+ \pi^-$ upper limit of 0.2% obs. 9-25454
 $B \rightarrow \omega \pi$, s- to d-wave coupling ratio 9-25457
 $D^0 \rightarrow \pi^+ \delta^-$ after production of D^0 from $\pi^+ d$ interaction 9-38543
 $D^0 \rightarrow \eta \pi^+ \pi^-$ decay at 8 GeV/c 9-48190
 $\delta^- \rightarrow \pi^+ \eta$, after production of δ^- from D^0 decay 9-38543
 ϵ charged mode decay in $K^- n$ interac. rel. to existence of $\eta(550)\pi$ resonance at 980 MeV 9-40433
 η , CP violation 9-22516
 η , cross-section, production, attempt to establish an upper limit, in 400 MeV mass region for neutral bosons, analysis of data 9-22573
 $\eta^0 \rightarrow \gamma\gamma$, $\pi^+ \pi^- \pi^0$, branching ratio meas., Dalitz plot obs. 9-36460
 $\eta^0 \rightarrow \pi^+ \pi^- \pi^0$, $\mu^- e$ branching ratio determ., e.m. C noninvariance 9-40416
 $\eta^0 \rightarrow \pi^0 \pi^0 \pi^0$, $\pi^+ \pi^- \pi^0$, branching ratio meas., Dalitz plot obs. 9-36460
 $\eta^0 \rightarrow \pi^+ \pi^- \pi^0$, T-odd and CP-noninvariant correlation 9-34278
 $\eta^0 \rightarrow \pi^+ \pi^- \pi^0$, T-odd and CP-noninvariant correlation 9-34278
 η and K_1 meson-pole models 9-32173
 $\eta^0 \rightarrow \pi^+ \pi^- \gamma$ and symm. violation 9-22542
 $\eta \rightarrow \pi^+ \pi^- \pi^0$, reduced spectra and sector distrib. calcs. 9-40418
 $\eta \rightarrow \pi^+ \pi^- \pi^0$ and $\eta \rightarrow \pi^+ \gamma$, soft-pion technique inapplicable because of infinite range character of e.m. forces 9-44005
 $\eta \rightarrow \pi^+ \pi^- \pi^0$, new two-angle theory of weak and e.m. interactions with $SU(3)$ symm. breaking 9-27480
 $\eta \rightarrow \pi\pi\gamma$ study using Veneziano model 9-38546
 $\eta \rightarrow \pi\pi\pi$ interference asymm. reduction 9-32165
 $\eta \rightarrow \pi\pi\pi$ $\pi-\pi$ scatt. lengths from veneziano formula 9-44038
 $\eta \rightarrow \mu^+ \mu^-$ obs., branching ratio calc. 9-22574
 $\eta(\eta) \rightarrow \gamma + 1^- + 1^+$, in context of e.m. form factors of hadrons 9-27497
 $I \rightarrow A_1 \pi$, partial width 9-25457
 $K^0 \rightarrow K^+ \gamma$, enhanced decay rate due to PVV interaction 9-38501
 $\lambda \rightarrow \pi N$ $O(4)$ symm. and particle mixing treatment 9-25472
 ω , continuum contribs. using octet-broken $U(3)$ symmetry 9-27536
 $\omega \rightarrow \eta\gamma$, branching ratio determ. by effective mass method 9-42095
 $\omega \rightarrow \pi^0 \pi^0 \pi^0$, branching ratio determ. by effective mass method 9-42095
 $\omega \rightarrow \pi\gamma$, Gell-Mann-Sharp-Wagner model corrections 9-46111
 $\omega \rightarrow \pi\pi\gamma$, analysis using current algebra 9-44042
 $\omega \rightarrow \pi\pi\pi$, Gell-Mann-Sharp-Wagner model corrections 9-46111
 $\omega \rightarrow \pi\pi\pi$ study using Veneziano model 9-38546
 $\rho^0 \rightarrow \pi^+ \pi^- \pi^0$ upper limit of 0.2% obs. 9-25454
 ϕ , continuum contribs. using octet-broken $U(3)$ symmetry 9-27536
 $\Gamma(h \rightarrow \gamma^0 \gamma)/\Gamma(\phi \rightarrow \text{all})$ ratio upper limit 9-44043
 $\phi \rightarrow KK$, radiation correction 9-36488
 $\phi \rightarrow \pi\pi\gamma$, analysis using current algebra 9-44042
 ρ , continuum contribs. using octet-broken $U(3)$ symmetry 9-27536
 $\rho^0 \rightarrow \pi^+ \pi^-$, upper limit 0.2% obs. 9-25454
 $\rho \rightarrow \pi\pi\gamma$, analysis using current algebra 9-44042
 $\rho \rightarrow \pi\pi\gamma$, radiative, investig. using four-point functions 9-29601
 W to 2 pseudoscalar mesons, a pseudoscalar and a vector meson 9-22607
 $W^- \rightarrow \mu^- \nu_\mu$ ang. anisotropy, polarization eff. 9-22606
 $W \rightarrow \pi\pi$, decay rate calc. 9-22607
 $X^0 \rightarrow \eta^0 \pi^0$, $\mu^- e$ branching ratio determ., e.m. C noninvariance 9-40416
 $X^0 \rightarrow \pi^+ \pi^- \eta$, Dalitz plot analysis, $\pi\pi$ mass dependence 9-44041
 2^+ , and $SU(6)$ -symmetry 9-36486

detection, measurement

telescope, meteorological effects and their correction 9-42116
 π , using ΔE detectors 9-44090

effects

π absorption in tissue-equivalent material 9-27123

interactions

see also *Nuclear reactions and scattering due to mesons*
 meson-baryon, by U_6 , peripheral absorpt. model 9-41996
 meson-baryon, multiprod. process cross-sections, asymptotic equalities 9-36459
 meson-baryon, quark model with production of positive parity meson 9-46085
 meson-meson, expressed in terms of canonical metric on $SU(3)$ 9-32162
 meson-N coupled systems soluble model 9-34277

Mesons continued**interactions continued**

meson-N form factor, one boson exchange model and L_2 interaction 9-34318
 neutral-spin-1-meson with parity- nonconserving interac., unrenormalizable theory, analysis 9-42060
 vector mes., Yang-Mill intermediate, weak, strong and e.m. interac. 9-25473
 ρN cross section meas., Glauber theory applic. 9-38483

magnetic moment
 ρ -N coupling magnetic moment as parameter in πN phase shift analysis 9-46103
 ρ agreement between quark model and vector dominance hypothesis 9-34315

mass
 e.m. mass shift in pseudoscalar octet due to vector-meson dominance 9-38501
 mass formula predicted for octet bosons 9-38540
 meson and baryon resonances, mass, spin and parity 9-36498
 nonets, general formulae 9-44004
 vector, axial-vector e.m. mass spectrum in broken $SU(3) \otimes SU(3)$ with quark model 9-44040
 δ^+ , obs. in decay of D^0 9-38543
 K_0 , mass prediction 9-46071
 ρ^0 determ. using $e^+e^- \rightarrow \pi^+ \pi^-$ 9-36474
 D^0 , obs. in $\pi^+ d \rightarrow p p D^0$ at 2.7 GeV 9-38543

production

acceleration, p linear as meson factory, popular article 9-48236
 E-meson, broken $SU_6(6)$ obs. 9-32167
 exotic, from apparent splitting of A_2 peak 9-48201
 high mass bosons, search for in $\pi^+ p \rightarrow p B^-$ at 16 GeV/c near 180° 9-38541
 in photoproduction interactions, new two-angle theory of weak and e.m. interactions with $SU(3)$ symm. breaking 9-27480
 photoproduction of mesons near threshold, using current commutation relations and PCAC 9-22526
 photoproduction of pseudoscalar mesons, moving cut contribs. 9-36463
 positive and negative, comparison of electroprod. cross sections giving pion form factor 9-22593
 positive parity in meson-baryon interac., quark model 9-46085
 pseudoscalar mesons, photoprod., moving cuts contrib. 9-36463
 rector, prod. from polarized targets 9-27443
 synchrocyclotron, 600 MeV, design of meson channel 9-46178
 vector mesons and other resonances photoproduction at 4.3 GeV 9-22609
 0 in $K^+ p$ interac., 4.6 and 9.0 GeV/c, double Regge description 9-29598
 A_1 , $\pi^+ d$ interaction at 8 GeV/c 9-44044
 A_1 in $\pi^- p \rightarrow p B^-$ at 16 GeV/c and near 180° 9-38541
 A_2 in $\pi^- p \rightarrow p B^-$ at 16 GeV/c and near 180° 9-38541
 D^0 , from $\pi^+ d \rightarrow p p D^0$ at 2.7 GeV/c 9-38543
 η , in $\pi p \rightarrow \pi\eta$ at 1050 and 1170 MeV/c 9-32166
 η^0 coherent photoprod. from deuteron 9-42059
 η^0 in $\pi^+ d \rightarrow p p \pi^+ \pi^0$, 3.65 BeV/c 9-34299
 η from (γd) , cross section, ang.-distrib. meas., $E_\gamma=850$ MeV 9-36462
 η^0 , from $\gamma p \rightarrow \pi^+ \eta$, between threshold and 900 MeV 9-44006
 η photoprod. from complex nuclei targets, eta-nucleon cross sections 9-44185
 η photoprod. on p, cross section meas. 9-36461
 η photoproduction < 2 GeV 9-22524
 η photoproduction on ^{12}C , energy below single nucleon production threshold 9-34279
 $\eta(X^0)$ photoprod. cross section calc. by dispersion-theoretic technique 9-36484
 η low-energy prod. in $\pi^- p \rightarrow \eta n$, reson. parameters calc. 9-29596
 $K^*(890)\pi^+$ intermediate state in $K^+ p \rightarrow K^+ \pi^+ \pi^+$, 12.7 GeV/c 9-36468
 $K^*(1300)$, in $K^+ p$ interac., 3.5 GeV/c 9-36489
 $K^*(1400)$, in $K^+ p$ interac., 3.5 GeV/c 9-36489
 ω^0 in $\pi^+ d \rightarrow p p \pi^+ \pi^0$, 3.65 BeV/c obs. 9-34299
 ω in $K^+ p$ interac., 4.6 and 9.0 GeV/c, double Regge description 9-29598
 by $IN \rightarrow VN$, and $eN \rightarrow eN II$, γV analogy model 9-34297
 in $\pi\pi$ diff. scatt. 9-27530
 ϕ photoproduction cross sections in γp , 6.5 17.8 GeV 9-25474
 ρ , in high energy $\pi N \rightarrow \rho \Delta$ reaction, conspiracy relations and $O(3,1)$ symm. 9-38527
 ρ in $\pi\pi$ diff. scatt., self-consistent width 9-27530
 ρ^0 photoproduction cross sections in γp , 6.5-17.8 GeV 9-25474

resonances
 2^+ , $U(6) \times U(6)$ kinematical transforms, and props. 9-32205
 axial vector dynamical calc. of parameters using Lipmann-Schwinger eqn. 9-38542
 boson resonances, review 9-40432
 classification into high-symmetry $SU(3)$ multiplets and suggested mass formula 9-25470
 coupling in 5-pt. Veneziano model, consts. calc. 9-36464
 e.m. corrections, 2nd order to G_0/G_V for β decay 9-38582
 energy relationships for resonance states 9-48177
 exotic, existence inferred, from apparent splitting of A_2 peak 9-48201
 exotic, systematic description 9-22603
 $I=1$, non strange meson, mass 1540 MeV, existence 9-38539
 mass, spin and parity review 9-36498
 mass relationships for resonance states, empirical derivation 9-46084
 mass spectra in quark model, mass depend. on quark-meson coupling const. 9-36458
 May 1966 classification 9-22633
 polarized target expts. 9-27535
 production in 2.7 GeV/c π^+ interactions on deuteron 9-32186
 quantum numbers for meson resonances 9-22605
 quark-antiquark-model with L excitation for $2^+, 1^+$ and 0^+ mesons 9-36485
 rector, prod. from polarized targets 9-27443
 Reggeization into high-symmetry $SU(3)$ multiplets 9-25470
 review 9-36443
 soft, neutral, exchange between nucleons, field theoretic model 9-38574
 spin, information from decay angles 9-44039
 $SU(3)$ multiplet structure for higher meson resonances 9-25471
 $SU(3)$ symmetry breaking, potential model 9-22604
 towers, direct-channel exchange-degenerate, rel. to absence of backward peaks 9-48200
 transformation into photons 9-27459

Mesons continued

resonances continued

tripion, rel. to hadronic corrections to Goldberger Treiman relation 9-38525

unstable particles, mass distribution, admissibility conditions 9-22602

vector \rightarrow pseudoscalar + pseudoscalar, in urbyrion model of hadrons 9-46109

vector, photoproduction, and other resonances photoproduction at 4.3 GeV 9-22609

vector, Yang-Mill intermediate, weak, strong and e.m. interac. 9-25473

vector and axial-vector e.m. mass spectrum in broken SU(3) \otimes SU(3) with quark model 9-44040

vector and tensor exchange processes, Regge pole model 9-32207

vector currents, partial conservation, and breaking of SU(3) 9-48160

vector dominance calc. of ρ mag. moment agreement with quark calc. 9-34315

vector dominance model anomaly found in π^\pm prod. by polarized photons 9-29581

vector mes. prod., Regge-pole model, applic. in $\pi N \rightarrow \rho N$ react. 9-40434

vector meson dominance, implications for photoabsorption in nuclear matter 9-48323

vector meson dominance in photoproduction, modifications 9-46057

vector meson-scalar meson, unequal mass, daughter sequences 9-32163

vector meson-vector meson scatt., coupling constraints determ. from super-convergence sum rules 9-46108

vector mesons obeying similar chiral transformation rules as other hadrons. 9-27478

vector-meson and e.m. fields coupled by current, consistency problem 9-36487

vector-meson decays and algebra of fields 9-32204

vector-meson dominance applic. to photon react. in nuclei, ρ mass eff. 9-22774

vector-meson universality, sensitivity of total X-section relations to small deviations 9-27484

vector-mesons decays, continuum contribs. using octet-broken U(3) symmetry model 9-27536

$\rightarrow \pi \gamma$ radiative decay, investig. using four-point functions 9-29601

0 prod. in K^+p interac., 4.6 and 9.0 GeV/c, double Regge description 9-29598

2^+ , decays and SU(6)-symmetry 9-36486

(K^+K^-) boson, isotopic-spin-1, search in 3.0 GeV K^+ interac. 9-27534

(K^+n) baryon, isotopic-spin-0 or -1, search in 3.0 GeV/c K^+ interac. 9-27534

($K^+\pi^+$) boson, isotopic-spin- $3/2$, search in 3.0 GeV/c K^+ interac. 9-27534

A_1^{++} production in K^+p interactions at 12.7 GeV/c 9-42092

$A_1^{++} \rightarrow \pi^+\gamma$ decay widths 9-32171

A_1 coherent prod. in Freon and H_2 comparison, A_1 -N cross section determ. 9-27541

A_1 -N interaction cross section determ. from A_1 coherent prod. in Freon and H_2 comparison 9-27541

$A_1(\rho\pi)$ enhancement, study using $\bar{K}N \rightarrow \Delta\pi$ 9-48202

$A_1 \rightarrow \pi\rho^0$ 9-25454

$A_1 \rightarrow \rho\pi$ decay, s- to d-wave coupling ratio, partial width 9-25457

$A_1\rho\pi$ decay amplitude spectral density sum rule and zero-mass extrapolation 9-38547

$A_1\rho\pi$ system, hard-pion calc., propagators single meson dominance 9-38549

$A_1\rho\pi$ system, Veneziano model 9-38550

$A_1\rho\pi$ system by current algebra calcs. 9-42089

A_2 , apparent splitting of peak rel. to existence of exotic mesons 9-48201

A_2 , eigenphase shift and double-humped resonances 9-38548

A_2 , structure in KK decay mode 9-44045

$A_2 \rightarrow \pi\rho$, crossing-symmetric Regge model applic. 9-38551

$A_2 \rightarrow \pi\eta$, crossing-symmetric Regge model applic. 9-38551

$A_2 \rightarrow \pi\nu\bar{\nu}$; branching ratio determ. 9-34316

A_2 decay, study using Veneziano model 9-38546

A_2 dipole model, basis for describing angular distribution of $\pi^+\rho \rightarrow \eta N^{*3/2}$ reaction 9-44046

$A_2(1300)$ mass region, $\Lambda\rho^0$ resonance in $K^+n \rightarrow \Lambda\rho^0\pi^-$, spin and parity analysis 9-42064

$A_2(1300)$ mass spectra, double pole explanation 9-25476

$A_2 \rightarrow KK$ decay mode suppression from $\pi K \rightarrow \rho K$ Veneziano amplitude determ. 9-42091

$A_2 \rightarrow \pi^+\pi^-\pi^+$, spin and parity anal. of Dalitz plot in A_2 region 9-29602

$A_2 f^0\pi \rightarrow \pi\pi\pi$, Dalitz-plot density and decay density, decay matrix elements 9-34314

$A_2 f^0\pi \rightarrow \pi\pi\pi$, f^0 Dalitz-plot density decay matrix elements 9-40435

$A_2\pi$ scatt., hard pion current algebra and dispersion relations results, comparison 9-32187

A_1 , kinematic-ambiguity-free test 9-22612

$A \rightarrow \pi^+\pi^-\pi^+\pi^-$ upper limit of 0.2% obs. 9-25454

$A\rho\pi$ system hard-pion calc., algebra-of-fields current commutators 9-38538

B, kinematic-ambiguity-free test 9-22612

$B \rightarrow \omega\pi$ decay, s- to d-wave coupling ratio 9-25457

$B \rightarrow \rho$ exchange in Regge pole model for $\pi N \rightarrow \omega N$ 9-32188

C^0 in $\pi^+p \rightarrow \pi^+C^0$ react., quark-model predictions for joint decay distrib., 8 GeV/c 9-38528

C in $pp \rightarrow KK\pi\pi$, width, mass, spin and parity determ. 9-22614

χ^0 SU(3) singlet-octet mixing angle, expression w.r.t. κ mass 9-25443

$D^0 \rightarrow \pi^+\pi^-\pi^0$ decay after production for D^0 from π^+d interaction 9-38543

D^0 , observed in $\pi^+p \rightarrow \pi^+\pi^+\pi^-\pi^0$ at 8 GeV/c 9-48190

$\delta^{\pm} \rightarrow \pi^+\pi^-$ decay, after production of δ^0 from D^0 decay 9-38543

η^0 prod. in $\pi^+d \rightarrow \pi\pi^+\pi^0$, 3.65 BeV/c 9-34299

$\eta(550\pi)$ at 980 MeV, found in the reaction $K^+n \rightarrow \Lambda\pi^-$ neutrals, absent when η decays by charged modes explained 9-40433

η^0 low-energy prod. in $\pi^+\pi^-\eta$, reson. parameters calc. 9-29596

F^0 in decay of $A_2 \rightarrow \rho^0\pi \rightarrow \pi\pi\pi$, Dalitz-plot density and decay matrix elements 9-40435

F^0 in decay of $A_2 \rightarrow \rho^0\pi \rightarrow \pi\pi\pi$, Dalitz-plot density and decay matrix elements 9-34314

$f \rightarrow A_1\pi$ decay, partial width 9-25457

$f(1260)$ rel. to Mandelstam representation of $\pi\pi$ scatt. 9-22601

G^0 in $\pi^+\rho \rightarrow \pi^+\pi^+\pi^0$, mass distrib. meas., $E_\pi=4.7, 5.74$ GeV/c 9-29603

$g(1650)$, spin $J^P=1^-$, from $\pi\pi$ scatt. 9-34311

K^0K^0 evidence for $I=0, J=0$ state 9-34291

K^+ in mass sum rule $K^2\pi^-\pi^0$ predicted from SU(3) \otimes SU(3) charge algebra 9-38540

$K^2\pi^0=K^+K^+2^-$ predicted sum rule for masses of octet bosons. 9-38540

Mesons continued

resonances continued

K^* (890) prod. in Kp interac. at 6 GeV/c 9-25449

$K^*(890)$, production and decay props., in $YK\pi$ final states 9-27522

$K^*(890)\pi^+$ intermediate state in $K^+\rho \rightarrow K^+\pi^+\pi^-$, 12.7 GeV/c 9-36468

$K^* \rightarrow K^+\pi^-$, enhanced decay rate due to PVV interaction 9-38501

$K^* \rightarrow K^+\pi^-$, rate determ. using effective Lagrangian 9-48203

K^* production in $pp \rightarrow K^+K^-\pi^+\pi^0$, $E_p=1.2$ GeV/c 9-32220

$K^* \rightarrow K\rho$ radiative corrections to the K -meson β decay 9-27545

$K^*(1420)$ splitting predicted from A_2 splitting using mass sum rule 9-38540

$K^*(1300)$ in $\pi N \rightarrow \Delta K^*(890)\pi$ reaction 9-48202

$K^*(1300)$ prod. in K^+p interac., 3.5 GeV/c, decay modes, widths, X-sections and branching ratios 9-36489

$K^*(1320)$ from K^-p 10 GeV/c interaction, spin-parity assignment 9-46112

$K^*(1400)$ prod. in K^+p interac., 3.5 GeV/c, decay modes, widths, X-sections and branching ratios 9-36489

$K^*(1420)$, $K\omega$ and $K\eta$ decays, upper limits, from K^+p collision obs. 9-36467

$K^*(890)$, from K^-p and K^+p , fit to production by Reggeized helicity amplitudes 9-34282

$K^*(890)$ production from KN interac., Regge pole anal., $M_K=2-13$ GeV/c 9-22583

$K^*(892)$ double-reson. prod. in K^+p 9-42094

$K^*(892)$ obs. from K^+p collisions, $K^*(892)\pi^+$ enhancement 9-36467

$K^*\pi$ and $\Delta\pi$ diff. prod. systems in 12.6 GeV/c K^+p interactions 9-22615

$K\pi$, evidence in 3.0 GeV/c K^+ interac. 9-27534

$K\pi$, near 1.1 GeV, evidence in $K^+\rho \rightarrow K^+\pi\Delta^{++}$ 9-25444

κ , and K_1 form factors 9-44009

κ , mass estimation from spectral function sum rules 9-34317

$\kappa(725)$, obs. in K^+p collisions 9-36467

L from K^-p 10 GeV/c interaction, spin-parity assignment 9-46112

$N^*(1240)$, description using Z=0 conditions 9-25475

ω^0 partial decay width, from e^+e^- annihilation obs. 9-29545

ω^0 prod. in $\pi^+d \rightarrow \pi\pi^+\pi^0$, 3.65 BeV/c 9-34299

ω decay, continuum contribs. using octet-broken U(3) symmetry model 9-27536

ω exchange in N-N scatt repulsive core and nonstatic effects in momentum space 9-44050

$\omega \rightarrow \eta\gamma$, branching ratio determ. by effective mass method 9-42095

$\omega \rightarrow \pi^+\pi^0$, branching ratio determ. by effective mass method 9-42095

ω photoprod., γp cross section and t distrib. meas., $E_\gamma=16$ GeV 9-27537

ω prod. in K^+p interac., 4.6 and 9.0 GeV/c, double Regge description 9-29598

ω production in $\pi N \rightarrow \omega N$, ρ -B Regge pole exchange model 9-32188

$\omega \rightarrow \pi\gamma$, Gell-Mann-Sharp-Wagner model corrections 9-46111

$\omega \rightarrow \pi\eta\gamma$ decay, analysis using current algebra 9-44042

$\omega \rightarrow \pi\pi\pi$, Gell-Mann-Sharp-Wagner model corrections 9-46111

$\omega \rightarrow \pi\pi\pi$ study using Veneziano model 9-38546

$\omega\pi\pi$ in $I=1$ state at mass of 1695 MeV, evidence 9-46110

$\omega\rho\pi$ vertex, Lagrangian chiral tensor determ. 9-22610

P production in $\pi N \rightarrow \pi\pi N$, interference effects 9-25477

$\pi^-\eta$, (mass of 0.98 GeV), prod. in $K^-n \rightarrow \Lambda^-\pi^-\eta$ reaction at 4.5 GeV/c 9-34313

$\pi^+\pi^-$ pairs, resonance search, photoproduction, in mass range 1360-1780 MeV 9-44024

$\Pi N \rightarrow V N$, and $eN \rightarrow eN \Pi$, γ -V analogy model 9-34297

$\pi(2190) \rightarrow \rho^0\rho^0\pi^0$, formation in pp interaction at 1.32 GeV/c 9-34312

$\pi\pi\pi$ diff. scatt., prod. 9-27530

$\pi\pi\pi$ decay, Dalitz plot 9-40424

$\pi\rho$ scatt. double charge exchange, existence of high mass resonances 9-29588

ρ^0 production from e^+e^- annihilation, $K^0K^0\pi^0$, 3π decay modes meas. 9-29599

$\Gamma(h \rightarrow \rho^0 \gamma)/\Gamma(\rho \rightarrow \text{all})$ ratio upper limit 9-44043

ρ decay, continuum contribs. using octet-broken U(3) symmetry model 9-27536

ρ photoprod., γp cross section and t distrib. meas., $E_\gamma=16$ GeV 9-27537

$\rho \rightarrow KK$ decay, radiation correction 9-36488

$\rho \rightarrow \pi\eta\gamma$ decay, analysis using current algebra 9-44042

ρ -hadron coupling constants from π, K, Ξ scatt. sum rules 9-22611

N coupling magnetic moment as parameter in πN phase shift analysis 9-46103

ρ -hadron coupling constants from π, K, Σ scatt. sum rules 9-29600

ρ , description using Z=0 conditions 9-25475

ρ , e.m. mass difference and tensor currents, spectral function sum rules 9-27538

ρ, f^0 , degenerate trajectories, bootstrap determ. by FESR 9-38545

ρ , first Regge recurrence, decay widths 9-38551

ρ , in quark model, Regge trajectory, N/D multichannel eqn. 9-38537

ρ , magnetic moment agreement between quark model and vector dominance hypothesis 9-34315

ρ , parameters determ. using $e^+e^- \rightarrow \pi^+\pi^-$ colliding beam expts. 9-36474

ρ^0 photoproduction, sum rules from field algebra 9-27542

ρ^0 prod. from $p\bar{p}$ interac., decay direction determ., $E_p(\text{polar})=2-2.5$ GeV 9-40436

$\rho^0 \rightarrow \pi^+\pi^-$, upper limit 0.2% obs. 9-25454

$\rho^0 \rightarrow \pi^+\pi^-\pi^0$, upper limit 0.2% obs. 9-25454

ρ^+ isovector form factors from vacuum- ρ^+ matrix elements 9-25426

$\rho^+ \rightarrow \rho^0$ mass difference, current-algebra and dispersion relations calc. 9-27539

$\rho^+ \rightarrow \rho^0$ e.m. mass difference, self-consistent calc. 9-27540

ρ bootstrap in $\pi\pi$ scatt., unitarized strip approx. method 9-27544

ρ decay, continuum contribs. using octet-broken U(3) symmetry model 9-27536

ρ dominance and PCAC consistency condition in πN scatt., dispersion-theoretic derivation 9-34308

ρ exchange in N-N scatt. repulsive core and nonstatic effects in momentum space 9-44050

ρ in mass sum rule $K^2\pi^-\pi^0$ predicted from SU(3) \otimes SU(3) charge algebra 9-38540

ρ O(4) expansion of Bethe-Salpeter eqn. 9-38520

ρ prod. in high energy $\pi N \rightarrow \rho\Delta$ conspiracy relations and O(3,1) symm. 9-38527

ρ prod. in $\pi\pi$ diff. scatt., self-consistent width 9-27530

ρ propagator, isovector hadron current applic. 9-27547

ρ trajectory coupling to $\pi\pi$ system 9-34311

$\rho \rightarrow \pi\eta\gamma$ decay, analysis using current algebra 9-44042

Mesons continued**resonances continued**

- ρ' new isovector reson., ω - ϕ mixing and vector dominance 9-32206
 $\rho \pm B$ Exchange in Regge pole model for $\pi N \rightarrow \omega N$ 9-32188
 $\rho\omega\pi$ vertex and Weinberg sum rules 9-42090
 $\rho\pi$ scatt., hard pion current algebra and dispersion relations results, comparison 9-32187
 $\rho\pi\pi$ decay amplitude spectral density sum rule and zero-mass extrapolation 9-38547
 $\rho\Sigma$ elastic scatt., superconvergence sum rules 9-42093
 σ -model renormalization in absence of baryon field 9-22608
 ΣK prod. in $\pi\pi$ reacts., two particle exchange model 9-29619
 V production from πN interaction, helicity amplitude reggeization, production cross section determ. 9-34304
 W , emission and reabsorption in quark model, matrix elements and Cabibbo angle 9-32203
 w , in $\pi^+p \rightarrow N^{*++}w$ react., quark-model predictions for joint decay distrib., 8 GeV/c 9-38528
 W partial decay rate, search 9-22607
 $W \rightarrow \mu^+ \nu_\mu$ ang. anisotropy, polarization eff. 9-22606
 x_0 , current algebra and branching ratios 9-38544
 X^0 width calc. by representing $X\pi \rightarrow \eta\pi$ amplitude with a Veneziano formula 9-42088
 $X^0(960) \rightarrow \gamma\gamma$, spin and parity determ. 9-29597
 $X^0 \rightarrow \eta\pi^+\pi^-$, $\mu\pi$ branching ratio determ., e.m. C noninvariance 9-40416
 $X^0 \rightarrow \pi^+\pi^-\eta$, Dalitz plot analysis, $\pi\pi$ mass dependence 9-44041
 C , relativistic many-channel reson. formula, test 9-22613

scattering

- broken-symmetry sum rules from superconvergent dispersion relations 9-27495
 finite energy sum rules for meson-meson scatt. 9-42056
 meson-baryon, backward differential cross section calc., N and Δ Regge trajectory exchange 9-27494
 meson-baryon, broken $SU_6(6)$ obs. 9-32167
 meson-baryon, charge-exchange and hypercharge-exchange react., analysis for total X -section relations sensitivity to deviations 9-27484
 meson-baryon, decouplet superconvergence relations 9-42057
 meson-baryon, static, Cutkosky bootstrap eqns. for degenerate baryon mass. 9-38557
 meson-baryon, SU_3 , continuous moment sum rules saturation 9-46086
 meson-baryon $35 \otimes 56$ low energy scatt., Lagrangian construction 9-38502
 meson-baryon scatt., superconvergent sum rules and J -plane singularities 9-29565
 meson-baryon total cross-section prediction, CHKN model energy depend. 9-36490
 meson-meson, finite energy sum rules 9-42056
 meson-meson scatt. length, chiral $SU(3) \times SU(3)$ calc. 9-25441
 meson-meson total cross-section prediction, CHKN model energy depend. 9-36490
 meson-nucleon, Regge pole model test 9-40417
 pseudoscalar mes., broken-symmetry sum rules from superconvergent dispersion relations 9-27495
 pseudoscalar octet-pseudoscalar octet, equal mass, unitarity, $SU(3)$ and selfbreaking 9-25442
 Regge and fixed poles in Veneziano model 9-27496
 scalar meson scatt., branch point and vanishing or total cross-section at infinite energy 9-38440
 soft-meson theorems, systematic tests and $SU(3) \otimes SU(3)$ symm. breaking theorem 9-22572
 two-particle, multichannel process in static limit, crossing and unitarity 9-22571
 vector meson-scalar meson, unequal mass, daughter sequences 9-32163
 vector meson-vector meson scatt., coupling constraints determ. from superconvergence sum rules 9-46108
 Veneziano model, algebraic realization of chiral symmetry 9-42036
 $\pi^+\rho \rightarrow \pi^+\rho^+$ Veneziano model 9-29588
 $\pi\omega \rightarrow \pi\omega$, Veneziano-type model 9-46101
 ρ bootstrap soln. and narrow width approx., equivalent-potential approach 9-27543
 $\rho O(4)$ expansion of Bethe-Salpeter eqn. 9-38520
- spin and parity**
 of abnormal charge parity, spin 0 and 1, props. and decay obs. 9-46087
 asymmetries of space and time in particle physics 9-22515
 isotopic spin rel. to nonelectronic decay, review 9-40398
 meson and baryon resonances, mass, spin and parity 9-36498
 ofresonance formed in πN and KN type react., spin-rot. parameter meas. method 9-22570
 triplet-odd nucleon-nucleon interaction 9-34378

Mesosphere see Atmosphere**Metal-insulator-metal structures see Semiconducting devices/tunnel and interface devices****Metal-insulator-semiconductor structures see Semiconducting devices/tunnel and interface devices****Metallo-organic compounds see appropriate metal compound headings****Metallurgy**

- see also Ageing; Zone melting and refining*
 alloys, applic. of elec. resistivity meas. 9-46932
 casting, u.s. 9-37275
 electron fractography, two-stage replica technique using Bioten 9-39151
 filamentary composite materials, developments and prospects 9-44796
 film preservation during specimen preparation by epoxy-sandwich technique 9-35193
 hot rolling of strip, slip-line fields and deformation 9-23944
 inclusion analysis by colour X-ray images 9-48851
 metallizing 9-46915
 Nimonic 80A, creep and fracture under static and superimposed cyclic stresses 9-33048
 orbital grinder-polisher for preparation of irrad. specimens 9-39465
 overstraining to reduce subsequent brittle failure risks 9-33070
 plaster moulds, capillary action 9-30703
 plastic/carbon two-stage replication of irrad. materials for electron microscopy 9-39445
 porous materials, resin-impregnation method of specimen mounting to isolate voids and microcracks 9-39485
 powder, applic. high energy rate densification applic. 9-35226
 solid-state reactions, kinetics, Cu and Cu-Be alloy, intense u.s. energy influence 9-28380

Metallurgy continued

- steel, 304, stainless, residual surface stresses, meas. technique and results 9-33102
 steel, Cr-Mn, equilibrium diagrams for weld metals 9-23976
 steel, electron probe microanalysis 9-49398
 steel, low C, explosively produced spall fractures, metallographic features 9-26354
 steel, Ni maraging, effect of shot peening on fatigue props. 9-26315
 steel, rail, structure effect on rate of propag. of fatigue cracks 9-33092
 steel strip, compacting from powder, popular article 9-48918
 steels, C, Mn-containing, determ. of N content 9-46940
 stresses, residual, surface of 304 stainless steel, meas. technique and results 9-33102
 superconductor, type II, hardening mechanism 9-49044
 vacuum chamber, large, performance during 10000 hour 2200°F test 9-38172
 welded clad metal diffusion layer structure 9-40983
 welding, electron beam, delineation and penetration 9-29380
 welding and cutting, gas flow mechanisms, flash Schlieren photography 9-33983
 AL-10wt.%Pu fuel elements, injection casting in Pyrex molds 9-22897
 AgCl sheets, high quality, prod. method 9-31723
 Al-Zn-Mg alloy, effect of shot peening on fatigue props. 9-26315
 Al-(30 at.%)Zn alloys, side-bands in Debye-Scherrer patterns 9-46936
 Al alloys, treatment for high strength, patent 9-26376
 AlN, hardness, infl. of high static and dynamic pressures 9-26361
 Be, improper preparation, effect on microstructure 9-39446
 Be foil, preparation for transmission electron microscopy using chemical saw 9-39256
 Cr-Mn steels, equilib. diag. for weld metals 9-23976
 Fe-(30 at.%)Ni-(5 at.%)Nb austenitic alloys, structure and hardening, comments 9-46934
 Fe-(30 at.%)Ni-(5 at.%)Nb austenitic alloys, structure and hardening, comments 9-46933
 Fe-Ni, treatment for low temp. use, patent 9-26362
 Fe grain growth, strain induced 9-42788
 Mg and alloys, book 9-39447
 Na, liquid, interactions with 304 stainless steel electron microscope observations 9-28209
 Nb alloy, diffusion-coated, preparation for optical metallography 9-35208
 Ni-Cr alloy ball-milling, addition of inorganic salts for prod. of very fine powder 9-23932
 Si-containing alloys, inclusions, i.r. absorpt. obs. 9-35213
 Sn-Pb, dilute alloys, electropolishing procedure to produce etched or polished surfaces 9-39959
 Sn, electropolishing procedure to produce etched or polished surfaces 9-39959
 SnTe-As₂Te₃ quasibinary system, metallographic exam. 9-42920
 Ti-(20 at.%)Nb alloy, props. determ. by electron and opt. microscopy, correlation with supercond. props. 9-39603
 U-(3.96 at.%)Si alloy, structures, effect of fabrication and heat treatment variables 9-33124
- Metals**
see also Alloys; Semiconductors; Semimetals
 acoustic resonances in plates, e.m. excitation 9-48957
 adhesive interaction with diamond 9-23930
 adsorption of CO, i.r. spectra obs., effect of other gases 9-35002
 anelasticity, improved meas. apparatus 9-35151
 antiferromagnetic, magnetic excitation spectrum in long wave limit 9-37669
 antiferromagnetic, magnetoresistance 9-26659
 antiferromagnetic, spin waves in mag. field 9-28638
 aqueous metal nitrates, Raman spectra, types of interaction 9-44569
 band structure from field emission meas. 9-37628
 b.c.c., flow stress at low temp. 9-33051
 b.c.c., glide band broadening at yield point 9-32938
 b.c.c., lattice geometry for time slip planes 9-33050
 b.c.c., low temp. strength, contrib. from interstitial solutes 9-41028
 b.c.c., screw dislocation mobility, effect of core structure 9-26284
 b.c.c., slip planes controlled by Peierls mechanism, geometry 9-44710
 b.c.c., slip problem 9-44769
 b.c.c., solution hardening, comments 9-46911
 b.c.c., solution hardening, comments 9-46912
 b.c.c., strain-hardening effects, plastic deform. 9-37239
 b.c.c., surface energy anisotropy and equilibrium shape 9-36937
 b.c.c., work hardening at low temp., theory 9-46924
 bearings, fatigue cracks by reciprocating rubbing 9-41032
 casting, u.s. 9-37275
 cavity erosion, from collapse of cavities formed by elec. discharge in liquid 9-48675
 charge model, screened uniform 9-44864
 chemisorption of CO, CN and hydrocarbons, π -electron systems and bond energies 9-39948
 cold working and annealing, struct. changes and effect on flow 9-46925
 composites, controlled solidification using monovariant eutectic reactions 9-36921
 conductivity, elec., temp. depend. at low temps. 9-44902
 contacts, metal-GaAs, resistance impurity conc. dependence 9-30953
 corrosion, meas. of atmospheric factors 9-24565
 corrosion protection by anodic metal dispersion, patent 9-23946
 crack strength calculation methods for sheet-metal parts 9-23919
 crystal, single, body centred, deformation by rolling, patent 9-28285
 crystallization kinetics and cryst. growth mechanism 9-36992
 crystals, melt-grown, microsegregation and cryst. perfection 9-37060
 cubic, face orientation determ. from dodecahedral etch pits 9-48784
 cubic, Gruneisen parameter determ. 9-24059
 cyclotron resonance expts. 9-35324
 deformation, high-speed mechanism 9-23875
 deformation of single cryst. during ion microscope exam. 9-39235
 diamagnetic resonance in mag. field normal to surface 9-31019
 dielec. functions of surfaces, freq. derivatives, apparatus for direct meas. 9-33367
 with dielectric coatings, reduction of photoelectron emission near u.v. region 9-26612
 dielectric const. determ., improved high reflectivity ellipsometry method 9-35462
 diffusion, meas by high temp. electrochem. method 9-46841
 diffusion (radiotracer) studies, use of microtome to obtain suitable surfaces 9-46843

Metals continued

- diffusion of interstitial H, phase diagrams and solubility meas. for gas to liquid transition 9-35122
 diffusion-coated, high-temp. oxidation 9-48870
 domain structure theory under de Haas-van Alphen effect conditions 9-30828
 ductile failure due to cup-and-cone fractures, scanning electron microscopy 9-48896
 elastic fatigue, reinterpretation 9-42897
 electrodes, anodic behaviour in 1M sulphamic acid-formamide solns., polarization curves 9-31202
 electron plasma, positron excitation and annihilation 9-30824
 electron radiation damage 9-30592
 e.m. wave transmission through slab, effect of boundary scatt. on helicon transmission near cut-off 9-26491
 emissivity rel. to surface roughness 9-43233
 inengineering and economy of industrial society 9-23958
 e.p.r. investigation, techniques, book 9-38338
 e.s.r., 'selective transmission', review of results 9-28743
 e.s.r., anisotropy effects 9-47427
 exchange effects, second-order, in localized moments 9-35527
 fatigue strength after deposition, combined effects of macro- and microstructures and residual stresses 9-39434
 fatigue strength in welded joints, effects of reactive stresses 9-23902
 f.c.c., accommodation of constrained deformation by slip and twinning 9-26281
 f.c.c., cyclic deformation and fatigue, eff. of slip character 9-30674
 f.c.c., elastic interaction between Frank dislocation loops and glide dislocations, activation energy 9-39359
 f.c.c., evaporated, nuclei shapes, stability obs. 9-32895
 f.c.c., ion-bombarded faceting influence on ejection patterns 9-44853
 f.c.c., neutron irradiated, voids 9-41119
 f.c.c., strain-hardening effects, plastic deform. 9-37239
 f.c.c., surface energy anisotropy and equilibrium shape 9-36937
 f.c.c. diffusion of H₂, activation energy 9-23841
 f.c.c. film, diffraction line broadening rel. to particle size and strain 9-44657
 ferromagnetic, hyperfine fields on impurities 9-45255
 ferromagnetic, multiband theory of inelastic neutron scatt. at low temp. 9-33447
 ferromagnetic, pore size effect on remanence ratios 9-43172
 ferromagnetic, spin wave theory corrections 9-45092
 ferromagnetic, spin-wave impurity excitations rel. to reduced susceptibility function 9-47235
 ferrous, corrosion tests after 7 years atmospheric exposure 9-24564
 film, monocrystalline, with lattice defects, elec. conductivity and thermoelec. power 9-37434
 film, quantum oscillations of thermodynamic props. in weak mag. field 9-30812
 film, thin, optical const. and thickness during deposition, continuous ellipsometric determination 9-32845
 film, ultra thin, elec. conduction by tunnelling through substrate 9-24122
 film, vacuum deposition prep. process on plastic, patent 9-28218
 films, discontinuous, electrical conduction by anomalous quantum-mechanical tunnelling 9-35331
 films, evaporated, energy loss of low energy protons and deuterons 9-28439
 films, thin, oxidation problems 9-39950
 fine grained, strength rel. to diffusion creep 9-46897
 in flames, fluoresc. yield rel. to underpopulation of doublet excited states 9-48379
 flow stress, temp. depend, rel. to plastic deform. 9-39418
 foil, e.m. compression for transient MOe mag. field prod. 9-47894
 foil, thin; ω_1 surface plasma waves prod. by light excitation 9-25941
 foil with oxidized stressed surface layer, bending 9-31189
 fracture criterion 9-44776
 fragmentation behaviour of explosively-loaded thin-walled cylinders, rel. to expansion velocity and material parameter dependence 9-42901
 friction coeff. with rocks, in air and u.v. vacuum, comparative estimate 9-26359
 galvanomagnetic tensor, approximate expression 9-37433
 h.c.p., Mossbauer hyperfine structure of ⁵⁷Fe 9-49255
 h.c.p., strain-hardening effects, plastic deform. 9-37239
 heat capacity, d.c. elec. pulse meas. technique 9-30779
 heat transfer between metallic surfaces in contact, surface roughness and waviness effect 9-24037
 heat transfer between two dissimilar surfaces in contact, effect of thickness 9-24035
 heat transfer between two metallic surfaces in contact, effect of surface oxidation 9-24036
 heat transfer between two similar surfaces in contact, theor. model 9-24034
 helicons, attenuation and polarization 9-39616
 hexagonal, elastic wave vibr. modes orientation depend. and assoc. dislocation damping 9-48890
 hexagonal, monocrystal growth 9-30515
 h.f. wave dispersion curves 9-44904
 high and low melting point, zone refining techniques review 9-23674
 hot workability and plastic deform. props. 9-35174
 impurity localized, mag. fields effects in s-d exchange model 9-47220
 with impurity localized moments sub-Mondo temp. props. 9-45041
 interface, model for electron structure 9-36936
 intermetallic cpds., D1₃ struct. type 9-39243
 interparticle distance correl. with interionic separation at melting point 9-35007
 ion beams, sputtering yields on polycryst. films 9-44854
 irradiated or quenched crystals, sweeping-up of dislocation loops by glide dislocations during deform. 9-32963
 Kubo formalism and relaxation of localized moments 9-35526
 laser beam effects on 28 pure subst., fracture zone depend. on conditions 9-48909
 laser beam interaction, time-dependent liquid-vapour ratio 9-48738
 magnetic moments, local correlation effect on occurrence 9-45042
 magnetic surface levels 9-49001
 magnetoresistance, microwave 9-35332
 mean free path, anisotropic, from galvanomagnetic meas. 9-37386
 metal, b.c.c., solute effect on low temp. strength 9-41028
 metal, skin effect in mag. field, rel. to h.f. conductivity 9-49018
 metal cyanides, magnetic susceptibilities meas. 9-24276
 molten bridge, microscopic, props. and rupture, rel. elec. contact 9-40799

Metals continued

- Mossbauer effect on impurity nuclei, linewidths, magnitude and isomer shifts 9-45284
 n.m.r. absorption in region of Doppler-shifted cyclotron edge 9-47441
 noble, Fermi surface, effect of elastic deform., determ. using thermoelec. power 9-44884
 non-transition, effect of nonmag. transitional impurities on supercond. critical temp. 9-24134
 nonferromagnetic, interaction of spin and cyclotron waves 9-33427
 nucleation phenomena in liq. to solid transform. 9-48736
 ordering, early stages, applic. of model for diffusion on cubic lattices 9-30622
 oxidation, logarithmic, Uhlig model 9-31190
 oxidation, logarithmic, Uhlig model 9-31191
 oxidation, parabolic law 9-39951
 oxidation kinetics, influence of vacancies 9-28794
 oxidation mechanism at elevated temp., in non-steady state range 9-41448
 oxide films, reactively sputtered, optical props. 9-30487
 oxide powders, partially reduced by Co²⁺ and Ni²⁺ high-coercivity 9-49212
 oxides, X-ray fluoresc. analysis, use of thin metal film standards 9-47483
 with paramagnetic impurities, spin density fluctuation spectrum 9-43149
 with paramagnetic impurity, inelastic electron scattering 9-37383
 with paramagnetic-impurity nuclei, spin relax. rate 9-28640
 particles, fine, prep. by gas evaporation method with plasma jet flame 9-33128
 particles in vacuum, field emission, effect on motion and energy of charged particles 9-31003
 phase stability, review 9-48936
 plasma contact, secondary emission electron energy spectrum 9-37633
 plastic behaviour, effect of superimposed vibrs. 9-39419
 plastic deform. props. in rel. to hot workability 9-35174
 plastic flow, rate-depend. constitutive relation w.r.t. dislocation motion 9-37257
 plastic working, introductory book 9-38286
 plates, ferromagnetic reson. field and linewidth, ang. depend. 9-45364
 polyvalent, non-transition, review of investigations on optical props. 9-31063
 positron annihilation, lifetime, γ pairs distribution 9-24112
 properties, practical limitations and industrial applications rel. to ceramics, book 9-23961
 pure, laser beam effects, fracture zone depend. on conditions 9-48909
 pure spectrochemical analysis of admixtures 9-49394
 quenching, explt. techniques and results 9-42907
 reflectivity, diffuse near i.r. 9-39800
 refractory, high temp., thermal and elec. conductivity, and total emissivity 9-39537
 review, crystals for research and technological applications 9-36971
 sandblasting rel. to glow-curve characts. of exo-electrons 9-47212
 seal, ceramic-to-metal, formation, patent 9-24995
 seal, ceramic-to-metal, composition, composition, patent 9-24996
 secondary multicharged ions prod. by bombardment, origin 9-47216
 sheet, anisotropic plasticity from stress/strain curves in tension 9-30657
 sheet, planar directionality and re-formability rel. to prestrain 9-35200
 single crystal growth from melt 9-23675
 solid, high temp., complex thermal characts. meas. 9-24039
 spectra, strong emission line shifts in compressed Ar, obs. 9-48377
 stability of 3-D elastic bodies 9-36165
 stacking fault energies, precise determination 9-32976
 strength rel. to diffusion creep 9-46897
 structural, corrosion in sea-water, fresh-water and tropical atmos., 16 year exposure exam. 9-24566
 structural anisotropy, stereology 9-46914
 superconductive, positron annihilation 9-26501
 surface, field ionization rel. to Fermi-surface struct., tunnelling probabilities obs. 9-47218
 surface, field ionization rel. to Fermi-surface struct., tunnelling probabilities obs. 9-43146
 surface, laser-heated, time-resolved temp. meas. 9-32835
 surface energy, rel. to vacancy concentration 9-32830
 surface energy anisotropy and equilibrium shape 9-36937
 surface impedance and boundary scattering anomalous stain depth conditions 9-37426
 surface impedance in weak mag. field, field strength and electron surface reflection depend. 9-26514
 surface microcraters prod. by laser pulse ordering rel. to purity 9-46715
 surface recomb. efficiencies of atomic O 9-28791
 surfaces, rough, reflectivity, plasmons coherent contrib. 9-35317
 testing by u.s. transducer, patent 9-38303
 thermal conductivity, metals, absolute method 38-345°C 9-39540
 thermal conductivity, related parameters 9-39535
 thermal conductivity, state of knowledge 9-39539
 thermal diffusivity meas., effect of pulse width 9-28432
 thermal radiation, e.m. tunneling between highly absorbing media 9-37372
 thermoelectric power meas. at low temp. using superconducting galvanometer 9-30982
 thermomigration 9-28309
 thin films, d.c. sputtering with r.f.-induced substrate bias 9-23634
 transformation o antiferromag. semiconductor in strong mag. field 9-24168
 transformation of antiferromag. semiconductor in strong mag. field 9-37505
 transport coeffs. meas. w.r.t. temp. 9-41157
 twin boundaries, coherent, free energy and surface free energy 9-44714
 u.s. direct generation 9-37321
 u.s. emission under stress, meas. and recording tech. 9-37324
 u.s. wave generation in metals electromagnetically 9-39513
 vapour press meas. by atomic absorpt. spectrophotometry 9-23608
 whiskers, axial screw-dislocation search 9-48853
 X-ray emission, 100-1000 eV electron bombard obs. 9-25013
 X-ray emission and absorpt. spectra, soft, threshold behaviour 9-49302
 X-ray emission spectra, behaviour near high-energy Fermi edge, theory 9-31119
 H content, n.m.r. determ. 9-43345
 O in Ti and refractory metals, conc. by fast neutron activation analysis 9-26851
 V₂O₃, positron lifetime spectra rel. to semiconductors to metal transition 9-47063

Metals continued

V_2V_3 , metal-semiconductor transition, critical pressure 9-44921

liquid *see Liquid metals***theory**

see also Crystals; Electron gas; Plasma

acoustic wave generation by e.m. radiation 9-26422

alkali metals, electron-ion interaction rel. to Fermi surfaces 9-26478

Anderson model, self-consistent solution 9-41130

Brillouin zones, occurrence and construct., influence on Fermi surface shape 9-39563

carrier density and mobility meas. for two-band model 9-39580

charged impurity screening, mag. field effect 9-33218

core electron spectra, characts. structure due to electron-plasmon coupling 9-44861

dilute, screening, nonlinear Thomas-Fermi eqn. soln. 9-47019

elastic constants of simple metals, pseudopotential calc. 9-46862

electrical conductivity in mag. field, hydrodynamic mechanism 9-30838

electron gas, approx. screening functions 9-41144

electron gas, shear viscosity 9-49011

electron liquid, screening of fixed charge 9-41124

electron relax. time from magnetoacoustic oscillations and tilt effect 9-47072

electron spin polarization around mag. impurity, calc. using Kondo effect 9-41287

electron work functions in free-electron model 9-41276

electron-gas model, size effects on diamagnetic susceptibility 9-24102

electronic struct. of random lattice, Green's function, coexistence of local and band character 9-33216

electronic structure of pure metals 9-47024

electronic structure of pure metals 9-47023

electronic transition model under high press. for groups IA and IIA 9-44873

e.m. oscillations, spontaneous excitation at freq. of several Hz 9-44862

e.m. waves absorpt. rel. to surface roughness 9-45268

energy, Wannier representation 9-35303

Fermi ellipsoid with anisotropic relax. time, magnetoconductivity 9-44903

Fermi energies, meas. for two-band model 9-39580

Fermi liquid, impure, charged and neutral, transport coeffs. 9-47785

Fermi momentum determ. from annihilation spectra, valence electrons calc. 9-33229

Fermi surface 9-48992

Fermi surface rel. to electronic props. of pure metals 9-47024

Fermi surface w.r.t. free electron model, Brillouin zone influence on shape, transport props. depend. 9-39563

Fermi-Thomas response of surface to external point charge 9-44620

field evaporation and ionization processes, static-field penetration and atomic polarization effects 9-43137

film, optical props., non-local theory 9-26703

galvanomagnetic effect, quantum mech. calc. in metals with mag. break-down 9-35333

galvanomagnetic phenomena in quantum limit 9-30837

helicon propag. in slab-shaped samples, quantum oscillations, dispersion relations 9-43049

hot-electron relax., Boltzmann eqn. study 9-47020

light scattering by itinerant spin-density excitation 9-47372

localized mag. moments, self-consistency conditions 9-37641

magnetic, time-reversal degeneracy in electronic band structure 9-47034

with magnetic impurities, orbital degeneracy effects 9-24269

with magnetic impurities, Kondo resistivity of interacting pair 9-24270

magnetic ordering, coupled spin-plasma waves, interaction with charged particles 9-41297

magnetite, double-exchange, electron-hopping process and metal-nonmetal transition 9-41168

monovalent, cohesive energies from virial theorem applic. 9-39179

oxides, covalency 9-44637

perturbation theory and alloying behaviour, Hg-Mg system 9-44860

perturbation theory and alloying behaviour formalism 9-44859

phonon frequencies from electron-phonon interaction modification with correlation effects 9-35308

phonon frequency and electron-phonon interaction in strong mag. field 9-26471

point defects, elec. props., Boltzmann eqn. soln., utilization of symmetry 9-32943

pseudo potentials, local, leading to effective interionic pot., rel. to analytic behaviour of electron-ion form factor 9-35305

pseudopotential calc. of elastic constants of simple metals 9-46862

Ruderman-Kittel-Kasuya-Yosida indirect-exchange interaction, temp. depend. 9-37639

sound absorpt. in quantizing mag. field for open trajectory case, giant oscillations 9-39517

spin waves, quantum, in non-ferromag. samples 9-47025

spin-orbit coupling of transition metal impurity in noble metal 9-47303

structure-dependent energy, cancellation of orthogonality charge 9-24088

surface, electron distrib., self-consistent props. 9-47052

surface, static-field penetration and atomic polarization effects 9-43137

surface pot. charact., in free-electron model 9-41276

surface roughness rel. to e.m. wave absorpt. 9-45268

transition metals, chemisorption of H, self-consistent model 9-24548

Wannier functions and interatomic forces 9-24080

X-ray absorpt. and emission, one-body theory exact solution 9-28706

X-ray absorpt. and emission singularities, first-order parquet calcs. 9-24435

X-ray absorpt. and emission singularities, self-consistent treatment of divergences 9-26760

X-ray emission spectrum, soft, electron-interaction effects, formalism and first-order theory 9-24434

Al, constant-energy surfaces, Korringa-Kohn-Rostoker calcs. 9-26479

Al, Hartree-Fock calc. of single-orthogonalized-plane-wave binding energy 9-24081

Au, electronic props and hyperfine interactions, pressure dependences, relativistic calc. in Wigner-Seitz model 9-26481

Bi, deform. pot. for electrons and holes 9-33252

C, dynamically compressed, metallic state existence 9-30847

Cu, core electrons, momentum distrib., anisotropy 9-30820

Cu Wannier function localization 9-26482

Hg-Mg system, perturbation theory and alloying behaviour 9-44860

LiH, pseudopotential approach, electron gas obs. 9-33222

Metamagnetism *see antiferromagnetism; Ferromagnetism***Meteorites**

see also Meteors

1969, April 25, path over British Isles, description of breakup 9-43639

1969, April 25 in N.Ireland, path and analysis of specimens 9-47680

age determ. of 2×10^7 yrs. from radioactive rare gas analysis 9-24889

Arizona crater fragments, applic. shock loaded Fe alloy obs. 9-43636

chondrite (C3 and C4), with opaque and microcryst. structure, Mexican fall (1969) 9-38088

chondrites, bronzite (H group), ^{87}Rb - ^{87}Sr age 9-43635

chondrites, rare earth abundances, radiochemical neutron activation analysis 9-29077

chondritic, N abundance 9-49586

dust, airborne collections at remote sites 9-37869

fall, Chihuahua, Mexico, (1969) specimen obs. 9-38088

ionization cross section, upper atmosphere ion distrib. determ. 9-31621

iron, transition from Widmanstätten & granular struct. in same sample 9-43637

isotopic composition, Kr and Xe 9-49393

microchondrules coalescence and decrease of volatiles in chondrites, cosmo-petrological significance 9-38087

micrometeorite flux on earth estimated from density of interplanetary particles 9-43645

minerals as detectors in study of chem. comp. of nuclei of $z > 22$ in cosmic rays 9-34343

olivine-granet transformation 9-27089

orgueil, magnetite content determ. by X-ray diffractometry 9-31622

Pueblito de Allende, anal. for organic constituents 9-43638

stony, composition, analytical data and assessment of quality 9-45672

stony, composition, sample preparation and x-ray fluorescence methods 9-45661

stony, composition some inter-element relationships 9-45673

Tungus meteorite fall of 1908, Dirac matter hypothesis 9-36028

Tunguska, rel. to upper atm. cond., airglow and geomag. field 9-26916

type I, carbonaceous, magnetite content determ. by X-ray diffractometry 9-31622

whitlockite, correlation between fission tracks and fission-type Xe from extinct radioactivity 9-34415

^{39}Ar in stone and iron meteorites 9-24888

Ca and ^{40}K produced by cosmic rays in iron meteorites, surface ionization mass spectrometric obs. 9-40182

Fe, search for Si in metal phase, rel. to Earth core models 9-41683

Fe, shock loading effects rel. to thermal history 9-24886

Fe, shocked, unshocked, Mossbauer spectra using reson. scatt. technique 9-24887

Fe, trace element distrib., analytical methods used 9-28835

^3H in stone and iron meteorites 9-24888

^{53}Mn in iron, neutron activation analysis 9-39974

N abundance in chondritic meteorites 9-49586

Ti stable nuclides, cosmic ray produced, surface ionization mass spectrometric obs. 9-38089

U content in stone meteorites, and Pu-Xe decay interval 9-45675

V stable nuclides, cosmic ray produced, surface ionization mass spectrometric obs. 9-38089

$^{50}\text{V}/^{51}\text{V}$ abundance ratio in chondrites and comparison with ratio in terrestrial matter 9-41681

Xe and Kr isotopic composition, anomalies 9-41682

Meteoroids *see Meteorites***Meteorological instruments**

see also Anemometers; Hygrometers; Ionosphere measuring apparatus

aerial sensing of atmospheric moisture concentration and movement 9-35810

dew point dynamic determ. method suitable for use on radiosondes 9-26895

Doppler radar system for wind turbulence meas., feasibility study 9-31308

radar, c.w. pseudorandom coded, for precipitation and cloud studies 9-43379

rain gauges, airflow around 9-49445

wind, remote sensing of vector velocity by optical heterodyne measurement of Doppler shifts 9-33766

Meteorology

air-sea interaction 9-26891

aircraft soundings of potential gradient, space charge and conduction current, relation to precipitation 9-26906

autumn rainfall correl. with winter temperatures 9-31287

balance equation, derivation of elliptic condition in spherical coordinates 9-24635

Baltic Sea, water level variations caused by meteorological effects 9-49436

baroclinic instability, presentation for forecasters 9-47526

barometric field numerical forecasting, orographic and frictional effects 9-49446

climatological studies, Dallas area 9-28864

clouds, precipitating, properties meas. by weather radar, feasibility 9-33752

cyclones, developing, energy conversions 9-49449

data rel. to Cosmos obs. of outgoing radiation spectra 9-31314

digital computer applications to weather forecasting 9-41479

energy exchange at earth's surface heat budget equation 9-26892

errors, observational, growth rate investigation methods 9-49444

field data analysis, automation 9-41480

field representation by polynomials and empirical orthogonal functions, possibility 9-41478

forecasting, extended range 9-49443

forecasting of night minimum surface temp. 9-49448

geostrophic wind field, northern hemisphere, zonal harmonic analysis 9-33765

heat and vapour propagation, analysis, Nolan, Pollak and Gardner type condensation nucleus counters 9-24634

heat balance, rad., sea-sky obs. 9-31317

infrared radiation analyses over Antarctic by Nimbus II satellite and balloon 9-24633

meson telescope, meteorological effects and their correction 9-42116

ozone soundings rel. to weather forecasting 9-41473

pairs of drops raised to equal and opposite potentials, comments 9-26899

parameters, analogy with effects of curvature on turbulent shear flow 9-41477

quasi-geostrophic flow, stability 9-24646

synoptic analysis, sequential for linear random fields 9-47527

Meteorology continued

troposphere, inversion layer study by simultaneous lidar and refractometer soundings 9-43380
troughs and ridges, wavelength vars., 500 mb mid. latitude 9-47525
visibility measurement using backscattered light 9-26903
weather modification, review 9-43394

Meteors

see also Meteorites

17 Sept. 1966, fireball photoelectric timing 9-38086
burst, communications absorpt. and multipath propag., Arctic 9-33791
CENFAM multistation radar system, receiving apparatus 9-41614
CENFAM Project for multistation radar system 9-41613
current effects on E_s 9-37983
dust in atmosphere, flux, concentration and collection 9-43384
echoes decay const., rotational motion due to wind gradients 9-36027
electronics, development and history 9-49585
height, beginning, summary of observational data 9-24885
Leonid shower, 1965, Aerobee sounding rocket, exposed surfaces, analyses of particles 9-40181
mass distribution index of meteoroids from amp. distrib. index of underdense radio echoes 9-24884
masses and luminosities 9-41680
meteoric interplanetary matter, piezoelec. detector obs., 10² to 10⁸ km 9-47679
micrometeoroid interaction with atmosphere, size and velocity of particles 9-43633
micron and submicron flux, upper limits, Gemini 12 obs. 9-31620
primaeval fireball, role in classical cosmology theory of galaxies formation 9-26999
radar detect., simultaneous, by spaced stations, probability 9-27088
radio echoes, persistent, wind structure from amplitude fluctuations 9-37933
radio ionization trail mea. 9-47678
radio scatt., communication technique 9-33832
radio-echoes, autocorrelation functions 9-43632
sporadic flow characteristics 9-33944
streams, mass influx and penetration rate 9-31619
trail group, daylight photo, red glow beneath possibly due to large conc. of small particles 9-43634
trail obs. of upper atm. winds 9-41547
trails, radiowave reflection calc. 9-31618

Metrology *see Measurement; Mechanical measurement*

Mica

Alpine, fission track ages 9-47509
etch-pit counter for neutrons 9-22914
fission track ages, 250 and 2500 m.y. 9-47510
and glass detectors for neutron beam recording 9-34360
kersantites, chem. composition and phys. props. 9-32898
lamproites, chem. composition and phys. props. 9-32898
minettes, chem. composition and phys. props. 9-32898
muscovite, as substrate for growth of ammonium iodide 9-37037
muscovite, cleavage study by spectrometry by Auger electrons 9-42742
muscovite, dislocation planes, electron microscopy 9-23748
muscovite, ruby, thermal expansion coeffs., anisotropy 9-44839
muscovite elec. conduction, breakdown, barrier action mechanism 9-37587
ruby muscovite, thermal expansion coeffs., anisotropy 9-44839
substrate for CdSe and CdTe vapour phase deposits growth on cleavage face 9-46726
substrate for epitaxial growth of SnTe 9-30492
surface conductivity, effects of annealing temp. and mag. field 9-47153
Ag film deposition, inclined fault concs. rel. to presence of various gases 9-35097
OH bonds, i.r. spectroscopic obs. 9-31099

Micelle systems *see Colloids*

Microanalysis *see Chemical analysis*

Microhardness *see Hardness*

Micrometeorites *see Meteorites*

Micrometry

see also Interferometry; Strain gauges; Thickness measurement

No entries

Microphones

see also Transducers

for musical instrument, ceramic reed mounted on instrument, patent 9-40277
sound ranging appl., square array, azimuth and elevation determ. 9-29284
switch, for pneumatic tube position indication in nuclear reactors 9-22913
toroidal, directional characteristics toroid shaped, design 9-43788

Microphotometers *see Densitometry*

Microprobe analysis *see Chemical analysis; X-ray*

Micropulsations *see Earth/magnetic field variations; Magnetic storms*

Microscopes

see also Electron microscopes; Ion microscopes

design, guiding factors 9-46011
flat-field objectives 9-36341
fluorescence, NUZ research instrument 9-48100
interference, double-refracting, variable image duplication and half-shade eyepiece 9-43923
i.r. polarizing 9-38409
objectives, image performance testing and optical transfer function meas. 9-46013
phase contrast, effect of varying conjugate area of phase plate 9-27400
school model 9-27399

Microscopy

see also Electron microscopy

chemical, in historical optical examination 9-26846
composite materials, analysis 9-46943
contrast developed by vapour-deposited multi-layer system 9-46764
electron-probe microanalysis, X-ray prod. and electron scatt. predictions using Boltzmann eqn. 9-36092
exit pupil holographic enlargement using partially coherent light 9-22466
ferrites, sintered, residual pores behaviour obs. 9-42921
field ion, improved contact procedure 9-30832
field-ion, applic. to particle size distrib. analysis 9-33117
field-ion micrographs, distinction of intrinsic from extrinsic stacking faults 9-32977

Microscopy continued

field-ion micrographs of lattice defects, computer interpretation 9-23808
forensic applic. 9-25333
in forensic science 9-27397
holographic, review 9-48061
holography, total internal reflection, applic. 9-41927
interferometry of thin films, replication method 9-23622
ion, sample with structural defects, method of formation 9-40936
particle size distribution determ. rel. to dynamic methods 9-48101
photo, for non-Newtonian velocity profiles determ. 9-46588
photomicrographs of inorg. chem. crystal precipitation 9-41458
polarized, for optical crystallography, book 9-48777
polymers, trace contamination identification 9-49391
specimen surface temp. meas. equipment 9-40288
steel, Fe-(2.0 wt.%)V-(0.2 wt.%)C alloy, field-ion study of carbide particle coarsening 9-33118
ultramicrophotography with microscope objectives 9-43934
X-ray materials science applic. bibliography 9-23721
Au film, on W, field-ion and field emission obs. of props. 9-23624
Co, field ion, observation of surface defects caused by chemisorbed layer 9-26827
Fe, a<110> dislocation, field-ion, evidence for existence 9-30609
Fe, field ion, observation of surface defects caused by chemisorbed layer 9-26827
Fe film, on Ir, field-ion and field emission obs. of props. 9-23624
Fe stacking fault, field-ion microscopic obs. 9-40962
Mn-Ni constitutional diagram, microstruct. obs. 9-39502
Mo-Zn alloys prepared by reduction of volatile halides, phase diagram obs. 9-39466
Nb, etch pits and sub-boundaries obs., contribution to diffusion 9-32985
Ni, field ion, observation of surface defects caused by chemisorbed layer 9-26827
Pb-Na solid solns., effect of Ag on discontinuous precip. 9-39500
Pt, quenched, secondary defect obs., e. microscopy and field ion microscope exam. 9-23815
Re surface phenomena obs. by field emission and field ion microscopes 9-46719
Si, precipitation of boron 9-37164
Ti-Al-Co alloy system, Ti-rich corner struct. obs. 9-40919
W-(1wt.%)Gd₂O₃ alloy, ion microscope exam. of matrix 9-41057
W, field evaporation from edges of (111) plane 9-26181
W polycrystalline, cold worked and annealed, preferred grain orientation from ion microscope exam. 9-40889

Microstructure of crystals *see Crystal structure/microstructure; X-ray examination of materials/microstructure*

Microtomes *see Biological technique and instruments; Laboratory apparatus and technique; Microscopy*

Microtrons *see Particle accelerators*

Microwave spectra *see Spectra*

Microwave spectrometers *see Spectrometers, radiofrequency*

Microwave techniques and devices

90° roof resonator, X-band model 9-27313
capacitor filled with plasma, microwave emission 9-38329
cavities, supercond. tuning 9-37482
cavity, cylindrical, eigenvalues from hollow-cathode discharge 9-36219
cavity perturbations by lossy dielectrics and plasmas 9-41859
cavity resonator for studying elec. susceptibility of ionized gases 9-34136
detector, gas, employing opto-acoustic eff. 9-28077
detector and a p-i-n reflection modulator for F band appl. 9-33354
dielectric thin rod, reflection coeff. at 9.3GHz 9-38341
Doppler shift demonstration apparatus, X-band, single antenna 9-43709
electron concentration decrease in air afterglow, meas. using cavity technique 9-44505
ferrite, development 9-43840
ferrites, props. 9-45172
ferrites waveguide resonator quick evaluation of characts. rel. to analog phase shifters 9-43815
ferroelectric ceramic subjected to strong field, parametric interaction mechanism 9-43111
frequency doubling, quantum mechanical, in ruby 9-25139
gas jet ionization for plasma production 9-30263
gas laser, submillimetre-wave, theory and construction 9-31937
generation and amplification, conference, Hamburg (1968) 9-31868
hologram, microwave, photoetching technique 9-34183
hypersonic waves in quartz, excitation by slow-wave structure, comparison with cavities 9-36236
interferometer, three-branch X-band, design and construction 9-38332
klystron, quasiperiodic focusing with permanent magnets 9-31869
klystron, reflex space charge effect on starting current and reflector voltage 9-41852
laser modulation by CS₂ Kerr cells 9-36285
LSA oscillator diode, analytic theory for ling samples 9-26573
magnetoplasma, microwave scatt. from fluctuations 9-23318
magnetoplasma scatt. diagnostics 9-23318
optical bench for undergraduate experiments 9-36218
parametric amplifier, band extension using two uncoupled resonators 9-36248
plasma blast-wave, laser-produced, cavity meas. 9-42499
plasma column electron distrib. meas. using microwave cavities 9-48584
plasma column profile meas. using resonant cavities 9-48583
for plasma diagnostics 9-34773
plasma electron heating method 9-30211
plasma excitation at upper hybrid resonance 9-32665
plasma phase shifter, theory and applic. 9-27993
polarimetry for permittivity meas. to 1200°C 9-38342
radar study of Venus at 3.8 cm 9-29071
rod deformation measurement 9-30636
second harmonic generation and sum and difference freqs. by inhomogeneous semiconductor 9-35387
for semiconductor carrier lifetime and mobility meas. 9-33292
Sommerfeld and Brillouin precursors in microwave domain, exptl. obs. 9-34116
sweep system for cyclotron beam 9-38626
travelling-wave semiconductor devices using space harmonic interactions in metal strip mosaic overlays 9-24207
velocity modulated tubes 9-47908
waveguide component, dielectric A/4-transformer, transformation parameters determ. 9-40294
zero bridge for e.p.r. superhet spectrometer 9-40298

Microwave techniques and devices continued

- Al laser-produced plasma, diagnostics 9-23319
 BaTiO₃, microwave absorpt. by free carriers 9-31101
 GaAs epitaxial diodes, fabrication and switching applic. 9-43085
 GaAs epitaxial microwave diodes, fabrication and switching applic. 9-43085
 GaAs filled waveguide, mm. wave generation by mixing CO₂ laser lines 9-31083
 GaAs Gunn oscillators with p-n junction contacts prod. and characteristics 9-39649
 Nb, superconducting TM₀₁₀ mode cavity with high electric field and Q₀ 9-24148
 ZnO thin film acoustic delay lines, prep. using vapour transport technique 9-48767

Mie theory see *Scattering*

Milky way see *Galaxies/the Galaxy*

Mineralogy see *Minerals*

Minerals

see also *Mica; Quartz; Ruby*

- aggregates, fine-grained, modal analysing using electron microprobe scanning pictures 9-39971
 albite, artificially produced alpha-recoil tracks for dating 9-47511
 alexandrite, (Al₂₋₃Cr₃BeO₄), anti-phase boundaries, electron microscope obs. 9-35104
 alkali feldspars, symmetry in granite of Plan de la Tour (Var) 9-28226
 allcharite, comparison with new species ruginite 9-30574
 analcite, piezoelec. effect 9-43121
 andalusite, from synthetic aggregates, isothermal compressibility 9-44761
 apatites, fission track ages 9-45462
 apophyllite, (KFCa₂Si₈O₂₀.8H₂O), p.m.r., rel. to position of protons and diffusion of H₂O mols. 9-47447
 aragonite, transformation to calcite to lime, electron microscope obs. 9-26385
 attapulgite, orientated, suspension in aqueous soln., light scattering studies rel. to effect of alt. elec fields 9-34929
 basalt, porphyritic alkali, Sr isotope disequilibrium 9-31276
 biotites, Mossbauer obs. of Fe ordering and ferrous-feric ratio 9-41367
 calcite, tunable four-photon optical parametric noise, 4300-5860 Å 9-49253
 calcite crystals, cleavage surface energy, infl. of Fe, Cu and S trace impurities 9-30479
 chalcopyrite, ⁵⁷Fe Mossbauer spectra, quadrupole splitting meas. 9-35634
 clinopentstatite, inversion at high temp. 9-42934
 clinopyroxenes, lattice parameter b, rel. to Al content and ionic substitution 9-30554
 coesite-tishovite transition, 550 to 1200°C and 82 to 98 kb 9-28399
 curienite, PB(UO₂)₂(VO₄)₂.5H₂O, analysis rel. to francevillite, cry. struct. props. 9-37147
 diorite, hornblende-biotite quartz, magnetization self reversal, nonreproducible 9-43501
 dolomite, cryst. defects, X-ray topographic obs. 9-32958
 elastic constants and rotated press. and temp. derivatives, data on 10 compounds 9-44748
 far i.r. spectrochem. analysis 9-45432
 faujasite, dehydrated La-exchanged, position of mols and cations at 420°C 9-32899
 faujasite, hydrated Ca-exchanged, positions of cations and molecules 9-30556
 faujasites, synthetic, rare earth ion exchange props. 9-24527
 feldspar separated from sands, thermoluminesc. rel. to accident dosimetry 9-49609
 feldspars, alkaline, Na-K exchange, microscopic obs. 9-37810
 ferromagnetic, demagnetization of remanent magnetization by pressure application 9-24710
 fluor-phlogopite, nucleation and growth from vapour polytypism obs. 9-37010
 fluorapatite, dislocation arrangements 9-42826
 fusain-argillite layers, impulse elec. breakdown, disruption of stronger component 9-45004
 geothite, occurrence on Mars 9-49580
 germanate albite under pressure, synthesis and phase change 9-42933
 grandidierite, (Mg, Fe)Al₃Si₃BO₆, crystal structure 9-30564
 granite of Plan de la Tour (Var), symmetry of alkali feldspars 9-28226
 gypsum, pulsed-n.m.r. line shapes, computation and analysis 9-43294
 gypsum, X-ray spectrochem. analysis, 2θ values 9-47484
 hematite single cryst., magnetoelectric props. 9-31049
 henritermierite, Ca₃(Mn_{1.5}Al_{0.5})(SiO₄)₂(OH)₄, tetragonal hydrogarnet, cryst. struct. 9-32905
 henritermierite, Ca₃(Mn_{1.5}Al_{0.5})(SiO₄)₂(OH)₄, chem., spectrographic and microprobe obs. 9-32906
 huebernite, MnWO₄, mag. struct. 9-43194
 Illite, Mossbauer effect obs. of Fe ion 9-37698
 ilvaite, iron oxidation states and site symmetries determ. by Mossbauer spectrometry 9-24381
 kersantite micas, chem. composition and phys. props. 9-32898
 kimirite (hydrated Ba feldspar), satellite occurrence in inverse lattice 9-46782
 koninckite, cry. symmetry, powder diag., X-ray obs. 9-37140
 kyanite, from synthetic aggregates, isothermal compressibility 9-44761
 laboratory spectra, rel. to interpretation of Martian surface composition 9-41678
 lamproite micas, chem. composition and phys. props. 9-32898
 leucophanite, crystal structure confirmation 9-39244
 light absorbing, birefractivity, sign inversion obs. 9-37688
 lucite single crystal, X-ray index of refraction obs. 9-39798
 magnesite, cryst. defects, X-ray topographic obs. 9-32958
 magnetic, thermodynamic props. 9-30776
 magnetite, 30 to 60% in quartz, galvanomagnetic effect 9-43500
 magnetite, inverse thermoremanent magnetization 9-35937
 magnetite, mag. props. change due to gamma radiation 9-37665
 magnetite, magnetic viscosity rel. to demagnetizing field 9-38011
 magnetite, remanent magnetization and coercive force, effect of annealing 9-45570
 magnetite dispersed powder susceptibility for low field intensity freq. independence 9-43502
 magnetostriction in weak fields at liquid nitrogen temps. 9-31476
 mawsonite, birefractivity, sign inversion obs. 9-37688

Minerals continued

- meteoritic, as detectors in study of chem. comp. of nuclei of z>22 in cosmic rays 9-34343
 miargyrite, artificial, struct. for n.q.r. meas. 9-47451
 Mica, heavy particle tracks 9-41123
 microcline, shock compression data, 670 to 580 kb 9-44759
 minette micas, chem. composition and phys. props. 9-32898
 molybdenite, dislocations at contact boundary with Mg films 9-32973
 Montmorillonite, Mossbauer effect obs. of Fe ion 9-37698
 monanite, PbFe₂(VO₄)₂(OH)₂, X-ray powder obs. 9-32925
 muscovite, cleavage study by spectrometry by Auger electrons 9-42742
 natrolite, etching of cleavage faces 9-42745
 oil shale, thermal conductivity, aboveground and in situ meas. 9-26436
 oligoclase, shock compression data, 670 to 580 kb 9-44759
 olivine in upper mantle beneath ocean, statistical orientation rel. to seismic anisotropy 9-33718
 olivine-garnet in meteorite 9-27089
 orthoclase electrostatic forces on faces cleaved in vacuum 9-37571
 periclase, eqns. of state and geophysical implications 9-28843
 perlite, elastic constants rel. to porosity 9-30635
 proustite, crystallization from melt 9-37064
 proustite, growth by Czochralski method 9-37065
 pyrrargyrite, crystallization from melt 9-37064
 pyrrargyrite, growth by Czochralski method 9-37065
 pyrrhotine, mag. props. change due to gamma radiation 9-37665
 pyrrhotite, Fe₇S₈, crystal structure 9-39281
 pyrrholites of Pierreite (Hautes-Pyrenees), thermochem. obs. 9-33657
 rancieite, chem. analysis, X-ray powder diff. and dehydration studies 9-32922
 Rhabdite meteoritic, crystal structure 9-30552
 rock, stratified, spectral analysis 9-28821
 rutile group, second-rank tensor anion polarizabilities 9-37576
 rutile polycrystalline, pressure derivatives of elastic props. 9-39394
 samsonite, crystal structure 9-39246
 sillimanite, from synthetic aggregates, isothermal compressibility 9-44761
 sodium faujasites, synthetic, lattice parameter Al content dependence, framework ion ordering 9-44669
 spectrochem. analysis of Zn, Nb, Be using C cavity electrodes, obs. 9-28828
 sphalerite of Pierreite (Hautes-Pyrenees), thermochem. obs. 9-33657
 spinel, Fe₂SiO₄, Fe_{1.5}Mg_{0.5}SiO₄ and Fe_{1.5}Mg_{0.5}SiO₄ lattice parameters rel. temp. and press. 9-30784
 spinel, thermodynamic stability calc. 9-30784
 β-spodumene, thermal expansion 9-26431
 ultrabasic rocks and carbonates, iodine and uranium contents, neutron activation method 9-45461
 ultramatic rock, elemental abundances and relationship with upper mantle 9-47505
 vermiculites, dehydration, i.r. spectroscopy 9-44658
 welinite (Mn⁴⁺MN₂²⁺SiO₄), crystal structure 9-23764
 wustite lattice parameters rel. to press. and temp. 9-30784
 yugawaralite, Ca₂Al₂Si₂O₇.8H₂O, cryst. struct. 9-39258
 zeolite, Linde L, with Fe³⁺ and FeCl₃, Mossbauer obs. 9-49258
 zeolite, synthetic Linde type-A, dielec. props. with adsorbed vapours 9-41233
 zeolite, Y, Mossbauer effect of exchangeable Fe²⁺ ions 9-43226
 zeolite A, crystallization kinetics 9-23685
 zeolite X and Y, sodium cation adsorption sites 9-24521
 zeolite Y, surface interactions from i.r. spectra of adsorbed aromatic hydrocarbons 9-24520
 zeolite Y, surface props. from i.r. spectra of adsorbed pyridine layers 9-24519
 zeolites, ²³Na and ²⁷Al quadrupole coupling constant changes on sorption 9-43300
 zeolites, A and X, synthetic, applic. in vacuum technology 9-25006
 zeolites, anhydrous, heat of exchange between gaseous ion and ion in zeolite 9-49368
 zeolites, rare earth faujasite-type, crystal chemistry 9-24522
 zeolites, rare earth ion exchange props. 9-24527
 zeolites with faujasite-type framework, distribution of cations and molecules 9-28776
 Ca-Amphiboles, Mossbauer obs. of comp. changes and ferrous-feric iron ratio 9-41367
 Ca₂Al₂Si₂O₇.H₂O, yugawaralite, cryst. struct. 9-39258
 CaO calcite crystals, heavy particle tracks 9-41123
 Fe-Ti oxides in volcanic lavas, model analysis using electron microprobe scanning pictures 9-39971
 Fe ore, sintered, reduction cracking 9-33093
 MgO polycrystalline periclase, elastic parameters rel. to press. 9-42867
 Mn, i.r. spectra obs. on 10 minerals 9-28690
 MnWO₄, huebernite, mag. struct. 9-43194
 MoS₂, rhombohedral, geological conditions of formation 9-48782
 Pb apatites, struct. and spectra study 9-37148
 Pb(UO₂)₂(VO₄)₂.5H₂O, curienite analysis rel. to francevillite, cry. struct., props. 9-37147
 Te compounds, isotopic anomalies of extracted Xe 9-42354
 TiFeS₂, ruginite, crystal struct. and reflection props. 9-30574

Minor planets see *Planets*

Mirages see *Atmospheric optics*

Mirrors

see also *Telescopes/astronomical*

- astronomical, fused silica lightweight blanks 9-25341
 astronomical, lightweight thermally stable blanks 9-25340
 continuous scanning system in high-speed cameras 9-31995
 deformable, with automatic figure control, for space telescopes 9-25339
 dielectric, high-reflectivity, light scattering 9-32020
 dielectric multilayer, phase anisotropy 9-34216
 differential reflecting X-ray filters 9-36337
 electron for beam monochromatization and emission image improvement 9-22351
 electron-optical, image of potential distributions at object surface 9-22352
 of foamed materials, for solar energy concentration, elastic modulus and specific weight 9-32029
 image scanning for high-speed photography, matrix theory 9-31994
 laser cavity, precision alignment 9-36271
 metal, refl. coeff. calorimetric meas. using laser 9-26701
 metal, selectively reflecting 9-32009
 parabolic, c.m. radiation pattern 9-36241
 parabolic, rays from off focal-point source, demonstration 9-29161

Mirrors continued

- parabolocylindrical and spherical concentrators for solar therapy device 9-32030
- paraboloidal surfaces, manufacture 9-32012
- parabolotoidal as solar energy concentrator elements 9-31993
- reflectivity changes due to oil contamination in vacuum rel. to space flight 9-22470
- rotatable for laser Q-switching, patent 9-31932
- segmented, with automatic figure control, for space telescopes 9-27369
- separated spherical, inverse Cassegrainian system, algebraic theory 9-32000
- single and double, geometrical image aberrations 9-36336
- single and double systems, image aberrations, theory 9-40375
- spherical reflector, focal regions 9-31992
- system of two, correction for spherical aberration, coma and astigmatism 9-32002
- Zenith, for astrometrical instruments 9-48102.
- Al, LiF coated, highest reflectance in vacuum ultraviolet 9-32011
- Al, protection from Hg acetate corrosion 9-33672
- Al with MgF₂ overcoating for space flight, optical degradation due to u.v. radiation and condensation obs. 9-40111
- GaAs injection laser, end-surface treatment 9-29432

Mixing see *Heat of solution; Solubility; Solutions*

Moderation see *Neutrons and antineutrons/moderation*

Moderators see *Nuclear reactors, fission/materials*

Modulation of light see *Light/modulation*

Moire fringes see *Interference/light*

Moisture

- see also *Atmosphere/humidity; Humidity; Permeability, mechanical*
- cement paste, drying under temp. gradients, role of moisture diffusion 9-34950
- neutron moderation meas. with depth and surface probes, soil and industrial appls. 9-35765
- in solids, content determ. by neutron moderation 9-39972

Molar volume see *Density*

Molecular beams

- see also *Particle velocity analysis*
- anisotropy parameters determ. from M depend. of total cross-section 9-42468
- beam generator 9-23028
- bimolecular reactions, mol. beam investigation 9-25792
- crossed, effect of speed distrib. on nonreactive scatt. 9-44388
- crossed mol.-electron, metastable species prod. 9-32478
- crystal growth, epitaxial, model 9-26216
- deflection at uncharged conducting surface 9-34575
- diatomic, scattered at solid surface, rotational transitions 9-42364
- focusing, alternate gradient technique, of neutral particles. 9-25728
- interhalogen exchange reactions, molec. beam kinetics 9-49367
- ion-molecule reaction, crossed-beam techniques 9-41442
- ion-molecule reactions, energy depend. of intermediate complex formation 9 49371
- methyl radical, thermal source 9-34606
- paramagnetic, spin wave amplification at interaction with ferromagnet 9-31028
- scattering data anal. 9-38933
- of supersonic origin, with plane symmetry distrib. intensity 9-48451
- Ar, supersonic, intermolecular binding 9-23035
- Ar monoenergetic, scattering by heated Pt 9-44316
- CO₂, supersonic, intermolecular binding 9-23035
- CsF, in selected vib.-rot. states, focused beam prod. 9-27849
- H₂ collision with Li⁺, vibr. excitation meas. 9-25796
- H isotopes, scatt. from Ag(111) surface 9-42713
- H triatomic high-energy, impact on D target, rel. to prod. of H ions 9-46328
- He, on LiF cryst. surface, scatt., theoretical 9-48751
- KBr, r.f. spectrum by elec. reson. 9-27862
- K⁺ oriented CF₃I reaction 9-43320
- Li hydrides, molec. consts. by molec. beam elec. reson. 9-30061
- N₂, atmos., sputtering of Ag and Au deposits at ≈200 km, rel. to surface binding energies 9-24076
- N₂ in metastable E³Σ_g⁺ state, emission spectrum amd radiative lifetime, mol.-beam meas. 9-38863
- NaCl, hyperfine spectrum by elec. reson. 9-44343
- Ni-modified molecular sieves, preparation 9-34605
- O₂, dissociative attachment of electrons, crossed beam expts., effect of O₂ source temp. 9-40623
- Xe, supersonic, intermolecular binding 9-23035

Molecular orbitals see *Molecules/electronic structure; Orbital calculation methods*

Molecular relaxation see *Molecules/relaxation*

Molecular spectra see *Spectra/inorganic molecules; Spectra/molecules; Spectra/organic molecules and substances*

Molecular structure see *Molecules/configuration and dimensions*

Molecular weight

- N-methyl-ethylenethiourea 9-48840
- N-methyl-trimethylenethiourea 9-48840
- polybutadienes, stereoregular Ziegler rel. to viscosity, obs. 9-30379
- polyethylene terephthalate, rel. to mech. props. 9-42863
- polymers, eff. on film-forming 9-25791
- regulation, at emulsion polymerization of butadiene with styrene 9-24551

Molecular weight determination

- air-sensitive compounds, method 9-23008
- copolymer solns. by Archibald ultra centrifugation method 9-28770
- polyindigo from i.r. spectra of soln. 9-27934
- polyisobutenes from gel permeation and gradient elution chromatography 9-32548
- polyisobutylene, calc. from diffusion meas. in very dilute solns. 9-32545
- polystyrene, by sedimentation transport in cyclohexane at Flory temp. 9-28771

Molecules

- see also *Kinetic theory; Spectra*
- chemical shifts of K-shell electron binding energies for first-row atoms in molecules 9-38821
- clathrates, p.m.r. lineshape and chem. shift of enclosed mols. 9-39924
- coordinate systems, relative, description of n particles 9-46255
- diamagnetic; mag. props. induced current density, susceptibility and shielding 9-29999

Molecules continued

- diamagnetic, elec. birefringence, quantum theory 9-46347
- diamagnetic susceptibility, approx. calc., perturbed Hartree-Fock theory 9-30010
- dimers, influence on thermal diffusion factor 9-36686
- dye, association, effect of binary solvents 9-27922
- electron scatt., relativistic scatt. factors 9-30017
- electron scattering, acute angle inelastic, and polarisability of scattering systems 9-44232
- energy levels excitation for energy transfer 9-23007
- ethylene-N₂ mixtures, influence of dimers on thermal diff. factor 9-36686
- field calculation, Fortran IV program, computation of magnetization of a molecular field ferromagnet 9-30013
- force and torque on nuclei of mol. subjected to external e.m. field 9-34600
- fractional parentage coeff., group theory reln. 9-36645
- hydrides, diatomic, first-row, config.-interaction studies 9-38828
- inert gases, neutral mols. prod. by electron-beam pulses 9-44345
- intramolecular reaction spins, NMR Boltzmann eqn. 9-25727
- ionicity, dielectric definition 9-38820
- linear polar, electric Sieflethen-Beenacker effect 9-48644
- matrix formation for kinematic coeffs., algorithm and computer tech. 9-36692
- methanes, halogen-substituted, force consts. ϵ_0 and r_0 9-36807
- moment distribution, case of wave functions with non-integer principal quantum number 9-27792
- monatomic, second order transport relations in fluid 9-46128
- multi-centre integrals; three- and four-centre, calc. 9-29998
- multilevel systems, transition rates 9-36644
- non-polar, randomly distributed in solid, dielectric theory 9-33365
- open-shell mol., effective rotational Hamiltonian, formalism, applic. 9-40582
- optical rotation, higher asymmetry 9-48095
- overlap integrals involving *f* orbitals, potentials for numerical integration 9-32455
- P and T invariance violation, high-precision mol.-beam resonance, proton electric dipole meas. 9-38568
- polar, orientation at solid-liq. interface, i.r. absorpt. spectra obs. 9-46341
- polarizability depend on nuclear co-ordinates, quantum and classical calcs. 9-27840
- polarized, relativistic dynamics 9-27793
- potential curves from spectroscopic data, WKB-method zero order approx. 9-23010
- Rayleigh scatt. of polarized photons 9-34589
- residual gas analysis and leak detection, metastable mols. time-of-flight meas. 9-38170
- resonance radiation and intersecting fields, influence of constant electric and magnetic fields 9-44303
- sensitizing dye, from substrate, regeneration 9-26553
- small polyatomic, wave function calc. 9-30011
- spectra, i.r., and charact. freqs. 700-300 cm⁻¹, a collection of spectra and interpretations 9-34592
- styrene-acrylic-melamine resins, quantitative infrared analysis 9-38914
- symmetric top, quadratic *f*-sum rules 9-23016
- target for negative ions, charge exchange cross-section meas. 9-22980
- triatomic, quantum mech. kinetic energy operator, separation of vib.-rot. motion 9-23021
- velocity distrib. in nonequil. flows, asymptotic solns. for weak shock case 9-30329
- water, dimeric, in atmosphere, presence shown by sub. mm absorpt. expts. 9-33755
- wave function calc. on small polyatomic mol. 9-30011
- Ar-CO₂, He mixtures, influence of dimers on thermal diff. factor 9-36686
- As compounds, infrared and Raman spectra 9-36695
- CO₂-Ar, Kr mixtures, influence of dimers on thermal diff. factor 9-36686
- CO electron reson. scatt., elastic and inelastic channel obs. 9-23057
- H₂, mag. props. 9-27859
- He-Ar mixtures, influence of dimers on thermal diff. factor 9-36686
- Kr-CO₂ mixtures, influence of dimers on thermal diff. factor 9-36686
- Li₂F₂ lin. dimer species, obs. in i.r. matrix spectra of LiF 9-23053
- N₂-ethylene mixtures, influence of dimers on thermal diff. 9-36686
- N₂, electron reson. scatt., elastic and inelastic channel obs. 9-23057
- N₂, electron scatt., low energy neutral bremsstrahlung cross section obs. 9-32423
- N₂ photoionization cross section, electron phase shift calc., simple model potential construction 9-46258
- No, vibr. relax., shock tube meas. 9-38861
- O₂ electron reson. scatt., scatt., elastic and inelastic channel obs. 9-23057
- O₂ electron reson. scatt., and inelastic channel obs. 9-23057
- Rb-rare gas mol. formation, Rb polarized atom relaxation in rare gas, theory 9-32534
- S-As, complexity in cryst., glassy and liq. phases, Raman obs. 9-35675
- S-Sc, complexity in cryst., glassy and liq. phases, Raman obs. 9-35675
- S, complexity in cryst., glassy and liq. phases, Raman obs. 9-35675

configuration and dimensions

- see also *Chemical structure; Crystal structure, atomic*
- bond angle in triatomic mols., determ. from isotopic shifts 9-42417
- p-bromobenzoyl, derivative of ϵ' -caesalpin, molecular structure 9-39324
- chain mols., Monte Carlo simulation 9-42462
- equilibrium geometry of polyatomic mols., *ab initio* calc. 9-40580
- floating spherical Gaussian orbital model 9-23020
- group theory application to structure determ., book 9-42368
- H-bond length, isotope effect 9-42370
- hexaoidobenzene, X-ray investigation, and cry. struct. 9-46799
- iterative calculation of geometry 9-30016
- methyl-pyridinium salts, configuration transformation in excited states obs. 9-34679
- polyatomic, displaying σ , π and 'three-centre' bonds, molecular wave-fn. calc. method 9-44314
- polyatomic, large change of shape transitions, applic. of Franck-Condon factors 9-42361
- polyatomic mols., equilibrium geometries, *ab initio* calc. 9-40580
- polymer, radius of gyration, excluded vol. effect 9-46427
- representation by drawing using digital plotter 9-40587
- symmetry models for undergraduate chemistry course 9-48447
- Fe(III)Cl₃ in methanol, solute structure obs. 9-34878
- N₂⁺ structure determ. using gas phase electron diff. 9-27867
- Pd complex, bis N-t-butylsilylaldiminato]palladium(II), conformation, and cryst. structure 9-23769
- Sb complex, tetraphenylantimony hydroxide, 3-dimen. X-ray diff. obs. 9-42418

Molecules continued

configuration and dimensions, inorganic

- alkali metal metaborates, M-O-B bond angle determ. from force constant analysis of i.r. spectral data 9-32463
 complexes with multidentate ligands, from ^{31}P n.m.r. 9-32460
 transition-metal complexes 9-23744
 $[\text{Cr}(\text{OH})(\text{en})_2]^+$ salts, from X-ray exam. 9-47224
 B_2Cl_4 , electron diffraction determ. 9-44319
 B_2H_6 , comparison of struct. determ. by electron diff. and spectroscopy 9-36713
 B_2O_3 , electron diffraction obs. 9-23029
 BeB_2H_6 9-44318
 BiF_3 , gaseous, thermodynamic functions calc. from molecular geometry and vibration freq. 9-30021
 COH^+ , protonated CO, non-empirical molecular orbital calc. of most stable configuration 9-34613
 ClO radical, equilib. internuclear distance from rotation spectrum 9-38836
 Co complex, bis(tricobalt enneacarbonyl)acetone, and crystal structure 9-39264
 Co complex, $\text{Co}(\text{H}(\text{N})_2[\text{P}(\text{C}_6\text{H}_5)_3])_3$ 9-46361
 Co complex, cobalt (III) tris (N,N-diethyldithiocarbamate, and crystal structure 9-30559
 Co complex, Trans-sulphiteisothiocyanate-bis(ethylenediamine)cobalt(III) dihydrate stereochemistry 9-39265
 Co complex, tris(diethyldithiocarbamate)cobalt (III), and crystal structure 9-44661
 CsOH , struct. refinement 9-44325
 Cu complex, bis-(3-amino-1-phenyl-2-buten-1-ono) copper (II), and crystal structure 9-30560
 Fe complex, (Fe bis-salicylidene- ethylenediamine):O pyridine; oxo-bridge five-co-ord struct. 9-33486
 Fe complex, iron (III)-benzhydryoxamate trihydrate 9-39276
 Fe complex, thio-p-toluoyldisulphidobis (dithio-p-toluato) iron (III), 3-dimen. diff. obs. 9-42785
 $\text{Fe}(\text{CO})_5$, gas phase, electron diff. data, structure refinement 9-38841
 $\text{H}_2\text{B}_2\text{O}_3$, bond lengths molecular-orbital treatment 9-39279
 H_2O , lower excited states, ab initio calc. 9-23046
 H_2O Coulomb and exchange integrals, from Slater type orbitals 9-23019
 H_2O ground state, Hartree-Fock SCF minimal basis calc. 9-38844
 HF gaseous polymers, electron diff. determ. 9-42395
 HNO_3 and DNO_3 , normal co-ord. treatment for physically true force const. in vapour and liquid states 9-46362
 K_2F_2 , from i.r. spectrum 9-25744
 LiBO_2 , electron diffraction obs. 9-23029
 LiO_2 , i.r. 9-44333
 N_4^+ , geometries by approx. SCF-MO theory which considers intermol. differential overlap 9-34637
 NF_3 , equilibrium struct. from microwave spectra in excited vib. states 9-34630
 $(\text{NH}_4)_2\text{Pt}(\text{S}_2)_2\cdot 2\text{H}_2\text{O}$ 9-39288
 NO_2^+ and NO_2^- , geometry 9-48467
 NS free radical, structure, by gas phase e.p.r. 9-46369
 NaAlF_4 , electron diffraction study 9-48473
 NaAlF_4 , electron diffraction study 9-44342
 Ni complex, bis(dimethyldithiophosphato)nickel(II) 9-39296
 Ni complex, dibromotetrapyrazolenickel(II), and crystal structure 9-26243
 Ni complex, hexakis(imidazole) nickel (II) nitrate 9-39295
 O_4^+ , O_4^- , geometries by approx. SCF-MO theory which considers intermol. differential overlap 9-34637
 PF_4 radical, isotropic hyperfine splittings and molec. struct. 9-23065
 PHF_2 , and microwave spectrum and dipole moments, obs. 9-30049
 Pb complex, lead (II) O, O-disopropylphosphorodithioate 9-42794
 Pd complex, diiodo-(N-methyl-o-ansidine) palladium (II) structure 9-25748
 RbOH , struct. refinement 9-44325
 RbOH and RbOD , from microwave spectra 9-38869
 $\text{S}_6(\text{NH}_2)_2$, three isomers 9-39305
 SO_2 , equilibrium structure refinement from rotational spectra 9-32485
 SO_2 in inert gas matrix, bond angles from vibration spectra 9-34641
 SO_2 isotopes, bond angle 9-42417
 SeO_2 in inert gas matrix, bond angles from vibration spectra 9-34641
 Si_2Cl_6 , D_{3h} or D_{3d} models, deduced from vibrational spectrum 9-30056
 SiCl_4 , electron diffraction determ. 9-44319
 Sn complex, dimethyltin dibenzoate, in organic solvents, n.m.r. obs. 9-27875
 Zn complex, 1:1 Zn(II)-malate geometry of ligand, n.m.r. study 9-46400
 poly-p-tolylisocyanate, structure from optical behaviour in soln. 9-27932

configuration and dimensions, macromolecules

- β -adenosine-2'- β -undine-5'-phosphoric acid 9-39316
 adsorbed polymer chain, conformation 9-30503
 biological in solution, conformation effects on gamma ray ang. correl. patterns 9-32536
 catalase, molecular structure 9-23780
 chain, config. correl. 9-44380
 chain config.—a path of quantum mechanical particle, mathematical principles 9-42458
 collagen, struct. study from models 9-43689
 collagen, thermal transconformation, calorimetric investig. 9-23184
 DNA, hydrodynamic properties 9-23415
 helix-coil transition in triple-stranded macromol. 9-48519
 keratins, α - β transformation, statistical mech. 9-36730
 ϵ -methylcaprolactam-caprolactam copolymers, conformational structure 9-32551
 nitroso rubber copolymer, structural study using ^{19}F NMR 9-27939
 poly(α -methacrolein), structure determ. by chem. reactions, n.m.r., i.r. 9-28793
 poly(ethylacrolein), structure determ. by chem. reactions, n.m.r., i.r. 9-28793
 poly(ethylacrolein), structure determ. by chem. reactions, n.m.r., i.r. 9-28793
 poly 1,1 dimethylsilylcyclobutane, i.r. spectrum and struct. 9-27935
 poly- ϵ -methylcaprolactam, structure in ordered state 9-32551
 poly-p-butylisocyanate, structure from optical behaviour in solns. 9-27932
 polybutadienes and polyisoprenes absorptivity determ. 9-30156
 1,3-polydioxalane, conformations in soln. 9-23187
 polyenes, photo and thermal isomerization mechanisms 9-35738
 polyethers, conformations in soln., theory 9-23185

Molecules continued

configuration and dimensions, macromolecules continued

- in polyethylene, irradi., free radicals config. rel. to decay, obs. 9-27936
 polyethylene oxide, conformations in soln. 9-23186
 polyindigo from i.r. spectra of soln. 9-27934
 polyisoprenes, from light scatt. and viscosity meas. in soln. 9-48524
 polymer in soln., math. model 9-30154
 polymers, linear, excluded vol. effect 9-27928
 polymers with polar groups, orienting effect of aqueous phase in emulsion on structure 9-32803
 polymethacrylic acid, viscosimetric investigation of conformation transition on ionisation 9-23196
 polymethylmethacrylate, peculiarity rel. to anomalous minimum in shear stress depend. of viscosity 9-32774
 polytetrahydrofuran, conformations in soln. 9-23186
 PVC, structural depend on precipitation conditions 9-32554
 random-walk model for hydrocarbon-type chains with short-range correlations 9-44379
 reviews 9-23183
 2,4,6-trichloroheptane from NMR and infrared spectra 9-32546
- configuration and dimensions, organic**
 1:2, 5:6-dibenzanthraquinone 9-39320
 3 β -acetoxy-5 β ,6 β -oxidocholestan-19-ol, vicinal H-C-O-H coupling consts., stereochem-depend. 9-46380
 adenosine 5'-monophosphate, from p.m.r., 100 MHz 9-32499
 adenosine 5'-triphosphate, from p.m.r., 100 MHz 9-32499
 alcohol solvation, structure of ion pairs 9-34880
 alkyl radicals, e.s.r. evidence for planar shape 9-44377
 aromatic systems, strained, conformation calc. 9-48487
 aromatic systems, strained, conformational analysis 9-48486
 benzene, molec. distortions and phosphoresc. 9-30081
 benzil in stilbene, trans-planar config. from polarization characs. of spectra 9-34660
 benzocyclopopyrpyran 9-39321
 1,2-benzodithiol-3-one oxime, and crystal structure 9-26258
 benzophenone, and crystal structure 9-46797
 bicyclo [1.1.0] butane, from microwave spectra 9-32504
 3,4'-biisoxazole, intermolecular and bond distances and angles 9-39338
 bis(diphenylphosphino)acetylene, and crystal structure 9-26261
 bis(diphenylmethyl) diselenide, X-ray analysis 9-39322
 α -bromine-anthraquinone, and crystal struct. 9-42799
 2 α -bromo-5 β -bromomethyl-5 α -methyl-2 β -oxo-1,3,2-dioxaphosphorinane, and crystal structure 9-26259
 6-bromoisoferrocene, and crystal structure 9-23784
 6 β -bromoprogesterone 9-39323
 t-butyl N, N-dimethylthiophosphorocarbamate 9-39325
 carboxylic acids, dimeric, in crystals, i.r. obs. 9-30093
 chloroacetaldehyde, n.m.r. study and conformational anal. 9-46655
 chloroacetaldehyde, n.m.r. study and conformational anal. 9-46655
 Chloroform-triethylamine system, dielec. props. rel. to mol. anisotropy 9-48712
 2-chlorotropane-cycloheptatriene adduct 9-39327
 cumene, e. diff. exam 9-23111
 cyclic, superposition links 9-26255
 cyclic phosphazene, $\text{N}_6\text{P}_6(\text{NMe}_2)_{12}$, and crystal structure 9-30583
 cyclohexadienes in gas phase, struct. and conformations by electron diff. meas. 9-46389
 cyclohexane, conformational energy, ab initio calc. 9-38886
 cyclopentane, conformational energy, ab initio calc. 9-38886
 cytosine, p-irrad., free radical produced, theoretical study 9-44354
 dibenzopentadiene, ground-state geometry and symmetry 9-36716
 trans-1,2-dibromide cyclohexane, equilib. conformation and vib. forms 9-36890
 1,2-dibromoethane, intensity temp. depend., energy difference of trans. and gauche configurations 9-44355
 trans-1,2-dichloride cyclohexane, equilib. conformation and vib. forms 9-36890
 3,5-dichloroanthranilic acid 9-35075
 1,2-dichloroethane, intensity temp. depend., energy difference of trans. and gauche configurations 9-44355
 1,1-difluoroethylene, full geometry, determ. from direct couplings in n.m.r. spectra in nematic solvent 9-30105
 digitoxigenin, and crystal structure 9-26260
 p-dihalobenzenes, min. potential config. in heterogeneous nucleation on cleaved alkali halide crys. 9-37105
 3,4-dihydro-2,4,6-triphenyl-s-tetrazin-1(2H)-yl, struct. by crystal-packing anal. and X-ray diff. 9-48516
 1:3-di-imines, N,N' disubstituted, conjugation and configuration from p.m.r. spectra 9-30106
 dimer stable conformation rel. to interaction energy surfaces, formic and acetic acid dimers 9-38822
 dimethoxytrimethylantimony, X-ray diff. determ. 9-30582
 anti-2,6-dimethyl-4-chloro-N-methylbenzaldazine 9-39341
 dimethylgermane 9-42430
 dimethyllead dihalides, I, and Raman obs., 4000-70 cm^{-1} 9-34675
 dimethylsulphoxide, r_s and r_o struct. 9-23138
 dimethyltin dibenzoate, in organic solvents, and n.m.r., obs. 9-27875
 2-(2,4'-dinitrobenzyl) pyridine, and crystal structure rel. to tautomeric reaction on light irrad. 9-30579
 1, 4-dinitroso-2, 3, 5, 6-tetramethylpiperazines, α , β , ϵ , γ , δ isomers, predominant conformations 9-32509
 1, 4-dinitrosopiperazine, conformation from n.m.r. spectrum 9-32509
 4,5-dioxo-2-thioxo-1,3-dithiolan, β form 9-39328
 $\gamma\gamma'$ -dipyridyl-di-N-oxide, internuclear bond angles 9-46392
 dodecadimethylaminocyclohexaphosphazehexaene, (N-P) $_6$ ring cpd., and crystal structure 9-30583
 ethane, r_{calc} / r_{exp} from n.m.r. in nematic phase 9-42433
 estriol, molecular packing and bonding 9-39333
 ethane, comparison of struct. determ. by electron diff. and spectroscopy 9-36713
 ethane, geometrical changes during internal rotation 9-36714
 ethyl fluoride dissolved in nematic liq. cry., structural const. NMR obs. 9-40613
 ethylene, -d $_4$, geometry from vibrational analysis of 1744 Å Rydberg transitions 9-44357
 ethylmercaptan, from microwave spectrum 9-27895
 formaldehyde -h $_2$, d $_2$ and hd, upper state geometrical parameters 9-48496
 glycylglycine hydrochloride, and crystal structure 9-26263
 halogenocyclohexanones, and deuterated derivatives, effects on i.r. spectra 9-23125

Molecules continued**configuration and dimensions, organic continued**

- heptalene, ground-state geometry and symmetry 9-36716
 heterocyclic systems containing 2.41 and 2.64 Å sulphur-oxygen distances, Huckel calcs. 9-46378
 hexameric phosphonitrilic dimethylamide, (N-P)_n ring cpd., and crystal structure 9-30583
 s-indacene, ground-state geometry and symmetry 9-36716
 as-indacene, ground-state geometry and symmetry 9-36716
 L-isoleucine, from crystal structure of bis-(L-isoleucinato) copper (II) 9-26228
 lead stearate, multilayer films, and crystal struct. 9-39349
 metal compounds of some group I, II and III elements, mol. orbital calcs. 9-46403
 methoxytetraphenylantimony, X-ray diff. determ. 9-30582
 methyl cephalonate bromoacetate, X-ray exam. 9-39340
 4-methyl-3-(p-bromophenyl)-1,2,5-oxadiazole, 5-oxide, X-ray diff. obs. 9-40924
 4-methyl-3-(p-bromophenyl)-1,2,5-oxadiazole, 2-oxide, X-ray diff. obs. 9-44678
 methyl diazine 9-34676
 methyl lithium, from n.m.r. meas. 9-46405
 methylthioethyne, bond lengths and angles, microwave spectra investigation 9-48501
 monobromomethylene, C-Br distance from rotational struct. of ν_1 and $2\nu_1$ bands 9-46408
 nitrosamines, heterocyclic, and conformations, n.m.r. studies 9-34682
 nitroxides, conformation effects on hyperfine structure of e.p.r. spectrum 9-44366
 oxalic acid, and -d₂, in gas, i.r. obs. 9-30133
 N-oximes, stereochemical eff. on absolute signs of geminal and vicinal N, H coupling constants 9-30134
 paraffins, linear and cyclic, structure effects on viscosity 9-25776
 pentalene, ground-state geometry and symmetry 9-36716
 pentaphenylantimony 9-23785
 phenylcyclobutane, e. diff. exam. 9-23111
 3-phenylisoxazolin-5-one, X-ray obs. 9-42801
 -3-phenylisoxazolin-5-one, X-ray obs. 9-35077
 2-phenylnaphthalene, rel. to pot. energy, and e struct. and spectra, calc. 9-27911
 phytochrome systems, in light absorpt. mechanism 9-40618
 piperidine iminoxyls, substituted, interconversion 9-38912
 polar mols in nematic solvents, orientation parameters from dielectric const. anisotropy 9-42371
 polymers, chain, in soln., random coil config. and light scatt. with intramol. interac. 9-34905
 polymers, high-resolution n.m.r. examination, review 9-42463
 polymers, structure eff. on film-forming 9-25791
 polypropylene, stereoregularity rel. to i.r. spectrum, obs. 9-30157
 potassium oxalate monohydrate, and crystal structure refinement 9-26265
 n-propyl alcohol, trans. form 9-46416
 propylene, barrier to internal rotation using Gaussian self-consistent field wave functions 9-48506
 propylene-ethylene copolymers, stereoregularity rel. to i.r. spectrum, obs. 9-30157
 pyridoxal phosphate oxime, and crystal structure 9-39344
 2-(2-pyridylmethylthio)benzoic acid 9-39348
 N-quinoline stereochemical eff. on absolute signs of geminal and vicinal N, H coupling constants 9-30134
 quinuclidinyl benzilate hydrobromide 9-35078
 n-radialenes and methyl derivatives, molecular orbital theory 9-32527
 rhodopsin systems, in light absorpt. mechanism 9-40618
 L-serine, chelation effects from crystal structure obs. of bis(L-serinato)cop- per(II) 9-26229
 L-serine, chelation effects from crystal structure obs. of diaquobis(L-seri- nato) nickel(II) 9-26241
 sodium 2-oxoacetate, and crystal structure 9-26268
 spermidine phosphate trihydrate, and crystal structure 9-26269
 terephthalbis(aminofluorobenzene) liq. cryst., config. from n.m.r. 9-28159
 terpenoids, C₂₅, X-ray exam. of methyl cephalonate bromoacetate 9-39340
 tetracyclohexyl- cyclotetraphosphine, symmetry 9-39351
 tricycloquinazoline 9-39353
 trimethylene selenide 9-42447
 trimethyllead halides, i.r. and Raman obs., 4000-70 cm⁻¹ 9-34675
 triphenylborates, from i.r. spectra 9-23164
 triphenylboron, from i.r. spectra 9-23164
 vinyl iodide 9-32533
 xanthone, 3-D symmetry 9-46802
 Fe_x(CO)₆[CH₃-C₆H₄-SO₂-N=C(OCH₃)-CH=CH-C(OCH₃)] 9-26262
 Ga complex, (C₂H₅)₂O.GaCl₃, symm. in solid and liquid states 9-24515
 (N-P) ring compounds, dodecadimethylamine cyclohexaphosphazexah- eane 9-30583
 with N sp²-hybridized, rel. to ¹⁴N n.m.r. shifts 9-25773
 P-F geminal coupling const. sign inversion 9-46412

dissociation*see also Heat of dissociation*

- absorption of line radiation as process of initiation 9-27921
 alcohol, solvation to radical ions, e.p.r. study 9-34880
 butyl benzene, tert., field ionised, vel. const. distrib. 9-25787
 butyrophenone, Norrish type II process during h.f. discharge 9-46545
 diatomic, high temp., photodissociation calcs. 9-23170
 diatomic mols., specific heat maximum caused by dissoc., position deriva- tion, simple calc. 9-39051
 in gas, effect on acoustic waves 9-48663
 H₂ in Venus atmosphere, photodissociation 9-49583
 n-heptane, field ionised, vel. const. distrib. 9-25787
 hydrocarbons, by fast electrons, excited H atom prod. 9-23174
 hydrocarbons C₃-C₈ double charged ions, kinetic energy release 9-40712
 methane + Ar⁺ → Ar + CH₃⁺ + H → Ar + CH₂⁺ + H₂, 1.5-4.2 eV, mechanism: 9-39936
 methanethiol, photodissociation 9-43336
 monocarboxylic acids, dissoc. consts., i.r. spect. study 9-23105
 organic field ionised mols., vel. const. distrib. 9-25787
 phenyldiazonium ions, meta and para substituted, thermal decomposition rates rel. to HMO calcs. 9-27914
 photodissociation translational spectroscopy 9-48513
 polyatomic, ensuing geometrical change and force consts. 9-44307

Molecules continued**dissociation continued**

- scattering products in dissociative attachment, angular dependence 9-34602
 solar facula-photosphere contrast in mol. lines, depend. on dissociation energy 9-41700
 specific heat maximum of diatomic mols. caused by dissoc., position deriva- tion, simple calc. 9-39051
 tetramethylsilane, adsorbed, by electron irradiat., thin Si films deposition obs. 9-44628
 transition-metal diatomic carbides, stability 9-32490
 CO₂-N₂-He-H₂O flowing laser, due to elec. discharge 9-40352
 CO₂-N binary syst., mass transfer cooling of flat plate, depend. 9-25789
 CO₂ in positive column of glow discharge 9-38919
 CO in He⁺-CO collisions, excited C ions form. obs. 9-36724
 CeC, stability 9-32490
 Cl₂, photodissoc. by translational spectroscopy 9-48513
 CoSO₄ in soln. rate determ. using u.s. absorption 9-30397
 CrH, predissociation of upper electronic state of 3680 Å transition 9-42449
 H₂, 2600-7000°K, three-at. recomb. reaction rates 9-25786
 H₂, photodissoc. 9-25785
 H₂⁺ by inelastic collisions between H₂ and H₂⁺, 3-20 keV 9-44375
 H₂⁺ collisional dissociation, ang. distrib. of protons, theory 9-40622
 H₂⁺ ions, angular depend. of dissoc. cross-section and rel. to internuclear distances 9-23169
 H₂ above 1000°K, kinetic props. 9-38920
 H₂ and D₂, by fast electron impact 9-23168
 H₂ dissociation zone in star, rel. to Hayashi effect 9-29021
 H₂O vapour by electron impact, excited H atoms prod. 9-30151
 H₂S, photodissociation 9-43336
 HBr dissociation kinetics in shock waves 9-47455
 (HeH)⁺, collision-induced dissoc. 9-38921
 N₂ atmospheric predissociation, influence on atomic N production 9-28908
 ND₃ electron capture obs. 9-25746
 NH₃, electron capture obs. 9-25746
 NH₃ and ND₃, dissociative attachment of electrons 9-46422
 NH₄Cl, gaseous, stability 9-36726
 NO₂, vac. u.v. photolysis 9-39961
 NiSO₄ in soln., rate determ. using u.s. absorption 9-30397
 O₂, dissociative attachment of electrons, crossed beam expts., effect of O₂ source temp. 9-40623
 O₂ dissociation and i.r. OH emission in aurora 9-33818
 P(V) acids, dissoc. constants 9-23171
 SF₆ in Ar, shock-tube kinetic studies 9-38923
 UC, stability 9-32490
- dissociation energies**
 diatomic mols., influence on position of sp. ht. maximum 9-39051
 specific heat maximum of diatomic mols., influence of dissoc. energy on position 9-39051
 sun photosphere mol. conc. determ. 9-31654
 AuB, mass spectrometric determ. 9-24528
 AuSi 9-46421
 BeCl and BeCl₂ 9-48511
 Ce-C system 9-32821
 Ce₂ 9-48512
 Cs halides, from high-temp. photoionization 9-44373
 F₂ 9-44374
 H₂, binding energies calc. for vibr. levels 9-36725
 He₂ 9-44332
 Na⁺, rel. to ion geometry calc. by approx. SCF-MO theory which considers intermol. differential overlap 9-34637
 Na₂ 9-38922
 O₄⁺, O₄⁺, rel. to ion geometry calc. by approx. SCF-MO theory which considers intermol. differential overlap 9-34637
 SF₆ from RRK theory analysis of shock-tube expts. 9-38923
 TiO 9-23172
 TiO 9-23173
- electronic structure**
see also Bonds
 acetonitrile, formation of solvated electron 9-27880
 asymmetrical pot. mols., vib. band envelopes, computer calc. 9-34622
 atomic electron populations, INDO-MO vs. SCF calc. 9-40586
 bonding, participation of d orbitals 9-40583
 CNDO calc. of small mols., spectra and ground-state props. 9-30007
 comprehensive university level text book 9-32395
 core model for simple-centre calc. 9-42398
 density distrib. calc., new expressions 9-40585
 diatomic homonuclear, three-dimens. FEMO model in term symbol, corre- spondence principle and e. distrib. calcs. 9-38824
 diatomic partition function calc., comparative study 9-44311
 effective electronegativity correlation with vib. freqs. 9-46346
 electron density semi-empirical determ., general eigenvalue theory 9-27841
 electron density semi-empirical determ., general eigenvalue theory 9-27841
 electronic-vibronic interaction, investig. using symmetry theory 9-30005
 energies of electronic transitions, estimation by new method 9-30015
 energy variances for simple mols., lower bounds calc. 9-38814
 floating spherical Gaussian orbital model 9-23020
 Franck-Condon band struct. and spectroscopic closure prop. 9-44304
 free electron model involving potential wells 9-30014
 Green's function for noninteracting particles 9-41735
 Hartree-Fock eqn. for mol. wavefunctions in infinite internuclear separation limit 9-38816
 Hartree-Fock eqn. in restricted Hilbert space 9-34598
 heteronuclear diatomic, bond-charge model for potential energy 9-38806
 homonuclear diatomic mols., bond order 9-42369
 Hulburt-Hirschfelder potential tested by calc. r-centroids of several diatom- ics 9-30018
 integral used in struct. calc. 9-44312
 intersystem crossing processes to individual zero-field levels of lowest triplet state, rate constant 9-42359
 local permutational symmetry and separated-atom limit 9-48368
 MO theory of X-ray K-absorpt. edges 9-39854
 multipole expansions and point charge models 9-44315
 orbital calc. method for alternant orbital calc. without spin projection 9-38815
 orbital calc. using multiple-scattering model 9-34597

Molecules continued

electronic structure continued

- orbitals, multicentre, systematic construction 9-44237
 orbits, localized, calc. by Hückel theory 9-32452
 polar mol., cry., electrons trapped in dipole fields, ESR studies 9-40584
 polyatomic, Gaussian-type functions 9-30008
 and properties, computation 9-42372
 pyridine complexes of iodine monohalides, from Mossbauer effect of ^{129}I 9-34688
 π -electron radicals, hyperfine coupling consts. of 2nd-row elements 9-42373
 radial distribution function, self-consistent equations 9-29892
 radiationless transitions in isolated mols. 9-44313
 radicals, self-consistent field calcs. 9-34601
 relaxation of excited states of large mol., radiative decay obs. 9-38823
 scattering model 9-34597
 spin degeneracy and stability of Hartree-Fock states 9-42317
 stability of configurations with almost degenerate electronic state 9-39788
 three-centre nuclear-attraction integrals via ellipsoidal coords. 9-30009
 transitions in slow atomic collisions, theory 9-34568
 triplet state electronic distribution, determ. by phosphorescence-microwave double-resonance 9-38804
 triplet-triplet energy transfer, relative orientation of involved molecules 9-42360
 two-photon transitions, resonance freq. shift 9-46342
 vibrational deficiency in polyatomic mols., electronic consequences 9-23015
 vibronic intensities, temp. depend. 9-44308
 wave function constructed from complex hybrids 9-38813
 wavefunctions, linear homogeneous constrained variation method 9-32451
 C_2 Hultburt-Hirschfelder calc. of r-centroid 9-30018
 CN, red system, r-centroid calc. by Hultburt-Hirschfelder method 9-30018
 Cl σ orbitals in molecules, s character determ. from n.q.r. and BEEM 9-32454
 H_2^+ , electron density variational calc. 9-27841
 H_2^+ , three parameter wave function, investigation 9-23048
 He electron density variational calc. 9-27841
 ^{14}N -containing mols., Mo wavefunctions and nuclear quadrupole coupling 9-27842
 N_2 Hultburt-Hirschfelder calc. of r-centroid 9-30018
 NiF_6^{4-} cluster, limited-basis set Hartree-Fock theory 9-32482
 OH r-centroid calc. by Hultburt-Hirschfelder method 9-30018
 $\text{Re}(\text{CO})_6^+$, assignment of electronic spectrum 9-32491

electronic structure, inorganic

- alkali diatoms, singlet potential 9-38866
 alkali halide diatomic molecules, binding energy calc. 9-48452
 alkali metal molecules, energies of electronic transitions, estimation by new method 9-30015
 bond-stretching-energy curves from integral Hellmann-Feynman method 9-30012
 chromophores, orthoaxial, parametrization of 'd' antibonding levels; orbital energy part 9-27843
 complexes, effect of ligand-field terms in MO calcs. 9-42378
 gases, photon echoes prod. by inhomogeneously broadened spectral line, polarization props. 9-30351
 group III halides, applicability of various potential functions 9-46352
 halides, triat., reaction with alkali ats., correl. with dynamics 9-25795
 hydrides, second-row diatomic, molec. charge distrib. and binding 9-48464
 iron-group cyanides, unique choices in energy level calcs., stability 9-34615
 one-centre expansion of H_2 molecule in fundamental state 9-23041
 sandwich complexes, hyperfine coupling consts. and covalency 9-42420
 small mols., long radiative lifetimes, theory 9-42377
 σ -bonded four-centre exchange reaction complexes 9-48463
 transition metal complexes, one and more step reactions, extension of Woodward-Hoffmann rules of stereoelectronic control 9-39932
 transition-metal complexes, MO theory of X-ray K-absorpt. edges 9-39854
 transition-metal fluorides, electron delocalization 9-42379
 p-xylene, vibrational structure 9-27920
 AlO , new bands in visible region 9-46354
 AlSe, electronic band system obs. in thermal emission 9-42380
 AsO^+ , (1,0) and (2,0) bands of A-X system, $^1\Pi$ - $^1\Sigma$ transition 9-46355
 BH, and mol. props., ground and excited states 9-38830
 BH, emission spectrum, Stark eff., $X(^1\sigma)$ and $A(^1\pi)$ dipole moments determ. 9-46357
 BO α system, rotational analysis of 0,2 band 9-44317
 C_2^+ , ab initio calc. 9-36696
 C_3^+ , C_3 , C_3^- , non-paired spatial orbital method 9-42388
 CCl_4 , SAVE-CNDO theory, semi-empirical all valence electron, effective field gradient 9-42413
 CN, $A^2\Pi_{3/2}$ state, microwave-optical double reson. 9-34609
 CN chemisorbed on metal surface 9-39948
 CN group 9-42386
 CN violet band system, electronic transition moment variation 9-38834
 CO , $c^2\Pi$ - $X^1\Sigma^+$ transition 9-44322
 CO , one-electron props. of near Hartree-Fock wavefunctions 9-32514
 CO_2 , population inversion and vibrational relax. in nonstationary conditions 9-48457
 CO_2 type, population inversion of energy levels rel. to energy of chem. reactions 9-48459
 CO^+ ion, new electr. band syst. assigned to $^2\Delta$ - $^2\Pi$ transition 9-25738
 CO chemisorbed on metal surface 9-39948
 CS_2 and Rydberg transitions in solid matrix, u.v. obs. 9-32466
 ClO_2^- transitions deduced from obs. u.v. spectrum in organic solns. 9-30039
 Co^+ , radiative lifetime of $B^2\Sigma^+$ state 9-44321
 Co complex, $\text{Co}(\text{II})$ of 1:3 bidentate Schiff's bases, spin density distrib. from isotropic proton resonance shifts 9-42411
 Co complex β - $\text{C}_2\text{O}(\text{II})$ phthalocyanine, ground state from paramag. anisotropy obs. 9-32470
 Cr complex, $\text{K}_2\text{Cr}(\text{NCS})_6$ in methanol-ethanol glass, 100°K, excited state absorption 9-38838
 Cu-8-hydroxyquinolate substituted in organic crystals, ligand ENDOR 9-45408
 CuF_6^{4-} octahedral ion, modified Wolfsberg-Helmholz molecular orbital calc. 9-36708
 Eu^{3+} , intensities of electronic transitions 9-39876
 F_2 and F_2^- , valence-bond and atoms-in-mols. calc. 9-38857
 $\text{FeCl}_3 \cdot 6\text{H}_2\text{O}$, oxidation state, pressure causes charge transfer 9-27851
 $\text{FeCl}_3 \cdot 6\text{NH}_3$, oxidation state, pressure causes charge transfer 9-27851
 $\text{FeF}_3 \cdot 3\text{H}_2\text{O}$, oxidation state, pressure causes charge transfer 9-30032
 H_2 , Franck-Condon factors for three band systems 9-32476
 H_2 , Franck-Condon factors for three band systems 9-32476
 H_2 , Franck-Condon factors for band systems 9-44330
 H_2 , fundamental state, study of one-centre expansion 9-23041
 H_2 , lowest double-minimum state E, $\text{F}^1\Sigma^+$, theoretical calc. 9-42394
 H_2 , model dipole spectrum 9-38849
 H_2 , one-centre calc. with unlimited radial basis 9-38846
 H_2 , projected Hartree product wavefunctions and CI calc. 9-29894
 H_2 , wavefunctions in infinite internuclear separation limit, Hartree-Fock eqn. 9-38816
 H_2 , $X^1\Sigma_g^+$ and $E^1\Sigma_g^+$ states, scaled atoms-in-molecules theory 9-34619
 H_2 , $^3\Sigma_u^-(2p\sigma)$ state 9-44328
 H_2^+ , geometric-mean variation function 9-42397
 H_2^+ , ns- σ Rydberg series, one-centre calc. 9-36698
 H_2^+ , relativistic theory 9-23047
 H_2 Lyman-band oscillator strengths 9-27856
 H_2 Lyman and Fulcher bands, vibr.-rot. interaction effects in Franck-Condon factors 9-30029
 H_2 quasi-bound states, calc. 9-48461
 H_2O , ground state binding energy, Hartree-Fock SCF minimal basis calc. 9-38844
 H_2O , lower excited states, ab initio calc. 9-23046
 H_2S , SCF calcs. 9-23075
 H_2S , wave-functions and d orbitals rel. to bonding 9-34617
 H_2^+ , bond-stretching-energy curves calc. 9-30012
 H_4 , configuration interaction in VB wavefunction for potential energy surfaces 9-48463
 H_4 , H_4^{3+} and H_4^{2+} , square and rectangular states 9-48462
 HD, n.m.r. spin coupling const. calc. 9-27857
 HDO^{17} , h.f.s. by beam maser 9-44329
 He_2 , $^3\Sigma_g^+$ state, quantum mechanical study 9-27860
 He_2 , $\text{F}^1\Pi_u$ and $\text{F}^3\Pi_u$ states, quantum-mechanical exam. 9-34626
 He_2 , $\text{F}^1\Pi_u$ states, quantum mechanical study 9-27861
 HeH^+ , bond-stretching-energy curves calc. 9-30012
 HeH^+ , one-centre calc. with unlimited radial basis 9-38846
 $\text{In}(\text{NCS})_6^{3-}$ complexes, electronic spectra 9-40593
 IrCl_6^{2-} , mag. circular dichroism in cryst. $(\text{CH}_3\text{NH}_3)\text{SnCl}_6$ 9-41353
 $\text{K}_2\text{Cr}(\text{NCS})_6$ in methanol-ethanol glass, 100°K, excited state absorption spectrum 9-38838
 KBr , hyperfine interaction consts. 9-27862
 Li_2 , state functions rel. to nucl. separation 9-48466
 Li_2 , diatomics-in-mols. theory 9-30034
 LiF , valence-bond and atoms-in-mols. calc. 9-38857
 LiH , calc. by generalization of valence-bond method 9-44334
 LiH , one-centre calc. with unlimited radial basis 9-38846
 LiH , self-consistent field eqn. in multicong. approx. 9-40592
 LiH , transcorrelated wave eqn. numerical soln. 9-34628
 LiH , wavefunctions in infinite internuclear separation limit, Hartree-Fock eqn. 9-38816
 LiH^+ 9-44335
 $\text{Mn}(\text{NCS})_4^{2-}$, $\text{Mn}(\text{NCS})_6^{4-}$, $\text{Mn}(\text{NCSe})_4^{2-}$, $\text{Mn}(\text{NCSe})_6^{4-}$, $\text{Mn}(\text{N}_3)_4^{2-}$ complexes, electronic spectra 9-40593
 N_2 , electronic band strengths of first positive system 9-48471
 N_2 , Franck-Condon factors for $v'=0$ progression of fourth positive band system 9-42407
 N_2^+ , e impact and emission, cross-sections for vibrational levels 9-32479
 N_2^+ , electronic band strengths of Meinel system 9-48471
 N_2^+ , matrix elements of electronic transition in first negative band system meas. by discharge in air flow 9-27865
 N_2^+ first negative bands excited by e impact obs. 9-32479
 N_2 first positive system, transition moment, r-centroid dependence 9-25745
 N_2 in metastable $\text{E}^3\Sigma_g^+$ state, emission spectrum and radiative lifetime, mol.-beam meas. 9-38863
 N_2O formed in vibrationally excited state in $\text{N} + \text{NO}_2 \rightarrow \text{N}^+ + \text{O}$ 9-24539
 N_4^+ , geometries by approx. SCF-MO theory which considers intermol. differential overlap 9-34637
 ND_3 electron total inelastic scatt. obs. 9-25746
 NF_3 , Gaussian basis SCF calc. 9-42403
 NF_3 , localized-orbital LCAO MO calc. of dipole moment and field gradient 9-42402
 NH , emission bands assigned to $d^1\Sigma^+b^1\Sigma^+$ transition 9-46368
 NH_3 , population inversion, adiabatic, obs. from laser chirped pulses transmission 9-44341
 NO_2^- , charge distrib. and orbital energies of ground state, CNDO calc. 9-44339
 NO_2^- transitions deduced from obs. u.v. spectrum in organic solns. 9-30039
 NO_2^+ and NO_2^- 9-48467
 NaCs, singlet ground state potential 9-38866
 Ni complex, $\text{Ni}(\text{II})$ of 1:3 bidentate Schiff's bases, spin density distrib. from isotropic proton resonance shifts 9-42411
 NiF_6 , hyperfine interaction and cryst. field splitting, SCF-MO calc. 9-33495
 No adsorbed on silica gel, mag. susceptibility 9-44631
 O_2 , simultaneous and induced electronic transitions 9-23060
 O_2 Schumann-Runge system, inc. high vibr. quantum nos., Frank-Condon factors 9-46373
 O_4^+ , O_4^- , geometries by approx. SCF-MO theory which considers intermol. differential overlap 9-34637
 O adsorbed on Ni, by ion-neutralization spectroscopy 9-32484
 OCS, and Rydberg transitions in solid matrix, u.v. obs. 9-32466
 OD^+ , $A^1\Pi/1X^2\Sigma^-$ transition, reanalysis 9-44346
 OH, shape and width of absorption lines by curve of growth method 9-48476
 OH^+ , $A^1\Pi/1X^2\Sigma^-$ transition, reanalysis 9-44346
 PCl_4^+ , SAVE-CNDO theory, semi-empirical all valence electron, effective field gradient 9-42413
 PF₅, radial, isotropic hyperfine splittings and molec. struct. 9-23065
 PH_3 , wave-functions and d orbitals rel. to bonding 9-34617
 PO, $D^2\Pi(a)$ and $D^2\Pi(a)$ states 9-40602

Molecules continued**electronic structure, inorganic continued**

- S₂, 0-0 band of system D-X $^3\Sigma_g^-$, analysis of incompletely resolved struct. and head struct. 9-48479
- S adsorbed on Ni, by ion-neutralization spectroscopy 9-32484
- SF₆ gas, photon echoes prod. By inhomogeneously broadened spectral line, polarization props. 9-30351
- SF₆, population inversion, adiabatic, obs. from laser chirped pulses transmission 9-44341
- SO₂, three electronic transitions, 1340-1190 Å region, vibr. analysis 9-30058
- SO₂F radical, CNDO-MO calc. 9-44326
- ScH₃NH₃, SCF calc. 9-42419
- Se adsorbed on Ni, by ion-neutralization spectroscopy 9-32484
- SeO₂, geometrical parameters of electronic transitions 9-23073
- SiH₄, SCF calcs. 9-23075
- SiH₄ wave-functions and d orbitals rel. to bonding 9-34617
- Sn₂, model for electronic states 9-42612
- Te₂, transition of $\Sigma-\Sigma$ type obs. in emission spectrum 9-34644
- TiF₆²⁻ octahedral ion, modified Wolfsberg-Helmholz molecular orbital calc. 9-36708
- Ti(H₂O)₆³⁺ octahedral ion, modified Wolfsberg-Helmholz molecular orbital calc. 9-36708
- TiH₃F, SCF calc. 9-42419
- TiO mol., spectra, four new bands in β system 1-0 sequence 9-32489
- VO(CO)₆⁺, assignment of electronic spectrum 9-32491
- VF₆²⁻ octahedral ion, modified Wolfsberg-Helmholz molecular orbital calc. 9-36708
- V(NCS)₆³⁻, V(NCSe)₆³⁻, V(N₃)₆³⁻ complexes, electronic spectra 9-40593
- VO(NCS)₆³⁻, VO(NCSe)₆³⁻, VO(N₃)₆³⁻ complexes, electronic spectra 9-40593
- WH₃ electron total inelastic scatt. obs. 9-25746
- XeF₂, mag. shielding of ¹⁹F 9-31172
- electronic structure, organic**
- o-, m- and p- anisaldehyde 9-46382
- O-, m-, p- bromobenzaldehyde vapours, electr. absorpt. spectra, longest wavelength $\pi^*-\pi$ syst. obs. 9-46387
- β -diketonate salts, triplet-state energy and zero-field splitting 9-23116
- 1-2,4,6-triphenylbenzene, anomalous N h.f.s. 9-27924
- acetylene-d₂, levels involved in absorpt. bands in 3-5 μ region, molec. consts. 9-34651
- trans-acrolein, CNDO CI study 9-32497
- allyl, configuration-interaction wavefunctions 9-38877
- allyl radical, and spectral characts. 9-30110
- amino acids, by X-ray diffraction analysis 9-34654
- p-aminobenzoic acid, orientation of transitions from dichroism of absorpt. bands 9-46386
- aniline, 2938 Å electronic system, rotational band contours 9-34656
- aniline, changes on excitation from dipole moment meas. by optical Stark effect 9-34686
- aniline, π -electron props. by MO-LCAO calc. 9-48504
- anthracene, nanosecond excited-state polarized absorption spectra in visible region 9-34657
- anthracene, triplet-triplet annihilation in vapour 9-38905
- anthracene adsorbed on NaY zeolite, luminesc. obs. 9-28222
- anthracene cation trapped in boric acid glass 9-42423
- anthraquinotetramethan and corresponding diquinone, CMO calc. for spectral and redox behaviour 9-23089
- aromatic aldehydes, vibronic interactions between $n\pi^*$ and $\pi\pi^*$ states 9-42426
- aromatic hydrocarbons, polarization of transitions 9-31137
- aromatic hydrocarbons, radiationless transitions, temp. depend. 9-23091
- aromatic hydrocarbons, triplet decay, temp. effect 9-23090
- aromatic hydrocarbons, triplet-state zero-field splittings 9-42425
- aromatic hydrocarbons in polymethylmethacrylate, phosphoresc. temp. effects 9-28723
- aromatic molecules, $\pi-\pi^*$ charge-transfer states 9-32495
- aza- naphthalenes, modified SCF treatment 9-32503
- azulene, dipole moments of excited states 9-30075
- azulene, singlet state in a solution, acceptance of energy from triplet state of another mol. 9-30076
- benzene, electron scattering, inelastic, rel. to excitation cross-sections 9-30082
- benzene, electronic vib. transition ¹A_{1g}→¹B_{2u} calc. 9-27888
- benzene, in triplet state, energy transfer to singlet state of azulene in solid soln. 9-30076
- benzene, molec. distortions and phosphoresc. 9-30081
- benzene, proton screening const. and mag. anisotropy, antisymmetrical MO calc. 9-23097
- benzene, Rydberg states in inert-gas matrices 9-46384
- benzene, vibronic intensity distrib. in phosphoresc. 9-30080
- benzene and derivatives, photoionization study of mol. orbitals 9-30078
- benzenes, methyl substituted, SCF-MO semiempirical calcs. 9-30092
- benzoic acid, orientation of transitions from dichroism of absorption bands 9-46386
- benzyl radical, delocalization of unpaired electron density 9-36728
- benzyl radicals, spin density distrib. 9-42427
- bicyclo [1.1.0] butane, microwave spectra 9-32504
- borazines, methyl substituted, SCF-MO semiempirical calcs. 9-30092
- bromoacetaldehyde, n.m.r. study and conformational anal. 9-46655
- butadiene, and spectral characts. 9-30110
- butadiene, cis- and trans-, SCF MO and CI calc. 9-27890
- butadiene, configuration-interaction wavefunction 9-38877
- butene, cis- and trans-, Rydberg progressions 9-38884
- charge-transfer between two π -electron systems in aromatic molecules 9-32495
- chloroacetaldehyde, n.m.r. study and conformational anal. 9-46655
- conjugated hydrocarbons, ring-current contrib. to mag. susceptibilities 9-36709
- α -copper phthalocyanine, MO calc. and e.s.r. line shape 9-33639
- coronene, spectral shifts of ¹L_a→¹A₁ transition with temp. and press. 9-30097
- correlatin effects of π electrons 9-44362
- correlation effects of π electrons 9-44363
- coumarin and related cpds., triplet state 9-30096
- cyano group 9-42386
- cyanogen, electronic spectrum 9-30098
- cyclic polyenes, vibronic borrowing 9-44353
- cyclobutanone vapour, u.v. spectrum, 3300°A resolution, ¹A₂ electronic state O vib. levels 9-42429

Molecules continued**electronic structure, organic continued**

- 4,4'-dichlorobenzophenone 9-31114
- 5,8-dihydroxynaphthaquinone, i.r. and visible spectrum obs., vib. and electronic structure deduced 9-30123
- dimer stable confirmation rel. to interaction energy surfaces, formic and acetic acid dimers 9-38822
- N,N-dimethylformamide, accidental near-degeneracies of n_o and π_2 MO's, photoelectron spectroscopy investig. 9-38898
- 4,5-dioxo-2-thioxo- 1,3-dithiolan, β form 9-39328
- 2,4-disubstituted thiazole derivatives, vibration spectra and structure 9-48508
- DNA, π -electronic structs. 9-48520
- DPPH free radical, MO-LCAO calc. 9-42453
- ethane and ethane-d₆, analysis of 1400 Å electronic transition 9-38893
- ethyl radical, spin polar. and delocalization, unrestricted Hartree-Fock method 9-27923
- ethylene, -d₄, vibrational struct. of 1744 Å Rydberg transitions 9-44357
- ethylene, and spectral characts. 9-30110
- ethylene amides, intramolec. charge transfer calc. 9-23118
- ethylene oxide, molec. g values and mag. anisotropy 9-42431
- fluoranthene, transitions from fine structure of absorption spectrum 9-30116
- fluorenone, electronic spectrum, 1680-2350Å, new band and comparison with SCF MO calc. 9-30117
- fluorinated radical anions, spin density distributions 9-38872
- fluorobenzene, molec. g values and mag. anisotropy 9-44359
- formaldehyde, one-electron props. of near-Hartree-Fock wavefunctions 9-32514
- formamide, accidental near-degeneracies of n_o and π_2 MO's, photoelectron spectroscopy investig. 9-38898
- formamide isomers, MO calc. 9-30119
- formic acid, accidental near-degeneracies of n_o and π_2 MO's, photoelectron spectroscopy investig. 9-38898
- formic acid and formate ion, ab initio SCF and CI calc. 9-30120
- fulvene 9-27897
- heterocycles, N and S containing, radical anions, spin density distributions 9-32518
- n -heterocyclics, ¹³C chem. shifts calc. 9-23127
- homopolynucleotides, energy band struct., SCF LCAO cryst. orbital calc. 9-48521
- hydrocarbons, alternant, triplet-triplet absorption spectra, correlation between SCFMO and HMO calcs. 9-38901
- hydrocarbons, MINDO calc. 9-30122
- hydrocarbons, saturated, ab. initio bond-orbital calc. 9-38900
- hydrocarbons chemisorbed on metal surface 9-39948
- m,p- hydroxybenzaldehyde, vapour, from emission spectra 9-34674
- ketene, SCF wavefunction, one-electron props., and electron-density maps 9-32521
- methane, wavefunctions in infinite internuclear separation limit, Hartree-Fock eqn. 9-38816
- methyl radical, spin polar. and delocalization, unrestricted Hartree-Fock method 9-27923
- methylene, evaluation by valence-bond treatment 9-46404
- N-methylformamide, accidental near-degeneracies of n_o and π_2 MO's, photoelectron spectroscopy investig. 9-38898
- 1-methylphenalenyl, spin densities, hyperconjugation eff. calc., e.s.r. study 9-34677
- 2-naphthaldehyde, ³A' assignment for lowest triplet state, from phosphorescence polarization meas. 9-34681
- naphthalene, in triplet state, energy transfer to singlet state of azulene in solid soln. 9-30076
- naphthalene, π -, non-paired spatial orbitals wave functions 9-34680
- naphthalene, triplet-triplet annihilation in vapour 9-38905
- naphthalene, triplet-triplet transitions, LCAO MO SCF calc. 9-23144
- naphthalene and monosubst. derivatives, low-energy triplet-triplet transitions 9-38906
- naphthalenes, partially deuterated, triplet lifetime, isotope effect calc. 9-40617
- 1-naphthol, triplet-triplet transitions, LCAO MO SCF calc. 9-23144
- 2-naphthol, triplet-triplet transitions LCAO MO SCF calc. 9-23144
- 2-naphthyl methyl ketone, ³A' assignment for lowest triplet state, from phosphorescence polarization meas. 9-34681
- nitro compounds, organic, of X-NO₂ type (X=C, N, O), electron distrib. from n.m.r. meas. 9-42440
- trans-1-nitro-1-propene, u.v. absorpt. obs. 9-27893
- p-nitroaniline, orientation of transitions from dichroism of absorption bands 9-46386
- nitroethylene, u.v. absorpt. obs. 9-27893
- nitrogen heterocycles, triplet-state zero-field splittings 9-42425
- nitrogen heterocyclics, π -electron charge densities and chem. shifts 9-44364
- nitrogen substitution effects in conjugated systems 9-23119
- nitrogen substitution effects in conjugated systems 9-23118
- p-nitrophenol, orientation of transitions from dichroism of absorption bands 9-46386
- oscillator strength distrib., correlation effects of π distrib. 9-44363
- oxocarbons, monocyclic, Huckel M.O. and (P-P-P) M.O. calcs. 9-30135
- p- π conjugation, rel. to hybridization of AO of nonbonding pair of electrons 9-48485
- pentadiene, and spectral characts. 9-30110
- pentadienyl, configuration-interaction wavefunction 9-38877
- pentafluorophenyl derivatives, chemical shifts, coupling consts., π -electron interactions correl. 9-42434
- pentafluorophenyl derivatives, π interactions and bonding in selected compounds 9-42435
- perylene in N-isopropylcarbazole, electronic excitation energy transfer 9-31138
- phenanthrene, triplet-triplet annihilation in vapour 9-38905
- phenol, changes on excitation from dipole moment meas. by optical Stark effect 9-34686
- phenol, configuration anal. 9-32450
- phenol, π -electron props. by MO-LCAO calc. 9-48504
- phenols, ortho-substituted, in dimethyl sulfoxide solns., n.m.r. study 9-42444
- phenothiazine, phosphoresc. triplet state 9-39888
- phenothiazine, phosphoresc. triplet state 9-39887
- phenoxazine, phosphoresc. triplet state 9-39888
- phenoxazine, phosphoresc. triplet state 9-39887

Molecules continued

electronic structure, organic continued

- phenyldiazonium ions, meta and para, substituted, HMO, rel to thermal decomposition, spectra and photolysis quantum yields 9-27914
 2-phenylnaphthalene, and spectra and pot. energy rel. to mol. config., calc. 9-27911
 4,4'-polarized cryst. absorpt. spectrum 9-31114
 poly(1-vinylnaphthalene), intramole. triplet energy transfer 9-24461
 polyacenes, linear, $^1A \rightarrow ^3L_a$ transition probabilities 9-38907
 polycyclic azines, vibronic interactions between $\pi\pi^*$ and $\pi\pi^*$ states 9-42426
 polycyclic hydrocarbons, correlation effects of π electrons 9-44362
 polyenes, spin-density waves, charge-density waves and bond alternation 9-44348
 polymer films, synthesized, vacuum u.v. absorpt. spectra obs. 9-31116
 polymers, self-consistent field theory 9-30153
 polypeptides, exciton band struct. 9-41456
 porphyrin, vibronic borrowing 9-44353
 propylene, rel. to internal rot. 9-48506
 pyrene, calc. from π electron spectra 9-30139
 quinoxaline, decay consts. of triplet subcomponents 9-39883
 quinoxaline, two $n \rightarrow \pi^*$ transitions 9-32525
 quinoxaline anions, spin densities 9-32526
 π -electron system of large conjugated mols., screened pots. calc. 9-38873
 n-radialenes and methyl derivatives, molecular orbital theory 9-32527
 rhodamine 6G mols., in soln., electronic absorption spectra and transitions 9-34690
 sandwich complexes, hyperfine coupling consts. and covalency 9-42420
 screened pots. in π -electron system of large conjugated mols., calc. 9-38873
 selenurea, applic. of random-phase-approx. method 9-40621
 spin-density waves, charge-density waves and bond alternation 9-44348
 stilbenes, para-substituted, first e transition freq., obs. 9-34692
 σ -bonded cpds, containing N or O, MINDO calc. 9-27899
 tetracyanobenzene complexes, charge-transfer triplet states 9-23158
 1,4,5,8-tetrahydroxyanthraquinone, from obs. visible spectra 9-30144
 tetraphenylcyclopentadienone radical anion, e.s.r. and molecular orbital study 9-30143
 thiophenol, π -electron props. by MO-LCAO calc. 9-48504
 thiourea, applic. of random-phase-approx. method 9-40621
 toluene ion radicals, spin delocalization and vibr.-electronic interaction 9-38917
 1,1,1-trichloroethane vapour, u.s. dispersion and relaxation obs. 30°C 9-32737
 trimethylene sulfide, electr. spectrum and transitions obs. 9-32524
 trimethylenemethane, zero-field splitting of ground triplet state 9-42448
 triphenylene triplet dianion, zero-field-splitting calc. 9-42446
 triphenylene triplet state from e.s.r. absorpt. meas. on oriented mol. in low mag. fields 9-38918
 triphenylmethyl radicals, spin density distrib. 9-42427
 triplet-triplet energy transfer in ordered and random media 9-28724
 urea, applic. of random-phase-approx. method 9-40621
 vinyl radical, spin polar, and delocalization, unrestricted Hartree-Fock method 9-27923
 CH_3^+ and CH_3^+ , potential energy surfaces 9-27903
 COH^+ , protonated CO, non-empirical molecular orbital calc. of most stable configuration 9-34613
 with N sp^2 -hybridized, rel. to ^{15}N n.m.r. shifts 9-25773
 NO_2-X compounds ($X=C, N, O$), electron distribution from n.m.r. meas. 9-42440

excitation

- 3,4-benzpyrene in aq. lauryl sulphate solns., excimer fluoresc. 9-40798
 acetylene, resonant scatt. of electrons, ang. distrib. 9-27855
 acridine dye adsorbates, pulse photoexcitation 9-48488
 anthracene, excited state mean lifetime and photolum. yield depend. on impurity conc. 9-26772
 anthracene, nanosecond excited-state polarized absorption spectra in visible region 9-34657
 anthracene, two-photon absorpt., energy depend. 9-39795
 aromatic, with symmetry π_g , by electron impact 9-30064
 aromatic mol. in soln., triplet-triplet interact. 9-40608
 aromatics, singlet state donor-acceptor complexes with aliphatic amines 9-23096
 benzanthracene, by electron impact 9-30083
 benzene, electron scattering, inelastic, rel. to cross-sections 9-30082
 benzene, resonant scatt. of electrons, ang. distrib. 9-27855
 benzene singlet state donor-acceptor complexes with aliphatic amines 9-23096
 bixinmethyl ester, static elec. polarizability change upon transition to first excited singlet-state 9-40611
 o-, m-bromo anilines, vapour, near u.v. absorpt. spectra, band obs. 9-25762
 CO_2 in laser, lifetime of 00V levels rel. to discharge current and power dissipation 9-43881
 complex mols., relaxation of upper triplet states, after light excitation, triplet-triplet absorption band obs. 9-25755
 crocetindimethylester, static elec. polarizability change upon transition to first excited singlet-state 9-40611
 p-dimethylaminop-nitrosilbene, static elec. polarizability change upon transition to first excited singlet-state 9-40611
 dipole moments, singlet excited states of naphthalene derivatives 9-27908
 dyes, photo-excited, redox reaction rel. to Fermi level 9-41973
 electron impact excitation, polarization of molecular line radiation, theory 9-32449
 electron scatt., improvement in the first Born theory 9-40572
 electron-molecule excitation, angular dependence of scattering products 9-34602
 energy degradation, Jablonski scheme 9-28814
 ethylene, halogen substituted, ionization potential, intra-molecular electric fields effects 9-42559
 ethylene, resonant scatt. of electrons, ang. distrib. 9-27855
 all-trans-, fluoresc. excitation 9-24460
 hydrocarbons by fast electrons, excited H atom prod. 9-23174
 ionization potential, intra-molecular electric fields effects 9-42559
 level calc. by many-electron pseudopotential formalism 9-32397
 lycopene, static elec. polarizability change upon transition to first excited singlet-state 9-40611
 methane gas, by fast electrons, glow spectra in i.r. region 9-38831
 methyl bromide, double irr. by i.r. and r.f. beams 9-46402

Molecules continued

excitation continued

- methyl-pyridinium salts, configuration transformation in excited states obs. 9-34679
 multiquantum transitions selection rules, laser beams applic. 9-22367
 naphthalene, by electron impact 9-30063
 naphthalene, radiative triplet lifetime and σ - π interaction 9-23143
 naphthalene, triplet states in pulse radiolysis of gaseous mixtures with benzene 9-49387
 naphthalene singlet state donor-acceptor complexes with aliphatic amines 9-23096
 organic solns., vac.-u.v.-excited, inter- and intramole. processes 9-42667
 perylene in N-isopropylcarbazole, electronic excitation energy transfer 9-31138
 2-phenyl-5-(4 biphenyl)-1,3,4-oxadiazole derivatives, excimer emission 9-44577
 photoexcitation and photoionization by off-reson. photons 9-34595
 polar molecules, rotational excitation by electrons 9-32448
 polycyclic hydrocarbons, low-lying excitations 9-44362
 polyvinyl carbazole, transfer of electronic excitation energy 9-39882
 pyrene, by electron impact 9-30063
 pyridine, temporary negative ion reson. 9-40619
 pyronine B soln. in ethanol, glycerol, Nd laser excitation, light generation, 550-650 nm, room temp. 9-30141
 radiationless transitions in isolated mols. 9-44313
 radiative decay of polyatomic mols. 9-42358
 radiative lifetime, effect of neighbouring identical mols. 9-36668
 relaxation of upper triplet states, after light excitation, triplet-triplet absorption band obs. 9-25755
 rhodamine 6J soln. in ethanol, glycerol, Nd laser excitation, light generation, 550-650 nm, room temp. 9-30141
 rhodamine 6Zh, reson. excitation energy transfer from 3-methoxybenzanthrone 9-25780
 rhodamine C, reson. excitation energy transfer from 3-methoxybenzanthrone and rhodamine 6Zh 9-25780
 rhodamine C soln. in ethanol, glycerol and polymethylmethacrylate, laser excitation, light generation, 550-650 nm, room temp. 9-30141
 rotational, in diatomic mol. collisions, distorted-wave approx. 9-30159
 saffranine T soln. in ethanol, glycerol, Nd laser excitation, light generation, 550-650 nm, room temp. 9-30141
 selenurea, applic. of random-phase-approx. method 9-40621
 p-terphenyl singlet state donor-acceptor complexes with aliphatic amines 9-23096
 tetrachloro-p-xylene, excimer emission in rigid organic glass, 280nm excitation, 77°K 9-32530
 thiourea, applic. of random-phase-approx. method 9-40621
 trimethylene sulfide, excited states shape from electr. spectrum obs. 9-32524
 triphenylene, by electron impact 9-30064
 urea, applic. of random-phase-approx. method 9-40621
 virtual, of energy levels for energy transfer 9-23007
 activation energies of glow curves, numerical calc. 9-27834
 BeF₃, a $\pi\pi^* \rightarrow \Sigma^+$ syst., character analysis 9-23031
 CO, e impact excitation structure obs. at 2.3 eV., electron affinity 9-34612
 CO, resonant scatt. of electrons, ang. distrib. 9-27855
 CO₂, metastable species prod. by electrons 9-32478
 CO₂, resonant scatt. of electrons, ang. distrib. 9-27855
 CO₂, vibr., by dipole interaction with slow electrons 9-36697
 CO₂[$A^1\Pi_u \rightarrow X^1\Pi_g$] bands obs., excitation by neutral mol. photons 9-27845
 CO₂ gas, by fast electrons, glow spectra in i.r. region 9-38831
 CO₂ in laser, 00°1 population level and obs. 9-43882
 CO₂ pulsed lasers, mechanisms 9-43880
 CO₂(v₂) vibrationally excited, deactivation by collisions with CO₂ or N₂ 9-42387
 CO gas, by fast electrons, glow spectra in i.r. region 9-38831
 CO*(001), deactivation rate determ. by meas. intensity of fluorescence radiation 9-25732
 Cr complex, K₃Cr(NCS)₆ in methanol-ethanol glass, 100°K, excited state absorption spectrum 9-38838
 D₂ singlet states, pot. function calc. 9-23042
 H₂, by slow e, rot. transitions with vibr. quantum excitation, calc. 9-38843
 H₂, electron scatt., differential elastic and rotational excitations calc. 9-46363
 H₂, electron scatt., low energy, polarization and exchange effects 9-40591
 H₂, excitation by low-energy electrons, cross section calc. 9-38853
 H₂, metastable species prod. by electrons 9-32478
 H₂, resonant scatt. of electrons, ang. distrib. 9-27855
 H₂, solid, i.r. absorption associated with orientational excitation 9-24410
 H₂⁺ electron scatt., $1s\sigma \rightarrow 2p\sigma$ transition, asymptotic closure cross section calc. 9-40573
 H₂⁺ ions, collision-induced, angular depend. of dissoc. cross-section and rel. to internuclear distances 9-23169
 H₂⁺-H₂ collisions, charge transfer and vibrational excitations 9-23051
 H₂ singlet states, pot. function calc. 9-23042
 H₂ vibrational, and charge transfer, in H₂⁺-H₂ collisions 9-23051
 H₂O gas, by fast electrons, glow spectra in i.r. region 9-38831
 H₂⁺ de-excitation by H₂, energy transfer 9-44494
 HD singlet states, pot. function calc. 9-23042
 I₂ fluoresc., by Kr⁺ laser 9-38855
 K₃Cr(NCS)₆ in methanol-ethanol glass, 100°K, excited state absorption spectrum 9-38838
 N₂-O₂ vibr. excitation and exchange in shock tube 9-30349
 N₂, 0-200 eV electrons collisions, vac. u.v. light emission 9-32480
 N₂, 1st positive band by electrons 9-40597
 N₂, by electron impact, production of metastable E Σ_g^+ state 9-38863
 N₂, metastable species prod. by electrons 9-32478
 N₂, resonant scatt. of electrons, ang. distrib. 9-27855
 N₂⁺, rotational lines in controlled temperature hollow cathode discharge 9-23055
 N₂⁺ 1st negative and Meinel bands by electrons 9-40597
 N₂⁺ first negative bands, electron impact excitation cross section 9-32479
 N₂⁺ first negative system, by low-energy electrons rot. temp. 9-30040
 N₂⁺ ions, rotational and vibrational motion, prod. in collisions between inert gas atoms and N₂ 9-42470
 of N₂B⁺ Π_g state, kinetic processes 9-42410
 N₂H⁺ → HN₂⁺, Balmer- α , N₂⁺(0,0) 1st-ve band photon emission, cross sections meas. 9-22985

Molecules continued**excitation continued**

- N_2O , metastable species prod. by electrons 9-32478
 $N_2(A^1\Sigma_u^+)$ deactivation 9-39961
 $N_2(B^3\Pi_u)$ deactivation 9-39961
N in metastable state, gas phase energy pooling 9-44338
 NH_3 gas, by fast electrons, glow spectra in i.r. region 9-38831
 NO , 3p mol. Rydberg state ($2\pi(V=O)$), spin-orbit coupling const. 9-40595
 NO , in pulse radiolysis 9-45425
 NO , resonant scatt. of electrons, ang. distrib. 9-27855
 NO_2 , by Ar^+ and Kr^+ lasers 9-40596
 $(NO)^+$, de-excitation cross-section in NO 9-34792
 NO gas, by fast electrons, glow spectra in i.r. region 9-38831
in O_2 - Ar mixture, of diatomic mols., by atom collision, calc. 9-40588
 O_2 , electronic, in photolysis of O_3 at 2537 Å 9-45423
 O_2 , resonant scatt. of electrons, ang. distrib. 9-27855
 O_2^+ , absolute excitation cross sections for emission of first negative bands under e. impact on O_2 9-42412
 O_2^+ , by electrons, spectral band cross sections meas. 9-23062
 O_2 in atmosphere, electron cooling by vibrational excitation 9-43444
 O_2 red, atmospheric spectral system electron transition probability 9-36706
 $O_2(^1\Delta_g)$ deactivation by O , N , benzene, obs. 9-34707
 SF_6 , vibr. induced by CO_2 laser rad. absorpt. 9-25750
 ThO , perturbed 1H state, rot. anal. 9-32488
 ZnS powder, activation energies of glow curves, numerical calc. 9-27834

intermolecular mechanics

- see also *Association; Collision processes/molecules; Kinetic theory/gases; Liquids/structure; Liquids/theory; Solids/theory*
acceptor-donor complexes, intermol. interaction influence on vib. spectra 9-32447
alcohols, association in soln. and in vapour phase 9-23507
alkali atom interactions with atoms and non-reactive diatomic mols., cross sections and van der Waals constants 9-42342
anisotropic cylindrically symmetric mols., Casimir-Polder asymptotic pot. 9-38929
anisotropic interaction effect on optical Kerr eff., field-induced phase transition 9-23498
arbitrary shape particles, scale particle theory 9-41783
atom-molecule potential-energy functions, determ. from scatt. of high-energy atomic beams 9-38794
benzene isotopic mixed crystals, intermol. Fermi reson. in vibr. spectrum 9-43007
Buckingham-Corner intermolec. potential in molec. beam scatt. 9-38933
constant for gauging suitability, ratio of Boyle volume and unit compressibility law volume 9-32729
crossed beams, effect of speed distrib. on nonreactive scatt. 9-44388
cyclohexane, conformational energy, ab initio calc. 9-38886
cyclopentane, conformational energy, ab initio calc. 9-38886
derivatives of classical deflection function 9-41742
diatomic mol. collision with atom, theory 9-36734
dichlorobenzene, o-, m- and n-, dipole-dipole forces in combinational scattering spectra, phase shift 9-46393
difluorobenzene, m- and n-, dipole-dipole forces in combinational scattering spectra, phase shift 9-46393
energy transfer, rot.-translational, classical mechanics 9-36735
force constants determ. from macroscopic props. 9-27836
between hydroxyl-containing substs. and O- and N- containing substs. investigated by i.r. abs. and Raman scatt. 9-27940
inert gas solids, triple-dipole forces eff. on Debye temp. 9-39530
inert gases, intermol. potential parameters from sound vel. data 9-36733
interaction, retarded of identical 2, 1 excited, cut-off determ. 9-34596
interaction energy, London- van der Waals, 2 unexcited axially symmetric mols. 9-36736
interaction potential calcs. rel. to thermal-diffusion column operation 9-34843
interaction second virial coeffs. from -125° to $50^\circ C$, meas. and correl. 9-44522
ion-molecule collision complexes, long-lived, evidence from numerical studies 9-36732
Kirkwood-Salsburg integral eqn. and virial coeff. of Lennard-Jones mols. 9-32557
Lennard-Jones gas, two-dimensional third virial coefficient 9-42605
Lennard-Jones params. of excited states, obs. 9-48528
linear mols., hard-core model, stat. mech. 9-27942
linear systems, decay of pair correlation function 9-34700
in liquid, non-uniform, molecular distributions 9-30367
methane, proton mag. shielding of interacting pair mols. 9-40630
methanes, halogen-substituted, second virial coeffs. and force consts. 9-36807
methyl siloxane polymers NMR studies 9-30471
mixtures of nonspherical mols., third virial coeffs. 9-42608
nonresonant vibr.-vibr. energy transfer due to dipole-dipole interactions 9-38934
orbiting collisions, phase shift 9-34704
organic liquids in aqueous binary mixtures, rel. to n.m.r. relax. meas. 9-46654
organic solns., vac. u.v.-excited, energy transfer 9-42667
pair distribution function for fluid hard spheres 9-30163
paraffins, linear and cyclic, effect on viscosity rel. to mol. structure 9-25776
Percus-Yevick equation, accuracy of numerical solutions 9-34702
Percus-Yevick equation accuracy of numerical solutions 9-34703
polymers, dil. solns., entanglement of molecules, computation using light scatt. and viscosity data 9-46615
potential function, from isotopic thermal diffusion factor 9-42466
Raman lines depolarization due to intermolecular interactions, perturbation calc. 9-40629
spectral changes during liq.-solid phase transition, vibrational spectroscopy method 9-44386
spherical and nonspherical molecules intermolecular forces from second virial coeff. 9-46428
o-terphenyl, mol. motion in liq., crystalline and glassy forms 9-39925
theory, mathematical, book 9-32555
vibrational energy exchange between diatomic mols. 9-32556
virial coeff., third, for intermolec. potentials with hard-sphere cores 9-44521
xylyl, o-, m- and n-, dipole-dipole forces in combinational scattering spectra, phase shift 9-46393
Ar-methane anisotropic intermolec. forces 9-38935

Molecules continued**intermolecular mechanics continued**

- Ar, 'effective' intermolec. pair potential 9-30339
Ar, gas, Lennard-Jones pot., deriv. of second virial coeff. 9-34833
Ar, pair potential 9-48657
Ar, pot. calcs. rel. to thermal diffusion column operation 9-34843
Ar supersonic jet, electron diff. obs. 9-23035
 CH_4 , second virial coeff. 9-34833
 CO_2 - N_2 reson. vibr. energy transfer between mode N_3 9-30164
 CO_2 , second virial coeff. 9-34833
 CO_2 supersonic jet, electron diff. obs. 9-23035
Cl crystal, intermolec. forces 9-43245
 CO_2 , deactivation of bending mode by H_2 and D_2 9-23034
DCN i.r. vibrational spectra depend. in intermolecular interactions, gas-soln. transition in solvent 9-30033
 H_2 -Kr intermolecular forces and (thermal) diffusion 9-46580
HCN i.r. vibrational spectra depend. on intermolecular interactions, gas-soln. transition in solvent 9-30033
He- H_2 intermolec. anisotropic 9-30354
Kr, pot. calcs. rel. to thermal diffusion column operation 9-34843
 N_2 - N_2 interaction rel. to O_4^+ , O_4^- geometries by approx. SCF-MO theory 9-34637
 N_2 - N_2O mixtures, vibration-vibration energy exchange, shock-tube study 9-34706
 N_2 - O_2 vibr. exchange in shock tube 9-30349
 N_2 , second virial coeff. 9-34833
Ne, pot. calcs. rel. to thermal diffusion column operation 9-34843
 O_2 - O_2 interaction rel. to O_4^+ , O_4^- geometries by approx. SCF-MO theory 9-34637
 O_2 - O_2 , simultaneous and induced electronic transitions 9-23060
OCS, line broadening of various rotational transitions due to dipole-dipole, dipole-quadrupole interac., obs. 9-34639
 SF_6 , dipole-quadrupole interaction rel. to light-echo obs. in gas 9-48481
Xe, pot. calcs. rel. to thermal diffusion column operation 9-34843
Xe supersonic jet, electron diff. obs. 9-23035
- internal mechanics**
acetaldoxime, cis- and trans-, barriers to internal rotation 9-40605
anthracene semiquinone derivatives, bridged, long-range e.p.r. coupling 9-34655
anthracene semiquinone derivations, bridged, long-range e.p.r. coupling 9-34655
benzenes, monosubstituted, substituent σ^0 rel. to i.r. ν_{16} intensities, obs. 9-30090
benzenes, para-disubstituted substituents direct interaction rel. to ν_{16} intensity, 1600 cm^{-1} 9-30091
borazane, internal rotational barrier computed 9-34670
trans-1-bromopropene, barrier to internal rotation 9-32505
chain molecules with segments interacting with Lennard-Jones' potential, Monte-Carlo computer simulation 9-42462
chloronitrobenzenes, steric effects of Cl substitution on u.v. spectra 9-30095
decafluorobiphenyl, steric repulsion between rings to explain discrepancies in assigned vib. spectrum 9-30100
dibromofluoroethane, heavy hindered rotator, neutron scatt. and far i.r. spectra 9-42432
1,4 dimethylanthrasemiquinone, anion radical, methyl group rotation, e.s.r. study 9-36718
divenes, monosubstituted, substituent σ^0 rel. to i.r. ν_{16} intensities, obs. 9-30090
energy transfer by virtual excitation of energy levels 9-23007
ethane, geometrical changes during internal rotation 9-36714
ethane, internal rotational barrier computed 9-34670
methane in Ar, neutron scatt., 5.3 Å, $86^\circ K$ 9-25771
methoxyethyne, internal rotation barrier 9-46406
methyl group in isoprene, internal barrier 9-30125
methyl siloxane polymers NMR studies 9-30471
di methylpolysilazanes, n.m.r. obs., internal motion temp. depend., 77-400°K 9-34697
methylsilane, internal rotational barrier computed 9-34670
methylthioethyne, centrifugal distortion 9-48501
monofluoroacetylene, CH deform.-GF stretching coupling, i.r. obs. 9-27882
naphthalene, σ - π interaction and radiative triplet lifetime 9-23143
organic liquids in aqueous binary mixtures, intramol. contrib., to n.m.r. relax. meas. 9-46654
phenol, height of potential barrier for ideal gas under harmonic oscillator 9-46414
2-phenylnaphthalene, pot. energy rel. to mol. config., calc. 9-27911
podosetin diacetate and dimethyl ether, n.m.r. study of hindered rotation 9-23152
polymers, chain, in soln., random coil config. and light scatt. with intramol. interac. 9-34905
ring puckering in five-membered rings, theory 9-36721
ring puckering in five-membered rings 9-38916
silacyclopentane, barrier to pseudorotation 9-32528
o-terphenyl, liq., EPR study of mol. motion 9-40805
tetrahydrofuran, ring puckering 9-38916
1,4,5,8-tetramethylanthrasemiquinone, anion radical, methyl group rotation, e.s.r. study 9-36718
1,1,2-trichloroethane, u.s. relax. and vol. change during internal rot. 9-42652
trifluoroacetaldehyde, i.r. vib. spectrum and internal rotation barrier 9-23123
trimethylene selenide, vibr. anal. and ring puckering 9-42447
XY, normal co-ordinate analysis on basis of Urey-Bradley force field, Coriolis coupling const. 9-30000
H-bond strengths, significance of i.r. freq. shifts 9-25726
HNO, pot. energy curves, unrestricted Hartree-Fock calc. 9-23044
 He_2 isotopic mols. interatomic potentials 9-38801
HeAr, interatomic potential 9-38854
HeNe, interatomic potential 9-38854
ICN, Fermi reson. const. 9-32467
 KNO_3 , polarized i.r. absorpt. spectra, internal-attice combination band region 9-47363
Li hydrides, molec. consts. by molec. beam elec. reson. 9-30061
 NH_3 , inversion spectrum, hyperfine structure 9-34632
NeAr, interatomic potential 9-38854
 Si_2Cl_6 , barrier to internal rotation, assessment from vibrational spectrum 9-30056

Molecules continued

moments

- acetaldoxime, *cis*- and *trans*-, quadrupole coupling const. 9-40605
 acetaldoxime *cis*- and *trans*-, dipole 9-40605
 p-amino-N-N-diethylaniline, elec. dipole moment using modified Higasi's eqn. 9-46410
 p-amino-N-N-dimethylaniline, elec. dipole moment using modified Higasi's eqn. 9-46410
 aniline, dipole moments of lowest singlet $\pi^* \leftarrow \pi$ states by optical Stark effect 9-34686
 anisidines, o-, m- and p-, dipole moments 9-36898
 aromatic molecules, substituted, dipole moment changes in excited states, rel. to $\pi \leftarrow \pi^*$ charge-transfer states 9-32495
 azulene, dipole moments of excited states 9-30075
 benzophenone, electric dipole moment determination by dielectrometer 9-45907
 bixinmethylester, static elec. polarizability change upon transition to first excited singlet-state 9-40611
 chloroform in electron donor solns. 9-23518
 crocetindimethylester, static elec. polarizability change upon transition to first excited singlet-state 9-40611
 di-n-butyl ether, electric dipole moment determination by dielectrometer 9-45907
 p-dimethylaminop'-nitrosilbene, static elec. polarizability change upon transition to first excited singlet-state 9-40611
 diphenyl ether, electric dipole moment determination by dielectrometer 9-45907
 N-N'diphenylaniline, elec. dipole moment using modified Higasi's eqn. 9-46410
 dipolar autocorrelation function rel. to complex dielec. permittivity 9-34599
 ethylene amides, dipole 9-23119
 ethylene oxide, quadrupole 9-42431
 ethylene sulfide, quadrupole moments 9-40612
 fluoroacetylene, mol. quadrupole moment 9-25764
 fluorobenzene, quadrupole 9-44359
 fulvene, dipole 9-27897
 Hulburt-Hirschfelder potential tested by calc. r-centroids of several diatomics 9-30018
 ketene, quadrupole 9-30126
 lycopenes, static elec. polarizability change upon transition to first excited singlet-state 9-40611
 methane, induced dipole moment in ν_3 vibr. mode, Stark effect obs. 9-34678
 methyldiazirine, dipole 9-34676
 naphthalene derivatives, singlet excited states, dipole moments 9-27908
 NH₃, elec. dipole, from Fourier dispersion spectra, 87-667 μ 9-30043
 nitroanisoles, o-, m- and p-, dipole moments 9-36897
 p-nitro-N-N'dimethylaniline, elec. dipole moment using modified Higasi's eqn. 9-46410
 m-nitro-N-N'dimethylaniline, elec. dipole moment using modified Higasi's eqn. 9-46410
 phenol, dipole moments of lowest singlet $\pi^* \leftarrow \pi$ states by optical Stark effect 9-34686
 polar gases, scatt. of electrons by rotating dipole 9-38819
 poly(4-methylstyrene), effective dipole moment 9-32550
 n-propyl alcohol, trans. form, dipole moment 9-46416
 propylene, dipole moment using Gaussian self-consistent field wave functions 9-48506
 pure polar liquid dipole moment computation, empirical eqn. 9-46646
 radiative decay, transition moments and oscillator strengths 9-36694
 tetrahydrofuran, dipole 9-38916
 triethylamine-naphthalene excited donor-acceptor complex dipole moment 9-23096
 BH, optical emission spectrum, Stark effect, X($^1\sigma$) and A($^1\pi$) dipole moments determ. 9-46357
 D₂Se, elec. dipole moment determ. from Stark effect on J=2₀₂ \rightarrow 2₁₁ and J=6₄₂ \rightarrow 6₅₁ lines 9-38850
 H₂O, ground state dipole moment, Hartree-Fock SCF minimal basis calc. 9-38844
 HBr, dipole, from far i.r. dispersion obs. 9-48460
 HCN, dipole moment variation with vibrational state 9-30047
 KBr, dipole, from molec. beam elec. reson. 9-27862
 N¹⁵N¹⁵O¹⁶, quadrupole 9-38862
 NF₃, localized-orbital LCAO MO calc. of dipole moment and field gradient 9-42402
 NF₃, quadrupole, SCF calc. 9-42403
¹⁵NH₃ quadrupole moment 9-42408
 OCS, dipole moment meas. using resonance cavity as absorption cell 9-34640
 OCS, dipole moment variation with vibrational state 9-30047
 OCS, elec. dipole and quadrupole 9-30046
 PHF₂, dipole, and microwave spectrum and struct., obs. 9-30049
 PHS, dipole moment from Stark components of microwave rotational transitions 9-30051
 SF₆, quadrupole moments of buffer mols. in gas from light-echo obs. 9-48481
 SiS, dipole moment from Stark components of microwave rotational transitions 9-30051
 SnS, dipole moment from Stark components of microwave rotational transitions 9-30051

nuclear coupling

- ¹³C-H coupling, expression using method of separated electron pairs 9-32496
 A₂B_x, homonuclear systems, modulation of Carr-Purcell spin-echo trains 9-48448
 acetaldoxime, *cis*- and *trans*-, quadrupole coupling constants 9-40605
 acetone, vicinal ¹³C-¹H and long-range ¹H-¹H coupling const., sign and magnitude 9-40606
 aldehydes, ¹³C-C-H spin-spin coupling constants involving formyl proton 9-44350
 benzaldehydes, aldehyde spin-spin coupling consts., Indor meas 9-46385
 benzaldehydes, monosubstituted, coupling constants, accurate values 9-30087
 benzenes, trisubstituted, proton-proton const., additivity of substituent effects 9-23100
 2,1,3-benzoselenadiazole, p.m.r. coupling constants 9-30088
 2,1,3-benzothiadiazole, p.m.r. coupling constants 9-30088
 2,1,3-benzoxadiazole, p.m.r. coupling constants 9-30088
 trans-1-bromopropene, quadrupole coupling tensor 9-32505

Molecules continued

nuclear coupling continued

- C-C spin coupling constants, geminal investigated in some representative mols. 9-46351
 core model for single-centre calc. of elec. field gradient 9-42398
 cyano group, constants, extended Huckel scheme 9-38890
 diethylaminotelluriumpentafluoride mag. double resonance, sign of Te-F spin-spin coupling const. 9-44356
 1,1-difluoroethylene, n.m.r. in nematic solvent, magnitudes and relative signs 9-30105
 dimethyltin dibenzoate, ¹¹⁹Sn-CH₃ coupling 9-27875
 e.p.r. hyperfine coupling consts., 'mixed basis' calc. 9-32458
 ethane, indirect coupling constants, absolute signs from n.m.r. in nematic phase 9-42433
 ethyl cyanide, ¹⁴N quadrupole coupling constants 9-38890
 ethylene, *trans*-d₂, strong Coriolis perturbation in i.r. spectrum 9-38894
 ethylenes, monosubstituted, J_{13-*r*} coupling constants 9-27894
 fluorobenzene derivatives, substituent effects on H-F couplings 9-38881
 fluorobenzenes, trifluoromethyl- and methoxy-substituted, eff. of trifluoromethyl substitution on F-F coupling constants 9-30118
 fluoromethanes, H-F spin-spin coupling const. 9-30434
 formaldehyde -h₂, D₂, and hd coriolis couplings 9-48496
 formamide-¹⁵N, coupling const. from obs. of heteronuc. double reson. using weak perturbing r.f. fields 9-40615
 group Coriolis coupling constants and group mean amplitudes of vibration 9-40579
 group IV hydrides and deuterides, Green's fn. calc. of Coriolis coupling and rotational distortion consts. 9-46353
 hydrocarbons, simple and derivatives, coupling constants, effect of one-centre exchange integrals 9-42437
 malate ion, proton coupling constants, ABX analysis 9-46400
 malic acid, proton coupling constants, ABX analysis 9-46400
 methane, solid; A and T nuclear spin systems mixture, phase transitions 9-35240
 methyldiazirine, quadrupole coupling consts. 9-34676
 methylquinolines, ¹H-¹H coupling constants 9-38904
 2-naphthaldehyde, vibronic spin-orbit interactions 9-34681
 2-naphthyl methyl ketone, vibronic spin-orbit interactions 9-34681
 nonmetal hexafluorides, force constants calc. 9-25743
 N-oximes, geminal and vicinal N, H coupling constants, absolute signs, stereochem. and medium eff. 9-30134
 pentafluorobenzene, relative signs from low-field n.m.r. 9-30136
 perfluorovinyl derivatives, F-F coupling consts. 9-23148
 phenoxy radicals, fluorinated, proton and fluorine coupling constants 9-34687
 proton spin coupling by π electrons 9-42376
 proton-proton coupling by π electrons 9-42375
 pyridazine, proton coupling constants 9-34689
 quadrupole coupling consts. relationship with force consts. 9-42363
 N-quinoline, geminal and vicinal N-H coupling constants, absolute signs, stereochem. and medium eff. 9-30134
 π -electron radicals, hyperfine coupling consts. of 2nd-row elements 9-42373
 spin-coupling parameters from low-field n.m.r. 9-30136
 spin-spin coupling, valence-bond theory by Penney-Dirac bond orders 9-46348
 2,4,6-trichloroheptane vicinal constants from 4-spin analysis of NMR spectra 9-32546
 trifluorochlorocyclobutanes, substituted, ¹H-¹⁹F and ¹⁹F-¹⁹F coupling constants from n.m.r. spectra 9-30148
 vinyl ethers, n.m.r. coupling consts. and chem. shifts temp. depend., obs. 9-27919
 vinyl halides, n.m.r. coupling consts. and chem. shifts temp. depend., obs. 9-27919
 vinyl iodide, quadrupole coupling const. 9-32533
 xenon fluorides and oxyfluorides, ¹²⁹Xe-¹⁹F coupling constant as function of ¹⁹F chemical shift 9-34646
 XY₂Z, Coriolis coupling constants calc. 9-30001
 XY₄ normal co-ordinate analysis on basis of Urey-Bradley force field, Coriolis coupling const. 9-30000
¹²⁹I₂ frozen solns., Mossbauer determ. 9-31089
¹¹⁹Sn-CH₃ coupling in dimethyltin dibenzoate 9-27875
¹²⁹Xe-¹⁹F coupling constant in Xenon fluorides and oxyfluorides, as function of ¹⁹F chem. shift 9-34646
 B-N cpds., field gradient calc. 9-23030
 B halides, solid, ¹¹B quadrupole coupling consts. 9-43296
 BaFPO₃, sign of F-P coupling const. 9-31169
⁸¹Br in KBrO₃ and NaBrO₃ chemical shift meas. in presence of strong nuc. quadrupole couplings 9-26670
¹³C-¹³C coupling, expression using method of separated electron pairs 9-32496
¹³CH coupling constants, effect of lone pairs 9-34649
³⁵Cl in NaClO₃ chemical shift meas. in presence of strong nuc. quadrupole couplings 9-26670
 Co(III) complexes, quadrupole coupling 9-45398
 D₃B(CN)₃, B-D quadrupole coupling 9-33643
 H₂, ortho hydrogen mols. linear chain, quadrupole interaction 9-25790
 H₂O, hyperfine structure on 6₁₆-5₂₃ transition, maser spectrometer obs. 9-34618
 HC¹³N, coupling consts., n.m.r. obs. 9-34621
 HD, n.m.r. spin coupling const. calc. 9-27857
 HDO¹⁷, quadrupole coupling 9-44329
 LiD, core model for single-centre calc. of elec. field gradients 9-42398
 N₂⁺ electron transition matrix element depend on internuclear distance 9-27865
¹⁴N, quadrupole, ab initio MO wavefunctions calc. 9-27842
¹⁴N in RCN and RCN⁻ mols. and ions, quadrupole coupling const. calc. 9-42400
 ND₃, constants of hyperfine interaction between D nuclei and intramolecular fields 9-38865
¹⁵N-¹H geminal and vicinal coupling constants in N-oximes and N-quinoline, absolute signs, stereochem. and medium eff. 9-30134
 NO₂⁻, ¹⁴N quadrupole coupling const. calc. 9-42401
 NS free radical, ¹⁴N quadrupole coupling const. from e.p.r. spectrum 9-46369
 NaI hyperfine coupling constants for sublevels of J=1, molecular beam electric resonance meas. 9-40600
 Ni²⁺ complex with dimethyl methylphosphonate, chemical exchange spin decoupling 9-28156
 RbOH, quadrupole coupling 9-38869

Molecules continued**nuclear coupling continued**

- TiCl₄, hyperfine interaction consts. 9-34645
Zn complex, 1:1 Zn (II)-malate, proton coupling constants, ABX analysis 9-46400

relaxation

see also Acoustic wave propagation; Dielectric phenomena; Liquids/theory; Nuclear magnetic resonance and relaxation; Paramagnetic resonance and relaxation

- benzene-carbon disulphide solns., acoustic relax. obs. and its mechanisms 9-46632
carbon tetrachloride, evidence of multiple vibrational-translational relax. 9-48702
complex mols., relaxation of upper triplet states, after light excitation, triplet-triplet absorption band obs. 9-25755
dielectric of mol. with inversion or internal rot. modes, correl. function treatment 9-42365
dipolar molecules, solvent depend., using microwave absorption 9-36900
electronic, in large mols., radiative decay and intramol. coupling 9-38823
gas flow, relaxation time determ. from config. of effective Mach line 9-46570
gas mixtures, vib. relax. rel. to u.s. dispersion 9-32734
non-polar polyatomic gases, rot. translational relax., role in thermal conductivity 9-26020
nonlinear, in polymer solutions 9-32773
polar molecule in dil. soln., relax. time eval., empirical eqn. 9-46645
polyamides relaxation obs., -140°C + 50°C 9-32544
polycaprolactam, relaxation obs., -140°C + 50°C 9-32544
polymers, dil. solns., computation using light scatt. and viscosity data 9-46615
polymers, treatment including co-operation in molecular motion 9-23189
polymethacrylic acid esters below glass transition point 9-32549
radiative decay of closely space levels, interference effects 9-40577
rigid mols. dielectric absorpt., meas 9-23088
small mols., long radiative lifetimes, theory 9-42377
upper triplet states, after light excitation, triplet-triplet absorption band obs. 9-25755
u.s. rot. relax., temp. depend. 9-23397
u.s. rot. relax., temp. depend. 9-23396
vibrational, of diatomic molecules excited by atom collision, calc. 9-40588
vibrational energy exchange between diatomic mols. 9-32556
CO₂, thermal relax. times of vib. levels 9-42385
CO₂, vib. freq. of asymmetric stretching mode, from shock wave meas. 9-34611
CO₂, vibrational, and population inversion in nonstationary conditions 9-48457
CO₂ rot. transition by collisions, relax. time calc. 9-44389
CO₂ thermal conductivity, shock heated, eff. of vibrational relaxation 9-36815
CO₂, deactivation of bending mode by H₂ and D₂ 9-23034
p-H₂, and mixtures with He, Ne, Ar, rot. relax. 9-42611
HBr, vibr. relax. in shock waves 9-42396
HCl, vibr. relax. behind shock waves 9-30030
HCl, vibrational 9-32474
HCl and DCl in shock waves, vibr. relax. 9-38847
HI, vibr. relax. in shock waves 9-42396
N₂ thermal conductivity, shock heated, eff. of vib. relax. 9-36815
NH₃ gas in bulk, time meas. w.r.t. press. from obs. of steady state transient 'wiggles' phenomenon 9-44528
NO, vibrational, negative temp. effect 9-42409
No, vibr. relax., shock tube meas. 9-38861
OCS gas in bulk, time meas. w.r.t. press. from obs. of steady state transient 'wiggles' phenomenon 9-44528

rotation

- acetonitrile, vibration-rotation interaction, Coriolis coupling constant 9-23085
acetonitrile in vibr. $v_8=2$ excited state, rot. spectrum 9-46379
acetylene-d₂, bands in 3-5 μ region, anal. rel. to molec. consts. of levels 9-34651
allene, pure rot. i.r. absorpt. 9-38879
allene, two rot. lines 9-38878
aniline, 2938 Å electronic system, rotational band contours 9-34656
aniline, Stark effect in fine structure in dipole moment meas. on excitation 9-34686
anisotropy meas. by n.g.r. relax. 9-39930
asymmetric rotation, reduced energy deriv. calc. using Hellman-Feynman theory 9-44305
bicyclo [1.1.0] butane, from microwave spectra 9-32504
butene-1, const. determ. from microwave spectra 9-23102
t-butyl chloride, freedom of orientation in cryst. 9-39670
centrifugal distortion consts., polyat. 9-40581
chloro-methylbenzenes, hexa-substituted crystals, librations 9-24418
chloroform, n.m.r. of ³⁵Cl, anisotropic molecular rotation in liquid 9-39119
chloromethane-d₃, v_1 band rotational structure, i.r. spectra 9-32507
2-chloropropene-1, 3-d, 9-40610
CO mol., i.r. bands, self and foreign gas broadening effects, comparison 9-27848
in collision between atom-diatom mol., rotational state rel. to anisotropy parameters 9-34701
cumene rotational isomerism from c. diff. exam 9-23111
cyanopropene, vibr. rot. anal. 9-23112
cyclopropane, vibr. rot. bands, computer anal. 9-38895
deuteriochloroform, n.m.r. of ²H and ³⁵Cl, anisotropic molecular rotation in liquid 9-39119
diatomic, analysis by computer 9-38827
diatomic, coherence between different j states rel. to h.f. effects in spin relax. in gases 9-34603
diatomic, quantitative correl. between rot. and vibr. spectroscopic consts. 9-30002
diatomic beam, transitions as result of scattering at solid surface 9-42364
diatomic mol., multiplet states with spin-orbit coupling intermediate between Hund's cases a and b 9-48442
diatomic potential curves, vibrational-rotational energy levels 9-48441
dibromofluoroethane, heavy hindered rotator, neutron scatt. and far i.r. spectra 9-42432
N, N-dimethylformamide, anisotropic molec. rot. in liq. 9-30433
dimethylgermane 9-42430
1,3-dioxolane, pseudorot. 9-38915

Molecules continued**rotation continued**

- ethane, rot. fine structure of perpendicular band v_1 9-34671
ethane-d₆, rotational contour in 0-0 band near 1406 Å 9-38893
ethanes, 1,2-disubstituted, barrier to internal rot. determ. from p.m.r. 9-30109
ethyl alcohol, microwave rot. spectrum, stable isomers, ground-state rot. and centrifugal distortion coeffs. 9-34668
ethyl alcohol, microwave spectrum 9-30150
ethylene, trans-d₂, anomalous struct. in v_1 band, strong Coriolis perturbation 9-38894
excitation, in diatomic mol. collisions, distorted-wave approx. 9-30159
1-fluoro-1, 1, 2, 2-tetrachloroethane, rot. isomerism, acoustic and i.r. determ. 9-27896
fluoroform, vibr.-rot. bands, computer anal. 9-38895
formaldehyde -h₂, d₂, and hd, absorp. spectra rotational fine structure analysis 9-48496
formic acid -d₂, spectrum 7.5 to 145 GHz, transition identification 9-44361
fulminic acid, ground state rotational constant from v_1 fundamental 9-34673
glycerine, liq., OH p- and d-hindered rot., cold n. scatt. obs. 9-28097
group IV hydrides and deuterides, Green's fn. calc. of Coriolis coupling and rotational distortion consts. 9-46353
Hartree-Fock theory appl. to oscillator and rot. strengths 9-38817
linear, spherical, and symmetric-top molecule, classical rotational time-correlation function obtained 9-46345
linewidth in microwave region in gases, graphical determ. 9-44310
liquid relaxation behaviour, and effect of chemical exchange 9-39117
methane, abundance and rot. temp. on Jupiter 9-40175
methane, gas and solid, inelastic neutron scatt. study 9-36717
methane-d₂, spectra, B type vibr.-rot. band analysis 9-30129
methoxyethylene, internal rotation barrier 9-46406
methyl acetylene, vibr.-rot. bands 9-23135
methyl acetylene-d₃, vibr.-rot. bands 9-23136
methyl cyanide, near i.r. spectra obs. 9-23128
methyl iodide, ¹³CH₃I, vibration-rotation bands 9-30131
methylbenzyl cyanides, diffusion consts. from n.m.r. study 9-46657
methyldiazirine 9-34676
2-methylfuran 9-48498
methylthioethyne, centrifugal distortion 9-48501
N-methylthiourea in nonpolar and polar solvents, rot. barrier about C-N bond from n.m.r. meas. 9-46658
monobromoacetylene, v_1 and $2v_1$ bands, rotational structures 9-46408
monohalobenzenes, doublet splitting in i.r. absorpt. spectrum indicating rot. structure 9-27887
NH₃, rot. line strengths, Fourier dispersion spectra, 87-667 μ 9-30043
organic compounds with three C rings, n.m.r., frequency and activation energy 9-31173
phenol, height of potential barrier for ideal gas under harmonic oscillator 9-46414
phenol, Stark effect in fine structure in dipole moment meas. on excitation 9-34686
phenylcyclobutane, rotational isomerism from c. diff. exam 9-23111
piperazine, anisotropy meas. by n.g.r. relax. 9-39930
polar liqs., rot. cor. rel. times 9-28111
polar mol., rot. transition by electron collisions 9-42465
polar molecules, rotational excitation by electrons 9-32448
polyatomic, rotational-vibrational spectra, sum rules determ. for nonrigid asymmetrical top 9-23013
polyoxyethylenes, internal rot. from mol. optical anisotropy calcs. 9-48526
polytetrafluoroethylene, torsional oscillations during room temp. crystallization 9-30472
prolate and oblate symmetric tops, far i.r. spectra 9-23079
propionyl fluoride, internal barrier functions 9-48505
n-propyl alcohol, trans. form, rot. constants 9-46416
propylene, internal rot. barrier calc. using Gaussian self-consistent field waves functions 9-48506
propylene imine, internal barrier 9-44369
propyne, mm. wave study, 68 to 119 GHz 9-44367
pseudorotation of five-membered rings 9-38916
pseudorotation of five-membered rings, theory 9-36721
reorientation in collisions between atom and diatomic mol. 9-27941
rotational excitation in collisions, closed channels and resonances 9-34699
silacyclopentane, barrier to pseudorotation 9-32528
spectra induced by vibrations, point groups examined 9-30006
spherical top mol. XY₄, vibr.-rot. Hamiltonian, tensor formulation 9-44309
tetrahedral mol. in octahedral cell, rotation-translation levels 9-38808
tetrahydrofuran, barrier to pseudorotation 9-38916
tetrahydrofuran, pseudorot. 9-38915
transition intensity for determ. of number mols./unit volume in lower level 9-27837
triatomic, linear, influence of Fermi reson. on rot. consts. 9-34593
triatomic mol., separation of vib.-rot. motion exhibited in quantum mech. kinetic energy operator 9-23021
1,1,2-trichloroethane, u.s. relax. and vol. change during internal rot. 9-42652
1,1,2-trifluoroethane, internal potential 9-44360
1, 1, 2-trifluoroethane, internal potential 9-48494
trifluoromethane, rotational microwave spectra obs. 9-30113
trifluoromethyl acetylene, rotational microwave spectra obs. 9-30113
trioxane, in v_2 excited decayed state, i.r. rotation spectrum 9-32532
vibrational-rotational energy of diatomic, calc. to 4th approx. by contact transformation method 9-27795
vibrational-rotational interactions, vib. angular momentum contrib. to normal freqs., calc. using zeta sum rules 9-30004
vibrational-rotational transitions in nonlinear mols. of XY₂ type, computation 9-27839
vibratory-rotational spectra, linewidth calc. 9-42362
vinyl iodide 9-32533
water vapour, vibrational-rotational energy levels quantum mechanical calcs., spectrum fine structure obs. 9-23049
AlO, rotational spectral lines, of (0-0) band 9-46354
AsH₃ vibration-rotation bands in 2 μ region 9-25731
AsO⁺, rot. analysis of (1,0) and (2,0) bands of A-X system 9-46355
B₂Cl₄, potential function 9-44319
BO α system, analysis of 0,2 band 9-44317

Molecules continued

- rotation continued
- BS, rotational structure of $^2\Delta_1\text{-}^2\Pi_1$ and two $^2\Sigma^+\text{-}^2\Pi_1$ transitions 9-30022
- BiF, 2250 Å system, rotational structure 9-42383
- CN, polar, transition by electron collisions, differential cross sections 9-46360
- CN, rot. transition by electron collisions 9-42465
- CO₂, constants from meas. of cw beats in bulk GaAs between CO₂ vib.-rot. lines 9-25737
- CO₂, rot. transition by collisions, relax. time calc. 9-44389
- CO₂, vibrational-rotational transitions, eff. of collisions on saturation nature 9-44323
- CO₂ isotopes, partition functions calc. 9-32468
- CaS gas, $A^1\Sigma^+\text{-}X^1\Sigma^+$ band rotational analysis, 1900°C, 6200-7200 Å 9-42389
- CIO radical, transitions in $^2\Pi_{3/2}$ and $^2\Pi_{1/2}$ states 9-38836
- D₂O, molecular g value determ. 9-34618
- D₂S, absorption spectra, far i.r. 9-27858
- D₂Se, Stark effect on $J=2_{02}\text{-}2_{11}$ and $J=6_{42}\text{-}6_{51}$ lines 9-38850
- p-H₂, and mixtures with He, Ne, Ar, rot. relax. 9-42611
- H₂, electron scatt., differential elastic and rotational excitations calc. 9-46363
- H₂, Heitler-London model, associated rotational props. 9-38848
- H₂, rot. excitation by electron impact, exchange and polarization effects 9-40591
- H₂, slow e excited, rot. transitions with vibr. quantum excitation, calc. 9-38843
- H₂¹⁸O, v_1 and v_2 bands, 2.5-3.0 μ , rotational structure 9-34624
- H₂¹⁶O, v_1 and v_2 bands, 2.5-3.0 μ , rotational structure 9-34623
- H₂ Lyman and Fulcher bands, vibr.-rot. interaction effects in Franck-Condon factors 9-30029
- H₂O, molecular g value determ. and hyperfine structure on $6_{14}\text{-}5_{23}$ transition 9-34618
- H₂S, spectra, far i.r. 9-27858
- HCN, rot. energy transfer rates, by microwave double reson. 9-30028
- HCl, polar, transition by electron collisions, differential cross sections 9-46360
- HCl, rot. transition by electron collisions 9-42465
- HF, perturbation of rot. lines by F₂, at 200 bar 9-36700
- He₂, rot. const. 9-44332
- K trioxalatoaluminate hydrated cryst., free rot. of proton pairs 9-28756
- MgBr, $A^2\Pi\text{-}X^2\Sigma^+$ system, rot. analysis of (0,0) bands 9-30036
- MgBr₂, $A^1\Pi\text{-}X^1\Sigma^+$ system (0,0) bands rotational analysis 9-42399
- N₂, in liq., Raman band shapes 9-30412
- N₂N₂⁺ 1st -ve system prod. by ion bombardment, rotational line intensities meas., 130°K 9-46429
- N₂⁺ excitation in rotational lines in controlled temperature hollow cathode discharge 9-23055
- N₂⁺ first negative system, excited by electrons, rot. temp. 9-30040
- N₂⁺ ions, motion prod. in collisions between inert gas atoms and N₂ 9-42470
- ¹⁵N₂¹⁸O, vibration-rotation bands, effects of Fermi resonance and l-type doubling 9-48470
- NF₃, equilibrium const., from vib.-rot. interactions 9-34630
- NF₃, from microwave spectra, l-type doubling and resonance in v_3 and v_4 states 9-34631
- NH, $d^2\Sigma^+\text{-}c^1\Pi$ bands, predissociations 9-34607
- NH₃, rotation-inversion spectrum 9-32481
- NH₄⁺ hindered rot. in NH₄I cryst. 9-35728
- NH₄ ion in NH₄ClO₄ 9-48970
- ¹⁵NH₃, spin rotation interaction, from Zeeman effect 9-42408
- NS free radical, rotational const. from e.p.r. spectrum analysis in gas phase 9-46369
- O₂, in liq., Raman band shapes 9-30412
- O₂, mag. dipole rot. spectrum, 12-65 cm⁻¹ 9-32483
- OCS, line broadening of various rotational transitions due to dipole-dipole, dipole-quadrupole interact., obs. 9-34639
- OD⁺, $A^3\Pi_1\text{-}X^3\Sigma^-$ transition, rot. analysis 9-44346
- OH⁺ trapped in KCl, KBr, NaCl and RbCl matrices, rot. barrier height 9-40935
- OH⁺, $A^3\Pi_1\text{-}X^3\Sigma^-$ transition, rot. analysis 9-44346
- OH excited A-doublet states, conditions for maser emission 9-34636
- OH ($^2\Sigma^+$) from photodecomp. of H₂O, initial rot. distrib. 9-38867
- PF₅, vibr.-rot. bands, computer anal. 9-38895
- PH₂ radical 9-23176
- PH₄⁺ hindered rot. in PH₄ halide cryst. 9-35728
- PO, D² Π_1 (a) and D² Π_2 (a) states 9-40602
- PbS, dipole moment from Stark components of microwave rotational transitions 9-30051
- PbTe, rot. spectrum, 11-15 GHz 9-48478
- PtCl₄ in solid K₂PtCl₆, investigation through press. depend. of ³⁵Cl NQR 9-31174
- IIF in defined rot. states, attractive interaction with rare gases, anisotropy factor 9-44390
- S₂, 0-0 band of system D-X $^3\Sigma^-$, analysis of incompletely resolved struct. and head struct. 9-48479
- SF₆, narrow reson. in Doppler line of rot.-vibr. transitions of v_3 band by CO₂-laser emission method 9-46375
- SF₆, v_3 and v_4 bands, rotational structure 9-34642
- SO₂, second and third-order changes of rot. constants by vibrations 9-32485
- SO spectrum $\beta^3\Sigma^+\text{-}X^3\Sigma^-$ and $A^3\Pi\text{-}X^3\Sigma^-$ band systems 9-38870
- SeF₄, gas-phase electron reson. 9-42416
- Sf, gas-phase electron reson. 9-42416
- SiS, dipole moment from Stark components of microwave rotational transitions 9-30051
- SnS, dipole moment from Stark components of microwave rotational transitions 9-30051
- Te₂, rot. constants suggesting $\Sigma\text{-}\Sigma$ transition from high resolution emission spectra 9-34644
- TiO, ν' system, rot. analysis of (0,0) band 9-40603
- TiF in β ,M 9-44390

vibration

- (R-O-): P(=O)H, P-H bending vibr. obs. 9-30066
- (R-O-): P(=S)(S-H), P-S-H vibr. and rot. isomers, obs. 9-30066
- acceptor-donor complexes, vib. spectra, influence of intermol. interaction 9-32447
- acetaldehyde, combination band of methyl group torsion and asymm. stretching vib. 9-25752

Molecules continued

- vibration continued
- acetic acid, anharmonicity of O-H stretching vib. rel. to dielec. const. of solvent 9-34650
- acetic acid, monomer and dimer, normal-coord. calc. 9-23083
- acetic acid and its ion, spectrum interpretation 9-42421
- acetonitrile, vibration-rotation interaction, Coriolis coupling constant 9-23085
- acetonitrile in vibr. $v_8=2$ excited state, rot. spectrum 9-46379
- acetylene, ¹²C₂D₂, ¹³C₂D₂ and ¹²C¹³CD₂ molecules, (v_4+v_5)⁰ bands 9-30068
- acetylene, force constants, cubic and quartic, calc. with general quartic force field and empirical anharmonic potential function 9-30069
- acridine, comparison with spectrum of anthracene 9-42422
- adsorbed molecules, i.r. spectra, review 9-42367
- alcohols, free and self-associated OH stretching, freqs. and anharmonicity const., depend. on deuterium substitution 9-30070
- alkali metal metabolates, force constant analysis of i.r. spectral data 9-32463
- alkali metals azides, new electronic and i.r. band after irradi., D_{3h} ion symmetry 9-27844
- alkanethiols, valence force field 9-38880
- n-alkyl acid, i.r. spectra, H bond stretching vib. determ. 9-23087
- n-alkyl chlorides series, C=2-6, vib. 9-40607
- n-alkyl cpds., combination band of methyl group torsion and asymm. stretching vib. 9-25753
- alkylarylsulphonium mixed cpds. 9-23086
- n-alkyltrimethylammonium bromides, end-group-chain coupling and force field, 1400,700 cm⁻¹ 9-44349
- amines, NH₂ group valence vibr. rel. to H bonding 9-34653
- angular momentum contrib. to normal freqs., calc. using zeta sum rules 9-30004
- anharmonic stretch-stretch interaction force const. of triatomic mols. 9-44306
- o-, m- and p-anisaldehyde in vapour phase, stretching mode 9-46382
- anthracene, comparison with spectrum of acridine 9-42422
- anthracene photodimer, i.r. spectrum analysis 9-32502
- 9,10-anthraquinone 9-23156
- aromatic aldehydes, vibronic interactions between $\pi\pi^*$ and $\pi\pi^*$ states 9-42426
- asymmetric-top energy eigenvalue sum rules based on fourth-order Hamiltonian 9-38810
- benzaldehyde, obs. 9-44352
- benzaldehyde from Raman and i.r. spectra 9-44352
- benzene, electronic vib. transition $A_{1g}\text{-}B_{2u}$ calc. 9-27888
- benzene, molec. distortions and phosphoresc. 9-30081
- benzene, vibronic intensity distrib. in phosphoresc. 9-30080
- benzenes, monosubstituted, i.r. v_{16} intensities rel. to substituent σ_p , ¹⁶obs. 9-30090
- benzenes, para-disubstituted substituents direct interaction rel. to v_{16} intensity, 1600 cm⁻¹ 9-30091
- benzenes, stretch vibrations, integral intensities of i.r. bands 9-30089
- benzimidazole, and metal complexes 9-23099
- benzine, CH-stretching overtone anharmonicity 9-27886
- benzophenone in solid state, from i.r. spectrum 9-30077
- p-benzoquinones, tetra substituted, i.r. spectra obs., vibrational frequencies calc. 9-30086
- benzo[a]anthracene photodimer, i.r. spectrum analysis 9-32502
- benzyl chloride, from Raman and i.r. spectra 9-44352
- benzyl chloride, obs. 9-44352
- benzyl formate, from Raman and i.r. spectra 9-44352
- benz[fl]indan impurity in fluorene, u.v. spectra, polarized fluorescence and absorption vibrational anal. 9-28697
- bicyclo (1.1.1)pentane from c diffraction data 9-25761
- 1,2-bis(dihaloboryl)ethanes 9-38882
- bis(trifluoromethyl)trioxide i.r. spectra, vib. modes degeneracy 9-25765
- bound states for weakly attractive potentials 9-32461
- o-, m-bromo anilines, vapour, vib. modes obs. in near u.v. absorpt. spectra 9-25762
- 0-, m-, p- bromobenzaldehyde vapours, longest wavelength $\pi\pi^*\text{-}\pi$ syst. in electr. spectra, vib. fundamentals 9-46387
- bromoform, C-H stretching vib. band, shape and width 9-48489
- β - bromophenotole, i.r. assignments 9-23101
- 2- bromopropene, combination band of methyl group torsion and asymm. stretching vib. 9-25752
- t- butylbenzene, alkyl derivative crystal, vibronic spectra, 20°K 9-31113
- γ - butyrolactone, ring deformations and i.r. and Raman spectra 9-48492
- carbon tetrabromide solute, i.r. vibrational band perturbation meas. 9-26123
- carbon tetrachloride, ν , fundamentals, chlorine isotopic splitting, using low temp. Raman cell 9-32068
- carbon tetrachloride solute, i.r. vibrational band perturbation meas. 9-26123
- carbon tetrafluoride in modified crystals., rel. to Fermi reson., 8 μ 9-28676
- chain molecules with end groups, intensities 9-34648
- chloro-methylbenzenes, hexa-substituted crystals, librational freq. 9-24418
- 2- chloroanthraquinone, vib. freq. and assignments, i.r. spectrum obs. 9-25763
- chloroform, C-H stretching vib. band, shape and width 9-48489
- α - chloronaphthalene in n-paraffin, quasiline spectra 9-46409
- 2- chloropropene, combination band of methyl group torsion and asymm. stretching vib. 9-25752
- 2-chloropropene-1,3-di, 9-40610
- CO mol., i.r. bands, self and foreign gas broadening effects, comparison 9-27848
- coherently excited, saturation and transient effects 9-25723
- crystal, combination scattering line width, temp. depend. 9-45304
- cyanogen halide-inorganic halide addition cpds., vibr. assignments, i.r. obs. 9-27847
- 2- cyanopropene, combination band of methyl group torsion and asymm. stretching vib. 9-25752
- cyanopropyne 9-23112
- cyclic polyenes, vibronic borrowing 9-44353
- cyclobutanes, vinyl, methyl and isopropenyl substituted 9-23114
- cyclobutanol, -di, -da, -ds, i.r. and Raman spectra, vib. assignment 9-23103
- cyclopentanone-da, ring deformations, and i.r. and Raman spectra 9-48492
- cyclopropane, group vibrations and vibrational analysis 9-23140
- cyclopropane, vibr.-rot. bands, computer anal. 9-38895

Molecules continued

vibration continued

- cyclopropane-H₆ and -D₆, force field and normal coordinates 9-38889
 decafluorobiphenyl, fundamentals computed using planar D_{2h} model, freq. assignment 9-30100
 deuteromethyl halide, force const., soln. of inverse eigenvalue problem 9-27838
 diatomic, quantitative correl. between rot. and vibr. spectroscopic consts. 9-30002
 diatomic molecules, predissociation probabilities for levels of bound state 9-32462
 diatomic potential curves, vibrational-rotational energy levels 9-48441
 trans-1,2-dibromide cyclohexane, normal forms and freqs. from i.r. spectra 9-36890
 p-dibromobenzene single crystals, polarized Raman spectra in intramolecular vibrational region 9-30104
 2,3-dibromobutane, assignments and force const. in liq. and solid 9-34663
 dibromofluoroethane, heavy hindered rotator, neutron scatt. and far i.r. spectra 9-42432
 dibromomethyl radical 9-44378
 2,3-dibromopentane, assignments and force const. in liq. and solid 9-34663
 p-dibromotetradeuterobenzene, i.r. and vib. spectral 9-27889
 trans-1,2-dichloride cyclohexane, normal forms and freqs. from i.r. spectra 9-36890
 2,5-dichloroaniline in solution, obs. of i.r. spectrum, assignments to vib. modes 9-32500
 2,6-dichloroaniline in solution, obs. of i.r. spectrum assignments to vib. modes 9-32500
 4,4'-dichlorobenzophenone 9-31114
 dichlorobenzene, o-, m- and n-, combinational scattering spectra, phase shift rel. to dipole-dipole intermolecular forces 9-46393
 p-dichlorobenzene single crystals, polarized Raman spectra in intramolecular vibrational region 9-30104
 1,2-dichloroethane, band envelopes rel. to struct. 9-34622
 dichloromethyl radical 9-46425
 2,4-dichlorotoluene, assignments, i.r. absorpt. spectra obs. 9-23109
 dideuteroacetylene, ¹²C₂D₂, ¹³C₂D₂ and ¹²C¹³CD₂ molecules, ($\nu_4 + \nu_5$)⁰ bands 9-30068
 difluoroacetaldehyde, F₂CO, vibrational intensity calcs. 9-38896
 2,5-difluoroaniline modes from obs. of i.r. absorption spectrum in liquid 9-32500
 difluorobenzene, m- and n-, combinational scattering spectra, phase shift rel. to dipole-dipole intermolecular forces 9-46393
 m-difluorobenzene, near u.v. absorpt. spectrum, band and fundamental vib. obs. 9-46394
 1,1-difluorocyclobutane, ring puckering 9-30101
 difluoromethyl radical 9-48517
 p-difluorotetradeuterobenzene, i.r. and Raman vib. spectra 9-27889
 2,4-difluorotoluene, assignments, i.r. absorpt. spectra obs. 9-23109
 1,2-dihalide substituted ethanes, spectra, calculation and interpretation 9-23120
 2,3-dihydrofuran, ring-puckering 9-30102
 5,8-dihydroxynaphthoquinone, i.r. and visible spectrum obs., vib. and electronic structure deduced 9-30123
 dimethylhydrogenphosphonate, P-H bending vibrs., Raman obs. 9-30066
 dimethyllead dihalides, i.r. and Raman obs., 4000-70 cm⁻¹ 9-34675
 N,N-dimethylthioacetamide, normal vib. analysis from i.r. and Raman spectra 9-46391
 N,N-dimethylthioformamide, normal vib. analysis from i.r. and Raman spectra 9-46391
 dimitrobenzenes, isomeric, vibrational spectra 9-48502
 diphenyl oxide hexane, heptane soln., quasiline absorption spectra, electronic-vibrational anal., 77°K 9-30114
 diphenyl phenylborate, frequencies from i.r. spectra 9-23151
 diphenyl sulfide hexane, heptane soln., quasiline absorption spectra, electronic-vibrational anal., 77°K 9-30114
 diphenyl sulphide and disulphide 9-23133
 diphenyl sulphoxide 9-23133
 diphenylethine and diphenylethine-d₁₀, i.r. spectra analysis 9-38909
 trans-1,2-diphenylethylene and trans-1,2-diphenylethylene, i.r. spectra analysis 9-38910
 γγ'-dipyridyl-di-N-oxide, i.r. spectrum, normal co-ord. analysis 9-46392
 dissociating polyatomic mol., ensuing geometrical change and force const. 9-44307
 2,4-disubstituted thiazole derivatives, vibration spectra and structure 9-48508
 1,3-dithian, i.r. spectrum, vibrational assignment 9-32510
 1,4-dithian, i.r. spectrum, vibrational assignment 9-32510
 durennes, monosubstituted, i.r. ν_{16} intensities re. to substituent σ_p , ¹⁶Obs. 9-30090
 eigenvector matrix properties 9-38812
 electronic-vibronic interaction, investig. using symmetry theory 9-30005
 energy exchange between diatomic mols. 9-32556
 energy operators reduction by use of symmetry 9-23014
 energy transfer in gases 9-23201
 ethane, rot. fine structure of perpendicular band ν_1 9-34671
 ethane and ethane-d₆, vib. analysis of ¹E_g-¹A_g, transition 9-38893
 ethanol, isotopic, monomers 9-38891
 ethanol, isotopic, self-associated 9-38892
 ethyl benzoate, liq. and soln., i.r. and Raman spectra, vib. freqs. assignment 9-25769
 ethyl chlorides, h_s, d₂, d₃, d_s, i.r. and Raman obs. 9-48490
 ethyl halides, combination band of methyl group torsion and asymm. stretching vib. 9-25753
 ethylene, -d₄, vibrational struct. of 1744 Å Rydberg transitions 9-44357
 ethylene, trans-D₂, ν_7 C-type perpendicular band, strong Coriolis perturbation 9-38894
 ethylene, vibr. intensity progression in V←N transition 9-30108
 ethylene carbonate, ring deformations and i.r. and Raman spectra 9-48492
 ethylene oxide, group vibrations and vibrational analysis and deuteration effects 9-23141
 ethylene sulphide, group vibrations and vibrational analysis and deuteration effects 9-23141
 ethylene thiourea, normal vibrations calc. by Wilson's GF matrix method 9-30112
 trans-ethylene-d₂, calc. of ν_7 9-48444
 ethylenes, monosubstituted, J_{13_{CH}} coupling constants 9-27894

Molecules continued

vibration continued

- Fermi resonance in mol. crystals, role of energy migration of vib. excitation along lattice 9-46344
 ferrocene, 1,1'-disubstituted cpds. 9-23121
 fluorene in hexane, heptane soln., quasiline absorption spectra, electronic-vibrational anal., 77°K 9-30114
 1-fluoro-1, 1, 2, 2-tetrachloroethane, torsional 9-27896
 2-fluoroaniline, modes from obs. of i.r. absorption spectrum in liquid 9-32500
 o-fluoroanisole, fundamental freqs. from near u.v. absorpt. spectrum 9-34672
 m-fluoroanisole, i.r. absorption spectra, vibrational 9-46395
 fluorobenzenes, NMR and i.r. correl., eff. of electronegativity 9-23122
 o- and m-fluorobenzonitriles, i.r. absorption spectra, vibrational 9-46395
 ortho- and meta-fluorobenzonitriles, u.v. absorption spectra 9-48493
 fluorobromobenzenes, o-, m- and p-, in-plane vibrations normal coordinate analysis 9-38897
 fluorochlorobenzenes, o-, m- and p-, in-plane vibrations normal coordinate analysis 9-38897
 fluoroform, vibr.-rot. bands, computer anal. 9-38895
 α-fluoronaphthalene-D₇ in n-paraffin, quasiline phosphoresc. spectra 9-46409
 α-fluoronaphthalene-D₇ in n-paraffin, quasiline phosphoresc. spectra 9-46409
 force const. matrix solns. 9-23018
 force constant calc. from observed frequencies 9-27838
 force constant solution of props. 9-30003
 force constants determ. by known ratio of freqs. 9-48445
 force constants determ. from macroscopic props. 9-27836
 force constants of mol. calc. by Urey-Bradley force field 9-30027
 force constants of mol. calc. by Urey-Bradley force field 9-30027
 force constants of polyatomic mols., *ab initio* calc. 9-40580
 force const., extremal props. 9-48446
 force const., matching method 9-34594
 force const., relationship with quadrupole coupling const. 9-42363
 Force field of Weinstock and Goodman and L Matrix method for octahedral hexafluorides 9-30019
 formaldehyde -h₂, d₂ and hd, excited state fundamental vib. frequencies 9-48496
 formic acid 9-24430
 frequencies of various bonds rel. to overall electronic environment 9-46346
 fulminic acid, p, fundamental 9-34673
 fundamental frequencies of 54 mols. 9-23017
 G matrices calc. in vibrational analysis, KDF-9 Algol program 9-30016
 gas mixtures, vib. relax. rel. to u.s. dispersion 9-32734
 glycine chelates, isomeric, far i.r. spectra, metal-O bond stretching vib. 9-27898
 group mean amplitudes and group Coriolis coupling constants 9-40579
 halides, force constants, mean-square quantities and bond energies, universal parameter 9-38840
 halogen hydrides, reduced potential curves 9-38835
 halogenated aromatic mol., out-of-plane vib., force fields 9-25768
 harmonic force-field calcs., redundant coordinates 9-36688
 heptane, frozen, fluoresc. spectra of coronene and 1,12-benzopyrene at high press., band obs. 9-32517
 heteronuclear diatomic, potential-energy, bond-charge model 9-38806
 hexafluorides, octahedral, force field of Weinstock and Goodman and L Matrix method 9-30019
 hydrides, pyramidal, mono- and deuterio-substituted, fundamental freq. and vib. forms calc. 9-25741
 hydroxy chromones, carbonyl stretching freqs. 9-30124
 i.r. absorption bands, integrated intensities, review 9-42366
 i.r. spectra, new method, use of symmetry to simplify calc. 9-27832
 isopropylbromide, assignments and force const. in liq. and solid 9-34663
 ketones, α-ethylenic, aliphatic and alicyclic, C=O and C=C stretching freqs., effect of alkyl subst. and stereochem. 9-32522
 linear triatomic, vibr.-rot. interactions 9-44325
 mercuric halide adducts of cyclic thio-ethers, ring vibrations 9-30107
 merocyanines, C-O stretching band behaviour and shape in mixed solvents 9-23137
 metal carbonyl cpds., and force const. calc., spectroscopic study 9-30020
 metal complexes with N-containing ligands, i.r. and Raman obs. of stretching and bending fund. 9-32459
 methane, induced dipole moment in ν_2 vibr. mode, Stark effect obs. 9-34678
 methane d₂ spectra, B type vibr.-rot. band analysis 9-30129
 methanethiol 9-23132
 methyl 2,3,4,5,6-pentafluorodiphenyls 9-23134
 methyl acetylene, vibr.-rot. bands 9-23135
 methyl acetylene-d₄, vibr.-rot. bands 9-23136
 methyl benzoate, liq. and soln., i.r. and Raman spectra, vib. freqs. assignment 9-25769
 methyl group tunneling splitting of torsional oscillator ground state used to calc. proton spin-lattice relaxation time 9-37671
 methyl halide, force const., soln. of inverse eigenvalue problem 9-27838
 methyl iodide, ¹³CH₃I, vibration-rotation bands 9-30131
 methylidifluoroamine, on basis of polarization and Raman spectra 9-27904
 methylene group-, group vibrations and vibrational analysis 9-23141
 methylene-group-, group vibrations and vibrational analysis 9-23140
 methylhydrazine 9-30127
 methylphenyl sulphide 9-23133
 methylphosphorodifluorodithioate 9-38902
 methylthioethyne, centrifugal distortion 9-48501
 modes assuming extremal force constants 9-36690
 monobromoacetylene, ν_1 and $2\nu_1$ bands, rotational structures 9-46408
 monofluoroacetylene, CH deform. CF stretching coupling Fermi reson., obs. 9-27882
 monohalobenzene, Fermi resonance during liquid-vapour phase transition 9-27887
 Morse oscillator, temp. depend. 9-32457
 2-naphthaldehyde, vibronic spin-orbit interactions 9-34681
 naphthalene, mean amplitudes, revised calc. 9-27907
 naphthalene in n-paraffin, quasiline phosphoresc. spectra 9-46409
 1,4-naphthoquinone 9-23156
 2-naphthyl methyl ketone, vibronic spin-orbit interactions 9-34681
 near symmetric tops, z axis coriolis coupling between perpendicular fundamentals 9-48444

Molecules continued

vibration continued
 nitrates, molten 9-39105
 nonresonant vibr.-vibr. energy transfer due to dipole-dipole interactions 9-38934
 nuclear, rel. to calc. of Raman spectrum 9-27840
 nylon, i.r. spectrum interpretation in terms of rocking-twisting and wagging 9-32552
 organic compounds with three C rings, n.m.r., frequency and activation energy 9-31173
 organogermanium cpds., spectra investigated rel. to electro-optical parameters 9-46397
 oxalic acid, and -d₂, carbonyl and C=O stretching freqs., 400-4000 cm⁻¹ 9-30133
 oxalyl bromide, band freqs. and assignments from i.r. and Raman spectra 9-34684
 oxalyl halides, attribution and analysis using normal coords. 9-46411
 pentacene, vibronic band position depend. on light polarization 9-27909
 pentafluorobenzonitrile 9-23147
 pentamethylene sulphide, i.r. spectrum, vibrational assignment 9-32510
 phenanthrene, totally symmetric vibronic perturbations rel. to 3400-Å spectrum 9-38911
 phenol, free and self-associated OH stretching, freqs. and anharmonicity const., depend. on deuterium substitution 9-30070
 phenylalanine and derivatives, vibr. struct. in near u.v., circular dichroism and absorpt. spectra 9-46415
 phenylboronic acid, frequencies from i.r. spectra 9-23151
 o-phenylenediamine, N-H frequencies in halide chelates 9-36719
 phosphiran, -1-d₁, -2,3-d₂; polarization, freq. shift meas., vib. assignment 9-23150
 phosphorescence spectrum, vibronic bands relative intensity, rel. to inter-system crossing route 9-40575
 photochemistry, vibronic effects 9-39960
 planar XY₃ mols., force consts. 9-36689
 poly 1,4-bis(β hydroxyethoxy) phenylene adipate, freqs. and forms 9-37734
 polyatomic, force consts. determ. 9-48440
 polyatomic, rotational-vibrational spectra, sum rules determ. for nonrigid asymmetrical top 9-23013
 polyatomic mol., calc. of matrix elements between vib. wavefunctions of ground and excited states 9-48443
 polyatomic mols., force constants, *ab initio* calc. 9-40580
 polycyclic azines, vibronic interactions between $n\pi^*$ and $\pi\pi^*$ states 9-42426
 polyenes, calc. of matrix elements between vib. wavefunctions of ground and excited states 9-48443
 polyethylene glycol chain, freq. distrib. 9-23194
 polymethylsiloxanes, Si-O-Si and Si-C bond stretching from i.r. vibr. absorpt. spectra 9-48510
 polypropylene, syndiotactic, Raman spectrum arising from A modes 9-30158
 polytetrafluoroethylene, vibr. anal. 9-42464
 porphyrin, vibronic borrowing 9-44353
 potential energy curve, empirical form 9-32461
 potential energy matrix, construction 9-38811
 propanoic acid far i.r. spectra, H bond stretching vib. determ. 9-23087
 propene and oxide, combination band of methyl group torsion and asymm. stretching vib. 9-25752
 propylene imine 9-44369
 propyne, rotation-vibration interac. consts., mm. wave study, 68 to 119 GHz 9-44367
 purine and deuterated derivatives 9-41397
 pyrene in methylcyclopentane at low temp., fundamental freqs. from quasi-linear fluorescence spectrum 9-38913
 pyridine-Br and BrCl complexes 9-23153
 pyridines, substituted, charge-transfer complexes with Br 9-23154
 quartic oscillator, 3-D, with $\epsilon=0, 1, 2$, energy levels 9-38809
 ring puckering in five-membered rings 9-38916
 ring puckering in five-membered rings, theory 9-36721
 rotational spectra induced point groups examined 9-30006
 selection rules for fundamentals, combinations and overtones, group theory applic., book 9-42368
 selenols, fundamental Se-H stretching freq. 9-34691
 silane, tetrahedral, spectroscopic mass and zero-order freq. calc. 9-30142
 silver nitrate adducts of cyclic thioethers, ring vibrations 9-32512
 spherical top mol. XY₄, vibr.-rot. Hamiltonian, tensor formulation 9-44309
 styrenes, o- and m-subst., fund. modes assignment from i.r. and Raman spectra obs. 9-32529
 sulphamate ion, internal vibr. calc., Urey-Bradley potential function 9-46419
 symmetric top, quadratic ζ -sum rules 9-23016
 symmetry coordinates, mixing in normal coordinates, eigenvector matrix investig. 9-38812
 tetracene photodimer, i.r. spectrum analysis 9-32502
 tetrafluorobenzoic acids, p-subst., OH stretching freqs. 9-30145
 tetraiodoethylene, i.r. and Raman vib. spectra, assignments 9-27902
 tetravinyltin, PMR spectrum, coupling const. for ¹³C, ¹¹⁹Sn and ¹¹⁷Sn satellites 9-27917
 thioalkanes, valence force field 9-38880
 thioethers, cyclic, mercuric halide adducts, ring vibrations 9-30107
 thioethers, cyclic, silver nitrate adducts, ring vibrations 9-32512
 thulium cyclopentadienides, coupling and struct. obs. in obs. spectra, low temp. 9-32531
 thulium methylcyclopentadienides, coupling and struct. obs. in obs. spectra, low temp. 9-32531
 toluene ion radicals, vibr.-electronic interaction 9-38917
 transition probability calc. in high energy collision using time-independent Schrödinger eqn. 9-34698
 transition-metal-ion complexes, EPR spectra, vib. struct. study 9-23024
 translational-vibrational energy transfer, steric factor 9-30162
 triatomic mol., separation of vib.-rot. motion exhibited in quantum mech. kinetic energy operator 9-23021
 triatomic mols., quantum dynamics 9-38807
 2,4,6-trichloroheptane, C-Cl stretching vib. in i.r. spectra 9-32546
 1,3,5 trichloropyrimidine and 4D derivative i.r. and Raman obs. 9-28139
 trifluoroacetaldehyde, i.r. vib. spectrum and internal rotation barrier 9-23123
 triglycine sulphate, H bond vibrations 9-32516
 α-2,4:6-trimethyl trithian, i.r. spectrum, vibrational assignment 9-32511

Molecules continued

vibration continued
 β-2,4:6-trimethyl trithian, i.r. spectrum, vibrational assignment 9-32511
 trimethylamine 9-30147
 trimethylamine, force field 9-23161
 trimethylamine charge-transfer complexes 9-23163
 trimethylene selenide, vibr. anal. and ring puckering 9-42447
 trimethylene sulfide, electr. spectrum, vib. struct. obs. of transitions 9-32524
 trimethyllead halides, i.r. and Raman obs., 4000-70cm⁻¹ 9-34675
 triphenylborates, force constants from i.r. spectra 9-23164
 triphenylboron, force constants from i.r. spectra 9-23164
 1:3:5-trithian, i.r. spectrum, vibrational assignment 9-32511
 undecanoic acid far i.r. spectra, H bond stretching vib. determ. 9-23087
 uranyl ion, absorption spectrum, vibronic analysis 9-25784
 vibrational deficiency in polyatomic mols., electronic consequences 9-23015
 vibrational-rotational energy of diatomic, calc. to 4th approx. by contact transformation method 9-27795
 vibrational-rotational transitions in nonlinear mols. of XY₂ type, computation 9-27839
 vibratory-rotational spectra, linewidth calc. 9-42362
 vibronic intensities, temp. depend. 9-44308
 water vapour, vibrational-rotational energy levels quantum mechanical calc., spectrum fine structure obs. 9-23049
 XY₂Z, mean square calc. 9-30001
 XY₄ normal co-ordinate analysis on basis of Urey-Bradley force field, Coriolis coupling const. 9-30000
 XY₆ molecules, force field of Weinstock and Goodman and L Matrix method 9-30019
 p-xylene, in excited electronic state 9-27920
 xylol, o-, m- and p-, combinational scattering spectra, phase shift rel. to dipole-dipole intermolecular forces 9-46393
 Ag chelates of glycine, DL α alanine, DL β phenylalanine and DL tyrosine, i.r. vib. spectra, assignments 9-23059
 AsH₃ vibration-rotation bands in 2μ region 9-25731
 AsS₃³⁻, orbital valence force field constants 9-32486
 BH₄⁻ vibrations, characts. and forms 9-42382
 BS, vibrational structure of ²Δ_g-A²Π_g and two ²Π⁺-²Π_g transitions 9-30022
 BaF₂ vapour, absorption spectra bands obs., ν₂ bending vib. assignment 9-23037
 BIF₃, gaseous, thermodynamic functions calc. from molecular geometry and vibration freq. 9-30021
 BrHBr, i.r. spectra at 20°K 9-44320
 CD₃, group-, group vibrations and vibrational analysis 9-23104
 CO₂-N₂ reson. vibr. energy transfer between mode N₂ 9-30164
 CO₂-N₂ vibrational thermal relax. times, determ. by stopping point, fluorescent and spectrophone methods 9-48455
 CO₂, relax. freq. of asymmetric stretching mode 9-34611
 CO₂, relaxation and population inversion in nonstationary conditions 9-48457
 CO₂, thermal relax. times 9-42385
 CO₂, vibrational-rotational transitions, eff. of collisions on saturation nature 9-44323
 CO₂, vibrational thermal relax. times, determ. by stopping point, fluorescent and spectrophone methods 9-48455
 CO₂ isotopes, partition functions calc. 9-32468
 CO₂ laser, temps. from visible sidelight emission, obs. 9-47977
 CO₂ vibr. excitation by dipole interaction with slow electrons 9-36697
 CO₂(ν₂) vibrationally excited, deactivation by collisions with CO₂ or N₂ 9-42387
 COS, mean amplitude and valence force consts. 9-23032
 CaF₂ vapour, absorption spectra bands obs., ν₂ bending vib. assignment 9-23037
 Ca(H₂PO₄)₂·H₂O, H₂PO₄ and H₂O vibrs., 4000-200 cm⁻¹ 9-44347
 Cd complexes with o-phenylenebisdimethylarsine 9-23078
 Cd halides 9-40589
 ClO₂, vib. analysis of 4750 Å band syst. 9-32469
 ClO₂F, E-species force consts. 9-30050
 Co₂, deactivation of bending mode by H₂ and D₂ 9-23034
 Co₃²⁺ in KCl cryst., i.r. absorpt. spectra 9-41382
 Co complex, Co(NCS)₂(p-picoline)₂, pC-H freqs. of clathrated mono- and di-subst. benzenes 9-48475
 Co(NH₃)₆³⁺, first band intensity 9-23039
 CsOH, vibr.-rot. interactions 9-44325
 Cu bistoplonate, single cry. electronic spectra, odd vib. obs. 9-24407
 Cu II tetrahalo-anions, ν₁(A₁) mode and force consts., Raman obs. 9-44327
 CuCl₂·2H₂O, vibrational analysis by i.r. spectra 9-38839
 D₂S, centrifugal distortion constants and inertia defects, calc. introducing anharmonicity influence 9-38851
 D₂Se, centrifugal distortion constants and inertia defects, calc. introducing anharmonicity influence 9-38851
 F₂CO, intensity calcs. 9-38896
 Fe II tetrahalo-anions, ν₁(A₁) mode and force consts., Raman obs. 9-44327
 Fe III tetrahalo-anions, ν₁(A₁) mode and force consts., Raman obs. 9-44327
 GeCl₄, ν, fundamentals, chlorine isotopic splitting, using low temp. Raman cell 9-32068
 GeD₇AsD₂, assignment of freqs. using normal co-ordinate calc. 9-30026
 GeD₇AsH₂, assignment of freqs. using normal co-ordinate calc. 9-30026
 GeD₇PD₂, assignment of freqs. using normal co-ordinate calc. 9-30025
 GeD₇PH₂, assignment of freqs. using normal co-ordinate calc. 9-30025
 GeF₂ in gas and solid Ar, Ne, i.r. obs. 9-27853
 GeH₇AsD₂, assignment of freqs. using normal co-ordinate calc. 9-30026
 GeH₇AsH₂, assignment of freqs. using normal co-ordinate calc. 9-30026
 GeH₇PD₂, assignment of freqs. using normal co-ordinate calc. 9-30025
 GeH₇PH₂, assignment of freqs. using normal co-ordinate calc. 9-30025
 GeH₇CN force constants of mol. calc. by Urey-Bradley force field 9-30027
 H-bond low-freq. vibr. assignments from far-i.r. studies 9-32453
 H₂D₂ mixed solid solutions, i.r. spectra induced into vibrational first harmonics, 4°K 9-33558
 H₂, disintegration of short-lived compound state in system e-H₂ C¹u V=0,1,2,3,... states 9-46364
 H₂, Franck-Condon factors for three band systems 9-32476
 H₂, Franck-Condon factors for three band systems 9-30032

Molecules continued
vibration continued

- H₂, slow e excited, rot. transitions with vibr. quantum excitation, calc. 9-38843
- H₂, vibr. terms of ground-state ($X^1\Sigma_g^+$) 9-36725
- H₂⁺, discrete vib. states due only to long-range forces 9-44328
- H₂¹⁶O, ν_1 and ν_2 bands, 2.5-3.0 μ , rotational structure 9-34624
- H₂¹⁸O, ν_1 and ν_2 bands, 2.5-3.0 μ , rotational structure 9-34623
- H₂ Lyman and Fulcher bands, vibr.-rot. interaction effects in Franck-Condon factors 9-30029
- H₂ mol. beam collision with Li⁺, vibr. excitation meas. 9-25796
- H₂CO, band envelopes rel. to struct. 9-34622
- H₂O, i.f. in ionic solns. 9-44547
- H₂S, centrifugal distortion constants and inertia defects, calc. introducing anharmonicity influence 9-38851
- H₂Se, centrifugal distortion constants and inertia defects, calc. introducing anharmonicity influence 9-38851
- HBr-HBr collisions, vib. transitions $P_{1,0}$ probabilities 9-25797
- HBr, vibr. relax. in shock waves 9-42396
- HCN, dipole moment variation with vibrational state 9-30047
- HCO radical, CH stretching, anharmonic potential constants 9-38852
- HCl-HCl and H₂Cl-H₂Cl collisions, vib. transitions $P_{1,0}$ probabilities 9-25797
- HCl, vibr. relax. 9-32474
- HCl, vibr. relax. behind shock waves 9-30030
- HCl and DCl in shock waves, vibr. relax. 9-38847
- HCl effect of inter-molecular interactions on vibrational spectra in i.r. region 9-23050
- HCl prod. in H+S₂, S₂Cl₂, SO₂, SO₂Cl₂ reactions, i.r. chemiluminesc. obs. 9-32473
- HDO, band envelopes rel. to struct. 9-34622
- HF-H₂FHe, Ar; collisions, vib. transitions $P_{1,0}$ probabilities 9-25797
- HF vibrational structure in the region of first ionization potential 9-34625
- HI-Ar, HI; collisions, vib. transitions $P_{1,0}$ probabilities 9-25797
- HNO₃, potential constns. 9-23058
- HNO₃ and DNO₃, normal co-ord. treatment for physically true force constns. in vapour and liquid states 9-46362
- He₂, $F^1\Pi_u$ and $F^3\Pi_u$ states, quantum-mechanical exam. 9-34626
- He₂, potential energy curve, empirical form 9-32461
- Hg (II) complex, o-phenanthroline, Raman and i.r. spectra, vib. freq. determ. 9-23052
- Hg complexes with o-phenylenebisdimethylarsine 9-23078
- Hg halides 9-40589
- HgCl₂, HgBr and HgI 9-34627
- Hi, vibr. relax. in shock waves 9-42396
- I₂, Morse oscillator, temp. depend. 9-32457
- I₂⁺, vib. freq. from resonance Raman spectrum 9-38856
- ICN, Fermi reson. const. 9-32467
- IF₄⁺, vibrational assignments 9-25743
- LiF₂ lin. dimer species, vib. assignments, obs. in i.r. matrix spectra of LiF 9-23053
- LiO₂, i.r. 9-44333
- MgF, Franck-Condon factors and r-centroids for A-X system 9-46367
- MgF₂ vapour, absorption spectra bands obs., ν_2 bending vib. assignment 9-23057
- Mn II tetrahalo-anions, $\nu_1(A_1)$ mode and force constns., Raman obs. 9-44327
- MoS₄²⁻, orbital valence force field constants 9-32486
- Mo(VI) dioxobis (acetylacetonate) 9-23076
- N₂-N₂O mixtures, vibration-vibration energy exchange, shock-tube study 9-34706
- N₂ O₂ vibr. exchange in shock tube 9-30349
- N₂⁺ Σ_u^+ perturbed level, deperturbed crossing Morse curves calc. 9-27863
- N₂⁺ ions, motion prod. in collisions between inert gas atoms and N₂ 9-42470
- N₂F₄ 9-23505
- N₂O, band profile determ. in various solvents and correlation function calcs. 9-44571
- N₂(A³ Σ_u^+), quenching in low vib. levels by N atoms 9-44340
- N containing anions, attenuated total refl. spectra, aqueous solns., i.r. vib. freq. 9-28135
- ¹⁵N₂¹⁶O, vibration-rotation bands, effects of Fermi resonance and l-type doubling 9-48470
- NCO, vibrationally excited, gas phase electron reson. spectrum 9-40599
- ND, revised vib. constants for b¹ Σ^+ state 9-46368
- NF₃, from microwave spectra, Σ^+ type doubling and resonance in ν_3 and ν_4 states 9-34631
- NH, revised vib. constants for b¹ Σ^+ state 9-46368
- NH₄ salts in liq. NH₃, conc. soln., i.r. spectra analysis 9-30042
- NH₄Cl₃NH₃, i.r. spectra analysis 9-30042
- NO₂, by Ar⁺ and Kr⁺ lasers 9-40596
- NO₂, near-i.r. vib.-rot. bands, Zeeman spectra 9-36702
- NO₂⁻ in KCl cryst., i.r. absorpt. spectra 9-41382
- NO formed in vibrationally excited state in N+NO₂O+NO 9-24539
- NOF, potential constns., refinement 9-30041
- Na salts of glycine, DL α alanine, DL β phenylalanine and DL tyrosine, i.r. vib. spectra, assignments 9-23059
- NaI, hyperfine-structure sublevels of J=1 state, r.f. transitions obs. 9-40600
- Na(SiO₃)₂ glass, spectral obs. 9-28674
- NbOBr₃, metal-O stretching vibr. freq. 4000-400 cm⁻¹ 9-27869
- NbOCl₃, metal-O stretching vibr. freq. 4000-400 cm⁻¹ 9-27869
- NbOI₃, metal-O stretching vibr. freq. 4000-400 cm⁻¹ 9-27869
- Ne₂ potential energy curve, empirical form 9-32461
- Ni complex, bis(monothioacetylacetonato) Ni(II), vibr. spectra 9-46370
- Ni complex, Ni(NCS)₂(p-pioline), γ -C-H freqs. of clathrated mono- and di-subst. benzenes 9-48475
- Ni(CN)₄ ion 9-24426
- No, relaxation, negative temp. effect 9-42409
- O, motion in condensed phases, Raman obs. 9-49296
- O₂, Schumann-Runge bands, predissociation 9-32462
- O₂, Schumann-Runge bands, predissociation 9-32462
- O₂⁻ luminescence centres in alkali halides, effect of hydrostatic press. 9-39864
- O₂⁻ luminescence centres in alkali halides 9-39862
- O₂⁻ luminescence centres in KBr, config. coordinate curves 9-39868
- O₂⁻ luminescence centres in alkali halides 9-39861
- O₂ in atmosphere, electron cooling by vibrational excitation 9-43444

Molecules continued
vibration continued

- O₂ Schumann-Runge system, inc. high vibr. quantum nos., Frank-Condon factors 9-46373
- OCS, dipole moment variation with vibrational state 9-30047
- OMO groups of inorganic complexes, stretch freq. selection rules 9-38868
- ONBr, isotropic species, vibrational spectra and force constants 9-46372
- P₄O₁₀, assignments and force constns. rel. to P-O bond orders 9-27871
- P₄O₆, assignments and force constns. rel. to P-O bond orders 9-27871
- PCl₃, potential energy constants and mean amplitudes of vibn., from vibr. spectral data 9-48477
- PD₃ force const. meas., freq. depend. on valence angle 9-25747
- PF₃, potential energy constants and mean amplitudes of vibn., from vibr. spectral data 9-48477
- PF₃, vibr.-rot. bands, computer anal. 9-38895
- PH₃ force const. meas., freq. depend. on valence angle 9-25747
- PO₄³⁻, coupled vib. in Ca₁₀(PO₄)₆F₂ cryst. 9-37317
- POF₃, E-species force constns. 9-30050
- POF₃, potential energy constants and mean amplitudes of vibn., from vibr. spectral data 9-48477
- PSCl₃, potential energy constants and mean amplitudes of vibn., from vibr. spectral data 9-48477
- PSF₃, E-species force constns. 9-30050
- PSF₃, potential energy constants and mean amplitudes of vibn., from vibr. spectral data 9-48477
- Pd complex, Pd(II)X₂Y₂ (X=Cl, Br or I, Y=Me₃P or Me₃As), metal-ligand and metal halogen stretching modes 9-30052
- Pd cpds. type PdX₂Y₂, effect of co-ordination on internal modes 9-23068
- cisPdII trimethyl-arsine, -phosphine, -stibine complexes, obs. 9-27872
- Pt complex, Pt(II)X₂Y₂ (X=Cl, Br or I, Y=Me₃P or Me₃As), metal-ligand and metal halogen stretching modes 9-30052
- Pt cpds. type PtX₂Y₂, effect of co-ordination on internal modes 9-23068
- cisPtII trimethyl-arsine, -phosphine, -stibine complexes, obs. 9-27872
- RbOH, vibr.-rot. interactions 9-44325
- Re complex, hexahalogen, K and Cs salts, force constns. 9-32487
- Re(CO)₆⁺, fundamental, combination and overtone freqs. assignment, CO stretching force constant calc. 9-32491
- ReClO₃, theoretical anal. 9-23069
- RuO₄, force field 9-42415
- S₂⁻ impurity centre in KBr, luminesc., config. coord. curves 9-39869
- S₂⁻ luminescence centres in alkali halides 9-39861
- S₂O₃²⁻ normal vibrations 9-27876
- SF₆, narrow reson. in Doppler line of rot.-vibr. transitions of ν_3 band by CO₂-laser emission method 9-46375
- SF₆, ν_3 and ν_4 bands 9-34642
- SF₆, Raman spectrum in solid, splitting of three fundamentals 9-30053
- SF₆, saturation of energy levels by absorpt. of i.r. laser rad. 9-48480
- SO₂, ν constants effect on harmonic and anharmonic potential constants 9-32485
- SO₂ in inert gas matrix, fundamental freqs. from i.r. spectrum 9-34641
- SO₂ isotopes in solid Kr matrices 9-42417
- SO₂⁺ in KCl cryst., i.r. absorpt. spectra 9-41382
- SPF₃, assignment using normal co-ordinate calcs. 9-30055
- SbS₄³⁻, orbital valence force field constants 9-32486
- SeO₂, bending vib. of ground state, vibrational analysis of three electronic transitions 9-23073
- SeO₂ in inert gas matrix, fundamental freqs. from i.r. spectrum 9-34641
- SiCl₆, eleven active fundamentals for D_{3h} or D_{3h}⁻ point groups, assignment 9-30056
- SiCl₄, force constns., mean amps., shrinkage effect and Coriolis coupling 9-48482
- SiCl₄, ν_1 fundamentals, chlorine isotopic splitting, using low temp. Raman cell 9-32068
- SiH₃CN force constants of mol. col. by Urey-Bradley force field 9-30027
- Sn complex, Et₃SnCl₃, Et₂SnCl₂ and Et₃SnCl liq. or soln., vib. spectra and normal coord. anal. 9-48484
- SnCl₄, ν_1 fundamentals, chlorine isotopic splitting, using low temp. Raman cell 9-32068
- SrF₂ vapour, absorption spectra bands obs., ν_2 bending vib. assignment 9-23037
- Tc complex, hexahalogen, K and Cs salts, force constns. 9-32487
- Ti complex, Ti(en)Cl₄ and Ti(en)Br₄ partial normal coord. analysis 9-38871
- UO₂²⁺, bend fundamental freq., from i.r. spectra of uranyl salts 9-49287
- V(CO)₆⁺, fundamental, combination and overtone freqs. assignment, CO stretching force constant calc. 9-32491
- VOF₃, E-species force constns. 9-30050
- VS₄²⁻, orbital valence force field constants 9-32486
- WS₄²⁻, orbital valence force field constants 9-32486
- W(VI) dioxobis(acetylacetonate) 9-23076
- Zn (II) complex, o-phenanthroline, Raman and i.r. spectra, vib. freq. determ. 9-23052
- Zn complexes with o-phenylenebisdimethylarsine 9-23078
- Zn II tetrahalo-anions, $\nu_1(A_1)$ mode and force constns., Raman obs. 9-44327
- ZnBr band spectrum in near u.v., vibr. constns. 9-46377
- Zr complex, tetrafluoride adducts of p-subst. pyridine-N-oxides, N-O and metal-ligand stretching freqs. 9-32493

Molecules, mesic and muonic

- mesic, large, model, and relevant expt. data 9-40571
- S-state matrix elements for muonic molecules 9-38928

Mollier diagrams see *Thermodynamic properties***Molybdenum**

- annealing under high vacuum, use of cryogenic vacuum pumps 9-26367
- cathode spot fixator, destruction mechanism 9-49169
- cold worked, recovery 9-39463
- in compounds, L level shifts and width changes 9-48400
- conductivity, elec., jump during melting 9-26156
- de Haas-van Alphen meas. 9-26499
- deformed by hydrostatic extrusion, dislocation struct. by electron microscopy 9-40950
- deformed struct., X-ray diff. topography 9-42815
- diffusion of P, interstitial mechanism, 2000-2220°C 9-35132
- diffusivity of N 9-40985
- dislocation structure, revealed by etching in hot Ar stream 9-32972
- dislocation velocity and macro-deformation 9-46823
- dislocations, large helical, X-ray obs., equilibrium vacancy conc. derivation 9-35094

Molybdenum continued

- ductile-brittle transition temp., depend. on strain rate, neutron irradi., press. and grain size 9-30742
electrochemical behaviour 9-31206
electron irradiated, dislocation pinning and depinning, 45° to 330°K 9-28294
electronic structure determ. from X-ray emission spectra 9-37755
emissive power and specific resistivity above 400°K, relationship 9-39547
emissivity, effect of oxide film 9-28435
energy levels in VII, VIII and IX spectra 9-46287
enthalpy and specific heat, 1000-2850°K 9-37356
films on BeO, thermal conductivity 9-24063
internal friction, effect of previous deform. in tension or torsion 9-41002
isotope effect on Mo₂B supercond. transition temp. 9-30872
K α X-radiation absorption by Pb in brass, depend on particle size in multiphase syst. 9-24440
lattice vibrations 9-35270
neutron irradi., elec. resistance recovery, effect of hydrostatic pressure 9-35342
neutron irradi., hydrostatic press. induced recovery of lattice parameter increases 9-40909
optical isotope shift, nucl. vol. and mass eff. 9-29988
phonon dispersion relations calc. from Sharma-Joshi theory, specific heat calc. 9-48946
plastic deformation, initial stage meas. by microstrain techniques 9-46891
recovery of lattice parameter increases due to neutron irradi., hydrostatic press. induced 9-40909
recrystallization, secondary, of foil, electron microscopy obs. 9-46923
reflection coefficient for near normal incidence of 1.4-11 eV photons 9-43230
rolling texture in single crystals, X-ray diff. exam. 9-41040
secondary ion scatt. by single crystal, angular relationships in energy spectra 9-47217
single crystal, thermal props. 9-41106
solubility of N, heat of soln. determ. 9-40985
spectral emittance, i.r. 9-45327
substrate for ZnS films, epitaxy 9-28216
as supporting structures for semiconductor devices 9-30935
surface interaction with O₂, low-energy electron diff. 9-42732
surface ionization, negative, of Br on (100) face 9-49179
surface ionization of Li atoms 9-44281
surface layers, work-hardened, crystal structure changes prod. by vacuum annealing 9-32932
target, bombarded by positive and negative ions of Cl, O and H, secondary electron emission 9-31010
thermal expansion at low temp. 9-37359
u.s. irradi. of single crystal producing increased dislocations and attenuation of 5-30 Mc/s u.s. 9-40952
work function and surface energy correlation 9-33414
X-ray M absorpt. spectra in u.s. region, absorpt., coeff. depend. 17-200 Å 9-37754
CaTiO₃:Fe-Mo, photobleachable electron-beam-induced colouration obs. 9-43201
Cs and Ba coated, total energy distrib. of field-emitted electrons 9-45031
Fermi surface investig. based on r.f. size effect, 1.7° to 4.2°K 9-37408
films, vacuum deposited, struct. and props. in rel. to deposition rate and temp. 9-36943
Mo, electron irradiated, rel. to dislocation pinning and depinning, 45° to 330°K 9-28294
Mo³⁺ absorpt. and fluoresc. spectra in aluminoboro-phosphate glasses 9-47350
Mo V in NaHSO₄-KHSO₄ melt and glass, spectra 9-37729

Molybdenum compounds

- alloys, supporting structures for semiconductor devices 9-30935
molybdenite, etch pit ion formations rel. to vacancy oxidation 9-28281
molybdenum permalloy tapes stress sensitivity and mag. squareness ratio. effect of comp. and heat treatment 9-49205
oxides, superconducting transition temp. determ. rel. to tungsten bronze type structure 9-26530
steel, carburized Cr-Mo, transform. features 9-41073
steel, Cr-Ni-Mo high C low alloy, fatigue strength rel. to hardness, obs. 9-26345
steels, embrittlement in temp. range of α - γ transformation 9-28369
Fe-(11 at.%)Mo alloy, precipitation eff. on mechanical behaviour 9-35173
Fe-Mo alloy, X-ray K-absorpt. edges of Fe, position investig. 9-33571
Fe-Mo alloy precipitates, fine faults and cryst. struct., electron microscope obs. 9-42787
Fe-Mo solid solns., creep behaviour, temp. and stress depend. 9-30669
Fe-(9.3 at. %)Mo alloy, ϵ -phase precip., superimposed deform. effect 9-39497
K₂MoO₃, with tungsten bronze type structure, superconducting transition temp. determ. 9-26530
Mo-Nb:Co alloy, Kondo temp. indepen. of host composition from resistivity and susceptibility meas. 9-45067
Mo-Nb alloys, electrical conductivity, theory and expt. 9-24127
Mo-(27 at.%)Re alloy single crystal, thermionic emission of (100) face 9-47211
Mo-Rh alloy, metal-metal carbide eutectic temp. determ. 9-34951
Mo-W alloys, electrotransport and diffusion, tracer technique 9-28320
Mo-Zn alloys prepared by reduction of volatile halides, phase diagram obs. 9-39466
Mo-(0.05-0.20wt.%)Ti₂Zr alloys, deformed, effect of annealing at 1100-2000°C on dislocation and mechanical props. 9-40951
Mo₂B, isotope effect on transition temp. 9-30872
Mo₂BC, crystal structure determ. of light atom positions 9-39286
Mo₂S single crystal, nucleation of Ag film 9-34992
Mo(10wt.%)Fe solid solutions, precipitation behaviour after rapid cooling 9-35207
MoO₃:V, e.s.r., hyperfine struct. lines 9-39907
MoO₃-CuO₃ phase diagrams in O₂, air, and under O₂ press. 9-35256
MoO₃-MgMoO₄ system, thermo-optical determ. of equilibrium diagram for new phase 9-23978
MoO₃:MoO₂ crystal growth, spiral-type, and microstruct. 9-30526
MoO₃, heated, crystallographic shear planes and non-stoichiometry obs. 9-35106
MoO₃, Moire pattern due to electron bombardment in microscope 9-42791
MoO₃, optical props. obs. 9-33536

Molybdenum compounds continued

- MoO₃ evaporated film, Au interface, capacitance depend. on geometry, a.c. meas. 9-37566
MoO₃ thin-film detector of H atoms 9-22987
MoS₂, dislocations at contact boundary with Mg film 9-32973
MoS₂, exciton absorption and band struct. eff. of pressure and temp. 9-28449
MoS₂, rhombohedral, geological conditions of formation 9-48782
MoS₂, exciton absorpt. spectrum, illustrating the spectrophotometric derivative method 9-27409
MoS₂²⁻, orbital valence force field constants 9-32486
 α -MoTe₂ single cryst., photovoltage obs. 9-33411
Mo(VI) dioxobis(acetylacetonate), i.r. spectrum 9-23076
Mo-Re alloys, field emission and surface struct. in α - and σ -phases 9-24250
Nb-Mo, solid solution alloys, lattice thermal conductivity, normal and superconducting state 9-30797
Nb-Mo alloy, thermal expansion at low temp. 9-37359
Nb-Mo alloys, thermal and elec. conductivities, Nernst-Ettinghausen coeffs. 9-47091
Ni-Mo alloy, solubility of H 9-39478
Ni-Mo alloys, eff. charge and diff. coeff. of Ni 9-26202
Ni-Mo alloys, metal surface atoms electronic interact. with anionic complexes in corrosion 9-28801
Ni₃(Fe, Mo) alloys, atomic ordering effects 9-32927
Ni₃(Fe, Mo) alloys, ferromag. ΔE -effect, Mo content depend. 9-47242
Ta-(20 at.%)Mo alloy single crystal, thermionic emission of (100) face 9-47211
Ti-(8wt.%)Al-(1wt.%)Mo-(1wt.%)V alloy sheet, hot-salt-stress-corrosion cracking and effect on tensile props. 9-23923
Ti-Mo alloys, effect of ω -phase precipitates on superconductivity and sp. ht. 9-35370
Ti-Mo dil. alloys, martensitic, supercond. transition temp. enhancement 9-37477
U-(0.45 wt.%)Mo, transform. kinetics rel. to cooling rates and overheating temp. 9-41069
U-UAl₂-Al₃Mo₃-Mo system, melting equil. 9-39133
W-Mo alloy, metal-metal carbide eutectic temp. determ. 9-34951
W-Mo alloy, secondary ion emission under effect of slow ions 9-24259

Monitoring see *Radiation monitoring*

Monochromators

- see also *Filters, optical; Light sources; X-ray monochromators*
aplanatic prisms, application 9-48120
attachment, for photoelec. absorption spectra recording 9-29489
bremsstrahlung for photon scatt. investig. 9-42007
electron, mirror application 9-22351
far u.v., SP-107 for 13-125 nm 9-32059
grating, concave vacuum with 1m variable range and translational scanning 9-41964
grazing-incidence vacuum u.v. type with fixed exit slit, for distant sources 9-25382
neutron, Ge monochromator, simple method of increasing mosaic spread 9-44082
single-beam, computer control, hardware 9-36397
spectroheliograph, rocket-borne, for Mg II line at 2802.7 Å 9-36396
ultra violet, with concave grating, determination of optical constants of uniaxial crystals 9-25385
u.v. grazing incidence vacuum type, with fixed exit slit for use with distant source 9-41966
vacuum, scattered light elimination and measurement 9-34230
X-ray crystallographic, focusing-type 9-23705

Monolayers see *Adsorbed layers*

Monomers see *Molecules*

Monomolecular layers see *Adsorbed layers*

Monte Carlo method see *Statistical analysis*

Moon

- 'mascons' at ringed maria rel. to acceleration residues and gravity field 9-33924
age of surface, rel. to obs. of ancient giant craters 9-38066
albedo, spectral, mid-u.v., Zond-3 probe obs. 9-33929
atmospheric constituents, coincidence mass spectrometer applic. feasibility 9-47668
auxiliary tables and related texts from late Babylonian period 9-41673
chemical composition of surface at Surveyor landing sites 9-29061
colour, differential, time depend., obs. and possible mechanisms 9-31586
composition, Surveyor V-VII obs. and interpretations 9-24844
composition calcs. 9-43621
cooling of cratered surface, infrared observations 9-31591
coordinates, absolute, of 906 lunar features 9-24837
Copernicus crater, photograph from Orbiter II misidentified 9-24841
Copernicus crater, volcanic theory 9-24838
craters, circularity of 487, and relations to formation 9-27072
craters, size, distrib. and location, of classes 1, 2 and 3625 km D. 9-47668
craters, size distrib. and location of classes 1, 2 and 3>25 km diameter on front face 9-47667
dark side, cartographic gridding of photographs received from Zond-3 9-43684
density rel. to nucleation of planets by heavy metallic elements 9-41674
dynamical figure, asymmetry prod. by mascons 9-33925
Earth-Moon system, mass rel. to sun, from obs. of Eros (1893-1966) 9-27075
earthshine and crescent, photographs at 2° solar elongation 9-33938
eclipse of 18 Oct 1967, 1.4 and 3.4 mm obs. 9-43611
exosphere, lateral transport of Ne and heavier constituents 9-29059
flashes from surface, obs. (in 1789) 9-24839
force function, deriv. using DOD-66 Selenodetic Control System 9-31587
full, enhancement of hydromag. emissions 9-41603
gamma ray investigation, and lunar rocks composition 9-33933
gravitational field, from lunar Orbiter tracking data 9-33937
gravity field, acceleration residues over ringed maria rel. to 'mascons' 9-33924
highland composition rel. to evolution of earth's crust 9-31593
influence on auroral periodicity 9-33809
interaction with solar wind 9-33953
internal composition models with pressure, temp., and compositional effects 9-45662
laser range measurements to lunar corner reflector 9-33927
libration clouds, detectability at small phase angles 9-33926

Moon continued

- luminescence, obs. correl. with K_p index, irrelevance of magnetospheric effects 9-47666
 magnetic fields induced inside rot. spherical conductor by external sources, calc. 9-31599
 magnetic induction from time varying interplanetary field 9-31594
 magnetic props., intrinsic, Explorer 35 obs. 9-29057
 mascons, information from spacecraft orbits, popular article 9-47607
 mascons, origin rel. to hypothesis of water presence 9-45663
 mascons, prod. of asymmetries in dynamical figure 9-33925
 moments of inertia and gravity field 9-49576
 multiple mountain, ring-like structures, model of 'frozen tsunamis' 9-31597
 occultation obs. 1960-1966, analysis 9-43615
 occultation of Sagittarius A 9-24818
 orbital history, integrals of motion 9-31596
 Orbiter 2 photographs, volcanic interpretation 9-24838
 origin due to fission of proto-earth 9-43614
 outermost layer, density-depth model 9-31592
 particles size-frequency distributions 9-45660
 photographic obs. from lunar Orbiter missions 9-33936
 plasma, low energy, Explorer 35 obs. 9-29095
 polarization-albedo relation for selected regions 9-31598
 radar ranging expt. for students 9-43706
 radiation, meas. at 1.2 mm 9-29104
 radiation and thermal models 9-27074
 radiation meas. at 3.2 cm, during 1964-1966 period 9-41672
 radio emission, effect of heat flux from interior 9-24835
 radio emissions, polarization characts. allowing for averaging by knife antenna pattern 9-40170
 radiocommunication via artificial lunar ionosphere 9-36017
 radius, from radar obs. 9-33928
 river dimensions, geometric and physical scaling from Earth systems 9-43616
 rock fragmentation on surface 9-43613
 rocks, composition, gamma-ray investigation 9-33933
 satellite orbit, first order changes and disturbing function 9-47605
 satellite orbit, secular and periodic changes, first and second order 9-47606
 scattering of radiowaves, 1.7 m, 'Luna-11' and 'Luna-12' observations 9-24840
 seismic refraction system 9-43610
 sinuous rilles, distrib. rel. to subsurface water and volatiles 9-36019
 soil, particulate thermophysical model 9-36016
 soil mechanics surface sampler 9-40171
 soil structure and mech. props. determ. by automatic stations 9-27071
 solar proton and electron shadowing (10-22 Nov., 1967) 9-29094
 solar wind detached compression wave, Explorer 35 obs. 9-29062
 solar wind interaction, kinetic theory 9-27100
 solar wind interaction, lab. simulation 9-31595
 solar wind interaction, wake at large distance 9-29058
 solar wind interaction and limb shock wave formation 9-36018
 space probe obs., and of planets, conference 9-33943
 spectra, 8-14 μ 9-24845
 spectra, comparison with Venus 9-38075
 spectroscopic observations in mid-i.r. region 9-29063
 surface, age, rel. to obs. of ancient giant craters 9-38066
 surface, correlation of surface material with temperature 9-43612
 surface, i.r. spectrophotometry from Zond-3 probe 9-33930
 surface, large-scale evolution 9-31588
 surface, mechanical props. from Surveyor III obs. around its landing site 9-33935
 surface, oblique-scattering radar reflectivity, Explorer 35 preliminary results 9-29060
 surface, spectral albedo in mid-u.v., Zond-3 probe obs. 9-33929
 surface, spectral reflectivity differences 9-49577
 surface and early history of the Earth's satellite system 9-31590
 surface and environment at Surveyor 1 landing site 9-33934
 surface and interior, recent spacecraft obs. 9-49578
 surface chemical composition analysis by direct methods 9-24836
 surface density, radiothermal and radar estimation 9-24842
 surface erosion by water, evidence 9-24843
 surface interaction with interplanetary matter 9-38067
 surface light-scattering, single-colour investigation of uniformity 9-31589
 surface soil, mechanical props. and density, Luna 13 instrumentation 9-33932
 surface structure at Luna 9 and Luna 13 landing sites 9-33931
 Surveyor III obs. around its landing site 9-33935
 temperature distribution 9-29064
 thermal anomalies in Mare Humorum, comment 9-47665
 thermal anomaly in Mare Humorum, internal heating rejected as the mechanism 9-47664
 thermal conductivity equation in presence of radiative energy transfer 9-27245
 thermal emission, meas. using balloon-borne instrument as part of far i.r. sky survey 9-29102
 tidal effect in F2-region of ionosphere, at low latitudes 9-47583
 topography representation, validity of truncated series of surface harmonics 9-27073
 Volume integrals relating form of surface to gravity harmonics 9-31587
 wake, dependence on solar wind characts. 9-49588
 wake, mag. field at large distances, Mariner 4 obs. 9-41697
 wake, perturbed interplanetary mag. field, Explorer 33 and 35, obs. 9-27090
Morse potential see *Kinetic theory; Molecules/intermolecular mechanics*
Mosaic structure see *Crystal structure/microstructure*
Mossbauer effect
 see also *Gamma-rays/absorption; Nuclear excitation*
 absorption spectra of single crystals, coherence and polarization effects 9-24376
 acoustic, theory and appl. 9-34088
 alkali dithioferates (III), tetrahedral 9-43220
 atomic, quantum treatment in book on approximation methods 9-40242
 biotites, Fe ordering and ferrous-feric ratio obs. 9-41367
 γ ray diffraction on crystals containing nuclei at lattice sites with nonuniform elec. field 9-31087
 Champeney and Moon's relativistic freq. shift expt., comments 9-45750
 conversion electrons prod. following γ bombard. used to investigate surface structure 9-30476
 corundum, of ^{57}Fe , eff. of hyperfine structure stabilization 9-26719

Mossbauer effect continued

- detection, simple method dispensing with multi-channel analyzer 9-29650
 diffusion of Mossbauer nuclei, influence on γ reson. scatt. 9-41363
 diocetylinoxide, lattice dynamic anisotropy and line asymmetry obs., 60-320°K 9-39822
 Doppler second-order shift and mass-change shift, difference 9-39815
 Dowex 50 resin, exchangeable Fe^{2+} ions 9-43226
 excited state mean lifetime determ. 9-22709
 Fayalite, shocked, unshocked, spectra using reson. scatt. technique 9-24887
 ferredoxin of Euglena, rel. to state of Fe atoms 9-32537
 glass and glass fibre, struct. obs. 9-45302
 glass soda-silica, Tm doped, Tm $^{3+}$ crystalline elec. field parameters 9-37702
 haematite, antiferromag., nuclear diff. of resonant radiation, rel. to mag. structure 9-49262
 hemoglobin, electronic struct. and quadrupole splittings of Fe^{2+} 9-42459
 ice: Fe^{2+} , Sn^{4+} , Eu^{3+} rel. to phase transform. conc. depend., obs. 9-33140
 Illite, Fe ion oxidation state, coordination symmetry and site distortion 9-37698
 ilvaite, iron oxidation states and site symmetries determ. 9-24381
 iodomethanes, iodine bond hybridization 9-32519
 line narrowing by u.s. vibrations with decaying amplitudes 9-26717
 magnetite, c. hopping mechanism 9-26724
 magnetite, stoichiometric and non-stoichiometric, struct. and fast electron-hopping process obs. 9-39818
 mass-change shift and second-order Doppler shift, difference 9-39815
 metals, h.c.p., of ^{57}Fe , hyperfine structure 9-49255
 metals, impurity nuclei, linewidths, magnitude and isomer shifts 9-45284
 Montmorillonite, Fe ion oxidation state, coordination symmetry and site distortion 9-37698
 nitrosyliron bis(N,N-diethyldithiocarbamate) 9-39823
 paramagnet with nonaxial symmetry of crystal field, hyperfine structure of Fe^{3+} spectra, mag. field effect 9-49257
 paramagnetic crystal, intensity, effect of ion-phonon interaction 9-33524
 paramagnets in weak ext. mag. field, hyperfine structure stabilization 9-28665
 polarization and opacity effs. on spectral area 9-28664
 polarization of Bragg reflected photons determ. from Mossbauer spectrum 9-30532
 pyridine complexes of iodine monohalides, of ^{129}I 9-34688
 radiation absorpt., rel. to conversion and photoeffect processes, interference 9-48270
 rare-earth iron garnets, Sc substituted, Fe ions canted spin struct. obs. 9-37667
 rare-earth stannates, ^{115}Sn spectra 9-33529
 recording using X-ray films or resistance of CdS 9-26716
 relaxation times, spin-spin and spin-lattice, meas. with Mossbauer effects 9-31053
 resonant γ radiation interaction with single crystal nuclei and electrons, inelastic channel suppression 9-24377
 rotating disc γ spectrometer 9-40454
 source of non-zero radius, cosine effect 9-44076
 spectra, analysis using versatile computer program 9-49256
 spectra, computer curve fitting, program 9-42198
 spectra computation for mixed multipolarity transitions, computer program extn. 9-34386
 spectrometer, constant acceleration, determ. of zero velocity 9-46134
 spectrometer, variable temp. absorber in longitudinal external mag. field 1.5-300°K 9-27585
 spectrometer for graduate laboratories 9-43712
 spectroscopy, basic characts., equipment and applics., reviews 9-47329
 transition metals, of ^{57}Fe , isomer shift 9-26718
 u.s. modulation, applic. to freq. meas. in highly attenuating mats. 9-37697
 velocity drive, vibration detector 9-36169
 vitamin B $_{12}$ and analogs, emission spectroscopy 9-27918
 zeolite, Linde L, with Fe^{3+} and FeCl_3 9-49258
 zeolite, Y, exchangeable Fe^{2+} ions 9-43226
 in ^{57}Fe and ^{151}Eu for study of pseudo-melting of doped ice at -65°C 9-28178
 ^{180}Hf meas. rel. to $2^+ \rightarrow 0^+$ γ -ray transitions study 9-35639
 ^{161}Dy , 43.8 keV γ transition following Coulomb excitation 9-36578
 ^{161}Dy , improved source for Mossbauer expts. 9-42227
 ^{211}Po , 84.2 keV 9-29743
 ^{181}Ta , 6.2 keV level, recoilless reson. absorpt. 9-32312
 ^{181}Ta γ -ray, 6.25 keV, absorpt. spectrum interference of electronic and nucl. reson. absorpt. obs. 9-35640
 ^{152}Sm , γ energy distrib. after β decay, showing down of nuclear recoil 9-45283
 ^{243}Am in AmO_2 and AmF_3 , isomer shift 9-44167
 ^{133}Ba , 7.2 yr. 9-33525
 ^{133}Cs , of 81 keV line in ^{133}Xe implanted iron 9-35632
 ^{183}W , 46.5 keV γ line absorpt., Debye-Waller f factor determ. 9-46795
 ^{143}Gd $2^+ \rightarrow 0^+$ rotational transition isomer shift determ. 9-27636
 ^{152}Gd in GdCl_3 , 86.5 keV level quadrupole moment, h.f.s. and spectra meas. 9-34402
 ^{195}Pt , of 129 keV state 9-48299
 ^{160}Er , 80.6 keV γ -transition for temp. depend. obs. of nuc. hyperfine splitting 9-24272
 ^{176}Hf , meas. rel. to $2^+ \rightarrow 0^+$ γ -ray transitions study 9-35639
 ^{187}Re , γ -energy distrib. after β decay, showing down of nuclear recoil 9-45283
 ^{176}Hf meas. rel. to $2^+ \rightarrow 0^+$ γ -ray transitions study 9-35639
 ^{148}Sm , γ energy distrib. after β decay, slowing down of nuclear recoil 9-45283
 ^{119m}Sn , u.s. modulation, applic. to freq. meas. in highly attenuating mats. 9-37697
 ^{129}I frozen solns. 9-31089
 ^{115}Sn charge radius determ. by Mossbauer spectroscopy 9-27632
 ^{119}Sn monomeric and polymeric cpds., bonding, influence on temp. depend. of Lamb-Mossbauer factor 9-27915
 Al, polarization of Bragg reflected photons from Mossbauer spectrum 9-30532
 Au-Fe alloys, of ^{57}Fe , mag. ordering obs. 9-39817
 Au-Fe alloys, hyperfine field of ^{197}Au 9-49259
 Au-Fe dilute alloys, absorpt. spectra of ^{57}Fe 9-45285
 Au, energy of resonance γ ray of ^{197}Au , pressure depend. 9-39816
 BaO \cdot F \cdot O $_2$, hyperfine struct., antiferromag. order 9-47283
 BaTiO $_3$, γ -rays scatt. by opt. phonons assoc. with paraelec.-ferroelec. phase transition 9-39691

Mossbauer effect continued

- C₁FeCl₃, spectra, electron charge transfer and quadrupole splittings obs. 9-24378
- C₂FeCl₃, spectra, electron charge transfer and quadrupole splittings obs. 9-24378
- Ca-amphiboles, comp. changes and ferrous-feric Fe ratio obs. 9-41367
- Ca₃Fe₂Ge₃O₁₂ paramagnetic garnet, spectra of ⁵⁷Fe, at room temp. 9-43221
- Ca₃Fe₂Si₃O₁₂ paramagnetic garnet, spectra of ⁵⁷Fe, at room temp. 9-43221
- CaO-Mn_{0.5}Zn_{0.5}Fe₂O₄ system 9-46958
- Cd₃Fe₂Ge₃O₁₂ paramagnetic garnet, spectra of ⁵⁷Fe, at room temp. 9-43221
- CdFe₂O₄, electric field gradient sign at octahedral site 9-35633
- CeFeO₃ orthoferrite, mag. props. and valence distrib. obs. 9-45055
- Co, hyperfine field at ¹¹⁹Sn, anomalous temp. depend. 900° to 1300°K 9-47330
- Co_{1-x}Fe_xS₂ 9-45286
- Co₃O₄? ⁵⁷Co, spectra of bulk material and ultra-fine particles 9-28666
- Co phthalocyanine, emission spectroscopy 9-27918
- CoCO₃? ⁵⁷Fe, antiferromag., Fe ion relax. and mag. hyperfine field obs. 9-41364
- CoF₂ of ⁵⁷Fe. rel. to magnetization of impurity Fe ²⁺ ions 9-45298
- CrO₂, of ⁵⁷Fe, internal mag. field temp. depend. coupling and spin direction obs. 9-45287
- CsFeF₃, of ⁵⁷Fe, hyperfine structure and magnetization meas. 9-45058
- Cu-(2wt.% Co alloy, structural transformations of precipitates on cold-rolling, obs. 9-30732
- Cu-Ni-Fe alloys, of ⁵⁷Fe, mag. ordering obs. 9-39817
- Cu-Ni alloys, dilute ⁵⁷Fe 9-47331
- Cu alloys, chem. shift. for ¹¹⁹Sn impurity, electronic props. obs. 9-43222
- CuFeS₂? ⁵⁷Fe, quadrupole splitting meas. 9-35634
- Cu-(12.6wt.% Be-(0.2wt.% Co)-(0.1wt.% Zn alloy 9-45288
- Dy silicides and germanides, chemical bond charact. 9-37696
- Dy(ClO₄)₃, solid solutions in ice 9-35352
- DyCrO₃, of ¹⁶¹Dy, hyperfine interactions and paramagnetic relax. 9-24379
- ErCrO₃, of ¹⁶⁶Er, hyperfine structure, 4-40°K 9-24380
- Eu, anomalous critical-point behaviour 9-45219
- Eu cpds., divalent, isomer shifts of ¹⁵¹Eu 9-45289
- Eu fluoride system, nonstoichiometry obs. 9-40915
- Eu silicides and germanides, oxidation states and chem. bond charact. 9-37696
- EuF₃·2H₂O isomer shift of ¹⁵¹Eu₂O₃ spectrum 9-35635
- EuFe garnet, anisotropy in exchange interac. obs. 9-33475
- Fe-Si, Bragg scattering of 14 KeV Mossbauer radiation of ⁵⁷Fe nuclei 9-37700
- Fe-Mn nodules, of ⁵⁷Fe, for determ. of particle size of Fe oxide phase 9-42786
- Fe-(48.2 at%)Ni, of ⁵⁷Fe, hyperfine mag. splitting, effect of texture 9-35636
- Fe-Sn dilute alloys, hyperfine field of ¹¹⁹Sn and resistivity study 9-47335
- Fe, ¹³³Cs spectra, positive mag. hyperfine field 9-37699
- Fe, absorpt. in ⁵⁷Fe from Curie pt. to γ - δ transition 9-41366
- Fe, high field studies of band ferromag. 9-43166
- Fe, of ¹³³Cs 81 keV line excited by implanted ¹³³Xe decay 9-35632
- Fe, of ¹⁷⁸Hf, hyperfine field determ. using Mossbauer expts. 9-35605
- Fe, of ⁵⁷Fe, hyperfine mag. splitting, effect of texture 9-35636
- Fe, r.f. sidebands, magnetically induced, in spectrum 9-47332
- Fe, spectra near triple pt., comparison bet. α , ϵ and γ Fe, isomer shifts 9-26722
- Fe_{1/2}Cu_{1/2}Cr₂S₄, spectroscopy for ionic ordering on A-sites 9-28588
- α -Fe₂O₃, spectrum shift, effect of exchange interaction of mag. ions 9-26720
- Fe₂P, consts. for Fe atom on each site, spin arrangements 9-33527
- Fe₂(MoO₄)₃, garnet-type, parameters for octahedral Fe³⁺ 9-49261
- Fe₃B₂O₁₁X(X=Cl,Br,I), spectra of ⁵⁷Fe, 80°-1100°K 9-35638
- Fe₃BO₆, weak ferromagnet, spin orientations for Fe sites 9-41314
- Fe₂O₄, spectral changes at low temp. phase transition, 85°-298°K 9-28668
- Fe₂O₄ linewidth study of ⁵⁷Fe rel. to electron hopping in octahedral sites 9-45294
- Fe₂O₄ magnetite ⁵⁷Fe hyperfine fields 9-45295
- Fe₃S₄, spectroscopy, ferromagnetic props. 9-33467
- Fe²⁺ in glasses, rel. to coordination 9-26199
- Fe complex, bis-dithioacetylacetone tetrachloroferrate (II), rel. to Fe^mII bonding, 78°K 9-38842
- Fe complex tetramethyl ammonium tetrachloro ferrate (II), rel. to FeII bonding, 78°K 9-38842
- Fe compounds, of ⁵⁷Fe, anomalous charge states of Fe, possible origin 9-35637
- Fe compounds, trivalent, contrib. to theory of quadrupole splitting 9-49260
- Fe compounds, trivalent, contrib. to theory of quadrupole splitting 9-45290
- Fe low-spin (d⁷) complex mols. 9-45296
- Fe meteorites, shocked, unshocked, spectra using reson. scatt. technique 9-24887
- Fe orthoclase, iron III in tetrahedral and octahedral environments 9-45291
- ⁵⁶Fe in putidaredoxin, ligand symm. and electronic configuration determ. 9-32538
- ⁵⁷Fe, following n capture by ⁵⁶Fe, recoil effects in metallic iron and alloys obs. 9-43224
- ⁵⁷Fe, u.s. modulation, applic. to freq. meas. in highly attenuating mats. 9-37697
- ⁵⁷Fe hyperfine params. analytical calc. from spectrum 9-24382
- ⁵⁷Fe in zeolites, spectra study 9-43223
- ⁵⁷Fe in magnetically ordered systems, spectral shape near disordering temp. 9-26721
- FeAs₂, resonance studies 9-45297
- FeCO₃, paramag. Fe²⁺ hyperfine interac. 9-26723
- FeCO₃ metamagnetic single crystal, 2.5°K to above Neel temp., rel. to order parameter and atomic-spin relax freq. 9-45293
- FeCl₂, metamagnetic transition 9-24328
- FeCl₂ hydrates, covalency eff., correl. betw. quadrupole splitting and isomer shift 9-28667
- FeCl₃, test for H₂O in anhydrous crysts. 9-45224
- FeCl₄(CH₃)₄N₂ 9-33526
- FeF₂, Fe²⁺ crystal-field splitting obs. in paramag. state 9-24383

Mossbauer effect continued

- Fe(OH)₃ gels, nuclear gamma resonance 9-31088
- α -, β -, γ -FeOOH, synthetic, electron spin axis direction obs. 9-47289
- FeP₂, resonance studies 9-45297
- FeS, resonance studies 9-45297
- FeSb₂, resonance studies 9-45297
- FeSb₂O₄, antiferromagnetic structure 9-41336
- FeSe, resonance studies 9-45297
- FeBr₂, metamagnetic transition 9-24328
- α -Ga₂O₃, spectrum shift, effect of exchange interaction of mag. ions 9-26720
- Ge, of ⁷⁶Ge Coulomb excited after recoil implantation 9-33531
- Ge compounds with B₈ structure 9-33528
- He refrigerator, closed cycle, for Mossbauer studies 20°K-300°K 9-27619
- Ho single crystals, mag. structure 9-47333
- I cpds. of ¹²⁷I rel. to nuclear decay effects on electronic structure of decaying atom and its bonding 9-38769
- (In-Ga)Fe garnet 9-49263
- K, recoilless fraction and thermal shift for 29.4 keV transition in ⁴⁰K 9-42952
- K₃Fe(CN)₆, hyperfine structure obs. 9-26725
- ⁴⁰K, radius change after 29.4 keV γ emission 9-34412
- ⁸³Kr, 9.3 keV level mag. moment from lines Zeeman splitting 9-27668
- ⁸³Kr gyromagnetic ratio and magnetic moment determ. 9-27667
- LiFe_{0.8}Mn_{0.2}PO₄ antiferromagnet, ⁵⁷Fe absorpt. spectrum 9-26726
- Mg₂SnO₄, thermal neutron capture, chem. eff. study 9-26852
- Mg₂? ⁵⁷Co, Fe multiple charge states, hyperfine interac. and relax. processes 9-33530
- MgO:Fe²⁺ quadrupole splitting spectroscopic obs., for quadrupole moment of ⁵⁷Fe^m determ. 9-44168
- Mn_{0.4}Zn_{0.6}Fe₂O₄, sublattice magnetizations and superexchange interactions obs. 9-39777
- Mn_{3-x}Fe_xO₄, quadrupole splitting temp. depend. 9-37701
- MnF₂ of ⁵⁷Fe, rel. to magnetization of impurity Fe²⁺ ions 9-45298
- MnSn₂, antiferromag., temp. depend. of effective mag. field 9-41368
- MnTe₂, antiferromag. and paramag., ¹²⁵Te obs. of electronic struct. and induced mag. features of ditelluride ligand 9-43225
- MnTiO₃ II high press. phase, antiferromag. obs. 9-44667
- Na₂Fe(CN)₅NO·2H₂O, nuclear effective-field-gradient and mean square displacement of Fe sites 9-24385
- Na₂Fe(CN)₅(NO)·2H₂O frozen solns. 9-45299
- Ni-Fe alloys, ⁵¹Ni hyperfine fields 9-45300
- Ni-Sn dilute alloys, hyperfine field of ¹¹⁹Sn and resistivity study 9-47335
- Ni, high-field studies of band ferromag. 9-43166
- Ni, of ⁵⁹Ni Coulomb excited after recoil implantation 9-33531
- Ni₃B₂O₁₁X(X=Cl,Br,I), spectra of ⁵⁷Fe, 80°-1100°K 9-35638
- NiFe₂O₄, substituted, rel. to mag. fields on Sn nuclei 9-26727
- NpAl₃, hyperfine field of ²³⁷Np, mag. props. 9-47334
- NpC hyperfine field of ²³⁷Np, mag. props. 9-47334
- PbTe: ⁵⁷Fe, impurity Fe ions obs. 9-39819
- PbTe:(In-La), of ¹²⁵Te, depend. of probability on degree of doping 9-39820
- PbTe, ¹²⁵Te emission spectra following thermal neutron capture in ¹²⁴Te 9-37703
- Pd-Co alloys, mag. props. of Sn nuclei from line splitting obs. 9-43179
- Pd-Fe alloys, spectrum rel. to quenching temp. in the range 820-950°K 9-41369
- Pt-(1 at%)Co alloy with plastic strain, spectrum widening obs. 9-43161
- Pt-Fe system near Pt₃Fe composition, magnetic behaviour determ. 9-24275
- Pt-(1 at%)Fe alloy with plastic strain, spectrum widening obs. 9-43161
- Pu₂Fe, quadrupole pairs and splittings, isomeric shift values 9-39821
- PuFe₂ in Perspex medium, growth of quadrupole split pair of lines 9-49264
- ⁹⁹Ru, isomer shift of 90 keV γ -rays in ruthenium compounds 9-45301
- Sb cpds. of ¹²⁵Sb, rel. to nuclear decay effects on electronic structure of decaying atom and its bonding 9-38769
- Sm₂Eu_{1-x}Fe mixed garnet, anisotropy in exchange interac. obs. 9-33475
- SmFe garnet, anisotropy in exchange interac. obs. 9-33475
- β -Sn, of ¹¹⁹Sn, thermal shift meas., 3.6-90°K 9-24386
- Sn, white, on ¹¹⁹Sn, anisotropy of emission probability and temp. and angular depend. 9-49265
- SnCl₂, solid solutions in ice 9-33532
- SnI₄, Mossbauer studies reveal nature of bond in molecular crystal 9-34643
- SnS lattice dynamic anisotropy and line asymmetry obs., 60-320°K 9-39822
- SnTe-GeTe, of ¹¹⁹Sn, temp. dependence rel. to ferroelec. phase transition 9-26592
- SnTe, of ¹¹⁹Sn, temp. dependence rel. to ferroelec. phase transition 9-26592
- SrFe_{1-x}Cr_xO_{3-y} perovskites, and mag. behaviour 9-47336
- Te: ⁵⁷Fe, impurity Fe ions obs. 9-39819
- Te, ¹²⁵Te emission spectra following thermal neutron capture in ¹²⁴Te 9-37703
- Te, anisotropy, at 80°K 9-31090
- Te cpds., of ¹²⁵Te, rel. to nuclear decay effects on electronic structure of decaying atoms and its bonding 9-38769
- TeO₂, ¹²⁵Te emission spectra following thermal neutron capture in ¹²⁴Te 9-37703
- U₂Fe, quadrupole pairs and splittings, isomeric shift values 9-39821
- UFeO₄, magnetic structures and props. study 9-45238
- Y_{0.3}Ca_{0.7}Fe_{0.45}V_{1.55}O₁₂ of ⁵⁷Fe, non-equivalency of Fe³⁺ octahedral-site 9-24387
- Y_{3-2x}Ca_{2x}Fe_{2-3x}V_xO₁₂ ferrite garnets, study using Fe⁵⁷, role of Fe³⁺ ions 9-41365
- YFe garnets, Ga-substituted, cation distrib. 9-45303
- Yb silicides and germanides, oxidation states and chem. bond charact. 9-37696
- ZnFe₂O₄, electric field gradient sign at octahedral site 9-35633

Motors see Electrical machines**Multiple stars see Stars****Muonic atoms see Atoms, mesic and muonic****Muonic molecules see Molecules, mesic and muonic****Muonium**

- hyperfine splitting, ground state, determ. from beat freq. in mag. field 9-36433
- in magnetic field, modulated μ^+ -spin precession (beats) 9-36433

Muons

- see also *Cosmic rays/muons; Nuclear reactions and scattering due to muons*
 angular distribution isotropy from π decay in nuclear emulsions 9-29577
 magnetic moment, anomalous, meas. 9-40406
 photomuons, ($<18\text{GeV}$), in Fe shield, transport calcs. 9-42984
 spin, anomalous torque eff. on g-2 expt. 9-38586
 spin and orbital motion in homogeneous mag. field, g-factor anomaly determ. 9-40404
 stopping power of matter, contribs. of spin, mag. moment and form factors 9-44855
 ϵ dominance in $I=J=1$ channel of $\pi\pi$ interac. rel. to $K\rightarrow\pi\pi\pi$ 9-38511
 ρ dominance in $I=J=1$ channel of $\pi\pi$ interac. rel. to $K\rightarrow\pi\pi\pi$ 9-38511
 Fe shield, transport of high energy ($<18\text{GeV}$) photomuons 9-42984

capture

- μ^- in $^3\text{He}(\mu^-, \nu)^3\text{H}$, capture rates, induced pseudoscalar form factor calc. using PCAC 9-27706
 μ^- nuc. capture rate in gaseous H_2 9-27705
 in $^3\text{He}(\mu^-, \nu)^3\text{H}$, capture rates, induced pseudoscalar form factor calc. using PCAC 9-27706
 ^{12}C , transition to ^{12}B g.s., probability calc. 9-36595
 $^{40}\text{Ca}(\mu, \nu)^{40}\text{K}$, $^{40}\text{Ca}(\mu, \nu)^{39}\text{K}$, products identified by γ decay of excited states 9-38694
 $^{40}\text{Ca}(\mu, \nu)^{39}\text{Ar}$, $^{40}\text{Ca}(\mu, \nu\text{pn})^{38}\text{Ar}$, products identified by γ decay of excited states 9-38694
 $^{12}\text{C}(\mu^-, \eta\mu)^{12}\text{B}$, capture rate, nuclear structure 9-34439
 $^{56}\text{Fe}(\mu^-, \nu)^{56}\text{Mn}$, prob. meas., theory comparison 9-29789
 in H_2 , gaseous, nuc. capture rate 9-27705
 ^3He , weak interaction theory 9-27704
 $^6\text{Li}\rightarrow^4\text{He}$, rate calc. from ^6Li magnetic form factor 9-36596
 $^{10}\text{O}(\mu, \nu)^{10}\text{N}^*$, partial capture rate, excitation level distrib. determ. 9-25616
 $^{10}\text{O}(\mu^-, \nu\mu)^{10}\text{N}$, RPA and Tamm-Dancoff model calc. of capture rate, nuclear structure 9-34439
 $^{28}\text{Si}(\mu, \nu)^{28}\text{Al}$, $^{28}\text{Si}(\mu, \nu\text{pn})^{27}\text{Al}$, products identified by γ decay of excited states 9-38694
 $^{28}\text{Si}(\mu, \nu\text{p})^{27}\text{Mg}$, $^{28}\text{Si}(\mu, \nu\text{pn})^{26}\text{Mg}$, products identified by γ decay of excited states 9-38694
 $^{32}\text{S}(\mu, \nu)^{32}\text{P}$, $^{32}\text{S}(\mu, \nu\text{pn})^{31}\text{P}$, $^{32}\text{S}(\mu, \nu\text{nn})^{30}\text{P}$, products identified by γ decay of excited states 9-38694
 $^{32}\text{S}(\mu, \nu\text{p})^{31}\text{Si}$, $^{32}\text{S}(\mu, \nu\text{pn})^{30}\text{Si}$, products identified by γ decay of excited states 9-38694

decay

- lifetime rel. to validity of special relativity tested in cosmic ray obs. 9-34022
 polarized, probability 9-41999
 radiative corrections to μ , β decay quantum electrodynamics 9-25403
 vector coupling const. equality with π , renormalizable weak interaction model 9-32124
 $\mu^+\text{-e}^+$ spectrum and asymm. of low energy positions, Hz bubble chamber obs. 9-42011
 μ^+ , time-reversal symm. 9-22542
 $\mu^+\text{-e}^+\text{-}\nu$, probabilities, effect of e.m. field 9-27469

detection, measurement

No entries

interactions

- bremstrahlung, for quantum electrodynamics testing 9-22540
 lepton no. conservation, investigation using pure muonic neutrino beam 9-43975
 $\mu^+\mu^-\rightarrow\lambda\lambda^-$ (λ =part. of arbitrary spin) obs. of timelike form factors and spectral function of photon 9-29534
 C and Fe targets, at 12 GeV/c, muon pair prod. 9-32135

production

- beam, high energy, small phase-space vol., design and performance 9-27470
 cosmic ray μ , e and μ pair production, energy spectra meas. 9-34348
 pair, by 12 GeV/c π^- and Kaons on C and Fe 9-32135
 pair, high energy production mechanism by fireballs 9-40407
 ultra-high energy, with nearly isotropic azimuthal distribution, mechanism of generation by cosmic rays 9-25498
 $e^+e^-\rightarrow\mu^+\mu^-$, search, upper limit 9-29541
 $\eta^0\rightarrow\mu^+\mu^-$ obs., branching ratio calc. 9-22574
 $\mu^+\mu^-$ pair, by high energy neutrinos in field of strong e.m. wave 9-29546
 $\mu^+\mu^-$ from e^+e^- , backward annihilation amplitude, s-antisymmetrical part double logarithmic asymptotics 9-34256
 ^{10}B , ^{10}B , muon and pion yields in 2p-1s X-ray transition 9-22716
 Be, μ and π yields in 2p-1s X-ray transitions 9-22716
 C, μ and π yields in 2p-1s X-ray transition 9-22716

scattering

- inelastic at 8.6-12.9 GeV/c, on carbon target 9-22539
 $\mu^+\text{p}$ or $\mu^-\text{p}$, elastic, high energy max. 17 GeV, one-photon exchange test 9-46065
 μp , elastic cross section in range $0.15 < q^2 < 0.85 (\text{GeV}/c)^2$, comparison with cp data 9-46066
 μp , polarization-odd effects, $E_{\mu}\approx 10\text{GeV}$ 9-25418

Music see *Acoustics/musical***Musical instruments**

- electronic device for reproduction of any musical scale 9-41829
 intervals, expt. determ. using 'visible speech' method 9-36185
 microphone with ceramic reed mounted on instrument, patent 9-40277
 organ pipe, using transmission line theory, analysis 9-43790
 piano, tonal props. rel. to bass bridge mechanical impedance 9-41830
 sonometer for musical expts. 9-36186

Navier-Stokes equations see *Flow; Hydrodynamics***Nebulae**

see also *Galaxies*

- 30 Doradus, spectrophotometric studies, emission line intensities analysis 9-27005
 Andromeda, globular clusters, comparison of those in M31 and in galaxy 9-33912
 collision strengths and photoionization cross section for N, O and Ne 9-29972
 comet-like, stellar spectra obs. 9-43544
 Crab, activity and changes 9-28994
 Crab, γ -ray detection by digitized spark chamber 9-35962
 Crab, center of symmetry obs. 9-31516
 Crab, cosmic X ray spectrum 9-24832
 crab, evidence of condensed supanova remnants rel. to continuous activity 9-40131

Nebulae continued

- Crab, filamentary envelope, proper motions, radial vels. and structure 9-27003
 Crab, intensity and spectral distrib. of high energy X-rays 9-38061
 Crab, optical and radio meas. of pulsar showing simultaneous emission of pulses 9-47657
 Crab, optical flashes study 9-40132
 Crab, optical pulsar, light curve shape rel-to colour and polarization 9-45644
 Crab, optical pulses, television detection 9-43591
 Crab, pulsed hard X-ray flux, attempt at detection 9-41669
 Crab, radiobrightness distribution, 2.16 and 8.2 mm 9-43524
 Crab, right ascension and flux density 9-43523
 Crab, synchrotron emission model, acceleration mechanism 9-49538
 Crab, two pulsating radio sources 9-27052
 Crab, X-rays from, and the diffuse background near the Galactic anticentre 9-28995
 Crab nebula and the diffuse background near the Galactic anticentre 9-28995
 Crab pulsar, generation of mag. flux and energy by rot mag. neutron star 9-45647
 Crab pulsar as cosmic ray source 9-33915
 crab remnant, 32.5 cm. spectrum, map produced using lunar occultation 9-31519
 gaseous, ^{20}Ne - ^{18}O lines intensities from O^+2p^3 electron impact obs. 9-34566
 gaseous, excitation of forbidden lines, formulation and calculations for 2p^2 ions 9-27004
 gaseous, general soln. of b_n problem 9-35960
 gaseous, H_α line contours obs. 9-41630
 gaseous, high-level populations of H 9-28992
 gaseous, three identification and intensities of faint emission lines 9-49539
 Grab acceleration of ultrarelativistic electrons 9-45602
 H II regions, effect on density of electrons and distance calcs. to pulsars 9-45605
 history of their obs. in astronomy 9-22027
 IC 418, planetary, radio obs. at 9.5 mm., electron temp. and density deduced 9-31510
 IC 443, supernova remnant, $\text{H}\alpha$ line obs, radial and expansion velocities, turbulence deduced 9-31518
 IC 4642, planetary, spectral line intensity variations, expt. and comments 9-41628
 IC 4997, identification and intensities of faint emission lines 9-49539
 IC 5217 planetary nebula, relative line intensities, spectrophotometric study 9-49536
 i.r. spectrum, electron density a d line intensities of abundant atoms determ. 9-45606
 M8, $\text{H}\alpha$ and NII line profiles, temp. and internal kinematics calcs. 9-41629
 M8, obs. of OII lines, electron density variation estimation 9-31517
 M-42 and M-43, radiomap at 1.94 cm 9-31515
 N6C 7027 planetary, radio obs. at 9.5 mm., electron temp. and density deduced 9-31510
 NGC 4361, planetary, high excitation, spectrophotometric studies 9-43522
 NGC 5189 emission-line spectra, classification 9-49537
 NGC 6302, spectroscopic study 9-43521
 NGC 6572, identification and intensities of faint emission lines 9-49539
 NGC 6857, 11 cm obs., group of compact H II regions hypothesis 9-41627
 NGC 7009, identification and intensities of faint emission lines 9-49539
 NGC 7023, spectrum of its illuminating star HD 200775 9-35961
 NGC 7662, planetary, ionization stratification and chemical abundances 9-35959
 observations by four 16th-17th century astronomers 9-34000
 Orion, investigation of the Bok globules 9-45633
 Orion, Paschen-line obs. reddening curve derived 9-28993
 Orion, temp. structure reexamination on basis of low electron temps. for H II regions 9-49540
 Orion A region, radiomap at 1.94 cm 9-31515
 planetary, 408 MHz emission, obs. 9-33900
 planetary, (O I) and (N II), excitation conditions 9-31514
 planetary, as possible X-ray sources in range 4-8 keV 9-33922
 planetary, efficiency of Bowen fluoresc. mechanism, comparison with that of Seyfert galaxies 9-49535
 planetary, evolution from ^{12}C stars 9-40141
 planetary, gas dynamical study 9-24754
 planetary, H Balmer emission lines and $\text{n}^2\text{D}^2\text{P}$ He series, strengths 9-27002
 planetary, IC 5217, relative line intensities, spectrophotometric study 9-49536
 planetary, in Magellanic Clouds, radial vel. meas. 9-31512
 planetary, NGC 7662, ionization and chemical abundances 9-35959
 planetary, nuclei early evolution in Galaxy, and Magellanic Clouds, photoelectric study 9-31513
 planetary, polarization of continuum background 9-24753
 planetary, southern; masses and galactic distrib., photoelectric study 9-31511
 planetary, southern, visual line strengths, short-term variations 9-27001
 planetary, spectral line intensity variations, expt. 9-41628
 planetary nucle emission-line spectra, classification 9-49537
 radio observations of HII regions 9-40134
 spectra, theories of their state, book 9-24741
 spherical, containing X-ray source, radiation field determ. 9-36014
 H I regions, ionization by cosmic rays and subsequent radiowave absorpt. 9-31520
 H II and H I regions, emission and absorpt. of radiowaves 9-31520
 H II diffuse regions, W1, W5, W13 and W16, radio obs. 9-49541
 H II region, compact, search at 15 GHz in regions of possible star formation 9-45603
 H II region, radio recombination lines, eff. of thermal equilibrium 9-24761
 H II region structure and props., arbitrary density distrib. model 9-24755
 H II regions, 74 MHz radio obs., mean e temp. derivation 9-31521
 H II regions, α - and β -radio recombination lines for $40 \leq n \leq 225$, prediction 9-35966
 H II regions, distrib. in irregular galaxies 9-35963
 H II regions, electron temps. 9-49540
 H II regions, galactic, rel. to 'dispersion measures' of pulsars 9-45604
 H II regions, H abundance from radio recombination lines obs. 9-35964
 H II regions, high-density and dust-filled, evolution 9-43526

Nebulae continued

H II regions, high density compact group, hypothesis for NGC 6857 11 cm obs. 9-41627
H II regions, radial vel. of the gas and associated stars 9-40133
H II regions, radio-line data analysis and interpretation 9-43525
H II regions in M33, radial vel. and ellipsoidal distrib. 9-47632
H spectrum, relative intensities, theory 9-45601
HII region, relation with OH condensations and protostars 9-33904
HII regions, motion in Galaxy, comparison with HI regions 9-35967
N II, excitation conditions in planetary nebulae 9-31514
O I, excitation conditions in planetary nebulae 9-31514
OH emission near HII regions, nebular filaments 9-27006

Neel temperature see Magnetic properties of substances

Negatons see Electrons

Negatrons see Electrons

Nematic phase see Liquid crystals

Neodymium

doped glass, pulsed laser with selected 2nd harmonic radiation 9-38382
double h.c.p. Fermi surface and generalized susceptibility 9-44889
elastic moduli, u.s. attenuation meas., 4.2-300°K, correl. with antiferromag. transitions 9-35146
Fermi surface and generalized susceptibility 9-44889
ferromagnet, f.c.c. phase, room temp. and liq. He temp. stabilization, electronic props. 9-35555
in garnet, Ce activated, fluorescent, energy transfer from Ce to Nd ion 9-26777
glass, absorbed pumping energy rel. to activator content 9-48029
glass, activated with trivalent Nd, photochemical stability 9-41455
glass, occlusions extraction and microanalysis 9-32956
glass, stimulated emission parameter deterioration during use 9-31109
glass laser, diffraction-limited high radiance 9-25295
glass laser, generation of i.r. radiation in polymethine dye 9-34168
glass laser, obs. 9-48028
glass laser, picosecond pulse width meas. by GaAs surface harmonic generation 9-34173
glass laser, picosecond pulses, evidence for self-focusing in gas breakdown 9-25983
glass laser, Q-switching by organic solvents 9-29423
glass laser focused radiation, conversion to X-rays in hot dense plasma 9-42517
glass laser rod oscillation patterns, streak camera obs. 9-45959
hyperfine interactions, calorimetric investigation 9-47305
isotope shift interpretation 9-34548
laser, stimulated combinational scattering of radiation in liq. N₂ 9-36879
laser, temporal struct. of emission in mode self-locking regime 9-45969
laser beam, monopulse sync. with ruby pulse using luminous liq. shutter 9-29421
laser radiation space time distribution, rel. to 2nd harmonic conversion coeff. 9-40361
laser second harmonic production in LiIO₃ 9-26691
resistivity, elec., due to exchange interaction and quadrupole scatt., temp. depend. 9-44901
spin lattice relax., optical detection, 1.28% to 2.15% 9-35595
X-ray absorption spectra K lines obs., effective co-ordination charges determ. 9-37745
LaNa(MoO₄)₂:Nd³⁺ crystals, use in c.w. laser 9-40359
LiNbO₃:Nd³⁺, absorpt. and luminesc. spectra, 4.2-295°K 9-28689
Nd³⁺ in LiYF₄ fluoresc. 9-39877
Na⁺ in silicate glass and CaWO₄, structure of stimulated emission bands 9-35650
Nd³⁺:CaWO₄ laser, fundamental longitudinal modes exam. 9-22419
Nd:glass laser, mode-locked, pulse duration 9-25285
Nd:LaMg (NO₃)₃ p relaxation time of several hundred hours at 0.3-0.4°K rel. to prod. of polarized samples 9-29524
Nd:YAl garnet, c.w., pumping efficiency using alkali additive lamps 9-31959
Nd:YAl garnet rods, index of refraction and thermal expansion coeff. 9-22412
Nd³⁺:YAl garnet, quasicontinuous giant pulse emission of ⁴F_{3/2}-⁴I_{3/2} transitions at 1.32 μm 9-22420
Nd:YAlG laser, mode-locked, stability by feed-back loop method 9-48027
Nd²⁺ (f-f) absorption spectrum obs. in CaF₂ 9-28682
Nd²⁺ in CaF₂, SrF₂ and BaF₂, thermal ionization potentials 9-46739
Nd³⁺:CaF₂:SrF₂ laser, stimulated emission, 300°K 9-29426
Nd³⁺: glass and ruby laser, ps. pulses with GW power, generation, meas. and applics. 9-31964
Nd³⁺:Ca(NbO₃)₃ laser, stimulated transitions, crystal field splitting terms, and absorpt. and luminescence spectra obs. 9-27332
Nd³⁺:LaF₃ laser, double freq. generation 9-40360
Nd³⁺, acoustic e.p.r. in LiNbO₃, for internal fields of ferroelec. crystals 9-28748
Nd³⁺, coherent emission from electro-optic crystals, obs. 9-26738
Nd³⁺, dispersion curves w.r.t. La³⁺ in aqueous chloride solutions 9-26111
Nd³⁺, e.p.r. and relax. processes in YAl garnet 9-24498
Nd³⁺, energy-level scheme in CaWO₄ 9-49232
Nd³⁺ coloration impurity in lanthanum glass, effect on light absorption 9-24372
Nd³⁺ doped glass laser, patent 9-48046
Nd³⁺ in CaF₂, ENDOR obs. of F- and H- interstitials 9-47449
Nd³⁺ in CaF₂ and CaWO₄, absorption spectra, visible, at liquid oxygen temp. 9-47352
Nd³⁺ in CaWO₄, Faraday effect obs. of ⁴I_{9/2}-²P_{1/2} transition 9-39805
Nd³⁺ in CaWO₄ laser, stimulated emission cross-section meas. 9-41916
Nd³⁺ in La₂Mg(NO₃)₁₂, e.s.r. temp. dependence, T₁/T₂ ratios 9-24483
Nd³⁺ in La₂Mg(NO₃)₁₂, Orbach relax. processes, T₁ and T₂ 9-24492
Nd³⁺ in LiNbO₃, Bi₄Ge₂O₁₂, Ba_{0.75}Ca_{0.25}Nb₂O₆ electro-optic crystals, coherent emissions obs. 9-43203
Nd³⁺ in RbMnF₃:Nd³⁺, fluorescence temp. dependence rel. to Mn²⁺→Nd³⁺ energy transfer 9-24456
Nd³⁺ in tysonite lanthanide fluorides far i.r. electronic and vibronic transitions obs. 9-35653
Nd³⁺ in tysonite lanthanide fluorides, far i.r. electr. and vibronic transitions, 9-39843
Nd³⁺ in vitreous matrix, effective amplification section of 1.06 transition 9-48399
Nd³⁺ in YAl garnet, methods for increasing concentration 9-37093
Nd³⁺ in YVO₄, absorption luminescence and stimulated emission spectra 9-26746

Neodymium continued

Nd³⁺ ions in disordered systems, e.p.r. line shapes 9-28742
Nd³⁺ metastable ion in mixed fluoride crystals, radiative lifetime, anomalous temp. dependence 9-41405
Nd²⁺-YAl garnet and Nd:glass, comparative pumping efficiencies of Xe, Ar and Kr flashlamps 9-31958
Nd³⁺(4fⁿ), spin-spin interactions determ. from matrix element expression 9-38774
Nd³⁺→Nd²⁺ photoreduction on SrF₂, under stimulated emission conditions 9-31960
Nd I arc spectrum, parametric calc. for electronic config. 9-29943
Nd³⁺ in aprotic SeOCl₂ soln., lum. and energy transfer to Yb³⁺ and Er³⁺ 9-22407
Nd³⁺ in La MN, hydrated enhancement of proton polarization due to 'solid effect' 9-24512
Neodymium compounds
monochalcogenides, antiferromag., mag. props. 9-49225
neodymium ethylsulphate, paramag. relaxation, phonon re-absorption and spectral spin diffusion 9-33491
Nd-glass laser, kinetics of free generation spectra in travelling-wave regime 9-27333
Nd-Co system, crystal structures of intermediate phases 9-28262
Nd₂O₃, self-diffusion coeffs. of O, by isotope exchange method 9-44741
Nd₂(MoO₄)₃-Nd₂(WO₄)₃ system, phase struct., differential thermal analysis and X-ray diffr. obs. 9-37305
α-Nd₂(MoO₄)₃, paramag., cryst. struct. 9-39292
Nd₃Fe₅-Sc₂P₁₂ garnets, (9<κ<1.5) 9-47247
Nd₂Ge₃, mag. susceptibilities rel. to D_{8h} structure 9-43157
Nd₂Si₃, mag. susceptibilities rel. to D_{8h} structure 9-43157
Nd₂Dy_{1-x}Sb_x, Neel and paramag. Curie temp., mag. exchange mechanisms 9-28595
Nd glass laser with plane-polarized emission 9-36308
NdAs, mag. props. w.r.t. cryst. field eff. 9-35590
NdBr₃, n.m.r. in paramagnetic state, freq. and temp. depend. 9-39921
NdCl₃, coupled Ising chains and magnetic ordering 9-33456
NdCl₃, paramagnetic susceptibilities, crystal field calc. 9-33440
NdCo₃, ferromag., press. effect on curie point 9-45154
NdF₃, polarized i.r. reflectance, optical phonons and mag. symmetry 9-47345
NdF₃ oriented single cryst., far i.r. electr. and vibronic transitions 9 39843
NdF₃ single cryst., far i.r. electronic and vibronic transitions obs. 9-35653
NDP, mag. props. w.r.t. cryst. field eff. 9-35590
NdSb, mag. props. w.r.t. cryst. field eff. 9-35590

Neon

atom, 2-electron energies transformation props., inter-orbital correlation energies 9-38773
atom, 2p₂ level, population relax. times, obs. using laser 9-46300
atom, absolute spontaneous transition probabilities 9-46281
atom, dipole polarizabilities, elec., and dipole shielding factors from Hartree-Fock wave eqns. 9-44241
atom, electron scatt., neutral bremsstrahlung cross section, shock tube obs. 9-29965
atom, excitation by electron impact, pulsed super-emittance from 2p-1s transition, mechanism 9-29959
atom, highly ionized, spectrum in plasma focus discharge 9-42329
atom, mean excitation energies upper and lower bounds calc. 9-38779
atom, three electron correl. effects 9-38772
atoms, charge state change for proton interaction, 5-50 keV 9 44483
atoms, metastable, in glow discharge, densities mes. rel. to press. and current 9-44508
atoms adsorbed on graphite, quasiharmonic freq. shifts. 9-48764
autoionizing levels, prod. by H⁺, He⁺ and Ne⁺ beams 9-23343
beam, ionized, spectra 2000 to 6000 Å 9-46320
breakdown pot. obs., secondary ionization coeffs. calc., mild steel electrodes 9-34811
collision strengths and photoionization cross sections 9-29972
collision with H₂-ve charge prod. cross section determ., 50-1000 eV 9-27826
conductivity ratio meas. in microwave resonant cavity discharge, 2.7 GHz 9-23288
density meas. over range 28°K-70°K pressures up to 240 at. 9-30325
diffusion in H₂O, coeffs., 10° to 60°C 9-26086
diffusion in inert-gas systems 9-42617
discharge, atom temp. meas., plasma inhomogeneity effects 9-34803
discharge, energy loss of primary electrons 9-48622
discharge, glow, metastable atom densities rel. to press. and current 9-44508
discharge, h.f., electron conc., temp. radial distrib., spectra emission intensity determ. 9-23355
discharge, ionization waves of type p 9-42603
discharge conditions for generation at λ=1.15 μ 9-25975
discharge negative glow, secondary and ultimate electron groups 9-48634
discharge plasma column, parameters 9-44507
discharge positive column, electron energy distribution 9-44506
electron elastic scatt., phase shifts, isoelectronic sequence extrapolation techniques 9-29964
electron elastic scattering from ²p metastable state, calc. 9-46307
electron scatt., elastic and inelastic, from ground state, first Born approx. calc. 9-32422
energy levels calc. using step-like model potential function and perturbation theory 9-44243
excitation cross section, total, determ. using Townsend's primary ionization coeff. 9-42561
excitation in hollow cathode discharge, balance eqn. for levels derivation 9-22961
excitations, collective, variational calc. 9-25704
excited levels, mag.-reson. expts. 9-29955
excited state, repulsive interaction with He, Ne, Ar ground state atoms 9-29968
flash tube, digitisation method for potential changes 9-27588
gas, viscosity calc. by eqn. 9-30355
gas target, traversed by He beam, charge equilb. fractions obs. 9-40559
gas viscosity meas. pot. fitted 9-36823
glow discharge, hollow cathode, with appl. mag. field, ionization waves, obs. 9-25982
in ice, selective doping 9-46814
intermolecular potential calcs. rel. to thermal-diffusion column operation 9-34843

Neon continued

- ion, collisionally excited u.v. and forbidden lines, intensity calcs. 9-25685
 ion acoustic waves rel. to moving striations 9-48636
 ion laser, u.v., c.w., 10 mW 9-27326
 ionization currents, pre-breakdown, spatial growth 9-48433
 laser 3.39 μm line width from Lamb-dip 9-27325
 line width of $3s_2$ - $3p_4$ transition in He-Ne mixture, press. depend. 9-42333
 liquid, compressibility and density up to 1000 kb/cm² 9-46593
 liquid, equation of state and interatomic potential 9-28093
 liquid, stability of electronic bubbles 9-46608
 luminescent lamp as light transformer 9-40386
 lunar exosphere, planetary, lateral transport 9-29059
 multi-ionized, transitions and decay meas. of levels 9-46299
 optical pumping of $^3\text{P}_2$ state and subsequent collisional depolarization 9-22973
 oscillator intensities for $\bar{\Gamma} \rightarrow \bar{\Gamma}^*$ transitions, and areas of electron impact excitation 9-36671
 phonon dispersion relations for cryst. at 2 densities, coherent inelastic neutron scatt. obs. 9-46978
 plasma, afterglow in mag., field, microwave scattering and noise emission 9-48568
 plasma, electron density in medium plane, determ. using transmission and reflection coeffs. formulae 9-23278
 plasma, excited level broadening due to interaction 9-23275
 plasma, partially ionized, transport and balance coefficients 9-44417
 plasma in homopolar rot. device, 10^{-2} mm Hg, electron collision freq. and current growth 9-25857
 plasma pulsed discharge, spectral absorptivity calc. from radiance spectral density 9-23301
 positive column in longitudinal mag. field, 0.5-4.0 mm pressure, comparison with binary collision theory 9-34809
 relative transition probabilities for twelve lines originating on $3s_2$ and $3s_3$ levels 9-25699
 r.f. discharge in non-resonant mag. field, breakdown characts. 9-25986
 separation from Ne-He mixture 9-23590
 shock waves, spectral distrib. of u.v. and visible radiation 9-48654
 solid, Buckingham potential, anharmonic parameters 9-33152
 solid, many-body corrections to isotopic volume differences 9-48778
 solid, phonon spectra theor. temp. depend., phonon Green function calc. 9-26412
 spark chamber gas recirculator-purifier 9-42154
 stellar abundance in A and B stars, search in spectra 9-43554
 thermal-diffusion column operation rel. to intermol. pot. calcs. 9-34843
 between vertical concentric cylinders, heat transfer and end effects for various temp. differences 9-40749
 Ar/Ne, solidified mixtures, e diff. study of crystallized phases 9-28255
 He-Ne, discharge, depolarizing and velocity-changing collision correl. 9-39026
 He-Ne, laser, localizer-beam flying application 9-31947
 He-Ne 6328 Å laser, external polarization technique using permanent magnet 9-29418
 He-Ne cw laser, temporal correlations in radiation at threshold 9-22400
 He-Ne laser, amplification and oscillation mechanism 9-29416
 He-Ne laser, freq. stabilization by external Ne absorpt. tube in mag. alternating field 9-25261
 He-Ne laser, gain coeff. temp. dependence calc. 9-41905
 He-Ne laser, generation intensity and inversion density rel. to hollow cathode diameter 9-25266
 He-Ne laser, h.f. pulse excited, characts., obs. 9-25267
 He-Ne laser, interference application for obtaining nonpolarized, single frequency radiation 9-25269
 He-Ne laser, Ne atoms density nonlinear depend. on saturation, Ne exchange collisions explanation exchange collision, saturation parameter nonlinear depend. on density 9-25271
 He-Ne laser, operating in TEM_{nm} modes, radiation divergence meas. 9-47992
 He-Ne laser, positive column calc. for dispersive effects eval. 9-43884
 He-Ne laser, pumping intensity, effect on relationship between gain and temperature 9-25268
 He-Ne laser, radiative power rel. to discharge gap geometry 9-47995
 He-Ne laser, self-locked, pulse velocity meas. 9-41903
 He-Ne laser Brewster angle attenuator within laser cavity, eqns. of polarization and attenuation 9-31969
 He-Ne laser construction for operation at 6328 Å 9-29415
 He-Ne laser in transverse mag. field, energy characts. 9-40354
 He-Ne laser multimode 0.63 μm output power and spectrum rel. to collisions 9-34164
 He-Ne laser radiation within hollow cathode 9-47994
 He-Ne laser resonator, $3s_2$ - $3p_4$ Ne transition line spectral width meas. 9-22960
 He-Ne laser with small discharge space, max. amplification depend. on tube axis position 9-29406
 He-Ne lasers for science and technology, operation 9-41906
 He-Ne mixture, He quenching rate calc. from He level population depend. on Ne atom conc. 9-25974
 He-Ne mixture, plasma production, N^{2+} ion production and loss during decay period, density time depend. 9-40666
 He-Ne mixtures, ionic analysis of cataphoresis 9-42569
 He-Ne single-mode laser, damping parameters of 0.63 μm line, nonlinear press. depend. 9-34165
 Ne-Ne mixtures, heat transfer from cylinders showing slip effects 9-46568
 Ne-Ar mixed gas plasma, generated by fission fragments, electron density 9-34751
 Ne-He laser interferometer for improvements of detections of fringe shifts in plasma density meas. 9-25910
 Ne-He mixture, ionization currents, pre-breakdown, spatial growth 9-48433
 Ne-Xe system, thermal diffusion factors 9-42616
 Ne^+ , recombination, electron temp. dependence obs. 9-32696
 Ne_2 potential energy curve, empirical form 9-32461
 Ne^+ producing autoionization levels of Ne 9-23343
 Ne^{3+} collision strengths for electron impact transitions 9-34563
 Ne I $2s_2$ laser level transition probabilities and mean lives 9-48413
 Ne I J=1 levels, radiative lifetimes, branching ratios and oscillator strengths determ. 9-27812
 Ne I J=1 levels, radiative lifetimes, branching ratios and oscillator strengths determ. 9-40547
 Ne II spectra, selected ranges between 10150 and 2500 Å 9-40546

Neon continued

- Ne VII and Ne VIII 3s-3p transitions, identification in high temp. plasma 9-48401
 NeI, line strength transitions and coupling coeffs. 9-27811
 O(¹D)-Ne interaction, electronic de-excitation of O(¹D) during vacuum u.v. photolysis of O₂ 9-35755
- Neon compounds**
 interatomic potential 9-38854
 He-Ne laser 3-mirror resonator, mirror motion influence on generation power 9-22399
 He-Ne laser in mag. field, nonlinear effects in output intensity 9-45954
 He-Ne mixture, conc. depend. on level meas. by absorption method in hollow cathode discharge 9-23354
- Neptunium**
 internal friction, meas. in l.f. inverted-torsion pendulum, 20-595°C 9-35158
 magnetic hyperfine coupling at low temp 9-47334
 ^{237}Np nucl. moment from e.p.r. on Np^{6+} in $\text{Cs}_2\text{UO}_2\text{Cl}_4\cdot\text{NpO}_2^{2+}$ and 2^+ 9-35712
 Np^{6+} , energy levels in PbMoO_4 9-31110
 Np^{4+} in ThO_2 , absorption spectrum, analysis of crystal field splitting of J levels 9-35665
 Np^{6+} e.p.r. in $\text{Cs}_2\text{UO}_2\text{Cl}_4\cdot\text{NpO}_2^{2+}$ and $\text{CsUO}_2(\text{NO}_3)_3\cdot\text{NpO}_2^{2+}$ 9-35712
 UF₆-WF₆ mixture, obs. to deviate from prediction of Schroder equation 9-34953
 UF₆-WF₆ mixture obs. deviate from prediction Schroder equation 9-23580
- Neptunium compounds**
 NpAl₂ ferromag. Mossbauer hyperfine field of ^{237}Np and susceptibility meas. 9-47334
 NpC Mossbauer hyperfine field of ^{237}Np and susceptibility meas. 9-47334
 NpO_2^{2+} absorpt. spectrum in $\text{Cs}_2\text{UO}_2\text{Cl}_4$ 9-33553
 NpO_2^{2+} e.p.r. in $\text{Cs}_2\text{UO}_2\text{Cl}_4$ and $\text{CsUO}_2(\text{NO}_3)_3$, Np^{6+} obs., ^{237}Np nucl. moment 9-35712
- Nernst effect** see *Magnetothermal effects*
Nernst-Ettinghausen effect see *Magnetothermal effects*
Neumann algebra see *Algebra; Elementary particles; Field theory, quantum*
Neutretto see *Neutrinos and antineutrinos*
Neutrinos and antineutrinos
 see also *Cosmic rays/neutrinos; Nuclear reactions and scattering due to/neutrinos*
 in astrophysics 9-38029
 baryons, 'electric', production 9-38556
 charge radius calc., eff. of weak interactions on lepton e.m. props. 9-38464
 Clifford algebra eqn., reduction to Dirac-type form 9-48156
 high energy, in field of strong e.m. field, rel. to lepton pair production 9-2954
 Mass upper limit from time of flight meas. in supernova explosions 9-38466
 mass zero allowed by quaternion soln. to Schwarzschild problem 9-31758
 muonic, beam for investigation of muonic lepton no. conservation 9-43975
 pair bremsstrahlung calc. for hot degenerate electron gas Coulomb scatt. on nuclei 9-42009
 solar flux, evidence from pp and $\text{p}e^-$ reactions in the Sun 9-29004
 solar flux rates, meas. by giant underground trap 9-47685
 solar neutrino fluxes, sensitivity 9-29092
 solar neutrino discrepancy, turbulent diffusion explanation 9-36029
 $e\nu$ scattering, elastic, detection possibility 9-22536
 ν_e dissociation of d, neutral weak-interac. search 9-27569
 $\nu\text{m} \rightarrow \text{l}^+\pi^0$ differential cross-section predicted by current algebra 9-46060
 $\nu_\mu(\nu_\mu)\bar{Z} \rightarrow W^+W^-\mu^{\pm}$, W-boson production in a neutrino beam, 2.30 GeV 9-27450
 $\nu\text{-}\mu\pi^+\pi^0$ total and differential cross sections for ν energy between 1 and 4 GeV 9-44021
 $\nu\text{N} \rightarrow \Lambda\pi\mu$, S-wave $\pi\Lambda$ phase shift information 9-32192
 $\nu\text{N} \rightarrow \mu^+\pi$, cross section derivation from Fermi-gas model 9-38467
 $\nu\text{N} \rightarrow \mu^+\mu^+$, quasilastic ν scatt., spark chamber detector obs. 9-32132
 $\nu\nu$ massless exchange scatt., high energy behaviour, calc. method 9-32130
 $\nu\nu$ massless exchange scatt., high energy behaviour, calc. method 9-32130
 8p8/176/5 9-38467
 W prod. 9-22607
- Neutron diffraction**
 computer-controlled diffractometer, operation crystall. 9-37128
 by ruled grating 9-28248
- Neutron diffraction crystallography**
 see also *Crystal structure, atomic*
 beam modulation by vibrating quartz crystal 9-30549
 chemical bonding influence on high energy n cross-sections 9-30547
 coherent scatt. amplitudes, table 9-23724
 Debye-Waller factors, anharmonic contribs. 9-26404
 diffractometer, time-of-flight, focusing expt. 9-30548
 diffractometer at Bucharest Institute of Atomic Physics 9-37130
 elastic diffr. applic. to struct. studies 9-48680
 electrostatic scatt. of thermal neutrons in mag. and non-magnetic crystals, theory 9-37129
 error analysis methods rel. to structure results comparison with X-ray diffr. technique 9-37121
 error sources, electronic and mechanical 9-23699
 free-atom form factor model as cause of errors in calculated structure factors 9-23735
 integrated intensity meas., geometrical aspects and errors due to non-monochromatic radiation 9-23727
 line profiles rel. to stacking faults in h.c.p. and f.c.c. polycrystals, general theory 9-23817
 monochromatization of neutrons at high-resolution by Bragg refl. in h.c.p. cryst. 9-30545
 mosaic spread, two-axis spectrometer meas. 9-30546
 optimization process for least-squares weighting schemes of diffractometer-collected data 9-39238
 powder specimen accurate relative intensity meas. techniques and apparatus 9-23700
 profile refinement method for nuclear and mag. structures 9-40891

Neutron diffraction crystallography continued

- quartz, mean intensity depend. on current and vibrating freq. 9-26247
 scalar wave dynamical diff. theory, matrix formalism 9-23701
 single-slit, between 21 and 4.1 μ width 9-35050
 smearing function rel. to Edgeworth map for vibr. atom in BaF₂ 9-42954
 spectroscopy methods 9-48824
 structure factor eqn., addition of higher cumulants rel. to generalized treatment for thermal-motion effects 9-23736
 structure factors, significance 9-23691
 symbolic addition, procedure applic. for signs eval. of struct. factors 9-40890
 time of flight statistical method, improvement 9-35051
 vibrating cryst., mean intensity increase and ν modulation obs. 9-48823
 and X-ray diff. data, joint refinement 9-30551
 and X-ray diff. data comparison, role of thermal diffuse scatt. 9-30537
 UC, neutron scatt. by C atoms, effect of chemical binding 9-23776

Neutron diffraction examination of materials

- alkaline-earth metal uranates, crystal structure and refinement from powder data 9-39253
 antiferromagnets with corundum structure, neutron scatt. by spin waves 9-41332
 Cr-Mn alloy, magnons and paramagnons, neutron mag. scatt. obs. 9-45215
 dimethylsulphoxide and dimethylsulphone aq. solns. 9-32763
 f.c.c. cryst. with point defects, force-const. changes effect on coherent scatt. 9-42953
 haematite, antiferromag., diff. of resonant γ radiation, rel. to mag. structure 9-49262
 Heisenberg antiferromagnet, mag. scattering 9-45202
 hexamethylenetetramine joint refinement of X-ray and neutron diff. data 9-30551
 liquid, scatt. rel. to mol. dynamics 9-48656
 liquid metals and alloys, review 9-36846
 liquids, elastic diff. for struct. obs. 9-48680
 liquids and solids, review 9-37785
 liquids and solids, review 9-47419
 magnetic and nuclear structs. determ. by profile refinement method, least-squares procedure 9-40891
 magnetic form factor determ. using polarized neutrons, error anal. 9-24268
 magnetic ions in crystals, scattering theory 9-45049
 magnetic materials, scatt. obs. 9-49188
 magnetic scatt., small angle behaviour of forward amplitude 9-31014
 magnetic scatt. of thermal neutrons, theory of electrostatic interactions 9-37129
 manganese formate dihydrate, deuterated, antiferromagnetic structure 9-24336
 4-nitroaniline, partly deuterated positional and thermal vibr. parameters 9-46801
 polarization analysis of thermal-neutron scatt. for triple-axis spectrometer 9-42780
 polyethylene, multiphonon contribs. to directional phonon freq. functions 9-46981
 powdered and single crystal samples, obs. using linear accelerator 9-42779
 quartz, synthetic crystals, quality determ. from diff. of vibr. and non-vibr. crystal 9-37150
 quasi-classical approx. for scatt. from systems and incorporating recoil effect 9-32894
 radiography, reciprocity-failure characteristics of films 9-43935
 silica glass, vitreous 9-28269
 solid, scatt. rel. to mol. dynamics 9-48656
 spectrometer, triple-axis, polarization analysis of thermal-neutron scatt. 9-42780
 spin-wave scatt. near Curie pt. 9-49201
 Ticonal X, magnetic microstructure obs. 9-49203
 uronium nitrate, crystal structure 9-26272
 and X-ray diff. data, joint refinement 9-30551
 and X-ray diff. data comparison, role of thermal diffuse scatt. 9-30537
 AgBiSe₂-AgBiS₂ system, high-temp. β -phase, rel. to cryst. structure order 9-42782
 Al powder patterns using linear electron accelerator 9-42779
 Al with point defects, force-const. changes effect on coherent scatt. 9-42953
 Ar liquid, atomic overlap 9-34875
 Au-X ordered alloys, X=transition elements and mixtures, and resistivity and specific heat studies 9-44659
 BaF₂, structure factor determ., anharmonicity and thermal diffuse scatt. corrections 9-24014
 BaF₂, vibr. atom, Edgeworth map. rel. to smearing function 9-42954
 BaOFe₂O₃, antiferromag. ordering 9-47283
 BaSc₂Fe₁₂-O₁₉ hexagonal ferrite single cryst., intensity anomalies due to superposition of reflex satellites 9-31043
 BaSc₂Fe₁₂-O₁₉(M), helicoidal antiphase spin ordering, neutron diffraction 9-37663
 Bi₂Te₃-Bi₂Se₃ pressed powder compacts, preferred orientation meas. 9-32862
 BiFeO₃-Pb(Fe_{0.5}Nb_{0.5})O₃, solid solution, spontaneous magnetic moment 9-33482
 BiFeO₃, atomic struct. 9-37135
 CaFe₂O₄ mag. peaks, obs. using linear electron accelerator 9-42779
 Co-(7.45 at.%)Fe solid soln., γ -phase precip. during ageing 9-41065
 Co-(8 wt.%)Fe, n depolarization and secondary extinction, obs. 9-39267
 Co, hexagonal, noncollinear spin density obs. 9-41304
 Co, hexagonal, noncollinear spin density, rel. to form factors, neutron polarization analysis 9-45121
 α -Co, search for anisotropy in magnon dispersion relation 9-41313
 Co film, magnetization studies 9-45167
 CoS₂, mag. props. 9-33437
 Co(S_{0.5}Se_{0.5})₂ system, mag. props. 9-33437
 CoSe₂, mag. props. 9-33437
 CoSeO₄, antiferromag. struct., Neel pt. 9-49223
 Cr₂BeO₄, spiral mag. structure, 4.5°K 9-45211
 Cr₂O₃, inelastic scatt. obs. of spin waves and mag. interactions 9-47285
 Cr alloys, coexistence of mag. phases obs. 9-39750
 Cr single crystal, spin directions, 122°K to 38.5°K, polarized neutron beam expts. 9-45214
 CrSb₂, marcasite-type, mag. props. obs. 9-35581
 Cs molten struct. 9-39075

Neutron diffraction examination of materials continued

- Cu-Mn-Al phase formation on heat treatment and ageing 9-37293
 CuMn₂O₄ spinel, cation distrib. determ. 9-40854
 Cu(NH₄)(SO₄)₂·6H₂O, structure parameter refinement 9-39270
 CuSO₄, antiferromag., moment density distrib., polarized-neutron determ. 9-41335
 EuSe single crystal, mag. phase transition, low temp. 9-47288
 Fe-Si alloys, spin-wave dispersion relationships determ. 9-24297
 Fe, spin wave modes 9-45110
 α -Fe₂O₃ mag. peaks, obs. using linear electron accelerator 9-42779
 Fe₂Se₄, magnetic structure 9-33477
 Fe film, magnetization studies 9-45167
 Fe single cryst. excited by magnetostructure resonator 9-48823
 FeMn₂O₄, magnetic structure at low temps. 9-45177
 GeO₂, vitreous 9-28269
 H₂O in ionic solns., l.f. molec. motions 9-44547
 H₂Fe(CN)₆ cryst. struct. 9-23756
 H₂Fe(CN)₆ cryst. struct., H-bonds and isotope eff. obs. 9-23756
 HCO₂ and DCO₂, bonding in crystals. 9-32908
 Ho, spin-wave excitations in conical and spiral mag. phases 9-45111
 Ho, spin wave dispersion relation in spiral mag. phase 9-45112
 K, anharmonic effects on vibr. normal modes, inelastic scatt. obs. 9-46975
 K(D_{0.35}H_{0.45})₂PO₄, pressure depend. of ferroelec. transition temp. 9-49143
 KD₂PO₄, pressure depend. of ferroelec. transition temp. 9-49143
 KH₂PO₄, intensity anomalies near phase transition pt. 9-40903
 KH₂PO₄, proton tunneling, n. scatt. obs. 9-24219
 MgCr₂O₄, magnetic structure 9-28630
 γ -Mn, antiferromagnetic structure confirmation 9-31051
 Mn_{0.6}Zn_{0.4}Fe₂O₄, sublattices magnetizations and superexchange interactions obs. 9-39777
 Mn₂GeS₄, orthorhombic, nucl. and mag. struct. 9-35589
 MnAlGe ternary alloy, atomic and ferromagnetic structure 9-35560
 MnAs(Sb,Bi), mag. form factors calc. from Bragg reflections 9-35553
 MnCr₂S₄ thiospinel, low temp. mag. transition obs. 9-47225
 ND₄2PO₄, pressure depend. of ferroelec. transition temp. 9-49143
 NH₄F, wurtzite type struct., space group P6₃mc, h.c.p. sublattices displacement, N-H bond distances 9-32923
 NH₄H₂PO₄, pressure depend. of ferroelec. transition temp. 9-49143
 Na molten struct. 9-39075
 NaCl, phonon dispersion relations from n. scatt. meas. at 80 and 300°K 9-24021
 NaCn, arrangement of (CN) group, model 9-28266
 NbC_{0.75}, ordering in struct. 9-40913
 Ni-Cu alloy, rel. to giant mag. moments near initial composition 4.2°K 9-45148
 Ni, phase transition investig., effect of mag. field 9-24305
 Ni, phase transition region near Curie pt., using polarized neutrons 9-37650
 Ni, spin-wave scatt. near Curie pt. 9-49201
 Ni, spin-wave spectrum 9-45115
 NiCl₂·6H₂O, cryst. struct., room temp. and 4.2°K 9-42793
 NiFe₂O₄, with polarized neutrons, for chemical and mag. struct. 9-48838
 NiS, pressure effect rel. to lattice compressibility, T>T_N and T<T_N 9-44672
 NiS₂, mag. props. 9-33437
 NiSe₂, mag. props. 9-33437
 NiSeO₄, antiferromag. struct., Neel pt. 9-49223
 Pb, phonon spectrum determ. by n. scatt. compared with tunneling meas. 9-26413
 Pb_{0.6}Tl_{0.4}, phonon spectrum determ. by n. scatt. compared with tunneling meas. 9-26413
 α -Pb(N₃)₂, crystal structure 9-39300
 PbZr_{0.1}Ti_{0.9}O₃, perovskitic ferroelec., atomic struct. for x=0.9 0.58 9-44673
 Pt-Mn ordered alloys, mag. structure 9-35563
 Rb liquid, atomic overlap 9-34875
 RbMnF₃, critical mag. scattering and sublattice magnetization 9-45234
 RbMnF₃, Heisenberg antiferromagnet, mag. scattering 9-45202
 SiO₂, vitreous 9-28269
 (Sr_{0.8}Ba_{0.2})₂Zn₂F₁₂O₂₂ hexagonal ferrite, localization of Zn²⁺ ions 9-42798
 Sr₂Fe₂O₇, antiferromag., mag. and cryst. struct. 9-41341
 TaC_{0.75}, ordering in struct. 9-40913
 Ti₂ZrO₃, antiferromag., existence, neutron-polarization analysis 9-45236
 Ti₂ZrO₃, crystal structure 9-26249
 UBi, magnetic structure and ordering 9-47294
 UBi antiferromag. struct. 9-39785
 UFeO₄, magnetic structures and props. 9-45238
 UP, low temp., magnetic transition 9-28590
 UP_{1-x}S_x system, (0<x<1), mag. phase diagram 9-45237
 USb and USb₄, magnetic structure and ordering 9-47294
 USb antiferromag. struct. 9-39785
 VF₂ single crystal and powdered samples, magnetic structure 9-45074
 W:C rhombic modification 9-32933
 YCo₃, YCo₅ and Y₂Co₇ single crystals, polarized-neutron diff. study of mag. moments 9-47250
 Zn, liq., expt. data anal. for ion-ion pot. determ. 9-23459
 Zn_{0.87}Mn_{0.13}Fe₂O₄, mag. struct. obs. 9-43189
 Zn_{0.8}Ni_{0.2}Fe₂O₄ ferrite system, chem. and mag. struct., Yafet-Kittel ordering 9-41329
 ZnFe₂O₄, oxygen parameter determ. 9-30576
- Neutron radiography** see Radiography
Neutron sources see Neutrons/production
Neutron spectra
¹⁸⁷Ta target, 80 MeV α bombard., FLUXPOS computer program calc. 9-34474
 atmospheric, in solar quiet period, geomag. latitude 46°N 9-41608
 C spheres pulsed with 14 MeV time spectra of emitted n. 9-34479
 epithermal spectrum meas. with resonance sandwich detectors 9-29891
 fast, in thermal reactors, by high resolution semicond. spectrometer 9-27791
 fission, exptl. determ., 0.6 to 24 MeV 9-22828
 gas proportional counter using p recoil, computer programme 9-22660
 graphite from spherical shell 9-27783
 hardness in fast breeder reactors, effect on gain 9-22866
 hyperfine structure of thermal spectrum across cluster-type fuel elements 9-22876
 leakage, time-dependent Monte Carlo, error estimation 9-22845

Neutron spectra continued

- line, graphical analysis from recoil proton proton proportional counter data 9-48218
 measurement with fast subcritical facility SUAK 9-29890
 methane, gas and solid, inelastic scatt. spectrum study of mol. dynamics 9-36717
 N_2 spheres pulsed with 14 MeV time spectra of emitted n. 9-34479
 polyethylene, from spherical shell 9-27783
 reaction rate determination, correction and smoothing parameters 9-27775
 reactor, energy analysis 9-25668
 theoretical and exptl., comparison for fast critical assemblies 9-29888
 water and A-water laminations, fast n, obs. 9-22896
 (n, γ), 'effective cross-section' concept for reactor neutrons 9-25636
 np interaction, channel cross section determ., $E_n=2-10$ GeV 9-29607
 p recoil spectrometer and meas. in core and blanket 9-29889
 p recoil telescope anal., response junction calc. 9-25532
 ^{242}Pu spontaneous fission 9-29859
 ^{244}Cm spontaneous fission 9-29859
 ^{235}U , time-of-flight meas. 9-29808
 ^{235}U in Cu container, energy distrib. of neutrons at 100 m 9-36621
 ^{238}Pu F α , obs. with ^6Li and ^3He fast n spectrometers 9-42290
 ^{239}Pu n induced fission 9-29859
 Am-Be source, calc. and expt. 9-22629
 Am-Be source use of He semiconducting spectrometer with sandwich diode detector 9-44084
 D $_2$ O-H $_2$ O mixture, poisoned, thermal spectra rel. to suitability of scatt. kernel 9-27788
 Ho, paramag., phonon dispersion relations 9-28415
 Na from spherical shell 9-27783
 Na scattering resonance, heterogeneity effect 9-27784
 Pu-Be source, calc. and expt. 9-22629
 Pu fuelled reactor, meas. and interpretation 9-29887
 U, natural-D $_2$ O lattices, obs. 9-32378
 U from spherical shell 9-27783
 U void effect on neutron spectrum indices and fast fission ratio 9-38737
 UC void effect on neutron spectral indices and fast fission ratio 9-38737
 W, time-of-flight meas. 9-29808

Neutron spectrometers

- boric filter method for collimated beams 9-40455
 combination n- γ detection 9-32249
 combination n- γ detection, below 4 MeV, PuBe new spectrum structure 9-32248
 diffractometer, time-of-flight, for crystal struct. analysis, focusing expt. 9-30548
 fast n time of flight spectrometer with n- γ discrimination 9-42131
 for fast neutrons, with CO $_2$ telescopes, Si detector and computer analysis 9-44083
 flight-time statistical method, struct. investigations 9-35051
 high flux, patent 9-38612
 proportional-counter, wall-effect correction calc. 9-29651
 scintillator, organic liquid FERDoR unfolding method and code, circuit 9-34353
 thick radiator, fast n, efficiency resolution and lpne shape anal. 9-32252
 time of flight, for fission neutron energy spectrum meas. 9-48216
 time of flight expts., efficiency improvement using random beam pulsing 9-42124
 time-of-flight methods, novel high-duty-cycle methods 9-29648
 triple axis, resolution function determ. method 9-42778
 triple-axis, polarization analysis of thermal-neutron scatt. 9-42780
 two-axis, crystal mosaic spread meas. 9-30546
 p recoil, investigation of energy loss in H 9-46137
 p recoil spectrometer and meas. in core and blanket 9-29889
 Ge monochromators, simple method of increasing mosaic spread 9-44082
 He semiconducting, with sandwich diode detector for Am-Be neutron source 9-44084
 ^3He semicond. spectrometer, n energy distrib. of Am-Be- and ^{252}Cf source 9-34355
 ^6Li semicond. sandwich, applic. in reactor, energy resolution and geometrical efficiency 9-34354
 Pb single crystal monochromator, efficiency and optimization 9-32251

Neutron transport theory

- see also Neutrons and antineutrons/diffusion; Neutrons and antineutrons/moderation*
 attenuation function calc. from exptl. curve 9-38729
 Boltzmann operator, semigroups, n slowing down in graphite 9-34054
 Chandrasekhar's X-, Y-functions for isotropic scatt. in thick slab 9-40528
 'die away' expt. in moderators, limited critical freq. of n wave 9-27781
 in ducts and other cavities in shields, modeling relationships 9-34481
 equation, time depend., with delayed n, analysis using matched asymptotic expansions 9-34480
 equation for arbitrary convex geometry, analytical solns. 9-44230
 leakage in small exponential cores, new method of analysis 9-27780
 monoenergetic, eqn. for finite slab, soln. by Laplace transformation 9-42316
 neutron wave propagation in an infinite moderating medium, using energy-depend. transport theory 9-34477
 one-speed, disadvantage factor rel. to anisotropic scatt. 9-34499
 random media effect on n transport 9-34483
 scattering law of asymmetric top molecule 9-34475
 streaming in moderator, effect of anisotropic hole systems 9-34502
 thermal, in moderating media, time behaviour 9-38986
 thermal flux flattening, in 1D geometry 9-34476
 thermal n flux filter, end effect 9-32393
 two-group time-dependent diffusion equation in reflected reactors, analysis of prompt n dieaway 9-27779
 wave propagation in moderator, point spectrum existence theorem 9-38732
 SiO $_2$ shields, calcs. for incident monoenergetic neutrons, 50-400 MeV 9-48234

Neutrons and antineutrons

- see also Cosmic rays/neutrons; Nucleons and antinucleons*
 beam collimation by rectangular tubes, Monte Carlo study 9-25180
 beam produced in $^3\text{H}(d,n)^4\text{He}$ with thick target, shape 9-29675
 CP violation model of decays with conservation and violation in second and third orders of primary interaction 9-32118
 decay, vector coupling const. equality with μ , renormalizable weak interaction model 9-32124

Neutrons and antineutrons continued

- decay of polarised neutrons, A and B coeff. determ. 9-42107
 electric dipole moment, exptl. obs. 9-27557
 electric dipole moment, upper limit determined 9-38585
 EURACOS fast irradi. facility 9-32223
 flux in reactor cell, energy and time depend., calc. using analytical Horowitz operator 9-22864
 magnetic charge, upper limits in Sun 9-24914
 magnetic extinction by polycrystals 9-41308
 magnetic moment, ratio to proton, nonrelativistic quark model 9-38584
 mean free path in Pb, meas. in energy region 1-10eV 9-22895
 moment, electric dipole, in the V-Ae 0 weak interactions theory 9-32221
 neutron flux in atmosphere produced by cosmic ray interactions, depth function 9-47551
 neutron single particle levels in Woods-Saxon pot. 9-42171
 neutron wave propagation, axial, in heterogeneous media 9-22855
 P-theory with axially variable parameters 9-22867
 polarised, decay, A and B coeff. determ. 9-42107
 pulse propagation in time-depend. P $_1$ -approx., soln. in short-time region 9-22847
 radiography, props. of films examined 9-25393
 resonance integrals for negative energy levels 9-44184
 resonance interaction effects, calc. by rational approx. to symmetric line shape function 9-22900
 Rossi- α meas. by dead-time method 9-34349
 solar neutron transport in earth's atmosphere, calc. 9-35829
 source, thermal/cold, using fast pulse moderation, temporal characts., 5-80 MeV 9-32377
 spin, anomalous torque meas., ^{13}C n.m.r. expt. 9-38586
 standard thermal flux facility, construction and calibration 9-22628
 thermal, decay in vac., assoc. proton recoil spectrum 9-44229
 thermal, gas., plane wave disturbance propag. theory 9-22842
 time and space relax. constants in proton gas model 9-27778
 transport equation, 3 dimen., for time independent monoenergetic neutrons, elementary solns. 9-22848
 transport in slab geometry, monoenergetic initial-value problem 9-22856
 transport theory, two-group, full range completeness theorem 9-22857
 ultracold neutrons, method of obtaining 9-48364
 wave propagation, one-speed, with source off interface 9-22843
 waves, rel. to sound waves 9-29860
 yttrium ferrite, ferromagnetic, mag. extinction 9-41308
 β -decay, axial vector coupling const., quasi-indep. quark model calc. 9-27552
 β decay, e.m. corrections, 2nd order, to G $_A$ /G $_V$ 9-38582
 β decay rate, effect of mag. field, astrophys. implications 9-44058
 $K \pi \rightarrow \Lambda(1520)\pi^-$ 9-25448
 n-p radius difference from π prod. by p on nuclei obs. 9-36472
 n- π^0 decay rate depend. determ. in const. uniform mag. field, 10G variation region 9-38583
 n- π^0 , parity violating amplitude determ. from ^{187}Ta transition γ circular polarization meas. 9-36580
 n-p mass difference and tadpole model 9-29613
 p-n mass differences, high and low energy contribs. 9-42061
 p-n mass diff. and form factor calc. by gravitational Ward-Takahashi identity 9-38577
 p-n mass difference from Reggeized tadpole model 9-40441
 ^{121}Sb capture cross section meas., resonant level parameters determ. 9-27633
 ^{252}Cf as radiographic source 9-42257
 ^{121}Sb capture cross section meas., resonant level parameters determ. 9-27633
 ^{121}Sb -Be source of thermal N, for precision anal. and tracer prod. 9-28834
 $^{10}\text{B}(d,n_0)^{11}\text{C}$; n polarization ang. distrib. meas., Ed=1.2-2.9 MeV 9-48341
 neutron, transmission of slow polarized beam 9-27280

absorption

- see also Nuclear excitation; Nuclear reactions and scattering due to neutrons*
 in cyclotron shielding, obs. during 80 MeV α bombard. of ^{187}Ta target 9-34474
 ferromagnetic perfect single cryst., anomalous capture of thermal polarized n by nuclei 9-26464
 local absorber in finite medium, perturbation effect of slowing down density 9-22850
 thermal neutrons in thin targets, calc. technique 9-42286
 ^{113}In and ^{115}In mixture, rel. to conc. of ^{115}In 9-45431
 ^{171}Lu and ^{175}Lu mixture, rel. to conc. of ^{175}Lu 9-45431
 D $_2$, thermal n absorpt. cross section, obs. 9-25617
 D $_2$ O, thermal n absorpt. cross section, obs. 9-25617
 Pb-polyethylene shields, fast-neutron attenuation, S_n calc. 9-33963
 SiO $_2$ shields, transport calcs. for incident monoenergetic neutrons, 50-400 MeV 9-48234
 U, natural, thermal neutron conversion ratio 9-44231

angular distributions

- Bi(γ ,n) fast photoneutrons 9-27697
 Pb(γ ,n), fast photoneutrons 9-27697
 Ta(γ ,n), fast photoneutrons 9-27697

capture *see* Nuclear reactions and scattering due to neutrons**detection, measurement**

- see also Dosimetry; Neutron spectrometers*
 beam modulation by vibrating quartz crystal 9-30549
 boric filter method for collimated beams 9-40455
 cosmic ray monitor for atmosphere, design 9-36500
 detector, large acceptance for simultaneous meas. of time-of-flight and co-ordinates of interaction point 9-34359
 detectors, polyethylene moderated, containing ^3He proportional counters 9-48227
 exponential decay constants, optimization of activation and counting times 9-25594
 fast flux testing in thermal reactor using spectrum-hardening filter 9-36642
 flux meas. by ionization chamber current fluctuations, patent 9-32253
 glass (mica) etch-pit counting method 9-22914
 Grey detector, efficiency determ. 9-48226
 line spectra, graphical analysis from recoil proton proton proportional counter data 9-48218
 miniature detector using plastic scintillator and photomultiplier 9-36515
 plastic scintillator, detection eff. for 20-170 MeV n 9-25515

**Neutrons and antineutrons continued
detection, measurement continued**

- prompt, fission emitted, average number, fission delayed γ -rays effect 9-25664
- in reactor, detectors positioning and flux meas. accuracy 9-27790
- reactor importance meas. methods, errors and optimization 9-32392
- reactor intensity distrib. rel. to shield composition 9-31688
- spectra and decay constants, meas. with fast subcritical facility SUAK 9-29890
- spectra of fast n in thermal reactors, by high resolution semicond. spectrometer 9-27791
- thermal and epithermal, glass and granular scintillators 9-42134
- thermal n incident on ^3He counter, wall effect 9-44091
- N detector, high temp., tests to 650°C 9-36508
- ^{243}Am slow neutron absorber, patent 9-38620
- ^{176}Lu - ^{164}Dy detector for thermal spectrum hyperfine structure obs. 9-22876
- BF_3 counter bank, improved, mixer circuit 9-29646
- BF_3 n detection system, radial array, investigation of response 9-25506
- Ge(Li) gamma spectrometric determ. fast/thermal ratio 9-25526
- $^3\text{H(d)}$, n / ^3He , time-of-flight neutron expt. for undergraduate laboratory 9-45718
- Li glass detection bank for time-of-flight neutron meas. with reactor 9-25516
- P-Au activation dosimetry 9-46141
- Rh self-powered neutron flux monitor calibration in simulated pressurised water reactor 9-36635
- S-Au 9-46141

diffusion

see also *Neutron transport theory*

- ^{235}U spherical shell transmission at 23 KeV, Monte Carlo interpretation 9-34482
- average potential model, dispersion of slow neutrons 9-29861
- average potential model, dispersion of slow neutrons 9-36619
- collision, anisotropic, in general cylindrical geometry 9-29862
- conduction eqn. solution appl. 9-26434
- dipyl diffusion length and age, static meas. 9-22891
- discrete decay const. exceeding $(\psi(E))_{\text{min}}$ 9-38730
- graphite, modulated wave asymptotic params., calc. 9-25665
- HB-40 diffusion length and age, static meas. 9-22891
- in heterogeneous reactor, anisotropic coeffs. calc., comparison with Benoist estimation 9-22863
- leakage in small exponential cores, new means of analysis 9-27780
- length in reactors 9-25668
- IN moderator, modulated wave asymptotic params. meas. above critical buckling and freq. 9-25665
- in reactors, reflected, decay of prompt neutrons, analysis 9-27779
- regulating cylinders covered with absorber in reactor reflector, efficiency 9-36624
- transport calculations, integral, polynomial approximations 9-22853
- transport eqn., soln. using material geometry parameter method 9-36620
- transport equation, consistency of certain approximate solutions 9-22852
- transport equation, time depend., of delayed n, analysis 9-34480
- transport in ducts and other cavities on shields, modeling relationships 9-34481
- in water, 18-280°C 9-30380
- water, diffusion length and age, static meas. 9-22891
- water moderating system, pulsed with thermal n, extrapolation length 9-34497
- in BeO assemblies, from $\lambda(B^*)$ curve 9-36629
- D_2O , diffusion and cooling coeffs., obs. 9-25617
- D_2O , thermal n coeffs., static and pulsed meas. 9-27776
- H_2O , thermal n coeffs., static and pulsed meas. 9-27776
- Pi-B source, through cylinder of water distrib. function calc. 9-34473
- Po-B source, through cylinder of water distrib. function calc. 9-22841

effects

see also *Nuclear reactions and scattering due to neutrons*

- β_1 -brass, metastable, on martensitic transformations 9-23981
- diffusion creep 9-28308
- fission, ternary, of ^{238}U and ^{232}Th , 29 MeV 9-44226
- graphite:B, irradi., effect of B on defect clustering, physical prop. meas. 9-30597
- graphite:B, irradi., effect of B on interstitial loop clustering, electron micro-scope obs. 9-30595
- graphite:B, irradi., nucleation of interstitial loops, effect of B 9-30596
- graphite, irradi., low temp., stored energy and elec. resistivity var. 9-24070
- graphite, irradi. at high temp., defect nucleation, cry. perfection influence 9-23794
- graphite, irradiated, 300°-1200°C, bulk expansion 9-46883
- graphite, pyrolytic, irradi., rel. to Young's modulus 9-46864
- graphite irradi. in CO_2 , uptake of Br and formation of lamellar cpds. with K obs. 9-28316
- graphite reactivity to O, n bombardment eff. 9-35743
- graphite-pyroc carbon composite mats. obtained by natural gas decomposition, n, irradi. eff. 9-28436
- Hastelloy N, post irradi. mech. props. rel. to strain rate 9-41030
- Inconel 625, creep strength reduction and embrittlement, 650°C 9-37250
- m.o.s.f.e.t.'s in pure neutron environment, theory and experiment 9-33360
- permalloy films, reactor irradi. and subsequent annealing effect on anisotropy field 9-47253
- plasma focus, anisotropies meas., n emission method 9-25866
- polyethylene dose absorbed in ^{235}U critical assembly 9-37284
- on Portevin-le Chatelier effect in carburised Ni-Cu alloys 9-28349
- steel, austenitic, irradi., He bubbles obs. 9-33108
- steel, ferritic, choice of parameter to meas. embrittlement 9-35299
- steel, ferritic, choice of parameter to meas. embrittlement 9-24071
- steel, stainless type 304L, fuel clad, tube burst tests of strength after irradi. 9-26339
- steel embrittlement rel. to microstruct., theory 9-37261
- steel stainless, irradiated, fatigue behaviour, review 9-23861
- swelling in austenitic stainless steel, reactor induced 9-28437
- teflon, dose absorbed in ^{235}U critical assembly 9-37284
- transistors, radiation tolerance, comparison of bipolar and f.e.t. types 9-30948
- voids in f.c.c. metals 9-41119
- water, cavitation threshold lowering 9-46592
- Zircaloy, creep props. during irradi. 9-28356
- Zircaloy, in-pile softening and hardening rel. to creep and strain rates 9-41023

**Neutrons and antineutrons continued
effects continued**

- Zircaloy-2 tubes, failure rel. to dose and stress appl. 9-39435
- Zircaloy-4, non-linear growth rel. to interstitial loops 9-37375
- ^{235}U fission, changes in fragment kinetic energy 9-40521
- Al, irradi., Kohler rule of magnetoresistance, validity at 4.2K 9-44906
- $\alpha\text{-Al}_2\text{O}_3$, hardness increase, dislocation formation on annealing 9-28310
- Al_2O_3 , irradi., e.p.r. spectrum of triplet ($S=Z$) state defect. 9-44689
- Al_3N_4 anisotropic growth 9-40857
- in Al foil, sputtering of U in-reactor, subsequent irradi. for fission track visualization 9-34489
- Al single crystal, plasticity and elec. cond. 9-46928
- Au-(0.1 wt.% Cu) alloy, irradi. at low temp., elec. resistivity recovery, effect of cold work 9-43025
- Au, irradi. at low temp., elec. resistivity recovery, effect of cold work 9-43025
- Au, irradiated, vacancy clusters 9-28279
- BaF_2 , irradi., e.s.r., F- and V-centres thermal stability obs. 9-43275
- Be impact resist. $1.75\text{--}4.39 \times 10^{21} \text{ n/cm}^2$ 9-28368
- C, dimensional changes and creep, rel. to strain and struct. 9-41022
- C, pyrolytic, effect of high exposure on dimensions 9-40992
- CaO , irradi., N centre, e.s.r. obs. 9-37794
- CaO calcite, thermal n tracks 9-41123
- $\text{CdCl}_2\text{:Ag}$, irradi., optical absorpt. and e.p.r. obs. 9-49272
- CdS , fast-irradi., radioactive decay and associated elec. changes 9-47104
- Cr-steels, embrittlement in temp. range of α - γ transformation 9-28369
- CsCl , irradi., rare gas diffusion and influence of α to β phase transform. 9-33004
- CsI , irradi., rare gas diffusion and influence of α to β phase transform. 9-33004
- Cu-B alloy, He bubble form., influence of precip. 9-41116
- β_1 -Cu-Zn alloy, irradiated, effect on martensitic transform. 9-37296
- Cu, behaviour at elevated temps. 9-28330
- Cu, irradi. at low temp., elec. resistivity recovery, effect of cold work 9-43025
- Cu 2 at % Al, behaviour at elevated temps. 9-28330
- Cu foil, spatial distrib. of damage spots 9-46806
- Cu 2 at % Mg, behaviour at elevated temps. 9-28330
- Cu(9.5 at %)Be-(0.2 at %)Zn, alloys, irradi., ageing characts. from resistivity meas. 9-33115
- Fe, irradi., dislocation channelling 9-48860
- Fe, irradi. at low temp., elec. resistivity recovery obs. 9-43027
- Fe embrittlement rel. to microstruct., theory 9-37261
- Ge, irradi., structural effects 9-44695
- n-Ge crystals, bombarded, for γ -ray spectrometers 9-46131
- InTe, high pressure polymorphs, influence on phase stability 9-35250
- KBr, irradi., effect on dislocation etch figure dimensions 9-40945
- KBr, low temp. annealing of induced defects 9-40967
- KCl, irradi., effect on dislocation etch figure dimensions 9-40945
- KH_2PO_4 , incoherent inelastic scattering cross section 9-28560
- $\text{Li}_2\text{O-2SiO}_2$ glass, on struct. and sequence of crystn. reactions 9-40833
- LiF, colour centres, F-band formation 9-35114
- LiF, e.p.r. linewidths of conduction electrons in Li particles 9-33630
- LiF, effect on i.r. absorption 9-39839
- LiF, irradi., effect on dislocation etch figure dimensions 9-40945
- LiF, thermal-neutron irradi. effect on elastic moduli 9-46865
- LiF vacancies formed by reactor radiation, detect. by annealing and elec. cond. meas. 9-32949
- Mg, damage and recovery, low temp. 9-32940
- MgF_2 single cryst., rad. damage, comparison with electron damage, optical absorpt. obs. 9-35117
- MgO , irradi., zero-photon line study 9-45325
- MgO , R-like centre production, Faraday rotation obs. 9-26295
- MgO , R-like centre production, Faraday rotation obs. 9-28306
- MgO single crystals, irradi., hardening 9-33099
- Mo-steels, embrittlement in temp. range of α - γ transformation 9-28369
- Mo, irradi., elec. resistance recovery, effect of hydrostatic pressure 9-35342
- Mo, irradi., hydrostatic press. induced recovery of lattice parameter increases 9-40909
- Mo, polycryst., irradi. depend. of ductile-brittle transition temp. 9-30742
- NaCl , irradi., effect on dislocation etch figure dimensions 9-40945
- NaNO_2 , neutron irradiated, ESR obs. 9-49354
- Nb, irradiated, dislocation channelling 9-42837
- Nb single cryst., rad. hardening, temp. depend. of yield stress 9-26371
- NBN type I superconductors, n irradi. enhancement of current carrying capacity 9-43039
- Ni, irradi., secondary defects formation 9-32959
- O reactivity to graphite, n bombardment eff. 9-35743
- P, high pressure polymorphs, influence on phase stability 9-35250
- Pb dose absorbed in ^{235}U critical assembly 9-37284
- PbO_2 , high pressure polymorphs, influence on phase stability 9-35250
- PbTe, thermal neutron capture in ^{124}Te , ^{125}Te Mossbauer emission spectra obs. 9-37703
- S, of orthorhombic S at 77K, prod. of unstable form. 9-30747
- Si(B(P), irradi. at 80°K, conductivity and Hall effect meas. rel. to carrier removal rates 9-44852
- p-Si, defect cluster formation and annealing, elec. meas. rel. to transport props. 9-47129
- p-Si, irradi., photoconductivity 9-41271
- p-Si, irradiated, donor-like centres production 9-47130
- Si, rad. induced atomic displacements 9-48844
- SiO_2 , high pressure polymorphs, influence on phase stability 9-35250
- Te, thermal neutron capture in ^{124}Te , ^{125}Te Mossbauer emission spectra obs. 9-37703
- TeO_2 , thermal neutron capture in ^{124}Te , ^{125}Te Mossbauer emission spectra obs. 9-37703
- Ti irradi. commercially pure, low temp. annealing effects on tensile props. 9-33112
- $\alpha\text{-U}$, defects, deviations from Matthiessen's rule 9-46805
- UO_2 , sintering pores and fission gas bubbles irradi. stability, obs. 9-37187
- V, defect clusters and loop prod. 9-39367
- V, irradi., cylindrical damage cells, transmission electron microscopy 9-44698
- W, irradiated, impurity segregation within dislocation array 9-28295
- Zr, damage, rate and distribution, effect of fast neutron spectrum 9-26469
- Zr, high pressure polymorphs, influence on phase stability 9-35250

interactions

- $\gamma\text{-}n\text{-}\pi\text{-}N^+$ cross-section predicted in quark model 9-29580

Neutrons and antineutrons continued interactions continued

- $\eta n \rightarrow \rho \pi^-$, differential cross section meas., $E_\eta=500-800$ MeV 9-32222
 $K^- n \rightarrow \lambda \pi^-$ neutrals, $\eta(550)\pi$, enhancement obs. 9-40433
 $K^- n \rightarrow \Lambda \pi^- \eta$, $\pi^- \eta$ reson., prod. at 4.5 GeV/c 9-34313
 $K^- n \rightarrow K^- \pi^+ \pi^-$ dominance of $N^* K^- \pi^+$ [(71±7)%], $E_K=2.24$ BeV/c 9-32178
 $K^- n \rightarrow \Lambda(1405)\pi^-$ 9-25448
 $K^- n \rightarrow \Lambda \rho^0 \pi^-$, $\rho^0 \pi^-$ resonance in $A_2(1300)$ mass region, 40 MeV width, spin and parity analysis 9-42064
 $K^- n \rightarrow \Sigma^- \pi^0$ in $K^- d \rightarrow \Sigma^- \pi^0$, 1600-1800 MeV, formation of Y^* (1665) 9-38596
 $K^- n \rightarrow \Sigma^- \pi^0$ in $K^- d \rightarrow \Sigma^- \pi^0$, 1600-1800 MeV, formation of Y^* (1665) 9-38596
 $K^- n \rightarrow \Sigma^- \pi^0$, cross section meas., $M_K=4.5$ GeV/c 9-27499
 $K^- n \rightarrow \lambda \pi^-$, λ polarization, diff. cross section meas., $M_K=4.5$ GeV/c 9-27499
 $K^- n \rightarrow K^0 p$ high energy charge-exchange reaction using Regge poles 9-44027
n-p, differential cross section and polarization, 200 MeV 9-25482
np, channel cross section and n spectra determ., $E_n=2-10$ GeV 9-29607
np, inelastic collisions at 20 GeV energies, analysis 9-25481
np, reaction channel separation at exposure of bubble chamber to 2-10 GeV neutron beam 9-27599
np- $\pi^+ \pi^- \pi^+ \pi^-$, 2-10 GeV, obs. of 730 events $\pi^+ \pi^- \pi^+$ explained as N^* isobar 9-25487
 $\nu n \rightarrow l^- \rho^0 \pi^-$ differential cross-section predicted by current algebra 9-46060
 $\nu n \rightarrow \pi^+ \mu^-$, quasielastic ν scatt., spark chamber detector obs. 9-32132
 ^{235}U spherical shell transmission at 23 KeV, Monte Carlo interpretation 9-34482

moderation

- see also Neutron transport theory*
density scaling of Boltzmann eqn., applic. in reactor physics 9-22849
diphenyl, static meas. of diffusion length and age of n 9-22891
discrete decay const. exceeding $(\nu(E)/E)_{\text{min}}$ 9-38730
fast, multigroup transport eqn., Fourier transform soln. for plane source 9-22846
in graphite, from Be (d,n) reaction, construction of standard thermal flux facility 9-22628
graphite, neutron wave propagation 9-34478
graphite, thermalization studied by time-step and Monte Carlo methods 9-22851
graphite, thermalization params., $2.99 < B^2 < 25.30$ 14 MeV 9-25666
HB-40, static meas. of diffusion length and age of n 9-22891
moderator assemblies for pulsed thermal neutron time-of-flight expts. 9-44059
for moisture content determ. 9-39972
moisture measurement with depth and surface probes, appls. 9-35765
neutron-wave propagation, application of Laguerre polynomials in analysis 9-22854
Placzek-type oscillations in one-isotope media for general elastic scatt. and absorpt. law 9-44193
pulsed neutron research, thermalization meas. 9-22869
reactor, moderator temp. eff. 9-25668
reactor fast pulse for thermal/cold source prod. 9-32377
in reactor textbook 9-34487
in reactors, heterogeneous, thermalization, P_1 multigroup calc. 9-22859
slowing down density, perturbation due to local absorber in pulsed finite medium 9-22850
temperature depend. on geometric parameter for water and loose diphenyl, meas., by pulse method 9-46251
ultracold neutrons 9-27558
water, static meas. of diffusion length and age of n 9-22891
wave propag. described by integrals over the continua 9-32373
wave propag. in crystalline and non-crystalline moderators 9-34477
waves in moderators, limiting critical freq., physical criteria 9-27781
waves in moderators, limiting critical freq., physical criteria 9-27782
BeO assemblies, pulsed, decay curves in region of Corngold's limit 9-22909
BeO assemblies, pulsed, extrapolation distances rel. to buckling 9-22908
D₂O, liquid, as moderator for cold neutron source 9-46252
D₂O-H₂O mixture, poisoned, thermal spectra rel. to scatt. kernel test 9-27788
H₂, liquid, as moderator for cold neutron source 9-46252
H₂O, neutron wave propagation 9-34478
Pb, thermalization process, study with pulsed source 9-22893
U-D₂O lattice with Pu, epithermal cross-sections 9-25672
U-H₂O assembly, n flux distrib. in slab elements 9-22879
U, natural-D₂O lattices params., obs. 9-32378

polarization

- $^3\text{H}(d,n)^3\text{He}$, n polarization energy and ang. distrib. meas., $E_d=0.5-2$ MeV 9-25653
Al, of 3.25 MeV neutrons, obs. 9-27733
 ^{12}C 2.33 MeV polarized neutron scatt. 9-27720
 $^{12}\text{C}(d,n)^{13}\text{N}$, n polarization meas., Mott-Schwinger scatt. method, $E_n=51.5$ MeV 9-22815
 ^{65}Cu , polarized n scatt., 2.33 MeV 9-27720
 ^{54}Fe , ^{56}Fe , scatt., 2.33 MeV 9-27720
 $^3\text{H}(d,n)^3\text{He}$, associated particle method production 9-36613
 $^3\text{H}(d,n)^3\text{He}$, meas. of gas recoil 9-25500
Mg of 3.25 MeV n, obs. 9-27733
 ^{58}Ni , ^{60}Ni , polarized neutron scatt., 2.33 MeV 9-27720
S of 3.25 MeV n, obs. 9-27733
Si of 3.25 MeV n, obs. 9-27733

production

- fast pulsed reactor Viper 9-25670
fast pulsed reactor Viper 9-25671
monoenergetic beam from $^{12}\text{C}(d,n)^{13}\text{N}$ at 1.2-4.5 MeV 9-42304
neutron selection by switch rotor, patent 9-34328
neutron tube, design and performance 9-40450
photoneutrons by bombarding heavy-metal targets with laser-accelerated electrons 9-34329
plasma, laser-heated 9-46120
plasma accelerator, coaxial, focus as intense source 9-25483
polyphenyl target, deuterated, obs. of $\text{D}(d,n)^3\text{H}$ reaction 9-25502
pulsed thermal n source for time-of-flight expts., moderator assemblies 9-44059
source reactor facility to operate -193° to 725°C 9-45922
ultracold neutrons 9-27558
(p,n) reactions on ^3H , ^3H , ^7Li and ^9Be , 30, and 50 MeV 9-29674

Neutrons and antineutrons continued production continued

- e, Be collision, yield meas., $E_n=10, 16$ GeV 9-29566
n, from 5 GeV/c p interactions in nuclear emulsions 9-48210
 $^{238}\text{PuF}_4$, from (α,n) reaction with ^{19}F , n spectrum obs. 9-42290
Am-Be neutron spectrum obs., comparison with spectra calc. from $^9\text{Be}(\alpha,n)$ reaction 9-22629
Kr isotopes fission, search 9-40527
Po-B source, scatt. in cylinder of water, distrib. function calc. 9-34473
Po-B source scatt. in cylinder of water, distrib. function calc. 9-22841
Pu-Be sources, calc. spectra compared with expt. data 9-22629
Xe isotopes fission, search 9-40527
- ## reflection
- reactor reflector spectrum calc. 9-34490
- ## scattering
- anharmonic crystal, interatomic pot. theory 9-30759
anisotropic, double P_1 method, further calc. step in treatment of scatt. integral 9-27777
antiferromagnets, critical magnetic, cross sections 9-24321
atmospheric, spherical, spatial distribution calc. 9-31475
Chandrasekhar's X-, Y-functions for thick slab 9-40528
in critical phenomena study 9-48926
crystal, coherent inelastic scatt., one-phonon reson., position and widths assignment, data analysis method 9-30764
dibromofluoroethane, heavy hindered rotator, n. scatt. spectra at two temps. 9-42432
dimethylsulphoxide and dimethylsulphone aq. solns. 9-32763
ferroelectric crystal, critical, rel. to lattice dynamics and dielec. props. 9-49141
ferroelectric crystal, one phonon differential scatt. cross section calc. 9-48943
ferromagnetic perfect single crystal, anomalous capture of thermal polarized n by nuclei 9-26464
gas, by molecules, theory 9-48656
general elastic scatt. law in one-isotope media, occurrences of Placzek-type oscs. 9-44193
glycerine, normal and deuterated liq. rel. to OH hindered rot., cold n obs. 9-28097
group IV-VI cpds., lattice dynamics rel. to ferroelectricity 9-39680
by harmonic oscillator, validity of the quasiclassical method 9-40254
hydrates, inelastic scatt. obs. of librational freqs. 9-42955
liquid, by mols., rel. to mol. dynamics 9-48656
by liquids, classical, effective field approxs. 9-39072
liquids, form prediction from collective motion theory 9-23456
liquids, optimal correl. functions 9-40773
liquids, slow n scatt. and molecular dynamics 9-26077
liquids classical, collective modes interpreted as zero sound 9-32761
by magnetic ions, differential cross section 9-24267
by magnetic ions in crystals, theory 9-45049
magnetic materials 9-49188
magnetic scatt., small angle behaviour of forward amplitude 9-31014
metals, ferromag., multiband theory of inelastic scatt. at low temp. 9-33447
in methane, gas and solid, inelastic scatt. spectrum study of mol. dynamics 9-36717
in methane, gaseous and solid 9-25772
methane in Ar, molecular dynamics at 5.3 Å, 86°K 9-25771
in moderators, effect on disadvantage factor calcs. 9-34499
in molecular spectroscopy, Raman and i.r. comparison 9-32456
paramagnets, rel. to short-range-order 9-24283
polyethylene glycol chain, freq. distrib. 9-23194
proton gas model, time and space eigenvalue problems 9-27778
quasi-classical approx. for scatt. from systems and incorporating recoil effect 9-32894
in reactor, energy-loss techs., improved counting efficiency using entire thermal spectrum 9-22877
in reactor textbook 9-34487
solid, by mols., rel. to mol. dynamics 9-48656
structure factor determ., lattice vibrations corrections 9-24014
thermal, in moderating media, time behaviour 9-38986
thermal neutrons in thin targets, calc. technique 9-42286
two-magnon inelastic scatt. of slow neutrons 9-43192
water, for 0.05 eV n, multiple scatt. and fit to McMurry-Russell model 9-27559
nd, low energy parameters, relationship with triton, investigation using N/D model 9-42115
nd polarization expt., rel. to 3N three-nucleon systems 9-27567
nd quartet scatt., applic. of method for calc. of lower bounds on phase shifts 9-27485
nd spin-dependence obs. 9-27560
np, differential cross section meas., $E_n=4-16$ GeV 9-42104
 π^- , backward elastic obs., 1.5-3.8 GeV/c 9-25465
 π , π backward, diff. cross section energy depend., $M_n=1.5-3.8$ GeV/c 9-25952
 π N peripheral absorpt. model modified with $U_{6,6}$ symmetry, appl. to backward data 9-42082
BaF₂, structure factor determ., anharmonicity and thermal diffuse scatt. corrections 9-24014
BaTiO₃, critical fluctuations obs. 9-33386
BaTiO₃ crystal, critical, rel. to lattice dynamics and dielec. props. 9-49141
C fibres, lattice vibrations obs. along c-axis 9-28414
CoF₂, two-magnon process 9-43192
Cu-Zn alloys, dispersion relations for lattice vibrations 9-30766
D₂O, inelastic at energies to 0.65 eV, energy-transfer cross-sections 9-28096
Fe-Si alloys, spin-wave dispersion relationships determ. 9-24297
Fe, critical and spin-wave scatt. 9-31030
Ga, phonon dispersion relation determination from inelastic scatt. 9-33160
H₂O and ice, slow inelastic 9-48681
KH₂PO₄ crystal, critical, rel. to lattice dynamics and dielec. props. 9-49141
MnO, paramagnetic, rel. to short-range order 9-24283
NH₄Cl, coherent inelastic scatt. meas. of normal modes of vibr. 9-46980
NaCl, phonon dispersion relations from meas. at 80 and 300°K 9-24021
NaNO₃ crystal, critical, rel. to lattice dynamics and dielec. props. 9-49141
Ne, phonon dispersion relations for cryst. at 2 densities from inelastic scatt. obs. 9-46978

Neutrons and antineutrons continued**scattering continued**

- Ni-Fe alloys, dispersion relations for lattice vibrations 9-30766
 Ni, critical magnetic scattering, intensity shift due to imperfections 9-26636
 Pb, phonon spectrum determ., comparison with tunneling meas. 9-26413
 Pb₄₈Ti₆₀, phonon spectrum determ., comparison with tunneling meas. 9-26413
 Po-B neutron source, scatt. in cylinder of water, distrib. junction calc. 9-34473
 Po-B source, scatt. in cylinder of water, distrib. function calc. 9-34473
 Po-B source scatt. in cylinder of water, distrib. junction calc. 9-22841
 SrTiO₃, antiferroelectric phase transition at 110°K rel. to normal vib. modes, obs. 9-24223
 SrTiO₃, lattice-dynamical exam. of phase transition at 110°K 9-23986
 SrTiO₃ cryst., due to excitation of soft optical phonon 9-35272

scattering, neutron-proton

- A_{np} meas in n-p scatt., 23.1 MeV 9-27554
 charge exchange process, contrib. to amplitude from moving cuts 9-38578
 cross section meas. below 3 MeV 9-29614
 differential cross section and polarization, 200 MeV 9-25482
 differential elastic cross section calc., 3-10 GeV 9-36496
 fluctuations in differential scattering cross section at few MeV n energies 9-44060
 Kohn variational principle, heuristic derivation 9-48209
 spin-independent scatt. amplitude from elastic dp scatt. obs., 1.69 GeV/c 9-22639

Newtonian fluids see *Fluids***Nickel**

- 3d-band shape from high-field susceptibility obs. 9-37406
 adsorption of N₂O, NO and CO₂, interactions and effect on work function 9-35003
 adsorption of O, S, and Se whose structure is examined by ion neutralization spectroscopy 9-32484
 in alkali halides, absorption and i.r. emission 9-33548
 amorphous film, ferromagnetic props. 9-26652
 atom, electronic configuration 9-25697
 atom, energy spectra calc. for 3d⁷ and 3d⁴4p configs. 9-38767
 atom form factor determ. by high voltage e. diff. 9-23722
 atomic spectrum, bibliography 9-38765
 atomic vibr. and relax. at (110) surface, calc. 9-35271
 band, ferromagnetism, high-field studies by Mossbauer and mag. moment meas. 9-43166
 Barkhausen and ΔE effects, rel. to applied stress 9-45147
 Barkhausen discontinuities size distrib., sample shape depend. in polycrystalline wires 9-41316
 brittleness, post-irrad. hot, rel. to He-filled deform. defects 9-37260
 cathode spot fixator, destruction mechanism 9-49169
 conductivity, elec., jump during melting 9-26156
 corrosion, atmospheric 9-37831
 corrosive surface reactions in field ion microscope 9-26827
 creep, stacking fault energy effect 9-39421
 creep at high temp., effect of low-temp. hardening 9-46913
 Debye-Waller factor and Debye temp. 9-28427
 deformation of single crystals, effect of continuous hydrogenation 9-46892
 density-of-states functions, X-ray photoelec. spectroscopy study 9-44886
 desorption of hydrogen on 100 surface, study of binding states 9-23646
 diffusion coeff. and eff. charge in Ni-Mo alloys 9-26202
 diffusion in MgO 9-44738
 dispersion curves, extended Bhatia model method 9-24012
 domain structure of single crystals, temp. depend., magneto optical Kerr technique 9-41317
 elastic const., third-order, sensitivity to changes in electron-to-atom ratio and mag. eff. 9-37217
 elec. resistivity and saturation magnetization damage rates 9-33205
 electrode erosion in high current discharge and cathode spot temp., obs. 9-34798
 electrodeposition parameters effect on growth habit and morphology 9-37034
 electrodes substrate for Co-P films, effect on coercive force and microstructure 9-31041
 electroless films on Si single crystal, internal stress 9-30654
 electron emission, second, total yield 9-31008
 electronic structure, ion-neutralization spectroscopy study 9-44890
 electronic structure determ. from X-ray emission spectra 9-37755
 eutectic melting at contact with diamond and graphite 9-26358
 explosion-shocked, thermal recovery process, electron microscope obs. 9-44696
 fatigue, high temp., rel. space charges 9-26318
 f.c.c. polycrystalline, flow stress and microstructure after shock-relief deformation 9-23879
 Fermi momentum determ. from annihilation spectra, valence electrons calc. 9-33229
 ferromagnetic anisotropy energy calc. by perturbation theory 9-47254
 ferromagnetic resonance, 20-380°K 9-24476
 ferromagnetic resonance, field, line width and temp. depend. determ., 9.2-26.2 Gc/s., -160 to 20°K 9-41419
 ferromagnetism explanation using correlation theory for narrow energy band 9-24287
 film, evaporated, intrinsic tensile stress meas., temp. depend. 9-37233
 film, on Cu, pseudomorphic growth of monolayer 9-34989
 film, optical and photoemissive props., in vacuum u.v. 9-45260
 film, thin, ultraclean, release of compressive intrinsic stress by gas adsorption 9-44758
 films, electrodeposited, magnetocryst. anisotropy, lattice distortion effect 9-39774
 films, electron tunnelling rel. to spin wave excitation 9-44995
 films, Faraday effect field depend., perpendicular anisotropy obs. 9-47322
 films, fine mag. struct. and coercive force 9-41321
 films, thin, struct. and conductance 9-39589
 foil, insulating material for space flight, outgassing behaviour 100-1800°F obs. 9-38173
 Gibbs free energy of self and impurity diffusion 9-33001
 growth, hydrothermal 9-37027
 growth of oriented bicryst. by electron beam floating-zone technique 9-46757
 growth of platelets and whiskers by thermal and chem. decomp. of NiI₂ and NiBr₂ 9-35018
 Hall effect, hydrostatic press. effects, 77 and 290°K, ≤7kbar 9-30852
 hardening, low-temp. effect on creep at high temp., electron microscope obs. 9-46913
 hysteresis, magnetostriction and magnetization reversal meas. in single crystal rod, room temp. 9-41315
 interband optical transitions investigation, low temp. magneto-optic meas. 9-41136
 internal friction studies, 77° to 298°K 9-26317
 internal stress effect on thermoremanence 9-45016
 ion bombarded, depth distrib. of vacancy clusters, 295°K and 80°K 9-30586
 ionic spectra, new classifications and corrected wavelengths of selected lines 9-34549
 i.r. absorpt. and reflectivity meas., rel. to virtual bound state 9-45269
 Jordan type after-effect, domain wall configuration during magnetization reversal 9-31034
 layer on thermocouple tip, by sputtering 9-33204
 low angle boundaries in large single cryst. 9-37185
 magnetic aftereffect due to dislocation displacement inside domain walls, effect of dissolved O 9-39766
 magnetic breakdown, band structure 9-47249
 magnetic excitations 9-45114
 magnetic moment and hyperfine constant, 4.2°K to 300°K 9-45150
 magnetic neutron scattering, temp. and intensity shift due to imperfections 9-26636
 magnetic response function calculation 9-26638
 magnetic saturation and magnetic moments of nuclei 9-26634
 magnetization, temp. variation calc. 9-47243
 magnetization by twisting in weak field, Matteucci effects 9-35566
 magneto-elastic hysteresis and internal friction 9-23863
 magneto-optical properties in visible and near infrared regions 9-39808
 magnetomechanical damping, 78° to 300°K 9-45157
 magnetomechanical damping, H influence 9-39401
 magnetomechanical damping effects 9-31036
 magnetostriction, effect of tensile stress 9-45156
 mechanical props., influence of oxidation 9-39424
 modification of molecular sieves 9-34605
 Mossbauer effect of ⁶¹Ni, Coulomb excited after recoil implantation 9-33531
 n.m.r. free induction decay amplitude depend. on r.f. field strength 9-43302
 optical absorpt. spectra in ZnWO₄ crystal 9-37731
 optical isotope shift, nucl. vol. and mass eff. 9-29988
 oriented bicryst., growth by electron beam floating-zone technique 9-46757
 oxidation, influence on mechanical behaviour 9-39424
 oxidation and cracking, effect of prior cold working 9-41450
 phase transition, effect of mag. field 9-24305
 phase transition region near Curie pt., investig. with polarized neutrons 9-37650
 photoemission from (111) surfaces, clean and Cs-covered 9-26617
 plastic deformation, X-ray investigation of initial stages 9-23888
 plastic deformation model based on near surface dislocation sources 9-41019
 platelets, growth by thermal and chem. decomp. of NiI₂ and NiBr₂ 9-35018
 polycrystal, effect of orientation-dependent solidification 9-46931
 positron annihilation, polarized, in (110) crystal 9-24114
 positron annihilation rel. to cryst. e. struct., obs. 9-35325
 potential and inner potential calc. from pseudopotentials applic. to low-energy electron diffraction 9-44654
 proton energy losses 9-30807
 quenched in vacancies, elec. resistivity 9-23796
 recrystallization, dynamic, during high temp. deform. 9-41020
 resistivity, temp. and mag. field depend. 9-24128
 secondary defects formation after neutron-irrad. 9-32959
 shock hardening in pressure range 820 to 1500 kbar, rel. to microstructure 9-30701
 shock wave hardened, softening and recrystallization during heating 9-33098
 shock-wave strengthened, final yield strength 9-35162
 specific heat of single cryst. near critical pt. 9-47005
 specific heats, extended Bhatia model method 9-24012
 spectral determ. in samples below reliable separation threshold, by plotting intensities of spectrogram lines 9-37854
 spherical single crystal, surface energy anisotropy determ. by thermal etch structures 9-46716
 spin waves, neutron scatt. near Curie pt. obs. 9-49201
 spin-wave spectrum, neutron scatt. meas. 9-45115
 stress relaxation, 20-300°K 9-48891
 structure after plastic deformation, X-ray diff. 9-23768
 thermal conductivity, 2-100°K 9-48976
 thermal recovery processes after explosive-shock loading, electron microscope obs. 9-44696
 thermoremanent magnetization, effect of plastic deform. 9-35568
 whiskers, growth by thermal and chem. decomp. of NiCl₂ and NiBr₂ 9-35018
 work function and surface energy correlation 9-33414
 X-ray scattering, diffuse, anomalously high intensities near Curie point 9-24304
 CO desorption by photon radiation 2.1-4.8 eV 9-23647
 in Fe-Ni-Co alloys, complexometric determination 9-45430
 α Fe, effect on N₂ diffusion and Fe₄N solubility 9-23840
 NaCl:Ni, precipitated particles obs. with electron microscope 9-40910
 neutron-irradiated, secondary defects formation 9-32959
 Ni-Mg system, contact fusion 9-26373
 Ni, III, selection rules for forbidden d⁷-d⁸ transitions, line strength calc. for 3d⁷p-d⁸ 9-40542
 Ni⁺ e.s.r. in AgCl:Ni²⁺ and AgBr:Ni²⁺ irradiated by light 9-33621
 Ni²⁺, absorpt. spectra in spinel 9-43242
 Ni²⁺, electron spin-lattice relaxation in La₂Mg₃(NO₃)₁₂·24H₂O 9-45245
 Ni²⁺, mag. susceptibility and spin-orbit coupling in ZnS 9-33435
 Ni²⁺, red fluorescence in reduced germanate glass 9-31134
 Ni²⁺ coloration impurity in lanthanum glass, effect on light absorption 9-24372
 Ni²⁺ crystal field eff. on paramagnetic behaviour 9-28645
 Ni²⁺ e.s.r. in AgCl and isotope effect in cry. field 9-43273

Nickel continued

- Ni²⁺ e.s.r. spectra in ZnWO₄ 9-37802
 Ni²⁺ in AgCl and AgBr, illuminated, e.s.r. obs. of Ni²⁺ 9-33621
 Ni²⁺ in ag. soln., indirect determ. of short relax. time 9-30426
 Ni²⁺ in MgO, molecular orbital theory of spin-phonon interactions 9-39787
 Ni²⁺ in NaCl, KCl, RbCl, optical absorption 9-39842
 Ni²⁺ in NiFe₂O₄, migration of ions to A-sites, X-band ferrimag. reson. obs. 9-35705
 Ni electrodeposits, struct. and ductility, effect of metallic contamination 9-37146
 Ni III, electric dipole transition 3d⁷p-d⁸, total line strengths and oscillator strengths 9-38768
 Ni strain-hardened by impulse leading, recovery behaviour 9-28348
 Ni²⁺ in MgO, e.p.r. line shape 9-24495
 on n-Si Schottky barrier, forward I-V characts. 9-43082
 ZnO:Ni, emission process mechanisms w.r.t. activator excitation energy transfer to electrons in traps 9-39874

Nickel alloys

see also *Nickel compounds*

- Alnico, Ti bearing, mag. props. rel. to structure 9-24310
 alnico alloy, mag. props. of α and α' phases, temp. instability of permanent magnets 9-45149
 alnico alloys single crystal precipitation and mag. props. 9-44792
 B-1900 high-temp, microstruct. effect on exposure at 980°C 9-48913
 brittleness, hot, rel. to He-filled deform. defects in irrad. precip.-hardened alloy 9-37260
 constantan, phonon emission spectra, thermal radiation obs. 9-42944
 creep-rupture characts., grain and specimen size effects 9-37245
 dilute, thermal conductivity, 2-100°K 9-48976
 dislocation complex rel. to deform. of γ' precipitation hardened samples 9-30613
 dispersion-hardening, grain size effects on yield point, strain hardening and creep resistance 9-33015
 eutectic melting at contact with diamond and graphite 9-26358
 Fe-Ni-Mn-Ti, martensitic, pre-precip. stage during ageing 9-37283
 films, wall coercive force, strain sensitivity, 200 Å to 1500 Å thickness 9-45163
 Hastelloy N, irrad., mech. props. variation with strain rate 9-41030
 invar, Curie temp., press. eff. for collective electron ferromagnet 9-28610
 Inconel 625, n irrad., creep strength reduction and embrittlement, 650°C 9-37250
 Invar, forced magnetostriction, absolute saturation magnetization press. coeffs., 4.2K 9-41320
 Invar, mag. anomaly in thermal expansion and spontaneous vol. magnetostriction 9-43177
 invar, sound vel. at low temp. 9-44817
 manganin coil press. gauge, calibration to 60 kbar under hydrostatic press. 9-40215
 mechanical properties, effect of low temps. 9-23905
 mechanical props., recovery by re-heat-treatment 9-23898
 molybdenum permalloy tapes stress sensitivity and mag. squareness ratio. effect of comp. and heat treatment 9-49205
 monel metal, effective atomic numbers for gamma interacts. 100-662 keV 9-24230
 Monel metal, for lecture demonstration of ferromag. curie point 9-22035
 M.S.O., mag. shunt props., C addition effect 9-45050
 mumetal, magnetomechanical damping effects 9-31036
 Ni-Co, magnetic moments, localized of Co, e.p.r. investg. 9-33634
 Ni-(20 wt.%)Cu, mag. moment distrib., mag. disorder neutron scatt. cross section meas. 9-35562
 nichrome, dispersion hardened, strengthening mechanism 9-23909
 Nimonic 80A, creep and fracture 9-33048
 nimonic single crystals, strain-hardening rel. to structural state of quenched alloy 9-33100
 Nimonic type, recrystn. 9-41044
 permalloy, Barkhausen and ΔE effects, rel. to applied stress 9-45147
 Permalloy, magnetic anisotropy, rotatable, in electron-microscope specimens 9-26646
 permalloy, ternary paramagnetic additions for production of magnetic film for memories 9-36252
 permalloy film, cathode-plasma-sputtered, struct. determ. by e. microscopy 9-40843
 permalloy film, high speed flux reversal and relaxation processes, dynamic Kerr obs. 9-45169
 permalloy films, anisotropy field, neutron irrad. and isothermal annealing effect 9-47253
 permalloy films, annealing behaviour of induced anisotropy, ageing and stabilization effects 9-37660
 Permalloy films, Bloch wall motion excited by fast-rising hard-axis pulses 9-45168
 Permalloy films, dynamic Kerr obs. of high-speed flux reversal and relax. processes 9-37661
 permalloy films, ferromag. reson. absorpt. at r.f.'s 9-47423
 permalloy films, fine mag. struct. and coercive force 9-41321
 Permalloy films, hysteresis magnetising angle, mag. anisometer meas. 9-43184
 Permalloy films, irradiated, spin wave resonance 9-45370
 Permalloy films, susceptibility, effect of surface roughness 9-49211
 Permalloy layers with non-mag. layer composite, mag. props. and struct. 9-43183
 permalloy single-crystal platelet, helical and other stripe structures 9-47248
 permalloy thin film effect of mag. annealing and elastic stress on mag. props. 9-41322
 permalloy thinfilms, electrodeposited, magnetism reduction 9-49191
 permalloy transducer, in magnetometer 9-34140
 Permalloy wires, magnetic domain nucleation and wall propagation, influence of structure and composition 9-35561
 phase structure, distortion from Cu-type substructure 9-35064
 plasticity theory, small-strain, dislocations coplanar motion 9-31834
 re-heat-treatment, mech. props. recovery 9-23898
 steel, Cr-Ni-Mo high C low alloy, fatigue strength rel. to hardness, obs. 9-26345
 steel-(18 wt.%)Ni maraging-steel, heat-treated, fatigue 9-30691
 yield point, strain hardening and creep resistance, grain size effects on dispersion-hardening specimen 9-33015
 zircaloy -2, low Ni, post-transition corrosion by steam at 300 and 340°C rel. to deuterium absorpt. and heat treatment 9-28806

Nickel alloys continued

- Ag-Ni solid solutions, initial states of Ni precipitation from superparamag. meas. 9-35212
 As and Bi impurities determ. 9-28830
 Au-(46 at.%)Cu-(4 at.%)Ni, order transform. of type $\alpha \leftrightarrow \beta$ order = β order, radiocrystallog. study 9-37304
 Au-Ni thin film thermocouples, vacuum-evaporated, thermoelec. power and Seebeck coeff. thickness depend. 9-45017
 Be-(1.3 wt.%)Ni, low-temp. and mixed ageing, struct. and hardness changes 9-39464
 C/Cr/Ni/Si system, controlled solidification using monovariant eutectic reactions 9-36921
 Co-Ni-Al-Cu-Nb-Fe, magnetostruct. analysis 9-47251
 Co-Ni-Al-Cu-Ti-Fe, magnetostruct. analysis 9-47251
 Co-Ni-Si, ferromag., internally oxidised, struct. obs. 9-48837
 Co-Ni alloys, internal friction during diffusionless phase transform. 9-37298
 Co-Ni internal friction and elec. resistivity near Curie pt. 9-47074
 Co-Ni internal friction meas. during $\alpha \leftrightarrow \beta$ transforms., -190° to 500°C 9-39400
 Co-Ni martensitic transform. under tensile stress 9-26386
 Co-(30.5 wt.%)Ni, allotropic transform., stress effects 9-23975
 20 wt.%Cr-35 wt.%Ni steel, creep-rate and grain boundary sliding 9-48901
 Cr-(49 wt.%)Ni-(1 wt.%)Ti, corrosion on exposure to pyrolysis conditions of sodium-base spent pulping liquors 9-28800
 Cr-(49 wt.%)Ni-(1 wt.%)Ti, corrosion on exposure to pyrolysis conditions of sodium-base spent pulping liquors 9-28799
 Cu-(14.5 wt.%)Al-(3.5 at.%)Ni with thermoelastic martensite, internal friction, amplitude depend. 9-42869
 Cu-Al-Fe-Ni aluminium bronzes, ductility rel. to microstructure 9-23894
 Cu-Ni-Fe, ⁵⁷Fe Mossbauer effect obs. of mag. ordering 9-39817
 Cu-Ni-Fe, hard-magnetic particle ensemble model, calc. 9-33453
 Cu-Ni-Fe, spinodal decomposition, electron microscope obs. 9-35242
 Cu-Ni, compress. rel. to para-ferromag. transition ordering obs. 9-35167
 Cu-Ni, damping behaviour and miscibility gap evidence 9-42870
 Cu-Ni, dilute ⁵⁷Fe Mossbauer studies 9-47331
 Cu-Ni, lattice thermal conductivity, temp. depend. at low temp. 9-26447
 Cu-Ni, near critical composition, magnetiz. polar. clouds of giant moments 9-26624
 Cu-Ni, rigid-band model and clustering eff. 9-26483
 Cu-Ni film, co-deposition by electron beam, struct., grain size and orientation 9-48763
 Cu-Ni i.r. absorpt and reflectivity meas., rel. to virtual bound state 9-45269
 Cu-Ni photoemission and optical studies rel. to electronic structure models 9-45033
 Cu-Ni surface, rel. to fatigue strength of Cu 9-33058
 Cu-(30 wt.%)Ni, substitutional Zener relaxation 9-26321
 Fe-Co-Ni fine particles prep. by evaporation in inert gases, mag. props. 9-33459
 Fe-(18 at.%)Cr-(20 at.%)Ni, dislocation damping and solute pinning 9-28292
 Fe-Cr-Ni, dislocation damping 9-39363
 Fe-Cr-Ni, extrinsic-intrinsic stacking-fault pairs 9-44711
 Fe-Mn-Ni with Ti added, ageing 9-48917
 Fe-(30 at.%)Ni-(5 at.%)Nb austenitic, structure and hardening, comments 9-46934
 Fe-(30 at.%)Ni-(5 at.%)Nb austenitic, structure and hardening, comments 9-46933
 Fe-Ni-Al-Co-Ti alloys, thermomech. treatment effect on mag. props. 9-47259
 Fe-Ni-Al-Ti, thermomech. treatment effect on mag. props. 9-47259
 Fe-Ni-Al, b.c.c., mag. moment behaviour rel. to composition changes 9-24274
 Fe-Ni-Al, decomp. of supersaturated solid solns., elastic stresses effect 9-39475
 Fe-Ni-C, shape strain for (259) γ martensitic transformation 9-28344
 Fe-Ni-Co alloys, complexometric determination of elements 9-45430
 Fe-Ni-Cr-Be, precip. processes, transmission electron microscopy obs. 9-39498
 Fe-Ni-Cr, dislocation mobility 9-39699
 Fe-Ni-Mn, f.c.c., intrinsic magnetization, 77°K to Curie temp. 9-45144
 Fe-(30 wt.%)Ni, b.c.c. and f.c.c., electron energy spectra, sensitivity to $\alpha \rightarrow \gamma$ transform. 9-39856
 Fe-(19 at.%)Ni, fracture during rolling 9-33066
 Fe-(40 at.%)Ni, invar, magnetostriction, effect of tensile stress 9-45156
 Fe-(30 wt.%)Ni, martensite, isothermal transform. rates, Kaufman and Cohenat's model 9-46950
 Fe-Ni, electrotransport and diffusion, tracer technique 9-28320
 Fe-Ni, high field susceptibility estimation at 0°K 9-47243
 Fe-Ni, in liq. Hg, ductility and toughness 9-42891
 Fe-Ni, invar, model, contrib. 9-37649
 Fe-Ni, magnetic domain wall distribution rel. to coherent boundaries of twin crystal 9-37651
 Fe-Ni, treatment for low temp. use, patent 9-26362
 Fe-(49 wt.%)Ni commercial, effect of S on initial permeability 9-49204
 Fe-(40 at.%)Ni oxidised at high temp., scale struct. and chem. composition 9-33669
 Fe-Ni films, ferromag., differential susceptibility obs. of struct. 9-43182
 Fe-Ni fine particles prep. by evaporation in inert gases, mag. props. 9-33459
 Fe-Ni r.f. magnetic susceptibility, effect of added electrons 9-28587
 Fe-Ni thin film, variation in mag. susceptibility with thickness 9-39773
 Fe-Ni thin films, Faraday effect field depend., perpendicular anisotropy obs. 9-47322
 Fe-(40 wt.%) Ni-(6 wt.%) Nb precipitation behaviour, ageing at 775°C 9-46951
 Fe-(48.2 at.%)Ni, Mossbauer effect of ⁵⁷Fe, hyperfine mag. splitting, effect of texture 9-35636
 Fe-(27 wt.%)Ni austenitic alloys, effect of Al, Si, Mn, and Cr on martensite form. during plastic deform. 9-41068
 Fe-Ni, eff. of Co on hardening, martensite ageing at high temp. 9-23942
 Fe-(31.4 at.%)Ni, magnetization, hydrostatic and shock-wave compression effects 9-43176
 Fe-Ni-Cr, eff. of Cr on martensitic transformation 9-23965
 Mn-(78.5 at.%)Ni galvanomagnetic effect, longitudinal 9-24278
 Mn-Ni constitutional diagram 9-39502
 Nb-C-Ni, liquid, carbide grain growth during sintering 9-34952
 Ni-10wt.% Cr, thermal conductivity, description of apparatus 9-26451

Nickel alloys continued

- Ni-(49-51 at.%)Al, electric and mag. props. 9-47069
 Ni-(1.18 at.%)Al, creep rate, 700°C, effect of ultrasonic vibrations 9-33047
 Ni-Al-Sc system, phase equilibria and solubility limits in Ni-rich region 9-30720
 Ni-Al, γ^1 phase, coherent solubilities 9-28403
 Ni-Al, shear stress, critical, temperature dependence 9-23908
 Ni-C eutectic, flake graphite struct. and defects obs., microscopy 9-44671
 Ni-C solid solns., Curie temps and residual resistivities 9-44914
 Ni-Co, K-state existence 9-26507
 Ni-Co, positron annihilation spectra 9-39576
 Ni-Co, self-diffusion of Co, rel. to Co conc. 9-39386
 Ni-Co films, electrochromically deposited, magnetocryst. anisotropy 9-41323
 Ni-Cr-Fe, atmospheric corrosion behaviour 9-37831
 Ni-Cr, non-collinear mag. structures with antiferromag. interaction between local mag. moments 9-45056
 Ni-Cr, oxidation and cation distrib. in NiO-Cr₂O₃ solid soln. formed 9-23656
 Ni-Cr, strain and fracture behaviour under cyclic loading 9-23915
 Ni-Cr, Ti oxide inclusions, predominating cpds. from fine structure microanalysis of emission X-ray spectra 9-37752
 Ni-Cr ball-milling, addition of inorganic salts for prod. of very fine powder 9-23932
 Ni-Cr film, vacuum-deposited, resistivity increase on heat treatment, 9-41043
 Ni-Cr films, Sn and solder whisker growth conditions and mechanism 9-48816
 Ni-Cu-H, low temp. elec. resistance anomalies 9-37450
 Ni-Cu, dilute, elastic consts., third-order, sensitivity to changes in electron-to-atom ratio and mag. eff. 9-37217
 Ni-Cu, ferro- and paramagnetic props., comparison 9-35539
 Ni-Cu, low temp. elec. resistance anomalies 9-37450
 Ni-Cu, minimum polarity models in mag. props. theory 9-45113
 Ni-Cu carburised, irradiation damage and the Portevin-Le Chatelier eff. 9-28349
 Ni-Cu giant moments near critical composition 4.2°K 9-45148
 Ni-Cu magnetic moments in ferromag. composition range determ. 9-43167
 Ni-Cu solid solns., ferro- to paramag. transition, sp.h., Curie temp. and moment obs. 9-35554
 Ni-Fe-Cu(Co) films, anisotropy components separation by temp. depend study of anisotropy field 9-45170
 Ni-Fe, creep, 550°-1000°C obs. 9-23897
 Ni-Fe, dynamic recrystn. during high temp. deform. 9-41020
 Ni-Fe, γ -radiation eff. on ordering transformations 9-23973
 Ni-Fe, low angle boundaries in large single cryst. 9-37185
 Ni-Fe, radiation enhancement of diffusion from directional ordering expts. 9-44742
 Ni-Fe, spin wave energies, press. depend. 9-33455
 Ni-(19 wt.%)Fe magnetic films, energy of combined Bloch and Neel type domain wall 9-28625
 Ni-(22 wt.%)Fe thin films, infl. of mech. stress on coercive force 9-24316
 Ni-Fe dispersion relations for lattice vibrations from neutron scattering 9-30766
 Ni-Fe film, electrodeposited, magnetization ripple wavelength meas., Lorentz microscopy 9-28624
 Ni-Fe films, magnetic annealing, effect of elastic stresses 9-33029
 Ni-Fe hyperfine fields meas. by ⁶¹Ni Mossbauer effect 9-45300
 Ni-Fe tapes, phase domain patterns, Kerr magneto-optic studies 9-26653
 Ni-Fe thin-films, 30 to 300Å thick, props. with creep observations 9-45068
 Ni-Fe thin films electrodeposited on scratched surfaces, uniaxial mag. anisotropy 9-28623
 Ni-Fe thin layers, effect of O on spin wave excitation 9-45369
 Ni-(17 wt.%)Fe, coercive force, previous loading rate effect 9-47241
 Ni-Ga-B, dil., phase equil. during solidification 9-39136
 Ni-Ge single crystals, mag. props. 9-47261
 Ni-Ge single crystals, prep. by Czochralski method 9-42758
 Ni-Ge single crystals, remagnetization hysteresis energy losses, field depend. 9-43175
 Ni-Mo, eff. charge and diff. coeff. of Ni 9-26202
 Ni-Mo, metal surface atoms electronic interact. with anionic complexes in corrosion 9-28801
 Ni-Mo, solubility of H 9-39478
 Ni-Pd films, electron tunnelling rel. to spin wave excitation 9-44995
 Ni-Re films, electro-deposited, phase and chemical composition 9-44791
 Ni-Si-Ti, microstruct. and tensile props. 9-48902
 Ni-Si, microstruct. and tensile props. 9-48902
 Ni-Si ferromag. internally oxidised, struct. 9-48837
 Ni-Si γ^1 phase, coherent solubilities 9-28403
 Ni-Si γ^2 phase, coherent solubilities 9-28403
 Ni-Sn dilute Mossbauer hyperfine field of ¹¹⁹Sn and resistivity study 9-47335
 Ni-Ti, grain boundary deformation rel. to temp. under constant strain 9-23889
 Ni-V, binary, α -phase, mag. props. 9-43158
 Ni-V, ferromagnetic resonance absorption, g-value temp. depend. 9-24477
 Ni-W, local ordering and elec. resistance, annealing effect 9-33255
 Ni-W, solubility of H 9-39478
 Ni-Zn-Si system, phase equilibria at 800°C 9-35209
 Ni-Zn, ferro- and paramagnetic props., comparison 9-35539
 Ni-rare earth cpds., role of RNi₂ cell in struct. determ. of other cpds. 9-30567
 Ni-rich binary, effect of small alloying additions on vol. diffusion at 900-1200°C 9-40986
 Ni₂Zn₃Si, cubic Ti₂Ni struct. type, calc. of interatomic distances and packing density 9-32924
 Ni₃Al single-cryst. elastic consts. 9-35140
 Ni₃Fe, annealed tin samples, antiphase boundary study 9-46791
 Ni₃Fe, Cr, atomic ordering effects 9-39297
 Ni₃(Fe, Mo), atomic ordering effects 9-39297
 Ni₃(Fe, W), atomic ordering effects 9-39297
 Ni₃(Fe, Cr), ferromag. ΔE -effect, Cr content depend. 9-47242
 Ni₃(Fe, Mo), ferromag. ΔE -effect, Mo content depend. 9-47242
 Ni₃(TiAl), hardened by coherent and ordered precip., yielding 9-39408
 β -NiAl, optical props. and energy band struct. 9-47367
 Pb and Sn impurities determ. 9-28830

Nickel alloys continued

- Pd-(~5at.%)Ni, ferromagnetic resonance and anisotropy 9-24478
 Pd-Ni, Curie temp., effect of hydrostatic pressure 9-28611
 Pd-Ni paramagnetic, spin fluctuations from sp. ht. and thermal expansion anomalies 9-45086
 Pt-Ni electrocatalysts for H₂/CO fuel cell anodes 9-29365
 Pt-Ni specific heat enhancement 1.15° to 4.2°K rel. to electron spin fluctuation interaction effects 9-44837
 Ru-Ni solid solutions, initial states of Ni precipitation from superparamag. meas. 9-35212
 Sn-Ni, dil., internal friction anomalies near melting pt. 9-39399
 Y-Ni, role of YNi₃ cell in struct. determ. of other cpds. 9-30567
- Nickel compounds**
see also Nickel alloys
 alumina whiskers/Ni composites, electron microscope obs. 9-33169
 aluminates, with spinel struct. sintering behaviour and microstruct. w.r.t. deviation from stoichiometry 9-30707
 diff. coeff. of cation vacancies, 750-1000°C 9-30588
 ferrite thin film, prep. and mag. props. 9-45184
 ferrites with spinel struct. sintering behaviour and microstruct. w.r.t. deviation from stoichiometry 9-30707
 ferrous ferrite, microstruct. control 9-48836
 sandwich complexes, hyperfine coupling consts. and covalency 9-42420
 [Ni(NH₃)₆]Cl₂, fine structure of Ni K X-ray absorpt. obs. 9-37747
 CdAs₂-NiAs eutectic, Hall effect, conductivity and magnetoresistance meas. 9-41196
 Co complex, Co(NCS)₂(γ -picoline)₄, γ C-H freqs. of clathrated mono- and di-subst. benzenes 9-48475
 Li₂Ni₂O solid solutions, energy states from photoelec. emission meas. 9-41284
 Ni-Al₂O₃ catalyst, D exchange between H and H₂O vapour, obs. 9-28790
 Ni-Fe ferrites, magnetization and magnetocrystalline anisotropy, infl. of O content 9-28633
 Ni-Rh alloy, paramagnetic, spin fluctuations from sp. ht. and thermal expression anomalies 9-45086
 Ni-Zn:Co²⁺ ferrites, Fe-rich, temp. spectra, mag. after-effects 9-28632
 Ni-Zn ferrite thin film, prep. and mag. props. 9-45184
 Ni-base superalloys, transmission electron microscopy study of microstructure 9-39298
 Ni, complex, dibromotetrapyrazolenickel(II), crystal and mol. structure 9-26243
 Ni, complex, N,N'-dimethyl-4,4'-dipyridinium tetracyanonickelate (II), crystal structure 9-26242
 Ni_{0.36}Ni_{0.64}Fe₂O₄, ferromagnetic resonance linewidth and shift from tensor susceptibility meas. 9-37666
 Ni_{0.9}Fe_{0.1}O₄, electrical conductivity, thermoelectric power, 20-100°C, effect of hydrostatic pressure 9-33300
 Ni_{1-x}Zn_xFe₂O₄, ferrimagnetically ordered, semiconductor props. 9-33310
 Ni_{1.18}, energy states from photoelec. emission meas. 9-41284
 Ni_{1.04}Si_{1.93} enthalpy changes at high temp. 9-39092
 Ni₂Nb₂O₇-BaTiO₃ solid soln., s.h.f. dielec. props. 9-39689
 Ni₂Nb₂O₇-BaTiO₃ solid soln., s.h.f. dielec. props. 9-47174
 Ni₃Al phase alloys, transition from exchange enhanced paramag. to weak ferromag. 9-45085
 Ni₃B₂O₁₃X (X=Cl, Br, I), ferroelec., crystal field and optical absorpt. characts. 9-45259
 Ni₃B₂O₁₃X (X=Cl, Br, I), Mossbauer spectra of ⁵⁷Fe, 80°-1100°K 9-35638
 Ni₃Fe, Ni hyperfine field and its application to the detection of long-range order 9-26637
 Ni₃Ga, magnetization of itinerant electrons, decrease by spin-orbit scatt. on impurities 9-26639
 Ni₃Ga phase alloys, transition from exchange-enhanced paramag. to weak ferromag. 9-45085
 Ni₃La₂(NO₃)₁₂·24H₂O, mag. phase transitions, obs. 9-39781
 Ni₃Mn, elec. resistivity and saturation magnetization damage rates 9-33205
 Ni²⁺ complex with dimethyl methylphosphonate, conc. and temp. depend. of n.m.r. spectra 9-28156
 Ni(II) complexes, dimethyldithio (seleno) carbamates, i.r. spectra, 2000-2500cm⁻¹ range, normal coordinate anal. 9-48474
 Ni complex, bis(monothioacetylacetonato)Ni(II), vibr. spectra 9-46370
 Ni complex, bis(dimethyldithiophosphato)nickel(II), crystal and molecular structure 9-39296
 Ni complex, bis(selenourethane)nickel(II) thiocyanate, X-ray powder data, i.r. spectra and crystal structure 9-26227
 Ni complex, diaquobis(L-serinato) nickel(II), crystal structure rel. to chelation effects on serine 9-26241
 Ni complex, hexakis(imidazole) nickel(II) nitrate, single cry. spectrum 9-35663
 Ni complex, hexakis(imidazole) nickel(II) nitrate, crystal and molecular structure 9-39295
 Ni complex, Ni(II) of 1:3 bidentate Schiff's bases, spin density distrib. from isotropic proton resonance shifts 9-42411
 Ni complex, Ni(NCS)₂(γ -picoline)₄, γ C-H freqs. of clathrated mono- and di-subst. benzenes 9-48475
 Ni complex, nickel(II) acetylacetonate, vapour u.v. electronic spectrum and matrix-isolated i.r. spectrum 9-27870
 Ni cyanide, magnetic susceptibility determ. by Faraday method, intermol. association 9-24276
 Ni faujasite zeolite, cryst. struct. and Ni(II) distrib., obs. 9-30568
 β -NiAl, elec. props. 9-37449
 NiAl, nonstoichiometric, lattice defects 9-40941
 NiAl, stoichiometric, creep behaviour 9-28355
 α -NiAs₂, crystal structure 9-23770
 NiBr₂, thermal and chem. decomp., Ni platelets and whiskers growth obs. 9-35018
 Ni(CN)₂·4H₂O, fine structure of Ni K X-ray absorpt. obs. 9-37747
 Ni(CN)₄ ion, laser Raman spectra 9-24426
 NiCl₂, antiferromag. reson. 9-47426
 NiCl₂·6H₂O, antiferromag., n.m.r. determ. of internal mag. fields at proton sites 9-47446
 NiCl₂·6H₂O, cryst. struct., room temp. and 4.2°K neutron diff. 9-42793
 NiCl₂·6H₂O, fine structure of Ni K X-ray absorpt. obs. 9-37747
 NiCo ferrite, mag. annealing, effect of Co ion conc. 9-47273
 NiCo ferrite, mag. annealing effect on magnetomechanical coupling coeff. 9-47273
 NiCo ferrites, dense, anisotropy broadening of ferromag. reson. 9-45368
 NiF₂, crystal growth from low melting flux 9-39207
 NiF₂, paramag. spin waves and correl. functions 9-33441

Nickel compounds continued

- NiF₂, phase transitions at pressures up to 160 kbar 9-44800
 NiF₂ thermal expansion determ. from room temp. to 600°C 9-44841
 NiF₆⁴⁻ cluster, limited-basin-cent Hartree-Fock theory 9-32482
 NiF₆ hyperfine interaction and cryst. field splitting, SCF-MO calc. 9-33495
 NiFe₂O₄, atomic vibration, mean square amplitude determ. 9-41081
 NiFe₂O₄, chemical and mag. struct. from polarised neutron diff. study 9-48838
 NiFe₂O₄, disordered, Ni²⁺ migration to A-sites, X-band ferrimag. reson. obs. 9-35705
 NiFe₂O₄, growth by pulling 9-37088
 NiFe₂O₄, single crystal growth from fluxed melts under pressure 9-35028
 NiFe₂O₄, substituted, mag. fields on Sn nuclei 9-26727
 NiFe₂O₄, spinel ferrite, absorpt. and Faraday rotation, 300°K, 1 to 8 μ 9-45277
 NiFe₂O₄, synthetic, chemical and thermal remanance relative stability 9-39776
 NiFe₂O₄ with [111] texture, anisotropy and ferromag. reson. 9-45367
 NiFe films, electrodeposited, stress meas. 9-37234
 Ni₂, thermal and chem. decomp., Ni platelets and whiskers growth obs. 9-35018
 Ni(II) complexes, with tetradentate Schiff base ligands, anomalous sign reversal in circular dichroism spectra 9-36703
 Ni(II) cyanopyridine and chloropyridine complexes, far i.r. spectra 9-23038
 β-Ni(IO₃)₂·2H₂O, 1-300 Oe, 2.2-20.5°K, observed to be ferromagnetic 9-47262
 NiMn_{0.85}Fe_{1.95}O₄, ferromagnetic resonance linewidth and shift from tensor susceptibility meas. 9-37666
 NiNb₂S₄, synthesis and lattice constants on basis of hexagonal unit cell 9-39284
 NiO:Li, dielec. const., interfacial polarization effect 9-35469
 NiO/MnO solid solns., dielec. loss, const. and conductivity meas. w.r.t. freq. 9-35465
 NiO-Cr₂O₃-O₂ system, phase equilibrium at high O pressures 9-28404
 NiO-Cr₂O₃ solid soln. on Ni-Cr alloys, cation distrib. on alloy oxidation 9-23656
 NiO-Fe₂O₃ system, solid-state reactions 1100 to 1300°C, kinetics rel. to reaction layer thickness 9-37820
 NiO, antiferromag., magnon energies 9-35591
 NiO, antiferromagnetic, coherent exchange scattering of low-energy electrons 9-45230
 NiO, catalytic activity, influence of metal support and u.v. irradi. 9-41446
 NiO, depend. of 10dq on metal-ligand distance 9-39789
 NiO, dielec. const., interfacial polarization effect 9-35469
 NiO, dielectric dispersion, 10¹⁰-10¹² Hz 9-45001
 NiO, elec. conductivity, press. depend., phase separation obs. 9-35338
 NiO, elec. conductivity and Seebeck coeff., temp. and O partial press. depend. 9-44966
 NiO, epitaxial growth on MgO, dislocation density rel. to growth conditions 9-35034
 NiO, fine structure of Ni K X-ray absorpt. obs. 9-37747
 NiO, fluxed-melt growth and elec. props. 9-37089
 NiO, highly mobile electrons obs., high temp. 9-44965
 NiO, impurity conduction, rel. to polaron theory 9-49009
 NiO, magnetic semiconductor, band structure 9-47118
 NiO, scales, mech. props. factorial expt. 9-23852
 NiO, self-diffusion of O, mechanism 9-44731
 NiO tilt angles of twin components in various lattice planes Berg-Barrett X-ray determ. 9-37145
 NiRh₂O₄-CuRh₂O₄ system, deformed spinel structs. 9-30704
 NiS, pressure effect rel. to lattice compressibility, T>T_n and T<T_n 9-44672
 NiS₂, mag. props. 9-33437
 NiSO₃·6H₂O, cryst. struct. 9-39294
 NiSO₄, u.s. absorption in ethylene glycol and water 9-30397
 NiSO₄ aq., dielec. props. 9-46648
 α-NiSO₄·6H₂O, circular dichroism meas. 9-26704
 NiSe₂, mag. props. 9-33437
 NiSeO₄, antiferromag. struct., Neel pt., neutron diff. powder obs. 9-49223
 NiSO₄·6H₂O, fine structure of Ni K X-ray absorpt. obs. 9-37747
 NiZn ferrite, ferromag. reson. linewidth, temp. depend. 9-33618
 Pd-Ni alloys, Stoner enhancement, paramag. susceptibility meas., rel. to field, depend. at high mag. field 9-45087
 Zn_{1-x}Ni_xFe₂O₄ ferrite system, Yafet-Kittel mag. ordering 9-41329

Night sky see *Airglow*

Nightglow see *Airglow*

Nilsson's model see *Nucleus/models*

Niobium

- see also *Superconducting materials/niobium*
 adsorption of Zr 2-d crystals, binding energy from temp. depend. of growth 9-23652
 annealed, low-temp. specific heat in mag. fields 9-37465
 atomic spectrum, a bibliography 9-38765
 in compounds, L level shifts and width changes 9-48400
 compression testing of high purity single crystals 9-46885
 deformed single crystals, mech. props., dislocation sub-structure and density, high strain rates 9-48898
 deuteron back-scattering, energy distribution 9-39549
 diffusion coefficients of C 9-35133
 diffusion of isotopes in W, lattice coeffs. meas. 9-40989
 diffusion of P, interstitial mechanism, 1300-1800°C 9-35132
 dislocation atmosphere formation rel. to strain-ageing 9-28381
 dislocation interaction, temp. depend. of flow and function stress 9-39366
 elastic constants and u.s. attenuation, eff. of O additions in single crystals, 4.2°-313°K 9-30634
 emissive power and specific resistivity above 400°K, relationship 9-39547
 energy levels in VI, VII and VIII spectra 9-46287
 etch pits sub-boundaries, optical microscope obs., contribution to diffusion 9-32985
 ferroelasticity due to H as lattice gas, obs. 9-23868
 fluxoid pinning by dislocations in single cryst. w.r.t. temp. and mag. field 9-39601
 hydride and deuteride solid solutions, interstitial ordering 9-23990
 lattice dynamics, Kohn anomalies 9-24017
 lattice dynamics, phonon freq. meas. 9-24016

Niobium continued

- magnetoacoustic effect, i.f., stiffness and attenuation, mag. field depend. 9-35283
 mechanical props., dislocation sub-structure and density in single crystals deformed at high strain rates 9-48898
 in minerals, spectrochem. analysis using C cavity electrodes, obs. 9-28828
 mixed state, attenuation of microwave phonons, 1.3°K 9-35279
 neutron irradiated, dislocation channeling 9-42837
 n.m.r. of ⁹¹Nb in single cryst. 9-45406
 optical constants 9-31069
 oxidation of single crystals, 550-925°C 9-49378
 oxidized surface, work function, contact potential difference method 9-31000
 plates, temp. depend. of sound vel. 9-46988
 potential and inner potential calc. from pseudopotentials applic. to low-energy electron diffraction 9-44654
 proton back-scattering, energy distribution 9-39549
 quenched, internal friction, eff. of quenching and annealing 9-30639
 radiation hardening in single cryst., eff. on temp. depend. of yield stress 9-26371
 solid solution hardening by Ta, V and W, theory and expt. 9-28385
 spectral emittance, i.r. 9-45327
 strain ageing, interstitial impurities obs. 9-35198
 strain amplitude dependence rel. mag. state 9-26316
 superconducting, surface magnetization 9-30876
 superconducting TM₀₁₀ mode cavity with high electric field and Q₀ 9-24148
 surface layers, work-hardened, crystal structure changes prod. by vacuum annealing 9-32932
 thermal expansion at low temp. 9-37359
 work function and surface energy correlation 9-33414
 X-ray M absorpt. spectra in u.s. region, absorpt., coeff. depend. 17-200 Å 9-37754
 Nb-N system, N precip. on dislocations, kinetics 9-30744
 Nb-S-Cu system, vapour growth of new single-crystalline phases 9-37007
 Nb, strain-ageing effects rel. to dislocation atmosphere formation 9-28381
 Nb₃Sn cryst. growth 9-44648
 Vilm., preparation for nuclear studies 9-48766
- Niobium compounds**
 alloy, diffusion-coated, preparation for optical metallography 9-35208
 alloys, superconducting, hysteresis rel. to dislocation pinning temp. and field dependence 9-24153
 Nb₃Sn, critical current density, correlation with impurity content and microstructure 9-41180
 niobates, tungsten-bronze-type ferroelectric crystals, electrooptic properties 9-28658
 alloys with V, Nb and Ta, electrical resistivity as a function of temperature 9-39584
 Co-Ni-Al-Cu-Nb-Fe alloys, magnetostruct. analysis 9-47251
 Cu-(2.5 wt. %)Zr-(0.5 wt. %)Nb alloy, radiation enhanced relaxation 9-41006
 Fe-(30 at.%)Ni-(5 at.%)Nb austenitic alloys, structure and hardening, comments 9-46934
 Fe-(30 at.%)Ni-(5 at.%)Nb austenitic alloys, structure and hardening, comments 9-46933
 Fe-(40 wt.%)Ni-(6 wt.%)Nb precipitation behaviour, ageing at 775°C 9-46951
 Mo-Nb:Co alloy, Kondo temp. indepnd. of host composition from resistivity and susceptibility meas. 9-45067
 Mo-Nb alloys, electrical conductivity, theory and expt. 9-24127
 Nb-Ti-Zr-Hf alloy system, constitution and supercond. props. 9-39597
 Nb₆O₃ added to borolanthanum, glasses immiscibility and catalytic crystallization 9-34971
 Nb-Al alloys, superconducting, alloys, positron annihilation, critical temp. eqn. parameters 9-39598
 Nb-Cr-Si system, θ-phase Nb₃Cr₂Si₃, cry. struct. 9-46790
 Nb-Mo, solid solution alloys, lattice thermal conductivity, normal and superconducting state 9-30797
 Nb-Mo alloy, thermal expansion at low temp. 9-37359
 Nb-Mo alloys, thermal and elec. conductivities, Nemst-Ettinghausen coeffs. 9-47091
 Nb-Sn superconducting alloys, mag. hysteresis and alloy constitution 9-37659
 Nb-Ta, solid solution hardening, theory and expt. 9-28385
 Nb-Ta alloys, normal state sp. ht. 9-33181
 Nb-Ta alloys, type II superconductors, anisotropic pinning and guided motion of vortices 9-43035
 Nb-Ta superconducting alloys, magnetization meas., temp. coeff. of electronic sp. heat and transition temp., conc. depend. 9-28478
 Nb-Ti-N alloy thin films, supercond. critical current-field meas. in continuous mag. fields 9-35362
 Nb-Ti alloys, supercond., cold working and precip. for effective flux pinning at high current densities 9-49053
 Nb-Ti supercond. sheets as stabilizing walls for levitated rings, flux penetration obs. 9-37493
 Nb-Ti supercond. tubes, steady-state flux jumping in superimposed a.c. and d.c. mag. fields 9-37471
 Nb-Ti supercond. tubes, steady-state flux jumping in superimposed a.c. and d.c. mag. fields 9-37471
 Nb-Ti superconducting wire, single core and twisted multi-strand, magnetization measurements 9-26526
 Nb-(25 at.%)Ti-(10 at.%)Zr alloy, solution-treated, ageing rel. to recrystallization 9-33122
 Nb-V, solid solution hardening, theory and expt. 9-28385
 Nb-W, solid solution hardening, theory and expt. 9-28385
 Nb-(40wt.%)Zr-(10wt.%)Ti superconducting hollow cylinders, mag. shielding in applied mag. fields at 4.2°K 9-43174
 Nb-(25 wt.%)Zr alloy, supercond., fluxoid pinning by second phases 9-49049
 Nb-Zr alloy, supercond., cellular decomp. and precipitation 9-39499
 Nb-Zr alloys, supercond., cold working and precip. for effective flux pinning at high current densities 9-49053
 Nb-(25 at.%)Zr alloy, a.c. energy losses around H_{c1} 9-35361
 Nb₃Cr₂Si₃, θ-phase in Nb-Cr-Si system, cry. struct. 9-46790
 Nb₂O₃-WO₃ system, non-periodic shear struct., electron microscope obs. and evaluation 9-39291

Niobium compounds continued

Nb₂O₅, emission spectra intensity, struct. modifications influence 9-33560
Nb₂O₅, film thickness meas. by electroreflectance interferometry 9-30486
Nb₂O₅, lattice energies, heat of atomization, bond energy and dissociation energies, rel. to fund. props. 9-30494
Nb₂O₅, thin films, growth and dielectric props. rel. to use as capacitor 9-30981
Nb₂Al-Nb₂Ge alloys, annealing effect on supercond. T_c 9-30877
Nb₂Al, hydrostatic pressure effect on superconductive transitions 9-49052
Nb₂Al, superconductivity 9-39599
Nb₂Al_{1-x}Ge_x alloys, critical fields obs. in liq. H₂ 9-35360
Nb₂Au_{1-x}Pt_{1-x} system, supercond. transition temp., annealing conditions influence 9-44942
Nb₂Ga-Nb₂Al system, supercond. transition temp. and effect of annealing 9-37469
Nb₂Ge-Nb₂Al system, supercond. transition temp. and effect of annealing 9-37469
Nb₂Sn, a.c. field-induced flux jumps 9-37468
Nb₂Sn, anisotropic supercond. energy gap 9-49051
Nb₂Sn, cubic-to-tetragonal transformation, volume change, 43°K 9-35249
Nb₂Sn, growth by solid Nb-liq. Sn reaction, diffusion and soln./deposition mechanisms 9-48764
Nb₂Sn, hydrostatic pressure effect on superconductive transitions 9-49052
Nb₂Sn, specific heat rel. to lattice transformation 9-24049
Nb₂Sn, supercond., cold working and precip. for effective flux pinning at high current densities 9-49053
Nb₂Sn, superconducting, production, patent 9-24155
Nb₂Sn, superconducting magnet, a.c. power loss meas. 9-37498
Nb₂Sn alloy, supercond., mag. hysteresis and cryst. struct. 9-39769
Nb₂Sn critical current density rel. to bombardment of protons and deuterons 9-41184
Nb₂Sn magnetic tape clad with OFHC Cu, Al; operating pt. and stabilizing cladding thickness determ. 9-39604
Nb₂Sn magnets, transiently stabilized, model, applic. to critical currents meas. 9-37484
Nb₂Sn supercond. alloy, magnetization, hysteretic loss and flux-jump stability obs. 9-35364
Nb₂Sn supercond. coils, persistent, critical conditions 9-35375
Nb₂Sn supercond. magnets, 15-cm-bore, pumped He tests 9-37491
Nb₂Sn supercond. quadrupole magnet system for IMP, comparison with NbTi system 9-37492
Nb₂Sn supercond. rings under isochroic conditions, levitation and stabilization against slide instability 9-37489
Nb₂Sn-Nb₂Al system, supercond. transition temp. and effect of annealing 9-37469
Nb₂(Al_{1-x}Ge_x), hydrostatic pressure effect on superconductive transitions 9-49052
NbC-Co system, microstructural development during liquid-phase sintering 9-42919
NbC-Fe(Ni,Co) liquid alloys, carbide grain growth during sintering 9-34952
NbC, elec. conductivity and thermo-e.m.f., 20°-2000°C, obs. 9-39588
NbC, hemispherical and monochromatic emissive power and specific resistivity, 1200-3500°K 9-39548
NbC, vaporization from open surface in vacuum, 2453-3428°K 9-26167
NbC_{0.9}, ordering in struct., neutron diff. obs. 9-40913
NbC_{0.9}, magnetic susceptibility, temp. and comp. depend., 20-300°K, x=0.70-0.98 9-43153
NbC emissivity and elec. conductivity obs. 9-37374
NbF₅, liquid, Raman spectra rel. to possible polymerization 9-26119
NbH, limiting composition, dissociation processes, and lattice transforms 9-31185
NbN, hydrostatic pressure effect on superconductive transitions 9-49052
NbN_x system, n.m.r., phase identification 9-35726
NbN film preparation, upper critical field H_{c2} 9-35359
NbN thin films, high-field supercond. props. 9-35363
NbN type II superconductors, n irradi. enhancement of current carrying capacity 9-43039
NbO, thermoelec. power and elec. conductivity meas. 9-37448
NbO₂, elec. and mag. props., 800°C region, phase transition obs. 9-33143
n-NbO₂, thermoelec. power and elec. conductivity meas. 9-37448
NbO₂ cryst. phase transition from deformed to normal rutile type struct. 9-35246
NbO⁺, hyperfine splittings in optical spectrum 9-44344
NbO films, preparation, optical and dielectric props. 9-30958
NbOCl₃, supercond. and metal-O stretching vibr., 4000-400 cm⁻¹ 9-27869
NbO_{1.5}, spectrum and metal-O stretching vibr., 4000-400 cm⁻¹ 9-27869
NbSe₂ lamellar struct., supercond., struct. determ. 9-41181
NbTi supercond. quadrupole magnet system for IMP, comparison with Nb₂Sn system 9-37492
NbX₆⁻ anions (X=Cl, Br or I), electronic absorption spectra 9-30060
Nb-(5 at.%)Ti alloy strip, supercond., peak effect in critical current w.r.t. temp. and field 9-39600
Nb-(75 at.%)Ti quenched alloy, phases and crystal structure by e. microscope and X-ray diffraction study 9-23767
Nbobr₃, spectrum and metal-O stretching vibr., 4000-400 cm⁻¹ 9-27869
Ta-Nb, solid solution alloys, lattice thermal conductivity, normal and superconducting state 9-30797
Ta-Nb alloys, spectral coeff. 1300 to 2000°K at 0.65 μ 9-40795
Ti-Nb supercond. alloy, magnetization, hysteretic loss and flux-jump stability obs. 9-35364
Ti-(20 at.%)Nb alloy, supercond. props. correlation with metallurgical props. 9-39603
Ti-22 at.%)Nb alloy, superconducting, critical currents 9-37478
type II superconductor, positron annihilation, electron-pairing eff., γ ang. distrib. meas. 9-30874
U-Nb system, monoclinic deform. of α-U lattice 9-40920
Zr-Nb alloy, α(α+β) boundary 9-41062
Zr-Nb system, α(α+β) boundary, microprobe determ. 9-28406
Zr-(1 at.%)Nb alloy, oxidation kinetics and corrosion behaviour in pressurized steam and air 9-35747

Nitrogen

absorption, effect on upper atmospheric composition meas. 9-28907
absorption by liquid iron plasma jet 9-46455
abundance in chondritic meteorites 9-49586

Nitrogen continued

adsorption by Pyrex at very low pressure 9-36969
adsorption on Be thick films obs. 9-36964
adsorption on silica aerogels 9-30498
adsorption on W(100) surface rel. to work function changes 9-42734
adsorption on W single crystal faces, surface potential determ. 9-48775
afterglow, pink, electrostatic probe obs. 9-44504
afterglow in mag. field 9-30315
arc in superimposed gas flow, arc-flow-electrode interacts and mode behaviour 9-23365
atmospheric predissociation, influence on atomic N production 9-28908
atom, core polarization and hyperfine structure calc. 9-46273
atom, correlation effects of non-closed shell many electron theory 9-38773
atom, electron scatt., low energy neutral bremsstrahlung cross section obs. 9-32423
atom, hyperfine structure calc., g.s. first-order wave function 9-32408
atom, polarization wave functions for ground state 9-34532
atom g(³S_{3/2}), calc. to 1 ppm 9-36657
atomic, night-time density in atm. 120 to 230 km, computation 9-41543
atomic beam, elastic scattering by NO and CO molecules, characts. 9-25712
atomic spectra, using Van de Graaff accelerator 9-22998
atoms, quenching of N₂(A³Σ_u⁺) in high vib. levels 9-44340
atoms in N₂-He mixture, pulsed laser radiation 9-41907
best-atom Slater orbital calcs., hybridized-promoted 9-48384
chemisorption on Re 9-49376
collision strengths and photoionization cross sections 9-29972
collisional broadening of spectral lines, comparison of other gases 9-25736
compressed gas, depolarization of Brillouin scattered light as function of gas density and laser power 9-28079
compressed gas, thermal conductivity, concentric cylinder meas. method 9-26027
dielectric const. of liquid at microwave frequencies in X-band 9-46647
diffusion and drift of K ions 9-40756
diffusion and flow in natural rocks 9-30332
diffusion in α-Fe, Ni effects 9-23840
diffusion in benzene and CCl₄, open-tube obs. 9-30383
diffusion in Zr-Al alloy, pumping speed meas., 10⁻⁶-1 torr, 300 and 500°C 9-37197
diffusivity in Mo 9-40985
discharge, decaying, e conc. by laser interferometry, 10⁻²-3 mm Hg 9-28050
in discharge, spectral line expansion and shift 9-46550
discharges, h.f. at lower than atmospheric press. 9-36788
dispersed flow film boiling, droplet breakup and heat transfer 9-26166
electric strength at elevated pressures and small gap spaces 9-42575
electron-ion recombination 9-34796
e.p.r. coupling consts. for σ radicals containing C, H, N and O atoms, extended Huckel calcs. 9-23025
e.p.r. in α-SiC polytypes 9-28750
forbidden transitions in isoelectronic sequence, relative line strengths 9-36653
gas, compressed, n.m.r., obs. of ¹⁴N spin relax. 9-40594
gas streams, concurrent injection of ethanol or water jets, max. drop dia. 9-34864
gas target, traversed by He beam, charge equilb. fractions obs. 9-40559
gas thermal conductivity meas. at 35 and 90°C 9-36814
ion, collisionally excited u.v. and forbidden lines, intensity calcs. 9-25685
ion irradiated, vacancy clusters 9-28279
ionization, Townsend coeffs., in gas containing radioactive impurities 9-39017
ions, radiative-lifetime meas. 9-36663
isoelectronic trap in GaAs₂P_{1-x}, determination of localization energy of excitons 9-28488
isotherms to 400°C and 10000 bar 9-44520
isotope separation in thermal diffusion column 9-46581
liquid, d.c., pre-breakdown phenom., study by electron field emission from metal electrode 9-44581
liquid, dielectric const. at microwave frequencies in X-band 9-46647
liquid, molec. motion and Raman band shapes 9-30412
liquid, nucleate pool boiling rel. to surface roughness and material 9-28189
liquid, stimulated combinational scattering of Nd laser radiation 9-36879
liquid jet, axisymmetric at supercritical press. 9-40765
mixture with O₂ and ether or methane, simultaneous HCN and H₂O laser emissions in pulsed discharge 9-22404
molecular, ionized, harmonic generation under alternating electric field 9-30300
molecular beam, meas. of emission spectrum and radiative lifetime in metastable E³Σ_u⁺ state 9-38863
molecule, A³Σ_u⁺, gas phase energy pooling 9-44338
molecule, electron scatt., low energy neutral bremsstrahlung cross section obs. 9-32423
molecule, vibrational perturbed ¹Σ_u⁺ level, deperturbed crossing Morse curves calc. 9-27863
muonic, 2p-1s X-rays obs., 2p pionic levels population determ. 9-44301
N²⁺+D⁺(or CD₄)->N₂D⁺+D(or CD₃), deviations from stripping model 9-27944
N²⁺, matrix elements of electronic transition in first negative band system meas. by discharge in air flow 9-27865
N²⁺, electron excitation of 1st negative and Meinel bands 9-40597
N²⁺, atmospheric formation rate rel. to press. 9-28910
in Nb-N system precipitation on Nb dislocations, kinetics 9-30744
NGC 5253 galaxy, N1 and N2 emission spectra obs. 9-35958
plasma, continuum radiation, 975-37000 Å 9000-13500°K, 1, 2 atm. press. obs. 9-23302
plasma, contrib. to emission by N⁻ 9-44442
plasma, emissivity meas., 110-300 nm, 2x10⁴°K and e density ~ 10¹⁷ cm⁻³ 9-48590
plasma, Stark-broadened H lines as temp. probes 9-48589
plasma, thermodynamic functions, approximate calc. 9-46464
plasma het, convective heat transfer 9-44460
plasma in homopolar rot. device, 10⁻²-mm Hg, electron collision freq. and current growth 9-25857
plasma jet, convective heat transfer 9-44459
plasma radiative power, total, 250-700 n.m. obs. 9-30261
quadrupole coupling to glyccool, n.m.r. determ. 9-49360
solid, α-N₂ absolute far-i.r. absorpt. intensities 9-49281

Nitrogen continued

- solid, defect structure, electron microscope obs. 9-37159
 solubility in Cu alloys 9-28384
 solubility in Mo, heat of soln. determ. 9-40985
 solubility in W, heat temp. 9-35136
 sp²-hybridized in organic cpds., ¹⁵N n.m.r. shifts 9-25773
 sphere, pulsed with neutrons (14 MeV), time spectra of emitted neutrons 9-34479
 stellar abundance in K grants 9-43528
 thermosphere, lower, conc. from mass spectrometer obs. 9-28906
 xx N₂ trapped in K halide crystals, e.s.r. 9-31166
 CO₂-N₂-He laser power enhancement by noncontracted discharge 9-22390
 CO₂-N₂-He-H₂O glow discharge, spectra, 2800-6500 Å, 3-7 torr 9-25979
 CO₂-N₂-He glow discharge, spectra, 2800-6500 Å, 3-7 torr 9-25979
 C+N atom collisions, interaction potts. 9-38792
 CO₂-N₂-He discharge, lasing action influence on electron energy distrib. 9-34800
 in GaP, isoelectronic trap, photoluminesc. spectrum, bound excitonic mol. obs. 9-39895
 H-N atomic collision, free scatt. model for e loss 9-46310
 H-N mixtures, diffusive separation using isotope solvents 9-28824
 N-Ar solid mixtures, thermodynamic props. 9-39528
 γ-N, adsorbed layer on W, tunneling of field emitted electrons 9-30960
 N₂O₂ mixture ionization and attachment irradiation by 1.5 MeV electrons 9-40710
 N₂-ethylene mixtures, influence of dimers on thermal diff. factor 9-36686
 N₂-C₂H₂ thermal conductivity of gas mixture meas. for investigation of Lennard-Jones potential 9-36803
 N₂-CO₂, vibrational thermal relax. times, determ. by stopping point, fluorescent and spectrophotom. methods 9-48455
 N₂-CO₂ gas mixture, Prandtl number meas., thermal conductivity calc. 9-36816
 N₂-CO₂ supersonic expansion in Laval nozzle, CO₂ population inversion 9-48648
 N₂-He mixtures, heat transfer from cylinders showing slip effects 9-46568
 N₂-N₂O mixtures, vibration-vibration energy exchange, shock-tube study 9-34706
 N₂-Ne mixtures, heat transfer from cylinders showing slip effects 9-46568
 N₂-O₂ gas discharge, ionic charge exchange 9-30303
 N₂-O₂ vibr. exchange in shock tube 9-30349
 N₂-methane-ethane system, form. of ethane rich middle layer on cooling below -225°F 9-42698
 N₂ breakdown under picosec. ruby-laser pulse 9-46544
 N₂ collisions with inert gas atoms, excitation of rotational and vibrational motion of N₂⁺ ions 9-42470
 N₂, electron energy-loss spectrum, perturbations due to config. interactions 9-38858
 N₂, electronic band strengths of first positive system 9-48471
 N₂, Franck-Condon factors for v'=0 progression of fourth positive band system 9-42407
 N₂, gas, second virial coeff. 9-34833
 N₂, impulse breakdown, secondary leader channels obs. 9-44511
 N₂, in mag. field, 5 shear viscosity coeffs. determ. 9-46577
 N₂, ionization by N⁺ and N₂⁺ ions, 0.2 to 1.8 and 0.5 to 1.8 MeV, resp. 9-28040
 N₂, ionization coeffs. meas. 9-32690
 N₂, K⁺ ion swarm, mobility, diffusion coeff. and reaction determ. 9-23203
 N₂, metastable peaks in mass spectra 9-42568
 N₂, metastable species prod. by electron excitation 9-32478
 N₂, microwave breakdown temp. depend. 9-32708
 N₂, primary specific ionization of relativistic particles 9-39015
 N₂, resonant scatt. of electrons, ang. distrib. 9-27855
 N₂, vacuum u.v. emission obs. 9-27866
 N₂, Li⁺ elastic differential scatt. cross section meas., 3-330 eV 9-46315
 N₂⁺ concentration in daytime F₂-region between 200 km and peak altitude, direct measurement 9-24701
 N₂⁺ concentration in daytime F₂-region between 200 km and peak altitude, direct measurement 9-31436
 N₂⁺ electron temp. depend. 9-32697
 N₂⁺ first negative bands, electron impact excitation cross section 9-32479
 N₂⁺ first negative system, excited by low-energy electrons, rot. temp. 9-30040
 N₂⁺ ion, excitation of λ=4278 Å band of first negative system by noble gas ions and atoms 9-30045
 N₂⁺ ions prod. in collisions between inert gas atoms and N₂, excitation of rotational and vibrational motion 9-42470
 N₂⁺ reactions with CH₄ and CD₄, dynamics 9-39940
 N₂⁺ rotational bands excited in hollow cathode discharge, Boltzmann distrib. 9-23055
 N₂⁺ structure determ. by electron diffraction 9-27867
 N₂⁺+D₂→N₂D⁺+D reaction, crossed-beam technique appl. 9-41442
 N₂⁺+O₂→N₂+O₂⁺ charge transfer in thermal and low eV region 9-42565
 N₂ absorption spectrum, 600-1100 Å 9-34625
 N₂ acoustic plane wave propag. 9-26033
 N₂ collision with incident beams of He, H, He⁺; electron and ion prod. cross section meas., 0.15-1.0 MeV 9-22982
 N₂ electron drift and resonance scatt. in terms of H₂⁺ temporary states 9-46578
 N₂ electron excitation of 1st positive bands 9-40597
 N₂ emission lines in u.v. spectrum of aurora 9-33817
 N₂ first positive system, transition moment, r-centroid dependence 9-25745
 N₂ first positive system, Einstein coeff., Halevi's correction application 9-27868
 N₂ gas viscosity meas. pot. fitted 9-36823
 N₂ and H₂ 9-23651
 N₂ Hulburt-Hirschfelder calc. of r-centroid 9-30018
 N₂ in F₂ layer max. rel. to seasonal anomaly 9-28956
 N₂ in thermosphere, midlatitude 150 to 450 km, concentration and temp. 9-28905
 N₂ in Venus atmosphere, upper limit to abundance 9-29070
 N₂ ionization in H-N₂ low energy collisions 9-34584
 N₂ laser systems, interaction between first and second positive systems 9-25239
 N₂ mol., electron reson. scatt., elastic and inelastic channel obs. 9-23057
 N₂ mol. excitation by 0-200MeV electron collisions, vac. u.v. light emission 9-32480

Nitrogen continued

- N₂ number densities in thermosphere, lower, day-night vars. 9-26920
 N₂ photoionization cross section, electron phase shift calc., simple model potential construction 9-46258
 N₂ radiating power in range 0.2 to 3 μ at 10⁴K, 1 atm. 9-40753
 N₂ radiation generated during B³πg A³Σ⁺u transition effect of inert gases 9-38864
 N₂ reaction with O⁺ ions, F region, rate calc. from loss coeff. 9-40091
 N₂ refractivity in far u.v., Pade summation of Cauchy dispersion eqn. 9-48666
 N₂ thermal conductivity, vibrational relaxation eff. 9-36815
 N₂A³Σ_u auroral green line excitation of atomic W 9-43424
 N₂H→HN₂⁺ Balmer-α, N₂(0,0) 1st -ve band photon emission, cross sections meas. 9-22985
 N₂-He mixture, thermal relaxation and heat transfer 9-48661
 N₂-O₂ mixture, thermal relaxation and heat transfer 9-48661
 N₂+H₂ ion-mol. reactions, using ion cyclotron reson. 9-31184
 N₂(A³Σ_u⁺), quenching in low vib. levels by N atoms 9-44340
 N₂(1st+) and N₂⁺(1st-) nonequilibrium region behind shock, radiation mechanism 9-42410
 N₂ radical in soln., spectroscopic obs. 9-38860
 N₂⁺, geometries by approx. SCF-MO theory which considers intermol. differential overlap 9-34637
 N₂⁺ extraction from plasma, space charge sheath effect 9-28016
 N₂⁺ formation in atmosphere 9-28909
 N₂⁺, atm., night time distrib. with incidence of aurora 9-28931
 N₂⁺, cosmic ray secondary e fluoresc. efficiency in 3914 Å band 9-46127
 N⁺ and N₂⁺ conc. in ionosphere 20 to 630 km obs. 9-43464
 N⁺ and N₂⁺ ions, ionization of He, Ne, Ar, Kr, H₂ and N₂, 0.2 to 1.8 and 0.5 to 1.8 MeV, resp. 9-28040
 N⁺ concentration in daytime F₂-region between 200 km and peak altitude, direct measurement 9-31436
 N⁺ in N₂, mobility, diffusion coeff. and reaction rates determ. 9-23347
 N⁺ recombination radiation in vacuum ultraviolet, shock tube studies 9-25968
 N²⁺ ion production and loss during decay period of He-Ne mixture plasma, density time depend. 9-40666
 N(D) deactivation in vac. u.v. photolysis of N₂O 9-49385
 N emission lines in u.v. spectrum of aurora 9-33817
 N I, laser lines, obs. 9-46280
 N I ⁴S_{3/2}-²D_{5/2,3/2} transitions at night, permanent feature of upper atm. 9-33804
 N I forbidden lines in nightglow at mag. equator 9-33806
 N II (III) u.v. multiplets, upper level decay scheme 9-44266
 N II line profile in M8 nebula 9-41629
 N III lines, absolute transition probabilities, meas and obs. 9-29941
 N VI, S and P state transitions, wavelength calc. and comparison with expt. 9-44257
 N VI, S and P state transitions, wavelength calc. and comparison with expt. 9-40540
¹⁴N, nuclear quadrupole moment, from MO calc. 9-27842
¹⁴N and ¹³³Cs, optically pumped, spin exchange 9-32418
 N root mean square charge radii 9-48415
³⁰N₂-²⁸N₂ mixture, equilibration by W catalysis, distrib. of active sites on W surface 9-33662
 N(³P)³(³P) vacuum u.v. emission obs. 9-27866
 N₂(v) relative intensities and exponential decay of ³P_{3/2} and ³P_{1/2} 9-44267
 O atomic, 2nd virial coeffs. 9-26019
 n-SiC:N electroluminesc. diodes, props. and anomalous nature of B and Al diffusion during prep. 9-37776
 in steels, C, Mn-containing, determ. 9-46940

Nitrogen compounds

- absorbance, i.r., 20 to 35 μ 9-40598
 nitrate powders, Raman spectra, absolute scatt. coeffs. 9-49295
 nitrates, molten, molec. vibr. 9-39105
 CO-N₂-He lasers, high power, high efficiency 9-22391
 CO₂-N₂-He-H₂O flowing laser, elec. discharge effect on mol. comp. 9-40352
 Cl₂BN(CH₃)₂, field gradient calc. 9-23030
 Co₂-N binary syst., mass transfer cooling of flat plate, dissociation depend. 9-25789
 Fe-N alloys, martensite transform. start temp. composition dependence 9-23982
 H₂BNH₂, field gradient calc. 9-23030
 HNO₃, potential const. 9-23058
 Li-NH₃ systems, low-temp. ht. capacities 9-39531
 N-α-Fe-C solid solution, permeability disaccommodation, -40°+180°C 9-26322
 N-O chemiluminescence, investigation of features 9-28737
 N-U-C-O system, phase relations at 1700°C 9-26400
 N₂-CO₂ gas discharge, aimnt depend. decay of CO₂ 00¹ level 9-34159
 N₂, electron scatt., elastic at 500 eV, absolute differential cross sections 9-38800
 N₂D₄ crystalline, Raman spectra, -70 to -195°C, crystal structure determ. 9-39853
 N₂F₄, liq., i.r. spectrum 9-23505
 N₂H₄ crystalline, Raman spectra, -70 to -195°C, crystal structure determ. 9-39853
 N₂H₄ decomp. in flow reactor 9-37819
 N₂H₄ molecule, spin-spin interaction between N nuclei 9-24513
 N₂O-H₂ flame properties for atomic absorption and emission spectroscopy 9-31224
 N₂O-N₂ mixtures, vibration-vibration energy exchange, shock-tube study 9-34706
 N₂O-N₂ molecular laser, central tuning dip on individual transitions 9-47999
 N₂O-acetylene flame stabilization technique 9-35745
 N₂O, adsorption and interactions on Ni (100), effect on work function 9-35003
 N₂O, metastable species prod. by electron excitation 9-32478
 N₂O, spectral linewidths for 2224 cm⁻¹ band 9-42406
 N₂O, vibration band profile determ. in various solvents and correlation function calcs. 9-44571
 N₂O adsorbed on silica gel and zirconia, radiolysis 9-24591
 N₂O liquid and solid refractive indices 9-44562
 N₂O natural convective heat transfer, comparison with, CO₂ and chlorotrifluoromethane 9-28170
 N₂O radiolysis with electron pulses, effect of temp. on yields 9-33685
 N₂O vac. u.v. photolysis, deactivation of N(D) 9-49385
 N₂O+CO bimolec. reaction in single pulse shock tube 9-43321

Nitrogen compounds continued

- $\text{N}_2\text{O} + \text{H}_2$ reaction kinetics 9-31183
 $\text{N}_2\text{O} + \text{O}^- \rightarrow \text{NO}^- + \text{NO}$, 0-3 eV obs. 9-46430
 $\text{N}^{15}\text{N}^{14}\text{O}$, mag. anisotropy, molec. g value and quadrupole moment 9-38862
 N containing anions, attenuated total refl. spectra aqueous soln., i.r. vib. freq. 9-28135
 $^{15}\text{N}_2^{16}\text{O}$, vibration-rotation bands, effects of Fermi resonance and l-type doubling 9-48470
 NCO , vibronically excited, gas phase electron reson. spectrum 9-40599
 NCS , gas phase electron reson. spectrum 9-40599
 NCS free radical, electronic absorpt. spectrum, rot. and vib. anal. 9-23175
 ND , emission bands assigned to $\text{d}^1\Sigma^+ - \text{n}^1\Sigma^+$ transition 9-46368
 NF_3 , equilibrium struct., from microwave spectra in excited vib. states 9-34630
 NF_3 , Gaussian basis SCF calc. 9-42403
 NF_3 , localized-orbital LCAO MO calc. of dipole moment and field gradient 9-42402
 NF_3 , thermal conductivity, mag. and elec. field effects 9-28076
 NF_3 , ν_3 and ν_4 states, Σ -type doubling and resonance, from anal. of microwave spectra 9-34631
 NF_3O , Raman spectrum 9-48468
 $\text{NH}_3\text{-N}_2$ mixture, i.r., absorptance, 20 to 35 μ 9-40598
 NH_4FeF_4 crystal growth from soln. X-ray diffraction powder study 9-26207
 NH mol., $\text{d}^1\Sigma^+ - \text{c}^1\Pi$ bands, predissociations 9-34607
 NO , 3p mol. Rydberg state ($2\pi(\nu=0)$), spin-orbit coupling const. 9-40595
 NO , absorption spectrum in vacuum u.v. and visible emission spectrum, 4d complex 9-23056
 NO , adsorbed on silica gel, mag. susceptibility 9-44631
 NO , adsorption and interactions on Ni (100), effect on work function 9-35003
 NO , adsorption on molec. sieve 9-39167
 NO , β , γ systems, transition dipole moment determ. 9-48472
 NO , diffusion in H_2O , coeffs., 10° to 60°C 9-26086
 NO , electron affinity 9-32693
 NO , mag. rot. spectrum of $\text{A}^2\Sigma^+ - \text{E}^2\Pi$ transition 9-44337
 NO , metastable peaks in mass spectra 9-42568
 NO , night-time density in atm. 120 to 230 km, computation 9-41543
 NO , paramagnetic molecules, energy splitting of core electron levels, ESCA spectra 9-34634
 NO , pulse radiolysis, NO_2 and N_2O_3 prod. 9-45425
 NO , resonant scatt. of electrons, ang. distrib. 9-27855
 NO , spectral emissivity in infrared region 9-36704
 NO , vib. relax., negative temp. effect 9-42409
 NO_2 , dissociative attachment of electrons 9-32693
 NO_2 , fluoresc. spectra excited by Ar^+ and Kr^+ lasers 9-40596
 $(\text{NO})_2$, matrix-isolated i.r. spectrum 9-42405
 NO_2 , near-i.r. Zeeman spectra 9-36702
 NO_2 , photochem. recoil spectra 9-43333
 NO_2 , vac. u.v. photolysis 9-39961
 NO_2^- , charge distrib. and orbital energies of ground state, CNDO calc. 9-44339
 NO_2^- , in solid soln. in KBr, infrared intensities 9-48469
 NO_2^- , N^{14} quadrupole coupling const. calc. 9-42401
 NO_2^- , absorption spectra in soln., transitions 9-30039
 NO_2^- in $\text{KCl}(\text{KBr})$, phonon resonant scatt. 9-28411
 NO_2^- luminescent centres in KBr, KCl and KI, yield depend. on exciting light freq. 9-31124
 $\text{NO}_2^- + \text{NO}_3^-$, isotope fractionation 9-41440
 NO_2^+ and NO_2^- , electronic struct. and geometry 9-48467
 NO_2^+ in air, production 9-43387
 NO_2 in gas mixture, nonlinear thermal Rayleigh scatt. of light 9-32738
 NO_2 reaction with atomic O, e.s.r. detect. 9-24534
 NO_2 spectral transition probability, absolute 9-23170
 NO_3^- ion, solvation by chloroform and water, i.r. spectroscopic evidence 9-42661
 NO_3^- ion in molten nitrates, Raman vibr. freqs. rel. to temp. 9-42662
 NO_3^- symmetry in solns., metal cations effects, obs. 9-36887
 NO_3^{2-} in KCl cryst., i.r. absorpt. spectra of ion vibrs. 9-41382
 NO^+ , appearance potential 9-32693
 $(\text{NO}^+)^*$, de-excitation cross-section in NO 9-34792
 NO^+ conc. in ionosphere 200 to 630 km, obs. 9-43464
 NO^+ concentration in daytime F₂-region between 200 km and peak altitude, direct measurement 9-24701
 NO^+ concentration in daytime F₂-region between 200 km and peak altitude, direct measurement 9-31436
 NO atmospheric, 60 to 96 km, evening twilight rocket obs. 9-31344
 NO lines in airglow burst, Cosmos 92 obs. 9-43422
 NO mol., electron reson. scatt., elastic and inelastic channel obs. 9-23057
 NO mol. gas, excited by fast electrons, glow spectra in i.r. region 9-38831
 NO molecules, rel. to scattering of O and N atoms 9-25712
 NO titration method chemiluminesc., reacts. 9-41445
 NOF , potential const., refinement 9-30041
 $\text{NO} + \text{NO}_2^-$, isotope fractionation 9-41440
 $\text{NO} + \text{O}^- \rightarrow \text{NO}_2^- + \text{O}$, 0-3 eV obs. 9-46430
 $\text{NPOCl}_2(\text{NSOCl})_2$, crystal structure 9-39287
 NS emission spectra, isotope shift studies 9-34635
 NS free radical, molecular structure by gas phase e.p.r. 9-46369
 Nb-Ti-N alloy thin films, supercond. critical current-field meas. in continuous mag. fields 9-35362
 No , vibr. relax., shock tube meas. 9-38861
 Ta-N film, electrical and optical meas. and electron diff. analysis 9-23625

ammonia

- adsorbed on synthetic Linde type-A zeolite, dielec. props. 9-41233
 adsorption and decomp. on W 9-48774
 adsorption and decomp. on W 9-48773
 alkali-metal- NH_3 solns., unpaired electron spin correl. times 9-44587
 amino-cupric ion, e.s.r. spectrum, -18°C \rightarrow 72°C 9-42391
 ammonium- ^{15}N heteronuc. double reson. using weak perturbing r.f. fields 9-40615
 emissivity, temp. range 6000-12000°K for 1,10 and 100 cm layers 9-26035
 gas, Fourier dispersion spectra, rot. line strengths and elec. dipole moment, 87-667 μ 9-30043
 gas in bulk, steady state transient 'wiggles' phenomenon, relax. times meas. 9-44528
 inversion spectrum, hyperfine structure 9-34632

Nitrogen compounds continued**ammonia continued**

- inversion spectrum, press. broadening 9-42404
 isotope exchange between liquid ammonia and H_2 , separation factor 9-31180
 Jovian, photolysis at 1350-2200 Å 9-41676
 line mixing by collision in far i.r. spectrum 9-38859
 liquid, complex dielec. const. at 3 GHz, as function of temp. 9-34918
 liquid, effect of dissolved salts on i.r. spectra 9-39106
 microwave emission in Sagittarius region, rel. to dust cloud conditions 9-43574
 molecular structure studied by totally inelastic electron scatt. 9-25746
 MPD arc config., energy fluxes to anode, heat transfer mech. responsible 9-32610
 n.m.r. ^{15}N shifts in liq. and vapour 9-32798
 oxidation and adsorption on silica-supported Pt and silica, i.r. spect. study 9-30044
 population inversion, adiabatic, obs. from laser chirped pulses transmission 9-44341
 rotation-inversion spectrum 9-32481
 spectra of gas emission in i.r. region of excited mol. 9-38831
 Stark spectroscopy by far i.r. masers 9-25767
 Gas Phase H-bonded complexes, i.r. spectra 9-25742
 K- NH_3 solns., viscosity, vacancy calc. 9-48686
 K- NH_3 solns. doped with KI, Knight shifts 9-44595
 ND_3 , hyperfine interaction between D nuclei and intramolecular fields 9-38865
 ND_3 , ND_2H , NDH_2 and NH_3 , ^{15}N n.m.r. chem. shifts 9-30430
 ND_3 and NH_3 , liquid and solid refractive indices 9-44562
 ND_3 dissociative electron capture obs. 9-25746
 ND_3 molecular structure studied by totally inelastic electron scatt. 9-25746
 $\text{NH}_3\text{-Na}$ solutions, complex dielec. constants as function of molar conc. 9-34918
 NH_3 adsorption and oxidation on silica-supported Pt and silica, i.r. spect. study 9-30044
 NH_3 and ND_3 , dissociative attachment of electrons 9-46422
 NH_4ClO_4 , thermal expansion mechanism 9-42973
 NH p chem. shift in protonation and Co(III) coordination rel. to neighbouring mag. anisotropy 9-28155
 $^{15}\text{NH}_3$, molecular g-values, mag. susceptibilities, quadrupole moment and spin interaction 9-42408
 Na-NH_3 gas mixtures, absorpt. spectra 9-34633
 Na-NH_3 solns., dielec. relaxs. 9-44582
 $\text{UC} + \text{NH}_3 \rightarrow \text{UN}_2 + \text{CH}_4 + \text{H}_2$ 9-31186
- ammonium compounds**
 ADP, in Ar-ion laser cavity, c.w. parametric u.v. generation 9-27363
 halides, melting curves and phase transitions to 40 kbar 9-30452
 NH_4Cl , stability of gaseous mol. 9-36726
 $\text{NH}_4\text{H}_2\text{PO}_4$, solution-grown crystals, mother-liquor inclusions formation at saturation 9-40862
 phase transitions, u.s. investigations 9-37302
 salts in liq. NH_3 , conc. soln., i.r. spectra analysis 9-30042
 ND_4Br , transition X-ray investigation, lattice parameters determ., -192 to 196°C 9-30743
 ND_4Br specific vol. determ. by hydrostatic weighing dilatometer, 20°-140°C 9-33141
 $\text{ND}_4\text{D}_2\text{PO}_4$, ferroelec., pressure dependence of transition temp. from neutron diff. 9-49143
 NH_3OHCl , X-irrad., optical and thermal conversions of V_k centres 9-32995
 $3(\text{NH}_4)_2 \cdot 0.7\text{MoO}_4 \cdot 4\text{H}_2\text{O}$, thermal decomposition, X-ray diff. and i.r. spectrophotometric exam. 9-30745
 $(\text{NH}_4)_2\text{MnF}_3$, cryst. struct. 9-30566
 $(\text{NH}_4)_2\text{Pt}(\text{S}_2)_3 \cdot 2\text{H}_2\text{O}$ crystal and molecular structure 9-39288
 $(\text{NH}_4)_2\text{SO}_4$, u.s. absorption meas. for suspension concentration 9-32802
 $(\text{NH}_4)_2\text{ClS}_2\text{O}_6$, crystal structure 9-39293
 $(\text{NH}_4)_2\text{HfF}_7$, relaxation determ. by γ - γ angular correlation 9-37675
 $(\text{NH}_4)_2\text{UO}_2\text{F}_6$ crystal structure and twinning 9-30565
 NH_4^+ , heat of formation by electron impact 9-32692
 NH_4ClO_4 burning, alone and in eff. of ionizing radiations 9-28787
 NH_4 ion, molec. freedom in NH_4ClO_4 9-48970
 NH_4AgI_3 , high ionic conductivity, room temp., prep., patent 9-30965
 NH_4Br , high-press. elastic const. and phase transitions, u.s. determ. 9-30633
 NH_4Br , III-IV transition X-ray investigation, lattice parameters determ., -192 to 196°C 9-30743
 NH_4Br , phase transitions, u.s. investigations 9-37302
 NH_4Br , recombination luminescence from self-trapped excitons 9-33586
 NH_4Br specific vol. determ. by hydrostatic weighing dilatometer, 20°-140°C 9-33141
 NH_4CN , polycryst., i.r. spectrum 9-49282
 $\text{NH}_4\text{Cl}:\text{CO}^{2+}$, Ni^{2+} , VO^{2+} , X-irrad., F-centres, e.p.r. obs. 9-32994
 NH_4Cl , coherent inelastic neutron scatt. meas. of normal modes of vibr. 9-46980
 NH_4Cl , e.p.r. spectrum due to radiation induced paramagnetic centre 9-33631
 NH_4Cl , lattice dynamics below -30.5°C 9-28413
 NH_4Cl , order-disorder phase transitions, critical exponent 9-33146
 NH_4Cl , phase transitions, u.s. investigations 9-37302
 NH_4Cl , recombination from luminescence from self-trapped excitons 9-33586
 NH_4Cl , sublimation mechanism of bubble migration in temp. gradient 9-35134
 NH_4Cl cryst., internal motions, n.m.r. and use of relax. function 9-31168
 NH_4Cl A-type phase transition Cu^{2+} impurity effects, e.s.r. and differential thermal analysis 9-33142
 NH_4ClO_4 , ht. capacity and thermodynamic props., 5°-350°K 9-48970
 NH_4ClO_4 , limiting press. and solid temp. for deflagration 9-33660
 NH_4ClO_4 , pressed-strands, burning vel. rel. to original particle size 9-26814
 $\text{NH}_4\text{Cl} \cdot 3\text{NH}_3$, i.r. spectra analysis 9-30042
 NH_4F , molecular form factors of NH_4^+ , X-ray diff. 9-32884
 NH_4F , segregation in ice single crystals 9-30518
 NH_4F , struct. and N-H bond obs., neutron and X-ray diff. 9-32923
 NH_4FeF_6 , crystal structure and mag. props. 9-35063
 $\text{NH}_4\text{H}_2\text{PO}_4$, ^{14}N nuclear quadrupole interactions by double resonance spectra 9-28768
 $\text{NH}_4\text{H}_2\text{PO}_4$, antiferroelectric, temp. depend. of induced electro-opt. eff. 9-31085

Nitrogen compounds continued
ammonium compounds continued

- NH₄H₂PO₄, electro- and piezooptical coeffs., dispersion and temp. depend. 9-33515
 NH₄H₂PO₄, electro-optical effect, transverse, and light modulation by crossed rods, obs. 9-33516
 NH₄H₂PO₄, ferroelec., pressure dependence of transition temp. from neutron diff. 9-49143
 NH₄H₂PO₄, glide elements and dislocation reactions 9-42838
 NH₄H₂PO₄ cryst., second harmonic generation 9-39791
 NH₄H₂PO₄ crystal, relative nonlinear coefficient, corrected value 9-33499
 NH₄H₂PO₄ crystal for modulating beam of He-Ne laser, design of production model 9-31988
 α-NH₄PO₃, nonlinear optical coeff. meas. relative to KH₂PO₄, LiNbO₃ and α-HIO₃ 9-26690
 NH₄I, nucleation and growth on muscovite mica 9-37037
 NH₄I, p.m.r. and hindered rot. 9-35728
 NH₄I, recombination luminescence from self-trapped excitons 9-33586
 NH₄NO₃-water solns., i.r. and Raman spectra rel. to NO₃⁻ symmetry, obs. 9-36887
 NH₄NO₃, nuc. mag. relax. time meas. of NH₄⁺ diffusion 9-30628
 NH₄PF₆.NH₄F, n.m.r. and spin-lattice relaxation times of ¹H and ¹⁹F, dielectric transitions 9-35727
 (NH₄)₂BeF₆, ferroelec. transition, n.m.r. study, mag. screening of ¹⁹F 9-43118
 (NH₄)₂PtCl₆, cross-relaxation between single and exchange-coupled Ir⁴⁺ ions, e.p.r. meas. 9-49356
 (NH₄)₂PtCl₆, hyperfine interactions of single and exchange-coupled Ir⁴⁺ ions, ENDOR investig., ⁴K 9-49364
 (NH₄)₂SO₄, ferroelec. order-disorder transition 9-33391
 (NH₄)₂SO₄, ferroelec. order-disorder transition 9-33390
 (NH₄)₂SO₄ single crystal, e.s.r. of Mn²⁺ in paraelec. and ferroelec. phases 9-31165
 NY₄ClO₄, u.v. photon induced colour centres 9-42853

Nobelium

No entries

Nobelium compounds

No entries

Noble gases *see Inert gases***Noctilucent clouds** *see Atmosphere/upper; Clouds***Noise**

- atmospheric h.f. bursts, pulse spacing 9-43401
 atmospheric radio noise measurements at 27 kHz, fixed stations in Europe 9-33786
 in centimetre range, due to tropospheric thermal rad. and precipitation 9-31316
 e.m. in sea, e.l.f. at depth 30 to 300 m (off Baja, Ca.) 9-45473
 e.m. wave scatt. on defects in a crystal 9-28708
 emissions from plasma resonances 9-39007
 energy-equivalent continuous sound level traffic noise, from street 9-34085
 film-grain, in holography 9-27353
 fluorescence as source in laser backscatter expt. 9-37920
 in Fourier emission spectroscopy of thermally excited gas, suppression 9-40576
 magnetospheric e.l.f., spatial extent and occurrence freq., OGO 3 obs. 9-31356
 magnetospheric v.l.f., triggering by Morse dots at 14.7 kHz 9-43415
 Markov photographic 9-40388
 in nuclear reactor ANNA, meas. and analysis 9-22878
 photon-bunching effects in spatially coherent noise field, enhancement 9-34153
 plasma, radiation at electroacoustic reson. freqs. 9-44423
 plasma afterglow, emission in mag. field 9-48568
 pulses in photomultipliers counting single photons 9-38360
 quantum optical 9-40346
 quantum phase in semiconductor diode laser obs. 9-43898
 reactor, analysis using covariance method via polarity detect. 9-34505
 seismic, structure estimation using arrays 9-37882
 seismic array, large aperture, long-period noise study 9-49414
 shot, thermal and ion current, for probe in quiescent plasmas 9-42536
 super l.f., in earth-ionosphere cavity, geomagnetic field effect 9-31395
 thermal, in spin-phonon system 9-30760
 thermal and shot, relation with fluctuating occupation numbers in statistical mechanics 9-47881
 underwater, beneath springtime sea-ice, diurnal variations 9-40003
 vibrations, random, of thin elastic plates 9-29252
 v.l.f. magnetospheric during whistler duct drift across mag. shell, triggering 9-43414

acoustic

- acceptability, criteria levels, two surveys aboard ship 9-22267
 adaptive optimum detect. theory, appl. to recurrence phenomena in noise 9-29287
 aircraft, judgment tests over past decade, analysis 9-29302
 amplitude discrimination, effect of duration 9-31705
 amplitude discrimination and freq. selectivity of signals in noise 9-40204
 broad-band, judged noisiness of moderated and multiple tones 9-27128
 bursts, reproducible, provided by average response computer 9-29301
 cavitation, from rot. bars in water, spectra 9-26059
 cavitation noise associated with bubble collapse 9-23489
 flow noise, nearfield, from vehicle/water boundary layers 9-45865
 Gaussian, white, detect. of known signal 9-29304
 Gaussian, white, detect. of known signal 9-29303
 identification of diesel engine seconds 9-24960
 non-Gaussian, known signal detect., three receiver designs 9-29300
 roller bearing, evaluation using axial testing technique 9-29299
 roller bearing, subjective response, establishment of objective criteria 9-29298
 sea, vertical directivity, integral equation analysis 9-28855
 semiconductors, piezoelectric, non-linear interaction of amplified u.s. noise 9-46994
 spatially incoherent, hydrophone optimum passive bearing estimation 9-43789
 in spin-phonon system, spacial correlation and spectral densities of noise field in infinite and bounded systems 9-30760
 thermal noise in spin-phonon systems 9-37309
 thresholds for l.f. octave bands of noise 9-43691

Noise continued**acoustic continued**

- transmission from turbulent boundary layer through flexible plate into closed cavity 9-45866
 u.s. attenuation and phase shift meas. in presence of noise 9-29273
 u.s. pulse vel. meas. in presence of noise 9-29272
 CdSe, photoconducting, and sound amplification 9-33176

electrical

- see also Cosmic radiation, radiofrequency; Sun/radiation, radiofrequency*
 i/f, proportionality to mobile charge carriers number 9-39614
 a.f. bands associated with ionospheric lower hybrid resonance phenomena, OGO 2 obs. 9-28943
 in beta-activity meas., reduction 9-44170
 coaxial cables, mechanisms producing noise and their elimination 9-29355
 contact, i.f. 9-47882
 cosmic, ionospheric absorption sudden increases 9-45524
 in electron scanning microscope, resolving power obs. 9-43854
 Green's function approach, and differential conductivity 9-47028
 homogeneous samples, noise rel. to mobile charge carriers number 9-39614
 ionospheric v.l.f. obs. during auroral absorption event 9-33830
 Josephson effect, D.C., calc. of thermal noise 9-37457
 memory systems, magnetic film, photon- and electron-beam-accessed, improvement of signal-to-noise ratio 9-43843
 microwave diodes, NBS report 9-33280
 m.o.s.f.e.t., generation-recombination model and experimental verification 9-26579
 m.o.s.f.e.t., p-channel, effect of crystallographic orientation 9-33361
 m.o.s.f.e.t. with n-type channel, h.f. excess noise and equivalent circuit representation 9-33349
 m.o.s.f.e.t. with n-type channel, h.f. excess noise and equivalent circuit representation 9-43092
 m.o.s.t., current noise spectrum, physical model 9-43090
 m.o.s.t., current noise spectrum, v.l.f. 9-43089
 in parametric amplifier, reduction using two uncoupled resonators 9-36248
 photoconductor, photon counting obs. 9-39704
 photodiode, photocurrent fluctuations and sensitivity threshold 9-37627
 probe, in quiescent plasma 9-28014
 in semiconductor current limiter diodes, meas. 9-33343
 semiconductor diodes, application of fluctuation-dissipation theorem 9-28536
 semiconductors, g-r noise relax. modes 9-39608
 spectral analysis at surface barriers by correlation method 9-36521
 in spectrometers, scintillation, electronic elimination 9-40456
 spectrum of irradiated photodetector, rel. to intra-Doppler spectral line structure 9-25689
 super l.f., in earth-ionosphere cavity, geomagnetic field effect 9-31395
 superconductor, quantum phase noise, temp. depend. meas. by interference techniques with point-contact Josephson junctions 9-37496
 superconductor, type-I, flux-flow noise 9-24152
 superconductors in mixed state, l.f. corresponding to voltage fluctuations produced by mag. flux changes 9-30856
 Al-Al₂O₃-Al thin films, meas. to verify tunnelling 9-33356
 Au films, current noise 9-28464
 CdSe, l.f. current noise illumination dependence 9-41260
 GaAs:Zn, spectra in thermal equil. and under optical excitation, electron fluctuations obs. 9-41198
 p-Ge, generation-recombination, and photo-Hall effect, in impurity centres 9-28513
 In-(2 at.%)Pb superconducting, type-I, films, flux-flow noise determ. 9-24152
 InSb, microwave noise emission 9-49085
 Si-Zn photoconductors, generation-recomb. type, spectrum, freq. and bias current depend. 9-41270
 Si, illuminated single crystals, 1/f noise without external voltage 9-26559
 Si single cryst., l.f., influence of opt. rad. 9-26561

Noise abatement

- see also Absorption/acoustic waves*
 acoustic filter characteristics expt. determination, for use in pulsating gas flows 9-43794
 energy-equivalent continuous sound level traffic noise, from street 9-34085
 insulation of a library and lecture rooms 9-34090

Nomenclature and symbols*see also Units*

- cinematography, international terminology 9-32075
 geomagnetic storms, world-substorm definition 9-35906
 high-speed photography, international terminology 9-32075
 photometry, units and definitions 9-32027

Nomograms*see also Graphs*

- stereographic and gnomonic projections, optical device for direct prod. and viewing 9-36152
 X-ray fluoresc. analysis grain-size effect 9-28833

Non-crystalline state *see Amorphous state; Vitreous state***Non-Newtonian fluids** *see Fluids***Nonlinear optics**

- advances, review 9-48077
 backward-travelling-wave parametric interactions, steady-state theory 9-34188
 bending of trajectories of asymmetrical light beams 9-27373
 bleach-out effect, nonlinear wave equations description 9-38365
 Brillouin scatt., large angle, heterodyne spectroscopy obs. 9-38393
 cavity with nonlinear crystal, 2nd harmonic generation, coherence and saturation props. 9-22374
 covalent cryst., nonlinear susceptibilities 9-49235
 crystal, variation of sum frequency power with crystal length, confirms existence of three pump frequencies 9-31064
 diffraction, self-focussing, self-action in nonlinear medium 9-25351
 dispersive media, quasi-monochromatic light pulses, evolution 9-26681
 elastic second harmonic generation by u.s. waves, Bragg diffraction study 9-26679
 e.m. wave interaction with medium with non-linear mag. susceptibility 9-45375
 e.m. waves, self-focusing, computer studies 9-34112
 entropy of effect in solids 9-47308

Nonlinear optics continued

- ferroelectric cryst., second harmonics generation 9-39791
 f.m., laser, harmonic generation for frequency stabilization, patent 9-41889
 frequency conversion, experiments using continuously pumped repetitivity Q-switched ruby laser 9-25320
 frequency conversion in Proustite, 10.6 μm to visible, spatial resolution obs. 9-26676
 frequency converters, travelling wave, derivation of Hamiltonian 9-31891
 gas spontaneous emission, interference effects 9-27804
 Group III-V compounds with zinc-blend structure, second order susceptibility 9-47309
 Group III-V compounds with zinc-blend structure, second order susceptibility 9-26678
 group III-V semiconductors, second-order susceptibilities 9-26684
 harmonic generation, props. of single crystals reviewed 9-28659
 III-V compounds, second order susceptibility, matrix element of solely spin orbit coupling 9-35610
 image-contrast amplifier 9-48111
 interactions in media with inversion symmetry 9-34189
 laser, Q-switched, intensity recovery from correl. data 9-43871
 laser applications, multiple scatt. processes 9-27344
 laser beam in dense plasma, penetration and self-focusing 9-48574
 laser frequency transforming by stimulated four-field parametric scatt. 9-29436
 laser radiation spectral charact. meas. method 9-31971
 liquid, refractive index, eff. of interaction betw. anisotropic mols. 9-23498
 materials, evaluation by powder technique 9-26677
 materials review 9-49233
 metal oxides with nonbonded electrons 9-45263
 modern, symposium, New York (1967) 9-27360
 in organic dye bleachable absorbers, for ruby lasers, abs. 9-26113
 parametric amplifier and freq. converter, P-representation 9-34150
 parametric luminescence, statistics of field and photocounts 9-28738
 photon echoes in gases, polarization props. 9-30351
 polarizabilities, averaged, in quasiopics, general props. 9-36332
 polarization in resonance media, perturbation theory 9-22365
 pulse amplification; ultrashort durations 9-29448
 quantum electronics conference, 1968, Miami, USA 9-25196
 quartz, second harmonic generation 9-39791
 Rayleigh thermal scatt., stimulated, time and freq. depend. 9-29434
 refraction, bending of trajectories of asymmetrical light beams 9-27373
 review of developments 9-41932
 review of developments 9-48078
 ruby, laser-enhanced two-photon decay 9-26766
 second harmonic generation at boundary of isotropic medium 9-22439
 second harmonic generation in crystals of space group $P3_1, 21^+1$ 9-26680
 second harmonic generator using organic molecular crystal, patent 9-41934
 second-harmonic generation in nonlinear crystals, enhancement using self-locked 0.63 μm He-Ne lasers 9-22437
 second-harmonic generation with diffraction-limited and high-spectral-radiance Nd:glass lasers 9-41917
 selective up-conversion in LiNbO_3 of broad-band i.r. source for tunable coherent light generator 9-27341
 selective up-conversion in LiNbO_3 of broad-band i.r. source for tunable coherent light generator 9-27341
 self-focusing of intense beams in nonlinear dielect. 9-48092
 self-trapped light filaments in liquids, obs. 9-26102
 semiconductor, resonance mixing of laser freqs. 9-41931
 semiconductors, absorption and restriction of laser radiation 9-26685
 semiconductors, bound-electron and conduction-electron nonlinearities, CO_2 laser obs. at 10.6 μ 9-28650
 semiconductors, multiphoton electron-hole pair prod., CO_2 laser obs. at 10.6 μ 9-28650
 semiconductors, polar, Stokes scatt. phonon-cyclotron broadening 9-28701
 susceptibility, electrodynamic bond-charge calc. 9-28649
 synchronization, 1st and 2nd harmonic freq. phases in anisotropic crystal 9-26683
 TE-wave propagation in isotropic nonabsorbing media, steady-state self-channeling theory 9-37676
 triglycine sulphate, second harmonic generation and scatt. by domains ferroelec. domains 9-45010
 wave theory close to exact soln. 9-36256
 wave theory close to exact soln. 9-47844
 Ag_3AsS_3 , synthetic proustite, properties and uses 9-31065
 Ag_3AsS_3 (synthetic proustite), props., upon conversion of i.r. 9-26686
 Ar, second-harmonic generation, c.w., 2572 Å 9-27318
 AsO_4^{2-} , geometric contribution to polarizability 9-35611
 $\text{Ba}_{0.75}\text{Ca}_{0.25}\text{Nb}_{20}\text{O:Nd}^{3+}$, parametric oscils. at room-temp 9-43203
 $\text{Ba}_2\text{NaNb}_5\text{O}_{15}:\text{Pr}^{4+}, \text{Ir}^{4+}$, absorpt. at 5300 Å due to impurities 9-28651
 $\text{Ba}_2\text{NaNb}_5\text{O}_{15}$, single crystal and single domain, props. study 9-26687
 $\text{Ba}_2\text{NaNb}_5\text{O}_{15}$, tetragonal, nonlinearity and parametric emission, 300-600°C 9-43202
 $\text{Ba}_2\text{NaNb}_5\text{O}_{15}$ 0.53 μm source continuous, in 1.06 μm YAIG:Nd laser cavity 9-40362
 $\text{Ba}_2\text{NaNb}_5\text{O}_{15}$ parametric oscillation and freq. doubling 9-37677
 $\text{Bi}_2\text{Ge}_3\text{O}_{12}:\text{Nd}^{3+}$, parametric oscils. at room temp. 9-43203
 Ca, (4s4p) $^3\text{P}_1$ state, coherence narrowing and shift of optical double reson. signals 9-29923
 CdS, intense ruby laser radiation effects on optical props. 9-35652
 GaAs, third-order mixing of laser radiation 9-26688
 GaAs 2nd. order electro-opt. coefficient at mm. wave difference frequencies 9-31083
 GaAs filled waveguide, mm. wave generation by CO_2 laser line mixing 9-31083
 GaAs laser parallelepiped, 5-cm., interference of 10.6 μ coherent radiation 9-43896
 GaAs surface harmonic generation, meas. of Nd glass laser picosecond pulse width 9-34173
 n-Ge, microwave harmonic generation at low temp. 9-49236
 Ge, third-order mixing of laser radiation 9-26688
 $\alpha\text{-HIO}_3$ coeff. meas. relative to KH_2PO_4 , $\text{NH}_4\text{H}_2\text{PO}_4$ and LiNbO_3 9-26690
 $\alpha\text{-HIO}_3$ coefficients, relative meas., corrected values 9-33499
 He-Ne laser in mag. field, nonlinear effects in output intensity 9-45954
 In As, third-order mixing of laser radiation 9-26688

Nonlinear optics continued

- InSb, difference-freq. generation, far i.r., temp.-depend. phase matching 9-31066
 InSb, inelastic scatt. from Landau level electrons in mag. fields, CO_2 laser obs. at 10.6 μ 9-28650
 InSb, mixing, third order, mag. field dependence 9-26689
 KH_2PO_4 , double refraction on second harmonic in thin crystals. 9-31076
 KH_2PO_4 , frequency doubling in crystal, effect of lwers radiation parameters 9-45280
 KH_2PO_4 , second-harmonic generation with diffraction-limited and high-spectral-radiance Nd-glass laser system 9-41917
 KH_2PO_4 coeff. meas. relative to $\text{NH}_4\text{H}_2\text{PO}_4$, LiNbO_3 and $\alpha\text{-HIO}_3$ 9-26690
 of KH_2PO_4 coefficients, relative measurement, corrected values 9-33499
 LiIO_3 , Nd laser second harmonic production 9-26691
 LiIO_3 , strong second harmonic generation of 3470 Å after ruby laser irradi. 9-26692
 $\text{LiNbO}_3:\text{Ho}^{3+}$, second-harmonic radiation obs. at 77°K 9-43203
 $\text{LiNbO}_3:\text{Nd}^{3+}$, second-harmonic radiation and parametric oscils. at room temp. 9-43203
 $\text{LiNbO}_3:\text{Tm}^{3+}$, second-harmonic radiation obs. at 77°K 9-43203
 LiNbO_3 , second-harmonic generation with mode-selection and high-spectral-radiance Nd-glass laser system 9-41917
 LiNbO_3 , surface harmonic generation from non-linear polarisation 9-29427
 LiNbO_3 , surface radiation from nonlinear optical polarization, obs. 9-26682
 LiNbO_3 coeff. meas. relative to KH_2PO_4 , $\text{NH}_4\text{H}_2\text{PO}_4$ and $\alpha\text{-HIO}_3$ 9-26690
 LiNbO_3 coefficients, relative meas., corrected values 9-33499
 $\text{NH}_4\text{H}_2\text{PO}_4$ coeff. meas. relative to KH_2PO_4 , LiNbO_3 and $\alpha\text{-HIO}_3$ 9-26690
 of $\text{NH}_4\text{H}_2\text{PO}_4$ coefficients, relative meas., corrected values 9-33499
 NaClO_3 , second-harmonic generation, total refl. phenomena 9-47310
 NaClO_3 crystals, transmitted and reflected second harmonic beams 9-26693
 PO_4^{2-} , geometric contribution to polarizability 9-35611
 SF_6 gas, photon echoes, polarization props. 9-30351
 SO_4^{2-} , geometric contribution to polarizability 9-35611
 Si, third-order mixing of laser radiation 9-26688
 ZnSe, mixing of CO_2 and He-Ne laser radiation 9-26694
 ZnTe, ruby laser lines mixing for submillimeter-wave generation 9-24353

Novae

- see also Stars*
 3C10 (Tycho's supernova) distrib. of polarized radiation obs. 9-24804
 3C358 (Kepler's supernova) distrib. of polarized radiation obs. 9-24804
 Cassiopeia A distrib. of polarized radiation obs. 9-24804
 Cassiopeia A, supernova remnant, search for energetic γ emission 9-29055
 Centaurus XR-2, nova model 9-41646
 Crab nebula, distrib. of polarized radiation obs. 9-24804
 crab remnant, 32.5 cm. spectrum, map produced using lunar occultation 9-31519
 Delphini, 1967, opt. telescope obs. 9-40151
 dynamical models, studied by means of a time-dependent hydro-dynamic computer program 9-29023
 HB 21, supernova remnant, contour map from obs. at 2695 MHz 9-47643
 IC 443, supernova remnant, H α line obs, radial and expansion velocities, turbulence deduced 9-31518
 North Polar Spur as supernova remnant 9-24800
 Nova Herculis, CN band analysis for moment of maximum, Dec, 1934 9-31547
 supanova condensed remnants in Crab Nebula, rel. to continuous activity 9-40131
 supanova dust as possible source of interstellar absorpt. bands 9-43578
 supernova, white dwarf, calculation 9-29025
 supernova explosion, apparatus for detect possible photon pulse above atmosphere 9-24805
 supernova explosions, upper limit of neutrino mass from time of flight meas. 9-38466
 supernova explosions in ancient Chinese records, assoc. with pulsars 9-43592
 supernova in NGC 2713, 1968, spectrum 9-24801
 supernova of 1006, evidence of European obs. 9-45628
 supernova remnant, Cassiopeia A, search for energetic γ emission 9-29055
 supernova remnants, 16, emission between 408 and 2700 MHz, spectra derivation 9-31544
 supernovae, Chuadez and Wild, photometric and spectral obs. 9-41645
 supernovae, early optical emission and luminosity 9-43560
 supernovae, type I, evolution from explosive ignition of C in stars of intermediate mass 9-24799
 supernovae, type I, rel. to white dwarfs 9-43559
 supernovae exponential brightness decreases rel. to ^{254}Cf spontaneous decay 9-49559
 V368 Aquilae 1936 observations 9-31549
 Vulpeculae 1968 No.2 (Kohoutek), light curve and spectra 9-49558
 ^{254}Cf /spontaneous decay rel. to supernovae brightness decreases 9-49559

Novoids *see Novae***Nuclear acoustic resonance** *see Absorption/acoustic waves, ultrasonic;***Nuclear magnetic resonance and relaxation****Nuclear alignment** *see Nuclear polarization***Nuclear bombardment targets**

- butanol polarized proton target 9-44078
 gas cell, mylar window, description 9-22655
 gas cell, with built-in slit geometry 9-22653
 gas target cell for scattering chamber 9-25501
 gaseous, scatt. chamber, description and operation 9-22654
 polarization meas., reversal by fast passage 9-27581
 polarized, method of prod. 9-27444
 polarized, nuclear spin refrigerators 9-27579
 polarized, technology 9-27445
 polarized for low energy nuclear expts. 9-27580
 polarized for p-p and π -p scatt. 9-27523
 polyphenyl target, deuterated, obs. of $\text{D(d,n)}^3\text{H}$ reaction 9-25502
 recoil on nucleon bombardment, rel. to kinetic energy of nucleon 9-29790
 BE, neutron yields following bombard. by 20 MeV ^3He , 14 MeV p and 7.5 MeV d 9-38607
 Cs, p irradiated, recoil radioiodine recoils 9-49388

Nuclear bombardment targets continued

- H, liquid, π^- interaction pt. localization 9-27591
 H; liq., thin-walled target, p scatt., uniform solid angle available 9-32244
 H; liq., thin parallel walled target 9-40452
 H target with cooling system for use with high power e and γ beams at SLAC 9-29677
³He, gaseous, polarized prod. using optical pumping and electron exchange 9-27583
³He dense, polarized, prod. methods 9-27582
 Li, thin, sealed in Ni for low O₂ contamination, technique 9-29647
 Li metal, transference from evaporator to target can, technique 9-48215
 LiF, incident p, α ; cross section meas. for calibration 9-32242
 Mg, in 3 MeV Van de Graaff accelerator, vacuum evaporation prep., thickness determ. 9-29680
 Nd:LaMg (NO₃): p relaxation time of several hundred hours at 0.3-0.4°K rel. to prod. of polarized samples 9-29524

Nuclear decay schemes *see Radioactivity/decay schemes***Nuclear decay theory**

- see also Beta decay theory; Nucleus/theory*
 α decay rates for actinide region, using shell-model 9-42239

Nuclear emulsions *see Nuclear track emulsions***Nuclear energy level lifetimes** *see Nucleus/energy level transitions***Nuclear excitation**

- see also Mossbauer effect; Nucleus/energy levels*
¹²C interaction with ¹⁴C, resons. obs. assuming quasimol. states 9-22827
²³Si in ²¹P(p,p₀), mean level width, excitation function meas., $E_p=8-10$ MeV 9-25591
⁹²Mo, low lying states excited via analog resonances produced in p scatt. 9-48289
 actinide nuclei, level density depend. on excitation energy 9-22738
 analog resonance excitation, analysis of fragmentation by coupled optical eqns. with effective nonlocal potentials 9-38642
 analogue resonance fine structure, (p,p') (p,n) reaction 9-25560
 atomic, quantum treatment in book on approximation methods 9-40242
 β^- vibrational state identification 9-40469
 collective motion and moments of inertia 9-44122
 collective motion theory in pairing- plus-quadrupole model 9-34379
 collective phenomenological potential, Schrodinger eqn. determ. 9-29702
 collision matrix, unitary pole resonance and compound nucleus 9-40468
 compound level average total width 9-22706
 compound nucleus sequential decays, statistical interference effects 9-46187
 Coulomb, of fission fragments 9-44228
 Coulomb and nuc. excitation process, interference 9-27614
 deformation parameters and nuclear r.m.s. radius 9-46191
 deformation-energy surface from single-particle levels, validity 9-22707
 deformed nucleus, shell corrections and effects 9-38637
 E2 transitions in doubly even sd shell from 2⁺ state, α induced 9-27618
 effect, on (d,p) stripping reactions 9-44213
 electroexcitation, subsequent particle and photon decay 9-42183
 function for radiative nuclides prod. by deuteron induced reaction on Fe 9-38715
 heavy-ion scatt., excitation of collective modes in a dynamic classical model 9-44221
 isobaric analog resonances, Lane eqn. analysis, exact s-matrix determ. 9-29699
 isobaric analog resonances popular article 9-46189
 isobaric analogue resonance prod. in (p, n) reactions, 30-50 MeV, microscopic theory of optical model 9-27710
 isobaric analogue states, Lane-Robson model, mechanical analogue 9-29703
 isobaric analogue states, rel. to theory of nuclear reactions 9-29796
 isomer production by ⁶⁰Co irradiation, laboratory teaching expt. 9-48261
 lifetime of levels, meas. using differential converter 9-42148
 lifetime of state determ. by Mossbauer eff. 9-22709
 light nuclei, classification of excited states in translation invariant shell models 9-44129
 multiple, interaction near Coulomb barrier 9-44119
 neutron-deficient nuclei, 50 < Z, N < 82, β, γ deformations, depend. of g.s. 9-25559
 optical potential, spin dependent, Born approx. for deformed nuclei 9-22701
 phonon description in Nilsson model 9-27615
 pion absorpt., radiative, validity of soft pion theorems 9-36609
 quadrupole moment, electric, static, of excited states, determ. 9-47306
 reviews 9-36555
 rotational and internal motion coupling 9-44123
 shell-model calc., single-particle level order and matrix elements determ. 9-22705
 single particle in rare earth region, charge radii change calc. 9-36567
 some-closed nuclei, four-particle two-hole core excitation 9-40467
 spin polarization in odd deformed nuclei, mag. dipole interaction, states $K=1/2$ 9-32301
 volume collective, theory contrib. 9-40465
 (p,n), analogue resonance fine structure, (p,p') (p,n) reaction 9-25560
 γ , neutron capture, as a means of studying nuclear levels 9-36573
 γ angular correlation following multiple Coulomb excitation, quantum mechanical effects 9-44126
¹¹⁰Cd(p,p') inelastic scatt. at 55 MeV, vibr. states investigation 9-22723
¹¹⁰Ce(p,p), p ang. distrib. meas., n particle-hole states, levels and parity determ., $E_p=9.4-11.7$ MeV 9-29734
¹⁴⁰Cg, rotational and quasi-rotational spectra 9-44155
¹⁶⁰Dy, resonance parameters and energy levels 9-22731
¹⁶¹Dy, Coulomb excitation Mossbauer effect of 43.8 keV transition 9-36578
²⁵²Cf, spontaneous fission, fragments mean kinetic energy and deformation energy determ. 9-34468
¹⁵²Gd, resonance parameters and energy levels 9-22731
¹⁹²Pt, 22 resonances of spin and parity 1⁻, spectra obs. 9-48300
¹³²Xg, rotational and quasi-rotational spectra 9-44155
¹¹⁰Cd(p,p') inelastic scatt. at 55 MeV, vibr. states investigation 9-22723
¹³⁴Cs, levels excited in ¹³³Cs(n,p) reaction 9-44156
¹⁵⁴Gd, resonance parameters and energy levels 9-22731
¹²⁴Te, and even isotopes to 130, isobaric analogue resonances 9-44196
¹⁶³Ho, giant dipole resonance, examined by photoneutron cross section in polarized state 9-38673
¹²⁷Te, Coulomb excitation of levels 9-44152
²⁰⁵Tl, resonance and de-excitation levels 9-46215

Nuclear excitation continued

- ²³⁵U, thermal fission, fragments mean kinetic energy and deformation energy determ. 9-34468
¹¹⁶Cd(p,p') inelastic scatt. at 55 MeV, vibr. states investigation 9-22723
¹²⁷In, Coulomb excitation with ¹⁶O in range 35-55 MeV 9-44154
¹²⁷I, resonance fluorescence from 375 KeV level obs. 9-29730
¹³⁸Ba, rotational and quasi-rotational spectra 9-44155
¹⁵⁸Gd, resonance parameters and energy levels 9-22731
²⁰⁸Pb, isobaric analogue state with ²⁰⁸Bi, energy level comparison 9-34405
²⁰⁸Pb proton decay of ground state isobaric analogue populated by (p,n) reaction 9-42232
²⁰⁸Pb(p,p')²⁰⁸Pb, low-lying states studied in p scatt. at resonance energy for isobaric analog, resonance 9-48302
²³⁸U, π photoproduction and quasideuteron interaction involved in excitation leading to fission 9-38726
¹⁴⁹Sm, Coulomb excitation of levels 9-42226
²⁵Al, 2nd excited state, cross-over/cascade branching ratio determ. 9-27652
²⁷Al,n bombardment, level-excitation cross section meas., $E_n=14.6$ MeV 9-36606
³⁸Ar, quadrupole and octupole deformations on 2s-1d shell, nuclear energy depend. 9-38657
¹¹⁷B, muon capture, to ¹¹Be(g.s.) and ¹¹Be*(320 keV) 9-44189
¹¹⁷B, resonances obs. in ¹¹B(p,p) reaction 15-31.5 MeV 9-25610
¹¹Be one-particle levels, at inelastic e scatt. 9-42275
¹¹Be, isobaric-spin mixing deduced from ¹¹Li(p,p')¹¹Be* 9-48272
¹¹Be \rightarrow ¹¹Be + γ e.m. transition rate calc. for ¹¹Be nuclear wavefns. information 9-44189
⁷⁹Br, Coulomb excitation of close-lying levels 9-46200
⁸¹Br, Coulomb excitation of close-lying levels 9-46200
¹²C, 10.8 MeV level, E1(AT=0) electroexcitation, form factors 9-25564
¹²C, by p scatt., α decay obs., levels determ., $E_p=57$ MeV 9-27715
¹²C, mag. excitations by inelastic electron scatt. at 180° 9-32302
¹²C giant reson., collective correl. model with surface-delta-interaction 9-29746
¹²C giant resonance region, continuum model based on config. mixing 9-25566
¹³C, 3.08 MeV level E1-electroexcitation, investigation 9-44132
¹³C giant resonance, excited by e scatt., compared to Kamimura-Ikeda-Arima model 9-44131
⁴⁰Ca, dipole resonance, effect of quadrupole vibrations 9-34411
⁴⁰Ca, giant dipole resonances, surface effects 9-40474
⁴⁰Ca giant reson., collective correl. model with surface-delta-interaction 9-29746
¹²(C,p), 2+ excitations, spin-flip prob. and diff. scatt. cross section meas. DWBA analysis 9-42278
¹²(C,p,p')¹²C*, diff. cross section and polarization scatt., $E=4.43-22.3$ MeV 9-34441
⁵²Cr,n bombardment, level-excitation cross section meas., $E_n=14.6$ MeV 9-36606
 Cu (A=59, 61, 63, 65 and 67, up to 2 MeV 9-38679
⁵⁹Cu from ⁵⁸Ni(d,n), isobar analogue states obs., spectroscopic factors determ. 9-29837
⁶¹Cu from ⁶⁰Ni(d,n), isobar analogue states obs., spectroscopic factors determ. 9-29837
¹⁸F low-lying even-parity levels, E2 decay strengths, deformed states calc. 9-22718
¹⁹F, discovery of new T=3/2 isobaric analog state 9-48262
¹⁹F, odd-parity levels wave function computation, E1 transitions 9-22717
¹⁹F by α bombardment, excited state lifetime meas., $E_\alpha=5.5$ MeV 9-29741
¹⁹F pear-shaped nuclei collective model calc. 9-22734
⁵⁶Fe 1.15 keV resonance, n scatt., n partial wave odd parity determ. 9-36588
 Cf, compound nucleus temporarily formed in various reaction, ang. mom. eff. in break-up 9-29757
⁴He, ground-state props. and effects of centre-of-mass motion 9-48279
⁴He(p,p')H, 1-7=1 states in He obs. 9-32305
⁴Li, form factor for excitation of 3.56 MeV level by e scatt. oscillator cluster model calc. 9-46193
⁶Li, giant resonance spectra from e scatt. 9-29784
⁶Li analysis using the 2-d bound state model and resonating group method 9-38709
⁷Li, one-particle levels, at inelastic e scatt. 9-42275
⁷Li giant resonance spectra from e scatt. obs. 9-29784
²³Mg discovery of new T=3/2 isobaric analog state 9-48262
²⁴Mg, Coulomb, at 61,57 and 52 MeV 9-48282
²⁴Mg, γ deformation, evidence from p scatt. 9-42230
²⁴Mg first excited state, static quadrupole moment obs. 9-29745
 Mn, by inelastic n scatt. 9-44145
 Mo isotopes, n resonances assigned 9-36574
¹³N E1 transitions bet. resonant states near 3.51 MeV(T=1/2-) and 2.37 MeV(1/2+) levels 9-27621
¹³Ne discovery of new T=3/2 isobaric analog state 9-48262
²⁰Ne, from (⁶Li,d) and (⁷Li,t) reactions, excitation of rotational bands 9-44223
²⁰Ne, hexadecapole deformation investigated by p scatt. 9-42230
²⁰Ne, wave function computation from g.s. value 9-22717
²⁰Ne from ¹⁹F(d,n), 10-14 MeV excitation states, C₂ factors determ., $E_d=5.1$ MeV 9-27744
⁵⁸Ni, electroexcitation of low-energy states 9-44147
⁵⁸Ni, excitation of giant resonance by means of high energy electrons 9-27665
⁵⁸Ni proton spin flip probability in ⁵⁸Ni(p,p')⁵⁸Ni(1.45 MeV) react. 9-27718
⁶⁰Ni, electroexcitation of low-energy collective states 9-44147
⁶⁰Ni, excitation of giant resonance by means of high energy electrons 9-27665
⁶²Ni, from ²⁸Si bombard, meas. of quadrupole moment of J $\pi=2^+$ state 9-44141
⁶⁴Ni, electroexcitation of low-energy collective states 9-44147
⁶⁴Ni, excitation of giant resonance by means of high energy electrons 9-27665
¹⁶O, ¹⁶O scatt. near Coulomb barrier, excitation functions and ang. distrib. at 13 MeV c.m. energy 9-38722
¹⁶O, 7.12 MeV level, E1(AT=0) electroexcitation, form factors 9-25564
¹⁶O, by γ , e; Goldhaber-Teller model, isospin and spin-isospin modes coupling, structure 9-34429

Nuclear excitation continued

- ¹⁴O, from (⁴Li,d) and (⁷Li,t) reactions, excitation of rotational bands 9-44223
¹⁶O, giant dipole resonances, nuclear surface effects 9-40474
¹⁶O, n bombardment, level-excitation cross section meas., $E_n=14.6$ MeV 9-36606
¹⁶O continuum shell model calc. of resonant particle-hole states 9-48276
¹⁶O giant reson., separability of residual two body interaction 9-42170
¹⁶O giant reson., collective correl. model with surface-delta-interaction 9-29746
¹⁶O giant resonance, quadrupole, evidence from ¹⁶O(α ,p)¹⁵N 9-44133
¹⁶O giant resonance region, continuum model based on config. mixing 9-25566
¹⁶O low-lying even-parity levels, E2 decay strengths, deformed states calc. 9-22718
¹⁸O(p, α ,^{1,2,3})¹⁸O, excitation functions, 3.2 to 5.4 MeV 9-22785
¹⁸O(p,p,¹)¹⁸O, excitation functions, 3.2 to 5.4 MeV 9-22785
⁸⁵Rb, Coulomb excitation of close-lying levels 9-46200
⁸⁵Sr giant reson., collective correl. model with surface-delta-interaction 9-29746
⁷⁷Se, Coulomb excitation of close-lying levels 9-46200
²⁸Si, evidence for hexadecapole deformation from p scatt. 9-42230
²⁸Si giant reson., collective correl. model with surface-delta-interaction 9-29746
²⁸Si projectiles incident on ⁶²Ni target, coulomb excitation, quadrupole moments determ. 9-44141
³⁰Si, quadrupole and octupole deformations on 2s-1d shell, nuclear energy depend. 9-38657
⁸⁹Sr isobaric analog resonance formation, comparison of coupled-channel formalism and R-matrix 9-44201
⁵¹T isobaric analogue resonances obs. in ⁵¹V formed as compound nucleus in ⁵⁰Ti(p,p)⁵⁰Ti 9-46199
⁹²Tc, isobaric analogue states, γ transitions to low lying states 9-29760
⁹²V, by inelastic n scatt. 9-44145
⁶⁸Zn to ⁶⁸Zn even isotopes, n bombardment, level-excitation cross section meas., $E_n=14.6$ MeV 9-36606
⁹⁶Zr(p,p)⁹⁶Zr, excitation function meas., isospin effects obs. 9-36603
⁹⁶Zr(p,p)⁹⁶Zr, excitation function meas., isospin effects obs. 9-36603

Nuclear explosions see *Explosions/nuclear***Nuclear field theory** see *Field theory, quantum***Nuclear fission**

- see also *Explosions/nuclear*; *Nuclear reactors, fission*
 asymmetric mass distrib., dynamic model 9-32366
 barrier structure and even-odd differences 9-27763
 barriers with two maxima, penetrability and energy depend. 9-32365
 by bremsstrahlung γ -quanta interaction with complex nucleus 9-22773
 bremsstrahlung-induced in heavy elements, γ photoproduction not necessary for cross-section 9-38726
 cross section energy depend., fluctuations of fission and n widths of scatt. 9-29843
 cross-section, new technique for meas. 9-44224
 delayed, probability at nucleon stability nuclear region boundaries 9-29842
 delayed events due to isomeric fission production by ³He and ⁴He beams 9-44227
 double barrier penetration 9-27607
 dynamical barrier, statistical model calc. 9-22830
 electron-induced in heavy elements, π photoproduction not necessary for cross-section 9-38726
 ellipsoidal drop, uniformly charged, γ -vibrational characteristics from hydrodynamical model 9-42313
 fission chamber for rapid calc. of ²³⁸U/²³⁵U ratio in fission fragments 9-22661
 fragmentation characteristics, effect of phase-space volume 9-27765
 Hamiltonian, single particle, self-consistent, fission proc. calc. 9-27653
 in meteorites, spontaneous, of superheavy elements 9-41682
 neutrons, prompt, average number emitted, fission delayed γ -rays effect 9-25664
 nuclear charge distribution in low-energy fission of thorium elements 9-48356
 optimization of activation and counting times 9-25594
 optimization of n cross-section data adjustments 9-29866
 phase-space integrals and distributions, methods of calculation 9-25660
 prompt n lifetime and temp. coeff. in Fuchs' model 9-27785
 quark-induced, quark capture and de-excitation obs., method to limit abund. 9-25491
 quasi-stationary states, role of, and the fission cross-section curve 9-27764
 reactor fuels, irradi., burnup, history, U and Pu content, nondestructive assay methods 9-25676
 single-particle theory 9-48357
 spontaneous, superheavy nuclei, stability 9-29845
 superheavy nuclei, limits of stability 9-42314
 symmetrical, geometric model, effective mass calc. 9-29844
 theory and props. introduced in book on atomic engineering 9-34368
 thorium elements, low energy fission, distrib. of nuclear charge 9-48356
 tripartite, induced by protons in range 600 MeV to 20 GeV 9-36615
 n spectrum, expl. determ. of number, 0/6 to 24 MeV 9-22828
²⁴¹Am, neutron fission analysis of odd-even nuclei 9-27770
¹⁹¹Ir, He ion induced, excitation func. and cross section meas. $E=42.2$ MeV 9-29857
²¹⁹Pa, neutron fission analysis of odd-even nuclei 9-27770
²⁴¹Pu fission cross-section for $E_n=1$ to 25 keV 9-29849
²⁴¹Pu thermal and fast n induced, yield 9-22836
²⁴¹Pu(d,p)²⁴²Pu, fission prob. depend. on excitation energy, resonance eff. 9-27773
²⁴²Am spontaneously fissioning, prod. by thermal neutron with ²⁴¹Am 9-44225
²⁵²Cf, fast n dosimetry meas. 9-38135
²⁵²Cf, spontaneous, K X-rays emission times and yields from fragments 9-38724
²⁵²Cf, spontaneous fission, fragments mean kinetic energy and deformation energy determ. 9-34468
²⁴²Pu, spontaneous, n spectra meas. 9-29859
²³²Th, by 20-85 MeV protons, yields and charge dispersion obs. 9-32368
²³²Th, n (14 MeV) induced, α decay prob., c.f. with ²³⁵U, n_{th} induced 9-29847
²³²Th, ternary, induced by 2.9 MeV neutrons, mechanism 9-44226

Nuclear fission continued

- ²³²Th by 9.5, 11.3 MeV p₂ and 11.5 MeV d, prods. Z distrib., obs. 9-29852
²³²Th fast n induced, yield 9-22836
²³²Th induced by 14.7 MeV neutron bombard. 9-27766
²³²Th n induced, cross section structure determ., $E_n=1-2.2$ MeV 9-27768
²³²Th(Ar,f), $E=230-380$ MeV, meas. ratio ternary to binary fission on 2π forward geometry 9-29854
²³²Th(γ ,f), mono-energetic γ -rays, 12 different energies, cross-sections 9-27771
¹⁹³Ir, He ion induced, excitation func. and cross section meas. $E=42.2$ MeV 9-29857
²⁴⁴Cm, spontaneous, n spectra meas. 9-29859
²⁴⁴Pu, Xe retention in meteoritic whitlockite, ²⁴⁴Pu/²³⁸U ratio 9-34415
¹⁵⁶Sm cross section, electron and bremsstrahlung induced, 60-1000 MeV 9-38726
¹⁷⁴Yb cross section, electron and bremsstrahlung induced, 60-1000 MeV 9-38726
¹⁸⁵Re, separated isotope, by 40 MeV α -particles angular distributions of fragments 9-40525
¹⁸⁵Re, separated isotope, by 40 MeV α -particles angular distributions of fragments 9-36617
¹⁹⁷Au, isotopically pure nuclei, by 40 MeV α -particles angular distributions of fragments 9-36617
¹⁹⁷Au, isotopically pure nuclei, by 40 Me α -particle angular distributions of fragments 9-40525
¹⁹⁷Au, isotopically pure nuclei, by 40 Me α -particles angular distributions of fragments 9-40525
¹⁹⁷Au, photofission, mass and energy distrib. of fragments 9-48362
¹⁹⁷Au(Ar,f), $E=230-380$ MeV, meas. ratio ternary to binary fission in 2π forward geometry 9-29854
²³⁷Np, n (14 MeV) induced, α decay prob., c.f. with ²³⁵U, n_{th} induced 9-29847
²³⁷Np, neutron fission analysis of odd-even nuclei 9-27770
¹⁸⁷Re, separated isotope, by 40 MeV α -particles angular distributions of fragments 9-40525
¹⁸⁷Re, separated isotope, by 40 MeV α -particles angular distributions of fragments 9-36617
²⁰⁸Pb cross section, electron and bremsstrahlung induced, 60-1000 MeV 9-38726
²³⁸Pu, n induced, fragment ang. distrib. meas., $E_n=0.06-7.20$ MeV 9-36618
²³⁸U, binary and ternary fission, ³He, and ⁴He induced 9-46247
²⁰⁹Bi, photofission, mass and energy distrib. of fragments 9-48362
²⁰⁹Bi cross section, electron and bremsstrahlung induced, 60-1000 MeV 9-38726
²⁰⁹Bi(Ar,f), $E=230-380$ MeV, meas. ratio ternary to binary fission in 2π forward geometry 9-29854
²³⁹Pu, cross-section near 83 eV, multilevel anal. 9-22833
²³⁹Pu, n induced, n spectra meas. 9-29859
²³⁹Pu, n induced, relative yield, energy spectra of light nuclei meas. 9-29846
²³⁹Pu, product activities and power output 9-22838
²³⁹Pu, slow-n induced, cross section correlation anal. 9-40522
²³⁹Pu, n_{th} induced, fragment nuclear charge distrib. calc. method 9-32371
²³⁹Pu capture-to-fission ratio for $E_n=20$ to 600 keV 9-32351
²³⁹Pu cross section and capture:fission ratio, 5 eV-23 keV 9-22831
²³⁹Pu fission cross-section for $E_n=1$ to 25 keV 9-29849
²³⁹Pu infinite dilution reson. integrals, multilevel effects 9-27767
²³⁹Pu thermal and fast n induced, yield 9-22836
²³⁹Pu(d,p)²⁴⁰Pu, fission prob. depend. on excitation energy, resonance eff. 9-27773
²³⁹Pu(n, f), delayed γ spectra meas., 2-80 μ sec, yield determ. 9-27769
²³⁹Pu(t,d), fission-fragment correlations 9-42315
 Ag, p induced, high energy cross section determ. by mica track detector 9-40523
 Ag photofission, 1 to 6 GeV photons 9-29855
 Au, by 40-140 MeV protons, cross-sections, inc. with energy 9-25663
 Au, p induced, high energy cross section determ. by mica track detector 9-40523
 BeO rapid fission factor determ. 9-34469
 Bi, by 40-140 MeV protons, cross-sections, inc. with energy 9-25663
 Bi, cross-section, induced by 600 MeV protons 9-36616
 Bi, p induced, high energy cross section determ. by mica track detector 9-40523
 Bi, tripartite, induced by protons in range 600 MeV to 20 GeV 9-36615
 Bi photofission, 1 to 6 GeV photons 9-29855
 Kr isotopes, search for n prod. 9-40527
 Pt, by 40-140 MeV protons, cross-sections, inc. with energy 9-25663
 Pt, Ir, Re, isotopes natural mixture, by MeV α particles angular distributions of fragments 9-40525
 Pt, Ir, Re, isotopes natural mixture, by 40 MeV α -particles angular distributions of fragments 9-36617
 Th, cross-section, induced by 600 MeV protons 9-36616
 Th, tripartite, induced by protons in range 600 MeV to 20 GeV 9-36615
 Th by γ , 200-1150 MeV 9-29851
 Th photofission, 1 to 6 GeV photons 9-29855
 Xe isotopes, search for n prod. 9-40527

products

- charge particle accompanied fission rel. to theoretical explanation for fission 9-32370
 containment after reactor accident 9-40529
 fragment charge dispersion excitation energy depend. for ²³⁸U(²⁰Ne,f) 9-29856
 fragment yields in terms of statistical model 9-46246
 fragments, Coulomb excitation 9-44228
 gas, radioactive, in-pile release rate determ. by mixing in He sweep-gas 9-25679
 gaussian curve for mass chains, tested 9-38728
 neutron energy spectrum, meas. by time of flight spectrometer 9-48216
 non-gaseous, escape behaviour of products recoiled into graphite 9-26299
 product activities and power output, influence of different props. of fissile nuclide and products 9-22838
 quark-content, method to limit abund. 9-25491
 shell effect on fragment deformation energy depend. on mass 9-32364
 short-lived, independent yield and nuclidic mass, on-line mass separator meas. 9-40530
 water vapour radiolysis by fission fragments, obs. 9-33684

Nuclear fission continued
products continued

- X-ray, K, emission after ^{252}Cf spontaneous fission, yield and emission time meas. 9-38724
- ^{92}Nb thermostable oxide diffusion in $\alpha\text{-Al}_2\text{O}_3$, obs. 9-30623
- /h, 9.5, 11.3 MeV p₂ and 11.5 MeV d induced, Z distrib., obs. 9-29852
- ^{235}U , β -decay kinetic energy obs. 9-22753
- ^{140}Ba yields for ^{235}U , ^{238}U fast and thermal fission, obs. 9-46248
- ^{141}Ce , thermostable oxide diffusion in $\alpha\text{-Al}_2\text{O}_3$, obs. 9-30623
- ^{131}I in L54M soln. reactor gas atm., obs. 9-46249
- ^{112}Ag from ^{235}U , n induced yield meas. 9-29848
- ^{252}Cf , energetics and mass distribution of fragments 9-48360
- ^{252}Cf , obs. of K-X-rays emitted in association with long-range α , rel. to emission products 9-38727
- ^{252}Cf fission, Xe and Kr yield examined on Al foil 9-40526
- ^{252}Cf spontaneous fission, n energy distrib. meas. 9-34355
- ^{232}Th , reactor-neutron fission yields 9-22837
- ^{232}Th photofission fragments, cross sections and ang. distrib., and struct. of fission barrier 9-48363
- ^{252}Th 14.8 MeV n-induced, study of low yield products 9-48361
- ^{143}Ba , ^{144}Ba gaussian curve for mass chains, tested from thermal induced neutron fission of ^{235}U 9-38728
- ^{153}Sm , thermostable oxide diffusion in $\alpha\text{-Al}_2\text{O}_3$, obs. 9-30623
- ^{115}Cd , from p induced ^{238}U fission, isomer yield ratio of $^{115\text{m}}\text{Cd}$ and $^{115\text{g}}\text{Cd}$ 9-34472
- ^{115}Pd from ^{235}U , n induced, yield meas. 9-29848
- ^{235}U neutron resonances, changes in kinetic energy 9-40521
- ^{206}Pb , ^4He induced, fragment ang. distrib. meas., pairing eff. at ^{210}Po saddle pt. 9-27772
- ^{157}Am , photofission, mass and energy distrib. of fragments 9-48362
- ^{207}Pb , ^4He induced, fragment ang. distrib. meas., pairing eff. at ^{211}Po saddle pt. 9-27772
- ^{147}Pm thermostable oxide diffusion in $\alpha\text{-Al}_2\text{O}_3$, obs. 9-30623
- ^{238}Pu , ^{240}Pu and ^{242}Pu photofission fragments, cross sections and ang. distrib., and struct. of fission barrier 9-48363
- ^{238}U , 9.5, 11.3 MeV p and 11.5 MeV d induced, Z distrib., obs. 9-29853
- ^{238}U , ang. distrib. of fragments, shadow patterns 9-40524
- ^{238}U , photofission, mass and energy distrib. of fragments 9-48362
- ^{238}U photofission fragments, cross sections and ang. distrib., and struct. of fission barrier 9-48363
- ^{138}Xe , 15 min., γ -ray obs. and spectra, ^{138}Cs levels 9-34471
- ^{209}Bi , photofission, mass and energy distrib. of fragments 9-48362
- Al film, fragments, prod. of secondary electrons, energy spectrum 9-49177
- Ba, gaseous, short-lived, mass-separated, half-life determ. 9-22765
- Be, from ^{235}U thermal n. fission, energy spectra and relative yields 9-29858
- Cs gaseous, short-lived, mass-separated, half-life determ. 9-22765
- ^{63}Cu , ^{238}U p induced fission cumulative form. yield, 20-85 MeV 9-29850
- ^{64}Ga , ^{238}U p induced fission yield, 20-85 MeV 9-29850
- ^{70}Ga , ^{238}U p induced fission yield, 20-85 MeV 9-29850
- ^{72}Ga , ^{238}U p induced fission yield, 20-85 MeV 9-29850
- ^{73}Ga , ^{238}U p induced fission cumulative form. yield, 20-85 MeV 9-29850
- ^3H from n-induced ^{233}U fission, yield and energy distrib. meas. 9-22839
- ^3He from n-induced ^{233}U fission, yield and energy distrib. meas. 9-22839
- ^4He from n-induced ^{233}U fission, yield and energy distrib. meas. 9-22839
- ^4He from n-induced ^{233}U fission, yield and energy distrib. meas. 9-22839
- Kr gaseous, short-lived, mass-separated, half-life determ. 9-22765
- Li, from ^{235}U thermal n. fission, energy spectra and relative yields 9-29858
- ^{60}Ni , ^{238}U p induced fission cumulative form. yield, 20-85 MeV 9-29850
- Rb gaseous, short-lived, mass-separated, half-life determ. 9-22765
- Sc in nuclear wastes, recovery by adsorpt-elution processes on TiPO₄ 9-24593
- Sn stable isotopes from fast n ^{233}U fission, relative yields, tandem mass spectrometer 9-38725
- Sr gaseous, short-lived, mass-separated, mass-separated, half-life determ. 9-22765
- U-Pu oxide fuel irradiated, solid fission product behaviour 9-41118
- U, fission gas induced swelling at high temp., effect of externally appl. hydrostatic press. 9-38735
- U sputtered in Al, fragments ejecting U, evidence of clusters and knock-ons 9-34489
- in UO_2 , gas bubbles irradi. stability, obs. 9-37187
- in UO_2 , gases, bubbles mobility rel. to release, obs. 9-37190
- Xe diffusion from UC , UO_2 , obs. 9-37214
- Xe gaseous, short-lived, mass-separated, half-life determ. 9-22765
- Xe isotopes, excess n-rich, in meteoritic whitlockite containing excess fission tracks 9-34415
- ^{72}Zn , ^{238}U p induced fission cumulative form. yield, 20-85 MeV 9-29850

uranium

- coupled cylinders, prompt n decay obs. 9-29881
- cross-section, induced by 600 MeV protons 9-36616
- natural uranium, thermal neutron conversion ratio 9-44231
- photofission, 1 to 6 GeV photons 9-29855
- solution, enriched, with natural boron poison, critical obs. 9-34498
- swelling induced by fission gas, effect of hydrostatic press. 0-1000 bar 9-38735
- tripartite, induced by protons in range 600 MeV to 20 GeV 9-36615
- p, 200-1150 MeV 9-29851
- p induced, 440 MeV, recoil props. of 20 nuclides 9-48358
- p induced, high energy cross section determ. by mica track detector 9-40523
- ^{233}U , n (14 MeV) induced, α decay prob., c.f. with ^{235}U , n⁹ induced 9-29847
- ^{233}U , n induced ^{112}Ag , ^{115}Pd yield meas 9-29848
- ^{233}U , n induced; Sn stable isotopes relative yields, tandem mass spectrometer 9-38725
- ^{233}U , thermal and fast n induced, yield 9-22836
- ^{233}U , n_{th} induced, fragment nuclear charge distrib. calc. method 9-32371
- ^{233}U fission cross-section for $E_n=1$ to 25 keV 9-29849
- ^{233}U (d,p) ^{234}U , fission prob. depend. on excitation energy, resonance eff. 9-27773
- ^{233}U (t,d), fission-fragment angular correlations 9-42315
- ^{235}U , 14.8 MeV n-induced, study of low yield products 9-48361
- ^{235}U , charge distribution gaussian in mass chain 9-38728
- ^{235}U , cross-section for n energies 6 eV to 3eV, study of resonances 9-22832
- ^{235}U , fast and thermal, ^{140}Ba yields, obs. 9-46248
- ^{235}U , n induced, ^{112}Ag , ^{115}Pd yield meas 9-29848

Nuclear fission continued
uranium continued

- ^{235}U , photo-induced; yield, K.E. and mass distrib. meas., $E_\gamma < 25$ MeV 9-32369
- ^{235}U , product activities and power output 9-22838
- ^{235}U , shielding factors, energy-dependent from transmission experiments on foils 9-25662
- ^{235}U , thermal fission, fragments mean kinetic energy and deformation energy determ. 9-34468
- ^{235}U , thermal n. function, energy spectra and relative yields of Li and Be nuclei 9-29858
- ^{235}U , n_{th} induced, asymmetric mass distrib., dynamic model 9-32366
- ^{235}U , n_{th} induced, fragment nuclear charge distrib. calc. method 9-32371
- ^{235}U cross section and capture:fission ratio, 0.15 eV-30 keV 9-22831
- ^{235}U fission cross-section, Doppler broadening, numerical treatment 9-32367
- ^{235}U fission cross-section for $E_n=1$ to 25 keV 9-29849
- ^{235}U in rod-cluster geometry, ratio of fission rate to that of ^{238}U 9-25661
- ^{235}U n induced cross section resonance parameters determ., $E_n=17$ -70 eV 9-22834
- ^{235}U neutron resonances, changes in fragment kinetic energy 9-40521
- ^{235}U thermal and fast n induced, yield 9-22836
- ^{235}U (d,p) ^{236}U , fission prob. depend. on excitation energy, resonance eff. 9-27773
- ^{235}U (n, \bar{n}), delayed γ , spectra meas., 2-80 μsec , yield determ. 9-27769
- ^{235}U (n, α) ^{232}Th , α particle spectrum, meas. of low energy part 9-22800
- ^{235}U (t,d), fission-fragment angular correlations 9-42315
- ^{238}U , ang. distrib. of fragments, shadow patterns 9-40524
- ^{238}U , fast and thermal, ^{140}Ba yields, obs. 9-46248
- ^{238}U , heavy ion induced, fragment charge, isotope distrib. meas. 9-29856
- ^{238}U , n-induced, light particle yield and energy distrib. meas. 9-22839
- ^{238}U , n (14 MeV) induced, α decay prob., c.f. with ^{235}U , n_{th} induced 9-29847
- ^{238}U , neutron induced 1.3, 1.4, 1.5, 2.9, 5.3, 6.9 MeV statistical model analysis 9-22835
- ^{238}U , p induced, $66 < A < 73$ nuclides yields, 20-85 MeV 9-29850
- ^{238}U , p induced, isomer yield ratio of $^{115\text{m}}\text{Cd}$ and $^{115\text{g}}\text{Cd}$ 9-34472
- ^{238}U , photofission, mass and energy distrib. of fragments 9-48362
- ^{238}U , π photoproduction and quasideuteron interaction involved in excitation leading to fission 9-38726
- ^{238}U , ternary, induced by 2.9 MeV neutrons, mechanism 9-44226
- ^{238}U (^{20}Ne , \bar{n}), fragment charge dispersion excitation energy depend. 9-29856
- ^{238}U by 9.5, 11.3 MeV p and 11.5 MeV d, prods. Z distrib., obs. 9-29853
- ^{238}U fast n induced, yield 9-22836
- ^{238}U in rod-cluster geometry, ratio of fission rate to that of ^{235}U 9-25661
- ^{238}U induced by 14.7 MeV neutron bombard. 9-27766
- ^{238}U photofission fragments asymmetry and anisotropy 9-34470
- ^{238}U photofission fragments, cross sections and ang. distrib., and struct. of fission barrier 9-48363
- ^{238}U proton induced, 40-85 MeV, recoil props. of ^{60}Ni , ^{67}Cu and ^{72}Zn 9-48359
- ^{238}U (Ar,f), $E=230$ -380 MeV, meas. ratio ternary to binary fission on 2π forward geometry 9-29854
- in Al, sputtered, ejection by fission fragments, evidence of clusters and knock-ons 9-34489
- U, natural-D₂O lattices, fast fission ratio, obs. 9-32378
- UC, fission gas swelling, bubble nucleation time and temp. depend. 9-38736

Nuclear fission reactors see *Nuclear reactors, fission*
Nuclear forces

- see also *Field theory, quantum/meson field*
- ^{44}Ar He binding energies by Hartree-Fock model 9-42209
- ^{210}Bi , low-energy spectra from shell model calc., vel.-depend. effective N-N potential 9-40480
- binding energies of open shell nuclei, from approx. HF soln., Yale and nonlocal pots. calcs. 9-44114
- binding energy, correction term in shell model 9-27608
- binding energy, modified Goldstone linked cluster expansion, convergence 9-38640
- binding energy and n and p half-density radii determ. 9-27606
- binding energy and nuclear radii correlation for light nuclei 9-44111
- binding energy calc. by hole line expansion method, 3-body contrib. 9-34377
- binding energy calc. using oscillatory wave functions 9-29696
- binding energy curve, maximum using variant of Weissacher-Bethe formula 9-46186
- cluster model, α -particles, role of Pauli principle 9-32297
- collective mode of high momentum transfer field 9-36558
- coulomb forces in the three-body problem, Faddeev-Lovelace modified eqns. 9-42168
- Coulomb interaction between states of definite isospin, average value of matrix elements calc. 9-36560
- deformed shell-model potential, P₊-dependent, deformation energy depend. 9-32295
- density matrix change on adding large number of particles to nucleus 9-34373
- effective interaction, energy dependence of mass operator 9-42178
- effective-interaction formulation of bound and continuum shell-model calc. 9-25556
- e.m. interaction between nucleons, rel. to volume collective excitations, theory contrib. 9-40465
- Faddeev eqn. for N-term separable potential 9-22698
- Faddeev eqn. soln., 3 spinless bosons with local Yukawa potential, binding energy comparison 9-36559
- four-body correlations, reduction of effective interaction due to Pauli principle 9-34374
- fractional parentage coeff., j -coupling states of p and n, shell theory 9-34376
- Gammel-Brueckner potential, 3-particle nuclei, E1 integrated photoabsorption cross section calc. 9-29716
- group-theoretical decomposition of effective interactions in sd-shell 9-42172
- Hamada-Johnston potential used to calc. coupling between single-particle and vibrational states 9-27648
- intranuclear cascades, conservation laws in elementary events 9-32290
- isobaric-spin potential simplified calc. method 9-44109
- K₁ X-ray energies, π , μ , meas. for elements Z=3 to Z=6, including nuclear force shifts 9-27803
- Lippmann-Schwinger eqn., 3-body, kernel props. 9-34371

Nuclear forces continued

- Majorana exchange forces and photodisintegration in three- particle nuclei 9-42270
- many body problems with strong forces, extension of Jastrow's method 9-43763
- meson-N coupled systems soluble model 9-34277
- models, review 9-44108
- multiple excitation near Coulomb barrier for interactions 9-44119
- neutron single particle levels in Woods- Saxon pot. 9-42171
- nonlocal potentials, sum rules 9-42167
- nucleon-nucleon scatt., phase shift analysis, 400 MeV- >10 GeV 9-40439
- open shell nuclei, binding energy calc. using projection technique 9-44114
- optical model neutron potential energy depend., 0-200 MeV 9-29687
- optical potentials in n strength function calc. 9-27612
- orbital rearrangement is sd-shell nuclei, single particle energy 9-29697
- pairing correlations, $T_3=1$, absence in 2s-1d shell intrinsic g.s., theory 9-22697
- pairing effects and n-p-surface delta interact. 9-29690
- pairing in LST scheme, exact soln. 9-29686
- potential, double barrier, parabolic, penetration formula 9-27607
- potential, hard-core, 3-body problem, Lippmann-Schwinger scatt. theory 9-29689
- potential, obs. of p.p. bremsstrahlung 65 MeV, various angles 9-40444
- potential, spin dependent optical. Born approx. for deformed nuclei 9-22701
- potentials, BCS functions rel. to n strength function calc. 9-27612
- potentials, separable, inversion problem 9-22696
- potentials, single particles from projected wave functions with/without charge term rel. to n strength functions 9-27612
- real and effective interactions, deformation, problems reviewed 9-36556
- real and effective interactions, deformation, problems reviewed 9-46185
- real central potential, radius parameter; energy dependence 9-48333
- repulsive core, review 9-40464
- residual, two body interactions, separability 9-42170
- residual interaction and conservation laws 9-42175
- review of modern models 9-44108
- sd-shell nuclei, single particle orbital rearrangement energy 9-29697
- separable-potential model of N-N interaction, partial waves, $J=4$, energy 0-400 MeV 9-29688
- single particle energies deduced from quasi-free scatt. 9-44113
- single particle energies deduced from quasi-free scatt. 9-36563
- space-parity violation in nuclear force, γ transitions, enhancement of admixture coeff. 9-36589
- spherical nuclei, schematic forces and number-conserving approach 9-44110
- spherical nuclei, shell model, residual interaction, spurious states soln. 9-32292
- spin-orbit interaction 9-22700
- spin-orbit potential, Thomas form, loss of surface-peaked character 9-48333
- square well potential, ellipsoidal, magic numbers 9-29694
- symmetry energy parameter calcs. for 35 heavy deformed nuclei 9-44109
- Tabakin interaction applic. to sd shell, nuclei $36 \leq A \leq 39$ 9-29750
- tensor forces in residual interaction of nucleous, use of shell model 9-42173
- tensor potential in optical model for d scatt. 9-22812
- tensorial interactions, effective, from nucleon-nucleon phase-shifts 9-29684
- three-nucleon problem using hard-core interaction 9-42174
- three-particle nuclei, photodisintegration and Majorana exchange forces 9-42270
- two body, in nuclei, and gauge invariance 9-42169
- two-body interaction in common harmonic- oscillator potential with hard core 9-38635
- two-body potential, stability condition 9-48249
- two-nucleon potential, non-relativistic 9-42166
- two-nucleon potential, non-relativistic 9-38634
- unified many-body theory of DWBA and optical model 9-32288
- velocity-dependent N-nuclear pot. used to calc. single-particle energy levels 9-48248
- Weizacher-Bethe formula for reproducing maximum binding energy curve 9-46186
- α - α interaction effective potential, repulsive core and Pauli principle 9-34375
- α four-body correlation and reduced width in heavy nuclei 9-34410
- N-N interpretation of short-range correlation 9-32291
- N-N scatt. phase shift, velocity depend. potential 9-32293
- n-p realistic local potential, hypertriton structure determ. 9-42208
- n binding energy rel. to energy dependence for level density of nuclei $A=30-65$ in Fermi gas model 9-27657
- N scatt. cross sections, narrow resonances from unbound states 9-40463
- NN correlations, π absorption and high energy scatt. expts. 9-36562
- NN interaction reviewed 9-36555
- NN phase shifts and mixing parameters, 0-400 MeV, separable potential fit 9-44048
- NN potential, Green's velocity dependent, inability to fit ^{210}Bi , ^{210}Pb , ^{210}Po 9-44166
- pp P wave phase shifts at low energies 9-48208
- pp scatt. triple, at 1.9 GeV obs., neither vector nor scalar meson exchange sufficient, spin important 9-38573
- π - nucleus scatt., π N chiral algebra and PCAC applic., sum rules determ. 9-42294
- π N interaction in nucleus, Foldy transformation 9-34303
- ^{210}Bi Green's velocity-dependent potential tested 9-44166
- ^{210}Pb , Green's velocity-dependent pot., shell model 9-44166
- ^{210}Pb , low-energy spectra from shell model calc., vel.-depend effective N-N potential 9-40480
- ^{210}Pb spectra calc., realistic interaction, eff. of Woods-Saxon wave function 9-38653
- ^{210}Po Green's velocity-dependent pot., shell model 9-44166
- ^{212}Th , μ -atomic h.f.s. in K, L and M lines, nuclear charge distrib. 9-38678
- ^{206}Pb spectra calc., realistic interaction, eff. of Woods-Saxon wave function 9-38653
- ^{116}Sn , $J=0^+$ states, pairing force and surface delta interaction, seniority 9-29756
- ^{117}Sn , p-n interac., n hole energy Z depend. 9-29732
- ^{208}Pb Hartree fock calc. in coord. space 9-34407
- ^{212}U , μ -atomic h.f.s. in K, L and M lines, nuclear charge distrib. 9-38678
- ^{139}Ce , p-n interac., n hole energy Z depend. 9-29732
- ^8Be , binding energy calc., 3-body potential model 9-42200

Nuclear forces continued

- ^{12}C , binding energy calc., 3-body potential model 9-42200
- ^{12}C , dynamic N-N correlations from elastic e scatt. 9-34398
- $^{40}\text{Ca(d,p)}^{41}\text{Ca}$ $I=1$ transition, tensor forces eff., cross section j -depend. determ. 9-27749
- ^{18}F spectra calc., realistic interaction, eff. of Woods-Saxon wave function 9-38653
- ^2H , nucleon correlation eff. in shell-model description 9-29714
- ^2H photodisintegration, influence of momentum- dependent potentials 9-34387
- ^3H , Faddeev eqn. soln., binding energy determ. 9-27622
- ^3H , irreducible tensor operator form for 3-body potential 9-25569
- ^3H , n-n potential stronger than p-p potential 9-32304
- ^4H binding energies by Hartree-Fock model 9-42209
- ^4He , bound state wave function, Coulomb energy and s'-state prob. calc. 9-38646
- ^4He , n-n potential stronger than p-p potential 9-32304
- ^4He , ^4He , ^6He binding energies for ΛN and $\Lambda\Lambda$ interaction parameters 9-44137
- ^4He binding energies by Hartree-Fock model 9-42209
- ^6He ground state binding energy calc. using 3-body model 9-22720
- ^6He , bound energy depend. on N-N interaction calc. 9-34389
- ^3K , sd shell, Tabakin interaction, e.m. transition rate, nuc. moment, spectroscopic factor calc. 9-29750
- ^6Li , dynamic N-N correlations from elastic e scatt. 9-34398
- ^6Li ground state binding energy calc. using 3-body model 9-22720
- N- nucleus potential calc., p,p scatt. in nuclear emulsion, strong-absorption model applic., $M_p=3\text{ GeV}/c$ 9-42280
- N-nuclear pot., velocity dependent, used to calc. single-particle energy levels 9-48248
- ^{62}Ni , $J=0^+$ states, pairing force and surface delta interaction, seniority 9-29756
- ^{16}O , binding energy calc., 3-body potential model 9-42200
- ^{16}O , dynamic N-N correlations from elastic e scatt. 9-34398
- ^{18}O spectra calc., realistic interaction. eff. of Woods-Saxon wave function 9-38653
- Sn isotopes, Tabakin potential and reaction matrix of Yale-Shakin used to calc. props. 9-46203
- ^{90}Y , low-energy spectra from shell model calc., vel.-depend. effective N-N potential 9-40480
- ^{92}Zr , p-n interac., n hole energy Z depend. 9-29732
- ^{92}Zr , low-energy spectra from shell model calc., vel.-depend effective N-N potential 9-40480

Nuclear fusion

see also *Explosions/nuclear; Nuclear reactors, fusion; Thermonuclear reactions*

controlled reactors, fusion-fission and fusion-reaction tube, approx. eqns. 9-46245

IMP, NbTi and Nb₃Sn supercond. quadrupole magnet systems comparison 9-37492

Japanese research review 9-22829

low- β research in open-ended magnetic mirrors, review 9-27762

plasma torus, mon. average-B stabilization, utilization 9-28037

solar, alpha fusion catalysis by quarks without neutrino prod., as energy source 9-45677

Nuclear induction see *Nuclear magnetic resonance and relaxation***Nuclear interactions** see *Collision processes; Field theory, quantum/interactions; Elementary particles; Nuclear reactions and scattering***Nuclear isomerism**

see also *Nucleus/energy levels*

- half-lives 0.02-15 msec, p- and α -excited isomers, obs. 9-27660
- new short lived isomers prod. by p, α bombard. 9-48332
- production of isomers by ^{60}Co irradiation, laboratory teaching expt, 9-48261
- ^{122}Sb formation by (γ ,n), yield meas., $E_\gamma \leq 19$ MeV 9-22725
- $^{113}\text{In}^m$, half-life determ. from γ spectra 9-27630
- ^{115}Cd , from p induced ^{218}U fission, isomer yield ratio of ^{115m}Cd and ^{115g}Cd 9-34472
- ^{145}Gd from $^{144}\text{Sm}(^3\text{He},2n)$; γ spectra meas., isomeric transition, M4 prob. determ. 9-29736
- ^{118}Ag , ^{120}Ag , radioact. decay obs. 9-44179
- ^{208}Bi , and ^{208}Pb , energy level comparison 9-34405
- ^{208}Pb , and ^{208}Bi , energy level comparison 9-34405
- Cd, p excited, half-life and γ -spectrum, obs. 9-27631
- ^{60}Co , n activation of 10.5 min. and 5.26 year states 9-22802
- Er, p excited, half-life and γ -spectrum, obs. 9-27631
- $\text{EuF}_3 \cdot 2\text{H}_2\text{O}$, Mossbauer spectrum of $^{151}\text{Eu}_2\text{O}_3$, shift obs. 9-35635
- ^{90m}Nb , β -activity examined 9-46222
- ^{90m}Nb half-life, effect of superconductivity 9-32329
- Sn, p excited, half-life and γ -spectrum, obs. 9-27631
- $^{94}\text{Tc}^{m-6}$ decay, excitation of ^{94}Mo energy levels 9-38680

Nuclear magnetic resonance and relaxation

see also *Molecules/nuclear coupling*

- o- dichlorobenzene, multiple-quantum transitions 9-30146
- AA BB' systems, multiple-quantum transitions 9-30146
- ABC spin- $1/2$ system, unambiguous analysis 9-34604
- acetone, vicinal ^{13}C -H and long-range ^1H - ^1H coupling const., sign and magnitude 9-40606
- acetylene, spin relax. 9-23402
- acetylglycine, irradiated, ENDOR study at 77°K 9-41436
- acrolein, variable temp. and variable solvent study 9-30431
- adenosine 5'-monophosphate, p.m.r., H_1 , H_2 , H_3 , H_4 ' bands assignment and chem. shifts 100 MHz 9-32499
- adenosine 5'-triphosphate, p.m.r., H_1 , H_2 , H_3 , H_4 ' bands assignment and chem. shifts, 100 MHz 9-32499
- alcohol mixtures at 1°K, proton polarization, obs. 9-28762
- aldehydes, ^{13}C -C-H spin-spin coupling constants involving formyl proton 9-44350
- alkali halide aqueous solns., ^{25}Cl , ^{81}Br and ^{127}I chem. shifts 9-34925
- alkali ions, hydrated, in aqueous soln., nuclear magnetic shielding 9-32797
- alkali metal alloys, liquid, Knight shift, rel. to conc. 9-30429
- alkali-metal chloride, aq. solns., spin-lattice relax. 9-44593
- alkylpyridines, chemical shifts of protons of alkyl substituents 9-38876
- alkylpyridines, chemical shifts of ring protons 9-36710
- alloys, dil. magnetic, nuclear spin relax. mechanism 9-24338
- alloys, dilute, nearly ferromagnetic, Korringa relation breakdown 9-24503

Nuclear magnetic resonance and relaxation continued

- alloys, solvent Knight shifts, changes on alloying and nonlinear effects 9-33642
- amines, NH p chem. shift in protonation and Co(III) coordination rel. to neighbouring mag. anisotropy 9-28155
- ammonium-¹⁵N mol., heteronuc. double reson. using weak perturbing r.f. fields 9-40615
- anthracene triplet exciton band-structure limits from n.m.r. 9-35667
- antiferromagnetic insulator, spin-lattice relax., exchange enhancement 9-47296
- apophyllite, (KFCa₂Si₂O₁₀.8H₂O), p.m.r., rel. to position of protons and diffusion of H₂O mols. 9-47447
- s-aryltetrazoles, and mass spectral properties 9-34658
- benzaldehydes, aldehyde spin-spin coupling const., Indor meas 9-46385
- benzaldehydes, monosubstituted, accurate chem. shifts and coupling constants 9-30087
- benzene, n.m.r. shift and quasicryst. struct. of liq. 9-30432
- benzene, proton spin relax. 23°C, 0.07 1.9 kbar 9-30121
- benzenes, monosubstituted P mag. reson., ring P chem. shifts, obs. 9-23536
- benzenes, trisubstituted, proton-proton coupling const., additivity of substituent eff. 9-23100
- 3,4-benzopyrene, at 220 and 100 MHz, computer analysis 9-34662
- 2,1,3-benzoselenadiazole, chem. shifts and coupling constants 9-30088
- 2,1,3-benzothiadiazole, chem. shifts and coupling constants 9-30088
- 2,1,3-benzoxadiazole, chem. shifts and coupling constants 9-30088
- binary mixtures of water and organic liquids spin-lattice relaxation time and self-diffusion coeff. 9-46654
- biopolymer study at high field strength, techs. and limitations 9-30155
- borate glasses, water content 9-26797
- borohydrides of Li, Na and K, internal rotations and phase transitions 9-43308
- bromoacetaldehyde, solvent and temp. depend. of vicinal spin-spin coupling const. 9-46655
- butadienenitrile rubbers, NMR, light scattering study of structure, vulcanization character 9-23789
- Carr-Purcell spin-echo trains in homonuclear A₂BX₂ systems 9-48448
- chemical exchange rates determ. moment method 9-24526
- chloroacetaldehyde, solvent and temp. depend. of vicinal spin-spin coupling const. 9-46655
- chloroform, of ³⁵Cl, anisotropic molecular rotation in liquid 9-39119
- chloropropene, NMR, light scatt. studies, of structure 9-23789
- clathrates, lineshape and chem. shift of enclosed mols. 9-39924
- collagen fibres, broad-line n.m.r. of H₂O and D₂O 9-43304
- complexes with multidentate ligands: ³¹P rel. to mol. struct., obs. 9-32460
- crystals, internal motions, relax. functions development and use in analysis 9-31168
- Cu-8-hydroxyquinolate substituted in organic crystals, Ligand ENDOR 9-45408
- cubic crystals, quadrupole broadening of screw and edge dislocations with (111) (110) slip system 9-32965
- cubic solids, spin echo signals, line shape 9-49362
- cupric formate tetrahydrate, DMR obs. of struct. and water mol. motion changes due to paraelec. antiferro. transition 9-35730
- 2-cyanoethylsilanes, spectra analyses and parameter predictions 9-38887
- p-cyanofluorobenzene, multiple quantum transitions and coupling const., obs. 9-23094
- cyclobutanone, of A₂B₂ spin system, iterative anal. of 60 MHz spectrum 9-48720
- 1,4-cyclohexadiene oriented in nematic solvent 9-36712
- cyclohexane in deuterated aniline, decay rate independent of pulse spacing 9-28157
- cyclohexane in deuterated aniline, decay rate independent of pulse spacing 9-44596
- cyclohexene cryst., molec. motions and phase transitions 9-43305
- cyclopropanes, monosubstituted, p.m.r. and ¹³C-H satellite spectra 9-38888
- cyclopropyl derivatives, p.m.r. spectra, high resolution 9-30099
- deutero-nitrobenzene liquids, electric field effects in ²D n.m.r. 9-46656
- deuteriochloroform, of ²H and ³⁵Cl, anisotropic molecular rotation in liquid 9-39119
- trans-dichloroethylene, spin-lattice relaxation 9-24344
- 2,4-dichlorophenyl methyl isopropylphosphoramidate, asymmetry rel. to intermol. H-bonding, obs. 9-27879
- 3,5-dichlorosalicylaldehyde, chemical shifts of protons in H bond, temp. depend. 9-34665
- 4, 4'-diethylbenzophenone, meas. 9-40614
- diethylaminoluriumperfluoride double resonance technique 9-44356
- p-difluorobenzene, parameters, ¹³C-H satellite spectrum 9-34666
- 1:3di-imines, N,N-disubstituted, conjugation and configuration from p.m.r. spectra 9-30106
- 4,4-dimethylbenzophenone, influence of electron transfer 9-42438
- N, N-dimethylformamide, anisotropic molec. rot. in liq. 9-30433
- dimethyltin dibenzoate, ¹¹⁹Sn-CH₃ coupling const. and mol. configs. in organic solvents, obs. 9-27875
- 1, 4-dinitropiperazine, conformation 9-32509
- 1, 4-dinitroso-2, 3, 5, 6-tetramethylpiperazines, α, β, ε, γ, δ isomers, predominant conformations 9-32509
- dioxolane-polydioxolane in equilibrium soln., meas. 9-28103
- DL-threonine and DL-allo-threonine 9-23165
- DL-valine 9-23165
- double resonance theory, mathematical approach 9-47877
- dynamic polarization eqns. rel. to shape of distant ENDOR signals 9-43309
- ethyl fluoride dissolved in nematic liq. cry. 9-40613
- electron nuclear triple resonance in liquids, prediction and meas. method 9-44590
- ethane, in nematic solvent 9-42433
- ethanes, 1,2-disubstituted, barrier to internal rot. determ. from p.m.r. 9-30109
- ethylene, spin-lattice relaxation 9-24344
- ethylene glycol with Cr (v) complex, proton dynamic polarizations 9-34926
- ferromagnetic insulator, spin-lattice relax., exchange enhancement 9-24341
- ferromagnets, amplification of signals, charact. features 9-43292
- field dependence of nuclear spin relaxation, observation of free precession of nuclear magnetization in earth's magnetic field 9-33855
- fluid, turbulent, decay of proton spin echoes, rel. to Kolmogorov scaling laws 9-30178

Nuclear magnetic resonance and relaxation continued

- fluids, intermol. contrib. to relax. of mol. spin density matrix 9-48449
- fluorobenzene derivatives, substituent effects on H-F couplings 9-38881
- fluorobenzenes, J_{13c-f} spin-spin coupling const., i.r. data correl., eff. of electronegativity 9-23122
- fluorobenzenes, trifluoromethyl- and methoxy-substituted 9-30118
- fluorocarbons, dynamic polarization in soln. 9-44597
- fluoromethanes, partially oriented, proton and ¹⁹F n.m.r. 9-30434
- formamide-¹⁵N mol., heteronuc. double reson. using weak perturbing r.f. fields 9-40615
- formic acid, ¹³C reson. enhancement by Overhauser effect, obs. 9-32513
- four nucleus molecule in a crystal, quantum mechanical calc. of spectrum 9-35721
- free radical solns., hydrogen bridge formation, study by dynamic nuclear polarization 9-42450
- gas, double reson. study using cavity spectrometer 9-45903
- gases, diatomic, h.f. effects in spin relax. 9-34603
- Gaussian line, distortion and width in presence of Overhauser effect 9-43821
- β-D-glucopyranosides, partially acylated 9-23124
- α-D-glucose penta-acetate, broad-line studies in crystalline and glassy states 9-28763
- glycerol, proton nucl. mag. relax., 450KHz to 120MHz 9-40808
- group III-V cpds., nuclear acoustic resonance meas. of gradient-elastic tensors 9-23851
- gypsum, p.m.r. and d.m.r. 9-28755
- gypsum crystals, pulsed-NMR line shapes, computation and analysis 9-43294
- halide ions, hydrated, in aqueous soln., nuclear magnetic shielding 9-32797
- n-heptane, liquid proton spin relax., press. and temp. depend. 23-190°C, 0.07-1.9 kbar 9-30121
- hetero-nuclear double resonance used to study geminal C-C spin-coupling constants 9-46351
- n-heterocyclics, ¹³C chem. shifts calc. 9-23127
- hexafluoro-1,3-butadiene, iterative anal. 9-47874
- hexamethylbenzene, proton relax. 9-43306
- hexamethylcyclotrisiloxane, solid state polymerization at low temps. 9-28766
- hexamethylphosphotriamide water mixture preferential solvation by diamagnetic cation ¹H and ³¹P n.m.r. spectroscopy 9-44600
- hydrate melts, viscosity and spin-lattice relax. time, temp. depend. 9-28105
- hydrated K-oxalatoaluminate cryst., free rot. of proton pairs 9-28756
- hydrocarbons, doped with diphenyl picrylhydrazil, proton polarization 9-28764
- hydrocarbons, simple and derivatives, coupling constants, effect of one-centre exchange integrals 9-42437
- 1-(β-hydroxyethoxy)-2,4-dinitrobenzene, intermol. H bonding detection 9-27900
- ice crystals, pulsed-NMR line shapes, computation and analysis 9-43294
- indole salts 9-44598
- intramolecular reaction spins, Boltzmann eqn. 9-25727
- Knight shift, rel. to conc. in liq. alkali alloys 9-30429
- Knight shift and quadrupole interaction for Mg single crystal 9-39920
- Kronig-Kramers relations under saturation conditions 9-26796
- Kronig-Kramers transforms, practical props. 9-24501
- lattice disorder effect on n.m.r. spin echo line shapes 9-30610
- liquid alloy, Knight shift calc. from pseudopotential formalism 9-23532
- liquid cryst. fluorinated Schiff base, molec. config. and order 9-28159
- liquids, equations of motion of nuclear magnetism, in presence of chemical exchange 9-44592
- liquids, molecular alignment induced by elec. field, eff. on spectrum 9-30435
- liquids, rotational relaxation and chemical exchange 9-39117
- malate ion, proton coupling constants and internal chemical shifts 9-46400
- malic acid, proton coupling constants and internal chemical shifts 9-46400
- metals, absorption in region of Doppler-shifted cyclotron edge 9-47441
- metals, spin relaxation rate of paramag. impurity nuclei 9-28640
- methane, solid, and deuterated modifications, nuclear spin-lattice relax. time temp. depend. 9-43198
- methanol and methanol-trimethylamine mixtures, vapour phase study of H bonding 9-48500
- methyl-*d*₅-acetylene, anisotropic molec. reorientation in liq. 9-40809
- methyl group, proton spin relaxation time, including tunneling splitting of torsional oscillator ground state 9-37671
- methyl halides, chem. shift anisotropy in liq.-cryst. solvents 9-38903
- methyl halides in liq.-cryst. solvents, chem. shift anisotropy 9-44599
- methyl siloxane polymers NMR studies, intra and inter-molecular movements 9-30471
- N-methylacetamide solns., aqueous solns. 9-28158
- 1- and 2-methylbenzotriazole, spectrum analysis, deuteration expt. 9-30130
- methylbenzyl cyanides, relax. times of ¹⁴N in neat liquids and m-xylene solns. 9-46657
- methylolithium, struct. and bonding 9-46405
- di methyl polysilazanes internal motion temp. depend., 77-400°K 9-34697
- 1-methylpyridinium ion, effect of solvent and anion 9-34927
- methylquinolines, chem. shifts and proton coupling constants 9-38904
- methylthionitrite, p.m.r. 9-23131
- N-methylthiourea in nonpolar and polar solvents, temp. depend., rot. barrier about C-N bond 9-46658
- montmorillonite aqueous gels, doublet splitting 9-23553
- α- and β-Naphthols, polycryst. 9-26801
- nitro compounds, organic, of X-NO₂ type (X=C, N, O), ¹⁴N quadrupolar relaxation and H line shapes 9-42440
- nitrobenzene, elec. field eff. in ¹⁴N NMR spectrum 9-34683
- nitrobenzene, of ¹⁴N, molecular alignment induced by elec. field, eff. on spectrum 9-30435
- nitromethane, in tetrachloroethylene near critical solution temp. 9-44596
- nitromethane, near critical solution temp. 9-28157
- nitromethane, of ¹⁴N, molecular alignment induced by elec. field, eff. on spectrum 9-30435
- nitrosamines, heterocyclic, studies on config. and conformations 9-34682
- non-polar molecules in liquids, proton resonance displacement, medium effects 9-40806
- ochotensimine, intramol. Overhauser effects, positive and negative, rel. to dipole-dipole relax. 9-25774

Nuclear magnetic resonance and relaxation continued

- organic compounds with three C rings, frequency and activation energy of molecular motion 9-31173
- organic liquids in aqueous binary mixtures, rel. to mol. motion 9-46654
- organic three-spin systems, analysis of complex spectra 9-23027
- oriented nuclei in alternating field, γ emission anisotropy 9-42192
- Overhauser effect, inter- and intramolecular, dependence on correlation times 9-48450
- Overhauser effect, positive and negative intramolecular, in all-proton system 9-25774
- N-oximes, geminal and vicinal N-H coupling constants, absolute signs, stereochem. and medium eff. 9-30134
- μ -oxobis(thiophosphoryl difluoride) 9-23064
- paramagnetic complexes, anomalous p.m.r. linewidths 9-38829
- paramagnetic crystals, dil., strong coupling bet. electron spin-spin interac. and nuc. spin systems 9-26664
- paramagnetic ions in soln., deuteron mag. reson. 9-46653
- pentaerythritol, p.m.r. 9-43307
- pentaerythritol, proton mag. reson. investig., mol. struct., motions and water diff. obs. 9-25777
- pentafluorobenzene, low-field n.m.r. spin-coupling signs 9-30136
- pentafluorophenyl derivatives, chemical shifts, coupling consts., π -electron interactions, correl. 9-42434
- pentafluorophenyl derivatives, π interactions and bonding in selected compounds 9-42435
- perfluorovinyl derivatives, ^{19}F reson. 9-23148
- phenols, ortho-substituted, in dimethyl sulfoxide solns., electronic effects 9-42444
- phenoxy radicals, fluorinated, spin densities from linewidths 9-34687
- phenylacetylene, spin-lattice relax. 9-39120
- phosphaes, solid, of ^{31}P 9-28759
- phosphorus organic cpds, high resolution spectra 9-34685
- podotarin diacetate and dimethyl ether, study of hindered rotation 9-23152
- polar liqs., self-diffusion coeffs. and rotational correl. 9-28111
- polymers, high-resolution n.m.r. examination review 9-42463
- polymethylmethacrylate, molecular motion in surface layers, study by impulse NMR methods 9-23191
- polystyrene, molecular motion in surface layers, study by impulse NMR methods 9-23191
- polytetrafluoroethylene, γ -irrad., rel. to irrad. atmos. effects 9-24511
- polytetrafluoroethylene room temp. crystallization NMR studies, molecular rotation 9-30472
- potassium oleate in D_2O soln., of smectic liq. cryst. phase 9-40775
- probe for spectrometers having internal reference nuclei, patent 9-36244
- proton spin coupling by π electrons 9-42376
- proton-proton coupling by π electrons 9-42375
- pulsed, line shapes of crystals, computation and analysis 9-43294
- pyridazine, proton coupling constants 9-34689
- quadrupole spin-lattice relaxation, two-freq. method of investig. 9-45246
- N-quinoline, geminal and vicinal N-H coupling constants, absolute signs, stereochem. and medium eff. 9-30134
- π -electron radicals, Cl hyperfine interactions 9-48515
- rare-earth group-VA intermetallic cpds., NaCl-type, P, As, Sb and Bi Knight shifts, temp. depend., signs, magnitudes 9-33648
- recoilless nuclear resonance spectra, pseudoquadrupole shift and asymmetric line broadening 9-24509
- relaxation effect on ang. correl. and distrib. of radiation from oriented nuclei 9-41351
- resonant nuclear disorientation expts., modulation effects, theory 9-24502
- RNA, *E. coli* ribosomal, aqueous soln. containing Mn^{2+} , proton mag. relax. obs. 9-40810
- Rochelle salt, ferroelectric, water mol. dynamics 9-28765
- Rochelle salt, ferroelectric ^{23}Na - and ^{2}D spin-lattice relax. 9-24345
- Rochelle salt, of ^{23}Na , rel. to ferroelec. props. 9-26593
- Rochelle salt, p.m.r., orientations of H_2O mols. 9-45405
- Rochelle salt, spin-lattice relaxation of ^{23}Na 9-26663
- rotating reference frames and effective mag. field 9-47873
- ruby, ENDOR saturation transfer mechanism rel. to thermal mixing of nuclear spins 9-43310
- saturation theory in diamag. materials with paramag. impurities 9-41432
- second moment, orientation depend. parameters determ. in structural investigation 9-41433
- selenols, proton shift of SeH group 9-34691
- solids, subsidiary resonances due to dipole interactions 9-39918
- solvent effects, Buckingham's Formula 9-30428
- spectra, computer program for calculation from parametric spin-Hamiltonian 9-36691
- spectrometer stabilization by lateral freq. spin generator 9-47876
- spin echoes, amplification and suppression, role of mode interaction 9-43195
- spin relaxation, multiple-time-scale method 9-38339
- spin ticking effect, new form of equation 9-42374
- spin-lattice relax. in axially symmetric ellipsoids with internal motion 9-23026
- spin-lattice relaxation by two-fold correlated spin reorientation 9-24340
- spin-ticking spectra, line splittings and splitting thresholds 9-38826
- spiropentane in nematic solvent 9-40620
- superconducting devices contrib. 9-35383
- terephthalbis(aminofluorobenzene) liq. cryst., molec. config. and order 9-28159
- o-terphenyl, relax. meas. in liq., crystalline and glassy forms and mol. correlation frequencies 9-39925
- tetracyclic phosphine hydrides 9-23146
- tetracyanoquinodimethane ion-radical salts, exciton-controlled proton relax. 9-39926
- tetravinyltin, PMR spectrum, coupling const. for ^{13}C , ^{117}Sn and ^{119}Sn satellites 9-27917
- thiophene, multiple-quantum transitions 9-30146
- three-spin $1/2$ system, unambiguous analysis 9-34604
- thulium ethylsulphate, spin-lattice relax. time of Tm^{6+} and protons 9-28641
- 2,4,6-trichloroheptane obs. structure 9-32546
- 1,3,5-trifluorobenzene in nematic liq. crystal, of proton and fluorine, spectra, analysis 9-34693
- trifluorochlorocyclobutanes, substituted, ^{19}F chemical shifts and coupling constants 9-30148
- trihalomethane-halide ion complexes in soln. 9-23537

Nuclear magnetic resonance and relaxation continued

- trimethylvinylammonium bromide and derivatives, ^{14}N -H and ^1H , ^1H spin couplings 9-48509
- triphenylmethyl radicals, methyl and fluorine substituted, ENDOR spectra 9-48721
- triple, in strong r.f. field 9-38340
- tungstates, metal heteropolytungstates, state of H obs. 9-43303
- vanadate powders, asymmetric quadrupole and chem. shift effects 9-43293
- vinyl ethers, coupling consts. and chem. shifts temp. depend., obs. 9-27919
- vinyl halides, coupling consts. and chem. shifts temp. depend., obs. 9-27919
- vinyl oleate, mesophases obs. 9-46659
- zeolites, effect of sorbed mols. on quadrupole coupling constants of ^{23}Na and ^{27}Al 9-43300
- ^{113}Cd m., frequencies rel. to ^{111}Cd 9-25575
- ^{113}Cd and ^{115}Cd m., frequencies rel. to ^{111}Cd 9-25575
- ^{119}In , in InP, InAs and InSb, rel. to β decay anisotropy 9-44177
- Ag-base solid solns., solute Knight shift and spin-lattice relax. 9-43295
- Ag single crystal, pulsed studies of ^{109}Ag , rel. to mag. domains due to de Haas-van Alphen effect 9-45393
- Al-Mn dilute alloys, low temp. phen., impurity obs. 9-28754
- Al-Ta alloys, dil., of ^{27}Al rel. to impurity-disloc. effects 9-24504
- Al, deformed, quadrupole broadening of reson. lines, dislocation density obs. 9-35723
- Al_2O_3 , double ^{53}Cr , ^{27}Al acoustic-nuclear mag. reson., 4.2°K 9-49359
- Al dil. alloys, of ^{27}Al , relax. rel. to atomic diffusion 9-47443
- Al sintering powders, cryst. lattice distortion rel. to oxidation obs. 9-47442
- Al supercond. films, dirty, Knight shift, BCS-Yosida depend. 9-45394
- AlF₃ modifications, ^{19}F n.m.r. chem. shift 9-48453
- AlSb, nuclear acoustic resonance meas. of gradient-elastic tensors 9-23851
- AsF₃, liquid and solid, molecular motion and ^{19}F spin-lattice relaxation time 9-44594
- Au-V dilute alloys, low-temp. mag. props. obs. 9-45395
- Au-base solid solns., solute Knight shift and spin-lattice relax. 9-43295
- B₂H₆, and B₃H₉, spin-lattice relax. 9-42681
- B halides, solid, ^{10}B quadrupole coupling consts. 9-43296
- ^{10}B - ^{19}F nmr coupling constant in various compounds, rel. to ^{19}F chemical shift 9-32464
- BaFPO₃, chem. shift anisotropies and sign of F-P coupling const. 9-31169
- BaS₂O₆·2H₂O, proton magnetic resonance obs. 9-24505
- Be intermetallic cpds., mag. behaviour at 4.2°K 9-45396
- Bi-Te alloys, nucleation 9-23583
- Bi, liquid, spin-lattice relax. of ^{209}Bi , electronic and magnetic contribs. 9-26134
- Bi, metallic, suppression of nuclear heat capacity by slow spin-lattice relax. 9-42967
- Bi nucleation obs. 9-23583
- ^{13}C -H coupling, expression using method of separated electron pairs 9-32496
- ^{13}C - ^{13}C coupling, expressions using method of separated electron pairs 9-32496
- ^{13}C , neutron anomalous torque and spin determ. 9-38586
- ^{13}C Overhauser effect 9-30062
- ^{13}C weak signals, recording using multichannel analyses 9-29352
- ^{13}CH coupling constants, effect of lone pairs 9-34649
- CaF_2 : $^{171}\text{Yb}^{3+}$, $^{173}\text{Yb}^{3+}$, endor obs. 9-35732
- CaF_2 :Nd $^{3+}$, ENDOR obs. of F- and H- interstitials 9-47449
- CaF_2 :Yb $^{3+}$, ENDOR on $^{173}\text{Yb}^{3+}$, electronic shielding by closed shells obs. 9-35731
- CaF_2 , ENDOR meas., comparison between Ce^{3+} -H- and Ce^{3+} -F- 9-37808
- CaF_2 , ENDOR obs. of Gd $^{3+}$, transferred hyperfine interaction 9-49363
- CaF_2 , H- and D- compensated tetragonal Ce^{3+} centres, ENDOR 9-39927
- CaF_2 crystals, pulsed-NMR line shapes, computation and analysis 9-43294
- Cd, spin-echo meas. of spin-spin interactions 9-47445
- Cd Knight shift, temp. depend. calc. 9-33644
- $\text{CdCr}_2\text{S}_4(\text{Se})_2$ of Cd, rel. to transferred spin polarization 9-47444
- CdCr_2S_4 , $^{111,113}\text{Cd}$ isotropic hyperfine fields, transferred spin polarization obs. 9-43297
- $\text{CdCr}_2\text{S}_4(\text{Se})_2$ chalcogenide spinels, hyperfine interac. of nuclei w.r.t. exchange interac. 9-31170
- CdCr_2Se_4 , $^{111,113}\text{Cd}$ isotropic hyperfine fields, transferred spin polarization obs. 9-43297
- CdF_2 :V $^{3+}$, ^{51}V ENDOR 9-47385
- CdS , of ^{113}Cd , spin-lattice relaxation time, $77-450^\circ\text{K}$ 9-47298
- CeF_3 , of ^{139}Ce , showing ionic diffusion 9-24506
- CeO_2 :Gd $^{3+}$ of ^{153}Gd and ^{157}Gd , ENDOR, nucl. mag. moments and hyperfine struct. anomaly obs. 9-35733
- CeO_2 , ENDOR studies of charge compensation mechanisms rel. to trigonal Dy $^{3+}$, Er $^{3+}$ and Yb $^{3+}$ centres 9-33652
- ^{55}Co in soln. with Co $^{2+}$ paramag. rare earths, obs. 9-40807
- Co $^{2+}$ in P-O containing solvents, chem.-exchange spin decoupling 9-23533
- Co complex, Co(II) of 1:3 bidentate Schiff's bases, spin density distrib. from isotropic shifts 9-42411
- Co films, relaxation times 9-33645
- $\text{CoCl}_2\cdot 6\text{H}_2\text{O}$, antiferromag., determ. of internal mag. fields at proton sites 9-47446
- Co(III) complexes, anisotropic chem. shifts 9-45398
- Co(III) complexes with α,α' -dipyridyl, proton magnetic resonance 9-32472
- CoS₂, mag. props. investigation 9-33437
- Co(S₂Se_{1-x})₂ system, mag. props. 9-33437
- CoSe₂, mag. props. investigation 9-33437
- Cr, of ^{53}Cr , Knight shift 9-24324
- CrB₂, antiferromagnetic behaviour 9-35583
- Cs, hyperfine interaction, relativistic analysis 9-24349
- Cs, Knight shift, pressure depend. calc. 9-33647
- Cs_2BeF_4 , of ^{19}F , rel. to retarded motion of tetrahedral group BeF₄ 9-43298
- $\text{Cs}_2\text{MnCl}_4\cdot 2\text{H}_2\text{O}$, antiferromag., hyperfine field and proton reson. obs. of mag. ordering 9-41333
- CsBr in aqueous soln., ^{81}Br relaxation times 9-32799

Nuclear magnetic resonance and relaxation continued

- CsCuCl₃, Cl³⁵ n.m.r. 9-45397
 CsF, free-induction-decay curves of ¹⁹F and ¹³³Cs spin systems, pulsed reson. obs. 9-35722
 CsNiCl₃, Cl³⁵ n.m.r. 9-45397
 Cu-Zn dilute alloys, ⁶³Cu lines conc. depend., 1st order quadrupole effect obs. 9-35724
 Cu, deformed, quadrupole broadening of reson. lines, dislocations density obs. 9-35723
 Cu, Fermi surface, hydrostatic press. effect, zero-press. de Haas-van Alphen freqs., in situ obs. 9-47041
 Cu₂CS₂·2H₂O single cry., magnetic ordering obs. in para- and antiferromag. states 9-37643
 Cu acetate, p relax. in H₂O, C₂H₅OH solns., obs. 9-48719
 Cu foils, elastically deformed, ⁶³Cu spectrum 9-24507
 Cu(NH₄)₂SO₄·H₂O, proton n.m.r. obs. of antiferromag. struct. 9-41334
 CuSO₄·5D₂O, d.m.r. 9-39919
 D₂B.N(CH₃)₃, d.m.r. 9-33643
 I, 1-difluoroethylene, ¹H and ¹⁹F spectra in nematic solvents 9-30105
 Dy, ferromag., spin-lattice relax. for ¹⁶³Dy 9-33490
 EuO ferromagnetic, ¹⁵¹Eu spin lattice relax., field and temp. depend 9-45244
 F₂, nuclear mag. shielding 9-42392
 F in organic solvents, Overhauser effect rel. to multiple interactions 9-48718
¹⁹F for structural determ. of nitroso rubber copolymer 9-27939
¹⁹F in MnF₂, freq. depend. on temp. thermometer, 10-40°K 9-40291
 Fe-Al(Co) alloys, Fe-rich, transverse relaxation times of ⁵⁷Fe, Suhl-Nakamura interaction 9-45240
 Fe, ^{198,199}Au hyperfine anomaly, non-contact contrib. to effective field obs. 9-37805
 Fe₂B detection of spin-wave gap 9-45109
 Fe transverse relaxation times of ⁵⁷Fe, rel. to emission or absorpt of magnon 9-45240
 FeCl₂ frozen aqueous solns., p.m.r. studies 9-33646
 FeF₂ antiferromagnet, ¹⁹F freq. temp. depend., 4.2K to critical region 9-35725
 FeF₂ critical fluctuations near Neel point, line width anomaly 9-45399
 Fe(II) complexes with α,α'-dipyridyl, proton magnetic resonance 9-32472
 Ga-In liquid alloy, Knight shift calc. from pseudopotential formalism 9-23532
 Ga, liquid, spin-lattice relax. of ^{69,71}Ga, Electronic and magnetic contribs. 9-26134
 GaAs, nuclear acoustic resonance meas. of gradient-elastic tensors 9-23851
 GaSb, nuclear acoustic resonance meas. of gradient-elastic tensors 9-23851
 H₂, solid, line shapes obs. 9-41434
 o-H₂, very dil. soln. in p-H₂, spin-lattice relaxation 9-34924
 H₂ gas, relaxation time meas., 293-738°K, 7-135 atm., J depend. on collisions 9-34616
 H₂S crystals, pulsed-NMR line shapes, computation and analysis 9-43294
 H in metals, content determ. 9-43345
¹H, spin lattice relaxation time in methyl group, including tunneling splitting of torsional oscillator ground state 9-37671
 HC¹³N, coupling const., obs. 9-34621
 HClO₄·H₂O, reorientation of H₃O⁺ ion 9-24508
³He, gas, surface-induced spin-lattice relax., nature and interpret. 9-26039
³He and ⁴He solutions, spin-lattice relaxation times, 1.4° to 2.1°K 9-30441
³He solid with ⁴He impurities, increase of exchange interac., eff. on heat capacity 9-28168
 Hg-In liquid alloy, Knight shift calc. from pseudopotential formalism 9-23532
 HgCr₂S₄(Se₄) chalcogenide spinels, hyperfine interac. of nuclei w.r.t. exchange interaction 9-33070
 HgCr₂S₄ spinel, of ¹⁹⁹Hg, ²⁰¹Hg and ⁵³Cr nuclei at 1.4°K, depend. on mag. structure 9-45400
 h(NO₃)₃ solvation in H₂O-acetone, p.m.r. 9-42682
 In-Tl liquid alloy, Knight shift calc. from pseudopotential formalism 9-23532
 In, liquid, of ¹¹⁵In, Knight shift and spin-lattice relax. rate temp. dependence 9-23534
 In liquid, spin-lattice relax. of ¹¹⁵In, electronic and magnetic contribs. 9-26134
 InAs, nuclear acoustic resonance meas. of gradient-elastic tensors 9-23851
 InBi, ¹¹⁵In spectrum, temp. depend., Knight shift and quadrupole coupling const. 9-45402
 InSb, acoustic, of ¹¹⁵In, ^{121,123}Sb, exchange line broadening 9-45401
 InSb, liquid, of ¹¹⁵In and ^{121,123}Sb, Knight shift and spin-lattice relax. rate temp. dependence 9-23534
 InSb, nuclear acoustic resonance meas. of gradient elastic tensors 9-23851
 K-Cs binary alloys, Knight shift 9-39116
 K-NH₃ solns. doped with KI, Knight shifts 9-44595
 K-Rb binary alloys, Knight shift 9-39116
 K₂CoF₆, of F⁻ transferred hyperfine interactions 9-41294
 K₂CoF₆, antiferromag., and transferred hyperfine interactions 9-45257
 K₂NiF₄, paramag., ¹⁹F NMR, hyperfine coupling and line width behaviour 9-37806
 K₂W₂O₁₃, p.m.r. investig. of structure 9-45404
 K₂Co(CN)₆·Cr³⁺, ENDOR saturation transfer mechanism rel. to thermal mixing of nuclear spins 9-43310
 K trioxalatoaluminate hydrate, p.m.r., free rot. of proton pairs 9-28756
 KBr, F-centres, ENDOR spectroscopy, elec. field effects 9-35734
 KCl, F-centre, electron wave function determ. from ENDOR 9-33237
 KCl, F-centres, ENDOR spectroscopy, elec. field effects 9-35734
 KCl, F-centres, ENDOR line intensities 9-33653
 KCl, superhyperfine interactions of H and D centres, zero-pt. vibr. influence, ENDOR obs. 9-45409
 KFCa₂Si₂O₂₈·8H₂O (apophyllite), p.m.r., rel. to position of protons and diffusion of H₂O molecules 9-47447
 KH₂PO₄, by double resonance method 9-28758
 KH₂PO₄, of ³¹P, rotary saturation and spin calorimetry 9-28757
 KMnF₃, of ¹⁹F, exchange narrowed hyperfine-broadened, discrepancies between theory and expt. 9-45388

Nuclear magnetic resonance and relaxation continued

- La, hexagonal metallic, ¹³⁹La reson., Knight shifts, spin relax. rates and quadrupole coupling consts. 9-31171
 La₂Mg₃(NO₃)₁₂·24H₂O Nd doped, proton spin relaxation time dependence on Nd concentration 9-47299
 La₂Mg₃(NO₃)₁₂·24H₂O·Nd³⁺ enhancement of proton polarization due to 'solid effect' 9-24512
 LaMg(NO₃)₃, radiation eff. on NMR proton relaxation 9-28767
 LiBr, chemical shifts and relax. time meas. in aq.-methanol mixture 9-30035
 LiBr in aqueous soln., ⁷Li relaxation times 9-32799
 LiCl-CrCl₃ system, phase study on fusion, by spin lattice relax. times 9-35259
 LiCl, chemical shifts and relax. time meas. in aq.-methanol mixture 9-30035
 LiD₂(SeO₃)₂ ferroelec. single cryst., deuteron mag. reson. obs. of H-bond networks 9-33389
 Mg simple crystal, quadrupole interaction and Knight shift 9-39920
 MgO, ENDOR meas. of F-containing trapped-hole centre, structure 9-39355
 Mn_{1.83}Fe_{1.97}O₄, single cryst., ⁵⁵Mn obs. of Mn³⁺ at B-site, anisotropic hyperfine field due to local Jahn-Teller distortion 9-43299
 Mn₂-Cr₂S₃ freqs. and nuclear relax times, 4° to 300°K, using nuclear spin echoes 9-45403
 Mn₂P₂O₇, of ³¹P, paramagnetic shift of resonance from γ H₀ 9-47448
⁵⁵Mn in CsMnF₃, field depend. of linewidth, 1.8 and 4.2°K 9-33649
⁵⁵Mn in RbMnF₃, field depend. of linewidth, 1.8 and 4.2°K 9-33649
 MnF₂, of ⁵⁵Mn, rel. to Suhl-Nakamura interaction 9-26798
 MnF₂ of ¹⁹F exchange-narrowed hyperfine-broadened discrepancies between theory and expt. 9-45388
 N, quadrupole coupling to glycolol, determ. 9-49360
 N, sp²-hybridized in organic cpds. ¹⁴N resonance shifts 9-25773
 ND₂ compressed gas, ¹⁴N spin relax. obs. 9-40594
 ND₃, ND₂H, NDH₂ and NH₃, ¹⁴N chem. shifts 9-30430
 NH₃, ¹⁵N shifts in liq. and vapour 9-32798
 NH₃, NH p chem. shift in protonation and Co(III) coordination rel. to neighbouring mag. anisotropy 9-28155
 NH₄Cl cryst., internal motions, relax. functions obs. 9-31168
 NH₄H₂PO₄, double resonance spectra for ¹⁴N quadrupole interactions 9-28768
 NH₄I, p.m.r. and hindered rot. 9-35728
 NH₄NO₃, relax. time meas. of NH₄⁺ diffusion 9-30628
 NH₄PF₆NH₄, of ¹H and ¹⁹F, spin-lattice relaxation times, dielectric transitions 9-35727
 (NH₄)₂BeF₄, ferroelec. transition, mag. screening of ¹⁹F 9-43118
 (NH₄)₂PtCl₂, ENDOR meas. of hyperfine interactions of single and exchange-coupled Ir⁴⁺, 4°K 9-49364
¹⁵N-¹H geminal and vicinal coupling constants in N-oximes and N-quinoline, absolute signs, stereochem. and medium eff. 9-30134
 Na-Cs binary alloys, Knight shift 9-39116
 Na, Knight shift, pressure depend. calc. 9-33647
 Na, liquid, spin-lattice relax. of ²³Na, electronic and magnetic contribs. 9-26134
 Na₂W₂O₁₃, p.m.r. structure investig. 9-45404
 NaBr in aqueous soln., ²³Na and ⁸¹Br relaxation times 9-32799
 NaCl, F-centres, ENDOR spectroscopy, elec. field effects 9-35734
 NaD₂(SeO₃)₂ ferroelec. single cryst., deuteron and ²³Na mag. reson. obs. of H-bond network and phase transition 9-33392
 NaF F-centre, electron wave function determ. from ENDOR 9-33237
 NaF-LiF mixed cryst., ²³Na first-order quadrupole splittings, double reson. obs. 9-35735
 NaIO₄·²³Na and ¹²⁷I, in single crystals. 9-33654
 NaNH₄SO₄·2H₂O ferroelec. leontite 9-43301
 Nb₂Al, supercond., Knight shift 9-39599
 Nb single cryst., of ⁹³Nb 9-45406
⁹³Nb in mixed state superconducting Nb, spin-lattice relax. time temp. and field depend. determ. 9-41348
 NbN, system, phase identification 9-35726
 Nd:LaMg(NO₃)₃ long p relaxation times at 0.3-0.4°K rel. to prod. of polarized samples 9-29524
 NdBr₃, paramagnetic state, freq. and temp. depend. 9-39921
 Ni, free induction decay amplitude depend. on r.f. field strength 9-43302
 Ni²⁺, spin echo meas. of Ni hyperfine field and its application to the detection of long-range order 9-26637
 Ni²⁺ complex with dimethyl methylphosphonate, conc. and temp. depend. of n.m.r. spectra 9-28156
 Ni complex, Ni(II) of 1:3 bidentate Schiff's bases, spin density distrib. from isotropic shifts 9-42411
 Ni single cryst. hyperfine const. and mag. moment 4.2°K to 300°K 9-45150
 NiCl₂·6H₂O, antiferromag., determ. of internal mag. fields at proton sites 9-47446
 NiS₂, mag. props. investigation 9-33437
 NiSe₂, mag. props. investigation 9-33437
 NO₂-X compounds (X=C, N, O), ¹⁴N quadrupolar relaxation and ¹H line shapes 9-42440
 P₂O₅F₄ 9-23064
³¹P in methyl- and phenyl phosphorus cpds., chemical shifts 9-25775
 PCl₃, polycrystalline, NMR line width, temp. eff. 9-26799
 PH₃ halides, p.m.r. and hindered rot. 9-35728
 Pb-Sn liquid alloy, Knight shift calc. from pseudopotential formalism 9-23532
 Pb liq. alloys, ²⁰⁷Pb Knight shift, electronic struct. of impurities obs. 9-32800
 p-PbTe, Knight shifts and band structure by helicon-nuclear-spin interaction 9-39910
 Ph₃ gas, proton spin-lattice relax. 9-48667
 Rb-Cs binary alloys, Knight shift 9-39116
 Rb, hyperfine interactions, relativistic analysis 9-24349
 Rb, Knight shift, pressure depend. calc. 9-33647
 Rb, liquid, spin-lattice relax. of ^{85,87}Rb, electronic and magnetic contribs. 9-26134
 Rb₂MnCl₂·2H₂O, antiferromag., hyperfine field and proton reson. obs. of mag. ordering 9-41333
 RbCl₂H, ENDOR meas. of U₂-centres 9-30621
 RbFeF₃, and spatial distrib. of spin density 9-41435
 RbFeF₃, of ¹⁹F, ⁸⁷Rb and ⁸⁵Rb, hyperfine interaction and spin-densities 9-28760
 RbH₂AsO₄, ⁸⁷Rb quadrupole coupling, elec.-field-gradient tensors and ferroelec. transition obs. 9-33393

Nuclear magnetic resonance and relaxation continued

- RbHSO₄, p.m.r. temp. dependence rel. to para- to ferroelec. phase transition mechanism 9-26800
- RbMnF₃, ⁵⁵Mn reson. modes 9-39922
- RbMnF₃, of ¹⁹F, exchange narrowed hyperfine broadened discrepancies between theory and expt. 9-45388
- RbMnF₃ ENDOR rel. to nuclear saturation, liq., helium temp. 9-45410
- Sb, liquid, of ^{121,123}Sb, Knight shift and spin-lattice relax. rate temp. dependence 9-23534
- Sb, liquid, spin-lattice relax. of ^{121,123}Sb electronic and magnetic contribs. 9-26134
- SbCl₃, quadrupole spin-lattice relaxation time, two-freq. investig. method 9-45246
- Sc single cryst., spin-lattice relax. rate, h.f.s. 9-49192
- ⁴⁵Sc, in aqueous solutions of Sc ions, Larmor freq. for magnetic moment calc. 9-25353
- Sc(NO₃), solvation in H₂O-acetone, p.m.r. 9-42682
- Si:P ENDOR obs. 9-35736
- Sn, spin-echo meas. of spin-spin interactions 9-47445
- Sn complex, dimethyltin dibenzoate, ¹¹⁹Sn-CH₃ coupling const. and mol. configs. 9-28757
- Th formate hydrates 9-41437
- Th oxalate hydrates 9-41437
- ThP, relaxation of ³¹P rel. to diamagnetic character of ThP 9-24343
- TiH_{1.6}, p nuclear spin relaxation time 9-28761
- TiH₄ cryst., internal motions, relax. functions obs. 9-31168
- Ti₃HGeO₁₆·4H₂O, adsorbed water and Ti obs. 9-33650
- TmAl garnet of ¹⁶⁹Tm and ²⁷Al 9-45407
- TmCl₃·6H₂O, recoilless nuclear resonance spectra, pseudoquadrupole shift and symmetric line broadening 9-24509
- U₁, para- and antiferromagnetic state, freq. and temp. depend. 9-39921
- U(IV) tetracyclopentadiene complex, isotropic ¹H-NMR shift, transferred hyperfine interac. mechanisms 9-27877
- UN paramag. state, ¹⁴N obs. 9-37807
- UP, relaxation of ³¹P rel. to paramagnetic character of UP 9-24343
- U₆, of ¹⁹F, dipolar broadening obs. 9-33651
- V-Cr cpds, ⁵¹V Knight shift and Neel temp 9-24324
- V, Knight shift pressure dependence 9-24510
- V₂Au, normal, quadrupole and anisotropic Knight shift effects, obs. 9-39923
- V₂Si, of ⁵¹V, quadrupole effects of second-order 9-49361
- V₂Sn type II supercond. V⁵¹ spin-lattice relax. time, temp. variation 9-35371
- VCl₄, liquid 9-39118
- XeF₂, mag. shielding of ¹⁹F 9-31172
- XeF₆, back of observed coupling, empirical explanation 9-34646
- Y(NO₃), solvation in H₂O-acetone, p.m.r. 9-42682
- Zn₃P₂, solid, chemical shift resolution by simple phase alternated multiple pulse sequence 9-35729
- Zn complex, 1:1 Zn (11)-malate, proton coupling constants and internal chem. shifts 9-46400
- ZnSiF₆·6H₂O:Fe²⁺, Mn²⁺, single cryst., spin-lattice relax. of ¹H and ¹⁹F 9-35594

Measurement

- adiabatic demagnetization expts., sample moving system 9-40303
- chemical shift in solid, resolution by simple phase alternated multiple pulse sequence 9-35729
- correction of imperfectly tuned wide-line signals 9-34128
- deuteron mag. reson. in soln. of paramag. ions 9-46653
- electron nuclear triple resonance in liquids, prediction and meas. method 9-44590
- iterative method for sets of mag. nonequiv., chem.-shift equiv. nuclei 9-47874
- liquids, adiabatic fast passage alteration by mag. field modulation 9-44591
- low-field, appl. to assignment of spin-coupling parameters 9-30136
- magnet for apparatus, patent 9-47878
- melting point lowering by surface molecular layers 9-40817
- multichannel analyses for time averaging of spectra 9-29352
- oscillator, stationary state behaviour 9-47875
- Overhauser effect, double resonance spectrometer for obs. 9-31883
- powder patterns, asymmetric quadrupole and chem. shift effects 9-43293
- proton relax. in solids, long T₁ 9-43306
- pulsed, by tone-burst generation 9-43822
- relaxometer, description and appl. to longit. and transverse relax. meas. 9-43824
- signal simulator for spectrometer adjustment without mag. field 9-31884
- spectrograph transmitting signal and field stabilization frequencies, patent 9-40304
- spectrometer, for high resolution spectra obs. of H and F reson. 9-47201
- spectrometer, operational details 9-41862
- spin-lattice relaxation time, mag. field asymmetric modulation about resonance 9-40302
- tube for use with milligram samples 9-22319

Nuclear matter see *Nucleus/theory*

Nuclear orientation see *Nuclear polarization*

Nuclear photoeffect see *Gamma-rays/effects; Nuclear reactions and scattering due to/photons*

Nuclear physics

- data acquisition, interactive graphics system 9-32285
- data library of UKAEA 9-22647
- electronic instrumentation 9-49613
- elements, collection of data, book 9-22026
- experimental methods, conference, 1968 9-38604
- graduate level textbook 9-22039
- integrated circuits, uses 9-29671
- laboratory computer system 9-27605
- magnetometers, remote-controlled 9-36251
- nucleonics in aerospace, symposium Columbus (1967) 9-26969
- pulse-height spectra, real-time data reduction technique 9-36554
- random phase approx. calc. method, problems 9-44121
- research, computer appl. at CERN, survey 9-32286
- research using quasi-monochromatic γ-rays, E>5 MeV 9-48246
- in Soviet society, influences 9-41720
- Sturm-Liouville functions use of expansions 9-44104
- textbook discursive for undergraduates with historical approach 9-38631
- theory and props. introduced in book on atomic engineering 9-34368
- van de Graaff accelerator expts. in teaching lab. 9-29153

Nuclear polarization

- core, after deformation, applic. of pairing-plus-quadrupole model 9-34379
- core polarization eff. on E2, M1 operators, Tabakin interaction 9-32294
- ENDOR spectrometer, for obs. of Overhauser effect 9-31883
- enhancement by dynamic cooling technique 9-31061
- ferromagnetic alloy, internal effective mag. field determ. by low-temp. nuclear orientation meas. 9-37654
- fluorocarbons in soln., dynamic 9-44597
- free radical solns., hydrogen bridge formation, study by DNP 9-42450
- line shape 9-27577
- of nuclear matter rel. to lifetimes of quasiparticles 9-48255
- polarized target prod. theory and methods 9-27444
- recoil nuclei, effect of atomic hyperfine quadrupole interactions 9-29708
- scattering, inelastic, of nucleon, second-quantized formulation 9-27707
- spin polarization eff. in deformed nuclei, Tamm-Dancoff analysis 9-22713
- target technology for high energy physics 9-27445
- ¹¹³Cd^m, orientation by optical pumping, n.m.r. frequencies 9-25575
- ¹¹³Cd and ¹¹⁴Cd^m, orientation by optical pumping, n.m.r. frequencies 9-25575
- ¹⁶⁵Ho, photoneutron cross section rel. to model for giant dipole resonance 9-38673
- ¹¹⁹In, monitoring by meas. of β anisotropy of decay of ground state 9-44177
- ⁷⁹Br/⁸¹Br nuclear quadrupole ratio determ. in LiBr, comparison with atomic Br 9-23054
- Ca isotopes, radius meas., excess n depend. 9-36572
- CaF₂:Yb³⁺ of ¹⁹F, spin-lattice relax. times meas. 9-47297
- CaF₂, of ¹⁹F nucl spins, antiferromag. state prod. and obs. 9-45207
- CuK₂(SO₄)₂·6H₂O, dynamic polarization of protons and their spin-lattice relaxation times 9-39786
- CuSO₄·4H₂O, of protons, spin-lattice relax. times of Cu²⁺ 9-47297
- Fe, orientation/mag. reson. of ¹s,¹⁹⁹Au, non-contact contrib. to effective field obs. 9-37805
- ³He, elastically scattered from ⁴He, polarization meas. by double-scatt. technique 9-46240
- ³He gas optically pumped, static mag. field detection, low-field magnetometer 9-23002
- ³He target for high energy scatt. expt. 9-27582
- ³He-⁴He solutions, conc.-dependent polarization 9-32807
- Nd:LaMg (NO₃), p relaxation time of several hundred hours at 0.3-0.4°K rel. to prod. of polarized samples 9-29524
- Ni isotopes, radius meas., excess n depend. 9-36572
- P compounds, dynamic nuclear polarization at 74 gauss 9-39115
- Sn isotopes, radius meas., excess n depend. 9-36572

Nuclear power see *Nuclear reactors, fission*

Nuclear quadrupole resonance

- alkali halide, quantum mechanical calculation 9-24514
- aniline: ¹⁴N, temp. depend. and chem. interpretation, 77-292°K 9-30071
- p-bromoaniline: ¹⁴N, temp. depend. and chem. interpretation, 77-292°K 9-30071
- p-bromophenol, Zeeman effect of ⁸¹Br 9-39929
- chlorinated hydrocarbons, solid, deuteron, quadrupole coupling 9-43311
- p-chloroaniline: ¹⁴N, temp. depend. and chem. interpretation, 77-292°K 9-30071
- p-chlorophenol, Zeeman effect of ³⁵Cl 9-39929
- p-chlorophenoxy acetic acid, of ³⁵Cl, temp. variation of freqs. 9-30103
- p-dibromobenzene, of ⁷⁹Br, temp. dependence 9-31175
- 2,4-dichloroaniline, of ³⁵Cl, temp. variation of freqs. 9-30103
- 2,6-dichloroaniline, of ³⁵Cl, temp. variation of freqs. 9-30103
- 4-fluoro-3-chloroaniline, of ³⁵Cl, temp. variation of freqs. 9-30103
- p-iodoaniline: ¹⁴N, temp. depend. and chem. interpretation, 77-292°K 9-30071
- molecular rotation anisotropy, meas. by relaxation 9-39930
- o-p-phenylene diamine: ¹⁴N, temp. depend. and chem. interpretation, 77-292°K 9-30071
- piperazine, anisotropy of molec. rot., meas. by relax. 9-39930
- powders, Zeeman patterns 9-43269
- quadrupole coupling const. relationship with force const. 9-42363
- rare-earth trihalides, hexagonal, Cl n.q.r., long-range order obs. 9-41340
- relaxation effect on ang. correl. and distrib. of radiation from oriented nuclei 9-41351
- spectra, in nuclear γ-ray reson. expts., analysis method 9-43825
- spin echoes form. and enhancement 9-47450
- urea, ¹⁴N n.q.r., saturation and relax. times 9-49366
- AgSbs, miargyrite, artificial, for low temp. α form 9-47451
- Ba(NO₃)₂·H₂O, of ¹⁴N, temp. depend. between 77°K and 300°K 9-37809
- Cl₂, in three substituted anilines and p-chlorophenoxy acetic acid, temp. variation of freqs. 9-30103
- ³⁵Cl in solid (C₂H₅)₂O·GaCl₃ to show mol. symm. rel. interpretation of i.r. spectrum of liquid 9-24515
- ³⁵Cl resonance freqs., Townes and Dailey interpretation, exam. by BEEM 9-32454
- CsPbCl₃, phase transitions determ. 9-41058
- ⁶⁹Ga in solid (C₂H₅)₂O·GaCl₃ to show mol. symm. rel. interpretation of i.r. spectrum of liquid 9-24515
- HgCl₂ powder, ³⁵Cl Zeeman pattern 9-43269
- K₂PtCl₆:³⁵Cl pressure depend., used to investigate rot. of PtCl₆ group 9-31174
- KClO₄:⁴⁹K, electric quadrupole moment, meas. using new steady-state double-resonance technique 9-29752
- KMnCl₃ polycryst., of ³⁵Cl 9-49365
- LiBr, ⁷⁹Br/⁸¹Br nuclear quadrupole ratio determ. 9-23054
- N₂H₄, spin-spin interaction between N nuclei 9-24513
- ¹⁴N in asymmetric field gradients, relax. times and saturation 9-49366
- NaBrO₃, press. and temp. depend. of ²³Na freq. 9-39928
- NaClO₄ powder, ³⁵Cl Zeeman pattern 9-43269
- RuCl₃ polycryst., of ³⁵Cl 9-49365
- TbCl₃ polycryst., of ³⁵Cl 9-49365
- UCl₄ polycryst., of ³⁵Cl 9-49365

Nuclear radius see *Nucleus/size*

Nuclear reactions and scattering

- see also *Chemical analysis/by nuclear reactions; Fallout; Nuclear bombardment targets; Nuclear excitation; Nuclear fission; Nuclear fusion; Nuclear spallation; Radioactivity; Thermonuclear reactions*
- 21+1 rule, refinement 9-42269
- amplitude exact representation, high energy approx. at medium energy 9-42267

Nuclear reactions and scattering continued

- analogue symmetry and broadening, multi-channel cancellation effects 9-42266
- beam defining slit mechanism, low background, for scatt. chambers 9-40497
- Bloch-Gillet formalism, K operator corrected 9-38692
- bremsstrahlung, internal in direct reactions, pole approx. 9-22771
- channels, elastic and inelastic, contribs. from a shell model description 9-42268
- charged particle absolute cross-section meas., expt. techniques 9-22767
- cluster channels, nucl. reactions above two-particle threshold 9-48322
- cluster representation framework, bound and resonance states theory 9-27689
- compound nucleus reactions, energy level density determ. from excitation functions of isolated levels 9-48287
- compound reactions, microscopic approach 9-22768
- near Coulomb barrier, interactions and multiple excitation 9-44119
- Coulomb excitation near Coulomb barrier, interference with nuc. excitation proc. 9-27614
- Coulomb multiple excitation, quantal corrections and WKB approx. 9-27690
- Coulomb mutual interaction energy for system of two ellipsoids with total symmetry-axis 9-46229
- cross sections, near threshold of reactions with giant-resonance form. 9-46230
- cross-section, average reaction, and transmission coefficients, relation 9-22772
- cross-sections, eigenchannel calc. for soluble model, accuracy of method 9-36594
- cross-sections, nuclear, problem of, and inelastic processes at high energies 9-25609
- deformed nuclei, one-nucleon transfer reactions 9-44117
- density matrix formalism, quantum theory of irreversible processes considerations 9-32334
- direct interactions in coupled channels 9-36592
- DWBA in (d,p) reactions, condition for obtaining in coupled channel theory 9-32355
- eigenchannel calc. for soluble model, accuracy of method 9-36594
- exchange reactions, T matrix approx. and DWBA, validity 9-32331
- excited state production cross-section in terms of imaginary part of integral involving wave function 9-36134
- extended R-matrix theory, tests 9-34425
- Fermi gas model, level-density, nonperiodic perturbations 9-38262
- fluctuation anal. for elastic scatt. cross sections 9-42263
- gas target cell for scattering chamber 9-25501
- inelastic processes at high energies and problem of nuclear cross-sections 9-25609
- ion implantation by nuclear reactions, techniques 9-33210
- K operator, corrected form in Bloch-Gillet formalism 9-38692
- K-matrix theory, applic. to soluble model 9-42265
- Lippmann-Schwinger eqn., scatt. soln. 9-22770
- multiparticle processes incorporation of two-particle Coulomb wave function 9-34426
- off-energy-shell effects, evidence from pp bremsstrahlung 9-38572
- optical model, book 9-42179
- optical model, computer ang. mom. approach to scatt., potential determ. 9-27691
- optical model, density depend. effects 9-34427
- optical model, particles with arbitrary spin, cross-sections and polarizations 9-29776
- optical model analysis of 20 MeV triton scatt. from 17 nuclides 9-48346
- optical model analysis of p scatt. on light 1p-shell nuclei, 10-50 MeV 9-48333
- optical model potential, spin orbit contribution to spin flip of polarized p 9-48334
- optical model potentials, criterion for equivalence 9-44211
- optical model treated with analogy to e.m. wave scatt. in mind 9-36561
- particle, charged, spectra. low energy, computer scanning method 9-27139
- rel. to particle focusing and channelling in crystals. 9-35294
- particle no. production depend. on incident energy calc. 9-29778
- particle spectra of 3-body break-ups, analytical expressions 9-27687
- particle transfer reactions, inelastic processes 9-42260
- phase shift definition when a separable potential has a bound state in the continuum 9-46228
- polarization, kinematic 9-36597
- polarization expts., performance method 9-44182
- polarization of spin-1/2 particles, elastic scatt. by strongly absorbing target 9-32333
- polarization prod. from unpolarized beam, target condition 9-40498
- potential, attractive monotonically decreasing, l=0 neutral particles, single channel scatt. resonance 9-32332
- Q-values, very high precision meas. 9-29775
- quasi-compound nucleus theory of inelastic scatt. 9-29804
- quasi-free scatt. and integration of single particle energies 9-44113
- quasi-free scatt. and integration of single particle energies 9-36563
- reaction chamber and associated experimental system 9-25607
- rearrangement, coupled channel method 9-22106
- resonance cross section calc. optimization 9-27692
- resonance integrals for negative energy levels, evaluation using Adler or Breit-Wigner formalism 9-44184
- resonating-group method 9-38709
- scattering chamber for Karlsruhe cyclotrons 9-25555
- shell bound-state method using truncated Hilbert space 9-44183
- spectroscopy, self-consistent, 2-nucleon transfer, J=0⁺ state wave function determ. 9-25606
- stripping reactions, BHMM theory, effect of exclusion-principle blocking 9-42264
- stripping reactions, sudden approx. validity 9-32331
- synthetic cross-sections, generation and statistical analysis by computer 9-27688
- t-matrix, separable approx. 9-36593
- theory taking channel coupling into account, review 9-42261
- thermal neutrons in thin targets, multiple scatt. and absorpt. 9-42286
- three body reactions, study using multiparametric recording system 9-22648
- three-body channels, new approach based on R-matrix formalism 9-46227
- transuranium element production 9-25608

Nuclear reactions and scattering continued

- U(3,1) non-compact group representation, scatt. amplitude analysis 9-29777
- (d,t) rel. to nucleus struct. meas., review 9-34380
- (α , xn), (a=n, p, α , γ or heavy ion), new method for study 9-29824
- (α , α') reaction, neutron and proton contribs. to nuclear excitation rates 9-42300
- (d,p) stripping reactions on deformed nuclei 9-44213
- γ emission, tables of coeffs. for ang. distrib. analysis 9-32300
- t optical potential determ. from fitting meas. of ⁴⁰Ca(t,d)⁴Ca 9-46198
- ⁴He, K⁺ capture, search for (Σ -n) and (Σ -nn) band states 9-29618
- Pb, 750, 1000, 2000 MeV, emission of n, p, π 9-27728
- chemical effects**
- see also *Chemical effects of radiations/ionizing radiations*
- ozone synthesis from O₂ in chemonuclear reactor, rel. to temp., ozone conc. and dose rate 9-37842
- thermal neutron capture in Mg₂SnO₄, chem. and Mossbauer study 9-26852
- high energy >1 GeV**
- 3.86 GeV, cross-section for strange particle prod. obs. in freon bubble chamber 9-25643
- fireball generation in quasinucleon interactions of 20-23 GeV p 9-42281
- fission, tripartite, induced by protons in range 600 MeV to 20 GeV 9-36615
- nucleus-nucleus, 3-26 GeV, cascade and evaporation studied in cosmic ray interactions with emulsion nuclei 9-22826
- structure investigated 9-32287
- structure probes with high energy particles 9-40461
- bye in emulsion, 10 and 16 GeV, inelastic interac. props. 9-29785
- K⁺, hyperfragments produced in 1.5, 3.0, 5.0 and 10.1 GeV/c interac. comparative study 9-48182
- K⁺ interaction with emulsion nuclei, at 10.1 GeV/c, hypernuclei prod. 9-40470
- by μ in emulsion, 10.5 GeV, inelastic interac. props. 9-29785
- p⁻ nucleus, 6.2-22.5 GeV, cascade and evaporation studied in cosmic ray interactions with emulsion nuclei 9-22826
- P-nucleus, in emission rel. to cascade-evaporation model 3 GeV/c 9-40507
- π reactions with emulsion nuclei at 200 GeV, 135 obs. 9-25640
- Be, p bombard 1-3 BeV, obs. of emitted p 9-48336
- Be(p, π^+), at 12.5 GeV/c, prod. cross sections 9-32184
- Bi, fission, tripartite, induced by protons in range 600 MeV to 20 GeV 9-36615
- C p bombard, 1-3 BeV, obs. of emitted p 9-48336
- Cl(π^- , Λ) 3.86 GeV, cross-section for strange particle prod. obs. in freon bubble chamber 9-25643
- C(π^- , Λ) 3.86 GeV, cross-section for strange particle prod. obs. in freon bubble chamber 9-25643
- Cu p bombard 1-3 BeV, obs. of emitted p 9-48336
- ²³Mg(p, 4 p)²⁴Na, cross section and excitation function meas., E_p=0.43-2.7 GeV 9-27717
- Pb, p bombard 1-3 BeV obs. of emitted p 9-48336
- Th, fission, tripartite, induced by protons in range 600 MeV to 20 GeV 9-36615
- U, fission, tripartite, induced by protons in range 600 MeV to 20 GeV 9-36615
- p-nucleus interactions, theoretical aspects 9-34445
- Nuclear reactions and scattering due to alpha-particles**
- A=6-209, ang. distrib. diffraction pattern obs., diff. cross section meas., E _{α} =104 MeV 9-29815
- deformed nuclei, nuclear non-rigidity effect 9-48347
- E2 transitions in doubly even sd shell, 2⁺ state excitation 9-27618
- energy struggling through gases 9-29818
- glass target, (⁴He,³H) stripping reaction at 120MeV, cross sections 9-42310
- isomers, new, short-lived, produced 9-48332
- optical model potentials, criterion for equivalence 9-44211
- optical potential microscopic description, cross section interaction depend. 9-29817
- Rutherford scatt. demonstrated with Al surface and ball bearings 9-22031
- S-matrix treatment using poles 9-34462
- scattering analysis inconsistency, remarks 9-46239
- superfluid model analysis of diffraction scatt. data 9-36610
- (α , n) reactions, level density depend. on mass number 9-34466
- (α , p) three nucleon transfer reactions 9-22814
- (α , α') reaction, isoscalar transition rates determ. 9-42300
- (α , α'), ⁹Be levels, pole representation from phase shift and potential meas. 9-27750
- (α , n), endoergic, and reverse reaction rates 9-46235
- (α , Np) in alpha emitters, γ spectra rel. to anal. of light element impurities 9-25603
- ⁴⁰Ca(α , α_0) ⁴⁰Ca, optical-model analysis, l-depend. absorption factor, 5.5-17.5 MeV 9-25646
- ¹⁶⁰Dy(α , α_0) ¹⁶¹Er, anomalous rotational band strong transitions obs. 9-36577
- ¹⁰⁰Mo(α , α_0) ¹⁰²Ru, γ -ray linear polarization obs. using Ge(Li) detector 9-38460
- ¹¹⁰Pd(α , α') Coulomb excitation, levels, spin, parity and E2 transitions determ., E _{α} \approx 10 MeV 9-22722
- ¹¹⁰Pd(α , d' γ), γ - γ ang. correlations following Coulomb excitation 9-36612
- ¹⁸¹Ta target, E _{α} =80 MeV., neutron ang. distrib. yield, spectra and shielding 9-34474
- ¹⁵⁶Dy(α , 5n)¹⁵³Er, creation of new isotope ¹⁵³Er 9-48436
- ²⁰⁶Pb(α , α'), ang. distrib. meas., phase anal., E _{α} =40 MeV 9-29829
- ²⁰⁶Pb(α , xn)²¹⁰⁻²Po, excitation functions, total cross-sections, compound-nucleus mechanism 9-44220
- ¹⁰⁶Pd(α , α') Coulomb excitation, levels, spin, parity and E2 transitions determ., E _{α} \approx 10 MeV 9-22722
- ¹¹⁸Sn(α , α'), diff. cross section meas., deformation lengths, 2⁺, 4⁺ states calc. E _{α} =65 MeV 9-40517
- ¹⁰⁷Ag(α , α' γ), γ - γ ang. correlations following Coulomb excitation 9-36612
- ²⁰⁷Pb(α , α'), ang. distrib. meas., phase anal., E _{α} =40 MeV 9-29829
- ¹¹⁷Sn(α , α' γ) γ - γ ang. correlations following Coulomb excitation 9-36612
- ²⁰⁸Pb(α , α'), ang. distrib. meas., phase anal., E _{α} =40 MeV 9-29829
- ¹⁰⁸Pd(α , α') Coulomb excitation, levels, spin, parity and E2 transitions determ., E _{α} \approx 10 MeV 9-22722

Nuclear reactions and scattering due to continued alpha-particles continued

- ¹⁰⁹Ag(α , γ)¹¹¹In, excitation function calc., n spectra, energy meas. 9-29824
¹⁰⁹Ag(α , n)¹¹²In, excitation function calc., n spectra, energy meas. 9-29824
¹⁰⁹Ag(α , n)^{112m}In, excitation function calc., n spectra, energy meas. 9-29824
 Al(⁴He, ³H) stripping reaction at 120 MeV, cross sections 9-42310
¹⁰⁸Ba(α , γ)¹⁰⁸Br γ cross-sections, 90° excitation curves for α , ¹⁴N deduced levels 9-27741
¹¹B(α , p)¹⁴C, differential cross section, ang. distrib., excitation function meas., $E_\alpha=10-25$ MeV 9-32356
¹⁰B(α , p)¹³C, 3.85 MeV γ source, ¹⁰B-PuO₂ mixture 9-29662
¹⁰B(α , p)¹³C, γ cross-sections, 90° excitation curves for α , ¹⁴N deduced levels 9-27741
⁹Be(α , n)¹²C, n energy distrib. meas. 9-34355
⁹Be(α , n) used for calc. of Am-Be neutron spectrum 9-22629
 C(⁴He, ³H) stripping reaction at 120 MeV, cross sections 9-42310
¹²C target, p-wave phase shift between 9.16 and 12.11 MeV, multilevel analysis 9-29819
⁴⁸Ca, phase shift analysis, unambiguous parameters, $E_\alpha=40$ MeV 9-34464
¹²C(α , α')¹²C, cross-section calc. utilizing S-matrix and poles 9-34462
¹²C(α , α')¹²Cm excitation functions and angular distribution at 20-24 MeV 9-22810
 Fe(⁴He, ³H) stripping reaction at 120 MeV, cross sections 9-42310
⁵²Cr(d, p)⁵³Cr, p polarization meas., DWBA calc. 9-27753
¹⁹F, excited state lifetime meas., $E_\alpha=5.5$ MeV 9-29741
⁵⁴Fe(α , p)⁵⁷Fe, 10.23 and 10.30 MeV, rel. to levels of ⁵⁷Co up to 1.90 MeV 9-29754
⁵⁴Fe(α , p)⁵⁸Co, 12-18.5 MeV thick target excitation function rel. to level density determination 9-48287
⁷⁴Ga(α , n) in search for ^{74m}As 9-32323
⁴He(⁴He, ⁴He)⁸He⁺, diff. cross section, excitation energy determ., $E_\alpha=64$ MeV 9-29820
³He(α , α')³He rel. to 7 MeV resonance 9-27739
³He(α , α')³He, cross section meas., $E_\alpha=164-245$ keV 9-27747
⁴¹K(³He, d)⁴²K α particle-hole state decay, γ -ray obs. 9-48284
³⁹K(α , α'), cross sections, ang. distrib. meas., $E_\alpha=22-29$ MeV 9-22811
⁶Li, elastic and inelastic scatt., ang. distrib. and deform. parameters, DWBA analysis, $E_\alpha=29.4$ MeV 9-42311
⁶Li α -d structure of ground state 9-44135
⁷Li elastic and inelastic scatt., ang. distrib. and deform. parameters, DWBA analysis, $E_\alpha=29.4$ MeV 9-42311
⁶Li(α , α')⁶He, α -d correlations, cross section meas., $E_\alpha=23.6$ MeV 9-27754
²⁴Mg, phase shift analysis, unambiguous parameters, $E_\alpha=40$ MeV 9-34464
²⁸Mg(α , n)²⁸Si, 8.543 MeV ²⁸Si level lifetime meas., $E_\alpha \sim$ threshold energy 9-38655
²⁴Mg(α , p)²⁷Al, p, γ spectra meas., levels, lifetime, spin and parity determ., $E_\alpha=9-13$ MeV 9-25656
⁵⁵Mn(α , α')⁵⁵Mn, 50 MeV, obs. of ang. distrib., DWBA analysis 9-34465
²³Na(α , γ)²⁷Al, $E_\alpha=2-3$ MeV, γ -ray spectra 9-46242
¹⁴N(α , α')¹⁴C, α spectra meas., levels determ., $E_\alpha=22.9$ MeV 9-38721
¹⁴N(α , α')¹³C, α p spectra meas., ¹³C decay determ., $E_\alpha=22.9$ MeV 9-38721
¹⁴N(α , γ)¹⁸F $1\frac{1}{2}^+$ level in resonance found 9-36569
¹⁴N(α , n)¹⁷O(5.00), ¹⁴N(α , p)¹⁷O(0.871) for estimation of isobaric-spin impurities of 18F states 9-42206
²³Nc(α , n)²⁵Mg, neutron source in stars 9-48329
²⁰Ne, 24 MeV α scatt. leading to 4.25 MeV state 9-46241
¹⁶O(α , α'), 5-10 MeV, phase-shift analysis 9-42305
⁴⁸Sc(α , α')⁴⁸Ti, 41 MeV, DWBA analysis 9-48351
²⁸Si(α , α')²⁸Si, excitation func. meas., $E_\alpha=14-25$ MeV 9-29831
²⁸Si(α , p)³¹P, excitation func., ang. distrib. meas., $E_\alpha=11-25$ MeV 9-29831
⁸⁸Sr, phase shift analysis, unambiguous parameters, $E_\alpha=40$ MeV 9-34464
⁸⁹Y(α , α'), diff. cross section meas., deformation lengths, 2⁺, 4⁺ states calc. $E_\alpha=65$ MeV 9-40517
⁶²Zn by ⁴He, reactions proceeding through ⁶⁸Ge, γ emission 9-27666
⁶²Zn reactions, ang. mom. eff. breakup in compound nucleus 9-29757
⁶²Zr(α , α'), diff. cross section meas., deformation lengths, 2⁺, 4⁺ states calc. $E_\alpha=65$ MeV 9-40517
⁶²Zr(α , α'), diff. cross section meas., deformation lengths, 2⁺, 4⁺ states calc. $E_\alpha=65$ MeV 9-40517
⁶²Zr(α , α'), diff. cross section meas., deformation lengths, 2⁺, 4⁺ states calc. $E_\alpha=65$ MeV 9-40517

cosmic rays

see also Cosmic rays/effects and interactions

- nucleus-nucleus collisions, 3-26 GeV, cascade and evaporation studies with emulsion nuclei 9-22826
 Pb, electron-photon cascade energy depend. on interacting particle energy 9-46244

deuterons

- ²H(d, n)³He, 83 MeV differential cross-section obs. 9-22817
⁴⁰Ca(d, p)⁴¹Ca (2.02 MeV), stripping form factors 9-22821
 diffraction interaction, nucleon pot. depth influence on disintegration 9-42297
 diffraction model analysis, amplitudes, phase shifts and spin-orbit effects determ. 9-42296
 inelastic collisions, mechanisms 9-25649
 polarizability of deuteron, influence on elastic scatt. 9-44210
 rare-earth nuclei, diff. cross section meas., optical model analysis, $E_d=12$ MeV 9-32354
 stripping reaction, 2-step, perturbation approach validity 9-27740
 stripping reactions on odd-A nuclei initiated by vector polarized deuterons 9-44217
 (d, ³He), ang. distrib. J and d spin-orbit potential depend. 9-29821
 (d, ³He), ang. distrib. meas., shell effects in potential radii 9-29822
 (d, p), rel. to nucleus struct. meas., review 9-34380
 (d, p) particle transfer reactions, inelastic processes 9-42260
 (d, p) stripping react., polariz. eff., applic. of generalized ring-locus model 9-25648
 (d, p) stripping reaction, negligible effect of repulsive core in DWBA 9-42299
 (d, p) total ang. momentum of transferred neutron calc. in weakly bound projectile model 9-38710
 (d, n, p) expts. with 4.5 MeV electrostatic accelerator 9-36545
 (d, p), type, mechanism 9-25647
 (d, p) reactions, vector analysing power and WBP model 9-22813

Nuclear reactions and scattering due to continued deuterons continued

- (d, p), close coupling eqns. obtained from variational principle 9-32355
⁸⁵Rb(d, p)⁸⁶Rb, study of ⁸⁶Rb low-lying levels 9-42217
¹⁷⁰Yb(d, p)¹⁷¹Yb, DWBA anal., $E_d=12$ MeV 9-25652
¹²¹Sb(d, nn)^{121m}Te, ¹²¹Te, isomeric cross section ratio calc., nuclear level, density derived, agreement with superconductor model 9-27743
¹¹²Cd(d, p)¹¹³Cd, 13 MeV, level structure of ¹¹³Cd determ. 9-38667
¹⁴²Nd(d, ³He)¹⁴⁴Pr, differential cross section, levels, spectroscopic factors determ., $E_d=29$ MeV 9-32311
¹⁰²Ru(d, p) excitation function meas., $E_d \leq 14$ MeV 9-29838
¹²⁷Sn(d, ³He), upto ¹²⁷Sn, even isotopes; In levels, spin and parity determ., $E_d=22$ MeV 9-29825
¹⁷²Yb(d, p)¹⁷³Yb, DWBA anal., $E_d=12$ MeV 9-25652
¹³³Cs(d, nn)^{133m}Ba, ¹³³Ba isomeric cross section ratio calc., nuclear level, density derived, agreement with superconductor model 9-27743
¹⁰⁴Pd(d, p)¹⁰⁵Pd, subbarrier d energy 9-44219
¹⁰⁴Ru(d, p) excitation function meas., $E_d \leq 14$ MeV 9-29838
¹⁷⁴Yb(d, p)¹⁷⁵Yb, DWBA anal., $E_d=12$ MeV 9-25652
²⁰⁶Pb(d, t)²⁰⁷Pb, t spectra meas., levels determ., $E_d=21.6$ MeV 9-27643
¹⁶⁷Er(d, t)¹⁶⁸Er levels determ. from t spectra, $E_d=12$ MeV 9-22816
¹³⁸Ba(d, p)¹³⁹Ba, p spectra meas., transitions and levels determ. 9-38705
²⁰⁸Pb(d, ³He)²⁰⁷Tl diff. cross section, excitation energy meas., level assignment, $E_d=50$ MeV 9-27746
²⁰⁸Pb(d, p)²⁰⁹Pb, cross section meas., levels, spectroscopic factors calc., $E_d=18.7$ MeV 9-27745
²⁰⁸Pb(d, p)²⁰⁹Pb; p, γ spectra meas., particle-vibration coupling, levels determ., $E_d=12$ MeV 9-29740
²⁰⁸Pb(d, t)²⁰⁷Pb diff. cross section, excitation energy meas., level assignment, $E_d=50$ MeV 9-27746
¹⁰⁹Ag(d, p)¹¹⁰Ag, angular distributions of 53 levels in ¹¹⁰Ag 9-29726
¹⁴²Nd(d, ³He)¹⁴³Mg, ³He energy spectra and ang. distrib. for $E_d=52$ MeV 9-22820
²⁷Al(d, ³He)²⁶Mg, proton pickup from 1p and 2s-1d shells of ²⁷Al 9-22820
²⁷Al(d, p)²⁸Al, 2.6 MeV stripping reaction obs. 9-22739
⁴⁰Ar(d, ³He)³⁹Cl, ³He spectra meas., levels, spin and parity determ., $E_d=52$ MeV 9-32358
¹¹B(d, α')⁹Be, 0.7 to 2.2 MeV, excitation functions 9-29839
¹⁰B(d, n)¹¹C; n polarization ang. distrib. meas., $E_d=1.2-2.9$ MeV 9-48341
 Be target, neutron yield 9-38607
 Be(d, n) construction of standard thermal in flux facility 9-22628
⁹Be(d, n)¹⁰B, at 4 MeV, excited levels of ¹⁰B determ. 9-44215
⁹Be(d, n)¹⁰B, γ -ray branching of ¹⁰B 3.59 MeV state 9-29711
⁹Be(d, p)¹⁰Be, p spectra meas., levels, spin, parity and spectroscopic factor determ., $E_d=2.8$ MeV 9-29712
⁴⁰Ca(d, p)⁴¹Ca 1.95 and 2.47 MeV reactions, proton polarization obs., comparison with theories 9-22822
 Ca, disintegration of 13.6 MeV deuterons on collision 9-48350
⁴⁰Ca(d, ³He), DWBA Predictions test at $E_d=82$ MeV 9-40520
⁴⁰Ca(d, n)⁴⁰Sc, charge exchange coupling eff. investigated 9-29835
⁴⁰Ca(d, p)⁴¹Ca, angular distribution, $E_d=2$ MeV 9-29823
⁴⁰Ca(d, p)⁴¹Ca, (α , α') $E_d=3.0-5.5$ MeV, excitation functions 9-29835
 Ca(d, d, p) Ca, tensor potential for optical model 9-22812
⁴⁰Ca(d, p)⁴¹Ca, 1e1 transition, tensor forces eff., cross section j -depend. determ. 9-27749
⁴⁰Ca(d, p)⁴¹Ca stripping cross-section calcs., comparison between coupled-channel method and DWBA 9-42306
⁴⁰Ca(d, p)⁴¹Ca (γ , 3.95 MeV) proton polarization near J-dependent cross-section min. 9-42307
⁴⁰Ca(d, p) vector analysing power calcs. using WBP model, comparison with obs. 9-22813
⁴⁰Ca(d, p)⁴¹Ca; p- γ delayed coincidence meas., half-life determ., $E_d=1.2$ MeV 9-34422
⁴⁰Ca(d, p)⁴¹Ca, branching ratio and spin of 3614 KeV level of ⁴¹Ca 9-48306
¹²C(d, d)¹²C double-scatt at 51 MeV, optical model prediction confirmed 9-34463
¹²C(d, α')¹⁰B differential cross section meas., $E_d=5-10$ MeV 9-27742
¹²C(d, α')¹⁰B Glendenning two-nucleon transfer theory analysis, $E_d=9.2-13.9$ MeV 9-48353
¹²C(d, d) differential cross section meas., $E_d=5-10$ MeV 9-27742
¹²C(d, n)¹³N, n polarization meas., Mott-Schwinger scatt. method, $E_d=51.5$ MeV 9-22815
¹²C(d, n)¹³N, total cross sections, at 1.2-4.5 MeV 9-42304
¹²C(d, n)¹³N α , γ , γ , p, n, p, ang. distrib. anal., unbound levels of N doublet determ. 9-25650
¹²C(d, p)¹³C, 7.0-26 MeV, behaviour rel. to weakly-bound-projectile model 9-42309
¹²C(d, p)¹³C differential cross section meas., $E_d=5-10$ MeV 9-27742
¹²C(d, p) vector analysing power calcs. using WBP model, comparison with obs. 9-22813
 Co disintegration of 13.6 MeV deuterons on collision 9-48350
⁵²Cr(d, p) vector analysing power calcs. using WBP model, comparison with obs. 9-22813
⁵³Cr(d, p)⁵⁴Cr* ($Q=6.71$ MeV), initiated by vector polarized deuterons 9-44217
⁶⁵Cu(d, p)⁶⁶Cu, ang. distrib., levels, spin and parity determ., $E_d=12$ MeV 9-38681
⁶³Cu(d, p)⁶⁴Cu, p spectra meas., $E_d=5.5$ MeV 9-25658
⁶³Cu(d, p)⁶⁴Cu, p spectra meas., $E_d=5.5$ MeV 9-25658
¹⁹F(d, n)²⁰Ne 10-14 MeV excitation states, C_p factors determ., $E=5.1$ MeV 9-27744
 Fe excitation functions for various nuclei obs. 9-38715
⁷⁴Ge(d, 2n) in search for ^{74m}As 9-32323
⁷⁴Ge(d, p), stripping reaction on enriched target 9-38716
⁷⁴Ge(d, p), stripping reaction on enriched target 9-38716
 H(d, d), ang. distrib., cross section, excitation curves determ., $E_d=3.5-12.25$ MeV 9-25645
²H(d, n)³He, n yield meas. in Cu single crystal 9-40518
²H(d, n)³He, time-of-flight neutron expt. for undergraduate laboratory 9-45718
²H(d, d)³He, vector analysing power meas., $E_d(\text{pol.})=10$ MeV 9-25654
²H(d, p)³He, differential cross section meas., $E_d=4-10$ MeV 9-42301
²H(d, n)³H n prod. from deuterated polyphenyl target 9-25502
²H(d, n)³He, low energies, threshold reson., spin, parity, isospin, coupling matrix element linking react. channels 9-22819
²H(d, n)³He, n polarization energy and ang. distrib. meas., $E_d=0.5-2$ MeV 9-25653
²H(d, n)³He, partially polarised neutron beam production by associated particle method 9-36613

Nuclear reactions and scattering due to continued electrons continued

- ³He(d,p)³He, vector analysing power meas., $E_d(\text{pol.})=10$ MeV 9-25654
³H(d,n)³He, as a beam source, shape of beam 9-29675
³H(d,n)⁴He, neutron bursts prod. using D⁺ ion burst apparatus 9-27604
³H(d,p)³He, 83MeV differential cross-section obs. 9-22817
³H(d,p)³He, low energies, threshold reson., spin, parity, isospin, coupling matrix element linking react. channels 9-22819
³H(d,p)³He, vector analysing power meas., $E_d(\text{pol.})=10$ MeV 9-25654
³H(d,p)³He 100-500 KeV analysis 9-22818
³He(d,d), ang. distrib. of vector analyzing power $E_d(\text{pol.})=4-10$ MeV 9-42302
³He(d,d)³He, resonating-group analysis 9-38709
³He(d,d)³He double scatt. at 11.5 MeV, d polarization obs. 9-44212
³He(d,p)³He, ang. distrib. of vector analyzing power $E_d(\text{pol.})=4-10$ MeV 9-42302
³He(d,p)³He, polarized d, asymmetry of p emission, $E_d=6-10$ MeV 9-44214
³He(d,p)³He, rel. to a stripping theory 9-27739
³K(d, p)⁴²K at 12 MeV, spin assignments to levels in ⁴²K 9-27751
⁴Li, elastic and inelastic scatt., ang. distrib. and deform. parameters, DEBA analysis, $E_d=14.7$ MeV 9-42311
⁴Li, elastic and inelastic scatt., ang. distrib. and deform. parameters, DWBA analysis, $E_d=14.7$ MeV 9-42311
⁷Li(d,n)² α , determ. of width of 4+(11.4 MeV) level of ⁸Be 9-42207
⁷Li(d,n)⁸Be, interference effects near 1 MeV resonance 9-27755
⁷Li(d,n)⁸Be, n, ang. distrib. meas., energy levels determ. 9-22824
²³Mg(d, α)²³Na, cross-section fluctuations, $E_d=1.5$ to 2.5 MeV, obs. 9-25657
²⁴Mg(d,p)²⁵Mg, stripping reactions on deformed nuclei, example 9-44213
²⁴Mg(d,p)²⁵Mg energy levels, spectroscopic factors determ., $E_d=2.02-4.22$ MeV 9-25655
²⁴Mg(d,p) vector analysing power calcs. using WBP model, comparison with obs. 9-22813
²⁵Mg(d,p) excitation functions, Ericson fluctuations, 1.5-2.9 MeV 9-48349
⁹⁸Mo(d, t), to ⁹⁸Mo, even isotopes, ang. distrib., DWBA, l value and spectroscopic factor, $E_d=23$ MeV 9-27759
¹⁴N(d, α)¹²C, applic. to ¹²C energy level determ. 9-48354
¹⁴N(d,d)¹⁴N diff. cross section meas., DWBA anal., $E_d=1-3.2$ MeV 9-25651
¹⁴N(d,p)¹⁵N diff. cross section meas., DWBA anal., spectroscopic factors determ., $E_d=1-3.2$ MeV 9-25651
²⁰Ne(d,n)²¹Na, γ spectra meas., levels, spin, parity, branching and mixing ratios determ., $E_d=2.37-5.32$ MeV 9-34409
Ni, disintegration of 13.6 MeV deuterons on collision 9-48350
⁵⁸Ni(d, ³He), DWBA predictions test at $e_d=82$ MeV 9-40520
⁵⁸Ni(d,n)⁵⁹Cu, isobar analogue states obs., spectroscopic factors determ. 9-29837
⁶⁰Ni(d,n)⁶¹Cu, isobar analogue states obs., spectroscopic factors determ. 9-29837
⁵⁸Ni(d,p)⁵⁹Ni, γ spectra meas., $E_d=5.5$ MeV 9-25658
⁵⁸Ni(d,p)⁶¹Ni, γ spectra meas., $E_d=5.5$ MeV 9-25658
⁵⁸Ni(d,t), form factors and config. mixing 9-34440
¹⁶O(d, ³He), DWBA predictions test at $e_d=82$ MeV 9-40520
¹⁶O(d, α)¹⁴N, isospin-forbidden, cross section, ang. distrib. meas., J^{*} assignment, $E_d=3-15$ MeV 9-29827
¹⁶O(d,n)¹⁷F, angular distributions leading to ¹⁹F ground and first excited states 9-29826
¹⁸O(d,n)¹⁹F energy levels determ., spin and parity assigned, $E_d=3$ MeV 9-36581
¹⁶O(d,p)¹⁷O: p-p delayed coincidence meas., half-life determ., $E_d=1.2$ MeV 9-34422
³¹P(d, α)²⁸Si, 7.3-12.02 MeV, cross-sections meas., Ericson fluctuation analysis 9-27748
Pd(d,p) spectroscopic factors ratio, states of same I- π , $e_d=8-17$ MeV 9-40519
⁸⁷Rb(d,t)⁸⁶, study of ⁸⁶Rb low-lying levels 9-42217
⁸⁹Ru(d,p); excitation junction meas., $E_d\leq 14$ MeV 9-29838
³⁴S(d,³He)³²P, 2-body interaction matrix elements, shell-model calc. 9-29832
³⁴S(d,n)³⁵Cl, 4.95 MeV, for spin and parity assignments to levels of ³⁵Cl 9-48283
⁷⁴Se(d,p) stripping reaction, $E_d=6.5$ MeV 9-44218
⁸⁰Se(d,p) stripping reaction $E_d=6.5$ MeV 9-44218
³⁰Si(d,p), cross-section meas. 9-27659
Ti disintegration of 13.6 MeV deuterons on collision 9-48350
⁴⁹Ti(d,t), spectroscopic study of resulting ⁴⁹Ti 9-22823
⁸⁹Y(d,p)⁹⁰Y, excitation curves, ang. distrib., spectroscopic factors, DWBA anal., $E_d=4$ MeV 9-22825
⁶²Zn(d, α)⁶⁴Cu, ang. distrib., levels, spin and parity determ., $E_d=12$ MeV 9-38681
⁹⁰Zr(d,p)⁹¹Zr, cross section, p polarization determ., optical model and DWBA analysis, $E_d=1$ MeV 9-38717
⁹⁰Zr(d, α)⁹¹Nb, excitation function, analyzing power determ. 9-27757
⁹⁰Zr(d, α)⁹¹Zr, excitation function, analyzing power determ. 9-27757
- electrons**
angular correlation formulas between inelastic scatt. and nuclear decay, after electroexcitation 9-42183
in emulsion, 10 and 16 GeV, inelastic interac. props. 9-29785
multipole moment, 1st order Born approx., cross section determ. 9-29787
scattering, inelastic energy and A dependence of cross sections 9-48325
scattering of fast electrons, cross sections calc. method 9-32338
spectra of scattered electrons, distortion by radiative effects, correction method 9-40503
transition radiation prod. by 20-50 MeV electrons in opt. freq. range, meas. of fast particle energy 9-40504
(e,e'p), on light nuclei, DWIA analysis, channel coupling, quasi-elastic high energies 9-32339
(e,e'p), p spectra meas., impulse approx. analysis 9-34437
e-N McVoy and Van Hove treatment for light nuclei 9-25614
e, Be, n, K⁺ production, yields meas., $E_e=10, 16$ GeV 9-29566
 ν pair bremsstrahlung calc. for hot degenerate electron gas Coulomb scatt. 9-42009
 π double production, mass-dispersion and current algebra theory 9-27515
⁵⁸Ni, elastic scatt. rel. to neutrons influence on charge distrib. 9-27703
¹⁶⁵Ho(e,e')¹⁶⁵Ho, 200 MeV obs. 9-27702
- ¹⁸N, elastic scatt. rel. to neutrons influence on charge distrib. 9-27703
Al(e⁺, e⁻); secondary emission, energy depend., $E_e=1.5-18$ GeV 9-42274
Au(e⁺, e⁻); secondary emission, energy depend., $E_e=1.5-18$ GeV 9-42274
Be(α , α)⁹Li, differential cross sections and angular distributions 9-27758
Be(α , α)⁹Li, differential cross sections and angular distributions 9-27758
Be(α , α)⁹Li, differential cross sections and angular distributions 9-27758
Be(α , α)⁹Li, one-particle levels excitation obs. 9-42275
¹²C, dynamic N-N correlations determ. 9-34398
¹²C, form factors, cluster model applic. 9-25570
¹²C, giant dipole resonance spectra, transition prob., 16.1 MeV level form factor determ., $E_e=115, 200$ MeV 9-34436
¹²C, pion prod., inelastic at 400-1100 MeV 9-48330
¹²C, quasi-elastic, e-N McVoy and Van Hove treatment 9-25614
¹²C, 1, 1', 2- scatt. spectra in continuum model based on configuration mixing 9-25566
¹²C, giant resonance, excited by e scatt., compared to Kamimura-Ikeda-Arima model 9-44131
¹²C(e,e), Born approx. analysis correlation structure and charge density, high energies 9-34438
¹²C(e,e') scatt. at 180°, mag. excitations of ¹²C 9-32302
¹²C(e⁺, e⁻) γ C, wide angle bremsstrahlung yield at 6.2°, $E_e=9.5$ GeV 9-25613
³He, 180° e scatt. at 56 MeV, nuclear mag. structure investigation 9-42273
⁴He, correlations and form factor meas., momentum transfer square $q^2 \leq 20 \text{ fm}^{-2}$ 9-34396
⁴He, elastic form factor calc. 9-25615
⁴He, quasi-elastic scatt., e-N McVoy and Van Hove treatment 9-25614
⁴He (e,e); Born approx. analysis, correlation structure and charge density, high energies 9-34438
⁶Li, dynamic N-N correlations determ. 9-34398
⁶Li, form factors, cluster model applic. 9-25570
⁶Li, short-range dynamical correlations 9-44130
⁶Li, inelastic scatt., one-particle levels excitation obs. 9-42275
⁶Li(e, e'), form factors obs., p-shell harmonic oscillation parameter determ. 9-29784
⁷Li(e, e') rel

Nuclear reactions and scattering due to continued helium-3 continued

- $^{12}\text{C}(\text{He}, \text{d})^{13}\text{N}$, 12-19 MeV, excitation functions, ang. distrib. meas. 9-38712
 $^{13}\text{C}(\text{He}, ^3\text{He})$, ^{14}O structure determ., ang. and energy distrib. meas., $E_{\text{He}}=2.8$ MeV 9-32357
 $^{12}\text{C}(\text{He}, \text{p})$, ^{14}O structure determ., ang. and energy distrib. meas., $E_{\text{He}}=2.8$ MeV 9-32357
 $^{13}\text{C}(\text{He}, \alpha)$, ^{14}O structure determ., ang. and energy distrib. meas., $E_{\text{He}}=2.8$ MeV 9-32357
 $^{40}\text{Ca}(\text{He}, \text{p})^{39}\text{Sc}$ ang. distrib., spin-orbit coupling, p polarization meas., levels determ. 9-32317
 $^{48}\text{Ca}(\text{He}, ^3\text{He})^{46}\text{Ca}$, ang. distrib. meas., spectroscopic factor, I_n determ., CWBA, $E=15$ MeV 9-32359
 $^{48}\text{Ca}(\text{He}, \alpha)^{44}\text{Ca}$, ang. distrib. meas., spectroscopic factor, I_n determ., DWBA, levels determ., $E=15$ MeV 9-32359
 $^{48}\text{Ca}(\text{He}, \text{t})^{46}\text{Sc}$, t spectra meas., levels, spin determ. 9-38719
 $^{48}\text{Ca}(\text{He}, \text{t})$ reaction for obs. of particle hole states in ^{48}Sc 9-44144
 $^{50}\text{Cr}(\text{He}, \alpha)^{48}\text{Cr}$, cross section, ang. distrib., spectroscopic factors determ., $E=18$ MeV 9-29836
 $^{50}\text{Cr}(\text{He}, \text{d})^{51}\text{Mn}$ and $^{52,54}\text{Cr}(\text{He}, \text{d})^{53,55}\text{Mn}$, 9.5, 10 MeV levels of $^{51,53,55}\text{Mn}$ investigated 9-40478
 $^{52}\text{Cr}(\text{He}, \alpha)^{51}\text{Cr}$, cross section, ang. distrib., spectroscopic factors determ., $E=18$ MeV 9-29836
 $^{52}\text{Cr}(\text{He}, \text{t})^{52}\text{Mn}$, t spectra meas., levels, spin determ. 9-38719
 ^{52}Cr 36 MeV inelastic scatt. obs., cross-section analysed 9-32352
 $^{53}\text{Cr}(\text{He}, \alpha)^{52}\text{Cr}$, cross section, ang. distrib., spectroscopic factors determ., $E=18$ MeV 9-29836
 $^{54}\text{Cr}(\text{He}, \alpha)^{53}\text{Cr}$, cross section, ang. distrib., spectroscopic factors determ., $E=18$ MeV 9-29836
 $^{19}\text{F}(\text{He}, \text{d})^{20}\text{Ne}$, Doppler-shift lifetime, transition energy meas., rotational props. level lifetime calc. 9-36582
 $^{54}\text{Fe}(\text{He}, \text{t})^{54}\text{Co}$, t spectra meas., levels, spin determ. 9-38719
 $^{54}\text{Fe}(\text{He}, \text{t})$ charge exchange reaction, effective two-body force study 9-38720
 $^4\text{He}(\text{He}, ^3\text{He})$, elastic, polarization of ^3He , meas. by double-scatt. technique 9-46240
 $^7\text{Li}(\text{He}, \alpha)^6\text{Li}$ for diagram of first excited levels of ^6Li 9-29719
 $^7\text{Li}(\text{He}, \text{p})^6\text{Be}$, ^7Be low-lying states obs. 9-32307
 $^{24}\text{Mg}(\text{He}, \text{n})^{26}\text{Si}$, n distrib. meas., DWBA calc., L , spin and parity determ., $E=7$ MeV 9-32315
 $^{24}\text{Mg}(\text{He}, \text{n})^{26}\text{Si}$ levels and spin determ. 9-32314
 $^{12}\text{N}(\text{He}, \text{d})^{14}\text{O}$, d ang. distrib. meas., DWBA fits, levels and spectroscopic factors determ., $E=11$ MeV 9-29738
 $^{23}\text{Na}(\text{He}, \text{d})^{24}\text{Mg}$, at 35 MeV, spectroscopic factors, first 7 states of ^{24}Mg 9-44138
 $^{23}\text{Na}(\text{He}, \text{d})^{24}\text{Mg}$, Doppler-shift lifetime, transition energy meas., rotational props. level lifetime calc. 9-36582
 ^{20}Ne 36 MeV inelastic scatt. obs., cross-section analysed 9-32352
 ^{58}Ni , optical-model analysis of elastic scatt. at 21.15, 27/64 and 34.14 MeV 9-46243
 ^{58}Ni 36 MeV inelastic scatt. obs., cross-section analysed 9-32352
 ^{58}Ni target, large angle scatt. obs. 9-42298
 $^{16}\text{O}(\text{He}, ^3\text{He})^{16}\text{O}$, 9.8-11.7 MeV range, energy dependence of angular distributions 9-29840
 $^{16}\text{O}(\text{He}, \alpha)^{16}\text{O}$, 9.8-11.7 MeV range, energy dependence of angular distributions 9-29840
 $^{16}\text{O}(\text{Li}, \alpha)^{18}\text{F}$, for precision meas. of levels in ^{18}F 9-36614
 $^{17}\text{O}(\text{He}, \text{n})^{18}\text{Ne}$ energy levels determ., spin and parity assigned, $E_{\text{He}}=3$ MeV 9-36581
 $^{18}\text{O}(\text{He}, \alpha)^{17}\text{O}$, $E(^3\text{He})=16$ MeV, for $T=3/2$ states in ^{17}O 9-44134
 $^{18}\text{O}(\text{He}, \text{d})^{19}\text{F}$ spectroscopic factors determ. 9-40475
 $^{31}\text{P}(\text{He}, \text{p})^{31}\text{S}$, 6 MeV obs., rel. to collective effects in ground and first three excited states of ^{31}S 9-44216
 ^{23}Si 27 MeV inelastic scatt. obs., cross-section analysed 9-32352
 ^{23}Si 36 MeV inelastic scatt. obs., cross-section analysed 9-32352
 $^{46}\text{Ti}(\text{He}, \text{d})^{47}\text{V}$, $^{48,50}\text{Ti}(\text{He}, \text{d})^{49,51}\text{V}$, 9.5, 10 MeV, energy levels calc., shell model confirmed 9-40478
 $^{50}\text{Ti}(\text{He}, \text{t})^{50}\text{V}$, t spectra meas., levels, spin determ. 9-38719
 $^{94}\text{Zr}(\text{He}, \text{d})^{95}\text{Nb}$, 34 MeV obs. rel. to nuclear structure in this region 9-38718

hyperons

No entries

mesons

see also *Cosmic rays/effects and interactions*

- pion absorpt., radiative, validity of soft pion theorems 9-36609
 (π^-, NN) , two-N pot. scatt. model 9-34430
 K^- nuclear optical potential, representation of inelastic cross section 9-34459
 K^- capture meas., implication of heavy nuclei neutron halo 9-40516
 K^- capture on complex nuclei 9-42293
 K^- interaction with emulsion nuclei, at 10.1 GeV/c, hypernuclei prod. 9-40470
 π^- nuclear interactions, peculiarities 9-34458
 π^- nucleus scatt., πN chiral algebra and PCAC applic., sum rules determ. 9-42294
 π -nucleus interac., coherent prod. of 17.2 GeV π , nuc. emulsion 9-22805
 π^- , high-energy, coherent inelastic interactions 9-48345
 π^- on emulsion nuclei 210-375 MeV, double charge exchange with π prod. cross sections obs. 9-22806
 $(\pi^+, 2p)$, quasi-free react., energy depend. 9-36608
 $\pi^+ \text{d} \rightarrow \pi^0 \text{pp}$ in nuclei, evidence 9-36608
 π interactions, soft-pion method, deviations and corrections 9-36607
 π reactions with emulsion nuclei at 200 GeV, 135 obs. 9-25640
 π with emulsion nuclei, 200 GeV, four-momentum transfer and effective mass. 9-25639
 π with emulsion nuclei, 200 GeV, four-momentum transfer and effective mass. 9-25639
 π^+ absorpt. in flight by complex nuclei, expt. set-up 9-22656
 Ag , K^- interaction at 1.5 GeV/c, hyperfragment prod. 9-40471
 $\text{Al}(\pi^-, \Lambda)$, $E_{\pi}=925$ MeV, obs. 9-29814
 $\text{Be}(\pi^-, \Lambda)$, $E_{\pi}=925$ MeV, obs. 9-29814
 $\text{Be}(\pi^-, \text{nn})$ energy spectra, momentum distrib. meas., π^- absorption determ. 9-25644
 $^{11}\text{B}(\pi^-, \pi^0)^{11}\text{C}$, single charge-exchange react., cross-section, $E_{\pi}=80$ to 200 MeV 9-25641
 Br , K^- interaction at 1.5 GeV/c, hyperfragment prod. 9-40471
 $\text{Cl}(\pi^-, \Lambda)$ 3.86 GeV, cross-section for strange particle prod. obs. in freon bubble chamber 9-25643
 $\text{C}(\pi^-, \Lambda)$, $E_{\pi}=925$ MeV, obs. 9-29814

Nuclear reactions and scattering due to continued mesons continued

- $\text{C}(\pi^-, \Lambda)$ 3.86 GeV, cross-section for strange particle prod. obs. in freon bubble chamber 9-25643
 $^{12}\text{C}(\pi^-, \text{nn})$ energy spectra, momentum distrib. meas., π^- absorption determ. 9-25644
 $^{12}\text{C}(\pi^-, \pi^+ \text{p})^{11}\text{B}$ mechanism characteristic identification conditions, $p_{\pi}=1.04$ GeV/c 9-34461
 $^{13}\text{C}(\pi^+, \pi^0)^{13}\text{N}$ charge exchange cross section meas., $E_{\pi}=80$ -280 MeV 9-25642
 $^{13}\text{C}(\pi^+, \pi^0)^{13}\text{N}$ cross section around 1st resonance in $\pi\text{-N}$ system meas. 9-22807
 $\text{Cu}(\pi^-, \Lambda)$, $E_{\pi}=925$ MeV, obs. 9-29814
 $\text{F}(\Pi^-, \Lambda)$ 3.86 GeV, cross-section for strange particle prod. obs. in freon bubble chamber 9-25643
 $^3\text{He}(\pi, \pi)$ scatt. meas., nuclear wave function components anal. 9-27737
 $^3\text{H}(\pi, \pi)$ scatt. meas., nuclear wave function components anal. 9-27737
 $^6\text{Li}(\pi^-, \text{nn})$, energy spectra, momentum distrib. meas., π^- absorption determ. 9-25644
 $^7\text{Li}(\pi^+, \pi^+)^7\text{B}$, double charge-exchange react., cross-section, $E_{\pi}=80$ to 200 MeV 9-25641
 $^{14}\text{N}(\pi^-, \pi^0)^{14}\text{O}$ charge exchange cross section meas., $E_{\pi}=80$ -280 MeV 9-25642
 $^{14}\text{N}(\pi^-, \pi^0)^{14}\text{O}$, 180 MeV obs. and comparison with calc. 9-22808
 $^{14}\text{N}(\pi, \text{p})^{12}\text{C}$ sequential decay processes 9-22809
 ^{16}O , π radiative capture, rate and Hamiltonian calc. by shell model 9-34460
 $^{16}\text{O}(\pi^-, \text{N})$ bound 1s and 2p π absorption rates calc. in shell model 9-42295
 $\text{W}(\pi^-, \Lambda)$, $E_{\pi}=925$ MeV, obs. 9-29814

muons

- ^3He , μ capture and pseudoscalar coupling constant 9-27704
 μ capture, SU(4) scheme matrix elements equality 9-29788
 μ in emulsion, 10.5 GeV, inelastic interac. props. 9-29785
 μ high-energy showers of penetrating part., analysis 9-25497
 μ quantum electrodynamics experimental test 9-22540
 μ^- nuc. capture rate in gaseous H_2 9-27705
 ^{11}B , μ on capture, to $^{11}\text{Be}(\text{g.s.})$ and $^{11}\text{Be}(320 \text{ keV})$ 9-44189
 C , inelastic scatt., $E_{\mu}=8.6$ to 12.9 GeV/c, obs. 9-22539
 ^{12}C , capture, transition to ^{12}B g.s., probability calc. 9-36595
 ^{12}C , μ capture, continuum model for nuclear excitation 9-25566
 $^{40}\text{Ca}(\mu, \nu)^{40}\text{K}$, $^{40}\text{Ca}(\mu, \text{nn})^{39}\text{K}$, products identified by γ decay of excited states 9-38694
 $^{40}\text{Ca}(\mu, \text{p})^{39}\text{Ar}$, $^{40}\text{Ca}(\mu, \text{vp})^{38}\text{Ar}$, products identified by γ decay of excited states 9-38694
 $^{12}\text{C}(\mu^-, \nu_n)^{12}\text{B}$, capture rate, nuclear structure 9-34439
 $^{59}\text{Co}(\mu, \nu)^{59}\text{Fe}$ due to cosmic rays 9-48331
 $^{56}\text{Fe}(\mu, \nu)^{56}\text{Mn}$, prob. meas., theory comparison 9-29789
 μ^- He capture of μ^- , probability calc., asymmetry of recoil 9-32340
 $^3\text{He}(\mu^-, \nu)^3\text{H}$, μ^- capture rates, induced pseudoscalar form factor calc. using PCAC 9-27706
 ^6Li - ^6He , capture rate calc. from ^6Li magnetic form. factor 9-36596
 ^{16}O , μ capture, continuum model for nuclear excitation 9-25566
 ^{16}O , partial capture rates and the induced, pseudoscalar, coupling constant 9-44190
 $^{16}\text{O}(\mu, \text{nn})^{15}\text{N}^*$, partial capture rate, excitation level distrib. determ. 9-25616
 $^{16}\text{O}(\mu, \nu_n)^{16}\text{N}$, RPA and Tamm-Dancoff model calc. of capture rate, nuclear structure 9-34439
 $^{28}\text{Si}(\mu, \nu)^{28}\text{Al}$, $^{28}\text{Si}(\mu, \text{nn})^{27}\text{Al}$, products identified by γ decay of excited states 9-38694
 $^{28}\text{Si}(\mu, \text{vp})^{27}\text{Mg}$, $^{28}\text{Si}(\mu, \text{pnn})^{26}\text{Mg}$, products identified by γ decay of excited states 9-38694
 $^{32}\text{S}(\mu, \nu)^{32}\text{P}$, $^{32}\text{S}(\mu, \text{nn})^{31}\text{P}$, $^{32}\text{S}(\mu, \text{nnv})^{30}\text{P}$, products identified by γ decay of excited states 9-38694
 $^{32}\text{S}(\mu, \text{vp})^{31}\text{Si}$, $^{32}\text{S}(\mu, \text{vp})^{30}\text{Si}$, products identified by γ decay of excited states 9-38694

neutrinos

No entries

neutrons

see also *Nuclear fission*

- ^{208}Pb , dose rate attenuation 9-22791
 ^{56}Fe , dose rate attenuation 9-22791
 (n, γ) , polarized thermal neutrons, γ polar meas. rel. to energy levels of several nuclei 9-27725
 μ activation anal., chemical separation methods 9-49402
 μ capture, complete unit for study of γ -ray spectra produced 9-44206
 μ capture, radiative, for intermediate-energy neutrons, validity of direct and collective mechanisms 9-29809
 μ capture cross sections, obs. rel. to statistical model, 5 keV-3 MeV 9-25638
 μ capture cross-sections, new technique for meas. 9-44224
 μ capture mechanism in the resonance region, entrance channel and doorway states 9-44205
 μ capture of polarized thermal n, μ emission circular polarization meas. 9-27736
 μ capture of thermal neutrons, partial widths of subsequent γ transitions 9-38643
 μ cross section meas. of (n, 2n), survey, 3-7 MeV 9-22794
 μ cross section of inelastic scatt. meas., using scintillation detector insensitive to γ -rays 9-22787
 μ detector to meas. elastic scatt. cross-section in the resonance region 9-46236
 μ elastic at 14.5 MeV determ. of nuclear matter rms radii 9-42196
 μ energy depend. of cross section oscillation for (n,p), low energy 9-22795
 μ Exothermic (n,n'), serach 9-34453
 μ Feynman-diagram tech. applic. to heavy-ion neutron transfer, below Coulomb barrier 9-42287
 μ foil, absorbing, in H_2O moderator, activity calc. 9-22844
 μ inelastic scattering, applic. of nuclear opt. model averaged potentials 9-22788
 μ interference between resonance parameters using R-matrix and Kapur-Peierls theories 9-25632
 μ isobaric analogue states, Lane-Robson model, mechanical analogue 9-29703
 μ by medium-heavy nuclei, at 3.25 MeV obs. 9-27734
 μ optical potential, nuclear structure props. 9-29806
 μ quasi-compound nucleus theory of inelastic scatt. comparison with expt. 9-29805

Nuclear reactions and scattering due to continued neutrons continued

- radiative strength function, excitation energy depend., heavy nuclei fast n capture 9-34450
- reaction rate, n spectra determ., correction and smoothing parameters 9-27775
- resonance capture, correlation and distribution of widths 9-42288
- resonance reaction theory, book 9-25633
- scattering, inelastic, technique for carbon meas., design 9-33700
- spectrum, fast-neutron, and dose-rate measurements in water and aluminum-water laminations 9-22896
- target nuclei in ferromag. perfect single cryst., anomalous absorpt. of thermal polarized n 9-26464
- thermal, n capture in Mg_2SnO_4 , chem. and Mossbauer study 9-26852
- thermal cross-section, mean and variance, calc. by picket fence model 9-27723
- thermal neutron transmission through target containing deuterium, nitrogen and lanthanum nuclei, spin depend. 9-42289
- time interval distributions in neutron detection, stochastic operator method of calculating 9-27786
- transition cross sections in residual nucleus for (n,α) , α spectra meas., $E_n=14.6$ MeV 9-27724
- (n,γ) , 'effective cross-section' concept for reactor neutrons 9-25636
- (n,γ) , spectrometer and spectra recording 9-36509
- (n,γ) emission meas., moderator chem. analysis 9-37865
- $(n,2n)$ in rare earth isotopes, at 14.2 MeV, cross sections 9-22793
- (n,α) , n generator pulsed source in Wilson cloud chamber 9-29672
- (n,α) in rare earth isotopes, at 14.2 MeV, cross sections 9-22793
- (N,α) reactions on isotopes of Ti, V, Zr, Nb, Ag, In, Sn and I, cross section determs. 9-44207
- (n,p) reactions exciting short lived states in ^{108}Ag , ^{134}Cs and ^{160}Tb 9-38666
- (n,nn) ; spin cut-off evaluation from isomeric cross section ratio, 14 MeV 9-32347
- (n,p) in rare earth isotopes, at 14.2 MeV, cross sections 9-22793
- (n,p) reactions on isotopes of Ti, V, Zr, Nb, Ag, In, Sn and I, cross section determs. 9-44207
- (n,p) spectra, various metals subject to high n flux 9-27726
- (n,t) reactions on light nuclei, cross-section meas. 9-22792
- ^{46}Fe , ^{56}Fe , 2.33 MeV, polarized 9-27720
- ^{240}Pu , cross sections, resonance parameters, radiative capture, fission, $E_n=0.01$ eV-15 MeV 9-34456
- ^{170}Yb (n, γ) ^{171}Yb , also capture by isotopes ^{172}Yb - ^{174}Yb , regularities capture to low-lying Nilsson levels 9-46238
- ^{141}Pr (n, γ) ^{142}Pr neutron resonance capture, γ -ray transitions, and capture levels 9-46237
- ^{241}Pu , cross sections, resonance parameters, radiative capture, fission, $E_n=0.01$ eV-15 MeV 9-34456
- ^{157}Gd to ^{160}Gd , even isotopes, transmission and radiative capture, resonance parameters meas. 9-34401
- ^{242}Pu , cross sections, resonance parameters, radiative capture, fission, $E_n=0.01$ eV-15 MeV 9-34456
- ^{242}Pu (n, γ) ^{243}Am , γ spectra meas., levels spin and parity determ. 9-27651
- ^{232}Th (n, n') cross section and excitation function meas., $E_n=1-2.2$ MeV 9-27768
- ^{133}Cs resonance n capture, γ spectra 9-25577
- ^{133}Cs (n, γ) ^{134}Cs , study of ^{134}Cs excited states 9-44156
- ^{103}Rh , n resonance region, scatt. cross-section meas. 9-46236
- ^{103}Rh (n, γ) ^{104}Tc cross section, 14.8 MeV 9-32348
- ^{103}Rh (n, $2p$) ^{102m}Tc cross section, 14.8 MeV 9-32348
- ^{103}Rh (n, n') ^{104m}Tc cross section, 14.8 MeV 9-32348
- ^{124}Te (n, γ) ^{125}Te , levels of ^{124}Te deduced 9-38668
- ^{145}Sm (n, γ) ^{146}Sm separation and γ spectrum, obs. 9-33688
- ^{124}Te (n, α), α decay obs., level width meas. 9-40515
- ^{134}Ba (n, γ) ^{135}Ba , γ -ray spectrum rel. to level structure of ^{135}Ba 9-42224
- ^{134}Ba (n, γ) ^{135}Ba neutron resonance capture, γ -ray transitions and capture levels 9-46237
- ^{157}Gd thermal n capture, conversion electron spectrum 9-32350
- ^{115}In (n, n') ^{116}In , M1 transitions obs. 9-29727
- ^{208}Pb (n, γ) ^{209}Pb , activation cross sections at 10-200keV 9-42292
- ^{105}Pd , max. α decay width determ. 9-40515
- ^{18}Re , total and capture cross-sections, resonant parameters 0.01 eV to 30 keV 9-22797
- ^{235}U and ^{236}U , ^{237}U production 9-44209
- ^{235}U capture-fission ratio and fission cross section, 0.15 eV-30 keV 9-22831
- ^{235}U (n, α) ^{232}Th , α particle spectrum, meas. of low energy part 9-22800
- ^{206}Pb (n, n), diff. cross section, excitation function calc., levels determ. 9-40513
- ^{197}Au n resonance region, scatt. cross-section meas. 9-46236
- ^{167}Er (n, γ) ^{168}Er , γ -ray spectra variation on resonant neutron capture 9-22796
- ^{127}I (n, 2n), angular correlations between neutrons 9-29813
- ^{207}Pb (n, n), diff. cross section, excitation function calc., levels determ. 9-40513
- ^{207}Pb (n, n') $^{207}Pb^*$ cross section and continuum coupling influence on ^{208}Pb , RPA anal. 9-22799
- ^{18}Re , total and capture cross-sections, resonance parameters 0.01 eV to 30 keV 9-22797
- ^{187}Re (n, γ) ^{188}Re , γ -ray spectra on absorpt. of thermal neutrons and 4.41 eV neutrons 9-22798
- ^{117}Sn , total cross section and neutron cross section 9-42291
- ^{148m}Pm (n, n), search 9-34453
- ^{138}Ba (n, γ) ^{139}Ba , γ spectra meas., transitions and levels determ. 9-38705
- ^{208}Pb (n, n) cross section meas., $E_n=5.3-6.3$ MeV 9-29807
- ^{238}U deformed, elastic and inelastic scatt. of fast n 9-40514
- ^{109}Ag (n, γ) ^{110}Ag , n capture by 5.2 eV resonance, levels of ^{110}Ag 9-27727
- ^{237}Bi (n, 2n), angular correlations between neutrons 9-29813
- ^{239}Pu capture-fission ratio and fission cross section, 5 eV-23 keV 9-22831
- ^{239}Pu capture-to-fission ratio for $E_n=20$ to 600 keV 9-32351
- ^{148}Sm , 0.099 eV reson. parameters 9-34454
- ^{157}Tb (n, n') γ , energy distribution of γ -rays 9-29810
- ^{129}Xe max. α decay width determ. 9-40515
- Al, 1000 MeV, n, p, π emission 9-27728
- Al, polarization of 3.25 MeV neutrons meas. 9-27733
- Al, radiative capture, resonance radiation width, cross section meas., $E_n=0.1-200$ keV 9-27731
- Al (n, γ) spectra when subject to high n flux 9-27726
- Al nuclei, polarized 1.5 MeV n scatt. in angle range 20-143° 9-36605

Nuclear reactions and scattering due to continued neutrons continued

- Al total cross-sections for very slow neutrons, 100 m/sec to 5 m/sec. 9-44204
- ^{27}Al level-excitation cross section meas., $E_n=14.6$ MeV 9-36606
- ^{27}Al (n, γ) ^{28}Al gamma-ray spectra study using Ge(Li) spectrometer 9-38706
- ^{27}Al (n, α) ^{24}Na , 13.8-14.8 MeV, cross-section meas. 9-27732
- ^{27}Al (n, γ) ^{28}Al , γ spectra meas., Q-value, excitation energy, decay scheme determ. 9-22801
- ^{40}Ar (n, α) ^{37}S activation cross section meas., $E_n=14.4$ MeV 9-29812
- ^{40}Ar (n, np+n; pn+n, d) ^{39}Cl , activation cross section meas., $E_n=14.4$ MeV 9-29812
- ^{38}Ar (n, γ) ^{39}Cl , activation cross section meas., $E_n=14.4$ MeV 9-29812
- ^{40}Ar (n, γ) ^{41}Ar , activation cross section meas. 9-29812
- ^{75}As (n, 2n), in search for ^{74m}As 9-32323
- Au, small-angle scatt. of n, differential cross-sections, polar., applic. 9-25634
- Au, total cross-sections for very slow neutrons, 100 m/sec to 5 m/sec. 9-44204
- 11B - 12B , 3.39 MeV resonance state obs., spin and parity assignment, $E_n=20.8$ keV 9-29729
- ^{9}Be (n, 2n), angular correlations between neutrons 9-29813
- ^{9}Be (n, α) 6He , α spectra, 6He excited states obs. 9-32306
- ^{9}Be (n, d) 8Li , eff. cross section, 16.3-18.7 MeV 9-22804
- ^{9}Be (n, nn), cross section energy depend. meas., $E_n=2.0-6.4$ MeV 9-34457
- ^{208}Bi (n, 2n), ang. correl. 9-34451
- ^{10}B (n, α) 7Li reaction on methylboric acid label in air, meas. of aeration 9-24609
- ^{10}B (n, α) cross-section and branching ratio from thermal energy to 1 MeV from evaluation of data 9-25637
- ^{10}B (n, γ) ^{11}B secondary γ -ray transition broadening 9-42201
- C, of polarized 2.33 MeV neutrons 9-27720
- C_2 (n, n') γ , γ spectra meas. 9-34452
- ^{12}C (n, α), α -part. angular distrib., amplitude of α -cluster, ground-state transition cross-section, $E_n=14.1$ MeV 9-32349
- ^{12}C (n, α) 9Be angular distrib., D.W.B.A. calc., 14 MeV 9-38703
- ^{12}C (n, n), cross section and resonance meas., $E_n=5.3-6.3$ MeV 9-29807
- Co, cross-sections, total neutron, 3.3-5.2 MeV 9-38702
- ^{59}Co , n_{res} transmission, intensity spin-spin interaction determ. 9-27722
- ^{60}Co cross section, meas., activation of 10.5 min. and 5.26 year states 9-22802
- ^{52}Cr level-excitation cross section meas., $E_n=14.6$ MeV 9-36606
- Cu, polarized 2.33 MeV n scatt. 9-27720
- Cu(n, γ) spectra when subject to high n flux 9-27726
- ^{19}F (n, α) ^{16}Na as source of neutrons from $^{238}PuF_6$ 9-42290
- Fe, cross section meas., comparison with theory 9-25635
- Fe, radiative capture, resonance radiation width, cross section meas., $E_n=0.1-200$ keV 9-27731
- ^{56}Fe inelastic scatt. cross sections, test of quasi-compound nucleus theory 9-29805
- Fe(n, γ) spectra when subject to high n flux 9-27726
- ^{57}Fe (n, γ) ^{58}Fe , γ spectra meas., decay scheme determ. 9-32320
- Fe(n, n') γ , γ spectra meas. 9-34452
- ^{69}Ga (n, γ) ^{70}Ga , 0.4-2.5 MeV, level and decay schemes determ. 9-38664
- ^{71}Ga (n, γ) ^{72}Ga , 0.4-2.5 MeV, level and decay schemes determ. 9-38664
- Gd, total cross-section for 16-19 MeV 9-22789
- Gd isotopes, s-wave n strength function, resonance parameter and potential scatt. radii 9-40484
- Gd rare isotopes, reson. transmission obs. using isotopic mixtures 9-38708
- Ge (n,n)Ge, 0.3-1.5 MeV. obs., interpretation using optical and compound nucleus models 9-48343
- ^{74}Ge (n, γ) ^{75}Ge , used to study levels of ^{74}Ge 9-48344
- ^{3}He (n, γ) 3H rel. to O^+ first excited state of 4He 9-27739
- Hg isotopes, activation cross section meas., $E_n=14.1$ MeV 9-27730
- ^{10}H (n, 2n) 9H coincident neutron spectra, n-n scatt., length determ. 9-44208
- ^{2}H (n, γ) 3H , γ transition meas., n separation energy determ. 9-38645
- ^{2}H (n, n), diff. cross section meas., $E_n=5.6-9.1$ MeV 9-27729
- ^{2}H (n, nn), cross section meas., $E_n=4.0-6.5$ MeV 9-34455
- Ho, spins of n resonances obs. 9-27560
- ^{39}K (n, γ) ^{40}K , 29.4 keV level lifetime determ. 9-27661
- ^{39}K (n, γ) ^{40}K , radius change of ^{40}K after γ emission, determ. using Mossbauer effect 9-34412
- La(n, γ) γ , γ spectra meas. 9-34452
- ^{6}Li (n, α) 3H fragment energy distrib. meas. and interpretation for Pu fuelled reactor 9-29887
- Mg nuclei, polarized 1.5 MeV n scatt. in angle range 20-143° 9-36605
- Mg polarization of 3.25 MeV n meas. 9-27733
- Mn, cross-sections, total neutron, 3.3-5.2 MeV 9-38702
- Mn(n, n), level excitation 9-44145
- Mo isotopes, n resonances assigned 9-36574
- ^{90}Mo (n, α), α decay obs., level width meas. 9-40515
- (n, γ), for intermediate energy neutrons, validity of direct and collective mechanisms 9-29809
- Na, radiative capture, resonance radiation width, cross section meas., $E_n=0.1-200$ keV 9-27731
- ^{23}Na , total cross section meas., ^{24}Na level structure determ., $E_n=300-900$ keV 9-38654
- ^{23}Na elastic and inelastic scatt. at 1.51, 2.47, 4.04, 6.40 MeV 9-22790
- ^{23}Na (γ , γ) ^{24}Na , gamma-ray spectra study using Ge(Li) spectrometer 9-38706
- Nb, cross-sections, total neutron, 3.3-5.2 MeV 9-38702
- Ni, radiative capture, resonance radiation width, cross section meas., $E_n=0.1-200$ keV 9-27731
- Ni cross section meas., comparison with theory 9-25635
- ^{58}Ni , ^{60}Ni , polarized neutron scatt., 2.33 MeV 9-27720
- Ni(n, γ) spectra when subject to high n flux 9-27726
- ^{10}N (n, γ) ^{11}N secondary γ -ray transition broadening 9-42201
- ^{15}N (n, n') ^{15}N , shell bound-state method using truncated Hilbert space 9-44183
- ^{15}N (n, n') $^{15}N^*$, elastic and inelastic cross sections calc., 1p-1h configuration space coupled channels, $E_n=0-12$ MeV 9-36604
- ^{15}N (n, n') ^{15}N , shell model calc. in continuum, S-matrix Humblet-Rosenfeld expansion 9-27721
- O, 1000 MeV, n, p, π emission 9-27728
- O level-excitation cross section meas., $E_n=14.6$ MeV 9-36606
- P, of 7 MeV neutrons, optical model calc. of cross-sections and polarizations 9-29776

Nuclear reactions and scattering due to continued**neutrons continued**

- Pb, 1000 MeV, n.p., π emission 9-27728
 Pb, small-angle scatt. of n, differential cross-sections, polar., applic. 9-25634
 Pb(n,n), ang. correl. 9-34451
⁸³Rb(n,p)⁸⁶Rb, study of ⁸⁶Rb low-lying levels 9-42217
 S polarization of 3.25 MeV n meas. 9-27733
⁴⁵Sc, effective absorption sections in d_{3/2}-f_{7/2} transitions 9-25592
 Se isotopes, radiative capture and transmission cross sections, levels determ. 9-38704
⁷⁴Se(n,2n)⁷³Se 14.7 MeV cross-section obs. and compared with theory 9-22803
⁷⁶Se(n, α)⁸¹Se 14.7 MeV cross section obs. and compared to theory 9-22803
⁸⁰Se(n,p)⁸¹mSe 14.7 MeV cross-section obs. and compared with theory 9-22803
⁷⁶Se(n,p)⁷⁴As, 14.7 MeV cross-section obs. and compared to theory 9-22803
⁷⁶Se(n,p)⁷⁸As 14.7 MeV cross-section obs. and compared to theory 9-22803
 Si nuclei, polarized 1.5 MeV n scatt. in angle range 20-143° 9-36605
 Si polarization of 3.25 MeV n meas. 9-27733
 Si(n,n), diff. cross section, γ spectra meas., E_x=4-7.67 MeV 9-29811
 Th. cross-sections, total neutron, 3.3-5.2 MeV 9-38702
 Th. small-angle scatt. of n, differential cross-sections, polar., applic. 9-25634
⁴⁶Ti(n,p)⁴⁶Sc, neutron cross section meas. by activation method 9-27735
⁴⁷Ti(n,p)⁴⁷Sc neutron cross section meas. by activation method 9-27735
⁴⁸Ti(n,p)⁴⁸Sc neutron cross section meas. by activation method 9-27735
 Tm(n,n') γ spectra meas. 9-34452
 U, small-angle scatt. of n, differential cross-sections, polar., applic. 9-25634
 U isotopes, 14 MeVn, Pa heavy isotope prod. 9-38707
 UO₂, neutron-irradiated, Pu isotopic analysis 9-43346
⁵¹V isotropic scatt., 32 Li-glass n₀ detectors array calibration 9-32263
 V(n,n), level excitation 9-44145
 W, small-angle scatt. of n, differential cross-sections, polar., applic. 9-25634
 W cross section meas., comparison with theory 9-25635
 Xe(n,p), cross section ratios for isomeric pairs 9-48293
⁸⁹Y, of 7 MeV neutrons, optical model calc. of cross-sections and polarizations 9-29776
 Y(n,n') γ spectra meas. 9-34452
⁶⁴Zn to ⁶⁸Zn even isotopes, level-excitation cross section meas., E_x=14.6 MeV 9-36606
 Zn(n,p) spectra when subject to high n flux 9-27726
 ZrH, single differential cross-section at 296° and 700°K 9-22901

nuclei of Z>2*see also Ions/scattering*

- 3-26 GeV, cascade and evaporation studied in cosmic ray interactions with emulsion nuclei 9-22826
¹¹B(¹²C, γ)²³Na obs. for first time 9-27761
⁶Li(¹⁶O, γ)²³Na obs. for first time 9-27761
 heavy ion bombardment of light nuclei, γ spectra meas. from compound nuclei 9-27760
 heavy-ion scatt., excitation of collective modes in a dynamic classical model 9-44221
 heavy-ion transfer, recoil damping, ang. distrib. meas. above Coulomb barrier 9-38723
 transfer of two neutrons in the semiclassical strong absorption model 9-32362
 two-nucleon, transfer, differential cross section expression 9-22779
 two-nucleon, transfer, form factors, overlap integral role 9-22779
 (³H,d), normalization const. calc. and S' state obs. 9-32353
 (³H,p), normalization const. calc. and S' state obs. 9-32353
¹¹⁰Pd(¹⁶O,¹⁶O) Coulomb excitation, levels, spin, parity and E2 transitions determ., E_x=42-49 MeV 9-22722
¹²⁶Sn (⁴⁰Ar, 4n)¹³⁶Er, lifetimes of rotational states of ¹³⁶Er 9-25581
¹²⁸Sn(⁴⁰Ar, 4n)¹³⁸Er, lifetimes of rotational states of ¹³⁸Er 9-25581
²³²Th, ¹²C diff. cross section, energy spectra, ang. distrib. meas., E_x=82 MeV 9-25659
²³²Th, ¹⁴N diff. cross section, energy spectra, ang. distrib. meas., E_x=110 MeV 9-25659
²³²Th, ¹⁵N diff. cross section, energy spectra, ang. distrib. meas., E_x=98.5 MeV 9-25659
¹²⁶Sn(Ar, 4n)¹⁴⁰Er, lifetimes of rotational states of ¹⁴⁰Er 9-25581
¹⁰⁶Pd(¹⁶O,¹⁶O) Coulomb excitation, levels, spin, parity and E2 transitions determ., E_x=42-49 MeV 9-22722
¹⁹⁷Au, ¹²C diff. cross section, energy spectra, ang. distrib. meas., E_x=82 MeV 9-25659
¹⁹⁷Au, ¹⁴N diff. cross section, energy spectra, ang. distrib. meas., E_x=110 MeV 9-25659
¹⁹⁷Au, ¹⁵N diff. cross section, energy spectra, ang. distrib. meas., E_x=98.5 MeV 9-25659
¹⁰⁶Pd(¹⁶O,¹⁶O) Coulomb excitation, levels, spin, parity and E2 transitions determ., E_x=42-49 MeV 9-22722
²⁴⁹Cf, ^{12,13}C, element 104 isotope production, α emission, isotope identification 9-42219
 Ag, bombarded by 86 MeV ¹²C, products obs. 9-48352
 Ag production of ³²P by ¹⁶O and ²⁰Ne induced reactions 9-44222
 Au production of ³²P by ¹⁶O and ²⁰Ne induced reactions 9-44222
⁹Be(⁷Li,⁸Li)⁸Be cross sections, optical potential, nucleon tunnelling theory anal. 9-32363
¹²C(¹²C, γ)²⁴Mg obs. for first time 9-27761
¹²C(¹²C,n)²³Mg at low energies, appl. to stellar C burning investigation 9-43540
¹²C(¹²C,p)²³Na at low energies, appl. to stellar C burning investigation 9-43540
¹²C(¹⁶O, γ)²⁸Si obs. for first time 9-27761
¹²C(⁶Li,d)¹⁶O, excitation of rotational bands in ¹⁶O, mechanism 9-44223
¹²C(⁷Li,t)¹⁶O, excitation of rotational bands in ¹⁶O, mechanism 9-44223
¹²C on ¹²C, resons. obs. assuming quasimol. states 9-22827
¹²C-¹²C reaction, appl. to stellar thermonuclear burning of C investigation 9-40142
⁴⁰Ca(γ ,p)³⁹K corals. in energies and width of structures 9-40502
⁵²Cr, by ¹⁶O reactions proceeding through ⁶⁸Ge γ emission 9-27666
⁵²Cr-¹⁶O, reactions, ang. mom.eff. in breakup in compound nucleus 9-29757
⁵⁶Fe, by ¹²C, reactions proceeding through ⁶⁸Ge, γ emission 9-27666
⁵⁶Fe+¹²C, reactions, ang. mom. eff. in breakup in compound nucleus 9-29757
¹²C(¹²C, α)²⁰Ne at low energies, appl. to stellar C burning investigation 9-43540
⁶Li(¹⁶O,d)²⁰Ne, double-scatt. model in α -clusters framework, forward peak in ang. distrib. determ. 9-42312
⁷Li, ⁷Li; diff. cross section, angle and energy depend. E=2.1-5.75 MeV 9-29841
⁷Li(¹⁶O, γ)²³Na obs. for first time, resonance like structure obs. 9-27761
¹⁶Mg, of ³⁵Cl, Coulomb excitation at 61, 57, 52 MeV, quadrupole moment 9-48282
¹⁴N(¹⁴N,¹³N)¹⁵N, cross sections, optical potential, nucleon tunnelling theory anal. 9-32363
²²Ne(³²S,³²S)²²Ne(2⁺) quadrupole moments of 2⁺ states deduced 9-22736
 Ni, production of ³²P by ¹⁶O and ²⁰Ne induced reactions 9-44222
⁶²Ni, ²⁸Si bombard, rel. to meas. quadrupole moment of excited states of both nuclei 9-44141
¹⁶O, ¹⁶O scatt., excitation functions, nuc. molecular potn., parameters estimation 9-29828
¹⁶O, ¹⁶O scatt. near Coulomb barrier, excitation functions and ang. distrib. at 13 MeV c.m. energy 9-38722
¹⁶O(⁶Li, α)¹⁸F 4.8-13.8 MeV, obs., interpretation in terms of cluster interaction and statistical fluctuation models 9-36614
¹⁶O(⁶Li,d)²⁰Ne, excitation of rotational bands in ²⁰Ne, mechanism 9-44223
¹⁶O(⁷Li,t)²⁰Ne, excitation of rotational bands in ²⁰Ne, mechanism 9-44223
¹⁶O(⁷Li,t)²²Ne, 0⁺ state excited, SU(3) (4, 4) rep., E=12 MeV 9-29742

Nuclear reactions and scattering due to continued**nuclei of Z>2 continued**

- core polarization, second-quantized formulation of scatt. 9-27707
 kinetic energy of scattered nucleon, rel. to recoil of target 9-29790
 optical-model parameters from analysing available data, for A>40, E<50 MeV 9-48355
 recoil of target 9-29790
 single-hole-nuclei, inelastic scatt. in theory of finite Fermi systems 9-44191
 surface coupling model multilevel structures, resonance interference and pole collision 9-40506
⁴He, non-relativistic crossed partial-wave expansion, E_x=66-312 MeV 9-22778
¹³N, Chew-Frautschi plot for scatt. 9-40505
- photons**
 bell metal, effective atomic numbers for photoelec., scatt. and total γ cross-sections 9-24230
 bremsstrahlung γ -quanta interaction with complex nuclei 9-22773
 bremsstrahlung monochromator for investig. 9-42007
 Cabibbo-Radicati sum rule applic. 9-34428
 complex nuclei targets, cross section of η mesons and nucleons prod. 9-44185
 cross-section at giant resonance energies, for ¹⁶O(γ ,n)¹⁵O 9-38693
 electric dipole photodisintegration cross section energy-weighted sums 9-40499
 form factors and config. mixing in direct reactions 9-34440
 isospin selection rules violated in photonuclear reactions on light nuclei 9-25612
 isospin sum rule, p and n mean-square radius reln., g.s. pair correlation function determ. 9-40499
 monel metal, effective atomic numbers for photoelec., scatt. and total γ cross-sections 9-24230
 photoabsorption, energy and A dependence of cross sections 9-48325
 photoabsorption in nuclear matter, implications of vector-dominance 9-48323
 photodisintegration and Majorana exchange forces in three-particle nuclei 9-42270
 photon absorption cross-section, vector-mes. dominance applic. and ρ mass eff. 9-22774
 photonuclear disintegration, 40-350 MeV, calc. 9-48324
 solder, effective atomic numbers for photoelec., scatt. and total γ cross-sections 9-24230
 sterling silver, effective atomic numbers for photoelec., scatt. and total γ cross-sections 9-24230
 three-particle nuclei, photodisintegration and Majorana exchange forces 9-42270
 (γ , NN), two-N pot. scatt. model 9-34430
 (γ ,p) on various nuclei, obs. 9-40501
 γ photoprod. from complex nuclei targets, eta-nucleon cross sections 9-44185
 γ reson. scatt. from Sn 9-40500
 γ reson. scatt. in mag. field, PT violations 9-29779
 π double production, mass-dispersion and current algebra theory 9-27515
¹³⁰Te, resonance scatt., γ spectra meas., level transitions obs. 9-27695
¹⁴¹Pr(γ , γ'), levels determ. from γ spectra, E_x=4.8-7.7 MeV 9-27634
¹⁸¹Ta(γ ,p),(p,d) and (γ ,t), E_x=400-1300 MeV 9-22776
²³²Th(γ ,t), mono-energetic γ -rays, 12 different energies, cross-sections 9-27771
¹⁰³Rh(γ ,n) cross section meas., E_x=1-5.5 GeV 9-25611
¹⁰³Rh(γ ,xn) processes, 0.4-0.9 GeV, obs. 9-42271
¹²³Sb(γ ,n)¹²²Sb isomeric state formation, yield meas., E_x≤19 MeV 9-22725
¹⁶⁵Ho(α ,n) and ¹⁶⁵Ho(γ ,nn) obs. with nucleus polarized in parallel and perpendicular positions rel. to model of giant reson. 9-38673
²⁰⁵Tl(γ ,p)²⁰⁵Tl, resonance scatt. used to investigate ²⁰⁵Tl energy levels 9-46215
²⁰⁶Pd(γ , n), cross section and resonances obs., γ and M1 transitions obs., E_x≤40 keV 9-27644
¹⁹⁷Au(γ ,n), E_x=0.4-0.9 GeV 9-32337
¹⁹⁷Au(γ ,n) cross section meas., E_x=1-5.5 GeV 9-25611
¹²⁷I(γ ,n) cross section meas., E_x=1-5.5 GeV 9-25611
²⁰⁷Pb(γ , n), cross section and resonances obs., γ and M1 transitions obs., E_x≤40 keV 9-27644
²⁰⁸Pb(γ , n), cross section and resonances obs., γ and M1 transitions obs., E_x≤40 keV 9-27644
²³⁸U(γ ,n) cross section meas., E_x=1-5.5 GeV 9-25611
²⁷Al(γ , n) ²⁶Al*, ²⁷Al(γ , 2n) ²⁵Al, photoneutron mass-sections meas., at 62 MeV 9-48327
⁹Be, absorption in giant dipole resonance region, cross section meas. E_x=250 MeV 9-34435

Nuclear reactions and scattering due to continued photons continued

- Bi(γ, n), angular distribution of fast photoneutrons 9-27697
¹¹⁸Bi(γ, p) resonances obs. at 21.6, 23.2, 25.5, 27.7, and 29.2 MeV, cross-section up to 31 MeV 9-25610
¹²C, total absorption cross section meas., $E_\gamma=9-31$ MeV 9-29780
¹²C (γ, d), excitation function and energy depend. meas., $E_\gamma=400-1400$ MeV 9-34432
¹²C (γ, p), excitation function and energy depend. meas., $E_\gamma=400-1400$ MeV 9-34432
¹²C $\rightarrow \gamma$, energy below single nucleon production threshold 9-34279
⁴⁰Ca(γ, n_0)³⁹Ca, corals. in energies and width of structures 9-40502
¹²C(γ, n), cross section meas., $E_\gamma=1-5.5$ GeV 9-25611
¹²C(γ, n)¹²C, elec. dipole cross-sections calc. 9-29781
¹²C(γ, p), (γ, d) and (γ, t), $E_\gamma=400-1300$ MeV 9-22776
¹²C(γ, π) 154 MeV rel. to magnetic quadrupole amplitude of π photoproduction N 9-25455
¹²C(γ, x)¹¹Be, high energy bremsstrahlung beam absolute monitor, cross section meas., $E_\gamma=0.4-0.9$ GeV 9-27694
⁶³Cu-75 wt%Sn, effective atomic number for pair prod., γ energy 2.6-17.6 MeV 9-24232
¹⁹F, total absorption cross section meas., $E_\gamma=9-31$ MeV 9-29780
⁵⁶Fe, absorption cross section energy depend. determ., $E_\gamma=10-26.5$ MeV 9-29782
¹⁴⁷Gd, γ -photoelectric cross-sections 9-24231
⁴He(γ, n)³He, at γ -quanta maximal energy of 120 MeV 9-27701
⁴He, photodisintegration, continuum model 9-44195
⁴He, π^0 -mesons coherent photoprod. 9-42272
³He(γ, π^0)³He, 340 MeV, section obs. 9-48326
⁴He(γ, K^+)⁴H, photoproduction of hypernuclei and cross-sections 9-29721
⁴He(γ, K^0)⁴He, photoproduction of hypernuclei and cross-sections 9-29721
⁴He(γ, p)³H, ⁴He excited states obs. 9-32305
⁴He(γ, p)³H, giant reson. fine struct. 9-48328
⁴He(γ, pn)²H, total cross-section 9-46231
³He(γ, π^+)³He, 340 MeV cross-section obs. and compared with impulse approx. calc. 9-27699
³He(γ, π^+) by Primakoff effect 9-38526
¹Hf complex as target, (n, γ) recoil, effect on γ - γ ang. correl. 9-35597
¹Hf γ -photoelectric cross-sections 9-24231
 (γ, d) , mass number dependence of reaction cross-section 9-22775
 (γ, p) , mass number dependence of reaction cross-section 9-22775
¹La, γ -photoelectric cross-sections 9-24231
⁷Li(γ, d) α , isospin selection rules violated 9-25612
⁷Li(γ, p), polarization depend., quasimonochromatic photons 9-29783
⁷Li(γ, p), (γ, d) and (γ, t), $E_\gamma=400-1300$ MeV 9-22776
²⁶Mg(γ, n)²⁵Mg, threshold cross-section data and source of stellar neutrons 9-48329
²⁶Mg(γ, n)²⁵Mg cross-section summed from threshold to 62 MeV using bremsstrahlung 9-27698
²⁶Mg(γ, nn)²⁵Mg cross-section summed from threshold to 62 MeV using bremsstrahlung 9-27698
¹⁴N, total absorption cross section meas., $E_\gamma=9-31$ MeV 9-29780
²³Na production from nuclei $A=27$ to 40, cross sections meas., $E_\gamma=100-1200$ MeV 9-34431
⁶⁰Ni, ⁶⁰Ni, photodisintegration in giant resonance region, anomalous features 9-44232
⁶⁰Ni, photoneutron cross section anomalies 9-44187
⁶⁰Ni, photoneutron cross section anomalies 9-44187
⁶⁰Ni inelastic scatt. cross sections, test of quasi-compound nucleus theory 9-29805
¹²N(γ, p)¹²C, elec. dipole cross-sections calc. 9-29781
¹⁰O, Goldhaber-Teller model, isospin and spin-isospin modes coupling, structure 9-34429
¹⁶O, total absorption cross section meas., $E_\gamma=9-31$ MeV 9-29780
¹⁶O(γ, n)¹⁵O, cross-section, calc. 9-48276
¹⁶O(γ, n)¹⁵O, cross-section at giant resonance energies 9-38693
¹⁶O(γ, n)¹⁵O, cross section between 35 and 65 MeV 9-27696
¹⁶O(γ, n)¹⁵O γ -decay of excited state 9-48280
¹⁶O(γ, p)¹⁵N cross-section, k-matrix calc. 9-48276
¹⁶O(γ, p)¹⁵N, energy and ang. distrib. 9-32336
¹⁶O(γ, p)¹⁵N*, γ -decay of excited state 9-48280
²⁰⁸Pb target, Delbruck scatt. of 10.8 MeV γ rays 9-32335
²⁰⁸Pb-33 wt%Sn, effective atomic number for pair production, for γ energy 2.6-17.6 MeV 9-24232
²⁰⁸Pb(γ, n), angular distribution of fast photoneutrons 9-27697
³¹P(γ, p)³⁰Si, photoproton spectra from 21.5 and 27 MeV bremsstrahlung 9-27693
²⁰¹Pt-20 wt%Rh, effective atomic number for pair prod., γ energy 2.6-17.6 MeV 9-24232
²⁰¹Pt-40 wt%Rh, effective atomic number for pair prod., γ energy 2.6-17.6 MeV 9-24232
²⁸Si (γ, n) ²⁷Si, ²⁸Si ($\gamma, 2n$) ²⁶Si, ²⁸Si (γ, pn), ²⁶Al*, 62 MeV, photoneutron cross-section meas. 9-48327
²⁸Si(γ, n)²⁷Si cross-section obs. 9-44186
³¹Si(γ, p)³⁰P, photoproton spectra 9-27700
³¹Si(γ, p)³⁰P, photoproton spectra 9-44188
²⁰⁸Ta(γ, n), angular distribution of fast photoneutrons 9-27697
²⁰⁸Ta γ -photoelectric cross-sections 9-24231
²³⁸U isotopes, 100 MeV bremsstrahlung irradiat., Pa heavy isotope prod. 9-38707
²³⁸U target, Delbruck scatt. of 10.8 MeV γ rays 9-32335
¹⁵¹V(γ, p) energy spectrum at 90°, $E_\gamma=26.6$ MeV 9-34433
⁵⁸W steel, effective atomic numbers for photoelec., scatt. and total γ cross-sections 9-24230
⁹⁰Y(γ, p), photoproton energy and ang. distrib., spin dipole reson., hole states 9-34434
⁹⁰Zr(γ, p), photoproton energy and ang. distrib., spin dipole reson., hole states 9-34434

protons

- 6.2-22.5 GeV, cascade and evaporation studied in cosmic ray interactions with emulsion nuclei 9-22826
¹⁴⁰Ce(p, d), n single-hole states in 50 $N \leq 82$ shell obs., $E_p=55$ MeV 9-48251
¹⁶O(p, α) ang. distrib., direct reaction mechanism, $E_p=38$ MeV 9-48337
⁶²Ni(p, α)⁵⁸Co, 6-13.5 MeV thick target excitation function rel. to level density determination 9-48287
 (p, n) 30-50 MeV with isobaric analogue prod., microscopic theory 9-27710

Nuclear reactions and scattering due to continued protons continued

- analog resonance excitation, analysis of fragmentation by coupled optical eqns. with effective nonlocal potentials 9-38642
 analogue resonances decay amplitude, p ang. correlation meas. 9-42285
 cosmotron expt. at Brookhaven, description 9-34444
 Coulomb interference in elastic scatt. of polarized p , phase-shift calc. 9-40508
 elastic at 14.5 MeV determ. of nuclear matter rms radii 9-42196
 elastic scatt., 6.14 MeV, ang. distrib., optical-model analysis 9-42276
 elastic scattering, Coulomb interference, phase-shift calc. 9-40508
 energy levels determ., spectra and ang. distrib. meas. of (p, d), $E_p=156$ MeV 9-25621
 extra-nuclear hadron cascade calculations using Passour's approx. 9-44197
 fireball generation, obs. in 20-23 GeV p quasinucleon interactions 9-42281
 inelastic, ang. distrib. and diff. cross section meas. and anal., $E_p=185$ MeV 9-36599
 inelastic scatt., exchange effects and realistic interaction, microscopic description 9-44194
 isobaric analogue states, Lane-Robson model, mechanical analogue 9-29703
 isomers, new, short-lived, produced 9-48332
 Kallio-Koltveit interaction tested in DWA analysis of p scatt. on two nuclei 9-29791
 Lane equations, solution, comparison between two methods 9-29803
 nuclear emulsions, strong-absorption model applic., N-nucleus potn. calc., $M_\pi=3$ GeV/c 9-42280
 nuclei, $N > 7$, in mag. field, ang. and mom. distrib. determ., $E_p=21$ GeV 9-27711
 O^{+2} cross section calc. for nuclei in 25-1d shell 9-46233
 optical model analysis of 11 MeV data, revision of potential radius, well depth dependence on mass number and isospin 9-44192
 optical-model parameters from analysing available data, for $A > 40$, $E < 50$ MeV 9-48355
 polarization, kinematic 9-36597
 resonances and energy depend. of diffraction peak, phenomenological reln., analysis 9-42277
 scattering from 1 p shell light nuclei 10-15 MeV, optical-model analysis 9-48333
 spectroscopic and form factors, DWBA determ., light nuclei, $E_p=156$ MeV 9-25622
 stellar reaction rates, effect of excited nuclear states 9-43541
 Theoretical aspects for $E_p < 10$ GeV 9-34445
 (p, He) , (p, t) simultaneous obs. on O^+ target, parentage of nuclear states determ. 9-38697
 (p, xn) , ($1 \leq x \leq 4$), cross sections at 400 MeV 9-27719
 (p, zp) localization in configuration space, di-proton model and kinetic energy approx. comparison 9-29795
 (p, p) , on heavy nuclei, resonance theory 9-29796
 (p, n) , endoergic, and reverse reaction rates 9-46235
 (p, n) , on heavy nuclei, resonance theory 9-29796
 (p, n) reactions on ²H, ³H, ⁷Li and ⁹Be, 30, and 50 MeV, n source 9-29674
 (p, n) threshold meas. rel. to calibration of beam analyzing system 9-25504
 (p, p) , on heavy nuclei, resonance theory 9-29796
 (p, pd) type, theoretical analysis 9-36600
 (p, t) , (p, He) simultaneous obs. on O^+ target, parentage of nuclear states determ. 9-38697
¹⁹F(p, α)¹⁶O, stellar rates, effect of excited nuclear states 9-43541
¹⁹F(p, p)²⁰Ne, stellar rates, effect of excited nuclear states 9-43541
 n production, from 5 GeV/c p interactions in nuclear emulsions 9-48210
 p -nucleus, in emission, rel. to cascade-evaporation model 3 GeV/c 9-40507
 (p, d) differential cross-section for light nuclei in terms of peripheral model 9-27712
 (p, p) expts. with 4.5 MeV electrostatic accelerator 9-36545
 (p, np) expts. with 4.5 MeV electrostatic accelerator 9-36545
¹¹⁶mCd(p, xn)¹¹¹In cross section meas., $E_p=70-400$ MeV 9-27714
¹¹⁶mCd(p, p) inelastic scatt. at 55 MeV, vibr. states investigation 9-22723
¹¹⁶mCd(p, p)¹¹⁶Pt, γ spectra meas., E_l transition and β matrix elements determ., $E_p=9-11$ MeV 9-29735
¹¹⁶Ce(p, p), p ang. distrib. meas., n particle-hole states, levels and parity determ., $E_p=9.4-11.7$ MeV 9-29734
¹⁹Os(p, p)¹⁹Os, Coloumb excitation γ - γ ang. correlations following 9-36612
¹¹¹Cd(p, n), differential cross section meas., spin change and symmetry obs. 9-38700
¹¹¹Cd(p, n)¹¹¹In, γ and n spectra meas., spin and ang. distrib. determ., $E_p=4.2-5.35$ MeV 9-42220
¹⁴²Ce(p, p)¹⁴³Pt quadrupole contribution to cross-section 9-34446
¹¹¹mCd(p, xn)¹¹¹In cross section meas., $E_p=70-400$ MeV 9-27714
¹¹¹Cd(p, n), differential cross section meas., spin change and symmetry obs. 9-38700
¹¹⁶Cd(p, p) inelastic scatt. at 55 MeV, vibr. states investigation 9-22723
¹²⁶Te and even isotopes to 130, isobaric analog resonances prod. 9-44196
¹⁰⁶Cd to ¹¹⁶Cd even isotopes, scatt. ang. distrib. meas., $B(E2)$ ratio calc., $E_p=14$ MeV 9-27713
¹¹⁶Cd(p, p) inelastic scatt. at 55 MeV, vibr. states investigations 9-22723
²⁰⁶Pb(p, d), n single-hole states in 82 $N \leq 126$ shell obs., $E_p=55$ MeV 9-48251
¹¹⁶Sn(p, n)¹¹⁶Sb, pre-compound particles at 10, 12, 14 MeV bombarding energies 9-29797
¹¹⁶Sn(p, p) cross section meas., optical model analysis, $E_p=21$ MeV 9-38695
¹¹⁶Xe(p, p), ¹³⁷Cs levels, isobaric analog resonances spectroscopic factors meas., $E_p=9-13$ MeV 9-40509
¹⁰⁷Ag, induced analog resonance reaction, excitation function meas., $E_p=5.9-7.25$ MeV 9-29725
¹⁹⁷Au(p, p), recoil ¹⁹⁶Au angular distrib. rel. to models, $E_p=30-85$ MeV 9-29800
¹⁹⁷Au(p, pn), recoil ¹⁹⁶Au angular distrib. rel. to models, $E_p=30-85$ MeV 9-29800
¹⁹⁷Au(p, pn)¹⁹⁶Au, av. recoil ranges of ¹⁹⁶Au, 20-85 MeV 9-25630
¹²⁷I(p, n), cross-section meas. 9-25626
¹²⁷I(p, pn), cross-section meas. 9-25626
¹¹⁷Sn(p, d) 17 MeV p , failure to obs. prod. of any singlet d 9-38698

Nuclear reactions and scattering due to continued

protons continued

- ¹¹⁷Sn(p,n), differential cross section meas., spin change and symmetry obs. 9-38700
- ¹¹⁷Sn(p,n)¹¹⁷Sb, excitation functions 9-38701
- ²⁰⁸Bi, 0⁺-isobaric analogue resonance, shell model description 9-44165
- ¹⁰⁸Cd(p,p'), analogue resonances decay amplitude, p ang. correlation meas. 9-42285
- ²⁰⁸Pb(p, p), around resonances which are analogues of single-particle bound states in ²⁰⁸Pb 9-29803
- ²⁰⁸Pb(p, p)²⁰⁸Pb, low-lying states studied in p scatt. at resonance energy for isobaric analog. resonance 9-48302
- ²⁰⁸Pb(p, d), n single-hole states in 82<N≤126 shell obs., Ep=55 MeV 9-48251
- ¹¹⁸Sn(p,n)¹¹⁷Sb, excitation functions 9-38701
- ²³⁸U fission by 40-85 MeV protons, recoil props. of prod. nuclei 9-48359
- ¹⁰⁹Ag, induced analog resonance reaction, excitation function meas., E_p=5.9-7.25 MeV 9-29725
- ¹¹⁹Sn(p,n), differential cross section meas., spin change and symmetry obs. 9-38700
- Ag(p,p), diff. cross section meas., diffuse-surface optical model anal., E_p=28 MeV 9-25623
- Al 750, 1000, 2000 MeV, emission of n, p, π 9-27728
- ²⁷Al 20 MeV polarized p asymmetric scatt. obs. 9-25619
- ²⁷Al spallation; ¹⁸F, ^{22,24}Na fragments energy distrib. and range determ. 9-40511
- ²⁷Al(p,3pn)²⁴Na, recoil nuclei ang. distrib. meas., E_p=660 MeV 9-34449
- ²⁷Al(p,α) ang. distrib., direct reaction mechanism, E_p=38 MeV 9-48337
- ²⁷Al(p,α)²⁸Si, E_p=1724 keV, for study of 9.699 MeV level in ²⁸Si 9-44140
- ²⁷Al(p,γ)²⁸Si, resonance energy and yield meas. by Ge(Li) detector 9-32258
- Al(p,p), diff. cross section meas., diffuse-surface optical model anal., E_p=28 MeV 9-25623
- ²⁷Al(p,p), rel. to excited core model for description of low-lying levels of ²⁷Al 9-44139
- ²⁷Al(p,p) elastic, low- and mediuk- energy 9-48340
- ⁴⁰Ar(p,n)⁴⁰K, for positive parity states of ⁴⁰K 9-44143
- ⁴⁰Ar(p,p) cross section meas., optical model analysis, E_p=21 MeV 9-38695
- Au(p,p) diff. cross section meas., diffuse-surface optical model anal., E_p=28 MeV 9-25623
- B isotope production by bombardment of O and C, mass spectrometry 9-22784
- Be isotope production by bombardment of O and C mass spectrometry 9-22784
- Be target, neutron yield 9-38607
- Be, elastic scatt. cross-sections for 100 MeV p, optical model anal. 9-22783
- BeO target, 28.5 BeV protons, α prod. 9-32345
- ⁹Be(p,α)⁶Li diff. cross section and ang. distrib. meas., E_p=38 MeV 9-25631
- ⁹Be(p,α) ang. distrib., direct reaction mechanism, E_p=38 MeV 9-48337
- ⁹Be(p,d), 12 and 17 MeV obs. of singlet d (S=0, T=1) prod. 9-38698
- ⁹Be(p,d), rel. to ⁹Be 2⁺ states 9-40473
- ⁹Be(p,α)⁶He, ang. correl. distrib. and quasi-free scatt., 55 MeV 9-40510
- ¹¹B(p,3α), α spectra meas., ¹²C resonances shape spin and parity depend., E_p=0.15-4 MeV 9-25625
- ¹¹B(p,α)⁸Be diff. cross section and ang. distrib. meas., E_p=38 MeV 9-25631
- ¹⁰B(p,n)¹⁰C, energy of first excited state of ¹⁰C obs. 9-46194
- C p bombard 1-3 BeV obs. of emitted p 9-48336
- ¹²C, elastic scatt. cross-sections for 100 MeV p, optical model anal. 9-22783
- ¹²C, scattering phase shifts 9-29792
- ⁴⁰Ca, elastic and inelastic scatt., spins partial widths and decay of 60 resons. 9-42279
- ⁴⁰Ca(p, p')⁴⁰Ca, DWBA analysis with code JULIE 9-27662
- ⁴⁰Ca(p, p')⁴⁰Ca, DWBA analysis with code JULIE 9-27662
- ⁴⁰Ca(p,p')⁴⁰Ca DWA analysis using Kallio-Koltveit interaction 9-29791
- ⁴⁴Ca(p,p'), p ang. distrib. meas., excitation function determ., E_p=10 MeV 9-29834
- ³⁵Cl(p,n)³⁵Ar, threshold determ. 9-42284
- ⁵⁹Co(p,α)⁵⁶Fe, 6-13.5 MeV thick target excitation function rel. to level density determination 9-48287
- ¹²C(p,α)⁹Be, ¹²C excited states and α decay obs., E_p=57 MeV 9-27715
- ¹²C(p,α)⁹Be diff. cross section and ang. distrib. meas., E_p=38 MeV 9-25631
- ¹²C(p,α) ang. distrib., direct reaction mechanism, E_p=38 MeV 9-48337
- ¹²C(p,n)¹³N, p transition mixing ratio, levels, spin and parity determ., E_p=352-634 keV 9-29713
- ¹²C(p,p')¹²C, at low energies, E₁ transitions bet. resonant states near 3.51 MeV(½⁺) and 2.37 MeV(½⁺) levels 9-27621
- ¹²C(p,p), polarization and ang. distrib. meas., E_p=11-23 MeV 9-27716
- ¹²C(p,p)¹²C, coupled channel, analysis in terms of doorway states 9-46234
- ¹²C(p,p) expt. and multiple collision and optical model theory comparison 9-25618
- ¹²C(p,p'), 2⁺ excitations, spin-flip prob. and diff. scatt. cross section meas. DWBA analysis 9-42278
- ¹²C(p,p'), polarization and ang. distrib. meas., E_p=11-23 MeV 9-27716
- ¹²C(p,p)¹²C DWA analysis using Kallio-Koltveit interaction 9-29791
- ¹²C(p,p)¹²C*, diff. cross section and polarization scatt., E=4.43-22.3 MeV 9-34441
- ¹²C(p,p')¹²C*, spin flip of polarized p., model 9-48334
- ¹²C(p,p), diff. cross section, polarization meas., optical parameters determ., E_p=7 MeV 9-32342
- ¹²C(p,p), diff. cross section, polarization meas., optical parameters determ., E_p=7 MeV 9-32342
- ¹²C(p,x) nuclear spallation production of ¹⁰B, ¹¹B 9-36601
- ⁵²Cr, scatt., elastic and inelastic rel. to nuclear models, 17.5 MeV 9-34443
- ⁵³Cr(d,d)⁵³Cr energy levels determ., Ed=7.5 MeV 9-48307
- ⁵²Cr(d,p)⁵³Cr energy levels determ., Ed=7.5 MeV 9-48307
- ⁵³Cr(p,p)⁵³Mn, ⁵⁴Mn level schemes 9-32360
- ⁵²Cr(p,p)⁵²Cr energy levels determ., Ep=7.5 MeV 9-48307
- ⁵³Cr(p,p)⁵³Cr energy levels determ., particles ang. distrib. obs., Ep=7.5 MeV 9-48307
- ⁵³Cr(p,p)⁵³Cr energy levels determ., particles ang. distrib. obs., Ep=7.5 MeV 9-48307
- Cu p bombard 1-3 BeV obs. of emitted p 9-48336

Nuclear reactions and scattering due to continued

protons continued

- ⁶³Cu inelastic scatt., final state spin depend. anomaly 9-32344
- ⁶³Cu, γ scatt., γ from ⁶⁰Co, 4000 Ci source, Compton scatt. 9-34413
- ⁶³Cu inelastic scatt., final state spin depend. anomaly 9-32344
- Cu(p,p), diff. cross section meas., diffuse-surface optical model anal., E_p=28 MeV 9-25623
- ⁶³Cu(p,pn), recoil ⁶⁴Cu angular distrib. rel. to models, Ep 30-85 MeV 9-29800
- ⁶³Cu(p,pn)⁶⁴Cu, av. recoil ranges of ⁶⁴Cu, 20-85 MeV 9-25630
- ¹⁹F spallation; ¹⁸F, ^{22,24}Na fragments energy distrib. and range determ. 9-40511
- Fe target, 1 and 3 GeV bombardment 9-27708
- ⁵⁶Fe, scatt., elastic and inelastic rel. to nuclear models, 17.5 MeV 9-34443
- ⁵⁶Fe(p, p')⁵⁶Fe, 5-6 MeV, spin-flip meas. reaction mechanism investigated 9-48335
- ⁵⁷Fe(p,p')⁵⁸Co, ⁵⁸Co level schemes 9-32360
- ⁵⁴Fe(p,p')⁵⁴Fe, energy levels, 2.56 MeV level spin determ. 9-29753
- ¹⁹F(p,α)¹⁶O diff. cross section and ang. distrib. meas., E_p=38 MeV 9-25631
- ¹⁹F(p,p')¹⁹F energy levels determ., Ep=9 MeV 9-36581
- ⁷²Ge(p, xn)⁷³⁻⁷⁵As, cross section, excitation func. meas., E_p=400 MeV 9-27719
- ⁷⁰Ge(p,p')(p,p'), ⁷⁰Ge deduced levels and assignments, E2 transitions, 7.0 MeV 9-25620
- ⁷⁰Ge(p,p')⁷⁰Ge*, reaction time meas. by blocking of energetic particle in single crystal 9-38696
- ⁷²Ge(p,p')⁷²Ge*, reaction time meas. by blocking of energetic particle in single crystal 9-38696
- ¹H, bremsstrahlung cross section, p-p time of flight diff., E_p=10 MeV 9-29798
- ³He, target polarized by optical pumping, left-right scatt. asymmetry, E_p=3.8-10.9 MeV 9-29793
- ⁴He, analyzing power and phase shift anal., E_p=70-80 MeV 9-36602
- ⁴He(p,d), pick-up and final state interactions obs., E_p=156 MeV 9-42282
- ⁴He(p,d)³He diff. cross section peripheral model anal., E_p=31-156 MeV 9-29718
- ³He(p,p)³He, continuum shell model 9-44195
- ³He(p,p)³He, phase shifts 9-27739
- ³He(p,p) expt. and multiple collision and optical model theory comparison 9-25618
- ³He(p, p'), polarization meas., phase-shift anal., E_p=4-11 MeV 9-25628
- ³He(p, p'), spin- correlation parameter meas., phase-shift anal., E_p=8.8 MeV 9-25629
- ³H(p,2p)n, 6.5-13.0 MeV, obs. of quasifree and sequential decay mechanisms 9-48338
- ³H(p,n)³He, 1 MeV flux meas., associated particle method, ³He no. and direction determ. 9-29640
- ²H(p,p), polarization and ang. distrib. meas., E_p=11-23 MeV 9-27716
- ²H(p,p)²H, p polarization meas., Ep=9.5 and 21.6 MeV 9-22781
- ²H(p,p)p, corrections to impulse approx., ang. distrib. meas., E_p=155 MeV 9-34448
- ²H(p,p)p, energy, ang. distrib. and cross section meas., 1st order impulse approx., E_p=155 MeV 9-32346
- ³⁹K(p, p')³⁹K*, p channels excitation functions meas., ⁴⁰Ca resonances obs. 9-29799
- ³⁹K(p,α)³⁶Ar, α channels excitation functions meas., ⁴⁰Ca resonances obs. 9-29799
- ³⁹K(p,p')³⁹K, α, and lifetime obs. on ⁴⁰Ca energy levels 9-44142
- ³⁹K(p,p')³⁹K, p-p delayed coincidence Meas., half-life determ., E_p=5.6 MeV 9-34422
- Li isotope production by bombardment of O and C mass spectrometry 9-22784
- ⁶Li, elastic scatt. cross-sections for 100 MeV p, optical model anal. 9-22783
- ⁶Li, elastic scatt. cross-sections for 100 MeV p, optical model anal. 9-22783
- ⁶Li, γ scatt., γ from ⁶⁰Co, 4000 Ci source, Compton scatt. 9-34413
- ⁶Li(p,He), cross section, spectroscopic factors determ., DWBA anal., E_p=30.3 MeV 9-22786
- ⁶Li(p,α), cross section, spectroscopic factors determ., DWBA anal., E_p=30.3 MeV 9-22786
- ⁶Li(p,α)³He ang. distrib., analyzing power, diff. cross section meas., E_p=2.7-10.6 MeV 9-25624
- ⁶Li(p,d), pick-up and final state interactions obs., E_p=156 MeV 9-42282
- ⁶Li(p,d), 12 MeV, obs. of singlet d (S=0, T=1) prod. 9-38698
- ⁶Li(p,d), cross section, spectroscopic factors determ., DWBA anal., E_p=30.3 MeV 9-22786
- ⁶Li(p,d), pick-up and final state interactions obs., E_p=156 MeV 9-42282
- ⁶Li(p,p)⁶He*, rel. to isobaric-spin mixing in ⁶He 9-48272
- ⁶Li(p,p)⁶Be-2α, E_p=1.5 MeV, ang. correl. derived and compared with expt. 9-48339
- ⁶Li(p,n), cross section energy dependence, determ. with Grey neutron detector 9-48226
- ⁶Li(p,p)⁶Li, phase shift and polarization ang. distrib. meas., E_p=0.5-5.6 MeV 9-32343
- ⁶Li(p,p)⁶Li ang. distrib., analyzing power, diff. cross section meas., E_p=2.7-10.6 MeV 9-25624
- ⁶Li(p,p)⁶Li* ang. distrib., analyzing power, diff. cross section meas., E_p=2.7-10.6 MeV 9-25624
- ⁶Li(p,p)d, first order analysis by PWBA calc. 9-44199
- ⁶Li(p,p)d⁶He, matrix element, calc. using fully antisymmetrized cluster-model wave function 9-44198
- ⁶Li(p,p), angular correlation meas., comparison with ⁶Li (p,p), E_p=30.3 MeV 9-22786
- ⁶Li(p,t), cross section, spectroscopic factors determ., DWBA anal., E_p=30.3 MeV 9-22786
- ²⁴Mg, ²⁵Mg, ²⁶Mg, 20 MeV polarized p asymmetric scatt. obs. 9-25619
- ²⁴Mg, relative p, γ yield determ., E_p=2010 keV 9-27652
- ²⁴Mg, Y_d deformation, evidence from p scatt. 9-42230
- ²⁴Mg spallation; ¹⁸F, ^{22,24}Na fragments energy distrib. and range determ. 9-40511
- ²⁴Mg(p,He)¹⁹Na, ¹⁹Na mass excess obs. 9-25568
- ²⁴Mg(p, 2p)²²Mg, cross section and excitation function meas., E_p=0.43-2.7 GeV 9-27717
- ²⁴Mg(p,d), 17 MeV p, failure to obs. prod. of any singlet d 9-38698
- ²⁴Mg(p,p) for study of 4.038 MeV state in ²⁴Al 9-25590
- ²⁴Mg(p,p)²⁴Mg, p polariz., E_p=3.14 MeV reson. obs., Al²⁵ 5.304 MeV level spin 9-25627

Nuclear reactions and scattering due to continued protons continued

- ⁵⁵Mn, scatt., elastic and inelastic rel. to nuclear models, 17.5 MeV 9-34443
- ⁵⁵Mn (p,α)⁵²Cr, 6-13.5 MeV thick target excitation function rel. to level density determination 9-48287
- ⁵⁵Mn(p,n)⁵⁵Fe, ⁵⁵Fe e capture decay energy, comparison 9-42244
- ⁹⁰Mo(p,γ)⁹⁰Tc, isobaric analogue states, γ transitions to low-lying states 9-29760
- ⁹⁰Mo(p,p')⁹⁰Mo excitation of low-lying states via isobaric analog resonances 9-48289
- ²³Na, γ scatt., γ from ⁶⁰Co, 4000 Ci source, Compton scatt. 9-34413
- ²³Na(p,γ)γγ correlation meas., levels deduced E_p=4.71, 5.12 MeV 9-48304
- ²⁰Ne and other s-d shell nuclei, evidence for Y₄ deformation from p scatt. 9-42230
- ²⁰Ne(p,γ)²¹Ne, second excited state mean lifetime 9-48281
- ²⁰Ne(p,p)²⁰Ne, cross-section calc. using 20 particle wave function 9-46233
- ²²Ne(p,p), cross section, ang. distrib. meas., ²³Na resonance deduced, E_p=4.8-14 MeV 9-22782
- ⁵⁸Ni, ⁶⁰Ni(p,p); optical model parameter differences determ., E_p=12-50 MeV 9-29692
- ⁶²Ni, p ang. distrib. meas., DWBA fits, γ spectra meas., levels determ., E_p=12 MeV 9-32322
- ⁶⁴Ni, p ang. distrib. meas., DWBA fits, γ spectra meas., levels determ., E_p=12 MeV 9-32322
- ⁵⁸Ni(p,d), form factors and config. mixing 9-34440
- ⁵⁸Ni(p,n)⁵⁸Cu, double-analog resonances 9-44200
- ⁵⁸Ni(p,p) cross section meas., optical model analysis, E_p=21 MeV 9-38695
- ⁵⁸Ni(p,p')⁵⁸Ni*(1.45 MeV), proton spin-flip probability, E_p=20 MeV 9-27718
- ¹⁴N(p,p)¹⁴N, 3.7-5.67 MeV obs. rel. to level structure of ¹⁵O 9-38649
- ¹⁴N(p,p) cross section meas., optical model analysis, E_p=21 MeV 9-38695
- O, 750, 1000, 2000 MeV, emission of n, p, n 9-27728
- ¹⁶O p spallation, formation cross sections for Li, Be and B 9-44203
- ¹⁶O proton scattering phase shifts 9-29792
- ¹⁶O(α,p)¹⁵N, quadrupole giant resonance evidence 9-44133
- ¹⁶O(p,α)¹³N diff. cross section and ang. distrib. meas., E_p=38 MeV 9-25631
- ¹⁸O(α,p)¹⁷O, excitation functions, 3.2 to 5.4 MeV 9-22785
- ¹⁸O(p,α)¹⁵N, excitation functions rel. to ¹⁹F resons., 1.39-3.20 MeV 9-34390
- ¹⁶O(p,p), collision with nucleus substructure, E_p=660 MeV 9-34447
- ¹⁶O(p,p), elastic low- and medium-energy 9-48340
- ¹⁶O(p,p) exp. and multiple collision and optical model theory comparison 9-25618
- ¹⁸O(p,p,γ)¹⁸O, excitation functions, 3.2 to 5.4 MeV 9-22785
- ¹⁸O(p,p)¹⁸O, excitation functions rel. to ¹⁹F resons., 1.39-3.20 MeV 9-34390
- ¹⁶O(p,p) cross section meas., optical model analysis, E_p=21 MeV 9-38695
- (p,α) on light nuclei, ang. distrib., direct reaction mechanism, E_p=38 MeV 9-48337
- Pb p bombard 1-3 BeV obs. of emitted p 9-48336
- ³¹P(p,α)²⁸Si, cross section energy depend., ³²S excited state parameters determ., E_p=10-12.5 MeV 9-29748
- ³¹P(p,α) ang. distrib., direct reaction mechanism, E_p=38 MeV 9-48337
- ³¹P(p,γ)³¹S lifetime and ang. distrib. meas. 9-42283
- ³¹P(p,p), cross section energy depend., ³²S excited state parameters determ., E_p=10-12.5 MeV 9-29748
- ³¹P(p,p,γ) ³²S mean level width, excitation function meas., E_p=8-10 MeV 9-25591
- ⁹⁰Se, effective absorption sections in d_{5/2}-f_{7/2} transitions 9-25592
- ²⁸Si, p polarization energy depend. meas., E_p=2.6-4.0 MeV 9-34442
- ²⁸Si 20 MeV polarized p asymmetric scatt. obs. 9-25619
- ²⁸Si spallation; ¹⁸F, ^{22,24}Na fragments energy distrib. and range determ. 9-40511
- ²⁸Si, γ scatt., γ from ⁶⁰Co source, Compton scatt. 9-34413
- ²⁸Si(p,He)²³Al, ²³Al mass excess obs. 9-25568
- ³⁰Si(p,p')³⁰P, p ang., energy distrib. meas., levels, spin and parity determ., E_p=3-4 MeV 9-27658
- Si(p,p), diff. cross section meas., diffuse-surface optical model anal., E_p=28 MeV 9-25623
- ²⁸Si(p,p), elastic low- and medium-energy 9-48340
- ²⁸Si(p,p), rel. to excited core model for description of low-lying levels of ²⁷Al 9-44139
- ²⁸Si(p,p)²⁸Si, evidence for hexadecapole deformation 9-42230
- ²⁸Si(p,p)²⁸Si*, reaction time meas. by blocking of energetic particle in single crystal 9-38696
- Sn(p,n) reactions, (E_p=3 to 5.5 MeV), proton strength functions, optical model analysis 9-44202
- ³⁶S(p,γ)³⁶Cl, rel. to levels of ³⁷Cl in 10.4 to 10.6 MeV range 9-42212
- ⁸⁸Sr/p, coupled eqns. solved numerically with optical-model parameters 9-38642
- ⁸⁸Sr(p,n)⁸⁸Y, excitation function, ang. distrib. meas., spin and parity determ. 9-29801
- ⁸⁸Sr(p,*) ⁸⁸Sr*, p ang. distrib. meas., antisymmetrized microscopic DWBA calc., levels, spin and parity calc., E_p=20 MeV 9-29794
- ⁸⁸Sr(p,n)⁸⁸Y, isobaric analog resonance formation, comparison of coupled-channel formalism and R-matrix 9-44201
- ⁸⁸Sr(p,n)⁸⁸Y, total cross section, S_{1/2} analog resonance meas., E_p≈6 MeV 9-38699
- Ti isotopes, elastic scatt. 9-36598
- ⁴⁸Ti(p,γ)⁴⁸V, ⁵⁰V level schemes 9-32360
- ⁴⁸Ti(p,p)⁴⁸Ti, study of analogue resonances of ⁵¹Ti in ⁵¹V 9-46199
- ⁴⁸Ti(p,p'), spectroscopic study of ⁴⁹Ti 9-22823
- ⁴⁸Ti(p,p)⁴⁸Ti, study of isobaric analogue states of ⁵¹Ti 9-46199
- ⁴⁸Ti(p,p,γ), levels lifetime branching ratio determ. by Doppler-shift attenuation method 9-38659
- ⁵¹V, scatt., elastic and inelastic rel. to nuclear models, 17.5 MeV 9-34443
- ⁶⁷Zn inelastic scatt., final state spin depend. anomaly 9-32344
- ⁹⁶Zr(p,d)⁹⁵Zr, excitation function meas., isospin effects obs. 9-36603
- ⁹⁶Zr(p,n)⁹⁵Nb*, charge exchange cross section calc. 9-40512
- ⁹⁶Zr(p,p')⁹⁶Zr, excitation function meas., isospin effects obs. 9-36603
- ⁹⁶Zr(p,p')⁹⁶Zr, 12 MeV, core-excitation model for ⁹¹Zr states 9-48342
- ⁹⁶Zr(p,p), p ang. distrib. meas., levels determ., E_p=18.7 MeV 9-27709
- ⁹⁶Zr(p,p')⁹⁶Zr, 12 MeV, core-excitation model for ⁹¹Zr states 9-48342

Nuclear reactions and scattering due to continued protons continued

- ⁹⁰Zr(p,t), L=0 transition obs., E_p=38 MeV 9-29802
- ⁹⁰Zr(p,t)⁸⁸Zr, rel. to excited levels of ⁸⁸Zr 9-42235
- ⁹⁰Zr(p,t)⁸⁸Zr, rel. to excited levels of ⁸⁸Zr 9-27670
- ⁹²Zr(p,t), L=0 transition obs., pair-vibrational like state excitation, e_p=38 MeV 9-29802
- ⁹²Zr(p,t), L=0 transition obs., E_p=38 MeV 9-29802
- ⁹²Zr(p,t), L=0 transition obs., E_p=38 MeV 9-29802
- ⁹⁶Zr(p,p)⁹⁶Zr, excitation function meas., isospin effects obs. 9-36603
- tritons
- diffraction interaction, splitting, diff. cross section formula 9-36570
- optical potential determ. from fitting meas. of ⁴⁰Ca(t,d)⁴¹Ca 9-46198
- well depth, real central and spin-orbit, light nuclei, E_p=2 MeV 9-29816
- ¹²C(α,¹H) reaction, degree of overlapping of ¹²C α substructures 9-48273
- ²³⁵U(t,d,f), fission-fragment angular correlations 9-42315
- ¹¹⁴Cd(d,t)¹¹³Cd, to determ. transitions in ¹¹³Cd 9-38667
- ²⁰⁷Tl(t,p)²⁰⁷Tl, p spectra meas., vib. levels, spin and parity determ., E_p=13 MeV 9-27646
- ²³⁵U(t,d,f), fission-fragment correlations 9-42315
- ²³⁸Pu(t,d,f), fission-fragment correlations 9-42315
- ¹⁹B(t,α)¹⁹Be, 1.00-2.10 MeV, ang. distrib. optical parameters by DWBA 9-42303
- ¹⁰B(t,p)¹²B, g.s. ang. distrib. meas., DWBA calc. 9-36611
- ⁴⁰Ca to ²⁰⁸Pb, 20 MeV analysis of optical model data from 17 nuclides 9-48346
- ⁴⁰Ca(t,d)⁴¹Ca, excitation of first two excited states of ⁴¹Ca 9-46198
- ⁴⁰Ca(t,p)⁴²Ca, ang. distrib., spin-orbit coupling, p polarization meas., levels determ. 9-32317
- ⁵³Cr(t,n)⁵²Mn, react. charact., ⁵⁴Mn level schemes 9-32360
- ¹²C(t,α)¹¹B, excitation functions and ang. distrib. for elastic scatt. 9-42308
- ¹²C(t,α)¹¹B, excitation functions and ang. distrib. for elastic scatt. 9-42308
- ¹²C(t,p)¹⁴C, excitation functions and ang. distrib. for elastic scatt. 9-42308
- ⁵⁷Fe(t,n)⁵⁸Co, react. charact., ⁵⁸Co level schemes 9-32360
- ⁷Li(t,He)⁷He, ³He spectra, cross section meas., ⁷He mass excess and g.s. determ. 9-27756
- ⁵⁸Mn(t,n)⁵⁷Fe, ⁵⁷Fe level schemes, spin distrib. 9-32360
- ¹⁵N(³He,t)¹⁵O, t ang. distrib. meas., E_p=11 MeV 9-29738
- ¹⁰Ne(t,³He)¹²F, energy spectra, excitation energy, Q-value determ., E_p=22 MeV 9-27639
- ¹⁰Ne(t,³He)¹⁸N, energy spectra, excitation energy, Q-value determ., E_p=22 MeV 9-27639
- ³¹P(t,p)³¹P, levels, spin and parity determ., p spectra meas., shell-model calc. 9-29832
- ⁴⁵Sc(t,α)⁴⁴Ca, ang. distrib. meas., levels, spectroscopic factors determ., E_p=12.95 MeV 9-29834
- ³⁰Si(t,α)²⁹Al, levels, spin and parity determ., E_p=11.8 MeV 9-38656
- ⁴⁹Ti(t,n)⁵⁰V, react. charact., ⁵⁰V level schemes 9-32360
- ⁵⁰V(t,α), spectroscopic study of resulting ⁴⁹Ti 9-22823
- X-rays see Nuclear reactions and scattering due to photons
- nuclear reactors, fission
- 710-CE fast critical expt. results 9-32379
- calorimeters, isothermal, CO₂/graphite rigs radiation dose rate meas. 9-22915
- chemonuclear, ozone synthesis from O₂ rel. to temp., ozone conc. and dose rate 9-37842
- cluster-type fuel elements, thermal spectrum meas. by activation of Ln-Dy 9-28786
- cylindrical moderator, change of cavity effective radius, effect on slow neutron flux 9-22887
- Doppler coeff. meas. at cryogenic temp. 9-29886
- Dragon, at 20MW, power/reactivity coeff. and temp. coeff. of resistivity determ. 9-22881
- energy-loss n scatt. techniques, improved counting efficiency using entire thermal spectrum 9-22877
- Enrico Fermi, dynamic characts. meas. 9-29878
- Enrico Fermi, static physics meas. to 200 MWt 9-32381
- epithermal spectrum meas. with resonance sandwich detectors 9-29891
- fast bursts, on-line mass separator, construction 9-40530
- fast critical, comparison of theoretical and exptl. n spectra 9-29888
- FRO zero-energy fast reactor, expt. and analysis 9-29875
- fuel resonance interact, effects, calc. by series expansion 9-22900
- gas-cooled, coolant flow and temps. rise, radial flux distrib. depend. 9-34491
- graphite-moderated CO₂ cooled, patent 9-46250
- with heat exchanger, patent 9-29873
- in-core disturbance localization with external detectors 9-22884
- in-core power meas. with external p detectors 9-22912
- in-core radiation detector for monitoring intense pulses 9-36641
- in-pile radiation and temp. effects on Inconel sheathed lead wires of chromel-alumel thermocouples 9-36637
- integral meas. application to n cross-section evaluation 9-29885
- irradiation projects at multipurpose research reactor, general survey 9-38738
- leakage in small exponential cores, new means of analysis 9-27780
- liquid effluent continuous monitor, natural radioactivity effects 9-22910
- materials liquid coolant laminar stream, heat flow studied, Nusselt no. determ. 9-22898
- MSCA fast critical expt. results 9-32379
- neutron flux filter, hollow-cylinder (d reson., end effect 9-32393
- neutron-wave propagation, application of Laguerre polynomials in analysis 9-22854
- neutrons, fast, spectra using high resolution semicond. spectrometer 9-27791
- noise anal., technique and apparatus 9-22878
- noise analysis, covariance method via polarity detect. 9-34505
- optimal control, corrections to soln. of integral eqn. 9-27787
- parameters meas., accuracy, auto- and cross-spectrum methods 9-34486
- Piqua Core I, fuel assembly performance, post-irrad. tests 9-36622
- pneumatic tube position indication using microphone switch 9-22913
- production type, pneumatic and mech. sample transfer systems for isotope irradiation 9-36643
- pulsed neutron research, thermalization meas. 9-22869
- radioactive gases, in-pile release rate, determ. by mixing in He sweep-gas 9-25679
- reactivity meter, noise-based with two-detector cross-correl. 9-22911
- research programs involving nuclear reactors, cost efficiency 9-22860

nuclear reactors, fission continued

- rod bundles and annuli, burnout correlations 9-22906
 spectrometer, ^4Li semicond. sandwich, energy resolution and geometrical efficiency 9-34354
 STARK coupled fast-thermal Argonaut reactor; evaluation of expts. 9-29874
 steam cooled, fast linear analytical dynamic model 9-34488
 temp. meas., u.s. method 9-36636
 theory, mathematical approach to formal collision theory 9-48365
 thermal, output power measurement with gamma-sensitive detectors 9-36639
 thermal test reactor, spectrum- hardening filter to provide region of fast n flux 9-36642
 thermocouple lead wires, Inconel sheathed, in-pile rad. and temp. effects 9-36637
 tubular fuel elements double sided cooling by boiling and superheating, simplified model 9-22865
 water speed in reactor container, meas. by thermocouple noise signal cross correl. 9-38740
 Zebra-6, capture-to-fission ratio in ^{239}Pu , obs. 9-32380
 ZPR-3 Assembly 48, dilute Pu fuel expt. 9-29876
 ZPR-6 Doppler meas. and theory 9-29877
 (n, γ), 'effective cross-section' concept for reactor neutrons 9-25636
 n diffusion length, moderation, energy spectrum analysis 9-25668
 n flux meas., detectors positioning and accuracy limits 9-27790
 n flux monitoring apparatus, alarm system, patent 9-32394
 n importance meas. methods, errors and optimization 9-32392
 n scattering, and moderation, the dynamics and evolution of the reactor, undergraduate book 9-34487
 n source reactor facility to operate -193° to 725°C 9-45922
 n spectra and decay constants, meas. with fast subcritical facility SUAK 9-29890
 p recoil spectrometer and meas. in core and blanket 9-29889
 ^{131}I in L54M soln. reactor gas atm., obs. 9-46249
 ^{41}Ar in exhaust air and oven core, IRT-1000 Sofia 9-22875
 Pu fuelled, n spectrum meas. and interpretation 9-29887
 Rh self-powered neutron flux monitor in simulated pressurised water reactor 9-36635
 U-H₂O assembly, n flux distrib. in slab elements 9-22879
 U, natural-D₂O lattices params., obs. 9-32378
 U alloyed tubes in EL 3 reactor, mechanical strength, creep resistance; neutron irradiation 9-34496

Nuclear reactors, fission materials

- alkali metals, liquid, plugging meter, exptl. continuous-indication, for impurity monitoring 9-24991
 Aluman, laser microprobe analysis, impurity emission rel. to matrix effects, obs. 9-24604
 ceramic fuels, radiation eff., review 9-22902
 coolant gas flow in rod clusters, transverse temp. diff., mixing rate determ. 9-34818
 coolant of Na, K, B Fluorides, Patent 9-25678
 cylindrical fuel element thermal stress analysis 9-25120
 diphenyl, loose, neutron temp.-depend. on geometric parameter, meas. by pulse method 9-46251
 diphenyl, n diffusion length and age 9-22891
 fuel aspects, wit particular ref. to U, Pu and Th, in reactor text book 9-34504
 fuel assembly, patent 9-29882
 fuel assembly materials, fundamental props., conference 9-32388
 fuel burn-up and n dose, meas. methods 9-22916
 fuel element bundles, liquid metal cooled, temp. non-uniformities calc. 9-22888
 fuel element fabrication 9-38733
 fuel elements, fission density distrib. meas. 9-34501
 fuel elements, patent 9-32390
 fuel elements, patent 9-46253
 fuel irradiation in multipurpose research reactor 9-38739
 fuel irradiation in multipurpose research reactor 9-38738
 fuel materials, nondestructive assay methods for various stages in fuel cycle 9-25676
 fuel particle, pyrocarbon- and silicon carbide coated, stress calc. using mathematical model 9-28340
 fuel swelling, calc. of gas content of bubbles using extrapolated Xe eqn. of state 9-40742
 fuels, thermal and elec. cond. and thermo-e.m.f., in-reactor meas. 9-28431
 graphite, ^{14}C labelled, oxidation, equipment for meas. by chemical and radiochemical methods 9-38734
 graphite, Cs sorption charact., high temp. and low Cs press. 9-39168
 graphite, dimensional variations during Br intercalation 9-26223
 graphite, I adsorpt., and desorpt. in vacuum and Ar, $27-1100^\circ\text{C}$ 9-28221
 graphite, lattice parameter and dimensional changes on irradi., 300 to 1350°C 9-28280
 graphite, microporosity changes during thermal and radiolytic oxidation 9-26224
 graphite, neutron irradiated in CO₂, uptake of Br and interstitial K cpd. formation 9-28316
 graphite, neutron wave propagation 9-34478
 graphite, nuclear grade for space applics., constitutive eqns. 9-33057
 graphite, thermal degassing after radiolytic oxidation in CO₂ or CO₂ + methane 9-28220
 graphite channel, air oxidation studies, radial diffusional effects 9-26824
 graphite powder, determ. of g. factor anisotropy 9-24484
 graphite tube, oxidation kinetics, effect of non-uniform burn off 9-26823
 HB-40, n diffusion length and age 9-22891
 impurity-doped, growth of gas-filled pores, effect of impurity atoms 9-32955
 Incology 800, He embrittlement, tensile strength obs. 9-35179
 isotopic heat source comprising mixture of isotopes, patent 9-22904
 liquid metals, transient boiling analysis rel. to fast reactor safety 9-39142
 looped channel cells, single element and 3-element compared 9-22889
 looped channel cells, single element and 3-element compared 9-32387
 methyl iodide detection upon heating irradiated fuels 9-34493
 moderator, neutron streaming, effect of anisotropic hole systems 9-34502
 moderator molecule, asymmetric top, neutron scatt. Law calc. 9-34475
 moderators, neutron scatt., linearly anisotropic, effect on disadvantage factor calcs. 9-34499
 polyethylene, n dose absorbed in ^{235}U critical assembly 9-37284

Nuclear reactors, fission materials continued

- shield composition effects on biological n, γ dose and intensity distrib. 9-31688
 spherical fuel element quenching with time dependent heat transfer coeff. 9-25677
 stainless steel fuel cladding, irradi., burst tests of strength 9-26339
 steel, mild, low temp. aqueous corrosion under reactor radiation 9-26826
 teflon, n dose absorbed in ^{235}U critical assembly 9-37284
 U-Pu oxide fuel irradiated in fast neutron flux, solid fission products behaviour 9-41118
 void effect on neutron spectrum indices and fast fission ratio 9-38737
 waste, disposal underground, economic method 9-37866
 water, n diffusion length and age 9-22891
 water, neutron temp.-depend. on geometric parameter, meas. by pulse method 9-46251
 - water laminations, fast neutron spectrum obs. 9-22896
 water moderating system, pulsed with thermal n, extrapolation length 9-34497
 Zircaloy, in-pile softening and hardening rel. to creep and strain rates 9-41023
 Zircaloy, oxidation behaviour, comments 9-37826
 Zircaloy tubes, hydride orientation rel. to deform., texture and stresses 9-39188
 Zircaloy-2, fracture in BWR and PWR conditions, obs. 9-37258
 Zircaloy-2 tubes, failure rel. to neutron irradi., hydride precip. and stress 9-39435
 Zircaloy-2, laser microprobe analysis, impurity emission rel. to matrix effects, obs. 9-24604
 ^{171}Tm , preparation by irradiating ^{169}Tm , then leaving to allow ^{170}Tm to decay and separating Yb, patent 9-22905
 ^{235}U in Cu container, energy distrib. of neutrons at 100 m 9-36621
 ^{239}Pu , in waste drums, γ -ray assay using intensity of 765 keV line 9-37864
 $^{238}\text{Pu}^{16}\text{O}_2$ as material suitable for space vehicle, patent 9-28971
 $^{238}\text{U}/^{235}\text{U}$ fission rates ratio in rod-cluster fuel elements, Monte Carlo calcs. 9-25661
 ^{238}U , resonance self-shielding factors for energy groups 5 eV to 2 keV 9-22890
 ^{239}Pu capture-to-fission ratio in Zebra-6 reactor 9-32380
 AL-10wt.%Pu fuel elements, injection casting in Pyrex molds 9-22897
 Al-reflected fast critical expt., meas. and analysis 9-29883
 Al₂O₃-reflected fast critical expt., meas. and analysis 9-29883
 Al reinforced with SiO₂ fibre, eff. of irradiation on strength 9-26338
 B, spectrum-hardening filter for fast flux testing in thermal test reactor 9-36642
 B,C cluster control calcs., applic. of effective boundary conds. 9-22885
 Be impact resist., $1.75-4.39 \times 10^{21}$ n/cm² 9-28368
 BeO-reflected fast critical expt., meas. and analysis 9-29883
 BeO assemblies, n decay const., deriv. of thermal n diffusion parameters from $\lambda(\text{B}^2)$ curve 9-36629
 BeO assemblies, pulsed, decay curves in region of Corngold's limit 9-22909
 BeO assemblies, pulsed, extrapolation distances rel. to buckling 9-22908
 BeO, pulsed assemblies, calc. of buckling corresponding to λ^* 9-22894
 Bi heat-transfer bonding betw. powder compacted ceramic fuel and cladding 9-22892
 C pyrolytic fuel coating, deposition technique 9-36633
 ^{60}Co , thermal neutron capture cross-section, activation of isomeric states 9-22802
 Cs recovery on TiPO₄ from nuclear wastes 9-24593
 D₂, liquid, as moderator for cold neutron source 9-46252
 D₂O-H₂O mixture, poisoned, thermal n spectra rel. to suitability of scatt. kernels 9-27788
 D₂O, inelastic n scatt. at energies ~ 0.65 eV, energy-transfer cross-sections 9-28096
 D₂O moderator, local boiling risk study via thermal exchanges 9-25673
 H₂, liquid, as moderator for cold neutron source 9-46252
 H₂O, neutron wave propagation 9-34478
 H liq. source for cold neutrons, thermal and hydrodynamic obs. of whirling layer under high heat flux 9-26052
 InGaSn alloy activation in generator elements of rad. loop in water reflector of IRT reactor 9-32384
 InGaSn alloy in activity generator elements of rad. loop, influence on active section of water reflector in IRT 9-32385
 Na void reactivity variations due to thin slab inhomogeneity 9-29884
 Pb, n mean free path meas. in energy region 1-10eV 9-22895
 Pb, n thermalization study with pulsed source 9-22893
 Pb, n dose absorbed in ^{235}U critical assembly 9-37284
 δ -Pu-(10 at %)Ce, thermal cond. in temp. range 75-300°K 9-41108
 δ -Pu-Ga alloys, thermal cond. in temp. range 75-300°K 9-41108
 Pu-(O-10at%)Zr, equilib. phase diagram 9-37306
 Pu, fission product heating, correction of fitting procedure 9-27789
 Pu, fission product heating, corrections expt fitting to empirical eqns. 9-27789
 Pu, oxidation in region of 400°C, PuO form. from α -Pu₂O₃ 9-39953
 Pu_{0.5}U_{0.5}O_{2-x}, O diffusion and stoichiometry in temp. gradient, 1200-2000°C 9-37207
 Pu ceramic compounds, physical props., data manual 9-22907
 Pu dilute fuel for ZPR-3 Assembly 48 expt. 9-29876
 Pu exothermic reaction of retained $\gamma \rightarrow \alpha$ transform. prior to $\alpha \rightarrow \beta$ transform. temp. 9-42935
 PuO₂/UO₂ fuel coolant temperature effects in steam generating heavy water reactors 9-25674
 PuO₂ dense micropheres, sol-gel process of prep. 9-36631
 SiO₂, vitreous pile-exposed, ionization expansion 9-35175
 Ta, reactions with Pu and U oxides at high temps. 9-28782
 Th lattices, D₂O moderated, in Siemens-Argonaut reactor 9-34500
 ThC-ThN solid solns., melting points in N₂ atmosphere 9-40819
 U-D₂O lattice with Pu, epithermal cross-sections 9-25672
 U-H₂O assembly, n flux distrib. in slab elements 9-22879
 U-(0.45 wt%)Mo, transform. kinetics rel. to cooling rates and overheating temp. 9-41069
 U-Nb system, monoclinization of α -U lattice 9-40920
 U-Pu systems, breeding gain in fast reactors, effects of spectral hardness 9-22866
 U-Zr alloys, specific heat meas. for various compositions 9-24052
 U-Zr alloys, specific heat meas. for various compositions 9-33185
 U, cavitation swelling, temp./exposure thresholds for small alloying additions (<1000 ppm) 9-41117

Nuclear reactors, fission continued**materials continued**

- U, fission gas induced swelling, effect of hydrostatic press. 0-1000 bar during annealing 9-38735
- U, laser microprobe analysis, impurity emission rel. to matrix effects, obs. 9-24604
- (U,Pu)O₂ fuel, thermal diffusion mechanisms rel. to stoichiometry 9-37213
- U,Si, irradi., X-ray diffraction patterns rel. to change in struct. 9-40921
- U,Si fuel, corrosion tests in 300°C water 9-28804
- U coupled cylinders, prompt n decay obs. 9-29881
- U isotopic analysis using X-ray fluorescence combined with A-activity meas. 9-33690
- U isotopic analysis using X-ray fluorescence combined with α -activity meas. 9-24598
- U metal turnings, detection of methyl iodide when heated 9-34493
- U void effect on neutron spectrum indices and fast fission ratio 9-38737
- UC, UN solid solns., melting points in N₂ atmosphere 9-40819
- UC, arc cast and sintered, thermal conductivity, irradiation eff., 150-1600°C 9-41111
- UC, bubble formation and swelling, nucleation time and temp. depend. 9-38736
- UC, chemical binding effect on n scatt. cross-section of C atoms 9-23776
- UC, fission gas swelling, calc. of bubble content using extrapolated Xe eqn. of state 9-40742
- UC, release of Rn and fission Xe, obs. 9-37214
- UC, synthesis by reaction and precipitation from liq. Zn-Mg alloy 9-36630
- UC_{1-x}N_x elec. resist. and Seebeck coeff., 80-1000°K obs. 9-35330
- UC large dilute cores, physical parameters 9-32391
- UC preparation from UF₄, Al and graphite 9-28772
- UF₄ prod. from UF₆ in fluidized bed reactor, 500-600°F, patent 9-22903
- UF₆-WF₆, melting point and eutectic props. 9-34953
- UF₆-WF₆, melting point and eutectic props. 9-23580
- UN_{2-x} preparation in UC+NH₃→UN_{2-x}+CH₄+H₂ 9-31186
- UO₂-PuO₂ fuels, heat flux distrib. in rods rel. to fissile material segregation 9-36632
- UO₂, 6% enriched, 0.05 wt % B₄C rel. irradi. stability, 1000 and 5000 MWd/te burnup 9-32389
- UO₂, dislocation behaviour in {100} {110} and {111}-glide planes 9-40956
- UO₂, fission gas bubbles and sintering pores irradi. stability, obs. 9-37187
- UO₂, fission gas release rel. to bubbles mobility, obs. 9-37190
- UO₂, irradiated, re-solution of fission gases 9-28326
- UO₂, laser microprobe analysis, impurity emission rel. to matrix effects, obs. 9-24604
- UO₂, O diffusion and comp. in temp. gradient, 1300-2500°C 9-37212
- UO₂, release of Rn and fission Xe, obs. 9-37214
- UO₂, sintered, thermal conductivity, irradiation eff., 150-1600°C 9-41111
- UO₂, sintered irradiated, detection of methyl iodide when heated 9-34493
- UO₂, small gas bubbles stability in irradiation environment near 1000°C 9-34495
- UO₂, surface diffusion, obs. review 9-37198
- UO₂, U self-diffusion, 1200-1600°C 9-37211
- UO₂, vibration compacted, eff. of sinusoidal vib. on compacted density 9-34494
- UO_{2.18x} flow stress depend. on nonstoichiometry at high temp. 9-33049
- UO_{2.18x} O and U self-diffusion rel. to comp., obs. review 9-37210
- UO_{2.18x} U self-diffusion, 1200-1600°C 9-37211
- UO_{2.18x} (0.005≤x≤0.217), U and O self-diffusion 780-1650°C 9-37215
- UO₂ fuel, irradi., isotopic anal. of U and Pu distrib., theory and expt. 9-25675
- UO₂ fuel, thermal diffusion mechanisms rel. to stoichiometry 9-37213
- UO₂ fuel coolant temperature effects in steam generating heavy water reactors 9-25674
- UO₂ irradiated fuels, preferential edge breeding of ²³⁹Pu 9-22899
- UO₂ porosity effect on kinetics of grain growth 9-26250
- UO₂ sintering rel. to O/U ratio, obs. 9-37287
- UO₂ void formation and migration in a single crystal subject to a temperature gradient 9-32950
- Zr-Cu claddings, oxidation and cracking in CO₂, obs. 9-37266
- ZrH, neutron single differential cross-section at 296 and 700°K 9-22901
- ZrH₄:U fueled, SNAP reactor, thermal conductivity 9-26459

operation

- activity generator elements of rad. loop influence on active section of water reflector of IRT 9-32385
- boiling water reactor stability range, obs. 9-22874
- burnout prediction, applic. of non-equilib. two-phase annular flow 9-34096
- control rod transient motion meas., eff. on AFRRI-TRIGA pulse reactor 9-32386
- control system, emergency, hydraulic 9-32382
- control system, emergency, hydraulic 9-22882
- critical assemblies, safety circuits design 9-36628
- dryout during flow and power transients, expt. and theory 9-22880
- fast or high flux, coolant boiling detection, acoustic method, tank wall effects 9-36640
- fast pulsed reactor Viper as source of neutron and γ radn., description 9-25671
- fast pulsed reactor Viper as source of neutron and γ radn., physical characteristics 9-25670
- fission product containment after accident 9-40529
- flowmeter for meas. on liquid metal coolant 9-36634
- heat transfer loop at Harwell, description 9-27242
- Hitachi training reactor (light water), Doppler-limited pulse operation tests 9-32383
- irradiation facility with heavy water circulation 9-38739
- isotope, high flux, reactivity and rod symmetry control system, on-line digital computer appln. 9-36626
- kinetic behaviour and control, in textbook 9-34492
- liquid metal fast breeder, fast flux test facility instrumentation requirements 9-36638
- operator identification by static programming 9-29879
- Pewee 1, integrated circuit control system for low power testing 9-36627
- pressurized-water reactor plant, on-line plant computers, applications and system configuration 9-36625
- prompt n decay obs. in delayed-critical coupled U cylinders 9-29881
- reflector spectrum calc. 9-34490
- regulating cylinders covered with absorber in reactor reflector, efficiency 9-36624

Nuclear reactors, fission continued**operation continued**

- shutdown, monitoring by Co target wire, patent 9-22886
 - start-up, computer-controlled, patent 9-29880
 - steam, initial conditions of thermodynamic cycle, optimal values 9-36623
 - textbook for undergraduates on the working reactor 9-32374
 - thermal problems, chapter in textbook on reactors 9-34503
 - ventilation systems, conference 9-34094
 - H₂ transport and reactivity applic. to control 9-22883
 - InGaSn alloy activation in generator elements of rad. loop in water reflector of IRT reactor 9-32384
 - InGaSn alloy in activity generator elements of rad. loop, influence on active section of water reflector in IRT 9-32385
 - Na vapour bubbles in cold liquid, sudden collapse 9-23595
 - N ejection by fission fragments, evidence for clusters and knock-ons 9-34489
- theory**
- analysis by CIAP and GLOBPERT codes with improved perturbation techniques 9-29871
 - binary cross-correlation meas., drift correction 9-22871
 - boiling water cell calcs. using P₁ theory with axially variable parameters 9-22867
 - burn-up-synthesis calcs., use of dynamic co-ordinate functions to save computer time 9-22862
 - Cadarache multigroup cross-section set presentation 9-29865
 - cell, space and energy depend. n flux calc., analytical use of Horowitz operator 9-22864
 - Cluster control calcs., applic. of effective boundary conds. 9-22885
 - core and reflector interface, n transport, boundary transients 9-22858
 - critical core volume and reactivity calc., multigroup cross-section sets, comparison 9-29868
 - cross-section sensitivity analysis for fast reactors 9-29869
 - density scaling of Boltzmann eqn. and applic. 9-22849
 - Doppler and Na void reactivity coeff. calc., allowance for inhomogeneity 9-29872
 - dryout during flow and power transients 9-22880
 - fast breeder problem, spectrum anal. using recent data 9-22866
 - fast critical assemblies, multigroup calc. comparison 9-29867
 - fast reactor analysis, multigroup cross-section prep. using MC² program 9-29864
 - Fuchs' model, temp. coeff., and prompt n lifetime, precise definitions 9-27785
 - heterogeneous, anisotropic diffusion coeffs. calc., comparison with Benoist estimation 9-22863
 - heterogeneous models, space-time kinetics 9-25667
 - heterogeneous reactors, P₁ multigroup calc. 9-22859
 - inhomogeneity effect on activation Doppler expt. 9-32376
 - model not requiring component temperatures for determ. of lumped heat-transfer and reactivity coeffs. 9-34485
 - Monte Carlo analysis of fast multicomponent critical systems 9-32375
 - Monte Carlo analysis of small fast critical assemblies 9-29870
 - neutron source, cold, model for high flux beam reactor 9-26052
 - optimization of n cross-section data adjustments 9-29866
 - pebble bed, power rel. to burnup and temp. reaction, model differences 9-22861
 - resonance integrals for negative energy levels 9-44184
 - rod cluster, hydraulic and burnout characteristics subchannel anal. by computer prog. 9-22870
 - with slab fuel elements, model for dynamics and time-depend. heat withdrawal 9-22868
 - space-time neutronics, multichannel synthesis method 9-29863
 - stochastic model of dynamics 9-34484
 - stress, force and strain distrib. in fuel element cladding, cracked pellets expansion 9-22873
 - Wigner-Seitz cell homogenisation in 2 group diffusion theory 9-22872

Nuclear reactors, fusion

- controlled, fusion-fission and fusion-reaction tube, approximate eqns. 9-46245
- thermonuclear reactor, pulsed, toroidal system for plasma compression 9-32628

Nuclear relaxation

see *Nuclear magnetic resonance and relaxation*

Nuclear scattering

see *Nuclear reactions and scattering*

Nuclear spallation

- Weisskopf evaporation theory, chains from highly excited nuclei, cross sections estimation 9-22769
- ²⁷Al, p induced; ¹⁸F, ^{22,24}Na fragments energy distrib. and range determ. 9-40511
- ¹²C(p,x) nuclear spallation production of ¹⁰B, ¹¹B 9-36601
- ¹⁹F, p induced; ¹⁸F, ^{22,24}Na fragments energy distrib. and range determ. 9-40511
- ²⁴Mg, p induced; ¹⁸F, ^{22,24}Na fragments energy distrib. and range determ. 9-40511
- ²⁸Si, p induced; ¹⁸F, ^{22,24}Na fragments energy distrib. and range determ. 9-40511

Nuclear structure

see *Nucleus/energy levels; Nucleus/theory*

Nuclear track emulsions

- digitized video track scanning and computer analysis 9-36539
- electron pairs, energy estimation 9-46142
- fading, parameters for films 9-48233
- latent image formation, ionization responsible rel. to recomb. of positive holes and electrons 9-34366
- Lexan polycarbonate detector, sensitivity enhancement by u.v. radiation in presence of oxygen 9-32272
- in magnetic field, 40 kG, relativistic tracks prod., part. sign determ. 9-36538
- relativistic tracks production in mag. field, particle sign determ. 9-36538
- separation of reaction tracks by the use of an applied electric field 9-48232
- β autoradiography in the presence of latent image fading 9-48233
- e, inelastic interac. props., 10 and 16 GeV 9-29785
- K⁻ meson capture in diamond loaded emulsions 9-44007
- μ , inelastic interac. props., 10.5 GeV 9-29785
- μ , p scatt., strong-absorption model applic., N-nucleus potn. calc., M_p=3GeV/c 9-42280
- pN interaction, grey track selection method, M_p=24 GeV/c 9-29608
- π coherent prod. at 17.2 GeV in π -nucleus interac., obs. 9-22805
- π slowing down charge difference effect 9-27533
- π - μ decays, isotropy in ang. distrib. 9-29577

Nuclear-solid interactions

see *Mossbauer effect; Solids*

Nucleation *see* **Clouds; Crystallization; Freezing****Nuclei with $150 \leq A$**

- ²⁰⁸Pb, dose rate attenuation 9-22791
²³²Th, cross-sections total neutron, 3.3-5.2 MeV 9-38702
²³⁵U enriched tubes, buckling in light water 9-23913
 A=104, isotope production from ²⁴⁹Cf, ^{12,13}C; α emission, isotope identification 9-42219
 A=135 to 151 odd nuclei, spins of (2f_{7/2})^{±1} ground states 9-46206
 Hamiltonian, single particle, self-consistent, fission proc. calc. 9-27653
 internal conversion coeffs., tables 9-46216
 k-forbidden transitions, systematic study in mass ranges 160 ≤ A ≤ 190, and A > 230 9-48265
 odd nuclei with 135 ≤ A ≤ 151, spins of (2f_{7/2})^{±1} ground states 9-46206
 quadrupole one-phonon states, energy, wave func., Saxon-Woods, Nilsson potn. calc. 9-29723
 rare-earth nuclei, d scatt., E_g=12 MeV 9-32354
 superheavy, stability against spontaneous fission 9-29845
 transuranium elements, nuclear charge distribution in low-energy fission 9-48356
 transuranic, n strength function calc. using strong coupling deformed nucleus 9-27612
 transuranium elements, production 9-25608
²¹⁰Bi, low-energy spectra from shell model calc., vel.-depend. effective N-N potential 9-40480
²¹⁰Bi Green's velocity-dependent potential tested 9-44166
²¹⁰Bi obs. with new β spectrometer 9-42130
¹⁶⁰Dy, low-lying E2 transitions, internal conversion-electron particle parameters 9-29737
¹⁶⁰Dy, nuclear g-factor, ang. correlation, Larmor precession freq. of 966 keV level 9-25582
¹⁶⁰Dy, odd levels, props. from angular correlation techniques 9-36576
¹⁶⁰Dy(α ,3n)¹⁶¹Er, anomalous rotational band strong transitions obs. 9-36577
¹⁶⁰Er prod. by (⁴⁰Ar, 4n) react., lifetimes of rotational states 9-25581
¹⁷⁰Er, n capture cross section, 5 keV-3 MeV 9-25638
¹⁶⁰Gd 2⁺ level lifetime meas. by Coulomb excitation 9-27637
¹⁶⁰Hf, hyperfine fields in Fe and Gd, IMPACT study 9-45256
¹⁶⁰Hf, Mossbauer effect meas. 9-35639
¹⁶⁰Hf in Fe hyperfine field determ. using Mossbauer expts. 9-35605
¹⁶⁰Hf nuclear structure effect on N- and O- shell electrons internal conversion 9-34384
²⁰⁰Hg, 1029 keV level spin 9-46214
²⁰⁰Hg, low-lying excited levels 9-34404
²⁰⁰Hg, quasirotational band, existence 9-48291
¹⁶⁰Ho → ¹⁶⁰Dy decay scheme 9-38691
¹⁷⁰Lu, decay scheme, conversion electron spectrum obs. 9-48317
¹⁷⁰Lu radioact. decay, γ spectra and transitions, ¹⁷⁰Yb obs. 9-25601
¹⁷⁰Lu → ¹⁷⁰Yb decay, γ spectra meas. 9-42252
²¹⁰Pb, energy levels and transitions, residual interaction model 9-40487
²¹⁰Pb, Green's velocity-dependent pot., shell model 9-44166
²¹⁰Pb, in surface air and precipitation, measurement 9-28900
²¹⁰Pb, low-energy spectra from shell model calc., vel.-depend effective N-N potential 9-40480
²¹⁰Pb spectra calc., realistic interaction, eff. of Woods-Saxon wave function 9-38653
²¹⁰Pb → ²⁰⁹Bi, L-subshell X-ray fluorescence yield and Coster-Kronig transition prob. 9-25602
²¹⁰Po Green's velocity-dependent pot., shell model 9-44166
²¹⁰Po, energy levels and transitions, residual interaction model 9-40487
²⁴⁰Pu, n scatt., cross sections, resonance parameters, radiative capture, fission, E_g=0.01 eV-15 MeV 9-34456
²²⁰Rn (thoron) meas. of atm. turbulent diffusion 9-37930
¹⁵¹Sm, internal conversion coeff. for E1, E2, M1, M2 transitions on K shell E_g=1.9 MeV 9-29765
¹⁵¹Sm, K-conversion coeff., E1, E2, M1, γ transitions 1-17 MeV multipolarities calc. 9-25576
¹⁵¹Sm type 'spherical' nuclei, E2+EO transitions 9-40481
¹⁵¹Sm type 'spherical' nuclei, E2+EO transitions 9-40482
¹⁵⁰Tb, γ spectrum 9-44180
¹⁶⁰Tb, short-lived states excited in (n,p) reaction 9-38666
¹⁷⁰Tm, β - γ directional correlation measurements 9-22732
¹⁷⁰Tm, transition $\beta(1^- \rightarrow 2^+)$, nuclear matrix elements, exptl. determ. 9-48297
¹⁷⁰Tm → ¹⁷⁰Er, EC decay, spectrum of K X-rays and γ -rays 9-29774
¹⁷⁰Tr 2⁺ level lifetime meas. by Coulomb excitation 9-27637
¹⁷⁰Yb, 84.3 keV transition, α meas. 9-29739
¹⁷⁰Yb, γ transitions and excited states obs. from ¹⁷⁰Lu decay 9-25601
¹⁷⁰Yb, level scheme from ¹⁷⁰Lu decay 9-48317
¹⁷⁰Yb (n, γ) ¹⁷¹Yb, also capture by isotopes ¹⁷²Yb-¹⁷⁴Yb, regularities capture to low-lying Nilsson levels 9-46238
¹⁷⁰Yb(d,p)¹⁷¹Yb, DWBA anal., E_g=12 MeV 9-25652
²⁴¹Am, neutron fission analysis of odd-even nuclei 9-27770
¹⁵¹Dy e capture energy prediction from ¹⁴⁷Gd e capture decay energy meas. 9-40493
¹⁶¹Dy, Coulomb excitation Mossbauer effect of 43.8 keV transition 9-36578
¹⁶¹Dy, half-life of 25.7 keV level, hindrance factor calcs. 9-42228
¹⁶¹Dy in DyCrO₃, Mossbauer effect obs. of hyperfine interactions and paramagnetic relax. 9-24379
¹⁶⁰Er from ¹⁶⁰Dy(α ,3n), anomalous rotational band strong transitions obs. 9-36577
¹⁷¹Er → ¹⁷¹Tm, γ spectra meas., energy levels determ. 9-32310
¹⁵¹Eu, isomer shifts of Mossbauer absorpt. in divalent Eu cpds 9-45289
¹⁵¹Eu, Mossbauer spectrum of ¹⁵¹Eu₂O₃ rel. to EuF₃·H₂O, isomer shift obs. 9-35635
¹⁵¹Eu²⁺ hyperfine coupling const. in CaF₂, SrF₂ and BaF₂, temp. depend. 9-33496
¹⁵¹Eu in rare earth-Fe garnets, Mossbauer eff., exchange interact. obs. 9-33475
²¹⁷Fr, conversion electron spectra, transition multipolarity level obs. 9-32313
¹⁵¹Gd decay, γ -ray and conversion electrons spectra 9-48313
¹⁵¹Gd → ¹⁵¹Eu, conversion electron and γ -ray spectra meas. 9-42251
²¹⁰Hg, n.m.r. in HgCr₂S₄ at 1.4°K, depend on mag. structure 9-45400
¹⁷¹Ir, He ion induced fission, excitation junc., cross section meas., E=42.2 MeV 9-29857
²¹¹Pa, Mossbauer effect, 84.2 keV 9-29743
²¹¹Pa, neutron fission analysis of odd-even nuclei 9-27770
²¹¹Pa coriolis interaction, between three Nilsson bands 9-27629
²⁴¹Pu fission cross-section for E_g=1 to 25 keV 9-29849

Nuclei with $150 \leq A$ continued

- ²⁴¹Pu scatt., cross sections, resonance parameters, radiative capture, fission, E_g=0.01 eV-15 MeV 9-34456
²⁴¹Pu thermal and fast n induced fission, yield 9-22836
²⁴¹Pu(d,p) ²⁴²Pu, fission prob. depend. on excitation energy, resonance eff. 9-27773
¹⁸¹Ta, 133-482 keV cascade, angular correlation meas. by differential method 9-38675
¹⁸¹Ta, 482 keV transition parity mixing, γ scatt., circular polarization meas. 9-27640
¹⁸¹Ta, 6.2 keV level, recoilless reson. absorpt. 9-32312
¹⁸¹Ta, E2- and M1-transitions and dipole moments mean values 9-36565
¹⁸¹Ta, transitions, γ circular polarization meas., n- π parity violating amplitude determ. 9-36580
¹⁸¹Ta 6.25 keV Mossbauer live absorpt. spectrum interference of electronic and nucl. reson. absorpt. obs. 9-35640
¹⁸¹Ta 80 MeV α bombard., neutron ang. distrib. yield, spectra and shielding 9-34474
¹⁸¹Ta in Hf cpds., quadrupole interaction, time differential ang. correl. studies 9-33497
¹⁸¹Ta(p,p),(p,d) and (γ ,t), E γ =400-1300 MeV 9-22776
¹⁷⁰Tb, decay scheme study by sum coincidence spectra 9-22760
²³¹Th from ²³²Th(α , α); α ang. distrib. meas., DWBA analysis, levels, spin and parity determ., E=30 MeV 9-29830
¹⁷¹Tm, preparation by irradiating ¹⁶⁹Tm, then leaving to allow ¹⁷⁰Tm to decay and separating Yb, patent 9-22905
¹⁷¹Tm from ¹⁷¹Er decay, γ spectra meas., energy levels determ. 9-32310
¹⁷¹Yb from ¹⁷⁰Yb(d,p), DWBA anal., E_g=12 MeV 9-25652
²⁴²Am → ²⁴²Am induced by n, negative result 9-48305
²¹²Bi in atmosphere, meas. and geophysical applications 9-24670
²⁵²Cf, fast n dosimetry meas. 9-38135
²⁵²Cf, fission, obs. of K X-rays in association with long-range α 9-38727
²⁵²Cf, proton and triton accompanied fission, energetics and mass distrib. of fragments 9-48360
²⁵²Cf, spontaneous fission, fragments mean kinetic energy and deformation energy determ. 9-34468
²⁵²Cf fission, Xe and Kr yield examined on Al foil 9-40526
²⁵²Cf as source for n radiography 9-42257
²⁵²Cf spontaneous fission, K X-rays emission times and yields from fragments 9-38724
²⁵²Cf spontaneous fission, n energy distrib. meas. 9-34355
¹⁶²Dy, half-life of 1490 KeV level meas. 9-40485
¹⁵²Eu, new transitions identified 9-44157
¹⁵²Eu allowed β -decay, meas. of β - γ circular polarization asymmetry 9-46221
¹⁵²Eu decay, β longit. polarization relative meas. 9-22759
¹⁵²Eu decay analysis used for determ. of γ intensities of β -vibrational → ground-state rotational band transitions 9-46211
¹⁵²Eu γ source used to calibrate Ge(Li) detectors 9-22673
¹⁵²Gd EO transition meas. 9-22730
¹⁵²Gd low-lying E2 transitions, internal conversion-electron particle parameters 9-29737
¹⁵²Gd to ¹⁶⁰Gd, even isotopes, n transmission and radiative capture, resonance parameters meas. 9-34401
¹⁶²Ho m → ¹⁶²Dy, half-lives of K-forbidden transitions 9-40485
¹⁹²Ir, β - γ directional correl. studies on two cascades 9-34423
¹⁹²Ir conversion electron obs. with double-focusing sector-type spectrometer 9-38610
¹⁹²Ir → ¹⁹²Os, ¹⁹²Pt; γ spectra meas., mag. dipole moment, E2/M1 mixing ratio determ. 9-32324
¹⁹²Ir → ¹⁹²Os, mixing ratio of 485 keV transition in ¹⁹²Os meas. 9-46213
²¹²Pb (Th B) meas. of atm. turbulent diffusion 9-37930
²¹²Pb in atmosphere, meas. and geophysical applications 9-24670
²¹²Po, α decay reduced width from α four-body correlation 9-34410
¹⁹²Pt, 22 resonances of spin and parity 1⁻, spectra obs. 9-48300
¹⁹²Pt, E2/M1 multipole mixing ratio from γ - γ meas. 9-25585
¹⁹²Pt, mixing ratios of transitions prod. by ¹⁹²Ir decay 9-46213
¹⁹²Pt, new level scheme obs. from ¹⁹⁶Au decay 9-48300
¹⁹²Pt from ¹⁹²Ir decay; levels, E2/M1 mixing ratio determ. 9-32324
²⁴²Pu scatt., cross sections, resonance parameters, radiative capture, fission, E_g=0.01 eV-15 MeV 9-34456
²⁴²Pu spontaneous fission, n spectra meas. 9-29859
²⁴²Pu(n, γ)²⁴³Am, γ spectra meas., levels spin and parity determ. 9-27651
²²⁸Ra, excited levels, from α -decay of ²²⁸Th 9-48303
¹⁵¹Sm, β -vibrational band → ground-state rotational band, attempt to meas. intensities 9-46211
¹⁵¹Sm, e.m. transitions in β - γ vibrational bands 9-40483
¹⁵¹Sm, from ¹⁵²Eu decay, γ transitions and γ - γ angular correlations 9-44157
¹⁵¹Sm, γ energy distrib. after β decay, slowing down of nuclear recoil 9-45283
¹⁵¹Sm, low-lying E2 transitions, internal conversion-electron particle parameters 9-29737
¹⁵¹Sm β vibrational bands and multipole mixing ratios 9-27635
¹⁵¹Sm EO/E2 intensity ratio determ., β - γ vib. band 9-22730
¹⁵¹Sm from n, ¹⁵²Gd; radiative capture meas. 9-34401
¹⁵¹Sm recoil nuclei due to ν emission from ^{152m}Eu in Eu₂(WO₄)₃, nucl. reson. fluoresc. obs. 9-35596
²³²Th, ¹²C reaction diff. cross section, energy spectra, ang. distrib. meas., E_g=82 MeV 9-25659
²³²Th, ¹⁴N reaction diff. cross section, energy spectra, ang. distrib. meas., E_g=110 MeV 9-25659
²³²Th, ¹⁵N reaction, diff. cross section, energy spectra, ang. distrib. meas., E_g=98.5 MeV 9-25659
²³²Th, charge distrib., intrinsic quadrupole moment, radius studied by obs. of muonic X-rays 9-38677
²³²Th, μ -atomic h.f.s. in K, L and M lines, nuclear charge distrib. 9-38678
²³²Th, n induced fission, 14 MeV, α decay prob., c.f. with ²³⁵U, n_{th} induced 9-29847
²³²Th, n spectra following bombardment with 147 MeV n, nuclear temp. and level density parameters 9-27766
²³²Th, ternary fission induced by 2.9 MeV neutrons, mechanism 9-44226
²³²Th(α ,He)²³³Th, α ang. distrib. meas., DWBA analysis, levels, spin and parity determ., E=30 MeV 9-29830
²³²Th fast n induced fission, yield 9-22836
²³²Th fission, n induced, cross section structure determ., E_g=1-2.2 MeV 9-27768
²³²Th fission by 9.5, 11.3 MeV p₂ and 11.5 MeV d, prods. Z distrib., obs. 9-29852

Nuclei with $150 \leq A$ continued

- ²³²Th photofission fragments, cross sections and ang. distrib., and struct. of fission barrier 9-48363
- ²³²Th 14.8 MeV n-induced, study of low yield products 9-48361
- ²³²Th fission by 20-85 MeV protons, yields and charge dispersion obs. 9-32368
- ²³²Th(γ, f), mono-energetic γ -rays, 12 different energies, cross-sections 9-27771
- ²³²Th(n, n') cross section and excitation function meas., $E_n = 1.2$ MeV 9-27768
- ¹⁶⁷Tm excited levels from ¹⁶²Yb decay 9-46225
- ¹⁸²W, multipole orders of low-energy γ transitions 9-44159
- ¹⁶²Yb decay to ¹⁶²Tm excited levels 9-46225
- ¹⁶²Yb(d,p)¹⁶³Yb, DWBA anal., $E_d = 12$ MeV 9-25652
- ²⁴¹Am, LX and γ emission 9-46226
- ²⁴¹Am from ²⁴²Pu(n, p), γ spectra meas., levels spin and parity determ. 9-27651
- ²⁴³Am from ²⁴⁷Bk, α spectra meas., levels spin and parity determ. 9-27651
- ²⁴³Am in AmO₂ and AmF₃, isomer shift 9-44167
- ²⁴³Am slow neutron absorber, patent 9-38620
- ²⁴³Am-²³⁹Np, γ transitions of ²³⁹Np, multiplicities 9-42256
- ¹⁶¹Dy, spin-lattice relax. in ferromagnetic Dy metal 9-33490
- ¹⁶³Er, ground-state spin obs. 9-36579
- ¹⁶³Er half life of 69.2 keV level, hindrance factor calc. 9-42228
- ¹⁵³Eu, from ¹⁵³Sm β decay 9-27675
- ¹⁵³Eu spin lattice relax in ferromag. EuO, field and temp. depend 9-45244
- ¹⁹³Ir, angular correlation in 253-461 KeV cascade 9-42229
- ¹⁹³Ir, He ion induced fission, excitation func., cross section meas., $E = 42.2$ MeV 9-29857
- ¹⁹³Ir, levels populated from β -decay of ¹⁹³Os, energies and spins obs. 9-34403
- ¹⁹³Ir levels, transitions, multiplicities, spin and parity assignments from ¹⁹³Os-¹⁹³Ir 9-48298
- ¹⁹³Os-¹⁹³Ir, β -decay obs. rel. to energy levels of ¹⁹³Ir 9-48298
- ²³³Pa Coriolis interaction, between three Nilsson bands 9-27629
- ¹⁸³Re-¹⁸³W electron capture decay energy determ. 9-29769
- ¹⁵¹Sm-¹⁵²Eu, γ -spectrum, higher precision meas. 9-40494
- ¹⁵³Sm-¹⁵³Eu, beta decay, levels of ¹⁵³Eu identified 9-27675
- ²⁰⁷Tl, E2-M1 279keV transition mixing ratio from γ - γ directional and linear polarization 9-48301
- ²³³U, n-induced fission, light particle yield and energy distrib. meas. 9-22839
- ²³³U, n induced fission, ¹¹²Ag, ¹¹⁵Pd yield meas. 9-29848
- ²³³U, n induced fission, 14 MeV, α decay prob., c.f. with ²³⁵U. n_{th} induced 9-29847
- ²³³U, n induced fission; Sn stable isotopes relative yields, tandem mass spectrometer 9-38725
- ²³³U, n_{th} induced fission, fragment nuclear charge distrib. calc. method 9-32371
- ²³³U fission cross-section for $E_n = 1$ to 25 keV 9-29849
- ²³³U thermal and fast n induced fission, yield 9-22836
- ²³³U(d,p)²³⁴U, fission prob. depend. on excitation energy, resonance eff. 9-27773
- ²³³U(t,d,f), fission-fragment angular correlations 9-42315
- ¹⁷³Yb³⁺, ENDOR in CaF₂, electronic shielding by closed shells obs. 9-35731
- ¹⁷³Yb from ¹⁷²Yb(d,p), DWBA anal., $E_d = 12$ MeV 9-25652
- ^{184m}Re-¹⁸⁴W decay scheme, γ -ray and conversion-electron spectra 9-40495
- ²²⁴Ac-²²⁰Fr, decay scheme 9-27679
- ¹³⁴Ba from ¹³⁴Cs decay, γ spectra meas., energy levels determ. 9-32310
- ²⁴⁴Cm spontaneous fission, n spectra meas. 9-29859
- ¹⁶⁴Dy 2⁺ level lifetime meas. by Coulomb excitation 9-27637
- ¹⁵⁴Gd 2⁺→0⁺ rotational transition isomer shift determ., Mossbauer meas. 9-27636
- ¹⁵⁴Gd β , γ vibrational bands and multipole mixing ratios 9-27635
- ¹⁵⁴Gd; e.m. transitions in β - γ vibrational bands 9-40483
- ²⁰⁴Hg, shell model study of β - γ correlations 9-48253
- ¹⁹⁴Ir-¹⁹⁴Pt, γ spectra meas., mag. dipole moment, E2/M1 mixing ratio determ. 9-32324
- ²³⁴Pa-²³⁴U, 1552 keV level half-life determ. 9-25588
- ²⁴⁴Pu fission, Xe retention in meteoritic whitlockite, ²⁴⁴Pu/²³⁸U ratio 9-34415
- ¹⁵⁴Sm fission cross section, electron and bremsstrahlung induced, 60-1000 MeV 9-38726
- ¹⁵⁴Sm from n, ¹⁵⁴Gd; radiative capture meas. 9-34401
- ¹⁵⁴Tb, decay of isomers obs. 9-34421
- ²⁴⁰Tl obs. with new β spectrometer 9-42130
- ²⁴⁰Tl target, ang. distrib. of matter evaporated by laser beam 9-41930
- ²⁴⁰U, half-life of 2-state at 990 keV 9-27649
- ²³⁴U from ²³⁴Pa decay, 1552 keV level half-life determ. 9-25588
- ²³⁴U from ²³⁸Pu decay, L _{α} M subshell ratios determ. of 43.5 E2 transition 9-25589
- ¹⁸⁴W, metastable excited level 9-44160
- ¹⁷⁴Yb fission cross section, electron and bremsstrahlung induced, 60-1000 MeV 9-38726
- ¹⁷⁴Yb(d,p)¹⁷⁵Yb, DWBA anal., $E_d = 12$ MeV 9-25652
- ²³⁵U n induced fission, cross section resonance parameters determ., $E_n = 17$ -70 eV 9-22834
- ¹⁵⁵Dy-¹⁵⁵Tb, associated γ -ray spectra rel. to ¹⁵⁵Tb energy level determ. 9-44158
- ¹⁵⁵Er, new isotope produced, life-time meas. 9-48436
- ¹⁶³Er, excited states, props. 9-38672
- ¹⁵⁵Gd, levels and transitions from ¹⁵⁵Tb decay γ - γ coincidence spectra anal. 9-25563
- ¹⁵⁵Gd, mag. moment from ENDOR obs. in CeO₂:Gd³⁺ 9-35733
- ¹⁵⁵Gd in GdCl₃, 86.5 keV level quadrupole moment, h.f.s. and spectra meas. 9-34402
- ¹⁵⁵Gd thermal n capture, conversion electron spectrum 9-32350
- ¹⁷⁵Hf-¹⁷⁵Lu, γ spectra meas., M1+E2 transitions, probabilities and mixing parameters determ. 9-22733
- ¹⁶⁰Ho, E2- and M1-transitions and dipole moments mean values 9-36565
- ¹⁶⁰Ho spins of neutron resonances, elec. and mag. moments meas. 9-27560
- ¹⁶⁵Ho(α, n) and ¹⁶⁵Ho(γ, nn) obs. with nucleus polarized in parallel and perpendicular positions rel. to model of giant reson. 9-38673
- ¹⁶⁵Ho(e,e')¹⁶⁵Ho, 200 MeV obs. 9-27702
- ¹⁷⁵Lu, E2- and M1-transitions and dipole moments mean values 9-36565
- ¹⁷⁵Lu, n capture cross section, 5 keV-3 MeV 9-25638

Nuclei with $150 \leq A$ continued

- ¹⁷⁵Lu from ¹⁷⁵Hf decay γ spectra meas., M1+E2 transitions, probabilities and mixing parameters determ. 9-22733
- ¹⁷⁵Lu internal conversion studies of 114 KeV transition 9-25584
- ¹⁸⁵Os decay scheme and energy 9-48318
- ²³⁵Pa, prod. and decay props. 9-38707
- ²⁰⁶Pb from ²⁰⁶Pb(d,t), t spectra meas., levels determ., $E_x = 21.6$ MeV 9-27643
- ¹⁹⁵Pt, Mossbauer effect of 129 keV state 9-48299
- ¹⁸⁵Re, n total and capture cross-sections, resonance parameters, 0.01 ev to 30 keV 9-22797
- ¹⁸⁵Re, separated isotope, fission by 40 MeV α -particles, angular distrib. of fragments 9-40525
- ¹⁸⁵Re, separated isotope, fission by 40 MeV α -particles, angular distrib. of fragments 9-36617
- ¹⁸⁵Re transition energy and intensities obs. 9-48318
- ¹⁵⁵Tb, energy levels from γ -ray spectra associated with ¹⁵⁵Dy-¹⁵⁵Tb decay 9-44158
- ¹⁵⁵Tb decay, γ - γ coincidence spectra, applic. of data processing method, ¹⁵⁵Gd level obs. 9-25563
- ²⁰⁵Tl, 2.61 and 2.69 MeV states, based on 3⁻ state in ²⁰⁶Pb 9-44163
- ²⁰⁵Tl, energy levels including resonance levels formed by γ scatt. 9-46215
- ²⁰⁵Tl level investigation using excitation with n-capture γ , anomalies 9-36573
- ²⁰⁵Tl(γ, p)²⁰⁵Tl, resonance scatt. used to investigate ²⁰⁵Tl energy levels 9-46215
- ²⁰⁵Tl(t,p)²⁰⁵Tl, p spectra meas., vib. levels, spin and parity determ., $E_x = 13$ MeV 9-27646
- ²²⁵U thermal and fast n induced fission, yield 9-22836
- ²³⁵U, 14.8 MeV n-induced, study of low yield products 9-48361
- ²³⁵U, charge distribution gaussian in mass chain 9-38728
- ²³⁵U, fission products, kinetic energy of β decay 9-22753
- ²³⁵U, fission products activities and power output 9-22838
- ²³⁵U, foils, energy-dependent shielding factors from transmission experiments 9-25662
- ²³⁵U, n capture-fission ratio and fission cross section, 0.15 eV-30 keV 9-22831
- ²³⁵U, n induced fission, ¹¹²Ag, ¹¹⁵Pd yield meas. 9-29848
- ²³⁵U, thermal fission, fragments mean kinetic energy and deformation energy determ. 9-34468
- ²³⁵U, thermal n. function, energy spectra and relative yields of Li and Be nuclei 9-29858
- ²³⁵U, thermal neutron fission, α particle spectrum, meas. of low energy part 9-22800
- ²³⁵U, time-of-flight meas. of n spectra 9-29808
- ²³⁵U, N, fission cross-sections for energies 6eV to 3keV, study of resonances 9-22832
- ²³⁵U, n_{th} induced fission, asymmetric mass distrib., dynamic model 9-32366
- ²³⁵U, n_{th} induced fission, fragment nuclear charge distrib. calc. method 9-32371
- ²³⁵U fission, fast and thermal, ¹⁴⁰Ba yields, obs. 9-46248
- ²³⁵U fission cross-section, Doppler broadening, numerical treatment 9-32367
- ²³⁵U fission cross-section for $E_n = 1$ to 25 keV 9-29849
- ²³⁵U in rod-cluster geometry, ratio of fission rate to that of ²³⁸U 9-25661
- ²³⁵U photon-induced fission; yield, K.E. and mass distrib. meas., $E_\gamma \leq 25$ MeV 9-32369
- ²³⁵U(d,p)²³⁶U, fission prob. depend. on excitation energy, resonance eff. 9-27773
- ²³⁵U(n, f), delayed γ spectra meas., 2-80 μ sec, yield determ. 9-27769
- ²³⁵U(t,d,f), fission-fragment correlations 9-42315
- ¹⁷⁵Yb, sum-pole coincidence spectrum, decay obs. 9-25583
- ¹⁷⁵Yb from ¹⁷⁴Yb(d,p), DWBA anal., $E_d = 12$ MeV 9-25652
- ²⁰⁶Pd(p, n), cross section and resonances obs., γ and M1 transitions obs., $E_p \leq 40$ keV 9-27644
- ¹⁵⁵Dy($\alpha, 5n$)¹⁵⁵Er, creation of new isotope ¹⁵⁵Er 9-48436
- ¹⁵⁶Er prod. by (40 Ar, 4n) react., lifetimes of rotational states 9-25581
- ¹⁶⁶Er, 80.6 keV transition, α_k meas. 9-29739
- ¹⁶⁶Er from ¹⁶⁷Er(d,t), levels, spin and parity determ. from t spectra, $E_d = 12$ MeV 9-22816
- ¹⁶⁶Er in ErCrO₃, Mossbauer hyperfine structure, 4-40°K 9-24380
- ¹⁶⁶Er, Mossbauer study of Ho single crystal mag. structure 9-47333
- ¹⁵⁵Gd/¹⁵⁸Gd isomer shift ratio determ., Mossbauer meas. 9-27636
- ¹⁷⁶Hf, half-life of 1227.4 keV level meas., K-forbidden transition 9-40485
- ¹⁷⁶Hf, Mossbauer effect meas. 9-35639
- ¹⁶⁰Ho 0⁺→0⁺ β transition, spectrum-shape factor and longitudinal polarization theory 9-29768
- ¹⁸⁶Ir-¹⁸⁶Os, γ -ray spectrum and transition multiplicities 9-42253
- ¹⁷⁶Lu, conc. in ¹⁷⁵, ¹⁷⁶Lu mixture, thermal neutron absorpt. method 9-45431
- ²⁵⁶Lw, properties, half-life and α spectra, review 9-36584
- ¹⁸⁶Os, E2/M1 mixing ratios of 2⁺-2⁺ transitions 9-32321
- ¹⁸⁶Os, level scheme from γ -ray spectrum of ¹⁸⁶Ir decay 9-42253
- ²³⁶Pa, prod. and decay props. 9-38707
- ²⁰⁶Pb, ⁴He induced fission, fragment ang. distrib. meas., pairing eff. at ²¹⁰Po saddle pt. 9-27772
- ²⁰⁶Pb, energy levels and transitions, residual interaction model 9-40487
- ²⁰⁶Pb 3⁻ state, basis of 2.61 and 2.69 MeV states in ²⁰⁵Tl 9-44163
- ²⁰⁶Pb(α, α), ang. distrib. meas., phase anal., $E_\alpha = 40$ MeV 9-29829
- ²⁰⁶Pb spectra calc., realistic interaction, eff. of Woods-Saxon wave function 9-38653
- ²⁰⁶Pb(α, xn)²¹⁰-²¹⁰Po, excitation functions, total cross-sections, compound-nucleus mechanism 9-44220
- ²⁰⁶Pb(d,t)²⁰⁶Pb, t spectra meas., levels determ., $E_p = 21.6$ MeV 9-27643
- ²⁰⁶Pb(n,n), diff. cross section, excitation function calc., levels determ. 9-40513
- ²⁰⁶Pb(p,d), n single-hole states in 82<N<126 shell obs., $E_p = 55$ MeV 9-48251
- ²⁰⁶Ra to ²¹⁴Ra from Pt(²²Ne, xn), isotope identification 9-27645
- ¹⁸⁶Re, β - γ directional correlation measurements 9-22732
- ¹⁸⁶Re from (d, p), (d, t), (n, p) and (n, e⁻) reactions, levels calc. 9-27641
- ²²⁶Rn, α -decay, rel. to excited levels of ²²²Ra 9-48303
- ¹⁷⁶Yb, n capture cross section, 5 keV-3 MeV 9-25638
- ^{197m}Hg, γ -spectrum, 50-1000keV 9-42254
- ²²⁷U-²²³Th-²²³Rg-²¹³Rn-²¹³Po, chain obs. 9-48319
- ¹⁹⁷Am, photofission, mass and energy distrib. of fragments 9-48362
- ¹⁹⁷Am, α , β C reaction, diff. cross section, energy spectra, ang. distrib. meas., $E_\alpha = 82$ MeV 9-25659

Nuclei with $150 \leq A$ continued

- ¹⁵⁷Au, ¹⁴N reaction, diff. cross section, energy spectra, ang. distrib. meas., $E_p=110$ MeV 9-25659
- ¹⁵⁷Au, ¹⁵N reaction diff. cross section, energy spectra, ang. distrib. meas., $E_p=98.5$ MeV 9-25659
- ¹⁵⁷Au, in Au-Fe alloys, hyperfine field 9-49259
- ¹⁵⁷Au, isotopically pure nuclei, fission by 40 MeV α -particles, angular distrib. of fragments 9-36617
- ¹⁵⁷Au, isotopically pure nuclei, fission b 40 MeV α particles, angular distrib. of fragments 9-40525
- ¹⁵⁷Au, resonance γ ray, pressure depend. of energy 9-39816
- ¹⁵⁷Au(γ , n), $E_\gamma=0.4-0.9$ GeV 9-32337
- ¹⁵⁷Au(γ , n) cross section meas., $E_\gamma=1-5.5$ GeV 9-25611
- ¹⁵⁷Au(p, p_{3n}), recoil ¹⁵⁴Au angular distrib. rel. to models, Ep 30-85 MeV 9-29800
- ¹⁵⁷Au(p, pn), recoil ¹⁵⁶Au angular distrib. rel. to models, Ep 30-85 MeV 9-29800
- ²⁰⁷Bi, isomeric state, high-spin, three-particle levels 9-42231
- ²⁰⁷Bi decay obs. using electron-gamma ang. correl. arrangement 9-25499
- ²⁰⁷Bi e capture decay, X-ray emission from L-subshells, ²⁰⁷Pb Coster-Kronig transition prob. 9-27678
- ²¹⁴Bk \rightarrow ²¹⁴Am, α spectra meas., levels spin and parity determ. 9-27651
- ¹⁶⁷Er, E2- and M1-transitions and dipole moments mean values 9-36565
- ¹⁶⁷Er, γ -ray spectra variation on resonant neutron capture 9-22796
- ¹⁶⁷Er(d, p) ¹⁶⁶Er levels determ. from t spectra, $E_t=12$ MeV 9-22816
- ¹⁵⁷Gd, mag. moment from ENDOR obs. in CeO₂:Gd³⁺ 9-35733
- ¹⁷⁷Hf, [624] $\frac{1}{2}$, rotational band, mag. moment of ground state 9-27638
- ¹⁷⁷Hf, E2- and M1-transitions and dipole moments mean values 9-36565
- ¹⁷⁷Hf in Fe, hyperfine field obs. and g factors of 321 keV level 9-35606
- ¹⁹⁷Hg decay, γ -spectra, 50-1000 keV 9-42254
- ¹⁷⁷Lu, E2- and M1-transitions and dipole moments mean values 9-36565
- ¹⁷⁷Lu, sum-peak coincidence spectrum, decay obs. 9-25583
- ²³⁷Np, Mossbauer hyperfine field in NpAl₃, NpC, Np and Am 9-47334
- ²³⁷Np, n induced fission, 14 MeV, in α decay, c.f. with ²³⁵U, n_{th} induced 9-29847
- ²³⁷Np, neutron fission analysis of odd-even nuclei 9-27770
- ²³⁷Np nucl. moment, e.p.r. on Np⁶⁺ in Cs₂UO₂Cl₄:NpO₂²⁺ and ²⁺ 9-35712
- ²³⁷Pb, prod. and decay props. 9-38707
- ²⁰⁷Pb, ⁴He induced fission, fragment ang. distrib. meas., pairing eff. at ²¹¹Po saddle point 9-27772
- ²⁰⁷Pb, hyperfine structure in e.p.r. spectrum of ZnTe:Pb 9-47439
- ²⁰⁷Pb Coster-Kronig transition, ²⁰⁷Bi e capture decay, L-subshell fluorescence yield 9-27678
- ²⁰⁷Pb from ²⁰⁸Pb(d, t), diff. cross section, excitation energy meas., level assignment, $E_d=50$ MeV 9-27746
- ²⁰⁷Pb Knight shift in Pb liq. alloys, electronic struct. of impurities obs. 9-32800
- ²⁰⁷Pb(α , α), ang. distrib. meas., phase anal., $E_\alpha=40$ MeV 9-29829
- ²⁰⁷Pb(γ , n), γ , cross section and resonances obs., γ and M1 transitions obs., $E_\gamma \leq 40$ keV 9-27644
- ²⁰⁷Pb(n, n), diff. cross section, excitation function calc., levels determ. 9-40513
- ¹⁸⁷Re, γ -ray spectra on absorpt. of thermal neutrons and 4.41 eV neutrons 9-22798
- ¹⁸⁷Re, γ energy distrib. after β decay, slowing down of nuclear recoil 9-45283
- ¹⁸⁷Re, n total and capture cross-sections, resonance parameters, 0.01 eV TO to 30 keV 9-22797
- ¹⁸⁷Re, separated isotope, disson by 40 MeV α -particles angular distrib. of fragments 9-40525
- ¹⁸⁷Re, separated isotope, disson by 40 MeV α -particles angular distrib. of fragments 9-36617
- ²²⁷Th obs, attachment to α spectrometer for separation of effects due to decay products 9-22752
- ²⁰⁷Tl from ²⁰⁷Tl(t, p), γ spectra meas., vib. levels, spin and parity determ., $E_t=13$ MeV 9-27646
- ²⁰⁷Tl from ²⁰⁸Pb(d, t), diff. cross section, excitation energy meas., level assignment, $E_d=50$ MeV 9-27746
- ²³⁵U, production by neutron irradiation of ²³⁵, ²³⁶U and accumulation in Pu 9-44209
- ¹⁷⁷W, production, identification and γ -ray spectra 9-38674
- ¹⁷⁷W β spectrum obs., decay scheme and log f_t determ. 9-27677
- ¹⁵⁹Au and ¹⁵⁹Au nucl. orientation/n.m.r. in Fe, non-contact contrib. to effective field obs. 9-37805
- ¹⁵⁹Au conversion electron obs. with double-focusing sector-type spectrometer 9-38610
- ¹⁵⁹Au foil, absolute disintegration rate by coincidence techniques 9-32325
- ²⁰⁸Bi, energy levels calc. from Hamada-Johnston pot. reaction matrix elements 9-34405
- ²⁰⁸Bi, multipole anal. of effective particle-hole interaction 9-34405
- ²⁰⁸Bi multipole analysis of particle-particle and particle-hole multiplets 9-38641
- ²⁰⁸Bi shell model description of the 0⁺- isobaric analogue resonance 9-44165
- ¹⁵⁹Er, prod. by (⁴⁰Ar, 4n) react., lifetimes of rotational states 9-25581
- ¹⁵⁹Gd, n capture cross section, 5 keV-3 MeV 9-25638
- ¹⁵⁹Gd, total cross section for 16-19 MeV 9-22789
- ¹⁵⁹Gd 2⁺ level lifetime meas. by Coulomb excitation 9-27637
- ¹⁷⁷Hf, Mossbauer effect meas. 9-35639
- ¹⁷⁷Hf in Fe hyperfine field determ. using Mossbauer expts. 9-35605
- ¹⁵⁸Ho decay scheme, γ and conversion electron spectra at energies above 1000 KeV obs. 9-48314
- ¹⁴⁸Lu \rightarrow ¹⁴⁸Yb, level, spin and parity determ., γ spectra meas. 9-27676
- ²³⁷Pa, prod. and decay props. 9-38707
- ²⁰⁸Pb, isobaric analogue state with ²⁰⁸Bi, energy level comparison 9-34405
- ²⁰⁸Pb, level investigation using excitation with n-capture γ ; anomalies 9-36573
- ²⁰⁸Pb, low-lying states studied in p scatt. at resonance energy for isobaric analog resonance 9-48302
- ²⁰⁸Pb, n thermalization study with pulsed-source 9-22893
- ²⁰⁸Pb, neutron and proton distributions 9-44164
- ²⁰⁸Pb, neutron radius obs. from analog state 9-34406
- ²⁰⁸Pb collective 3⁺ state, g-factor calc. 9-42233
- ²⁰⁸Pb core ± 2 nucleons, semi-realistic structure calc. of levels 9-22735
- ²⁰⁸Pb coupling of single particle and collective octupole states 9-27648
- ²⁰⁸Pb Hartree fock calc. in coord. space 9-34407
- ²⁰⁸Pb proton decay of ground state isobaric analogue populated by (p, n) reaction 9-42232

Nuclei with $150 \leq A$ continued

- ²⁰⁸Pb(α , α), ang. distrib. meas., phase anal., $E_\alpha=40$ MeV 9-29829
- ²⁰⁸Pb(d, ³He) ²⁰⁷Tl diff. cross section, excitation energy meas., level assignment, $E_d=12$ MeV 9-27746
- ²⁰⁸Pb(d, p) ²⁰⁹Pb, cross section meas., levels, spectroscopic factors calc., $E_d=18-17$ MeV 9-27745
- ²⁰⁸Pb(d, p) ²⁰⁹Pb, γ spectra meas., particle-vibration coupling, levels determ., $E_d=12$ MeV 9-29740
- ²⁰⁸Pb(d, t) ²⁰⁷Pb diff. cross section, excitation energy meas., level assignment, $E_d=50$ MeV 9-27746
- ²⁰⁸Pb(γ , n), cross section and resonances obs., γ and M1 transitions obs., $E_\gamma \leq 40$ keV 9-27644
- ²⁰⁸Pb(n, γ) ²⁰⁹Pb, activation cross sections at 10-200 keV 9-42292
- ²⁰⁸Pb(n, n) cross section meas., $E_n=5.3-6.3$ MeV 9-29807
- ²⁰⁸Pb(p, p), around resonances which are analogues of single-particle bound states in ²⁰⁹Pb 9-29803
- ²⁰⁸Pb(p, p) ²⁰⁸Pb, low-lying states studied in p scatt. at resonance energy for isobaric analog resonance 9-48302
- ²⁰⁸Pb(p, d) n single-hole states in 82 < N \leq 126 shell obs., Ep=55 MeV 9-48251
- ²³⁸Pu, ²⁴⁰Pu and ²⁴²Pu photofission fragments, cross sections and ang. distrib., and struct. of fission barrier 9-48363
- ²³⁸Pu, γ -ray assay in waste drums from intensity of 765 keV line 9-37864
- ²³⁸Pu, light element impurity anal. by reaction γ spectra 9-25603
- ²³⁸Pu, n induced fission, fragment ang. distrib. meas., $E_n=0.06-7.20$ MeV 9-36618
- ²³⁸Pu helium generation, thermal power and spontaneous fission 9-29770
- ²³⁸Pu \rightarrow ²³⁴U, L, M subshell ratios determ. of 43.5 E2 transition 9-25589
- ¹⁶⁷Tm \rightarrow ¹⁶⁶Er decay, e- γ coincidence spectra 9-40492
- ²³⁸U, binary and ternary fission, ³He, and ⁴He induced 9-46247
- ²³⁸U, n induced fission, 16 MeV α decay prob., c.f. with ²³⁵U, n_{th} induced 9-29847
- ²³⁸U, n spectra following bombardment with 147 MeV n, nuclear temp. and level density parameters 9-27766
- ²³⁸U, neutron induced 1.3, 1.4, 1.5, 2.9, 5.3, 6.9 MeV statistical model analysis 9-22835
- ²³⁸U, photofission, mass and energy distrib. of fragments 9-48362
- ²³⁸U, π photoproduction and quasideuteron interaction involved in excitation leading to fission 9-38726
- ²³⁸U, resonance self-shielding factors for energy groups 5 eV to 2 keV 9-22890
- ²³⁸U, ternary fission, induced by 2.9 MeV neutrons, mechanism 9-44226
- ²³⁸U charge distrib., intrinsic quadrupole moment, radius studied by obs. of muonic X-rays 9-38677
- ²³⁸U deformed, elastic and inelastic scatt. of fast n 9-40514
- ²³⁸U deformed nucleus in muonic atoms, exact calc. of eigenvalues 9-40570
- ²³⁸U fast n induced fission, yield 9-22836
- ²³⁸U fission, fast and thermal, ¹⁴⁰Ba yields, obs. 9-46248
- ²³⁸U fission, p induced, isomer yield ratio of ^{115m}Cd and ^{115g}Cd 9-34472
- ²³⁸U fission by 9.5, 11.3 MeV p and 11.5 MeV d, prods. Z distrib., obs. 9-29853
- ²³⁸U fission fragments, ang. distrib., shadow patterns 9-40524
- ²³⁸U fission heavy ion induced, fragment charge, isotope distrib. meas. 9-29856
- ²³⁸U in rod-cluster geometry, ratio of fission rate to that of ²³⁵U 9-25661
- ²³⁸U photofission fragments asymmetry and anisotropy 9-34470
- ²³⁸U photofission fragments, cross sections and ang. distrib., and struct. of fission barrier 9-48363
- ²³⁸U proton induced, 40-85 MeV, recoil props. of ⁶⁴Ne, ⁶⁷Cu and ⁷²Zn 9-48359
- ²³⁸U spherical shell transmission at 23 KeV, Monte Carlo interpretation 9-34482
- ²³⁸U, μ -atomic h.f.s. in K.L. and M lines, nuclear charge distrib. 9-38678
- ²³⁸U(γ , n) cross section meas., $E_\gamma=1-5.5$ GeV 9-25611
- ^{199m}Hg, conversion coefficients and fluorescence yields obs. 9-42255
- ²⁰⁹Bi, in liquid Bi, spin-lattice relax. 9-26134
- ²⁰⁹Bi, particle-vibration (3⁻) coupling, one-particle structure determ. 9-25587
- ²⁰⁹Bi, particle vibration coupling 9-27648
- ²⁰⁹Bi, photofission, mass and energy distrib. of fragments 9-48362
- ²⁰⁹Bi, quadrupole moment calc. from h.f.s. of 6p_{7/2} ³P, and ¹P, 9-40488
- ²⁰⁹Bi fission cross section, electron and bremsstrahlung induced, 60-1000 MeV 9-38726
- ²⁰⁹Bi from ²¹⁰Pb decay, L-subshell X-ray fluorescence yield and Coster-Kronig transition prob. 9-25602
- ²⁰⁹Bi level investigation using excitation with n-capture γ ; anomalies 9-36573
- ²⁰⁹Bi single-particle structure determ. by particle-core coupling model 9-36583
- ²⁰⁹Bi(n, 2n), angular correlations between neutrons 9-29813
- ²⁴⁹Cf, ^{12,13}C bombardment, element 104, isotope production, α emission, isotope identification 9-42219
- ¹⁵⁹Dy \rightarrow ¹⁵⁹Tb angular correlation between K and L X-rays from ¹⁵⁹Tb 9-46212
- ¹⁵⁹Er decay scheme new data 9-48316
- ¹⁵⁹Gd Ge(Li)-Ge(Li) gamma ray coincidence studies 9-38690
- ¹⁵⁹Hg, n.m.r. in HgCr₂S₄ at 1.4^oK, depend on mag. structure 9-45400
- ¹⁵⁹Hg 158 keV E2 transition, N-subshell internal conversion coeff. meas. 9-40486
- ¹⁵⁹Ho decay scheme, γ -ray and conversion electron spectra obs. 9-48315
- ¹⁵⁹Ir \rightarrow ¹⁵⁹Os, γ spectra meas., ¹⁵⁹Os Mossbauer eff. obs. 9-38676
- ²³⁹Np, gamma transitions studied by α - γ coincidences 9-42256
- ¹⁵⁹Os from ¹⁸⁹Ir, γ spectra meas., Mossbauer eff. obs. 9-38676
- ²⁰⁸Pb from ²⁰⁸Pb(d, p) γ ; p, γ spectra meas., particle vibration coupling, levels determ., $E_d=12$ MeV 9-29740
- ²⁰⁸Pb from ²⁰⁸Pb(d, p); cross section meas., levels, spectroscopic factors calc., $E_d=18-17$ MeV 9-27745
- ²⁰⁸Pb particle-vibration (3⁻) coupling, one-particle structure determ. 9-25587
- ²⁰⁸Pb single-particle structure determ. by particle-core coupling model 9-36583
- ²³⁹Pu, fission cross-section near 83 eV, multilevel anal. 9-22833
- ²³⁹Pu, fission products activities and power output 9-22838
- ²³⁹Pu, infinite dilution fission reson. integrals, multilevel effects 9-27767
- ²³⁹Pu, n capture:fission ratio and fission cross section, 5 eV-23 keV 9-22831
- ²³⁹Pu, n induced fission, relative yield, energy spectra fo light nuclei meas. 9-29846

Nuclei with $150 \leq A$ continued

- ^{239}Pu , n , induced fission, fragment nuclear charge distrib. calc. method 9-32371
- ^{239}Pu capture-to-fission ratio in Zebra-6 reactor 9-32380
- ^{239}Pu capture-to-fission ratio for $E_n=20$ to 600 keV 9-32351
- ^{239}Pu fission, slow- n induced, cross section correlation anal. 9-40522
- ^{239}Pu fission cross-section for $E_n=1$ to 25 keV 9-29849
- ^{239}Pu n induced fission, n spectra meas. 9-29859
- ^{239}Pu separation with strongly basic anion-exchange resin paper 9-28819
- ^{239}Pu thermal and fast n induced fission, yield 9-22836
- $^{239}\text{Pu}(d,p)^{240}\text{Pu}$, fission prob. depend. on excitation energy, resonance eff. 9-27773
- $^{239}\text{Pu}(n, f)$, delayed p , spectra meas., 2-80 μsec , yield determ. 9-27769
- $^{239}\text{Pu}(t, df)$, fission-fragment correlations 9-42315
- ^{157}Tb , from ^{159}Dy decay, angular correlation between K and L X-rays 9-46212
- ^{157}Tb , quadrupole moment, from Tb II spectrum 9-38671
- $^{157}\text{Tb}(n, n'p)$, energy distribution of p -rays 9-29810
- ^{169}Tm , Mossbauer effect in Tm^{3+} -doped soda-silica glass, crystalline elec. field parameters determ. 9-37702
- ^{169}Tm n.m.r. in TmAl garnet, $<4^\circ\text{K}$ 9-45407
- ^{169}Tm spin-lattice relax. in thulium ethylsulphate 9-28641
- Al, total cross-sections for very slow neutrons, 100 m/sec. to 5 m/sec. 9-44204
- Au, p induced fission, high energy cross section determ. by mica track detector 9-40523
- Au, small-angle scatt. of n , differential cross-sections, polar., applic. 9-25634
- Au, total cross-sections for very slow neutrons, 100 m/sec. to 5 m/sec. 9-44204
- Au, e^+ ; secondary emission, energy depend., $E=1.5$ –18 GeV 9-42274
- Au(p, p) diff. cross section meas., diffuse-surface optical model anal., $E_p=28$ MeV 9-25623
- Bi, fission, cross-section, induced by 600 MeV protons 9-36616
- Bi, fission, tripartite, induced by protons in range 600 MeV to 20 GeV 9-36615
- Bi, p induced fission, high energy cross section determ. by mica track detector 9-40523
- Bi, photofission induced by 1 to 6 GeV photons 9-29855
- Bi(γ, n), angular distributions of fast photoneutrons 9-27697
- Cd, small-angle scatt. of n , differential cross-sections, polar., applic. 9-25634
- Dy, Tb, Gd, Eu isotopes, α decay 9-42259
- Er isomer, p excited, half-life and γ -spectrum, obs. 9-27631
- Gd isotopes, s -wave n strength function, resonance parameter and potential scatt. radii 9-40484
- Gd rare isotopes, reson. transmission obs. using isotropic mixtures 9-38708
- Hg isotopes, neutron activation cross section meas., $E_n=14.1$ MeV 9-27730
- Hg odd-mass isotopes, nuclear spectra number conserving calc. 9-27647
- ^{41}K decay, obs. of γ -ray emissions 9-40490
- Os isotopes ($A=178$ –181), production, identification and γ -ray spectra 9-38674
- Os transition matrix elements, E2, M1, signs of 9-44161
- Pb, cosmic-ray collision, electron-photon cascade energy depend. on interacting particle energy 9-46244
- Pb, Delbruck scatt. of 10.8 MeV γ rays 9-32335
- Pb, N reactions, 750–2000 MeV, with N, π emission 9-27728
- Pb, odd-mass isotopes, nuclear spectra number conserving calc. 9-27647
- Pb, small-angle scatt. of n , differential cross-sections, polar., applic. 9-25634
- Pb p bombard 1-3 BeV obs. of emitted p 9-48336
- Pb(γ, n), angular distributions of fast photoneutrons 9-27697
- Pt, Ir, Re, natural mixture, fission by 40 MeV α -particles, angular distrib. of fragments 9-36617
- Pt, Ir, Re, natural mixture, fission by 40 MV α particles, angular distrib. of fragments 9-40525
- Pt transition matrix elements, E2, M1, signs of 9-44161
- Pu dilute fuel for ZPR-3 Assembly 48 expt. 9-29876
- PuO_2 — ^{10}B mixture as source of 3.85 γ 9-29662
- Re isotopes ($A=177$ –179), production, identification and γ -ray spectra 9-38674
- Rn in atmosphere, meas. method and its validity 9-41538
- Sn nuclear-structure probs. investigated with inverse-gap-eqn. method 9-46203
- Ta, stopping power, 5–13.5 MeV protons, deuterons, 8–20 MeV ^3He , ^4He 9-22780
- Ta(γ, n), angular distributions of fast photoneutrons 9-27697
- Th, fission, cross-section, induced by 600 MeV protons 9-36616
- Th, fission, tripartite, induced by protons in range 600 MeV to 20 GeV 9-36615
- Th, photofission induced by 1 to 6 GeV photons 9-29855
- Th, small-angle scatt. of n , differential cross-sections, polar., applic. 9-25634
- Tl, odd-mass isotopes, nuclear spectra number conserving calc. 9-27647
- Tm(n, p) γ spectra meas. 9-34452
- U, fission, cross-section, induced by 600 MeV protons 9-36616
- U, fission, tripartite, induced by protons in range 600 MeV to 20 GeV 9-36615
- U, natural, thermal neutron conversion ratio 9-44231
- U, p induced fission, 440 MeV, recoil props. of 20 nuclides 9-48358
- U, p induced fission, high energy cross section determ. by mica track detector 9-40523
- U, photofission induced by 1 to 6 GeV photons 9-29855
- U, small-angle scatt. of n , differential cross-sections, polar., applic. 9-25634
- V, Delbruck scatt. of 10.8 MeV γ rays 9-32335
- W, small-angle scatt. of n , differential cross-sections, polar., applic. 9-25634
- W, time-of-flight meas. of n spectra 9-29808
- W transition matrix elements, E2, M1, signs of 9-44161
- W(n, n) cross section meas., comparison with theory 9-25635

Nuclei with $20 \leq A \leq 49$

- ^{23}Na in ferroelectric rochelle salt, spin-lattice relax. 9-24345
- $^{23}\text{P}(p, p)$, ^{32}S mean level width, excitation function meas., $E_p=8$ –10 MeV 9-25591
- ^{41}K , quadrupole moment determ. by resonance scatt. of light investig. of hyperfine struct. of $4p$ and $5p^2P_{3/2}$ -states 9-29751

Nuclei with $20 \leq A \leq 49$ continued

- $^{48}\text{Ca}(^3\text{He}, p)^{50}\text{Sc}$, levels, spin, parity determ. from p spectra, $E_{\text{He}}=18.5$ MeV 9-27752
- $A=39$, core polarization eff. on M1 operator, f corrections calc. 9-32294
- $A=41$, core polarization eff. on M1 operator, f corrections calc. 9-32294
- Tabakin interaction applic. to sd shell, nuclear $36 \leq A \leq 39$ 9-29750
- well depth, real central and spin-orbit, elastic t scatt., $E_n=2$ MeV 9-29816
- $^{27}\text{Al}(n, p)^{28}\text{Al}$ gamma-ray spectra study using Ge(Li) spectrometer 9-38706
- ^{49}V energy levels determ. from ^{49}Cr positron decay γ spectra meas. 9-48320
- ^{32}P , width of 3.51 MeV level 9-48274
- ^{208}Pb , g factor of 3-octopole state vibr. 9-34408
- Al, n polarization analyzing power at 3.25 MeV 9-27733
- Al, n radiative capture, resonance radiation width, cross section meas., $E_n=0.1$ –200 keV 9-27731
- Al, polarized 1.5 MeV neutron scattering, angle range 20–143° 9-36605
- Al, stopping power, 5–13.5 MeV protons, deuterons, 8–20 MeV ^3He , ^4He 9-22780
- Al, e^+ ; secondary emission, depend., $E=1.5$ –18 GeV 9-42274
- Al ($^4\text{He}, ^3\text{H}$) stripping reaction at 120 MeV, cross sections 9-42310
- ^{23}Al , mass excess obs. in $^{28}\text{Si}(p, ^4\text{He})^{23}\text{Al}$ 9-25568
- ^{25}Al , 2nd excited state, cross-over/cascade branching ratio determ. 9-27652
- ^{25}Al , props. of 4.038 MeV state from $^{24}\text{Mg}(p, \gamma)$ react. 9-25590
- ^{25}Al , spin of 5.304 MeV level, $^{24}\text{Mg}(p, p)^{25}\text{Al}$ Mg scatt. obs. 9-25627
- ^{26}Al , cosmogenic, in estimation of terrestrial cosmic dust accretion rate 9-31279
- ^{27}Al , from $^{23}\text{Na}(\alpha, \gamma)$, new excited levels 9-46242
- ^{27}Al , low-lying levels, excited core model description 9-44139
- ^{27}Al , n.m.r. relax. in dil. Al alloys 9-47443
- ^{27}Al , n bombardment, level-excitation cross section meas., $E_n=14.6$ MeV 9-36606
- ^{27}Al 20 MeV polarized p asymm. scatt. obs. 9-25619
- ^{27}Al 36 MeV ^3He scatt. obs. 9-32352
- ^{27}Al (γ, n) ^{26}Al , ^{27}Al ($\gamma, 2n$) ^{25}Al , photoneutron mass-sections meas., at 62 MeV 9-48327
- ^{27}Al from $^{24}\text{Mg}(\alpha, p)$, p spectra meas., levels, lifetime, spin and parity determ., $E_n=9$ –13 MeV 9-25656
- ^{27}Al n.m.r. in dilute Al-Mn alloys 9-28754
- ^{27}Al n.m.r. in zeolites, effect of sorbed mols. on quadrupole coupling constants 9-43300
- ^{27}Al n.m.r. lines in bulk deformed Al, quadrupole broadening obs. 9-35723
- ^{27}Al n.m.r. TmAl garnet, 1.5° to 300°K 9-45407
- ^{28}Al , new levels found in $^{27}\text{Al}(d, p)^{28}\text{Al}$, 2.6 MeV 9-22739
- ^{28}Al from $^{27}\text{Al}(n, p)$, γ spectra meas., Q -value, excitation energy, decay scheme determ. 9-22801
- ^{29}Al from $^{30}\text{Si}(t, \alpha)$ levels, spin and parity determ., $E_n=11.8$ MeV 9-38656
- $^{27}\text{Al}(d, ^3\text{He})^{26}\text{Mg}$, ^3He energy spectra and ang. distrib. for $E_n=52$ MeV 9-22820
- $^{27}\text{Al}(d, ^3\text{He})^{26}\text{Mg}$, proton pickup from $1p$ and $2s$ - $1d$ shells of ^{27}Al 9-22820
- $^{27}\text{Al}(d, p)^{28}\text{Al}$, 2.6 MeV stripping reaction obs. 9-22739
- $^{27}\text{Al}(n, \alpha)^{24}\text{Na}$, 13.8–14.8 MeV, cross-section meas. 9-27732
- $^{27}\text{Al}(n, \gamma)^{28}\text{Al}$, γ spectra meas., Q -value, excitation energy, decay scheme determ. 9-22801
- $^{27}\text{Al}(p, ^3\text{He})^{24}\text{Mg}$, recoil nuclei ang. distrib. meas., $E_p=660$ MeV 9-34449
- $^{27}\text{Al}(p, \alpha)$ ang. distrib., direct reaction mechanism, $E_p=38$ MeV 9-48337
- $^{27}\text{Al}(p, \gamma)^{28}\text{Si}$, $E_p=1724$ keV, for study of 6.999 MeV level in ^{28}Si 9-44140
- $^{27}\text{Al}(p, \gamma)^{28}\text{Si}$, resonance energy and yield meas. by Ge(Li) detector 9-32258
- Al(p, p) diff. cross section meas., diffuse-surface optical model anal., $E_p=28$ MeV 9-25623
- $^{27}\text{Al}(p, p)$, $^{28}\text{Si}(p, p)$, rel. to excited core model for description of low-lying levels of ^{27}Al 9-44139
- $^{27}\text{Al}(p, p)$, elastic low- and medium energy 9-48340
- ^{33}Ar — ^{33}Cl ($T=3/2$) level, shell-model calc. 9-29832
- ^{39}Ar — ^{39}Cl , β endpoint and vector coupling const. determ. 9-42284
- ^{36}Ar , $T=0$ pairing correlations, Hartree-Fock-Bogoliubov eqn. 9-29744
- $^{36}\text{Ar}(^3\text{He}, n)^{38}\text{Ca}$, levels, spin and parity determ., $E=9$ MeV 9-29833
- ^{38}Ar , quadrupole and octupole deformations in $2s$ - $1d$ shell, reduced $E3$ transition rate calc. 9-38657
- ^{41}Ar oven reactor core and in exhaust air, IRT-1000 Sofia 9-22875
- $^{40}\text{Ar}(d, ^3\text{He})^{39}\text{Cl}$, ^3He spectra meas., levels, spin and parity determ., $E_n=52$ MeV 9-32358
- $^{40}\text{Ar}(n, \alpha)^{37}\text{S}$ activation cross section meas., $E_n=14.4$ MeV 9-29812
- $^{40}\text{Ar}(n, np+n; pn+n, d)^{39}\text{Cl}$, activation cross section meas., $E_n=14.4$ MeV 9-29812
- $^{38}\text{Ar}(n, p)^{38}\text{Cl}$, activation cross section meas., $E_n=14.4$ MeV 9-29812
- $^{40}\text{Ar}(n, p)^{40}\text{Cl}$, activation cross section meas., $E_n=14.4$ MeV 9-29812
- $^{40}\text{Ar}(n, n)^{41}\text{Ar}$, activation cross section meas. 9-29812
- $^{40}\text{Ar}(p, n)^{40}\text{K}$, for positive parity states of ^{40}K 9-44143
- $^{40}\text{Ar}(p, p)$ cross section meas., optical model analysis, E_{21} MeV 9-38695
- ^{39}CC from $^{40}\text{Ar}(d, ^3\text{He})$; ^3He spectra meas., levels spin and parity determ., $E_p=52$ MeV 9-32358
- Ca, disintegration of 13.6 MeV deuterons on collision 9-48350
- Ca isotopes; Coulomb energy, anomalous isotope shift of radii, core polarization, excess n depend. 9-36572
- ^{38}Ca , positron decay, γ transitions obs. 9-44181
- ^{38}Ca from $^{36}\text{Ar}(^3\text{He}, n)$; levels, spin and parity determ., $E=9$ MeV 9-29833
- ^{40}Ca , $1d_{3/2}=1f_{7/2}$ energy splitting, expt. and theor. comparison 9-27663
- ^{40}Ca , dipole resonance, effect of quadrupole vibrations 9-34411
- ^{40}Ca , lifetime obs. using $^{39}\text{K}(p, p)^{40}\text{Ca}$ reaction 9-44142
- ^{40}Ca , surface effects in dipole resonances matrix element calc. for dipole transitions 9-40474
- $^{40}\text{Ca}(^3\text{He}, p)^{42}\text{Sc}$ ang. distrib., spin-orbit coupling, p polarization meas., levels determ. 9-32317
- ^{40}Ca compound nuclei from ^{39}K , p ; resonances obs., channel excitation func. meas. 9-29799
- ^{40}Ca elastic and inelastic proton scatt. 9-42279
- ^{40}Ca giant reson., collective correl. model with surface-delta-interaction 9-29746
- ^{40}Ca levels deduced from p scatt. expt. 9-27662
- ^{40}Ca lifetimes, γ -decay spectra 9-42213
- ^{41}Ca — ^{41}Sc mirror pair, nuclear matter radii calc. from Coulomb energy, comparison 9-38658
- ^{41}Ca , 3614 KeV level, branching ratio and spin 9-48306
- ^{41}Ca , angular distributions for levels from $^{40}\text{Ca}(d, p)^{41}\text{Ca}$ reaction 9-29823

Nuclei with $20 \leq A \leq 49$ continued

- ⁴¹Ca, first two excited states obs. 9-46198
⁴¹Ca low-lying parity states, transition rates, spectra calc., phonon-particle coupling model 9-32316
⁴²Ca, γ -ray ang. distrib., reaction independent analysis using Ge(Li) detector 9-42262
⁴²Ca, $J=0^+$ states, shell model calc. 9-40489
⁴²Ca, particle-hole state decay, γ -ray obs. 9-48284
⁴²Ca configuration and analogue states obs. m ⁴¹Ca(³He, α) ⁴²Ca 9-27751
⁴²Ca from ⁴⁰Ca(t,p), ang. distrib., spin-orbit coupling, p polarization meas., levels determ. 9-32317
⁴²Ca lifetime of 3.19 MeV (6^+) state from decay of (7^+) 615 keV in ⁴²Sc 9-42214
⁴³Ca, level scheme, from ⁴³K decay obs. 9-40490
⁴³Ca, $J=0^+$ states, shell model calc. 9-40489
⁴³Ca from ⁴⁵Sc(t, α) α ang. distrib. meas., levels, spectroscopic factors determ., $E_x=12.95$ MeV 9-29834
⁴³Ca from ⁴⁴Ca(d,p) γ ; p- γ delayed coincidence meas., half-life determ., $E_x=2.3$ MeV 9-34422
⁴³Ca, $J=0^+$ states, shell model calc. 9-40489
⁴³Ca from ⁴⁸Ca(He, α); ang. distrib. meas., spectroscopic factor, I_n determ., DWBA, energy levels determ., $E_x=15$ MeV 9-32359
⁴³Ca, double β -decay, possible interference due to $\beta\gamma$ correlation of ²¹⁴Bi in equilibrium with ²²⁶Ra impurity 9-22763
⁴³Ca, phase shift analysis, unambiguous parameters, $E_\alpha=40$ MeV 9-34464
⁴³Ca(³He, ³He)⁴³Ca, ang. distrib. meas., spectroscopic factor, I_n determ., DWBA, $E_x=15$ MeV 9-32359
⁴³Ca(³He, α)⁴³Ca, ang. distrib. meas., spectroscopic factor, I_n determ., DWBA, levels determ., $E_x=15$ MeV 9-32359
⁴³Ca(³He,t)⁴³Sc, α spectra meas., levels, spin determ. 9-38719
⁴³Ca(³He,t) reaction for obs. of particle hole states in ⁴⁸Sc 9-44144
⁴³Ca levels deduced from p scatt. expt. 9-27662
⁴³Ca(α , α_0) ⁴⁰Ca, optical-model analysis, l-depend. absorption factor, 5.5-17.5 MeV 9-25646
⁴³Ca(α ,p)³⁹K reaction, correls. in energies and width of structures 9-40502
⁴³Ca(d,³He) reaction, DWBA predictions test at $E_d=82$ MeV 9-40520
⁴³Ca(d,n)⁴⁵Sc, charge exchange coupling eff. investigated 9-29835
⁴³Ca(d,p)⁴¹Ca, angular distribution, $E_d=2$ MeV 9-29823
⁴³Ca(d,p) ⁴⁰Ca(0), $E_d=3.0$ -5.5 MeV, excitation functions 9-29835
⁴³Ca(d,d)Ca, tensor potential for optical model 9-22812
⁴³Ca(d,p)⁴¹Ca (2.02 MeV), stripping form factors 9-22821
⁴³Ca(d,p)⁴¹Ca $l=1$ transition, tensor forces eff., cross section j -depend. determ. 9-27749
⁴³Ca(d,p)⁴¹Ca stripping cross-section calcs., comparison between coupled-channel method and DWBA 9-42306
⁴³Ca(d,p)⁴¹Ca(³He,3.95 MeV) proton polarization near J -dependent cross-section min. 9-42307
⁴³Ca(d,p)⁴¹Ca 1.95 and 2.47 MeV reactions, proton polarization obs., comparison with theories 9-22822
⁴³Ca(d,p)⁴¹Ca; p- γ delayed coincidence meas., half-life determ., $E_d=1.2$ MeV 9-34422
⁴³Ca(d,p)⁴¹Ca, branching ratio and spin of 3614 KeV level of ⁴¹Ca 9-48306
⁴³Ca(γ n)³⁹Ca reaction, correls. in energies and width of structures 9-40502
⁴³Ca(μ , ν)⁴⁰K, ⁴⁰Ca(μ , ν)³⁹K, products identified by γ decay of excited states 9-38694
⁴³Ca(μ , ν)³⁹Ar, ⁴⁰Ca(μ , ν)³⁸Ar, products identified by γ decay of excited states 9-38694
⁴³Ca(p,p')⁴⁰Ca DWA analysis using Kallio-Koltveit interaction 9-29791
⁴³Ca(p,p'), p ang. distrib. meas., excitation function determ., $E_p=10$ MeV 9-29834
⁴³Ca(t,d)⁴¹Ca, excitation of first two excited states of ⁴¹Ca 9-46198
⁴³Ca(t,p)⁴²Ca, ang. distrib., spin-orbit coupling, p polarization meas., levels determ. 9-32317
³¹Cl ($T=3/2$) from ³³Ar decay, shell-model calc. 9-29832
³¹Cl, 1.763 MeV level props. 9-46197
³¹Cl, B(E2) of first two excited states and lifetimes meas. 9-29749
³¹Cl, lifetime meas. of six lowest lying levels 9-42236
³¹Cl, n.m.r. in alkali halide aqueous solns., chem. shift 9-34925
³¹Cl, n.m.r. in chloroform and deuteriochloroform, anisotropic molecular rotation in liquid 9-39119
³¹Cl, n.m.r. in CsNiCl₂ and CsCuCl₂ 9-45397
³¹Cl, n.m.r. in soln. with Co²⁺ paramag. rare earths, obs. 9-40807
³¹Cl, n.q.r. freqs., Townes and Dailey interpretation, exam. by BEEM 9-32454
³¹Cl, n.q.r. in p-chlorophenol, Zeeman effect 9-39929
³¹Cl, n.q.r. in three substituted anilines and p-chlorophenoxy acetic acid, temp. variation of freqs. 9-30103
³¹Cl in K₂PtCl₆, NQR, pressure depend. rel. to rot. of PtCl₆ group 9-31174
³¹Cl in Li Cl, n.m.r. relax. time and chemical shift meas., aq-methanol mixture 9-30035
³¹Cl in solid (C₂H₅)₂O, GaCl₃ to show mol. symm. rel. interpretation of i.r. spectrum of liquid 9-24515
³¹Cl level assignments 9-48283
³¹Cl n.q.r. in TbCl₃, RuCl₃, UCl₄ and KMnCl₃ 9-49365
³¹Cl, levels in 10.4 to 10.6 MeV range, from ³⁶S(p, γ) ³¹Cl reaction 9-42212
³¹Cl(p,n)³⁵Ar, threshold determ. 9-42284
³¹Cl(π^- , λ) 3.86 GeV, cross-section for strange particle prod. obs. in freon bubble chamber 9-25643
⁴⁸Cr, positron decay, ⁴⁹V energy levels determ. from γ spectra meas. 9-48320
⁴⁸Cr from ⁵⁰Cr(³He, α), energy levels, cross section, ang. distrib., spectroscopic factors determ., $E_x=18$ MeV 9-29836
⁴⁸Cr-²⁷Al, double acousto-nuclear mag. reson. in Al₂O₃, 4.2°K 9-49359
⁴⁹F(³He,d)⁵⁰Ne, Doppler-shift lifetime, transition energy meas., rotational props. level lifetime calc. 9-36582
⁵⁰F-²⁰Ne, β -decay to 4.97 MeV level 9-38684
⁵⁰F from ²²Ne(t,³He); g.s. mass excess determ. from Q-value, $E_x=22$ MeV 9-27639
Fe excitation functions for various nuclei obs. 9-38715
Fe(³He,t) charge exchange reaction, effective two-body force study 9-38720
Fe inelastic neutron scatt. cross sections, test of quasi-compound nucleus theory 9-29805

Nuclei with $20 \leq A \leq 49$ continued

- ⁵⁷Fe quadrupole moment from Mossbauer spectroscopy of Fe²⁺ in MgO 9-44168
⁵⁷K, sd shell, Tabakin interaction, e.m. transition rate, nuc. moment, spectroscopic factor calc. 9-29750
⁵⁷K positron decay, γ transitions obs. 9-44181
⁵⁷K, n.m.r. in KH₂PO₄, rotary saturation and spin calorimetry 9-28757
⁵⁷K, quadrupole moment determ. by hyperfine struct. of 4p and 5p²P_{3/2} states 9-29751
⁵⁷K from ⁵⁹K(p,p') γ ; p- γ delayed coincidence meas., half-life determ., $E_x=5.6$ MeV 9-34422
⁵⁷K low-lying parity states, transition rates, spectra, calc., phonon-particle coupling model 9-32316
⁴⁰K, positive parity states 9-44143
⁴⁰K, recoilless fraction and thermal shift for 29.4 keV transition, rel. to K lattice dynamics Mossbauer obs. 9-42952
⁴⁰K from ³⁹K(n, γ), 29.4 keV level lifetime determ. 9-27661
⁴⁰K quadrupole moment detect. by new double resonance technique in KClO₄ 9-29752
⁴⁰K radius change after 29.4 keV γ emission, determ. using Mossbauer effect 9-34412
⁴¹K, $7/2^-$ state, g -factor, mag. moment, half-life meas., spin precession method., 1.29 MeV 9-36586
⁴¹K, n capture cross section, 5keV-3 MeV 9-25638
⁴¹K spin assignments using ⁴¹K(d,p)⁴²K, 12 MeV 9-27751
⁴¹K(α , α), cross sections, ang. distrib. meas., $E_\alpha=22$ -29 MeV 9-22811
⁴¹K(n, γ)⁴⁰K, 29.4 keV level lifetime determ. 9-27661
³⁹K(p, α)³⁶Ar, α channels excitation functions meas., ⁴⁰Ca resonances obs. 9-29799
³⁹K(p, γ)⁴⁰Ca, and lifetime obs. on ⁴⁰Ca energy levels 9-44142
³⁹K(p,p')³⁹K*, p channels excitation functions meas., ⁴⁰Ca resonances obs. 9-29799
³⁹K(p,p')K; p- γ delayed coincidence Meas., half-life determ., $E_p=5.6$ MeV 9-34422
⁷¹Ta dil. alloys, n.m.r. 9-24504
Mg, n polarization analyzing power at 3.25 MeV 9-27733
Mg, polarized 1.5 MeV neutron scattering, angle range 20-143° 9-36605
²⁴Mg, ²⁵Mg, ²⁶Mg 20 MeV polarized p asymm. scatt. obs. 9-25619
²⁴Mg, γ -decay of levels, from (³He,d) γ reaction, lifetimes of 5 states 9-36582
²⁴Mg, K-2+ band, first 7 states, obs. using ²³Na(³He,d)²⁴Mg reaction 9-44138
²⁴Mg, p scatt., relative p', γ yield determ., $E_p=2010$ keV 9-27652
²⁴Mg, phase shift analysis, unambiguous parameters, $E_\alpha=40$ MeV 9-34464
²⁴Mg, structure, importance of space correls. 9-44127
²⁴Mg, T=0 pairing correlations, Hartree-Fock-Bogoliubov eqn. 9-29744
²⁴Mg, Y₄ deformation, evidence from p scatt. 9-42230
²⁴Mg(³He,n)²⁶Si, n distrib. meas., DWBA calc., l, spin and parity determ., $e=7$ MeV 9-32315
²⁴Mg(³He,n)²⁶Si levels and spin determ. 9-32314
²⁴Mg level order, interface on effective interaction 9-42210
²⁴Mg quadrupole moment, Coulomb excited at 61, 57, 52 MeV 9-48282
²⁴Mg static quadrupole moment of first excited state, obs. 9-29745
²⁴Mg from ²⁴Mg(d,p), energy levels, spectroscopic factors determ., $E_d=2.02$ -4.22 MeV 9-25655
²⁴Mg hyperfine interaction with vacancy-pair centre in MgO, e.s.r. obs. 9-47438
²⁴Mg structure, importance of space correls. 9-44127
²⁴Mg level order, interface on effective interaction 9-42210
²⁴Mg(α ,n)²⁸Si, 8.543 MeV ²⁸Si level lifetime meas., E_α ~ threshold energy 9-38655
²⁴Mg(α ,p)²⁷Al p, γ spectra meas., levels, lifetime, spin and parity determ., $E_\alpha=9$ -13 MeV 9-25656
²⁴Mg(d,p)²⁵Mg energy levels, spectroscopic factors determ., $E_d=2.02$ -4.22 MeV 9-25655
²⁴Mg(d,p) excitation functions, Ericson fluctuations, 1.5-2.9 MeV 9-48349
²⁴Mg(γ , n)²⁵Mg, threshold cross-section data and source of stellar neutrons 9-48329
²⁴Mg(p,n)²³Mg cross-section summed from threshold to 62MeV using bremsstrahlung 9-27698
²⁴Mg(p,n)²³Mg cross-section summed from threshold to 62MeV using bremsstrahlung 9-27698
²⁴Mg(p,³He)¹⁹Na, ¹⁹Na mass excess obs. 9-25568
²⁴Mg(p, 2p)²⁴Na, cross section and excitation function meas., $E_p=0.43$ -2.7 GeV 9-27717
²⁴Mg(p,d), 17 MeV p, failure to obs. prod. of any singlet d 9-38698
²⁴Mg(p,p')²⁴Mg, 3-4 MeV, p polariz 9-25627
N reactions, 750-2000 MeV, with N, π emission 9-27728
Na, n radiative capture, resonance radiation width, cross section meas., $E_n=0.1$ -200 keV 9-27731
²¹Na from ²⁰Ne(d,n) γ , γ spectra meas., levels, spin parity, branching and mixing ratios determ., $E_d=2.37$ -5.32 MeV 9-34409
²¹Na second excited state mean lifetime 9-48281
²¹Na, diffusion in RbCl, 377-707°C 9-23842
²¹Na, K electron capture and β^+ emission ratio meas. 9-32326
²¹Na excitation by ¹⁹F α bombardment, level lifetime meas., $E_\alpha=5.5$ MeV 9-29741
²¹Na excitation by ¹⁹F α bombardment, level lifetime meas., $E_\alpha=5.5$ MeV 9-29741
²¹Na, lifetimes of 7 states below 5 MwV meas. by Doppler shift method 9-22737
²¹Na, n total cross section meas., ²⁴Na level structure determ., $E_n=300$ -900keV 9-38654
²¹Na, n.m.r. in NaIO₄ single crystals. 9-33654
²¹Na, n.m.r. relaxation times in NaBr aqueous solns. 9-32799
²¹Na, n.q.r. in NaBrO₃, press. and temp. depend. 9-39928
²¹Na, spin-lattice relaxation in ferroelectric Rochelle salt 9-26663
²¹Na, γ scatt., γ from ⁶⁰Co, 4000 Ci source, Compton scatt. 9-34413
²¹Na(³He,d)²⁴Mg, at 35 MeV, spectroscopic factors, first 7 states of ²⁴Mg 9-44138
²¹Na(³He,d)²⁴Mg, Doppler-shift lifetime, transition energy meas., rotational props. level lifetime calc. 9-36582
²¹Na first-order quadrupole splittings in NaF-LiF mixed cryst., nucl. double reson. obs. 9-35735
²¹Na in liquid Na, spin-lattice relax. 9-26134
²¹Na in Rochelle salt, n.m.r. obs. of ferroelectricity 9-26593
²¹Na mag. reson. of NaD₃(SeO₃)₂ ferroelec. single cryst. 9-33392

Nuclei with $20 \leq A \leq 49$ continuedNuclei with $20 \leq A \leq 49$ continued

- ²¹Na n.m.r. in zeolites, effect of sorbed mols. on quadrupole coupling constants 9-43300
- ²³Na neutron elastic and inelastic scatt. at 1.51, 2.47, 4.04, 6.40 MeV 9-22790
- ²³Na resonance meas., from ²²Ne(p,p'), $E_p=4.8$ -14 MeV 9-22782
- ²⁴Na, spin values of doublet at 1.34 MeV 9-27650
- ²⁴Na from ²⁵Mg(p, 2p), cross section and excitation function meas., $E_p=0.43$ -2.7 GeV 9-27717
- ²⁴Na level structure from ²³Na, n total cross section, $E_n=300$ -900 keV 9-38654
- ²⁴Na production by γ reactions, nuclei $A=27$ to 40, cross sections meas., $E_\gamma=100$ -1200 MeV 9-34431
- ²⁴Na recoil nuclei from ²¹Al(p,3pn), ang. distrib. meas. 9-34449
- ²⁴Na tracer, cooling-water flow of power station pump, meas. 9-28084
- ²⁷Na(³He,d)²⁸Si, Doppler-shift lifetime, transition energy meas., rotational props. level lifetime calc. 9-36582
- ²⁷Na(α , γ)²⁷Al, $E_\alpha=2.3$ MeV, γ -ray spectra 9-46242
- ²⁷Na(n, γ)²⁸Na, gamma-ray spectra study using Ge(Li) spectrometer 9-38706
- ²⁷Na(p,p' γ) $\gamma\gamma$ correlation meas., levels deduced $E_p=4.71$, 5.12 MeV 9-48304
- ²⁸Ne, 4.25 MeV state due to ²⁴MeV α scatt 9-46241
- ²⁸Ne, E2 transition rate calc, Hartree-Fock wave func. 9-25586
- ²⁸Ne, from (²Li,d) and (⁷Li,t) reactions, excitation of rotational bands 9-44223
- ²⁸Ne, from β -decay of ²⁸F 9-38684
- ²⁸Ne, γ -decay of levels, from (²He,d γ) reaction, lifetime of 3 states 9-36582
- ²⁸Ne, s-d shell, calculations with realistic interactions 9-29693
- ²⁸Ne, wave function computation from g.s. value 9-22717
- ²⁸Ne 36 MeV ³He scatt. obs. 9-32352
- ²⁸Ne and other s-d shell nuclei, evidence for Y_4 deformation from p scatt. 9-42230
- ²⁸Ne energy spectrum, using Hartree-Fock and Tamm-Dancoff wave functions 9-44162
- ²⁸Ne from ¹⁹F(d,n), 10-14 MeV excitation states, C_p factors determ., $E_d=5.1$ MeV 9-27744
- ²⁸Ne g.s. rot. band excitation energy calc., cluster model theory 9-27642
- ²⁸Ne, quadrupole moments of 2^+ levels deduced from ³²S scatt. 9-22736
- ²⁸Ne excitation by ¹⁹F α bombardment, level lifetime meas., $E_\alpha=5.5$ MeV 9-29741
- ²⁸Ne excitation by ¹⁹F α bombardment, level lifetime meas., $E_\alpha=5.5$ MeV 9-29741
- ²⁸Ne from ¹⁸O(²Li, t), 0^+ state excited, SU(3) (4, 4) rep., $E=12$ MeV 9-29742
- ²⁸Ne level order, interface on effective interaction 9-42210
- ²⁸Ne-²⁴Na, delayed γ -ray spectrum study of β decay 9-42243
- ²⁸Ne(d,n γ)²¹Na, γ spectra meas., levels, spin, parity, branching and mixing ratios determ., $E_d=2.37$ -5.32 MeV 9-34409
- ²⁸Ne(p,p')²⁸Ne, cross-section calc. using 20 particle wave function 9-46233
- ²⁸Ne(p,p'), cross section, ang. distrib. meas., ²³Na resonance deduced, $E_p=4.8$ -14 MeV 9-22782
- ²⁸Ne(t, ³He)²⁸F, energy spectra, excitation energy, Q-value determ., $E_t=22$ MeV 9-27639
- ²⁸Ni static quadrupole moment of first excited $J^\pi=2^+$ state 9-44141
- ²⁸Ni, ³He large angle scatt. obs. 9-42298
- ²⁸Ni static quadrupole moment of first excited $J^\pi=2^+$ state 9-44141
- ¹⁶O- α , rotational band near decay threshold energy, molecule-like structure 9-34388
- ²⁸O, s-d shell, calculations with realistic interactions 9-29693
- ³¹P, in ³¹P(p, γ)³²S, lifetime and ang. distrib. meas. 9-42283
- ³¹P, n.m.r. in complexes with multidentate ligands 9-32460
- ³¹P, n.m.r. in Mn₂P₂O₇, paramagnetic shift of resonance from γ H₂ 9-47448
- ³¹P, n.m.r. in solid phosphates 9-28759
- ³¹P, parity determ., $E_p=3$ -4 MeV 9-27658
- ³¹P, photoproton spectra from 21.5 and 27 MeV bremsstrahlung 9-27693
- ³¹P(³He,p)³²S, 6 MeV obs., rel. to collective effects in ground and first three excited states of ³²S 9-44216
- ³¹P in methyl- and phenyl phosphorus cpds., chemical shifts 9-25775
- ³¹P in ThP diamagnet., nuclear mag. relax. 9-24343
- ³¹P in UP paramagnet., nuclear mag. relax. 9-24343
- ³¹P mag. moment, M1, E2 transition prob. calc. from shell model wave functions 9-36585
- ³¹P n.m.r. spectroscopy 9-44600
- ³¹P, β -decay in fast-n.-irrad. CDs, associated elec. changes 9-47104
- ³¹P, production by ¹⁶O and ²⁰Ne induced reactions on Ni, Ag and Au 9-44222
- ³¹P β decay, bremsstrahlung spectra obs. 9-22532
- ³¹P obs. with new β -spectrometer 9-42130
- ³¹P spectrum measurement and β -ray spectrometers characteristics 9-36511
- ³¹P from ³¹P(t,p); levels, spin and parity determ., shell model calc., p spectra meas. 9-29832
- ³¹P prod. as air mass exchange indicator 9-45499
- ³¹P, scattering of 7 MeV neutrons, optical model calc. of cross-sections and polarizations 9-29776
- ³¹P(d, α)²⁹Si, 7.3-12.0 MeV, cross-sections meas., Ericson fluctuation analysis 9-27748
- ³¹P(p, α)²⁸Si, cross section energy depend., ³²S excited state parameters determ., $E_p=10$ -12.5 MeV 9-29748
- ³¹P(p, α) ang. distrib., direct reaction mechanism, $E_p=38$ MeV 9-48337
- ³¹P(p,p), cross section energy depend., ³²S excited state parameters determ., $E_p=10$ -12.5 MeV 9-29748
- ³¹P(t,p)³²P, levels, spin and parity determ., p spectra meas., shell-model calc. 9-29832
- ³¹Rb 150 KeV level lifetime meas. 9-48285
- S, n polarization analyzing power at 3.25 MeV 9-27733
- ³¹S β decay, log f calc. from shell model wave functions 9-36585
- ³¹S, photoproton spectra 9-44188
- ³¹S, T=0 pairing correlations, Hartree-Fock-Bogoliubov eqn. 9-29744
- ³¹S 4.46 MeV level, lifetime, spin, parity meas., B(E2) calc. 9-29748
- ³¹S excited state parameters determ. from ³¹P, p, $E_p=10$ -12.5 MeV 9-29748
- ³²S giant reson., collective correl. model with surface-delta-interaction 9-29746
- ³²S in ³¹P(p,p0), mean level width, excitation function meas., $E_p=8$ -10 MeV 9-25591
- ³³S, collective effects in ground and first three excited states, using ³¹P(³He,p)³³S 9-44216
- ³³S β activity on planar surface, distrib. meas. using scanning device 9-27593
- ³³S diffusion in Fe-C, C effect on mobility in grain boundaries 9-37203
- ⁴⁰Sc-⁴⁰Ca, β -decay, obs. of delayed protons 9-29771
- ⁴¹Sc-⁴¹Ca mirror pair, nuclear matter radii calc. from Coulomb energy, comparison 9-38658
- ⁴¹Sc, two particle one hole states 9-42279
- ⁴¹Sc from ⁴⁰Ca(t,p), ang. distrib., spin-orbit coupling, p polarization meas., levels determ. 9-32317
- ⁴¹Sc, dipole giant resonance, effective absorption for neutrons and protons in $d_{3/2}$ - $f_{7/2}$ transition 9-25592
- ⁴¹Sc, in aqueous solutions of Sc ions, Larmor freq. for magnetic moment calc. 9-23535
- ⁴³Sc ground state spectroscopic factors 9-48351
- ⁴³Sc decay, β - γ circular polarization correlation in decay Fermi/Gamow-Teller matrix element ratio determ. 9-32328
- ⁴³Sc from ⁴⁸Ca(³He,t) γ spectra meas., level spin and parity determ. 9-38719
- ⁴³Sc levels, particle-hole configurations 9-44144
- ⁴³Sc obs. with new β -spectrometer 9-42130
- ⁴⁶Sc from ⁴⁸Ca(³He,p) 9-27752
- ⁴⁶Sc(α ,t)⁴⁶Ti, 41 MeV, DWBA analysis 9-48351
- ⁴⁶Sc(α , γ)⁴⁶Ca, ang. distrib. meas., levels, spectroscopic factors determ., $E_\alpha=12.95$ MeV 9-29834
- ³⁴S(d,³He)³³P, 2-body interaction matrix elements, shell-model calc. 9-29832
- ³⁴S(d,n)³³Cl, 4.95 MeV, for spin and parity assignments to levels of ³³Cl 9-48283
- Si, n polarization analyzing power at 3.25 MeV 9-27733
- Si, polarized 1.5 MeV neutron scattering angle range 20-143° 9-36605
- ²⁶Si from ²⁴Mg(³He,n), n distrib. meas., DWBA calc., L, spin and parity determ., $E=7$ MeV 9-32315
- ²⁶Si from ²⁴Mg(³He,n γ), levels and spin determ. 9-32314
- ²⁷Si, low-lying levels studied in ²⁸Si(³He, α)²⁷Si 9-27654
- ²⁸Si, decay of 9.699 MeV level 9-44140
- ²⁸Si, evidence for hexadecapole deformation from p scatt. 9-42230
- ²⁸Si, γ -decay of levels, from (³He,d γ) reaction, lifetimes of 8 states 9-36582
- ²⁸Si, p elastic scatt., polarization energy depend. meas., $E_p=2.6$ -4.0 MeV 9-34442
- ²⁸Si 20 MeV polarized p asymm. scatt. obs. 9-25619
- ²⁸Si 36 MeV ³He scatt. obs. 9-32352
- ²⁸Si (γ , n) ²⁷Si, ²⁸Si (γ , 2n) ²⁶Si, ²⁸Si (γ , pn), ⁶²MeV, photoneutron cross-section meas. 9-48327
- ²⁸Si (p,p), rel. to excited core model for description of low-lying levels of ²⁷Al 9-44139
- ²⁸Si from ²³Mg(α ,n γ), 8.543 MeV level lifetime meas., $E_\alpha \sim$ threshold energy 9-38655
- ²⁸Si giant reson., collective correl. model with surface-delta-interaction 9-29746
- ²⁸Si moment of inertia determ. by modified Peierls-Urbano method 9-42193
- ²⁸Si prolate and oblate intrinsic state, (s,d) shell coupled-vib. model 9-27655
- ²⁸Si spherical and deformed states, inverted coexistence 9-42234
- ²⁸Si structure using 37.7 MeV (³He,d) and 21.2 MeV (p,p') scatt. studies 9-27656
- ²⁸Si, mean lives of states below 5 MeV by Doppler shift attenuation method 9-42211
- ²⁸Si, γ scatt., γ from ⁶⁰Co, 4000 Ci source, Compton scatt. 9-34413
- ²⁸Si spins of $4u$, $5u$ and $6u$ excited states 9-27748
- ³⁰Si, quadrupole and octupole deformations in 2s-1d shell, reduced E3 transition rate calc. 9-38657
- ³¹Si β decay, log f from shell model wave functions 9-36585
- ³¹Si levels, transition mixing ratios, collective model for excitation 9-27659
- ³²Si spherical and deformed states, inverted coexistence 9-42234
- ³¹Si allowed β decay, meas. of B- γ circular polarization asymmetry 9-46221
- ²⁸Si(α , α)²⁸Si, excitation func. meas., $E_\alpha=14$ -25 MeV 9-29831
- ²⁸Si(α ,p)³¹P, excitation func., ang. distrib. meas., $E_\alpha=11$ -25 MeV 9-29831
- ²⁸Si(γ ,n)²⁷Si cross section obs. 9-44186
- ²⁸Si(μ , ν)²⁸Al, ²⁸Si(μ , ν)²⁷Al, products identified by γ decay of excited states 9-38694
- ²⁸Si(μ , ν)²⁷Mg, ²⁸Si(μ , ν)²⁶Mg, products identified by γ decay of excited states 9-38694
- Si(n,n), diff. cross section, γ spectra meas., $E_n=4$ -7.67 MeV 9-29811
- ²⁸Si(p,³He)²¹Al, ²¹Al mass excess obs. 9-25568
- ³¹Si(p, γ)³¹P, γ ang., energy distrib. meas., levels, spin and parity determ., $E_p=3$ -4 MeV 9-27658
- Si(p,p), diff. cross section meas., diffuse-surface optical model anal., $E_p=28$ MeV 9-25623
- ²⁸Si(p,p), elastic, lo- and medium-energy 9-48340
- ²⁸Si(p,p')²⁸Si*, reaction time meas. by blocking of energetic particle in single crystal 9-38696
- ²⁸Si(t, α)²⁹Al, levels, spin and parity determ., $E_t=1.8$ MeV 9-38656
- ³²S(p, γ)³¹P, photoproton spectra 9-27700
- ³²S(μ , ν)³²P, ³²S(μ , ν)³¹P, ³²S(μ , ν)³⁰P, products identified by γ decay of excited states 9-38694
- ³²S(μ , ν)³¹Si, ³²S(μ , ν)³⁰Si, products identified by γ decay of excited states 9-38694
- ³⁶S(p, γ)³⁷Cl, rel. to levels of ³⁷Cl in 10.4 to 10.6 MeV range 9-42212
- Ti, disintegration of 13.6 MeV deuterons on collision 9-48350
- Ti isotopes, elastic p scatt. 9-36598
- ⁴²Ti, projected Hartree-Fock method and stretch scheme calc. 9-32318
- ⁴²Ti, shell-model study of n-p correlations 9-48253
- ⁴²Ti possible levels, shell model 9-22740
- ⁴²Ti low-lying triplet, Hartree-Fock description with band mixing 9-36587
- ⁴²Ti(³He, d)⁴²V, ⁴⁸Sc(³He, d)⁴⁹Si, 9.5, 10 MeV, energy levels calc., shell model confirmed 9-40478
- ⁴²Ti five low-lying states, spectroscopic factors 9-48351
- ⁴²Ti structure using 37.7 MeV (³He,d) and 21.2 MeV (p,p') scatt. studies 9-27656
- ⁴²Ti, levels, lifetime, branching ratio determ. by Doppler-shift attenuation method 9-38659
- ⁴⁹Ti, spectroscopic study 9-22823

Nuclei with $20 \leq A \leq 49$ continued

- ⁵⁰Ti(d,t) spectroscopic study of resulting ⁴⁹Ti 9-22823
⁴⁶Ti(n,p)⁴⁶Sc neutron cross section meas. by activation method 9-27735
⁴⁷Ti(n,p)⁴⁷Sc neutron cross section meas. by activation method 9-27735
⁴⁸Ti(n,p)⁴⁸Sc, neutron cross section meas. by activation method 9-27735
⁴⁸Ti(p,p)⁵⁰V, ⁵⁰V level schemes 9-32360
⁴⁷Ti(t,n,p)⁵⁰V reaction charac., ⁵⁰V level schemes 9-32360
⁴⁷V, ⁵¹V from ^{46,48,50}Ti(³He,d) Ti(³He,d) ^{47,49,51}V reactions, shell model fit to energy levels 9-40478
⁴⁸V, high-energy γ radiation obs. 9-36591
⁵⁰V(t, α), spectroscopic study of resulting ⁴⁹Ti 9-22823

Nuclei with $50 \leq A \leq 89$

- ⁵²Cr, n bombardment, level-excitation cross section meas., $E_n=14.6$ MeV 9-36606
⁵³Cr(d,p)⁵⁴Cr* (Q=6.71 MeV) reaction initiated by vector polarized deuterons 9-44217
⁵⁶Fe, dose rate attenuation 9-22791
⁶⁰Cu, decay scheme, γ -ray spectrum 9-42245
⁶²Ni(p, α)⁵⁹Co, 6-13.5 MeV thick target excitation function rel. to level density determination 9-48287
⁸⁷Kr-⁸⁷Rb, γ spectra meas., levels determ. 9-27685
 internal conversion coeffs. for Z \geq 30, tables 9-46216
⁶³Cu, γ scatt., γ from ⁶⁰Co, 4000 Ci source, Compton scatt. 9-34413
⁸⁵Rb(d,p)⁸⁶Rb, study of ⁸⁶Rb low-lying levels 9-42217
⁷⁰As decay scheme, γ -ray and relative intensities 9-46223
⁷¹As decay scheme, γ -ray and relative intensities 9-46223
⁷²As decay scheme, γ -ray and relative intensities 9-46223
⁷⁵As Coriolis-coupling calc. low-lying states, theor. level spectra 9-22746
⁷⁵As, 199 KeV, 280 KeV level lifetimes meas. 9-48285
⁷⁵As Coriolis-coupling calc. low-lying states, theor. level spectra 9-22746
⁷⁵As from ⁷⁵Se decay, M1-E2 mixing ratio and conversion electron particle parameter determ. 9-40479
⁷⁵As half-life, times of three excited levels by delayed γ γ coincidences 9-48288
⁷⁵As Coriolis-coupling calc. low-lying states, theor. level spectra 9-22746
⁷⁶Br, from (¹²C, ⁶²Cu), γ spectra, β^+ endpoint energy meas. decay scheme determ. 9-38666
⁷⁸Br decay scheme, half life determ., γ spectra meas. 9-25605
⁷⁹Br/⁸¹Br nuclear quadrupole ratio determ. in LiBr 9-23054
⁷⁹Br, Coulomb excitation of close-lying levels 9-46200
⁷⁹Br 217 KeV level lifetime meas. 9-48285
⁷⁹Br n.q.r. in p-dibromobenzene, temp. dependence 9-31175
⁸¹Br, Coulomb excitation of close-lying levels 9-46200
⁸¹Br, n.m.r. in alkali halide aqueous solns., chem. shift 9-34925
⁸¹Br, n.m.r. relaxation times in LiBr, NaBr and CsBr aqueous solns. 9-32799
⁸¹Br, n.q.r. in p-bromophenol Zeeman effect 9-39929
⁸¹Br in LiBr, n.m.r. relax time and chemical shift meas. in aq-methanol mixtures 9-30035
⁷⁴Se, decay, γ spectrum and level diagram for ⁷⁴Se 9-38685
⁷⁴Se disintegration of 13.6 MeV deuterons on collision 9-48350
⁷⁴Se isotopes, retention in rat 9-24949
⁵⁴Co from ⁵⁴Fe(³He,t) t spectra meas., levels spin and parity determ. 9-38719
⁵⁵Co energy levels calcs. by modified Tamm-Dancoff approximation 9-42215
⁵⁶Co from ⁵⁶Ni decay, slow rate to 1+ 2p-2h state, higher energy giant spin-isospin resonance 9-27680
⁵⁷Co, excited through ⁵⁶Fe(α ,p), deduced levels up to 1.90 MeV 9-29754
⁵⁷Co, Mossbauer spectra in MgO rel. to determ. of multiple charge states, hyperfine interactions and relax. processes of ⁵⁷Fe 9-33530
⁵⁷Co, Mossbauer spectra in Co₃O₄ bulk material and ultrafine particles 9-28666
⁵⁷Co from ⁵⁷Ni decay, γ spectra meas., levels, spin determ. 9-38660
⁵⁸Co level schemes from (t,n) and (p,p) reactions 9-32360
⁵⁸Co, cross-sections, total neutron, 3.3-5.2 MeV 9-38702
⁵⁸Co, η_{total} transmission, intensity spin-spin interaction determ. 9-27722
⁵⁸Co, revised A-chains 9-22743
⁵⁸Co E2 transition obs. following excitation due to bombardment 9-22741
⁵⁸Co E2 transition obs. following excitation due to bombardment 9-22741
⁶⁰Co, revised A-chains 9-22744
⁶⁰Co, thermal neutron capture cross-section, activation of isomeric states 9-22802
⁶⁰Co 400 Ci radioactive source nuclear resonance fluorescence, γ Compton scatt. 9-34413
⁶⁰Co in Co-Pd alloy, mag. field on nuclei meas. by nuclear orientation 9-28620
⁶⁰Co γ spectrum, Monte Carlo calc. 9-25597
⁶⁰Co within shell-shaped air-gap shield, dose build up factor 9-34506
⁶¹Co, γ spectrum 9-42246
⁶¹Co, revised A chains 9-22745
⁶¹Co-⁶¹Ni, γ spectra meas. 9-34416
⁶¹Co-⁶³Ni, γ spectra meas., β spectrum endpoint determ. 9-34416
⁵⁹Co(μ , γ)⁵⁹Fe due to cosmic rays 9-48331
⁶⁰Co(p, α)⁵⁸Fe, 6-13.5 MeV thick target excitation function rel. to level density determination 9-48287
⁵⁸Cr(³He, α)⁵⁹Cr, cross section, ang. distrib., spectroscopic factors determ., E=18 MeV 9-29836
⁵⁸Cr(³He,d)⁵¹Mn and ^{52,54}Cr(³He,d)^{53,55}Mn, 9.5, 10 MeV levels of ^{51,53,55}Mn investigated 9-40478
⁵³Cr from ⁵²Cr(³He, α), energy levels, cross section, ang. distrib., spectroscopic factors determ., E=18 MeV 9-29836
⁵³Cr, by ¹⁸O reactions proceeding through ⁴⁸Ge γ emission 9-27666
⁵³Cr, γ scatt., elastic and inelastic rel. to nuclear models, 17.5 MeV 9-34443
⁵³Cr by ¹⁸O, reactions, ang. mom. eff. in breakup of compound nucleus 9-29757
⁵²Cr(³He, α)⁵¹Cr, cross section, ang. distrib., spectroscopic factors determ., E=18 MeV 9-29836
⁵²Cr(³He,t)⁵²Mn, γ spectra meas., levels spin determ. 9-38719
⁵²Cr 36 MeV ³He scatt. obs. 9-32352
⁵²Cr from ⁵³Cr(³He, α), energy levels, cross section, ang. distrib., spectroscopic factors determ., E=18 MeV 9-29836
⁵²Cr-²⁷Al, double acousto-nuclear mag. reson. in Al₂O₃, 4.2°K 9-49359
⁵³Cr, in pure Cr, mag. resonance, Knight shift 9-24324
⁵³Cr(³He, α)⁵²Cr, cross section, ang. distrib., spectroscopic factors determ., E=18 MeV 9-29836

Nuclei with $50 \leq A \leq 89$ continued

- ⁵³Cr E2 transitions obs. following excitation due to bombardment 9-22741
⁵³Cr from ⁵²Cr(d,p), energy levels determ. Ed=7.5 MeV 9-48307
⁵³Cr from ⁵⁴Cr(³He, α), energy levels, cross section, ang. distrib., spectroscopic factors determ., E=18 MeV 9-29836
⁵⁴Cr(³He, α)⁵³Cr, cross section, ang. distrib., spectroscopic factors determ., E=18 MeV 9-29836
⁵³Cr(d,p)⁵³Cr, γ polarization meas., DWBA calc. 9-27753
⁵³Cr(d,d)⁵³Cr energy levels determ., Ed=7.5 MeV 9-48307
⁵³Cr(p,p)⁵⁴Mn, ⁵⁴Mn level schemes 9-32360
⁵²Cr(p,p)⁵²Cr energy levels determ., Ep=7.5 MeV 9-48307
⁵²Cr(p,p)⁵³Cr energy levels determ., particles ang. distrib. obs., Ep=7.5 MeV 9-48307
⁵³Cr(p,p)⁵³Cr energy levels determ., particles ang. distrib. obs., Ep=7.5 MeV 9-48307
⁵³Cr(t,n)⁵⁴Mn reaction charac., ⁵⁴Mn level schemes 9-32360
 Cu (A=59, 61, 63, 65 and 67), excitation energies, spins, parities, e.m. moments transition rates calc. 9-38679
 Cu p bombard 1-3 BeV obs. of emitted γ 9-48336
⁵⁹Co, revised A-chains 9-22743
⁵⁹Cu and double-analog resonances in ⁵⁸Ni(p,n)⁵⁸Cu, ⁵⁹Co analog 9-44200
⁵⁹Cu from ⁵⁸Ni(d,n), isobar analogue states obs., spectroscopic factors determ. 9-29837
⁶⁰Cu, revised A-Chains 9-22744
⁶⁰Cu-⁶⁰Ni, γ transitions meas., levels, spin and parity determ. 9-27681
⁶¹Cu, half-life and energy levels meas. 9-27682
⁶¹Cu, γ transition induced by space-parity violation, enhancement of admixture coeff. 9-36589
⁶¹Cu, revised A chains 9-22745
⁶¹Cu from ⁶⁰Ni(d,n), isobar analogue states obs., spectroscopic factors determ. 9-29837
⁶²Cu decay, γ -ray spectrum 9-38683
⁶²Cu, γ transition induced by space-parity violation, enhancement of admixture coeff. 9-36589
⁶³Cu hyperfine lines in ZnO:Cu e.p.r. obs. 9-35718
⁶³Cu in Cu foils, elastically deformed, n.m.r. 9-24507
⁶³Cu n.m.r. in Cu-Zn dil. alloys, 1st order quadrupole effect obs. 9-35724
⁶³Cu n.m.r. lines in bulk deformed Cu, quadrupole broadening obs. 9-35723
⁶³Cu proton inelastic scatt., final state spin depend. anomaly 9-32344
⁶⁴Cu, diffusion in α - and γ -Fe rel. to defect interactions 9-46851
⁶⁴Cu from ⁶³Cu(d,p); ang. distrib. meas., DWBA analysis, levels determ., E_d=12 MeV 9-38663
⁶⁴Cu from ⁶²Zn(d, α); ang. distrib. meas., DWBA analysis, levels determ., E_d=12 MeV 9-38663
⁶⁴Cu half-life in metal and CuSO₄, Cu(NH₃)₂ solns., obs. 9-27683
⁶⁴Cu, polarized n scatt., 2.33 MeV 9-27720
⁶⁴Cu hyperfine lines in ZnO:Cu e.p.r. obs. 9-35718
⁶⁴Cu proton inelastic scatt., final state spin depend. anomaly 9-32344
⁶⁴Cu from ⁶³(d,p); ang. distrib., levels, spin and parity determ., E_d=12 MeV 9-38683
⁶⁴Cu from ⁶²Zn(d, α); ang. distrib., levels, spin and parity determ., E_d=12 MeV 9-38681
⁶⁴Cu-⁶⁶Zn, 2.37 MeV O⁺ level population, γ spectra meas. 9-27684
⁶⁴Cu, ²³Na p induced fission cumulative form. yield, 20-85 MeV 9-29850
⁶⁴Cu, prod. in proton induced ²³U fission, recoil props. 9-48359
⁶⁴Cu(d,p)⁶⁴Cu, ang. distrib., levels, spin and parity determ., E_d=12 MeV 9-38681
⁶⁴Cu(d,p)⁶⁴Cu, G spectra meas., Ed=5.5 MeV 9-25658
⁶⁴Cu(d,p)⁶⁴Cu, γ spectra meas., Ed=5.5 MeV 9-25658
⁶⁴Cu(p,p), diff. cross section meas., diffuse-surface optical model anal., E_p=28 MeV 9-25623
⁶⁴Cu(p,pn), recoil ⁶⁴Cu angular distrib. rel. to models, Ep 30-85 MeV 9-29800
⁶⁴Cu(p,pn)⁶⁴Cu, av. recoil ranges of ⁶⁴Cu, 20-85 MeV 9-25630
⁶⁴Fe, n radiative capture, resonance radiation width, cross section meas., E_n=0.1-200 keV 9-27731
⁶⁴Fe(³He, ³H) stripping reaction at 120MeV, cross section 9-42310
⁶⁴Fe target, 1 and 3 GeV proton bombard., residual nuclei, Monte Carlo calc. 9-27708
⁶⁴Fe target, Kaons and π bombard., muon pair prod. 9-32135
⁵⁶Fe-⁵⁸Fe isotope pair in self-diffusion studies in δ , γ and α -phases 9-26301
⁵⁶Fe, ⁵⁶Fe, polarized neutron scatt., 2.33 MeV 9-27720
⁵⁶Fe(³He,t)⁵⁶Co, t spectra meas., levels spin determ. 9-38719
⁵⁶Fe Mossbauer effect following n capture by ⁵⁶Fe, recoil effects in metallic iron and alloys obs. 9-43224
⁵⁶Fe, liquid scintillation counter meas., variations 9-25512
⁵⁶Fe, reactor produced, use in obtaining X-ray diff. patterns of powders 9-40907
⁵⁶Fe electron capture decay, inner - bremsstrahlung spectrum endpoint, decay energy meas. 9-42244
⁵⁶Fe from ⁵⁵Mn(p,n); e capture decay energy comparison 9-42244
⁵⁶Fe, by ¹²C, reactions proceeding through ⁴⁸Ge, γ emission 9-27666
⁵⁶Fe, p scatt., elastic and inelastic rel. to nuclear models, 17.5 MeV 9-34443
⁵⁶Fe by ¹⁶C, reactions, ang. mom. eff. in breakup of compound nucleus 9-29757
⁵⁶Fe 1.15 keV resonance, n scatt., n partial wave odd parity determ. 9-36588
⁵⁶Fe energy gap, self-consistency and pairing calc. 9-32319
⁵⁶Fe in cosmic rays, photodisintegration by universal radiation field, E<10¹⁰ GeV, 10¹⁰ years eff. 9-43511
⁵⁶Fe in putidaredoxin, ligand symm. and electronic configuration determ. from Mossbauer study 9-32538
⁵⁶Fe proton inelastic scatt. for implantation perturbed ang. correl. expts. 9-33494
⁵⁶Fe stellar nucleosynthesis in Si quasi-equilibrium and the ⁵⁸Ni problem 9-49547
⁵⁷Fe, 14 KeV Mossbauer radiation, Bragg scattering by Fe:Si ideal crystal 9-37700
⁵⁷Fe, E2/M1 mixing ratios lifetimes of levels from Coulomb excitation 9-27664
⁵⁷Fe, electric quadrupole interactions in garnets, Mossbauer line spectra splitting 9-43221
⁵⁷Fe, γ transition induced by space-parity violation, enhancement of admixture coeff. 9-36589

Nuclei with $50 \leq A \leq 89$ continued

- ⁵⁷Fe, Mossbauer effect in Cu-Ni-Fe and Au-Fe alloys rel. to mag. ordering determ. 9-39817
- ⁵⁷Fe, Mossbauer effect in Fe compounds, anomalous charge states of Fe, possible origin 9-35637
- ⁵⁷Fe, Mossbauer effect in Fe-Mn nodules rel. to particle size determ. of Fe oxide phase 9-42786
- ⁵⁷Fe, Mossbauer effect in Fe-(48.2 at %)Ni and pure Fe, hyperfine mag. splitting, effect of texture 9-35636
- ⁵⁷Fe, Mossbauer effect in $Y_{0.22}Ca_{2.78}Fe_{3-2}V_{0.12}O_{12}$ ferrite garnets 9-41365
- ⁵⁷Fe, Mossbauer spectra in $Y_{0.2}Ca_{2.8}Fe_{3.65}V_{1.35}O_{12}$, non-equivalency of Fe³⁺ octahedral-site 9-24387
- ⁵⁷Fe, Mossbauer spectra in Fe₃B₇O₁₃X (where X=Cl,Br,I) 9-35638
- ⁵⁷Fe, Mossbauer spectra in Ni₃B₇O₁₃X (where X=Cl,Br,I) 9-35638
- ⁵⁷Fe, Mossbauer studies in CsFeF₃, hyperfine structure ad magnetization meas. 9-45058
- ⁵⁷Fe, n.g.r. in (Fe,Mg_{1-x})SiO₃ 0.269 $\leq x \leq$ 1.0, 300° to 1.7°K 9-45292
- ⁵⁷Fe E2-M1 absorption in Mossbauer spectra, transition probabilities calc. 9-22742
- ⁵⁷Fe E2 transition obs. following excitation due to bombardment 9-22741
- ⁵⁷Fe electron spin density determ. using internal conversion 9-48383
- ⁵⁷Fe in CoCO₃, Mossbauer obs. of Fe ion relax. 9-41364
- ⁵⁷Fe in corundum, eff. of hyperfine structure stabilization 9-26719
- ⁵⁷Fe in CuFeS₂, Mossbauer spectra, quadrupole splitting meas. 9-35634
- ⁵⁷Fe in dilute Au-Fe alloys, Mossbauer absorpt. spectra 9-45285
- ⁵⁷Fe in FeF₃, hyperfine struct., critical temp. depend. 9-24384
- ⁵⁷Fe in h.c.p. metals, Mossbauer hyperfine structure 9-49255
- ⁵⁷Fe in haematite, antiferromag., nuclear diff. of resonant γ radiation, rel. to mag. structure 9-49262
- ⁵⁷Fe in LiFeC₆, Mn₂, PO₄ antiferromagnetic, Mossbauer effect 9-26726
- ⁵⁷Fe in MnF₂ and CoF₂, Mossbauer effect meas. rel. to magnetization of impurity Fe²⁺ ions. 9-45298
- ⁵⁷Fe in Na₂Fe(CN)₅NO₂H₂O, effective-field-gradient mean square displacements 9-24385
- ⁵⁷Fe in Pt(Pd,Cu), Debye-Waller factor 9-41082
- ⁵⁷Fe in rare earth-Fe garnets, Mossbauer eff., exchange interac. obs. 9-33475
- ⁵⁷Fe in Te and PbTe, Mossbauer obs. of Fe ions 9-39819
- ⁵⁷Fe in transition metals, isomer shift in Mossbauer spectra 9-26718
- ⁵⁷Fe in YFe garnets, Ga-substituted, cation distrib. by Mossbauer effect spectroscopy 9-45303
- ⁵⁷Fe in zeolites, Mossbauer spectra study 9-43223
- ⁵⁷Fe level schemes and spin distrib. from (t,n γ) reaction 9-32360
- ⁵⁷Fe in magnetically ordered systems, Mossbauer spectra near disordering temp. 9-26721
- ⁵⁷Fe Mossbauer absorpt. in pure Fe from Curie pt. to γ - δ transition 9-41366
- ⁵⁷Fe Mossbauer effect in CrO₂ 9-45287
- ⁵⁷Fe Mossbauer effect in Fe, hyperfine fields obs. and band ferromag. 9-43166
- ⁵⁷Fe Mossbauer linewidth study in Fe₂O₃ electron hopping in rel. to octahedral sites 9-45294
- ⁵⁷Fe Mossbauer spectroscopy, hyperfine params. analytical calc. 9-24382
- ⁵⁷Fe Mossbauer spectrum hyperfine fields in Fe₃O₄, magnetite 9-45295
- ⁵⁷Fe Mossbauer studies in Cu-Ni alloys 9-47331
- ⁵⁷Fe multiple charge states, hyperfine interactions and relax. processes in MgO from ⁵⁷Co Mossbauer spectrum 9-33530
- ⁵⁷Fe nuclear transverse relation times in Fe and Fe-rich alloys, Suhl-Nakamura interaction 9-45240
- ⁵⁷Fe, E2/M1 mixing ratios of 2⁺-2⁺ transitions 9-32321
- ⁵⁷Fe from ⁵⁷Fe(n, γ); γ spectra meas., decay scheme determ. 9-32320
- ⁵⁷Fe, revised A-chains 9-22743
- ⁵⁷Fe liquid scintillation counter meas. variations 9-25512
- ⁵⁷Fe Nilsson model fit to energy levels 9-38661
- ⁶⁰Fe, revised A-chains 9-22744
- ⁶⁰Fe, revised A chains 9-22745
- ⁶⁰Fe-⁶⁰Co, half-life, β and γ spectra 9-44174
- ⁵⁴Fe proton inelastic scatt. for implantation perturbed ang. correl. expts. 9-33494
- ⁵⁴Fe(α ,p)⁵⁷ 10.23 and 10.30 MeV, rel. to levels of ⁵⁷Co up to 1.90 MeV 9-29754
- ⁵⁴Fe(α ,p)⁵⁹Co, 12-18.5 MeV thick target excitation function rel. to level density determination 9-48287
- ⁵⁴Fe(μ^- , ν)⁵⁸Mn, prob. meas., theory comparison 9-29789
- ⁵⁴Fe(n, γ)⁵⁸Fe, γ spectra meas., decay scheme determ. 9-32320
- ⁵⁴Fe(n,n) γ cross section meas., comparison with theory 9-25635
- ⁵⁴Fe(n,n' γ) γ spectra meas. 9-34452
- ⁵⁴Fe(p, γ)⁵⁶Fe, 5-6 MeV, spin-flip meas. reaction mechanism investigated 9-48335
- ⁵⁷Fe(p, γ)⁵⁸Co, ⁵⁸Co level schemes 9-32360
- ⁵⁴Fe(p, γ) γ , energy levels, 2.56 MeV level spin determ. 9-29753
- ⁵⁷Fe(t,n) γ ⁵⁸Co reaction charact., ⁵⁸Co level schemes 9-32360
- ⁶⁰Ga decay, γ spectrum 9-42247
- ⁶⁰Ga from ⁶⁰Ge decay, γ spectra meas., levels determ. 9-38662
- ⁶⁰Ga decay, γ spectrum 9-42247
- ⁶⁰Ga determ. from hyperfine structure 9-36661
- ⁶⁰Ga, ²³⁸U p induced fission yield, 20-85 MeV 9-29850
- ⁶⁰Ga, levels studied by inelastic n scatt. 9-38664
- ⁶⁰Ga 320 KeV level lifetime meas. 9-48285
- ⁶⁰Ga in liquid Ga, spin-lattice relax. 9-26134
- ⁶⁰Ga in solid (C₂H₂), O₂GaCl₃ to show mol. symm. rel. interpretation of i.r. spectrum of liquid 9-24515
- ⁷⁰Ga, ²³⁸U p induced fission yield, 20-85 MeV 9-29850
- ⁷¹Ga, levels investigated, spins and parities determ. using inelastic n scatt. 9-38664
- ⁷¹Ga in GaAs, Gunn domain interaction 9-35391
- ⁷¹Ga in liquid Ga, spin-lattice relax. 9-26134
- ⁷²Ga, ²³⁸U p induced fission yield, 20-85 MeV 9-29850
- ⁷²Ga decay, γ spectrum 9-42247
- ⁷²Ga determ. from hyperfine structure separation 9-36661
- ⁷³Ga, ²³⁸U p induced fission cumulative form. yield, 20-85 MeV 9-29850
- ⁶⁹Ga(n,n' γ)⁶⁹Ga, 0.4-2.5 MeV, level and decay schemes determ. 9-38664
- ⁶⁹Ga(n,n' γ)⁷¹Ga, 0.4-2.5 MeV, level and decay schemes determ. 9-38664
- ⁶⁹Ge (n,n) γ , 0.3-1.5 MeV, obs., interpretation using optical and compound nucleus models 9-48343
- ⁶⁶Ge-⁶⁶Ga, γ spectra meas., levels determ. 9-38662
- ⁶⁶Ge, compound nucleus formed in various reactions, γ emission 9-27666
- ⁶⁶Ge, compound nucleus temporarily formed in various reaction, ang. mom. eff. in break up 9-29757

Nuclei with $50 \leq A \leq 89$ continued

- ⁷⁰Ge high resolution study from ⁷⁰Ge(p,p'), levels and assignments, E2 transitions 9-25620
- ⁷²Ge energy gap, self-consistency and pairing calc. 9-32319
- ⁷³Ge, Coulomb excited after recoil implantation, Mossbauer studies 9-33531
- ⁷⁴Ge, E2/M1 mixing ratios of 2⁺-2⁺ transitions 9-32321
- ⁷⁴Ge, levels spin, parity assignments made 9-48344
- ⁷⁴Ge(d,p), stripping reaction on enriched target 9-38716
- ⁷⁴Ge(d,p), stripping reaction on enriched target 9-38716
- ⁷⁴Ge(n, γ)⁷⁴Ge, used to study levels of ⁷⁴Ge 9-48344
- ⁷²Ge(p, π)⁷²⁻⁷³As, cross section, excitation func. meas., E_p=400 MeV 9-27719
- ⁷⁰Ge(p, γ)⁷⁰Ge*, reaction time meas. by blocking of energetic particle in single crystal 9-38696
- ⁷²Ge(p, γ)⁷²Ge*, reaction time meas. by blocking of energetic particle in single crystal 9-38696
- Kr gaseous, short-lived, mass-separated fission products, half-life determ. 9-22765
- ⁸⁰Kr, 1.320 MeV α and 1.256 MeV 2⁺ levels obs. from ^{80m}Br decay 9-42216
- ⁸²Kr from ⁸²Rb decay, γ spectra obs. 9-22747
- ⁸³Kr, 1st excited state mag. mom. determ., Mossbauer eff. 9-27667
- ⁸³Kr, 9.3 keV level mag. moment from Mossbauer lines Zeeman splitting 9-27668
- ^{74m}As search using ⁷⁵As(n,2n), ⁷¹Ga(α ,n) and ⁷⁴Ge(d,2n) reactions 9-32323
- ^{80m}Br decay, β and γ spectroscopy 9-42216
- Mn excitation of levels by inelastic n scatt. 9-44145
- ⁵¹Mn, ⁵³Mn, ⁵⁵Mn, levels obs. from ^{50,52,54}Cr(³He,d)^{51,53,55}Mn 9-40478
- ⁵²Mn from ⁵²Cr(³He,t); t spectra meas., levels spin and parity determ. 9-38719
- ⁵³Mn, level at 1290 keV, γ -ray cascades 9-44146
- ⁵³Mn energy levels calcs. by modified Tammi-Dancoff approximation 9-42215
- ⁵⁴Mn level schemes from (t,n γ) and (p, γ) reactions 9-32360
- ⁵⁵Mn, cross-sections, total neutron, 3.3- 5.2 MeV 9-38702
- ⁵⁵Mn, n capture cross section, 5 keV-3 MeV 9-25638
- ⁵⁵Mn, p scatt., elastic and inelastic rel. to nuclear models, 17.5 MeV 9-34443
- ⁵⁵Mn, resonant acoustic coupling, in nuclear acoustic resonance of RbMnF₃ 9-46993
- ⁵⁵Mn (p, α)⁵²Cr, 6-13.5 MeV thick target excitation function rel. to level density determination 9-48287
- ⁵⁵Mn ENDOR resonant freq., rel. to nuclear saturation 9-45410
- ⁵⁵Mn in CsMnF₃, n.m.r. linewidth, field depend., 1.8 and 4.2°K 9-33649
- ⁵⁵Mn in MnF₂, n.m.r., rel. to Suhl-Nakamura interaction 9-26798
- ⁵⁵Mn in RbMnF₃, n.m.r. linewidth, field depend., 1.8 and 4.2°K 9-33649
- ⁵⁵Mn n.m.r. in dilute Al-Mn alloys 9-28754
- ⁵⁵Mn n.m.r. modes in RbMnF₃ 9-39922
- ⁵⁵Mn n.m.r. of Mn³⁺ in Mn_{1-x}Fe_xO₄ 9-43299
- ⁵⁵Mn isomer, of Mn³⁺ activity examined 9-46222
- ⁵⁵Mn(α , α)⁵⁵Mn, 50 MeV, obs. of ang. distrib., DWBA analysis 9-34465
- ⁵⁵Mn(p,n)⁵⁵Fe, ⁵⁵Fe capture decay energy, comparison 9-42244
- ⁵⁵Mn(t,n)⁵⁵Fe, ⁵⁵Fe level schemes, spin distrib. 9-32360
- Ni(n,n) cross section meas., comparison with theory 9-25635
- Ni, disintegration of 13.6 MeV deuterons on collision 9-48350
- Ni, n radiative capture, resonance radiation width, cross section meas., E_p=0.1-200 keV 9-27731
- Ni isotopes; Coulomb energy, anomalous isotope shift of radii, core polarization, excess n depend. 9-36572
- ⁵⁶Ni-⁵⁶Co(1⁺) slow rate to 2p-2h state, higher energy giant spin-isospin resonance 9-27680
- ⁵⁷Ni-⁵⁷Co, γ spectra meas., levels, spin determ. 9-38660
- ⁵⁸Ni, ⁶⁰Ni, polarized neutron scatt., 2.33 MeV 9-27720
- ⁵⁸Ni, ⁶⁰Ni(p,p); optical model parameter differences determ., E_p=12-50 MeV 9-29692
- ⁵⁸Ni, ⁶⁰Ni, photodisintegration in giant resonance region, anomalous features 9-46232
- ⁵⁸Ni, charge distrib., effects of neutrons, from elastic electron scatt. meas. 9-27703
- ⁵⁸Ni, elastic scatt. of ³He at 21.15, 27.64 and 34.14 MeV, optical-model analysis 9-46243
- ⁵⁸Ni, electroexcitation of low-energy collective states 9-44147
- ⁵⁸Ni, excitation of giant resonance by means of high energy electrons 9-27665
- ⁵⁸Ni, inelastic e scatt., 2⁺-states excitation 9-22777
- ⁵⁸Ni, γ -ray ang. distrib., reaction independent analysis using Ge(Li) detector 9-42262
- ⁵⁸Ni, lifetimes of excited states produced by 7-9 MeV p scatt. obs. 9-48286
- ⁵⁸Ni, photoneutron cross section anomalies 9-44187
- ⁵⁸Ni 36 MeV γ -He scatt. obs. 9-32352
- ⁵⁸Ni proton spin flip probability in ⁵⁸Ni(p,p')⁵⁸Ni*(1.45 MeV) react. 9-27718
- ⁵⁸Ni, γ transition induced by space-parity violation, enhancement of admixture coeff. 9-36589
- ⁵⁸Ni, n strength function and imaginary optical potential, model 9-29755
- ⁵⁸Ni, revised A-chains 9-22743
- ⁶⁰Ni, charge distrib., effects of neutrons, from elastic electron scatt. meas. 9-27703
- ⁶⁰Ni, electroexcitation of low-energy collective states 9-44147
- ⁶⁰Ni, excitation of giant resonance by means of high energy electrons 9-27665
- ⁶⁰Ni, photoneutron cross section anomalies 9-44187
- ⁶⁰Ni, revised A chains 9-22744
- ⁶⁰Ni from ⁶⁰Co decay, E2 M1, transitions, obs. 9-27681
- ⁶⁰Ni from ⁶⁰Co decay, γ spectra meas., levels spin and parity determ. 9-27681
- ⁶⁰Ni inelastic neutron scatt. cross sections, test of quasi-compound nucleus theory 9-29805
- ⁶⁰Ni structure using 37.7 MeV (³He,d) and 21.2 MeV (p,p') scatt. studies 9-27656
- ⁶¹Ni, Coulomb excited after recoil implantation, Mossbauer studies 9-33531
- ⁶¹Ni, levels obs. in ⁶¹Cu decay 9-27682
- ⁶¹Ni, revised A chains 9-22745
- ⁶¹Ni 67 KeV 320 level lifetime meas. 9-48285
- ⁶¹Ni E2 transitions obs. following bombardment 9-22741
- ⁶¹Ni in Ni-Fe alloys, Mossbauer hyperfine fields 9-45300

Nuclei with $50 \leq A \leq 89$ continued

- ⁶²Ni, $J=0^+$ states, pairing force and surface delta interaction, seniority 9-29756
- ⁶²Ni, p. ang. distrib. meas., DWBA fits, γ spectra meas., levels determ., $E_\gamma=12$ MeV 9-32322
- ⁶³Ni volume diffusion in Ni-rich binary alloys at 900-1200°C 9-40986
- ⁶⁴Ni, charge distrib., effects of neutrons, from elastic electron scatt. meas. 9-27703
- ⁶⁴Ni, electroexcitation of low-energy collective states 9-44147
- ⁶⁴Ni, excitation of giant resonance by means of high energy electrons 9-27665
- ⁶⁴Ni, inelastic e scatt., 2^+ -states excitation 9-22777
- ⁶⁴Ni, p. ang. distrib. meas., DWBA fits, γ spectra meas., levels determ., $E_\gamma=12$ MeV 9-32322
- ⁶⁵Ni allowed β -decay, meas. of β - γ circular polarization asymmetry 9-46221
- ⁶⁶Ni, ^{238}U p induced fission cumulative form. yield, 20-85 MeV 9-29850
- ⁶⁶Ni, prod. in proton induced ^{238}U fission, recoil props. 9-48359
- ⁶⁸Ni(d, ^3He), DWBA predictions test at $E_d=82$ MeV 9-40520
- ⁶⁸Ni(d,n) ^{68}Cu , isobar analogue states obs., spectroscopic factors determ. 9-29837
- ⁶⁰Ni(d,n) ^{60}Cu , isobar analogue states obs., spectroscopic factors determ. 9-29837
- ⁵⁸Ni(d,p) ^{59}Ni , γ spectra meas., $E_d=5.5$ MeV 9-25658
- ⁶⁰Ni(d,p) ^{61}Ni , γ spectra meas., $E_d=5.5$ MeV 9-25658
- ⁵⁸Ni(d,t), form factors and config. mixing 9-34440
- ⁵⁸Ni(p,d), form factors and config. mixing 9-34440
- ⁵⁸Ni(p,n) ^{58}Cu , double-analog resonances 9-44200
- ⁵⁸Ni(p,p) cross section meas., optical model analysis, $E_p=21$ MeV 9-38695
- Rb gaseous, short-lived, mass-separated fission products, half-life determ 9-22765
- Rb isotopes ($A=81, 82, 83, 84$ and 86), γ spectra 9-38687
- ⁸²Rb decay to ^{82}Kr , γ spectra obs. 9-22747
- ⁸⁵Rb, Coulomb excitation of close-lying levels 9-46200
- ⁸⁵Rb, half-life of 514 KeV state obs. 9-40491
- ⁸⁵Rb, n capture cross section, 5 keV-3 MeV 9-25638
- ⁸⁵Rb in liquid Rb, spin-lattice relax. 9-26134
- ⁸⁶Rb, low-lying levels from (d,p), (d,t) and (n,p) reactions 9-42217
- ⁸⁷Rb, ^{87}Rb in RbFeF_3 , n.m.r. and spatial distrib. of spin density 9-41435
- ⁸⁷Rb from ^{87}Kr decay, γ spectra meas., levels determ. 9-27685
- ⁸⁷Rb in liquid Rb, spin-lattice relax. 9-26134
- ⁸⁷Rb n.m.r. quadrupole coupling in RbH_2AsO_4 , ferroelec. transition obs. 9-33393
- ⁸⁸Rb decay, levels of resulting ^{88}Sr 9-22748
- ⁸⁷Rb(d,t) ^{86}g , study of ^{86}Rb low-lying levels 9-42217
- ⁸⁵Rb(n,p) ^{86}Rb , study of ^{86}Rb low-lying levels 9-42217
- Se isotopes n radiative capture and transmission cross sections, levels determ. 9-38704
- ⁷¹Se- ^{71}As decay obs. 9-42258
- ⁷⁴Se from decay of ^{74}Br , level diagram 9-38685
- ⁷⁵Se decay, γ spectra energy and rel. intensities meas. 9-48321
- ⁷⁵Se- ^{75}As , M1-E2 mixing ratio and conversion-electron particle parameter determ. 9-40479
- ⁷⁵Se, Coulomb excitation of close-lying levels 9-46200
- ⁷⁸Se energy gap, self-consistency and pairing calc. 9-32319
- ⁸⁰Se, 1.478 MeV level obs. from ^{80}Br decay 9-42216
- ⁷⁴Se(d,p) stripping reaction, $E_d=6.5$ MeV 9-44218
- ⁸⁰Se(d,p) stripping reaction, $E_d=6.5$ MeV 9-44218
- ⁷⁴Se(n,n') ^{74}Se 14.7 MeV cross-section obs. and compared with theory 9-22803
- ⁷⁸Se(n, α) ^{75}Ge 14.7 MeV cross section obs. and compared to theory 9-22803
- ⁸⁰Se(n,p) ^{81}Se 14.7 MeV cross-section obs. and compared with theory 9-22803
- ⁷⁴Se(n,p) ^{74}As , 14.7 MeV cross-section obs. and compared to theory 9-22803
- ⁷⁸Se(n,p) ^{78}As 14.7 MeV cross-section obs. and compared to theory 9-22803
- ⁸⁸Sr/p, coupled eqns. solved numerically with optical-model parameters 9-38642
- ⁸⁵Sr, e capture decay 9-40491
- ⁸⁵Sr, e. capture decay energy from inner bremsstrahlung end-point energy meas. 9-29772
- ⁸⁶Sr decay of two 3^- states, E(3) transitions meas. 9-27669
- ⁸⁵Sr, 2^+ and 3^- states, behaviour, Green function study 9-36590
- ⁸⁸Sr, phase shift analysis, unambiguous parameters, $E_\alpha=40$ MeV 9-34464
- ⁸⁸Sr isobaric analog resonance formation, comparison of coupled-channel formalism and R-matrix 9-44201
- ⁸⁸Sr levels from decay of ^{88}Br 9-22748
- ⁸⁸Sr positive-parity states, proton orbitals 9-42218
- ⁸⁹Sr/ ^{90}Sr in rain, effect of Chinese nuclear explosions (Dec 1966 and June 1967) 9-43406
- ⁸⁹Sr, diffusion in SrF_2 , BaF_2 , and CaF_2 , to study cation defects 9-39382
- ⁸⁹Sr, positive-parity states, neutron-neutron hole states 9-42218
- ⁸⁸Sr(p, n) ^{89}Y , excitation function, ang. distrib. meas., spin and parity determ. 9-29801
- ⁸⁸Sr(p, $^{89}\text{Sr}^*$), p. ang. distrib. meas., antisymmetrized microscopic DWBA calc., levels, spin and parity calc., $E_p=20$ MeV 9-29794
- ⁸⁸Sr(p,n) ^{89}Y , isobaric analog resonance formation, comparison of coupled-channel formalism and R-matrix 9-44201
- ⁸⁸Sr(p,n) ^{89}Y , total cross section, $S_{1/2}$ analog resonance meas., $E_p \approx 6$ MeV 9-38699
- ⁵¹T isobaric analog resonances obs. in ^{51}V formed as compound nucleus in $^{50}\text{Ti}(p,p)^{50}\text{Ti}$ 9-46199
- Ti isotopes, elastic p scatt. 9-36598
- ⁵⁰Ti($^3\text{He}, t$) ^{50}V , γ spectra meas., levels, spin determ. 9-38719
- ⁵⁰Ti(p,p) ^{50}Ti , study of isobaric analogue states of ^{51}Ti 9-46199
- V, excitation of levels by inelastic n scatt. 9-44145
- ^{50}V from $^{50}\text{Ti}(^3\text{He}, t)$; t spectra meas., levels spin and parity determ. 9-38719
- ^{50}V level schemes from (t,n

) and (p,p) reactions 9-32360

^{51}V , n isotropic scatt., 32 Li-glass n_{Li} detectors array calibration 9-32263

^{51}V , n.m.r. in normal V_3Al , quadrupole and anisotropic Knight shift effects, obs. 9-39923

^{51}V , n.m.r. in V_3Si , quadrupole effects of second-order 9-49361

^{51}V , p scatt., elastic and inelastic rel. to nuclear models, 17.5 MeV 9-34443

^{51}V 320 KeV level lifetime meas. 9-48285

Nuclei with $50 \leq A \leq 89$ continued

- ^{51}V energy levels calcs. by modified Tamm-Dancoff approximation 9-42215
- ^{51}V in V-Cr alloys, Knight shift and Neel temp. 9-24324
- ^{51}V spin-lattice relax. time in V_3Sn type II supercond., temp. variation 9-35371
- $^{51}\text{V}(p,p)$ energy spectrum at 90° , $E=26.6$ MeV 9-34433
- ^{88}Y , e capture decay 9-40491
- ^{88}Y from $^{88}\text{Sr}(p, n)$; excitation function, ang. distrib. meas., spin and parity determ. 9-29801
- ^{89}Y , n capture cross section, 5 keV-3 MeV 9-25638
- ^{89}Y , scattering of 7 MeV neutrons, optical model calc. of cross-sections and polarizations 9-29776
- $^{89}\text{Y}(\alpha, \alpha)$, diff. cross section meas., deformation lengths, 2^+ , 4^+ states calc. $E_\alpha=65$ MeV 9-40517
- $^{89}\text{Y}(d,p)^{90}\text{Y}$, excitation curves, ang. distrib., spectroscopic factors, DWBA anal., $E_d=4$ MeV 9-22825
- $^{89}\text{Y}(p,p)$, photoproton energy and ang. distrib., spin dipole reson., hole states 9-34434
- $\text{Y}(n,n')\gamma$, γ spectra meas. 9-34452
- ^{60}Zn , revised A chains 9-22744
- ^{61}Zn , revised A chains 9-22745
- ^{63}Zn - ^{63}Cu decay, γ -transitions and level scheme 9-34417
- ^{64}Zn by ^4He , reactions proceeding through ^{68}Ge , γ emission 9-27666
- ^{64}Zn by ^4He , reactions, ang. mom. eff. in breakup of compound nucleus 9-29757
- ^{64}Zn shell-model study of n-p correlations 9-48253
- ^{64}Zn to ^{68}Zn even isotopes, n bombardment, level-excitation cross section meas., $E_n=14.6$ MeV 9-36606
- ^{65}Zn , L/K capture ratio 9-22764
- ^{65}Zn , origin after 1967 Chinese nuclear tests 9-24668
- ^{66}Zn , ground-state transition width of 7368 keV level by nuclear resonant scatt. 9-46217
- ^{66}Zn from ^{66}Cu decay, 2.37 MeV O^+ level population, γ spectra meas. 9-27684
- ^{67}Zn proton inelastic scatt., final state spin depend. anomaly 9-32344
- ^{72}Zn , ^{238}U p induced fission cumulative form. yield, 20-85 MeV 9-29850
- ^{72}Zn , prod. in proton induced ^{238}U fission, recoil props. 9-48359
- $^{66}\text{Zn}(d, \alpha)$ ^{64}Cu , ang. distrib. meas. DWBA analysis, levels determ., $E_d=12$ MeV 9-38663
- $^{68}\text{Zn}(d, \alpha)^{66}\text{Cu}$, ang. distrib., levels, spin and parity determ., $E_d=12$ MeV 9-38681
- ^{88}Zr , excited levels, from $^{90}\text{Zr}(p,t)^{88}\text{Zr}$ 9-27670
- ^{88}Zr , excited levels, from $^{90}\text{Zr}(p,t)^{88}\text{Zr}$ 9-42235

Nuclei with $6 \leq A \leq 19$

- $^{11}\text{B}(^{12}\text{C}, \gamma)^{23}\text{Na}$ obs. for first time 9-27761
- ^{12}C , isospin-nonconserving decays 9-34392
- ^{13}C , isospin-nonconserving decays 9-34392
- ^{13}N , isospin-nonconserving decays 9-34392
- ^{14}N , (p,p) cross section meas., optical model analysis, $E_p=21$ MeV 9-38695
- ^{14}N in organic nitro-compds, with sp^2 -hybridized N, n.m.r. shifts 9-25773
- ^{16}O , binding energy calc., 3-body potential model 9-42200
- ^{19}F in RbFeF_3 , n.m.r. and spatial distrib. of spin density 9-41435
- ^{6}Li , nuclear associations from data on high energy reactions 9-25571
- $^6\text{Li}(^{16}\text{O}, \gamma)^{22}\text{Ne}$ obs. for first time 9-27761
- A-6 nuclei, realistic nonsingular potentials and level spectra 9-38648
- atomic hfs calc. by many-body theory 9-22962
- Be^9 (t, α) Li^8 , differential cross sections and angular distributions 9-27758
- differential cross sections of reactions (p,d) and (He^3, α) in terms of peripheral model 9-27712
- Li , from ^{235}U thermal n. fission, energy spectra and relative yields 9-29858
- short-range dynamical correlations from elastic electron scatt. 9-44130
- well depth, real central and spin-orbit, elastic t scatt., $E_t=2$ MeV 9-29816
- $^{19}\text{F}(p, \alpha)^{16}\text{O}$, stellar rates, effect of excited nuclear states 9-43541
- $^{19}\text{F}(p, \gamma)^{20}\text{Ne}$, stellar rates, effect of excited nuclear states 9-43541
- (n,t) reaction cross-sections, meas. 9-22792
- $^{14}(\alpha, \alpha)^{12}\text{C}$, α d spectra meas. levels determ., $E_\alpha=22.9$ MeV 9-38721
- ^{27}Al , p induced spallation; ^{18}F , $^{22,24}\text{Na}$ fragments energy distrib. and range determ. 9-40511
- B, isotope production by bombardment of O and C mass spectrometry 9-22784
- ^9B , quadratic isobaric multiplet mass eqn., perturbations, excitation energies determ. 9-32308
- ^{10}B - ^{10}Be isobaric analogue state from $^9\text{Be}(d,p)$, $E_d=2.8$ MeV, γ spectra meas. 9-29712
- ^{10}B , ^{11}B , production in p nuclear spallation of ^{12}C 9-36601
- ^{10}B , ^{10}B , muon and pion yields in 2p-1s X-ray transition 9-22716
- ^{10}B , energy of excitation of first 4 excited states reported 9-46194
- ^{10}B , excited levels determ. from $^{9}\text{Be}(d,n)^{10}\text{B}$ reaction 9-44215
- ^{10}B , from $^9\text{Be}(d,n,p)$, γ -ray branching of 3.59 MeV state 9-29711
- ^{11}B - ^{19}F nmr coupling constant in various compounds, rel. to ^{19}F chemical shift 9-32464
- ^{11}B , muon capture, to $^{11}\text{Be}(g.s.)$ and $^{11}\text{Be}^*(320 \text{ keV})$ 9-44189
- ^{11}B , recoil broadening of secondary transition following neutron capture in ^{10}B 9-42201
- $^{10}\text{B}(^3\text{He}, \alpha)^{10}\text{B}$, ang. distrib., cross section, excitation function meas. $E=33$ MeV 9-38711
- ^{11}B in $^{12}\text{C}(\pi, \pi\pi)$, reaction mechanism, characteristic identification conditions, $p_\pi=1.04$ GeV/c 9-34461
- ^{12}B from $^{10}\text{B}(t,p)$ g.s. ang. distrib. meas., DWBA calc. 9-36611
- ^{12}B resonance from ^{11}B , n; 3.39 NeV state, spin and parity assignment, $E_n=20.8$ keV 9-29729
- $^{11}\text{B}(\alpha, p)^{14}\text{C}$, differential cross section, ang. distrib., excitation function meas., $E_\alpha=10.25$ MeV 9-32356
- $^{10}\text{B}(\alpha, p)^{13}\text{C}$, 3.85 MeV γ source, ^{10}B - PuO_2 mixture 9-29662
- $\text{Be}(\beta^-)^9\text{Be}(\alpha, ^4\text{He})$, rel. to $^9\text{Be}(2^+)$ states 9-40473
- $^{11}\text{B}(d, \alpha)^9\text{Be}$, 0.7h0 2 MeV, excitation functions 9-29839
- Be , e collision, n, K_α^0 production, yields meas., $E_e=10, 16$ GeV 9-29566
- Be , from ^{235}U thermal n. fission, energy spectra and relative yields 9-29858
- Be , isotope production by bombardment of O and C, mass spectrometry 9-22784
- Be , μ and π yields in 2p-1s X-ray transitions 9-22716
- Be , p bombard 1-3 BeV, obs. of emitted p 9-48336
- Be^9 (t, α) Li^8 , differential cross sections and angular distributions 9-27758
- $\text{Be}^9(t, d_0)$ Be^{10} , differential cross sections and angular distributions 9-27758

Nuclei with $6 \leq A \leq 19$ continued

- Be target, 12.5 GeV/c proton bombard., pion prod. cross sections 9-32184
- ⁹Be d+ α model, analysis using resonating group method 9-38709
- ⁷Be, excitation of one-particle levels at inelastic e scatt. 9-42275
- ⁷Be in galactic cosmic radiation, stability 9-40116
- ⁷Be, Λ binding energy 4.93 ± 0.55 MeV 9-22721
- ⁹Be, 17.64-16.63 MeV transition nearly pure M1 9-48339
- ⁹Be, 2⁺ states from ⁹Be(p,d), α - α scatt. and ⁸Li, ⁹Be β -decay 9-40473
- ⁹Be, binding energy calc., 3-body potential model 9-42200
- ⁹Be, isobaric-spin mixing deduced from ⁷Li(p,p)⁹Be* 9-48272
- ⁹Be 4+(11.4 MeV) level, width, from ⁷Li(d,n) 2α reaction 9-42207
- ⁹Be from ⁷Li-p, levels determ. from ang. distrib. energy depend., $E_{\text{pot.}}=2.7-10.6$ MeV 9-25624
- ⁹Be from ⁷Li(d,n), ang. distrib. meas., energy levels determ. 9-22824
- ⁹Be levels, pole representation from α - α scatt. phase shift and potential meas. 9-27750
- ⁹Be, 17.28 MeV level studied through ⁷Li+d- α + α +n 9-27627
- ⁹Be, elastic scatt. cross-sections for 100 MeV p, optical model anal. 9-22783
- ⁹Be, photoabsorption in giant dipole resonance region, cross section meas., $E_{\gamma}=250$ MeV 9-34435
- ⁹Be, quadratic isobaric multiplet mass eqn., perturbations, excitation energies determ. 9-32308
- ⁹Be(³He,⁴Li)⁶Li, ang. distrib., excitation func. meas., $E=4-10$ MeV 9-32361
- ⁹Be(⁷Li,⁸Li)⁹Be cross sections, optical potential, nucleon tunnelling theory anal. 9-32363
- ⁹Be Adler's self-consistency condition, charge symmetric π -nucleon forward dispersion reln. 9-34301
- ⁹Be low-lying states obs. from ⁷Li(³He,p)⁹Be 9-32307
- ⁹Be odd-parity states projected Hartree-Fock calc. 9-27626
- ¹⁰Be from ⁹Be(d,p); γ spectra meas., levels, spin, parity and spectroscopic factor determ., $E_{\gamma}=2.8$ MeV 9-29712
- ⁹Be(α , n)¹²C, n energy distrib. meas. 9-34355
- ⁹Be(d,n)¹⁰B, at 4 MeV, excited levels of ¹⁰B determ. 9-44215
- ⁹Be(d,n)¹⁰B, γ -ray branching of ¹⁰B 3.59 MeV state 9-29711
- ⁹Be(d,p)¹⁰Be, γ spectra meas., levels, spin, parity and spectroscopic factor determ., $E_{\gamma}=2.8$ MeV 9-29712
- ⁹Be(n,2n), angular correlations between neutrons 9-29813
- ⁹Be(n, α)⁶He, α spectra, ⁶He excited states obs. 9-32306
- ⁹Be(n,d)⁸Li, eff. cross section, 16.3-18.7 MeV 9-22804
- ⁹Be(n,nn), cross section energy depend. meas., $E_n=2.0-6.4$ MeV 9-34457
- ⁹Be(p, α)⁶Li diff. cross section and ang. distrib. meas., $E_p=38$ MeV 9-25631
- ⁹Be(p, α) ang. distrib., direct reaction mechanism, $E_p=38$ MeV 9-48337
- ⁹Be(p,d), 12 and 17 MeV obs. of singlet d (S=0, T=1) prod. 9-38698
- ⁹Be(p,d), rel. to ⁹Be 2⁺ states 9-40473
- ⁹Be(p,p α)⁷He, ang. correl. distrib. and quasi-free scatt., 55 MeV 9-40510
- ⁹Be(π , nn) energy spectra, momentum distrib. meas., π -absorption determ. 9-25644
- ¹¹B(p,p) resonances obs. at 21.6, 23.2, 25.5, 27.7, and 29.2 MeV, cross-section up to 31 MeV 9-25610
- ¹⁰B(n, α)⁷Li reaction on methylboric acid label in air, meas. of aeration 9-24609
- ¹⁰B(n, α) cross-section and branching ratio from thermal energy to 1 MeV from evaluation of data 9-25637
- ¹⁰B(n, γ)¹¹B, secondary γ -ray transition broadening 9-42201
- ¹¹B(p,3 α), α spectra meas., ¹²C resonances shape spin and parity depend., $E_{\alpha}=0.15-4$ MeV 9-25625
- ¹¹B(p, α)⁹Be diff. cross section and ang. distrib. meas., $E_p=38$ MeV 9-25631
- ¹⁰B(p,n)¹⁰C, energy of first excited state of ¹⁰C obs. 9-46194
- ¹¹B(π , π')¹¹C, double charge-exchange react., cross-section, $E_{\pi}=80$ to 200 MeV 9-25641
- ¹¹B(t, α)⁹Be, 1.00-2.10 MeV, ang. distrib. optical parameters by DWBA 9-42303
- ¹⁰B(t,p)¹²B, g.s. ang. distrib. meas., DWBA calc. 9-36611
- ¹²C-H coupling, expression using method of separated electron pairs 9-32496
- ¹²C- α , rotational band near decay threshold energy, molecule-like structure 9-34388
- C, μ and ν yields in 2p-1s X-ray transition 9-22716
- C(³He,³H) stripping reaction at 120 MeV, cross sections 9-42310
- C p bombard 1.3 BeV obs. of emitted p 9-48336
- C target, Kaons and π bombard., muon pair prod. 9-32135
- ⁹C, quadratic isobaric multiplet mass eqn., perturbations, excitation energies determ. 9-32308
- ¹²C, energy of first excited state of ¹⁰C obs. 9-46194
- ¹²C, ¹³C 36 MeV ³He scatt. obs. 9-32352
- ¹²C, 10.8 MeV level, E1 ($\Delta T=0$) electroexcitation, form factors 9-25564
- ¹²C, α elastic scatt., p-wave phase shift between 9.16 and 12.11 MeV, multilevel analysis 9-29819
- ¹²C, binding energy calc., 3-body potential model 9-42200
- ¹²C, dynamic N-N correlations from elastic e scatt. 9-34398
- ¹²C, elastic scatt. cross-sections for 100 MeV p, optical model anal. 9-22783
- ¹²C, fundamental and first excited levels from ¹⁴N(d, α)¹²C reaction 9-48354
- ¹²C, γ total absorption cross section meas., $E_{\gamma}=9-31$ MeV 9-29780
- ¹²C, new level at 18.1 MeV 9-27761
- ¹²C, e scatt., giant dipole resonance spectra, transition prob., 16.1 MeV level form factor determ., $E_{\gamma}=115, 200$ MeV 9-34436
- ¹²C, e scatt. form factors, cluster model description 9-25570
- ¹²C(¹²C,¹²C)²⁰Ne react. at low energies, appl. to stellar C burning investigation 9-43540
- ¹²C(¹²C, γ)²⁴Mg obs. for first time 9-27761
- ¹²C(¹²C,n)²³Mg react. at low energies, appl. to stellar C burning investigation 9-43540
- ¹²C(¹²C,p)²³Na react. at low energies, appl. to stellar C burning investigation 9-43540
- ¹²C(¹⁶O, γ)²⁸Si obs. for first time 9-27761
- ¹²C 2.33 MeV polarized neutron scatt. 9-27720
- ¹²C(³He, ³He), ang. and energy distrib. meas., $E_{\text{He}}=2.8$ MeV 9-32357
- ¹²C(³He, α_0)¹⁴C, ang. distrib., excitation curves, resonances meas., ¹⁵O structure determ., $E=5-8$ MeV 9-32303
- ¹²C(³He, α_0)¹⁴C, ang. distrib. excitation curves, resonances meas., ¹⁵O structure determ., $E=5-8$ MeV 9-32303
- ¹²C(³He, d)¹⁴N, 12-19 MeV, excitation functions, ang. distrib. meas. 9-38712

Nuclei with $6 \leq A \leq 19$ continued

- ¹²C(⁴Li,d)¹⁶O, excitation of rotational bands in ¹⁶O, mechanism 9-44223
- ¹²C(⁷Li,t)¹⁸O, excitation of rotational bands in ¹⁶O, mechanism 9-44223
- ¹²C (t, α)¹¹B reaction, degree of overlapping of ¹²C α substructures 9-48273
- ¹²C Adler's self-consistency conditions, charge symmetric π -nucleon forward dispersion reln. 9-34301
- ¹²C bombardment of Ag nuclei, products obs. 9-48352
- ¹²C dipole resonance calc., g.s. fractional parentage structure influence on photodisintegration 9-42202
- ¹²C double-scatt. of 51 MeV d, optical mode prediction confirmation 9-34463
- ¹²C electron inelastic scatt. at 400-1100 MeV, π prod. 9-48330
- ¹²C from ¹⁴N(α , α d); α d spectra meas., level determ., $E_{\alpha}=22.9$ MeV 9-38721
- ¹²C giant reson., collective correl. model with surface-delta interaction 9-29746
- ¹²C interaction with ¹²C, reson. obs. assuming quasimol. states 9-22827
- ¹²C muon capture, transition to ¹²B g.s., probability calc. 9-36595
- ¹²C nuclear excitation due to e scatt., μ capture, continuum model based on configuration mixing 9-25566
- ¹²C proton scattering phase shifts 9-29792
- ¹²C resonance in ¹¹B(p,3 α) reactions, shape depend. on spin and parity $E_{\alpha}=0.15-4$ MeV 9-25625
- ¹²C spherical and deformed states, inverted coexistence 9-42234
- ¹³C-¹³C coupling, expression using method of separated electron pairs 9-32496
- ¹³C, 3.08 MeV level E1-electroexcitation, investigation 9-44132
- ¹³C, lowest T=3/2 states, γ decay modes and obs. 9-25565
- ¹³C, n.m.r., neutron anomalous torque and spin determ. 9-38586
- ¹³C, n.m.r. absorption spectra, time averaging with adapted multichannel analyser 9-29352
- ¹³C, n.m.r. in methyl lithium, struct. and bonding determ. 9-46405
- ¹³C(+, π)¹³N charge exchange cross section meas., $E_{\pi}=80-280$ MeV 9-25642
- ¹³C(³He, ³He), ¹⁶O structure determ., ang. and energy distrib. meas., $E_{\text{He}}=2.8$ MeV 9-32357
- ¹³C(³He, p), ¹⁶O structure determ., ang. and energy distrib. meas., $E_{\text{He}}=2/8$ MeV 9-32357
- ¹³C(³He, α), ¹⁶O structure determ., ang. and energy distrib. meas., $E_{\text{He}}=2.8$ MeV 9-32357
- ¹³C from ¹⁴N(α , α p); α p spectra meas., level determ., $E_{\alpha}=22.9$ MeV 9-38721
- ¹³C giant resonance, excited by e scatt., compared to Kamimura-Ikeda-Arima model 9-44131
- ¹³C Overhauser effect 9-30062
- ¹³C width of 3.68 MeV level meas. 9-48274
- ¹⁴C, activity variation with time and location in South Pacific and Antarctic Oceans 9-37902
- ¹⁴C age of tree rings 9-39991
- ¹⁴C β activity on planar surface, distrib. meas. using scanning device 9-27593
- ¹⁴C diffusion in TiC_{0.67}, anomalous 9-46858
- ¹⁴C particulate tracers of stratospheric motion 9-28896
- ¹⁵C-¹⁵N, β -decay obs. 9-38684
- ¹³CH coupling constants, effect of lone pairs 9-34649
- ¹²C-¹²C react., appl. to stellar thermonuclear burning of C investigation 9-40142
- ¹²C(α , α)¹²C cross-section calc. utilizing S-matrix and poles 9-34462
- ¹²C(α , α)¹²Cm excitation functions and angular distribution at 20-24 MeV 9-22810
- ¹²C(d, α)¹⁰B differential cross section meas., $E_d=5-10$ MeV 9-27742
- ¹²C(d, α)¹⁰B Glendenning two-nucleon transfer theory analysis, $E_d=9.2-13.9$ MeV 9-48353
- ¹²C(d,d) differential cross section meas., $E_d=5-10$ MeV 9-27742
- ¹²C(d,n)¹³N, n polarization meas., Mott-Schwinger scatt. method, $E_d=51.5$ MeV 9-22815
- ¹²C(d,n)¹³N, total cross sections, 1.2-4.5 MeV 9-42304
- ¹²C(d,n)¹³N*¹²C,n,p ang. distrib. anal., unbound levels of N doublet determ. 9-25650
- ¹²C(d,p)¹³C, 7.0-26 MeV, behaviour rel. to weakly-bound-projectile model 9-42309
- ¹²C(d,p)¹²C differential cross section meas., $E_d=5-10$ MeV 9-27742
- ¹²C(e, α)¹²C, quasi-elastic, e-N McVoy and Van Hove treatment 9-25614
- ¹²C(e,e') scatt. at 180°, mag. excitations of ¹²C 9-32302
- ¹²C(e,e); Born approx. analysis, correlation structure and charge density, high energies 9-34438
- ¹²C(γ ,d), excitation function and energy depend. meas., $E_{\gamma}=400-1400$ MeV 9-34432
- ¹²C(γ ,n), cross section meas., $E_{\gamma}=1-5.5$ GeV 9-25611
- ¹²C(γ ,n)¹²C, elec. dipole cross-sections calc. 9-29781
- ¹²C(γ ,p), excitation function and energy depend. meas., $E_{\gamma}=400-1400$ MeV 9-34432
- ¹²C(γ ,p), (γ ,d) and (γ ,t), $E_{\gamma}=400-1300$ MeV 9-22776
- ¹²C(γ ,x)⁷Be, high energy bremsstrahlung beam absolute monitor, cross section meas., $E_{\gamma}=0.4-0.9$ GeV 9-27694
- ¹²C(μ , ν_{α})¹²B, capture rate, nuclear structure 9-34439
- ¹²C(n, α), α -part. angular distrib., amplitude of α -cluster, ground-state transition cross-section, $E_n=14.1$ MeV 9-32349
- ¹²C(n, α)⁹Be angular distrib., D.W.B.A. calc., 14 MeV 9-38703
- ¹²C(n,n), cross section and resonance meas., $E_n=5.3-6.3$ MeV 9-29807
- ¹²C(p, α)⁹Be, ¹²C excited states and α decay obs., $E_p=57$ MeV 9-27715
- ¹²C(p, α)⁹B diff. cross section and ang. distrib. meas., $E_p=38$ MeV 9-25631
- ¹²C(p, α) ang. distrib., direct reaction mechanism, $E_{\alpha}=38$ MeV 9-48337
- ¹²C(p, γ)¹⁵N, γ transition mixing ratio, levels, spin and parity determ., $E_{\gamma}=352-634$ keV 9-29713
- ¹²C(p,p), polarization and ang. distrib. meas., $E_p=11-23$ MeV 9-27716
- ¹²C(p,p)¹²C, coupled channel, analysis in terms of doorway states 9-46234
- ¹²C(p,p) expt. and multiple collision and optical model theory comparison 9-25618
- ¹²C(p,p), 2⁺ excitations, spin-flip prob. and diff. scatt. cross section meas. DWBA analysis 9-42278
- ¹²C(p,p), polarization and ang. distrib. meas., $E_p=11-23$ MeV 9-27716
- ¹²C(p,p)¹²C DWA analysis using Kallio-Kolttvit interaction 9-29791
- ¹²C(p,p)¹²C*, diff. cross section and polarization scatt., $E=4.43-22.3$ MeV 9-34441
- ¹²C(p,p)¹²C*, spin flip of polarized p., model 9-48334

Nuclei with $6 \leq A \leq 19$ continued

- $^{12}\text{C}(\text{p},\text{p})$, diff. cross section, polarization meas., optical parameters determ., $E_p=7\text{ MeV}$ 9-32342
- $^{13}\text{C}(\text{p},\text{p})$, diff. cross section, polarization meas., optical parameters determ., $E_p=7\text{ MeV}$ 9-32342
- $^{12}\text{C}(\text{p},\text{x})$ nuclear spallation production of ^{10}B , ^{11}B 9-36601
- $\text{C}(\pi^-, \Lambda)$ 3.86 GeV, cross-section for strange particle prod. obs. in freon bubble chamber 9-25643
- $^{12}\text{C}(\pi^-, \text{n})$ energy spectra, momentum distrib. meas., π^- absorption determ., 9-25644
- $^{13}\text{C}(\pi^+, \pi^0)^{13}\text{N}$ cross section around 1st resonance in $\pi\text{-N}$ system meas. 9-22807
- $^{12}\text{C}(\text{t}, \alpha)^{11}\text{B}$, excitation functions and ang. distrib. for elastic scatt. 9-42308
- $^{12}\text{C}(\text{t}, \alpha)^{11}\text{B}$, excitatooon functions and ang. distrib. for elastic scatt. 9-42308
- $^{12}\text{C}(\text{t}, \text{p})^{11}\text{C}$, excitation functions and ang. distrib. for elastic scatt. 9-42308
- $\text{e}^-, \text{e}^+ \text{p}$ C wide angle bremsstrahlung yield at 6.2° , $E_e=9.5\text{ GeV}$ 9-25613
- ^{17}F , from $^{16}\text{O}(\text{d}, \text{n})$, spectroscopic factors 9-29826
- $^{17}\text{F} \rightarrow ^{17}\text{O}$, limit of β branching to 871 keV state of ^{17}O 9-38684
- ^{17}F , to 5 MeV using $^{16}\text{O}(\text{He}, \text{p})^{18}\text{F}$ meas. 9-36614
- ^{18}F isobaric spin impurities, from cross-section ratios of $^{14}\text{N}(\alpha, \text{n})^{17}\text{F}(0,500)$ and $^{14}\text{N}(\alpha, \text{p})^{16}\text{O}(0,871)$ 9-42206
- ^{18}F low-lying even-parity levels, E2 decay strengths, deformed states calc. 9-22713
- ^{18}F spectra calc., realistic interaction, eff. of Woods-Saxon wave function 9-38653
- ^{18}F discovery of new $T=3/2$ isobaric analog state 9-48262
- ^{18}F , γ total absorption cross section meas., $E_\gamma=9\text{-}31\text{ MeV}$ 9-29780
- ^{18}F , level lifetimes obs. 9-48277
- ^{18}F , lifetime of first excited state meas. 9-48278
- ^{18}F , magnetic screening in $(\text{NH}_4)_2\text{BeF}_4$, rel. to ferroelec. transition 9-43118
- ^{18}F , n.m.r. in 1,1-difluoroethylene, in nematic solvent 9-30105
- ^{18}F , n.m.r. in Cs_2BeF_4 , rel. to retarded motion of tetrahedral group BeF_4 9-43298
- ^{18}F , n.m.r. in K_2CoF_4 , and transferred hyperfine interactions 9-45257
- ^{18}F , n.m.r. in partially oriented fluoromethanes 9-30434
- ^{18}F , n.m.r. in trifluoromethyl- and methoxy-substituted fluorobenzenes 9-30118
- ^{18}F , n.m.r. in xenon fluorides and oxyfluorides, chem. shift ref. to ^{129}Xe - ^{19}F coupling 9-34646
- ^{18}F , n.m.r. study of critical fluctuations near Neel point in FeF_2 9-45399
- ^{18}F , odd-parity levels wave function computation, E1 transitions 9-22717
- ^{18}F , p induced spallation; ^{18}F , $^{22,24}\text{Na}$ fragments energy distrib. and range determ. 9-40511
- ^{18}F , s-d shell, calculations with realistic interactions 9-29693
- ^{18}F , spin-lattice relaxation time in solid and liquid AsF_3 as fn. of temp. 9-44594
- ^{18}F dynamic polarization in $\text{CaF}_2:\text{Yb}^{3+}$, spin-lattice relax. times meas. 9-47297
- ^{18}F excitation by α bombardment, level lifetime meas., $E_\alpha=5.5\text{ MeV}$ 9-29741
- ^{18}F from $^{18}\text{O}(\text{He}, \text{d})$, spectroscopic factors determ. 9-40475
- ^{18}F from $^{18}\text{O}(\text{d}, \text{n})$, energy levels spin and parity determ., $\text{Ed}=3\text{ MeV}$ 9-36581
- ^{18}F from $^{19}\text{F}(\text{p}, \text{p})$, energy levels determ., $\text{Ep}=9\text{ MeV}$ 9-36581
- ^{18}F hyperfine coupling in $\text{LiF}:\text{Mn}^{2+}$, phonon-induced corrections 9-33628
- ^{18}F hyperfine splittings in e.s.r. spectra of fluorinated aromatic free radicals 9-46396
- ^{18}F in MnF_2 , n.m.r. freq. depend. on temp., thermometer, $10\text{-}40^\circ\text{K}$ 9-40291
- ^{18}F in RbF_3 , n.m.r. obs. of spin density and hyperfine interac. 9-28760
- ^{18}F NMR meas. for structural determ. of nitroso rubber copolymer 9-27939
- ^{18}F n.m.r. exchange narrowed hyperfine-broadened in MnF_2 , KMnF_3 and RbMnF_3 9-45388
- ^{18}F n.m.r. in AlF, modifications, chem. shift 9-48453
- ^{18}F n.m.r. in FeF_3 , antiferromagnet 9-35725
- ^{18}F n.m.r. in Uf_6 , dipolar broadening obs. 9-33651
- ^{18}F n.m.r. of substituted trifluorochlorocyclobutanes, chemical shifts and coupling constants 9-30148
- ^{18}F n.m.r. spectra in pentafluorophenyl derivatives 9-42434
- ^{18}F n.m.r. spectra in pentafluorophenyl derivatives, π interactions and bonding 9-42435
- ^{18}F pear-shaped nuclei collective model calc. 9-22734
- ^{18}F reson., shell model rel to obs., $\leq 3.2\text{ MeV}$ 9-34391
- ^{18}F resonance in $^{14}\text{N}(\alpha, \text{p})$ reaction, $^{11/2}^+$ state found 9-36569
- ^{18}F reson. from $^{16}\text{O}(\text{p}, \text{p})^{16}\text{O}$, $^{16}\text{O}(\text{p}, \alpha)^{13}\text{N}$, $1.39\text{-}3.20\text{ MeV}$ 9-34390
- ^{18}F spin-lattice relax. in $\text{ZnSiF}_6 \cdot 6\text{H}_2\text{O} \cdot \text{Fe}^{2+} \cdot \text{Mn}^{2+}$ 9-35594
- ^{18}F spin system in CsF , pulsed n.m.r. obs. of free-induction-decay curves 9-35722
- ^{18}F spins in CaF_2 , polarised, antiferromag. state prod. and obs. 9-45207
- $^{18}\text{F}(\text{d}, \text{n})^{18}\text{O}$ 10-14 MeV excitation states, C_p factors determ., $E=5.1\text{ MeV}$ 9-27744
- $^{18}\text{F}(\text{p}, \alpha)^{18}\text{O}$ diff. cross section and ang. distrib. meas., $E_p=38\text{ MeV}$ 9-25631
- $^{18}\text{F}(\text{p}, \text{p})^{18}\text{F}$ energy levels determ., $\text{Ep}=9\text{ MeV}$ 9-36581
- $\text{F}(\pi^-, \Lambda)$ 3.86 GeV, cross-section for strange particles prod. obs. in freon bubble chamber 9-25643
- $^4\text{He}-\alpha$, rotational band near decay threshold energy, molecule-like structure 9-34388
- ^4He , d + α model, analysis using resonating group method 9-38709
- ^4He , ground state binding energy calc. using 3-body model 9-22720
- ^4He , nucleon associations from data on high energy reactions 9-25571
- ^4He excited states obs. from $^8\text{Be}(\text{n}, \alpha)^8\text{He}$ α spectra 9-32306
- ^4He from n-induced ^{233}U fission, yield and energy distrib. meas. 9-22839
- $^4\text{He} \rightarrow ^6\text{Li}$ β transition probability calc. using Green's and Tabakin's potentials 9-38648
- ^4He from $^7\text{Li}(\text{t}, ^4\text{He})$, ^3He spectra, cross section meas., mass excess and g.s. determ. 9-27756
- ^4He , bound energy depend. on N-N interaction calc. 9-34389
- $^6\text{He}(\text{p}, \text{K}_\alpha)^4\text{He}$, photoproduction of hypernuclei and cross-sections 9-29721
- Li, isotope production by bombardment of O and C mass spectrometry 9-22784
- ^6Li , 14.7 MeV d and 29.4 MeV α -part. elastic and inelastic scatt., DWBA analysis 9-42311
- ^6Li , charge form factor calc. in Born approx. 9-44130

Nuclei with $6 \leq A \leq 19$ continued

- ^6Li , collective α -d and α -t models, information from e scatt. 9-29784
- ^6Li , diagram of first excited levels from $^7\text{Li}(\text{He}, \alpha)^6\text{Li}$ reaction 9-29719
- ^6Li , dynamic N-N correlations from elastic e scatt. 9-34398
- ^6Li , e scatt., form factors, cluster model description 9-25570
- ^6Li , elastic scatt. cross-sections for 100 MeV p, optical model anal. 9-22783
- ^6Li , first two excited levels investigated by e scatt. 9-27625
- ^6Li , form factor for excitation of 3.56 MeV level by e scatt. oscillator cluster model calc. 9-46193
- ^6Li , magnetic and quadrupole moments calc. 9-38648
- ^6Li , with 3.56 MeV level 9-48274
- $^6\text{Li}, \mu \rightarrow ^6\text{He}$, capture rate calc. from ^6Li magnetic form. factor 9-36596
- $^6\text{Li}(^{16}\text{O}, \text{d})^{20}\text{Ne}$, double-scatt. model in α -clusters framework, forward peak in ang. distrib. determ. 9-42312
- ^6Li analysis using the 2-d bound state model and resonating group method 9-38709
- ^6Li charge form factor, calc. using exponential wave function 9-29720
- ^6Li ground state, α -d structure 9-44135
- ^6Li semicond. sandwich n spectrometer, applic. in reactor, energy resolution and geometrical efficiency 9-34354
- ^6Li , 14.7 MeV d and 29.4 MeV α -part. elastic and inelastic scatt., DWBA analysis 9-42311
- ^7Li , elastic scatt. cross-sections for 100 MeV p, optical model anal. 9-22783
- ^7Li , excitation of one-particle levels at inelastic e scatt. 9-42275
- ^7Li , γ scatt., γ from ^{60}Co , 4000 Ci source, Compton scatt. 9-34413
- ^7Li , n.m.r. in methylthilium, struct. and bonding determ. 9-46405
- $^7\text{Li}(^{16}\text{O}, \text{p})^{23}\text{Na}$ obs. for first time, resonance like structure obs. 9-27761
- $^7\text{Li}(\text{He}, \alpha)^6\text{Li}$ for diagram of first excited levels of ^6Li 9-29719
- $^7\text{Li}(^3\text{He}, \text{p})^6\text{Be}$, ^6Be low-lying states obs. 9-32307
- ^7Li bombardment by ^7Li , diff. cross section, angle and energy depend. $E=2\text{-}5.75\text{ MeV}$ 9-29841
- ^7Li collective α -d and α -t models, information from e scatt. 9-29784
- ^7Li field-gradient tensor in ferroelec. $\text{LiD}_3(\text{SeO}_3)_2$; deuteron mag. reson. obs. 9-33389
- ^7Li , quadratic isobaric multiplet mass eqn., perturbations, excitation energies determ. 9-32308
- ^7Li ground state binding energy calc. using 3-body model 9-22720
- $^7\text{Li}(\alpha, \alpha\text{d})^4\text{He}$, α -d correlations, cross section meas., $E_\alpha=23.6\text{ MeV}$ 9-27754
- $^8\text{Li}(\beta^-)^8\text{Be}(\alpha)^4\text{He}$, rel. to ^8Be 2^+ states 9-40473
- $^7\text{Li}(\text{d}, \text{n})$ 2α reaction, determ. of width of $4+(11.4\text{ MeV})$ level of ^8Be 9-42207
- $^7\text{Li}(\text{d}, \text{n})^8\text{Be}$, interference effects near 1 MeV resonance 9-27755
- $^7\text{Li}(\text{d}, \text{n})^8\text{Be}$, n ang. distrib. meas., energy levels determ. 9-22824
- $^7\text{Li}(\text{e}, \text{e})$; Born approx. analysis, correlation structure and charge density, high energies 9-34438
- $^7\text{Li}(\text{p}, \text{d})$ α isospin selection rules violated 9-25612
- $^7\text{Li}(\text{p}, \text{p})$, polarization depend., quasimonochromatic photons 9-29783
- $^7\text{Li}(\text{p}, \text{p})$, (p, d) and (p, t), $E_p=400\text{-}1300\text{ MeV}$ 9-22776
- $^7\text{Li}(\text{He}, ^3\text{He})$, cross section, spectroscopic factors determ., DWBA anal., $E_p=30.3\text{ MeV}$ 9-22786
- $^7\text{Li}(\text{p}, \alpha)$, cross section, spectroscopic factors determ., DWBA anal., $E_p=30.0\text{ MeV}$ 9-22786
- $^7\text{Li}(\text{p}, \alpha)^4\text{He}$ ang. distrib., analyzing power, diff. cross section meas., $E_{\text{pot}}=2.7\text{-}10.6\text{ MeV}$ 9-25624
- $^7\text{Li}(\text{p}, \text{d})$, pick-up and final state interactions obs. $E=156\text{ MeV}$ 9-42282
- $^7\text{Li}(\text{p}, \text{d})$, 12 MeV, obs. of singlet d ($S=0$, $T=1$) prod. 9-38698
- $^7\text{Li}(\text{p}, \text{d})$, cross section, spectroscopic factors determ., DWBA anal., $E_p=30.3\text{ MeV}$ 9-22786
- $^7\text{Li}(\text{p}, \text{d})$, pick-up and final state interactions obs. $E_p=156\text{ MeV}$ 9-42282
- $^7\text{Li}(\text{p}, \gamma)^8\text{Be}-2\alpha, E_p=1.5\text{ MeV}$, ang. corrs. derived and compared with expt. 9-48339
- $^7\text{Li}(\text{p}, \text{n})$, cross section energy dependence, determ. with Grey neutron detector 9-48226
- $^7\text{Li}(\text{p}, \text{p})^6\text{Li}$, phase shift and polarization ang. distrib. meas., $E_p=0.5\text{-}5.6\text{ MeV}$ 9-32343
- $^7\text{Li}(\text{p}, \text{p})^6\text{Li}$ ang. distrib., analyzing power, diff. cross section meas., $E_{\text{pot}}=2.7\text{-}10.6\text{ MeV}$ 9-25624
- $^7\text{Li}(\text{p}, \text{p})^6\text{Li}^*$ ang. distrib., analyzing power, diff. cross section meas., $E_{\text{pot}}=2.7\text{-}10.6\text{ MeV}$ 9-25624
- $^6\text{Li}(\text{p}, \alpha\text{d})$, first order analysis by PWBA calc. 9-44199
- $^6\text{Li}(\text{p}, \text{pd})^4\text{He}$, matrix element, calc. using fully antisymmetrized cluster-model wave function 9-44198
- $^7\text{Li}(\text{p}, \text{pd})$, angular correlation meas., comparison with $^6\text{Li}(\text{p}, \text{pd})+E_p=30.3\text{ MeV}$ 9-22786
- $^7\text{Li}(\text{p}, \text{t})$, cross section, spectroscopic factors determ., DWBA anal., $E_p=30.3\text{ MeV}$ 9-22786
- $^7\text{Li}(\pi^-, \text{n})$, energy spectra, momentum distrib. meas., π^- absorption determ. 9-25644
- $^7\text{Li}(\pi^+, \pi^-)^7\text{B}$, double charge-exchange react., cross-section, $E_\pi=80\text{ to }200\text{ MeV}$ 9-25641
- $^7\text{Li}(\text{t}, ^4\text{He})^4\text{He}$, ^7He spectra, cross section meas., ^7He mass excess and g.s. determ. 9-27756
- ^{23}Mg discovery of new $T=3/2$ isobaric analog state 9-48262
- ^{23}Mg , p induced spallation; ^{18}F , $^{22,24}\text{Na}$ fragments energy distrib. and range determ. 9-40511
- N, spin-spin interaction in N_2H_4 molecule 9-24513
- ^{13}N , excited in $^{12}\text{C}(\text{He}, \text{d})^{13}\text{N}$ reaction, obs. 9-38712
- ^{13}N , lowest $T=1/2$ states, γ decay modes and obs. 9-25565
- ^{13}N E1 transitions bet. resonant states near $3.51\text{ MeV}(3/2^-)$ and $2.37\text{ MeV}(1/2^+)$ levels 9-27621
- ^{14}N , γ total absorption cross section meas., $E_\gamma=9\text{-}31\text{ MeV}$ 9-29780
- ^{14}N , NO_2 , solid soln. in KBr, infrared intensities 9-48469
- ^{14}N , n.m.r. in nitromethane and nitrobenzene, eff. of molecular alignment induced by elec. field 9-30435
- $^{14}\text{N}(^{14}\text{N}, ^{13}\text{N})^{13}\text{N}$, cross sections, optical potential, nucleon tunnelling theory anal. 9-32363
- ^{14}N in $\text{Ba}(\text{NO}_3)_2 \cdot \text{H}_2\text{O}$, n.q.r. temp. depend. between 77°K and 300°K 9-37809
- ^{14}N doublets, excitation obs., in ^3He and d bombard of ^{12}C , ^{16}O and ^{15}N 9-48275
- ^{14}N excited levels from $^{10}\text{B}+\alpha$ react. 9-27741
- ^{14}N from $^{14}\text{N}(\text{d}, \text{d})$, diff. cross sections meas., DWBA anal., $E_d=1\text{-}3.2\text{ MeV}$ 9-25651
- ^{14}N from $^{16}\text{O}(\text{d}, \alpha)$, isospin-forbidden, cross section, ang. distrib. meas., J⁺ assignment, $E_\alpha=3\text{-}15\text{ MeV}$ 9-29827
- ^{14}N in RCN and RCN^- mol. and ions, quadrupole coupling const. calc. 9-42400

Nuclei with $6 \leq A \leq 19$ continued

- ¹⁴N n.m.r. in trimethylvinylammonium bromide and derivatives, ¹⁴N, ¹H spin couplings 9-48509
¹⁴N n.m.r. in UN in paramag. state 9-37807
¹⁴N n.m.r. relax. times in methylbenzyl cyanides effect of fast internal rot. 9-46657
¹⁴N nuclear hyperfine const. and quadrupole coupling const. in NS 9-46369
¹⁴N nuclear quadrupole relaxation in organic nitro compounds of X-NO₂ type (X=C, N, O) 9-42440
¹⁴N quadrupole coupling const. in NO₂-calc. 9-42401
¹⁴N quadrupole coupling in N(SO₃)₂⁻ in potassium aminedisulphonate from c.s.r. 9-39916
¹⁴N quadrupole interaction in NH₄H₂PO₄ by double resonance spectra 9-28768
¹⁴N spin relax. in compressed N₂ gas 9-40594
¹⁴N, even-parity levels 9-42203
¹⁴N, NO₂-solid soln. in KBr, infrared intensities 9-48469
¹⁴N, recoil broadening of secondary transitions following neutron capture in ¹⁴N 9-42201
¹⁴N(³He,d)¹⁴O, d ang. distrib. meas., DWBA fits, levels and spectroscopic factors determ., E=11 MeV 9-29738
¹⁴N Chew-Frautschi plot for scatt. of nucleons 9-40505
¹⁴N from ¹⁴C(p,γ), γ transition mixing ratio, levels, spin and parity determ., E_γ=352-634 keV 9-29713
¹⁴N from ¹⁴N(d,p), diff. cross sections meas., DWBA anal., spectroscopic factors determ., E_p=1-3.2 MeV 9-25651
¹⁴N lifetimes and branching ratio of excited states 9-48280
¹⁴N obs. in β decay of ¹⁴C 9-38684
¹⁴N→¹⁴O, β decay to 0⁺ 6.05 MeV excited state obs. through e⁺e⁻ pair emission 9-44173
¹⁴N from ¹⁴O(t,³He); g.s. mass excess determ. from Q-value, E_γ=22 MeV 9-27639
¹⁴N-H geminal and vicinal coupling constants in N-oximes and N-quinoline, absolute signs, stereochem. and medium eff. 9-30134
¹⁴N→¹²Cnp, from ¹²C(d,n), p ang. distrib. anal., N doublet unbound levels determ. 9-25650
¹⁴N* from ¹⁶O(μ,nν), partial capture rate, excitation level distrib. determ. 9-25616
¹⁴Na, mass excess obs. in ²⁴Mg(p,⁶He)¹⁴Na 9-25568
¹⁴N(α,αp)¹²C, αp, spectra meas., ¹³C decay determ., E_α=22.9 MeV 9-38721
¹⁴N(α,p)¹⁵F 1¹/₂⁺ level in resonance found 9-36569
¹⁴N(α,n)¹⁷F(0.500)/¹⁴N(α,p)¹⁷O(0.871) for estimation of isobaric-spin impurities of 18F states 9-42206
¹⁴N(d,α)¹²C, applic. to ¹²C energy level determ. 9-48354
¹⁴N(d,d)¹⁴N diff. cross section meas., DWBA anal., E_d=1-3.2 MeV 9-25651
¹⁴N(d,p)¹⁵N spectroscopic factors determ., E_p=1-3.2 MeV 9-25651
¹⁴Ne discovery of new T=1⁺, isobaric analog state 9-48262
¹⁴Ne from ¹⁴O(³He,n), energy levels spin and parity determ., E_{he}=3 MeV 9-36581
¹⁴Ne from ¹⁶O(³He,n); γ spectra meas., levels lifetimes, spin, decay modes determ. 9-25567
¹⁴N(p,p)¹²C, elec. dipole cross-sections calc. 9-29781
¹⁴N(n,p)¹⁵N secondary γ-ray transition broadening 9-42201
¹⁴N(n,n)¹⁵N, shell bound-state method using truncated Hilbert space 9-44183
¹⁴N(n,n)¹⁵N*, elastic and inelastic cross sections calc., 1p-1h configuration space coupled channels, E₀-12 MeV 9-36604
¹⁴N(n,n)¹⁵N, shell model calc. in continuum, S-matrix Humblet-Rosenfeld expansion 9-27721
¹⁴N(p,p)¹⁴N, 3.7-5.67 MeV obs. rel. to level structure of ¹⁵O 9-38649
¹⁴N(π⁺,π⁰)¹⁴O charge exchange cross section meas., E_π=80-280 MeV 9-25642
¹⁴N(π⁺,π⁰)¹⁴O, 180 MeV obs. and comparison with calc. 9-22808
¹⁴N(τ, pa)¹²C sequential decay processes 9-22809
¹⁴O N reactions, 750-2000 MeV, with N, π emission 9-27728
¹⁴O, lifetimes of excited states from Doppler broadening 9-48280
¹⁴O energy levels obs. from ¹⁴N(p,p)¹⁴N 9-38649
¹⁴O structure determ. from ¹²C,³He; optical-model plus-resonance analysis, E=5-8 MeV 9-32303
¹⁴O, ¹⁶O scatt., excitation functions, nuc. molecular potn., parameters estimation 9-29828
¹⁴O, ¹⁶O scatt. near Coulomb barrier, excitation functions and ang. distrib. at 13 MeV c.m. energy 9-38722
¹⁴O, 0⁺ state evidence from e scatt., monopole matrix element, transition radius and width determ., E_γ=14 MeV 9-42205
¹⁴O, 7.12 MeV level, E1(ΔT=0) electroexcitation, form factors 9-25564
¹⁴O, dynamic N-N correlations from elastic e scatt. 9-34398
¹⁴O, four-particle, four-hole band, phenomenological approach 9-34393
¹⁴O, from (⁶Li,d) and (⁷Li,t) reactions, excitation of rotational bands 9-44223
¹⁴O, γ total absorption cross section meas., E_γ=9-31 MeV 9-29780
¹⁴O, mean lifetime of 10.94 MeV state meas. 9-46195
¹⁴O, muon partial capture rates and the induced, pseudoscalar, coupling constant 9-44190
¹⁴O, parity non conserving alpha decays, theory 9-42242
¹⁴O, π radiative capture, rate and Hamiltonian calc. by shell model 9-34460
¹⁴O, surface effects in dipole resonances, matrix element calc. for dipole transitions 9-40474
¹⁴O, e scatt. form factors, cluster model description 9-25570
¹⁴O,n bombardment, level-excitation cross section meas., E_n=14.6 MeV 9-36606
¹⁴O +ve parity states, shell model calc., B(E2) values 0-0 transition matrix element determ. 9-42204
¹⁴O(³He,³He)¹⁴O, 9.8-11.7 MeV range, energy dependence 9-29840
¹⁴O(³He,α)¹⁵O, 9.8-11.7 MeV range, energy dependence of angular distributions 9-29840
¹⁴O(³He,n)¹⁸Ne γ spectra meas., levels lifetimes, spin, decay modes determ. 9-25567
¹⁴O(⁶Li,α)¹⁸F, for precision meas. of levels in ¹⁸Fe 9-36614
¹⁴O(⁶Li,α)¹⁸F 4.8-13.8 MeV, obs., interpretation in terms of cluster interaction and statistical fluctuation models 9-36614
¹⁴O(⁶Li,d)²⁰Ne, excitation of rotational bands in ²⁰Ne, mechanism 9-44223
¹⁴O(⁷Li,t)²⁰Ne, excitation of rotational bands in ²⁰Ne, mechanism 9-44223
¹⁴O continuum shell model calc. of resonant particle-hole states 9-48276

Nuclei with $6 \leq A \leq 19$ continued

- ¹⁴O excitation by p, e; Goldhaber-Teller model, isospin and spin-isospin modes coupling, structure 9-34429
¹⁴O from ¹⁵N(³He,d); d ang. distrib. meas., DWBA fits, levels and spectroscopic factors determ., E=11 MeV 9-29738
¹⁴O giant reson., collective cor. model with surface-delta-interaction 9-29746
¹⁴O nuclear excitation due to e. scatt., μ capture, continuum model based on configuration mixing 9-25566
¹⁴O phase conspiracy in unoccupied Hartree-Fock orbitals 9-42199
¹⁴O proton scattering phase shifts 9-29792
¹⁴O quasi-elastic, e-N McVoy and Van Hove treatment 9-25614
¹⁴O structure determ. from (¹³C,³He), E_{he}=2-8 MeV 9-32357
¹⁴O, from ¹⁷F β-decay 9-38684
¹⁴O, T=1⁺ states 9-44134
¹⁴O(³He,n)¹⁹Ne energy levels determ., spin and parity assigned, E_{he}=3 MeV 9-36581
¹⁴O calc. of nuclear quadrupole moment 9-22962
¹⁴O from ¹⁶O(d,pp); p-γ delayed coincidence meas., half-life determ., E_d=1.2 MeV 9-34422
¹⁴O, low-lying levels, calc. within shell model 9-38650
¹⁴O(³He,α)¹⁷O, E(³He)=16 MeV, for T=1⁺ states in ¹⁷O 9-44134
¹⁴O(³He,d)¹⁹F spectroscopic factors determ. 9-40475
¹⁴O(⁷Li,t)²²Ne, 0⁺ state excited, SU(3) (4, 4) rep., E=12 MeV 9-29742
¹⁴O low-lying even-parity levels, decay strengths, deformed states calc. 9-22718
¹⁴O spectra calc., realistic interaction, eff. of Woods-Saxon wave function 9-38653
¹⁴O, s-d shell, calculations with realistic interactions 9-29693
¹⁴O(α,α), 5-10 MeV, phase-shift analysis 9-42305
¹⁴O(α,p)¹⁵N, quadrupole giant resonance evidence 9-44133
¹⁴O(d,³He) reaction, DWBA predictions test at E_d=82 MeV 9-40520
¹⁴O(d,α)¹⁴N, isospin-forbidden, cross section, ang. distrib. meas., J^π assignment, E_d=3-15 MeV 9-29827
¹⁴O(d,n)¹⁷F, angular distributions leading to ¹⁷F ground and first excited states 9-29826
¹⁴O(d,n)¹⁹F energy levels determ., spin and parity assigned, E_d=3 MeV 9-36581
¹⁴O(d,pp)¹⁷O; p-γ delayed coincidence meas., half-life determ., E_d=1.2 MeV 9-34422
¹⁴O(e,e), 0⁺ state evidence, monopole matrix element, transition radius and width determ., E_e=14 MeV 9-42205
¹⁴O(e,e); Born approx. analysis, correlation structure and charge density, high energies 9-34438
¹⁴O(γ,n₀)¹⁵O, cross-section, calc. 9-48276
¹⁴O(γ,n₀)¹⁵O, cross-section at giant resonance energies 9-38693
¹⁴O(γ,n₀)¹⁵O, cross section between 35 and 65 MeV 9-27696
¹⁴O(γ,n)¹⁵O*, γ-decay of excited state 9-48280
¹⁴O(γ,p)¹⁵N cross-section, k-matrix calc. 9-48276
¹⁴O(γ,p)¹⁵N, energy and ang. distrib. 9-32336
¹⁴O(γ,p)¹⁵N*, γ-decay of excited state 9-48280
¹⁴O(μ,nν)¹⁵N*, partial capture rate, excitation level distrib. determ. 9-25616
¹⁴O(μ,ν)¹⁴N, RPA and Tamm-Dancoff model calc. of capture rate, nuclear structure 9-34439
¹⁴O(p,α)¹³N diff. cross section and ang. distrib. meas., E_p=38 MeV 9-25631
¹⁴O(p,α) ang. distrib., direct reaction mechanism, E_p=38 MeV 9-48337
¹⁴O(p,α)_{1,2}¹³O, excitation functions, 3.2 to 5.4 MeV 9-22785
¹⁴O(p,α)¹⁵N, excitation functions rel. to ¹⁹F reson., 1.39-3.20 MeV 9-34390
¹⁴O(p,p), collision with nucleus substructure, E_p=660 MeV 9-34447
¹⁴O(p,p), elastic low- and medium-energy 9-48340
¹⁴O(p,p) cross section meas., optical model analysis, E_p=21 MeV 9-38695
¹⁴O(p,p) expt. and multiple collision and optical model theory comparison 9-25618
¹⁴O(p,p,p)¹⁸O, excitation functions, 3.2 to 5.4 MeV 9-22785
¹⁴O(p,p)¹⁸O, excitation functions rel. to ¹⁹F reson., 1.39-3.20 MeV 9-34390
¹⁴O(π-,n) bound 1s and 2p π absorption rates calc. in shell model 9-42295
¹⁴O(t,³He)¹⁴N, energy spectra, excitation energy, Q-value determ., E_t=22 MeV 9-27639
²⁸Si, p induced spallation; ¹⁸F, ^{22,24}Na fragments energy distrib. and range determ. 9-40511
⁹⁰Zr(p,p)⁹⁰Zr, 12 MeV, core-excitation model for ⁹¹Zr states 9-48342
⁹¹Zr(p,p)⁹¹Zr, 12 MeV, core-excitation model for ⁹¹Zr states 9-48342

Nuclei with $90 \leq A \leq 149$

- ¹⁰⁹Cd, m/l orbital-electron capture ratio, l and k X-ray escape points calc. 9-38689
¹³⁹La, from decay of ¹³⁹Ba, structure of 1/2⁺ state 9-29767
⁹¹Zr, spectrum, core excitation model predictions 9-48342
⁹²Mo, low lying states excited via analog resonances produced in p scatt. 9-48289
A=135 to 151 odd nuclei, spins of (2f_{7/2})³ ground states 9-46206
A=90 region, spectra of particle-hole type excitations 9-38665
coupling in dimethyltin dibenzoate 9-27875
differential cross section, levels, spectroscopic factors determ., E_d=29 MeV 9-32311
internal conversion coeffs., tables 9-46216
isotopes; Coulomb energy, anomalous shift of radii, core polarization, excess n depend. 9-36572
odd mass nuclei, pairing effects and n-p-surface delta interact. 9-29690
odd nuclei with 135 ≤ A ≤ 151, spins of (2f_{7/2})³ ground states 9-46206
rare-earth nuclei, d scatt., E_d=12 MeV 9-32354
⁹⁰Y from ⁸⁹Y (d,p) excitation curves, ang. distrib., spectroscopic factors, DWBA anal., E=4 MeV levels determ. 9-22825
¹¹⁰Ag diffusion in Zn 9-23845
^{110m}Ag decay, energies and intensities of transitions obs. 9-22756
¹¹²Cd(p, xn)¹¹¹In cross section meas., E_p=70-400 MeV 9-27714
¹¹⁰Ag, angular distributions of 53 levels, analysis by (d,p) reactions 9-29726
¹¹⁰Ag, level diagram, 0-2 MeV deduced from ¹⁰⁹Ag(n,p)¹¹⁰Ag 9-27727
¹³⁰Ba, neutron resonances 9-22727
¹⁴⁰Ba yields of ²³⁵U, ²³⁸U fission, fast and thermal, obs. 9-46248
¹⁴⁰C, rotational and quasi-rotational spectra 9-44155
¹⁴⁰Cd(p,p') inelastic scatt. at 55 MeV, vibr. states investigation 9-22723
¹⁴⁰Ce, two-quasiparticle states of proton system, evidence for, from ¹⁴⁰Pr decay 9-48296

Nuclei with $90 \leq A \leq 149$ continued

- $^{140}\text{Ce}(^3\text{He},\alpha)^{138}\text{Ce}$ spectroscopic factors calc., unified model 9-25578
 $^{140}\text{Ce}(\text{p},\text{d})$, n single-hole states in $50 < N \leq 82$ shell obs., $E_p = 55$ MeV 9-48251
 $^{140}\text{Ce}(\text{p},\gamma)^{141}\text{Pr}$, γ spectra meas., E1 transition and β matrix elements determ., $E_p = 9-11$ MeV 9-29735
 $^{140}\text{Ce}(\text{p},\text{p})$, γ ang. distrib. meas., n particle-hole states, levels and parity determ., $E_p = 4.9-11.7$ MeV 9-29734
 $^{100}\text{Mo}(\alpha,2n)^{102}\text{Ru}$, γ -ray linear polarization obs. using Ge(Li) detector 9-38460
 ^{129}Sn , excitation of seniority 0, 2 and 4 in quasi-particle theory 9-29728
 ^{130}Te , γ resonance scatt., spectra meas., level transitions obs. 9-27695
 $^{140}\text{Tr} \rightarrow ^{140}\text{Ce}$ evidence for two-quasiparticle states of proton system 9-48296
 $^{111\text{m}}\text{Pd} \rightarrow ^{111}\text{Ag}$, γ spectra meas., levels, spin and parity determ. 9-34419
 ^{111}Ag from $^{111\text{m}}\text{Pd}$, γ spectra meas., levels, spin and parity determ. 9-34419
 $^{131}\text{Ba} \rightarrow ^{131}\text{Cs}$, rel. to angular correlations in ^{131}Cs 9-29731
 ^{111}Cd E2 transitions obs. following bombardment 9-22741
 ^{111}Cd n.m.r. in CdCr_2Se_4 and CdCr_2S_4 , isotropic hyperfine fields and transferred spin polarization obs. 9-43297
 $^{111}\text{Cd}(\text{p},\text{n})$, differential cross section meas., spin change and symmetry obs. 9-38700
 $^{111}\text{Cd}(\text{p},\text{n})^{111}\text{In}$, γ and n spectra meas., spin and ang. distrib. determ., $E_p = 4.2-5.35$ MeV 9-42220
 $^{141}\text{Ce} \rightarrow ^{141}\text{Pr}$, γ spectra meas., levels determ. 9-32311
 ^{131}Cs , angular correlations determ. 9-29731
 ^{131}Cs and ^{132}Cs nuclear electric quadrupole moments, optical double reson. obs. 9-42223
 ^{121}I from ^{121}Xe decay, γ spectra meas. 9-29766
 ^{121}I , half life in solid and liquid sources, obs. 9-25600
 ^{121}I in biosphere in 1968, contamination meas. by thyroid testing 9-43405
 ^{121}I in L54M soln. reactor gas atm., obs. 9-46249
 ^{121}I in milk, Midwest USA obs. and explanation 9-26913
 $^{131}\text{I} \rightarrow ^{131}\text{Xe}$ in $\text{CH}_3^{131}\text{I}$, molecule Coulomb fragmentation, nuclear resonance-fluorescence scatt. 9-25599
 $^{131}\text{I} \rightarrow ^{131}\text{Xe}$ in I^{131} , molecule Coulomb fragmentation, nuclear resonance-fluorescence scatt. 9-25599
 ^{111}In , in nucleus of biomols., conformation from γ ang. correl. patterns 9-32536
 ^{111}In from $^{111}\text{Cd}(\text{p},\text{n})$; γ and n spectra meas., $E_p = 4.2-5.35$ MeV 9-42220
 ^{141}Pr , muonic X-rays magnetic h.f.s. parameter meas. 9-36575
 ^{141}Pr , n capture cross section, 5 keV-3 MeV 9-25638
 ^{141}Pr from ^{141}Ce decay, γ spectra meas., levels determ. 9-32311
 ^{141}Pr from $^{142}\text{Nd}(\text{d},\text{He})$, differential cross section, levels, spectroscopic factors determ., $E_p = 29$ MeV 9-32311
 ^{141}Pr isobaric analogue resonance in $^{140}\text{Ce}(\text{p},\gamma)$, γ spectra meas., E1 transition, $E_p = 9-11$ MeV 9-29735
 ^{141}Pr isobaric resonances, n particle-hole states in ^{140}Ce obs., p bombardment, 9.4-11.7 MeV 9-29734
 ^{141}Pr structure, expt. cf. with shell model calc. 9-42225
 $^{141}\text{Pr}(\gamma, \gamma')$, levels determ. from γ spectra., $E_p = 4.8-7.7$ MeV 9-27634
 $^{141}\text{Pr}(\text{n},\gamma)^{142}\text{Pr}$ neutron resonance capture, γ -ray transitions, and capture levels 9-46237
 ^{121}Sb , ^{123}Sb E2 transitions obs. following bombardment 9-22741
 ^{121}Sb , acoustic nuclear mag. reson. in InSb , exchange line broadening 9-45401
 ^{121}Sb , n and radiative capture total cross sections meas. 9-27633
 ^{121}Sb in liquid Sb, spin-lattice relax. 9-26134
 ^{121}Sb in liquid Sb and InSb , n.m.r. 9-23534
 $^{121}\text{Sb}(\text{d},\text{nn})^{121\text{m}}\text{Te}$, ^{121}Te , isomeric cross section ratio calc., nuclear level, density derived, agreement with superconductor model 9-27743
 ^{121}Sn , spin and hyperfine struct. 9-42222
 $^{121}\text{Xe} \rightarrow ^{121}\text{I}$, γ spectra meas. 9-29766
 ^{131}Xe , from I^{131} and $\text{CH}_3^{131}\text{I}$ β decay levels nuclear resonance-fluorescence scatt. 9-25599
 ^{112}Ag from $^{233,235}\text{U}$, n induced, yield meas. 9-29848
 ^{132}Ba , neutron resonances 9-22727
 $^{112}\text{Cd}(\text{d},\text{p})^{113}\text{Cd}$, 13 MeV, level structure of ^{113}Cd determ. 9-38667
 ^{142}Ce , lowest isobaric analogue resonance in (d,p) spin $1/2$ 9-25579
 $^{142}\text{Ce}(\text{p},\gamma)^{143}\text{Pr}$ quadrupole contribution to cross-section 9-34446
 ^{132}La , spin and parity of ground state 9-38669
 $^{142}\text{Ru}(\text{d},\text{p})$ excitation function meas., $E_d \leq 14$ MeV 9-29838
 ^{123}Sb isomeric state formation by (γ,n) , yield meas., $E_\gamma \leq 19$ MeV 9-22725
 ^{123}Sn , charge distrib., effects of neutrons, from elastic electron scatt. meas. 9-27703
 $^{125}\text{Sn}(\text{d},^3\text{He})$, upto ^{122}Sn , even isotopes; In levels, spin and parity determ., $E_p = 22$ MeV 9-29825
 ^{122}Xe , rotational and quasi-rotational spectra 9-44155
 ^{122}Xe , γ - γ ang. correls. 9-22728
 $^{113+}\text{Xe}(\text{cd}, \text{xn})$ $^{114\text{m}}\text{In}$ in cross section meas., $E_p = 70-400$ MeV 9-27714
 ^{122}Te isomeric transitions, investig. of accompanying radiation 9-46205
 ^{103}Rh from $^{103}\text{Rh}(\text{p},\text{p}')$, decay scheme, levels, spin, parity, BCE2) determ. 9-25574
 ^{131}Ba , Mossbauer effect, 7.2 yr. half-life 9-33525
 ^{131}Ba , ^{144}Ba gaussian curve for mass chains, tested from thermal induced neutron fission of ^{235}U 9-38728
 ^{113}Cd , n.m.r. in CdS , spin-lattice relaxation time, 77-450°K 9-47298
 ^{113}Cd investigated by means of $^{114}\text{Cd}(\text{d},\text{p})^{113}\text{Cd}$ 9-38667
 ^{113}Cd levels studied using $^{112}\text{Cd}(\text{d},\text{p})^{113}\text{Cd}$ 9-38667
 $^{113}\text{Cd}^{\text{m}}$, nuclear orientation by optical pumping, n.m.r. frequencies 9-25575
 ^{113}Cd n.m.r. in CdCr_2Se_4 and CdCr_2S_4 , isotropic hyperfine fields and transferred spin polarization obs. 9-43297
 $^{113}\text{Cd}(\text{p},\text{n})$ differential cross section meas., spin change and symmetry obs. 9-38700
 ^{133}Cs , 82 and 160 KeV states lifetimes 9-48294
 ^{133}Cs mag. hyperfine field in Fe, Mossbauer spectra 9-37699
 ^{133}Cs Mossbauer spectra of 81 keV line in ^{133}Xe implanted iron 9-35632
 ^{133}Cs resonance neutron capture γ spectra, transition obs. 9-25577
 ^{133}Cs spin system in CsF , pulsed n.m.r. obs. of free-induction-decay curves 9-35722
 $^{133}\text{Cs}(\text{d},\text{nn})^{133\text{m}}\text{Ba}$, ^{133}Ba , isomeric cross-section ratio calc., nuclear level density derived, agreement with superconductor model 9-27743
 $^{133}\text{Cs}(\text{n},\gamma)^{134}\text{Cs}$, study of ^{134}Cs excited states 9-44156
 ^{121}I from ^{121}Xe decay, γ spectra meas. 9-29766
 $^{131}\text{In}^{\text{m}}$ from ^{131}Sn decay, isomeric state half-life determ. from γ spectra 9-27630
 $^{103}\text{Pd} \rightarrow ^{103}\text{Rh}$, X and γ -ray yield obs., decay scheme 9-38688
 ^{143}Pm decay, 742 KeV transition, conversion line coeffs. 9-46207

Nuclei with $90 \leq A \leq 149$ continued

- ^{143}Pm single-particle self-energies, 2-body matrix elements calc. 9-29733
 ^{103}Rh , 53 keV γ -ray K-shell internal conversion coeff. 9-46202
 ^{103}Rh , n resonance region, scatt. cross-section meas. 9-46236
 ^{103}Rh from ^{102}Pd decay 9-38688
 ^{103}Rh recoiled nuclei in Fe-C4815 at. %Rh alloy, anomalous hyperfine field 9-35564
 $^{103}\text{Rh}(\text{p},\text{n})$ cross section meas., $E_p = 1-5.5$ GeV 9-25611
 $^{103}\text{Rh}(\text{p},\text{xn})$ processes, 0.4-0.9 GeV, obs. 9-42271
 $^{103}\text{Rh}(\text{n},^3\text{He})^{101}\text{Te}$ cross section, 14.8 MeV 9-32348
 $^{103}\text{Rh}(\text{n},\alpha)^{99\text{m}}\text{Tc}$ cross section, 14.8 MeV 9-32348
 $^{103}\text{Rh}(\text{n},2\text{p})^{102\text{m}}\text{Te}$ cross section, 14.8 MeV 9-32348
 ^{103}Ru , decay scheme study by sum coincidence spectra 9-22760
 ^{103}Ru radioactive decomposition, obs. 9-34418
 ^{123}Sb , 160 KeV level lifetime meas. 9-48285
 ^{123}Sb , acoustic nuclear mag. reson. in InSb , exchange line broadening 9-45401
 ^{123}Sb , n and radiative capture total cross sections meas. 9-27633
 ^{123}Sb in liquid Sb, spin-lattice relax. 9-26134
 ^{123}Sb in liquid Sb and InSb , n.m.r. 9-23534
 $^{123}\text{Sb}(\text{p},\text{n})^{122}\text{Sb}$ isomeric state formation, yield meas., $E_p \leq 19$ MeV 9-22725
 ^{133}Sn , spin and hyperfine struct. 9-42222
 ^{131}Sn L and K X-ray escape points calc. 9-38689
 $^{131}\text{Sn} \rightarrow ^{131\text{m}}\text{In}$, isomeric state half-life determ. from γ spectra 9-27630
 ^{127}Te E2 transitions obs. following bombardment 9-22741
 $^{127}\text{Te}(\text{n},\gamma)^{128}\text{Te}$, levels of ^{128}Te deduced 9-38668
 $^{127}\text{Xe} \rightarrow ^{127}\text{I}$, γ spectra meas. 9-29766
 ^{131}Xe diffusion in CsI, trapping rel. to defects, obs. 9-37202
 ^{131}Xe implanted in iron, Mossbauer spectra of subsequently excited ^{133}Cs 9-35632
 ^{134}Ba , 1580 KeV level not obs. 9-48295
 ^{134}Ba , levels from decay of ^{134}Cs 9-22758
 ^{134}Ba to ^{138}Ba isotopes, charge radii meas. by X-ray line isotopic shift 9-34399
 ^{144}Ce , internal conversion coeff. for E1, E2, M1, M2 transitions on K shell, $E_p = 1-9$ MeV 9-29765
 ^{144}Ce , K-conversion coeff., E1, E2, M1, γ transitions 1-17 MeV multipolarities calc. 9-25576
 ^{144}Ce , levels deduced from ^{144}In decay 9-29764
 ^{144}Ce , quasirotational band, existence 9-48291
 $^{144}\text{Ce}(\text{d},\text{t})^{143}\text{Cd}$, to determ. transitions in ^{133}Cd 9-38667
 $^{144}\text{Ce}(\text{p},\text{p}')$ inelastic scatt. at 55 MeV, vibr. states investigation 9-22723
 ^{134}Cs , decay to levels of ^{134}Ba , γ -ray and conversion line spectra 9-22758
 ^{134}Cs , levels excited in $^{133}\text{Cs}(\text{n},\gamma)$ reaction 9-44156
 ^{134}Cs , short-lived states excited in (n,γ) reaction 9-38666
 $^{134}\text{Cs} \rightarrow ^{134}\text{Ba}$, γ spectra meas., energy levels determ. 9-32310
 ^{140}Gd , 123 keV transition, K-shell particle parameter 9-38670
 ^{141}In , double decay process, internal conversion studies, 192 keV transition 9-44150
 $^{141\text{m}}\text{In} \rightarrow ^{141}\text{Cd}$, $\log f/\text{values}$, γ spectra meas. 9-29764
 $^{141\text{m}}\text{In} \rightarrow ^{141}\text{Sn}$, $\log f/\text{values}$, γ spectra meas. 9-29764
 ^{141}Nd lowest isobaric analogue resonance in (d,p) spin $1/2$ 9-25579
 $^{105}\text{Pd}(\text{d},\text{p})^{106}\text{Pd}$, subbarrier d energy 9-44219
 ^{144}Pr , ground state spin, angular correlation studies 9-46208
 ^{144}Pr $0 \rightarrow 0^+$ β transition, spectrum-shape factor and longitudinal polarization theory 9-29768
 $^{104}\text{Ru}(\text{d},\text{p})$ excitation function meas., $E_d \leq 14$ MeV 9-29838
 ^{123}Sb -Be source of thermal N, for precision anal. and tracer prod. 9-28834
 ^{123}Sb decay scheme, conversion electron spectra obs. 9-48292
 $^{123}\text{Sb} \rightarrow ^{124}\text{Te}$, levels of ^{124}Te by decay of 60d and 1.5 min isomers of ^{124}Sb 9-27673
 $^{145}\text{Sm}(\text{He},2\text{n})^{143}\text{Gd}$, isomeric transition, M4 prob. determ. from γ spectra 9-29736
 $^{145}\text{Sm}(\text{n},\gamma)^{146}\text{Sm} \rightarrow ^{145}\text{Pm}$, separation and γ spectrum, obs. 9-33688
 ^{131}Sn , levels deduced from ^{141}In decay 9-29764
 ^{124}Te , and even isotopes to 130, isobaric analogue resonances 9-44196
 ^{124}Te , energy level scheme determ. from $^{123}\text{Te}(\text{n},\gamma)^{124}\text{Te}$ 9-38668
 ^{124}Te , levels from ^{124}Sb decay, 60d and 1.5 min isomers 9-27673
 ^{124}Te and even isotopes to 130, isobaric analogue resonances prod. 9-44196
 ^{124}Te level scheme from ^{124}Sb decay 9-48292
 $^{124}\text{Te}(\text{n},\alpha)$, α decay obs., level width meas. 9-40515
 $^{105}\text{Ag} \rightarrow ^{105}\text{Pd}$ electron capture decay, γ radiation 9-46224
 ^{134}Ba , hyperfine const. and quadrupole interac. for F-centre in BaO 9-35109
 $^{134}\text{Ba}(\text{n},\gamma)^{135}\text{Ba}$, γ -ray spectrum rel. to level structure of ^{136}Ba 9-42224
 $^{134}\text{Ba}(\text{n},\gamma)^{135}\text{Ba}$ neutron resonance capture, γ -ray transitions and capture levels 9-46237
 ^{113}Cd , and $^{113}\text{Cd}^{\text{m}}$, nuclear orientation by optical pumping, n.m.r. frequencies 9-25575
 ^{113}Cd , β -decay in fast-n.irrad. CdS, associated elec. changes 9-47104
 ^{113}Cd , from p induced ^{238}U fission, isomer yield ratio of $^{115\text{m}}\text{Cd}$ and ^{115}Cd 9-34472
 ^{145}Eu single-particle self-energies, 2-body matrix elements calc. 9-29733
 ^{145}Gd from $^{145}\text{Sm}(\text{He},2\text{n})$; γ spectra meas., isomeric transition, M4 prob. determ. 9-29736
 $^{121}\text{I} \rightarrow ^{122}\text{Te}$ 35 keV transition, K/L and L subshell conversion ratio determ., Auger spectra 9-25598
 ^{111}In , 35.6 keV transition, K-conversion coefficient meas. 9-42221
 ^{111}In , acoustic nuclear mag. reson. in InSb , exchange line broadening 9-45401
 ^{111}In , conc. in 113 , ^{115}In mixture, thermal neutron absorpt. method 9-45431
 $^{111}\text{In}(\text{n},\text{np})^{110}\text{In}$, M1 transitions obs. 9-29727
 ^{111}In in liquid In and InSb , n.m.r. 9-23534
 ^{111}In in liquid In, spin-lattice relax. 9-26134
 ^{111}In n.m.r. spectrum in InBi , temp. depend. 9-45402
 ^{111}In spin system in InSb , rel. to generation of ultrasound 9-46984
 ^{145}Nd , spin and magnetic moment of 72.5 keV state, multipolarity of transition M1 9-25580
 ^{102}Pd , 344 keV level lifetime 9-29724
 ^{102}Pd , from $^{104}\text{Pd}(\text{d},\text{p})$, determ. of spectroscopic factors 9-44219
 ^{102}Pd , N; max- α decay width determ. 9-40515
 ^{112}Pd from $^{233,235}\text{U}$, n induced, yield meas. 9-29848
 ^{145}Pm , prep. by $^{145}\text{Sm}(\text{n},\gamma)^{145}\text{Sm} \rightarrow ^{145}\text{Pm}$ and γ spectrum, obs. 9-33688
 ^{123}Sb , nuclear decay effects on electronic structure of decaying atom and its bonding in cpds. from Mossbauer meas. 9-38769
 ^{123}Sb decay, γ spectra meas. 9-22757
 ^{127}Te , Coulomb excitation of levels 9-44152

Nuclei with $90 \leq A \leq 149$ continued

- ¹²⁵Te, Mossbauer effect in metals, linewidths, magnitude and isomer shifts 9-45284
- ¹²⁵Te, Mossbauer effect in Te single crystal 9-31090
- ¹²⁵Te, Mossbauer effect in PbTe:In (La), depend. of probability on degree of doping 9-39820
- ¹²⁵Te, nuclear decay effects on electronic structure of decaying atom and its bonding in cpds. from Mossbauer meas. 9-38769
- ¹²⁵Te, nuclear g-factor of 322 keV intruder state 9-44153
- ¹²⁵Te, superhyperfine structure in e.p.r. spectrum of ZnTe:Pb 9-47439
- ¹²⁵Te from ¹²⁵I, 35 keV transition, K/L and L subshell conversion ratio determ., Auger spectra 9-25598
- ¹²⁵Te Mossbauer effect in MnTe₂, paramag. and antiferromag. 9-43225
- ¹²⁵Te Mossbauer spectra in PbTe, Te and TeO₂ following thermal neutron capture in ¹²⁴Te 9-37703
- ¹⁰⁶Rh→¹⁰⁶Pd, γ spectra meas., levels determ. 9-22755
- ¹⁰⁶Ag→¹⁰⁶Pd decay, γ spectrum 9-42248
- ¹³⁶Ba, level structure from ¹³⁵Ba(n, γ)¹³⁶Ba reaction 9-42224
- ¹⁰⁶Cd to ¹¹⁶Cd even isotopes, p scatt. ang. distrib. means., B(E2) ratio calc., $E_\gamma=14$ MeV 9-27713
- ¹¹⁶Cd(p, γ) inelastic scatt. at 55 MeV, vibr. states investigation 9-22723
- ¹⁴⁶Eu→¹⁴⁶Sm, γ spectra internal conversion coeffs. determ., levels, deduced 9-48312
- ¹¹⁶In, polarized, β decay anisotropy 9-44177
- ¹¹⁶In from ¹¹⁵In(n_{th} , γ) M1 transitions obs. 9-29727
- ¹⁴⁶Nd from ¹⁴⁶Pm decay, γ spectra meas., energy levels determ. 9-34420
- ¹⁴⁶Nd lowest isobaric analogue resonance in (d,p) spin 7/2 9-25579
- ¹⁴⁶Pd from ¹⁰⁶Rh, γ spectra meas. levels determ. 9-22755
- ¹⁴⁶Pm→¹⁴⁶Nd γ spectra meas., energy levels determ. 9-34420
- ¹⁴⁶Pm→¹⁴⁶Sm γ spectra meas., energy levels determ. 9-34420
- ¹⁴⁶Sm from ¹⁴⁶Eu γ decay, levels determ., spin and parity assigned 9-48312
- ¹⁴⁶Sm from ¹⁴⁶Pm decay, γ spectra meas., energy levels determ. 9-34420
- ¹¹⁶Sn, J=0⁺ states, pairing force and surface delta interaction, seniority 9-29756
- ¹¹⁶Sn, low-lying excited states, Tamm-Dancoff approx., particle conservation 9-29701
- ¹¹⁶Sn(α , α), diff. cross section meas., deformation lengths, 2⁺, 4⁺ states calc. $E_\gamma=65$ MeV 9-40517
- ¹¹⁶Sn(p,n)¹¹⁶Sb, pre-compound particles at 10,12,14 MeV bombarding energies 9-29797
- ¹¹⁶Sn(p,p) cross section meas., optical model analysis, $E_p=21$ MeV 9-38695
- ¹³⁶Xe(p, γ), ¹³⁷Cs levels, isobaric analog resonances spectroscopic factors meas., $E_\gamma=9-13$ MeV 9-40509
- ¹²⁷In, Coulomb excitation with ¹⁶O in range 35-55 MeV 9-44154
- ¹²⁷Te isomeric transitions, investig. of accompanying radiation 9-46205
- ¹⁰⁹Ag, p induced analog resonance reaction, excitation function meas., $E_p=5.9-7.25$ MeV 9-29725
- ¹⁹⁷Au n resonance region, scatt. cross-section meas. 9-46236
- ¹⁹⁷Au(p,n)¹⁹⁶Au, av. recoil ranges of ¹⁹⁶Au, 20-85 MeV 9-25630
- ¹³⁷Ba, hyperfine const. and quadrupole interac. for F-centre in BaO 9-35109
- ¹⁰⁷Cd, γ radiation 9-44149
- ¹⁰⁷Cd decay scheme 9-44151
- ¹³⁷Cs compound nucleus in ¹³⁶Xe(p,p); levels, isobaric analog resonances spectroscopic factors meas., $E_\gamma=9-13$ MeV 9-40509
- ¹³⁷Cs conversion electron obs. with double-focusing sector-type spectrometer 9-38610
- ¹⁴⁷Gd e capture, energy meas., ¹⁵¹Dy e capture decay energy prediction 9-40493
- ¹⁴⁷Gd→¹⁴⁷Eu, β^+ - γ coincidence meas. 9-40493
- ¹⁴⁷Gd→¹⁴⁷Eu, decay, e- γ coincidence spectra 9-40492
- ¹¹⁷I→¹¹⁷Te, β decay and assoc. γ rays, rel. to excited states in ¹¹⁷Te 9-44178
- ¹²⁷I, core and particle parameters of low-lying levels, in core-excitation model 9-22726
- ¹²⁷I, n.m.r. in alkali halide aqueous solns., chem. shift 9-34925
- ¹²⁷I, nuclear decay effects on electronic structure of decaying atom and its bonding in cpds. from Mossbauer meas. 9-38769
- ¹²⁷I, resonance fluorescence from 375 KeV level obs. 9-29730
- ¹²⁷I n.m.r. in NaIO₄ single crystals. 9-33654
- ¹²⁷I(p,n) cross section meas., $E_p=1-5.5$ GeV 9-25611
- ¹²⁷(n,2n), angular correlations between neutrons 9-29813
- ¹²⁷(p,n), cross-section meas. 9-25626
- ¹²⁷(p,pn), cross-section meas. 9-25626
- ¹⁴⁷Nd γ spectra dis. 9-27682
- ¹⁴⁷Nd→¹⁴⁷Pm, γ - γ ang. correlations meas., multipole admixtures determ. 9-40496
- ¹⁰⁷Pd, obs. in ¹⁰⁷Rh, lifetime of 115.6 keV and other levels determ. 9-48311
- ¹⁴⁷Pm from ¹⁴⁷Nd decay, γ - γ ang. correlation meas., spin determ. 9-40496
- ¹⁰⁷Rh→¹⁰⁷Pd, 22 min., obs., β -branching ratios meas. 9-48311
- ¹¹⁷Sn, p-n interac., n hole energy Z depend. 9-29732
- ¹¹⁷Sn, total cross section and neutron cross section 9-42291
- ¹¹⁷Sn(p,d) 17 MeV, p, failure to obs. prod. of any singlet d 9-38698
- ¹¹⁷Sn(p,n), differential cross section meas., spin change and symmetry obs. 9-38700
- ¹¹⁷Sn(p,n)¹¹⁷Sb, excitation functions 9-38701
- ¹¹⁷Te, excited state study by β decay of ¹¹⁷I 9-44178
- ¹³⁸Pr→¹³⁸Ce, β^+ decay 9-44250
- ¹⁴⁸Pr(m,n), search 9-34453
- ¹⁰⁸Ag, short-lived states excited in (n, γ) reaction 9-38666
- ¹³⁸Ba, rotational and quasi-rotational spectra 9-44155
- ¹³⁸Ba(d,p)¹³⁹Ba, γ spectra meas., transitions and levels determ. 9-38705
- ¹³⁸Ba(n, γ)¹³⁹Ba, γ spectra meas., transitions and levels determ. 9-38705
- ¹⁰⁸Cd(p, γ), analogue resonances decay amplitude, p ang. correlation meas. 9-42285
- ¹³⁸Cs, level struct. from ¹³⁸Xe 15 min fission product γ spectra 9-34471
- ¹¹⁸I, ¹²⁰I and isomeric states radioactivity obs. 9-44179
- ¹⁴⁸I decay scheme 9-44171
- ¹⁴⁸Sm, γ energy distrib. after β decay, slowing down of nuclear recoil 9-45283
- ¹¹⁸Sn, charge distrib., effects of neutrons, from elastic electron scatt. meas. 9-27703
- ¹¹⁸Sn(p,2n)¹¹⁷Sb, excitation functions 9-38701
- ¹³⁸Xe 15 min fis. product, γ spectra, ¹³⁸Cs levels 9-34471
- ¹³⁹Nd→¹³⁹Pr, three-quasiparticle multiple in ¹³⁹Pr 9-34400

Nuclei with $90 \leq A \leq 149$ continued

- ¹⁰⁹Ag, p induced analog resonance reaction, excitation function meas., $E_p=5.9-7.25$ MeV 9-29725
- ¹⁰⁹Ag from ¹⁰⁹Pd, γ spectra meas., levels, spin and parity determ. 9-34419
- ¹⁰⁹Ag pulsed n.m.r. in Ag single crystal, rel. to mag. domains due to de Haas-van Alphen effect 9-45393
- ¹⁰⁹Ag(α , γ)¹¹¹In, excitation function calc., n spectra, energy meas. 9-29824
- ¹⁰⁹Ag(α , n)¹¹²In, excitation function calc., n spectra, energy meas. 9-29824
- ¹⁰⁹Ag(α , n)¹¹²Nm, excitation function calc., n spectra, energy meas. 9-29824
- ¹⁰⁹Ag(d,p)¹¹⁰Ag, angular distributions of 53 levels in ¹¹⁰Ag 9-29726
- ¹⁰⁹Ag(n, γ)¹¹⁰Ag, n capture by 5.2 eV resonance, levels of ¹¹⁰Ag 9-27727
- ¹³⁹Ba from ¹³⁸Ba(d,p); γ spectra meas., transitions and levels determ. 9-38705
- ¹³⁹Ba from ¹³⁸Ba(n, γ); γ spectra meas., transitions and levels determ. 9-38705
- ¹³⁹Ba→¹³⁹La, nuclear matrix elements in 2.14 MeV β group 9-29767
- ¹³⁹Ba→¹³⁹La, γ spectra meas., levels determ. 9-27674
- ¹³⁹Ce, p-n interac., n hole energy Z depend. 9-29732
- ¹³⁹Ce, unified model calc. for energy spectrum, level lifetimes 9-25578
- ¹⁴⁹Eu, γ spectrum 9-44180
- ¹⁴⁹Gd, γ spectrum 9-44180
- ¹²⁹I, Mossbauer effect in pyridine complexes of iodine monohalides 9-34688
- ¹²⁹I, Mossbauer effect in SnI₄ molecular crystal, rel. to chemical bonding in molecule 9-34643
- ¹²⁹La, n capture cross section, 5 keV-3 MeV 9-25638
- ¹²⁹La, single-particle self-energies, 2-body matrix elements calc. 9-29733
- ¹²⁹La from ¹³⁹Ba, γ spectra meas., levels and decay scheme determ. 9-27674
- ¹³⁹La n.m.r. in hexagonal La metal, Knight shifts, spin relax. rates and quadrupole coupling consts. 9-31171
- ¹⁴⁹Pm, gyromag. ratio of 114 keV state 9-46209
- ¹⁴⁹Pm, mag. moments of 114 and 270 keV levels 9-46210
- ¹³⁹Pr, multiplet of six high-lying, high-spin, odd parity states 9-34400
- ¹¹⁹Sb, excited states 9-22724
- ¹⁴⁵Sm, 0.099 eV n reson. parameters 9-34454
- ¹⁴⁵Sm, 286 KeV state life time 9-48294
- ¹¹⁹Sm, Coulomb excitation of levels 9-42226
- ¹¹⁹Sm, in white Sn, Mossbauer effect, anisotropy of emission probability and temp. and angular depend. 9-49265
- ¹¹⁹Sm, Mossbauer effect in SnI₄ molecular crystal, rel. to chemical bonding in molecule 9-34643
- ¹¹⁹Sn (p,n), differential cross section meas., spin change and symmetry obs. 9-38700
- ¹¹⁹Sn charge radius determ. by Mossbauer spectroscopy 9-27632
- ¹¹⁹Sn in β -Sn, Mossbauer thermal shift meas., 3.6-90°K 9-24386
- ¹¹⁹Sn in antiferromag. MnSn₂, Mossbauer effect 9-41368
- ¹¹⁹Sn in Co-Pd and Fe-Pd alloys, mag. field on nuclei meas. 9-28620
- ¹¹⁹Sn in Co, hyperfine field, anomalous temp. depend. 900° to 1300 °K 9-47330
- ¹¹⁹Sn in Fe(Ni-Sn) dilute alloys, Mossbauer hyperfine field and resistivity study 9-47335
- ¹¹⁹Sn in NiFe₂O₄, Mossbauer obs. of mag. field at nuclei 9-26727
- ¹¹⁹Sn Mossbauer effect in Cu alloys, electronic props. obs. 9-43222
- ¹¹⁹Su, Mossbauer spectra in rare-earth stannates (R₂Sn₂O₇) 9-33529
- ¹²⁹Tb, γ spectrum and conversion electron spectrum 9-44180
- ¹²⁹Xe-¹⁹F coupling constant in Xenon fluorides and oxyfluorides, as function of ¹⁹F chem. shift 9-34646
- ¹²⁹Xe, n; max= α decay width determ. 9-40515
- ⁹⁰Nb, half-life of the first metastable state 9-22766
- ⁹⁴A nuclear structure in this region using ⁹⁴Zr(He³,d)⁹⁵Nb 9-38718
- Ag, bombarded by 86 MeV ¹²C, products obs. 9-48352
- Ag, p induced, high energy cross section determ. by mica track detector 9-40523
- Ag, photofission induced by 1 to 6 GeV photons 9-29855
- Ag(p,p), diff. cross section meas., diffuse-surface optical model anal., $E_p=28$ MeV 9-25623
- Ba gaseous, short-lived, mass-separated fission products, half-life determ. 9-22765
- Ba isotopes (A=131, 133, 135 and 139), from (n, γ) reactions, γ ray spectra 9-42249
- Cd, small-angle scatt. of n, differential cross-sections, polar., applic. 9-25634
- Cd isomer, p excited, half-life and γ -spectrum, obs. 9-27631
- Ce(n,n'), γ spectra meas. 9-34452
- Cs, odd mass, mag., quadrupole moments, energy spectra, M1, E2 transition rates, unified-model calc. 9-32309
- Cs gaseous, short-lived, mass-separated fission products, half-life determ. 9-22765
- Fe, γ absorption cross section energy depend. determ., $E_\gamma=10-25.5$ MeV 9-29782
- In A=111-121, odd; from ¹¹²⁻¹²²Sn(d,³He); levels, spin and parity determ., $E_\gamma=22$ MeV 9-29825
- Kr gaseous, short-lived, mass-separated fission products, half-life determ. 9-22765
- La, odd mass, mag., quadrupole moments, energy spectra, M1, E2 transition rates, unified-model calc. 9-32309
- La(n,n'), γ spectra meas. 9-34452
- ^{90m}Nb half-life, effect of superconductivity 9-32329
- Mo isotopes, n resonances assigned 9-36574
- Mo odd mass isotopes, low energy props. using intermediate coupling approach 9-22749
- ⁹²Mo, energy levels calc. 9-29759
- ⁹²Mo, excitation energy, spin, parity, lifetime meas. by in-beam γ spectroscopy 9-29758
- ⁹⁴Mo energy levels, excited in the decay of the ⁹⁴Tcm⁺ isomeric pair 9-38680
- ⁹⁷Mo from ⁹⁷Nb decay; γ spectra meas., levels determ. 9-32330
- ⁹⁸Mo, n capture cross section, 5 keV-3 MeV 9-25638
- ⁹⁸Mo from ⁹⁸Nb decay, γ - β spectra and coincidence meas., levels determ. 9-34414
- ⁹⁹Mo→⁹⁹Tc, K-shell conversion coeff. of 40.58 keV transition 9-29773
- ⁹²Mo(d, t), to ⁹²Mo, even isotopes, ang. distrib., DWBA, t value and spectroscopic factor, $E_d=23$ MeV 9-27759
- ⁹²Mo(n, α), α decay obs., level width meas. 9-40515
- ⁹²Mo(p, γ)⁹²Mo excitation of low-lying states via isobaric analog resonances 9-48289

Nuclei with $90 \leq A \leq 149$ continued

- ⁹⁰Nb, level spectra calc. treating excited states as particle-hole excitations of ⁹⁰Zr core 9-38665
⁹¹Nb, cross-sections, total neutron, 3.3-5.2 MeV 9-38702
⁹¹Nb, spin-lattice relax. time in mixed state superconducting Nb 9-41348
⁹¹Nb n.m.r. in Nb single cryst. 9-45406
⁹⁶Nb-⁹⁶Mo, γ and β spectra 9-44176
⁹⁷Nb-⁹⁷Mo, γ spectra meas., levels determ. 9-32330
⁹⁸Nb-⁹⁸Mo, γ , β spectra and coincidence meas., levels determ. 9-34414
Pd(d,p) spectroscopic factors ratio, states of same I- π , $e_p=8-17$ MeV 9-40519
Rb gaseous, short-lived, mass-separated fission products, half-life determ. 9-22765
⁸⁹Ru, energy levels calc. 9-29759
⁸⁹Ru, excitation energy, spin, parity lifetime meas. by in-beam γ spectroscopy 9-29758
⁹⁷Ru-⁹⁷Tc, γ spectra meas., level structure determ. 9-27686
Ru(d,p); excitation function meas., $E_d \leq 14$ MeV 9-29838
Sb isotopes, moving triton model used to calc. magnetic moment 9-46204
Sn isomer, p excited, half-life and γ -spectrum, obs. 9-27631
Sn stable isotopes from fast n ²³⁵U fission, relative yields, tandem mass spectrometer 9-38725
Sn(p,n) reactions, ($E_p=3$ to 5.5 MeV), proton strength functions, optical model analyses 9-44202
Sr gaseous, short-lived, mass-separated fission products, half-life determ. 9-22765
⁸⁸Sr content in seawater, radiometric measuring device 9-22751
⁸⁸Sr particulate tracers of stratospheric motion 9-28896
⁸⁸Sr yield, Chinese thermonuclear explosion (1967) 9-28898
⁹³Tc, isobaric analogue states, γ transitions to low lying states 9-29760
⁹³Tc and ^{93m}Tc, γ -ray spectra, half-life obs. 9-48290
⁹³Tc and ^{94m}Tc, γ -ray spectra, half-life obs. 9-48290
⁹⁴Tc m.s. isomeric pair, decay, excitation of ⁹⁴Mo energy levels 9-38680
⁹⁶Tc-⁹⁶Mo γ -spectra and conversion electron spectra 9-44175
⁹⁷Tc from ⁹⁷Ru decay, γ spectra meas., level structure determ. 9-27686
⁹⁷Tc, multipolarity of 40.584 keV transition 9-29773
Xe, fission-type, from extinct radioactivity, in meteoritic whitlockite, correlation with fission tracks 9-34415
Xe gaseous, short-lived, mass-separated fission products, half-life determ. 9-22765
Xe isotopes, isomeric cross sections ratios 9-48293
⁹⁰Y, level spectra calc. treating excited states as particle-hole excitations of ⁹⁰Zr core 9-38665
⁹⁰Y, low-energy spectra from shell model calc., vel.-depend. effective N-N potential 9-40480
⁹¹Y from ⁸⁹Y(t,p) and ⁹²Zr(t, α), energy levels, spin and parity assignments 9-48308
⁶⁵Zn diffusion in Zn:Ag 9-23845
⁹⁰Zr, level investigation using excitation with n-capture γ , anomalies 9-36573
⁹¹Zr, p-n interac., n hole energy Z depend. 9-29732
⁹¹Zr E2 transitions obs. following bombardment 9-22741
⁹²Zr, ⁹⁴Zr E2 transitions obs. following bombardment 9-22741
⁹²Zr, low-energy spectra from shell model calc., vel. depend. effective N-N potential 9-40480
⁹²Zr, spin determ. for resonances decaying to excited J=0 states 9-46201
⁹²Zr(³He,d)⁹²Nb, 34 MeV obs. rel. to nuclear structure in this region 9-38718
⁹²Zr (p,t), L=0 transition obs., $E_p=38$ MeV 9-29802
⁹²Zr-⁹²Nb gamma-ray spectrum, branching ratio determ. 9-27671
⁹²Zr(α , α'), diff. cross section meas., deformation lengths, 2⁺, 4⁺ states calc., $E_\alpha=65$ MeV 9-40517
⁹²Zr(α , α'), diff. cross section meas., deformation lengths, 2⁺, 4⁺ states calc., $E_\alpha=65$ MeV 9-40517
⁹²Zr(α , α'), diff. cross section meas., deformation lengths, 2⁺, 4⁺ states calc., $E_\alpha=65$ MeV 9-40517
⁹²Zr(d,p)⁹²Zr, cross section, p polarization determ., optical model and DWBA, analysis, $E_p=1$ MeV 9-38717
⁹²Zr(³He,p,n)⁹²Nb, excitation function, analyzing power determ. 9-27757
⁹²Zr(³He,p,n)⁹²Zr, excitation function, analyzing power determ. 9-27757
⁹²Zr(γ +p), photoproton energy and ang. distrib., spin dipole reson., hole states 9-34434
⁹²Zr(p,d)⁹²Zr, excitation function meas., isospin effects obs. 9-36603
⁹²Zr(p,n)⁹¹Nb*, charge exchange cross section calc. 9-40512
⁹²Zr(p,p')⁹²Zr, excitation function meas., isospin effects obs. 9-36603
⁹²Zr(p,p')⁹²Zr, excitation function meas., isospin effects obs. 9-36603
⁹²Zr(p,p'), p ang. distrib. meas., levels determ., $E_p=18.7$ MeV 9-27709
⁹²Zr(p,t), L=0 transition obs., $E_p=38$ MeV 9-29802
⁹²Zr(p,t)⁸⁸Zr, rel. to excited levels of ⁸⁸Zr 9-27670
⁹²Zr(p,t)⁸⁸Zr, rel. to excited levels of ⁸⁸Zr 9-42235
⁹²Zr(p,t), l=0 transition obs., pair-vibrational like state excitation, $E_p=38$ MeV 9-29802
⁹²Zr(p,t), L=0 transition obs., $E_p=38$ MeV 9-29802

Nuclei with $A \leq 5$

- ⁴He binding energies by Hartree-Fock model 9-42209
¹H-¹⁵N geminal and vicinal coupling constants in N-oximes and N-quinoline, absolute signs, stereochem. and medium eff. 9-30134
H(d,n)³He, 83 MeV differential cross-section obs. 9-22817
H(d,n)³He, n polarization energy and ang. distrib. meas., $E_d=0.5-2$ MeV 9-25653
alpha particle cluster structure 9-48271
deuterons, disintegration in a pulse approximation 9-27568
differential cross sections of reactions (p,d) and (He³, α) in terms of peripheral model 9-27712
energy levels from translation-invariant shell model calc. for A=4,5 9-27624
⁴He binding energy depend. on 3π exchange ANN force 9-25573
three-body simple model, energy calc. by Monte Carlo method 9-22719
three-particle nuclei, Gammel-Brueckner potential, E1 integrated photoabsorption cross section calc. 9-29716
three-particle nuclei, photodisintegration and Majorana exchange forces 9-42270
two-nucleon potential, non-relativistic 9-42166
two-nucleon potential, non-relativistic 9-38634
(¹H, p) normalization const. calc. and S' state obs. 9-32353
(¹H, d) normalization const. calc. and S' state obs. 9-32353
(¹He, d) normalization const. calc. and S' state obs. 9-32353
¹H in ¹³C, n.m.r., neutron anomalous torque and spin determ. 9-38586
⁴HeC, $\pi^+\pi^-$ mesonic decays ratio determ. 9-25572
(n,t) reaction cross-sections, meas. 9-22792

Nuclei with $A \leq 5$ continued

- ⁴H³ mesonic decay, lifetime meas. 9-38651
⁴He, π^+ decay obs. and branching ratio rel to π decay 9-38652
⁴He⁴ mesonic decay, lifetime meas. 9-38651
⁴He⁵ mesonic decay, lifetime meas. 9-38651
⁴He⁶ mesonic decay, lifetime meas. 9-38651
¹H, in 2,1,3-benzoselenadiazole, p.m.r. spectra and parameters 9-30088
¹H, in 2,1,3-benzothiadiazole, p.m.r. spectra and parameters 9-30088
¹H, in 2,1,3-benzoxadiazole, p.m.r. spectra and parameters 9-30088
¹H, in benzene, proton spin lattice relax. time, 23°C 9-30121
¹H, n.m.r. in methylquinolines 9-38904
¹H, n.m.r. in pentaerythritol 9-43307
²D in ferroelectric rochelle salt, spin-lattice relax. 9-24345
²D NMR in deuterio-nitrobenzene, electric field effects 9-46656
¹⁹F, n.m.r. in NH₄PF₆·NH₄F, spin-lattice relaxation times anomaly rel. to dielectric phase transitions 9-35277
¹H, in liquid n-heptane spin relax., press. and temp depend 23-190°C, 0.07-1.9 kbar 9-30121
¹H, n.m.r. in benzaldehyde, monosubstituted, chem. shift and coupling const. 9-30087
¹H-¹⁹F coupling in fluorobenzene derivatives, substituent effects 9-38881
¹H, p, p-p bremsstrahlung cross section, time of flight diff., $E_p=10$ MeV 9-29798
¹H, in solid methane and deuterated modifications, nuclear spin-lattice relax. time temp. depend. 9-43198
¹H, N.M.R. in 1,1-difluoroethylene, in nematic solvent 9-30105
¹H, n.m.r. in Co(II) complexes of 1:3 bidentate Schiff's bases, spin density distrib. from isotropic shifts 9-42411
¹H, n.m.r. in Cu acetate, relax. in H₂O, C₂H₅OH solns., obs. 9-48719
¹H, n.m.r. in 1:3-di-imines, N:N disubstituted 9-30106
¹H, n.m.r. in monosubstituted cyclopropanes, ¹³C-H spectra 9-38888
¹H, n.m.r. in NH₄PF₆·NH₄F, spin-lattice relaxation times anomaly rel. to dielectric phase transitions 9-35277
¹H, n.m.r. in Ni(II) complexes of 1:3 bidentate Schiff's bases, spin density distrib. from isotropic shifts 9-42411
¹H, n.m.r. in organic nitro compounds of X-NO₂ type (X=C, N, O), line shapes 9-42440
¹H, n.m.r. in pyridazine, proton coupling constants 9-34689
¹H, n.m.r. in selenols, proton shift of SeH group 9-34691
¹H, n.m.r. in very dil. solns. of o-H₂ in p-H₂ spin lattice relaxation 9-34924
¹H, p.m.r. in trimethylvinylammonium bromide and derivs., ¹⁴N, ¹H and ¹⁹F spin couplings 9-48509
¹H, spin lattice relaxation in La₂Mg₃(NO₃)₁₂·24H₂O dependence on Nd concentration 9-47299
¹H, spin lattice relaxation time in methyl group, including tunneling splitting of torsional oscillator ground state 9-37671
¹H in H₂ gas, n.m.r. relaxation time meas., 293-738°K, 7-135 atm., J depend. on collisions 9-34616
¹H, n.m.r. in non-polar liquids, medium effects on proton chemical shifts 9-40806
¹H n.m.r. spectroscopy 9-44600
¹H spin-lattice relax. in ZnSiF₆·6H₂O·Fe²⁺, Mn²⁺ 9-35594
¹H, in solid methane and deuterated modifications, nuclear spin-lattice relax. time temp. depend. 9-43198
¹H, magnetic dipole moment, calc. with baryons resons. in ground state 9-34394
¹H, minimum percent D state calc. 9-34395
¹H, n.m.r. in deuteriochloroform, anisotropic molecular rotation in liquid 9-39119
²H, nucleon correlation eff. in shell-model description 9-29714
²H, vibrational analysis with trial that is a linear combination of oscillator states 9-40472
²H mag. resonance of paramag. ions in soln. 9-46653
²H photodisintegration, momentum-dependent potentials influence, off-energy-shell effects study 9-34387
²H scatt. cross-section rel. to spin polarization 9-29629
²H, binding energy, double scatt. length calc. from Hamada-Johnston potential 9-29715
²H, Faddeev eqn. soln., binding energy determ. 9-27622
²H, form factors of energy levels 9-36571
²H, improved S-state wave function 9-27623
²H, improved S-state wave function 9-40476
²H, irreducible tensor operator form for 3-body potential 9-25569
²H, nucleus diffraction interaction, splitting, diff. cross section formula 9-36570
²H, π scatt. meas., nuclear wave function components anal. 9-27737
²H, π , decay rates and branching ratios by separable-potential model wave functions 9-44136
²H(γ + π^0) by Primakoff effect 9-38526
²H isospin admixture polar vector matrix for β -decay and charge form factor 9-32304
²H thin sources, prod. by glow discharge 9-42238
³H binding energy depend. on 3π exchange ANN force 9-25573
⁴He, decay rates and branching ratios by separable-potential model wave functions 9-44136
⁴He binding energies by Hartree-Fock model 9-42209
³H-³H, n separation energy determ. from ²H(n, γ)³H γ transition meas. 9-38645
³H-²H n separation energy determ. from ²H(n γ)³H γ transition meas. 9-38645
¹H-¹³C coupling constants, effect of lone pairs 9-34649
H(d, d), ang. distrib., cross section, excitation curves determ., $E_d=3.5-12.25$ MeV 9-25645
H(d, n)³He, n yield meas. in Cu single crystal 9-40518
H(d,d)²H, vector analysing power meas., $E_d(\text{pol.})=10$ MeV 9-25654
H(d,p)³He, differential cross section meas., $E_d=4-10$ MeV 9-42301
H(d,n)³He, low energies, reson. obs., coupling matrix element linking react. channels 9-22819
H(d,n)³He, vector analysing power meas., $E_d(\text{pol.})=10$ MeV 9-25654
H(d,n)³He, as n beam source, shape of beam 9-29675
H(d,p)³He, 83 MeV differential cross-section obs. 9-22817
H(d,p)³He, low energies, reson. obs., coupling matrix element linking react. channels 9-22819
H(d,p)³H, vector analysing power meas., $E_d(\text{pol.})=10$ MeV 9-25654
He(γ ,n)He⁴, at γ -quanta maximal energy of 120 MeV 9-27701
He, 180° e scatt. at 56 MeV, nuclear mag. structure investigation 9-42273
He, bound state wave function, Coulomb energy and s'-state prob. calc. 9-38646

Nuclei with $A \leq 5$ continued

- ³He, elastically scattered from ⁴He, polarization meas. by double-scatt. technique 9-46240
- ³He, form factors of energy levels 9-36571
- ³He, nucleus diffraction interaction, splitting, diff. cross section formula 9-36570
- ³He, π absorption, capture rate and coupling const. determ. 9-27517
- ³He, π scatt. meas., nuclear wave function components anal. 9-27737
- ³He, weak interaction theory 9-27704
- ³He beam causing delayed fission events due to isomeric fission 9-44227
- ³He capture of μ^- , probability calc., asymmetry of recoil 9-32340
- ³He from n-induced ²³⁵U fission yield and energy distrib. meas. 9-22839
- ³He from n-induced ²³⁵U fission, yield and energy distrib. meas. 9-22839
- ³He isospin admixture Coulomb energy rel. to n-n potential and charge form factor 9-32304
- ³He optical model of scatt. on nuclei at 15 MeV 9-48348
- ⁴He, binding energy determ. from Λ N potential 9-42111
- ⁴He, 1-, T=0 new state obs. 9-34397
- ⁴He, Adler's self-consistency conditions, charge symmetric π -nucleus forward dispersion reln. 9-34301
- ⁴He, coherent photoprod. of π^0 -mesons 9-42272
- ⁴He, e scatt., correlations and form factor meas., momentum transfer square $q^2 \leq 20 \text{ fm}^{-2}$ 9-34396
- ⁴He, excited 0⁺ level, formation mechanism 9-38647
- ⁴He, form factors of energy levels 9-36571
- ⁴He, ground-state props. and effects of centre-of-mass motion 9-48279
- ⁴He, independent-pair wave function from energy variational principle 9-29717
- ⁴He, odd-parity states 9-40477
- ⁴He, p scatt., analyzing power and phase shift anal., $E_p=70-80 \text{ MeV}$ 9-36602
- ⁴He, phase conspiracy in unoccupied Hartree-Fock orbitals 9-42199
- ⁴He, photodisintegration, continuum model 9-44195
- ⁴He(³He, ³He), elastic, polarization of ³He, meas. by double-scatt. technique 9-46240
- ⁴He(⁴He, ⁴He)⁺, diff. cross section, excitation energy determ., $E_a=64 \text{ MeV}$ 9-29820
- ⁴He (e,e); Born approx. analysis, correlation structure and charge density, high energies 9-34438
- ⁴He beam causing delayed fission, events due to isomeric fission 9-44227
- ⁴He cosmic rays, modulation near solar minimum, obs. 9-27573
- ⁴He excited states obs. from ⁴He(γ , p)³H 9-32305
- ⁴He from n-induced ²³⁵U fission, yield and energy distrib. meas. 9-22839
- ⁴He in cosmic rays, photodisintegration by universal radiation field, $E < 10^{10} \text{ GeV}$, 10^{10} years eff. 9-43511
- ⁴He target in deuteron scatt., polarization obs. 9-44212
- ⁴He-³He n virtual process coupling const. determ. from ⁴He(p,d)³He, $E_p=31-156 \text{ MeV}$ 9-29718
- ⁴He first excited state of 3MeV obs. in ⁹Be decay 9-27627
- ⁴He, binding energy determ. from Λ N potential 9-42111
- ⁴He binding energies by Hartree-Fock model 9-42209
- ⁴He(N,n) non-relativistic crossed partial-wave expansion, $E_n=66-312 \text{ MeV}$ 9-22778
- ³He(α , γ)³He, cross section meas., $E_a=164-245 \text{ keV}$ 9-27747
- ³He(d,d), ang. distrib. of vector analyzing power E_d (pol.)=4-10 MeV 9-42302
- ³He(d,d)⁴He, resonating-group analysis 9-38709
- ³He(d,p)⁴He, ang. distrib. of vector analyzing power E_d (pol.)=4-10 MeV 9-42302
- ³He(d,p)⁴He, polarized d, asymmetry of p emission, $E_d=6-10 \text{ MeV}$ 9-44214
- ³He(γ , π^0)³He, 340 MeV, section obs. 9-48326
- ³He(γ , K⁺)⁴H, photoproduction of hypernuclei and cross-sections 9-29721
- ³He(γ , p)³H, ⁴He excited states obs. 9-32305
- ³He(γ , p)³H, giant reson. fine struct. 9-48328
- ³He(γ , pn)³H, total cross-section 9-46231
- ³He(γ , π^0)³He, 340 MeV cross-section obs. and compared with impulse approx. calc. 9-27699
- ³He(p,d), pick-up and final state interactions obs., $E_p=156 \text{ MeV}$ 9-42282
- ³He(p,d)⁴He diff. cross section peripheral model anal., $E_p=31-156 \text{ MeV}$ 9-29718
- ³He(p,p), target polarized by optical pumping, left-right scatt. asymmetry, $E_p=3.8-10.9 \text{ MeV}$ 9-29793
- ³He(p,p)³He, continuum shell model 9-44195
- ³He(p,p) expt. and multiple collision and optical model theory comparison 9-25618
- ³He(p, ρ), polarization meas., phase-shift anal., $E_p=4-11 \text{ MeV}$ 9-25628
- ³He(p, ρ), spin- correlation parameter meas., phase-shift anal., $E_p=8.8 \text{ MeV}$ 9-25629
- ²H(n, $2n$)³H coincident neutron spectra, n-n scatt. length determ. 9-44208
- ²H(n, γ)³H, γ transition meas., n separation energy determ. 9-38645
- ²H(n,n), diff. cross section meas., $E_n=5.6-9.1 \text{ MeV}$ 9-27729
- ²H(n,nn), cross section meas., $E_n=4.0-6.5 \text{ MeV}$ 9-34455
- ²H(p, $2p$), 6.5-13.0 MeV, obs. of quasifree and sequential decay mechanisms 9-48338
- ³H(p,n)³He, 1 MeV flux meas., associated particle method, ³He no. and direction determ. 9-29640
- ²H(p,p), polarization and ang. distrib. meas., $E_p=11-23 \text{ MeV}$ 9-27716
- ²H(p,p)³H, p polarization meas., $E_p=9.5$ and 21.6 MeV 9-22781
- ²H(p,pp)n, corrections to impulse approx., ang. distrib. meas., $E_p=155 \text{ MeV}$ 9-34448
- ²H(p,pp)n, energy, ang. distrib. and cross section meas., 1st order impulse approx., $E_p=155 \text{ MeV}$ 9-32346

Nucleic acids see *Macromolecules***Nucleons and antinucleons**

- see also *Cosmic rays/nucleons; Neutrons and antineutrons; Nuclear reactions and scattering due to/nucleons; Protons and antiprotons*
- charge commutation relation matrix elements, arbitrary momentum 9-22618
- e.m. form factor and n electric dipole moment 9-22542
- e.m. form factors, quasi-independent quark model 9-48206
- e.m. form factors expression in terms of ρ , ω and ϕ resonances 9-22619
- e.m. mass and coupling-constant shifts of N and Δ (1238) in bootstrap model 9-46115
- flux intensity in atmosphere, calculated specific yield functions for neutron monitors 9-29634
- form factors, e.m. evidence for q^{-6} depend. 9-46114
- form factors, superconvergence and asymptotic behaviour 9-27547

Nucleons and antinucleons continued

- formfactor, e.m., decrease exponential character, lower bound determ. 9-29576
- isovector magnetic moment from low energy sum rules 9-27479
- magnetic moment, anomalous, calc. from sidewise dispersion reln. 9-38560
- magnetic moments in strong coupling meson theory 9-32209
- meson-nucleon Lagrangians, chiral SU(2) \times SU(2) symmetric, construct. 9-27493
- resonances, simple phenomenological model 9-38559
- structure determ. from NN and π N collision multiplicity distrib. functions 9-38563
- weak axial vector amplitudes generalized sum rules, π N spin-flip sum rule determ. 9-38558
- Λ KN coupling constant g_{Λ}^2 from KN dispersion relations disagrees with SU(3) symmetry 9-34294
- N mag. moments and g_{μ}/g_V , rel. bet. sidewise dispersion relation calc. using $J=1/2$ baryon reson. model 9-22622
- N-N* transition, γ NN* vertex momentum-transfer depend., dispersion theor. model 9-29605
- p-n mass diff. and form factor calc. by gravitational Ward-Takahashi identity 9-38577
- ρ -N coupling magnetic moment as parameter in π N phase shift analysis 9-46103
- antinucleons**
- No entries
- interactions**
- Baryons resonances [dd D₁₃ prod in π N \rightarrow π D₁₃ and π D₁₃ D₁₃] coupling constant 9-44026
- internucleon parity violating pot. negligibility on using field-current identity 9-34319
- meson-N coupled systems soluble model 9-34277
- meson-N form factor, one boson exchange model and L₂ interaction 9-34318
- photoproduction of π on N, magnetic quadrupole amplitude 9-25455
- π N production mechanism 9-29583
- eN \rightarrow π N, γ NN* vertex momentum-transfer depend., dispersion theor. model 9-29604
- γ NN \rightarrow NN π , soft π prod. at threshold, theory, S-matrix element 9-38562
- γ N, π production, dispersion analysis 9-38519
- γ N with π prod., evaluation of multipoles 9-22592
- γ N \rightarrow N π , kinematically free amplitude Reggeization method applic. 9-27519
- γ N \rightarrow VB, photon-vector-meson analogy model, diff. cross section, polarization, helicity density matrix reln. 9-34320
- γ N \rightarrow γ B, photon-vector-meson analogy model, diff. cross section, polarization, helicity density matrix reln. 9-34320
- γ N \rightarrow π , cross section, threshold determ., PCAC theory, $E_\gamma=160-230 \text{ MeV}$ 9-29606
- γ N \rightarrow π_0 N, photoproduction at low energy limit in chiral dynamics 9-48188
- KN, production mechanisms 9-29583
- KN \rightarrow Δ π , vertex function, nature rel. to Deck effect 9-48202
- KN \rightarrow K \bar{K} , superconvergence and Y₁^{*}(1385)BP coupling 9-22636
- KN \rightarrow K⁺(890) π Regge pole anal., $M_K=2-13 \text{ GeV/c}$ 9-22583
- Λ N, from data on bound energies of Λ He⁴, Λ He³ and Λ He⁶ 9-27628
- Λ N, π -photon exchange, charge symmetry violating eff. 9-34332
- Λ N reviewed, forces, models 9-36497
- Λ N \rightarrow Σ N, virtual transition eff. on Λ d binding energy, Faddeev theory applic. 9-44061
- N₁N₂ \rightarrow π π , isospin matrices and projection operators 9-38561
- N₁ π \rightarrow N₂ π , isospin matrices and projection operators 9-38561
- pN, 22.6 and 24 GeV/c, multiple particle production 9-32214
- pN, in nuclear emulsion, grey track selection method, $M_p=24 \text{ GeV/c}$ 9-29608
- pN, secondary charged particles ang. distrib., $E_p=20 \text{ GeV}$ 9-34322
- pN 16 GeV/c, effective-target-mass calc. 9-40438
- π photoproduction from nucleon, dispersion analysis 9-44022
- π N, 28 GeV/c, effective-target-mass calc. 9-40438
- π N, in nucleus, Fock transformation 9-34303
- π N, multiplicity distrib. regularity determ., threshold to 27 BeV 9-38563
- π N 3.86 GeV in freeon bubble chamber 9-25643
- π N \rightarrow Δ K⁺(890) π , study of K⁺(1300) 9-48202
- π N \rightarrow Δ π , or Δ π ; kinematically free amplitude Reggeization method applic. 9-27519
- π N \rightarrow VN, V Δ helicity amplitude reggeization, production cross section determ. 9-34304
- π N \rightarrow ω N, ρ +B Regge pole exchange model 9-32188
- π N \rightarrow π D₁₃, superconvergent relation and π D₁₃D₁₃ coupling constant 9-44026
- π N \rightarrow π N π , Treiman-Yang angle anisotropies explained 9-25477
- π N \rightarrow ρ Δ , at high energy, conspiracy relations and O(3,1) symm. 9-38527
- π N \rightarrow ρ Δ , forward peak existence, explanation 9-34300
- ρ N cross section meas., Glauber theory applic. 9-38483

interactions, nucleon-nucleon

- elastic, strong-coupling solns. of mes. field theory with hard core 9-27548
- in intranuclear cascades, asymmetry in energy distrib. 9-32290
- multiplicity distrib. regularity determ., threshold to 27 BeV 9-38563
- and nuclear forces, repulsive core 9-40464
- partial-wave scatt. amplitudes, off-energy-shell behaviour of potential models 9-38564
- review 9-36555
- triplet-odd, and spin-orbit splitting 9-34378

interactions, pion-nucleon see *Pions/interactions, pion-nucleon***scattering**

- Compton dominated by Pomeranchukon exchange, evidence from e-N scatt. 9-32128
- Compton scatt., invariant amplitudes and 3rd-order low-energy theorem 9-22522
- electron-nucleon inelastic scatt., field theoretical model 9-22534
- lepton-nucleon, asymptotic sum rules at infinite momentum 9-38566
- meson-nucleon, Regge pole model test 9-40417
- narrow resonances from unbound states in cross sections 9-40463
- parity-degenerate N Regge trajectory, residue zeros 9-27551
- phase-shifts, low-energy calc. with model including only N, N*, ρ , intermediate states 9-46103
- e-N for scatt. on light nuclei 9-25614
- γ N \rightarrow γ N, at high energies, space-time picture 9-48207
- KN, data for possible determ. π Λ σ couplings 9-46104

Nucleons and antinucleons continued**scattering continued**

- KN, small angle, Regge-pole eikonal theory 9-38516
 KN low energy, finite-energy sum rule check of Kim's analysis 9-32179
 KN sum rules based on Khuri amplitude, degeneracy of Regge trajectories 9-48178
 KN→KN, S-wave scatt. length calc. taking into account symmetry breaking of chiral SU(3)⊗SU(3) 9-27511
 AN, potentials and ^3He , ^4He binding energies determ. 9-42111
 N-d, d polarization, in impulse approx. framework 9-32210
 NN, absence of backward peaks, rel. to existence of meson towers 9-48200
 Nd, in $S=1/2$ state, effective range expansion 9-42099
 Np→ $\Delta\pi$, static multipole moments of Δ_{1236} ($3/2, 3/2$) from superconvergence 9-38595
 $\pi N \rightarrow \Lambda \pi \mu$, S-wave $\pi\Lambda$ phase shift information 9-32192
 πN , multichannel-potential model applic. to $I=1/2$, $J=1/2^+$ state 9-36478
 π , B $^+$ forward spin flip amplitudes asymptotic behavior 9-46102
 πN , amplitude, $E_\pi < 2$ GeV, parametrization 9-27527
 πN , charge exchange scatt., dip mechanisms at $J=1$ 9-32211
 πN , chiral algebra and PCAC applic., sum rules determ. 9-42294
 πN , dispersion sum rules analysis at intermediate and high energies 9-34310
 πN , inelasticity functions and partial-wave driving forces at large energies 9-46107
 πN , low-energy parameters calc. 9-34309
 πN , low-energy parameters calc. 9-48195
 πN , partial wave analysis of Regge amplitudes using Regge-pole model 9-44031
 πN , Regge-pole parameter dispersion sum rules applic. 9-22562
 πN , Regge pole generalized interference model for resonance region 9-29589
 πN , ρ dominance, PCAC consistency condition, dispersion-theoretic derivation 9-34308
 πN , S-wave scatt. length, tree-diagram calc. method 9-38475
 πN , s-wave scatt. length Fubini-Furlan on-shell formula 9-34286
 πN , sum rules for backward direction 9-40427
 πN , u-channel Regge pole exchanges, structure energy and total cross section depend. 9-40429
 πN , virasoro model for representation of amplitude containing Regge behaviour, crossing symmetry and analyticity 9-48192
 πN , low energy theorems from dispersion relations and crossing symm. 9-32194
 πN baryon trajectory derivatives at $W=0$ 9-48194
 πN Coulomb corrections to phase shifts by dispersion theoretical calc. 9-40428
 πN crossed channel Regge pole study of scatt. amplitudes 9-32195
 πN dispersion relations and low energy parameters derived 9-32196
 πN N/D eqn. solved, inclusion of Castillejo-Dalitz-Dyson poles 9-32197
 πN partial waves at low energies and in unphysical region 9-25466
 πN polarization and spin-rotation predictions from Regge poles 9-45571
 πN resonance widths, evaluated in the SL(2, C) model of Regge poles 9-42081
 πN S and P waves in πN δ approx. and 33-resonance dominance 9-29593
 πN three-channel model including πN and σN 9-48193
 $\pi\pi$ isovector form factors, momentum transfer depend. distant contrib. 9-48191
- scattering, nucleon-nucleon**
 $^1\text{S}_0$ phase shift, soln. of Nambu-Salpeter-Bethe equation 9-44049
 dynamical theory using universal coupling scheme of primary interac. 9-27550
 elastic cross-section, new formula 9-25480
 flow energy eff. of structure and high energy phenom. 9-22620
 form factors eff. in one-boson-exchange model, K-matrix method 9-34321
 formalisms, relativistic, non-relativistic and angular momentum 9-40440
 meson, heavy pseudoscalar, coupling const. determ. 9-42055
 meson exchange, repulsive core and nonstatic effects in momentum space 9-44050
 non-relativistic 2-nucleon potential, general representation 9-42166
 non-relativistic 2-nucleon potential, general representation 9-38634
 O_4 propagators, Toller poles reduction to Regge poles 9-36492
 off-forward, high-energy, $O(3,1)$ partial-wave analysis, qualitative aspects 9-22621
 one-boson exchange, and 2 or 3π exchange, $T=O$ states 9-32212
 phase shift analysis, 400 MeV→10 GeV, review 9-40439
 phase shift analysis at 400 MeV 9-27549
 phase shift analysis near 20 MeV, use of τ -criterion for discrimination 9-46047
 phase shift contributions, 2π exchange, Feynman diagram calc. 9-38565
 phase shifts analysis of effective tensorial interaction 9-29684
 phase shifts and mixing parameters, 0-400 MeV, separable-potential fit 9-44048
 polarization effects rel. to phase shift and Regge trajectory determ. 9-27443
 Regge amplitude limit for large values of s and k_{\perp}^2 9-29561
 NN, possible dip mechanisms at $J=1$ 9-32211
 $\pi\pi$ and $\pi\pi\pi$ exchange-contributions one-boson exchange mode, elimination of scalar meson 9-44051

scattering, pion-nucleon *see Pions/scattering, pion-nucleon***Nucleus**

- see also Elements/origin; Hypernuclei; Radioactivity; Scattering, particles*
 charge distrib., energy-density formalism applied to isotope shift 9-42197
 charge distribution, investigations with muonic atoms 9-38632
 heavy, relativistic, refined formula for charges 9-46196
 many-body problem by variational method 9-42188
 nuclear effective charge calc. from valence electron spectra 9-38761
 stable nuclei, systematic classification method 9-40462
 structure from (d,p), (d,t), reactions, review 9-34380
 structure investigations by means of high-energy probes 9-32287
 vibrational and rotational motion, even nuclei, unified microscopic theory 9-34381
 d clustering, Hartree-Bogoliubov theory, Pauli principle and single particle potential 9-34369
 ^{192}Pt , from ^{191}Ir decay, E_2/M_1 mixing ratio determ. 9-32324
 ^6Li , charge form factor calc. in Born approx. 9-44130
 Sn isotopes, structure props. investigated using inverse-gap-equation and quasiparticle theories 9-46203

Nucleus continued**electric moment***see also Molecules/nuclear coupling*

- core polarization eff. on E2 operator, Tabakin interaction 9-32294
 E2 transitions in doubly even sd shell, 2^+ state excitation 9-27618
 E1c reduced probabilities calc. using Nilsson and Saxon-Woods potentials 9-48257
 even nuclei, quadrupole transition probabilities 9-27617
 even-even spherical nuclei, elc. quadrupole transition probabilities 9-42191
 hexadecapole moment in electrostatic triple field gradient, classical calc. of precession 9-36566
 multipole growth of low-lying excited state, RPA, Thouless theorem extension 9-22714
 odd non-axial nuclei, E2-transitions and dipole mean values 9-36565
 odd non-axial nuclei, sum rules for dipoles and E2-transitions 9-34385
 quadrupole, static, of excited states, determ. 9-47306
 quadrupole couplings of β -radioactive nuclei 9-29708
 quadrupole moment of $N=Z$, $Z+2$, $Z+4$ even-even nuclei, with 2s, 1d shell filled 9-48252
 quadrupole moment ratio for even-even spherical nuclei, description from phonon model 9-44112
 quadrupole transition probabilities in even nuclei 9-27617
 spin-quadrupole interactions, influence on 2^+ vibrational states 9-44120
 sum rules for dipoles and E2-transitions of non-axial odd nuclei 9-34385
 transitions, E2, and dipole mean values in non-axial odd nuclei 9-36565
 ^{140}Ce , $(p,p')^{141}\text{Pr}$, γ spectra meas., E1 transition and β matrix elements determ., $E_\gamma=9-11$ MeV 9-29735
 ^{160}Dy , low-lying E2 transitions, internal conversion-electron particle parameters 9-29737
 ^{15}Sm E1, E2 multiplicities calc. from relativistic Hartree-Fock-Slater wave functions 9-25576
 ^{15}Sm γ internal conversion, E1, E2 transitions on K shell, $E_\gamma=1-9$ MeV 9-29765
 ^{15}Sm type 'spherical' nuclei, E2+E0 transitions 9-40481
 ^{15}Sm type 'spherical' nuclei, E2+E0 transitions 9-40482
 ^{13}Cs and ^{132}Cs quadrupole moments, optical double reson. obs. 9-42223
 ^{12}Sn , from spin and hyperfine struct. 9-42222
 ^{181}Ta , E2-transitions and dipole mean values 9-36565
 ^{152}Gd low-lying E2 transitions, internal conversion-electron particle parameters 9-29737
 ^{193}Pt , E2:M1 multipole mixing ratio from γ - γ meas. 9-25585
 ^{15}Sm , multipolarity of γ -transitions 9-44157
 ^{152}Sm E0/E2 intensity ratio determ., β - γ vib. band 9-22730
 ^{23}Th , charge distrib., intrinsic quadrupole moment, radius studied by obs. of muonic X-rays 9-38677
 ^{11}Sn , from spin and hyperfine struct. 9-42222
 ^{207}Tl , E2:M1 279keV transition mixing ratio from γ - γ directional and linear polarization 9-48301
 ^{114}Cd E1, E2 multiplicities calc. from relativistic Hartree-Fock-Slater wave functions 9-25576
 ^{114}Cd , γ internal conversion, E1, E2 transitions on K shell, $E_\gamma=1-9$ MeV 9-29765
 ^{234}U E2 43.5 keV transition, K, M subshell ratio determ. 9-25589
 ^{153}Gd , ^{157}Gd , from atomic beam mag. resonance obs. 9-22952
 ^{153}Gd in GdCl_3 , 86.5 keV level quadrupole moment, meas. 9-34402
 ^{160}Ho , E2-transition and dipole mean values 9-36565
 ^{160}Ho , electric quadrupole moment of resonant states meas. 9-27560
 ^{175}Lu , E2-transitions and dipole mean values 9-36565
 ^{175}Lu from ^{175}Hf decay, γ spectra meas., E2+M1 transitions, probabilities and mixing parameters determ. 9-22733
 ^{116}Cd to ^{116}Cd even isotopes, p scatt. ang. distrib. means., B(E2) ratio calc., $E_\gamma=14$ MeV 9-27713
 ^{167}Er , E2-transitions and dipole mean values 9-36565
 ^{177}Hf , E2-transitions and dipole mean values 9-36565
 ^{177}Lu , E2-transitions and dipole mean values 9-36565
 ^{208}Pb , E2 transition obs. in (γ , n) reaction, $E_\gamma < 40$ keV 9-27644
 ^{238}U charge distrib., intrinsic quadrupole moment, radius studied by obs. of muonic X-rays 9-38677
 ^{209}Bi , quadrupole moment calc. from h.f.s. of $6p7s^3P_1$ and $1P_1$ 9-40488
 ^{13}Ce E2 transition probability, unified model calc. 9-25578
 ^{19}Hg 158 keV E2 transition, N-subshell internal conversion coeff. meas. 9-40486
 ^{189}Os from ^{189}Ir , γ spectra meas., E2/M1 determ. 9-38676
 ^{159}Tb , quadrupole moment, from Tb II spectrum 9-38671
 ^{38}Ar , reduced E3 transition rate calc. 9-38657
 ^{75}As from ^{75}Se decay M1-E2 mixing ratio determ. 9-40479
 ^8Be , g.s. quadrupole moment from projected Hartree-Fock calc. for odd-parity state 9-27626
 ^{12}C , 10.8 MeV level, E1($\Delta T=0$) electroexcitation, form factors 9-25564
 ^{35}Cl , B(E2) of first two excited states and lifetimes meas. 9-29749
 Cs, odd mass, quadrupole moment and E2 transition rate, unified-model calc. 9-32309
 ^{18}F E2 decay strength determ. deformed states calc. 9-22718
 ^{19}F E1 transitions, wave functions and structure of odd parity states determ. 9-22717
 ^{57}Fe , E2/M1 mixing ratios lifetimes of levels from Coulomb excitation 9-27664
 ^{39}K , quadrupole moment determ. by resonance scatt. of light investig. of hyperfine struct. of $4p$ and $5p^2P_{3/2}$ -states 9-29751
 ^{40}K quadrupole moment determ. by new double resonance technique in KClO_4 9-29752
 ^{41}K , quadrupole moment determ. by resonance scatt. of light investig. of hyperfine struct. of $4p$ and $5p^2P_{3/2}$ -states 9-29751
 La, odd mass quadrupole moment and E2 transition rate, unified-model calc. 9-32309
 ^6Li , quadrupole moment, calc. using Green's and Tabakin's potentials 9-38648
 ^{24}Mg , quadrupole moment 9-48282
 ^{24}Mg static quadrupole moment of first excited state, obs. 9-29745
 N, quadrupole, from SCF calc. of NF_3 9-42403
 ^{13}N E1 transitions bet. resonant states near 3.51 MeV($3/2^-$) and 2.37 MeV($1/2^-$) levels 9-27621
 ^{14}N , quadrupole 9-42400
 ^{14}N , quadrupole, from MO calc. 9-27842
 ^{20}Ne , E2 transition rate calc., Hartree-Fock wave func. 9-25586
 ^{22}Ne , quadrupole moments of 2^+ levels deduced from ^{23}S scatt. 9-22736
 ^{60}Ni from ^{60}Cu decay, E2 transitions meas. 9-27681
 ^{62}Ni static quadrupole moment of first excited $J^\pi=2^+$ state 9-44141
 ^{160}O , 7.12 MeV level, E1($\Delta T=0$) electroexcitation, form factors 9-25564

Nucleus continued electric moment continued

- ¹⁰O, B(E2) values 0-0 transition matrix element determ. 9-42204
- ¹⁷O calc. of nuclear quadrupole moment 9-22962
- ¹⁸O E2 decay strength determ., deformed states calc. 9-22718
- ³¹P E2 transition prob. calc. from shell model wave functions 9-36585
- ²⁸Si, static quadrupole moment of first excited J⁼2⁺ state 9-44141
- ³⁰Si, reduced E3 transition rate calc. 9-38657
- ⁸⁶Sr decay of two 3⁺ states, E(3) transitions meas. 9-27669

energy level transitions

- ¹⁴³Nd 72.5 keV level, M1 with possible E2 admixture 9-25580
- anomalous conversion, e- γ angular correl. meas. 9-32299
- collective and two-particle (isomeric) states in 'spherical' even-even nuclei, props. 9-42189
- core polarization eff. on E2, M1 operators, Tabakin interaction 9-32294
- correlation of γ from energy level transitions summing effect correction 9-29639
- dipole and quadrupole γ transition, angular correl. coeffs. 9-48267
- E1, $\Delta K=0$ systematic difference between odd proton and odd neutron nuclei 9-42228
- E2 and M1 transitions and dipole moment calcs. for six non-axial odd nuclei 9-36565
- E2 transition probability ratios for transitions between low-lying rotational states 9-44124
- E2 transitions in doubly even sd shell, 2⁺ state excitation 9-27618
- e.m. and isoscalar transition rates, comparison for N>Z even-even nuclei 9-42187
- E1 and M1, reduced probabilities calc. using Nilsson and Saxon-Woods potentials 9-48257
- E1 in rare earth region using Saxon-Wood potential 9-22729
- even-even nuclei, 'spherical', collective and two-particle (isomeric) states props. 9-42189
- even-even spherical nuclei, e.m. transition probability 9-42191
- excited states, exponential decay, anomaly, field model soln. 9-22704
- isomers, p- and α -excited, with half-lives 0.02-15 msec, obs. 9-27660
- K-forbidden systematic study in mass ranges 160<A<190, and A>230 9-48265
- L subshell conversion intensities, meas. by 50-cm Fe-free β spectrometer at Uppsala, Sweden 9-38608
- lifetime meas. in picosecond range using coincidence techniques 9-42150
- lifetime measurements using Doppler effect on various nuclei with A=10 to A=21 9-36568
- lifetime of short-lived stat3s, effects of time-analyser sensitivity on errors 9-48268
- lifetimes, meas. using differential converter 9-42148
- M1, forbidden, probabilities for odd-A spherical nuclei 9-42195
- M1, meas. by 50-cm Fe-free β spectrometer at Uppsala, Sweden 9-38608
- magnetic dipole, between lowest rotational states of even-even nuclei 9-44125
- N>Z even-even nuclei, comparison of e.m. and isoscalar transition rates 9-42187
- nuclear state mean lifetimes, Doppler shift meas. method 9-29706
- odd, non-axial nuclei, E2 and M1 transitions calc. 9-36565
- photonicuclear reactions, isospin-selection forbidden, reasons for E1 transitions 9-25612
- radiation prod. by 20-50 MeV electrons in opt. freq. range, meas. of fast particle energy 9-40504
- rotational band levels γ transitions, ratio of reduced probabilities 9-42190
- vibrational states, core particle-hole excitations, transition prob. calc. 9-29705
- γ -transition probabilities, single particle, spherical harmonic oscillator pot. 9-34383
- γ transitions between levels of rotational bands, ratio of reduced probabilities 9-42190
- γ transitions following thermal neutron capture, partial widths 9-38643
- γ transitions induced by space-parity violation in nuclear forces 9-36589
- ³P, width of 3.51 MeV level 9-48274
- ¹⁴⁰Ce(p, γ), ¹⁴¹Pr, γ spectra meas., E1 transition and β matrix elements determ., E_g=9-11 MeV 9-29735
- ¹⁶⁰Dy, low-lying E2 transitions, internal conversion-electron particle parameters 9-29737
- ¹⁷⁰Er 2⁺ lifetime meas. by Coulomb excitation 9-27637
- ¹⁶⁰Er prod. by (⁴⁰Ar, 4n) react., lifetimes of rotational states 9-25581
- ¹⁶⁰Gd 2⁺ lifetime meas. by Coulomb excitation 9-27637
- ²¹⁰Pb, residual interaction model 9-40487
- ²²⁰Po, residual interaction model 9-40487
- ¹⁵⁰Sm, γ internal conversion, E1, E2, M1, M2 transitions on K shell, E_g=1-9 MeV 9-29765
- ¹⁵⁰Sm, K-conversion coeff., E1, E2, M1, γ transitions 1-17 MeV multipolarities calc. 9-25576
- ¹⁵⁰Sm type 'spherical' nuclei, E2+EO transitions 9-40481
- ¹⁵⁰Sm type 'spherical' nuclei, E2+EO transitions 9-40482
- ¹⁰⁷Te, γ resonance scatt., spectra meas., transitions obs. 9-27695
- ¹⁷⁰Tm, β (1 \rightarrow 2⁺), nuclear matrix elements, exptl. determ. 9-48297
- ¹⁷⁰Yb, 84.3 keV transition, α _g meas. 9-29739
- ¹⁷⁰Yb, γ transitions from ¹⁷⁰Lu radioact. decay obs. 9-25601
- ¹¹¹Cd E2 transitions obs. following bombardment 9-22741
- ¹⁶¹Dy, Coulomb excitation Mossbauer effect of 43.8 keV transition 9-36578
- ¹⁶¹Dy, half-life of 25.7 keV level, hindrance factor calcs. 9-42228
- ¹⁶¹Er, anomalous rotational band strong transitions obs. 9-36577
- ²²¹Fr, conversion electron spectra, transition multipolarity level obs. 9-32313
- ¹²¹Sb, ¹²¹Sb E2 transitions obs. following bombardment 9-22741
- ¹⁸¹Ta, 133-482 keV cascade, angular correlation meas. by differential method 9-38675
- ¹⁸¹Ta, 482 keV transition parity mixing, γ scatt., circular polarization meas. 9-27640
- ¹⁸¹Ta, γ circular polarization meas., n- $\pi\pi$ parity violating amplitude determ. 9-36580
- ^{242m}Am-²⁴²Am induced by n, negative result 9-48305
- ¹⁶²Dy, half-life of 1490 KeV level meas. 9-40485
- ¹⁵²Eu, new transitions identified 9-44157
- ¹⁵²Gd E0 transition meas. 9-22730
- ¹⁵²Gd low-lying E2 transitions, internal conversion-electron particle parameters 9-29737
- ¹⁹²Os, mixing ratio of 485 keV transition populated in ¹⁹²Ir decay 9-46213
- ¹⁹²Pt, mixing ratios of transitions prod. by ¹⁹²Ir decay 9-46213
- ¹⁹²Pt; from ¹⁹²Ir decay, E2/M1 mixing ratio determ. 9-32324

Nucleus continued energy level transitions continued

- ¹⁵²Sm, β -vibrational band \rightarrow ground-state rotational band, attempt to meas. intensities 9-46211
- ¹⁵²Sm, e.m. transitions in β - γ vibrational bands 9-40483
- ¹⁵²Sm, γ transitions, multipole mixing ratios not agreeing with single parameter hand-mixing theory of strong coupling model 9-27635
- ¹⁵²Sm, low-lying E2 transitions, internal conversion-electron particle parameters 9-29737
- ¹⁵²Sm, multipolarity mixing ratio of γ cascades 9-44157
- ¹⁸²W, multiple orders of low-energy γ transitions 9-44159
- ^{123m}Te isomeric transitions, investig. of accompanying radiation 9-46205
- ²⁴³Am γ and M1 transitions meas. 9-27651
- ¹¹³Cd investigated by means of ¹¹⁴Cd(d,t)¹¹³Cd 9-38667
- ¹³³Cs, 82 and 160 KeV states lifetimes 9-48294
- ¹³³Cs, from γ spectra following resonance n capture 9-25577
- ¹⁶³Er half life of 69.2 keV level, hindrance factor calc. 9-42228
- ¹¹³In^m, isomeric state half-life determ. from γ spectra 9-27630
- ¹⁹³Ir, angular correlation in 253-461 KeV cascade 9-42229
- ¹⁹³Ir γ -intensities meas., multipolarities calc., comparison with models 9-48298
- ¹⁴³Pm, 742 Kev transition, conversion line coeffs. 9-46207
- ¹⁰³Rh, 53 keV γ -ray K-shell internal conversion coeff. 9-46202
- ¹⁰³Rh(p,p') ¹⁰³Rh decay scheme obs., B(E2) determ. 9-25574
- ¹²³Sb, 160 KeV level lifetime meas. 9-48285
- ¹²³Te E2 transitions obs. following bombardment 9-22741
- ¹¹⁴Cd, K-conversion coeff., E1, E2, M1, γ transitions 1-17 MeV multipolarities calc. 9-25576
- ¹¹⁴Cm, γ internal conversion, E1, E2, M1, M2 transitions on K shell, E_g=1-9 MeV 9-29765
- ¹⁶⁴Dy 2⁺ lifetime meas. by Coulomb excitation 9-27637
- ¹⁴²Gd, 123 keV transition, K-shell particle parameter 9-38670
- ¹⁴²Gd 2⁺ \rightarrow 0⁺ rotational transition isomer shift determ., Mossbauer meas. 9-27636
- ¹⁵⁴Gd γ transitions, multipole mixing ratios not agreeing with single parameter hand-mixing theory or strong coupling model 9-27635
- ¹⁵⁴Gd; e.m. transitions in β - γ vibrational bands 9-40483
- ¹¹⁴In, double decay process, internal conversion studies, 192 keV transition 9-44150
- ²³⁴U, half-life of 2⁺ state at 990 keV 9-27649
- ²³⁴U 1552 keV level from ²³⁴Pu decay 9-25588
- ²³⁴U E2 43.5 keV transition, K, M subshell ratio determ. 9-25589
- ¹⁴⁵Gd from ¹⁴⁵Sm(^{He,2n}); γ spectra meas., isomeric transition, M4 prob. determ. 9-29736
- ¹⁵⁵Gd, from ¹⁵⁵Tb decay γ - γ coincidence spectra anal. 9-25563
- ¹⁵⁵Gd in GdCl₃, 86.5 keV level quadrupole moment meas., Mossbauer absorption 9-34402
- ¹¹⁵In, 35.6 keV transition, K-conversion coefficient meas. 9-42221
- ¹⁷⁵Lu from ¹⁷⁵Hf decay γ spectra meas., M1+E2 transitions, probabilities and mixing parameters determ. 9-22733
- ¹⁷⁵Lu directional correlation and conversion probability meas. for 114 KeV M1+E2 transition meas. 9-25584
- ¹⁰⁵Pd, 344 keV level lifetime 9-29724
- ¹⁸⁵Re, energy and intensities obs. 9-48318
- ¹⁵⁷Tb decay, γ - γ coincidence spectra, applic. of data processing method, ¹⁵⁷Gd level obs. 9-25563
- ¹⁷⁵Yb decay, 396 and 251 keV levels, fractional intensities for crossover and cascade 9-25583
- ¹⁰⁶Cd to ¹¹⁶Cd even isotopes, p scatt. ang. distrib. means., B(E2) ratio calc., E_g=14 MeV 9-27713
- ¹⁵⁶Er prod. by (⁴⁰Ar, 4n) react., lifetimes of rotational states 9-25581
- ¹⁶⁶Er, 80.6 keV transition, α _g meas. 9-29739
- ¹⁷⁶Hf, half-life of 1227.4 keV level meas., K-forbidden transition 9-40485
- ¹¹⁶In from ¹¹⁵In(n, α ,p) M1 transitions obs. 9-29727
- ¹⁴⁶Nd from ¹⁴⁶Pm decay, γ spectra meas., energy levels determ. 9-34420
- ¹⁴⁶Nd from ¹⁴⁶Pm decay, γ spectra meas. 9-34420
- ¹⁸⁶Os, E2/M1 mixing ratios of 2⁺ \rightarrow 2⁺ transitions 9-32321
- ²⁰⁶Pb, residual interaction model 9-40487
- ²⁰⁶Pd(p, n), cross section and resonances obs., γ and M1 transitions obs., E_g=40 keV 9-27644
- ¹⁴⁶Pm \rightarrow ¹⁴⁶Sm, γ spectra meas., energy levels determ. 9-34420
- ¹⁴⁶Sm from ¹⁴⁶Pm decay, γ spectra meas., energy levels determ. 9-34420
- ^{127m}Te isomeric transitions, investig. of accompanying radiation 9-46205
- ²⁰⁷Bi, isomeric state, high-spin, three-particle levels 9-42231
- ¹⁰⁷Cd, γ radiation 9-44149
- ¹¹⁷Cd decay scheme 9-44151
- ¹⁷⁷Hf [624] γ /2, rotational band, E2/M1 mixing ratios determ. 9-27638
- ¹²⁷Lu, resonance fluorescence from 375 KeV level obs. 9-29730
- ¹⁷⁷Lu decay, 208, 250 and 321 keV peaks, fractional intensities for crossover and cascade 9-25583
- ²⁰⁷Pb(p, n), cross section and resonances obs., γ and M1 transitions obs., E_g=40 keV 9-27644
- ¹⁰⁷Pd, obs. in ¹⁰⁷Rh, lifetime of 115.6 keV and other levels determ. 9-48311
- ¹³⁸Ba(n, γ)¹³⁹Ba, γ spectra meas., levels. determ. 9-38705
- ¹⁵⁸Er prod. by (⁴⁰Ar, 4n) react., lifetimes of rotational states 9-25581
- ¹⁵⁸Gd, 2⁺ lifetime meas. by Coulomb excitation 9-27637
- ²⁰⁸Pb, E2 transition obs. in (p, n) reaction, E_g=40 keV 9-27644
- ²⁰⁸Pb(p, n), cross section and resonances obs., γ and M1 transitions obs., E_g=40 keV 9-27644
- ¹³⁹Ba from ¹³⁸Ba(d,p); γ spectra meas. 9-38705
- ¹³⁹Ce M1, E2 moments and transition probability, unified model calc. 9-25578
- ¹⁹⁹Hg 158 keV E2 transition, N-subshell internal conversion coeff. meas. 9-40486
- ¹⁸⁹Os from ¹⁸⁹Ir, γ spectra meas., E2/M1 determ. 9-38676
- ¹⁴⁹Pm, 114 KeV state, gyromag. ratio obs. 9-46209
- ¹⁴⁹Sm, 286 KeV state life time 9-48294
- ¹⁵⁹Tb, from ¹⁵⁹Dy decay, angular correlation between K and L X-rays 9-46212
- ²¹Al from ²⁴Mg(α ,p) γ , p γ spectra meas., 4.58 MeV level obs., E_g=9-13 MeV 9-25656
- ³⁶Ar, reduced E3 transition rate calc. 9-38657
- ⁷⁵As, 199 KeV, 280 KeV level lifetimes meas. 9-48285
- ⁷⁵As from ⁷⁵Se decay M1-E2 mixing ratio determ. 9-40479
- ⁷⁵As half-life, times of three excited levels by delayed γ coincidences 9-48288
- ^{10B}, ^{nat}B, muon and pion yields in 2p-1s X-ray transition 9-22716
- ^{10B}, from ⁹Be(d,n) γ , γ -ray branching of 3.59 MeV state 9-29711

Nucleus continued

energy level transitions continued

- ¹¹B, recoil broadening of secondary transition following neutron capture in ¹⁰B 9-42201
- Be, μ and π yields in 2p-1s X-ray transitions 9-22716
- ⁸Be, 17.64-16.63 MeV transition nearly pure M1 9-48339
- ¹¹Be α -¹¹Be + γ e.m. transition rate calc. for ¹¹Be nuclear wavefn. information 9-44189
- ⁷⁹Br, Coulomb excitation, γ transition, E2 transition prob. determ. 9-46200
- ⁷⁹Br 217 KeV level lifetime meas. 9-48285
- ⁸¹Br, Coulomb excitation, γ transitions, E2 transition prob. determ. 9-46200
- C, μ and π yields in 2p-1s X-ray transition 9-22716
- ¹²C, prob. determ. from e scatt. data 9-34436
- ¹²C from ¹⁴N (α, α_d); α spectra meas., $E_\alpha=22.9$ MeV 9-38721
- ¹³C, 3.08 MeV level E1-electroexcitation, investigation 9-44132
- ¹³C, lowest $T=3/2$ states, γ decay modes and obs. 9-25565
- ¹³C from ¹⁴N (α, α_p); α p spectra meas., $E_\alpha=22.9$ MeV 9-38721
- ¹³C width of 3.68 MeV level meas. 9-48274
- ³⁸Ca, with positron decay, obs. 9-44181
- ⁴⁰Ca, lifetime obs. using ³⁹K(p, γ)/⁴⁰Ca reaction 9-44142
- ⁴⁰Ca, lifetimes, γ -decay spectra 9-42213
- ⁴⁰Ca, matrix elements calc. for dipole transitions 9-40474
- ⁴¹Ca low-lying parity states, transition rates, spectra calc., phonon-particle coupling model 9-32316
- ⁴²Ca from $6^+(3.19 \text{ MeV})$ to $4^+(2.75 \text{ MeV})$ state, from decay of $(7+)$ 6.15 keV in ⁴²Sc 9-42214
- Cd isomer, p excited, half-life and γ -spectrum, obs. 9-27631
- ³⁵Cl, B(E2) of first two excited states and lifetimes meas. 9-29749
- ³⁵Cl, $\delta(E2/M1)$ determ. for decay of 1.763 MeV level to ground state 9-46197
- ³⁵Cl, lifetime meas. of six lowest lying levels 9-42236
- ⁵⁷Co, excited through ⁵⁴Fe(α, p), between levels up to 1.90 MeV 9-29754
- ¹⁴C(p, γ)/¹⁵N, γ spectra meas., mixing ratio determ., $E_\gamma=352-634$ keV 9-29713
- ⁵³Cr E2 transitions obs. following excitation due to bombardment 9-22741
- Cs, odd mass, magnetic moment and M1 transition rate unified model calc. 9-32309
- Cu ($CA=59, 61, 63, 65$ and 67), calc. 9-38679
- Cu, induced by space-parity violation, enhancement of admixture coeff. 9-36589
- Cu, induced by space-parity violation, enhancement of admixture coeff. 9-36589
- Er isomer, p excited, half-life and γ -spectrum, obs. 9-27631
- ¹⁸F E2 decay strength determ., deformed states calc. 9-22718
- ¹⁹F, level lifetimes obs. 9-48277
- ¹⁹F, lifetime of first excited state meas. 9-48278
- ¹⁹F E1 transitions, wave functions and structure of odd parity states determ. 9-22717
- ¹⁹F excitation by α bombardment, level lifetime meas., $E_\alpha=5.5$ MeV 9-29741
- ⁵⁷Fe, E2/M1 mixing ratios lifetimes of levels from Coulomb excitation 9-27664
- ⁵⁷Fe, induced by space-parity violation, enhancement of admixture coeff. 9-36589
- ⁵⁷Fe E2-M1 absorption in Mossbauer spectra, transition probabilities calc. 9-22742
- ⁵⁷Fe E2 transition obs. following excitation due to bombardment 9-22741
- ⁵⁷Fe, E2/M1 mixing ratios of 2^+-2^+ transitions 9-32321
- ⁵⁸Fe from ⁵⁷Fe(n, γ); γ spectra meas., decay scheme determ. 9-32320
- ⁶⁹Ga, from inelastic n scatt. 9-38664
- ⁶⁹Ga 320 KeV level lifetime meas. 9-48285
- ⁷¹Ga, studied following inelastic n scatt. 9-38664
- ⁷¹Ga, formed in compound nuclear reactions, γ emission 9-27666
- ⁷⁴Ge, E2/M1 mixing ratios of 2^+-2^+ transitions 9-32321
- ⁷⁴Ge, E1+E2-transitions, integrated, total and differential cross sections 9-34387
- ⁸⁴K, sd shell, Tabakin interaction, e.m. transition rate, nuc. moment spectroscopic factor calc. 9-29750
- ³⁹K low-lying parity states, transition rates, spectra, calc., phonon-particle coupling model 9-32316
- ⁴⁰K from ³⁹K(n, γ) + 29.4 keV level lifetime determ. 9-27661
- La, odd mass, magnetic moment and M1 transition rate, unified model calc. 9-32309
- ⁶¹Li, form factors for 2.184 MeV C2 transition and 3.562 MeV M1 transition 9-27625
- ⁶¹Li, with of 3.56 MeV level 9-48274
- ^{80m}Br decay, energies and rel. intensities of β and γ transitions 9-42216
- ²⁴Mg, γ -decay of levels, from (³He, $d\gamma$) reaction, lifetimes of 5 states 9-36582
- ⁵³Mn, level at 1290 keV, γ -ray cascades 9-44146
- ⁵³Mn, found from α scatt., 50 MeV 9-34465
- ⁹²Mo, in-beam γ spectroscopy meas. 9-29758
- ¹³N, lowest $T=3/2$ states of decay modes and obs. 9-25565
- ¹³N E1 transitions bet. resonant states near 3.51 MeV ($3/2^-$) and 2.37 MeV ($1/2^-$) levels 9-27621
- ¹⁵N, recoil broadening of secondary transitions following neutron capture in ¹⁴N 9-42201
- ¹⁵N lifetimes and branching ratio of excited states 9-48280
- ²¹Na from ²⁰Ne ($d, n\gamma$), γ spectra meas. branching and mixing ratios determ. 9-34409
- ²¹Na second excited state mean lifetime 9-48281
- ²¹Na, lifetimes of 7 states below 5 Mw meas. by Doppler shift method 9-22737
- ²³Na($p, p'\gamma$) $\gamma\gamma$ correlation meas., levels deduced $E_p=4.71, 5.12$ MeV 9-48304
- ²⁰Ne, E2 transition rate calc, Hartree-Fock wave func. 9-25586
- ²⁰Ne, γ -decay of levels, from (³He, $d\gamma$) reaction, lifetimes of 3 states 9-36582
- ¹⁸Ne from ¹⁶O(³He, n); γ spectra meas., levels lifetimes, spin, decay modes determ. 9-25567
- ⁵⁸Ni, lifetimes of excited states produced by 7-9 MeV p scatt. obs. 9-48286
- ⁵⁸Ni, quadrupole and octupole transitions after electroexcitation, formfactors 9-44147
- ⁵⁸Ni induced by space-parity violation, enhancement of admixture coeff. 9-36589

Nucleus continued

energy level transitions continued

- ⁶⁰Ni, quadrupole and octupole transition after electroexcitation, formfactors 9-44147
- ⁶⁰Ni from ⁶⁰Cu decay, E2 M1, transitions, obs. 9-27681
- ⁶¹Ni 67 KeV 320 level lifetime meas. 9-48285
- ⁶¹Ni E2 transitions obs. following bombardment 9-22741
- ⁶¹Ni from ⁶¹Cu decay, obs. 9-27682
- ⁶²Ni, p ang. distrib. meas., meas., DWBA fits, γ spectra meas., levels determ., $E_\gamma=12$ MeV 9-32322
- ⁶⁴Ni, p ang. distrib. meas., DWBA fits, γ spectra meas., levels determ., $E_\gamma=12$ MeV 9-32322
- ⁶⁴Ni, quadrupole and octupole transitions after electroexcitation, formfactors 9-44147
- ¹⁵O lifetimes of excited states from Doppler broadening 9-48280
- ¹⁶O, B(E2) values 0-0 transition matrix element determ. 9-42204
- ¹⁶O, four-particle, four-hole band, phenomenological approach, e.m. transition probabilities 9-34393
- ¹⁶O, mean lifetime of 10.94 MeV state meas. 9-46195
- ¹⁶O, new 0^+ state, evidence from e scatt. data, $E_x=14$ MeV, monopole matrix element, transition radius and width determ., $E_x=14$ MeV 9-42205
- ¹⁶O giant resonance in ¹⁶O(γ, n_0) ¹⁵O 9-38693
- ¹⁶O matrix elements calc. for dipole transitions 9-40474
- ¹⁸O E2 decay strength determ., deformed states calc. 9-22718
- Os transition matrix elements, E2, M1, signs of 9-44161
- ³¹P M1, E2 transition prob. calc. from shell model wave functions 9-36585
- Pt transition matrix elements, E2, M1, signs of 9-44161
- ²³Rb 150 KeV level lifetime meas. 9-48285
- ⁸⁵Rb, Coulomb excitation, γ transitions, E2 transition prob. determ. 9-46200
- ⁸⁵Rb, half-life of 514 KeV state obs. 9-40491
- ⁸⁴Ru, in-beam γ spectroscopy meas. 9-29758
- ²³S B(E2) determ. from meas. lifetime of 4.46 MeV level; compared with theor. calc. 9-29747
- ⁴³Sc, $d_{3/2}$ - $f_{7/2}$, effective absorption for neutrons and protons 9-25592
- ⁷²Se, Coulomb excitation, γ transitions, E2 transition prob. determ. 9-46200
- ²⁶Si levels, spins, γ -branching and mixing ratios determ. from γ spectra 9-32314
- ²⁷Si decay and γ -ray spectra of various levels 9-27654
- ²⁸Si, decay of 9.699 MeV level 9-44140
- ²⁸Si, γ -decay of levels, from (³He, $d\gamma$) reaction, lifetimes of 8 states 9-36582
- ²⁸Si from ²⁵Mg($\alpha, n\gamma$), 8.543 MeV level lifetime meas., $E_\alpha \sim$ threshold energy 9-38655
- ²⁹Si, mean lives of states below 5 MeV by Doppler shift attenuation method 9-42211
- ³⁰Si, reduced E3 transition rate calc. 9-38657
- ³¹Si multiple mixing ratios, γ -ray branching ratios 9-27659
- Sn isomer, p excited, half-life and γ -spectrum, obs. 9-27631
- ⁸⁶Sr decay of two 3^- states, E(3) transitions meas. 9-27669
- ⁸⁶Sr, half-lives and energies of 2^+ and 3^- states 9-36590
- ⁹⁷Tc, isobaric analogue states, γ transitions to low lying states 9-29760
- ⁹⁷Tc and ^{98m}Tc γ -ray spectra, half-life obs. 9-48290
- ⁹⁷Tc and ^{98m}Tc γ -ray spectra, half-life obs. 9-48290
- ⁹⁷Tc, multipolarity of 40.584 keV transition 9-29773
- ⁴⁸Ti($p, p'\gamma$), lifetimes and branching ratios determ., Doppler-shift attenuation method 9-38659
- ⁵¹V 320 KeV level lifetime meas. 9-48285
- W transition matrix elements, E2, M1, signs of 9-44161
- ⁶⁶Zn, ground-state transition width of 7368 keV level by nuclear resonant scatt. 9-46217
- ⁹¹Zr E2 transitions obs. following bombardment 9-22741
- ⁹²Zr, γ E2 transitions obs. following bombardment 9-22741

energy levels

see also Radioactivity/decay schemes

- 2^+ vibrational states, influence of spin-quadrupole interactions 9-44120
- ¹³⁹La, from decay of ¹³⁹Ba, structure of $5/2^+$ state 9-29767
- ⁹²Mo, low lying states excited via analog resonances produced in p scatt. 9-48289
- from (n, γ) reactions using polarized thermal n and meas. γ polar 9-27725
- A=30-65, level density energy dependence, Fermi gas model corrections 9-27657
- A=6 nuclei, realistic nonsingular potentials and level spectra 9-38648
- A=90 region, spectra of particle-hole type excitations 9-38665
- actinide nuclei, level density depend. on excitation energy 9-22738
- anharmonic, of spherical nucleus, description from phonon model 9-44112
- anisotropic oscillator model calc. 9-29694
- β -vibrational state in deformed nuclei, identification 9-40469
- γ -band inertial parameter in even-even nuclei 9-25561
- classification and description 9-46185
- classification and description 9-36556
- collective excitations phenomenological potential, Schrodinger eqn. determ. 9-29702
- collective vibrations in theory of finite Fermi systems 9-22710
- collective-model theory 9-29704
- coupling between single-particle and vibrational states using Hamada-Johnston pot. 9-27648
- deformed nuclei, equilibrium deformations of states, shape isomers 9-48258
- deformed nuclei wave function symmetry under time reversal and change in sign K 9-48256
- deformed odd-odd nuclei, magnetic props. of rotational levels 9-48266
- density calc., agreement between (d, n) reaction isomeric ratio calc. and superconductor model 9-27743
- density parameters and mass shell corrections, relationship 9-38636
- distributions at low energy for A \leq 70, Fermi gas model calc. 9-27613
- energies and eigenfunctions in average field, using nonlocal potential calc. 9-48259
- even nuclei, collective quadrupole states 9-44115
- even nuclei $16 \leq A \leq 254$, lower states using collective degrees of freedom 9-48263
- fine structure, splitting estimated, P and CP violation 9-32298
- form factors 9-36571
- giant-resonance form., cross sections near threshold of reactions 9-46230
- ground state correlations for model Hamiltonian 9-44116

Nucleus continued

energy levels continued

- ground-state energy, upper bound of many-body system 9-48249
isobaric analogue resonances, energy- asymmetry, model-independent descrip. 9-42182
isolated level, description in terms of effective range theory 9-46188
level densities from excitation functions of isolated levels 9-48287
level density, mass no depend., investigation using (α , n) reactions 9-34466
level density of a Fermi system, nonperiodic perturbations of the energy-level scheme 9-38262
light closed-shell nuclei, ground state props., reaction matrix eqn. soln 9-40466
light nuclei, classification of excited states in translation invariant shell models 9-44129
light nuclei, classification of states, orthogonal group O_{n-1} representation, reduction to symmetrical group S_n representation 9-29709
light nuclei, classification of states, p- and sd-shell nuclei 9-29710
many-body system, variational method for ground state props. 9-42188
mass number 6, 7, 8, 12, 13, energy level and magnetic moment calc. using central interaction plus spin-orbit interaction 9-27616
multiple analysis of particle-particle and particle-hole multiplets 9-38641
Nilsson model calc. 9-29694
odd non-axial nuclei, sum rules 9-34385
one-nucleon transfer reactions on deformed nuclei 9-44117
phenomenology, review 9-36555
probes using high-energy particles 9-40461
Racah coefficient multiple analysis of particle-particle and particle-hole multiplets 9-38641
seniority and quasispin, relation, generalization to arbitrary groups 9-44118
seniority-1 states of the Hamiltonian 9-42184
shell model, translation-invariant, calc. for $A=4,5$ 9-27624
shell-model theory, correlation effects 9-29704
some-closed nuclei, four-particle two-hole core excitation 9-40467
spectra and ang. distrib. meas. from (p, d) reaction, $E_p=156$ MeV 9-25621
spherical odd-A nuclei, quasiroational band existence 9-48260
sum rules for non-axial odd nuclei 9-34385
surface cluster states, at 10-30 MeV 9-46190
Tamm-Dancoff modified approx., unfilled n and p shell description 9-29700
variable-moment-of-inertia model, g.s. band, even-even nuclei anal. 9-27609
variational calc., based on method of steepest descent in Hilbert space 9-22708
vibrational and rotational motion in even nuclei, a unified microscopic approach 9-25562
vibrational nuclei, calc. of ground-state correlations, methods 9-44121
vibrational states, core particle-hole excitations, energy levels, transition prob. calc. 9-29705
 γ emission, tables of coeffs. for ang. distrib. analysis 9-32300
 $^{11}_2$ Na from 20 Ne(d, γ), γ spectra meas. 9-34409
 50 Y from 89 V(d,p) excitation curves, ang. distrib., spectroscopic factors, DWBA anal., $E_p=4$ MeV levels determ. 9-22825
 110 Ag, angular distributions of 53 levels, analysis by (d,p) reactions 9-29726
 110 Ag, level diagram, 0-2 MeV deduced from 109 Ag(n, γ) 110 Ag 9-27727
 110 Ba, neutron resonances 9-22727
 210 Bi low-energy spectra from shell model calc., vel.-depend. effective N-N potential 9-40480
 140 Ce, two-quasiparticle states of proton system, evidence for, from 140 Pr decay 9-48296
 140 Ce(p,p), p ang. distrib. meas., $E_p=9.4-11.7$ MeV 9-29734
 160 Dy, nuclear g-factor, ang. correlation, Larmor precession freq. of 966 keV level 9-25582
 160 Dy, odd levels, props. from angular correlation techniques 9-36576
 170 Er from electron capture decay of 170 Tm 9-29774
 180 Gd, rel. to resonance parameters 9-22731
 200 Hg, 1029 keV level spin 9-46214
 200 Hg, low-lying excited levels 9-34404
 200 Hg, quasiroational band, existence 9-48291
 210 Pb, low-energy spectra from shell model calc., vel.-depend. effective N-N potential 9-40480
 210 Pb, residual interaction model 9-40487
 210 Pb spectra calc., realistic interaction, eff. of Woods-Saxon wave function 9-38653
 110 Pd from 110 Pd(16 O, γ), Coulomb excitation, γ spectra meas., $E_o=42-49$ MeV 9-22722
 210 Po, residual interaction model 9-40487
 160 Tb, short-lived states excited in (n, γ) reaction 9-38666
 170 Yb, excited states obs. from 170 Lu radioact. decay 9-25601
 170 Yb, from 170 Lu decay, scheme obs. 9-48317
 111 Ag from 110 Pd, γ spectra meas. 9-34419
 113 Cs, angular correlations determ. 9-29731
 131 Cs and 132 Cs, $7F_{3/2}$ state, hyperfine splitting, optical double reson. obs. 9-42223
 111 In from 111 Cd(d,n); γ and n spectra meas., $E_p=4.2-5.35$ MeV 9-42220
 211 Pa coriolis interaction, between three Nilsson bands 9-27629
 141 Pr from 142 Nd(d, 3 He); 3 He energy, ang. distrib. meas., $E_d=29$ MeV 9-32311
 141 Pr structure, expt. cf. with shell model calc. 9-42225
 141 Pr(p, γ), γ spectra meas., $E_p=4.8-7.7$ MeV 9-27634
 121 Sn, hyperfine struct. determ. by atomic-beam magnetic resonance technique 9-42222
 231 Th from 232 Th(3 He, α); α ang. distrib. meas., $E=30$ MeV 9-29830
 171 Tm from 171 Er decay, γ spectra meas. 9-32310
 110 Ba, neutron resonances 9-22727
 152 Gd, rel. to resonance parameters 9-22731
 142 Pr, from 141 Pr(n, γ) 142 Pr obs. 9-46237
 192 Pt from 192 Ir decay, γ spectra meas. 9-32324
 192 Pt, from 196 Au decay, partial radiative widths obs. 9-48300
 222 Rn, spin 3- vibrational level and second rot. term of fundamental band, from α -decay of 226 Th 9-48303
 152 Sm, from 152 Eu decay, revised level scheme 9-44157
 232 Th, level density following bombardment with 14.7 MeV 9-27766
 121 Tm excited levels from 162 Yb decay 9-46225
 241 Am from 242 Pu(n, γ), γ spectra meas. 9-27651
 241 Am from 247 Bk decay, α spectra meas. 9-27651
 113 Cd studied using 112 Cd(d,p) 113 Cd 9-38667

Nucleus continued

energy levels continued

- 163 Er, ground-state spin obs. 9-36579
 153 Eu, from 153 Sm β decay 9-27675
 191 Ir structure determ. from β -decay of 192 Os 9-48298
 193 Os- β - 193 Ir, energies and spins of Ir 9-34403
 231 Pa Coriolis interaction, between three Nilsson bands 9-27629
 141 Pm single-particle self-energies, 2-body matrix elements calc. 9-29733
 109 Rh from 109 Pd decay 9-38688
 109 Rh(p, γ) 109 Rh decay scheme obs. 9-25574
 113 Sn, hyperfine struct. determ. by atomic-beam magnetic resonance technique 9-42222
 134 Ba, 1580 KeV level not obs. 9-48295
 134 Ba, from decay of 134 Cs 9-22758
 134 Ba from 134 Cs decay, γ spectra meas. 9-32310
 114 Cd, from 114 In decay 9-29764
 114 Cd, quasiroational band, existence 9-48291
 134 Cs, levels excited in 133 Cs(n, γ) reaction 9-44156
 134 Cs, short-lived states excited in (n, γ) reaction 9-38666
 154 Gd, rel. to resonance parameters 9-22731
 204 Hg, shell model study of n-p correlations 9-48253
 114 Sn from 114 In decay 9-29764
 124 Te, energy level scheme determ. from 123 Te(n, γ) 124 Te 9-38668
 124 Te, from 124 Sb decay, 60d and 1.5 min isomers 9-27673
 124 Te scheme, from 124 Sb decay 9-48292
 184 W, metastable excited level 9-44160
 163 Er, excited states, props. 9-38672
 149 Eu single-particle self-energies, 2-body matrix elements calc. 9-29733
 155 Gd, from 155 Tb decay γ - γ coincidence spectra anal. 9-25563
 175 Lu, Coriolis coupling between $7/2^+$ and $5/2^+$ bands 9-22733
 205 Pb from 206 Pb(d,t), t spectra meas., levels determ., $E_t=21.6$ MeV 9-27643
 193 Pt, Mossbauer effect of 129 keV state 9-48299
 157 Tb, from γ -ray spectra associated with 157 Dy- 157 Tb decay 9-44158
 127 Te, Coulomb excitation of levels 9-44152
 127 Te, nuclear g-factor of 322 keV intruder state 9-44153
 208 Tl, 2.61 and 2.69 MeV states, based on 3- state in 206 Pb 9-44163
 208 Tl, resonance and de-excitation levels 9-46215
 208 Tl level investigation using excitation with n-capture γ , anomalies 9-36573
 136 Ba, from 135 Ba(n, γ) 136 Ba obs. 9-46237
 136 Ba, level structure from 135 Ba(n, γ) 136 Ba reaction 9-42224
 168 Er from 167 Er(d,t), t spectra meas., $E_d=12$ MeV 9-22816
 146 Nd from 146 Pm decay, γ spectra meas. 9-34420
 206 Pb, 3- state, basis of 2.61 and 2.69 MeV states in 207 Tl 9-44163
 206 Pb, residual interaction model 9-40487
 206 Pb spectra calc., realistic interaction, eff. of Woods-Saxon wave function 9-38653
 206 Pb(n,n), diff. cross section, excitation function calc., levels determ. 9-40513
 166 Pd from 166 Rh, γ spectra meas. 9-22755
 166 Pd from 166 Pd(16 O, γ), Coulomb excitation, γ spectra meas., $E_o=42-49$ MeV 9-22722
 186 Re from (d, p), (d, t), (n, p) and (n, e $^+$) reactions 9-27641
 146 Sm from 146 Eu γ decay, internal conversion coeff. calc. 9-48312
 146 Sm from 146 Pm decay, γ spectra meas. 9-34420
 118 Sn, J=0 $^+$ states, pairing force and surface delta interaction, seniority 9-29756
 118 Sn, low-lying excited states, Tamm-Dancoff approx., particle conservation 9-29701
 127 In, three new levels, identification with 16 O in range 35-55 MeV 9-44154
 137 Cs compound nucleus in 136 Xe(p,p); isobaric analog resonances meas., $E=9-13$ MeV 9-40509
 171 Hf, [624] γ , rotational band, mag. moment of ground state 9-27638
 171 Lu, low-lying, prop. determ. in core-excitation model, core and particle parameters 9-22726
 147 Nd γ spectra dis. 9-27682
 207 Pb from 208 Pb(d,t), diff. cross section, excitation energy meas., level assignment, $E_o=50$ MeV 9-27746
 207 Pb(n,n), diff. cross section, excitation function calc. levels determ. 9-40513
 117 Te, excited states at 274.4 and 325.9 keV, from 117 I decay study 9-44178
 207 Tl from 207 Tl(t,p), p spectra meas., $E_t=13$ MeV 9-27646
 207 Tl from 208 Pb(d,t), diff. cross section, excitation energy meas., level assignment, $E_o=50$ MeV 9-27746
 108 Ag, short-lived states excited in (n, γ) reaction 9-38666
 208 Bi, calc. from Hamada-Johnston pot. reaction matrix elements 9-34405
 138 Cs from 138 Xe 15 min fission product γ spectra 9-34471
 152 Gd, rel. to resonance parameters 9-22731
 208 Pb, 3- octupole vibr. state, g factor obs. 9-34408
 208 Pb, coupling of single particle and collective octupole states 9-27648
 208 Pb, level investigation using excitation with n-capture γ ; anomalies 9-36573
 208 Pb, low-lying states studied in p scatt. at resonance energy for isobaric analog resonance 9-48302
 208 Pb, neutron radius obs. from analog state 9-34406
 208 Pb collective 3- state, g-factor calc. 9-42233
 208 Pb Hartree-Fock calc. in coord. space 9-34407
 208 Pb core ± 2 nucleons, semi-realistic structure calc. 9-22735
 108 Pd from 108 Pd(16 O, γ), Coulomb excitation, γ spectra meas., $E_o=42-49$ MeV 9-22722
 238 U, level density following bombardment with 14.7 MeV 9-27766
 168 Yb from 168 Lu decay, γ spectra meas. 9-27676
 209 Bi single-particle structure determ. by particle-core coupling model 9-36583
 209 Pb single-particle structure determ. by particle-core coupling model 9-36583
 109 Ag from 109 Pd, γ spectra meas. 9-34419
 139 Ba from 138 Ba(d,p); γ spectra meas. 9-38705
 139 Ba from 138 Ba(n, γ); γ spectra meas. 9-38705
 209 Bi, particle-vibration (3-) coupling, one-particle structure determ. 9-25587
 209 Bi coupling of single particle and collective octupole states 9-27648
 209 Bi level investigation using excitation with n-capture γ ; anomalies 9-36573
 139 Ce 11/2- lifetime, unified model calc. 9-25578
 139 La, single-particle self-energies, 2-body matrix elements calc. 9-29733

Nucleus continued
energy levels continued

- ¹³⁹La from ¹³⁹Ba, γ spectra meas., decay scheme determ. 9-27674
¹⁹⁰Os from ¹⁸⁹Ir decay, γ spectra meas. 9-38676
²⁰⁸Pb from ²⁰⁸Pb(d,p, γ); p, γ spectra meas., $E_x=12$ MeV 9-29740
²⁰⁸Pb from ²⁰⁸Pb(d,p γ); cross section meas., $E_x=8-18.7$ MeV 9-27745
²⁰⁹Pb particle vibration (3-) coupling, one-particle structure determ. 9-25587
¹⁴⁹Pm, gyromag. ratio of 114 keV state 9-46209
¹⁴⁹Pm, mag. moments of 114 and 270 keV levels 9-46210
¹³⁹Pr, multiplet of six high-lying, high-spin, odd parity states 9-34400
¹¹⁸Sb, excited states 9-22724
¹⁴⁸Sm, Coulomb excitation of levels 9-42226
⁹⁴A nuclear structure in this region using ⁹⁴Zr(He³,d)⁹⁵Nb 9-38718
²¹Al, 4.038 MeV state, study from ²⁴Mg(p,p) react. 9-25590
²¹Al, from ²³Na(α , γ), new excited levels 9-46242
²¹Al, low-lying levels, excited core model description 9-44139
²¹Al from ²⁴Mg(α ,p γ), γ spectra meas., $E_x=9-13$ MeV 9-25656
²¹Al, new levels found from ²¹Al(d,p)²⁸Al, 2.6 MeV 9-22739
²¹Al from ³⁰Si(α , γ), $E_x=11.8$ MeV 9-38656
⁷¹As, obs. from the decay of ⁷¹Se 9-42258
⁷¹As Coriolis-coupling calc. low-lying states, theor. level spectra 9-22746
⁷¹As Coriolis-coupling calc. low-lying states, theor. level spectra 9-22746
⁷¹As Coriolis-coupling calc. low-lying states, theor. level spectra 9-22746
¹⁰B, energy of excitation of first 4 excited states reported 9-46194
¹⁰B, excited levels determ. from ⁹Be(d,n)¹⁰B reaction 9-44215
¹⁰B, from ⁹Be(d,n γ), γ -ray branching of 3.59 MeV state 9-29711
¹⁰B d + α model, analysis using resonating group method 9-38709
⁸Be, isobaric-spin mixing deduced from ⁷Li(p, γ)⁸Be* 9-48272
⁸Be 2+ states, from ⁹Be(p,d), α - α scatt. and ⁷Li, ⁸B β -decay 9-40473
⁸Be 4+(11.4 MeV) level, width, from ⁷Li(d,n) 2 α reaction 9-42207
⁸Be compound nucleus from ⁷Li,p, ang. distrib. energy depend., $E_{pot}=2.7-10.6$ MeV 9-25624
⁸Be from ⁷Li(d,n), n ang. distrib. meas. 9-22824
⁸Be, 17.28 MeV level studied through ⁷Li+d- α + α +n 9-27627
¹⁰Be from ⁹Be(d,p); γ spectra meas. 9-29712
¹⁰C, energy of first excited state of ¹⁰C obs. 9-46194
¹²C, 10.8 MeV level, EI(ΔT=0) electroexcitation, form factors 9-25564
¹²C, 16.1 MeV level form factor determ. from e scatt. data 9-34436
¹²C, fundamental and first excited levels from ¹⁴N(d, α)¹²C reaction 9-48354
¹²C, new level at 18.1 MeV 9-27761
¹²C dipole resonance calc., g.s. fractional parentage structure influence on photodisintegration 9-42202
¹²C from ¹⁴N(α , α d); α d spectra meas., $E_x=22.9$ MeV 9-38721
¹²C spherical and deformed states, inverted coexistence 9-42234
¹²C from ¹⁴N(α , α p); α p spectra meas., $E_x=22.9$ MeV 9-38721
⁵⁵Co, shell-model calc. by quasiparticle method 9-42215
³⁶Ca from ⁴⁰Ar(d,³He), γ spectra meas., $E_x=52$ MeV 9-32358
³⁶Ca from ³⁶Ar(³He,n); n spectra meas., $E_x=9$ MeV 9-29833
⁴⁰Ca, $1d_{3/2}=1f_{7/2}$ energy splitting, expt. and theor. comparison 9-27663
⁴⁰Ca from ⁴⁰Ca(p,p γ)⁴⁰Ca, 7.40, 7.68 MeV levels 9-27662
⁴⁰Ca, 3614 keV level, branching and spin 9-48306
⁴⁰Ca, angular distributions for levels from ⁴⁰Ca(d,p)⁴¹Ca reaction 9-29823
⁴¹Ca, first two excited states obs. 9-46198
⁴¹Ca low-lying parity states, transition rates, spectra calc., phonon-particle coupling model 9-32316
⁴²Ca, particle-hole state decay, γ -ray obs. 9-48284
⁴²Ca configuration and analogue states obs. m ⁴²Ca(³He, α) ⁴²Ca 9-27751
⁴²Ca from ⁴⁰Ca(t,p), ang. distrib., spin-orbit coupling, p polarization meas. 9-32317
⁴³Ca, level scheme, from ⁴³K decay obs. 9-40490
⁴³Ca from ⁴⁵Sc(t, α), α ang. distrib. meas., $E_x=12.95$ MeV 9-29834
⁴³Ca from ⁴³Ca(³He, α); ang. distrib. meas., spectroscopic factor, I_n determ., DWBA, determ., $E_x=15$ MeV 9-32359
⁴³Ca, 5.15 MeV level probably 5- 9-27662
³⁵Cl, 1.763 MeV level props. 9-46197
³⁵Cl, 10.4 to 10.6 MeV, from ³⁶S(p, γ) ³⁵Cl reaction 9-42212
⁴⁰Co from ⁴⁵Fe(³He,t); t spectra meas. 9-38719
⁵⁷Co, excited through ⁵⁴Fe(α ,p), deduced levels up to 1.90 MeV 9-29754
⁵⁷Co from ⁵⁷Ni decay, γ spectra meas. 9-38660
⁵⁷Co level schemes from (t,n γ) and (p,p γ) reactions 9-32360
¹²Cp, ρ ²Be, ¹²C excited states meas., α decay obs., $E_p=57$ MeV 9-27715
⁵⁹Cr from ⁵⁰Cr(³He, α), cross section, ang. distrib., spectroscopic factors determ., $E=18$ MeV 9-29836
⁵¹Cr from ⁵²Cr(³He, α), cross section, ang. distrib., spectroscopic factors determ., $E=18$ MeV 9-29836
⁵²Cr, from p scatt., 17.5 MeV 9-34443
⁵²Cr from ⁵²Cr(³He, α), cross section, ang. distrib., spectroscopic factors determ., $E=18$ MeV 9-29836
⁵²Cr from ⁵²Cr(d,p), $E_d=7.5$ MeV 9-48307
⁵²Cr from ⁵⁴Cr(³He, α), cross section, ang. distrib., spectroscopic factors determ., $E=18$ MeV 9-29836
⁵³Cr(d,d)⁵³Cr; $E_d=7.5$ MeV 9-48307
⁵²Cr(p,p)⁵²Cr; $E_p=7.5$ MeV 9-48307
⁵²Cr(p,p)⁵²Cr; $E_p=7.5$ MeV 9-48307
⁵²Cr(p,p)⁵³Cr; $E_p=7.5$ MeV 9-48307
Cs, odd mass, unified-model calc., expt. comparison 9-32309
⁶³Cu from ⁶³Cu(d,p); ang. distrib. meas., DWBA analysis, $E_d=12$ MeV 9-38663
⁶³Cu from ⁶⁶Zn(d, α); ang. distrib. meas. DWBA analysis, $E_d=12$ MeV 9-38663
⁶³Cu from ⁶⁵Cu(d,p); p spectra meas., $E_p=12$ MeV 9-38681
⁶³Cu from ⁶⁸Zn(d, α); α spectra meas., $E_d=12$ MeV 9-38681
¹⁷F, from ¹⁶O(d,n), spectroscopic factors 9-29826
¹⁷F, to 5 MeV using ¹⁶O(³He,p)¹⁸F, meas. 9-36614
¹⁸F isobaric-spin impurities, from cross-section ratios of $6a,p^{17}$ O(0.871) 9-42206
¹⁸F low-lying even-parity levels, deformed states calc. 9-22718
¹⁸F spectra calc., realistic interaction, eff. of Woods-Saxon wave function 9-38653
¹⁹F, $1/2^+$ level discovery 9-36569
¹⁹F from ¹⁸O(d,n), $E_d=3$ MeV 9-36581
¹⁹F from ¹⁹F(p,p), $E_p=9$ MeV 9-36581
¹⁹F reson.,

Nucleus continued**energy levels continued**

- ¹⁶O, from ⁶Li(d, α) and ⁷Li(t, α) reactions, excitation of rotational bands 9-44223
- ¹⁶O from ¹³N(³He, d); d ang. distrib. meas., spectroscopic factor determ., $E=11$ MeV 9-29738
- ¹⁷O, from ¹⁷F β -decay 9-38684
- ¹⁷O, T= $\frac{1}{2}$ states 9-44134
- ¹⁸O, low-lying levels, calc. within shell model 9-38650
- ¹⁸O low-lying even-parity levels, deformed states calc. 9-22718
- ¹⁸O spectra calc., realistic interaction, eff. of Woods-Saxon wave function 9-38653
- ³¹P from ³¹P(p, p); p spectra meas. 9-29832
- ³¹P from ³⁰Si(p, γ), γ spectra meas., $E_{\gamma}=3.4$ MeV 9-27658
- Pb, odd-mass isotopes, nuclear spectra number conserving calc. 9-27647
- ⁸⁶Rb, low-lying levels from (d, p), (d, t) and (n, γ) reactions 9-42217
- ⁸⁷Rb from ⁸⁷Kr decay, γ spectra obs. 9-27685
- ⁸⁸Ru, calculation 9-29759
- ⁹⁴ru, in-beam γ spectroscopy meas. 9-29758
- ³²S, 4.46 MeV level lifetime meas. 9-29747
- ³²S excited state parameters determ. from ³¹P, p, $E_p=10-12.5$ MeV 9-29748
- ³²S in ³¹P(p, p α), mean level width, excitation func, meas., $E_p=8-10$ MeV 9-25591
- ³³S, collective effects in ground and first three excited states, using ³¹P(³He, p)³³S 9-44216
- ⁴¹Sc, two particle one hole states 9-42279
- ⁴²Sc from ⁴⁰Ca(²He, p), ang. distrib., spin-orbit coupling p polarization meas. 9-32317
- ⁴³Sc g.s. structure, (t, α) reaction 9-29834
- ⁴³Sc ground state spectroscopic factors 9-48351
- ⁴⁸Sc, particle hole states, spin assignment on basis of angular distrib. 9-44144
- ⁴⁸Sc from ⁴⁸Ca(⁴He, t); t spectra meas. 9-38719
- ⁵⁰Sc from ⁴⁸Ca(³Ca(²He, p), p spectra meas., $E_{\text{pr}}=18.5$ MeV 9-27752
- Se isotopes, n radiative capture and transmission, cross sections meas. 9-38704
- ⁷⁴Se from decay of ⁷⁴Br, level diagram 9-38685
- ⁸⁰Se, 1.478 MeV level obs. from ^{80m}Br decay 9-42216
- ²⁶Si from ²⁴Mg(²He, n γ), levels and spin determ. 9-32314
- ²⁷Si, low-lying levels studied in ²⁸Si(³He, α)²⁷Si 9-27654
- ²⁸Si prolate and oblate intrinsic state, (s, d) shell coupled-vib. model 9-27655
- ²⁸Si spherical and deformed states, inverted coexistence 9-42234
- ³¹Si, with ³¹Si³⁰ (d, p) reaction 9-27659
- ³²Si spherical and deformed states, inverted coexistence 9-42234
- Sn isotopes, structure props. investigated using inverse-gap-equation and quasiparticle theories 9-46203
- ⁸⁸Sr, 2⁺ and 3⁺ states, behaviour, Green function study 9-36590
- ⁸⁸Sr, from ⁸⁸Rb decay, obs. 9-22748
- ⁸⁸Sr, positive-parity states, neutron-neutron hole states 9-42218
- ⁸⁹Sr, positive-parity states, neutron-neutron hole states 9-42218
- ⁸⁹Sr(p, p)⁸⁹Sr⁺, p ang. distrib. meas., $E_p=20$ MeV 9-29794
- ⁹²Tc^{m-4} isomeric pair, decay, excitation of ⁴²Mo energy levels 9-38680
- ⁹⁷Tc from ⁹⁷Ru decay, γ spectra meas. 9-27686
- ⁴⁴Ti, projected Hartree-Fock method and stretch scheme calc. 9-32318
- ⁴⁴Ti, shell-model study of n-p correlations 9-48253
- ⁴⁴Ti possible levels, shell model 9-22740
- ⁴⁵Ti low-lying triplet, Hartree-Fock description with band mixing 9-36587
- ⁴⁶Ti five low-lying states, spectroscopic factors 9-48351
- ⁴⁷Ti, spectroscopic study 9-22823
- ⁴⁷Ti(p, p' γ), levels up to 3.74 MeV excitation energy determ. 9-38659
- Tl, odd-mass isotopes, nuclear spectra number conserving calc. 9-27647
- V, excitation of levels by inelastic n scatt. 9-44145
- ⁴⁷V, ⁵¹V, from ^{46, 48, 50}Ti(²He, d)^{47, 49, 51}V reactions, shell model fit 9-40478
- ⁴⁹V, γ spectra meas. of ⁴⁹Cr positron decay 9-48320
- ⁵⁰V from ⁵⁰Ti(²He, t); t spectra meas. 9-38719
- ⁵⁰V level schemes from (t, n γ) and (p, γ) reactions 9-32360
- ⁵¹V, from p scatt., 17.5 MeV 9-34443
- ⁵¹V, shell-model calc. by quasiparticle method 9-42215
- Xe isotopes, isomeric cross sections ratios 9-48293
- ⁸⁸Y from ⁸⁸Sr(p, n); excitation function, ang. distrib. meas., spin, parity determ. 9-29801
- ⁹⁰Y, level spectra calc. treating excited states as particle-hole excitations of ⁹⁰Zr core 9-38665
- ⁹⁰Y, low-energy spectra from shell model calc., vel. depend. effective N-N potential 9-40480
- ⁹¹Y from ⁸⁹Y(tip), spin and parity assigned, $F_T=12.1$ MeV 9-48308
- ⁹¹Y from ⁹²Zr(t, α), spin and parities assigned $E_t=12.1$ MeV 9-48308
- ⁶⁶Zn shell-model study of n-p correlations 9-48253
- ⁶⁶Zn from ⁶⁶Cu decay, 2.37 MeV O⁺ level population, γ spectra meas. 9-27684
- ⁸⁸Zr, from ⁹⁰Zr(p, t)⁸⁸Zr 9-27670
- ⁸⁸Zr, from ⁹⁰Zr(p, t)⁸⁸Zr 9-42235
- ⁹⁰Zr, level investigation using excitation with n-capture γ , anomalies 9-36573
- ⁹¹Zr, p inelastic scatt., ang. distrib. meas., $E_p=18.7$ MeV 9-27709
- ⁹¹Zr, spectrum, core excitation model predictions 9-48342
- ⁹²Zr, low-energy spectra from shell model calc., vel.-depend. effective N-N potential 9-40480
- ⁹⁴Zr, spin determ. for resonances decaying to excited J=0 states 9-46201

excitation *see* Nuclear excitation**magnetic moment**

see also Gyromagnetic ratio; Molecules/nuclear coupling; Nuclear magnetic resonance and relaxation

- 1p shell, M1 transition rates, Gemow-Teller transition, spectroscopic factors 9-22702
- core polarization eff. on M1 operator, Tabakin interaction 9-32294
- deformed odd-odd nuclei, rotational levels 9-48266
- even-even spherical nuclei, mag. dipole transition probabilities 9-42191
- Ho, magnetic dipole moment of resonant states meas. 9-27560
- of lowest rotational states of even-even nuclei Krutov model 9-44125
- M1 transitions meas. by 50-cm Fe-free β spectrometer at Uppsala, Sweden 9-38608
- magnetic dipole moments analysed using magnetic dipole interaction effects on energy shift of one-particle levels 9-22713
- mass number 6, 7, 8, 12, 13, energy level and magnetic moment calc. using central interaction plus spin-orbit interaction 9-27616

Nucleus continued**magnetic moment continued**

- mirror nuclei, with β -decay, ft values, used to determ. ang. momentum distrib. between orb. ang. mom. and spin 9-46220
- M λ , reduced probabilities calc. using Nilsson and Saxon-Woods potential 9-48257
- odd non-axial nuclei, M1-transitions and dipole mean values 9-36565
- odd non-axial nuclei, sum rules for dipoles and M1-transitions 9-34385
- odd-A spherical nuclei, ground state moments from study of *f*-forbidden M1 transitions 9-42195
- spin polarization in odd deformed nuclei, mag. dipole interaction, states $K=\frac{1}{2}$ 9-32301
- sum rules for dipoles and M1-transitions of non-axial odd nuclei 9-34385
- ¹⁶⁰Dy, nuclear g-factor, ang. correlation, Larmor precession freq. of 966 keV level 9-25582
- ¹⁵²Sm, γ internal conversion, M1, M2 transitions on K shell, $E_{\gamma}=1.9$ MeV 9-29765
- ¹⁵²Sm M1 multipolarity calc. from relativistic Hartree-Fock-Slater wave functions 9-25576
- ¹²¹Sn, from spin and hyperfine struct. 9-42222
- ¹⁸¹Ta, M 1-transitions and dipole mean values 9-36565
- ¹⁹²Ir-¹⁹²Os, ¹⁹²Pt, dipole moment, γ spectra meas., E2/M1 mixing ratio determ. 9-32324
- ¹⁹²Pt, E2:M1 multipole mixing ratio from γ - γ meas. 9-25585
- ¹⁹²Pt; from ¹⁹²Ir decay, E2/M1 mixing ratio determ. 9-32324
- ²⁴³Am p and M1 transitions meas. 9-27651
- ¹¹³Sn, from spin and hyperfine struct. 9-42222
- ²⁰⁹Tl, E2:M1 279keV transition mixing ratio from γ - γ directional and linear polarization 9-48301
- ¹¹⁴Cd M1 multipolarity calc. from relativistic Hartree-Fock-Slater wave functions 9-25576
- ¹¹⁴Cm, γ internal conversion, M1, M2 transitions on K shell, $E_{\gamma}=1.9$ MeV 9-29765
- ¹⁹⁴Ir-¹⁹⁴Pt, dipole moment, γ spectra meas., E_{γ} /M1 mixing ratio determ. 9-32324
- ¹⁴⁵Gd from ¹⁴⁵Sm(³He, 2n); γ spectra meas., isomeric transition, M4 prob. determ. 9-29736
- ¹⁵⁵Gd, from ENDOR obs. in CeO₂:Gd³⁺ 9-35733
- ¹⁶³Ho magnetic dipole moment of resonant states 9-27560
- ¹⁷⁵Lu from ¹⁷⁵Hf decay, γ spectra meas., E2-M1 transitions, probabilities and mixing parameters determ. 9-27233
- ¹⁴¹Nd, 72.5 keV level, $\mu=-1.121(\pm 0.013)$ 9-25580
- ¹¹⁶In, evaluation from n.m.r. in InP, InAs and InSb 9-44177
- ¹¹⁶In from ¹¹⁵In(n, α , γ) M1 transitions obs. 9-29727
- ²⁰⁶Pd(p, n), cross section and resonances obs., γ and M1 transitions obs., $E_p<40$ keV 9-27644
- ¹⁵⁷Gd, from ENDOR obs. in CeO₂:Gd³⁺ 9-35733
- ¹⁷⁷Hf, [624] $\frac{1}{2}$, rotational band, mag. moment of ground state 9-27638
- ¹⁷⁷Hf, M 1-transitions and dipole mean values 9-36565
- ¹⁷¹Lu, M1-transitions and dipole mean values 9-36565
- ²⁰⁷Pb(p, n), cross section and resonances obs., γ and M1 transitions obs., $E_p<40$ keV 9-27644
- ²⁰⁶Pb(p, n), cross section and resonances obs., γ and M1 transitions obs., $E_p<40$ keV 9-27644
- ¹³⁹Ce M1 transition probability, unified model calc. 9-25578
- ¹⁸⁹Os from ¹⁸⁹Ir, γ spectra meas., E2/M1 determ. 9-38676
- ¹⁴⁹Pm, 114 and 270 keV levels 9-46210
- ⁷⁵As from ⁷⁵Se decay M1-E2 mixing ratio determ. 9-40479
- ⁸Be, 17.64-16.63 MeV transition nearly pure M1 9-48339
- Cs, odd mass, magnetic moment and M1 transition rate, unified model calc. 9-32309
- Cu (CA=59, 61, 63, 65 and 67), calc. 9-38679
- ⁵⁷Fe, E2/M1 mixing ratios lifetimes of levels from Coulomb excitation 9-27664
- ⁵⁷Fem quadrupole, from Mossbauer spectroscopy of Fe²⁺ in MgO 9-44168
- ⁶⁷Ga, determ. from hyperfine structure separation 9-36661
- ⁷²Ga, determ. from hyperfine structure separation 9-36661
- ²H, dipole moment and D*-state components 9-34394
- ³He, M1 continuum from 6 to 20 MeV, 180° electron scatt. obs. 9-42273
- ⁴K $\frac{1}{2}$ -state, spin precession method, 1.29 MeV 9-36586
- ⁸³Kr, 9.3 keV level, Mossbauer lines Zeeman splitting 9-27668
- ⁸³Kr, g.s. and 1st excited state mag. mom., g-determ., Mossbauer eff. 9-27667
- La, odd mass, magnetic moment and M1 transition rate, unified model calc. 9-32309
- ⁶Li, calc. using Green's and Tabakin's potentials 9-38648
- ⁶⁰Ni from ⁶⁰Cu decay, M1 transitions meas. 9-27681
- ³¹P, μ and M1 transition prob. calc. by shell model wave functions 9-36585
- Sb isotopes, calc. using nuclear model with moving triton 9-46204
- ⁹⁷Tc, multipolarity of 40.584 keV transition 9-29773

magnetic resonance *see* Nuclear magnetic resonance and relaxation models

- 1p shell, M1 transition rates, Gemow-Teller transition, spectroscopic factors 9-22702
- α -particle model, necessary symmetries of Hartree-Fock Hamiltonian 9-42177
- anisotropic oscillator mode, energy level calc., magic numbers deduced 9-29694
- cluster, applic. to form factor description of ⁶Li, ¹²C, ¹⁶O, e scatt. 9-25570
- cluster configurations, applications to nuclear spectroscopy and nuclear fission 9-25557
- cluster model, α -particles, role of Pauli principle 9-32297
- collective, energy level theory 9-29704
- continuum shell model rel. to p scatt. from ³He and the photodisintegration of ⁴He 9-44195
- core excitation, for structure of ⁹¹Zr 9-48342
- Davydov, deformed heavy nuclei collective spectrum, parametrization 9-32296
- Davydov-Chaban and Davydov-Filippov energy level transition test 9-44124
- energy level density parameters and mass shell corrections, relationship 9-38636
- excited core model and nature of energy levels of ²⁷Al 9-44139
- Fermi gas, backshifted, for level densities of compound nuclei determ. 9-48287
- Fermi gas, ground state agreement for doubly even nuclei 9-27657
- Krutov, for deformed nuclei, magnetic moments and dipole transitions 9-44125

Nucleus continued
models continued

- light nuclei, classification of excited states in translation invariant shell models 9-44129
- Lipkin-Meshkov-Glick, importance of ground state correlations 9-44116
- M-scheme of shell model calcs., group theoretic approach 9-22703
- Nilsson, energy level calc., magic numbers deduced 9-29694
- Nilsson, fit to levels of ^{56}Fe 9-38661
- Nilsson, phonon description of deform. 9-27615
- optical, ^3He scatt. on Nuclei at 15 MeV 9-48348
- optical, analysis of 14.5 MeV n elastic scatt. data, rel. to nuclear matter radii 9-42196
- optical, density depend. effects 9-34427
- optical, differences in parameters between pairs of isotopes, found from difference functions of scatt. data 9-29692
- optical, failure to predict polarization of 3.25 MeV neutrons by various nuclei 9-27733
- optical, tensor pot. in d scatt. 9-22812
- optical, treated with analogy to e.m. wave scatt. in mind 9-36561
- optical, unified many-body theory 9-32288
- optical and shell models, book 9-42179
- optical cross-sections and polarizations of scattering of particles with arbitrary spin by nuclei 9-29776
- optical isobaric analogue resonance production in (p, n) reactions, new microscopic theory 9-27710
- optical model averaged potentials, applic. to neutron inelastic scattering 9-22788
- optical potential, spin dependent, Born approx. for deformed nuclei 9-22701
- optical-model analysis of $^{40}\text{Ca}(\alpha, \alpha_0)^{40}\text{Ca}$, l-depend. absorption factor 9-25646
- pairing-plus-quadrupole, nuclear deformations, collective motion theory 9-34379
- particle-core coupling model, for single-particle structure of ^{209}Bi and ^{209}Pb 9-36583
- phonon model of spherical nucleus 9-44112
- poles due to particle-particle and particle-hole collective motions isolated 9-42178
- review paper for teaching 9-22036
- shell, ^{18}O low-lying energy levels calc. 9-38650
- shell, continuum, of ^{16}O , used to calc. particle-hole resonant states 9-48276
- shell, description of 0^+ -isobaric analogue resonance in ^{208}Bi 9-44165
- shell, description of deuteron, nucleon correlation eff. 9-29714
- shell, doubly closed, with 2n and 2p outside, study of n-p correlation 9-48253
- shell, energy level and correlation theory 9-29704
- shell, fit to levels in $^{47,49,51}\text{V}$ and $^{51,53,55}\text{Mn}$ 9-40478
- shell, for ^{205}Tl 9-46215
- shell, for elastic and inelastic channel contribs. 9-42268
- shell, Green's velocity-dependent N-N pot. tested on ^{210}Bi , ^{210}Pb and ^{210}Po 9-44166
- shell, mass formula and binding energy 9-27608
- shell, residual interaction, spurious states soln. 9-32292
- shell, s-d, calculations with realistic interactions 9-29693
- shell, s-d, calculations with realistic interactions 9-29693
- shell, SU(3) algebra in mixed-shell space (0p, 0d, 1s) 9-38638
- shell and optical models, book 9-42179
- shell corrections and effects 9-38637
- shell model for first p shell 9-27616
- shell nuclei, s-d, evidence for Y_4 hexadecapole deformation 9-42230
- shell review 9-36555
- soft core model, nucleon matter calc. 9-48254
- statistical, energy-temp. reln. correlation eff. 9-27610
- strong coupling deformed rel. to calc. of n strength functions for transuranic elements 9-27612
- superconductor for energy level density calc. Agreement with derivation from isomeric ratios from (d, 2n) reactions 9-27743
- superfluid, α diffraction scatt. analysis 9-36610
- surface delta interaction models and pairing effects 9-29690
- three-body simple model, energy calc. by Monte Carlo method 9-22719
- variable-moment-of-inertia, g.s. band, even-even nuclei anal. 9-27609
- α -particle model, superfluid transition in nucleus 9-29691
- t, moving in nucleus, tested in calc. of magnetic moments of Sb isotopes 9-46204
- ^{51}V , and p elastic, inelastic scatt., 17.5 MeV 9-34443
- ^{210}Bi , shell model, Green's velocity-dependent potential 9-44166
- ^{210}Pb shell, Green's velocity-dependent pot. 9-44166
- ^{210}Po Green's velocity-dependent pot., shell model 9-44166
- ^{208}Bi shell model description of the 0^+ -isobaric analogue resonance 9-44165
- ^{12}C α substructure recovery determ. by $^{12}\text{C}(\text{t}, \alpha)^{11}\text{B}$ reaction 9-48273
- ^{52}Ce inadequacy of weak coupling model for lowest states 9-29749
- ^{52}Cr , and p elastic, inelastic scatt., 17.5 MeV 9-34443
- ^{19}F pear-shaped nuclei collective model calc. 9-22734
- ^{56}Fe and p elastic, inelastic scatt., 17.5 MeV 9-34443
- ^6Li , ^7Li , collective, α -d, α -t models, evidence from e scatt. 9-29784
- ^{55}Mn , and p elastic, inelastic scatt., 17.5 MeV 9-34443
- ^{59}Ni , n strength function and imaginary optical potential 9-29755
- ^{31}P , optical model of 7 MeV neutron scattering, calc. of cross-sections and polarization 9-29776
- ^{52}Sc , shell model for dipole giant resonance 9-25592
- ^{89}Y , optical model of 7 MeV neutron scattering, calc. of cross-sections and polarization 9-29776

size

- ($1d_{5/2}$) shell nuclei, mass prediction 9-48262
- charge radii change in rare earth region, single particle excitation 9-36567
- radii and binding energy correlation, for light nuclei 9-44111
- radius and shape meas. 9-46192
- radius parameter deduced from 2 n transfer heavy ion reactions 9-32362
- r.m.s. radius, dependence on deformation parameters 9-46191
- rms radius of matter from 1.45 MeV proton and neutron scatt. 9-42196
- shapes, Y_2 and Y_4 , correl. 9-44127
- strong absorption radius and its relation to the optical model wave function 9-44211
- Y_4 deformation in ^{20}Ne and other s-d shell nuclei, evidence from p scatt. 9-42230
- $Z=3$ to $Z=6$, from muonic X-ray data 9-27803
- ^{112}Sn , charge distrib., effects of neutrons, from elastic electron scatt. meas. 9-27703

Nucleus continued
size continued

- ^{232}Th , charge distrib., intrinsic quadrupole moment, radius studied by obs. of muonic X-rays 9-38677
- ^{134}Ba to ^{138}Ba isotopes, charge radii meas. by X-ray line isotopic shift 9-34399
- ^{208}Pb , neutron and proton distributions 9-44164
- ^{208}Pb Hartree fock calc. in coord. space 9-34407
- ^{118}Sn , charge distrib., effects of neutrons, from elastic electron scatt. meas. 9-27703
- ^{238}U charge distrib., intrinsic quadrupole moment, radius studied by obs. of muonic X-rays 9-38677
- ^{119}Sn charge radius determ. by Mossbauer spectroscopy 9-27632
- Ca isotopes, Coulomb energy, radii anomalous isotope shift, excess n depend. 9-36572
- ^{41}Ca - ^{41}Sc mirror pair, nuclear matter radii calc. from Coulomb energy, comparison 9-38658
- ^3H S' probability and change form factor obs. in e scatt. 9-32304
- ^3He charge form factor compared to ^3H in e scatt. 9-32304
- ^4He radius change after 29.4 keV γ emission, determ. using Mossbauer effect 9-34412
- ^6Li charge form factor, calc. using exponential wave function 9-29720
- ^{24}Mg , structure, importance of space correls. 9-44127
- ^{25}Mg , structure, importance of space correls. 9-44127
- ^{20}Ne and other s-d shell nuclei, evidence for Y_4 deformation from p scatt. 9-42230
- Ni isotopes, Coulomb energy, radii anomalous isotope shift, excess n depend. 9-36572
- ^{58}Ni , charge distrib., effects of neutrons, from elastic electron scatt. meas. 9-27703
- ^{60}Ni , charge distrib., effects of neutrons, from elastic electron scatt. meas. 9-27703
- ^{64}Ni , charge distrib., effects of neutrons, from elastic electron scatt. meas. 9-27703
- ^{41}Sc - ^{41}Ca mirror pair, nuclear matter radii calc. from Coulomb energy, comparison 9-38658
- ^{31}Si an oblate spheroid in Single-particle collective model 9-27659
- Sn isotopes, Coulomb energy, radii anomalous isotope shift, excess n depend. 9-36572
- spin and parity
see also *Gyromagnetic ratio; Molecules/nuclear coupling*
- $^{103}\text{Rh}(p, p')^{103}\text{Rh}$ decay scheme obs. 9-25574
- ^{50}Sc from $^{48}\text{Ca}(\text{He}, p)$, p spectra meas., $E_{\text{He}}=18.5$ MeV 9-27752
- ^{63}Cu γ transition induced by space-parity violation, enhancement of admixture coeff. 9-36589
- A=135 to 151 odd nuclei, spins of $(2f_{7/2})^{2,3}$ ground states 9-46206
- bases summary (1968) 9-22712
- energy levels fine structure, splitting estimated, P and CP violation 9-32298
- isospin purity rel. to Fermi matrix elements 9-48310
- isospin selection rules violated in photoneuclear reactions on light nuclei 9-25612
- J=0 $^+$ state wave function determ. in 2-nucleon transfer reaction by self-consistent spectroscopy 9-25606
- j-j coupling states of p and n, fractional parentage coeff., shell theory 9-34376
- mirror nuclei, β -decay ft values used with magnetic moment to determ. ang. momentum distrib. between orb. ang. mom. and spin 9-46220
- moment of inertia determ. method 9-42193
- moment of inertia of N=Z, Z+2, Z+4 even-even nuclei, with 2s, 1d shell filled 9-48252
- odd nuclei with $135 \leq A \leq 151$, spins of $(2f_{7/2})^{2,3}$ ground states 9-46206
- polarization of γ meas. after nucleus n capture 9-27736
- rotation, 3 dims. description using collective variables 9-48269
- rotation, theory employing 2 dims. soft rotator 9-48264
- rotation of deformed nuclei and moments of inertia, collective model 9-29707
- rotation of non-axial nuclei, theory 9-44124
- rotational states in large single j-shell, quadrupole-quadrupole interaction 9-34382
- rotational states of even-even nuclei, magnetic moments and dipole transitions 9-44125
- space-parity violation in nuclear force, γ transitions, enhancement of admixture coeff. 9-36589
- spin polarization eff. in deformed nuclei, Tamm-Dancoff analysis 9-22713
- spin polarization in odd deformed nuclei, mag. dipole interaction, states $K=\frac{1}{2}$ 9-32301
- spin-quadrupole interactions, influence on 2^+ vibrational states 9-44120
- spinning particle, classical treatment, book 9-41766
- $^{140}\text{Ce}(\alpha, p, p)$, p ang. distrib. meas., $E_{\alpha}=9.4$ -11.7 MeV 9-29734
- ^{206}Hg , 1028.7 keV third excited level 9-34404
- ^{206}Hg , 1029.7 keV level spin 9-46214
- ^{110}Pd from $^{110}\text{Pd}(\text{He}, \text{He})^{110}\text{Pd}$, Coulomb excitation, γ spectra meas., $E_{\alpha}=42$ -49 MeV 9-22722
- ^{126}Sn , excitation of seniority 0, 2 and 4 in quasi-particle theory 9-29728
- ^{111}Ag from $^{111}\text{Ag}(\text{p}, d)$, γ spectra meas. 9-34419
- ^{111}In from $^{111}\text{Cd}(p, n)$; γ and n spectra meas., $E_{\gamma}=4.2$ -5.35 MeV 9-42220
- ^{141}Pr from $^{141}\text{Nd}(d, \text{He})$; ^3He energy, ang. distrib. meas., $E_{\alpha}=29$ MeV 9-32311
- ^{121}Sn , constants by atomic-beam magnetic-resonance technique 9-42222
- ^{187}Ta , 482 keV transition parity mixing, γ scatt., circular polarization meas. 9-27640
- ^{237}Th from $^{237}\text{Th}(\text{He}, \alpha)$; ang. distrib. meas., $E=30$ MeV 9-29830
- ^{142}Ce , lowest isobaric analogue resonance in (d, p) spin $\frac{1}{2}$ 9-25579
- ^{132}La , ground state 9-38669
- ^{222}Ra , spin 3^- octapolar vibrational level 9-48303
- ^{152}Sm , transition rates from negative parity levels disagree with strong coupling model 9-27635
- ^{243}Am from $^{243}\text{Pu}(n, \gamma)$, γ spectra meas. 9-27651
- ^{243}Am from ^{243}Bk decay, α spectra meas. 9-27651
- ^{113}Cd levels studied using $^{112}\text{Cd}(d, p)^{113}\text{Cd}$ 9-38667
- ^{163}Er , ground-state spin obs. 9-36579
- ^{193}Ir , assignments 9-48298
- ^{193}Ir , energies and spins from β -decay of ^{193}Os 9-34403
- ^{113}Sn , constants by atomic-beam magnetic-resonance technique 9-42222
- ^{154}Gd transition rates from negative parity levels disagree with strong coupling model 9-27635
- ^{146}Nd lowest isobaric analogue resonance in (d, p) spin $\frac{1}{2}$ 9-25579
- ^{147}Pr , ground state spin, angular correlation studies 9-46208

Nucleus continued

spin and parity continued

- ¹²⁴Te, from ¹²⁴Sb decay, 60d and 1.5 min isomers 9-27673
¹⁴⁵Nd, 72.5 keV level, spin determ. $\frac{1}{2}$ 9-25580
²⁰³Tl, spin of γ -scattering level 9-46215
²³⁵U n induced fission, cross section resonance parameters determ., $E_n=17-70$ eV 9-22834
¹⁶⁶Er from ¹⁶⁷Er(d,t), t spectra meas., $E_d=12$ MeV 9-22816
¹⁴⁶Nd lowest isobaric analogue resonance in (d,p) spin $\frac{1}{2}$ 9-25579
¹⁰⁶Pd from ¹⁰⁶Pd(¹⁶O, ¹⁶O), Coulomb excitation, γ spectra meas., $E_\alpha=4\alpha-49$ MeV 9-22722
¹⁴⁶Sm from ¹⁴⁶Eu β decay, internal conversion coeff. calc. 9-48312
¹¹⁶Sn, $J=0^+$ states, pairing force and surface delta interaction, seniority 9-29756
¹⁴⁷Pm from ¹⁴⁷Nd decay, γ - γ ang. correlation meas., spin determ. 9-40496
²⁰⁷Tl from ²⁰⁵Tl(p,p), p spectra meas., $E_p=13$ MeV 9-27646
^{138m}Pr, determ. from β^+ decay 9-42250
¹⁰⁸Pd from ¹⁰⁸Pd(¹⁶O, ¹⁶O), Coulomb excitation, γ spectra meas., $E_\alpha=42-49$ MeV 9-22722
¹⁶⁸Yb from ¹⁶⁸Lu decay, γ spectra meas. 9-27676
¹⁰⁹Ag from ¹⁰⁹Ag, γ spectra meas. 9-34419
²⁵Al, 4.038 MeV state, spin-parity assignments 9-25590
²⁵Al, spin of 5.304 MeV level, $^{24}\text{Mg}(p,p)^{25}\text{Mg}$ scatt. obs. 9-25627
²⁷Al from ²⁴Mg(α, p), $p\gamma$ spectra meas., $E_\alpha=9-13$ MeV 9-25656
²⁹Al from ²⁸Si(t, α), $E_t=11.8$ MeV 9-38656
¹²³B, 3.39 MeV resonance state from ¹¹B, n; transmission and scatt. meas., $E_n=20.8$ keV 9-29729
⁸Be, isobaric-spin mixing deduced from ⁷Li(p, γ)⁸Be* 9-48272
⁹Be ground, 2nd and 3.04 MeV excited states 9-32307
⁹Be odd-parity states projected Hartree-Fock calc. 9-27626
¹⁰Be from ⁹Be(d,p), γ spectra meas. 9-29712
³⁸CC from ⁴⁰Ar(d, ²He), ³He spectra meas., $E_d=52$ MeV 9-32358
³⁸Ca from ³⁶Ar(³He, n), n spectra meas., $E_n=9$ MeV 9-29833
³¹Ca low-lying parity states, transition rates, spectra calc., phonon-particle coupling model 9-32316
⁴²Ca, $J=0^+$ states, shell model calc. 9-40489
⁴⁴Ca, $J=0^+$ states, shell model calc. 9-40489
⁴⁶Ca, $J=0^+$ states, shell model calc. 9-40489
³⁵Cl, of 1.763 MeV level 9-46197
³⁵Cl level assignments 9-48283
⁵⁴Co from ⁵⁴Fe(³He, t), t spectra meas. 9-38719
⁵⁷Co, excited through ⁵⁴Fe (α, p), deduced levels up to 1.90 MeV 9-29754
⁵⁷Co from ⁵⁷Ni decay, γ spectra meas. 9-38660
⁵⁹Co, n_{opt} transmission, intensity spin-spin interaction determ. 9-27722
⁶³Cu ($E_\alpha=59, 61, 63, 65$ and 67), calc. 9-38679
⁶³Cu, γ transition induced by space-parity violation, enhancement of admixture coeff. 9-36589
⁶⁴Cu from ⁶³Cu(d,p), ang. distrib. meas., DWBA analysis $E_d=12$ MeV 9-38663
⁶⁴Cu from ⁶⁴Zn(d, α), ang. distrib. meas., DWBA analysis, $E_d=12$ MeV 9-38663
⁶⁶Cu from ⁶⁵Cu(d,p), p spectra meas., $E_d=12$ MeV 9-38681
⁶⁶Cu from ⁶⁶Zn(d, α), α spectra meas., $E_d=12$ MeV 9-38681
¹⁹F $\frac{1}{2}^+$ state in resonance in ¹⁸N(α, p) reaction 9-36569
¹⁹F from ¹⁸O(d,n), $E_d=3$ MeV 9-36581
⁵⁴Fe from ⁵⁴Fe($p, p'\gamma$), 2.56 MeV level spin determ. 9-29753
⁵⁷Fe, γ transition induced by space-parity violation, enhancement of admixture coeff. 9-36589
⁵⁷Fe spin distrib. in ⁵⁵Mn(t,n γ)⁵⁷Fe 9-32360
⁶⁶Ga from ⁶⁶Ge decay, γ spectra meas. 9-38662
⁶⁸Ga, ⁷¹Ga, of nuclear energy levels, determ. in n scatt. expt. 9-38664
⁶⁸Ge, compound nucleus temporarily formed in various reaction, ang. mom. eff. in break-up 9-29757
⁷⁴Ge, assignments made 9-48344
⁷H isospin admixture induced by violation of charge independence hypothesis 9-32304
²H scatt. cross-section rel. to spin polarization 9-29629
³He, isospin admixture due to Coulomb force and violation of charge independence hypothesis in nuclear forces 9-32304
⁴He, first excited state 0^+ 9-27739
⁴He, odd-parity states 9-40477
⁴He, odd-mass isotopes, nuclear spectra number conserving calc. 9-27647
¹¹A=¹¹¹-¹²¹, odd from ¹¹²-¹²²Sn(d, ³He); levels, spin and parity determ., $E_d=22$ MeV 9-29825
³⁹K low-lying parity states, transition rates, spectra, calc., phonon-particle coupling model 9-32316
⁴⁰K, positive parity states 9-44143
⁴²K spin assignments using ⁴¹K(d, p)⁴²K, 12 MeV 9-27751
⁵²Mn from ⁵²Cr(³He, t), t spectra meas. 9-38719
⁹²Mo, in-beam γ spectroscopy meas. 9-29758
¹⁴N, 7.97 MeV level, not of negative parity, isospin assignments 9-48275
¹⁴N from ¹⁴O(d, α), isospin-forbidden, cross section, ang. distrib. meas., $E_\alpha=3-15$ MeV 9-29827
¹⁵N from ¹⁴C(p, γ), γ spectra meas., $E_p=352-634$ keV 9-29713
²¹Na from ²⁰Ne(d,n γ), γ spectra meas. 9-34409
¹⁶Ne from ¹⁶O(³He, n), γ spectra meas. 9-25567
¹⁶Ne from ¹⁷O(³He, n), $E_n=3$ MeV 9-36581
²²Ne from ¹⁸O(Li, t), 0^+ state excited, SU(3) (4, 4) rep., $E=12$ MeV 9-29742
⁵⁹Ni, γ transition induced by space-parity violation, enhancement of admixture coeff. 9-36589
⁶⁰Ni from ⁶⁰Cu decay, γ spectra meas. 9-27681
⁶²Ni, $J=0^+$ states, pairing force and surface delta interaction, seniority 9-29756
¹⁶O, new 0^+ state, evidence from e scatt. data, $E_\alpha=14$ MeV 9-42205
¹⁶O +ve parity states, shell model calc. 9-42204
¹⁶O from ¹³C, ³He, 3^+ assignment to resonance state 9-32357
³¹P from ³¹P(t,p), p spectra meas. 9-29832
³¹P from ³⁰Si(p, γ), γ spectra meas., $E_p=3-4$ MeV 9-27658
¹³Pb, odd-mass isotopes, nuclear spectra number conserving calc. 9-27647
⁸Ru, in-beam γ spectroscopy meas. 9-29758
³S, 4.46 MeV level, $J^\pi=4^+$ 9-29747
⁴⁸Sc, particle hole states, spin assignment on basis of angular distrib. 9-44144
⁴⁸Sc from ⁴⁸Ca(³He, t), t spectra meas. 9-38719
²⁴Si from ²⁴Mg(³He, n) n distrib. meas., DWBA calc., L, spin and parity determ., $E=7$ MeV 9-32315
²⁴Si from ²⁴Mg(³He, n γ), levels and spin determ. 9-32314

Nucleus continued

spin and parity continued

- ²⁷Si $\frac{1}{2}^+$ for 0.96 MeV $\frac{1}{2}^+$ for 2.17 MeV, $\frac{1}{2}^+$ for 2.65 MeV, $\frac{1}{2}^+$ for 3.8 MeV 9-27654
²⁸Si moment of inertia determ. by modified Peierls-Urbano method 9-42193
²⁹Si spins of 4^{th} , 5^{th} and 6^{th} excited states 9-27748
³¹Si, with ³¹Si⁰(d,p) reaction 9-27659
⁸⁸Sr(p, p')⁸⁸Sr*, p ang. distrib. meas., $E_p=20$ MeV 9-29794
¹⁷¹Tl, odd-mass isotopes, nuclear spectra number conserving calc. 9-27647
⁵⁶V from ⁵⁶Ti(²He, t), t spectra meas. 9-38719
⁸⁸Y from ⁸⁸Sr(p, n); excitation function, ang. distrib. meas. 9-29801
⁹¹Y from ⁸⁹Y(t, p), energy levels obs., $E_t=12.1$ MeV 9-48308
⁹¹Y from ⁹²Zr(t, α), energy levels obs., $E_t=12.1$ MeV 9-48308
- theory**
see also Nuclear forces
 binding energy anal., $J=0$, $T=1$ and $T=0$, J odd 9-29698
 binding energy and n and p half density radii determ. 9-27606
 binding energy calc. using oscillatory wave functions 9-29696
 centre-of-mass motion in Hartree-Fock solutions 9-38633
 charge distrib., model independent description, high energy electron scatt. appl. 9-32338
 collective motion and moments of inertia of deformed nuclei 9-44122
 collective motion as change in density of nuclear matter 9-29707
 collision matrix, unitary pole resonance and compound nucleus 9-40468
 complex system whose Hamiltonian contains small interaction odd under time-reversed 9-45787
 core polarization eff. on E2, M1 operators, Tabakin interaction 9-32294
 Coulomb nuclear S-matrix Regge trajectories 9-34372
 current conversation, effect 9-42169
 deformed nuclei, collective motion and moments of inertia 9-44122
 deformed nuclei, coupling of rotational and internal motions 9-44123
 deformed nuclei wave function symmetry under time reversal and change in sign K 9-48256
 deformed shell-model potential, P_4 -dependent, deformation energy depend. 9-32295
 deformed two-dimens. nucleus, rot., random phase approx. 9-44106
 density matrix change on adding large number of particles to nucleus 9-34373
 effective interaction between quasiparticles in nuclei, origin and form of long-range parts 9-48250
 excitations, volume collective, of nuclear matter, theory contrib. 9-40465
 Faddeev eqn. for N-term separable potential 9-22698
 Fermi system, density matrix variation due to addition of large number of particles 9-44107
 Fermi theory for low-lying nonrotational states in even-even nuclei 9-22710
 fragments and hyperfragments with $Z \geq 4$ prod. in 1.5 GeV/c K⁻ interac. with Ag and Br nuclei 9-40471
 Hamiltonian, single particle, self-consistent, fission proc. calc. 9-27653
 Hamiltonian of independent particle system, separation of centre of mass 9-34370
 harmonic oscillators, relativistic 9-36557
 Hartree-Bogoliubov, validity in exactly solvable n-body problem model 9-25558
 Hartree-Fock and Hartree-Bogoliubov eqns. with exact symmetries 9-27189
 Hartree-Fock approximation, convergence of modified Goldstone linked-cluster expansion 9-38640
 Hartree-Fock formulas for moment of inertia 9-42194
 Hartree-Fock solutions, centre-of-mass motion 9-38633
 Hartree-Fock spectra, projected, basis states truncation eff. 9-29683
 Hartree-Fock-Bogoliubov calcs. on N=Z, Z+2, Z+4 even-even nuclei with 2s, 1d shell filled 9-48252
 intranuclear cascades, conservation laws in elementary events 9-32290
 inverse gap equation method, tested on tin isotopes 9-46203
 light nuclei, spectroscopy from single charge exchange of π^+ mesons 9-22715
 matter, recent developments 9-38639
 meson-N coupled systems soluble model 9-34277
 nuclear matter, dense, conditions for ferromag. transition, neutron star appl. 9-41642
 orbital rearrangement is sd-shell nuclei, single particle energy 9-29697
 oscillator basis Sussex matrix elements and on- and off-shell plane wave matrix elements, connection 9-42181
 overlap functions, single particle, related to spectroscopic factors 9-42185
 potential, hard-core, 3-body problem, Lippmann-Schwinger scatt. theory 9-29689
 quadratic isobaric multiplet mass eqn., perturbations, excitation energies determ. 9-32308
 quadrupole one-phonon states, energy, wave func., Saxon-Woods, Nilsson potn. calc. 9-29723
 quasiparticle lifetimes in dielectric model of nucleus 9-48255
 Racah coefficient multipole analysis of particle-particle and particle-hole multiplets 9-38641
 reaction matrix calc. for matter by exact method, ³S₁-³D₁ states geometric series 9-29695
 residual interaction and conservation laws 9-42175
 review of recent developments 9-36556
 review of recent developments 9-46185
 rotational and internal motions, coupling in deformed nuclei 9-44123
 RPA, inadequacy for calc. of quasiparticle lifetimes 9-48255
 s-d shell, calculations with realistic interactions 9-29693
 s-d shell, effective interactions and SU(3) symm. 9-22699
 Saxon-Woods potential rel. to allowed β -decay and E.A. transitions in rare-earth region 9-22729
 sd-shell nuclei, single particle orbital rearrangement energy 9-29697
 separation energies and single particle states, Hartree-Fock equations 9-42186
 Slater determinants and quasiparticle vacuum states, criteria 9-42165
 stability of nuclear matter 9-36564
 statistical, for medium and heavy nuclei 9-42176
 SU(3) \times R₃, polynomial bases and Wigner coefficients 9-29682
 superfluid transition in nuclear matter 9-29691
 symmetry and shape of Hartree-Fock density, even-even N=Z light nuclei 9-27620
 Tamm-Dancoff approx., spherical superconductor nuclei, particle conservation 9-29701

Nucleus continued
theory continued

- Tamm-Dancoff modified approx., unfilled n and p shell description 9-29700
- tensorial interactions, effective, from nucleon-nucleon phase-shifts 9-29684
- three-body problem, isotropic harmonic-oscillator forces, exact quantum-mechanical soln. 9-41764
- three-body problem coordinates and observables, SU(3) representation on 6-dimens. sphere 9-29685
- two-nucleon potential, non-relativistic 9-38634
- two-nucleon potential, non-relativistic 9-42166
- unified many-body theory of DWBA and optical model 9-32288
- variational calc., based on method of steepest descent in Hilbert space 9-22708
- vibrational and rotational motion in even nuclei, a unified microscopic approach 9-25562
- wave functions, shell- model, structure 9-29722
- wave functions in Fermi systems, normalization condition 9-32289
- Λ binding energy in nuclear matter 9-42180
- n halo implication in heavy nuclei due to K⁻ capture meas. 9-40516
- n strength function calc. using strong coupling deformed nucleus 9-27612
- n strength functions calc. for transuranic elements with strong coupling deformed nucleus and various potentials 9-27612
- ¹⁸⁰Hf internal conversion of N- and O- shell electrons, nuclear structure effect 9-34384
- ²⁰⁸Pb, neutron and proton distributions 9-44164
- ²⁰⁸Pb core+2 nucleons, semi-realistic structure calc. of levels 9-22735
- ³⁶Ar, T=0 pairing correlations, Hartree-Fock- Bogoliubov eqn. 9-29744
- ⁵⁶Fe energy gap, self-consistency and pairing calc. 9-32319
- ⁷²Ge energy gap, self-consistency and pairing calc. 9-32319
- ⁷Li, binding energy, double scatt. length calc. from Hamada-Johnston potential 9-29715
- ⁴He, independent-pair wave function from energy variational principle 9-29717
- ²⁴Mg, T=0 pairing correlations, Hartree-Fock-Bogoliubov eqn. 9-29744
- Mo off-mass isotopes, low energy props. using intermediate coupling approach 9-22749
- ¹⁶O structure determ. from (¹³C, ³He), E_{lab}=2.8 MeV 9-32357
- ³²S, T=0 pairing correlations, Hartree-Fock- Bogoliubov eqn. 9-29744
- ⁷⁸Se energy gap, self-consistency and pairing calc. 9-32319

Oceanography

- see also Liquid waves; Seawater*
- acoustic holography, underwater 9-43793
- acoustic measurements 9-24631
- acoustic spectrum broadening due to ocean wave interference 9-29269
- acoustic wave propag. in presence of stochastic boundaries, theory 9-36873
- acoustic wave propag. in shallow isovelocity water 9-30390
- air-sea interaction 9-26891
- air-sea interaction, macroscale, model 9-43378
- Arctic Ocean sediments, magnetic stratigraphy and faunal patterns 9-45566
- Australia and Antarctica, morphological continental drift fit 9-43368
- Baltic Sea, water level variations caused by meteorological effects 9-49436
- bottom irregularities 9-43375
- bottom irregularities, determ. using short duration acoustic signal back-scatt. 9-22262
- Chile Rise, sea floor spreading shown by mag. anomalies and seismicity pattern 9-41472
- circulation, wind-driven, three-dimensional model 9-26889
- cold water off Somalia, time of appearance 9-45476
- conductivity, elec. of sea bed in shallow waters, determ. 9-35792
- confused seas, wavelength and period 9-28856
- current velocity meas. with e.m. meter, Mediterranean obs. 9-39993
- currents associated with internal short period waves, statistical anal. 9-45465
- deep currents and channels, Pacific, preliminary results 9-40002
- deep sea photographic techniques 9-37907
- deep sound scattering layers, obs. 9-47524
- deep submergence rescue vehicle photo- instrumentation 9-36412
- DEEPSTAR 4000 submersible for biol. and geophys. obs. 9-37906
- diffraction of sea waves 9-49431
- double Kelvin waves in rotating shallow ocean, trapping modes 9-23434
- e.m. noise, e.l.f. at depth 30 to 300 m (off Baha, Ca.) 9-45473
- exploration, sonar applications 9-37905
- floor sediments, thermal conductivity obs. 9-31282
- floor spreading rel. to heat flow and gravity 9-31274
- floor topography, description by statistical method 9-45471
- fracture zone topography rel. to sea floor spreading and plate tectonics 9-47522
- global numerical ocean model 9-35804
- gravimetry at sea in towed gondola 9-31238
- gravity longwaves, amplification by circular islands, model 9-35798
- gravity surveys by deep submersibles 9-37874
- gravity waves, internal, temp. oscils. on shelf and open sea 9-39998
- gravity waves, linear, seismic generation 9-35803
- gravity waves, long crested random, mass transport 9-28857
- gravity waves, multiple, due to shallow water interaction with submerged bars 9-45470
- Gulf Stream, kinematic waves 9-31284
- heat-flow meas. in N. Atlantic, tech. and failings 9-24628
- hydroacoustic signals from CHASE V explosion of Cape Mendocino 9-29268
- inertial motion, coherence and band structure 9-45477
- internal gravity waves, interact. trapping rel. to variation in degree of stratification 9-26888
- internal gravity waves, progressive shape in fluids 9-25824
- internal waves, wave numbers and group vels., freq. depend., model 9-47516
- Irish Sea floor, geological survey, rocks found 9-43369
- isostatic floor-spreading with glacio-eustatic fluctuations test of hypothesis based on tectonic events 9-47518
- Kelvin waves, diffraction by sharp bend on rotating earth 9-28858
- Laplace's tidal eqns. over sphere, eigenvalue calcs. 9-49428
- light scatt. obs. in central Arctic ocean 9-24629
- lithodynamics of sea 9-43361
- Love modes for oceanic and continental earth model tables of amplitudes, phase velocity and group velocity, variational parameters 9-26867
- Oceanography continued**
- lunar-tidal effects, amplitude error in the L vector from noisy data 9-37868
- magnetic field, anomalous, statistical characts. 9-31451
- magnetic field, marine secular variation 9-31448
- magnetic variations at surface and bottom 9-40097
- mid-oceanic ridges, seismicity rel. to characts. of crust and upper mantle 9-33716
- N. Atlantic and adjacent seas, pole tide 9-43370
- Newfoundland and Labrador areas, shelf and continental slope, morphology 9-43365
- noise, acoustic, vertical directivity, integral equation analysis 9-28855
- non-tidal seas, free water surfaces oscillations, probability distribution of random variables 9-49432
- North Atlantic, heat flow meas., tech. and failings 9-24628
- oceanic rises in reln. to expanding Earth hypothesis 9-41470
- oscillations, inertial period, in deep sea 9-49441
- Pacific and marginal seas, bathymetric curves at 500 m relief intervals 9-45475
- Pacific temperature, surface, seasonal vars. 9-47523
- parameters affecting sound propagation 9-37899
- photometer transparency meter, multiple reflection, for meas. attenuation of directed beam in seawater 9-36369
- power spectrum methods applied to variations of parameters of sea 9-49433
- radar altimetry from spacecraft 9-35808
- radiowave propag., e.l.f., zonal harmonic calc. 9-45459
- Rayleigh waves, dispersion analysis method 9-45446
- Red Sea bottom 1795 to 2195 m depth, temp. salinity and chlorinity 9-43372
- Rossby waves, time periodic, effect of random currents 9-43377
- salt fingers instability rel. to internal gravity waves and collective instability 9-33748
- sea floor spreading off Chile rel. to tectonic evolution 9-45474
- sea level control rel. to continents, effect of vol. changes of oceanic rises 9-41471
- sea level forced oscills., S, Baltic and rel. to atm. press. and wind vars. 9-37900
- sea reflection spectra, photographic obs. 9-43367
- sea surface spatial wavy structure, radar determ. 9-39995
- sea-air interactions, long range prediction of large scale motion, simplified model 9-24648
- sea-floor spreading 9-24630
- sediment meas. by submersibles 9-37904
- sediment props. determ. from Rayleigh waves on ocean floor 9-45472
- short-period water waves, hydrodynamic theories and their applics. 9-49429
- short-period waves causing hydrodynamic pressure forces 9-49437
- slow-scan television applications 9-37908
- sofar speeds, Pacific, comments on previous determs. 9-29271
- Somali coast, cold water, time of appearance 9-45476
- sound propag., surface channel, surface-coupled losses 9-31281
- sound speed in seawater, simple accurate eqns. development 9-47521
- sound vel. fluctuations, spatial correl. with ocean movements 9-31280
- sound vel. in distilled and sea water, comments on previous determs. 9-29271
- strobe light source with pressure-equalized electronics 9-36381
- surface reverberation, relative contribs. of surface air bubbles and waves 9-24610
- surface temp. patterns and their synoptic charges, satellite data optimal processing 9-49442
- surface waves, acoustic pings reflection, intensity fluctuations 9-47520
- survey of Ross's original deep sea sounding site 9-31283
- telemetry system 9-24632
- telluric current, effect on GEK meter obs. 9-43373
- temperature meas. of sea, time variation at four points simultaneously 9-35809
- temperature of surface, effect of ice concentration 9-43371
- thermohaline circulation for finite depth, applic. of one-parameter density model 9-35799
- tidal current turbulent boundary layer 9-39996
- tidal eqn., Laplace, asymptotics of eigenfunctions 9-39999
- tidal investigations, precise declination meas. method 9-43363
- tidal parameters, satellite determ. 9-28854
- tidal records, harmonic analysis, data filtering 9-43366
- tidal waves, harmonic constants 9-43374
- tides, deep sea, elec. and mag. fields induced in earth 9-31275
- tides, effect on lunar variations of vertical component of geomag. field 9-37999
- tides, littoral, applic. of expression for oscill. perfect liq. w.r.t. mean level of free surface 9-26065
- turbulence, small scale, obs. 9-40001
- turbulence, velocity and temp. fluctuations in and above thermocline, meas. techs. 9-35806
- turbulence of sea waters, special ref. to wave motion 9-49435
- turbulent energy dissipation at sea surface 9-35800
- turbulent flow, spectra of temp. and velocity fluctuations 9-35805
- turbulent processes, sampling interval choice for discrete obs. 9-49426
- under water noise beneath springtime sea-ice, diurnal variations 9-40003
- underlying surface temp. from aircraft obs. of outgoing i.r. 9-35830
- underwater acoustic wavefront variations caused by internal waves 9-30391
- water basins, proper gravitational and planetary vibrations, numerical determ. 9-37903
- water waves in channels and around islands, spectra calc. 9-30361
- water waves mechanics, tests under laboratory conditions 9-49439
- wave diffraction due to step in bottom topography for two superimposed fluids 9-40763
- wave generated by single pressure impulse 9-49438
- wave measurements using wave recorders 9-49440
- wave transformation with changing depth 9-49430
- waves, unusually high, Poisson's law applic. 9-49427
- waves, wind generated, breaking and equilib. spectrum 9-31285
- waves generated by turbulent wind, freq. power spectra 9-39994
- waves on sea surface for continuously changing density, 3D problem 9-37901
- wavy surface, finite difference determ. of slopes 9-39997
- wind drift currents, equatorial region 9-45469
- wind generated lead during freezing, max. size 9-49424
- wind wave development, initial, lab. expt. 9-40000

Oceanography continued

- wind waves, length modification in narrow coastal zone, calc. 9-35801
- wind-wave generation 9-49434
- wind-wave interactions investigation, of shear stresses 9-44541
- ²³⁴Th/²³⁸U ratios and distribution 9-47519
- Ar concentrations in the Pacific, comparison of data 9-45467
- ¹⁴C, activity variation with time and location in South Pacific and Antarctic Oceans 9-37902
- O distribution, and effect of advection, turbulence and biochemical demand 9-43376
- Si, total rate of removal of dissolved Si in biogenous deposits 9-33749

Octet theory *see* *Elementary particles/symmetry; Field theory, quantum*

Omegatrons *see* *Leak detection; Mass spectrometers; Vacuum technique*

Onsager relations *see* *Statistical mechanics; Thermodynamics*

Optical activity *see* *Optical rotation*

Optical communication *see* *Laser beams/applications*

Optical constants

- see also* *Absorption/light; Reflectivity*
- bulk materials, from reflectance on transmittance data 9-26695
- carbon tetrachloride, i.r., exptl. determ., consistency of results 9-23500
- chloroform, i.r., exptl. determ., consistency of results 9-23500
- coals and soots, i.r. region 9-24357
- crystals, biaxial and uniaxial 9-47312
- diamond particles, and extinction curves, showing nonexistence in interstellar dust 9-43575
- elasto-optical, improved ultrasonic meas. methods 9-36366
- film, thin metal, calc. from complex refl. and transmitted amplitudes, series expansion 9-32013
- films, from reflectance on transmittance data 9-26695
- films, thin, slightly absorbing, ellipsometric meas., thickness 9-37678
- graphite, anisotropy rel. to band structure 9-26697
- lithium acetate dihydrate monocrystal, effect of temp. 9-47315
- metal thin film during deposition, continuous ellipsometric determination 9-32845
- metallic thin film, opt. const. and thickness, hill-climbing technique 9-39804
- mixture, computation by graphical method 9-35612
- non-ideal surface sample, determ. 9-49239
- pr(FeO_4), H_2O 9-39302
- pyrographite, i.r. region 9-24357
- α -quartz, photoelastic const. obs. 9-37683
- rare-earth borides, from plasma refl. edge obs. 9-39802
- reflection coeff. for laser radiation on solid surfaces, reduction 9-43208
- tetracyanoquinodimethan, absorpt. coeff. calc. from reflection and transmission meas. 9-39796
- thin films, determination using polarization measurements 9-47311
- triglycine sulphate, i.r. range, applic. to pyroelec. 9-35615
- uniaxial crystals, use of u.v. monochromator with concave grating 9-25385
- ZnSnP_2 , and vibrational frequencies from i.r. reflection spectra 9-35614
- Ag thin evaporated films 9-47313
- Ag thin film during deposition, continuous ellipsometric determination 9-32845
- Ag thin films near plasma freq., influence of struct. 9-37680
- Au thin evaporated films 9-47313
- C and coals, i.r. region 9-24357
- CdO , effect of lattice vibrations, 300° and 85°K 9-35613
- Cu_3PSe_4 films, 0.4-15 μ 9-35398
- Cu_3PSe_4 films, 0.4-15 μ 9-35398
- Cu_3PSe_4 films, 0.4-15 μ 9-35398
- Cu and Cu:Ni alloys, optical transitions, nature 9-24354
- CuCl , crystals, near excitonic absorpt. region, refl. spectra obs. at 4.2°K 9-37710
- EuSe single cryst. 9-49238
- Ga single crystals, refractive index and extinction coeff. 9-33502
- GaAs, non-ideal surface, determ. 9-49239
- GeTe, imaginary part. of freq. dependent dielec. function calc. 9-39794
- In, thin films, far, u.v. 9-37681
- InP, transverse and longit. freqs., dielec. consts. 9-47314
- K, 0.5-4.0 eV, by split-beam ellipsometry 9-49240
- KCl single cryst., conductivity and energy loss spectra, temp. depend. 9-33559
- Mg₂Ge, from reflectance meas., 0.6-11.0 eV at 77°K 9-24355
- Mg₂Ge, and electronic band structure calcs. 9-24356
- Mg₂Si, and electronic band structure calcs. 9-24356
- Mg₂Si, from reflectance meas., 0.6-11.0 eV at 77°K 9-24355
- Mg₂Sn, and electronic band structure calcs. 9-24356
- Mg₂Sn, from reflectance meas., 0.6-11.0 eV at 77°K 9-24355
- Mo permittivity, real and imaginary, depend on photons of 1.4-11 eV, from reflection coeff. meas. 9-43230
- Na, 0.5-4.0 eV, by split-beam ellipsometry 9-49240
- Nb, rel. to elec. props. 9-31069
- S, orthorhombic in vacuum u.v. 9-37682
- Se single cryst., from reflectivity spectrum calc. from ellipsometric meas. 9-43204
- SnS_2 , and electronic band structure calcs. 9-26485
- SnSe_2 , and electronic band structure calcs. 9-26485
- SnTe , imaginary part. of freq. dependent dielec. function calc. 9-39794
- Zn, rel. to elec. props. 9-31070
- ZnS epitaxial films 9-37684
- ZnSe epitaxial films 9-37684

Optical dispersion *see* *Dispersion, optical*

Optical fibres *see* *Fibres/optical*

Optical films *see* *Films/liquid; Films, solid/optical properties*

Optical filters *see* *Filters, optical*

Optical images

- see also* *Aberrations, optical; Holography; Resolving power, optics*
- blur in propagation through random media, ratio of short-time to long-time blur widths 9-26904
- colour, photoelectrophoresis imaging method 9-40389
- degrees of freedom, max. number for coherent and incoherent illum. 9-48083
- diffraction defocusing of coherently illuminated edge 9-36355
- diffraction images of coherently illuminated objects 9-34207
- enhancement technique by using coherent system without spatial filter 9-29455
- evaluation, Lunar Orbiter application 9-32044

Optical images continued

- on ferromagnetic thin films, thermal recording resolving power 9-28662
- formation processes, exceeding normal limit of resolution 9-34197
- formation with arbitrary holographic type surfaces 9-34198
- Fourier transform of intensity distrib. for partially illuminated object 9-22442
- Fresnel zone plate, image formation in visible and soft X-ray region 9-27385
- glass imaging device, refr. index controlled change by ion exchange treatment 9-49241
- hologram imaging by ray tracing, evaluation 9-36323
- holograms, incoherent, bias level reduction 9-36321
- holographic, degradation by atmospheric turbulence 9-40366
- holographic, function rel. photographic film to image brightness 9-27346
- holographic digital reconstruction 9-36330
- holographic sharpness restoration 9-40370
- intensifier, statistical brightness gain 9-32045
- laser, formed by matrix control, patent 9-34180
- loss of resolution due to multiple small-angle scatt. in water 9-36878
- microscope objectives, image performance testing and optical transfer function meas. 9-46013
- motion, errors in photographic investigation 9-22444
- partially coherent, transfer functions 9-2347
- of periodic bar pattern through aberration-free annular aperture 9-43909
- photographic, growth of small images of point sources rel. to emulsion, lens and camera 9-22483
- point image of point source, mode of introduction 9-34193
- pseudoscopic in holography, appearance and location rel. to diffraction operator 9-47852
- quality, work survey of Technical Univ. Berlin 9-48085
- quality definition 9-45984
- ray tracing, algebraic, by digital computer 9-36345
- reconstruction of X-ray hologram with visible light 9-46003
- reflected from rot. mirror, motion for point, line and plane objects 9-41936
- resolution limit for line objects, diffraction-limited circular aperture 9-43918
- restoration, band-limited, by linear mean-square estimation 9-32001
- restoration, uncertainty and information 9-27374
- restoration by spatial filtering 9-32039
- rotation by prism, methods 9-34196
- rotation by revolving prism 9-38410
- scattering by seawater particles and turbulence, imaging props. 9-44564
- Schmidt camera, image quality exam. using spot diagrams 9-49596
- thermal recording on thin ferromag. films 9-47265
- thermograph, applic. of columnar thermopile and photoelec. multiplier 9-38397
- transfer function, effect of coherent illum. 9-48084
- transfer function variation with focus 9-32003
- of u.s. beams, multiple microwave, in solids, by Bragg diffraction 9-36189

Optical instrument testing

- lens focal length and flange focal distance, electronic meas. 9-46033
- lens transfer function meas., computer applic. 9-31997
- resolvometer, resolutions determinations of photographic systems films 9-34236
- resolvometry, error analysis 9-27412
- spot diagram generator for lens aberrations 9-22467
- transfer function, effect of coherent illum. 9-48084

Optical instruments

- Some instruments are listed separately, e.g. Refractometers*
- acousto-optic deflectors, wideband, using acoustic beam steering 9-36188
- analogue computer for Fourier transform spectroscopy 9-29487
- apertures, circular, 'knife-edge', prod. method 9-45708
- application to investigation of reflecting surfaces and transparent insulation in solar devices 9-32010
- beam splitter, ZnSe coated NaCl, for CO₂ laser 9-48099
- cavity, enhancement of internal refl. spectroscopic sensitivity 9-36389
- collimator, improved, for extreme u.v. and X-rays 9-48103
- colorimeters, tristimulus 9-34212
- correlator for Fresnel images 9-36352
- correlators, noise reduction by ultrasonic shutter 9-36371
- dichroism, linear, measuring device, and study of dichroism under stress 9-46010
- electro-optic modulator, patent 9-40374
- evaporographic converter for i.r. glass Schlieren exam. 9-38408
- excitation-function meas., polarization corrections elimination 9-36372
- Fresnel zone plate, variable pattern, moiré synthesis 9-27386
- goniometric projection production and viewing 9-36152
- image rotation by revolving prism 9-38410
- for improving electron diffractometer intensity profile record 9-27283
- light modulator, variable freq., for u.s. telescopes 9-46012
- microdensitometer, computer-linked for analysis of X-ray plates 9-32031
- mirrors, oil contamination changes of reflectivity rel. to space flight 9-22470
- modulation transfer factor for instrument made stigmatic by deposition of dielec. thin film on lens 9-46009
- phototheodolite, ballistic, multiple-frame camera 9-32089
- polishers, Teflon, for precision optical flats 9-38405
- reflecting astrolabe, 25 cm aperture 9-33961
- reflectometer, absolute, for flat specular samples, visible and vacuum u.v. region 9-38406
- reflectometer, measurement of principal angle of incidence and principal azimuth of reflecting surface 9-32028
- reflectometer with normal incidence scanning 9-36370
- scattered-light intensity from gases 9-39052
- solar therapy device with parabolocylindrical and spherical concentrators 9-32030
- spectrum analyzer for power spectral density meas. 9-27398
- stereographic projection production and viewing 9-36152
- for straightness test on slides or flat surface 9-38411
- stray light eliminated in Rayleigh scatt. expts. 9-36359
- thermograph, applic. of columnar thermopile and photoelec. multiplier 9-38397
- upper atm. temp. variations with height, meas. by space vehicles 9-41542
- u.v. (extreme) collimator, improved 9-48103
- Zenith mirror, for astrometrical instruments 9-48102

Optical materials

- see also* *Filters, optical*
- behaviour in extreme environments 9-32032
- crystal, achromatization for plane polarized light rotation 9-24361

Optical materials continued

- crystallochemical selection of mats. for i.r. beam control, data 9-38394
dielectrics, isotropic, dispersion obs. in absorption bands 9-35617
films, stress production during deposition, mechanism and control 9-28341
glass, refractive index and expansion coefficient, temperature dependence 9-26698
glass, silicate and sulphur selenide, mechanical strength 9-26341
glass composition for fibre-optic device core 9-41957
glass-ceramics, new properties and applications 9-33500
glass-ceramics, transparent 9-49234
glasses, new properties and applications 9-33500
glasses for fibres, chem. compatibility definition and meas. 9-38412
i.r. glass examination by evaporographic converter 9-38408
mat. surface, refl. of light, physical mechanism of the specular peak 9-41945
metal oxides with nonbonded electrons, as nonlinear optical materials 9-45263
nonlinear, evaluation by powder technique 9-26677
nonlinear, review 9-49233
photochromic, for quantum electronics, review 9-26705
photochromic, photobleachable electron-beam-induced colouration 9-43201
rough surface, coherent light scatt., speckle pattern formation 9-37735
AgCl photochromic glasses 9-33521
Ba₂NaNb₂O₁₅, single crystal and single domain, nonlinear optical props. study 9-26687
Ba₂NaNb₂O₁₅ 0.53 μ m source, continuous, in 1.06 μ m YACG:Nd laser cavity 9-40362
CaTiO₃:Fe-Mo, photochromic, photobleachable electron-beam-induced colouration 9-43201
Ge windows for CO₂ laser 10.6 μ m radiation., power transmission 9-26675
Ge windows for CO₂ laser 10.6 μ m radiation., power transmission 9-26675
LiF transparency in the u.v. reduced by formation of surface film in air 9-33523
NaCl windows for CO₂ laser 10.6 μ m radiation., power transmission 9-26675
Se glass for i.r. 8-15 μ m transmission, patent 9-24352
Sr(NO₃)₂, photochromic, refractive index changes meas., coherent light illumination 9-26700
Y₂O₃:TbO₂ sintered ceramic, prep., props. and applic. 9-33501

Optical mode, crystals see *Crystals/lattice mechanics*

Optical model see *Nucleus/models*

Optical properties of substances

see also *Optical constants; Optical materials*

- 9-27932
acoustic pulse prod. by gas, as microwave detector and for gas analysis 9-28077
air, heated, basic radiative proc. and spectral props. 9-23400
air, heated, integral props. for spectrum and intervals, 4000-20000°K 9-23401
alkali halides, XUV spectrophotometer 9-29485
alkali-halides, absorption of U₂-centres, effect of external stresses 9-49251
atmospheres, finite, isotropically scatt., with specular reflectors, refl. and transmission functions 9-29531
birefringent crystal plates, cascade sets, path difference and polarization directions effect on wave fronts 9-45270
blood, scattering and absorption constants 9-47694
castor oil, acoustically induced birefringence study 9-23495
chlorophyll solns., eff. of laser light on optical transmission coeff. 9-28131
cholesteric liq.-cryst. films 9-39103
coated glass sheets, optical and energy parameters 9-32038
corundum crystal, light scatt. effects 9-33522
crystal, ADP-type, electrooptical eff., optical beam discrete deviation meas. 9-26708
crystal, non-opaque, using polarizing microscope, book 9-48777
crystal optical const. and dispersion reln., i.r. region 9-26115
crystal optics taking into account magnetoelectric effect 9-24350
crystals, biaxial and uniaxial, principal constants 9-47312
n-decane- β,β' dichloroethyl ether opalescence at critical mixing point 9-36877
diamond-type crystals, critical-point structure, strain effects 9-24395
dielectric media on opaque substrate, absorbing, emitting and scattering 9-26671
dinucleoside phosphates, model calc. 9-48523
electronic structure selection rules and densities of states, photoemission studies 9-44876
elements, collection of data, book 9-22026
films on semiconducting backings 9-24351
fluid, statistical props. of scattered radiation 9-42474
gases, absorpt. coeffs. meas. using Fabry-Perot interferometer 9-29465
gases, microwave rotational lines, width determ. using graphical method 9-44310
glass, high pressure effects 9-28193
glass, photochromatic, reversible photochemical reactions 9-26714
glass-ceramics, new properties and applications 9-33500
glasses, new properties and applications 9-33500
III-V compounds, second order susceptibility, matrix element of solely spin orbit coupling 9-35610
impurity center in crystals, effect of vibrational mixing of two close-lying levels 9-28677
isogyre eqn. for triclinic mag. crystal 9-24362
Kerr cell, linearity improved with four electrodes 9-34907
liquid, molecular, laser-induced secondary beam absorpt. obs. 9-32506
liquid, optical const. and dispersion reln., i.r. region 9-26115
liquids, laser beam self focusing and stimulated Mandelstam Brillouin and Raman scattering 9-42654
liquids, molecular, nonlinear effects induced by laser light 9-26103
liquids, nonfocusing, and quartz, stimulated Brillouin scattering 9-26098
liquids, organic, temp. depend. of absorption and dispersion, cell for meas. 9-28130
liquids, refractive index, absolute, intensity-dependent var. 9-26105
liquids, refractive index, nonlinear, local field theory 9-26107
liquids, self-trapping interpretation of small scale light filaments 9-28125
liquids, small-scale filaments prod. by laser beams, explanation 9-32784

Optical properties of substances continued

- liquids with high time resolution, Raman scattering, backward stimulated, investigation 9-26114
lossy media, higher-order coherence function propag. 9-35608
metals, polyvalent, non-transition expt. and theor. investigations, review 9-31063
oscillations, long-wave, in ionic crystals 9-26407
paint-like coatings computer calc. incorporating Fresnel's law, Snell's law, Bier's law and kinetic theory 9-37689
paramagnetic salts, rel. to crystal field parameters 9-33498
photochromic materials, photobleachable electron-beam-induced colouration 9-43201
plastics, anisotropic, produced by polymer reticulation in liq. crystal diluent 9-26078
poly-p-butylisocyanate, structure from optical behaviour in solns. 9-27932
polymers, model calcs. 9-48523
polystyrene, optical polarization obs. of stressed state and effect of ultrasound 9-46880
porcelain enamels, TiO₂ opacified adjustment of controlling parameters by crystallization rates and TiO₂ solubility 9-37687
pseudobinary (III-V)-(II-VI) systems, energy gaps, and solid solubilities 9-35205
radiation rotational effect upon nonlinear crystal 9-24363
resonance line radiative transfer from a point on the boundary of a half-space 9-44272
ruby crystals, optical homogeneity rel. to laser emission characts. 9-26674
scattering fluctuation theory 9-23497
seawater, dependence of apparent optical properties on inherent optical properties 9-30403
semiconductor, hexagonal, elasto-optic and electro-optic props., effect of bandgap 9-35623
semiconductor, low-mobility and disordered, rel. to e transport 9-30902
semiconductor, rel. to band struct. 9-49091
semiconductors, magnetic, and elec. and mag. props. 9-49064
solids, absorpt. meas., elimination of surface refl. effects 9-33519
solids, inelastic-electron-scattering and optical data, parametric calc. 9-37679
spiropyranes in soln., photochromy obs., by means of triplet-triplet absorption 9-34910
triglycine sulphate-isomorphous ferroelec. solid soln., rotatory thermo-optical effect 9-47371
turbulent media, homogeneous, spherical wave propag. 9-40752
water, short light pulse propag. 9-39101
Ag-Mn alloy, studies rel. to electronic structure models 9-45033
Ag thin evaporated films, opt. const., transmittance 9-47313
AgCl photochromic glasses 9-33521
Al thin film, extreme u.v., photoelec. emission rel. polarization and angle of incidence 9-31072
Al wire exploded in vacuum, plasma 9-44440
Ar, liq., with Xe and Kr doping, far i.r. absorpt. 9-34908
Ar arc, high press. 9-40727
Au thin evaporated films, opt. const., transmittance 9-47313
Au thin film, extreme u.v., photoelec. emission rel. polarization and angle of incidence 9-31072
Ba_{(41)Na₂₋₂₀Nb₁₀O₃₀}, rel. to crystallographic data, and thermal expansion coeffs. 9-37134
Bi₁₂GeO₂₀ piezoelec., elasto-optic matrix elements 9-33394
Bi₁₂SiO₂₀ piezoelec., elasto-optic matrix elements 9-33394
CaCO₃, calcite, tunable four-photon optical parametric noise, 4300-5860Å 9-49253
CaF₂:Tr³⁺ (Tr³⁺=trivalent rare-earth), optical centres, thermodynamics 9-30614
CaFPO₄ spectroscopic props. and laser characts. 9-26673
CaTiO₃:Fe-Mo, photobleachable electron-beam-induced colouration 9-43201
CdS plate, d.c. driven, focusing effect 9-26707
Cr, refractive index and absorption spectra 9-24359
Cu-Ni alloy, studies rel. to electronic structure models 9-45033
(87wt.%Cu)-(13wt.%Ni) optical transitions, nature 9-24354
Cu and Cu:Ni alloy, optical transitions nature 9-24354
Cu wire exploded in vacuum, plasma 9-44440
Eu benzoylacetonate solutions at -150°C energy of threshold rel. spectral compos. stimulating light 9-28134
Eu chalcogenides, long wavelength/phonon freqs. and dielec. dispersion from i.r. reflectivity meas. 9-39799
Fe, and transverse Kerr magneto-optic effect, 0.35 to 1.0 μ m 9-45274
Fe³⁺ in glasses, rel. to coordination 9-26199
GaAs, Franz-Keldysh effect light modulation 9-39810
GaSb 9-47119
GdFe₃, and transverse Kerr magneto-optic effect, 0.35 to 1.0 μ m 9-45274
Ge, interband props. of grain boundaries 9-26737
He liquid, absorption of u.v. radiation 9-44565
InTe layers, tetragonal phase, anisotropy 9-41200
K₂Nb₂O₇, mica-like single cryst. 9-30522
KH₂PO₄ crystals, optical rectification of mode-locked pulses 9-26712
KNb₂O₇ mica-like single cryst. 9-30522
LiF: effect of thermal treatment, X- and γ -irradiation 9-28546
LiNbO₃ crystals, optical rectification of mode-locked laser pulses 9-26712
MgO single crystal, electron and neutron irr., colouration and flow stress 9-33099
Ni films in vacuum u.v., correl. with photoemission obs. 9-45260
Pb-Ge chalcogenide alloys, and solid solution range 9-30721
PbMoO₄ crystal, melt grown, acousto-optic props. 9-49254
RbFeF₃, orthorhombic, behaviour during antiferromag. to ferromag. transition 9-47293
SF₆, continuous parametric amplifications of 10.6 μ m signals from CO₂ laser 9-27340
SF₆, cross saturation of 10.6 μ m signals from CO₂ laser 9-28081
SF₆ gas, transmission of coherent optical pulses 9-46574
Sb₂S₃ single crystals, in ferroelec. phase transition temp. range 9-45261
a-SiC:N, dichroic crystal-optical device, patent 9-28653
Sr_{1-x}Ba_xNb₂O₆, ferroelec., elasto-optic matrix elements 9-33394
YFe garnet, Si doped, optical dichroism 9-24307

Optical pumping

- alkali atom, depolarization cross sections significance from D₂ pumping 9-34558
alkali metals, spin relaxation, optical obs. in buffer gas 9-29942

Optical pumping continued

- atomic vapour, rel. between ang. charact. of ground state and absorpt. and dispersion props. 9-32416
 with black body radiation, threshold conditions 9-27309
 cavities, close coupling geometry, efficiency 9-29394
 chambers, elliptic-cylindrical, for solid lasers, optimum design 9-22415
 coherent, monomode giant pulse generation 9-34172
 detection signal optimization 9-22970
 dye lasers, use of second harmonic of Q-switched ruby laser for pumping 9-31949
 flashlamp for organic dye lasers pumping 9-48005
 flashlamp source, time-resolved spectroscopy 9-29483
 gases, mol., by own radiation 9-34157
 Hertzian coherence, used to meas. dephasing collisions in atomic vapour with buffer gas 9-29966
 homopolar generator as energy store for large laser 9-29428
 i.r., of interstellar OH 9-27048
 laser, giant pulse production by coherent pumping 9-31934
 laser, inverted state, patent 9-47949
 laser, possible characts. of bremsstrahlung source from gas discharge plasma 9-22369
 laser, powerful nsec. pulse prod. using Mandel'shtam-Brillouin and stimulated Raman scatt. 9-27302
 laser, Q-switched, spinning-prism, flash tube firing time control 9-27294
 laser, rod and lamp alignment within spherical reflector 9-27295
 laser, solid tunable, beam-pumped, patent 9-48050
 laser efficiency enhanced by enclosing ionisable gas within transparent enclosure surrounding laser crystals patent 9-31925
 monochromatic, effect on Mandel'shtam-Brillouin scatt. 9-46343
 multiphoton ionization, perturbed propag. kernel, theory 9-25202
 nonlinear resonator, parametric generation without reflecting dielec. coating 9-47945
 organic dyes, xanthene and coumarin groups, lasing action, flashlamp-pumped 9-45960
 parametric oscillator, steady state oscillation analysis 9-47924
 pulse-train propagation in resonant medium, Maxwell-Schrodinger eqn. soln. 9-25705
 quantum electronics, vol.1. of book 9-47918
 relaxation process theory 9-34555
 resonance structures and pumps, various forms 9-41912
 rods, solid lasers, optical path changes, analysis by holographic interferometry and high speed photography 9-48088
 ruby, intensely excited, emission power and time constant obs. 9-45941
 ruby laser, regular spiking, spectral output and far-field pattern as influenced by resonator mirror vibrations 9-41913
 ruby laser refr. index change during pumping 9-29424
 ruby laser rod, temp. distrib. 9-22418
 ruby laser with Ar ion laser, operation at room temp. and 77°K 9-25288
 selective excitation spectroscopy 9-46019
 sequential, use in atomic clocks 9-47720
 solid laser, through disc end face, patent 9-36300
 threshold microwave-field amplitude for unstable growth of spin waves under oblique pumping 9-43186
¹¹³Cd^m, for nuclear orientation, n.m.r. frequencies 9-25575
¹¹⁵Cd and ¹¹⁵Cd^m, for nuclear orientation, n.m.r. frequencies 9-25575
 Ar, ³P₂, metastable state depolarization cross-sections 9-22973
 Ar, population inversion, excitation mech. for transitions in Ar III and IV 9-28041
 Ar atoms in ³P₂ metastable state 9-27814
 Ar II saturation phenom. in active transitions 9-36287
 CO₂ laser, pulsed, inversion as time function, theory and experiment 9-36291
 Cs-6³P_{1/2} states distrib. due to sat. hydrocarbon collisions, eff. cross sections 9-44279
 Cs, 8521 Å line display utilizing swept GaAs laser 9-48408
 Cs and Cu, spin exchange 9-40548
 Eu benzoylacetate solutions at -150°C, energy of threshold rel. to spectral compos. stimulating light 9-28134
 He-Xe gas mixture, stimulated conc. scatt. of light by super-regenerative amplification 9-46286
 He, ³P→¹D excitation, prob. calc. 9-23000
 He, metastable, ion polarization via Penning collisions 9-38803
 He discharges, production of intense polarized electron beams 9-28045
 He θ -pinch, possible population inversion 9-36771
³He⁺ polarization by optical pumping, ion source appl. 9-40335
³He gas, nuclear polarization static mag. field detection, low-field magnetometer 9-23002
³He polarized target prod. with electron exchange 9-27583
 Li atoms, hyperfine splittings and press. shifts of ⁶Li and ⁷Li 9-40550
 Li vapour, Dehmelt-type transients for ⁷Li, obs. 9-36669
 LiNbO₃, parametric oscillation, pumped with ruby laser 9-28663
¹⁴N and ¹³³Cs spin exchange, app. for high ¹⁴N signals 9-32418
 Na vapour with Ar buffer, in Hertzian coherence rel. to obs. of dephasing collisions 9-29966
 Nd glass, absorbed energy rel. to activator content 9-48029
 Nd glass stimulated emission parameter deterioration during use 9-31109
 Ne, ³P₂ metastable state depolarization cross-sections for collisions with He and Ne 9-22973
 O²⁺, prod. of population inversion by optical pumping from He⁺ 9-34167
 Rb, transition probabilities between magnetic sublevels 9-46301
 Rb nonlinear hyperfine pressure shift induced by optical pumping 9-36664
⁸⁵Rb, optical pumping in inert gases, excited state mixing obs. 9-34561
⁸⁷Rb atoms in inert gases, excited state mixing obs. 9-34561
 V³⁺, Al₂O₃ mm wave maser, rate equation analysis 9-31926
 Xe, ³P₂ metastable state 9-22973
 Xe atoms in ³P₂ metastable state 9-27814
 YAl garnet: Nd laser, Kr lamp pumping, 105 W output 9-48033
 YAl garnet: Nd lasers, diode pumped, c.w. operation, 46 mW output at 1.0614 μ m with 1% efficiency 9-48034
 YAl garnet: Nd using K-Hg discharge lamp 9-25201
 YAl garnet: Nd laser, continuous operation by injection luminescent pumping 9-25301

Optical quantum generators *see Lasers***Optical rotation**

- see also Magneto-optical effects; Optical constants; Polarimeters; Polarized light*
 activity, quantum statistical-mech. theory 9-48698
 p-azoxyanisole nematic liq. crystals. 9-30405
 by crystals, stress effects and rel. to symmetry 9-47318

Optical rotation continued

- higher asymmetry, molec. theory 9-48095
 molecules, inactive, induced activity, role of H bonding 9-48700
 non-enantiomorphous class 4 crystal, optical activity 9-49242
 photoelectric measurement, errors 9-27393
 plane polarized light, achromatization of crystal-optical components 9-24361
 tertiary alcohols, specific rotation and mag. rotary dispersion 9-48697
 uniaxial crystals, activity 9-43211
 uranylpropionate crystals, 3500-10000 Å 9-43213
 Bi₂SiO₂₀, photoactivity and field-induced changes 9-35621
 CdGa₂S₄, class 4, activity and rotatory power at 4872 Å 9-31074
 CdGa₂S₄, non-enantiomorphous class 4, optical activity 9-49242
 MgO, paramagnetic Faraday-rotation pattern of F centre, 1.8°K 9-35116
 Rb₂S₂O₈ crystals, dispersion over range 250-1050nm 9-43212

Optical systems

- see also Aberrations, optical; Lenses; Optical images; Optical instruments; Optical materials; Resolving power, optics*
 aberrations automatic correction 9-36344
 aberrations automatic correction in composite systems 9-34217
 alignment practice in production 9-45985
 array for use in noncoherent space-to-ground laser communications 9-31966
 autocollimating, alignment for quality control of 2nd order aspherical surfaces of revolution 9-38401
 cavities, degenerate, comprising lenses 9-25344
 coherent, defocussing for partial defocus correction 9-29455
 coherent, with ideal lens, Fourier transform representation and approximations 9-45981
 complex, design, aberration corrections by computer 9-34194
 condensing cones, hollow, ray tracing 9-29454
 contrast reproduction for two lines darker than surrounding field, resolution limit 9-41956
 corners, right-angle, hollow, ray tracing 9-29454
 design for quasi-monochromatic partially coherent illumination 9-25343
 design guide, book 9-29456
 detector response in polychromatic light 9-48082
 differentiation of cross grating, applic. to strain meas. 9-25068
 digital switchable deflector 9-27368
 encoder, decimal to binary 9-41955
 Faraday rotator, low mag. field, using glass rectangular parallelepiped 9-25345
 fibre, grazing total internal reflection ray obs. 9-38400
 filters, spatial, realization with polarized light 9-36379
 for Golyal cell, compact rugged, stable 9-29473
 imaging, resolution, statistical estimation 9-27375
 interferometric method for generation of contour lines on opaque objects 9-36932
 inverse Cassegrainian system, two separated spherical mirrors, algebraic theory 9-32000
 lens, rotationally symmetric, maximum modulation transfer function 9-29453
 lever, for fibre mech. props., appl. of light sensitive potentiometer 9-28328
 light pipes, cylindrical, with total internal refl. transmission coeff. 9-34215
 minimal astigmatism surfaces, calc. 9-36346
 modulation transfer function, effect of wave aberration 9-27364
 modulation transfer function, estimation by Rayleigh criterion analogy 9-38399
 modulation transfer functions, determ. from power spectrum of random chart and its image 9-43910
 multi-component, investigation with Christiansen filter 9-22473
 performance specification, choice of methods 9-34195
 point image of point source, mode of introduction 9-34193
 polarizing pile of dielectric plates, optical characts. 9-29472
 possibilities for gasdynamics 9-29458
 prism, minimum deflection for symmetric ray paths, elementary proof 9-36338
 quantum limited, detection of incoherent objects 9-45982
 quasi-, with nonquadratic phase correctors 9-38396
 radiometry with spectrally selective sensors 9-32026
 ray tracing, algebraic, by digital computer 9-36345
 reflectometer, u.v. vacuum, for use with extreme u.v. synchrotron radiation 9-27396
 refracting, 2 surfaces, with zero 3rd order spherical aberration 9-40376
 relay lens f/3, 245 mm, high resolution design 9-41938
 resonator, cylindrical, lens inside matched to mirror, field and natural freq. calc. 9-25227
 scanning, resonant multiplex, for circular beam 9-25374
 skew invariant 9-22446
 spatial filtering system alignment 9-34221
 spherical aberration, 7th order, optimum correction 9-22443
 stresses, internal, due to differential expansion 9-36373
 telecentric, for vocal cord cinematography 9-33964
 telemetry, appl. to shock tube meas. 9-29306
 testing, using wavefront shearing interferometers 9-27379
 thin, with simple lenses, props. 9-38398
 third-order aberration coeff. partial derivatives, evaluation 9-31998
 toroidal right-angle bends, ray tracing 9-29454
 total internal reflection micro-holography 9-41927
 tracking, photon counting by multi-coincidence method 9-45574
 transfer function, effect of coherent illum. 9-48084
 transfer function, theory interpret. rel. to its moments 9-25346
 transfer function, white modulation, rel. colour correction 9-22445
 transfer function determ. with 3rd and 5th order spherical aberration 9-22468
 transfer function in region of low spatial freqs. 9-45986
 transfer function meas. techniques 9-29452
 transfer function variation with focus 9-32003
 transilluminated partially coherent, quadratic filter theory 9-45983
 two mirror, correction for spherical aberration, coma and astigmatism 9-32002
 of visual pyrometers rel. to temp. meas. accuracy 9-41845
 wave-aberration difference function variance magnitude, correlation with relative modulation function 9-36347
 Ag-glass-Cu waveguide, coaxial 9-34218

Optical waveguides *see Electromagnetic wave propagation/guided waves*

Optics

- see also Aberrations, optical; Atmospheric optics; Lenses; Mirrors, etc.; Optical images; Quantum optics*
- acoustic generation by electrostrictive mixing of light beams 9-34083
 applications, paintings, dating and analysis 9-28820
 applied to crime detection 9-25332
 coherent, high-resolution spectral analysis 9-29392
 crystal, magnetoelectric effect 9-24350
 degrees of freedom of image for coherent and incoherent illum. 9-48083
 design guide to modern optical systems, book 9-29456
 flow visualization 9-46450
 fluctuating signal, aperture averaging factor 9-45976
 forensic applic. 9-25333
 Institut d'Optique (Orsay), research projects (1964-7) 9-31991
 mirage creation in the laboratory 9-25349
 modern, symposium, New York (1967) 9-27360
 modulation transfer functions, determ. from power spectrum of random chart and its image 9-43910
 pathology, applic. 9-29112
 physical, book 9-29463
 physical, inverse diffraction, using Bojarski identity on e.m. far field back-scattered 9-47851
 planetary radar data, processing 9-31603
 polarized narrow, beam, e.m. field intensity and properties 9-29459
 resonance line rad. transfer in finite homogeneous cylinders, effects of geometry 9-45801
 signal processing by acoustic Bragg diffraction and optical heterodynings 9-27365
 space-limited functions, multiple reprod. 9-48086
 systems and transforms for engineering students, book 9-40377
 temperature functions of optical fields 9-27358
 transfer function, theory in terms of moments, and expt. meas. 9-25346
 two-dimensional synchronous detection techniques 9-29447
 undergraduate lab. facilities 9-27155
 undergraduate text 9-38188
 wave theory and its applications, textbook 9-40227

geometrical

- of acoustic waves in mag. and piezoelec. media 9-27227
 of astigmatic beam waveguide and resonator 9-27401
 Fermat's principle, analytical consequence 9-43906
 field of view, elliptical geometry and parallel postulate 9-33971
 first-order, arbitrary ray coordinate behaviour, consistency 9-25338
 image aberrations of single and double mirrors 9-36336
 laser, liquid, amplification coeff., calc. 9-22406
 quasiisotropic approximations 9-45979
 radiation of open cylinder of infinite length, characts. 9-40282
 rectangular aperture, calc. of solid angle subtended at point opposite one corner 9-22440
 sign convention 9-45977
 sign convention 9-45978
 spectrometer experiment, improved computer version 9-43700
 undergraduate text 9-38188

nonlinear *see* Nonlinear optics**Orbital calculation methods**

- ab initio bond-orbital method 9-38900
 for alternant mol. orbitals without spin projections 9-38815
 approximate MO scheme for metal complexes 9-42378
 atom, Gaussian-orbital approx. by minimization of variance 9-29974
 best-atom Slater orbitals for first-row elements, hybridized-promoted 9-48384
 bipolar expansion, molec. multicentre integrals 9-36646
 Born-Oppenheimer treatment, appl. to H atom 9-46323
 Breit-Pauli Hamiltonian, one- and two-centre expansions 9-27794
 Brillouins' theorem extension used to calc. atomic spin-extended wave-functions 9-34526
 chromophores, orthoaxial, rel. to parametrization of 'd' antibonding levels 9-27843
 CNDO, in spectroscopy, small mols. 9-30007
 CNDO/2 used to determ. wave function coupling constants 9-42437
 configuration anal. in LCAO-MO theory 9-32450
 configuration interaction, two-body density function 9-32396
 configuration-interaction wavefunctions for small π systems 9-38877
 contact transformation method, eqn. for n-times transformed operator, method for calc. S-functions 9-27795
 for defect-solid electronic structure exam., applic. to divacancy in diamond 9-46810
 diatomics-in-mols. theory 9-30034
 using different orbitals for different spins method for alternant mol. orbitals calc. 9-38815
 electron shells, equivalent, wave functions 9-29915
 energy levels distrib., inversion and bond orders alteration anal. 9-23022
 energy variances for simple mols., lower bounds calc. 9-38814
 FEMO three-dimens. model for calc. term symbols, correspondence principle and e. distrib. in diatomic homonuclear mols. 9-38824
 floating spherical Gaussian orbital model 9-23020
 Gaussian expansions of atomic orbitals 9-38755
 Gaussian-type functions for polyatomic systems 9-30008
 Hartree-Fock, coupled perturbed, diagrammatic analysis 9-34512
 Hartree-Fock energies, saddle point character 9-29896
 Hartree-Fock eqn. for mol. wavefunctions in infinite internuclear separation limit 9-38816
 Hartree-Fock orbitals long-range behaviour 9-22925
 Hartree-Fock wave functions, inaccuracies in use of explicit angular momentum coupling 9-34511
 Hartree-Fock-Slater method, electron binding energy calc. 9-34529
 Hulbert-Hirschfelder potential tested by calc. r-centroids of several diatomics 9-30018
 Hulthén approximations to 1s and 2p orbitals of atoms 9-44245
 Hulthén type radial functions, generalized, as approximation to Hartree-Fock 2p functions 9-38752
 hydrocarbons, alternant, triplet-triplet absorption spectra, correlation between SCFMO and HMO calcs. 9-38901
 hypervirial theorems for transition multipole matrix elements calc. 9-29895
 INDO-MO vs. SCF calc. of atomic electron populations in mols. 9-40586
 INDO-SCF methods used to determ. wave function coupling constants 9-42437
 integral used in variational method 9-44312
 interacting geminals, natural orbital expansion 9-46260

Orbital calculation methods continued

- L-S eigenfunctions, construction and use by a computer program 9-36655
 LCAO theory, improved foundations 9-22919
 local exchange approx. in self-consistent-field, scaling procedure to agree with virial theorem 9-46259
 local permutational symmetry and separated-atom limit 9-48368
 localized-orbital LCAO MO wavefunction 9-42402
 many-electron systems, inhomogeneous, statistical exchange approximation 9-25043
 MINDO method 9-27899
 MINDO method 9-30122
 molecular, multicentre, systematic construction 9-44237
 molecular localized orbits, quantum theory, one-electron Huckel parameter determ. 9-32452
 molecular orbital calc. using multiple scattering model 9-34597
 molecular orbital orthogonality conditions rel. to stability of iron-group cyanides 9-34615
 molecule of C_{2v} symmetry, SCF one-centre expansion method for integral anal. 9-23019
 molecules, Hartree-Fock eqn. in restricted Hilbert space 9-34598
 multicentre electron repulsion integrals, convergence props. 9-44235
 multicentre electron repulsion integrals convergence props. 9-44234
 multicentre integrals, evaluation by polished brute-force techniques 9-44233
 natural orbital Hamiltonian derivation and appl. 9-38743
 natural orbitals, direct calc. by many-body perturbation theory 9-38742
 natural orbitals, divergences, and variational principles 9-48369
 natural orbitals of multiconfigurational wave functions, Hamiltonian 9-40532
 nitrobenzene, molecular isomers calc. 9-44365
 nitrochlorobenzene, molecular isomers calc. 9-44365
 non-paired spatial orbital Functions, generation methods, applic. to C_3 electr. struct. calc. 9-42388
 octahedral complexes, modified Wolfsberg-Helmholz calc. 9-36708
 optimized Gaussian basis SCF wavefunctions for first-row atoms 9-48375
 overlap integrals, tight-binding model applied to band structure of solids 9-35316
 perturbation theory, many-electron and adiabatic approximation 9-25684
 Pirac treatment contrasted with Schrodinger, rel. to zero probability positions of electrons 9-24523
 polarization wave function defined 9-34532
 polyatomic molecules wave-fn calc. method combining advantages of Slater and gaussian orbitals 9-44314
 polymers, SCF-SCAO theory 9-30153
 projected Hartree product wavefunctions 9-29894
 projected Hartree product wavefunctions, Young operators 9-29893
 pseudopotential approach atomic and mol. systems 9-22920
 pseudopotential method 9-27799
 quasi-bound states 9-48461
 radial distribution function, self-consistent equations 9-29892
 radial transition integrals and wave functions rel. to atomic transition probabilities 9-27802
 rare-earth complexes, overlap and Coulomb integral calcs. 9-45248
 Rayleigh-Schrodinger multiple perturbation theory 9-48367
 scattering model for molecular orbitals 9-34597
 SCF formalism, general 9-32398
 SCF-MO calc. ground state 1s orbital energies, for determ. of chemical shifts 9-38821
 Schrodinger eqn. soln. for arbitrary atom 9-34510
 self-consistent field method, Hartree-Fock eqns., further approximation 9-29913
 semi-empirical SCF scheme for small polyatomic mol. 9-30011
 Slater-type atomic orbitals, two-centre exchange integrals 9-38741
 SO-SCF function, determ. 9-40544
 spin degeneracy and stability of Hartree-Fock states 9-42317
 symmetry-projected single-determinant wavefunctions, density matrices 9-47755
 three-centre nuclear-attraction integrals via ellipsoidal coords. 9-30009
 three-parameter orbitals generalized from Slater and Gaussian functions 9-36684
 tight-binding band calc. of solids, eff. of inclusion of overlap integrals 9-47033
 time-reversal operator 9-34513
 Townes-Dailey theory, reliability check 9-42400
 transition metal complexes, overlap and Coulomb integral calcs. 9-45248
 two-electron systems variational perturbation theory calculations 9-42326
 valence-bond method, generalization 9-44334
 wave function constructed from complex hybrids 9-38813
 Wolfsberg-Helmholz, modified, for octahedral complexes 9-36708
 $\rho(0)$ electron density of heavy effects of screening incorporated 9-34527
 P-H collisions, a new orbital to allow for intermediate molecular state 9-32436
 BH mol. props. and electronic structure in ground and excited states 9-38830
 Li atom g.s. anal., spin orbitals and Fermi contact term 9-22959
 LiH, mol. transcorrelated wave eqn. numerical soln. 9-34628

Orbitals *see* Molecules/electronic structure**Order-disorder transformations *see* Phase transformations/solid-state****Ordered structure *see* Crystal/structure; Solids/structure****Organic compounds**

- see also Free radicals; Macromolecules; Plastics; Polymers; Waxes*
- 2-[2',4' dinitrobenzyl], cryst. struct. 9-30579
 (R-O)₂P(=O)H, P-H bending vibrs., obs. 9-30066
 (R-O)₂P(=S)(S-H), P-S-H vibrs. and rot. isomers, obs. 9-30066
 0-, m-, p- bromenzaldehyde vapours, electr. absorpt. spectra, longest wavelength $\pi \leftarrow \pi^*$ syst. obs. 9-46387
 β -diketonate salts, triplet-state energy and zero-field splitting 9-23116
 1,2,3,7,8,9-hexachlorodibenzo-p-dioxin, crystal structure and identification as hydropercaradium-producing factor 9-39335
 1,4,5,8-tetramethylanthrasemiquinone, anion radical, e.s.r. 9-36718
 p-azophenylidiphenylcarbamyl chloride, interconversion of cis and trans isomers under effect of light 9-24589
 3,4-benzpyrene in aq. lauryl sulphonate solns., excimer fluoresc. 9-40798
 α - ω -diphenylpolyene ketone charge transfer complexes with tetracyanethylene and chloranil, spectra 9-42443

Organic compounds continued

acetaldehyde, ^{13}C -H spin-spin coupling constants involving formyl proton 9-44350
 acetaldehyde, combination band of methyl group torsion and asymm. stretching vib. 9-25752
 acetaldehyde, i.r. spectra absolute band intensities, theor. and expt. 9-25756
 acetaldehyde(d_1), Raman line intensity, obs. 9-27884
 acetaldoxime, cis- and trans-, microwave spectra, molec. consts. 9-40605
 acetic acid, monomer and dimer, normal-coord. calc. 9-23083
 acetic acid and its ion, vibrational spectrum interpretation 9-42421
 acetic acid in nonpolar and polar solvents, anharmonicity of O-H stretching vib. 9-34650
 acetone, $-d_6$, Raman polarization meas., skeletal bending mode determ., He-Ne laser excitation 9-28136
 acetone, and acetone- d_6 absolute intensities of Raman lines meas., electro-optic parameters calc. 9-27883
 acetone, boiling, heat transfer depend. on e.m. field 9-23597
 acetone, i.r. bands, electrooptical parameters meas., intensity theor. calc. 9-32498
 acetone, i.r. bands, electrooptical parameters meas., intensity theor. calc. 9-27881
 acetone, photoionization efficiency curves for parent and fragment ions 9-39021
 acetone, u.v. absorpt. spectra, effects of temp. and salt additions 9-36888
 acetone, vicinal ^{13}C -H and long-range ^1H -H coupling const., sign and magnitude 9-40606
 acetone-chloroform, heat of mixing continuous determ. 9-40784
 acetonitrile, formation of solvated electron 9-27880
 acetonitrile, rotational spectrum in vibrational ground and excited state 9-23085
 acetonitrile and acetonitrile- d_3 , i.r. spectra 9-28696
 acetonitrile in vibr. $v_8=2$ excited state, rot. spectrum 9-46379
 3 β -acetoxy-5 β ,6 β -oxidocholestan-19-ol, vicinal H-C-O-H coupling consts., stereochem-depend. 9-46380
 1-acetyl 2-ethoxynaphthalene, cryst. struct 9-32934
 acetyl system, spectra and mol. orbital calc., electronic, steric eff. of substituent 9-23084
 acetylene, $^{12}\text{C}_2\text{D}_2$, $^{13}\text{C}_2\text{D}_2$ and $^{12}\text{C}^{13}\text{C}_2\text{D}_2$ molecules, ($\nu_4+\nu_3$) bands 9-30068
 acetylene, flash decomp. on W 9-43327
 acetylene, force constants, cubic and quartic, calc. with general quartic force field and empirical anharmonic potential function 9-30069
 acetylene, inelastic collisions with Na, total cross sections for $3^2\text{P}_{1/2}$ - $3^2\text{P}_{3/2}$ mixing 9-44288
 acetylene, nuclear spin relax. 9-23402
 acetylene, oxidation mechanism 9-33661
 acetylene, pyrolysis over Pt and Ni, rel. to growth of single-crystal graphite 9-39192
 acetylene derivatives with conjugated bonds, effect of intramolecular interactions on i.r. spectra 9-46381
 acetylene production from natural gas, patent by combustion, patent 9-47458
 acetylene-air flames, low press., ionization and recombination processes 9-42563
 acetylene- d_2 , i.r. absorpt. spectra, anal. of bands in 3-5 μ region, molec. consts. of levels 9-34651
 acetylene- O_2 -Ar mixture, spin detonation anal. and shock wave confluences 9-34093
 acetylglycine, irradiated, ENDOR study at 77°K 9-41436
 acetylene, resonant scatt. of electrons, ang. distrib. 9-27855
 N-acetyl-N'-phenylselenourea, crystal structure 9-26256
 acids, vapour spectra, band freq. 9-32445
 acridine, vibr. spectrum, comparison with anthracene 9-42422
 acridine dye absorption, luminescence and polarized luminescence spectra, 77°K 9-23113
 acridine dye adsorbates, triplet-triplet absorption spectra 9-48488
 acriflavine, emission spectra in solution 9-26122
 trans-acrolein, electronic structure CNDO CI study 9-32497
 acrolein, liq. and solns. of various concs. in cyclohexane, n.m.r. studies 9-30431
 acrolein ^{13}C -H spin-spin coupling constants involving formyl proton 9-44350
 acrylic monomers, polymerization in thin layers in presence of oxygen 9-24550
 adenosine, i.r. absorption spectra, 230-30 cm^{-1} , 20 to -175°C , crystal lattice vib. anal. 9-25783
 adenosine 5'-monophosphate, p.m.r. rel. to mol. struct., 100 MHz 9-32499
 adenosine 5'-triphosphate, p.m.r. rel. to mol. struct., 100 MHz 9-32499
 adenosine triphosphate, storage by polyhydric compounds addition, patent 9-24939
 β -adenosine-21- β -undec-5'-phosphoric acid cryst. and mol. struct. 9-39316
 adipic acid crystal, i.r. spectra, room and liq. N_2 temp., Raman spectra 9-34652
 β -alanine, γ -irrad., low temp. photoconversion 9-31208
 L-alanine-1- ^{13}C , irrad. at low temp., e.s.r. 9-33686
 alcohols, normal, heats of mixing and thermodynamics 9-23484
 alcohol, solvation to radical ions, e.p.r. study 9-34880
 alcohol, u.s. absorption at 25°C, relax curves due to LiCl in soln 9-23493
 alcohol mixtures at 1°K, proton polarization obs. 9-28762
 alcohols, association in soln. and in vapour phase 9-23507
 alcohols, dielectric props. over wide temp. range, time domain meas. 9-47885
 alcohols, thermal conductivity data considerations for standard reference materials 9-42703
 alcohols, vapour spectra, band freq. 9-32445
 aldehydes, ^{13}C -C-H spin-spin coupling constants involving formyl proton 9-44350
 aliphatic amines donor-acceptor complexes with aromatics singlet excited states 9-23096
 aliphatic monocarboxylic acids, i.f. infrared spectra 9-38885
 aliphatic normal alcohol, adsorption on silica gel 9-23649
 alkali halides-thiourea mixed cry., i.r. absorption spectra, interac. obs. 9-24420
 alkane mixtures, critical state, Prigogine corresponding states theory and cell model prediction 9-42691
 alkanes, liq., mol. sound vel. and compress., variation with temp. and press. 9-34904

Organic compounds continued

alkanes, liq., mol. sound vel. and compressibility, temp. and press. depend. 9-42650
 alkanes, radiolysis, charge separation and ionic processes 9-31214
 n-alkanes + cyclic hydrocarbons, Soret coeffs. 9-30382
 alkanethiols, valence force field 9-38880
 n-alkoxy ethanol monomolecular films, surface viscosity at various temp. and pressures 9-23448
 n-alkyl acid, i.r. spectra, H bond stretching vib. determ. 9-23087
 alkyl acrylate and fluoroalkyl acrylate copolymer, viscosity index improvers for lubricating oil, patent 9-23192
 alkyl ammonia anions-nonyl alcohol H-bonds, i.r. obs. 9-27885
 alkyl bromides, solid-phase radiolysis, e.p.r. of radicals 9-39912
 n-alkyl chlorides series, $\text{C}=2-6$, vib. 9-40607
 n-alkyl cpds., combination band of methyl group torsion and asymm. stretching vib. 9-25753
 alkyl ethers, microwave dielec. relax. 9-42671
 alkyl phosphinates, unsaturated monomer and oligomer, vibr. analysis, 400-4000 cm^{-1} 9-25757
 alkyl radicals, e.s.r. evidence for planar shape 9-44377
 alkyl radicals, unimolec. decomp., neopentyl rupture 9-39943
 alkylarylsulphonium mixed cpds., i.r. spectra 9-23086
 alkylchlorosilane on Ge surface, adhesion and elec. charact. variation 9-48924
 n-alkyltrimethylammonium bromide mols. end group freqs. and band progression rel. to chain length, 1400-700 cm^{-1} 9-44349
 allene, pure rot. i.r. absorpt. 9-38879
 allene, two rot. lines 9-38878
 allosteric enzymes. Monod-Wyman-Changeux, model, quaternary structure and cooperative ligand binding 9-34695
 allyl, configuration-interaction wavefunctions 9-38877
 allyl radical molecules, spectral characts. and electronic structures 9-30110
 amides, liquid, dielectric relax. rel. to intermol. association 9-26128
 amides, N-monosubstituted, deuteroderivatives, i.r. spectra 9-42663
 amines, NH_2 group valence vibrs. rel. to H bonding 9-34653
 amines, NH p chem. shift in protonation and Co(III) coordination rel. to neighbouring mag. anisotropy 9-28155
 amines and amides, vapour spectra, band freq. 9-32445
 amino acids, aromatic, u.v. induced photochem. transforms., obs. 9-28816
 amino acids, electronic structure determ. by X-ray diffraction analysis 9-34654
 m-aminobenzoic acid, crystals and soln. i.r. spectra 9-45332
 p-aminobenzoic acid, oriented, polarized absorption spectrum 9-46386
 p-amino-N-N'-diethylaniline, elec. dipole moment using modified Higasi's eqn. 9-46410
 p-amino-N-N'-dimethylaniline, elec. dipole moment using modified Higasi's eqn. 9-46410
 aminoethanolamine, dielec. props. rel. to mol. struct., -70 to 60°C 9-30417
 3-amino-1,4-naphthoquinone, crystal structure 9-26267
 p-aminophthalimide soln., electronic-absorption-band region, Einstein-coeff. spectra obs. 9-30072
 anilene, deuterated, doped with cyclohexane, NMR, molecular diffusion effect 9-28157
 anilene-cyclohexane mixture, shear viscosity obs. near critical point 9-32771
 aniline, 2938 Å electronic system, rotational band contours 9-34656
 aniline, ^{14}N n.g.r. temp. depend., 77-292°K 9-30071
 aniline, deuterated, doped with cyclohexane, NMR, molecular diffusion effect 9-44596
 aniline, dielectric studies at microwave freq., relaxation data and dipole moments 9-48711
 aniline, dipole moments of lowest singlet $\pi^* \leftarrow \pi$ states by optical Stark effect 9-34686
 aniline, halide substituted, i.f. Raman spectra 9-42424
 aniline, π -electron props. 9-48504
 aniline molecules, surface thermal ionization, proof 9-33426
 5-anilino-3-oxo-2-phenyl-2,3-dihydro-1H-pyrazolo [3,4-d] thiazole crystal structure 9-39317
 anisidines, o-, m- and p-, dielectric constants and dipole moments 9-36898
 anisole-benzene mixtures, dielec. props., internal field effects 9-46649
 anthracene soln., electronic-absorption-band region, Einstein-coeff. spectra obs. 9-30072
 anthracene: tetracene radiation damage rel. to optical absorption 9-26747
 anthracene, 185, 250 nm absorpt. in benzene, toluene 9-34912
 anthracene, anisotropy of triplet exciton diffusion 9-35137
 anthracene, crystalline, radiating-centres inhomogeneity, fluorometric phase spectra, -196°C 9-39879
 anthracene, current carriers mobilities, temp. depend. 9-33312
 anthracene, delayed fluorescence, charge-transfer excitons 9-33599
 anthracene, dipole Davydov splittings 9-49006
 anthracene, dipole Davydov splittings 9-49006
 anthracene, direct electron-hole recomb. 9-44971
 anthracene, elastic constants determ. from u.s. meas. 9-35143
 anthracene, electrolum. diode characts. 9-49336
 anthracene, electron and hole mobilities, high-temp. depend. 9-24087
 anthracene, electron photoemission 9-49176
 anthracene, electron-bombarded, carrier generation process obs. 9-33226
 anthracene, excited state mean lifetime and photolum. yield depend. on impurity conc. 9-26772
 anthracene, exciton-photon (polariton) dispersion curve 9-39571
 anthracene, fluoresc., singlet excitons diffusion coeff. obs. 9-41410
 anthracene, fluorescence spectra, excited by giant-pulse ruby laser 9-35691
 anthracene, formed by pyrolysis in presence of AlCl_3 , CuCl_2 9-26819
 anthracene, intrinsic photoconductivity 9-39728
 anthracene, low-lying valence states and intrinsic photocond. 9-24239
 anthracene, low-temp. hole injection and hole trap distrib. 9-44970
 anthracene, nanosecond excited-state polarized absorption spectra in visible region 9-34657
 anthracene, oriented growth in electric field 9-37097
 anthracene, photo-e.m.f. sign inversion 9-24238
 anthracene, photoemission of metallic electrons, conducting levels obs. 9-47215
 anthracene, pure and doped single cryst., line defects distrib. 9-37182

Organic compounds continued

- anthracene, recomb. radiation temp. depend. 9-39894
 anthracene, temp. depend. of steady current theory 9-28450
 anthracene, tight binding calc. of current carrier mobilities 9-33313
 anthracene, transfer of excitation energy to new-type excitons 9-47055
 anthracene, trap charact. and optical de-trapping obs. from photo-electron emission from alkali metal contacts obs. 9-33232
 anthracene, triplet excitons interaction with trapped electrons 9-39729
 anthracene, triplet-triplet annihilation in vapour 9-38905
 anthracene, two-photon absorpt., energy depend. 9-39795
 anthracene, vibr. spectrum, comparison with acridine 9-42422
 anthracene adsorbed on NaY zeolite, rel. to σ state, 77 and 290°K, mol. state, luminesc. obs. 9-28222
 anthracene and deuterated anthracene, rad. induced paramag. centres, EPR obs. 9-24499
 anthracene cation trapped in boric acid glass 9-42423
 anthracene crystals, hole injection from liquid redox electrodes 9-26475
 anthracene crystals, photocurrent excitation spectrum, exciton mechanism 9-35509
 anthracene crystals, tetracene doped, evidence for long-range exciton-impurity interactions 9-24457
 anthracene crystals, fluorescence spectrum 9-45351
 anthracene derivatives, polarization spectra rel. to oscill. orientation, 20°C 9-25758
 anthracene in glycerol solns., fluorescence, emission anisotropy 9-23513
 anthracene in mixed crystals (also containing naphthalene), triplet-triplet energy transfer 9-43262
 anthracene in soln., naphthalene addition, non variation of absorption spectrum 9-32501
 anthracene mixed crystal, guest-host interaction eff. on spectra 9-35643
 anthracene molecules in cyclohexane, radiation-induced fluorescence, effect of elec. field 9-44351
 anthracene photodimer, i.r. spectrum analysis 9-32502
 anthracene scintillator screens, prep. and props. 9-39860
 anthracene semiquinone derivatives, bridged long-range e.p.r. coupling 9-34655
 anthracene semiquinone derivatives, bridged, long-range e.p.r. coupling 9-34655
 anthracene single cryst., radical recomb. kinetics 9-32535
 anthracene solidified vitreous solns., absorpt. spectra, aggregates existence obs. 9-46701
 anthracene thin film, crystalline phase, fluorescence spectra and X-ray diffraction 9-35689
 anthracene triplet exciton band-structure limits from n.m.r. 9-35667
 anthracene-liquid relax electrode system, temp. depend. of saturation currents 9-24585
 9,10-antraquinone, thermodynamic props. 9-46418
 9,10-antraquinone, vibr. spectra 9-23156
 anthraquinotetramethan and corresponding diquinone, CMO calc. for spectral and redox behaviour 9-23089
 antimony trichloride:naphthalene, 2, 1 complex, crystal and molecular structure 9-39343
 aromatic, π - π^* charge-transfer states 9-32495
 aromatic aldehydes, vibronic interactions between $\pi\pi$ and $\pi\pi^*$ states 9-42426
 aromatic amines, disubstituted, dielectric studies at microwave freq., relaxation data and dipole moments 9-48711
 aromatic cpds. in halogenated liqs., molec. cations obs. by pulse radiolysis 9-31215
 aromatic free radicals, fluorinated, ^{19}F hyperfine splitting in e.s.r. spectra 9-46396
 aromatic hydrocarbon mixtures, anal. by selective fluoresc. 9-24605
 aromatic hydrocarbons, adsorption on zeolite Y, i.r. spectroscopy rel. to surface interactions 9-24520
 aromatic hydrocarbons, polarization of electronic transitions 9-31137
 aromatic hydrocarbons, radiationless transitions, temp. depend. 9-23091
 aromatic hydrocarbons, triplet decay, temp. effect 9-23090
 aromatic hydrocarbons, triplet-state zero-field splittings 9-42425
 aromatic hydrocarbons, triplet-triplet absorpt. polarized excitation spectra, obs. 9-23082
 aromatic hydrocarbons in polymethylmethacrylate, phosphoresc. temp. effects 9-28723
 aromatic mol. in soln., triplet-triplet interac. 9-40608
 aromatic molecules, diamagnetic susceptibility and anisotropy 9-30065
 aromatic mols., conformational analysis 9-48486
 aromatic mols., strained, conformation calc. 9-48487
 aromatic monomers and dimers, luminesc., high-energy electron excitation 9-43259
 aromatic rings of phenylalanine, tyrosine and tryptophan, H-addition radical formation 9-46423
 N-arylcarbazoles, u.v. absorpt. and luminescence 9-25759
 ON-aryl carbazoles, intramol. triplet energy transitions 9-23108
 arylamide, Cl substituted, steric effects in i.r. spectra, obs. 9-25760
 arylphenylacrylic acid i.r. spectra, carbonyl stretching freq. 9-23092
 arylpyrazolines, electronic absorption and luminescence spectra, structure depend. 9-30074
 s-aryltetrazoles, n.m.r. and mass spectral properties 9-34658
 p-azoxyanisole liquid crystal in nematic phase, Rayleigh scatt. of laser light 9-40793
 aza-naphthalenes, modified SCF treatment 9-32503
 azapyridocyanines, u.v. absorpt., fluorescence and phosphorescence transitions 9-23093
 p-azoxyanisole, liquid crystals, X-ray structure study in alternating elec. fields 9-42634
 p-azoxyanisole, nematic mesophase, perturbation of order by second component, e.s.r. study 9-42633
 p-azoxyanisole liq. cry., trans. liq. temp. depend. and electro opt. eff., nematic mesophase obs. 9-26112
 p-azoxyanisole nematic liq. crystals, optical rot. and electro-optic effect 9-30405
 p-azoxyphenetole, liquid, liquid crystal and solid states, for i.r. meas. 9-34913
 azulene, dipole moments of excited states 9-30075
 azulene molecule, in singlet state in solid solution, energy transfer from triplet state of another mol. 9-30076
 azulenes, protonated 1-substituted, solns. fluoresc., 20°C 9-28143
 batrachotoxinin A, structural formula and crystal structure using O-p-bromobenzoyl derivative 9-26257
 1,2-benzanthracene cryst., photoioniz. threshold meas. 9-33424

Organic compounds continued

- benzalacetophenone-mesityl oxide reaction, Li-catalysed condensation, obs. 9-47461
 benzaldehyde, Raman spectra, i.r. spectra obs. 9-44352
 benzaldehydes, aldehyde spin-spin coupling consts., Indor meas 9-46385
 benzaldehydes, monosubstituted, n.m.r. spectral parameters 9-30087
 benzanthracene molecules, excitation by electron impact 9-30083
 benzene, $^3B_{1u} \rightarrow ^1A_{1g}$ transition, factor-group splitting in vibrationless zero-zero absorption band 9-35692
 benzene, absorption spectra, noise intensity from fluctuations in readings 9-36889
 benzene, cryst. struct. at high-pressure 9-32903
 benzene, diffusion in cyclohexane meas. 9-44553
 benzene, doped crystals, triplet states 9-24098
 benzene, effect of deuteration on fluoresc. lifetime of liq. 9-48706
 benzene, electron scatt., cross section and spin polarization meas., $E_0=60$ 1600 eV 9-23167
 benzene, electron scattering, inelastic, rel. to excitation cross-sections 9-30082
 benzene, electronic spectrum calc. 9-44304
 benzene, electronic vib. transition $^1A_{1g} \rightarrow ^1B_{2u}$ calc. 9-27888
 benzene, fluoresc. of low-pressure vapour 9-30079
 benzene, halide substituted, l.f. Raman spectra 9-42424
 benzene, hypersonic absorpt. determ. from Brillouin line breadth 9-44560
 benzene, isotopically mixed crystals, singlet excited states 9-24097
 benzene, liquid, far i.r. absorptions 9-40796
 benzene, molec. distortions and phosphoresc. 9-30081
 benzene, mols. photoionization, π system contribution, calc. 9-34669
 benzene, N_2 and Ar diffusion, open-tube obs. 9-30383
 benzene, n.m.r. shift and quasicryst. struct. of liq. 9-30432
 benzene, proton screening const. and mag. anisotropy, antisymmetrical MO calc. 9-23097
 benzene, proton spin relax. 23°C, 0.07 1.9 kbar 9-30121
 benzene, Raman line intensities as function of conc. and solvent type 9-48701
 benzene, relative phosphoresc. radiative rates in two cyclohexane sites 9-28725
 benzene, resonant scatt. of electrons, ang. distrib. 9-27855
 benzene, Rydberg states in inert-gas matrices 9-46384
 benzene, self-diffusion in benzene-toluene liquid mixture 9-36856
 benzene, sorption and dielectric isotherm on acid-purified silica gel after 6 month storage, 1 Mc/sec, 25°C 9-42735
 benzene, sublimation energy 9-46691
 benzene, sublimation energy 9-44618
 benzene, vibronic intensity distrib. in phosphoresc. 9-30080
 benzene and acetylene derivatives, T-T* absorption spectra by 2-quantum photosensitized reactions 9-42428
 benzene and derivatives, photoionization study of mol. orbitals 9-30078
 benzene anion solns., ion pairing and temp. depend. of linewidth 9-42680
 benzene carbonic acid, u.v. electron absorption spectra 9-30085
 benzene crystals, doped, absorption spectra of localized exciton states 9-31112
 benzene derivatives, liquid, spectrum of depolarized light scattering 9-26117
 benzene derivatives, phosphoresc. lifetime rel. to σ , π -mixing and C-H vibr. 9-23095
 benzene in perdeuterobenzene cry., ESR of phosphorescent state, hyperfine and fine struct. obs. 9-35719
 benzene ion-mol. reactions 9-24541
 benzene isotopic mixed crystals, site effects in vibr. spectrum 9-43007
 benzene molecule, in triplet state, energy transfer to singlet state of azulene mol. 9-30076
 benzene sorption and diffusion in vinyl acetate methyl acrylate 9-33010
 benzene-carbon disulphide solns., acoustic relax. obs. and its mechanisms 9-46632
 benzene-carbon tetrachloride, liquid mixture thermal conductivity 9-36865
 benzene-toluene, liq. mixture thermal conductivity 9-36865
 benzene/benzene- d_6 , excess enthalpy and volume of mixing 9-23485
 benzene- o,o' -ditolyl (or diphenyl or diphenyl methane) mixing effects 9-48683
 benzenes, methyl substituted, SCF-MO semiempirical calcs. 9-30092
 benzenes, monosubstituted, i.r. ν_{16} intensities rel. to substituent σ_p^0 , ^{16}O s. 9-30090
 benzenes, monosubstituted, ring P chem. shifts, P mag. reson. obs. 9-23536
 benzenes, para-disubstituted, ν_{16} intensity rel. to substituents direct interaction, 1600 cm^{-1} 9-30091
 benzenes, stretch vibrations, integral intensities of i.r. bands 9-30089
 benzenes, substituted; spectra and lum. depend. on charge-transfer state 9-30084
 benzenes, trisubstituted, proton-proton coupling const., additivity of substituent effects 9-23100
 benzil, hexagonal cry., circular dichroism meas. 9-26704
 benzil in stilbene cryst., trans-planar config. from polarization characts. of spectra 9-34660
 benzimidazole, and metal complexes, i.r. spectra 9-23099
 benzine, CH-stretching overtone anharmonicity 9-27886
 benzo-[g,h,i]-perylene, absorpt. and fluorescence spectra 9-34661
 benzocyclopropapyran, crystal and molecular structure 9-39321
 benzodioxane-1,4, 6-substituted, u.v. and i.r. absorpt. spectra 9-40609
 1,2-benzodithiol-3-one oxime, crystal and mol. structure 9-26258
 benzoic acid, Cl substituted, steric effects in i.r. spectra, obs. 9-25760
 benzoic acid, oriented, polarized absorption spectrum 9-46386
 benzoic acid adsorption on glass, rate and magnitude meas. 9-30502
 benzol, boiling, heat transfer depend. on c.m. field 9-23597
 benzol [cd] pyrene-6-one, negative ion 9-30305
 1,12-benzoperylene in heptane, frozen, fluoresc. spectra 9-32517
 benzophenone, crystal and mol. structure 9-46797
 benzophenone, electric dipole moment determination by dielectrometer 9-45907
 benzophenone, e.s.r. of triplet state 9-49358
 benzophenone, phosphoresc. spectrum 9-39886
 benzophenone derivatives with donor and acceptor substituents, u.v. absorpt. spectra, obs. 9-30413
 benzophenone in solid state, i.r. spectrum 9-30077
 benzophenone-naphthalene, triplet energy transfer in cryst. and glassy state 9-28724
 3, 4-benzopyrene conc. quenching and quasi-line luminescence spectra temp. depend. obs. 9-23098

Organic compounds continued

- 3,4-benzopyrene p.m.r. spectra at 220 and 100 MHz 9-34662
 p-benzoquinone, ionization by nondissoc. e attachment in ground and excited state fields 9-32694
 p-benzoquinone, luminesc., triplet-singlet- $n\pi^*$ in cryst. and e-donor-acceptor complexes, -180°C 9-31142
 p-benzoquinones, tetra substituted, i.r. spectra obs., vibrational frequencies calc. 9-30086
 2,1,3-benzoselenadiazole, p.m.r. spectra and parameters 9-30088
 2,1,3-benzothiadiazole, p.m.r. spectra and parameters 9-30088
 2,1,3-benzoxadiazole, p.m.r. spectra and parameters 9-30088
 benzoyl system, spectra and mol. orbital calc., electronic, steric eff. of substituent 9-23084
 benzo[a]anthracene photodimer, i.r. spectrum analysis 9-32502
 benzyl acetate, chloroform, heat of mixing continuous determ. 9-40784
 benzyl chloride, Raman spectra, i.r. spectra obs. 9-44352
 benzyl chloride in cyclohexane, gas-phase pulse radiolysis, benzyl radicals 9-43339
 benzyl formate, Raman, and i.r. spectra obs. 9-44352
 benzyl radical, emission spectrum in vapour state rel. to symm. and transitions 9-34694
 benzyl radicals, spin density distrib. 9-42427
 benzylidene impurity in fluorene, u.v. spectra, polarized fluorescence and absorption vibrational anal. 9-28697
 bi(anthracene-9,10-dimethylene) photo-isomer, diamag. susceptibilities and anisotropies 9-45081
 bicyclo (2,2,1) heptane radical, E.S.R. 9-46398
 bicyclo [1.1.0] butane, microwave spectrum 9-32504
 bicyclo [1.1.0] butane, microwave spectrum and struct. 9-32504
 3,4'-biisoxazole, crystal and molecular structure 9-39338
 biphenyl, photocond. spectrum 9-30996
 1,2-bis(dihaloboryl)ethanes, vibr. spectra 9-38882
 bis(diphenylphosphino)acetylene, crystal and mol. structure 9-26261
 bis(perfluoromethyl) nitroxide, gas-phase e.s.r. relax. 9-32739
 bis(diphenylmethyl) diselenide, cryst. and mol. struct. 9-39322
 1,4-bis(methylthio)naphthalene cation-radical, electronic and e.s.r. spectra 9-38883
 1,4-bis-2-(5-phenyloxazolyl)-benzene (POPOP) as medium for rendering light isotropic in Cherenkov counter 9-29656
 bis(trifluoromethyl)trioxide i.r. spectra, vib. modes degeneracy 9-25765
 bitumens, between liquid and solid, u.s. absorption and dispersion 9-30450
 bixinmethyl ester, static elec. polarizability change upon transition to first excited singlet-state 9-40611
 borazane, internal rotational barrier computed 9-34670
 borazines, methyl substitute, SCF-MO semiempirical calcs. 9-30092
 α -bromine anthraquinone, cryst. and molecular struct. 9-42799
 α -, m-bromo anilines, vapour, near u.v. absorpt. spectra 9-25762
 α -bromo chloro benzene, solid, near u.v. absorpt. spectrum 9-46383
 α -bromo iodo benzene, vapour, near u.v. absorpt. spectrum 9-46383
 bromoacetaldehyde, n.m.r. study and conformational anal. 9-46655
 β -bromoaniline, ^{14}N n.g.r. temp. depend. $77-292^\circ\text{K}$ 9-30071
 4-bromobenzonitrile in liq. cryst. solvent, i.r. absorption spectra 9-48682
 p-bromobenzoyl derivative of ϵ' -casealpin, crystal and molecular structure 9-39324
 2 α -bromo-5 β -bromomethyl-5 α -methyl-2 β -oxo-1,3,2-dioxaphosphorinane crystal structure 9-26259
 bromoform, C-H stretching vibr. band, shape and width 9-48489
 bromoform, in CCl_4 and CS_2 soln., integrated intensity of i.r. absorption band 9-23110
 6-bromoisofenchone, crystal and mol. structure 9-23784
 β -bromophenotol, u.v. and i.r. spectra rel. to transitions and vib. 9-23101
 p-bromophenol, Zeeman effect of ^{81}Br n.g.r. 9-39929
 6 β -bromoprogesterone, crystal and molecular structure 9-39323
 2-bromopropene, combination band of methyl group torsion and asymm. stretching vib. 9-25752
 trans-1-bromopropene, microwave spectrum and molec. consts. 9-32505
 busmuth triphenyl, electron scatt., cross section and spin polarization meas., $E_g=60-1600\text{ eV}$ 9-23167
 butadiene, cis- and trans-, SCF MO and CI calc. 9-27890
 butadiene, configuration-interaction wavefunctions 9-38877
 butadiene, mols. photoionization, π system contribution, calc. 9-34669
 butadiene molecules, spectral characts. and electronic structures 9-30110
 butadiene with styrene, regulation of molecular weight in polymerization 9-24551
 n-butane, isotope effects in photoionization yields and absorpt. cross-sections 9-30298
 butane- d_{10} , reaction with atomic H 9-39944
 butanes, methyl-substituted, p-irrad., free radical e.s.r. spectra 9-48499
 1- and 2-butanol, dielec. relaxation at high pressures 9-32791
 butanol polarized proton target 9-44078
 butanol-water NaCl solns., liq.-liq. equilibrium 9-32765
 butanols, acoustic relax., $10-300\text{ kHz}$ 9-28123
 butene, cis- and trans-, Rydberg progressions 9-38884
 butene-1, rotational const. determ. from microwave spectra 9-23102
 butene-2, Cd-photosensitized isomerization, energy transfer by benzene 9-31212
 butyl alcohol, dielec. const. freq.-temp. meas. by helical resonator method 9-36895
 n-butyl alcohol, film condensation, heat flux meas. and Nusselt soln. 9-39141
 n-butyl alcohol, low temp. phase transitions, luminescence obs. 9-42692
 n- and iso-butyl alcohol, sound velocity, temp. depend. 9-30401
 t-butyl alcohol-water mixtures, small angle X-ray scatt., conc. and temp. depend. 9-28101
 butyl benzene, tert., field ionised, unimol. decomp. 9-25787
 t-butyl chloride, liq. and solid, microwave absorpt. 9-39670
 t-butyl N, N-dimethylthiopericarbamate, crystal and molecular structure 9-39325
 t-butylbenzene, alkyl derivative crystal, vibronic spectra, 20°K 9-31113
 γ -butyrolactone, i.r. and Raman spectra of gas and liq. rel. to mag. deform. 9-48492
 butyrophenone, h.f. discharge and dissoc. processes 9-46545
 calcium 1,3-diphosphorylimidazole, crystal structure 9-30580
 calcium formate, crystalline, Raman spectra 9-47378
 calcium stearate Langmuir film, electric conduction 9-37583
 calcium tartrate, nucleation and growth in gels 9-37029
 camphor, fcc, mobility of non-coherent twin boundaries 9-40963

Organic compounds continued

- camphor (*d* and *dl*), dielec. props. as function of temp., at 1, 10 and 100 kHz 9-49135
 carbazole, copolyolysis with aryne precursors, and enhanced graphitization 9-26811
 carbazole, N-heterocyclic, space group determ. 9-30581
 carbinols u.v. electron absorption spectra 9-30085
 carbon disulphide, dielec. props., press., vol., and temp. effects 9-39109
 carbon disulphide, liquid, far i.r. absorptions 9-40796
 carbon tetrabromide solute, i.r. vibrational band perturbation meas. 9-26123
 carbon tetrachloride, cohesion energy, vapour press. and molar vol., obs. 9-28094
 carbon tetrachloride, cryst. struct. at high press. 9-32903
 carbon tetrachloride, dielec. props., press., vol., and temp. effects 9-39109
 carbon tetrachloride, electron scatt., cross section and spin polarization meas., $E_g=60-1600\text{ eV}$ 9-23167
 carbon tetrachloride, equilibria of assoc. bet. pyridine deriv. and alcohols 9-23106
 carbon tetrachloride, evidence of multiple vibrational-translational relax. 9-48702
 carbon tetrachloride, frozen, forced Raman scatt. 9-37737
 carbon tetrachloride, hypersonic absorpt. determ. from Brillouin line breadth 9-44560
 carbon tetrachloride, i.r. optical constants, exptl. determ., consistency of results 9-23500
 carbon tetrachloride, liquid, absorption and dispersion in $740-820\text{ cm}^{-1}$ range, temp. depend. 9-48703
 carbon tetrachloride, liquid, far i.r. absorptions 9-40796
 carbon tetrachloride, N_2 and Ar diffusion, open-tube obs. 9-30383
 carbon tetrachloride, ν_1 fundamentals, CI isotopic splitting, using low temp. Raman cell 9-32068
 carbon tetrachloride, positron lifetimes in liquid 9-44583
 carbon tetrachloride, Raman spectra determ. using He-Ne laser as excitation source 9-49293
 carbon tetrachloride, shock compressed, elec. cond. and permitt., microwave technique 9-30419
 carbon tetrachloride solute, i.r. vibrational band perturbation meas. 9-26123
 carbon tetrafluoride, cryst., modified, absorpt. and refl. rel. to Fermi reson., 8μ 9-28676
 carbonyl cpds., vapour spectra, band freq. 9-32445
 carboxylic acids, dilute, aqueous, u.s. absorpt. rel. to dissoc. equilib. 9-48695
 carboxylic acids, dimeric, mol. config. in crystals, i.r. obs. 9-30093
 carboxylic acids, in vapour phase, heat of dimerization, spect. obs. 9-23107
 carboxy methyl cellulose, aqueous soln., laminar flow, heat transfer studies 9-26088
 castor oil, acoustically induced birefringence study 9-23495
 cellulose, e.p.r. parameters rel. to charring 50 to 600°C 9-26810
 cerium ethyl sulphate $\cdot \text{ND}$, spin lattice relax. and cross-relax., optical detection, $1.28-2.15^\circ\text{K}$ 9-35595
 cetyl dimethylbenzylammonium chloride, influence on $\text{Na}_2\text{P}_2\text{O}_{10}$ crystal growth 9-37038
 chain molecules with end groups, vibrational intensities 9-34648
 charge-transfer-complex formation, use of hexafluorobenzene and pentafluorobenzonitrile as acceptors 9-28784
 charged insoluble monolayers, influence of monovalent counterions 9-23447
 chloral hydrate, e.p.r., e and γ irradiated, rel. to conc. of produced paramag. centres 9-33638
 p-chloranil, electron injection into single cryst. by aqueous electrolyte contact 9-41203
 chlorinated hydrocarbons, solid, deuteron. quadrupole coupling 9-43311
 m-chloro ethyl benzenes, solid, near u.v. absorpt. spectra 9-46383
 p-chloro iodo benzene, vapour, near u.v. absorpt. spectrum 9-46383
 chloro-methylbenzenes, hexa-substituted crystals, i.r. spectra and molec. librations 9-24418
 chloroacetaldehyde, n.m.r. study and conformational anal. 9-46655
 chloroacetyl halides, rot. isomerism 9-30094
 p-chloroaniline, ^{14}N n.g.r. temp. depend. $77-292^\circ\text{K}$ 9-30071
 2-chloroanthraquinone, i.r. and visible emission spectra 9-25763
 2-chlorobiphenyl-4-carboxylic acid, cry. struct., X-ray diff. obs. 9-35073
 chloroform, C-H stretching vibr. band, shape and width 9-48489
 chloroform, in CCl_4 and CS_2 soln., integrated intensity of i.r. absorption band 9-23110
 chloroform, i.r. optical constants, exptl. determ., consistency of results 9-23500
 chloroform, n.m.r. of ^{35}Cl , anisotropic molecular rotation in liquid 9-39119
 chloroform, solvation of nitrate ion, i.r. spectroscopic evidence 9-42661
 chloroform in electron-donor solns. 9-23518
 Chloroform-triethylamine system, dielec. props. rel. to mol. anisotropy 9-48712
 chloromethane, i.r. spectra, ν_1 band rotational structure 9-32507
 chloromethane-CO and CO $_2$ systems, composition dependence of thermal diffusion factor 9-39058
 α -chloronaphthalene, two-photon absorpt. obs. 9-32506
 α -chloronaphthalene in n-paraffin, quasiline phosphoresc. spectra 9-46409
 chloronaphthalene, 1,4-, 1,5-, 2,6-, e spectra, obs. 9-27891
 chloronated, h.f. mech. props. 9-39098
 chloronitrobenzenes, u.v. spectra in THF and cyclohexane 9-30095
 p-chlorophenol, Zeeman effect of ^{35}Cl n.g.r. 9-39929
 p-chlorophenoxy acetic acid, n.g.r. ^{35}Cl , temp. variatn. of freqs. 9-30103
 chlorophyll and derivatives, use in Q-switching of ruby laser 9-36303
 chlorophyll solns., eff. of laser light on optical transmission coeff. 9-28131
 chlorophyll solutions, a and b type, excitation energy transfer and luminesc. 9-36892
 2-chloropropene, combination band of methyl group torsion and asymm. stretching vib. 9-25752
 2-chloropropene-1,3-d, internal rot. and vib. 9-40610
 2-chloroquinoline, cryst. struct. refinement at -140°C 9-46798
 chlorotrifluoromethane, natural convective heat transfer, comparison with CO_2 and N_2O 9-28170
 2-chlorotripropene-cycloheptatriene adduct, crystal and molecular structure 9-39327
 cholesteric liq.-cryst. films, optical props. 9-39103

Organic compounds continued

- incholester benzoate liq. crystals, pyrene fluoresc. decay time, obs. 9-32786
- cholesterol derivatives, liq. crystals. elec. field induced orientation 9-34876
- cholesterol liquid crystals, texture, rel. to domain occurrence 9-40774
- cholestery-2-(2-ethoxyethoxy) ethyl carbonate, Brillouin scatt. 9-46644
- chromium phthalocyanin, reduced, hyperfine struct. in e.s.r. spectra 9-42445
- citric acid, anhydrous, cryst. struct., X-ray diff. obs. 9-35074
- citric acid, anhydrous, cryst. struct., X-ray diff. obs. 9-44677
- citric acid, supersaturated aqueous solns., molecular cluster formation 9-30374
- clathrates, p.m.r. lineshape and chem. shift of enclosed mols. 9-39924
- cojugated hydrocarbons, ring-current contrib. to mag. susceptibilities 9-36709
- complex mols., relaxation of upper triplet states, after light excitation, triplet-triplet absorption band obs. 9-25755
- constituents in Pueblito de Allende meteorite, anal. 9-43638
- copper (II) benzoate, e.p.r. meas. at 9.1 and 12.0 GHz, spin Hamiltonian parameters 9-49350
- copper acetate, p. relax. in H_2O , C_2H_5OH solns., obs. 9-48719
- copper acetate monohydrate, γ -irrad., conversion of Cu^{2+} to Cu^+ 9-49386
- copper chloride cpds., $Cu(C_4H_{21}N_3)_2Cl_4$, transition temp. from a.c. susceptibility data 9-45107
- copper formate tetrahydrate, antiferromag. reson., 1.4 to 15°K 9-45378
- copper formate tetrahydrate, two-dimensional antiferromagnet behaviour 9-26661
- copper phthalocyanine, atomic planes bordering a crack config. 9-42904
- α -copper phthalocyanine, e.s.r. powder line shape and MO calc. 9-33639
- Copper porphyrins, quartet luminescence 9-26773
- copper (II) salicylate adducts, e.p.r. and mag. susceptibility 9-37804
- coronene, absorption shifts with press. and temps. 9-30097
- coronene, oscillator strength distrib. correlation effects of π distrib. 9-44363
- coronene, phosphorescence in hexyl alcohol frozen soln., infl. of soln. struct. and oxygen 9-49325
- coronene in heptane, frozen, fluoresc. spectra 9-32517
- coronene in n-dodecane, phosphorescence temp. depend., centre formation, O sensitivity 9-23515
- coronene in n-octane, phosphorescence temp. depend., centre formation, O sensitivity 9-23515
- coumarin and related cpds., triplet state, e.p.r. 9-30096
- creatine phosphokinase, storage by polyhydric compounds addition, patent 9-24939
- crocetindimethylester, static elec. polarizability change upon transition to first excited singlet-state 9-40611
- crysene, heat capacity anomaly 9-33186
- cumene, mol. structure from e. diff. exam. 9-23111
- cumene hydroperoxide solution, H-bonding investigated by i.r. absorpt. 9-27892
- cupric formate tetrahydrate, DMR obs. of struct. and water mol. motion changes due to paraelec. antiferro. transition 9-35730
- cyanides, γ -irrad. crystals, e.s.r. of trapped electrons 9-47440
- cyanine dye absorption, luminescence and polarized luminescence spectra, 77°K 9-23113
- cyanine dye in methanol soln. laser 9-36296
- cyanine dyes, conditions for and characs. of lasing action 9-41909
- ciano group, coupling constants, extended Huckel scheme 9-38890
- ciano group, electronic struct. 9-42386
- 9-cyanoanthracene, polarised u.v. absorpt. spectrum at 4.2°K 9-33566
- ciano-1(9) anthracene vitreous solns., absorpt. spectra, aggregates struct. obs. 9-46702
- 4-cyanobenzoic acid in liq. cryst. solvent, i.r. absorption spectra 9-48682
- 2-cyanoethoxysilanes, NMR spectra, analyses 9-38887
- cyanogen, electronic spectrum 9-30098
- 2-cyanopropene, combination band of methyl group torsion and asymm. stretching vib. 9-25752
- cyanopropyne, vibr. spectra 9-23112
- p-cyanofluorobenzene, n.m.r. multiple quantum transitions and coupling consts., obs. 9-23094
- cyclic molecules, superposition links 9-26255
- cyclic phosphazene, $N_4P_4(NMe_2)_{12}$, crystal and mol. structure 9-30583
- cyclic phosphazene, $N_4P_4(NMe_2)_{12}$, crystal and mol. structure 9-30583
- cyclic polyenes, vibronic borrowing 9-44353
- 1,3,5,7-cyclo-octatetraene, low energy e impact excitation spectrum, obs. 9-23126
- cyclobutane-1,3-dione, i.r. and Raman spectra 9-23115
- cyclobutanes, vinyl, methyl and isopropenyl substituted, i.r. spectra 9-23114
- cyclobutanol, -d₁, -d₄, -d₅, i.r. and Raman spectra, vib. assignment 9-23103
- cyclobutanone, n.m.r. parameters of A_2B_2 spin system, anal. 9-48720
- cyclobutanone vapour, u.v. spectrum, 3300°A resolution, 1A_2 electronic state O vib. levels 9-24229
- cyclobutanones, photochem. decomp. 9-33682
- 1,3,5-cycloheptatriene, low energy e impact excitation spectrum, obs. 9-23126
- 1,4-cyclohexadiene oriented in nematic solvent, n.m.r. 9-36712
- cyclohexadienes in gas phase, struct. and conformations by electron diff. meas. 9-46389
- cyclohexane, conformational energy, ab initio calc. 9-38886
- cyclohexane, diffusion of benzene in liquid meas. 9-44553
- cyclohexane, liquid, far i.r. absorptions 9-40796
- cyclohexane, polymorphic transition at -86°C, positron annihilation obs. 9-32859
- cyclohexane, reaction with hot-H-atoms 9-43344
- cyclohexane, self-diffusion in cyclohexane-toluene liquid mixture 9-36856
- cyclohexane in deuterated anilene, NMR near critical soln. temp. 9-28157
- cyclohexane in deuterated anilene, NMR near critical soln. temp. 9-44596
- cyclohexane-anilene mixture, shear viscosity obs. near critical point 9-32771
- cyclohexane-carbon tetrachloride, liquid mixture thermal conductivity 9-36865
- cyclohexane/cyclohexane-d₁₂, excess enthalpy and volume of mixing 9-23485
- cyclohexanexime, substituted, crystal structure 9-39336

Organic compounds continued

- cyclohexanol, phase transformations, growth rates and morphology 9-35251
- cyclohexene, liquid, far i.r. absorptions 9-40796
- cyclohexene cryst., molec. motions and phase transitions, n.m.r. 9-43305
- cyclooctatetraene anion radical, temp. dependent e.s.r. 9-44589
- π -cyclopentadienyl derivatives of cpds., mass spectra 9-34515
- cyclopentane, conformational energy, ab initio calc. 9-38886
- cyclopentane, mass spectrometric investigation of products of radiolysis 9-24592
- cyclopentanone-d₄, i.r. and Raman spectra of gas and liq., rel. to mag. deofms. 9-48492
- cyclopropane, group vibrations and vibrational analysis 9-23140
- cyclopropane, vib.-rot. bands, computer anal. 9-38895
- cyclopropane-H₂ and -D₂, force field and normal coordinates 9-38889
- cyclopropanes, monosubstituted, p.m.r. and ^{13}C -H satellite spectra 9-38888
- cyclopropyl derivatives, p.m.r. spectra, high resolution 9-30099
- cytidine, i.r. absorption spectra, 230-30 cm⁻¹, 20 to -175°C, crystal lattice vib. anal. 9-25783
- cytosine, γ -irrad., free radical produced, structure 9-44354
- cytosine monohydrate, e.s.r. of γ -irrad. cryst. 9-45390
- decafluorobiphenyl, vibrational spectrum, below 200 cm⁻¹ 9-30100
- n-decane, liq., negative-carrier mobility meas. 9-42672
- n-decane- β,β' dichloroethyl critical opalescence investigated by light and X-ray scatt. 9-36877
- 3-deoxy-2-c-hydroxymethyl-D-erythro-pentate, crystal structure 9-39345
- detergent films, interface props. 9-23446
- deuterated formaldehyde, Stark spectroscopy by i.r. lasers 9-25767
- deutero-nitrobenzene liquids, electric field effects in 2D n.m.r. 9-46656
- deuterochloroform, n.m.r. of 2H and ^{35}Cl , anisotropic molecular rotation in liquid 9-39119
- Deuteromethyl halides, force consts., soln. of inverse eigenvalue problem 9-27838
- per-deuterophenazine, triplet state, e.p.r., obs. 9-48503
- diacetylenes: heteroaromatic substituted carbonyl cpds., absorpt. spectra, 1637-1630 cm⁻¹ 9-30067
- dialkylacetylenes, straight-chain, i.r. absorpt. rel. to struct., obs. 9-27878
- diamides, electron conduction, model 9-33249
- 10,10'-dianthranyl, diama. susceptibilities and anisotropies 9-45081
- diaryl N oxides, methoxy-substituted, e spectra, obs. 9-27912
- 1,2,5,6-dibenzanthraquinone, crystal and molecular structure 9-39320
- dibenzocyclohexadienyl radical in anthracene single crystal, radiation induced, ENDOR studies 9-39913
- dibenzodimethoxy compound, polycyclic cryst. struct., obs. 9-30577
- dibenzooquinene, polycyclic cryst. struct., obs. 9-30577
- dibenzopentalene, ground-state geometry and symmetry 9-36716
- dibenzthiophene, surface photocond., activation energy and characs. 9-49165
- p-dibromobenzene, ^{79}Br n.q.r. and l.f. Raman lines, temp. dependence 9-31175
- p-dibromobenzene single crystals, polarized Raman spectra in intramolecular vibrational region 9-30104
- 2,3-dibromobutane, liq., solid, conformations, vib. assignments and force consts. 9-34663
- 1,2-dibromoethane liquid, Raman spectra intensity temp. depend., energy difference of trans. and gauche configurations 9-44355
- dibromofluoroethane, heavy hindered rotator, neutron scatt. and far i.r. spectra 9-42432
- 11 β ,12 α -dibromo-3 α -9-oxidocholeonic acid methyl ester, crystal structure 9-39329
- 2,3-dibromopentane, liq., solid, conformations, vib. assignments and force consts. 9-34663
- p-dibromotetrauterobenzene, i.r. and Raman vib. spectra 9-27889
- di-n-butyl ether, electric dipole moment determination by dielectrometer 9-45907
- dicalcium strontium propionate-acetate mixed cryst., $6(1-\frac{1}{2})(CH_3CO_2)_{2x}$, ferroelec. hysteresis loops 9-35481
- 1,1'-dichloro-2-methyl propane, rotational isomerism, NMR investig. 9-23162
- 2,4-dichloroaniline, n.q.r. of ^{35}Cl , temp. variation of freqs. 9-30103
- 2,6-dichloroaniline, n.q.r. of ^{35}Cl , temp. variation of freqs. 9-30103
- 2,6-dichloroaniline in solution, obs. of i.r. spectrum assignments to vib. modes 9-32500
- 2,6-dichloroaniline in solution, obs. of i.r. spectrum assignments to vib. modes 9-32500
- 9,10-dichloroanthracene, Urbach rule and long-wave tail of exciton band 9-39849
- 9,10-dichloroanthracene with chlorinil, absorption spectra 9-30073
- 3,5-dichloroanthranilic acid, cryst. struct. 9-35075
- dichlorobenzene, o-, m- and n-, combinational scattering spectra, phase shift rel. to dipole-dipole intermolecular forces 9-46393
- o-dichlorobenzene, n.m.r. multiple-quantum transitions 9-30146
- p-dichlorobenzene single crystals, polarized Raman spectra in intramolecular vibrational region 9-30104
- 1-(2,6-dichlorobenzyl)-6-hydroxy-1,4,5,6-tetrahydronicotinamide dihydrate, crystal structure 9-39330
- 1,2-dichloroethane, vib. band envelopes rel. to molec. struct. 9-34622
- 1,2-dichloroethane liquid, Raman spectra intensity temp. depend., energy difference of trans. and gauche configurations 9-44355
- trans-dichloroethylene, nuclear spin-lattice relaxation 9-24344
- meso-3,3'-di-(p-chlorophenyl) bi-3-phthalidyl, crystal structure refinement 9-39331
- 2,4-dichlorophenyl methyl isopropylphosphoramidate, n.m.r. asymmetry rel. to intermol. H-bonding, obs. 9-27879
- 3,5-dichlorosalicylaldehyde, chemical shifts of protons in H bond, temp. depend. 9-34665
- 2,4-dichlorotoluene, i.r. absorpt. spectra, vib. assignments 9-23109
- 9-dicyanomethylene-2,7-dinitrofluorene, crystal structure 9-30578
- dideuteracetylene, $^{12}C_2D_2$, $^{13}C_2D_2$ and $^{13}C^{13}CD_2$ molecules, ($\nu_4 + \nu_3$)⁰ bands 9-30068
- didodecyl sulphide, microwave dielec. relax. 9-42671
- diethanolamine, dielec. props. rel. to mol. struct., -70 to 60°C 9-30417
- diethyl ether, light scatt. near crit. pt., gravity effects 9-30406
- 4,4'-diethyl-benzophenone, ESR and NMR obs. 9-40614
- diethylaminotelluriumpentaffluoride magnetic double resonance study 9-44356
- diethyldithiocarbamates of uranyl, two monoclinic polymorph phases, crystallography and chemical study 9-23787

Organic compounds continued

- diethylthiatricarbocyanin dye, stimulated Raman scatt. 9-28137
 difluoroacetaldehyde, F_2CO , vibrational intensity calcs. 9-38896
 2,5-difluoroaniline liquid, i.r. absorption spectrum, vibration modes 9-32500
 p-difluorobenzene, n.m.r. parameters, ^{13}C -H satellite spectrum 9-34666
 difluorobenzene m- and n- combinational scattering spectra, phase shift rel. to dipole-dipole intermolecular forces 9-46393
 m-difluorobenzene vapour, near u.v. absorpt. spectrum, band obs. 9-46394
 1,1-difluorocyclobutane, microwave spectrum and ring puckering 9-30101
 1,1-difluoroethylene, n.m.r. in nematic solvents 9-30105
 difluoromalealdehyde, band intensities, 2.0-6.0 μ 9-46390
 p-difluorotetrafluorobenzene, i.r. and Raman vib. spectra 9-27889
 2,4-difluorotoluene, i.r. absorpt. spectra, vib. assignments 9-23109
 digitoxigenin, crystal structure 9-26260
 diglycerides analysis by coupled mass spectrometry-gas chromatography 9-31221
 1,2-dihalide substituted ethanes, vibration spectra, calculation and interpretation 9-23120
 p-dihalobenzenes, heterogeneous nucleation on cleaned alkali halide cryst., molecular config. obs. 9-37105
 4,4'-dihydroxyazobenzene a liq. cryst. solvent in i.r. spectroscopy 9-48682
 2,3-dihydrofuran, ring-puckering vibr. 9-30102
 5,10-dihydrophenazine, near-u.v. absorpt. spectrum 9-32508
 2,5-dihydrothiophene l.r. and Raman vib. spectra meas., freq. assignment 9-27901
 dihydrothymine, radicals formed by H-atom bombard. 9-43324
 3,4-dihydro-2,4,6-triphenyl-s-tetrazin-1(2H)-yl, struct. by crystal-packing anal. and X-ray diff. 9-48516
 5,8-dihydroxynaphthoquinone, i.r. and visible spectrum obs., vib. and electronic structure deduced 9-30123
 1,3-di-imines, N,N'-disubstituted, spectroscopic study 9-30106
 dimethoxytrimethylantimony, crystal and molec. struct. 9-30582
 dimethyl aniline-chloranil effect 9-45281
 dimethyl aniline-tetracyanoquinodimethane complexes, electro-optical effect 9-45281
 dimethyl ether, SO_2 and methylchloride, binary and ternary mixtures, thermal conductivity and viscosity 9-36817
 dimethyl formamide, in mixture of benzene and liq. paraffin, internal field at microwave freqs. 9-46650
 dimethyl formamide, thermal conductivity meas., 20-160°C 9-30388
 dimethyl sulfoxide, Raman line displacement of S=O related to acidity of hydroxyl-containing substs. 9-27940
 dimethyl terephthalate, ionization potential and electron affinity rel. to conducting and valence bands 9-37417
 dimethylacetylene, liquid, far i.r. absorptions 9-40796
 1,4-dimethylanthracemiquinone, anion radical, e.s.r. spectrum obs. 9-36718
 4,4-dimethyl-benzophenone, electron transfer effect on n.m.r. of ring protons 9-42438
 anti-2, 6-dimethyl-4-chloro-N-methylbenzaldoxime, crystal and molecular structure 9-39341
 N,N-dimethylformamide, accidental near-degeneracies of n_σ and π_2 MO's, photoelectron spectroscopy investig. 9-38898
 N,N-dimethylformamide, anisotropic molec. rot. in liq., n.m.r. 9-30433
 dimethylgermane, microwave spectrum 9-42430
 dimethylglyoxime, crystal, van der Waals interact. and H bonding 9-40853
 dimethylhydrogenphosphonate, P-H bending vibrs., Raman obs. 9-30066
 dimethyllead dihalides, l.r. Raman spectra and mol. struct. obs., 9-34675
 2,9-dimethyl-1,10-phenanthroline, crystal structure 9-39342
 α , α -dimethyl- β -propiolactone, polymerization 9-26820
 dimethylsulphoxide, r, s, and r_s struct. 9-23138
 dimethylsulphoxide-water system, phase diagram and stable hydrate form 9-32815
 N,N-dimethylthioacetamide, i.r. and Raman spectra and normal vibrations 9-46391
 N,N-dimethylthioformamide, i.r. and Raman spectra and normal vibrations 9-46391
 2, 5- and 3, 4-dimethylthiophene and 2, 3, 4, 5-tetramethylthiophene, vibrational spectra, calculation and interpretation 9-25770
 N, N'-dimethylurea, i.r. spectra bands and vib. determ., normal co-ord. anal. 9-23130
 dinitrobenzenes, isomeric, vibrational spectra 9-48502
 3,5-dinitro-4-methylbenzoic acid, crystal structure 9-23781
 1, 4-dinitrosopiperazine, conformation from n.m.r. spectrum 9-32509
 1, 4-dinitroso-2, 3, 5, 6-tetramethylpiperazines, α , β , ϵ , μ , δ isomers, predominant conformations from n.m.r. 9-32509
 dioctyltin oxide, lattice dynamic anisotropy and line asymmetry obs., 60-320°K, Mossbauer effect investig. 9-39822
 1,4-dioxan, liquid, far i.r. absorptions 9-40796
 dioxane binary soln., excess vol. of mixing 9-34881
 p-dioxane-water, dilute solns., dielec. props. 9-34928
 dioxane-water NaCl solns., liq.-liq. equilibrium 9-32765
 4,5-dioxo-2-thioxo-1,3-dithiolan, β form cryst. and mol. struct. 9-39328
 1,3-dioxolane, far-i.r. spectra and pseudorotation 9-38915
 diphenyl, appearance and growth of non-singular crystal surfaces 9-37014
 diphenyl, cryst. growth from vapour, diffusion along substrate surface 9-48796
 diphenyl, loose, neutron temp.-depend. on geometric parameter, meas. by pulse method 9-46251
 diphenyl derivatives, phosphoresc., fluoresc. in of one-, multi-component solvents 9-34915
 diphenyl ether, electric dipole moment determination by dielectrometer 9-45907
 diphenyl methane-o,o'-ditolyl, mixing effects 9-48683
 diphenyl phenylboronate, i.r. spectra rel. to vibrational frequencies 9-23151
 2,2-diphenyl-1-l-picyrhydrazyl, e.s.r. in low fields using simple apparatus 9-45901
 diphenyl sulphide and disulphide, vibr. spectra 9-23133
 diphenyl sulphoxide, vibr. spectra 9-23133
 diphenyl surface crystals, formation and growth from vapour phase 9-40861
 2,5-diphenyl-1,3,4-oxadiazol dioxo derivatives of scintillator activators, intermol. H-bonds, fluoresc. and i.r. obs. 9-30414
 diphenylamine derivatives, methoxy-substituted e spectra, obs. 9-27912

Organic compounds continued

- N-N'diphenylaniline, elec. dipole moment using modified Higasi's eqn. 9-46410
 diphenylethine and diphenylethine- d_{10} , i.r. spectra analysis 9-38909
 trans-1,2-diphenylethylene and trans-1,2-diphenylethylene, i.r. spectra analysis 9-38910
 diphenylmercury, Hg radioisotope enrichment by neutron irradi. 9-37843
 diphenylmethyl neutral radicals, e.s.r. study 9-48495
 diphy, neutron diffusion length and age 9-22891
 α , α -dipyridyl, luminesc. at 55°K, using cylindrical cryostat 9-38168
 γ -dipyridyl-di-N-oxide, i.r. spectrum, normal co-ord. analysis 9-46392
 2,4-disubstituted thiazole derivatives, vibration spectra and structure 9-48508
 1,4-dithian, i.r. spectrum, vibrational assignment 9-32510
 1,3-dithian, i.r. spectrum, vibrational assignment 9-32510
 dithiocarbamates, and acid derivs., electronic spectra, $\eta \rightarrow \pi^*$, $\eta \rightarrow \sigma^*$, $\pi \rightarrow \pi^*$ transitions in u.v. 9-36711
 dithiocarbamates, eff. on corrosion of tinplate 9-28803
 DL-threonine and DL-allothreonine, n.m.r. 9-23165
 DL-valine n.m.r. 9-23165
 DNA helix-coil transition, thermal props. determ. 9-22138
 dodecadimethylaminocyclohexaphosphazene, (N-P) $_6$ ring cpds, crystal and mol. structure 9-30583
 dodecadimethylaminocyclohexaphosphazene, crystal and mol. structure 9-30583
 durene, doped cryst., electronic energy transfer 9-24458
 duren, e.s.r., of triplet state of photochem. oxidation product, fine struct. obs. 9-33640
 duren crystal, e.p.r. signals after gamma radiolysis and u.v. photolysis 9-47421
 duren, monosubstituted, i.r. ν_{16} intensities rel. to substituent σ_p , ^{10}B obs. 9-30090
 dye, flashlamp-excited laser, gain analysis 9-48007
 dye, source of losses in lasers 9-25277
 dye lasers, near 4000 Å wavelength, pumping with second harmonic of Q-switched ruby laser 9-31949
 dye solution lasers, flashlamp excitation, measurement of critical population inversion 9-27328
 dye solutions, excited with impulse lamps, optical generation 9-29419
 dye-laser, cw operation 9-25278
 dye-photosensitizers, flash investigation 9-24182
 dyes, photodiode effect, formation and dissociation mechanisms 9-28572
 dyes, solutions for lasers review 9-43887
 dyes, xanthene and coumarin groups, lasing action, flashlamp-pumped 9-45960
 electroflashed radiation induced by strong elec. fields in liqs. 9-26124
 1,5-endomethylenequinolizidinium p-toluenesulphonate, cryst. struct. 9-35076
 epoxy resin, critical surface tension rel. to adhesion with SiC 9-23620
 epoxy resin adhesive films, transparency changes due to u.v. irradiation 9-47328
 1,2-epoxycyclohexane, spectral component parameters 9-40578
 erbium ethylsulphate, spin-lattice relaxation anisotropy 9-26665
 estril, crystal and molecular structure 9-39333
 estril structure, phase determ., computer program for least squares method 9-39332
 estrone, intrinsic fluoresc. spectrum interpretation 9-34667
 ethane, C_2D_6 , $C_2D_2H_4$, charge exchange mass spectra, H/D isotope effect 9-25722
 ethane, comparison of struct. determ. by electron diff. and spectroscopy 9-36713
 ethane, derivatives, fluorine-chlorine, thermal cond., -125→+100°C, meas. by unsteady state relative method 9-36866
 ethane, flash decomp. on W 9-43327
 ethane, geometrical changes during internal rotation 9-36714
 ethane, inelastic collisions with Na, total cross sections for $3^2P_{1/2}$ - $3^2P_{3/2}$ mixing 9-44288
 ethane, internal rotational barrier computed 9-34670
 ethane, n.m.r. in nematic solvent 9-42433
 ethane, rot. fine structure of perpendicular band ν_2 9-34671
 ethane and ethane- d_6 , analysis of 1400 Å electronic transition 9-38893
 ethane-methane- N_2 system, form. of ethane rich middle layer on cooling below -225°F 9-42698
 ethanes, 1,2-disubstituted, barrier to internal rot. determ. from p.m.r. 9-30109
 ethanol, boiling, heat transfer depend. on e.m. field 9-23597
 ethanol, i.r. spectra of isotopic monomers 9-38891
 ethanol, isotopic, self-associated, i.r. spectra 9-38892
 ethanol, max. drop size on jet injection into N_2 or He gas streams 9-34864
 ethanol, shocked-state refr. index 9-44566
 ether, mixture with N_2 and O_2 , simultaneous HCN and H_2O laser emissions in pulsed discharge 9-22404
 ether, Raman spectra lines intensity var. with exciting light freq., oscillator strength determ. 9-30111
 ethyl acetate, enriched, $^{13}C/^{12}C$ isotope ratio meas., method 9-34588
 ethyl alcohol, dielec. const. freq.-temp. meas. by helical resonator method 9-36895
 ethyl alcohol, diethyl carbonate, diethyl oxalate determination in ternary mixture 9-39966
 ethyl alcohol, microwave rot. spectrum, stable isomers, ground-state rot. and centrifugal distortion coeffs. 9-34668
 ethyl alcohol, microwave spectrum 9-30150
 ethyl alcohol vapour, eff. on surface conductivity of Ge 9-49101
 ethyl alcohol, bubble growth on glass surface during boiling 9-30465
 ethyl benzoate, liq. and soln., i.r. and Raman spectra, vib. freqs. assignment 9-25769
 ethyl chlorides, H_2 , D_2 , D_3 , D_4 , i.r. and Raman spectra vibr. analysis 9-48490
 ethyl cinnamate-mesityl oxide reaction, Li-catalysed condensation, obs. 9-47461
 ethyl cyanide, ^{14}N quadrupole coupling constants 9-38890
 ethyl ether decomposition in presence of ethylene, laser irradiated 9-31187
 ethyl fluoride dissolved in nematic liq. cry., NMR study 9-40613
 ethyl halides, combination band of methyl group torsion and asym. stretching vib. 9-25753
 ethyl iodide, electron scattering cross section and spin polarization meas., $E_e=200-600$ eV 9-23166

Organic compounds continued

- ethyl methyl ketone, u.v. absorpt. spectra, effects of temp. and salt additions 9-36888
- ethyl radical, spin polar, and delocalization, unrestricted Hartree-Fock method 9-27923
- ethyl vinyl ether-Al(*i*-C₄H₉)₃ complexation and i.r. spectrum, obs. 9-48491
- ethylene, -d₄, vibrational struct. of 1744 Å Rydberg transitions' 9-44357
- ethylene, copolymerization with propylene and 4-vinylcyclohexane-1, and effect of catalyst 9-31188
- ethylene, flash decomp. on W 9-43327
- ethylene, halogen substituted, ionization potential, intra-molecular electric fields effects 9-42559
- ethylene, inelastic collisions with Na, total cross sections for 3²P_{1/2}-3²P_{3/2} mixing 9-44288
- ethylene, isotope effects in photoionization yields and absorpt. cross-sections 9-30298
- ethylene, isotopic, meas. of 2nd virial coeffs. at 236.04°K. 9-48660
- ethylene, mols. photoionization, σ , π system contribution, calc. 9-34669
- ethylene, nuclear spin-lattice relaxation 9-24344
- ethylene, photoionization 9-32695
- ethylene, reaction with atomic O, e.s.r. detect. 9-24534
- ethylene, resonant scatt. of electrons, ang. distrib. 9-27855
- ethylene, trans-d₂, i.r. spectrum, strong Coriolis perturbation 9-38894
- ethylene, vibr. ch₂ intensity progression in V-N transition 9-30108
- ethylene amides, electronic struct. calc. 9-23118
- ethylene amides, u.v. spectra and dipole moments 9-23119
- ethylene and ethylene-d₄ cryst., far i.r. spectra 9-45333
- ethylene carbonate, i.r. and Raman spectra of gas and liq., rel. to mag. deforms. 9-48492
- ethylene glycol with Cr (v) complex, proton dynamic polarizations 9-34926
- ethylene molecules, spectral characts. and electronic structures 9-30110
- ethylene oxide, group vibrations and vibrational analysis 9-23141
- ethylene oxide, i.r. Raman scattering spectra 9-28705
- ethylene oxide, molec. g values, mag. anisotropy and quadrupole moment 9-42431
- ethylene oxide-oxygen flame, mass spectrometric study 9-28785
- ethylene sulfide, mol. g values, mag. susceptibility anisotropies, quadrupole moments 9-40612
- ethylene sulphide, group vibrations and vibrational analysis 9-23141
- ethylene sulphide, i.r. Raman scattering spectra 9-28705
- ethylene thiourea, normal vibrations calc. by Wilson's GF matrix method 9-30112
- trans-ethylene-d₂, 2 axis Coriolis perturbations in i.r. spectra 9-48444
- ethylene-d₂, Cd-phosensitized cis-trans-geminal interconversion 9-31213
- ethylene-N₂ mixtures, influence of dimers on thermal diff. factor 9-36686
- ethylenes, monosubstituted, J_{13,14} coupling constants 9-27894
- ethylmercaptan, microwave spectrum and mol. structure. 9-27895
- ethyltoluene photodissociation products, fluorescence spectra of trapped radicals in crystalline matrices 9-47402
- explosive, polycrystalline, strain-rate sensitive, compressive wave propag. behaviour 9-39409
- fatty acids on Hg surface, test of two-dimensional scaled-particle theory 9-40782
- ferrocene, 1,1'-disubstituted cpds., i.r. and Raman spectra 9-23121
- ferrocene, γ -irrad., e.s.r. of free radicals 9-43288
- ferrocene and its molecular complexes, single crystals polarized absorption spectra 9-47370
- fluoranthene, electronic spectrum and electron affinity 9-30116
- fluorene, benz[*f*]indan impurity u.v. spectra, polarized fluorescence and absorption vibrational anal. 9-28697
- fluorene, copolyolysis with arylene precursors, and enhanced graphitization 9-26811
- fluorenone, electronic spectrum, 1680-2350 Å, new band and comparison with SCF MO calc. 9-30117
- fluorenone ketyl solns. evidence for existence of paramagnetic and diamagnetic ion clusters 9-34923
- fluorenyl neutral radicals, e.s.r. study 9-48495
- all-trans-, fluoresc. yields and absorpt. 9-24460
- fluorescein in glycerine soln., conc. effect on luminesc. 9-42668
- fluorinated radical anions, spin density distributions 9-38872
- fluorinated solvents, Overhauser effect study of multiple interactions 9-48718
- 1-fluoro-1, 1, 2, 2-tetrachloroethane, acoustic and i.r. determ. of internal rot. 9-27896
- fluoroacetylene, mag. susceptibility anisotropy and mol. quadrupole moment 9-25764
- 2-fluoroaniline, liquid, i.r. absorption spectrum, vibration modes 9-32500
- m-fluoroanisole, i.r. absorption spectra, vibrational 9-46395
- o-fluoroanisole, near u.v. absorpt. spectrum 9-34672
- fluoroaromatic cpds., metastable transitions obs. 9-24532
- fluorobenzene, molec. g values mag. anisotropy and quadrupole moment 9-44359
- fluorobenzene crystal u.v. absorption spectra near 1st electronic transition, polarized light, 20°K. 9-26748
- fluorobenzene derivatives, n.m.r. spectra, substituent effects in H-F coupling 9-38881
- fluorobenzenes, trifluoromethyl- and methoxy-substituted, n.m.r. spectra 9-30118
- fluorobenzenes, vib. data, NMR and i.r. correl. 9-23122
- o- and m-fluorobenzonitriles, i.r. absorption spectra, vibrational 9-46395
- ortho- and meta-fluorobenzonitriles, u.v. absorption spectra 9-48493
- fluorobromobenzenes, o-, m- and p-, in-plane vibrations normal coordinate analysis 9-38897
- fluorocarbons, dynamic nuclear polarization in soln. 9-44597
- fluorocarbons, glory scatt. of Li 9-42471
- 4-fluoro-3-chloroaniline, n.q.r. of ³⁵Cl, temp. variation of freqs. 9-30103
- fluorochlorobenzenes, o-, m- and p-, in-plane vibrations normal coordinate analysis 9-38897
- fluorodichloromethane (Freon 22), pVT behaviour in gaseous and liq. states 9-36805
- fluoroform, vibr., rot. bands, computer anal. 9-38895
- fluoromethanes, partially oriented, proton and ¹⁹F n.m.r. 9-30434
- β -fluoronaphthalene-D₇ in n-paraffin, quasiline phosphoresc. spectra 9-46409
- α -fluoronaphthalene-D₇ in n-paraffin, quasiline phosphoresc. spectra 9-46409
- formaldehyde, gas-phase reaction with H atoms, kinetic isotope effects 9-28781

Organic compounds continued

- formaldehyde, interstellar, microwave detection 9-29037
- formaldehyde, i.r. laser irrad., Stark spectrum obs. 9-25766
- formaldehyde, obs. using mol. jet spectrometer 9-43928
- formaldehyde, one-electron props. of near-Hartree-Fock wavefunctions 9-32514
- formaldehyde, Stark spectroscopy by i.r. lasers 9-25767
- formaldehyde -h₂, d₂ and hd, 3500 Å 1A₂-x 1A₁ transition, vibrational and rotational analyses 9-48496
- formaldehyde in solid low-temp. solns. fluoresc. 9-39880
- formamide, accidental near-degeneracies of n_g and π_2 MO's, photoelectron spectroscopy investig. 9-38898
- formamide, thermal conductivity meas., 20-160°C 9-30388
- formamide isomers, MO calc. 9-30119
- formamide-¹⁵N mol., heteronuc. double reson. using weak perturbing r.f. fields 9-40615
- formate ions, counter current electromigration ¹⁴C isotope effect 9-48439
- formic acid, ¹³C n.m.r. enhancement by Overhauser effect, obs. 9-32513
- formic acid, accidental near-degeneracies of n_g and π_2 MO's, photoelectron spectroscopy investig. 9-38898
- formic acid, i.r. laser irrad., Stark spectrum obs. 9-25766
- formic acid, liq. and solid, l.f. Raman spectra 9-24430
- formic acid, u.s. propag. temp. coeff. meas. 9-23494
- formic acid and formate ion, ab initio SCF and CI calc. 9-30120
- formic acid, -d₃, rotation spectrum 7.5 to 145 GHz, identification of transitions 9-44361
- formyl fluoride, 2670 Å absorption spectrum analysis 9-32515
- freon 113, temp. profile of thermal sublayer on Cu horizontal surface during pool boiling 9-23598
- Freon 114, natural convection in supercritical region 9-26150
- Freon 13 liq. in critical region, boiling by Pt wire, obs. 9-28186
- Freon 22, pVT behaviour in gaseous and liquid states 9-36805
- Freon-12, boiling in region of centrifugal forces, heat transfer coeffs. 9-23603
- Freon-21 vapour, P-T relations, exptl. investigation 9-40816
- Freon-22, critical heat flux modeling, comparison with water 9-34736
- fulminic acid, high resolution i.r. spectra 9-34673
- fulvene, microwave spectrum, dipole moment, electr. struct. 9-27897
- fulvenes, heterosubstituted, lattice parameters and space groups 9-39334
- gaseous, conc. in Arctic atmospheres 9-43386
- glasses, trapped e.s.r. and optical absorpt. rel. to matrix polarity, 77°K 9-28695
- β -D-glucopyranosides, partially acylated, synthesis and n.m.r. 9-23124
- glucose, storage by polyhydric compounds addition, patent 9-24939
- D-glucose frozen aqueous solns., e.s.r. study of free radicals formed by gamma-irrad. 9-42454
- α -D glucose penta-acetate, broad-line n.m.r. studies in crystalline and glassy states 9-28763
- glucose-b-phosphate dehydrogenase, storage by polyhydric cpds. addition, patent 9-24939
- glycerine, fluorescein conc. effect on luminesc. of soln. 9-42668
- glycerine, normal and deuterated liq., OH hindered rot., cold n scatt. obs. 9-28097
- glycerine in water, low-level excitation of sonoluminescence 9-36871
- glycerol, proton nucl. mag. relax., 450KHz to 120MHz 9-40808
- glycerol, shocked-state, refr. index 9-44566
- glycerol solns., Couette flow between rot. cylinders, relax. effects 9-32749
- glycine chelates, isomeric, far i.r. spectra, metal-O bond stretching vib. 9-27898
- glycine hydrochloride, X-irrad., radical formation 9-43340
- glycine irrad., anisotropic hyperfine splitting of e.s.r. 9-23178
- glycocol, quadrupole coupling of N₁, n.m.r. determ. 9-49360
- glycol, heat transfer, non-Newtonian, in non-circular tubes, theory and expt. 9-44559
- glycol-water solutions of CuSO₄, u.s. absorpt. rel. to temp. 9-34903
- glycylglycine hydrochloride, crystal structure 9-26263
- β -gorgonene-AgNO₃, cryst. struct. 9-23782
- gramicidin C bromohydrate, synthesis and crystal. study 9-42800
- guanidium aluminium sulphate hexahydrate, ferroelec., dehydration nuclei rel. to dislocation sites 9-37115
- guanosine, i.r. absorption spectra, 230-30 cm⁻¹ 20 to -175°C, crystal lattice vib. anal. 9-25783
- H-bonding, inter- and intra-mol., rel. to absorpt., fluoresc. band widths, obs. 9-23081
- Hafner's hydrocarbons, protonated, solns. fluoresc., 20°C 9-28143
- halide conductivity cell dosimeter 9-29665
- m-halobenzaldehyde, rotational isomerism 9-42436
- halobenzene series, u.v. absorption spectra variation, polarized light, 20°K 9-26748
- halogenated aromatic mol., out-of-plane vib., force fields 9-25768
- halogenated ethylenes, two-bond, C-proton coupling consts. 9-44358
- halogenocyclohexanones, and deuterated derivatives, i.r. spectra 9-23125
- HB-40, neutron diffusion length and age 9-22891
- helixenes in 1,4-dioxan. soln., fluorescence spectra 9-40616
- heptalene, ground-state geometry and symmetry 9-36716
- heptamethylbenzene tetrachloroaluminate, cryst. struct. 9-23783
- n-heptane, field ionised, unimol. decomp. 9-25787
- heptane, frozen, fluoresc. spectra of coronene and 1,12-benzoperylene at high press. 9-32517
- heptane, frozen, phase transform. rel. to quinoline-heptane solns. phosphoresc., 55-123°K 9-28726
- n-heptane, liq., negative-carrier mobility meas. 9-42672
- n-heptane, liquid proton spin relax., press. and temp. depend. 23-190°C, 0.07-1.9 kbar 9-30121
- 4,4'-di-n-heptyloxyazobenzene smectic mesophase, solute e.p.r., obs. 9-32796
- heterocycles, N and S containing, radical anions, spin density distributions 9-32518
- heterocyclic amine N-oxides, anion radicals, polarography rel. to e.s.r. 9-36715
- heterocyclic systems containing 2.41 and 2.64 Å sulphur-oxygen distances, Huckel calcs. 9-46378
- n-heterocyclics, ¹³C chem. shifts calc. 9-23127
- hexadecanol monolayers, in retardation of water evaporation rate 9-23591
- hexafluoro-1,3-butadiene, iterative anal. of n.m.r. spectrum 9-47874
- hexafluorobenzene as acceptor in charge-transfer-complexes 9-28784
- hexafluorobenzene scintillator dosimeter, for use in mixed γ and n fields 9-36531
- hexaoidobenzene, crystal and molecular struct. 9-46799

Organic compounds continued

hexameric phosphonitric dimethylamide, (N-P)₆ ring cpds, crystal and mol. structure 9-30583
 hexamethylbenzene, proton relax. 9-43306
 hexamethylenetetramine crystals from soln. and vapour phase 9-39202
 hexamethylenetetramine-borine, crystal structure 9-26264
 hexamethylphosphorotriamide water mixture preferential solvation by diamagnetic cation ¹H and ³¹P n.m.r. spectroscopy 9-44600
 hexane, frozen, phase transition. rel. to quinoline-hexane solns. phosphoresc., 55-123°K 9-28726
 hexane, liq. charge collection from moving stream 9-42669
 n-hexane, liq., negative-carrier mobility meas. 9-42672
 hexane, liquid, charge carriers which are probably free electrons obs. 9-28151
 hexane, liquid, elec. conduction using crossed-wire electrode system 9-40804
 n-hexane, superheated specific vol. and speed of sound near saturation line 9-23466
 of hexavalent S, charge of S ions determ. from S Kα_{1,2} line chem. shift 9-37751
 hydrazinium hydrogen oxalate, cryst., D-substitution effects rel. to H-bond symmetry, 3600-200 cm⁻¹ 9-24393
 hydrides, tetrahedral, spectroscopic mass and zero-order freq. calc. 9-30142
 hydrocarbon ions, e.s.r. proton hyperfine splitting relations 9-38899
 hydrocarbon liquid, flowing through tube, electric current generation 9-26129
 hydrocarbon oil breakdown in a.c. arc, growth of pyrocarbon 9-23364
 hydrocarbons, alternant, triplet-triplet absorption spectra, correlation between SCFMO and HMO calcs. 9-38901
 hydrocarbons, aromatic, in solid matrix, flash excited luminescence, triplet lifetime meas., 77°K 9-43255
 hydrocarbons, dissociative excitation by fast electrons 9-23174
 hydrocarbons, doped with diphenyl picrylhydrazil, proton polarization 9-28764
 hydrocarbons, glory scatt. of Li 9-42471
 n-hydrocarbons, irrad., pairwise trapping of radicals 9-45427
 hydrocarbons, MINDO calc. 9-30122
 hydrocarbons, rate const. for scavenging of electrons in radiolysis 9-43341
 hydrocarbons, sat., collision induced distrib. of Cs-62P_{1/2} states 9-44279
 hydrocarbons, saturated, ab. initio bond-oriental. calcs. 9-38900
 hydrocarbons, saturated liq. density, b.p. mol. wt. cf. with Ar 9-32758
 hydrocarbons, simple and derivatives, coupling constants, effect of one-centre exchange integrals 9-42437
 hydrocarbons, thermal conductivity, at normal pressures 9-40751
 hydrocarbons C₃-C₈ double charged ions decomp., kinetic energy release 9-40712
 hydrogen bonds, bifurcated 9-23653
 hydroxy chromones, carbonyl stretching freqs. 9-30124
 hydroxy crystals, evidence for non-H-bonded hydroxyl groups 9-42739
 α-(2-hydroxy-3,5-dibromobenzylidene)-p- butyrolactone, cryst. struct., diff. obs. 9-39337
 m,p- hydroxybenzaldehyde, vapour, emission spectra 9-34674
 N(4)-hydroxycytosines, H-bond association with purines 9-42635
 1-(β-hydroxyethoxy)-2,4-dinitrobenzene, intermol. H bonding, NMR detect. 9-27900
 hydroxyurea, X-irrad., e.s.r. of radical pairs 9-45426
 n- hyptil alcohol, thermal conductivity 20-160°C 9-30388
 as-indacene, ground-state geometry and symmetry 9-36716
 s-indacene, ground-state geometry and symmetry 9-36716
 indigoidal pigments, ionization by u.v. in dioxane and acid solns., obs. 9-28153
 indole salts, n.m.r. study 9-44598
 p-iodoaniline, ¹⁴N n.g.r. temp. depend., 77-292°K 9-30071
 iododurene, Raman and i.r. spectra rel. to lattice vibrs. 9-44813
 iodoform, in CCl₄ and CS₂ soln., integrated intensity of i.r. absorption band 9-23110
 iodomethanes, iodine bond hybridization, Mossbauer determ. 9-32519
 ions in crystals, e.p.r. investigation, techniques, book 9-38338
 i.r. absorption bands spontaneous emission probability determ. 9-38875
 i.r. absorption bands spontaneous emission probability determ. 9-25754
 iron phthalocyanin, reduced, hyperfine struct. in e.s.y. spectra 9-42445
 isobutane, reaction with excited O¹D₂ atoms 9-24543
 isobutyric acid-water binary liq. mixture at critical conc., anomalous shear viscosity 9-48687
 isopentane, dielec. props., press., vol., and temp. effects 9-39109
 isopentane-3 methyl pentane mixture, a low temp. acoustic bond for mercury 9-31722
 isoprene, trans form identification, microwave spectrum 9-30125
 isopropenyl groups, =CH₂ stretching vibr. bands splitting rel. to isomerism, obs. 9-44370
 isopropyl alcohol, solvation to fluorenone ketyl 9-34880
 isopropyl bromide, liq., solid, conformations, vib. assignments and force consts. 9-34663
 isopropyl chem. activated radicals, competitive unimolec. decomp. 9-24546
 kerosene, rheology near solid boundary 9-39069
 ketene, molec. g values, mag. susceptibilities and quadrupole moments 9-30126
 ketene, SCF wavefunction, one-electron props., and electron-density maps 9-32521
 ketones, α-ethylenic, aliphatic and allylic, C=O and C=C stretching freqs., effect of alkyl subst. and stereochem. 9-32522
 ketones, i.r. spectrum at transition liq.-solid 9-32520
 ketones, Raman line displacement of C=O and acidity of hydroxyl containing cpds. 9-27940
 labelled, gas chromatographic anal. method using interrupted elution 9-24600
 lanthanum ethyl sulphate:Nd, spin lattice relax., optical detection, 1.28° to 2.15°K 9-35595
 lanthanum ethyl sulphate, e.s.r. spectra, Gd³⁺ zero-field splitting anomaly 9-39914
 laser emission in u.v. 9-27303
 laser passive shutters for Q switching, molecular triplet-triplet transitions 9-25279
 laurylpyridinium bromide (iodide), u.s. vib. potentials as function of conc. 9-48694
 lead stearate, multilayer films, structure 9-39349
 ligand quenching of fluoresc. of CeCl₃ in aqueous soln. 9-42665

Organic compounds continued

lipid-cholesterol spherical, normal mode vibrs. 9-41816
 liquid, dielectric breakdown due to laser radiation 9-48710
 liquid, evaporation, retardation, partial ester of polyhydric ether alcohol addition, patent 9-23589
 liquids, absorption and dispersion in i.r. absorption bands region 9-46643
 liquids, cohesion energy-vol.-temp. relations, obs. 9-28094
 liquids, Raman spectra width and shape of lines 9-46642
 liquids, steady-state and transient space-charge-limited currents by injection from tunnel cathode 9-34919
 liquids, stimulated Brillouin scattering steady-state gain 9-42659
 liquids, viscosity, effect of ultrasound 9-42637
 liquids in aqueous binary mixtures n.m.r. meas. and molecular motion 9-46654
 lithium acetate dihydrate monocrystal, optical consts., temp. depend 9-47315
 lithium formate monohydrate, crystalline, Raman spectra 9-47378
 luminophor solns., characts. of stimulated radiation 9-43886
 luminors, rigid solns., e. excitation energy transfer 9-35688
 malate ion, n.m.r., proton coupling constants and internal chemical shifts 9-46400
 maleic hydrazide in soln. in dimethylsulfoxide, Raman spectrum 9-46399
 maleimide monomer-fluorene, radiation-induced polymerization 9-26821
 malic acid, n.m.r., proton coupling constants and internal chemical shifts 9-46400
 malonamide, X-irrad., e.s.r. of σ-electron radical 9-38924
 manganese formate dihydrate, deuterated, antiferromagnetic structure from n. diff. obs. 9-24336
 manganese formate dihydrate antiferromagnet with weak canting interaction, mag. phase transition 9-33489
 mercuric halide adducts of cyclic thio-ethers, ring vibrations 9-30107
 merocyanines, C-O stretching band behaviour and shape in mixed solvents 9-23137
 mesitylene, e. irrad., e.s.r. study of radical formed 9-42439
 mesitylene, temp. depend. of phosphoresc. lifetime 9-31143
 mesitylene in B-trimethylborazole cry., EPR of phosphorescent state, fine and hyperfine struct. obs. 9-24500
 metal compounds of some group I, II and III elements, mol. orbital calcs. 9-46403
 methad absorption in Jovian atmosphere, rotational temp. from 3ν₃ band 9-43623
 methane+Ar⁺→Ar+CH₃⁺+H→Ar+CH₂⁺+H₂, 1.5→4.2 eV, mechanism 9-39936
 methane, α-irrad., ion-mol. reactions 9-45428
 methane, absorpt., coeff., far u.v. obs. 9-28078
 methane, abundance and rot. temp. on Jupiter 9-40175
 methane, CD₄, CD₂H₂ charge exchange mass spectra, H/D isotope effect 9-25722
 methane, CH₃⁺+CH₄ reaction, direct mechanism 9-49375
 methane, compressed gas, thermal conductivity, concentric cylinder meas. method 9-26027
 methane, deuterated (CD₄)+CH₃OH⁺→CD₃+CH₃OH⁺, stripping→complex transition 9-38936
 methane, deuterated (CD₄)+X⁺→CD₃+XD⁺, deviations from stripping model 9-27944
 methane, electron drift vel., press. depend. 9-48616
 methane, flash decomp. on W 9-43327
 methane, gas and solid, inelastic neutron scatt. study of mol. dynamics 9-36717
 methane, halogen substituted, saturated vapour, specific heat calc. 9-26030
 methane, ion-mol. reactions 9-24544
 methane, i.r. laser irrad., Stark spectrum obs. 9-25766
 methane, Jovian, photolysis at 1216 Å and 1350-1450 Å 9-41676
 methane, liq., mol. sound vel. and compressibility, temp. and press. depend. 9-40789
 methane, liquid and solid refractive indices 9-44562
 methane, mixture and N₂ and O₂, simultaneous HCN and H₂O laser emissions in pulsed discharge 9-22404
 methane, mol. wavefunctions in infinite internuclear separation limit, Hartree-Fock eqn. 9-38816
 methane, neutron scatt. in gas and solid 9-25772
 methane, ν₃ spectral band near 3000 cm⁻¹ in night airglow 9-24679
 methane, orthorhombic density in critical region 9-48739
 methane, photoionization, threshold electrons 9-44485
 methane, pressure-induced i.r. spectrum 9-32523
 methane, proton mag. shielding of interacting pair mols. 9-40630
 methane, reaction dynamics of N₂⁺ 9-39940
 methane, reaction with H atoms, kinetics, e.s.r. determ. 9-47454
 methane, reactions with tritium atoms 9-47474
 methane, solid; A and T nuclear spin systems mixture, phase transitions 9-35240
 methane, solid, and deuterated modifications, nuclear spin-lattice relax. time temp. depend. 9-43198
 methane, solid, h.p. stress gradient obs. at 77°K 9-26323
 methane, solid, lattice consts. and thermal expansion meas. 9-40926
 methane, spectral emissivity of 3.3 μ band at 297, 673 and 923°K 9-46401
 methane, Stark effect of absorpt. line, maser obs. 9-34678
 methane, Stark spectroscopy by i.r. lasers 9-25767
 methane, stimulated Rayleigh scatt., critical absorption coeffs. and anti-Stokes shift, density depend. 9-46573
 methane, thermal cond., 25°C-450°C and up to 1000 bars 9-46569
 methane, vibration-rotation spectra, pressure broadening of ν₃ band meas. 9-23129
 methane, Xe-photosensitized decomp. 9-24590
 methane + O, reaction rate coeffs. 9-39939
 methane and fluorinated derivatives, Kerr const., hyperpolarizability determ., 632.8 nm 9-42613
 methane and methane-d₄, inelastic collisions with Na, total cross sections for 3P_{1/2} 3P_{3/2} mixing 9-44288
 methane and methane-d₄, phys. props., theory 9-39143
 methane and methane-d₄, phys. props., theory 9-44617
 methane-d₄, spectra, B type vib.-rot. band analysis 9-30129
 methane derivatives, fluorine-chlorine, thermal cond., -125→+100°C, meas. by unsteady state relative method 9-36866
 methane in Ar, neutron scatt., 5.3 Å, 86°K, molecular dynamics 9-25771
 methane mol. gas excited by electrons, glow spectra in i.r. region 9-38831
 methane-Ar anisotropic intermolec. forces 9-38935
 methane-Ar phase diagram 9-44803

Organic compounds continued

- methane-d₃, upper transition, quantum statistical treatment 9-48933
 methane-d₄, threshold energy for substitution of T for D 9-39965
 methane-d, upper transition, quantum statistical treatment 9-48933
 methane-ethane-N₂ system, form. of ethane rich middle layer on cooling below -225°F 9-42698
 Methane-methane-d₄ solid soln., upper transition, quantum statistical treatment 9-48933
 methane-Xe, charge exchange obs. by ion-cyclotron double reson 9-44495
 methane-Xe ionic reactions 9-42566
 methane-XeF₄, SbF₅ mixture photolysis, HF chem. laser emission, obs. 9-31944
 methane/He mixture, vibration-rotation spectra, pressure broadening of ν₃ band meas. 9-23129
 methane/N₂ mixture, vibration-rotation spectra, pressure broadening of ν₃ band meas. 9-23129
 methanes, halogen-substituted, second virial coeffs. and force consts. 9-36807
 methanethiol, photodissociation 9-43336
 methanethiol, vibr. spectra 9-23132
 methanol, adsorpt. or sorption on W, photoelectron spectroscopy rel. to orbitals involved in bonding 9-44634
 methanol, mass spectrometry 9-31220
 methanol, n.m.r. meas., vapour phase study of H bonding 9-48500
 methanol temp. profile of thermal sublayer on Cu horizontal surface during pool boiling 9-23598
 methanol-d₄, microwave spectrum 18-38 GHz 9-23508
 methanol-trimethylamine mixtures, n.m.r. meas., vapour phase study of H bonding 9-48500
 methanolions+D₂ (or CD₄)-CH₃OHD+D (or CD₂), stripping→complex transition 9-38936
 3-methoxybenzanthron, reson. excitation energy transfer to rhodamines C, 6Zh 9-25780
 methoxyethyne, internal rotation barrier, reinvestigation of microwave spectrum 9-46406
 methoxytetraphenylantimony, crystal and molec. struct. 9-30582
 methyl 2,3,4,5,6-pentafluorodiphenyls, i.r. spectra 9-23134
 methyl-d₃-acetylene, anisotropic molec. reorientation in liq. 9-40809
 methyl acetylene, vibr.-rot. bands 9-23135
 methyl acetylene-d₃, vibr.-rot. bands 9-23136
 methyl alcohol, dielec. const. freq.-temp. meas. by helical resonator method 9-36895
 methyl alcohol, i.r. laser irradi., Stark spectrum obs. 9-25766
 methyl alcohol, low temp. phase transitions, luminescence obs. 9-42692
 methyl benzoate, liq. and soln., i.r. and Raman spectra, vib. freqs. assignment 9-25769
 methyl bromide, double irradi. by i.r. and r.f. beams 9-46402
 methyl cephalonate bromoacetate, X-ray study of crystal and molecular structure 9-39340
 methyl chloride, i.r. laser irradi., Stark spectrum obs. 9-25766
 methyl chloride dimethyl ether, SO₂, binary and ternary gas mixtures, thermal conductivity and viscosity 9-36817
 methyl chloride-He mixture, thermal diffusion 9-32740
 methyl cyanide, i.r. laser irradi., Stark spectrum obs. 9-25766
 methyl cyanide, near i.r. spectra obs., rotational const. determ. 9-23128
 methyl derivatives of n-radicals, structural and electronic props. by molecular orbital theory 9-32527
 methyl diphenyl-thio-(seleno-) phosphinite, crystal structure 9-39339
 methyl ether decomposition in presence of ethylene, laser irradiated 9-31187
 methyl ethyl ketone-water NaCl solns., liq.-liq. equilibrium 9-32765
 methyl ethyl ketone-water NaCl solns., liq.-liq. equilibrium 9-32765
 methyl fluoride matrix-isolated u.v. photolysis, free radicals prod. 9-45424
 methyl group, proton spin relaxation time, including tunneling splitting of torsional oscillator ground state 9-37671
 methyl halides, force consts., soln. of inverse eigenvalue problem 9-27838
 methyl halides, n.m.r. chem.-shift anisotropy in liq. cryst. solvents 9-38903
 methyl halides in liq.-cryst. solvents, chem. shift anisotropy 9-44599
 methyl iodide, ¹³CH₃I, vibration-rotation bands 9-30131
 methyl iodide, collisions with K, cross-sections 9-27823
 methyl iodide, detection after heating of irradiated nuc. fuels 9-34493
 methyl methacrylate, u.v.-induced polymerization 9-33666
 β-methyl naphthalene, anisotropic growth velocity from morphological-kinetic data 9-40860
 methyl phosphorus cpds., ³¹P-resonance, chem. shifts 9-25775
 methyl radical, spin polar. and delocalization, unrestricted Hartree-Fock method 9-27923
 4-methyl-3-(p-bromophenyl)-1,2,5-oxadiazole, 2-oxide, cryst. and mol. struct. 9-44678
 4-methyl-3-(p-bromophenyl)-1,2,5-oxadiazole, 5-oxide, cryst. and mol. struct. 9-40924
 N-methyl-ethylenethiourea, cry. struct. spectra and phys. props. 9-48840
 3-methyl-pyridine heavy water system, critical opalescence, temp. depend. 9-42656
 methyl-pyridinium salts, anomalous Stokes shifts and fluorescence decay times 9-34679
 methyl-styrene, isometric, u.v. vapour absorpt. spectra, rel. to electronic band systems 9-23142
 N-methyl-trimethylenethiourea, cry. struct., spectra and phys. props. 9-48840
 N-methylacetamide solns., aqueous, p.m.r. study 9-28158
 methylammonium ions, counter current electromigration ¹⁴C isotope effect 9-48439
 N-methylaniline vapour, near u.v. absorption spectrum 9-30128
 9-methylanthracene vapour, discrete fluorescence spectrum 9-46407
 methylbenzene derivatives, phosphoresc. lifetime rel. to σ, π-mixing and C-H vibr. 9-23095
 1- and 2-methylbenzotriazole, n.m.r. spectrum analysis, deuteration expt. 9-30130
 methylbenzyl cyanides, ¹⁴N n.m.r. relax. times effect of fast internal rot. 9-46657
 methylchloroform, cryst. and plastic, far i.r. absorpt. rel. to lattice motions, obs. 9-24419
 methyl-cyclopentadienyl nickel nitrasyl, i.r. and laser Raman spectra 9-30132
 methylidiazirine, microwave rotational spectra 9-34676

Organic compounds continued

- methylidifluoroamine, vibrational spectrum on basis of polarization meas. and Raman spectra 9-27904
 methylene, electronic struct. determ. by valence-bond treatment 9-46404
 methylene chloride, vapour and liq., i.r. band intensities calc. 9-48497
 methylene group-, group vibrations and vibrational analysis 9-23141
 methylene-group-, group vibrations and vibrational analysis 9-23140
 N-methylformamide, accidental near-degeneracies of n₂ and π₂ MO's, photoelectron spectroscopy investig. 9-38898
 2-methylfuran, microwave spectrum 9-48498
 methylhydrazine, i.r. and Raman spectra 9-30127
 methylmethacrylate sensitized by photoreduced dye, polymerization 9-24552
 3-methylpentane, ionic processes from irradi. liq. and solid 9-28720
 3-methylpentane- nitroethane, coexistence curve near crit. pt. 9-23577
 1-methylphenalenyl, spin densities, hyperconjugation eff. calc., e.s.r. study 9-34677
 N-methyl-3-phenyl-4-bromoisoaxazolin-5-one, crystal structure 9-40925
 methylphenyl sulphide, vibr. spectra 9-23133
 N-methyl-4-phenylisoaxazolin-5-one, crystal structure 9-26266
 methylphosphorodifluorodithioate, i.r. and Raman spectra 9-38902
 methylpolyisiloxanic oils, electrohydrodynamical behaviour at -20-80°C 9-36896
 1-methylpyridinium ion, p.m.r. spectrum, effect of solvent and anion 9-34927
 methylquinolines, chem. shifts and proton coupling constants 9-38904
 methylsilane, internal rotational barrier computed 9-34670
 methylthioethyne, molecular structure and centrifugal distortion 9-48501
 methylthionitrite, i.r., Raman, and p.m.r. spectra 9-23131
 N-methylthiourea in nonpolar and polar solvents, n.m.r. temp. depend. rot. barrier about C-N bond 9-46658
 molecular motions in compounds with three C rings, n.m.r. 9-31173
 monoalkylacetylenes, straight-chain, i.r. absorpt. rel. to struct., obs. 9-27878
 monobromoacetylene, ν₁ and 2ν₂ bands, rotational structures 9-46408
 monocarboxylic acids, i.r. spectra study of dissoci. const. and monomer and dimer c=O bands 9-23105
 monochloroethyl radicals, chemically activated, decomposition 9-39947
 monodeuterotropylenyl radical, e.s.r. spectra obs., empirical resonance energy estimation 9-23177
 monoethanolamine, dielec. props. rel. to mol. struct., -70 to 60°C 9-30417
 monofluorides, aliphatic, fluorine chemical shift, effect of solvent 9-44549
 monofluoroacetylene, CH deform.-CF stretching coupling Fermi reson., i.r. obs. 9-27882
 monohalobenzenes, vapour and liquid, investigation of i.r. absorption spectra 9-27887
 monomethylammonium trichloromercurate, space group and unit cell dims. 9-46800
 mylar films, high field conduction 9-37585
 mylar films, non-destructive breakdown 9-47162
 myoglobin, e.p.r. zero field splitting, 4 mm obs. 9-43818
 n-pentane, adsorbed on synthetic Linde type-A zeolite, dielec. props. 9-41233
 naphthalene molecules, excitation by electron impact 9-30063
 2-naphthaldehyde, vibronic spin-orbit interactions 9-34681
 naphthalene, dark injection and radiative recomb. of electrons 9-41212
 naphthalene, delayed fluoresc. and triplet exciton life 9-24459
 naphthalene, dipole Davydov splittings 9-49006
 naphthalene, dipole Davydov splittings 9-49006
 naphthalene, fluoresc. quantum yield 9-33600
 naphthalene, fluorescence spectra, excited by giant-pulse ruby laser 9-35691
 naphthalene, intensifying effect of violet and green light on photocurrent for red light 9-47207
 naphthalene, low freq. phonons near Brillouin zone boundaries 9-24020
 naphthalene, luminesc. and absorpt., added ethyl bromide effects, obs. 9-28138
 naphthalene, magnetoelectret state 9-30979
 naphthalene, molecular admixture, relation between emission spectrum and solubility 9-28719
 naphthalene, optical detect. of e.s.r. in phosphoresc. triplet states 9-37770
 naphthalene, optical spin polarisation intriplet state 9-45391
 naphthalene, phosphoresc. decay time in solns., conc. depend. 770°K 9-35697
 naphthalene, π- system non-paired spatial orbitals wave functions 9-34680
 naphthalene, radiative triplet lifetime and σ-π interaction 9-23143
 naphthalene, singlet-triplet absorpt. by photoexcitation spectra 9-31115
 naphthalene, spin relax. and optical spin polarization of triplet excitons 9-39915
 naphthalene, triplet states in pulse radiolysis of gaseous mixtures with benzene 9-49387
 naphthalene, triplet-triplet annihilation in vapour 9-38905
 naphthalene, triplet-triplet transitions, LCAO MO SCF calc. 9-23144
 naphthalene, vibration, mean amplitudes, revised calc. 9-27907
 naphthalene and monosubst. derivatives, low-energy triplet-triplet transitions 9-38906
 naphthalene derivatives, singlet excited states, dipole moments 9-27908
 naphthalene in n-paraffin, quasiline phosphoresc. spectra 9-46409
 naphthalene molecule, in triplet state, energy transfer to singlet state of azulene mol. 9-30076
 naphthalene phosphoresc. in mixed crystals also containing anthracene guest mols. 9-43262
 naphthalene thermoelectret, pure and doped glow-peak analysis 9-37606
 naphthalenes, 1- and 2-substituted, triplet-triplet absorpt. spectra, calc. 9-23144
 naphthalenes, α-phenylated, fluoresc. and phosphoresc. spectra 9-42441
 naphthalenes, disubstituted, i.r. spectra 9-23145
 naphthalenes, partially deuterated, triplet lifetime, isotope effect calc. 9-40617
 naphthalenes-d₂, phosphoresc. lifetimes 9-46609
 naphthazarin metal complexes, elec. conductivity 9-43022
 naphthalene, isotopically mixed crystals, singlet excited states 9-24097
 2-naphthol, triplet-triplet transitions, LCAO MO SCF calc. 9-23144
 1-naphthol, triplet-triplet transitions, LCAO MO SCF calc. 9-23144
 α- and β-Naphthols, polycryst., proton mag. reson. spectra 9-26801
 1,4-naphthoquinone, thermodynamic props. 9-46418
 1,4-naphthoquinone, vibr. spectra 9-23156
 naphthoquinonic cpds, bifurated hydrogen bond existence 9-23653

Organic compounds continued

- 2-naphthyl methyl ketone, vibronic spin-orbit interactions 9-34681
 naphthacene, sensitized fluorescence excitation spectrum obs. 9-32501
 naphthacene, sensitized fluorescence excitation spectrum obs. 9-32501
 naphthalene frozen soln. in hexane, phosphorescence spectra depend. on conc. 9-26781
 neodymium ethylsulphate, paramag. relaxation, phonon re-absorption and spectral spin diffusion 9-33491
 nitro compounds, organic, of X-NO₂ type (X=C, N, O), ¹⁴N quadrupolar relax, ¹H line shapes and electron distrib. 9-42440
 3-nitro-1-propene, u.v. absorpt. obs. 9-27893
 trans-1-nitro-1-propene u.v. absorpt. rel. to e struct., obs. 9-27893
 p-nitroaniline, oriented, polarized absorption spectrum 9-46386
 4-nitroaniline, partly deuterated, two-dimensional neutron diff. study of crystal struct. 9-46801
 p-nitroaniline and related compounds, stimulated and spontaneous Raman spectra 9-45335
 nitroanisoles, o-, m- and p-, dielectric constants and dipole moments 9-36897
 nitrobenzene, ¹⁴N NMR spectrum, elec. field eff. 9-34683
 nitrobenzene, dielectric saturation in dipolar and nondipolar organic solvents 9-32792
 nitrobenzene, molecular isomers calc. by orbital method 9-44365
 nitrobenzene, n.m.r. of ¹⁴N, molecular alignment induced by elec. field, eff. on spectrum 9-30435
 nitrobenzene, Raman line intensities as function of conc. and solvent type 9-48701
 nitrobenzene in hexane, soln. decomposition, effects of γ irradiation 9-30368
 1-p-nitrobenzeneazo-2-naphthol (Para Red), twinning, X-ray diff. obs. 9-32863
 nitrochlorobenzene, molecular isomers calc. by orbital method 9-44365
 p-nitro-N,N'-dimethylaniline, elec. dipole moment using modified Higasi's eqn. 9-46410
 m-nitro-N,N'-dimethylaniline, elec. dipole moment using modified Higasi's eqn. 9-46410
 nitroethane Na salts, geometrical isomers, i.r. and Raman obs. 9-27905
 nitroethylene, u.v. absorpt. rel. to e struct., obs. 9-27893
 nitrogen heterocycles, triplet-state zero-field splittings 9-42425
 nitrogen heterocycles, lowest ionization potential 9-39016
 nitrogen heterocycles, π -electron charge densities and chem. shifts 9-44364
 nitromethane, n.m.r. of ¹⁴N, molecular alignment induced by elec. field, eff. on spectrum 9-30435
 nitromethane, u.v. absorpt., obs. 9-27893
 nitromethane in tetrachloroethylene NMR near critical soln. temp. 9-44596
 nitromethane in tetrachloroethylene NMR near critical soln. temp. 9-28157
 nitromethane Na salts, geometrical isomers, i.r. and Raman obs. 9-27905
 p-nitrophenol, oriented, polarized absorption spectrum 9-46386
 1-nitropropane Na salts, geometrical isomers, i.r. and Raman obs. 9-27905
 2-nitropropane Na salts, geometrical isomers, i.r. and Raman obs. 9-27905
 nitrosamines, heterocyclic, configs. and conformations, n.m.r. studies 9-34682
 nitrosyliron bis(N,N-diethyldithiocarbamate, Mossbauer effect 9-39823
 nitroxides, e.p.r. spectrum, hyperfine structure, effect of conformation 9-44366
 n.m.r. of three-spin systems, analysis of complex spectra 9-23027
 n-nonane, cohesion energy, vapour press. and molar vol., obs. 9-28094
 norvaline in acid sulphate electrolyte, rel. to Cu cathode growth at air-soln. interface 9-28810
 ochotensimine, intramol. Overhauser effects, positive and negative, rel. to dipole-dipole relax. 9-25774
 n-octane, liq., negative-carrier mobility meas. 9-42672
 n-octane liq. at const. density, mol. sound vel. and compressibility 9-40790
 octanol isomers, dielec. relax. press. effect 9-30418
 1-octyne, liquid, far i.r. absorptions 9-40796
 olefines, reaction rates with H atoms 9-43334
 olefins, reaction rates olefins 9-43335
 ooligonitraniline donor-acceptor complexes, carrier conductivity, thermoelec. props. 9-33225
 organophosphoryl compounds containing N-P and S-P bonds, hydrogen bonding ability 9-30138
 oxalate ions, counter current electromigration ¹⁴C isotope effect 9-48439
 oxalic acid, and -d₂, gas, spectra rel. to mol. struct., 400-4000 cm⁻¹ 9-30133
 oxalic acid, use in multimegarad γ dosimetry 9-24950
 oxalyl bromide, i.r. and Raman spectra, band freqs. and assignments 9-34684
 oxalyl halides, attribution and analysis using normal coords. 9-46411
 oxidation by Co³⁺ 9-24560
 N-oximes, geminal and vicinal N, H coupling constants, absolute signs, stereochem. and medium eff. 9-30134
 oxocarbons, monocyclic, electronic struct. calc. 9-30135
 3-oxo-, 4-phenyl, 1,2-benzfluorenone solutions, fluorescence spectra 9-32785
 oxybenzoic acids u.v. electron absorption spectra 9-30085
 oxydiethanoic acid, free radical formed on e irradi., in e.s.r. in zero field 9-42442
 paraffins, linear and cyclic, viscosity rel. to mol. structure 9-25776
 paraffins in β,β' -dichlorodiethyl ether, critical opalescence, light-scatt. studies 9-34909
 pentacene, vibronic band position depend. on light polarization 9-27909
 pentachlorobiphenyl, vitrons, detect. at 40 MHz 9-39098
 pentachloroethoxyacetic acid, struct. formula and cryst. struct. 9-39346
 pentadiene molecules, spectral characts. and electronic structures 9-30110
 pentadienyl, configuration-interaction wavefunctions 9-38877
 pentaerythritol, p.m.r. 9-43307
 pentaerythritol, proton mag. reson. investig. 9-25777
 pentaerythritol tetranitrate, thermal decomp. prod. by fracture 9-30531
 pentafluorobenzene, low-field n.m.r. spin-coupling signs 9-30136
 pentafluorobenzonitrile, i.r. and Raman spectra 9-23147
 pentafluorobenzonitrile, microwave absorpt. spectrum obs. 9-27910
 pentafluorobenzonitrile as acceptor in charge-transfer-complexes 9-28784

Organic compounds continued

- pentafluorophenyl derivatives, chemical shifts, coupling consts., π -electronic interactions, correl. 9-42434
 pentafluorophenyl derivatives, π interactions and bonding in selected compounds 9-42435
 pentalene, ground-state geometry and symmetry 9-36716
 pentamethylene sulphide, i.r. spectrum, vibrational assignment 9-32510
 n-pentane liq. at const. density, mol. sound vel. and compressibility 9-40790
 n-pentane near critical pt., light scatt. under gravitational effect 9-23501
 pentanol, primary, secondary and tertiary, dielectric polarization and saturation 9-46651
 pentaphenylantimony, cryst. and molec. struct. 9-23785
 perchlorodiphenylmethyl free radical, e.s.r. 9-38908
 perchlorotriphenylmethyl free radical, e.s.r. 9-38908
 perfluoro-1,3,5-triazacyclohexane, i.r. spectrum 9-25778
 perfluorovinyl derivatives, ¹⁹F n.m.r. 9-23148
 perinaphthyl neutral radicals, e.s.r. study 9-48495
 perpyrhen, eff. of heavy atoms on intercombination transitions 9-25779
 perylene, injection of defect electrons in dark and under illumination 9-30995
 perylene, intrinsic photoconductivity 9-39728
 perylene cryst., photoioniz. threshold meas. 9-33424
 perylene in N-isopropylcarbazole, electronic excitation energy transfer 9-31138
 perylene molecular crystals, 'effective molecule' model in electronic spectrum calc. 9-41392
 phenanthrene, dipole Davydov splittings 9-49006
 phenanthrene, phosphoresc. decay time in solns., conc. depend. 770°K 9-35697
 phenanthrene, triplet-triplet annihilation in vapour 9-38905
 phenanthrene 3400-Å spectrum rel. to totally symmetric vibronic perturbations 9-38911
 phenanthrene determination in anthracene 9-35762
 phenanthrene frozen soln. in hexane, phosphorescence spectra depend. on conc. 9-26781
 Phenanthrene frozen soln. in octane, phosphorescence spectra depend. on conc. 9-26781
 phenanthrene oriented in biphenyl, deuterium isotope effect in zero-field splittings 9-43289
 phenanthrene soln., electronic-absorption-band region, Einstein-coeff. spectra obs. 9-30072
 phenazine, triplet state, e.p.r., obs. 9-48503
 phenanthrene, dipole Davydov splittings 9-49006
 phenol, dipole moments of lowest singlet $\pi^* \leftarrow \pi$ states by optical Stark effect 9-34686
 phenol, height of potential barrier for ideal gas under harmonic oscillator 9-46414
 phenol, LCAO-MO configuration anal. 9-32450
 phenol, π -electron props. 9-48504
 phenol-water mixture, light scatt. meas. of conc. fluctuations near critical point 9-40794
 phenolic-nylon chars, thermal conductivity 9-26460
 phenols, excited, dissoci. consts. from fluoresc. quenching 9-39108
 phenols, ortho-substituted, in dimethyl sulfoxide solns., n.m.r. study 9-42444
 phenols, vapour spectra, band freq. 9-32445
 phenothiazine, phosphoresc. triplet state 9-39888
 phenothiazine, phosphoresc. triplet state, e.s.r. 9-39887
 phenoxazine, phosphoresc. triplet state 9-39888
 phenoxazine, phosphoresc. triplet state, e.s.r. 9-39887
 phenoxyl radicals, fluorinated, spin densities from n.m.r. linewidths 9-34687
 2-phenyl-5-(4 biphenyl)-1,3,4-oxadiazole derivatives, excimer emission 9-44577
 phenylacetylene, nuclear spin-lattice relax. 9-39120
 phenylalanine and derivatives, near u.v. circular dichroism and absorpt. spectra, vibr. struct. anal. 9-46415
 phenylalanine fluorescence spectrum excited by vacuum U.V. obs. 9-30149
 phenylboronic acid, i.r. spectra rel. to vibrational frequencies 9-23151
 phenylcyclobutane, mol. structure from c. diff. exam. 9-23111
 phenyldiazonium ions, meta and para. substituted, HMO calc. 9-27914
 o-p-phenylene diamine, ¹⁴N n.g.r. temp. depend., 77-292°K 9-30071
 o-phenylenediamine, N-H frequencies in halide chelates 9-36719
 2-phenylindole, self-quenching 9-44576
 3-phenylisoxazolin-5-one, cryst. and mol. struct., X-ray obs. 9-35077
 3-phenylisoxazolin-5-one, cryst. and mol. struct., X-ray obs. 9-42801
 2-phenylnaphthalene, phot. energy rel. to mol. config., e struct. and spectra, calc. 9-27911
 1-phenylphenalenyl radical, spin densities, hyperconjugation eff. calc., e.s.r. study 9-34677
 1-phenylphenalenyl radical, spin densities, hyperconjugation eff. calc., e.s.r. study 9-34677
 phosphiran, -1-d₂, -2,3-d₂; gas i.r. and liquid Raman vib. spectra, freq. shift meas. 9-23150
 phosphorescence, non-exponential decay 9-23512
 phosphorus, high-resolution NMR spectra 9-34685
 photochemistry, excitation energy degradation, Jablonski scheme 9-28814
 photochromic spiropyran layers, coloration by u.v. laser radiation 9-27916
 phthalimide solutions, fluorescence decay and depolarization 9-23514
 phthalates, zinc and cadmium, luminesc. 9-47399
 phthalic esters, electrohydrodynamic behaviour at -20-80°C 9-36896
 phthalimide derivatives, spectral and fluorometric characteristics depend. on oxygen 9-23149
 phthalimide solns. in alcohols and glycerine, fluoresc. polarization, temp. depend. 9-36893
 phthalimide solutions, anisotropy in fluorescent emission obs. 9-23509
 phthalocyanine, free base, matrix isolated, absorpt. and fluoresc. spectra 9-49289
 phthalocyanine, metal-free β -form single cryst., electron trapping and bulk conduction in vacuum 9-28462
 phthalocyanine soln. phototropic laser shutters, transmission, obs. 9-36277
 phthalocyanines, origin of photocarriers 9-43131
 phthalocyanines, trapping levels obs. 9-49166
 photochrome systems, light absorpt. mol. mechanism 9-40618
 piperazine, anisotropy of molec. rot. meas. by n.g.r. relax. 9-39930

Organic compounds continued

- podototarinate diacetate and dimethyl ether, n.m.r. study of hindered rotation 9-23152
- polar gases, thermal conductivity in elec. field 9-42610
- 4,4'-polarized cryst. absorpt. spectrum 9-31114
- poly-n-butylacrylates, four viscoelastic relax. obs. -40 to 148°C 9-23430
- polyacenes, linear, $^1A \rightarrow ^1L_g$ transition probabilities 9-38907
- polycyclic hydrocarbons, correlation effects of π electrons 9-44362
- polycyclicazines, vibronic interactions between $\pi\pi^*$ and $\pi\pi^*$ states 9-42426
- polyenes, bond alternation 9-44348
- polyenes, photo and thermal isomerization mechanisms 9-35738
- polyenes, vibrational struct. of electronic spectra 9-48443
- polyethylacrylates, four, viscoelastic relax. obs. -40 to 148°C 9-23430
- polyethylene absorber, slow positron emission measurable flux 9-24244
- polymethylmethacrylate, transient radiation, spatial distribution 9-37764
- polymethyn dye solns. for ruby laser freq. conversion 9-34171
- polystyrene sulfonic acid membrane, elec. conductivity rel. to temp. and water absorption 9-28463
- porphyrin, vibronic borrowing 9-44353
- positron annihilation, lifetime rel. to mol. first ionization pot. 9-33239
- potassium acid phthalate, diamag. susceptibilities and anisotropies 9-45081
- potassium aminedisulphenate, quadrupole coupling in $(\text{NO}_3)_2^{2-}$ from e.s.r. meas. 9-39916
- potassium caprate, crystal structure refinement 9-39326
- potassium hydrogen malonate, cryst. struct., ambiguity in least-squares analysis 9-39347
- potassium oleate in D_2O soln., n.m.r. meas. of smectic liq. cryst. phase 9-40775
- potassium oxalate monohydrate, crystal and mol. structure, refinement 9-26265
- potassium thiocyanate, gamma-irrad., e.p.r. spectrum of radical species 9-45392
- potassium trioxaloferrate, Fe(III) activity transfer process 9-39185
- proflavin in rigid org. medium, delayed fluorescence, one- or two-photon mechanisms 9-47403
- propane, heat capacity Joule-Thomson coeff. Isothermal throttling coeff. latent heat of vaporization meas. 9-36818
- propane O_2 mixture, pressure var. behind shock front, eff. of tube diam. 9-28061
- propane-air flame, electrically augmented, temp. and heat transfer meas. in discharge zone 9-25131
- propane-air mixtures, constant volume, combustion, effect of containing wall linings 9-45881
- propanoic acid far i.r. spectra, H bond stretching vib. determ. 9-23087
- i-propanol on Al oxides, catalytic decomposition, apparatus for obs. 9-37823
- propargyl aldehyde ^{13}C -C-H spin-spin coupling constants involving formyl proton 9-44350
- propene and oxide, combination band of methyl group torsion and asymm. stretching vib. 9-25752
- propionic acid, u.s. propag. temp. coeff. meas. 9-23494
- propionyl fluoride, microwave spectrum, rotational isomerism 9-48505
- propionophenone, time-resolved phosphoresc., spectra identification 9-44368
- propyl alcohol, dielec. const. freq.-temp. meas. by helical resonator method 9-36895
- n-propyl alcohol, low temp. phase transitions, luminescence obs. 9-42692
- n-propyl alcohol, trans. form, rot. constants, dipole moment and structure 9-46416
- propylene, barrier to internal rot. using Gaussian self-consistent field wave functions 9-48506
- propylene, copolymerization with ethylene and 4-vinylcyclohexane-1, and effect of catalyst 9-31188
- propylene, oxidation by photolysis with NO_2 9-43338
- 1,2-propylene glycol, liq., hypersound propag. obs. from stimulated Mandelstam-Brillouin scatt. 9-30399
- propylene glycol solvent effect on pyrene luminesc. 9-48708
- propylene imine, vibr. spectra 9-44369
- propylene polymerization on complex catalysts in the presence of alcohols and diethylethoxyaluminum 9-26822
- propylene-1- d_3 , thermal and NO catalyzed cis-trans isomerization 9-43328
- propyne, rotation and rotation-vibration interac. consts., mm. wave study, 68 to 119 GHz 9-44367
- pseudo-isocyanine soln. fluoresc. meas. with 200 MHz modulated fluorometer 9-48707
- purine, and deuterated derivatives, Raman and i.r. spectra 9-41397
- purines, H-bond assoc. with N(4)-hydroxycytosines 9-42635
- pyrazine, absorpt. and phosphoresc. spectra, excitonic struct. 9-47405
- pyrazine, fine struct. of Phosphoresc. at 4.2°K 9-24463
- pyrazine in acid medium, nature and symmetry of phosphorescent state, e.p.r. and luminescent meas. 9-46417
- pyrazine in durene and 1:4 dichlorobenzene, phosphorescence decay obs. 9-31144
- 2-pyrazolin-5-one derivatives, i.r. spectral analysis 9-30140
- pyrazoline dye recognition using spectral correl. 9-30140
- pyrene, delayed fluoresc. in ethanol rel. to solute re-encounter probability 9-34916
- pyrene, fluoresc. decay time in cholesterol benzoate liq. crystals, obs. 9-32786
- pyrene, quantum mechanical calc. of π -electron spectra and electronic structure 9-30139
- pyrene cryst., photoioniz. threshold meas. 9-33424
- pyrene fluoresc. in frozen solns. rel. to excimer form, obs. 9-48507
- pyrene in ethanol, soln., Fluorescence spectra, isobestic pts. 9-40574
- pyrene in methylcyclopentane at low temp., fundamental vib. freqs. from quasilinear fluorescence spectrum 9-38913
- pyrene molecular crystals, 'effective molecule' model in electronic spectrum calc. 9-41392
- pyrene molecules, excitation by electron impact 9-30063
- pyrene molecules in cyclohexane, radiation-induced fluorescence, effect of elec. field 9-44351
- pyrene in propylene glycol, phosphoresc., normal, M^* and D^* fluoresc. 9-48708
- pyrene-d-10, in photo-excited triplet state, e.s.r. anisotropic saturation 9-44371
- pyridazine, proton coupling constants 9-34689

Organic compounds continued

- pyridine, adsorption on zeolite Y, i.r. spectroscopy rel. to adsorbent surface props. 9-24519
- pyridine, cohesion energy, vapour press. and molar vol., obs. 9-28094
- pyridine, temporary negative ion reson. 9-40619
- pyridine adsorpt. by $\gamma\text{-Al}_2\text{O}_3$ rel. to active centres nature, obs. 9-26192
- pyridine complexes of iodine monohalides, Mossbauer effect of ^{129}I 9-34688
- pyridine derivatives and alcohols in CCl_4 , equilibria of assoc. 9-23106
- pyridine sorbed on porous glass, i.r. spectra 9-26196
- pyridine-Br and BrCl complexes, vibr. spectra 9-23153
- pyridine-chloroform, heat of mixing continuous determ. 9-40784
- pyridines, substituted, charge-transfer complexes with Br, far i.r. spectra 9-23154
- pyridinium H-bonded halides, i.r. and Raman spectra 9-49290
- 2-pyridone, ^{18}O and ^{16}O labelled, i.r. spectra 9-23155
- pyridoxal phosphate oxime, crystal and molecular structure 9-39344
- 2-(2-pyridylmethylthio) benzoic acid, crystal and molecular structure 9-39348
- pyritinol/ $5'$ -thiopyridoxine, redox pot. 9-28809
- pyronine B soln. in ethanol, glycerol, Nd laser excitation, light generation, 550-650 nm, room temp. 9-30141
- pyrylium salts as Q-switches 9-47933
- quaternary ammonium salts in acetone, elec. conductivity ion-pair formation 9-23524
- quaternary ammonium salts in acetone, elec. conductivity, pressure and temp. effects 9-23522
- quaternary ammonium salts in acetone, elec. conductivity transport mechanism 9-23523
- N-quinoline, geminal and vicinal N,H coupling constants, absolute signs, stereochem. and medium eff. 9-30134
- quinoline in hexane and heptane, frozen, phosphoresc. rel. to phase transforms., 55-123°K 9-28726
- quinone, effect on Ge surface props. 9-43093
- quinoxaline, optical detect. of e.s.r. in phosphoresc. triplet states 9-37770
- quinoxaline, radiative and radiationless decay consts. 9-39883
- quinoxaline, two $n \rightarrow \pi^*$ transitions 9-32525
- quinoxaline anions, spin densities 9-32526
- quinuclidinyl benzilate hydrobromide, cryst. and mol. struct. 9-35078
- π -electron radicals, MO theory of hyperfine interactions 9-38874
- n-radialenes, structural and electronic props. by molecular orbital theory 9-32527
- Rao's constant and molecular compressibility in liquids and their mixtures 9-30398
- rare earth complexes with tenoyltrifluoro- acetone and rhodamine-C, benzene solns., fluoresc. 9-42664
- rare-earth ethylsulphates, covalency eff. 9-35008
- Rayleigh scattering spectrum, energy distribution, liquids far from melting point 9-26121
- relaxation of rigid mols. dielectric absorpt. meas. 9-23088
- rhodamin-B cryst., photoioniz. threshold meas. 9-33424
- rhodamine, i.r. absorption spectra 9-23157
- rhodamine, i.r. absorption spectrum, 400-3500 cm^{-1} 9-23157
- rhodamine 3B, emission spectra in solution 9-26122
- rhodamine 6G, methanolic, laser cw operation 9-25278
- Rhodamine 6G dye laser, threshold inversion and triplet state conc., wavelength depend. 9-34888
- rhodamine 6G mols., in soln., electronic absorption spectra and transitions 9-34690
- rhodamine 6J soln. in ethanol, glycerol, Nd laser excitation light generation, 550-650 nm, room temp. 9-30141
- rhodamine 6Zh, reson. excitation energy transfer from 3-methoxybenzantron 9-25780
- rhodamine C, reson. excitation energy transfer from 3-methoxybenzantron and rhodamine 6Zh 9-25780
- rhodamine C soln. in ethanol, glycerol and polymethylmethacrylate, Nd laser excitation, light generation, 550-650 nm, room temp. 9-30141
- rhodamine dye laser, flashlamp pumped spectral output 9-22408
- rhodamine GZh molecules, association, effect of binary solvents 9-27922
- rhodopsin systems, light absorpt. mol. mechanism 9-40618
- rosin films, light sensitive volume changes, spectral characts. 9-28698
- saffranine T soln. in ethanol, glycerol, Nd laser excitation, light generation, 550-650 nm, room temp. 9-30141
- salol, cryst. growth from melt in capillary tubes, retardation of growth rate 9-37273
- salol, liq., Rayleigh line wing fine struct. and transversal hypersound propag. 9-44573
- samarium ethylsulphate, spin-lattice relaxation anisotropy 9-26665
- sandwich complexes, hyperfine coupling consts. and covalency 9-42420
- Schiff base, fluorinated, liq. cryst., molec. config. and order from n.m.r. 9-28159
- scintillator, combined with Si photodiode for high energy charged particle detect. 9-42139
- secondary ammonium halides, long-chain, X-ray study 9-37154
- selenols, $^1\text{H}(\text{Se-H})$ n.m.r. chem. shift and fundamental Se-H stretching freq. 9-34691
- selenurea, applic. of random-phase-approx. method 9-40621
- semiconducting, conductivity behaviour and suitability for devices 9-41193
- semiconductor p-n junctions, diffusion doped 9-35436
- semiconductors, conduction mechanism in band and hopping models 9-28503
- sideramines, e.s.r. 9-39917
- silacyclopentane, far i.r. spectrum and barrier to pseudorot. 9-32528
- silane, tetrahedral, spectroscopic mass and zero-order freq. calc. 9-30142
- silicone fluids, positron lifetimes 9-27467
- silicone oils, convection on non-uniformly heated, rotating plane 9-22289
- silver nitrate adducts of cyclic thio-ethers, ring vibrations and Ag-S bond 9-32512
- sodium caprylate-water-ethylene glycol (glycerol) (tetraethylene glycol), system, phase equilibrium 9-23547
- sodium dodecylbenzene sulphate, influence on $\text{Na}_3\text{P}_2\text{O}_{10}$ crystal growth 9-37038
- sodium formate, crystalline, Raman spectra 9-47378
- sodium laurylsulphate solns., u.s. vib. potentials as function of conc. 9-48694
- sodium naphthalenide solns. in tetrahydrofuran, anomaly in e.s.r. spectrum 9-30427
- sodium-2-oxovalerate, crystal and mol. structure 9-26268
- solasodane derivatives, e.s.r. spectra 9-44372

Organic compounds continued

- solutions, binary dilute, Brillouin intensity ratios and Landau-Placzek law deviations, obs. 9-30408
 solvents for laser Q-switching 9-29423
 sorbitan tristearate ultrathin black films, elec. resistivity 9-37580
 spermidine phosphate trihydrate, crystal structure 9-26269
 spiropentane in nematic solvent, n.m.r. study 9-40620
 spiropyran layers, photochromic, coloration by u.v. laser radiation 9-27916
 spiropyranes in soln., photochromy obs., by means of triplet-triplet absorption 9-34910
 steroids, CH_2 , CH_3 -groups i.r. deform. vibr. bands, obs. 9-25781
 steroids, oxide, 11 β ,12 α -dibromo-3 α ,9-oxidocholeonic acid methyl ester, crystal structure 9-39329
 stilbene, acoustic impedance calc., use as high temp. acoustic bond 9-26416
 stilbene, photoisomerism, theory 9-43337
 stilbene, Raman scatt. cross-sections 9-41396
 stilbene crystal, 2-photon light absorpt. depend. on light polarization 9-24375
 stilbene in dil. toluene soln., γ -ray-induced trans \rightarrow cis isomerization, temp. depend. 9-40560
 stilbenes, para-substituted, first ϵ transition freq., obs. 9-34692
 strontium formate dihydrate, crystalline, Raman spectra 9-47378
 styrenes, o- and m-subst., i.r. and Raman spectra 9-32529
 succinic acid crystal, i.r. and Raman spectra, rel. to H bonding 9-35668
 sucrose, diffusion in water 9-23476
 sucrose, growth rate curves rel. to surface diffusion model 9-37098
 sucrose crystals, growth from aqueous soln. at 0°C 9-39203
 sulfonamides, i.r. spectra 9-36720
 sulphamate ion, internal vibr. calc., Urey-Bradley potential function 9-46419
 σ -bonded cpds. containing N or O, MINDO calc. 9-27899
 p-TCNQ, anisotropy of electrical conductivity 9-30914
 teflon films, high field conduction 9-37585
 terephthalbis(aminofluorobenzene) liq. cryst., molec. config. and order from n.m.r. 9-28159
 terpenoids, C_{25} , crystal structure of methyl cephalonate bromoacetate 9-39340
 p-terphenyl, cryst. struct. 9-32935
 o-terphenyl, liq., EPR study of mol. motion 9-40805
 o-terphenyl, mol. motion in liq., crystalline and glassy forms 9-39925
 p-terphenyl crystals, hole injection from liquid redox electrodes 9-26475
 tertiary alcohols, specific rotation and mag. rotatory dispersion 9-48697
 tertiary phosphine hydrobromides, n.m.r. 9-23146
 1,1,2-tetrabromo and tetrachloroethane, rotational isomerism, NMR investig. 9-23162
 tetracene, charge carrier mobility meas. 9-30817
 tetracene, dipole Davydov splittings 9-49006
 tetracene, dipole Davydov splittings 9-49006
 tetracene, fission of singlet excitons into triplet ones obs. 9-35320
 tetracene, intrinsic photoconductivity 9-39728
 tetracene, low-lying valence states and intrinsic photocond. 9-24239
 tetracene, space-charge-limited currents, trapping levels and quasi-Fermi-level obs. 9-41204
 tetracene crystal, fission of singlet excitons into pair of triplet excitons 9-49007
 tetracene photodimer, i.r. spectrum analysis 9-32502
 tetracene single cry., fluorescence efficiency, mag. field eff. 9-26779
 tetracene thin film, temperature-independent conducting state 9-33284
 tetrachloro-p-xylene, excimer emission in rigid organic glass, 280nm excitation, 77°K 9-32530
 tetrachloroethylene, cohesion energy, vapour press. and molar vol., obs. 9-28094
 tetrachloroethylene, doped with nitromethane, NMR, molecular diffusion eff. 9-44596
 tetrachloroethylene, doped with nitromethane, NMR, molecular diffusion eff. 9-28157
 tetracyanobenzene complexes, e.s.r. of charge-transfer triplet states 9-23158
 tetracyanoquinodimethan, absorpt. coeff. calc. from reflection and transmission meas. 9-39796
 tetracyanoquinodimethan complexes, mag. susceptibility from 2.5°K to room temp. 9-47233
 tetracyanoquinodimethane ion-radical salts, exciton-controlled proton relax. 9-39926
 tetracyanoquinodimethane complex with benzthiocarbocyanine dye, electron double resonance 9-28753
 tetracyclohexylcyclotetraphosphine, molecular and crystal structure 9-39351
 tetrafluorobenzoic acids, p-subst., ν_{OH} , and πK_{a} values 9-30145
 tetrahydrofuran, complex formation with dissolved chloronitrobenzenes, evidence from u.v. spectra 9-30095
 tetrahydrofuran, far-i.r. spectra and pseudorotation 9-38915
 tetrahydrofuran, microwave spectrum, barrier to pseudorotation 9-38916
 tetrahydrofuran-water NaCl solns., liq.-liq. equilibrium 9-32765
 1,4,5,8-tetrahydroxyanthraquinone, visible emission and abs. spectrum, analysis of bands 9-30144
 tetraiodoethylene, i.r. and Raman vib. spectra, assignments 9-27902
 tetrakis-(dimethylamino)-ethylene, electronic spectrum and chemiluminesc. 9-23159
 tetramethyl ammonium tri-iodomercurate, electro-optical props. 9-43217
 2,2,6,6-tetramethyl-4-hydroxypiperidine-1-oxyl radical, mag. susceptibility and e.s.r. spectra 9-45091
 3,5,8,10-tetramethylcycloheptazulene, monoclinic form, cryst. struct. 9-39350
 2,2,4,4-tetramethyl-3-oxoglutaric acid, cryst. and mol. struct. 9-48788
 tetramethylsilane, adsorbed, electron-irrad., thin Si films deposition obs. 9-44628
 tetramethylurea, i.r. spectra bands and vib. determ., normal co-ord. anal. 9-23130
 tetraphenylcyclobutadiene molybdenum dicarbonyl bromide, from X-ray diff. meas. 9-48841
 tetraphenylcyclopentadienone radical anion, e.s.r. and molecular orbital study 9-30143
 tetraphenylhydrazine, diphenylamino radical dimer as colour centre 9-42855
 tetrapropylammonium tetrafluoroborate, anomalies of viscosity of analogues 9-42640

Organic compounds continued

- tetraynylidyne, PMR spectrum, coupling const. for ^{13}C , ^{117}Sn and ^{119}Sn satellites 9-27917
 1,4-thallose benzoate-thiourea complex, crystal structure 9-39319
 thallose formate aqueous soln., saturated, density determ. 20-28°C 9-28329
 2- and 3-phenyl radicals, e.p.r., inequivalence of CH_2 protons 9-36722
 thermodynamic props. of 12 substs. in their ideal gas state 9-26024
 thiacyanocyanine dye absorption, luminescence and polarized luminescence spectra, 77°K 9-23113
 thioalkanes, valence force field 9-38880
 thioamide cpds., SH group determ. from $\text{SK}\alpha_{1,2}$ line chem. shift 9-37751
 thiocyanate cpds. identification from $\text{SK}\alpha_{1,2}$ line chem. shift 9-37751
 thio-ethers, cyclic, mercuric halide adducts, ring vibrations 9-30107
 thio-ethers, cyclic, silver nitrate adducts, ring vibrations and Ag-S bond 9-32512
 thiol esters, complex, i.r. absorption freq. determ. 9-23160
 thiophene, n.m.r. multiple-quantum transitions 9-30146
 thiophenol, π -electron props. 9-48504
 thiourea, applic. of random-phase-approx. method 9-40621
 thiourea, ferroelec. phase transitions, effect of hydrostatic pressure on dielec. const. 9-28567
 thiourea-alkali halides mixed cry., i.r. absorption spectra, interac. obs. 9-24420
 thorium formate hydrates, n.m.r. 9-41437
 thorium oxalate hydrates, n.m.r. 9-41437
 L-threonyl-L-phenylalanine-p-nitrobenzyl ester hydrobromide, crystal structure 9-26270
 thulium cyclopentadienides, visible and i.r. absorption spectra, low temp. 9-32531
 thulium ethylsulphate, spin-lattice relax. time of Tm^{169} and protons 9-28641
 thulium methylcyclopentadienides, visible and i.r. absorption spectra, low temp. 9-32531
 thymidine, i.r. absorption spectra, 230-30 cm^{-1} , 20 to -175°C, crystal lattice vib. anal. 9-25783
 thymine, radicals formed by H-atom bombard. 9-43324
 thymine anhydride, cryst. struct. 9-39352
 TMPD-TCNQ, spin-lattice relax., temp. depend. 9-41347
 toluene, absorption spectra, noise intensity from fluctuations in readings 9-36889
 toluene, acoustic relax., 10-300 kHz 9-28123
 toluene, bubble growth on glass surface during boiling 9-30465
 toluene, dielec. props., press., vol., and temp. effects 9-39109
 toluene, liq. at const. density, mol. sound vel. and compressibility 9-40790
 toluene, self-diffusion in benzene-toluene, cyclohexane-toluene liquid mixtures 9-36856
 toluene, sound velocity at constant density 9-46633
 toluene, sound velocity meas. along saturation line 9-44561
 toluene, thermal conductivity meas., 20-200°C 9-30388
 toluene, viscosity, effect of ultrasound 9-42637
 toluene ion radicals, spin delocalization and vibr.-electronic interaction 9-38917
 toluene Raman spectra determ. using He-Ne laser as excitation source 9-49293
 toluene-carbon tetrachloride, liquid mixture thermal conductivity 9-36865
 toluenes, polydeuterated, spectral charact., correls. in 900-500 cm^{-1} region 9-46420
 trenchloride, primary electro-optical effect 9-35629
 triacetin, liq., hypersound propag. obs. from stimulated Mandelstam-Brillouin scatt. 9-30399
 1,1,2-tribromo and trichloroethane, rotational isomerism, NMR investig. 9-23162
 2,4,6-tribromoaniline, crystal structure 9-39318
 1,1,2-trichloroethane, u.s. relax. and vol. change during internal rot. 9-42652
 1,1,1-trichloroethane vapour, u.s. dispersion and relaxation obs. 30°C 9-32737
 1,3,5-trichloropyrimidine and 4D derivative, vibr. i.r. and Raman obs. 9-28139
 tricycloquinazoline, crystal and molecular structure 9-39353
 trideuteronitromethane Na salts, geometrical isomers, i.r. and Raman obs. 9-27905
 triethylamine and water, soln. decomposition, effects of γ irradiation 9-30368
 triethylamine-naphthalene excited donor-acceptor complex dipole moment 9-23096
 trifluoroacetaldehyde, i.r. vib. spectrum and internal rotation barrier 9-23123
 1,3,5-trifluorobenzene in nematic liq. crystal, proton and fluorine mag. reson. spectra 9-34693
 trifluoroethoxyethoxybutanes, substituted, n.m.r. studies of ^{19}F chemical shifts and coupling constants 9-30148
 1,1,2-trifluoroethane molecule, internal rotation potential 9-44360
 trifluoromethane, rotational microwave spectra obs. 9-30113
 trifluoromethyl acetylene, rotational microwave spectra obs. 9-30113
 trifluoromethyl iodide, oriented molec. beam reaction with K atoms 9-43320
 1,1,2-trifluoroethane molecule, internal rotation potential 9-48494
 triglycerides, recrystallization at low supercooling 9-37106
 triglycine sulphate, γ -irrad., e.s.r., hindered motion of CH_2 in CH_2COO^- obs. 9-35720
 triglycine sulphate, dielec. behaviour 0.5 to 4.5 Mc/s 9-30975
 triglycine sulphate, dielectric props. over wide freq. range 9-47181
 triglycine sulphate, elec. and spectral charact., effect of γ -irradiation 9-47182
 triglycine sulphate, ferro-paraelectric transition, pressure depend. of Curie point, 0.23 kbar 9-41248
 triglycine sulphate, ferroelec. domains boundaries, X-ray topography obs. 9-28556
 triglycine sulphate, ferroelec. props., eff. of electrode material 9-33387
 triglycine sulphate, ferroelec. transition, Pippard scheme for sp. ht., thermal expansion and isothermal compressibility 9-30970
 triglycine sulphate, ferroelectric, visualization of domain structure at electron microscope level 9-41249
 triglycine sulphate, ferroelectric properties, influence of ^{60}Co γ rays 9-47179
 triglycine sulphate, H bond vibrations 9-32516

Organic compounds continued

- triglycine sulphate, i.r. transmission and refl., spectra, optical consts., applic. to pyroelec. 9-35615
- triglycine sulphate, polarization switching processes, effect of u.s. vibrations 9-47183
- triglycine sulphate, second harmonic generation and scatt. by domains ferroelec. domains 9-45010
- triglycine sulphate, thermal conductivity, influence of d.c. field in phase transition region 9-39545
- triglycine sulphate, X and γ irradiated, Barkhausen effect 9-47180
- triglycine sulphate crystals, pyroelectric effect 9-39684
- triglycine sulphate group ferroelectrics in polar and nonpolar cuts, pyroelec. coeff. and dielec. const. deriv. 9-43122
- triglycine sulphate pyroelec. detector, h.f. response 9-45014
- triglycine sulphate substrate, effect on conduction of Te films 9-28502
- triglycine sulphate-isomorphous ferroelec. solid soln., optical investig. 9-47371
- triglycinefluoroberyllate ferroelec. crystal, l.f. Raman spectra at 80 to -140°C 9-49299
- triglycinesulphate ferroelec. crystal, l.f. Raman spectra at 80 to -140°C 9-49299
- triglycinesulphate ferroelec. crystal, l.f. Raman spectra at 80 to -140°C 9-49299
- trihalomethane-halide ion complexes in soln. association, n.m.r. and i.r. spectra 9-23537
- β -2,4,6-trimethyl trithian, i.r. spectrum, vibrational assignment 9-32511
- α -2,4,6-trimethyl trithian, i.r. spectrum, vibrational assignment 9-32511
- trimethylamine, molec. force field 9-23161
- trimethylamine, Raman spectra and vibr. assignments 9-30147
- trimethylamine charge-transfer complexes, i.r. spectra 9-23163
- N-trimethylborazines, isotopically substituted, i.r. spectra, band obs. 9-27906
- trimethylene selenide, vibr. anal. and ring puckering 9-42447
- trimethylene sulfide, electr. spectrum obs. 9-32524
- trimethylenediammonium dichloride, crystal structure 9-32936
- trimethylenemethane, zero-field splitting of ground triplet state 9-42448
- trimethylead halides, i.r. Raman spectra and mol. struct., obs. 9-34675
- trimethylvinylammonium bromide and derivatives, ^{14}N , ^1H spin couplings from n.m.r. study 9-48509
- trinitrotoluene, glass transition from undercooled melt at 258°C 9-39137
- trioxane, cryst. struct. at low-temp., X-ray obs. 9-44679
- trioxane, polymerization to polyoxymethylene, struct. obs. 9-37824
- trioxane molecule in ν_2 excited decayed state, i.r. rotation spectrum 9-32532
- trioxymethylene, ionization potential 9-22359
- triphenyl antimonide, i.r. and Raman spectra 9-30137
- triphenyl arsenide, i.r. and Raman spectra 9-30137
- triphenyl bismuthine, i.r. and Raman spectra 9-30137
- triphenyl phosphide, i.r. and Raman spectra 9-30137
- triphenylarsine and oxide, i.r. spectra, assignments 9-25782
- triphenylborate, i.r. spectra 9-23164
- triphenylboron, i.r. spectra 9-23164
- triphenylene, oriented, e.s.r. absorpt. in phosphorescent state at low mag. fields 9-38918
- triphenylene molecule, excitation by electron impact 9-30064
- triphenylene phosphoresc., matrix site effects 9-49326
- triphenylene triplet dianion, zero-field-splitting calc. 9-42446
- 2,4,5-triphenylimidazolyl radical e.s.r. spectrum interpretation 9-27913
- triphenylmethane base dyes, in plexiglass, triplet-triplet absorpt. spectra 9-41393
- triphenylmethane base dyes, in plexiglass, triplet-triplet absorpt. spectra 9-49291
- triphenylmethane dye absorption, luminescence and polarized luminescence spectra, 77°K 9-23113
- triphenylmethyl radicals, methyl and fluorine substituted, ENDOR study for substituent effects 9-48721
- triphenylmethyl radicals, spin density distrib. 9-42427
- triphenylmethyl trapped in methylcyclopentane, fluorescence spectrum at very low temp. 9-46413
- triphenylmethylarsonium 7-, -7, 8-, 8- tetracyanoquinodimethan, elec. conductivity and thermoelec. power anisotropy 9-33314
- triphenylphosphine oxide complexes, i.r. spectra, assignments 9-25782
- trisethylsulphoniomethane, crystal structure 9-26271
- 1:3:5-trithian, i.r. spectrum, vibrational assignment 9-32511
- tropenyl radical, e.s.r. spectra obs., empirical resonance energy estimation 9-23177
- tryglycine sulphate, dielec. const. by thermal noise method 9-49145
- tryglycine sulphate lab. expt. to demonstrate ferroelec. props. 9-37590
- tryptophan, fluoresc. quenching and solvent isotope effect 9-32787
- tryptophan fluorescence spectrum excited by vacuum U.V. obs. 9-30149
- L-tryptophan, crystal structure from powder patterns 9-39354
- L-tyrosine, crystal structure from powder patterns 9-39354
- tyrosine fluorescence spectrum excited by vacuum U.V. obs. 9-30149
- undecanoic acid far i.r. spectra, H bond stretching vib. determ. 9-23087
- uranyl ion, absorption spectrum, vibronic analysis 9-25784
- uranylpropionate crystals, 3500-10000 Å opt. rot. 9-43213
- uranylpropionate crystals, dichroism and polarization of luminescent rad. 9-43213
- urea, ^{14}N n.q.r., saturation and relax. times 9-49366
- urea, adsorption in NaCl pellets 9-48771
- urea, applic. of random-phase-approx. method 9-40621
- urea, crystal lattice vibrations, i.r. Raman meas. 9-48948
- urea, diffusion in water 9-23476
- urea nitrate, crystal structure 9-23788
- ureas, di-substituted symmetric, whisker growth 9-39219
- uridine, i.r. absorption spectra, 230-30 cm^{-1} , 20 to -175°C, crystal lattice vib. anal. 9-25783
- uronium nitrate, crystal structure by n. diff. exam. 9-26272
- vanadyl acetylacetonate paramagnetic probe alignment in p-azoxyanisole, isotropic-nematic transition, e.s.r. 9-42633
- vanadyl phthalocyanine 9-41430
- vapour diffusion in air, coeff. meas. 9-30326
- vinyl ethers, n.m.r. coupling consts. and chem. shifts temp. depend., obs. 9-27919
- vinyl halides, n.m.r. coupling consts. and chem. shifts temp. depend., obs. 9-27919
- vinyl iodide, microwave spectrum and molec. consts. 9-32533
- vinyl oleate, mesophases, n.m.r. obs. 9-46659
- vinyl radical, spin polar, and delocalization, unrestricted Hartree-Fock method 9-27923

Organic compounds continued

- 4-vinylcyclohexane-1, copolymerization with propylene and ethylene, effect of catalyst 9-31188
- vinyltrimethyl(phenyl)-silanes, copolymerization with styrene in the presence of butyllithium 9-24549
- vitamin B₁₂ and analogs, emission Mossbauer spectroscopy 9-27918
- xanthene dye, absorption, luminescence and polarized luminescence spectra, 77°K 9-23113
- xanthone, crystal and molecular structure 9-46802
- p-xylene, vibrational structure of electronic spectra 9-27920
- p-xylene-carbon tetrabromide complex, polarized i.r. spectrum 9-24394
- xylo, o-, m- and n-, combinational scattering spectra, phase, shift rel. to dipole-dipole intermolecular forces 9-46393
- m-xylo, sound velocity at constant density 9-46633
- yttrium yttrium ethyl sulphate crystal for nuclear spin refrigerator 9-27579
- yttrium ethyl sulphate single cryst., Gd³⁺ e.s.r. spin-Hamiltonian parameters 9-43290
- zinc phthalocyanine, matrix isolated, absorpt. and fluoresc. spectra 9-49289
- 4-F-stilbene, i.r. absorpt. and fluoresc. spectra, vibr. analysis, 77°K 9-28699
- ¹¹⁹Sn monomeric and polymeric cpds., influence of bonding on temp. depend. of anisotropic Lamb-Mossbauer factor 9-27915
- Ar-alcohol Geiger counter, photon spectrum in discharge obs. 9-25507
- Ar-ethyl alcohol two-phase flow, adiabatic, phase and vel. distrib., obs. 9-46558
- 4-Br-stilbene, i.r. absorpt. and fluoresc. spectra, vibr. analysis, 77°K 9-28699
- C₂H₄⁺+C₂H₆→C₂H₄⁺+C₂H₆ intermediate-complex reaction obs. at ~1 eV 9-41443
- C₆H₆, stimulated Brillouin scattering threshold and line shift, temp. dependence 9-26110
- CCl₄, stimulated Brillouin scattering threshold and line shift, temp. dependence 9-26110
- CD₃, group-, group vibrations and vibrational analysis 9-23104
- CD₄⁺+CD₄→CD₃⁺+CD₃ collision mechanism at ~1 eV, obs. 9-41443
- CN, electron oscillator strength of violet system, basic meas. technique 9-46388
- 4,4'-di-Cl-stilbene, i.r. absorpt. and fluoresc. spectra, vibr. analysis, 77°K 9-28699
- 4-Cl-stilbene, i.r. absorpt. and fluoresc. spectra, vibr. analysis, 77°K 9-28699
- Cr-Al acetylacetonate mixed single crystals, spin-lattice relax. props. 9-49227
- Fe₂(CO)₉(CH₃)₂C₆H₄SO₂n=C(OCH₃)₂-CH=CH-C(OCH₃)₂ 9-26262
- Ga complex (C₂H₅)₂ O.GaCl₃ mol. symm. in solid and liquid states 9-24515
- Ge cpds., vibrational mol. spectra investigated rel. to electro-optical parameters 9-46397
- HD⁺+HD→H₂D⁺+D collision mechanism at ~1 eV, obs. 9-41443
- HD⁺+HD→HD₂⁺+H collision mechanism at ~1 eV, obs. 9-41443
- hydrocarbons, chemisorption on metal surfaces π -electron system and bond energies 9-39948
- 4-I-stilbene, i.r. absorpt. and fluoresc. spectra, vibr. analysis, 77°K 9-28699
- methane, second virial coeff. 9-34833
- methylithium, n.m.r. study of struct. and bonding 9-46405
- (N-P), ring compounds, dodecadimethylaminocyclohexaphosphazehexaene, cry. and mol. struct. 9-30583
- with N sp²-hybridized, ^{14}N n.m.r. shifts 9-25773
- NO₂-X compounds (X=C, N, O), ^{14}N quadrupolar relaxation and ^1H line shapes and electron distribution 9-42440
- Na ethyl sulphate monohydrate, Raman and i.r. spectra 9-24431
- Na uranyl acetate, eff. of deuteration of acetate group 9-23005
- O₂-acetylene flames, turbulent, atoms fluoresc. power efficiencies, obs. 9-24601
- O₂-acetylene flames, absorpt. and emission enhancement rel. to free-atom form., obs. 9-22936
- Pb- polyethylene shields, fast-neutron attenuation, S_n calc. 9-33963
- Organometallic compounds** see Under appropriate metal compound heading
- Orthicons** see Electron tubes
- Oscillations** see also Electromagnetic oscillations; Liquid oscillations; Piezoelectric oscillations; Vibrations
- atmosphere, microbarographic, due to nuclear explosions 9-33761
- in atmosphere, semidiurnal 9-41496
- atmospheric, response curves 9-31303
- beam-column with finite elec. conductivity in constant transverse mag. field 9-27215
- betatrons for particles passing through a resonance vertical damping eff. 9-46146
- cavity containing fluid, nonlinear equations 9-41790
- cylindrical sample in transverse mag. field, magnetomorph, in isothermal elec. conductivity 9-37427
- cylindrical shell, axisymmetrical motions, anal. method of characteristics 9-22227
- Duffing eqn., soln. with large damping 9-22179
- of earth, free, perturbation theory 9-37870
- fluid, differentially heated, amplitude vacillation characteristics determined by multi-probe technique 9-27947
- fluid in viscous incompressible sphere, own gravitation and surface stress, viscosity eqn. 9-23214
- at fluid interface in presence of transverse electrostatic field 9-32569
- foil in plunging or pitching modes, flow and lifting problem 9-23410
- Fourier series solns., demonstration using combination tones 9-43708
- framed structure, existence of dual with same natural frequencies 9-22239
- of galaxies, cold thin disk models, WKB analysis 9-40127
- Helmholtz, in pulsating combustion chambers 9-45838
- ionic crystals, long-wave 9-26407
- i.f., in low pressure discharge 9-44497
- Lorentzian, heavily damped, refraction spectrum 9-28133
- magnetosheath, frequency calc. 9-43421
- nonplanar osc. surface problem., complex cross-flow representation 9-22229
- pendulum, horizontal, effect of atm. density 9-40263
- photon behaviour in coupled systems 9-37612

Oscillations continued

- quartz-crystal viscometer, resonant freq. changes with pressure to 8000 atm. 9-41809
 in rotating fluids, instability, effects of radial law of depth 9-25801
 of scattering amplitude and restrictions on high-energy behaviour 9-25030
 sphere in compressible viscous fluid in slip regime 9-40634
 steel, microcracks, initiated by 178 Kc/sec. 9-35190
 string oscillator, relaxation 9-43749
 system, non-linear with two degrees of freedom, subharmonic instability 9-27212
 thermal, in multilayer walled media, theory and expt. 9-24033
 toroidal, earth eigenvibrations, finite dislocation excitation 9-33731
 torsional, of elastic half-space 9-27214
 u.s. waves in magnetized media 9-44814
 CF₄ capillary, ion oscillations, intensity determination, first, second, third and fourth stages of ionization 9-25973
 Cd single crystal, Sondheimer, in Hall resistivity 9-37441
 in CdS elastic bending, in elec. conducting sample 9-44763
 CdSe, photoconducting, temp.-elec. instability 9-39711
 GaAs, photoexcited current oscillations by two bulk negative resistance effects 9-28489
 H₂ laser at 7525 Å 9-47986
 He-Ne laser, amplification and oscillation mechanism 9-29416
 He-Ne laser, detection technique at 3.39 μ 9-47987
 LiNbO₃, optical parametric, pumped with ruby laser 9-28663
 in Si p-n devices after irradiation with one-MeV electrons 9-24193

Oscillators

- classical ensemble, nonlinear with self losses affected by harmonic force 9-38328
 damped oscillating circuit, approx.-equiv. to lossless line with reactive load 9-43831
 field, two, interacting in circular laser, quantum investig. without perturbation theory 9-29407
 frequency variation spectra, automatic tracing and numerical anal. 9-41865
 with inertial nonlinearity, natural fluctuations 9-38327
 n.m.r., stationary state behaviour 9-47875
 optical parametric, output locking to absorbing atomic transition 9-47926
 Osaka cold cathode discharge tube used as an oscillation prod. e.m. waves 9-36785
 transistor, frequency stability 9-30947
 transistorized, current-controlled nonlinear negative resistance type, design and appls. 9-34131

Oscillator effect *see Semiconductors***Oscillators** *see Semiconducting devices***Oscillographs** *see Electrical measurement***Oseen method** *see Flow; Hydrodynamics***Osmium**

- implanted in Fe, meas. of internal mag. field 9-39765
 thermal and electrical resistivity, 2 to 20°K 9-41169
¹⁸⁹Os, hyperfine struct. and nucl. quadrupole moment, arc spectrum obs. 9-29929

Osmium compounds

- OsF₆ spectrum, i.r., Jahn-Teller effect 9-34647
 OsSe₂, crystal structure 9-23770

Osmosis

- anomalous, interpret using model including eqn. for motion of local centre of mass 9-23478
 dilute soln. in ⁴He, osmotic pressure 9-23565
 electro-osmotic meas. of membrane charact. 9-23477
 Fermi-Bose mixtures, osmotic pressure of dil. solns. 9-36146
 ion transport across membrane, noise spectra and relax. times obs. 9-34892
 polystyrene-polybutadiene block copolymers, viscosity and osmotic press. meas., 34.2°C 9-39086
³He-⁴He mixtures, degenerate, osmotic press. down to 0.027°K 9-42687

Overhauser effect *see Nuclear magnetic resonance and relaxation***Oxidation**

- acetylene, mechanism 9-33661
 alloys, and cation distrib. in metal oxide/metal sulphide solid solutions formed 9-23656
 charcoal, in CO₂, kinetics, 10⁻³ to 40 atm., 700 to 1300°C 9-41449
 diamond, surface oxides formation, props., struct. 9-24555
 dielectric constant obs. of normal and reduced crystal at various temp. and various fields 9-30961
 diffusion-coated mats at high temps. 9-48870
 dyes, photo-excited, redox reaction rel. to Fermi level 9-41973
 graphite, ¹⁴C labelled, in reactors, equipment for meas. by chemical and radiochemical methods 9-38734
 graphite, boronated, react. obs., B₂O₃ formation and behaviour 9-28795
 graphite, in CO₂, kinetics, 10⁻³ to 40 atm., 700 to 1300°C 9-41449
 graphite, radiolytic in CO₂ or CO₂ + methane, thermal degassing studies 9-28220
 graphite, thermal and radiolytic, charges in microporosity 9-26224
 graphite channel, long, in air, kinetics and radial diffusional effects 9-26824
 graphite tube, with O₂ access in bore, kinetics rel. to non-uniform burn off 9-26823
 graphite vacancies, rel. to etch pit ion formations 9-28281
 logarithmic, Uhlig model, modification for surface effects 9-31190
 logarithmic, Uhlig model, modification to surface effects, comment 9-31191
 metal, fine particles, prep. by gas evaporation method with plasma jet flame 9-33128
 metal, parabolic law for growth kins of coherent films 9-39951
 metal films, thin, problems 9-39950
 metal foil, bending due to stressed surface layer 9-31189
 of metal surfaces in contact, heat transfer anal. 9-24036
 metals, at elevated temp., analysis of non-steady state range 9-41448
 metals, eff. of vacancies on kinetics 9-28794
 molybdenite vacancies, rel. to etch pit ion formation 9-28281
 of organic compounds by Co³⁺ 9-24560
 polymers, early free-radical stage 9-26825
 propylene, by photolysis with NO₂ 9-43338
 pyritinol/5⁺-thiopyridoxine, redox pot. 9-28809
 rare earth metals, rel. to chem. shifts of K_{α1} X-ray lines, role of f-electrons 9-37750

Oxidation continued

- redox method, applic. to meas. of mass transfer coeffs., in two-phase systems 9-34882
 rutile single crystals, reduction, nature of defects formed 9-32945
 stainless steel at high temp., electron probe microanalysis of thin films 9-24607
 steel, Fe₃O₄ film growth characteristics in dil LiOH soln. at 300°C 9-39952
 steel, mild, in O₂/H₂O vapour mixtures at 950°C 9-33668
 steel, mild and low-alloy, in CO₂ based atmospheres 9-24558
 tetrakis-(dimethylamino)-ethylene, chemiluminesc. 9-23159
 Zircaloy, pre-transition behaviour for individual piece, comments 9-37826
 Zr alloys, at high temps. 9-41451
 Ag, anodic oxidation 9-49382
 Ag, anodic oxidation 9-49383
 Al, infl. of light on rate for estimation of Al₂O₃ film band structure parameters 9-31000
 Al fine wires, mech. effects during growth of anodic oxide films 9-31192
 BaTiO₃, reduced and reoxidized, phase comp. 9-42939
 C black, thermal, study of porosity and size of cry. domains 9-28258
 CO, anodic discharge in 6N KOH on Ni₂S₂ 9-31193
 CO over Au, spectroscopic obs. 9-35001
 Co-(10 wt.%)Cr, high temp., formation of oxide scales, microstructure 9-31194
 Co-(10 wt.%)Cr alloys, high temp. kinetics 9-31195
 Co-Ni-Si alloys, ferromag., internally oxidised, struct. obs. 9-48837
 Co, dilim struct. and composition rel. to temp. > or < phase transform temp. 9-32841
 Cr 9-24556
 Cs₂O, CsOH and Cs₂O₂, oxidation products studied by differential thermal analysis 9-26609
 Cu-Ag alloys, and cation distrib. in Cu₂S-Ag₂S solid soln. formed 9-23656
 Cu-Pd alloys, internal oxidation by diffusion process, 850-1000°C 9-24557
 Cu-Pt alloys, internal oxidation by diffusion process, 850-1000°C 9-24557
 Cu-(26 wt.%)Zn alloy, ZnO films establishment and growth 9-26191
 Cu, rate increased by prior cold working, mechanism 9-41450
 Cu, thin film oxidation, kinetics 9-43329
 Cu faces under oxygen ion bombardment 9-44640
 Cu single crystals in water, electron diffraction observations 9-31196
 Fe-(2 wt.%)Al alloy, Ge effect on internal oxidation 9-46740
 Fe-C alloy, effect of surface contamination during H₂ annealing 9-36938
 Fe-C alloys, 500°C, kinetics 9-31197
 Fe-Cr alloy effect of Y and Gd 9-24559
 Fe-(50 wt.%)Cr alloy 9-24556
 Fe-(40 at.%)Ni alloy, scale struct. and chem. composition 9-33669
 Fe-(1 wt.%)Si alloy, Ge effect on internal oxidation 9-46740
 Fe, in O₂/H₂O vapour mixtures at 950°C 9-33668
 Fe, rate increased by prior cold working, mechanism 9-41450
 Fe ore, sintered, reduction cracking 9-33093
 FeCl₃·6H₂O, oxidation state, pressure causes charge transfer 9-27851
 FeCl₃·6NH₃, oxidation state, pressure causes charge transfer 9-27851
 FeF₃·3H₂O, oxidation state, pressure causes charge transfer 9-27851
 Fe(III) reduction to Fe(II) in solids at high press., reversible 9-37825
 FeS₂, mechanism in O₂, and in neutral or reducing gases 9-33670
 GaP electrodes, redox processes, charge transfer reactions, photoexcitation and electroluminesc. obs. 9-30990
 p-GaSb, effect on photoemission 9-43145
 H₂/CO fuel cell mixtures, use of Pt-Ni catalysts as anodes 9-29365
 Mo(100) surface, low-energy electron diff. obs. 9-42732
 NH₃ on silica-supported Pt and silica, i.r. spect. study 9-30044
 Nb single crystals, 950-925°C 9-49378
 Nd³⁺→Nd²⁺ photoreduction on SrF₂, under stimulated emission conditions 9-31960
 Ni-Cr alloys, and cation distrib. in NiO-Cr₂O₃ solid soln. formed 9-23656
 Ni-Si alloys, ferromag., internally oxidised, struct. obs. 9-48837
 Ni, influence on mechanical behaviour 9-39424
 Ni, rate increased by prior cold working, mechanism 9-41450
 Pb, anodic passivation mechanism in various media obs. 9-33678
 PbO-Cr₂O₃ ternary system, and phase equilibria 9-28405
 Pu, near 400°C, PuO form. from α-Pu₂O₃ reaction with metal 9-39953
 Sb³⁺, photochemical in HCl, LiCl soln., Bunsen-Roscoe law break- down 9-29939
 Si-SiO₂ structures, of, rel. to density of surface states 9-26560
 p-Si-on-sapphire films, effect on elec. charact. 9-35405
 p-Si, effect of method from e.p.r. meas. 9-49357
 Si, thermally, SiO₂ film transmission and reflection spectra, thickness depend, 7-11 μ 9-24374
 n-Si epitaxial films on sapphire, and subsequent annealing, effects on elec. props. 9-49111
 SiH₄-oxidant systems in SiO₂ film formation, study 9-23639
 Ti, kinetics, effect of annealing 9-33671
 Ti, kinetics analysis rel. to phenomenological scheme for nonsteady-state range 9-47462
 Ti films, thermal oxidation, for prep. of TiO₂ layers 9-36962
 UO₂ powders with high surface area, oxidising and reducing atmospheres on sintering 9-33113
 W, secondary ion emission method obs., sputtering probability with Ar⁺ 9-42982
 ZnO on Ag support, by CO, photosensitized 9-28796
 B ZnS, electron microscope obs. 9-49379
 Zr-Cu reactor fuel claddings in CO₂, and cracking, obs. 9-37266
 Zr, gas flow rate effect on kinetics 9-45420
 α-Zr, O₂ diffusivity and parabolic oxidation kinetics 9-26306
 Zr-(1 at.%)Nb alloy in pressurized steam and air, corrosion behaviour, 400-700°C 9-35747

Oxide cathodes *see Cathodes/oxide***Oxygen**

- absorption, effect on upper atmospheric composition meas. 9-28907
 absorption on CdSe films, rel. to conductivity and space charge region variation 9-30905
 absorption spectra, Lyman-alpha 9-23061
 adsorption and diffusion on oriented Pt field emitters 9-23648
 adsorption on Be thick films obs. 9-36964
 adsorption on CdS and ZnO {0001} surfaces, LEED obs. 9-28211
 adsorption on SbSi, eff. on elec. conductivity, photoconductivity and work function 9-30496

Oxygen continued

- adsorption on W(100) surface rel. to work function changes 9-42734
 adsorption on W single crystal faces, surface potential determ. 9-48775
 adsorption on ZnO polar surface, effect on props. 9-42741
 atom, core polarization and hyperfine structure calc. 9-46273
 atom, correlation effects of non-closed shell many electron theory 9-38773
 atom, electron scatt., low energy neutral bremsstrahlung cross section obs. 9-32423
 atom, hyperfine structure calc., g.s. first-order wave function 9-32408
 atom, polarization wave functions for ground state 9-34532
 atomic, exposure-depend. surface recomb. 9-28791
 atomic, red line, predawn enhancement over U.K. (1965-1968) 9-47562
 atomic beam, elastic scattering by NO and CO molecules, characts. 9-25712
 atomic beam, values of $4p^2P$ levels using new high intensity spectroscopic source 9-42344
 atoms, interstitial, in Ta, diffusion coeff. and activation energy 9-28284
 atoms, London dispersion forces 9-25714
 atoms, mag. moment of $(2p^4)^3P_{1,2}$ levels, precision calc. 9-36656
 aural green line excitation by $N_2(A^3\Sigma_u^+)$ rate const. calc. 9-43424
 auroral 5577 Å line transition probability lab. obs. 9-46282
 auroral green line, absolute transition probability, lab. meas. 9-31373
 B-band lines, parameters rel. to atmospheric temp. 9-40011
 best-atom Slater orbital calcs., hybridized-promoted 9-48384
 boiling-point reproducibility, press.-temp. relation near 1 atm. 9-26168
 $CaCO_3$, self-diffusion in calcite by isotope exchange with CO_2 9-46844
 chemisorption on CdS sintered layers, effect on photoelectronic behaviour 9-47200
 chemisorption on PbS(100) surface 9-39949
 collision strengths and photoionization cross sections 9-29972
 condensed phases, molec. motion, Raman obs. 9-49296
 dielectric const. of liquid at microwave frequencies in X-band 9-46647
 diffusion in CeO_2 and $CeO_2:Gd^{3+}$ single crystals, 1040° to 1535°K, and elec. conductivity and thermoelec. power 9-33246
 diffusion in Cu-Pd(Pt) alloys, internal oxidation, 850-1000°C 9-24557
 diffusion in liquid Fe at 1560°C 9-48691
 diffusion in $Pu_{0.7}U_{0.8}O_{2-x}$ rel. to stoichiometry in temp. gradient, 1200-2000°C 9-37207
 diffusion in rare-earth oxides 9-26304
 diffusion in n-Si:P, γ -irradiated, rel. to thermal donor formation 9-32951
 diffusion in UO_2 , rel. to comp. in temp. gradient, 1300-2500°C 9-37212
 discharges, h.f. at lower than atmospheric press. 9-36788
 distribution in 70 to 150 km region of atmosphere, X-ray and EUV photometric determinations of latitudinal and temporal variations 9-31341
 electrolysis, liberation with H on electrode, electrode glow 9-41454
 electron scattering, shape resonance, cross section and collision strength determ. 9-38786
 electron swarm expts. anal., Boltzmann transport equation appl. 9-23344
 e.s.r. spectra, formation and decay proc. in r.f. discharge 9-29350
 forbidden transitions in isoelectronic sequence, relative line strengths 9-36653
 gas laser simplified 9-22386
 gas weak density, 7640 Å band, effect of temp. and pressure 9-46371
 hemoglobin saturation, opt. determ. 9-45703
 impurity in Nb₃Sn correlation with critical current density, and microstructure 9-41180
 interaction with n-Ge atomically clean surface 9-46718
 interdiffusion in Cu₂O, obs. from elec. conductivity meas. 9-44733
 ion, collisionally excited u.v. and forbidden lines, intensity calcs. 9-25685
 ion energy levels, radiative lifetimes 9-36659
 ion line radial intensity distribution for pulse discharge with confined channel 9-41968
 ion-mol. reactions 9-24544
 ionization and attachment coeffs. 9-39018
 in ionosphere, night over Arecibo 9-24685
 in ionosphere E-F regions, atoms excitation rel. to e, ion and neutral gas cooling 9-47581
 ionosphere F region equilibrium distributions, atoms and ions 9-24700
 ions, negative, electron detachment using ion beams with energies 3 to 100 eV 9-34572
 ions, positive, drift vel. in oxygen, obs. 9-23348
 l.r. vibration spectrum, effect of precip. of solid soln. of Au in Si 9-45315
 isotope exchange with CO in shock waves 9-49370
 isotope separation in thermal diffusion column 9-46581
 isotopic concentration gradient determination, ion mass analyzer 9-24596
 K-shell X-ray prod. in Al_2O_3 thin films by 20-100 keV protons 9-24073
 laser, oscillographic and interferometric obs. 9-41908
 line near 63 μ , thermal effect of radiative transfer in thermosphere 9-40081
 liquefier apparatus 9-24993
 liquid, dielectric const. at microwave frequencies in X-band 9-46647
 liquid, molec. motion and Raman band shapes 9-30412
 liquid, refractive index 9-44562
 liquid, use in Saturn V, problems 9-45572
 liquid, viscosity, rel. to press and temp. 9-46619
 liquid-vapour system, sp. hts. along coexistence path 9-34897
 magnetic first-order transitions in FeRh films, role 9-45223
 mesospheric, polar at night, distribution 9-31343
 mixture with N_2 and ether or methane, simultaneous HCN and H_2O laser emissions in pulsed discharge 9-22404
 molecular parameters of O_2 0.7620 μ absorption and transmission function calc. 9-36705
 molecule adsorbed on Ni, structure determ. by ion neutralization spectroscopy 9-32484
 molecules, mag. props. in O_2 -Ar solid mixtures 9-45231
 molecules, simultaneous and induced electronic transitions 9-23060
 NGC 5253 galaxy, O II emission spectra obs. 9-35958
 nightglow 6300 Å emission, post-midnight peak obs. and theory 9-40054
 O_2 atmospheric i.r. bands in airglow, temporal variations, balloon obs. 9-45509
 O^+ collision strengths for electron impact transitions 9-34563
 O^+ recombination radiation in vacuum ultraviolet, shock tube studies 9-25968
 O_2 number densities in thermosphere, lower, day-night vars. 9-26920
 paramagnetic molecules, energy splitting of core electron levels, ESCA spectra 9-34634
 photolysis, vacuum u.v., and electronic de-excitation of $O(^1D)$ by inert gases 9-35755

Oxygen continued

- plasma, emissivity meas., 110-300 nm, 2×10^4 °K and e density $\sim 10^{17}$ cm⁻³ 9-48590
 plasma, thermodynamic functions, approximate calc. 9-46464
 plasma radiative power, total, 250-700 n.m. obs. 9-30261
 pulse radiolysis at v. high dose rate, yield of O_3 9-39963
 quenching of coronene phosphorescence in hexyl alcohol frozen soln. 9-49325
 reactivity to graphite eff. of neutron bombardment 9-35743
 red-line emission in night airglow, total intensity formula 9-49472
 seawater distribution and effect of advection, turbulence and biochemical demand 9-43376
 self-diffusion in CoO and NiO, mechanism 9-44731
 self-diffusion in Na_2O_3 , Sm_2O_3 and Er_2O_3 , coeffs. calc. by isotope exchange method 9-44741
 self-diffusion in $UO_{2.12}$ 0.005 $\leq x \leq 0.217$, 780-1250°C 9-37215
 self-diffusion in $UO_{2.12}$ rel. to comp., obs. review 9-37210
 solar photosphere, abundance and local thermodynamic equilibrium 9-24917
 solar photospheric spectrum, center-to-limb analysis 9-31656
 solid, defect structure, electron microscope obs. 9-37159
 solid, temps. at transition points, obs. 9-40289
 sorption on Ti, study at 273, 195 and 77°K 9-48772
 specific heats C_p , triple point to 300K, at press. up to 350 atm 9-34898
 specific heats of liq.-vapour system along coexistence path 9-34897
 spectroheliograms, i.r. interpretation 9-41691
 spin wave excitation depend. in thin Ni-Fe layers 9-45369
 stellar abundance in K giants 9-43528
 supercooled, water drop nucleation 9-26075
 surface distribution by 3He activation and autoradiography 9-26849
 thermodynamic props. at temps. to 250 K and press. to 350 atm, along isochores 9-34899
 thermosphere mol. o density, Ariel III obs. 9-47554
 u.v. vacuum absorpt. spectra, rel. to evaluation in N_2 , H_2 and inert gases 9-37858
 Al powder-oxygen mixtures, detonation investigation 9-27234
 Fe-O system, phase boundaries and thermodynamic props. by e.m.f. meas. 9-30741
 in GaP:Zn, solubility, red luminesc. generation obs. 9-33321
 in p-GaP, red emission, config. coordinates applic. 9-37761
 in LiF, effect on low temp. ionic conductivity 9-39671
 N_2 - O_2 gas discharge, ionic charge exchange 9-30303
 N^+ , electron scattering, shape resonance, cross section and collision strength determ. 9-38786
 in Ni single cryst. effect on mag. aftereffect due to dislocations displacement in domain walls 9-39766
 O^- , electrons photodetachment cross section, pseudopotential calc. method 9-46257
 O_2 -Ar mixture, vibrational excitation of diatomic mols. by atom collision, calc. 9-40588
 O_2 -Ar solid mixtures, mag. props. of O_2 molecules 9-45231
 O_2 - C_2H_2 thermal conductivity of gas mixture meas. for investigation of Lennard-Jones potential 9-36803
 O_2 - H_2 flames, turbulent, atoms fluoresc. power efficiencies, obs. 9-24601
 O_2 -acetylene flames, turbulent, atoms fluoresc. power efficiencies, obs. 9-24601
 O_2 , atmospheric spectrum, 1-1 and 2-0 bands, rel. to rotational, oscillational and kinetic temps. 9-26893
 O_2 , electron affinity 9-32693
 O_2 , ionization and attachment, irradiation by 1.5 MeV electrons 9-40710
 O_2 , Li⁺ elastic differential scatt. cross section meas., 3-330 eV 9-46315
 O_2 , microwave line broadening, contrib. of London dispersion force 9-36707
 O_2 , predissociation in Schumann-Runge band system, lab. obs. and atm. effects 9-49487
 O_2 , primary specific ionization of relativistic particles 9-39015
 O_2 , refractivity in far u.v., Pade summation of Cauchy dispersion eqn. 9-48666
 O_2 , Schumann-Runge bands, predissociation 9-32462
 α - O_2 , solid far i.r. absorption and antiferromagnetic resonance mode at 4.2°K 9-28691
 O_2 , Venus, upper limit 9-24895
 O_2^- , appearance potential 9-32693
 O_2^- , ground state photodetachment by sunlight, obs. 9-42562
 O_2^- , impurity centre in KBr, luminesc., config. coordinates of local vibr. 9-39868
 O_2^- , impurity centres in alkali halides, luminesc., thermal quenching 9-39863
 O_2^- , impurity centres in alkali halides, luminesc. spectra 9-39861
 O_2^- , impurity centres in alkali halides, luminesc. spectra 9-39862
 O_2^- , impurity centres in alkali halides, luminesc., effect of hydrostatic press. 9-39864
 O_2^+ , absolute excitation cross sections for emission of first negative bands under e. impact on O_2 9-42412
 O_2^+ , recombination, electron temp. depend. 9-32697
 O_2^+ , concentration in daytime F₂-region between 200 km and peak altitude, direct measurement 9-31436
 O_2^+ , concentration in daytime F₂-region between 200 km and peak altitude, direct measurement 9-24701
 O_2^+ , excitation by electrons, cross sections spectral band meas. 9-23062
 O_2^+ , recombination with ionospheric electrons 9-37958
 O_2^+ , second negative bands, isotope shift study, revised rot. and vib. const. 9-23063
 O_2 (Δ_g) quenching by O_2 , N_2 collisions and air, obs. 9-23206
 O_2 acoustic plane wave propag. 9-26033
 O_2 at 100 to 150 km, u.v. absorption rocket obs., Woomera 9-37932
 O_2 in atmosphere, 100 to 130 km at night, densities 9-43411
 O_2 in atmosphere, electron cooling by vibrational excitation 9-43444
 O_2 atmospheric density, rocket obs. 9-31346
 O_2 , dissociation and i.r. OH emission in aurora 9-33818
 O_2 in thermosphere, midlatitude 150 to 450 km concentration and temp. 9-28905
 O_2 , ionization in H- O_2 low energy collisions 9-34584
 O_2 lines, spin-rotational, absorption coefficient in geomagnetic field 9-45495
 O_2 , mag. dipole rot. spectrum, 12-65 cm⁻¹ 9-32483
 O_2 , mol., electron reson. scatt., elastic and inelastic channel obs. 9-23057
 O_2 , optical absorpt. coeff. near 1215 Å, and rel. to press. (100 to 760 torr) 9-34638
 O_2 , pulse discharge loss rel. to applied voltage 9-30309

Oxygen continued

- O₂ Schumann-Runge system, inc. high vibr. quantum nos., Frank-Condon factors 9-46373
 O₂ spectral system, red atmospheric, electron transition probability 9-36706
 O₂ spectral transition probability, absolute 9-23170
 O₂-propane mixture, pressure var. behind shock front, eff. of tube diam. 9-28061
 O₂-He mixture, thermal relaxation and heat transfer 9-48661
 O₂-N₂ mixture, thermal relaxation and heat transfer 9-48661
 O₂(Δ_2 - Σ_2)(0,0), (0,1) transitions, ratio 9-40601
 O₂(Δ_2) deactivation by O, N, benzene, obs. 9-34707
 O₂(Δ_2)+O₂→O₂+O, reaction rate const. 9-43322
 O₂ resonant scatt. of electrons, ang. distrib. 9-27855
 O₂⁺, O₄⁺, geometries by approx. SCF-MO theory which considers intermol. differential overlap 9-34637
 O⁺, formation in dissociative attachment of electrons to O₂, crossed beam expts. 9-40623
 O₂ centre in KCl, paramag. reson., pulse saturation 9-47437
 O⁺+N₂O→NO⁺+NO, 0-3 eV obs. 9-46430
 O⁺+NO₂→NO₂⁺+O, 0-3 eV, obs. 9-46430
 O⁺, shape resonance, cross section and Collision strength determ. 9-38786
 O⁺ and O₂⁺ conc. in ionosphere 200 to 630 km obs. 9-43464
 O⁺ and O⁻, bombardment of Mo, secondary electron emission 9-31010
 O⁺ collision, inelastic, with Ar, energy transfer distrib. meas., 50-200 keV 9-46313
 O⁺ concentration and temp. at 1000-1200km, cosmos 5 obs. 9-45505
 O⁺ concentration in daytime F2-region between 200 km and peak altitude, direct measurement 9-31436
 O⁺ concentration in daytime F2-region between 200 km and peak altitude, direct measurement 9-24701
 O⁺ ions production, ionosphere F region 9-24697
 O⁺ reaction with O₂ and N₂, ions F region, rate calc. from loss coefficient 9-40091
 O²p³ excitation by electron impact, ²D_{3/2}-²S_{1/2} transition, collision strengths resons. 9-34566
 O²D₂ excited atoms, reaction with isobutane 9-24543
 O(1D), electronic de-excitation by inert gases during vacuum u.v. photolysis of O₂ 9-35755
 O²⁺, electron scattering, shape resonance, cross section and collision strength determ. 9-38786
 O²⁺, prod. of population inversion by optical pumping from He⁺ 9-34167
 O²⁺ forbidden lines excitation, resons. in cross sections 9-22974
 O atomic, 2nd virial coeffs. 9-26019
 O emission lines in u.v. spectrum of aurora 9-33817
 O I, line intensity in aurora from spectrograms 9-43425
 O I 5577 and 6300 Å intensity ratio in quiet aurora 9-47565
 O I (5577 Å) in sunlit aurora, and He I (1.083 μ), brightnesses, obs. 9-45766
 O I (6300 Å) auroral emission in F-region, mechanism 9-26952
 O I forbidden lines in nightglow at mag. equator 9-33806
 O I Å6300 line in nightglow, Doppler shifts 9-45514
 O I solar emission line profile, 1302-1306 Å, rocket obs. 9-41689
 O II lines in M8 nebula, brightness 9-31517
 O II to VI electronic states lifetime meas. by beam-foil technique 9-22975
 O in Venus atmosphere, upper limit to abundance 9-29070
 O V, 2p² 1D level, mean life 9-25708
 O VII, S and P state transitions, wavelength calc. and comparison with expt. 9-40540
 O VII, S and P state transitions, wavelength calc. and comparison with expt. 9-44257
¹⁶O muonic, 2p-1s X-rays obs., 2p pionic levels population determ. 9-44301
¹⁶O root mean square charge radii 9-48415
¹⁶O small-angle scatt. in C, BeO, Al₂O₃ thin foils 9-35298
¹⁸O muonic 2p-1s X-rays obs., 2p pionic levels population determ. 9-44301
¹⁸O self-diffusion in CoO and CoO:Al(Li) 9-40982
 OI 6300 Å twilight airglow, enhancement rel. to latitude 9-28924
 Oz-acetylene flames, absorpt. and emission enhancement rel. to free-atom form., obs. 9-22936
 in PbS photoconducting films, effect on props. 9-37622
 in PbS photosensitized films, oxide centre exam. 9-37615
 SiLi, O, dopant interaction with electron-irrad. produced defects 9-42813
 spectral lines, Stark broadening and displacement rel. plasma high temp. meas. 9-25913
 in Ti and refractory metals, fast neutron activation analysis 9-26851
 Yb³⁺-O²⁻-Fe³⁺ system, superexchange integrals 9-45076
 Zn/O secondary battery, use of fluidized bed Zn anode 9-37839
 n-Zn_{0.8}Cd_{0.2}Sb effect of oxygen and conduction 9-49098
 in ZnO₂, ion conductivity by electrolysis in Cu solutions 9-35754

Oxygen compounds

- adsorption on W, effect on thermal faceting and work function 9-35012
 chalcogenides AⁿB^mC^v with perovskite structure, synthesis 9-42755
 ethylene oxide-oxygen flame, mass spectrometric study 9-28785
 metal oxides, irradiation effects, e.s.r. obs. rel. to catalytic behaviour 9-35709
 metal oxides, nonstoichiometric, chem. diffusion coeffs. 9-44727
 OH bonds in mica, i.r. spectroscopic obs. 9-31099
 OH microwave emission in Cygnus, positions and spectra of four new sources 9-47655
 oxide crystals, melt-grown, developments, review 9-37048
 oxide impurities in Ca₁₀(PO₄)₆F₂ giving rise to specific absorpt. fluoresc., and colour and paramag. centres form. 9-40933
 oxide systems, effect of cationic field strengths in liquids 9-23579
 oxides, diffusion, ideal conditions for direct meas. 9-44743
 oxides, effective ionic radii 9-39182
 oxides, electronic states of defects 9-44689
 oxides, ionic conductivity, survey and exptl. problems 9-45003
 oxides, mass transfer conf. 9-44726
 oxides, mixed valence-type, phase transitions due to electronic ordering 9-41127
 oxides, Nd³⁺-doped, radiative lifetime of metastable ion, anomalous temp. dependence 9-14105
 oxides, point defect form. energy calc. 9-44688
 oxides, point defects characterization 9-44687
 oxides with nonbonded electrons, as nonlinear optical materials 9-45263
 ozone synthesis in chemonuclear reactor 9-37842

Oxygen compounds continued

- tetrahedra, geometric contrib. to non-linear polarizability 9-35611
 C-O complexes in Si, vibr. absorpt. 9-41390
 CO-N₂-He lasers, high power, high efficiency 9-22391
 Cu-O liquid alloys, wetting of sapphire 9-26179
 N-O chemiluminescence, investigation of features 9-28737
 Na-C-O system, three-phase equil., thermodynamic analysis 9-39127
 O-U-N-C system, phase relations at 1700°C 9-26400
 O₂-Ar-acetylene mixture, spin detonation anal. and shock wave confluences 9-34093
 OCS, dipole moment meas. using resonance cavity as absorption cell 9-34640
 OCS, dipole moment variation with vibrational state 9-30047
 OCS, line broadening of various rotational transitions due to dipole-dipole, dipole-quadrupole interact., obs. 9-34639
 OCS, Mag. susceptibility anisotropy and quadrupole moment 9-30046
 OCS, resonance, third order, anharmonic 9-30048
 OCS gas in bulk, steady state transient 'wiggles' phenomenon, relax. times meas. 9-44528
 OCS mol., trapped, e and Rydberg transitions, u.v. obs. 9-32466
 OCS reaction with atomic O, e.s.r. detect. 9-24534
 OD⁺, A³Π₁-X³Σ⁻ transition, reanalysis 9-44346
 OH, absorption lines, shape and width by curve of growth method 9-48476
 OH, galactic, pumping mechanisms for maser action 9-24740
 OH, spectral bands in night airglow, Δv=1 sequence 9-24679
 OH⁻, trapped in KCl, KBr, NaCl and RbCl, rot. barrier height 9-40935
 OH⁻ in alkali halides, i.r. absorpt. spectrum 9-24403
 OH⁻ in KCl, splitting in impurity motional spectrum rel. to dielectric behaviour at low temp. 9-26583
 OH⁻ in KCl, tunnel splitting of impurity motional ground states rel. to elec. cooling 9-27143
 OH⁻ in NaCl:Ca²⁺m impurity assoc. effects on optical absorpt. 9-37728
 OH⁺, A³Π₁-X³Σ⁻ transition, reanalysis 9-44346
 OH absorpt. line profile in flames, atm. and reduced press., Zeeman scanning 9-28786
 OH anomalous emission, possible protostar source, reln. with HII regions 9-33904
 OH clouds, microwave line optical depths and excitation temps. 9-43567
 OH contamination of nightglow obs. 9-41560
 OH emission near HII regions, nebular filaments 9-27006
 OH galactic emission sources, time variations 9-35952
 OH galactic radiosources, anomalous emission in satellite lines 9-41655
 OH groups in molecular crystals, evidence for non-H-bonding 9-42739
 OH i.r. emission in aurora 9-33818
 OH impurities in Ca₁₀(PO₄)₆F₂ giving rise to specific absorpt. fluoresc., and colour and paramag. centres form. 9-40933
 OH interstellar clouds, 1665 Mhz long-baseline interferometric obs. 9-38052
 OH ion liberation in alkali halides, direct absorpt. band obs. 9-43236
 OH mol., excited Λ-doublet states, conditions for maser emission 9-34636
 OH r-centroid calc. by Hulbert-Hirschfelder method 9-30018
 OH radicals, galactic, radio emission 9-24829
 OH radicals, reson. radio waves, polarization parameters and amplification and attenuation coeffs. 9-38053
 OH*(²Σ⁺) from photodecomp. of H₂O, initial rot. distrib. 9-38867
 OMO groups of inorganic complexes, stretch freq. selection rules 9-38868
 ONBr, isotropic species, vibrational spectra and force constants 9-46372
 ONF₃, Raman spectrum 9-48468
 SiO₂ thermally oxidised, crystallographic symmetry of surface state density 9-23773
 Ti-O alloys, magnetic susceptibility, var. with temp. and alloying rel. to electronic struct. 9-35533
 V-O solid soln., degassing kinetics 9-39942
 Zr-O solid solns., sintered, electron work function 9-39734

Ozone

- atmosphere, content rel. to nightglow intensity 9-41561
 atmosphere, stationary regime effective temp., vars. day and night 9-40006
 atmosphere, upper layers, vertical distribution from u.v. scattering satellite obs. 9-40012
 atmosphere distribution, estimation by inverting radiative transfer equation for pure molecular scattering 9-28870
 atmospheric, coeffs. of absorption in Hartley band, verification 9-41524
 atmospheric, horiz. and vertical distrib., special cases 9-41487
 atmospheric, photochemical theory 9-24641
 atmospheric, photochemistry in presence of water vapour 9-31298
 atmospheric, soundings rel. to weather forecasting 9-41473
 atmospheric, temp. determ. from solar spectrum obs. 9-31288
 atmospheric, total characts. and station network effectiveness 9-41492
 atmospheric determ. from 1043 cm⁻¹ spectra by satellites 9-41490
 atmospheric dynamics 9-41495
 atmospheric optical sonde with simultaneous meas. 9-41474
 atmospheric photochem. 30 to 35 km, parameters determ. 9-41491
 atmospheric production by silent discharges 9-41544
 atmospheric total obs., computer evaluation 9-41493
 atmospheric steady regime, short period vars. 9-31296
 atmospheric vertical distrib., comparison of Umkehr and electrochem. sonde obs. 9-41488
 atmospheric vertical distrib., simultaneous Umkehr obs. with two Dobson photometers 9-41489
 atmospheric vertical distrib. from 9.6 μ emission and absorpt. spectra 9-41486
 auroral decrease in geomag. storm, X-ray ionization effect 9-41570
 concentration above 40 km, anomaly 9-41494
 Dobson spectrophotometer, improved solid-state amplifier 9-41475
 in earth's atmosphere, reactions with Fe⁺, Mg⁺, Ca⁺, Na⁺ and K⁺ ions, measurements 9-40044
 i.r. absorption spectra in O₂ matrix at 10° K 9-45329
 layer in upper atm., photochemistry 9-35834
 liquid, i.r. absorpt. spectra 9-46641
 meridional distrib., chem., atm. and solar effects 9-41485
 ozonosphere, u.v. spectra of reflected solar light, obs. from space 9-40033
 ozonosphere disturbance, height determ. 9-43383
 photolysis at 2537 Å electronically excited O₂ 9-45423
 planetary distribution, satellite u.v. spectral obs. 9-40013
 sensors, Brewer-Mast, accuracy 9-41476
 in stratosphere, effect on twilight polarization 9-41556

Ozone continued

- stratosphere, ozone and temp. vertical profiles 9-41540
 in stratosphere, perturbations during solar eclipse (12 Nov 1966) 9-31294
 stratospheric, concentration rel. to photochemical processes 9-47532
 Venus atmosphere, distribution 90 km to cloud top 9-40177
 vertical distrib. in upper stratosphere, satellite obs. 9-41545
 yield from O₂ in proposed chemonuclear reactor, rel. to temp., ozone conc. and dose rate 9-37842
 yield in pulse radiolysis of O₂ at v. high dose rate 9-39963

Ozonosphere *see* Atmosphere**p-n junctions** *see* Semiconducting devices/junctions**P-V-T relations** *see* Equations of state**Pair creation** *see* Electron pairs; and under individual particles, e.g. Mesons**Palaeomagnetism** *see* Rock magnetism**Palladium**

- creep, stacking fault energy effect 9-39421
 crystal growth and annealing process 9-39213
 Debye-Waller factor of $\frac{3}{2}\epsilon$ 9-41082
 density of states and electronic sp. ht. 9-37357
 dispersion hardening, patent 9-26391
 Fermi radius, velocity and g factor, exptl determ 9-47046
 film, electrical conductivity and Hall consts. 9-30848
 films, electron tunnelling rel. to spin wave excitation 9-44995
 films, thin, struct. and conductance 9-39589
 LEED beam scattering, non-specular by (100) face 9-46778
 photoelectric cross-section bs. for 662 keV γ 9-29962
 susceptibility, unenhanced paramag. 9-45088
 thermal diffusivity and conductivity, at 675-1750°K 9-41107
 thermal expansion at low temp. 9-33188
 X-ray absorpt. spectra, L_{III} white line obs., band levels filling determ. 9-37749
 X-ray emission spectra band shape anal., valence e level diagram determ. 9-36665
 X-ray M absorpt. spectra in u.s. region, absorpt., coeff. depend. 17-200 Å 9-37754
 X-ray absorpt. spectra L series obs., e states studied 9-37748
 D₂ solubility and diffusion meas. 250-350°C 9-37206
 H₂ solubility and diffusion meas. 250-350°C 9-37206
 in KCl, impurity eff. on growth of F and M optical absorption bands 9-28686
 in Na, molten, spin-slip scatt. of conduction electrons 9-32793
 Pd/H₂ syst., susceptibility meas., 50°-100°C 9-41295
 Pd₂ system, elec. resistivity D conc. dependence 9-24129

Palladium compounds

- alloys, crystal growth and annealing process 9-39213
 alloys, dispersion hardening, patent 9-26391
 alloys, phase structure, distortion from Cu-type substructure 9-35064
 Ag-Pd alloys, plasma freq., residual resistivity, sp. ht. 9-37436
 Ag-Pd alloys, stacking fault densities from X-ray diff. line profiles 9-40961
 Ag(Pd) alloys, photoemission expts. rel. to virtual resonant bound states 9-45032
 Co-Pd alloys mag. fields on ⁶⁰Co and ¹¹⁹Sn nuclei, electron polarization 9-28620
 Cu-Pd alloys, interdiffusion, effect of coherency strains 9-35128
 Cu-Pd alloys, internal oxidation by diffusion process, 850-1000°C 9-24557
 Cu₃Pd alloy, diffusion of H 9-23838
 Fe-Pd alloys, thin films, coercive force rel. to grain size 9-28622
 Fe-Pd alloys, mag. fields on ⁶⁰Co and ¹¹⁹Sn nuclei, electron polarization 9-28620
 Mn-Pd alloy system near MnPd₃, cryst. and mag. struct. 9-35588
 Ni-Pd alloy films, electron tunnelling rel. to spin wave excitation 9-44995
 PbS, relativistic band structure 9-39629
 Pd-Ag alloy films, effective surface coeffs., vol. diffusion effect in electron diff. obs. 9-39379
 Pd-Ag alloys, anisotropic impurity scattering rel. to Hall coeff. 9-37451
 Pd-Ag alloys, thermal expansion at low temp. 9-33188
 Pd-Ag dilute alloys, mag. susceptibility meas 9-45069
 Pd-(50 wt.%)Au alloy, Young's modulus temp. depend. 9-44752
 Pd-Co-Sn alloys, ferromag., mag. props., Mossbauer obs. 9-43179
 Pd-Co alloy, local ordering and elec. resistance annealing effect 9-33255
 Pd-Cr alloy, annealed at 510°C, weak ferromagnetism 9-49202
 Pd-Cr dilute mag. alloy, elec. resistivity below Kondo temp., eff. of coherence length 9-26508
 Pd-Cr dilute magnetic alloys, specific heat, temp. depend. below Kondo temp. 9-24050
 Pd-Fe, γ solid solutions, thermodynamic props. 9-30753
 Pd-(14 at.%)Fe alloy, low-temp. sp.ht. changes due to short-range order changes 9-33183
 Pd-Fe alloys, elec. resistivity, critical behaviour near mag. ordering temp. 9-44915
 Pd-Fe alloys, ferromag., conc. depend, magnetization 9-45151
 Pd-Fe alloys, Mossbauer spectrum rel. to quenching temp. in the range 820-950°C 9-41369
 Pd-Fe dilute alloy, ferromagnetic, $\partial m/\partial T$ meas., temp. and mag. field depend., rel. to spin-wave exchange stiffness coeff. 9-47263
 Pd-Fe dilute alloy, spin polarization range, conc. depend 9-45116
 Pd-Fe dilute alloys, low temp. elec. resistivities 9-44916
 Pd-H system, elec. resistance rel. to H content, temp. depend. 9-33256
 Pd-In alloys, lattice spacings and mag. susceptibilities, solid-solubility of In 9-30571
 Pd-(~5at.%)Ni alloy, ferromagnetic resonance and anisotropy 9-24478
 Pd-Ni alloy, Curie temp., effect of hydrostatic pressure 9-28611
 Pd-Ni alloy, paramagnetic, spin fluctuations from sp. ht. and thermal expansion anomalies 9-45086
 Pd-Ni alloys, Stoner enhancement field depend. at high mag. fields, paramag. susceptibility meas. 9-45087
 Pd-Pt, γ solid solutions, thermodynamic props. 9-30753
 (50at.%)Pd-Pt alloy, diffusive dispersion at high temps. short range order 9-44674
 Pd-Rh dilute alloys, ma. susceptibility, field-depend at high-mag. fields 9-45070
 Pd-Rh dilute alloys, mag. susceptibility, meas 9-45069
 Pd-Rh exchange enhanced alloys, field-depend, mag. susceptibility, 200 kG 9-26625
 Pd-Si based alloy glasses, form stability and struct. 9-42706
 Pd₂Ag_{1-x} doped with transition elements, torsional speed of sound obs. 9-30771

Palladium compounds continued

- Pd alloys, H diff. coeff. and variation with H conc. 9-28322
 Pd co-ordination cpds, type PdX₂Y₂, vibr. spectra 9-23068
 Pd complex, bis (N-t-butylsalicylaldimino) palladium(II), crystal struct. and molecular conformation 9-23769
 Pd complex, diiodo-(N-methyl-o-anisidine) palladium (II), structure 9-25748
 Pd complex, Pd(II)X₂Y₂ (X=Cl, Br or I, Y=Me₂P or Me₂As), square planar, vibrational spectra 9-30052
 cis-PdII trimethyl-arsine, -phosine, -stibene complexes, vibr. spectra obs. 9-27872

Paper

- conducting, analogue in the study of incompressible fluid flow problems 9-30176
 onionskin, acoustic decoupling props. 9-46991
 reflectance spectra, discrepancies in Kubelka-Munk eqn. applic. 9-37712

Paraelectric materials *see* Dielectric properties of substances**Paramagnetic resonance and relaxation***see also* Lasers; Masers

- β -diketonate salts, triplet-state energy and zero-field splitting 9-23116
 absorption curves, moments, errors in numerical calc. 9-35707
 absorption curves, moments calc., errors 9-39902
 absorption curves for complex ions, second moments, covalence effect 9-31167
 acetyl glycine, irradiated, ENDOR study at 77°K 9-41436
 L-alanine-1-¹³C irradi. at low temp. 9-33686
 alcohol, solvations to radical ions, e.p.r. study 9-34880
 alkali halide-B₂O₃ γ -irrad. glasses, stable V centres 9-24480
 alkali halides, electrolytically coloured, Cd centres obs. 9-40970
 alkali-metal-NH₃ solns., unpaired electron spin correl. times 9-44587
 alkaline earth fluorides, of V_k centres, eff. of polarized bleaching light 9-23826
 alkyl bromides, radicals formed in solid-phase radiolysis 9-39912
 alkyl radicals, evidence for planar shape 9-44377
 amino-cupric ion, -18°C → +72°C 9-42391
 anisotropic transition probability factor 9-31157
 anthracene and deuterated anthracene, rad. induced paramag. centres, spectra obs. 9-24499
 anthracene semiquinone derivations, bridged, long-range coupling 9-34655
 anthracene semiquinone derivatives, bridged, long-range coupling 9-34655
 anthracene single cryst., radical recomb. kinetics rel. to mol. motion from annealing obs. 9-32535
 aromatic free radicals, fluorinated, ¹⁹F hyperfine splittings 9-46396
 aromatic stable radical intermediates in pyrolysis 9-40604
 benzene anion free radical, relax. 9-46424
 benzene anion solns., ion pairing and temp. depend. of linewidth 9-42680
 benzene in perdeuterobenzene cry., phosphorescent state, hyperfine and fine struct. obs. 9-35719
 benzophenone, triplet state 9-49358
 biological mats., techniques, book 9-38338
 biomolecules, photosensitization, e.s.r. study of solvent effect 9-47472
 bis (perfluoromethyl) nitroxide, gas-phase relax. 9-32739
 1,4-bis(methylthio)naphthalene cation radical 9-38883
 1,3-butadiene, aq. soln., propagating type free radicals, spectra obs., density determ. 9-27925
 butanes, methyl-substituted, γ -irrad., spectra of free radicals 9-48499
 I₂ quartet under uniaxial stress 9-39906
 cadmium chalcogenides, of rare-earth ions, rel. to atomic environment 9-47430
 cavities, high temp. reactor for meas. 9-40300
 cellulose char, g-factor and line parameters rel. to initial state and carbonization temp. 9-26810
 chloral hydrate, e and γ irradiated, rel. to conc. of produced paramag. centres 9-33638
 chromium phthalocyanine, reduced, hyperfine struct. 9-42445
 cohelle salt: Cu²⁺, dynamic proton polarization 9-33632
 conduction-electron g shift, derivation 9-41423
 copper acetate monohydrate, γ -irrad., conversion of Cu²⁺ to Cu⁺ 9-49386
 α -copper phthalocyanine, powder line shape and MO calc. 9-33639
 copper (II) salicylate adducts, and mag. susceptibility 9-37804
 Cotton-Mouton r.f. resonance, Lorentzian absorpt., graphical representation 9-43922
 Cotton-Mouton-Voigt effect in X band 9-45379
 coumarin and related cpds., triplet state 9-30096
 crystals with colour centres, techniques, book 9-38338
 cyclooctatetraene anion radical, temp. dependent e.s.r., ion pairing effects 9-44589
 cytosine monohydrate, γ -irrad. cryst. at 77°K 9-45390
 per-deuterophenazine, triplet state, in diphenyl crystals, obs. 9-48503
 diamonds, effect of heat and pressure treatment 9-26366
 dibenzocyclohexadienyl radical in anthracene single crystal, radiation induced, ENDOR studies 9-39913
 4,4'-diethyl-benzophenone, spectrum 9-40614
 diffusion, spectral, in nonuniformly broadened lines 9-49345
 1,4-dimethylanthrasemiquinone, anion radical 9-36718
 N,N'-dimethylpyrazine cation radical, e.s.r. relax 9-23117
 2,2-diphenyl-1-picrylhydrazyl, in low fields using simple apparatus 9-45901
 diphenyl/methyl neutral radicals 9-48495
 dipolar lineshifts in free-radical crystals, theory 9-43287
 double resonance theory, mathematical approach 9-47877
 duren, signal comparison after gamma and u.v. irradi. 9-47421
 duren, triplet state of photochem. oxidation product, fine struct. obs. 9-33640
 dynamic polarization eqns. rel. to shape of distant ENDOR signals 9-43309
 electron nuclear triple resonance in liquids, prediction and meas. method 9-44590
 electron-nucleus system, relaxation time expressing derivation 9-41343
 electron-transfer rates in soln., errors in meas. 9-45412
 erbium ethylsulphate, spin-lattice relaxation anisotropy 9-26665
 ferrimyoglobin, electron spin-echo obs. of relax. processes 9-42457
 ferrocene, γ -irrad., free radicals 9-43288
 fluorenone ketyl soln., existence of paramagnetic and diamagnetic ion clusters 9-34923
 fluorenyl neutral radicals 9-48495

Paramagnetic resonance and relaxation continued

- fluorinated radical anions, one-parameter relation between isotropic F splitting and π -electron spin density 9-38872
 fluoroberyllate glass, of divalent Mn 9-45385
 free electrons, use in meas. of (g-2) anomaly 9-29540
 free radical solns., hydrogen bridge formation, study by dynamic nuclear polarization 9-42450
 free radicals, gas phase, spin trapping techniques for detection 9-42451
 free radicals prod. at potential-modulated electrodes, synchronous detection 9-25788
 β -Ga₂O₃:Fe³⁺ of Fe³⁺, theoretical and expt. symmetry effects 9-41427
 gases, techniques, book 9-38338
 Gaussian, graphic representation of r.f. Cotton-Mouton effect, rel to Lorentzian case 9-47872
 glass, barium silicate containing Ti, gamma-induced optical absorpt., Ti³⁺ formation 9-37693
 glass, Fe reson. 9-37797
 glass, photosensitive, neutral Au atom obs. 9-39911
 glass, soda-boric oxide, Cu²⁺ spectra 9-37800
 glasses, of Fe³⁺, rel. to coordination 9-26199
 glasses, organic, trapped e spectra rel. to matrix polarity, 77°K 9-28695
 D- glucose aqueous ice gamma-irrad., study of free radicals 9-42454
 glycine hydrochloride, X-irrad., radical formation 9-43340
 glycine irrad., anisotropic hyperfine splitting 9-23178
 graphite, withrhombohedral phase, g-factor anisotropy determ 9-24484
 group II-VI compounds, of defect centres 9-37803
 group II-VI compounds, of ionized donor, to monitor compensation 9-37531
 group II-VI compounds, of rare-earth ions, rel. to atomic environment 9-47430
 group II-VI compounds, zincblende and wurtzite struct., of Fe³⁺, theory 9-47429
 haemoglobin, of Fe and Cu 9-33641
 of (2,2,1) heptane radical 9-46398
 4,4'-di-n-heptyloxyazobenzene smectic mesophase, of solute, obs. 9-32796
 heterocyclic amine N-oxides anion radicals, rel. to polarography 9-36715
 high-spin d⁵ systems 9-39917
 hydrocarbon ions, proton hyperfine splittings, comparison of relations 9-38899
 n-hydrocarbons, irrad., pairwise trapping of radicals 9-45427
 hydroxyurea, X-irrad., radical pairs 9-45426
 hyperfine coupling consts., 'mixed basis' calc. 9-32458
 hyperfine splitting, rot. H₂ and p-electron interact. 9-23178
 ice, irradiated, H atom yields, effect of O on determ. 9-31164
 ice single crystals, X-irrad., OH radicals 9-47436
 impurity ions with spin 1, 3/2 and 5/2, angular variation 9-31156
 in-plane g values in low-symmetry d¹ and d⁹ systems 9-31163
 ion-radical salts, electron double resonance of triplet excitons 9-28753
 ionic crystals, recombination luminescence investigated by EPR relaxation 9-33576
 iron phthalocyanin, reduced, hyperfine struct. 9-42445
 Jahn-Teller system containing Cu²⁺.6H₂O, relax. behaviour 9-31159
 Jahn-Teller system containing Cu²⁺.6H₂O, relax. behaviour, model 9-31160
 lanthanum ethyl sulphate, Gd³⁺ zero-field splitting anomaly 9-39914
 line widening by internal deform. in cryst. 9-35708
 line widths, angular dependences 9-31158
 lines, forbidden transitions and discrete saturation 9-37790
 liquids, techniques, book 9-38338
 liquids in communicating vessels for vertical variable loadings 9-42678
 magnetic resonance lines, dipolar-broadened, saturation, in presence of phonon bottleneck 9-49347
 magnetic resonance lines, saturation, rel. to thermodynamics 9-49348
 magnetic resonance lines, saturation, rel. to thermodynamics 9-49349
 magneto-optical meas. method of ion relaxation 9-40299
 malonamide, X-irrad., of σ -electron radical 9-38924
 mesitylene, study of radical formed on e. irradiation 9-42439
 mesitylene in B-trimethylborazole cry., phosphorescent state, fine and hyperfine struct. obs. 9-24500
 metal oxides, irradiation effects obs. rel. to catalytic behaviour 9-35709
 metals, 'selective transmission' technique, review of results 9-28743
 metals, anisotropy effects 9-47427
 metals, techniques, book 9-38338
 methyl and methyl-d₃ radicals in aq. soln. 9-42455
 methyl methacrylate free radicals, spectrum obs. to investigate polymerization 9-33666
 methyl radical, proton hyperfine splitting temp. depend. 9-36729
 1-methylphenalenyl, e.s.r. meas. of spin densities, hyperconjugation eff. calc. 9-34677
 monocarboxylic acid radical anions, 77°K 9-42452
 monodeuteroisopropenyl radical, empirical resonance energy estimation 9-23177
 multilevel systems, relax. by conduction-electron spins, spin-lattice line-widths 9-43196
 myoglobin zero field splitting 4 mm obs. 9-43818
 naphthalene, optical spin polarisation tripletstate 9-45391
 naphthalene, phosphoresc. triplet states, optical detect. 9-37770
 naphthalene, spin relax. and optical spin polarization of triplet excitons 9-39915
 nematic liq. crystals, e.s.r. of spin-labelled nematogenlike probes 9-44588
 neodymium ethylsulphate, paramag. relaxation, phonon re-absorption and spectral spin diffusion 9-33491
 1-nitro-2,4,6-triphenylbenzene, anomalous N h.f.s. 9-27924
 nitropolyarylvinylenes, superfine struct. 9-44384
 nitroxides, conformation effects on hyperfine structure 9-44366
 non-insulated paramagnetic subst., g factor determ. by rapid modulation method 9-43271
 nuclear polarization enhancement by dynamic cooling 9-31061
 Orbach relax. processes, T₁ and T₂ 9-24492
 organic cpds, techniques, book 9-38338
 organic cyanides, γ -irrad. crystals, N hyperfine coupling and g factor of trapped electrons 9-47440
 oxydiethanoic acid, free radical formed on e irrad., in zero field 9-42442
 paramagnetic crystals, dil., strong coupling bet. electron spin-spin interact. and nuc. spin systems 9-26664
 paramagnetic species, point symmetry and expt. Hamiltonian 9-39222
 perchlorodiphenylmethyl free radical 9-38908
 perchlorotriphenylmethyl, free radical 9-38908
 perinaphthenyl neutral radicals 9-48495

Paramagnetic resonance and relaxation continued

- phenanthrene oriented in biphenyl, deuterium isotope effect in zero-field splittings 9-43289
 phenazine, triplet state, in diphenyl crystals, obs. 9-48503
 phenothiazine, phosphoresc. triplet state 9-39887
 phenoxazine, phosphoresc. triplet state 9-39887
 phenoxyl radicals, fluorinated, alternation in linewidths to assign n.m.r. ¹⁹F coupling constants 9-34687
 1-phenylphenalenyl radical, spin densities, hyperconjugation eff. calc., e.s.r. study 9-34677
 piperidine iminoxyls, substituted, interconversion 9-38912
 polar molecules, cry., study of electrons trapped in dipole fields 9-40584
 polyethylene, irradiated, discrete line saturation 9-37790
 polymers, irrad., pairwise trapping of radicals 9-33687
 polytetrafluoroethylene, oriented, electron pulse irrad. 9-43291
 potassium aminedisulphonate, quadrupole coupling in N(SO₃)₂⁻ 9-39916
 potassium thiocyanate, gamma-irrad., spectrum of radical species 9-45392
 principles and experimental techniques 9-49346
 proteins, study of irradiation induced radical states 9-24941
 pyrazine in acid medium, meas. rel. to nature and symmetry of phosphorescent state 9-46417
 pyrene-d-10, in photo-excited triplet state, e.s.r. anisotropic saturation 9-44371
 quartz, brown synthetic, of Fe³⁺ 9-41426
 quartz, zero-field e.p.r. of Fe³⁺ 9-43279
 quinoxaline, phosphoresc. triplet states, optical detect. 9-37770
 quinoxaline anions, spin densities 9-32526
 π -electron radicals, hyperfine coupling consts. of 2nd-row elements 9-42373
 π -electron radicals, MO theory of hyperfine interactions 9-38874
 rare earth ions in disordered systems, line shapes 9-28742
 rare earth metals, expression for acoustic resonance coeffs. 9-41422
 relaxation 9-49226
 relaxation, and applic., book 9-47222
 Rochelle salt, ferroelec. phase transitions, study 9-30972
 rotational, macroscopic aspects of expts. 9-43819
 ruby: Cr³⁺, g-factor and fine structure lines up to 7 kbar 9-33655
 ruby crystals, relaxation time meas. for spin-phonon interaction Hamiltonian parameter 9-45242
 ruby crystals with symmetry T_{2h} line from in elec. fields 9-24481
 samarium ethylsulphate, spin-lattice relaxation anisotropy 9-26665
 saturation of nonuniformly broadened lines, role of spectral diffusion and dipole-dipole reservoir 9-29349
 scheelite-type crystals, of Er³⁺ 9-41424
 semiconductors, techniques, book 9-38338
 sideramines 9-39917
 sodium naphthalenide solns. in tetrahydrofuran, spectral anomaly 9-30427
 solasodane derivatives 9-44372
 spectra, computer program for calculation from parametric spin-Hamiltonian 9-36691
 spectra line analysis, described by composition of Gaussian and Lorentz profiles 9-25156
 spectra of complex compounds in solns., effect of ligand field on hyperfine splitting 9-32795
 spectrometer, computer control 9-31881
 spectrometers, magnetic field modulation influence on paramagnetic absorption line width 9-38825
 spin systems, strongly polarized, population transfer obs. 9-39901
 spin tickling effect, new form of equation 9-42374
 spin-phonon interaction in external elec. fields 9-45243
 structural information 9-46350
 sucrose aqueous ice gamma-irrad., study of free radicals 9-42454
 o-terphenyl, liq., mol. motion study, linewidth obs. 9-40805
 tetracyanobenzenes complexes, charge-transfer triplet states 9-23158
 tetracyanquinodimethane complex with benzthiocarbocyanine dye 9-28753
 1,4,5,8-tetramethylanthraquinone, anion radical 9-36718
 2,2,6,6-tetramethyl-4-hydroxypiperidine-1-oxyl radical, absorpt. spectra 9-45091
 tetraphenylcyclopentadienone radical anion, and molecular orbital study 9-30143
 tetraphenylhydrazine, diphenylamino radical dimer as colour centre 9-42855
 2- and 3-phenyl radicals, inequivalence of CH₂ protons 9-36722
 three-level system, double quantum transition 9-49344
 transition metal ions in complex, π state, in soln e.s.r., solvent induced fluctuations 9-30038
 transition metal ions in crystal, techniques, book 9-38338
 transition-metal-ion complexes, spectra, vib. struct. study 9-23024
 trichloromethyl radical in soln., spectrum 9-40624
 triglycine sulphate, γ -irrad., hindered motion of CH₂ in CH₂COO⁻ 9-35720
 trimethylenemethane, zero-field splitting of ground triplet state 9-42448
 triphenylene, oriented, absorpt. in phosphorescent state at low mag. fields 9-38918
 triphenylene triplet dianion, zero-field-splitting calc. 9-42446
 2,4,5-triphenylimidazolyl radical, spectrum interpretation 9-27913
 triphenylmethyl radicals, substituted 9-36723
 tropenyl free radical, relax. 9-46424
 tropenyl radical, empirical resonance energy estimation 9-23177
 ultramarines, investigation of S radicals 9-36727
 vanadyl acetylacetonate paramagnetic probe alignment in p-azoxyanisole, isotropic-nematic transition 9-42633
 vanadyl phthalocyanine 9-41430
 vinyl acetate, aq. soln., propagating type free radicals, spectra obs., density determ. 9-27925
 vinyl propionate, aq. soln., propagating type free radicals, spectra obs., density determ. 9-27925
 yttrium ethyl sulphate, of Gd³⁺ spin-Hamiltonian parameters 9-43290
 zinc chalcogenides, of rare-earth ions, rel. to atomic environment 9-47430
 Ag₂CO₃ γ -irrad. crystals 9-37791
 AgBr:Ni²⁺, illuminated, Ni⁺ obs. 9-33621
 AgCl:Ni²⁺, illuminated, Ni⁺ obs. 9-33621
 AgCl of Ni²⁺ and isotope effect in cry. field 9-43273
 Al, of Cr³⁺, with and without doping 9-37796
 Al₂O₃:Cr³⁺, spin-phonon interaction in ext. elec. fields 9-45243

Paramagnetic resonance and relaxation continued

- Al₂O₃, neutron irradi., triplet (S=Z) state defect obs. 9-44689
 α -AlOOH:Fe³⁺ of Fe³⁺, theoretical and exp. symmetry effects 9-41427
 AsO₄³⁻ in γ -irrad. calcite 9-39903
 n-BaB₆, single cryst., conduction-e.s.r. 9-37793
 BaF₂:U³⁺, spin-lattice relaxation examined by paramagnetic resonance 9-35710
 BaF₂, h.f.s. const. of V_K and V_L centres, lattice vibr. influence 9-43274
 BaF₂, hyperfine interactions of H atoms, temp. depend. 9-31060
 BaF₂, neutron-irrad., F- and V-centres thermal stability obs. 9-43275
 BaO, F-centre obs., isotropic and anisotropic hyperfine const. and quadrupole interac. for ¹³⁵Ba 9-35109
 BaWO₄:Er³⁺, ground and first excited states of tetragonal Er³⁺ centres 9-41424
 BiLi:Cr³⁺, spectrum for Cr³⁺ single ions and exchange-coupled Cr³⁺ pairs 9-24482
 C, turbostratic, B and Na doped, effect of heat treatment 9-26791
 C black, heat treatment effect of g-shift 9-24485
 C fibres, struct. determ., g values rel. to preferred orientation 9-32904
 C film, evaporated, effect of water vapour 9-39904
 CO complexes, quadrupole effects 9-43278
 3Ca₃(PO₄)₂:Ca(F_{1-x}Cl_x)₂:Mn²⁺, synthetic, rel. to effect of incorp. of Cl on Mn²⁺ positions 9-47431
 n-CaB₆, polycryst., conduction-e.s.r. 9-37793
 CaCO₃:Pb²⁺, hyperfine interaction 9-41425
 CaF₂:Dy²⁺, investig. at T=4.2°K in wavelength range 1.7-35 mm 9-33622
 CaF₂:Dy³⁺, under uniaxial stress 9-39906
 CaF₂:Eu²⁺ Γ_8 level, effect of nearby Jahn-Teller tunneling level 9-45383
 CaF₂:Gd³⁺, spin-lattice coeff. determ. from uniaxial stress effects on e.p.r. spectra 9-33492
 CaF₂:Gd³⁺ spin-lattice coeffs. determ. from uniaxial stress studies 9-45380
 CaF₂:R³⁺, H⁻, (R=rare earth), spectra obs. 9-47353
 CaF₂:Tm³⁺, anomalous population distrib. in optically excited metastable level 9-31161
 CaF₂:U³⁺, spin-lattice relaxation examined by paramagnetic resonance 9-35710
 CaF₂:U³⁺ system, strongly polarized, population transfer among spin packets obs. 9-39901
 CaF₂:U⁴⁺, and UPR spectra, superhyperfine interactions 9-39905
 CaF₂:Yb³⁺, ENDOR on ¹⁷³Yb³⁺, electronic shielding by closed shells obs. 9-35731
 CaF₂, ENDOR meas., comparison between Ce³⁺-H⁻ and Ce³⁺-F⁻ 9-37808
 CaF₂, ENDOR obs. of Gd³⁺, transferred hyperfine interaction 9-49363
 CaF₂, h.f.s. const. of V_K and V_L centres, lattice vibr. influence 9-43274
 CaF₂, hyperfine interactions of H atoms temp. depend. 9-31060
 CaF₂:Eu²⁺, spin-lattice coeff. determ. from uniaxial stress effects on e.p.r. spectra 9-33492
 CaF₂:U⁴⁺, spin-phonon interaction from u.s. paramag. resonance 9-33623
 CaO:Gd³⁺, spin-lattice coeff. determ. from uniaxial stress effects on e.p.r. spectra 9-33492
 CaO, F⁻ and F centres, paramag. reson. linewidth and hyperfine interactions obs. 9-45382
 CaO, impurity effects and hyperfine struct. obs. 9-45381
 CaO, N-centre due to neutron irradi. 9-37794
 CaWO₄:Eu²⁺ crystal field splittings and hyperfine structure const., 4.2 and 78°K 9-43200
 CdCl₂:Ag, irradi., paramag. centre obs. 9-49272
 CdF₂:Cr³⁺ 9-47385
 CdF₂:Eu²⁺, 300, 77 and 1.5°K 9-28745
 CdF₂:V³⁺, V²⁺ 9-47385
 CdF₂, of Gd³⁺ 9-37795
 CdS, of photoinduced Cu and Ag centres 9-47433
 CdS, paramag. reson. of Fe³⁺:Cu associated centres, 77°K 9-47432
 CdTe:Co²⁺, electrically induced e.p.r. transitions 9-35711
 CdTe:Yb,Er, effects of P and Li compensation on rare earth doping 9-47434
 CdWO₄:Cu²⁺, spectra, linear elec. field effects 9-24486
 CdWO₄:Mn²⁺, spectrum hyperfine structure, effect of external elec. field 9-31162
 (Ce₂La_{1-x})₂Mg₃(NO₃)₁₂·24H₂O, dipolar-broadened electron resonance lines of Ce³⁺ ions, saturation, in presence of phonon bottleneck 9-49347
 Ce³⁺ in ag. soln., indirect determ. of short relax. time 9-30426
 CeMg(NO₃)₆, ground-state g factor obs., mag. field depend. 9-43276
 CeMg(NO₃)₆, high field magnetization, calibration error correct. 9-43277
 Cl atoms adsorbed on silica gel 9-39174
 Cl atoms adsorbed on silica gel 9-30497
 Co²⁺ in ag. soln., indirect determ. of short relax. time 9-30426
 Cr complex, tris (oxalatogromium) (III), zero-field splittings 9-24487
 Cs₂UO₂Cl₂:NpO₂²⁺, Np⁶⁺ spectrum, ²³⁷Np nucl. moment obs. 9-35712
 Cs₂UO₂:AsO₄³⁻, γ -irrad. 9-39903
 CsUO₂(NO₃)₃:NpO₂²⁺, Np⁶⁺ spectrum, ²³⁷Np nucl. moment obs. 9-35712
 Cu-Mn dilute alloys, 1.8° to 300°K 9-26792
 Cu²⁺ in NH₃ soln., -18°C→+72°C 9-42391
 Cu²⁺ in ZnO 9-33637
 Cu (II) benzoate, 9.1 and 12.0 GHz, spin Hamiltonian parameters 9-49350
 Cu chelates, in-plane g values 9-31163
 Cu complex, bis(ethylenediamine) copper(II) nitrate, single crystal ESR spectrum, g value calc. 9-28744
 Cu complex, CuCa acetate hexahydrate 9-33484
 Cu complex, Cu(II) hydrogen o-phthalate dihydrate 9-48829
 Cu complex, Cu(II) tetramethylene diamine chloride 9-33624
 Cu complex, diphenyl sulphoxide perchlorate, spectra obs., hyperfine lines 9-24488
 Cu complexes, quadrupole effects 9-43278
 Cu(II) complexes, principal g factors calc. 9-33625
 CuK₂(SO₄)₆·6H₂O, dynamic polarization of protons and their spin-lattice relaxation times 9-39786
 Cu(NH₃)₄(SCN)₂, principal g factors calc. 9-33625
 Cu(NO₃)₂·2.5H₂O, cross relax. among Cu²⁺ ion pairs 9-26662
 3CuO, P₂O₅, 24MoO₃, 58H₂O single cryst. 9-35713
 CuSO₄, Cu²⁺ diffusion in aq. soln., e.p.r. obs. 9-34890
 EuAlO₃:Cr³⁺ 9-47435
 EuCl₃:Gd³⁺ pair and Gd³⁺:Eu³⁺ interac. const. 9-33439
 F, of colour centre on u.v. irradi., identification of Y impurity 9-40971

Paramagnetic resonance and relaxation continued

- Fe³⁺ in corundum, angular dependence obs. 9-47428
 Fe³⁺ in quartz, zero-field e.p.r. 9-43279
 Fe³⁺ in synthetic brown quartz 9-41426
 (FeF₆)³⁻ in aq. solns., spectra 9-36901
 GaAs, g-factor shift of Fe³⁺ and Mn²⁺, covalency influence 9-43280
 GaAs, of transition metal impurities, line width 9-45384
 GaP:Mn, Li diffused, Li tripple ion detection 9-24493
 Gd₂(SO₄)₃·8H₂O, Faraday eff. 9-28746
 Gd³⁺, in ZnO, hyperfine interaction with odd Gd isotopes 9-33636
 H-addition radicals formed in aromatic rings of phenylalanine, tyrosine and tryptophan, spectra obs. 9-46423
 H₂S⁻ hyperfine coupling const., d orbitals effect 9-32458
 H₂S⁺ hyperfine coupling const., d orbitals effect 9-32458
 H and N coupling const. for σ radicals containing C, H, N and O atoms, extended Huckel calc. 9-23025
 H atom reaction with methane, kinetics meas. 9-47454
 HFO₂, monoclinic, Fe³⁺ spectrum 9-33627
 H+C₂H₄ reaction, e.s.r. detect. 9-24534
 HSiO₂:Gd³⁺, ground-state splitting 9-33626
 K₂SO₄ crystal, X-irradiated, spectra obs. 9-24491
 K₂ZnF₆:Co²⁺, and superhyperfine interaction const. 9-45257
 K₂ZnF₆:Mn single crystal, and transferred hyperfine interactions 9-45387
 K₂ZnF₆, of Co²⁺, rel. to mag. struct. 9-41294
 K halide crystals, trapped N₂⁻ 9-31166
 KBr, F centre spin-lattice relax. theory and optical meas., 0-50 kG 9-24342
 KCl:Ca, F centres obs. 9-37191
 KCl:Mg, additively coloured, props. 9-48868
 KCl, F centres obs. 9-37191
 KCl, hyperfine and superhyperfine struct. const. of stabilized and Ag atoms, temp. depend. 9-35714
 KCl, paramag. reson. of O⁻ centre, pulse saturation 9-47437
 KCl, simultaneous optical bleaching and X-irrad. obs. 9-42848
 KCl, superhyperfine interactions of H and D centres, zero-pt. vibr. influence, ENDOR obs. 9-45409
 KClO₃, X-irrad. at low temp., of ClO₂, ($\delta M_1=1$, $\Delta M_1=\pm 1$ or ± 2) 9-49352
 KH₂PO₄:Cu²⁺, ferroelec. 9-26793
 KLi, F centre spin-lattice relax., theory and optical meas., 0-50 kG 9-24342
 KMnF₃, of Mn²⁺ exchange-narrowed, discrepancies between theory and expt. 9-45388
 KZnF₆:Mn²⁺, nearest-neighbor exchange const. determ. 9-45386
 La₂Mg₃(NO₃)₁₂:T³⁺, (T=Ce, Nd, Sm), Orbach relax. processes, T₁ and T₂ 9-24492
 La₂Mg₃(NO₃)₁₂:T³⁺, (T=Ce, Nd, Sm), temp. dependence, T₁/T₂ ratios 9-24483
 La₂Mg₃(NO₃)₁₂·24H₂O:Cu²⁺·6H₂O, relaxation behaviour 9-31159
 La₂Mg₃(NO₃)₁₂·24H₂O, Ni²⁺ electron spin-lattice relaxation rate by direct process 9-45245
 LaBr₃ and LaCl₃, of coupled Ce³⁺ and Nd³⁺ rel. to high degree electrostatic and exchange interactions. 9-47227
 Li, conduction-electron spins, pulsed-microwave studies 9-33629
 Li, spin-flip scatt. cross-section for conduction electrons of impurity atoms 9-41345
 Li, spin-flip scatt. cross-section for conduction electrons of impurity atoms 9-41346
 Li₄RhH₈ (x=4,5), structure and bonding obs. 9-48834
 LiCl-KCl eutectic: MnCl₂, and K₂MnCl₆ form., obs. 9-28749
 LiCl, hyperfine and superhyperfine struct. const. of stabilized Cu and Ag atoms, temp. depend. 9-35714
 LiCl, of Cu²⁺ centres, g-values and h.f.s. 9-43281
 LiF:Mn²⁺m 9.5 GHz, hyperfine interactions 9-37798
 LiF:Si, X-irrad., paramag. fault 9-49353
 LiF, n-irrad., linewidths of conduction electrons in Li particles 9-33630
 LiNbO₃:Cr³⁺(Nd³⁺) acoustic, for internal fields of ferroelec. crystals 9-28748
 MgAl₂O₄:Cr³⁺ spinel, theory of strong trigonal field 9-28644
 MgO:Cu²⁺, dynamic Jahn-Teller effect at 4.2°K from Cu²⁺ spectrum 9-24494
 MgO:Mn⁴⁺, rel. to tetragonal and octahedral sites of Mn⁴⁺ 9-24496
 MgO:Ni²⁺, spectral line shape 9-24495
 MgO:Ni²⁺, spin-phonon interactions, molecular orbital theory 9-39787
 MgO, acoustic paramag. reson. of Cr²⁺, interpret. taking account of Jahn-Teller effect 9-24346
 MgO, from F⁺ vacancy-pair centre 9-47438
 Mn²⁺, impurities in monticellite (MgCaSiO₄) 9-24497
 Mn²⁺ in (NH₄)₂SO₄ single cry., paraelec. and ferroelec. phases investig. 9-31165
 Mn²⁺ in aq. soln., 3.2 cm and 10 cm spectra, comparison 9-34922
 Mn complex, ⁵S state of Mn²⁺ in soln. X-band spectra obs. 9-30038
 Mn⁴⁺, of [Mn(IV)₆O₆]₂⁶⁻ in dil. (NH₄)₆ [Ni(IV)₆O₆]₂·8H₂O 9-43283
 MnCl₂·H₂O in organic solvents, spectra in 10 cm band 9-42679
 MnCl₂²⁻ tetrahedral complexes, covalent bonding 9-37799
 MnCl₄²⁻ octahedral complexes, covalent bonding 9-37799
 MnF₂, of Mn²⁺ exchange-narrowed, discrepancies between theory and expt. 9-45388
 Mn(II) complexes of spin- $\frac{1}{2}$ with large ligand field splittings 9-41428
 MnTiO₃, II high press. phase, antiferromag. obs. 9-44667
 MoO₃:V, hyperfine struct. lines 9-39907
 NCO, vibrationally excited, gas phase electron reson. spectrum 9-40599
 NCS, gas phase electron reson. spectrum 9-40599
 NH₄OHCl, X-irrad., optical and thermal conversion of V_K centres 9-32995
 NH₄Cl, due to radiation induced paramagnetic centre 9-33631
 NH₄Cl λ -type phase transition, Cu²⁺ impurity effects 9-33142
 (NH₄)₂PtCl₆, cross-relaxation between single and exchange-coupled Ir⁴⁺ ions 9-49356
 NO, adsorbed on molec. sieve 9-39167
 NS free radical, molecular structure, analysis in gas phase 9-46369
 N(SO₃)₂⁻, quadrupole coupling meas. 9-39916
 Na, conduction-electron spins, pulsed-microwave studies 9-33629
 Na, liquid, conduction, -200°C TO +300°C 9-26133
 Na, molten, spin-flip scatt. of conduction electrons obs. 9-32793
 Na, spin-flip scatt. cross-section for conduction electrons of impurity atoms 9-41345

Paramagnetic resonance and relaxation continued

- Na, spin-flip scatt. cross-section for conduction electrons of impurity atoms 9-41346
- $\text{Na}_2\text{S}_2\text{O}_3 \cdot 5\text{H}_2\text{O}$ p-irrad. single cryst., g- and ^{33}S hf-tensor parameters for trapped radicals 9-35716
- Na_2SO_4 , SO_4^{2-} , SO_3^{2-} , O_2^- identified by ESR following X-irradiation 9-30616
- $\text{Na}_4[\text{Cu}(\text{NH}_3)_4]$ $[\text{Cu}(\text{S}_2\text{O}_3)_2]$ single cryst., absorption curves, covalence effect on second moments 9-31167
- Na atom in ammonia-ethylamine mixture solvents, electron spin resonance absorption 9-49355
- Na germanate, glasses, Nd activated, spectra 9-39909
- $\text{NaBr}:\text{Ca}^{2+}$ single cryst., paramag. centres obs. 9-33633
- $\text{NaCl}:\text{Ca}^{2+}$, V-centres, X-ray irrad. temp. effects 9-30618
- $\text{NaCl}:\text{Ca}^{2+}$ single cryst., paramag. centres obs. 9-33633
- $\text{NaCl}:\text{Cu}:\text{NaCl}:\text{Cu}:\text{Ag}$ recombination luminescence, trapping of electrons and holes detect. by EPR meas. 9-33587
- $\text{NaCl}:\text{Mn}^{2+}$, irrad., X- and K-band spectra, paramag. Mn centre 9-35715
- NaCl, diffusion of Mn^{2+} , coeff. determ. 9-30627
- NaCl, ground state splitting of Mn^{2+} , elec. field effect 9-43284
- NaCl, hyperfine and superhyperfine struct. consts. of stabilized Cu and Ag atoms, temp. depend. 9-35714
- NaF , of Mn^{2+} , 4 spectra obs., spin-Hamiltonian method analysis, 93-573K 9-39908
- $\text{NaMgAl}[\text{Cr}](\text{C}_2\text{O}_4)_2 \cdot 9\text{H}_2\text{O}$ single crystal, triplet molecules and Cr III, X and P band 9-49351
- NaNO_2 , neutron irradiated, ESR obs. 9-49354
- Ni-Co alloys, of Co, localized mag. moments investig. 9-33634
- Ni^{2+} crystal field eff. on paramagnetic behaviour 9-28645
- Ni^{2+} in ag. soln., indirect determ. of short relax. time 9-30426
- O, spectra, formation and decay proc. in r.f. discharge 9-29350
- $\text{O}+\text{OCS}$, $\text{O}+\text{CS}_2$, $\text{O}+\text{NO}$, reactions, e.s.r. detect. 9-24534
- PbTiO_3 , of Fe^{3+} at Q band and 70GHz 9-45389
- $\text{Rb}_2\text{SO}_4:\text{VO}^{2+}$ single cryst., preferred orientations and spin Hamiltonian parameters at X-band 9-41429
- RbMnF_6 , of Mn^{2+} exchange-narrowed, discrepancies between theory and expt. 9-45388
- S, used to follow conversion of unstable to stable form. 9-30747
- S unstable forms prod. by condensation, studied by paramagnetic resonance 9-30746
- SO_2^- in aq. soln., linewidth depend on temp. viscosity 9-30054
- $\text{SbI}_3:\text{Cr}^{3+}$, spectrum for Cr^{3+} single ions 9-24482
- Si:Li-diffused, rel. to Li-O complex 9-26794
- Si:P, absorpt. intensity 9-35717
- Si:P, method for spectral depend. of photoionization of impurity atoms and colour centre 9-37636
- Si:P ENDOR obs. 9-35736
- Si- SiO_2 interface, at 77°K, effect of heat treatment in H_2 or He 9-49357
- p-Si, at 77°K, effect of heat treatment in H_2 or He 9-49357
- Si, study of donor electron magnetic interaction, 4.2°K, 10 GHz 9-43285
- p-SiC:B,N, rel. to interimpurity recombination obs. 9-28712
- α -SiC polytypes, of N atoms 9-28750
- n- SrBa_2 polycryst., conduction-e.s.r. 9-37793
- $\text{SrF}_2:\text{Er}^{3+}$, conc. depend. of site symmetry 9-24490
- $\text{SrF}_2:\text{U}^{3+}$ spin-lattice relaxation examined by paramagnetic resonance 9-35710
- SrF_2 , h.f.s. consts. of V_F and V_C centres, lattice vibr. influence 9-43274
- SrF_2 , hyperfine interactions of H atoms, temp. depend. 9-31060
- $\text{SrMoO}_4:\text{Er}^{3+}$ second excited state of Er^{3+} centres 9-41424
- $\text{SrTiO}_3:\text{Fe}:\text{Mo}$ and $\text{Ni}:\text{Mo}$, photochromic, and optical spectra studies 9-26742
- SrTiO_3 , of Fe^{3+} at Q band and 70GHz 9-45389
- Te anisotropic chemical shift 9-43272
- $\text{ThSiO}_4:\text{Ce}^{3+}$, ground-state splitting 9-33626
- $\text{ThSiO}_4:\text{Gd}^{3+}$, ground-state splitting 9-33626
- TiO_2 , Fe^{3+} spin-lattice relaxation for X- and F-band transitions 9-47300
- TiO_2 , of Cr^{3+} ions coupled with O vacancies 9-37801
- VO^{2+} chelates, in-plane g values 9-31163
- YAl garnet, spectra and relax. processes of Nd^{3+} 9-24498
- $\text{YAsO}_4:\text{Gd}^{3+}$ spectra in X-band 9-43286
- $\text{YCl}_3 \cdot 6\text{H}_2\text{O}:\text{Gd}^{3+}$ 9-28747
- $\text{YPO}_4:\text{Gd}^{3+}$ spectra in X-band 9-43286
- $\text{YVO}_4:\text{Gd}^{3+}$ spectra in X-band 9-43286
- ZnAl_2O_4 , of Cr^{3+} and Fe^{3+} , rel. to single-ion mag. interactions 9-45080
- $\text{Zn}(\text{BrO}_3)_2 \cdot 6\text{H}_2\text{O}:\text{Cu}^{2+}$, relaxation behaviour 9-31159
- ZnGa_2O_4 , of Cr^{3+} and Fe^{3+} , rel. to single-ion mag. interactions 9-45080
- $\text{ZnO}:\text{Cu}$ single cryst., $^{63,65}\text{Cu}$ hyperfine lines obs. 9-35718
- $\text{ZnO}:\text{Fe}^{3+}$, meas. rel. to g tensor anisotropy 9-26795
- ZnO of Co^{2+} substitutional divalent ions 9-28752
- $\text{ZnS}:\text{Cu}$, paramagnetic centres 9-28751
- $\text{ZnS}:\text{Mn},\text{Li}$, spin-lattice relaxation time of Mn^{2+} 9-47301
- ZnS/ZnSe mixed crystal, of defect centres 9-37803
- ZnS , of defect centres 9-37803
- $\text{ZnSO}_4:\text{Mn}^{2+}$, fine struct. and cryst.-field interac. obs. 9-33635
- $\text{ZnSe}:\text{Ge}(\text{Pb})$ impurities as hole traps, hyperfine and superhyperfine struct. obs. 9-35706
- $\text{ZnSe}:\text{V}$, for monitoring compensation 9-37531
- ZnSe , of defect centres 9-37803
- $\text{ZnSiF}_6 \cdot 6\text{H}_2\text{O}:\text{Fe}^{2+},\text{Mn}^{2+}$, single cryst., spin-lattice relax. of ^1H and ^{19}F 9-35594
- $\text{ZnTe}:\text{Pb}$, photo-induced resonance of Pb^{3+} 9-47439
- ZnTe , Er^{3+} and acceptor co-doped, spectrum and photoluminesc. obs. 9-41431
- ZnWO_4 , Cr^{3+} anisotropic spin-orbit coupling obs. 9-33564
- ZnWO_4 , of Cu^{2+} and Ni^{2+} , spectra obs. 9-37802
- Zr-Co alloys, of Co, localized mag. moments investig. 9-33634
- ZrO_2 , monoclinic, Fe^{3+} spectrum 9-33627
- $\text{ZrSiO}_4:\text{Gd}^{3+}$, ground-state splitting 9-33626

Measurement

- apparatus for low fields, simple 9-45901
- dielectric resonator cavity, TE_{011} design curves and quality factor, spectrometer input 9-38326
- electron nuclear triple resonance in liquids, prediction and meas. method 9-44590
- flash photolysis spectrometer for paramagnetic species existing in a chemical reaction 9-33680
- high temperature maintenance of sample, method 9-45902
- spectrometer, for large zero field splittings meas. 4 mm 9-43818
- spectrometer, superhet $\lambda=10$ cm., microwave zero bridge 9-40298

Paramagnetic resonance and relaxation continued measurement continued

- spectrometer, two-transistor modulation amplifier 9-34127
- spectrometer and computer of average transients for transient paramag. species 9-29350
- techniques and applications, book 9-38338
- temperature control of samples, 10 to 80 K, automatic equipment 9-31882
- u.s. electron nuclear double reson. technique 9-29351
- Cu-Mn dilute alloys, electron spin resonance over 1.8°K to 300°K range 9-24489

Paramagnetism

- see also *Magnetic properties of substances/paramagnetic*
- alkali metals Raman scattering of light by spin waves 9-37738
- ferromagnet with domain structure, thermodynamic transition theory 9-31031
- field diffusion in nonlinear ferromag. medium 9-47895
- maghemite, Curie temp. estimation 9-35537
- magnetization curves, numerical calc. 9-26631
- metals, anomalous Hall eff. through ferroparamagnetism transition 9-28593
- spin-phonon modes, coupled, interpret. of excitation energies 9-49193
- spin-phonon system, thermal noise analysis 9-30760
- susceptibility, high field independence using Van Vleck formalism 9-24280
- ternary additions to permalloy for production of magnetic film for memories 9-36252
- thermodynamic and h.f. props. of paramagnet with negative anisotropy const. at low temp. 9-31022
- titanomagnetics, Curie temp. estimation 9-35537
- transient species, ESR spec. and computer of average transients for recording spectra 9-29350
- Co(III) complexes, residual paramag. obs. 9-35535
- CoCs_2Cl_4 , magnetic anisotropy 9-47230

Parametric amplifiers see Amplifiers**Parent see Nucleus; Radioactivity****Parity**

- see also *individual particles, e.g. Mesons/spin and parity*
- CP violation, superweak model supported 9-38509
- hadrons, K-parity for systems with SU(3) and charge-conjugation symmetry 9-42013
- non-conservation in axial interaction 9-36424

Particle accelerators**see also Ion beams**

- AGS gradient correction 9-46176
- beam loss due to ν_e - $N_e=1$ and $3\nu_e$ - $\nu_e=3$ resonances 9-46149
- coaxial Hall accelerator, analysis 9-22684
- conference, 1968 9-38604
- cybernetic, development of research 9-27602
- electrical technology, conference, New York, USA (1968) 9-29353
- electron, using electrodynamic space-charge effect 9-32278
- electron beam loading effect on parameters of accelerating systems 9-44096
- electron ring, 1000 GeV, use of static magnetic field 9-46170
- electron ring, method for static-field compression 9-46169
- electron ring 25 MeV beam injected into static magnetic field 9-46171
- electron rings suitable for ion accel., formation 9-22692
- electrostatic, ion-electron change-over type, ion beam energy determ. 9-22683
- engineering and technology, conference, Washington, USA(1969) 9-46145
- fast neutrons shielding, exp. studies 9-32274
- ferrites, nonlinear effects at high r.f. fields 9-47270
- heavy ion, 'double tube' version suggested 9-46155
- heavy ion, problems and techniques, review 9-46151
- heavy ion, sources, isochronous cyclotron at Dubna USSR, Tandatron, charge-change type, outline 9-46167
- high-energy, review, including those in operation, under construction, and proposed 9-36540
- ion, suitability and formation of electron rings 9-22692
- ions, heavy, Hartig accelerator, induced betatron oscills. and mag. deflectors 9-46164
- linear, formation of electron beam, calculations of transverse oscillations 9-29382
- liquid hydrogen target for 30Ma, 20GeV, electron beam 9-46181
- liquid hydrogen target techniques, improvements 9-46180
- low-energy facility data acquisition and analysis, time-shared computer complex 9-36543
- nuclear magnetometers, remote-controlled 9-36251
- nuclear research applic., performance characteristics and requirements 9-36541
- for nuclear spectroscopy, review 9-36555
- orbits and nonlinear effects in terms of field coefficients in the median plane 9-46147
- phase space dynamics of particles, book 9-40313
- proton, energies above 1000 GeV using collective interaction and coherent effects 9-46165
- proton linacs, beam dynamics 9-46157
- relativistic-electron rings, static compression 9-25547
- review of development since Veksler (1944) 9-25548
- shielding of 15 MeV neutrons 9-32273
- strong-focusing, limiting proton currents 9-32282
- synchrocyclotron, 600 MeV, design of meson channel 9-46178
- synchrocyclotron, Dubna, radial and axial betatron oscillations 9-44102
- synchrotron oscillations in storage ring, stability and growth rates 9-42163
- Van de Graaff, atomic spectroscopy by means of spectra of He and N 9-22998
- very high energy for isotope production, proposals 9-36542
- zero gradient synchrotron, refrigerated liquid hydrogen targets 9-46182
- e, low energy, utilizing photoelectric effect 9-46172
- p, the Los Alamos meson factory, popular article 9-48236
- d polarized sources and targets 9-38579
- p polarized sources and targets 9-38579

accessories

- beam (proton) profile monitor, non-destructive, using wire planes 9-25553
- beam extraction system, regenerative, for 180 cm synchrocyclotron 9-25554

Particle accelerators continued**accessories continued**

- beam transport in 300 MeV linac 9-46156
- cavities, r.f. Nb, fabrication 9-39605
- cavities, supercond. microwave, tuning 9-37482
- current monitors, non-intercepting, for 30 MeV electron linac drift tubes 9-36549
- deflecting maze-structure for obtaining short life e packets for injection 9-44097
- injector of negative polarized ions 9-38362
- instrumentation, conference, Montreal, Canada, Oct (1968) 9-32238
- integrator and meter with low input impedance, 10^{-8} - 10^{-4} A, current meas. 9-32284
- linac beam loss detection system using self-powered γ -ray detectors 9-36546
- magnets with vertical symmetry planes for ring accelerators 9-48245
- monitor for high energy electron beams, utilising detection of Cerenkov light from N_2 gas 9-29681
- particle accumulators, circular, autophase for relativistic motion 9-48244
- scattering chamber for Karlsruhe cyclotrons 9-25555
- storage ring for Orsay linac, electron-positron collision obs. 9-38630
- storage rings, stability and growth rates of relativistic bunch 9-42163
- sweep system for cyclotron beam 9-38626
- transfer system, 6 second, for cyclotron activated short lived isotopes 9-44300
- voltage divider of composite C resistors for accelerator terminal volts. meas. 9-40306
- zero gradient targetry syst. for ZGS 9-46183
- p beam monitor wire plane for zero gradient synchrotron 9-29678
- D³ bursts, prod. apparatus and use for producing neutron bursts from $^3H(d,n)^4He$ react. 9-27604
- Mg target, vacuum evaporation prep., thickness determ., 3 MeV Van de Graaff 9-29680

betatrons

- bremsstrahlung, determ. of time, correlation component of intensity envelope 9-27603
- design and polar determ. of e.m. field 9-42160
- electron ring beams, high current, dynamics, self field effects 9-36553
- magnetic contractor mechanism 9-42158
- oscillations for particles passing through a resonance, vertical damping eff. 9-46146
- plasma, axial field, runaway electron beam obs. 9-32280
- radiation generator for radiotherapy 9-46173

cyclotrons

- AVE, beam time structure, burst width control 9-22690
- AVF, external target irradiation 9-46179
- beam chopper for 60" fixed freq. cyclotron 9-48242
- beam collimator and shutter assembly with rotating radiation cooled elements 9-46150
- beam current spectral density and number of accidental coincidences, calc. 9-22689
- beams, energy measuring device 9-42159
- heavy ion isochronous, at Dubna USSR 9-46167
- ion, variable energy, Orsay, operation and heavy ion injection obs. 9-38629
- for ions A740, multi-charged, strong focusing ring cyclotron 9-22693
- isochronous, microstructure beam pulses intensity distrib. meas. 9-32279
- isochronous, with tandem injector for heavy ions 9-46166
- isochronous with separated homogeneous field magnets, orbit dynamics 9-44100
- Karlsruhe isochronous, scatt. chamber 9-25555
- Karlsruhe, energy resolution and distribution of external beam 9-25550
- Karlsruhe isochronous, beam property measurements 9-48243
- monoenergetic, for prod. of p, d, α , 3He , 6Li small energy spread beams 9-42161
- sub-nanosecond bursts in AVF cyclotron 9-22690
- sweep system for cyclotron beam 9-38626
- synchrocyclotron, 180 cm, regenerative beam extraction system 9-25554
- synchrocyclotron, beam extraction system 9-36551
- Li ion acceleration in the Kurchatov cyclotron (USSR) 9-42162
- Li ions, multicharged, acceleration in the Kurchatov cyclotron (USSR) 9-42162
- p, variable energy, Grenoble, design and operation 9-38628

linear

- 10 MeV/ft, two miles long, r.f. superconducting materials research 9-47093
- 20 GeV, 2-mile unit, special features 9-36548
- 30 MeV electron, non-intercepting current monitors for drift tubes 9-36549
- 50 MeV as injector for proton synchrotron NIMROD 9-46175
- ALS electron beam bunching 9-46148
- beam loss detection system using self-powered γ -ray detectors 9-36546
- deflecting maze-structure for obtaining short life e packets for injection 9-44097
- electron, 300 MeV, beam transport 9-46156
- electron, 300 MeV, construction and operation at Tohoku Univ. Japan 9-22688
- electron, 300 MeV, design, construction and tests 9-48238
- electron, 5 MeV, for X-ray generation 9-48239
- electron, appl. to neutron diff. obs. 9-42779
- electron, superconducting, 100 GeV, two mile, feasibility study 9-46163
- electron, superconducting, design of structures 9-47066
- electron beam in longitudinal magnetic field 9-48240
- electrons, 2 GeV, bunching of output 9-44098
- electrostatic, 4.5 MeV, description 9-36545
- EVA, 85 MeV electron accelerator at Amsterdam 9-22687
- heavy, from tandem linac with 20 MV at terminal and 60 μ A ion current 9-46162
- heavy ion, designing for 7 MeV/AMU for all stable elements 9-46160
- heavy ion, system for 7.5 MeV nucleon for elements from hydrogen to uranium 9-46161
- induction type, calculations 9-42157
- ion, with collective acceleration 9-22685
- ion longitudinal Coulomb repulsion, high beam phase space density 9-36544
- iris, electron packet beam along guide axis, transitional phenomena 9-46158
- MP tandem Van der Graaf, Yale, operating charact. 9-40460
- multisection, raising of current impulse limit 9-48237
- pre-accelerators, recent progress 9-22695

Particle accelerators continued**linear continued**

- proton, 10 MeV, focusing system, radial acceptance 9-34367
- proton, 50 MeV, injector voltage and r.f. fields setting-up method 9-44103
- proton, focusing syst., high field gradient 9-48241
- RPI, operation of vacuum system components when subject to intense radiation 9-36547
- shielding for electron accelerator as pulsed neutron source 9-32277
- SLAC, H target with coding system to prevent boiling 9-29677
- SLAC, time-of-flight system for use with 1.6 GeV/c spectrometer 9-29676
- storage ring for Orsay linac, electron-positron collision obs. 9-38630
- superconducting resonators, r.f. absorption measurements for TE and TM modes 9-47092
- tandem, 20 MV at terminal, 60 μ A ion current, for heavy ions 9-46162
- tandem Van de Graaff, energy calibration 9-25549
- tandem Van der Graaf, MP, Yale, operating charact. 9-40460
- tank tuning error sensitivity anal. 9-22686
- van de Graaff, suitable for teaching lab. 9-29153
- Van der Graaf, MP tandem, Yale, operating charact. 9-40460
- Au-W thick target bremsstrahlung spectra meas. with large NaI scintillation spectrometer 9-32276
- e, Saclay, design and performance tests 9-38625

synchrotrons

- 6 GeV Hamburg expts. (1965-66) 9-22525
- 50 MeV as injector for proton synchrotron NIMROD 9-46175
- 200 BeV unit, technical problems and design considerations 9-36552
- accelerated current depend. on pressure in Sirius vacuum compartment, exptl. determ. 9-44099
- background analysis for NASA 600MeV proton synchrocyclotron of short- and long-lived gamma rays 9-46159
- beam density distribution, measurement by means of flipping targets 9-46153
- beam detection, non-destructive, using residual gas ionization 9-46152
- beam profile, dynamic measurement using visible radiation 9-46154
- bremsstrahlung prod. on internal target, efficiency 9-25551
- heavy ion, beam dynamics problems 9-46168
- magnetic contractor mechanism 9-42158
- nucroton with plasma injector 9-22691
- oscillations in high-energy synchrotrons 9-44101
- proton, 45 GeV project 9-38627
- proton, computer studies of vertical beam blow-up during resonant ejection, Nimrod 9-29679
- proton, 70 GeV, applications and present status 9-46174
- proton current, internal, thermistor probe for meas., theory, design and results 9-25552
- quantum fluctuations of radiation and electron dynamics 9-47067
- resonance injection with two degrees of freedom 9-32283
- shielding embankment effectiveness meas. using cosmic ray μ , obs. 9-22694
- shielding layout, 300 GeV 9-32281
- spectrum in space charge cluster, mode instability 9-36550
- superconducting, replacing magnet pulsing by magnet rotation 9-46177
- Zero Gradient Synchrotron, wire plane profile monitor for p beams 9-29678

Particle beams

- 50 MeV line injector for 7 GeV proton synchrotron 9-46175
- analyzing system calibration using (p,n) threshold 9-25504
- beam-plasma interaction, asymptotic behaviour 9-48596
- beam-plasma interaction, nonlinear Vlasov theory 9-46472
- charged, Cherenkov plasma excitation, nonlinear theory 9-46466
- charged, near curvilinear emitter, formation 9-40314
- chopper, for use with 60" fixed freq. cyclotron 9-48242
- collimator and shutter assembly with rotating radiation cooled elements 9-46150
- collision damping in non relativistic case 9-45921
- from cyclotron, energy measuring device 9-42159
- cyclotron microstructure beam pulses intensity distrib. meas. 9-32279
- density distribution, measurement by means of flipping targets 9-46153
- double slit collimation system, improvements 9-29379
- gradient corrections for AGS 9-46176
- laboratory beam emission cross sections, systematic errors 9-41959
- loss due to ν - ν =1 and 3ν - ν =3 resonances 9-46149
- magnetosphere, oblique incidence streams, space-time relationships 9-31351
- matching with quadrupole lenses 9-41875
- motion in wind tunnel 9-39040
- neutron, partially polarised, associated particle method production 9-36613
- neutron collimation by rectangular tubes, Monte Carlo study 9-25180
- neutron source, reactor facility to operate -193 to 725°C 9-45922
- nonlaminar, with axial symmetry, internal structure 9-31911
- orbits and nonlinear effects in terms of field coefficients in the median plane 9-46147
- phase space dynamics, book 9-40313
- polarization expts., performance method 9-44182
- profile measurement, dynamic, using visible synchrotron radiation 9-46154
- proton, beam pulse system capable of prod. 4 MeV pulses of 0.15 ns duration 9-25194
- proton linacs, beam dynamics 9-46157
- slit mechanism for scatt. chambers, low background 9-40497
- spreading due to space charge forces, relativistic soln. 9-42155
- time of flight expts., efficiency improvement using random beam pulsing 9-42124
- α , with small energy spread, prod. 9-42161
- d, with small energy spread, prod. 9-42161
- n, fast, directional, from collimator, investigations 9-32275
- n, polarized, prod. from polarized p target 9-27560
- p, with small energy spread, prod. 9-42161
- p beam monitor wire plane for zero gradient synchrotron 9-29678
- 3He , with small energy spread, prod. 9-42161
- Li ions, multicharged, acceleration in the Kurchatov cyclotron (USSR) 9-42162
- 6Li , with small energy spread, prod. 9-42161
- neutron, transmission of slow polarized beam 9-27280

Particle detectors

- see also *Bubble chambers; Cloud chambers; Counters; Ionization chambers; Nuclear track emulsions; Particle track visualization*
- angular correlation, perturbed meas., finite time-resolution eff. 9-27578
- associated particle method, $^3\text{H}(\text{p},\text{n})^3\text{He}$, 1 MeV n flux meas., ^3He no. and direction determ. 9-29640
- association in nucl. reaction obs. 9-38605
- blocking patterns in solids, scanning by Ge, Ta 9-25529
- γ , avalanche-diode, high temp. charact. 9-25524
- conference, 1968 9-38604
- conference, Montreal, Canada, Oct (1968) 9-32238
- correlation techniques, appl. to locating structure in expt. data 9-44075
- cosmic ray neutron, for balloon and rocket expts., design and calibration 9-38602
- dosimeter, spherical, capsule type glass, improvements 9-27595
- electrometer, wideband integrating, for weak fluxes 9-25528
- electrostatic analyzer, (Hughes-McMillen 127°), energy resolution improvement 9-29642
- electrostatic analyzers, spherical plate, ang. response 9-29641
- gas discharges 9-38614
- identification of particles, on-line computer method 9-40451
- in-core, for monitoring intense rad. levels in pulsing reactor cores 9-36641
- n, covariance method of reactor-noise analysis via polarity detect. 9-34505
- neutron, cylindrical, with moderator, one-dimensional diffusion equation code PMC 9-44077
- particle-gamma angular correl. apparatus 9-44074
- photon, windowless, for soft X-ray and extreme UV, Spiraltron matrices 9-36527
- photoneutrons, (γ , xn) reactions simultaneous study, scintillation system 9-34362
- primary electron, for OGO-E satellite experiments 9-38022
- scintillation, for cosmic ray telescope of large area, high charge resolution 9-27571
- for Vela 4 satellite energetix particle experiment 9-38020
- β , γ , X-radiation, simultaneous, selective and versatile low level assembly 9-25530
- α , recording electrostatic energy analyzer 9-25535
- γ - ν angular correlation expt., resolution eff., energy calibration 9-34361
- n, Grey detector, efficiency determ. 9-48226
- N, high temp., tests to 650°C 9-36508
- n, polyethylene moderated ^3He detectors 9-48227
- n_{eff} , calibration of 32 Li-glass detectors array by ^{21}V , n isotropic scatt. 9-32263
- n diffractometer, time-of-flight, for cry. structure anal., focusing expt. 9-30548
- n flux distributions recording device for use in reactors 9-29643
- n flux monitoring apparatus, nuclear reactor alarm system, patent 9-32394
- p recoil telescope, n energy spectra anal., response junction 9-25532
- AgBr pure thin film 9-48231
- CsI(Tl) scintillator-Si photodiode, combination for γ -ray spectrometry, 180 keV to 1.5 MeV 9-27590
- Ge migration and precipitation of Li, control for detector production 9-26557
- Ge(Li) rise in isotopic ratio determination of U 9-27830
- ^3H monitor based on scintillation 9-25593
- Li ion implantation technique rel. to prod. 9-28532
- Ne flash tube, digitisation method for potential changes 9-27588
- Si, surface barrier type, for low energy H^+ , He^+ , N^+ , Ne^+ and Ar^+ 9-36518
- Si ΔE detector for π energy meas. 9-44090
- Si pn junction for high temp. operation 9-25525
- Si(Li), spherical segment shape, use in cosmic ray telescope 9-22645

Particle focusing see *Particle optics***Particle optics**

- see also *Electron optics; Ion optics*
- adiabaticity trajectories in cusped mag. field 9-44453
- apertures, circular, 'knife-edge', prod. method 9-45708
- beams of charged particles, theor. and expt. optics 9-38348
- betatron oscillations, radial and axial, of Dubna synchrocyclotron 9-44102
- biprism expt. with particles other than electrons 9-41874
- biprism expts. for particles other than electrons 9-38349
- charged particle motion in spatially homogeneous mag. field with exponential time decay 9-29378
- grid of r.f. mass spectrometer electrostatic analysis 9-25681
- lenses, electrostatic, axial pot., approx. calc. 9-41878
- magneto-optic systems with plane symmetry, propr. 9-45920
- mirror trap, particle motion 9-40682
- nonlinear, wave theory close to exact soln. 9-36256
- normal rotating quadruplet, acceptance phase 9-27279
- plasma, fast, injection into double bend mag. field, drift and purification 9-44413
- proton linac focusing syst., high field gradient 9-48241
- quadrupolar lenses in succession, focusing and aberrations 9-36257
- quadrupole doublets and triplets, waist-to-waist transfer props. 9-25179

Particle range see *Energy loss of particles***Particle size**

- see also *Surface measurement*
- aerosol, atmospheric, using light scatt. counters, influence of refr. index 9-28889
- aerosol, distrib. from spectral attenuation meas. 9-36905
- aerosol size classifier, sub-micron, calibration 9-34932
- aerosols, apparatus, patent 9-34934
- analysis and analyzers, average diameter techniques 9-26378
- Antarctic ice media, grain size rel. to extinction coeff. in rad. transfer 9-39992
- in colloid, distrib. from X-ray scatt. 9-36904
- rel. to crystal growth vel. of small particles 9-48791
- determination by composite method for particle size $<45 \mu$ 9-23611
- distrib. determ. X-ray small angle scatt. 9-40878
- distribution, opt. microscopy determ. rel. to dynamic methods 9-48101
- distribution analysis from field-ion microscope data 9-33117
- distribution in volume diffusion-controlled Ostwald ripening 9-39460
- effect on electron work function, theoretical 9-49155
- emulsions, by light scatt. 9-36906
- grain size distribution analysis 9-35225
- haematite, rel. to Morin transition and lattice spacing 9-32914

Particle size continued

- ice, grain size determ. from density and one of light attenuation coeffs. 9-45464
- lunar, size-frequency distributions 9-45660
- metal fine, prep. by gas evaporation method with plasma jet flame, lattice imperfection 9-33128
- in moving stream, size, velocity and position, technique 9-47719
- powder flowability, depend. 9-23610
- Saharan dust falling in Britain, July 1968 9-26900
- snow, grain size determ. from density and one of light attenuation coeffs. 9-45464
- steel, Fe(2.0 wt.%)V-(0.2 wt.%)C alloy, carbide coarsening, field-ion study 9-33118
- transport processes in particulate systems, and residence time distrib. effects 9-23539
- AlN, microcryst., surface modes and finite size effects, i.r. absorpt. meas. 9-37717
- Cu-Co single cryst. with precipitates 9-39428
- Fe-Mn nodules, of Fe oxide phase, determ. by Mossbauer effect 9-42786
- Fe, pure, grain size effect on lower yield stress 9-42881
- α -FeOOH, rel. to Neel temp. 9-47290
- LiF, effect on thermoluminesc. 9-41412
- LiF thermoluminescent dosimeter, efficiency depend. on grain size 9-22674
- NH_4ClO_4 , in pressed-strand prod., rel. to burning velocity 9-26814
- Nb₃Sn alloy, supercond., grain size, correl. with hysteresis charact. 9-39769
- Ni₃(TiAl) alloy, w.r.t. hardening by coherent and ordered precip. and yield-ing, model 9-39408
- Pb in brass, determ. from Cu K α X-ray absorption 9-24440
- ZnS:Ag, thermal recrystallization effects 9-30555

Particle spectrometers

- see also *Alpha-particle spectrometers, etc.*
- Browne-Buechner, magnetic, tangent focal plane approx. 9-44080
- channel multiplier, 0.5 to 500 keV electrons and protons, for ATS-E satellite 9-38023
- cosmic-ray muon, scattering correction, 6-316 GeV/c 9-22642
- directional analyser, electrostatic, for ion and electron velocity distributions 9-29372
- in electron linac, 300 MeV, beam transport 9-46156
- ion, design 9-37978
- magnetic, position-sensitive detector signal division by on-line computer 9-25503
- magnetic, uniform field with screens, fringing field distrib. 9-34352
- missing mass, with detect of 2 outgoing particles 9-22656
- n.m.r. instrument, operational details 9-41862
- photoproton, for use with high intensity electron accelerators 9-42129
- recoil proton, data, decomposition of empirical functions 9-32250
- scintillation, effective resolution improvement method 9-34350
- scintillation, electronic elimination of noise pulses 9-40456
- scintillation, random-summing effects, direct compensation 9-42128
- SLAC, time-of-flight system for use with 1.6 GeV/c spectrometer 9-29676
- solid state, random-summing effects, direct compensation 9-42128
- π^+ absorpt. in flight by complex nuclei, expt. set-up 9-22656
- Ge(Li) 2 crystal Compton spectrometer, γ spectra meas. 9-27584
- ^6Li , high resolution, for fast neutron spectra in thermal reactors 9-27791

Particle symmetry see *Elementary particles/symmetry***Particle track visualization**

- see also *Bubble chambers; Cloud chambers; Luminescence chambers; Nuclear track emulsions; Spark chambers*
- deuterium target within Ne-H bubble chamber 9-25542
- plastics, charged particle registration by restricted energy loss criteria 9-25540
- polycarbonate film, etching rate enhancement by photo-oxidation effect 9-32271
- reaction channel separation at exposure of bubble chamber to 2-10 GeV neutron beam 9-27599
- relativistic tracks prod. in emulsions in 40 kG mag. field, part. sign determ. 9-36538
- streamer chamber, Ne-He gas purifier 9-46143
- K $^-$, hyperfragments produced in 1.5, 3.0, 5.0 and 10.1 GeV/c interac. comparative study 9-48182
- AgBr pure thin film 9-48231
- U fission fragment tracks in Al foil, microscope exam. 9-34489

Particle tracks

- see also *Energy loss of particles*
- charged particle moving in a medium with ionization losses and in a non-uniform magnetic field 9-44094
- formation in solids, review 9-24067
- on polycarbonate film, enhancement of etching rates by photo-oxidation effect 9-32271
- scanning, digitized video, and computer analysis 9-36539
- α -particle scatt. from crystals, cellulose nitrate plastic for track recording 9-42763
- in CaO calcite, determ. 9-41123

Particle velocity analysis

- see also *Alpha-particle spectrometers; Beta-ray spectrometers; Energy loss of particles; Ion velocity; Mass spectrometers*
- charged, Lorentz force equation for orbital motion, numerical solution 9-31923
- directional analyser, electrostatic, for electrons 9-29372
- momentum in inhomog. mag. field calc. 9-31910
- Pb and In evaporated particles in vacuum, distribution 9-32818
- suspensions in liquids colloidal electrophoretic mobility meas. 9-46662
- p beam monitor wire plane for zero gradient synchrotron 9-29678

Particles see *Elementary particles; Energy loss of particles; Scattering, particles; and under individual particles, e.g. Protons and antiprotons***Paschen-Back effect** see *Spectra***Patterson diagrams** see *X-ray crystallography/calculation methods***Peierls-Nabarro force** see *Crystal imperfections/dislocations; Internal friction***Peltier effect** see *Thermoelectricity***Pendelösung fringes** see *X-ray crystallography***Pendulums**

- horizontal, oscillation period rel. to atm. density 9-40263
- length, humidity effect 9-45803
- seismograph, vertical, long periods, improved stability 9-24616

Pendulums continued

- spherical, analogue of dipole field motion 9-29164
torsion, precision, with electronic resetting mechanism, period weight sensitivity 9-34058

Periodic system

- see also *Elements*
No entries

Permalloy see *Iron alloys*; *Nickel alloys***Permeability, magnetic** see *Magnetic properties of substances*; *Magnetization process***Permeability, mechanical**

- see also *Diffusion in solids*
membrane, transport parameters 9-26087
phase separation, vapour-liquid, through wall at supersonic velocities 9-26163
polymers, of low mol. wt. penetrants, models, mechanisms and laws, review 9-39389
porous media, dusty-gas theory for thermal transpiration 9-39380
porous medium, effect on filtered mixing of mutually soluble liquids, with one-sided miscible displacement 9-39079
Pyrex glass, permeation of deuterium 9-40987
rubber, gas desorption and permeability in vacuum 9-39178
sinter bodies by non-wetting liquids, topological approach 9-23962
 α -Fe-C-N solid solution, disaccommodation, -40° to $+180^{\circ}$ C 9-26322
SiO₂, vitreous, of H₂, H⁺ transport contrib. 9-46856

Permittivity see *Dielectric properties of substances***Perturbation theory** see *Field theory, quantum*; *Quantum theory***pH** see *Electrochemistry***Phase diagrams** see *Phase equilibrium*; *Phase transformations***Phase equilibrium**

- see also *Solubility*; *Solutions*
Al-Si eutectic alloy, banding explanation 9-44613
alloy ternary and quaternary systems, temp.-conc. sections along curves or surfaces where a melt is saturated w.r.t. 2 phases 9-39130
alnico alloy, α and α' phases, saturation magnetization, temp. instability of permanent magnets 9-45149
ceramics, carbide-boride-graphite, fusion-cast, phase assemblages 9-30729
ceramics, stability of highly defective phases, review 9-30727
cholesterol propionate + n-azoxyanisole, melting and solidification diagram 9-40774
critical phenomena diluted solutions, thermodynamic props. near solvent critical point 9-26093
critical point of pure subst., asymmetry of density deflections 9-36915
cyclohexane-methanol mixtures, near-critical, interfacial tension 9-34886
eutectics, solidification, theory 9-46684
eutectics, solidification, theory comments 9-46685
Fermi-Bose mixture, isotopic, phase separation 9-36146
ferrimagnetic spinels, cation distrib., temp. depend. 9-35737
gas dynamics during volume heating and cooling 9-30344
glass, microheterogeneous, phase connectivity origin 9-26173
group II-VI compounds, solid-vapour and solid-liquid-vapour, rel. to crystal growth technique 9-36995
group IV-VI cpds. and alloys, deviations from stoichiometry and lattice defects 9-39483
high temperature, bibliography 9-41718
ice, vitreous, short ordering range 9-46699
III-V group ternary phase diagrams, quasi-chem. equil. model 9-44610
iron, lattice stability, review 9-48936
isothermal ternary systems, interphase stability 9-36934
lamellar eutectics, morphological interface stability 9-36935
liquid binary mixture, critical, diffuse interface, optical reflectivity obs., 9-39084
liquid-gas critical pt., theory 9-48679
liquid-vapour system, sound propag. near critical point 9-40824
liquids, immiscibility phase boundaries determ. from density meas. 9-40778
metal, liq. melts, vol. diffusion coeffs. rel. to equilb. charact. 9-39131
metal, stability, review 9-48936
Mg-Al eutectic alloy, superplastic deform. mechanism 9-42883
mutually soluble liquids, filtered mixing in porous medium with one-sided miscible displacement 9-39079
oxide systems, effect of cationic field strengths in liquids 9-23579
in polymer solutions 9-23463
rare-earth silicates, di- and trivalent 9-30752
sodium caprylate-water-ethylene glycol (glycerol) (tetraethylene glycol) system 9-23547
steel, austenitic containing Al and Ti, soln.-treated, equil. precip. formed on ageing obs. 9-46949
steel, C, mag. fields effect on martensitic pt. location 9-46959
steel, Cr-Mn, equilibrium diagrams for weld metals 9-23976
steel, Cr-Ni-Mo, orientation relationship between χ -phase and austenite 9-23951
ternary critical states, diffusion at and near 9-24518
Ticonal 600 alloy, comp. of α_1 and α_2 phases from mag. props. and microstructure evolution 9-44804
transition metal diagram computation, review 9-48936
transition metal difluorides, high-pres. stability obs. 9-37299
two-phase random medium, variational bounds on bulk props. 9-43754
water-dimethylsulphoxide system, phase diagram and stable hydrate form 9-32815
Ag-Bi eutectic, struct. of Ag-rich phase 9-37131
Ag-Ca, alloys, over whole comparison range by thermal anal., X-ray diff. 9-48937
Ag₂Te phase diagram 9-46956
AgBiSe₂-AgBiS₂ system, high-temp. β -phase, X-ray and neutron diff. studies 9-42782
Al-Bi system, thermodynamic obs. 9-46679
Al-In system, thermodynamic obs. 9-46679
Al-O system, P-T-x diagram, and existence of suboxides 9-26158
Al₂O₃-Y₂Al₂O₁₂ system, eutectic point position, microstruct. obs. 9-35254
Al₂O₃-SiO₂ system, metastable liquid immiscibility 9-32826
(1-x)Al₂LiO₃-xGeAlLiO₄ solid soln., spinel phase, stability domain boundaries 9-33119
Ar-methane, phase diagram 9-44803
Ar, liq.-gas phases coexistence curves 9-46688
Au-Cu-Zn alloys, β stability, and elastic anisotropy 9-46957

Phase equilibrium continued

- Au-Sn system, metastable γ -brass and non-equilib. Hume-Rothery phases 9-35255
BaCl₂-H₂O and BaCl₂-D₂O systems, polymorphic and dehydration boundaries to 40 kbar 9-28171
BaMnO₃, perovskite-like struct., stability relations at high pressure 9-35241
BaSO₄-SrSO₄-PbSO₄, subsolidus phase relations and lattice constants 9-23949
BaTiO₃, reduced and reoxidized, phase comp. 9-42939
Bi-(50-60at%)Te, characterization by X-ray diff. patterns 9-28394
Bi III-V and IV-V boundaries obs. from elec. resistance changes in piston-cylinder apparatus 9-41071
C, phase diagram, artificial diamonds prep. 9-33135
Ca-Yb system, f.c.c. and b.c.c. solid solns. in temp. range 900-400°C 9-30716
CaF₂-AlF₃ system, phase diagram, DTA and X-ray powder obs. 9-44805
CaO-MnO₂-ZnO₂-Fe₂O₄ system, phase diagram 9-46958
CaO-Ta₂O₅ system, to melting points 9-39494
CaO-ZrO₂ system, cubic phase existence, 1300° to 1700°C 9-23974
CaO.SiO₂-2CaO.SiO₂-ZrO₂ compositions and melting points of four ternary invariant points 9-33147
Cd-Hg alloys, thermodynamic investigations 9-48878
Cd(NO₃)₂-glycine-water system, exp. existence from viscometric and densimetric obs. 9-23461
CdO-Cr₂O₃-O₂ system, at high O pressures 9-28404
Cr-Mn steels, diag. for weld metals 9-23976
Cr alloys with Pt-series metals, similar ordering and mag. props. 9-33438
CsMnF₃, perovskite-like struct., stability relations at high pressure 9-35241
 α -Cu-Al alloys, short-range ordered state and stable superlattice phase obs. 9-39275
Cu-Nb-S system, vapour growth of new single-crystalline phases 9-37007
Cu-Th system, thermodynamic obs. 9-46679
Cu-MoO₃ phase diagrams in O₂, air and under O₂ press. 9-35256
CuRb(PO₃)₃, cry. struct. in Cu(PO₃)₂-RbPO₃ system 9-30561
CuTi(PO₃)₃, cry. struct. in Cu(PO₃)₂-TiPO₃ system 9-30561
Eu-Ti-O system, phase relations in portion of 1400°C isotherm 9-35257
Fe-(25 at%)Al alloys, electron microscope investig., magnetiz. and magnetocrystalline anisotropy 9-26648
Fe-Al alloys, long-range ordered phase, X-ray diff. obs. 9-44664
 α -Fe-Al superlattice phases, phase diagram and first order transforms 9-46952
Fe-Cr system, pressure infl. 9-41059
Fe-O system, phase boundaries 9-30741
Fe₂-O₂ transitions in single phase region, thermodynamic props. 9-28402
Fe₂O₃/Mg₂Fe_{2-x}O₄-(x-1)/2 spinel system, ferrimag., cation distrib. and temp. depend. in magnesioferrite 9-35737
(1-x)Fe₂LiO₃-x(GeFeLiO₄) solid soln., spinel phase, stability domain boundaries 9-33119
Fe alloys, effect of alloying element 9-33148
Ga-GaAs-GaP system, liquidus-solidus isotherms, GaAs₂P_{1-x} soln. growth obs. 9-36917
Ga-Sb system, liquidus curve 9-30449
Ga₂Te₃-impurity system, phase diagram 9-40934
Gd-Co system, intermetallic cpds. over whole conc. range and lattice const. 9-48921
Gd-Pb, determination by differential thermal analysis, metallographic and X-ray methods 9-41060
x(Ge₂Li₂O₁₂)-GeZn₂O₄ solid soln., spinel phase, stability domain boundaries 9-33119
Ge-Te-Ga-Te system, constitution diagram by conc. depend. of u.s. propagation velocity 9-28417
H₂O, modification at high pressure and temp. 9-26076
Hf-Cr binary system, diag. 9-33149
Hf-Si binary system, diag. 9-35258
Hf-V binary system, diag. 9-33149
HfO₂-Sc₂O₃ system, study by thermal and X-ray anal. 9-39476
Hg-Ga liq. alloy, form. enthalpies 9-30369
Hg-Sn liq. alloy, form. enthalpies 9-30369
In-As-Sb phase diagrams, quasi-chem. equil. model 9-44610
In-Ga-As phase diagrams, quasi-chem. equil. model 9-44610
In-Te system, thin films, phase composition rel. to conc. 9-30484
In₂Te₃-impurity system, phase diagram 9-40934
InSb, P-T diagram at high temps. and pressures 9-42922
K₂O-GeO₂ system, thermal expansion data for crystalline compounds 9-26398
KCl-AlCl₃-MgCl₂-H₂O quaternary syst., phase rule study, 25°C 9-23977
KTAO₃-K₂NbO₃ system, subsolidus stability relations 9-26157
Li/Na/KCO₃ eutectic mixture, diffusion of ²²Na and ¹⁴C 9-30625
Li-Na system, immiscibility phase boundaries determ. from density meas. 9-40779
Li₂SO₄-K₂SO₄ phase diagram from differential thermal anal. 9-48923
Li₂V₂O₇-O₂ phase relations 9-35328
LiCl-CrCl₃ system, on fusing 500-700°C, n.m.r. study 9-35259
Mg-Eu system, phase diagram 9-33150
MgO-Cr₂O₃-O₂ system, at high O pressures 9-28404
Mn-Ge alloys, phase diagram determ. using magneto-thermal methods 9-48938
Mn-In alloys, solid and liquid 9-31017
Mn-Ni constitutional diagram 9-39502
MnF₂, phase diagram 9-39184
Mo-Zn alloys prepared by reduction of volatile halides, phase diagram 9-39466
MoO₃-MgMoO₄ system, new phase from equilibrium diagram by thermo-optical method 9-23978
N₂-methane-ethane system, form. of ethane rich middle layer on cooling below -225°F 9-42698
Na-C-O system, three-phase, thermodynamic analysis, activities calc. 9-39127
(Na_{1-x}Li_x)NbO₃ solid solution ceramics, phase diagram 0° to 600°C 9-26389
NaNbO₃-BaNb₂O₇ system, liquidus and solidus equil. 9-39503
Nb₂O₅-Li₂O, rel. to stoichiometry of LiNbO₃ 9-36977
Nb₂O₅-WO₃ system, non-periodic shear struct., electron microscope obs. and evaluation 9-39291
NbN_x system, n.m.r. obs. 9-35726

Phase equilibrium continued

- $\text{Nd}_2(\text{MoO}_4)_3$ - $\text{Nd}_2(\text{WO}_4)_3$ system, differential thermal analysis and X-ray diff. obs. 9-37305
 Ni-Al-Sc system, Ni-rich, at 1000°C, identification, and solid solubility limits 9-30720
 Ni-Al, Si, Ti, alloys, γ' phase, coherent solubilities 9-28403
 Ni-Ga-B dil. alloys, during solidification 9-39136
 Ni-Re alloy films, electro-deposited, and chemical composition 9-44791
 Ni-Zn-Si system at 800°C, β and two ternary phases 9-35209
 Ni alloys, structure distortion from Cu-type 9-35064
 $\text{NiO-Cr}_2\text{O}_3\text{-O}_2$ system, at high O pressures 9-28404
 Pb-Sn-Te system, diagram 9-36918
 Pb alloys, binary, equil. partition coeff. rel. to strength 9-44772
 Pb binary alloys, partition coefficient relation with strength 9-26399
 $\text{PbF}_2\text{-AlF}_3$ system, phase diagram, DTA and X-ray powder obs. 9-44805
 $\text{PbO-Cr}_2\text{O}_3\text{-O}_2$ ternary system, relations and reactions at high temps. 9-28405
 PbTe-CdTe alloys 9-42923
 PbTe-EuTe system, investigation by thin film techniques 9-39486
 Pd-Si based alloy glasses, stability 9-42706
 Pd alloys, structure distortion from Cu-type 9-35064
 Pt alloys, structure distortion from Cu-type 9-35064
 Pu-(0-10at%)Zr, equil. phase diagram 9-37306
 RbNiF₂, perovskite-like struct., stability relations at high pressure 9-35241
 $\text{Rh}_2\text{Cu}_2\text{Ni}_{1-x}\text{O}_8$, new orthorhombic phase with $0.12 \leq x \leq 0.175$ 9-30704
 Sc-Ni system, (Ni-rich), phase identification at 1000°C 9-30720
 SiC-B₂C-C system, struct. of SiC phase from 2200 to 2550°C 9-48939
 Sn-Zn eutectic alloy system, morphology changes 9-46681
 SrMnO₃, perovskite-like struct., stability relations at high pressure 9-35241
 Th-ThO₂, thermal, X-ray and microscopic techniques analysis 9-41061
 Ti-Al-Ce alloy system, diagram for Ti-rich corner, struct. obs. 9-40919
 Ti-Al alloy, diagram, study on Ti-rich region 9-26381
 Ti-(8 wt.%)Mn alloy, ω and martensite, microstructures, electron micro-scope obs. 9-35214
 Ti-(5 at.%) Mn alloy martensites, electron microscope obs. 9-39311
 Ti-Se system, immiscibility phase boundaries determ. from density meas. 9-40779
 TiNiF₃, perovskite-like struct., stability relations at high pressure 9-35241
 U-C-O-N system, relations at 1700°C 9-26400
 U-Al₂-Al₃Mo₂-Mo system, melting equil. 9-39133
 S-U₂O₈, existence of δ phase 9-28271
 UF₆-WF₆, eutectic mixture props. obs. at liquid-solid transition 9-23580
 UF₆-WF₆, eutectic mixture props. obs. at liquid-solid transition 9-34953
 UO₂-Cu alloy, phase diagram and investigation of system 9-28395
 Zn-Cd alloys, solute trapping by rapid solidification 9-26160
 ZnO-B₂O₃ syst., lamellar glass-cryst. structures from eutectic solidification 9-36930
 Zr-C system, phase and lattice parameter ranges 9-30754
 Zr-Nb system, $\alpha/(\alpha+\beta)$ boundary, microprobe determ. 9-28406
 Zr-Si binary system, diag. 9-35258
 Zr-(25 at.%) Ti alloy, ω phase, as-quenched form, electron diff. and micro-scopy obs. 9-37307
 Zr-W system, high-temp. relationships, m.p. and X-ray data anal. 9-48940
 Zr(HPO₄)₂, rel. to ion-exchange props. 9-26208
 Zr(HPO₄)₂·2H₂O, rel. to ion-exchange props. 9-26208

Phase flow see *Flow/two-phase*

Phase meters see *Electrical measurement*

Phase transformations

- Al-Si eutectic alloy, banding explanation 9-44613
 binary mixtures near critical point, kinetic phen. 9-48735
 bitumens in rubber transition zone, u.s. absorption and dispersion 9-30450
 Bose gas, condensation 9-47783
 Bose liqs., two models giving first order phase transition 9-40258
 bubbles and continuous phase, gas interchange in gas-solid fluidized bed 9-40823
 n-butyl alcohol determ. by luminescence obs. 9-42692
 cement mortar, hardening obs. of stress-strain curves 9-37230
 CO₂ exchange at air-water interface, effect of hydration 9-30453
 critical phenomena, dynamic, scaling laws 9-22127
 near critical point, laminar Couette flow, wall heat transfer and skin friction 9-23374
 crystal, new-phase nucleus, growth kinetics, theory 9-48811
 crystal at liquid-solid transition at T=0, sound wave 9-35273
 crystallization of solid cylinder in supercooled liq., stability of shape 9-35023
 drop, centre of mass fluctuations, and homogeneous nucleation theory, embryo equil. distrib. 9-36923
 drop, centre of mass fluctuations, and homogeneous nucleation theory, embryo equil. distrib. 9-46683
 in earth's mantle at 200 to 1200km depth. 9-45455
 eutectoid and eutectic transf., solute diff., distrib., boundary value problem, soln. 9-26149
 F model, low-temp. series 9-41778
 f.c.c. crystals, stability limits 9-44611
 in flow, 2 phase 9-25822
 fluid binary systems, high press. and temps., apparatus 9-28182
 gas of long thin rods, two-dimensional, order-disorder 9-34828
 gas separation, from mixture, to solid phase, patent 9-23606
 gas-liquid critical point, lattice gas model 9-36924
 glasses, Na₂O-SiO₂, primary and secondary phase separation 9-30455
 He, near λ point transport coeffs. determ. by single frequency 9-26147
 ice-water vapour, ice-water, ice-ice boundaries, surface free energies, exptl. determ. 9-39153
 ketones, i.r. spectrum at transition liq.-solid 9-32520
 Kirkwood instability for hard rods 9-29219
 Lennard-Jones system 9-46687
 liquid, field-induced, mol. interaction and optical Kerr effect 9-23498
 macromolecules, multistranded, first-order transitions 9-23181
 macromolecules, two-stranded, higher-order transitions 9-23180
 many-body system condensing in periodic and homogeneous states 9-34040
 mesophase-forming materials, depolarized light intensity and optical micro-scopy 9-32764
 metal matrix composites, controlled solidification using monovariant eutectic reactions 9-36921
Phase transformations continued
 metals, gas to liquid transition of interstitial H, phase diagrams and solubility meas. 9-35122
 metals, laser beam interaction, time-dependent liquid-vapour ratio 9-48738
 metals and alloys, liq. to solid, nucleation phenomena 9-48736
 methane, orthobaric density in critical region 9-48739
 methyl alcohol, determ. by luminescence obs. 9-42692
 NaCl-H₂O system, phase entropy diagrams for different compositions 9-26161
 phase transition, second-order, impurity effects near critical point 9-46678
 poly(β -naphthyl methacrylate) in 4 solvents, critical opalescence 9-28144
 poly(β -vinyl naphthalene) in 3 solvents, critical opalescence 9-28144
 poly(butyl methacrylate) in isopropanol, critical opalescence 9-28144
 poly(dimethyl siloxane) in tetralin, critical opalescence 9-28144
 polyethylene-diphenyl ether; critical point determ. method 9-28173
 polypropylene, pressure-crystallized, structure and thermal behaviour of phases formed 9-46711
 polystyrene-cyclohexane; critical point determ. method 9-28173
 n-propyl alcohol determ. by luminescence obs. 9-42692
 second order, generalized Landau ansatz appl. 9-26153
 second order phase transitions, Landau theory modified near critical point 9-31782
 second-order exact thermodynamics and rigorous exponent equalities near transition line 9-23575
 semiconductor-metal transition in SmB₆ and transition metal oxides, model 9-33279
 statistical theory 9-47773
 superfluid, in one and two dimensions 9-34048
 of systems, propagation of acoustic waves 9-29270
 thermodynamic perturbation theory applied 9-34036
 thermodynamics quantities at transition points, averaging of singularities 9-47775
 two-phase media, nonequilibrium thermodynamics 9-46677
 vapour and liquid solutions, entropy determ. 9-26161
 vapour-liq. equil., binary and ternary mixtures, vapour composition graphical determ. 9-23587
 water, transition obs. using sound velocity meas. 9-40772
 water-argon system, high press. and temps., apparatus 9-28182
 Ag/Au/Si system, controlled solidification using monovariant eutectic reactions 9-36921
 Al₂O₃/Y₂Al₂O₇ system, eutectic solidification 9-34960
 Ar, critical region P-V-T meas., theory and expt. 9-28174
 Bi-Te alloys, nucleation, NMR obs. 9-23583
 Bi nucleation, eff. of small addition of solute 9-28180
 Bi nucleation, NMR obs. 9-23583
 Bi nucleation, supercooling depend. on liq. drop size 9-28179
 C/Cr/Ni/Si system, controlled solidification using monovariant eutectic reactions 9-36921
 C, graphitizing, formation by solidification from liq. or plastic state 9-48743
 Fe alloys, solidification, growth morphology and solute segregation 9-23952
 H, supercond. solid to liq. under influence of zero pt. energy 9-42738
³He-⁴He mixtures, liquid-solid transition obs., freezing curve drawn 9-32804
 KH₂PO₄, slater model, first order transition 9-45008
 Na₂O-SiO₂ glasses, primary and secondary phase separation 9-30455
 Na borosilicate glasses, phase-separated, viscosity and transform. temp. 9-46680
 O₂, molec. motion in condensed phases, Raman obs. 9-49296
 O₂, solid, temps. at transition points, obs. 9-40289
 Pb nucleation, supercooling depend. on liq. drop size 9-28179
 Pb nucleation, eff. of small addition of solute 9-28180
 Pd-Si based alloy glasses, glass-liq. obs. 9-42706
 SbSI, hysteresis, nonequilibrium carrier effects 9-24233
 Sn-Zn eutectic alloy system, morphology changes 9-46681
 Sn nucleation, eff. of small addition of solute 9-28180
 Sn nucleation, supercooling depend. on liq. drop size 9-28179
 SrTiO₃, at 108°K, lattice parameters change, meas. and obs. 9-30748
 Zn-Cd alloys, solute trapping by rapid solidification 9-26160
 Zr-W system, high-temp. relationships, m.p. and X-ray data anal. 9-48940
solid-state
 see also *Ageing*
 $\alpha/(\alpha+\beta)$ boundary in the Zr-Nb system 9-41062
 alkali metal nitrates, temp. depend. of elec. conductivity during phase transitions 9-24115
 alloys, eff. of radiation 9-24068
 alloys, ordering strains, relief by twinning 9-35252
 alnico, decomposition of solid soln. from X-ray diff. anal. 9-39473
 aluminium methylammonium alum., in phases I and II, elementary cell parameters, temp. depend. 9-42927
 ammonium halides, to 40 kbar 9-30452
 aragonite to calcite to lime, electron microscope obs. 9-26385
 binary system, diffuseness growth of new phase 9-35015
 binary system forming eutectic mixture, crystallization dynamics 9-23963
 borohydrides of Li, Na and K 9-43308
 β -brass, metastable, martensitic transformations, heat treatment, n. irradi. and deformation effects 9-23981
 β -brass, neutron-irrad., thermal cycling, martensitic start temp. obs. 9-42928
 t-butyl chloride 9-39670
 carbon tetrachloride 9-32903
 ceramic systems, effect of very high pressure 9-30553
 ceramics, press-forging 9-35216
 clinostatite, inversion at high temp., rel. to all Mg pyroxenes 9-42934
 coesite-stishovite, 550 to 1200°C and 82 to 98 kb 9-28399
 copolymers of butene with α -olefins, obs. 9-32880
 critical phenomena, neutron scatt. applic. 9-48926
 crystal growth mechanism 9-23661
 crystal lattice change detection by technique based on shadow effect 9-28242
 cubic to tetragonal, macroscopic periodicity theory 9-26384
 cupric formate tetrahydrate, struct. changes rel. to paraelec.-antiferro. transition, DMR obs. 9-35730
 cyclohexanol, growth rates and morphology 9-35251
 cyclohexene 9-43305

Phase transformations continued
solid-state continued

- diamond formation from graphite in presence of metals, mechanism 9-41064
- f.c.c. ternary alloys, order-disorder critical temp., conc. depend. 9-28401
- first order, resembling 2nd order, thermodynamic derivatives 9-39488
- germanate albite under pressure 9-42933
- graphite, graphitization and chem. structure, X-ray diffraction studies, samples from polynuclear aromatics 9-39257
- group IV-VI cpds., rocksalt structure, theory 9-39487
- hafnia-rare-earth oxides solid soln., metastable to stable phase separation 9-30723
- hard sphere cell model 9-48925
- heptane rel. to quinoline-heptane frozen solns. phosphoresc., 55-123°K 9-28726
- hexane rel. to quinoline-hexane frozen solns. phosphoresc., 55-123°K 9-28726
- ice, vitreous, short ordering range and transform. to diamond cubic struct. 9-46699
- internal friction at low temps. 9-41005
- limestones and marbles, compressional velocity data representation near Lambda transition 9-46884
- magnetic, double-shock method for pressure limit detection 9-35524
- (225), martensite transf., plastic accommodation 9-26383
- martensitic, crystallography rel. to fine structure in transmission electron micrographs 9-28397
- martensitic, effect of stresses in mechanism 9-33134
- methane, A and T nuclear spin systems mixture 9-35240
- methane-d₂, upper transition, quantum statistical treatment 9-48933
- methane-d₄, upper transition, quantum statistical treatment 9-48933
- Methane-methane-d₄ solid soln., upper transition, quantum statistical treatment 9-48933
- molecular crystals, order-disorder, theory 9-41070
- nucleation models for 1st-order transition front 9-42924
- nylon 66, rel. to double melting obs. 9-34954
- olivine-garnet in meteorite 9-27089
- ordering, early stages, applic. of model for diffusion on cubic lattices 9-30622
- oxide particles in metal matrix, coagulation 9-44787
- perovskite, cell deformation parameter behaviour near transition pt. rel. to elec. ordering 9-33032
- polybutene II-polybutene I accelerated by comonomers 9-32880
- polyethyleneglycoladipate, α -, p-bis-(β -hydroxy-ethoxyphenyl)enediadipeate) copolymers, glass temp. rel. to component concs. 9-30473
- polymers, cryst., shock wave induced, obs. 9-30733
- polyoxypropylene, rupture and change in supermolecular structure 9-28362
- polypropylene, low-molecular-weight fractions on crystallization 9-46714
- polyvinylfluoride, dielec. props. rel. to glass-rubber transition, obs. 9-30962
- pressure-induced transf., behaviour, visual obs. 9-30735
- pyrites, exoelectron emission during transformations, 300°-650°K 9-24248
- quantum -Coulomb plasmas, first-order phase transitions' mechanism, model 9-23574
- quartz, shock-induced preferred disorder 9-42938
- quartz α - β transition, small-angle X-ray scatt. 9-39931
- rare-earth oxides, high temp. obs. 9-30736
- refractory oxides, high-temp. obs. 9-30736
- Rochelle salt, ferroelec. phase transitions, e.s.r 9-30972
- second order, in crystals of space group O_h 9-42925
- silica, vitreous, metastability of high cristobalite 9-48932
- specific heat, singularities at transition points of second kind, qualitative characts. 9-44832
- spinel, high pressure and temp. rel. to earth's mantle 9-44793
- spinel decomposition in tetragonal system 9-33144
- steel, (Cr,Fe), C₂ identification and transform. obs. 9-48831
- steel, austenitic, initial state eff. on martensitic transformation 9-23966
- steel, austenitic stainless, metastable, austenite to martensite transform, during plastic straining 9-35178
- steel, carburized Cr-Mo, behaviour and C content effect 9-41073
- steel, Cr-Mo, isothermal and continuous cooling transform. diagrams 9-23968
- steel, Fe-Mn-C, austenite-martensite transform., charact., X-ray diff. obs. 9-46948
- steel, martensite (225), habit plane line lengths comparison with austenite before transform. 9-42931
- steel, martensite decomposition at low temp. 9-23964
- steel, martensite transf., obs. using hot-stage X-ray diff. meas. 9-39495
- steel, martensitic transform., twinning obs., electron microscopy 9-46744
- steel, pearlite, growth, alloying elements and press. effect 9-42930
- steel, plastic deform., ferrite recryst. p- α transf. 9-37295
- steel, quenched, carbide phase formation during low-temp. tempering, mechanism 9-33137
- steel, structural recrystallization, effect of phenomena in α -phase 9-33136
- steel, Widmanstätten ferrite form 9-46947
- steel castings, 18-8 Mo stainless, rel. to high temp. strength props. 9-44771
- sulphospinel, pressure-temp. relations 9-26392
- tetragonal system, spinodal decomposition 9-33144
- transition metal difluorides, high-press. stability obs. 9-37299
- transition metal molybdates, anion coordination and volume changes 9-35244
- transparent mats., pressure-induced transf. behaviour, visual obs. 9-30735
- two-phase system, rel. to internal friction theory 9-33018
- vinyl acetate methyl acrylate copolymer possible glass transition at 21°C 9-33010
- zirconia, high-temp. obs. 9-30736
- zirconia-rare-earth oxides solid soln., metastable to stable phase separation 9-30723
- AGi, p- to β -phase, decrease in conductivity 9-33379
- Ag-Cd β -phase alloys, order-disorder transf., Hall coeffs., elec. resistivity 9-35253
- Ag-Zn β -phase alloys, order-disorder transf., Hall coeffs., elec. resistivity 9-35253
- Ag-Zn equiatomic alloy, β '- α ' transform., stress effect 9-30737
- Ag-Zn equiatomic alloys, β '- α ' and β '- α ' transform. 9-33145
- Ag₂S, order-disorder and ht. capacity 9-39526
- Ag₂S, thin film, comparison with bulk state 9-48927

Phase transformations continued
solid-state continued

- Ag₂Se, thin film, comparison with bulk state 9-48927
- Ag₂Te, thin film, comparison with bulk state 9-48927
- Ag halides, B1-type, press.-induced struct. changes, X-ray diff. obs. 9-41063
- AgI, ht. capacity and order-disorder transition 9-39527
- AgNO₃, orthorhombic-rhombohedral at 159°C, thermal expansion data 9-35287
- Al(15wt.%Ag) alloys, h.c.p. γ plates formation mechanism, e microscopy 9-30738
- Al-Cu-Ag alloy, resistivity charges rel. to formation and dissolution of Ag-rich zones 9-46758
- Al-Fe alloys, Fe-rich, transf. diagram constant., applic. of dark ground e microscope 9-33131
- Al-Si subeutectic alloy, thermal stresses calc. by phase suspension model 9-23948
- Al-Zn alloys, spinodal decomp. rel. to yield and tensile strengths, ductility and hardening 9-37289
- Al-Zn alloys, spinodal struct. formation, stability and breakdown rel. to Zn conc. 9-37290
- Al₂O₃-SiO₂ glasses, amorphous- cryst., and metastable glass-in-glass separation 9-32826
- Al₂O₃-3H₂O, to Al₂O₃ by treatment with plasma jet 9-46945
- Ar-N mixtures, enthalpies 9-39528
- Au/Pb supercond. layered films, composition and transition obs. 9-26528
- Au(50 at.%)Cd alloy, martensite, influence of plastic deformation 9-39491
- Au(46 at.%)Cu(4 at.%)Ni alloy, order transform. of type $\alpha_{\text{disorder}} \rightarrow I_{\text{order}}$ radiocrystallog. study 9-37304
- Au-Mn alloy, martensitic, near equiatomic composition 9-26379
- AuCu₃, order-disorder eff., reflectivity and photoemission 9-26395
- AuCu₃, order transform. of type $\alpha_{\text{disorder}} \rightarrow I_{\text{order}}$ radiocrystallog. study 9-37304
- B₂O₃-PbO-Al₂O₃ system glasses, spinodal decomposition 9-39492
- BN, pyrolytic, from compression annealing and hot working 9-41041
- BaMnO₃, perovskite-like struct. at high press., stability relations 9-35241
- BaTiO₃, annealed and glassy, four fold coordination in glassy struct. 9-32827
- BaTiO₃, high resistivity, cubic-tetragonal transitions obs. 9-43115
- BaTiO₃, nucleation models for 1st-order transition front 9-42924
- BaTiO₃, reduced and reoxidized, phase comp. 9-42939
- BaTiO₃, tetragonal-cubic, rel. to chain structure 9-32901
- Bi, supercond. amorphous, transition temp. obs. from phonon spectrum 9-41076
- C, dynamically compressed, metallic state existence 9-30847
- C, hard, partial graphitization above 2000°C, structures present 9-28396
- C fibre, polyacrylonitrile based, stress graphitization 9-39493
- C film, evaporated, graphitization under heat treatment, 1000° to 2200°C 9-39453
- C glassy, graphitization, role of strain 9-23980
- Ca-3wt.%Al-0.6wt.%Cu alloy, structural changes during precipitation of a hard solution 9-44789
- CaAl₂O₄, high pressure transformations 9-44799
- CaO-Ta₂O₅ system, diagram 9-39494
- Cd-Hg alloys, thermodynamic investigation 9-48878
- Ce, p- α transition, positron annihl. obs. 9-46946
- Ce, low-temp., effect on elastic moduli, adiabatic compressibility and Debye temp. 9-40997
- Ce, transition to tetravalent state under press. 50 kbar 9-41072
- Co-Ni alloy, martensitic, under tensile stress 9-26386
- Co-Ni alloys, $\alpha = \beta$ friction meas., -190° to 500°C 9-39400
- Co-Ni alloys, kinetics and internal friction 9-37298
- Co(30.5wt.%)Ni alloy, allotropic transform., stress effects 9-23975
- Co, $\beta = \alpha$, eff. on constitutional, fine structure and conc. of structural defects. 9-23804
- Co, h.c.p.-f.c.c., effect on oxide film struct. 9-32841
- Co, polymorphism rel. to atomic size factor 9-46954
- Co₂La₂(NO₃)₁₂·24H₂O, mag. ordering, obs. 9-39781
- CoF₃, pressures up to 160 kbar 9-44800
- CoO:Li monoxide to spinel, role of cation vacancy density 9-48929
- CoO, from elec. conductivity press. depend. obs. 9-35338
- Cr-Mo steels, isothermal and continuous cooling transform. diagrams 9-23968
- Cr-steels, α - γ phase, embrittlement by neutron irradiation 9-28369
- CrCl₃, neutron-irrad., effect of α to β transform. on rare gas diffusion 9-33004
- CsFeF₃ hexagonal to lower symmetry at 83°K, rel. to magnetiz. and Mossbauer studies of ⁵⁷Fe 9-45058
- CsI, neutron-irrad., effect of α to β transform. on rare gas diffusion 9-33004
- CsMnF₃ perovskite-like struct. at high press., stability relations 9-35241
- CsPbCl₃, rel. to crystal growth 9-39211
- CsPbCl₃, n.q.r. determ. 9-41058
- Cu(14.95 wt.%)Sn alloy, b.c.c. to orthorhombic γ_1' martensitic, crystallography 9-30739
- Cu-Al alloys, martensitic, effect on strength and deform. behaviour 9-35172
- Cu-Al martensitic cryst. struct. stability, solute content effect 9-42929
- Cu-Be-Co dil. alloys, constitution and behaviour 9-39274
- Cu-Fe dilute alloys, martensite nucleation in Fe precipitates 9-37300
- Cu-Ga alloys, massive and martensitic transform. temp. 9-41066
- Cu-Mn-Al on heat treatment and ageing 9-37293
- Cu-Ni-Fe alloys, spinodal decomposition, electron microscope study 9-35242
- Cu-Sn alloys, martensitic, effect on strength and deform. behaviour 9-35172
- Cu-Ti-Al aluminium additions, effect on decomp. kinetics 9-37292
- β_1 -Cu-Zn alloy, martensitic, effect of neutron irradiation 9-37296
- Cu-Zn β -phase alloys, order-disorder transf., Hall coeffs., elec. resistivity 9-35253
- Cu₂Se, thin film, comparison with bulk state 9-48927
- Cu₂Te, thin film, comparison with bulk state 9-48927
- Cu₂La₂(NO₃)₁₂·24H₂O, mag. ordering, obs. 9-39781
- Cu₂-Te, tetragonal, γ and γ' disordering modifications 9-42937
- CuAu II alloy, from CuAu II of disorder 9-30750
- CuFe₂O₄- α -Fe₂O₃ mixture, reaction and phases formed on heating, rel. to Cu₂Fe₂O₄ spinel formation 9-30740
- CuO-MoO₃ phase diagrams in O₂ air and under O₂ press. 9-35256
- CuPt alloys, energy of ordering tin soln. calorimetry 9-48934

Phase transformations continued
solid-state continued

- α -Fe-Al, superlattice phase changes and equilib. 9-46952
 Fe-Al alloys, Fe-rich, transf. diagram construct., applic. of dark ground electron microscope 9-33131
 Fe-C alloy, (225) γ , martensitic shape strain 9-28344
 Fe-C alloys, during tempering and cold plastic deform., singularities 9-39496
 Fe-Cr system, pressure infl. 9-41059
 Fe-(30.50wt.%)Ir alloys, $\gamma \rightarrow \alpha$ and $\gamma \rightarrow \epsilon$ transform. rel. to Ir content, dilatometric meas. 9-41067
 Fe-Mn-C alloy, (225) γ , martensitic shape strain 9-28344
 Fe-N alloys, martensite transform. start temp. composition dependence 9-23982
 Fe-Ni-Al alloys, decomp. of supersaturated solid solns., elastic stresses effect 9-39475
 Fe-Ni-C alloy, (259) γ , martensitic shape strain 9-28344
 Fe-Ni-C martensites, twinning during phase transf. in fine struct. obs. from electron micrograph 9-26233
 Fe-Ni-Mn-Ti martensitic alloys, pre-precip. stage obs. during ageing 9-37283
 Fe-(30wt.%) Ni alloy, martensite, isothermal transform., use of Kaufman and Cohen's model 9-46950
 Fe-(30 wt.%)Ni alloy, electron energy spectra sensitivity to $\alpha \rightarrow \gamma$ transform. 9-39856
 Fe-(27wt.%)Ni austenitic alloys, effect of Al, Si, Mn, and Cr on martensite form. during plastic deform. 9-41068
 Fe, $\alpha \rightarrow \gamma$ rel. to diffusion kinetics of Cu 9-46851
 Fe, $\alpha \rightarrow \gamma$ transformation, internal friction singularities 9-23857
 α -Fe, kamacite, shock-induced preferred disorder 9-42938
 Fe, polymorphism rel. to atomic size factor 9-46954
 Fe, shock-compressed, $\alpha \rightarrow \epsilon$ -phase transition, conductivity and demagnetization obs. 9-26388
 Fe₃Al, long-range order variation near transition temp. 9-26397
 Fe₃C, cohenite, shock-induced preferred disorder 9-42938
 Fe₃O₄, low temp. transition, Mossbauer spectra changes, 85°-298°K 9-28668
 Fe₃P, schreibersite, shock-induced preferred disorder 9-42938
 Fe alloys, (225) γ , martensite transf., role of plastic accommodation 9-26383
 Fe alloys, effect of alloying element on allotropic transform. 9-33148
 FeLiO₂, α , α_{II} and β phases, order-disorder transf., differential thermal analysis 9-26396
 FeLiO₂, ordered and disordered phases, short range order, from X-ray diff. meas. 9-48935
 Fe-Ni-Cr alloys, martensitic, eff. of Cr content 9-23965
 Ga, supercond. amorphous, transition temp. obs. from phonon spectrum 9-41076
 Ge-As solid solution, new phase precipitation mechanism 9-35243
 H₂-D₂ mixtures, phase separation 9-23983
 o-H₂, orientational order-disorder obs. 9-46955
 H₂, solid, rel. to $(\partial P/\partial T)_V$ meas. 9-26424
³He, cubic to hexagonal form 9-34948
 HfO₂-Sc₂O₃ system, phase diagram study by thermal and X-ray anal. 9-39476
 HfO₂-ZrO₂ phase diagram determination 9-23991
 ice:Fe²⁺, Sn⁴⁺, Eu³⁺, conc. depend., Mossbauer obs. 9-33140
 In-Th alloys, elastic and anelastic behaviour during martensitic transform. 9-42865
 In-Tl alloys, f.c.c.-f.c.t. transition, thermal expansion in vicinity 9-28434
 In, and structural changes, use of coordinate correlation of valence electrons 9-46741
 In₂O₃, anion coordination and volume changes 9-35244
 InSb-GaSb alloy, press-induced transform, behaviour 9-37301
 InSb-InAs alloy, press-induced transform, behaviour 9-37301
 InTe, high-pressure polymorph, neutron effects on phase stability 9-35250
 K₂Fe(CN)₆, rel. to polarization, dielec. props. and stability criteria, theoretical analysis 9-41240
 KH₂PO₄, u.s. attenuation obs. of critical points 9-37302
 KMnF₃, due to softening of phonon modes 9-33155
 KNO₃ 9-32903
 KNbO₃, tetragonal-cubic, rel. to chain structure 9-32901
 (KPO₃)_n, Weissenberg photographs obs. 9-35245
 [(1-x)La, x Ca]MnO₃ 9-33127
 Li-NH₃ systems, low-temp. 9-39531
 (Li₂O.MgO).Al₂O₃-nSiO₂, thermally crystallized, high-quartz solid soln. phases 9-28398
 Mg-Sn alloys, solution hardening, room temp. 9-23984
 Mg-Zn-Zr cast alloy system, conversion of non-equilib. dendritic growth forms of phase ZnZr 9-41056
 Mg₂SiO₄, high press. phase, cry. struct. and chem., geophys. implications 9-40908
 Mg pyroxenes, from study of inversion in clinoenstatite 9-42934
 MgCd, recrystallization rel. to grain size 9-23969
 Mn-Ge alloys, phase diagram determ. using magneto-thermal methods 9-48938
 Mn, polymorphism rel. to atomic size factor 9-46954
 Mn₃La₂(NO₃)₁₂.24H₂O, mag. ordering, obs. 9-39781
 Mn₂O₄, high pressure transformations 9-44799
 MnF₂, pressures up to 160 kbar 9-44800
 MnF₂, two phase transform. obs. at high press. and temp. 9-39184
 MnTiO₃ I to MnTiO₃ II, struct. obs. 9-44667
 Mo-steels, $\alpha \rightarrow \gamma$ phase, embrittlement by neutron irradiation 9-28369
 Mo, polycryst., ductile-brittle transition temp., depend. on strain rate, neutron irradi., press. and grain size 9-30742
 ND₂Br, I-II molar vol. change determ. by hydrostatic weighing dilatometer 9-33141
 ND₂Br, transition X-ray investigation, lattice parameters determ., -192 to 196°C 9-30743
 NH₄ salts, single cryst., u.s. investigations 9-37302
 NH₄Br, high-press. 9-30633
 NH₄Br, III-IV transition X-ray investigation, lattice parameters determ., -192 to 196°C 9-30743
 NH₄Br, new ordered phase from u.s. obs. 9-37302
 NH₄Cl, u.s. attenuation obs. of critical points 9-37302
 NH₄Cl, λ -type transition, Cu²⁺ impurity effects, e.s.r. and differential thermal analysis 9-33142
 NH₄Cl, order-disorder, critical exponent 9-33146
 (NH₄)₂SO₄, ferroelec. order-disorder transition 9-33390

Phase transformations continued
solid-state continued

- (NH₄)₂SO₄, ferroelec. order-disorder transition 9-33391
 NY₂Br, I-II molar vol. change determ. by hydrostatic weighing dilatometer 9-33141
 Na, effect on spin susceptibility 9-35538
 NaCl-KCl, differential thermal microanal. 9-28391
 NaNH₂.SO₄.2H₂O ferroelec. leconteite 9-43301
 NaNO₃, thermal conductivity, diffusivity and permittivity anisotropy at phase transition 9-30796
 NaNO₃, structural change under shock compression 9-37303
 Nb-Zr alloy, supercond., cellular to isostructural, and precipitation 9-39499
 Nb₃Sn, cubic-to-tetragonal, volume change, 43°K 9-35249
 Nb₃Sn, specific heat meas. 9-24049
 Nb hydrides and deuterides, interstitial ordering in solid solutions 9-23990
 NbH, rel. to heat treatment 9-31185
 NbO₂, deformed to normal rutile type struct., lattice parameters, temp. depend. 9-35246
 NbO₂, rel. to collapse of long-range ordering of Nb-Nb bonds, from mag. and elec. obs. 9-33143
 Ni-Fe alloys, ordering transformation, eff. of γ -radiations 9-23973
 Ni₂La₂(NO₃)₁₂.24H₂O, mag. ordering, obs. 9-39781
 NiF₂, pressures up to 160 kbar 9-44800
 NiO, from elec. conductivity press. depend. obs. 9-35338
 3(NH₄)₂.0.7MoO₃.4H₂O, thermal decomposition, X-ray diff. and i.r. spectrophotometric exam. 9-30745
 oxides, mixed valence-type, due to electronic ordering, energy obs. 9-41127
 P, high-pressure polymorph, neutron effects on phase stability 9-35250
 Pb-Bi alloys, d.h.c.p. phase form under h.p. 9-44802
 PbO-SiO₂ system, crystallization sequences in silica phase 9-26390
 PbO₂, high-pressure polymorph, neutron effects on phase stability 9-35250
 Pb(Sr_{1/2}Nb_{1/2})₂-Ti₂O₃ system, rel. to ferroelec. phase transitions 9-28563
 PbZrO₃, enthalpy changes, impurity eff. 9-26584
 Pd-Si based alloy glasses, electron microscope obs. 9-42706
 Pd, $\alpha \rightarrow \beta$, thermal effect prior to equilib. temp. rel. to exothermic retained $\gamma \rightarrow \alpha$ transform. 9-42935
 Pu, α, β , is differential enthalpic study 9-44801
 Pu, β to α transform. at high press., α -Pu single crystal growth 9-35247
 RbNO₃, struct. changes 160°C to melting pt., elec. conductivity meas. 9-46962
 RbNiF₂, perovskite-like struct. at high press., stability relations 9-35241
 S unstable-stable transition followed by paramagnetic resonance 9-30747
 Se, hexagonal, growth kinetics from α - and β -monoclinic single crystals 9-42936
 SiO₂, high-pressure polymorph, neutron effects on phase stability 9-35250
 SrMnO₃, perovskite-like struct. at high press., stability relations 9-35241
 SrTiO₃, at 110°K, lattice-dynamical exam. 9-23986
 Ta hydrides and deuterides, interstitial ordering in solid solutions 9-23990
 TaH, rel. to heat treatment 9-31185
 Tb, irreversible from h.c.p. at about 25 kb at 22°C 9-39501
 ThC, order disorder transformation, evidence for substructure existence 9-28270
 Ti-Cr binary alloys, martensite react., morphology and substruct. 9-26393
 Ti (5 at.%) Mn alloy martensites, electron microscope obs. 9-39311
 Ti-(13.5-14 at.%)V alloys, α -from ω -phase formation 9-23987
 Ti₂Al ordered and disordered alloys, low temp. electronic sp. ht. coeff. 9-30751
 Ti alloys, β - α kinetics rel. to fracture toughness and strength props. 9-37252
 TiO, Madelung potentials and ordering energy 9-30508
 TiO₂-SnO₂ system, spinodal decomposition 9-33144
 TiO₂, rutile- α -PbO₂ form, high press. and temp. obs. 9-23988
 TiO₂, under dynamic loading 9-39482
 Ti binary and ternary solid solns., supercond. transition temp. 9-23989
 TiNiF₂, perovskite-like struct. at high press., stability relations 9-35241
 U-(0.45 wt.%)Mo, kinetics rel. to cooling rates and overheating temp. 9-41069
 U-Nb system, monoclinization of cryst. lattice of α -U after quenching from γ solid soln. 9-40920
 U₃Si, plastic deformation and 60°C irradiation, X-ray diffraction analysis of structure 9-35248
 U₃O₈, due to electronic ordering, energy obs. 9-41127
 U alloys, martensitic, type II twinning 9-30512
 α -U low-temp. transition, depend. on impurities, cold-working and annealing 9-26394
 U multilayers on W, effect on work function 9-32850
 V₂O₅, metal-semiconductor transitions on excitonic phase change, pressure depend. studies 9-30892
 V₂Si, cubic-to-tetragonal, volume change, 21°K 9-35249
 V₂Si, suppression by uniaxial stress c V₂Si, structural transformation suppression rel. to change in critical density 9-24162
 V hydrides and deuterides, interstitial ordering in solid solutions 9-23990
 Xe, u.s. attenuation obs. of critical points 9-37302
 Yb Martensitic near room temp. from resistivity meas. 9-46953
 ZnF₂, pressures up to 160 kbar 9-44800
 ZnS, hexagonal-cubic, kinetics 9-23970
 ZnS polytypes, 2H-4H, electron microscope contrast effs. at interface 9-28275
 ZnS powders, and lattice dimensions, effect of point defects 9-40923
 Zr-Nb alloy, $\alpha/(\alpha+\beta)$ boundary 9-41062
 Zr, high-pressure polymorph, neutron effects on phase stability 9-35250
 ZrO₂-HfO₂, phase diagram determination 9-23991
 ZrSiO₄, high pressure transformations 9-44799

Phase transitions see Phase transformations

Phase-contrast microscopy see Microscopy

Phonographs see Sound reproduction

Phonon bottleneck see Crystals/lattice mechanics

Phonon drag see Crystal electron states/transport processes; Crystals/lattice mechanics

Phonon-electron interactions see Crystal electron states/transport processes; Crystals/lattice mechanics

Phonons *see Crystals/lattice mechanics*

Phosphorescence *see Luminescence*

Phosphors *see Luminescence; Luminescent devices*

Phosphorus

- black, growth at very high gas pressures 9-37001
diffusion in Mo and Nb, interstitial mechanism, 2000-2220 and 1300-1800°C respectively 9-35132
diffusion in Si 9-48877
diffusion in Si, induced defects obs. 9-32975
diffusion in Si, strain compensation rel. to dislocation generation obs. 9-46824
diffusion through SiO layers into Si 9-48876
ENDOR obs. in doped Si 9-35736
e.s.r. absorption intensity in Si 9-35717
growth using equipment for very high gas pressures 9-37001
implantation in silicon, range 9-44856
n.m.r. Knight shifts in rare-earth group-VA intermetallic cpds. 9-33648
poly- γ -benzyl-L-glutamate conc. soln. in dioxane, supermolecular structure formation obs. 9-28102
polymorphs, stability of high-pressure phases, effect of neutron irradiation 9-35250
red, X-ray K-absorpt. spectrum obs. 9-31120
solubility, with Fe in Cu(36 wt%)Zn 9-30717
in CdTe:Yb,Er, effect of charge compensation on rare-earth doping, e.p.r. study 9-47434
in Cu(36wt%)Zn, influence on recrystallization 9-30718
Si:P, ESR, absorpt. intensity 9-35717
Si:P, Hall coeff. obs. of semicond.-to-metal transition rel. to impurity conc. 9-49095
in steel, spectroscopic examination using Ar discharge source 9-47480
in ZnTe, luminescence rel. to shallow acceptor centres 9-26769

Phosphorus compounds

- calcium halophosphate luminescence, activated by Sb, temperature quenching 9-26780
dynamic nuclear polarization at 74 gauss 9-39115
 μ -oxobis(thiophosphoryl difluoride) 9-23064
phosphate glasses, Nd³⁺-doped, radiative lifetime of metastable ion anomalous temp. dependence 9-41405
phosphates, solid, n.m.r. of ³¹P 9-28759
phosphates, tetragonal, electro-optic parameter in 400-700 nm range at room temperature 9-31086
phosphates of type MNH₂PO₄·H₂O (M=Cd,Co, Mg,Mn,Fe,Ni) and MKPO₄·H₂O (M=Cd,Co,Mg,Mn and Ni), crystal structure and density 9-37138
pnictides, binary, with marcasite type struct. mag. props. 9-31016
Co-P alloys, amorphous layers, characterisation by very low coercive force 9-24311
Fe-P alloys, amorphous layers, characterisation by very low coercive force 9-24311
Fe₈₀P₁₃C₇ alloy, amorphous ferromag., resistivity minimum 9-37429
Fe₈₀P₁₃C₇ amorphous ferromag. alloy, Hall effect 9-39578
H₃PO₄·1/2H₂O crystal structure and refinement 9-39278
In_{1-x}Ga_xP alloys, band structure and direct transition electroluminescence 9-24467
NPCL₂(NSOCl)₂, crystal structure 9-39287
P-Au neutron activation dosimetry in reactors 9-46141
P₂O₅F₃, n.m.r. 9-23064
P₂O₅-BaO-MgO system, luminescence of Eu²⁺ 9-31131
P₂O₁₀, vibr. assignments, force consts. and P-O bond orders 9-27871
P₂O₆, vibr. assignments, force consts. and P-O bond orders 9-27871
P(V) acids, dissociation constants 9-23171
PCl₃, potential energy constants and mean amplitudes of vibn., from vibr. spectral data 9-48477
PCl₄⁺, SAVE-CNDO theory, semi-empirical all valence electron, effective field gradient 9-42413
PCl₃, polycrystalline, NMR line width, temp. eff. 9-26799
PD₂, force const. meas., freq. depend. on valence angle 9-25747
PDF₂, microwave spectrum, mol., struct. and dipole moment, obs. 9-30049
PF₃, potential energy constants and mean amplitudes of vibn., from vibr. spectral data 9-48477
PF₃, radical, isotropic hyperfine splittings and molec. struct. 9-23065
PF₃, Raman spectrum of solid 9-24427
PF₃, vibr.-rot. bands, computer anal. 9-38895
PH₃, radical, emission bands, rot. anal. 9-23176
PH₃, mol. wave-functions and d orbitals rel. to bonding 9-34617
PH₃ force const. meas., freq. depend. on valence angle 9-25747
PH₃ halides, p.m.r. and hindered rot. 9-35728
PHF₃, microwave spectrum, mol. struct. and dipole moment, obs. 9-30049
PO, D²Π_g(a) and D²Π_g(a) states 9-40602
PO₄²⁻, non-linear polarizabilities 9-35611
PO₄²⁻, coupled vib. in Ca₁₀(PO₄)₆F₂ cryst. 9-37317
PO mol., β system, struct. and analysis of bands 9-23066
PbCl₂, SnCl₄, Nd₂O₃ soln., laser emission charact. 9-45956
POCl₃, potential energy constants and mean amplitudes of vibn., from vibr. spectral data 9-48477
POF₃, E-species force consts. 9-30050
POF₃, potential energy constants and mean amplitudes of vibn., from vibr. spectral data 9-48477
PSe emission spectra, isotope shift studies 9-34635
PSCl₃, potential energy constants and mean amplitudes of vibn., from vibr. spectral data 9-48477
PSF₃, E-species force consts. 9-30050
PSF₃, potential energy constants and mean amplitudes of vibn., from vibr. spectral data 9-48477
Ph₃ gas, proton spin-lattice relax. 9-48667

Photochemistry

- see also Photographic process*
p-azophenyldiphenylcarbonyl chloride, interconversion of cis and trans isomers under effect of light 9-24589
 β -alanine, γ -irrad., low temp. photoconversion 9-31208
amino acids, aromatic, u.v. irrad., photochem. transforms., obs. 9-28816
anthracene, nanosecond excited-state polarized absorption spectra in visible region 9-34657
anthracene-doped boric acid glass, spectra 9-42423
atmospheric ozone, 30 to 35 km, parameters derived. 9-41491
biomolecules, photosensibilization process, e.s.r. study 9-47472

Photochemistry continued

- butene-2, Cd-photosensitized isomerization, energy transfer by benzene 9-31212
butyrolphenone, processes in h.f. discharge 9-46545
capillary technique for liquid phase experiments 9-33681
copper acetate monohydrate, γ -irrad., conversion of Cu²⁺ to Cu⁺ 9-49386
cyclobutanones 9-33682
2-(2',4'- dinitrobenzyl) pyridine tautomeric reaction rel. to crystal and mol. structure 9-30579
durene, u.v. irrad., e.p.r. signal comparison with 9-47421
dye methylene blue, photoreduced for polymerization sensitization of methylmethacrylate 9-24552
electrolytes in aq. soln, glass-like, γ -irrad., electron trapping at -196°C 9-24399
ethylene, γ -induced polymerization 9-33665
ethylene-d₂, Cd-photosensitized cis-trans-geminal interconversion 9-31213
ethyltoluene photodissociation products, fluorescence spectra of trapped radicals in crystalline matrices 9-47402
flash kinetic meas., suppression of disturbing light signals 9-26834
flash photolysis, thermal effects 9-26835
flash photolysis, nanosecond, using Q-switched laser, and excited singlet states 9-39964
glass, photochromatic, reversible photochemical reactions 9-26714
of Jupiter above 1000 Å 9-41676
latent image distrib. in granular vols. 9-22484
methane, Jovian, photolysis at 1216 Å 9-41676
methane, Xe-photosensitized decomp. 9-24590
methanethiol, photodissociation 9-43336
methyl fluoride matrix-isolated u.v. photolysis, free radicals prod. 9-45424
methyl methacrylate, u.v.-induced polymerization 9-33666
NH₃ and methane, Jovian, photolysis at 1350-1450 Å 9-41676
NH₃ Jovian, photolysis at 1450-1700 Å 9-41676
organic molcs., excitation energy degradation, Jablonski scheme 9-28814
ozone in upper atmosphere 9-35834
phenyldiazonium ions, meta and para substituted, photolysis quantum yields, rel. to HMO calcs. 9-27914
photochromic materials, props. 9-28815
photoisomerism, molec. rearrangements theory 9-43337
photoluminescence of solutions theory and expt., book 9-31209
photomutagenic-dye-solvent interactions, photosensibilization process, e.s.r. study 9-47472
photopolymers, for hologram recording 9-25324
pigment solution generation during ruby laser 2nd harmonic irradiation 9-43332
polypeptides, exciton band struct. 9-41456
polytetrafluoroethylene, photo-decomposition 9-33069
propylene, oxidation by photolysis with NO₂ 9-43338
recoil spectroscopy 9-43333
all-trans- retinal, fluoresc. yields 9-24460
spiropyranes in soln., photochromy obs., by means of triplet-triplet absorption 9-34910
stilbene, photoisomerism, theory 9-43337
N,N,N',N'- tetramethyl phenylenediamine and indole in acetonitrile, flash photolysis, formation solvated electron, obs. 9-27880
triphenylhydrazine, diphenylamino radical dimer as colour centre 9-42855
triphenylene-dodecahydrotriphenylene mixed crystal on u.v. irrad. 9-38918
turbidity layers, microphotometric meas., Schwarzschild-Villiger effect 9-23540
U.V. irradiation ESR spectrometer for obs. of eff. 9-33680
vibronic effects 9-39960
water, OH*(²Σ⁺) radicals, rot. distrib. 9-38867
AgBr phosphor, photolysis 9-33602
AgBr-Ag₂S phosphor, photolysis 9-33602
Br atom recombination, thermal effects in flash photolysis 9-26835
C₂ molecules, photodissociation in comets' atmosphere 9-24882
C₂O₂, photolysis at 1470 Å in presence of CH₃F 9-47473
Cl-O mixtures, photolysis, absorption spectrum of ClOO intermediate radical 9-30152
Cl₂, photochem. recoil spectra 9-43333
H₂, decomp. and reaction of H atoms with olefins 9-43335
H₂ molcs., photodissoc. 9-25785
H₂O₂, vac. u.v. photolysis, mechanism 9-31210
H₂S, photodissociation 9-43336
H₂S photolysis, H-atom prod. and addition to olefins 9-43334
IBr photodissoc. by flash photolysis, reversible laser system obs. 9-34166
N₂O vac. u.v. photolysis, deactivation of N(²D) 9-49385
N₂ radical in soln., spectroscopic obs. 9-38860
NH₃ Jovian, photolysis at 1700-2200 Å 9-41676
NO₂, vac. u.v. photolysis 9-39961
NaCl, coloured and annealed, colloid evolution 9-26296
NaNO₃, solms., u.v. decomposition, temp. eff. 9-24588
Nd (trivalent) activated glass, stability 9-41455
NO₂, photochem. recoil spectra 9-43333
NO₂, vacuum u.v. photolysis and electronic de-excitation of O(¹D) by inert gases 9-35755
O₃ in presence of water vapour 9-31298
O₃ photolysis at 2537 Å, electronically excited O₂ 9-45423
Sb³⁺ oxidation in HCl, LiCl, soln., Bunsen-Roscoe law breakdown 9-29939
SbF₃-H₂, methane mixtures photolysis, HF chem. laser emission, obs. 9-31944
Si₃N₄ layers deposition at low temp. 9-46728
UF₆-H₂, HF chem. laser, operation and chem. 9-36292
Xe F₄-H₂, methane mixtures photolysis, HF chem. laser emission, obs. 9-31944

Photoconducting devices

- electrophotography, photoconductive compositions for plates, patent 9-22489
photocell, multistage, maximum efficiency 9-47196
photoconductor, film, with CdS-Cu²⁺ heterojunctions, charact. 9-46845
photoconductor, for high sensitivity image pick-up tubes, patent 9-33405
photoconductor, photocurrent fluctuations and sensitivity threshold 9-37627
photon counting, noise sources obs. 9-39704
square barrier-limited, collection efficiency rel. to carrier diffusion into electrode 9-47210
Ag-GaAs Schottky-barrier u.v. detector 9-43125

Photoconducting devices continued

- CdS:Cu sintered coordinate-sensitive photoresistors, prep. 9-35513
 CdS-CdSe variable composition photoresistors 9-35501
 p-n-CdSe heterojunctions as photoelements, prep. 9-35505
 CdTe thin-film photocells, fabrication 9-33413
 CuTe thin-film photocells, fabrication 9-33413
 GaAs receiving devices, construct., fabrication and props. 9-45021
 GaAs Schottky barrier avalanche photodiodes 9-26575
 Ge diode detector for 1.54 μ , high speed 9-49159
 (Hg, Cd)Te photodetectors for 1.5 μ 9-49160
 (Hg,Cd)Te as i.r. detector material 9-47204
 Pb salt detectors, development reviewed 9-45026
 PbO layers as photodetectors, conductivity mechanism and band struct. 9-39722
 Si photocell, optical characts. for thermophotoelect. conversion 9-39731
- Photoconductivity**
see also Photoconducting devices
 Ionic cryst., conf. 9-39702
 A^{IV}C^{VI} semiconducting cpds., spectrum, peculiarities 9-37715
 alkali halides, spin depend. 9-41257
 anthracene, intrinsic, photon energy depend. 9-39728
 anthracene, spin inversion of photo-emf. 9-24238
 anthracene, triplet excitons interaction with trapped electrons 9-39729
 anthracene crystals, exciton mechanism of excitation spectrum 9-35509
 anthracene single cryst., intrinsic 9-24239
 biphenyl, photocond. spectrum 9-30996
 p-radiation field perturbation at barrier due to hole-type inhomogeneity 9-26599
 CdSe short-wavelength quenching of photocond. between 400 and 700 nm 9-37616
 chalcogenide glasses, photo-excited carriers transport and generation 9-39709
 charge carriers recomb. kinetics 9-41255
 conference 9-39702
 diamond, semicond., oscillatory spectrum, role of phonons 9-41258
 diamond, substitutional N donor obs. 9-37401
 dibenzothiophene, surface, activation energy and characts. 9-49165
 dye-photosemiconds., org., flash investigation 9-24182
 electron-hole plasma interactions with lattice vibrations 9-26415
 electrophotographic imaging layers, Lewis acid, phenol-aldehyde resin, patent 9-22491
 exciton dissociation by localized elec. fields, vibr. struct. obs. 9-41138
 field-dependent conductivity parameters determ. using high-field domains 9-39705
 frozen-in conductivity extinction by elec. field 9-28577
 high resistivity materials, conf. 9-39702
 materials with 0.1 eV band gap, intrinsic performance, sensitivity limits 9-41254
 m.i.s. systems, transient photocurrents and internal photoemission 9-39656
 molecular photoconductors, field controlled quantum efficiency, models 9-39707
 multi-photon, mechanisms 9-41256
 multi-photon, mechanisms 9-39706
 muscovite mica, pulse-photoconductivity obs. of carrier mobility 9-37587
 ohmic contact for group II-VI photoconductors 9-47197
 oscillatory, Monte Carlo simulation 9-35499
 p-n junctions, photo-emf. due to ionization of impurity centres 9-37626
 perylene, injection of defect electrons in dark and under illumination 9-30995
 perylene, intrinsic, photon energy depend. 9-39728
 photon density relax. 9-37612
 phthalocyanines, origin of photocarriers 9-43131
 phthalocyanines, trapping levels obs. 9-49166
 poly(N-vinylcarbazole), carrier mobility 9-43133
 poly-N-vinylcarbazole, dye sensitization of photocond., quantum yield 9-49167
 polystyrene, depend. on voltage and illumination intensity 9-43132
 powder, fine for electrophotography, preparation method, patent 9-22487
 response characts. of extrinsic photoconductors 9-43129
 semiconductor, and screened Coulomb interaction 9-39703
 semiconductor, illuminated, occupation ratio of dislocation acceptor levels 9-26556
 semiconductor, impurity absorpt. in carrier self-oscill. excitation 9-37512
 semiconductor, impurity photocurrent and photocapacitive methods for carrier emission rate and cross-sections determ. 9-39636
 semiconductor, multi-phonon, mechanisms 9-39706
 semiconductor, n-type, degenerate and nondegenerate, theoretical analysis 9-33412
 semiconductor, photoionization spectrum of deep impurities 9-39634
 semiconductor, two-photon vol. excitation, effect of induced light absorpt. by nonequil. holes 9-39708
 semiconductor e.m. field effect on electron scatt., theory 9-30901
 semiconductor films, III-V and II-VI, mechanism 9-33404
 semiconductor population inversion connection 9-35394
 semiconductor with bipolar mechanism of conductance, negative differential resistance obs. 9-37517
 semiconductors, at large light intensity 9-28574
 semiconductors, electron irradiation and subsequent photocond. studies, low-temp. set up 9-31724
 semiconductors, manyvalley 9-24226
 semiconductors, struct., barriers and junctions, conf. 9-39702
 in semiconductors, two-photon absorption process 9-28570
 semiconductors containing traps and recombination centres, relaxation 9-28573
 spectra, data representation method 9-22477
 stationary surface, analysis 9-45020
 study using Lallemand electron camera with special electron multiplier 9-47903
 Ternary cpds., conf. 9-39702
 tetracene, intrinsic, photon energy depend. 9-39728
 tetracene single cryst., intrinsic 9-24239
 Ag₂As₂S₃, occurrence of electronic conduction from obs. 9-39662
 AgBr dye-sensitized single crystals, mechanism 9-43126
 AgI, sensitization by adsorbed pigments, obs. 9-26764
 As-Se alloy system, photo-excited carriers transport and generation 9-39709
 B single crystals and films 9-35500
 CaF₂:Gd, photochromic, study 9-24227
 CaWO₄, photoelectret state obs. of local trapping levels 9-39890

Photoconductivity continued

- n-Cd₃P₂, low temp., response obs. 9-39712
 Cd_{0.9}Hg_{0.1}-Te graded-gap structures, 77°K and 300°K 9-49156
 Cd_{0.9}Mg_{0.1}-Te:Cl, double-acceptor defects and hole traps 9-41263
 CdI₂, spectral distribution 9-28576
 CdS-BaTiC₂ boundary, transient photocurrents obs. 9-43128
 CdS-SiO₂ film system, frozen-in conductivity extinction by elec. field 9-28577
 CdS-metal contacts, work function at higher current densities 9-39733
 CdS, electron bombarded, i.r. attenuation of induced photocond. current 9-47198
 CdS, excitation spectra obs. in intrinsic absorpt. range near fund. edge, coeff. correl. 9-39710
 CdS, excited by ruby laser 9-47199
 CdS, exciton dissociation and photocarrier recomb. 9-41261
 CdS, h.f. oscillations cry. with induced neg. diff. conductivity 9-33407
 CdS, hole injection by electrolytic contact 9-24172
 CdS, impurity photoeffect meas. of radiative capture of electrons by activated recombination r-centres 9-30798
 CdS, magnetomicrowave effects at 38 GHz, charge carrier density control by photogeneration 9-30922
 CdS, non-equil. contact pot. difference on surface 9-33409
 CdS, oscillatory photoconductive and exciton spectra 9-39713
 CdS, phonon-assisted exciton transitions in spectral response 9-43127
 CdS, pos. and neg. conduction under i.r. irradiation 9-26600
 CdS, residual conductivity effect at room temp. 9-35504
 CdS, residual conductivity effect at room temp. 9-35504
 CdS, residual conductivity effect at room temp. 9-35504
 CdS, response at low temp. and high excitation intensities 9-49313
 CdS, saturation, and appearance of fast-decay photocurrents, under laser excitation 9-49157
 CdS, stationary characts., and kinetics of photocurrent and its i.r. quenching 9-37759
 CdS, thermally-stimulated-current curves determ. of electron traps 9-41259
 CdS, two channel capture mechanism of holes at sensitizing recomb. centres 9-41262
 CdS, CdSe_{1-x}, excited by ruby laser 9-47199
 CdS film, frozen-in conductivity extinction by elec. field 9-28577
 CdS single cryst., carrier dragging due to laser rad. 9-28578
 CdS single cryst., internal photoeff. in exciton region of absorpt. spectrum 9-26603
 CdS single cryst., intrinsic excitonic absorpt., correl. 9-35503
 CdS single cryst., photo- and e-conductance comparison 9-37617
 CdS single crystals grown from controlled atmospheres of constituent elements 9-37006
 CdS sintered layers, photoelectronic behaviour ambient-dependence 9-47200
 CdS surfaces, discrete trapping levels, rel. to detection 9-28575
 CdS X-ray conductivity 9-24173
 CdSe, acoustic noise and sound amplification 9-33176
 CdSe, electron-bombarded and u.v. radiation illum., electron-hole pair form. energy determ. 9-47133
 CdSe, I-V characts. of photo-current caused by trapping of carriers 9-26602
 CdSe, stationary characts., and kinetics of photocurrent and its i.r. quenching 9-37759
 CdSe, temp.-elec. instability 9-39711
 CdSe short-wavelength quenching eff. between 400 and 700 nm 9-37616
 CdSe textured films, recombination processes 9-31123
 CdTe, rel. to electronic props. of defect centres 9-49158
 CdTe APN films, photocurrent kinetics and relax. time relax. time 9-26601
 CdTe films, of anomalously high photovoltage, number of microphotoelements determ. 9-37613
 CdWO₄, photoelectret state obs. of local trapping levels 9-39890
 Cu₂O, i.r.-induced, 110°K 9-24229
 Cu₂O, slow, explanation assuming existence of three types of traps 9-30989
 Cu₂O, temp. dependence, 160-120°K, excitonic processes 9-24228
 CuAlS₂(Se₂), single cryst. prepared by vapour transport with iodine 9-48797
 CuCl, exciton dissociation by localized elec. fields, vibr. struct. obs. 9-41138
 EuS effect of mag. order 9-45266
 EuSe, mag. polaron effects, temp. depend. rel. to mag. ordering 9-39714
 GaAs:Si, photocurrent meas., effects due to energy band tails caused by impurities 9-39716
 GaAs:Zn, noise spectra under optical excitation, electron fluctuations obs. 9-41198
 GaAs-poly-N-vinyl carbazole-Au systems transient photocurrents and internal photoemission 9-39656
 n-GaAs, epitaxial, oscillatory spectra at 2°K 9-26604
 n-GaAs, epitaxial far-i.r., mag. field effects on hydrogenic donor states 9-45022
 GaAs, i.r. spectra of shallow donors in mag. fields 9-41265
 p-GaAs, lifetime of majority carriers rel. to temp. and hole density 9-37618
 n-GaAs, meas. in optical probing of inhomogeneities and acoustoelect. instabilities 9-49080
 GaAs, semi-insulating, mag. field effect 9-39715
 n-GaAs, spectral photosensitization, high area in fundamental absorption region 9-30991
 GaAs epitaxial layers, donor magnetospectroscopy 9-39717
 GaP:S, extrinsic, electron-phonon interaction obs. 9-41264
 GaP electrodes, redox processes, photoexcitation obs. of charge transfer 9-30990
 GaS(Se, Te), spectral distribution, eff. of hydrostatic pressure 9-28579
 GdS crystals, generated by e beam 9-33408
 Ge:Au, hopping mechanism, depend. on temp. and Au conc. 9-35506
 n-Ge:Au, injecting contacts influence on impurity photocond. kinetics 9-47203
 Ge:Ga, bipolar photoeffect due to anomalous Cu distrib. in and near diffused layer 9-45024
 n-GeSb, injecting contacts influence on impurity photocond. kinetics 9-47203
 p-Ge-Be, impurity spectra 9-37619
 n-Ge-p-GaAs heterojunctions, photoeffects under reverse bias 9-41222
 Ge, extrinsic, response characts. 9-43129
 Ge, extrinsic photocond. from edge dislocations 9-45023
 p-Ge, high temp. photodiode. effect 9-47202

Photoconductivity continued

- Ge, i.r. photoresponse for impurity and defect energies and conc. determ. 9-39644
- Ge, illuminated, occupation ratio of dislocation acceptor levels 9-26556
- Ge, magnetomicrowave effects at 38 GHz, charge carrier density control by photogeneration 9-30922
- Ge, oscillatory magneto-photoconductivity 9-39718
- p-Ge, photocond. spectra in fields of 0.5-100 V/cm at temp. 8-15°K 9-37620
- p-Ge, plastically bent, steady state transient photocond., trapping effect due to dislocations 9-35507
- Ge, recombination centres formation by ^{60}Co γ -radiation 9-30994
- Ge single crystals, decay, effects of heat treatments 9-37538
- (Hg,Cd)Te as i.r. detector material 9-47204
- Hg_{0.8}Cd_{0.2}Te, sweep-out of minority carriers 9-39719
- Hg_{1-x}Cd_xTe alloys, 1 eV band gap, responsivity photoabsorpt., equil. charge carrier transport and photo-Hall effect 9-41267
- Hg_{1-x}Cd_xTe alloys, and material parameters 9-41266
- Hg₂, synthetic single crystals, quenching, determ. of localized levels in energy gap 9-28580
- InAs, pot. barrier interaction of depletion regions 9-39720
- InP, current carrier lifetimes, 78°-300°K 9-37621
- InSb, field effect and surface photocond. obs. 9-43130
- n- and p-InSb, impurity spectra 9-30992
- n-InSb, negative, in impurity absorpt. region 9-47205
- n- and p-InSb, surface effs. due to x-irradiation 9-30993
- InSb, two-photon vol. excitation, effect of induced light absorpt. by nonequil. holes 9-39708
- InSb m.o.s. devices, photoresponse props. 9-39658
- K,CsSb photocathode, energy band scheme 9-28584
- KCl, F₂ centres, a.c. meas. 9-39376
- KI, assoc. with two quantum absorpt. processes 9-41268
- MnO single crystals 9-28581
- Pb_{1-x}Sn_xTe(Se), thickness dependence 9-38386
- PbBr₂ at liq. N₂ temp. 9-39721
- PbCl₂ at liq. N₂ temp. 9-39721
- PbO-SnO mixed cryst. layers 9-41269
- PbO, yellow, in polarized light 9-49284
- PbO layers, vapour-deposited 9-39722
- PbS epitaxial films, photosensitivity mechanism 9-49161
- PbS film, absolute quantum yield due to internal photoelec. effect 9-33410
- PbS photosensitized film, dark cond., steady-state photocond. and photoresponse time 9-37615
- PbS polycrystalline film, props. rel. to chemisorption of O 9-37622
- S, orthorhombic, e. and hole traps energy distrib. 9-37623
- Sb₂S₃, single crystals, i.r. and thermal quenching effect 9-49162
- SbSI, eff. of O₂ adsorption 9-30496
- SbSI, hysteresis, nonequilibrium carrier effects 9-24233
- Se, amorphous, photo-excited carriers transport and generation 9-39709
- Se, trapping and capture levels rel. to space charge and surface voltage on exposure to light 9-39727
- Se films, amorphous role of Hg in inducing anomalous phenomenon 9-47206
- Si:Al(B), electron-irrad., defects effect on spectra 9-44985
- n-Si:As, low temp. 9-39723
- n-Si:As(P,Sb), extrinsic; electron-phonon interaction obs. 9-41264
- Si:Au, photocurrent and photocapacitive meas. of electron and hole emission rates at centres 9-39636
- Si:B, quenched-in defects obs. 9-39357
- Si:Zn, noise, spectrum, freq. and bias current depend., changing recomb. traffic w.r.t. doping and temp. 9-41270
- n-Si, high purity, recombination lifetimes, 4.2°K to room temp. 9-35508
- Si, high temp. photodiodec. effect 9-47202
- Si, illuminated single crystals, 1/f noise without external voltage 9-26559
- Si, impurity-doped, effects of Li, Na, Be, Cl, Al and O on carrier lifetime 9-24234
- Si, intrinsic oscillatory spectra obs. 9-39724
- p-Si, neutron-irrad. 9-41271
- Si, optical excitation at 1.06 μ , function of intensity and elec. field 9-37624
- Si, recombination centres formation by ^{60}Co γ -radiation 9-30994
- p-Si, spectra at 100°K, rel. to deuterium-induced radiation defects 9-30589
- p-Si, stationary surface photo conductivity, analysis 9-45020
- Si neutron-irradiated, divacancy formation study 9-49108
- Si p-n junction, photoresponse edge, effect of elec. field in space charge layer 9-37558
- p-SiC:B, N, decay rel. to interimpurity recombination obs. 9-28712
- SrTiO₃, excitation spectra investigation 9-45025
- SrTiO₃, pulsed and CW meas., trapping phenomena obs. 9-39725
- Ta₂O₅ films, negative photocond. 9-24235
- TiO₂, final photocurrent, calc. using field emission concept 9-24236
- TlBr, photocarrier polaron mass and relax. time from cyclotron reson. obs. 9-39726
- TiCl, band struct. and polaron transport props. obs. 9-41272
- TiCl, photocarrier polaron mass and relax. time from cyclotron reson. obs. 9-39726
- TlInS₂(Se₂Te₂) single cryst. 9-44969
- ZnO, contact with rhodamine B dye, mechanism of dye sensitization 9-49163
- ZnO, trapping and capture levels rel. to space charge and surface voltage on exposure to light 9-39727
- ZnS, excited by ruby laser 9-47199
- ZnS, photocapacitive effects 9-37625
- ZnS, self-activated, i.r. induced photoconductivity, correl. with luminesc. obs. 9-41273
- p-ZnSe:Cu, investig. of imperfections responsible 9-49164
- ZnSe, oscillatory photoconductive and exciton spectra 9-39713
- ZnSe as-grown cryst. with Cu impurity, excitation spectra and luminesc. comparison 9-43254
- ZnWO₄, photoelectret state obs. of local trapping levels 9-39890

Photodisintegration see *Deuterons/photodisintegration; Nuclear reactions and scattering due to photons*

Photodissolution see *Photochemistry*

Photoeffect, nuclear see *Gamma-rays/effects; Nuclear reactions and scattering due to photons*

Photoelasticity

- see also *Double refraction/mechanical*
- alkali-halides, absorption of U₂-centres, effect of external stresses 9-49251
- application to shock wave analysis in saturated granular matter 9-30643
- book, selected papers of Max M. Frocht 9-41803
- box girder, study of stress distrib. 9-36163
- coefficients meas. by u.s. light diffraction technique liqs. and solids 9-26308
- crystals, piezo- and elasto-optical coeffs., temp. depend. 9-39813
- disk subjected to many compressive concentrated radial loads on periphery, stress analysis 9-31829
- dynamic recording using sequentially modulated ruby laser system 9-29232
- elasto-optical and piezo-optical coeffs. of cryst., temp. depend. 9-39813
- high-speed framing photography by ruby laser 9-32095
- holographic nondestructive testing 9-42862
- holographic strain detection 9-42873
- measurement by ultrasonics, improved methods 9-36366
- Perovskite-type crystals, phenomena accompanying orthorhombic deformation of cubic lattice 9-28558
- photographic display of principal stress directions 9-31830
- photoviscoelastic analysis for determ. of stress strain and strain-birefringence relations 9-35159
- piezo-optical and elasto-optical coeffs. of cryst., temp. depend. 9-39813
- α -quartz, constants obs. 9-37683
- sum of principal stresses by holographic interferometry 9-31818
- two-dimensional, use in minimising stress conc. in design of solid propellant rocket grains 9-47811
- u.s. delay-line crystals, constants 9-49148
- α -Ag-In dil. alloys, piezoreflectance 9-47325
- AgBr, piezo-optic study of exciton and polaron states 9-39814
- Ge, piezoreflective spectra 9-35646
- α -HfO₂, soln. grown cryst. 9-37326
- KCl cryst., piezo- and elasto-optical coeffs., temp. depend. 9-39813
- LiF cryst., piezo- and elasto-optical coeffs., temp. depend. 9-39813
- NaCl, cryst., piezo- and elasto-optical coeffs., temp. depend. 9-39813
- ZnO, flow stress increase under illumination 9-26329

Photoelectrets see *Electrets; Photography*

Photoelectric cells see *Photoconducting devices; Photoconductivity; Photoelectricity; Photovoltaic effects*

Photoelectric effect, atomic see *Atoms*

Photoelectric emission see *Electron emission/photoelectric*

Photoelectricity

- see also *Electron emission/photoelectric; Photoconductivity; Photovoltaic effects*
- anisotropic effects 9-30987
- electrophotographic layers, photoinduced discharge, effect of capture 9-30967
- fireball timing meas., 17 Sept., 1966 9-38086
- ionic cryst., photo-Hall mobility, strong phonon interactions obs. 9-39701
- liquid Raman spectra, lines polarization and intensity 9-30409
- optical rotation meas. applic., errors 9-27393
- organic dyes, photodipole effect, formation and dissociation mechanisms 9-28572
- photodiodelectric eff. in cooled semiconductors, applic. to laser detector 9-34186
- photon counting techniques and applications 9-47921
- polarimeter with visual compensation 9-46006
- study using Lallemand electron camera with special electron multiplier 9-47903
- turbulence in high-temp. flow, photoelec. meas. 9-36744
- e accelerator, low energy, utilizing photoelectric effect 9-46172
- AgCl, and luminescence props. of crystal 9-33603
- CdS, photoadsorption of oxygen, surface photovoltage and work function changes 9-28211
- CdS with blocking Au contacts, effect of increasing photocurrent on work function 9-39732
- CdS-CdTe film heterojunction, effects 9-30988
- CdSe, i.f. current noise illumination dependence 9-41260
- GaAs:Si p-n junctions, photo-e.m.f. spectra at 300 and 77°K 9-37614
- GaP, responses meas. 9-35434
- n-Ge-p-CdTe heterojunctions, props., and elec. props. 9-37557
- n-Ge-p-ZnTe heterojunctions, props., and elec. props. 9-37557
- Ge(Li) detector, meas. of photoelectric cross section as college expt. 9-36522
- In-Te system, thin films, depend. on conc. 9-30485
- Sb₂S₃ and Sb₂Se₃, props., effect of high hydrostatic pressure 9-28571
- SbSi photopyro-effect 9-24243
- ZnO electrophotographic layers, space charge density, effect of elec. field 9-30963
- ZnS:Cu:Cl, photodiodelectric effect 9-24237
- ZnS, photocapacitive effects 9-37625
- Photoelectromagnetic effects**
- Dember potential, effect of sample thickness 9-35512
- Gurevich-Firsov oscillations 9-47208
- photomagnetic oscillations, Gurevich-Firsov type 9-47208
- semiconductors, oscillations due to variation of mag. field, model 9-30998
- semiconductors, photomagnetic effect in impurity absorption region 9-33412
- Bi thin films 9-47209
- Cd,Hg_{1-x}Te graded-gap structures, 77°K and 300°K 9-49156
- CdS single crystal, photo Hall mobility at high electric field, temperature dependence 9-28582
- n-InSb, oscillations due to variation of mag. field, model 9-30998
- n-Si:As, low temp. 9-39723
- n-Si:As, photomagneto- and photoconductive effects 9-39723
- Photofission** see *Nuclear fission*
- Photographic light sources** see *Light sources; Photography*
- Photographic materials**
- see also *Nuclear track emulsions*
- colour infrared film, remote sensor, quality improvement 9-38419
- electrophotographic imaging layers, Lewis acid, phenol-aldehyde resin, patent 9-22491
- electrophotography, photoconductive compositions for plates, patent 9-22489
- emulsion, effect on small image growth 9-22483

Photographic materials continued

- emulsion calibration, digital computer program for anal. 9-43933
- emulsions, density and exposure relationship, linearity conditions 9-29494
- film, function which relates to brightness of holographic images 9-27346
- film, incorporating a photopolymerisable component, fabrication technique, patent 9-32078
- films, transmittance fluctuations rel. to r.m.s. density 9-34235
- fluorescent layers for plates, formation method, patent 9-27414
- in holography, nonlinear effects due to polynomial reln. between exposure and amp. transmittance 9-25327
- Ilford Q-2 plate on double focusing spark source mass spectrograph, charact. curve 9-42355
- i.r. emulsions, chemical hypersensitization in water-alcohol soln. with 6% NH_3 9-25390
- layers, antihalation or receiving, in diffusion transfer process, composition, patent 9-27419
- multilevel-grain model 9-29495
- photochromic, props. 9-28815
- photoconductive fine powder for electrophotography, preparation method, patent 9-22487
- photopolymers, hologram recording 9-25324
- plates, photometric calibration by double refracting crystal filter 9-40390
- Ag halide emulsion, spontaneously developable, amine borane constituent, patent 9-32077
- Ag halide emulsions rapid development method, patent 9-27420
- Ag halide film and developing agents, exposed, activator and stabilizing solns. added, patent 9-22486
- Ag halides, high resolution prod. of fine line originals, patent 9-27415
- AgBr:l luminescent excitation spectra of single crys. and of nucl. emulsion type Ya-2 9-43251
- AgBr pure thin film, as particle detector 9-48231
- PbI₂ films, holographic recording 9-38390

sensitivity

- composition, relief image formation for printed circuit boards, patent 9-29497
- electric field, pulsating effect on latent image formation 9-48126
- electron microscope emulsion, energy depend. for 100 to 600kV electrons 9-38356
- emulsion on glass or mylar film base, edge sharpness and halation for 100kV electron beam 9-38357
- films, for use in neutron radiography 9-25393
- films used with light emitting screens in neutron beam radiography, reciprocity failure characts. 9-43935
- information sensitivity rel. Markov noise 9-40388
- to laser long-wave radiation, blackening rel. to two-photon process, obs. 9-27413
- multicolour, 3 colour oscillograph trace recording, composition and prod., patent 9-27418
- multicolour, oscillograph trace recording, composition and production, patent 9-27416
- multicolour, rapid access recording, composition and production, patent 9-27417

Photographic process

see also *Photochemistry*

- latent image distrib. in granular vols. 9-22484
- metal halide decomposition by ionising radiation, Zn evaporation, patent 9-29496
- photometallic image production in thin films by photo decomposition 9-38421
- reversal colour film, for broadcast transmission 9-32076
- spectral sensitization, redox reaction due to photo-excited dye mols., rel. to Fermi level of dyes 9-41973
- Ag halide film and developing agents, exposed, activator and stabilizing solns. added, patent 9-22486
- Ag image conversion to dielec. image for improved diff. efficiency in interference pattern recording 9-27411
- AgBr:l luminescent excitation spectra of single crys. and of nucl. emulsion type Ya-2 9-43251

development

- acceleration in u.s. sound field 9-23615
- colour-forming chemicals, volatile photosensitizer, plate heated, patent 9-22485
- electric field, pulsating effect on latent image formation 9-48126
- electrophotography, aqueous electrolytic developer solutions, patent 9-32099
- washing unit for prints improved 9-36411
- Ag halide emulsions rapid development method, patent 9-27420
- AgBr crystals, photographic behaviour 9-25389

Photography

see also *Cameras; Cinematography; Lenses/photographic; Radiography*

- 2ns, with super radiant light, X-rays or electron 9-48124
- bubble chamber, reliability of Fraunhofer holograms 9-27600
- differential interferometer, photographs and their evaluation 9-32022
- distance, applic. of regulated-pulsed lasers 9-29438
- electro-optical multichannel recorder for pulse signals 9-27421
- electrophotographic printing obs. of C colloidal suspensions electrostatic charge images development 9-44604
- electrophotography, colour recording by 3 colour filter and thermoplastics, patent 9-22490
- electrophotography photoconductive fine powder, preparation method, patent 9-22487
- flare in objectives, meas. 9-38420
- forensic applic. 9-25333
- in forensic science 9-27397
- Gaussian pictorial fields and their definition by means of correlator 9-41972
- growth of small images, influence of emulsion, lens and camera 9-22483
- image deblurring and aperture synthesis with Fourier transform holography 9-48063
- image formation using laser brightening, charact. 9-36326
- image restoration by spatial filtering 9-32039
- interference pattern recording, 3 dimens., diff. efficiency improvement by bleaching 9-27411
- long-distance i.r. flash, source design 9-32074
- noise, Markov 9-40388
- phase objects, use of freq. modulation and spatial filtering 9-43932

Photography continued

- resolvometer, resolutions determinations of photographic systems films 9-34236
 - resolvometry, error analysis 9-27412
 - Schlieren, with mode-locked laser as light source 9-48125
 - solar granulation, review of early observations 9-27101
 - stereo, coherent imaging for data processing 9-36410
 - ultramicrophotography with microscope objectives 9-43934
 - Schlieren, of gas flow in elec. arc or plasma, use and props. of Ar laser 9-22384
- applications**
- analysis of composite materials photomicrographic 9-46943
 - characteristic curves, photometric 9-41947
 - cinematography of solar flare kinematics 9-38118
 - conjunctival determ. of flow of blood 9-49605
 - deep oceanographic techniques 9-37907
 - deep submergence rescue vehicle instrumentation 9-36412
 - diffraction grating production using triangular interferometer 9-27380
 - electrical breakdown at small gaps in vac. 9-39030
 - electron microbeam probe samples, colour photography appl. 9-31234
 - electron micrographic images, radial symm. testing and recording device 9-33982
 - electron microscope density curve checking 9-43857
 - emission detector, r.m.s. error in radiometric meas. 9-25391
 - emulsion for electron microscopy at 1000kV, sensitivity, edge sharpness and halation 9-38357
 - fixed focus camera 9-46030
 - flame propag. in elec. field, obs. 9-31861
 - flash, of spherical waves in detonated gas mixtures 9-31856
 - multiple picture prod. by filter with percussion response represented by dot network 9-40387
 - optical image motion investigation, errors 9-22444
 - photoelastic principal stress directions, display 9-31830
 - photometallic image production in thin films by photo decomposition 9-38421
 - photometry, linearization of characteristic curves 9-32025
 - photomicrographs of inorg. chem. crystal precipitation 9-41458
 - photoresist exposure, design of projection system 9-27422
 - picosecond pulse measurement by two-photon excitation of photographic film 9-22482
 - plates, astronomical, device for comparing 9-31682
 - recording channels, superposition on emulsion by spatial freq. modulation 9-25392
 - sea reflection spectra obs. 9-43367
 - solar coronal emission line photographs, image quality improvement 9-41711
 - solar granulation, effect of finite resolution 9-36062
 - spark in air, 4-m length, study using high-speed image-converter photography 9-46546
 - spectral emission anal., sensitivity limits rel. to film characts. and region of spectral line 9-37849
 - stars, faint, background exposure density and detect. limit, relationship 9-31672
 - stars, flare, multiple exposure photographic techniques 9-27035
 - strobe photos with 'Big Swinger' camera 9-46031
 - sun, in extreme u.v., pin hole camera instrumentation on rockets and results 9-43654
 - transient radiation originating at electron transience from vacuum to dielectric, photographic registration 9-24208
 - U.S. waves in plane solid sheets, impact excited, visualization techniques 9-34057
- colour**
- high-speed, modified Schlieren apparatus 9-32096
 - imaging method using photoelectrochromism 9-40389
 - i.r. remote sensor, quality improvement 9-38419
 - photochromic materials, props. 9-28815
 - reversal film processing, for broadcast transmission 9-32076
 - reversed film reproduction fidelity in photomicrography 9-48127
 - X-ray images obtained from microprobe rel. to metal inclusion analysis 9-48851
- high-speed**
- 70 mm drum camera 9-29502
 - ballistic, applic. of laser beams 9-31986
 - camera, continuous access framing, 45 ns exposure 9-32092
 - camera, foil-shutter multi-lens prototype 9-32084
 - camera, rotating-mirror, continuous access for 250000 frames/sec. 9-32091
 - camera, rotating-prism, with registration sprocket 9-29503
 - camera PhC-I with high aperture ratio 9-29504
 - capacitor discharge circuit for magneto-optical 100 ns shutter 9-29500
 - capping shutter with independent operating solenoids 9-32086
 - Chronolite camera, variable spark-gap with gas pressure chamber 9-32094
 - colour, modified Schlieren apparatus 9-32096
 - conference, Stockholm (1968) 9-29493
 - continuous mirror scanning system for cameras 9-31995
 - drum shutter for ribbon-frame camera 9-32083
 - electromechanical 200 μ s shutter 9-32085
 - electronic shutter tube 9-31919
 - framing, ruby laser application 9-32095
 - framing drum spectrograph 9-32069
 - image intensifier for high-speed spectrography 9-32049
 - integral image camera, 1 ns exposure time 9-29499
 - international terminology 9-32075
 - with laser, pulsed, light source and smear camera 9-46034
 - laser beam applications 9-29505
 - laser syst. for aeroballistic range photography 9-46035
 - of liquid drop impact and cavitation 9-32754
 - mirror image scanning, matrix theory 9-31994
 - motion blur, holographic compensation by shutter modulation 9-45973
 - for optical path changes analysis in solid laser rods by pumping 9-48088
 - shock-wave compression, problems of rotating-mirror streak cameras 9-32087
 - shutters, collapsing-foil, exploding-wire and carbon injection 9-29501
 - spark, of shape of fracture front in glass plate 9-30681
 - spectrophotochronograph 9-29491
 - stereoscopic grid camera applic. 9-32081
 - streak camera attachments for stereoscopy, spectrography and image dissection 9-32090
 - test equipment for 5 to 500 ns exposures 9-29498

Photography continued
high-speed continued

- time-resolving grazing-incidence spectrograph 9-29490
- welding and cutting, gas flow mechanisms, flash Schlieren methods 9-33983
- W controlled fracture, possibility for elec. current switching 9-33068

Photoionization

- anthracene, cryst., intrinsic, mechanism 9-39728
- atom, cross section calc. 9-23339
- atoms, heavy, using nonrelativistic model with central pot. 9-44276
- benzene and derivatives, photoionization study of mol. orbitals 9-30078
- benzene mol., π system contribution, calc. 9-34669
- butadiene mol., π system contribution, calc. 9-34669
- cycloheptatrienyl radical 9-23345
- ethylene mol., σ , π system contribution, calc. 9-34669
- halogens, photodetachment cross-section calc. from electron capture meas. 9-27817
- molecular photoelectrons, angular distribution 9-34591
- molecules by off-reson. photons, equilib. conc. 9-34595
- perylene, cryst. intrinsic, mechanism 9-39728
- semiconductor deep impurities, spectrum 9-39634
- tetracene, cryst., intrinsic, mechanism 9-39728
- Ba I, $6s^2$ 1S_0 , $65d^1D_2$ cross sections, Many-Channel Quantum Defect calc. 9-48406
- H, two-photon ionization in ground state 9-34580
- H₂, angular distribution of photoelectrons, calc. 9-34591
- Li, cross-section, many-body calc. 9-34571
- Li⁺ photodetachment cross-section calc. 9-46297
- Li⁺, ground and four excited levels as function of energy of expelled electron 9-36674
- Li cross section 9-42338
- N, collision strengths and photoionization cross-sections 9-29972
- Ne, collision strengths and photoionization cross-sections 9-29972
- O, collision strengths and photoionization cross-sections 9-29972
- Xe, cross-sections for Xe⁺, Xe²⁺ and Xe³⁺ production, 28-83 eV 9-40551

gases

- diatomic, high temp., cross section and transition probability calc. 9-23170
- ethylene, efficiency and mass anal. 9-32695
- ethylene, isotope effects in yields and absorpt. cross-sections 9-30298
- mass spectrometric study, apparatus and techniques 9-39021
- methane, threshold electrons 9-44485
- nn-butane, isotope effects in yields and absorpt. cross-sections 9-30298
- O₂, ground state photodetachment by sunlight, obs. 9-42562
- in shock wave precursor 9-46553
- Ar, cross section in Hartree-Fock approx., calc. 9-40549
- Ar, discrete structure in 40-60 Å region of continua 9-34531
- (CH₃)₂CO parent and fragment ions, photoionization efficiency curves 9-39021
- Cs halides, dissociative, high-temp. 9-44373
- Fe X line strength in Seyfert galaxy model 9-45599
- Fe XIV line strength in Seyfert galaxy model 9-45599
- HCN 9-30296
- Kr, discrete structure in 40-60 Å region of continua 9-34531
- S₂, high-temp. vapour 9-44484
- Se₂, high-temp. vapour 9-44484
- Te₂, high-temp. vapour 9-44484
- Xe, discrete structure in 40-60 Å region of continua 9-34531
- Zn atoms, cross sections wavelength dependences, 247-1242 Å 9-34562

Photolysis *see Photochemistry***Photomagnetic effects** *see Photoelectromagnetic effects***Photomagnetolectric effects** *see Photoelectromagnetic effects***Photometers**

- see also Spectrophotometers*
- a.c. without amplifiers, using multistage photomultiplier 9-22463
- airglow, with improved red sensitivity 9-45512
- colour system, wide baseline, for galaxy synthesis, stellar photometric obs. 9-29013
- Elko II photometer for iron and steel lab. 9-47481
- flame for spectrochemical analysis 9-41459
- forward scatter, patent 9-40381
- integrating, for meas. virus suspension absorption 9-31685
- integrating, IPM2 for submicroscopic weighing 9-46008
- light-scattering, low-angle, for solns. meas., 17-150° 9-30407
- sky, calibration 9-26901
- for spectral irradiance meas. 9-32057
- spiral scanner with optical viewfinder 9-36368
- stellar, synchronous three colour 9-31681
- teletphotometers for Cosmos 149 satellite 9-45577
- tilting-filter, performance optimization, design 9-36367
- transparency meter, multiple reflection, for meas. attenuation of directed beam in seawater 9-36369

Photometry

- see also Brightness; Densitometry; Illumination; Spectrophotometry*
- autocollimators with beam splitters, selection of photodetectors 9-36408
- characteristic curves, photographic 9-41947
- δ Scuti variables 9-45627
- Delta Scuti type variable, observations of five 9-45626
- electrophotometry of light fluxes, use of photomultiplier operating as photon counter 9-25370
- flare in photographic objectives, meas. 9-38420
- galaxies, bright, 64, mainly in Virgo Cluster region 9-31502
- galaxies, normal, radio and radio quiet, and QSO's, UVB data 9-31565
- glass, transmission props., effect of false flashes 9-35630
- heavy water, isotope content determ. 9-49392
- introduction from radiometry considerations 9-29151
- linearization of characteristic curves in photographic photometry 9-41946
- microphotometer measurements of stellar radial meas. 9-31671
- moon, surface light-scattering, single-colour investigation of uniformity 9-31589
- mosaic prism for star field photometric calibration 9-24936
- occultation of stars, photometrical observation from the moon 9-31674
- optical fibre bundle filling factor, meas. 9-38413
- Orion Belt region, H γ photometry of B stars 9-24790
- photographic, linearization of characteristic curves 9-32025
- photographic plates, photometric calibration by double refracting crystal filter 9-40390

Photometry continued

- photosynthesis, meas. of radiant energy acting on plants 9-27122
- planet Mars, analysis 9-49580
- radiometry, optical resource letter 9-40380
- rectangular aperture, calc. of solid angle subtended at point opposite one corner 9-22440
- rocket-borne auroral meas. 9-31366
- SI units and conversion tables 9-41948
- stars, 10 new horizontal branch, obs. using 4-colour system of Stromgren 9-29015
- stars, A type, 146, K line strengths 9-27024
- stars, δ Scuti, new, periods and amplitudes calc. 9-29012
- stars, G, K and M, i.r. region emission spectra obs. 9-31539
- stars, high polarized, wavelength depend. of polarization 9-31534
- stars, variable in Large Magellanic Cloud, $\alpha=5^h12^m$, $\delta=-67.5^\circ$ region 9-38044
- stellar, 12 colour, wide-baseline colour system and appl. 9-29013
- stellar open clusters, Coma and Ursa Major, 4-colour and H β photometry 9-31554
- TZ Bootis, star, yellow and blue light photoelec. obs. 9-29016
- units and definitions 9-32027
- V502 Ophiuchi, star, yellow and blue light photoelec. obs. 9-29017
- virus suspension absorption meas. with integrating photometer 9-31685
- O₂ density distributions, X-ray and EUV determinations of latitudinal and temporal variations in 70 to 150km region of atmosphere 9-31341

light sources

No entries

Photomultipliers

- channel multiplier, operation at -78.5°C 9-40333
- continuous channel, use in obtaining pulse counting mode mass spectra 9-42320
- counting single photons, nature of noise pulses 9-38360
- crossed elec. and mag. field secondary electron, high speed response, multiplier 9-41884
- fluctuations of dark current in 1p21 cell 9-34147
- high-gain, with first dynode of Cs-activated GaP, performance 9-36264
- in Lallemand electron camera, for use in photoelec. studies 9-47903
- photoelectrons time distrib. from laser and pseudo-gaussian sources 9-45933
- photon counter electrophotometry of light fluxes 9-25370
- for photon counting in optical tracking of satellite, multicoincidence method, sampling technique 9-38014
- pulse height resolution, with high gain 1st-GaP(Cs) dynode 9-29386
- sensitivity enhancement by optical method 9-43858
- soft X-ray, open mag. and channel multipliers 9-48225
- solar-blind, use in flame spectroscopy 9-31226
- stability criterion of amplification coeff. in single electron meas. mode 9-36265
- thermionic emission shot noise equation, dynode emission 9-31920
- Cs₂Te photocathode, props. 9-25190

Photons

- see also Cosmic rays/photons; Gamma-rays; Nuclear reactions and scattering due to photons; X-rays*
- attenuation by air, 5.9 keV 9-43864
- beam, information content 9-43865
- beam coherence, experimental meas. 9-27290
- bunching effects in spatially coherent noise field, enhancement 9-34153
- collisions with 550 MeV relativistic electrons, ang. and energy distrib. of γ -quanta 9-29542
- counting, multi-coincidence method, for optical tracking of satellite, sampling technique 9-38014
- counting, photoconductive 9-39704
- counting correlations for field statistical analysis 9-27293
- counting for optical tracking, multi-coincidence method 9-45574
- counting with slowly modulated light beams 9-47922
- emission cross-section, Poisson formula applic. 9-36431
- emission from hot dense plasma by conversion of focused laser radiation 9-42517
- interaction with matter, energy rel. to refractive index 9-43907
- interference effects due to low-intensity beams through Fabry-Perot interferometer 9-41943
- laser, gas, photon distrib. function after rapid switching on 9-29409
- laser beams, independ., correl., stimulated refl. expt. 9-43901
- mass, review of latest expts. 9-43967
- mixed thermal and coherent radiation, twofold joint photocount statistics 9-45940
- one-photon corrections to interactions between atomic states 9-25680
- optical, by atom interacting with radio freq. photons 9-22969
- phonon-photon signal generation by lasers under pulsed and continuous regimes 9-29402
- polarized, π^+ and π^- mesons prod., agreement with vector dominance model 9-42073
- propagator, iso-vector hadron current applic. 9-22547
- radiative transfer from magnetic monopole to elec. charge 9-38438
- radiative transport in finite homogeneous cylinders, Monte Carlo anal. 9-45801
- rest mass, radiophysical meas. method 9-48153
- spectral function, contrib. from part.-antipart. states w.r.t. timelike form factors, mass spectra obs. 9-29534
- spectrum and target parameters of positron annihilation in flight system 9-25422
- statistics 1st-Born, matter-field correl. depend. 9-47923
- transformation into vector mesons 9-27459
- virtual longitudinal, search for contribution in ep scatt. 9-38471
- wave eqn. derived from symmetric spinor formulation multipole solns. 9-48136
- $\gamma d \rightarrow \eta p n$ cross section, ang.-distrib. meas., $E_\gamma=850$ MeV 9-36462

interactions

- absorption, E1, cross section calc. in 3-particle nuclei, Gammel-Brueckner potential 9-29716
- with charged particles, S-matrix theory study 9-25413
- experiments at 6 GeV e Hamburg acceleration 9-22525
- fixed poles in photoproduction amplitudes 9-29535
- hadron photoproduction reaction, Glauber theory applic. 9-38483
- photoeffect at high energy 9-29533
- one photon interaction with matter, quantum statistics 9-29393
- photoproduction, Veneziano-like parametrizations 9-48175
- photoproduction at threshold, helicity amplitude behaviour 9-38458
- photoproduction at threshold by current algebra sum rules 9-43968

Photons continued**interactions continued**

- photoproduction of composite particles, asymptotic behaviour in some models 9-46056
 photoproduction of mesons near threshold 9-22526
 photoproduction of mesons near two-angle theory of weak and e.m. interactions with $SU(3)$ symm. breaking 9-27480
 photoproduction of π , kinematic discussion and dynamical model. 9-25460
 photoproduction of π on N, magnetic quadrupole amplitude 9-25455
 photoproduction proc., Regge-pole model kinematic constraints and factorization 9-38457
 photoproduction processes by $U_{6,6}$ peripheral absorpt. model 9-41996
 r.f. with atoms, absorption and scattering of optical photons 9-22969
 shielding, transverse, of 4 and 5 GeV beams, calcs. 9-42156
 with stars, relativistic, delays rel. to position of origin on disc 9-29018
 transition effect for electron-photon shower, calc. 9-43973
 vector meson dominance in photoproduction, modifications 9-46057
 α photodisintegration, tensor forces and vel. depend. potential for cross section calc. 9-38601
 d, π photoprod., backward, $E_{\gamma} \sim 1$ GeV, pion-nucleon final state interaction effect 9-44025
 Δ (1238) isobar, photoproduction at photon energies below 1 GeV 9-22635
 η photoprod. on p, cross section meas. 9-36461
 η photoproduction, below 2 GeV 9-22524
 $\eta(X^0)$ photoprod. cross section calc. by dispersion-theoretic technique 9-36484
 $\gamma NN \rightarrow NN\pi$, soft π prod. at threshold, theory, S-matrix element 9-38562
 $\gamma N, \pi$ production, dispersion analysis 9-38519
 γ prod of π, γ , first reson. region, investigation 9-25456
 $\gamma N \rightarrow N\pi$, kinematically free amplitude Reggeization method applic. 9-27519
 $\gamma N \rightarrow VB$, photon-vector-meson analogy model, diff. cross section, polarization, helicity density matrix reln. 9-34320
 $\gamma N \rightarrow \gamma B$, photon-vector-meson analogy model, diff. cross section, polarization, helicity density matrix reln. 9-34320
 $\gamma n \rightarrow p\pi, 0.2 \rightarrow 2.0$ GeV, cross-sections, comp. with theor. predictions 9-40422
 $\gamma n \rightarrow \pi^+\pi^-\pi^0$ as test for A_1 and B mes. as reson. or kinematic eff. 9-22612
 $\gamma N \rightarrow \pi$, cross section, threshold determ., PCAC theory, $E_{\gamma}=160-230$ MeV 9-29606
 $\gamma N \rightarrow \pi_0 N$, photoproduction at low energy limit in chiral dynamics 9-48188
 $\gamma n \rightarrow \pi^- N^+$ cross-section predicted in quark model 9-29580
 $\gamma n \rightarrow \rho\pi^0$, differential cross section meas., $E_{\gamma}=500-800$ MeV 9-32222
 $\gamma p \rightarrow K^0 \Sigma, E(\gamma)$ up to 5 GeV 9-44008
 $\gamma p \rightarrow p\pi^0 \rightarrow p\pi^+, \rho^0$ decay direction determ., $E(\gamma)$ polar $= 2.5$ GeV 9-40436
 $\gamma n \rightarrow \pi^+$, ang. distrib. meas., 230-350 MeV 9-22523
 $\gamma p \rightarrow \omega$ cross section and t distrib. meas., $E_{\gamma}=16$ GeV 9-27537
 $\gamma p \rightarrow p\eta$, between threshold and 900 MeV 9-44006
 $\gamma p \rightarrow p\pi^0$, production cross section meas., recoil p obs., $E_{\gamma}=220-400$ MeV 9-40423
 $\gamma p \rightarrow p\pi^0$ below $E_{\gamma}=222$ MeV, ang. distrib. obs. 9-29578
 $\gamma p \rightarrow p\pi^0$ backward angles between 700 and 150 MeV 9-44020
 $\gamma p \rightarrow p\rho^0$, sum rules and convergence 9-27542
 $\gamma p \rightarrow \pi^+ \pi^0$ double p prod. form factor in vertex 9-36470
 $\gamma p \rightarrow \pi^+ n$, cross section determ., helicity amplitude Reggeization method 9-34304
 $\gamma p \rightarrow \pi^+ p$ baryonic resonance contributions, quark model 9-29580
 $\gamma p \rightarrow \eta$ cross section and t meas., $E_{\gamma}=16$ GeV 9-27537
 π^+ , photoproduction by polarized photons, vector dominance, cross section and asymmetry 9-42075
 π^+ photoprod. in Regge-pole model, exchange-degenerate conspirators 9-32185
 π^+ photoproduction, vector dominance anomaly 9-29581
 π photoproduction, below 2 GeV 9-22524
 π photoproduction from nucleon, dispersion analysis 9-44022
 π photoproduction in γN interac. multipole amplitudes evaluated 9-22592
 π photoproduction on 3H , impulse approx. calc. in elastic channel, $E_{\gamma}=200-500$ MeV 9-25453
 π photoproduction on 3He , impulse approx. calc. in elastic channel, $E_{\gamma}=200-500$ MeV 9-25453
 π photoproduction on d, impulse approximation tested, d wave-function meas. 9-42074
 $^{12}C \rightarrow \eta$, energy below single nucleon production threshold 9-34279
 γp 6.5-17.8 GeV, vector meson prod. differential cross-section 9-25474
 $\gamma p \rightarrow \pi^+ n$, linearly polarized photons 9-44018
 N_2 photoionization cross section, electron phase shift calc., simple model potential construction 9-46258
 O_2 , electrons photodetachment cross section, pseudopotential calc. method 9-46257

polarization

- Bragg reflected from a crystal, polarization determ. from Mossbauer spectrum 9-30532
 circular, and π form factor calc. in $e^+ \rightarrow \pi^+ \pi^- \gamma$ 9-29548
 nucleus polarized thermal n capture, γ emission meas. 9-27736
 Al single crystal, deduced from Mossbauer spectrum 9-30532
 Ge(Li) detector, γ -ray linear polarization sensitivity 9-38460

scattering

- bremsstrahlung monochromator for investig. 9-42007
 Cabibbo-Radicati sum rule, applic. in nuclear physics 9-34428
 Compton, forward, contrib. of pole at $\alpha=0$ 9-32158
 Compton, from bound K-shell electron, matrix element calc. 9-38459
 Compton process, polarization of Dirac output particle 9-22527
 Maxwellian electron gas, rel. to radiant heat transfer calcs. 9-22109
 nucleus, vector meson prod. and radiative capture, amplitude, cross section calc. 9-27460
 photon-photon, cross section, graviton exchange, classical and quantum linearized theory of gravitation calc., comparison 9-32127
 photon-scalar particle cross section, graviton exchange, classical and quantum linearized theory of gravitation calc., comparison 9-32127
 plasma electrons, thermodynamic Green function technique, cross section calc. 9-32599
 Rayleigh scatt. of polarized photons by molecules 9-34589
 e, relativistic, Compton scatt., γ polarization meas. 9-36430
 $e\gamma$, elastic, amplitude in quantum electrodynamics at infinite energy 9-40403

Photons continued**scattering continued**

- $\gamma\gamma$, elastic, amplitude in quantum electrodynamics at infinite energy 9-40403
 $N\gamma \rightarrow \Delta\pi$, static multipole moments of $\Delta_{1236} (3/2, 3/2)$ from superconvergence 9-38595
 on H atoms, amplitude, exact expression, and Lamb shift in nonrelativistic approx. 9-36683
 $^{90}K, 4p$ and $5p^2P_{3/2}$ states, hyperfine struct. investig. by resonance scatt. 9-29751
 $^{41}K, 4p$ and $5p^2P_{3/2}$ states, hyperfine struct. investig. by resonance scatt. 9-29751

Photonicuclear reactions see Nuclear reactions and scattering due to photons**Photophoresis**

No entries

Photoproduction see Gamma-rays/effects; Nuclear reactions and scattering due to photons; Photons/interactions**Photoresistors see Photoconducting devices; Semiconducting devices****Photosphere see Sun****Photovoltaic effects**

- dielectric crystals, transient effect as function of wavelength 9-47207
 dye-photoconductor interfaces 9-43135
 heterodyne detection of scatt. i.r. radiation, quantum theory 9-38366
 naphthalene, intensifying effect of violet and green light on current for red light 9-47207
 polymer films, in vacuum u.v. 9-43136
 semicond. heterojunctions, analysis 9-49168
 AgBr, nonlinearities 9-43134
 Cd, Hg, γ -Te alloys, assoc. with effective mass gradient 9-39730
 CdS-Pt, impurity effect, photo. e.m.f. stimulation mechanism in i.r. spectral region 9-30997
 in CdS-Cu, S heterojunctions 9-24240
 CdS ceramic solar cell, props. and model 9-25171
 CdTe film, anomalously high, nature 9-26605
 Cu₂S-CdS heterojunctions, heat-treated, mechanism and hole-trapping obs. 9-39650
 GaP-Cu diodes, charge-carrier capture and effect on transition capacitance 9-35510
 α -MoTe, single cryst., spectral distrib. of photovoltage 9-33411
 Se polycrystalline layer junction with In-AgSe solid soln., photocell for i.r. 9-41274
 Si films, high voltage eff. 9-24241
 Te-Ag thin films on contact, obs. 9-35511
 Te-Bi thin films on contact, obs. 9-35511
 Zn_xCd_{1-x} ternary system film 9-24242

Physical chemistry

- dielectric constant, uses and measurement 9-24214
 flow, laminar stream, over reactive surface, periodic fluctuation of chemical species mass fraction 9-25815
 thermodynamic systems under non-hydrostatic stresses, chemical potential 9-22272
 transport processes, simplified models, review 9-37816
 Ne-He mixture, separation in liquefier 9-23590

Physical effects of radiations

see also Under individual radiations. e.g. Neutrons and antineutrons/effects

- alkali halide whiskers, shape depend. of radiation induced defects 9-32941
 alkali metal azides, D_{3h} symmetry of ion, explanation of new electronic and i.r. band 9-27844
 alkaline earth oxides, irradi., electronic states of defects obs. 9-44689
 alloys, eff. on rate processes 9-24068
 anthracene: tetracene radiation damage rel. to optical absorption 9-26747
 austenitic alloys, foil induced swelling due to void formation 9-48755
 breakdown time-lags, statistical distrib. by Townsend mechanism under high-energy particle irradi. 9-48637
 calcite, thermoluminescence mechanisms following α and reactor irradiation 9-31147
 ceramic nuclear fuels, Review 9-22902
 charged-particle track formation, review 9-24067
 chemical damage, photoannealing, influence of crystal defects. 9-23933
 crystal growth, equi. surface struct. changes 9-37021
 crystal macrodefects, radiation produced, electron microscope investigation 9-32984
 crystals, model of radiation damage involving thermal vibrs. of atoms 9-41114
 crystals, particle focusing and channeling, review 9-35294
 crystals, rad. damage, anisotropic effects 9-33202
 defect formation by channeling particles 9-33203
 diffusion creep due to neutrons 9-28308
 diffusion enhancement in solids by ionizing radiation 9-42856
 electron spectra, low energy, established within and emitted from irradiated conducting materials 9-26466
 epoxy resin film, transparency changes due to u.v. irradiation 9-47328
 excitons, photodissociation by i.r. radiation, continuum model 9-28452
 fog dissipation 9-31313
 glasses, laser damage 9-33520
 graphite, irradi., diffusion mechanism 9-40981
 ice, irradi., trapping of electrons 9-42980
 in-pile, and temp., on Inconel sheathed lead wires of chromel-alumel thermocouples 9-36637
 ionization by u.v. radiation from target in laser beam focus 9-36780
 laser damage in glasses 9-33520
 laser radar, eye hazards, analysis and reduction 9-38152
 lasers, space radiation effects 9-22422
 linear accelerator vacuum components, technological problems 9-36547
 metal crystals, irradi., sweeping-up of loops by glide dislocations during deform. 9-32963
 metals, f.c.c., voids due to neutrons 9-41119
 mirror for space flight, optical degradation due to u.v. radiation and condensation obs. 9-40111
 neutron irradiation and Portevin-Le Chatelier effect in carburised Ni-Cu alloys 9-28349
 oxides, irradi., electronic states of defects obs. 9-44689
 Permalloy films irradi., spin wave resonance 9-45370
 polycarbonate film, charged-particle irradi., etching rate accel. by u.v. irradi. in O₂ atmos 9-32271
 quartz, γ -irradi., glow curves rel. to dose, defect synthesis 9-26273

Physical effects of radiations continued

- relaxation apparatus for use in radiation fields 9-46872
 RNA, ribosomal soln. γ irradi. effects 9-26132
 rubber adhesive film, transparency changes due to u.v. irradiation 9-47328
 semiconducting compounds, damage determ. by optical reflectivity technique 9-37503
 space environment effects on materials 9-48977
 styrene, polymerization and post-polymerization 9-24554
 swelling in austenitic stainless steel, reactor induced 9-28437
 thermocouple lead wires, Inconel sheathed, in-pile rad. and temp. 9-36637
 thermocouples, irradiated, decalibration by self-annealing scatt. centres 9-22301
 water, cavitation threshold lowering by fast neutrons 9-46592
 zirconolite-4, radiation enhanced relaxation 9-41006
²³⁹Pu edge breeding in irradiated UO₂ 9-22899
 Ag crystals, Xe ions bombard., threshold of damage obs. 9-30800
 Al-(10 wt.%)Zn alloy, irradiated at 78°K, pre-precipitation rate 9-30715
 Al, in-reactor U sputtering, subsequent irradiation for fission fragments track etching and obs. 9-34489
 Al₂N₃ neutron irradi., anisotropic growth 9-40857
 Al reinforced with SiO₂ fibre, eff. of irradiation on strength 9-26338
 Al single crystal, yield, plasticity and elec. cond., macrosound and n effects 9-46928
 Au crystals, Xe ions bombard., threshold of damage obs. 9-30800
 BaTiO₃ crystals and ceramics, mixed pile radiation effect on electrophysical props. 9-41238
 Be, hot pressed, release of gas 9-37282
 Be and BeO, damage mechanisms, eff. on macroscopic props., review 9-24069
 CaCO₃, fission fragment tracks, structure and healing 9-26467
 CaF₂, X-ray diffraction profiles broadening 9-46784
 CdS i.r. photoconductivity 9-26600
 Cr-steels, embrittlement in temp. range of α - γ transformation 9-28369
 Cu-(2.5 wt.%)Zr-(0.5 wt.%)Nb alloy, radiation enhanced relaxation 9-41006
 n-Ge, i.r. wavelength depend. of electrical breakdown current 9-30926
 Ge, irradiation rel. to diffusion mechanism and point defects, review 9-37209
 p-InSb, defects formation by illumination 9-28283
 Ir, fission-fragment damage and formation mechanism 9-42810
 LaMg(NO₃)₃, proton relaxation time in NMR 9-28767
 LaMg(NO₃)₃, radiation damage eff. 9-28438
 LiCl, reactor-irradiated, X-ray- and thermoluminescence 9-28729
 LiF, fission fragment tracks, structure and healing 9-26467
 LiF thermal conductivity changes following irradiation induced imperfections 9-33198
 MgF₂, overcoated Al mirrors for space flight optical degradation due to u.v. radiation and condensation obs. 9-40111
 Mo-steels, embrittlement in temp. range of α - γ transformation 9-28369
 NH₄OHCl, X-irradiated, optical conversion of V_k centres 9-32995
 Nd: glass, damage threshold improvement by chemical polishing 9-26171
 Ni-Fe alloys, enhancement of diffusion and directional ordering expts. 9-44742
 Ni, desorption of CO by photons, 2.1-4.8 eV 9-23647
 NiO, u.v. irradi., effect on catalytic activity 9-41446
 Pu and alloys, self-irradiation eff. 9-24072
 Si:Li-diffused, electronic level changes on irradiation, e.s.r. obs. 9-26794
 Si, absorption edge modification by radiation-induced defects 9-47132
 Si, irradiation rel. to diffusion mechanism and point defects, review 9-37209
 Si p-n junction, defect isochronal annealing temp. 9-24199
 Si solar cell assemblies, proton-induced damage 9-24077
 U, anisotropic grain growth and cavitation swelling rel. to alloying additions 9-33206
 U₂Si, 60°C phase change, X-ray diffraction analysis 9-35248
 U alloys, dilute, temp./exposure thresholds for cavitation swelling 9-41117
 UC, arc cast and sintered, on thermal conductivity, 150-1600°C 9-41111
 UO₂, irradiated, growth of fission gas bubbles 9-28152
 UO₂, sintered, on thermal conductivity, 150-1600°C 9-41111
 Zr, damage, rate and distribution, effect of fast neutron spectrum 9-26469

Physics

- see also Biographies; History; Nuclear physics; Teaching*
 american college textbook, introductory 9-36104
 causality, follows from existence of asymptotic causality 9-43695
 college textbook for non-scientist 9-31735
 college textbook for US students 9-31734
 definition of physical system 9-29142
 education for industry, specialist versus generalist 9-41725
 education of physicists for work in industry 9-41721
 educational requirements of physicists in industry 9-41722
 experiment-oriented general course 9-29144
 extramural, post-graduate, and refresher courses, responsibilities of industry and universities 9-41726
 Feynman course, exercises complementary to pt. I 9-47717
 Goethe's Farbenlehre, physicists views 9-45711
 graphs, least-squares adjustment of weighted to data general linear eqn. 9-45802
 the great experiments of physics, book 9-22029
 IEEE Northeast Electronics Research and Engineering Meeting Boston (1968) 9-36096
 introductory American physics textbook 9-34001
 Iowa Academy of Science, 77th session, Des Moines (1967) 9-36095
 Italian Physical Society, 52nd Congress Oct. 1966 9-33998
 manual, programmed, to accompany American physics text 9-31736
 N-bug problem, path traversed 9-45717
 navigation, inertial; accelerometers on pendulum on object, multiple integration 9-45714
 practical, new teaching techniques 9-22033
 practical physics, text book of methods 9-40226
 research programs involving nuclear reactors, cost efficiency 9-22860
 science conference, Des Moines, IA, USA (1968) 9-43696
 seminar, 'Perspective on science' 9-27154
 teaching at middle level, scheme for new plan 9-29145
 teaching in biological sciences 9-29147
 teaching laboratory as place of research 9-36097

Physics continued

- teaching science of materials at U.N.A.M. (Universidad Autonoma de Mexico) 9-29146
 textbook, American college, produced by physical science study committee 9-41730
 U.N.A.M. (Universidad Nacional Autonoma de Mexico) general physics course, lab. work importance 9-36098
 university cooperation with industry, effect on physicists career 9-41723
 university courses adaptation to industrial needs 9-41724
- Physics fundamentals**
see also Cosmology; Elementary particles; Field theory, classical; Field theory, quantum; Indeterminancy; Mechanics; Parity; Probability; Quantum theory; Relativity; Thermodynamics; Units
 atomic physics, college textbook 9-48370
 atomic physics textbook 9-48371
 causality, non-violation by tachyons 9-45751
 causality aspects of relativistic plasma 9-32591
 causality of energy density propagation 9-25031
 collections of excerpts by authors who have written on basics 9-31733
 definition of physical system 9-29142
 dipole field motion and analogy with spherical pendulum 9-29164
 2e/h meas. by a.c. Josephson effect 9-39593
 entropy, derivatives at absolute zero 9-29159
 ground state of spherically symmetric potentials 9-29160
 heat, definitions, review 9-45721
 heat conduction problem, eigenfunction soln. 9-29154
 Heisenberg two-spin model exact soln by Green's junction methods 9-29148
 invariability of velocity of light, expt. to test validity of Einstein's second postulate 9-41744
 maser model dynamics 9-29163
 m.h.d. conversion, introductory paper 9-25018
 Planck's const., lower bound theoretical estimation 9-47756
 potential, central; phase shift, scatt. length, discrete and continuous spectrum props. 9-45767
 quantum mechanics phase eqn. derivation 9-45766
 radiometry and photometry, introduction 9-29151
 SI units scheme 9-22038
 Snelshaw and gravitational deflection of light, corpuscular theory justification 9-29155
 textbook of the physics of elementary processes 9-38185
 time, its nature rel. to first law of thermodynamics 9-45729
- Physiology**
see also Biological technique and instruments; Blood; Hearing; Vision
 aortic valve, fluid mechanics and closure mechanism 9-49601
 pathology, optical, X-ray and electron microscopic 9-29112
- Piezo-optical effects** *see Photoelasticity*
- Piezoelectric oscillations**
 crystal, vibrating, spectral characts. rel. to direction of exciting elec. field 9-41251
 linear theory, fully coupled, exact solns. for waves in plates 9-22247
 plates, thickness vibrations, electromech. coupling const. rel. to fundamental material const. 9-37593
 quartz, Bechmann's number for harmonic overtones of thickness-shear vibrs. 9-31848
 α -quartz, excitation of elastic surface waves giving rise to light scatt. 9-47307
 quartz, plates, AT-cut, beveled, thickness-twist vibrs. 9-29259
 quartz crystal, singly rotated, force-freq. coeff. chart 9-37596
 shaker, piezoelec., for calib. of vibr. pickups 9-38295
 surface elastic waves, excitation and detection 9-43784
 surface wave propag., e.m. boundary conditions effect 9-45013
 vibrator, piezoelec., remotely controlled, for low temp. region of cryostat. 9-34080
 LiNbO₃, microwave frequency acoustic surface wave propagation losses 9-33173
 ZnO:Li, u.s. wave attenuation, temp. and freq. depend. 9-37339
- Piezoelectricity**
see also Electrostriction; Piezoresistance
 acoustic surface wave propag. in piezoelec. substrates, eqns. and soln. 9-37320
 acoustoelectric domains propag. in piezoelec. III-V semicond., evolution 9-37349
 alkali metal niobates based highly dense piezoelec. material 9-39676
 analcite 9-43121
 bending rectangular plate, theory 9-36160
 blood vessel walls 9-38129
 ceramic plate coupled to n-Si, acoustic wave amplification 9-26419
 ceramics, accurate method for coeffs. meas. 9-37592
 ceramics, Na₂O, Li₂O, and Nb₂O₅ composition, patent 9-30725
 ceramics, rel. to orientational dielec. polarization 9-47187
 coefficients, accurate meas. method 9-37592
 crystal-vacuum boundary, reflection of acoustic wave 9-44819
 electroacoustic surface wave propag. 9-28425
 electromechanical characts. of piezoelec. materials in strong excitation fields, under high press. 9-47185
 electron-hole plasma interactions with lattice vibrations 9-26415
 heterojunction characteristics, modulation by field-independent piezoelectrically-induced polarization discontinuity 9-28527
 magnetically ordered, induced ferroelec. mag. obs. 9-39748
 materials, literature digest, 1967 9-33368
 materials, surface wave without counterpart in elastic homogeneous material 9-24224
 nematic liquid crystal, polarization and curvature strain rein. 9-28148
 nonhomogeneous transducers and filters, acoustic response w.r.t. piezoelec. stress 9-37348
 parameters of new materials and properties of devices 9-43120
 Perovskite-type crystals, accompanying orthorhombic deformation of cubic lattice 9-28558
 piezoelectric converter for cardiac assistance device 9-38130
 piezoelectric effect 9-47191
 piezosemiconductors, acoustic wave generation 9-28419
 polaron, strong-coupled, effective mass calc. 9-39572
 polarons, piezoelec., effective mass and energy calcs. by Feynman method 9-41139
 quartz, piezoelec. const., temp. variation 9-33397
 quartz, X-cut, elec. breakdown and recovery under shock wave compression 9-47189

Piezoelectricity continued

- semicond. tapered surfaces, acoustic domain studies 9-37521
 semiconductor, acoustoelectric, domain theory, nonlinear interactions 9-48963
 semiconductor, acoustoelectric domain theory, domain soln. 9-48964
 semiconductor, acoustoelectric domain theory, linear regime 9-48962
 semiconductor mechanical sensors using piezoelectric effect 9-47191
 semiconductors, acoustic amplification under large signal conditions 9-33177
 semiconductors, electromechanical transducers, modification of energy conversion process by effects due to carriers 9-34084
 semiconductors, III-V, evolution of propag. acoustoelec. domains 9-37349
 semiconductors, multiple wave interactions 9-49065
 semiconductors, nonlinear limiting of acoustic wave amplification, use of perturbation technique 9-28422
 semiconductors, root-locus analysis of electroacoustic amplifiers 9-28423
 semiconductors, static domain 9-37350
 semiconductors piezoelec. amplification and generation of acoustic waves 9-30774
 semiconductors with piezoelec. interactions, hypersound absorpt. by carriers 9-48952
 solid, effect of charged dislocations 9-48856
 sound generation by non-uniform piezoelec. materials 9-34082
 static domain in piezo-semicond. 9-37350
 surface wave propag., e.m. boundary conditions effect 9-45013
 thin-film transducers, development and results 9-30980
 transducers, bonded, high performance for freqs. beyond 100 MHz 9-36184
 transducers, semicond., reson. freqs. 9-25105
 transducers, thin-film, electromech. coupling factors, elec. meas. tech. 9-37594
 transverse wave interaction in materials 9-35459
 α -Ag-In dil. alloys, piezoreflectance 9-47325
 $\text{BaTiO}_3\text{:Co}$, electromechanical props. 9-47171
 $\text{Bi}_{1-x}\text{Ge}_x\text{O}_{20}$, elasto-optic matrix elements 9-33394
 $\text{Bi}_{1-x}\text{Si}_x\text{O}_{20}$, elasto-optic matrix elements 9-33394
 CdS, calculation of constant using phonon dispersion model 9-46972
 CdS, permittivity components and strain modulus, 1.5-300°K 9-33395
 CdS semiconducting crystal acoustic amplifier, temp. depend. of characts. 9-44815
 CdS semiconducting crystal acoustic amplifier, temp. depend. of characts. 9-44815
 CdSe, acoustoelec. eff. rel. to current saturation and oscillation mechanism 9-26543
 CdSe semicond., attenuation of transverse u.s. waves, action of photons 9-28420
 GaAs, current saturation induced by sound amplification, nonlinear theory 9-47111
 n-GaAs acoustoelec. domains, Brillouin scatt. studies 9-37352
 n-InSb-Ge, amplitude depend. u.s. attenuation at liq.-He temp. 9-44825
 n-InSb, films, contribution to energy scattering of conduction electrons 9-26549
 KD_2PO_4 , ferroelec. anomalies in dielec. and piezoelec. props. 9-41244
 LiIO_3 , and electrical behaviour 9-37595
 LiNbO_3 , acoustic surface wave coupling across air gap 9-26594
 LiNbO_3 , electro-optic coeffs., signs 9-33396
 LiNbO_3 , plane longit. elastic wave with vector along Y-axis of rod, vel. and energy propag. direction 9-37228
 LiNbO_4 sputtered films, coupling factors 9-42725
 LiTaO_3 , microwave u.s. attenuation 9-44826
 $(\text{Na}_{1-x}\text{Li}_x)\text{NbO}_3$ solid solutions ceramics, disappearance of properties at transition temp. 9-26389
 $\text{PbTiO}_3\text{-PbZrO}_3\text{-PbMg}_{0.5}\text{W}_{0.5}\text{O}_3$ solid solns., piezoelec. props. 9-47188
 $\text{Pb}(\text{Zr,Ti})\text{O}_3$ ceramic, adulterated, high-field losses 9-26585
 $\text{Pb}(\text{La}_{0.5}(\text{M}^{3+})_{0.5}\text{Ti}_{1-x}\text{O}_3)$, (M=Nb or V), electromech. coupling coeff. 9-24220
 RbH_2AsO_4 , normal and deuterated 9-39696
 RbH_2PO_4 , ferroelec. anomalies in dielec. and piezoelec. props. 9-41244
 RbH_2PO_4 , single cryst., consts. 9-44749
 SbSI orientated fibroform cryst., constants 9-48808
 Te, piezoelec. consts., strain-induced electronic displacement rel. to cores obs. 9-35493
 ZnO attenuation of compressional and shear piezoelectrically active u.s. waves, freq. depend. 9-37340
 ZnO epitaxial thin film on CdS, sapphire; perfection depend. on substrate polish, temp. 9-36953

Piezomagneto-optical effects see *Magneto-optical effects***Piezoresistance**

- see also *Piezoelectricity*
 m.o.s.t., strain effect 9-26581
 thin films, oriented, longit. and transverse isotropy 9-35326
 InSb, coeffs., deformation potential shift consts. 9-43046

Piles, nuclear fission see *Nuclear reactors, fission***Pinch effect** see *Discharges, electric; Plasma/confinement; Semiconducting materials***Pions**

- absorption in tissue-equivalent material 9-27123
 atom, $7\text{S}_{1/2}$ state, lifetime, depend. on exciting conditions 9-29960
 charged, lifetimes, comparison for test of CPT theorem 9-27513
 decoupling theory, gemel families in Bethe-Salpeter eqn. 9-36435
 e.m. form factor, bounds 9-27514
 e.m. form factor in ρ^0 resonance region from $e^+e^- \rightarrow \pi^+\pi^-$ cross section meas. 9-29544
 e.m. formfactor determ. in space-like region from modulus in time-like region 9-34296
 e.m. mass differences and sum rules in Lagrangian model 9-29554
 e.m. radius determ. from phase-shift analysis of $\pi^+\pi^-$ diff. scatt. cross section data, $E_\pi=51.75$ MeV 9-38521
 exchange in N-N scatt repulsive core and nonstatic effects in momentum space 9-44050
 F.(s) form factor, parametrizations using either Omnes function or N/D method 9-36474
 fields, equal-time commutators calc. giving superconvergence sum rule 9-27524
 form factor, calc. and use in determ. of isovector electromag. form factors 9-38479
 form factor, dispersion sum rules 9-22589
 form factor and γ circular polarization calc. in $e^+e^- \rightarrow \pi^+\pi^- \gamma$ 9-29548

Pions continued

- form factor by comparing cross sections of positive and negative mesons electromag. 9-22593
 formfactor, e.m., decrease exponential character, lower bound determ. 9-29576
 kinematic parameters from p interact. with photo-emulsion nuclei in mag. field, Ep=21 GeV 9-27711
 one-pion exchange compared with expt. in π prod. expt. 9-48186
 radius, mean square, continuum contribs., calc. 9-32182
 self-consistency conditions for coupling constants from applying gauge conditions to production 9-46096
 slowing down in nuclear emulsions, charge difference effect 9-27533
 soft-pion technique inapplicable to relationship between $\eta \rightarrow \pi^+\pi^-\pi^0\gamma$ and $\eta \rightarrow \pi^0\gamma\gamma$ 9-44005
 SU(2) \otimes SU(2), non-linear realizations describing π field 9-38434
 two and three π exchange contrib. to N-N scatt. 9-44051
 zero-mass π theories invariant under c-number translations of π field, general framework study 9-48185
 $K^2\pi^2=K^{*2}2$ predicted sum rule for masses of octet bosons. 9-38540
 NN scatt., $T=0$ state $2,3\pi$ exchange 9-32212
 π - $\Lambda\sigma$ coupling from FSDR evaluated at KN scatt. threshold 9-46104
 π^+ capture in H_2D_2 gas mixture 9-36473
 $\pi^+\pi^-$ pairs, resonance search, photoproduction, in mass range 1360-1780 MeV 9-44024
 π^+ , single charge exchange rel. to spectroscopy of light nuclei 9-22715
 Si(Li), energy-loss and straggling by π^+ 9-30810
- decay**
 damping of charged pion beams due to decay in flight, lifetime comparison 9-27513
 lifetime rel. to validity of special relativity tested in cosmic ray obs. 9-34022
 model incorporating a time reversal invariance violation 9-32183
 weak radiative decays, sum rules, F_π/F_π eval. 9-32171
 π_{12} appl. of algebraic model describing symm. breaking 9-32174
 π_{13} appl. of algebraic model describing symm. breaking 9-32174
 π^0, π^+, π^- , Cherenkov counter for lifetime meas. 9-29655
 π^+ Goldberger-Treiman relation, hadronic corrections 9-38525
 $\pi^0 \rightarrow \pi^+\pi^-$ weak interactions of urbarions, pseudoscalar coupling magnitude determ. 9-27471
 $\pi^+e^- \rightarrow \pi^0e^+\nu$, model incorporating a time reversal invariance violation 9-32183
 $\pi^+e^- \rightarrow \pi^0e^+\nu$, probabilities, effect of e.m. field 9-27469
 $\pi^0 \rightarrow e^+e^-$, analysis, rate comp. to 2 photon mode 9-22590
 $\pi^0 \rightarrow \gamma\gamma$ and symm. violation 9-22542
 $\pi \rightarrow \gamma\gamma$, relevance of axial-vector current anomalies 9-48138
 $\pi \rightarrow \mu$ in nuc. emulsions, isotropy, in ang. distrib. 9-29577
 $\pi \rightarrow \mu\nu$, e.m., probabilities, effect of e.m. field 9-27469
 π_{12} and K_{12} decay consts., f_K and f_π equality 9-22548
 $\pi^0 \rightarrow \gamma\gamma$, matrix element sign and model depend. 9-38518
 ρ lifetime meas. from Primakoff effect obs. 9-46094
 $\pi \rightarrow \gamma\gamma$, Gell-Mann-Sharp-Wagner model corrections 9-46111
 $\pi \rightarrow \mu\nu$, V-A theory deviations 9-41999
- interactions**
 A_1 production in 8 GeV/c $\pi^+\pi^-$ interactions 9-44044
 and C targets, at 12 GeV/c, muon pair prod. 9-32135
 low-energy, by equal-time commutators of current algebra 9-44017
 nuclear absorpt. of pions, radiative, validity of soft pion theorems 9-36609
 $\gamma\pi \rightarrow \gamma\pi$ Compton scattering, threshold behaviour 9-29582
 $\gamma\pi \rightarrow \pi\pi\pi$ photoproduction amplitudes 9-29582
 $\pi^0 \rightarrow (\rho^+\pi^-\pi^0)$, evidence against prod. of $I=5/2$ baryon reson. of mass 1640 MeV/c² 9-42114
 $\pi^0 \rightarrow \rho^+\pi^-\pi^0$, $I=3/2$ baryon resonance obs., 1640 MeV/c²; $M\pi=2.26$ GeV/c 9-27562
 $\pi^2\text{H}$, A_1 production at 8 GeV/c 9-44044
 π^0 , $E_\pi=2.7$ GeV/c, four-charge-particle final states 9-32186
 π^0 neutral ρ enhancements at 8 GeV/c 9-46095
 $\pi^0 \rightarrow \rho^+\rho^0$, 2.7 GeV/c, $D^0 \rightarrow \pi^+\pi^-$ study 9-38543
 $\pi^0 \rightarrow \rho^+\rho^0$, 3.65 GeV/c, $\pi^+\pi^-\pi^0$ in ω^0 and η^0 regions obs. 9-34299
 $\pi^0 \rightarrow \rho^+\rho^0$ in nuclei, evidence 9-36608
 $\pi^0 \rightarrow \pi^+\pi^-\pi^0$, π^0 ang. distrib. determ., $E_\pi=600-1300$ MeV 9-40426
 π^+ absorption by ^3He , capture rate and coupling const. determ. 9-27517
 $\pi K \rightarrow \rho K$, Veneziano amplitude determ., $A_2 \rightarrow K\bar{K}$ decay mode suppression determ. 9-42091
 $\pi\Lambda$, solub. model, $Y_1^*(1385)$ resonance amplitude domination 9-22595
 $\pi N \rightarrow \bar{N}N$, VA helicity amplitude reggeization, production cross section determ. 9-34304
 π with 50 GeV/c momentum, charact. 9-46098
- interactions, pion-nucleon**
 $\pi \rightarrow \pi^+\pi^-$ diff. cross section data extrapolation, $t \rightarrow 2$ 9-22596
 $\pi^0 \rightarrow \rho^+\rho^-$, 16 GeV/c search for high mass bosons produced near 180° 9-38541
 $\pi^0 \rightarrow \pi^+\pi^0$, neutral final states obs., 1.71-2.46 GeV/c 9-27521
 $\pi\rho$, 7.0 GeV/c, distrib. of transverse and longitudinal meas. obs. in bubble chamber expt. 9-32191
 $\pi\rho$, transversal and longitudinal momenta of secondaries, distrib. and mass depend., $M_\pi=4$ GeV/c 9-32190
 $\pi\rho$ in nuclei, $E_\pi=925$ MeV, Λ^0 prod., cross sections 9-29814
 $\pi \rightarrow \pi^0$, π^0 backward emission, p-quanta meas., $M_\pi=1.55-3.8$ GeV/c 9-34305
 $\pi \rightarrow K^+\Lambda^0$, K^* exchange particle and trajectory determ., O(3,1) symmetry analysis 9-32189
 $\pi \rightarrow K^+\Sigma^0$, K^* exchange particle and trajectory determ., O(3,1) symmetry analysis 9-32189
 $\pi \rightarrow K^+\Lambda^0$, Reggeized Σ_π , Σ_γ exchange model 9-29585
 $\pi \rightarrow \Lambda^0 \Sigma^0 K^0$, 4.0 GeV, cross sections 9-27522
 $\pi \rightarrow \Lambda^0 \Sigma^0 K^0$, 4.0 GeV, cross sections 9-27522
 $\pi \rightarrow N^* \pi^+ \pi^-$, 11 GeV/c, $\pi^+\pi^-$ elastic scatt. study 9-25461
 $\pi \rightarrow \Sigma^+ K^0$, Σ^- polariz. meas., 1130 MeV/c 9-29621
 $\pi \rightarrow \eta^0 n$, neutral final states obs., 1.71-2.46 GeV/c 9-27521
 $\pi \rightarrow \eta^0 n$ high energy charge-exchange reaction, using Regge poles 9-44027
 $\pi \rightarrow \pi^+\pi^-$, 11 GeV/c, analysis of reaction 9-44029
 $\pi \rightarrow \rho\Lambda_2$, $A_2 \rightarrow \pi^+\pi^-\pi^0$, spin and parity anal. of Dalitz plot in A_2 region 9-29602
 $\pi \rightarrow \pi^+\pi^0$, 1.7 GeV/c, 2244 bubble chamber events 9-44028
 $\pi \rightarrow \pi^0 n$, neutral final states obs., 1.71-2.46 GeV/c 9-27521
 $\pi \rightarrow \pi^0 n$, energy depend. and composite model analysis, quark rearranging mechanism 9-42078
 $\pi \rightarrow \pi^0 n$, neutral final states obs., 1.71-2.46 GeV/c 9-27521

Pions continued

interactions, pion-nucleon continued

- $\pi^- p \rightarrow \pi^0 n$ high energy charge-exchange reaction, using Regge poles 9-44027
 $\pi^- p \rightarrow \pi^+ \pi^- \pi^+ \pi^- n$, g^0 resonance obs. in mass distrib., $E_\pi=4.7, 5.74$ GeV/c 9-29603
 $\pi^- p \rightarrow \pi^+ \pi^- n$, di-pion system in ρ mass region considered as $\pi\pi$ scatt. process 9-46100
 $\pi^+ p$, low-energy η reson. parameters calc. 9-29596
 $\pi^+ p$, diff. cross sections obs., channels comparison via baryon resonances, $E_\pi=8$ GeV/c 9-46099
 $\pi^+ p \rightarrow K^+ \Sigma^+$, K^+ exchange particle and trajectory determ., $O(3,1)$ symmetry analysis 9-32189
 $\pi^+ p \rightarrow N^{*++} C^0$, quark-model predictions for joint decay distrib., 8 GeV/c 9-38528
 $\pi^+ p \rightarrow N^{*++} w$, quark-model predictions for joint decay distrib., 8 GeV/c 9-38528
 $\pi^+ p \rightarrow \eta N_{\rho^0}$, η angular distrib. of high energy reaction, on basis of dipole model for A_2 meson 9-44046
 $\pi^+ p \rightarrow \rho^+ \pi^+ \pi^+ \pi^- \pi^- \pi^0$, D^0 meson prod. at 8 GeV/c 9-48190
 $\pi^- p \rightarrow K^- Z^0$, 6, 8 GeV/c search for strangeness +1 baryon 9-22634
 $\pi^+ p$ polarization data, Regge exchange models, $0 < -t < 4$ (GeV/c)² 9-22596
 $\pi p \rightarrow K \Sigma$ K - Σ relative parity determ. 9-27523
 $\pi p \rightarrow \Lambda K + n\pi$, $n=0, 1, 2, 3, 4$, 5.95 BeV/c obs. 9-27518
 $\pi p \rightarrow n, P$; $n=3, 5, 7$; effective mass spectrum of multipion system, Monte Carlo calc., high-energy 9-34306

interactions, pion-pion

- phase-shift from Faddeev relativistic eqn. appl. to $\bar{p}p \rightarrow \pi\pi\pi$ 9-36476
 Veneziano model, unitarized, appl. to expt. data 9-36477
 $\pi^- p \rightarrow \eta n$, continuous-moment sum rules and absorptive Regge cuts 9-48189
 $\pi^- p$, peripheral model near 1 BeV 9-29584
 $\pi^- p$ charge-exchange differential x -section at 180°, energy depend. 9-25462
 $\pi^- p \rightarrow \Lambda K^0$ cross sections 790-1060 MeV, structure near Σ threshold 9-42079
 $\pi^- p \rightarrow \Lambda \bar{\Lambda} n$ phenomenological treatment of props. of $\Lambda \bar{\Lambda}$ system 9-42110
 $\pi^- p \rightarrow \eta n$, η branching ratio and coupling const. determ., cross sections fit, partial-wave analysis 9-40425
 $\pi^- p \rightarrow \eta n$ Regge pole model with absorptive corrections 9-32201
 $\pi^- p \rightarrow \rho A_2 \rightarrow \pi\rho\eta, \pi\rho\rho$; branching ratio and cross section determ., $M_\pi=3.25$ GeV/c 9-34316
 $\pi^- p \rightarrow \pi^- X p$, where $X \rightarrow \pi^+ \pi^-$, incident pion energy of 25 BeV, multi-Reggeism consistency 9-25463
 $\pi^- p \rightarrow \pi^- \rho \eta$ at 1170 MeV/c, η prod. 9-32166
 $\pi^- p \rightarrow \pi^0 n \rightarrow \pi\rho\eta, \rho$ 9-27520
 $\pi^+ p \rightarrow \Sigma^+ K^+, 3.23$ GeV/c Regge pole model of strange vector and tensor meson exchange 9-32207
 $\pi^+ p \rightarrow \pi^+ \eta$ at 1050 and 1170 MeV/c, η prod. 9-32166
 $\Pi^- p \rightarrow Y^+ K^+ + 2$ to 4 GeV/c, peripheral peaking in $Y_1^*(1385)$ ang. distrib. 9-25467
 $\pi\pi \rightarrow \pi\pi$ meson resonance, bootstrap of meson trajectories from superconvergence 9-38529
 $\pi\pi \rightarrow \pi\omega$, Veneziano model consistency 9-44030
 ρ dominance in $I=J=1$ channel and ϵ dominance in $I=J=0$ channel rel. to $K-\pi\pi\pi$ 9-38511
 $\pi^- p \rightarrow K^0 \Delta$ cross section calc., new model 9-43983
 π^\pm transverse momentum distrib. in two and six prong events at 7.0 GeV/c 9-22591

interactions, pion-proton

No entries

production

- charged, photoprod., and finite energy sum rules 9-34298
 electro- and photoproduction, mass-dispersion and current algebra theory 9-27515
 electroproduction, vertex depend. on momentum-transfer, dispersion theor. model 9-29604
 electroproduction in polarized- p target, ang. distrib. calc. 9-42164
 multiple, in $K^+ p$ collisions, 3.5 GeV/c 9-36467
 multiple, in $p-p$ collisions at 4 GeV/c, cross-sections, $N^*(1236)$ isobar dominance 9-38569
 on nuclei by $p, n-p$ radius difference obs. 9-36472
 photo. electro and weak, kinematic discussion and dynamical model. 9-25460
 photoproduction, backward, from deuterium, $E_\gamma \sim 1$ GeV, pion-nucleon final state interaction effect 9-44025
 photoproduction, sum rules, high energy contribs., evaluation 9-32139
 photoproduction, vector dominance anomaly 9-29581
 photoproduction < 2 GeV 9-22524
 photoproduction amplitudes, fixed poles 9-29535
 photoproduction at low energy limit in chiral dynamics 9-48188
 photoproduction from nucleons, dispersion analysis 9-44022
 photoproduction from nucleons, dispersion analysis 9-38519
 photoproduction in polarized- p target, ang. distrib. calc. 9-42164
 photoproduction of π on N , magnetic quadrupole amplitude 9-25455
 photoproduction on 3H , impulse approx. calc. in elastic channel, $E_\gamma=200$ -500 MeV 9-25453
 photoproduction on 4He , impulse approx. calc. in elastic channel, $E_\gamma=200$ -500 MeV 9-25453
 photoproduction on d , cross-section calc. in relativistic impulse approximation 9-42074
 photoproduction on nucleons, threshold determ., PCAC theory, $E_\gamma=160$ -230 MeV 9-29606
 photoproduction process, Regge parametrization of formulas 9-27516
 Pomeranchuk exchange and multi-pion production 9-44016
 in proton-beryllium collisions at 12.5 GeV/c 9-32184
 single- and double- π prod. by π exchange, comp. with expt. 9-48186
 transverse momentum distrib. in two and six prong events, from π^\pm collisions at 7.0 GeV/c 9-22591
 zero energy theorems relating $A \rightarrow B\pi$ to $A \rightarrow B$ 9-22594
 e inelastic scatt. from nuclei 9-29786
 $eN \rightarrow eN\pi$, and $IIN \rightarrow VN$, ν - ν analogy model 9-34297
 νN interactions, multipoles evaluated 9-22592
 $\nu p \rightarrow \pi^+ N^+$ cross-section predicted in quark model 9-29580
 $\nu p \rightarrow \pi^+ \Delta^{++}$, form factor in vertex 9-36470
 $\nu p \rightarrow \pi^+ p$ baryonic resonance contributions, quark model 9-29580
 $\Lambda n \rightarrow \pi p, 0.2$ - 2.0 GeV, cross-sections, comp. with theor. predictions 9-40422

Pions continued

production continued

- $\nu \rightarrow \mu^+ \pi^+ p$ total and differential cross sections for ν energy between 1 and 4 GeV 9-44021
 $\bar{p}p \rightarrow n\pi$ angular and momentum distrib. by a Reggeized multiperipheral model 9-42106
 in π -nucleus interac., coherent prod. at 17.2 GeV, nuc. emulsion tech. 9-22805
 π^- , photoprod. 0.2-2.0 GeV, cross-sections 9-40422
 π^- , yields at small angles, by 70 GeV proton-aluminium interactions 9-44019
 π^- by polarized photons, agreement with vector dominance model 9-42073
 π^- interactions on emulsion nuclei, 210-375 MeV 9-22806
 π^- from ηn , first reson region, investigation 9-25456
 π^- photoprod. off N , four-trajectory model using π evasion and cut conspiracy 9-29579
 π^0 from $ep \rightarrow \eta p^*(1236), f_2, f_3, f_4$ determ. from excitation curve 9-36471
 π^0 from νp interaction, production cross section meas., recoil p obs., $E_\nu=220$ -400 MeV 9-40423
 π^0 photoprod. below $E_\gamma=222$ MeV, ang. distrib. obs. 9-29578
 π^0 photoprod. on 4He 9-42272
 π^+ , by polarized photons, agreement with vector dominance model 9-42073
 π^+ , photoproduction by polarized photons, vector dominance, cross section and asymmetry 9-42075
 π^+ from $K^+ \rightarrow \pi^+ \pi^0 \pi^0$, energy spectrum meas., fit to σ -resonance model 9-38506
 π^+ high-energy forward photoproduction in Regge-pole model, cross section determ. 9-38507
 π^+ photoprod. in Regge-pole model, exchange-degenerate conspirators 9-32185
 π^+ photoprod. off N , four-trajectory model using π evasion and cut conspiracy 9-29579
 π^+ prediction by scaling law, 20-70 GeV and 300 GeV p 9-48187
 $\pi^+ \pi^- \pi^+ \pi^-$ coherent prod. cross-section in 16 GeV π^\pm collisions with C_2F_5Cl 9-25454
 π from pNN at threshold, theory 9-38562
 π^0 from $\nu p \rightarrow \pi^0 \nu$, backward angles between 700 and 1150 MeV 9-44020
 π^0 photoproduction model based on exchange of w trajectory plus Regge cut 9-46097
 $\pi\pi\pi$ from decays, $\pi\pi$ scatt. amplitude determ. from Dalitz plot 9-40424
 from $^{12}C+e$ inelastic scatt. at 400-1100 MeV 9-48330
 4He , π^+ decay obs. and branching ratio rel. to π decay 9-38652
 $^{10}B, ^{11}B$, muon and pion yields in 2p-1s X-ray transition 9-22716
 Be, μ and π yields in 2p-1s X-ray transitions 9-22716
 Be target bombarded by 12.3 BeV/c p 9-38580
 C, μ and π yields in 2p-1s X-ray transition 9-22716
 Gd target bombarded by 12.3 BeV/c p 9-38580
 $^3He(p, \pi^0)^4He, 340$ MeV, section obs. 9-48326
 π^+ from $\nu p \rightarrow \pi^+ n$ reaction, linearly polarized photons 9-44018
 π^0 from ν^3He by Primakoff effect 9-38526

scattering

- chiral symmetry, algebraic restrictions 9-29587
 Compton scatt., use of current algebra combined with Lovelace-Veneziano amplitude 9-48184
 low-energy, by equal-time commutators of current algebra 9-44017
 Pade approx. to s -matrix, resonances and Regge trajectories calc. 9-25458
 superconvergence relations, algebraic structure 9-32193
 three-pion scatt., enhanced A , mass by a kinetic mechanism, Bose statistics 9-44023
 A, π hard pion current algebra and dispersion relations results, comparison 9-32187
 $P\rho O(4)$ expansion of Bethe-Salpeter eqn. 9-38520
 π -hadron, π scatt. length expression derivation 9-38523
 $\pi^- \Sigma^+ \rightarrow \pi^+ \Sigma^-$, sum rules for amplitudes, $\pi\Lambda\Sigma$ and $\pi\Sigma\Sigma$ coupling const. obs. 9-29586
 $\pi^- d$, differential cross section meas., $M_\pi=2$ -5.5 GeV/c 9-38524
 $\pi^+ K^-$, absence of backward peaks, rel. to existence of meson towers 9-48200
 $\pi^+ p \rightarrow \pi^+ \rho^+ \pi^+$ Veneziano model 9-29588
 $\pi^\pm \Delta$, differential cross section meas., phase-shift analysis, π e.m. radius determ., $E_\pi=51$ -75 MeV 9-38521
 $\pi\alpha$ cross section determ., Coulomb interference corrections determ. 9-38522
 $\pi d, 895$ MeV/c, cross section obs. 9-25459
 πd , Glauber shadow, inelastic contrib. estimated with Regge-pole theory 9-34307
 $\pi d \rightarrow \nu n \pi$, at high energies with large momentum transfer to neutron 9-42077
 $\pi\Delta(1236)$ sum rules in $O(3,1)$ dynamical group model 9-36499
 $\pi\Delta \rightarrow \pi f$, saturating superconvergence relations 9-25457
 πK , amplitude by chiral Lagrangian calc. K_4 decay axial-vector form-factor determ. 9-38504
 πK , sum rules and ρ -hadron coupling const. determ. 9-22611
 πK , sum rules and ρ -hadron coupling const. determ. 9-29600
 πK , Veneziano type amplitude calc. 9-42076
 πK Veneziano-type amplitudes construction nonet scheme 9-42058
 $\pi\Lambda$, Veneziano model, S -wave scatt. length found 9-42080
 $\pi\Lambda$ phase shift information from $\bar{E} \rightarrow \Lambda \pi \bar{\nu}$ and $\bar{\nu} N \rightarrow \Lambda \pi \bar{\nu}$ processes 9-32192
 $\pi\Lambda$ σ term evaluation, consistency with current divergence algebra 9-22597
 $\pi n, \pi$ backward, diff. cross section energy depend., $M_\pi=1.5$ -3.8 GeV/c 9-29592
 πN , Regge-pole parameter dispersion sum rules applic. 9-22562
 $\pi\omega-\pi\Delta$, saturating superconvergence relations with qq - and p -wave bound states 9-25457
 $\pi\omega-\pi\Delta$, Veneziano-type model 9-46101
 $\pi\rho \rightarrow \pi f$, saturating superconvergence relations 9-25457
 $\pi\Sigma$ sum rules and ρ -hadron coupling const. determ. 9-29600
 $\pi\Sigma$ sum rules and ρ -hadron coupling const. determ. 9-22611
 $\pi\Sigma$ σ term evaluation, consistency with current divergence algebra 9-22597
 $\pi\Sigma$ sum rules and ρ -hadron coupling const. determ. 9-22611
 $\pi\Sigma$ sum rules and ρ -hadron coupling const. determ. 9-29600
 $\pi\pi$ hard pion current algebra and dispersion relations results, comparison 9-32187

Pions continued

scattering, pion-nucleon

- 898 MeV/c differential cross-section obs. 9-46105
 high energy, correlation between polarization and the complex zeros of elastic amplitudes 9-44000
 peripheral absorpt. model modified with $U_{6,6}$ symmetry, appl. to backward data 9-42082
 polarized targets 9-27523
 π -p, 1-2.5 GeV/c, optical and Regge pole models 9-27529
 π -p, 1.7 GeV/c, 3094 bubble chamber events, cross-section found 9-44028
 π -p, interference model for backward data 9-42051
 π -p, phase-shift analysis solutions compared to experimental data 9-36481
 π -p \rightarrow π^0 n, p exchange 9-27443
 π -p \rightarrow π^0 n, polarization meas. 9-27523
 π -p, 8-22 BeV/c, quantum electrodynamic representation 9-38440
 π -p, Coulomb correction on the $3/2, 1/2^-$ scatt. length 9-44033
 π -p hybrid model explanation 9-36469
 π -p \rightarrow π^0 π^0 π^0 π^0 , effective mass distribution, applic. of modified phase spaces model, 8 GeV/c 9-32198
 π -p \rightarrow π^0 π^0 π^0 π^0 π^0 , effective mass distribution, applic. of modified phase spaces model, 8 GeV/c 9-32198
 $\sigma(\pi^0$ - π^0 Δ^0)=0 9-29575
 $3\sigma(\pi^0$ - π^0 Δ^+)+ $2\sigma(\pi^0$ - π^0 Δ^0)= $16\sigma(K^-$ - π^0 η) π^0 9-29575
 $\sigma(\pi^0$ - π^0 Δ^+)+ $6\sigma(\pi^0$ - π^0 Δ^0)= $4\sigma(K^-$ - π^0 Δ^+) 9-29575
 π -p, ang. distrib. meas., 5.2 and 6.9 GeV/c 9-40421
 π -p, elastic differential cross section meas., M_{π^0} =1.7-2.8 GeV/c 9-38531
 π -p, polarization rotation prediction, amplitude calc., high energy 9-25468
 π -p elastic, polarized protons at large momentum transfer 9-42083
 π -p elastic differential cross section meas., E_{π^0} >8 GeV 9-36480

scattering, pion-pion

- amplitude, signature and asymptotic props., generalization 9-36483
 amplitude, Weinberg's of-mass-shell dependence, expl. test 9-48198
 baryon compressibility coeff., calc. from cross section 9-44047
 bootstrap of ρ and Pomeranchuk trajectories using unitarized strip approximation 9-48196
 Chew-Mandelstam equation analysis of low-energy scatt. 9-48197
 current algebra, scattering lengths and the Veneziano model 9-22598
 current algebra calc. of scatt. lengths 9-48199
 Dalitz plot of 3π decays, amplitude determ. 9-40424
 in di-pion mass region 1.0 to 1.4 GeV/c, phase shifts 9-44036
 di-pion production π^0 - π^0 π^0 considered as $\pi\pi$ scatt. process 9-46100
 diffraction scatt., large angle, amplitude calc. 9-43989
 dispersion calc. of scatt. lengths 9-40430
 effective mass spectrum of π^0 π^0 π^0 system 9-42086
 elastic, constrained phase shift analysis for $N^{*1/2}$ resonances in mass range 7800-2200 MeV 9-44064
 finite energy sum rules with Cheng-representation 9-32202
 finite-energy sum rules and unitarity for $I=1$ state 9-40431
 graphical anal. of data, σ -resonance search 9-22600
 inelasticity functions and partial-wave driving forces at large energies 9-46107
 lengths, from current algebra 9-25469
 lengths of scatt. from Veneziano formula and $\eta \rightarrow 3\pi$, $K \rightarrow 3\pi$ decays 9-44038
 Logunov-Tavkhelidze equations, soln. for partial wave amplitudes 9-38533
 low-energy, scatt. lengths by pole-dominance model 9-42085
 Mandelstam representation ruled out due to props. of $f(1260)$ resonance 9-22601
 Pade approximation in σ model, current algebra constraints, exact unitarity 9-36482
 phase shift, S-wave, current-algebra-constrained single-pole approx. 9-38534
 phase shifts analysed by forward dispersion relations 9-38535
 Regge behaviour, Veneziano-type model 9-38532
 resonances, vector, prod., diff. model 9-27530
 S wave phase shifts, one parameter fit using current algebra 9-44035
 S-matrix calc. 9-27532
 S-matrix theory, a one parameter model 9-42084
 S-wave, $I=0$ and $I=2$, model constructed from dispersion relations 9-29595
 s-wave scatt. lengths and a universal partial width for a Regge trajectory 9-38533
 S-waves in isospin $I=0$ and $I=2$, simple models 9-38536
 scattering length and low energy phase shift determ. from forward dispersion reln. 9-27531
 sum rules, Adler-Weisberger type, high energy contrib. evaluation 9-32139
 sum rules based on Khuri amplitudes, degeneracy of Regge trajectories 9-48178
 Veneziano's formula results compared with current algebra results 9-44034
 Veneziano model, higher resonances contrib. to current-algebra sum rules 9-22599
 Veneziano terms with negative residue 9-43991
 Veneziano-Lovelace model, infinite series of Regge poles 9-46081
 Veneziano-type amplitudes construction, nonet scheme 9-42058
 π -p, at 300 MeV, proton polarization 9-46106
 π -, elastic, near 1.04 GeV/c, momentum-depend. fluctuations, absence 9-32199
 π -p \rightarrow σ - K^{*0} ang. distrib., two particle exchange model 9-29619
 π -p \rightarrow π^0 Δ^+ $3/2$ -isobar prod. reaction, M1 dominance hypothesis 9-32200
 π -p \rightarrow σ - K^{*0} ang. distrib., two particle exchange model 9-29619
 π -p, 6, 8, 10 and 12 GeV/c polarization parameter 9-27528
 π - π elastic cross-sections and distrib. of scatt. angle, from π -p \rightarrow N^{*++} π obs. 9-25461
 π -p, 6, 10 and 12 GeV/c, polarization parameter 9-27528
 π -p \rightarrow π^0 η Δ^{++} $3/2$ -isobar prod. reaction, M1 dominance hypothesis 9-32200
 $\pi^+\pi^-$, absence of backward peaks, rel. to existence of meson towers 9-48200
 $\pi^+\pi^-$, determ. of sign of scatt. amplitude 9-42087
 $\pi^+\pi^-$, δ_0^0 phase shifts, π^0 π^0 mass spectrum 9-44037
 π -p elastic scatt., momentum depend. of diff. slopes 9-38530
 $\pi\pi \rightarrow \pi\pi\Delta$, saturating superconvergence relations 9-25457
 $\pi\pi \rightarrow \pi\pi\omega$, Regge amp. partial waves, 'top positions' of loops 9-40411

Pions continued

scattering, pion-pion continued

- ρ bootstrap in unitarized strip approx. 9-27544
 ρ prod., self-consistent width, diff. model 9-27530
 ρ trajectory coupling to π - π system 9-34311
 π^0 π^0 elastic cross sections, meas. from pole extrapolation of $pp \rightarrow \Delta^{++}$ reaction 9-44056
 scattering, pion-proton
 No entries
 Pitch detection see Acoustical measurement; Hearing
 Plages see Sun
 Planetary nebulae see Nebulae; Stars
 Planets
 see also Solar system
 accumulation, relative sizes of largest bodies 9-27077
 albedo and illuminance calc. 9-31601
 asteroid, (48) Doris, definitive orbit based on provisional reciprocal mass of Jupiter 9-38070
 asteroid belt colliding objects, model 9-43622
 asteroids, jet streams formation 9-38069
 asteroids, Kirkwood gaps, statistical explanation 9-47671
 asteroids, resonant, in Kirkwood gaps 9-47671
 atmosphere motion and mechanics, estimation 9-47537
 atmospheres, gray and nongray, structure, convective instability and Greenhouse effect 9-43618
 atmospheres, half-space appl. to equation of transfer 9-36020
 atmospheres, nongray, temperature structure 9-43619
 atmospheres, nongray, temperature structure 9-24848
 Cassini's second and third laws, generalization to include effects of axial symmetry and rotation rates 9-31600
 comet encounters, close 9-40180
 constitution, essay in book 9-41671
 convection of interiors 9-27076
 Cytherean upper atmosphere model, calculation 9-27085
 Earth-Moon system, mass rel. to Sun from obs. of Eros (1893-1966) 9-27075
 Earth-to-Moon trajectories, asymptotic soln., errata and addenda 9-26970
 Eros, motion obs. rel. to mass of Earth-Moon system 9-27075
 exosphere, rotating neutral, model 9-47670
 Icarus, analysis of radar and optical obs., sun oblateness, Mercury mass determ. 9-31604
 Icarus, asteroid, Belgian obs. 9-31605
 1566-Icarus, obs. 9-29066
 interior, convection 9-27076
 interiors, convection dependence on the magnitude of the Rayleigh number 9-29065
 ion-exosphere with variable conditions at baropause 9-27078
 i.r. observations on planetary atmospheres 9-45666
 Jupiter, 6 cm radiation, polarization and rotation period determ. 9-31608
 Jupiter, asteroids in resonance with, secular motion 9-24850
 Jupiter, brightness temp., 8-14 μ 9-24845
 Jupiter, brightness temp. at 2.25 and 8 mm 9-24846
 Jupiter, changes in r.f. rot. period, two component model 9-40176
 Jupiter, decametric rad., 'fifth' source on or near visible planetary disk, non-lo-controlled 9-36021
 Jupiter, decametric rad., apparent control by Europa 9-36022
 Jupiter, decametric radiation obs. rel. to Galilean satellite rad. belts 9-24853
 Jupiter, decametric radio bursts, orientation of polarization ellipse, Faraday effect obs. 9-43624
 Jupiter, exospheric temperature as function of solar cycle 9-40173
 Jupiter, flux density at 81.5 MHz 9-24852
 Jupiter, Io, unipolar inductor 9-24851
 Jupiter, magnetosphere interaction with heliosphere boundary 9-47683
 Jupiter, mass determ. from motion of four minor planets 9-47673
 Jupiter, methane abundance and rot. temp. 9-40175
 Jupiter, minor constituents in its atmosphere 9-24854
 Jupiter, motion of fifth satellite, revised values of mean motion and regression of nodes 9-27080
 Jupiter, new moons suggested to explain periodic modulations of radio emission 9-31607
 Jupiter, nucon spectrum, 2.8-14 μ 9-43625
 Jupiter, periodic orbits for resonance $1/12$ 9-29069
 Jupiter, photochemistry above 1000 Å 9-41676
 Jupiter, radiation observations 9-29104
 Jupiter, Red Spot, evidence of vorticity 9-24855
 Jupiter, Red Spot prominence correl. with Zurich sunspot number 9-40174
 Jupiter, red spot visibility correl. with sunspot activity 9-47672
 Jupiter, right ascension, 1967 obs. 9-33942
 Jupiter, rocket spectra from 2000 to 3000 Å 9-43629
 Jupiter, rotational temp. of methane from 3μ absorption band 9-43623
 Jupiter, surface temp. calc. of Galilean satellites 9-33940
 Jupiter, wavelength depend. of polarization, aerosol scatt. effect 9-29068
 Jupiter's satellites, mutual perturbation, elementary book 9-43512
 Jupiter system, mass from motion of (48) Doris 9-38070
 mantles, thermal and nonthermal convection 9-31602
 Mars, atmospheric model rel. to Mariner 4 obs. 9-29070
 Mars, average surface temperature and vertical temperature profile, seasonal and latitudinal variations 9-24861
 Mars, brightness surface distrib., changes 9-31610
 Mars, brightness temp., 8-14 μ 9-24845
 Mars, composition calc. 9-43621
 Mars, grid system 9-33941
 Mars, hypothesis for S. Mayeda's flare 9-41677
 Mars, internal structure 9-49579
 Mars, lower ionosphere 9-24859
 Mars, Mariner-6 probe results 9-47674
 Mars, meas. by Mariner spacecraft 9-49515
 Mars, optical parameters of surface and atmosphere 9-41675
 Mars, photometric and polarimetric obs. 9-49580
 Mars, recent ground obs. 9-33939
 Mars, review 9-27086
 Mars, right ascension, 1967 obs. 9-33942
 Mars, simulated atmosphere, optical radiation behind shock wave 9-23385
 Mars, simulation of surface materials using the optical props. of those on earth 9-43627

Planets continued

- Mars, spectra 8-14 μ , CO₂ 10.4 μ 'hot' band obs. and interpretation 9-24845
- Mars, surface, comparison of reflectivity and colour of bright and dark regions 9-24856
- Mars, surface, optical comparison with earth materials 9-43626
- Mars, topography, radar meas. 9-31609
- Mars, visible and i.r. spectra rel. to nature of surface 9-41678
- Mars atmosphere, upper, recombination mechanism of CO and O 9-24860
- Martian surface features, identification, Mars Mariner IV 9-24858
- mass, information from spacecraft orbits, popular article 9-47607
- Mercury, anomalous spin rate, radar obs. 9-24932
- Mercury, Cassini's second and third laws, generalization to include effects of axial symmetry and rotation rates 9-31600
- Mercury, composition calc. 9-43621
- Mercury, iron in core and mantle, models 9-45669
- Mercury, mass, determ. from radar and optical observations of Icarus 9-31604
- Mercury, nonsynchronous rotation 9-29072
- Mercury, radial speed optical meas., aberration const. obs. 9-47687
- Mercury, recent ground obs. 9-33939
- Mercury, review 9-27086
- Mercury, rot. period from photographic obs. of surface features 9-24862
- Mercury, thermal history, new calcs. 9-45664
- minor, motion analysis of four, giving mass of Jupiter 9-47673
- motion of triaxial rigid body orbiting oblate primary, first-order theory 9-31496
- Neptune, its discovery, book 9-41671
- Neptune, photographic obs. of occultation April 1968 rel. to radius 9-49581
- Neptune, radius determ. from BD-17°4388 occultation obs. 9-24863
- Neptune, radius determ. from BD-17°4388 occultation obs. 9-24864
- Neptune mass from Uranus orbit analysis 9-47675
- nucleation from heavy metallic elements rel. to observed density of Moon 9-41674
- opposition effect and its implications 9-24857
- orbits, perfectly plane, determination 9-47619
- orbital inclination, elementary book on perturbation 9-43512
- Pluto, magnitude 9-27081
- radar data, optical processing 9-31603
- rotating and non-rotating, Hadley regime props. 9-38068
- rotation, from gravitational accretion of small masses from large distances 9-49587
- rotation, review 9-29072
- satellites, commensurability evolution 9-31611
- Saturn, dynamical structure of ring, theory 9-49582
- Saturn, equatorial zone, variations in intensity 9-24865
- Saturn, exospheric temperature, as function of solar cycle 9-40173
- Saturn, Mimas-Tethys commensurability, evolution 9-31611
- Saturn, ring disappearance in 1966, photometry of condensations 9-24867
- Saturn, stability anal. of rings with differential rot. 9-24866
- space probe obs., and of moon, conference 9-33943
- thermal conductivity equation in presence of radiative energy transfer 9-27245
- Uranus, orbit analysis for calc. of Neptune's mass 9-47675
- Venera 4 impact, deductions from Mariner 5 and radioastronomical obs. 9-38071
- Venus, 8-13 μ emission, telescope obs. 9-38075
- Venus, albedos and monochromatic phase curves, terrestrial photoelec. obs. 9-38078
- Venus, anomalous spin rate, radar obs. 9-24932
- Venus, appl. theory growth curve and phase effects in cloudy atmosphere 9-38077
- Venus, atmosphere, nonlinear Hadley regime motion 9-38068
- Venus, atmosphere, optical and radar refraction 9-38065
- Venus, atmosphere, sources of HCl and HF 9-24880
- Venus, atmosphere minor constituents spectral search 9-24873
- Venus, atmospheres nongray CO₂-H₂O greenhouse model 9-43620
- Venus, atmospheric, chemical composition, based on Venera 4 obs. 9-24868
- Venus, atmospheric composition, Venera 4 obs. 9-24869
- Venus, atmospheric model rel. to Mariner 5 obs. 9-29070
- Venus, atmospheric optical thickness found 9-31601
- Venus, atmospheric radar signal absorption 9-38072
- Venus, atmospheric water vapour, microwave spectroscopy 9-24878
- Venus, brightness temp. and negligible phase variation at 4.52 cm, rel. to atmos. 9-36023
- Venus, brightness temp. and spectra, 8-14 μ 9-24845
- Venus, brightness temp. at 2.25 and 8 mm 9-24846
- Venus, CO₂ bands and water vapour line, effect of cloud scattering 9-41679
- Venus, composition calc. 9-43621
- Venus, dust particles in lower atmosphere, terminal velocities 9-49584
- Venus, evolution model for dense CO₂ atmosphere 9-45671
- Venus, far u.v., Venera 4 obs. 9-38083
- Venus, H₂ photodissociation 9-49583
- Venus, H content in upper atmosphere 9-40172
- Venus, high dispersion spectroscopic observations of CO₂ band at 7820 Å 9-43630
- Venus, high resolution interferometric obs. of brightness and polarization distrib. 9-40178
- Venus, i.r. reflectivity compared with ice clouds 9-38080
- Venus, linear polarization of scattered sunlight, obs. 9-31615
- Venus, Lyman α , Mariner 5 obs. 9-31614
- Venus, Mariner 5 Lyman α obs. interpretation 9-24870
- Venus, microwave opacity of atmosphere, radar obs. 9-31612
- Venus, model atm. for investigation of phase effect on brightness temp. 9-31613
- Venus, O₂ upper limit 9-24895
- Venus, optical polarization 9-38081
- Venus, ozone distribution 90 km to cloud top 9-40177
- Venus, phase curve rel. nature of clouds 9-38079
- Venus, polarization of scattered sunlight, comparison with calculation 9-31616
- Venus, radar obs., determ. of interplanetary plasma densities 9-33946
- Venus, radar obs. at 3.8 cm. 9-29071
- Venus, radar radius, Mariner 5 and Venera 4 combined obs. rel. earth based obs. 9-38073

Planets continued

- Venus, radar time-of-flight obs. 9-27082
- Venus, radiation obs. rel. Venera 4 obs. 9-24896
- Venus, radio obs. at 21.3 cm 9-27084
- Venus, recent ground obs. 9-33939
- Venus, retrograde rotation 9-29072
- Venus, review 9-27086
- Venus, right ascension, 1967 obs. 9-33942
- Venus, rocket spectra from 2000 to 3000 Å 9-43629
- Venus, scattering of visible radiation by atmosphere 9-24879
- Venus, spectrum absolute, 2.8 to 14 μ 9-38076
- Venus, structure of atmosphere, comparison of Mariner 5 and Venera 4 results 9-45667
- Venus, thermal history, new calcs. 9-45664
- Venus, upper atmosphere, CO₂ model rel. Mariner 5 obs. 9-24872
- Venus, upper atmosphere, structure 9-38074
- Venus, upper atmosphere model, calculation 9-27085
- Venus, variation in radar cross-section due to terrain at point of obs. 9-38084
- Venus, water vapour escape mechanism 9-24876
- Venus, water vapour variations, high-dispersion spectroscopic studies 9-27083
- Venus and Mars, radio wave absorption by water vapour in atmosphere 9-47676
- Venus atmosphere, 8-14 μ limb darkening rel. radiative transfer 9-24874
- Venus atmosphere, cm and decim-cm propagation 9-45670
- Venus atmosphere, D/H ratio, deductions from Lyman α Mariner 5 obs. 9-43628
- Venus atmosphere, review 9-24875
- Venus atmosphere, upper, recombination mechanism of CO and O 9-24860
- Venus spectrum, CO₂, comparison of procedures used to analyze spectroscopic observations 9-31617
- Venus upper atmosphere, review 9-24871
- Venus vicinity, 'Venus-4' plasma measurements 9-24877
- Venus, radio and radar spectra rel. surface conditions 9-38082
- Vesta, mass determ. from Arete perturbation obs. 9-24849

Plasma

- see also Discharges, electric; Electrons; Ions; Space charge; Thermonuclear reactions
- absorption of laser radiation, transparency effect 9-25888
- a.c. conductivity, steady elec.-field-induced anisotropy, in slightly ionized plasma 9-46482
- acceleration by e.m. surges, development of plasma wind tunnels and propulsion devices 9-32623
- acceleration by local electron cyclotron reson. 9-42492
- advances in plasma physics, book 9-27971
- air, contrib. to emission by N⁻ 9-44442
- alkali metal, computation of thermo props. 9-36755
- anisotropic, electron spatial distribution, for axial mag. field and microwave excitation 9-27981
- antenna, thin cylindrical, elec. field penetration, surface current and impulse 9-48571
- arc-heater, enthalpy distrib. of hot-core and cold-gas regions 9-23393
- axisymmetric column, temp. profile 9-38958
- with body at large positive potential, neighbouring particles velocities and electron temps. 9-42551
- Bohm diffusion, toroidal plasma sustained by fusion reaction products 9-27977
- boundary layers, two-dimensional, similarity solutions 9-40654
- bounded, one-dimens., dynamics and approach to equilibrium 9-25843
- Burnout-V turbulently heated plasma, Doppler broadened spectra emission 9-44443
- in capillary discharge, elec. resistance, flow and heat transfer 9-40714
- Champan-Enskog series, calc. of first two terms 9-47764
- Cherenkov excitation by modulated particle beam, nonlinear theory 9-46466
- classical, pair distrib. function, quantum corrections 9-46458
- classical, second order current response and conductivity 9-23272
- clusters interaction with axially symmetric mag. field 9-36750
- cold, condensation prod. of thin films 9-34995
- collision-free, gravity-supported, ion acoustic waves propag., Landau damping 9-46525
- collisionless, one-dimensional free expansion, Vlasov equations 9-30210
- collisionless approx., hydrodynamic eqns. and moments of distrib. function 9-27985
- collisionless in uniform field, covariant dispersion theory 9-32590
- collisionless thermalization of injected electron beam 9-48599
- Compton effect, induced of waves under astrophysical conditions 9-43581
- conductivity, elec., 'nonlinear' for appl. e.m. field near plasma freq. 9-23282
- conductivity, elec. for partially ionized case, calc. 9-38969
- conductivity in steady mag. field 9-32611
- conductivity of many component plasma 9-40661
- current sheet produced by induction, stability rel. to density 9-27972
- current-voltage characs., scanner and data processing system 9-30256
- cyclotron harmonic wave propag., hot plasma in uniform mag. field 9-23285
- cylindrical wave diffraction at semi-plane 9-23261
- d.c. arc, magnetic intensification of close cathode intensified spectral lines 9-25988
- density and velocity distributions, magnetic wells method 9-30222
- density increase in stationary deionizing flux, effect 9-40660
- density meas. with H₂⁺ probe 9-32638
- diffusion, resistance and rotation about magnetic axis in toroidal system 9-48609
- diffusion and friction coeffs., test particle in two-dimens. plasma 9-38961
- diffusion coeff., transverse, in mag. field, electron temp. depend. 9-46469
- diffusion coeff., transverse, of high electron temp. plasma in mag. field, meas. 9-46468
- diffusion in toroidal stellarator 9-40678
- diffusion in uniform magnetic field 9-40658
- diffusion modes across uniform magnetic field, pressure dependence 9-42493
- dipole transition probabilities, effect of intermolecular elec. fields 9-46459
- discharge, anisotropies of focus, neutron emission method 9-25866
- discharge, straight turbulent, dynamic characteristics 9-27975
- discharge, toroidal, runaway current intensity 9-28043
- discharge by exploding wire, expansion vel. 9-25852

Plasma continued

- discharge positive column, Tonks-Dattner resonances, nonlinear behaviour due to r.f. generation 9-44424
- 'dressed particles' models in microfield theory 9-23265
- in Earth's magnetosphere, plasmopause plasma sheet and energetic trapped electrons, satellite obs. 9-37941
- eigenfunctions use in solving problems 9-42488
- electroacoustic waves, dynamics 9-40788
- electric microfield, Gaussian 9-23283
- electric microfield, joint probability distribution, with neglect of interactions between particles 9-27987
- electrical conductivity, meas. with high time resolution 9-38970
- electrical conductivity, scalar average, in Lorentzian gas 9-25846
- electro-gas-dynamic equations, investigations of systems 9-30186
- electrodes in flowing plasma, elec. breakdown investig. 9-40724
- electron, warm, drifting, lossy, equivalent dielectric tensor, model 9-32594
- electron beam radial self-focussing under beam instability conditions 9-30214
- electron concentration determ. using self-reversed Stark-broadened spectral line 9-44445
- electron density in strong mag. field from spectral line intensity 9-34774
- electron density meas. using He-Ne laser interferometric technique 9-46478
- electron density meas. using r.f. impedance method 9-46506
- electron energy distributions in electric discharges, microwave frequency excitation 9-30232
- electron extraction in vacuum 9-30208
- electron formation in slightly dissociated gaseous media, equilibrium diagram 9-39013
- electron heating at cyclotron freq. in nonuniform mag. field 9-27974
- electron temp., time behaviour in plasma-beam discharge, meas. 9-42489
- electron temp. near absorbing and emitting surfaces for weak ionization 9-44408
- electron velocity distribution with oscills. present 9-42491
- electron-beam generated, cylindrical, density and potential distribution theory 9-32602
- electron-hole, weak turbulence of helicons 9-48550
- electron-ion, non-isothermic, statistical structure 9-32593
- electrons, diffusion in velocity space 9-44414
- electrons, microwave heating, method 9-30211
- electrons energy distributions, Boltzmann-equation, Lorentz-plasma, periodic e.m. fields 9-30220
- electrons leaving at electrode boundary, angular distribution 9-46462
- electrostatic wave propag. in medium with negative dielec. const. 9-46487
- e.m. acceleration of plasma conugulation in reisonron 9-30262
- e.m.f., static, magnitude 9-30231
- energy distribution of free electrons, low temp. nonequilibrium 9-40659
- equilibrium composition statistical mechanics calc. for partially ionized state, review 9-22141
- equivalent impedance in travelling mag. field, and reactive energy prod. 9-30224
- exospheric trans-polar, unified model 9-37940
- expansion anisotropy, interpretation in terms of drifting and expanding sphere model 9-23271
- expansions in Laval nozzles, approximate methods of calculation 9-46471
- exploding wire, light emission at low pressures 9-30241
- fast, injection into double bend mag. field, drift and purification 9-44413
- first order phase transitions in a quantum plasma 9-25053
- flame, electron temp., probe meas. 9-30252
- flame, thermo electric effect at thermodynamic equilibrium 9-36763
- focus, dense, on coaxial gun axis, 90° laser light scatt. 9-25886
- formation under microwave action 9-42511
- gas flow, Schlieren obs., properties of Ar laser 9-22384
- generation in discharge pressed out to wall by mag. field 9-40715
- guiding center theory, high order corrections 9-44406
- guiding centre theory 9-40655
- gyroresonance of electron in limit of large number of revolutions 9-25847
- heating, turbulent, by current energy loss and efficiency investig. 9-36752
- heating, turbulent, in toroidal system with current, diamagnetism, h.f. behaviour and radiation investig. 9-36751
- heating in high-pressure electrodeless discharges 9-34748
- h.f. discharge pot. difference between plasma and electrodes 9-44425
- h.f. heating by ext. stochastic field 9-23269
- high temperature, physics, book 9-23262
- hot, dense, keV range, conversion of focused laser radiation to X-rays 9-42517
- hot, joint probability distribution of the electronic microfield, with neglect of interactions between particles 9-27987
- impulse response to obliquely reflected e.m. wave 9-48569
- inert gas afterglow, dielec. props. 9-34805
- inhomogeneous, with almost monoenergetic component, dielec. const. 9-48559
- interaction of electrons or ions with atoms 9-29970
- interaction of pulsed moving plasma with stationary plasma of quasi-stable discharge 9-38981
- interaction with laser radiation, nonlinear confining forces 9-25887
- interface, electron ion temp. relaxation 9-23268
- interplanetary, charged particle acceleration obs. rel. to fast proton peak 9-43651
- interplanetary, current density at null points 9-38092
- interplanetary, density determ. from radar obs. of Venus 9-33946
- interplanetary, Explorer 10 obs. 9-38094
- interplanetary, irregularities, radioastronomical investigations of motions and dimensions 9-24890
- interplanetary, motion rel. to theoretical models 9-38091
- interplanetary penetration of magnetosphere 9-37952
- interplanetary flows, velocity and width calcs. from probe obs. 9-33945
- interstellar, turbulence and cosmic ray acceleration 9-24728
- ion conc., negative, determ. by lightning- photodetachment method 9-46476
- ion-sound waves, finite amplitude, in unstable plasma 9-48601
- ionization and recombination rates, electron diffusion concept 9-40708
- ionized, weakly, neutral waves with large amplitude, decay stability 9-30269
- ionospheric resonances, periodicities in amplitude 9-31410
- isotropic, impedance of immersed thin cylinder antenna 9-38976
- Italian work reviewed for year 1966-67 9-27970
- jet in toroidal magnetic field, motion 9-30250

Plasma continued

- kinetic BBGKY eqns., mathematical basis 9-23266
- kinetic Boltzmann eqn. with isotropic distribution function and reflecting boundary conditions 9-46462
- kinetic equations, book 9-30338
- kinetic theory 9-32730
- kinetic theory, review 9-40657
- laser, in θ pinch plasma, rel. concentration 9-23299
- laser beam produced, heating, model and expt. data 9-46511
- laser beam self-focusing effect by ponderomotive forces 9-43902
- laser light scatt., theory and expt. considerations 9-42516
- laser light scatt. at 90° by dense plasma focus 9-25886
- laser light scatt. in dense, cold plasma 9-46488
- laser produced, expansion anisotropy 9-23271
- laser-heated, neutron generation 9-46120
- laser-produced, condensed products, i.r. spectra 9-30209
- layers near electrode, quasi neutral and space charged 9-48560
- lifetimes of energy levels, depend, on system parameters, influence of synchrotron amplification 9-44407
- light scattering spectrum, relativistic corrections 9-34764
- Lorentz, Tensor expansion in spherical surface harmonics in Boltzmann eqn. 9-44402
- Lorentz sc, electron effective mobility in transverse mag. field 9-40662
- Lorentzian, under freq. modulated elec. field, electron distrib. function 9-48556
- Lorentzian, under freq. modulated elec. field, nonlinear electron conductivity 9-44410
- Lorentzian in elliptical magnetic field, soln. to Boltzmann eqn. 9-48547
- low density, high temp., ionization equilb. and radiative cooling calcs. 9-48545
- low temp., elec. arc source 9-40725
- low temperature, electron energy distrib. and conc., reson. radiation yield effect 9-36758
- low-temp., electrical conductivity, temp. pulsations effect 9-38968
- magneto-, r.f.-excited, ambipolar diffusion 9-32596
- magneto-active, finite amplitude e.m. wave beams, self-action 9-48570
- magnetoactive, cold, interaction with relativistic rotating electrons, synchrotron radiation temporal growth rate 9-25840
- magnetoactive weakly ionized, diffusion of electron conc. inhomogeneities 9-38960
- magnetoplasma, collisionless, local ion heating due to trapped electrons 9-44411
- magnetoplasma, time-varying, e distrib. function 9-38956
- magnetospheric, structure, waves and energetic particles 9-28919
- magnetostatic field perturbation caused by waves 9-46457
- many body system, development of quasi-particle concept 9-40656
- many component, transport props. 9-40661
- master equation and quasi-linear equations 9-38955
- material state at up to 10¹⁷ atm. and 10⁸°K 9-25052
- metagalactic, macroscopic motion, cause of microwave background ang. variations 9-38037
- metal contact, secondary emission electron energy spectrum 9-37633
- metal surface disintegration debris rel. to screening of incident radiation 9-29437
- microwave heating, electron cyclotron, stochastic model 9-25851
- motion in time depend, mag. field 9-42490
- multicomponent, with space charge, in electric field, equations 9-44487
- in neutral sheet of Earth's magnetotail, two-dim. model 9-31358
- noise radiation at electroacoustic reson. freqs. 9-44423
- non-equilibrium, in supersonic spherical source, stationary motion 9-38963
- non-equilibrium, ionization relaxation 9-46456
- non-isothermic electron-ion, characteristic magnitudes 9-25845
- non-Maxwellian, light scatt. 9-48576
- non-thermal, stationary, atoms and ions, excited levels population theory 9-25860
- non-uniform, h.f. electrostatic wave propagation in magnetic field 9-25867
- nonequilibrium, total and local radiative energy losses rates 9-32627
- nonisothermal, disturbance by body moving with supersonic velocity 9-48542
- nonisothermal, fully ionized, unified transport theory 9-46465
- nonlinear motion in strong h.f. field in quasistatic approx. 9-38962
- nonthermal, diffusion (in rel. to ions.) 9-31403
- nonuniform dispersing medium, wave evolution 9-38982
- nonuniform flow, velocity determination by measurement of induced potential 9-25854
- optical properties of plasma from electrode-less discharge in air stream 9-40674
- optical thickness distrib. of instationary columns, meas. technique 9-46489
- pair distribution function 9-30221
- parameters determ. from intensity of continuous spectra 9-44441
- partial, Ohm's law in crossed mag. and elec. fields, for high diffusion vels. 9-30230
- partially degenerated, transport theory 9-25853
- partially ionized, elec. conductivity calc. 9-38969
- particle acceleration in random fields, statistical 9-25850
- particle density and velocity, in longitudinal mag. field, plasmascope obs. 9-32603
- in Penning discharge with heated cathode, outflow into vacuum region free of mag. field 9-46540
- perturbation theory in a moving frame for calc. of stationary solutions of Vlasov equation 9-23264
- PIG discharges in various field configs. 9-25839
- pinch experiments, resistive instabilities, finite- β equilibria, Fokker-Planck and Vlasov equations, numerical calculations 9-42487
- plasma-beam discharge, time behaviour of electron temp. meas. 9-42489
- positive column, effect of cathode props. 9-48631
- power radiated by oscillating mag. and elec. dipoles in cold, streaming plasma 9-42514
- Prigogine's master eqn., infinities in statistical theory 9-44404
- Prigogine-Resibois master equation and quasi-linear equations 9-38955
- probes, electrostatic cooled, continuum theory extension 9-25912
- in pulse high current discharge, near-electrode obs. 9-40718
- quantum, cluster internal calc. 9-48544
- quantum, partition function, free energy, calc. 9-48543
- quantum-Coulomb, first-order phase transitions' mechanism, model 9-23574
- quiescent, longit. dielec. permeability 9-34754

Plasma continued

quiescent, probe noise 9-28014
 radial distribution function, calc. for small particle separations, including quantum effects 9-32589
 radiation, transverse and longitudinal, generation and absorption 9-28001
 radiation and transport coefficients, quasi-particle concept applic. 9-40656
 radiation from highly ionized dense plasma, dynamic spectrum 9-46470
 radiation interaction, emission-absorpt. processes determ. 9-38985
 radiation spectrum from gas discharge as possible source for laser pumping 9-22369
 radiative transfer in optically thick, hot plasma outer layer 9-48664
 recombination, dielectric, reviewed 9-44496
 reflex discharge, anomalous diffusion rel. to instabilities 9-46526
 relativistic, aspects of causality 9-32591
 relativistic, concentric regions interstreaming in cylindrical waveguide, interactions 9-48551
 relativistic, conference, Coral Gables (1968) 9-32587
 relativistic, with e.m. interactions, perturbative approach to ring equations 9-40652
 relativistic ring equations, non-perturbative approach 9-46460
 resonances, non-linear effects 9-32588
 r.f., ion extraction, r.f. discharge 9-39022
 ring equations, relativistic, for plasma with e.m. interactions, perturbative approach 9-40652
 Schlieren photography mode-locked laser light meas. by collision with foreign gases 9-27321
 Schlieren photography mode-locked laser light source, synchronization with spark-producing laser 9-27403
 semiconductor, electron beam interaction with (helicon) whistler wave 9-24104
 in semiconductors, n-type, screening effect on electron energy spectrum 9-49099
 shell, superconducting, expansion into vacuum mag. field 9-46483
 in shock tube, flow parameters rel. working channel construction 9-27976
 single-particle distribution function in a high temp. plasma. relativistic corrections 9-25842
 slab, electron density profile, determ. via a.c. resistance and frequency 9-46477
 solar, geomag. tail region, at 500 and 1000 Earth radii, characts. 9-38109
 solar, interplanetary, radio scintillation obs. 9-38108
 solar, near orbit of Jupiter, characts. 9-31646
 in solar flares, turbulence and accompanying phenomena, Petschek's model appl. 9-43674
 solid-plasma interface polarization, theory 9-34976
 sound velocity in multi-temp. plasma 9-23267
 spectral line broadening by Stark effect, effects of dynamic ion shielding 9-48575
 spectral line parameters, effect of plasma in homogeneity 9-28002
 spectral lines of ions in stochastic varying fields, Doppler broadening 9-40663
 sputtering process, r.f. inductive, for film surface coating 9-46720
 near stationary equilib., e.m. perturbation and induced charges, linear relationship 9-44431
 stellar, viscosity and prod. of stars magnetic field 9-45608
 stream, stationary ion-sound waves 9-44403
 streamer propag. and props., qualitative theory 9-36786
 striations, moving, large amplitude 9-34749
 structure, light laser source, spectrum preexcitation by an electric discharge 9-25241
 supersonic spherical source, stationary motion of non-equilib. plasma 9-38963
 temperature and density, electron and ion, Thomson scattering determ. with low resolution monochrometer 9-25858
 temperature modulation for acoustic wave generation 9-23303
 thermal, radius as function of wall thickness and material 9-38959
 thermal props. treated in conference 9-26014
 in thermionic convertor, ionization equilibrium in low voltage arc 9-47893
 thermodynamic functions, approximate methods of calculation 9-46464
 thermodynamic functions and Coulomb interaction, partially ionized plasma, quantum-statistical calc. 9-38957
 thermodynamics; free energy, density fluctuation energy in relativistic and collisional states 9-36753
 thetatron, radiation interpreted as bremsstrahlung 9-23300
 time dependent axisymmetric collisionless finite β , numerical simulation 9-44449
 time varying, elec. conduction and Hall const. rel. to freq. 9-42498
 toroidal, stationary, classical diffusion 9-25849
 transparent layer in strong h.f. field, nonlinear motion in quasistatic approx. 9-38962
 transport coefficients, approximate calculations 9-42486
 transport cross sections for screened and cutoff Coulomb potentials 9-25848
 transport equations, 13-moment solutions 9-42606
 transport properties, calculation using cross-sections derived from collision term of Boltzmann equation 9-40664
 transport properties, experimental and analytical studies 9-23274
 transport properties, integral calc. using Debye shielded Lande potential 9-23270
 transport theory, unified, for fully ionized, nonisothermal 9-46465
 turbulence 9-23325
 turbulence, quantum mechanical interpretation 9-30213
 turbulent, elec. d.c. conductivity decrease during propag. of ion waves 9-34753
 turbulent, energy of e.m. and kinetic fluctuations 9-27973
 turbulent, interaction between Langmuir and acoustic waves 9-40698
 turbulent, longit. dielec. permeability 9-34754
 turbulent, one-particle distribution function and elec. field spectrum 9-48546
 turbulent, weakly, dielec. const., Langmuir freq. correction 9-32612
 turbulent flow, space-time correl. function and wave-number frequency depend. spectral function 9-23289
 turbulent heating in a torus, after the cessation of heating current 9-46463
 turbulent jets, book 9-40737
 turbulent magnetosonic wave attenuation 9-48553
 two-temperature, dielectric constant, analysis and applic. 9-27990
 Venus vicinity, 'Venus-4' measurements 9-24877

Plasma continued

viscosity, thermal conductivity and electrical conductivity, approximate solutions 9-42486
 Vlasov and Maxwell eqns., time independent soln. symmetry props. 9-44412
 Vlasov equation, uniform perturbation theory 9-32586
 Vlasov turbulence, class of exact solns. 9-48549
 Vlasov turbulence, closure conditions 9-48548
 wave evolution in nonuniform dispersing medium 9-38982
 waves, self-action, in rarefied plasma in mag. field 9-25938
 waves scattered power and radar cross-section of space vehicle 9-34123
 weakly ionized gases, theory, book 9-25841
 weakly unstable, charged-particle scattering theory 9-30242
 weakly unstable, kinetic theory 9-46532
 z-pinch, high density, radiative losses, obs. 9-40653
 air, emissivity meas., 110-300 nm, 2×10^4 K and e density $\sim 10^{17}$ cm $^{-3}$ 9-48590
 Al, prod. by laser impact on Al target, u.v. emission spectrum obs. 9-36769
 Al emission lines, 5000 to 10000°K 9-40675
 Al spectrum for excitation by ruby laser 9-38781
 of Al wire exploded in vacuum, optical and spectral 9-44440
 Ar, expansions in Laval nozzles, approximate methods of calculation 9-46471
 Ar, spectral absorptivity of pulsed discharge calc. from radiance spectral density 9-23301
 Ar, thermal induction, energy balance equation, analytical solution of Heller-Elenbass equations 9-28004
 Ar, thermodynamic functions, approximate methods of calculation 9-46464
 Ar, Z-pinch, ion density and current distributions 9-32604
 Ar afterglow, electron temp. gradient, spatially nonuniform parameters effect on transport processes 9-34755
 Ar discharge, flowing, NaK seeded, electron temp. meas. 9-27978
 Ar flow in presence of boundary layer, volt amp. characts. 9-44426
 Ar induction coupled, modification of B microcryst. particles passing through 9-37133
 in Ar Knudsen arc, density and electron temperature 9-42585
 C line radiation energy, 10^4 to 10^5 K 9-40676
 CO $_2$ laser, properties 9-47972
 Cs, diagnostics using laser interferometry 9-46510
 Cs, electron density meas. under collision conditions comparative study by Langmuir probe and spherical h.f. probe 9-46479
 Cs, ionization and simultaneous free-electron Maxwellization 9-34750
 Cs, mass-spectrometer analysis of dominant ionic species 9-42485
 Cs I lines electronic excitation cross section meas. in gas discharge 9-27816
 Cs population of excited atomic states, and ionization at low pressure 9-42484
 Cs thermionic discharge, electron energy distrib. 9-34756
 Cs vapour, ionic composition of arc-discharge plasma 9-36759
 Cs vapour, ionic composition of arc-discharge plasma 9-36759
 of Cu wire exploded in vacuum, optical and spectral 9-44440
 D, ion heating in very fast theta pinch 9-30212
 F line radiation energy, 10^4 to 10^5 K 9-40676
 H-C at 40 000°K and 70 at., coeff. of continuous absorpt. calc. 9-44444
 H, eqn. of state and ionization degree, calc. 9-38957
 H, finite partition functions 9-46461
 H, highly ionised, relaxation theory applies. 9-40651
 H, highly ionized, decay, spectral and microwave obs. 9-40665
 H, nonthermal, ions and atoms density ratios 9-32605
 H, radiative energy transfer, Planck and Rosseland coeffs., live and continuum rad. 9-48554
 H $_2$, electron-cyclotron resonance, 200 W microwave power, parameter determ. under steady-state conditions 9-42511
 H $_2$, fast pulsed discharge, properties 9-39025
 H $_2$ expansions in Laval nozzles, approximate methods of calculation 9-46471
 H $_2$ thermodynamic functions, approximate methods of calculation 9-46464
 H discharge column, low press., distribution of ionization states 9-46542
 H in impulse tube, electron density and temp. meas. by rapid scan spectrometer 9-44419
 2 H, laser produced, electron temperature 9-44409
 2 H theta-pinch, cross-sectional electron distribution, using Mach-Zehnder interferometer 9-42483
 He-Ne, N $^{2+}$ ion production and loss during decay period, density time depend. 9-40666
 He, afterglow, decay props. 9-23286
 He, diff. and mass flow effect on ioniz. degree 9-32597
 He, electron density and kinetics of heating from acoustic oscillations obs. at low temp. 9-39010
 He, electron density and radiation of atoms, effect of optical orientation of 4 He atoms 9-38984
 He, formation of molecular He in afterglow 9-23263
 He, He $^+$ and He $^{++}$ existence, mass spectra obs. 9-36760
 He, high-freq. elec. fields, spect. meas. 9-23287
 He, in linear Z-pinch tube, spectroscopic studies 9-23306
 He, laser-produced, line and continuum emission 9-34776
 He, population of highly excited states, effect of stepwise ionization 9-46539
 He, thermodynamic functions, approximate method of calculation 9-46464
 He, H $^+$ existence at room-temp., mass spectrometric obs. 9-25969
 He afterglow, electron temp. gradient, spatially nonuniform parameters effect on transport processes 9-34755
 He afterglow, production of He $^+$ in collisions between metastable atoms 9-46336
 He cryogenic, sound oscillations, excitation and damping 9-48606
 He decay of e temp. investigated 9-32592
 He excitation in +ve column discharge 9-25721
 He II, ionization displacement due to particle currents in temp. gradient direction 9-48552
 He laser induced breakdown, plasma evolution 9-28053
 He partially ionized, transport and balance coefficients 9-44417
 HeI, local thermodynamic equilib., validity criteria 9-23277
 Hg:Cs arc, probe obs. 9-38972
 Hg-vapour discharges, current rise slow rates, correlation with pinch 9-42523

Plasma continued

- Hg, current-modulated column, internal semiconducting materials/GaAs [p-n junctions, avalanche breakdown] electron density and radial distribution meas. 9-38965
- Hg thermal, 1000 to 15000°K and 10 torr to 50 atm, conc. of ionization states 9-44420
- Li, expansions in Laval nozzles, approximate methods of calculation 9-46471
- Li, high-density, linear Stark broadening 9-34765
- Li emission lines, 5000 to 100000°K 9-40675
- N, absorpt. by liquid iron from plasma jet 9-46455
- N, contrib. to emission by N⁻ 9-44442
- N₂, emissivity meas., 110-300 nm, 2×10⁴°K and e density ~ 10¹⁷ cm⁻³ 9-48590
- N₂, first positive system, transition moment, r-centroid dependence 9-25745
- N₂, thermodynamic functions, approximate methods of calculation 9-46464
- N²⁺ ion production and loss during decay period, He-Ne mixture, density time depend. 9-40666
- N continuum radiation, 975-37000 Å 9000-13500°K, 1.2 atm. press. obs. 9-23302
- N jet laminar, convective heat transfer 9-44459
- N laminar jet, convective heat transfer 9-44460
- N thermal conductivity and viscosity calc. 9-36754
- Na I 5682-88 Å and 4978-82 Å lines, Stark broadening 9-32413
- Ne-Ar mixed gas, generated by fission fragments, electron density 9-34751
- Ne, electron density in medium plane, determ. using transmission and reflection coeffs. formulae 9-23278
- Ne, spectral absorptivity of pulsed discharge calc. from radiance spectral density 9-23301
- in Ne discharge, diffusion of plasma column 9-44506
- Ne discharge column parameters 9-44507
- Ne excitation in hollow cathode discharge, balance eqn. for levels derivation 9-22961
- Ne partially ionized, transport and balance coefficients 9-44417
- O₂, emissivity meas., 110-300 nm, 2×10⁴°K and e density ~ 10¹⁷ cm⁻³ 9-48590
- O₂, thermodynamic functions, approximate methods of calculation 9-46464
- Si in capillary discharge, optical absorption for laser irradiation 9-42518
- Xe, absorpt. coeffs. in continuum, obs. 9-34766
- Xe fast neutrals in plasma beam projected from coaxial gun 9-32606
- collision processes**
- between atoms and ions, effect on I-V curves of spherical Langmuir probe 9-28015
- BBGKY hierarchy, truncation procedure 9-25855
- beam, multicomponent, pair collisions effects 9-46531
- beam injected into electron plasma, energy loss rate time var. 9-44479
- beam-plasma interaction, h.f. instability collisional damping 9-44480
- charge exchange, accidentally resonant and ion momentum transfer 9-46467
- charged particle beam interaction, nonlinear Vlasov theory 9-46472
- charged particle motion in nonlinear plasma, energy losses 9-30215
- charged particle-neutral, effect on e.m. scattering by free electrons 9-46485
- collision freqs., circ. polarized microwave reflection obs. 9-44434
- Compton scatt. by electrons, thermodynamic Green function technique, cross section calc. 9-32599
- damping, of plasma longitudinal waves 9-44468
- damping of electron waves, small amplitude 9-44469
- Debye shielded Lande potential for integral calc. of transport props. 9-23270
- dense low temp., rel. to ion recombination 9-46474
- drift waves, finite amplitude collisional 9-32657
- drift waves, identification, stabilization and enhanced transport 9-30218
- effect on ion current at Tonks-Langmuir boundary 9-46509
- electron beam, weak, in inhomogeneous plasma, Vlasov eqn. solved 9-46473
- electron beam energy transfer to longitudinal waves 9-44470
- electron beam-plasma system, electrostatic waves propagation, transformation and absorption 9-27988
- electron plasma four-wave interactions, kinetic eqns. 9-30216
- electrons, slow, diffusion cross section in inert gas, microwave obs. 9-23273
- energy loss of fast test ions 9-48555
- excitation, parametric, in mag. field, Vlasov eqn., Bernstein mode growth rate 9-27979
- Fokker-Planck model contribution to spin wave echoes 9-32600
- frequency meas. using r.f. impedance method 9-46506
- hydrogenic ion plasma, recombination and ionization coeffs. according to collisional-radiative model 9-42494
- inert gases, collisional-radiative electron-ion recomb. rate 9-30219
- ion-ion in low pressure gas rel. to shock wave passage 9-27991
- Lorentz gas response to a.c. pulse 9-44437
- low-frequency, Fokker-Planck equation, asymptotic solution 9-27980
- magnetic traps, toroidal, transfer processes 9-25899
- in magnetoplasma drift wave instability, anomalous collision freq. 9-44427
- many-body simulation, clouds-in clouds, clouds-in-cells physics 9-36757
- nonlinear wave interaction, stabilization by means of dissipation 9-32675
- quantum interaction between plasma and rad. field 9-32598
- scattering of atomic beams, collective effects 9-25856
- shock waves with rigid obstacles, in mag. fields parallel to dirn. of propag. 9-25870
- transport across a strong mag. field 9-36756
- wave echo, Coulomb collisions and microturbulence effect 9-30217
- waves, electron and ion, for Maxwellian and shifted Maxwellian cases 9-44418
- waves, longitudinal, absorption and emission 9-30270
- waves, longitudinal damping 9-44468
- in weakly ionized gases, book 9-25841
- Ar in homopolar rot. device, 10⁻²-mm Hg, electron collision freq. and current growth 9-25857
- H, homogeneous plasma, recombination and ionization coeffs. according to collisional-radiative model 9-42494
- H₂ in homopolar rot. device, 10⁻²-mm Hg, electron collision freq. and current growth 9-25857

Plasma continued**collision processes continued**

- H plasmas, collisional-radiative recombination and ionization coeffs., effect of atomic collision 9-42495
- He, decaying, neutral particles collisions effect on excited molecules densities 9-46475
- He in homopolar rot. device 10⁻² mm Hg, electron collision freq. and current growth 9-25857
- Hg-Kr discharge positive column afterglow, 2nd kind collisions cross section estimation 9-25981
- N₂ in homopolar rot. device, 10⁻² mm Hg, electron collision freq. and current growth 9-25857
- Ne, excitation by electron impact, optical transitions 9-36671
- Ne, excited level broadening due to interaction with gas 9-23275
- Ne in homopolar rot. device 10⁻² mm Hg, electron collision freq. and current growth 9-25857
- confinement**
- 'Tokamak' type mag. config., possible future in thermonuclear reactor 9-44452
- Astron, rotational and tearing modes, numerical simulation 9-44449
- ballooning effects in closed systems, effect on stability 9-28007
- capture into divertor aperture at asynchronous injection of two plasma streams 9-42556
- closed magnetic traps, with average minimum-B 9-48579
- compression in toroidal mag. field, parameters 9-40691
- constrictions in finite conductivity plasma 9-25957
- cross-field transport, magnetically confined, low-beta collisions dominated plasma 9-25902
- cusp geometry 9-44456
- cusped geometries, Chalice project, experiment and interpretation 9-44457
- cusped geometries, Chalice project, review 9-42525
- in cusped mag. field, adiabaticity of charged particle trajectories 9-44453
- discharge, beam-plasma, wall potential effs., stability obs. 9-23310
- in divertor mag. field, interaction of two plasma fluxes 9-25889
- dynamic stability, variational approach 9-25946
- E layer, magnetic field pattern and Bohm confinement time 9-48580
- E layer, plane relativistic with imbedded shearing mag. field, stability 9-44405
- electric field penetration of plasma with fractionally accommodating boundary 9-36770
- electron flow in spherical geometry, negative electrostatic potential well, experimental studies 9-30243
- of electrons, in mag. mirror supplemented by r.f. field 9-25898
- electrons in cylindrical geometry, stability 9-44481
- flute modes, low-β, instability rel. to transverse anisotropy 9-46500
- flute modes inducing particle diffusion in plasma with T_e > T_i 9-46491
- fusion research, survey of USAEC'S program 9-23313
- Hall acceleration in polyptron machine 9-28011
- Heliotron and biconical cusp fields, superposed, equation of motion 9-32629
- hot, in spherical multipole mag. field, conditions 9-25900
- hot, in spherical multipole mag. field, experimental results 9-25901
- hot electron, cyclotron, in magnetic mirror field 9-42524
- hydromagnetic equilibrium double toroidal configurations within perfectly conducting sphere 9-44451
- hydromagnetic systems, geodesic acoustic waves, modes analysis 9-30266
- θ pinch, high β mirror instabilities 9-44448
- θ pinch, rot., mode growth and stability 9-23307
- θ pinch coil, magnetic field disturbance measurements, h.f. analogue model 9-25896
- θ pinch dynamics, two dimensional, transverse magnetic fields 9-23309
- θ-pinch, concentration and laser scattering simultaneous obs. 9-23299
- θ-pinch, curved, grad B drift suppression 9-25895
- θ-pinch, very fast, low-density D plasma, ion heating 9-30212
- θ-pinch eff. of small amp. ripples of mag. field 9-38987
- θ-pinch mirror modes, numerical simulation 9-44449
- injection and containment of charged particles in cusp mag. field 9-48578
- interaction with magnetic containment fields, theory and experiment 9-46512
- jet in toroidal magnetic field, motion 9-30250
- laser radiation interaction, nonlinear forces 9-25887
- of laser-produced plasma 9-23323
- by longitudinal mag. field, e.m. wave phase velocity variation in resonator 9-30238
- Lorentz trapping, use in hot electron plasma formation 9-32646
- magnetic, dynamic stability, variational approach 9-42552
- magnetic, high density, dynamically stable structure, variational method 9-46504
- magnetic dipole guard field, initial acceleration calc. 9-30244
- magnetic field helical, calculation of symmetry 9-28010
- magnetic mirror, axisymmetric and multipolar, eqns. of motion and mag. moment variation 9-28009
- magnetic mirror, high-β, two-dimensional equilibrium including particle loss 9-30247
- magnetic mirror, particle density and velocity, plasmascope obs. 9-32603
- magnetic trap, micro-stability theory 9-30293
- magnetic trap, rotating plasma characs. 9-23330
- magnetic traps, toroidal, particle and energy fluxes across mag. field 9-25899
- magnetic well, asymmetric minimum B config, with toroidal multipole and resonantly coupled helical field 9-40681
- magnetic well, existence of field min. line with arbitrary curvature and torsion 9-46498
- magnetic wells, critical pressure 9-23311
- magnetic wells, method for distribution calc. in adiabatic invariant terms 9-30222
- measurement, using superhigh frequency radiation range and detection equipment 9-40693
- mirror, electron cyclotron heating 9-25851
- mirror, h.f. electrostatic instability propag. transverse to mag.-field 9-40683
- mirror, hot, stabilization by adding warm plasma 9-23337
- mirror cusp fields, polynomial representation 9-28008
- mirror machine, cyclotron heating due to modulated beam 9-44458
- mirror trap, particle motion 9-40682
- in mirror trap at e cyclotron reson., 9050 MHz 9-34770
- multipole, 2 dimens-, mag. field closed expressions 9-28006
- multipoles with shear, MHD 9-23336

Plasma continued**confinement continued**

- negative energy waves in mirror machines, destabilization 9-30248
- negative V'' system with 80% well depth 9-32630
- negative V'' wavy toroidal field with helical multipole 9-32631
- open-ended mirrors for fusion research, review 9-27762
- phase space dynamics of particles, book 9-40313
- pinch, inverse, hydromagnetic model, numerical studies 9-28005
- pinch discharge laser, electron temp. and conductivity 9-47958
- pinch effect, magnetic, in thermal r.f. induction plasma 9-42521
- pitch curvature effect on stability 9-44446
- plasmoid r.f., resonance props. reviewed 9-36783
- preheating in megajoule theta-pinch experiment 1 9-23308
- in Q machine with symmetrically heated end plates 9-25904
- in quadrupole, linear, containment time rel. to mag. field and electron temp. 9-44455
- radiation pressure of laser-produced plasma 9-46490
- rarefied plasma surrounded by surface of complex conductivity, potential oscillations, instability 9-30292
- screw pinch stability 9-38988
- sheath, Rosenbluth-Ferraro-Dungey, evaluation 9-25892
- sheath, transient, ion-acoustic wave form. 9-23304
- sheet pinch, finite-resistivity instabilities 9-30280
- sheet pinches, relativistic with current shear 9-44447
- short mirror machine, ion cyclotron instability anal. 9-46502
- snowplough model, 2-dimens. axisymmetric, current sheath dynamics 9-46493
- snowplough model, 2-dimens. axisymmetric, current sheath dynamics 9-46492
- stability and drift motion of plasma with loss from ends of axially symmetric mag. bottle 9-34787
- stabilization due to oscillating e.m. field 9-25949
- stellar equilibria determ. using guiding centre eqns. 9-23312
- stellarator, confinement time and loss due to turbulent transport across mag. field 9-30245
- theta pinch, high- β , tearing mode instabilities 9-30285
- theta pinch, interchange instabilities of higher modes, and stabilization effects 9-32669
- theta pinch ISAR 3, ion temperature measurement by laser forward scattering 9-25897
- theta pinches, use of M and S configuration 9-44450
- thetatron, plasma wave excitation and dissipation 9-25936
- times, alternative law to 'Bohm' 9-34767
- Tokamak-3, discharge current pulse effect 9-28003
- toroidal, compression probing using fast-atom beam 9-42531
- toroidal equilibrium with helical windings, low and finite β 9-46503
- toroidal θ -pinch, collapse, snowplough model 9-25894
- toroidal mag. surfaces 9-44454
- toroidal pinch, superimposed multiple-cusp magnetic field, particle motion 9-25177
- toroidal shape for MHD, curvature effects, properties 9-42497
- toroidal system with conducting walls, pulsed, as thermonuclear reaction 9-32628
- toroidal systems, trapped particle instabilities 9-46499
- toruses, min. average-B stabilization 9-28037
- upper bounds for total particle energy rel. to given confining field 9-46501
- waveguides, e.m. modes 9-42504
- Z pinch discharge, conical 9-40680
- z-pinch, high density, radiative losses, obs. 9-40653
- Z-pinch, plasma focus and neutron emission mechanism 9-38989
- Z-pinch tube, linear, spectroscopic studies of He plasma 9-23306
- Ar column, axial current density meas. 9-34768
- Ar inverse pinch, m.h.d. prod. of collisional shocks 9-46495
- Ar or He, magnetically confined column 9-25891
- Cs, thermally ionized, collisionless sheaths between field modified emitters and plasma 9-25893
- H, θ -pinch, density, temp. and mag. field structs of plasma shock fronts 9-46497
- H inverse pinch, m.h.d. prod. of collisional shocks 9-46495
- He, θ -pinch, excitation, ionization and recomb., spectroscopic exam. 9-36771
- He inverse pinch, m.h.d. prod. of collisional shocks 9-46495
- Hg, sheath growth, dynamic 9-40679

devices

- accelerator, coaxial, focus as neutron source 9-25483
- accelerator with linear electrodes, experimental study 9-38999
- accelerators, short-pulsed, high voltage prod. by pulsed charging of capacitors by exploding wires 9-42519
- alkali plasma diode, d.c. props. 9-38359
- anode of generator, film-cooling 9-22336
- Ar beam prod. in Laval nozzle, calcs. 9-39001
- Astron, relativistic electron injection, modified computer code 9-32632
- Astron, stability with rigid E-layer electrons 9-38991
- beam-plasma system, parametric amplification 9-42503
- beams interfering at mutual intersection with axis of cylindrical tube, patent 9-25906
- betatron, axial field, runaway electron beam obs. 9-32280
- coaxial electrode gun, spectra of highly ionized Ne and Ar, up to 4 keV 9-42329
- diode, volt-ampere characteristics calculation 9-30246
- discharge, emitting material protection from excessive ion bombardment, patent 9-48593
- display, influence of gas composition and signal waveform, for computer controlled teaching system 9-29136
- gun, coaxial, with positive central electrode, simple model 9-30249
- homopolar, three-dimens. flow distrib., secondary flaws effects 9-48582
- θ pinch coil, magnetic field disturbance measurements, r.f. analogue model 9-25896
- induction torch, thermal r.f., magnetic pinch effect 9-42521
- jet, Ar, N, used to produce active η -type alumina from aluminium hydroxide 9-46945
- jet, cutoff by transverse mag. field 9-34771
- jet, electric field exam., effect of easily ionizable elements 9-48122
- jet as cathode for Ar laser 9-40351
- jet flame, use in gas evaporation method of fine metal particle prep. 9-33128
- jet generator, patent 9-48594
- jets, use for amplifying radiation 9-32633
- jets, vel. profiles meas. 9-42526
- Laval nozzle for beam prod., calcs. 9-39001

Plasma continued**devices continued**

- lens for focusing ion beams 9-27288
 - magnetic field pattern and Bohm confinement time 9-48580
 - m.h.d. shock tubes, scalar gas cond. calc. rel. to current sheet growth 9-46494
 - mirror machine, cyclotron heating due to modulated beam 9-44458
 - mirror machine, flute oscillations 9-48581
 - mirror machines, destabilization of negative energy waves 9-30248
 - mirror trap, e confinement at cyclotron reson., 9050 MHz 9-34770
 - MPD accelerator, oscillations and possible nonaxisymmetric current distrib. 9-25903
 - MPD arc jet, energy fluxes to anode, determ. of heat transfer mech. responsible 9-32610
 - parametric resonator with impulsive parameter modulation, instability 9-30277
 - plasmatron for heating Ar with K admixture 9-38993
 - plasmatron with arc stabilized by Ar flux, energy relationships 9-38992
 - plasmatrons, variable current, emission of W electrodes 9-43141
 - polytron machine, Hall acceleration in 9-28011
 - probe, sampling, examination of ion intake 9-25915
 - pulsed e.m. gas acceleration, spontaneous transition of a parallel plate accelerator 9-25890
 - Q machine with symmetrically heated end plates, confinement improvement 9-25904
 - Q-machines, longitudinal inhomogeneities 9-40684
 - reflex discharge for plasma physics expts. 9-43711
 - resonance probe sheath capacity theory applied to the cathode dark space 9-44501
 - r.f. probe for conductivity meas. 9-34772
 - rotating homopolar with mirror mag. field, discharge growth obs. 9-25857
 - sheath diode, microwave nonlinear effects 9-23305
 - short mirror machine, ion cyclotron instability anal. 9-46502
 - stabilization by arc discharge tube rotation, patent 9-34790
 - stellarator, confinement time and loss due to turbulent transport across mag. field 9-30245
 - stellarator, MHD energy principle applic. for equilibrium 9-32678
 - stellarator, strongly turbulent microwave-heated plasmas, fluctuation properties 9-28028
 - stellarator, toroidal, diffusion of plasma 9-40678
 - stellarator sirius, vacuum system 9-46505
 - technology, book 9-42520
 - thermionic diodes, electron instabilities 9-47892
 - thermonuclear reactor, possible use of 'Tokamak' type mag. apparatus 9-44452
 - theta pinch ISAR 3, ion temperature measurement by laser forward scattering 9-25897
 - torch, induction, patent 9-46513
 - toroidal screw pinch, theory and experiment 9-46496
 - toroidal stellarator, collisional diff., const. calc. 9-25905
 - tube, gas lasers, with variable cross-section and discharge current, patent 9-48009
 - waveguides, e.m. modes 9-42504
 - wind tunnel, Mach 3, using magnetic nozzle 9-32724
 - ZETA, Si II multiplet intensities rel. to solar spectra 9-27094
 - Ar-heating plasmatron with K admixture 9-38993
 - Ar, induction torch, temp. and electron density distribution 9-25907
 - Ar arc jet, temp. meas. at atm. pressure 9-30251
 - Ba, Q-device, low-density meas. rel. to verification of 'equilibrium' theory 9-28018
 - Cs diode, electron and ion oscillations, simultaneous excitation obs. 9-25943
 - Cs thermionic diodes, emitter and collector sheaths, properties 9-34769
 - H, jets, equations when chemical reactions resulting from methane decomposition take place, dissipation terms calc. 9-38994
- diagnostics**
- absorption coefficient meas. using laser pulses 9-28000
 - absorption coefficients determ. using gas laser 9-42530
 - accelerating plasma, comparisons of current sheet velocities in two groups of coaxial accelerators 9-28017
 - air flow behind shock, elec. conductivity determ. using cold electrodes 9-40669
 - alkali metals, quadrupole transitions 9-23320
 - arc, high pressure, transport coeff. determ. 9-32635
 - atomic phenomena using laser heterodyne interferometer 9-36349
 - boundary layer, mobility-controlled, charge distrib. obs. by ion collection probe 9-25908
 - charged particle concentration determ. 9-42529
 - charged particle energy distribution e.s. analyzer for moving and resting plasma 9-40677
 - compression, adiabatic, in toroidal device, fast-atom beam probe 9-42531
 - compression in toroidal mag. field, parameters 9-40691
 - computer, experiments, fast numerical procedures 9-33980
 - conductivity meas. by r.f. probe 9-34772
 - cylindrical probe, calcs. for a collisionless magnetized plasma 9-46508
 - density meas., laser methods 9-44461
 - density meas. by e.m. propag. at small angle to mag. field 9-25879
 - density of charged particles, measurement, moving plasma cloud 9-30258
 - in dipolar magnetic field, properties 9-32644
 - using dipole antenna admittance calculation 9-42527
 - electric fields, measurement using surface charge induction method 9-42537
 - electrical conductivity, meas. with high time resolution 9-38970
 - electrodeless conductivity probe, impedance changes rel. to applied mag. field 9-23314
 - electron concentration and temp. of plasma in local thermodynamic equilibrium 9-38996
 - electron concentration in hypersonic flows, laser interferometry meas. 9-48588
 - electron cone, distribution, effect of refraction on radio interferometric meas. 9-48587
 - electron density, opt. interferometric meas., improvements of detections of fringe shifts using He-Ne laser as source 9-25910
 - electron density and temp., Langmuir probe analysis 9-42538
 - electron density in strong mag. field from spectral line intensity 9-34774
 - electron density meas. by CO₂ laser interferometer 9-23315
 - electron density profile of slab, determ. by a.c. resistance as function of freq. 9-46477
 - electron distrib. meas. using microwave cavities 9-48584

Plasma continued**diagnostics continued**

electron mean free path and drift velocity meas. 9-30253
 electron temp. from absorption meas. of X-radiation from plasma 9-30260
 electron temperature measurement of weakly ionized alkali seeded rare gas plasma, line reversal method 9-25917
 enthalpy and pressure meas. probes, description 9-40694
 flame, probe meas. of electron temp. 9-30252
 flowing, electrical properties meas., experiment and theory 9-32634
 h.f. discharge in cylindrical and spherical geometries, calorimetric meas. 9-32640
 high-speed processes, optical methods 9-32645
 using holography, survey of investigation (1966-1967) 9-30257
 θ -pinch, Faraday rotation meas. 9-38995
 θ -pinch coil, mag. field disturbances with h.f. analogue model 9-40690
 interferometers, focused, design charts for source and antenna parameter selection 9-30254
 ion-acoustic-wave potential and density perturbation, meas. and correlation 9-30255
 ionospheric density profiles from phase-freq. obs. 9-31414
 ions, positive, extraction, wall space charge 9-28016
 Langmuir probe, circular planar, guarding type, theory 9-25914
 Langmuir probe, r.f. response variation with amplitude and freq. 9-40686
 Langmuir probe, single, advances in theory 9-23316
 Langmuir probe, spherical, effect of elastic collisions between atoms and ions on I-V curves 9-28015
 Langmuir probe automatic second derivative plotters, audio signal injection 9-32639
 Langmuir probe data, techniques for reduction to obtain comparison with current theories 9-30259
 Langmuir satellite probe in collisionless ionosphere with mag. field, current voltage characts. 9-43455
 laser beam scattering method 9-32636
 laser heterodyne meas., dispersion-corrected, three-wavelength, of electron densities 9-42528
 laser interferometric meas. of e. density 9-23315
 laser interferometry for electron concentration in hypersonic flows 9-48588
 laser interferometry technique 9-46510
 laser light scatt. technique using scattering spectrum at 90° 9-46488
 laser scattering, cooperative, at 90° from cold, dense plasma 9-32687
 linear hard-core configuration, meas. results 9-27998
 low-density beams, ion velocity distributions 9-28013
 magnetic field meas. by Faraday effect using resonant laser radiation 9-38998
 magnetic field to electron conc. ratio meas. by Voigt effect using resonant laser rad. 9-40687
 in magnetic field with thin cylindrical probes 9-32641
 maser interferometer, $337 \mu\text{m}$ c.w. for electron density and collision freq. 9-25909
 medium-pressure, probe charact. 9-42532
 MHD-generator plasmas 9-28012
 microwave, of laser produced Al plasma 9-23319
 microwave cavity method, analysis of perturbations caused by plasma 9-41859
 microwave scatt. from magnetoplasma, enhancement at cyclotron resonance and from an electron beam 9-23318
 microwave scattering enhancement by instability in mag. field 9-28033
 microwave techniques 9-34773
 non-uniform, resonance probe charact. 9-32624
 optical probing of cylindrical weak current arc 9-39034
 Penning discharge charact., local mag. field deformation effect 9-32642
 of pinch discharge laser, spectroscopic 9-47958
 plasmascope operation, design and applic. 9-48585
 probe, cylindrical, effect of mag. field and collisions on ion current 9-46509
 probe, flush electrostatic, edge effect 9-32637
 probe coil excited by plasma cluster, flux moving in axially symmetric mag. field 9-36750
 probe impedance in warm plasma 9-40685
 probe noise in quiescent plasma 9-28014
 probe with electrostatic separation, distrib. functions 9-44462
 probes, hot diffusion, spherical and cylindrical 9-23317
 probes, multi-electrode with positive potentials use 9-42533
 probes and effect on volt ampere characts. of plasma 9-42534
 profile meas. in columns using microwave resonant cavities 9-48583
 quiescent, probe noise investigation and mechanism for reduction of shot noise 9-42536
 radiation, correlation radiometry applic. 9-25916
 resonance of capacitor system containing warm plasma, quasistatic approx. value 9-46507
 r.f. impedance method for electron density and collision freq. meas. 9-46506
 scanner and data processing system for current-voltage characts. 9-30256
 Scylla IA θ pinch density meas. by CO_2 laser beam interferometer 9-40353
 by selective excitation spectroscopy 9-46019
 sonic probe 9-40688
 temperature, by Stark broadening of spectral lines, effects of dynamic ion shielding 9-48575
 temperature, high, by Stark broadening and displacement 9-25913
 temperature and density, electron and ion, Thomson scattering determ. with low resolution monochromator 9-25858
 temperature and electron concentration of plasma in local thermodynamic equilib. 9-38996
 temperature meas. by absorption of resonant laser radiation 9-38997
 temperature meas. by gamma ray resonance scattering 9-40689
 temperature meas. during production and heating by laser pulses 9-48586
 temperatures, Stark-broadened H lines as probe 9-48589
 theoretical and practical aspects, and quantitative spectroscopy, book 9-32643
 torsional Alfvén wave application 9-23281
 turbulent flow, space-time correl. function useful for probe anal. 9-23289
 velocity, Doppler determ. with photoelec. recording 9-40692
 velocity measurement by inductive probes, distortions rel. to space charge, temp. distrib. and press. grads. 9-25911
 Z-pinch, preionization, meas. of Thomson and Rayleigh scatt. 9-44415
 Al laser produced plasma, microwave diagnostics 9-23319

Plasma continued**diagnostics continued**

Ar, viscosity obs. up to $12 \times 10^8 \text{K}$ 9-38964
 Ar and Ar-He jets, electron conc. determ. using v.h.f. Fabry-Perot interferometer and opt. Stark effect 9-42522
 Ar arc jet, temp. meas. at atm. pressure 9-30251
 Ar arc with K added, weak current cylindrical, light probing 9-39034
 Ba, Q-device, density meas. in low density range, rel. to verification of 'equilibrium' theory 9-28018
 of Ba⁺ using tunable dye laser 9-44463
 CO_2 laser interferometer, transient low-density plasma meas. 9-40353
 Cs, Langmuir probe and spherical h.f. probe, comparative studies of electron density meas. under collisional conditions 9-46479
 H_2^+ probe for meas. plasma density 9-32638
 H_β Balmer line, particle density meas. through Stark broadening 9-25859
 H temperature from intensity ratio $\text{H}\beta$ to background 9-30261
 He, inductive, electric conductivity as function of time and space, spectroscopic measurements 9-42535
 He electron conc. from He I 4922 and 4472 Å line widths 9-30261
 He θ -pinch, spectroscopic exam. of excitation, density and temp., and possible population inversion 9-36771
 Hg vapour, transient, abnormally high electron density confirmation, laser-interferometer meas. 9-48557
 N, Stark-broadened H lines as temp. probes 9-48589
 U matrix in opt. d.c. arc plasma, core dimensions, temp., voltage and elec. field distrib. 9-25918

electromagnetic waves
 absorption analysis in anomalous dispersion region 9-48564
 absorption coefficient meas. using laser pulses 9-28000
 absorption of powerful wave in collisionless plasma 9-46486
 amplitude modulation by modulated mag. fields, modified theory and applic. to communications during blackout 9-32617
 amplitude modulation by modulated mag. fields, modified theory and applic. to communications during blackout 9-32617
 anisotropic, point charge in motion, Cerenkov radiation spectrum 9-34759
 antenna in plasma, book 9-25942
 beam-plasma system, parametric amplification 9-42503
 Born scattering from finite volume turbulent plasma 9-48562
 boundary value problems 9-25878
 bounded by mag. field, phase velocity variation for existence of region of slow waves 9-30238
 bremsstrahlung, relativistic correction 9-44435
 cold, composed of one type of atom, relativistic nonlinear interact. with e.m. waves 9-27997
 cold column, wave-mixing and weak non-linear resonance phenom. 9-27996
 cold plasma in constant longitudinal magnetic field nonlinear interaction of steady-state circularly polarized e.m. wave 9-23297
 in cold plasma in long. mag. field, nonlinear interaction of circularly polarized wave 9-23295
 column, excitation by external ring source 9-27994
 compressible with a homogeneous drift vel. and mag. field 9-40673
 coupling between 3 waves with different freqs., non-mag. medium 9-30234
 cyclotron harmonic waves, parametric amplification 9-32619
 detector design for space and in-flight operation 9-38027
 on dielectric rod, analysis with diagnostic applic. 9-45899
 dielectric susceptibility of free electron gas on interaction with e.m. wave field 9-25884
 in dipolar magnetic field, microwave interaction, properties 9-32644
 dispersion front, reflection and refraction, waveguide props. 9-48561
 Doppler eff. due to uniformly moving radiator 9-38978
 from electric point dipole in isotropic and uniaxial plasma 9-48573
 electron heating, energy calc. from Boltzmann transport eqn. 9-32618
 electron plasma waves, e.m. radiation 9-30239
 electron stream-plasma system, synchrotron radiation amplification 9-25882
 electron-hole, slightly noncompensated, cutoff 9-26492
 electrostatic wave propag. in medium with negative dielec. const. 9-46487
 electrostatic, propagation, soln. 9-32674
 energy transfer mode between field and plasma 9-27995
 field penetration, cylindrically bounded, anomalous skin eff. 9-25881
 field pressure effect on propag., dispersion equations 9-42510
 finite amplitude, in magneto-active medium, self-action 9-48570
 generate by electrons gyrating in magnetized plasma, theory and expt. 9-27999
 guided, in magnetized plasma, dispersion props. 9-42508
 harmonic generation, second, due to incidence 9-30240
 helicon wave amplifier, using semi-metals doped semiconductors, patent 9-48577
 h.f., penetration in slightly ionized plasma, freq. and mass ratios 9-42507
 h.f. radiative transfer, quasilinear theory 9-32621
 hybrid resonances h.f., in non-uniform plasma, non-linear theory 9-42509
 interacting, statistical treatment 9-30235
 interaction, l.f. field with plane non-isothermal layer 9-48566
 laser beam interactions with ionized gases 9-34793
 laser penetration and self-focusing in dense plasma 9-48574
 l.f., in linear hard-core configuration, stability and propagation conditions 9-27998
 Lorentz gas response to a.c. pulse 9-44437
 magneto, compressible lossy, fields and propag. unified approach 9-47870
 magnetoionic homogeneous medium, infinitely long conductive circular cylinder, e.m. waves eigen values 9-46484
 magnetoplasma, bounded, space-charge waves generation by nonlinear interaction of microwave signals 9-30237
 magnetoplasma, microwave scatt. from fluctuations 9-23318
 magnetoplasma, semicond. drifting, instabilities 9-48567
 Maxwell's equations solution in approximation to geometrical optics 9-29333
 microwave cavity, cylindrical, eigenvalues from hollow-cathode discharge 9-36219
 microwave diagnostic techniques 9-34773
 microwave electron-cyclotron heating in ELMO 9-32626
 microwave phase shifter, theory and applic. 9-27993
 microwave pulse absorption and parameters variation 9-42512
 microwave pulse amplification 9-34763
 microwave scattering, enhanced, by plasma instability in mag. field 9-28033

Plasma continued**electromagnetic waves continued**

- microwave transmission coeffs., variations with 'nominal cut-off' 9-38975
- microwaves, circ. polarized electron cyclotron damping 9-44434
- monochromatic high amp. wave, non-linear damping 9-38979
- monochromatic travelling waves, nonlinear behaviour by asymptotic method 9-32625
- moving plasma, delay and distortion effects 9-40297
- non-linear circularly polarized, with speed of light, in multicomponent plasma 9-34762
- nonlinear sum and difference freq. generation in inhomogeneous magneto-plasma 9-38980
- nonlinear Vlasov eqn., relativistic regime 9-44436
- oblique reflection of impulsive wave from half-space, response rings 9-48569
- partially ionized, acoustic wave propagation, modulation of discharge parameters 9-36765
- penetration into cylinder 9-48565
- perturbation and induced charges, linear relationship, near stationary equilib. 9-44431
- plasmoid r.f., resonance props. reviewed 9-36783
- polarized, circularly R.H. and L.H., along uniform mag. field in hot plasma 9-40192
- polarized, reflection in mag. field, ray displacement 9-44430
- propagation; soln. via matrix formulation of Maxwell's eqns. 9-40671
- propagation, book 9-25862
- propagation, group velocity and energy transport 9-25143
- propagation at small angle to mag. field for density meas. 9-25879
- propagation of TE wave with large amplitude 9-47869
- radiation mechanisms, plasma waves conversion into e.m. waves 9-41617
- radiation pressure on plasma-vacuum boundary 9-23290
- radiative processes infinities in statistical theory 9-44404
- reflected wave in vacuum at plasma boundary, nonlinear deviations 9-23296
- reflection, incoherent, effect of surface waves in vacuum boundary 9-44439
- reflection and absorpt. coeffs. for acute angle incident waves from magneto-active plasma 9-32622
- reflection incident at arbitrary angle, kinetic theory 9-44438
- relativistic collisionless plasma, e.m. waves trans. and refl. at boundary, exact soln. 9-23293
- r.f. energy density and velocity of energy transport, wave frequency close to frequency of damped oscillations 9-23292
- r.f. energy density and velocity of energy transport, wave frequency close to frequency of damped oscillations 9-23291
- r.f. power transmission, non-uniform density distribution effect 9-32624
- scattering, multiple, in underdense plasma, transport equation for intensity 9-42513
- scattering, multiple in underdense plasma 9-34761
- scattering, nonlinear effects 9-44432
- scattering, Thomson with unequal electron and ion temp., effect of collisions 9-42515
- scattering by free electrons, effect of charged particle-neutral collisions 9-46485
- scattering by hydrodynamic pulsations 9-38977
- scattering by small ellipsoid moving in external static mag. field 9-42505
- scattering from sphere, comparison between geometrical optics approximation and rigorous method 9-36768
- sinusoidally stratified media, propagation, analytical treatment 9-42506
- slab in waveguide, nonlinear interaction of microwave field 9-36767
- strong-field e.m. wave propag. near electron cyclotron freq. 9-25880
- synchrotron radiation from gyrating single electrons 9-34758
- TE wave non-linear focussing in two-level system 9-22316
- Tonks-Dattner resonances, subharmonic generation 9-23294
- transient radiation in plane stratified dispersive medium, similarity principle appl. 9-42502
- transmission for normal incidence in moving layer, kinetic theory 9-44438
- transverse electron beam fast-wave interactions, small-signal propagation, growing waves 9-36766
- transverse modes in moving medium, steady-state behavior and power relationships 9-30236
- turbulent flow scattering, wave-number freq. spectrum anal. 9-23289
- two counterstreaming electron plasmas, e.m. wave propag. 9-32595
- two counterstreaming electron plasmas thermal stabilization of modified ordinary wave 9-32620
- two-stream magnetoplasma, wave and dispersion equations 9-48563
- uniaxial compressible, containing infinite cylindrical antenna, charact. 9-25154
- warm plasmas with heat flow and tensor press. disturb. 9-34760
- in waveguide, cylindrical with relativistically interstreaming concentric regions 9-48572
- waveguide, non-uniform, phase rels. of symmetric modes 9-25883
- waveguide, with strong transverse magnetic field, propagation characteristics 9-25153
- waveguide filled with warm uniaxial plasma, characteristics 9-25152
- waveguide for whistler freq. range, theory 9-34126
- waveguides, e.m. modes 9-42504
- whistler mode excitation during interaction of electron beam 9-25885
- whistlers, amplitude dispersion and nonlinear instability 9-44433
- Ar afterglow in mag. field, microwave scattering and noise emission 9-48568
- Ar dense low temp., total radiation obs. 9-40672
- CS, near hybrid ion-electron resonant freq. 9-23298
- He afterglow in mag. field, microwave scattering and noise emission 9-48568
- Hg and Xe, radiation portion, high pressure, stable 9-30323
- Ne afterglow in mag. field, microwave scattering and noise emission 9-48568

magnetohydrodynamics

- accelerator, oscillations and possible nonaxisymmetric current distrib. 9-25903
- Alfven and magnetoacoustic wave propagation in helicoidal systems 9-36777
- channel flow, own mag. field effects, and fringe field resistance 9-27983
- channels, single-pair, electrode current distributions determ. 9-25863
- cold collision-face plasma, weak non-linear hydromag. waves 9-42541
- collisionless, hypothetical system expressions for motion 9-32608
- collisionless approx. and moments of distrib. function 9-27985

Plasma continued**magnetohydrodynamics continued**

- collisionless flow past slender bodies, effect of tensor conductivity 9-25865
 - collisionless heating of solar-wind plasma by damping hydromag. waves 9-24913
 - coupling oscillations and drift instabilities 9-46516
 - dissociated real gas in thermal equilib., channel flow in generator 9-25165
 - duct, current and voltage distrib. around normal shock wave 9-25875
 - effect on hydrodynamic turbulence and motion of particle suspensions in viscous fluids, singular-perturbation methods 9-27986
 - energy principle, applic. for stellarator equilibrium 9-32678
 - energy storage and transfer, experiment and theory 9-41174
 - finite Larmor radius eqns. with nonuniform elec. fields and velocities 9-46480
 - flow, stationary self-contracting, effect of finite conductivity 9-23279
 - flow in inhomogeneous transverse magnetic field 9-42496
 - flow in transverse magnetic field in tube of square cross-section with conducting walls 9-30198
 - flux transport in elec. shock tube, interaction expt. 9-23280
 - focus, dense, pinch curvature effect on stability 9-44446
 - generator, transport processes 9-27982
 - generator-plasma, diagnostic techniques 9-28012
 - geomagnetic disturbance propag. in unevenly magnetized cold plasma 9-31352
 - gyroscopically stabilized plasma in strong mag. field, exchange invariance 9-42475
 - Hall voltage nonlinearity 9-36762
 - hybrid mode, upper, dispersion in spatially inhomogeneous plasma 9-25861
 - interplanetary disturbances, magnetoacoustic and Alfven velocities 9-43642
 - loss-cone flute mode, single harmonic, nonlinear evolution 9-46528
 - low- β , penetration across mag. field 9-30227
 - in magnetic mirror, axisymmetric and multipolar, non-adiabatic behaviour 9-28009
 - magnetospheric wave amplification, 0.2 to 5.0 Hz and rel. to Pc 1 micro-pulsations 9-28966
 - Ohm's law in crossed mag. and elec. fields, for high diffusion vels. 9-30230
 - particle-wave interaction, weak turbulence theory 9-34752
 - power generation 9-27270
 - purification by electrostriction, patent 9-40668
 - radiative energy losses, total and local, rates in nonequil. plasmas 9-32627
 - reactive energy prod. in travelling mag. field, calc. from equiv. impedance 9-30224
 - relativistic, applic. of symmetry concepts 9-32609
 - shock production, scalar cond. calc. rel. to current sheet growth 9-46494
 - shock wave, collisionless, formation 9-36761
 - shock wave, collisionless, formation 9-30228
 - shock wave, non-evolutionary, stability 9-42501
 - shock wave collisions with rigid obstacles in mag. fields parallel to propag. dirn. 9-25870
 - solar wind interaction with moon, lab. simulation 9-31595
 - solar-wind, collisionless heating by damping hydromag. waves 9-24913
 - stability and equilib. of plasma-current multipole configuration, expt. demonstration 9-40702
 - stability multipoles with shear 9-23336
 - stationary electric arc in cross flow and transverse mag. field, anal. 9-46549
 - stationary plane flow of electrically conducting, non-heat conducting, non-viscous perfect gas in transverse magnetic field 9-30226
 - string with a.c. stabilisation with quadrupole mag. field 9-40667
 - superconducting shell, expansion into ambient mag. field, soln. 9-46483
 - supersonic, flow, around 2 dims. mag. dipole 9-38966
 - toroidal shape, curvature effects, properties 9-42497
 - torsional Alfven waves, obs. 9-23281
 - transverse injection of dense plasma into linear octupole magnetic field 9-25864
 - turbulent, weakly, conservation equations, inclusion of magnetic fields 9-38967
 - velocity meas. by inductive probes, possible sources of distortion 9-25911
 - Vlasov, magnetogravitational instability 9-27984
 - vortex flows, double, axially traversing multipole fields 9-32607
 - waves, 3 dims., emission characts. 9-30223
 - waves, plane coherent, propag. in presence of density fluctuations 9-46481
 - waves, solitary in collisionless warm plasma 9-44421
 - Z-pinch, plasma focus and neutron emission mechanism 9-38989
 - Ar, collisional shock prod. in inverse pinch, characts. 9-46495
 - Ar, impulse drives, interactions with transverse magnetic field 9-30229
 - Ar, K seeded, effects of auxiliary d.c. discharges on performance of linear MHD generator 9-48558
 - Ar, MPD arc, heat transfer mech. responsible for energy fluxes to anode 9-32610
 - H, collisional shock prod. in inverse pinch, characts. 9-46495
 - He, collisional shock prod. in inverse pinch, characts. 9-46495
 - NH₃, MPD arc, heat transfer mech. responsible for energy fluxes to anode 9-32610
- measurement technique** see *Plasma/diagnostics*
- oscillations**
- acoustic wave propag. in elec. disturbance near-field 9-32656
 - acoustic waves, interaction with Langmuir waves in turbulent plasma 9-40698
 - Alfven wave in cold collision-free plasma 9-42541
 - Alfven waves, torsional; attenuation and propagation in nonuniform, resistive, cylindrical plasma; conducting boundary 9-36776
 - Alfven waves propag. in non-homogeneous plasma with gravit. field 9-28026
 - Alfven waves propag. in nonhomogeneous two-dims. plasma 9-23326
 - Alfven waves through the Earth's bow shock 9-45507
 - alkali metal, noise due to radial electric field 9-28029
 - anisotropic, moving, energy and power-flow density of wave, transf. laws 9-34783
 - anisotropic, waves, quasi-linear theory 9-32654
 - axially magnetised column with hollow and perfectly conducting cores, resonance 9-32647
 - beam, multicomponent, pair collisions effects 9-46531
 - beam-plasma interaction, asymptotic behaviour 9-48596

Plasma continued
oscillations continued

beam-plasma system, bounded with finite temperature, dispersive properties 9-39006
 Bernstein modes, radiation-induced decay instability 9-25944
 with body at large positive potential, neighbouring longitudinal waves, amplification and instability 9-42551
 bounded, electron waves and resonances, book 9-25942
 bremsstrahlung calc. in freq. region 9-36772
 in bubble, surface 9-39574
 capacitor filled with plasma, microwave emission 9-38329
 cavity modes of partially filled spherical cavity 9-34779
 charged particle beams transit thro' non-adiabatic mag. field 9-25175
 cold, composed of one atom type, due to nonlinear relativistic interact. with e.m. waves 9-27997
 cold collision-face plasma, weak non-linear hydromag. waves 9-42541
 cold column, weak nonlinear resonance phenom. due to scatt. of plane incoming waves 9-27996
 collective, electron vel. distribution 9-42491
 collisional damping, perturbed electron distribution function, linearized kinetic equation 9-32660
 collisionless, wave trains propag. at angle to mag. field, soln. 9-34781
 collisionless thermalization of injected electron beam, rel. to wave modes 9-48599
 compression waves, nonlinear in multicomponent collisionless plasma, laminar structure 9-46515
 cosmic ray accelerating mechanism in space 9-35949
 current, spontaneous large amplitude in thermionic diodes 9-47892
 cyclotron harmonic ion waves, stop- and pass-band charact. 9-28025
 cyclotron harmonic waves, resonant mode coupling 9-44471
 cyclotron waves, ion, in mirror confined plasma propag. and damping 9-44467
 cylinder, inhomogeneous, in mag. field rel. to drift instability suppression by feedback 9-23327
 with diffusion in velocity space, variational study 9-25929
 drift waves, finite amplitude collisional 9-32657
 drift waves, partly ionized plasma, dispersion relation 9-28038
 drift waves and rel. to stability problems 9-28032
 drift waves in inhomogeneous resistive medium, parametric excitation 9-48598
 echo soln. of Vlasov eqn. 9-30272
 echo wave, transverse with transverse excitation 9-25926
 echoes generation process 9-32662
 echoes of ion-wave spatial, theory and experiment 9-34785
 eigenmodes of partially filled spherical cavity 9-34779
 electron, collisional time damping evaluation 9-30267
 electron, dipole and quadrupole bremsstrahlung calc. 9-30267
 electron, dispersion eqn. soln. 9-42540
 electron concentration, l.f. 9-25928
 electron is v.h.f. filed, time averaged force 9-48607
 electron waves, small amplitude, relativistic damping calc. 9-44469
 electron-cyclotron resonance, 200 W microwave power, parameter determin. under steady-state conditions 9-42511
 electron-plasma oscillations, resonant four-wave interaction 9-34784
 electron-sound waves, induced scatt. and disintegrations 9-42547
 electronic wave disintegration 9-40697
 electrostatic, for Fermi electron energy distribution in mag. field 9-25921
 electrostatic in a.c. external field 9-25927
 electrostatic l.f. collisional in rot. plasma cylinder, dispersion rels. 9-25950
 electrostatic non-linear quasi-neutral waves 9-48600
 electrostatic waves, book 9-25862
 electrostatic waves from Maxwellian plasma, emission intensity distrib. 9-32650
 energy and momentum of waves 9-32666
 enhanced oscill., scatt. laser light obs. from arc discharge 9-39004
 excitation, parametric, in mag. field, Vlasov eqn., Bernstein mode growth rate 9-27979
 excitation by modulated electron beams 9-46521
 excitation by modulated ion beam 9-48602
 excitation energy comparison with average kinetic electron energy 9-46520
 in external elec. field, initial value problem 9-23324
 field fluctuations, elec., and convective modes 9-26040
 flute, instability, effect of resonance particle drift due to mag. field inhomogeneity 9-28030
 flute mode, nonlinear evolution of single harmonic loss-cone 9-46528
 flute modes in scaled down mirror machine 9-48581
 flute modes inducing particle diffusion in plasma with $T_e \geq T_i$ 9-46491
 geodesic acoustic waves modes analysis, in hydromagnetic systems 9-30266
 gravitational mode and finite-resistivity of sheet pinch 9-30280
 group velocity and index determ. from implicit function 9-40695
 h.f. vibrations, stimulation by electron beam interaction 9-44474
 hollow-cathode discharge 9-44422
 hydromagnetic, coupling modes between Alfvén and magnetosonic waves, drift instabilities 9-46516
 hydromagnetic, torsional, electron motion effects along mag. field lines 9-37935
 inhomogeneous, electrostatic waves, propagation and linear transformation 9-32651
 inhomogeneous, parametric eff. of alternating elec. field 9-34782
 inhomogeneous, Vlasov eqn. numerical soln. 9-25935
 inhomogeneous bounded, Vlasov-Poisson eqns. self-consistent soln. 9-44465
 intensive waves, nonlinear interaction 9-39002
 ion, second harmonics generation and attenuation 9-40696
 ion acoustic, long wavelength, Landau damping 9-25920
 ion acoustic waves, large amplitude, in Cs plasma, collisionless damping 9-40701
 ion acoustic waves, transient sheath obs. by leading edge extrapolation 9-23304
 ion acoustic waves in turbulent plasma 9-42543
 ion cyclotron oscillations, electrostatic, excitations in weakly ionized plasma in external d.c. field 9-28024
 ion plasma oscillations in discharge produced by back diffusion plasma sources 9-28022
 ion sound, suppression and parametric amplifications 9-48604
 ion wave damping in nonuniform plasma 9-48597
 ion wave modes, three, propag. and wave-wave coupling 9-46518

Plasma continued
oscillations continued

ion waves, oblique, slightly turbulent, excitation 9-36774
 ion-acoustic, excited, ion distrib. function perturbed part obs. 9-30273
 ion-acoustic, nonlinear scatt. by electrons 9-46523
 ion-acoustic and ion-plasma, parametric coupling and energy transfer 9-42542
 ion-acoustic waves, propagation in plasma subject to ambipolar drift 9-34780
 ion-cyclotron wave generation, dominant influence of electron inertia 9-42545
 ion-sonic vibrations in mag. field at low press. 9-42550
 ion-sound waves, finite amplitude, in unstable plasma 9-48601
 ionosphere F region, electron resonance wave propag. 9-31441
 ionospheric resonances, subsidiary 9-40082
 isotropic, homogeneous, enhanced bremsstrahlung radiation calc. 9-30268
 Landau damping and echo review 9-42546
 Landau modes, higher order 9-25930
 Langmuir, role in resonance luminescence capture 9-22918
 Langmuir waves, interaction with acoustic waves in turbulent plasma 9-40698
 l.f., at upper hybrid resonance, microwave excitation 9-32665
 l.f., non-linear excitation, non-isothermal isotropic plasma 9-30276
 l.f. in rarefied cylindrical magnetoplasma 9-46524
 l.f. self excited and forced waves in d.c. discharge 9-44472
 linear waves, small amplitude, phase vel. and polarization 9-25922
 longitudinal, and Landau damping 9-40700
 longitudinal waves, collisional absorption and emission 9-30270
 longitudinal waves, energy transfer from electron beam 9-44470
 longitudinal waves collision damping 9-44468
 magnetized, hot, bounded plasma, ion-electron resonances 9-36775
 magnetized plasma in strong h.f. field, short wave and vibrational instabilities 9-44476
 magneto-acoustic wave in cold collision-free plasma 9-42541
 magneto-plasma, low freq. non-linear mixing of ion wave with applied e.m. wave 9-32655
 magnetoacoustic waves, periodic, instability 9-30275
 magnetoactive, in h.f. electric field, electrostatic oscillations, dispersion relations 9-40699
 magnetoactive inhomogeneous, nonlinear effects near resonance 9-42548
 magnetoactive relativistic, polarization of normal waves and synchrotron radiation transfer 9-27989
 magnetoplasma; collisionless, Maxwellian, nonrelativistic boundless, Landau damping of longitudinal electron oscillations, external mag. field 9-39009
 magnetoplasma, alkali, electron temp. eff. on l.f. oscillations 9-42544
 magnetoplasma, weakly ionised, h.f., characts. of unstable waves 9-32682
 magnetosonic wave propag. across mag. field in warm collisionless plasma 9-24675
 Maxwellian plasma, electrostatic waves, emission intensity distrib. 9-32650
 modified and hybrid, prediction on discriminating, gyro-plasma probe experiment 9-34786
 multimode, and amplification in pinched electron-hole plasmas 9-48595
 non-uniform, h.f. electrostatic wave propagation in mag. field 9-30278
 nonisothermal streaming, l.f. electrostatic oscillations 9-42549
 nonlinear, low-freq. spectra of anisotropic plasma 9-25939
 nonlinear periodic waves in dispersive medium, instability 9-25940
 nonlinear theory, review 9-39005
 nonlinear theory, review 9-30274
 nonlinear wave interaction, stabilization by means of dissipation 9-32675
 parametric excitation and high order mode coupling 9-32659
 parametric resonator with impulsive parameter modulation, instability 9-30277
 positive column, l.f., asymmetric modes 9-25933
 positive column, l.f., axisymmetric modes 9-25932
 positive column oscillations in external e.m. field 9-36789
 in Q-machine, stabilization of pot. oscillations by h.f. mag. field 9-48605
 quasistatic, radiation damping calc. 9-44473
 rarefied, kinetics, simple waves and nonstationary solns. 9-39008
 rarefied plasma surrounded by surface of complex conductivity, instability 9-30292
 relativistic, in magnetic field, covariant treatment 9-30264
 resonance, in bounded inhomogeneous plasmas, central freqs., elec. fields and Landau damping 9-44465
 resonances, noise emission and Landau damping 9-39007
 resonant, pulsed dipole excitation growth and decay 9-32653
 resonant 3-wave coupling, kinetic eqn. 9-25923
 resonant power absorption from externally driven elec. field, zero temp. 9-30271
 self-action of waves in rarefied plasma in mag. field 9-25938
 semiconductor, free carrier transport props., study by magneto-plasma waves 9-28511
 in semiconductor p-n junction, l.f. in elec. and mag. fields 9-44987
 in semiconductor with non-standard dispersion law in presence of elec. and mag. fields 9-37504
 sum and difference freq. generation by two nonuniform elec. fields in static mag. field 9-32648
 sum and difference frequencies generation due to applied non-uniform microwave fields, analysis 9-46514
 supersonic flow around cylinder with oscillating surface 9-30265
 supra-luminous waves and radiation from density inhomogeneities 9-32667
 surface modes excited by electron beam 9-36773
 surface waves, instabilities caused by beam-plasma interaction 9-25937
 surface waves at vacuum boundary, effect on incoherent reflection of e.m. waves 9-44439
 temporal echoes, computer simulation testing theoretical prediction 9-46519
 tensor pressure plasma, Navier-Stokes form for div. p 9-25924
 transverse waves, temporal damping rate by Landau equation 9-32661
 transverse waves in hot collisionless magnetized plasma 9-44466
 turbulent, in current instability case, anomalous transverse diffusion obs. 9-30289
 turbulent, weakly, dielec. const., Langmuir freq. correction 9-32612
 turbulent microwave-heated stellarator plasmas, fluctuation properties 9-28028
 turbulent plasma, book 9-28027

Plasma continued**oscillations continued**

- turbulent plasma, ion acoustic waves 9-42543
- v.h.f. excited by electron beams 9-46522
- wave diffusion, effect of collisions 9-48603
- wave echo excited by two cyclotron waves 9-46517
- wave echoes, collisional eff. in Su Oberman and Fokker-Planck models 9-32600
- wave in moving anisotropic medium, energy and power-flow density, transf. laws 9-34783
- wave motion, evolution, nonlinear interaction with weak electron beam 9-25925
- wave regeneration in inhomogeneous medii, WKB approximation 9-32658
- waves, electrostatic large amplitude, constants of motion for perturbation 9-25934
- waves, e.s., particle acceleration in mag field due to spatially varying phase vel. 9-28023
- waves, induced conversion into e.m. waves 9-41617
- waves, quasi-linear problems 9-44475
- waves, stable and weakly unstable plasma, damping 9-25947
- waves excitation and Landau damping, mag. field effects, Thomson scatter meas. 9-32663
- waves in homogeneous plasma, temp. relax. effects 9-32649
- waves in magnetized plasma with particle drift motions, nonlinear coupling 9-32652
- waves in thetatron discharge, excitation and dissipation 9-25936
- weakly ionized, ion-acoustic standing waves excitation 9-32664
- weakly ionized, three-fluid hydrodynamics equations 9-32684
- weakly ionized plasma, perturbation theory of nonlinear oscillations 9-34778
- ω_s surface waves excitation by light in thin metal layers 9-25941
- Cs diode, electron and ion oscillations, simultaneous excitation obs. 9-25943
- Cs noise due to radial electric field, meas. 9-28029
- Cs thermally ionized plasma, large amplitude ion acoustic waves, collisionless damping 9-40701
- Ga liquid foils 9-41148
- He, acoustic l.f. oscillations at low temp., kinetics of heating and electron density calc. 9-39010
- He cryogenic, sound oscillations, excitation and damping 9-48606
- Hg, vapour, frequency in terms of discharge conditions 9-39003
- K noise due to radial electric field, meas. 9-28029
- Sn liquid foils 9-41148
- Xe, electrostatic ion waves in mag. field due to He contamination, Landau damping 9-30279

production

- current sheet, by induction, stability rel. to density 9-27972
- discharge plasma development in H spark at small pd values 9-39032
- duoplasmatron-type discharge, emitted particle, energy spectra 9-38990
- electron, hot, by MeV ion injection and Lorentz trapping 9-32646
- flow, long duration and high velocity, generation in multi-segmented tube by gas injection method 9-28019
- frequency-shifting method, exciting plasma is resonant cavity 9-23321
- generator, vortex linear, discharge chamber wall and electric arc column heat transfer 9-29322
- generator with bilateral outflow, and variable diameter electrodes 9-23322
- hot, in spherical multipole mag. field, experimental results 9-25901
- by laser, high power Q switched 9-28020
- laser, ionization by u.v. radiation from target in beam focus 9-36780
- by laser beam absorpt., theoretical model and expt. data 9-46511
- laser generation, physical mechanism 9-48611
- by laser irradiation of solid surfaces 9-23323
- laser prod., temp. meas. 9-48586
- laser-plasma system, production from single solidified gas particle 9-39000
- laser-produced, optical absorption and expansion 9-38983
- laser-produced gas breakdown, elec. field distrib. along beam axis 9-28055
- by microwave ionization in gas jet 9-30263
- pinch device, inverse, numerical studies 9-28005
- by Q-switched laser on Al sphere as target 9-42539
- shock heated gases, ionization rate measurements, investigation for use of Lecher wire method 9-25919
- u.v. initiated directional gas breakdown 9-28052
- Al, by laser impact on Al target, u.v. emission spectrum obs. 9-36769
- Al surface, optically excited resonance under u.h. vacuum conditions in reflection and photoemission 9-48591
- Al wire explosion in vacuum 9-44440
- Ar, by microwaves, strongly ionised low press. plasma 9-48592
- Cu wire explosion in vacuum 9-44440
- D, by subnanosec. laser pulses 9-34775
- D₂ by giant laser pulse irradi. of solid, conds for isotropic plasma 9-28021
- H, transient, by normal ionizing shock wave, electron density obs. 9-23276
- H₂ by giant laser pulse irradi. of solid, cords for isotropic plasma 9-28021
- H₂ solid, thin foil prod. for laser beam target 9-27147
- He, laser-induced breakdown, spectroscopic studies 9-34776
- He, laser induced breakdown, plasma development analysis 9-25844
- Li by giant laser pulse irradi. of solid, conds for isotropic plasma 9-28021
- LiH laser irradi., electron-ion recombination 9-44464
- LiH solid particles irradiated by laser beam, for thermonuclear research 9-46512

shock waves

- air, ionization relaxation zone length behind strong shock front 9-25961
- air flow behind shock, elec. conductivity 9-40669
- attenuation in low pressure gas, snow-plough model anomaly 9-27991
- calculations, approximate methods 9-44428
- collision-free, turbulence, lab. obs. rel. space data 9-25873
- collisionless, formation due to supersonic flow around 2 dimens. mag. dipole 9-38966
- collisionless, in rarefied plasma 9-36764
- collisionless, ion sound instability 9-25871
- collisionless shock wave heating obs. 9-38973
- collisions with rigid obstacles and other shock waves, depend. of density on Mach number 9-25870
- density of charged particles, measurement, moving plasma cloud 9-30258
- electron concentration in hypersonic flows, laser interferometry meas. 9-48588

Plasma continued**shock waves continued**

- e.m. production in tube, by sudden applic. of crossed mag. and elec. fields 9-28071
 - exothermic waves in magnetic field, calculations 9-30225
 - gas density and time depend. of laser produced blast waves, image converter photographs and probe data 9-34757
 - gasdynamic, formation between plasma flow and magnetic barrier 9-42500
 - generation by ions 9-29314
 - hydromagnetic non-evolutionary, stability 9-42501
 - inert gases, microwave-induced ionization wave propagation 9-32616
 - ionizing, switch-on, structure calc. using Navier-Stokes eqns. 9-25874
 - laser induced breakdown, enhanced heating at shock front of blast wave 9-30233
 - laser-produced blast waves, microwave meas. 9-42499
 - magnetic field interactions 9-27992
 - magnetohydrodynamic, structure 9-25877
 - in magnetoplasma, drift wave instability effect on elec. resistivity 9-44427
 - MHD, in collisionless plasma, formation 9-36761
 - MHD, in collisionless plasma, formation 9-30228
 - MHD, in non-aligned flow 9-25869
 - MHD duct, current and voltage distribution around normal wave 9-25875
 - MHD interaction expt., flux transport 9-23280
 - m.h.d. production, scalar cond. calc. rel. to current sheet growth 9-46494
 - non-linear quasi-neutral 9-48600
 - precursor ions and electrons, diffusion 9-25872
 - profile models, differential equations soln. 9-25876
 - structure in steady flow 9-40670
 - turbulence, role of ballistic term 9-32614
 - turbulent, collisionless 9-32615
 - Vlasov and Poisson eqn. shock-like solns. 9-25868
 - Ar, thermodynamic parameters of gas behind shock wave, calc. 9-38974
 - Ar inverse pinch, m.h.d. prod. of collisional shocks, characts. 9-46495
 - H, normal ionizing waves, electrode config. effects 9-44429
 - H, transient, electron density and homogeneity obs. 9-23276
 - H inverse pinch, m.h.d. prod. of collisional shocks, characts. 9-46495
 - H θ -pinch, density, temp. and mag. field structs. of shock fronts 9-46497
 - He inverse pinch, m.h.d. prod. of collisional shocks, characts. 9-46495
- stability**
- against i.f. interchange modes, conditions same as for max. entropy function 9-46530
 - algorithm for investigation of instabilities 9-25948
 - anisotropic, moving, energy and power-flow density of wave, transf. laws 9-34783
 - with anisotropic pressure, approximation 9-32683
 - with anisotropic velocity distribution, computer expt. 9-30284
 - Astron-type devices, with rigid E-layer electrons 9-38991
 - rel. to auroral fine structure 9-45515
 - axial-symmetric, in finite conductivity discharge 9-25957
 - ballooning effects in closed systems 9-28007
 - beam, multicomponent, pair collisions effects 9-46531
 - beam-plasma, linear instab. in mag. field, obs. 9-25951
 - beam-plasma, nonlinear effects and turbulent behaviour 9-32677
 - beam-plasma interaction, h.f. instability collisional damping 9-44480
 - Bernstein modes, radiation-induced decay 9-25944
 - bound, finite length, mechanism with frequencies connected with particles transit time 9-23331
 - bounded, one-dimens., dynamics and approach to equilibrium 9-25843
 - Burnout-V turbulently heated plasma, Doppler broadened spectra emission 9-44443
 - cold, in magnetic field, periodic waves stability 9-30283
 - collisional, in curved mag. field, kinetic theory 9-32671
 - collisionless drift waves stabilization 9-30218
 - collisionless, transverse instabilities 9-32672
 - collisionless microinstability 9-40706
 - column current, feedback stabilization 9-36778
 - confined plasma, stabilized by oscillating e.m. field 9-25949
 - crossed field instability rel. to ionospheric charge density irregularities 9-43461
 - current convective instability in presence of feedback 9-48610
 - current instability, effect of nonlinear scatt. of waves and weak plasma inhomogeneity 9-30290
 - current instability, turbulent diffusion and ion heating 9-30289
 - current of plasma between conducting deflectors in transverse magnetic field 9-30282
 - current sheet produced by induction, rel. to density, and final destruction 9-27972
 - cyclotron harmonics, cut-off, rel. to energy losses 9-30287
 - cyclotron instability of anisotropic cold ions 9-32685
 - cylinder, uniformly rot., drift instabilities 9-25950
 - density gradient drift instabilities, mag. curvature effect 9-30281
 - diocotron instability in presence of cold plasma 9-32670
 - discharge, magnetized positive column in turbulence 9-42554
 - discharge, weakly ionized, helical instability onset 9-25959
 - drift instabilities in plasma column, effect of surface dissipation 9-30291
 - drift instability of inhomogeneous plasma, suppression by feedback 9-23327
 - drift temperature instability in time modulated mag. field, eff. of elec. and mag. h.f. field 9-23335
 - rel. drift waves 9-28032
 - drift waves, partly ionized plasma, dispersion relation 9-28038
 - drift-convection and channel instabilities, stabilization by h.f. press. vars. 9-48607
 - drift-type instability, feedback stabilization 9-34777
 - drifting-dissipative in non-uniform plasma, modulation influence 9-34789
 - dynamic, in magnetic containment devices, variational approach 9-42552
 - dynamic, magnetic confinement, structure by variational method 9-46504
 - E×B instability, non-linear theory 9-32679
 - E layer, plane relativistic with imbedded shearing mag. fields 9-44405
 - electron, and injected beam, originally stable, nonstationary props. 9-44479
 - electron beam instability, h.f. modulation effect on energy and temp. of accelerated electrons 9-30286
 - electron gas in a magnetic field, Vlasov description 9-28035
 - electrons, in cylindrical geometry, analytic study 9-44481
 - electrostatic wave propagation boundary conditions effect 9-32674
 - feedback stabilization of drift-type instability 9-34777

Plasma continued**stability continued**

fire-hose instability in relativistic plasma, growth rate, rel. to cosmic ray liberation 9-48608
 flute instability, for axisymmetric plasma with finite ion Larmor radius 9-28031
 flute oscil., effect of resonance particle drift due to mag. field inhomogeneity 9-28030
 gravitational, Hall current, finite Larmor radius and conductivity effects 9-24815
 gravitational rotating discharge with crossed elec. and mag. field 9-25954
 heating, turbulent, of ions during electron-sonic instability 9-30288
 h.f. electrostatic instability propag. transverse to mag. field 9-40683
 hot, mirror confined, improvement by adding warm plasma 9-23337
 hot electron, microinstabilities characts. 9-34791
 of hydromagnetic shock wave 9-42501
 θ pinch, high β mirror instabilities 9-44448
 θ pinch, rotating 9-23307
 inhomogeneous, parametric eff. of alternating elec. field 9-34782
 instabilities, density gradient drift, magnetic curvature effects 9-32686
 instability, drift, collisionless, growth rate calc. 9-32681
 instability, parametric resonator with impulsive patemeter modulation 9-30277
 instability condition for ion flute mode with temperature gradients 9-32680
 instability due to electron beam-plasma interac. 9-34788
 instability of beam-plasma discharge and time charact. 9-32673
 interchange stability and drift motion of plasma with loss from ends of axially symmetric mag. bottle 9-34787
 ion cyclotron instability anal. in short mirror machine 9-46502
 ion interaⁿtion, temp. depend., no mag. field 9-36266
 ion plasma oscillations in discharges produced by back diffusion plasma sources 9-28022
 ion sound, in collisionless shock wave 9-25871
 ion-ion velocity space instability 9-32676
 ionization instability, numerical simulation possibility 9-23334
 ionospheric instabilities rel. to radar aurora, review 9-33822
 ionospheric wave motions during particle precip. 9-47576
 Kadomtsev-Nedospasov current-convective instability, effect of longit. dimensions of column on development 9-25956
 Kelvin-Helmholtz instability, effects of rotation and an oblique magnetic field 9-39011
 kinetic theory 9-46532
 kinetic theory, stable and weakly unstable plasmas 9-25947
 Larmor radius, finite ion. effect on stability of rotating superposed fluids 9-23328
 laser-produced, interaction with magnetic field, enhanced resistivity in wave front obs. 9-40703
 l.f. waves in linear hard-core configuration, stability and propagation conditions 9-27998
 loss-cone flute mode, nonlinear evolution 9-46528
 in magnetic containment device, variational approach 9-25946
 magnetic flute modes, low- β , instability due to transverse anisotropy 9-46500
 magnetized plasma in strong h.f. field 9-44476
 magnetoacoustic wave instability in strong mag. field 9-28036
 magnetoacoustic waves, periodic, instability 9-30275
 magnetogravitational, Vlasov 9-27984
 magnetoplasma, suppression of drift type instability by feedback technique 9-36779
 magnetoplasma, weakly ionised, h.f., characts. of unstable waves 9-32682
 magnetostatic field perturbation caused by waves 9-46457
 maximum-J configuration, temp. gradient instabilities 9-46529
 m.h.d. equilb. and stability of plasma-current multipole configuration, expt. demonstration 9-40702
 MHD generators, with cathode and anode duct of refractory material in inert gas, patent 9-45913
 micro-stability in magnetic traps, theory 9-30293
 microwave scattering enhancement by instability in mag. field 9-28033
 multipoles with shear, MHD 9-23336
 negative energy waves in mirror machines, destabilization 9-30248
 nonlinear interaction, stabilization by dissipation effects 9-23333
 nonlinear periodic waves in dispersive medium 9-25940
 nonlinear wave interaction, stabilization by means of dissipation 9-32675
 oscillations at surface due to electron beam interaction 9-36773
 periodic quadrupole min. B field, optimum config. 9-32668
 in Q-machine, stabilization of pot. oscillations by h.f. mag. field 9-48605
 quasi-particle concept applic. 9-40656
 in radiogalaxies and quasars, mechanism 9-41651
 rarefied plasma surrounded by field of complex conductivity, potential oscillations, instability 9-30292
 Rayleigh-Taylor instabilities, obs. 9-42553
 reflex discharge, instabilities rel. to anomalous diffusion 9-46526
 for resistive dissipation vanishingly small 9-40705
 resistive instabilities in toroidal plasma 9-25958
 resistive instability, growth and damping rate meas. 9-23332
 resistive instability, numerical calc. methods 9-42487
 r.f., centrifugal instability 9-25955
 of screw pinch 9-38988
 sheet pinch, finite resistive m.h.d. case, gravitational mode 9-30280
 spatial harmonics at harmonic frequencies of half cyclotron frequency 9-44477
 stabilization by arc discharge tube rotation patent 9-34790
 stabilization in presence of radial electric field 9-23330
 stellarators with sharp surfaces 9-32678
 stream-plasma system, radiative instability problem, solutions 9-40704
 string with a.c., using quadrupole mag. field 9-40667
 supersonic spherical source, stationary motion of non-equilib. plasma 9-38963
 synthesized from neutralized beam 9-39012
 in thermionic diodes, electron instabilities 9-47892
 thermodynamic, of dense nondegenerate plasma 9-42555
 theta pinch, high- β , tearing mode instabilities 9-30285
 theta pinch, interchange instabilities of higher modes, and stabilization effects 9-32669
 toroidal systems, drift-acoustic wave stability rel to resistive diffusion and rotn. about mag. axis 9-48609
 toroidal sysvems, trapped particle instabilities 9-46499
 toroidal with radial electric field, electron diffusion 9-25952

Plasma continued**stability continued**

toruses, min. average-B stabilization 9-28037
 transport processes with microinstability present 9-44416
 trapped particle stabilization in dense plasma 9-25945
 trough-shaped, stabilization through feedback system 9-23329
 turbulence, charact. meas. by laser beam scattering 9-46533
 turbulent magnetized, drift instabilities 9-44478
 turbulent plasma, book 9-28027
 two counterstreaming electron plasmas thermal stabilization of modified ordinary wave 9-32620
 two-stream instability, convective and absolute at equal temps. 9-28034
 velocity space, electron instab., obs. 9-23338
 wave evolution in nonuniform dispersing medium 9-38982
 wave in moving anisotropic medium, energy and power-flow density, transf. laws 9-34783
 weakly ionized, drift oscillations analysis 9-32684
 weakly turbulent plasma, nonlinear theory 9-46527
 Cs, thermal ionization and Li ion beam penetration, velocity space instabilities 9-48611
 H, current instability in strong alternating elec. field 9-25960
 Hg, vapour, free-fall decay in early afterglow 9-34810

Plasma diodes

see Electricity/direct conversion; Electron tubes; Plasma/devices

Plasma guns

see Plasma/devices

Plasma in solids

see Crystal electron states/plasma; Electron gas; Semiconductor; Solids

Plasma jets

see Plasma/devices

Plasma sheath

see Plasma confinement

Plasma thermocouples

see Electricity/direct conversion; Plasma/devices

Plasma torches

see Plasma/devices

Plasma waves

see Plasma oscillations

Plasmoids

see Plasma

Plasmons

see Crystal electron states/plasma

Plastic deformation

see also Slip
 alkali halides, conductivity enhancement (Gyulai-Hartly effect), a.c. dielec. meas. 9-33373
 alloys, substitutional, serrated yielding 9-39411
 anisotropic media, shear deform, Coulomb's criterion invariant form 9-45826
 austenite, recrystallization kinetics 9-33107
 book, introductory 9-38286
 brass, anneal, propag. of large amplitude waves 9-42872
 β -brass, metastable, effect on martensitic transformations 9-23981
 brass plate, cross-shaped, yield surface after prestraining or cold rolling, explt., study 9-26327
 α -brass wire, internal friction study by torsional oscill. method 9-35154
 collapse pressure of cylindrical nozzle intersecting conical pressure vessel 9-38285
 complementary work theorems in piecewise-linear elastoplasticity 9-41807
 compressive, effect of plastic buckling 9-37236
 concrete, reinforced, orthotropic, plastic flexure analysis 9-41806
 cryostate for expts. down to 77°K 9-27144
 crystals, dislocation rich surface layer form. 9-46896
 crystals, dislocation rich surface layer form. 9-46895
 diaphragm, circular, bulging by hydrostatic pressure 9-31833
 dislocations, continuous distribution, review of expt. results rel. to theory 9-23807
 ductile fracture, mechanics by internal necking between adjacent cavities 9-30676
 Duralumin, reduction in stress on applic. of oscillatory energy 9-37286
 duraluminium, 77°K, recovery of elec. resistivity 9-39581
 elasto-plastic deform. of bar by longit. torsion, variational methods for calc. 9-45830
 energy dissipation due to penny-shaped crack 9-33033
 f.c.c. metals, cyclic, eff. of slip character 9-30674
 rel. to fracture and mechanical strength, interdisciplinary approach, book 9-39431
 graphite, nuclear grade for space applics., constitutive eqns. 9-33057
 in hot rolling of strip 9-23944
 initial microstresses influence on polycrystals macroscopic strain 9-37237
 inverse strain-rate effects 9-35169
 (225)-martensite transf., role of plastic accommodation 9-26383
 metal, in uniaxial tension, effect of mode of unloading on residual lattice strains 9-39410
 metal shaping using alternating mag. field 9-41013
 metals, b.c.c., f.c.c. and h.c.p., due to strain-hardening 9-37239
 metals, ductile failure due to cup-and-cone fractures 9-48896
 metals, flow stress, temp. depend., effect on mechanism 9-39418
 metals, props. in rel. to hot workability 9-35174
 metals, tensile tests, effect of superimposed vibrs. 9-39419
 metals, work-hardening processes 9-35196
 missiles, metal cylindrical flat ended, longit. impact 9-41808
 Moire and grid method of meas. 9-35168
 polycapromide, mechanical damage, accumulation under static load 9-33039
 polycarbonate craze, yield stress from cyclic stress strain behaviour 9-46879
 polyethylene, yield strength, dislocation loops motion obs. 9-30734
 polyethylene, oriented, tensile deformation 9-46894
 polyethylene terephthalate, heat generation, model 9-33034
 polyethylene-stainless-steel lap joints, yield strength, dislocation loops motion obs. 9-30734
 polymethylmethacrylate, stress and strain softening in yielding under constant load 9-46887
 polystyrene, mechanical damage, accumulation under static load 9-33039
 projectile impact on viscoplastic circular plate, finite deflection 9-25065
 propellant, plastic yield stress determ. by simple test 9-23876
 quartz, synthetic dislocations assoc. with deform. and recovery, transmission electron microscope obs. 9-40955
 rigid circular plate, large deflection, influence of geometry changes 9-31831
 shell, 120° conical, edge constraint eff. on buckling 9-40269
 shell, ring-stiffened cylindrical, buckling 9-40270

Plastic deformation continued

- silicon iron, effect of twin and grain boundaries, 185 and 300°K 9-41018
solids with differing props. in compression, tension and torsion theory 9-26307
- stationary, rate depend. on stress and activation area determ. 9-42878
steel, austenitic, effect on structure and mech. props. 9-33059
steel, austenitic, TiC particles 9-33045
steel, austenitic stainless, metastable, transform. obs. 9-35178
steel, austenitic stainless and EN25, cycling effect on stress range 9-23867
steel, reduction in stress on applic. of oscillatory energy 9-37286
steel, transformer, strain effects on coercive force and magnetostriction 9-45140
steel plate with circular hole, under cyclic loading 9-23886
steels, props. in rel. to hot workability 9-35174
strain rate equation applicability, back stress term inclusion for transient and steady-state validity 9-30656
structural systems, symmetric, with first and second order imperfections, buckling 9-27196
thermodynamic activation parameters evaluation, review 9-44765
thermodynamics of rate sensitive plastic materials 9-22217
truss, shallow, effect on dynamic buckling 9-45827
wedge, by rigid flat die, under action of tangential force 9-25083
yield and reverse yield waves generated by impulsive e.m. radiation 9-45829
yield point load of conical shell 9-36168
A, dislocation density depend. on primary recrystallization 9-40947
Ag-Cu alloys, pressure hardening against H₂S corrosion 9-30659
Ag single cryst. stored energy values, rel. to work hardening theories 9-26325
AgCl:Mn, potential difference at defects 9-23877
Al-Cu-Mg-Al alloys, effect on S precip. 9-48928
Al-Cu-Mg alloys, effect on S precip. 9-48928
Al-Mg-Zn alloy, dislocation distrib. w.r.t. ageing time 9-37280
Al-Zn solid soln. and precip. hardened alloy cryst., dislocation distrib. 9-39364
Al-(0.5wt.%)Zr, infl. of precipitated particles 9-44794
Al, 1100, under u.s. vibration, isothermal recrystallization kinetics invest. 9-37238
Al, alloys, structural instability, strain-induced 9-26326
Al, amplitude depend. of damping, rel. to dislocations 9-30661
Al, f.c.c. polycrystalline, flow stress after shock-relief deformation 9-23879
Al, polycryst., tensile deform., work hardening curve obs. 9-41014
Al, u.s. wave attenuation due to dislocations meas. 9-37332
Al, w.r.t. quadrupole broadening of n.m.r. lines 9-35723
Al₂O₃, at crack tip, rel. to fracture below 1000°C 9-33084
Al cycling effect on stress range 9-23867
Al fibres, mechanical damage, accumulation under static load 9-33039
Al single crystal, macroscopic and n. irradi. effects 9-46928
Al wires, changes in crystallite orientation 9-35170
 α -As single crystals, rel. to dislocations 9-46889
Au-(50 at.%)Cd alloy, martensite, influence of plastic deformation 9-39491
 β' AuZn, comp., temp., strain-rate and grain size dependence 9-23881
Be, isothermally hot-pressed, microyield and flow stress rel. to microstrain 9-35181
Bi, Bauschinger effect in twinning 9-42880
C, pyrolytic, basal plane distortion 9-39412
CdS single cryst., optical spectra depend. on dislocations density due to plastic flow 9-35644
Co, eff. on constitution, fine structure and conc. of structural defects. 9-23804
Co hexagonal crystal, magnetization and magnetostriction 9-37657
CoO scales, effect of stoichiometry 9-23882
Cu-Al alloys, martensitically transformed 9-35172
Cu-Fe two-phase mats., prod. of internal microstresses 9-46881
Cu-Sn alloys, martensitically transformed 9-35172
Cu-Ti, Cu-Ti-Al alloys, after low-temp. ageing 9-37292
 α -Cu-Zn alloys, activation vol. analysis at yield point w.r.t. dislocation intersection processes 9-39413
Cu, by shock compression, rel. to final yield strength 9-35162
Cu, dislocation density depend. on primary recrystallization 9-40947
Cu, f.c.c. polycrystalline, flow stress after shock-relief deformation 9-23879
Cu, microyielding, dislocation arrangement 9-48897
Cu, strain bursts, coarse slip and cyclic hardening 9-28357
Cu cyclically deformed, elec. resistivity change w.r.t. defects 9-33254
Cu cycling effect on stress range 9-23867
Cu electroplated Cr coatings effect 9-26328
Cu polycryst., preyield dislocation motion and multiplication obs. 9-35171
Cu polycrystalline, effect on mech. props. at about 77°K 9-37240
Cu single cryst., cyclically deformed, slip bursts 9-33052
Cu single cryst., fatigue crack formation during cyclic deform. 9-30682
Cu single crystal, electrodeposited, mech. props. and structure, rel. to deposition conditions 9-46786
Cu single crystals, mech. props., dislocation configs. and densities, effect of strain rate 9-41010
Cu w.r.t. quadrupole broadening of n.m.r. lines 9-35723
Cu whiskers below yield pt. 9-39407
Cu wire, internal friction study by torsional oscill. method 9-35154
Cu-Au ordered alloy, dislocation structure formation 9-23813
Fe-C alloys, cold, phase transform. singularities 9-39496
Fe-(0.05 wt.%)C alloy, recovery processes, dislocation-interstitial interactions obs. 9-30594
Fe-(11 at.%)MO alloy, mechanism rel. to temp., 295°-700°K, 700°-950°K and 950°-1100°K 9-35173
Fe-(27 wt.%)Ni austenitic alloys, effect of Al, Si, Mn and Cr on martensite form. during deform. 9-41068
Fe-(3 wt.%)Si, yielding dislocation configs. obs., delay-time model 9-44766
Fe, armoc, by twinning mechanism, eff. on ductile-brittle transition temp. 9-28345
Fe, Ferovac-E, shock-loaded, dynamic yielding mechanism by dislocation twinning 9-41017
Fe, pressurization effects on yield behaviour, effect of grain size 9-28347
Fe, pressurization effects on yield behaviour, effect of grain size 9-28346
Fe, pure, grain size and strain rate effect on lower yield stress 9-42881

Plastic deformation continued

- Fe alloys, (225), martensite transf., role of plastic accommodation 9-26383
Fe single crystals, dislocation and slip mechanism 9-23884
Fe- $\leq(0.04 \text{ wt.}\%)$ C quench aged alloy, hardening and softening obs. under cyclic straining 9-33079
Ge layers, epitaxially grown on GaAs 9-37241
Ge single cryst., dislocation distrib., etch pit obs. 9-42832
K-Na alloys, tensile deformation, yielding and flow mechanisms, conc. depend. 9-30664
K-Rb alloys, tensile deformation, yielding and flow mechanisms, conc. depend. 9-30664
KCl, strain bands introduced by indentation, decoration with F-centres 9-37242
LiF, recovery of amplitude independ. damping 9-42882
LiNbO₃, due to mech. twinning, crack nucleation obs. 9-23887
Mg-Al eutectic alloy, superplastic, mechanism 9-42883
Mg-(5 at.%)Li-(1.5 at.%)Al alloy, during rolling, mechanism 9-33035
Mg(5.1 wt.%) Zn alloy, twinning, inhibition by precipitates 9-46827
Mo, polycryst., microstrain meas. rel. to initial stages 9-46891
Mo, stress rel. to dislocation velocity 9-46823
Mo extruded hydrostatically, disloc. struct. by electron microscopy 9-40950
Mo single crystals, rolling texture exam. by X-ray diff. 9-41040
NaCl, conductivity enhancement (Gyulai-Hartly effect), a.c. dielec. meas. 9-33373
NaF, eff. on R absorption bands and M-colour centres of γ -irrad. crystals 9-26297
Nb, yield point return meas. of strain-ageing rel. to dislocation atmosphere formation 9-28381
Nb alloys, superconducting, dislocation pinning temp. and field dependence from hysteresis meas. 9-24153
Nb single cryst., temp. depend. of yield stress, eff. of neutron irradi. 9-26371
Nb single crystal deformed at high strain rates, mech. props., dislocation sub-structure and density 9-48898
Ni-Fe alloys, high temp., dynamic recryst. obs. 9-41020
Ni, by shock compression, rel. to final yield strength 9-35162
Ni, creep strength increase 9-46913
Ni, electrochemically polarized single crystals, model based on near surface dislocation sources 9-41019
Ni, f.c.c. polycrystalline, flow stress after shock-relief deformation 9-23879
Ni, high temp., dynamic recryst. obs. 9-41020
Ni, initial stage X-ray investigation 9-23888
Ni, rel. to internal frictions studies, 77° to 298°K 9-26317
Ni, effect on thermoremanent magnetization 9-35568
Ni polycrystalline, structure by X-ray diff. 9-23768
Ni single crystals, serrated yielding under continuous hydrogenation 9-46892
Ni strain-hardened by impulse loading, recovery behaviour 9-28348
Si-P single cryst., yield stresses, dislocation distrib., temp. and strain rate depend. 9-30665
Si, dislocation struct. obs. 9-42840
Ta, low temp. strain ageing, hardening obs. 9-44767
TiC particles in austenitic steel during creep 9-33045
Ti, h.c.p., slip modes 9-44770
U₂Si, phase change, X-ray diffraction analysis 9-35248
W-Rh alloys, yielding rel. to Rh conc. and ductile-brittle transition temp. 9-39415
W, polycryst. cast, tensile and compressive yield stresses, temp. and pressurization effects 9-44757
Zn, Bauschinger effect in twinning 9-42880
Zn bicryst., grain-boundary crack formation during deform. at high temp. 9-30698
Zn single cryst., X-ray diff. topography 9-35096

Plastic flow

see also Rheology

- anisotropic medium under plane deform., constraint fields 9-41804
armco iron, temp. and strain rate depend., 150° to 250°K 9-33044
clay suspensions, surface prop. dependence 9-23548
elastic-plastic flow eqns formulated and applied 9-22198
extrusion, Moore and grid method of meas. 9-35168
Ferrovac E iron, flow stress temp. dependence 9-41011
flow stress, strain-rate sensitivity for Peierls mechanism 9-39404
fracture, criterion of 9-30697
rel. to fracture and mechanical strength, interdisciplinary approach, book 9-39431
Incoloy 800, He embrittlement, tensile Strength obs. 9-35179
linear, basic eqns. reduced to generalization of Hamilton's canonical formalism 9-27198
metal, b.c.c., flow stress at low temp. 9-33051
metal, b.c.c., yield point considerations rel. to interstitial solutes 9-41028
metals, effect of superimposed vibr. 9-39419
metals, influence of struct. changes due to cold working and reverse annealing 9-46925
metals, polycryst., rate-depend. constitutive relation w.r.t. dislocation motion 9-37257
metals, stress, temp. depend., rel. to plastic deform. 9-39418
metals, true stress/true strain curve from indentation hardness meas. 9-23865
microscopic processes, to distinguish between solid and high-viscosity liquids 9-28353
necking in axis-symmetric tension specimens 9-34074
Nb superconductor, flow stress increase and electron dislocation interaction 9-44939
polyethylene, yield strength, dislocation loops motion obs. 9-30734
polyethylene-stainless-steel lap joints, yield strength, dislocation loops motion obs. 9-30734
steel, austenitic stainless, metastable, transform. obs. 9-35178
steel, C-Mn, quenched and tempered, ductility from Charpy-V notch tests 9-30690
steel, nonmetallic inclusions, critical size 9-48905
Ag, by dislocation motion, contrib. to mat. transport observed in sintering 9-46916
Al, quenched and aged, mechanism, 86°K 9-48900
Al, surface layer stress effect 9-23880
Al flow-stress relation to strain and strain-rate, drop-hammer test 9-39406

Plastic flow continued

- Al single crystals, dislocation motion during tensile or creep tests 9-30675
 CdS single cryst., optical spectra depend. on dislocations density due to plastic flow 9-35644
 Co-Fe-V alloys, high strength, high ductility rel. to partially-recrystallized structure 9-34790
 Cr, pressurized at 10-25 kbars, ductile/ brittle transition, dislocation distrib. change 9-39427
 Cu-Al-Fe-Ni aluminum bronzes, ductility rel. to microstructure, 20-800°C 9-23894
 α -Cu-Zn alloys, activation vol. analysis at yield point w.r.t. dislocation intersection processes 9-39413
 Cu, shock-wave strengthened, final yield strength 9-35162
 Cu deformed single crystals, flow stress, two region strain-rate sensitivity 9-41010
 Cu flow-stress relation to strain and strain-rate, drop-hammer test 9-39406
 Cu polycrystalline, ductility at about 77°K 9-37240
 Er, flow-stress temp. depend., 77 to 750°K 9-30663
 Fe-Ni alloys in liq. Hg, ductility and toughness 9-42891
 Fe-(3 wt.6%)Si, yielding dislocation configs. obs., delay-time model 9-44766
 Fe, pure, lower yield stress, effect of grain size and strain rate 9-42881
 α -Fe, strain-rate sensitivity, 0° to 900°C 9-30671
 α -Fe, thermally activated, analysis, 78°-320°K 9-23883
 α -Fe, thermally activated, stress relaxation and use of Johnston-Gilman eqn. in analysis 9-30672
 In superconductor, flow stress increase and electron dislocation interaction 9-44939
 K-Na alloys, yield and flow mechanism, conc. depend. 9-30664
 K-Rb alloys, yield and flow mechanism, conc. depend. 9-30664
 LiF ductility at low temp. 9-33038
 MgO single crystals, electron and neutron irradi., hardening flow stress and optical colouration 9-33099
 Mn-(11 at.5%)Cu alloy, relax. peak obs. w.r.t. twinning surface disloc. 9-35156
 NaCl powder, densification in air during sintering by plastic flow 9-35232
 Nb, single crystal of high purity in compression, effect of specimen dimensions 9-46885
 Ni-Si-Ti alloys, ductility 9-48902
 Ni-Si alloys, ductility 9-48902
 Ni, shock-wave strengthened, final yield strength 9-35162
 Ni electrodeposits, ductility, effect of metallic contamination 9-37146
 Ta, low temp. strain ageing, hardening obs. 9-44767
 UO₂, nonstoichiometry and temp. depend. 9-33049
 W, b.c.c. single crystal, flow stress temp. dependence 9-41011
 ZnO, flow stress increase under illumination 9-26329

Plasticity

see also *Viscoelasticity*

- anisotropic, sheet metal axisymmetric plane stress, strain-hardening 9-34075
 anisotropic medium under plane deform., constraint fields 9-41804
 bar, circular, elasto-plastic props. under axial load and torque 9-36167
 book, introductory 9-38286
 cones, solid truncated, yielding under quasistatic and dynamic loading 9-22219
 Cosserat surface, elastic-plastic theory 9-22209
 cyclic loading of tube, incremental calc. 9-23893
 diaphragm, circular, bulging by hydrostatic pressure 9-31833
 dislocations coplanar motion, small strain theory, Ni-base alloy 9-31834
 elastic-plastic and rigid-plastic plates of arbitrary thickness and flat bars of arbitrary width, stability 9-47809
 elastic-plastic continua with simple force dipole 9-25082
 elastic-plastic cylindrical shell under axial compression, instability 9-34071
 elastic-plastic deformation, strain components finite, thermomechanical coupling 9-34069
 elastic-plastic plates, impulsively loaded, bending waves 9-41796
 elastic-plastic stress distrib. near crack tip effect on fatigue crack propag. nucleation theory 9-46909
 elastic-plastic structures, iterative soln. of incremental problem 9-31827
 elastic-plastic tube, instabilities under internal pressure and axial pressure 9-45808
 elastic-plastic wave generation by absorpt. of e.m. radiation in thin surface layer 9-45846
 elastoplasticity, linear, complementary plastic work theorems 9-41807
 energy dissipation due to penny-shaped crack 9-33033
 failure criteria of plastic solids in the space of stress-invariants 9-39433
 fracture, effect 9-48910
 rel. to fracture and mechanical strength, interdisciplinary approach, book 9-39431
 graphite, EGCR-type AGOT, props. at room temp., 1000, 2000 and 4500°F 9-41009
 index determination reliability 9-35148
 junction growth, basic eqn. 9-31802
 limit analysis, convergence theorems for minimal sequences 9-45828
 lower bounds on structural performances under cyclic loading and temp., use of elastic solns. 9-22210
 metal, sheet anisotropic, from stress/strain curves in tension 9-30657
 metals, ductile failure due to cup-and-cone fractures 9-48896
 metals, effect of superimposed vibrs. 9-39419
 plane shear-pressure wave in elastic-plastic half-space, closed form solution 9-22218
 plastic-elastic matrix, elastic-fibre reinforced, continuum model 9-31823
 plates, circular and annular sandwich, with piecewise constant cross section, optimal design 9-31832
 polycrystalline solid, continuum stress-plastic strain relation 9-41805
 rigid circular gate, large deflections, influence of geometry changes 9-31831
 rigid-viscoplastic strain hardening annular plate, impulsively loaded 9-22240
 shell, 120° conical, edge constraint eff. on buckling 9-40269
 shell, cylindrical circular, instability expt. 9-40264
 shell, ring-stiffened cylindrical, buckling 9-40270
 slip, development of concept 9-41024
 steel, austenitic stainless, metastable 9-35178
 steel, ferrite-pearlite, ductile fracture resistance 9-46899
 steel cylinders, ductility under explosive loading conds., strain rate effects 9-30660

Plasticity continued

- stress waves uniaxially prestressed plastic viscoplastic unbounded media, harmonic dispersion analysis 9-31846
 structural systems, symmetric, with first and second order imperfections, buckling 9-27196
 superplasticity of certain metal alloys, popular article 9-48903
 thermodynamics of rate sensitive plastic materials 9-22217
 torsion, elastic-plastic of hollow bars, stress analysis by quadratic programming 9-36166
 unstable elastic-plastic fracture brittle criterion rel. to energy balance considerations 9-44775
 viscoplastic circular plate, finite deflection under projectile impact 9-25065
 Al-Zn eutectoid, superplastic behaviour, rel. to grain boundary sliding and grain rotation 9-23900
 Al-Zu alloys, ductility impaired by spinodal decomp. 9-37289
 Al, polycryst., tensile deform., work hardening curve obs. 9-41014
 Al alloy cylinders, ductility under explosive loading conds., effect of strain rate 9-30660
 Al oxide anodic films, oxide enhancement during growth on fine wires 9-31192
 Be sheet, ductility behaviour around transition temp., rel. to orientation, ageing and grain refinement effects 9-26333
 Co-(30.5wt.%)Ni alloy, allotropic transform., stress effects 9-23975
 Co-W alloy, superplasticity, strain rate tests, structural effects 9-26343
 Cu-Co single cryst. w.r.t. precip. state 9-39428
 Er, ductility from 77 to 750°K 9-30663
 LiF ductility at low temp. 9-33038
 Ni-Si-Ti alloys, ductility 9-48902
 Ni-Si alloys, ductility 9-48902
 Ti alloys, structural ductility 9-37243
 W-Rh alloy, ductile-brittle transition rel. to Rh conc., and yield stress 9-39415
 Zn-Al alloy, superplasticity 9-26330
 Zn, commercial purity, extended 9-28352

Plastics

see also *Polymers*

- adhesive at low temp., props. 9-26382
 anisotropic, production by reticulation of polymers in liquid crystal diluent 9-26078
 cellulose nitrate, for α -particle track recording, crystal scatt. appl. 9-42763
 degradation, environmental, under stressed conditions 9-26342
 diffraction gratings with restricted thermal expansion, production method 9-25364
 electrically conducting, elec. uniformity evaluation technique 9-43023
 electrodeposit-supporting, effect on corrosion of electrodeposits 9-28797
 electron beam absorpt., 20 to 50000 eV, and in air 9-37376
 F32L fluoroplastic, films, photovoltaic effect in vacuum u.v. 9-43136
 fiber reinforced, elec. and luminescent effs. of fracture 9-26351
 light scatt and absorption 9-36363
 particle track visualization and registration by energy loss criteria 9-25540
 plastics, filament wound reinforced, technology 9-35237
 plate, reinforced, input impedance determ. 9-37227
 polymethylmethacrylate, acoustic velocities, press. and temp. depend. 9-35276
 propellant, yield stress determ. 9-23876
 reinforced, thermal props. up to 150°C, meas. by i.r. method 9-33187
 scintillation, μ^+ depolarization, mag. field depend. 9-29995
 scintillator for neutron detection 20-170 MeV, efficiency 9-25515
 stiff-bonded; stability of 3-D elastic bodies 9-36165
 Al metallized polycarbonate and polyethylene terephthalate capacitors 9-39698
 Zn, Al metallized polycarbonate and polyethylene terephthalate capacitors 9-39698

Platinum

- adsorption and diffusion on oriented field emitters 9-23648
 adsorption phenomena, investig. by potentiostatic method 9-46731
 annealed wire, internal friction, shear modulus and transient creep rate 9-33024
 atomic scatter factor for electrons, 50-2.5 keV 9-46793
 atoms, ionization coeffs. determ. on W and Pt surfaces 9-45034
 atoms and at. groups, e optical phase contrast calcs. 9-32893
 chemisorption of CO, i.r. spectra, temp. effect 9-43325
 chemisorption of gases, LEED study 9-26818
 conductivity, elec., jump during melting 9-26156
 creep, stacking fault energy effect 9-39421
 Debye-Waller factor of ⁵⁷Fe 9-41082
 deformed, state I recovery by residual elec. resistivity meas. 9-26277
 density-of-states functions, X-ray photoelec. spectroscopy study 9-44886
 depth distributions, low-energy, obtained by sputtering 9-47013
 dispersion hardening, patent 9-26391
 electron emission, secondary, total yield 9-31008
 electron scattering obs. on (100) face 9-46746
 Fermi radius, velocity and g factor, exptl determ. 9-47046
 film, electrical conductivity and Hall consts. 9-30848
 galvanic platinizing of stainless steel, effect on passivity in H₂SO₄ 9-24574
 growth, hydrothermal 9-37027
 heated, scattering of monoenergetic Ar beam 9-44316
 horizontal wire in water, large step change in temp. rel. to transient film boiling 9-28188
 interaction with alkali halide crystals, capacitance enhancement 9-49134
 internal friction, shear modulus and transient creep rate of annealed wire 9-33024
 Ohm's law verification up to 10⁹ A/cm² current densities 9-24126
 photoelectric cross-section of atom obs. at 84, 100 KeV 9-44282
 thermionic emission in Cs vapour, report on various aspects 9-25170
 thermometer, resistance, comparison with H vapour press. thermometer 9-45885
 thermometers, accuracy in determ. of temps. between 2 and 14 K 9-40290
 thin film on glass, elec. conductivity 9-24121
 vacancies, quenched resistivities and Matthiessen's rule 9-35336
 wire at 1080°C, positive ion emission from alkali metal iodides on surface, time var. 9-39745
 wires, resistivity, size-depend. deviations from Matthiessen's rule, 1.2° to 4.2°K 9-49026
 in Na, molten, spin-slip scatt. of conduction electrons 9-32793

Platinum continued

- Pt/Pt contacts, adhesion w.r.t. contact resistance 9-33132
 Pt-Al₂O₃ catalyst, surface transport of various gases 9-26195
 Pt, quenched, secondary defect obs., e. microscopy and field ion microscope exam. 9-23815
 Pt⁴⁺ in Ba₂NbNb₂O₁₅, optical defect 9-28651
 Si:Pt, elec. props. 9-49110
 WO₃, activated fuel cell electrodes, mechanism and performance 9-47891

Platinum compounds

- alloys, dispersion hardening, patent 9-26391
 alloys, phase structure, distortion from Cu-type substructure 9-35064
 Pt-Pd, γ solid solutions, thermodynamic props. 9-30753
 Au-Pt, precipitation kinetics, coherent and incoherent, study by resistivity changes 9-28382
 Co-Pt equiatomic alloy, magnetostriction, effect of tensile stress 9-45156
 Cr alloys with Pt-series metals, structural and magnetic similarities 9-33438
 Cu-Pt alloys, internal oxidation by diffusion process, 850-1000°C 9-24557
 CuPt alloys, energy of ordering by tin soln. calorimetry 9-48934
 Fe-(32 at.%)Pt alloy, quenched, fine struct., X-ray diff. obs. 9-46787
 Nb₃Au_{1-x}Pt_x system, supercond. transition temp., annealing conditions influence 9-44942
 Pt-(0.07 at.%)Co alloy, low-temp. elec. resistivity 9-33257
 Pt-Co alloys, double ageing rel. to coercive force increase 9-26372
 Pt-Co dilute alloy, magnetoresistivity 9-44917
 Pt-(1 at.%)Co alloy with plastic strain, paramag. susceptibility, elec. resistivity and Mossbauer effect behaviour 9-43161
 Pt-(23 wt.%)Co equi-atomic alloy single crystal having [111] orientation, mag. props. 9-45152
 Pt-Fe, γ solid solutions, thermodynamic props. 9-30753
 Pt-Fe dilute solid soln., interac. of quenched in vacancies with Fe atoms 9-26278
 Pt-Fe system near Pt₃Fe composition, magnetic behaviour from Mossbauer effect meas. 9-24275
 Pt-(1 at.%)Fe alloy with plastic strain, paramag. susceptibility, elec. resistivity and Mossbauer effect behaviour 9-43161
 Pt-In alloys, lattice spacings and solid solubility of In 9-30571
 Pt-Mn alloys, ordered, magnetic structure, n. diff. analysis 9-35563
 Pt-Ni alloys, specific heat enhancement 1.15° to 4.2°K rel. to electron spin fluctuation interaction effects 9-44837
 Pt-Ni electrocatalysts for H₂/CO fuel cell anodes 9-29365
 Pt-SiO cermet thin films, resistances obs. 9-47155
 Pt-Sn alloys, lattice spacing and solid solubility of Sn 9-30571
 Pt-40 wt% Rh, effective atomic number for pair prod. for γ energy 2.6-17.6 MeV 9-24232
 Pt-20 wt%Rh, effective atomic number for pair prod. for γ energy 2.6-17.6 MeV 9-24232
 Pt₃Mn alloy, spontaneous magnetization, atomic ordering effect 9-39770
 Pt co-ordination cpds. type PtX₂Y₂, vibr. spectra 9-23068
 Pt complex, [Pt Cl₂ (C₂H₄)₂], Raman and i.r. vib. spectra, solid and aq. soln. 9-27873
 Pt complex, K[Pt Cl₃ (C₂H₄)₂].H₂O, Raman and i.r. vib. spectra, solid and aq. soln. 9-27873
 Pt complex, K[Pt Cl₃ (C₂D₄)₂].H₂O, Raman and i.r. vib. spectra, solid and aq. soln. 9-27873
 Pt complex, potassium aminotrichloroplatinate monohydrate, crystall. struct. 9-26244
 Pt complex, Pt(II)X₂Y₂ (X=Cl, Br or I, Y=Me₃P or Me₃As), square planar, vibrational spectra 9-30052
 Pt complex, trans-bisglycinatoplatinum(II), cryst. struct. 9-39303
 PtAs₂, crystal structure 9-23770
 cisPtII trimethyl-arsine, -phosphine, -stibine complexes, vibr. spectra, obs. 9-27872

Pleochroism

- alkali halides, Ag⁺ doped, Ag⁻ mag. circular dichroism obs. 9-33508
 benzil, hexagonal cry., circular dichroism meas. 9-26704
 circular dichroism tensor parameter in uniaxial cry. 9-26704
 Cotton-Mouton effect through absorpt. band 9-39100
 dichroism, linear, measuring device, and study of dichroism under stress 9-46010
 polychloroprene films, i.r. dichroism and stress rel. to crystallinity and orientation, obs. 9-30650
 polyvinylchloride films, stretched, i.r. dichroism of dioctyl-, diethyl phthalate plasticizers rel. to orientation, obs. 9-28654
 uranylpropionate crystals, luminescen. rad. dichroism 9-43213
 α -NiSO₄·6H₂O, circular dichroism meas. 9-26704
 Cu(II) complexes, with tetradentate Schiff base ligands, anomalous sign reversal in circular dichroism spectra 9-36703
 IrCl₄²⁻, mag. circular dichroism in cryst. (CH₃NH₂)₂SnCl₆ 9-41353
 KBr:Ti³⁺, dichroism, influence of uniaxial compressive stress 9-31075
 KCl:Ag⁺ stress-induced dichroism in u.v. absorpt. bands, temp. depend. 9-45322
 KCl:Ti³⁺, dichroism, influence of uniaxial compressive stress 9-31075
 KCl, mag. circular dichroism of F band, orbital Lande factor 9-47362
 KI:Ti³⁺, dichroism, influence of uniaxial compressive stress 9-31075
 LiNbO₃:Cr³⁺ single crystals, dichroism 9-39803
 NaCl:Cu²⁺, stress-induced dichroism in u.v. absorpt. bands, temp. depend. 9-45322
 Ni(II) complexes, with tetradentate Schiff base ligands, anomalous sign reversal in circular dichroism spectra 9-36703
 RbNi(CO)₂F₃ spectra, dispersion of magneto-opt. eff. in absorption line region 9-33513
 Si:Al(B) electron-irrad., stress induced dichroism of photoconductivity spectra, valence band-defect level obs. 9-44985
 α -SiC:N, dichroic crystal-optical device, patent 9-28653
 Zn complex, bis (L-aminoacid) (II), circular dichroism and far U.V. spectra 9-23077

Plexiglas see Plastics**Plutonium**

- α - β transform., differential enthalpic study 9-44801
 alpha counters, in-line, for extraction from irradiated fuel monitoring 9-32256
 anion exchange determ. of contamination in blood 9-29113
 etching, a.c. through inorganic acid, Pu electrode, patent 9-23803
 exothermic reaction of retained γ - α phase transform. prior to α - β transform. temp. 9-42935

Plutonium continued

- isotopes, photon to alpha particle ratio in radiation 9-25604
 isotopic distribution in irradiated UO₂ fuel rods, expt. and theory 9-25675
 magnetic and electrical props. rel. to Mossbauer effect in cpds. 9-39821
 in-neutron-irradiated UO₂, isotopic analysis 9-43346
 oxidation near 400°C, PuO form. from α -Pu₂O₃ reaction with metal 9-39953
 self-irradiation eff. 9-24072
²⁴⁰Pu isotopic analysis in Pu by optical emission spectroscopy 9-32443
²⁴⁴Pu abundance in early solar system, rel. to continuous galactic nucleosynthesis theory 9-45658
²³⁹Pu edge breeding in irradiated UO₂ 9-22899
 α -Pu, growth of single cryst. from β to α solid-state phase transform. at high press. 9-35247
 α -Pu, new electrolytic polishing and etching for revealing microstructure 9-39304
- Plutonium compounds**
 alloys, self-irradiation eff. 9-24072
 ceramics, physical props., data manual 9-22907
 δ -stabilized alloys, % of α -Pu by X-ray meas. 9-39479
 oxides and Ta reactions at high temps. 9-28782
²³⁹Pu¹⁴⁰O, as suitable α -emitting power source (evolving no neutrons) for space vehicle, patent 9-28971
 Al-10wt.%Pu, fuel elements, injecting casting in Pyrex molds and encapsulating in Zircaloy 9-22897
 Pu-Al alloy, diffusion in stabilized δ -Pu 9-28323
 Pu-Al alloys, electron microprobe anal. 9-49400
 Pu-Al delta-stabilized alloys elastic and anelastic behaviour at low temp. 9-37224
 Pu-Be neutron spectrum, calc. and expt. 9-22629
 Pu-Ce delta-stabilized alloys elastic and anelastic behaviour at low temp. 9-37224
 δ -Pu-(10 at.%)Ce, thermal cond. in temp. range 75-300°K 9-41108
 Pu-Ga alloy, delta-stabilized, % of α -Pu by X-ray meas. 9-39479
 δ -Pu-Ga alloys, thermal cond. in temp. range 75-300°K 9-41108
 Pu-Nd, solubility of binary system 9-28386
 Pu-Pr, solubility of binary system 9-28386
 Pu-Sm, solubility of binary system 9-28386
 Pu-(O-10at.%)Zr, equilib. phase diagram 9-37306
 Pu_{0.2}U_{0.8}O_{2-x}, O diffusion and stoichiometry in temp. gradient, 1200-2000°C 9-37207
 α -Pu₂O₃ reaction with Pu 400°C to form PuO 9-39953
 Pu₃Si₄, paramagnetic susceptibility, transition to antiferromagnetism 9-24284
 Pu₃Fe, Mossbauer effect and relevance to Pu behaviour 9-39821
 PuC(P,S) powders, densification 9-35238
 PuFe₂, Mossbauer spectra, in Perspex medium 9-49264
 PuN, heat of formation and thermal functions, 700° to 3040°K 9-26809
 PuO, formation by α -Pu₂O₃ reaction with metal near 400°C 9-39953
 PuO_{1.52}, paramagnetic susceptibility, transition to antiferromagnetism 9-24284
 PuO₂/UO₂ fuel coolant temperature effects in steam generating heavy water reactors 9-25674
 PuO_{2-x}, hypostoichiometric, evaporation, 2070° to 2380°K 9-26169
 PuO₂, ht. capacity, 300-1100°K 9-35285
 PuO₂ dense microspheres, prep. by sol-gel process 9-36631
 PuS, paramagnetic susceptibility, transition to antiferromagnetism 9-24284
 PuS₂, paramagnetic susceptibility, transition to antiferromagnetism 9-24284
 U-Pu oxide fuel irradiated, solid fission product behaviour, neutron flux 9-41118
 UO₂-PuO₂ fuels, heat flux distrib. in rods rel. to fissile material segregation 9-36632

Pockels effect see Electro-optical effects**Point defects see Crystal imperfections****Point groups see Crystal structure, atomic****Poiseuille flow see Flow; Hydrodynamics****Poisson ratio see Elastic constants****Polar cap absorption see Electromagnetic wave propagation/ionosphere****Polar cap flow see Airglow****Polarimeters**

- far atmospheric light depolarization meas. 9-48093
 ellipsometric quantities, determ. 9-40379
 ellipsometry, precision, Poincare's applic. 9-36365
 Glan-Thompson crossed polarizers, defect obs. 9-25368
 microwave, permittivity meas. to 1200°C 9-38342
 photoelec., with visual compensation 9-46006
 photoelectric, linear and circular polarization 9-27391
 photoelectric spectropolarimeter, with microscope, performance 9-48094
 scattered light from gases 9-39052

Polarized light

see also *Double refraction; Optical rotation; Photoelasticity; Polarimeters*

- alkaline earth fluorides, bleaching eff. on opt. and e.p.r. spectrum of V_k centres 9-23826
 in Cary Model 14 spectrophotometer, effect on transmittance measurements of anisotropic materials 9-32056
 circularly, piezo-opt. production 9-46007
 crystal, rel. to magnetoelec. effect 9-43218
 9-cyanoanthracene, u.v. absorpt. spectrum, 4.2°K 9-33566
 degree of polarization, meas. 9-43920
 depolarization at 6328 Å due to atmospheric transmission 9-37916
 depolarization properties of surfaces illuminated by coherent light 9-32023
 dielectrics, ellipsometric analysis of radiation damage 9-35295
 diffraction by two parallel strips in a plane 9-32019
 diffuse refl. from roughened surfaces, depolarization obs. 9-33507
 in electrooptic cubic crystals, phase and polarization 9-41357
 incident on lossless mat., magneto-optical effects rel. to propag. and impedance perturbations 9-25369
 instrumental, excitation-function meas., polarization corrections elimination 9-36372
 interstellar, use in interstellar cloud models investigation 9-29033
 from Jupiter, wavelength depend., aerosol scatt. effect 9-29068
 laser backscatt. imagery, polarization effects 9-36364
 from Mira variable stars 9-33907
 mirrors, dielectric multilayer, phase anisotropy 9-34216

Polarized light continued

- modulation technique, high-reflectivity ellipsometry appl., for elec. const. of metals determ. 9-35462
- molecular crystals with defect levels, ratio, and absorpt intensity 9-33541
- monochromatic, propagation in Riemann space 9-29471
- monochromatic beam, c.m. field intensity and properties 9-29459
- Mueller matrices, use in polarization determ. 9-43921
- Mueller matrices for polarizing system characterization 9-32024
- naphthalene, spin polarization of triplet excitons 9-39915
- optical const. thin films, determination using polarization measurements 9-47311
- pentacene, vibronic band position var. with direction 9-27909
- photoelectric instrument for measuring linear and circular polarization 9-27391
- physorption at low temps., ellipsometric investigation 9-42730
- pile of dielectric plates, optical characts. 9-29472
- plane, rotation, achromatization of crystal-optical components 9-24361
- quartz rod depolarization effectiveness 9-43210
- Rayleigh scatt. of polarized photons by molecules 9-34589
- in resonator, open with plane circular mirrors 9-43876
- rubber, uniaxially oriented, fluorescence meas. 9-39881
- scattered by gases and vapours 9-39052
- scattered from cloud during formation, changes 9-28887
- scattered from haze and clouds 9-33768
- scattered from uneven surfaces with high absorptivity rel. incidence angle 9-31073
- scattering by polymer soln., supermolecular order formation obs. 9-28102
- scattering in slab of randomly oriented particles, symmetry relations 9-41528
- for spatial filters realization 9-36379
- spectropolarimeter, automatic, for Faraday effect meas. in visible and u.v. 9-48118
- stilbene crystal 2-photon absorption, ang. distrib. determ. 9-24375
- twilight, effect of O₃ stratospheric quantity 9-41556
- u.v. incident on thin film, photoelec. emission rel. polarization 9-31072
- Venus, linear polarization of scattered sunlight, obs. 9-31615
- Venus, polarization of scattered sunlight, comparison with calculation 9-31616
- Versus, obs. 9-38081
- visibility in, horizontal range 9-40038
- p-xylene-carbon tetrabromide complex, i.r. spectrum 9-24394
- 6328 Å laser, external polarization technique using permanent magnet 9-29418
- CaWO₄:Nd³⁺, absorpt. obs. of ⁴I_{9/2}→²P_{1/2} transition assignments of ground-state sub-levels 9-39805
- H 3²D→2²P transition radiation 9-32430
- He-Ne, with Brewster windows, elliptical polarization of output 9-25314
- He-Ne laser Brewster angle attenuator within laser cavity, eqns. of polarization and attenuation 9-31969
- from He atoms excited by electron impact 9-29958
- KCl, absorpt. in u.v. band of V_k centres, effect on V_k centre reorientation 9-35113
- KH₂PH crystal, optical rectification effect dispersion 9-47326
- NaCl single crystal, investig. of plastic props., 300° to 1.4°K 9-33036
- YF₃, i.r., spectrum, phonon assignment 9-42951
- YFe garnet, rel. to investigation of dislocation effects on magnetiz. processes 9-47276

Polarography see *Chemical analysis/electrochemical*

Paralons see *Crystal electron states/paralons*

Polishing see *Surface structure*

Polonium

- Po-B neutron source, scatt. in cylinder of water, distrib. function calc. 9-34473
- Po-B neutron source, scatt. in cylinder of water, distrib. junction calc. 9-22841
- Po-B neutron source, scatt. in cylinder of water, distrib. junction calc. 9-34473

Polonium compounds

- chalcogenides A^xB^yC^z with perovskite structure, synthesis 9-42755

Polyelectrolytes see *Electrochemistry; Polymers; Solutions*

Polymerization

- α-ethylacrolein, intrinsic viscosity increase, structure studied 9-28793
- α-methacrolein, intrinsic viscosity increase, structure studied 9-28793
- acrylic monomers, in thin layers, in presence of oxygen 9-24550
- anthracene, formed by pyrolysis in presence of AlCl₃, CuCl₂ 9-26819
- butadiene with styrene, regulation of molecular weight 9-24551
- copolymerization in solid state, review 9-28792
- copolymerization of ethylene, propylene and 4-vinylcyclohexane-1, effect of catalysts 9-31188
- crystalline matrix 9-33663
- α, α-dimethyl-β-propiolactone to a polyester 9-26820
- dimethylvinylethynylcarbinol, with high acetylene bond content 9-24553
- dioxolane-polydioxolane in equilibrium soln., 300-28103
- ethylene, γ-induced polymerization obs. 9-33665
- free radical, dynamics in continuous stirred tank reactor 9-33664
- gas discharge, prod. of thin films 9-40845
- gelation, mol. size distrib. change due to crosslinking, math. theory 9-41447
- hexamethylcyclotrisiloxane, NMR low temps. 9-28766
- maleimide monomer-fluorene, radiation induced 9-26821
- methyl methacrylate polymerization from ESR of free radicals 9-33666
- methylmethacrylate sensitized by photoreduced dye 9-24552
- network polymers, equilibrium deformation 9-32543
- polyisoprene on γ-TiCl₃, struct., i.r. obs. 9-27937
- propylene on complex catalysts in the presence of alcohols and diethylethoxyaluminum 9-26822
- styrene, following irradiation 9-24554
- terlonitrile, polymerization and preparation 9-33667
- trioxane to polyoxymethylene by electron beam, struct. obs. 9-37824
- vinyltrimethyl(phenyl)-silanes, copolymerization with styrene in the presence of butyllithium 9-24549
- water, temp. depend. obs. from stimulated Raman spectrum 9-34911

Polymers

see also *Plastics*

- acoustic spectrometer for dynamical mechanical props. of solids at low temp. 9-46871
- adsorbed chain, conformation 9-30503

Polymers continued

- alkyl acrylate and fluoroalkyl acrylate, viscosity index improvers for lubricating oil, patent 9-23192
- amorphous, reversible deformations, singularities in development curve 9-26331
- amorphous linear high, orientation anisotropy of heat conductivity 9-35292
- benzenes, monesubst., formed in elec. discharges, spectra 9-48522
- biopolymer, n.m.r. study at high field strength, tech. and limitations 9-30155
- birefringence of stretched semicryst. networks rel. to crystallinity 9-31077
- 1, 3-butadiene, aq. soln., propagating type free radicals, e.s.r. spectra obs. 9-27925
- carbonyl and carboxylic groups, importance in photodestruction 9-40627
- Cellofas dil. solns., flow through tubes and granular beds, relax. effects. 9-32748
- cellulose acetates in dilute soln., compressibility and solvation 9-32769
- cellulose tricarbanilates in benzophenone, flow birefringence, 55-110°C 9-39102
- cellulosic fuels, effect of organic impurities, chemical kinetics 9-35746
- chain, configurational correl. 9-44380
- chain, distrib. functions 9-44382
- chain, excluded vol., monomer units mutual interaction 9-32542
- chain, in soln., random coil config. and light scatt. with intramol. interac. 9-34905
- chain, moments of chain vectors for four models 9-44381
- chain molecules, Monte Carlo computer simulation 9-42462
- chains with excluded vol. effects, light scatt. and viscosity 9-36731
- condensation type, semicond., electric transport props. rel. to mol. struct. 9-47097
- conformational structures 9-32551
- contaminations, trace, microscopic identification 9-49391
- copolymer scintillators, styrene with vinyl derivatives of 2, 5-diaryloxazoles and 2, 5-diphenyl-1, 3, 4-oxadiazole 9-31149
- copolymer solns. mol. wt. meas. by Archibald ultracentrifugation method 9-28770
- copolymers of butene with α-olefins, cocrystallization behaviour, and polybutene II→polybutene I phase transition 9-32880
- copolymers of ethylene, propylene and 4-vinylcyclohexane-1, structure 9-31188
- cotton fibres birefringence, obs. 9-28656
- cross-linked, chemical structure thermostabilization during crystallization 9-46703
- crystalline, gas diffusion 9-23846
- crystalline, nonoriented, 'silver' crack formation during creep 9-23925
- crystalline, shock wave induced struct. transition, obs. 9-30733
- crystallinity of drawn polymers, by density meas. 9-46706
- crystallization of linear high polymers, chain-folding and molecular-species segregation 9-46705
- dextran, u.s. absorpt. in aq. solns. 9-42653
- dextran aqueous soln., u.s. relaxation 9-36874
- dielectric film, prep. and characts. 9-33399
- dielectric props. of laminar materials, multiparameter control 9-33364
- dielectric relaxation of some crystalline heterochain polymers 9-24216
- diffusion of low mol. wt. penetrants, review 9-39389
- dinucleoside phosphates, optical props., model calcs. 9-48523
- 4, 4-diphenylphthalidedicarboxylic acid, synthesis and props. 9-28191
- disordered cryst., X-ray scatt. 9-35072
- Dowex 50 resin, Mossbauer effect of exchangeable Fe²⁺ ions 9-43226
- dynamic mechanical characteristics evaluation method 9-26309
- electrets, in aqueous solutions, interfacial phenom. 9-37608
- electron microscope examination, sample preparation method 9-23190
- electronic struct., self-consistent field theory 9-30153
- emulsion, orienting effect of aqueous phase on structure with polar groups 9-32803
- epoxy, polarization charact. features 9-40834
- equation of state for solid, uses 9-37361
- ethylene-propylene, storage and loss moduli meas. by glueing to steel 9-33020
- excluded volume, Percus-Yevick type integral eqn. 9-32540
- excluded volume effect on radius of gyration 9-46427
- film, oriented, birefringence effect on low-angle lights- scatt. patterns 9-49243
- film, polycrystalline, deformation characterization rel. to molecular orientation 9-30666
- film, this, birefringence effect on light scatt., classical treatment 9-49244
- film-forming, melt rheology 9-26048
- film-forming, molecular constitution 9-25791
- films, dielectric breakdown rel. to electromechanic deformation 9-43110
- films, friction and lubrication 9-26360
- films, photovoltaic effect in vacuum u.v. 9-43136
- films, solid, light scatt. theories 9-37694
- films, synthesized, vacuum u.v. absorpt. spectra, electr. struct. obs. 9-31116
- flow of dil. solns. through tubes and granular beds, relax. effects 9-32748
- fracture initiation, kinetic theory using elastic networks of various degrees of orientation 9-46908
- glasslike, high elastic states, friction depend. on temp. 9-27931
- graft copolymers, hydrodynamic and optical props. of solns. 9-32553
- growth, simplified treatment including chain folding, review 9-36989
- Gruneisen const. in crystalline and glassy, and thermal props. 9-46979
- heat coefficients during thermal destruction 9-41112
- helical mols., hyperpolarizability and i.r. phonon dispersion 9-32541
- hexafluoropropene-tetrafluoroethylene copolymer, rupture, tensile strength hardness following γ-irradiation 9-33069
- hexafluoropropene-vinylidene fluoride copolymer, rupture, tensile strength hardness following γ-irradiation 9-33069
- high linear amorphous, orientation anisotropy of heat conductivity 9-35292
- high polymer mol., mechanical entanglements, stat. analysis 9-23188
- high polymer physics, selected papers from conference 9-46704
- hydrodynamic interaction, variational calc. 9-42460
- i.r. spectra, influence of defects 9-47379
- irradiated, pairwise trapping of radicals, e.s.r. 9-33687
- latex samples, scattering of coherent and incoherent light 9-42658
- lattice-model chains, Brownian motion 9-34696
- linear system with nearest-neighbour interactions, mean first passage time 9-41779
- long polymer backbone, dynamics 9-42461

Polymers continued

- luminescence, high-energy electron excitation 9-43259
 mechanical props., dynamic, meas. using support 9-23864
 melt viscosity, hydrostatic press. depend., extrusion rheometer, 190°C 9-39082
 melts, cone and plate rheometer for viscosity meas. 9-46618
 methyl methacrylate polymerization from ESR of free radicals 9-33666
 methyl siloxane polymers NMR studies 9-30471
 in methylene series, i.f. absorpt. spectra 9-48525
 di methylpolysilazanes, internal motion, n.m.r. obs., 77-400°K 9-34697
 molecule, config. change in soln., math. model 9-30154
 molecules, linear, excluded vol. effect 9-27928
 Monte-Carlo calc., non-self-intersecting random walk model, side groups eff. 9-38927
 mylar films, non-destructive elec. breakdown 9-49139
 network, deformational behaviour effect of diluent content during polymerization 9-32543
 nitropolyarylvinylenes, e.s.r. spectra, superfine struct. 9-44384
 n.m.r., high-resolution, as tool for examination, review 9-42463
 nylon, i.r. spectrum interpretation in terms of rocking-twisting and wagging 9-32552
 nylon, mechanism of water sorption 9-32851
 nylon 66, double melting rel. to phases, obs. 9-34954
 nylon 66 fibres, fractographic analyses and prelim. obs. 9-42895
 nylon 66 fibres, i.r. study of structural change due to heat treatment 9-27938
 nylon 6.6 fibres, oriented, elastic anisotropy, expt. values compared with aggregate theory 9-35147
 nylon 66 yarns, drawn, effect of annealing condition on struct. 9-46707
 Nylon-6, friction and wear props., γ irradi. effects, obs. 9-39444
 nylon-6, surface and bulk crystallinity, i.r. spectroscopy 9-48843
 optical props., model calcs. 9-48523
 oxidation, initiation of free-radicals by rupture and subsequent processes 9-26825
 permeability of low mol. wt. penetrants, review 9-39389
 Perspex, non-crystalline, fracture 9-26357
 phase equilibrium and light scattering 9-23463
 photopolymers, for hologram recording 9-25324
 photoresist films, scattering effects is ion beam exposure, comments 9-32846
 polystyrene films, photovoltaic effect in vacuum u.v. 9-43136
 poly(α -methacrolein), structure determ. by chem. reactions, n.m.r., i.r. 9-28793
 poly(β -naphthyl methacrylate) in 4 solvents, critical opalescence 9-28144
 poly(β -vinyl naphthalene) in 3 solvents, critical opalescence 9-28144
 poly(butyl methacrylate) in isopropanol, critical opalescence 9-28144
 poly(diethylene glycol methacrylate) and its copolymers, effect of side groups on thermomechanical behaviour 9-32547
 poly(dimethyl siloxane) in tetralin, critical opalescence 9-28144
 poly(ethylacrolein), structure determ. by chem. reactions, n.m.r., i.r. 9-28793
 poly(ethylene glycol methacrylate) and its copolymers, effect of side groups on thermomechanical behaviour 9-32547
 poly(N-vinylcarbazole), carrier mobility 9-43133
 poly(1-vinylnaphthalene), intramolec. triplet energy transfer 9-24461
 poly(propylene oxide) solutions, conc. depend. of viscosity 9-28109
 poly- α -amino acid solns., laser light scatt. 9-42657
 poly 1,1 dimethylsilylcyclobutane, i.r. spectrum and struct. 9-27935
 poly 1,4bis(hydroxyethoxy) phenylene adipate, i.r. spectra rel. to forms of vibrations 9-37734
 poly-p-benzyl-L-glutamate conc. soln. supermolecular structure formation, low-angle polarized light scatt. 9-28102
 poly- ϵ -methylcaprolactam, amorphous and ordered states, conformational structure 9-32551
 poly-N-isobutylmaleinimide, number of monomeric units, segmental anisotropy 9-23193
 poly-N-vinylcarbazole, dye sensitization of photocond., quantum yield 9-49167
 poly-p-butylisocyanate, structure from optical behaviour in solns. 9-27932
 poly-p-chlorostyrene, isotactic, chain struct. stability in solns. and gels, i.r. obs. 9-28140
 poly-p-tolylisocyanate, structure from optical behaviour in solns. 9-27932
 polyacrylamide dil. solns., flow through tubes and granular beds, relax. effects 9-32748
 polyacrylamide solns., Couette flow between rot. cylinders, relax. effects 9-32749
 polyacrylonitrile, rheo-optical behaviour from creep, creep recovery and birefringence meas. 9-46900
 polyacrylonitrile and its copolymers, properties in solution and solid state review 9-28200
 polyamide (6 nylon) pyrolytic products, mass spectrometric analysis 9-43347
 polyamides, crystallization in alcohol suspensions of mineral particles 9-35030
 polyamides relaxation obs., -140°C-+50°C 9-32544
 polybutadienes, absorptivity determ. 9-30156
 polybutadienes, stereoregular Ziegler viscosity rel. to mol. wt., microtacticity, obs. 9-30379
 polybutene-1, high-speed deform., exam. by photographic light-scatt. technique 9-46901
 polybutene-1 single crystal, annealing, 70-90°C, stability 9-39458
 polybutene-1 single crystal, annealing, 70-90°C, stability 9-39458
 polycapraamide, chemical bonds, effect of mechanical load, obs. by i.r. spectroscopy 9-32829
 polycapraamide, cracks, submicroscopic, formation under load 9-33096
 polycapraamide, mechanical damage, accumulation under static load 9-33039
 polycapraamide fibres, sound velocity temp. depend., infl. of processing method 9-24024
 polycapraamide in γ -form, thermal expansion 9-24058
 polycaprolactam, elastic relaxation, effect of water content 9-33027
 polycaprolactam, relaxation obs., -140°C-+50°C 9-32544
 polycaprolactam without thermal history, crystallization obs. by nephelometry 9-32874
 polycarbonate film, charged-particle irradi., etching rate accel. by photo-oxidation effect 9-32271
 polycarbonates, crystallization kinetics 9-32873

Polymers continued

- polycapraamide, cracks, submicroscopic, charact, features of growth 9-33097
 polychloroprene, crystalline orientation in stretched networks 9-48746
 polychloroprene, films, i.r. dichroism and stress rel. to crystallinity and orientation, obs. 9-30650
 polydimethylsiloxanes, vibrational Raman spectra 9-23511
 1,3-polydioxalane, conformations in soln. 9-23187
 polyelectrolyte soln. with mono- and divalent counter ions, rodlike model 9-42636
 polyelectrolytes, intrinsic viscosity 9-32772
 polyesters and polyamides in amorphous state, solubility and heat resistance 9-28191
 polyethers, conformations in soln., theory 9-23185
 polyethylene, optical modes by neutron scatt. 9-46981
 polyethylene, amorphous, surface tension, significant structs. model 9-34887
 polyethylene, crystalline and fold structure from lattice freq. analysis 9-46710
 polyethylene, crystallites mol. and textural orientation, applied stress eff. 9-30584
 polyethylene, dielectric loss angle at low temp., calorimetric meas. 9-33375
 polyethylene, drawn, crystallinity by density meas. 9-46706
 polyethylene, electron mobility determ. by injection through cathode method 9-47156
 polyethylene, films surface crystallinity rel. to substrate surface energy, i.r. obs. 9-34986
 polyethylene, fold structure changes on annealing 9-46712
 polyethylene, friction and wear props., γ irradi. effects, obs. 9-39444
 polyethylene, high density, ageing under mechanical stresses 9-46930
 polyethylene, irradi., free radicals decay rel. to steric config. and matrix mol. motion, obs. 9-27936
 polyethylene, irradiated, e.p.r. line, discrete saturation 9-37790
 polyethylene, linear, in p-xylene, crystallization optical investigation 9-28238
 polyethylene, low-density deformation process study by stress, strain, i.r. absorpt. meas. 9-27933
 polyethylene, molten; stress function of rate of shear, thegoniometer design 9-39065
 polyethylene, neutron dose in critical assembly 9-37284
 polyethylene, neutron spectra from spherical shell obs. 9-27783
 polyethylene, nonoriented, 'silver' crack formation during creep 9-23925
 polyethylene, oriented, shear resist. rel. to lamellae out-of-plane deform. mechanism, obs. 9-28358
 polyethylene, oriented, tensile deformation 9-46894
 polyethylene, screw dislocation mobility, Peierls stress 9-46825
 polyethylene, surface structure different when crystallized in contact with Au or Teflon 9-23614
 polyethylene, thermal conductivity below 1°K, modification to theory 9-28433
 polyethylene, thermal expansion of unit cell 9-48842
 polyethylene, thermal props. from Grueneisen const. 9-46979
 polyethylene, unit cell dimensions, variations rel. to crystallization, annealing and deformation conditions 9-46803
 polyethylene, yield strength 9-30734
 polyethylene annular spherulites, fine structure and mechanism of deformation, direct electron microscopic investig. 9-26254
 polyethylene dissolution in xylene and octadecane 9-46616
 polyethylene extended chain cryst. growth and morphology 9-26213
 polyethylene fibers, oriented, elastic anisotropy, expt. values compared with aggregate theory 9-35147
 polyethylene film, crack, zone structure near tip 9-28373
 polyethylene film, decay processes of surface charges 9-49136
 polyethylene films, biaxially oriented and cast, elec. transport, obs. 9-35463
 polyethylene glycol chain, freq. distrib. and neutron scatt. 9-23194
 polyethylene glycol soln., u.s. relaxation 9-36874
 polyethylene oxide, chain folding from i.r. spectra 9-46713
 polyethylene oxide, conformations in soln. 9-23186
 polyethylene oxide dilute behaviour rel. to conc. 9-44538
 polyethylene pellets, laboratory preparation 9-38415
 polyethylene single crystals, fold structure investigated by various methods 9-32828
 polyethylene terephthalate, dielectric loss angle at low temp., calorimetric meas. 9-33375
 polyethylene terephthalate, effect of mech. load, obs. by i.r. spectroscopy 9-32829
 polyethylene terephthalate, mech. props. rel. to molecular wt., temp. and crystallinity 9-42863
 polyethylene terephthalate, plastic deformation, heat generation, model 9-33034
 polyethylene terephthalate), oriented drawn films, tensile and shear yield stress 9-30667
 polyethylene terephthalate fibres, oriented, elastic anisotropy, expt. values compared with aggregate theory 9-35147
 polyethylene terphthalate, chemical bonds, effect of mechanical load, obs. by i.r. spectroscopy 9-32829
 polyethylene-diphenyl ether; critical point determ. method 9-28173
 polyethylene-polyisobutene mixtures, struct., X-ray obs. 9-30474
 polyethylene-stainless-steel lap joints, yield strength 9-30734
 polyethyleneglycoladipate, o-, p-bis-(β -hydroxy-ethoxyphenylenediadipate) copolymers, glass temp. rel. to component concs. 9-30473
 polyethyleneglycoladipate, thermooptic obs. of melting 9-23195
 polyethylenes, dielectric loss depend. on crystalline structure 9-28550
 polyimide:Ag films, i.r. absorpt. spectra, obs. 9-26749
 polyindigo solutions, i.r. spectra, structural anal. and mol. wt. determ. 9-27934
 polyisobutene-polystyrene-cyclohexane(benzene) system, light scatt. rel. to solute interaction parameter 9-23510
 polyisobutenes, mol. wt. determ. from gel permeation and gradient elution chromatography 9-32548
 polyisobutylene, compressibility 9-46886
 polyisobutylene, diffusion in very dilute solns. obs., mol. wt. calc., polydispersity characterized 9-32545
 polyisoprene, polymerized on β -TiCl₃, i.r. absorpt. and struct., obs. 9-27937
 polyisoprenes, absorptivity determ. 9-30156

Polymers continued

- polyisoprenes, mol. struct. determ. from light scatt. and viscosity meas. in soln. 9-48524
- polymethacrylic acid, laser-excited Raman spectra 9-44383
- polymethacrylic acid, viscosimetric investigation of conformation transition on ionisation 9-23196
- polymethacrylic acid esters below glass transition point, relaxation behaviour 9-32549
- polymethine dye, i.r. radiation generation using Nd glass laser 9-34168
- polymethylmethacrylate, block, microstruct. 9-42802
- polymethylmethacrylate, viscoelastic plate, calc. of temp. stresses and contraction 9-28334
- polymethylmethacrylate, acoustic velocities, press. and temp. depend. 9-35276
- polymethylmethacrylate, elec. breakdown development investig. 9-43109
- polymethylmethacrylate, molecular motion in surface layers, study by impulse NMR methods 9-23191
- polymethylmethacrylate, nanosec. pulse radiolysis 9-31216
- polymethylmethacrylate, stress and strain softening in yielding under constant load 9-46887
- polymethylmethacrylate soln., minimum in shear stress depend. of viscosity 9-32774
- polymethylmethacrylates, orientation anisotropy of heat conductivity 9-35292
- polymethylsiloxanes, cyclic, integral intensities in vibr. absorpt. spectra 9-48510
- poly(4-methylstyrene), effective dipole moment 9-32550
- poly α methylstyrene-benzene soln., light scatt., excluded vol. effect, obs. 9-30407
- polyolefines, crystallization from dil. soln., optical investigation by light scatt. 9-28238
- polyoxyethylenes, mol. optical anisotropy from rot. isomers 9-48526
- polyoxypropylene, rupture and change in supermolecular structure 9-28362
- polypeptides, exciton band struct. 9-41456
- polyphenyl target, deuterated, obs. of D(d,n)³H reaction 9-25502
- polypropylene, chemical bonds, effect, effect of mech. load, obs. by i.r. spectroscopy 9-32829
- polypropylene, cracks, submicroscopic, charact. features of growth 9-33097
- polypropylene, cracks, submicroscopic, formation under load 9-33096
- polypropylene, crystallinity influence on relax. phenomena 9-34974
- polypropylene, crystallization, melting effect on nuclei 9-32878
- polypropylene, dielectric loss angle at low temp., calorimetric meas. 9-33375
- polypropylene, effect of mech. load, obs. by i.r. spectroscopy 9-32829
- polypropylene, i.r. spectrum rel. to stereoregularity, obs. 9-30157
- polypropylene, isotactic, chain struct. stability in solns. and gels, i.r. obs. 9-28140
- polypropylene, isotactic, light scatt. obs. 9-37695
- polypropylene, isotactic, mechanical relax. rel. to polymorphism and lamella orientation 9-48745
- polypropylene, linear, in 1-chloronaphthalene, crystallization, optical investigation 9-28238
- polypropylene, low-molecular-weight fractions, crystallization rel. to morphology and phase transformations 9-46714
- polypropylene, oriented, shear resist. rel. to lamellae out-of-plane deform. mechanism, obs. 9-28358
- polypropylene, pressure-crystallized, structure and thermal behaviour of phases formed 9-46711
- polypropylene, syndiotactic, D₂ symmetry, laser-excited Raman spectrum 9-30158
- polypropylene fibre deformation during prep., spinning, drawing and heat setting 9-39416
- polypropylene fibres, oriented, elastic anisotropy, expt. values compared with aggregate theory 9-35147
- polypropylene film, crack, zone structure near tip 9-28373
- polystyrene, compressibility 9-46886
- polystyrene, depolarization meas. by Raman spectra rel. to orientation 9-47380
- polystyrene, effect of ultrasound on stressed state 9-46880
- polystyrene, electroconductivity, solvent and ionic conc. effects 9-23525
- polystyrene, isotactic, chain struct. stability in solns. and gels, i.r. obs. 9-28140
- polystyrene, isotactic, crystallite orientation rel. to crystallinity, obs. 9-30475
- polystyrene, isotactic, spherulitic growth rate, obs. 9-28202
- polystyrene, mechanical damage, accumulation under static load 9-33039
- polystyrene, mol. wt. meas. by sedimentation transport in cyclohexane at Flory temp. 9-28771
- polystyrene, molecular motion in surface layers, study by impulse NMR methods 9-23191
- polystyrene, nanosec. pulse radiolysis 9-31216
- polystyrene, photocond. 9-43132
- polystyrene, plasticized with esters of aromatic dicarboxylic acids, viscosity and glass temp. 9-23901
- polystyrene dielectric in gamma-electric cell, high voltage operation 9-31897
- polystyrene foams, heat transfer, eff. of thickness and tempo. 9-41113
- polystyrene latex particles suspended in air, elec. charge obs. 9-46661
- polystyrene sol, electroviscous effects in dispersions of monodisperse latices 9-23551
- polystyrene solns., dynamical mech. props. 23-300 MHz 9-48688
- polystyrene storage and loss moduli meas. by glueing to steel 9-33020
- polystyrene-cyclohexane; critical point determ. method 9-28173
- polystyrene-polybutadiene block copolymers, dilute soln. viscosity and osmotic press. meas. 34.2°C 9-39086
- polystyrenes, amorphous, orientation anisotropy of heat conductivity 9-35292
- polytetrafluoroethylene, γ -irrad., effects of irrad. atmos. from n.m.r. obs. 9-24511
- polytetrafluoroethylene, oriented, electron pulse irrad., e.s.r. 9-43291
- polytetrafluoroethylene, photo-decomposition 9-33069
- polytetrafluoroethylene, Raman band assignments 9-44385
- polytetrafluoroethylene, vibr. anal. 9-42464
- polytetrafluoroethylene films, morphology and light-scattering patterns 9-42707
- polytetrafluoroethylene films, morphology rel. to light-scatt. patterns 9-46709

Polymers continued

- polytetrafluoroethylene room temp. crystallization NMR studies, molecular rotation 9-30472
- polytetrahydrofuran, conformations in soln. 9-23186
- polythene cavity under high direct electric stresses at elevated temperatures, discharge-repetition rate 9-28054
- polyurethane, birefringence, stress, photoviscoelastic analysis 9-35159
- polyurethane, linear, high mol. rot. prep., characterization by viscosity and light scatt. 9-27929
- polyurethane, nonlinear viscoelastic, stress relax., torsion creep 9-31838
- polyurethane, thermal conductivity, guarded hot plate apparatus 9-26461
- polyurethanes linear, crystallization from melt 9-26212
- polyvinyl butyrol, cracks, submicroscopic, formation under load 9-33096
- polyvinyl acetate acrylate copolymers, infrared spectrophotometry 9-37861
- polyvinyl acetate pyrolytic products, mass spectrometric analysis 9-43347
- polyvinyl butyral, cracks, submicroscopic charact. features of growth 9-33097
- polyvinyl carbazole, transfer of electronic excitation energy 9-39882
- polyvinyl chloride, cracks, submicroscopic, charact. features of growth 9-33097
- polyvinyl chloride, cracks, submicroscopic, formation under load 9-33096
- polyvinyl chloride, positron lifetime, anomalous 9-43016
- polyvinyl chloride, stress-optical behaviour temp. dependence and effect of plasticizer content 9-47319
- polyvinyl chloride, unplasticized, mech. props. and viscosity, 100-180°C 9-30652
- polyvinyl chloride film, radiation dosimeter, by luminescence meas. under high press., patent 9-22677
- polyvinyl chloride-acetate copolymer very thin films, prep. and meas. 9-34981
- polyvinylalcohol gel, light scatt. obs. 9-37695
- polyN-vinylcarbazole, energy migration study from spectra 9-48527
- polyvinylchloride films, stretched, dioctyl-, diethyl phthalate plasticizers i.r. dichroism rel. to orientation, obs. 9-28654
- polyvinylcyclopropane, crystalline, oriented fibre and film scruples, unit cell determ. by X-ray diff. meas. 9-46804
- poly-3-vinyl-9-ethylcarbazole, elec. behaviour on γ -irradiation 9-24120
- polyvinylfluoride, dielec. props., 10-150°C 9-30962
- positron lifetimes, correl. with intermol. forces 9-33240
- propylene-ethylene copolymers, i.r. spectrum rel. to stereoregularity, obs. 9-30157
- PTFE, dielectric loss angle at low temp., calorimetric meas. 9-33375
- PVC, structural depend. on precipitation conditions 9-32554
- radii of gyration of random-flight chains, probability density functions 9-38926
- ramie fibres birefringence, obs. 9-28656
- random-walk model for hydrocarbon-type chains with short-range correlations 9-44379
- Rayleigh scatt. fine structure 9-36881
- relaxation, treatment including co-operation in molecular motion 9-23189
- reticulation in liquid crystal diluent, rel. to anisotropic plastic mat. production 9-26078
- rheological properties, acoustic meas. methods 9-36835
- ross-linked, statistical thermodynamics 9-34973
- sedimentation const., conc. depend. 9-32539
- semiconducting, condensation type, electric transport props. 9-47097
- semicrystalline, mechanical anisotropy rel. to molecular orientation 9-36929
- solid, light scattering technique for structure determ. 9-28199
- solid, positron lifetimes, correl. with intermol. forces 9-33240
- solubility of low mol. wt. penetrants, review 9-39389
- solution, dil., intrinsic viscosity depend., on shear rate calc. method 9-28107
- solutions, dil., relax. effects in flow through tubes and granular beds 9-32748
- solutions, dilute, light scatt. and viscosity rel. to molecular entanglement and relaxation time 9-46615
- solutions, equivalent rigid spheres of solute suspended in liq., temp. depend. 9-34877
- solutions, excluded-vol. effects on equilib. props. 9-36848
- solutions, excluded-vol. effects on limiting viscosity number 9-36849
- solutions, intrinsic viscosity, theory and expt. 9-48684
- solutions, intrinsic viscosity and Huggins const., extrapolation calcs. comparison 9-34884
- solutions, light scatt. 9-39099
- solutions, multicomponent, critical point determ. method 9-28173
- solutions, Rayleigh fine structure theory 9-36881
- solutions, solvent depend. of rheological behaviour 9-28108
- solutions, stat. thermodynamics, pairwise interactions of linear chains 9-32766
- solutions, supermolecular order formation by polarized light low-angle scatt. 9-28102
- solutions and melts, nonlinear viscoelastic model 9-23432
- solutions optical activity, model for depend. on mol. wt. and stereoregularity 9-28132
- spheres in monolayer, diff. of laser light, for demonstrating crystal structure techniques 9-47712
- storage and elastic moduli, meas. method 9-33020
- storage and loss moduli meas. by glueing to steel 9-33020
- stressed, cracks, submicroscopic, charact. features of growth 9-33097
- structure and props., artificial nucleating agents mechanism 9-27930
- tar solution in tube, lowering of turbulent heat exchange during flow 9-40785
- Teflon, neutron dose in critical assembly 9-37284
- Teflon, thin film capacitor, breakdown studies 9-37586
- tetrafluoroethylene-hexafluoropropylene copolymers, γ -irrad., dielec. relax. 78°-300°K 9-26586
- telonitrite, polymerization and preparation 9-33667
- thermoelastic behaviour of networks swollen in n-dexane 9-23850
- 2,4,6-trichlorophenol, NMR and infrared spectra obs. rel. to conformational structure 9-32546
- vinyl acetate, aq. soln., propagating type free radicals, e.s.r. spectra obs. 9-27925
- vinyl acetate-methyl acrylate, sorption and diffusion of benzene obs. 9-33010

Polymers continued

- vinyl propionate, aq. soln., propagating type free radicals, e.s.r. spectra obs. 9-27925
viscoelastic props. of crosslinked, effects of blending sol. and gel fractions 9-46708
viscosity, intrinsic, in mixed solvents 9-46620
viscosity, intrinsic, of low mol. wt. polymers, obs. 9-28106
viscosity of solutions, extension of Zimm's theory 9-32773
water vapour adsorption 9-42736
wormlike chains, intrinsic viscosity 9-27927
X-ray scatt. by disordered cryst. 9-35072
¹¹³Sn polymeric cpds., influence of bonding on temp. depend. of anisotropic Lamb-Mossbauer factor 9-27915
Au-poly-N-vinyl carbazole-GaAs systems, transient photocurrents and internal photoemission 9-39656
CS₂ structural and elec. props. investigation 9-34975
HF gaseous, struct. determ. by electron diffr. 9-42395
SO potential energy calc. Van der Waals interac. 9-46736

Polymorphism

- see also Crystal structure*
chlorites, two-packet unit cell, systematic derivation of possible polytypes 9-39263
cyclohexane, polymorphic transition at -86°C, positron annihilation obs. 9-32859
fluor-phlogopite, nucleation and growth from vapour polytypism obs. 9-37010
hafnia, additions of rare-earth oxides, effects 9-30723
lanthanide metals and alloys, stacking sequence and influence of 4f electrons 9-30509
layer sequences in polytypes with close-packed structures, determ. using Patterson method 9-23743
opal, SiO₂·nH₂O, polytypism and stacking faults rel. to packing imperf. 9-42843
P, high-pressure polymorph, influence of neutron irradiation on phase stability 9-35250
polypropylene, effect on mechanical relax. 9-48745
polytypes, mechanism of growth from obs. of dissoc. dislocations in CdI 9-48859
polytypism, epitaxial theory 9-44638
sulphospinel, pressure induced 9-26392
zirconia, additions of rare-earth oxides, effects 9-30723
Ag₂Te, phase diagram 9-46956
BaCl₂-H₂O and BaCl₂-D₂O systems, and dehydration phase boundaries 9-28171
CaB₂O₄ 9-39260
CdSnAs, supercond. polymorph, high-pres. 9-41178
Co, influence of atomic size 9-46954
Fe, eff. of alloying elements 9-35009
Fe, influence of atomic size 9-46954
InTe, high-pressure polymorph, influence of neutron irradiation on phase stability 9-35250
KCuF₃, single cryst., polytype struct., X-ray diffr. exam. 9-32917
Mn, influence of atomic size 9-46954
MnF₂, high-pres. and temp., X-ray diffr. phase diagram and transforms. obs. 9-39184
NaCl, transition pressure for NaCl-CsCl struct., quantum mech. calc. 9-23985
NaF, transition pressure for NaCl-CsCl struct., quantum mech. calc. 9-23985
PbI₂, polytypism 9-46742
PbO₂, high-pressure polymorph, influence of neutron irradiation on phase stability 9-35250
2H-SiC, polytype whiskers, growth rate than β-SiC rel. to presence of O₂ 9-35032
SiC, polytypism 9-36975
SiC polytypes, 6H, 4H, 15R, X-ray diffr. lines intensities, revised 9-40916
SiC polytypism, review 9-26245
SiO₂, high-pressure polymorph, influence of neutron irradiation on phase stability 9-35250
SiO₂·nH₂O, opal, polytypism and stacking faults rel. to packing imperf. 9-42843
β-Ta₂O₅, from unit cell meas. 9-39309
TaSe₂, X-ray diffraction of new polymorph. 9-35011
TiO₂, X-ray diffraction examination 9-32860
TiO₂, phase transform. at high press. and temp., X-ray diffr. obs. 9-23988
TiO₂ under dynamic loading 9-39482
WO₃ structures stable at room temp. rel. to symmetry 9-23655
ZnS, polytypism 9-36982
ZnS, polytypism rel. to growth in vac. or inert atm., correl. with luminesc. 9-35099
ZnS grown from vapour, tendency towards polytypism and stacking faults distrib. 9-37184
ZnS polytypes of 10l, 22l and 26l families 9-32861
Zr, high-pressure polymorph, influence of neutron irradiation on phase stability 9-35250

Polynomials *see Algebra; Functions***Polytypism** *see Polymorphism***Pomeranchuk rule** *see Elementary particles/scattering***Population inversion** *see Lasers; Masers; Optical pumping***Porosity** *see Porous materials***Porous materials**

- see also Permeability, mechanical; Surface measurement*
beds of mixed beads, thermal conductivity meas. using probe 9-39541
cements, porosity, for chemical bonding of alumina powders 9-35229
ceramics, brittle, micromech. thermal stresses and thermal stress resistance 9-48968
convective flow in, stability 9-44535
dielectrics, permittivity meas., accuracy 9-24213
ductile, dynamic compaction, constitutive eqn. 9-35166
electrode systems, effect of finite-contact-angle meniscus 9-31203
electrodes, two-phase, anomalous distrib. of current conversion 9-49381
ferrites, porosity and mag. anisotropy, determ. from approach to saturation 9-37662
fluid filtration, chem. reaction with media, simulation problems 9-38947
formation resistivity factor of unconsolidated porous media, effect of particle shape 9-30831
glass, sorption of pyridine, i.r. spectra 9-26196

Porous materials continued

- glass containing supercond. metals as granular superconductors 9-47083
graphite, Hg porosimetry and He intrusion determ., limitations of Hg method 9-26225
graphite, microporosity changes during thermal and radiolytic oxidation 9-26224
graphite, polycrystalline, microporosity eff. on elastic modulus and yield curve 9-28343
graphite, pore size variation effect on rate of radiolytic corrosion by CO₂ 9-41452
graphite artificially densified by natural gas decomposition, pore size distrib. changes, new porosimeter obs. 9-23753
graphite channel, air radial diffusional effects on oxidation kinetics 9-26824
heated, internal heat transfer to cold air 9-28074
inhomogeneous media, marginal stability 9-34102
layer, gas filtration, non-stationary, for nonlinear resistance layer, numerical solns. 9-40736
magnetic, pore size effect on remanence ratios 9-43172
marginal stability in inhomogeneous media 9-34102
perlite, elastic constants rel. to porosity 9-30635
plaster moulds, capillary action 9-30703
polystyrene sulfonic acid membrane, elec. conductivity rel. to temp. and water absorption 9-28463
pore diffusion in solids, kinetics, review 9-37188
pore struct. analysis by water vapour adsorption, t-curves 9-35052
pore-grain boundary interactions rel. to grain growth 9-32897
porosimeter, Hg, using γ-beam absorpt., design and applic. to graphite meas. 9-23753
Rayleigh flow, 2-dim, viscous, incompressible, past infinite porous flat plate 9-23422
refractories, mech. deterioration due to thermal cycling 9-33014
refractories, periclase-spinelide, microstruct. 9-42781
resin-impregnation method of specimen mounting to isolate voids and microcracks 9-39485
rocks, natural, diffusions and flow of N₂ 9-30332
semiconductor smoke, resistivity 9-44951
silica, microporous, prep. by freeze-thawing technique 9-46732
surface area and pore size distrib. from adsorbed gas weighting, automatic apparatus 9-38189
surfaces, two mutual attraction, determination method 9-39484
thermal transpiration, dusty-gas theory 9-39380
vertical slab, stability of convection 9-34733
viscosity variation of gas flow 9-26042
Vycor glass, containing superfluid fraction of liquid helium 9-34943
water movement, evap. during second stage of drying 9-34854
Al alloys, porosity, depend. on grain size and composition 9-28393
C black, thermal, closed porosity study by oxidation 9-28258
C blacks, surface area and porosity eval. 9-23645
Fe, dynamic compaction props. 9-44762
KCl, He filled pores temp. induced migration, obs. 9-37189
Ni_{0.36}Zn_{0.64}Fe₂O₄, ferromagnetic resonance linewidth and shift from tensor susceptibility meas. 9-37666
Ni Mn_{0.05}Fe_{1.95}O₄, ferromagnetic resonance linewidth and shift from tensor susceptibility meas. 9-37666
UO₂, irradiated, re-solution of fission gases 9-28326
UO₂, sintering pores irradi. stability, obs. 9-37187
UO₂ cermet from UO₂-Mo system, impact and bending strength depend. 9-35222
UO₂ porosity effect on kinetics of grain growth 9-26250
YFe garnet, and Ca-V substituted, effective linewidth due to porosity and anisotropy, field depend., microwave freqs. 9-45371
YFe garnet, effective linewidth and relax. obs. 9-31055

Porter-LeChatelier effect *see Stress/strain relations***Positive column** *see Discharges, electric***Positive ray sources** *see Ion sources***Positive rays** *see Chemical analysis/by mass spectrometry; Ion beams***Positons** *see Positrons***Positronium**

- chemical interactions in sq. KMnO₄ solids. 9-45429
cross-section for formation from e⁺ collisions in H calc. 9-46064
formation by passage of positrons through electron gas 9-44898
inmolecular materials, decay, free volume model 9-22537
positronium hydride, variational wave function, soln. 9-22538

Positrons

- see also Electron pairs; and Electrons, which include both negative and positive electrons when the differences between them are of no special significance*

- annihilation in bE foil, with γ prod., shielding studies 9-22528
annihilation in Ar, models 9-38785
annihilation in Ar, rel. to applied elec. field and Ar density 9-38784
annihilation in Bi single crystal, temp. effect on γ ang. distrib. 9-24113
annihilation in flight system, target parameters and photon spectrum 9-25422
annihilation in metals, lifetime, γ pairs distribution 9-24112
annihilation in Nb₃Sn type II superconductor, e-pairing eff., γ ang. distrib. meas. 9-30874
annihilation in Ne-iso-electronic series, diamond, and solid I₂ 9-30830
annihilation of secondary cosmic-ray positrons in the galaxy, resulting γ-ray spectrum 9-31492
double-electron capture, on passing through He, cross section calc., E_{max} < 250 eV 9-46335
electron flux meas. from polyethylene absorber 9-24244
falling, gravitational force, exptl. determ. 9-25421
lifetime in PVC, anomalous 9-43016
lifetimes in silicone fluids 9-27467
metals, thermalization, effect of superconducting transition 9-24111
passage through electron gas, positronium formation 9-44898
in polymers, solid, lifetimes meas., intermol. forces correl. 9-33240
positron beam production and expts., popular review 9-43847
production during mutual approach of heavy nuclei and vacuum polarization 9-48158
in silicone fluids, decay lifetime 9-27467
superconductive metals, annihilation 9-26501
yield from thick target 9-22535
e⁺p scatt., radiative corrections, N⁺(1236) resonance contrib. calc. 9-40402
μ⁺-e⁺ spectrum and asymm., Hz bubble chamber obs. 9-42011

Positrons continued

- Cu-Zn alloy single cryst., annihilation 9-33241
 Cu, annihilation in single cryst., temp. effect 9-33242
 Nb-Al superconducting alloys, annihilation, critical temp. eqn. parameters 9-39598
 Ni (110) crystal polarized annihilation 9-24114
 RbBr single cryst., anisotropic penetration, X-ray spectrum obs. 9-35300
- Potassium**
 absorption, optical, electron-electron interaction effect 9-49279
 anharmonic effects on normal modes of vibr. neutron scatt. obs. 9-46975
 arcs in various gases containing 1 mol. % k, temp. and radiation 9-42583
 atom, $4^2P_{3/2}$ state, hyperfine structure, atomic beam mag. reson. obs. 9-44252
 atom, deformation of K, L and M due to interaction with optical electron 9-44268
 atom, electron scattering, effect of long-range forces 9-27819
 atom, impact ionization by electrons and protons, cross section obs. 9-34556
 atom, octopole-allowed transitions in electron energy-loss spectra 9-40543
 atomic absorption spectrum, shift and splitting in laser radiation field 9-29937
 atomic beam, gravitational deflection obs. 9-43725
 atomic beam, intense, used as source of polarized electrons 9-40459
 atomic beam, scatt. by various compounds 9-42469
 atomic beam reaction with oriented CF_3I 9-43320
 atomic cluster, ionization pot. obs. 9-29956
 atoms, excited, induced collisions in Rb vapour $4^2P_{1/2}$ - $4^2P_{3/2}$ mixing 9-34574
 atoms, excited, induced collisions in Rb vapour causing sensitized fluoresc., energy transfer obs. 9-34573
 boiling in tubes, heat transfer coeffs. mean and local 9-23487
 charge-transfer cross section for He^+ and Ar^+ meas. 10-1500 eV 9-46316
 colloidal particles in KCl, light attenuation, spectral dependence of coeffs. 9-49278
 deformation in commercial and high purity, mechanism at low temp. 9-46893
 diffusion and drift of K ions in N_2 9-40756
 diffusion of Na, vacancy and interstitial mechanisms, computer calc. 9-44736
 diffusion of Rb 9-40984
 electron mean free path, meas. by r.f. size effect 9-30816
 electron-electron interaction effects on optical absorpt. 9-49279
 g-factor meas., atomic structure parameters derived 9-29936
 Hall coeff., accurate determ. from helicon waves and surface mode loss 9-24124
 helicon wave resonant damping 9-26494
 hyperfine interaction and Fermi surface electron wave depend. on cellular potential 9-39566
 ion, earth's atmosphere, measurement of reaction with ozone 9-40044
 line strengths in 146 A stars 9-27024
 liquid, incipient boiling superheat meas. 9-26165
 liquid, self-diffusion coeff. 9-42643
 liquid, viscosity up to 1500°C 9-40780
 magnetoplasma mode, correlation-proc., exptl. evidence 9-26495
 magnetoresistance, strain dependence 9-35343
 magnetoresistive effects, saturation and linear 9-37447
 MHD, thermodynamic props. of combustion products of methane and oil with ionizing K seeds 9-36748
 Mossbauer obs. of lattice dynamics, recoilless fraction and thermal shift for 29.4 keV transition in ^{40}K 9-42952
 optical consts., 0.5-4.0 eV, by split-beam ellipsometry 9-49240
 phonon frequencies from electron-phonon interaction modification with correlation effects 9-35308
 plasma, oscillations, noise due to radial elec. field obs. 9-28029
 polarized atomic beam, ionization ω with u.v. light to produce polarized e beam 9-27282
 resistivity, low temp. 9-37437
 in rocks, gamma spectrometer surface obs. 9-37893
 scattering by alkali atom, spin-exchange cross section calc., partial-wave anal. 9-22984
 size effect, r.f., in cylindrically shaped samples 9-43028
 spectra, radiative splitting of atomic levels in laser rad. field 9-27809
 spectrum, electron impact, generalized oscillator strengths 9-34543
 in upper atmosphere, abundance and theory of origin 9-35832
 vapour diffusion in He and Ar 9-39059
 vapour liquid mixtures, hydrodynamic and elec. props. 9-23487
 vapour press., const. vol. piezometer obs. 9-40829
 vibration normal modes, anharmonic effects, neutron scatt. obs. 9-46975
 vibrational spectrum, calcs. 9-39510
 X-ray K emission spectra from KCl cry., lattice defects determ. 9-36693
 K/H and K/Li ion exchange in synthetic resin, kinetics 9-41438
 K/Hg, amalgam, fuel cell potential and thermo-dynamic props. 9-36926
 K-Ar, Xe, methyl iodide, collisions, cross-sections 9-27823
 K-NH₃ solns., vacancy calc. of viscosity 9-48686
 K-NH₃ solns. doped with KI, Knight shifts 9-44595
 K⁺ concentration in Antarctic ice, obs. 9-33729
 K⁺ ion swarm in N₂, mobility, diffusion coeff. and reaction, determ. 9-23203
 K⁺ new model potential, suitable for liquids and solids 9-34518
 K($^2P_{1/2}$)+Rb($^2S_{1/2}$)-K($^2S_{1/2}$)+Rb($^2P_{1/2}$)+ ΔE , fluorescence detected, cross-section calcs. 9-32429
 K, 1, $3p^4s^3d$ configuration, intermediate coupling matrices, transitions obs. 9-32412
 K vapour, induced versus parametric scattering processes 9-47998
 ^{39}K , self spin-exchange cross-section meas. using microwave absorption between Zeeman sublevels 9-46314
 ^{40}K produced by cosmic rays in iron meteorites, surface ionization mass spectrometric obs. 9-40182
 K+HBr(DBr)-KBr reactive collisions, crossed mol. beam expts., angular and vel. distrib. of KBr 9-35741
 Na-K mixture, ionization pot. of atomic cluster, obs. 9-29956

Potassium compounds

- acid phthalate, diamag. susceptibilities and anisotropies 9-45081
 apophyllite, (KFCa₂Si₄O₁₀·8H₂O), p.m.r., rel. to position of protons and diffusion of H₂O mols. 9-47447
 caprate, crystal structure refinement 9-39326
 dielectric constant at high temps. of KI 9-39665
 halide crystals, e.s.r. of trapped N₂⁻ 9-31166
 halides, F-centre emission energies and lifetimes 9-32999

Potassium compounds continued

- halides, P-activated, luminescence 9-33583
 KDP, in Ar-ion laser cavity, c.w. parametric u.v. generation 9-27363
 lucite, energy-loss spectra for high-energy electrons as function of depth 9-37377
 muscovite, dislocation planes, electron microscopy 9-23748
 potassium thiocyanate, gamma-irrad., e.p.r. spectrum of radical species 9-45392
 potassium trioxalatoferrate, Fe (III) activity transfer process 9-39185
 K-Cs binary alloys, electron spin susceptibilities, Knight shift 9-39116
 K-Na(Rb) alloys, tensile deformation, yield and flow stress, conc. depend. 9-30664
 K-Rb binary alloys, electron spin susceptibilities, Knight shift 9-39116
 K_{0.14}NiO₂, crystal structure, and effect of replacing K by Rb and Cs 9-40905
 K_{0.30}MoO₃, anisotropic elec. behaviour, X-ray diff. obs. 9-37446
 K₂C₂O₄H₂O, neutron inelastic scatt. obs. of librational freqs. 9-42955
 K₂C₄H₄O₆·1/2H₂O cryst., second harmonic generation 9-39791
 K₂CF₄, n.m.r. of F⁻ transferred hyperfine interactions 9-41294
 K₂CoF₄, antiferromag., n.m.r. and transferred hyperfine interactions 9-45257
 K₂CoF₄ single cry., nature of ionic conductivity 9-35471
 K₂CoF₄ two-dimensional antiferromagnet, optical absorpt., 4.2° TO 300°K 9-45321
 K₂Cr₂O₇, single crystal, Raman spectra, rel. to symmetry class 9-47374
 K₂CsB photoacathode, energy band scheme from photoelec. emission, optical absorpt., photo- and elec. cond. props. 9-28584
 K₂CuCl₂·2H₂O, ferromagnet, anomalous resonance, nature 9-45366
 K₂MoO₃, with tungsten bronze type structure, superconducting transition temp. determ. 9-26530
 K₂NiF₆, paramag., NMR 9-37806
 K₂NiF₆, static dielec. const. at various d.c. field strengths 9-37582
 K₂NiF₆ neutron scatt., two-dimen. Heisenberg antiferromagnet model 9-26660
 K₂NiF₆, electronic abs. spectrum study 9-32477
 K₂NiF₆, solid, i.r. and Raman abs. spectra study 9-32494
 K₂O-GeO₂ system, phase equilibria and thermal expansion data 9-26398
 K₂O-PbO-SiO₂ glasses, luminescence centres 9-31129
 K₂O-SiO₂ glass, alkali-ion movement, electron-probe microanalysis 9-34968
 K₂O-SiO₂ glass, luminescence spectra 9-39872
 K₂O-SiO₂ vitreous solids, elec. conduction and phase separation by electron microscopy 9-41156
 K₂O·Al₂O₃·6SiO₂, meas. of Al₂O₃ fragments at surface by molec. emission 9-42709
 K₂PtCl₆, interaction between quadrupolar relaxation of ³⁵Cl and molecular rotation of PtCl₆ 9-31174
 K₂SO₄-Li₂SO₄ phase diagram from differential thermal anal. 9-48923
 K₂SO₄, cry., thermal expansion coeffs., exptl. method applic. 9-24053
 K₂SO₄, morphology of cryst. faces, by Hartman method 9-46745
 K₂SO₄ crystal, X-irradiated, e.p.r. spectra obs. 9-24491
 K₂W₂O₈, structure, p.m.r. investig. 9-45404
 K₂ZnF₄·Co²⁺, e.p.r., super-hyperfine interaction const. 9-45257
 K₂ZnF₄, Mn single crystal, e.s.r. and transferred hyperfine interactions 9-45387
 K₂ZnF₄, e.p.r. of Co²⁺, rel. to mag. struct. 9-41294
 K₂[Ni(CN)₄](H₂O)₂, fine structure of Ni K X-ray absorpt. obs. 9-37747
 K₂Co(CN)₆·3H₂O, ENDOR saturation transfer mechanism rel. to thermal mixing of nuclear spins 9-43310
 K₂Cr(NCS)₆ in methanol-ethanol glass, 100°K, excited state absorption 9-38838
 K₂Fe(CN)₆, Mossbauer effect obs. 9-26725
 K₂MoCl₆ crystal structure 9-40904
 K₂Y(Si₂O₇(OH))₂, crystal structure 9-23762
 K₃[Co(CN)₆]₄ X-ray absorpt. spectra, fine struct., effect of absorber thickness and tube voltage 9-39857
 K₄Fe(CN)₆, phase changes rel. to polarization, dielec. props and stability criteria, theoretical analysis 9-41240
 K₃MnCl₆ form. in LiCl-KCl eutectic: MnCl₂, e mag. reson. obs. 9-28749
 K₄Nb₆O₁₇, growth and props. 9-26238
 K₄Nb₆O₁₇, mica-like single crystal, growth, optical, elec., mech. and struct. props. 9-30522
 K₂Pb₂La₂Nb₁₀O₃₀, crystal growth and dielectric constant 9-23682
 K₂ReO₅, with tungsten bronze type structure, superconducting transition temp. determ. 9-26530
 K₂Sr₂La₂Nb₁₀O₃₀, crystal growth and dielectric constant 9-23682
 K complex, tris-oxalato-chromate trihydrate, mag. behaviour 300-90°K 9-26623
 K trioxalatoaluminate hydrate, p.m.r., free rot. of proton pairs 9-28756
 KAl(SiO₃)₂, energy-loss spectra for high-energy electrons as function of depth 9-37377
 KBr:Sm²⁺ vibronic side bands calc. 9-49285
 KBr-KCl solid solution films, fundamental absorpt. spectra 9-28685
 KBr-NaBr solid solution films, fundamental absorpt. spectra 9-28685
 KBr-RbBr solid solution films, fundamental absorpt. spectra 9-28685
 KBr, r.f. spectrum by molec. beam elec. reson. 9-27862
 KCO₂/Li/Na, diffusion of ²²Na and ¹⁴C near eutectic mixture 9-30625
 β-K₂FeF₄, crystal structure 9-26237
 KClO₃, single crystal, ⁴⁰K elec. quadrupole moment meas. by new resonance technique 9-29752
 KClO₃ X-irrad., e.p.r. of ClO₂, (ΔM₁=1, ΔM₂=±1 or ±2) 9-49352
 KCoF₃, crystal growth from low melting flux 9-39207
 KCuF₃, polytype struct., X-ray diff. exam. 9-32917
 K(D_{0.55}H_{0.45})₂PO₄, ferroelec., pressure depend. of transition temp. from neutron diff., up to 10 kbar 9-49143
 KD₂PO₄, detection of photon- photon scattering, interaction of microwave and laser beams 9-24358
 KD₂PO₄, electro-optical effect, transverse, and light modulation by crossed rods, obs. 9-33516
 KD₂PO₄, ferroelec., pressure depend. of transition temp. from neutron diff., up to 10 kbar 9-49143
 KD₂PO₄, ferroelec. anomalies in dielec. and piezoelec. props. 9-41244
 KD₂PO₄, ferroelec. phase transition obs. and KH₂PO₄ comparison 9-41242
 KD₂PO₄, H atom potentials rel. to phase transition mechanism, i.r. spectra obs. 9-26589
 KD₂PO₄, Ising spin system, relaxation process near Curie temp. 9-35483
 KD₂PO₄ crystal, dielectric permittivity, effect of strong elec. field 9-41241
 KD₂PO₄ crystal, electro-optical effect, fourth-order 9-41358

Potassium compounds continued

- KD₃(SeO₃)₂, ferroelec. single cryst. dielec. const. temp. depend., H-bond role in phase transition 9-32855
 KF:U, luminesc. decay and fundamental series emission 9-35695
 KF, surface phenomena and dislocations 9-23618
 KF F-centres, Stark effect of relaxed excited states 9-24392
 KFCa₂Si₂O₃·8H₂O, (apophyllite) p.m.r., rel. to position of protons and diffusion of H₂O mols. 9-47447
 KH₂AsO₄ and isomorphs, to 42 m symmetry, electro-optic effect, half-wave retardation voltage 9-35628
 KH₂PO₄:Cu²⁺, ferroelectric, e.s.r. 9-26793
 KH₂PO₄, 45° Z cut, light modulation, and isomorphs 9-35620
 KH₂PO₄, Curie pt. obs. with and without tunnel effect 9-33388
 KH₂PO₄, electro- and piezooptical coeffs., dispersion and temp. depend. 9-33515
 KH₂PO₄, electro-optical effect, transverse, and light modulation by crossed rods, obs. 9-33516
 KH₂PO₄, electrocaloric effect 9-35482
 KH₂PO₄, ferroelec. phase transition obs. and KD₂PO₄ comparison 9-41242
 KH₂PO₄, ferroelec. transition dilatometric invest. 9-28561
 KH₂PO₄, ferroelectric domains boundaries, X-ray topography obs. 9-28556
 KH₂PO₄, H atom potentials rel. to phase transition mechanism, i.r. spectra obs. 9-26589
 KH₂PO₄, heat capacity anomaly near ferroelec. transition 9-43117
 KH₂PO₄, linear electro-optic effect, theory 9-33517
 KH₂PO₄, n.m.r. by double resonance method 9-28758
 KH₂PO₄, neutron diff. intensity anomalies near phase transition pt. 9-40903
 KH₂PO₄, neutron incoherent inelastic scattering cross section 9-28560
 KH₂PO₄, partially deuterated, ferroelectric mode obs. 9-26756
 KH₂PO₄, phase transitions, u.s. investigations 9-37302
 KH₂PO₄, proton tunneling, n. scatt. obs. 9-24219
 KH₂PO₄, rotatory saturation and spin calorimetry assoc. with ³⁹K NMR 9-28757
 KH₂PO₄, second-harmonic generation with diffraction-limited and high-spectral-radiance Nd-glass laser system 9-41917
 KH₂PO₄, second harmonic double refraction using He-Ne laser 9-31076
 KH₂PO₄, Slater model, first order phase transition 9-45008
 KH₂PO₄, specific heat determ. by pyroelectric method 9-30783
 KH₂PO₄, u.s. wave propag. near ferroelec. phase transition 9-48949
 KH₂PO₄ cryst., second harmonic generation 9-39791
 KH₂PO₄ crystal, freq. doubling, effect of lasers radiation parameters 9-45280
 KH₂PO₄ crystal, relative nonlinear optical coefficient, corrected value 9-33499
 KH₂PO₄ crystals, dynamical, scattering and dielec. props. 9-49141
 KH₂PO₄ crystals, optical rectification of mode-locked laser pulses 9-26712
 KH₂PO₄ ferroelec. transition, Pippard scheme for sp. ht., thermal expansion and isothermal compressibility 9-30970
 KH₂PO₄ frequency converter for pulse laser, design 9-38382
 KH₂PO₄ nonlinear optical coeff. meas. relative to NH₄H₂PO₄, LiNbO₃ and α-HIO₃ 9-26690
 KH₂PO₄, ferroelec. domain struct. by Frauhoffer diffraction and Toepler shadow methods 9-47175
 KH₂(SeO₃)₂, H-bond role, dielec. anomaly in KD₃(SeO₃)₂, obs. 9-32855
 KH₂PO₄ crystal, dispersion of optical rectification effect 9-47326
 KHgBr₃·H₂O, crystal structure 9-39280
 KI:Ag⁺, stress-induced shifts of lattice resonant modes 9-24015
 KI:CdI₂, thermoelec. power and ionic conductivity 9-41253
 KI:(Ga³⁺), centers, absorpt. bands obs. 9-35111
 KI:In, X-ray luminesc. build-up, obs. 9-35698
 KI:(In³⁺), centers, absorpt. bands obs. 9-35111
 KI:Ti, F centre prod. by impurities, α and ν_K centre motion importance 9-44718
 KI:Ti, intercentre luminescence, elec. field effs. 9-39871
 KI:Ti³⁺, dichroism, influence of uniaxial compressive stress 9-31075
 KI:(Ti³⁺), centers, absorpt. bands obs. 9-35111
 KI:Ti phosphors, kinetics of thermal decomposition of activator hole centres 9-33582
 KI:AgI, luminescence 9-47404
 KI-KBr mixed crystals, Faraday rotation in high mag. fields 9-26706
 KI-KCl mixed crystal phosphors, luminescence behaviour obs. 9-33588
 KI, dielectric constant at high temps. 9-39665
 KI, dislocation visualization by condensation method 9-44708
 KI, dispersion relations 9-30762
 KI, F centre, electronic structure calc. 9-40973
 KI, F centre, lattice dynamics rel. to electronic Raman spectra and lattice and electronic absorptions 9-35118
 KI, F centre spin-lattice relax., theory and optical meas., 0-50 kG 9-24342
 KI, luminescent yield of NO₂⁻ centres, exciting light freq. depend. 9-31124
 KI, Raman spectrum of S₂⁻ and Se₂⁻ mols. 9-49294
 KI, shock polarization, rel. to lattice characts. 9-30957
 KI, thermoelec. power and ionic conductivity 9-41253
 KI, two quantum photoconductivity 9-41268
 KI, U₂ centre Faraday rotation 9-33512
 KI 2-photon absorption spectra, optical transition in Brillouin zone, 0-7.5 eV 9-39838
 KI and KI(In) self-luminesc. decay, additional traps 9-37784
 KI containing CN⁻, u.s. velocity and attenuation 9-37329
 KI containing F-aggregate centres, α-band increase w.r.t. time, M-centres formation 9-32990
 KI solution, ultrasonic cavitation, relaxation phenomena 9-46629
 KI thin film, far u.v. absorption spectrum obs. and interpreted 9-37730
 KI:Ti³⁺, electron-lattice interaction, absorption spectra meas. 9-41386
 KLiSO₄ cryst., second harmonic generation 9-39791
 K(MgCoF₃)₂ with paramagnetic ion impurities, electron states group theoretical classification 9-28443
 KMnCl₃, broadband fluoresc., temp. depend. 9-49319
 KMnCl₃, n.g.r. of ³⁵Cl 9-49365
 KMnF₃, soft phonon modes, neutron scatt. obs. 9-33155
 KMnF₃, e.p.r. of Mn²⁺ and ¹⁹F n.m.r. exchange narrowed discrepancies between theory and expt. 9-45388
 KMnF₃, single crystal slab, absorption spectra in far i.r. and visible, multiple magnons 9-45326
 KMnO₄, semiconducting props., temp. depend. 9-33282

Potassium compounds continued

- n-KMnO₄, thermal decomposition in solid phase 9-37818
 KMnO₄ aq. solns., positronium interactions 9-45429
 KN₃, thermoluminescence meas., trapping levels, 10²-525°K 9-47407
 KNO₃, cryst. struct., high-pressure 9-32903
 KNO₃, molten, Raman vib. freqs. of NO₃⁻ ion rel. to temp. 9-42662
 KNO₃, polarized i.r. absorpt. spectra, internal-lattice combination band region 9-47363
 KNO₃, solid state battery, form. 9-47890
 KNO₃ film, ferroelec. phenomena 9-49144
 KNa Pt(CN)₄·3H₂O, crystal structure 9-23761
 KNb₂O₆ mica-like single cryst., growth, optical elec., mech. and struct. props. 9-30522
 KNbO₃, atomic chain structure rel. to phase transition 9-32901
 KNbO₃, ferroelec., cry. struct., X-ray and micro-electron diffraction invest. 9-46788
 KNiF₃, crystal growth from low melting flux 9-39207
 KOH aqueous electrolytic soln. with zincate ions, flow effect on morphology of electrodeposited Zn 9-33679
 KOH in KCl as-grown and annealed cryst., paraelec. reson., tunnelling behaviour obs. 9-39673
 (KPO₃)_n glassy and crystalline, valence angles and dihedral angles rel. to structure 9-40906
 (KPO₃)_n phase transform., Weissenberg photographs obs. 9-35245
 KTa_{1-x}Nb_{1-x}O₃, dielectric properties 9-35473
 KTa_{1-x}Nb_{1-x}O₃ crystal, growth from melt, patent 9-48805
 KTaO₃-KNbO₃ system, subsolidus stability relations 9-26157
 KTaO₃, ferroelec., electron scatt. 9-37591
 KTaO₃, polariton obs. by small-angle light scatt. 9-24429
 KTaO₃, u.s. attenuation and vel., interpret. of temp. and freq. depend. 9-37328
 KTaO₃, u.s. attenuation by interaction with soft optic mode 9-24025
 KZnF₂:Mn²⁺, e.p.r. determ. of nearest-neighbour exchange const. 9-45386
 KZnF₂, single crystal with perovskite structure, hydrothermal synthesis 9-42746
 K₂[Cd(NO₃)₆], u.v. and i.r. absorpt. and Raman spectra 9-49288
 K₂[Hg(NO₃)₆], u.v. i.r. and Raman spectra 9-49288
 Ki, F-centre prod. by two-photon absorpt., quantum efficiency 9-44719
 KTa_{1-x}Nb_xO₃, ferroelec., electron scatt. 9-37591
 Na-K, liquid, turbulent in temp. fluctuations in flow field 9-23426
 Na-K liquid alloys, electromigration 9-30416
 NaHSO₄-KHSO₄ melt and glass, Mo V spectrum 9-37729
- potassium bromide**
 cleavage surface, substrate for CdS film, rel. to structure 9-40840
 colour centres, colloidal and F aggregate, optical and thermal stability, elec. conductivity obs. 9-46835
 defects, n and γ induced, low temp. annealing 9-40967
 dislocation etch figures, effect of neutron irradiation on dimensions 9-40945
 dislocation interactions with pinning centres, from Young's modulus invest. 9-32971
 dislocation visualization by condensation method 9-44708
 electrical conduction, pure and doped, anion contrib. at high temp. 9-35472
 electrical conductivity, effect of M centres 9-32988
 electrostrictive coeffs., calc. using theory for ionic non-piezoelec. ionic crystal composed of point charges 9-47186
 F centre, electronic structure calc. 9-40973
 F centre spin-lattice relax., theory and optical meas., 0-50 kG 9-24342
 F centres formation, thermoluminesc. obs. 9-33606
 F-centre prod. by two-photon absorpt., quantum efficiency 9-44719
 F-centre production on vacuum u.v.-irradiation, photostimulated e. emission obs. 9-30617
 F-centres, ENDOR spectroscopy, elec. field effects 9-35734
 F-centres, Stoke's shift, electronic absorption and emission bands, temp. depend. 9-24411
 Faraday rotation in high magnetic fields using high speed integrators 9-31080
 heat capacity, 30°-500°K 9-24047
 interstitial H⁻, H⁻ and V₁ centres, radiation-induced, form. kinetics 9-42849
 interstitials, ionizing rad. induced, prod. rate at low temp. 9-32948
 i.r. absorpt. of Li⁺, particle in curved box model 9-47364
 lattice expansion following F-centre formation 9-28304
 luminescent yield of NO₂⁻ centres, exciting light freq. depend. 9-31124
 phonon scatt. by O⁻ centres in pure and doped cryst., thermal conductivity obs. 9-42949
 photoemission from metal contact 9-26611
 photoluminescence, room-temperature, electric-field-enhanced 9-45359
 proton energy distribution and channelling in lattice 9-38089
 reflection spectrum in extreme u.v., dielectric const. and loss function 9-28673
 scattering parameters in crossed mol. beam expts. on K+HBr(DBr) reactive collisions 9-35741
 surface phenomena and dislocations 9-23618
 thermodynamic props., anharmonic effects, data analysis 9-24048
 thermoluminescence and F centres formation obs. 9-33606
 U₂ centre Faraday rotation 9-33512
 u.s. velocity and attenuation in crystals containing CN⁻ 9-37329
 vacancies, ionizing rad. induced, prod. rate at low temp. 9-32948
 window material for i.r. spectroscopy under high pressure 9-32065
 KBr:CN, phonon resonant scatt. 9-26408
 KBr:Ca(Cl), F-centre prod. rate due to electron irradiation 9-46834
 KBr:Ca(Cl), F-centre prod. rate due to electron irradiation 9-46834
 KBr:Cd, thermoluminesc. and optical absorpt. obs., F centres formation 9-33606
 KBr:H⁻ lattice vibration local mode frequency computation 9-28410
 KBr:KH, U₁-α centre pairs conversion into U₂-F centre pairs 9-35112
 KBr:Li⁺, stress-induced shifts of lattice resonant modes 9-24015
 KBr:NO₂⁻, phonon resonant scatt. 9-28411
 KBr:Na, colour centre production at 80°K 9-23827
 KBr:Na⁺, radiation-induced interstitial centres, form. kinetics 9-42849
 KBr:O₂⁻, luminescence; config. coordinate curves of local vibr. of centre 9-39868
 KBr:OH⁻, rot. barrier height 9-40935
 KBr:Pb²⁺, electrolytically coloured, prod. and optical props. of centres 9-32992
 KBr:S₂⁻, luminescence spectra, config. coordinate curves 9-39869
 KBr:Ti, activator incorporation and luminesc. 9-39870
 KBr:TiIn, X-ray luminesc. build-up, obs. 9-35698

Potassium compounds continued**potassium bromide continued**

- KBr:Ti⁴⁺, dichroism, influence of uniaxial compressive stress 9-31075
 KBr:Ti modulated absorption spectrum, triplet struct. and Stark eff. obs. 9-41381
 KBr:Zn, thermoluminesc. and optical absorpt. obs., F centres formation 9-33606
 KBr-KCl mixed crystals, Faraday rotation in high mag. fields 9-26706
 KBr-KI, mixed crystals, Faraday rotation in high mag. fields 9-26706
 KBr:Ti⁴⁺, electron-lattice interaction, absorption spectra meas. 9-41386
 KCl:Li⁺, off-centre behaviour lattice parameter dependence 9-35087
 KCl-KBr-Tl crystal, symmetry of Ti centres 9-42852
 KI, F centre, lattice dynamics rel. to electronic Raman spectra and lattice and electronic absorptions 9-35118

potassium chloride

- anharmonic thermal vibrations, X-ray meas., 300° to 800°K 9-44812
 aqueous soln., elec. conductivity 300-1000°C, up to 12 kbar 9-48717
 band structure and polaron theory, F-centre electron wave function determ. 9-33237
 cleavage surface, substrate for CdS film, rel. to structure 9-40840
 rel. to coal vacuum discharge spectral analysis, sensitivity improvement by KCl addition 9-26845
 colour centre obs. from photostimulated thermoluminescence in additively coloured crystals 9-47408
 colour centre production by 5keV electrons 9-23829
 colour centres, optical conversion of F to M centres with repetitive light pulses 9-46833
 colour centres formation, F₂ and Z₂, by anion vacancy migration 9-39375
 conductivity and energy loss spectra, temp. depend. exciton states obs. 9-33559
 crystal X-ray K emission spectra of potassium obs., lattice defects determ. 9-36693
 defect production by X-irrad. at 20°K, electron-hole recombination mechanism 9-26276
 depth distributions, low-energy, obtained by sputtering 9-47013
 dielectric relaxation effects due to air-gaps in specimen electrode contacts 9-37581
 diffusion annealing of bent crystal at 550-750°C causing straightening 9-42884
 diffusion coeff. of soln., determ. by pulsation method 9-44555
 dislocation etch figures, effect of neutron irrad. on dimensions 9-40945
 dislocation study by etching cleavage planes 9-37177
 dislocations in melt-grown cryst., thermal etching obs. 9-37178
 elasto-optical and piezo-optical coeffs., temp. depend. 9-39813
 electret behaviour and ionic thermal currents 9-37605
 electrical conductivity, effect of M centres 9-32988
 electrical conductivity of pure cryst. 9-47154
 electron-irradiated during microscope exam., point defect coagulates obs. 9-42808
 electronic spectra, 5-40 eV region, complex dielec. const. determ. 9-37711
 electronic structure calcs., point defects in ionic crystals 9-40928
 electrostrictive coeffs., calc. using theory for ionic non-piezoelec. ionic crystal composed of point charges 9-47186
 energy parameters of In⁺ and Ti⁺ 9-31052
 e.s.r. obs. of simultaneous optical bleaching and X-irrad. 9-42848
 F₂ centres, a.c. photoconductivity meas. 9-39376
 F' colour centres, electronic props. 9-28296
 F and M optical absorption bands, eff. of Ca, Cd, Mn and Pb impurities on growth 9-28686
 F centre formation by pulsed electron beam at 80°K 9-35110
 f centre, lattice dynamics rel. to electronic Raman spectra and lattice and electronic absorption 9-35118
 F centres, ENDOR line intensities 9-33653
 F centres, e.s.r. and optical absorpt. obs. 9-37191
 F centres excited states, orbital Lande factor 9-47362
 F-centre build-up due to p irradiation, source of vacancies 9-32987
 F-centre colouring first-stage, expld. separation of two exponential components 9-30615
 F-centre hyperfine interaction constants, temp. depend. 9-46836
 F-centre production on vacuum u.v.-irradiation, photostimulated e. emission obs. 9-30617
 F-centres, ENDOR spectroscopy, elec. field effects 9-35734
 F-centres, Stark effect of relaxed excited states 9-24392
 Faraday rotation in high magnetic fields using high speed integrators 9-31080
 formation and luminescence of Eu⁺ 9-26768
 fracture surface energy, ionizing irrad. effects 9-28372
 heat capacity, 30°-500°C 9-24047
 interstitial H⁺, H⁻ and V_i centres, radiation-induced, form. kinetics 9-42849
 ion spherical symmetry determ. from structure factor meas. 9-23760
 ionic conductivity, possible trivacancy mechanism 9-28552
 KCl:SO₄²⁻, i.r. absorpt. spectra of impurity ion vibrs. 9-41382
 lattice defects, X-ray diff. study 9-46815
 lattice dynamics at 115°K 9-46976
 light, attenuation by colloidal K particles, spectral dependence of coeffs. 9-49278
 luminescent yield of NO₂⁻ centres, exciting light freq. depend. 9-31124
 nucleation of supersaturated solns., eff. of various substrates 9-32876
 optical bleaching and X-irrad., simultaneous, e.s.r. obs. 9-42848
 paramag. reson. of O₂⁻ centre, pulse saturation 9-47437
 phonon scatt. by O⁻ centres in pure and doped cryst., thermal conductivity obs. 9-42949
 piezo-optical and elasto-optical coeffs., temp. depend. 9-39813
 point defect coagulates due to electron irrad. during microscope exam. 9-42808
 pores, He filled, temp. induced migration, obs. 9-37189
 proton energy distribution and channelling in lattice 9-30809
 radiation damage stabilization by trapped Xe, obs. 9-37205
 screw dislocations revealed by etching on (100) cleavage faces 9-48861
 specific heat at low temp., adiabatic meas. 9-25135
 Stark effect of Z₁ and Z₂ centres in electric field modulated absorpt. spec. 9-23828
 strain bands decoration with F-centres in cryst. deformed by indentation 9-37242
 stress relaxation, dislocations mechanism, -196°-150°C 9-33026
 structure factor determ. by elastic scatt. of X-rays, lattice vibrations correction 9-24014

Potassium compounds continued**potassium chloride continued**

- superhyperfine interactions of H and D centres, zero-pt. vibr. influence, ENDOR obs. 9-45409
 thermal etch figures of vac. heated crystals at 150-500°C 9-40855
 thermal expansion meas. by liq. Ga immersion dilatometer rel. to anharmonic effects 9-47007
 thermodynamic props., anharmonic effects, data analysis 9-24048
 thermoluminescence, photostimulated, in additively coloured crystals 9-47408
 U₂ centre, continuum theory 9-41380
 U₂ centre, wave function and isotropic h.f.s. 9-42850
 u.s. velocity and attenuation in crystals containing CN⁻ 9-37329
 V_k centre optically stimulated orientation 9-35113
 vaporization of single cryst., mass spectrum 9-48741
 X-irradiation and optical bleaching, simultaneous e.s.r. obs. 9-42848
 Au evaporated film, effects of forced high nucleation densities 9-32843
 colour centres, V and F, optical growth at 295°K, impurity eff. 9-23830
 KBr:Ca(Cl₂), F-centre prod. rate due to electron irrad. 9-46834
 KBr:Li⁺ off-centre behaviour lattice parameter dependence 9-35087
 KCl: NO₂⁻, i.r. absorpt. spectra of impurity ion vibrs. 9-41382
 KCl:Ag, X-irrad., photostimulated luminesc., due to hole release from V_k centres 9-39897
 KCl:Ag,Tl, X-ray luminesc. build-up, obs. 9-35698
 KCl:Ag⁺ stress-induced dichroism in u.v. absorpt. bands, temp. depend. 9-45322
 KCl:Ag phosphors, types I and II luminescence, two competing recombination processes 9-35381
 KCl:Ag(Ca, Cd, Co, Ti), F-centre prod. rate due to electron irrad. 9-46834
 KCl:Au, absorpt. bands, mechanism of form. 9-49277
 KCl:CN, phonon resonant scatt. 9-26408
 KCl:CO₃²⁻, i.r. absorpt. spectra of impurity ion vibrs. 9-41382
 KCl:Ca, F centres, e.s.r. and optical absorpt. obs. 9-37191
 KCl:Ca²⁺, elec. conductivity 9-47154
 KCl:Cd, Raman scatt. by F centres 9-33569
 KCl:Cd²⁺, F-centre mobilities, 540-700°C 9-40972
 KCl:KOH, as-grown and annealed, paraelec. reson., tunneling behaviour obs. 9-39673
 KCl:Li, microwave freq. phonon generation 9-26409
 KCl:Li, phonon reson. scatt. obs. from thermal conductivity meas., isotope and elec. field effects 9-42948
 KCl:Li⁺(OH⁻), electric cooling rel. to tunnel splitting of impurity motional ground states 9-27143
 KCl:Li⁺(OH⁻)(CN⁻), dielectric behaviour at low temp. rel. to splitting in impurity motional spectrum 9-26583
 KCl:Li F₂ centres, elec. field modulated absorpt., off-axis centre model 9-42851
 KCl:Mg, additively coloured, optical, elec. and e.s.r. obs. 9-48868
 KCl:Mn, F-centres growth and thermoluminescence 9-28303
 KCl:Mn, F colour centre formation inhibited by Mn impurities, thermoluminescent investigation 9-31148
 KCl:NO₂⁻, phonon resonant scatt. 9-28411
 KCl:Ni²⁺, absorption spectrum 9-39842
 KCl:OH, specific heat at 0.3°K 9-44834
 KCl:OH⁻, rot. barrier height 9-40935
 KCl:Pb, F centre prod. by impurities, α and V_k centre motion importance 9-44718
 KCl:Pb²⁺, dielectric loss, optical absorption and emission spectra, effect of vacancy pairs aggregation 9-31108
 KCl:Pb²⁺, electrolytically coloured, prod. and optical props. 9-32992
 KCl:Sm²⁺, vibronic side bands calc. 9-49285
 KCl:Sr²⁺, F-centre mobilities, 540-700°C 9-40972
 KCl:Ti⁴⁺, dichroism, influence of uniaxial compressive stress 9-31075
 KCl-AlCl₃-MgCl₂-H₂O quaternary syst., phase rule study, 25°C 9-23977
 KCl-KBr mixed crystals, Faraday rotation in high mag. fields 9-26706
 KCl-KI mixed crystal phosphor, luminescence obs. 9-33588
 KCl-NaCl mixed crystal phosphors, luminescence behaviour obs. 9-33588
 KCl-NaCl solid soln., enthalpies of crystallisation, anomalies in struct. obs. 9-37161
 KCl, e.p.r. of stabilized Cu and Ag atoms, hyperfine and superhyperfine struct. const., temp. depend. 9-35714
 KCl, F-centre luminesc., decay time and quantum efficiency, temp. depend. 9-35685
 KCl, M-centre singlet-triplet splitting, calc. 9-35107
 KCl, phonon dispersion relations at 80 and 300 K 9-33161
 KCl:Ti⁴⁺, electron-lattice interaction, absorption spectra meas. 9-41386
 KCl-KBr-Tl crystal, symmetry of Ti centres 9-42852
 KI, F centre, electronic structure calc. 9-40973
 KCl:OH, electrocaloric phenomena, thermodynamics, paraelec. cooling obs. 9-37588
 KCl:TiCl₃, lattice defects, X-ray diff. study 9-46815
 RbCl, F₁-centre accumulation due to proton irrad., 78°-380°K 9-30620

Potential energy, gaseous molecules see *Molecules/intermolecular mechanics*

Potential energy, single molecules see *Molecules/internal mechanics; Molecules/vibration*

Potentiometers see *Electrical measurement*

Powder diffraction cameras see *X-ray crystallography/apparatus*

Powder metallurgy see *Metallurgy; Sintering*

Powders

see also *Granular structure; Particle size; Sintering; Surface measurement*

absorption spectra rel. to that of massive substance 9-39829

adhesion of particles, electrostatic contrib. 9-44798

alumina, binary mixtures, sintering kinetics 9-35230

alumina, cements for chemical bonding 9-35229

alumina, hot-pressing technique 9-35201

ceramic, prep. by cryochem. method 9-33125

ceramic, vibration pressing 9-35217

compacted, variables in reflectance spectra 9-37706

cubic, X-ray intensities of patterns, thermal diffuse scatt. contrib. 9-32885

e.s.r., anisotropic transition probability factor 9-31157

ferromagnetic, sintered, residual pores behaviour obs. 9-42921

ferromagnetic, use in visualiz. of boundaries and domains 9-28612

flowability, particle size depend., eff. of adding glidant 9-23610

fluidization, solid-phase entrainment, mathematical description 9-25808

glass, shrinkage, sintering by viscous deformation 9-35227

Powders continued

- glass compacts, sintering during constant rates of heating 9-33130
 i.r. absorpt. spectra, interpretation 9-31111
 i.r. internal reflection spectroscopy, patent 9-38416
 isostatic hot pressing technique 9-35228
 metal oxides, partially reduced high-coercivity 9-49212
 metallurgical, high energy rate densification applic. 9-35226
 nitrates, Raman spectra, absolute scatt. coeffs. 9-49295
 oxides, calcination process, electron microscope exam. 9-35221
 PbCrO₄-C, BaSO₄ mixtures, diffuse reflectance 9-24360
 photoconductive, fine, for electrophotography, preparation method, patent 9-22487
 quarts comminution, net energy input rel. to fineness 9-26375
 quartz comminution, net energies input rel. to fineness 9-26374
 Raman spectra, absolute scatt. coeffs. 9-49295
 reflectance spectroscopy, high resolution 9-47340
 silicates, i.r. emissivities, obs. and cloudy atmosphere model of spectral emission from condensed powder 9-28693
 soda lime glass compacts, shrinkage isotherms rel. to water vapour partial press. 9-33129
 spectra excitation by spark rel. to granule size 9-39967
 spectrochemical anal. by spark excitation technique 9-48114
 spheres of controlled size, fabrication by planetary rolling 9-35199
 stimulated Raman scatt., forced combination dissipation obs. 9-34170
 sulphates, Raman spectra, absolute scatt. coeffs. 9-49295
 superconducting, type II, echo formation 9-24147
 vacuum-powder insulation, thermal conductivity at high temp. 9-41096
 X-ray diffraction examination, protection with polymer coating 9-46767
 AgO, effect of added impurities on elec. resistivity 9-28545
 Al, absolute X-ray scatt. factors from transmission meas. 9-28254
 Al, sintered, control of fretting wear 9-41035
 Al, sintering, n.m.r. obs. of cryst. lattice distortions rel. to oxidation 9-47442
 BaSO₄-C mixtures, diffuse reflectance 9-24360
 BaSO₄-PbCrO₄ mixtures, diffuse reflectance 9-24360
 BeO, sintering to high density 9-35231
 Be(OH)₂, calcination process, electron microscope exam. 9-35221
 Bi₂Te₃-Bi₂Se₃ pressed compacts, preferred orientation meas. by pulsed neutron diff. 9-32862
 C-PbCrO₄ mixtures, diffuse reflectance 9-24360
 CoSe₂-S₇₋₈ magnetization, and susceptibility meas. 4.2° to 300°K 9-47245
 Fe, high purity prod. by sintering and zone melting 9-39448
 In amalgam, electrochemical props. 9-49380
 LiF, X-ray diff. patterns using ⁵⁷Fe sources 9-40907
 MgO in contact with high refractive index glass 9-43209
 MnTiO₃ II high press. struct. obs. 9-44667
 Ni-Cr alloy ball-milling, addition of inorganic salts for prod. of very fine powder 9-23932
 Pb-(10wt.%) In oxide coated, type II supercond., flux pinning by oxide films 9-49045
 SnO₂, i.r. absorpt. spectra, interpretation 9-31111
 ThO₂, calcination process, electron microscope exam. 9-35221
 TiO₂, i.r. absorpt. spectra, interpretation 9-31111
 UO₂ high-surface-area, sintering, influence of atmosphere 9-33113
 UP_{0.75}Se_{0.25}, metamag. obs. 9-34344
 W, substruct. and block size distrib., X-ray diff. obs. 9-46796
 ZnS:Mn,Cu,Cl phosphors, preparation and d.c. electroluminescent props. 9-37781
 ZnS, lattice dimensions and phase transitions, effect of point defects 9-40923
 ZnS, triboluminesc., jet powder technique 9-26788

Praseodymium

- b.c.c., self-diffusion and solute diffusion of La, Ho and In 9-33007
 diffusivity of Co, Ag and Au 9-44745
 double h.c.p. Fermi surface and generalized susceptibility 9-44889
 elastic moduli, ν , attenuation meas., 4.2-300°K, correl. with antiferromag. transitions 9-35146
 Fermi surface and generalized susceptibility 9-44889
 ferromagnet, f.c.c. phase, room temp. and liq. He temp. stabilization, electronic props. 9-35555
 hyperfine field on implantation in Fe, obs. using nuclear orientation 9-35604
 resistivity, elec., due to exchange interaction and quadrupole scatt., temp. depend. 9-44901
 Pr³⁺, cryst. field in LaCl₃ 9-28643
 Pr³⁺ coloration impurity in lanthanum glass, effect on light absorption 9-24372
 Pr³⁺(4f²), spin-spin interactions determ. from matrix element expression 9-38774
 Pr III 4f²6s, 4f²5d, and 4f²6p configurations, level energies, interpretation 9-22964

Praseodymium compounds

- La-Pr dilute solns., elec. resistivity and effective mag. moment rel. to Pr conc. 9-45066
 Pr₂O₃, B-type monoclinic, lattice parameters and cell volumes 9-30562
 Pr₂La_{1-x}Al_x, magnetization and crystallographic data 9-28597
 Pr₂La_{1-x}Al_x, magnetization and crystallographic data 9-28597
 PrAl₃ cubic laves cpd., mag. moment from heat capacity meas. 0.1° to 1.0°K 9-45071
 PrBi, paramag., nuclear ordering, exptl. evidence 9-26669
 PrCl₃, coupled Ising chains and magnetic ordering 9-33456
 PrCo₃ cubic laves cpd., mag. moment from heat capacity meas. 0.1° to 1°K 9-45071
 PrCo₃, ferromag., press. effect on curie point 9-45154
 Pr₂F₃·Nd³⁺ oriented single cryst., far i.r. electr. and vibronic transitions 9-39843
 Pr₂F₃·Nd³⁺ single cryst., far i.r. electronic and vibronic transitions obs. 9-35653
 PrF₃, polarized i.r. reflectance, optical phonons and mag. symmetry 9-47345
 PrNi₂ cubic laves cpd., mag. moment from heat capacity meas. 0.1° to 1.0°K 9-45071
 PrP, magnetic props., depend. on nonstoichiometry 9-28268
 PrP, transport reaction for growth 9-39197
 Pr(ReO₄)₃·3H₂O, crystal structure, optical constants, density 9-39302

Precipitation

- see also Atmosphere/precipitation
 alnico alloy single crystals and mag. props. 9-44792
 chemical crystals, inorg., photomicrographs 9-41458

Precipitation continued

- conditions affecting PVC structure 9-32554
 in diffusion channel rel. to precipitate-membrane formation and structure 9-24517
 dissolution kinetics of precipitate, depend. on growth mode 9-30749
 electron, in auroral zone, IQSY obs. 9-26931
 grain-boundary allotriomorphs, growth 9-35101
 hardening of mats. by a second phase, recovery creep model 9-28354
 w.r.t. internal friction 9-33021
 martensite, of VC, during tempering mechanism 9-33121
 nucleation rates, effect of excess vacancies 9-42926
 Saharan dust falling in Britain, July 1968 9-26900
 solid solution, supersaturated interstitial, effect of vacancies 9-32955
 spherical, coherency loss, theory 9-33133
 steel, 0.095%V, precip. reactions during heat treatment 9-33138
 steel, 12% Cr-Co-Mo, struct. changes during tempering 9-42932
 steel, austenitic containing Al and Ti, soln.-treated, equil. precip. formed on ageing obs. 9-46949
 steel, carbide precip. kinetics, role of W diffusion 9-39383
 steel, mild, containing 1½%Cu, interface precip. 9-33055
 steels, Mo, quenched and tempered, B influence on carbide precip. 9-48931
 in superconductor alloys, for effective flux pinning at high current densities 9-49053
 Zircaloy tubes, of hydride, orientation rel. texture and stresses 9-39188
 Zircaloy-2 tubes, hydride precip. rel. to failure 9-39435
 Ag-Ni solid solns., of Ni, initial state and vel. consts., superparamag. meas. 9-35212
 Al-(0.06 at.%) Si, Si atoms clustering during ageing rel. to resist., 300°C 9-30712
 Al-(0.13 at.%) Si, Si atoms clustering during ageing rel. to resist., 300°C 9-30712
 Al-(1 at.%) Ag alloys, p¹ phase for model verification of dissociated prismatic dislocation loops 9-35091
 Al-Ag alloys, of p¹ phase causing internal friction peak 9-35152
 Al-(18wt.%) Ag alloys, dissolution kinetics, depend. on growth mode 9-30749
 Al-(1 wt.%) Cd alloy, pre-precipitation, rel. to recovery after quenching and cold-working 9-23936
 Al-Cu-Mg-Ag alloys, S laths size obs. 9-48928
 Al-Cu-Mg alloys, S laths size obs. 9-48928
 Al-(4 at.%) Cu, grain-boundary allotriomorphs, growth 9-35101
 Al-(4wt.%) Cu, transition structures formation, effect of cyclic straining 9-39490
 Al-Cu alloy θ' precipitate, as-aged, stacking faults 9-35098
 Al-(4.3 wt.%) Cu alloy, effect of pressure 9-42917
 Al-Mg-Si alloys, precipitates influence on recryst. behaviour 9-39452
 Al-Zn-Mg alloys, near grain boundaries, distribution rel. to boundary misorientation 9-39489
 Al-Zn-Mg alloys, preprecip., hardness and X-ray scatt. meas. 9-23979
 Al-(10 wt.%) Zn, alloy, irradiated at 78°K, pre-precip. rate 9-30715
 Al-Zn alloys, of Zn, breakdown mechanism of spinodal structs. 9-37291
 Al-(6wt.%) Zn(2wt.%) Mg alloy, precipitate nature and morphology 9-28390
 Al-(0.5wt.%) Zr, particles infl. on plastic deformation and recrystallization 9-44794
 Au-Co alloys, rel. to mag. hardness 9-41055
 Au-Pt, coherent and incoherent, kinetics study by resistivity changes 9-28382
 Au-Si solid soln., effect on i.r. vibration spectrum of O 9-45315
 Ca-3wt.%Al-0.6wt.%Cu alloy, structural changes during precipitation of hard soln. 9-44789
 CaCO₃, fractionation of Ca isotopes 9-42356
 Co-(7.45 wt.%) Ti solid soln., γ -phase, precip. during ageing, neutron diff. and chem. analysis 9-41065
 Cu-B alloy, influence on He bubble formation during irradiation 9-41116
 Cu-Co alloys, containing coherent precipitates, critical resolved shear stress 9-44755
 Cu-Co alloys containing coherent particles, critical resolved shear stress 9-44756
 Cu-Co single cryst., plastic behaviour 9-39428
 Cu-(2wt.%) Co alloy, structural transformations in precipitates on cold-rolling, Mossbauer obs. 9-30732
 Cu-Fe dilute alloys, martensite nucleation in Fe precipitates 9-37300
 Cu-Fe solid solns., homogeneous decomposition 9-48930
 Cu-Ti-Al alloys, electron microscope obs. 9-46938
 Cu-Ti alloys, electron microscope obs. 9-46938
 Cu-(39.8wt.%) Zn alloy, uniaxial tensile stress effect 9-46939
 Cu(1wt.%)Co, loss of Co precipitate coherency by electron irradiation in micro-scope 9-28383
 CuFe₂O₄- α -Fe₂O₃ mixture, reaction and phases formed on heating, rel. to Cu_{0.9}Fe_{2.1}O₄ spinel formation 9-30740
 Cu(36wt.%)Zn, of Fe and P, rel. to solubility and max. saturation 9-30717
 Cu(36wt.%)Zn, two-phases with Fe and P, rel. to softening and grain growth inhibition in recryst. 9-30718
 Fe-Mo alloy precipitates, fine faults and cryst. struct. obs. 9-42787
 Fe-(40wt.%) Ni-(6wt.%) Nb alloy, behaviour on ageing at 775°C 9-46951
 Fe-Ni-Al alloys, elastic stresses effect during decomp. of saturated solid solns. on precipitated phase particles orientation 9-39475
 Fe-Ni-Cr-Be alloy, transmission electron microscopy obs. 9-39498
 Fe-Ni-Mn-Ti martensitic alloys, pre-precip. stage during ageing 9-37283
 Fe-W alloy precipitates, fine faults and cryst. struct. obs. 9-42787
 (FeMn)₂AlC in Fe-Al alloy, X-ray diff. obs. 9-33139
 Fe-(9.3 at.%) Mo alloy, ϵ -phase precip., superimposed deform. effect 9-39497
 Ge-As solid soln., rel. to defects 9-44682
 Ge-As solid solution, new phase, mechanism 9-35243
 Ge, from solid solutions rel. to diffusion mechanism and point defects, review 9-37209
 K₂AmO₄(CO₃)₂, for separation of ²⁴³Am from ²⁴⁴Cm 9-26802
 Li₂O-SiO₂ glass, metastable precipitate formation and effect on conductivity 9-24215
 Mg-Mn alloys, creep specimens and thermally aged, of α -Mn, e. microscope exam. 9-28265
 Mg-(5.1 wt.%) Zn alloy, rel. to deform. twinning inhibition 9-46827
 Mg (0.7 at.%) Mn, in worked, and aged samples, effect on fatigue 9-30638
 Mo-(10wt.%) Fe solid solutions, after rapid cooling, rel. to annealing time and temp. 9-35207

Precipitation continued

- NaCl:Ca, rel. to low temp. conductivity 9-37577
 NaCl:Ni, electron microscope visualisation of precip. particles 9-40910
 NaCl-BaCl₂ single cryst. pulled from melt, oriented impurity precipitates 9-30601
 Nb-N system, N on Nb dislocations, kinetics 9-30744
 Nb-Zr alloy, supercond., quenched, grain boundary precip. prior to cellular decomp. 9-39499
 Ni₂ (TiAl) alloy, w.r.t. hardened by coherent and ordered precip., yielding 9-39408
 Ni alloy B-1900 high-temp., effects on exposure at 980°C 9-48913
 Pb-Na solid solns., discontinuous precip., Ag effect 9-39500
 Pb-(8.2 wt.%)Na solid solns., three mechanisms 9-35210
 Ru-Ni solid solns., of Ni, initial state and vel. const., superparamag. meas. 9-35212
 Si, from solid solutions rel. to diffusion mechanism and point defects, review 9-37209
 Ti-Mo alloys, ω -phase precipitates, effect on superconductivity and sp. ht. 9-35370
 Ti-V alloys, ω -phase precip. 9-23987
 Ti₃Al in Ti-Al alloys, t. Lp. eff. on growth, particle size line broadening 9-28400
 U-Al alloy, kinetics 9-28378
 U-Al alloy, morphology 9-28377
 U-Fe-Al alloy, kinetics 9-28378
 U-Fe-Al alloy, morphology 9-28377
 UC, from liquid Zn-Mg alloy with suspended C and dissolved U 9-36630
 UC in U-Mo 1.5% alloy, high temp. anneal, rapid quench gamma phase 9-35260
 Zn-(2 wt.%)Cu alloy, grain boundary reaction type precipitation from obs. of cracking in Cu films deposited on alloy surface 9-23957

Pressure

- see also Atmospheric pressure and density; High pressure phenomena and effects; Radiation pressure; Vapour pressure*
 in channel at onset of supersonic jet outflow 9-28067
 cylinder, circular, in cross-flow up to $Re=5 \times 10^6$, local distrib. and skin friction 9-25805
 distrib. on flow surface of deep heavy fluid, rel. to stationary waves of finite amplitude 9-23245
 distribution over front hemisphere in sphere-cylinder combination in m.h.d. flow 9-34743
 flow of water past smooth wall with single projection, wall press. fluctuations 9-46583
 flow past rough wall, press. fluctuations 9-46584
 Hartree-Fock solids and atoms, modified, calc. and virial theorem 9-39554
 hot gas in cooled channel, subsonic, stagnation press. rel. to flow profile 9-23372
 in nozzle intersecting pressure vessel, collapse analysis 9-38285
 propane -O₂ mixture, var. behind shock front, eff. of tube diameter 9-28061
 severe favourable gradient, rel. to reversion of turbulent to laminar flow 9-39036
 sonic boom shock pressure rise and overpressure level 9-40740
 streamwise gradient in turbulent flow, effect on law of wall 9-34725
 on surface in motion, due to isotropic atmospheric turbulence 9-46560

Pressure measurement

- see also Manometers; Vacuum gauges; Vapour pressure measurement*
 gas, rarefied stream, measuring systems time delay 9-43715
 gases, PVT meas. up to 10 kilobars, apparatus 9-30333
 manganin coil gauge, calibration to 60 kbar under hydrostatic pressure 9-40215
 manometer working by changes in refraction of laser beam 9-32717
 shock, by flash radiography 9-29316
 surface balance design suitable for oil-water, air water interfaces 9-34006
 transducer, capacitive 9-22045
 transducer, pneumatically operated calibrator 9-45731
 transducer, strain-gauged diaphragm type 9-25024
 transducer for infrared measurements at high pressure 9-34005
 He two-phase flow, meas. device 9-46664

Prisms, optical

- aplanatic, applic. to monochromators and spectrographs 9-48120
 deviation representation by series 9-43908
 half-, symmetrically crossed, geometrical spectra 9-27370
 image rotation methods 9-34196
 mosaic, for star field photometric calibration 9-24936
 refractive index distrib. of inhomogeneous optically transparent media 9-22469
 revolving, for image rotation 9-38410
 schlieren, formation using thermal gradients 9-34199

Probability

- see also Random processes; Statistical analysis*
 cellulose, microcrystalline, disperse system, flow birefringence study 9-34930
 collision, anisotropic, in general cylindrical geometry 9-29862
 computer program for probability density calc. of ionospheric obs. 9-43770
 distribution functions, reduced 9-45774
 distributions, joint, of the electric microfield in hot plasmas, with neglect of interactions between particles 9-27987
 generalised discrete and continuous schemes, Renyi's entropy 9-45740
 photoelectrons assoc. with thermal optical field with Lorentzian spectrum, distrib. of time intervals 9-45937
 stochastic processes, linear passive transformations 9-47767
 wave function determ. by given position and momentum probability densities 9-34028
 γ -ray dose determination from internal emitters by Monte Carlo determinations 9-27118

Procopiu effect *see Films, solid; Magnetoelectric effects; Magnetomechanical effects*

Programming *see Calculating apparatus/digital computer programmes*

Projectiles *see Ballistics*

Projectors, optical

- panoramic, for large high luminance display 9-25373

Promethium

No entries

Promethium compounds

No entries

Prominences, solar *see Sun/prominences*

Propagation *see Acoustic wave propagation; Electromagnetic wave propagation*

Propagators *see Field theory, quantum; Quantum electrodynamics*

Proportional counters *see Counters/proportional*

Prospecting *see Geophysical prospecting*

Protactinium

No entries

Protactinium compounds

No entries

Proteins

- adsorbed layers, hysteresis and stress-relax. 9-23450
 albumin bovine serum, dielec. props. of aq. solns., r.f. and microwave obs. 9-28147
 allosteric enzymes, Monod-Wyman-Changeux, model, quaternary structure and cooperative ligand binding 9-34695
 Borden acetyl cellulose, two-stage replica technique for electron fractography 9-39151
 blood vessel walls, piezoelec. eff. 9-38129
 casein colloidal solns., iso-electronic points, study with streaming current detector 9-23550
 collagen, first-order phase transition 9-23181
 collagen, molecular struct. 9-43689
 collagen, thermal transconformation, calorimetric investig. 9-23184
 collagen fibres, broad-line n.m.r. of H₂O and D₂O 9-43304
 colloidion, substrate for vapour phase deposits growth of CdSe and CdTe 9-46726
 connective tissues, eutectic struct. from electron micrographs 9-48839
 DNA, heat- and alkali-denatured spectra comparison 9-23182
 DNA in phages, filament struct. from lum. with orange acridine, obs. 9-27926
 electron microscopy of microdroplets electronically deposited from sprayed suspensions 9-42686
 e.s.r. of high-spin d⁵ systems 9-39917
 ferredoxin of Euglena, Mossbauer spectroscopy rel. to state of Fe atoms 9-32537
 ferrihaemoglobin azide, low-spin, anisotropy in g-values 9-35600
 ferrimyoglobin, electron spin-echo obs. of relax. processes 9-42457
 gelatin colloidal soln., iso-electronic points, study with streaming current detector 9-23550
 globin colloidal solns., iso-electronic points, study with streaming current detector 9-23550
 haemoglobin, e.p.r. of Fe and Cu 9-33641
 hemoglobin, electronic struct. and quadrupole splittings of Fe²⁺ 9-42459
 hemoglobin nitric oxide, Mossbauer effect 9-45296
 homopolynucleotides, energy band struct., SCF LCAO cryst. orbital calc. 9-48521
 L-isoleucine, configuration from crystal structure of bis(L-isoleucinato) copper (II) 9-26228
 keratins, statistical-mech. of α - β transformation 9-36730
 methionine shown incorporated in rhodopsin of frog by ¹⁴C labelling 9-24988
 muscle action, theory 9-41779
 muscular tissues, eutectic struct. from electron micrographs 9-48839
 n.m.r. at high field strengths, techniques and limitations 9-30155
 putidaredoxin, ⁵⁶Fe Mossbauer study, ligand symm. and electronic configuration determ. 9-32538
 radical states, irradi. induced, e.s.r. study 9-24941
 ribosomes, e. microscope exam., statistical anal. to determ. length 9-29110
 RNA, *E. coli* ribosomal, aqueous soln. containing Mn²⁺, proton mag. relax. obs. 9-40810
 L-serine, chelation effects from crystal structure obs. of bis(L-serinato)copper(II) 9-26229
 L-serine, chelation effects from crystal structure obs. of diaquobis(L-serinato)nickel(II) 9-26241
- Proton magnetic resonance** *see Nuclear magnetic resonance and relaxation*
- Proton spectra**
 computer program for proportional counter analysis 9-22660
 radiation belt, $2 \leq L \leq 3$, obs. 9-35860
 recoil proportional counting, spectrum distortion from amplifier overloads 9-42133
 recoil spectrometer data, decomposition of empirical functions 9-32250
³¹P(p,p)³⁰Si, photoproton, from 21.5 and 27 MeV bremsstrahlung 9-27693
³²S(p,p)³¹P, photoproton 9-44188
- Protonium** *see Protons and antiprotons*
- Protonosphere** *see Atmosphere/upper*
- Protons and antiprotons**
see also Cosmic rays/protons; Nuclear reactions and scattering due to protons; Nucleons and antinucleons
 auroral, obs. (1964-7) 9-35848
 beam pulse system capable of prod. 4 MeV pulses of 0.15 ns duration 9-25194
 charge exchange on alkali atoms 9-44254
 charge form factor from polarization phenomena in electron scattering in high energy region 9-25417
 diamond-type lattices, channeling charact. 9-47012
 electric dipole moment determ. from high-precision mol.-beam resonance 9-38568
 elements Z₂=20 to Z₂=30, stopping-power meas., excitation pot. and shell corrections calc. 9-33208
 e.m. form factors correl. with pp scatt. 9-29611
 energy loss in evaporated metal film 9-28439
 form factor of p, expt.-determination 9-44052
 gravitational moment 9-22624
 hadronic and electromagnetic structure of proton 9-32213
 hadronic structure of proton, from high energy pp scatt. investigation 9-32216
 internal structure hypothesis 9-22623
 Larmor freq. gravity shift meas. 9-38567
 magnetic charge, upper limits in Sun 9-24914
 magnetic form factor, from high energy large angle pp scatt. 9-32213
 magnetic moment, ratio to neutron, nonrelativistic quark model 9-38584
 motion in strong-focusing accelerator 9-32282
 pseudopotential form factor 9-48424
 radiography, contrast and resolution quality 9-22488
 radius, quasi-independent quark model calc. 9-27552

Protons and antiprotons continued

stopping power of matter, contribs. of spin, mag. moment and form factors 9-44855
K⁺p, 12 GeV/c, K $\pi\pi$ enhancement at 1780 MeV 9-34284
K⁺p, cross section meas., diffractive peak obs., M_K=7.3 GeV/c 9-25452
n-p radius difference from π prod. by p on nuclei 9-36472
N~p mass difference and tadpole model 9-29613
p-n mass differences, high and low energy contribs. 9-42061
p-n mass diff. and form factor calc. by gravitational Ward-Takahashi identity 9-38577
p-n mass difference from Reggeized tadpole model 9-40441
Al, energy losses by 0.5-30 keV p 9-30807
Al, range and ionization energy losses, Bragg's curve method meas., E_p=100-660 MeV 9-33213
Au, transmission through thin crystals, 400keV 9-42979
Bi, energy losses by 0.5-30 keV p 9-30807
C, energy losses by 0.5-30 keV p 9-30807
C, range and ionization energy losses, Bragg's curve method meas., E_p=100-660 MeV 9-33213
Cu, energy losses by 0.5-30 keV p 9-30807
Cu, range and ionization energy losses, Bragg's curve method meas., E_p=100-660 MeV 9-33213
Cu target, 12.3 BeV/c, cross sections for π , k, \bar{p} prod 9-38580
Fe, energy losses by 0.5-30 keV p 9-30807
Ge, energy distribution and channelling 9-30809
Ge, energy losses by 0.5-30 keV p 9-30807
G, stopping power for p of 0.35-5.50 MeV 9-30808
³He(p, p_{pol}), polarization meas., phase-shift anal., E_p=4-11 MeV 9-25628
KBr, energy distribution and channelling 9-30809
KCl, energy distribution and channelling 9-30809
NaCl, energy distribution and channelling 9-30809
Ni, energy losses by 0.5-30 keV p 9-30807
Pb, range and ionization energy losses, Bragg's curve method meas., E_p=100-660 MeV 9-33213
Sb, energy losses by 0.5-30 keV p 9-30807
Si, energy distribution and channelling 9-30809
Si, energy losses by 0.5-30 keV p 9-30807
Si cryst., planar channelling, energy spectrum temp. effects 9-37378
Si(Li), energy-loss and straggling, spectrum 9-30810
Sn, range and ionization energy losses, Bragg's curve method meas., E_p=100-660 MeV 9-33213
Ti, energy losses by 0.5-30 keV p 9-30807

absorption

No entries

angular distribution

photoprotons from ⁸⁹Zr(γ ,p), spin dipole reson. and isobaric splitting eff. 9-34434
¹²C(d,n)¹²N $\pi^+\pi^0$ ang. distrib. anal., unbound levels of N doublet determ. 9-25650

antiprotons

No entries

detection, measurement

beam monitor wire plane for zero gradient synchrotron 9-29678
recoil, gas proportional counter, computer programme for analysis 9-22660
H proportional counter, p energy loss through ionization 9-46137

effects

LiF accumulation of F₁-centres, 78°-380°F 9-30620
Al, stopping power for 0.6-2.4 MeV protons 9-33212
Ar, excitation induced by 0.15-1.0 MeV PROTONS 9-42337
CaO calcite, 3 GeV tracks 9-41123
Cs atom, impact ionization, cross section obs. 9-34556
Cs compound target bombard., radioiodine recoils 9-49388
GaAs, bombardment, rel. to isolation of junction devices 9-30938
H atom excitation in 2s or 2p states, asymptotic expressions for cross sections 9-34579
³He and ⁴He, proton bombardment, charge exchange and ioniz. cross sections 9-48614
In, stopping power for 0.6-2.4 MeV protons 9-33212
Ir, point defect clusters, field ion microscope exam. 9-35085
K atom, impact ionization, cross section obs. 9-34556
KCl, accumulation of F₁-centres, 78°-380°K 9-30620
KCl F-center build-up under p irradiation, vacancy source 9-32987
LiH, absorption and luminescence spectra, radiation eff. 9-33585
Na atom, impact ionization, cross section obs. 9-34556
NaCl, accumulation of F₁-centres, 78°-380°K 9-30620
NaCl F-center build-up due to p irradiation, source of vacancies 9-32987
Nb₂Sn, 1-3 MeV, on critical current density of superconducting layers 9-41184
on Si solar cell assemblies, proton induced damage 9-24077
O K-shell X-ray prod. in Al₂O₃ thin films by 20-100 keV protons 9-24073
Rb atom, impact ionization, cross section obs. 9-34556
RbCl, accumulation of F₁-centres, 78°-380°K 9-30620
Si, localised radiation damage, observation 9-33332
Si, rad. induced atomic displacements 9-48844
Zn, stopping power for 0.6-2.4 MeV protons 9-33212
Zn/Su, luminesc. decay times after proton-excitation 9-49318

interactions

see also Nuclear reactions and scattering due to protons
annihilation in hydrogen, K₁⁰K₂⁰ enhancements prod. 9-34292
gravitational moment search 9-22624
e scatt., radiative corrections 9-46061
ep- π^0 (1236), π^0 prod. meas., f_e, f₋, F₁ determ. from excitation curve 9-36471
 γ p-K₁², E(γ) up to 5 GeV 9-44008
 γ p- π^+ , ang. distrib. meas., 230-350 MeV 9-22523
 γ p- π^0 cross section and t distrib. meas., E_p=16 GeV 9-27537
 γ p- ω cross section and t distrib. meas., E_p=16 GeV 9-27537
 γ p- η η' , between threshold and 900 MeV 9-44006
 γ p- π^0 , production cross section meas., recoil p obs., E_p=220-400 MeV 9-40423
 γ p- π^0 backward angles between 700 and 150 MeV 9-44020
 γ p- ρ^0 , sum rules and convergence 9-27542
 γ p- π^+ δ^{++} double π prod. form factor in vertex 9-36470
 γ p- π^0 n, cross section determ., helicity amplitude Reggeization method 9-34304
 γ p- π^0 p baryonic resonance contributions, quark model 9-29580
K-p-K⁰(890) π -p, 7.3 GeV/c, double-Regge-pole analysis 9-48183

Protons and antiprotons continued

interactions continued

K-p at 10GeV/c, ω -prd. 9-34334
K-p- Ξ^0 K⁰ cross-section, polarization, 1.7, 2.1, 2.4-2.7 GeV/c 9-38590
K-p, 1.33 GeV/c, resonance prod. in γ π π final states 9-40447
K-p, 3-body final state, double peripheral production mechanism, 6 GeV/c 9-34283
K-p, 6 GeV/c, prod. of 3 strange particles with strangeness -1 9-36466
K-p-K⁰ ω p, modified double-Regge analysis, momentum and particle distrib. determ. 9-42063
K-p-K⁺p, K⁰n partial and differential cross sections meas., M_K=0.6-1.2 MeV/c 9-46092
K-p-K⁺ π^+ π^+ at 2.24 BeV/c 9-32178
K-p-K⁰+ neutrals, production cross section meas., M_K=7.7 GeV/c 9-38513
K-p-K⁰ π -p, Deck virtual-diffraction background calc., E_K=6, 10 GeV/c 9-42062
K-p-K⁰n high energy charge-exchange reaction using Regge poles 9-44027
K-p-K⁰(890)p, diff. cross section, spin density matrix element energy transfer depend., Reggeized helicity amplitude 9-34282
K-p-K⁰(890)n, diff. cross section, spin density matrix element energy transfer depend., Reggeized helicity amplitude 9-34282
K-p- Λ^0 + neutrals, production cross section meas., M_K=7.7 GeV/c 9-38513
K-p- Σ π partial-wave analysis, resonance formation in mass region, 1.6-1.8 GeV/c 9-46093
K-p- Ξ -K⁺, 1.7-2.7 GeV/c, cross-section and polarization obs., I=0 baryon exchange and Y^{*}(2100) prod. 9-38590
K-p- Ξ -K⁺ π^0 , Ξ + (1930) enhancement obs. 9-38590
K-p- Ξ K⁰ π^- , 1.7, 2.1, 2.4-2.7 GeV/c cross-section and polarization obs. 9-38590
K-p- π^- , K⁰ exchange particle and trajectory determ., O(3,1) symmetry analysis 9-32189
K⁰p- Λ π^+ , observation of Y^{*}(1616) 9-44065
K⁰p- Λ $\pi^+\pi^0$, observation of Y^{*}(1700) 9-44065
K⁺-p-K⁰(890) π^+ -K⁺ π^+ π^+ , 12.7 GeV/c comparison of data with diffractive prod. model 9-36468
K⁺p, 12.7 GeV/c, A₁+ Λ production 9-42092
K⁺p, 5 GeV/c, double reson. prod. of K⁰(892) and N⁰(1236) 9-42094
 σ (K⁺p-K⁰ Δ^+)=3 σ (K⁺p- π^+ Y^{*})=3 σ (K⁺p-K⁰ Δ^+) 9-29575
K⁺p-K⁰ π^+ π^+ , Regge pole exchange analysis, M_K=7.3 GeV/c 9-40420
K⁺p-K⁰(f890)p, diff. cross section, spin density matrix element energy transfer depend., Reggeized helicity amplitude 9-34282
K-p-K⁰ Ξ^0 total and differential cross sections meas., resonance formation, 1.26-1.84 GeV/c 9-22584
K-p-K⁺ Ξ^- , total and differential cross sections meas., resonance formation, 1.26-1.84 GeV/c 9-22584
K⁺p-K⁰(890)p, π , ω class determ., O(3,1) symmetry 9-22582
 Λ p, potential model analysis, effective range parameter determ. 9-38588
np, channel cross section and n spectra determ., E_n=2-10 GeV 9-29607
np, reaction channel separation at exposure of bubble chamber to 2-10 GeV neutron beam 9-27599
np- $\pi^+\pi^+\pi^-\pi^0$, 2-10 GeV, obs. of 730 events $\pi^+\pi^-\pi^0$ explained as N^{*} isobar 9-25487
 ν - μ - $\pi^+\pi^0$ total and differential cross sections for ν energy between 1 and 4 GeV 9-44021
p interactions with emulsion nuclei, 5 GeV/c \bar{n} prod. 9-48210
pd-ppn, 6.5-13.0 MeV, obs. of quasifree and sequential decay mechanisms 9-48338
pN, 16 GeV/c, effective-target-mass calc. 9-40438
pN, 22.6 and 24 GeV/c, multiple particle production 9-32214
pN, in nuclear emulsion, grey track selection method, M_p=24 GeV/c 9-29608
pn, inelastic collisions at 20 GeV energies, analysis 9-25481
pN, secondary charged particles ang. distrib., E_p=20 GeV 9-34322
pp- $\pi^+\pi^+\pi^-\pi^0$, ang. correlations correlations and distrib. meas., M_p=5.7 GeV/c 9-38581
 π p- η n, continuous-moment sum rules and absorptive Regge cuts 9-48189
 π p- π B⁻, 16 GeV/c search for high mass bosons produced near 180° 9-38541
 π p, 7.0 GeV/c, distrib. of transverse and longitudinal meas. obs. in bubble chamber expt. 9-32191
 π p, transversal and longitudinal momenta of secondaries, distrib. and mass depend., M_K=4 GeV/c 9-32190
 π p peripheral model near 1 BeV 9-29584
 π p- η n, π^0 backward emission, p_{quant} meas., M_K=1.55-3.8 GeV/c 9-34305
 π p-K⁰ Λ^0 , K⁰ exchange particle and trajectory determ., O(3,1) symmetry analysis 9-32189
 π p-K⁰ Σ^0 , K⁰ exchange particle and trajectory determ., O(3,1) symmetry analysis 9-32189
 π p-K⁰ Λ , Reggeized Σ ₀₁, Σ ₇ exchange model 9-29585
 π p- Λ (Σ)K⁰, 4.0 GeV, cross sections 9-27522
 π p- Λ (Σ)K⁰ \bar{K}^0 , 4.0 GeV, cross sections 9-27522
 π p- Λ K⁰ cross sections 790-1060 MeV, structure near Σ threshold 9-42079
 π p- Λ $\bar{\Lambda}$ n phenomenological treatment of props. of $\Lambda\bar{\Lambda}$ system 9-42110
 π p- η n high energy charge-exchange reaction, using Regge poles 9-44027
 π p- η n, η n branching ratio and coupling const. determ., cross sections fit, partial-wave analysis 9-40425
 π p- η n Regge pole model with absorptive corrections 9-32201
 π p- π^0 $\pi^+\pi^-$, 11GeV/c, analysis of reaction 9-44029
 π p- π A₂⁻, A₂- $\pi^+\pi^-\pi^+$, spin and parity anal. of Dalitz plot in A₂ region 9-29602
 π p- π A₂⁻- π^0 $\pi^+\pi^-$; branching ratio and cross section determ., M_K=3.25 GeV/c 9-34316
 π p- π p \bar{n} at 1170 MeV/c, η prod. 9-32166
 π p- $\pi^+\pi^0$, 1.7 GeV/c, 2244 bubble chamber events 9-44028
 π p- π η , energy depend. and composite model analysis, quark rearranging mechanism 9-42078
 π p- $\pi^+\pi^-\pi^0$ $\pi^+\pi^-$, g⁹ resonance obs. in mass distrib., E_K=4.7, 5.74 GeV/c 9-29603
 π p- π^0 n high energy charge-exchange reaction, using Regge poles 9-44027
 π p- π^0 nN, di-pion system in ρ mass region considered as $\pi\pi$ scatt. process 9-46100

Protons and antiprotons continued
interactions continued

- $\pi^+ \rightarrow e_1 \mu^+$ angular distrib. of high energy reaction, on basis of dipole model for A_2 meson 9-44046
 $\pi^+ p \rightarrow K^+ \Sigma^+$, K^+ exchange particle and trajectory determ., O(3,1) symmetry analysis 9-32189
 $\pi^+ p \rightarrow \Sigma^+ K^+ 3.23 \text{ GeV/c}$ Regge pole model of strange vector and tensor meson exchange 9-32077
 $\pi^+ p \rightarrow \pi^+ \pi^+ \pi^+ \pi^+ \pi^0 D^0$ meson prod. at 8 GeV/c 9-48190
 $\sigma(\pi^+ p \rightarrow \pi^0 \Delta^0) = 0$ 9-29575
 $3\sigma(\pi^+ p \rightarrow \pi^+ \Delta^+) + 2\sigma(\pi^+ p \rightarrow \eta \Delta^0) = 16\sigma(K^- p \rightarrow \eta Y^{*0})$ 9-29575
 $\sigma(\pi^+ p \rightarrow \pi^+ \Delta^+) + 6\sigma(\pi^+ p \rightarrow \eta \Delta^0) = 4\sigma(K^- p \rightarrow K^+ \Delta^+)$ 9-29575
 $\pi^+ p \rightarrow \pi^+ \eta$ at 1050 and 1170 MeV/c, η prod. 9-32166
 $\pi^+ p \rightarrow \pi^+ \pi^+ \pi^0$ ang. distrib. determ., $E_{\pi^+} = 600-1300 \text{ MeV}$ 9-40426
 $\pi^+ p \rightarrow K^+ Z^0$, 6, 8 GeV/c search for strangeness +1 baryon 9-22634
 $\pi^+ p \rightarrow \Lambda K + n\pi$, $n=0, 1, 2, 3, 4$, 5.95 BeV/c obs. 9-27518
 $\pi^+ p \rightarrow \pi^+ F$; $n=3, 5, 7$; effective mass spectrum of multipion system, Monte Carlo calc., high-energy 9-34306
 $\Sigma^+ p$, potential model analysis, 3S_1 resonance, effective range parameter determ. 9-38588
 Y_p , review of data 9-29625
Al target, 70 GeV proton bombard, search for quarks 9-34259
Be target, 12.5 GeV/c proton bombard., pion prod. cross sections 9-32184
H, proton collision, 0.5-50 KeV, parametric treatment 9-40563
H atom, proton collision, parametric treatment, quantum considerations 9-40564
He atoms ionization, 5-50 keV 9-44483
 γp 6.5-17.8 GeV, vector meson prod. differential cross-section 9-25474
 $\gamma p \rightarrow \pi^+ n$, linearly polarized photons 9-44018
Kr atoms ionization 5-50 keV 9-44483
Ne atoms ionization, 5-50 keV 9-44483
 $\pi^+ p \rightarrow K^0 \Delta$ cross section calc., new model 9-43983
Xe atoms ionization, 5-50 keV 9-44483

protons and antiprotons**interactions, proton-proton**

- bremsstrahlung, 30-200 MeV, pot. model 9-46116
bremsstrahlung at 48 and 30 MeV, using Hamada-Johnson potential 9-42100
bubble-chamber study, 4 GeV/c, $N^*(1236)$ isobar dominance 9-38569
energy, angular distrib., multiplicities of secondaries, thermodynamic model 9-42101
fireball production, parameters from quantum field theory, $E=30-250 \text{ GeV}$ 9-32215
P wave phase shifts in the nucleus at low energies 9-48208
particle spectra produced, calculation by computer program 9-36493
 $pp \rightarrow p\pi^0$, U(6, 6) symmetry and Regge-pole model, coupling const., cross section energy and ang. distrib. determ. 9-44054
 $pp \rightarrow K^+ K^- \pi^+ \pi^- (\pi^0)$ cross sections meas., K^* resonances obs., $E_p = 1.2 \text{ GeV/c}$ 9-32220
 $pp \rightarrow KK\pi\pi$, C meson width, mass, spin and parity determ. 9-22614
 $pp \rightarrow N^*(1238)p\pi^+$, 6 GeV/c, comp. with one-pion-exchange proc. including absorpt. eff. 9-40442
 $pp \rightarrow \Sigma K p$, 6 BeV cross-section obs. 9-27553
 $pp \rightarrow X^0 p^+ \pi^-$, $X^0 \rightarrow \eta \pi^+ \pi^-$ followed by η decay, individual rates determ. 9-46118
 $pp \rightarrow \eta \pi^+ \pi^-$, followed by η decay, individual rates determ. 9-46118
 $pp \rightarrow nn$, partial cross section meas., structure search, $M_p = 1.3 \text{ GeV/c}$ 9-36495
 $pp \rightarrow n\pi$ angular and momentum distrib. by a Reggeized multiperipheral model 9-42106
 $pp \rightarrow p\Lambda K^+$, cross section determ. from soft-kaon approx., $P_{lab} = 2.4 \text{ GeV/c}$ 9-38570
 $pp \rightarrow pN_{1/2}$, $I=1/2$ baryon reson. prod., diffraction dissc. mechanism 9-27566
 $pp \rightarrow \pi^+ \pi^- \Delta^+$, double-Regge-pole-exchange model. Pomeron $\pi\pi$ exchange, $E_p = 28.5 \text{ GeV/c}$ 9-38571
 $pp \rightarrow \pi^+ d$, (N_π, N_p) exchange degeneracy model, diff. cross section explanation 9-42102
 $pp \rightarrow \pi^+ \pi^- \pi^0$, Veneziano model analysis 9-46119
 $pp \rightarrow \pi\pi\pi$, Faddeev relativistic eqn. soln., $\pi\pi$ phase-shift 9-36476
 $pp \rightarrow \rho^0 \rho^0 \pi^0$ at 1.32 GeV/c, of $\pi(2190)$ mesonic state 9-34312
 $pp \rightarrow \Lambda K p$, 6 BeV cross-section obs. 9-27553
 $pp \rightarrow \Sigma^+ K^+ n$, 6 BeV, cross-section obs. 9-27553
 $pp \rightarrow m\pi$, behaviour of mean square of matrix element for annihilation determ. 9-36494

Protons and antiprotons**magnetic moment**

- quark quasilinear-independent model calc. 9-27552

polarization

- alcohol mixtures at 1°K, proton polarization obs. 9-28762
in double scatt. arrangement 9-44053
double scatt. expts. with 4.5 MeV electrostatic accelerator 9-36545
in dp scatt. at 9.5 and 21.6 MeV 9-22781
ethylene glycol with Cr (ν) complex, dynamic polarizations 9-34926
hydrocarbons, doped with diphenyl picrylhydrazil, proton polarization 9-28764
in nuclear reactions, kinematics 9-36597
source using Stern-Gerlach separation and resonant charge transfer methods 9-27555
sources and targets 9-38579
target for expts with 4 GeV 9-27556
pp scatt., multidirectional 9-44057
 π elastic scatt. at 300 MeV, recoil proton 9-46106
 $^{40}\text{Ca}(d,p)^{41}\text{Ca}$ 1.95 and 2.47 MeV reactions, comparison with three theories 9-22822
 $\text{La}_2\text{Mg}_2(\text{NO}_3)_{12} \cdot 24\text{H}_2\text{O} : \text{Nd}^{3+}$ enhancement of proton polarization due to 'solid effect' 9-24512
 $^{24}\text{Mg}(p,p)^{24}\text{Mg}$, 3-4 MeV 9-25627

production

- polarized, double scatt. arrangement 9-44053
polarized sources using Stern-Gerlach separation and resonant charge transfer methods 9-27555
yields at small angles, 70 GeV proton-aluminium interac 9-44019
p, yields at small angles, by 70 GeV proton-aluminium interactions 9-44019
P⁺, photoprod. in Coulomb field obs., lifetime meas. 9-46094
Be target bombarded by 12.3 BeV/c p. 9-38580
Cu target bombarded by 12.3 BeV/c p. 9-38580

Protons and antiprotons continued
scattering

- $A_{\pi\pi}$ meas in p-p scatt., 11-27 MeV 9-27554
 $A_{\pi\pi}$ meas in p-p scatt. at 73.5, 98 and 143 MeV, and 11-27 MeV 9-27554
back-scattering from Ti and Nb, energy distribution 9-39549
double scatt. arrangement for prod. of polarized protons 9-44053
filter, mathematical, capture yield distortion and anomalies anal. 9-32341
inelastic, field-theory calcs. rel. to scaling laws, cross-sections and momentum of the virtual photon 9-38472
meson exchange, field theoretic model, electromag. form. factors 9-38574
Regge behaviour at large angle 9-29561
regge cuts coupled, signature determ. 9-38493
Regge pole asymptotics in large angle scatt. 9-29561
target for expts with 4 GeV 9-27556
e-p, vector-meson dominance model, longitudinal and transverse cross section calc. 9-29543
e-p, p.e.m. form factors determ., 15-50 fm⁻² 9-40445
e⁺p, radiative corrections, $N^*(1236)$ resonance contrib. calc. 9-40402
ep, polarization-odd effects, $E_{\pi^+} \approx 10 \text{ GeV}$ 9-25418
ep- ηp 3.963 and 5.159 GeV obs. 9-25420
ep- ηp , differential cross section meas., wide-angle bremsstrahlung, $E_{\pi^+} = \text{GeV}$ 9-36432
 $\gamma p \rightarrow \gamma p$, space-time picture 9-48207
K-p backward scatt., double Regge pole exchange 9-34295
K-p, hybrid model explanation 9-36469
K-p, parameterizations reviewed 9-34294
K-p, scatt. length and K-matrix parametrization, Λ KN coupling const. prediction 9-42066
 $K^+ p$ backward, elastic, exchange degenerate Λ -trajectory interpretation 9-38514
 $K^+ p$, backward, Regge trajectories, exchange degenerate pairs, interference, dip cancellation 9-38508
 $K^+ p$, polarization ang. distrib. meas., $M_K = 1.2-2.5 \text{ GeV/c}$ 9-25451
 $K^+ p$ elastic scattering at 864, 969 and 1207 MeV/c 9-44015
 $K^+ p$, ang. distrib. meas., 5.2 and 6.9 GeV/c 9-40421
 $K^+ p$, on-mass shell evaluation of scatt. amplitude 9-38515
 $K^+ p$, u-channel Regge pole exchanges, structure energy and total cross section depend. 9-40429
 $K^+ p$ elastic differential cross section meas., $E_p > 8 \text{ GeV}$ 9-36480
 $K^+ p$ elastic scatt., momentum depend. of diff. slopes 9-38530
Kp, baryon compressibility coeff., calc. from cross section 9-44047
Kp, coupling const. $g_{\Lambda K n}$ and $g_{\Sigma K n}$ calc. using kaon-nucleon dispersion relations 9-32181
 $K^+ p$, s-wave scatt. length and effective range determ. 9-22586
 $K^+ p$, elastic, cross section and ang. distrib. meas. $M_K = 3.55 \text{ GeV/c}$ 9-22588
 $\mu^+ p$ or $\mu^- p$, elastic, high energy max. 17 GeV, one-photon exchange test 9-46065
 μp , elastic cross section in range $0.15 < q^2 < 0.85 (\text{GeV/c})^2$, comparison with ep data 9-46066
 μp , polarization-odd effects, $E_{\mu} 10 \text{ GeV}$ 9-25418
n-p, Kohn variational principle, heuristic derivation 9-48209
np, $A_{\pi\pi}$ meas. at 23.1 MeV 9-27554
np, differential cross section meas., $E_{\pi^+} = 4-16 \text{ GeV}$ 9-42104
np, fluctuations in differential scattering cross section at few MeV n energies 9-44060
pd, polarization expt., rel. to 3N three-nucleon systems 9-27567
pn charge exchange process, contrib. to amplitude from moving cuts 9-38578
 π -p, at 300 MeV, proton polarization 9-46106
 π -p, 1-2.5 GeV/c, optical and Regge pole models 9-27529
 π -p, 1.7 GeV/c, 3094 bubble chamber events, cross-section found 9-44028
 π -p, interference model for backward data 9-42051
 π -p, phase-shift analysis solutions compared to N_xperimental data 9-36481
 π -p elastic, near 1.04 GeV/c, momentum-depend. fluctuations, absence 9-32199
 π -p, 6, 8, 10 and 12 GeV/c polarization parameter 9-27528
 $\pi^+ p$, 6, 10 and 12 GeV/c, polarization parameter 9-27528
 $\pi^+ p$, 8-22 BeV/c, quantum electrodynamic representation 9-38440
 $\pi^+ p$, Coulomb correction on the $3/2, 1/2$ scatt. length 9-44033
 $\pi^+ p$ hybrid model explanation 9-36469
 $\pi^+ p$, ang. distrib. meas., 5.2 and 6.9 GeV/c 9-40421
 $\pi^+ p$, elastic differential cross section meas., $M_{\pi^+} = 1.7-2.8 \text{ GeV/c}$ 9-38531
 $\pi^+ p$ elastic, polarized protons at large momentum transfer 9-42083
 $\pi^+ p$ elastic differential cross section meas., $E_{\pi^+} > 8 \text{ GeV}$ 9-36480
 $\pi^+ p$ elastic scatt., momentum depend. of diff. slopes 9-38530
 πp , 898 MeV/c differential cross-section obs. 9-46105
 πp , baryon compressibility coeff., calc. from cross section 9-44047
 πp diffraction scatt., large angle, amplitude calc. 9-43989
 πp high energy, correlation between polarization and the complex zeros of elastic amplitudes 9-44000
 πp peripheral absorpt. model modified with $U_{6,6}$ symmetry, appl. to backward data 9-42082
Ar, low-energy differential elastic scatt. 9-44287
 ^{54}Fe target, subsequent implantation perturbed ang. correl. expts. 9-33494
 ^{56}Fe target, subsequent implantation perturbed ang. correl. expts. 9-33494
np cross section meas. below 3 MeV 9-29614
 $\pi^+ p$ elastic cross sections, meas. from pole extrapolation of $pp \rightarrow \Delta^+ \pi^+$ reaction 9-44056

scattering, proton-proton

- baryon compressibility coeff., calc. from cross section, slope changes for $\ln(d\sigma/dt)$ 9-44047
bremsstrahlung, prod. and obs. at 65 MeV at various angles, rel. to nuclear matter 9-40444
bremsstrahlung calcs. rel. to off-energy-shell contribs. 9-38572
cross section, differential, angular depend., $M_{\pi^+} = 8.1-12.1 \text{ GeV/c}$ 9-22625
differential cross section, phase-shift analysis, $E_{\pi^+} = 6-10 \text{ MeV}$ 9-38575
dispersion relations, broad area, subtraction for forward scatt. 9-32218
dispersion relations, forward, computed by expanding unphysical part in Chebyshev polynomials 9-34323
elastic, high energy, small momentum transfer scatt., model 9-46117
elastic, interpretation using self-consistent multiple-quark-scatt. analysis 9-27482
elastic, large angle, new formula 9-25480
elastic, Pomeronon exchange and multiple scatt. corrections 9-42105
elastic at large momentum transfers 9-34327

Protons and antiprotons continued
scattering, proton-proton continued
elastic at large momentum transfers 9-34325
helicity amplitudes, relations between them in high energy elastic scatt. 9-46117
high energy, correlation between polarization and the complex zeros of elastic amplitudes 9-44000
high energy, elastic, optical model, implications 9-32217
high energy, elastic, using phenomenological formula 9-42031
high energy (8-21 GeV/c) large angle, optical-model description 9-32216
high energy, struct., p.e.m. form factors correl. 9-29611
incoherent dplet model, N subunits decomposition and recombination, high energy, large angle 9-38576
inelastic, and interpretation 9-22626
interaction energy and repulsive core in high energy elastic scatt. 9-40446
multi-Regge baryon exchange and central interactions 9-34324
optical model for high energy elastic scatt., implications 9-32217
phase shift uncertainties at 95 MeV, new Harwell data, analysis 9-32219
polarization data, 6-12 GeV/c. b//c// 9-27528
polarization effects in high energy elastic scatt. 9-44057
pomeronchon exchange and multiple scatt. corrections for elastic scatt. 9-42105
Regge Pole, single, model; large angle, high energy, $E > 10\text{GeV}$ 9-22627
Regge pole contrib. at large angle 9-32155
triple, at 1.9 GeV obs., neither vector nor scatter meson exchange sufficient, spin important 9-38573
vacuum polarization interaction, effective range params. and triplet phases 9-40443
Yeneziano model, for large angle scatt. 9-44055
pn and pp elastic scatt. at 0.3-2.0 GeV/c. S and t channel effects 9-34326
pn, values of real and imaginary at zero energy 9-34323
pp and pn elastic scatt. at 0.3-2.0 GeV/c, S and t channel effects 9-34326
pp $\rightarrow \Delta^+ n$ at 6.6 GeV/c, pole extrapolation results for $\pi^+ p$ cross sections 9-44056
pp $\rightarrow \pi^+ p$, diff. cross section, ang. distrib., d momentum spectra meas., $M_p = 21.1\text{ GeV/c}$ 9-29612
polarized targets 9-27523
scattering proton-deuteron
cross section meas., d contains $N^*(1688)$, $E_p = 1\text{ GeV}$ 9-42103
inelastic, 200 MeV, expt. test of impulse approx. 9-29610
d aligned high energy beam production 9-29628
pd $\rightarrow p\pi\pi^-$, $N^*(1470)$ prod. at 7.0 GeV/c 9-25486
pn total cross-section by Chew-Low extrapolation tech., $E_p = 89\text{ MeV}$ 9-29609
Pseudopotential methods see *Crystal electron states*
Pulsars see *Cosmic radiations, radio/frequency*
Pulse generators see *Circuits*
Pulse-height analysers see *Counting circuits*
Pumps
see also *Vacuum pumps*
performance, application of rocket effect on bubbles 9-39068
Purkinje effect see *Vision*
Pyroelectricity
ceramics, ferroelec., pyroelec. effect study 9-39684
ferroelectric crystals, rel. to electrooptic coeff. 9-24225
ferroelectrics, pyroelec. coeff. in infrafreq. range, method and calc. rels. 9-37589
KH₂PO₄, specific heat determ. by pyroelectric method 9-30783
signal reproduction in ferroelec. recording using pyroelec. effect 9-47167
and thermoelectric effect, in. in cryst. 9-28568
triglycine sulphate, ferroelec., pyroelec. effect study 9-39684
triglycine sulphate, pyroelectric effect under γ -irradiation 9-47182
triglycine sulphate detector, i.f. response 9-45014
triglycine sulphate detector, h.f. response 9-45014
triglycine sulphate group ferroelectrics in polar and nonpolar cuts, pyroelec. coeff. and dielec. const. deriv. 9-43122
triglycine sulphate i.r. spectra, static dielec. const. and ferroelec. transition obs. 9-35615
BaTiO₃, pure and doped single crystals, pyroelec. effect study 9-39684
CSNO₃, dipole moment in elec. field and pyroelec. coeff. rel. to crystal space group 9-30977
Gd₂(MoO₄)₃, phenomenon analogous to Barkhausen effect 9-30976
RbH₂PO₄, high-temp. phase transition 9-47176
RbNO₃, dipole moment in elec. field and pyroelec. coeff. rel. to crystal space group 9-30977
Sb₂S₃ ferroelectric semicond., pyrocurrent max. at 320°K spontaneous polarization 9-41246
SbSi photopyro-effect 9-24243
TiNO₃, dipole moment in elec. field and pyroelec. coeff. rel. to crystal space group 9-30977
Pyrolysis see *Chemical reactions*
Pyrometers
use in arc solar furnace simulator power characts. determ. 9-40283
suitable cavity radiator, emissivity meas. 9-27251
microsuction, for true gas temps. 9-44523
photoelectric NPL, and International practical Temp. scale meas., 1063-2700°C 9-43803
pyroelectric detectors, temperature below phase transition region 9-27238
visual, temp. meas. accuracy 9-41845
Quadrupole crystal field interactions see *Crystals/hyperfine field interactions*
Quadrupole moments, molecular see *Molecules/moments*
Quadrupole moments, nuclear see *Nucleus/electric moment*
Quanticle theory (of chemical binding) see *Bonds*
Quantization see *Field theory, quantum/quantization; Quantum theory/quantization*
Quantum chemistry
approximate wave functions, new class, construct. by integral transform 9-40531
electronegativity in covalent systems, quantum dielec. theory, electronic dielectronic constant 9-46735
exchange reactions, coupled-channels approach 9-45413
natural orbitals, divergences, and variational principles 9-48369
Pirac treatment contrasted with Schrodinger, rel. to zero probability positions of electrons 9-24523

Quantum chemistry continued
proton in H-bonds, lingering time in wells of double-minimum potential 9-23023
three-body rearrangement scatt., solvable model 9-27174
triatomic reactions, Hamiltonian 9-39935
wave function approx., error 9-46254
C, hot atom reaction with O₂ 9-24538
Quantum counters see *Photons; Radiation detectors*
Quantum electrodynamics
see also *Electrodynamics; Electromagnetism*
atoms, excited syst., radiation emission 9-38436
broken symmetries, gauge invariance and the Goldstone theorem 9-41980
in comprehensive textbook on the theory of elementary particles 9-32116
in cosmology 9-24722
Coulomb gauge and reformulated Lorentz gauge equivalence 9-48134
Dirac electron and hidden momentum forces 9-22531
Dirac equation, transformation generalization 9-29538
Dirac particle, one-particle operators 9-29539
direct particle theory and universe response rel. to total transition rate of atomic electron 9-28982
dressed stationary states 9-34241
eikonal expansion, relativistic, rel. to elastic scatt. 9-41983
elastic scattering, high energy 9-22509
electron dynamical mass and renormalization const., bare charge and photon nonexistence 9-29518
electron interacting with e.m. field, Rayleigh-Ritz method used to derive field eqns. 9-46043
equal time commutators for the renormalized current 9-43952
Feynman rules at infinite momentum, mag. moment and 2nd-order self-energies determ. 9-41986
field theory, self-consistent; comment 9-32110
Gupta-Bleuler theory, existence of unphysical states in form of ghost couples 9-43953
heavy electron, theory 9-48133
Heisenberg Lee model, existence of unphysical states in form of ghost couples 9-43953
impossibility of quantizing Maxwell's eqns by means of a potential $A_\mu(x)$ 9-46044
impulse-energy conservation principle, variational, in Wheeler-Feynman theory 9-45758
i.r. divergences and states with definite charge parity 9-29519
Kapitza-Dirac eff. 9-34242
Lagrangian theory in new formulation 9-29517
macroscopic 9-46042
magnetic monopoles Feynman-Dyson perturbation theory 9-38438
metric, indefinite; covariant and consistent 9-38439
with modified fermion propagator, asymmetrical pair prod. 9-36420
molecules, 2, identical, 1 excited, retarded interaction long range cut-off 9-34596
nonlinear gauge 9-34243
optical rotation, higher asymmetry 9-48095
radiative corrections to μ, β decay 9-25403
radiative processes, description in terms of cosmology and direct particle theory 9-47614
scalar, gauge invariance and mass 9-32111
scalar meson scatt., branch point and vanishing or total cross-section at infinite energy 9-38440
scattering amplitudes, elastic, at infinite energy 9-40403
spin-1/2, Lagrangian extended to nonlocal but gauge-invariant form 9-43954
spinor, axial-vector current in perturbation theory 9-41985
spinor electrodynamics, axial-vector current, e.m. correct. to divergence, deriv. from field eqn. 9-27438
spinor electrodynamics, axial-vector vertex, anomalous props. 9-27437
spontaneous emission and time-symmetric electrodynamics with zero-point oscils. 9-41984
rel. to Universe 9-47612
vacuum polarization, fourth order, calc. 9-41988
vertex $\gamma\gamma$ evaluated using S-matrix theory 9-38452
Wheeler-Feynman theory, variational impulse-energy conservation principle 9-45758
e in multilevel atom interacting with radiation, derivation of kinetic eqn. 9-25402
 μ bremsstrahlung experimental test 9-22540
Quantum electronics see *Lasers; Masers; Photons; Quantum optics*
Quantum field theory see *Field theory, quantum*
Quantum fluids
criterion for distinguishing 9-34043
electron liquid in metal, screening of fixed charge 9-41124
entropy differences between ideal and non-ideal systems 9-41780
evaporation rate, temp. depend. 9-26144
hard-sphere gas, relax. times from eigenvalues calc. in Boltzmann eqn. 9-43767
hydrodynamics, quantum employing current-current commutation relations 9-46436
interacting part. syst., rigorous evolution eqn. for one-body density matrix, closing 9-34053
pair distrib. function, 0°K, and rel. to liq. ⁴He 9-41784
phase transition of homogeneous and periodic systems 9-34040
quantum gas, props. 9-34043
spin-1/2, XY model on f.c.c. lattice, partition function and specific heat, high temp. series expansion 9-39759
superfluid, macroscopic effects 9-30447
superfluidity, macroscopic wave eqns. 9-47780
velocity field definition 9-47778
⁴He liq. theory, three problems 9-23554
HeII, electron extraction from quantized vortex lines 9-34944
boson systems
Bose condensation, generalized, resulting from broken symmetry 9-38259
Bose condensation, rel. to mag. flux quantization of superconducting rings 9-28483
Bose gas, hard sphere, at low temp., pair distrib. function 9-22161
Bose gas, hard sphere, dilute, thermodynamical functions 9-47783
Bose-Einstein condensation, critical temp., effect of exciton-exciton interaction 9-45791
Bose-Einstein syst., fluctuations 9-36145
charged gas, oscillation spectrum of vortex filaments 9-38261

Quantum fluids continued
boson systems continued

- collective methods for systems with long-range coherence 9-25053
- condensed, low temp. behaviour of interacting liquid 9-22159
- degenerate, condensate stability and equilibrium fluctuations in
 - homogeneous thermodynamic equilibrium 9-45792
- energy transfer between electronic states and boson field, model 9-39562
- excitation energy calc., quasi-linear canonical transformation method 9-43765
- Fermi-Bose mixture, isotopic, phase separation 9-36146
- Fermion-Bose gas interacting, dilute, mixture, ground state props. 9-31789
- fluid, degenerate cancellation of $1/r$ and $1/r^2$ behaviour of pair distrib. functions 9-47784
- gauge-invariant formulation of grand-canonical systems, velocity invariance 9-34049
- gravitational forces, nonsaturation for N-boson systems 9-43734
- ground state energy, 1-dimens. syst. pair approx. calc. 9-22158
- ground state energy, 1-dimens. syst. pair approx. calc. 9-41785
- Hartree-Fock 2-dimens. gas, condensation in low-temp., strong-interaction region 9-45793
- hydrodynamics, quantum commutators for interacting system 9-45794
- ideal gas, condensation, generalised scaling and critical eigenvector 9-31788
- interacting, low momentum excitation spectrum using currents and densities as coordinates 9-38260
- liquid, general response props. at 0°K and at a finite temp. 9-22160
- liquid, response props., symmetry breakdown rel. to superfluid density 9-38258
- pair-correlation theory, sum rules and momentum distrib. 9-22157
- particle fluctuations 9-31787
- partition function invariance to operator similarity transformation, excitation and Einstein condensation 9-29215
- quasi linear canonical transformation method 9-47779
- quasi-free states product form, generation factors 9-22162
- relativistic quantum theory of perfect gas 9-27187
- superfluid, Green's functions and relns. between kinetical coeffs. 9-22155
- superfluid, Green's functions in hydrodynamical approx., identities 9-22156
- superfluid phase transitions in one and two dimensions 9-34048
- superfluidity, coherent state formalism 9-45795
- surface waves in presence of second sound 9-27186
- thermodynamic props. of two models, first order phase transitions 9-40258
- thermodynamics of one-dimensional system with δ junction interactions 9-47782
- treated in quantum mechanics textbooks 9-41756
- He II, boson gas model for core radius of quantum vortices 9-26145
- He II, excitation spectrum derivation, repulsive core and attractive well 9-28165
- ⁴He, liquid and superconductors, Fermi versus Bose condensation 9-24140

fermion systems

- density matrix of N-fermion system, expansion 9-38263
- effective interaction calc. using functional differentiation of Brueckner theory 9-46671
- electrons, N, one electron Hamiltonian deriv. 9-38743
- Fermi liquid theory of linear antiferromag. chains 9-49221
- Fermi-Bose mixture, isotopic, phase separation 9-36146
- Fermi-Dirac relativistic gas at high temp., equation of state, calc. methods 9-34050
- Fermi-Dirac syst., fluctuations 9-36145
- Fermion-Bose gas interacting, dilute, mixture, ground state props. 9-31789
- ferromagnetism in dense neutron Fermi liquids 9-45796
- gas, helicons' Cheronkov and collision absorpt. coeff. 9-39616
- gas, magnetized, eqn. of state, thermodynamic approach 9-25054
- gravitational forces, nonsaturation for N-fermion systems 9-43734
- hard-sphere gas rel. to ferromag. in neutron stars 9-49556
- Hartree-Fock and Hartree-Bogoliubov eqns. with exact symmetries 9-27189
- impurity ion mobility in Fermi liquid 9-46666
- ion mobility, in interacting Fermi liqs., in temp. depend. 9-40259
- level density of a Fermi system, nonperiodic perturbations of the energy-level scheme 9-38262
- liquid, impure, charged and neutral, transport coeffs. 9-47785
- liquid, nearly ferromag., effective mass in paramagnon theory 9-47786
- liquid in random scatt. centres, transport eqn., quasiparticle description in macroscopic and low temp. limit 9-25055
- liquids, thermodynamic props. in Hartree-Fock approx. 9-29216
- magnetized gas, equations of state 9-25056
- nuclear collective vibrations in low-lying nonrotational states in even-even nuclei 9-22710
- nuclear matter, with scalar boson exchange, quasiparticle lifetimes 9-48255
- nuclei, atomic, normalization of single particle wave functions in Fermi systems 9-32289
- pairing vibrs. described by generator coordinate method 9-43766
- quasi-free states product form, generation factors 9-22162
- relativistic quantum theory of perfect gas 9-27187
- specific heat of finite Fermi system with random levels, low temp. 9-27188
- spin interaction, antiparallel, two-body, variational theory 9-31790
- superconductor, transport eqns. and Fermi-liq. effects 9-35347
- treated in quantum mechanics textbooks 9-41756
- ³He, Fermi-liquid parameters in Brueckner theory 9-46671
- ⁴He, liquid and superconductors, Fermi versus Bose condensation 9-24140

Quantum generators see *Lasers; Masers***Quantum mechanics** see *Quantum theory***Quantum optics**

- 0.34m.m. wave generation by beating ruby laser R_1 and R_2 lines 9-25283
- atomic clocks 9-43866
- coherence props. of fields 9-40346
- cross-spectral densities, props. 9-34151
- crystal rotatory dispersion 9-35616
- damped harmonic oscillator, Liouville eqn., density operator eqn. equiv. to Fokker-Planck semiclassical eqn. 9-27289
- e.m. field density operator, P representation regularization 9-41755

Quantum optics continued

- e.m. field density operator, pure states and P representation 9-38225
 - equivalence theorem, reformulation in terms of Laguerre polynomials 9-47920
 - generation and amplification, conference, Hamburg (1968) 9-31868
 - heterodyne detection of scatt. i.r. radiation 9-38366
 - laser, quantum and classical stochastic processes 9-45945
 - laser amplifiers and oscillators 9-40345
 - mixed thermal and coherent radiation, twofold joint photocount statistics 9-45940
 - modern, symposium, New York (1967) 9-27360
 - molecular amplifier electronics, review 9-47908
 - multiphoton ionization, perturbed propag. kernel, theory 9-25202
 - multiquantum transitions selection rules, laser beams applic. 9-22367
 - nonlinear effects 9-47918
 - operators representation in terms of coherent states 9-45939
 - parametric amplifier and freq. converter, P-representation 9-34150
 - parametric excitation of quantum oscillator 9-29957
 - parametric gain near lattice resonance 9-25197
 - parametric generator with feedback in only one wave 9-45938
 - parametric oscillator, doubly resonant, steady-state oscillation analysis 9-47924
 - parametric oscillators, doubly and singly resonant pulsed, spectral properties 9-22364
 - phase space formulation, master equation, derivation and appl. 9-31924
 - photochemical materials, review 9-26705
 - photoelectrons assoc. with thermal optical field with Lorentzian spectrum, probability distrib. of time intervals 9-45937
 - of photomixing, double and sum frequency components do not appear 9-25355
 - one photon interaction with matter, quantum statistics 9-29393
 - photon statistics, 1st-Born, matter-field corrls. depend. 9-47923
 - polarization in resonance media, perturbation theory 9-22365
 - pulse shaping by self-focusing effect 9-47916
 - pulsed coherent radiation, self-induced transparency obs. 9-43863
 - quantum parametric amplifier, saturation in pulse regime 9-38367
 - quasistationary optical fields 9-47917
 - radiation statistics rel. to two quantum photocurrent spectra 9-29389
 - review, parametric devices and pulsed lasers 9-48011
 - scattering of partially coherent radiation, Heisenberg calc. of intensity 9-34152
 - theory, book 9-22363
 - two-layered, diffuse refl. and transmission from scatt. and transmission functions 9-24662
 - ultrashort pulse width determination by two-photon fluorescence patterns 9-25195
 - GaAs laser diodes, dependence of differential external quantum efficiency and gain on reflectivity 9-45963
 - parametric emission, spontaneous, power and bandwidth 9-25198
- Quantum statistics** see *Statistical mechanics/quantum*
- Quantum theory**
- see also *Electron theory; Field theory, quantum; Elementary particles*
 - action principle, general, using Lie algebra, interaction picture appl. 9-38267
 - algebraic, basic concepts 9-22090
 - anharmonic oscillator, uniformly valid asymptotic approx. 9-29201
 - anharmonic oscillator in functional space 9-22102
 - atom, two-level, driven, zero-temp. bath damping, density operator time evolution 9-29189
 - atomic correlation integrals, recursive and analytical evaluation 9-34031
 - atomic system, transition operator in radiative damping theory 9-32399
 - axiomatic foundation 9-22089
 - basic treatment questioned, book 9-25038
 - blackbody radiation spectrum, derivation without quantum assumptions 9-47830
 - bound states, new iteration method 9-22171
 - Breit-Pauli Hamiltonian, one- and two-centre expansions 9-27794
 - γ angular correlations, following multiple Coulomb excitation, quantum mechanical effects 9-44126
 - coherence theory 9-22305
 - complete set of observables in Hilbert space formalism, related theorems 9-29190
 - complex functional manifold, non-linear, and related Hilbert space, physical interpretation 9-43742
 - Compton scatt., intensity-depend. freq. shift 9-48131
 - critique of customary interpretation probabilistic approach 9-43738
 - cyclotron and hydrogenic orbital, overlap integral 9-37381
 - defect theory, analysis of atomic reson. struct. 9-22979
 - discrete-state continuum and continuum-continuum interac., creation of low-energy discrete state 9-38805
 - disordered systems, average propagator and density of states path integral approach 9-22101
 - early papers compilation of 17 famous articles, book 9-27172
 - effective rotational Hamiltonian for open-shell molecules 9-40582
 - eigenvalues of eigenvectors of perturbed special-function operators using matrix methods 9-38236
 - eigenvalues upper and lower bounds 9-47749
 - of electrical residual resistance, low impurity 9-41126
 - and electromagnetic background radiation, relationship 9-22100
 - electron behaviour at low levels in mag. field 9-22530
 - electron gas anomalous mag. moment in intense field 9-38264
 - electron gas with anomalous magnetic moments in intense magnetic fields 9-29217
 - electron in screened coulomb potential, high-order perturbation theory for bound states 9-45771
 - e.m. field density operator, P representation regularization 9-41755
 - e.m. field density operator, pure states and P representation 9-38225
 - expectation values, lower bounds, two new formulae 9-40241
 - formulation using currents and densities as coordinates 9-25039
 - groups theoretical treatment of non-maximally degenerate systems 9-43746
 - Hamilton's equations, Hamilton-Dirac theory 9-43745
 - Hamiltonian g.s. energy, complementary bounds determ. by integral Schrodinger eqn. 9-36130
 - Hamiltonian of independent particle system, separation of centre of mass 9-34370
 - Hamiltonian theory, search for 3-dimensional potentials 9-43751
 - harmonic classical operator, 3-dimens., SU(3) group theory, Hilbert space generators 9-31770

Quantum theory continued

- harmonic oscillator, phase representation 9-43740
- harmonic oscillators, relativistic, in nuclear physics 9-36557
- Hartree-Fock, coupled perturbed, diagrammatic analysis 9-34512
- Hartree-Fock eqn. for mol. wavefunctions in infinite internuclear separation limit 9-38816
- Hartree-Fock theory appl. to oscillator and rot. strengths 9-38817
- hidden-variable, violation of propositions quantum ordering 9-27170
- hydrogenic and cyclotron orbital, overlap integral 9-37381
- hypergeometric difference equations and Coulomb relativistic problem 9-27171
- idealized expts. and the light they shed on meas., popular article 9-47752
- integral representation, phase shifts, relativistic 9-29199
- irreversible processes, nuc. reactions as an example 9-32334
- Klein-Gordon multiparticle states, measure-theoretical description 9-41982
- of lattice dynamics 9-24000
- of lattice dynamics, condensed systems, total electronic energy rel. to nuclear displacements 9-24003
- of lattice dynamics, electron total energy expansion 9-24001
- of lattice dynamics, electronic contrib. to dynamical tensor 9-24002
- left inversed of certain definite operators in space of test functions 9-31768
- limit to the physical meas. of length relative to the form of the theory 9-43741
- linear operators for quantum mechanics, book 9-31763
- Liouville eqn. for damped harmonic oscillator 9-27289
- logic approach, quantum, to mechanics 9-22091
- many body problem with repulsive potential 9-38456
- Markov processes, relation with quantum mechanics 9-29196
- Markovian process in quantum mechanics 9-22093
- of measurement 9-31737
- measurement, single sequences, empirical acceptability conditions 9-40229
- measurement process, axioms in quantum mechanics 9-34027
- measurement theory fundamentals, density operator and wave packet reduction 9-31762
- mechanics, impossibility in Hilbert space over finite field 9-40238
- mechanics, N-body problem, quantum mechanical 9-40253
- mechanics phase eqn. derivation 9-45766
- molecular localized orbits, Hückel theory 9-32452
- multiquantum transitions selection rules, laser beams applic. 9-22367
- N-body problem, analyticity in non-relativistic quantum mechanics 9-27173
- noncanonical transition from one Hamiltonian to another 9-29192
- n.q.r. in alkali halides 9-24514
- nuclear reactions as an example of quantum theory or irreversible processes 9-32334
- orbital angular momentum, why it cannot be half-integral 9-43739
- orthodox interpretation, alternative 9-45768
- p-density matrices, necessary and sufficient conditions for N-representability 9-38224
- of paraparticles 9-31771
- particle affected by gravitational and e.m. actions, quantum relativistic energy 9-47748
- perturbation theory geometric approximation, derivation 9-46264
- phase shifts, relativistic, integral representation 9-29199
- photons, single, interference effects 9-41943
- Planck's const., lower bound theoretical estimation 9-47756
- potential, central; phase shift, scatt. length, discrete and continuous spectrum props. 9-45767
- quasiparticle and eigenfunction of inhomog. syst. w.r.t. core-electron state 9-22092
- quasiprobabilities and correlation from functions 9-27182
- Rayleigh-Schrodinger multiple perturbation theory 9-48367
- relativistic, gravitational interactions study 9-47733
- relaxation of systems with equidistant spectra 9-29193
- rotation operators, teaching methods 9-43705
- rotations, ang. coord. in regular and phase space w.r.t. kq-representation 9-43740
- spectral decompositions of functionals for quantum-mechanical sums, Dirac formalism 9-31761
- spin eigenfunctions, projection 9-38237
- spin systems, infinite vol., correl. functionals 9-22118
- spinning particle, classical treatment, book 9-41766
- spinor fields, 8-component, in lattice space, symmetry props. 9-40392
- stochastic processes in quantum mechanics, new formulation of theory 9-29197
- superposition principle modification 9-43742
- superselection rules and commutativity, operator spectrum discreteness 9-34240
- superselection rules continuous, developed from the calculus of propositions 9-29191
- system of identical particles, lower bounds to ground-state energy 9-38247
- system with infinitely degenerate bound states 9-41754
- textbook, introductory for university students 9-40239
- textbook for second course 9-40240
- textbook theoretical with emphasis on particle motion in field, scatt. and transition 9-41756
- three-body problem, isotropic harmonic-oscillator forces, exact analytic soln. 9-41764
- time of arrival meas., formal considerations 9-36127
- time of arrival meas., statistical aspects 9-31765
- time of arrival meas., suitable apparatus and soln. to relevant Schrodinger equation 9-31764
- time operation and covariant 4-dimensional commutation relations in super Hilbert space 9-47750
- turbulence in plasma, quantum mechanical interpretation 9-30213
- water vapour, vibrational-rotational energy levels quantum mechanical calc., spectrum fine structure obs. 9-23049
- WKB approximation, sufficiency condition for validity 9-38235
- WKB generalised method, second approx 9-29198
- H two-dimens. atom, symm., discrepancy in recent treatments 9-22990
- H wave mechanical, heuristic model, solns. 9-22991
- He-like ions, $2p^2ID$ and 3P weakly quantized states, Hartree-Fock eqn. perturbation treatment 9-32438
- Li atom, crystal construction 9-26239
- N_2 , $^1\Sigma_g^+$ perturbed level, deperturbed crossing Morse curves calc. 9-27863

Quantum theory continued**application methods**

- approximation methods described, book 9-40242
- asymptotic evaluation of WKB matrix elements 9-38234
- atom (bound state) in spherically symm. pot., phase integral approx. of Green's functions 9-38748
- atomic and molecular excited-state calc., many-electron pseudopotential formalism 9-32397
- atomic system, matrix elements of operators between two degenerate levels, calc. using field form of perturbation theory 9-44244
- atoms with 3-10 electrons, nonrelativistic eigenvalues of some states 9-40536
- bremsstrahlung, cross section calc. using Sommerfeld-Maue eigenfunctions 9-38462
- conical potential well, quasistationary states 9-47762
- correlation, effects and multiplet oscillator strengths for electric dipole transitions in atoms 9-42323
- Coulomb interaction in finite state 9-47763
- crystal defects, flow of defectons and impurities at low temp. 9-40927
- double-minimum potential adjustment by sums of Morse-potentials 9-22103
- eigenvalues, improved eqn. for lower bounds 9-36131
- e.m. field in gyrotropic medium 9-41849
- Feynman amplitudes, renormalized, parametric integral representation 9-41988
- Feynman diagrams, high energy behaviour via electric circuit analogy 9-41990
- Fock space of single Bose operator, generalized Bose operators 9-45747
- frequency converters, travelling wave, nonlinear dielec., derivation of Hamiltonian 9-31891
- galaxies, cold thin disk models, WKBJ analysis of free oscills. 9-40127
- galaxies and gas spheres, stability, Schrodinger operator criterion 9-35956
- gravitational interactions, gauge conditions 9-47742
- Hankel-transformed perturbation theory functions 9-29520
- harmonic oscillator, anisotropic three dimen., normalization of wavefunction, calc. of $\langle r^2 \rangle$ 9-47760
- harmonic oscillator, ladder operators appl. by means of Ostrogradsky variables 9-47759
- harmonic oscillator, linearly forced, transition probability 9-45770
- harmonic oscillator chains, momentum correlations and distrib., relaxation 9-38246
- Hartree-Fock calc, multiconfig., for lowest 3P , 1D and 1S states of C atom 9-25693
- Hartree-Fock energies, saddle point character 9-29896
- Hellman-Feynman theorem use in reduced energy deriv. calc. for asymmetric rotator mol. 9-44305
- hypervirial theorems for transition multipole matrix elements calc. 9-29895
- infinite tilted well 9-43748
- isospin crossing matrix props. 9-38490
- Kepler problem, using quantum group dynamics, Fock variables and Bacry's generators 9-43750
- laser radiation, single mode 9-43875
- laser system, time depend. soln. of master equation 9-29397
- laser theory, applic. of multi-time-correlation functions 9-43868
- linear potential problem, simple soln. 9-45772
- local moments method, energy eigenvalues calc. 9-29200
- macromolecules, quantum mechanical particle path interpretation of chain config. 9-42458
- magnetism, book 9-47223
- many body problems with strong forces, extension of Jastrow's method 9-43763
- many particle correlated integral transform trial functions construction 9-44237
- matrix elements of operators between states of two degenerate levels 9-22929
- molecular wavefunctions, linear homogeneous constrained variation method 9-32451
- molecules, diamagnetic, elec. birefringence 9-46347
- multi-time-correlation functions applied to laser theory 9-43868
- multipole moment operators, hypervirial theorems 9-29895
- operator perturbation theory applied to simple systems 9-38239
- oscillator, parametric excitation 9-29957
- Ostrogradsky variables with ladder operations used to find eigenvalues of harmonic oscillator 9-47759
- perturbation approach to Bloch electron wave functions and energy levels in mag. field 9-44865
- perturbation method, canonical, for motion integrals 9-31769
- perturbation theory and spin problem 9-34032
- perturbation theory based on exactly localized states 9-22099
- perturbation theory of nonlinear boundary value problems 9-22098
- perturbation treatment of Hartree-Fock equations, ground states in boron-like ions 9-34520
- perturbed rigid rotor, operator anal. by commutator method 9-36132
- phase operator method used in new derivation of Josephson plasma resonance 9-44927
- potential scattering, Orear behaviour 9-41772
- quantum-thermodynamic defn. of electronegativity of atoms 9-44239
- quartic oscillator, 3-D, with $e=0$, 1, 2, energy levels 9-38809
- Ramshauer effect, classical analogy 9-47713
- resonance problems, applic. of general perturbation method in wave mechanics 9-38230
- Rutherford scattering, complete correspondence identity for electron-proton system 9-41769
- Rutherford scattering, derivation of correspondence identities, development of relevant classical theory 9-41768
- scattering amplitudes, invariant, determ. from experimental observables 9-41771
- scattering amplitudes, properties, macroscopic causality conditions, formulation and consequences 9-41770
- scattering from real multipoles 9-47761
- second quantization treated in quantum mechanics textbook 9-41756
- stars, electron scatt. opacities, effect of quantum free-electron correls. 9-35972
- string oscillator relaxation 9-43749
- tachyons and their interactions, quantum mechanical description 9-43735
- transmission factor through barrier, Feynman quantum mech. calc. 9-34033

Quantum theory continued**application methods continued**

- transport equation, neutron, time depend., singular perturbation theory treatment 9-34480
- transport phenomena in moderately dense gas, quantum corrections 9-34834
- triatomic mols., vibr. dynamics 9-38807
- tunnelling used to explain electrical conduction in discontinuous metal films 9-35331
- two-body problems vibrational analysis with trial wave function that is a linear combination of oscillator states 9-40472
- two-particle amplitudes, absorptive part. as a scalar product 9-41765
- two-point function, lowest poles calc. by functional integration 9-43747
- velocity-dependent potentials in Lagrangian and Hamiltonian formalisms 9-41761
- wave function determ. by given position and momentum probability densities 9-34028
- wavefunctions for bound states and scattering 9-47754
- Wigner rotational phase-space distribution-function 9-34030
- H, photon scattering, using infinite component wave equations 9-41757
- H atom, interaction with light wave field in second order perturbation theory 9-42347
- H atom, proton collision, parametric treatment, quantum considerations 9-40564
- He atom, appl. of two new formulae for expectation values lower bounds 9-40241
- ⁶Li charge form factor, calc. using exponential wave function 9-29720

many-particle systems see *Helium/liquid; Quantum fluids; Statistical mechanics/quantum; Superconductivity; Superfluidity*

quantization

see also *Field theory/quantum/quantization*

- crystal nonlinear effects, theoret. treatment in second-quantization representation 9-23997
- of gravitational field from modified theory of general relativity 9-29184
- magnetic charge, and angular momentum 9-34026
- magnetic monopole electric charge from Hamiltonian's unitarity equivalence, interacting particles 9-38429
- magnetic monopoles, model 9-45888
- massor fields, one-component 9-45757
- non-uniform, applic. to closed-loop digital systems 9-27138
- second quantization, Hamiltonian diagonalization method 9-47751
- superconducting hollow cylinders, quantized mag. flux obs. with electron interferometer 9-41187
- superfluid circulation and flux, condensate wave function theory 9-30447
- tunnel capacitor, for charge-quantization studies 9-37548

wave equations

- anharmonic oscillators, energy eigenvalues, analytical evaluation 9-41762
- approximate wave functions, new class, construct. by integral transform 9-40531
- atoms and molecules, distribution of moments, case of wave functions with non-integer principal quantum number 9-27792
- Bohr's freq. law and Schrodinger's emission law, conflict in resonance predictions 9-45769
- condensate, theory of superfluid system quantization 9-30447
- Dirac, Klein-Gordon and Schrodinger eqns., transport eqns. in Minkowski space 9-41763
- Dirac, solution by invariant decomposition 9-41760
- Dirac eqn., intrinsic spinor tech. applic. 9-25040
- Dirac eqn. for rectilinear periodic motion of e. 9-32134
- Dirac equation, transformation generalization 9-29538
- Dirac equations at high energies, different aspects 9-29195
- Dirac particle, one-particle operators 9-29539
- discrete least squares method for solution, nuclear three-body problem applic. 9-36129
- double perturbation theory for He-like systems 9-38756
- energy variances for simple mols., lower bounds calc. 9-38814
- field theory analytic representation 9-22494
- finite and infinite component fields generated from Dirac eqn. 9-43950
- first order, for half-odd-integral spin particles 9-32122
- Hamiltonian ground level, nodelessness and symmetry 9-22096
- Heisenberg's uncertainty principle experimental violation envisagement 9-38223
- infinite component, interpretation outline of an application 9-41757
- Kemmer particle in electromagnetic field, Hamiltonian 9-38226
- Lorentz group over finite field, Dirac spinors related props. 9-22062
- lower bounds to energy eigenvalues 9-41759
- massless particle canonical wave eqn. derived from symmetric spinor formulation multiple solns. 9-48136
- molecular wavefunctions, linear homogeneous constrained variation method 9-32451
- multicentre integrals computation method 9-47758
- nucleons, binding energy calc. 9-29696
- out-of-phase scatter, asymptotic behaviour in Dirac's radial system 9-40243
- particle shock, permanent localized station hypothesis and wave train limitations 9-43744
- particles, spin $1/2$, relativistic eqns. in Pauli algebra 9-25406
- perturbation method in wave mechanics and applic. to resonance problems 9-38230
- perturbation theory for improvement of approximate wavefunctions 9-41753
- relativistic eqn. for particles with spin j in the $2[2j+1]$ -component formalism 9-22512
- scattering amplitude, analytical behaviour in Dirac theory 9-41767
- Schrodinger's eqn. soln. for dressed stationary states 9-34241
- Schrodinger, exponential soln. for potential scatt. 9-38229
- Schrodinger, for many particle systems, in spherical coord. systems 9-47753
- Schrodinger, from theory of motion of particle subject to stochastic forces 9-29197
- Schrodinger, N-body, suitability for describing nucleus 9-36556
- Schrodinger, N-body, suitability for describing nucleus 9-46185
- Schrodinger, nonrelativistic 3-body bound-state problem approx. and perturbation 9-34029
- Schrodinger, one-dimens. time-independent 9-29201
- Schrodinger coupled equations, resolution of system 9-38231
- Schrodinger eqn., approx. separation 9-27796
- Schrodinger eqn., de Vogelaere's method for integration 9-36128

Quantum theory continued**wave equations continued**

- Schrodinger eqn., proper-time, covariant space-time operators and infinite-component wave functions 9-29194
- Schrodinger eqn., validity rel. to wave normalisation 9-31766
- Schrodinger eqn. soln. for arbitrary atom 9-34510
- Schrodinger eqn. with Thomas-Fermi potential 9-25686
- Schrodinger equation, relativistic corrections 9-22094
- Schrodinger equation with Woods-Saxon potential, solution 9-38232
- Schrodinger for two oppositely charged particles in a magnetic field, partial separation 9-38233
- Schrodinger non-selfadjoint scattering eqn., solution expansions 9-31767
- Schrodinger quantum mech., fluid analogy 9-22097
- Schrodinger rel. to tensors in Hilbert space 9-45732
- Schrodinger representations, generalized, and appls. 9-38227
- Schrodinger time independent used to calc. molecular vibrational transition in high energy collision 9-34698
- spin, Schrodinger eqn. derived from classical concept 9-47757
- spinor formalism, intrinsic, development, applic. 9-25040
- superfluid, macroscopic eqns. 9-47780
- symmetry-projected single-determinant wavefunctions, density matrices 9-47755
- three-dimensional analytic potential, WKB method 9-25042
- two-centre Coulomb integrals, analytic expression 9-44236
- variational principle applied to density matrix 9-25041
- variational wavefunctions, sum rules 9-41758
- wave function approximation error in quantum chemistry 9-46254
- wave function determ. by given position and momentum probability densities 9-34028
- wave picture of matter criticised 9-43738
- wavefunctions for bound states and scattering 9-47754
- wavefunctions of identical particles, para- and nonpara-statistical 9-38228
- H, functions describing levels with width 9-29977
- H₂⁺ three parameter wave function, investigation 9-23048
- ³H, improved S-state wave function 9-27623
- ³H, improved S-state wave function 9-40476
- He-like atom, Schrodinger soln., new coord. system 9-40567
- for He liq. variational calcs., Bose-Einstein condensation 9-39122

Quarks

- alpha fusion catalysis in sun, without neutrino prod., rel. to energy output 9-45677
- baryon resons. classification into broken SU(6)×O(3) scheme using quark-diquark model 9-32227
- boson resonances, quark model, a review 9-40432
- commutation relations abstracted from quark-model commutators 9-22543
- cosmic ray, inducing nuc. fis., method to limit abund. in products 9-25491
- in cosmic rays at sea level, search procedure and results 9-32137
- and dualities, categorizing 9-46067
- fermion of spin $1/2$, quark model new predictions 9-38477
- field theory, bilocal, appl. to quark and antiquark composite systems 9-43977
- generalized model based on tower of quarks with all possible spins and parities 9-43976
- interactions, weak, pseudoscalar coupling magnitude 9-27471
- Maki-Hara model for elementary particles, comment 9-46068
- meson model, relativistic formulation 9-44002
- meson-baryon interac. with production of positive parity meson 9-46085
- model, nonstatic relations between baryon mag. moments 9-48205
- model for 0⁺, 1⁺, 2⁺ meson resonances decay 9-36485
- model for baryon-baryon and baryon-antibaryon scattering 9-22559
- model of baryons mass spectra, eigenfunctions 9-27546
- parafermi statistics outlined, review 9-22544
- polarization expts. and additivity assumption of model 9-43978
- search, using 70GeV proton bombard. of Al 9-34259
- stable, search by u.v. spectroscopy and oil-drop charge meas. tech. 9-38476
- stellar spectra, transitions prediction 9-38773
- SU(3) triplet particles responsible for cosmic-ray observations 9-44067
- three-triplet model, for elementary particles, comment 9-46068
- vector mesons, e.m. mass spectrum in broken SU(3) ⊗ SU(3) with quark model 9-44040
- $p\bar{n} \rightarrow \pi^+ N^+$ cross-section predicted in quark model 9-29580
- $p\bar{p} \rightarrow \pi^0 p$ baryonic resonance contributions, quark model 9-29580
- ρ magnetic moment calc., agreement with vector dominance calc. 9-34315

Quartz

- 30 to 60% magnetite, galvanomag. effect 9-43500
- α , photoelastic constants obs. 9-37683
- α - β transition, small-angle X-ray scatt. 9-39931
- acoustic surface wave mixing on α -quartz, obs. 9-48950
- acoustic surface wave propag., 30-800 MHz 9-37319
- Bechmann's number for harmonic overtones of thickness-shear vibs. 9-31848
- birefringence and appl. $\lambda/2$ and $\lambda/4$ plates 9-28655
- at boiling temp., loss of u.v. transparency, causes 9-36880
- bonds, broken on fresh surface, conc. 9-46734
- Brillouin scattered lines, polarization levels 9-33570
- brown synthetic, e.p.r. of Fe³⁺ 9-41426
- ceramics, strength as influenced by caking and crystn. 9-48908
- commutation, net energy input rel. to fineness 9-26374
- crystal vibrator, singly rotated, force-freq. coeff. chart 9-37596
- crystal viscometer, resonant freq. changes with pressure to 8000 atm. 9-41809
- crystalline, stimulated Brillouin scattering at liquid M₂ temp. 9-26098
- Dauphine twin boundaries, electron and X-ray diffraction contrasts 9-30572
- defect synthesis for γ irradiation 9-26273
- dielectric breakdown and recovery under shock wave compression 9-47189
- diffusion paths of ions during electrolysis, rel. to conductivity 9-39387
- dislocation centers on 0001 surface, struct. 9-42839
- e.p.r. of Fe³⁺ in brown synthetic quartz 9-41426
- fibres, fused, for u.v. transmission 9-48104
- films, pyrolytic, nature of breakdown, 77° to 223°K 9-33382
- fused, i.r. spectrum compared with that of BeF₂ glasses 9-41375
- fused, stimulated Brillouin scattering at room temp. 9-26098
- fused, thermal conductivity 9-41098

Quartz continued

- fused, thermal conductivity, $0 \rightarrow 650^\circ\text{C}$, precise meas. 9-37371
 fused, transient colour centres 9-42854
 glass, crystn. and struct., i.r. refl. spectroscopy obs., 1000-1300°C 9-26175
 growth, trapping of colloidal inclusions 9-37043
 incorporation of di- and trivalent Co interstitials 9-28282
 i.r. absorption spectra meas. in fused amorphous quartz, $9\ \mu$ 9-26740
 lattice defects, meas. by X-ray moiré topography giving mismatch between two crystals 9-26287
 neutron diffraction, mean intensity depend. on crystal current and vibrating freq. 9-26247
 optical activity 9-43211
 paper, insulating material in space, outgassing behaviour obs., 100-1800°F 9-38173
 phonon interactions at degeneracies of acoustic phonon branches 9-48947
 phonons, thermally emitted, obs. 9-30761
 piezoelectric const., temp. variation 9-33397
 plate, AT-cut, with metallic electrode strip, shear-flexure-twist vibrs. 9-22236
 plates, AT-cut, beveled, thickness-twist vibrs. 9-29259
 plates, temp. depend. of sound vel. 9-46988
 polycrystalline, pressure derivatives of elastic props. 9-39394
 pulsed-radiation-induced current in cryst. and fused samples 9-44998
 as Q modulator, electro-optical, advantages 9-40347
 α -quartz, light scatt. by elastic surface waves 9-47307
 α -quartz, longit. hypersonic damping, obs. 9-26759
 quartz comminution, net energy input rel. to fineness 9-26375
 α -quartz, Raman spectrum at high press. 9-31118
 radiolysis cells, gas phase, effect of temp. on saturation currents 9-33683
 Raman linewidth and shift temp. dependence in α -quartz 9-24428
 Rayleigh wave dispersion 9-48959
 rod, light depolarization effectiveness 9-43210
 second harmonic generation 9-39791
 shock-induced preferred disorder 9-42938
 silica, fused, longit. hypersonic damping, obs. 9-26759
 spores and terraces occurring on hydrothermally grown crystals 9-44642
 synthetic, dislocations assoc. with plastic deform. and recovery, transmission electron microscope obs. 9-40955
 synthetic, growth, hydrothermal method 9-39201
 synthetic cryst., inhomogeneities, optical investig. 9-37165
 synthetic crystals, quality determ. by neutron diff. 9-37150
 thermometers, ranges, sensitivity and fidelity limits 9-25134
 twin boundaries, Brazil, X-ray topographic obs., diff. contrast effects 9-42845
 u.s. waves, collinear longit., interaction 9-46986
 vibrating crystal, modulation of monoenergetic neutron beam 9-30549
 wetting by hydrophobic liqs., effect of adsorbed water 9-34978
 in whitewares, particle strain meas. by X-ray technique 9-23869
 X-ray spectrochem. analysis, 2θ values 9-47485
 zero-field e.p.r. of Fe^{3+} 9-43279
 Sm activated glass, luminescence and absorption 9-41407

Quartz resonators see *Piezoelectric oscillations; Resonators; Transducers*

Quasars

- see also *Cosmic radiations, radiofrequency; Cosmology; Galaxies; Stars*
 3C230, new radio position shows it is not optically identified 9-41652
 3C273, fluctuating component, estimation of intensity 9-43582
 3C454.3, periodic optical var. with possible period approx. 340 days 9-45639
 3C 270, 3C 278, flux density at 40 cm. obs. and calc. using computer program 9-24821
 3C 48, estimate of angular dimensions from interplanetary scintillations 9-45636
 absorption lines in spectra rel. to red-shift and screening hypothesis 9-31567
 brightness increases of two new sources 9-38054
 extragalactic radio sources in the i.r. 9-29051
 faster-than-light particles as explanation, popular article 9-45748
 flux variations of 5 sources at 6.6 cms, obs. and model 9-24820
 Hoyle-Fowler model 9-27055
 Hoyle-Fowler model 9-27057
 Hubble plot anomaly explained by gravitational lens image model 9-41654
 interferometer obs. with trans-Pacific baseline at 2.300 MHz 9-41667
 i.r. emission, review of present knowledge 9-29044
 linear polarization obs., 11-20 cm wavelength 9-24830
 linear polarization props. and analysis, 11-20 cm wavelength 9-24831
 number density, models and ionization of intergalactic H 9-36004
 plasma stability mechanism 9-41651
 positions, accurate, by plate overlap method 9-31566
 positions for 41 sources between declinations $+20^\circ$ and -33° 9-31568
 quasi-stellar objects considered as radio-galaxies, applic. of fluctuating mag. field mechanisms of ionized clouds 9-29043
 radio spectra of revised 3C catalogue sources 9-40157
 red-shift anal., method rel. to combination of cosmological and gravitational factors 9-43583
 red-shifts, emission and absorption, expanded list 9-41653
 redshifts, distance dependent? 9-27058
 redshifts beyond $z=2$, detectability 9-45638
 redshifts distribution 9-45637
 review 9-38055
 review 9-36005
 scintillation of 3C273, intensity of fluctuating component 9-43582
 scintillation of 3C 48 giving its angular dimensions 9-45636
 spectra, expected strengths of 21 cm redshifted absorpt. lines, possibility of detect. 9-49565
 spectra, radio, distinguishability from radio galaxies 9-29040
 stability of quasistatic solns. for gravitationally interacting mass system 9-24734
 synchrotron rad., Scheuer luminosity meas. method queried for moving sources and quasars 9-27054
 synchrotron radiation losses in self-absorbed radio sources 9-27056
 UVB system data for 14 sources south of $+20^\circ$ declination 9-31565

Quasi-particles see *Excitons; Magnons, Phonons, Polarons, etc.*

Quenching, optical see *Luminescence*

Quenching, thermal see *Heat treatment*

Racah coefficients see *Quantum theory*

Radiation

- see also *Acoustic radiations; Bremsstrahlung; Cherenkov radiation; Electromagnetic waves; Electrons/radiation; Emissivity Radiative transfer; Stars/radiation; Sun/radiation; Sunlight*
 from accelerated charge, at rest or freely falling rel. to gravitational field 9-38214
 amplification by plasma jet 9-32633
 atmospheric, net, study over five years, Delhi, India 9-28883
 atmospheric and solar, Kew Observatory work review 9-47545
 black-body, in transparent medium, relativistic coherence theory 9-22076
 blackbody cavity, distrib. in moving frame of reference 9-40156
 from bosons in field of two plane linearly polarized e.m. waves moving towards each other 9-41851
 of a charge under influence of constant external force 9-25178
 colloid, capillary-porous, distrib. and energy absorbed for bilateral irradiation 9-23546
 cylindrical targets, attenuation factor for scattered radiation 9-44850
 from density inhomogeneities in plasma 9-32667
 from dipole, vertical, placed on boundary of H-plane semi-infinite impedance system 9-43817
 from elements of cylindrical arch rectangular base, local angular coeff. calc. 9-40281
 field, nonstationary, direct line solution of transfer equation 9-25060
 fluid, statistical props. of scattered radiation 9-42474
 flux, 0.3 to $3\ \mu$, Cosmos 149 meas. 9-40031
 gas, non-isothermal, radiant energy emission calc. 9-36687
 gravitational, investigation by successive approximations 9-45749
 interacting with electron system, Green's function analysis 9-32402
 interaction with two level system 9-25701
 i.r. gaseous radiation interaction with thermal conduction 9-30341
 magnetospheric cyclotron, Doppler shifted calc. 9-49471
 molecular resonance, and intersecting fields, influence of constant electric and magnetic fields 9-44303
 from plasma, transverse and longitudinal generation and absorption 9-28001
 plasma-radiation field quantum interaction 9-32598
 rectangular surfaces intersecting, angular coeff. calc. 9-25025
 rotational effect on nonlinear crystal 9-24363
 scalar, e.m. or gravitational, jets, extended source construct. 9-22067
 solar e.m., total downward flux rel. to height 9-41519
 source image, investigation using multielement radio interferometer with autonomous reception 9-43810
 sources, cavity type with specular or diffuse wall reflection, comparison 9-40280
 total at earth's surface, time var. rel. to cloudiness 9-40027
 transient, originating at electron transience from vacuum to dielectric, photographic registration 9-24208
 tunable far-i.r. rad. generated from difference freq. between two ruby lasers 9-31955
 v.l.f., from subsequent return strokes in multiple stroke lightning 9-37922
 Ag thin films, roughness, correl. with plasma resone. radiation 9-44621
 from Nd laser, 2nd harmonic conversion coeff. rel. to space time distribution 9-40361
 from SiC and GaP pulsed diodes, props. 9-38387
 SnI₂ vapour, spectral and temp. depend. 9-42612
- heat**
 absorption, gross and net, rel. to rad. laws 9-48087
 from air behind shock wave 9-42560
 atmospheric i.r. flux divergence, 12-44.44, μ spectral and vertical distribution 9-35822
 from black body cylindrical cavity with temp. gradient, radiating power 9-41837
 blackbody radiation spectrum, derivation without quantum assumptions 9-47830
 blackbody radiation with transparent medium, relativistic coherence theory 9-38312
 Earth, Cosmos 149 rad. surface temp. obs. 9-40030
 emissivity of materials, up to 100°C , meas. 9-28678
 emissivity of non-diffuse cavity sources, calc. 9-31859
 far-i.r. background rad. in explanation of galactic γ flux, eff. on cosmic rays 9-26989
 field calc. allowing for transmission functions 9-40028
 field characts. for triangular duct 9-22167
 field of open cylinder of infinite length 9-40282
 to finite sized bodies, calc. of inside temp. via surface temp. 9-22297
 flame characts., layer-wise obs. 9-22294
 flux, 3 to $14\ \mu$, Cosmos 149 meas. 9-40031
 flux formation in cloudy conditions 9-35821
 in gap between core and cladding; cylindrical nuclear fuel element thermal stress analysis 9-25120
 interchange between surfaces, effect of direction and wavelength depend. surface props. 9-22273
 i.r. radiative equilibrium under large path length conditions 9-23392
 i.r. sky flux obs. and correl. with local conditions 9-41523
 i.r. spectra, computer analysis 9-41460
 laws rel. to stimulated emission 9-45872
 mixed thermal and coherent radiation, twofold joint photocount statistics 9-45940
 with photon scattering effects, transport eqn. soln. 9-22109
 polarization in anisotropic media 9-43800
 radiant exchange in chamber of square cross section, local charact., calc. 9-38313
 sea-sky balance obs. 9-31317
 shock layer, non-gray, stagnation-point, cooling and self-absorpt. effects 9-23383
 solid body, rel. surface props. 9-22275
 solids, 1-dimens., treated, transient surface temp. and conduction soln. 9-22286
 surface normal irradiation, characteristic reflection curve analysis 9-22276
 terrestrial, 7-15 μ , spectra, Cosmos 45 obs. 9-31315
 terrestrial outgoing spectra, Cosmos obs. rel. to meteorological data 9-31314
 transfer, nongray, nonisothermal, in optically thin region 9-22274
 transfer to ablation heat shields of entry vehicles 9-22304
 Wien displacement law, wavelength rel. to wavenumber derivation 9-31858
 He II quasiparticle radiation, pulsed carbon film heater obs. 9-23569
 W strip lamp spectral radiance standard 9-25377
- Radiation belts** see *Atmosphere/radiation belts*

Radiation chemistry *see* *Chemical effects of radiations/ionizing radiations; Radiochemistry*

Radiation damage *see* *Physical effects of radiation*

Radiation detectors

see also *Bolometers; Photometry; Radioactivity measurement*
 absolute radiometer, 0.4-2.0 μm 9-27239
 acousto-optical, selectivity and sensitivity in gas analysers 9-37851
 air gap conditioning system, patent 9-32240
 bolometer, thermistor, for monochromatic light meas. 9-47832
 γ ray telescope with large area wire spark chambers, balloon-borne 9-38128
 γ -ray, self-powered, in linac beam loss detection system 9-36546
 γ -ray, suitability of GaP-GaAs system at room temp. 9-26539
 computers in radiation meas. 9-22649
 dosimeter, thermoluminescent phosphor, 10^{-3} - 10^3 R, patent 9-29666
 dynamic properties, probability analysis 9-45873
 gamma, semiconductor material requirements 9-25522
 Golay cell, compact rugged, stable optical system 9-29473
 heterodyne detection of scatt. i.r. radiation, quantum theory 9-38366
 infrared, thin film, transient temp. response 9-36207
 i.r., chopper-modulated system, error analysis 9-29321
 i.r., use 9-41839
 i.r., very-far, bolometer with high-responsivity, theory construction and performance 9-40284
 i.r. analyser, two-wavelength, patent 9-38314
 i.r. photocell, Se heterojunction with AgSe-In solid soln. 9-41274
 photo-, for autocollimators with beam splitters, selection 9-36408
 photographic emulsion, r.m.s. error in meas. 9-25391
 photon, windowless, for soft X-ray and extreme UV, Spiraltron matrices 9-36527
 photovoltaic, quantum heterodyne detection of scatt. i.r. radiation 9-38366
 pyroelectric, triglycine sulphate, h.f. response 9-45014
 pyroelectric, triglycine sulphate, h.f. response 9-45014
 radiometer, continuously recording, for night sky 1 to 2 μm emissions 9-33807
 radiometer based on thermopile 9-22277
 radiometry, optical resource letter 9-40380
 semiconductor, thermal, spectral characts. improvement 9-43235
 for space, review 9-45578
 spectral reflection factor meas. equipment for use in 15-2100°C and 4000-12000 Å range 9-38311
 superconducting, based on Josephson effect, operating characts. 9-49059
 for surface radioactive contamination, patent 9-48229
 thermograph, applic. of columnar thermopile and photoelec. multiplier 9-38397
 thermoluminescent dosimeter of $\text{CaSO}_4\text{:Mn}$ +impurity ions, preparation, patent 9-27596
 thermoreceiver transient response calc. 9-47831
 triglycine sulphate pyroelec., h.f. response 9-45014
 triglycine sulphate pyroelec., h.f. response 9-45014
 tubes, high voltage supply, using Cockcroft-Walton multiplier, patent 9-48228
 u.v. ZnS Schottky barrier 9-33347
 Ag-GaAs Schottky-barrier u.v. detector 9-43125
 Ge, impurity and defect energies and conc. determ. by highly sensitive photosensitive technique 9-39644
 Ge, specification, NBS report 9-33280
 Ge i.r. imaging sensor, monolithic using large scale integration 9-47833
 Ge(Li), coaxial, charge trapping effects 9-36517
 Ge(Li), coaxial, well-type, for sum spectra of coincident gamma rays 9-36524
 Ge(Li), energy linearity and resolution, theory and experiment 9-36516
 Ge(Li), signal time meas., filter and discriminator techniques comparison 9-36519
 Hg-CdTe alloy system, magneto-optical obs. of band struct. and cyclotron reson. 9-39807
 LiF dosimeter system performance, lattice defect structures effect 9-49610
 Pb-SnTe alloy system, magneto-optical obs. of band struct. and cyclotron reson. 9-39807
 Si, nuclear, NBS report 9-33280
 Si amplifying, for portable gamma-ray survey meters 9-36525
 Si(Li), energy linearity and resolution, theory and experiment 9-36516
 Sn thin supercond. films as high-speed detectors 9-35367

Radiation effects *see* *Biological effects of radiations; Chemical effects of radiations; Physical effects of radiations*

Radiation monitoring

see also *Dosimetry*
 in-core detector, for intense pulsed rad. 9-36641
 pulse radiolysis apparatus for monitoring at 2000 Å 9-32239
 reactor, liquid metal fast breeder, fast flux test facility instrumentation requirements 9-36638
 reactor, pressurised water, simulated, for Rh self-powered neutron flux monitor calibration 9-36635
 for reactor engineer, in textbook 9-34507
 splash protection of large-area water-viewing detector 9-48366
 thermoluminescent dosimeters as personnel monitors 9-24948
 ^{235}U in Cu container, energy distrib. of neutrons at 100 m 9-36621

Radiation pressure

see also *Acoustic streaming*
 acoustic, on gas bubble ascending in liquid 9-23438
 array, periodic, plane infinite, near field calc. 9-22248
 liquid thermal diffusion, force orientation depend. on speed of sound and conductivity 9-46622
 plasma, laser produced, confined 9-46490
 solar, forces induced on satellite mats, reflectance model estimation 9-24712

Radiation protection

see also *Radiation monitoring*
 6 MV X-ray source, leakage radiation 9-24944
 aerospace nuclear safety 9-25669
 barytes concrete, props. 9-24945
 cylindric shell-shaped iron shield with air-gap, containing ^{60}Co , dose build-up 9-34506
 fast neutrons shielding, exp. studies 9-32274
 fission product containment after reactor accident 9-40529
 high energy particle accelerators shielding 9-32281
 neutron shielding during 80 MeV α bombard. of ^{187}Ta target 9-34474

Radiation protection continued

neutron shielding for pulsed source from electron linear accelerator 9-32277
 packaging for radioactive liquids and gases 9-22917
 personnel shield, movable, for access to hot cells 9-24947
 photon beams, 4 and 5 GeV, transverse shielding calcs. 9-42156
 for reactor engineer, in textbook 9-34507
 screens, for reactor engineer in textbook 9-34509
 secondary, due to 6 MV X-ray source 9-24943
 shield composition effects on n, γ intensity distrib. 9-31688
 shielding, review 9-32372
 shielding of 15 MeV neutrons 9-32273
 synchrotron shielding embankment effectiveness meas. using cosmic ray μ , obs. 9-22694
 techniques reviewed in textbook for reactor engineer 9-34508
 in X-ray diffraction of substs., by means of a polymer coating 9-46767
 X-ray equipment in hospitals, regular surveys for safety 9-24946
 γ shielding studies at 10 MeV with γ from positron annihilation 9-22528
 ^{238}U , resonance self-shielding factors for energy groups 5 eV to 2 keV 9-22890
 Pb- polyethylene shields, fast-neutron attenuation, S, calc. 9-33963
 SiO_2 shields, transport calcs. for incident monoenergetic neutrons, 50-400 MeV 9-48234

Radiative recombination *see* *Luminescence*

Radiative transfer

air, end-wall heat transfer, shock-tube meas. 9-23395
 air, heated, basic radiative proc. and spectral props. 9-23400
 air, heated, integral props. for spectrum and intervals, 4000-20000°K 9-23401
 Antarctic ice, diffusion, extinction coeff. rel. to grain size 9-39992
 atmosphere, planetary, long wave, calc. 9-31332
 atmosphere, solution to integral equations 9-31293
 atmospheric, measurements used in indirect sensing, statistical information content 9-24660
 atmospheric heat exchange, determ. from strong and weak water vapour absorption 9-24638
 configuration factors vector properties and influence charts 9-34056
 IN dielectric media on opaque substrate 9-26671
 diffuse refl. and transmission of time-dependent collimated light, by a finite inhomogeneous atm. 9-45582
 diffusion of high-density radiation in unidimens. medium 9-41788
 dissipation function by the invariant imbedding eqn. 9-45583
 duct, triangular, radiation field characts. 9-22167
 electron gas, Maxwellian, relativistic Boltzmann eqn., for photon transport with noncoherent scatt. 9-31792
 e.m. waves scatt., spectral theory 9-29346
 exponential integral approxs., accurate and efficient solns. 9-47792
 furnace, radiative heat transfer between gas and wall, Monte Carlo 3D analysis 9-34832
 gas, hot optically thick, in outer layer 9-48664
 in gas, of heat, effect on acoustic waves 9-48663
 gas, resonance rad., higher decay modes, eigenvalue problem 9-34839
 heat, cryst. growth interface stability in presence of rad. transfer 9-37057
 heat, in closed system of bodies separated by light transmitting medium 9-25113
 heat transfer simultaneous with conduction, 2 absorbing media, intimate contact 9-36210
 heat-transfer equation for scattering medium, numerical solution 9-22279
 in homogeneous cylinders, effects of geometry on source functions and emergent line intensity profiles 9-45801
 inhomogeneous atmosphere, soln. without redistrib. of freq. 9-47791
 integral eqn., analytically solvable, line shapes and h.f.s., high optical depth 9-31798
 inverse bremsstrahlung cross-sections in screened potentials, classical calcs. 9-46271
 i.r., equilibrium under large path length conditions 9-23392
 irreversibility, study of spectral line emission from two discrete levels with influence of continuum 9-46272
 magnetic monopole to elec. charge 9-38438
 molecular scatt., eqn. inversion for atm. ozone distrib. 9-28870
 non-scattering medium, moment and discrete ordinate methods 9-47789
 nongray absorbing and emitting medium, exact soln. 9-31797
 photon, atmosphere-ocean system 9-36149
 photon scattering effects, transport eqn. soln. 9-22109
 in plane parallel homogeneous medium, numerical method applicable to nonconservative scatt. 9-36223
 plane parallel source illuminated by external source, multiple scatt. 9-36360
 plane shock wave in homogeneous medium, changes in boundary conds. 9-22269
 plane-parallel atmospheres, multiple scatt. 9-36362
 in plane-parallel media, e.m. wave multiple scatt., conference 9-25151
 planetary atmospheres, radiative terms in thermal conduction equation from O and CO net emission 9-26894
 plasma, nonequilibrium, total and local radiative energy losses rates 9-32627
 pure radiation news function in general relativity 9-38220
 regular thermal conditions in solid bodies 9-44844
 resonance line, from a point on the boundary of a halfspace 9-44272
 resonance rad., higher decay modes, eigenvalue problem 9-34839
 resonance radiation through optically thick layer 9-36150
 semiclassical theory of atom in its own radiation field 9-38437
 solids in contact with one another, by e.m. tunneling 9-37372
 in spectral line, nonlinear, nonstationary problem 9-43924
 statistical simulation of diffusion by Russian roulette technique 9-22166
 surface interchange, effect of direction and wavelength depend. surface props. 9-22273
 surface to surface, energy, conference 9-34094
 thermal, transfer functions of atmosphere 9-40030
 thermal conductivity equation in presence of radiative energy transfer 9-27245
 thermophysical aspects, conference 9-26014
 Thomas-Fermi potential for atomic cross sections for continuous radiation emission and absorption 9-46271
 transfer equation for nonstationary radiation field, direct lines solution 9-25060
 tropospheric and stratospheric aerosol attenuation 9-40014
 Venus atmosphere, rel. 8-14 μ limb darkening 9-24874
 X and Y functions, calc. using soln. of integral eqn. 9-47790

Radiative transfer continued

- X-ray source in optically thick environment, spherical nebula case 9-36014
- Ar discharge plasma numerical soln. rel. to self-absorption eff. 9-27978
- CO₂-H₂O mixtures emissivity, analytical calc. 9-26028
- H plasma, Planck and Rosseland coeffs., emissivity, line and continuum rad. 9-48554
- O line near 63 μ , thermosphere, thermal effect 9-40081

Radiators see *Electromagnetic waves/radiators; Transducers*

Radicals see *Free radicals*

Radioactive dating

- Alpine micas, fission track ages 9-47509
- apatites, fission track ages 9-45462
- artificially produced alpha-recoil tracks in albite 9-47511
- chondrites (H group), ⁸⁷Rb-⁸⁷Sr age 9-43635
- fission track etch pits studies of australite 9-45463
- foraminiferal ooze deposits in Southern Ocean 9-47508
- glacier, ²¹⁰Pb small-sample method 9-47512
- micas, 250 and 2500 m.y., fission track ages 9-47510
- time scale calibration, corrections applic. 9-24623
- tree rings, ¹⁴C age determ. 9-39991
- k-Ar geochronology, residual gas in mass spectrometers 9-43362
- Pu-Xe decay intervals for stone meteorites, and U content 9-45675

Radioactive tracers

- storm runoff, instrumentation 9-24659
- turbulent flow of water in a pipe, tracer mixing obs. 9-28086
- ¹⁴¹Ce diffusion of fission products in α -Al₂O₃, obs. 9-30623
- ¹¹¹In, in biological macromols. in soln., conformation from gamma ang. correl. patterns 9-32536
- ¹⁵³Sm, diffusion of fission products in α -Al₂O₃, obs. 9-30623
- ¹⁴⁷Pm, diffusion of fission products in α -Al₂ obs. 9-30623
- As diffusion in Si 9-37208
- Bi:Sn, distrib. coeff. and acceptor valency determ. 9-43002
- ¹⁴C, particulate, of stratospheric motion 9-28896
- Cu diffusion in Li, interstitial-like 9-39384
- ²⁴Na, cooling-water flow of power station pump meas. 9-28084
- ⁹⁰Nb, diffusion of fission products in α -Al₂O₃, obs. 9-30623
- ⁹⁰Sr, particulate, of stratospheric motion 9-28896

Radioactivity

- see also *Alpha-particles; Beta-rays, Gamma-rays; Atmosphere/radioactivity; Beta-decay theory; Chemical analysis, radioactive; Chemical effects of radiations/ionizing radiations; Fallout; Geophysical prospecting; Nuclear decay theory; Nuclear bombardment targets; Nuclear excitation; Nuclear reactions and scattering; Radiochemistry*
- Earth, estimation from thermal data 9-31253
- gamma ray activity at rock outcrop surface, spectrometer obs. 9-37893
- global pollution, meas. by airborne gamma ray spectrometry 9-37894
- isotope thermal source, internal heat flow effects 9-26437
- laboratory demonstration 9-25017
- meteoritic whitlockite, correlation between fission tracks and fission-type Xe from extinct radioactivity 9-34415
- neutron activated foil in H₂O moderator, calc. 9-22844
- recoil nuclei, polarization, effect of atomic hyperfine quadrupole interactions 9-29708
- theory and props. introduced in book on atomic engineering 9-34368
- waste disposal underground, earth crust study 9-37866
- α -active aerosols, charging by secondary e emission 9-26139
- β -decay in rare earth region, Saxon-Woods potential 9-22729
- ¹⁵⁶Tb, γ spectrum 9-44180
- ¹⁷¹Tm, preparation by irradiating ¹⁶⁹Tm, then leaving to allow ¹⁷⁰Tm to decay and separating Yb, patent 9-22905
- ¹⁵²Eu, β longit. polarization relative meas. 9-22759
- ¹⁵²Eu decay analysis used for determ. of γ intensities of β -vibrational \rightarrow ground-state rotational band transitions 9-46211
- ²⁵⁴Cf spontaneous decay rel. to supernovae brightness decreases 9-49559
- ¹⁵³Dy \rightarrow ¹⁵⁵Tb, associated γ -ray spectra rel. to ¹⁵⁵Tb energy level determ. 9-44158
- ¹²¹ \rightarrow ¹²²Te 35 keV transition, K/L and L subshell conversion ratio determ., Auger spectra 9-25598
- ²³²Pa, decay props. 9-38707
- ¹²⁵Te from ¹²⁵I, 35 keV transition, K/L and L subshell conversion ratio determ., Auger spectra 9-25598
- ¹⁴⁵U, fission products, kinetic energy of β decay 9-22753
- ²³⁵U \rightarrow ¹⁴⁶Sm, internal conversion coeffs. determ., levels deduced, spin and parity assignment 9-48312
- ¹¹⁶In, polarized, β decay anisotropy 9-44177
- ²³⁶Pa, decay props. 9-38707
- ^{197m}Hg, γ -spectra, 50 \rightarrow 1000 keV 9-42254
- ¹⁹⁷Hg, γ -spectra, 50 \rightarrow 1000 keV 9-42254
- ²³⁷Pa, decay props. 9-38707
- ¹⁷¹W, γ spectra 9-38674
- ¹⁹⁸Au foil, absolute disintegration rate by coincidence techniques 9-32325
- ²³⁸Pa, decay props. 9-38707
- ²³⁸Pu, light element impurity anal. by reaction γ spectra 9-25603
- ^{199m}Hg, conversion coefficients and fluorescence yields obs. 9-42255
- ¹⁴⁹Eu, γ spectrum 9-44180
- ¹⁴⁹Gd, γ spectrum 9-44180
- ¹⁴⁹Tb, γ spectrum and conversion electron spectrum 9-44180
- Ba isotopes (A=131, 133, 135 and 139), from (n,p) reactions, γ ray spectra 9-42249
- ¹³C, activity variation with time and location in South Pacific and Antarctic Oceans 9-37902
- ⁴⁸Ca, double β -decay, possible interference due to $\beta\gamma$ correlation of ²¹⁴Bi in equilibrium with ²²⁶Ra impurity 9-22763
- ⁶¹Co, γ spectrum 9-42246
- Dy isotopes, α decay 9-42259
- Eu isotopes, α decay 9-42259
- ⁵⁹Fe as X-ray diffraction source 9-26847
- ⁶⁶Ga, γ spectrum 9-42247
- ⁶⁷Ga, γ spectrum 9-42247
- ⁷²Ga, γ spectrum 9-42247
- Gd isotopes, α decay 9-42259
- ³H, β -decay, polar vector matrix element 9-32304
- ³H thin sources, prod. by glow discharge 9-42238
- ⁵⁸Mn isomer, β -activity examined 9-46222
- ¹⁶O, parity non conserving alpha decays, theory 9-42242
- Os isotopes, (A=178 \rightarrow 181), γ spectra 9-38674
- ³²P β decay, bremsstrahlung spectra obs. 9-22532

Radioactivity continued

- ³²P prod. as air mass exchange indicator 9-45499
- Rb isotopes (A=81, 82, 83, 84 and 86), γ spectra 9-38687
- Re isotopes (A=177 \rightarrow 179), γ spectra 9-38674
- Rn decay products, transport proc. in air 9-32327
- Rn decay products transport proc. in air 9-22762
- Tb isotopes, α decay 9-42259
- ⁴⁸V, high-energy γ obs. 9-36591
- ⁸⁸Y, positron decay obs. 9-40491

dating see *Radioactive dating*

decay periods

- radio-nuclides, 13, short-lived, by isotope separator techniques 9-42237
- ¹³¹I sources, solid and liquid, comparison, obs. 9-25600
- ¹¹⁴In-¹¹⁴Cd, γ spectra, log f /t values 9-29764
- ¹¹⁴In-¹¹⁴Sn, γ spectra, log f /t values 9-29764
- ¹⁵⁴Tb, decay of isomers obs. 9-34421
- ²³⁴U 1552 keV level from ²³⁴Pu decay 9-25588
- ¹¹⁵Cd, β -decay in fast n-irrad. CdS, associated elec. changes 9-47104
- ¹⁵²Er new isotope half-life, α -decay energy meas. 9-48436
- ²⁵⁶Lw, α spectra obs., review 9-36584
- ¹⁴⁷Nd-¹⁴⁷Pm, p - γ ang. correlations meas., log f /t determ. 9-40496
- ¹⁷W β spectrum obs. 9-27677
- ⁹⁰Nb, half-life of the first metastable state 9-22766
- Ba short-lived mass-separated gaseous fission products 9-22765
- ⁷²Br, γ spectra meas. 9-25605
- ⁴⁴Ca from ⁴⁴Ca(d, pp); p - γ delayed coincidence meas., E_d=32.3 MeV 9-34422
- Cs short-lived mass-separated gaseous fission products 9-22765
- ⁶¹Cu-⁶¹Ni half-life meas. 9-27682
- ⁶²Cu-⁶²Ni, half-life meas. and assignments 9-38683
- ⁶⁴Cu in metal and CuSO₄, Cu(NH₃)₄ solns., obs. 9-27683
- ⁵⁹Fe, liquid scintillation counter meas. variations 9-25512
- ⁵⁹Fe liquid scintillation counter meas. variations 9-25512
- ⁵⁶Fe, half-life determ. 9-44174
- ³⁹K from ³⁹K(p,p' γ); p - γ delayed coincidence meas., E_p=5.6 MeV 9-34422
- ⁴K $\frac{1}{2}$ state, spin precession method, 1.29 MeV 9-36586
- Kr short-lived mass-separated gaseous fission products 9-22765
- ^{90m}Nb half-life, effect of superconductivity 9-32329
- ⁵⁶Ni-⁵⁶Co(1⁺) slow rate to 2p-2h state, higher energy giant spin-isospin resonance 9-27680
- ¹⁷⁰O from O(d,pp); p - γ delayed coincidence meas., E_d=1.2 MeV 9-34422
- ³²P, β decay in Fast-N-irrad. CdS, associated elec. changes 9-47104
- Rb short-lived mass-separated gaseous fission products 9-22765
- ³¹S β decay, log f /t calc. from shell model wave functions 9-36585
- ⁴⁰Sc-⁴⁰Ca, T_{1/2} meas., obs. of delayed protons 9-29771
- ³¹Si β decay, log f /t calc. from shell model wave functions 9-36585
- Sr short-lived mass-separated gaseous fission products 9-22765
- Xe short-lived mass-separated gaseous fission products 9-22765

decay schemes

- ¹³¹I-¹³¹Xe in II¹³¹Xe in II¹³¹, molecule Coulomb fragmentation, nuclear resonance-fluorescence scatt. 9-25599
- ¹³C, isospin-nonconserving decays 9-34392
- ¹³N, isospin-nonconserving decays 9-34392
- radio-nuclides, 13, short-lived, by isotope separator techniques 9-42237
- ^{110m}Ag, energies and intensities of transitions obs. 9-22756
- ¹⁶⁰Ho-¹⁶⁰Dy 9-38691
- ¹⁷⁰Lu, γ spectra and transitions 9-25601
- ¹⁷⁰Lu-¹⁷⁰Yb 9-42252
- ¹⁷⁰Lu-¹⁷⁰Yb conversion electron spectrum obs. 9-48317
- ²⁰⁹Pb-²⁰⁹Bi, L-subshell X-ray fluorescence yield and Coster-Kronig transition prob. 9-25602
- ¹⁴⁰Pr-¹⁴⁰Ce evidence for two-quasiparticle states of proton system, evidence for 9-48296
- ¹⁶⁰Tb-¹⁶⁰Dy, p - γ and p -conversion e sequences, angular correlation coeffs., rel. to odd levels in ¹⁶⁰Dy 9-36576
- ¹⁷⁰Tm, β - γ directional correlation measurements 9-22732
- ¹⁷⁰Tm \rightarrow ¹⁷⁰Er, EC decay, spectrum of K X-rays and γ -rays 9-29774
- ¹¹⁰Pd-¹¹¹Ag, γ spectra meas., levels, spin and parity determ. 9-34419
- ¹¹⁰Pd-¹¹¹Ag, γ spectra meas., levels, spin and parity determ. 9-34419
- ¹³¹Ba-¹³¹Cs, rel. to angular correlations in ¹³¹Cs 9-29731
- ¹⁴¹Ce-¹⁴¹Pr, γ spectra meas., levels determ. 9-32311
- ¹⁷¹Er-¹⁷¹Tm, γ spectra meas., levels determ. 9-32310
- ¹⁵¹Gd, γ -ray and conversion electrons spectra 9-48313
- ¹⁵¹Gd-¹⁵¹Eu, conversion electron and γ -ray spectra 9-42251
- ¹³¹I-¹³¹Xe in CH₃¹³¹I, molecule Coulomb fragmentation, nuclear resonance-fluorescence scatt. 9-25599
- ¹⁶¹Tb, study by sum coincidence and 4 π sum-probe coincidence spectra 9-22760
- ¹²¹Xe-¹²¹I, γ spectra meas. 9-29766
- ¹⁵²Eu allowed β -decay, meas. of β - γ circular polarization asymmetry 9-46221
- ¹⁶²Ho-¹⁶²Dy, half-lives of K-forbidden transitions 9-40485
- ¹⁹²Ir, β - γ angular correl. meas. on two cascades 9-34423
- ¹⁹²Ir-¹⁹²Os, ¹⁹²Pt; γ spectra meas., mag. dipole moment, E2/M1 mixing ratio determ. 9-32324
- ¹⁹²Ir-¹⁹²Os, mixing ratio of 485 keV transition in ¹⁹²Os meas. 9-46213
- ¹⁹²Ir-¹⁹²Pt, mixing ratios of transitions in ¹⁹²Pt 9-46213
- ¹⁶²Yb to ¹⁶²Tm excited levels 9-46225
- ²⁴³Am, LX and γ emission 9-46226
- ²⁴³Am-²³⁹Np, γ transitions of ²³⁹Np, multipolarities 9-42256
- ¹⁹³Os-¹⁹³Ir, β -decay obs. rel. to energy levels of ¹⁹³Ir 9-48298
- ¹⁰³Pd-¹⁰³Rh, X and γ -ray yield 9-38688
- ¹⁸³Re-¹⁸³W electron capture decay energy determ. 9-29769
- ¹⁰⁰Ru, obs. 9-34418
- ¹⁰⁰Ru, study by sum coincidence and 4 π sum-peak coincidence spectra 9-22760
- ¹⁵³Sm-¹⁵³Eu, γ -spectrum, higher precision meas. 9-40494
- ¹⁵³Sm-¹⁵³Eu, beta decay, levels of ¹⁵³Eu identified 9-27675
- ¹²³Te, conversion electron, spectra conversion coeff. and γ spectra obs. 9-46205
- ¹²³Xe-¹²¹I, γ spectra meas. 9-29766
- ^{184m}Re-¹⁸⁴W, γ -ray and conversion-electron spectra 9-40495
- ²²⁴Ac-²²⁰Fr 9-27679
- ¹³⁴Cs, to levels of ¹³⁴Ba, from γ -ray and conversion line spectra 9-22758
- ¹³⁴Cs \rightarrow Ba, γ spectra meas., levels determ. 9-32310
- ¹¹⁴In-¹¹⁴Cd, log f /t values, γ spectra meas. 9-29764
- ¹¹⁴In-¹¹⁴Sn, log f /t values, γ spectra meas. 9-29764
- ¹⁹⁴Ir-¹⁹⁴Pt; γ spectra meas., levels determ. 9-32324

Radioactivity continued**decay schemes continued**

- ¹⁴⁴Pr 0⁺→0⁺ β transition, spectrum-shape factor and longitudinal polarization theory 9-29768
- ¹²⁴Sb, conversion electron spectra rel. to nature of γ transition and ¹²⁴Te level scheme 9-48292
- ¹²⁴Sb→¹²⁴Te, levels of ¹²⁴Te by decay of 60d and 1.5 min isomers of ¹²⁴Sb 9-27673
- ¹⁵⁴Tb, decay of isomers obs. 9-34421
- ¹⁰⁵ag→¹⁰⁵pd, γ radiation 9-46224
- ¹⁷⁵Hf→¹⁷⁵Lu, γ spectra meas., M1+E2 transitions, probabilities and mixing parameters determ. 9-22733
- ¹⁸⁵Os→¹⁸⁵Re, energy obs. 9-48318
- ¹²⁵Sb, γ spectra meas. 9-22757
- ¹⁰⁶Rh→¹⁰⁶Pd, γ spectra meas. 9-22755
- ^{106m}Ag→¹⁰⁶Pd, γ spectrum 9-42248
- ¹⁶⁶Ho 0⁺→0⁺ β transition, spectrum-shape factor and longitudinal polarization theory 9-29768
- ¹⁸⁶Ir→¹⁸⁶Os, γ -ray spectrum and transition multiplicities 9-42253
- ¹⁴⁶Pm→¹⁴⁶Nd, γ spectra meas. 9-34420
- ¹⁴⁶Pm→¹⁴⁶Sm, γ spectra meas. 9-34420
- ¹⁸⁶Re, β - γ directional correlation measurements 9-22732
- ¹⁷⁶Ta→¹⁷⁶Hf half-life of 1227.4 keV level meas. 9-40485
- ²²⁶Th→²²²Ra, rel. to excited levels of ²²²Ra 9-48303
- ^{127m}Te, conversion electron spectra, conversion coeff. and γ spectra obs. 9-46205
- ²²⁷U→²²³Th→²¹⁹Rg→²¹⁵Rn→²¹¹Po, chain obs. 9-48319
- ²⁰⁷Bi e capture decay, X-ray emission from L-subshells, ²⁰⁷Pb Coster-Kronig transition prob. 9-27678
- ²⁴⁷Bk→²⁴³Am, α spectra meas., levels spin and parity determ. 9-27651
- ¹⁴⁷Gd→¹⁴⁷Eu, β → γ coincidence meas. 9-40493
- ¹⁴⁷Gd→¹⁴⁷Eu, e- γ coincidence spectra 9-40492
- ¹¹⁷Lu→¹¹⁷Te, rel. to excited states of ¹¹⁷Te isotope at 274.4 and 325.9 keV 9-44178
- ¹⁴⁷Nd→¹⁴⁷Pm, γ - γ ang. correlations meas., multipole admixtures determ. 9-40496
- ¹⁰⁷Rh→¹⁰⁷Pd, 22 min., obs., β -branching ratios meas. 9-48311
- ¹⁸⁷W β spectrum obs. 9-27677
- ^{138m}Pr→¹³⁸Ce, β decay 9-42250
- ¹⁵⁸Ho, γ and conversion electron spectra at energies above 1000 KeV obs. 9-48314
- ¹¹⁹I, ¹²⁰I, and isomeric states, obs. 9-44179
- ¹¹⁸I, from γ -ray obs. associated with β^+ emission and electron capture 9-44171
- ¹⁶⁸Lu→¹⁶⁸Yb, level, spin and parity determ., γ spectra meas. 9-27676
- ²³⁸Pu→²³⁴U, L, M subshell ratios determ. of 43.5 E2 transition 9-25589
- ²³⁸Pu helium generation, thermal power and spontaneous fission 9-29770
- ¹⁶⁸Tm→¹⁶⁸Er, e- γ coincidence spectra 9-40492
- ¹⁰⁹Pd→¹⁰⁹Ag, γ spectra meas., levels, spin and parity determ. 9-34419
- ^{139m}Nd→¹³⁹Pr, three- quasicaparticle multiple in ¹³⁹Pr 9-34400
- ¹³⁹Ba→¹³⁹La, nuclear matrix elements in 2.14 MeV β group 9-29767
- ¹³⁹Ba→¹³⁹La, γ spectra meas., levels determ. 9-27674
- ¹⁵⁹Dy→¹⁵⁹Tb angular correlation between K and L X-rays from ¹⁵⁹Tb 9-46212
- ¹⁵⁹Er, new data 9-48316
- ¹⁵⁹Gd Ge(Li)-Ge(Li) gamma ray coincidence studies 9-38690
- ¹⁵⁹Ho, γ -ray and conversion electron spectra obs. 9-48315
- ¹⁸⁹Ir→¹⁸⁹Os, γ spectra meas. 9-38676
- ²⁸Al from ²⁷Al (n,p), γ spectra meas. 9-22801
- ³⁵Ar→³⁵Cl (T=3/2⁺) level, shell-model calc. 9-29832
- ³⁵Ar→³⁵Cl, β endpoint and vector coupling const. determ. 9-42284
- ⁷⁰As, γ -ray energies and relative intensities 9-46223
- ⁷¹As, γ -ray energies and relative intensities 9-46223
- ⁷²As, γ -ray energies and relative intensities 9-46223
- ⁸B(β)→⁸B(α)He, rel. to ⁸Be 2⁺ states 9-40473
- ⁷⁴Br, from (¹²C, ⁶²Cu), γ spectra, β endpoint energy meas. 9-38686
- ⁷⁴Br→⁷⁴Se, γ spectrum and level diagram for ⁷⁴Se 9-38685
- ⁷⁵Br, γ spectra meas. 9-25605
- ¹²C, isospin-nonconserving decays 9-34392
- ¹²C→¹²C(β , p) α Be reaction, excited states determ., E_p=57 MeV 9-27715
- ¹⁴C age of tree rings 9-39991
- ¹³C→¹³N, β -decay obs. 9-38684
- ³⁸Ca, positron decay, γ transitions obs. 9-44181
- ⁶¹Co→⁶¹Ni, γ spectra meas. 9-34416
- ⁶¹Co→⁶¹Ni, γ spectra meas., β spectrum endpoint determ. 9-34416
- ⁶⁰Cu, γ -ray spectrum 9-42245
- ⁶⁰Cu→⁶⁰Ni, γ transitions meas., levels, spin and parity determ. 9-27681
- ⁶¹Cu→⁶¹Ni obs. levels of ⁶¹Ni 9-27682
- ⁶²Cu→⁶²Ni, γ -ray spectrum 9-38683
- ⁶⁶Cu→⁶⁶Zn, 2.37 MeV 0⁺ level population, γ spectra meas. 9-27684
- ¹⁷F→¹⁷O, limit of β branching to 871 keV state of ¹⁷O 9-38684
- ²⁰F→²⁰Ne, β -decay to 4.97 MeV level 9-38684
- ⁶¹Fe→⁶¹Co, β and γ spectra 9-44174
- ⁶⁶Ge→⁶⁶Ga, γ spectra meas., levels determ. 9-38662
- ⁶He→⁶Li β transition probability calc. using Green's and Tabakin's potentials 9-38648
- ³⁹K positron decay, γ transitions obs. 9-44181
- ⁴³K γ -ray emissions 9-40490
- ⁸⁷Kr→⁸⁷Rb, γ spectra meas., levels determ. 9-27685
- ⁸Li(β)→⁸Be(α)He, rel. to ⁸Be 2⁺ states 9-40473
- ⁹⁰Mo→⁹⁰Tc, K-shell conversion coeff. of 40.58 keV transition 9-29773
- ¹⁶Ni→¹⁶O, β decay to 0⁺ 6.05 MeV excited state obs. through e⁺e⁻ pair emission 9-44173
- ²²Na β^+ emission, 0.87 keV K electron capture peak, ratio meas. 9-32326
- ⁹⁶Nb→⁹⁶Mo, γ and β spectra 9-44176
- ⁹⁷Nb→⁹⁷Mo, γ spectra meas., levels determ. 9-32330
- ⁹⁸Nb→⁹⁸Mo, β spectra and coincidence meas. 9-34414
- ²⁴Ne→²⁴Na, delayed γ -ray spectrum study of β decay 9-42243
- ⁷¹Ni→⁷¹Co, γ spectra meas., levels, spin determ. 9-38660
- ⁶⁵Ni allowed β -decay, meas. of β - γ circular polarization asymmetry 9-46221
- ⁸²Rb decay to ⁸²Kr, γ spectra obs. 9-22747
- ⁸²Rb, levels of resulting ⁸²Sr 9-22748
- ⁹⁷Ru→⁹⁷Tc, γ spectra meas., level structure determ. 9-27686
- ⁴⁰Sc→⁴⁰Ca, β -decay, obs. of deuterium protons 9-29771
- ⁶Sc, β - γ circular polarization correlation in decay, Fermi/Gamow-Teller matrix element ratio determination 9-32328
- ⁷¹Se→⁷¹As, obs. and levels of ⁷¹As 9-42258

Radioactivity continued**decay schemes continued**

- ⁷⁵Se→⁷⁵As, M1-E2 mixing ratio and conversion-electron particle parameter determ. 9-40479
- ⁴⁸Si allowed β decay, meas. of B- γ circular polarization asymmetry 9-46221
- ⁸⁵Sr→⁸⁵Rb, decay energy from inner bremsstrahlung end-point energy meas. 9-29772
- ⁹⁶Tc→⁹⁶Mo γ -spectra and conversion electron spectra 9-44175
- ⁶³Zn→⁶³Cu, γ -transitions and level scheme 9-34417
- electron capture**
- ¹⁰⁹Cd, m/I orbital-electron capture ratio, I and K X-ray escape points calc. 9-38689
- K capture, K electron ejection, momentum spectra calc., relativistic corrections 9-29762
- L/K capture ratios in terms of internal conversion coeffs. 9-27672
- ¹⁷⁰Tm→¹⁷⁰Er, spectrum of K X-rays and γ -rays 9-29774
- ¹⁸³Re→¹⁸³W, decay energy determ. 9-29769
- ¹¹⁴In→¹¹⁴Cd, $\log f$ values, γ spectra meas. 9-29764
- ¹⁰⁵ag→¹⁰⁵pd, γ radiation 9-46224
- ¹²⁵Sb, K capture effects on electronic structure of decaying atom and its bonding in cpds. from Mossbauer meas. 9-38769
- ¹²⁵Te, K capture effects on electronic structure of decaying atom and its bonding in cpds. from Mossbauer meas. 9-38769
- ²⁰⁷Bi decay, X-ray emission from L-subshells, ²⁰⁷Pb Coster-Kronig transition prob. 9-27678
- ¹⁴⁷Gd, decay energy meas., ¹⁴⁷Dy e capture energy prediction 9-40493
- ¹²⁷I, K capture effects on electronic structure of decaying atom and its bonding in cpds. from Mossbauer meas. 9-38769
- ^{139m}Nd→¹³⁹Pr, three- quasicaparticle multiple in ¹³⁹Pr 9-34400
- ⁶Cu in metal and CuSO₄, Cu(NH₃)₂ solns., obs. 9-27683
- Dy, energy prediction from ¹⁴⁷Ge e capture decay energy meas. 9-40493
- ⁵⁷Fe, inner-bremsstrahlung spectrum endpoint, decay energy meas. 9-42244
- ²²Na, 0.87 keV K peak obs., ratio to β^+ emission rate meas. 9-32326
- ⁸⁵Sr, decay energy from inner bremsstrahlung end-point energy meas. 9-29772
- ⁸⁵Sr, obs., derivation of fluorescence yield 9-40491
- ⁸⁸Y obs., derivation of fluorescence yield 9-40491
- ⁶Zn, L/K capture ratio 9-22764
- protection** see *Radiation protection*
- Radioactivity measurement**
- see also *Dosimetry; Radiation monitoring; and the specific radiation, e.g. Gamma rays*
- amplitude spectra, preliminary processing on Minsk-2 computer using light-pencil oscillograph 9-42123
- human body, rotational technique, patent 9-41715
- least-squares analysis of γ spectra, computer prog. 9-38682
- lower limit of detection for very short-lived radioisotopes 9-25596
- optimization of activation and counting times 9-25594
- parent-daughter decay interval, meas. of distrib. to determine half-life 9-25595
- radionuclides absorbed dose, formalism for calculation 9-27124
- reactor liquid effluent continuous monitor, natural radioactivity effects 9-22910
- scintillating granules, disperse system, soln. for β -emitting liquids 9-22670
- ⁹⁰Mo→⁹⁰Tc, analysis of γ spectra with computer programme 9-38682
- Rn in atmosphere, meas. method and its validity 9-41538
- RnA and RnB, distrib. of decay products calc. in different shaped volumes of air 9-34424
- RnA and RnB, distrib. of decay products calc. in different shaped volumes of air 9-22761
- ⁹²Zr→⁹²Nb, analysis of γ spectra with computer programme 9-38682
- apparatus**
- see also *Particle detectors*
- coincidence techniques for meas. of level lifetimes in picosecond range 9-42150
- multichannel analyser in combination with on-line computer 9-27598
- pulse shaping network, use in improving signal-to-noise ratios in β activity meas. 9-44170
- sample changer automatic for use in α -spectroscopy 9-29761
- scintillation counter for transparent liquids 9-34358
- β - γ emitters, coincidence method, automatic correction digital apparatus 9-22750
- for ⁹⁰Sr content in seawater determ. 9-22751
- ²²⁷Th decay meas. attachment for separation of decay product background 9-22752
- ¹⁴C β activity on planar surface, scanning device 9-27593
- ¹⁴C in atm. CO₂, activity meas. 9-26912
- γ ionization chamber, well type, for rapid activity determ. 9-44169
- ⁵S β activity on planar surface, scanning device 9-27593
- Radioastronomy**
- see also *Cosmic radiations, radiofrequency; Sun/radiation, radiofrequency*
- astronomical unit, determ. from galactic H line source (r.f.) radial vel. meas. 9-29100
- astronomical unit, radio determ. method, agreement with dynamical method 9-47688
- astronomical unit, radio determ. method, agreement with dynamical method 9-43686
- brightness distrib. of a source, by method of regularization 9-41712
- Canadian long-baseline interferometer 9-38124
- CENFAM multistation radar system, receiving apparatus 9-41614
- CENFAM Project for multistation radar system 9-41613
- compound interferometer, 160 MHz at Nobeyama 9-36078
- CP 0950 pulsar obs., test for mass effect on freq. 9-27053
- Culgoora 158 MHz solar interferometers 9-36051
- Culgoora obs. programme of observations 9-36075
- Culgoora spectrograph, specifications 9-36050
- digital autocorrelation spectrometer, description 9-45692
- dispersion removal technique, pulsar obs. appl. 9-36010
- and Doppler effect 9-33914
- for earth exploration, microwave techniques 9-38127
- extragalactic sources, observed and intrinsic parameters, relationship 9-29040
- Flours compound interferometer, correlating receiver system 9-36077
- Flours compound interferometer, preliminary obs. 9-36076
- flux density scale at 408 MHz 9-24822

Radioastronomy continued

- gain horns, employment of standard type 9-36053
- Galactic central region, comparison with Galaxies showing nuclear structure 9-24747
- galactic HII regions, observations at 4170 MHz 9-40134
- image forming technique suitable for radioastronomy 9-36079
- intensity interferometer applic. 9-45998
- interferometer investigation of radio brightness distribution over source 9-45691
- interferometry, long-baseline, popular article 9-49595
- interplanetary plasma, investigation of motions and dimension of irregularities 9-24890
- interplanetary radio scintillation obs. of solar plasma 9-38108
- interstellar plasma inhomogeneities, discrete source scintillation investigation 9-43571
- interstellar atomic hydrogen radiation, investigation by 1.4 GHz parametric amplifier with closed-cycle cooling 9-33957
- ionospheric inhomogeneities, spaced receiver obs. 9-45533
- ionospheric inhomogeneity obs. at 13.54 MHz 9-33844
- ionospheric irregularities, comparison of scintillation depths of radio star and satellite scintillations 9-24692
- Italian cross radio telescope operation 9-45693
- Jupiter, decametric rad., 'fifth' source on or near visible planetary disk, non-to-controlled 9-36021
- Jupiter, flux density at 81.5 MHz 9-24852
- Jupiter decametric radiation, apparent control by Europa 9-36022
- long-baseline, 'absolute' direction, possible determination 9-38126
- long-baseline interferometer, bandwidth extension 9-38125
- lunar emissions, polarization characts. allowing for averaging by knife antenna pattern 9-40170
- meteor echoes, underdense, amp. distrib. rel. to initial radius of train 9-24884
- microwave detection of interstellar formaldehyde 9-29037
- Molonglo cross solar obs. 9-36045
- Moon, meas. at 3.2 cm, during 1964-1966 9-41672
- North Liberty observatory, Iowa, apparatus 9-31679
- radar astronomy, development 9-45689
- radar astronomy, development 9-45690
- radiation field, 3°K , black-body radiation obs. by mdvng observers 9-24719
- radio pulses from cosmic ray air showerx at 44, 105, 239 and 408 MHz 9-42120
- radiotelescopes suitable for more detailed exam. of radio sources 9-33958
- Sagittarius A, occultation by moon 9-24818
- scintillation of satellite 40 MHz signals, variation with observers latit. 9-31393
- solar radioastronomy, review 9-36043
- spectral-line receiver, multi-channel, design and operation 9-31676
- time and freq. standards for long-baseline interferometry 9-36107
- Venus, obs. at 4.52 cm, negligible phase variation and mean brightness temp. tel. to atmos. 9-36023
- Venus, radio obs. at 21.3 cm 9-27084
- W3, maser radiation sources in 1665 and 1667 OH lines 9-24784
- Weissenau solar observatory, apparatus 9-31678

Radiocarbon dating *see* Radioactive dating**Radiochemistry**

- see also* Chemical analysis/radioactive; Chemical effects of radiations/ionizing radiations; Radioactive tracers
- hot reactions, integral eqns., special solns. 9-43342
- hot-H-atom reactions with cyclohexane, beam method 9-43344
- isotope irradiation in production reactor, sample transfer systems 9-36643
- methane- d_4 , threshold energy for substitution of T for D 9-39965
- molecular plating, appl. to electrodeposition of americium 9-43331
- radiolysis, pulse, 2000 Å monitoring apparatus 9-32239
- radiolysis cells, gas phase, pyrex and quartz, effect of temp. on saturation currents 9-33683
- tritium β -decay, probability of formation of $[(\text{He})^+]_4$ 9-48432
- ^{243}Am separation from ^{243}Cm by precipitation of $\text{K}_3\text{AmO}_4(\text{CO}_3)_2$ 9-26802
- ^{145}Pm prep. by $^{144}\text{Sm}(n,p)^{145}\text{S} \rightarrow ^{145}\text{Pm}$, separation and γ spectrum obs. 9-33688
- ^{239}Pu separation with strongly basic anion-exchange resin paper 9-28819
- C, hot atom reaction with O_2 , quantum chem. 9-24538
- Cl hot atom reaction with alkanes 9-43343
- Cs compounds, p bombarded, radioiodine recoils 9-49388
- $\text{Fe}(\text{NH}_4)_2(\text{SO}_4)_6 \cdot \text{H}_2\text{O} \cdot ^{57}\text{Co}^{2+}$, daughter Fe^{3+} stabilization rel. to H_2O radiolysis by Auger e, obs. 9-23801
- Hg, enrichment of isotopes by neutron irradiation of diphenylmercury solns. 9-37843
- KMnO_4 aq. solns., positronium reaction 9-45429
- T-atom reactions with methane 9-47474

Radiography

- see also* Luminescent devices; X-ray tubes
- C and O surface distribution determ. 9-26849
- cineradiography with field-emission tube 9-32097
- composite, electron and X-ray image production, patent 9-48128
- direct electron beam fluorography 9-32098
- display system, three-dimensional with full-color 9-49615
- flash, meas. of shock pressure 9-29316
- flash timing improvement 9-33994
- gamma-ray, comparison of imaging devices using three dimensional phantom 9-49606
- image production system, three-dimensional 9-49614
- of liquid dielec. breakdown compression headwaves 9-32768
- modulation transfer function of radiologic system 9-27423
- neutron, medical applications 9-49607
- neutron, properties of different films 9-25393
- neutron beam, reciprocity failure characts. of films used with light emitting screens 9-43935
- neutron scintillators, glass and granular, optimization 9-42134
- proton, contrast and resolution quality 9-22488
- spectrometer, transportable, for spectra from various X-ray machines 9-25012
- X-ray diagnostic equipment, radiologic survey 9-24946
- X-ray hologram, plane-grating, construction with electron microprobe 9-38391
- β autoradiography in the presence of latent image fading 9-48233
- ^{232}Cf as neutron source 9-42257

Radiolysis *see* Chemical effects of radiations/ionizing radiations**Radiometer gauges** *see* Vacuum gauges**Radiosondes** *see* Meteorological instruments**Radiosources** *see* Cosmic radiations, radiofrequency**Radiostars** *see* Cosmic radiations, radiofrequency; Stars**Radiotelescopes** *see* Radioastronomy**Radio wave propagation** *see* Electromagnetic wave propagation**Radio wave spectra** *see* Nuclear magnetic resonance and relaxation; Paramagnetic resonance and relaxation; Spectra**Radium**

No entries

Radium compounds

No entries

Radium emanation *see* Radon**Rain**

- atmospheric, radioactive equilibrium with short lived decay products at 2m above ground, obs. 9-47552
- daughter products, systematic errors in meas. by filter method 9-40042
- diffusion from UC , UO_2 , obs. 9-37214
- diffusion in NaCl, after irradi. by 10^8 to 2×10^{16} ions/cm 2 9-48875
- interstitial diffusion of recoil atoms in UC 9-28325
- transport of decay products in air 9-32327
- transport of decay products in air 9-22762
- RnA and RnB, distrib. of decay products calc. in different shaped volumes of air 9-22761
- RnA and RnB, distrib. of decay products calc. in different shaped volumes of air 9-34424

Rain

- see also* Condensation; Snow
- artificial modification 9-43393
- autumn rainfall correl. with winter temperatures 9-31287
- drops on mountain slope melting layer, size distribution 9-41514
- effect on extraterrestrial mm. wave propagation 9-31331
- e.m. wave scattering and attenuation 9-40040
- fallout obs. (Jan. June 1967) 9-31335
- freezing, fragmentation in free fall 9-26898
- frontal, warm, advected changes in melting layer height 9-47542
- gauges, aerodynamic characts. 9-49445
- intensity and reflectivity standard deviations values calc. from drops size distribution 9-41515
- internal circulation and shape of large drops 9-28880
- millimeter e.m. wave propagation attenuation 9-33795
- onset, rel. to ice nuclei 9-41517
- radio attenuation, mm wavelengths, radiometry for earth space links 9-37927
- radioactivity of individual drops, results of measurements 9-28899
- radioisotopic tracing of storm runoff 9-24659
- salinity, instantaneous meas. via elec. cond., effects of temp., dust and elec. discharge 9-34879
- spherical cap approximation, validity in heterogeneous nucleation 9-28875
- vertical motions, Doppler radar determ. 9-40026
- Sr^{90} stratospheric residence time and interhemispheric mixing 9-40041
- $^{87}\text{Sr}/^{86}\text{Sr}$ ratio, effect of Chinese nuclear explosions (Dec 1966 and June 1967) 9-43406

Raman spectra *see* Scattering/light, Raman spectra**Ramsauer effect** *see* Electron beams; Electrons/absorption; Energy of particles**Random functions** *see* Random processes**Random processes**

- see also* Brownian motion; Fluctuations; Statistical analysis
- atoms in gas, effect of random motion on coherence of emitted radiation 9-38747
- electric field in dielectric with statistically homogeneous random permittivity 9-22111
- Markov approximation, rel. to light propag. in medium with random refractive index inhomogeneities 9-41939
- Markov noise, photographic 9-40388
- Monte Carlo leakage spectra, time-dependent, error estimation 9-22845
- motion of particle, Lagrangian formulation 9-27176
- nonlinearly correlated walk processes in multidimns. signal space 9-41773
- oscillator, nonlinear, Fokker-Planck equation, expt. confirmation of applicability 9-22110
- oscillator ensemble, classical, self losses rel. to harmonic force 9-38328
- seismic wave interferences, damping law distortion 9-26873
- self-avoiding walks on tetrahedral lattice 9-45776
- self-avoiding lattice polygons, number estimation 9-41777
- steady-state random walks, appl. to homogeneous nucleation 9-41776
- stochastic point processes, sequent. correls. 9-22172
- systems, equilib. props. 9-22123
- time interval distributions in neutron detection, stochastic operator method of calculating 9-27786
- two correlated random walk processes in 2TW-dimns. space as model for intensity fluctuation of two random signals 9-31886
- two correlated random walk processes in 2TW-dimns. space as model for intensity fluctuations of two random signals 9-31887
- vibrations of thin elastic plates 9-29252
- walks, inhomogeneous, passage-time property 9-29204

Range of particles *see* Energy loss of particles**Rare earth compounds**

- see also* The compounds of the individual metals; Ferrites
- alloy of Co-Sm system, high-coercive-force, prep. by getter sputtering 9-44627
- aluminates, perovskite type structure and rhombohedral lattice distortion 9-42795
- binary alloys, growth of single crystals by three methods 9-37078
- borides, plasma refl. edge and u.v. reflectivity obs. 9-39802
- chlorides, coupled Ising chains and magnetic ordering 9-33456
- cobaltides, T_2CO_3 ($\text{T}=\text{Gd}, \text{Tb}, \text{Dy}, \text{Ho}, \text{Er}$ and Tm) crystal structure 9-39313
- complexes, solid, overlap and Coulomb integral calcs. 9-45248
- complexes with tenoyltrifluoro-acetone and rhodamine-C, benzene solns., fluoresc. 9-42664
- dialuminides, s-f exchange interaction effects on elec. conductivity 9-24119
- diselenides, mag. susceptibility temp. depend. 9-43154
- double oxides, heat capacity obs. below 2°K 9-47004
- electrostatic and exchange interactions, high degree 9-47227

Rare earth compounds continued

- ethylsulphates, covalency eff. 9-35008
 ethylsulphates, sm^{+3} spin-lattice relaxation time calc. 9-43197
 ferrites, ferrimag. reson., mag. anisotropy effect 9-39898
 fluoride systems, nonstoichiometry 9-40915
 fluorides, in ZnS Lumocem devices, electroluminesc. 9-35700
 gallium garnets, magnetic transitions rel. to sp. ht. 9-24051
 garnet single crystals, Raman and far i.r. spectra, comparison 9-39850
 garnets, ferrite, monocrystals, magnetization near Curie points 9-45175
 group-VA intermetallic, NaCl-type, P, As, Sb and Bi n.m.r. Knight shifts 9-33648
 indium intermetallics, R_2In and R_3In_3 , crystal structure and lattice constants 9-28252
 iron borates, synthesis, X-ray powder diffraction patterns and cell parameters 9-37149
 iron garnets, exchange resonance and optical Faraday effect 9-45278
 lanthanide chelates of 1,10-phenanthroline, triplet exciton migration 9-31135
 lanthanide-nickel cpds., Ln_2Ni_{17} , mag. characts. 9-47260
 molybdates, lattice parameters rel. to temp. 9-35067
 niobate-alkali metal niobate solid soln., dielec. props. rel. to crystal chemistry 9-24210
 niobates, mag. props. in strong pulsed fields 9-35592
 noble metal equiatomic cpds., antiferromag. ordering rel. to band structure 9-24334
 orthoferrite, domain wall mobility by direct stroboscopic obs. of moving domain walls 9-45233
 orthoferrites, Bi-substituted, (R_1 - Bi_xFeO_3), synthesis and composition-dependent mag. props. 9-32869
 orthoferrites, flux grown crystals, Pb substitution 9-28237
 orthoferrites, magnetic and spectroscopic props. review 9-45232
 orthoferrites, specific heat, 1.5-20°K, magnetic ordering, magnetization orientation and Zeeman effect 9-33184
 oxides, added to zirconia and hafnia, effects on polymorphism 9-30723
 oxides, cathode applications 9-41279
 oxides, diffusion of O 9-26304
 oxides, doping of EuO films, rel. to mag., magneto-optical, optical and transport props. 9-47266
 oxides, nonstoichiometric, defect complexes and microdomains 9-44685
 oxides, solid solns. in binary systems, behaviour during crystallization by Verneuil method 9-37062
 oxides, struct. transform., high temp. 9-30736
 oxides-zirconia solid solns., preheating products obs. 9-30724
 oxy sulphates (Ln_2SO_4), fluoresc., phosphors obs. 9-43258
 rare earth-Zn cpds. with CsCl struct., mag. obs. 9-35556
 rare-earth iron garnets, Sc substituted, Fe ions canted spin struct., Mossbauer effect obs. 9-37667
 rare-earth-transition metal Laves phase, lattice parameters 9-35066
 salts, anomalous paramag. susceptibility caused by crystal field 9-45089
 silicates, di- and trivalent, struct. and phase obs. 9-30752
 singlet crystal-field ground state systems, collective excitations and mag. props. 9-45253
 stannates ($R_2Sn_2O_7$), Mossbauer spectra of ^{119}Sn 9-33529
 trihalides, hexagonal, heat capacity, mag. susceptibility, Cl n.q.r., low-temp. 9-41340
 vanadate crystals, RVO_4 -type, flux growth 9-26211
 vanadates, solubility in Na_3VO_4 , Li_3VO_4 and V_2O_5 , crystn. conditions 9-40777
 - BF_3 derivatives, ^{11}B - ^{19}F nmr coupling constant rel. to ^{19}F chemical shift 9-32464
 In-rare earth cpds., mag. props. and cryst. struct. 9-39751
 Ni-rare earth system, RNi_5 cell role in struct. determ. of other cpds. 9-30567
 $RCrTeO_6$ preparation and cryst. struct. 9-32919
 $RO-TiO_2$ glassy systems, Ti^{4+} coordination 9-32827

Rare earth metals

- see also The individual metals*
 acoustic paramag. reson., coeffs. derivation 9-41422
 activators in YOCr, fluoresc. and luminesc. props. 9-37768
 central ions in complexes in solid-state, quantum calcs. 9-45248
 chemical shifts of $K_{\alpha 1}$ X-ray lines during oxidation, role of f-electrons 9-37750
 configurations, $4f^{n-1}5d$, in fluorite type crystal, strong-field approx. 9-41350
 critical scatt. of sound 9-37333
 doping in $BaTiO_3$, effects on elec. props. 9-39685
 growth of single crystals by three methods 9-37078
 ion exchange of synthetic faujasites 9-24527
 ion impurities in group II-VI compounds, e.p.r. rel. to atomic environment 9-47430
 ions, $4f^2$ shell crystalline field screening effects and nuclear moments 9-22955
 ions, antiresonance phenomena in crystals irradiated by X-rays 9-49271
 ions, Hartree-Fock wave functions, inaccuracies in use of explicit angular momentum coupling 9-34511
 ions, in germanate and gallate garnets, mag. props. 9-47231
 ions, S-state, hyperfine coupling const. in cubic cryst., temp. depend., theory 9-33496
 ions in $CaF_2:H$, spectra 9-47353
 ions in garnets, selection rules in absorpt. spectra 9-24416
 magnetism, book 9-47223
 in meteoritic chondrites, abundances, radiochemical neutron activation analysis 9-29077
 powders, high resolution reflectance spectroscopy 9-47340
 in rocks, average content and distribution 9-37896
 semiconductors, magnetic, elec., opt. and mag. props. 9-49064
 solar abundances 9-41687
 spectra, extra lines obs. 9-47339
 spectral intensities of trivalent ions in soln. 9-36885
 trivalent ion spectra, Stark structure analysis by stimulated radiation spectroscopy technique 9-31092
 X-ray absorpt. coeff. determ. for $4d$ e, N_{IV} edge studied, 50-500 MeV 9-37744
 Zener diffusion parameter rel. to atomic number 9-33008
 (n, p) reactions in 8 isotopes at 14.2 MeV, cross sections 9-22793
 (n, α) reactions in 8 isotopes at 14.2 MeV, cross sections 9-22793
 (n, α) reactions in 8 isotopes at 14.2 MeV, cross sections 9-22793
 in CaF_2 , activated, spectrochem. determination 9-33695
 ^{35}Cl n.m.r. in solns. rel. to Ln-Cl complexes struct., obs. 9-40807
 in GaAs, ultra-trace determination 9-33696

Rare earth metals continued

- ions in disordered systems, e.p.r. line shapes 9-28742
 in LaF_3 , trivalent ion doped, phosphorescence 9-43260
- Rare gases** *see Inert gases*
- Rayleigh scattering** *see Scattering/light*
- Rayleigh waves** *see Elastic waves; Seismic waves*
- Re(b)inder effect** *see Mechanical strength; Surface phenomena*
- Reaction kinetics**
see also Catalysis; Chemical reactions; Exchanges, Chemical; Explosions
 acetylene, flash decomp. on W 9-43327
 acetylene oxidation 9-33661
 activated reorientational processes, pre-exponential factor 9-39933
 alkali at beam with triat. halide mols. 9-25795
 alkyl radicals, unimolec. decomp., neopentyl rupture 9-39943
 benzene ion-mol. reactions 9-24541
 bimolecular reactions, mol. beam investigation 9-25792
 bimolecular reactions, theory 9-25793
 binary gas mixture, rate effect on temp. and conc. distrib. 9-28777
 body rotating in ionized air stream, destruction kinetics 9-47452
 Boltzmann chem.-kinetic eqn., variational soln. 9-39934
 chemical equilibrium, analog. computer calc. 9-37811
 corrosion, linear 9-24563
 ethane, flash decomp. on W 9-43327
 ethylene, flush decomp. on W 9-43327
 exchange reactions, quantum mech., coupled channels approach 9-45413
 1-fluoro-1, 1, 2, 2-tetrachloroethane, rotational isomerization 9-27896
 gas-phase reactions, kinetic isotope effects, temp. depend. 9-28780
 gas-surface interactions, continuum and discrete lattice models 9-40836
 gaseous mixture, thermal equilibrium, Monte-Carlo method 9-39044
 gases in discharge flow systs., at and free radical conc. meas. 9-26805
 graphite single cry. react. with H_2O in He, rates, activation energy var., e microscopic investig. 9-24537
 graphite tube oxidation, effects of non-uniform burn off 9-26823
 heterogeneous reactions, press. effects 9-24531
 hot reactions, integral eqns., special solns. 9-43342
 hot-H-atom reactions with cyclohexane, beam method 9-43344
 hydration energies of ions, gas phase 9-24530
 hydrocarbon radiolysis, rate const. for scavenging of electrons 9-43341
 ion exchanger, film diffusion 9-45414
 ion-atom slow interchange reactions, temp. depend. 9-43312
 ion-molecule reaction rates meas. by ion cyclotron reson. 9-45415
 ion-molecule reactions, anomalous low-energy behaviour 9-33659
 ion-molecule reactions, electron density rearrangement theory 9-28778
 ion-molecule reactions, energy depend. of intermediate complex formation 9-49371
 ion-molecule reactions in methane, Kr, and O_2 , using pulsed mass spectrometer 9-24544
 isopropyl chem. activated radicals, competitive unimolec. decomp. 9-24546
 light scatt. as probe of fast reactions 9-24529
 light scatt. from reactive fluids 9-31181
 $M+XC(2D)$, exothermic, product distrib. 9-45416
 $M+XC(3D)$, exothermic, product distrib. 9-45417
 methane, CH_3^+ + CH_4 reaction, direct mechanism 9-49375
 methane, flash decomp. on W 9-43327
 methane-d₄, threshold energy for substitution of T for D 9-39965
 monochloroethyl radicals, chemically activated, decomposition 9-39947
 nonequilibrium effects in gas reactions 9-37815
 i-propanol on Al oxides, catalytic decomposition, apparatus for obs. 9-37823
 propylene-1-d₂, thermal and NO catalyzed cis-trans isomerization 9-43328
 pyrrhotites of Pierrefitte (Hautes-Pyrenees), thermochem. obs. 9-33657
 radical intermediate, high temp. chem. reactions, consecutive-parallel and Rice-Herzfeld mechanisms 9-35739
 rate constant evaluation at high temp. 9-26817
 reaction-rate treatment of extrapolation methods in creep testing 9-33042
 reaction-rate treatment of life fraction hypothesis in creep testing 9-33041
 rearrangement reactions, photoisomerism 9-43337
 resonance theory of termoelec. recomb. kinetics 9-48426
 spherulites of Pierrefitte (Hautes-Pyrenees), thermochem. obs. 9-33657
 stochastic and deterministic formulation of rate eqns. 9-41441
 three-body rearrangement scatt., solvable model 9-27174
 transport processes, simplified models, review 9-37816
 triatomic, quantum, mech. Hamiltonian 9-39935
 water radiolysis, nanosecond pulse expts., nonhomogeneous kinetics rel. to $e[H_2O]$ behaviour 9-37556
 Zircaloy, pre-transition oxidation behaviour, comments 9-37826
 ∞ gas phase reaction rate data at high temperature 9-49373
 AIP, thermal decomposition 9-36927
 BH_3CO , pyrolysis energetics 9-43314
 C-CO₂, role of sublimation and self-diff. of C, temp. >2000°K 9-28779
 C hot atom reaction with O_2 , quantum chem. 9-24538
 C vitreous, combustion in low O_2 press. 9-26815
 CD_4^+ + CD_4 + CD_4 , collision mechanism at ~1 eV, obs. 9-41443
 CO₂-C, role of sublimation and self-diff. of C, temp. >2000°K 9-28779
 CO₂ dissociation, in positive column of glow discharge 9-38919
 CS₂, thermal decomp., shock heated CS₂-aR emission spectrum obs. 9-35740
 C + CO₂, rate constant evaluation at high temp. 9-26817
 Cl hot atom reaction with alkanes 9-43343
 Cl + Br₂ → ClBr + Br, energy disposal 9-39938
 Co (10 wt.%) Cr alloys, high temp. oxidation 9-31195
 D₂, transfer reactions with CO₂⁺, D₂O⁺ and H₂S⁺ 9-49374
 D + D₂ = D₃ + D 9-41439
 D + H₂ = DH + H 9-41439
 Graphite to O, eff. of neutron bombardment 9-35743
 H-atom-formaldehyde gas-phase reaction, kinetic isotope effects 9-28781
 H-atom reaction rates with olefins 9-43334
 H-atom reaction rates with olefins 9-43335
 H₂, D₂ and HD gaseous ion-mol. reactions, ion cyclotron reson. 9-43313
 H₂ combustion, shock-initiated 9-39946
 H₂ mols., photodissoc. 9-25785
 H₂ reactivity to atomic N and O 9-43317
 H₂O vapour react with graphite single cry. in He, rates, activation energy var., e microscopic investig. 9-24537
 H₂O + D₂O = 2HDO equilib., zero-point energy 9-31179

Reaction kinetics continued

- H atom reactions with Cl_2 and F_2 , mass spectra 9-43316
 H atoms with methane, e.s.r. meas. 9-47454
 HBr dissociation in shock waves 9-47455
 $\text{H} + \text{C}_2\text{H}_4$, using e.s.r. detect. 9-24534
 $\text{H} + \text{C}_2\text{D}_4 \rightarrow \text{HD} + \text{C}_2\text{D}_3$, translational-energy depend. 9-39944
 $\text{H} + \text{D}_2 = \text{HD} + \text{D}$ 9-41439
 $\text{H} + \text{H}_2 = \text{H}_3 + \text{H}$ 9-41439
 K/H and K/Li ion exchange in synthetic resin, kinetics 9-41438
 K molec. beam reaction with oriented CF_3I 9-43320
 Li aluminosilicate glass, pyroceramic formation 9-36922
 N_2^+ with CH_4 and CD_4 , dynamics 9-39940
 N_2H_4 decomp. in flow reactor 9-37819
 $\text{N}_2\text{O} + \text{CO}$ in single-pulse shock tube, and recomb. of O and CO 9-43321
 $\text{N}_2\text{O} + \text{H}_2$ 9-31183
 $\text{N}_2 + \text{H}_2$ ion-mol. reactions, using ion cyclotron reson. 9-31184
 $\text{Na}_2\text{S}_2\text{O}_8$ isothermal decomposition, concentration oscillations 9-24540
 NaCl, additive coloration by metal 9-32997
 $\text{NiO} \cdot \text{Fe}_2\text{O}_3$ solid-state reaction 1100 to 1300°C, from reaction layer thickness anal. 9-37820
 $\text{O}_2 + \text{CO}$, isotope exchange in shock waves 9-49370
 $\text{O}_2(\Delta_g) + \text{O}_2 \rightarrow 2\text{O}_2 + \text{O}$, rate const. 9-43322
 O^{16}D_2 excited atoms, reaction with isobutane 9-24543
 O reactivity to graphite, eff. of neutron bombardment 9-35743
 $\text{O} + \text{CH}_4$, rate coeffs. 9-39939
 $\text{O} + \text{H}_2$, rate coeffs. 9-39939
 $\text{O} + \text{OCS}$, $\text{O} + \text{CS}_2$, $\text{O} + \text{NO}_2$, using e.s.r. detect. 9-24534
 SF_6 dissociation in Ar, shock-tube expts. 9-38923
 SO_2 , chemiluminesc. afterglow, temp. depend. 9-43323
 T-atom reactions with methane 9-47474
 Ti oxidation, effect of annealing 9-33671
 V-O solid solns., degassing kinetics 9-39942
 Xe-methane system, ionic reactions 9-42566

Reactors see *Nuclear reactors, fission; Nuclear reactors, fusion*

Recombination see *Ions, recombination; Semiconductor*

Recombination radiation see *Luminescence*

Recording

- electro-optical, multichannel, high data rates, for pulse signals 9-27421
 electron diffractometer intensity profile, optical improvement 9-27283
 ferroelectric, signal recording by polarizing ferroelectrics 9-47167
 holograms, acoustic, laser flying spot technique 9-29293
 holograms, using temporal modulation 9-25325
 of holograms on photopolymer materials 9-25324
 holographic storage of 1 re-dimens. meas. information, appls. 9-45971
 laser beam, recording of digital information on thin mag. film 9-45159
 magnetic, oriented coating on substrate, patent 9-22341
 magnetic recording medium, patent 9-47899
 magneto-optical 9-45271
 Mossbauer effect, X-ray film and CdS detector appls. 9-26716
 neutron flux distributions recording device for use in reactors 9-29643
 nuclear reactions, three body, using multiparametric system 9-22648
 photoelectric absorpt. spectra, monochromator attachment 9-29489
 photographic, superposition of channels on emulsion by spatial freq. modulation 9-25392
 seismic processes, by long-period galvanometer 9-31259
 shear waves, continuous-signal methods, early development 9-37876
 shear waves, continuous-signal methods, later experimentation 9-37877
 spectra, optical, methods using image intensifiers 9-27405
 spectrophotometric system 9-41965
 susceptibility of superparamag. substs., recording instrum. 9-38345
 transient event holography, reconstruction and evaluation 9-31982
 ultrasonic images, 3-dimensional, holographic 9-27350
 u.s. attenuation, high sensitivity logarithmic recorder 9-38299

Recrystallization (metals) see *Heat treatment*

Rectifiers

- see also *Electron tubes; Semiconducting devices*
 p-s-n diodes at high injection levels, effective carrier lifetime 9-30942
 three-phase bridge, current decrease in load at const. firing angle 9-43830
 three-phase bridge, current in load for variable firing angle 9-43829
 Ag alloy on Se, conductivity asymmetry in impulse regime 9-41158
 CdS, voltage, ambient gas effect on rectification at free surface 9-39640
 Se, C-V charact., recurrent changes 9-49116
 Se, capacity meas. 9-26562

Red giants see *Stars*

Red shifts see *Astronomical spectra; Cosmology; Relativity/general*

Reflectance see *Reflectivity*

Reflection

- see also *Neutrons/reflection; X-ray reflection*
 direct of plane wave by transparent sphere 9-29177
 electrons, from metal surface, rel. to surface impedance in weak mag. field 9-26514
 inert gas beam on surface of W ribbon 9-48754
 internal gravity waves in stratified fluids with shear flow, at critical levels 9-27958
 mirrors, metal, calorimetric meas. using laser 9-26701
 plane waves from stratified medium 9-22066
 seismic waves, from discontinuities within Earth's upper mantle 9-49416
 SH waves at solid-firmoviscous boundary in earth 9-35791
 shock wave, on interaction with mag. field of current grid, theoretical analysis 9-38305
 surface normal irradiation, characteristic reflection curve analysis 9-22276
 of surface waves by movable strip, theory 9-30360
 vectors, an illustration 9-22050
 C, stacking faults, 001 reflections, analysis 9-37183
- acoustic waves**
 see also *Echo; Reverberation*
 acoustic filter performance, reflection factor determination 9-43794
 critical angle refl. min., prediction method for liq.-solid interface 9-22257
 magnetoacoustic, on free boundary of conducting porous medium 9-42961
 ocean surface, intensity fluctuations 9-47520
 from piezoelectric crystal-vacuum boundary 9-44819
 plane, from elastic plate reinforced with stiffness members 9-22256
 plane sawtooth waves decay inside tubes 9-45854
 sea, surface reverberation, relative contribs. of surface air bubbles and waves 9-24610
 at shear layer in fluid 9-45856

Reflection continued**acoustic waves continued**

waveguides, cylindrical, asymmetries 9-45855

acoustic waves, ultrasonic

No entries

electromagnetic waves

- circularly polarized, from imperfect spheres, radar cross section calc. 9-34120
 dielectric bounded layer, phase shift 9-34118
 e.l.f. radio waves, ionospheric reflection coeffs. calc. under effect of ions 9-24686
 inhomogeneous region, total reflection phase shift 9-36226
 ionosphere, electron collisions effect on polarisation 9-49481
 ionosphere, lower, phase of partially reflected waves, recording method 9-49482
 ionosphere, reflected wave envelope correl. coefficient and spectrum width 9-31384
 limited wave by dioptr. plane, calc. of resurgent wave field 9-43808
 metal, rel. to surface roughness 9-45268
 by moving uniaxially anisotropic slab 9-34119
 nonlinear deviations, in vacuum at plasma boundary 9-23296
 paint films on black substrate, 0.8-2.0 μ range 9-43206
 plasma boundary, exact soln. for relativistic collisionless plasma 9-23293
 plasma half-space, oblique refl. of impulse wave, response rings 9-48569
 plasma waveguide props. 9-48561
 plasma-vacuum boundary, effect of surface waves 9-44439
 polarized in plasma, ray displacement in mag. field 9-44430
 pulse distortion, totally reflecting layers 9-45894
 pulse distortion, totally reflecting layers comments 9-45895
 radio, by meteor trails, calc. 9-31618
 reflection coeff. determ. without introducing boundary conditions 9-36225
 reflection-refraction at interface bet. isotropic mats. under applied static elec. field, electro-opt. eff. theory applc. 9-25145
 from thin conducting sheet on curved surface, mode conversion problem 9-22313
 total reflection of limited wave, and Goos-Hanchen effect, strict formulation 9-41854
 Venus, radar obs., variations 9-38084
 $\text{Cd}_x\text{Ca}_{1-x}\text{O}$ Reststrahlenbands and intrinsic absorption edge 9-47342
- light**
 see also *Films, solid/optical properties; Mirrors*
 anisotropic transfer problems in thick layers, asymptotic fitting method for solution 9-34209
 antiferromagnetic semiconductors, rel. to magnon drag contrib. to transport props. 9-24332
 bulk materials, reflectance data rel. to optical constants. determ. 9-26695
 coatings, three layer anti-reflection, design 9-27377
 dielectric three-layer medium 9-48099
 diffuse, from roughened surfaces, depolarization obs. 9-33507
 diffuse, of time-dependent collimated, by a finite inhomogeneous atm. 9-45582
 diffusion rel. to angle of incidence 9-48080
 direction vector from series of reflectors, tensor expression 9-25352
 fibre optical system, grazing total internal reflection ray obs. 9-38400
 films, thin, reflectance data rel. to optical consts. determ. 9-26695
 Fresnel coeffs., generalized, as linear fractional transforms. and representation in Smith chart 9-32008
 glass, soda-boric oxide, Cu^{2+} spectra 9-37800
 glasses, low loss, ellipsometric determ. of surface reflectances 9-39801
 group II-VI compounds, spectra near fundamental band edge 9-37708
 from inhomogeneous layer (E vector normal to plane of incidence), general theory 9-45990
 laser, holography of diffusely reflecting objects 9-27339
 laser beam, from plane parallel plates, equally inclined interference fringes effect 9-36316
 mat. surfaces, physical mechanism of the specular peak 9-41945
 3-methyl-pyridine heavy water system, critical opalescence, temp. depend. 9-42656
 mirrors, oil contamination changes of reflectivity rel. to space flight 9-22470
 molecular complexes, adsorbed, dissoc. equil. obs. 9-39166
 multilayer resonant reflectors 9-32007
 multiple, of laser beam, maximum vel. process photography 9-31972
 parabolic mirror, rays from off focal-point source, demonstration 9-29161
 porcelain enamels, TiO_2 opacified, reflectance and colour 9-37687
 rare-earth borides, plasma refl. edge, opt. const. and dielec. parameters determ. 9-39802
 reflectometer, u.h. vacuum, for use with extreme u.v. synchrotron radiation 9-27396
 reflectometer with normal incidence scanning 9-36370
 from rotating mirror, image motion for point, line and plane objects 9-41936
 self-insulation of materials in medium against intense light 9-27343
 sapphire, coeff. rel. to temp. distrib. 9-42964
 satellite, spherical, irradiated by Lambertian earth, photon radiance angular distribution 9-27376
 by sea, spectra, photographic obs. 9-43367
 selective, by metal mirror 9-32009
 semiconductor surface, internal spectra 9-43229
 single axis crystal boundary isotropic medium 9-28652
 skylight, effect of surface reflection on angular and spectral distribution 9-24661
 solid surfaces, laser beam, coeff. dependence on radiation parameters 9-43208
 solids, absorpt. meas., elimination of surface refl. effects 9-33519
 spectroscopy, internal refl., effect of angle of incidence change 9-32053
 steel in water, self-insulation against intense light 9-27343
 surface roughness meas. 9-43207
 by surfaces in solar devices, applc. opt. instruments 9-32010
 tetrayanoquinodimethan, meas., 0.29-2.5 μ rel. to absorpt. coeff. calc. 9-39796
 thin layer on metal surface, i.r. spectrum determ. 9-35648
 total, role of lateral wave 9-45989
 total internal, digital deflector, switchable 9-27368
 triglycine sulphate, i.r. spectra, optical const. and pyroelec., obs. 9-35615
 Venus, spectral, terrestrial photoelec. obs. 9-38078
 Al coating on ground pyrex, diffusion rel. to incidence angle 9-48080

Reflection continued
light continued

- Bi₂O₃ layers, evaporated band gap obs. for optical and valence-conduction band transitions 9-39162
 CdS, Se_{1-x}S_x single cryst. in fund absorpt. region 9-47341
 CdS plastically deformed single cryst., spectra depend. on dislocation density 9-35644
 Cr film, grown by molecular beam incidence crystallite shape 9-32909
 CuCl, transverse magneto refl. in near u.v. 9-35622
 CuCl crystals, refl. spectra, optical const. determ. near excitonic absorpt. region 9-37710
 EuO, energy range 1-9 eV 9-26702
 EuO reflectance 69K-1.5K, spin-polarized splitting of peaks 9-37690
 Ga_{1-x}In_xSb, electroreflectance, variation with composition 9-45307
 GaAs, reflectance modulation by optical carrier injection 9-28672
 GaS, spectra meas. rel. to interband transitions 9-28671
 GaSe, spectra meas. rel. to interband transitions 9-28671
 Ge, combination with transparency for elec. resistivity calc. 9-24190
 Ge, heavily doped, u.v. spectrum 9-35645
 Ge reflectance modulation by optical carrier injection 9-28672
 InAs_{1-x}P_x, electroreflectance, variation with composition 9-45307
 InAs_{1-x}Sb_x, electroreflectance, variation with composition 9-45307
 InSe, spectra meas. rel. to interband transitions 9-28671
 KBR single crystal, extreme u.v. spectrum 9-28673
 Mg₂Sn, spectra, for energy band structure 9-35647
 MgO powder in contact with high refractive index glass 9-43209
 MnTe, rel. to magnon drag contrib. to transport props. 9-24332
 Na₂WO₃, specular and diffuse reflectance spectra 9-31094
 NaClO₃, total refl. phenomena in second-harmonic generation due to laser beam 9-47310
 PbO-GeO₂ glass system, with 0 to 55 mol % PbO, spectra 9-28675
 Sb₂S₃, spectrum, 2.2-0.6 eV 9-39825
 Si, combination with transparency for elec. resistivity calc. 9-24190
 Si, heavily doped, u.v. spectrum 9-35645
 SiO₂ film spectra, interference influence in SiO₂-Si system, 9 μ region 9-35619
 SnO₂ semiconducting layers on glass, i.r. reflection depend. on surface resistivity 9-26729
 TiO₂/MgF₂ films, double anti-reflective system for optical glass surface 9-36962
 TiFeS₂, power const. 9-30574
 W₁₈O₄₉, specular and diffuse reflectance spectra 9-31094
 W₁₈O₄₉, specular and diffuse reflectance spectra 9-31094
 ZnO, i.r. electroreflectance, elec. Gruneisen const. calc. 9-33540
 ZnO, spectra for excitons exhibiting spatial dispersion 9-45309
 ZnO crystals, polar surfaces, and elec. conductivity meas. 9-42741
 ZnSnP₂, i.r. spectra, optical constants and vibrational frequencies 9-35614

reflectivity

- see also Diffusion/light; Films, solid/optical properties; Optical constants*
 absolute specular, meas. spectrophotometer attachment 9-32067
 albedo vars., calc. from satellite obs. 9-43395
 albedo vats., calc. from satellite obs. 9-37914
 brick, reflectivity, diffuse near i.r. 9-39800
 crystal surface, polariton modes soln. obs. 9-49010
 diffuse reflectance spectra, theoretical interpretation 9-36386
 flat, specular samples, meas. using absolute reflectometer 9-38406
 group IV-VI cpds, electroreflectance 9-39809
 ice clouds, i.r., comparison with Venus obs. 9-38080
 internal reflectance spectroscopy, review 9-36388
 liquid binary mixture, critical, diffuse interface obs. 9-39084
 lunar surfaces, colour differences 9-49577
 mawsonite, birefractivity, sign inversion obs. 9-37688
 metal films, self-supporting, covered by oxide layers, eff. of plasma oscils. 9-26672
 metal surfaces, rough, plasmons coherent contrib. 9-35317
 metals, improved high reflectivity ellipsometry method for dielec. const. determ. 9-35462
 Metals, reflectivity, diffuse near i.r. 9-39800
 microsamples, i.r. reflectance spectroscopy 9-36390
 minerals, absorbing, birefractivity, sign inversion obs. 9-37688
 paint-like coatings computer calc. incorporating Fresnel's law, Snell's law, Bier's law and kinetic theory 9-37689
 paints, reflectivity, diffuse near i.r. 9-39800
 paper, discrepancies in Kubelka-Munk reflectance eqn. applic. 9-37712
 of plate, homogeneous plane parallel, rel. to transmission 9-41940
 powders, compacted, variables in reflectance spectra 9-37706
 radar, for raindrops, standard deviation of values calc. from size distribution 9-41515
 rare-earth borides, u.v., and plasma refl. edge obs. 9-39802
 reflectance spectroscopy, high-temp. and dynamic modes 9-36387
 reflectance spectroscopy, symposium, Chicago (1967), proceedings in book 9-29482
 semiconducting compounds, optical technique for determ. of radiation damage 9-37503
 semiconductor, photorefectance and screened Coulomb interaction 9-39703
 semiconductors, high resolution meas., new method 9-37705
 slab with random complex dielec. const., statistical treatment 9-40249
 slate, reflectivity, diffuse near i.r. 9-39800
 solids, modulated reflectance, effect of spatially dependent perturbations 9-24396
 spectrophotometers 9-32062
 spectrophotometric meas. precision and accuracy 9-36393
 stratified media, electroreflectance 9-35624
 tree bark, reflectivity, diffuse near i.r. 9-39800
 white reflectance standards, prep. and calibration 9-34201
 α -Ag-In dil. alloys, piezorefectance 9-47325
 Al₂SiO₅-coated, determ. 9-37373
 AuCu₃ order-disorder eff. obs. 9-26395
 BaSO₄-C powder mixtures, diffuse reflectance 9-24360
 BaSO₄-PbCrO₄ powder mixtures, diffuse reflectance 9-24360
 BaTiO₃, absolute reflectance spectra, 0.325-0.7 μ 9-33537
 Bi₂Se₃(Te₂), reflectivity spectra, 0.7 to 12.5eV 9-33538
 C-BaSO₄ powder mixtures, diffuse reflectance 9-24360
 C-PbCrO₄ powder mixtures, diffuse reflectance 9-24360
 Cd_{1-x}Zn_xS, i.r. active lattice modes from spectra 9-47343
 Cd₂Ca_{1-x}O mixed crystals prepared by sintering 9-47342
 Cd₂Hg_{1-x}Te, intra-band, rel. to semimetal-semiconductor transition 9-49078

reflectivity continued

- Cd₂Hg_{1-x}Te solid solns., fund. spectrum 1.5-4 eV, band struct. obs. 9-45306
 CdS₂Ag, effective mass of free holes determ. 9-39618
 CeF₃, polarized i.r. spectral analysis rel. to optical phonons and mag. symmetry 9-47345
 Cu-Ni alloys, and i.r. absorpt., rel. to virtual bound state 9-45269
 Cu and i.r. absorpt. rel. to virtual bound state 9-45269
 Eu chalcogenides, i.r., dielec. dispersion and phonon freqs. obs. 9-39799
 Eu chalcogenides single cryst. 9-49238
 FeS₂, i.r. spectra, lattice vibration obs. 9-46974
 FeSi₂, i.r. 9-33505
 GaAs, and modulated reflectivity 9-49268
 GaAs, reflectance and photorefectance spectra, intense exciton struct. obs. 9-41377
 GaP, and modulated reflectivity 9-49268
 GaSb 9-47119
 Ge, piezorefective spectra 9-35646
 Hg liquid, normal and at 45° 9-46638
 In thin films, reflectance meas., far u.v. optical const., obs. 9-37681
 p-InSb, spectra, conductivity effective mass of holes meas. 9-35407
 KCl single cryst., conductivity and energy loss spectra, temp. depend. 9-33559
 LaF₃, polarized i.r. spectral analysis rel. to optical phonons and mag. symmetry 9-47345
 Mg₂Ge, 0.6-11.0 eV at 77°K rel. to optical and dielec. constant calcs. 9-24355
 Mg₂Si, 0.6-11.0 eV at 77°K rel. to optical and dielec. constant calcs. 9-24355
 Mg₂Sn, 0.6-11.0 eV at 77°K rel. to optical and dielec. constant calcs. 9-24355
 MnO, dielec. and Reststrahlen parameters determ. 9-45308
 NaNO₂ cryst., far-i.r. spectra, temp. depend. 9-41370
 NdF₃, polarized i.r. spectral analysis rel. to optical phonons and mag. symmetry 9-47345
 Ni, and i.r. absorpt., rel. to virtual bound state 9-45269
 PbCrO₄-C-BaSO₄ powder mixtures, diffuse reflectance 9-24360
 PbTe, in band structure parameter determ. 9-39630
 PrF₃, polarized i.r. spectral analysis rel. to optical phonons and mag. symmetry 9-47345
 S, orthorhombic in vacuum u.v. 9-37682
 Sb₂Te₃, spectra, 0.7 to 12.5eV 9-33538
 Se-Te mixed cryst., far-i.r. spectra, lattice vibr. eigenfreqs. and oscillator strengths 9-39826
 Se single cryst., spectrum calc. from ellipsometric meas., optical const. and interband transitions rel. to fine struct. 9-43204
 Si, charges induced by 40 keV Sb ion bombardment 9-33506
 Si photorefectance spectrum and rel. to electroreflectance 9-43231
 SiO film on Si, corrections for thickness meas. by variable angle monochromatic fringe obs. 9-34982
 Sn₄As₃, conduction obs. 9-37474
 Sn₄P₃, conduction obs. 9-37474
 Ti_{1-x}Pa_x, and optical props., lattice const., obs. 9-35070
 ZnS, and modulated reflectivity 9-49268
 ZnSe, and modulated reflectivity 9-49268
 ZnSe film as NaCl 9-48099

Refraction

- critical internal refraction condition in tetragonal and hexagonal cry. 9-30641
 seismic in continental margin, correl. analysis of data 9-45450
 surface waves and microseisms in North Atlantic 9-28840
 wavefronts, a special case 9-25342

acoustic waves

- see also Dispersion/acoustic*
 lenses, fluid, Luneberg-Gutman, wave analysis 9-29297
 lenses, underwater, nearly spherical, low aberration 9-27233
 at shear layer in fluid 9-45856

acoustic waves, ultrasonic

- birefringence in stressed crystals 9-30642

electromagnetic waves

- see also Electromagnetic wave propagation*
 ionospheric, i.f., 60 to 6000 km 9-31387
 by moving uniaxially anisotropic slab 9-34119
 plasma waveguide props. 9-48561
 reflection-refraction at interface bet. isotropic mats. under applied static elec. field, electro-opt. eff. theory applic. 9-25145
 Venus atmosphere, radio and optical 9-38065

refraction**light**

- see also Double refraction*
 atmospheric rel., holographic image degradation 9-40366
 in electrooptic cubic crystal 9-41357
 film, nonabsorbing, on isotropically absorbing substrate ellipsometric obs. 9-33504
 half-prisms, symmetrically crossed, geometrical spectra 9-27370
 merit gases, in far u.v., Pade summation of Cauchy dispersion eqn. 9-48666
 porcelain enamels, TiO₂ opacified, reflectance and colour 9-37687
 prism, minimum deflection for symmetric ray paths, elementary proof 9-36338
 system, 2 surface with zero 3rd order spherical aberration 9-40376
 Snell's law and gravitational deflection of light, corpuscular theory justification 9-29155
 turbulent atmosphere with Gaussian correl. index fluctuations 9-31323
 Venus atmosphere 9-38065
 H₂, in far u.v., Pade summation of Cauchy dispersion eqn. 9-48666
 H in far u.v., Pade summation of Cauchy dispersion eqn. 9-48666
 K₂D₂PO₄ crystal, double, induced by elec. field, fourth-order effect 9-41358
 N₂, in far u.v., Pade summation of Cauchy dispersion eqn. 9-48666
 O₂ in far u.v., Pade summation of Cauchy dispersion eqn. 9-48666
 RbH₂PO₄ crystal, double, induced by elec. field, fourth-order effect 9-41358

Refractive index

- differential-prism method of distrib., inhomogeneous optically transparent media 9-22469
 effective for coherent field in random medium 9-27257
 liquid, variation due to continuous distrib. of resonances, Debye and Gaussian type 9-32782

Refractive index continued

- liquids, absolute, intensity-dependent var. 9-26105
- liquids, nonlinear, local field theory 9-26107
- lucite, X-ray index obs. 9-39798
- radio, atmosphere, 1965, India 9-28895
- radio, upper troposphere over India 9-28894
- Ag colloidal particles, electron m.f.p. limitation, wavelength depend 9-41115
- Be X-ray index obs. 9-39798
- Cr, 293 and 420°K rel. to mag. props. 9-24359
- KZnF₃ single crystal perovskite structure, hydrothermally synthesized 9-42746
- LiF X-ray index obs. 9-39798
- NaF X-ray index obs. 9-39798

light

- see also Dispersions, optical; Double refraction; Optical constants*
- aerosol particles, atmospheric, influence on size determ. 9-28889
- atmosphere, vertical spectra rel. to stability 9-41526
- atmospheric variation, rel. to laser beam propag. 9-31968
- beryl, press. depend., rel. to photo elasticity 9-47317
- coals and soots, i.r. region 9-24357
- crystal, rel. to magnetoelec. effect 9-43218
- dielectrics, changes rel. to radiation damage, ellipsometric analysis 9-35295
- dielectrics, isotropic, dispersion in absorption bands 9-35617
- effective for coherent field in random medium 9-27257
- ethanol, shocked-state 9-44566
- eye lens, refr. index distrib. 9-47702
- films, thin, slightly absorbing, ellipsometric meas., thickness 9-37678
- glass, changes production by Na-Li ion-exchange techniques 9-49241
- glass, temperature dependence 9-26698
- glass, various types, function of wavelength and temperature 9-37685
- glycerol, shocked-state 9-44566
- homogeneity meas. by two angle method 9-48091
- ice I, complex refr. index 4000-30 cm⁻¹ 9-45264
- inelastic-electron-scattering and optical data, parametric calc. 9-37679
- inert gases, condensed 9-47316
- liquid and solid state of some gases 9-44562
- of liquid medium, complex, relationship of real and imaginary parts 9-44563
- liquids, relation with density 9-23496
- nonlinear, of liquid, eff. of interaction betw. anisotropic mols. 9-23498
- nonpolar fluids, elec.-induced anisotropy 9-38938
- photon-matter interaction energy 9-43907
- pyrographite, i.r. region 9-24357
- ruby, changes during pumping 9-29424
- waves in nonlinear medium, e.m. theory 9-25351
- As₂S₃, amorphous, 0.6-2μ 9-39797
- C and coals, i.r. region 9-24357
- α-CdS, press. depend., rel. to photo elasticity 9-47317
- Cu₂S films, for forbidden band width 9-44949
- CuAlS₂(Se₂), single cryst. prepared by vapour transport with iodine 9-48797
- o-D₂, liq., 3200Å Cherenkov radiation, 24.2°K 9-40791
- EuO, effect of mag. order 9-45266
- EuS effect of mag. order 9-45266
- Ga single crystals, meas. along principal axes 9-33502
- HBr, far I.R., obs. 9-48460
- LiYF₄, of cry. grown from melt 9-23683
- (Mg,Fe):SiO₂, olivine, and absorpt. spectra, 1.7° to 290°K 9-45324
- MnO, from reflectivity obs. 9-45308
- Na₃AlF₆ films, evaporated, influence of various parameters on refractive index 9-33503
- Se, amorphous, electric field influence 9-35618
- Se single crystal 9-26699
- Si film, on isotropically absorbing substrate, ellipsometric obs. 9-33504
- Sr(NO₃)₂, photochromic, change meas. 9-26700
- of TeO₂ based glass 9-41352
- ThF₄ films, evaporated, influence of various parameters on refractive index 9-33503
- TiO₂, reactively vacuum-evaporated layers, rel. to structure 9-42729
- ZnO, press. depend., rel. to photo elasticity 9-47317
- α-ZnS, press. depend., rel. to photo elasticity 9-47317
- ZnTe, semicond., interpretation in quantum mech. model 9-39811

Refractive index measurement

- liquids, linear refractometer design 9-34906
- solutions, and conc., shadow-optical meas. 9-46636
- solutions, two simple methods requiring only microscope and spectroscopic cell 9-46635
- thin films, meas. method 9-31071
- Nd:YAl garnet rod laser 9-22412
- Sr(NO₃)₂, photochromic, changes with coherent light illumination 9-26700

Refractometers

- for atmosphere obs., portable 9-38407
- critical angle, linear, for liqs. 9-34906
- interferometric, automatic, for liquids and gases 9-22465
- shadow-optical, for solution refr. index and conc. 9-46636

Refractories *see High-temperature phenomena and effects***Refrigerators** *see Low-temperature production***Regge poles** *see Elementary particles/scattering***Relativity**

- Champeney and Moon's rotating Mossbauer expt., comments 9-45750
- communications effects associated with fast-moving space antennas 9-47736
- cosmology 9-26983
- dynamics, analytic, 2nd-order eqns. deriv. methods 9-40236
- earth's motion through ether detection null result explanation 9-29179
- Einstein cosmological eqns., Schwarzschild metric generalization 9-22075
- e.m. field correl. in presence of random sources 9-25137
- energy density propag., causality 9-25031
- evaluation of some aspects 9-34020
- faster-than-light particles, popular article 9-47737
- faster-than-light particles, popular article 9-45748
- field theory, commutator expectation value weakening, local field theorem 9-22505
- heat, engines, relativistic, Planck's and Ott's formulation 9-43798

Relativity continued

- invariability of velocity of light, expt. to test validity of Einstein's second postulate 9-41744
- lever problem, non-rotating, viewed from different systems 9-27164
- Lorentz electron theory, history of his work 9-43697
- magnetohydrodynamics, circulation and related topics 9-30196
- mass and momentum transformation under special conformal transformations of space-time conformal group 9-43730
- Maxwell rels. and Riemann space characts. 9-22077
- plasma wave nonlinear Vlasov eqn., relativistic regime 9-44436
- quantum theory, relativistic, gravitational interactions study 9-47733
- radiation, black body, in transparent medium, coherence props. 9-22076
- relativistic motion in straight line, comments 9-47735
- Schrodinger equation corrections 9-22094
- space, topological struct. 9-43729
- spinning particle, classical treatment, book 9-41766
- spinning particle with structure, eqns. of motion 9-34019
- tachyons do not violate causality 9-45751
- temperature, relativistic transformation 9-45780
- thermodynamics foundations and space dynamics 9-38308

general

- see also Cosmology; Gravitation; Space-time configurations*
- accelerated charge, at rest or freely falling rel. to gravitational field, radiation 9-38214
- action principle, quadratic 9-38218
- Alfvén shock, necessary and sufficient conditions 9-30184
- Bondi-Sachs analysis of empty space fields, pure radiation news function 9-38220
- charge and mass distrib., exact fields of Einstein eqn. 9-31759
- closed time-like lines, paths in universes 9-43733
- clusters of point masses, models with large red shift 9-45584
- conservation laws, review 9-34024
- conserved quantities obtained by Newman-Penrose formalism group theoretic approach 9-38215
- coordinates, co-moving, junction conditions for spherically symmetric matter 9-31756
- covariant tetrad conservation-law generators 9-41750
- cylindrical thin shells, soln. 9-45759
- de Broglie wavefield, eqns. in the case of spherical symmetry 9-45761
- Einstein's eqns., approx. radiative solns., construction 9-45763
- Einstein's eqns., source specification, soln. without metric 9-38221
- Einstein's equations, exact static exterior and interior soln. for thick plane plate 9-31757
- Einstein's field eqns. first order approx. to spherically symmetric soln. 9-38217
- Einstein empty space field eqns. soln., Newman-Penrose method for twist-degenerate metrics 9-45760
- Einstein field eqns., Reissner-Nordstrom soln. generalization 9-45762
- Einstein spaces of second embedding class 9-22082
- Einstein vacuum field eqns. in Weyl co-ordinates, exact soln. 9-41751
- Einstein vacuum field equations, stationary 'noncanonical' solns. 9-41749
- Einstein-Maxwell eqns., mass dipole problem of Weyl soln., study using calculus of delta functions 9-45765
- Einstein-Maxwell eqns., use of delta functions for integration consts. eval. 9-45764
- e.m. momentum in matter, relativistic aspects, 'try simplest cases' resolution 9-29374
- equations of motion and structure of singularities 9-34025
- equations of motion in internal central symmetric field 9-22083
- gravitation, Birkhoff's theory, four-vector force 9-29187
- gravitation, Einstein's equations in mixed initial and boundary value problems 9-25037
- gravitation, spherical symmetric distributions 9-25036
- gravitational field equations in Birkhoff's theory, from potential of point mass 9-36126
- gravitational fields, stationary axial symmetric, internal solution 9-25035
- gravitational radiation theory, invariant formulation 9-22084
- gravitational waves, Einstein-Maxwell field 9-29186
- Greens theorem generalization appl. 9-22086
- inertia and cosmology, reln. 9-47741
- Kundt gravitational waves 9-22085
- light propagation, influence of gravitational field 9-22080
- mass, relative 9-22081
- mass dipole problem of Weyl soln. in Einstein-Maxwell theory, study using calculus of delta functions 9-45765
- massor fields, one-component, model, charges, props., Lagrangians 9-45757
- matter evolution, surface distrib. 9-47747
- modification for gravitational field quantization 9-29184
- one-body problem, solns obtained by Lorentz-invariant theories of gravitation 9-27166
- particle affected by gravitational and e.m. actions, quantum relativistic energy 9-47748
- particle model, spherically charged, extension 9-22087
- perturbations of arbitrary spherically symmetric metric, rel. to collapse 9-31491
- photon delays near relativistic stars 9-29018
- predictions, verification from radar and optical observations of minor planet Icarus 9-31604
- radiating spheres, zero-limb darkening, exterior solution 9-24782
- radiation field, 3°K, black-body radiation obs. by moving observers 9-24719
- relativistic, Doppler eff. in spectral lines, ambiguity 9-22436
- Schwarzschild's incompressible sphere, relativistic, iterative scheme for soln. 9-45591
- Schwarzschild problem, quaternion soln. allowing for zero neutrino mass 9-31758
- spinning particle dynamics 9-47739
- spinning three-leg propagating in association with pole-dipole-like mass distribution 9-47740
- stars, isentropic, evolution 9-45609
- static homogeneous formations and planckneons 9-36125
- stellar models, adiabatic fluid spheres, struct. and stability 9-24764
- superluminal behaviour, causality, and stability 9-47744
- T-models, spherically-symmetric, in theory 9-41620
- T-models of 'sphere' 9-43507
- tachyons and their interactions, quantum mechanical description 9-43735
- test in radar obs. on planets 9-24932
- theory test using pulsars 9-24825

Relativity continued**general continued**

validity, possible meas. via Doppler effect in transmission from Earth satellites 9-41615

Weyl gravitational and zero-rest-mass scalar fields, coupled 9-43736

special

angular-momentum flux for gravitational radiation to octupole order 9-45755

clock paradox 9-34023

clock paradox, inconsistencies 9-41747

clock paradox, thought expt. 9-36124

disproof of Dingle reply and criticism 9-34021

dynamics of variable rest mass systems 9-43771

Einstein's eqn. of motion of test part in 'weak gravitational field' modification 9-34016

Einstein-Maxwell equations, solution for a cylindrical, electric current 9-22078

expanding wavefronts demonstrated on computer-generated film 9-43698

extension to hold for expanded electrodynamic theories, universal const. problem 9-22079

heat transformation in relativistic thermodynamics 9-22270

lever, right-angled, stress; Laue soln. review 9-41745

lever, right-angled, stressed 9-41746

metric, conditions for fixing 9-47738

Michelson-Morley expt., fringe shift and wave-train superposition and interference 9-45754

Michelson-Morley expt., phase shift upon 90° rotation 9-45752

Michelson-Morley expt. performed in solid transparent medium as test 9-43732

space and time meas. in flat space 9-45743

speed transformation between inertial frames 9-45753

teaching, four new approaches, survey 9-43707

teaching, relationship between rest mass and pot. field 9-47715

tested in cosmic ray obs. of π , μ lifetimes 9-34022

thermodynamics relativistic, appl. of dynamics with variable rest mass 9-43731

time dilation and length contraction examples 9-29183

torques and angular momentum of a system in equilibrium 9-38213

two-particle collision kinematics, convenient 4-vector eqn. 9-36123

validity of theory 9-25034

validity of theory 9-25032

validity of theory, Lorentz transformation, underlying physics 9-25033

velocity addition formula, representation in circular functions 9-38212

unified field theories

Birkhoff's theory and potential of point mass 9-22088

Einstein's space-time, beginning of unified formalism 9-43737

gravitation and c.m., geometric description 9-27167

massor fields, one-component, model, charges, props., Lagrangians 9-45757

strong, c.m., weak and gravitational interactions, relation in value of G 9-41752

vector meson interacting with gravitational field 9-38222

Relaxation

see also *Acoustic wave propagation. Dielectric phenomena; Elastic relaxation; Ferroelectric phenomena; Ferromagnetic relaxation; Molecules/relaxation; Nuclear magnetic resonance and relaxation; Paramagnetic resonance and relaxation*

air ionization relax. behind shock waves 9-42560

alkali halide crystals, rate, effect of dislocations 9-33026

alkali metal atom, spin relaxation, optical obs. in buffer gas 9-29942

alkali-borosilicate glass, spectrum and fluctuation theory 9-26096

autofretted cylinders, effect of time and temp. on residual stresses 9-33030

Brownian particle, quantum corrections to momentum relax. time 9-43756

Cellofas, solns., dil., relax. effects in flow through tubes and granular beds 9-32748

collision-induced, anisotropic, in gas, of multipole moments, cross section determ. 9-32426

dielectric, of γ -irrad. tetrafluoroethylene-hexafluoropropylene copolymers, 78°-300°K obs. 9-26586

dielectric material, relaxation times distribution calc. from experimental data 9-35464

dielectric relaxation of some crystalline heterochain polymers 9-24216

dielectrics, distributions of relaxation times, Argand diagrams 9-33370

dispersion struct., and creep under humidity fluctuations 9-44601

electron ion temperature, at plasma interface 9-23268

ferroelectrics, Gaussian distrib. of relax. times in paraelec. large signal susceptibility obs. 9-24217

ferromagnetic metals, elastic relaxation, influence on viscosity phenomena of intercrystalline layers, and mag. field effect 9-33013

ferromagnetic metals, elastic relaxation, influence on viscosity phenomena of intercrystalline layers, and mag. field effect 9-23848

gas laser in mag. field, collision-induced anisotropic relax. 9-31940

glass, mixed alkali, non-linear variation due to alkali oxide replacement 9-39148

glycerol solns., relax. effects in Couette flow between rot. cylinders 9-32749

hard-sphere gas, relax. times 9-43767

ice, mechanism, diffusion theory 9-28318

ionization, of non-equilibrium plasma 9-46456

multilevel systems, transition rates 9-36644

oscillations of photons in inverted, coupled systems 9-37612

Pb₂MgNb₂O₇-Pb₂NiNb₂O₇ system, dielectric, accompanied by correlated dispersion of mechanical props. 9-28564

permalloy film, process, dynamic Kerr obs. 9-45169

polyacrylamide, solns., dil., relax. effects in flow through tubes and granular beds 9-32748

polyacrylamide solns., relax. effects in Couette flow between rot. cylinders 9-32749

polymer solns., dil., relax. effects in flow through tubes and granular beds 9-32748

polymers, crystalline heterochain, dielectric relax. 9-24216

polypropylene, crystallinity influence 9-34974

polyurethane, nonlinear viscoelastic, stress relax., torsion creep 9-31838

quantum systems with equidistant spectra 9-29193

rubber vulcanizates, stress relax, simple viscoelastic model 9-30645

steel, Si, mechanical and magnetic, infl. of H impurity 9-30644

string oscillator 9-43749

u.s., in liq., theory with vib. point as group of mols. 9-30389

Relaxation continued

viscoelastic materials, linear, relax. tests, error functions 9-33019

zircalloy-4, radiation enhanced relaxation 9-41006

Ag-(0.26 at.%)Cu alloy, stress relax. from internal friction meas. 9-48885

Ag-Cl-Cd single cryst., vacancy-dipoles 9-33372

AgCl transition-metal doped single cryst., vacancy-dipoles 9-33372

CO₂ lasers, effect on gain saturation 9-47969

CaF₂:Eu²⁺ spin lattice time, rel. to magnetic field, Faraday rot. obs. 9-49228

CaF₂:NaF, electrical and mechanical 9-28548

Cu-(2.5 wt.%) Zr-(0.5 wt.%)Nb alloy, radiation enhanced relaxation 9-41006

Cu-base α -solid solns., elastic fields, rel. to splitting and distrib. of dislocations 9-32968

α -Fe-C-N solid solution, permeability disaccommodation, -40°-+180°C 9-26322

α -Fe, stress, and use of Johnston-Gilman eqn. in analysis of thermally activated flow 9-30672

n-Ge, electrical conductivity 9-30925

KCl, dielec., effects due to air-gaps in specimen-electrode contacts 9-37581

KD₂PO₄, Ising spin system near Curie temp. 9-35483

MnO₂:Li, dipole relaxation and loss 9-35466

(NH₄)₂HfF₆, γ - γ angular correlation determ. of relaxation constant 9-37675

NaCl, dielec., effects due to air-gaps in specimen-electrode contacts 9-37581

Ni, stress relax. at 20, 77, 200 293°K 9-48891

Rb-rare gas mol. formation, Rb polarized atom relaxation in rare gas, theory 9-32534

Ti, relaxation tests for thermally activated deformation parameters 9-28350

α -Ti, spectrum, effect of H content, comment 9-30647

α -Ti, spectrum, effect of H content, comment 9-30648

TiO₂, reduced rutile, ionic defects rel. to mech. and dielec. relax. of hopping electrons 9-44690

Zn-Ag dilute alloys, time of electrons, de Haas-van Alphen studies 9-37424

Zn-Mn dilute alloys, time of electrons, de Haas-van Alphen studies 9-37424

Zn, pure, grain boundary relax. 9-44715

Remanence see *Magnetization state*

Renner effect see *Molecules*

Replica techniques see *Electron microscopy*

Reproduction see *Sound reproduction*

Resistance, electrical see *Conductivity, electrical*

Resistance thermometers see *Thermometers/resistance*

Resistivity see *Conductivity, electrical*

Resolving power, optics

see also *Optical instrument testing*

diffraction gratings and telescopes 9-22464

diffraction limited for line objects and circular aperture 9-43918

electron scanning microscope 9-43854

eye, dependence on various combinations of aberrations 9-27129

frequency conversion in Proustite, 10.6 μ m to visible spatial resolution obs. 9-26676

grazing-incidence spectrometer, optimum adjustment 9-34229

of imaging sensors for low light-level 9-29477

imaging system, statistical estimation 9-27375

incoherent objects seen through turbulent medium 9-41531

lens, improvement using Hoppe zoneplate 9-22441

of mass spectrometer, elec. deflection type 9-38746

in microscope design 9-46011

microscope exit pupil holographic enlargement using partially coherent light 9-22466

solar granulation, possible 'smearing' effects 9-36062

testing in electron microscopy 9-40324

Resonance, elementary particles see *Baryons/resonances;*

Hyperons/resonances; Mesons/resonances

Resonance, magnetic see *Magnetic resonance and relaxation*

Resonance spectra see *Spectra*

Resonators

active crystal, orientation rel. to ruby laser generation spectrum 9-38379

astigmatic, intrinsic freq. and field distrib. on mirrors, geometrical optics approx. 9-27306

beams response under concentrated moving masses 9-31828

cavity, superconducting Pb, r.f. absorption measurements for TE and TM modes 9-47092

cavity resonator for studying elec. susceptibility of ionized gases 9-34136

circular, in gas laser, emission modes 9-25234

confocal, with ring-shaped aperture, eigenfunction system 9-47942

confocal unstable, with CO₂-N₂-He laser, properties 9-47973

confocal-mirror, multislit coupling structure, sampling theorem applic. 9-36220

dielectric, radiation Q factor, theory 9-25138

dielectric cavity, TE_{01n}; design curves, quality factor, e.s.r. spectrometer input 9-38326

Fabry-Perot, asymptotic expansion theorem 9-47944

Fabry-Perot, mode control 9-47943

Fabry-Perot, review 9-25226

Fabry-Perot, review and literature survey 9-25225

Fabry-Perot, transverse, stimulated Raman scattering in 9-25724

ferrite sphere, electromagnetic resonances, axial-symmetric modes 9-27256

lase with rotated directions of principal curvatures, c.m. oscillations determ. 9-27307

laser, 2-mirror cavities, unfolded directions of principal curvatures 9-25228

laser, adjustment effect on beam output angle 9-29403

laser, axial mode freq. computation 9-22377

laser, geometry rel. to power output, calc. 9-25221

laser, mode structure theory 9-48014

laser, ring, phase reln. for mode capture different Q factors 9-27308

laser, spectrum transient behaviour 9-25224

laser, temp. dependent incidence of optical radiation; patent 9-47946

laser, transverse modes, competition and stimulated switching effects 9-25223

laser cavity, u.s. beam transmission, patent 9-47947

Resonators continued

- laser optimization rel. to minimal pulse-width generation by Q-switching 9-34156
- laser with rotated directions of principal curvatures, e.m. oscillations determ. 9-31935
- lasers, coupled, operating conditions as function of relative detuning 9-41891
- lasers with resonator mirrors with variable transmission over cross-section, spatial and energy charact. 9-29401
- length shifts meas. down to 10^{-3} Å with two-mode laser 9-47941
- microwave 90° roof model 9-27313
- with mirror, for laser structure, patent 9-47948
- multicavity optical 9-45947
- open, with spherical mirrors, Q-factor determ. 9-34115
- open with plane mirrors, vibrations rel. to angular distrib. selector 9-36279
- optical, astigmatic, 3-dimensional, ray theory 9-27401
- optical, cylindrical, lens inside matched to mirror, field and natural freq. calc. 9-25227
- optical, different types 9-40340
- optical, Huygens' principle in inhomogeneous isotropic media and integral equation 9-29398
- optical, mode selection by thin scatt. film in standing wave field 9-25229
- optical, non-planar end reflectors, normal modes 9-27314
- optical, off-axis, stimulated Brillouin scatt. 9-25219
- optical, open with plane circular mirrors, polarization state 9-43876
- optical, small calibrated damping introduction method 9-22376
- optical, stimulated combination emission of Raman light 9-36278
- optical, with absorbing film, for mode selection 9-36276
- optical cavities, degenerate, comprising lenses 9-25344
- optical nonlinear, parametric generation without reflecting dielec. coating 9-47945
- parametric, impulsive parameter modulation, instability 9-30277
- in particle accumulator, tuning 9-48244
- plane mirror, coupled, diff. losses 9-45892
- quartz, synthetic, growth and properties 9-39201
- spherical laser with passive shutter, pulse duration obs. 9-27305
- T-shaped, four-mirror, in He-Ne laser, longitudinal mode selection 9-43885
- three-mirror, in He-Ne laser, mirror motion influence on generation power 9-22399
- CO₂ laser cavity, Q switching 9-29414
- GaAs junction laser, dependence of total stimulated light power and gain factor on length 9-48041
- GaAs junction lasers, spectra at currents 1.5 to 3 times threshold level 9-48042
- GaAs laser, coherence, intensity distrib. of emitted radiation 9-45965
- GaAs laser diodes, differential quantum efficiency and gain dependent on length 9-45964
- He-Ne laser, $3s_2$ - $3p$, Ne transition line spectral width meas. 9-22960
- of He-Ne laser containing GaAs diode laser, absorption by non equilibrium carriers 9-38383
- He-Ne lasers, for mode quenching to obtain high bit-rate pulses 9-31945
- Pb cavities, supercond., technology of prod. 9-39607

acoustic *see* Acoustic resonators

electromagnetic *see* Electromagnetic oscillations

Reverberation

- see also Architectural acoustics; Echo*
- curve, of several rooms, integrated tone bust method 9-36198
- in library and lecture rooms 9-34090
- power meas. in chambers 9-45864
- rooms separated by solid and hollow walls 9-25107
- sea, surface reverberation, relative contribs. of surface air bubbles and waves 9-24610

Reviews

- ³He props. and solns. in ⁴He 9-23562
- accelerators, cybernetic 9-27602
- approximation theory of complex functions 9-22046
- astronomical instruments 9-31680
- atmosphere, upper, semi-annual density vars. 9-49461
- atmosphere remote sensing using radiometric techniques at microwave frequencies, review 9-33780
- atmospheric aerosol 9-43385
- atmospheric electricity 9-31327
- atomic and molecular theory related to lasers 9-40344
- atomic collisions between excited and unexcited atoms 9-36679
- atomic transition probabilities, theoretical 9-27802
- aurora's rel. to polar substorms, expt. and theory 9-37957
- aurora, optical morphology 9-35847
- auroral spectroscopy and excitation mechanisms 9-31371
- baryon resonances 9-42112
- Boltzmann eqn., approx. methods of soln. 9-47764
- Boltzmann equation solution methods 9-47765
- boson resonances 9-40432
- ceramic nuclear fuels, radiation effects 9-22902
- charge of state, popular article 9-48734
- charged-particle tracks in solids 9-24067
- cloud physics 9-31312
- color meas. in USA 9-41949
- colorimetry in Europe 9-41950
- comet tails 9-24883
- conservation laws in general relativity 9-34024
- continental drift described, popular article 9-49403
- copolymerization in solid state, review 9-28792
- cosmic ray variations, diurnal and sidereal 9-35918
- cosmological constant Λ rel. to the theory of elementary particles 9-45593
- cosmology, isotropy of 3 deg. background radiation 9-38031
- crystal growth, high-temp. and high-pressure solution 9-37015
- crystal growth, morphological stability at interface separating solid and liq., review 9-37016
- crystals, for research and technological applications 9-36971
- current algebra 9-40396
- current algebra 9-22541
- current algebra and sum rule methods 9-36423
- current algebra results in weak decays of metastable hadrons 9-42024
- dielectric breakdown in solids, research trends 9-30968
- dielectronic recombination 9-44496
- diffusion mechanism and point defects in silicon and germanium 9-37209

Reviews continued

- dislocation climb mechanism 9-28287
- divergent X-ray method, principle technique and applics. 9-32888
- DNA, hydrodynamic properties 9-23415
- double, star evolution 9-38051
- earth's outer geomag. field, particle flux obs. 9-37965
- earth's outer radiation belt particle dynamics 9-37964
- earth's radiation belt, formation 9-37963
- electric dipole moment of elementary particles 9-43960
- electro- and magneoptical props. of solids 9-31078
- electro-optical properties and harmonic generation in single crystals 9-28659
- electrolysis and simple cells, non-technical 9-35753
- electron-diffraction, low-energy, band structure and dispersion surfaces in 3-dimens. mixed Laue and Bragg reflections 9-37126
- elementary particles, conference report (1967) 9-46045
- elements, their origin, popular article 9-49522
- e.m. interactions, applic. of symmetry and current algebra 9-25427
- e.m. wave scatt. by spheres 9-36357
- equations of state, analytical and experimental, isothermal data fit for Hg, water 9-36844
- eutectic growth, lamellar and rod-like 9-37049
- extragalactic research, review 9-40194
- Fabry-Perot resonator 9-25226
- faster-than-light particles, popular article 9-45748
- ferroelectricity of solids, recent developments 9-33384
- ferromagnetic thin film saturation magnetism 9-49209
- fibre optics 9-29474
- fluids at supercritical press., forced convection heat transfer 9-26151
- Fourier transform spectroscopy 9-32051
- fracture toughness in predicting low-stress failure in materials 9-28363
- friction, dry, testing, basic principles 9-36157
- fusion, low- β research 9-27762
- fusion research, survey of USAEC'S program 9-23313
- galaxies of local group 9-38039
- gas breakdown, laser induced 9-25985
- gas laser developments and uses 9-36284
- gas sorption analysis techniques 9-35758
- geomagnetic conjugate-point phenomena 9-35901
- geomagnetic field, diurnal vars. and associated upper atmos. phenomena 9-47591
- geomagnetic field diurnal vars. and their meas. 9-49508
- glass, high pressure effects at different temps. 9-28193
- Goldstone theorem. 9-41980
- group theory in atomic physics 9-46266
- group theory in solid state 9-46694
- growth from metal solutions 9-37017
- hadrons, metastable, weak decays 9-36438
- heat resistivity and heat-resistant metallic materials 9-33179
- helicon waves in solids 9-26489
- holographic microscopy 9-48061
- holography, capabilities and applications 9-34182
- holography (1969), book 9-40372
- holography and coherent imaging 9-25321
- ice, structure and point defects, effect on elec. and mech. props. 9-48832
- image enhancement technique 9-29443
- image formation by the eye 9-29125
- image intensifier systems 9-24937
- intergalactic matter 9-26993
- internal reflectance spectroscopy, review 9-36388
- interplanetary plasma, observed props. 9-24894
- interstellar dust grains 9-27051
- interstellar grains, nucleation and growth 9-24817
- interstellar medium, structure and dynamics 9-29038
- ion charge transfer in gaseous discharges 9-32699
- i.r. absorption bands, integrated intensities, review 9-42366
- i.r. spectra of adsorbed molecules 9-42367
- isobaric analog resonances popular article 9-46189
- isotopes and elements, synthesis 9-44105
- Josephson effects, experimental work 9-33277
- Landau damping and echo review in a plasma 9-42546
- lasers, organic dye 9-43887
- light scatt. near critical point for fluids and non-fluids 9-36876
- light waves in nonlinear medium, e.m. theory 9-25351
- lightning, e.m. radiation from developments in Japan since 1963 9-37925
- liquid metal structure studies by means of X-ray, neutron and electron diffraction 9-36846
- macromolecular 9-23183
- magnetic materials, soft 9-39753
- magnetosphere, quantitative models 9-37945
- magnetospheric, 100 to 10^5 Hz 9-37947
- magnetospheric convection and rel. to storms, aurora and rad. belts, review 9-37951
- magnetospheric electrons, pitch angle diffusion 9-37948
- magnetospheric low energy plasma 9-37949
- measurement in quantum mechanics 9-43743
- melt-growth of oxide crystals, developments 9-37048
- Mercury, Venus, and Mars, surfaces, atmospheres, radiation 9-27086
- meson, baryon resonances in May 1966 9-22633
- meson and baryon resonances, mass, spin and parity 9-36498
- metal oxides surface diffusion 9-37198
- metal phase stability 9-48936
- metals, e.s.r., results of 'selective transmission' technique 9-28743
- MHD power generation in Japan 9-22332
- Mossbauer spectroscopy, charact., equipment and applics. 9-47329
- neutron diffraction examination of liquids and solids 9-47419
- neutron diffraction examination of liquids and solids 9-37785
- new thermophysical meas. instruments 9-41846
- non-linear optics 9-41932
- non-linear optics 9-48078
- nonleptonic decay 9-40398
- nuclear forces, repulsive core 9-40464
- nuclear fusion, Japanese research 9-22829
- nuclear physics, experimental 9-36555
- nuclear physics, theoretical problems 9-46185
- nuclear physics, theoretical problems 9-36556
- nuclear reaction theory taking channel coupling into account, review 9-42261
- nuclear struct. from (d,p), (d,t) reactions 9-34380
- nuclear-force models 9-44108

Reviews continued

- nucleon-nucleon scatt., phase shift analysis, 400 MeV > 10 GeV 9-40439
 optical parametric devices and pulsed lasers 9-48011
 oxide crystals, melt-growth, developments 9-37048
 particle accelerators since Veksler 9-25548
 particle focusing and channelling in cryst. 9-35294
 photoelasticity, selected papers of Max M. Frocht 9-41803
 photon mass. 9-43967
 physical chemistry of transport processes 9-37816
 planetary rotation 9-29072
 plasma, partially ionized equilibrium composition statistical mechanics calc. 9-22141
 plasma kinetic theory 9-40657
 plasma physics, Italian work reviewed for year 1966-67 9-27970
 plasmoids r.f., and resonance-sustained gas discharges 9-36783
 polarons in transition-metal oxides, present status 9-28454
 polyacrylonitrile and its copolymers, props. in solution and solid state 9-28200
 polymer growth, simplified, treatment including chain folding 9-36989
 polymer solids, diffusion, permeability and solubility of low mol. wt. penetrants 9-39389
 polymers, high-resolution n.m.r. examination 9-42463
 pore diffusion in solids 9-37188
 positron beam production and expts., popular review 9-43847
 pulsars, review of models 9-38059
 pulsars discovery 9-45654
 quantum fluids, descriptive 9-34043
 quasars 9-36005
 quasars speculative theories 9-38055
 radar aurora and ionospheric plasma instabilities 9-33822
 radiation detectors for space 9-45578
 radiation shielding 9-32372
 radio aurora research (1963-7) 9-35854
 radio sources, variable 9-29052
 radio spectra 9-29042
 rare earth orthoferrites, mag. and spectroscopic props 9-45232
 Regge pole theory 9-22568
 Regge pole theory, systematic review of recent developments 9-48168
 regge pole theory, systematic review of recent developments 9-48167
 scanning electron microscope, applic. to semiconductor devices 9-32892
 semiconducting material physics 9-41191
 semiconductor doping by ion implantation 9-35411
 semiconductors, amorphous, popular review 9-44948
 solar active regions, statistics 9-24921
 solar plasma 9-45686
 solar radiation integral absorption coefficient determ. 9-41841
 solar radioastronomy 9-36043
 solar system origin, collection of popular reviews, book 9-49575
 solar wind interaction with magnetosphere, lab. expts. 9-37944
 space probe orbital information on planet masses and lunar mascons, popular article 9-47607
 spherical shell, buckling 9-22212
 stars, rotating, atmospheres 9-24772
 stellar evolution, collection of popular papers, book 9-45613
 stellar spectra, collection of reprinted popular articles, book 9-45621
 sun decimetres whole-sum observations 9-36052
 sunspots 9-24922
 superconducting magnets 9-28482
 superconductors, new 9-44924
 surface meas. in tribology 9-36105
 telescopes for the amateur astronomer, book 9-49597
 thermal conductivity of 46 gases at atmos. press. 9-26025
 thermal decomposition of irradiated materials 9-24533
 thin films, optical properties in vacuum u.v. 9-26696
 time, astronomical and atomic standards 9-29168
 transition metal phase diagram computation 9-48936
 transition metals, b.c.c., point defects 9-26274
 transport coeff. for moderately dense gas, theory 9-36802
 u.s. holography 9-48066
 u.s. meas., diff. effects 9-25099
 vacuum u.v., spectroscopy, optics, apparatus, techniques and applics. 9-46017
 variable stars, research 9-40150
 Venus atmosphere 9-24875
 Venus upper atmosphere 9-24871
 vision, energetic theory aspects 9-31715
 wear testing of dry and lubricated systems 9-37267
 weather modification 9-43394
 white dwarfs 9-27019
 Wolf-Rayet stars, review of population I type 9-24793
 X-ray astronomy modulation collimators 9-47690
 X-ray astronomy observational techniques 9-29107
 zodiacal light 9-38096
 zone refining, techniques and applications 9-23674
 ΛN interaction 9-36497
 v in astrophysics 9-38029
 ^{226}Lw , properties, half-life and α spectra 9-36584
 Al_2O_3 , specific heat of solid 9-37355
 Al corrosion 9-26828
 Be and BeO, radiation effs. 9-24069
 H atom energy level nuclear corrections calc. by effective potential model 9-36681
 He solid, second sound obs. 9-42689
 Hg arc Raman spectra of gases 9-46340
 OH clouds in space, popular review 9-45635
 SiC, structure 9-26245
 UO_2 , O and U self-diffusion rel. to comp., obs. 9-37210

Reynolds number *see Flow; Hydrodynamics***Rhenium**

- chemisorption of N_2 and CO 9-49376
 electrodeposition 9-37841
 paramagnetic susceptibility, 20.4° to 293°K 9-31024
 pyrolytic deposition from ReCl_5 9-39199
 surface phenomena obs. by field emission and field ion microscopes 9-46719
 surface vaporization of Sr atoms and ions 9-37637
 wire, Young's modulus at high temp., u.s. meas. 9-42966
 work function, effect of surface oxidation and effects on Na, Na halides and LiCl ionization 9-35522
 work function and surface energy correlation 9-33414

Rhenium continued

- W-Re thermocouple, type-VR 5/20, calibration characts. 9-34105

Rhenium compounds

- oxides, superconducting transition temp. determ. rel. to tungsten bronze type structure 9-26530
 Cr-Re alloys coexistence of mag. phases, neutron diff. obs. 9-39750
 K_2ReO_3 , with tungsten bronze type structure superconducting transition determ. 9-26530
 Mo-(27 at.%)Re alloy single crystal, thermionic emission of (100) face 9-47211
 Mo-Re alloys, field emission and surface struct. in α - and σ -phases 9-24250
 Ni-Re alloy films, electro-deposited, phase and chemical composition 9-44791
 $\text{Re}_2(\text{CO})_{10}$ nematic soln., polarization of absorpt. bands in i.r. region 9-44336
 Re complex, hexahalogen, K and Cs salts, vibration spectra and force constants 9-32487
 $\text{Re}(\text{CO})_6^+$, vibrational and electronic spectra and bonding 9-32491
 ReClO_4 , vibr. freq., theoretical anal. 9-23069
 ReF_6 spectrum, i.r., Jahn-Teller effect 9-34647
 ReO_3 , band struct. and Fermi surface 9-47048
 ReO_3 , band struct. in tight-binding approximation 9-47047
 W-(5 at.%)Re alloy single crystal, thermionic emission of (100) face 9-47211
 W-(5 at.%)Re single cryst., deform. prod. during ion microscope exam. 9-39235

Rheology*see also Plasticity; Viscoelasticity*

- balance rheometer theory for meas. of complex viscosity, elasto-viscous liq. 9-32755
 continuous media, microstructure analysis examples 9-45806
 cylinder-sphere intersecting shell, under internal pressure, complete soln. 9-45809
 dispersion systems, structured, translocated by vibr. 9-42683
 elasto-viscous liq., balance rheometer theory for meas. of complex viscosity 9-32755
 elastoplasticity, linear, duality from problems of cause and effect 9-29225
 fatigue strength rel. to stress waveform, model and obs. 9-26346
 glass, alkali borate and B_2O_3 , Newtonian viscous flow, deviations 9-28197
 glasses, behaviour 9-28194
 kerosene, near solid boundary 9-39069
 polymer solution, solvent depend. of behaviour 9-28108
 polymers, film-forming, melt rheology 9-26048
 polymers, liquid, properties, acoustic meas. 9-36835
 rheometer, cone-and-plate, for meas. viscosity of polymer melts 9-46618
 shear layer effect on plane sound waves in fluid 9-45856
 soil, creep considering structural transformations 9-26332
 suspensions, dilute orientated 9-44603
 tube, elastic-plastic, under internal pressure and axial tension, instability conditions 9-45808

Rhodium

- chemisorption of CO, i.r. spectra, temp. effect 9-43325
 crystal, single, growth by electron-beam zone melting, microhardness 9-48807
 crystal growth and annealing process 9-39213
 dispersion hardening, patent 9-26391
 X-ray absorpt. spectra L series obs., e states studied 9-37748
 X-ray emission spectra band shape anal., valence e level diagram determ. 9-36665

Rhodium compounds

- alloys, dispersion hardening, patent 9-26391
 Mo-Rh alloy, metal-metal carbide eutectic temp. determ. 9-34951
 Pd-Rh dilute alloys, ma. susceptibility, field-depend at high-mag. fields 9-45070
 Pd-Rh dilute alloys, mag. susceptibility meas. 9-45069
 Pd-Rh exchange enhanced alloys, field-depend. mag. susceptibility, 200 kG 9-26625
 Rh-Fe dilute alloy magnetoresistance, 1.3° to 20° fields up to 200 kG 9-44910
 $\text{Rh}_2\text{Cu}_2\text{Ni}_2\text{O}_4$, new orthorhombic phase with $0.12 \leq x \leq 0.175$ 9-30704
 $\text{Rh}_2\text{Pd}_2\text{Zr}_2$, doped with transition elements, torsional speed of sound obs. 9-30771
 Rh-Ru-Fe alloys resistivity and susceptibility as function of temp. 9-44918
 Ti-Rh alloy, supercond. transition temp., determ. by sp. ht. meas. 9-30880
 W-Rh alloy, metal-metal carbide eutectic temp. determ. 9-34951
 W-Rh alloys, yielding rel. to Rh conc. and ductile-brittle transition temp. 9-39415

Riemann-Cristoffel tensors *see Relativity; Tensors***Righi-Leduc effect** *see Magnetothermal effects***Ring currents** *see Atmosphere; Ionosphere***Riometers** *see Ionosphere measuring apparatus***Rochelle salt**

- Barkhausen effect in X and γ irradiated crystals 9-47180
 crystal faces, nonisothermicity investig. during growing and dissolving from solns. 9-26203
 dielectric props. over wide freq. range 9-47181
 dielectric relaxation and crystal water stoichiometry, activation energy determ. 9-41234
 electro-optical effect, rel. to light modulator use 9-43216
 ferroelectric, spin-lattice relaxation of ^{23}Na 9-26663
 ferroelectric phase transitions, e.s.r. 9-30972
 ferroelectric properties, ^{23}Na n.m.r. 9-26593
 ferroelectric properties, influence of ^{60}Co γ rays 9-47179
 ferroelectric props. used in laboratory demonstration expt. 9-37590
 orientations of H_2O mols., p.m.r. determ. 9-45405
 spin-lattice relax. of ^{23}Na and ^2D rel. to ferroelectric mode contrib. 9-24345
 water molecule dynamics from n.m.r. exam. in ferroelectric state 9-28765
 Cu^{2+} -doped, dynamic proton polarization 9-33632
 e.p.r. spectra of Cu^{2+} -doped material, linear elec. field effects 9-24486

Rock magnetism

- anomalies due to 2 dimensional structure, interpretation by least squares method 9-38007
 baked contacts, lava flow on sedimentary rock, mag. props. 9-33876
 basalts, submarine thermoremanent magnetisation, self-reversal 9-38008

Rock magnetism continued

- data analysis, precision parameter κ , confidence limits 9-45568
 deep-sea sedimentary cores, short period polarity events 9-45567
 diorite, hornblende-biotite quartz, nonreproducible self reversal 9-43501
 ferromagnetic minerals, demagnetization of remanent magnetization by pressure application 9-24710
 field intensity determ. through polarity reversal 9-41611
 grains, single domain, thermal fluctuations of magnetic moments 9-33874
 igneous rocks, anisotropy 9-31477
 lavas and sediments, rel. to reversals of geomag. field, 1967 Bakerian lecture 9-24709
 lithosphere drift estimation rel. to polar wandering 9-31479
 magnetite, 30 to 60% in quartz, galvanomagnetic effect 9-43500
 magnetite, inverse thermoremanent magnetization 9-35937
 magnetite, mag. props. change due to gamma radiation 9-37665
 magnetite, remanent magnetization and coercive force, effect of annealing 9-45570
 magnetite dispersed powder susceptibility for low field intensity freq. independence 9-43502
 magnetite magnetic viscosity rel. to demagnetizing field 9-38011
 magnetite magnetostriction in weak fields at liquid nitrogen temps. 9-31476
 magnetite-containing rocks, transitional thermoremanent magnetization in rel. to low temp. treatment 9-33877
 magnetostriction, from liquid nitrogen temp. to Curie point, meas. 9-31476
 magnetotelluric analysis, inverse, to determ. earth's resistivity structure 9-37891
 magnetotelluric sounding, inversion to determ. resistivity of earth layers 9-37890
 measurements rel. to history of Earth's field 9-45547
 natural chemical magnetization, laboratory studies 9-24711
 paleomagnetic data analysis 9-49514
 paleomagnetic reconstruction of lithospheric plate rotations 9-40109
 paleomagnetic stability of baked contact rocks 9-33876
 parameters determ. by differential thermal analysis 9-28970
 Pleistocene andesite and scoria samples from Usami Volcano, Japan, intensity 9-38009
 pyrrhotine, mag. props. change due to gamma radiation 9-37665
 remanent, orientation and intensity, effect of shock 9-45569
 remanent magnetization stability 9-47603
 sedimentary rocks, post-deposited remanent magnetization 9-38005
 semimantary, natural remanent magnetization 9-35938
 stability, evaluation of meas. methods 9-31478
 susceptibility, borehole meas. with coil pairs 9-38006
 susceptibility for low field intensity freq. independence obs. 9-43502
 tertiary age, secondary natural magnetization, nature 9-38010
 thermoremanence of Ni, internal stress effect 9-45016
 thermoremanent magnetization, effect of plastic deformation 9-35568
 variations, pressure-induced, complex interpretation 9-33873

Rockets

- engine chamber insulation mats., thermal conductivity 9-38013
 in evacuated tubes, mag. suspension and guidance by supercond. magnets 9-37499
 gyro-plasma probe experiment, modified and hybrid plasma resonances, prediction on discrimination 9-34786
 propellant, plastic yield stress determ. by simple test 9-23876
 Saturn V, problem of liquid H_2/O_2 propellants 9-45572
 trajectory determ., image orthicon television system appl. 9-38012

Rolling *see Forming processes***Rotating bodies**

- see also Angular velocity measurement; Centrifuges; Earth/rotation; Gyroscopes*
 anode, electrochem. cell, cathode ionic mass transfer obs. 9-47466
 disc, unstable motion of electrically conducting liquid presence of strong axial magnetic field 9-30206
 disc in viscous fluid, moment of resistance 9-42619
 dynamical linearized eqns. with matrix formalisms 9-47799
 ellipsoid in viscous fluid, moment of resistance 9-42619
 Euler angles, a generalization 9-45735
 infinite disc, unstable motions of electrically conducting liquid, presence of strong axial magnetic field 9-30207
 libration, soln. of ideal reson. problem 9-31495
 libration, soln. of ideal reson. problem 9-31495
 membranes, circular, response to simultaneous const. spin and precessional motion 9-29246
 slip between rolling ball and track, factors affecting contact conditions 9-31801
 spinning body without gravitational waves 9-22180
 stagnation flow against rotating magnetized disc 9-42482

Rotation, molecular *see Molecules/rotation***Rotatory power, dispersion** *see Optical rotation***RS coupling** *see Atoms; Spectra/atoms***Rubber**

- adhesive films, transparency changes due to u.v. irradiation 9-47328
 bitumens in rubber transition zone, u.s. absorption and dispersion 9-30450
 butadienitrile rubbers, NMR, light scattering study of structure, vulcanization character 9-23789
 charge transport mechanism from elec. props. meas. 9-41128
 chloropropene, NMR, light scatt. studies, of structure 9-23789
 constitutive relation for rubber-like mats. 9-39393
 crystallization, stress-induced, in rapidly stretched natural rubber, obs. 9-28201
 elasticity, energy contrib. analysis 9-46860
 elasticity, general random network bead-spring model 9-35144
 free retraction of stretched rubber obs. with cine-camera 9-39390
 gas bubbles nucleation and growth 9-34972
 gas desorption and permeability in vacuum 9-39178
 latex particles, sulfonated, secondary electroviscous effect calc. from zeta pot. 9-32801
 natural, vulcanizates, dynamic modulus rel. to trapped and untrapped entanglements 9-30651
 neoprene film, constitutive relation 9-39393
 nitroso rubber copolymer structural study using ^{19}F NMR 9-27939
 1,4-polybutadiene, dynamic modulus rel. to trapped and untrapped entanglements 9-30651
 raw and finished, spectrochemical analysis by impurity method 9-43348

Rubber continued

- rubber-sulphur systems, comparison of viscoelastic and dielectric props. 9-33376
 SBR, fracture obs. -57°C -40°C, and at rates 9-35187
 storage and elastic moduli, meas. method 9-33020
 structural effects of irradiation 9-24079
 styrene, butadiene, in cross-linked rubbers 9-30651
 styrene-butadiene, dynamic modulus rel. to trapped and untrapped entanglements 9-30651
 styrene-butadiene, nonlinear non-isothermal viscoelastic behaviour 9-28333
 tensile strength rel. to crosslinkage lability and relax., obs. 9-28361
 uniaxially oriented, fluorescent light polarization meas. 9-39881
 vulcanizates, stress relax., simple viscoelastic model 9-30645

Rubidium

- atom, electron impact, generalized oscillator strengths 9-29963
 atom, electron scatt., low-energy, phase-shift calc. 9-22978
 atom, impact ionization by electrons and protons, cross section obs. 9-34556
 atom, nonlinear hyperfine pressure shift obtained by optical pumping 9-36664
 atom, octopole-allowed transitions in electron energy-loss spectra 9-40543
 atomic beam, comparison meas. with UHV microbalance, quartz osc. and ionization foil 9-22988
 atomic spectrum, bibliography 9-38765
 charge-transfer cross section for He^+ and Ar^+ meas. 10-1500 eV 9-46316
 diffusion in K 9-40984
 elastic consts., pressure derivatives 9-23853
 g-factor meas., atomic structure parameters derived 9-29936
 hyperfine interaction, relativistic analysis 9-24349
 Knight shift, pressure depend. calc. 9-33647
 laser, short-term frequency stability of frequency standard 9-36297
 liquid, atomic overlap, neutron diff. obs. 9-34875
 liquid, nuclear spin-lattice relax. of $^{85,87}Rb$ 9-26134
 liquid, sound speed and isothermal compressibility meas., 56-260°C 9-23465
 liquid, thermal conductivity in temp. range 87-788°C 9-40787
 optical pumping, transition probabilities between magnetic sublevels 9-46301
 phonon frequencies from electron-phonon interaction modification with correlation effects 9-35308
 scattering by alkali atom, spin-exchange cross section calc., partial-wave anal. 9-22984
 sunspot abundance from sunspot spectra 9-31657
 vapour, sensitized fluoresc. by collisions with K atoms, $^{42}P_{1/2}$ - $^{42}P_{3/2}$ mixing in K 9-34574
 vapour, sensitized fluoresc. by induced collisions with K atoms, energy transfer obs. 9-34573
 vapour, stimulated three-photon scattering 9-22954
 $K(^2P_{1/2}) + Rb(^2S_{1/2}) \rightarrow K(^2S_{1/2}) + Rb(^2P_{1/2}) + \Delta E$, fluorescence detected, cross-section meas. 9-32429
 Rb-rare gas mol. formation, Rb polarized atom relaxation in rare gas, theory 9-32534
 Rb^+ , electronic dipole polarizabilities calc. 9-40545
 ^{85}Rb , ^{87}Rb , self spin-exchange cross-section meas. using microwave absorption between Zeeman sublevels 9-46314
 ^{85}Rb atoms optical pumping in inert gases, excited state mixing obs. 9-34561
 ^{87}Rb , reson. freq. and optical pumping rel. to atomic clocks 9-47720
 ^{87}Rb atoms optical pumping in inert gases, excited state mixing obs. 9-34561
 ^{87}Rb in cell, filter efficiency for doublet hyperfine components 9-29945
 ^{87}Rb main doublet hyperfine components, filtration conditions 9-38770
 RbI, II, excited levels g factor spectral determ. 9-29944

Rubidium compounds

- halides, F-centre emission energies and lifetimes 9-32999
 molten, self-diff. coeff., 318-499°C 9-30381
 K-Rb alloys, tensile deformation, yield and flow stress, conc. depend. 9-30664
 K-Rb binary alloys, electron spin susceptibilities, Knight shift 9-39116
 RbH_2PO_4 , ferroelec. anomalies in dielec. and piezoelec. props. 9-41244
 Rb-Cs binary alloys, electron spin susceptibilities, Knight shift 9-39116
 $Rb_{1-x}Ni_xO_3$ crystal structure 9-40905
 Rb_2BeF_4 , dielec. props. rel. to ferroelec. transition in $(NH_4)_2BeF_4$ 9-43118
 $Rb_2MnCl_4 \cdot 2H_2O$, antiferromag., n.m.r. obs. of mag. ordering 9-41333
 $Rb_2O \cdot SiO_2$ glass, luminescence spectra 9-39872
 $Rb_2S_2O_6$ crystals, rotation of plane of polarisation of light 9-43212
 $Rb_2SO_4 \cdot VO^{2+}$ single cryst., e.s.r. spectrum 9-41429
 Rb_2CoCl_4 , heat capacity meas., mag. phase transition obs., comparison with Ising model 9-39532
 $RbAg_4I_6$, high ionic conductivity, room temp., prep., patent 9-30965
 RbBr-KBr solid solution films, fundamental absorpt. spectra 9-28685
 RbBr-RbI solubility gap, equilib. phases for moist solid soln. 9-35211
 RbBr, lattice disorder effect on n.m.r. spin echo line shapes 9-30610
 RbBr, orientation in thin films, study by electron diffraction 9-39229
 RbBr single cryst., positron anisotropic penetration, X-ray spectrum obs. 9-35300
 $RbCl:CN^-$, electric cooling rel. to tunnel splitting of impurity motional ground states 9-27143
 $RbCl:H$, ENDOR meas. of U_2 -centres 9-30621
 $RbCl:Ni^{2+}$, absorption spectrum 9-39842
 $RbCl:OH^-$, rot. barrier height 9-40935
 RbCl, diffusion of ^{22}Na , 377-707°C 9-23842
 RbCl, F_1 -centre accumulation due to proton irradi., 78°-380°K 9-30620
 RbCl, ionic conductivity, possible trivacancy mechanism 9-28552
 RbCl, orientation in thin films, study by electron diffraction 9-39229
 RbCl, specific heat at low temp., adiabatic meas. 9-25135
 RbCl F-centres, Stark effect of relaxed excited states 9-24392
 RbD_2PO_4 , permittivity, anomalous behaviour below Curie point 9-47177
 $RbFeF_3$, ferromagnet, domain wall dislocation interactions 9-45126
 $RbFeF_3$, magneto-optical effects, origin and magnitude 9-24366
 $RbFeF_3$, n.m.r. of ^{19}F , ^{87}Rb and ^{85}Rb , hyperfine interaction and spin-densities 9-28760
 $RbFeF_3$, orthorhombic, cubic-magnetic and optical behaviour 9-47293
 $RbFeF_3$, spatial distrib. of spin density and n.m.r. 9-41435
 $RbFeF_3$, crystal growth from soln., X-ray diffraction powder study 9-26207
 RbH_2AsO_4 , normal and deuterated, electropt. and dielec. props. 9-39697

Rubidium compounds continued

- RbH₂AsO₄, normal and deuterated, piezoelec. and elastic props. 9-39696
 RbH₂AsO₄ cryst., second harmonic generation 9-39791
 RbH₂AsO₄ ferroelec. transition, ⁸⁷Rb n.m.r. quadrupole coupling and elec. field-gradient obs. 9-33393
 RbH₂PO₄, elastic, piezoelec. and dielec. const. 9-44749
 RbH₂PO₄, electro-optical effect, transverse, and light modulation by crossed rods, obs. 9-33516
 RbH₂PO₄, high-temp. phase transition 9-47176
 RbH₂PO₄ cryst., second harmonic generation 9-39791
 RbH₂PO₄ crystal, electro-optical effect, fourth-order 9-41358
 RbHSO₄, p.m.r. temp. dependence rel. to para- to ferroelec. phase transition mechanism 9-26800
 RbI, orientation in thin films, study of electron diffraction 9-39229
 RbMgF₂-RbCoF₃, prep. and props. of ferrimags. 9-47274
 RbMgF₂-RbCoF₃ system, ferrimagnetic comps., mag. and opt. props. 9-45186
 RbMnCl₃, broadband fluoresc., temp. depend. 9-49319
 RbMnF₃:Na⁺, fluorescence temp. dependence of Mn²⁺ and Na⁺ rel. to Mn²⁺→Na⁺ energy transfer 9-24456
 RbMnF₃:Nd³⁺ fluorescence characts., temp. effects, 5 to 300°K 9-28718
 RbMnF₃, ⁵⁵Mn n.m.r. modes 9-39922
 RbMnF₃, ⁶A₁→⁴A₁, ⁴(G) pure electr. transition, thermal shift and broadening 9-39845
 RbMnF₃, ⁶A₁→⁴A₁, ⁴(G) pure electr. transition, thermal shift and broadening 9-39844
 RbMnF₃, critical magnetic scattering of neutrons and sublattice magnetiz. 9-45234
 RbMnF₃, ENDOR rel. to nuclear saturation liq. helium temp. 9-45410
 RbMnF₃, flopped antiferromagnet, excitation of electronic and nuclear spin waves 9-47282
 RbMnF₃, n.m.r., ⁵⁵Mn linewidth, field depend., 1.8 and 4.2°K 9-33649
 RbMnF₃, u.s. attenuation near mag. phase transitions freq., and temp. depend 9-48958
 RbMnF₃, antiferromagnetic, nuclear acoustic resonance 9-46993
 RbMnF₃ e.p.r. of Mn²⁺ and ¹⁹F n.m.r., exchange narrowed discrepancies between theory and expt. 9-45388
 RbNO₃, pyroelectric props. rel. to crystal space group 9-30977
 RbNO₃, struct. transform. 160°C to melting pt., elec. conductivity meas. 9-46962
 RbNO₃, mollen, diffusion and ionic mobility of ²²Na, ¹³⁷Cs obs., temp. depend. 9-34891
 RbNi(Co)F₃, ferromagnetic, opt. and magneto-opt. props. 9-33513
 RbNiF₃, ferrimagnetic resonance, 77-200°K 9-28740
 RbNiF₃, hexagonal ferrimag., mag. resonance and anisotropic g factors 9-45361
 RbNiF₃, magneto-optical effects, origin and magnitude 9-24366
 RbNiF₃, Raman scatt. by mag. excitations 9-45336
 RbNiF₃ perovskite-like struct., phase transf. and stability relations at high press. 9-35241
 RbOH, microwave spectra and struct. 9-38869
 RbOH, vibr.-rot. interactions and struct. refinement 9-44325

Ruby

- absorption bands, multiplet impurity, method of moments applic. to calc. 9-45313
 colour centres, influence on lasing threshold 9-39372
 colour centres, optical and γ -ray colouring 9-39371
 crystal field theory 9-28642
 crystals, optical homogeneity rel. to laser emission characts. 9-26674
 c.p.r. of Cr³⁺, g-factor and fine structure lines up to 7 kbar 9-33655
 ENDOR saturation transfer mechanism rel. to thermal mixing of nuclear spins 9-43310
 energy transport mechanisms 9-45305
 e.p.r. line form in elec. fields, crystals with T_d symmetry 9-24481
 filamentary damage formation by laser beam 9-48847
 fluorescence excitation process 9-47400
 as fluorescing and laser material 9-31954
 glass laser focused radiation, conversion to X-rays in hot dense plasma 9-42517
 growth, flame fusion method, infl. of molten film thickness on crystal perfection 9-23677
 growth of 0° boules with hexagonal maphology, Verneuil method 9-37066
 growth of single cryst. by thermal imaging tech. 9-36993
 intensely excited, emission power and time constant obs. 9-45941
 inversion coefficient, theoretical and exptl. investg. 9-31928
 i.r. reflection spectrum of synthetic rubies, 5-25 μ 9-28669
 laser, ²E metastable population kinetics and Q-switched reson. losses obs. 9-36302
 laser, applic. to high-speed framing photography 9-32095
 laser, distribution of temperature during pumping 9-22418
 laser, film deposited on metal plate, patent 9-48048
 laser, for pumping LiNbO₃, parametric oscillation 9-28663
 laser, generation spectrum. rel. to resonator active crystal orientation 9-38379
 laser, giant pulse form. registration by multiframe image converter 9-31956
 laser, kinetics of free generation spectra in travelling-wave regime 9-27333
 laser, mode-locked, picosecond pulse production 9-43891
 laser, mode-locked, pulse duration 9-25285
 laser, modification of pulsed refl. mode for high-power-pulse transmission mode operation 9-48071
 laser, oscillator-amplifier, pulse transmission mode, design and charact. 9-48019
 laser, output energy degradation due to colour centre formation 9-38377
 laser, partial giant pulse prod. for stroboscopy 9-29425
 laser, passive Q-switching based on stimulated Mandel'shtam- Brillouin scattering of light 9-36306
 laser, picosecond pulses, evidence for self-focusing in gas breakdown 9-25983
 laser, pulse parameters rel. to spectral and luminesc. props. of passive filters 9-36305
 laser, Q switched single pulse 9-41914
 laser, Q-switched, emission charact. and pulse stretching 9-48018
 laser, Q-switched, in motion picture holography 9-25322
 laser, Q-switched, travelling-wave oscillations, method 9-48020
 laser, Q-switched for dynamic event holography 9-36329
 laser, Q-switching by natural chlorophyll and derivatives 9-36303
 laser, Q-switching by organic solvents 9-29423

Ruby continued

- laser, radiation field in active rod, effect of nonuniformity on dynamics 9-36304
 laser, reflection holograms, pulsed, single-mode 9-22425
 laser, regular spiking, spectral output and far-field pattern as influenced by resonator mirror vibrations 9-41913
 laser, resonator ended by a rectangular prism 9-22416
 laser, ring single-direction, construction method 9-48021
 laser, self-Q-switching at 77°K and 300°K 9-36309
 laser, sequentially modulated system, for recording dynamic photoelasticity 9-29232
 laser, single freq., with variable radiation freq., spectral characts. under giant pulse operation conditions 9-41915
 laser, single-mode high-power, using multi-elements 9-36307
 laser, stable freq. monochromatic mode 9-45957
 laser, transverse-mode selection effects on wavefront 9-48052
 laser, with resonator having Q-factor modulation 9-29422
 laser beam, monopulse sync. with Nd pulse using luminous liq. shutter 9-29421
 laser freq. conversion by polymethyn dyes 9-34171
 laser pulse power amplification during induced Mandelstam-Brillouin back-scatt. 9-22417
 laser with external mirrors for discrimination mode exclusion, kinetic spectrum 9-48022
 laser-enhanced two-photon decay 9-26766
 lasers, repetitively Q-switched, continuously pumped, applications in frequency conversion experiments 9-25320
 lasers, space field structure, h.f. modulation 9-43892
 lasers, two, tunable far-i.r. rad. generated from difference freq. 9-31955
 lasing threshold, influence of colour centres 9-39372
 luminescence, R line duration and width rel. to Cr³⁺ concentration 9-31122
 magnetic resonance lines intensities and distrib. of paramag. ions in matrix 9-49340
 microwave frequency doubling, quantum mechanical 9-25139
 pink, resonance fluorescence, sharp line excitation 9-26775
 refractive index change during opt. pumping 9-29424
 relaxation time constant between ⁴T_{1,2} and ²E states, determ. 9-26776
 relaxation time meas. for spin-phonon interaction Hamiltonian parameter 9-45242
 two-photon stimulated processes, study 9-26731
 u.s. attenuation of longit. waves at microwave freqs., temp. depend. 9-39518
 wetting by molten Al, alloys, Cu and Au, contact angle meas., sessile drop technique 9-34977
 Cr³⁺ ²E level, population density measurement by excited state absorption 9-33534

Russell-Saunders coupling *see Atoms; Spectra/atoms***Ruthenium**

- X-ray absorpt. spectra L series obs., e states studied 9-37748

Ruthenium compounds

- Mossbauer effect of ⁹⁰Ru, isomer shift of 90 keV γ -rays 9-45301
 Fe-Ru h.c.p. alloys, e-phase, mag. props. 9-43159
 Li-Ru-Fe alloys resistivity and susceptibility as function of temp. 9-44918
 Ru-Ni solid solutions, initial states of Ni precipitation from superparamag. meas. 9-35212
 Ru complex, tris(2,2'-bipyridine)ruthenium(II) dichloride, luminesc. 9-42414
⁹⁰Ru, isomer shift of 90 keV γ -rays in various compounds 9-45301
 RuCl₃, n.q.r. of ³⁵Cl 9-49365
 RuF₆ spectrum, i.r., Jahn-Teller effect 9-34647
 RuO₂, ht. capacity 0.54°10°K 9-48971
 RuO₂, thermal expansion from X-ray determ. of lattice constants, 30-702°C 9-24056
 RuO₄, vibr. spectra and force field 9-42415
 RuSe₂, crystal structure 9-23770

Rutile *see Titanium compounds***S-matrix theory**

- see also Dispersion relations*
 α -condition for singularity equivalent to requirement that discontinuity round each threshold be given by Cutkosky integral 9-22499
 bootstrap models, principle of complementarity, small hadronic parameters 9-34274
 bosons, zero-mass, soft coupling to other particles 9-32115
 Cayley transform, physical-region struct. 9-25404
 leads to classical description of interactions 9-48152
 of composite particles, rel. to S-matrix theory 9-32229
 corrected amplitudes, behaviour on arcs of Landau curves 9-38423
 Coulomb nuclear, Regge trajectories 9-34372
 Coulomb potential screening by exponential tail 9-22498
 of current, integral representations of third and fourth order current elements obtained 9-34261
 currents and off-mass-shell scatt. amplitude extension, determ. 9-32149
 dimer problem, partition function rederivation using S-matrix method 9-43755
 electromagnetic long-range forces incorporation in theory 9-38240
 electron (quantized Dirac field) in classified time-dependent e.m. field, theory 9-38346
 function S-matrix rel. to function theory of scatt. 9-43752
 gauge invariance in self-coupled generalized Yang-Mills fields 9-25401
 interactions involving photons, one-part. singularity, cluster decomposition props. 9-25413
 isobaric analogue resonances, energy- asymmetry, model-independent descrip. 9-42182
 nuclear α particle scatt., applic. 9-34462
 product structure of measurements 9-43966
 quantum electrodynamics, vertex $ey\bar{e}$ evaluated 9-38452
 quantum field theory, causality and locality 9-36419
 scattering amplitude, many-particle physical- region discontinuity eqn. 9-36429
 singularities and discontinuities of unitarity integrals expressed in terms of M diagrams 9-38422
 static, 3-particle unitarity eqns., class of exact solns. 9-25434
 two-body S-matrix, approximate model 9-46107
 unitarity of renormalized matrix in axiomatic field theory, problems of 'dressing' of the operators 9-27439
 K_r-K_s decay, new unitary sum rule obtained using S-matrix 9-29570
 π - π scattering, one-parameter model 9-42084

S-matrix theory continued

- $\pi\pi$ scatt. calc. 9-27532
 $12(C, \alpha)^{12}C$, cross-section calc. utilizing S-matrix and poles 9-34462

Safety precautions see *Radiation protection***Sakata model** see *Elementary particles***Samarium**

- activated quartz glass, luminescence 9-41407
 configuration in SmB_6 rel. to mag. ordering 9-45072
 elastic moduli, u.s. attenuation meas., 4.2-300°K, correl. with antiferromag. transitions 9-35146
 hyperfine interactions, calorimetric investigation 9-47305
 spectrum, L emission, weak lines study 9-34550
 vapour, i.r. laser lines 9-29947
 Sm^{+3} in rare-earth ethylsulphates, spin-lattice relaxation time calc. 9-43197
 Sm^{2+} , fluoresc. in crystals, thermal effects 9-41409
 Sm^{2+} in alkali halides, vibronic side bands calc. 9-49285
 Sm^{2+} , dispersion curves w.r.t. La^{3+} in aqueous chloride solutions 9-26111
 Sm^{3+} , field in Sm Ga and Sm Al garnets calc. from absorption and emission spectra 9-43244
 Sm^{3+} in CaF_2 type I, trigonal crystal field energy levels 9-33244
 Sm^{3+} in $\text{La}_2\text{Mg}_2(\text{NO}_3)_{12}$, Orbach relax. processes, T_1 and T_2 9-24492
 Sm^{3+} in $\text{La}_2\text{Mg}_2(\text{NO}_3)_{12}$, e.s.r. temp. dependence, T_1/T_2 ratios 9-24483
 Sm I spectrum, level lifetimes, Hanle effect meas. 9-29950

Samarium compounds

- ethylsulphate, spin-lattice relaxation anisotropy 9-26665
 $\text{CaF}_2:\text{Sm}^{2+}$ crystal laser, characts. 9-38380
 $\text{Sm}_{1-x}\text{Bi}_x\text{FeO}_3$, synthesis, mag. reorientation temp. rel. to Bi substitution 9-32869
 Sm_2O_3 , self-diffusion coeffs. of O, by isotope exchange method 9-44741
 $\text{Sm}_2\text{Eu}_{1-x}\text{Fe}$ mixed garnet, garnet, anisotropy in exchange interac., Mossbauer obs. 9-33475
 SmAl garnet levels of Sm^{2+} calc. from absorption and emission spectra 9-43244
 SmB_6 , semicond.-metal transition, model 9-33279
 SmB_6 , nonmagnetic divalent config. of Sm ion at low temp. 9-45072
 SmCo_5 , mag. props. influence of absorbed H 9-45073
 SmCo_5 , co-rich part permanent magnets, energy products $20 \times 10^6 \text{ G.Oe}$ 9-33433
 SmCo_5 pressed-powder magnets, high energy product 9-49213
 SmFe garnet, anisotropy in exchange interac. Mossbauer obs. 9-33475
 SmFeO_3 , DyFeO_3 solid soln. single crystal, spin reorientation, 2° to 500°K 9-45235
 SmGa garnet levels of Sm^{3+} calc. from absorption and emission spectra 9-43244

Sampling see *Statistical analysis***Sand**

- clay-sand mixtures, elec. resistivities 9-49017
 durability of luminescent tracers 9-41399
 failure criterion, angle of internal friction 9-39433
 thermal conductivity as function of moisture temp. and porosity, obs. in Rajasthan 9-30789

Satellites, artificial

- ATS-E, channel multiplier spectrometer for 0.5 to 500 keV electrons and protons 9-38023
 attitude stability in circular and elliptical orbits 9-40110
 charge and pot. distrib. around Explorer 31, depend. on ionic composition 9-31481
 comic ray intensity monitoring recorder 9-29632
 communication, Doppler effects in ionospheric and tropospheric communications computer program 9-45575
 Cosmos 149, equipment for earth brightness obs. 9-45577
 Cosmos 149, expt. problems and instrumentation 9-45576
 Cosmos 149 instruments for flux meas. in range 0.3 to 40μ 9-40031
 for determining tidal parameters and rotatory deceleration 9-28854
 eclipses, book 9-33893
 e.m. wave emission, trajectories through anisotropic ionosphere 9-41573
 energy integral, study of earth's gravity field from satellite 9-33878
 E.S.R.O., for general survey of sky in i.r. 9-29106
 ESO 1/Aurora experiments 9-33814
 Explorer 22 electron meas. in ionosphere, evaluation 9-35865
 forces induced by solar rad., reflectance model estimation 9-24712
 gas-surface energy transfer experiment in upper atmosphere 9-35831
 geodetic triangulation, Polish experiments 9-31249
 geomag. tail meas. at 1000 earth radii, obs. with Pioneer 7, Explorer 28 and 33 9-40047
 geopotential resonant perturbations on orbits 9-33881
 gravity gradient, program to analyse dynamic behaviour 9-26971
 high sensitivity TV camera for detection of auroras 9-33812
 Inclination Removal Ionospheric Beacon, design 9-49490
 infrared radiation analyses over Antarctic 9-24633
 ionization production, upper atmosphere 9-31353
 ionospheric gas dynamics 9-49495
 ionospheric waveguide communication channel, averaged field 9-43436
 i.r. spectrometer, design 9-25387
 laser meas. of earth satellites position 9-35939
 laser tracking system 9-28972
 low degree earth gravity harmonics, effects on 12 and 24 hour satellites 9-31239
 Luna 11, solar cosmic rays recording, (1966) 9-22644
 lunar, first- and second order changes in orbit, secular and periodic 9-47606
 lunar, orbit under attraction of Moon, Earth and Sun, first order changes and disturbing function 9-47605
 luni-solar perturbations of earth satellite orbits 9-47604
 manned, astronomy programme plan 9-38025
 manned Earth satellites, Russian, absorbed radiation doses, obs. 9-45573
 motion of triaxial rigid body orbiting oblate primary, first-order theory 9-31496
 Nimbus II meas. of solar radiation bidirectional reflectance from clouds over snow, charact. 9-35819
 observations (Jan to Dec 1968) 9-33879
 optical tracking, orbits forecasting and obs. reduction 9-28973
 orbit disturbances, explanation from evidence of natural terrestrial satellites 9-27079
 orbit expansion by microthrust, formula analysis 9-28975
 orbital parameters of 16 satellites, teaching paper 9-45725
 orbital perturbations as function of gravity anomalies 9-24716

Satellites, artificial continued

- orbital resonances due to general geopotential, asymptotic solns. 9-38015
 orbits, Doppler effect in r.f. transmission rel. to validity of relativity 9-41615
 orbits, perturbations due to sun and moon 9-35940
 orbits, polar, spheroidal calc. method, improvement 9-31482
 orbits in rotating coord. system, perturbation terms correction 9-31483
 pulse height analyzer and associated equipment for general appl. 9-42149
 radio signals, severe amplitude scintillations during sunrise 9-24713
 radiocommunication, scintillation boundary obs. 9-31391
 S^3 small scientific, operating program and nuclear instrumentation payload 9-38019
 secular accel., solar radiation press. effects rel. to Echo 2 9-28974
 small astronomy satellite programme 9-33880
 for solar atmosphere structure, feasibility 9-47609
 spherical, irradiated by Lambertian earth, photon radiance angular distribution 9-27376
 spheroidal polar orbit calc. method, improvement 9-31482
 station keeping problems 9-24715
 swept frequency sounders, study of ionization maximum in polar latitudes 9-33828
 thermal control, coating stability and Earth refl. sunlight obs. 9-24714
 tracking, optical, using multi-coincidence method of photon counting 9-45574
 tracking, optical multi-coincidence method of photon counting, sampling technique 9-38014
 tracking cameras, three East German instruments 9-27115
 Vela 4, nuclear instrumentation for energetic particle experiment 9-38020
 Vela 5, multiplier for E. de/dx particle identifier 9-38016

SC (sudden commencement) see *Magnetic storms***Scalars** see *Counting circuits***Scandium**

- magnetic susceptibility and anisotropy 9-49192
 magnetic susceptibility between 0.36-300°K 9-49190
 magnetization of itinerant electrons, decrease by spin-orbit scatt. on impurities 9-26639
 n.m.r., spin-lattice relax. rate, h.f.s. 9-49192
 in rare-earth iron garnets, Fe ions, canted spin struct., Mossbauer effect obs. 9-37667

Scandium compounds

- alloys with nonmagnetic metals, mag. susceptibility between 0.36 and 300°K 9-49190
 Gd-Sc alloys, magnetic structure props., 4° to 300°K 9-45125
 $\text{HfO}_2\text{-Sc}_2\text{O}_3$ system, phase diagram and equilibria, solubility 9-39476
 Ni-Al-Sc system, phase equilibria and solubility limits in Ni-rich region 9-30720
 Sc-Gd dil. alloy, at 1000 ppm, mag. saturation moment 9-49190
 $\text{Sc}_2\text{O}_3:\text{Bi}^{3+}$, luminescence 9-31125
 Sc_2O_3 , high-pressure transformation, molar volume relationships 9-48779
 Sc_2O_3 added to borolanthanum, glasses immiscibility and catalytic crystallization 9-34971
 ScBO_4 (where B=P, V, Nb), as phosphor host lattices 9-45352
 ScH_3NH_3 , SCF calc. 9-42419
 $\text{Sc}(\text{NO}_3)_3$, solvation in H_2O -acetone, p.m.r. 9-42682

Scattering

- amplitude, analytical behaviour in Dirac theory 9-41767
 amplitude, analytical props for long-range forces 9-38240
 amplitude construction from differential cross-sections 9-36416
 amplitude determination from differential cross-sections by unitarity 9-22104
 amplitudes, invariant, determ. from experimental observables 9-41771
 amplitudes, properties, macroscopic causality conditions, formulation and consequences 9-41770
 asymptotic behaviour of out-of-phase scatter under central pot., in Dirac's theory 9-40243
 atom by rigid rotor, resonance widths 9-23197
 atom-atom glory scatt., quantum effects 9-38787
 atom-diatom, inelastic transitions and quenching of glory extrema 9-38931
 atomic collisions, time-dependent semiclassical theory 9-31773
 using Bethe-Salpeter eqn., correction 9-27442
 cluster expansion and N-body scatt. Faddeev type integral eqn. 9-22126
 Coulomb potential screening by exponential tail, S-matrix theory 9-22498
 crossed molec. beams, effect of the speed distrib. on nonreactive scatt. 9-44388
 derivatives of classical deflection function 9-41742
 Faddeev equations, sufficient conditions for stability 9-38238
 fluid, function near critical point 9-34709
 functional quantum theory 9-43752
 gravity waves in water, by circular dock 9-26069
 inelastic, anomaly-free variational method 9-22105
 inelastic wave functions, non-arbitrary method for calc. by expansion technique 9-31774
 ion motion in electrostatic dipole fields 9-31921
 Kohn variational method convergence, s-wave particle in potential 9-29202
 in liquids, absorbing, stimulated thermal Raleigh, obs. 9-26101
 Mandelstam representation double spectral function in potential scatt. theory 9-38427
 Mandelstam representation for logarithmically singular potentials, proof 9-38426
 Mandelstam symmetries in complex angular momentum plane, logarithmic FESR 9-38241
 Mie, with logarithmic Gauss distrib., collective scatt. and polarization functions 9-29176
 molecular beam scatt. data anal. 9-38933
 molecules, diatomic, beam incident at solid surface, rotational transitions 9-42364
 N-body problem, analyticity in non-relativistic quantum mechanics 9-27173
 oscillations of scattering amplitude and restrictions on high-energy behaviour 9-25030
 phase shift definition when a separable potential has a bound state in the continuum 9-46228
 plane wave by transparent sphere, direct reflection and transmission Debye terms 9-29177
 in plasma, of cyclotron harmonic waves 9-44471
 potential, quantum, possible equivalent statistical potential 9-29208

Scattering continued

- potential, time-dependent semiclassical theory from Feynman's path integral formulation 9-31772
- potential scattering, Orear behaviour 9-41772
- potentials, singular, high energy cross section 9-36133
- quantum mechanical theory of scattering from real multipoles 9-47761
- quantum-mechanical three-particle nonrelativistic theory, stability of Faddeev equations 9-38238
- of radiation by cylindrical targets, attenuation, correction factor 9-44850
- Rutherford scattering, complete correspondence identity for electron-proton system 9-41769
- Rutherford scattering, derivation of correspondence identities, development of relevant classical theory 9-41768
- Schrodinger eqn. for potential scatt., exponential soln. 9-38229
- seismic P waves, by randomly inhomogeneous elastic half space 9-45442
- semiclassical limit of inelastic scatt. amplitude 9-22095
- SL(2, C)/SU(2) harmonic functions, partial wave analysis of amplitudes 9-36120
- small angle, from anisotropic potentials 9-23200
- square well, 3-dimens., S-wave phase shift and resonance analysis 9-29203
- stimulated thermal Raleigh, in absorbing liquids, obs. 9-26101
- Thomson, plasma waves, meas. for electron-density fluctuation in ionosphere 9-32663
- three-body rearrangement scatt., solvable quantum-mech. model 9-27174
- by transparent sphere of scalar waves, Glory and Rainbow 9-29178
- two-particle amplitudes, absorptive part, as a scalar product 9-41765
- two-point function, lowest poles calc. by functional integration 9-43747
- wavefunctions, construction method 9-47754
- Ar atomic beam, preferential scatt. from LiF(001) surface 9-42714
- Ar from solid surface, spatial distribution of 0.30-0.54 eV gaseous atoms 9-27821
- Cs by HBr 9-42469
- Fe:Si, Bragg scattering of 14 KeV Mossbauer radiation of ^{57}Fe nuclei 9-37700
- H molec. beams, isotopic, from $\alpha\text{g}(111)$ surface 9-42713
- He isotope beams from Ag(111) surface 9-42713
- He metastable atoms by He 9-29984
- K in crossed molec. beams 9-42469
- Li, glory scatt. by fluorocarbons and hydrocarbons 9-42471
- acoustic waves**
- creeping waves, expt. evidence for rigid sphere and cylinder scattered 9-38300
- creeping waves propag. theory and expt. 9-47823
- cylinders, solid, aluminium, in water, 'creeping waves' obs. 9-29275
- ferromagnets, combination scatt. 9-48961
- interface, liquid-solid, uneven, Kirchhoff principle appl. 9-45857
- ion-acoustic oscill. in plasma, nonlinear scatt. by electrons 9-46523
- matrix formulation, new 9-38301
- nonlinear, of ion-acoustic oscill. in plasma 9-46523
- ocean bottom irregularities determ. using short duration signals 9-22262
- by ocean deep layers, obs. 9-47524
- piezoelectric rod, semicond., circular sound amplification 9-25101
- pulses, by rigid sphere immersed in fluid 9-29276
- pulses, by solid aluminium cylinders in water, 'creeping waves' obs. 9-29275
- rare-earth metals, critical scatt. 9-37333
- sphere, rigid, immersed in fluid, pulse scatt. 9-29276
- from statistically rough known surface, bistatic scatt. pattern 9-29274
- by uneven interface, resonance effects 9-22258
- acoustic waves, ultrasonic**
- gas mixtures, rel. to vib. relax. 9-32734
- testing of inhomogeneities in heterogeneous media 9-29279
- Dy, critical scatt. in paramag. region near Neel temp. 9-24027
- Ho, critical scatt. in paramag. region near Neel temp. 9-24027
- Tb, critical scatt. in paramag. region near Neel temp. 9-24027
- electromagnetic waves**
- bistatic, inverse scatt. technique, plane-wave representation 9-43812
- by body of arbitrary shape and arbitrary, but homogeneous props. 9-38336
- in bounded media, parametrically modulated 9-47848
- in bounded plasma, nonlinear effects 9-44432
- coordinate transformation application 9-34122
- correlation function methods reviewed 9-36233
- crystal, by local centers near excitation zone, level shift and band width 9-28708
- cylinder, infinite; line focus props. determ. 9-31873
- from cylinder, metallic, with inhomogeneous dielectric sheath 9-40292
- by cylinder, tilted, infinite, dielectric 9-36229
- by cylinder uniformly moving along its axis in fill space and in refractive media 9-25148
- by cylinders, infinitely long 9-36357
- dielectric media on opaque substrates 9-26671
- dispersive medium, time-space periodically-modulated, theory 9-25150
- double scatt. and its application to the critical behaviour of fluids 9-36233
- by electrons, free in plasma, effect of charged particle-neutral collisions 9-46485
- field scatt. by long imperfectly conducting wire, soln. 9-41858
- field singularities distribution, Rayleigh hypothesis 9-47856
- by free electrons, harmonic generation study 9-22314
- by gas-like distribution of spheres, electronic averaging of phase quadrature components 9-36234
- by hydrodynamic pulsations of turbulent plasma 9-38977
- interaction with nonmagnetic dielectric particles immersed in infinite homogeneous isotropic nonmagnetic medium 9-27259
- for inverse diffraction problem, using Bojarski identity 9-47851
- by ionization in atmosphere, mag. field aligned 9-31392
- by ionized spherical cloud in atmosphere, artificial 9-31329
- ionosphere, disturbed, lower, forward-scatter observations 9-33833
- ionosphere, induced and mixed, properties 9-31389
- magnetosphere, induced and mixed, properties 9-31389
- microwaves, enhancement by plasma instability in mag. field 9-28033
- Mie and Rayleigh-Gans theories compared for inhomogeneous particles 9-36231
- Mie multiple scatt. in plane parallel homogeneous medium 9-36223
- by molecular assembly 9-36232
- moving media, radially, first order vector wave equation solution 9-38335
- multiple, in underdense plasma, transport equation for intensity 9-42513
- multiple in plasma parallel layers 9-36224

Scattering continued**electromagnetic waves continued**

- multiple rel. to radiative transfer in plane-parallel atmospheres 9-36362
- non-spherical particles, of the order of the wavelength 9-36229
- paint films on black substrate, coefficients for 0.8-2.0 μ range 9-43206
- partially coherent radiation, Heisenberg calc. of intensity 9-34152
- particulate, in media and multiple, conference 9-25151
- for perfectly conducting prolate spheroid echo area 9-47857
- by plasma, underdense, intensity transport eqn. 9-34761
- by plasma afterglow in mag. field 9-48568
- plasma sphere, comparison between geometrical optics approximation and rigorous method 9-36768
- by prolate spheroids 9-36229
- 1,2-propylene glycol, liq., stimulated Mandelstam-Brillouin scatt. for obs. of hypersound propag. 9-30399
- radar backscatter calc. transport eqn. 9-34761
- radar echoes, clear-air origins and use in investigation atmospheric structures 9-33783
- radio, 1.7 m, Moon's surface, 'Luna-11' and 'Luna-12' observations 9-24840
- radio, by moving body trail in ionosphere 9-31388
- radiowaves, by ionos. small scale inhomogeneities polarization 9-41860
- by rain of various origins 9-40040
- Rayleigh-Gans and Mie theories compared for inhomogeneous particles 9-36231
- in rectangular waveguide, by cylindrical post parallel to electric field vector of dominant mode 9-25147
- resonance, polarized radiation in weak mag. fields, Monte Carlo treatment 9-38333
- single-body, impulse response concept 9-36230
- space vehicle in warm plasma, power and radar cross-section evaluation 9-34123
- sphere, absorbing, wave charact. evaluation 9-36228
- by spheres, review 9-36357
- on spherical polydispersions, book 9-40293
- by spherically symmetric inhomogeneous particles 9-36231
- stimulated thermal scatt. in isotropic media 9-43813
- stimulated thermal scatt. in isotropic media 9-43814
- from thin conducting sheet on curved surface, mode conversion problem 9-22313
- Thomson, applic. to ionospheric temp. and density meas. 9-31413
- Thomson, with unequal electron and ion temp., effect of collisions 9-42515
- transfer eqns. and spectral field densities 9-29346
- triacetin, liq., stimulated Mandelstam-Brillouin scatt. for obs. of hypersound propag. 9-30399
- turbulent plasma, finite volume, in first Born approx. 9-48562
- by vibrating interface between media 9-38334
- by wedges, perfectly conducting, for transversely polarized line source excitation 9-47858
- ^4He , Rayleigh scatt. at $T < 0.6\text{K}$ 9-39123
- ^3He - ^4He weak solns., Rayleigh scatt. 9-39123
- light**
- see also Diffusion, light
- aerosol spherical atmosphere 9-37917
- aerosols, size distribution from spectral attenuation meas. 9-36905
- amorphous media, expt. 9-28199
- angular distribution coefficients, evaluation 9-46004
- anisotropic in semi-infinite atmosphere 9-43617
- anisotropic transfer problems in thick layers, asymptotic fitting method for solution 9-34205
- Arctic ocean, central, obs. 9-24629
- by atmosphere, cloudy and hazy 9-41527
- atmosphere, Rayleigh, intensity of radiation 9-28933
- atmosphere-ocean system, radiative transfer 9-36149
- atmospheres, flnite, with specular reflectors, refl. and transmission functions 9-29531
- atmospheric, model calc. 9-33776
- atmospheric, polarization and angular distribution changes during cloud formation 9-28887
- atmospheric hygroscopic particles, effect on backscattered power of laser beam 9-41529
- atmospheric laser beam backscatter rel. to visibility 9-28885
- by atoms in resonant freq. region for investigation of excited atomic energy levels, review of exptl. techniques 9-29908
- attapulgite, orientated, suspension in aqueous soln., effect of alternating elec. fields 9-34929
- p-azoxyanisole liquid crystal, quasielastic Rayleigh scatt. 9-40793
- backscatter effects in active night vision systems, effect of phase function at forward angle 9-41530
- beam emerging from scatt. medium, structure 9-37919
- benzene derivatives, liquid, depolarized light, spectrum 9-26117
- binary solns., theory 9-28126
- biomolecules in soln., rotn. and translation meas. using laser beat freq. spectroscopy 9-48113
- birefringence effect, using classical theory, appl. to thin polymer films and gaseous molecules 9-49244
- by black paint surface, polarization rel. to incidence angle 9-31073
- blood, for highly collimated light 9-45703
- blood, parameters 9-47694
- at boundaries to parametrically modulated media 9-34210
- Brillouin, stimulated, experimental investigations review 9-25367
- Brillouin, stimulated, in nonfocusing liquids and quartz 9-26098
- butadienenitrile rubbers, NMR, light scattering study of structure, vulcanization character 9-23789
- by fluids, fluctuation theory 9-23497
- chain molecules, comb. cascade and star cascade and star models 9-42456
- chemically reacting medium, depolarization spectrum 9-24529
- chemically reactive fluids 9-31181
- chloropropene, NMR, light scatt. studies, of structure 9-23789
- from clouds and haze, radiance and polarization 9-33768
- coherent, from a rough surface, speckle pattern formation, theory and expt. 9-37735
- by colloidal spheres 9-36357
- colloids, effect of orientation of particles by laser field 9-23543
- conducting cylinders, at normal incidence 9-33518
- cornea, theory 9-38155
- corundum crystal, due to defects 9-33522

Scattering continued**light continued**

- near critical point in fluids and non-fluids, review 9-36876
- crystals, second-order combinational, and i.r. absorpt., selection rules 9-41371
- n-decane- β,β' dichloroethyl critical opalescence investigated by light and X-ray scatt. 9-36877
- dichlorobenzene, o-, m- and n-, combinational spectra, phase shift rel. to dipole-dipole intermolecular forces 9-46393
- dielectric cylinders, at normal incidence 9-33518
- dielectric mirrors, high-reflectivity 9-32020
- diethyl ether, near crit. point, gravity effects 9-30406
- diffuorobenzene, m- and n-, combinational spectra, phase shift rel. to dipole-dipole intermolecular forces 9-46393
- by elastic surface waves in α -quartz 9-47307
- emulsions, part. size meas. 9-36906
- fibres, large, at normal incidence 9-33518
- fibres immersed in liquid rel. to birefringence meas. 9-28656
- fluid, correlation and fluctuation props., single-mode laser input 9-32561
- fluids, multicomponent, theory 9-39099
- flux equivalences among Rayleigh, isotropic and other models 9-36356
- gas, Rayleigh scatt. cross section and normal depolarization meas. 9-48665
- gas, resonance rad. transfer, higher decay modes, eigenvalue problem 9-34839
- gas mixtures, nonlinear thermal Rayleigh scatt. 9-32738
- gas mols., birefringence effect, classical treatment 9-49244
- gases, dilute monatomic, hydrodynamic theory using Burnett equations 9-30352
- gases and vapours, intensity and polarization 9-39052
- gases of nonpolar linear mol., depolarized Rayleigh scatt. and tensor polariz. reson. 9-39053
- Gaussian intensity-fluctuation distribution 9-29470
- glass, back scatter rel. to surface roughness and spatial scatter 9-37692
- by glass cylinders, long thin, angular distribution at oblique incidence 9-26713
- by glass surface, polarization rel. to incidence angle 9-31073
- granulation phenomenon of laser illuminated surface 9-43919
- helical polymer mols., hyperpolarizability and i.r. phonon dispersion 9-32541
- ice clouds, in near infrared, theory 9-47541
- inert gases, collision-induced 9-32432
- interface props. of particle scatterers 9-23503
- i.r. radiation, quantum heterodyne detection 9-38366
- laser, by fog and smoke, polarization obs. 9-35824
- laser, in β -pinch plasma, rel. concentration 9-23299
- laser backscatt. imagery, polarization effects 9-36364
- laser beam expt. for plasma turbulence meas. 9-46533
- laser beams, 0.63 μ , in artificial fogs, wood smokes and model media 9-28886
- laser light scatt. in plasmas, theory and exptl. considerations 9-42516
- laser radiation propag., spotted background structure 9-44602
- laser tech. for liquid spect. 9-36882
- liquid, depolarization and orientational correlations 9-23499
- liquid, meas. of rotational diffusion 9-28128
- liquid mixtures, binary, critical opalescence 9-34909
- liquid surface, stimulated, theory 9-26109
- liquids, by thermally excited capillary waves 9-28088
- liquids, isotropic and anisotropic in simple systems and binary mixtures 9-36875
- liquids, theory, treatment of field fluctuations 9-48699
- liquids, viscous, from shear waves, 0 to 15 GHz, 9-26104
- liquids and gases, stimulated Rayleigh-wing and thermal Rayleigh, theory, review 9-26034
- liquids in external resonator, stimulated scatt. of Rayleigh line using 9-46637
- liquids near crit. point, gravity effects 9-30406
- macromolecules, semirigid, statistical zigzag model 9-23179
- macromolecules in soln., rotary-diffusion broadening of Rayleigh lines 9-39104
- Mandelsham-Brillouin, stimulated, effect of monochromatic pumping 9-46343
- mat. surfaces, physical mechanism of the specular peak 9-41945
- metals, by itinerant spin-density excitation 9-47372
- methane, stimulated Rayleigh scatt., critical absorption coeffs, and anti-Stokes shift, density depend. 9-46573
- Mie total and differential backscattering cross-sections for Junge aerosol models 9-22459
- milk, for highly collimated light 9-45703
- modulated, in semi-infinite medium 9-38395
- by molecular assembly 9-36232
- molecular crystal, line width temp. depend. 9-45304
- by molecular system, condensed unified theory 9-36361
- moon, surface light-scattering, single-colour investigation of uniformity 9-31589
- multiple, rel. to radiative transfer in a plane parallel medium illuminated by an external source 9-36360
- multiple scatt. processes in nonlinear optics 9-27344
- optical coherent waves by curved rough bounded surface, spatial correlation determ. 9-22461
- organic liquids far from melting point, energy distribution in Rayleigh spectrum 9-26121
- paint-like coatings, Mie scatt. theory 9-37689
- paraffins in β,β' -dichlorodideethyl ether, critical opalescence 9-34909
- partially coherent-radiation scatt., by discrete scatterers, Heisenberg operator determ. of intensity 9-34152
- patterns and morphology for polytetrafluoroethylene films 9-42707
- n-pentane near critical pt., under influence of gravitational eff. 9-23501
- phenol-water mixture, meas. of conc. fluctuations near critical point 9-40794
- plasma, non-Maxwellian 9-48576
- plasma, of laser light at 90° 9-46488
- plasma, relativistic corrections to spectrum 9-34764
- by plasma focus, laser light scatt. at 90° 9-25886
- polariton resonant scatt., composite particle treatment 9-45334
- polarized, in slab of randomly oriented particles, symmetry relations 9-41528
- poly- α -amino acid solns., laser light 9-42657
- polybutene-1, high-speed deform., exam. by photographic light-scatt. technique 9-46901

Scattering continued**light continued**

- polyethylene, high-speed deform., exam. by photographic light-scatt. technique 9-46901
- polyethylene, linear, in p-xylene, crystallization optical investigation 9-28238
- polyisobutene-polystyrene-cyclohexane (benzene) system, rel. to solute interaction parameter 9-23510
- polyisoprene solns., meas. for mol. struct. determ. 9-48524
- polymer chains with excluded vol. effects 9-36731
- polymer fil, birefringence effect, classical treatment 9-49244
- polymer films, solid, theory 9-37694
- polymer films low-angle patterns, effect of birefringence 9-49243
- polymer solns., dilute, rel. to molecular entanglement and relaxation time 9-46615
- polymer solns., theory 9-39099
- in polymer solutions 9-23463
- polymer structure determ. 9-28199
- polymeric soln., supermolecular order formation by polarized light low-angle scatt. 9-28102
- polymers, chain, in soln. with intramol. interac., rel. to random core config. 9-34905
- polyolefines crystallization from dil. soln., optical investigation 9-28238
- polypropylene, isotactic, obs. 9-37695
- polypropylene, linear in 1-chloronaphthalene, crystallization optical investigation 9-28238
- polytetrafluoroethylene films, morphology rel. to light-scatt. patterns 9-46709
- polyvinylalcohol gel, large rise in H_v 9-37695
- α -quartz, by elastic surface waves 9-47307
- Raman and Rayleigh, in terms of oscillator strengths and refr. indices 9-25690
- random orientation fluctuation model for solid polymer films 9-37694
- Rayleigh, off spherical molecules at right angles, elimination of stray light 9-36359
- Rayleigh assumption, scattering by periodic surface 9-22462
- Rayleigh from dilute polymer solutions, fine structure theory 9-36881
- Rayleigh scatt., nonlinear, thermal, in gases 9-32738
- Rayleigh scatt. by 3d magnetized transition metal, scatt. amplitude and spin depend. determ. 9-41361
- Rayleigh scatt. of polarized photons by molecules 9-34589
- Rayleigh thermal scatt., stimulated, time and freq. depend. 9-29434
- resonance rad. transfer, higher decay modes, eigenvalue problem 9-34839
- rodlike macromols. oriented in a.c. fields 9-23502
- ruby, characterization of Verneuil grown crystals 9-37066
- ruby, pink, resonance fluorescence, sharp line excitation 9-26775
- ruby laser, stimulated Mandel'shtam-Brillouin scattering for passive Q-switching 9-36306
- salol, liq., Rayleigh line wing fine struct. and transversal hypersound propag. 9-44573
- seawater, directional charact., relation with apparent optical properties, model 9-30403
- by seawater particles and turbulence 9-44564
- in semi-infinite medium asymptotic formula 9-45595
- semiconductors, polar, Stokes scatt., phonon-cyclotron broadening 9-28701
- semiconductors in strong elec. field, by hot electrons, and fluctuations 9-49063
- semiconductors without inversion centre, by charged centres 9-28700
- semiconductors without inversion centres, by current carriers 9-49292
- soap film, peristaltic mode rel. to frequency analysis 9-46634
- solids, inelastic-electron-scattering and optical data, parametric calc. 9-37679
- by soot surface, polarization rel. to incidence angle 9-31073
- spectrometer, self-beat, for laser light scatt. by solns. 9-42657
- by spheres, polydispersed, coherent and incoherent 9-42658
- by spheres, two components, randomly distributed 9-22458
- by spherical particles, particle spectrum information determ. 9-36358
- spheroidal particles oriented by streaming 9-36903
- statistical correlation function theory for solid polymer films 9-37694
- statistical props. of light scatt. by fluid 9-42474
- stimulated, at surface of highly viscous liq. 9-42655
- stimulated thermal Rayleigh, in fluids 9-25309
- stimulated thermal scatt. in isotropic media 9-43814
- stimulated thermal scatt. in isotropic media 9-43813
- styrene-butyl methacrylate graft copolymer 9-32553
- styrene-methyl methacrylate graft copolymer 9-32553
- surface emission rel. to macroscopic roughness 9-41359
- Thomson and Rayleigh scatt. in preionization Z-pinch 9-44415
- Thomson scatt., eff. of phase of incident high intensity rad. 9-34208
- transfer function of scatt. media 9-25366
- in turbid media, new equation 9-36363
- turbidity layers, microphotometric meas., Schwarzschild-Villiger effect 9-23540
- by uneven surfaces with high absorptivity, polarization rel. to incidence angle 9-31073
- upper atmosphere, infrared, observations 9-47561
- u.v., from rough surfaces, experiments 9-45267
- in vacuum monochromators, and measurement elimination 9-34230
- Venus, by clouds, effect on CO₂ bands and water vapour lines 9-41679
- by Venus, linear polarization obs. 9-31615
- by Venus, polarization, comparison with calculation 9-31616
- Venus, props. atmospheric particles rel. cloud models 9-38079
- by Venusian atmosphere 9-24879
- Verneuil crystals, uncommon, characterization 9-37066
- water, loss of resolution in images due to multiple small-angle scattering 9-36878
- water droplets, intensity and polarization 9-28888
- water Kerr cell, wavelength shifts, r.f. excitation 9-40792
- xylol, o-, m- and n-, combinational spectra, phase shift rel. to dipole-dipole intermolecular forces 9-46393
- Ag, nonradiative surface plasma waves excitation 9-41145
- Al atoms, Raman and Rayleigh cross sections 9-25690
- Al coating on ground pyrex, reflection diffusion rel. to incidence angle 9-48080
- C₆H₆, stimulated Brillouin scattering threshold and line shift, temp. dependence 9-26110
- CCl₄, stimulated Brillouin scattering threshold and line shift, temp. dependence 9-26110

Scattering continued**light continued**

- CO₂, stimulated Rayleigh scatt., critical absorption coeffs. and anti-Stokes shift, density, depend. 9-46573
 CS₂, stimulated Brillouin scattering threshold and line shift, temp. dependence 9-26110
 Ca, (4s4p)¹P, state, coherence narrowing and shift of optical double reson. signals 9-29923
 Cr, by itinerant spin-density excitation 9-47372
 Cs atoms, Rayleigh cross section 9-25690
 He, liquid stimulated Mandel'shtam-Brillouin scatt. 9-48725
 He-Xe gas mixture, laser stimulated, conc. scatt. 9-46286
 at He laser-prod. breakdown front, mechanism 9-23362
 He liquid, electron trapped in bubble 9-23560
 I₂ in gas mixture, nonlinear thermal Rayleigh scatt. 9-32738
 InSb, cross-section in presence of free carriers 9-33306
 K vapour, induced versus parametric processes 9-47998
 N₂, liquid, stimulated combinational, from Nd laser 9-36879
 NO₂ in gas mixture, nonlinear thermal Rayleigh scatt. 9-32738
 NaCl:Pb, Rayleigh scatt. correl. with u.v. absorpt. spectra 9-45328
 NiF₂, inelastic mag., paramag. spin waves and correl. functions obs. 9-33441
 O₂ layers of atmosphere, u.v. rel. to vertical distributions 9-40012
 Rb vapour, stimulated three-photon 9-22954
 V phthalocyanide, forced Mandel'shtam-Brillouin scatt., ruby laser pulse length reduction 9-28129
 YFe garnet, i.r. scatt. by two-magnon processes 9-24421

light, Brillouin spectra

- benzene, line breadth and hypersonic absorption 9-44560
 carbon tetrachloride, evidence of multiple vibrational-translational relax. 9-48702
 carbon tetrachloride, line breadth and hypersonic absorption 9-44560
 cholesteryl-2-(2-ethoxyethoxy) ethyl carbonate, liquid crystal, temp. dependence 9-46644
 dispersive liquids, stimulated scatt., phonon-freq. depend. of steady-state gain 9-44568
 heterodyne spectroscopy of large angle scatt. 9-38393
 large angle, heterodyne spectroscopy obs. 9-38393
 laser-induced stimulated 9-41394
 liquid crystal, temp. dependence 9-46644
 liquids, hypersonic velocity determ. 9-30393
 liquids, organic, ruby laser light, Stokes light and hypersound generation at room temperature 9-39107
 liquids, steady-state gain 9-42659
 Mandel'shtam-Brillouin scatt. in laser powerful nsec. pulses prod. 9-27302
 off-axis resonator, quantitative theory of stimulated scatt. 9-25219
 quartz, fused, ruby laser light, Stokes light and hypersound generation at room temperature 9-39107
 α quartz, longit. hypersonic damping, obs. 9-26759
 quartz, polarization levels of scattered lines 9-33570
 Rayleigh component attenuation using interferometric filtering 9-40385
 solutions, binary dilute, Brillouin intensity ratios and Landau-Placzek law deviations, obs. 9-30408
 stimulated, for self focused laser beam in liquid 9-42654
 CS₂, line breadth and hypersonic absorption 9-44560
 CdS, acoustic shear-waves generated by supersonic electrons study 9-46996
 CdS, acoustoelec. domain form. obs. 9-43055
 CdS, electron-phonon packets obs. 9-47106
 CdS, semicond., acoustic domains obs. 9-35397
 CdS, stimulated Brillouin scattering, threshold and direction control 9-48960
 GaAs, acousto-electric domains 9-44958
 n-GaAs, acoustoelec. domains 9-37352
³He-He II system, line shape 9-34941
 KI 2-photon absorption spectra, optical transition in Brillouin zone, 0-7.5 eV 9-39838
 LiNbO₃, u.s. microwave pulses 9-35278
 N, compressed gas, depolarization as function of gas density and laser power 9-28079
 NaBrO₃ single crystal, study 9-47381
 ZnO, acoustic shear-waves generated by supersonic electrons study 9-46996

light, Raman spectra

- anharmonic crystal, interatomic pot. theory 9-30759
 apparatus using laser excitation and polarization 9-29484
 atom, reson. effect rel. to Autler-Townes effect 9-46268
 backward-stimulated in liquids with high time resolution, investigation 9-26114
 in broad-band i.r. source for tunable coherent light generation 9-27341
 in broad-band i.r. source for tunable coherent light generator 9-27341
 cell, low-temp. 9-22480
 depolarization ratio of lines due to intermolecular interactions, perturbation calc. 9-40629
 dimethyl sulfoxide, Raman line displacement of S=O related to acidity of hydroxyl-containing subs. 9-27940
 excitation in laser dispersing cavity 9-22410
 in Fabry-Perot resonators, transverse 9-25724
 frozen liquids, forced by ruby laser rad., skeletal vibs. 9-37377
 gases, detection of laser scattering, trail arrangement 9-48117
 gases, with Hg arc irr., intensities and depolarization ratios 9-46340
 intensities of lines calc. by averaging method 9-32444
 laser-induced, spontaneous and stimulated bubble 9-41394
 liquid, polarization and intensity of lines photoelectric study 9-30409
 liquid, with laser excitation, intensities and depolarization ratios of lines 9-46640
 liquid and solid substances, production with laser beam 9-36883
 liquids and binary mixtures, line intensities as function of conc. and solvent type 9-48701
 longitudinal modes in molec. crystrs. 9-37736
 low temperature cell for sublimed films and solid samples 9-32068
 magnetic crystals, matrices determ. from mag. point groups irreducible corepresentations 9-24422
 molecular, calc. method when nuclei undergo harmonic vibrations 9-27840
 overtone and combination bands, symmetry of scatt. tensor for higher orders 9-34523
 plasma, semicond., scatt. by coupled plasmon-cyclotron-harmonic modes 9-33238
 light, Raman spectra continued
 powders, forced combination dissipation obs. 9-34170
 quantitative understanding of stimulated Raman scattering, results 9-25729
 quantum electronics conference, 1968, Miami, USA 9-25196
 semiconductor, free carrier distrib. functions determ. 9-49071
 spectrometer with conventional or laser source 9-22478
 spectroscopy, latest achievements, review 9-40384
 spontaneous and induced, connection 9-27833
 stimulated, gain pressure dependence 9-27835
 stimulated, for self focused laser beam in liquid 9-42654
 stimulated, time dependence anomalies, obs. 9-25730
 stimulated combinational emission in optical resonator 9-36278
 stimulated oscillation threshold condition 9-27342
 stimulated Raman scatt. in laser powerful nsec. pulses prod. 9-27302
 substance in Cuvette, determ. using He-Ne laser as excitation source 9-49293
 three-level system, and Orbach process, rel. to double quantum transition 9-49344
 triglycinefluoroberyllate ferroelec. crystal, l.f. at 80° to -140°C 9-49299
 triglycinesulphate ferroelec. crystal, l.f. at 80 to -140°C 9-49299
 vacuum shift, conversion tables for air obs. 9-27406
 variable temp. cell design for use with Raman spectrophotometer 9-32063
 vibrational Raman eff., inner and outer scatt. tensors 9-27831
 DyAl garnet, electronic transitions rel. to Dy³⁺ 9-24425
 exciton-enhanced by optical phonons 9-35670
 He liq., rotors, spectrum intensity and polarization 9-32805
 MnF₂, antiferromag., matrices determ. from mag. point groups irreducible corepresentations 9-24422
 Pt complex, K [Pt Cl₂(C₂D₂)]₂.H₂O aq. soln. depolarizations, vib. fundamentals assignment 9-27873
 Pt complex, K [Pt Cl₂(C₂H₄)]₂.H₂O aq. soln. depolarizations, C-C stretching freq. determ. 9-27873
 Pt complex [Pt Cl₂(C₂H₄)]₂ aq. soln. depolarizations, vib. fundamentals assignment 9-27873
 light, Raman spectra, inorganic
 α -gravity at high press. 9-31118
 alkali halide crystals with defects, obs. 9-33568
 alkali metals, scattering by spin waves 9-37738
 aqueous metal nitrates, types of interaction 9-44569
 centrosymmetric crystals, polariton obs. 9-24429
 diamond, stimulated Raman gain meas. 9-25734
 ferroelectrics with tungsten-bronze struct., lattice vibr. obs. 9-41079
 metal complexes with N-containing ligands, stretching and bending fund. 9-32459
 nitrate powders, absolute scatt. coeffs. 9-49295
 nitrates, molten 9-39105
 powders, absolute scatt. coeffs. 9-49295
 α -quartz, linewidth and shift temp. dependence, 5-300°K 9-24428
 rare earth garnet single crystals, comparison with far i.r. 9-39850
 ruby, anti-Stokes photon emission associated with laser enhanced two-photon decay 9-26766
 silica, vitreous, Stokes-Raman spectrum, temp. depend 9-49297
 stilbene cross-sections using Ar laser line at 4880 Å 9-41396
 sulphate powders, absolute scatt. coeffs. 9-49295
 water, distilled, stimulated emission obs. 9-34911
 zincblende type crystals, intensities, magnitude and trends 9-47377
 As₂S₃, He-Ne laser excitation 9-31117
 As₂S₃, He-Ne laser excitation 9-31117
 As compounds, infrared and Raman studies 9-36695
 BaTiO₃, tetragonal, by polaritons 9-35671
 BeO, wurzite-type, 1st-order scatt. 9-47373
 BeSO₄.4H₂O, low freq. vib. and lattice modes 9-24423
 CS₂, backward-stimulated, investigation 9-26114
 CS₂, backward stimulated pulses 9-23504
 CS₂, backward stimulated pulses 9-23504
 CS₂, and i.r. spectrum 9-34614
 Ca₁₀(PO₄)₆F₂, coupled PO₄³⁻ vib. in cryst. 9-37317
 CdS, multiple-phonon-resonance eff., reln. with fluorescent-emission spectrum 9-26754
 CdS, multiple-phonon resonant scatt., frequency spectra of higher orders 9-26753
 CdS, wurzite-type, 1st-order scatt. 9-47373
 CdS, Se_{1-x}S_x crystals, photon-phonon interactions 9-26752
 CdS, Se_{1-x}S_x mixed-crystal system, LO phonon freqs. determ. 9-46971
 CeCl₃, electronic and phonon Raman effects, asymmetry 9-26755
 CeCl₃, electronic effect rel. to f¹ config. electronic states 9-24424
 Cl crystal 9-43245
 Cs₂[Zn(NO₃)₆]₄ 9-49288
 Cu₂O, first order, active mode determ. and symmetry props. 9-39851
 Cu II tetrahalo-anions, $\nu_1(A_1)$ mode and force consts., obs. 9-44327
 Fe II tetrahalo-anions, $\nu_1(A_1)$ mode and force consts., obs. 9-44327
 Fe III tetrahalo-anions, $\nu_1(A_1)$ mode and force consts., obs. 9-44327
 GaAs, by longitudinal cyclotron waves in electron gas 9-33567
 GaP, indirect gap semicond., resonant scatt. obs. 9-41395
 GeCl₄, ν_1 fundamentals, chlorine isotopic splitting patterns, using low temp. cell 9-32068
 GeD₃AsD₂, liquid phase, vibrational assignment 9-30026
 GeD₃AsH₂, liquid phase, vibrational assignment 9-30026
 GeD₃PD₂, liquid phase, vibrational assignment 9-30025
 GeD₃PH₂, liquid phase, vibrational assignment 9-30025
 GeH₃AsD₂, liquid phase, vibrational assignment 9-30026
 GeH₃AsH₂, liquid phase, vibrational assignment 9-30026
 GeH₃PD₂, liquid phase, vibrational assignment 9-30025
 GeH₃PH₂, liquid phase, vibrational assignment 9-30025
 H₂, freq. shift, focused laser beam induced 9-25740
 H₂ gas, laser excited, width of Q(1) line 9-30031
 HBr and DBr crystrs. 9-43246
 HCl and DCl crystrs. 9-43246
 HNO₃ and DNO₃ intensities, bond polarisability theory calcs. 9-46362
 He liquid, two-roton, amplitude calc. 9-32808
 Hg (II) complex, o-phenanthroline, vib. freq. determ. 9-23052
 HgCl₂, HgBr and HgI 9-34627
 H₂g, He-Ne laser excitation 9-31117
 I₂⁺, resonance spectrum in solution 9-38856
 InP, optical freqs. and dielec. consts. meas. 9-47314
 InSb, by longitudinal cyclotron waves in electron gas 9-33567
 K₂Cr₂O₇, single crystal, rel. to symmetry class 9-47374

Scattering continued

light, Raman spectra, inorganic continued

- K₂NiF₆, solid, abs. spectra study 9-32494
 KBr, F centre, electronic, rel. to lattice dynamics 9-35118
 KCl: Cd, due to F centres 9-33569
 KCl, F centre, electronic, rel. to lattice dynamics 9-35118
 KH₂PO₄, partially deuterated, ferroelectric mode obs. 9-26756
 KI, F centre, electronic, rel. to lattice dynamics 9-35118
 KI, of S₂⁻ and Se₂⁻ mols. 9-49294
 KNO₃, molten, vibr. freqs. of NO₃⁻ ion rel. to temp. 9-42662
 KTaO₃, polariton obs. 9-24429
 K₂[Cd(NO₃)₆] 9-49288
 K₂[Hg(NO₃)₆] 9-49288
 LiNbO₃, tunable stimulated Raman oscillator, Q-switched ruby laser excitation 9-35672
 MgNO₃-water solns. rel. to NO₃⁻ symmetry, obs. 9-36887
 Mn II tetrahalo-anions, $\nu_1(A_1)$ mode and force consts., obs. 9-44327
 N₂, liq., band shapes and molec. motion 9-30412
 N₂D₂, crystalline, -70 to -195°C, crystal structure determ. 9-39853
 N₂H₄, crystalline, -70 to -195°C, crystal structure determ. 9-39853
 NH₄NO₃-water solns. rel. to NO₃⁻ symmetry, obs. 9-36887
 Na₂K_{1-x}TaO₃, 4-600°K. phonon modes rel. to dielec. phase transitions 9-47366
 NaBa₂Nb₂O₁₅ and related ferroelectrics, lattice vibr. obs. 9-41079
 NaCl-AgCl crystals, by resonant modes of Ag⁺ 9-28702
 NaCl, F centre, electronic, rel. to lattice dynamics 9-35118
 NaCl, second-order, assignments and dispersion curves 9-39852
 NaClO₃ single crystals near critical temp., combination dispersion 9-28703
 NaF, second-order, and lattice dynamics 9-35673
 NaNO₃ cross-section using Ar laser line at 4880 Å 9-41396
 NaNO₃-Ca(NO₃)₂ molten, vibr. freqs. of NO₃⁻ ion rel. to temp. 9-42662
 NaNO₃-water solns. rel. to NO₃⁻ symmetry, obs. 9-36887
 NaNO₃, molten, vibr. freqs. of NO₃⁻ ion rel. to temp. 9-42662
 NbF₅, liquid, rel. to polymerization possibility 9-26119
 Ni(CN)₄ ion in crystals and soln., laser excited 9-24426
 PF₅, solid 9-24427
 O₂, condensed phases, molec. motion determ. 9-49296
 O₂, liq., band shapes and molec. motion 9-30412
 ONF₃ 9-48468
 PbO-GeO₂ glass system with 0 to 55 mol % PbO 9-28675
 PbS and PbSe, spin-flip, by carriers 9-35674
 PbS(Se)(Te), from single-particle excitations of carriers, charge-density and spin-density fluctuations contribs. 9-47375
 PbTe, spin-flip, by carriers 9-35674
 Pd complex, Pd(II)X₂Y₂ (X=Cl, Br or I, Y=Me₃P or Me₃As), square planar mol. 9-30052
 cisPdII trimethyl-arsine, -phosphine, -stibine complexes, stretching vibrs., obs. 9-27872
 Pt complex, Pt(II)X₂Y₂ (X=Cl, Br or I, Y=Me₃P or Me₃As), square planar mol. 9-30052
 cisPtII trimethyl-arsine, -phosphine, -stibine complexes, stretching vibrs., obs. 9-27872
 RbNiF₃, ferrimagnetic by mag. excitation 9-45336
 Re complex, hexahalogen, K and Cs salts, 1000 to 45 cm⁻¹ 9-32487
 Re(CO)₆⁺, vibrational and electronic spectra and bonding 9-32491
 S-As mixtures, cryst., glassy and liq. rel. to mol. complexity, obs. 9-35675
 S-Se mixtures, cryst., glassy and liq. rel. to mol. complexity, obs. 9-35675
 S, cryst. glassy and liq. rel. to mol. complexity, obs. 9-35675
 SF₆, solid, splitting of three fundamentals 9-30053
 SbI₃ in soln. and solid phases, band assignments 9-26758
 Si₂Cl₆ in liquid phase, vibrational assignment, structure and internal rotation study 9-30056
 SiCl₄ ν , fundamentals, chlorine isotopic splitting patterns, using low temp. cell. 9-32068
 Sn complex, EtSnCl₃, Et₂SnCl₂ and Et₃SnCl, liq. or soln., depolarization degrees 9-48484
 Sn complex, of type cis-SnX₄2L 9-30057
 SnCl₄ ν , fundamentals, chlorine isotopic splitting patterns, using low temp. cell. 9-32068
 SnHPO₄·1/2H₂O, assignment 9-28704
 SrTiO₃ polariton obs. 9-24429
 TaF₅, liquid, rel. to polymerization possibility 9-26119
 Tc complex, hexahalogen, K and Cs salts, 1000 to 45 cm⁻¹ 9-32487
 Ti complex, TiX₄bipy (X=Cl or Br and bipy=2,2'-bipyridyl) 9-30057
 V(CO)₆⁻, vibrational and electronic spectra and bonding 9-32491
 YAl garnet, laser-excited, 100 100-800 cm⁻¹, compared with YGa and YbAl garnets 9-49298
 YFe garnet, i.r. radiation, scatt. by two magnon processes 9-45337
 YGa garnet:Yb, electronic Raman scatt. to crystal field levels of $^2F_{7/2}$ manifold 9-49300
 YbAl garnet, laser-excited, 100-800 cm⁻¹, compared with YAl and YGa garnets 9-49298
 Yga garnet, laser-excited, 100-800 cm⁻¹, compared with YAl and YbAl garnet 9-49298
 Zn (II) complex, o-phenanthroline, vib. freq. determ. 9-23052
 Zn II tetrahalo-anions, $\nu_1(A_1)$ mode and force consts., obs. 9-44327
 ZnO, wurtzite-type, 1st.-order scatt. 9-47373
 ZnS, by Mn impurities, vibr. resonant modes obs. 9-43247
 ZnS, cubic, first- and second-order rel. to electro-optic and lattice dynamics effects 9-47376
 ZnS, intensities 9-47377
 ZnS, wurtzite-type, 1st.-order scatt. 9-47373
 ZnSe, intensities 9-47377
 ZnTe, intensities 9-47377
 9-47373

light, Raman spectra, organic

- p-dibromotetradeuterobenzene, vibrational spectra study 9-27889
 2,5-dihydrothiophene, vib. freq. assignment, 4000-70 cm⁻¹ 9-27901
 1,3,5-trichloropyrimidine and 4D derivative rel. to vibr. assignments, obs. 9-28139
 tri-phenyl compounds of As, Sb, Bi and P, Raman and i.r. obs. 9-30137
 acetaldehyde and acetaldehyde-d₂, meas. of abs. intensities of Raman lines 9-27884
 acetone, -d₆, polarization meas., skeletal bending mode determ., He-Ne laser excitation 9-28136
 adipic acid crystal, and i.r. spectra 9-34652
 benzaldehyde, obs. 9-44352
 benzene, line intensities as function of conc. and solvent type 9-48701

Scattering continued

light, Raman spectra, organic continued

- benzene and aniline, halide substituted, i.f. 9-42424
 benzene isotopic mixed crystals, site effects in vibr. spectrum 9-43007
 benzyl chloride, obs. 9-44352
 benzyl formate obs. 9-44352
 γ -butyrolactone, rel. to ring deformations 9-48492
 calcium formate, crystalline 9-47378
 carbon tetrachloride, ν , fundamentals, chlorine isotopic splitting patterns, using low temp. cell 9-32068
 chloroacetyl halides, rot. isomerism 9-30094
 cyclopentanone-d₄, rel. to ring deformations 9-48492
 cyclobutane-1,3-dione 9-23115
 cyclobutanol, -d₁, -d₂, -d₃, depolarization meas., vib. assignment 9-23103
 p-dibromobenzene, low freq. lines, temp. dependence 9-31175
 p-dibromobenzene single crystals, polarized Raman spectra in intramolecular vibrational region 9-30104
 1,2-dibromomethane, intensity temp. depend., energy difference of trans. and gauche configurations 9-44355
 p-dichlorobenzene single crystals, polarized Raman spectra in intramolecular vibrational region 9-30104
 1,2-dichloroethane, intensity temp. depend., energy difference of trans. and gauche configurations 9-44355
 diethylthiaticarbocyanin dye, SRS amplification 9-28137
 p-difluorotetradeuterobenzene, vibrational spectra study 9-27889
 dimethyllead dihalides, and i.r. spectra mol. struct., 4000-70 cm⁻¹ 9-34675
 dimethylhydrogenphosphonate, rel. to P-H bending vibrs., obs. 9-30066
 N,N-dimethylthioacetamide, normal vibrations analysis 9-46391
 N,N-dimethylthioformamide, normal vibrations analysis 9-46391
 diphenyl sulphide and disulphide 9-23133
 ether, intensity var. with exciting light freq., oscillator strength determ. 9-30111
 ethyl benzoate, liq., vib. freqs. assignment 9-25769
 ethyl chlorides, h₂, d₂, d₃, vib. analysis 9-48490
 ethylene carbonate, rel. to ring deformations 9-48492
 ethylene oxide, i.r. 9-28705
 ethylene sulphide, i.r. 9-28705
 ferrocene, 1,1'-disubstituted cpds. 9-23121
 formic acid, liq. and solid, i.f. spectra 9-24430
 iodicurene, rel. to crystal-lattice vibrs. 9-44813
 ketones, Raman line displacement of C=O and acidity of hydroxyl containing cpds. 9-27940
 liquids, width and shape of lines 9-46642
 lithium formate monohydrate, crystalline 9-47378
 maleic hydrazide in soln. in dimethylsulfoxide 9-46399
 methanethiol 9-23132
 methyl benzoate, liq., vib. freqs. assignment 9-25769
 methyl-cyclopentadienyl nickel nitrosyl 9-30132
 methyldifluoroamine, vib. spectrum 9-27904
 methylhydrazine 9-30127
 methylphosphorodifluoridodithioate 9-38902
 methylthionitrite 9-23131
 p-nitroaniline and related compounds, stimulated and spontaneous spectra 9-45335
 nitrobenzene, line intensities as function of conc. and solvent type 9-48701
 nitroethane Na salts, rel. to geometric isomers, obs. 9-27905
 nitromethane Na salts, rel. to geometric isomers, obs. 9-27905
 1-nitropropane, Na salts, rel. to geometric isomers, obs. 9-27905
 2-nitropropane Na salts, rel. to geometric isomers, obs. 9-27905
 oxalyl bromide, rel. to band freqs. and assignments 9-34684
 pentafluorobenzonitrile 9-23147
 phosphiran, -1-d₁, -2,3-d₂, polarization, freq. shift meas., vib. assignment 9-23150
 polydimethylsiloxanes, scatt. factor, tensor components, polarizability 9-23511
 polymethacrylic acid, laser-excited 9-44383
 polypropylene, syndiotactic, D₂ symmetry, laser-excited Raman spectrum 9-30158
 polystyrene, depolarization meas. rel. to orientation 9-47380
 polytetrafluoroethylene, band assignments 9-44385
 propylene imine 9-44369
 purine and deuterated derivatives 9-41397
 pyridine-Br and BrCl complexes 9-23153
 pyridinium H-bonded halides 9-49290
 sodium formate, crystalline 9-47378
 strontium formate dihydrate, crystalline 9-47378
 styrenes, o- and m-subst., vib. fund modes assignment 9-32529
 succinic acid crystal, rel. to H bond vibrs. and strength 9-35668
 tetraiodoethylene, vib. spectra and assignments 9-27902
 trideuterionitromethane Na salts, rel. to geometric isomers, obs. 9-27905
 trimethylamine 9-30147
 trimethylene selenide, vibr. anal. and ring puckering 9-42447
 trimethyllead halides, and i.r. spectra mol. struct., 4000-70 cm⁻¹ 9-34675
 urea, i.r. meas. of crystal lattice vibrations 9-48948
 Na ethyl sulphate monohydrate, bond obs. 9-24431

X-rays see X-ray scattering

Scattering, elementary particles see Elementary particles/scattering

Scattering, nuclear see Nuclear reactions and scattering

Scattering, particles

- see also Collision processes; Energy loss of particles; Field theory, quantum/interactions; Elementary particles/scattering; Nuclear forces; Nuclear reactions and scattering; Particle tracks; S-matrix theory; and under individual particles, e.g. Alpha-particles
 anisotropic with absorption, Milne problem exact analytical solution and numerical treatment 9-38206
 chamber with gaseous target description and operation 9-22654
 Coulomb, rel. to effective radius of positive column 9-48633
 cross sections calc. with arbitrary spin, canonical method 9-36425
 density emitted by point source in homogeneous medium with general anisotropic scatt. 9-36122
 elastic, high energy, quantum electrodynamics 9-22509
 excited state production cross-section in terms of imaginary part of integral involving wave function 9-36134
 high-energy, statistical model 9-42039
 Levinson's theorem in Lee model with ghosts 9-46040
 magnetospheric electrons, pitch angle mechanisms 9-37948

Scattering, particles continued

- Milne problem with absorption and anisotropic scattering, exact analytical solution and numerical treatment 9-38206
- relativistic theories, multi-trajectory operators 9-48147
- trapped in earth's mag. field, bound resonant scatter 9-28936
- Ar beam, monoenergetic, by heated Pt 9-44316

Schizons see *Elementary particles; Field theory, quantum/interactions, weak*

Schlieren systems

- collision exchange interferometry on steel and glass models 9-29457
- density gradient meas. in transparent media 9-32006
- diffraction theory of methods 9-32005
- high-speed colour photography 9-32096
- i.r. glass examination by evaporographic convertor 9-38408
- mode-locked laser as light source 9-48125
- photographs of lasers-induced sparks, mode-locked laser light source, synchronization 9-27403
- prism formation using thermal gradients 9-34199
- projectile hypersonic wake, obs. 9-30331
- shock wave damping by multiple refl. at slits, spark cinematography 9-29315
- three-dimensional, description 9-32004
- velocity meas. with combined Doppler principle 9-38191
- welding and cutting, gas flow mechanisms, flash Schlieren photography 9-33983
- Ω wave optics 9-39066
- use of Ar laser in study of gas flow in elec. arc, or plasma 9-22384
- ^4He , photography of thermal pulses 9-48728

Schottky defects see *Crystal imperfections/vacancies*

Schottky effect (noise) see *Electron tubes; Noise/electrical; Semiconducting devices*

Schrodinger equation see *Quantum theory/wave equations*

Schwarzschild space see *Cosmology; Gravitation; Relativity/general*

Scintillation see *Luminescence*

Scintillation chambers see *Luminescence chambers*

Scintillation counters see *Counters/scintillation*

Seals

- ceramic-to-metal, formation, patent 9-24995
- ceramic-to-metal conductive, composition, patent 9-24996
- mechanical, avoidance of limiting conditions by makers 9-27148
- vacuum, for elec. leads 9-33992

Seawater

- beach bathymetric meas., airborne pulsed laser applic. 9-35807
- and clays, chemical equilibrium 9-45466
- confused seas, wavelength and period 9-28856
- English Channel, geoides, deviations from mean level 9-24611
- inert gas contents 9-47517
- interface with air, wind stress coefficient and boundary layer flow 9-31307
- light scatt. obs. in central Arctic ocean 9-24629
- light scattered by particles and turbulence, imaging props. 9-44564
- parameters affecting sound propagation 9-37899
- Red Sea bottom 1795 to 2195 m depth, temp. salinity and chlorinity 9-43372
- salt fingers instability rel. to internal gravity waves and collective instability 9-33748
- shallow, 1120 Hz signal propag. fluctuation obs. 9-26097
- sound speed calculation, accurate simple eqns. development 9-47521
- state equations 9-35802
- submarine viewing situation, modulation transfer function dependent on range and seawater properties 9-30404
- temperature, surface, effect of ice concentration 9-43371
- temperature meas., time variation at 4 points simultaneously 9-35809
- turbulence and temperature microstruct. in and above thermocline 9-35806
- turbulent flow, temp. and velocity fluctuations, and power spectra 9-35805
- volume attenuation coefficient and volume scattering function, rel. to apparent optical properties 9-30403
- wind-wave interactions investigation, of shear stresses 9-44541
- ^{14}C , activity variation with time and location in South Pacific and Antarctic Oceans 9-37902
- ^3He excess, terrestrial primordial abundance evidence 9-45468
- O distribution, and effect of advection, turbulence and biochemical demand 9-43376
- Sr concentration latit. 4° to 34°N in Atlantic, spectral obs. 9-45479
- ^{90}Sr content, radiometric measuring device 9-22751

Second sound see *Helium/liquid, sound propagation*

Secondary electron emission see *Electron emission/secondary*

Sedimentation

- anisotropy in packing of random spheres, computer simulation 9-30438
- fluid sphere, slow unsteady settling toward flat fluid interface 9-23538
- gelatin gels. 9-23552
- in graphite, glide and rotation 9-39368
- ocean meas. by submersibles 9-37904
- polymer mols., conc. depend. 9-23539

Seebeck effect see *Thermoelectricity*

Seidel theory see *Aberrations, optical*

Seignette salt see *Rochelle salt*

Seignettelectric materials see *Ferroelectric materials*

Seismic waves

- see also *Seismology*
- anomalies and dynamic evolution of the Earth's crust and upper mantle 9-31263
- asthenospheric layer waveguide simulation, internal inhomogeneities 9-26871
- atmospheric pressure waves coupled to Rayleigh wave, from distant earthquake 9-28849
- attenuation and dispersion in low velocity zone 9-26872
- attenuation in upper mantle and lithosphere discontinuities, lateral vars. 9-45449
- rel. to auroral bursts periodicity 9-26930
- body and surface, investigations and theory 9-43357
- body waves, travel times, velocities and amplitudes 9-26862
- body-wave observations, Monte Carlo inversion 9-49413
- coda of small local earthquakes, analysis as scattered waves 9-31267

Seismic waves continued

- for communications, c.w. 80 Hz information carrier, instrumentation 9-24627
- in crust, law of longit. waves for Marche-Poitou region 9-47503
- damping law, distortion by random interferences 9-26873
- data, at Dourbes (Belgium), during April (1968) 9-49509
- detection system for lunar use 9-43610
- discrimination using strain seismographs 9-41465
- dT/dA, direct meas. 9-41467
- elastic, in quarter plane, propag. eqn. finite difference soln. 9-35778
- elastic wave scattering by random field of surface scatterers 9-39983
- head and reflected, in presence of stratified overlying rock mass 9-33708
- headwaves and reflection in supercritical region, model investigations 9-39987
- heterogeneous sphere, body waves amplitude, wave and ray theories comparison 9-45445
- interference, in case of well logging 9-35788
- ionospheric continuous travelling coupling, May 1968 Japan earthquake obs. 9-43355
- in layered sphere due to explosive point source 9-45447
- local activity induced by the Mangla Dam, Pakistan 9-45454
- longitudinal, between 105° and 115° , received after P waves arrival diffracted by mantle-core boundary, analysis 9-28842
- longitudinal in thinly layered media, phase velocity dispersion 9-33715
- Love modes for oceanic and continental earth model tables of amplitudes, phase velocity and group velocity, variational parameters 9-26867
- Love surface, dispersion of group velocities 9-33721
- in mantle, Love, excitation and wave magnitude definition 9-39981
- medium with random inhomogeneity distrib., distortion theory 9-26874
- microseism propagation velocity, dependence on period 9-24615
- multiple reflection within outer core 9-24620
- optical stimulation with coherent light 9-25103
- P, core diffraction, long period amplitudes near shadow edge 9-28845
- P, long period and SH waves rel. to determ. earthquakes 9-39977
- P, low velocity layer at 800 km depth, evidence 9-45439
- P, S and Rayleigh in Athabasca glacier, obs. 9-31277
- P, spherical, scattering by randomly inhomogeneous elastic half space 9-45442
- P, SV and SH diffracted, and shadow boundary shifts 9-28844
- P'P' reflections from upper mantle structure, remarks 9-47502
- P and Rayleigh data, linear phase filtering 9-37879
- P and S travel times rel. to upper mantle vel. structure 9-35784
- P and S waves as mantle reconnaissance tool, relative amplitudes 9-47494
- P codes, short period, compressional and shear phases 9-41463
- P velocities in lower mantle, array meas. 9-41469
- P wave travel times, search for standard showing little source bias 9-45453
- PcP, transit times and amplitude for surface foci 9-33706
- plane, effect of prestressed state on propagation 9-33714
- power spectrum and covariance function for underwater explosions, model 9-45436
- power spectrum and covariance function for underwater explosions, model 9-49409
- primary, refraction profile, travel time and amplitude interpretation 9-31266
- primary, transmission and attenuation 100 to 600 km 9-35774
- propagation in 'gradient media', model 9-31260
- propagation in self-gravitating anisotropic Earth, mathematical theory 9-26877
- pulse meas. of rock salt elastic props. 9-26311
- Rayleigh, 1st shear mode on ocean floor, sediment props. determ. 9-45472
- Rayleigh, horizontal refraction, amplitude variation 9-47499
- Rayleigh, in surface layers, theory and obs. 9-49417
- Rayleigh, oceanic dispersion analysis method 9-45446
- Rayleigh, particle motion ellipticity rel. to crustal structure 9-35790
- Rayleigh, propag. across continental margin, amplitude variations 9-45437
- Rayleigh and Stonely waves in common spectrum for source in a layered sphere 9-39984
- in real media with low velocity gradient 9-33710
- reflected from transition zone, field pattern estimation 9-49418
- reflected with velocity dependent on 2 variables inverse geometrical seismology problem 9-33711
- reflection from discontinuities within Earth's upper mantle 9-49416
- refracted, amplitude obs. rel. to heterogeneity of crust and upper mantle 9-31272
- S from nuclear explosion (Nevada), travel times and amplitudes 9-35780
- S velocity at core-mantle boundary, diffracted S observations 9-47500
- scattering by surface imperfections, perturbation method 9-45438
- sea, association with New England, earthquake (Nov., 1755) 9-26868
- SH reflection and transmission at solid-firmoviscous boundary 9-35791
- SH waves, spectral behaviour for crustal thickness determ. 9-47497
- shear wave recording by continuous signal methods, early development 9-37876
- shear wave recording by continuous signal methods, later experimentation 9-37877
- short period P waves, crustal characteristics, Central Alberta 9-26870
- spherically symmetric compressible media, discrete Eulerian model 9-37888
- surface, attenuation and moment, simultaneous determ. 9-35777
- surface, excitation by earthquakes and underground explosions 9-28846
- surface, use in selecting crustal structure models 9-37889
- surface components in microseisms 9-35783
- T-phase radiators, Western Aleutians 9-26858
- thin low velocity layers in upper mantle, hypothesis 9-43360
- thinly layered random medium, transmission and reflection 9-22246
- transverse, spherical emitter 9-35787
- transverse and longitudinal, cylindrical radiator freq. characts. 9-35786
- travel time, changes with stress variations at depth 9-26869
- travel time anomalies 9-35781
- travel time anomaly due to heat flow and density 9-31264
- velocity and absorpt. variation due to spalling 9-31258
- velocity and attenuation in imperfectly elastic rock 9-39985

Seismographs see *Seismology*

Seismology

- see also *Geophysical prospecting; Seismic waves*
- accelerometer error in dynamic analysis, correction 9-41466
- acoustic emission prior to rockbursts and earthquakes 9-47498

Seismology continued

- aftershock sequence, heat liberation calc. 9-26857
 alluvium, dynamic amplification of seismic response 9-35775
 analogue computer correction of records obtained in presence of nonstationary oscillations 9-31262
 anisotropy in upper mantle beneath ocean, ocean, rel. to statistical orientation of olivine cryst. 9-33718
 asymmetric active regions, gravity anomalies and seismicity 9-39986
 attenuation in upper mantle and lithosphere discontinuities, lateral vars. 9-45449
 Chile Rise, seismicity pattern showing sea floor spreading 9-41472
 common spectrum computed for source in a layered sphere 9-39984
 cross section, upper part, parameter determ. 9-33709
 crustal movements rel. to mag. axis over 600 M.yr. 9-31271
 crustal structure, refraction methods, Missouri 9-26879
 Dashti Biaz earthquake, Aug. 1968, fault data and engineering aspects 9-33717
 data analysis, high resolution velocity technique 9-45441
 depth computation, 3 dimensional, using space sampled velocity logs 9-37881
 diagnostic value of seismic energy 9-35785
 displacements around deep earthquake epicentre, effect of focal radiation asymmetry 9-33705
 $dT/d\Delta$, direct meas. 9-41467
 dynamic evolution of the Earth's crust and upper mantle, seismic anomalies 9-31263
 Earth, anisotropic spherical model, stress discontinuities propagation, ray paths and travel times 9-47490
 earth, free oscillations spectra 9-31286
 earth motions and seismic sources, analysis by power spectral density 9-47492
 earthquake, Eastern Turkey, Varto area, 1966 9-26859
 earthquake, New England, Nov. 1755 assoc. with sea wave 9-26868
 earthquake, Turkey, Varto Ustukran, 1966 9-26860
 earthquake accelerograms, nonstationary random process model 9-47493
 earthquake fault plane, fault area and rupture vel. determ. 9-39977
 earthquake foci, inverse problem 9-33713
 earthquake focus, 2 dims. model 9-33707
 earthquake focus 2-shear surface development 9-37887
 earthquake frequency minima at equinoxes 9-43354
 earthquake hypocentre location using small networks 9-47495
 earthquake prediction, criterion on rock resistivity variation with time 9-26876
 earthquake source mechanism, propagating phase boundary 9-24619
 earthquake statistics, coefficient p rel. to stress state 9-26875
 earthquakes, fault plane solns. rel. to principal stress direction 9-35782
 earthquakes, large shallow, magnitude rel. to rupture parameters 9-35776
 earthquakes, no. rel. to magnitude (1964-5) 9-39982
 earthquakes, observed intensity-epicentral distance relations 9-47496
 earthquakes, occurrence rel. to presence of relatively acidic rock 9-33719
 earthquakes, source parameters, discrimination from nuclear explosions 9-24614
 earthquakes associated with underground nuclear explosions 9-49415
 elastic layer over homogeneous half-space, spectral transfer functions 9-28841
 elastic wave propag. in rocks, automatic u.s. pulse meas. system 9-37884
 elastic waves, propagations in layered media, finite difference methods, seismograms 9-26863
 elastodynamic source fields dynamical theory, basic rupture parameters 9-26878
 e.m. seismograph constants, least-squares inversion method 9-49410
 energy release by faulting 9-35779
 epicenters and origin times of surface focus events 9-39978
 epicentre determ. by seismic arrays, comment on 'azimuth only' soln. 9-43356
 epicentre source bias, existence 9-24618
 epicentric event location using several arrays 9-24617
 equations of state, high temp., examination of suitability 9-30777
 fault travelling, elastic displacements in the near-field 9-39979
 faults dip angle calc. from surface deformation 9-45452
 field pattern of reflected body waves, determ. by stationary phase method 9-49418
 filtering, linear phase, of multicomponent data 9-37879
 filters, time varying deconvolution 9-37880
 focal mechanism determ. from P and S data, computer program 9-41464
 geology rel. to seismic response 9-35775
 geomagnetic variations and absorption in Scotland 9-47587
 geyser, Old Faithful, deduction of inner workings 9-31255
 h.f. microseisms, known source 9-26861
 ice near melting point, internal friction from seismic obs. of Athabasca glacier 9-31277
 international seismological centre research, review 9-37886
 Iran earthquake, Aug. 1968, fault rupture study 9-28848
 L-shaped Gauribidanur seismic array, tables for reading apparent signal velocity across array 9-28850
 Laplace transform numerical inversion of discontinuous original, applic. 9-36111
 layered medium synthesis from acoustic transmission response 9-37878
 logging in cased wells 9-35788
 magnet for transducers in seismometer, optimum size determ. 9-41468
 mantle, upper, structure rel. to P and S travel times 9-35784
 marine refraction profile, primary waves, travel time and amplitude interpretation 9-31266
 measurement and errors, optimization 9-35772
 microfracture in rocks, rel. to earthquakes 9-26864
 microseisms, and Rayleigh surface waves, lateral refraction, North Atlantic 9-28840
 mid-oceanic ridges, rel. to rift and fracture zones of crust 9-33716
 Mohorovicic discontinuity, investigation 9-33721
 multiple-storey structures on flexible foundations, seismic response 9-47491
 noise structure estimation using arrays 9-37882
 north pole, geographic, trajectory over 1200 M.yr. 9-31271
 observed motion of rotation pole, effect of earthquakes on Chandler wobble 9-31265
 in oceanic wave-guides, diagnostic diagrams and transfer functions 9-26866
 P codes composition determ. using mag. tape seismograms 9-41463

Seismology continued

- P wave travel times, search for standard showing little source bias 9-45453
 P-velocity models to fit restricted sets of travel-time data 9-47501
 pendulum seismographs, vertical, long periods, improved stability 9-24616
 pericline, eqns. of state and geophysical implications 9-28843
 radiator, cylindrical finite length, freq. character 9-35786
 real acoustic sections, continuous logging expt. 9-31261
 recording by long-period galvanometer 9-31259
 records, inverse filtration 9-33712
 reflection arrivals identification using velocity filtering 9-49411
 refraction in continental margin, data interpretation using correl. analysis 9-45450
 response spectra calc. from strong motion earthquake records 9-39980
 rock elastic velocity anisotropy rel. to stress 9-31257
 rugosity-insensitive density logging system for rough holes 9-37885
 seismic activity, local, induced by the Mangla Dam, Pakistan 9-45454
 seismic array, large aperture, long-period noise study 9-49414
 seismic array, large aperture, short-period P-wave signal variations, nature 9-49412
 seismic efficiency rel. to stress 9-28847
 seismic events location, systematic error 9-45444
 seismicity maps, Iranian Plateau and Hindu Kush Region, 1967 9-26865
 signal processing results, long period for large aperture array 9-45440
 signals, multi mode dispersed, multiple filter analysis technique 9-37875
 sonic boom effects, obs. 9-45448
 source model from spectral analysis of Love and Rayleigh waves 9-35777
 spherical emitter of transverse waves 9-35787
 spherically symmetric compressible media, discrete Eulerian model 9-37888
 strain seismograph, interferometric, with high magnification, sensitivity 9-31268
 strain seismographs, applic. wave discrimination 9-41465
 stress accumulation at depth, determ. 9-35773
 teleseismic data for earthquakes and explosions identification 9-45451
 underground seismic reflection meas., reflected point method 9-45443
 velocities, mean and interval, effect of phase velocity dispersion on meas. by logging 9-35789
 wave velocity and absorpt. variation due to spalling 9-31258
- Selenium**
 absorption spectrum of thin single crystals near fundamental edge 9-28692
 amorphous, i.r. absorpt. and multiphonon processes 9-45330
 amorphous, propagation velocity of mechanical waves rel. to Ge content 9-30646
 amorphous, refractive index, influence of electric field 9-35618
 amorphous, transient photoconductivity 9-39709
 amorphous, X-ray intensity curves rel. to dimensions of struct. element 9-32824
 atomic spectrum, bibliography 9-38765
 charge accumulation 9-33377
 defects in single cryst., X-ray topography 9-44709
 electrophotographic layers, photodischarge kinetics, influence of trapping and capture 9-39727
 etch pit observations, single, trigonal crystal of Se 9-28228
 film, crystal structure 9-42796
 film, lateral diffusion of Ag rel. to thin-film couple behaviour 9-42859
 films, amorphous, electron bombardment-induced crystallization 9-32842
 glass preparation, i.r. transmission 8-15 microns, patent 9-24352
 growth of single crystals in gels at ambient temp. 9-37042
 Hall effect in trigonal cryst., d.c. meas. 9-44968
 hexagonal, growth kinetics from α - and β -monoclinic single crystals during structural transform. 9-42936
 molecule adsorbed on Ni, structure determ. by ion neutralization spectroscopy 9-32484
 photoconductivity amorphous films, role of Hg in inducing anomalous phenomenon 9-47206
 photoluminescence of trigonal single cryst. 9-41414
 polycrystalline layer junction with In-AgSe solid soln., photocell for i.r. 9-41274
 rectifiers, capacity meas. 9-26562
 rectifiers, critical breakdown voltage from I-V characts. under hydrostatic pressure 9-26564
 rectifiers, recurrent changes in C-V charact. 9-49116
 reflectivity spectrum from ellipsometric meas., optical const. and interband transitions rel. to fine struct. 9-43204
 refractive index of single crystal, ordinary and extraordinary 9-26699
 resistance limited currents with blocking contacts 9-26509
 thermoelectric properties, infl. of crystallization method, 250°-360°C 9-30986
 trigonal, double Schottky-barrier capacitance meas. 9-49130
 trigonal, exponential absorpt. edge rel. to crystal orientation w.r.t. incident light 9-41388
 trigonal, Hall effect d.c. meas. 9-44968
 vitreous, hole Hall mobility and trap parameters determ. in multiple trapping case 9-39668
 X-ray K-absorpt. edges in ZnSe and CdSe, shifts 9-39858
 Se:Pd film, crystal structure 9-42796
 α -Se, monoclinic cryst., optical absorpt., comparison in solns. 9-39846
 Se₂, photoionization 9-44484
 Se₂⁻ Raman spectrum in KI 9-49294
 Se amorphous films, effect of condensation velocity on crystn. 9-44649
 Se I transition probabilities, near vacuum u.v., obs. 9-23366
⁷⁵Se in GaP, vapour-grown, substrate orientation effect on dopant incorporation 9-30920
- Selenium compounds**
 chalcogenides A^{IV}B^{VI}C^{VI} with perovskite structure, synthesis 9-42755
 glasses, elec. conductivity and opt. absorpt. 9-30956
 sulphur selenide glass, mechanical strength 9-26341
 Ag₂Se, thin films, struct. transforms compared with solid state 9-48927
 As₂Se alloy system, transient photoconductivity 9-39709
 Se-As system, laser-induced vaporization, mass spectra 9-28187
 Se-Te mixed cryst., long wavelength optical lattice vibrs., i.r. reflectivity obs. 9-39826
 Se-Te solid solns., edge absorpt. and band gap obs. 9-43250
 Se-Te system, single cryst. growth phenomena 9-36997
 SeCd thin film transistor 9-49125
 SeF₄ gas-phase electron reson. spectra 9-42416

Selenium compounds continued

- SeO₂, mol. absorption spectrum 2000-4500 Å 9-23073
 SeO₂ in inert gas matrix, i.r. spectra and geometry 9-34641
 SeOCl₂, aprotic soln., luminesc. and energy transfer of rare earth ions 9-22407
 Te-Se system, immiscibility phase boundaries determ. from density meas. 9-40779

Self-diffusion *see Diffusion in gases, in liquids, in solids***Semi-insulating materials (high-resistivity semiconductors)** *see Semiconducting materials***Semiconducting devices**

- see also Counters/semiconductor; Lasers/semiconductor; Masers*
 amplifier, travelling wave, loss charact. 9-47135
 bolometer, range i.r. to mm 9-41840
 chalcogenide glass element with fused-in electrodes, hynamic and static I-V characts. 9-26563
 dielectric films in semiconductor technology 9-37550
 diode laser, interference prevention, patent 9-48047
 doping by ion implantation, review 9-35411
 electrical behaviour using scanning electron microscope 9-30544
 n-GaP, Schottky barriers of silver, current-voltage charact. 9-49119
 glasses, props. rel. to use as switches 9-30934
 guard ring structure for planar p-n junction 9-28525
 guard ring structure for planar p-n junction 9-28525
 Gunn effect, voltage modulation across travelling domain, patent 9-44993
 Hall generators, null voltage compensation methods 9-39648
 impurity concentration deduction from Schottky-barrier (C,V) characts., possible errors 9-30918
 injection electroluminescent behaviour 9-28734
 laser Q-switching mirror mechanism 9-36275
 metal-n-Si contacts, minority carrier injection 9-26565
 microwave detector and a p-i-n reflection modulator for F band appl. 9-33354
 organic semiconductors suitability 9-41193
 oscillators, geometrical dimens. influence on charact. 9-47134
 with p-n junction, lateral retrograded, at surface, patent 9-49114
 review of various types 9-47908
 scanning electron microscope appls., review 9-32892
 sealing, using synthetic resin, for metal housing, patent 9-49133
 switching and conduction in non-crystalline materials 9-28485
 thermal props. 9-33280
 thermistor applic. to high temp. meas. 9-22302
 thermistor bolometer for monochromatic light meas. 9-47832
 thermistor with high temp. coefficient of resistance, stable up to 10³°C in air, patent 9-28524
 thin films, modes of propagating light waves 9-35386
 thyristor, turn-on with lateral field in emitter 9-37549
 transducers, piezoelec., reson. freqs. 9-25105
 transistor oscillator, frequency stability 9-30947
 tunnel capacitor, for charge-quantization studies 9-37548
 CdSe Schottky barriers, barrier heights rel. to preparation 9-24194
 GaAs, optical modulation device 9-33352
 GaAs Gunn oscillators with p-n junction contacts prod. and characteristics 9-39649
 Ge, semi-infinite base, magnetic field effect on I-V characts. and transient processes 9-43083
 Ge rod with lateral probe, potential instability 9-35433
 Ge triode, construction and characts. 9-43087
 InSb, thin film Hall transducers, props. in strong mag. field at liq. He temps. 9-24195
 n-InSb waveguide, dimensional resonances of helicon waves 9-41201
 Mo and alloys, supporting structure 9-30935
 Pb_{1-x}Sn_x Se diodes, mag. field depend. of i.r. laser emission 9-41922
 (Sb₂Te₃-Bi₂Te₃)-(Bi₂Te₃-Bi₂Se₃) thermocouple, transient response of thermoelectric cooling 9-28569
 Se rectifier, barrier capacity, interpretation of results 9-30936
 Se rectifiers, I-V characts. under hydrostatic pressure 9-26564
 Si-SiO₂ m.i.s. structs., surface states density rel. to thermal oxidation conds. of Si 9-26560
 Si, eff. of dislocations on performance 9-37551
 Si, fabrication, doped SiO₂ diffusion sources deposited from SiH₄ and B₂H₆ or PH₃ 9-23638
 Si, fabrication, doped SiO₂ diffusion source deposited from SiH₄ 9-23637
 Si, meas. using three-point probe breakdown technique, theoret. model 9-30928
 Si p-i-n, current oscillations after irradiation with one-MeV electrons 9-24193
 Si photodiode-CsI(Tl) scintillator combination for γ-ray spectrometry, 180 keV to 1.5 MeV 9-27590
 SiN advantages and applications 9-35435
 W and alloys, supporting structure 9-30935
- Diodes**
 chalcogenide glass base, thin film, dynamic V-I characts. 9-24201
 current limiters, noise meas. 9-33343
 electroluminescent, non-coherent, frequency response at low injection levels, derivation 9-31151
 GaP electroluminesc. diodes, prod. characts. and appls. 9-49333
 Gunn, vibrs. and low-freq. oscillations, mag. field influence 9-39654
 high resistance, electronic differentiation of c-v charact. 9-49120
 I-V characteristics, diodes made of compensated semiconductors 9-28533
 IMPATT, performance under gamma and neutron radiation effect 9-49118
 junction, field factor meas. 9-49117
 laser, peak emission shift with cavity Q, temp. and doping depend. 9-27334
 laser, radiative recomb. quantum efficiency, temp. depend. 9-25302
 LSA oscillator diode, analytic theory for ling specs 9-26573
 metal-Si Schottky barrier, transport props. 9-47143
 microwave, noise, NBS report 9-33280
 noise, nonequilibrium, application of fluctuation-dissipation theorem 9-28536
 with nonhomogeneous cathodes, transient processes during switching 9-30941
 p-n, C-V relations, depend. on conc. of shallow and deep impurities 9-35448
 p-s-n, at high injection levels, effective carrier lifetime 9-30942
 photodiode, operation kinetics under barrier conditions 9-33341

Semiconducting devices continued**diodes continued**

- photodiode, photocurrent fluctuations and sensitivity threshold 9-37627
 pulsed laser, streak camera time resolution meas. 9-32088
 relativistic planar, space-charge- limited flow, Poisson's eqn. soln. 9-37560
 reverse current, spontaneous, due to Brillouin e.m.f. 9-24200
 Schottky, C-V relations, depend. on conc. of shallow and deep impurities 9-35448
 Schottky, hot electrons production in metal by forward bias injection, barrier recombination effect 9-44990
 Schottky barrier, metal-Si, transport props. 9-47143
 Schottky barrier, uniaxial stress eff. 9-33344
 Schottky contacts, metal-semicond., barrier energies 9-44991
 Schottky-Barrier diodes, Au-doped and p-irrad., stress eff. 9-24202
 SiC diffused, alloyed and point-contact current and electrolum. brightness rel. to reverse bias 9-37561
 speed of operation, determ. from physical parameters 9-30940
 speed of operation of low inertia types and those with abrupt restoration of inverse resistance 9-30939
 thermionic emission current due to strong elec. field, filamentation 9-33342
 thermometer for low temp. 9-26572
 tunnel, resolution stability of subnanosecond coincidence circuit 9-30945
 tunnel effect, thin film, negative resistance 9-47142
 V-I characteristics, use for meas. of mag. fields >500 Oe 9-29368
 Al-GaAs Schottky barrier u.v. detector 9-43125
 Al_{0.4}Ga_{0.6}As:Si electroluminesc. p-n junctions, props. and efficiency 9-37775
 Al_{0.4}Ga_{0.6}As:P, prep. by liq. phase epitaxy, electroluminesc. obs. 9-47413
 As₂Se₃, switching, filamentary conduction 9-35449
 CdS-CdTe film, photoelec. effects 9-30988
 CdTe, coaxial construction and characts. 9-35443
 GaAs-AlAs, diffused, injection electroluminesc. 9-37780
 GaAs, avalanche, high power and efficiency 9-35447
 GaAs, epitaxial, microwave parameters, switching application 9-43085
 GaAs, ion-implanted, I-V characts., resistance and breakdown voltage 9-30944
 GaAs, laser, topography of absorptivity and emissivity 9-23306
 GaAs, luminescence rel. to mismatch dislocations obs. 9-24448
 GaAs, p-n junction and Schottky barrier, epitaxial growth of guard rings 9-30943
 GaAs, tunnel, high reverse currents, theory 9-28541
 GaAs_{1-x}P_x, vapour grown, electroluminescent efficiencies optimization 9-31153
 GaAs_{1-x}P_x, diffused, electroluminescence 9-37779
 GaAs epitaxial microwave, fabrication and switching applic. 9-43085
 GaAs epitaxial microwave diodes, fabrication and switching applic. 9-43085
 GaAs Gunn, small-signal cond. freq. independence, obs. 9-49129
 GaAs i.r. emitters 9-22423
 GaAs laser, spontaneous emission line breadth, doping depend. 9-27336
 GaAs Schottky barrier avalanche photodiodes 9-26575
 GaAsP, yellow emission 9-41225
 GaP-ZnO, electroluminescent, output charact. 9-41403
 GaP-Cu, induced photoavalanche effect, charge-carrier capture, effect on transition capacitance 9-35510
 GaP, electroluminescent, negative resistance 9-26574
 GaP green-light-emitting, grown by liq. phase epitaxy, spectral props. 9-49121
 GaP injection electroluminesc. reduction by reverse operation, obs. 9-26784
 GaP p-n, electroluminesc. 9-33610
 GaP pulsed, radiation props. 9-38387
 GaP Schottky barrier, props. at 25-500°C 9-33345
 n-GaP Schottky barrier diodes, I-V characts., analysis 9-35434
 n-GaP vapour grown epitaxial electroluminesc. diodes with green emission at room temp. 9-41224
 GaSb, tunnel, high reverse currents, theory 9-28541
 Gap photodiodes for optical modulation 9-39651
 p-Ge:As, I-V characts., influence of radial carrier currents 9-35444
 Ge photodetector for 1.54 μ, high speed 9-49159
 MgTe-CdTe visible light-emitting, new material 9-47418
 PbS, stimulated recombination radiation 9-33595
 Si:As, I-V characts., anomalous, with negative resistance region, 77° to 370°K 9-28534
 Si:Hg, I-V characts., 77 and 300°K 9-43084
 Si:Hg, I-V characts., 77 and 300°K 9-35445
 Si:Pt, with negative resistance characts. 9-47144
 Si, anode-cathode space plasma, light emission during second breakdown 9-39652
 n-Si, characts. rel. to trap filling mechanism 9-26577
 Si, compensated, negative resistance and reversible switching phenomenon 9-49122
 Si, p-n junction imaging, evaporation of AgCl film on C replica 9-32847
 Si, pressure eff. on parameters 9-24203
 Si, pulsed 10 MeV electron irradi., rapid annealing of damage from voltage meas. 9-35446
 Si, punch-through, transit-time effects 9-28537
 Si n⁺-p-n⁺ SCL, small-signal high-freq. impedance 9-33346
 Si punch-through epitaxial Schottky barrier diodes, avalanche breakdown voltages, computer calc. 9-26576
 n-Si with Au, Ni or Cr, Schottky barriers, forward I-V characts. 9-43082
 n-SiC:N, electroluminesc., props. and anomalous nature of B and Al diffusion during prpe. 9-37776
 SiC pulsed, radiation props. 9-38387
 ZnS Schottky barrier u.v. detectors 9-33347

junctions

- avalanche current elec. suppression 9-41220
 avalanche p-n, weak multiplication factors calc. 9-47136
 breakdown mechanism, Zener current meas. 9-28528
 capacitance, diffusion, calc. 9-26567
 capacitance var. determined by exciting radiation of energy less than forbidden band width 9-37552
 degenerate heterojunctions, band diagram analysis 9-33337
 delineation and dislocation revealing by HIO₄-HF-H₂O system 9-33339
 emitter-base, reverse bias stress rel. to transistor h_{FE} degradation 9-35452
 p-nGaAs, avalanche breakdown, temperature dependence 9-35439
 heterojunction characteristics, modulation by field-independent polarization discontinuity induced by physical effect 9-28527

Semiconducting devices continued
junctions continued

- heterojunction solar cells, max. energy conversion efficiencies calc. 9-29367
- heterojunctions, impurity equil. distrib. rel. to temp. effective mass, lattice consts. and binding energy diff. 9-24198
- heterojunctions, photovoltaic effects analysis 9-49168
- heterojunctions, transistor and laser actions possibility 9-35453
- i.r. transient radiation, use in device diagnostics 9-37554
- m.i.m., phonon emission and self-energy effects in tunnelling 9-43095
- organic p-n, diffusion doped 9-35436
- p⁺/n planar, breakdown voltage by SiO₂ diffusion masks 9-41223
- p-n, abrupt, at arbitrary injection levels, 1-dimens. transport eqns. soln. 9-33338
- p-n, avalanche, weak multiplication factors calc. 9-47136
- p-n, elec. breakdown mechanism, Zener current meas. 9-28528
- p-n, error function diffused, depletion layer calcs. 9-30937
- p-n, forward biased, oscillatory magneto-current 9-28526
- p-n, lasers, emission in near-infrared and visible portion, review 9-48036
- p-n, lateral retrograded, at surface of semicond. device, patent 9-49114
- p-n, oblate hemi-spheroidal, two-dimensional field theory 9-35437
- p-n, organic, diffusion doped 9-35436
- p-n, planar breakdown voltage, increase using punch-through controlled surface 9-28525
- p-n, planar breakdown voltage, increase using punch-through controlled surface 9-28525
- p-n, plasma oscillations, l.f. in elec. and mag. fields 9-44987
- p-n, space charge region boundary-conditions 9-26566
- p-n, space-charge-limited currents 9-44986
- p-n, transient characts. analysis 9-44988
- p-n step, avalanche breakdown rel. to structural irregularities 9-43078
- photo-e.m.f. due to ionization of impurity centres 9-37626
- photoconductivity, conf. 9-39702
- piezoelectric mechanical sensors 9-47191
- potential distribution approx. expressions 9-29162
- semiconductor metal, excess tunneling current due to electron-plasmon interac. calc. 9-37553
- thermal detector, spectral characts. improvement 9-43235
- thermographic mapping with liquid crystals, techniques 9-37555
- Al-I-Bi tunnel, pressure effects up to 30 kbar, 77°K 9-37556
- Al_{0.5}Ga_{0.5}As:Si electroluminesc. diodes, props. and efficiency 9-37775
- Cd_{0.5}Mg_{0.5}Te p-n, prep. and electroluminescent props. 9-26569
- CdS-Cu₂S heterojunctions in film photoelect. charact. 9-46845
- CdS-Cu₂S heterojunctions, photovoltaic effect study 9-24240
- CdS-CdTe film heterojunction photoelec. effects 9-30988
- p-n-CdSe heterojunctions as photoelements, prep. 9-35505
- CdTe, p-n, capacitance charact. 9-47137
- Cu₂S-CdS heterojunctions, heat-treated, photovoltaic effect mechanism 9-39650
- p-nGaAs, avalanche breakdown 9-47139
- p-GaAs:Fe, p-n junction construction for fast switching 9-35438
- GaAs:Ge, p-n structure, reverse-biased, light emission charact. 9-49332
- GaAs:Si epitaxial p-n, radiative recomb. mechanism 9-47138
- GaAs:Si epitaxial p-type films grown on n-GaAs substrate, photo-e.m.f. spectra at 300 and 77°K 9-37614
- GaAs:Si(Ge) p-n, elec. and optical characts. 9-26570
- GaAs-GaP heterojunctions, charact. 9-44989
- GaAs-Pb, Cu²⁺-z. doped at interface, zero bias anomalies 9-24197
- GaAs, isolation using proton bombardment 9-30938
- GaAs, laser, stripe geometry 9-25304
- GaAs_{0.5}Px heterojunction, misfit dislocations, form., propag., interaction and densities 9-47140
- GaAs abrupt asymmetrical junctions, radiative tunneling 9-43253
- GaAs p-n, electron emission into vacuum 9-28529
- GaP, p-n, reverse-biased, electro-optic and waveguide props. 9-24196
- GaSb-ZnTe heterojunction, fabrication and props. 9-49067
- Ge-Al_{0.5}In_{0.5}O₂ heterojunctions, switching effect 9-47141
- Ge-CdS single crystal film systems, switching effect 9-43079
- n-Ge-p-CdTe, elec. and photoelec. props. 9-37557
- n-Ge-p-GaAs heterojunctions, photoeffects under reverse bias 9-41222
- Ge-In_{0.5}O₂ heterojunctions, switching effect 9-47141
- pGe-nSi alloyed heterojunctions, current-voltage and current-temp. charact. 9-28530
- n-Ge-p-ZnTe, elec. and photoelec. props. 9-37557
- Ge, characteristics, influence of anisotropic deformation 9-35440
- Ge(Li), p-i-n detector reproducible method of chemically forming surface 9-46140
- p-Ge-n-Si epitaxial tunnel heterojunctions obtained by vacuum evaporation, I-V charact. 9-41221
- Nb-Ga-As, mech. contacted, supercond. tunnelling effects 9-33340
- Nb-Si, mech. contacted, supercond. tunnelling effects 9-33340
- Pb-Si, mech. contacted, supercond. tunnelling effects 9-33340
- Se, trigonal, double Schottky-barrier capacitance meas. 9-49130
- Si:Au p-n, breakdown voltage rel. to conditions of prep. by zone melting method 9-43080
- Si, Au-diffused planar p⁺/n junction, lifetime profile 9-37559
- Si, p-n, surface replication using interfacial amorphous films 9-32840
- Si, radiation-induced defect isochronal annealing temp. 9-24199
- Si degenerate p-n, numerical estimate of transport properties, use of Fermi-Dirac statistics 9-26568
- Si n⁺-p-n structures, localization of breakdown under emitter dip effect conditions 9-35441
- Si p-n, epitaxial growth for photoelec. converters 9-31904
- Si p-n, photoresponse edge, effect of elec. field in space charge layer 9-37558
- Si p-n, reverse I-V characts., instability under low-energy electron irradiation 9-28531
- Si p-n detector, prod. by Li ion implantation method 9-28532
- Si pn junction radiation detection, high temp. 9-25525
- n-Si with Au, Ni or Cr, Schottky barriers, forward I-V characts. 9-43082
- SiC, p-n junctions, luminescent brightness rel. to temp. 9-26785
- SiC diffusional p-n, temp. depend. of injection luminescence 9-45357
- SiC p-n, electroluminescence, tunnelling and avalanche processes 9-43081
- SiC p-n, epitaxial, avalanche breakdown 9-35442
- ZnTe, ion-implanted, type conversions and p-n junction formation 9-26571

transistors

- base-collector junction behaviour at high collector current densities 9-35455

Semiconducting devices continued
transistors continued

- bipolar, minority-carrier density rel. to injection level 9-49124
- bipolar, with lightly doped collectors, series resistance meas. techniques 9-37565
- bipolar and f.e.t., comparison of neutron radiation tolerance, comments 9-30948
- breakdown, second, meas. 9-33280
- capacitance, diffusion, calc. 9-26567
- cylindrical geometry, edge injection and pinch-in effect 9-26578
- diffused impurity in emitter and base regions, patent 9-41227
- double-diffused, low to high injections 9-28538
- double-diffused with Gaussian impurity distrib., intrinsic transport parameters 9-33350
- drift, with circular emitter, effect of base distrib. resistance on emitter current density 9-43091
- driftless, current amplification factor, depend. on surface recombination velocity 9-44992
- f.e.t., effect of carrier mobility on capacity 9-49123
- f.e.t. and bipolar, stress phenomena transducer applic. 9-49126
- field, BaTiO₃ deposit, small control coercive field strength, composition, patent 9-30950
- fluorescent-coated phototransistor dosimeter 9-36528
- h.f. power, with increased reverse breakdown voltage, patent 9-41226
- junction, effect of negative resistance 9-30949
- low current d.c. gain, effect of heat treatment with various ambient atmospheres and contamination 9-28539
- measurement of diffusion parameters 9-43088
- m.o.s., charge pumping phenomena, gate pulse induced, first-order theory 9-30955
- m.o.s., enhancement n-channel, with high electron mobility, prep. and stability 9-37563
- m.o.s., substrate doping effect on gain 9-28543
- m.o.s.f.e.t.'s, neutron radiation effects, theory and experiment 9-33360
- m.o.s.f.e.t.'s, surface degeneracy effects 9-43066
- m.o.s.f.e.t., electron mobility, cryst. orientation effect 9-33351
- m.o.s.f.e.t., generation-recombination noise, model and experimental verification 9-26579
- m.o.s.f.e.t., p-channel, crystallographic orientation effect on mobility, surface state density and noise 9-33361
- m.o.s.f.e.t. with n-type channel, h.f. excess noise and equivalent circuit representation 9-33349
- m.o.s.f.e.t. with n-type channel, h.f. excess noise and equivalent circuit representation 9-43092
- m.o.s.t., current noise spectrum, physical model 9-43090
- m.o.s.t., current noise spectrum, v.l.f. 9-43089
- planar h₀ degradation due to reverse bias emitter-base junction stress 9-35452
- shallow diffused, dislocations influence on props. 9-35451
- spreading resistance in multi-emitter struct. 9-37564
- switching, time lags, for different current densities and impurity distributions 9-47145
- in temperature regulating system for 4-300°K 9-27142
- CdSe-SiO₂ thin films, C-U characts. at semiconductor-insulator boundary 9-30951
- CdSe thin film 9-49125
- GaAs, field-effect transistor with Schottky-barrier gate, design and fabrication 9-24205
- Ge p-n-p, effect of quinone on surface props. 9-43093
- n-p-n-Si:B,P, h.f. operation, dopant diffusion anomalies 9-39653
- Si-SiO₂ m.o.s.f.e.t., electron mobility, cryst. orientation effect 9-33351
- Si, field-effect transistor with Schottky-barrier gate, design and fabrication 9-24205
- Si n-p-n structures, diffusion pipes, location at structural defects 9-30603

tunnel and interface devices

- diode, Esaki tunnelling probability 9-33348
- diode, switching-time calc., transient analysis 9-35450
- diodes, advanced laboratory tunnelling experiment 9-28535
- diodes, thin film, negative resistance 9-47142
- electronic switching eff., tunnelling barrier decrease, polyconductivity existence 9-30933
- equivalent circuit with a negative diffusion capacitance, derivation from continuity equation 9-24204
- Esaki tunnelling probability of diode 9-33348
- group IV-VI cpds. in m.l.s. structures, tunnelling characts. 9-39655
- heterocontact, semicond-dielectric, with potential trap for electrons in contact layer 9-26580
- junctions, metal-semicond., zero bias anomalies 9-35456
- lamellar structures, superconductivity 9-37458
- metal-GaAs contacts, variation of contact resistance with impurity conc. and implications 9-30953
- metal-semiconductor barriers, thermionic-field resistance maxima 9-33353
- metal-semiconductor contact, perturbation, C-V charact. and equiv. cct 9-47146
- metal-semiconductor interface, interpretation of elec. props. meas. 9-43094
- metal-semiconductor sandwich, magneto-plasma wave propagation 9-30952
- metal-SiO₂-metal, current mechanism 9-28549
- m.g.o.s. structures, polarization process of thin phosphosilicate glass films 9-33363
- MoO₃, memory element, charge storage model, variable threshold 9-24206
- m.i.m. junctions phonon emission and self-energy effects in tunnelling 9-43095
- m.i.m. struct., carrier transport 9-41228
- m.i.m. structure, injected electron currents through insulator 9-35457
- m.i.m. structures, electroluminescent phenom. 9-47411
- m.i.m. tunnel junctions, effect of deep traps on barrier heights 9-44994
- m.i.s., heavy inversion region, capacitance 9-28542
- m.i.s. capacitors, non-equil. C-V and I-V charact. 9-44996
- m.i.s. struct., n-type, v.l.f. response of inversion layer 9-47147
- m.i.s. structure surface state meas. device 9-43096
- m.i.s. system (m=Al, Ag), I-V characts. 9-44997
- m.i.s. systems, transient photocurrents and internal photoemission 9-39656
- m.o.s., flame spectrophotometric analysis of Na content in processing materials 9-31223

Semiconducting devices continued**tunnel and interface devices continued**

- m.o.s. capacitors, low current d.c. gain, effect of heat treatment with various ambient atmospheres and contamination 9-28539
- m.o.s. charge pumping phenomenon with applied gate pulses, first-order theory 9-30955
- m.o.s. struct., electron irradi., continuous polarizing voltage effect on props. 9-47149
- m.o.s. struct., surface states densities evaluation 9-49131
- m.o.s. structure, inversion layer carrier mobility 9-37567
- m.o.s. structure Ge with pyrolytic SiO₂ films, charge motion 9-28544
- M.O.S. system, use in expansion of temp. range of Cu₂O electroluminesc. 9-37778
- m.o.s.f.e.t. generation-recombination noise, model and experimental verification 9-26579
- m.o.s.f.e.t. with n-type channel, h.f. excess noise and equivalent circuit representation 9-33349
- m.o.s.f.e.t. with n-type channel, h.f. excess noise and equivalent circuit representation 9-43092
- m.o.s.t., current noise spectrum, physical model 9-43090
- m.o.s.t., current noise spectrum, v.l.f. 9-43089
- m.o.s.t., strain effects 9-26581
- multilayered struct., pot. distrib. applic. to spreading resistance correction factors 9-47148
- noise meas. to verify tunnelling 9-33356
- photoconductivity, conf. 9-39702
- tunnel diode, effect on capacitive loading 9-37562
- Ag-PrO₂-M structure, electron emission 9-45029
- Al-Al₂O₃ triodes, hot-electron transport 9-49128
- Al-Al₂O₃-Bi_{1-x}Sb_x film, oscillatory effects on electron tunnelling 9-39657
- Al-Al₂O₃-ZnTe, I-V characs. of tunnelling junction 9-33357
- Al-GaSe-Au struct., carrier transport 9-41228
- Al-I-Bi junctions, pressure effects up to 30 kbar, 77°K 9-37556
- Al-I-M films, (M=Ni, Pd, NiPd alloys, Fe, Gd) electron tunnelling, rel. to spin wave excitation 9-44995
- Al-PrO₂-M structure, electron emission 9-45029
- Al-Si₃N₄-Si structure, prep. and elec. props. 9-43097
- Al₂O₃-Si, m.o.s., d.c. reactive sputtered, interface characs. 9-49132
- Al-Al₂O₃-Au(Ag) structure, I-V characs. 9-30954
- Al-Al₂O₃-Al thin films, noise meas. to verify tunnelling 9-33356
- Au-MoO₃-Au, m.i.m. structure, capacitance depend. on geometry, a.c. meas. 9-37566
- Au-PrO₂-M structure, electron emission 9-45029
- GaAs-Cs-Sb, heterojunction, mechanism of photoemission 9-49175
- GaAs-poly-N-vinyl carbazole-Au systems transient photocurrents and internal photoemission 9-39656
- GaAs, tunnel diodes, high reverse currents, theory 9-28541
- GaAs die in case with Au bonded connector, patent 9-43086
- GaAsP diodes, yellow emission 9-41225
- GaSb, tunnel diodes, high reverse currents, theory 9-28541
- Ge-Al alloy dot on n-type Ge, h.f., low resistance, capacitance, prod., patent 9-39046
- Ge die in case with Au bonded connector, patent 9-43086
- p-Ge-n-Si epitaxial heterojunctions obtained by vacuum evaporation, I-V charact. 9-41221
- InSb m.o.s., surface charge wave propag. in mag. field 9-47150
- InSb m.o.s. devices, photoresponse props. 9-39658
- p-InSb m.o.s. struct., conductivity in n-type surface inversion layer, low temp. 9-44963
- NbO films, m.o.s. behaviour from evaluation of dielectric props. 9-30958
- Se, trigonal, double Schottky-barrier capacitance meas. 9-49130
- Si/SiO₂/Si₃N₄ double-layer films, Na diffusion and distrib. 9-26305
- Si/SiO₂/Si₃N₄ double-layer films, Na diffusion and distrib. 9-26305
- Si-Si₃N₄ films, trapping levels obs. 9-33359
- Si-SiO₂, e.p.r. rel. to heat treatment in H₂ or He, and to p-Si oxidation method 9-49357
- Si-SiO₂ interface, surface recombination velocity, surface potential effects 9-33355
- with Si₃N₄ single-layer film, Na diffusion and distrib. 9-26305
- with Si₃N₄ single-layer films, Na diffusion and distrib. 9-26305
- Si epitaxial MOS structure, relax. effects 9-35458
- n-Si surface barrier detector mag. fields up to 60 kOe, 4.2°K 9-41229
- SiO₂-Si m.o.s. struct., diffused Zn effects on C-V characs. 9-33362
- SiO₂, doping with P for m.o.s. device stabilization 9-37568
- SiO₂, thermally grown, in m.i.m. structure, Fowler-Nordheim tunneling 9-43098
- SiO₂ thermal growth, use of Si₃N₄ as alkali barrier liner 9-33358
- Sn-PrO₂-M structure, electron emission 9-45029
- Zr-ZrO₂-metal structure, I-V charact. 9-30954

Semiconducting materials

see also *Magnetoelectric effects; Photoconductivity; Photovoltaic effects; Semimetals*

- Al₂BY cpds., optical effective mass of free carriers 9-47117
- A^{IV}B^{IV}C^{III} chain compounds, energy spectrum and edge absorption spectra, peculiarities 9-37715
- acoustic wave interac., nonlinear theory 9-37351
- acoustoelectric domains propag. in piezoelec. III-V semicond., evolution 9-37349
- acoustoelectric static domain in piezo-semicond. 9-37350
- admixtures with stoichiometric vacancies 9-47095
- Ag₂Te, solid and liq., transport props. 9-37519
- amorphous alloys, band model 9-33316
- amorphous popular review 9-44948
- anthracene, current carriers mobilities, temp. depend. 9-33312
- anthracene, direct electron-hole recomb. 9-44971
- anthracene, electrolum. diode characs. 9-49336
- anthracene, low-temp. hole injection and hole trap distrib. 9-44970
- anthracene, tight binding calc. of current carrier mobilities 9-33313
- antiferromagnetic, current carrier mobility, spin-electron interac. effect 9-37516
- antiferromagnetic electron-magnon interac., conduction band shift 9-28504
- antiphase boundaries, geometry, props. and interactions with grain boundaries and dislocations 9-40937
- band structure determination using photoemission studies 9-37397
- binary, atomic displacement threshold energy of electron, calc. and expt. 9-35297
- binary compound, diffusion data, review 9-26298

Semiconducting materials continued

- carrier emission rates and cross-sections impurity photocurrent and photo-capacitive methods 9-39636
- carrier lifetime and mobility meas. by microwave techniques 9-33292
- carriers mixed scatt. on acoustic lattice vibrs. and ionized impurities, parameters determ. 9-37509
- chalcogenide amorphous films, conduction and elec. switching 9-28491
- chalcogenide glass base, thin film diodes, dynamic V-I characs. 9-24201
- chalcogenide glasses, bulk and thin film switching and memory effects 9-49062
- chalcogenide thin films, amorphous, negative capacitance 9-33283
- charge distrib. within surface space-charge region 9-43068
- p-chloranil, electron injection into single cryst. by aqueous electrolyte contact 9-41203
- with conductance bipolar mechanism, negative differential resistance obs. 9-37517
- conduction electrons interac. with phonons, effective mass of carriers 9-26473
- conductivity, phonon drag, effect contrib. 9-33288
- diamond, oscillatory photoconductivity, role of phonons 9-41258
- dopant conc. and conductivity relation, meas. technique 9-37532
- doping, ion bombardment by exploding wire technique 9-28509
- dye-photosemiconds., org., flash investigation 9-24182
- effective mass determ. from i.r. plasma refl., carriers degeneration depend. 9-44972
- electroabsorption coeff., excitonic effects 9-43051
- electroabsorption coeffs., excitonic effects 9-43052
- electroluminescence, polarization, of pure cryst. with narrow forbidden band 9-47412
- electron irradiation and subsequent photocond. studies, low-temp. set up 9-31724
- electron-hole interac., screened 9-26541
- excitons, diamag. detect of states 9-30823
- extrinsic, mag. freeze-out of electrons 9-43060
- extrinsic magneto-optical effects theory 9-43061
- ferromagnetic, current carrier mobility, spin-electron interac. effect 9-37516
- ferromagnetic, electron-magnon interac., conduction band shift 9-28504
- ferromagnetic, spin-plasma surface wave interaction 9-33323
- field emission depend. on space-charge-limited currents 9-33416
- film, thin, dimensionless n-type negative resistance 9-35393
- films, thermogalvanomagnetic effect, influence of inelastic carrier scattering 9-35494
- films, thin, non-homogeneity controlling 9-35389
- free carrier distrib. functions determ. by Raman scatt. 9-49071
- galvanomagnetic effects in strong elc. fields 9-47098
- glasses, props. rel. to use as switches 9-30934
- glasses, V₂O₅-P₂O₅, internal friction, elastic moduli and densities, elec. conductivity, 100° to 400°K 9-35155
- group II-IV-V₂ compounds, solution and vapour-growth 9-37063
- group II-VI compounds, band structure, pseudopotential calcs. 9-37398
- group II-VI compounds, band structure and optical spectra 9-37399
- group II-VI compounds, defect characterization rel. to elec. meas. 9-37156
- group II-VI compounds, donor-doped, incorporation mechanism 9-37531
- group II-VI compounds, electroluminescence 9-49331
- group II-VI compounds, exciton electroluminescence spectra 9-37707
- group II-VI compounds, growth, general aspects 9-36995
- group II-VI compounds, lattice vibrations, optical studies 9-46982
- group III-V, freqs. of localised modes due to substitutional impurities 9-35265
- group III-V, second-order optical susceptibilities 9-26684
- group III-V compounds, growth from metal solns., infl. of solvent and impurities on habit and morphology 9-36981
- group III-VI, layered, reflection spectra meas. rel. to interband transitions 9-28671
- group IV-VI cpds., tunneling characs. 9-39655
- group IV-VI cpds., electroluminescence 9-39809
- growth from melt, homogeneous impurity incorporation 9-30520
- growth from solution of homogeneous single crystals 9-37054
- Gunn oscillations, coherence 9-33291
- Hall effect meas. using an extension of Goldsmid's bridge 9-44979
- heat capacity, d.c. elc. pulse meas. technique 9-30779
- helicons, attenuation and polarization 9-39616
- hypersound absorpt. by carrier in materials with screened deform. and piezoelec. pots. 9-48952
- ice, dopant conc. and conductivity relation, meas. technique 9-37532
- II-VI cpds., cham. polishing 9-44977
- III-V, II-VI and IV-VI compounds, props. suitable for sensors 9-49066
- III-V, localised modes due to impurities 9-44810
- illuminated, occupation ratio of dislocation acceptor levels 9-26556
- impedance in presence of acoustic instability 9-43050
- impurities, deep, photoionization spectrum calc. 9-39634
- impurity atom distributions meas., differential capacitance technique 9-28508
- impurity centres, deep, theory and i.r. props. 9-39635
- impurity concentration deduction from Schottky-barrier (C,V) characs., possible errors 9-30918
- impurity diffusion via vacancy mechanism, theory 9-44975
- light absorption in strong mag. field 9-39828
- luminescence, intrinsic and shallow intrinsic, in wide band-gap semiconductors 9-49309
- magnetoresistance tensor components, Sondheimer oscillations, transverse elc. field effect 9-39617
- molecular cryst. thin layers with intermol. H-bonds, charge carrier generation mechanism 9-33366
- muonium mechanism of μ^+ depolarization 9-29996
- n-type, current-voltage charact. and elc. field distrib. 9-37514
- naphthalene, dark injection and radiative recomb. of electrons 9-41212
- negative resistance mechanism due to space charge injection 9-28493
- noise, 1/f, rel. to mobile charge carriers number 9-39614
- non-crystalline, conduction and switching 9-28485
- noncompensated quasimonopolar, carrier conc. distrib. on 'light-darkness' boundary 9-43056
- oligonitrilic donor-acceptor complexes, carrier conductivity, thermoelec. props. 9-33225
- optical absorption, saturated, through band filling 9-24167
- optical mixing by mobile carriers 9-44952
- organic, conduction mechanism in band and hopping models 9-28503

Semiconducting materials continued

- oxides, scanning electron microscope appls., review 9-32892
 p-type, field emission theory 9-31004
 perylene, injection of defect electrons in dark and under illumination 9-30995
 phonon drag effect, contrib. to elec. conductivity 9-33288
 photo-Hall e.m.f., polarity inversions 9-33290
 photo-ionization spectrum of deep impurities 9-39634
 photoconductivity, conf. 9-39702
 photoconductivity, two-photon, effect of induced light absorpt. by nonequil. holes 9-39708
 photomagnetic effect oscillations due to variation of mag. field, model 9-30998
 piezo-semiconductors, static domain 9-37350
 piezoelectric, acoustic, amplification under large signal conditions 9-33177
 piezoelectric, electromechanical transducers, modification of energy conversion process by effects due to carriers 9-34084
 piezoelectric, nonlinear limiting of acoustic wave amplification, use of perturbation theory 9-28422
 piezoelectric, root-locus analysis of electroacoustic amplifiers 9-28423
 piezoelectric III-V semicond., evolution of propag. acoustoelec. domains 9-37349
 plasma, electron-hole, instability of pinch effect 9-39575
 plasma, finite-amplitude helical mode 9-47102
 plasma, Raman scatt. by coupled plasmon-cyclotron-harmonic modes, nonlocal effects 9-33238
 plasmon-optical-phonon coupled system, sum rules 9-43048
 polar, direct-band, photon optical absorption in crossed electric and mag. fields 9-28484
 polishing, optimum abrasive sizes for minimizing polishing times 9-30883
 polymers, condensation type, electric transport props. 9-47097
 properties suitable for sensors 9-49066
 quantizing films with granulated metallic coating, supercond. 9-49038
 radiation damage, determ. by optical reflectivity technique 9-37503
 radiative recombination rate of donor-acceptor pairs 9-49306
 reflectance, light-modulated 9-37705
 requirements for p-ray detectors 9-25522
 resistivity, carrier lifetime, inhomogeneities, Hall effect meas. 9-33280
 review, crystals for research and technological applications 9-36971
 review or props. 9-41191
 rutile, Hall mobility temp. dependence, 300-1250°K 9-24181
 shock strained, acousto-electric effect, Boltzmann equation and wave-particle drag 9-37513
 smoke, resistivity 9-44951
 space charge, non-equil. surface effects for arbitrary ionization degree of impurities 9-33318
 space-charge wave instability, materials field-dependent diffusion coefficient and saturated drift velocity 9-43047
 spectra, universal relation between absorpt. and luminesc. at high pumping densities 9-47346
 Stokes scattering, phonon-cyclotron broadening in polar mats. 9-28701
 p-TiCN, anisotropy of electrical conductivity 9-30914
 tetracene, space-charge-limited currents, trapping levels and quasi-Fermi-level obs. 9-41204
 tetracene, thin film, temperature-independent conducting state 9-33284
 thermoelectric polycrystalline alloys, calc. of thermal, elec., conductivities and thermoelec. e.m.f. 9-37609
 thin films, vacuum-evaporated on flexible substrates, props. 9-35388
 three-dimensional systems of solns., phase-space analysis in subspaces 9-35392
 triphenylmethylarsonium 7-, 7-, 8-, 8- tetracyanoquinodimethane, elec. conductivity and thermoelec. power anisotropy 9-33314
 AgSb_{0.9}Fe_{0.1}Te₂, resistivity and Hall coeff. determ. 9-24171
 AgSbTe₂, Peltier coeff. at boundary between solid and liq. phases, determ. 9-45019
 Al_{1-x}Ga_xAs solid solns. with forbidden band width gradient, recomb. radiation 9-47389
 Al_{1-x}Ga_xP diodes prep. by liq. phase epitaxy, electroluminesc. obs. 9-47413
 Al_{1-x}Ga_xAs:Si electroluminesc. diodes, props. and efficiency 9-37775
 p-AlSb, acceptor photoexcitation spectra, uniaxial stress eff. on lines 9-39832
 AlSb, chemical and isoelectronization diffusion of Zn, Longini's interstitial/substitutional model 9-35125
 AlSb, diffusion in AlSb, chemical and isoelectronization, depend. 9-35124
 AlSb films, condensation 9-28487
 As₂S₃ conductivity, effect of Ag and Cu impurities 9-33295
 As₂SeTe₂ diode, switching, filamentary conduction 9-35449
 B, thermally stimulated current, trapping processes obs. 9-43062
 B carrier mobility, trapping levels and temp. depend. 9-28494
 Ba_{1-x}La_{2x/3}TiO₃ props. validity from Ba_{1-x}Ce_{2x/3}TiO₃ data 9-37506
 Ba_{1-x}Ce_{2x/3}TiO₃ props., validity for Ba_{1-x}La_{2x/3}TiO₃ 9-37506
 (Ba_{1-x}La_{2x/3})TiO₃ superconductivity, review of expt. data 9-41179
 n-BaB₆ single cryst., conduction-e.s.r. 9-37793
 BaTiO₃-SrTiO₃-BaSnO₃ system solid solns. 9-41192
 BaTiO₃, doped, origin of semicond. props. 9-39610
 Bi-Sb alloys, magnetoresistance anomalies in strong mag. fields, 4.2° to 10°K 9-30890
 Bi₂Se₃ films, properties 9-30889
 Bi₂Te₃, band structure, pseudopotential approach 9-44885
 Bi₂Te₃ films, properties 9-30889
 BiSeI, energy spectrum and edge absorption spectra, peculiarities 9-37715
 (Ca_{1-x}Sr_x)TiO₃ superconductivity, review of expt. data 9-41179
 n-CaB₆, polycryst., conduction-e.s.r. 9-37793
 Cd_{1-x}Mg_xTe p-n junctions, prep. and electroluminescent props. 9-26569
 n-Cd_{1-x}Mg_xTc(Al) mixed cryst., Hall coeff. and resistivity w.r.t. electron mobility, carrier conc. and donor ioniz. energy 9-43054
 Cd₃As₂-NiAs eutectic, Hall effect, conductivity and magnetoresistance meas. 9-41196
 Cd₃As₂, effective mass of electrons from thermoelectric power and Hall coeff. data 9-35313
 Cd₃P₂, field emission anomalous temp. depend. 9-43139
 n-Cd₃P₂ photoconductivity 9-39712
 n-Cd₃P₂, recomb. radiation, optically excited, and stimulated emission, obs. 9-49312
 Cd₃Hg_{1-x}Te alloys, electronic props. in vicinity of semimetal-semiconductor transition 9-49078
 Cd₃Hg_{1-x}Te, effective mass for composition range 0-30% 9-48995

Semiconducting materials continued

- Cd₃Hg_{1-x}Te, from melt, stoichiometry control rel. to props. 9-46756
 Cd₃Hg_{1-x}Te, Shubnikov-de Haas effect 9-47061
 Cd₃Zn_{1-x}S mixed cryst., phonon vibr. spectrum 9-42947
 n-CdCr₂S₄, ferromagnetic, magnetoresistance effect of exchange interaction 9-44956
 n-CdCr₂Se₄In, resistivity, normal Hall coeff. and Seebeck coeff. 9-45018
 Cd₃Y_{1-x}I_x, i.r. absorpt. and transport props. rel. to trapped electron theories 9-47354
 CdF₂Y₂, resistivity and Hall coeff. 9-49077
 CdF₂, effective mass and scatt. mech. 9-41205
 CdGeAs₂, amorphous thermal conductivity, phonons mean free path from Debye model 9-37367
 CdS:Pt, impurity photovoltaic effects, stimulation mechanism in i.r. spectral region 9-30997
 CdS:Se mixed alloy system, band structure, pseudopotential calc. 9-37404
 CdS-Cu₂S heterojunctions in film photocells, charact. 9-46845
 CdS, acoustic domains, Brillouin scatt. meas. 9-35397
 CdS, acoustic shear-waves generated by supersonic electrons, Brillouin scattering study 9-46996
 CdS, acoustoelec. domain form., Brillouin scatt. obs. 9-43055
 CdS, acoustoelectric domain formation at high elec. fields 9-46998
 CdS, after-sounding effect 9-37522
 CdS, band structure, pseudopotential calc. 9-37404
 CdS, behaviour of holes and electrons revealed by laser excitation 9-49157
 CdS, beta-excitation, charge pulses obs., carrier mobility and lifetimes, electron-hole prod. energy 9-33298
 CdS, carrier trapping effects resolving by use of supercond. cavities 9-41209
 CdS, conductivity and luminescence induced by intensive electron bombardment, 300°K 9-30903
 CdS, current oscil. stimulated by external u.s. signal 9-48965
 CdS, current saturation and oscillation, nonlinear theory 9-47105
 CdS, dark cond. rel. to S vapour press. during heat treatments 500 to 700°C 9-49076
 CdS, elec. and mag. field depend. 9-33297
 CdS, electron-phonon packets, observation by microwave transmission and Brillouin scattering meas. 9-47106
 CdS, electron bombardment, i.r. attenuation of induced photocond. current 9-47198
 CdS, emission spectrum, donor-acceptor pair lines obs. 9-49273
 CdS, exciton-phonon interaction 9-37709
 CdS, exciton line widths and phonon interaction 9-37766
 CdS, fast-neutron-irrad., elec. changes associated with radioactive decay 9-47104
 CdS, growth of single crystals, controlled composition, from vapour phase 9-37005
 CdS, hole-trap depletion layer form. 9-41210
 CdS, hole injection by electrolytic contact 9-24172
 CdS, intrinsic excitons, phonon-assisted emission 9-37765
 CdS, I⁻ point valence band, spin-orbit corrections 9-37403
 CdS, laser transitions 9-36312
 CdS, lattice scattering of electrons 9-47031
 CdS, light emissions from acoustoelec. domain 9-45344
 CdS, magnetomicrowave effects at 38 GHz, charge carrier density control by photogeneration 9-30922
 CdS, parametric amplification of acoustic shear waves 9-37343
 CdS, phonon. spectra of acoustic domains 9-37312
 CdS, photocond., conductivity variation of non-ohmic behaviours 9-43053
 CdS, photoconductivity of cryst. excited by ruby laser 9-47199
 CdS, photoluminesc. field quenching at elec. breakdown 9-35703
 CdS, photoluminescence, low-temperature 9-49314
 CdS, recombination and luminescence processes in single crystals 9-37759
 CdS, recombination kinetics at low temp. and high excitation intensities 9-49313
 CdS, recombination processes under high excitation 9-37758
 CdS, residual photoconductivity effect at room temp. 9-35504
 CdS, residual photoconductivity effect at room temp. 9-35504
 CdS, second current saturation of non-ohmic behaviour 9-47107
 n-CdS, second sound-acoustic electron-wave interaction, effect on distributed acoustic amplification 9-30775
 CdS, tapered smaples, acoustic domain studies 9-37521
 CdS, valence band structure calc. 9-48994
 CdS, vapour growth from controlled atmospheres of constituent elements 9-37006
 CdS_{1-x}Se_x, g-factor of conduction band electrons 9-47040
 CdS_{1-x}CdSe_x photocond. of cryst. excited by ruby laser 9-47199
 CdS_{1-x}Se_x refl. in fund absorpt. region, band struct. 9-47341
 CdS acoustoelectric phonon generation observed in X-ray diffraction microscopy 9-46997
 CdS detector for observing Mossbauer effect 9-26716
 CdS elec. current rel. to temp. 9-37520
 CdS films cond. rel. to intercryst. barriers, >500 V cm⁻¹ 9-26542
 CdS films on Ge plates, switching effect 9-43079
 CdS high-field domains, transition between stationary and moving 9-33324
 CdS laser, electron beam pumped, high power and efficiency 9-34177
 CdS layers, currents bounded by space charge 9-30906
 CdS photoconductive single cryst., electroacoustic props. correl. with resistivity inhomogeneities 9-35502
 CdS photoconductivity under i.r. irradiation 9-26600
 CdS piezoelectric crystal acoustic amplifier, temp. depend. of characts. 9-44815
 CdS piezoelectric crystal acoustic amplifier, temp. depend. of characts. 9-44815
 CdS rectification by high-resistance barrier layer in various gaseous media at -20-80°C 9-39640
 CdS resistivity inhomogeneities in single crystal 9-37507
 CdS single cryst., photo- and e-conductance comparison 9-37617
 CdS single cryst. alloyed with In and Ga impurities, luminesc. 9-37756
 CdS single crystal, space charge limited current, temp. depend. 9-44955
 CdS thin layers, current fluctuations due to elastic waves 9-35396
 CdS X-ray conductivity 9-24173
 CdSb:Ag, effective mass of free holes from reflectivity meas. 9-39618
 p-CdSb, Hall coeff. and specific resistance rel. to temp. in strong elec. field 9-24174

Semiconducting materials continued

- CdSb, Peltier coeff. at boundary between solid and liq. phases, determ. 9-45019
 CdSe-SiO₂ thin films, C-U characts. at semiconductor-insulator boundary 9-30951
 CdSe, acoustoelec. effects 9-47103
 CdSe, acoustoelectric current fluctuations, spectral power 9-33296
 CdSe, after-sounding effect 9-37522
 CdSe, band structure, pseudopotential calc. 9-37404
 CdSe, current saturation and oscillation, mechanism rel. to acoustoelec. eff. in piezoelec. mats. 9-26543
 CdSe, electron-bombarded and u.v. radiation illum., electron-hole pair form. energy 9-47133
 CdSe, high-temp. defect equilibria, investigation by self-diffusion and electrical transport props. meas. 9-37200
 CdSe, I-V characts. of photo-current caused by trapping of carriers 9-26602
 CdSe, Γ -point valence band, spin-orbit corrections 9-37403
 CdSe, piezoelec., attenuation of transverse u.s. waves, action of photons 9-28420
 CdSe, recombination and luminescence processes in single crystals 9-37759
 CdSe, valence band structure calc. 9-48994
 CdSe evaporated films, conductivity and Hall effect 9-33299
 CdSe film, change density reduction by surface alloying of In 9-33319
 CdSe films, interface-related conductivity and space charge region variation 9-30905
 CdSe films, props. of Au contacts 9-41211
 p-n-CdSe heterojunctions as photoelectrons, prep. 9-35505
 CdSe laser, electron beam pumped, high power and efficiency 9-34177
 CdSe Schottky barriers, barrier heights rel. to preparation 9-24194
 p-CdSiAs₃, conductivity, Hall effect mobility 9-44957
 n-CdTe:In (Al, Cd), heat treated, multiply charged acceptors, photo-Hall effect obs. 9-49075
 CdTe, band structure determination using photoemission studies 9-37397
 CdTe, defect centres, electronic props. 9-49158
 CdTe, Gunn effect 9-49090
 CdTe, photoluminescence, 20-80°K, fine structure of spectra 9-37760
 CdTe coaxial diode, construction and characts. 9-35443
 CdTe film, d.c. electromotive force caused by microwave field, investig. 9-30885
 CdTe film, elec. conductivity, investig. at microwave freq. 9-30904
 CdTe films, electroabsorption oscillations magnitude, elec. field strength depend. 9-49248
 CdTe films, stimulated recrystn., effect on conductivity 9-39163
 CdTe laser, excited by electron bombardment, characts. 9-34176
 CdTe p-n junctions, capacitance charact. 9-47137
 Ce hydride nonstoichiometric crystals, resistivities 9-44907
 CeS, influence of 10-45 MHz u.s. waves on conductivity 9-39619
 p-CoCr₂S₄, ferromagnetic, magnetoresistance effect of exchange interaction 9-44956
 p-CoO:Li, drift mobility w.r.t. temp. from conductivity and Seebeck coeff. meas. 9-37518
 CoO magnetic, band structure 9-47118
 CrO₂-Cr₂O₃ system, elec. conductivity of non-stoichiometric oxides, 100° to 450°C 9-28495
 CrSb₂, marcasite-type resistivity 9-35581
 Cte film heterojunction, photoelec effects 9-30988
 Cu₂O, elec. conductivity and thermoelec. power 9-28496
 Cu₂-CdS heterojunctions, heat-treated, photovoltaic effect mechanism 9-39650
 Cu₃PSe films, cond., thermo e.m.f. and optical props., obs. 9-35398
 Cu₃PSe₂ films, cond., thermo e.m.f. and optical props., obs. 9-35398
 Cu₃PSe₂ films, cond., thermo e.m.f. and optical props., obs. 9-35398
 β -Cu₂V₂O₇, evolution of props. w.r.t. increasing x 9-41197
 CuAlS₂(Se), energy gaps from optical transmission meas. and resistivity meas. 9-48797
 EuS, energy gap temp. depend., mag. sp. ht. and Curie const. calc. 9-37529
 EuS(Se), band structure from optical reflection and absorption data 9-28505
 p-FeCr₂S₄, ferromagnetic, magnetoresistance effect of exchange interaction 9-44956
 FeO₂ (45 mol.%) P₂O₅ glass, conduction mechanism from mechanical loss data 9-30640
 FeSi₂, i.r. reflectivity 9-33505
 n γ , α -Ga₂O₃, elec. cond., O adsorpt. dependence 9-49081
 Ga₂Te, thermal conductivity, solid and liquid, phonon and carrier mechanism, temp. depend. 9-33194
 Ga₂In_{1-x}Sb alloys, Gunn effect and conduction band struct. 9-41199
 GaAs-Cs-Sb, heterojunction, mechanism of photoemission 9-49175
 GaAs-GaP heterojunctions, charact. 9-44989
 GaAs_{1-x}, absorption spectra and Hall coeff., temp. depend. 9-33554
 GaAs_{1-x}P_x, vapour grown diodes, electroluminescent efficiency optimization 9-31153
 GaAs_{1-x}P_x, low-level interband optical absorpt. 9-47358
 GaAs diodes, ion-implanted, I-V characts., resistance and breakdown voltage 9-30944
 GaAs photoconductivity spectra of shallow donors i.r. obs. in mag. 9-41265
 GaAs platelet lasers, time behaviour of modes 9-36314
 n-GaAs single cryst., external photoemission, work function 9-41283
 GaAsP diodes, yellow emission 9-41225
 GaP:⁶³Zn(75Se), vapour-grown, substrate orientation effect on dopant incorporation 9-30920
 GaP:Bi, Zeeman splitting of recomb. radiation from excitons 9-45347
 GaP:S, electron-phonon interaction in extrinsic photoconductivity 9-41264
 GaP:Zn-O electroluminescent diodes, output charact. 9-41403
 GaP:Zn, resistivity and Hall coeff. variation with dopant conc. 9-44954
 GaP:Zn soln.-grown, O solubility 9-33321
 p-GaP:Zn(O), red emission, config. coordinates applic. 9-37761
 GaP:Zn(O), photoluminescence, Hall effect and conductivity 9-33604
 GaP-Cu diodes, induced photovoltaic effect, charge-carrier capture, effect on transition capacitance 9-35510
 GaP-GaAs system, suitability for room temp. gamma ray counters 9-26539
 GaP, band struct. and reflectivity 9-49268
 GaP, chemical and isoelectronic diffusion of Zn, Longini's interstitial/substitutional model 9-35125

Semiconducting materials continued

- GaP, donor and acceptor multipole fields and effects 9-43063
 n-GaP, electron mobility and impurity conc., crystals grown by cooling of Ga soln. 9-26544
 GaP, energy gap temp. dependence, 297-1273°K 9-43249
 GaP, indirect gap, resonant Raman scatt. 9-41395
 GaP, interimpurity recombinations involving isoelectronic trap Bi 9-39866
 GaP, localized vibrational modes of impurities, i.r. absorpt. obs. 9-35657
 GaP, p-n junction, reverse-biased, electro-optic and waveguide props. 9-24196
 GaP, pair spectra involving Si donors 9-45358
 GaP, photoluminescence, i.r. radiation effect 9-24472
 GaP, two-photon excitation, intensity behaviour of recomb. radiation of excitons 9-47393
 GaP, work function, giant temp. depend. 9-35514
 GaP diodes, green-light-emitting, grown by liq. phase epitaxy, spectral props. 9-49121
 GaP p-n diodes, electroluminescence 9-33610
 n-GaP Schottky barrier diodes, I-V characts., analysis 9-35434
 GaP Schottky barrier diodes, props at 25-500°C 9-33345
 n-GaP vapour grown epitaxial electroluminesc. diodes with green emission at room temp. 9-41224
 GaP(Sb), channeling charact. of protons and He ions 9-47012
 GaS, prep., purity and conductivity 9-39611
 GaS, reflection spectra meas. rel. to interband transitions 9-28671
 GaSb:Te, conduction band structure, Hall coeff. and resistivity temp. depend. 9-37530
 GaSb-InSb, e. scatt. mode 9-24085
 GaSb-ZnTe heterojunction, fabrication and props. 9-49067
 GaSb, band struct. calc. by empirical pseudopot. method, and optical props. 9-47119
 GaSb, cathodoluminescence, investig. by scanning electron microscope with modulated beam 9-24471
 GaSb, cathodoluminescence, investig. by scanning electron microscope with modulated beam 9-24471
 GaSb, covalent charge transfer 9-33302
 GaSb, e.s.catt. mode 9-24085
 GaSb, energy band structure, semi-empirical Kohn-Rostoker method 9-30923
 n-GaSb, magnetoresistance oscillations, energy gaps between valleys in conduction band 9-39620
 p-GaSb, photoemission caesiating and oxidation effects 9-43145
 GaSb, tunnel diodes, high reverse currents, theory 9-28541
 GaSe, energy structure, effect of Br impurity, absorpt. spectra 9-35412
 GaSe layer semiconductor, existence of two dimensional exciton observed 9-35319
 GaSe reflection spectra meas. rel. to interband transitions 9-28671
 Ge-Al₂O₃-In₂O₃ heterojunctions, switching effect 9-47141
 Ge-In₂O₃ heterojunctions, switching effect 9-47141
 Ge-Mg₂Sb₂, amorphous films, reordering diffusion process under annealing 9-34985
 Ge-Si-As-Te, glassy films, breakdown mechanism 9-33305
 Ge alloyed, strongly, donor complex forms, mechanisms 9-49096
 Ge films, heteroepitaxy on GaAs 9-36946
 Ge(Li) cylindrical detector efficiencies calc. 9-32257
 GeS, elec. card. activation energy in solid and liquid, 20-750°C 9-30909
 GeTe, carrier energy spectrum changes due to solid solns. form. 9-47113
 GeTe, k.p. band model 9-39628
 GeTe, relativistic band structure 9-39629
 GeTe, relativistic band struct. and electr. props. 9-43057
 GeTe, superconductivity, review of exp. data 9-41179
 HfC, conductivity, thermoelec. power, Hall coeff., rel. to C content 9-47114
 Hg_{1-x}Cd_xTe, helicons and nonreson. cyclotron absorpt. method of props. determ. 9-47101
 p-HgCr₂Se₄, ferromag., resistivity and mobility 9-44961
 HgS, synthetic single crystals, photoelectronic props. for band structure 9-28580
 HgSe, band structure and transport parameters 9-48997
 HgSe, electron and hole effective mass 9-24094
 HgSe, g-factor from de Haas-van Alphen effect 9-47062
 HgSe, homogeneity range and concentration-pressure isotherms 9-37508
 HgSe, ionized-impurity-limited mobility and band struct. 9-49092
 HgSe, powdered, propagation and dimensional resonances of helicon-like waves 9-30891
 HgSe, Shubnikov-de Haas effect, inversion asymmetry splittings 9-49013
 HgTe-ZnTe, conduction band struct. and electron scatt. mechanism rel. to semimetal-semicond. transition 9-35307
 HgTe, band structure, temp. dependence from pressure meas. 9-48998
 HgTe, band structure and transport parameters 9-48997
 HgTe, electron and hole effective mass 9-24094
 n-HgTe, galvanothermoelectric effects 9-35497
 HgTe, interband magneto-optical transitions, low temp. reflection and electrorefraction study 9-47344
 HgTe, magnetoresistance oscillations 9-49014
 HgTe, powdered, propagation and dimensional resonances of helicon-like waves 9-30891
 HgTe, resistivity rel. to crystn. temp. 9-44960
 HgTe, two helicon resonances obs. 9-43014
 HgTe, valence band, hole effective mass, rel. to temp. 9-30917
 HgTe epitaxial films, transport props. 9-28214
 In, Fermi electron surface, model calc. 9-43005
 InAs-ZnSe solid solns., conductivity, carrier mobility and conc. and thermo-e.m.f. 9-4962
 InAs, covalent charge transfer 9-33302
 n-InAs, meas. of elec. cond. thermoelec. power, magnetothermo-e.m.f. and Nerst-Ettingshausen coeff. 9-39622
 InAs, optical mixing of laser radiation, third-order 9-26688
 InAs, pot. barrier interaction of depletion regions 9-39720
 InAs, powdered, propagation and dimensional resonances of helicon-like waves 9-30891
 InAs, third harmonic generation, mobile carrier nonlinearity, interband proc. 9-26547
 InAs_{1-x}P_x epitaxial layers prep. by vapour-deposition, electron mobilities and n-, p-doping obs. 9-30910
 p-InP:Zn(Cd), Hall coefficient and elec. cond. meas. at 4-700°K 9-39623
 InP, current carrier lifetimes, 78°-300°K 9-37621
 n-InP, diffusion of Au 9-46853

Semiconducting materials continued

- p-InP, doped into n-type, Hall coeff., elec. conductivity and hole mobility, temp. depend 9-28500
 InP, optical freqs. and dielec. const. meas. 9-47314
 InP bulk ionized, recombination radiation rel. to elec. field 9-49315
 InSb-GaSb alloy, press-induced transform behaviour 9-37301
 InSb-InAs alloy, press-induced transform behaviour 9-37301
 InSb_{1-x}Bi_x alloys, optical absorpt. and gap obs. 9-43240
 InSb_{1-x}Bi_x solid solns., Hall effect, conductivity, band gap obs. 9-43058
 InSe, mobility of charge carriers from conductivity and Hall coeff. meas., temp. depend. 9-35404
 InSe, reflection spectra meas. rel. to interband transitions 9-28671
 InTe, layers, tetragonal phase, electronic and optical props 9-41200
 K_{0.16}MoO₄, resistivity anisotropy from X-ray diffr. and cryst. struct. obs. 9-37446
 KMnO₄, conductivity and thermo- e.m.f., temp. depend 9-33282
 n-KMnO₄, thermal decomposition in solid phase 9-37818
 p-n-LaCoO₃, conductivity temp. coeff., mobility activation energy, Seebeck coeff. w.r.t. resistivity 9-37527
 LaTe₂-LaSb, solid soln., Sb substitution effect on resistivity and thermoelec. power 9-39639
 MgSiP₂, growth and energy gap meas. 9-44974
 Mn Te magnon drag contrib. to transport props. 9-24332
 MnO, highly mobile electrons obs., high temp. 9-44965
 n-NbO₂, thermoelec. power and conductivity meas. 9-37448
 NiCrO₃, preparation, crystal, magnetic and electric properties 9-43160
 NiCrO₃, resistivity and activation energy meas. 9-43160
 NiO, elec. conductivity and Seebeck coeff., temp. and O partial press. depend. 9-44966
 NiO, highly mobile electrons obs., high temp. 9-44965
 NiO, magnetic, band structure 9-47118
 On- 9-43069
 Pb_{1-x}Sn_xSe diodes, mag. field depend. of i.r. laser emission 9-41922
 Pb_{1-x}Sn_xTe, band structure from Hall effect and Seebeck coeff. hole conc. dependences 9-39632
 Pb_{1-x}Sn_xTe, emission in mag. fields, band struct. obs. 9-41406
 PbRe, bandstructure, parameters from optical reflectivity, transmission and Faraday effect 9-39630
 PbS, band structure and scattering mechanism from transport props. meas. 9-39631
 PbS, conductivity and luminescence induced by intensive electron bombardment, 300°K 9-30903
 PbS, relativistic band structure 9-39629
 PbS, spin-flip Raman scattering by carriers 9-35674
 PbSe, band structure and scattering mechanism from transport props. meas. 9-39631
 p-PbSe, electrical props., depend. on carrier density and temp., indication of two valence bands 9-35409
 PbSe, relativistic band structure 9-39629
 PbSe, spin-flip Raman scattering by carriers 9-35674
 PbSe epitaxial films, field effect meas. at 30 Hz-70 kHz small and large signal meas. 9-41190
 PbSe epitaxial films, field effect meas. at 30 Hz-70 kHz small and large signal meas. 9-41190
 n-PbSe epitaxial films, layered distrib. of charge carriers from transverse magnetoresistance meas. 9-42996
 PbTe:In(La), Mossbauer effect of ¹²⁵Te, depend. of probability on degree of doping 9-39820
 p-PbTe-CdTe alloy, scattering of light-mass from magnetoresist. meas. 9-41206
 PbTe, band structure and scattering mechanism from transport props. meas. 9-39631
 p-PbTe, band structure from helicon-nuclear-spin interaction 9-39910
 PbTe, fund. energy gap, press. coeffs. 9-33317
 n-PbTe, magnetoplasma effects, local and non-local 9-47059
 PbTe, n- and p-types, prep. of low conc. high mobility mats. 9-39624
 p-PbTe, oscillatory magnetoresistance, effective mass of holes calc. 9-44967
 PbTe, relativistic band structure 9-39629
 PbTe, relativistic band struct. and electr. props. 9-43057
 PbTe, spin-flip Raman scattering by carriers 9-35674
 PbTe, valence band structure 9-39633
 PbTe epitaxial films, field effect meas. at 30 Hz-70kHz small and large signal meas. 9-41190
 PbTe polycryst. layers, surface props. 9-33325
 PbTe thick layers, transport props., heat treatment effects 9-39625
 Sb₂Se₃-Sb(Te) liquid alloy, thermal conductivity mechanisms 9-34900
 Sb₂Se₃, liquid, thermal conductivity mechanisms, electronic contribution 9-34900
 Sb₂Te₃ Peltier coeff. at boundary between solid and liq. phases, determ. 9-45019
 Se, rectifiers, critical breakdown voltage from I-V characts. under hydrostatic pressure 9-26564
 Se, trigonal, double Schottky-barrier capacitance meas. 9-49130
 Se rectifier, barrier capacity, interpretation of results 9-30936
 Se trigonal single cryst., Hall effect d.c. meas. 9-44968
 Si:Pt, elec. props. 9-49110
 Si-Al₂O₃, m.o.s., d.c. reactive sputtered, interface characts. 9-49132
 Si, eff. of Au doping on surface characts. 9-37535
 n-Si, electron mobility, field depend., 77K 9-35429
 Si alloyed, strongly, donor complexes form. mechanisms 9-49096
 Si-C:B, N, interimpurity recombination, obs., from photocond. decay and e.p.c. signals after illumination 9-28712
 n-SiC:N electroluminesc. diodes, props. and anomalous nature of B and Al diffusion during prep. 9-37776
 n-SiC, deep donor level obs. 9-49097
 SiC, diffusion data, review 9-26298
 p-SiC, radiative recombination at deep impurity states 9-28711
 SiC diffusional p-n junctions, temp. depend. of injection luminescence 9-45357
 SiC epitaxial p-n junctions, avalanche breakdown 9-35442
 SiC p-n junctions, tunnelling and avalanche processes at electroluminescence 9-43081
 SiN advantages and applications 9-35435
 SiP₂, orthorhombic, single cryst. growth from soln., p-type semicond. obs. 9-35022
 SmB₆ and transition metal oxides, semicond.-metal transitions, model 9-33279
 SmB₆ and transition metal oxides, semicond.-metal transitions, model 9-33279

Semiconducting materials continued

- α-Sn, covalent bond in rel. to neutral pseudo atom concept 9-28507
 SnO₂, electrical properties, stoichiometric relationship 9-35329
 SnO₂ films, negative magnetoresistance 9-33311
 SnO₂ layers on glass, i.r. reflection depend. on surface resistivity 9-26729
 SnTe, fund. energy gap, press. coeffs. 9-33317
 SnTe, k.p. band model 9-39628
 SnTe, relativistic band structure 9-39629
 SnTe, relativistic band struct. and electr. props. 9-43057
 SnTe superconductivity, review of expt. data 9-41179
 n-SrB₆ polycryst., conduction-e.s.r. 9-37793
 SrTiO_{3-x}, degenerate, soft-mode supercond. obs. 9-33275
 SrTiO₃ superconductivity, review of expt. data 9-41179
 Ta₂O₅ films, negative photocond. 9-24235
 Te, Fermi surface of holes, shape, Shubnikov-de Haas eff. meas. 9-26552
 Te, p-type, cyclotron resonance, quantum effects 9-44896
 Te, piezoelec. const., strain-induced electronic displacement rel. to cores obs. 9-35493
 p-Te, warm hole energy relax. time 9-49087
 Te film, elec. resistance, effect of ferroelec. substrate on temp. depend 9-28502
 TiC, conductivity, thermoelec. power, Hall coeff., rel. to C content 9-47114
 TiO₂-VO₂ sintered pseudobinary system, semiconductor-to-semiconductor transition from elec. conductivity and thermoelectric power meas. 9-49088
 TiO₂-VO₂ sintered pseudobinary system, semiconductor-to-semiconductor transition from conductivity and thermoelec. power meas. 9-49088
 TiInS₂(Se₂Te₂), struct., elec. conductivity, Hall effect, photocond. and optical props. 9-44969
 p-TiSe:Pb, conductivity and thermoelec. power, rel. to valence-band structure 9-43059
 UO₂ nearly stoichiometric single cryst., thermoelec. power and elec. conductivity, activation energies obs., 170-1250°K 9-33403
 V₂O₃, positron lifetime spectra rel. to semiconductors to metal transition 9-47063
 V₂O₃ metal-semiconductor transitions on excitonic phase change, pressure depend. studies 9-30892
 VO₂, semiconducting-metallic transition 9-28230
 VO₂ elec. props. comp. dependence 9-28272
 WO₃ single crystal, conduction mode study 9-49089
 Zn, Hg_{1-x}Te solid solutions, elec. conductivity and Hall coeff., 77°-400°K, 250-10000 G 9-30913
 n-Zn_{0.5}Cd_{0.5}Sb effect of oxygen and conduction 9-49098
 ZnO, acoustic shear-waves generated by supersonic electrons, Brillouin scattering study 9-46996
 ZnO single crystals, high electric field effects 9-47116
 ZnP₂, I-V characts., 90° to 350°K 9-35609
 ZnS:Cu²⁺, valence band structure, correlation with absorption and excitation spectra 9-37732
 ZnS, afterglow due to tunneling 9-37763
 ZnS, band struct. and reflectivity 9-49268
 ZnS, electrical props. of single crystal grown from Ga and In melts 9-37095
 ZnS, Γ-point valence band, spin-orbit corrections 9-37403
 ZnS, photoconductivity of cryst. excited by ruby laser 9-47199
 ZnS single cryst., electro-absorpt. 9-39812
 ZnSb:Te, effect of doping on elec. props., and crystn. process 9-42757
 n-ZnSb, prep. and props. 9-39612
 p-ZnSe:Cu, photoelectric props. 9-49164
 ZnSe:V, incorporation mechanisms of donors 9-37531
 ZnSe, band struct. and reflectivity 9-49268
 ZnSe, Gunn effect 9-49090
 ZnSe, Γ-point valence band, spin-orbit corrections 9-37403
 ZnSiP₂, recombination radiation spectrum, forbidden, band location 9-26770
 p-ZnSnSb₂, electro-physical props. 9-35410
 ZnTe, ion-implanted, type conversions and p-n junction formation 9-26571
 ZnTe, Pockels' coeff., refr. index and absorpt. coeff., dispersion 9-39811
 ZrC, conductivity, thermoelec. power, Hall coeff., rel. to C content 9-47114

gallium arsenide

- acoustic wave generation, subharmonic 9-30908
 acousto-electric domains, Brillouin scatt. obs. 9-44958
 acoustoelec. domains, Brillouin scatt. studies 9-37352
 acoustoelectric domains, trap-controlled bunching of electrons 9-44976
 acoustoelectric interaction, piezoelec. and elastic anisotropy 9-41090
 avalanche diode, high power and efficiency 9-35447
 band struct. and reflectivity 9-49268
 bulk ionized, recombination radiation rel. to elec. field 9-49315
 cathodoluminescent studies of striations, dislocation-induced defects and doping behaviour 9-43267
 coated with CsO, photoemission, low work function, heat treated 9-35518
 conductivity and luminescence induced by intensive electron bombardment, 300°K 9-30903
 covalent charge transfer 9-33302
 current instability and threshold field under acoustic amplification 9-28499
 current oscillations connected with acoustoelectric domain motion 9-35399
 current saturation induced by sound amplification, nonlinear theory 9-47111
 deep level conc. from Hall eff. meas., n-type, 300-700°K 9-30916
 degenerate, carrier lifetime meas. 9-24175
 die in case with Au bonded connector, patent 9-43086
 diffusion of Cu in annealed cryst., effect of dislocations 9-44734
 diffusion of Zn, chemical and isoconcentration, Longini's interstitial/substitutional model 9-35125
 diode base for injection lasers, spectral characteristics rel. to impurity energy states near conduction band 9-34178
 diode laser in gas laser resonator, absorption by non equilibrium carriers 9-38383
 effective mass of carriers, determ. from temp. depend. of ultrasound vel. 9-46999
 electroabsorption spectra of n-type crystals at 300 and 77.3°K 9-39837
 electroabsorption spectra of plane-parallel, n-type crystals at low free-carrier density 9-37723

Semiconducting materials continued**gallium arsenide continued**

electroluminescence in single cry. by tunnel injection of minority carriers 9-24178
 electron capture cross section by Cu ion centres 9-49106
 electron distrib. func., Boltzmann eqn., Gunn eff. threshold field calc. 9-33304
 electron drift velocity for different temperatures, analytical approach 9-49079
 electron heating influence on instability of elec. current 9-47109
 electron population inversion induced by high elec. fields 9-26545
 electroreflectance interpretation of Λ_3 - Λ_1 transitions 9-31084
 electroreflectance interpretation of Λ_3 - Λ_1 transitions 9-31084
 electroreflectance of impurities, Mn, Si, Cd 9-28661
 energy gap temp. dependence, 300-973°K 9-43249
 energy minima near Brillouin zone boundary location method 9-48988
 epitaxial layers, chemically-deposited growth and perfection 9-36951
 epitaxial layers, extrinsic photoconductivity spectral meas. in mag. fields, donor obs. 9-39717
 epitaxial diodes for switching application 9-43085
 exciton reflectance and photorefectance 9-41377
 excitons, hyperbolic, stress-induced exchange splitting of optical structure 77°K 9-28453
 gamma detection props. 9-25523
 Gunn diode, small-signal cond. freq. independence, obs. 9-49129
 Gunn domains interaction with ^{74}Ga nuclei 9-35391
 Gunn oscillators with p-n junction contacts, forward and reverse characteristics 9-39649
 Gunn-eff. charact., ionized impurity scatt. effect 9-39637
 Gunn-effect optical modulator 9-33352
 Hall constant, conductivity and thermoelectric power, n-type 9-33301
 Hall effect in slightly doped n-type crystals, low temp. 9-33303
 high-ohmic, volt-ampere charact., electron heating effect 9-37523
 high-resistivity, with nonlinear I-V characts., impedance investig. 9-28498
 hot carrier cond. anisotropy and Gunn oscill. threshold obs. 9-47108
 hot electron diffusion rate, anisotropy 9-47112
 hot electron effects at microwave frequencies 9-24177
 implantation profiles of ^{85}Kr ions, rel. to energy, cryst. direction and dose 9-47120
 inhomogeneities of Ohmic resistivity rel. to acoustoelec. instabilities in n-type, from optical probing 9-49080
 ion implanted, properties 9-37524
 i.r. absorption spectra, after irradi., rel. to doping or struct. defects 9-37725
 i.r. emitter diodes 9-22423
 junction devices isolation using proton bombardment 9-30938
 junction laser, optimum stripe width for continuous operation 9-36313
 junction laser, Q-switched, pulse spiking 9-41919
 junction laser, resonant mode spectra at high injection level 9-48042
 laser, continuous wave, optical pulsations 9-48039
 laser, diffused junction, annealing effects, optimum temp. rel. to impurity conc. 9-45958
 laser, dislocation-free, electron-beam- pumped, nonuniform emission charact. 9-41920
 laser, under e. beam excitation 9-22421
 laser, features and operation, applic. in communication syst. 9-45962
 laser, injection, displacement of stimulated emission beam in mag. field 9-45961
 laser, injection, dynamics of emission in continuous and pulsed regions 9-48044
 laser, injection, end-surface mirror production 9-29432
 laser, injection, modulation at 1 GHz 9-38385
 laser, injection, noncatastrophic degradation of power output 9-31963
 laser, injection type, efficiency and characts. at 300°K 9-36310
 laser, injection-type, radiation power hysteresis 9-27337
 laser, optically coupled injection-type, quenching effect 9-38388
 laser, p-n junction diode, superradiance spectra and inhomogeneity distribution 9-36315
 laser, photon loss in active and passive regions 9-29433
 laser diode, damped relaxation oscillations, regular pulse train 9-31961
 laser diode emission, spatial coherence 9-43897
 laser diode spontaneous emission line breadth, doping depend. 9-27336
 laser diodes, dependence of differential external quantum efficiency and gain on reflectivity 9-45963
 laser parallellepiped, 5-cm., interference of 10.6 μ coherent radiation 9-43896
 layer formation, Cr diffusion through SiO_2 , patent 9-28219
 magnetoresistance, magnetophonon oscillations, 77 to 340°K 9-28497
 metal-GaAs contacts, variation of contact resistance with impurity conc. and implications 9-30953
 microwave permittivity, temperatures between 100°K and 600°K 9-24169
 modulation of CO_2 laser at 10.6 μ 9-37691
 n-type, acoustoelec. domains, Brillouin scatt. studies 9-37352
 n-type, annealing under excess As vapour 9-33281
 n-type, bulk element, current instabilities, dielectric surface loading effect 9-28540
 n-type, deep level conc. from Hall eff. meas., 300-700°K 9-30916
 n-type, degenerate, magnetoresistance giant peak 9-44959
 n-type, edge photoluminesc. band profiles 9-47394
 n-type, epitaxial layers prep., resistivity and Hall coeff. obs. 9-30907
 n-type, external photoemission in single cryst., work function 9-41283
 n-type, field-emitted electrons, energy distrib. band and surface obs. 9-35517
 n-type, generation and detection of 10^{12} Hz phonons 9-49083
 n-type, Hall const., conductivity and thermoelectric power 9-33301
 n-type, Hall effect in slightly doped cryst. at low temp. 9-33303
 n-type, h.f. phonon generation and detection 9-39520
 n-type, microwave emission study of acoustic freqs. in acoustoelec. domains 9-48966
 n-type, non-degenerate, epitaxial, negative longit. magnetoresist. and displacement of longit. magnetophonons 9-26546
 n-type, radiation, near i.r., modulation by acoustoelec. domains at room temp. 9-37724
 n-type, radiative lifetimes and time-resolved spectra 9-26538
 n-type, second sound-acoustic electron-wave interaction, effect on distributed acoustic amplification 9-30775
 n-type, spectral photosensitivity, high area in fundamental absorption region 9-30991

Semiconducting materials continued**gallium arsenide continued**

n-type, transport processes, displaced Maxwellian calcs. 9-24176
 n-type, with impurity band, space charge layer capacitance 9-35400
 n-type epitaxial, far-i.r. photocond. mag. field effects on hydrogenic donor states 9-45022
 optical mixing of laser radiation, third-order 9-26688
 p-n junction, electron emission into vacuum 9-28529
 p-n junction and Schottky barrier diodes, epitaxial growth of guard rings 9-30943
 p-n junctions, avalanche breakdown 9-47139
 p-n junctions, avalanche breakdown, temp. dependence 9-35439
 p-type, Cs coated, transport props. from photoemission meas. 9-49082
 p-type, luminesc. involving As vacancy-acceptor centers 9-45346
 p-type, temp. dependence of photocond. lifetime in single crystals 9-37618
 photoconductivity spectral meas. of epitaxial layers in mag. fields, donor obs. 9-39717
 photodiode, Schottky barrier avalanche 9-26575
 photoelectric receiving devices, construct., fabrication and props. 9-45021
 photoemission, external, in n-type single crystal, work function 9-41283
 photoexcited, current oscillations by two bulk negative existence effects 9-28489
 photorefectance and reflectance spectra, intense exciton struct. obs. 9-41377
 radiative efficiency and deep-level luminescence in n-type crystals grown by liquid-phase epitaxy, dopant conc. effects 9-47396
 radiative recombination from photoexcited hot carriers, effective temp. Maxwellian distrib. 9-41404
 Raman scattering of light by cyclotron waves in degenerate electron gas 9-33567
 semi-insulating, photoconductivity, mag. field effect 9-39715
 space charge, two- and three-dimens., growth from negative differential resistivity 9-47110
 spectral photosensitivity, high area in fundamental absorption region, n-type 9-30991
 surface inhomogeneities form contact potential meas. on etched faces 9-26554
 transport processes, displaced Maxwellian calc. for n-type material 9-24176
 tunnel diodes, high reverse currents, theory 9-28541
 vapour-grown, facet effect 9-30921
 Cd diffusion profiles as a function of temp. and As vapour pressure 9-46852
 Cu substitutional impurities, electroabsorption study 9-35413
 epitaxial diodes for switching application 9-43085
 (Ga, In) As alloys, electroreflectance of Λ_3 - Λ_1 transitions 9-31084
 (Ga, In) As alloys, electroreflectance of Λ_3 - Λ_1 transitions 9-31084
 GaAs: Cd, electron-irrad., intrinsic and annealed, luminesc. 9-49316
 p-GaAs: Cd, epitaxial, photoluminesc. w.r.t. conduction band-acceptor recombination theory 9-37783
 GaAs: Cd ion implanted layers, surface resistivity, annealing depend. 9-33320
 GaAs: Cr, epitaxial growth, electronic concs. and mobilities 9-48760
 p-GaAs: Fe, p-i-n struct. construction for fast switching 9-35438
 p-GaAs: Fe, radiative transitions between deep acceptors and valence band 9-47395
 GaAs: Ge, p-n junction, reverse-biased, light emission charact. 9-49332
 GaAs: Si, energy band tails and photoconductivity 9-39716
 n-GaAs: Si, epitaxial, photoluminesc. w.r.t. conduction band-acceptor recombination theory 9-37783
 GaAs: Si epitaxial p-n junctions, radiative recomb. mechanism 9-47138
 GaAs: Si p-n junctions, photo-e.m.f. spectra at 300 and 77°K 9-37614
 GaAs: Si(Ge) p-n junction, elec. and optical characts. 9-26570
 GaAs: Zn, noise spectra in thermal equil. and under optical excitation, electron fluctuations obs. 9-41198
 GaAs: Zn ion implanted layers, surface resistivity, annealing depend. 9-33320
 GaAs-AlAs diffused diodes, injection electroluminesc. 9-37780
 GaAs-Cs-O, photoemission, low work function, heterojunction model 9-35520
 GaAs-GaP heterojunctions, charact. 9-44989
 p-GaAs-n-Ge heterojunctions, photoeffects under reverse bias 9-41222
 GaAs-Pb junctions, Cu^{2+} -doped at interface, zero bias anomalies 9-24197
 GaAs-poly-N-vinyl carbazole-Au systems transient photocurrents and internal photoemission 9-39656
 n-GaAs, electron bombardment damage, thermally stimulated conductivity meas. 9-35079
 GaAs_{1-x}P_x, diffused diodes, electroluminescence 9-37779
 GaAs_{1-x}P_{1-x}, N isoelectronic trap, determination of localization energy of excitons 9-28488
 GaAs_{1-x}P_{1-x} hot carrier cond. anisotropy and Gunn oscill. threshold obs. 9-47108
 GaAs junction laser, dependence of total stimulated light power and gain factor on length 9-48041
 GaAs laser diodes, differential quantum efficiency and gain dependent on length 9-45964
 GaAs surface harmonic generation, meas. of Nd glass laser picosecond pulse width 9-34173
 GaP(Sb), channeling charact. of protons and He ions 9-47012
 Ge doped, laser transition to band edge or impurity states 9-25303
 p-type, Ge-doped, injection luminescence 9-49337

germanium
 breakdown, depend. on i.r. irradiation wavelength 9-30926
 carrier diffusion, enhanced, rel. to carrier density wave instability 9-26555
 carriers, hot, nonequil., exclusion 9-47125
 channeling charact. of protons and He ions 9-47012
 crystal copper-staining method, nonuniformities obs. 9-24186
 current oscillations, frequency and amplitude due to gradient instability 9-33328
 deformed, influence on anisotropy of thermoelectric power 9-35496
 die in case with Au bonded connectors, patent 9-43086
 diodes with semi-infinite base, magnetic field effect on I-V characts. and transient processes 9-43083
 dislocation acceptor level position, n-type 9-37540
 dislocations obs., carrier conc. decrease after deformation p-type 9-35424
 doped, i.r. emission from free carriers 9-47359

Semiconducting materials continued

germanium continued

- electro-reflectance spectra, low-temp., 0.7-2.6 eV fine struct. 9-35627
 energy bands, strain-split 9-24187
 exciton gas, condensation 9-47127
 excitonic condensation 9-41218
 excitons, diamag. detect of states 9-30823
 Fano factor determ. at 77°K in Ge(Li) detector 9-42145
 field effect mobility in n-type, frequency and temperature dependence 9-47126
 film, plasma anodized, voltage drop meas. model 9-26188
 films, Hall coeff. and conductivity, influence of surface states on temp. depend. 9-33326
 galvanomagnetic effects in strong elec. fields, theory 9-28486
 growth from metal solns., infl. of solvent and impurities on habit and morphology 9-36981
 Hall effect anisotropy of n-type in strong non-quantizing mag. fields 9-39643
 high-field conductivity in n-type at room temp., longit. anisotropy 9-24188
 hot carrier cond. anisotropy and Gunn oscill. threshold obs. 9-47108
 hot carriers, conductivity, review 9-33329
 hot current carrier surface recombination velocity and diffusion constant dependence on high elec. field 9-41213
 illuminated, occupation ratio of dislocation acceptor levels 9-26556
 implanted p-type dopants, influence of n-type dopants on lattice location 9-26558
 impurity and defect energies and conc. determ. by highly sensitive photo-sensitive technique 9-39644
 impurity centres, photo-Hall effect and generation-recombination noise 9-28513
 impurity-assisted intervalley electron scatt. under uniaxial compression 9-35421
 i.r. imaging sensor, monolithic using large scale integration 9-47833
 junctions, influence of anisotropic deformation on characteristics 9-35440
 magneto-electro-reflectance in crossed and parallel-field config. 9-39806
 magnetoconcentration effect due to carriers redistrib. at impurity centres, Hall const. temp. depend. obs. 9-39645
 magnetomicrowave effects at 38 GHz, charge carrier density control by photogeneration 9-30922
 magnetopiezotransmission obs. of effective masses 9-44982
 magnetoresistance, transverse, in n-type sample in strong elec. and mag. fields, 16.6°K 9-33327
 Magnetoresistance in intermediate mag. field region 9-24189
 melting curve to 65 kbar 9-39132
 n-type, 'fast' surface states temperature and frequency dependence 9-47126
 n-type, degenerate, density of states rel. to impurity conc. 9-41217
 n-type, dislocation high-density saturation effects 9-43072
 n-type, dislocation obs. and effects, acceptor level position 9-37540
 n-type, electrical conductivity relax. 9-30925
 n-type, electron emission due to high microwave field 9-39737
 n-type, electron irradiated, fast recovery 9-33331
 n-type, free electron density, mobility and Hall coeff., 4.2° to 7.9°K 9-28512
 n-type, Hall coeff. depend. on carrier conc., in low mag. fields 9-24180
 n-type, Hall effect anisotropy in strong non-quantizing mag. fields 9-39643
 n-type, high-field conductivity at room temp., longit. anisotropy 9-24188
 n-type, hot current carrier surface recombination velocity and diffusion constant dependence on high elec. field 9-41213
 n-type, magnetoresistance in intermediate mag. field region 9-24189
 n-type, microwave harmonic generation at low temp. 9-49236
 n-type, phonon scatt. by neutral donors 9-44983
 n-type, recombination radiation spectrum 9-35684
 n-type, recombination-generation equilibrium several states in hot electron system 9-35422
 n-type, surface props. after 50 keV ion irradi. 9-47124
 n-type, thermal pinch effect 9-43073
 n-type, thermoelectric power, influence of elastic deform. 9-37611
 n-type, transverse magnetoresistance, elec. field strength depend. 9-49103
 n-type, transverse magnetoresistance in strong elec. and mag. fields, 16.6°K 9-33327
 n-type exposed to H₂ in 10⁻¹⁰mm Hg vacuum, effect on elec. props. 9-39642
 non-ohmic conduction under strong mag. field 9-35420
 nonequilibrium carriers, condensed phase 9-47128
 ohmic point contacts, study of I-V relation 9-37539
 optical field eff. on surface, modulated absorption, spectra meas. 9-41215
 optical mixing of laser radiation, third-order 9-26688
 p-type, dislocations obs., carrier conc. decrease after deform. 9-35424
 p-type, heavily doped, forbidden band width from Hall effect meas. and resistivity, 600° to 800°K 9-28514
 p-type, high-field energy distrib. and heavy hole diffusion coeffs. 9-24179
 p-type, impurity centres, photo-Hall effect and generation-recombination noise 9-28513
 p-type, minority carrier mobility strain depend. 9-49105
 p-type, photocond. spectra in fields of 0.5-100 V/cm at temp. 8-15°K 9-37620
 p-type, photodiode effect, high temp. 9-47202
 p-type, plastically bent, photocond. obs., trapping effect due to dislocations 9-35507
 p-type, with deep impurities, recombination and scattering of carriers, effect of elec. field 9-28516
 particle detectors, ion-implanted, preparation and performance 9-42144
 phonon mean free path from transmitted phonon drag data 9-35423
 photoconductivity, extrinsic, from edge dislocations 9-45023
 photodetector for 1.54μ, high speed 9-49159
 plastically bent, steady state and transient photocond., trapping effect due to dislocations, p-type 9-35507
 plate substrate for CdS films, switching effect 9-43079
 polarization state of an electrode from electroreflectance meas., at semi-cond-electrolyte interface 9-49102
 properties suitable for sensors 9-49066
 quenched, thermal acceptors and associated vacancy behaviour 9-49107
 for radiation detectors, characterization 9-27592
 recombination and scattering of carriers, p-type material with deep impurities 9-28516
 recombination centres formation by ⁶⁰Co γ-radiation 9-30994

Semiconducting materials continued

germanium continued

- recombination radiation obs. of condensed phase of nonequil. carriers 9-47128
 recombination radiation spectrum, n-type 9-35684
 recombination-generation equilibrium, several states, n-type 9-35422
 recovery in electron irradiated n-type material 9-33331
 reflection spectra, u.v., effect of heavy doping, band struct. critical points obs. 9-35645
 relaxation of elec. cond., n-type 9-30925
 resistance changes in thin samples at high elec. fields, space-charge region surface conductivity effects 9-41214
 resonance absorpt. at 36 Ge/s, 100-1500 Oe, 2-50°K, in p-type 9-43071
 rod, potential instability of attached lateral probe 9-35433
 scattering mechanisms, hot-electron studies 9-37541
 Schottky diode contacts, metal-semicond., barrier energies 9-44991
 shallow impurity states under elec. breakdown, far i.r. absorpt. studies 9-28517
 single crystals, resistivity, photoconductive decay and λ_i drift props., heat treatments effects 9-37538
 specification of props. rel. to radiation detector performance, NBS report 9-33280
 spectrometers, Walford-Doust rapid calibration method, some corrections 9-22657
 splits, internal recontacted, elec. props., gas adsorption and X-ray studies 9-42846
 surface, atomically clean, model of spectrum of levels 9-47123
 surface, effect of atomic H on elec. props. 9-28515
 surface, slow potential change mechanical 9-30927
 surface conductivity, eff. of alcohol vapours 9-49101
 surface mobility and scattering of carriers 9-35419
 surface modified by alkylchlorosilane, adhesion and elec. charact. variation 9-48924
 surface props., effect of quinone 9-43093
 surface states, donor and acceptor character, effect of CO adsorption 9-43074
 surface states rel. to thermal desorption of water in ultra high vac. 9-35425
 surfaces, SiO₂-passivated, dominant surface electronic props. rel. to annealing treatment 9-49104
 three-valley model for electrons in conduction band to explain obs. bulk negative differential conductivity 9-30924
 triode, solid-state, construction and characts. 9-43087
 Cs-coated, electron emission due to high microwave field 9-39737
 electron capture cross section by Cu ion centres 9-49106
 Fe as recombination centre, study by transient p-n junction technique 9-33330
 films, surface centres, elec. instabilities and ionization 9-47122
 p-Ge: Au, diode, I-V characts., influence of radial carrier current 9-35444
 Ge: Au, hopping photoconductivity mechanism, depend. on temp. and Au conc. 9-35506
 Ge: Au, i.r. absorpt. rel. to hole transitions from impurity levels to valence band 9-44981
 n-Ge: Au, injecting contacts influence on impurity photocond. kinetics 9-47203
 Ge: Au(Au, Sb) single crystals, specific resistance, carrier conc. and Hall mobility, rel. to inclusions 9-42807
 Ge: B, i.r. absorpt. rel. to hole transitions from impurity levels to valence band 9-44981
 p-Ge: Be, impurity photoconductivity spectra 9-37619
 Ge: Ga, bipolar photoeffect due to anomalous Cu distrib. in and near diffused layer 9-45024
 p-Ge: GaAs, radiative recomb., influence of local pot. fluctuations, low-temp. 9-39867
 n-Ge: Mn, spontaneous current oscillations due to excitation of recomb. waves 9-41216
 Ge: Sb, far i.r. absorpt. spectra, excitation lines shift, conc. depend. 9-35659
 Ge: Sb, Hall coeff. obs. of semicond.-to-metal transition rel. to impurity conc. 9-49095
 n-Ge: Sb, injecting contacts influence on impurity photocond. kinetics 9-47203
 n-Ge: Sb, microwave Faraday rot. 9-41355
 n-Ge: Sb Hall effect distortion by Nernst-Ettingshausen and Righi-Leduc effects 9-37537
 Ge: Sn, radiative recomb. 9-37762
 Ge-Al alloy dot on n-type Ge, h.f. tunnel diode, low resistance, capacitance, prod., patent 9-30946
 n-Ge-p-CdTe heterojunctions, elec. and photoelec. props. 9-37557
 n-Ge-p-GaAs heterojunctions, photoeffects under reverse bias 9-41222
 p-Ge-n-Si alloyed heterojunctions, current-voltage and current-temp. characts. 9-28530
 n-Ge-p-ZnTe heterojunctions, elec. and photoelec. props. 9-37557
 p-Ge, forbidden band width from Hall effect meas. and resistivity, 600° to 800°K 9-28514
 p-Ge, high-field energy distrib. and heavy hole diffusion coeffs. 9-24179
 p-Ge, light holes effect on galvanomagnetic effects 9-44980
 n-Ge crystals, bombarded with thermal and fast neutrons, for γ-ray spectrometers 9-46131
 n-Ge scanning electron micrograph using beta conductive signal, elec. field distrib. 9-46773
 Ge(Li) 2 crystal Compton spectrometer, γ spectra meas. 9-27584
 Ge(Li) coaxial detector, undepleted region eff. on Doppler-broadened line shape 9-32260
 Ge(Li) detector, efficiency calibration, 8-98 keV, using X-ray machines 9-44086
 Ge(Li) detector, γ-ray response characts., 0.1 to 2 MeV. expt. determ. 9-42141
 Ge(Li) detector, resonance energy and yield meas. in ²⁷Al(p, γ)²⁸Si 9-32258
 Ge(Li) detector, semi-empirical efficiency curve for 50 to 1400 keV γ-rays 9-42140
 Ge(Li) detectors, line shape anal. of γ-ray spectra 9-22711
 Ge(Li) rectangular detector drifted from 5 sides, collimated γ beam, pulse shape characteristics 9-32261
 Ge(Li) detector, NaI(Tl) small split annulus anti-Compton spectrometer meas. 9-32247
 p-Ge-n-Si epitaxial tunnel heterojunctions obtained by vacuum evaporation, I-V charact. 9-41221

Semiconducting materials continued**germanium continued**

- Li-ion drift mobility, 23.8° and 61.2°C 9-35131
- Li migration and precipitation control for radiation detector production 9-26557
- P doped epitaxial film production by spark doping 9-39159
- resistivity calc. from reflection and transparency obs. 9-24190
- ZnSe epitaxial layer prep. process 9-34991
- ZnSe epitaxial layers, elec. and photoelec. props. 9-35417

indium antimonide

- absorpt. spectra between 50-1400 μ at 1.5°K 9-37727
- absorption spectrum and energy levels of impurity centres 9-35408
- acoustic nuclear mag. reson. of ^{115}In , $^{121,123}\text{Sb}$, exchange line broadening 9-45401
- acoustoelectric domain and microwave emission, decay 9-35402
- bulk quantum efficiency, rel. to doping conc. and temp. 9-35414
- conductivity effective mass of holes, p-type 9-35407
- deep level compensation, influence on electrical props. of p-type material 9-35406
- deformation potential constants, hole scattering mechanism 9-33307
- deformation potential shift consts. 9-43046
- donor action of β dislocations, p- to n-type conductivity change 9-33322
- donor-impurity excitation spectra in high mag. fields 9-45320
- energy levels and absorpt. spectrum of impurity centres 9-35408
- Faraday rotation at 23.4 GHz in n-type films at room temp. 9-49250
- field effect and surface photocond. obs. 9-43130
- films, energy scattering of conduction electrons, piezoelectric contribution 9-26549
- films, thin, transport props. 9-33309
- films on substrates, attenuation of elastic surface waves 9-47121
- in GaSb, e. scatt. mode 9-24085
- heat treated, Hall effect obs. of deep acceptor level 9-39638
- helicons and nonreson. cyclotron absorpt. techniques of props. determ. 9-47100
- hot carrier cond. anisotropy and Gunn oscill. threshold obs. 9-47108
- hot-electron relaxation times, n-type 9-30912
- impurities, deep-lying, props., NBS report 9-33280
- light scatt., inelastic, from Landau level electrons in mag. fields, CO₂ laser obs. at 10.6 μ obs. 9-28650
- magnetoacoustic absorpt., longitud., Landau levels effects 9-26420
- microwave conductivity in hot electron region in n-type, anisotropy 9-30911
- microwave emission, low-field, contacts effects 9-49068
- microwave emission in crossed mag. and low electric fields, nitrogen temp. 9-37536
- microwave third harmonic generation at low temp. 9-35403
- m.o.s. devices, photoresponse props. 9-39658
- n-type, acoustoelec. domain and microwave emission, decay 9-35402
- n-type, anisotropic microwave conductivity in hot-electron region 9-30911
- n-type, carrier recombination and trapping effects 9-35401
- n-type, combined reson. absorpt. line obs. 9-47115
- n-type, electron cyclotron resonance, quantum effects 9-26540
- n-type, electron-hole prod. Gunn effect, conduction band minima props. 9-41202
- n-type, hot electron temp. w.r.t. elec. field 9-33308
- n-type, hot-electron microwave incremental conductivity 9-49084
- n-type, hot-electron relaxation times 9-30912
- n-type, magnetoresistance and Hall effect anomalies rel. to absence of inversion centre 9-26550
- n-type, microwave emission enhanced by acoustic cyclotron resonance 9-48967
- n-type, microwave emission in crossed mag. and low electric fields, nitrogen temp. 9-37536
- n-type, microwave permittivity of atomic lattice at 77°K 9-37526
- n-type, minority carrier lifetime, temp. depend. 80°-210°K 9-39621
- n-type, photoconductivity, negative 9-47205
- n-type, photomagnetic effect oscillations due to variation of mag. field, model 9-30998
- n-type, sound amplification in transverse mag. field 9-24028
- n-type, thermoelectric power and conductivity, eff. of hydrostatic pressure up to 16 Katm. 9-28501
- n-type, X-ray irradiat., elec. and thermal conductivity changes, energy band bending 9-49086
- n-type waveguide, dimensional resonances of helicon waves 9-41201
- n-type Z-pinch time evolution determ. from conductivity meas. 9-44964
- noise emission, microwave 9-49085
- optical mixing, third order, mag. field dependence 9-26689
- oscillation, continuous coherent, freq. depend. on applied transverse mag. field 9-26548
- p-type, conductivity effective mass of holes 9-35407
- p-type, conductivity in n-type surface inversion layer, low temp. 9-44963
- p-type, high-resistivity, compensated, current instability obs. 9-37525
- p-type, influence of deep level compensation on electrical props. 9-35406
- p-type, nonlinear effects rel. to elec. field, for impurity concs. $< 10^{14} \text{ cm}^{-3}$ 9-28510
- p-type, X-ray irradiat., elec. and thermal conductivity changes, energy band bending 9-49086
- permittivity, microwave, of atomic lattice at 77°K 9-37526
- photoconductivity, impurity spectra, in n- and p-InSb 9-30992
- photoconductivity, two-photon, effect of induced light absorpt. by nonequil. holes 9-39708
- photoconductivity changes under X-irradiation, surface effs. 9-30993
- photomagnetic effect oscillations due to variation of mag. field, model for n-type 9-30998
- pinch effect in n-type 9-41147
- plasma, electron-hole, radial Hall voltage 9-37416
- powdered, propagation and dimensional resonances of helicon-like waves 9-30891
- Raman scattering of light by cyclotron waves in degenerate electron gas 9-33567
- scattering mechanism and effective mass of electrons 9-44973
- scattering of light due to free carriers 9-33306
- sound amplification in transverse mag. field, n-type sample 9-24028
- sound wave amplification, 0.5-2 GHz 9-39522
- surface photoconductivity and field effect obs. 9-43130
- surface props. of polycryst. layers 9-33325
- thermoelectric power and conductivity, eff. of hydrostatic pressure up to 16 Katm., n-type 9-28501

Semiconducting materials continued**indium antimonide continued**

- thin film Hall transducers, props. in strong mag. field at liq. He temps. 9-24195
 - Z-pinch time evolution determ. in n-type, from conductivity meas. 9-44964
 - n-InSb:Ge, amplitude-depend. u.s. attenuation at liq.-He temp. 9-44825
 - InSb, electron state theory of deep donor levels 9-26551
 - p-InSb cyclotron resonance at 137 Gc/s 9-37420
 - n-type, surface charge wave propag. in m.o.s. layer, in mag. field 9-47150
 - YFe Garnet hybrid structure, interaction between spin waves and electrons 9-24320
- silicon**
- 1/f noise without external voltage at illuminated single crystals 9-26559
 - absorption edge modification by radiation-induced defects 9-47132
 - anodically oxidised, aging effect on surface states 9-39641
 - band struct., empirical pseudopot. approach 9-49000
 - breakdown, three-point probe technique, theoretical model 9-30928
 - carriers, hot, nonequil., exclusion 9-47125
 - channeling charact. of protons and He ions 9-47012
 - conductivity anisotropy of polycryst. due to differing vapour deposition conditions 9-35428
 - conductivity charges rel. to thermal defect investig. 9-32944
 - contacts, metal-n-Si, minority carrier injection 9-26565
 - cooling of hot electrons in mag. field 9-49109
 - counter using preamplifier for detection of low energy nuclear radiation 9-29660
 - deposition of gaseous transport species of B 9-37534
 - detector, surface barrier, for charged particles at relativistic energies 9-42146
 - devices, eff. of dislocations on performance 9-37551
 - diffusion of As, isoconcentration studies 9-37208
 - diode, anode-cathode plasma radiation in second breakdown 9-39652
 - diode, compensated, negative resistance and reversible switching phenomenon 9-49122
 - diodes, I-V charact., anomalous, with negative resistance region 77° to 370°K 9-28534
 - diodes, n⁺-p-n⁺ SCL, small-signal high-freq. impedance 9-33346
 - diodes, pressure eff. on parameters 9-24203
 - dislocations, effect on carrier lifetime 9-30931
 - dislocations, effect on conductivity 9-30932
 - doped, float-zone, electrical conductivity before and after γ -irradiation 9-28520
 - doping, solid soln. prop. and behaviour 9-44984
 - effective mass equations, breakdown due to rapidly varying potentials 9-44878
 - electron capture coeffs. of group III acceptors 9-39647
 - electron mobility field depend. in n-type at 77K 9-35429
 - electroreflectance rel. to photoreflectance spectrum 9-43231
 - epitaxial layers, chemically-deposited growth and perfection 9-36951
 - epitaxial MOS structure, relax. effs. 9-35458
 - etched by H₂S gas, surface exam. 9-32837
 - Faraday rotation, microwave in doped single cry. 9-24367
 - field emission, nonlinear, depend. on temp. and light intensity, p-type 9-26608
 - film, epitaxial, on spinel substrate, Hall effect and resistivity meas. 9-36950
 - film, high voltage photovoltaic eff. 9-24241
 - film on sapphire, electrically and optically active defects 9-37545
 - growth from metal solns., infl. of solvent and impurities on habit and morphology 9-36981
 - hot carrier cond. anisotropy and Gunn oscill. threshold obs. 9-47108
 - hot carriers, conductivity, review 9-33329
 - implanted p-type dopants, influence of n-type dopants on lattice location 9-26558
 - impurities interact. with radiation defects in p-Si during high-temp. annealing 9-37547
 - impurity-assisted intervalley electron scatt. under uniaxial compression 9-35421
 - integrated circuit fabrication, X-ray detection of bulk and surface defects 9-30604
 - interface with SiO₂, charge density and electron donor sites 9-43099
 - p-inversion layer, magnetoelec. charact. 9-37542
 - ion implantation damage, observed by optical reflection spectroscopy 9-28518
 - ion implanted profile build-up, radiotracer studies 9-37533
 - l.f. noise in single crystal, opt. rad. influence 9-26561
 - localised radiation damage, observation 9-33332
 - magnetoresistance, 77°K 9-28522
 - minority carrier lifetime, effect of dislocations 9-24191
 - minority carrier lifetime rel. to dislocation density, n-type 9-35430
 - minority carrier lifetimes of γ irradiated, annealed, interactions of point defects with impurities 9-46807
 - n⁺-p-n structures, localization of breakdown under emitter diode effect conditions 9-35441
 - n-p-n structures, diffusion pipes, location at structural defects 9-30603
 - n-type, Al implanted, temperature dependence of R_{sh} 9-35426
 - n-type, coupled to piezoelec. plate, acoustic wave amplification 9-26419
 - n-type, degenerate, density of states rel. to impurity conc. 9-41217
 - n-type, dislocation density, eff. on minority carrier lifetime 9-35430
 - n-type, electron mobility, field depend., 77K 9-35429
 - n-type, epitaxial, resist. rel. to e. bombardment between 12-18 keV 9-37543
 - n-type, e.p.r. study of donor electron magnetic interaction, 4.2°K, 10 GHz 9-43285
 - n-type, heavily-doped, enhanced Au solubility effect 9-30929
 - n-type, magnetoresistance, 77°K 9-28522
 - n-type, photoengraving and effect of illumination 9-33334
 - n-type, room temp. magnetoresistance at high elec. field 9-41219
 - n-type epitaxial films on sapphire formed by vacuum evaporation, elec. props. 9-49111
 - n-type transverse magnetoresistance of hot carriers rel. to scattering, n-type 9-30930
 - neutron irradiation induced defect clusters and annealing, elec. meas. and effect on transport props. in p-type material 9-47129
 - neutron-irradiated, divacancy formation study photoconductivity study 9-49108
 - optical mixing of laser radiation, third-order 9-26688
 - p⁺-n-p⁺ structures, hole velocity determination from current-voltage characteristics 9-24192

Semiconducting materials continued

silicon continued

- p-n devices, current oscillations after irradiation with on-MeV electrons 9-24193
- p-n junction, photoresponse edge, effect of elec. field in space charge layer 9-37558
- p-n junction detector, prod. by Li ion implantation method 9-28532
- p-n junctions, degenerate, numerical estimate of transport properties, use of Fermi-Dirac statistics 9-26568
- p-n junctions, epitaxial growth for photoelec. converters 9-31904
- p-n junctions, reverse I-V characs., instability under low-energy electron irradiation 9-28531
- p-type, galvanomag. anisotropy and energy-depend. warping of valence bands 9-43075
- p-type, interaction between radiation defects and impurities during high-temp. annealing 9-37547
- p-type, neutron irradiation effects from Hall effect and carrier lifetimes 9-47130
- p-type, neutron-irrad., photoconductivity 9-41271
- phonon drag transmitted, in diffused N-P-N and P-N-P structures 9-37546
- photocell for thermophotoc. converter 9-39731
- photoconductivity, intrinsic oscillatory 9-39724
- photoconductivity, stationary surface, of p-Si, obs. and theory 9-45020
- photoelectric effect, high temp. 9-47202
- photorefectance spectrum and rel. to electroreflectance 9-43231
- properties suitable for sensors 9-49066
- punch-through diode, transit-time effects 9-28537
- radiation damage on low temp. irrad. of degenerate crystals 9-28277
- Radiation defects interact. with impurities in p-Si during high-temp. annealing 9-37547
- for radiation detectors, characterization 9-27592
- recombination centres formation by ^{60}Co β -radiation 9-30994
- reflection spectra, u.v., effect of heavy doping, band struct. critical points obs. 9-35645
- resistance changes in thin samples at high elec. fields, space-charge region surface conductivity effects 9-41214
- resonance absorpt. at 36 Gs, 100-1500 Oe, 2-50°K 9-43071
- Schottky barriers of Au, Ni or Cr on n-type, forward I-V characs. 9-43082
- Schottky diode contacts, metal-semicond., barrier energies 9-44991
- splits, internal recontacted, elec. props., gas adsorption and X-ray studies 9-42846
- surface, slow potential change mechanism 9-30927
- surface anomalous magnetoconductance 9-28523
- surface barrier detector, mag. field up to 60kOe, 4.2°K, n-Si 9-41229
- surface contamination by large angle ion scattering 9-33333
- surface resistivity of base region, method and suitable struct. 9-33336
- thermal conductivity anisotropy of polycryst. due to differing vapour deposition conditions 9-35428
- thin films, with diffusion mask of SiO_2 , X-ray topography of strains 9-26246
- thin slices, minority carrier lifetime meas., three methods, comparison 9-39646
- three-point probe heating effects 9-49112
- transverse magnetoresistance of hot carriers rel. to scattering, n-type 9-30930
- trap filling mechanism 9-26577
- Au-diffused planar p-n junction, lifetime profile 9-37559
- Au-doped, injection currents and negative resistance 9-28521
- Au doped, noise spectrum and spectra with voltage variable relaxation time 9-35427
- GaAs:Si epitaxial p-n junctions, radiative recomb. mechanism 9-47138
- p-Ge-n-Si alloyed heterojunctions, current-voltage and current-temp. charact. 9-28530
- p-Ge-n-Si epitaxial tunnel heterojunctions obtained by vacuum evaporation, I-V charact. 9-41221
- implanted layers, post-annealing conductance behaviour 9-28519
- resistivity calc. from reflection and transparency obs. 9-24190
- Si:Al, electron-irrad., defects effect on photoconductivity spectra 9-44985
- n-Si:As, electron-phonon interaction in extrinsic photoconductivity 9-41264
- n-Si:As, photomagnetoec. and photoconductive effects, low temp. 9-39723
- Si:Au, electron and hole emission rates at centres from photocurrent and photocapacitive meas. 9-39636
- Si:Au p-n junctions, breakdown voltage rel. to conditions of prep. by zone melting 9-43080
- Si:B, electron-irrad., defects effect on photoconductivity spectra 9-44985
- Si:B, i.r. absorpt. rel. to hole transitions from impurity levels to valence band 9-44981
- Si:B, impurity-assisted intervalley electron scatt. 9-43076
- n-p-n-Si:B,P h.f. transistors, dopant diffusion anomalies 9-39653
- Si:B(P), irrad. at 80°K, conductivity and Hall effect meas. rel. to carrier removal rates 9-44852
- Si:Bi, resonant phonon interactions effect on absorpt. line shapes 9-26741
- Si:Hg diodes, I-V characs., 77 and 300°K 9-35445
- Si:Hg diodes, I-V characs., 77 and 300°K 9-43084
- n-Si:Li, electron-irrad., defects obs. using Hall coeff. and resistivity meas. 9-49113
- Si:Li, pulled-crucible and float-zone samples, Hall effect meas., thermal ionization energies 9-47131
- Si:Na, ionization energy obs. from resistivity and Hall coeff. temp. depend. meas. 9-43077
- Si:P, ESR, absorpt. intensity 9-35717
- n-Si:P, electron-phonon interaction in extrinsic photoconductivity 9-41264
- Si:P, Hall coeff. obs. of semicond.-to-metal transition rel. to impurity conc. 9-49095
- Si:P dislocation-free single cryst., plastic deform. initial stage 9-30665
- Si:Pt diodes with negative resistance characs. 9-47144
- n-Si:Sb electron-phonon interaction in extrinsic photoconductivity 9-41264
- Si:Zn photoconductors, noise 9-41270
- Si-Ge layers, transient response for minority carrier lifetime 9-35431
- Si-SiO₂, interface, surface recombination velocity, surface potential effects 9-33355
- Si-SiO₂, structures, surface states density rel. to thermal oxidation conds. of Si 9-26560

Semiconducting materials continued

silicon continued

- Si-SiO₂-Al system, C-V hysteresis curve 9-35432
- p-Si-on-sapphire films, oxidation effect on elec. characs. 9-35405
- n-Si, high purity, recombination lifetimes, 4.2°K to room temp. 9-35508
- p-Si, minority carrier mobility meas., bulk and surface recombination, analytical treatment 9-37544
- n-Si, pulsed 10 MeV electron irrad., rapid annealing of damage 9-35446
- SiC diodes, current and electrolum. brightness rel. to reverse bias 9-37561
- Si(Li), electric field profile and electron drift velocity in $\langle 111 \rangle$ direction, room temp., 2-48 kV/cm 9-33335
- Si(Li), energy-locc and straggling by high energy electrons, π^+ , and protons 9-30810
- Si(Li) detectors, spherical segment shape, cosmic ray telescope appl. 9-22645
- SiO₂/Si m.o.s. struct., diffused Zn effects on C-V characs. 9-33362
- Semiconductor lasers** *see Lasers/semiconductor*
- Semiconductors**
- see also Crystal electron states; Magnetolectric effects; Photoconductivity; Photovoltaic effects*
- A^{III}B^V, impurity behaviour, thermodynamic predictions 9-49093
- acceptor impurities, deep levels in forbidden band, theoretical model 9-41207
- acoustic wave interac., nonlinear theory 9-37351
- acoustic waves, nonlinear interaction, theory 9-41088
- acoustoelectric domains propag. in piezoelec. III-V semicond., evolution 9-37349
- acoustoelectric static domain in piezo-semicond. 9-37350
- anisotropic, effect of impurities 9-26595
- antiferromagnetic, current carrier mobility, spin-electron interac. effect 9-37516
- antiferromagnetic, magnon drag contrib. to transport props. 9-24332
- antiferromagnetic, transform. into metal in strong mag. field 9-24168
- antiferromagnetic, transform. into metal in strong mag. field 9-37505
- band struct., rel. to optical and transport props. 9-49091
- band structure of compound semiconductors 9-37396
- bands of electronic surface states, calc. 9-30899
- binary compounds, p- and n-type, self-potentials rel. to deviation from stoichiometry 9-36974
- bounded, Lorentz-field amplification, computer solutions 9-37502
- bulk ionized, recombination radiation rel. to elec. field 9-49315
- carrier emission rates and cross-sections impurity photocurrent and photo-capacitive methods 9-39636
- carrier lifetime and mobility meas. by microwave techniques 9-33292
- carrier lifetime meas., bibliography 9-33293
- carrier lifetimes in the presence of trapping 9-47096
- carriers and excitons, fieldless heating 9-39615
- carriers mixed scatt. on acoustic lattice vibrs. and ionized impurities, parameters determ. 9-37509
- cathodoluminescence, monochromatic image obs. in scanning electron microscope, rel. to microanal. 9-43266
- chalcogenide amorphous films, conduction and elec. switching 9-28491
- charge distrib. within surface space-charge region 9-43068
- charging-discharging method, thermally stimulated, trapping levels calcs. 9-39613
- compensated, scattering of carriers by ionized impurities 9-39557
- complex band structure, free carriers, transport properties, study by magneto-plasma waves 9-28511
- with conductance bipolar mechanism, negative differential resistance obs. 9-37517
- conductivity, phonon drag, effect contrib. 9-33288
- contacts, a.c. test method for separating contact influence from bulk props. 9-44978
- continuity equation for probability that allowed state of energy is occupied by an electron 9-24204
- cooled, photodiode, eff. appl. to laser detector 9-34186
- crystal imperfections, theory expt., book 9-48792
- crystals with high permittivity, acoustoelec. waves interaction with carriers 9-28424
- current fluctuations in strong elec. fields 9-33286
- current oscillations in mag. field in case of inelastic scattering 9-33287
- current saturation due to electron-phonon interaction, theory 9-44953
- degenerate, electron-plasma interaction and tunneling meas. 9-41195
- degenerate, recombinations via defects, rate expressions 9-30888
- degenerate to arbitrary degree, u.s. amplification 9-35281
- diamond-type, band structure and covalency 9-30915
- diamond-type, effective carrier mass, contrib. of electron interaction with short-wavelength vibrations 9-44874
- dielectric dispersion, three-layer description 9-24209
- dielectric function, microscopic, model calc. 9-26582
- diffusion source using doped oxide 9-37195
- disordered, e transport and related optical phenomena 9-30902
- dispersion, variation in laser beam field 9-35390
- doped, semicond.-to-metal transition rel. to impurity conc. 9-49095
- doping by ion implantation 9-41208
- doping by ion implantation, review 9-35411
- effective mass determ. from i.r. plasma refl., carriers degeneration depend. 9-44972
- effective mass equations, breakdown due to rapidly varying potentials 9-44878
- elastic lattice wave interaction with electron fluxes 9-30774
- electric drift instability criterion 9-35322
- electroabsorption coeff., excitonic effects 9-43051
- electroabsorption coeffs., excitonic effects 9-43052
- electroluminescence, polarization, of pure cryst. with narrow forbidden band 9-47412
- electron elastic scattering, effect of e.m. field 9-30901
- electron heating and phonon bottleneck in crossed elec. and quantising mag. fields 9-33278
- electron scatt. by neutral acceptors 9-28490
- electron shielding in heavily-doped mats. 9-24183
- electron-hole interac., screened 9-26541
- electron-hole interaction, dielec. screening 9-49069
- electron-phonon interaction, expt. investigation, using acoustic propag. 9-33294
- electron-phonon interaction screening for case with complex band structure 9-37510
- electronic spectrum, effect of dislocations, quantum mechanical treatment 9-33315

Semiconductors continued

- electronic states of homogeneous and inhomogeneous mixed semiconductors 9-37528
 for electronics industry, fabrication techniques 9-37501
 electrons, hot, in crossed elec. and quantizing mag. fields 9-47029
 energy minima near Brillouin zone boundary location method 9-48988
 entropy of fusion, excess due to configuration of bonding electrons 9-28175
 e.p.r. investigation, techniques, book 9-38338
 excitation binding to ionized impurities 9-24184
 excitonic insulator transition temp., in terms of mathematical parameter 9-30884
 excitons and carriers, fieldless heating 9-39615
 extrinsic, mag. freeze-out of electrons 9-43060
 extrinsic magneto-optical effects theory 9-43061
 ferroelectric, instability phenomena, nonlinear eqn. for electric induction 9-41237
 ferromagnetic, current carrier mobility, spin-electron interac. effect 9-37516
 ferromagnetic, spin-plasma surface wave interaction 9-33323
 field emission depend. on space-charge-limited currents 9-33416
 film, current-carrying, interface with ferrite, amplification of magnetostatic surface waves 9-43816
 film, thin, dimensionless n-type negative resistance 9-35393
 films for electrochemical work, conference 9-33676
 fluctuations in strong elec. field and scatt. of light by hot electrons 9-49063
 free carrier sweep-out in space charge field after pulse injection 9-30896
 g-r noise relax. modes 9-39608
 galvanomagnetic effects in strong elec. fields 9-47098
 galvanomagnetic effects in strong elec. fields, theory 9-28486
 group III-V, second-order optical susceptibilities 9-26684
 group IV-VI cpds., band edge structure 9-39627
 group IV-VI cpds., cubic, dielec. props. 9-39666
 Gunn effect domains, microscope probing 9-24185
 Gunn-instability, two-valley model, soft plasma modes, critical fluctuations and optical props. 9-30895
 Hall coeff. meas. method, 80-375°K 9-24171
 Hall effect and elec. conductivity, four-probe meas. methods 9-44950
 Hall effect in impurity semiconductors 9-49072
 heavily doped, energy-scale of localized levels near surfaces 9-35416
 helicon propag. in slab-shaped samples, quantum oscillations, dispersion relations 9-43049
 helicons, attenuation and polarization 9-39616
 helicons interferometry and monreson. cyclotron absorpt. methods for props. determ. 9-47100
 hexagonal, elasto-optic and electro-optic props., effect of bandgap 9-35623
 hypersound absorpt. by carrier in materials with screened deform. and piezoelec. pots. 9-48952
 III-V and II-VI films, photoconduction mechanism 9-33404
 impedance in presence of acoustic instability 9-43050
 impure, optical absorption, internal electric field effects 9-24402
 impurities, deep, photoionization spectrum calc. 9-39634
 impurity absorpt. line shapes, effect of resonant phonon interactions 9-26741
 impurity bombardment produced ionization under arbitrary elec. fields 9-30900
 impurity centres, deep, theory and i.r. props. 9-39635
 impurity diffusion via vacancy mechanism, theory 9-44975
 indirect-gap, field-excited electroluminescence 9-30887
 inhomogeneous, generation of second harmonic and sum and difference freqs. in microwave range 9-35387
 inorganic binary, correlation between bond energies and forbidden bands 9-48780
 instabilities in semicond. with nonequilibrium carrier density 9-41194
 isotropic, electrical conductivity anisotropy in contact region 9-24170
 kinetic eqn. soln. for semiconductors with narrow conductivity band in strong elec. field 9-26537
 laser frequencies resonance mixing 9-41931
 light intensity, nonlinear absorpt. and restriction of laser radiation 9-26685
 light scattering by charged centres in crystals without inversion centre 9-28700
 light scattering by current carriers in sample without inversion centres 9-49292
 liquid, conduction, localized states in pseudogap and near extremities of conduction and valence bands 9-33243
 liquid, Hall coeff. and conductivity, temp. depend 9-40800
 localized levels near surfaces, energy scale rel. to heavy doping and bulk values 9-35416
 low-mobility, e transport and related optical phenomena 9-30902
 low-resistivity, trap determination technique 9-49094
 magnetic, and e.s.r. and exchange interac., book 9-47222
 magnetic, band structure 9-47118
 magnetic, elec., opt. and mag. props. 9-49064
 magnetic ordering, coupled spin-plasma waves interaction with charged particles 9-41297
 magneto-optical oscillations, interband splitting of absorption coeff. 9-33509
 magnetoactive, electrons, indirect exchange and localized magnons 9-28607
 magnetoresistance, contribution of screened ionized impurities 9-30919
 magnetoresistance tensor components, Sondheimer oscillations, transverse elec. field effect 9-39617
 many-valley, phonon-assisted cyclotron resonance 9-28492
 many-valley, with anisotropic scattering time, h.f. transport props. 9-47099
 manyvalley, photoconductivity 9-24226
 mixed binary dissociable conductors, thermodynamic diagram of electrochemical equilibrium 9-39609
 molecular cryst. thin layers with intermol. H-bonds, charge carrier generation mechanism 9-33366
 multivalley, transverse volume e.m.f. and stretching of diffusion lengths 9-49073
 n-type, current-voltage charact. and elec. field distrib. 9-37514
 n-type degenerate, plasma screening effect on surface charge electron energy spectrum 9-49099
 narrow gap, conference report 9-39626

Semiconductors continued

- noise and differential conductivity of hot electrons, Green's function approach 9-47028
 non-polar, electronic mobility at intermediate and high elec. fields 9-37515
 noncompensated quasimonopolar, carrier conc. distrib. on 'light-darkness' boundary 9-43056
 nonlinear galvanomagnetic phenomena in crossed elec. and mag. fields, transport eqn. 9-37511
 nonlinear optics, CO₂ laser obs. at 10.6 μ 9-28650
 nonpiezoelectric, with ambipolar conduction, sound amplification by elec. field 9-33175
 nonpolar, long-wavelength phonon scatt. of carriers 9-49070
 optical mixing by mobile carriers 9-44952
 organic, conductivity behaviour 9-41193
 organic, with narrow conductivity band, kinetic eqn. soln. 9-26537
 piezoelectric, acoustoelectric domain theory, linear regime 9-48962
 phonon drag effect, contrib. to elec. conductivity 9-33288
 photo-Hall e.m.f., polarity inversions 9-33290
 photo-ionization spectrum of deep impurities 9-39634
 photoconductivity, conf. 9-39702
 photoconductivity, multi-phonon, mechanisms 9-39706
 photoconductivity, photoreflectance and screened Coulomb interaction 9-39703
 photoconductivity, two-photon, effect of induced light absorpt. by nonequil. holes 9-39708
 photoconductivity, two-photon absorption process 9-28570
 photoconductivity at large light intensity 9-28574
 photoconductivity relaxation in semiconductors containing traps and recombination centres 9-28573
 photodeformation effect in crystals of cubic symmetry 9-44764
 photon absorpt. coeff. at low-temp., indirect two-photon transitions 9-37714
 piezo, acoustic wave amplification, inhomogeneities 9-48953
 piezo-semiconductors, static domain 9-37350
 piezoelectric, acoustic, amplification under large signal conditions 9-33177
 piezoelectric, acoustoelectric domain theory, domain soln. 9-48964
 piezoelectric, acoustoelectric domain theory, nonlinear interactions 9-48963
 piezoelectric, multiple wave interactions 9-49065
 piezoelectric, non-linear effects in u.s. amplification 9-46994
 piezoelectric III-V semicond., evolution of propag. acoustoelec. domains 9-37349
 piezjunction effects 9-47191
 piezosemiconductors, acoustic wave generation 9-28419
 plasma, electron-hole, instability of pinch effect 9-39575
 plasma, finite-amplitude helical mode 9-47102
 plasma oscillations in semicond. with non-standard dispersion law in presence of elec. and mag. fields 9-37504
 plasmon-optical-phonon coupled system, sum rules 9-43048
 polishing, optimum abrasive sizes for minimizing polishing times 9-30883
 population inversion between free carrier zone and local centre levels by field effect 9-35394
 prediction of properties from atomic disposition and interactions 9-30894
 properties suitable for sensors 9-49066
 recombination process, self-oscillation of carriers in a unipolar mat. 9-37512
 recombination radiation during pinch effect for strong degeneracy of electron gas 9-49307
 resistivity, carrier lifetime, inhomogeneities, Hall effect meas. 9-33280
 resistivity meas. method, 80-375°K 9-24171
 review of props. 9-41191
 screening, effect of carrier-wavelength 9-30886
 self-transparency effect, by ultra short pulse of coherent light 9-49252
 semiconductor-electrolyte interface, impedance meas. 9-43067
 space charge, non-equil. surface effects for arbitrary ionization degree of impurities 9-33318
 Stokes scattering, phonon-cyclotron broadening in polar mats. 9-28701
 strongly compensated, Hall coeff., anomalous temp. depend 9-33285
 superconducting, transition temp. shifts with elec. charging 9-37461
 superconducting energy-gap eqn., derivation by Green's function method 9-26521
 surface, electroreflectance meas. rel. to band structure 9-43215
 surface, internal reflection spectra 9-43229
 surface, non-equil. phenomena 9-43065
 surface, optical absorpt. due to bands in energy gap 9-39827
 surface channels, anisotropy of kinetic phenomena w.r.t. cryst. symmetry and thermodynamics 9-33289
 surface elastic wave instability, current carriers with low recombination rate 9-30897
 surface phenomena 9-43064
 surface properties, photoelec. emission determ. 9-43142
 surface sensitizing-dye mol. regeneration 9-26553
 surface states, quasi-continuous spectrum of levels in forbidden band 9-35415
 surface states, theory 9-49100
 surfaces, degeneracy effects 9-43066
 thermal conductivity, meas. techniques 9-30791
 three-dimensional systems of solns., phase-space analysis in subspaces 9-35392
 threshold current rel. to losses, model of interzonal transitions without selection rules 9-43070
 U.S. absorption, in uniform electric fields 9-41085
 u.s. amplification, nonlinear effects explained by an approx. model 9-37347
 u.s. amplification, rel. to arbitrary degree of degeneracy 9-35281
 u.s. propagation in h.f. electric field, re-derivation of dispersion relationship 9-41086
 zone refining techniques, review 9-23674
 V₂V₃, metal-semiconductor transition, critical pressure 9-44921

Semimetals

- conductivity, classical size effect theory in relax. time approx. 9-39579
 conference report 9-39626
 elastic lattice wave interaction with electron fluxes 9-30774
 e.m. properties near cyclotron resonance 9-37418
 entropy of fusion, excess due to configuration of bonding electrons 9-28175
 excitonic insulator transition temp., in terms of mathematical parameter 9-30884

Semimetals continued

- graphite, pyrolytic, negative magnetoresistance 9-41163
 helicons interferometry and moneson. cyclotron absorpt. methods for props. determ. 9-47100
 magnetic impurities, dynamical effect on excitonic phase in temp. region $T > K_*$ 9-49183
 molten, absorption of sound, from melting to 900°C 9-30394
 potential difference quantum oscillations 9-30825
 sound absorption oscillations, ang. depend. of amplitude 9-48955
 superconducting energy-gap eqn., derivation by Green's function method 9-26521
 U.S. absorption, in uniform electric fields 9-41085
 As, de Haas-Shubnikov oscillations in magnetoresistance, Fermi surface obs. 9-43024
 As, magneto-acoustic attenuation, giant quantum oscillations, spin splitting 9-35335
 Bi-Pb, band structure determ. from magnetoresistance and Hall eff. meas. 9-30843
 Bi-Te, second-harmonic generation by damped Alfvén waves and helicons 9-41160
 Bi-Sb alloys, magnetoreflection obs. of band struct. 9-41162
 Bi, deform. pot. for electrons and holes 9-33252
 Bi, electron relax. time from magnetoacoustic oscillations and tilt effect 9-47072
 Bi, electron relax. time from magnetoacoustic oscillations and tilt effect 9-47072
 Bi, films, anomalies in resistivity 9-49020
 Bi, low-field galvanomag. coeffs. temp. depend. 9-49019
 Bi, magnetoresistance anisotropy, carrier influence 9-41161
 Bi, second-harmonic generation by damped Alfvén waves and helicons 9-41160
 Bi film, resistivity oscillations upon deform., 78° and 300°K 9-30845
 Bi thin films, elec. conductivity and Hall effect, thickness dependence, 4.2°-300°K 9-33251
 Bi thin films, photoelectromagnetic effect meas. 9-47209
 Cd₂Hg_{1-x}Te alloys, electronic props. in vicinity of semimetal-semiconductor transition 9-49078
 HgTe-ZnTe, conduction band struct. and electron scatt. mechanism rel. to semimetal-semicond. transition 9-35307
 Sb, Peltier coeff. at boundary between solid and liq. phases, determ. 9-45019
 Sb, resistivity, reluctance, Hall const., differential thermo. e.m.f., 300-750K 9-47076

Series

- Chebyshev polynomial expansion of 'well-behaved' function, coeffs. evaluation 9-36114
 Stieltjes, Convergent series, best error bounds for Pade approximants 9-41733

Sferics *see Atmospheric***Shadow universe** *see Cosmology; Elementary particles***Shear strength** *see Mechanical strength/shear***Shell model** *see Nucleus/model***Shielding** *see Radiation protection***Shock tubes**

- aerodynamic, for diffusor study 9-42599
 boundary layers, dependence on shock strength 9-45868
 diameter eff. on pressure var. of propane-O₂ mixture behind shock front 9-28061
 end-wall radiative heat transfer in air 9-23395
 flow diagnosis by ionic laser beam 9-45867
 gas flow near diaphragm, shock waves motion and stream parameters 9-41833
 hypersonic wake diagnostics, electrostatic probes, use and calibration 9-48649
 optical telemetry appl. 9-29306
 plasma flow parameters rel. working channel construction 9-27976
 precursor phenomena, experiment and theory 9-43795
 reflected shock interaction, expt. study 9-23382
 T-tube and tube with coaxial electrodes, wave propagation 9-40741
 thermal parameter meas. of insulating solid films 9-39524
 two phase, using powder-gas aerosol, development and testing 9-28161
 Ar-He mixture, heat transfer rates meas., thermal conductivity calc., 650-5000 °K 9-26026
 Ar heat transfer rates meas., thermal conductivity calc., 650-5000 °K 9-26026
 N⁺ and O⁺ shock tube studies, recombination radiation in vacuum ultraviolet 9-25968
 NO, β , γ systems, transition dipole moment determ. 9-48472
 Xe heat transfer rates meas., thermal conductivity calc., 650-5000 °K 9-26026

Shock waves

- see also Detonation; Explosions; Plasma/shock waves; Supersonic flow*
 acoustic-gravity, single perturbation analysis 9-31854
 air, emission spectra and luminance temp. 9-36202
 air, hypersonic, energy transfer between different degrees of freedom 9-46564
 air blast on vertical wall, overpressure peak at foot 9-34823
 Alfvén, in relativistic MHD 9-30184
 atmospheric ground-pressure waves from nuclear explosion, rel. to winds, models 9-24645
 blast, electrically driven, shock tube experiments 9-29312
 blunt body critical point, heat exchange, radiation effect 9-42597
 boundary layers in tube, dependence on shock strength 9-45868
 bow, in lab. simulation of solar wind interaction with magnetosphere 9-37944
 in classical fluid, particular soln. of Enskog eqn. 9-44395
 collision with supersonic slender body, analytical soln. and press. distrib. 9-25109
 compression flow in non-axially-symmetric annular nozzle 9-40641
 compression photography, problems of rotating-mirror streak cameras 9-32087
 curved unsteady, with tangential and normal vels., gradients of flow variables 9-31851
 damped mechanical systems, book 9-25087
 damping by multiple refl. at slits, spark cinematography 9-29315
 decay, MHD wave 9-23258
 demonstration model 9-36200
 design of body to produce specified sonic-boom signature 9-26013
 diffraction by sharp wedge, blast race analysis 9-46561

Shock waves continued

- divergent spherical, formation and propagation on production by exploding wires in air 9-43796
 dust-gas systems behind reflected waves, burning 9-47457
 enthalpy of gas calc., press., density, temp. and speed meas. 9-31850
 equations of state, reduction to isothermal eqns. of state 9-28335
 equations of state rel. to Gruneisen's parameter 9-28430
 expansion rates, prod. from spark discharges 9-30317
 exploding wires, dwell time gas dynamics 9-27235
 explosion of spherical charge in air, parameters calc. 9-45870
 from explosions of condensed detonators, interaction with external e.m. field in near zone 9-38306
 failing nonequilibrium region in argonlike gas, physical processes 9-46553
 flow past wedge-shaped profile 9-42598
 in fluid sphere of variable internal friction, propagation 9-38298
 in fluids, development from finite amplitude plane waves 9-29309
 formation in supersonic nozzle, boundary layer differential eqns. soln. 9-22049
 gas behind shock wave in Ar, thermodynamic parameter calc. 9-38974
 gas binary mixtures, components of diff. mol. wt., propag. 9-26012
 gas flow, axisymmetric hypersonic, over slender body 9-25999
 gas flow around cylinders and spheres, shock detachment distance 9-32601
 in gas mixtures, struct. and separation of component vels. and temps. 9-34826
 gas at rest, elec. cond., production by sudden applic. of crossed mag. and elec. fields 9-28071
 gas supersonic flow around segmented bodies 9-42591
 gases, monotonic; compression discontinuity 9-44518
 gases, rel. to inelastic collisions, 10 °K 9-34841
 in gases with density and temperature variation, amplitude expression 9-32725
 generation by ions 9-29314
 generation in liqs. by gas detonation 9-46627
 granular materials, saturated, analysis from photoelastic images 9-30643
 heat and mass transfer, transient, non-linear, high-intensive; wave formation 9-22282
 ice crystal nucleation by lightning discharge 9-26908
 interaction due to combined two shear loadings 9-40278
 interplanetary mag. field, IMP 3 obs. (1965, 1966, 1967) 9-24893
 in ionized gas, due to steady radiation front 9-44482
 lamellar media, energy cumulation 9-37229
 by laser interaction with solid target, luminous fronts obs. 9-41910
 in lattice, finite amplitude waves, mass points chain model 9-36201
 liquids under high pressure, for determ. of eqn. of state 9-36843
 MHD, relativistic, existence and uniqueness theorems 9-46453
 MHD duct, current and voltage distribution around normal wave 9-25875
 MHD formation by reflection 9-23259
 motion and stream parameters, at start of gas flow near shock tube diaphragm 9-41833
 oblique, interaction with a turbulent boundary layer 9-22268
 oblique, linear waves interaction, amplitude formulas 9-29311
 particle, in wave mech. 9-43744
 plane, attenuation in free space and in presence of rigid or interfacial boundaries 9-29310
 plane, obliquely impinging on obtuse wedge, drift accompanying reflection 9-34092
 plane, step, transient response of rigid sphere 9-29307
 plane radiative, propagation in homogeneous medium with boundary at optical depth $\tau = 5$ initially 9-22269
 from point explosion, propag. into cold atm. with density varying exponentially with altitude 9-34091
 polyatomic gas propag., applic. of Chapman-Enskog theory 9-46566
 precursor in argonlike gas, physical processes 9-46553
 pressure meas. by flash radiography 9-29316
 propagation in a T-tube and a tube with coaxial electrodes 9-40741
 propagation in inhomogeneous gases 9-32723
 propagation in inhomogeneous gases, time development of shock 9-48651
 radiating nongray shock layer, cooling and self-absorpt. effects 9-23383
 radiation from explosion in circular disk 9-35160
 reflected shock interaction in shock tube, expt. study 9-23382
 reflection by magnetic field of current grid, theoretical analysis 9-38305
 S waves from Nevada nuclear explosion, travel times and amplitudes 9-35780
 insolar corona, propag. oblique 9-32723
 solar wind, double structure, effect of high electron proton temp. ratios 9-31645
 solar wind, elapsed-time obs. of Earth's bow shock 9-24930
 in solid, motion in near zone 9-39402
 in solid plate-space system, anal. rel. to Gruneisen coeff. and eqn. of state determ. 9-48972
 sonic boom, minimum shock strengths and overpressures, eqn. for given conditions 9-40740
 from spin detonation, three-wave confluences represented in three-dimens. hodograph 9-34093
 star, outer part 9-24774
 in stellar atmospheres, stability, dissipation and propag. in atomic H 9-24762
 structure in expansion flows, expt. investigation 9-31853
 structure in expansion flows, numerical calc. 9-31852
 thermal in spherical shell, soln. using image technique 9-22223
 vibration relaxation eff. on limiting layer 9-45869
 Ar, spectral distrib. of u.v. and visible radiation 9-48654
 for atoms recombination with H, Ar, H₂, obs., 2500-7000°K 9-29978
 H, partially ionized, structure 9-48653
 H₂ driver gas, time of arrival at end plate rel. to reflected shock interacts 9-23382
 Kr, spectral distrib. of u.v. and visible radiation 9-48654
 Ne, spectral distrib. of u.v. and visible radiation 9-48654
 O₂-propane mixture, pressure var. behind shock front, eff. of tube diameter 9-28061
 Pb-plexiglass layers, shock wave energy cumulation 9-37229
 Xe, spectral distrib. of u.v. and visible radiation 9-48654

effects

- in air, ionizational relaxation 9-42560
 Alfvén, inviscous fluid of finite elec. cond. 9-34747
 alkali metals, compression data 9-46882

Shock waves continued
effects continued

- boundary layer flow on flat plate, heat transfer and transition to turbulence 9-40739
- α -brasses, dislocations distrib. rel. to stacking fault energy in shock-deformation 9-23879
- compression estimation at high press. 9-23873
- diatomic mol.s., vibr. energy exchange 9-32556
- double-shock method for pressure limit detection in magnetic phase transitions 9-35524
- ethanol, refr. index obs. 9-44566
- exploding wires, plasma light emission at low pressure 9-30241
- explosive, organic polycrystalline, strain-rate sensitive, compressive wave propag. behaviour 9-39409
- flux compression, similitude 9-29313
- gas, monatomic, ionizing shock structure 9-30294
- gas, spherocylindrical molecules, trimodal shock structure solutions 9-30336
- gas flows, containing arbitrarily large number of shocks, calculation 9-36795
- gas heating, role in envelope of close binary stars 9-27038
- geological, on remanent magnetism orientation and intensity 9-45569
- glycerol, refr. index obs. 9-44566
- hallstones, induction of cavitation by u.s. waves 9-45491
- Hugoniot for condensed media 9-23455
- hydromagnetic, oblique, in gas, transition through two successive shocks 9-46575
- ideal gas flow, compressible, patterns 9-40734
- interpolation formula for relationship between shock velocity and particle velocity 9-42871
- ion-electron pairs production, diffusion in shock tube walls 9-43797
- ionic crystals, polarization, rel. to lattice characts. 9-30957
- ionization, normal wave; gas velocity variation 9-36801
- magnetic line, curvature behind pseudo-stationary shock 9-25834
- metal cylinders, thin-walled, explosively-loaded, fragmentation behaviour expansion velocity and material parameter dependence 9-42901
- optical radiation behind wave in simulated Martian atmosphere 9-23385
- plasma heating by strong collisionless shock waves obs. 9-38973
- polymers, cryst., struct. transition, obs. 9-30733
- polymers, shock compression 9-37361
- quartz, preferred disorder prod. 9-42938
- quartz, X-cut, elec. breakdown and recovery under shock wave compression 9-47189
- semiconductor, shock strained, Boltzmann equation and wave-particle drag 9-37513
- shock tube, diaphragm, shock waves motion and stream parameter 9-41834
- shock-turbulence interaction, acoustic energy flux from unit area downstream of shock 9-34825
- sonic bangs, acoustic-elastic effects in reponse of large windows 9-41835
- sonic boom, energy spectral density derivation 9-29308
- sonic booms, subjective magnitude, calc. procedure 9-47828
- sphere, rigid, transient response to plane, step shock wave 9-29307
- steel, low C, explosively produced spall fractures, metallographic features 9-26354
- steel cylinders, ductility under explosive loading conditions 9-30660
- steel shells, closed, response to blast of internal explosive charges 9-40279
- turbulence environment interaction, acoustic waves production, experiment 9-42602
- vapour-gas mixture, boundary layer at a tube wall behind a wave 9-39140
- water droplets nucleation and supercooling, obs. 9-39134
- Ag, shock velocity, u_p , and particle velocity, u_p , in hydrostatic compression, applic. of interpolation formula for relationship between u_p and u_p 9-42871
- AgN₃, explosion initiation by collapsing air bubble 9-28788
- Al, f.c.c. polycrystalline, shock-relief deformation effects on mech. strength and microstructure 9-23879
- Al alloys, ductility under explosive loading conditions 9-30660
- Al layer, anodized, rel. to elec. output 9-24117
- Ar, ionizing, behind reflected shock wave, shock reflection process and thermal layer 9-48662
- Au shock velocity, u_p , and particle velocity, u_p , in hydrostatic compression, applic. of interpolation formula for relationship between u_p and u_p 9-42871
- CO₂-N₂ reson. vibr. energy transfer between mode N₂ 9-30164
- CO₂, blue continuum emission, 1900-2400°K, shock tube study 9-38837
- CO₂, heated to 1294-2670°K, thermal conductivity 9-36815
- CO₂, i.r. emission near 4.2 μ , meas. of relax. freq. of asymmetric stretching mode 9-34611
- Cu, f.c.c. polycrystalline, shock-relief deformation effects on mech. strength and microstructure 9-23879
- Cu, hardened, softening and recrystallization during heating 9-33098
- Cu, strengthened, rel. to final yield strength 9-35162
- α -Fe, kamacite, preferred disorder prod. 9-42938
- Fe, porous, dynamic compaction props. 9-44762
- Fe, prestrained, substructural changes obs. 9-32915
- Fe, shock-compressed, α - to ϵ -phase transition, conductivity and demagnetization obs. 9-26388
- Fe₃C, cohenite, preferred disorder prod. 9-42938
- Fe₃P, schreibersite, preferred disorder prod. 9-42938
- Fe meteorites, shock loading effects rel. to thermal history 9-24886
- Fe-(31.4at.%)Ni alloy, compression rel. to magnetization 9-43176
- H₂ combustion, chem. kinetics 9-39946
- H plasma prod. by normal ionizing shock wave 9-23276
- HBr, vibr. relax. 9-42396
- HBr dissociation kinetics 9-47455
- HCl, vibr. relax. behind shock waves 9-30030
- HCl and DCl, vibr. relax. 9-38847
- HI, vibr. relax. 9-42396
- He gas in T-tube, obs. of refl. shock 9-30324
- KI, polarization, rel. to lattice characts. 9-30957
- Li⁷H and Li⁶D, polarizattice characts. 9-30957
- N₂-O₂ vibr. exchange 9-30349
- N₂, heated to 1294-2670°K, thermal conductivity 9-36815
- N₂O+CO bimolec. reaction in single pulse shock tube 9-43321
- N₂O+H₂ reaction 9-31183
- N₂(1+) and N₂⁺(1-) nonequilibrium region behind shock, radiation mechanism 9-42410

Shock waves continued
effects continued

- N plasmas, Stark-broadened H lines as temp. probes 9-48589
- NaNO₃ structural change under shock compression 9-37303
- Ni, explosion-shocked, thermal recovery processes, electron microscope obs. 9-44696
- Ni, f.c.c. polycrystalline, shock-relief deformation effects on mech. strength and microstructure 9-23879
- Ni, hardened, softening and recrystallization during heating 9-33098
- Ni, hardening in pressure range 820 to 1500 kbar, rel. to microstructure 9-30701
- Ni, strengthened, rel. to final yield strength 9-35162
- No, vibr. relax., shock tube meas. 9-38861
- ¹⁸O₂+CO, isotope exchange 9-49370
- β -PbN₆, explosion initiation by collapsing air bubble 9-28788
- RbI, polarization, rel. to lattice characts. 9-30957
- SF₆ dissociation in Ar, kinetics 9-38923
- SO₂, chemiluminesc. afterglow, temp. depend. 9-43323
- TiO₂, polymorphism 9-39482
- Shot noise** see *Noise/electrical*
- Showers** see *Cosmic rays/showers and bursts*
- Shubnikov-de Haas effect** see *Magnetoresistance*
- Silicon**
see also *Semiconducting devices; Semiconducting materials/silicon*
- adsorption of H rel. to atom recombination kinetics on differently oriented planes 9-36968
- burning in stars, conditions for explosive nucleosynthesis 9-49546
- channeling charact. of protons and the ions 9-47012
- cracks, partial, chem. etching 9-44780
- crystal grown in (100) direction, dislocation reaction 9-48863
- crystal grown in (100) direction, dislocation struct. by chemical etching and microscopy 9-48862
- Crystal growth mechanism, from reduction of SiCl₄ by hydrogen 9-48794
- crystal in uniaxial compression, deform. const. determ. from absorpt. spectra 9-41012
- crystalline layer growth on Al₂O₃ substrate, method, patent 9-23667
- defects, rad. induced, mechanisms, and interaction with Li impurities 9-48844
- defects, X-ray detection, applic. in integrated circuit fabrication 9-30604
- deformation by thermal gradient, effect on X-ray propag. 9-23772
- deuteron-irradiated, energy spectra of radiation defects, p-type 9-30589
- diffusion mechanism and point defects, review 9-37209
- diffusion of As, isoconcentration studies 9-37208
- diffusion of As using AsH₃ 9-28324
- diffusion of P, induced defects obs. 9-32975
- diodes, punch-through epitaxial Schottky barrier, avalanche breakdown voltages 9-26576
- dislocation generation, strain compensation by diffused impurities 9-46824
- dislocation struct. after plastic deform. 9-42840
- dislocations, quantitative relation in 14 mm slice using chem. etching and X-ray topography 9-40954
- dislocations formation mechanism due to ϵ bombardments 9-26286
- electron inelastic scatt., interband transition excitation, E_g=30-200 eV 9-40887
- electroreflectance rel. to photorefectance spectrum 9-43231
- epitaxial layers, chemically-deposited, growth and perfection 9-36951
- e.p.r. in LiF, rel. to paramag. fault 9-49353
- etched by H₂S gas, surface exam. 9-32837
- field emission, nonlinear, depend. on temp. and light intensity, p-type 9-26608
- film, thin, deposited by electron irradi. of tetramethylsilane, electron diff. and microscopy obs. 9-44628
- film epitaxial deposition by H₂ reduction of chlorosilanes, gas press. and velocity effects 9-28215
- film on isotropically absorbing substrate, ellipsometric obs. 9-33504
- film on sapphire, electrically and optically active defects 9-37545
- film on sapphire, orientation selection for substrate 9-23658
- foil, ion irradi., defect prod. 9-44683
- growth from metal soln., habit and morphology, infl. of solvent and impurities 9-36981
- impurity-doped, effects of Li, Na, Be, Cl, Al and O on carrier lifetime 9-24234
- inclusions in Si-containing alloys, i.r. absorpt. obs. 9-35213
- interaction with diamond at high pressures and temps. 9-26807
- ion implanted crystals, investigation using directional effects in charged particle reaction yields 9-30598
- in iron meteorites, search in metal phase rel. to Earth core models 9-41683
- Laue reflected and refracted beams, rocking curve oscillations 9-32928
- layer epitaxial growth from vapour phase through liq. alloy, low temp. deposition, patent 9-30530
- optical excitation at 1.06 μ , photocond. rel. to intensity and elec. field 9-37624
- optical mixing of laser radiation, third-order 9-26688
- optical reflectivity changes induced by 40 keV Sb ion bombardment 9-33506
- oxidised substrate adhesion to Au underlayer by adherent layer, mechanism determ. 9-39480
- p-type, deuteron-irradiated, energy spectra of radiation defects 9-30589
- p-type, field emission, nonlinear, depend. on temp. and light intensity 9-26608
- photorefectance spectrum and rel. to electroreflectance 9-43231
- plastically deformed, dislocation struct. obs. 9-42840
- point defects generated by quenching, density, lattice parameter and elec. props. investig. 9-32944
- polycrystalline deposition from SiCl₄ reduction, on graphite 9-37011
- precipitation of boron 9-37164
- proton channeling in thin cryst., energy spectrum, temp. effects 9-37378
- proton energy distribution and channelling in lattice 9-30809
- proton energy losses 9-30807
- radiation damage on low temp. irradi. of degenerate crystals 9-28277
- radiative Auger effect, simultaneous emission of X-ray photon and L-shell electron 9-40553
- range of implanted B, P and As 9-44856
- reflection spectra, u.v., effect of heavy doping 9-35645
- removal from ocean by biogenous deposits, total rate 9-33749
- SiI, relative transition probabilities, in the Sun 9-24899

Silicon continued

- solar cell assemblies, proton induced damage 9-24077
 solubility of Cu, effect of grain-boundaries 9-42797
 solubility of Na 9-40988
 splints, internal recontacted, elec. props. gas adsorption and X-ray studies 9-42846
 structure, (111) 7×7, cleaving at 850°C 9-35068
 structure of ion-implanted Au layer in single crystal 9-39307
 substrate for SiO₂ film, m.o.s. and radiochemical analysis of impurities 9-42814
 surface, physisorption at low temps., ellipsometric investigation 9-42730
 surface perccussion marks on single crystals, divergent X-ray diff. pattern 9-33037
 surface struct. of (111) and (100) by reflection high energy electron diff. 9-48752
 surfaces, stacking fault nucleation, growth and annihilation mechanisms 9-42844
 thermal conductivity anisotropy of polycryst. due to differing vapour deposition conditions 9-35428
 thermal expansion, 20°-300°K, interferometric meas. up to 800°K 9-30787
 thermal stresses prod. by electron beam melting, source image distortion obs. 9-35164
 vibrational absorpt. of C and C-O complexes 9-41390
 X-ray anomalous transmission, 100° to 650°K 9-33573
 X-ray crystallographic determ. of accurate absolute scatt. factor determ. 9-23771
 X-ray diff. topographs of bicryst., fringe contrast and geometry 9-32982
 X-ray satellite theory based on sudden approx. only, exptl. evidence against 9-35676
 in Al-(2.5 at.%)Cu-(1.2 at.%)Mg alloy, effect on ageing 9-48915
 Al₂Ga₂As₂Si electroluminesc. diodes. props. and efficiency 9-37775
 B implanted and annealed, condensed defect structure distrib. 9-32953
 B and P diffusion through SiO layers 9-48876
 Band-P diffusion 9-48877
 in Cu-(0.2 wt.%)Al internally oxidised alloy, effect on mech. props. 9-46903
 Fe-Si frame single crystal, negative Barkhausen jumps, existence, character and rate during magnetization 9-37658
 GaAs:Si, energy band tails and photoconductivity 9-39716
 in GaP, pair spectra obs. 9-45358
 Si:B(P), irradi. at 80°K, conductivity and Hall effect meas. rel. to carrier removal rates 9-44852
 Si:Bi, impurity absorpt. line shapes, effect of resonant phonon interactions 9-26741
 Si:C i.r. absorption bands rel. electron irradiation 9-26739
 Si:Li-diffused, e.s.r. 9-26794
 Si:Li, O, dopant interaction with electron-irrad. produced defects 9-42813
 Si:O i.r. absorption bands rel. electron irradiation 9-26739
 Si:O single crystals, periodicity by X-ray transmissions 9-32926
 Si:P, ESR, absorpt. intensity 9-35717
 n-Si:P, γ irradiated, thermal donor formation 9-32951
 Si:p, photoionization of impurity atoms and colour centres using e.p.r. 9-37636
 Si:P cylinder, with coil round it, impedance change as function of applied axial mag. field 9-23314
 Si:P dislocation-free single cryst., plastic deform. initial stage 9-30665
 Si:P ENDOR obs. 9-35736
 Si/SiO₂/Si₃N₄ double-layer films, Na diffusion and distrib. 9-26305
 Si-B, quenched in defects. elec. and photo-conductivity obs. 9-39357
 n-Si-WSi₂ interface, barrier height reaction-process dependence rel. to interface structure 9-42715
 n-Si, high purity, recombination lifetimes, 4.2°K to room temp. 9-35508
 Si, lattice deform. due to high-energy ion implantation, X-ray exam. 9-35103
 Si I-, Si II-, Si III- lines 1100-2600 Å, oscill. strength meas. 9-44269
 Si I transition probabilities, near vacuum, obs. 9-23366
 Si II, in the Sun and ZETA, relative intensities of selected multiplets 9-27094
 Si III oscillator strengths calc. and many electron correl. problem approxs. 9-29946
 Si III solar emission line profile, 1206.52 Å, rocket obs. 9-41689
 Si primary spherulite growth and morphology in Al-(20wt.%)Si alloys 9-23775
 Si XI ions, grazing incidence spectra, emitted by laser produced plasma 9-38758
 Si XII ions, grazing incidence spectra, emitted by laser produced plasma 9-38758
 spectral lines, Stark broadening and displacement rel. plasma high temp. meas. 9-25913
 thermal expansion, Gruneisen parameters 9-33190

Silicon compounds

- see also Quartz
 Al-Si eutectic alloy, banding explanation 9-44613
 coesite-stishovite transition, 550 to 1200°C and 82 to 98 kb 9-28399
 faujasite, dehydrated La-exchanged, position of mols and cations at 420°C 9-32899
 for semicond. devices 9-35435
 monosilane, halogen substituted, saturated vapour, specific heat calc. 9-26030
 opal, SiO₂·nH₂O, packing imperf. rel. to stacking faults and polytypism 9-42843
 opals, electron microscopy study, 3-dimens. packing of spheres, stereopictures determ. 9-40917
 perlite, elastic constants rel. to porosity 9-30635
 Si₃N₄-P films, surface potential drifting 9-37579
 silica, Brazil quartz, viscosity, 1600-2480°C 9-30470
 silica, cryochem. method for prep. 9-33125
 silica, fused, longit. hypersonic damping, obs. 9-26759
 silica, microporous, prep. by freeze-thawing technique 9-46732
 silica, vitreous, acoustoelastic effect 9-35141
 silica, vitreous, metastability of high cristobalite 9-48932
 silica, vitreous, Stokes-Raman spectrum, temp. depend 9-49297
 silica gel, benzene sorption and dielectric isotherm, 1 Mc/sec, 25°C 9-42735
 silica gel, desorption rates of CO₂, Ar mixtures at various temps. 9-46663
 silica gel, mag. susceptibility of adsorbed NO mols. 9-44631
 silica gels, vacuum freeze-dried, struct. rel. to cryst. nucleation 9-34936
 silica glass, densified, energy spectrum 9-46700

Silicon compounds continued

- silicate glass, mechanical strength 9-26341
 silicate glasses, K₂O-PbO-SiO₂, luminescence centres 9-31129
 silicate glasses, Na₂O-SiO₂, primary and secondary phase separation 9-30455
 silicate glasses containing Ti gamma-induced optical absorpt. 9-37693
 silicates, rotating-disc solution spectrochem. analysis 9-35764
 siliceous materials, surface conc. of broken bonds on fresh face 9-46734
 silicone resin films on Si, Elec. props. 9-30959
 soda-silica glasses, Tm doped, Mossbauer effect obs. of Tm³⁺ crystalline elec. field parameters 9-37702
 Ag/Au/Si system, controlled solidification using monovariant eutectic reactions 9-36921
 Al(0.06 at.%) Si, resist. rel. to Si atoms clustering in ageing, 300°C 9-30712
 Al(0.13 at.%) Si, resist. rel. to Si atoms clustering in ageing, 300°C 9-30712
 Al-0.12 at. %Si dil. alloy, clustering of Si atoms during step aging 9-23940
 Al-Mg-Si alloys, recrystn. behaviour, influence of precipitates 9-39452
 Al-Mg-Si alloys containing Mg₂Si, 2-stage ageing effect 9-39461
 Al-Mg-si alloy, electron microscope images, quality deterioration with specimen thickness, 50-100 KeV 9-23747
 Al-Si, subeutectic, thermal stresses calc. by phase suspension model 9-23948
 Al-Si dilute alloys, cold-worked, isochronal annealing obs., recovery process 9-33104
 Al-Zr-Si alloys, recrystn. and age hardening, influence of Si 9-42910
 Au-Si solid soln., Precipitation effect on i.r. vibration spectrum of O 9-45315
 C/Cr/Ni/Si system, controlled solidification using monovariant eutectic reactions 9-36921
 CaF₂, longit. hypersonic damping, obs. 9-26759
 CaO-SiO₂-2CaO-SiO₂-ZrO₂ system, phase equilibria 9-33147
 Co-Ni-Si alloys, ferromag., internally oxidised struct. obs. 9-48837
 Cr-(2 wt.%)Ta-(0.5 wt.%)Si alloy guide vane specimens, thermal fatigue testing 9-33075
 Fe-(3 wt.%)Si transformer sheet, domain wall motion, freq. depend. and wall bowing 9-39764
 Fe-(3.25 wt.%)Si, alloy, domain width, thickness depend., critical thickness 9-39763
 Fe-(3 wt.%)Si, alloy, polycrystalline, slip, twinning and fracture, effect of pressurization 9-33053
 Fe-(3 wt.%)Si, alloys, ferromag. domains, X-ray topographic obs., diff. contrast on walls 9-26643
 Fe-(3 at.%)Si, polycrystalline, nucleation of mechanical twins 9-46826
 Fe-(3 wt.%)Si, yielding dislocation configs. obs., delay-time model 9-44766
 Fe-Si, grain-oriented, with high permeability, mag. props. characts. 9-45145
 Fe-Si, primary recryst., ageing effect on texture form. 9-46921
 Fe-(3 wt.%) Si alloy, domain shape, comparison between calc. and obs. 9-41307
 Fe-Si alloy, domain wall width meas. in thin sections by electron interference method 9-41310
 Fe-Si alloys, antiphase boundaries, crystallographic charact., electron microscopy study 9-37142
 Fe-Si alloys, Fe-rich, mass spontaneous magnetization, 298 K 9-39768
 Fe-Si alloys, ferromag. domain walls, image contrast, origin, X-ray topography obs. 9-28614
 Fe-Si alloys, magnetic props., infl. of galvanically deposited Ni films 9-26647
 Fe-Si alloys, microinhomogeneities in cast worked and annealed samples 9-48846
 Fe-Si alloys, ordered, antiphase boundaries, props. 9-26231
 Fe-Si alloys, spin-wave dispersion relationships determ. 9-24297
 Fe-Si alloys, textured mag. props. for Si>3.25% 9-45124
 Fe-Si dil. alloy, secondary recrystn., grain growth rate orientation depend. 9-39456
 Fe-Si ferromag. domain walls, visibility on diff. topographs and comparison with BaTiO₃ ferroelec. walls 9-39682
 Fe-Si grain-oriented, soft mag. materials review 9-39753
 Fe-Si secondary recrystallization by solute-induced boundary restraint 9-44785
 Fe-Si single cryst., lattice distortion and X-ray topographic contrast due to 90° ferromag. domain wall 9-33460
 Fe-Si solid solns., resistivity and Matthiessen's rule deviations 9-41167
 Fe-(0.6 wt.%)Si alloy, Barkhausen and ΔE effects, rel. to applied stress 9-45147
 Fe-(3-7 wt.%) Si alloy, magnetomechanical damping 78° to 300°K 9-45157
 Fe-(3 wt.%)Si alloy, edge and screw dislocation mobilities, h.v. electron transmission microscopy meas. 9-42829
 Fe-(1 wt.%) Si alloy, Ge effect on internal oxidation 9-46740
 Fe-(3 at.%)Si alloy, magnetoelastic internal friction, anisotropy 9-33023
 Fe-(3 wt.%)Si alloy single crystal, surface energy relative variation for (110) and (100) planes, under annealing atmosphere 9-26180
 Fe-(3 wt.%)Si alloys of different impurities, recrystn. during high-temp. annealing 9-39474
 Fe-(3wt.%)Si alloy, surface energy of (110) and (100) planes infl. of annealing 9-34979
 Fe-(3 wt.%) Si cold-rolled-(119) [001]-oriented single crystals, primary recrystallization textures, effects of AlN 9-44784
 Fe-(3 wt.%)Si single crystals, crack nucleation, effect of stress concentrations 9-48911
 Fe79Si3, eddy current losses rel. to thickness 9-26506
 K₂O-SiO₂, vitreous solids, elec. conduction and phase separation by electron microscopy 9-41156
 Li₂O-SiO₂ glass, metastable precipitate formation and effect on elec. props 9-24215
 Na-B-Si glass, spectra, Raman, e.p.r., i.r. and electronic 9-26757
 Ni-Si-Ti alloys, microstruct. and tensile props. 9-48902
 Ni-Si alloys, ferromag., internally oxidised, struct., obs. 9-48837
 Ni-Si alloys, γ phase, coherent solubilities 9-28403
 Ni-Si alloys, microstruct. and tensile props. 9-48902
 Ni-Zn-Si system, phase equilibria at 800°C 9-35209
 Ni₂Zn₃Si phase, cubic Ti₂Ni struct. and interatomic distance calc. 9-32924
 Pd-Si based alloy glasses, form stability and struct. 9-42706
 Pt-SiO₂ cermet thin films, resistances obs. 9-47155

Silicon compounds continued

- Si/SiO₂/Si₃N₄ double-layer films, Na diffusion and distrib. 9-26305
 Si-Fe, dislocation theory of susceptibility and coercive force 9-33457
 Si-Hf binary system, phase equilib. diag. 9-35258
 Si-Si₃N₄ films, trapping levels obs. 9-33359
 Si-SiO₂ structures, surface states density rel. to thermal oxidation conds. of Si 9-26560
 Si-Zr binary system, phase equilib. diag. 9-35258
 Si₂Cl₆, vibrational spectrum, structure and internal rotation 9-30056
 Si₃N₄, impurity-doped, electrical and physicochemical props. 9-37578
 Si₃N₄, instability in H₂-H₂O and H₂-HCl mixtures during Si etching 9-32866
 Si₃N₄ as alkali barrier liner for SiO₂ thermal growth 9-33358
 Si₃N₄ films, dielectric props. and appls. 9-24212
 Si₃N₄ layers, deposition using photochem. reaction 9-46728
 Si₃N₄ single-layer film, Na diffusion and distrib. 9-26305
 SiBr₄ vapours, glow discharge spectrum 9-48483
 p-SiC:B,N, interimpurity recombination obs. from photocond. decay and e.p.r. signals after illumination 9-28712
 SiC:Be, luminescence spectra rel. to Be conc., 77 to 500K 9-28713
 α-SiC:N, dichroic crystal-optical device, patent 9-28653
 n-SiC:N electroluminesc. diodes, props. and anomalous nature of B and Al diffusion during prep. 9-37776
 SiC, band struct., empirical pseudopot. approach 9-49000
 β-SiC, compressibility, meas. by use of X-ray diffr. camera for high pressure studies 9-48820
 SiC, cubic, lattice dynamics 9-24019
 n-SiC, deep donor level obs. 9-49097
 SiC, diffusion of Al by heating to 1800-2400°C for 2-30 hours 9-33009
 SiC, etching, improved technique 9-46749
 SiC, H₂ etching 9-26204
 SiC, p-n junctions, luminescent brightness rel. to temp. 9-26785
 SiC, polytypism 9-36975
 SiC, positron annihilation 9-30830
 p-SiC, radiative recombination at deep impurity states 9-28711
 SiC, satellite theory based on sudden approx. only. exptl. evidence against 9-35676
 SiC, semiconducting diffusion data review 9-26298
 SiC, structure, review 9-26245
 SiC, vapour-deposition and microstructure 9-23774
 SiC, vapour-deposition and microstructure 9-39306
 α(6H)-SiC absorption spectrum at 86°K in vicinity of 3 eV 9-41389
 n-SiC α(6H) crystals, optical absorpt. in 0.6 μ range from 80 to 1100°K 9-43243
 SiC coating on B filament, elevated temp. strengths after exposure to air 9-30679
 SiC diffusional p-n junctions, temp. depend. of injection luminescence 9-45357
 SiC diode, pulsed, radiation props. 9-38387
 SiC epitaxial p-n junctions, avalanche breakdown 9-35442
 α-SiC etching in H at high temp., variation with susceptor mat. and inert gas atmospheres 9-30514
 SiC fibres, critical surface tension of wetting, rel. to interact. with resins and coupling agents 9-23620
 SiC filament, vapour deposited on W, macrostruct. 9-48866
 SiC films, cubic, reactive deposition procedure 9-42727
 SiC films, formation by reactive deposition and chem. conversion processes 9-42728
 SiC p-n junctions, tunnelling and avalanche processes at electroluminescence 9-43081
 α-SiC polytypes, e.p.r. of N atoms 9-28750
 SiC polytypes 6H, 4H, 15R, X-ray diffr. line intensities, revised 9-40916
 SiC whisker reinforced composite materials 9-35236
 2H-SiC whiskers, growth rel. to presence of O₂ 9-35032
 β-SiC whiskers, struct. obs. by X-ray diffraction, comments 9-32927
 SiCl₄, Coriolis coupling force consts., mean amps of vib. and shrinkage effect 9-48482
 SiCl₄, molec. struct. 9-44319
 SiCl₄, positron lifetimes in liquid 9-44583
 SiCl₄, vibr. freqs. and stretching force consts., i.r. obs. 9-27874
 SiCl₄, ν, fundamentals, Cl isotopic splitting using low temp. Raman cell 9-32068
 SiD₃CN force constants of mol. calc. by Urey-Bradley force field 9-30027
 SiF, Franck-Condon factors and r-centroids for β syst. 9-23074
 SiF₃, free radical, I.R. spectrum 9-31211
 SiH₃CN, force constants of mol. calc. by Urey-Bradley force field 9-30027
 SiH₄, mol. wave-functions and d orbitals rel. to bonding 9-34617
 SiH₄, SCF calcs. 9-23075
 SiHF₃ matrix-isolation vac. u.v. photolysis 9-31211
 α-SiN whiskers, vapour deposition production method, patent 9-23688
 SiO, evaporated films, thermal conductivity 9-39543
 SiO₂-BaO₃ glass films, two-phase structure development 9-26174
 SiO₂-C fibre reinforced, Young's modulus, rupture modulus and fracture toughness 9-44773
 SiO₂-Na₂SO₄-Gd, use in Gd microquantities determ. 9-49323
 SiO₂-PbO system, crystallization sequences in silica phase 9-26390
 SiO₂, absorption of light, Rosseland and Planck mean coeffs. 9-49548
 SiO₂, doped, deposited from SiH₄, diffusion characts. and appls. 9-23637
 SiO₂, doped, deposited from SiH₄ and B₂H₆ or PH₃, diffusion sources for Si device fabrication 9-23638
 SiO₂, doping with P, m.o.s. device stabilization 9-37568
 SiO₂, glassy state, vibrational analysis 9-28198
 SiO₂, instability in H₂-H₂O and H₂-HCl mixtures during Si etching 9-32866
 SiO₂, natural, electron irradi., 'A' band and absorpt. in near i.r. correl. 9-41391
 SiO₂, polymorphs, stability of high-pressure phases, effect of neutron irradiation 9-35250
 SiO₂, thermally grown, in m.i.m. structure, Fowler-Nordheim tunneling 9-43098
 SiO₂, thermally oxidised, crystallographic symmetry of surface state density 9-23773
 SiO₂, vitreous, H⁺ transport during H₂ permeation 9-46856
 SiO₂, vitreous, n diff. patterns 9-28269
 SiO₂, vitreous pile-exposed, ionization expansion 9-35175
 SiO₂ aerogels, adsorpt. of Ar and N₂ 9-30498

Silicon compounds continued

- SiO₂, amorphous films, anodic growth, dielec. breakdown and carrier transport 9-45006
 SiO₂ coated Al film, reflectance, solar absorptivity and thermal emissivity 9-37373
 SiO₂ film, loss tangent and permittivity, incomplete data, analysis 9-47158
 SiO₂ film, transmission and reflection spectra, thickness depend., 7-11 μ 9-24374
 SiO₂ film interference influence on reflection spectrum in SiO₂/Si system, 9 μ region 9-35619
 SiO₂ film on Si, impurities, combined m.o.s. and radiochemical analysis 9-42814
 SiO₂ film on Si, thickness meas. by variable angle monochromatic fringe obs., reflectivity corrections 9-34982
 SiO₂ films, chemical vapour deposition apparatus 9-26189
 SiO₂ films, electron-gun deposited, effects of heat treatment in air 9-48765
 SiO₂ films, I-V characts. rel. to temp., dielectric constant and loss, freq. depend. 9-28549
 SiO₂ films in semiconductor devices 9-37550
 SiO₂ films on Si, surface and interface elec. props. 9-43099
 SiO₂ fused, γ irradi., current-voltage depend. 9-49138
 SiO₂ gel, e.s.r. of adsorbed Cl atoms 9-30497
 SiO₂ gel, e.s.r. of adsorbed Cl atoms 9-39174
 SiO₂ glass, effect of ⁴He and ³He on low temp. ht. capacity 9-42733
 SiO₂ low loss glass attenuation coeff. using double beam spectrophotometer 9-25383
 SiO₂ on Si films, characterization by electron microprobe and ellipsometry 9-23628
 SiO₂ oscillator strength of (A'²E-X⁺) band system, shock tube study 9-28161
 SiO₂ particles-Cu matrix interface, generation of dislocations, local shear stresses 9-30611
 SiO₂ particles in strained Cu single crystals, lattice rotations assoc. with structure, electron microscope obs. 9-32911
 SiO₂ satellite theory based on sudden approx. only. exptl. evidence against 9-35676
 SiO₂ shields, neutron transport calcs. for incident monoenergetic neutrons, 50-400 MeV 9-48234
 SiO₂ in Si-SiO₂-Al structure, elec. strength rel. to thickness 9-35475
 SiO₂ thermal growth, use of Si₃N₄ as alkali barrier liner 9-33358
 xSiO₂-(1-x)Al₂O₃:Eu²⁺ phosphors, luminesc. 9-47390
 SiO₂-GeO₂ glass, i.r. spectra 9-49267
 SiO₂-nH₂O, opal, packing imperf. rel. to stacking faults and polytypism 9-42843
 SiO₂-CdS film system, frozen-in conductivity extinction by elec. field 9-28577
 SiO_x diffusion masks, breakdown voltage of p⁺/n planar junctions 9-41223
 SiO_x film, annealed, a.c. and d.c. cond. processes at high and low fields 9-47160
 SiO added to borolanthanum glasses, immiscibility and catalytic crystallization 9-34971
 SiO capacitor, thermal conductivity calc. from breakdown meas. 9-26463
 SiO films, elec. pulse breakdown 9-45005
 SiO thin film, breakdown mechanism, surface irregularities 9-41236
 SiO thin film capacitor, break-down studies 9-37586
 SiP₂, de Haas-van Alphen effect 9-49015
 SiP₂, orthorhombic, single cryst. growth from soln., p-type semicond. obs. 9-35022
 SiS, dipole moment from Stark components of microwave rotational transitions 9-30051
 SiSe₂, optical transmission 9-28694
 SrO, phonon dispersion curves 9-39509
 SrTiO₃, photoconductivity and photoluminesc. excitation spectra, electroluminescence spectra 9-45025
 Ti₂O-SiO₂ glasses, cation distrib. 9-48781
 U-(3.96 at.%)Si alloy, structure, effects of fabrication and heat treatment variables 9-33124
 UO₂-SiO₂ system, thermal conductivity, with varying UO₂ concentrations over the range 100-800°C 9-26456
- Silver**
- adsorption lifetimes and binding energies on W surfaces 9-39177
 in alkali halide crystals, theoretical anal. of hyperfine and superhyperfine interactions of stabilized atoms 9-37792
 alloying additions to Be, influence on microyield strength 9-35181
 atomic absorpt. spectra in solid Ar, Kr and Xe matrices 9-27805
 band structure, APW cal. 9-30819
 condensation, coeff., 600-900°C 9-39083
 crater formation by Fe microspheres at 0.5 to 10 km/sec. 9-30700
 creep, stacking fault energy effect 9-39421
 crystals, Xe ions bombard., threshold of damage obs. 9-30800
 crystals grown by electrodeposition, large step-height spirals on surface, origin 9-23825
 cyclotron resonance in thin slab, mass of neck orbits and orbital diameters 9-26496
 Debye-Waller factors, temp. depend. 9-35261
 deposits on satellites, sputtering by atmos. N₂ beams, rel. to surface binding energy 9-24076
 diffusion in Ag-Au alloys, high temp. electrochem. method meas. 9-46841
 diffusion in CdS in prep. of shear-mode-evaporated u.s. transducers 9-42957
 diffusion in Pb, Sn, In, and Tl, rapid, interstitial mechanism 9-28321
 diffusion in Se film, rel. to thin-film couple behaviour 9-42859
 diffusion in Zn and effect on Zn self-diffusion 9-23845
 diffusion of Sb, intercryst., temp. depend. 9-46846
 diffusion on Te thin film in Ag-Te couple, lateral diffusion 9-35135
 diffusivity in Pr 9-44745
 in discharge, evaporated from filament into He stream excitation and effect of Cu on emission 9-31222
 dislocation density depend. on primary recrystallization after large plastic deformation 9-40947
 dislocation loops, complex Frank, stacking fault steps form. rel. to fault climb 9-40943
 dislocation motion, etch pit obs. 9-40944
 dislocations, Frank, disloc. in quenched Ag, e diff. obs. 9-40959
 electrical resistivity rel. to temp., calc. using lattice dynamics model 9-35339

Silver continued

- electrode, differences during charging after five full charge-discharge cycles. 9-26833
- electrodeposition parameters effect on growth habit and morphology 9-37034
- electron emission, second., total yield and charact. energy losses 9-31008
- electron energy loss spectra in i.r. region 9-28441
- electron maximum range, 15 MeV, explt. determ. 9-26470
- epitaxy and nucleation on NaCl 9-23689
- epitaxy on MgO, in electron microscope, (100) cleaved surface mechanism determ. 9-39220
- excited levels, spectroscopic study by electron bombardment 9-29955
- exploding wire phenomena, effect of nature and dimens. 9-45419
- Fermi surface, effect of elastic deform., determ. using thermoelec. power 9-44884
- film, growth in ultra high vac. on mica, influence of air, O₂, N₂ and H₂O vapour 9-34993
- film, growth on alkali halides 9-23636
- film, optical properties, plasma resonance emission, temp. depend., 90-770°K 9-23641
- film, thin, optical const. and thickness during deposition, continuous ellipsometric determination 9-32845
- film on mica, inclined fault concs. rel. to presence of H₂, O₂ or H₂O during deposition 9-35097
- film optical properties and foil thickness determ. by curves of constant transmission 9-23640
- films, hypersonic attenuation, 8.4-10.0GHz 9-44821
- films, nucleation on MoS₂ single crystal 9-34992
- films, rough, optical stimulation of non-radiative plasmons 9-37415
- films, thin, abnormal absorpt. in vacuum and gas atmosphere 9-47347
- films, thin, surface roughness correl. with proton reson. radiation 9-44621
- films, thin evaporated, optical props. 9-47313
- films on plastic substrate, thermal conductivity 9-33192
- foil target, attenuation of heavy ions, obs. 9-28440
- fusing wires surrounded by air, energy balance 9-42694
- gamma ray scatt., 145 keV, differential elastic scatt. X-section 9-46263
- Gibbs free energy of self and impurity diffusion 9-33001
- growth, hydrothermal 9-37027
- Hall effect and phonon drag 9-43026
- hardening, stage III, temp. and strain rate depend. 9-39459
- impurities in As₂S₃ on conductivity 9-33295
- impurity in Cu, eff. on initial stages of growth 9-30525
- light scatt., nonradiative surface plasma waves excitation 9-41145
- magnetic domains due to de Haas-van Alphen effect pulsed n.m.r. studies of ¹⁰⁹Ag in single crystal 9-45393
- magnetoreflection meas. and optical dielec. function change 9-49246
- magnetoresistance, 4.2°K 9-44912
- microporous, in catalyst electrode for fuel cell, patent 9-31898
- m.l.s. system, I-V characts. 9-44997
- nucleation, heterogeneous, on W field emitter tip, electron microscopic obs. 9-48812
- phonon dispersion relation for symmetry directions 9-46970
- photoelectric emission in fair u.v. 9-43143
- photoelectric yield meas. with Laldem and electronic camera 9-45028
- photoemission, plasma resonance 9-33422
- plastic deform. of single cryst., stored energy 9-26325
- shock velocity, u_s , and particle velocity, u_p , in hydrostatic compression, applic. of interpolation formula for relationship between u_p and u_s 9-42871
- sintered electrode, microstructure changes after repeated low current cycling 9-31205
- sintering, role of plastic flow by dislocation motion in material transport 9-46916
- sintering of spherical particles under high press. 9-30728
- sols, prepared in nitrate melts, electron micrographs 9-36907
- solubility of C 9-44788
- spectral determ. in samples below reliable separation threshold, by plotting intensities of spectrogram lines 9-37854
- sputtering yield at low energies 9-33204
- stage I recovery, elec. resistivity and annealing 9-35083
- surface, (111), scatt. of isotopic He and H₂ beams 9-42713
- surface atoms in (100) and (110) faces of single crystal, mean displacement studies at low temps. 9-39248
- surface tension, 1300-2200°K 9-28110
- thermal diffusivity from linear dimens. changes 9-41097
- thermal expansion at low temp. 9-33188
- thin film on glass, elec. conductivity 9-24121
- thin films, opt. const. near plasma freq., influence of struct. 9-37680
- thin optical films, preparation method 9-22449
- work hardening between 77 and 1200°K, three stage curve 9-46926
- X-ray, K and L absorpt. spectra fine structure investigation 9-39855
- X-ray M absorpt. spectra in u.s. region, absorpt., coeff. depend. 17-200 Å 9-37754
- ϵ states energy band structure calc. by orthogonalized plane wave method 9-37400
- Ag-GaAs Schottky-barrier u.v. detector 9-43125
- Ag-Pb normal metal-superconductor junctions, proximity effect by electron tunneling 9-24166
- (Ag₂)_n clusters emerging from surface on bombard. with Kr ions 9-26618
- Ag⁺ centres in alkali halides, excitation and emission spectra, hydrostatic press. eff. 9-41401
- Ag⁺ mag. circular dichroism in Ag⁺-coped alkali halides 9-33508
- Ag⁺ activator in alkali halide crystals, optical struct. of luminescence centres 9-47387
- Ag⁺ centres in alkali halides, u.v. absorpt. spectra 9-43237
- Ag⁺ diffusion in borosilicate glass under elec. field, dendritic growth obs. 9-48872
- Ag⁺ in alkali halides, Ag⁺ mag. circular dichroism obs. 9-33508
- Ag⁺ in KCl, stress-induced dichroism in u.v. absorpt. bands, temp. depend. 9-45322
- Ag⁺ ion, analytical self-consistent-field wave function, cusp condition 9-22938
- Ag²⁺ in CdS, e.p.r. of photoinduced centres 9-47433
- Ag I spectrum, isotope shift meas., error sources and soln. 9-29987
- CdCl₂, Ag⁺ irradi., optical absorpt. and e.p.r. obs. 9-49272
- CdS:Ag, effective mass of free holes from reflectivity meas. 9-39618
- KCl:Ag, X-irrad., photostimulated luminesc., due to hole release from V_K centres 9-39897
- in KCl, e.p.r. spectra of stabilized atoms, temp. depend. 9-35714

Silver continued

- in LiCl, e.p.r. spectra of stabilized atoms, temp. depend. 9-35714
- in Na, molten, spin-slip scatt. of conduction electrons 9-32793
- NaCl:Ag, X-irrad., photostimulated luminesc. due to hole release from V_K centres 9-39897
- in NaCl e.p.r. spectra of stabilized atoms, temp. depend. 9-35714
- in Pb-Na solid solns., effect on discontinuous precip. 9-39500
- Te-Ag photovoltaic eff. on contact of thin films 9-35511
- Zn:Ag, diffusion of ¹¹⁰Ag, effect of dopant 9-40990
- Silver compounds**
- AgCl-AgI, molten eutectic mixture, thermoelec. props. 9-39089
- alloy, Se based, rectifier, conductivity asymmetry in impulse regime 9-41158
- alloys, dilute, Hall coeff., room temp. to 1.5°K 9-44911
- alloys, dilute, Hall coeff. and transport props. 9-37442
- chelates of glycine, DL α alanine, DL β phenylalanine and DL tyrosine, i.r. vib. spectra, assignments 9-23059
- halide phosphors, temp. quenching of luminescence, mechanism 9-33601
- halide photographic emulsion, spontaneously developable, amine borane constituent, patent 9-32077
- halides, aggregate centres, absorpt. spectra, oscillatory effect and fine struct. obs. 9-39370
- halides, B1-type, press.-induced phase transform., X-ray diffr. obs. 9-41063
- halides, diffusion by divalent ions 9-28314
- halides, f.c.c., mass transport 9-44729
- halides, flash and afterglow kinetics, ionic processes 9-33577
- halides, high resolution prod. of fine line originals, patent 9-27415
- halides, induced i.r. absorpt. due to bound polarons 9-46829
- halides, induced i.r. absorpt. due to excitons generated by band-to-band excitation 9-39830
- halides, melting curves at h.p. 9-44615
- halides, polaron effective mass, translational energy depend., cyclotron reson. obs. 9-39573
- molten alloys, elec. resist. from partial interf. functions 9-30422
- oxides, anodic formation 9-49383
- oxides, anodic formation 9-49382
- solid-solns., solute Knight shift and spin-lattice relax. 9-43295
- stirling Ag, effective atomic numbers for gamma interacts. 100-662 keV 9-24230
- Ag/Au/Si system, controlled solidification using monovariant eutectic reactions 9-36921
- Ag/Cu eutectic, rel. sputtering rates, temp. depend. 9-44851
- Ag-Au alloy, liq., elec. resistivity, form factors 9-39112
- Ag-Au alloys, diffusion of Ag, high temp. electrochem. method meas. 9-46841
- Ag-Au alloys, Kirkendall shift, press. and vacancy-flow effects 9-46848
- Ag-Au dilute alloys, de Haas-van Alphen effect studies, rel. to scattering temp. 9-37422
- Ag-Au layered struct. solid soln., X-ray diffr. static atomic displacements influence on diffuse intensity 9-37132
- Ag-Au solid soln., vibrational entropy and thermal vibrations, correlation 9-33151
- Ag-Au solid solns., lattice parameters 9-39247
- Ag-Bi eutectic, struct. of Ag-rich phase 9-37131
- Ag (0.26 at.%)Cu alloy, oxidized at 250 or 300°C, stress relaxations from internal friction spectra 9-48885
- Ag-Ca alloys, phase diagram over whole composition range 9-48937
- Ag-Cd alloys, activity meas., by atomic absorption 9-37855
- Ag-Cd β -phase alloys, order-disorder transf., Hall coeffs., elec. resistivity 9-35253
- Ag-Cs-O photocathodes, external field enhanced photoemission 9-37631
- Ag-Cu alloys, H₂S corrosion resistance enhanced by pressure deformation 9-30659
- Ag-Cu alloys, liq. and vapour quenched, metastable struct. obs. 9-40899
- Ag-Ge alloys quenched from melt, formation of faulted close-packed structures 9-40938
- Ag-Ge films, vapour-quenched on vitreous SiO₂, struct. anal by X-ray scatt 9-28213
- α -Ag-In dil. alloys piezoreflectance 9-47325
- Ag-In liq. alloy system, thermodynamics, Knudsen cell and mass spectrometric obs. 9-36860
- Ag-Mg solid solution alloys, Ag-rich, stored energy of cold work and elec. resistivity 9-48920
- Ag-Mn alloys, photoemission and optical studies rel. to electronic structure models 9-45033
- Ag-Ni solid solutions, initial states of Ni precipitation from superparamag. meas. 9-35212
- Ag-Pd alloys, plasma freq., residual resistivity, sp. ht. 9-37436
- Ag-Pd alloys, stacking fault densities from X-ray diffr. line profiles 9-40961
- Ag-Sn h.c.p. alloys, stacking fault energies 9-40960
- Ag (31 at.%)Zn alloy, elastic after-effect kinetics, resistance meas. 9-35161
- Ag-Zn alloys, thermodynamic activity of Zn, effect of free electron concentration 9-26477
- Ag-Zn alloys in solid soln., cold-worked state, X-ray diffr. study 9-46935
- Ag-Zn β -phase alloys, order-disorder transf., Hall coeffs., elec. resistivity 9-35253
- Ag-Zn equiatomic alloy, β' - β transform., stress effect 9-30737
- Ag-Zn equiatomic alloys, β' - β and β' - β' transform. 9-33145
- Ag-Zn system, mag. susceptibility of ϵ and η phase alloys 9-43150
- Ag (0.2-0.4 at.%)Al alloys, oxidized, internal friction meas. 9-48885
- Ag₂-S-Cu₂S solid solution on Cu-Ag alloy, cation distrib. on alloy oxidation 9-23656
- Ag₂CO₃, e.s.r. of γ -irrad. crystals 9-37791
- Ag₂O, elec. conductivity at high oxygen pressure 9-24116
- Ag₂S, heat capacity 9-39526
- Ag₂S, struct. transforms in thin films, compared with bulk state 9-48927
- Ag₂S, thermal conductivity, anomalous temp. depend. 9-30793
- β -Ag₂S defective order of cations 9-40929
- Ag₂S evaporated layer, diffusion processes obs. with photoemission electron microscope 9-40980
- Ag₂S formation, influence of AgBr surface structure on mechanism 9-37024
- Ag₂Se, struct. transforms in thin films, compared with bulk state 9-48927
- Ag₂Te, polymorphism, phase diagram determ. 9-46956
- Ag₂Te, solid and liq., transport props. 9-37519
- Ag₂Te, struct. transforms in thin films, compared with bulk state 9-48927
- Ag₂AsS₃, (proustite), crystallization from melt 9-37064

Silver compounds continued

- Ag₃AsS₃, (proustite), growth by Czochralski method 9-37065
 Ag₃AsS₃, elec. conductivity, dielec. const. and photoconductivity 9-39662
 Ag₃AsS₃, electro-optical coefficients meas. 9-31082
 Ag₃AsS₃, synthetic proustite, nonlinear optical props. and uses 9-31065
 Ag₃AsS₃ (synthetic proustite), nonlinear optical props. and upconversion of i.r. 9-26686
 Ag₃AsS₃, acoustic properties 9-30770
 Ag₃SbS₃, (pyrrargyrite), growth by Czochralski method 9-37065
 Ag₃SbS₃, (pyrrargyrite), crystallization from melt 9-37064
 Ag halide film and developing agents, exposed, activator and stabilizing solns. added, patent 9-22486
 Ag halide photographic emulsions rapid development method, patent 9-27420
 Ag halide vapours, u.v. absorpt. cross-sections 9-46376
 AgBiSe-AgBiS₂ system, high-temp. β -phase, X-ray and neutron diffr. studies 9-42782
 AgBr-I luminescent spectra of single crys. and of nucl. emulsion type Ya-2, photographic process 9-43251
 AgBr: Ni²⁺, illuminated, e.s.r. obs. of Ni⁺ 9-33621
 AgBr, brominated, acceptor ionization of neutral Ag vacancies from optical absorpt. obs. 9-41373
 AgBr, diffusion of chloride and iodide tracers 9-40979
 AgBr, edge emission spectrum temp. depend., 42-50°K 9-35680
 AgBr, epitaxial growth from melt, form. of oriented bubbles 9-48817
 AgBr, exciton and polaron states, dynamic piezo-optic study of absorpt. edge 9-39814
 AgBr, interstitial motion in diffusion 9-28312
 AgBr, optical absorpt. edge press. shifts 9-45312
 AgBr, photovoltaic effect nonlinearities 9-43134
 AgBr, polaron mobility, high temp. 9-43012
 AgBr, surface structure influence on mechanism of Ag₂S formation 9-37024
 AgBr crystals, photographic behaviour in developing process 9-25389
 AgBr dye-sensitized single crystals, photocond. mechanism 9-43126
 AgBr membranes, elec. cond. and diffuse double layer 9-31200
 AgBr phosphors, temp. quenching of luminescence Schon-Klasens and Lambe-Klick mechanisms 9-33602
 AgBr pure thin film, as particle detector 9-48231
 AgBr-Ag₂S phosphors, temp. quenching of luminescence Schon-Klasens and Lambe-Klick mechanisms 9-33602
 α -AgCd, Zener relaxation, activation energies 9-33025
 AgCd dil. alloys, electronic specific heat 9-26426
 AgCl: Cd single cryst., relax. of vacancy-dipoles 9-33372
 AgCl: Mn, potential difference at defects during plastic deformation 9-23877
 AgCl: Ni²⁺, illuminated, e.s.r. obs. of Ni⁺ 9-33621
 AgCl, absorpt. spectrum, exciton-phonon coupling effects 9-39831
 AgCl, crystal luminescence and photoelec. props. 9-33603
 AgCl, deform. of ions, X-ray obs. 9-30507
 AgCl, diffusion of Au⁺, low temp. suppression by chlorine 9-46847
 AgCl, diffusion of bromide and iodide tracers 9-40979
 AgCl, e.s.r. of Ni²⁺ and isotope effect in cry. field 9-43273
 AgCl, interstitial motion in diffusion 9-28312
 AgCl, latent hardening due to dislocations interact. 9-35191
 AgCl, luminescence, temp. quenching mechanism 9-28709
 AgCl, luminescence, u.v. laser excitation, spectral distrib. and decay, low temp. meas. 9-47388
 AgCl, optical absorpt. edge press. shifts 9-45312
 AgCl, Sr²⁺ diffusion, activation energy 9-46857
 AgCl, vacancy diffusion condition factor 9-28313
 AgCl, velocity of ultrasound, eff. of pressures up to 100 kbar 9-24023
 AgCl, vibration spectrum and thermodynamic functions 9-24009
 AgCl, zone refining indicating that blue lum. band is due to defects 9-35679
 AgCl aqueous solution, space charge limited ionic transport at solution interface 9-32833
 AgCl film, evaporation on C replica for NaCl electrical surface relief obs. 9-32848
 AgCl film, evaporation on C replica of Si p-n junctions for imaging 9-32847
 AgCl luminesc., u.v. excited, and photon multiplication, 80°K 9-26765
 AgCl photochromic glasses, properties 9-33521
 AgCl plates for infrared spectroscopy, restoration of transmission 9-36402
 AgCl sheets, high quality, prod. method 9-31723
 AgCl single crystals, etch pits, rel. to dislocation structure 9-46748
 AgCl transition-metal doped single cryst., relax. of vacancy-dipoles 9-33372
 γ , β -AgI, elec. conductivity and cryst. struct. 9-33379
 AgI, ht. capacity and order-disorder transition 9-39527
 AgI, luminesc. and photocond. sensitization by adsorbed pigments, obs. 9-26764
 AgI, nucleation and growth in gels 9-37029
 AgI crystals, ice and water nucleation 9-41510
 AgI crystals in large water drops, freezing temp. effect on 9-42697
 AgI cumulus seeding, effect on width-height ratios 9-33769
 AgI particles in supercooled water drops, de-activation 9-42696
 AgI sols., prepared in nitrate melts, electron micrographs 9-36907
 AgMn alloy, photoemission energy distrib. meas. rel. to impurity bound states 9-26613
 Ag(Mn) alloys, photoemission expts., rel. to virtual resonant bound states 9-45032
 AgN₃, explosion initiation by collapsing air bubble 9-28788
 AgNO₂, spin polarization in triplet state 9-37769
 AgNO₃-alkali nitrate molten mixtures, elec. cond. and density 9-23520
 AgNO₃, thermal expansion of orthorhombic and rhombohedral forms 9-35287
 AgO powders, electric resistivity, effect of added impurities 9-28545
 AgO soln. in acid, spectra resolution, 8000-13000 cm⁻¹ 9-27850
 Ag(Pd) alloys, photoemission expts. rel. to virtual resonant bound states 9-45032
 AgPd dil. alloys, electronic specific heat 9-26426
 AgSb₉Fe₁₀Te₂, semicond., resistivity and Hall coeff. determ. 9-24171
 AgSbS₃, miargyrite, artificial, n.g.r. of low temp α form 9-47451
 AgSbTe₃, Pelier effect at boundary between solid and liq. phases, determ. 9-45019
 AgSe-In solid soln. forming junction with Se layer, i.r. photocell 9-41274
 AgTe monocrystals, growth by chemical transport reaction 9-42759

Silver compounds continued

- α -Ag-Cd alloys, self-diffusion 9-33002
 Al(1 at.%) Ag alloys, dissociated prismatic dislocation loops, model verification 9-35091
 Al-Ag alloy, δ formation, small angle X-ray diffraction study 9-23947
 Al-Ag alloys, internal friction peak due to γ' phase precipitation 9-35152
 Al-Ag alloys, strength increase by strain-induced solute disposition stability control, eff. of additions 9-28360
 Al-Ag dilute alloy, impurity resistance, 1.2° to 300°K 9-30840
 Al-Ag dilute solid solutions, vibrational entropy, electronic influences 9-39508
 Al(15wt.%)Ag alloys, growth of h.c.p. γ plates, mechanism, e microscopy 9-30738
 Al-Cu-Ag, resistivity changes rel. to growth and dissolution of Ag-rich zones and vacancies 9-46758
 Al-Cu-Mg-Ag alloys, S precip. obs. 9-48928
 Au-Ag alloys, interdiffusion, effect of gradient energy 9-37199
 Cu-Ag alloys, oxidation and cation distrib. in Cu₂S-Ag₂S solid solution formed 9-23656
 Cu-Ag spectral lines, analytical, effect of additives 9-31228
 Cu-Ag surface alloy, rel. to fatigue strength of Cu 9-33058
 Cu₂Se, struct. transforms in thin films, compared with bulk state 9-48927
 Cu₂Te, struct. transforms in thin films, compared with bulk state 9-48927
 Li-Ag alloys, lattice parameters 9-42789
 NaCl-AgCl crystals, Raman scattering by resonant modes of Ag⁺ 9-28702
 NaNO₃-AGNO₃ melt, thermo-chains 9-30386
 Pd-Ag alloy films, effective surface coeffs., vol. diffusion effect in electron diff. obs. 9-39379
 Pd-Ag alloys, anisotropic impurity scattering rel. to Hall coeff. 9-37451
 Pd-Ag alloys, thermal expansion at low temp. 9-33188
 Pd-Ag dilute alloys, mag. susceptibility meas. 9-45069
 Zn-Ag dilute alloys, relax. time meas. from de Haas-van Alphen studies 9-37424

Sinanoglu's theory see Atoms/structure**Sintering**

- alumina powders, binary mixtures, kinetics 9-35230
 ceramics, phase-inversion and liquid-phase 9-35216
 diffusion coefficients determ., volume, grain-boundary and surface 9-42857
 ferrites, residual pores behaviour obs. 9-42921
 glass powder compacts, at constant rates of heating, from shrinkage data 9-33130
 glass powder compacts, shrinkage isotherms rel. to water vapour partial press. 9-33129
 glass powders, shrinkage by viscous deformation 9-35227
 liquid-phase, of two-phase alloy, microstructural development 9-42919
 topological approach 9-23962
 topology, algebraic and network, applic. 9-23934
 vacancy gradients generated, solute segregation obs. 9-23791
 wires, by surface diffusion 9-44783
 wires, by surface diffusion 9-44782
 Ag, material transport mechanisms, contrib. of creep 9-46916
 Ag spherical particles under high press. 9-30728
 Al₂O₃, recrystallization kinetics 9-33105
 Al₂O₃, irregular cryst. under high press. 9-30728
 Al powders, n.m.r. obs. of cryst. lattice distortions rel. to oxidation 9-47442
 Au particles, behaviour by electron microscopy 9-26365
 BeO powders, to >99% density 9-35231
 CoO, pure and doped, kinetics, O self-diffusion mechanism obs. 9-44731
 Cr₂O₃, surface and fracture study rel. to metal content 9-37279
 CuCr₂Se₄-Br₂ spinels, press. sintering 9-33126
 Fe, high purity prod. 9-39448
 Fe₂O₃, surface and fracture study rel. to metal content 9-37279
 Fe ore, reduction cracking obs. 9-33093
 Fe solid solns., isothermal shrinkage obs. 9-39449
 MgAl₂O₄ spinel, hot pressing behaviour 9-37076
 MgAl₂O₄ spinel ceramics 9-28389
 MgO, recrystallization kinetics 9-33105
 MgO irregular cryst. under high press. 9-30728
 NaCl, compared with related materials 9-35233
 NaCl, pressure, comments 9-26368
 NaCl powder, densification in air by plastic flow or volume diffusion 9-35232
 NbC-Co system, liquid-phase, rel. to microstructural development 9-42919
 NbC-Fe(Ni-Co) liquid alloys, carbide grain growth 9-34952
 Ni aluminates and ferrites, behaviour w.r.t. deviation from stoichiometry 9-30707
 NiO, pure and doped, kinetics, O self-diffusion mechanism obs. 9-44731
 PuC(P,S) powders, densification 9-35238
 ThC₂, coated particles preparation fluidized Bed. 9-41053
 UC₂, coated particles preparation fluidized Bed. 9-41053
 UC(P,S) powders, densification 9-35238
 UO₂-UN mixtures, behaviour 9-30730
 UO₂, initial phase study by Dorn method, comment 9-26369
 UO₂, sintered, thermal diffusivity and conductivity 9-26457
 UO₂ powders with high-surface-area, influence of atmosphere 9-33113
 UO₂, rel. to O/U ratio, obs. 9-37287
 W spherical particles under high press. 9-30728
 Y₂O₃:ThO₂, optical ceramic, prep., props. and applic. 9-33501
 ZnO, surface area decrease with isothermal heating to constant value characteristic at treatment temp. 9-35234
 ZrO₂, recrystallization kinetics 9-33105

Skin effect

- acoustic generation in conductors, approx. theory 9-42962
 in ferromagnetic conductors 9-38325
 metal, in mag. field, conductivity electrons collision with surface rel. to h.f. conductivity 9-49018
 metals, anomalous, surface impedance and boundary scattering 9-37426
 nonlinear, in plasma cylinder 9-48565
 plasma, cylindrical, e.m. field penetration 9-25881
 resistivity distributions, spatially inhomogeneous, skin effect obs. at various frequencies 9-27262
 skin depth determination by r.f. size effect 9-24110
 Bi, skin depth determination by r.f. size effect 9-24110
 Sn, supercond., freq. depend. of depth 9-37473
 Sn, superconducting, freq. depend. of depth 9-37473

Sky brightness

see also *Airglow; Twilight*

- angular and spectral distribution, effect of surface reflection 9-24661
- daytime above water, rel. to cloudiness and wind velocity 9-40025
- i.r. flux obs. and correl. with local conditions 9-41523
- noctilucent clouds, contrast with sky 9-45513
- photometers, calibration 9-26901
- radiance, model calc. 9-33776
- restoration of true fields, calc. 9-35823
- sun size influence on light distribution 9-33773

Slidrules see *Calculating apparatus***Slip**

- alloys, B2 type, fault energy created 9-42841
- b.c.c. metals, lattice geometry for true slip planes 9-33050
- between rolling ball and track, factors affecting contact conditions 9-31801
- cantilever laminated vibrating beam, energy dissipation 9-25090
- in crystals, dislocation movement as basic process 9-41025
- dislocation glide and climb motion superposition at high temps. 9-37180
- f.c.c., metals, character depend. on dislocation confinement, eff. on cyclic deformation and fatigue 9-30674
- hot rolling of strip, slip-line fields 9-23944
- links connection with stress distribution, dislocation structure and crack formation 9-26335
- in martensitic phase transformations under stress mechanism 9-33134
- in metals, b.c.c. 9-44769
- metals, b.c.c., controlled by Peierls mechanism, geometry 9-44710
- metals, f.c.c., accommodation of constrained deformation by slip and twinning 9-26281
- nucleation of persistent slip bands 9-33071
- Peierls mechanism controlled, geometry 9-44710
- plastic, developments of the concept 9-41024
- polyethylene, oriented, glide rel. to lamellae, out-of-plane deform. mechanism, obs. 9-28358
- polypropylene, oriented, glide rel. to lamellae, out-of-plane deform. mechanism, obs. 9-28358
- steel, martensite, internally twinned, slip dislocations movement 9-42828
- steel, mild, surface-rolled, slip line formation during fatigue, electron microscope obs. 9-35189
- surface layer form. during plastic deform., effect of steps 9-46895
- surface layer form. during plastic deform., role of steps 9-46896
- systems rel. to atomic/crystal structure 9-42888
- wedge, plastic, line field for deform. by rigid flat die under action of tangential force 9-25083
- Al-alumina alloys, slip bands and glide planes 9-37246
- Al-Zn-Mg-Cu alloy, deformed, rel. to intergranular stress corrosion cracking 9-23811
- Al single crystals, coarse model of crack formation and propag., rel. to fatigue 9-48904
- CdS, orientation effect on transient and steady-state creep 9-42885
- (92wt.%)Co-(8wt.%)Fe constrained deformation accommodation by slip and twinning 9-26281
- 20 wt.%Cr-35 wt.%Ni steel, creep-rate at low stress rel. to grain boundary sliding 9-48901
- Cu, coarse associated with strain bursts and cyclic hardening 9-28357
- Cu, cross-slip of screw components in fatigue-cell formation 9-23914
- Cu alloys, active volume of clusters 9-32983
- Cu single cryst., slip bursts during cyclic deform. 9-33052
- Cu single cryst., traces on surfaces, microscopy exam., w.r.t. non-conservative motion of dislocations 9-39365
- Cu single crystals, coarse model of crack formation and propag., rel. to fatigue 9-48904
- Fe-(49wt.%)Cr-(2wt.%)V, mode effects in brittle fracture 9-26356
- Fe-(3 wt.%)Si, alloy, polycryst., pressurization effect 9-33053
- Fe, neutron irradiated, analysis of band geometry 9-48860
- Fe single crystals, mechanism of plastic deformation 9-23884
- Fe single crystals hardness tests 9-35192
- Mg₃Cd single crystal, basal, 77° to 500°K, critical resolved shear stress 9-33054
- Mg single crystals, coarse model of crack formation and propag., rel. to fatigue 9-48904
- NH₄H₂PO₄, glide elements and dislocation reactions 9-42838
- NaCl, rel. to dislocation glide and climb motion superposition at high temps. 9-37180
- NaCl single crystal, formation during bending, optical polarization investig. 300° to 1.4°K 9-33036
- NaAl, stoichiometric, rel. to creep 9-28355
- Tl, h.c.p., modes 9-44770

Smectic phase see *Liquid crystals***Smokes** see *Aerosols***Snoek effect** see *Crystal imperfections/interstitials; Elastic relaxation***Snow**

- Antarctic, structure and composition with fissure detection, e.m. methods 9-33730
- fallout on ground attenuation of γ radiation by snow-cover 9-33797
- fallout on ground attenuation of γ radiation by snow-cover 9-24666
- flakes on mountain slope melting layer, size distribution 9-41514
- grain size determ. from density and one of light attenuation coeffs. 9-45464

Sodium

- absorption, optical, electron-electron interaction effect 9-49279
- arc temp. profile and radiation efficiency calc., relax. method 9-48643
- atmospheric, abundance and distrib. meas. by tuned laser radar at night 9-49466
- atom, 3p²P state, cross section for de-excitation by Ar 9-38780
- atom, deformation of K, L and M due to interaction with optical electron 9-44268
- atom, electron scattering, effect of long-range forces 9-27819
- atom, five-photon ionization, role of structure and radiation field 9-48412
- atom, impact ionization by electrons and protons, cross section obs. 9-34556
- atom, proton charge exchange bombard., H atom formation cross section 9-27813
- atom, spin-extended wavefunction 9-34547
- atom 3p^{1/2}-3p^{3/2} mixing induced in collisions with CH₄, CD₄, C₂H₂, C₂H₄ and C₂H₆ 9-44288
- atom in ammonia-ethylamine mixture solvents, electron spin resonance absorption 9-49355
- atomic cluster, ionization pot. obs. 9-29956

Sodium continued

- atoms collision ionization of H excited atoms 9-22992
- band structure parameters calc. from overlap integrals 9-35316
- binding energy of b.c.c. and h.c.p. phases 9-42737
- bubbles in cool liquid, sudden collapse 9-23595
- compressibility of b.c.c. phase 9-42737
- conduction-electron spin reson., pulsed-microwave studies 9-33629
- Debye-Waller factors, temp. depend. 9-35261
- diffusion and solubility of Au, 0° to 77°K 9-42861
- diffusion in RbCl, 377-707°K 9-23842
- diffusion in Si₃N₄ single-layer and Si/SiO₂/Si₃N₄ double layer films 9-26305
- diffusion of K, vacancy and interstitial mechanisms, computer calc. 9-44736
- elastic constants, temp. and pressure dependence 9-28332
- electron excitation from core bands during collision with fast primary electrons, energy and angular distribution of 9-31011
- electron-electron interaction effects on optical absorpt. 9-49279
- e.s.r., spin-flip scatt. cross-section for conduction electrons of impurity atoms 9-41345
- films, anomalous absorpt., rel. to bulk metal and effect of temp. 9-35631
- fluorescence quenching by Ar 9-38780
- forbidden transitions in isoelectronic sequence, relative line strengths 9-36653
- Hall coeff., accurate determ. from helicon waves and surface mode loss 9-24124
- heat transfer medium in capsules for fuel pins under irradiation 9-38739
- hyperfine interaction and Fermi surface electron wave depend. on cellular potential 9-39566
- interstellar, D line profiles in 77 stars 9-40154
- interstellar, D lines in spectra of 75 stars 9-43547
- isoelectronic series, theoretical ionization energies and oscillator strengths 9-22927
- in KBr, effect on colour centre production at 80°K 9-23827
- Knight shift, pressure depend. calc. 9-33647
- lattice bond energy and lattice constant, construction of crystal using quantum mechanics 9-42950
- liquid, conduction e.p.r., -200°C to +300°C 9-26133
- liquid, diffusion and electromigration of Cd and In 9-31201
- liquid, flow, rel. to induced e.m.f. along external mag. field (α -effect) 9-36899
- liquid, heat transfer from sphere during forced convection 9-26092
- liquid, nuclear spin-lattice relax. of ²³Na 9-26134
- liquid, optical absorpt., plasmon effect 9-44572
- liquid, self-diffusion coeff. 9-42643
- liquid, viscosity up to 1500°C 9-40780
- liquid suspensions with high solid concentration, flow properties 9-23544
- magnetoresistance, strain dependence 9-35343
- magnetoresistive effects, saturation and linear 9-37447
- muonic, 2p-1s X-rays obs., 2p pionic levels population determ. 9-44301
- optical absorpt. in new i.r., calc. 9-24414
- optical consts., 0.5-4.0 eV, by split-beam ellipsometry 9-49240
- resistivity, low temp. 9-37437
- scattering by alkali atom, spin-exchange cross section calc., partial-wave anal. 9-22984
- scattering resonance, on neutron spectrum, heterogeneity effect 9-27784
- in semiconductor device processing materials, flame spectrophotometric analysis 9-31223
- solubility in Si 9-40988
- spectrum, electron impact, generalized oscillator strengths 9-34543
- spin susceptibility, phase transform. effect 9-35538
- spin-flip scatt. of conduction electrons from impurities 9-32793
- structure when molten, neutron beam exam. 9-39075
- subcooled, heat transfer from hot spheres, and vaporization at surfaces 9-28116
- surface ionization on Re and oxygenated Re surface 9-35522
- thermal and electrical conductivity meas. between 35-98°K 9-42978
- in upper atmosphere, abundance and theory of origin 9-35832
- vapour, orientated, mag. reson., second order modulation of transversal light beam 9-22438
- vapour with Ar buffer, obs. of atomic dephasing collisions 9-29966
- void reactivity variations due to thin slab inhomogeneity in nuclear reactors 9-29884
- X-ray diffraction intensities, temp. depend. in range 115-353°K 9-23766
- yellow doublet in H-O-Ar flame, rel. to fluoresc. yield and excitation temp. 9-48379
- neutron spectra from spherical shell obs. 9-27783
- in Al₂O₃, sintered alumina, effect on glow curve 9-28728
- on Ar (100) surface, equilib. conc. 9-23616
- and Cs atomic beams, interaction 9-25713
- e.s.r., spin-flip scatt. cross-section for conduction electrons of impurity atoms 9-41346
- in N₂ arc discharge, spectral effects 9-46550
- Na-H₂, radiation generation depend. on Na and electron conc. in discharge 9-27324
- Na-H₂ laser, Na 4S_{1/2} population inversion and gain calc. 9-36293
- Na-He atomic collision, Na in ²P state, cross-section behaviour 9-29973
- Na-NH₃ gas mixtures, absorpt. spectra 9-34633
- Na-NH₃ solutions, complex dielec. constants as function of molar conc. 9-34918
- Na-NaCl system, light attenuation coeffs. calc. 9-39790
- Na-O₂ collision, obs. of charge transfer, ionization and rearrangement 9-23204
- Na, molten, spin-flip scatt. of conduction electrons from impurities 9-32793
- Na₂ dissociation energy 9-38922
- Na⁺, earth's atmosphere, measurements of reaction with ozone 9-40044
- Na⁺, in CaF₂, luminescence spectra, 4.2° and 77°K 9-33578
- Na⁺ concentration in Antarctic ice, obs. 9-33729
- Na⁺ energy levels calc. using step-like model potential function and perturbation theory 9-44243
- Na⁺ new model potential, suitable for liquids and solids 9-34518
- Na⁺ collision strengths for electron impact transitions 9-34563
- Na I 5682-88 Å and 4978-82 Å lines of plasma, Stark broadening 9-32413
- ²²Na and ²⁴Na diff. in f.c.c. Li₂SO₄ 9-33006
- ²²Na diffusion in Li/Na/KCO₃ near eutectic mixture 9-30625
- ²²Na in molten alkali nitrate salts, diffusion and ionic mobility meas. 9-34891

Sodium continued

- ^{23}Na , self spin-exchange cross-section meas. using microwave absorption between Zeeman sublevels 9-46314
 NaI multicounter goniometer, γ - γ angular correlation meas. 9-32262
 NaI(Tl) crystal, γ anticoincidence shielding at 0.661 MeV meas. 9-32243
 NaI(Tl) crystal counter, dimensions, background and peak efficiency, 0.2-4 MeV 9-32259
 Na-K mixture, ionization pot. of atomic cluster, obs. 9-29956
 Si-Na, ionization energy obs. from resistivity and Hall coeff. temp. depend. meas. 9-43077
 spectral lines, Stark broadening and displacement rel. plasma high temp. meas. 9-25913
 in Xe solid, absorption spectrum, multiplet struct. 9-22956

Sodium compounds

- additions to acetone and ethyl methyl ketone effect on u.v. absorpt. spectra 9-36888
 borosilicate glass, phase-separated, viscosity and transform. temp. 9-46680
 faujasites, synthetic, lattice parameter Al content dependence, framework ion ordering 9-44669
 formate, crystalline, Raman spectra 9-47378
 halides, F-centre emission energies and lifetimes 9-32999
 halides, $\text{Na}^+\text{L}_{2,3}$ absorpt. spectra 9-41385
 halides, surface ionization on Re and oxygenated Re surface 9-35522
 laurylsulphate solns., u.s. v.b. potentials as function of conc. 9-48694
 Na^{24}Cl , diffusion in $\text{NaCl}\cdot\text{H}_2\text{O}$, theory and meas. 9-23476
 NaBr-KBr solid solution films fundamental absorpt. spectra 9-28685
 NaN_3 , thermoluminescence, 15° to 300°K 9-43264
 $\text{NaNH}_4\text{SO}_4\cdot 2\text{H}_2\text{O}$ ferroelec. leconteite, n.m.r. 9-43301
 n.m.r. in single crystals. 9-33654
 rocksalt, thin films, electrical breakdown 9-33381
 salicylate, mag. field-dependent fluorescence 9-37767
 salts of glycine DL α -alanine DL β phenylalanine 9-23059
 soda-boric oxide glass, e.s.r. and optical spectra of Cu^{2+} 9-37800
 soda-lime glass diffusion of water near and within transform range 9-46854
 soda-silica glasses, Tm doped, Mossbauer effect obs. of Tm^{3+} crystalline elec. field parameters 9-37702
 sodium naphthalenide solns. in tetrahydrofuran, anomaly in e.s.r. spectrum 9-30427
 solid and molten, elec. cond. 9-30835
 substrate for CdSe and CdTe vapour phase deposits growth on cleavage face 9-46726
 thermal expansion meas. by liq. Ga immersion dilatometer rel. to anharmonic effects 9-47007
 zeolites, ^{23}Na and ^{27}Al quadrupole coupling constant changes on sorption 9-43300
 K-Na alloys, tensile deformation, yield and flow stress, conc. depend. 9-30664
 Li-Na system, immiscibility phase boundaries determ. from density meas. 9-40779
 Na/Li/KCO₃, diffusion of ^{22}Na and ^{14}C near eutectic mixture 9-30625
 Na-B-Si glass, spectra, Raman, e.p.r., i.r. and electronic 9-26757
 Na-C-O system, three-phase equil., thermodynamic analysis 9-39127
 Na-Cs binary alloys, electron spin susceptibilities, Knight shift 9-39116
 Na-K, liquid, turbulent in temp. fluctuations in flow field 9-23426
 Na-K liquid alloys, electromigration 9-30416
 $(\text{Na}_3\cdot\text{Li}_2)\text{NbO}_3$ solid solution ceramic, structure, dielectric and piezoelectric props. 9-26389
 $\text{Na}_2\text{Al}_2\text{Si}_2\text{O}_{10}\cdot 2\text{H}_2\text{O}$, natrolite, etching of cleavage faces 9-42745
 $\text{Na}_2\text{Fe}(\text{CN})_6\cdot 2\text{H}_2\text{O}$, nuclear effective-field-gradient and mean square displacement of Fe sites 9-24385
 $\text{Na}_2\text{Fe}(\text{CN})_6(\text{NO})\cdot 2\text{H}_2\text{O}$ frozen solns., Mossbauer effect 9-45299
 $\text{Na}_2\text{Mn}_2\text{Si}_2\text{O}_7$, crystal structure determ. by superposition method 9-40911
 $\text{Na}_2\text{O}\cdot\text{Al}_2\text{O}_3\cdot\text{SiO}_2\cdot\text{H}_2\text{O}$, hydrothermal crystallization, 250° , 350° , 450° , 550°C , pressures between 200 and 2000 9-40867
 $\text{Na}_2\text{O}\cdot\text{SiO}_2$ glass, alkali-ion movement, electron-probe microanalysis 9-34968
 $\text{Na}_2\text{O}\cdot\text{SiO}_2$ glass, luminescence spectra 9-39872
 $\text{Na}_2\text{O}\cdot\text{SiO}_2$ glasses, primary and secondary phase separation 9-30455
 $\text{Na}_2\text{O}\cdot\text{R}_2\text{O}_3\cdot\text{GeO}_2\cdot\text{H}_2\text{O}$ system (R=rare earth element), hydrothermal crystallization and crystal structure studies 9-40866
 $\text{Na}_2\text{Pd}(\text{CN})_4\cdot 3\text{H}_2\text{O}$ stacking of heavy atoms in crystals structure 9-35062
 $\text{Na}_2\text{S}_2\text{O}_3\cdot 5\text{H}_2\text{O}$ γ -irrad. single cryst., e.s.r. obs. of trapped radicals 9-35716
 $\text{Na}_2\text{S}_2\text{O}_4$, isothermal decomposition, concentration oscillations 9-24540
 Na_2SO_4 , X-irradiated, paramagnetic colour centers identified by ESR at 77°K 9-30616
 $\text{Na}_2\text{TeO}_3\cdot\text{Na}_2\text{CO}_3\cdot\text{H}_2\text{O}$ system, solubility at 25°C , obs. 9-40776
 $\text{Na}_2\text{W}_2\text{O}_{11}$, structure, p.m.r. investg. 9-45404
 Na_3AlF_6 evaporated film, refractive index, influence 9-33503
 Na_3VO_4 , solubility of YVO_4 and rare earth vanadates, crystn. conditions and structure 9-40777
 $\text{Na}_4[\text{Cu}(\text{NH}_3)_4][\text{Cu}(\text{S}_2\text{O}_3)_2]$, e.s.r. absorpt. curves, covalence effects on second moments 9-31167
 $\text{Na}_4\text{P}_2\text{O}_{10}$, glassy and crystalline, valence angles and dihedral angles rel. to structure 9-40906
 $\text{Na}_4\text{P}_2\text{O}_{10}\cdot 6\text{H}_2\text{O}$ growth from aqueous soln., influence of surface-active agents 9-37038
 $\text{Na}_4\text{P}_2\text{O}_{10}\cdot 14\text{H}_2\text{O}$, cryst. struct. 9-35061
 $\text{Na}_4\text{K}_{1-x}\text{TaO}_3$, optical phonons from i.r. Raman spectra, 4-600°K, rel. to dielectric phase transitions 9-47366
 Na_4WO_3 , reflectance spectra, specular and diffuse, rel. to electronic props. 9-31094
 Na salicylate, fluorescence radiation, angular distribution 9-45350
 NaAlF₆ molecule, electron diffraction study 9-48473
 NaAlF₆ molecule, electron diffraction study 9-44342
 NaBa₂Nb₂O₁₅, absorpt. spectra H impurity content obs. 9-41374
 NaBa₂Nb₂O₁₅, ferroelectric transition temp. variations on quenching 9-28562
 NaBa₂Nb₂O₁₅ and related mats., lattice vibr. spectra, Raman meas. 9-41079
 NaBi supercond. 9-49034
 NaBr:Ca²⁺ single cryst., paramag. centres, e.s.r. obs. 9-33633
 NaBr in aqueous solution, ^{23}Na and ^{81}Br n.m.r. relaxation times 9-32799
 NaBrO₃, n.a.r., press. and temp. depend. of ^{23}Na freq. 9-39928
 NaBrO₃ single crystal, Brillouin effect study 9-47381
 NaCl:Pr³⁺, electrolytically coloured, prod. and optical props. of centres 9-32992

Sodium compounds continued

- NaCl-KCl, differential thermal microanal. 9-28391
 NaCl, ionic conductivity, possible trivacancy mechanism 9-28552
 NaCl windows for CO₂ laser 10.6 μm radiation, power transmission 9-26675
 NaClO_3 , ^{35}Cl Zeeman quadrupole reson. 9-43269
 NaClO_3 , second-harmonic generation of light, total refl. phenomena 9-47310
 NaClO_3 , solution-grown crystals, mother-liquor inclusions formation at saturation 9-40862
 NaClO_3 crystals, transmitted and reflected second harmonic beams 9-26693
 NaClO_3 single crystals near critical temp., combination dispersion in Raman spectra 9-28703
 NaCn, neutron diffraction investig. rel. to model 9-28266
 NaCs, singlet ground state potential 9-38866
 $\text{NaD}_3(\text{SeO}_3)_2$ ferroelec. single cryst., H bond network and phase transition obs. from deuteron and ^{23}Na mag. reson. 9-33392
 $\text{Na}(\text{D}_2\text{H}_4)_2(\text{SeO}_3)_2$ system, phase diagram 9-30973
 $\text{NaF}\cdot\text{H}_2\text{O}$ (D₂), i.r. absorption due to localized vibrations of ions 9-30619
 NaF:U, luminesc. decay and fundamental series emission 9-35695
 NaF-LiF mixed cryst., ^{23}Na first-order quadrupole splittings, nucl. double reson. obs. 9-35735
 NaF, dislocation identification by electrolytic coloration and chem. etching 9-23814
 NaF, ENDOR hyperfine consts. and lattice distortion of V_K-type centres 9-46837
 NaF, e.p.r. of Mn^{2+} 4 spectra obs., spin-Hamiltonian method analysis, 93-573K 9-39908
 NaF, F centre fluorescence in single cryst., thermal quenching 9-33598
 NaF, γ -irrad., R=F₁⁺ centre conversion 9-40975
 NaF, lattice dynamics 9-46977
 NaF, M-centres reorientation, R-bands absorption decrease due to uniaxial plastic deformation of γ -irrad. crystals 9-26297
 NaF, positron annihilation 9-30830
 NaF, Raman spectrum, second-order, and lattice dynamics 9-35673
 NaF, surface phenomena and dislocations 9-23618
 NaF, thermal etching at 860-930°K 9-48787
 NaF, transition pressure for NaCl-CsCl struct., quantum mech. calc. 9-23985
 NaF, valence band calc. by tight binding method 9-48999
 NaF band structure and polaron theory F-centre electron wave function determ. 9-32327
 NaF F-centres, Stark effect of relaxed excited states 9-24392
 NaF X-ray photo effect of refraction of single crystal 9-39798
 NaF(u) phosphor, absorpt. and fluoresc. spectra 9-24455
 $\text{NaH}_2(\text{SeO}_3)_2$ crystals, unusual H isotopic effect 9-30973
 $\text{NaHSO}_4\cdot\text{KHSO}_4$ melt and glass, Mo V spectrum 9-37729
 NaI:Ga(In,Sn,Pb), absorpt., excitation and photoluminescence spectra 9-33590
 NaI:In centres due to O-containing impurities which reduce activator luminescence 9-33613
 NaI:NaCl, far-i.r. absorpt. spectrum rel. to gap and resonant modes assoc. with Cl-impurity 9-24413
 NaI:TI, recombination luminesc., characts. associated with fine substructure 9-39873
 NaI:TI centres due to O-containing impurities which reduce activator luminescence 9-33613
 NaI, energy-band calc. using combined plane-wave tight-binding, method 9-42998
 NaI, hyperfine structure, molecular beam electric resonance meas. 9-40600
 NaI slabs, γ -ray imaging props., detector scatt. effects, Monte Carlo calcs. 9-40458
 NaI thin film, far u.v. absorption spectrum obs. and interpreted 9-37730
 NaI(Tl), γ detection, photopoke efficiency meas. 9-29663
 NaI(Tl) detectors, imbedded into or external to cylindrical gamma source, efficiency 9-42135
 NaI(Tl) scintillation crystal, gamma photofraction functions 9-26782
 NaI(Tl) scintillation crystal calc. of no. of photons emitted per scintillation 9-29654
 NaI(Tl) total absorption detector for electrons and gamma-rays in 4-14 GeV range 9-32255
 NaK as heat transfer medium in capsules for fuel pins under irradiation 9-38739
 $\text{NaLa}(\text{MoO}_4)_2$ and $\text{NaLa}(\text{MoO}_4)_2\cdot\text{H}_2\text{O}$, prep. and X-ray structure study 9-40912
 NaNO_2 , far-i.r. reflectivity spectra, temp. depend. 9-41370
 NaNO_2 , ferroelec., i.r. absorption, temp. depend. 9-33163
 NaNO_2 , ferroelec., phase transition at -95°C , thermal expansion and dielec. const. obs. 9-35486
 NaNO_2 , neutron irradiated, ESR obs. 9-49354
 NaNO_2 , u.s. attenuation near critical pts. 9-44827
 NaNO_2 crystals, dynamical, scattering and dielec. props. 9-49141
 NaNO_2 ferroelec. transition, Pippard scheme for sp. ht., thermal expansion and isothermal compressibility 9-30970
 $\text{NaNO}_3\cdot\text{AgNO}_3$ melt, thermo-chains 9-30386
 $\text{NaNO}_3\cdot\text{Ca}(\text{NO}_3)_2$, molten, Raman vibr. freqs. of NO_3^- ion rel. to temp. 9-42662
 NaNO_3 -water solns., i.r. and Raman spectra rel. to NO_3^- symmetry, obs. 9-36887
 NaNO_3 -water solns., rel. to NO_3^- symmetry, obs. 9-36887
 NaNO_3 , cryst. surface distortion, i.r. data 9-48750
 NaNO_3 , growth of large single crystal by Kyropoulos method 9-35027
 NaNO_3 , molten, Raman vibr. freqs. of NO_3^- ion rel. to temp. 9-42662
 NaNO_3 , solns., u.v. decomposition, temp. eff. 9-24588
 NaNO_3 , thermal conductivity, diffusivity and permittivity anisotropy at phase transition 9-30796
 NaNO_3 molten, diffusion and ionic mobility of ^{23}Na , ^{133}Cs obs., temp. depend. 9-34891
 NaNO_3 molten, doped with monovalent nitrates, cationic mobilities 9-44586
 NaNO_3 structural change under shock compression 9-37303
 NaNbO_2F_2 , crystal structure and refinement 9-39289
 $\text{NaNbO}_3\cdot\text{BaNb}_2\text{O}_6$ system, liquidus and solidus equil. 9-39503
 $\text{NaNbO}_3\cdot\text{CdTiO}_3$ solid solns., struct. and dielec. props. 9-39695
 NaNbO_3 , crystal structure, comparison with ferroelec. phase 9-39290
 NaNiF_3 , orthorhombic canted antiferromag., mag. resonance and anisotropic g factors 9-45361
 NaNiF_3 , two forms obs. 9-44670

Sodium compounds continued

- NaNiF₂ single crystal, antiferromag. reson. in wavelength range 1.2-10 mm, fields up to 150 kOe, temp. 77-150°K 9-41421
 NaNO₃ crystalline powders, Raman scatt. cross-sections using Ar laser line at 4880 Å 9-41396
 NaOH-doped ice, dielec. props 9-39669
 NaOH dilute solns., heat transfer, from Pt wire, variation 9-46625
 Na-NH₃ solns., dielec. relaxs. 9-44582
 Pb-Na solid solns., discontinuous precip., Ag effect 9-39500
 Pb-(8.2 wt.%)Na solid solns., precip., three mechanisms 9-35210
 SiO₂-Na₂SO₄-Gd, use in Gd microquantities determ. 9-49323

sodium chloride

- additive coloration 9-32997
 adsorption of urea and PbCl₂ in octahedral pellets 9-48771
 anharmonic thermal vibrations, X-ray meas., 300° to 800°K 9-44812
 breakdown, intrinsic electronic to $\approx 240^\circ$, including thermal instability above 9-28554
 cleavage fracture along (110) faces and their etch patterns 9-48785
 cleavage surface, substrate for CdS film, rel. to structure 9-40840
 rel. to coal vacuum discharge spectral analysis, sensitivity improvement by NaCl addition 9-26845
 colloid evolution, mechanism 9-26296
 colour centre form. by 25 keV electron bombardment, colouration depth 9-44720
 colour centres due to ^{60}Co - γ -irrad. effect of gas adsorpt. 9-48869
 conductivity enhancement following plastic deformation (Gyulai-Hartly effect), a.c. dielec. meas. 9-33373
 containing CN $^-$, u.s. velocity and attenuation 9-37329
 crystal field in Na vacancy, appl. of lattice self-potential 9-36974
 crystal growth by Czochralski method, form. of two-dimensional nuclei on {001} faces 9-39212
 defect production by X-irrad. at 20°K, electron-hole recombination mechanism 9-26276
 dielectric relaxation effects due to air-gaps in specimen electrode contacts 9-37581
 diffusion annealing of bent crystal at 550-750°C causing straightening 9-42884
 diffusion coeff. of soln., determ. by pulsation method 9-44555
 diffusion of Kr, Xe and Rn, after irradi. by 10^8 to 2×10^{16} ions/cm² 9-48875
 diffusion of Mn²⁺, coeff. determ. by e.p.r. 9-30627
 diffusion of Na and ionic conductivity rel. to vacancy pairs, obs. in applied elec. field 9-44740
 dislocation density in deformed single cryst. 9-32974
 dislocation etch figures, effect of neutron irrad. on dimensions 9-40945
 dislocation glide and climb motion superposition at high temps. 9-37180
 dislocations, viscous drag and densities 9-37179
 elasto-optical and piezo-optical coeffs., temp. depend. 9-39813
 electric breakdown development investig. 9-43109
 electrical conductivity, low temp. of Ca-doped crystal, precipitation influenced 9-37577
 electrical relief of surface by AgCl evaporation on C replica 9-32848
 electron-irradiated during microscope exam., point defect coagulates obs. 9-42808
 electronic structure calcs., point defects in ionic crystals 9-40928
 electrostrictive coeffs., calc. using theory for ionic non-piezoelec. ionic crystal composed of point charges 9-47186
 e.p.r. obs. of Mn²⁺ ground state splitting, elec. field effect 9-43284
 etching mechanism, interdependence of poison and undersaturation of solvent 9-28227
 evaporation fronts in (100) surfaces, movements 9-30517
 F centre, electronic structure calc. 9-40973
 f centre, lattice dynamics rel. to electronic Raman spectra and lattice and electronic absorption 9-35118
 F centres formation, thermoluminesc. obs. 9-33606
 F-aggregate centres, charged, absorpt. and emission band obs. 9-35119
 F-center build-up due to π irradiation, source of vacancies 9-32987
 F-center production on vacuum u.v.-irradiation, photostimulated e. emission obs. 9-30617
 F-centres, ENDOR spectroscopy, elec. field effects 9-35734
 F-centres, Stark effect of relaxed excited states 9-24392
 formation and luminescence of Eu⁺ 9-26768
 grain boundary structure and mechanical strength, infl. of crystal orientation 9-26340
 growth, vapour phase, molecular processes involved 9-37009
 growth in H₂O soln. with Mn²⁺, X-ray diffr. topographs 9-37144
 growth surfaces, effect of surface-active impurities on microstructure 9-2376z
 heat capacity, 30°-500°C 9-24047
 hyperfine spectrum by molec.-beam elec. reson. 9-44343
 ions deform., X-ray obs. 9-30507
 irradiated, stored energy and release rel. to colour centre conc. 9-46839
 laser beam self-bending in cryst. 9-47327
 nucleation in (100) orientation, electron microscope study 9-37103
 phonon dispersion relations from n.scatt. meas. at 80 and 300°K 9-24021
 piezo-optical and elasto-optical coeffs., temp. depend. 9-39813
 plasma instability during electrical breakdown, formation of gas bubbles 9-41235
 plastic properties of single crystal, optical polarization investig., 300° to 1,4°K 9-33036
 point defect coagulates due to electron irrad. during microscope exam. 9-42808
 point defects in crystals producing cellular substruct. 9-44686
 polygonization of single crystal surfaces by electron bombardment 9-30513
 powder, densification in air, during sintering by plastic flow or volume diffusion 9-35232
 pressure sintering, comments 9-26368
 proton energy distribution and channelling in lattice 9-30809
 Raman spectra, second-order 9-39852
 rock salt crystals, tensile strength rel. to surface preparation 9-41027
 sintering compared with related materials 9-35233
 solubility of free Cd²⁺, ionic conductivity meas. 9-30626
 solution, weak aqueous, heat of vaporization 9-26161
 solution in water-organic mixtures, liq.-liq. equilibrium 9-32765
 stress relaxation, dislocations mechanism, -196°-150°C 9-33026
 substrate for Ag epitaxy and nucleation 9-23689
 substrate for CdSe and CdTe vapour phase deposits growth on cleavage face 9-46726

Sodium compounds continued**sodium chloride continued**

- substrate for epitaxial growth of PbTe thin films, substructural transitions in early stages 9-26186
 surface phenomena and dislocations 9-23618
 thermal expansion, X-ray diffr. meas. temp. depend. rel. to Schottky defects conc. 9-37360
 thermal expansion at high-temp., X-ray diffraction study 9-30786
 thermodynamic properties, anharmonic effects, data analysis 9-24048
 thermoluminescence, F centres formation 9-33606
 thermoluminescence glow curves, kinetic order and actuation energy anal. 9-49328
 transition pressure for NaCl-CsCl struct., quantum mech. calc. 9-23985
 U₂-centre, wave function and isotropic h.f.s. 9-42850
 vacancies, cationic, formation energies 9-42811
 void formation and migration in a single crystal subject to a temperature gradient 9-32950
 whiskers, elec. conductivity, 150-600°C 9-28551
 whiskers, regrowth from pure and poisoned solutions 9-37039
 Au evaporated film, effects of forced high nucleation densities 9-32843
 Au film epitaxial and polycryst., rel. to H₂O contamination 9-46724
 Ca-doped, low temp. conductivity precip. influenced 9-37577
 elec. fields and polariz. prod. by defect charge density, lattice summations 9-33215
 KCl-NaCl solid soln., enthalpies of crystallisation, anomalies in struct. obs. 9-37161
 KCl, e.p.r. of stabilized Cu and Ag atoms, hyperfine and superhyperfine struct. consts., temp. depend. 9-35714
 Na-NaCl system, light attenuation coeffs. calc. 9-39790
 Na nucl. mag. energy levels in rotating frame, acoustic excitation 9-35601
 NaCl:Ag, recombination luminesc., characts. associated with fine substructure 9-39873
 NaCl:Ag, X-irrad., photostimulated luminesc. due to hole release from V_k-centres 9-39897
 NaCl:Ag, X-ray luminesc. build-up, obs. 9-35698
 NaCl:BaCl₂ crystals, dislocation density effect on ageing, elec. conductivity meas. at 550°C 9-46929
 NaCl:Ca²⁺, OH $^-$, optical absorpt., impurity assoc. effects 9-37728
 NaCl:Ca²⁺, V-centres rel. to x-ray irrad. temp., e.s.r. obs. 9-30618
 NaCl:Ca²⁺, single crystal, paramag. centres, e.s.r. obs. 9-33633
 NaCl:Ca(Cd), Na⁺ diffusion and ionic conductivity 9-39672
 NaCl:Ca(Cd), thermoluminesc., F centres formation 9-33606
 NaCl:CdCl₂, dipole aggregation, kinetics 9-39356
 NaCl:Cu, additively coloured with Na vapour, colloidal absorpt. bands 9-32998
 NaCl:Cu, recombination luminesc., characts. associated with fine substructure 9-39873
 NaCl:Cu, NaCl:Cu:Ag recombination luminescence, trapping of electrons and holes detect. by EPR meas. 9-33587
 NaCl:Cu⁺, i.r. absorption, resonant mode broadening 9-33164
 NaCl:Cu⁺, stress-induced dichroism in u.v. absorpt. bands, temp. depend. 9-45322
 NaCl:Dy³⁺ luminescence spectra obs. to gauge changes taking place during electrolytic colouring 9-32996
 NaCl:Fe from melt, X-ray luminesc. 9-37772
 NaCl:Mn²⁺, irrad., X- and K-band spectra, paramag. Mn centre 9-35715
 NaCl:Ni, influence of impurity on dielectric loss 9-35467
 NaCl:Ni, precipitated particles obs. with electron microscope 9-40910
 NaCl:Ni²⁺, absorption spectrum 9-39842
 NaCl:OH $^-$, rot. barrier height 9-40935
 NaCl:Pb, u.v. absorpt. spectrum correl. with Rayleigh scatt. 9-45328
 NaCl:Pb²⁺, dielectric loss, optical absorption and emission spectra, effect of vacancy pairs aggregation 9-31108
 NaCl:Pb phosphor, luminescence obs. 9-33593
 NaCl:Sr²⁺, thermoluminesc., glow curves and phosphoresc. centres form. obs. 9-37773
 NaCl:Ti³⁺, electron-lattice interaction, absorption spectra meas. 9-41386
 NaCl:BaCl₂ single crystal, pulled from melt, oriented impurity precipitates 9-30601
 NaCl-KCl mixed crystal phosphor, luminescence obs. 9-33588
 NaCl, electrostatic pots. and spatial deriv. about pt. defects 9-33214
 NaCl-AgCl crystals, Raman scattering by resonant modes of Ag⁺ 9-28702
 RbCl, F $^-$ -centre accumulation due to proton irrad., 78°-380°K 9-30620
 ZnS structures, i.r. localized modes, shell models 9-23800
 ZnSe coated beam-splitter for CO₂ laser 9-48099

Sofar see Sound ranging**Sogicons** see Semiconducting devices**Soil**

- basalt on steel, friction obs. at ultrahigh vacuum 9-37271
 creep, rheological model considering structural transformations 9-26332
 failure criterion, angle of internal friction 9-39433
 filtering parameters effect on horizontal drainage 9-42644
 heat flux and temp. profile calc. from thermal diffusion model 9-31254
 inhomogeneous, friction of air currents 9-31301
 lunar, particular thermophysical model 9-36016
 lunar, structure and mech. props. determ. by automatic stations 9-27071
 lunar, surface sampler 9-40171
 moisture measurement by neutron moderation, depth and surface probes 9-35765
 permeability determinations in Rumania 9-35797
 psychrometer for meas. relative humidity 9-33732
 stratified, nonhomogeneous, water filtering 9-43364
 water evaporation, vertical flow eqn. and flow meas. 9-34854

Solar activity see Sun; Sunspots**Solar batteries** see Electricity, direct conversion**Solar cells** see Electricity, direct conversion/solar cells**Solar constant** see Sunlight**Solar corona** see Sun/corona**Solar corpuscular streams** see Sun/radiation corpuscular**Solar eclipses** see Sun/eclipses**Solar flares** see Sun/flares**Solar furnaces** see Heating; High-temperature phenomena and effects**Solar noise** see Sun/radiation, radiofrequency**Solar prominences** see Sun/prominences

Solar system

- see also *Planets, etc.*
 asteroids in resonance with Jupiter, secular motion analysed 9-24850
 eclipses, book 9-33893
 essays on origin, the earth's interior, comets, tektites and Neptune 9-41671
 evolution, modern theories 9-43609
 exploration, collection of popular review articles, book 9-49574
 formation, from the mechanism of loss of angular momentum from proto-sun 9-45659
 origin, collection of popular reviews, book 9-49575
 perturbations in the solar system, elementary book 9-43512
 spectrum, 21 cm line emission, 1200 profiles 9-31585
²⁴⁴Pu abundance in early system, rel. to continuous galactic nucleosynthesis theory 9-45658
¹²⁹I abundance in early system, rel. to continuous galactic nucleosynthesis theory 9-45658

Solar wind see *Sun/radiation, corpuscular*

Solid solutions

- see also *Alloys; and under compounds of the individual elements. Solid solutions such as Au-Cu, Au-Cu-Zn are indexed under compounds of the named elements, i.e. 'Gold compounds', 'Copper alloys', 'Zinc compounds' in these examples*
 alkali chlorides, fund. absorpt. in extreme u.v. 9-35662
 alkali-rare earth niobates, dielec. props. rel. to crystal chemistry 9-24210
 alnico, decomposition of alloy from X-ray meas. 9-39473
 BaTiO₃-SrTiO₃ dielec. const., reversible, depend. on field strength above Curie point 9-41239
 benzil in stilbene, trans-planar config. of benzil from polarization characts. of spectra 9-34660
 binary, coherency loss during ageing, X-ray exam. 9-30711
 β brass, X-ray diffr., static atomic displacements influence on diffuse intensity 9-37132
 (CuMn₂O₄)₂(AFe₂O₄)_(1-x), magnetic and electrical props., where A=Cu²⁺, Ni²⁺, Zn²⁺, Co²⁺ or Ni²⁺ 9-30834
 dendrites, axial parts, effect of cooling rate during crystn. on composition 9-48814
 dicalcium strontium propionate-acetate mixed cryst., 6(1-x)(CH₃COO)_{6x}, ferroelec. hysteresis loops 9-35481
 dilute, in alloys, equations of general appl. 9-42914
 dilute, in alloys, equations of general appl. 9-42915
 dilute, in alloys, equations of general appl. 9-42913
 elastic free energy, microscopic theory 9-37288
 energy transfer by virtual excitons, Agranovich expression averaged for ensemble of mols. 9-49003
 (α-Fe₂O₃)_{1-x}(Cr₂O₃)_x, magneto-chem. study of formative conditions 9-49189
 ferrimagnetic spinels, cation distrib., temp. depend. 9-35737
 ferroelectric with perovskite struct., u.s. wave absorption and velocity, temp. depend. 9-41084
 hafnia-rare-earth oxides, separation of metastable to stable phase 9-30723
 hardening due to size effect 9-46927
 internal friction due to precipitation 9-33021
 metal oxide, formed on alloy oxidation, cation distrib. 9-23656
 Metal sulphide, formed on alloy oxidation, cation distrib. 9-23656
 Methane-methane-d, solid soln., upper transition, quantum statistical treatment 9-48933
 naphthalene, molecular admixture, relation between emission spectrum and solubility 9-28719
 ordered, equilb. vacancy conc. 9-42809
 organic luminors, e excitation energy transfer 9-35688
 oxide particles in metal matrix, coagulation 9-44787
 periclase solid soln. containing Li⁺ and R³⁺ (Cr, Al, Fe) ions 9-23955
 perovskites, complex, s.h.f. dielec. props. 9-39678
 pseudobinary (III-V)-(II-VI) systems, and optical energy gaps 9-35205
 rare earth oxides, in binary systems, behaviour during crystallization by Verneuil method 9-37062
 solute segregation in vacancy gradients generated by sintering and temp. changes 9-23791
 β-spodumene-silica, thermal expansion, lattice parameters of spodumene 9-26431
 (Sr, Bi_{2/3})TiO₃-CaTiO₃ system, dielec. props. 9-41231
 substitutional, relax. time model for short-range order changes and Zener relax. 9-46870
 supersaturated, in Mg alloys, effect of decomposition on u.s. attenuation 9-46990
 thermodynamic activities calc. using point defect conc. 9-30714
 transition metal phosphides, crystallographic and mag. props. 9-44676
 zirconia-rare-earth oxides, preheating products obs. 9-30724
 zirconia-rare-earth oxides, separation of metastable to stable phase 9-30723
¹²⁹I, frozen solns., Mossbauer determ. effect 9-31089
 Ag-Au, lattice parameters 9-39247
 Ag-Au layered struct. X-ray diffr., static atomic displacement influence on diffuse intensity 9-37132
 Ag-Mg alloys, Ag-rich, stored energy of cold work and elec. resistivity 9-48920
 Ag-Ni, precipitation of Ni, initial state, and vel. const. from superparamag. meas. 9-35212
 Ag-Zn alloys, X-ray diffr. study of cold-worked state, faults and dislocations 9-46935
 Ag-base, solute Knight shift and spin-lattice relax. 9-43295
 α-AgCd, Zener relaxation, activation energies 9-33025
 Al-($<0.22\text{at.}\%$)Ti, lattice parameter comp. dependence 9-42918
 Al-Cr, dil., mag. susceptibility and sp. ht. w.r.t. localized d-state props. 9-33269
 Al-Cu-Cr, supersaturated, kinetics of decomp. 9-46937
 Al-Mn, dil. mag. susceptibility and sp. ht. w.r.t. localized d-state props. 9-33269
 Al-V, dil., mag. susceptibility and sp. ht. w.r.t. localized d-state props. 9-33269
 Al-Zn, plastically deformed single cryst., dislocation distrib. 9-39364
 (1-x)Al_{1-x}LiO₃-xGeAlLiO₄ spinel phase, stability domain boundaries 9-33119
 Al₂Ga_{1-x}As_x, with forbidden band width gradient, recomb. radiation 9-47389
 Al-Fe, enhanced Fe solubility by rapid quenching 9-42916
 Au-Si, precipitation effect on i.r. vibration spectrum of O 9-45315
 Au-base, solute Knight shift and spin-lattice relax. 9-43295
 (Ba,Sr)TiO₃, u.s. wave absorption and velocity, temp. depend. 9-41084

Solid solutions continued

- BaSO₄-SrSO₄-PbSO₄, subsolidus phase relations and lattice constants 9-23949
 Ba(Ti,Zr)O₃, u.s. wave absorption and velocity, temp. depend. 9-41084
 BaTiO₃-CdTiO₃ single crystals, elec. props. 9-47172
 BaTiO₃-Co-Ta₂O₇, s.h.f. dielec. props. 9-47174
 BaTiO₃-Co-Ta₂O₇, s.h.f. dielec. props. 9-39689
 BaTiO₃-Ni₂Nb₂O₇, s.h.f. dielec. props. 9-47174
 BaTiO₃-Ni₂Nb₂O₇, s.h.f. dielec. props. 9-39689
 BaTiO₃-SrTiO₃-BaSnO₃, semiconducting props. 9-41192
 Bi₂Te₃(20 Mol.%)Bi₂Se₃, thermoelec. props., conc. inhomogeneities influence 9-41252
 BiFeO₃-Pb(Fe_{1-x}Nb_x)₃O₇, spontaneous magnetic moment by neutron diffraction 9-33482
 Ca-Al, stacking fault energy influence on high temp. creep 9-42886
 Ca-Yb system, b.c.c. and f.c.c. characts., 900-400°C 9-30716
 Ca-3wt.%Al-0.6wt.%Cu alloy, structural changes during precipitation of hard soln. 9-44789
 CaF₂-AlF₃ system, phase diagram, DTA and X-ray powder obs. 9-44805
 CaTiO₃-based, conc. depend. and temp. coeff. of dielec. const. 9-39663
 Cd-Hg alloys, phase equl. and transform., thermodynamic investigations 9-48878
 Cd_{1-x}Hg_xTe, fund. reflectivity spectrum, 1.5-4 eV, band struct. obs. 9-45306
 Cd_{1-x}Hg_xTe cryst., prep. by vertical-zone melting method 9-46755
 Ce-S, transition metal doped, thermal conductivity, temp. depend. 9-37368
 Co-(7.45 wt.%)Ti, γ-phase precip. during ageing, neutron diffr. and chem. analysis 9-41065
 CoSe₂-S₂ single crystals and powder magnetiz. and susceptibility meas. 4.2° to 300°K 9-47245
 Cu-(16 at.%)Al, high temp. creep behaviour 9-33043
 Cu-Al, stacking fault energy influence on high temp. creep 9-42887
 Cu-Co, magnetic hysteresis rel. to ageing time 9-26622
 Cu-Co single cryst., plastic behaviour w.r.t. precip. state 9-39428
 Cu-Fe, homogenous decomposition 9-48930
 Cu-Ga, width of split dislocations, effect of near order 9-42827
 Cu-Mg, dilute, binding energy between dislocation and Mg atom 9-37175
 Cu-Zn, Ge-Ga solid soln. hardening 9-39472
 Cu-base, dislocations, degree of splitting and anomalous after-effect 9-32968
 Cu₂S-Ag₂S on Cu-Ag alloys, cation distrib. on alloy oxidation 9-23656
 Cu₂Al, X-ray diffr., static atomic displacements influence on diffuse intensity 9-37132
 Cu(36wt.%)Zn, with Fe and P, boundaries between 600 and 350°C 9-30717
 Dy(ClO₄)₃ in ice, Mossbauer spectra 9-33532
 α-Fe-CN-N, permeability disaccommodation, -40° to +180°C 9-26322
 Fe-Mo, creep behaviour, temp. and stress depend. 9-30669
 in Fe-Ni-Al alloys, decomp. of supersaturated solns., elastic stresses effect 9-39475
 Fe-Si, resistivity and Matthiessen's rule deviations 9-41167
 Fe, sintering procedure contrib. 9-39449
 Fe₂O₃/Mg₂Fe₂O₄(x-1/2) spinel system, ferrimag., cation distrib. and temp. depend. in magnesioferrite 9-35737
 Fe₂Ge₂Mn₂Ge₂, saturation magnetiz. meas. and Curie temp. 9-45065
 (1-x)Fe_{1-x}LiO₃-x(GeFeLiO₄) spinel phase, stability domain boundaries 9-33119
 Ga_{1-x}In_xSb, growth and characterization using temp.-gradient zone melting 9-30719
 GaAs_{1-x}P_x cryst. growth from Ga-rich soln., lattice distortion and atomic struct. obs. 9-35206
 Ge-As, defects during precip., nature 9-44682
 Ge-As, new phase precipitation mechanism 9-35243
 x(GeLiO₂)₂-GeZn₂O₄ spinel phase, stability domain boundaries 9-33119
 GeTe-Sb(Bi)Te, carrier energy spectrum of GeTe, changes due to soln. form. 9-47113
 H₂C-TaC system thermal expansion 9-26430
 InAgSe, forming junction with Se layer, i.r. photocell 9-41274
 InAs-ZnSe, conductivity, carrier mobility and conc. and thermo-e.m.f. 9-44962
 InSb_{1-x}Bi_x, Hall effect, elec. conductivity, band gap obs. 9-43058
 KBr-KCl film, fundamental absorpt. spectra 9-28685
 KBr-NaBr film, fundamental absorpt. spectra 9-28685
 KBr-RbBr film, fundamental absorpt. spectra 9-28685
 KCl-KaCl, enthalpies of crystallization, anomalies in struct. obs. 9-37161
 La-Ce dilute, Kondo phenomenon 9-44913
 La-Pr dilute, elec. resistivity and effective mag. moment, rel. to Pr conc. 9-45066
 LaTe₂-LaSb₂, Sb substitution effect on resistivity and thermoelec. power 9-39639
 Mg-Sn alloys, hardening, room temp. 9-23984
 Mg₂Ge-Mg₂Sn, lattice thermal conductivity 9-33199
 Mg₂Si-Mg₂Sn(Ge), lattice thermal conductivity 9-33199
 MgO-chromite, lattice spacings rel. to chromite addition 9-32921
 in MgO, cation solns., Mg_{1-x}(R⁺R²⁺)O type 9-39477
 MgTe-CdTe, new material for visible light-emitting diodes 9-47418
 Mn₂Cr_{1-x}S_x, sign and size of exchange integral, evaluation from neutron diffr. and magnetic structure study 9-28615
 MnO/CoO, dielec. const., loss and conductivity meas. w.r.t. freq. 9-35465
 MnO/NiO, dielec. const., loss and conductivity meas. w.r.t. freq. 9-35465
 Mo-(10wt.%)Fe, precipitation processes after rapid cooling 9-35207
 NaCl-KCl, differential thermal microanal. 9-28391
 NaNbO₃-CdTiO₃, struct. and dielec. props. 9-39695
 Nb, hardening eff. of Ta, V and W additives, theory and expt. 9-28385
 Nb hydrides and deuterides, interstitial ordering 9-23990
 Ni-C, Curie temps. and residual resistivities 9-44914
 Ni-Cu, ferro- to paramagnetic transition obs. 9-35554
 Ni-Re alloy film, electro-deposited, phase and chemical composition 9-44791
 Ni₂Fe, alloyed with Cr, Mo and W, atomic ordering effects 9-39297
 NiO-Cr₂O₃ on Ni-Cr alloys, cation distrib. on alloy oxidation 9-23656
 Pb-Ge chalcogenide alloys, and optical props. 9-30721
 Pb-Na, discontinuous precip. Ag effect 9-39500
 Pb-(8.2 wt.%)Na, precipitation three mechanisms 9-35210
 PbF₂-AlF₃ system, phase diagram, DTA and X-ray powder obs. 9-44805
 PbTe-EuTe system, investigation by thin film techniques 9-39486

Solid solutions continued

- PbTiO₃-LaFeO₃ magnetic props. 9-39784
 PbTiO₃-PbZrO₃-PbMg_{0.5}W_{0.5}O₃ piezoelec. props. 9-47188
 Pb(Zr,Ti)₂O₇ atomic struct. of 2 rhombohedral ferroelec. phases 9-44673
 Pd-Fe system, γ -phase, thermodynamic props. 9-30753
 Pd-Pt system, γ -phase, thermodynamic props. 9-30753
 Pt-Fe, dil., interac. of quenched-in vacancies with Fe atoms 9-26278
 Pt-Fe system, γ -phase, thermodynamic props. 9-30753
 Pu-Nd, thermal, micrographic and X-ray diffraction examinations 9-28386
 Pu-Pr, thermal, micrographic and X-ray, diffraction examinations 9-28386
 Pu-Sm, thermal, micrographic and X-ray diffraction examinations 9-28386
 RbBr-RbI solubility gap, equilb. phases for moist solid soln. 9-35211
 Rh₂Cu₃Ni_{1-x}O₄, new orthorhombic phase with $0.12 \leq x \leq 0.175$ 9-30704
 Ru-Ni, precipitation of Ni, initial state and vel. const. from superparamag. meas. 9-35212
 Se-Te, edge absorpt. and band gap obs. 9-43250
 Si, epitaxial, behaviour of group III-V impurities 9-44984
 SmFe₂-DyFe₂ single crystal, spin reorientation, 2° to 500°K 9-45235
 SnCl₂ in ice, Mossbauer spectra 9-33532
 (Sr,Bi,Li)₂MnO₃ new ferroelec.-ferromag. material 9-47178
 (Sr,Bi)₂MnO₃ new ferroelec.-ferromag. material 9-47178
 (Sr,Bi_{2/3})TiO₃ u.s. wave absorption and velocity, temp. depend. 9-41084
 Ta hydrides and deuterides, interstitial ordering 9-23990
 ThC-ThN m.p. and excess free energy of mixing at 2820°C 9-40819
 ThC-UC, 3, 8 and 15 metal % U, elec. props. 9-26510
 ThP-UP, synthesis, lattice parameters and melting points 9-33123
 in TI, binary and ternary, supercond. transition temp. 9-23989
 UC-UN m.p. and excess free energy of mixing at 2820°C 9-40819
 UP-US, mag. props. 9-45117
 V-O, degassing kinetics 9-39942
 V hydrides and deuterides, interstitial ordering 9-23990
 Zn-Cd alloys, solute trapping by rapid solidification 9-26160
 Zn,Hg_{1-x}Te, Hall coeff. and elec. conductivity 77°-400°K, 250-10000 Gs 9-30913
 Zr-O, sintered, electron work function 9-39734

Solidification *see* Freezing**Solids**

- see also Crystals; Films, solid; Metals; Plastics; Powders; Semiconductors; Vitreous state*
 dimethylglyoxime, van der Waals forces and H bond calcs. 9-40853
 high temperature, bibliography 9-41718
 optical absorpt. meas., elimination of surface refl. effects 9-33519
 spectra, calculating method 9-24390

structure

- see also Crystal structure; Electron diffraction examination of materials; Electron microscope examination of materials; Granular structure; Neutron diffraction examination of materials; X-ray examination of materials*
 alkali halides, at m.p., interparticle distance correl. with interionic separation 9-35007
 alkali halides, ionic radii deriv. using repulsive energy method 9-35006
 amorphous substs., Madelung const. and dispersion 9-42705
 borohydrides of Li, Na and K, internal rotations 9-43308
 cyclohexene, molec. motions 9-43305
 glasses, non-oxide chalcogenide, i.r. reflectance structure spectroscopy 9-36928
 glassy metastable oxide phases, rel. to quenching 9-23612
 Hartree-Fock, pressure calc. and virial theorem 9-39554
 ice, slow inelastic neutron scatt. 9-48681
 inert gas bubble growth, constant rate of gas generation 9-32823
 ionic crystals, lattice self-potentials and Madelung const. 9-36973
 ionic radii, radii, multivalent self-consistent set derivation 9-32854
 lunar soil, determ. by automatic stations 9-27071
 Madelung energies of centrosymmetric struct., direct summation, computerized procedure 9-30506
 metal, energy in Hartree-Fock approximation, Wannier representation 9-35303
 metals, at m.p., interparticle distance correl. with interionic separation 9-35007
 metals, stereological anisotropy 9-46914
 neutron diffraction examination, applications 9-47419
 neutron diffraction examination, applications 9-37785
 nylon 66 yarn, drawn, annealing conditions 9-46707
 pentaerithritol, molec. motions 9-43307
 polyethylene single crystals, fold structure investigated by various methods 9-32828
 polymer, light scatt. technique for determ. 9-28199
 threads, synthetic complex 9-44795
 β -Al₂O₃, lattice self-potentials and Madelung const. 9-36974
 As, amorphous, dimensions of struct. element from X-ray intensity curves 9-32824
 BaO-SiO₂ glass films, two-phase development 9-26174
 BaO-TiO₂ glassy systems four fold coordination of Ti ions 9-32827
 C monofilaments, glassy, prep. struct. isotropy 9-28195
 Ca-Yb system, f.c.c. and b.c.c. characts. in temp. range 900-400°C 9-30716
 CaF₂, interstitial and lattice sites, similarity 9-36974
 Cr steels, hardened, from sound vel. meas. 9-23755
 (KPO₃)_n glassy, rel. to valence angles and dihedral angles in PO₄ tetrahedra 9-40906
 Li₂O-2SiO₂ glass, effect of neutron irradiat. 9-40833
 Mg₂P₂O₇ glassy, rel. to valence angles and dihedral angles in PO₄ tetrahedra 9-40906
 Na₂P₂O₇ glassy, rel. to valence angles and dihedral angles in PO₄ tetrahedra 9-40906
 NaCl, crystal field in Na vacancy 9-36974
 Se, amorphous, dimensions of struct. element from X-ray intensity curves 9-32824
 TiO, Madelung potentials and ordering energy 9-30508

theory

- condensed matter, conference 9-48981
 correlation functions and Green functions, zero-frequency anomalies 9-42987
 crystalline order in two dimensions 9-34044
 diamond-type crystals, optical critical-point structure, strain effects 9-24395

Solids continued**theory continued**

- dielectric constant, rel. to shell model of lattice dynamics 9-35262
 electronic nature, fundamental covalent-ionic transition 9-39183
 Goldstone-type model with antiferromagnetic props. 9-25405
 Green's function, one-particle, for completely disordered system 9-44857
 group theory in the solid state 9-46694
 quantum solids, short- and long-range correlations, self-consistent treatment 9-23993
 statistical mechanics, book 9-40252
 surface tension in ionic cryst. in presence of dipole moments 9-32831
 tight-binding model for energy bands 9-35316
 treated in quantum mechanics textbooks 9-41756
 Ne, many-body corrections to isotopic volume differences 9-48778

Solitions *see* Transducers**Sols***see also Colloids; Sedimentation*

- Ag prepared in nitrate melts, electron micrographs 9-36907
 Au prepared in nitrate melts, electron micrographs, and absorpt. and scatt. spectra 9-36907
 blending fractions effect on viscoelastic props. of crosslinked polymers 9-46708
 polystyrene, electroviscous effects in dispersions of monodisperse lattices 9-23551
 Schiller layers, inter-particle distance 9-30440
 silica, freeze-thawing, for microporous silica prep. 9-46732
 zirconia, sol-gel process for prep. of stabilized particles 9-30731
 AgI prepared in nitrate melts, electron micrographs 9-36907
 Au, u.s. wave induced birefringence 9-36908
 PuO₂, gel formation and calcination to produce dense microspheres 9-36631
 ThO₂, ionic solvation and growth 9-23549

Solubility*see also Phase equilibrium*

- t-butyl alcohol-water soln., mutual solubilities, comparison with methyl cyanide-water 9-42651
 Deuterium in Pyrex glass 9-40987
 gas bubbles 9-48677
 gases in liq., reduction in sound fields, mechanism 9-46612
 methyl cyanide-water soln., mutual solubilities, comparison with t-butyl alcohol-water 9-42651
 polyesters and polyamides in amorphous state, solubility and heat resistance 9-28191
 polymers, of low mol. wt. penetrants, models, mechanisms and laws, review 9-39389
 pseudobinary (III-V)-(II-VI) systems, solid, and optical energy gaps 9-35205
 Pyrex glass, of deuterium 9-40987
 surface tension effects on rate of dissolution of solid surface in thin liquid film flowing past in laminar motion 9-48668
 water-methyl cyanide soln., mutual solubilities, comparison with t-butyl alcohol-water 9-42651
 Ag, of C. equil. solid solubility temp. depend. 9-44788
 Al, of Fe, enhanced value obtained by rapid quenching 9-42916
 AlP in Al, rel. to temp., for crystal growth 9-37025
 AlP in molten Al, 900°-1200°C 9-30372
 Au, of C, equil. solid solubility temp. depend. 9-44788
 BaH₂, limit in Ba, 200 to 620°C 9-28315
 C in U, UC precipitation in U-Mo 1.5% alloy 9-35260
 Ca₁₀(PO₄)₆Cl₂, of Sb³⁺ 9-42740
 Cu, of C, equil. solid solubility temp. depend. 9-44788
 Cu₃Pd of H during diffusion 9-23838
 Cu alloys, of N 9-28384
 Cu in Si, effect of grain-boundaries 9-42797
 Cu(36wt%)Zn, of Fe and P, max. saturation and precipitation 9-30717
 α -Fe, of Fe₂N, rel. to N₂ diffusion, effect of Ni 9-23840
 K₄Nb₂O₁₁, in conc. HF and water 9-26238
 Li₃VO₄, of YVO₄ and rare earth vanadates, crystn. conditions and structure 9-40777
 Mo, of N, heat of soln. determ. 9-40985
 Na, of Au, and diffusion, 0° to 77°C 9-42861
 Na₂TeO₃-Na₂CO₃-H₂O system at 25°C, obs. 9-40776
 Na₂VO₄, of YVO₄ and rare earth vanadates, crystn. conditions and structure 9-40777
 NaCl, of Cd²⁺, ionic conductivity meas. 9-30626
 NaCl in water-butanol mixtures, liq.-liq. equilibrium 9-32765
 NaCl in water-dioxane mixtures, liq.-liq. equilibrium 9-32765
 NaCl in water-methyl ethyl ketone mixtures, liq.-liq. equilibrium 9-32765
 NaCl in water-tetrahydrofuran mixtures, liq.-liq. equilibrium 9-32765
 Ni-Al-Sc system, solid solubility limits at 1000°C, for Ni-rich region 9-30720
 Ni-Al, Si, Ti, alloys, γ phase, coherent solubilities 9-28403
 Ni-Mo alloy, of H, conc. depend. of enthalpy and entropy of soln. 9-39478
 Ni-W alloy, of H, conc. depend. of enthalpy and entropy of soln. 9-39478
 Pd-In alloys, primary solid solubility of In 9-30571
 Pd, of H₂ and D₂ 9-37206
 Pt-In alloys, primary solid solubility of In 9-30571
 Pt-Sn alloys, primary solid solubility of Sn 9-30571
 RbBr-RbI solubility gap, equilb. phases for moist solid soln. 9-35211
 Sc-Ni system, solid solubility limits at 1000°C for Ni-rich systems 9-30720
 SeO₃, of HFO₂, at elevated temp., and vice versa 9-39476
 Si₃B₂C system, of B in α -SiC at 2450 to 2500°C 9-48939
 of TiO₂ in opacified porcelain enamels, control for adjustment of parameters controlling optical props. 9-37687
 V₂O₅, of YVO₄ and rare earth vanadates, crystn. conditions and structure 9-40777
 W, of N₂, high. temp. 9-35136

Solution energy *see* Heat of solution**Solutions***see also Heat of solution; Liquids; Solid solutions*

- ⁴He superfluid-³He, phonon-quasiparticle interactions, microscopic theory 9-34942
 acetic acid in polar soln., anharmonicity of O-H stretching vib. rel. to solvent dielec. const. 9-34650
 alcohol, solvations to radical ions, e.p.r. study 9-34880
 alkali-metal chloride aq. solns., nuclear spin-lattice relax. 9-44593

Solutions continued

- aqueous alkali hydroxides, thermal cond. meas. as a function of conc. 9-44558
 benzene-carbon disulphide, acoustic relax. obs. and its mechanisms 9-46632
 benzene-o,o'-ditolyl (or diphenyl or diphenyl methane), mixing effects 9-48683
 binary, continuous sensitivity to particle traversal, physical conditions 9-30373
 binary solvents, effect on dye molecule association 9-27922
 cellulose acetates in dilute solns., solvation estimated from compressibility 9-32769
 citric acid, supersaturated aqueous solns., molecular cluster formation 9-30374
 colloidal part. in 1-1 plus 2-1 electrolyte mixture, stability props., mutual antagonism 9-23545
 critical opalescence, nonlocal hydrodynamic eqns. 9-23576
 cumene hydroperoxide solution, H-bonding investigated by i.r. absorpt. 9-27892
 d.c. transport coeffs., dynamics 9-23519
 diffusion in mixed dense fluids 9-30167
 dilute polymer solutions, conc. effect on grid turbulence 9-44536
 diluted, thermodynamic props. near solvent critical point 9-26093
 dimethyl formamide, in mixture of benzene and liq. paraffin, internal field at microwave freqs. 9-46650
 dimethylsulphoxide and dimethylsulphonic aq. solns., neutron scatt. and X-ray data 9-32763
 dioxane binary soln., excess vol. of mixing 9-34881
 p-dioxane-water, dielec. props. 9-34928
 dioxolane-polydioxolane in equilibrium soln. 9-28103
 diphenyl methane-d,o'-ditolyl, mixing effects 9-48683
 electrolyte, extension of Debye-Huckel theory 9-37838
 electrolytes, aqueous 1-1, at 25°C, integral eqn. computations, error analysis 9-35748
 fluorenone ketyl, existence of paramagnetic and diamagnetic ion clusters 9-34923
 gases in water, behaviour 9-39080
 ionic, l.f. motions of H₂O mols. 9-44547
 light scatt. by binary solns. 9-28126
 liquid, sound absorpt. due to conc. fluctuations calc. 9-28119
 3-methyl-pyridine heavy water system, critical opalescence, temp. depend. 9-42656
 mixed salts, u.s. parameters, conc. dependence, rel. to complex formation 9-23491
 mixing of liquids, rapid, energetic model 9-33656
 mono-molecular, equivalent rigid spheres of solute suspended in liq., temp. depend. 9-34877
 mutually soluble liquids, filtered mixing in porous medium with one-sided miscible displacement 9-39079
 nitrobenzene in dipolar and nondipolar organic solvents, dielectric saturation 9-32792
 n.m.r., solvent effects formula 9-30428
 organic, vac.-u.v.-excited, inter- and intramolec. processes 9-42667
 poly(β -naphthyl methacrylate) in 4 solvents, critical opalescence 9-28144
 poly(β -vinyl naphthalene) in 3 solvents, critical opalescence 9-28144
 poly(butyl methacrylate) in isopropanol, critical opalescence 9-28144
 poly(dimethyl siloxane) in tetralin, critical opalescence 9-28144
 poly- α -amino acid, laser light scatt. 9-42657
 polyelectrolyte, with mono- and divalent counterions, rodlike model 9-42636
 polyethylene dissolution in xylene and octadecane 9-46616
 polymer, equivalent rigid spheres of solute suspended in liq., temp. depend. 9-34877
 polymer, excluded-vol. effects on equilib. props. 9-36848
 polymer, excluded-vol. effects on limiting viscosity number 9-36849
 polymer, hydrodynamic interaction, variational calc. 9-42460
 polymer, in tube, lowering of turbulent heat exchange during flow 9-40785
 polymer, intrinsic viscosity, theory and expt. 9-48684
 polymer, light scatt. 9-39099
 polymer, mol. config. change, math. model 9-30154
 polymer, Rayleigh fine structure theory 9-36881
 polymer, sedimentation const., conc. depend. 9-32539
 polymer, solvent depend. of rheological behaviour 9-28108
 polymer, stat. thermodynamics, pairwise interactions of linear chains 9-32766
 polymer dilute, critical Taylor number rel. to conc. 9-44538
 polymer optical activity, model for depend. on mol. wt. and stereoregularity 9-28132
 polystyrene, electroconductivity, solvent and ionic conc. effects 9-23525
 polystyrene-polybutadiene block copolymers, viscosity and osmotic press. meas. 34.2°C 9-39086
 potassium oleate in D₂O, n.m.r. meas. on smectic liq. cryst. phase 9-40775
 rainwater, salinity meas. by elec. cond., effects of temp., dust and de-ionization 9-34879
 refractive index and conc., shadow-optical meas. 9-46636
 refractive index meas., two simple methods requiring only microscope and spectroscopic cell 9-46635
 salt, stratified, axisymmetric internal waves generated by moving oscillating sphere 9-34861
 salt in water, collective instability of salt fingers rel. to molecular diffusivity 9-33748
 semigrand isobaric-isothermal ensemble distrib. functions 9-40247
 solute flow across membranes, hydrodynamic irreversible thermodynamic approaches, comparison 9-36857
 spiropyranes in soln., photochromy obs., by means of triplet-triplet absorption 9-34910
 stabilizing gradient of solute, effect on onset of thermal convection 9-39087
 sucrose, non-cavitating u.s. effects on hydrolysis 9-37821
 tar, in tube, lowering of turbulent heat exchange during flow 9-40785
 thermodynamic props., effect of external fields 9-48692
 trapped dielectron, theory 9-46613
 urea, aq., ultrasonics and water struct. 9-30400
²³⁵U (93.19 wtx), with natural boron poison, critical obs. 9-34498
 Co(II) chloride solns. in water and alcohols, X-ray diff. 9-44548
 CuSO₄ in glycol-water mixtures, u.s. absorpt. rel. to temp. and conc. 9-34903

Solutions continued

- Eu salts, radiationless transitions of Eu³⁺ with excitation of H₂O vib. deuterated and undeuterated 9-28141
 FeCl₃ frozen aqueous, p.m.r. studies 9-33646
 Fe(III)Cl₃ in methanol, solute structure obs. 9-34878
³He in ⁴He, review 9-23562
 InCl₃-alkali-metal chloride molten mixtures, Raman spectra 9-44570
 K-NH₃, doped with KI, Knight shifts 9-44595
 K-NH₃, viscosity, vacancy calc. 9-48686
 MnSO₄ mixture in H₂O-ethylene glycol, u.s. absorpt. obs. 9-39097
 N₂O, vibration band profile determ. in various solvents and correlation function calcs. 9-44571
 NH₃ liq., effect of dissolved salts on i.r. spectra 9-39106
 Tb salts, radiationless transitions of Tb³⁺ with excitation of H₂O vib., deuterated and undeuterated 9-28141
 UO₂, of fission gas atoms from bubbles, re-solution process into irradiated material 9-28326
 ZnSO₄ mixture in H₂O-ethylene glycol, u.s. absorpt. obs. 9-39097

Sonar see Sound ranging**Sonic boom see Aerodynamics; Shock waves/effects****Sonoluminescence see Luminescence/liquids and solutions****Soret effect see Diffusion in liquids, thermal****Sorption**

- see also Adsorption
 accommodation coeff. calc., virtual phonon processes effects 9-23644
 adatom interactions, indirect, through AB-type cryst., rel. to surface states 9-34998
 benzene in vinyl acetate-methyl acrylate 9-33010
 body with variable porosity, high temp. reaction kinetics 9-26817
 chemisorption energy, influence of lattice vibrations calc. 9-47460
 chemisorptive luminesc. 9-43326
 desorption from glass following Ar⁺ bombardment 9-39172
 dissociative chemisorption formation of immobile films 9-26816
 gas-condensate system, differential eqns. of filtration 9-48673
 gases, analysis techniques, general review 9-35758
 glass, desorption of conically pumped noble gases, pre-exponential factor 9-39171
 glass, desorption of H following Ar⁺ bombardment 9-39172
 glass, desorption of ionically pumped Ar from clean and metallized surfaces 9-30495
 glass, porous, of pyridine, i.r. spectra 9-26196
 graphite, I desorpt. in vacuum and Ar, and adsorpt., 27-1100°C 9-28221
 graphite, neutron irradiated in CO₂, uptake of Br 9-28316
 graphite, of H, temp. desorp. obs. 9-39169
 graphite, thermal desorption studies after radiolytic oxidation in CO₂ or CO + methane 9-28220
 hydrocarbons on metal surfaces, π -electron system and bond energies 9-39948
 inert gases desorpt. curves, numerical calc. 9-23642
 nylon, of water, molecular mechanism 9-32851
 phonic desorption of impurities from walls of a vacuum vessel 9-40217
 silica gel, of benzene, after 6 month storage, 25°C 9-42735
 solids diffusion coeff. determ. from sorption data 9-46840
 transition metals, chemisorption of H, self-consistent model 9-24548
 zeolites, A and X, synthetic, applic. in vacuum technology 9-25006
 zirconia, deuterium absorption rel. to post-transition corrosion by steam at 300°C and 340°C 9-28806
 C active, of SO₂, 50 to 650°C, interact. and regeneration of C 9-26806
 CO on metal surfaces, π -electron system and bond energies 9-39948
 CO on metal surfaces, π -electron system and bond energies 9-39948
 CO on Ni, desorption induced by photon radiation 2.1-4.8 eV 9-23647
 CDS chemisorption, effect on rectification props. of high-resistance barrier layer 9-39640
 CDS sintered layers, of ambient oxygen, effect on photoelectronic behaviour 9-47200
 Co, surface defects caused by chemisorbed layer 9-26827
 Cs-graphite system, characts. at high temp. and low Cs pressures 9-39168
 D₂ desorption from Ti-sponge 9-30499
 Fe, surface defects caused by chemisorbed layer 9-26827
 on Fe effect friction and adhesion props. 9-37272
 Ge, thermal desorption of water in ultra high vac. rel. to surface states 9-35425
 n-Ge atomically clean surface, interaction with O 9-46718
 Ge surface, physisorption at low temps., ellipsometric investigation 9-42730
 Ge surface layer, thermodesorption and mass spectra analysis of desorbing particles 9-36967
⁴He adsorbed monolayer, quantum theory 9-23557
 I, chemisorption of CO, i.r. spectra, temp. effect 9-43325
 K₄Nb₆O₁₇, of water, volume expansion obs. and water release on compression 9-26238
 Ni, chemisorption of H on films, static capacitor examination of surface potential 9-24547
 Ni, surface defects caused by chemisorbed layer 9-26827
 O chemisorption on Fe, Fe-Al and Fe-Cr oxides in high vacuum conditions, eff. on surface conductivity 9-37822
 PbS (100) surface, O₂ chemisorption 9-39949
 PbS films, of O₂, effect on photoconductivity 9-37622
 Pt, chemisorption of CO, i.r. spectra, temp. effect 9-43325
 Pt, chemisorption of gases, LEED study 9-26818
 Re, chemisorption of N₂ and CO 9-49376
 Rh, chemisorption of CO, i.r. spectra, temp. effect 9-43325
 Si surface, physisorption at low temps., ellipsometric investigation 9-42730
 SiO₂ gel, desorption rates of CO, Ar mixtures at various temps. 9-46663
 SiO₂ glass, effect of ⁴He and ³He on h.t. capacity at low temp. 9-42733
 W, chemisorptive luminesc. 9-43326
 W, desorption of Y in strong elec. field, 300° to 630°K 9-46733
 W, desorption spectrum of trapped rare gas ions obs. 9-36970
 W, inert gas thermal release from (110) and (211) surfaces 9-44633
 W, of methanol, photoelectron spectroscopy rel. to orbitals involved in bonding 9-44634
 W single crystal, adsorpt. of Y on (121), (111) and (021) faces, investig. using electron field-emission projector 9-44632
 ZnO, surface states assoc. with chemisorbed species 9-43008
 Zn(PO₃)₂ gels, chemisorpt. and ion exchange rel. to comp., obs. 9-28789

Sound see Acoustics

Sound field *see Acoustic radiators; Acoustics; Intensity measurement/acoustics*

Sound ranging

- atmospheric ultrasonics 9-33800
- azimuth and elevation errors for square array of microphones 9-29284
- ocean bottom irregularities determ. using short duration signal backscatt. 9-22262
- ocean exploration applications 9-37905
- potentialities, as research and commercial tool 9-22263
- sonar echoes, automatic distinction between hard and soft objects, fish detect. appl. 9-41831
- sonar system, domed, S/N 9-29296
- u.s. pulse refl. method as mobility and for the blind 9-22265

Sound recording *see Recording*

Sound reproduction

see also Acoustic radiators; Recording; Transducers

No entries

Space charge

- anthracene, transient photo-enhanced limited current obs. of triplet excitons interaction with trapped electrons 9-39729
- atmosphere, rel. to precipitation, pot. gradient and conduction current, aircraft soundings 9-26906
- bipolar space charge limited current between coaxial cylinders and concentric spheres 9-47907
- charge clusters localized in given space, eqns. for e.m. field distrib. and density of subst. 9-25191
- density of charged particles, measurement, moving plasma cloud 9-30258
- diode, relativistic planar, Poisson's eqn. of space-charge-limited flow, soln. 9-37560
- electrodynamic, effect on electron acceleration 9-32278
- in gas, externally ionized, effect on elec. conductivity 9-44489
- klystron, reflex space charge effect on starting current and reflector voltage 9-41852
- layers associated with bulk, negative differential conductivity, analytic results 9-43105
- liquids, organic steady-state and transient space-charge-limited currents by injection from tunnel cathode 9-34919
- magnetoplasma, waves generation by nonlinear interaction of microwave signals 9-30237
- metal interfaces, effective dielec. const. determ. 9-41230
- neutralization due to positive ion injection into cylinders and spheres 9-33417
- and Ni fatigue, high temp. 9-26318
- oxidation, logarithmic, effect, and modification of Uhlig model for surface effects 9-31190
- oxidation, logarithmic, effect, and modification of Uhlig model for surface effects, comment 9-31191
- plasma layer near electrode 9-48560
- semi-insulator, localized levels obs. from meas. of ohmic and space-charge-limited conduction 9-43106
- semiconductor, field emission depend. on space-charge-limited currents 9-33416
- semiconductor p-n junctions, space-charge-limited currents 9-44986
- semiconductors, non-equal. surface charge for arbitrary ionization degree of impurities 9-33318
- semiconductors, trapped field, free carrier sweep-out after pulse injection 9-30896
- tetracene, space-charge-limited currents 9-41204
- upper atmosphere, equilibrium 9-35859
- wave instability in semiconductor with field-dependent diffusion 9-43047
- CdS, trap conc. determ. by space charge currents 9-37402
- CdS layers, currents boundary 9-30906
- CdSe films, simultaneous variation with conductivity, from depletion depth meas. 9-30905
- CdTe p-n junctions, nonuniform distrib. rel. to capacitance relax. 9-47137
- Fe-Ni, alloys, r.f. magnetic susceptibility, effect of added electrons 9-28587
- n-GaAs, with impurity band, space charge layer capacitance 9-35400
- Si, anodically oxidized, aging effect on surface states 9-39641
- Si p-n junction, photoresponse edge, effect of elec. field in space charge layer 9-37558
- Zn:Li single cryst., space charge limited currents between asymmetric contacts 9-33378
- ZnO electrophotographic layers, density, effect of elec. field 9-30963

plane air-gap, distortions of field inc. in breakdown voltage due to additional space charges 9-23361

- vacuum gauge, ion-focussing 9-25003

solid

- p-chloranil, limited currents prod. by electron injection by aqueous electrolyte contact 9-41203
- p-n junction, boundary conditions 9-26566
- semiconductor, p-type, injection causing negative resistance mechanism 9-28493
- trapping level non-exponential distrib. determ. by space-charge-limited currents using differential method 9-41125
- CdS single crystal, limited current, temp. depend. 9-44955
- GaAs, two- and three-dimens., growth from negative differential resistivity 9-47110
- MnO/CoO solid solns., dielec. const. and loss large values at low freq. due to space charge polarization 9-35465
- MnO/NiO solid solns., dielec. const. and loss large values at low freq. due to space charge polarization 9-35465
- NiO:Li, interfacial polarization effect w.r.t. dielec. const. 9-35469
- NiO, interfacial polarization effect w.r.t. dielec. const. 9-35469
- Se electrophotographic layers, kinetics on exposure to light 9-39727
- ZnO electrophotographic layers, kinetics on exposure to light 9-39727

Space groups *see Crystal structure, atomic*

Space research

see also Atmosphere

- aerospace simulation facilities instrumentation, conference, Farmingdale (1969) 9-49516
- Apollo 8 flight, problems solved 9-45572
- CENFAM multistation meteor radar system, receiving apparatus 9-41614
- CENFAM Project, multistation radar system for meteors and upper atmosphere 9-41613
- flight, permissible radiation doses, substantiation 9-31687

Space research continued

- gamma ray spectrometer for space instrument appls. 9-25505
- health physics support program 9-27121
- ionosphere, from space vehicles 9-37979
- luminous particles phenomenon 9-31480
- Lunar Orbiter image evaluation 9-32044
- lunar soil mechanics surface sampler 9-40171
- Mariner 5 and Venera 4 combined obs. Venus radius rel. earth radar obs. 9-38073
- nuclear experiment design for electron flux meas. 9-38026
- nucleonics in aerospace, symposium Columbus (1967) 9-29699
- probes and the exploration of solar system, popular review articles, book 9-49574
- small scientific satellite, nuclear instrumentation payload 9-38019
- solar atmosphere structure, satellite feasibility 9-47609
- u.v. radiation, scattered, in earth's neighbourhood, observations by interplanetary stations Venera 2 and Venera 3 9-24847
- Venera 4 impact, deductions from Mariner 5 and radioastronomical obs. 9-38071

Space vehicles

see also Rockets; Satellites, artificial

- ablation heat shield, anal. of convective and radiative heat transfer 9-22304
- attitude stability in circular and elliptical orbits 9-40110
- drag data correlation on re-entry, for spheres and cones 9-26005
- Earth-to-Moon trajectories, asymptotic soln., errata and addenda 9-26970
- environment, effects on materials 9-48977
- IMP F and G, solar cosmic ray particle identifier, design and calibration 9-38021
- insulation materials, multifoil, outgassing behaviour obs., 100-1800°F 9-38173
- ionospheric research 9-37979
- isotopic α -emitting power source materials evolving no neutrons, patent 9-28971
- luminous particles phenomenon 9-31480
- manned Earth satellites, Russian, absorbed radiation doses, obs. 9-45573
- nuclear system safety 9-25669
- orbital information on planet masses and lunar mascons, popular article 9-47607
- POGO, ion chamber experiment, total ionization measurements in outer radiation zone 9-40067
- Saturn V (1967), infrared emission soon after launch 9-27228
- sun elevation angles and times of rising and setting, computation procedure 9-43503
- Venera 2 and Venera 3, u.v. radiation in earth's neighbourhood, scattered, observations 9-24847
- ²³⁸Pu¹⁶O, isotopic α -emitting power source materials evolving no neutrons, patent 9-28971

instrumentation

see also Rockets; Satellites, artificial

- Ariel III, cosmic noise meas., 2-4.2 MHz 9-47608
- Ariel III, e density, temp. probes 9-45527
- atmosphere density gauge, γ scatt., design by multivariable search method 9-24636
- γ spectrometry, satellite data processing system 9-38018
- channel multiplier spectrometer, 0.5 to 500 keV electrons and protons, for ATS-E satellite 9-38023
- Cosmos 149, expt. problems and instrumentation 9-45576
- electron trap behaviour on slowly moving charged spacecraft 9-43454
- ESRO I/Aurora satellite experiments 9-33814
- ionization chamber for Kosmos 19, 25 cosmic ray meas. 9-38101
- ionosphere irregularity direct detection, satellite instrument 9-49499
- for Luna 13, mechanical props. and density of surface soil determ. 9-33932
- magnetometer, rocket released, construction and preliminary results 9-41593
- magnetometer, rocket-released, attitude stabilized 9-41592
- Mariner apparatus for Mars meas. 9-49515
- mass spectrometer, non-magnetic 9-43688
- meteoroid sensors of Explorer 16 and Lunar Orbiter, comparison of obs. 9-29076
- mirror for space flight, optical degradation due to u.v. radiation and condensation obs. 9-40111
- mirrors, oil contamination changes in u.v. reflectance 9-22470
- nuclear, for research on board small scientific satellites 9-38019
- optical apparatus for upper atm. temp. distrib. meas. 9-41542
- particle detectors for Vela 4 satellite energetic particle experiment 9-38020
- particle identifier, E. dE/dx, two pulse multiplier 9-38016
- plasma wave detector, design and in-flight operation 9-38027
- primary electron detector system forOGO-E satellite experiments 9-38022
- pulse weight analyser, multichannel, with memory 9-38024
- radiometric apparatus reviewed 9-45578
- satellite cosmic ray intensity monitoring recorder 9-29632
- solar cosmic ray particle identifier for IMP F and G spacecraft, design and calibration 9-38021
- solar u.v. and X-rays atm. absorpt., non dispersive detectors for rocket 9-31346
- spectrometer, scintillation, rocket borne, for cosmic ray obs. 9-31584
- swept frequency sounders, study of ionization maximum in polar latitudes 9-33828
- telescope, astronomical, balloon-borne, operating characts. 9-27111
- telescope, rocket-borne, liquid He cooling 9-38123
- telescope, satellite, coupled to crew compartment, attitude stabilization 9-26974
- telescope, solar, balloon-borne, guiding system 9-26975
- telescopes, optical, astronomical programmes review 9-29673
- u.v. telescope, automated, for satellite observatory 9-28976
- γ spectrometers, satellite on-board calibration system using Co⁶⁰ and Am²⁴¹ sources 9-38017

Space-time configurations

- automorphisms of a general Minkowski space forming a group 9-43727
- axisymmetric stationary, using 3.dimens. relativity theory 9-29180
- Bianchi type IX closed space rel. to the presence of homogeneity of the universe 9-33889
- Birkhoff's theory, four-vector force 9-29187
- complex functional manifold, non-linear, and related Hilbert space, physical interpretation 9-43742

Space-time configurations continued

- coordinates, co-moving, junction conditions for spherically symmetric matter 9-31756
- curvature collineations, a prop. of space-times defined by the vanishing Lie derivative of the Riemann curvature tensor 9-38216
- de Broglie wavefield, eqns. in the case of spherical symmetry 9-45761
- Einstein's space-time, rel. to unified field theory 9-43737
- Einstein space, exact soln. of gravitational waves 9-45746
- flat space, space and time meas. in special relativity framework 9-45743
- Fock space of single Bose operator, generalized Bose operators 9-45747
- Friedmann universes, covariant e.m. potentials and fields 9-47731
- Friedmann universes, soln. of Maxwell's classical electrodynamic equations 9-22347
- generalized concept of space 9-22074
- Hilbert space, super which allows time operator in quantum mechanics 9-47750
- Hilbert spaces with kernel functions, theory and applics. 9-31744
- Lorentz and other groups, comparative study 9-47728
- Lorentz group extended to describe integral or half-integral spin states 9-25407
- mass and momentum transformation under special conformal transformations of space-time conformal group 9-43730
- minkowski metric, asymmetric non-static deviation 9-47746
- non-singular metric for Galilei group 9-31753
- nonlocal field theory, 2-dimensional, source of isospin freedom 9-34238
- null networks in flat space-time 9-22073
- odd-dimensional, and CPT theorem 9-34247
- Petrov classification of stationary axisymmetric empty space-times 9-43728
- Petrov type D metrics all derived 9-47730
- Poincare and Galilei groups, projective extensions rel. to 5-dim. space 9-31753
- relativistic, Hamiltonians construct. from hyper-regular Lagrangians 9-40236
- Riemann, propagation of monochromatic polarized light 9-29471
- Riemann spaces, 4-dimensional, algebraic classification 9-38207
- Riemannian manifolds, locally symmetric K-contact, theorems 9-27158
- Riemannian spaces, embedding in Euclidean or Minkowskian spaces 9-43726
- state space decomposition in some field theory models 9-38424
- state vector spaces with indefinite metric in quantum field theory 9-32108
- stress-function space-time theory rel. to time-depend. and moment stresses expressions 9-45812
- subspace, 4-dimens., isometries group of tangent spaces 9-22070
- symmetric spaces, general theory, book 9-34010
- transformation, space-time, time order preservation 9-38211
- U(3) symmetry breaking caused by zero mass particles in unified theory of gravitation 9-38219
- zero-mass fields, Jost-Schroer theorem 9-22072

Spallation *see Nuclear spallation***Spark chambers**

- digitized, search for Crab nebula γ emission 9-35962
- discharges, electronic elimination of subsequent radiation pick-up 9-42152
- electrical breakdown, ionization growth, inclined spark development 9-29673
- fast, sonic, description 9-25546
- magnetostriuctive, in mag. field ≤ 15 kOe, particle detection efficiency and accuracy meas. 9-25543
- streamer, 20 cm gap, and circuitry, meas. anal. and ang. resolution 9-25545
- streamer, specific primary ionization meas. and relativistic increase 9-25544
- streamer chambers, Ne-He gas purifier, cryogenic 9-46143
- triggering by missing mass techniques 9-44095
- wire, data analysis using on-line computer 9-36536
- wire, four thyratrons for h.v. pulse generation 9-22682
- wire, high-energy experiments, data acquisition, analysis and control, real-time computer system 9-36537
- wire, large, construction and uniform magnetostriuctive readout 9-42153
- wire, large area, with ferrite core readout, in γ ray telescope 9-38128
- wire, on-line, used as mass spectrometer 9-27601
- He streamer chamber, ionization meas. 9-46144
- Ne gas recirculator-purifier 9-42154

Spark counters *see Counters/spark***Sparks, electric***see also Breakdown, electric; Lightning*

- 4-m, in air 9-46546
- air, breakdown, primary and secondary streamer dendrites 9-28051
- air, impulse testing in nanosecond range, current and tension 9-42577
- air gap, polarity effects of breakdown triggered by a laser 9-32706
- air spark gap, dispersion of sparking voltage under high current successive discharges 9-48639
- atmospheric, 250 c, 40 kv 9-32710
- cathode erosion mechanism 9-43330
- Chronolite camera, variable spark-gap with gas pressure chamber 9-32094
- cross-excitation in laser microprobe emission spectroscopy for samples 10-25 μ dram. 9-47476
- Cu-Ag alloy, spectral lines, effect of additives 9-31228
- discharges, prod. of shock waves 9-30317
- gap, laser-triggered, for kilovolt pulses of accurately variable timing 9-29390
- gas breakdown by laser picosecond pulses, evidence for self-focusing 9-25983
- H, development of discharges, streak photography obs. 9-30319
- laser, discharge through two separate 9-46547
- laser, image structure 9-43867
- laser-produced, multiple collinear, in gases 9-28055
- l.v. pulse discharge triggering in vacuum, aid of sliding spark 9-23363
- machining, application of rocket effect on bubbles 9-39068
- metal alloy emission processes, vibrational effect 9-45311
- pressurized two-electrode spark gap, saturable inductance, experiments with various ferrite materials 9-30318
- spectroscopic light source for extreme u.v. 9-36407
- trigger, effect on breakdown of water gap 9-32709
- two-electrode gap, pressurized, saturable, inductance 9-25987
- Ar h.p. 20 ns spark channel, radiance saturation and afterglow emission 9-30314

Sparks, electric continued

- Cl, in various gases, 10 mm Hg to 6 atm, spectral line intensities rel. to Cu or graphite electrodes 9-36792
 - H, small pd valves, plasma discharge development 9-39032
 - He h.p. 20 ns spark channel, radiance saturation and afterglow emission 9-30314
 - S, in various gases, 10 mm Hg to 6 atm, spectral line intensities rel. to Cu or graphite electrodes 9-36792
- Specific heat**
see also Thermodynamic properties
 anharmonic crystal, interatomic pot. theory 9-30759
 of antiferromagnetic linear chain in Fermi liquid theory 9-49221
 azeotropic mixture, at critical pt. 9-46624
 of atoms, electronic, calc. 9-38750
 Bose gas at transition point 9-47783
 calorimeter assembly for adiabatic meas. at low temp. 9-25135
 equations of state rel. to Gruneisen's parameter 9-28430
 finite Fermi system with random levels, low temp. 9-27188
 Gruneisen parameters of cubic metals 9-24059
 Ising model, high-temp. 9-35542
 Ising model, three-dimensional array of 27 points 9-36142
 metals, calc. from eqns. of state 9-39090
 superconducting ellipsoid, finite jumps when it enters or leaves intermediate state 9-44922
 Al-Cr dil. solid soln., w.r.t. localized d-state props. 9-33269
 Al-Mn dil. solid soln., w.r.t. localized d-state props. 9-33269
 Al-V dil. solid soln., w.r.t. localized d-state props. 9-33269
 Pb calc. from eqns. of state 9-39090
 TiO₂, Debye temp. and elastic const., calc. from force field 9-35142

gases

- 9,10-anthraquinone 9-46418
- azeotropic mixture, at critical pt. 9-46624
- diatomic molecules, position of sp. ht. maximum, simple calc. 9-39051
- methane, halogen substituted, saturated vap., calc. 9-26030
- monosilane, halogen substituted saturated vap., calc. 9-26030
- 1,4-naphthoquinone 9-46418
- propane, meas. 9-36818
- steam, 0-800°C, 0-1000 bar, using a new eqn. of state 9-34831
- Au-(10 at %)In, specific heat meas. at 3°K, nuclear term obs., cry. elec. field studied 9-30780

liquids

- air, quantitative calc. from model of vibr. mols. with some translatory motion 9-34869
- azeotropic mixture, at critical pt. 9-46624
- at constant volume, square well with infinite walls calc. 9-30385
- gravity effect on meas. and position of phase interface near critical pt. 9-36859
- propane, meas. 9-36818
- singularity of temp. depend. near critical points 9-36858
- water, at constant press., maxima fitting neither Ehrenfest's nor thermodynamic stability theory 9-36861
- water, Monte Carlo calc. using Rowlinson's intermolecular pair pot 9-34874
- Ar, quantitative calc. from model of vibr. mols. with some translatory motion 9-34869
- BiF₃, heat capacity meas. for heat and entropy of fusion calc. 9-30021
- CO₂, quantitative calc. from model of vibr. mols. with some translatory motion 9-34869
- H, quantitative calc. from model of vibr. mols. with some translatory motion 9-34869
- He³/He⁴ mixture near junction of lambda and phase-separation curve 9-40812
- O, C, from triple point to 300K, at press. up to 350 atm 9-34898
- O liq-vapour system, along coexistence path 9-34897

solids

- adsorbed surface layer on model cryst., change due to layer 9-37311
- alloys, dilute, electronic contrib. 9-26426
- apparatus for meas. down to 0.015°K 9-24040
- cast vitreous-crystalline materials in different compositions 9-39525
- cementite, 2° to 20°K 9-24045
- crysene, heat capacity anomaly 9-33186
- Cu containing hydrogen, 0.4° to 3.0°K, anomaly 9-42969
- diamond, Debye temp. at low temps., X-ray meas. 9-24043
- diamond-like structures, heat capacity 9-33180
- of Fermi atoms adsorbed on a close-packed substrate at low temp. 9-46730
- ferromagnet in finite applied field, heat capacity singularity 9-44831
- ferromagnets, impure, mag. field effects 9-44830
- Gruneisen coefficient, from anal. of shock wave flow in system of plates and spaces 9-48972
- Gruneisen parameters rel. to elastic moduli in low symmetry cryst. 9-39392
- impure crystal at low temp., with tunneling 9-47037
- inert gas crystals, surface, in quasiharmonic approximation 9-39190
- inert gas solids, Debye temp., eff. of triple-dipole forces 9-39530
- Ising model above Curie temp., Pade approximant analysis 9-37645
- metals, under press., d.c. elec. pulse meas. technique 9-30779
- metals localized moments sub-Kondo temp. study 9-45041
- metals near melting point, meas. method employing i.r. laser 9-37354
- Ni single cryst. near mag. critical pt. 9-47005
- noble metal alloys, α -phase, Debye charact. temp. 9-44836
- plastics, reinforced, heat capacity, temp. dependence up to 150°C, meas. by i.r. method 9-33187
- polymers, organic, Gruneisen parameter expressions from eqn. of state 9-37361
- rare earth double oxides, heat capacity obs. below 2°K 9-47004
- rare earth gallium garnets, magnetic transitions 9-24051
- rare-earth orthoferrites, 1.5-20°K, magnetic ordering, magnetization orientation and Zeeman effect 9-33184
- rare-earth trihalides, hexagonal, low-temp. heat capacity meas. 9-41340
- refractory metal oxides, heat capacity rel. to bond energy values and dissociation energies 9-30494
- semiconductors, under press., d.c. elec. pulse meas. technique 9-30779
- singularity nature near second kind phase transition points, imperfections eff. 9-44832
- steel, stainless austenitic, magnetic contribution, low temp. 9-33171
- transition metal borides, heat capacity meas. for bonding and band structure theory, 1.5-18°K 9-28445
- triglycine sulphate, near ferroelec. transitions, Pippard scheme 9-30970

Specific heat continued
solids continued

- Van Hove singularities, anomaly typical of second-order transition 9-41091
- Ag-Au solid soln., Debye-Waller factor, -ve excess entropy, determ. 9-33151
- Ag-Pd alloys, conc. depend. 9-37436
- Ag₂S 9-39526
- AgCd dil. alloys, electronic contrib. 9-26426
- AgI, ht. capacity and order-disorder transition 9-39527
- AgPd dil. alloys, electronic contrib. 9-26426
- Al₂O₃, ht. capacity, 300°-1100°K 9-35285
- α-Al₂O₃, corundum, heat capacity, 2-25 K 9-44833
- Al₂O₃, review of values 9-37355
- Al alloys, commercial, 1.6 to 4°K 9-35293
- Ar-N mixtures 9-39528
- Ar, 0.4-12°K meas. and extrapolation to 0°K 9-24041
- Au-V dilute magnetic alloys, temp. depend. below Kondo temp. 9-24050
- Au-(10 at %)Zn, specific heat meas. at 3°K, nuclear terms obs., crystal electric field studied 9-30780
- Au_{1-x}Pd_xGa₂ heat capacity as function of Pd content 9-49047
- Au_xX ordered alloys, X-transition elements and mixtures, and electron and neutron diff. and resistivity studies 9-44659
- BaTiO₃, near ferroelec. transitions, Pippard scheme 9-30970
- Be, low temps., rel. to impurities 9-24042
- Bi, 1-30°K 9-47006
- Bi, Gruneisen parameters 9-33189
- Bi, metallic, 0.05-0.8K, and suppression of nuclear heat capacity 9-42967
- BiFe₃, heat capacity meas. for heat and entropy of fusion calc. 9-30021
- CO, heat capacity low temp., from freq. distrib. calc. of lattice vibrs. 9-41077
- CaWO₄, Cp, thermal conductivity and diffusivity meas. 9-26427
- Cd, 1-30°K 9-47006
- Cd, Debye temp. by X-ray reflections from powders 9-28428
- CdGeAs₂, semicond. amorphous, Debye model calc. of phonons mean free path 9-37367
- CdS, Debye temp. calculation using phonon dispersion model 9-46972
- Ce, Debye temp., low-temp. phase transform. effect 9-40997
- CeBr₃, at constant magnetization, from adiabatic susceptibility meas. 9-47229
- Co₂La₂(NO₃)₁₂·24H₂O rel. to mag. phase transitions, obs. 9-39781
- Co(S_{Se})₂ system, thermostatical investigation, heat capacity 9-31029
- Cr, anomalous heat capacity and resistivity meas. near T_g 9-48969
- Cr, enthalpy and heat capacity at high temp. 9-39529
- Cr₂(CH₃COO)₄·OC₂H₅O, low temp. 9-28426
- CrCl₃, anhydrous, below 4°K 9-30781
- CrSb₃, marcasite-type, mag. props. obs. 9-35581
- CsCuCl₃, rel. to bonding 9-24044
- CsPbCl₃, temp. dependence 9-39211
- Cu-Al-Fe dilute alloy, 1.2° to 14°K 9-47001
- Cu-Be alloys, determ. by an adiabatic calorimeter rel. to ageing 9-37285
- Cu, extended Bhatia model method 9-24012
- Cu, meas. near melting point using infra-red laser 9-37354
- Cu, pure single-crystal and polycrystalline, below 3°K 9-42968
- Cu₂La₂(NO₃)₁₂·24H₂O rel. to mag. phase transitions, obs. 9-39781
- Dy, hyperfine interactions obs. 9-47305
- EuS, comparison with classical Heisenberg model 9-30782
- EuS, mag. sp. ht. from energy gap temp. depend. obs. 9-37529
- Fe-Be alloys, and magnetization 9-45143
- α-Fe, from phonon dispersion calc. 9-48946
- Fe₂Te₃, electronic contrib., d-band struct. obs. 9-39565
- FeRh system, rel. to first-order antiferromag. to ferromag. transition mechanism 9-45222
- GaP, heat capacity 55°K-300°K 9-33180
- Gd-(9wt.%)La alloy, nuclear component for effective mag. field at impurity nuclei 9-33461
- Gd-(10wt.%)Lu alloy, nuclear component for effective mag. field at impurity nuclei 9-33461
- Ge heat capacity, 30° to 500°C, anharmonic effects in thermodynamic props. 9-47002
- He, Deluie temp. calc. 9-23573
- ³He, bcc, anomalous, source uncertain 9-46676
- ³He solid with ⁴He impurities, effect on heat capacity of exchange system 9-28168
- HgTe-CdTe crystal, composition depend. rel. to lattice dynamics 9-26450
- IrO₂, ht. capacity 0.54°-10°K 9-48971
- KBr, heat capacity, 30°-500°K 9-24047
- KBr, heat capacity and Gruneisen function, exptl. data analysis 9-24048
- KCl:OH, at 0.3°K rel. to OH tunnelling states 9-44834
- KCl, adiabatic meas. at low temp. 9-25135
- KCl, heat capacity, 30°-500°K 9-24047
- KCl, heat capacity and Gruneisen function, exptl. data analysis 9-24048
- KD₂PO₄, heat capacity assoc. with ferroelec. phase transition, KH₂PO₄ comparison 9-41242
- KH₂PO₄, by pyroelectric method 9-30783
- KH₂PO₄, heat capacity assoc. with ferroelec. phase transition, KD₂PO₄ comparison 9-41242
- KH₂PO₄, heat capacity anomaly near ferroelec. transition 9-43117
- KH₂PO₄, near ferroelec. transitions, Pippard scheme 9-30970
- Kr, 0.4-12°K meas. and extrapolation to 0°K 9-24041
- La₂O₃, in temp. range 298.15 to 1600°K 9-41105
- LaB₆, low temp. 9-47003
- LaB₆, heat capacity, 1100-2200°K 9-26428
- Li-NH₃ systems, low-temp. ht. capacities 9-39531
- Li, Gruneisen parameters, pseudopotential calcs. 9-26410
- Lu₂O₃, in temp. range 298.15 to 1600°K 9-41105
- Mn₂La₂(NO₃)₁₂·24H₂O rel. to mag. phase transitions, obs. 9-39781
- MnCl₂·4H₂O, ht. capacity, 0.4°-4.2°K in mag. fields 9-44835
- MnCo₂·4H₂O, high-resolution meas. near Neel temp. 9-24046
- Mo, from phonon dispersion calc. 9-48946
- Mo, near melting point 9-37356
- NH₄ClO₄, ht. capacity 5°-350°K 9-48970
- NaCl, heat capacity, 30°-500°K 9-24047
- NaCl, heat capacity and Gruneisen function, exptl. data analysis 9-24048
- NaNO₂, near ferroelec. transitions, Pippard scheme 9-30970
- Nb-Ta alloys, normal state 9-33181
- Nb-Ta superconducting alloys, temp. coeff. of electronic component, depend. on Ta conc. 9-28478

Specific heat continued
solids continued

- Nb, annealed, low-temp. sp. ht. in mag. fields 9-37465
- Nb, deformed type II superconductor, eff. of dislocation distribution 9-30875
- Nb₂Al, supercond. 9-39599
- Nb₂Sn, rel. to lattice transformation 9-24049
- Nd, hyperfine interactions obs. 9-47305
- Ni-Cu solid solns., at ferro- to paramagnetic transition 9-35554
- Ni-Rh alloys paramagnetic anomalies at low temp. rel. to spin fluctuations 9-45086
- Ni, Debye temp. 9-28427
- Ni, extended Bhatia model method 9-24012
- Ni₃La₂(NO₃)₁₂·24H₂O rel. to mag. phase transitions, obs. 9-39781
- Ni meas. near melting point using infra-red laser 9-37354
- Pb-In alloys, normal and superconducting state 9-33182
- PbTiO₃, near ferroelec. transitions, Pippard scheme 9-30970
- Pd-Cr dilute magnetic alloys, temp. depend. below Kondo temp. 9-24050
- Pd-(14 at %)Fe alloy, low-temp., changes due to short-range order changes 9-33183
- Pd-Ni alloy, paramagnetic, low-temp anomalies rel. to fluctuations 9-45086
- Pd, density of states and electronic sp. ht. 9-37357
- PrAl₃, cubic Laves cpd., heat capacity meas., rel. to mag. moment, 0.1° to 1.0°K 9-45071
- PrCo₃, cubic Laves cpd. heat capacity meas. rel. to mag. moment 0.1° to 1.0°K 9-45071
- PrNi₃, cubic Laves cpd., heat capacity meas. rel. to mag. moment 0.1° to 1.0°K 9-45071
- Pt-Ni alloys, enhancement 1.15° to 4.2°K, rel. to electron spin fluctuation interactions effects. 9-44837
- Pu-Al delta-stabilized alloys, Debye temp., temp. depend. 9-37224
- Pu-Ce delta-stabilized alloys, Debye temp., temp. depend. 9-37224
- α-Pu rel. to self-irradiation effs. 9-24072
- PuO₂, ht. capacity, 300-1100°K 9-35285
- Rb₂CoCl₄, heat capacity meas., mag. phase transition obs., comparison with Ising model 9-39532
- RbCl, adiabatic meas. at low temp. 9-25135
- RuO₂, ht. capacity 0.54°-10°K 9-48971
- Sb, Gruneisen parameters 9-33189
- SiO₂, glass, effect of ⁴He and ³He on ht. capacity at low temp. 9-42733
- Sm, hyperfine interactions obs. 9-47305
- Sn, 1-30°K 9-47006
- Te, Debye temp. by X-ray reflections from powders 9-28428
- ThB₆, low temp. 9-47003
- Ti-Mo alloys, effect of ω-phase precipitates on electronic component 9-35370
- Ti-Rh alloy, and supercond. transition temp. determ. 9-30880
- Ti₃Al ordered and disordered alloys, low temp. electronic sp. ht. coeff. 9-30751
- Ti₂Te, polycrystal, temp. dependence 9-26598
- Ti₂Te, polycrystal, temp. dependence 9-26598
- TiCl₃, temp. depend., vibr. spectrum obs. 9-30763
- U-Zr alloys, specific heat meas. for various compositions 9-33185
- U-Zr alloys, specific heat meas. for various compositions 9-24052
- UC_{1-x}O_x, heat capacity, from thermochem. study 9-28783
- UO₂, ht. capacity, 300-1100°K 9-35285
- W, X-ray Debye temp. meas. 9-35286
- W from phonon dispersion calc. 9-48946
- Y, 1-30°K 9-47006
- YbB₆, low temp. 9-47003
- Zn, 1-30°K 9-47006

Spectra

- see also Absorption/light; Astronomical spectra; Atmospheric spectra; Chemical shift; Colour; Mass spectra; Scattering/light; Raman spectra; Spectrochemical analysis; Spectroscopy; Stark effect; X-ray spectra; Zeeman effect
- absorption, component parameters determ. by statistical processing of curve 9-40578
- absorption, due to impurity centres in solid, long wavelength edge of absorpt. curve obs. 9-33546
- absorption, isobestic pts., conditions 9-40574
- absorption-concentration relationship calcs. for spectral lines 9-25696
- air, emission, and luminance temp., of shock waves 9-36202
- air radiating power in range 0.2 to 3 μ at 10°K, 1 atm. 9-40753
- antiferromagnet, spin-forbidden resonance energy transfer mechanism 9-24323
- auroral electron energy, extended to 45 eV 9-28929
- background intensity, random deviation from mean level, rel. to photographic anal. of spectral emission 9-37849
- bands, overlapping, mathematical expansion 9-48116
- bandwidth for partially coherent slit illumination 9-43925
- bremsstrahlung energy spectrum, near asymptotic expression 9-38461
- cosmic ray, proton and He Nuclei, 100 to 2000 MeV 9-32237
- crystal optical const. and dispersion reln., i.r. region 9-26115
- crystals, electronic transitions between local and zone states in impurity centres 9-43227
- crystals, second-order combinational, and i.r. absorpt., selection rules 9-41371
- crystals with mixed linear chains, i.r. absorpt. rel. to lattice vibrations 9-24401
- d.c. arc plasma, close-cathode intensified, mag. intensification 9-25988
- dielectric crystal, excitation of interacting polariton waves 9-47057
- discrete-state continuum and continuum-continuum interac., creation of low-energy discrete state 9-38805
- electron, low energy, established within and emitted from irradiated conducting materials 9-26466
- electronic absorption and emission bands moments temp. depend. 9-24411
- emission, excitation and photoconductivity, data representation methods 9-22477
- emission, isobestic pts., conditions 9-40574
- emission-concentration relationship calcs. for spectral lines 9-25696
- energy transfer between electronic states interacting with boson field 9-39562
- ESR, computer program for calculation from parametric spin-Hamiltonian 9-36691
- exciton polarizability and magnetic field reversal in yellow series spectrum 9-26728
- extra-galactic, low frequency spectra of radio sources 9-27059

Spectra continued

- false, from plane grating, laser illumination 9-32018
 fluorescence spectra of cpd. emitting from monomer and excimer states, isobestic pts. 9-40574
 galaxies, Markarian's, with u.v. continuum, spectral observations 9-26997
 Heavy elements, L_2 - and L_3 -subshell fluorescence yields 9-34525
 Heisenberg ferromagnet, optical surface spin-waves 9-26628
 impurity absorption, long-wavelength edge shape, Green's function invest. 9-45310
 of impurity light absorpt. centres with local oscill., broadening electron-vib. bands mechanisms 9-26730
 i.r., condensed products of laser produced plasma 9-30209
 Joshi effect, sensitivity under visible radiations 9-30310
 Lande interval rule deviations and isotropic exchange 9-33428
 laser, solid-state, kinetics of free generation spectra in travelling-wave regime 9-27333
 laser beams, amp. and/or phase modulated, analysis by holographic method 9-25330
 line analysis, described by composition of Gaussian and Lorentz profiles 9-25156
 linear molec. crystals, absorpt. by charge-transfer excitons 9-24400
 lines, nonuniformly expanded, effect of strong fields upon contours 9-48115
 liquid, optical const. and dispersion reln., i.r. region 9-26115
 liquids, scattering by thermally excited capillary surface waves 9-28088
 liquids, submillimetre wave refraction 9-28133
 liquids and glasses at high temp., vibr., i.r. reflectance spectrometer 9-46020
 Lorentzian curves containing arbitrary mixtures of absorption and dispersion, line parameters 9-41960
 macroscopic particle spectrum obtainable from light scatt. 9-36358
 molecular cry., i.r., 'oriented gas model' applic. 9-24389
 Mossbauer, computer curve fitting, program 9-42198
 opaque substance, emittance rel. to surface porosity 9-49269
 optical, recording using image intensifiers 9-27405
 organic liquids far from melting point, energy distribution in Rayleigh scattering spectrum 9-26121
 paramagnetic salts, rel. to crystal field parameters 9-33498
 photoluminescent materials, quantum efficiency spectra 9-31154
 plasma, charged arc, in Cs vapour, line intensity and complexity 9-38971
 plasma, highly-ionized dense, dynamic spectrum of radiation prod. 9-46470
 plasma from electrode-less discharge in air stream, 0.2 to 0.8 microns, 9800°K and 1 kg/cm². 9-40674
 powders, high resolution reflectance spectroscopy 9-47340
 power, of object flux transmittance, holographic determ. 9-40368
 rare earth ion, trivalent, Stark structure analysis by stimulated radiation spectra technique 9-31092
 reflection, frost and Venus clouds, in 0.9 to 3.4 μ range 9-47540
 reflection, rel. to surface roughness 9-43207
 resonance, oscillator distrib., calc. method 9-22652
 resonance lines oscillator strengths for np^2 - $npms$ transition calc. of GeI, AsII, SnI, SbII, PbI and BiII 9-38762
 resonance nonadiabatic transitions 9-46256
 salol, liq., Rayleigh line wing fine struct. and transversal hypersound prop. 9-44573
 sea reflection, directional energy, photographic obs. 9-43367
 semiconductor, impure, internal electric fields effects 9-24402
 semiconductor surface, internal reflection 9-43229
 semiconductors, light-modulated reflectance 9-37705
 semiconductors at high pumping densities, universal relation between absorpt. and luminesc. 9-47346
 single-particle, of degenerate electron gas, ground state energy 9-47058
 solid, absorption, effect of vibrational mixing of two close-lying levels of an impurity center 9-28677
 solids, calculating method 9-24390
 solids, modulated reflectance and absorpt., effect of spatially dependent perturbations 9-24396
 86102/6/5 9-40753
 spontaneous emission and time-symmetric quantum electrodynamics 9-41984
 superconductors, weakly coupled, singularities 9-24131
 synchrotron emission with components flying apart at relativistic velocities 9-33916
 time, of spheres pulsed with 14 MeV neutrons 9-34479
 Urbach's rule impurity absorption for insulators and semiconductors 9-45310
 Venus, 8-13 μ emission, telescope obs. 9-38075
 Venus, absolute, 2.8 to 14 μ 9-38076
 Venus, albedos and monochromatic phase curves, terrestrial photoelec. obs. 9-38078
 Venus, far u.v., Venera 4 obs. 9-38083
 Venus, radio and radar spectra rel. surface conditions 9-38082
 Venus, search for minor atmospheric constituents 9-24873
 Al plasma prod. by laser impact on Al target, u.v. emission obs. 9-36769
 Ar, shock waves, distrib. of u.v. and visible radiation 9-48654
 GaAs, p-n junction diode, superradiance spectra and inhomogeneity distribution 9-36315
 H plasma, expanding, electron density and temp. meas. by rapid scan spectrometer 9-44419
 He, laser-produced plasma, line and continuum emission studies 9-34776
 He plasma, high-freq. elec. field meas. 9-23287
 Kr, shock waves, distrib. of u.v. and visible radiation 9-48654
 Ne, shock waves, distrib. of u.v. and visible radiation 9-48654
 8z22/8/5 9-28675
 Xe, shock waves, distrib. of u.v. and visible radiation 9-48654

Ions

see also Atoms/excitation; Atoms/structure

- absorption from excited levels, low-temperature suppression 9-29907
 alkali vapour, h.f. spectrum, saturation eff. of Zeeman transitions 9-27806
 Ar II transitions in range 1900-4500 Å, radiative lifetimes 9-32407
 Ar III, 4s levels new radiative lifetime values 9-25706
 Autler-Townes and Raman reson. effects 9-46268
 bielectronic interactions for $(d+s)^n$ configs., spin depend., symmetry props. 9-38757
 Burnout-V turbulently heated plasma, Doppler broadened spectra emission 9-44443
 C plasma, line radiation energy, 10^4 to 10^5 °K 9-40676

Spectra continued

atoms continued

- calculation allowing for configuration mixing in N=4 electron isoelectronic sequence 9-34521
 Cd vapour, vacuum u.v., absorpt. cross section obs. 9-22946
 complex, for different types of coupling 9-40344
 comprehensive university level text book 9-32395
 continuous spectra of complex atoms 9-30261
 coupling, LS to LL for d^n config., transform. matrices 9-29910
 CS g-factor meas., atomic structure parameters derived 9-29936
 $(d+s)^n$ configurations and R_e group 9-22931
 dielectronic recombination following electron capture by positive ion, radiation damping in optical continuum 9-44248
 Doppler-broadened transitions, coupled, laser-induced line-narrowing effects 9-22934
 effective operators, use and derivation 9-29909
 electron isoelectronic sequences, self consistent field calc. for energy levels 9-32400
 electronic, line by line calc. for voigt profile 9-48378
 emission intensity at 3914 Å rel. to cosmic noise absorption 9-43430
 exploding wires at low pressure 9-30241
 F plasma, line radiation energy, 10^4 to 10^5 °K 9-40676
 fine structure, components, collisional broadening and shift, ang. quantum number depend. 9-44247
 forbidden transitions in isoelectronic sequence, relative line strengths 9-36653
 gas, phonon echo polarization and amplitude 9-42327
 inert-gas afterglows, line shapes 9-44503
 interacting, resonance radiation 9-38789
 inverse bremsstrahlung cross-sections in screened potentials, classical calcs. 9-46271
 ionic electrode, dynamics of lines close by during pulsed elec. discharge 9-36791
 ions, non-hydrogen-like, width and shifts of spectral lines 9-44250
 isoelectronic sequence $Z=N+4$, $N+5\ldots 20$, splitting of terms of $1s^2 2s^2 2p_n$ configs. 9-38760
 isoelectronic series with $1s^2 2s^2 2p^n$ config., fine structures calc. using extended method 9-44251
 isotope shift due to neutron number, n charge distrib. effect first-order perturbation approach 9-44242
 isotope shifts, simple and complex spectra, electronic quantities 9-29986
 Lamb shift obs. by quantum beats 9-22999
 level-crossing effects, zero-field, in cascade process induced by highly saturated laser field 9-32415
 level-crossing signals, time-constant effects and modulation correction 9-36654
 line broadening by electron impact, perturber radiation contribution to lineshape 9-32403
 line emission from two discrete levels under influence of continuum, rel. to radiative transfer irreversibility 9-46272
 line intensity rel. to thermochemical reactions of SiC oxides and compounds of Ti, Zr, V, Ta, Mo and W 9-49372
 line structure, intra-Doppler, from noise spectrum of coherently amplified radiation 9-25689
 linewidth, natural, coherent enhancement 9-40538
 Lyman α anisotropic galactic emissions 9-43516
 many-electron, lamp shift, variational principle for Bethe's average excitation energy 9-38763
 matrix elements of operators between states of two degenerate levels 9-22929
 metals, in compressed Ar, strong emission line shifts, obs. 9-48377
 metals in flames, underpopulation of doublet excited states and fluoresc. yield 9-48379
 microwave spectral tables, listing 9-29920
 one-electron radiative transitions, relativistic expressions for matrix elements 9-29917
 oscillator strengths, relative, meas. technique 9-45678
 oscillator strengths for electric dipole transitions of H 9-29976
 oscillator strengths of p^2 - p^2 transitions 9-22933
 photon echo polarization and amplitude in gas medium 9-42327
 in plasma, dipole transitions probabilities, effect of intermolecular elec. fields 9-46459
 pressure broadening in gases, theory 9-29906
 radiative process with excessive Doppler broadening, noise spectral contour determ. 9-38764
 Raman and Autler-Townes reson. effects 9-46268
 resonance line radiative transfer from a point on the boundary of a half-space 9-44272
 Si^2 matrix, internal consistency of its signs 9-29912
 Si II, in the Sun and ZETA, relative intensities of selected multiplets 9-27094
 spectral line coeffs. from Fabry-Perot profiles, Doppler, dispersion broadening and instrum. effects 9-34586
 spontaneous emission, nonlinear interference effects 9-27804
 spontaneous emission, nonlinear interference effects with allowance for collisions 9-29919
 super heavy atoms, ground state, spectrum energy predictions 9-22937
 two-particle scalar operators for $(d+s)^n$ config., symmetry props. 9-32401
 ultrafine struct. in excited levels, meas. method 9-46269
 X-ray, L-series satellites, $30 < Z \leq 50$ 9-22928
^{151,153}Eu, hyperfine struct., nucl. quadrupole moments, spark spectrum obs. 9-29929
²⁰¹Hg, 6¹P, level, hyperfine struct. and Lande factor 9-29931
¹¹³Cd resonance line, λ 3261 Å, temp. depend. of broadening effects 9-29934
²³³U arc spectrum, hyperfine struct., ground 1L_0 level deduced 9-29952
¹¹⁴Cd resonance line, λ 3261 Å, collision broadening by pressure of inert gases, temp. effects 9-40557
¹⁵⁵Gd, ¹⁵⁷Gd, 4f⁷5d⁵ ⁹D multiplets, hyperfine struct. meas. by atomic beam mag. reson., nucl. mom. calc. 9-22952
²⁰⁸Pb, ²⁰⁷Pb, 208Pb, 7229A isotope shifts in 7229A transition 9-22963
⁹⁸Hg green line profile from photometric meas. of Fabry-Perot rings 9-27808
¹⁹⁸Hg source, photon time-of-arrival distrib. obs. 9-27292
^{199,201}Hg, 6¹P, 6³D_{1,2} and 6¹P, 6¹D₂ transitions, hyperfine struct. 9-29932
¹⁹⁹Hg, 6¹P, level, hyperfine struct. and Lande factor 9-29931
¹⁸⁰Os, hyperfine struct., nucl. quadrupole moment, arc spectrum obs. 9-29929
¹⁵⁷Tb, hyperfine struct. and g_J values of low levels 9-48403

Spectra continued
atoms continued

- ¹²⁹Xe, hyperfine struct. of i.r. laser lines, interpretation on visible and i.r. 9-29954
- Ag, in solid Ar, Kr and Xe matrices, u.v. absorpt. 9-27805
- Ag excited levels, spectroscopic study by electron bombardment 9-29955
- Ag I, isotope shift meas., error sources and soln. 9-29987
- Al, series perturbations and oscillator strengths, ²D series, Hartree-Fock approx. 9-22939
- Al, Stark broadening and displacement, plasma high temp. meas. 9-25913
- Al I, ^{3s}³3d³²S_{1/2} and ²D_{3/2} hyperfine structure, Stark effect investigations 9-40539
- Al in plasma excited by ruby laser 9-38781
- Al plasma emission lines, 5000 to 100000°K 9-40675
- Ar, 40-60 Å photoionization continua region, discrete structure 9-34531
- Ar, highly ionized, in a plasma focus discharge 9-42329
- Ar, low press. gas-jet source, vacuum ultra-violet region 9-22941
- Ar, spectrum emitted as result of proton impact 9-42337
- Ar discharge, 1s and 2p level population, electronic temp., conc. meas., 9500 MHz 9-32702
- Ar excited levels, mag.-reson. expts. 9-29955
- Ar I 7635.10 Å emission profile and self-absorpt. correction, obs. 9-48386
- Ar II, III, IV, cascade-free transitions, radiative lifetimes 9-25691
- Ar II lines, widths and shifts calc. 9-44250
- Ar II optical transition probabilities, arc obs. 9-46292
- Ar pulsed discharge in plasma, spectral absorptivity calc. from radiance spectral density 9-23301
- Ar I 6965.8, 7067.3 and 7345.5 Å lines at 0.03-0.07 torr 9-29921
- Au I, 6p²P_{3/2} state, hyperfine structure investigation by reson. scatt. 9-44255
- B III, mean lives of 2p²P⁰ levels, oscillator strengths 9-44256
- Ba, vapour density determ. 9-42702
- Ba excited levels, spectroscopic study by electron bombardment 9-29955
- Ba I, isotope shift meas., error sources and soln. 9-29987
- Ba I, resonance line broadening by inert gases, effective cross-sections 9-48388
- Ba II lines emitted by discharge along surface of liquid jet, Stark width 9-40716
- Be, far u.v., 2000-500 Å, auto-ionized line series 9-42330
- Be II, mean lives of 2p²P⁰ levels, oscillator strengths 9-44256
- Bi, pulsed discharge, excitation and transitions, obs. 9-25692
- C, 247.8 Å line emission, in shock-heated mixtures of CO, CH₄ and CF₄ in Ar and Ne 9-48387
- C, in arc plasma, Stark broadening of lines 9-44258
- C collisionally excited u.v. and forbidden lines, intensity calcs. 9-25685
- in C d.c. arc, ion and atom persistent lines intensities, calc. 9-24602
- C energy levels, radiative lifetimes 9-36659
- C I, laser lines, obs. 9-46280
- C V, S and P state transitions, wavelength calc. and comparison with expt. 9-40540
- C V, S and P state transitions, wavelength calc. and comparison with expt. 9-44257
- CO₂ vibration-rotation transitions for 00¹1-10⁰ band, collision effects on saturation characteristics 9-22972
- CS g-factor meas., atomic structure parameters derived 9-29936
- Ca, ionized, solar H and K lines 9-31635
- Ca, laser-pumped, abs. from excited states 9-46274
- Ca I, resonance line broadening by inert gases, effective cross-sections 9-48388
- Ca II, K line profile, comparison of models for chromosphere 9-31636
- Ca II line in solar spectrum rel. to non-uniform model of chromosphere 9-36070
- Ca XV, fine structure obs. 9-31628
- ⁴²Ca, 4s4p¹P₁ state, hyperfine struct., level crossing meas. 9-29922
- Cd, excited at 53p₁ level, Hertzian coherence conservation in sensitized fluoresce. 9-46275
- Cd, resonance broadening temp. dependence 9-40541
- Cd II, laser c.w. transition, 3250 Å 9-47983
- Cd in solid Xe, absorption, multiplet struct. obs. 9-22956
- Cd reson. line λ 3261 Å, press. effects, obs. 9-48389
- Cd I absorption spectrum obs. in vacuum u.v. 9-27798
- Ce I, II, infrared lines, isotope shifts 9-29989
- Ce II solar lines, 4000 Å-4700 Å, non-coherent scatt. explanation 9-29089
- Ce IV isotope shift obs. 9-34533
- Cl, (³P_{1/2}) and (³P_{3/2}) states, kinetic spectroscopic studies in vac. u.v. 9-34534
- Cl, spark in various gases, line intensities rel. to press. and Cu or graphite electrodes 9-36792
- Cl I, neutral, wavelengths, energy levels and analysis 9-29925
- Cl II, cascade-free transitions, radiative lifetimes 9-25691
- Co, for 3d/7 and 3d/74p configs., calc. of radial integrals 9-38767
- Co, K α lines in metal and cpds., chem. combination effect on asymmetry indices 9-25695
- Co II, selection rules for forbidden d⁷p⁸ transitions, line strength calc. for 3d⁷4p-d⁸ 9-40542
- Co II, total line strengths and oscillator strengths for 3d⁷4p-d⁸ transitions 9-38768
- Cr³⁺ in ruby, population density in ²E levels, measurement by excited state absorption 9-33534
- Cr I, absolute gf-values from shock tube meas. 9-42322
- Cr I in compressed Ar, He, emission line shifts, 3014-5328 Å 9-48390
- Cr with electronic configurations 3d³ and 3d³4p, energy, theoretical invest. 9-29940
- Cr-Nb, a bibliography for 18 elements 9-38765
- Cr-6³P_{3/2} states distrib. due to sat. hydrocarbon collisions, eff. cross sections 9-44279
- Cs, 8521 Å line display utilizing swept GaAs laser 9-48408
- Cs, hyperfine freq., effects of molec. buffer gases 9-22948
- Cs, quenching of reson. radiation by He 9-42343
- Cs, red shift, broadening and asymmetry in the presence of Xe, Cf₄ 9-46276
- Cs, Stark eff., 7P_{3/2} state hyperfine levels meas. 9-25694
- Cs absorpt. lines shift due to inert gas presence, obs., model 9-29926
- Cs I, 4555 Å line broadening by Ar 9-34535
- Cs I, isotope shift meas., error sources and soln. 9-29987
- Cs in low pressure discharge, level population determ. 9-34536
- Cs ionized atoms, absorption spectra 9-44253

Spectra continued
atoms continued

- Cu, excited and oriented by electron impact, in mag. field, polarization of spectral lines w.r.t. electron energies 9-29928
- Cu, ionic, new classifications and corrected wavelengths of selected lines 9-34549
- Cu 3d⁴4s4p configuration, g_J and hyperfine structure calc. 9-44260
- Cu I, quadratic Stark shifts in some transitions 9-22950
- Cu II 3d⁹4s1D and ³D levels, isotope shift w.r.t. specific-mass effect, exchange polarization of 3d-shell 9-29927
- Cu vapour source, half-life after emission, meas. by atomic absorpt. spectrometry 9-48391
- D and H₂ in Venus atmosphere, concentration ratio from Lyman α obs. 9-43628
- Eu I oscillator strength, f-values determ. by hook method 9-34537
- Fe, for 3d⁷ and 3d⁷4p configs., calc. of radial integrals 9-38767
- Fe⁺, 3d⁴4p config., energy spectrum 9-48397
- Fe group, energy spectra of config. 3d⁴4p 9-48395
- Fe group, energy spectra of configs. 3d⁴s, 3d⁴s₂, 3d⁴s₃ and 3d⁴s₄ 9-48393
- Fe group energy spectra of configs. 3d⁴d and 3d⁴d₂ 9-48396
- Fe group isoelectronic series, energy spectra of configs. 3d⁴s, 3d⁴s₂ and 3d⁴s₃ 9-48394
- Fe I, oscillator strengths and transition probabilities, 2100-9900 Å 9-29930
- Fe I, selection rules for forbidden d⁷p-d⁸ transitions, line strength calc. for 3d⁷4p-d⁸ 9-40542
- Fe I, total line strengths and oscillator strengths for 3d⁷rp-d⁸ transitions 9-38768
- Fe I and Fe II lines, 3190 to 3315 Å, absolute gf-values 9-34538
- Fe I relative oscillator strength obs. 9-45678
- Fe XII solar emission lines, relative intensity as function of temp. and electron density 9-43683
- Ga V, elec. dipole transition configs. obs. 9-48398
- Gd³⁺ in 5 hexagonal crystals, optical absorption 9-33555
- Ge, absorpt. characteristics, obs. 9-28829
- Ge VI, elec. dipole transition configs. obs. 9-48398
- H-C plasma at 40 000°K and 70 atm., coeff. of continuous absorpt. calc. 9-44444
- H, 2S_{1/2}-2P_{1/2} interval, meas. 9-25715
- H, Balmer emission lines for planetary nebulae 9-27002
- H, Lamb shift in nonrelativistic approx. using formulas for photon scattering amplitude 9-36683
- H, Lamb shifts obs. using spatially periodic potentials 9-42346
- H, oscillator strengths for electric dipole transitions 9-29976
- H, solar, Jefferies-Thomas computation and obs. rel. to photosphere and chromosphere models 9-31637
- H_α, H_β Balmer line profiles emission in vortex-cooled arc, broadening meas. 9-27825
- H_α auroral, obs. 9-31372
- H_β Balmer line, plasma particle conc. meas. through Stark broadening 9-25859
- H_γ, Stark broadening of line profile in plasma column 9-42345
- H⁺N₂→HN₂⁺, Balmer-α, N₂⁺(0,0) 1st -ve band photon emission, cross sections meas. 9-22985
- H Balmer lines, asymmetry in transverse elec. field 9-48423
- H beam emerging from C foil, periodic intensity fluctuations in Balmer spectrum 9-46332
- H level populations, double-resonance method 9-47925
- H Lyman α, Venus, Mariner 5 obs. 9-31614
- H plasma, line and continuum rad. 9-48554
- H solar Lyman α profile rel. to geocorona, rocket obs. 9-29084
- ²H, u.v. absolute spectral energy distrib. 9-36666
- H³D→2²P, polarization 9-32430
- H_α Balmer line, emission and absorption coefficient in arc plasma 9-34576
- H_α line in solar spectrum rel. to non-uniform model of chromosphere 9-36070
- H_β line intensity ratio to background at same wavelength, appl. to plasma temp. determ. 9-30261
- He-like ions, long wavelength satellites to resonance lines, applic. to solar spectrum 9-42351
- He, 1S-2¹P transition, oscillator strength calc. using Hanle method 9-38776
- He, 2S_{1/2}-2¹P, line isotope shift meas. 9-25719
- He, laser transitions, lifetimes of upper and lower excited-state levels as fn. of press. 9-48431
- He, n³D-2³P series, for planetary nebulae 9-27002
- He, singlet-triplet transition prob. variational calc. 9-29981
- He, transitions between doubly excited states and 2S² state, line strengths calc. 9-42350
- He, Van de Graaff accelerator, use of 9-22998
- He I, Stark broadening of allowed and forbidden transitions, calcs. 9-42349
- He I 4922 and 4472 Å line widths, appl. to plasma electron conc. determ. 9-30261
- He II, 303.8 to 230.7 Å and 206.2 to 120 Å, production 9-44298
- He like ions from He I to Ne IX, intercombination oscillator strengths 9-36662
- He line coeffs. from Fabry-Perot profiles, Doppler, dispersion broadening and instrum. effects 9-34586
- He magnetic splitting determ. 9-29936
- ³He, ultrafine struct. meas. in 1D levels 9-46269
- ⁴He⁺, 4S_{1/2} and 4²P_{1/2} levels, observation of resonance effect, in modulated fluorescent light 9-25720
- He+p charge-transfer collisions, polarization of Balmer-α radiation 9-22989
- Hg, 1.5295 mμ laser line, isotopic struct., obs. 9-34541
- Hg, absorpt.-conc. relationships 9-25696
- Hg, electron-impact spectrum 9-44263
- Hg, line shift by high power laser pulse 9-25709
- Hg, relative brightness and optical excitation functions meas. 9-29933
- Hg, resonance broadening temp. dependence 9-40541
- Hg in solid Xe, absorption, multiplet struct. obs. 9-22956
- Hg vapour, two-photon stimulated processes, study 9-26731
- Hg I absorption spectrum, 600-950 Å new resonance window obs. 9-27798
- N₂H⁺→HN₂⁺, Balmer-α, N₂⁺(0,0) 1st -ve band photon emission, cross sections meas. 9-22985
- Ho³⁺, (f-f) absorption obs. in CaF₂ 9-28682

Spectra continued
atoms continued

- I, Zeeman effect for forbidden line and emission spectrum 1.31-2.24 μ obs. 9-29935
- In I-spectrum, hyperfine struct. of $5s^25d^2D_{3/2}$ and $5s^26d^2D_{3/2}$ states 9-44264
- In I, hyperfine struct. of $5s^25d^2D_{3/2}$ and $5s^26d^2D_{3/2}$ states, Stark eff. investig. 9-29938
- K, absorption, shift and splitting in laser beam radiation field 9-29937
- K, electron impact, generalized oscillator strengths 9-34543
- K, g-factor meas. atomic structure parameters derived 9-29936
- K, octopole-allowed transitions in electron energy-loss spectra 9-40543
- K vapour, radiative splitting of atomic levels in laser rad. field 9-27809
- ^{39}K , 4p and $5p^2P_{3/2}$ -states hyperfine struct. investig. by resonance-scatt. of light 9-29751
- ^{41}K 4p and $5p^2P_{3/2}$ -states, hyperfine struct. investig. by resonance-scatt. of light 9-29751
- Kr 1236 Å resonance beam, disturbances by inert gases and H_2 9-44265
- Kr 40-60Å photoionization continua region, discrete structure 9-34531
- Kr 5871 Å line shape determ. by correlation method 9-43926
- Kr discharge, 1s and 2p level population, electronic temp., conc. meas., 9500 MHz 9-32702
- Kr ionized, transitions competition 9-45955
- krII lines at 0.02-0.08 torr 9-29921
- Li, 2934 Å 3714 Å multiplets due to decay to $^4\text{P}^0$ of lowest-lying $^4\text{S}^e$ and $^4\text{P}^e$ states 9-25698
- Li, hyperfine splittings and press. shifts of ^6Li and ^7Li , optical pumping expt. 9-40550
- Li atom energy levels splitting calc., transition from quadratic to linear Stark eff. for spectral lines 9-22957
- Li I, mean lives of $2p^2\text{P}^0$ levels, oscillator strengths 9-44256
- Li in solid Xe, absorption, multiplet struct. obs. 9-22956
- Li plasma, high-density, linear Stark broadening 9-34765
- Li plasma emission lines, 5000 to 10000°K 9-40675
- Mg, far u.v., 2000-500 Å, auto-ionized line series 9-42330
- Mg, Stark broadening and displacement, plasma high temp. meas. 9-25913
- Mg II, H and K line profiles, comparison of models for chromosphere 9-31636
- Mg vapour source, half-life after emission, meas. by atomic absorpt. spectrometry 9-48391
- Mn $^{2+}$ ion, analysis, 600-9300 Å 9-38771
- Mo in compounds, L level shifts and width changes 9-48400
- Mo VII, VIII and IX energy levels 9-46287
- N, radiative-lifetime meas. 9-36663
- N, Van de Graaff accelerator, use of 9-22998
- N $^-$ emission in nitrogen and air plasmas 9-44442
- N collisionally excited u.v. and forbidden lines, intensity calcs. 9-25685
- N I, laser lines, obs. 9-46280
- N II (III) u.v. multiplets, upper level decay scheme 9-44266
- N III lines, absolute transition probabilities, meas and obs. 9-29941
- N VI, S and P state transitions, wavelength calc. and comparison with expt. 9-40540
- N VI, S and P state transitions, wavelength calc. and comparison with expt. 9-44257
- N(^3P)3s(^2P) vacuum u.v. emission obs. 9-27866
- Na, Stark broadening and displacement, plasma high temp. meas. 9-25913
- Na electron impact, generalized oscillator strengths 9-34543
- Na I 5682-88 Å and 4978-82 Å lines of plasma, Stark broadening 9-32413
- Na in solid Xe, absorption, multiplet struct. obs. 9-22956
- Nb in compounds, L level shifts and width changes 9-48400
- Nb VI, VII and VIII energy levels 9-46287
- Nd, isotope shift, interpretation 9-34548
- Nd $^{2+}$, (f-f) absorption obs. in CaF_2 9-28682
- Nd $^{3+}$ in vitreous matrix, effective amplification section of 1.06 transition 9-48399
- Nd I arc spectrum, electronic configs., parametric calc. 9-29943
- Ne, discharge conditions for generation at $\lambda=1.15\mu$ 9-25975
- Ne, highly ionized, in a plasma focus discharge 9-42329
- Ne, multi-ionized, transitions and decay meas. of levels 9-46299
- Ne, oscillator intensities for $\Gamma-\Gamma^*$ transition, areas of electron excitation 9-36671
- Ne, pulsed super-emittance from 2p-1s transition, mechanism 9-29959
- Ne, transition probabilities study with laser excitation 9-25699
- Ne 3s-3p, transition in He-Ne laser resonator meas. 9-22960
- Ne collisionally excited u.v. and forbidden lines, intensity calcs. 9-25685
- Ne emission, intensity in h.f. discharge determ. 9-23355
- Ne excited levels, mag.-reson. expts. 9-29955
- Ne II selected ranges between 10150 and 2500 Å 9-40546
- Ne ionized beam, 2000 to 6000 Å 9-46320
- Ne pulsed discharge in plasma, spectral absorptivity calc. from radiance spectral density 9-23301
- Ne VII and Ne VIII 3s-3p transitions, identification in high temp. plasma 9-48401
- Ni, for 3d 7 and 3d 4 4p configs., calc. of radial integrals 9-38767
- Ni, ionic, new classifications and corrected wavelengths of selected lines 9-34549
- Ni I in compressed Ar, He, emission line shifts, 3050-3619 Å 9-48390
- Ni III, selection rules for forbidden d 9 p-d 8 transitions, line strength calc. for 3d 7 4p-d 8 9-40542
- Ni III, total line strengths and oscillator strengths for 3d 7 4p-d 8 transitions 9-38768
- N(v) relative intensities and exponential decay of $^2\text{P}_{3/2}$ and $^2\text{P}_{1/2}$ 9-44267
- O, solar photosphere, center-to-limb analysis 9-31656
- O, Stark broadening and displacement, plasma high temp. meas. 9-25913
- O, VII, S and P state transitions, wavelength calc. and comparison with expt. 9-40540
- O, VIII, S and P state transitions, wavelength calc. and comparison with expt. 9-44257
- O, values of 4p ^2P levels using new high intensity spectroscopic source 9-42344
- O auroral green line excitation by $\text{N}_2(\text{A}^3\Sigma_u^+)$, rate const. calc. 9-43424
- O collisionally excited u.v. and forbidden lines, intensity calcs. 9-25685
- O energy levels, radiative lifetimes 9-36659
- OI 6300 Å twilight airglow, enhancement rel. to latitude 9-28924
- O5577 Å auroral line transition lab. obs. 9-46282
- in Oz-acetylene flames, absorpt. and emission enhancement rel. to free-atom form., obs. 9-22936

Spectra continued
atoms continued

- Pr III 4f 6 s, 4f 5 d, and 4f 6 p configurations, level energies, interpretation 9-22964
- Rb, octopole-allowed transitions in electron energy-loss spectra 9-40543
- Rb g-factor meas., atomic structure parameters derived 9-29936
- Rb nonlinear hyperfine pressure shift induced by optical pumping 9-36664
- Rb vapour, stimulated three-photon scattering 9-22954
- ^{85}Rb replacement by ^{87}Rb and ^{87}Rb mixture for filtration 9-38770
- ^{87}Rb principal doublet hyperfine components, filtration efficiency 9-29945
- RbI, II, excited levels g factor determ. 9-29944
- S, spark in various gases, line intensities rel. to press. and Cu or graphite electrodes 9-36792
- S I transition probabilities, near vacuum u.v., obs. 9-23366
- S II, cascade-free transitions, radiative lifetimes 9-25691
- S II, level excitation by beam-foil technique 9-48402
- S III level excitation by beam-foil technique 9-48402
- S isotope abundances by band spectroscopy 9-46283
- Sb^{3+} in HCl, LiCl soln., Bunsen-Roscoe law breakdown 9-29939
- Se I transition probabilities, near vacuum u.v., obs. 9-23366
- Si, Stark broadening and displacement, plasma high temp. meas. 9-25913
- Si I, Si II, Si III-lines 1100-2600 Å, oscil. strength meas. 9-44269
- Si I transition probabilities, near vacuum u.v., obs. 9-23366
- Si III oscillator strengths calc. and many electron correl. problem approx. 9-29946
- Si XI ions, grazing incidence spectra, emitted by laser produced plasma 9-38758
- Si XII ions, grazing incidence spectra, emitted by laser produced plasma 9-38758
- SiI relative transition probabilities in the Sun 9-24899
- Sm, L emission, weak lines study 9-34550
- Sm I, level lifetimes, Hanle effect meas. 9-29950
- Sm vapour, i.r. laser lines 9-29947
- Sn, odd-even isotope shifts 9-34542
- Sn II laser c.w. transitions, 6453 and 6844 Å 9-47983
- Sr I, resonance line broadening by inert gases, effective cross-sections 9-48388
- Sr II absorpt. oscillator strengths, 1400-1900 Å and 4000-4400 Å 9-32414
- SrI, in 1646-2028 Å region 9-22965
- Sm^{3+} in CaF_2 , type I, trigonal crystal field energy levels 9-33244
- TC I, energy levels and classified lines, tables 9-34551
- Tb, structure of spectrum, 4f 8 5d 6 s 9-38775
- Th I, Slater integrals, Hartree-Fock soln. 9-25700
- Th lines, 2747 to 4572 Å, interferometric obs. 9-46284
- Ti I, odd configurations 9-29948
- Ti II, line strengths for the transition array (3d 3 +3d 2 4s)-3d 2 4p, calc. 9-34522
- Ti with electronic configurations 3d 2 and 3d 3 4p, energy, theoretical investigation 9-29940
- Ti, 6 $^2\text{P}_{3/2}$ state, lifetime and effective quenching cross section, r.f. discharge obs. 9-29949
- Ti I spectra, 6d $^2D_{3/2}$ -state, influence of electric field on level crossings 9-48404
- Tm $^{2+}$, (f-f) absorption obs. in CaF_2 9-28682
- Tm I, level lifetimes and crossings, Hanle effect meas. 9-29950
- Tm vapour, i.r. laser lines 9-29947
- UII spark spectrum, A and B systems unification 9-29951
- V $^+$ ion, new lines 2500-8800 Å 9-38777
- V with electronic configurations 3d 3 and 3d 3 4p, energy, theoretical investigation 9-29940
- vapour source, meas. by atomic absorpt. spectrometry involving pulse technique 9-48391
- W I, energy levels and classified lines, tables, 2000-10500 Å 9-34552
- W I, even energy levels, theor. interpretation, tables 9-34553
- W line transitions, probability determ. 9-46302
- Xe, discharged 1s and 2p level population, electronic temp., conc. meas., 9500 MHz 9-32702
- Xe, isotopic variation (132, 130) of thirteen i.r. laser lines, relative isotopic displacement 9-48438
- Xe, u.v. absolute spectral distrib. 9-36666
- Xe 1295 Å resonance beam, disturbances by inert gases and H_2 9-44265
- Xe 40-60Å photoionization continua region, discrete structure 9-34531
- Xe adsorbed on LIF films, u.v. absorpt. 9-44630
- Xe excited levels, mag.-reson. expts. 9-29955
- Xe highly saturated laser field, zero-field level-crossing effects in cascade process. 9-32415
- Xe I, radiative lifetimes for excited states 9-48405
- Xe II radiative lifetimes for excited states 9-48405
- Xe isotopes, i.r. laser lines, isotope shift meas. 9-29991
- Xe photoabsorption near $\text{N}_{IV,V}$ edge, comparison with solid Xe 9-26745
- Y in compounds, L level shifts and width changes 9-48400
- Yb I, absorpt., line obs. 9-44270
- Yb isotopes, stable, 656p ^1P , level h.f.s. determ., level-crossing and anticrossing spectroscopy 9-22967
- Yb vapour, i.r. laser lines 9-29947
- Zn, ^3P , state, collision broadening of double resonance line empirical formula for resonance curve 9-34554
- Zn, ionic, new classifications and corrected wavelengths of selected lines 9-34549
- Zn electrode, line dynamics nearby during pulsed elec. discharge 9-36791
- Zn II laser c.w. transitions, 7479 and 7588 Å 9-47983
- Zn IV, elec. dipole transition configs. obs. 9-48398
- Zn isoelectronic series, oscillator strengths energy eigenvalues, mean radii, calcs. 9-44271
- ZnI absorption spectrum obs. in vacuum u.v. 9-27798
- Zr V, VI and VII energy levels 9-46287

inorganic liquids and solutions

- alkali-metal nitrates, molten, i.r. absorpt. band shapes 9-30411
- binary solns., dilute, Brillouin intensity ratios and Landau-Placzek law deviations, obs. 9-30408
- complex compounds in solns., effect of liquid field on e.s.r. hyperfine splitting 9-32795
- inert solns. of diatomic mol., i.r., theory 9-44567
- ozone, i.r. absorpt. 9-46641
- rare earths, trivalent, in soln., intensities 9-36885
- AgO in acid, transition bands assignment, 8000-13000 cm^{-1} 9-27850

Spectra continued

inorganic liquids and solutions continued

- Br₂, i.r. absorption temp. depend., induced dipole moment and correlation function determ. 9-42660
 Br₂/I₂, i.r. absorption temp. depend., induced dipole moment and correlation function determ. 9-42660
 Co(H₂O)₆²⁺, electronic, interpret. 9-48458
 CuCO₃, in acid, transition bands assignment, 8000-13000 cm⁻¹ 9-27850
 Gd³⁺ in aq. soln., electronic energy levels 9-26118
 H₂O and D₂O, vac. u.v. 9-36884
³He impurity quasipart. in superfluid ⁴He, excitation spectrum, effective interac. energy 9-23563
 I₂, i.r. absorption temp. depend., induced dipole moment and correlation function determ. 9-42660
 K₂[Cd(NO₃)₄], u.v. and i.r. absorpt. and Raman spectra 9-49288
 MgNO₃-water, vibr., rel. to NO₃⁻ symmetry, i.r. absorpt. obs. 9-36887
 N₂F₄ liq., i.r. 9-23505
 N₂O, vibration band profile determ. in various solvents and correlation function calcs. 9-44571
 N containing anions, attenuated total refl. spectra, aqueous soln., i.r. vib. freq. 9-28135
 NH₃ liq., effect of dissolved salts on i.r. spectra 9-39106
 NH₄ salts in liq. NH₃, conc. soln., i.r. spectra, vib. freq. shifts, H-bonds study 9-30042
 NH₄NO₃-water, vibr., rel. to NO₃⁻ symmetry, i.r. absorpt. obs. 9-36887
 NO₃⁻ ion, solvation of nitrate ion, i.r. spectroscopic evidence 9-42661
 Na, plasmon effect on absorpt. 9-44572
 NaHSO₄-KHSO₄, melts, Mo V obs. 9-37729
 NaNO₃-water, vibr., rel. to NO₃⁻ symmetry, i.r. absorpt. obs. 9-36887
 Nd³⁺: SeOCl₂ laser liq. rel. to Nd ion conc., acidity and temp. 9-26120
 Pt complex, [Pt Cl₂ (C₂H₄)₂], Raman and i.r. vib. 9-27873
 Pt complex, K [Pt Cl₂ (C₂D₄)₂].H₂O, Raman and i.r. vib. 9-27873
 Pt complex K [Pt Cl₂ (C₂H₄)₂].H₂O, Raman and i.r. vib., C-C stretching freq. determ. 9-27873
 Tb³⁺ in aq. soln., electronic energy levels 9-36886

inorganic molecules

see also Molecules

- air, effect of halogen compounds 9-34629
 anthracene soln., electronic absorption- band region, Einstein-coeff. spectra obs. 9-30072
 bands, electron excited, use in intensity calibration 9-25380
 gases, photon echoes, polarization props. 9-30351
 inert-gases, prod. by electron-beam pulses 9-44345
 microwave spectral tables, listing 9-29920
 polyenes, vibration struct. of electronic spectra 9-48443
 rare earth complexes with tenoyltrifluoro- acetone and rhodamine-C, benzene solns., fluoresc. 9-42664
 transition metal pyridine-2- carboxamide chelates, far, i.r., normal coord. treatments 9-25751
 vaporization of solids, using matrix isolation techniques 9-28190
 water vapour, ν₂ band, twenty lines, strength meas. 9-36699
 As compounds, infrared and Raman studies 9-36695
 CO₂, 00¹ level decay in pulsed CO₂-N₂ gas discharges 9-34159
 CSe₂, i.r. and Raman 9-34614
 GaAs:Cu, of bound excitons, vib. structure analysis and effect of uniaxial compression rel. to impurity centre structure 9-33231
 H₂¹⁸O, ν₁ and ν₂ bands, 2.5-3.0 μ, rotational structure 9-34623
 Li hydrides, molec. consts. by molec. beam elec. reson. 9-30061
 LiF, i.r. matrix spectra, dimer Li₂F, obs. 9-23053
 N₂, radiation generated during B³Πg A²Σ⁺u transition effect of inert gases 9-38864
 NO, paramagnetic, energy splitting of core electron levels 9-34634
 Na-NH₃ gas mixtures, absorpt. 9-34633
 O₂, paramagnetic, energy splitting of core electron levels 9-34634
 PbTe, reflectivity, transmission and Faraday effect in determ. band structure parameters 9-39630
 S Kβ₁ line shape in metal sulphides, X-ray microprobe, curved quartz crystal spectrograph 9-25749
 SF₆, ν₂ and ν₄ bands 9-34642

inorganic molecules, diatomic

- electronic, line by line calc. for voigt profile 9-48378
 predissociation probabilities for vibrational levels of bound state 9-32462
 radiative decay, transition moments and oscillator strengths 9-36694
 rotational analysis, computer application 9-38827
 Ag halide vapours, u.v. absorpt. cross-sections 9-46376
 AlO, visible region, new bands 9-46354
 AlO exploding wire obs., book 9-29138
 AlSe, electronic band system obs. in thermal emission 9-42380
 AsO, electronic band systems obs. 9-46356
 AsO⁺, (1,0) and (2,0) bands of A-X system, ¹Π-¹Σ transition 9-46355
 BH, emission, Stark effect, X(¹σ) and A(¹π) dipole moments determ. 9-46357
 BS, ²Δ-A²π and two ²Σ⁺-²π transitions 9-30022
 BaD absorpt., 6100-7300 Å. 9-32465
 BaO, recorded in Ba release expt. for atm. temp. determ. 9-26917
 BeF, A²π-X²Σ⁺ syst., abs. spectra, character analysis 9-23031
 BeF, Franck-Condon factors and r-centroids for bands of A²Π-X²Σ syst. 9-46358
 BiF, 2250 Å system, rotational structure 9-42383
 BiF, A-X, syst., Franck-Condon factors and r-centroids 9-23074
 C₂, extension of (A²Π-X²Π_g) band system 9-34610
 C₂, transition probabilities for the Swan and Mulliken bands 9-42384
¹²C¹³P, B²Σ⁺-A²Σ⁺ band syst., Franck-Condon factors and r-centroids 9-23033
 CN, mag. dipole transitions between excited electronic states obs., 10.5-11.5 GHz 9-23036
 CN violet band system, electronic transition moment variation 9-38834
 CO, absorpt. lines, collisional broadening coeffs. of foreign gases 9-25736
 CO, fundamental, self- and foreign-gas broadening, ratio of collision cross-sections 9-25735
 CO, reclassification of upper state of 3A bands 9-44322
 CO₂ gas, excited by fast electrons, glow spectra in i.r. region 9-38831
 CO₂ rotational constants, from meas. of cw beats in bulk GaAs between CO₂ vibrational-rotational lines 9-25737
 CO⁺ ion, new electr. band syst. assigned to ²Δ_g-A²Π_g transition 9-25738
 CO adsorbed on LiF films, u.v. absorpt. 9-44630
 CO adsorbed on metal films, i.r. absorption 9-26193
 CO chemisorbed on Rh, Ir and Pt, i.r. obs., temp. effect 9-43325
 CO gas, excited by fast electrons, glow spectra in i.r. region 9-38831

Spectra continued

inorganic molecules, diatomic continued

- CO i.r. absorptance down to 113°K 9-32471
 CO i.r. rot.-vibr. bands, self and foreign gas broadening effects, comparison 9-27848
 CS, new band system in near u.v. region, seen in diffusion flames 9-48456
 CaF, A-X and B-X syst., Franck-Condon factors and r-centroids 9-23074
 CaS gas, A¹Σ⁺-X¹Σ⁺ band rotational analysis, 1900°C, 6200-7200 Å 9-42389
 Cl₂, press.-induced fundamental i.r. absorpt. band 9-30023
 ClO radical, microwave, rot. transitions Q=3/2-1/2 in ²Π_{1/2} state 9-48514
 Co⁺, radiative lifetime of B²Σ⁺ state 9-44321
 CrH, predissociation of upper electronic state of 3680 Å transition 9-42449
 CuI absorption edge, donor-acceptor interactions and adsorption of organic molts. 9-25739
 D₂, emission in extreme u.v. from autoionizing levels 9-28042
 DCl cry., i.r. absorpt. 9-47360
 F₂, compressed, rot. and translational induced spectra 9-36700
 F₂ oscillator strengths, corrections to recent results 9-30037
 F₂ rotational, obs. 9-29484
 H₂-D₂ mixed solid solutions, i.r. induced into vibrational first harmonics, ⁴K 9-33558
 H₂, emission in extreme u.v. from autoionizing levels 9-28042
 H₂, Franck-Condon factors for three band systems 9-30032
 H₂, Franck-Condon factors for three band systems 9-32476
 H₂, Franck-Condon factors for band systems 9-44330
 H₂, model dipole spectrum 9-38849
 H₂, transition moments for Lyman band 9-24810
 H₂ laser excited Raman scatt., width of Q(1) line 9-30031
 H₂ Lyman-band oscillator strengths 9-27856
 H₂ Lyman and Fulcher bands, vibr.-rot. interaction effects in Franck-Condon factors 9-30029
 HCl, emission of vibration-rotation lines from hot vapour, conc. dependences 9-25696
 HCl i.r. region, vibrations, effect of inter-molecular interactions 9-23050
 HF, perturbation of rot. lines by F₂, at 200 bar 9-36700
 HF absorption spectrum in 600-1100 Å region 9-34625
 HF chem. laser emission in XeF₄, SbF₅-H₂, methane mixtures photolysis, obs. 9-31944
 He₂, 510-611 Å absorpt. 9-44332
 He₂, absorption spectrum 600-620 Å 9-34625
 He₂, spectroscopic constants for F¹Π_u and f³Π_u states, quantum-mechanical exam. 9-34626
 HgBr, band spectrum in u.v. region, analysis and new vib. consts. of systems 9-46184
 HgCl, HgBr and HgI, i.r. 9-34627
 I₂, 11-5 band R (127) line hyperfine components, saturated absorpt., 633 nm 9-48465
 I₂⁺, vib. freq. from resonance Raman spectrum 9-38856
 I₂ beam resonance line reference for Ar laser frequency stabilization 9-25245
 La₂, visible 9-46366
 LaO, emission, rot. analysis of indigo system 9-46365
 LiF crystal, absorption determ. 2-25 μ 9-24373
 MgBr, A²Π-X²Σ⁺ system, rot. analysis of (0,0) bands 9-30036
 MgF, Franck-Condon factors and r-centroids for A-X system 9-46367
 MgO oscillator strengths, corrections to recent results 9-30037
 N₂, ¹Σ_g⁺ vib. levels, deperturbed crossing Morse curves calc. 9-27863
 N₂, 1st positive bands, electron excitation 9-40597
 N₂, electron energy-loss spectrum, perturbations due to config. interactions 9-38858
 N₂, electronic band strengths of first positive system 9-48471
 N₂, Franck-Condon factors for v'=0 progression of fourth positive band system 9-42407
 N₂, pink afterglow in mag. field 9-30315
 N₂, N₂⁺ 1st -ve system prod. by ion bombardment, rotational line intensities meas., 130°K 9-46429
 N₂⁺, 1st negative and Meinel bands, electron excitation 9-40597
 N₂⁺, electronic band strengths of Meinel system 9-48471
 N₂ ion, excitation of λ=4278 Å band of first negative system by noble gas ions and atoms 9-30045
 N₂⁺ rotational bands excited in hollow cathode discharge, Boltzmann distrib. 9-23055
 N₂⁺m first negative bands excited by e impact obs. 9-32479
 N₂ absorption, dipole-allowed; lowest valence and Rydberg states 9-27864
 N₂ absorption spectrum, 600-1100 Å 9-34625
 N₂ first positive system, Einstein coeff., Halevi's correction application 9-27868
 N₂ in arc discharge, effect of Na addition 9-46550
 N₂ in metastable B²Σ⁺ state, emission spectrum amdg radiative lifetime, mol.-beam meas. 9-38863
 N₂ radiating power in range 0.2 to 3 μ at 10⁴K, 1 atm. 9-40753
 N₂ vacuum u.v. emission 9-27866
 N₂ yellow afterglow at low pressures, visible emission rel. to atomic recombination kinetics 9-39029
 N₂(1+) and N₂⁺(1-) nonequilibrium region behind shock, radiation mechanism 9-4210
 N₂ mixture with O₂ and ether or methane, simultaneous HCN and H₂O laser emissions in pulsed discharge 9-22404
 ND, emission bands assigned to d¹Σ⁺-b¹Σ⁺ transition 9-46368
 NH, emission bands assigned to d¹Σ⁺-b¹Σ⁺ transition 9-46368
 NH d¹Σ⁺-c¹Π bands, predissociations 9-34607
 NO, β, γ systems, transition dipole moment determ. 9-48472
 NO, infrared region 9-36704
 NO, mag. rot. spectrum of A²Σ⁺-²Π_g transition 9-44337
 NO formed in vibrationally excited state in N+NO₂O+NO 9-24539
 NO gas, excited by fast electrons, glow spectra in i.r. region 9-38831
 NS, isotope shift studies, microwave discharge emission spectra 9-34635
 NaCl, h.f.s. by molec.-beam elec. reson. 9-44343
 NbO⁺, hyperfine splittings of 0,0 sub-bands 9-44344
 No, the 4d complex 9-23056
 O₂, atmospheric 1-1 and 2-0 bands, rel. to rotational, oscillational and kinetic states 9-26893
 O₂, mag. dipole rot., 12-65 cm⁻² 9-32483
 O₂, Schumann-Runge bands, predissociation 9-32462
 O₂, u.v. vacuum absorpt., rel. to evaluation in N₂, H₂ and inert gases 9-37858

Spectra continued

inorganic molecules, diatomic continued

- O₂ 0.7620 μ absorption and transmission function calc., molecular parameters 9-38832
 O₂⁺ absolute excitation cross sections for emission of first negative bands under e. impact on O₂ 9-42412
 O₂⁺ second negative bands, isotope shift study, revised rot. and vib. const. 9-23063
 O₂ 7640 Å band, effect of temp. and pressure 9-46371
 O₂ absorption near 1215 Å, press. range 100 to 760 torr 9-34638
 O₂ atmospheric i.r. bands in air glow 9-45509
 O₂ B-band lines, parameters rel. to atmospheric temp. 9-40011
 O₂ lines, spin-rotational, absorption coefficient in geomagnetic field 9-45495
 O₂ Lyman-alpha absorption 9-23061
 O₂ spectral system, red atmospheric, electron transition probability 9-36706
 O₂ transition probability, absolute 9-23170
 O₂ u.v. absorption, 100 to 150 km, Woomera 9-37932
 O₂(¹ Δ_g →³ $\Sigma_g^-) (0, 0), (0, 1) transitions, ratio 9-40601
 O₂ mixture with N₂ and ether or methane, simultaneous HCN and H₂O laser emissions in pulsed discharge 9-22404
 OD⁺ rot. analysis of high-resolution spectrum of A³ Π_1 -X³ Σ^- transition 9-44346
 OH, absorption lines, shape and width by curve of growth method 9-48476
 OH⁺ rot. analysis of high-resolution spectrum of A³ Π_1 -X³ Σ^- transition 9-44346
 OH bands in emission spectrum of night airglow, 2 to 4 μ m 9-28922
 PO, visible and u.v. bands 9-40602
 PO β syst., rot. analysis of bands, vib. assignments of new bands 9-23066
 PS isotope shift studies, microwave discharge emission spectroscopy 9-34635
 PbCl, rotational analysis of A-X bands 9-23067
 S₂, 0-0 band of system D-X ³ Σ_g^- , analysis of incompletely resolved struct. and head struct. 9-48479
³²S₂, C³ Σ_u^- →X³ Σ_g^- system, rot. anal. 9-23070
 SF₆ gas, photon echo, polarization props. 9-30351
 SO, β ² Σ^- →X³ Σ^- and A³ Π_1 -X³ Σ^- band systems 9-38870
 SBO, fine structure analysis and isotope effect studies in B-X, C-X and D-X systems 9-23072
 SeF₄ gas-phase electron reson. 9-42416
 SiF₄ β system, Franck-Condon factors and r-centroids 9-23074
 SiO, oscillator strength of (A¹ Π →X² Σ^+) band system, shock tube study 9-28161
 Te₂, emission spectra, high resolution, rot. constants suggesting Σ - Σ transition 9-34644
 ThO perturbed ¹I state, rot. anal. 9-32488
 TiO, γ system, rot. analysis of (0,0) band 9-40603
 TiO four new bands in β system 1-0 sequence 9-32489
 Tl halide vapours, u.v. absorpt. cross-sections 9-46376
 ZnBr, band spectrum in near u.v., vibr. const. 9-46377$

inorganic molecules, diatomic, radiofrequency

see also Nuclear magnetic resonance and relaxation; Paramagnetic resonance and relaxation

- BrO free radical 9-44376
 CN, A² $\Pi_{3/2}$ state, microwave-optical double reson. 9-34609
 ClO radical, rotational transitions in ² $\Pi_{3/2}$ and ² $\Pi_{1/2}$ states 9-38836
 H₂⁺, vibrational levels 9-27854
 KBr, molec. beam elec. reson. 9-27862
 O₂ line broadening, contrib. of London dispersion force 9-36707
 OH excited A-doublet states, conditions for maser emission 9-34636
 PbS, dipole moment from Stark components of microwave rotational transitions 9-30051
 SF₆ gas-phase electron reson. 9-42416
 SIS, dipole moment from Stark components of microwave rotational transitions 9-30051
 SnS, dipole moment from Stark components of microwave rotational transitions 9-30051
 TiCl, h.f.s. 9-34645

inorganic molecules, polyatomic

- alkali metal metabolates, i.r. spectra in solid Ar or Kr matrix 9-32463
 alkali metals azides, new electronic and i.r. band after irradiation, D_{3h} ion symmetry 9-27844
 cyanogen halide-inorganic halide addition cpds., vibr. assignments, i.r. obs. 9-27847
 DNA, heat- and alkali-denatured, comparison 9-23182
 group IV and V boron hydrides, i.r. absorpt. 9-42381
 heavy water, i.r. laser irradiation, Stark spectrum obs. 9-25766
 metal complexes with N-containing ligands, i.r. and Raman obs. of stretching and bending fund. 9-32459
 NH₃, Fourier dispersion, rel. to rot. line strengths and elec. dipole moment, 87-667 μ 9-30043
 ozone, coeffs. of absorption in Hartley band, verification 9-41524
 ozone, liq., i.r. absorpt. 9-46641
 SiF₄ free radical, i.r. 9-31211
 transition-metal fluorides, theory 9-42379
 water vapour, vibrational-rotational energy levels quantum mechanical calc., spectrum fine structure obs. 9-23049
 Ag chelates of glycine, DL α alanine, DL β phenylalanine and DL tyrosine, i.r. vib. spectra, assignments 9-23059
 AsH₃, i.r., effect of accidental Coriolis-type reson. 9-34608
 AsO, emission bands 9-48454
 BaF₂ vapour, absorption bands, ν_2 bending vib. assignment 9-23037
 HBrBr, i.r. at 20°K 9-44320
 CF₄, oscillator strengths, 2250-3000 Å absorpt. 9-27846
 CO₂-N₂-He-H₂O glow discharge, 3-7 torr, 2800-6500 Å 9-25979
 CO₂-N₂-He glow discharge, 3-7 torr, 2800-6500 Å 9-25979
 CO₂-N₂, vibrational thermal relax. times, determ. by stopping point, fluorescent and spectrophone methods 9-48455
 CO₂, 10.6 μ m line, saturation of absorption 9-25733
 CO₂, blue continuum emission, 1900-2400°K, shock tube study 9-38837
 CO₂, i.r. emission in shock waves rel. to relax. freq. of asymmetric stretching mode 9-34611
 CO₂ < P₅₆ > absorpt. ray anomalies for ν_1 - ν_2 transition, laser source spectroscopy obs. 9-46359
 CO₂, 00⁰1-10⁰ and 00⁰1-02⁰ transitions amplification coeff., obs. 9-25255
 CO₂+A¹ Π_u →X² Π_g bands obs., excitation by neutral mol. photons 9-27845

Spectra continued

inorganic molecules, polyatomic continued

- CO₂, 15 μ m band narrow intervals, transfer function numerical modelling 9-38832
 CO₂ band, 15 μ m, use in yropospheric temp. soundings 9-41483
 CO₂ band, Venus, effect of cloud scattering 9-41679
 CO₂ bands in emission spectrum of night airglow, 2 to 4 μ m 9-28922
 CO₂ glow discharge, 3-7 torr, 2800-6500 Å 9-25979
 CO₂ radiating power in range 0.2 to 3 μ m at 10°K, 1 atm. 9-40753
 CO₂ spectral line strengths, P(20) and P(16) 9-42390
 CO₂ vibrational thermal relax. times, determ. by stopping point, fluorescent and spectrophone methods 9-48455
 CO₂(001)→CO₂(000) fluorescence radiation intensity rel. to deactivation rate 9-25732
 CS₂-Ar, shock heated, rel. to CS₂ thermal decomp., obs. 9-35740
 CaF₂ vapour, absorption bands, ν_2 bending vib. assignment 9-23037
 Ca(H₂PO₄)₂·H₂O and deuterated analogue, H₂PO₄⁻ and H₂O vibr., 4000-200 cm⁻¹ 9-44347
 in CaSO₄·2H₂O, HDO vibr. rel. to pot. environment, obs. 9-24391
 Cd complexes with o-phenylenebisdimethylarsine, i.r. 9-23078
 Cd halides, i.r. 9-40589
 ClO₂, 4750 Å band syst., vib. analysis 9-32469
 ClO₂ in organic soln., obs., transitions deduced 9-30039
 ClOO radical absorpt. 2100-3000 Å 9-30152
 Co lines near 7000, 3800 and 2400 cm⁻¹, collision broadened, shapes 9-40590
 Co complex, Co(NCS)₂(γ -picoline), ν C-H freqs. of clathrated mono- and di-subst. benzenes 9-48475
 Co complex, cobalt (II) acetylacetonate, matrix-isolated, rel. to struct., 650-2200 cm⁻¹ 9-27870
 Co(H₂O)₂²⁺, electronic, interpret. 9-48458
 Co(II) cyanopyridine and chloropyridine complexes, far i.r. 9-23038
 Co(NH₃)₆³⁺, first band intensity, contrib. of odd vib. 9-23039
 Cr complex, K₂Cr(NCS)₆ in methanol-ethanol glass, 100°K, excited state absorption 9-38838
 CrH₂P₂O₇·2H₂O, i.r., ionic dissoc. of constituent water obs. 9-44324
 Cs, trapped, e. and Rydberg transitions, u.v. obs. 9-32466
 Cu complex, copper (II) acetylacetonate, matrix-isolated, rel. to struct., 650-2200 cm⁻¹ 9-27870
 CuCl₂·2H₂O, vibrational analysis 9-38839
 Cu(II) complexes, with tetradentate Schiff base ligands, anomalous sign reversal in circular dichroism spectra 9-36703
 Cu(II) cyanopyridine and chloropyridine complexes, far i.r. 9-23038
 D₂O, laser transitions, self-correlations 9-42393
 D₂S, absorption, far i.r. 9-27858
 D₂Se, Stark effect on J=2₀₂→2₁₁ and J=6₄₂→6₅₁ lines 9-38850
 DCN i.r. vibration intensity depends on intermolecular interactions, gas-soln. transition in solvent 9-30033
 GaAsO₄·2H₂O, (4000-200 cm⁻¹) 9-30024
 GaPO₄·2H₂O, (4000-200 cm⁻¹) 9-30024
 GeCl₄ vibr. freqs. and stretching force const., i.r. obs. 9-27874
 GeD₃AsD₃, i.r. spectra in gas and solid phase, Raman spectra in liq. phase 9-30026
 GeD₃AsH₃, i.r. spectra in gas and solid phase, Raman spectra in liq. phase 9-30026
 GeD₃PD₃, i.r. spectra in gas and solid phase, Raman spectra in liquid phase 9-30025
 GeD₃PH₃, i.r. spectra in gas and solid phase, Raman spectra in liquid phase 9-30025
 GeF₂, i.r., in gas and solid Ar, Ne, vibr. params. 9-27853
 GeH₃AsD₃, i.r. spectra in gas and solid phase, Raman spectra in liq. phase 9-30026
 GeH₃AsH₃, i.r. spectra in gas and solid phase, Raman spectra in liq. phase 9-30026
 GeH₃PD₃, i.r. spectra in gas and solid phase, Raman spectra in liquid phase 9-30025
 GeH₃PH₃, i.r. spectra in gas and solid phase, Raman spectra in liquid phase 9-30025
 H₂¹⁸O, ν_1 and ν_3 bands, 2.5-3.0 μ m, rotational structure 9-34624
 H₂¹⁸O weak features in atm. absorption 9-44331
 H₂O, absorption between 0.5 and 36 cm⁻¹, line parameters 9-34620
 H₂O, laser transitions, self-correlations 9-42393
 H₂O absorption lines, 475-692 cm⁻¹ position, intensity and width 9-36701
 H₂O gas, excited by fast electrons, glow spectra in i.r. region 9-38831
 H₂O vapour, in lowest vib. excited state, due to rot. transitions, rel. to atm. absorption 9-44331
 H₂O vapour line, Venus, effect of cloud scattering 9-41679
 H₂S, absorption, far i.r. 9-27858
 HCN, i.r. vibration, intensity depend. on intermolecular interactions, gas-soln. transition in solvent 9-30033
 (HCN)₂ gas phase H-bonded complexes, i.r., band study 9-25742
 HCN gas phase H-bonded complexes, i.r., band study 9-25742
 HCP 9-23043
 HDO, weak features in atm. absorption 9-44331
 HfX₂⁻ anions (X=Cl or Br), electronic absorption spectra 9-30060
 Hg (II) complex, o-phenanthroline, i.r. region, vib. freq. determ. 9-23052
 Hg complexes with o-phenylenebisdimethylarsine, i.r. 9-23078
 Hg halides, i.r. 9-40589
 In(NCS)₃⁻ complexes, electronic spectra 9-40593
 K₂NiF₆, electronic abs. spectrum study 9-32477
 K₂Cr(NCS)₆ in methanol-ethanol glass, 100°K, excited state absorption 9-38838
 KrF₂, i.r., obs. rel. to structure elucidation 9-25744
 LiO₂, i.r. 9-44333
 MgBr₂, A² π →X² Σ^+ system (0,0) bands rotational analysis 9-42399
 MgF₂ vapour, absorption bands, ν_2 bending vib. assignment 9-23037
 Mn(CO)₅, nematic soln., polarization of i.r. absorpt. bands 9-44336
 Mn(NCS)₃²⁻, Mn(NCS)₅⁴⁻, Mn(NCSe)₅⁴⁻, Mn(NCSe)₆⁴⁻, Mn(N₃)₆²⁻ complexes, electronic spectra 9-40593
 Mo(VI) dioxobis(acetylacetonate), i.r. 9-23076
 NiO, linewidths for 2224 cm⁻¹ band 9-42406
 NiO formed in vibrationally excited state in N+NO₂→N⁺+O 9-24539
¹⁵N, ¹⁴O, vibration-rotation bands, effects of Fermi resonance and l-type doubling 9-48470
 NCS radical, electronic absorpt., bands, rot. and vib. anal. 9-23175
 NF₃, microwave, rel. to Σ -type doubling and resonance in ν_3 and ν_4 states 9-34631
 NF₃, microwave in excited vib. states, rel. to equilib. struct. 9-34630
 NH₃, far L_r line, line mixing by collisions 9-38859

Spectra continued

inorganic molecules, polyatomic continued

- NH₃, rotation-inversion spectrum 9-32481
 NH₃, adsorption and oxidation on silica-supported Pt and silica, i.r. spect. study 9-30044
 NH₃ gas, excited by fast electrons, glow spectra in i.r. region 9-38831
 NH₃ gas in bulk, steady state transient 'wiggles' phenomenon, relax. times meas. 9-44528
 NH₃ gas phase H-bonded complexes, i.r., band study 9-25742
 NH₃ i.r. absorption, 20 to 35 μ 9-40598
 (NO)₂, matrix-isolated i.r. spectrum 9-42405
 NO₂, near-i.r. Zeeman spectra 9-36702
 NO₂⁻, in solid soln. in KBr, infrared intensities 9-48469
 NO₂⁻ in organic soln., obs., transitions deduced 9-30039
 NO₂ excited by Ar⁺ and Kr⁺ lasers 9-40596
 NO₂ transition probability, absolute 9-23170
 Na salts of glycine, DL α alanine, DL β phenylalanine and DL tyrosine, i.r. vib. spectra, assignments 9-23059
 NbOBr₃, metal-O stretching vibr. freq., 4000-400 cm⁻¹ 9-27869
 NbOCl₃, metal-O stretching vibr. freq., 4000-400 cm⁻¹ 9-27869
 NbOBr₃, metal-O stretching vibr. freq., 4000-400 cm⁻¹ 9-27869
 NbX₆⁻ anions (X=Cl, Br or I), electronic absorption spectra 9-30060
 Ni (II) complexes, dimethylidithio (seleno) carbamates, normal coordinate anal. 9-48474
 Ni (II) complexes, with tetradentate Schiff base ligands, anomalous sign reversal in circular dichroism spectra 9-36703
 Ni complex, bis(monothioacetylacetonato) Ni(II), vibr. spectra 9-46370
 Ni complex, Ni(NCS)₂(γ -picoline)₄, γ -C-H freqs. of clathrated mono- and di-subst. benzenes 9-48475
 Ni complex, nickel (II) acetylacetonate, vapour u.v. electronic spectrum and matrix isolated i.r. spectra 9-23059
 Ni(II) cyanopyridine and chloropyridine complexes, far i.r. 9-23038
 OCS, resonance, third order, anharmonic 9-30048
 OCS gas in bulk, steady state transient 'wiggles' phenomenon, relax. times meas. 9-44528
 OCS trapped e and Rydberg transitions, u.v. obs. 9-32466
 ONBr, isotropic species, vibrational spectra and force constants 9-46372
 OsF₆, i.r., Jahn-Teller effect 9-34647
 P₄O₁₀, vibr. assignments and force consts. 9-27871
 P₄O₆, vibr. assignments and force consts. 9-27871
 PCl₃, potential energy constants and mean amplitudes of vibn., from vibl. spectral data 9-48477
 PDF₂, microwave spectrum, struct. and dipole moment, obs. 9-30049
 PF₃, potential energy constants and mean amplitudes of vibn., from vibl. spectral data 9-48477
 PF₅, vibr.-rot. bands, computer anal. 9-38895
 PH₂ radical, emission bands 9-23176
 PHF₂, microwave spectrum, struct. and dipole moment obs. 9-30049
 POCl₃, potential energy constants and mean amplitudes of vibn., from vibl. spectral data 9-48477
 POF₃, potential energy constants and mean amplitudes of vibn., from vibl. spectral data 9-48477
 PSCl₃, potential energy constants and mean amplitudes of vibn., from vibl. spectral data 9-48477
 PSF₃, potential energy constants and mean amplitudes of vibn., from vibl. spectral data 9-48477
 Pd co-ordination cpds. type PdX₂Y₂, i.r. spectra 9-23068
 Pd complex, Pd(II)X₂Y₂(X=Cl, Br or I, Y=Me₃P or Me₃As, square planar, i.r. and Raman spectra 9-30052
 cisPdII trimethyl-arsine, -phosphine, -stibine complexes, stretching vibrs., i.r. obs. 9-27872
 Pt co-ordination cpds. type PtX₂Y₂, i.r. spectra 9-23068
 Pt complex, [PtCl₂(C₂H₅)₂], Raman and i.r. vib. 9-27873
 Pt complex, K[PtCl₂(C₂H₅)₂].H₂O, Raman and i.r. vib., C-C stretching freq. determ. 9-27873
 Pt complex, K[PtCl₂(C₂D₅)₂].H₂O, Raman and i.r. vib. 9-27873
 Pt complex, Pt(II)X₂Y₂(X=Cl, Br or I, Y=Me₃P or Me₃As, square planar, i.r. and Raman spectra 9-30052
 cisPtII trimethyl-arsine, -phosphine, -stibine complexes, stretching vibrs., i.r. obs. 9-27872
 Re₂(CO)₁₀ nematic soln., polarization of i.r. absorpt. bands 9-44336
 Re complex, hexahalogen, K and Cs salts i.r. spectra 1000 to 45 cm⁻¹ 9-32487
 Re(CO)₆⁺, i.r. and Raman spectra in solution and solid 9-32491
 ReF₆, i.r., Jahn-Teller effect 9-34647
 RuF₆, i.r., Jahn-Teller effect 9-34647
 RuO₄, i.r. 9-42415
 S₂O₃²⁻ normal vibrations 9-27876
 SF₆, fine struct., 10.5 μ 9-46374
 SF₆, light-echo intensity distrib. calcs. on gas 9-48481
 SF₆, narrow reson. in Doppler line of rot.-vibr. transitions of ν_3 band by CO₂-laser emission method 9-46375
 SF₆, Raman spectrum in solid, splitting of three fundamentals 9-30053
 SF₆, saturation of absorpt. of i.r. laser rad. rel. to press. and buffer gases 9-48480
 SO₂ in inert gas matrix, vibrational spectrum 9-34641
 SO₂ isotopes in solid Kr matrices, i.r. 9-42417
 SO₂ three electronic transitions, 1340-1190 Å region, vibr. analysis 9-30058
 SeO₂, absorption spectrum 2000-4500 Å 9-23073
 SeO₂ in inert gas matrix, vibrational spectrum 9-34641
 Si₂Cl₆, i.r. and Raman spectra in liquid phase 9-30056
 SiBr₄ vapours, glow discharge spectrum 9-48483
 SiCl₄, vibr. freq. and stretching force consts., i.r. obs. 9-27874
 SiCl₄, i.r., rel. to Coriolis coupling and force consts. 9-48482
 SiO₂ film transmission and reflection, thickness depend., 7-11 μ 9-24374
 Sn complex, EtSnCl₃, Et₂SnCl₂ and Et₃SnCl liq. or soln., vib. spectra and normal coord. anal. 9-48484
 SnCl₄, vibr. freqs. and stretching force consts., i.r. obs. 9-27874
 SrF₂ vapour, absorption bands, ν_2 bending vib. assignment 9-23037
 TaX₆⁻ anions (X=Cl, Br or I), electronic absorption spectra 9-30060
 Tc complex, hexahalogen, K and Cs salts i.r. spectra 1000 to 45 cm⁻¹ 9-32487
 TcF₆, i.r., Jahn-Teller effect 9-34647
 TiCl₄, vibr. freqs., i.r. obs. 9-27874
 V(CO)₆⁺, i.r. and Raman spectra in solution and solid 9-32491
 V(NCS)₃⁺, V(NCS)₂⁺, V(N₃)₃⁺ complexes, electronic spectra 9-40593
 VO(NCS)₃⁺, VO(NCS)₂⁺, VO(N₃)₃⁺ complexes, electronic spectra 9-40593
 W(VI) dioxobis(acetylacetonate), i.r. 9-23076

Spectra continued

inorganic molecules, polyatomic continued

- Zn (II) complex, o-phenanthroline, i.r. region, vib. freq. determ. 9-23052
 Zn complex, bis (L-aminoacid) (II), circular dichroism and far U.V. spectra 9-23077
 Zn complex, zinc (II) acetylacetonate, matrix-isolated, rel. to struct., 650-2200 cm⁻¹ 9-27870
 Zn complexes with o-phenylenebisdimethylarsine, i.r. 9-23078
 ZnBr₂ emission spectrum in visible region, analysis and vib. consts. of B² Σ -X² Σ syst. 9-32492
 Zr complex, tetrafluoride adducts of p-subst. pyridine-N-oxides, i.r. spectra 9-32493
 ZrX₆²⁻ anions (X=halogen), electronic absorption spectra 9-30060
inorganic molecules, polyatomic, radiofrequency
 see also Nuclear magnetic resonance and relaxation; Paramagnetic resonance and relaxation
 H₂O, 22 GHz line, foreign-gas broadening 9-23045
 HCN, microwave double reson., rot. energy transfer rates 9-30028
 HDO¹⁷, h.f.s. by beam maser 9-44329
 N¹⁵N¹⁵O¹⁶, Zeeman effect 9-38862
 NH₃, inversion spectrum, hyperfine structure 9-34632
 NH₃ Stark spectroscopy by far i.r. masers 9-25767
 OCS, line broadening of various rotational transitions due to dipole-dipole, dipole-quadrupole interact., obs. 9-34639
 RbOH and RbOD, for structure determ. 9-38869
 SO₂, microwave spectra in doubly excited vibrational states and γ constants determ. 9-32485
inorganic solids
 A^{VB}B^{VC} semiconducting cpds., energy and egde absorpt., peculiarities 9-37715
 absorption, valence electron model of atom 9-33545
 alkali, halides: Ni(Cu), rel. to coordination props. 9-33548
 alkali chloride solid solns., fund. absorpt. in extreme u.v. 9-35662
 alkali halide phosphors, absorpt. spectrum, vib. analysis 9-24455
 alkali halides: Eu²⁺ (Sm²⁺), absor. and emission, -175°K, rel. to zero-phonon transitions theory 9-37716
 alkali halides, absorpt., of aggregate centres, fine struct. and oscillatory effect obs. 9-39370
 alkali halides, electrolytically coloured, Cd centres obs. 9-40970
 alkali halides, OH⁻-doped, i.r. stretching band obs. 9-24403
 alkali halides, Sm²⁺ vibronic side bands calc. 9-49285
 alkali halides, two-photon absorpt. 9-47349
 alkali halides, u.v. absorpt. of Ag⁺, Cu⁺ and Tl⁺ centres, band electronic fine struct. obs. 9-43237
 alkali metals azides, new electronic and i.r. band after irradiation, D_{3h} ion symmetry 9-27844
 alkali-halides, absorption of U₂-centres, effect of external stresses 9-49251
 alkaline earth fluorides, of V₁ centres, eff. of polarized bleaching light 9-23826
 alkaline earth tungstates, Bi doped, u.v.-induced colouration, darkening and fading processes 9-45282
 alkaline-earth fluorides, H and F bands 9-28302
 aluminoboro-phosphate glasses, absorpt. of Mo³⁺ 9-47350
 anharmonic effects in ionic crystals with weak vibrational-electronic coupling 9-33574
 crystal electron interacting system, optical and energy loss spectra, dynamical theory 9-37385
 diamond, u.v. absorpt. rel. to platelet defects, obs. 9-26732
 diamond-type crystals, critical-point structure, strain effects 9-24395
 diamonds, effect of heat and pressure treatment 9-26366
 electrolytes in aq. soln., glass-like, γ -irrad., absorpt. at -196°C 9-24399
 excitonic absorpt. in high mag. fields 9-43232
 exploding wires, fast-explosion striations, mechanical mechanism 9-47337
 ferromagnetic thin film magnetic spectrum 9-43180
 fluorapatite, activated by rare earth, Mg lamp excitation, fluorescence spectra obs. 9-31133
 garnets: rare earth ions, selection rules 9-24416
 glass, i.r., structure examination 9-30469
 glass, soda-boric oxide, Cu²⁺ obs. 9-37800
 glass, weak phosphorescence, characts. 9-38360
 glasses, K₂O-PbO-SiO₂, absorpt. spectra 9-31129
 glasses, non-oxide chalcogenide, i.r. reflectance structure 9-36928
 group II-VI compounds, absorption and reflection near fundamental band edge 9-37708
 group II-VI compounds, exciton electroreflectance spectra 9-37707
 group II-VI compounds, rel. to band structure 9-37399
 ice, orientationally ordered and disordered phases far-i.r. absorpt. obs. 9-33557
 impurity atoms, two-electron-eigenstates of (sp)³ P multiplet and phonon-induced optical transitions 9-41372
 ionic crystals, Reststrahlen frequency 9-30756
 i.r. absorpt. i.r. lines due to lattice vib. modes, temp. depend. 9-33157
 i.r. absorption, true-freq. determ. from internal reflection data 9-37713
 laser, based on electron-vibrational transitions in CaF₂:Sm²⁺ cryst. 9-37704
 leucosapphire, i.r. refl., 5-25 μ 9-28669
 magnetic ion pairs, exchange interaction effect 9-39824
 metal carbonyl cpds., vib. freq. and force const. calc. 9-30020
 metallic alloys, emission processes, vibrational character due to electric spark 9-45311
 metallic surfaces, charact. energy loss, method for clean surface maintenance in vacuum 9-32832
 metals, core electron spectra, characts. structure due to electron-plasmon coupling 9-44861
 metals, i.r. obs. of Co adsorption and effect of other gases 9-35002
 mica, i.r., due to OH bonds 9-31099
 minerals, Mn i.r. spectra obs. on 10 minerals 9-28690
 molecular cryst., exciton phenomena, book 9-49005
 nitrate glass, Co (II)-doped, rel. to Co coordination 9-26735
 non-conducting cryst., interband absorpt. change in elec. field, Stark effect obs. 9-33547
 optical absorption of impurities, applic. to metal-ion activated alkali halide phosphors 9-31098
 optical absorption of impurities, theory 9-31097
 ozone, i.r. absorpt. at 10°K, in O₂ matrix 9-45329
 permanganates, i.r. 9-24412
 phosphor particles in systems, emission under 2537 Å excitation 9-31139
 powder and massive substance, rel. between absorption spectra 9-39829

Spectra continued

inorganic solids continued

- powders, compacted, reflectance variables 9-37706
 powders, i.r. absorpt., interpretation 9-31111
 quartz, fused amorphous, i.r. absorption meas., $9\ \mu$ 9-26740
 quartz glass rel. to cry. struct., i.r. refl., 1000-1300°C 9-26175
 rare earth garnet single crystals, Raman and far i.r. spectra, comparison 9-39850
 rare earth orthoferrite spectroscopic and mag. props. 9-45232
 rare earth spectra, extra lines obs. 9-47339
 rare-earth complexes, overlap and Coulomb integral calcs. 9-45248
 Reststrahlen frequency in ionic crystals 9-30756
 ruby, energy transport mechanisms 9-45305
 ruby, laser-enhanced two-photon decay 9-26766
 ruby, synthetic, i.r. refl., 5-25 μ 9-28669
 ruby, two-photon stimulated processes, study 9-26731
 ruby laser, rel. to resonator active crystal orientation 9-38379
 semiconductors, impurity absorpt. line shapes, effect of resonant phonon interactions 9-26741
 silicate glass with Nd^{3+} ions, structure of stimulated emission bands 9-35650
 silicates, i.r. emissivity, obs. and cloudy atmosphere model of emission from condensed powder 9-28693
 spinel, Ni^{2+} doped 9-43242
 structure of stimulated emission bands 9-35650
 superconducting film containing mag. impurities, far-i.r. study of energy-gap props. 9-41185
 transition metal complexes, overlap and Coulomb integral calcs. 9-45248
 transition metal ions, from effective Hamiltonians obtained by cryst. field theory 9-47304
 transition metals, absorption in 3p transition region 9-33561
 vermiculites, dehydration, i.r. spectroscopy 9-44658
 wurtzite type crystals, absorption and emission bands polarization 9-33544
 zeolite, La-exchanged type X, cations and mol. positions at 25, 425 and 735°C 9-39249
 Ag atoms in Ar, Kr and Xe matrices, u.v. absorpt. 9-27805
 Ag halides, absorpt., of aggregate centres fine struct. and oscillatory effect obs. 9-39370
 AgBr:I luminescent spectra of single crys. and of nucl. emulsion type Ya-2 9-43251
 AgBr, brominated, absorpt., acceptor ionization energy of neutral Ag vacancies obs. 9-41373
 AgCl, absorpt., exciton-phonon coupling effects 9-39831
 Al, L shell contrib. to total absorpt. cross-section 9-45314
 $\gamma\text{-Al}_2\text{O}_3$ i.r., 1370-1390 cm absorption band rel. to AlOH stretch vibration 9-49270
 $\text{Al}_2\text{O}_3\text{:Ti(V, Cr)}$, far-i.r. absorpt. in applied mag. field, Zeeman splitting of lines, single d electrons obs. 9-31100
 Al garnet, rare earth, i.r. lattice spectra 9-47338
 AlN, phonon structure of Mn^{4+} activator centres 9-24010
 p-AlSb, acceptor photoexcitation spectra, uniaxial stress eff. on lines 9-39832
 As, i.r. magnetoreflexion data for trigonal face rel. to band parameters 9-47320
 Au, isotope shift pressure dependences, relativistic calc. in Wigner-Seitz model 9-26481
 Au films, dispersed, light and electron emission centres 9-26606
 Au surfaces, adsorption of CO and H₂ obs. 9-35001
 $\beta\text{-B}$, rhombic, lattice vibr., band edge and free carrier absorpt. 9-39834
 BaF₂ crystal, i.r. absorption meas., $50\ \mu$ 9-26740
 Ba(OD)₂.D₂O, i.r. absorpt. spectrum 9-33167
 BaTiO₃, absolute reflectance, 0.325-0.7 μ 9-33537
 BaTiO₃, i.r. bands for defect structure identification 9-35105
 BeF₂-XF glass system with X=alkali ion 9-41375
 BeO, u.v. for reflectance and band struct. 9-28670
 BeSO₄.4H₂O, i.r. vib. spectra, cry. struct. and H bonding schemes obs. 9-24423
 Bi₂O₃-B₂O₃-(R₂O) glass systems, i.r. absorpt. rel. to chem. struct. 9-46698
 Bi₂Se₃(Te₂), reflectivity, 0.5 to 12.5eV 9-33538
 Bi₂Ge₂O₁₂:Nd³⁺ coherent emission obs. 9-26738
 BiSBr, transmission around absorption edge of polarized light, internal photoeffect 570-650 nm, 93-293°K 9-32870
 CS₂ polymer, i.r. structural studies 9-34975
 (Ca, Cd)₂(PO₄)₂FCl structural and optical props., Pb and Mn activated 9-47382
 Ca₁₀(PO₄)₆F₂, i.r., coupled PO₄³⁻ vib. 9-37317
 CaF₂:Gd³⁺, crystal field splitting of ⁶P_{7/2} and ⁶I_{7/2} terms of Gd³⁺ 9-31056
 CaF₂:Gd³⁺, u.v. absorpt. 9-43238
 CaF₂:Gd³⁺ lifetimes of levels, prob. of radiative transitions 9-28681
 CaF₂:GdF₃ mixed cryst., Gd³⁺ absorpt. and fluoresc., energy levels obs. 9-35660
 CaF₂:H absorption spectrum, use, of polarized bleaching light 9-26293
 CaF₂:Ho³⁺ luminescence absorption and relaxation spectra 9-35681
 CaF₂:Nd³⁺, visible absorption spectra of Nd³⁺ at liquid oxygen temp. 9-47352
 CaF₂:R³⁺.H⁺, (R=rare earth), electronic, i.r. absorpt., vibronic and e.s.r. spectra 9-47353
 CaF₂:Sm²⁺ crystal, electron-vibrational transitions, rel. to laser spectrum 9-37704
 CaF₂:Yb³⁺, optical, and lifetimes of ²F_{5/2} energy level 9-31091
 CaF₂:Yb³⁺, Zeeman effect rel. to different site symmetries of Yb³⁺ 9-31103
 CaF₂:rare earth ions, asymmetric lines stronger when doped crystal irradiated by X-rays 9-49271
 CaF₂, thermal radiation and spectral emissivity, obs. 9-35651
 CaF₂:Ho³⁺, Nd³⁺, Tm³⁺ (f-f) absorption spectrum of con. obs. 9-28682
 Ca(NbO₃)₂:Nd³⁺ crystal, absorption, luminescence and generation spectra, 77 and 300°K 9-27332
 CaO:Bi, absorption and emission, Zeeman splitting 9-33549
 CaO:Ni²⁺, electronic absorpt., 5000 to 33300 cm⁻¹ 9-28680
 CaQO₂:Nd³⁺, visible absorption spectra of Nd³⁺ at liquid oxygen temp. 9-47352
 CaSO₄.2H₂O crystal, i.r. absorption, H bond vib., electronic spectra meas., structural imperfection determ. 9-23799
 CaSO₄.2H₂O, HDO mol. vibrs. rel. to pot. environment, obs. 9-24391
 CaWO₄:Tb³⁺, absorpt. and fluorescence, rel. to crystal field parameters 9-33550
 Cd_{1-x}Zn_xS, i.r. active lattice modes from reflectivity spectra 9-47343

Spectra continued

inorganic solids continued

- Cd₂Ca_{1-x}O Reststrahlenbands and intrinsic absorption edge 9-47342
 Cd₂Hg_{1-x}Te solid solns., fund. reflectivity, 1.5-4 eV, band struct. obs. 9-45306
 Cd complex, bis(selenourea) cadmium (II) thiocyanate, rel. to crystal structure 9-26227
 CdCl₂:Ag, irradi., absorpt. obs. 9-49272
 CdF₂:V³⁺, V²⁺ 9-47385
 CdF₂:Y, i.r. absorpt. donor conc. and temp. depend. rel. to trapped electron theories 9-47354
 CdI², excitonic transitions stimulated by adsorption of organic molecules 9-26194
 CdO, i.r. absorpt., phonon and polaron effects 9-24404
 CdS, absorption, intrinsic, associated with longitudinal optical-phonon assisted 'direct' exciton creation 9-37719
 CdS, absorption, rel. to exciton-phonon interaction 9-37709
 CdS, donor-acceptor pair lines obs. 9-49273
 CdS, emission lines at low temp. and high excitation intensities 9-49313
 CdS, thin films on Al, i.r. reflectivity showing absorption peaks 9-26733
 CdSe_{1-x}S_x mixed-crystal system, phonon freqs. from i.r. reflectance and transmittance spectra 9-46971
 CdS crystals, generation during ruby laser 2-photon excitation 9-49283
 CdS films, absorpt., intense ruby laser radiation effect 9-35652
 CdS plastically deformed single cryst., refl. fluoresc. and absorpt., depend. on dislocation density 9-35644
 CdS single cryst., absorpt. spectrum, internal photoeff. in exciton region 9-26603
 CdS single cryst., excitation spectra of photoconductivity, correl. with exciton absorpt. 9-35503
 CdS(Se), electroabsorption in exciton region, band structure 9-35625
 CdSe, emission and absorpt., of bound exciton complexes, 4.2°K 9-37718
 CdSe, optical absorption edge, structure 9-47355
 n-CdTe:Br, i.r. absorpt. 9-26734
 CdTe, optical absorption edge, structure 9-47355
 CdTe films, absorpt. in high elec. fields 9-41376
 CdTe semiconductor films, photosensitivity spectrum, influence of temp. 9-33535
 Ce C_{2v} centre, Stark structure of the 5d¹ config. in MeF₂ type crystals 9-43228
 CeF₃:Nd³⁺, oriented single cryst. far i.r. electr. and vibronic transitions, Zeeman study 9-39843
 CeF₃:Nd³⁺ single cryst., far i.r. electronic and vibronic transitions obs. 9-35653
 CeF₃, polarized i.r. reflectance, optical phonons and mag. symmetry 9-47345
 Co complex, bis(selenourea) cobalt (II) thiocyanate, rel. to crystal structure 9-26227
 CoCl₂.2H₂O far i.r. studies of magnon-phonon interaction 9-45077
 CoF₂, antiferromagnetic, far i.r. studies, rel. to magnon-optical phonon interaction 9-47356
 Cr, absorption, 293 and 420°K rel. to mag. props. 9-24359
 Cr₂O₃, absorpt. spectrum of excitons, mag. Davydov splittings 9-33552
 Cr³⁺ in Al-line glass, absorpt., obs. 9-35655
 Cr complex, hexaurea Cr(III) ion in crystals 9-33551
 Cs₂UO₂Cl₂:NpO₂²⁺ absorpt. spectrum, energy level obs. 9-33553
 CsLi:(Na⁺, K⁺, Rb⁺, Tl⁺) impurity induced far i.r. absorpt., rel. to phonon density 9-37720
 CsI, two-photon spectrum rel. to even-parity X-exciton 9-26736
 CsI thin film, far u.v. absorption spectrum obs. and interpreted 9-37730
 Cs₂[Zn(NO₃)₆], u.v., i.r. and Raman spectra 9-49288
 Cu-Ag alloys, effect of additives on analytical lines 9-31228
 Cu₂O, absorpt. line contours, line broadening and asymmetry w.r.t. exciton-phonon interac. 9-35656
 Cu₂O, exciton line at λ_2 =5817 Å 9-33235
 Cu₂O, quenched, absorpt. 9-28683
 Cu₂O, u.v. electroreflectance 9-35626
 Cu (II) glycyl-glycylglycine chloride sesquihydrate single cry. spectra, band obs. 9-24405
 Cu bisacetylacetonate, single cry. electronic spectra 9-24407
 Cu bistopolonate, single cry. electronic spectra, d-d transitions obs. 9-24407
 CuCl, absorption, study of lines ν_4 (25571.5 cm⁻¹) and ν_5 (25501 cm⁻¹), 4.2°K 9-49274
 CuCl, Zeeman effect of bound excitons, absorpt. and emission obs. 9-37721
 CuCl crystals, reflection near excitonic absorpt. region, optical consts. determ. 9-37710
 CuCl evaporated films, Faraday rotation due to excitons 9-24370
 CuI, excitonic transitions stimulated by adsorption of organic molecules 9-26194
 Cu(II) complex bis (prolinato), polarized single cry. electronic spectra 9-24406
 DCl, i.r. absorpt. 9-47360
 DyAlO₃, absorpt., mag. structure and metamag. translations investigation 9-31105
 Eu₂(WO₄)₃ single cryst., nucl. reson. fluoresc. of 3 eV ¹⁵²Sm recoil atoms, anisotropic pot. obs. 9-35596
 Eu³⁺ absorpt. intensities 9-39876
 EuAlO₃:Cr³⁺, Cr³⁺-Eu³⁺ pair emission 9-39835
 EuO:R³⁺ film, (R=rare earth oxide), absorpt. bands 9-47266
 Fe-(30 wt %Ni) alloy, f.c.c. and b.c.c., electron energy spectra, sensitivity to $\alpha\text{-}\gamma$ transform. 9-39856
 Fe Garnet, rare earth, i.r. lattice spectra 9-47338
 FeCl₂.2H₂O far i.r. studies of magnon-phonon interaction 9-45077
 Fe(II) fluoro and bromo complexes, d-d spectra 9-24409
 FeS₂, i.r. reflectivity, lattice vibration obs. 9-46974
 FeSi, i.r. reflectivity 9-33505
 Ga₂In_{1-x}Sb, electroreflectance, variation with composition 9-45307
 Ga film, absorpt. in different gaseous media 9-45265
 Ga garnet, rare earth, i.r. lattice spectra 9-47338
 GaAs:Si, compensated, local mode absorpt. and defects 9-47357
 GaAs:Si p-n junctions, photo-e.m.f. spectra at 300 and 77°K 9-37614
 n-GaAs, electroabsorpt. at 300 and 77.3°K 9-39837
 n-GaAs, electroreflection characs. in electroabsorpt. spectra rel. to low free carrier density 9-37723
 GaAs, high resistivity, i.r. abs. at 82°K 9-49276
 GaAs, i.r. absorpt., rel. to doping or structural defects, after irradi. 9-37725

Spectra continued

inorganic solids continued

- n-GaAs, microwave emission study of acoustic freqs. in acoustoelec. domains 9-48966
 n-GaAs, reflectance and photorelectance, intense exciton struct. obs. 9-41377
 GaAs_{1-x}P_x solid solutions, absorption from conduction bands or donor levels, temp. depend. 9-33554
 GaP absorption spectrum at 4.2-500°K, fine struct. 9-43239
 GaP crystal, reflection and photolum. spectra obs., 77.3°K 9-24397
 GaS, reflection meas. rel. to interband transitions 9-28671
 GaSe, absorpt. for Br impurity effect on energy structure 9-35412
 GaSe, reflection meas. rel. to interband transitions 9-28671
 GaSe layer semiconductor, existence of two dimensional exciton observed 9-35319
 Gd, emission, M_{IV} and M_V absorption 9-28707
 Gd₂O₃, emission, M_{IV} and M_V absorption of Gd 9-28707
 GdF₃, Gd³⁺ absorpt. and fluoresc., energy levels obs. 9-35660
 GdFe garnet, optical absorption, 2000-5000 Å 9-35658
 p-Ge:Be, impurity photoconductivity 9-37619
 Ge:Sb, far i.r. absorpt. spectra, excitation lines shift, conc. depend. 9-35659
 Ge, doped, i.r. emission from free carriers 9-47359
 Ge, electro-reflectance spectra, low-temp., 0.7-2.6 eV 9-35627
 Ge, electroreflectance, satellite structure 9-31093
 Ge, for i.r. studies on shallow impurity states under elec. breakdown 9-28517
 Ge, heavily doped, u.v. refl. spectrum 9-35645
 Ge, interband optical props. of grain boundaries 9-26737
 Ge, piezorefractive 9-35646
 p-Ge, resonance absorpt. at 36 Gc/s, 100-1500 Oe, 2-50°K 9-43071
 Ge amorphous, sharp absorption edge at 0.5 eV 9-31106
 GeO₂, vitreous state, vibrational analysis using i.r. absorpt. and reflection spectra 9-28196
 H₂-D₂ mixed solid solutions, i.r. induced into vibrational first harmonics, 4°K 9-33558
 H₂-D₂ solid solution, fundamental bands at 4°K 9-28684
 H₂, i.r. absorption associated with orientational excitation 9-24410
 HCoO₂ and DCoO₂, i.r. 9-32908
 Hg, absorpt., from cyclotron reson. 9-35323
 HgCl, HgBr and HgI, i.r. 9-34627
 HgI, excitonic transitions stimulated by adsorption of organic molecules 9-26194
 α-HgS, absorption meas. rel. to valence band splitting 9-28448
 HgS, fundamental absorption edge 9-47361
 HgTe, interband magneto-optical transitions, low temp. reflection and electrorefraction study 9-47344
 In film, absorpt. in different gaseous media 9-45265
 InAs_{1-x}P_x, electroreflectance, variation with composition 9-45307
 InAs_{1-x}Sb_x, electroreflectance, variation with composition 9-45307
 p-InSb, absorpt. spectra between 50-1400 μ at 1.5°K 9-37727
 InSb, absorpt. spectrum and energy levels of impurity centres 9-35408
 InSb, donor-impurity excitation spectra in high mag. fields 9-45320
 n- and p-InSb, impurity photoconductivity 9-30992
 p-InSb, reflectivity, conductivity effective mass of holes meas. 9-35407
 n-InSb microwave emission, low-field 9-26763
 InSe, reflection meas. rel. to interband transitions 9-28671
 K₂NiF₆, i.r. and Raman abs. spectra study 9-32494
 K₂O-PbO-SiO₂ glasses, absorpt. spectra 9-31129
 K₂O-SiO₂ glass, luminescence 9-39872
 KBr:Li⁺, vibration, stress-induced shifts of lattice resonant modes 9-24015
 KBr:Sm²⁺ vibronic side bands calc. 9-49285
 KBr:Ti⁴⁺, absorption band shifts under infl. of uniaxial compressive stress 9-31075
 KBr:Ti modulated absorption spectrum, triplet struct. and Stark eff. obs. 9-41381
 KBr-KCl solid solution film, fundamental absorpt. 9-28685
 KBr-NaBr solid solution film, fundamental absorpt. 9-28685
 KBr-RbBr solid solution film, fundamental absorpt. 9-28685
 KBr, electronic absorption and emission bands moments temp. depend. 9-24411
 KBr, F centre spin-lattice relax., theory and meas., 0-50 kG 9-24342
 KBr single crystal, reflection in extreme u.v. 9-28673
 KBr:Ti⁴⁺, electron-lattice interaction, absorption spectra meas. 9-41386
 KCl:Ag, absorption bands, mechanism of form. 9-49277
 KCl:Mg, additively coloured, absorpt. band obs. 9-48868
 KCl:Ni²⁺, optical absorption 9-39842
 KCl:Pb²⁺, emission and absorption, effect of vacancy pairs aggregation 9-31108
 KCl:Sm²⁺ vibronic side bands calc. 9-49285
 KCl:Ti⁴⁺, absorption band shifts under infl. of uniaxial compressive stress 9-31075
 KCl, attenuation by colloidal K particles, spectral dependence of coeffs. 9-49278
 KCl, orbital Lande factor for excited states of F centres 9-47362
 KCl, Stark effect of Z₁ and Z₂ centres in electric field modulated absorpt. spectrum 9-23828
 KCl containing NO₃⁻, CO₃²⁻ and SO₄²⁻, i.r. absorpt. obs. of ion vibrs. 9-41382
 KCl single cryst., conductivity and energy loss spectra, temp. depend. 9-33559
 KCl single crystallites, electronic spectra, 5-40 eV region, complex dielec. const. determ. 9-37711
 KCl:Ti⁴⁺, electron-lattice interaction, absorption spectra meas. 9-41386
 KD₂PO₄, i.r. temp. dependence rel. to H atom potential determs. 9-26589
 KH₂PO₄, i.r., temp. dependence rel. to H atom potential determ. 9-26589
 KI:Ag⁺, vibration, stress-induced shifts of lattice resonant modes 9-24015
 KI:(Ga³⁺)₂, absorpt. bands, electr. struct. of ion centres obs. 9-35111
 KI:(In³⁺)₂, absorpt. bands, electr. struct. of ion centres obs. 9-35111
 KI:Ti⁴⁺, absorption band shift under infl. of uniaxial compressive stress 9-31075
 KI:(Ti³⁺)₂, absorpt. bands, electr. struct. of ion centres obs. 9-35111
 KI, 2-photon absorption, optical transition in Brillouin zone, 0-7.5 eV 9-39838
 KI, F centre spin-lattice relax., theory and meas., 0-50 kG 9-24342
 KI thin film, far u.v. absorption spectrum obs. and interpreted 9-37730
 KI:Ti⁴⁺, electron-lattice interaction, absorption spectra meas. 9-41386

Spectra continued

inorganic solids continued

- KNO₃, polarized i.r. absorpt. for three cryst. phases 9-47363
 K₂[Cd(NO₃)₆], u.v. and i.r. absorpt. and Raman spectra 9-49288
 K₂[Hg(NO₃)₆], u.v., i.r. and Raman spectra 9-49288
 LaF₃:Nd³⁺ oriented single cryst. far i.r. electr. and vibronic transitions, Zeeman study 9-39843
 LaF₃:Nd³⁺ single cryst., far i.r. electronic and vibronic transitions obs. 9-35653
 LaF₃, Gd³⁺ absorpt. and fluoresc., energy levels obs. 9-35660
 LaF₃, polarized i.r. reflectance, optical phonons and mag. symmetry 9-47345
 Li₂O-SiO₂, glass, luminescence 9-39872
 LiF, i.r. absorpt., subsequent to n- and γ-irradiation 9-39839
 LiF, irradiated, γ-absorpt. band obs. 9-37726
 LiF, N-region absorpt. at 3°K 9-28688
 LiF with MgF₂ and MgO impurities, opt. absorption 9-41383
 LiH, absorption and luminescence spectra, radiation eff. 9-33585
 LiNO₃, i.r. reflect. from surface distorted cryst. 9-48750
 LiNbO₃:Cr³⁺ 9-31104
 LiNbO₃:Nd³⁺, polarized light absorpt., 4.2-295°K 9-28689
 LiNbO₃, absorption spectra of clear, yellow and bleached crystals 9-28687
 LiTaO₃:Cr³⁺ 9-31104
 LiYF₄:Er³⁺, absorption and fluorescence, Er³⁺ energy levels 9-31107
 Mg₂Su, reflection, for energy band structure 9-35647
 MgAl₂O₄:Cr³⁺ spinel, theory of strong trigonal field 9-28644
 MgF₂:Co²⁺, far i.r. absorpt., exchange interactions obs. 9-41384
 MgF₂ single cryst., absorpt., colour centres due to electron and neutron irradi. 9-35117
 MgO-Al₂O₃:Cr³⁺ absorption and fluorescence spectra 9-26778
 Mn₂Fe₂-O₄ ferrites, cubic and tetragonal, i.r. absorpt., lattice vibrs. classification and band splitting obs. 9-39841
 MnF₂:Fe²⁺, near i.r. absorpt. 9-49280
 MnF₂, absorpt. spectrum, magnon sidebands obs. 9-35661
 MnF₂, antiferromag., behaviour under spin-flop from critical Zeeman effect anisotropy obs. 9-35642
 MnO, absorpt. 300-1.7°K 9-47365
 MnO, crystal-field absorpt. bands obs. 9-39840
 MnO, restrahlen spectrum analysis 9-24398
 α-MnS, single cryst., fine struct. 9-43241
 Mo reflection coefficient for near normal incidence of 1.4-11 eV photons 9-43230
 MoO₃, optical props. obs. 9-33536
 α-MoTe, single cryst., photovoltage obs. 9-33411
 α-N₂, absolute far-i.r. absorpt. intensities 9-49281
 N₂D₄, Raman spectra, -70 to -195°C, crystal structure determ. 9-39853
 N₂H₄, Raman spectra, -70 to -195°C, crystal structure determ. 9-39853
 NH₄CN, polycryst., i.r. absorption 9-49282
 NH₄Cl:3NH₃, i.r. spectra analysis, H-bonds study 9-30042
 Na-Bi glass, Raman, e.p.r., i.r. and electronic spectra 9-26757
 Na, near i.r. absorpt., calc. 9-24414
 Na₂O-SiO₂ glass, luminescence 9-39872
 Na₂K₂Ta₂O₇, i.r. and Raman, 4-600°K, phonon modes rel. to dielec. phase transitions 9-47366
 Na₂WO₄, reflectance, diffuse and specular, rel. to electronic props. 9-31094
 NaBa₂Nb₂O₁₀, absorpt., H impurity content obs. 9-41374
 NaCl:Cu, additively coloured with Na vapour, colloidal absorpt. bands 9-32998
 NaCl:Cu⁺, i.r. obs., resonant mode broadening 9-33164
 NaCl:Ni²⁺, absorpt. 9-39842
 NaCl:Pb, u.v. absorpt. correl. with Rayleigh scattering 9-45328
 NaCl:Pb²⁺, emission and absorption, effect of vacancy pairs aggregation 9-31108
 NaCl:Ti⁴⁺, electron-lattice interaction, absorption spectra meas. 9-41386
 NaCl, charged F-aggregate centres obs., absorpt. and emission band obs. 9-35119
 NaF(u) phosphor, absorpt. spectrum, vib. analysis 9-24455
 NaHSO₄-KHSO₄ glass, Mo V obs. 9-37729
 NaI:NaCl far-infrared absorpt. rel. to gap and resonant modes assoc. with Cl-impurity 9-24413
 NaI thin film, far u.v. absorption spectrum obs. and interpreted 9-37730
 NaNO₃, far-i.r. reflectivity, temp. depend. 9-41370
 NaNO₃, ferroelec., far i.r. abs., temp. depend. 9-33163
 NaNO₃, i.r. reflect. from surface distorted cryst. 9-48750
 Na(SiO₃)₂ glass, changes over range 548-850°C vibration 9-28674
 Nb₂O₅, emission, structural modifications influence on intensity 9-33560
 NdF₃, oriented single cryst. far i.r. electr. and vibronic transitions, Zeeman study 9-39843
 NdF₃, polarized i.r. reflectance, optical phonons and mag. symmetry 9-47345
 NdF₃ single cryst., far i.r. electronic and vibronic transitions obs. 9-35653
 Ni complex, bis(selenourea)nickel (II) thiocyanate, rel. to crystal structure 9-26227
 Ni complex, hexakis (imidazole) nickel (II) nitrate, single cry. spectrum, band obs. and assignments 9-35663
 3(NH₄)₂0.7MoO₃·4H₂O, thermal decomposition, i.r. spectrophotometric exam. 9-30745
 αO₂, far i.r. absorption 9-28691
 O₂, vibration, effect of precip. of solid solution of Au in Si 9-45315
 Pb:Gd(Mn) films, quenched supercond., far-i.r. study of energy-gap props. 9-41185
 Pb apatites, mineral, freqs. shift of vibrs. 9-37148
 PbI₂, electroabsorption in exciton region 9-33539
 PbMoO₄:Np⁴⁺, energy-level scheme for Np⁴⁺ 9-31110
 PbO-GeO₂ glass system, with 0 to 55 mol % PbO, reflection 9-28675
 PrF₃:Nd³⁺, oriented single cryst. far i.r. electr. and vibronic transitions, Zeeman study 9-39843
 PrF₃:Nd³⁺ single cryst., far i.r. electronic and vibronic transitions obs. 9-35653
 PrF₃, polarized i.r. reflectance, optical phonons and mag. symmetry 9-47345
 Rb₂O-SiO₂ glass, luminescence 9-39872
 RbCl:Ni²⁺, optical absorption 9-39842
 RbMnF₃, ⁶A₁→⁴A₁, ⁴E(G) pure electr. transiion, thermal shift and broadening 9-39844

Spectra continued

inorganic solids continued

- RbMnF₃, ⁶A₁→⁴A₁, ⁶E(4G) pure electr. transition, thermal shift and broadening 9-39845
- Sb₂O₃, transmission, 0.4-0.06 eV 9-39825
- Sb₂S₃, reflection, 2.2-0.6 eV, and transmission, 0.4-0.06 eV 9-39825
- Sb₂S₃, transmission, 0.4-0.06 eV 9-39825
- Sb₂Te₃, reflectivity, 0.5 to 12.5eV 9-33538
- Se-Te mixed cryst., far-i.r. reflectivity, lattice vibr. eigenfreqs. and oscillator strengths 9-39826
- Se-Te solid solns., edge absorpt. and band gap obs. 9-43250
- Se, amorphous, i.r. absorpt. and multiphonon processes 9-45330
- Se, thin single crystals, absorption near fundamental edge 9-28692
- Se single cryst., reflectivity, from ellipsometric meas., optical const. and interband transitions rel. to fine struct. 9-43204
- Si:Bi, impurity absorpt. line shapes, effect of resonant phonon interactions 9-26741
- Si:C i.r. absorption bands rel. electron irradiation 9-26739
- Si:O i.r. absorption bands rel. electron irradiation 9-26739
- Si-containing alloys, i.r. absorpt. obs. of inclusions 9-35213
- Si, heavily doped, u.v. refl. spectrum 9-35645
- p-Si, resonance absorpt. at 36 Gs, 100-1500 Oe, 2-50°K 9-43071
- Si absorption 1.17-1.27 eV under uniaxial compression 9-41012
- Si photorefractance, and rel. to electrorefractance 9-43231
- α(6H)-SiC absorption spectrum at 86°K in vicinity of 3 eV 9-41389
- SiO₂, i.r. spectra interpreted in glassy state 9-28198
- SiO₂, natural, electron irradi., 'A' band and absorpt. in near i.r. correl. 9-41391
- SiO₂.GeO₂ glass, i.r. transmission 9-49267
- SmAl, garnet, absorption and emission used to calculate field of Sm³⁺ ion 9-43244
- SmGa garnet, absorption and emission used to calculate field of Sm³⁺ ion 9-43244
- SnHPO₄·1/2H₂O, vibrational, assignment 9-28704
- SnO₂ powders, i.r. absorpt., interpretation 9-31111
- SnO₂ semiconducting layer, i.r. reflection depend. on surface resistivity 9-26729
- SnO in Ar, Kr, Xe matrices, D-X absorpt. system, matrix induced intersystem crossing 9-49286
- SnS in Ar, Kr, Xe matrices, D-X absorpt. system, matrix induced intersystem crossing 9-49286
- Sr₂VO₄.Cl:Mn, absorpt., transition rel. to site symmetry and cry. field parameter 9-35664
- Sr(OD)₂.D₂O, i.r. absorpt. spectrum 9-33167
- SrTiO₃:Cr³⁺, line shifts, thermal- and elec.-field-induced, rel. to dielectric constant behaviour 9-24415
- SrTiO₃:Cr³⁺(Mn²⁺), absorpt. and fluorescence 9-26743
- SrTiO₃:Fe:Mo and Ni:Mo, photochromic, and EPR studies 9-26742
- SrTiO₃, absorption rel. to colour centres produced by elec. field 9-40976
- Ta₂O₅, emission, structural modifications influence on intensity 9-33560
- TbAlO₃:Cr³⁺, emission of Cr³⁺-Th³⁺ pairs 9-39878
- TeO₂·V₂O₅-BaO glass forming region, transmission 9-39847
- ThO₂:Np⁴⁺, absorpt., analysis of crystal field splitting of J levels 9-35665
- Ti complex, hexaurea Ti(III) iodide, Jahn-Teller effect 9-39848
- TiO₂ powders, i.r. absorpt., interpretation 9-31111
- UO₂(NO₃)₂·6H₂O, i.r. rel. to bending fundamental freq. of UO₂²⁺ 9-49287
- V complex, hexaurea V(III) ion in crystals 9-35654
- W₁₈O₄₉, reflectance, diffuse and specular, rel. to electronic props. 9-31094
- W₂₀O₅₈, reflectance, diffuse and specular, rel. to electronic props. 9-31094
- Xe photoabsorption near N_{IV,V} edge, comparison with solid Xe 9-26745
- Y₂O₃:E³⁺ emission and absorpt. transitions, Eu³⁺ emission from two symmetry sites obs. 9-33562
- Y₃Al₅₂, absorpt., 10- to 55000 cm⁻¹ wave no. 9-35666
- YAl garnet:Nd³⁺, using Jarrell-Ash Im Ebert scanning spectrometer 9-26751
- YCrO₃, antiferromagnetic, Davydov splitting direct obs. 9-24335
- YF₃, polarized i.r., phonon assignment 9-42951
- YFe garnet, emission and absorpt. studies of Ho³⁺ ions 9-45331
- YFeO₃ powder, absorpt. and refl. spectra obs. of h.f. lattice vib. 9-41080
- YGa garnet:Tm³⁺, selection rules 9-24416
- YVO₄:Nd³⁺, absorption, luminescence and stimulated emission 9-26746
- Yga garnet, emission and absorpts studies of Ho³⁺ ions 9-45331
- α-Zn₃(VO₄)₂:Co²⁺, crystal field study 9-26668
- Zn sulfates, infrared absorpt. obs. 9-47368
- ZnO, absorption, intrinsic, associated with longitudinal, optical-phonon assisted 'direct' exciton creation 9-37719
- ZnO, i.r. electroabsorption in multi-phonon region 9-33565
- ZnO, i.r. electroreflectance, elec. Gruneisen const., calc. 9-33540
- ZnO, refl. and transmission for excitons exhibiting spatial dispersion 9-45309
- ZnS:Bi, reflection 9-24462
- ZnS:Cu, Zeeman effect in absorpt. line at 1.44 μm 9-24417
- ZnS:Cu²⁺, absorption and excitation, correlation with valence band structure 9-37732
- ZnS epitaxial films, absorpt. 9-37684
- ZnS single crystals grown from Ga and In melts, absorption and emission 9-37095
- ZnSe:Al, Li, i.r. absorption of localized vibration 9-47369
- ZnSe epitaxial films, absorpt. 9-37684
- ZnSnP₂, i.r. reflection, optical constants and vibrational frequencies 9-35614
- ZnTe, absorption, exciton interpretation 9-37733
- ZnWO₄:C, optical absorpt. 9-37731
- ZnWO₄:Cr³⁺, absorption i.r. emission and excitation 9-33563
- ZnWO₄:Cr³⁺ anisotropic spin-orbit coupling obs. 9-33564

inorganic solids, radiofrequency

see also Nuclear magnetic resonance and relaxation; Paramagnetic resonance and relaxation

BiSb alloys, emission of microwave radiation in weak electric field 9-31102

PbTe, rot. spectrum, 11-15 GHz 9-48478

V³⁺ ion in corundum, sub-millimetre absorption, at liquid He temps. 9-46692

molecules

acceptor-donor complexes, vib. spectra, influence of intermol. interaction 9-32447

adsorbed molecules, i.r. spectra, review 9-42367

Spectra continued

molecules continued

- air, heated, basic radiative processes and spectral props. 9-23400
- air, heated, integral props. for spectrum and intervals, 4000-20000°K 9-23401
- asymmetric rotator, reduced energy deriv. calc. using Hellman-Feynman theory 9-44305
- atmospheric, far i.r., identification of rot. absorpt. lines 9-31361
- CNDO calc. of small mols. 9-30007
- CNDO-MO theory 9-44326
- comprehensive university level text book 9-32395
- diatomic, e spectra, line by line calc. for Voigt profile 9-48378
- diffuse reflectance, characterization of ligand field spectra 9-37672
- Einstein absorpt. coeff. in condensed medium, calc. 9-34590
- energies of electronic transitions, estimation by new method 9-30015
- excited singlet states, absorpt., nanosec. flash photolysis tech. 9-39964
- Fermi resonance in mol. crystals, role of energy migration of vib. excitation along lattice 9-46344
- fluorescence rotational depolarization depend. in viscous soln. 9-23012
- Fourier emission, thermally excited gas, background suppression 9-40576
- Franck-Condon band struct. and spectroscopic closure prop. 9-44304
- group theory application to spectral analysis, book 9-42368
- i.r., and charact. freqs. 700-300 cm⁻¹, a collection of spectra and interpretations 9-34592
- intermolecular, changes during liq.-solid phase transition, vibrational spectroscopy method 9-44386
- i.r., characteristic frequencies ~ 700-300 cm⁻¹, collection of spectra, interpretation and bibliography 9-34592
- i.r., new method, use of symmetry to simplify calc. 9-27832
- i.r. absorption bands, integrated intensities, review 9-42366
- i.r. adsorption, information from derivative of energy distribution of field omitted electrons 9-25725
- i.r. low-temp. technique for improving resolution 9-32446
- laser Raman scattering in gases, detection, trial arrangement 9-48117
- methods of molecular spectroscopy expolided in studying the transition dipole moment of NO. 9-48472
- microwave rotational lines of gases, width determ. using graphical method 9-44310
- near symmetric tops, z axis coriolis perturbations in i.r. spectra 9-48444
- neutron scatt., technique, Raman and i.r. comparison 9-32456
- polar mol. orientation at solid-liq. interface, i.r. absorpt. spectra obs. 9-46341
- polar molecules in polar-non-polar solvent mixtures, absorption band shift 9-30410
- polarized electronic spectroscopy of oriented mols. by liquid crystal 9-46349
- polyatomic, i.r. region intensities and dipole moment derivative, parametric theory 9-23011
- polyatomic, large change of shape transitions, applic. of Franck-Condon principle 9-42361
- polyatomic, rotational-vibrational mode, sum rules determ. for nonrigid asymmetrical top 9-23013
- polyatomic mol., calc. of matrix elements between vib. wavefunctions of ground and excited states 9-48443
- polyelectrolytes, effect of hydration on the ion-water interac. 9-46639
- prolate and oblate symmetric tops, far i.r. 9-23079
- radiative decay of closely space levels, interference effects 9-40577
- radiant energy emission procedure for approx. calcs. 9-36687
- Raman, stimulated, gain pressure dependence 9-27835
- rotational spectra induced by vibrations point groups examined 9-30006
- saturable absorption 9-23009
- tetrahedral mol. in octahedral cell, rotation-translation levels 9-38808
- theory related to laser 9-40344
- two-photon transitions, resonance freq. shift 9-46342
- vapour, i.r., band freq. shift obs. 9-32445
- vibrational-rotational transitions in nonlinear mols. of XY₂ type, computation 9-27839
- vibratory-rotational, linewidth calc. 9-42362
- CH line spectrum solar center-to-limb behavior 9-31633
- C₂ line spectrum solar center-to-limb behavior 9-31633
- CN line spectrum solar center-to-limb behavior 9-31633
- CO line spectrum solar center-to-limb behavior 9-31633
- H-bonding, far-i.r. obs., vibr. assignments 9-32453
- MgH line spectrum solar center-to-limb behaviour 9-31633

organic molecules and substances

see also Molecules

- o-, m- and p- bromaldehyde, electronic transitions 9-46382
- O-, m-, p- bromobenzaldehyde vapours, electr. absorpt. spectra, longest wavelength π*→π syst. obs. 9-46387
- all-trans, retinal, rel. to fluorenc. 9-24460
- tri-phenyl compounds of As, Sb, Bi and P, Raman and i.r. obs. 9-30137
- α-ω-diphenylpolyene ketone charge transfer complexes with tetracyanethylene and chloranil 9-42443
- AB₂C_{1-x} type, persistence and amalgamation type 9-35641
- acetic acid and its ion, vibrational 9-42421
- acetone, u.v. absorpt., effects of temp. and Li or Na salt additions 9-36888
- acetone and acetone-d₆, meas. and calc. of absolute intensities of Raman lines 9-27883
- acetonitrile in vibr. ν₈=2 excited state, rot. transitions 9-46379
- acetyl system, substituent electronic and steric eff. 9-23084
- acridina dye absorbances, triplet-triplet absorption 9-48488
- acridine and anthracene, mols. of similar structure and mass but different synum. 9-42422
- acridine dye absorption, luminescence and polarized luminescence spectra, 77°K 9-23113
- acriflavine, emission spectra in solution 9-26122
- adenosine, i.r. absorption spectra, 230-30 cm⁻¹, 20 to -175°C, crystal lattice vib. anal. 9-25783
- n-alkyl acid, far i.r. study, H bond stretching vib. determ. 9-23087
- allyl radical, characts., and electronic structures 9-30110
- amides, N-monosubstituted, deuterio derivatives, i.r. spectra 9-42663
- amino acids, aromatic, rel. to u.v. induced photochem. transforms. 9-28816
- p-aminobenzoic acid, oriented, polarized absorption spectrum 9-46386
- 3-aminophthalimide soln., electronic-absorption-band region, Einstein-coeff. spectra obs. 9-30072
- aniline, Stark effect meas. of dipole moments of lowest singlet π*→π states 9-34686

Spectra continued

organic molecules and substances continued

- anthracene: tetracene radiation damage rel. to optical absorption 9-26747
- anthracene, crystalline, radiating-centres inhomogeneity, fluorometric phase spectra, -196°C 9-39879
- anthracene, nanosecond excited-state polarized absorption spectra in visible region 9-34657
- anthracene cation trapped in boric acid glass 9-42423
- anthracene crystals, photocurrent excitation spectrum, exciton mechanism 9-35509
- anthracene derivatives, polarization, rel. to oscill. orientation, 20°C 9-25758
- anthracene in benzene, toluene, 185, 250 nm absorpt. 9-34912
- anthracene in mixed crystals (also containing naphthalene), triplet-triplet energy transfer 9-43262
- anthracene mixed crystal, guest-host interaction eff. 9-35643
- anthracene solidified vitreous solns., absorpt., aggregates existence obs. 9-46701
- anthracene thin film, crystalline phase, fluorescence spectra and X-ray diffraction 9-35689
- anthracene triplet exciton band-structure limits from n.m.r. 9-35667
- anthraquinotetramethan and corresponding diquinone, CMO calc. for spectral and redox behaviour 9-23089
- aromatic hydrocarbons, polarization of electronic transitions 9-31137
- aromatic hydrocarbons, triplet-triplet absorpt. polarized excitation spectra, obs. 9-23082
- N-aryloxy carbazoles, u.v. absorpt. and luminescence 9-25759
- aryphenylacrylic acid i.r. spectra, carbonyl stretching freq. 9-23092
- arypyrazolines, electronic absorption and luminescence, structure depend. 9-30074
- azapyridocyanines, u.v. absorpt., fluorescence and phosphorescence transitions 9-23093
- azines, transition metal (II) complexes 9-34659
- benzene, electronic spectrum calc. 9-44304
- benzene, electronic vib. transition ${}^1A_{1g} \rightarrow {}^1B_{2g}$ calc. 9-27888
- benzene, standard solution, absorpt., noise intensity 9-36889
- benzene, substituted; charge-transfer state eff. 9-30084
- benzene and acetylene derivatives, T-T* absorption spectra by 2-quantum photosensitized reactions 9-42428
- benzene carbonic acid, u.v. electron absorption 9-30085
- benzene crystals, doped, absorption of localized exciton states 9-31112
- benzene derivatives, liquid, depolarized light scattering 9-26117
- benzil in stilbene cryst., absorpt., polarization charact. rel. to trans-planar config. 9-34660
- benzine, CH-stretching overtone anharmonicity 9-27886
- benzo-[g,h,i]-perylene, absorpt. and fluorescence spectra 9-34661
- benzodioxane-1,4,6-substituted, u.v. and i.r. absorpt. 9-40609
- benzoic acid, oriented, polarized absorption spectrum 9-46386
- benzophenone derivatives with donor and acceptor substituents, u.v. absorpt., obs. 9-30413
- 3,4-benzopyrene conc. quenching and quasi-line luminescence spectra temp. depend. obs. 9-23098
- benzoyl system, substituent electronic and steric eff. 9-23084
- benzyl radical from toluene and ethyl benzene, emission spectrum in vapour state 9-34694
- benzylindan impurity in fluorene, v. spectra, polarized fluorescence and absorption vibrational anal. 9-28697
- 1,4-bis(methylthio)naphthalene cation-radical, electronic and e.s.r. spectra 9-38883
- o-, m- bromo anilines, vapour, near u.v. absorpt. spectra, band obs., excited and ground state freq. 9-25762
- O-bromo chloro benzene, solid, near u.v. absorpt. spectrum, band and freq. obs. 9-46383
- p-bromo iodo benzene, vapour, near u.v. absorpt. spectrum, band and freq. obs. 9-46383
- bromoform, C-H stretching vibr. band, shape and width 9-48489
- β -bromophenol, u.v. and i.r. rel. to transitions and vib. 9-23101
- butadiene, charact., and electronic structures 9-30110
- butene, cis- and trans-, Rydberg progressions 9-38884
- butene-1, rotational isomerism, microwave obs. 9-23102
- t-butylbenzene, alkyl derivative crystal, vibronic spectra, 20°K 9-31113
- carbinols, u.v. electron absorption 9-30085
- carbonium ions, internal reflection spectroscopy 9-34664
- carbonyl and carboxylic groups, effect of U.V. on charact. 9-40627
- o-m-chloro ethyl benzenes, solid, near u.v. absorpt. spectra, band and freq. obs. 9-46383
- p-chloro iodo benzene, vapour, near u.v. absorpt. spectrum, band and freq. obs. 9-46383
- 2-chloroanthraquinone, visible emission spectrum, bands and freq. 9-25763
- chloroform, C-H stretching vibr. band, shape and width 9-48489
- α -chloronaphthalene in n-paraffin, quasiline phosphorescence spectra 9-46409
- chloronaphthalene, 1,4-, 1,5-, 2,6-, e spectra, obs. 9-27891
- chloronitrobenzenes, u.v. spectra in THF and cyclohexane 9-30095
- coronene, spectral shifts of ${}^1L_a \rightarrow {}^1A_1$ transition with temp. and press. 9-30097
- cumene hydroperoxide solution, H-bonding investigated by i.r. absorpt. 9-27892
- cyanine dye absorption, luminescence and polarized luminescence spectra, 77°K 9-23113
- 9-cyanoanthracene, polarised u.v. absorpt. spectrum at 4.2°K 9-33566
- cyano-1(9) anthracene vitreous solns., absorpt., aggregates struct. obs. 9-46702
- 2-cyanoethylsilanes, NMR, analyses and parameter predictions 9-38887
- cyanogen, electronic spectrum 9-30098
- 1,3,5,7-cyclo-octatetraene, low energy e impact excitation, obs. 9-23126
- cyclobutanol, d₁-, d₂-, i.r. vib. assignment 9-23103
- cyclobutanone vapour, u.v. spectrum, 3300°A resolution, 1A_2 electronic state O vib. levels 9-42429
- 1,3,5-cycloheptatriene, low energy e impact excitation, obs. 9-23126
- cytidine, i.r. absorption spectra, 230-30 cm⁻¹, 20 to -175°C, crystal lattice vib. anal. 9-25783
- diaryl N oxides, methoxy-substituted, e spectra, obs. 9-27912
- di bromofluoroethane, heavy hindered rotator, far i.r. 9-42432
- 9,10-dichloroanthracene with chlorin absorption 9-30073
- dichlorobenzene, o-, m- and n-, combinational scattering, phase shift rel. to dipole-dipole intermolecular forces 9-46393
- 4,4'-dichlorobenzophenone, polarized cryst. absorpt. 9-31114

Spectra continued

organic molecules and substances continued

- difluorobenzene m- and n-, combinational scattering, phase shift rel. to dipole-dipole intermolecular forces 9-46393
- m-difluorobenzene vapour, near u.v. absorpt. spectrum, band obs. 9-46394
- 1,2-dihalide substituted ethanes, vibration freq., calculation and interpretation 9-23120
- 5,10-dihydrophenazine, near-u.v. absorpt. spectrum 9-32508
- 2,5-dihydrothiophene i.r. and Raman vib. spectra meas., freq. assignment 9-27901
- 5,8-dihydroxynaphthaquinone, i.r. and visible spectrum obs., vib. and electronic structure deduced 9-30123
- 1,3-di-imines, N,N' disubstituted, electronic spectra in methanol 9-30106
- 2,5- and 3,4-dimethylthiophene and 2,3,4,5-tetramethylthiophene, vibrational spectra, calculation and interpretation 9-25770
- diphenyl oxide in hexane, heptane soln., quasiline absorption, electronic-vibrational anal. 77°K 9-30114
- diphenyl sulfide in hexane, heptane soln., quasiline absorption, electronic-vibrational anal. 77°K 9-30114
- diphenylamine derivatives, methoxy-substituted, e spectra, obs. 9-27912
- dithiocarbamates, and acid derivs., maxima in u.v. region rel. to $\eta \rightarrow \pi$, $\eta \rightarrow \sigma^*$ $\pi \rightarrow \pi^*$ transitions 9-36711
- dye laser, dependence on conc. and dye length 9-36295
- 1,2-epoxycyclohexane, component parameter determ. by statist. processing of absorption curve 9-40578
- ether, N₂, O₂ mixture, simultaneous HCN and H₂O laser emissions in pulsed discharge 9-22404
- ethyl alcohol, microwave rot. spectrum, stable isomers, ground-state rot. and centrifugal distortion coeffs. 9-34668
- ethyl alcohol, microwave spectrum 9-30150
- ethyl methyl ketone, u.v. absorpt., effects of temp. and Li or Na salt additions 9-36888
- ethylene, d₂ vibrational struct. of 1744 Å Rydberg transitions 9-44357
- ethylene, charact., and electronic structures 9-30110
- ethylene amides, u.v. 9-23119
- excitation energy degradation, Jablonski scheme 9-28814
- ferrocene and its molecular complexes, single crystals polarized absorption spectra 9-47370
- fluoranthene, electronic spectrum and electron affinity 9-30116
- fluorene in hexane, heptane soln., quasiline absorption, electronic-vibrational anal. 77°K 9-30114
- fluorenone, electronic spectrum, 1680-2350 Å, new band and comparison with SCF MO calc. 9-30117
- fluorenone ketyl optical, existence of paramagnetic and diamagnetic ion clusters 9-34923
- o-fluoroanisole, near u.v. absorpt., rel. to fundamental vibr. freqs. 9-34672
- fluorobenzene crystal u.v. absorption near 1st electronic transition, polarized light, 20°K 9-26748
- ortho- and meta-fluorobenzonitriles, u.v. absorption spectra 9-48493
- α -fluoronaphthalene-D₂ in n-paraffin, quasiline phosphoresc. spectra 9-46409
- β -fluoronaphthalene-D₂ in n-paraffin, quasiline spectra 9-46409
- formaldehyde, using mol. jet spectrometer 9-43928
- formaldehyde-d₂, d₃ and hd, 3500 Å 1A_2 - 1A_1 transition 9-48496
- formaldehyde in solid low-temp. solns. 9-39880
- formic acid-d₃ rotation spectrum, transition identification 9-44361
- formyl fluoride, 2670 Å absorption system analysis 9-32515
- glasses, trapped e spectra rel. to matrix polarity, 77°K 9-28695
- glasses and crystals, for laser 9-41912
- guanidine, i.r. absorption spectra, 230-30 cm⁻¹, 20 to -175°C, crystal lattice vib. anal. 9-25783
- rel. to H-bonding, inter- and intra-mol., absorpt. and fluoresc. band widths, obs. 9-23081
- halobenzene series, u.v. absorption variation, polarized light, 20°K 9-26748
- helixenes in 1,4-dioxan. soln., fluorescence spectra 9-40616
- hydrocarbons, alternant, triplet-triplet absorption spectra, correlation between SCFMO and HMO calcs. 9-38901
- m,p-hydroxybenzaldehyde, vapour, emission type 9-34674
- indigoidal pigments in dioxane and acid solns., obs. 9-28153
- i.r. absorption bands spontaneous emission probability determ. 9-25754
- i.r. absorption bands spontaneous emission probability determ. 9-38875
- linear molec. crystals, absorpt. by charge-transfer excitons 9-24400
- liquid, absorption i.r. bands intensity temp. depend. meas. 9-23506
- luminescence, aromatic compounds, n-paraffin solutions, effect of rate of freezing and concentration 9-28142
- merocyanines, C-O stretching band behaviour and shape in mixed solvents 9-23137
- methane, emissivity of 3.3 μ band at 297, 673 and 923°K 9-46401
- methane, N₂, O₂ mixture, simultaneous HCN and H₂O laser emissions in pulsed discharge 9-22404
- methane, vib.-rot., pressure broadening of ν_3 meas. 9-23129
- methane/He mixture, vib.-rot., pressure broadening of ν_3 meas. 9-23129
- methane/He mixture, vib.-rot., pressure broadening of ν_3 meas. 9-23129
- methane/N mixture, vib.-rot., pressure broadening of ν_3 meas. 9-23129
- methanol-d₄, microwave 18-38 GHz, and transition assignments 9-23508
- methoxyethylene, internal rotation barrier, reinvestigation of microwave spectrum 9-46406
- methyl bromide, double irr. by i.r. and r.f. beams 9-46402
- N-methyl-ethylenethiourea, u.v. and i.r. 9-48840
- methyl-pyridinium salts, anomalous charge transfer fluorescence and Stokes shifts 9-34679
- N-methyl-trimethylenethiourea, u.v. and i.r. 9-48840
- N-methylaniline vapour, near u.v. absorption spectrum 9-30128
- 9-methylanthracene, discrete fluorescence spectrum 9-46407
- methylthiouramine, vib. spectrum 9-27904
- methylstyrene, isomeric, u.v. vapour absorpt., rel. to band systems 9-23142
- naphthalene, molecular admixture, relation between emission spectrum and solubility 9-28719
- naphthalene, singlet- singlet and triplet-triplet absorpt., added ethyl bromide effects, obs. 9-28138
- naphthalene, singlet-triplet absorpt. by photoexcitation spectra 9-31115
- naphthalene and monosubst. derivatives, low-energy triplet-triplet transitions 9-38906
- naphthalene in n-paraffin, quasiline phosphoresc. spectra 9-46409
- naphthalenes, 1- and 2-substituted, triplet-triplet absorpt., calc. 9-23144
- trans-1-nitro-1-propene, rel. to e struct., u.v. absorpt. 9-27893

Spectra continued

organic molecules and substances continued

- 3-nitro-1-propene, u.v. absorpt. 9-27893
 p-nitroaniline, oriented, polarized absorption spectrum 9-46386
 nitroethylene, rel. to e struct., u.v. absorpt. 9-27893
 nitromethane, u.v. absorpt. 9-27893
 p-nitrophenol, oriented, polarized absorption spectrum 9-46386
 p-nitrosodimethylamine soln., electronic-absorption-band region, Einstein-coeff. spectra obs. 9-30072
 organogermanium cpds., investigated rel. to electro-optical parameters 9-46397
 oxalyl halides, attribution and analysis using normal coords. 9-46411
 3-oxo, 4-phenyl, 1,2-benzofluorenone solutions 9-32785
 oxybenzoic acids, u.v. electron absorption 9-30085
 paper, discrepancies in Kubelka-Munk reflectance eqn. applic. 9-37712
 pentacene, vibronic band position depend. on light polarization 9-27909
 pentadiene, characts., and electronic structures 9-30110
 perylene molecular crystals, 'effective molecule' model in electronic spectrum calc. 9-41392
 phenanthrene 3400-Å spectrum rel. to totally symmetric vibronic perturbations 9-38911
 phenanthrene soln., electronic-absorption-band region, Einstein-coeff. spectra obs. 9-30072
 phenol, Stark effect meas. of dipole moments of lowest singlet $\pi^* \leftarrow \pi$ states 9-34686
 phenothiazine, polarized absorpt. 9-39888
 phenoxazine, polarized absorpt. 9-39888
 phenylalanine and derivatives, absorpt. at 298 and 77°K 9-46415
 phenylalanine fluorescence spectrum excited by vacuum U.V. radiation 9-30149
 phenyldiazonium ions, meta and para substituted, rel. to HMO calcs. 9-27914
 2-phenylnaphthalene, and e struct. and pot. energy rel. to mol. config., calc. 9-27911
 phosphate glasses, absorpt. of first row transition metal ions 9-33543
 phosphiran, -1-d₃, -2,3-d₃; i.r., vib. assignment, freq. shift meas. 9-23150
 phthalimide derivatives, spectral and fluorometric characteristics depend. on oxygen 9-23149
 phthalocyanine, free base, matrix isolated, absorpt. 9-49289
 polymer films, synthesized, vacuum u.v. absorpt., electr. struct. obs. 9-31116
 polymers in methylene series, i.f. spectra absorpt. 9-48525
 polynucleotides, vacuum u.v. absorpt., rel. to electronic structure 9-26750
 polyvinyl alcohol films, ultraviolet absorption spectra 9-35669
 poly-n-vinylcarbazole, energy energy migration study 9-48527
 propanoic acid far i.r. spectra, H bond stretching vib. determ. 9-23087
 pyrazine, absorpt. $B_{2u}(\pi-\pi^*) \leftarrow A_{1g}$, excitonic struct. 9-47405
 pyrene, π -electron, group theory study 9-30139
 pyrene in ethanol soln., Fluorescence spectra, isobestic pts. 9-40574
 pyrene molecular crystals, 'effective molecule' model in electronic spectrum calc. 9-41392
 pyridinyl radical dimers, u.v. absorpt. spectra, exciton splitting 9-40626
 pyronine B soln. in ethanol, glycerol, Nd laser excitation, light generation, 550-650 nm, room temp. 9-30141
 quinoxaline, u.v. spectrum, two $n \rightarrow \pi^*$ transitions 9-32525
 report on CN, CO and organogermanium cpds. 9-46321
 rhodamine 3B, emission spectra in solution 9-26122
 rhodamine 6G mols., in soln., electronic absorption spectra and transitions 9-34690
 rhodamine 6J soln. in ethanol, glycerol, Nd laser excitation, light generation, 550-650 nm, room temp. 9-30141
 rhodamine C soln. in ethanol, glycerol and polymethylmethacrylate, Nd laser excitation, light generation, 550-650 nm, room temp. 9-30141
 rosin films, characts. of light sensitive volume changes 9-28698
 soffranine T soln. in ethanol, glycerol, Nd laser excitation, light generation, 550-650 nm, room temp. 9-30141
 solutions, binary dilute, Brillouin intensity ratios and Landau-Placzek law deviations, obs. 9-30408
 spiropyranes in soln., photochromy obs., by means of triplet-triplet absorpt. 9-34910
 stilbenes, para-substituted, first e transition freq., obs. 9-34692
 tetrachloro-p-xylene, excimer emission in rigid organic glass, 280nm excitation, 77°K 9-32530
 1,4,5,8-tetrahydroxyanthraquinone, visible emission and abs. spectrum, analysis of bands 9-30144
 tetrakis(dimethylamino)-ethylene, electronic spectrum 9-23159
 thiocarbocyanine dye absorption, luminescence and polarized luminescence spectra, 77°K 9-23113
 thiol esters, complex, i.r. absorption freq. determ. 9-23160
 thulium cyclopentadienides, visible and i.r. absorption, vib. coupling and struct. obs., low temp. 9-32531
 thulium methylcyclopentadienides, visible and i.r. absorption, vib. coupling and struct. obs., low temp. 9-32531
 thymidine, i.r. absorption spectra, 230-30 cm⁻¹, 20 to -175°C, crystal lattice vib. anal. 9-25783
 toluene, standard solution, absorpt., noise intensity 9-36889
 trifluoroacetaldehyde, i.r. vib. spectrum and internal rotation barrier 9-23123
 trifluoromethane rotational microwave spectra obs. 9-30113
 trifluoromethyl acetylene, rotational microwave spectra obs. 9-30113
 trimethylene sulfide, electr. spectrum, vib. struct. of transitions, ground and excited states shape obs. 9-32524
 triphenylmethane dye absorption, luminescence and polarized luminescence spectra, 77°K 9-23113
 tryptophan fluorescence spectrum excited by vacuum U.V. radiation 9-30149
 tryptophan fluorescence spectrum excited by vacuum U.V. radiation 9-30149
 undecanoic acid far i.r. spectra, H bond stretching vib. determ. 9-23087
 uranyl ion, absorption spectrum, vibronic analysis 9-25784
 uridine, i.r. absorption spectra, 230-30 cm⁻¹, 20 to -175°C, crystal lattice vib. anal. 9-25783
 xanthene dye absorption, luminescence and polarized luminescence spectra, 77°K 9-23113
 xylol, o-, m- and n-, combination scattering, phase shift rel. to dipole-dipole intermolecular forces 9-46393
 zinc phthalocyanine, matrix isolated, absorpt. 9-49289
 CN, electron oscillator strength of violet system, basic meas. technique 9-46388

Spectra continued

organic molecules and substances continued

- Na uranyl acetate, ligand isotope eff. 9-23005
 spectra
 organic molecules and substances, infrared
 2-pyrazolin-5-one derivatives 9-30140
 (R-O)₂P(=O)H, P-H bending vibrs., obs. 9-30066
 (R-O)₂P(=S)(S-H), P-S-H vibrs. and rot. isomers, obs. 9-30066
 2-chloroanthraquinone, vib. freq. and assignments 9-25763
 p-dibromotetradeuterobenzene, vibrational spectra study 9-27889
 trans-1,2-diphenylethylene and trans-1,2-diphenylethylene, solid and soln. samples 9-38910
 o- and m-fluorobenzenitriles, absorption, vibrational 9-46395
 1,3,5 trichloropyrimidine and 4D derivative, vibr. assignments, obs. 9-28139
 N-trimethylborazines isotopically substituted, band obs. 9-27906
 acetaldehyde, absolute band intensities determ., expt. and theor. 9-25756
 acetaldehyde, combination band of methyl group torsion and asymmetrical stretching vib. 9-25752
 acetone, bands and electrooptical parameters meas., intensity theor. calc. 9-27881
 acetone, bands and electrooptical parameters meas., intensity theor. calc. 9-32498
 acetonitrile and acetonitrile-d₃ 9-28696
 acetylene derivatives with conjugated bonds, C≡C absorpt. band intensity, intramolecular interactions effect 9-46381
 acetylene-d₂, absorption, anal. of bands in 3-5 μ region, molec. consts. of levels involved 9-34651
 acids, vapour spectra, band freq. 9-32445
 adipic acid crystal, at room and liq. N₂ temp. 9-34652
 alcohols, association in soln. and in vapour phase 9-23507
 alcohols, vapour spectra, band freq. 9-32445
 alkali-halides-thiourea mixed cry., abs. spectra, interac. and band obs. 9-24420
 n-alkyl chlorides series, C=2-6, vib. 9-40607
 n-alkyl cpds., combination band of methyl group torsion and asymm. stretching vib. 9-25753
 alkyl phosphinates, unsaturated monomer and oligomer, vibr. analysis, 400-4000 cm⁻¹ 9-25757
 alkylarylsulphonium mixed cpds. 9-23086
 n-alkyltrimethylammonium bromide mols. and group freqs. and band progression rel. to chain length, 1400-700 cm⁻¹ 9-44349
 allene, search for pure rot. absorpt. 9-38879
 allene, two rot. lines 9-38878
 amines, N-H, group valence vibrs. rel. to H bonding 9-34653
 amines and amides, vapour spectra, band freq. 9-32445
 m-aminobenzoic acid, crystals and soln. 9-45332
 anthracene photodimer, and correl. between bands and proposed structure 9-32502
 9,10-anthraquinone 9-23156
 aromatic hydrocarbons adsorbed on zeolite Y, rel. to surface interactions 9-24520
 arylanilide, Cl substituted, steric effects, obs. 9-25760
 p-azoxyphenetole, liquid, liquid crystal and solid states, for i.r. meas. 9-34913
 benzaldehyde, obs. 9-44352
 benzene isotopic mixed crystals, site effects in vibr. spectrum 9-43007
 benzenes, monosubstituted ν intensities rel. to substituent obs. 9-30090
 benzenes, para-disubstituted ν_{16} intensity rel. to substituents direct interaction, 1600cm⁻¹ 9-30091
 benzenes, stretch vibrations, integral intensities of i.r. bands 9-30089
 benzimidazole, and metal complexes 9-23099
 benzoic acid, Cl substituted, steric effects, obs. 9-25760
 benzophenone in solid state, obs. and assignments 9-30077
 p-benzoquinones, tetra substituted, i.r. spectra obs., vibrational frequencies calc. 9-30086
 benzo[a]anthracene photodimer, and correl. between bands and proposed structure 9-32502
 benzyl chloride, obs. 9-44352
 benzyl formate, obs. 9-44352
 1,2-bis(dihaloboryl)ethanes 9-38882
 bis(trifluoromethyl)trioxide, vib. modes degeneracy 9-25765
 4-bromobenzonitrile in liq. cryst. solvent 9-48682
 β -bromophenetole, and vibration assignment 9-23101
 2-bromopropene, combination band of methyl group torsion and asymmetrical stretching vib. 9-25752
 t-butyl alcohol-water soln., abs. spectra, comparison with methyl cyanide-water 9-42651
 to-butylchloride, far i.r. absorpt. 9-39670
 γ -butyrolactone, gas and liq., rel. to ring deforms. 9-48492
 carbon disulphide, liquid, far i.r. absorptions 9-40796
 carbon tetrabromide solute, vibrational band perturbation meas. 9-26123
 carbon tetrachloride, assoc. of pyridine deriv. and alcohols, i.r. study 9-23106
 carbon tetrachloride, liquid, absorption and dispersion in 740-820 cm⁻¹ range, temp. depend. 9-48703
 carbon tetrachloride, liquid, far i.r. absorptions 9-40796
 carbon tetrachloride solute, vibrational band perturbation meas. 9-26123
 carbon tetrafluoride, cryst., modified, absorpt. and refl. rel. to Fermi reson., 8 μ 9-28676
 carbonyl cpds., vapour spectra, band freq. 9-32445
 carboxylic acids, dimeric, rel. to mol. config. in crystals, >77°K 9-30093
 chloro-methylbenzenes, hexa-substituted crystals 9-24418
 chloroacetyl halides, rot. isomerism 9-30094
 chloroform, in CCl₄ and CS₂ soln., integrated intensity of i.r. absorption band 9-23110
 chloromethane, ν_2 band rotational structure 9-32507
 2-chloropropene, combination band of methyl group torsion and asymmetrical stretching vib. 9-25752
 2-chloropropene-1,3-d₂ 9-40610
 4-cyanobenzoic acid in liq. cryst. solvent 9-48682
 2-cyanopropene, combination band of methyl group torsion and asymmetrical stretching vib. 9-25752
 cyanopropene 9-23112
 cyclobutane-1,3-dione 9-23115
 cyclobutenes, vinyl, methyl and isopropenyl substituted 9-23114
 cyclohexane, liquid, far i.r. absorptions 9-40796
 cyclohexene, liquid, far i.r. absorptions 9-40796
 cyclopentanone-d₄, gas and liq., rel. to ring deforms. 9-48492
 cyclopropane, vibr.-rot. bands, computer anal. 9-38895

spectra continued

organic molecules and substances, infrared continued

- decafluorobiphenyl, vibrational spectrum below 200 cm^{-1} 9-30100
 deuterated formaldehyde, Stark spectroscopy by i.r. lasers 9-25767
 diacetylenes: heteroaromatic substituted carbonyl cpds., absorpt., 1637-1630 cm^{-1} 9-30067
 dialkylacetylenes, straight-chain, absorpt. rel. to struct., obs. 9-27878
 trans-1,2-dibromide cyclohexane, rel. to freqs. and vib. forms and conformation equilb. 9-36890
 2,3-dibromobutane, liq., solid, rel. to conformation, vibs. and force consts. 9-34663
 dibromomethyl radical, matrix isolated 9-44378
 2,3-dibromopentane, liq., solid, rel. to conformation, vibs. and force consts. 9-34663
 trans-1,2-dichloride cyclohexane, rel. to vib. forms and conformation equilb. 9-36890
 2,6-dichloroaniline, in solution, obs. of i.r. spectrum assignments to vib. modes 9-32500
 2,5-dichloroaniline in solution, obs. of i.r. spectrum, assignments to vib. modes 9-32500
 dichloromethyl radical, matrix isolated 9-46425
 2,4-dichlorotoluene, liq., absorpt. spectra, vib. assignments 9-23109
 2,5-difluoroaniline liquid, i.r. absorption spectrum, vibration modes 9-32500
 difluoroformaldehyde, band intensities, 2.0-6.0 μ 9-46390
 difluoromethyl radical in solid Ar 9-48517
 p-difluorotetradecarobenzene, vibrational spectra study 9-27889
 2,4-difluorotoluene, liq. absorpt. spectra, vib. assignments 9-23109
 2,3-dihydrofuran, ring-puckering vibr. 9-30102
 dimethylacetylene, liquid, far i.r. absorptions 9-40796
 dimethylhydrogenphosphonate, P-H bending vibrs., Raman obs. 9-30066
 dimethyllead dihalides, and Raman spectra mol. struct. 4000-70 cm^{-1} 9-34675
 N,N-dimethylthioacetamide, normal vibrations analysis 9-46391
 N,N-dimethylthioformamide, normal vibrations analysis 9-46391
 N, N'-dimethylurea, normal co-ord. anal., bands and vib. determ. 9-23130
 dinitrobenzenes, isomeric, vibrational spectra 9-48502
 1,4-dioxan, liquid, far i.r. absorptions 9-40796
 1,3-dioxolane, pseudorotation 9-38915
 diphenyl phenylborate, rel. to vib. frequencies 9-23151
 diphenyl sulphide and disulphide 9-23133
 diphenyl sulphoxide 9-23133
 2,5-diphenyl-1,3,4-oxadiazol dioxy derivatives of scintillator activators, rel. to intermol. H-bonds, obs. 9-30414
 diphenylethene and diphenylethene- d_8 , soln. and solid samples, vibr. assignments and dichroic behaviour 9-38909
 γ -dipyridyl-di-N-oxide, normal co-ord. analysis 9-46392
 1,4-dithian, 4000-40 cm^{-1} , vibrational assignment 9-32510
 1,3-dithian, 4000-40 cm^{-1} , vibrational assignment 9-32510
 durennes, monosubstituted v intensities rel. to substituent obs. 9-30090
 ethane, rot. fine structure of perpendicular band ν_1 9-34671
 ethanol, isotopic, monomers 9-38891
 ethanol, isotopic, self-associated 9-38892
 ethyl benzoate, liq. and soln., vib. freqs. assignment 9-25769
 ethyl chlorides, h_3 , d_3 , d_5 , d_7 , vibr. analysis 9-48490
 ethyl halides, combination band of methyl group torsion and asymm. stretching vib. 9-25753
 ethyl vinyl ether- $\text{Al}(\text{C}_2\text{H}_5)_3$, rel. to complexation, obs. 9-48491
 ethylene, trans- d_2 , strong Coriolis perturbation 9-38894
 ethylene and ethylene- d_4 cryst., far i.r. 9-45333
 ethylene carbonate, gas and liq., rel. to ring deform. 9-48492
 trans-ethylene- d_2 , 2 axis Coriolis coupling calc. 9-48444
 ferrocene, 1,1'-disubstituted cpds. 9-23121
 1-fluoro-1,1,2,2-tetrachloroethane, internal rot. and isomerism 9-27896
 2-fluoroaniline, liquid, i.r. absorption spectrum, vibration modes 9-32500
 m-fluoroanisole, absorption, vibrational 9-46395
 fluorobenzenes, C-F stretching and bending vib. freq., NMR data correl., eff. of electronegativity 9-23122
 fluoroform, vibr.-rot. bands, computer anal. 9-38895
 formaldehyde, i.r. laser irradi., Stark spectrum obs. 9-25766
 formaldehyde, Stark spectroscopy by i.r. lasers 9-25767
 formic acid, i.r. laser irradi., Stark spectrum obs. 9-25766
 fulminic acid 9-34673
 glycine chelates, isomeric, metal-O bond stretching vib. 9-27898
 m-halobenzaldehydes, rotational isomerism 9-42436
 halogenocyclohexanones, and deuterated derivatives 9-23125
 hydrazinium hydrogen oxalate, cryst., D-substitution effects rel. to H-bond symmetry, 3600-200 cm^{-1} 9-24393
 hydrogen bonding between OH and nitro groups 9-23080
 hydroxy chromones, carbonyl stretching freqs. 9-30124
 N(4)-hydroxycytosine soln. with purines, rel. to H-bond assoc. 9-42635
 iodoform, absorpt., rel. to cryst. lattice vibrs. 9-44813
 iodoform, in CCl_4 and CS_2 soln., integrated intensity of i.r. absorption band 9-23110
 iodoform, in CCl_4 and CS_2 soln., integrated intensity of i.r. absorption band 9-23110
 isopropenyl groups, $=\text{CH}_2$ stretching vibr. bands splitting rel. to isomerism, obs. 9-44370
 isopropyl bromide, liq., solid, rel. to conformation, vibs. and force consts. 9-34663
 ketones at transition liq.-solid, temp. lowering effect 9-32520
 l.f. aliphatic monocarboxylic acids 9-38885
 liquids, absorption and dispersion in i.r. absorption bands region 9-46643
 low-temp. technique for improving resolution 9-32446
 mercuric halide adducts of cyclic thio-ethers, ring vibrations 9-30107
 methane, abundance and rot. temp. on Jupiter 9-40175
 methane, i.r. laser irradi., Stark spectrum obs. 9-25766
 methane, pressure induced 9-32523
 methane, Stark effect of absorpt. line, maser obs. 9-34678
 methane, Stark spectroscopy by i.r. lasers 9-25767
 methane d_3 , b type vibr.-rot. band analysis 9-30129
 methane gas excited by electrons, glow spectra in i.r. region 9-38831
 methanethiol 9-23132
 methyl 2,3,4,5,6-pentafluorodiphenyls 9-23134
 methyl acetylene, vibr.-rot. bands 9-23135
 methyl acetylene- d_3 , vibr.-rot. bands 9-23136
 methyl alcohol, i.r. laser irradi., Stark spectrum obs. 9-25766
 methyl benzoate, liq. and soln., vib. freqs. assignment 9-25769
 methyl chloride, i.r. laser irradi., Stark spectrum obs. 9-25766

spectra continued

organic molecules and substances, infrared continued

- methyl cyanide, i.r. laser irradi., Stark spectrum obs. 9-25766
 methyl cyanide, rotational const. determ. 9-23128
 methyl cyanide-water soln., abs. spectra study, comparison with t-butyl alcohol-water 9-42651
 methyl iodide, $^{13}\text{CH}_3\text{I}$, vibration-rotation bands 9-30131
 ϵ -methylcaprolactam-caprolactam, conformational structure 9-32551
 methylchloroform, cryst. and plastic, absorpt. rel. to lattice motions, far i.r. 9-24419
 methyl-cyclopentadienyl nickel nitrosyl 9-30132
 methylene chloride, vapour and liq., band intensities calc. 9-48497
 methylhydrazine 9-30127
 methylphenyl sulphide 9-23133
 methylphosphorodifluorodithioate 9-38902
 methylthionitrite 9-23131
 monoalkylacetylenes, straight-chain, absorpt. rel. to struct., obs. 9-27878
 monobromocacetylene, ν_1 and $2\nu_1$ bands, rotational structures 9-46408
 monocarboxylic acids, dissoci. const. and integrated intensities of monomer and dimer C=O bands 9-23105
 monofluoroacetylene, CH deform.-CF stretching coupling Fermi reson., obs. 9-27882
 monohalobenzenes, liquid and vapour doublet splitting indicates rot. structure 9-27887
 naphthalenes, disubstituted 9-23145
 1,4-naphthoquinone 9-23156
 new method, use of sym. to simplify calc. 9-27832
 2-nitropropane Na salts, rel. to geometric isomers, obs. 9-27905
 nitroethane Na salts, rel. to geometric isomers, obs. 9-27905
 nitromethane Na salts, rel. to geometric isomers, obs. 9-27905
 1-nitropropane Na salts, rel. to geometric isomers, obs. 9-27905
 nylon, i.r. spectrum interpretation in terms of rocking-twisting and wagging 9-32552
 nylon 66 fibres, spectral study of structural change due to heat treatment 9-27938
 nylon-6, total refl. obs. of surface crystallinity 9-48843
 nylon-6, transmission obs. of bulk crystallinity 9-48843
 1-octyne, liquid, far i.r. absorptions 9-40796
 oxalic acid, and $-d_2$ gas, rel. to mol. struct., 400-4000 cm^{-1} 9-30133
 oxalyl bromide, rel. to band freqs. and assignments 9-34684
 pentafluorobenzonitrile 9-23147
 pentamethylene sulphide, 4000-40 cm^{-1} , vibrational assignment 9-32510
 perfluoro 1,3,5-triazacyclohexane 9-25778
 phenanthrene determination in anthracene 9-35762
 phenols, vapour spectra, band freq. 9-32445
 phenylboronic acid, rel. to vib. frequencies 9-23151
 o-phenylenediamine, N-H frequencies in halide chelates 9-36719
 poly(α -ethylacrolein), structure depend. on temp. determ. 9-28793
 poly(α -methacrolein), structure depend. on temp. determ. 9-28793
 poly 1,4-bis(β hydroxyethoxy) phenylene adipate, rel. to vibration forms 9-37734
 poly 1,1 dimethylsilylcyclobutane, i.r. spectrum and struct. 9-27935
 poly- ϵ -methylcaprolactam, conformational structure 9-32551
 poly-p-chlorostyrene, isotactic, solns. and gels rel. to chain struct. stability, obs. 9-28140
 polycapromide, shift and profile of vibration absorpt. bands, effect of mechanical load 9-32829
 polyethylene, thermal expansion of unit cell 9-48842
 polyethylene oxide, chain folding obs. 9-46713
 polyethylene terephthalate, shift and profile of vibration absorpt. bands, effect of mechanical load 9-32829
 polyimide:Ag films, obs. 9-26749
 polyindigo solns., structural anal. and mol. wt. determ. 9-27934
 polyisoprene, polymerized on $\beta\text{-TiCl}_3$, rel. to struct., obs. 9-27937
 polymers, influence of defects 9-47379
 polymers of monosubst. benzenes formed in elec. discharges 9-48522
 polymethylsiloxanes, cyclic, integral intensities in vibr. absorpt. spectra 9-48510
 polypropylene, isotactic, solns. and gels rel. to chain struct. stability, obs. 9-28140
 polypropylene, rel. to stereoregularity, obs. 9-30157
 polypropylene, shift and profile of vibration absorpt. bands, effect of mechanical load 9-32829
 polystyrene, isotactic, solns. and gels rel. to chain struct. stability, obs. 9-28140
 prolate and oblate symmetric tops 9-23079
 propene and oxide, combination band of methyl group torsion and asymmetrical stretching vib. 9-25752
 propylene imine 9-44369
 propylene-ethylene copolymers, rel. to stereoregularity, obs. 9-30157
 purine and deuterated derivatives 9-41397
 pyridine adsorbed on zeolite Y, rel. to adsorbent surface props. 9-24519
 pyridine sorbed on porous glass 9-26196
 pyridine-Br and BrCl complexes 9-23153
 pyridines, substituted, change-transfer complexes with Br 9-23154
 pyridinium H-bonded halides 9-49290
 2-pyridone, ^{16}O and ^{18}O labelled, i.r. spectra 9-23155
 rhodamine, absorption 9-23157
 rhodamine, absorption, 400-3500 cm^{-1} 9-23157
 rubbers, structural changes after irradiation and role of sulphurs 9-24079
 selenols, fundamental Se-H stretching freq. 9-34691
 silacyclopentane, far i.r. 9-32528
 silver nitrate adducts of cyclic thio-ethers, ring vibrations and Ag-S bond 9-32512
 stearyl methacrylate-cetyl methacrylate copolymer in waxes, infrared determination 9-37860
 steroids, deform. vibr. band intensities rel. to number of CH_2 , CH_3 -groups, obs. 9-25781
 styrene-acrylic-melamine resins, quantitative analysis 9-38914
 styrenes, o- and m-subst., vibr. fund. modes assignment 9-32529
 succinic acid crystal, rel. to H bond vibs. and strength 9-35668
 sulfonamides 9-36720
 tetracene photodiode, and correl. between bands and proposed structure 9-32502
 tetrahydrofuran, pseudorotation 9-38915
 tetraiodoethylene, vib. spectra and assignments 9-27902
 tetramethylurea, normal co-ord. anal., bands and vib. determ. 9-23130
 thio-ethers, cyclic, mercuric halide adducts, ring vibrations 9-30107
 thio-ethers, cyclic, silver nitrate adducts, ring vibrations and Ag-S bond 9-32512

spectra continued**organic molecules and substances, infrared continued**

- thiourea-alkali halides mixed cry., abs. spectra, interac. and band obs. 9-24420
- thulium cyclopentadienides, absorption, vib. coupling and struct. obs., low temp. 9-32531
- thulium methylcyclopentadienides, absorption, vib. coupling and struct. obs., low temp. 9-32531
- toluenes, polydeuterated, characts., and correls. in 900-500-cm⁻¹ region 9-46420
- 2,4,6-trichloroheptane, structure from C-Cl stretching vib. 9-32546
- trideuteriomethane Na salts, rel. to geometric isomers, obs. 9-27905
- trifluoro-s-triazine-tris(trifluoromethyl)-s-triazine series, NaCl region 9-30115
- triglycine sulphate, γ -irradiated, rel. to changes in ferroelec. props. 9-47182
- triglycine sulphate, transmission and refl. spectra, optical const. and pyroelec. obs. 9-35615
- triglycine sulphate-isomorphous ferroelec. solid soln., anomalous behaviour in phase transition region 9-47371
- trihalomethane-halide ion complexes in soln. 9-23537
- β -2:4:6-trimethyl trithian, 4000-40cm⁻¹, vibrational assignment 9-32511
- α -2:4:6-trimethyl trithian, 4000-40cm⁻¹, vibrational assignment 9-32511
- trimethylamine charge-transfer complexes 9-23163
- trimethylene selenide, vibr. anal. and ring puckering 9-42447
- trimethyllead halides, and Raman spectra mol. struct. 4000-70 cm⁻¹ 9-34675
- trioxane, in ν_s excited decayed state, rotation 9-32532
- triphenylarsine and oxide, assignments 9-25782
- triphenylborate, structure and force constant determ. 9-23164
- triphenylboron, structure and force constant determ. 9-23164
- triphenylmethane deriv. dyes, in plexiglass, triplet-triplet absorpt. 9-41393
- triphenylmethane deriv. dyes, in plexiglass triplet-triplet absorpt. 9-49291
- triphenylphosphine oxide complexes, assignments 9-25782
- 1:3:3-trithian, 4000-40cm⁻¹, vibrational assignment 9-32511
- p-xylene-carbon tetrabromide complex, polarized 9-24394
- 4-Br-stilbene, absorpt. and fluoresc., vibr. analysis, 77°K 9-28699
- CF matrix-isolated radical 9-45424
- 4-Cl-stilbene, absorpt. and fluoresc., vibr. analysis, 77°K 9-28699
- 4,4'-di-Cl-stilbene, absorpt. and fluoresc., vibr. analysis, 77°K 9-28699
- 4-F-stilbene, absorpt. and fluoresc., vibr. analysis, 77°K 9-28699
- H-bonding, far-i.r. obs., vibr. assignments 9-32453
- H₂C matrix-isolated spectra 9-45424
- HCF matrix-isolated radical 9-45424
- 4-I-stilbene, absorpt. and fluoresc., vibr. analysis, 77°K 9-28699
- Na ethyl sulphate monohydrate, bond obs. 9-24431
- OH absorption band shift rel. to -log (acidity constant) in hydroxyl-containing substs. 9-27940

Spectra**organic molecules and substances, radiofrequency**

- see also *Nuclear magnetic resonance and relaxation; Paramagnetic resonance and relaxation*
- 1,4,5,8-tetramethylanthrasemiquinone, anion radical, e.s.r. 9-36718
- acetaldoxime, cis, and trans- 9-40605
- acetonitrile, rotational, in vibrational ground and excited state 9-23085
- bicyclo [1.1.0] butane, microwave spectra 9-32504
- trans-1-bromopropene 9-32505
- 1,1-difluorocyclobutane 9-30101
- 1,4-dimethylanthrasemiquinone, anion radical, e.s.r. spectrum obs. 9-36718
- dimethylgermane 9-42430
- dimethylsulphoxide isotopes, rot. spectra, r_s and r_0 struct. 9-23138
- ethylmercaptan, and structure 9-27895
- fulvene 9-27897
- isoprene 9-30125
- methyl diazine 9-34676
- 2-methylfuran 9-48498
- methylthioethyne, microwave spectra 9-48501
- microwave detection of interstellar formaldehyde 9-29037
- microwave spectral tables, listing 9-29920
- n.m.r. of three-spin systems, analysis of complex spectra 9-23027
- perfluorobenzonitrile, microwave absorpt. obs. 9-27910
- phosphorus organic cpds., high-resolution NMR spectra 9-34685
- propionyl fluoride 9-48505
- tetrahydrofuran 9-38916
- vinyl iodide 9-32533

Spectral line breadth**see also Doppler effect; Stark effect; Zeeman effect**

- absorption line shape theory as a special case of kinetic theory 9-32406
- atom system, radiative process with excessive Doppler broadening, noise spectrum 9-38764
- benzene, Brillouin line breadth and hypersonic absorption 9-44560
- broadening, laser light in liquids, obs. compared with theory 9-25315
- carbon tetrachloride, Brillouin line breadth and hypersonic absorption 9-44560
- CO mol., l.r. bands, self and foreign gas broadening effects, comparison 9-27848
- coherent enhancement of natural linewidth 9-40538
- Doppler broadened emission from Burnout-V turbulently heated plasma 9-44443
- Doppler-broadened transitions, coupled, laser-induced line-narrowing effects 9-22934
- electron impact broadening, perturber radiation contribution to lineshape 9-32403
- emulsion calibration, math. approach 9-32052
- e.p.r., angular dependences on mag. field rotation 9-31158
- ferromagnetic resonance lines, inhomogeneous broadening 9-45363
- gas laser transitions, determ. with hole-burning technique 9-25238
- impurity absorption in ionic crystals, calc. of shape function of phonon part 9-33574
- inert-gas afterglows 9-44503
- instrumental line width and transmission factor for partially coherent slit illumination 9-43925
- ions in stochastic varying fields in plasma, Doppler broadening 9-40663
- laser, gas, and two-mode beating calc. 9-41893
- of laser beam, quantum mechanical estimate 9-48051
- line broadening ability of various gases relative to N₂, meas. on CO 9-25736

Spectral line breadth continued

- linewidth meas. with microwave spectrometer employing source modulation technique 9-47871
- methane, vibration-rotation spectra, pressure broadening of ν_3 band meas. 9-23129
- methane/He mixture, vibration-rotation spectra, pressure broadening of ν_3 band meas. 9-23129
- methane/N mixture, vibration-rotation spectra, pressure broadening of ν_3 band meas. 9-23129
- microwave rotational lines of gases, width determ. using graphical method 9-44310
- molecular crystal, combination scattering, temp. depend. 9-45304
- molecular vibratory-rotational spectra, calc. 9-42362
- Mossbauer line narrowing by u.s. vibrations with decaying amplitudes 9-26717
- nuclear dynamic polarization eff. 9-27577
- organic cpds. absorpt. and fluoresc. bands rel. to inter-, intra-mol. H-bonding, obs. 9-23081
- for plasma, inhomogeneous 9-28002
- plasma, Stark broadening, effects of dynamic ion shielding 9-48575
- plasma electron conc. determ. using self-reversed Stark-broadened profiles 9-44445
- Raman lines in organic liquids 9-46642
- resonances, weak, assignment of positions and widths, data analysis method 9-30764
- spectral pressure broadening in gases, theory 9-29906
- spectrometers with circular aperture, diffraction theory calc. 9-25384
- spectrophotometry, analytical, rel. to instrum. and film props. 9-26843
- Stark-broadened, self-reversed profiles in plasma electron conc. determ. 9-44445
- o-terphenyl, liq., EPR, Mol. motion from electron resonance 9-40805
- ¹¹³Cd resonance line, λ 3261 Å, temp. depend. of broadening effects 9-29934
- ¹¹⁴Cd resonance line, λ 3261 Å, collision broadening by pressure of inert gases, temp. effects. 9-40557
- Al, Stark broadening and displacement, plasma high temp. meas. 9-25913
- Ba I, resonance line broadening by inert gases, effective cross-sections 9-48388
- CN, A² $\Pi_{1/2}$ state, microwave-optical double reson. 9-34609
- CO, foreign-gas broadening coeffs., rel. to N₂ 9-25736
- CO, self-broadening, ratio of collision cross-sections to foreign-gas broadening 9-25735
- CO, collision-broadened line shapes 9-40590
- CS₂, Brillouin line breadth and hypersonic absorption 9-44560
- Ca I, resonance line broadening by inert gases, effective cross-sections 9-48388
- Ca II, H and K line profiles in solar flares 9-36069
- Ca II in sun, computation rel. to non-uniform chromosphere 9-36070
- Cd, resonance broadening temp. dependence 9-40541
- Cs, red shift, broadening and asymmetry in the presence of Xe, Cf₄ 9-46276
- Cs I, 4555 Å line, effect of Ar 9-34535
- EuTe, antiferromagnetic resonance linewidth, temp. depend. 9-45376
- Fe₂O₄, Mossbauer study of ⁵⁷Fe rel. to electron hopping in octahedral sites 9-45294
- GaAs laser diode spontaneous emission, doping depend. 9-27336
- H₂O, 22 GHz line, foreign-gas broadening 9-23045
- H α , H β Balmer line profiles emission in vortex-cooled arc, broadening meas. 9-27825
- H β Balmer line broadening in plasma, particle conc. meas. 9-25859
- HCN laser, meas. technique 9-41900
- H α in sun, computation rel. to non-uniform chromosphere 9-36070
- ³He-He II system, Brillouin light spectrum 9-34941
- Hg, resonance broadening temp. dependence 9-40541
- Li plasma, high-density, linear Stark broadening 9-34765
- Mg, Stark broadening and displacement, plasma high temp. meas. 9-25913
- Mg₂Cd, ordered and disordered, soft X-ray L₂₃ emission edge-breadth 9-43248
- Mo in compounds, L β_1 line 9-48400
- of N₂ in arch discharge, expansion 9-46550
- N₂O, linewidths for 2224 cm⁻¹ band 9-42406
- NH₃ inversion spectrum, press. broadening 9-42404
- Na, Stark broadening and displacement, plasma high temp. meas. 9-25913
- Na I 5682-88 Å and 4978-82 Å lines of plasma, Stark broadening 9-32413
- Nb in compounds, L β_1 line 9-48400
- Ne 3s₂-3p₄ transition in He-Ne mixture press. depend. 9-42333
- Ne 3s₂-3p₄ transition in He-Ne laser resonator meas. 9-22960
- O, Stark broadening and displacement, plasma high temp. meas. 9-25913
- O₂, microwave, contrib. of London dispersion force 9-36707
- O₂ pure, and air, half width mean values 9-36705
- OCS, line broadening of various rotational transitions due to dipole-dipole, dipole-quadrupole interac., obs. 9-34639
- OH, absorption lines, shape and width by curve of growth method 9-48476
- Si, Stark broadening and displacement, plasma high temp. meas. 9-25913
- Sr I, resonance line broadening by inert gases, effective cross-sections 9-48388
- Y in compounds, L β_1 line 9-48400
- Zn, ³P, state, collision broadening of double resonance line empirical formula for resonance curve 9-34554

Spectrochemical analysis

- see also *Chemical analysis/by mass spectrometry; Spectroscopy*
- absorption, integral, rel. to specimen conc. in pulsed evaporation formulae 9-26841
- acousto-optical radiation detectors in gas analysers, sensitivity and selectivity 9-37851
- addition method, tabulation of analytical data 9-33691
- of admixtures in pure metals using internal standards 9-49394
- air pollution analysis by correlation spectrometer 9-33693
- alkali elements in discharge, by introducing oxides of Co, Ti and V 9-31229
- alkaline earth oxides and aluminates, flame spectroscopy, thermodynamic stability 9-33692
- alkylpyridines, NMR spectra, chemical shifts of protons of alkyl substituents 9-38876

Spectrochemical analysis continued

- alkylpyridines, NMR spectra, chemical shifts of ring protons 9-36710
 Aluman, by laser microprobe, impurity emission rel. to matrix effects, obs. 9-24604
 arc analysis, servocontroller for sample vaporization 9-28827
 aromatic hydrocarbon mixtures, by selective fluoresc. 9-24605
 ashed biological materials, advantages of high-current d.c. arc 9-47477
 ASTM methods 9-33694
 atom and ion persistent lines intensities in d.c. C arc, calc. 9-24602
 atomic absorpt., voigt eqn. model and precision burner construction rel. to absolute meas. 9-24603
 carbonate content of bone, use of d.c. arc 9-35759
 coal, vacuum discharge, sensitivity improvement by NaCl, KCl addition 9-26845
 detection improved by additional exposure of plate, time determ. 9-31225
 differentiating samples containing Ag, Ga or Ni, qualitative determ. 9-37854
 Elko II photometer for iron and steel lab. 9-47481
 emission, forensic applic. 9-25333
 flame photometer with attachment for spectrophotometer 9-41459
 flame photometric methods 9-47479
 flame photometry, atomic absorpt., fluctuational conc. limits criterion 9-47478
 garnets, using laser microprobe 9-37848
 gas mixtures, diffusion separated using isotope solvents 9-28824
 GeCl₄ rel. to contamination by ampoules, obs. 9-31231
 henritermierite, Ca₃(Mn_{1.5}Al_{0.5})(SiO₄)(OH)₂ 9-32906
 in historical object examination 9-26846
 internal reflection applic., gas chromatography, pyrolysis and skin analysis 9-37853
 i.r., computer analysis 9-41460
 i.r. absorption continuous on-line techniques 9-26840
 laser applic., emission microspectroscopic elemental analysis using Q-switched ruby laser 9-22411
 by laser microprobe, impurity emission rel. to matrix effects, obs. 9-24604
 laser microprobe emission spectroscopy, elec. spark cross-excitation 9-47476
 metals, ASTM methods 9-33694
 microanalysis using high-current impulse Ar arc method 9-24599
 minerals, far i.r. spectroscopic anal. 9-45432
 minerals, Zn, Nb and Be meas. using C cavity electrodes, obs. 9-28828
 organic compounds, without spectral decomposition of fluorescence 9-33698
 paintings, dating and analysis 9-28820
 phenanthrene determination in anthracene, infrared method 9-35762
 photoelectron spectroscopy and adsorbed species, rel. to orbitals involved in surface bonding 9-44634
 photographic methods of spectral emission anal., practical sensitivity limits 9-37849
 photometric, line width rel. to instrum. and film props. 9-26843
 photomultipliers, solar-blind, use in flame spectroscopy 9-31226
 polychromator, direct reading photomultiplier tube, for laser microprobe emission spectroscopy 9-46021
 polyvinyl acetate acrylate copolymers, infrared spectrophotometry 9-37861
 powders, spark excitation technique, transport mechanism of materials 9-48114
 qualitative determ. below threshold of reliable element separation, by plotting intensities of spectrogram lines 9-37854
 of radioisotope solutions, with two lead shielded cells 9-28826
 reaction products, short-lived, streak-camera recording technique 9-32071
 reflectance spectra in thin-layer chromatography 9-37852
 resonance lines, modulation in spectral lamp by means of pulsating vapour cloud 9-31227
 rock, stratified 9-28821
 of rubber, raw and finished, impurity method 9-43348
 sensitivity rel. to discharge gap length and arc current intensity 9-49395
 silicates, rotating disc solution technique 9-35764
 solids microanalysis, applic. of ionoluminesc. techniques 9-49329
 spark excitation of powders rel. to granule size 9-39967
 spark spectrography, sensitivity improvement 9-28823
 spectrometer, direct-reading, computer program for emission data evaluation 9-46026
 spectrometer, direct-reading emission, design 9-32061
 standard spectra construction by fractional exposure 9-26842
 stearyl methacrylate-cetyl methacrylate copolymer in waxes, infrared determination 9-37860
 steel, c type, vacuum photoelectric instruments 9-49396
 Steel, stainless, by laser microprobe, impurity emission rel. to matrix effects, obs. 9-24604
 steel examination for C, P and S using Ar discharge source 9-47480
 steels, determ. Pb, Bi, Sn and As impurities 9-28830
 styrene-acrylic-melamine resins, quantitative infrared analysis 9-38914
 of trace impurities in Cu 9-35760
 two-component mixtures, absorpt. coeff. and optical density rel. to minimum conc. of particular component 9-37850
 X-ray fluorescence, calc. methods, empirical coeffs. and fundamental parameters 9-31233
 X-ray fluorescence, quantitative, X-ray tube spectral distrib. 9-31232
 X-ray spectrometer total reflection, for fluorescent analysis of light elements 9-31235
 Zircaloy-2, by laser microprobe, impurity emission rel. to matrix effects, obs. 9-24604
²⁴⁰Pu isotopic analysis in Pu by optical emission spectroscopy 9-32443
 Ag-Cd alloys, activity meas., by atomic absorption 9-37855
 Ag evaporated from filament into He stream of r.f. discharge, excitation and effect of Cu on emission 9-31222
 Al determination in presence of fluoride by emission spectroscopy 9-37856
 Ar discharge source for solns. excitation, 2450 MHz 9-28822
 C electrodes, photographic methods of anal., practical sensitivity limits 9-37849
 CaF₂, rare earths amounts used in activation 9-33695
 ClO₃⁻, spectrophotometric determ. 9-31230
 ClO₄⁻, spectrophotometric determ. 9-31230
 Cu-Ag alloy discharge, effect of additives 9-31228
 Ga determination in CdTe, use of alumina-cup electrode 9-35761
 GaAs, rare-earths determination by ultra-trace method 9-33696

Spectrochemical analysis continued

- Ge, absorpt. spectroscopy, flame and solvent effects, obs. 9-28829
 H-N mixtures, diffusion separated using isotope solvents 9-28824
 H₂-Ar-arc flames, turbulent, atoms fluoresc. power efficiencies, obs. 9-24601
 In determination in CdTe, use of alumina-cup electrode 9-35761
 Li in N₂O₃, flame photometry, suitable acid for quenching Li radiation 9-37857
 N₂O-H₂ flame properties for atomic absorption and emission spectroscopy 9-31224
 Na content in materials assoc. with semiconductor device processing 9-31223
 Ni alloys, determ. Pb, Bi, Sn and As impurities 9-28830
 O₂-H₂ flames, turbulent, atoms fluoresc. power efficiencies, obs. 9-24601
 O₂-acetylene flames, turbulent, atoms fluoresc. power efficiencies, obs. 9-24601
 O₂, in N₂, H₂ and inert gases, by u.v. vacuum absorpt. spectra 9-37858
 Pb²⁺ in HCl, LiCl, HBr, LiBr, by luminesc., 77°K 9-33697
 S, combined action of thermochemical reagents and carriers, sulphidization of MoO₃ 9-28831
 Sn-Cu alloy vacuum condensates, e.vap., obs. 9-28832
 Sr in seawater, latit. 4° to 34° N in Atlantic, isotopic dilution technique 9-45479
 Ti⁴⁺ in HCl, LiCl, HBr, LiBr, by luminesc., 77°K 9-33697
 U, by laser microprobe, impurity emission rel. to matrix effects, obs. 9-24604
 U alloys, of Fe and Al, flame anal. without previous separation 9-26839
 U isotopic analysis using X-ray fluorescence combined with α -activity meas. 9-24598
 U isotopic analysis using X-ray fluorescence combined with A-activity meas. 9-33690
 UO₂, by laser microprobe, impurity emission rel. to matrix effects, obs. 9-24604
 Y₂O₃, luminesc., using YVO₄:lanthanide phosphors 9-28714
 ZnSe, in hollow cathode or d.c. arc, determ. of excess Zn or Se by blackening of lines 9-37859

Spectrometers

- see also Mass spectrometers; Monochromators; Particle spectrometers; Spectrophotometers; X-ray spectrometers*
 absorption for 600-1100 Å region 9-34625
 Bass-Kessler spectrograph modifications 9-43927
 circular aperture, diffraction theory of line breadth 9-25384
 correlation type for air pollution analysis 9-33693
 Czerny-Turner, 4m plane grating asymmetric, optimization 9-46023
 Czerny-Turner, multiply diffracted light expt. 9-32055
 Czerny-Turner spectrograph, grating position rel. to coma 9-46024
 direct-reading, computer program to evaluation of emission data 9-46026
 direct-reading, computer-aided design and manufacture 9-32060
 double-pass, performance on observing the Arcturus stellar spectrum 9-41639
 Ebert, vacuum, double beam grating spectrometer for 10-200 cm⁻¹ region 9-43929
 emission, direct-reading, design 9-32061
 Fabry-Perot polyetalon, effect of plate defects 9-41963
 grazing incidence, adjustment for maximum resolution 9-34229
 hertzian for mol. jets 9-43928
 high speed exploration, with twin channel network, design and operation 9-46022
 high-speed, 1.5-6 micron region, off-axis parabolic mirrors and cooled detector 9-25386
 for ions (heavy) energy loss spectra, 20-250 keV 9-34149
 i.r., far region, double pass optical system 9-36394
 i.r., for meteorological satellite, design 9-25387
 i.r. reflectance types, for vibr.-spectra of liqs. and glasses at high temp. 9-46020
 Jarrel-Ash 1m Ebert scanning, YAl G:Nd³⁺ optical transition props. 9-26751
 Karl Zeiss company, Leipzig Fair exhibits, 1968 9-27407
 narrow band, seeing and transparency variations compensated, stellar photometry appl. 9-27024
 optical and mech. design book 9-29486
 photoelectric spectropolarimeter, with microscope, performance 9-48094
 Raman, high resolution, with conventional or laser source, construct. and use 9-22478
 reflectance, standardization 9-36399
 self-beat, for laser light scatt. by solns. 9-42657
 SISAM, use in atomic spectroscopy 9-29935
 spectropolarimeter, automatic, for Faraday effect meas. in visible and u.v. 9-48118
 split-pole magnetic spectrograph, theory for performance 9-27408
 two-beam i.r., correction for thermal background in temp. meas. 9-36215
 for u.v. airglow meas. of earth between 1100 and 3400 Å 9-37953
 X-ray fluorescent, for multielement trace analysis, sensitivity 9-26848
 NaI, scintillation, in Linac thick target bremsstrahlung spectra meas. 9-32276

accessories

- aplanatic prisms 9-48120
 arc, d.c., anode and excitation conditions 9-30320
 beam condenser for i.r. spectrophotometer 9-36395
 for Cary 14 spectrophotometer colorimetric 9-41954
 Cary Models 14 and 15, spectrophotometer, diffuse and specular reflectance accessories 9-36406
 cell, low-temp., for Raman laser spectra 9-22480
 charge image detector for extended spatial distrib. 9-27263
 collimator, mechanical, with wide spacing 9-41967
 electromechanical syst. for meas. ratio of 2 continuous signals 9-29488
 far-infrared cells, fixed and variable pathlengths, method of making 9-36403
 filters, interferometric for Rayleigh component attenuation in Brillouin spectroscopy 9-40385
 flame spectrophotometer attachment 9-41459
 Fourier transform optical analogue computer 9-29487
 framing drum spectrograph 9-32069
 frequency selector for laser spectroscopy 9-45948
 graphite crucible method in atomic absorpt. spectroscopy 9-48121
 image intensifier for high-speed spectrography 9-32049
 image slicers 9-48119
 i.r. cell, low temp., using gas diffusion and heat gate principle 9-34234
 i.r. reflectance, hohlraum-type, techniques and attachments 9-36401
 laser-Raman cell for pressurized liquids 9-34233

Spectrometers continued**accessories continued**

- line centring device, automatic digital, for direct reading emission spectrometers 9-36404
- monochromator attachment for photoelec. absorption spectra recording 9-29489
- optical and mech. design book 9-29486
- photodetectors for autocollimators with beam splitters, selection 9-36408
- polychromator, direct-reading, for laser microprobe emission spectroscopy 9-46021
- Raman cell, low temp., for sublimed films and solid samples 9-32068
- Raman cell, variable temp., design 9-32063
- rotating disc shutter for time-resolved spectrograph 9-29492
- slit dissector and its appl. 9-43930
- spectrographic plate position indicators, punched cards 9-34231
- spectrophotocronograph 9-29491
- spectrophotometer attachment for absolute specular refl. coeff. meas. 9-32067
- streak camera technique in spectrochem. analytic recording of short-lived reaction products 9-32071
- table, high precision, with removable arms 9-22479
- time-resolved film spectrograph 9-32070
- time-resolving grazing-incidence spectrograph 9-29490
- wedge filters with variable absorpt. for emission spectral anal., preparation and use 9-46028
- windows, thin, for flow proportional counters in X-ray fluoresc. spectrometers 9-32066
- KBr window for I.R. spectroscopy under high pressure 9-32065

Spectrometers, radiofrequency

- see also Nuclear magnetic resonance and relaxation/measurement; Paramagnetic resonance and relaxation/measurement*
- cavity type for double reson. study of gases 9-45903
- ENDOR spectrometer, for obs. of Overhauser effect 9-31883
- e.p.r., computer-instrument interface and control programs 9-31881
- e.p.r., Karl Zeiss Leipzig Main exhibits, 1968 9-27407
- e.p.r., superhet $\lambda=10$ cm., zero bridge 9-40298
- e.p.r. for large zero field splittings meas. 4 mm 9-43818
- ESR, magnetic field modulation influence on paramagnetic absorption line width 9-38825
- e.s.r. for obs. of flash photolysis 9-33680
- e.s.r. spectrometer and computer of average transients for transient paramag. species 9-29350
- e.s.r. two-transistor modulation amplifier 9-34127
- mass analyzer, electrostatic field analysis of grid 9-25681
- microwave, for linewidth meas. employing source modulation technique 9-47871
- n.m.r., for high resolution spectra obs. of H and F reson. 9-47201
- n.m.r., stabilization by lateral freq. spin generator 9-47876
- probe for internal reference nuclei, patent 9-36244
- spectrograph transmitting signal and field stabilization frequencies, patent 9-40304
- sub-millimetre, for solids absorption at liquid He temp. 9-46692
- for whistlers and v.l.f., multichannel spectral analyser 9-26907

Spectrophotometers

- abridged, international standardization techniques 9-36398
- attachment for absolute specular refl. coeff. meas. 9-32067
- Cary 14, accessories for colour meas. 9-41954
- Cary Model 14, polarization, effect on transmittance measurements of anisotropic materials 9-32056
- Cary Models 14 and 15, diffuse and specular reflectance accessories 9-36406
- use in colorimetry, photometric accuracy 9-41952
- Dobson ozone, improved solid-state amplifiers 9-41475
- double beam, for ultra low loss optical glasses 9-25383
- dual beam design, drift free direct reading 9-48112
- goniophotometer for appearance props. and scatt. 9-36400
- i.r., beam condenser, design and performance 9-36395
- i.r. reflectance, hohlraum-type, techniques and attachments 9-36401
- monochromatic, international standardization techniques 9-36398
- photometer, simple, without amplifiers 9-22463
- prism, derivative attachment 9-27409
- Raman, variable temp. cell design 9-32063
- recording spectrophotometric system 9-41965
- reflectance instruments 9-32062
- for spectral irradiance meas. 9-32057
- spectrophotocronograph 9-29491
- wide-range system, control and data acquisition functions, automation, software 9-32058
- XUV, for alkali halide optics 9-29485
- MoS₂ exciton absorpt. spectrum, illustrating the derivative method 9-27409

Spectrophotometry*see also Colorimetry*

- analytical, line width rel. to instrum. and film props. 9-26843
- atomic absorpt. by pulse technique 9-48391
- atomic absorption, for vapour press. meas. of metals 9-23608
- ATR, i.r., sample pyrolysis technique 9-36391
- colorimetry, Polish organic pigment exam. 9-25371
- flame photometric analysis 9-47479
- flame photometry, atomic absorpt., fluctuational conc. limits criterion 9-47478
- forensic appl. 9-25333
- in forensic science 9-27397
- Galaxy gradients 9-24750
- glasses, low loss, optical, ellipsometric determ. of surface reflectances 9-39801
- infrared polyvinyl acetate acrylate copolymers 9-37861
- i.r. reflectance, independent of emitted flux at controlled temp. 9-36392
- light sources, tilting-filter photometer appl. 9-36367
- molten salt, resistance heated low thermal gradient furnaces appl. 9-36090
- of moon's surface, i.r., from Zond-3 probe 9-33930
- non stable stars study, flare of SS Cygni 9-27113
- radiation statistics rel. to two quantum photocurrent spectra 9-29389
- radiometry with spectrally selective sensors 9-32026
- reflectance instruments 9-32062
- reflectance meas. precision and accuracy 9-36393
- standard spectra construction by fractional exposure 9-26842
- stars, early type, energy distrib. in u.v. 9-31535
- stellar, instrument profile effects, reference to the Arcturus Atlas 9-41638

Spectrophotometry continued

- u.v., extreme, lab. simulation of solar emission for calibration 9-38417
 - wavenumber plotting of output 9-29481
 - ¹⁹⁸Hg green line profile from meas. of Fabry-Perot rings 9-27808
 - N₂O-acetylene flame stabilization technique 9-35745
- Spectroscopy**
- see also Spectra; Spectrometers; Spectrophotometry*
 - absorption from excited levels, low-temperature suppression 9-29907
 - apparatus function, elimination by spectroscopic method 9-41961
 - applied spectroscopy reviews, book 9-41962
 - atomic absorpt., graphite crucible method 9-48121
 - Auger electron, retarding field analyzer based on display LEED optics 9-32246
 - bands, overlapping, mathematical expansion 9-48116
 - beam emission cross sections determ., systematic errors 9-41959
 - beam foils, charge deflection expts. 9-22476
 - Brillouin, Rayleigh component attenuation using interferometric filtering 9-40385
 - buffer selection for melting diagram determ. 9-28176
 - calibration of fluorescence apparatus 9-34232
 - chemically reacting medium, depolarization spectrum of scatt. light 9-24529
 - correlation methods for narrow line shape determ. 9-43926
 - cryostat for crystals under uniaxial compression 9-38167
 - Czerny-Turner spectrometer, multiply diffracted light, experimental confirmation of theory 9-32055
 - diffraction gratings, holographically made, spectrographic performance 9-34214
 - diffuse reflectance, characterization of ligand field spectra 9-37672
 - diffuse reflectance, theoretical interpretation 9-38386
 - double resonance experiment, correlated intensity fluctuations 9-36670
 - electronic instrumentation 9-49613
 - emission, emulsion calibration, math. approach 9-32052
 - emission spectrography, selected buffer compounds, influence on d.c. arc 9-36382
 - exploding wire, book 9-29138
 - false spectra from plane grating, laser illumination 9-32018
 - far-i.r., conference 9-32050
 - Faraday rot., contour distortion rel. to non-monochromaticity 9-34228
 - Fourier, fast, of large arrays of data. 9-25379
 - Fourier, real time operation and performance 9-36384
 - Fourier, emission, thermally excited gas, background suppression 9-40576
 - Fourier spectrography, high luminosity and low noise, using holographic techniques 9-46018
 - Fourier transform, far i.r., simple analogue computer 9-36405
 - Fourier transform, review 9-32051
 - gas lasers, double resonance theory 9-38370
 - half-prisms, symmetrically crossed, geometrical spectra 9-27370
 - heterodyne, for large angle Brillouin scatt. 9-38393
 - infrared, adsorption of low vapor pressure materials on solid surfaces 9-36383
 - instrumental line width and transmission factor for partially coherent slit illumination 9-43925
 - intensity calibration using electron excited molecular bands 9-25380
 - internal reflectance, review 9-36388
 - internal reflection, determ. of i.r. absorpt. true freq. 9-37713
 - internal reflection, effect of angle of incidence change 9-32053
 - internal reflection, obs. of electrochem. reaction 9-37840
 - internal reflection, sensitivity enhancement by optical cavities 9-36389
 - interpretation, statistical probability method and white noise assumption 9-36889
 - ion-neutralization spectroscopy of O, S, Se adsorbed on Ni 9-32484
 - i.r., application in chromatography 9-26844
 - i.r., internal reflection method for powders, patent 9-38416
 - i.r., thin layer on metal surface, reflection method 9-35648
 - i.r. cell, low temp., using gas diffusion and heat gate principle 9-34234
 - laser, frequency selector 9-45948
 - laser, in liquids 9-36882
 - laser beat frequency, applic. to rotation and translation of biomolecules in soln. 9-48113
 - laser Raman scattering in gases, detection, trial arrangement 9-48117
 - using lasers 9-40344
 - lightning, return stroke, high speed time resolved, qualitative analysis 9-26909
 - lightning, return stroke, high speed time resolved, quantitative analysis 9-26910
 - lightning, return stroke, high speed time resolved, time-dependent model 9-26911
 - line curvature, radius allowance for in meas. 9-36385
 - Lorentzian curves containing arbitrary mixtures of absorption and dispersion, line parameters 9-41960
 - using Michelson interferometer 9-46025
 - optical, cryogenic systems 9-34226
 - optical reflection, obs. of ion implantation damage in Si 9-28518
 - phosphorescence-microwave double-resonance 9-38804
 - photodissociation translational spectroscopy 9-48513
 - plasma, velocity, Doppler determ. with photoelec. recording 9-40692
 - plasma charged particle concentration determ., limits to different methods 9-42529
 - polyethylene pellets, laboratory preparation 9-38415
 - powders, i.r. internal reflection method, patent 9-38416
 - power spectra, coherence and bispectra of geophysical data, estimation, Fourier Transform application 9-26853
 - Raman, excitation sources and other recent achievements, review 9-40384
 - Raman apparatus using laser excitation and polarization 9-29484
 - Raman chamber for high temp. compressed fluids 9-46027
 - Raman shift in vacuum, conversion tables for abs. obs. 9-27406
 - reflectance, high-temp. and dynamic modes 9-36387
 - reflectance, i.r., of microsamples 9-36390
 - reflectance, symposium, Chicago (1967), proceedings in book 9-29482
 - saturable absorption effects. Exptl. methods 9-23009
 - selective excitation, and applics. 9-46019
 - slit broadening, effects from broad spectra 9-32064
 - spectral line contour uniform expansion, effect of strong fields 9-48115
 - spectral power density meas., opt. spectrum analyzer 9-27398
 - spectrography, graphic ultrapurification by preburning 9-34227
 - spectrometer params. rel. to meas. errors 9-25381

Spectroscopy continued

- spectropolarimetric studies, elimination of instrument polarization 9-32054
- time and space resolved measurements of particle density, temperature, and electrical conductivity in He plasma 9-42535
- time-resolved, applic. to laser pumping flashlamp 9-29483
- u.s., in liquids 9-36882
- vacuum u.v., absorpt. and emission review of optics, instrumentation and applics. 9-46017
- AgCl plates, restoration of transmission infrared 9-36402
- Ar ion laser, vacuum ultraviolet perturbation 9-22382
- He, Van de Graaff accelerator, use of 9-22998
- He II spectra production, 303.8 to 230.7 Å and 206.2 to 120 Å 9-44298
- N, Van de Graaff accelerator, use of 9-22998
- Ni ion-neutralization study rel. to electronic structure 9-44890
- O ion line radial intensity distribution, for pulse discharge with confined channel 9-41968
- Rb filter cell efficiency rel. to temp. and press. of Ar content 9-29945

light sources

- adjustable-waveform h.v. spark source for emission spectrometry 9-22481
- exploding wire, light emission, time depend. obs. 9-46029
- h.f. spectral lamps for non-readily volatile elements 9-41971
- high intensity, for obs. of O atomic beam 9-42344
- hollow cathode lamps for use in emissions and absorption 9-38418
- hollow-cathode lamp, pulsating atomic vapour cloud to produce modulation of resonance lines 9-31227
- inter-element effect by easily ionizable elements 9-48122
- i.r. gas discharge emitters 9-32072
- i.r. lasers and far i.r. masers for Stark spectroscopy of molecules 9-25767
- lamps, h.f. electrodeless and power packs, characts. 9-48123
- laser for Raman spectrometer 9-22478
- spark, for extreme u.v. region, performance 9-36407
- u.v., intensity control system 9-43931
- Ar arc calibration, vac. u.v. and C arc standards 9-44269
- H₂-Ar-air flames, turbulent, atoms fluoresc. power efficiencies, obs. 9-24601
- He plasma, for vacuum u.v., radiative power, calc. 9-27410
- He plasma, recombination radiation as brightness standard 9-48590
- N₂-O₂ flame properties for atomic absorption and emission spectroscopy 9-31224
- Ne luminescent lamp as light transformer 9-40386
- O₂-H₂ flames, turbulent atoms fluoresc. power efficiencies, obs. 9-24601
- O₂-acetylene flames, turbulent, atoms fluoresc. power efficiencies, obs. 9-24601
- Oz-acetylene flames, absorpt. and emission enhancement rel. to free-atom form., obs. 9-22936
- W lamps, standard, rel. to errors in absolute intensity meas. 9-25388
- Xe lamp, low voltage, spectral investigation 9-41970
- Xe pulsed lamp, radiation rel. energy supplied 9-41969

Spectroscopy, radiofrequency

- see also Nuclear magnetic resonance and relaxation; Paramagnetic resonance and relaxation; Spectrometers, radiofrequency*
- application to astronomy 9-27109
- far i.r. masers for Stark spectroscopy of molecules 9-25767
- microwave, of water vapour in Venus atmosphere 9-24878
- n.m.r. spectrometer adjustment without mag. field using signal simulator 9-31884
- refraction spectroscopy of foreign-gas broadening 9-23045
- spin generator, lateral freq. 9-47876

Speech

- see also Hearing*
- articulation tests in auditorium studies 9-29305
- babies, deaf palate, cry characts. 9-24954
- coding, automatic, and recognition procedure, digital code pattern construction 9-41716
- communication, underwater, wide-band liq. modulation device 9-27231
- consonants (Hindi) in clipped speech, perceptual confusions 9-40198
- consonants (Hindi) perception, significant features and errors 9-24956
- cutaneous recognition as function of channel capacity in discrete set of channels 9-31690
- fatigue, auditory, during articulation, obs. 9-24955
- fundamental freq., rate of change rel. to subglottal air press. during sustained phonation 9-40197
- intonation contours, synthetic, influence of fundamental freq. cues on their perception 9-29114
- joint distrib. indicator device, training the deaf, appl. 9-38136
- Laryngeal disease patients, vowel amplitude modulation 9-31691
- larynx, study by transillumination during running speech 9-38139
- motor control of coarticulation in CVC monosyllables 9-29115
- recognition, automatic, infrasonic cues 9-27125
- running, study of larynx by transillumination 9-38139
- spectral props. of individual voices 9-38138
- synthesizers, vocal track, voiced and voiceless excitation representation 9-24952
- telecentric optical system for vocal cord cinematography 9-33964
- telephone, separation of noiselike sounds from vowel/vowellike sounds 9-31689
- transmission, narrowing of frequency band 9-29280
- u.s. components 9-38137
- vocal track excitation at lips, generation of speech like signals 9-31692
- voice circuits, quality judgments, multidim. analyses 9-24953
- vowel amplitude modulation in patients with Laryngeal diseases 9-31691

Spherical aberration *see Aberrations, optical***Spicules** *see Sun/prominences***Spin** *see Elementary particles; Hyperons/spin and parity;**Mesons/spin and parity; Nucleus/spin and parity; Rotating bodies***Spin echo** *see Nuclear magnetic resonance and relaxation***Spin waves** *see Ferromagnetism/spin-wave theory***Spin-lattice relaxation** *see Crystals/lattice mechanics; Magnetic resonance and relaxation***Spinors** *see Quantum theory, wave equations***Spions (pions with spin)** *see Pions***Spirality** *see Elementary particles; Field theory, quantum***Sporadic-E** *see Ionosphere/E-region***Sprays**

- see also Aerosols; Drops; Jets*
- No entries

Spurions *see Elementary particles***Sputtering**

- apparatus, high capacity, design and construction 9-39155
- cathodic in vibrating arc ion source 9-27286
- cleaning electrodeplated small engineering parts 9-28812
- computer simulation 9-35296
- d.c., metal deposition r.f.-induced substrate bias 9-23634
- electrodes in vacuum impulse discharge, strain and thermoelastic waves 9-48620
- film, thin multilayer, deposition rate and uniformity, r.f. power 9-36955
- films, multicomponent thin, composition model 9-44623
- gas discharge, r.f., conductance and capacitance, mag. field depend. meas. 9-36784
- laser, of absorbent titanium oxide-magnesium oxide film at u.h.f. for vacuum reduction 9-43693
- low energy 9-33204
- magnetron type system, low press., new design 9-31728
- metal ion low-energy beams on polycryst. films, yield meas. 9-44854
- metal oxide films, optical props. 9-30487
- metals, f.c.c., ion-bombarded, faceting influence on ejection patterns 9-44853
- rel. to particle focusing and channelling in crystals. 9-35294
- plasma, r.f. inductive, for film surface coating 9-46720
- rare-earth alloy films, high-coercive-force, prep. by getter sputtering 9-44627
- r.f., for cleaning substrate surfaces 9-23634
- r.f. sputter etching 9-46747
- r.f. sputtering apparatus for material coating, patent 9-46551
- sputter-ion diode pump, cathode post geometry, pumping speed depend. 9-40218
- sputter-ion pump, noble gas pumping enhancement depend. on cathode geometry 9-38177
- substrate bombardment, r.f., parameters calc., secondary electrons meas. 9-36956
- surfaces, ion-eroded, microtopography 9-35048
- Ag/Cu eutectic, rel. sputtering rates, temp. depend. 9-44851
- Ag deposits at satellite attitudes, by N₂ beam, rel. to surface binding energies and composition 9-24076
- Al, low-energy depth distrib. 9-47013
- Al of U in-reactor, subsequent irradi. for fission fragment track etching and obs. 9-34489
- AlN films grown by reactive sputtering, dielectric props. 9-35755
- Au deposits at satellite attitudes, by N₂ beam, rel. to surface binding energies and composition 9-24076
- GdFe garnet epitaxial film, prep. by r.f. sputtering mag. and structural props. 9-49210
- Ge [100] surfaces, ejection pattern of atoms, temp. depend. 9-35301
- H II regions, chemical sputtering of ice grains and mantles 9-24759
- inert gas atoms, ion induced re-emission from polycryst. W 9-33207
- KCl, low-energy depth distrib. 9-47013
- Nb thin films, getter-sputtering for fabrication of Nb-NbO-Pb Josephson junctions 9-35377
- NbN film preparation, upper critical field H_{c2} 9-35359
- Ni film on Li nuclear bombard. target for low O₂ contamination 9-29647
- Pt, low-energy depth distrib. 9-47013
- Ta, reactive, in mixed Ar/O atmospheres, mechanism 9-42716
- W, inert gas atom re-emission on inert gas ion bombardment 9-33207
- W, re-emission, ion-induced, of noble gas atoms 9-30799
- W oxide secondary ions, sputtering probability with Ar⁺ 9-42982
- ZnO epitaxial thin film on CdS, sapphire; perfection depend. on substrate polish, temp. 9-36953
- ZnO film deposition by triode sputtering, crystallographic orientation 9-39187
- ZnO thin film on CdS, sapphire; perfection depend. on deposition rate, substrate polish, temp., 100-500°C 9-36953

Stacking faults *see Crystal imperfections***Standards***see also Constants; Units*

- alcohols, thermal conductivity data considerations for standard reference materials 9-42703
- frequency, Cs, U-shaped resonators applic. 9-34004
- mass, metrological progress 9-31739
- reflectance spectroscopy, instruments 9-36399
- spectrophotometers, monochromatic and abridged, international standardization techniques 9-36398
- temperature, International Practical Scale 1063-2700°C, by NPL photoelec. pyrometer 9-43803
- thermometry, calibration standards, triple point temp. meas. system 9-22295
- thin film, use for X-ray fluorescence analysis of metal oxides 9-47483
- time and freq. for long-baseline interferometry 9-36107
- white reflectance, prep. and calibration 9-34201
- Cs frequency, U-shaped resonators applic. 9-34004

Stark effect

- (in) plasma, electron con. using self-reversed, Stark-broadened spectral line 9-44445
- alkali halides, F-centre, relaxed excited states 9-24392
- aniline, in rotational fine structure rel. to dipole moment meas. of lowest singlet states 9-34686
- antiferromagnets, rutile, in d.c. elec. field 9-45197
- azulene, dipole moments of excited states 9-30075
- broadening of H lines as temp. probes in N plasmas 9-48589
- crystals, non-conducting, theory 9-33547
- deuterated formaldehyde, Stark spectroscopy by i.r. lasers 9-25767
- electron in uniform strong elec. field, exact propagator, applic. to Stark eff. calc. 9-29911
- formaldehyde, i.r. laser irradi., spectrum obs. 9-25766
- formaldehyde, Stark spectroscopy by i.r. lasers 9-25767
- formic acid, i.r. laser irradi., spectrum obs. 9-25766
- heavy water, i.r. laser irradi., spectrum obs. 9-25766
- laser light splitting, dynamics, interaction 9-43903
- methane, i.r. laser irradi., spectrum obs. 9-25766
- methane, Stark spectroscopy by i.r. lasers 9-25767
- methane absorpt. line, maser obs., dipole moment evaluation 9-34678
- methyl alcohol, i.r. laser irradi., spectrum obs. 9-25766
- methyl chloride, i.r. laser irradi., spectrum obs. 9-25766
- methyl cyanide, i.r. laser irradi., spectrum obs. 9-25766
- phenol, in rotational fine structure rel. to dipole moment meas. of lowest singlet states 9-34686
- plasma, high temp. meas. 9-25913

Stark effect continued

- plasma, spectral line broadening, effects of dynamic ion shielding 9-48575
 rare earth ion, trivalent, spectra, structure analysis by stimulated radiation spectra technique 9-31092
 solids, energy level connection with lattice parameters, electric field and periodic potential 9-24092
 Al I, $3s^2 3d^2 D_{3/2}$ and $3D_{3/2}$ hyperfine structure, Stark effect investigations 9-40539
 Al spectral lines, broadening and displacement rel. plasma high temp. meas. 9-25913
 BH emission spectrum, $X(^1\sigma)$ and $A(^1\pi)$ dipole moments determ. 9-46357
 Ba II lines emitted by discharge along surface of liquid jet, Stark width 9-40716
 C spectra line broadening in arc plasma 9-44258
 $\text{CaF}_2:\text{Gd}^{3+}$, splitting of 6P_1 and 4I_1 terms of Gd^{3+} 9-31056
 $\text{CaF}_2:\text{Gd}^{3+}$ equilibrium distrib. of ions in Stark levels 9-48481
 Cd, shifts in 3P_1 excited states 9-36660
 Ce $3d$ centre in MeF_2 type crystals, Stark structure of $5d^1$ config. 9-43228
 ClO radical, in rotational spectra of ^{35}ClO and ^{37}ClO 9-38836
 Cs, $7P_{3/2}$ state hyperfine levels meas. 9-25694
 Cu I quadratic shifts in some transitions 9-22950
 D, Se, on $J=2_{1/2} \rightarrow 2_{1/2}$ and $J=6_{3/2} \rightarrow 6_{3/2}$ lines, rel. to μ determ. 9-38850
 H α , H β Balmer line profiles emission in vortex-cooled arc, broadening meas. 9-27825
 H β Balmer line profiles in plasma, particle conc. meas. 9-25859
 H γ , broadening of line profile in plasma column 9-42345
 H Balmer lines, asymmetry in transverse elec. field 9-48423
 H beam emerging from foil, Stark mixing causing periodic intensity fluctuations in Balmer lines 9-46332
 H transient plasma, broadening obs. of H β rad., electron density obs. 9-23276
 He I, electron and ion broadening of allowed and forbidden transitions, calcs. 9-42349
 He plasma, high-freq. elec. field strength meas. 9-23287
 Hg, shifts in 3P_1 and 3P_2 excited states 9-36660
 In I, investig. of hyperfine struct. of $5s^2 5d^2 D_{3/2}$ and $5s^2 6d^2 D_{3/2}$ states 9-29938
 KBr:Ti modulated absorption spectrum, quadratic Stark eff. obs. 9-41381
 KCl, F-centre, relaxed excited states 9-24392
 KCl, Z₁ and Z₂ centres, in electric field modulated absorpt. spectrum 9-23828
 KF, F-centre, relaxed excited states 9-24392
 Li, energy levels splitting calc. 9-22957
 Li plasma, high-density, linear Stark broadening 9-34765
 Mg Spectral lines, broadening and displacement rel. plasma high temp. meas. 9-25913
 NH₃ Stark spectroscopy by far i.r. masers 9-25767
 Na I 5682-88 Å and 4978-82 Å lines of plasma, Stark broadening 9-32413
 Na Spectral lines, broadening and displacement rel. plasma high temp. meas. 9-25913
 NaCl, F-centre, relaxed excited states 9-24392
 NaF, F-centre, relaxed excited states 9-24392
 O spectral lines, broadening and displacement rel. plasma high temp. meas. 9-25913
 PBS, dipole moment from Stark components of microwave rotational transitions 9-30051
 RbCl, F-centre, relaxed excited states 9-24392
 Si spectral lines, broadening and displacement rel. plasma high temp. meas. 9-25913
 SIS, dipole moment from Stark components of microwave rotational transitions 9-30051
 SnS, dipole moment from Stark components of microwave rotational transitions 9-30051
 Tl spectra, Stark parameter determination, level crossings 9-48404
 Y₂O₃:Eu³⁺ emission spectrum, splitting of $^3D_0 \rightarrow ^3F_1$ 9-33562
 Zn, shifts in 3P_1 excited states 9-36660

Stars

- see also *Nebulae; Novae; Sun*
 5 parsecs outer range 9-33901
 A-type, 1700 bright stars north of -21° , two-dimens. spectral classifications 9-31537
 ADS 11680, improved orbit 9-31551
 ADS 1223, optical binary, motion 9-49560
 ADS 12447, visual binary, orbit deduced graphically 9-36000
 ADS 16326 visual binary, parallaxes and masses 9-47645
 ADS 1865, K6 dwarf binary system, parallax and mass ratio obs. 9-28997
 ADS 3475, visual binary, parallaxes and masses 9-47645
 ADS 8862, visual binary, parallaxes and masses 9-47645
 ADS 9392, improved orbit 9-29032
 ADS 9617, visual binary, parallaxes and masses 9-47645
 ADS 9756, visual double star, orbital elements 9-49560
 apical acceleration, galactic motion 9-43536
 atmosphere, model for O-type stars with u.v. line blanketing 9-27010
 atmosphere, non-LTE, effects of Balmer α 9-29002
 atmospheres, model, computation by Monte Carlo relaxation method 9-41632
 atmospheres, radiation intensity expression for isotropic coherent scatt. plus absorpt. 9-45607
 atmospheres, shock front in atomic H, stability, dissipation and propag. 9-24762
 atmospheres for rotating, review 9-24772
 B2, causing anomalously low polarization, regions in stellar neutral hydrogen 9-40155
 Barnard's, alternate dynamical analysis 9-47633
 Barnard's star, parallax, proper and orbital motion, acceleration from photographic obs. 9-29031
 BD +20°2465, astrometric study, comparison of two measuring machines 9-31522
 BD +4°4510, visual binary parallax and mass ratio 9-31553
 Be and shell stars, relationship from Balmer line spectrum form. in extended atms. 9-47641
 binaries, above main sequence, masses and spectrograms 9-40152
 binaries, eclipse observations 9-45629

Stars continued

- binaries, orbit planes of nine determ. from obs. of polarized radiation 9-31557
 binaries, spectroscopic, single line, absence of secondary spectrum 9-35996
 binaries, visual, four, parallaxes and masses determ. 9-47645
 binary, eclipsing; Russell's ψ -method applic. to minima 9-33913
 binary, visual, ADS 12447, orbit deduced graphically 9-36000
 binary, with intrinsic variables 9-40153
 binary close systems, appreciation of time darkening laws 9-31559
 binary system, close, applic. of restricted problem of two rigid spheroids 9-38036
 binary systems, spectroscopic, large masses and props. 9-27040
 BL Tel, eclipsing variable 9-45630
 Blanco 1 cluster, four-colour photoelec. photometry 9-27041
 blue, proper motion in field of pulsar CP 1919 9-27065
 carbon stars, detection in survey centred on south galactic pole 9-31523
 η Cas, orbit calc. 9-47634
 catalogue of the positions and proper motions of stars between declinations -35° and -40° 9-28998
 Cepheid variables, pulsating, oscillations of atmosphere 9-24797
 Cepheids, faint, in Cygnus and Monoceros, photoelectric (UBV) photometry 9-29024
 Cepheids, Oort's const. A determ. 9-31545
 Cepheids relation between mass and period 9-45623
 Cepheid SU Cas, absolute magnitude and distance determ. using field stars 9-27034
 chromosphere temp. rise due to dominance of H $^-$ opacity 9-40135
 clusters, colour magnitude diagrams, tNory and obs. 9-43549
 clusters, globular, surface brightness by ring diaphragm and narrow slit 9-41647
 clusters, open, NGC 6475(M7), rot. vels. 9-35994
 clusters, relativistic, spherically symmetric, sufficient conditions for stability against radial perturbation 9-29000
 clusters, spectral studies, progress review 9-40129
 clusters in Magellanic clouds, UVB photometry, compared with those in the Galaxy 9-27043
 CoD -35° 4257, new long period variable 9-40149
 collisionless one-dimens. system, Lynden-Bell statistics, numerical expt. check 9-35975
 convection starting depths in normal and metal-deficient stars 9-31527
 Cygnus, photoelectric (UBV) photometry of eighteen faint Cepheids 9-29024
 δ Scuti variables, photometry 9-45627
 Delta Scuti type variable, observations of five by photometry 9-45626
 densities in regions of intermediate galactic latitude, survey of early type stars 9-38040
 diameter meas. from apparent angular diameter and occultation by moon 9-24775
 Don 91, visual double star, orbital elements 9-49560
 double, evolution reviewed 9-38051
 DQ Her short-period variations due to oscillations of shock wavefront 9-45624
 dwarfs, white, effect of neutronization on critical parameters 9-27032
 early type, intermediate galactic latitude regions, finding list 9-38040
 electron thermal conduction theory 9-43534
 energy prod. w.r.t. proton-proton reaction and C-N cycle 9-35969
 Et Pegasi, photoelectric observations 9-27011
 faint, background exposure density and photographic detect. limit, relationship 9-31672
 flare, BD +51°2402, EV Lac, and PZ Mon, 1967 activity obs. 9-33908
 flare, multiple exposure photographic techniques 9-27035
 giants, K2-M6, high dispersion classification at high and low velocities 9-24780
 globular cluster M15, age and initial He abundance 9-27044
 globular clusters, age rel. to Galactic mass and gravit. const. vars. 9-33895
 globular clusters in Andromeda nebula, comparison between those in galaxy and M31 9-33912
 gravitational instability, non-Jeans type 9-41648
 gravitational wave emission and vibr. damping in relativistic starlike objects 9-28979
 gravitational-to-inertial mass ratio from Einstein and Brans-Dicke theories 9-40140
 group in line of sight with Large Magellanic cloud, BV photometry rel. to reality, and distance modulus 9-27042
 η Carinae, intrinsic reddening greater than surroundings, from relative intensities of Fe II lines 9-40148
 Hayashi effect, modifications due to high-opacity atms. or H₂ dissociation zone 9-29021
 HD 147889, max. polarization wavelength correl. with interstellar extinction 9-31534
 HD 204827 max. polarization wavelength correl. with interstellar extinction 9-31534
 HD 3035, binary, companion a K O star 9-45631
 high temp. hydrostatic instability, general relativistic eff. 9-45611
 horizontal branch, at high Galactic latits., positrons magnitudes and spectra 9-47626
 Hyades, distance modulus 9-31550
 Hyades low luminosity members, proper motions and photoelec. obs. 9-31550
 hydrostatic instability in high temp. stars, general relativistic eff. 9-45611
 IC 4499 cluster, variable stars coords 9-35998
 M13 variables, period changes 9-31546
 M3, M5 globular clusters, membership, size, relationship to RR Lyrae variables 9-31558
 M stars, grant, space density in Galactic anticentre 9-47625
 magnetic variables, model of absorpt. line spectrum originating in circumstellar envelope 9-33909
 main sequence, upper, differential rot., models 9-35971
 masses of stars above main sequence 9-40152
 massive, in He burning phase, pulsational props. 9-24798
 massive, pulsating, models and stability 9-24803
 massive high-velocity (rogue), existence and freq. explanation by cosmological model 9-31490
 Melotte 227 cluster, four-colour photoelec. photometry 9-27041
 metal deficient, atmospheric models 9-43535
 m.h.d. toroidal oscillations, decay time 9-31524
 MK classification of 314 F and G type 9-49542
 models, polytropic, by nonrelativistic generalization theory 9-27008

Stars continued

- Monoceras, photoelectric (UBV) photometry of ten faint Cepheids 9-29024
 neutron, conductive instability in presence of small perturbing forces 9-49557
 neutron, degenerate, nonradial gravity wave rel. to pulsar periodicity 9-47658
 neutron, ferromag., hard-sphere Fermi gas obs. 9-49556
 neutron, mag., radio emission data indicating new pulsar model 9-24795
 neutron, magnetic, rot. and oscillating, model accounting for optical and radio emissions of pulsars 9-41659
 neutron, magnetic and rotating, generation of mag. flux and energy as in Crab Nebula 9-45647
 neutron, oblique rotator model rel. to pulsar emission mechanism 9-41660
 neutron, rotating, hypothesis for pulsar origin 9-31577
 neutron, rotating, model of rad. mechanism for pulsars 9-31581
 neutron, rotating rel. to mag. models of pulsars 9-41666
 neutron, rotational slowing rel. to sudden decrease in period of pulsar PSR 0833-45 9-43598
 neutron and pulsars 9-33915
 neutron as pulsar 9-38059
 neutron star, criteria for ferromagnetism 9-45796
 neutron starquakes, rel. to pulsar periods 9-47642
 NGC 6397 globular cluster, atmospheric parameters of 19 blue-horizonal-branch stars 9-29009
 NGC 6475 (M7) open cluster, Rot. vels. 9-35994
 NGC 7492 globular cluster, search for variables 9-27033
 NGP, A0-AZ, vel. and space density distrib., galactic force law calc. 9-28987
 NML Cygnus, graphite particle circumstellar shell model, rel. to i.r. rad. 9-33902
 in Norma region of Milky Way, space densities rel. to spectral type and distance from Sun 9-26994
 nuclear Q values in dense stellar plasma, correction using modified ionic cluster expansion 9-49550
 nuclear reaction rates, effect of excited nuclear states 9-43541
 O-type, model atmospheres, with u.v. line blanketing 9-27010
 OB, southern and supergiants; 4-9 magnitude range, radial velocities determ. 9-31529
 OB classifications, Cleveland system, related to MK system 9-29014
 OB faint stars between Carina and Centaurus, a survey and catalogue 9-47639
 occultation by Earth, observed from moon 9-31674
 Omicron Andromedae 1961-1966, radial vels. 9-49555
 opacities, electro n-scatt., effect of quantum corrls. 9-35972
 orbits in galactic plane, evaluation in generalized Kepler motion 9-24760
 parallax obs. with two different refractors, discrepancies 9-40193
 parallaxes, relative and proper motions of 14 stars 9-40136
 polarization, wavelength depend. 9-31534
 polytrope, mag., precession formulation 9-27015
 population rel. to galaxy classification 9-38038
 pressure w.r.t. hydrodynamic theory 9-35969
 pulsars, acceleration of cosmic rays 9-24729
 pulsars, two band emission model, from neutron stars radio emission data 9-24795
 pulsating, non-adiabatic linear oscillations of atmosphere 9-24797
 pulsation hypothesis for massive red supergiants 9-29001
 pulsations, interaction between high and low frequency 9-45622
 R-type, detection in survey centred on south galactic pole 9-31523
 radial vel., micromphotometer meas. technique 9-31671
 red supergiants, pulsating, oscillations of atmosphere 9-24797
 relativistic, photon delays rel. to position of origin on disc 9-29018
 reutron source, photon-neutron reaction of ^{24}Mg as primary production mechanism 9-48329
 rotation, differential, in upper main sequence stars 9-35971
 rotation during gravitational contraction hydrodynamical theory 9-41633
 rotational energy and radiation press., equivalence principle, rotating star in equilb. 9-40140
 RR Lyrae variables, relationship to globular clusters 9-31558
 Schrodinger operator criterion for stability of stellar system 9-35956
 Sco X-1, model 9-38062
 Sco X-1 region, 83 stars, positions and proper motions 9-31583
 α Serpents, strong CN K2 III star, curve of growth analysis 9-35982
 shock phenomena in outer part 9-24774
 space density and luminosity in Solar neighbourhood 9-27039
 spherical system, insufficiency of Boltzmann assumption 9-27046
 stability of clusters, sufficient conditions for stability against radial perturbation 9-29000
 stability of self-gravitating gaseous mass, for non-adiabatic perturbation 9-47637
 stability of stellar systems, Schrodinger operator criterion 9-35956
 statistical mechanics of violent relaxation, numerical expt. check 9-35975
 stellar system, computer expt. on one dimensional model of self-gravitating system 9-27000
 stellar system model constructed from numerical experiment 9-43563
 stellar systems, stability and the Hartree-Fock exchange operator 9-45600
 subluminal, luminosity calibration and space density of blue subluminal stars 9-41635
 supergiants, red, massive, pulsation hypothesis 9-29001
 supergiants, yellow, model atmospheres 9-40138
 supernova, discovery of pulsar at suspected supernova position, possible association 9-27064
 systems, stellar distrib. function, Chapman-Enskog treatment 9-31507
 α 1785 visual binary, parallax and mass ratio 9-31552
 Tau Persei, parallax and orbital motion, obs. (1945-64) 9-29030
 temperature and opacity to black body radiation 9-35969
 transit, objectivization of obs. 9-45688
 transit obs. complete reduction by computer 9-33956
 twinkling absence when seen from outside Earth's atm., implications 9-41641
 variable, blue sequence, energizing mechanisms for instabilities 9-43542
 variable, research review 9-40150
 variables, positions in IC 4499 cluster 9-35998
 variables, search in globular cluster NGC 7492 9-27033
 variables round 6 Comae, optical obs. 9-29027
 Vega, surface gravity and temp. as model atmosphere parameters 9-27031

Stars continued

- AI Velorum stars, colours, space motions and statistical parallaxes 9-43562
 white dwarf supernova, calculation 9-29025
 white dwarf with H burning in envelope, as model for pulsating radio source 9-31575
 white dwarfs, adiabatic atm. pulsations as pulsar model 9-31579
 white dwarfs, dense, radial oscill. period ion gas contrib. near min. 9-35990
 white dwarfs and pulsars, supercond. 9-24763
 Wolf-Rayet envelopes, Bappu and Ganesh method for electron temp. determ., comment 9-41631
 X-ray, model 9-38062
 young, distrib. in small Magellanic cloud, correl. with neutral H distrib. 9-31500
 zero-limb darkening, exterior solution for radiation spheres in general relativity 9-24782
 H pure, early type stars, model atmosphere computation 9-41632
 He burning phase of massive star, pulsational props. 9-24798
- composition**
see also Elements/origin
 A field stars, model-atmosphere abund. analysis 9-43527
 A stars, peculiar, heavy-element abundances 9-31526
 A stars, peculiar and normal, search for neon in spectra 9-43554
 Arcturus, forbidden Ca II 9-27013
 atmospheric models, source function mean intensity, flux, calcs. using matrix methods 9-29003
 B3 HD 37058, Ti and Sr abundance determ., Wrubel's curve of growth 9-33903
 B stars, peculiar and normal, search for neon in spectra 9-43554
 Cepheids, Li and Be abund. 9-24796
 chemical, limitations of instrumentation and theory 9-40139
 elements synthesis and distrib. 9-35969
 G8-K2 giants, metal abundances, use of BVR photometry 9-27012
 γ Gem, model-atmosphere abund. analysis 9-43527
 globular cluster M15, initial He abundance and age 9-27044
 globular clusters M3, M13, M15 and M92, helium abundance 9-43548
 HD 101013 from differential curve of growth analysis 9-41640
 HD 2421, model-atmosphere abund. analysis 9-43527
 β Her, from differential curve of growth analysis 9-41640
 lb supergiants, Li and Be abund. 9-24796
 K giants, abundances of C, O and N 9-43528
 K giants, supermetallicity 9-49543
 late-type evolved stars, supermetallicity, technique for obtaining differential abundances 9-49543
 light element abundances 9-35968
 M, near sun and in nucleus of Galaxy, pulsation characts. difference rel. to He and heavy element abundance 9-38045
 δ Bootis stars, chemical composition, possibly a type of Ap star 9-28999
 molecular weight of matter w.r.t. hydrodynamic theory 9-35969
 oPeg, model-atmosphere abund. analysis 9-43527
 red giants, H, He, C, composition 9-43534
 Sirius, reappraisal 9-24771
 γ Tau, from differential curve of growth analysis 9-41640
 θ^1 Tau, from differential curve of growth analysis 9-41640
 θ Vir, model-atmosphere abund. analysis 9-43527
 C stars, Merrill-Sanford bands due to overabundance of ^{28}Si 9-24792
 Li depletion in main sequence stars, observational time-scales 9-35973
 Si burning, role of weak decays rel. to p/n densities 9-49549
- evolution**
 1M_{\odot} star, first hydrostatic contraction phase 9-27018
 Be stars, simple model for evolution of circumstellar envelope 9-43530
 binaries, close syst., mass exchange, dynamical eff. 9-24808
 binary, in galactic field, statistical test 9-27037
 binary components, visual, evolutionary stages 9-24807
 binary system, effects of mass exchange and ejection on orbit 9-27017
 collection of popular papers, book 9-45613
 collisionless self-gravitating system, statistical mech. rel. to quasi-equilib. state approach 9-27016
 contraction, hydrostatic, first, of 1M_{\odot} star 9-27018
 convective region exam. by Henyey theory 9-45612
 density and temp. limits at centre of massive sphere 9-40137
 diffusion of energy in the stellar interior, time scale 9-29005
 double stars, review 9-38051
 electron gas, relativistic, entropy 9-47787
 explosive ignition of C in stars of intermediate mass 9-24799
 explosive nucleosynthesis conditions for C burning and Si burning 9-49546
 extreme population I, 0.85 and 0.95 M_{\odot} stars 9-29007
 extreme population I 1.5 and 2.0 M_{\odot} stars 9-29006
 in globular clusters, H-R diagrams, characteristic features 9-31556
 globular clusters, M3, M13, M15 and M92, age difference 9-43548
 globular clusters, primeval, mass computation 9-49518
 gravitational collapse, coupling of ang. mom. with grav. field 9-31532
 horizontal branch stars, evolutionary tracks computation 9-38041
 isentropic stars, general relativistic effects 9-45609
 late history 9-26982
 M supergiants, hypothesis 9-24778
 magnetopolytropes, gaseous, equilb. and stability 9-47635
 masses of stars formed from clouds of solid hydrogen grains, freq. distrib. 9-35976
 massive high-velocity (rogue), existence and freq. explanation by cosmological model 9-31490
 massive star in the burning phase, pulsational props. 9-45625
 massive stars, occurrence of semi-convection 9-43537
 neutrino emitting URCA process, model 9-31531
 neutron, from massive O stars, rel. to pulsar formation 9-43595
 nucleosynthesis, ^{56}Fe prod. and the ^{58}Ni problem 9-49547
 population II stars, He abundance determ. rel. to cosmological model 9-43539
 pre-protostar stage, dissipation of mag. energy prod. non-thermal radio sources 9-41634
 proto stars, from fragmentation of thin toroid formed in initial contraction of gas 9-45610
 protostar, spherically symm., collapsing, dynamics 9-29008
 protostars, possible source of anomalous OH emission, reln. with HII regions 9-33904
 protostars collapse and flare-up, radiation and convection energy flow 9-43543
 pulsation props. of massive star in He burning phase 9-45625

Stars continued
evolution continued

- random splitting model for protostar formation 9-24779
- regions of formation searched at 15 GHz for compact H II regions 9-45603
- Rosseland and Planck mean absorpt. coeffs. for ice, graphite and SiO₂ 9-49548
- of subcritical mass and high density existence and formation 9-40137
- theory and obs., comparison 9-31533
- theory including magnetoturbulence applied to explain nature of pulsars 9-27063
- water-bag model of spherical symm. system 9-35997
- white dwarfs, interpretation, review 9-27019
- white dwarfs, plasma transitions 9-25053
- white dwarfs, rel. to type I supernovae 9-43559
- pe-p²D_v, detailed rate calc. 9-29004
- pp-²De^{1/2}, detailed rate calc. 9-29004
- C-rich stars, models, C burning and flashes with and without neutrinos 9-24765
- C burning, expt. investigation of ¹²C-¹²C reacts. 9-43540
- C thermonuclear burning in stars, synthesis of elements and energy generation 9-40142
- ¹²C stars, and prod. of planetary nebulae 9-40141
- ⁵⁶Fe nucleosynthesis in Si quasi-equilibria and the ⁵⁸Ni problem 9-49547
- H condensation onto interstellar grains, role in stellar formation 9-35977
- H grains, isothermal clouds, formation and freq. distrib. of masses of stars 9-35976
- Li depletion in main sequence stars, observational time-scales 9-35973
- Si burning, abundances A=28 to A=62, quasi-equilibrium configurations 9-49549

magnetism*see also Sun/magnetism*

- axisymmetric mag. field with differential rotations in spherical fluid shell 9-43533
- 53 Cam, spectroscopic evidence for mag. field in atm. 9-38049
- dipole field at angle to rotation axis, as possible source of pulsar rad. 9-33917
- dissipation of mag. energy in collapsing interstellar cloud to form non-thermal radio sources 9-41634
- ferromagnetism, in neutron stars, neutron Fermi liquids 9-45796
- field generated by convective surface motion 9-31528
- field generation by convective zones 9-27007
- field of star due to viscosity of plasma atmosphere 9-45608
- HD 152107, abnormal line intensities in hydrogen spectrum 9-27021
- HD 173650, light curves 9-31540
- HD 188041, mag. field variations for various elements, Zeeman obs. 9-41643
- HD 215441, periodic variations 9-35970
- neutron, ferromag. transition conditions for dense nuc. matter 9-41642
- neutron, rotating, oblique dipole field rel. to pulsar emission 9-43589
- white dwarfs, electron gas in envelope, behaviour 9-31525

radiation*see also Cosmic radiations, radiofrequency; Sun/radiation*

- A stars, 146, K line strengths 9-27024
- Be-type, wavelength dependence of polarization 9-38046
- binaries, close, gas heated by shock wave, role in envelope of systems 9-27038
- binaries, visual, magnitude differences, photometric determ. 9-47644
- 44i Bootis, photoelec. obs. using blue and yellow filters 9-38048
- brightness distrib. of stellar transits by photoelec. means 9-43555
- Carina, photometric standard sequences 9-47638
- Carina-Centaurus region, 135 OB stars, photoelec. UVB obs. 9-35983
- CE Cas, double Cepheid, period-luminosity-colour relation calibration and instability strip 9-43550
- VW Cephei, photoelec. obs. using blue and yellow filters 9-38048
- cephheids, influence of line blanketing on colour 9-24787
- Cepheids, remarks on pulses 9-24802
- CH Cygni, photoelectric scanner observations and possibility of radio wave emission 9-24781
- cluster, open, NGC 7128, UVB photometric obs. 9-35999
- clusters, globular, NGC 2808, NGC 1851, UVB photoelec. investigation 9-35993
- VZ Cnc, i.r. colours 9-43562
- Coma Cluster, 38 stars, 4-colour and H β photometry 9-31554
- coma sluster, short period variability search for δ scuti stars 9-31555
- cosmic 3°K background radiation, star light thermalization interpretation 9-28980
- ϵ CrA, light and colour curves 9-38047
- Cygnus, OH microwave emission, positions and spectra 9-47655
- δ Del, photoelec. continuum obs., 3390-10400 Å 9-43561
- Delta Scuti stars, photoelec. continuum obs., 3390-10400 Å 9-43561
- diffuse refl. and transmission of time-dependent collimated light, by a finite inhomogeneous atm. 9-45582
- dissipation function by the invariant imbedding eqn. 9-45583
- DQ Her, synchronous photometric obs. of 71.1 s periodic variations 9-35992
- early type, u.v. spectrophotometry 9-31535
- electron energy distrib. calc. from obs. synchrotron radiation 9-29041
- F5-G0 stars, catalogue of *uvby* photometry 9-40145
- G8-K0, type giants, reddening lines in the UVB system 9-41636
- globular clusters, four brightest in Fornax, integrated magnitudes and colours 9-38050
- globular clusters, H-R diagrams, characteristic features 9-31556
- globular clusters M3, M13, M15 and M92, reddening values 9-43548
- Hayashi effect, modifications due to high-opacity atmos. or H₂ dissociation zone 9-29021
- HD 125924, 9th magnitude B star, obs. 9-24789
- HD 19216, nature of its variability 9-35989
- HD 199757, spectrophotometric and spectroscopic analysis of variations 9-43562
- HD 217312 in III Cephei association, photometric obs. 9-24809
- HDE 310376, rapid irregular variable, spectroscopic obs., photometric obs. 9-43551
- horizontal-branch, 10 new stars, positions, spectral type, B magnitudes 9-29015
- IC 1805, extinction characts. of surrounding absorbing matter 9-43564
- IC 1805 absorpt. to reddening ratio of stellar light, UVB obs. 9-43564
- interstellar reddening, function of heliocentric distance and galactic latitude and longitude 9-47649
- i.r., photographic-photoelec. obs. 9-27030

Stars continued
radiation continued

- i.r. object in region of IC 1805, obs. 9-27027
- i.r. region photometric study; G, K and M late-type stars, H ion emission 9-31539
- isophotal wavelength of U, B, V, R systems for photometry meas. 9-35987
- Lacerta OB1 region, spectral classes and photographs magnitudes, 3621 stars 9-31536
- Large Magellanic Cloud, $\alpha=5^{\circ}12'$, $\delta=-67.5^{\circ}$ region, variable stars photometry 9-38044
- late type stars, press. induced opacity of mol. hydrogen 9-35978
- late-type stars, near i.r. photometry 9-29019
- long-period variables, UVB obs. 9-31541
- luminosity resolution, colour index for G5 and later stars 9-29013
- RR Lyrae stars, photometric and spectroscopic obs. 9-41637
- RR Lyrae variables in field of M2, periods and photographic magnitudes B and V 9-49545
- M7 giants in nuclear bulge of the Galaxy, colour and TiO strengths 9-38045
- magnitude, absolute; recalibration consistent with photometric distance moduli of clusters 9-35988
- magnitude extinction rel. to Earth's atm. density 9-33905
- massive hot non-rotating stars, with adiabatic temp. grad., general-relativistic models, ideal gas and rad. config. 9-24764
- Milky Way, southern, photometric programme 9-47638
- Mira variables, polarization of emitted light 9-33907
- narrow slit in photometry for brightness meas. of stellar systems 9-43685
- neutron star, e.m. emission spectrum calc. 9-31543
- NGC 1851, globular cluster, UVB photoelec. investigation 9-35993
- NGC 2808, globular cluster, UVB photoelec. investigation 9-35993
- NGC 7128, open cluster, UVB photometric obs. 9-35999
- NGC 752 cluster, short period variability search for δ scuti stars 9-31555
- NML Cygnus, i.r., graphite particle shell model for origin 9-33902
- O-type, six, luminosity and temp. criteria from spectrograms 9-35984
- OB stars in Carina-Centaurus region, photoelec. UVB obs. 9-35983
- OH 1665 and 1667 lines in W3, sources of maser radiation 9-24784
- open clusters, 4-colour and H β photometry 9-31554
- P Cygni, photometry, interpretation 9-27026
- photometry, 12 colour, wide baseline colour system and appl. 9-29013
- plane-parallel atmospheres, multiple scatt. 9-36362
- Polaris, intrinsic colour index and absolute magnitude 9-35991
- protostars, associated i.r. radiation 9-29020
- ρ Pup, photoelec. continuum obs., 3390-10400 Å 9-43561
- relativistic stars, photon delays rel. to position of origin on disc 9-29018
- Ros 4, distant open cluster associated with nebulosities, position and distance, UVB photometry 9-47647
- S x Phe, spectrophotometric and spectroscopic anal. of variations 9-43562
- Sco X-1, intensity and time variation, rocket obs. 9-38063
- Sco X-1, polarization of X-rays, search 9-27028
- δ Sct, photoelec. continuum obs., 3390-10400 Å 9-43561
- δ Scuti, new, photometry, periods and amplitudes 9-29012
- F-K supergiants, influence of line blanketing on colour 9-24787
- supernova remnants, 16, radio emission between 408 and 2700 MHz, spectra derivation 9-31544
- synchrotron, losses in self-absorbed radio sources 9-27056
- Taurus A, 21 cm absorpt line, frequency decrease near sun, gravitational or e.m. effect? 9-33906
- TZ Bootis, light variation and orbital elements 9-29016
- Ursa Major Cluster, 10 stars, 4-colour and H β photometry 9-31554
- W Ursae Majoris, photoelec. obs. using blue and yellow filters 9-38048
- V1389 Sgr, M 8.5 III star, colour and TiO strength 9-38045
- V502 Ophiuchi, yellow and blue light photoelec. obs. 9-29017
- variables and other, period viewing (1967) 9-29026
- AI Vel, spectrophotometric and spectroscopic analysis of variations 9-43562
- W3, maser radiation sources in 1665 and 1667 OH lines 9-24784
- white dwarf, opacity due to electron behaviour in envelope 9-31525
- Y2 Canis Minoris, prolonged radio emission 9-45617
- YC Canis Minoris, visual and photoelec. obs. of flare 9-45618
- K line strengths in 146 A stars 9-27024

spectra

- α Centauri, He line strengths in the spectrum variable 9-24788
- A stars, peculiar and normal, search for neon in spectra 9-43554
- A-type, 1700 bright stars north of -21° , two-dimens. spectral classifications 9-31537
- absorption band, $\lambda 4430$, image tube obs. 9-27025
- absorption lines of quasi-stellar, rel. to red-shift and screening hypothesis 9-31567
- Arcturus, performance of a double-pass spectrometer 9-41639
- Arcturus, forbidden Ca II 9-27013
- β Aurigae, binary, eclipsing, orbital elements, 3900-4500 Å 9-33911
- auto-ionization lines, contrib. to Rosseland opacity, calc. 9-40144
- β Urae, He I $\lambda 10830$ line 9-27045
- B stars, peculiar and normal, search for neon in spectra 9-43554
- Balmer series, limiting resolved line 9-27020
- BD +10°2179, helium-carbon star, spectra of atmosphere 9-43553
- BD +42°2173, a new C star 9-45620
- Be stars, Balmer line spectrum form. in extended atm. 9-47641
- binary, close, HR 5317, curve of growth analysis 9-35995
- binary β Aurigae, eclipsing, orbital elements, 3900-4500 Å 9-33911
- α Boo, λ 8500 region, obs. at reciprocal dispersion of 8 Å/mm 9-31683
- 12 Cam, calcium emission in giant binary 9-43552
- 53 Cam, partial resolution of Zeeman patterns 9-38049
- κ Cancri, magnetic field and light variations 9-29011
- α^2 Canum Venaticorum, 5000 to 6650 Å 9-29010
- Cepheids, faint, in Cygnus and Monoceros, photoelectric (UVB) photometry 9-29024
- Cepheids, line spectrum computation method 9-24787
- CH Cygni, absorpt. and emission, July 1967 9-29028
- collection of popular reprinted articles, book 9-45621
- 17 Comae Berenices, magnetic field and light variations 9-29011
- in comet-like nebulae, obs. on 8 9-43544
- CU Virginis (HD 122424), variations 9-31548
- curves of growth, effect of electron scatt. 9-47636
- α^2 CVn, spectral evidence for oblique-rotator model 9-43529
- cygnus, photoelectric (UVB) photometry of eighteen faint Cepheids 9-29024
- δ Persei, weak absorption lines 9-35981

Stars continued

spectra continued

- distortions due to atmospheric composition 9-24786
 double systems, UVB observations 9-29022
 eclipsing and spectroscopic binary HD 161783 9-49553
 effectively thin approx. 9-38043
 Et Pegasi, photoelectric observations 9-27011
 F and G - tpe, MK classification 9-49542
 F-M, total line and band absorption 9-45614
 FG Sagittae, variable, energy distribution 9-27611
 η Carinae, relative intensities of [Fe II] lines rel. to intrinsic reddening 9-40148
 HD 101013 differential curve of growth analysis, using Arcturus (K2 III) as reference 9-41640
 HD 152107, abnormal line intensities in hydrogen spectrum 9-27021
 HD 173650, magnetic, observations 9-31540
 HD 188041, mag. field variations for various elements, Zeeman obs. 9-41643
 HD 191980, peculiar B-type 9-24783
 HD 199757 spectrophotometric and spectroscopic analysis of variations 9-43562
 HD 200775, illuminating star of NGC 7023 nebulae 9-35961
 HD 204411, cool Ap star, line identifications and equivalent widths, model atmosphere analysis 9-49552
 HD 217312 in III Cephei association, spectrographic orbit obs. 9-24809
 HD 30353, He star, i.r. photometry 9-45631
 HDE 310376, rapid irregular variable, spectroscopic obs. 9-43551
 β Her, differential curve of growth analysis, using Arcturus (K2 III) as reference 9-41640
 horizontal branch at high galactic latitudes 9-47626
 hot model atm., neutral He lines and departures from LTE 9-45615
 HR 5317, close binary, curve of growth analysis 9-35995
 HR 7484, spectrographic and photometric analyses 9-27022
 IC 1805 region, interstellar absorpt., spectrophotometric obs. 9-47650
 interstellar extinction curves for graphite particles coated with solid H 9-40147
 K-Line absolute magnitudes, effect of metal abundances 9-31542
 late type stars, press. induced opacity of mol. hydrogen 9-35978
 line shifts effect on temp. distrib. in stellar atmosphere 9-49544
 β -Lyr, slow variations in brightness 9-33910
 RR Lyrae stars, photometric and spectroscopic obs. 9-41637
 δ CMa(F81a), observed and computed spectrum comparison 9-24787
 magnetic variables, absorpt. line, origin in different layers of circumstellar envelope 9-33909
 Merrill-Sanford bands in carbon stars due to overabundance of ^{28}Si 9-24792
 metal abundances, effect on K-line absolute magnitudes 9-31542
 metallic-line, Zeeman observations 9-43546
 metallic-line, Zeeman observations 9-43545
 MH α , 328-116, M-giant + nebula composition, emission lines spectrogram obs. 9-24806
 MH α 328116 possible presence of Fe IV lines 9-35979
 Mira variables, new TiO bands, $\lambda\lambda$ 9725-10250 identification, structure and variations 9-41644
 Monoceros, photoelectric (UBV) photometry of ten faint Cepheids 9-29024
 nebulae, gaseous, excitation of forbidden lines, formulation and calculations for $2p^2$ ions 9-27004
 NGC 2516, open cluster, H-R diagram 9-47646
 NGC 6231 cluster in Sco OB I spectral classifications and UVB photometry 9-29029
 NGC 6397 globular cluster, 19 blue-horizontal-branch stars 9-29009
 nominal S-4 magnitudes calc., extra-atmospheric 9-38042
 Nova Herculis, CN band analysis for moment of maximum, Dec, 1934 9-31547
 OB bright, stars south of -20° , MK spectral classification 9-40143
 OB stars, southern, 121, line strengths from spectrograms 9-43556
 OB stars, southern, 380 earlier than class A7 absolute visual magnitudes 9-43557
 opacity, Rosseland, contrib. of auto-ionization lines, calc. 9-40144
 Orion, bright stars, far u.v. spectrophotometry, rocket obs. 9-49551
 Orion Belt region, Hy photometry of B stars 9-24790
 Paschen rays for H, intensity variation rel. to spectral type and luminosity class 9-47640
 α Per (F51b), observed and computed spectrum comparison 9-24787
 SX Phe, spectrophotometric and spectroscopic analysis of variations 9-43562
 praesepe, open cluster, photoelectric obs. of 97 stars 9-47648
 quark transitions prediction 9-38773
 red variables, 51, variations in near i.r. 9-31538
 RY Draconis, Merrill-Sanford bands, possibly due to ^{28}Si abundance 9-24792
 α Sco, λ 8500 region, obs. at reciprocal dispersion of 8 Å/mm 9-31683
 Sco OB 1, spectral classifications and UVB photometry 9-29029
 in selected area 193, magnitudes, colours and spectral classes 9-27029
 α Serpents, strong CN K2 III star, curve of growth analysis 9-35982
 shell, of Zeta Tauri, radial vel. variations 9-35986
 shell stars, 4, changing spectra 9-31338
 shell stars, Balmer line spectrum form in extended atm. 9-47641
 solar type, line statistics in 3100 < λ < 8200 Å region 9-45616
 spectrophotometry, instrument profile effects, reference to the Arcturus Atlas 9-41638
 SS Cygni flare - study of non stable stars 9-27113
 F-Supergiants, line spectrum computation method 9-24787
 supernova in NGC 2713, (1968) 9-24801
 γ Tau, differential curve of growth analysis, using Arcturus (K2 III) as reference 9-41640
 θ 1 Tau, differential curve of growth analysis, using Arcturus (K2 III) as reference 9-41640
 Taurus A, continuous rad. at 1.2 mm in far i.r. 9-43558
 (U-B) and (B-V) colours, theoretical 9-27023
 U.B.V., system, corrections of response curves and parameters 9-40146
 AI Vel, spectrophotometric and spectroscopic analysis of variations 9-43562
 Wolf 359, dM8e, spectrum of a flare 9-35980
 Wolf-Rayet, review of population I type 9-24793
 Wolf-Rayet star in Small Magellanic Cloud 9-24791
 WY Gem, (1967-68) 9-35985
 WZ Cassiopeiae, atomic and mol. absorpt. lines 9-49554

Stars continued

spectra continued

- γ Canum Venaticorum Merrill-Sanford bands, possibly due to ^{28}Si abundance 9-24792
 Zeeman observations of metallic-line stars 9-43545
 Zeeman observations of metallic-line stars 9-43546
 Zeta Tauri, shell spectrum, radial vel. variations 9-35986
 β -Lyr, He I 10830 Å line investigation 9-24785
 C-Cu, theoretical wavelengths for K α -type X-ray emission 9-24432
 Cr I, absolute gf-values 9-42322
 Fe IV lines in MH α 328116 spectrum 9-35979
 Na D lines, interstellar, in spectra of 75 stars 9-43547
 Na D lines, interstellar, profiles in 77 stars 9-40154
 OH anomalous emission, protostar source, reln. with HII regions 9-33904
structure
 40 Eridani B, white-dwarf atmosphere 9-27009
 atmosphere, effect of line shifts on temp. distrib. 9-49544
 atmosphere, model, matrix method for calculating source function, mean intensity and flux 9-24768
 atmosphere model of late-type stars 9-43531
 axisymmetric mag. field with differential rotations in spherical fluid shell 9-43533
 BD+10°2179, helium-carbon star, atmosphere from spectra 9-43553
 Be stars, simple model for struct. of circumstellar envelope 9-43530
 Chandrasekhar mass limit, estimated from gravitational forces in fermion and boson systems 9-43734
 chromospheres and polarization in late-type stars 9-24769
 convective envelopes, rotating, excitation of nonspherical waves 9-43532
 coordinate stretching and interface location, PL expansion 9-35974
 α^2 CVn, oblique-rotator model, new evidence 9-43529
 general-relativistic models of massive hot non-rotating stars with adiabatic temp. grad. 9-24764
 late-type stars, model atmospheres 9-43531
 magnetic field generated by convective motion, and convection-magnetic interaction 9-31528
 main-sequence, equilibrium models 9-31530
 massive hot non-rotating stars, with adiabatic temp. grad., general-relativistic models, ideal gas and rad. config. 9-24764
 matter equilb. state at high temps. and densities 9-24777
 neutron star, gas accretion theory, including proton retardation by plasma waves and in pair collisions 9-31543
 neutronization of matter with high densities 9-24794
 P Cygni, expanding atmosphere 9-43538
 polytropes, rotationally distorted 9-24773
 polytropic, with strong mag. fields, perturbation method of determ. 9-27014
 population II main-sequence stars, phys. conditions in convective envelopes 9-24770
 rotating, atmospheres, review 9-24772
 RR Lyrae, model atmospheres 9-24776
 RR Lyrae type, model atmospheres 9-24766
 YZ Canis Minoris, corona struct. based on flare obs. 9-45619
 H/He ratio, effect on atmospheric structure-radiative capacity in stellar atmospheres 9-24767

Stars (nuclear) see Particle track visualisation

Statistical analysis

- see also *Measurement/errors; Probability; Random processes*
 causal processes, distribution of density of intervals between neighbouring events 9-36507
 Debye-Waller type thermal averages evaluation method 9-38248
 ergodic theory, entropy and generators, book. 9-27793
 for experimental, book 9-33979
 Lorentzian parameters, propag. of statistical counting errors 9-42127
 many-body systems, common approximations 9-22146
 Markov processes, relation with quantum mechanics 9-29196
 Monte Carlo simulation of oscillatory photoconductivity 9-35499
 photon field, counting correlation meas. 9-27293
 random walks, inhomogeneous, passage-time property 9-29204
 stochastic point processes, sequent. corrls. 9-22172
 stochastic processes in quantum mechanics, new formulation of theory 9-29197
applications
 see also *Counters/statistical analysis*
 adsorbed monomer cluster distrib. on one-dimens. lattice, matrix method calcs. 9-34997
 atmospheric temp. profile, regularization 9-40009
 binary alloys, generalized spherical model 9-24292
 chain molecules, Monte Carlo computer simulation 9-42462
 chemical kinetics, stochastic formulation 9-41441
 column under axial stochastic load, dynamic stability, Lyapunov-type anal. 9-22228
 cosmic ray intensity increases 9-24708
 creep, stochastic model 9-33040
 dislocation distrib. in linear elastic medium 9-23806
 distribution function, radial, form rel. to collision operators 9-29210
 droplet condensation mechanism, model 9-39139
 earthquake statistics, coefficient γ rel. to stress state 9-26875
 elastic beams, natural frequency, with random imperfections 9-43782
 electrolytes, aqueous 1-1, at 25°C, integral eqn. computations, error analysis 9-35748
 electron sums over atomic states and electron specific heat calc. 9-38750
 e.m. radiation, polarized, reson. scatt. in weak mag. fields, Monte Carlo treatment 9-38333
 exchange approximation for inhomogeneous many-electron systems 9-25043
 fayrites, polycrystalline, initial microwave tensor susceptibility 9-49215
 ferromagnetic thin films, reduced matrix procedure 9-31038
 filter, mathematical, proton elastic scatt. anomalies anal. 9-32341
 filtering, low pass, influence on corrl. meas. for non-Gaussian processes 9-29221
 gas discharges, Monte Carlo simulation 9-42570
 gases, electrical breakdown at medium pressures 9-30316
 geomagnetic anomalies, source depth determ. 9-31453
 geomagnetic D_{st} field for storm 18-19 June 1936, new analysis 9-43486
 geomagnetic storm fluctuations 9-35905
 geomagnetic variations, classification of days 9-33859
 geomagnetic world charts 9-33857
 geophysical interpretation efficiency, estimation 9-33701

Statistical analysis continued
applications continued

- glacial drift topographies, differentiation 9-37895
 high polymer molecules, mech. entanglements 9-23188
 imaging system resolution, estimation theory 9-27375
 inert-gas crystals, Monte Carlo simulation 9-23795
 information content of radiations measurements used in indirect sensing 9-24660
 interferometry of transonic currents 9-29468
 ionosphere, F2, horizontal drifts and anisotropy of irregularities, correl. analysis 9-41591
 ionospheric magnetoionic wave components in oblique incidence, statistical chars. 9-43442
 mechanical behaviour of solids 9-39431
 microcrack linking, model 9-30693
 mixed thermal and coherent radiation, twofold joint photocount statistics 9-45940
 modelling of narrow beam propagation in scattering medium adjoining reflecting surface 9-29460
 monatomic gases, distribution-function autocorrelations calc. 9-34045
 Monte Carlo analysis of fast multicompartment critical nuclear reactors 9-32375
 Monte Carlo computer simulation of chain molecules 9-42462
 Monte Carlo method for small fast critical nuclear reactors 9-29870
 Monte Carlo technique in quantum statistics 9-25051
 Monte-Carlo method, simulation of random walks and reacts. of point defects 9-30590
 Monte-Carlo method, simulation of walks and reacts. of point defects 9-30591
 Monte-Carlo method for solving physical and chemical kinetics problems 9-39044
 Nakagami m-distrib. for scintillation of signals from S66 satellite 9-47573
 nonequilibrium operator applied to energy exchange between subsystems 9-23390
 ocean floor topography 9-45471
 oceanographic turbulence sampling interval choice 9-49426
 paleomagnetic data 9-49514
 phase shift analysis, use of τ -criterion, applic. to nucleon-nucleon scatt. 9-46047
 phase-shift analysis, use of τ -criterion 9-46046
 photon counting for optical tracking of satellite sampling technique of multi-coincidence method 9-38014
 plasma, turbulent, formulation of stat. theory 9-48546
 polar auroras, pre-IGY obs. 9-41569
 polymer chains with excluded vol. effects 9-36731
 probability distribution functions, reduced 9-45774
 radiative transport in finite homogeneous cylinders, Monte Carlo anal. 9-45801
 Raman lines intensities calc. by averaging method 9-32444
 random die problem 9-36151
 random motion of particle, Lagrangian formulation 9-27176
 rooms and structures, acoustic input power and response 9-25106
 Russian roulette technique applied to statistical simulation of radiative diffusion 9-22166
 sea surface, wavy, finite difference determ. of slopes 9-39997
 seismic refraction in continental margin, correl. analysis of data 9-45450
 smoothing, linear, of marine gravimeter obs. 9-37873
 sound transmission through partition, using statistical energy analysis 9-41825
 spectra, 2-quantum photocurrent 9-29389
 spectral component parameters determ. by processing of absorption curve 9-40578
 spectroscopic meas. interpretation, probability method and white noise assumption 9-36889
 steel, brittle fracture, model 9-35186
 structural phase factors, determ. using conditional probability laws 9-48819
 thermal detector dynamic properties, probability analysis 9-45873
 thermal neutron cross-sections, mean and variance calc. by picket fence model 9-27723
 time correlation func. of dynamical variable, statistical error due to finite time averaging 9-45782
 time interval distributions in neutron detection, stochastic operator method of calculating 9-27786
 two-phase random medium, variational bounds on bulk props. 9-43754
 viscosity coeffs. tensor determination 9-36746
²³⁵U/²³⁸U fission rates ratio in rod-cluster fuel elements, Monte Carlo calcs. 9-25661
 Ar, liq., Monte Carlo calc. of thermodynamic props. 9-39070
 DyAl garnet, antiferromag., Monte Carlo calc. rel. to interpret. of optical absorpt. spectrum 9-24408
 Fe-C alloy, microcrack formation 9-30694
 Fe-III atom and ions up to 15000°K, sums and distribution over electron states 9-38751

Statistical mechanics

- see also Lattices, theory and statistics; Quantum fluids*
 anharmonic oscillators, coupled, 2D, approach to thermal equilb., computer studies 9-31777
 arbitrary shape particles, scale particle theory 9-41783
 automorphism groups induced on lattices by interactions 9-45775
 Bogoliubov inequality used to determ. depend. of free energy 9-31786
 Boltzmann's gas model, ergodicity 9-22145
 Boltzmann's H function convexity 9-47766
 Boltzmann collision integral approx. representation by Fock-Planck type operator 9-36148
 Boltzmann distrib., partition function development, exchange corrections 9-22115
 Boltzmann distrib., partition function development formula for $\ln Z$ 9-22116
 Boltzmann eqn., approx. methods of soln. 9-47764
 Boltzmann eqn., inelastic scatt. prob. and collision freq. determ., slightly ionized gas 9-22150
 Boltzmann eqn. asymptotic soln. for Maxwellian molecules 9-32731
 Boltzmann equation solution methods review 9-47765
 Boltzmann eqs, BBGKY hierarchy structure 9-22142
 Boltzmann transfer eqn. to derive response of Lorentz gas to a.c. pulse 9-44437
 Born approximation validity considered using a non-Markoffian master eqn. 9-38242
 broken symm. and decay of order in restricted dimensionality 9-43764

Statistical mechanics continued

- canonical distribution and Archimedes principle 9-27178
 Casimir-Onsager reciprocal relations, phenomenological derivation 9-43761
 classical fluid, single-particle distrib. function derived from relaxation-fluctuation theory 9-31778
 classical perturbation theory, all order invariants determ. by averaging method 9-36139
 continuum gas, thermodynamic and distrib. functions, analytic and clustering props. 9-22112
 correlation functions in non-homogeneous charged region of electrolytic ions 9-22140
 covariant, relativistic four vector 9-22134
 critical exponents, renormalization by hidden variables 9-36144
 critical phenomena, dynamic, scaling laws 9-22127
 Debye-Waller type thermal averages evaluation method 9-38248
 density matrix, low temp. expansion for systems described by a potential 9-31779
 diffusion in mixed dense fluids 9-30167
 dimensional analysis problems, systematic determ. of no. of independent values 9-43758
 dislocations with jogs in cubic crystal, distribution functions 9-32961
 distribution functions representation by functional integrals 9-38249
 Dzyaloshinsky-Moriya ferromagnet, stat. model w.r.t single cryst. 9-33448
 electro energy distribution in moving slightly ionized gas 9-48615
 entropy differences between ideal and non-ideal systems 9-41780
 entropy of crystallized solid of long chain mols. 9-22139
 entropy throughout the domain of kinetic equations 9-43762
 equation of state of Gaussian mols. 9-29218
 equilibrium, textbook dealing with the master eqn. and partition functions 9-40252
 F model, low-temp. series 9-41778
 field theory classically with special reference to e.m. fields 9-38203
 fluid with square-well potential, radial distrib. function 9-42473
 gas of hard rods, one-dimens., zeros of grand partition function, Yang-Lee distrib. 9-34052
 gas of long thin rods, two-dimensional 9-34828
 gaseous suspensions; dynamic and spectral eqns. 9-36902
 Gibb's entropy law validity in strongly coupled systems 9-38251
 hard sphere cell model, cryst. transform. 9-48925
 hard sphere infinite system, variational principle for equilibrium 9-29213
 hard-disk fluid, radial distrib. functions and eqn. of state 9-30168
 hard-sphere distrib. functions and augmented van der Waals theory 9-31794
 hard-sphere gas, relax. times from eigenvalues applic. calc. 9-43767
 harmonic oscillator damped, applic. of Markoffian theories, non-Markoffian master eqn. 9-38243
 Heisenberg model, finite 9-34038
 Heisenberg model, general spin anisotropic, high temp. series expansion 9-47770
 Hermite reciprocity law and ang. mom. states, equivalent particle configurations, boson and fermion state reln. 9-36143
 hydrodynamics and time-correlation functions 9-34055
 imperfect gases, cluster theory 9-32728
 irreversible, most probable path 9-47774
 Ising model, 3D, 2D point array 9-36142
 Ising model, Bogoliubov inequality applic. 9-25047
 Ising model, generating functional and Green's function hierarchy 9-41774
 Ising model, Green's function approach 9-35540
 Ising model, thermodynamic quantities, self-consistent field near critical pt. 9-39758
 Ising model with general spin and phase transition, theorems 9-22114
 Ising model with long-range interac., expansion of free energy per spin 9-25045
 Ising system dynamic behaviour 9-47234
 keratins, α - β transformation 9-36730
 kinetic eqn. derivation, quasi-particles and entropy 9-22143
 Kirkwood instability for hard rods 9-29219
 Kondo problem, equivalence to a classical one-dimensional Coulomb gas 9-41782
 Kramers eqn., exact time-depend. analysis 9-43768
 laser signal, single mode gas, model 9-43878
 lattice gas, thermodynamic and distrib. functions, analytic and clustering props. 9-22112
 lattice gas, zeros of great canonical distrib. functions 9-40246
 lattices, new approximation method 9-31775
 Lennard-Jones fluid, hypernetted-chain approx. 9-29209
 linear mols., hard-core model 9-27942
 linear system with nearest-neighbour interactions, mean first passage time 9-41779
 linear systems of interacting molecules, decay of pair correlation functions 9-34700
 linearly associated system with random elements, thermal props. 9-22138
 Liouville equation eigenvalues, one dimens. system 9-22153
 liquid, orientational correlations and depolarization of scattered light 9-23499
 liquid transport proc., approximate theories and models 9-26079
 Lorentz gas diffusion coeff. density expansion 9-22165
 macromolecules, quantum mechanical particle path interpretation of chain config. 9-42458
 many particle systems, near equilb., described by Hartree-Fock approx. 9-38252
 Master eqn. derivation, macroscopic observables characterization 9-22108
 master equation, non-Markoffian, used to examine the validity of the Born approximation 9-38242
 material state at up to 10^{17} atm. and 10^8 °K 9-25052
 Mayer's graphical expansions, estimation methods 9-22130
 Mayer's graphical expansions, estimation methods 9-22131
 melting 9-30451
 metastable states decay rate calc. 9-47773
 molecular collisions which bring equilb. closer also increase available phase space, teaching paper 9-45777
 molecules, diatomic partition function calc., comparative study 9-44311
 movement theorem for resonance line shapes arising from decoupled Green's function eqns. 9-34034
 n-particle phase space in terms of invariant momentum transfers 9-22149

Statistical mechanics continued

- non-equilib., kinetic equations deriv. using projection techniques, construction of new hierarchy 9-40250
 - non-equilib., kinetic equations on introducing outside fields, projection method 9-40251
 - non-equilibrium, thermodynamically- equivalent Hamiltonian calc. method 9-22144
 - nonconserved mutual exchange systems, kinetic eqn. soln. 9-38257
 - nonconserved mutual exchange systems kinetic eqn. 9-38256
 - one dimen., infinitely many particle system, time evolution of states 9-22147
 - Ornstein-Zernike systems, critical props. 9-45783
 - pair distribution function of classical fluids, interpolation of HNC and PY eqns. 9-32562
 - pair-correlation function, long-range 9-30166
 - particles in external pot. instead of box, theory 9-31780
 - particles mixture, equation of state based on canonical ensembles theory 9-39046
 - perturbation theory and critical phenomena 9-34036
 - perturbing body, parameter calc. using Monte Carlo and linear programming methods 9-43352
 - phase functions of systems, non-ergodicity 9-45784
 - phase space increase with equilibrium producing molecular collisions, teaching paper 9-45777
 - plasma, collective interactions between c.m. waves 9-30235
 - plasma, partially ionized, equilibrium composition calc., review 9-22141
 - plasma, Prigogine's master eqn., two kinds of infinities 9-44404
 - polar fluid, dynamical Langevin eqn. 9-42472
 - polymer excluded vol., Percus-Yevick type integral eqn. 9-32540
 - polymer solns., pairwise interactions of linear chains 9-32766
 - polymers, crossed-linked 9-34973
 - polymers, random-flight chains 9-38926
 - quasi-linear canonical transformation method applied to boson systems 9-43765
 - quasi-unitary algebras, attached to temperature states 9-22120
 - random matrix, with random bias, eigenvalue distrib. calc. 9-27184
 - of random systems, equilib. props. 9-22123
 - rubber elasticity, general random network bead-spring model 9-35144
 - scaling laws, microscopic foundation 9-36141
 - semigrand isobaric-isothermal ensemble distrib. functions 9-40247
 - Senffleben-Beenakker effects for rough sphere gas in a magnetic field 9-45798
 - single-particle distribution function in a high temp. plasma, relativistic corrections 9-25842
 - stellar systems, Lynden-Bell statistics, numerical expt. check 9-35975
 - stochastic types of motion in system of coupled harmonic oscillators 9-45789
 - surface layer at large distance, asymptotics of correlation functions 9-27185
 - system of harmonic oscillators, calc. of low-temperature limit 9-31779
 - system of interacting particles, mean number of occupations and thermodynamic functions 9-22121
 - system quantities, technique for transformation 9-43760
 - textbook, undergraduate level 9-40244
 - thermal noise, shot noise and fluctuating occupation numbers relationship 9-47881
 - thermodynamic prop. from equilb. statistics, high temp. expansion and error bounds 9-45778
 - thermodynamics, equivalence problem, stability conditions 9-31783
 - thermodynamics, statistical foundations 9-22133
 - thermodynamics existence for real matter with Coulomb forces 9-22132
 - thermodynamics of small systems, replacement free energy 9-27179
 - time correlations, equivalence of description methods 9-27182
 - violently agitated self gravitating systems, generalized statistical thermodynamics 9-41622
 - viral expansion treatment of physical adsorption 9-40847
 - Voltzmann eqn. elastic collision integral, conversion into differential form 9-45773
 - Walden, product rule for electrolytes, generalized 9-28808
 - water clusters in vapour phase, H-bond energy determ. 9-44616
 - Yvon-Born-Green hierarchy and its truncations, consistency 9-46432
- quantum**
- autocorrelation functions, one-particle momentum, study of their kinetic equations 9-38250
 - auxiliary variables w.r.t. variational principle for log. of partition function 9-22124
 - boson amplitude operators, ordered expansions 9-29211
 - boson field interac. with electr. states, model of energy transfer 9-39562
 - cluster expansion and N-body scatt. Faddeev type integral eqn. 9-22126
 - co-ordinate probabilities, calc. by Gibbs method 9-34042
 - configurational integral in separable Hilbert space, analyticity props. 9-22129
 - correlation functions and Green functions, zero-frequency anomalies 9-42987
 - correlations decay, relaxation of momentum correlations and distributions in harmonic oscillator chains 9-38246
 - coupling-parameter expansions convergence, distrib. and thermodynamic functions 9-27181
 - covariant equilibrium distribution of a system rel. to relativistic transformation of temperature 9-45780
 - crystal electron interacting system, optical and energy loss spectra, dynamical theory 9-37385
 - density matrix eqn. rel. to master eqn. 9-27175
 - density operator expansions, quasiprobability distrib. 9-29212
 - diatomic gas in contact with diatomic crystal, rel. to thermodynamic equilib. 9-32834
 - Ehrenfests' wind-tree model, normal and abnormal diffusion of particles 9-36138
 - equilibrium states of infinite systems at $T \neq 0$ 9-22137
 - ergodic, abstract mean, theorems applic. 9-36140
 - fluctuations far from equilb., theory 9-22135
 - Fokker-Planck eqn. discussed 9-34042
 - gas, moderately dense, quantum corrections to classical Enskog collisional transfer corrections 9-34834
 - gases, many-body T matrix, application 9-40257
 - gases, many-body T matrix, application 9-40256
 - ground-state wave function symmetry 9-34046
 - hard sphere gas at high temp., expression for quantum-mechanical free energy 9-45790
 - hard-sphere gas free energy eqn., high temp. 9-22128

Statistical mechanics continued

- quantum continued**
 - impurity resistance in quantum systems, two approaches 9-47777
 - infinite quantum lattice systems, ground state investigation 9-22119
 - Ising model, field-theoretic and functional- integral aspects 9-31776
 - Ising model, recurrence formulas for graphs 9-34037
 - kinetics, variational principle 9-25049
 - many-body phase-space integrals computation method 9-27180
 - many-particle system, response to quasistatic changes in vol., correl.-function expressions for viscosity coeff. and shear and bulk moduli 9-22148
 - many-state collision problem scatt. matrix. approx. formula and extension of B II approx. 9-32424
 - master equation in phase space formulation of quantum optics 9-31924
 - methane, solid; A and T nuclear spin systems mixture, phase transitions 9-35240
 - methanes, solid, theory of phase transitions 9-48933
 - momentum relax. time of Brownian particle 9-43756
 - nonequilibrium, axiomatic field theory for mutation 9-45779
 - one-dimensional XY model, exact time dependent analysis, Liouville eqn. 9-45785
 - one-particle propagator self-energy and virial coeff. in lorentz model 9-45781
 - operators, boson amplitude, ordered expansions 9-29211
 - operators, density, expansions and quasiprobability distrib. 9-29212
 - optical activity 9-48698
 - ordered and disordered systems, localization of electrons, bound bands 9-44879
 - paraparticles, quantum mechanics 9-31771
 - partition function invariance to operator similarity transformation, excitation and Einstein condensation 9-29215
 - phase-space distrib. generalized, relationships 9-22122
 - one photon interaction with matter, quantum statistics 9-29393
 - plasma, partially ionized, thermodynamic functions and Coloumb interaction 9-38957
 - plasma-radiation field quantum interaction 9-32598
 - polarization kinematics in nuclear reactions 9-36597
 - potential, quantum, possible equivalent statistical potential 9-29208
 - pseudo-oscillator, phase space representation 9-31781
 - saturation investig. of nonuniformly broadened lines, role of spectral diffusion and dipole-dipole reservoir 9-29349
 - semiconductors, effect of dislocations on band structure 9-33315
 - Sp_4 algebra, irreducible representations construction by para-boson operator 9-41781
 - spin, wave eqn. derived from classical concept 9-47757
 - spin systems, infinite vol., correl. functionals 9-22118
 - system of identical particles, lower bounds to ground-state energy 9-38247
 - system quantities, technique for transformation 9-43760
 - system with stochastic Hamiltonian and given initial state time evolution 9-22117
 - thermodynamics, harmonic oscillators infinite system 9-22136
 - variational principle for log. of partition function employing auxiliary variables 9-22124
 - waves in random media, averages of various props. 9-40249
 - Wiener integral for obtainings form suitable for Monte Carlo technique 9-25051
 - He, Lennard-Jones gas, quantum mechanical second virial coeff. 9-39049
- Statistical thermodynamics** *see* *Statistical mechanics*
- Steady-state theory** *see* *Cosmology*
- Steam**
- air-steam convection currents, u.s. anemometer design 9-36794
 - condensation heat transfer in forced convection, effect of superheating 9-26162
 - conductivity, elec., high press. and temp., multiwire lead-in and meas. cell design 9-26038
 - dissociation, 1000-5000°K, 0.001-100b, thermodynamic functions 9-30458
 - equation of state for 0-800°C and 0-1000 bar 9-34831
 - fast breeder reactor initial conditions, optimal 9-36623
 - Prandtl number and thermal conductivity at one atmos. 9-28075
 - spectra of gas emission in i.r. region of excited mol. 9-38831
 - water heat transfer loop at Harwell, description 9-27242
- Sidel**
- adhesion of Al chemically vapour deposited coating 9-28376
 - aging rel. to weldability 9-30713
 - AlSi 304, 304L, 316 and 347, stress corrosion cracking 9-26355
 - austenite, orientation relationship between χ -phase and matrix 9-23951
 - austenite nucleation sites 9-26387
 - austenite retention, X-ray diff. determ. 9-23953
 - austenitic, creep, TiC particles plastic deform. and recrystn. 9-33045
 - austenitic, eff. of initial state on martensitic transformation under infl. of mag. field 9-23966
 - austenitic, H-charged, internal friction and embrittlement 9-33085
 - austenitic, irradi. and annealed, He bubbles obs. 9-33108
 - austenitic, stainless, swelling induced by fast reactor irradiation 9-28437
 - austenitic 1Kh18N9, structure and strength and hardness, effect of previous deformation. 9-33059
 - austenitic containing Al and Ti, soln.-treated, equil. precip. formed on ageing obs. 9-46949
 - austenitic stainless, fracture paths of stress corrosion cracks 9-39441
 - austenitic stainless, metastable, plastic behaviour 9-35178
 - austenitic stainless and EN25, strain hardening and softening by cycles of plastic deform. 9-23867
 - Bauschinger effect in quench-hardened spring steel, effect of tempering temperature 9-23885
 - beam, composite with concrete, partial interaction between elastically connected elements 9-26380
 - brittle cracking susceptibility, effects of residual stresses and strain ageing 9-39439
 - brittle fracture, statistical model 9-35186
 - brittle fracture with interaction between elastic crack and slip band, criterion 9-44779
 - brittleness, n irradi. induced, rel. to microstruct., theory 9-37261
 - carbon, brittleness caused by boron-rich phase precip. from superheated austenite 9-41042
 - carbon and low alloy cast, atmospheric corrosion 9-24580
 - carbonitrided, fatigue strength, effect of retained austenite 9-30688
 - carburized Cr-Mo, transform. features 9-41073
 - cast, fatigue crack propag., microfractographic investig. 9-33080

Steel continued

cast, fatigue fracture, effect of size distrib. of internal defects 9-35188
 castings, continuous, microstruct. and effects on mech. props. 9-39467
 cementite, specific heat, 2° to 20°K 9-24045
 cleavage strength, microstructure effects in C-Mn steels of varying comp. after austenizing, quenching and tempering 9-39432
 cold-rolled transformer, processes during final annealing 9-39455
 compacting from powder, popular article 9-48918
 composition, Seebeck effect determ. 9-37846
 contact, pot., stress induced shifts, obs. 9-43019
 corrosion, atmospheric, of carbon and low alloy cast steels 9-24580
 corrosion, low temp. aqueous, in mild steel under reactor irradiation 9-26826
 corrosion, u.s. influence 9-37829
 corrosion of precipitation-hardened low-C martensitic steel, tempering effects on anodic polarization 9-24578
 corrosion rate in various districts of Northern California 9-37830
 corrosion resistance of stainless steel, H₂SO₄ 9-24574
 crack initiation and propag. under sinusoidal loading, carbon steel, obs. 9-30695
 creep at 550° and 565°C 9-35177
 creep rupture, double notch, of 5Cr-0.5Mo steels 9-33046
 creep rupture of 347 stainless steel at high temp. 9-33064
 Crystal growth mechanism in struct. form. 9-48794
 cylinder, ductility under explosive loading cond., strain at fracture 9-30660
 diffusion of Cr in low C steel, mechanism 9-46849
 elastic-plastic deformation of plate with circular hole under cyclic loading 9-23886
 En 25 and En 32B, fatigue, push-pull low endurance, 20°C and 450°C 9-23859
 En 25 and En 32B, fatigue behaviour, uniaxial, and biaxial low-endurance, comparison 9-23858
 equilibrium diagrams for weld metals in Cr-Mn steels 9-23976
 fatigue, low-endurance, studies under cyclic torsion 9-23860
 fatigue, push-pull low endurance, 20°C and 450°C 9-23859
 fatigue behaviour, uniaxial and biaxial low-endurance, comparison of two specimens 9-23858
 fatigue crack propagation, effect of mean stress and material yield stress 9-30696
 fatigue crack propagation, effect of structure on rate 9-33092
 fatigue failure in high strength steel, fractographic investigation 9-33081
 fatigue fracture, hardening and softening obs. 9-30689
 fatigue limit, optimal tensile strength level for maximum limit in high-strength steel 9-33082
 fatigue limit and branch point, size effects, carbon steel 9-33078
 fatigue strength of induction hardened steel rel. to retained ferrite microstruct., obs. 9-26348
 fatigue strength rel. to hardness of Cr-Ni-Mo high C low alloy steel, obs. 9-26345
 fatigue strength rel. to stress waveform, 0.3% C steel obs. 9-26346
 fatigue tests in heat-treated 18% Ni-steel 9-30691
 fatigue tests in heat-treated 5%Cr-steel 9-28365
 ferrite-pearlite, ductile fracture resistance 9-46899
 fracture, brittle, with interaction between elastic crack and slip band 9-44779
 fracture, explosively produced spall, metallographic features in low C steel 9-26354
 fracture, neck-and-split tensile, of anisotropic plate steel 9-33065
 fracture, notch brittle, and dynamic strain aging 9-33114
 fracture toughness and crack propagation in 300M steel 9-33067
 fracture toughness of 0.36 wt.% C steel, instrumented Charpy impact test 9-28366
 fracture toughness rel. to precracked Charpy W/A in high-strength steels 9-35182
 freezing from plane chill, analytical solutions, exact and approx., comparison 9-39135
 frictional behaviour up to 500°C 9-41039
 frictional coeff. with ground basalt obs. at ultrahigh vacuum 9-37271
 H-11, vacuum-melted, prestraining and ageing effect on mech. props. 9-46904
 hardened ball-bearing, residual austenite determ. from u.s. sound vel. obs. 9-42911
 heat resistivity and mech. props., review 9-33179
 high strength, fatigue failure, fractographic investig. 9-33081
 high-pressure effects on microstructure and hardness 9-23967
 high-speed cutting, vol. and grain-boundary diffusion of W, role in carbide precip. kinetics 9-39383
 high-strength, fatigue limit, optimal tensile strength level for maximum limit 9-33082
 high-strength, fracture toughness and uniaxial tensile props. relationship 9-33060
 hot workability and plastic deform. props. 9-35174
 impurity redistribution, effect of heat treatment 9-23939
 inclusion anal. using colour X-ray images 9-48851
 inclusions, nonmetallic, effect on strength 9-48905
 Incoloy 800, He embrittlement, tensile strength obs. 9-35179
 isothermal and continuous cooling transform. diagrams in Cr-Mo steel 9-23968
 laser-irradiated, self-insulation in water against intense light 9-27343
 low C, explosively produced spall fractures, metallographic features 9-26354
 magnetostriction, effect of tensile stress 9-45156
 martensite, C-bearing, ageing kinetics 9-39462
 martensite, internally twinned, slip dislocations movement 9-42828
 martensite, low-C internally twinned, tempering character. 9-41052
 martensite, microtwins, electron microscope obs. 9-46744
 martensite, VC precip. during tempering, mechanism 9-33121
 martensite (225), habit plane line lengths comparison with austenite before transform. 9-42931
 martensite decomposition at low temp. 9-23964
 χ -martensite rel. to carbon content, X-ray diff. meas. 9-37294
 martensite transf., obs. using hot-stage X-ray diff. meas. 9-39495
 (225)-martensite transf., role of plastic accommodation 9-26383
 martensites, Co- and Cr-bearing, decomposition kinetics of martensite extracted by anodic dissolution from steels 9-37274
 martensitic, low-C, precip.-hardened, corrosion (anodic polarization meas.), tempering effects 9-24578
 martensitic wires, Mattencci effect 9-33454
 mechanical properties, effect of low temps. 9-23905

Steel continued

microanalysis, electron probe applic. 9-49398
 mild, containing 1 1/2%Cu, interface precip. 9-33055
 mild, corrosion rates in various districts of Northern California 9-37830
 mild, dynamic yield strength, mean, from strain meas. on 'mushroomed' ends of projectile 9-30662
 mild, electron beam floating zone melting 9-33109
 mild, fatigue crack propag., effect of corrosive environment and stress history 9-37262
 mild, low temp. aqueous corrosion under reactor irradiation 9-26826
 mild, oxidation in O₂/H₂O vapour mixtures at 950°C 9-33668
 mild, plastic deform., stress reduction on applic. of oscillatory energy 9-37286
 mild, surface-rolled, slip line and crack formation during fatigue, electron microscope obs. 9-35189
 mild, tube-bulge method to determ. stress-strain relns. 9-28338
 mild and low-alloy, oxidation in CO₂ based atmospheres 9-24558
 neutron radiation embrittlement, choice of parameter for meas. 9-35299
 neutron radiation embrittlement choice of parameter for meas. 9-24071
 nitrided, nature of hardness 9-23927
 nucleation of metallic and sulphide phases on high m.p. oxide precipitates within silicate inclusions 9-23954
 oscillatory wire drawing, reduced stress and friction 9-37286
 oxidation in CO₂ based atmospheres 9-24558
 oxidation in O₂/H₂O vapour mixtures at 950°C 9-33668
 oxide films <4 μ m, electron probe microanalysis method 9-24607
 passivity breakdown in borax soln. 9-24579
 pearlite, growth, alloying elements and press. effect 9-42930
 plastic deform. props. in rel. to hot workability 9-35174
 plate, anisotropic, neck-and-split tensile fracture 9-33065
 plate abnormal portions, non-destructive mag. detecting method 9-28589
 plate with circular hole, elastic-plastic deform. under cyclic loading 9-23886
 quenched, carbide phase formation during low-temp. tempering, mechanism 9-33137
 rail, fatigue crack propagation, effect of structure on rate 9-33092
 recrystallisation of ferrite in plastically deformed steel 9-37295
 shells, closed, response to blast of internal explosive charges 9-40279
 spring, quench-hardened, tempering temp. influence on Bauschinger effect 9-39391
 stainless, 304, electron microscope observations of interactions with liquid Na 9-28209
 stainless, 304, emittance at cryogenic temp., cyclic incident radiation technique 9-24064
 stainless, 304, interfacial free energies, electron microscopy 9-28297
 stainless, 304, interfacial free energies, electron microscopy 9-28298
 stainless, 304, residual surface stresses, meas. technique and results 9-33102
 stainless, austenitic, metastable, plastic behaviour 9-35178
 stainless, electron scatt. diagram modification due to defects 9-48845
 stainless, galvanic platinizing and passivity in H₂SO₄ 9-24574
 stainless, H adsorption and Ar exchange 9-39170
 stainless, in MgCl₂ soln., transgranular stress-corrosion cracking, interpret. 9-26349
 stainless, irradi., hot brittleness rel. to He-filled deform. defects 9-37260
 stainless, irradiated, fatigue behaviour, review 9-23861
 stainless, laser microprobe analysis, impurity emission rel. to matrix effects, obs. 9-24604
 stainless, sliding of graphite, interface geometry rel. to wear 9-41036
 stainless, stacking fault energies, intrinsic:extrinsic ratio 9-23821
 stainless, thermal conductivity 9-41098
 stainless, type 347, creep rupture at high temp. 9-33064
 stainless, type-304L, fuel element cladding, irradi., burst tests of strength 9-26339
 stainless, types 304 and 347, irradi., void volume fractions 9-48755
 stainless austenitic, magnetic contribution to low temp. specific heat 9-33171
 stainless-steel-polyethylene lap joints, yield strength 9-30734
 steel, stainless SUS 29, thermal fatigue cracks, 200-700°C 9-26353
 steel, transformer grade with S coated surface, secondary recrystn., role of surface energy 9-46917
 stress corrosion cracking susceptibility in chloride-containing high temp. water, effect of composition 9-26355
 stress/strain diagram rel. to stress rate in elastic range 9-41008
 stresses, residual, surface, of 304 stainless steel, meas. technique and results 9-33102
 structural recrystallization, effect of recrystallization phenomena in α -phase 9-33136
 structure and mech. props., effect of previous deform. of austenitic sample 9-33059
 surface-hardened, effective case depth, error probability 9-39442
 tempering medium carbon St.40 at 250-700°C, effect on dislocation redistribution, electron microscopy 9-40948
 thermal conductivity meas. 9-42975
 thermal fatigue cracks, 200-700°C 9-26353
 thermomechanically treated and quench-hardened, inherited strength character. obs. 9-46920
 transformer, annealed, dispersed inclusions, eff. on core losses 9-23802
 transformer, covered with Ni film, initial permeability, infl. of tensile stress 9-28618
 transformer, deformed, strain effects on coercive force and magnetostriction 9-45140
 transformer, magnetostriction, effect of tensile stress 9-45156
 unlubricated sliding with Cu surface, high speed 9-41038
 unlubricated surfaces, wear and friction variation 9-41037
 Widmanstätten ferrite form. 9-46947
 yielding, delayed related to strain rate as is immediate yield 9-39414
 As and Bi impurities determ. 9-28830
 C-Mn, cleavage strength, microstructure effects in various compositions after different heat treatments 9-39432
 C-Mn, quenched and tempered, fracture tests 9-30690
 0.36 wt.%C, fracture toughness, instrumented Charpy impact test 9-28366
 C, Mn-containing, determ. of N content 9-46940
 C, P and S presence, spectroscopic examination 9-47480
 C, u.s. wave velocities, elastic const. 9-35275
 C mag. fields effect on martensitic pt. location 9-46959
 C type, spectral analysis, vacuum photoelectric instruments 9-49396
 20 wt.%Cr-35 wt.%Ni, austenitic, creep-rate at low stress, and grain boundary sliding 9-48901

Steel continued

- (12 wt.%) Cr-Co-Mo, precip. obs. during tempering 9-42932
 Cr-Mn, equilib. diag. for weld metals 9-23976
 Cr-Mo, carburized, transform. features 9-41073
 Cr-Mo, isothermal and continuous cooling transform. diagrams 9-23968
 Cr-Ni-Nb, stainless, annealing of creep fracture damage for irradiated samples 9-39457
 Cr-Ni-Nb stainless, annealing of creep fracture damage, irradiated and unirradiated 9-39457
 (Cr,Fe),C, form. and identification in alloy steels 9-48831
 Cr, embrittlement by neutrons in α - γ phase transf. region 9-28369
 Cr, hardened, struct. obs. from sound vel. meas. 9-23755
 Cr, heat treated, shot-peening and Cr-plating effects on fatigue 9-28365
 Cr martensitic, strain and fracture behaviour under cyclic loading 9-23915
 Fe-C martensite crystal, diffuse electron scattering due to short-range order 9-32912
 Fe-Mn-C, austenite-martensite transform., charact., X-ray diff. obs. 9-46948
 Fe-Ni-C martensites, twinning during phase transf. in fine struct. obs. from electron micrograph 9-26233
 Fe-(2.0 wt.%)V-(0.2 wt.%)C alloy, carbide particle coarsening, field-ion study 9-33118
 Fe microcracks initiated by 17.8 kc/sec oscillations 9-35190
 MO, embrittlement by neutrons in α - γ phase transf. region 9-28369
 Mo, 18-8, stainless, castings, high temp. strength 9-44771
 Mo, quenched and tempered, B influence on carbide precip. 9-48931
 Ni maraging-steel, heat-treated, fatigue tests 9-30691
 Ni maraging, fatigue props., effect of shot peening 9-26315
 Pb and Sn impurities determ. 9-28830
 Si, {111}<211> texture, secondary recrystallization 9-46922
 Si, mechanical and magnetic after effects, infl. of H impurity 9-30644
 Si grain-oriented static and 60Hz domain structures, effect of longitud. tensile stress 9-45122
 V mild steel, precip. reactions and hardness changes during heat treatment 9-33138
 W steel, effective atomic numbers for gamma interacts. 100-662 keV 9-24230
 X40MnCr22 mag. susceptibility at 5°-1800°K 9-24330

Stellar atmospheres *see Stars***Stellar clusters** *see Stars***Stellar composition** *see Stars/composition***Stellar evolution** *see Stars/evolution***Stellar motion** *see Celestial mechanics; Stars***Stellar structure** *see Stars/structure***Stellarator** *see Plasma/devices***Stereoisomerism** *see Isomerism***Stereophonic sound** *see Acoustics***Steroscopy** *see Vision***Stimulated emission** *see Lasers; Luminescence; Masers***Stimulated Raman scattering** *see Lasers; Scattering/light, Raman spectra***Stochastic processes** *see Probability; Random processes; Statistical analysis***Stokes flow** *see Flow; Hydrodynamics***Stokes law, fluids** *see Flow; Viscosity***Stokes law, optical** *see Luminescence***Stokes lines** *see Luminescence; Scattering/light, Raman spectra; Spectral molecules***Stopping power** *see Energy loss of particles***Storage devices**

- film, permalloy, with ternary paramagnetic additions 9-36252
 holographic storage of three-dimens. meas. information, applics. 9-45971

Storage rings *see Particle accelerators/accessories***Storms** *see Atmosphere/movements; Magnetic storms; Thunderstorms***Strain effects** *see Deformation; Elastic deformation; Plastic deformation***Strain gauges**

- diaphragm pressure transducer 9-25024
 frictional type, assessment under static and dynamic strain conditions 9-47723
 Hopkinson split bar, strain gauge-quartz crystal instrumented 9-46876
 optical (coherent) processing techniques in strain detection 9-42873
 relaxation apparatus for use in radiation fields 9-46872
 rosette misalignment, errors in evaluation of stresses 9-28337
 special purpose long narrow foil gauge 9-47724
 thin film, with high gauge factor, and associated transducer design 9-46861

Strain hardening *see Work hardening***Strange particles**

- $\Delta \neq 0$ violation in weak interactions, avoidance 9-34260
 Regge pole model of strange vector and tensor meson exchange 9-32207
 spurion + baryon $\rightarrow \pi$ + baryon, model for P-wave decay of hyperons 9-46121
 K \bar{p} , 6 GeV/c, prod. of 3 strange particles with strangeness -1 9-36466
 Z*, strangeness +1 baryon, search for in $\pi\pi \rightarrow K^+Z^*$, 6, 8 GeV/c 9-22634

Strangeness *see Elementary particles; Field theory, quantum***Stratosphere** *see Atmosphere***Streamers** *see Discharges, electric***Strength** *see Electric strength; Mechanical strength***Stress analysis**

- see also Bending; Photoelasticity; Strain gauges; Torsion*
 aeolotropic shell, spherical stresses due to radial and rotatory vibs. 9-22230
 anisotropic materials in Hertzian contact, stresses due to indentation and sliding 9-41793
 assemblages, thin walled, consistent matrix formulation 9-45805
 bar, rectangular infinite, wave propag. 9-43783
 bar-mass system subjected to rectangular force pulse, approx. using spring mass 9-45819
 bending and membrane, elliptic hole in cylindrical shell, axial tension 9-31812
 bonded materials containing cuts on interface, thermal stresses 9-38289
 box girder, study of stress distrib. 9-36163
 buckling, local, of thin flat-walled structures combined shear and stress: stability function 9-36158

Stress analysis continued

- buckling, under arbitrary membrane loading, discrete element method applic. 9-38269
 cable, two-material, subjected longitudinally excitation waves 9-45843
 circular elastic cylinder, exponential decay of stresses for axisymmetric end loads 9-31826
 column under axial stochastic load, dynamic stability, Lyapunov-type anal. 9-22228
 compressed vessels, rotationally symmetric, on symmetric compression by two constant and opposite pressures 9-26063
 conducting plate in mag. field, critical pressure and stability 9-29224
 conical shell, shallow, with circular hole 9-22188
 in continuous isotropic medium 9-43775
 coplanar circular cracks in infinite solid under shear loading 9-47813
 crack problem, two-dimensional elasticity theory 9-29231
 crack propagation monitoring techniques for polycrystalline ceramics 9-33091
 crack running in quasi-brittle material, thermoelastic anal. at tip 9-33087
 cracks, penny shaped, dynamic intensity factor for axisymmetric loading 9-22201
 cracks and dislocation arrays in heterogeneous media, anti-plane strain behaviour 9-33090
 cylinders, elastic hollow finite, under axially symmetric deform. 9-31816
 cylindrical shell of varying wall thickness, under edge loading, influence coeffs. 9-25070
 cylindrical shell-core syst., elastic stress wave propag. and refl., transient response formulae 9-22191
 cylindrical shells, creep under combined lateral and axial press. 9-31805
 cylindrical thick stiffened shell, in-vacuo natural freq., strain distrib. at resonance 9-38272
 disc, finite, quasi-static thermal stresses due to instantaneous point heat source 9-31839
 disk subjected to many compressive concentrated radial loads on its periphery, photo-elastic investigation 9-31829
 dislocations, graphical representation of stress distrib. and forces acting 9-32967
 displacement, general theory, Lagrange function 9-31804
 elastic body, notch effects interference, approx. calc. 9-25072
 elastic body, semi-infinite, under step-wide conc. surface impact load 9-29227
 elastic continuum, doubly periodic array of material discontinuities, uniaxial loading, stress displacement fields 9-34073
 elastic Cosserat surface, static and dynamic solns. for finite deform 9-38280
 elastic cylinder, constrained, thermal expansion 9-37358
 elastic infinite medium, travelling load in cylindrical bore, response 9-34072
 elastic medium with stress couple, equil. problem, soln. in linear theory 9-25073
 elastic plate containing rigid rectangular inclusion, parametric study of complex variable method 9-25077
 elastic plate with two equal reinforced circular openings 9-25079
 elastic solid containing external elliptical crack, stress-intensity factors and pot. functions 9-33088
 elastic-plastic axisymmetric impact of circular plates 9-38271
 elastic-plastic continua with simple force dipole 9-25082
 elastic-plastic cylindrical shell under axial compression, instability, critical stress determ. 9-34071
 elastic-plastic structures, iterative soln. of incremental problem 9-31827
 elasto-plastic props. of circular bar under axial load and torque 9-36167
 elastostatic two-dimensional problems, equilibrium stress field model for finite elements 9-22207
 for elliptical vacuum chamber 9-47708
 errors due to misalignment of rosettes in strain gauges 9-28337
 fatigue strength rel. to stress waveform 9-26346
 fibres, viscous, tearing 9-33061
 film, evaporated dielectric, as optical coating 9-37231
 film, evaporated metal, as optical coating 9-37231
 fixed points method, applic. 9-34062
 flexible shell, concept of finite elements, rotations and small strains 9-31807
 flexure of flat plate, electrical analogue 9-27205
 fuel particle, pyrocarbon- and silicon carbide-coated, mathematical model 9-28340
 girders, continuous, critical axial load 9-34062
 glass, chemically strengthened, profile, rel. to strength and fracture behaviour 9-28336
 half-plane with edge crack, Wiener-Hopf technique, stress and displacements determ. 9-38281
 holes drilled at ends of crack, stress distribution 9-47801
 incompressible and near-incompressible material, assumed stress hybrid finite element method 9-41797
 infinite body with partially bonded circular cylindrical inclusion under longitudinal shear 9-45813
 infinite plate with circular hole subject to pressure by rivet, eff. of couple stresses on distribution 9-22194
 initial microstresses influence on polycrystals macroscopic strain 9-37237
 interference stress in half plane containing elastic disc, same material 9-31813
 inverse strain-rate effects 9-35169
 isotropic spherical bodies in Hertzian contact, stresses due to indentation and sliding 9-41793
 Kantorovich method, extended, for soln. of eigenvalue problems 9-41798
 limit, convergence theorems for minimal sequences 9-45828
 lower bounds on structural performances under cyclic loading and temp., use of elastic solns. 9-22210
 metals, b.c.c., f.c.c. and h.c.p., strain-hardening effects 9-37239
 metals, mech. oscillations effect on plastic behaviour 9-39419
 micro-elastic materials, uniqueness theorems in static and dynamical case 9-38278
 microthermoelastic materials, uniqueness theorems in coupled case 9-38278
 neutron irradi., low temp., of deformed specimens under tensile stress, sample carrier 9-29137
 normal and tangential forces on moving strip 9-29226
 Parallelepiped, compressed neo-Hookean rectangular, stability 9-25080
 penny shaped crack in elastic medium, response to plane harmonic shear wave 9-29228

Stress analysis continued

- photoelastic materials, principal stress directions, photographic display 9-31830
- plane deformation with uniform transverse stretch, soln. of deform. fields 9-31825
- plane with elliptical hole, stress and strain fields produced by heat source 9-25069
- plastic solids, failure criteria in space of stress invariants 9-39433
- plastic-elastic matrix, reinforced with elastic fibres, continuum model 9-31823
- plasticity, anisotropic, sheet metal axisymmetric plane stress, strain-hardening 9-34075
- plate, elastic, transient plane bending wave propag., three-dimensional methods applicability 9-45815
- plate, rectangular, symmetrical circular hole under tension, hoop stress 9-25067
- polyethylene, molten; stress function of rate of shear, teogoniometer design 9-39065
- polyethylene terephthalate, oriented drawn films, tensile and shear yield stress 9-30667
- polymers, liquid, properties, acoustic meas. 9-36835
- postbuckling behaviour and imperfection sensitivity, effect of nonlinear prebuckling state 9-25071
- pressure vessel, elliptical cross section, deforms. and stresses 9-31803
- principle stresses along sections of symmetry, separation using isopachic patterns 9-47800
- propellant, plastic yield stress determ. by simple test 9-23876
- quartz particles in whitewares, strain meas. by X-ray technique 9-23869
- radial, circumferential and axial for circular elastic rod ramp unloading 9-29230
- rectangular plate with circular perforations along 2 bonded edges, subject to restrained shrinkage 9-47811
- rectangular strips, end problem when narrow side under fractions and shearing forces 9-34063
- relaxation apparatus for use in radiation fields 9-46872
- residual surface stresses of 304 stainless steel, meas. technique and results 9-33102
- rigid-plastic circular plate, combined distributed loads and geometry changes 9-31831
- ring, compressed, elastic and plastic stress distrib., expt. determ. 9-25081
- rod, thin, elastic, rectang. stress pulse damping 9-27204
- rods, elastic, nonhomogeneous, longit. wave propag. 9-27223
- rubber, stress-temp. meas. at different strains in analysis of internal-energy contribs. to elastic stress 9-46860
- semi-infinite plate compressed with elastic flat punch, time depend. variation of stress distrib. 9-45811
- shallow circular arch, large deflection behaviour using Rayleigh-Ritz finite element method 9-31806
- shell, cylindrical circular, instability expt. 9-40264
- shell arches, lateral stability with tie rods 9-34061
- shells, creep buckling 9-31808
- shells, elastic cylindrical, load diffusion from axially loaded stiffeners 9-29229
- shells, two cylindrical, of equal diameter, at intersection 9-47808
- shells, two cylindrical intersecting normally and subject to internal pressure 9-31817
- shells and plates, three-dim. and two-dim., of transient waves, effective applic. regions 9-41801
- shock wave interaction due to combined two shear loadings 9-40278
- spheres, hollow and complete, residual stress meas. 9-31811
- spherical shells, homogeneous differential eqns. particular solns. 9-34060
- St. Venant flexure, narrow beams, including couple stresses 9-36164
- stability of heterogeneous orthotropic axially compressed cylindrical shells 9-38270
- steel, 304, stainless, residual surface stresses, meas. technique and results 9-33102
- stiffened cylinders with symmetrically distributed stringers, comp. program 9-22241
- strain meas. by opt. Differentiation of cross grating 9-25068
- stress redistribution time in creep in mechanical structures 9-22189
- stress-function space-time theory rel. to time-depend. and moment stresses expressions 9-45812
- structural systems, discrete, general theory for branching analysis 9-43774
- structural systems, discrete perfect and imperfect, branching analysis 9-31809
- structural systems, symmetric, with first and second order imperfections, buckling 9-27196
- thermal, in solid with external circular crack 9-45836
- thermal, inversion transformation soln., with variable heat transfer 9-25085
- thermal, of nuclear reactor cylindrical fuel element 9-25120
- thermal stress fields, interferometric determ. 9-29469
- thermal stress in long cylinder containing penny-shaped crack 9-38288
- thermoelastic stress distributors. near external crack of infinite solid 9-27211
- thermostructural, initial in two-dimensional medium with isotropic components 9-45817
- torsion, elastic-plastic, of hollow bars, by quadratic programming 9-36166
- transmission associated with subsurface characts. of Rayleigh waves 9-31844
- variational principle and convergence of finite-element method based on assumed stress distribution 9-40266
- vibrational strain effect on internal friction, calc. method 9-31810
- viscoelastic mats., numerical methods 9-27210
- viscoelastic media, relative deform. anal stress due to temp. changes 9-28334
- wave propagation, two-dimensional, in nonlinear media, development of computer program 9-41819
- waves in uniaxially prestressed plastic, viscoplastic unbounded media, harmonic dispersion analysis 9-31846
- wedge, elastic, mixed boundary conditions 9-47805
- Al-(11 wt.%)Mg age-hardening alloy, stress and stress-corrosion resistance, effect of deform. by hydrostatic extrusion 9-41051
- Al-Si subeutectic alloy, thermal stresses calc. by phase suspension model 9-23948
- Au-(46.1 at.%)Cd alloy, intrinsic resistive stress of twinning surface dislocations 9-35157

Stress analysis continued

- Cu-Co alloys containing coherent precipitates, critical resolved shear stress 9-44755
- Cu-Co alloys containing coherent particles, critical resolved shear stress 9-44756
- Cu whiskers, elastic and plastic behaviour below yield pt. 9-39407
- Fe, pure, lower yield stress, effect of grain size and strain rate 9-42881
- α -Fe, relaxation and use of Johnston-Gilman eqn. rel. to thermally activated flow 9-30672
- p-Ge, minority carrier mobility strain depend. 9-49105
- KCl deformed by indentation, strain bands decoration with F-centres 9-37242
- Mn-(11 at.%)Cu alloy, intrinsic resistive stress of twinning surface dislocations 9-35157
- Mn-(11 at.%)Cu alloy, intrinsic resistive stress of twinning surface dislocations 9-35157
- Mo, polycryst., ductile-brittle transition temp., strain rate depend. 9-30742
- Na liquid suspensions with high solid concentration, shear rate-shear stress characts. 9-23544
- Nb single cryst., dislocation interaction, temp. depend. of flow and function stress 9-39366
- NiFe, electrodeposited films 9-37234
- Si films with SiO₂ diffusion mask, X-ray topographic technique 9-26246
- Si single cryst. wafers, thermal stresses prod. by electron beam melting, source image distortion obs. 9-35164
- Sn epitaxial film, residual strains rel. to mismatch at interface 9-39160
- Stress effects**
- alkali halides deformation potential determ. from piezobirefringence meas. 9-24364
- alkali-halides, absorption of U₂-centres, effect of external stresses 9-49251
- armco iron, plastic flow stress, strain rate and temp. depend., 150° to 250°K 9-33044
- bar, infinite cylindrical, embedded in elastic medium, diffusion of axial load 9-41800
- α - brass, enhanced diffusion during cyclic straining 9-44732
- α - brass, stress-corrosion cracking in CuSO₄/(NH₄)₂SO₄ soln. 9-26352
- brass plate, cross-shaped, yield surface after prestraining or cold rolling, expt., study 9-26327
- I₈ quartet e.p.r. under uniaxial stress 9-39906
- carbonaceous materials, laser-induced stress waves, homogenization and dispersion 9-48888
- ceramic/glass mats., two-phase, crack formation and strength 9-30677
- ceramics, porous, micromech. thermal stresses and stress resistance 9-48968
- collapse pressure of cylindrical nozzle intersecting conical pressure vessel 9-38285
- compressed vessels, rotationally symmetric, on symmetric compression by two constant and opposite pressures 9-26063
- cones, solid truncated, yielding under quasistatic and dynamic loading 9-22219
- coplanar circular cracks in infinite solid under shear loading 9-47813
- couple stresses eff. on distribution in infinite plate with circular hole subject to pressure by rivet 9-22194
- creep const. determ. from stress relaxation tests with inhomogeneous stress 9-35176
- creep rupture of 347 stainless steel at high temp. 9-33064
- crystals, elastic wave propag. and acoustical birefringence 9-30642
- in crystals, piezo-optical rotation and rel. to symmetry 9-47318
- current-induced, in solid cylindrical conductors 9-45837
- cyclic loading, crack growth in elasto-plastic bodies 9-39437
- cyclic loading of tube, thermal strains, incremental calc. 9-23893
- cylindrical body, dislocations, mean square stress for restricted random distrib. 9-48854
- diamond-type crystals, on optical critical-point structure 9-24395
- dislocation array, planar, in displacement depend. stress field, stress intensification at tip 9-32962
- dislocation velocities, depend. 9-44702
- dislocation velocity, periodic internal fields influence 9-39361
- displacement due to shear of pivot tubes with rectangular mouths 9-38942
- distribution in solids, effect of inclusions 9-42877
- elastic waves, effect of couple-stresses on diffraction by cylindrical discontinuities 9-41818
- elastic-plastic and rigid-plastic plates of arbitrary thickness and flat bars of arbitrary width, stability 9-47809
- elastic-plastic plates, impulsively loaded, bending waves 9-41796
- elastically anisotropic half-space, and deform. field 9-38282
- energy conversion, chemical to kinetic, by active stress 9-29318
- energy release by faulting 9-35779
- explosive, organic polycrystalline, strain-rate sensitive, compressive wave propag. behaviour 9-34049
- fatigue crack propagation under dynamic stress 9-44777
- fatigue cracks form, by rolling, effect of surface-active subst. on origin 9-46907
- Ferrovac E iron, strain ageing behaviour rel. to applied ageing stress and interstitial conc. in soln. 9-41050
- in f.e.l. and bipolar transistor, transducer applic. 9-49126
- fracture in bending, torsion and radial fluid pressure, interpret. 9-26350
- geological shock effect on remanent magnetism orientation and intensity 9-45569
- glass, sheet, internal friction under high stress 9-46868
- glass/ceramic mats., two-phase, crack formation strength 9-30677
- graphite, stress relax. at high temps. 9-46874
- graphite, stress relax. at high temps. 9-46873
- inverse strain-rate effects 9-35169
- in martensitic phase transitions mechanism 9-33134
- materials under inhomogeneous strain, amplitude-dependent internal friction, evaluation 9-35150
- metal, mode of unloading on residual lattice strains in plastic deformation 9-39410
- metal, oscillatory energy applic. in plastic deform. and stress reduction 9-37286
- metal shaping, alternating magnetic field applic. 9-41013
- metals, b.c.c., f.c.c., and h.c.p., strain-hardening effects, plastic deform. 9-37239
- metals, mech. oscillations effect on plastic behaviour 9-39419
- metals, reactive, effect on fatigue strength in welded joints 9-23902
- meteorite, Arizona fragment, applic. of Fe alloys shock load obs. 9-43636

Stress effects continued

- m.o.s.t. 9-26581
 Nimonic 80A, static and superimposed cyclic stresses, creep and fatigue behaviour 9-33048
 overstraining to reduce subsequent brittle failure risks 9-33070
 permalloy, rel. to Barkhausen and ΔE effects 9-45147
 permalloy thin film, effect of elastic stress on mag. props. 9-41322
 permeability, anomalous, induced by stress var. after weak-field demagnetization 9-31012
 plastics, degradation, environmental 9-26342
 plate, elastic, response to cyclic longit. force 9-29254
 polycapromide, cracks, submicroscopic, charact. features of growth 9-33097
 polycapromide, cracks, submicroscopic, formation under load 9-33096
 polycapromide, effect of mechanical load on chem. bonds, i.r. spectroscopy obs. 9-32829
 polycapromide, mechanical damage, accumulation under static load 9-33039
 polyethylene, high density, mechanical, rel. to ageing 9-46930
 polyethylene crystallites, applied stress eff. on mol. and textural orientation 9-30584
 polyethylene terephthalate effect of mechanical load on chem. bonds, i.r. spectroscopy obs. 9-32829
 polymer relaxation, treatment including co-operation in molecular motion 9-23189
 polymers, cracks, submicroscopic, charact. features of growth 9-33097
 polymethylmethacrylate, stress and strain softening in yielding under constant load 9-46887
 polypropylene, cracks, submicroscopic, charact. features of growth 9-33097
 polypropylene, cracks, submicroscopic, formation under load 9-33096
 polystyrene, mechanical damage, accumulation under static load 9-33039
 polyurethane, nonlinear viscoelastic, stress relax., torsion creep 9-31838
 polyvinyl butyral, cracks, submicroscopic, charact. features of growth 9-33097
 polyvinyl butyral, cracks, submicroscopic, formation under load 9-33096
 polyvinyl chloride, cracks, submicroscopic, charact. features of growth 9-33097
 polyvinyl chloride, cracks, submicroscopic, formation under load 9-33096
 polyvinyl chloride, stress-optical behaviour temp. dependence and effect of plasticizer content 9-47319
 precipitates, spherical, effect on coherency loss, theory 9-33133
 rock-salt type cryst., latent hardening due to interac. of dislocations 9-35191
 rubber, natural, induced crystn. in rapid stretching, obs. 9-28201
 Schottky barrier diodes, uniaxial stress, eff. 9-33344
 Schottky-Barrier diodes, Au-doped and γ -irrad. 9-24202
 si impurity-assisted intervalley electron scatt. under uniaxial compression, reson. linewidth broadening 9-35421
 Snock relax, internal stresses effect 9-44754
 solid contact area 9-28208
 stability of undistorted states of loaded body 9-22199
 steel, austenitic stainless, corrosion cracking susceptibility in chloride-containing high temp. water, effect of composition 9-26355
 steel, austenitic stainless, fracture paths of stress corrosion cracks 9-39441
 in steel, case hardened, repeated bending 9-42892
 steel, H-11, vacuum-melted, prestraining effect on mech. props. 9-46904
 steel, mean stress and yield stress effect on fatigue crack propagation 9-30696
 steel, nonmetallic inclusions, static and dynamic loading 9-48905
 steel, residual stresses and strain ageing effects on brittle cracking susceptibility 9-39439
 steel, Si, grain-oriented longit. tensile on static and 60Hz domain structures 9-45122
 steel, stainless, type 347, creep rupture at high temp. 9-33064
 steel, stainless, in $MgCl_2$ soln. transgranular stress-corrosion cracking, interpret. 9-26349
 steel, thermomech. treated and quench-hardened, inherited strength charact. obs. 9-46920
 steel, transformer, covered with Ni film, tensile stress effect on initial permeability 9-28618
 steel, transformer, deformed, rel. to coercive force and magnetostriction 9-45140
 steel, transformer, tensile, rel. to magnetostriction 9-45156
 steel cylinders, ductility under explosive loading conds. 9-30660
 steel plate with circular hole, elastic-plastic deform. under cyclic loading 9-23886
 stress-corrosion cracking, transgranular, interpret. 9-26349
 tangential, variable, on surface of water waves 9-32756
 uniform transverse strength, and plane deform., soln. of Ericksen's problem for deform. fields 9-31825
 vibrational strain effect on internal friction, calc. method 9-31810
 wires under axial tension, torsional stiffness 9-34059
 Zircaloy-2 tubes, fatigue stress rel. to neutron irradi. and hydride precip. 9-39435
 (36wt.%) Zn, stress-corrosion cracking, electrochem. factors 9-23920
 α -Ag-In dil. alloys, piezoeffectance 9-47325
 Ag-Zn equitatomic alloy $\beta \rightarrow \epsilon$ transform. 9-30737
 AgCl, latent hardening due to interac. of dislocations 9-35191
 Al(4wt.%)Cu, cyclic straining effect on transition precipitate structure formation 9-39490
 Al-Mg alloy, -induced knitting of dislocation networks with four-fold nodes 9-44706
 Al-Zn-Mg-Cu alloy, deformed, intergranular corrosion cracking, rel. to dislocation structure 9-23811
 Al, surface layer effect on fatigue resistance and brittle fracture 9-23880
 Al alloy cylinders, ductility under explosive loading conds. 9-30660
 Al alloys, corrosion cracking, stress conc. influence 9-44778
 Al alloys, stress-corrosion induced prop. changes, nondestructive eval. 9-26829
 Al fibres, mechanical damage, accumulation under static load 9-33039
 Al notched columns with fixed ends, failure under load 9-48906
 Al single cryst., cyclically strained, surface microrelief changes, diff. method obs. 9-46777
 Al supercond. thin films, strain effect on T_c 9-41177
 AlZnMg 1 alloy sheet, stress corrosion susceptibility 9-46779

Stress effects continued

- BaTiO₃, phase transitions in single crystals, influence of uniaxial compression 9-47169
 BaTiO₃, nonlinear properties of of single crystals under linear compression 9-39690
 C, glassy m strain role in promoting graphitization 9-23980
 C, graphitization, effect on dynamic elastic mod. and internal friction 9-26320
 CaF₂:Dy³⁺ γ quartet e.p.r. under uniaxial stress 9-39906
 Co-Ni alloy, martensitic transform. 9-26386
 Co-(30.5wt.%)Ni, allotropic transform. 9-23975
 Co-Pt equitatomic alloy, tensile, rel. to magnetostriction 9-45156
 Cu-(14.5 wt.%)Al-(3.5 at.%)Ni alloy with thermoelastic martensite, internal friction 9-42869
 Cu-Co alloys containing coherent precipitates, critical resolved shear stress 9-44755
 Cu-Co alloys containing coherent particles, critical resolved shear stress 9-44756
 Cu-Mn alloys, stress-corrosion cracking, electrochem. factors 9-23920
 Cu-(39.8wt.%) Zn alloy, effect of uniaxial tensile stress on precipitation 9-46939
 Cu, modulation of x-ray emission band due to alternating elastic strain 9-49303
 Cu, strain bursts, coarse slip and cyclic hardening 9-28357
 Cu alloys, transgranular stress-corrosion cracking, interpret. 9-26349
 Cu and alloys, stress cracking by liq. metals 9-48941
 Cu deformed single crystals, effect of strain-rate of mech. props. and dislocation substructure 9-41010
 Cu polycrystalline, effect of torsional prestrain 9-46877
 Cu single cryst., slip bursts during cyclic deform. 9-33052
 Fe-Ni-Al-Co-Ti, thermomech. treated, effect on mag. props. 9-47259
 Fe-Ni-Al-Ti, thermomech. treated, effect on mag. props. 9-47259
 Fe-Ni-Al alloys, elastic stresses effect on decomp. of supersaturated solid solns. 9-39475
 Fe-(0.6 wt.%)Si alloy, rel. to Barkhausen and ΔE effects 9-45147
 Fe-(3.7 wt.%)Si magnetic domain movements of mech. vibration 78° to 300°K 9-45157
 Fe-(3 wt.%)Si single crystals, effect of stress concentrations on crack nucleation 9-48911
 Fe, pure, lower yield stress, effect of grain size and strain rate 9-42881
 Fe alloys, shock load obs., applic. to Arizona meteorite fragments 9-43636
 Fe grain growth, strain induced 9-42788
 Fe magnetic domain boundary movements, of mech. vibration damping 78° to 300°K 9-45157
 Fe(40 at.%)Ni invar alloy, tensile, rel. to magnetostriction 9-45156
 Fe-(9.3 at. %)Mo alloy, ϵ -phase precip., superimposed deform. effect 9-39497
 Fe-(31.4at.%)Ni alloy, hydrostatic and shock-wave compressions, effect on magnetization 9-43176
 GaAs:Cu, uniaxial compression, rel. to structure of impurity centres 9-33231
 Ge, dislocation behaviour during thermocyclic treatment 9-37176
 p-Ge, minority carrier mobility strain depend. 9-49105
 Ge, piezoelectric spectra 9-35646
 Ge, strain-split energy bands 9-24187
 Ge on anisotropy of thermoelectric power 9-35496
 Ge impurity-assisted intervalley electron scatt. under uniaxial compression, reson. linewidth broadening 9-35421
 Ge junction, anisotropic deformations effect on characteristics 9-35440
 In supercond. thin films, strain effect on T_c 9-41177
 InSb, rel. to dislocation mobility 9-42833
 K, strain depend. of longit. magnetoresistance 9-35343
 KBr:Ti⁴⁺, dichroism, influence of uniaxial compressive stress 9-31075
 KCl:Ag⁺, uniaxial stress-induced dichroism in u.v. absorpt. bands, temp. depend. 9-45322
 KCl:Ti⁴⁺, dichroism, influence of uniaxial compressive stress 9-31075
 KCl deformed by indentation, strain bands decoration with F-centres 9-37242
 KI:Ti⁴⁺, dichroism, influence of uniaxial compressive stress 9-31075
 LiF, latent hardening due to interac. of dislocations 9-35191
 LiF single crystals, periodic and increasing, rel. to dislocation multiplication 9-40949
 Mg,Cd single crystal, critical resolved shear stress for basal slip, 77° to 500°K 9-33054
 MgO polycrystalline periclase, elastic parameters rel. to press. 9-42867
 Na, strain depend. of longit. magnetoresistance 9-35343
 NaCl:Cu⁺, uniaxial stress-induced dichroism in u.v. absorpt. bands, temp. depend. 9-45322
 NaCl, deformed, single cryst., dislocation density obs. 9-32974
 NaCl single crystal, rel. to bending, 300° to 1.4°K 9-33036
 Nb, strain-ageing effects rel. to dislocation atmosphere formation 9-28381
 Nb single cryst., dislocation interaction, temp. depend. of flow and function stress 9-39366
 Nb single crystal deformed at high strain rates, mech. props., dislocation sub-structure and density 9-48898
 Nb wire, superconducting, tension effect on magnetization curve 9-35532
 Ni-Cr alloy, strain behaviour, cumulative, under cyclic loading 9-23915
 Ni-(22 wt.%)Fe, thin films, infl. on coercive force 9-24316
 Ni-(17 wt.%)Fe alloy, coercive force, previous loading rate effect 9-47241
 Ni-Fe films, elastic, rel. to annealing in mag. field 9-33029
 Ni, dislocations, effect on thermoremanence 9-45016
 Ni, magnetic domain boundary movements, of mech. vibrations damping 78° to 300°K 9-45157
 Ni, rel. to Barkhausen and ΔE effects 9-45147
 Ni, tensile, rel. to magnetostriction 9-45156
 Ni strain-hardened by impulse loading, recovery behaviour 9-28348
 Sn epitaxial film, residual strains rel. to mismatch at interface 9-39160
 Sn supercond. thin films, strain effect on T_c 9-41177
 steel, martensitic Cr, strain behaviour, cumulative, under cyclic loading 9-23915
 Ta, diffusion of interstitial O, relax. eff. 9-28284
 Tb, magnetization changes rel. to micro-eddy currents, internal friction damping 9-26319
 Te, strain-induced electronic displacement rel. to cores, piezoelec. const. obs. 9-35493
 Ti(6 wt.%)Al-(4 wt.%)V, stress-corrosion cracking in anhydrous methanol 9-48894

Stress effects continued

- Ti-(8wt.%)Al-(1wt.%)Mo-(1wt.%)V alloy sheet, hog-salt-stress-corrosion cracking and effect on tensile props. 9-23923
 Ti, relaxation tests for thermally activated deformation parameters 9-28350
 Ti alloys, stress corrosion in methanolic soln. 9-23922
 U foils <2000 Å, preparation for electron microscopy rel. to stress corrosion cracking 9-23777
 V₃Si, structure transformation suppression rel. to change in critical current density 9-24162
 W, polycryst. cast, tensile and compressive yield stresses, temp. and pressurization effects 9-44757
 W micro-strain, temp. depend., and transition to macro-strain 9-23890
 Zn, critical shear stress, dislocation forest density depend. 9-46878
 Zn bicrystals, shear, rel. to grain-boundary slide-hardening 9-42889

Stress measurement *see Strain gauges***Stress/strain relations***see also Elastic constants*

- brass, annealed, propag. of large amplitude waves 9-42872
 α -brass, enhanced diffusion during cyclic straining 9-44732
 brass, stress rate depend. in elastic range 9-41008
 brass plate, cross-shaped, rel. to yield surface after prestraining 9-26327
 brittle materials, strain-energy and size effects in brittle materials 9-28367
 cement mortar, hardening obs. of stress-strain curves 9-37230
 circular rod in plane strain and with suddenly removed radial pressure 9-22216
 crystal system, rel. to orientation vector and scalar moduli 9-39403
 explosive, organic polycrystalline, strain-rate sensitive, compressive wave propag. behaviour 9-39409
 films, magnetic, strain sensitivity of wall coercive force, 200 Å to 1500 Å thickness 9-45163
 force-distance diagrams in forest-cut processes, critique of methods 9-30653
 graphite, EGCR-type AGOT, curves at room temp., 1000, 2000 and 4500°F 9-41009
 graphite, nuclear grade for space applics., constitutive eqns. 9-33057
 graphite single-crystal, direct basal-plane shear 9-46875
 Hastelloy N, irradi., fracture strain rel. to temp. and strain rate 9-41030
 metal, sheet, curves in tension, rel. to anisotropic plasticity 9-30657
 metal plastic deform., stress reduction on applic. of oscillatory energy 9-37286
 metals, true stress/true strain curve from hardness meas. 9-23865
 metals b.c.c., at low temp., theory 9-46924
 microstrain region, during hysteresis 9-23866
 molybdenum permalloy tape, stress sensitivity and mag. squareness ratio, effect of comp. and heat treatment 9-49205
 Nimonic 80A, creep and fracture rel. to static and superimposed cyclic stresses 9-33048
 nuclear fuel element cladding, cracked pellets expansion 9-22873
 plastic yield and reverse yield waves generated by impulsive e.m. radiation 9-45829
 polycarbonate craze, cyclic tensile testing 9-46879
 polychloroprene films, and i.r. dichroism rel. to crystallinity and orientation, obs. 9-30650
 polycrystalline solid, continuum stress-plastic strain relation 9-41805
 polyurethane, by photoviscoelastic analysis 9-35159
 rigid-viscoplastic strain hardening annular plate, impulsively loaded 9-22240
 rubber, SBR, fracture obs. -57°C and at different strain rates 9-35187
 rutile polycrystalline, pressure derivatives of elastic props. 9-39394
 steel, austenitic stainless and EN25, strain hardening and softening prod. by plastic deform. cycling 9-23867
 steel, cyclic strain hardening and softening at various strain ratios, rel. to fatigue damage 9-23860
 steel, martensitic Cr, strain and fracture behaviour under cyclic loading 9-23915
 steel, mean dynamic yield strength from strain meas. on 'mushroomed' ends of projectiles 9-30662
 steel, mild, delayed yield, relation to strain rate 9-39414
 steel, uniaxial and biaxial cyclical curves, comparison 9-23858
 steel, uniaxial strain cycling, 20°C and 450°C 9-23859
 steels, stress rate depend. in elastic range 9-41008
 strain rate equation applicability, back stress term inclusion for transient and steady-state validity 9-30656
 strain-rate sensitivity of flow stress for Peierls mechanism 9-39404
 stress-strain-strain rate, Hopkinson split bar adaption for meas. 9-46876
 tubular materials, tube-bulge method of determ. 9-28338
 yielding, serrated, rel. to initiation at high temp. 9-42874
 Zircaloy-4 tensile props. at low strain rates, in-pile, un- and post-irrad. obs. 9-37256
 Al, polycryst., in work hardening curve for tensile deform. 9-41014
 Al, strain hardening and softening prod. by plastic deform. cycling 9-23867
 Al alloy, cyclic strain hardening and softening at various strain ratios, rel. to fatigue damage 9-23860
 Al dynamic stress-strain release paths up to 200 kb 9-39405
 Al flow-stress relation to strain and strain-rate, drop-hammer test 9-39406
 Al stress rate depend. in elastic range 9-41008
 Al subject to tensile creep with stress variation 9-39422
 β AuZn, in plastic deformation, comp., temp., strain-rate and grain size dependence 9-23881
 Cu-Co single cryst. with precipitates, curves 9-39428
 Cu-W fibre-reinforced composite, curve 9-42875
 Cu, mean dynamic yield strength from strain meas. on 'mushroomed' ends of projectiles 9-30662
 Cu, parameters, effect of electroplated Cr coatings 9-26328
 Cu, strain hardening and softening prod. by plastic deform. cycling 9-23867
 Cu flow-stress relation to strain and strain-rate, drop-hammer test 9-39406
 Cu polycrystalline, effect of unidirectional or cyclic twist 9-46877
 Cu stress rate depend. in elastic range 9-41008
 Er, strain-rate sensitivity, and flow-stress temp. depend., 77 to 750°K 9-30663
 Fe, grey cast, 4-295°K 9-48893
 Fe, pure, lower yield stress, effect of grain size and strain rate 9-42881
 α -Fe, relaxation and use of Johnston-Gilman eqn. in analysis of thermally activated flow 9-30672

Stress/strain relations continued

- α -Fe, strain-rate sensitivity of flow stress, 0° to 900°C 9-30671
 Fe, strain rate behaviour in pure shear 9-42876
 Fe single crystals, produced by strain-anneal method, relation between stretching amount and preferred orientation 9-35163
 Fe single crystals deformed at -75°C, yield drop orientation dependance 9-33028
 Mg-Zn-Zr alloy, strain-rate hardening, grain-size depend. 9-39443
 Mg-Zr alloy, constant-load tests, creep curve anal. 9-30673
 Mg, dynamic stress-strain release paths up to 200 kb 9-39405
 Mn-(11 at.%)Cu alloy, relax. peak obs. w.r.t. twinning surface disloc. 9-35156
 Mo, polycryst., microstrain meas. of initial stages of plastic deform. 9-46891
 Ni-Cr alloy, strain and fracture behaviour under cyclic loading 9-23915
 Pb, work hardening and injected dislocation density determ. 9-41046
 SiO₂ quartz polycrystalline, pressure derivatives of elastic props. 9-39394
 W, yield stress, temp. and strain rate depend., effect of Rh additions 9-39415
 W micro-strain, temp. depend., and transition to macro-strain 9-23890

Stresses, internal

- alkali halide crystals, relax. rate, effect of dislocations 9-33026
 alloys, ordering strains, relief by twinning 9-35252
 autofrettaged cylinders, effect of time and temp. on residual stresses 9-33030
 back stress term inclusion in strain rate equation for transient and steady-state validity 9-30656
 effect on Bordoni peak width in internal friction 9-44753
 ceramic/glass mats., two phase, stresses around spheres and crack formation obs., strength meas. 9-30677
 ceramics, brittle, porous, thermal stress resist. and micromech. stresses 9-48968
 conical shell, shallow, with circular hole 9-22188
 crack, Griffith, with asymmetrically loaded surfaces, intensity factors 9-41792
 cylindrical shell-core syst., elastic stress wave propag. and refl., transient response formulae 9-22191
 disk subjected to many compressive concentrated radial loads on its periphery, photo-elastic investigation 9-31829
 rel. to dislocation distribution 9-42822
 effect on dislocation velocity 9-39361
 in dispersed barrier hardening temp. dependence analytical model 9-46818
 distribution, connection with slip lines 9-26335
 distribution in solids, effect of inclusions 9-42877
 elastic-plastic stress distrib. near crack tip effect on fatigue crack propag. nucleation theory 9-46909
 films, optical thin, production during deposition, mechanism and control 9-28341
 films, polycrystalline, relief mechanism 9-28339
 films, residual 9-37232
 films, thin, on Si substrates, Twyman-Green interferometry meas. 9-35165
 fuel particle, pyrocarbon- and silicon carbide-coated, mathematical model 9-28340
 glass/ceramic mats., two phase, stresses around spheres and crack formation obs., strength meas. 9-30677
 during hysteresis, in microstrain region 9-23866
 metal, residual lattice strains after deformation, effect of unloading 9-39410
 metals, residual stresses after deposition, combined effects with other factors on fatigue strength 9-39434
 methane, solid, h.p. stress gradient obs. at 77°K 9-26323
 microresidual stress-field around inclusions, meas. 9-26642
 Ni evaporated film intrinsic tensile stress meas., temp. depend. 9-37233
 in optical systems, due to differential expansion 9-36373
 optically-sensitive materials, effect of ultrasound, optical polarization obs. 9-46880
 polystyrene, effect of ultrasound, optical polarization obs. 9-46880
 rubber vulcanizates, relax., simple viscoelastic model 9-30645
 seismic, accumulation at depth, determ. 9-35773
 shell, perforated ribbed cylindrical, under internal pressure 9-41799
 rel. to Snoek relax. 9-44754
 spheres, hollow and complete, residual stress meas. 9-31811
 steel, residual stresses effect on brittle cracking susceptibility 9-39439
 superlattice B2, starting stress of glissile superdislocation 9-26282
 viscoelastic solids, u.s. meas. technique 9-37222
 waves in viscoelastic solid, thermodynamic influences 9-22221
 Zircaloy tubes, orientation of hydride precip. 9-39188
 Ag-(0.26 at.%)Cu alloy, oxidized at 250 or 300°C, stress relaxations from internal friction meas. 9-48885
 Al₂O₃ particles-Cu matrix interface, local shear stresses causing dislocation generation 9-30611
 Al alloys, corrosion cracking, stress conc. influence 9-44778
 Al evaporated film intrinsic tensile stress meas., temp. depend. 9-37233
 Au films, sputtered, stress relief rel. to hillock growth 9-42717
 Co electroless film on Si single crystal 9-30654
 Co hexagonal crystal magnetization and magnetostriction 9-37657
 Cu-Fe two-phase mats, microstresses rel. to plastic deform. 9-46881
 Cu evaporated film intrinsic tensile stress meas., temp. depend. 9-37233
 Ga₂Te₃ crystal with stoichiometric vacancies, local elastic stresses and solubility of impurities 9-40934
 Gd films, thermal stresses due to electron irradi., nucleation mechanism of twinning 9-35100
 In₂Te₃ crystal with stoichiometric vacancies, local elastic stresses and solubility of impurities 9-40934
 Mo, microstrain meas. of initial stages of plastic deform. 9-46891
 Ni, relaxation, 20-300°K 9-48891
 Ni electroless film on Si single crystal 9-30654
 Ni films, electrodeposited, lattice distortion effect on magnetocryst. anisotropy 9-39774
 Ni thin films, ultraclean, release of compressive intrinsic stress by gas adsorption 9-44758
 NiFe, electrodeposited films 9-37234
 Pt-(1 at.%)Co alloy with plastic strain, paramag. susceptibility, elec. resistivity and Mossbauer effect behaviour 9-43161
 Pt-(1 at.%)Fe alloy with plastic strain, paramag. susceptibility, elec. resistivity and Mossbauer effect behaviour 9-43161
 Si single cryst. wafers, thermal stresses prod. by electron beam melting, source image distortion obs. 9-35164

Stresses, internal continued

- SiO₂ particles-Cu matrix interface, local shear stresses causing dislocation generation 9-30611
W, polycryst. cast, tensile and compressive yield stresses, temp. and pressurization effects 9-44757

Striations *see Discharges, electric***Stripping reactions** *see Nuclear reactions and scattering***Stroboscopes**

- holograms, stroboscopic, using mode-locked laser 9-48059
rare earth orthoferrites, obs. of moving domain walls rel. to domain wall mobility 9-45233
ruby laser, partial giant pulse prod. 9-29425
selective design with adjustable period 9-29475
ultrasonic, variable freq. light modulator design 9-46012

Strong interactions *see Elementary particles/Interactions, strong; Field theory, quantum/Interactions, strong***Strontium**

- absorpt. oscillator strengths, 1400-1900 Å and 4000-4400 Å 9-32414
atomic spectrum, a bibliography 9-38765
atoms and ions, vaporization from SrO surface on W and Re 9-37637
B3 HD 37058 star abundance determ., Wrubel's curve of growth 9-33903
field emission through atoms adsorbed on W surface 9-24251
ion polarization via Penning collisions with optically pumped metastable He 9-38803
isotopes in porphyritic alkali basalt, disequilibrium and rel. to magmatic processes 9-31276
in NH₃, conc. >6 MPM, electrical conductivity meas., 200-300°K 9-23521
optical isotope shift, nucl. vol. and mass eff. 9-29988
in seawater, latit. 4° to 34°N in Atlantic, spectral obs. 9-45479
Sr²⁺, diffusion in AgCl, activation energy 9-46857
Sr²⁺ in KCl, effect on F-centre mobility, 540-700°K 9-40972
Sr²⁺ in NaCl, thermoluminesc. 9-37773
Sr⁹⁰, stratospheric residence time and interhemispheric mixing from fallout in rain 9-40041
Sr I, absorption spectrum, 1646-2028 Å 9-22965
Sr I, resonance line broadening by inert gases, effective cross-sections 9-48388
SrO₄B₂O₃·Sm₂O₃, photoluminescence and absorption, synthesized at diff. temp. 9-31155

Strontium compounds

- formate dihydrate, crystalline, Raman spectra 9-47378
In-SrTiO₃ junctions, surface pot. barrier and supercurrent flow obs. 9-49056
SnF₂-CaF₂:Nd³⁺, stimulated emission from Nd³⁺, luminescence of ⁴F_{3/2}→⁴I_{11/2} transition, 300°K 9-29426
(Sr,Bi_{1/2})MnO₃ solid solns., new ferroelec.-ferromag. material 9-47178
(Sr,Bi)MnO₃ solid solns., new ferroelec.-ferromag. material 9-47178
(Sr, Bi_{1/2})TiO₃-CaTiO₃ system solid solns., dielec. props. 9-41231
(Sr,Bi_{1/2})TiO₃ solid soln, u.s. wave absorption and velocity temp. depend. 9-41084
Sr_{0.5}Ba_{0.5}Nb₂O₆, ferroelec., spontaneous polarization, room-temp., pulsed-field method 9-35478
(Sr_{0.8}Ba_{0.2})₂Zn₂Fe₂O₄, hexagonal ferrite, magnetization curves rel. to critical fields 9-26657
(Sr_{0.8}Ba_{0.2})₂Zn₂F₁₂O₃₂, hexagonal ferrite, localization of Zn²⁺ ions, neutron scatt. meas. 9-42798
Sr₂DuSi₂O₇, akermanite analog, growth and X-ray obs. of distorted tetrahedra of Cu²⁺ 9-35010
Sr₂Fe₂O₇, antiferromag., mag. and cryst. struct., neutron diff. obs. 9-41341
α-Sr₂P₂O₇, crystal struct., in group Pnam 9-30573
Sr₂SiO₆-Ba₂SiO₄ system, fluorescence of Eu²⁺, depend. on composition 9-28717
Sr₂SiO₆-Ca₂SiO₄ system, fluorescence of Eu²⁺, depend. on composition 9-28717
Sr₂TiO₄, radioactive heat source material, thermal conductivity 9-26453
Sr₂(AsP₂)Cl₃, synthesis, unit cell dimensions 9-35664
Sr₂(VO₄)Cl₃, synthesis, and optical spectra with Mn-doping 9-35664
Sr₂Ba_{1-x}Nb₂O₆, ferroelectric, optical effect, temp. dependence 9-26710
Sr₂Ba_{1-x}Nb₂O₆, electro-elastic, elasto-optic matrix elements 9-33394
SrB₂O₆, III and IV high pressure phases, crystal data 9-39308
n-SrB₂ polycryst., conduction e.s.r. 9-37793
SrF₂:¹⁵¹Eu²⁺ hyperfine coupling const., temp. depend. 9-33496
SrF₂:Er³⁺, e.s.r., conc. depend. of site symmetry 9-24490
SrF₂:Er³⁺, quantum efficiencies and lifetimes 9-24453
SrF₂:Sm²⁺, fluoresc., temp. effects 9-41409
SrF₂:Tb³⁺,Yb³⁺, luminescence, quanta summation processes 9-45342
SrF₂:Tm²⁺ acoustical phonon tunable detector 9-26403
SrF₂:U³⁺ spin-lattice relaxation examined by paramagnetic resonance 9-35710
SrF₂:U neutron-irrad. single cryst., diffusion of Kr and Xe 9-35127
SrF₂, h.f.s. consts. of V_K and V_L centres, lattice vibr. influence 9-43274
SrF₂, hyperfine interactions of H atoms, temp. depend. 9-31060
SrF₂, M center, optical absorption 9-26292
SrF₂, photoreduction Nd³⁺→Nd²⁺ under stimulated emission conditions 9-31960
SrF₂, thermal ionization potentials of Nd²⁺, Dy²⁺, He²⁺ and Er²⁺ 9-46739
SrF₂, with and without H doping, X-ray prod. of centers 9-26293
SrF₂, cathode, photoelec. yield in vacuum u.v. 9-26616
SrF₂, diffusion of ⁸⁷Sr, study of cation defects 9-39382
SrF₂, neutron-irrad. single cryst., diffusion of Kr and Xe 9-35127
SrF₂, vapour, absorption spectra bands obs., ν₂ bending vib. assignment 9-23037
SrFe_{1-x}Cr_xO_{3-y}, perovskites, Mossbauer study and mag. behaviour 9-47336
SrFe₁₂O₁₉ single crystals M₁ and K₁ as functions of temp. from mag. meas. 9-47256
SrKNb₂O₆, ferroelec., spontaneous polarization, room-temp., pulsed-field method 9-35478
SrMnO₃, perovskite-like struct., phase transf. and stability relations at high press. 9-35241
SrMoO₄:Er³⁺ e.p.r. spectrum, second excited state of Er³⁺ centres 9-41424
Sr(NO₃)₂, photochromic, refractive index changes meas., coherent light illumination 9-26700
SrO, additive coloration, absorpt. band and F' centres obs. 9-44721

Strontium compounds continued

- SrO, elastic props. and lattice dynamics 9-48883
SrO, electrical conductivity, electric field effects 9-30833
SrO cathodoluminescence obs. 9-28731
SrO radioactive heat source material, thermal conductivity 9-26453
SrO surface on W and Re, vaporization of Sr atoms and ions 9-37637
Sr(OD)₂D₂O, i.r. absorpt. spectrum 9-33167
SrO(Sr_{1-x}La_xMn_{1/2}³⁺Mn_{1/2}⁴⁺O₃) layered structure, chemical and mag. study. 1.4°-300°K 9-45153
SrS:Cu, phosphoresc. decay curves and thermal glow curves, rel. to trap levels 9-35693
SrS:Cu,Zr, phosphoresc. decay and thermoluminesc. rel. to trap levels 9-35694
SrSO₄-BaSO₄ system, subsolidus phase relations and lattice constants 9-23949
SrTiO₃:Cr³⁺, optical line shift, dielectric-related 9-24415
SrTiO₃:Cr³⁺(Mn⁴⁺), absorpt. and fluorescence spectra 9-26743
SrTiO₃:Eu³⁺, impurity-lattice coupling to optical phonons 9-33166
SrTiO₃:Fe:Mo and Ni:Mo, photochromic, optical and EPR studies 9-26742
SrTiO₃:Nb, supercond. transition temp. obs. 9-49055
SrTiO₃:Zr, supercond., transitions from large to nearly- small polarons 9-47056
SrTiO₃-BaSnO₃-BaTiO₃ system solid solns., semiconducting props. 9-41192
SrTiO₃-BaTiO₃ solid soln., dielec. const. reversible depend. on field strength above Curie Point. 9-41239
SrTiO₃, antiferroelectric phase transition at 110°K rel. to normal vib. modes 9-24223
SrTiO₃, dielectric constant obs. of normal and reduced crystal at various temp. and various fields 9-30961
SrTiO₃, displacive-type ferroelec., dynamics of soft mode 9-41247
SrTiO₃, displacive-type ferroelec., sound attenuation near Curie point, anomalous behaviour 9-35277
SrTiO₃, e.s.r. studies of Fe³⁺ at Q band and 70GHz 9-45389
SrTiO₃, ferroelec., electron scatt. 9-37591
SrTiO₃, in one para., and two ferroelectric states simultaneously at 0°K 9-28566
SrTiO₃, O deficient, paramag. centres effect on supercond. transition temp. 9-37475
SrTiO₃, phase transition at 110°K, lattice-dynamical exam. 9-23986
SrTiO₃, polariton obs. by small-angle light scatt. 9-24429
SrTiO₃, pseudo-cubic, anomalous hypersonic absorpt. 9-37337
SrTiO₃, single crystals, dielec. const., loss tangent and conductivity, temp. depend. 9-39694
SrTiO₃, soft optical phonon, neutron scatt. obs. 9-35272
SrTiO₃, trapping phenomena, photoconductivity meas. 9-39725
SrTiO_{3-x}, soft-mode supercond. 9-33275
SrTiO₃, colour centres prod. by fields of 20 V/mm at 100-165°C 9-40976
SrTiO₃, degenerate semiconductor, review of exptl. data on superconductivity 9-41179
SrTiO₃, lattice parameters change near phase transform, at 108°K, meas. and obs. 9-30748
SrTiO₃, radioactive heat source material, thermal conductivity 9-26453
SrTiO₃, single cryst., elastic compliance temp. depend. 9-41000
SrTiO₃, single cryst., elastic compliance temp. depend. 9-40999
SrTiO₃, superconducting ceramic, Zr-doped, effective masses determ. 9-26532

Structure factors *see Crystal structure, atomic; X-ray crystallography***Structure of matter** *see Crystal structure; Liquids/structure; Solids/structure***SU(3) group theory** *see Elementary particles/symmetry; Field theory, quantum/Interactions, strong; Group theory***Sublimation**

- see also Heat of sublimation; Vaporization*
benzene, energy, molec. calc. 9-46691
benzene, energy, molec. calc. 9-44618
dehydration, heat and mass transfer mechanisms 9-28183
heatproof materials, thermal conductivity rel. temp. determ. 9-25122
of plate lying in a half-space 9-42701
rotating sphere in rarefied air, heat and mass transfer processes 9-23607
As crystal, (111) cleavage face pit growth at spiral dislocation site 9-30467
BiF₃, enthalpy and entropy, calc. from vapour pressures 9-30021
C, role in C-CO₂ interac., temp. >2000°K 9-28779
CdO single cryst., vel. temp. depend., optimum growth conditions derivation 9-34967
Sb crystal, (111) cleavage face, pit growth at spiral dislocation site 9-30467

Sudden commencement *see Magnetic storms***Suhl effect** *see Hall effect; Semiconductors***Sulphur**

- diffusion in liquid Fe at 1560°C 9-48691
epitaxial layers, C conc. obs. 9-46725
free radicals in ultramarines, e.p.r. investigation 9-36727
gas plane layer, radiant convective heat exchange with solid substrate 9-40750
K_{0.2} lines chem. shift in cpds. 9-37751
microdistribution in malleable cast irons during annealing 9-23950
molecular complexity in cryst., glassy and liq. phases, obs. 9-35675
molecule adsorbed on Ni, structure determ. by ion neutralization spectroscopy 9-32484
orthorhombic, energy distribution of electron and hole traps 9-37623
orthorhombic, optical props. in vacuum u.v. 9-37682
orthorhombic, X-ray K-absorpt. spectrum obs. 9-31120
plasma in capillary discharge, optical absorption for laser irradiation 9-42518
radiative Auger effect, simultaneous emission of X-ray photon and L-shell electron 9-40553
spark spectra in various gases, line intensities rel. to press. and Cu or graphite electrodes 9-36792
spectrographic analysis, combined action of thermochemical reagents and carriers, sublimization of MoO₃ 9-28831
thermal expansion between -170°-70°C for S₈ 9-39533
trace impurity in calcite, infl. on cleavage surface energy 9-30479
unstable-stable transition followed by paramagnetic resonance 9-30747
unstable forms prod. by condensation, studied by paramagnetic resonance 9-30746

Sulphur continued

- X-ray K-absorpt. in ZnS and CdS, zincblende and wurtzite structures, obs. 9-31121
 Ce-S solid solution, transition metal doped, thermal conductivity, temp. depend. 9-37368
 Fe-49 wt.%(Ni) alloys, commercial effect on initial permeability 9-49204
 S-Cu-Nb system, vapour growth of new single-crystalline phases 9-37007
 S₂, 0-0 band of system D-X Σ_g^- analysis of incompletely resolved struct. and head struct. 9-48479
 S₂, photoionization 9-44484
 S₂, impurity centre in KBr, luminesc., config. coord. curves 9-39869
 S₂, impurity centres in alkali halides, luminesc. spectra 9-39861
 S₂, Raman spectrum in KI 9-49294
 S₈, thermal expansion between -170°-70°C 9-39533
 S²⁻ X-ray K-absorpt. in CaS, obs. 9-24438
 α -S elastic and thermoelastic const. meas. 9-48882
 S I transition probabilities, near vacuum u.v., obs. 9-23366
 S II, level excitation by beam-foil technique 9-48402
³²S, C³²S₂-X³²S₂ system, rot. anal. 9-23070
³²S small-angle scatt. in C, BeO, Al₂O₃ thin foils 9-35298
³²S diffusion in Fe-C, C effect on mobility in grain boundaries 9-37203
 SIII, level excitation by beam-foil technique 9-48402

Sulphur compounds

- As-S glass/Al composite system, bonding mechanism 9-32852
 chalcogenides AY^{IV}C^{VI} with perovskite structure, synthesis 9-42755
 glasses, elec. conductivity and opt. absorpt. 9-30956
 metal sulphides, S K β_1 line shape meas., X-ray microprobe, curved quartz crystal spectrograph 9-25749
 pyrrhotites of Pierrefitte (Hautes-Pyrenees), thermochem. obs. 9-33657
 rubber-sulphur systems, comparison of viscoelastic and dielectric props. 9-33376
 sphalerites of Pierrefitte (Hautes-Pyrenees), thermochem. obs. 9-33657
 sulphate powders, Raman spectra, absolute scatt. coeffs. 9-49295
 sulphospinel, pressure induced polymorphism, pressure-temp. phase relations 9-26392
 sulphur selenide glass, mechanical strength 9-26341
 Ag₂S, thin films, struct. transforms compared with solid state 9-48927
 NPCl₂(NSOC)₂, crystal structure 9-39287
 S-As mixtures, mol. complexity in cryst., glassy and liq. phases, Raman obs. 9-35675
 S-Au neutron activation dosimetry in reactors 9-46141
 S-Se mixtures, mol. complexity in cryst., glassy and liq. phases, Raman obs. 9-35675
 S₂O₃²⁻ normal vibrations 9-27876
 S₆(NH)₂, crystal structure of the three isomers 9-39305
 SF₆, gas-phase electron reson. spectra 9-42416
 SF₆-C₂F₃Cl mixture for Q-switching of CO₂ laser 9-27319
 SF₆, continuous parametric amplifications of 10.6 μ signals from CO₂ laser 9-27340
 SF₆, cross saturation of 10.6 μ signals from CO₂ laser 9-28081
 SF₆, drift velocity of ions, time-of-flight meas. 9-42564
 SF₆, fine struct. of spectrum at 10.5 μ 9-46374
 SF₆, i.r. absorpt. saturation rel. to press. and added buffer gases 9-48480
 SF₆, narrow reson. in Doppler line of rot.-vibr. transitions of ν_3 band by CO₂-laser emission method 9-46375
 SF₆, ν_3 and ν_4 bands 9-36462
 SF₆, Raman spectrum in solid, splitting of three fundamentals 9-30053
 SF₆+HCl→F₂Cl+(SF₅H), 0.3 eV obs. 9-46430
 SF₆ dissociation in Ar, shock-tube expts. 9-38923
 SF₆ gas, transmission of coherent optical pulses 9-46574
 SF₆ mol. vibr. induced by CO₂ laser rad. absorpt. 9-25750
 SF₆ scavenger for electron scatt. on He 9-29982
 SF₆+HCOO→SF₅•+(HCOOF) 9-46430
 SH, interstellar, search for 111-MHz lines 9-49562
 SO, polymeric, potential energy calc. Van der Waals interac. 9-46736
 SO₂, chemiluminesc. afterglow, temp. depend. 9-43323
 SO₂, dimethyl ether, methyl chloride, binary and ternary mixtures, thermal conductivity and viscosity 9-36817
 SO₂, microwave spectrum in doubly excited vibrational states and γ constants determ. 9-32485
 SO₂, sorption and interact. on active C, 50 to 650°C 9-26806
 SO₂ in aq. soln., e.p.r. linewidth depend on temp., viscosity 9-30054
 SO₂ adsorbed on synthetic Linde type A zeolite, dielec. props. 9-41233
 SO₂ in inert gas matrix, i.r. spectra and geometry 9-34641
 SO₂ isotopes in solid Kr matrices, i.r. spectra and geometry 9-42417
 SO₂ mol., three electronic transitions, 1340-1190 Å region, vibr. analysis 9-30058
 SO₃[•] radical, CNDO-MO calc. 9-44326
 SO₃²⁻, non-linear polarizabilities 9-35611
 SO₃²⁻ in KCl cryst., i.r. absorpt. spectra of ion vibrs. 9-41382
 SO spectrum β^2 -X³²S₂ and A¹IT-X³²S₂-band systems 9-38870
 SPFs, vibrational assignment using normal co-ordinate calcs. 9-30055
 SR₆, population inversion, adiabatic, obs. from laser chirped pulses transmission 9-44341
 SiC cryst., prod. by vapour transport react. 9-28231
 So₄[•] concentration in Antarctic ice, obs. 9-33729

Sum rules see *Elementary particles/theory*

Sun

see also *Sunsports*

- 1967, activity in photosphere, (1967) 9-31651
 'seeing', meas. in solar observation instruments 9-36038
 abundances, and Si burning 9-49549
 active region, statistics 9-24921
 activity, correlational-spectral analysis of periodicity 9-41704
 activity, effect on atmospheric circulation 9-31300
 activity, MHD explanation 9-31658
 activity, rel. to 11-year modulation of cosmic rays 9-31647
 activity, solar and geophysical (Feb. 1965 and March 1966) 9-41703
 activity during 1967, obs. 9-24919
 activity rel. to ionospheric r.f. absorpt. freq. depend. 9-28941
 angular momentum loss due to solar wind, effect of finite elec. cond. 9-38095
 arch filament systems, prod. and motions 9-41702
 atmosphere, Bilderberg model, modification improves representation of obs. 9-31665
 atmosphere, dynamical problems 9-38120
 atmosphere, non-divergent oscillation 9-36071
 atmosphere, simplified model 9-31666
 atmosphere, theories, initial-value methods for integral equations 9-27106

Sun continued

- atmosphere, vortex motion of ions, mag. field due to vortices 9-24914
 atmospheric oscillations, 5-minute 9-31661
 chromosphere, flares and phenomena in upper layer of active region 9-41710
 chromosphere, model construction from emission lines in non-coherent scatt. 9-24928
 chromosphere, non-uniform model, line profiles of H α , H and K lines of Ca II 9-36070
 chromosphere, short period pulsations in mag. field 9-31663
 chromosphere temp. rise due to dominance of H γ opacity 9-40135
 chromosphere transport coefficients, thermal conductivity 9-29097
 chromospheric plagues, calcium, decay curves 9-31652
 chromospheric spicules, mechanism of formation 9-31662
 composition, H, He, C, from electron thermal conductivity 9-43534
 Culgoora solar observatory, optical programme 9-36030
 cycle, eleven year, possible relation with null neutrino flux 9-41699
 cycle of 2600 years, from glaciation data since fifth century BC 9-26884
 disc brightness temp. distrib., May 20 1966 partial eclipse, 3.1 cm 9-33948
 equatorial zone of avoidance, effect on interplanetary mag. field and cosmic ray distribution 9-35920
 evolution, eff. of Brans-Dicke theory 9-29080
 filaments, Kippenhahn-Schluter model, stability analysis 9-43670
 fusion catalysis by quarks without neutrino prod., as energy output source 9-45677
 granulation, effect of finite resolution 9-36062
 granulation, morphological study 9-36061
 granulation, review of early photographic observations 9-27101
 Hubble constant and motion w.r.t. galaxies 9-43653
 image on airborne ice crystals 9-33775
 interior, rot. ang. momentum w.r.t. oblateness 9-43655
 ionosphere conductivity variations near dip equator (Nov., 1966) 9-24690
 limb, freq. analysis of image motion 0.5 to 50 Hz 9-36031
 MHD gravity coupled waves in solar atmosphere 9-27107
 motion w.r.t. galaxies, and kinematics of local supercluster 9-33896
 Mount Wilson and Palomar observatory, solar research, apparatus 9-31484
 Oblateness, determ. from radar and optical observations of Icarus 9-31604
 oblateness, max., from secular stability of differential rot. 9-40183
 oblateness, theor. upper bound 9-43655
 observatory, high altitude, at Boulder, Co., USA 9-36074
 periodic activity due to tidal forces created by planets 9-36033
 photography in extreme u.v., pin hole camera instrumentation on rockets and results 9-43654
 photosphere, elec. cond. calcs. using precise electron-neutron interaction cross section value 9-24916
 photosphere, granulation models 9-41701
 photosphere, neutral atomic O, abundance and local thermodynamic equilibrium 9-24917
 photosphere and low chromosphere, Bilderberg model 9-31655
 photosphere mol. conc., dissociation equilibrium 9-31654
 photospheric paths in granular material between spot groups 9-36060
 plasmasphere map of chromosphere and spots 9-29098
 quiet and active, research development, review 9-40185
 rare earths abundances 9-41687
 rotation, differential, origin 9-24897
 rotation, twice yearly Doppler compensator meas., 1966-8 9-31625
 size influence on sky light distribution 9-33773
 solar activity, magnetohydrodynamic mechanism 9-49592
 solar physics at Arcetri Astrophysical Observatory 9-40184
 solar-terrestrial environment, conference 9-29096
 solar-terrestrial relations, historical survey 9-38107
 surface oblateness, model atm. calc. rel. to difference between polar and equatorial flux 9-41688
 surges, Jul. 1957 to Dec. 1967, statistical props. 9-38116
 temperature determ. from obs. on γ flux, review 9-38029
 turbulent diffusion explanation of surdace Li depletion and neutrino discrepancy 9-36029
 velocity map, obtained directly in one spectroheliogram 9-36032
 Weissenau solar observatory, apparatus 9-31678
 X-ray and extreme u.v. bursts from flares, effect on ionos. sudden freq. deviations 9-43438
 CO layer, thickness deduced from spectrum 9-31627
 He abundance, rel. to ν detection by ³⁷Cl(ν ,e⁻)³⁷Ar 9-45682
 Li depletion at surface, turbulent diffusion explanation 9-36029
 O lines photosphere center-to-limb analysis 9-31656

corona

- composition of lower corona, trends due to mixing and diffusion 9-36072
 delay, fluctuation and 'smearing' effects on pulsar signals 9-31576
 dielectronic recombination, effects of electron and radiation density 9-42567
 electron density in condensation estimated from variation in S-component of radio emission 9-36054
 electron plasma waves, e.m. radiation 9-30239
 electron temp. calc. 1-1.5 $\times 10^6$ K 9-36044
 emission line photographs, image quality improvement 9-41711
 enhancement in extreme u.v. 9-43680
 gas, transport coefficients, thermal conductivity 9-29097
 in geomagnetic activity forecasting, method 9-24704
 geomagnetic storms rel. to corona activity 9-47592
 green and red lines, polar., 1965-66 eclipses data, interpretation 9-43678
 heating, as result of Landau damping of ion-acoustic waves 9-36073
 in i.r. region 9-43679
 lower, composition, trends due to mixing and diffusion 9-36072
 A5303 emission regions, A5303, physical properties 9-29099
 A5303 emission regions, physical properties 9-29099
 magnetic field calc. from variations in the growth of type III radiobursts 9-31639
 nonspherical shape, effect on interplanetary mag. field and cosmic ray distribution 9-35920
 occultation of radio sources by the sun, refraction and scatt due to corona 9-31564
 phenomena accompanying flares 9-38119
 physical processes, radar exploration 9-38121
 polar rays exam. for pole positions, during 1961, 1966 eclipses 9-27093
 prediction compared with photographic obs. for eclipse of Sept. 22, 1968 9-43681

Sun continued**corona continued**

- radio echoes from active regions 9-38121
- recombination spectra of highly charged ions, failure to obs. at 5 cm 9-31667
- red and green lines, polar., 1965-66 eclipses data, interpretation 9-43678
- shock wave propag, magnetogas dynamics 9-32723
- spectral obs. for cm wavelengths during eclipse meas. 9-27108
- streamers, 'open' configs. 9-24929
- structure at eclipse of Sept 22, 1968, prediction compared with obs. 9-43682
- structure prediction in eclipse of Sept. 1968 9-40186
- super-corona and solar plasma, review 9-45686
- white light, brightness variations (1964-67) 9-38122
- Ca XV laboratory obs. of fine structure confirms presence 9-31628
- Fe XII emission lines, relative intensity as function of temp. and electron density 9-43683

eclipses

- 1965-66, polar. in green and red coronal lines obs. 9-43678
- 1966, May 20, obs. of X-ray emission sources 9-36035
- 1966, May 20, partial, measurements 9-29104
- 1966, May 20, radio observation 9-36034
- 1966, November 12, photoelectric obs. of continuum at the extreme solar limb 9-43656
- 1968, Sept. 22, Siberian observations 9-29082
- 1968, Sept. 22, corona prediction compared with photographer obs. 9-43681
- 1968, Sept. 22, coronal struct., prediction compared with obs. 9-43682
- 1968, Sept. 22, coronal structure prediction 9-40186
- ancient records, reliability 9-29081
- effect on equatorial electrojet in Pacific, N-S cross section 9-37960
- effect on geomagnetic field near dip equator, (Nov., 1966) 9-35916
- ionospheric E-layer variations explained by quasi-equilibrium between electron density and soft X-rays emission on sun 9-24898
- observation from aircraft 9-45687
- observations and influence on ionosphere theory 9-47570
- pole positions from corona ray exam., (1961, 1966) 9-27093
- total (1968), effect on long path v.l.f. transmissions 9-37975

flares

- 1966, Sep. 2, chromospheric, by spectroscopic obs. 9-41709
- active longitudes 9-36063
- activity during March and April 1968, radio obs. 9-24923
- activity forecasting, review of methods 9-41708
- bursts, microwave and hard X-ray, theory 9-43676
- chromospheric, phenomena in upper layer of active region 9-41710
- coronal and prominence accompaniments 9-38119
- cosmic particles of energy below geomagnetic threshold, and heavy nuclei, Kosmos 19 and Kosmos 25 obs. 9-38101
- cosmic ray effects of small flares 9-38105
- cosmic ray n component dependence obs. 9-38106
- cosmic rays, solar, anisotropies following flares 9-38110
- data by incidence sounding techniques 9-49593
- gas flow due to a flare, hydrodynamical description 9-38117
- geomagnetic associated events including shock waves, IMP 3 obs. (1965, 1966, 1967) 9-24893
- geomagnetic variation association, clarifying dynamo wind structure 9-35915
- geophysical activity rel. to form, height in atm. 9-26964
- ionizing radiation increase during two flares, May (1967) 9-43677
- kinematics, from high time-resolution cinematography 9-38118
- mag. fields, 21 and 23 May 1967 obs 9-24926
- rel. to magnetic storm 21-28 May (1967) 9-43492
- mechanism for build-up of flare energy 9-43675
- microwave burst rel. to ionospheric sudden freq. deviations 9-49591
- model based on force free currents in atm. 9-38115
- plasma turbulence and associated phenomena, Petschek's model appl. 9-43674
- proton, 7 July 1966, rel. to geomag. micropulsations 9-40105
- proton, of 9 Jun (1968) 9-43672
- proton and electron event (16-19 July 1966) cause 9-24915
- proton injection, spectrum 9-40191
- proton obs. in magnetotail and magnetosheath following flare of July 7, 1966 9-27105
- and r.f. bursts 3 August 1967 correl., obs. 9-33950
- soft X-ray obs., Explorer 33 and 35, (8 July 1968) 9-43673
- solar wind disturbances generated by flares, numerical simulation 9-43666
- sunspot size relationship 9-24924
- X-bremsstrahlung, longit. distrib. on solar disc at time of flare 9-43660
- X-ray and extreme u.v. bursts, effect on ionos. sudden freq. deviations 9-43438
- X-ray and cm wavelength emission, correl. and mechanism 9-36065
- X-ray line and continuum spectra, 0.5 to 8.5 Å 9-24905
- X-ray spectra, OSO-III satellite (1967) obs. 9-24906
- X-rays, OGO-III ion chamber obs., 23 May (1967) 9-24927
- Ca II, H and K line profiles 9-36069

magnetism

- chromosphere, short period pulsations in mag. field 9-31663
- coronal field calc. from variations in the growth of type III radiobursts 9-31639
- field distrib., recurrences and solar activity 9-31626
- field extent over 2000 gauss deduced from varying component of radio emission 9-36054
- field line eff. on cosmic ray daily variation 9-28968
- field structure obs. on supergranulation boundaries rel. to origin of chromospheric spicules 9-49594
- fields during sunspot activity, magnetographs, no shift assoc. with const. monopole contrib. obs. 9-24914
- flare and prominence fields, 21 and 23 May 1967 obs 9-24926
- Hale's work, biographical review 9-22028
- hydromagnetic model of sunspot cycle 9-38114
- magnetic pressure in the formation of spicules 9-31662
- photospheric mag. field polarity, rel. to interplanetary field polarity 9-38113
- pole positions from corona polar ray exam. during 1961, 1966 eclipses 9-27093
- prominence and flare fields, 21 and 23 May 1967 obs. 9-24926
- sunspot, field line structure and depend. on spot area 9-31660
- sunspot, Zeeman triplet obs., region intensity and structure determ. 9-31659

Sun continued**magnetism continued**

- vector magnetograph, simul. direction meas., calibration techniques 9-31684

prominences

- 1967 observations 9-24925
- active, mag. fields, 21 and 23 May 1967 obs. 9-24926
- chromospheric spicules, mechanism for origin 9-49594
- eruptions, flare unconnected, Jan (1968) 9-36068
- phenomena accompanying flares 9-38119
- quiescent, with bright metallic lines, structure, temp. 9-27104
- splintering loop 9-36067
- H and He emissions in outer regions of prominences, photometric comparison 9-36066

radiation

- see also Sunlight*
- absorption by water layer with variable coeff. of heat exchange, temp. distrib. 9-45478
- bursts from flares, microwave and hard X-ray, theory 9-43676
- eclipse, 1966, May 20, obs. of X-ray emission sources 9-36035
- e.m., spectral distribution 9-33947
- energy output without neutrinos via alpha fusion catalysis by quarks 9-45677
- energy received on ground, in Uccle (Belgium). data 9-49453
- flux from limb, difference between polar and equatorial, rel. to surface oblateness 9-41688
- forces induced on satellite mats., reflectance model estimation 9-24712
- integral absorption coefficient determ., review 9-41841
- in interplanetary mag. field sectors, thermal and e.m. flux 9-27099
- ionizing, increase during two flares, May (1967) 9-43677
- Kew Observatory, review of work 9-47545
- luminosity decrease due to Brans-Dicke theory 9-29080
- neutrino, null flux relation with eleven year solar cycle 9-41699
- photometry of XUV images, units methods and some results 9-43659
- polarization rate for continuous radiation 9-47682
- sea level meas. of submillimetre radiation 9-29087
- slowly varying component, from obs. at 8.6 mm. 9-43657
- solar brightness at far infrared, observations of center-to-limb variation 9-31668
- spectral distribution in 0.3-3 Å region during flare based on v.l.f. propagation effects 9-38097
- u.v., extreme, 260-1300 Å, OSO-III satellite (1967) obs. 9-24902
- u.v., extreme, solar cycle variations 9-49590
- u.v. heating of thermosphere F region 9-31428
- X-ray emission, quiescent period, rocket and satellite obs. 9-45679
- X-bremsstrahlung, longit. distrib. on solar disc 9-43660
- X-ray activity, peak characts. (Mar-Apr 1966) 9-41692
- X-ray burst, homology 9-43661
- X-ray burst of 7 July 1966, mechanism 9-24908
- X-ray bursts, hard, directivity 9-36041
- X-ray and cm wavelength emission from flares, correl. mechanism 9-36065
- X-ray emission, impulsive, satellite observations 9-36040
- X-ray fluxes, Solrad satellite obs. March-December (1968) 9-36039
- X-ray spectra during flares, OSO-III satellite (1967) obs. 9-24906
- X-rays, 8-12 Å, ion chamber photometer obs. 9-24907
- X-rays, flare, OGO-III ion chamber obs., 23 May (1967) 9-24927
- X-rays, soft, from flare 8 July 1968, Explorer 33 and 35 obs. 9-43673
- XUV, systematic photometry, units methods and some results 9-43659
- H and He emissions in outer regions of prominences, photometric comparison 9-36066
- He and H emissions in outer regions of prominences, photometric comparison 9-36066

radiation, corpuscular

- alphas, low energy, use in interplanetary medium investigation (28 May 1967) 9-43647
- cosmic ray 27 day variation, origin and direction of corpuscular streams 9-36058
- cosmic rays, galactic, effect on isotropy of change in solar wind velocity 9-36059
- cosmic rays, heavy nuclei, flux rises 9-22646
- cosmic rays, recording by lunar satellite Luna 11 (1966) 9-22644
- cosmic rays from exponential source, energy spectrum at earth 9-25494
- electric field, v.l.f., Pioneer 8 obs. 9-24891
- geophysical effects 9-38111
- gradient, radial, Mariner 4 and 5 obs. 9-49589
- heavy nuclei from sun not reflecting composition of solar atmosphere 9-38104
- heliosphere boundary interact. with magnetosphere of Jupiter 9-47683
- incidence affecting geomag. disturbance field asymmetry 9-35914
- in interplanetary mag. field vectors, plasma flux 9-27099
- interplanetary plasma obs. 9-47681
- rel. to ionospheric electron production rate 9-45523
- ions, electrostatic heating beyond 0.1 AU 9-43667
- linear interaction with wind, lab. simulation 9-31595
- lunar interaction and limb shock wave formation 9-36018
- lunar interaction with solar wind 9-31594
- lunar wind interaction, wake at large distance 9-29058
- magnetic storm active periods diurnal distrib. rel. to corpuscular streams, obs. 9-26966
- in magnetic storms, interaction with magnetosphere rel. to short-period pulsations 9-28964
- modulation of galactic rad. in interplanetary space, stratospheric obs. 9-31493
- neutrino fluxes, eff. of Brans-Dicke theory 9-29080
- neutrino fluxes, sensitivity 9-29092
- neutrons, upper limits on mag. charge 9-24914
- noise storms, relative positions of type I sources and assoc. continuum 9-29090
- particle event, OGO-III ion chamber obs., 23 May (1967) 9-24927
- plasma inhomogeneous structure, review 9-45686
- plasma, geomag. tail region, at 500 and 1000 Earth radii, characts. 9-38109
- plasma, interplanetary, radio scintillation obs. 9-38108
- plasma, low energy near moon, Explorer 35 obs. 9-29095
- plasma emission, electronic thermal conduction role 9-31643
- plasma flow around magnetosphere 9-37943
- pressure on magnetosphere rel. to horizontal geomag. field increase during storm 9-31457

Sun continued**radiation, corpuscular continued**

- proton and electron event 16-19 July 1966, association with flare 9-24915
- proton fluxes, satellite obs., correl. with riometer obs. of polar cap absorpt. 9-31394
- proton obs. in magnetotail and magnetosheath following flare of July 7, 1966 9-27105
- proton penetration to four Earth radii (1965-6) 9-41695
- protons, 1-30 MeV experiments 9-38112
- protons, 5-21 and 21-70 MeV, penetration to synchronous altitude 9-43417
- protons, E>100MeV incident over Antarctica January-February (1967) 9-43669
- protons, energetic, earth's magnetotail penetration Vela 4 obs. (21 May-8 June 1967) 9-43665
- protons, energetic rel. to auroral substorm activity 9-43433
- protons, energy spectrum meas. method 9-45685
- protons, halo and energetic storm, props. and origin 9-43668
- protons, low energy, magnetospheric entry (26 May 1967) 9-41551
- protons, low energy, use in interplanetary medium investigation (28 May 1967) 9-43647
- protons, satellite obs. at 1100km altitude (March 1966) 9-41696
- protons, upper limits on mag. charge 9-24914
- protons and electrons, shadowing by Moon (10-22 Nov., 1967) 9-29094
- protons over earth's polar caps, nonuniformity (24 March 1966) 9-41609
- quiet component of 9.1 cm emission and M-regions, rel. to geomag. activity 9-38100
- satellites, artificial, secular accel., radiation press. effects 9-28974
- shock wave structure, double, effect of high electron proton temp. ratios 9-31645
- solar-terrestrial relations, historical survey 9-38107
- viscous magnetospheric boundary layer, analysis 9-33802
- rel. to warming of Antarctic stratosphere (Spring 1963) 9-41484
- wind, and magnetic clouds in interplanetary space which disturb cosmic rays 9-35950
- wind, anisotropy, calc. using Boltzmann's theory with Krook's collision term. 9-47684
- wind, azimuthal motion, effect of finite elec. cond., ang. momentum loss of sun 9-38095
- wind, effect of cosmic rays 9-45683
- wind, effect of its speed on cosmic ray intensity, theory 9-45565
- wind, elapsed-time obs. of Earth's bow shock 9-24930
- wind, energetic terrestrial electrons behind bow shock and upstream 9-28917
- wind, flare generated disturbances, numerical simulation 9-43666
- wind, fluctuating, effect on motion of cosmic rays 9-35948
- wind, interaction with geomag. field 9-31644
- wind, interaction with moon, kinetic theory 9-27100
- wind, interactions with Moon and geomag. field 9-33953
- wind, interplanetary, Mariner 2 obs. 9-38090
- wind, inviscid eqn., convergent soln. 9-31648
- wind, ions angular distrib., Pioneer 6 obs. 9-29093
- wind, large velocity discontinuities, Explorer 34 obs. 9-31650
- wind, long wavelength turbulence and heating 9-36055
- wind, longitudinal anisotropy and obs. on 27-day cycle in cosmic-rays 9-38003
- wind, lunar detached compression wave, Explorer 35 obs. 9-29062
- wind, lunar wave mag. field at large distances, Mariner 4 obs. 9-41697
- wind, near orbit of Jupiter, plasma and field parameters 9-31646
- wind, quiet, energy flux densities rel. to geomag. activity 9-26965
- wind, rel. to auroras 9-26929
- wind, related to magnetic storms features 9-35911
- wind, scintillations of radio sources near the sun 9-29091
- wind, thermal anisotropies and e.m. instabilities 9-40192
- wind, turbulent fluctuations, effect on cosmic ray intensity 9-35944
- wind, viscous eqn., asymptotic soln. 9-31649
- wind, with mag. field, model and ang. momentum calc. 9-36056
- wind boundary, observations of magnetosheath 9-40190
- wind direction, IMP 1 obs. (27 Nov 1963 to 24 Feb 1964) 9-45684
- wind effects on cosmic ray variations, 'delay' caused by clash between solar and galactic magnetic fields 9-38102
- wind interaction with galactic cosmic rays 9-43664
- wind interaction with geomag. field 9-37942
- wind interaction with magnetosheath, Vela 3 obs. 9-41549
- wind interaction with magnetosphere 9-28914
- wind interaction with magnetosphere, lab. expts., review 9-37944
- wind interactions with geomag. field at various dipole axis inclinations, magnetopause surfaces and fields 9-43493
- wind near earth, obs. rel. to cause of sudden mag. commencements and impulses 9-41607
- wind plasma, collisionless heating by damping hydromag. waves 9-24913
- wind plasma characts. rel. to lunar wake 9-49588
- wind protons and neutral part. charge-transfer interac. 9-24812
- wind velocity, E-W asymmetry 9-41698
- wind velocity variations rel. to const. of troposphere and ionosphere 9-28859
- wind velocity variations rel. to const. of troposphere and ionosphere 9-45480
- wind-comet interaction model predicting size and shape of the contact discontinuity 9-47677
- e plasma oscillations, Pioneer 8 obs. 9-24891
- ν , detection by $^{37}\text{Cl}(\nu, e^-)$ ^{37}Ar rel. to solar He abundance 9-45682
- ν flux rates, meas. by giant underground trap 9-47685

radiation, radiofrequency

- activity, July-Sept. 1966 obs. 9-31641
- brightness centroid at 15.375GHz obs. 9-27098
- burst at 4.2 mm, assoc. with class 2B flare of July 6, 1968 9-43662
- bursts, 13 January 1968, 239 MHz 9-33949
- bursts, 3 August 1967, and flare correl., 9825 MHz 9-33950
- bursts, fine structure in 25-100 MHz spectra 9-31638
- bursts, periodic struct., rel. to peak intensity and total energy 9-41694
- bursts, polarization obs. at 2.8 GHz 9-38098
- bursts, type IV, nature of high frequency cutoffs 9-45680
- bursts, uneven intensity growth used to determ. mag. field in corona 9-31639
- Culgoora 158 MHz solar interferometers 9-36051
- Culgoora radioheliograph, prog. of observations 9-36075
- Culgoora spectrograph, specifications 9-36050

Sun continued**radiation, radiofrequency continued**

- decimetre and metre wavelengths, distrib. over the quiet sun, calc. 9-36044
- decimetre whole-sun observations review 9-36052
- disc brightness temp. distrib., May 20 1966 partial eclipse, 3.1 cm 9-33948
- eclipse, 1966, May 20, 3.2 and 9.1 cm obs. 9-36034
- emission at 1 mm. wavelength, model 9-27103
- fluctuations, low-freq. quasiperiodic 9-24910
- gain horns, employment of standard type 9-36053
- high resolution observations at 408, 696 and 1424 MHz 9-36046
- microwave, polarized, from solar hemispheres 9-27096
- microwave, slowly varying component, height during Quiet Sun Years 9-24912
- microwave (9.1cm) emission, statistical investigation of slowly varying components 9-43663
- microwave burst spectra (March and July 1966) 9-41693
- microwave bursts, 1 to 5GHz, 29 Oct (1968) 9-36042
- microwave bursts, obs. in circular polarization, origin rel. to mag. field changes 9-33952
- microwave bursts rel. to ionospheric sudden freq. deviations 9-49591
- Molongo cross observations 9-36045
- observations from Torun Observatory 9-24911
- plages and bursts, technique for decimetre obs. at Fleurs field station 9-36049
- power spectra of bursts at microwavelengths 9-40189
- quasi-periodic intensity variation at 3.3 cm wavelength 9-31640
- quiet and slowly varying components of 9.1 cm emission during solar min. 9-38099
- relative fluxes from active regions at 2 and 3 cm 9-45681
- review of solar radioastronomy 9-36043
- S-component, around 1 cm. wavelength 9-36054
- sun noise radio meas. at 7 GHz, tropospheric and ground effects 9-24664
- sun/rad., r.f. 10700, 2700, 960 MHz, July 1 to Sept. 30, 1967 9-27097
- time splitting of solar bursts 9-24909
- type II bursts new explanation for band splitting 9-36047
- type IV microwave bursts, evolution and decay 9-36048

spectra

- see also *Sun/corona; Sun/flares; Sun/prominences*
- absorption band at 0.43μ 9-45494
- anomalous absorption regions in 7-9 cm^{-1} and 21-24 cm^{-1} ranges 9-33951
- atmosphere structure, satellite feasibility 9-47609
- brightness temperature measurements near 1cm wavelength 9-31642
- chromosphere emission lines, rel. to effectively thin model construction 9-24928
- chromospheric flare, Sep 2, 1966, spectroscopic obs. 9-41709
- chromospheric spectrum outside of eclipse, $\lambda\lambda 3040$ to 9266 \AA 11500 lines 9-33955
- continuum in far-i.r. and mm. regions 9-29088
- corona, outer, i.r. obs. 9-43679
- corona at cm wavelengths during eclipse meas. 9-27108
- coronal emission regions, $\lambda 5303$, physical properties 9-29099
- coronal enhancement in extreme u.v. 9-43680
- coronal recombination spectra of highly charged ions, failure to obs. at 5 cm 9-31667
- e.m., spectral distribution 9-33947
- facula-photosphere contrast in mol. lines, depend. on dissociation energy 9-41700
- far ultraviolet, predictions compared with rocket obs. 9-31631
- of flare protons 9-40191
- flares, X-ray line and continuum spectra, 0.5 to 8.5 \AA 9-24905
- Fraunhofer i.r. lines, source function from equivalent width 9-31629
- Fraunhofer lines, limb effect 9-41690
- Hale's work, biographical review 9-22028
- high resolution, work at Univ. Liege, Belgium 9-29085
- image motion of solar limb, frequency analysis, 0.5 to 50 Hz 9-36031
- infrared Fraunhofer lines, source functions in cores 9-31634
- intensity profile, far infrared and mm regions, observational studies 9-31669
- i.r., balloon observation, variation with altitude in 2.2 to $13 \mu\text{m}$ region 9-29086
- Liege solar atlas, instrumental profile 9-41685
- limb darkening observations between 1800 and 2900 \AA 9-31670
- limb effect of Fraunhofer lines 9-41690
- line source function in atmosphere, freq. depend. 9-43658
- molecular conc.-optical depth curves for CH, NC, OH, C₂, CN and CO 9-41700
- photospheric temperature model, 900 to 130000 \AA continuum 9-31632
- radio power, bursts at microwavelengths 9-40189
- satellite lines classified as forbidden $\text{Is}^2 \text{ } ^1\text{S}_0$ - $\text{Is2s}^2\text{S}$, line of He-like ion 9-42351
- solar filter, series of Fabry-Perot interferometers 9-36037
- spectroheliograph, rocket-borne, for Mg II line at 2802.7 \AA 9-36396
- sunspots, umbral intensities, i.r. continuum spectrophotometric obs., thermal model construct. 9-24918
- temperature meas. of atmospheric ozone 9-31288
- Utrecht Solar Atlas, instrumental profile 9-41686
- u.v. continuous, high dispersion, Balmer jump 9-31630
- u.v. extreme, lab. simulation 9-38417
- windings, effects of line blanketing, high flux predicted <4500 \AA 9-31664
- X-ray, below 20 \AA , spatial variability 9-24904
- X-ray, hard, obs. from OSO-III 9-40188
- Be II lines, isotropic wavelength shifts 9-27095
- C₂ lines, center-to-limb behaviour 9-31633
- CH lines, center-to-limb behaviour 9-31633
- CN lines, center-to-limb behaviour 9-31633
- CO, thickness of layer in atmosphere, deduced 9-31627
- CO lines, center-to-limb behaviour 9-31633
- Ca, ionized, H and K lines 9-31635
- Ca autoionizing lines, oscillator strength obs. m shock tube 9-22944
- Ca II, H and K line profiles in disc flares 9-36069
- Ca II, K line profile, comparison of models for chromosphere 9-31636
- Ca II transition, Fraunhofer line, photoelectric obs. 9-31653
- Ca XV laboratory obs. of fine structure confirms presence in corona 9-31628
- Ce II lines, 4000 \AA -4700 \AA , non-coherent scatt. explanation 9-29089
- Ce II lines, reversal from absorpt. to emission 9-40187

Sun continued**spectra continued**

- Fe, highly ionized oscillator strengths and wavelengths of some X-ray and extreme u.v. spectrum lines 9-24903
 Fe I relative oscillator strength, laboratory obs. 9-45678
 Fe II lines, theoretical equivalent widths calc. 9-36036
 Fe XII emission lines, relative intensity as function of temp. and electron density 9-43683
 FeI in sunspot, red displacement obs at certain heights 9-33954
 Ga II line profile computed rel. to non-uniform chromosphere 9-36070
 H Ly α profile at 1206.52 Å, rocket obs. 9-41689
 H Lyman α profile rel. to geocorona, rocket obs. 9-29084
 H α , Jefferies-Thomas computation and obs. rel. to photosphere and chromosphere comps. 9-31637
 H α line profile computed rel. to non-uniform chromosphere 9-36070
 He II line intensity meas. for electron temp. and optical thickness determ. 9-24901
 Mg b-lines, computed profiles 9-29083
 Mg II, H and K line profiles, comparison of models for chromosphere 9-31636
 MgH, lines, center-to-limb behavior 9-31633
 MgII doublet lines, high resolution, balloon obs. 9-24900
 Na D-lines, computed profiles 9-29083
 O, i.r. spectroheliograms, interpretation 9-41691
 O I profile at 1302-1306 Å, rocket obs. 9-41689
 Si I, relative transition probabilities 9-24899
 Si II, multiplets, selected, relative intensities in the Sun and ZETA 9-27094
 Si III profile at 1206.52 Å, rocket obs. 9-41689

Sunlight

see also *Sky brightness*

- beam attenuation by aerosols 9-47544
 duration rel. to total cloud amount 9-47543
 Earth refl., obs. satellite thermal control appl. 9-24714
 energy received on ground, in Uccle (Belgium), data 9-49453
 green flash development with time, pictures from 10.6 km altitude 9-41521
 Kew Observatory work, review 9-47545
 polarization of sky at sunset, neutral points, Mar-July (1968) 9-43396
 scattered by Venus, linear polarization obs. 9-31615
 scattered by Venus, polarization, comparison with calculation 9-31616
 scattered sky rad., absorption band at 0.43 μ 9-45494
 effect on skylight and angular and spectral distribution on reflection 9-24661
 total downward flux rel. to height, calc. and aircraft obs. 9-41519

Sunspots

- 1967 observations 9-24920
 active longitudes for activity 9-36063
 activity correl. with visibility of the Jupiter red spot 9-47672
 activity during 1967, obs. 9-24919
 activity during March and April 1968, radio obs. 9-24923
 activity forecasting, review of methods 9-41708
 autocorrelation functions 9-43671
 conductivity, elec., calcs. using precise Electron-neutron interaction cross section value 9-24916
 cosmic ray effects, use of sunspot number W as relevant parameter 9-38102
 cosmic ray variation eff. 9-36057
 cycle, 11 year, rel. geomag. Pc I pearl pulsations 9-45561
 cycle, hydromagnetic model 9-38114
 data by incidence sounding techniques 9-49593
 dependence of lunar daily geomag. variation 9-33871
 far i.r. observation 9-36064
 flares as function of sunspot size 9-24924
 groups, photospheric paths in granular material between them 9-36060
 hydromagnetic waves, thermal generation 9-43652
 magnetic field, fine structure and depend. on spot area 9-31660
 magneto-kinematic model of solar cycle 9-27102
 number, correl. with radiowave fluctuations on Earth 9-31382
 observation through clouds, optics 9-43397
 penumbrae, photoelec. obs. of intensity 9-41707
 periodic activity due to tidal forces created by planets 9-36033
 plasmasphere map of chromosphere and spots 9-29098
 radio-aurora, rate of occurrence in eastern Canada over eleven-year period, statistical charact. 9-24680
 relative number rel. to geomag. $S_p(h)$ vars. 9-43491
 structure, review 9-24922
 thermal generation of hydromagnetic waves 9-43652
 umbra, thermal model based on i.r. continuum spectrophotometric obs. 9-24918
 umbrae, chromospheric inhomogeneities, props. 9-41705
 umbrae normal Zeeman triplet π component origin, region intensity velocity and mag. structure 9-31659
 umbral flashes, visual and photometric obs. on K-line filtergrams 9-41706
 Zurich number, correl. with prominence of Jupiter's Red Spot 9-40174
 Zurich sunspot number and daily variation in cosmic rays 9-26967
 Cs abundance from sunspot spectra 9-31657
 FeI line red displacement obs. at certain heights 9-33954
 In abundance from sunspot spectra 9-31657
 Rb abundance from sunspot spectra 9-31657

Superconducting devices

- advances, conference report 9-49028
 antenna 9-37480
 bolometer, equiv. cct. 9-44947
 cavities, microwave, tuning 9-37482
 cavities, use in resolving carrier trapping effects in CdS 9-41209
 cavity resonators, automatic tuning using optical feedback 9-37479
 coil, forced-cooled, hydrodynamics and current stability 9-26535
 composites, heat transfer, and stability, transient 9-49041
 conference, 1968 9-35344
 depth gauge for liq. He 9-44606
 energy storage and transfer, experiment and theory 9-41174
 film, across rectangular waveguide, propag. effects 9-30881
 filters, multiresonator band-pass and band-reject 9-37483
 flux pumping into circuits, efficiency 9-39606
 galvanometer, rel. to meas. of thermoelec. power in metals at low temp. 9-30982
 hard slabs, tubes and solenoids, power dissipation and flux jumps 9-26533
 Josephson barriers, maximum tunnelling supercurrents 9-37495

Superconducting devices continued

- Josephson effect at junction, athermal fluctuations effect on radiation line broadening 9-41188
 Josephson effects, review of experimental work 9-33277
 Josephson junctions, thin film Nb-Nb-Pb, fabrication by use of getter-sputtering 9-35377
 Josephson junctions, thin film Pb-PbO-Pb, barrier-thickness depend. on d.c. quantum interference effect 9-35378
 Josephson junctions zero-voltage current depend. on mag. fields 9-35373
 lenses, for 500-kV electron microscope column 9-36258
 linear struct., kinetic inductance meas. 9-35349
 magnetometer based on Josephson effect, operating characts. 9-49059
 metal junctions, stimulated radiative emission at gap freq., measurement method 9-44946
 metal junctions, stimulated radiative emission at gap freq., lasing conditions 9-43043
 modulator, use in voltmeter with 10^{-12} resolution 9-40214
 in n.m.r. detection, contrib. 9-35383
 point contacts, d.c. and microwave behaviour 9-35418
 point contacts, Josephson effect 9-49061
 proximity effect by electron tunneling in normal metal-superconductor junctions 9-24166
 quantum interference, stable point-contact, SQUID 9-35379
 quantum phase noise, temp. depend. meas. by interference techniques with point-contact Josephson junctions 9-37496
 quantum supercond. applic. 9-41189
 radiation detector based on Josephson effect, operating characts. 9-49059
 rings, magnetic flux quantization and Bose condensation 9-28483
 sandwiches, ferromag.-supercond.-ferromag. 9-24165
 solenoids, uniform current density, optimum shapes 9-35385
 solenoids, use of multi-strand cable 9-26534
 switches using Pb pressure contacts, device characteristics 9-30882
 thin-film bridges, vortex fluctuations 9-24164
 transmission lines, geometric arrangement for maximizing power transmission capability 9-35382
 transmission lines, thin-film, slow-wave propag. of e.m. waves obs. 9-37481
 tunnel junctions, fabrication on Nb films 9-37494
 tunnel junctions containing small Sn particles, elec. charact., zero-bias anomalies and supercond. of particles 9-43045
 tunneling, thin film, theoretical and exptl. investig., and applic. to e.h.f. 9-26536
 vibrating plane for shuttling flux in persistent current magnetometer 9-35374
 vitmeter based on Josephson effect, operating characts. 9-49059
 Ag-Pb normal metal-superconductor junctions proximity effect by electron tunneling 9-24166
 Cd-Al₂O₃-Al junctions, electron tunnelling charact. 9-37497
 Cu-Pb normal-metal-superconductor junctions proximity effect by electron tunneling 9-24166
 In-SrTiO₃ junctions, surface pot. barrier and supercurrent flow obs. 9-49056
 NB microwave TM₀₁₀ mode cavity with high electric field and Q₀ 9-24148
 Nb-GaAs junctions, tunnelling effects 9-33340
 Nb-Nb₂O₅-V thin film tunneling junction, theoretical and exptl. investig., and applic. to e.h.f. 9-26536
 Nb-NbO-Pb thin film Josephson junctions, fabrication by use of getter-sputtering 9-35377
 Nb-Si junctions, tunnelling effects 9-33340
 Nb-Ti wire, single core and twisted multi-strand, magnetization measurements 9-26526
 Nb₃Sn, magnet, a.c. power loss meas. 9-37498
 Nb r.f. cavities, fabrication 9-39605
 Pb-PbO-Pb thin film Josephson junctions, barrier-thickness depend. on d.c. quantum interference effect 9-35378
 Pb-Si junctions, tunnelling effects 9-33340
 Pb-terfon-Nb, coaxial line, freq. and time depend. using BCS theory 9-37487
 Pb_{0.7}In_{0.3}:GaAs:Zn junction, initial resistivity ang. depend. in mag. field 9-43044
 Pb resonating cavities, technology of prod. and vacuum system 9-39607
 Sn-Pb normal metal-superconductor junctions proximity effect by electron tunneling 9-24166
 Sn thin films as high-speed radiation detectors 9-35367
 Ta-Al point contacts, radiative emission at Ta energy gap freq. 9-25300
 Ta-Ta₂O₅-Nb thin film tunneling junction, theoretical and exptl. investig., and applic. to e.h.f. 9-26536

Superconducting magnets

- 30 kG, 8-ft.-diam., for Brookhaven Nat. Lab. bubble chamber 9-37490
 55 kG, stabilized, with one inch bore 9-49046
 150 kG, modular three-section 1.5-in.-bore 9-35376
 for bubble chamber, Brookhaven Nat. Lab. 9-37490
 conference, 1968 9-35344
 cooled, stability 9-35384
 critical currents meas., applic. of model of transiently stabilized Nb₃Sn magnets 9-37484
 dipole, new winding techniques 9-26525
 energy loss meas. on twisted multifilamentary wires 9-37485
 field meas., torque magnetometer 9-49060
 field trapped in hollow cylinder, electron optical meas. 9-25172
 flux jumps, dynamic stabilization by composite supercond.-normal metal tape windings 9-37486
 flux jumps in nonideal type II slabs 9-35354
 for intravascular navigation of catheter 9-35380
 modular three-section 1.5-in.-bore 150 kG 9-35376
 multifilamentary wires, twisted, energy losses meas. 9-37485
 in particle accelerators, high-energy, possible uses 9-36540
 in pulse generators, high energy, using flux displacers 9-36249
 for rockets mag. suspension and guidance in evacuated tubes 9-37499
 solenoid, inside-notch-corrected for high homogeneity, design 9-35357
 solenoid, stabilizing materials efficient use 9-39604
 superconductor with highly conducting substrate, behavioural analysis 9-43037
 technology reviewed 9-28482
 8.8 tesla, 51-cm.-bore coil system, tests 9-37488
 for train mag. suspension and guidance 9-37500
 for vehicles mag. suspension and guidance 9-37500

Superconducting magnets continued

- Nb-Ti sheets as stabilizing walls for levitated rings, magnetization meas., flux penetration 9-37493
- Nb₃Sn, 51-cm-bore, pumped He tests 9-37491
- Nb₃Sn, transiently stabilized, model, applic. to critical currents meas. 9-37484
- Nb₃Sn coils, persistent, critical conditions 9-35375
- Nb₃Sn quadrupole system for IMP, comparison with NbTi system 9-37492
- Nb₃Sn rings under isochroic conditions, levitation and stabilization against slide instability 9-37489
- Nb₃Sn tape clad with OFHC Cu, Al; operating pt. and stabilizing cladding thickness determ. 9-39604
- NbTi quadrupole system for IMP, comparison with Nb₃Sn system 9-37492

Superconducting materials

- advances, conference report 9-49028
- alloy with rigid vortex lattice, critical currents 9-37478
- alloys, binary, transition temp. increase, mechanism 9-24139
- alloys in high mag. fields, nonequib. thermodynamics 9-33263
- alloys in rapidly alternating mag. field of large amplitude, behaviour of parameter Δ 9-37463
- alloys in strong alternating field, dynamic props. of parameter Δ in T_c region 9-30864
- Amperian mag. systems, shape and orientation effects 9-30859
- anisotropic type-II, flux penetration 9-47087
- clean material, upper critical field temp. depend. determ. 9-33267
- composite, magnetoresistance of Cu at 4.2°K in transverse fields up to 100 kG 9-41166
- composite, stabilized current density expression 9-49027
- composite, undergoing flux jumping, transient stability limits prediction 9-35348
- critical currents in low fields, technique for obtaining 9-44923
- critical currents meas., applic. of model of transiently stabilized Nb₃Sn magnets 9-37484
- critical field ratio, temp. depend. 9-33265
- diamagnetic susceptibility above transition temp., large anomaly 9-39592
- diamagnetic susceptibility at transition, fluctuating Cooper pairs contrib. 9-33260
- DNA, double-stranded, room-temp. supercond. 9-49057
- 2e/h meas. by a.c. Josephson effect 9-39593
- electrical stability, in resistive state 9-35351
- film, nonlinear h.f. props. 9-49030
- film containing mag. impurities, far-i.r. study of energy-gap props. 9-41185
- films, thin, critical current for diffuse refl. of electrons from walls 9-39594
- films, thin, effect of thickness on d.c. Josephson current 9-37462
- films, ultra-thin, high T_c obs. and enhanced electro-phonon coupling 9-37459 *
- films, weakly coupled, resistive transition 9-35345
- flux jumping in composite supercond., transient stability limits prediction 9-35348
- flux-line arrangement 9-41173
- gapless, anomalous scatt. due to magnetic impurities, Suhl's dispersion eqn. 9-35346
- granular, 'Ball array' model, 'dirty limit' Ginzburg-Landau eqn. deriv. 9-30861
- granular, metals in porous glass, critical field obs. 9-47083
- s-d interband impurity scatt., d-band transition temp. decrease 9-33261
- Josephson effect at junction, athermal fluctuations effect on radiation line broadening 9-41188
- lamellar struct., transition and critical field obs. 9-39747
- linear struct., kinetic inductance meas. 9-35349
- magnetically induced structural modifications, u.s. meas. 9-37464
- magnetization meas. by electronic integrator 9-39591
- metal, conductivity above transition temp., nonlinear effects 9-30860
- metals, microwave phonon-electron interac., conversion of e.m. into sound energy 9-37384
- metals, non-transition, nonmag. transitional impurities effect on critical temp. 9-24134
- metals, nontransition, press. depend. of transition temp. 9-30858
- metals, positron annihilation 9-26501
- mixed state, flux motion, electrical resistance and noise 9-30856
- molybdenum oxides, with tungsten bronze type structure, superconducting transition temp. determ. 9-26530
- multistrand compound conductors, steady-state performance 9-35350
- new materials, review 9-44924
- phonon microwave excitation 9-26405
- positron thermalization, effect of normal metal-supercond. transitions 9-24111
- preparation of high current density ribbons by elements co-condensation in vacuum 9-39590
- resistive microstrip, inductive behaviour 9-35353
- in resistive state, elec. and thermal stability 9-35351
- rhenium oxides, with tungsten bronze type structure, superconducting transition temp. determ. 9-26530
- semiconducting films, quantizing, with granulated metallic coating 9-49038
- semiconductors, energy-gap eqn., derivation by Green's function method 9-26521
- semimetals, energy-gap eqn., derivation by Green's function method 9-26521
- single-zone, isotropic with paramag. impurities 9-37455
- spectrum, energy gaps obs. 9-43032
- spin fluctuations assoc. with form. of localized mag. moments 9-47082
- stabilization into resistive state 9-26520
- strong coupling, surface-sheath nucleation field, temp. depend. 9-35366
- strong coupling, time depend. Ginzburg-Landau eqns. 9-24143
- superconducting, skin depth, freq. depend. 9-37473
- surface critical current, anisotropy near H_{c2} 9-30865
- thermal stability, in resistive state 9-35351
- as thermometric fixed points 9-35381
- thin films, Josephson eff. at r.f., props. and applic. 9-28471
- transition metal alloys, transition temps. rel. to electron interaction in 3d band 9-24151
- transition metal compound thin films with rocksalt struct. 9-36959
- two-band, paramag. impurities influence on thermodynamic props. 9-33264
- two-band, with nonmag. impurities, upper critical field 9-30857
- type II, alternating mag. field effect on current flow 9-28473

Superconducting materials continued

- type II, dirty, transition temp., effect of small superparamag. grains 9-44932
- type II, e.m. radiation from moving vortices due to fluctuating currents 9-35355
- type II, hardening mechanism for carrying high currents in high mag. fields 9-49044
- type II, nonideal, flux jumps in slabs 9-35354
- type-I, current-carrying intermediate state obs., elec. resistance due to flux motion 9-30867
- type-I, II, book 9-47081
- type-I thick slab, field penetration, intermediate-state config. 9-30866
- type-II, anisotropic, flux penetration 9-47087
- type-II, defects in flux-line lattices 9-28286
- type-II, pinning effect on nonlinear resistance in mixed state 9-49042
- u.s. attenuation in normal and superconducting states, non-free-electron behaviour 9-26417
- vortex filaments, oscillation spectrum 9-38261
- weakly coupled, spectral props. 9-24131
- Al-Cr dil. solid soln., residual resistance, sp.ht., mag. susceptibility and transition temp. change w.r.t. localized d-state 9-33269
- Al-Mn dil. solid soln., residual resistance, sp. ht. mag. susceptibility and transition temp. change w.r.t. localized d-state 9-33269
- Al-V dil. solid soln., residual resistance, sp. ht. mag. susceptibility and transition temp. change w.r.t. localized d-state 9-33269
- Al, 35-80Å film, enhanced transition temp. obs. 9-30869
- Al, critical temp., hydrostatic press. effect 9-37467
- Al, lifetime of excitations, calc. 9-44935
- Al, quasiparticle recombination rate, calc. 9-44934
- Al₂Th₃, rel. to Si₂U₃-type structure 9-39596
- Al films, dirty, Knight shift, BCS-Yosida depend. 9-45394
- Al films, granular, transition temp. enhancement 9-24149
- Al fine particles prepared by evaporation in He gas, enhanced superconductivity 9-33270
- Al granular film, transition temp. enhancement mechanism, expt. evidence 9-24150
- Al granular films, fluctuations in 3-d regime causing excess conductivity 9-26527
- Al granular films, microwave conductivity 9-37466
- Al thin films, granular, microwave conductivity 9-28481
- Al thin films, strain effect on T_c 9-41177
- Al thin films, strain effect on T_c 9-41177
- Au/Pb layered films, phase composition and transition obs. 9-26528
- Au_{1-x}Pd_xGa_{1-x}, effect of Pd additions on critical temps. 9-49047
- (Ba₂Sr_{1-x})TiO₃ degenerate semiconductor, review of expt. data on supercond. 9-41179
- Ba under pressure at 1.3°K and 5°K 9-24146
- Be, theoretical transition temps. 9-35358
- Be₂Nb₃, rel. to Si₂U₃-type structure 9-39596
- Be₂Ta₃, rel. to Si₂U₃-type structure 9-39596
- Bi-Sn alloys, phase formation and structure, high pressures 9-23752
- Bi, amorphous, phonon spectrum by electron tunneling, transition temp. obs. 9-41076
- Bi₂K, transition temp. press. depend 9-49048
- Bi films, transition curves in perpendicular field, superconducting fluctuations 9-44931
- Bi films, transition temp. size dependence 9-30870
- (Ca₂Sr_{1-x})TiO₃ degenerate semiconductor, review of expt. data on supercond. 9-41179
- Cd-Al₂O₃ Al junctions, electron tunnelling charact. 9-37497
- Cd, isotope effect coeff. from transition temp. meas. 9-44936
- Cd, theoretical transition temps. 9-35358
- Cd, u.s. attenuation, anisotropy, rel. to Fermi surface and deform. parameter 9-37338
- CdSnAs₂, polymorph, high-press., prep., cryst. struct. and transition temp. 9-41178
- Cr₂Rh critical mag. field data 9-24163
- Cr₂Tr critical mag. field data 9-24163
- CuSe_x, marcasite type superconductor, nature, cry. struct. 9-28261
- Ga, amorphous, phonon spectrum by electron tunneling, transition temp. obs. 9-41076
- Ga, isotope effects 9-28475
- δ -Ga, props. 9-44937
- Ga₂Nb₃, rel. to Si₂U₃-type structure 9-39596
- Ga films, transition temp. size dependence 9-30870
- Ga single cryst., energy gap temp. depend., tunnelling meas. 9-33271
- GeTe, transition temp. carrier conc. dependence 9-39794
- GeTe degenerate semiconductor, review of expt. data on supercond. 9-41179
- In-Bi alloys, metastable states obs. 9-44938
- In-Cd dil. alloy, transition temp. pressure dependence rel. to Fermi surface topology determ. 9-47043
- In-(3.9 at.%)Pb alloy, type I-II transition obs. 9-47089
- In-(2 at.%)Pb films, type-I, flux-flow noise determ. 9-24152
- In-SrTiO₃ junctions, surface pot. barrier and supercurrent flow obs. 9-49056
- In, electronic density of states, nonlinear pressure effect, H_c change 9-37407
- In, enclosed, coalescence 9-28476
- In, high purity, elec. and thermal conductivities, 1.5 to 4.2°K 9-30871
- In, supercurrent decrease in gapless region 9-43038
- In, T_c obs. by shear-wave attenuation amplitude dependence 9-26418
- In, thin film, effect of preferred cryst. growth on ang. depend. of critical field 9-47088
- In (3at.%)Bi alloys, magnetization curves, demagnetization coeff. dependence 9-26529
- In flow stress increase and electron dislocation interaction 9-44939
- In thin films, strain effect on T_c 9-41177
- In thin films, strain effect on T_c 9-41177
- InBi foil, effect of cold working on transition temp. 9-47078
- Ir, press. effect on transition temp. 9-44940
- K₂MoO₃, with tungsten bronze type structure, transition temp. determ. 9-26530
- K₂ReO₃, with tungsten bronze type structure, transition temp. determ. 9-26530
- La:Ce Kondo superconductor, quasibound states obs. 9-33268
- La-Ce dilute alloy, Kondo supercond. quasibound states 9-44941
- La_{1-x}Ce_xAl₂ alloys, pressure eff. on supercond. transition temp. 9-28477
- La_{1-x}Gd_xAl₂ alloys, pressure eff. on supercond. transition temp. 9-28477

Superconducting materials continued

- La₂C₃, bicr. structure, superconducting over entire homogeneity range 9-33272
- La_{2-x}Ce_xIn alloys, supercond., transition temp. rel. to pressure, 0-23kbar 9-47090
- Mo, B, isotope effect on transition temp. 9-30872
- Nb-Al alloys, positron annihilation, critical temp. eqn. parameters 9-39598
- Nb-Mo, solid solution alloys, lattice thermal conductivity in normal and superconducting states 9-30797
- Nb-Mo alloys, thermal and elec. conductivities, Nernst-Ettinghausen coeffs. 9-47091
- Nb-Sn alloys, mag. hysteresis and alloy constitution 9-37659
- Nb-Ta alloys, magnetization meas., temp. coeff. of electronic sp. heat and transition temp., conc. depend. 9-28478
- Nb-Ta alloys, type II, anisotropic pinning and guided motion of vortices 9-43035
- Nb-Ti-N thin films, critical current-field meas. in continuous mag. fields 9-35362
- Nb-Ti-Zr-Hf alloy system, critical current density and fields, conc. depend. 9-39597
- Nb-Ti alloys, cold working and precip. kinetics for high critical current densities 9-49053
- Nb-Ti sheets as stabilizing walls for levitated rings, magnetization meas., flux penetration 9-37493
- Nb-Ti tubes, steady-state flux jumping in superimposed a.c. and d.c. mag. fields 9-37471
- Nb-(40wt.%)Zr-(10wt.%)Ti hollow cylinders, mag. shielding in applied mag. fields at 4.2°K 9-43174
- Nb-(25 wt.%)Zr alloy, fluxoid pinning by second phases 9-49049
- Nb-Zr alloys, cold working and precip. kinetics for high critical current densities 9-49053
- Nb-(25 at.%)Zr alloy, a.c. energy losses around H_{c1} 9-35361
- Nb₂Al-Nb₂Ge alloys, heat treatment effect on T_c 9-30877
- Nb₂Al, sp.h.t., mag. susceptibility and Knight shift obs. 9-39599
- Nb₂Al_{1-x}Ge_x alloys, critical fields obs. in liq. H₂ 9-35360
- Nb₂Au_{1-x}Pt_x system, annealing conditions influence on T_c 9-44942
- Nb₂Ga-Nb₂Al system, transition temp., effect of low-temp. annealing 9-37469
- Nb₂Ge-Nb₂Al system, transition temp., effect of low-temp. annealing 9-37469
- Nb₂O₃, critical mag. field data 9-24163
- Nb₂Sn, a.c. field-induced flux jumps 9-37468
- Nb₂Sn, anisotropy in energy gap 9-49051
- Nb₂Sn, cold working and precip. kinetics for high critical current densities 9-49053
- Nb₂Sn, critical current density, correlation with impurity content and microstructure 9-41180
- Nb₂Sn, magnet, a.c. power loss meas. 9-37498
- Nb₂Sn, mechanism and formation kinetics from elemental components 9-48764
- Nb₂Sn alloy, mag. hysteresis and cryst. struct. 9-39769
- Nb₂Sn alloy, magnetization, hysteretic loss and flux-jump stability obs. 9-35364
- Nb₂Sn coils, persistent, critical conditions 9-35375
- Nb₂Sn critical current density rel. to bombardment of protons and deuterons 9-41184
- Nb₂Sn magnets, 51-cm-bore, pumped He tests 9-37491
- Nb₂Sn magnets, transiently stabilized, model, applic. to critical currents meas. 9-37484
- Nb₂Sn quadrupole magnet system for IMP, comparison with NbTi system 9-37492
- Nb₂Sn rings under isochroic conditions, levitation and stabilization against slide instability 9-37489
- Nb₂Sn type II, positron annihilation, electron-pairing eff., γ ang. distrib. meas. 9-30874
- Nb₂Sn-Nb₂Al system, transition temp., effect of low-temp. annealing 9-37469
- Nb alloys, hysteresis rel. to dislocation pinning temp. and field dependence 9-24153
- NbN, enhancement of current carrying capacity by fast neutron irradiation 9-43039
- NbN film prepared by reactive sputtering, upper critical field H_{c2} 9-35359
- NbN thin films, high-field props. 9-35363
- NbSe₂, lamellar struct., occupation of sublattice sites rel. to critical temp. 9-41181
- NbTi quadrupole magnet system for IMP, comparison with Nb₂Sn system 9-37492
- Nb-(5 at.%)Ti alloy strip, peak effect in critical current w.r.t. temp. and field 9-39600
- Pb-(0.565at.%)Bi alloys, type I and II, critical field comp. dependence 9-43041
- Pb-(0.25 wt.%)Bi, surface-sheath nucleation field, temp. depend. 9-35366
- Pb-(10wt.%)In alloy, powder, oxide coated type II, flux pinning by oxide films 9-49045
- Pb-In alloys, critical field and generalized Ginzburg-Landau parameter, κ₂ determ. 9-24156
- Pb-In alloys, second generalized Ginzburg-Landau parameter, temp. dependence 9-24157
- Pb-In alloys, specific heat 9-33182
- Pb-(1.6wt.%)Ti, type II, rectangular flux line lattice 9-28479
- Pb-Ti alloy, fluxons, nucleation and propagation in thin cylindrical specimens 9-44933
- Pb, intermediate state, effect of transport current 9-49054
- Pb_{0.9}La_{0.3}GaAs_{0.7}Zn junction, initial resistivity ang. depend. in mag. field 9-43044
- Pb₄₀Ti₆₀, tunneling meas. in phonon spectrum determ. 9-26413
- Pb alloys, preparation, patent 9-24158
- Sb, high press. phase, transition temp. 9-39602
- Sn-Cd, lattice thermal conductivity, dopant-conc. dependence, rel. to normal and superconducting states 9-26452
- Sn, narrow thin-films, quantum phase correlations and fluctuations 9-24159
- Sn, skin depth, freq. depend. 9-37473
- Sn, skin depth, freq. depend. 9-37473
- Sn, u.s. absorption in supercond. transition rel. to cryst. orientation 9-37336
- Sn, As₃, and carrier conc. and ionic model obs. 9-37474
- Sn, P₃, and carrier conc. and ionic model obs. 9-37474
- Sn films, conductivity temp. dependence at 20 GHz 9-43042

Superconducting materials continued

- Sn films, upper critical field meas. 9-35368
- Sn films, upper critical field rel. to deposition on substrates held at low temps. 9-28480
- Sn small particles in tunnel junctions 9-43045
- Sn thin films, microwave conductivity 9-28481
- Sn thin films, strain effect on T_c 9-41177
- Sn thin films, strain effect on T_c 9-41177
- Sn thin films as high-speed radiation detectors 9-35367
- Sn u.s. absorpt. in supercond. transition rel. to cryst. orientation 9-37336
- SnTe, critical mag. fields rel. to varying carrier conc. 9-33274
- SnTe, transition temp. carrier conc. dependence 9-39794
- SnTe degenerate semiconductor, review of expt. data on supercond. 9-41179
- SnTiO₃:Nb, transition temp. obs. 9-49055
- SnTiO₃:Zr, transitions from large to nearly-small polarons 9-47056
- SnTiO₃, O deficient, paramag. centres effect on transition temp. 9-37475
- SnTiO_{3-x}, degenerate semiconductor, soft-mode supercond. obs. 9-33275
- SnTiO₃, ceramic, Zr-doped, effective masses determ. 9-26532
- SnTiO₃, ceramic, Zr-doped, effective masses determ. 9-26532
- SnTiO₃, degenerate semiconductor, review of expt. data on supercond. 9-41179
- Su granular films, fluctuations in 3-d regime causing excess conductivity 9-26527
- Ta-Nb, solid solution alloys, lattice thermal conductivity in normal and superconducting states 9-30797
- Ta-Ta₂O₅-Nb thin film tunneling junction, theoretical and exptl. investig., and applic. to e.h.f. 9-26536
- Ta, resistance meas. during supercond.-normal transition 9-37476
- Ta₈₁Pt₁₉, Tc vs. c/a correlation 9-24163
- Tc, for 10 MeV/ft two mile linac, r.f. properties and fabrication techniques 9-47093
- Th-C, anisotropy of energy gap 9-30879
- Th-Gd alloys, anisotropy effect on critical field curves 9-30879
- Th_{1-x}Er_x, transition temp. comp. dependence rel. to spin-spin correlations among Er impurities 9-24160
- Ti-Mo alloys, effect of ω-phase precipitates on transition temp. 9-35370
- Ti-Mo dil. alloys, martensitic, transition temp. enhancement 9-37477
- Ti-Nb, multifilament, and Cu composites, magnetiz., coupling obs. 9-35369
- Ti-Nb alloy, magnetization, hysteretic loss and flux-jump stability obs. 9-35364
- Ti-(20 at.%) Nb alloy, props. correlation with metallurgical props. 9-39603
- Ti-(22 at.%)Nb alloy, critical currents 9-37478
- Ti-Rh alloy, transition temp. determ. from sp. ht. meas. 9-30880
- Ti-Pb-Bi alloys, tunneling meas. 9-24161
- V_{1-x}Ni_x, T_c vs. c/a correlation 9-24163
- V₂Ga, critical fields temp. depend. from magnetiz. obs. 9-44945
- V₃Pd, T_c vs. c/a correlation 9-24163
- V₂Si, pressure, hydrostatic, effect on transitions 9-49052
- V₂Sn, type II, V⁵¹ nucl. spin-lattice relax. time, temp. variation 9-35371
- V anisotropy temp. dependence, 1.7-4.2°K 9-24154
- W₂B isotope effect on transition temp. 9-30872
- Y₂C₃, high pressure synthesis, magnetic susceptibility meas. 9-35372
- Zn, microwave absorpt. obs., mag. field depend. 9-47094
- Zn, theoretical transition temps. 9-35358
- Zn, u.s. attenuation, anisotropy, rel. to Fermi surface and deform. parameter 9-37338
- Zr₂Co-Zr₂Ni mixed cryst., transition temp. 9-33276
- Zr films, 2.10³-12.10³ Å with substrate temp. below 100°C 9-37452
- ZrB₁₂, B isotope eff. on transition temp. 9-24132
- lead**
- for 10 MeV/ft two mile linac, r.f. properties and fabrication techniques 9-47093
- alloys, r.f. absorption in cavity resonators, measurements for TE and TM modes 9-47092
- critical temp., hydrostatic press. effect 9-37467
- film, transition temp. determ. from tunneling and resistive meas. 9-43040
- films, fluctuation rounding of resistive transition 9-41186
- films, flux flow and critical current, Nernst effect obs. 9-41183
- films, thin, resistivity and crit. temp., eff. of imperfections 9-26531
- films, upper critical field rel. to deposition on substrates held at low temps. 9-28480
- flow stress increase and electron dislocation interaction 9-44939
- hollow cylinders, quantized mag. flux obs. with electron interferometer 9-41187
- Landau-level widths effective masses and magnetic-interaction effects 9-26500
- Nernst effect and flux flow in films 9-41183
- pressure contacts in switches, device characteristics 9-30882
- r.f. absorption in cavity resonators, measurements for TE and TM modes 9-47092
- transition temp., press. effects 9-33273
- u.s. shear-wave attenuation 9-24026
- Ag-Pb normal metal-superconductor junctions, proximity effect by electron tunneling 9-24166
- Au/Pb layered films, phase composition and transition obs. 9-26528
- Cu/Pb layers, proximity effect, induced excitation spectrum, density of states meas. 9-44944
- Cu-Pb normal metal-superconductor junctions, proximity effect by electron tunneling 9-24166
- electron tunneling data for pressure depend. of phonon spectrum 9-24018
- Nb-NbO-Pb thin film Josephson junctions, fabrication by use of getter-sputtering 9-35377
- Nb-Pb thin film tunnel junctions, method for fabricating 9-28471
- Pb-Gd films, quenched, far-i.r. study of energy-gap props. 9-41185
- Pb-Mn films, quenched, far-i.r. study of energy-gap props. 9-41185
- Pb-PbO-Pb thin film Josephson junctions, barrier-thickness depend. on d.c. quantum interference effect 9-35378
- Pb-Si junctions, tunnelling effects 9-33340
- Pb-terfon-Nb, coaxial line, freq. and time depend. using BCS theory 9-37487
- Pb, tunneling meas. in phonon spectrum determ. 9-26413
- Sn-Pb normal metal-superconductor junctions, proximity effect by electron tunneling 9-24166
- niobium**
- for 10 MeV/ft two mile linac, r.f. properties and fabrication techniques 9-47093
- a.c. energy losses around H_{c1} 9-35361

Superconducting materials continued

- niobium continued
- anisotropy temp. dependence, 1.7-4.2°K 9-24154
- deformed type II, dislocation distribution eff. on specific heat rel. to fluxoid pinning 9-30875
- energy gap anisotropy rel. to temp. depend. of Ginzburg-Landau parameters in upper critical field 9-28478
- film, thin, a.c. losses 9-30878
- films, thin, critical fields, coherence lengths, temp. depend. 9-35365
- films, tunnel junctions fabrication 9-37494
- flux flow and critical current, Nernst effect obs. 9-41182
- flux pinning, anisotropic, in single cryst. 9-37470
- fluxoid pinning by dislocations in single cryst. w.r.t. temp. and mag. field 9-39601
- magnetization curve, effect of tension 9-35532
- magnetization curve shape, effect of purity 9-44943
- Nernst effect and flux flow obs. 9-41182
- resistivity, temp. depend. 9-49050
- r.f. cavities, fabrication 9-39605
- surface layers, critical currents, nature 9-37472
- surface magnetization 9-30876
- thermal conductivity near upper critical field 9-33200
- vortex lattice, elastic consts. and search for collective oscillations 9-30873
- ^{90m}Nb half-life, effect of superconductivity 9-32329
- Nb-GaAs junctions, tunnelling effects 9-33340
- Nb-Nb₂O₅-V thin film tunneling junction, theoretical and exptl. investig., and applic to e.h.f. 9-26536
- Nb-NbO-Pb thin film Josephson junctions, fabrication by use of getter-sputtering 9-35377
- Nb-Pb thin film tunnel junctions, method for fabricating 9-28471
- Nb-Si junctions, tunnelling effects 9-33340
- Nb-Zr, flux pinning by grain boundaries 9-28474
- Nb₂Al, pressure, hydrostatic, effect on transitions 9-49052
- Nb₂Sn, pressure, hydrostatic, effect on transitions 9-49052
- Nb₂Sn, production, patent 9-24155
- Nb₂(Al_{1-x}Ge_x), pressure, hydrostatic, effect on transitions 9-49052
- ⁹³Nb spin-lattice relax. time temp. and field depend. determ. 9-41348
- NbN, pressure, hydrostatic, effect on transitions 9-49052
- Pb-terfon-Nb, coaxial line, freq. and time depend. using BCS theory 9-37487
- in SrTiO₃, transition temp. obs. 9-49055
- Ti-Nb, multifilament, and Cu composites, magnetiz., coupling obs. 9-35369
- Superconductivity**
- alkali and alkaline-earth metals, nonsupercond. status 9-43031
- alloy, dilute, transition temp. pressure dependence rel. to Fermi surface topology determ. 9-47043
- alloys, dilute magnetic, influence of mag. impurities on T_c 9-44925
- alloys in strong alternating field, dynamic props. of parameter Δ in T_c region 9-30864
- alloys with paramagnetic impurities, gapless region 9-43033
- alloys with rigidly pinned vortex lattice, temp. depend. of critical current 9-47080
- annealed, low temp. specific heat in mag. fields 9-37465
- applied, conference, 1968 9-35344
- in arbitrary interaction spin systems 9-49037
- BCS-Tamm-Dancoff approximation for spherical nuclei, conservation of number of particles 9-30862
- Bernoulli potentials rel. to Meissner current, temp. depend. 9-43029
- book 9-47081
- boson and quantum plasma transitions 9-25053
- causes, confirmation by examples 9-49034
- conference, 1968 9-35344
- critical current of film in mixed state 9-49032
- critical field, upper, theory, symmetry considerations 9-24138
- critical field ratio, temp. depend. 9-33265
- critical-field ratio H_{c2}/H_{c1} for pure superconductors outside Landau-Ginzburg region, T_c > 0°K 9-24137
- crystals, non-ideal, critical temp. of transition, using ion density correlation functions 9-49033
- current, stability conditions 9-30863
- cylinder, singly-connected, quantum effects rel. to surface-current layer 9-44926
- density-matrix methods and time dependence of order parameter 9-44928
- dirty two-band superconductors, current density in limiting case of large non-mag. impurity conc. 9-26522
- DNA, double-stranded, room-temp. 9-49057
- e/h determ. using macroscopic quantum phase coherence, expt. 9-24135
- 2e/h meas. by a.c. Josephson effect 9-39593
- in electron linac, 100 GeV, two mile, feasibility study 9-46163
- in electron linacs and r.f. separators, design of structures 9-47066
- electron tunneling between superconductors through paramagnetic impurity barrier, Kondo eff. influence 9-44929
- enhancement eff. in very thin films, theory unsatisfactory 9-30869
- enhancement mechanism, expt. evidence 9-24150
- Fermi versus Bose condensation 9-24140
- film, nonlinear h.f. props. 9-49030
- films, narrow, quantum phase correlations and fluctuations 9-24159
- films, thin, critical current for diffuse refl. of electrons from walls 9-39594
- films, ultra-thin, high T_c obs. and enhanced electro-phonon coupling 9-37459
- flux jumping in composite supercond., transient stability limits prediction 9-35348
- flux jumps in magnets, dynamic stabilization by composite supercond.-normal metal tape windings 9-37486
- flux-line arrangement 9-41173
- fluxoid lattice near upper critical field, elastic constants 9-35139
- Fulde-Ferrel model, with molecular field acting on electron spin 9-33262
- gapless superconductor, anomalous scatt. due to magnetic impurities, Suhl's dispersion eqn. 9-35346
- Ginzburg-Landau 'dirty limit' eqn. for granular supercond. 9-30861
- Ginzburg-Landau eqn. to third order, fluctuation corrected, higher moments of distribution function 9-24142
- Ginzburg-Landau eqns. sufficient near critical point 9-28469
- Ginzburg-Landau parameter, second generalized, temp. dependence 9-24157
- hollow cylinders, quantized mag. flux obs. with electron interferometer 9-41187

Superconductivity continued

- introductory article to supercond., Josephson effect and tunnelling 9-49058
- Josephson barriers, maximum tunnelling supercurrents 9-37495
- Josephson current, d.c., film thickness influence 9-37462
- Josephson current for barrier transparency near T_c 9-26523
- Josephson eff., a.c. 9-28470
- Josephson eff., r.f., props. and applic. 9-28471
- Josephson effect, a.c., simple undergraduate apparatus for its obs. 9-47714
- Josephson effect, D.C., calc. of thermal noise 9-37457
- Josephson effect, d.c., thermal fluctuation effect 9-47079
- Josephson effect, stationary, effect of fluctuations 9-24145
- Josephson effect at weak junction 9-49039
- Josephson effects, review of experimental work 9-33277
- Josephson plasma resonance, deriv. using quantum phase operators 9-44927
- Kondo, quasibound states 9-44941
- Kondo effect, pressure of energy gap in state density function 9-44930
- lamellar struct., transition and critical field obs. 9-39747
- magnetic field near surface simulated by electrolytic flow 9-24130
- multistrand compound conductors, steady-state performance 9-35350
- Nb, flux pinning, anisotropic, in single cryst. 9-37470
- nonlinear effects above transition temp. 9-30860
- one-dimensional systems, Peierls doubling and Cooper pairing vertices, evaluation and role using Green function formalism 9-37460
- order parameter, dynamical critical fluctuation above the transition point 9-33259
- order parameter, fluctuations, effect on tunneling density of states 9-49036
- near paramagnetic impurity, effect of electron scatt. 9-49031
- plasma shell, expansion into vacuum mag. field 9-46483
- popular article on change of state 9-48734
- quantum, applic. to instrumentation 9-41189
- quantum phase fluctuations of order parameter, eff. on superfluidity 9-24141
- rings containing 1-dimens. weak links, dissipative fluctuations and quantum transitions 9-43030
- semiconducting films, quantizing, with granulated metallic coating 9-49038
- in semiconducting structures, lamellar 9-37458
- semiconductor, transition temp. shifts with elec. charging 9-37461
- in semiconductors, energy-gap eqn., derivation by Green's function method 9-26521
- in semimetals, energy-gap eqn., derivation by Green's function method 9-26521
- solenoids, thermoelectric generator 9-31900
- specific heat jumps when ellipsoid enters or leaves mixed state in a constant applied field 9-44922
- spin fluctuations assoc. with form. of localized mag. moments 9-47082
- strong coupling, time depend. Ginzburg-Landau eqns. 9-24143
- supercurrent, idealized model 9-24133
- superfluid systems, macroscopic quantum effects 9-30447
- surface critical current, anisotropy near H_{c2} 9-30865
- surface layer, critical currents, nature 9-37472
- surface nucleation and boundary conditions 9-47078
- surface sheath, induced persistent currents 9-49035
- in synchrotrons, replacing magnet pulsing by magnet rotation 9-46177
- in textbook of quantum mechanics 9-41756
- theory 9-49040
- theory 9-30855
- in thermal expansion phonon-enhancement contrib. calcs., use of T_c press. depend. calcs. 9-44838
- thermoelectric and thermomag. eff. in superconductors, existence 9-37456
- transition temp., effect of cond. electron density 9-24144
- transition temp., variational calc. 9-35352
- transition temp. press. depend. for nontransition metals 9-30858
- transport eqns. and Fermi-liq. effects 9-35347
- tunnelling proc., one- and two-part. 9-28470
- two-zone with mag. impurities, thermodynamic critical mag. field derivation 9-41172
- type I, flux distribution observations in thin films of varying thickness 9-28472
- type I, superheated states, obs. method 9-39595
- type-I, flux-flow noise 9-24152
- type-I, resistance of current-carrying intermediate state due to flux motion 9-30867
- type-I thick slab, field penetration, intermediate-state config. 9-30866
- undergraduate experiment demonstrating flux quantization and superconductivity 9-27156
- upper critical field for all electron mean free paths 9-26524
- vortex filaments, oscillation spectrum 9-38261
- vortex line interaction force with parallel dislocation 9-44704
- vortex nucleation near second-order phase transition and excited states of sheath near H_{c2} 9-24136
- white dwarfs and pulsars 9-24763
- Al₂O₃-Bi₂-Sb₂ film junctions, oscillatory effects on electron tunnelling 9-39657
- Al, lifetime of excitations, calc. 9-44935
- Al, quasiparticle recombination rate, calc. 9-44934
- Al fine particles prepared by evaporation in He gas, enhanced superconductivity 9-33270
- Al granular films, microwave conductivity 9-37466
- As, search 9-39602
- δ-Ga, props. 9-44937
- Ga single cryst., energy gap temp. depend., tunnelling meas. 9-33271
- H solid in metallic phase rel. to distorted h.c.p. lattice 9-42738
- In-Bi alloys, metastable states obs. 9-44938
- In, supercurrent decrease in gapless region 9-43038
- La₂C₃, bicr. structure, superconducting over entire homogeneity range 9-33272
- Mg, theoretical transition temps. 9-35358
- Nb-GaAs junctions, tunnelling effects 9-33340
- Nb-Si junctions, tunnelling effects 9-33340
- Nb-Ti-Zr-Hf alloy system, critical fields and current density, conc. depend. 9-39597
- Nb-Ti supercond. tubes, steady-state flux jumping in superimposed a.c. and d.c. mag. fields 9-37471

Superconductivity continued

- Nb-Ti tubes, steady-state flux jumping in superimposed a.c. and d.c. mag. fields 9-37471
 Nb₃Al, s.p.h.t., mag. susceptibility and Knight shift obs. 9-39599
 NbN thin films, high-field props. 9-35363
 Pb-(0-1.1at.%)Bi alloys, type I, critical field comp. dependence 9-43041
 Pb-Si junctions, tunnelling effects 9-33340
 Pb-tenon-Nb, coaxial line, freq. and time depend. using BCS theory 9-37487
 Pb, intermediate state, effect of transport current 9-49054
 Sb under press. 9-39602
 Sn₄As₃, and carrier conc. and ionic model obs. 9-37474
 Sn₄P₃, and carrier conc. and ionic model obs. 9-37474
 Sn small particles in tunnel junctions 9-43045
 SrTiO_{3-x} degenerate semicond., soft-mode supercond. obs. 9-33275
 Ti-(20 at.%) Nb alloy, props. correlation with metallurgical props. 9-39603
 Ti binary and ternary solid solns., supercond. transition temp. 9-23989
 V-Si, critical current density change on structural transformation suppression by uniaxial stress 9-24162

type II

- alloy with rigid vortex lattice, critical currents 9-37478
 anisotropic pinning and guided motion of vortices 9-43035
 book 9-47081
 clean material, upper critical field temp. depend. determ. 9-33267
 current flow, alternating mag. field effect 9-28473
 dirty supercond., transition temp., effect of small superparamag. grains 9-44932
 e.m. radiation from moving vortices due to fluctuating currents 9-35355
 films, equilib. config. of flux lines 9-43034
 flux jumps in slabs of nonideal supercond. 9-35354
 flux line, density and arrangement, depend. on specimen radius vector due to lattice defects 9-35356
 flux line lattice, rectangular 9-28479
 flux mobility props. assoc. with diamagnetism 9-41175
 flux pinning in thermodynamically reversible superconductors 9-47084
 flux vortices, pinned, response to l.f. fields 9-49029
 flux-creep mechanisms, irreversible magnetization evanescent decay obs. 9-43036
 fluxoid pinning in nonideal material, force between a fluxoid and a lattice defect 9-47086
 fluxons, nucleation and propagation in thin cylindrical specimens 9-44933
 flux penetration in anisotropic superconductor 9-47087
 hardening mechanism for carrying high currents in high mag. fields 9-49044
 magnetic instabilities in hard superconductors, adiabatic critical state 9-47085
 magnetostriction due to surface currents, elastic consts. calc. 9-26620
 mixed-state thermal resistivity in irreversible supercond. 9-33266
 nonlinear resistance in mixed state, theory of pinning effect 9-49042
 pinning effect on the nonlinear resistance in mixed state, theory 9-49042
 powders, echo formation 9-24147
 pressure, hydrostatic, effect on transitions 9-49052
 spin diffusion 9-24339
 susceptibility meas. in l.f. fields, phase sensitive detector 9-49029
 theory 9-49040
 thermodynamically reversible superconductors, flux pinning 9-47084
 transport currents when in resistive state in high magnetic fields, flow resistivity and Hall angle 9-49043
 vortex oscillations, damping 9-30868
 vortices, single, electronic and magnetic structure eqns. 9-41176
 In-(3.9 at.%)Pb alloy, type I-II transition obs. 9-47089
 Nb-Mo alloys, thermal and elec. conductivities, Nernst-Ettinghausen coeffs. 9-47091
 Nb, deformed, dislocation distribution eff. on specific heat rel. to fluxoid pinning 9-30875
 Nb₃Sn, a.c. field-induced flux jumps 9-37468
 Nb₃Sn, positron annihilation, electron-pairing eff., γ ang. distrib. meas. 9-30874
 Pb-(10wt.%) In oxide coated powder, flux pinning by oxide films 9-49045
 Pb-Tl alloy, fluxons, nucleation and propagation in thin cylindrical specimens 9-44933
 Pb-(1.1-56.5at.%)Bi alloys I critical comp. dependence 9-43041
 Ti-(22 at.%)Nb alloy critical currents 9-37478
 V₃Sn, V⁵¹ nucl. spin-lattice relax. time, temp. variation 9-35371

Supercooling

- of fog to cause ice nucleation, rel. to velocity and growth rate of falling crystals 9-41511
 rel. to nucleation of ice and water on AgI crystals 9-41510
 nucleation of water in He, H₂, O₂, Ar and CO₂ 9-26075
 triglycerides, recrystallization at low supercooling 9-37106
 vapour in expanding flow, number of condensation centres 9-28184
 water, dynamically induced freezing, physical stimuli obs. 9-34957
 water, growth rates of ice dendrites 9-39200
 water, ice nucleation, time lag activation energy, formation probability 9-32814
 water, single cryst. ice cyl. growth, interfacial free energy and morphological stability 9-37102
 water, vitrification temp. estimate 9-23584
 water droplets, rel. to shock waves, pre-heating, aeration and elec. field, obs. 9-39134
 water drops, AgI particle de-activation 9-42696
 Bi-Te alloys, nucleation, NMR obs. 9-23583
 Bi nucleation, NMR obs. 9-23583
 Bi nucleation, supercooling depend. on liq. drop size 9-28179
 Ga, X-ray scatt. obs. at 19°C 9-30371
 Na, subcooled, heat transfer from hot spheres, vapour formation at surfaces 9-28116
 Pb nucleation, supercooling depend. on liq. drop size 9-28179
 Sn nucleation, supercooling depend. on liq. drop size 9-28179

Superexchange see *Antiferromagnetism; Exchange interactions***Superfluidity**

- see also *Helium/liquid; Quantum fluids*
 Bose liquid, superfluid density 9-22160
 Bose superfluid, Green's functions and relns. between kinetical coeffs. 9-22155
 Bose superfluid, Green's functions in hydrodynamical approx. identities 9-22156

Superfluidity continued

- Bose system, coherent state formalism 9-45795
 corrections to β -decay of deformed nucleus 9-42240
 dense liq., shear, flow, vortex waves and rings, eqn. at zero temp. 9-30446
 Josephson effects, review of experimental work 9-33277
 phase transitions in one and two dimensions 9-34048
 popular article on change of state 9-48734
 quantum macroscopic effects 9-30447
 superconductors, eff. of quantum phase fluctuations of order parameter 9-24141
 in textbook of quantum mechanics 9-41756
 wave equations, macroscopic 9-47780
 He, entropy of superfluid component 9-23567
 He, flow, pressure-driven; press.-vel. depend. determ. 9-36912
 He, liq., superfluid fraction contained in porous Vycor glass 9-34943
 He, relaxation function expressions for thermal conductivity χ 9-32811
 He adsorbed films, third-sound obs. 9-34946
 He II, counterflow in rot. channel 9-48731
 He II, positive ion mobility, scatt. by elementary excitations 9-40814
 He II, thermal quenching in long channels, critical state condition 9-44608
 He II, thermodynamic functions, analytic expressions and macroscopic props. 9-23564
 He II temp. depend. of critical heat current 9-39125
 He unsaturated films, model describing onset of superfluidity and third sound 9-40813
³He solns. in ⁴He, concentration depend. nuclear spin polarizations 9-32807
⁴He containing ³He impurity quasipart., excitation spectrum, effective inter. energy 9-23563
³He-⁴He solns., fourth sound propag., λ point to 0.5°K 9-26146

Superlattice structure see *Alloys; Crystal structure, atomic; Solid solutions***Supernovae** see *Novae***Superparamagnetism** see *Ferromagnetism***Supersonic flow**

- see also *Shock waves*
 aerodynamics, drag minimization, stability of delta wings and boundary layer transitions 9-32727
 air, energy transfer between different degrees of freedom behind hypersonic shock 9-46564
 around two parting bodies 9-44514
 control surfaces, at Mach 6, turbulent heat transfer for attached or separated flow 9-26006
 in ducts with statistically roughened walls 9-28068
 electron concentration meas. two-wavelength laser interferometry method 9-48588
 front structure, turbulent, of axisymmetric compressible wake 9-28070
 gas, ionised around cylinder with oscillating surface 9-30265
 in gas, steady plane, containing arbitrarily large number of shocks, calculation 9-36795
 of gases, finite-difference technique for numerical computation 9-36796
 hypersonic flow around blunt body, heating theory 9-26007
 hypersonic near wake flow, FORTRAN program for calculation of solutions 9-40632
 hypersonic over slender cone, circumferential nonuniform heating 9-44517
 hypersonic round a slender body, laminar boundary layers 9-26003
 interferometry of transonic currents 9-29468
 jet, flow around infinite wedge 9-44515
 jet outflow into channels, calc. of min. press. and press. in front of flow at onset 9-28067
 laminar boundary layer for Mach nos. to 15 9-46433
 laminar separated, heat transfer calc., integral method 9-40729
 leading edge, sharp, kinetic theory 9-26009
 light diffraction by supersonic waves, Raman-Nath eqns., exact soln. 9-22457
 light diffraction by supersonic waves, Raman-Nath eqns., soln. 9-27390
 magnetohydrodynamic generator, optimisation, restriction of angle of mouth of duct, 9-30192
 plasma around 2 dims. mag. dipole 9-38966
 plasma wind tunnel, Mach 3, using magnetic nozzle 9-32724
 projectile wake, L.P., Schlieren obs. 9-30331
 sandwich plates, flutter evaluation 9-47807
 around segmented bodies, gas quality effect 9-42591
 shock wave interact. with superphonically moving body. soln. 9-25109
 shock waves flow past wedge-shaped profile 9-42598
 skin friction measurement using heated film gauges 9-42595
 spatial, around elliptical paraboloids and cones, calc. by finite-difference method 9-42589
 thin film gauge for meas. of skin friction in supersonic flow 9-23244
 trail behind blunt bodies 9-42590
 turbulent jet from axisymmetric nozzle with underexpansion 9-42594
 viscous heat conducting gas, asymptotic damping of disturbances, second approx. derivation 9-23384
 wake, 2 dims., turbulent mean-flow obs. 9-26008
 wake, laminar compressible, behind long slender cylinder, theory and expt. 9-23381
 wings of complex shape, aerodynamic characts. 9-42600
 He, visualisation by electron beam fluorescence probe 9-46559
 N₂-CO₂ in Laval nozzle, expansion, CO₂ population inversion 9-48648

Supersonics see *Ultrasonics***Surface diffusion** see *Diffusion in liquids; Diffusion in solids; Surface phenomena***Surface energy**

- see also *Crystal electron states/surface*
 alkali halides, (100) face 9-30478
 alloys, twin boundaries, coherent, free energy 9-44714
 calcite crystals, cleavage energy, infl. of Fe, Cu and S trace impurities 9-30479
 diamond, entropy, phonon contribution 9-23617
 droplets, embryonic, in liquid nucleation from vapour 9-39138
 excess solid-liquid free energy, calc. from dendritic growth obs. 9-37107
 glass, fracture surface energy 9-42903
 ice, at ice-water vapour, ice-water, ice-ice boundaries, exptl. determ. 9-39153
 ice-water interfacial free energy and morphological stability theory 9-37102

Surface energy continued

- ionic crystal, potential of half-crystals bounded by plane built-up with point ions 9-32831
- liquid binary mixture, critical, diffuse interface obs. 9-39084
- metal, self-consistent calc. for semi-infinite electron gas model 9-47052
- metals, f.c.c., evaporated, on substrate, interfacial energy in stability and shape calcs. of nuclei 9-32895
- metals, f.c.c. and b.c.c., anisotropy and equilibrium shape 9-36937
- metals, rel. to vacancy concentration 9-32830
- metals, twin boundaries, coherent, free energy 9-44714
- mixed crystals, equilibrium form, surface composition and surface free energy 9-36931
- pyrographite 9-42712
- in recrystallization, secondary, role 9-46917
- steel, transformer grade with S coated surface, role in secondary recryst. 9-46917
- transition metals, correlation with work function 9-33414
- twin band-grain boundary junctions, relative interfacial free energy meas. 9-44712
- twin/grain boundary relative free energy ratio meas., role of misorientations 9-44713
- Al liquid, polytherms 9-40781
- Cd, anisotropy, from equil. shapes of Ar bubbles 9-46717
- CdS, photovoltage and work function changes on exposure to oxygen 9-28211
- Fe(3 wt.%Si) alloy, relative variation for (110) and (100) planes, under annealing atmosphere 9-26180
- Fe(3wt.%Si) alloy, changes on (110) and (100) planes infl. of annealing 9-34979
- Fe, solid, determ. by inert sessile drop method 9-32836
- KCl fracture, ionizing irradi. effects 9-28372
- Mg, anisotropy, from equil. shapes of Ar bubbles 9-46717
- Ni spherical single crystal, anisotropy determ. by thermal etch structures 9-46716
- PbTe, charge distrib. from adsorption meas. 9-39173
- Ti, 'zero creep' method, 1600°C 9-23621
- W, anisotropy meas. of tips with field ion microscope 9-34980
- W single crystal, <100> axis, determ. from fracture stress and crack length, 77°K 9-33095
- WSi₂-n-Si interface, barrier height reaction-process dependence rel. to interface structure 9-42715
- Zn, cleavage, of basal plane 9-30481
- Zn interfacial energy of (0001) plane in contact with liq. Hg, 298°K 9-40837

Surface ionization *see Ionization, surface***Surface measurement**

- see also Area measurement*
- emission, microscope, surface material determ. from electron energy distribution 9-22357
- interface, solid-liquid, temp. and vel. meas. by thermoelec. probe 9-39210
- interference microprofilometer with single objectives 9-36350
- lenses, testing by non-contacting interferometer 9-34203
- molecular scanner, by spatial variations in emission of atoms or mols. 9-42709
- optically rough, interferometric meas. using CO₂ laser source 9-45993
- pressure, surface balance design suitable for oil-water, air water interfaces 9-34006
- roughness, reflectometric method 9-43207
- spherical deep, and microscope objectives, absolute, by laser interferometry 9-26176
- temperature of microscopic specimens, equipment 9-40288
- tribology, review 9-36105
- W polycrystalline electrode of thermionic converter, electron mirror microscopic investigation 9-24254

Surface phenomena

- see also Adsorption; Capillarity; Catalysis; Electron emission; Films; Ionization, surface; Liquid waves/surface; Sorption*
- adsorbed layer on model cryst., influence on vibr. props. 9-37311
- acoustic wave scatt. by uneven liquid-solid interface 9-45857
- acoustic waves on solids, attenuation due to interaction with phonons 9-28416
- air-solution interface, cathode growth in Cu electrodeposition 9-28810
- air-water interface, wind stress coeffs. 9-41503
- of alkali halide crystals, surface phenomena, decoration method with electron microscopy 9-23619
- alkali halides, etching dislocations 9-23618
- alkali halides, tension of (100) face 9-30478
- alkali halides, topography change due to temp. effects (thermal attack) 9-30477
- alloy, binary, thin films, effective surface diffusion coeffs., vol. diffusion effect in electron diff. obs. 9-39379
- alloy, dilute binary, freezing, interface stability analysis 9-36920
- alloy melt, binary, interface stability during solidification 9-34958
- Auger e spectrometer for analysis of contaminants on the surface in ultrahigh vacuum work 9-39150
- Auger electron study 9-29961
- bimetallic interface, partially bonded, forces of interaction with stationary screw dislocation 9-35089
- bubble, plasma oscillations 9-39574
- charge, distribution on dielectric capacitive probe for meas. 9-31892
- charged monolayer at liq. interface, ideal eqn. of state 9-34873
- during chemical diffusion 9-35120
- clay suspensions, effect on plastic flow behaviour 9-23548
- conducting, deflection of neutral atomic or molecular beam 9-34575
- crystals, anisotropic, pseudosurface waves, characts. 9-27222
- crystals, layer form. during plastic deform., role of slip steps 9-46896
- crystals, layer form. during plastic deform., role of slip steps 9-46895
- defect prod. due to ion bombardment in single crystal. 9-26177
- diamond, entropy, phonon contribution 9-23617
- diatomic gas in contact with diatomic crystal, thermodynamic equilib. 9-32834
- dielectric, charge density meas. 9-37574
- dielectric, nuclei formation around point charges 9-42747
- dielectrics, resist., meas. apparatus 9-22322
- diffusion, effect of non-equilib. segregation 9-48871
- diffusion of tracers in metal surfaces use of microtome to obtain suitable surfaces 9-46843
- dye-photoconductor interfaces, photovoltaic effect 9-43135
- elastic waves, charact. and props. 9-36171
- electrets, surface charge, eff. of atmospheric pressure 9-37602

Surface phenomena continued

- electroacoustic surface waves in piezoelec. or conducting solids 9-28425
- emulsion film, curvature at oil/water interface 9-34935
- enthalpy, relationship with characteristic temp. 9-28205
- equilibrium surface struct. changes of cryst. grown under irradiation 9-37021
- erosive rupture due to friction and fluid flow around surface, mechanism 9-23912
- exoelectronic emission of layers during sliding friction 9-24247
- f.c.c. cryst., surface atoms mean square displacements and vels., temp. depend. 9-44806
- Fermi atoms adsorbed on substrate at low temp., specific heat 9-46730
- Fermi-Thomas response of metal surface to external point charge 9-44620
- films on Ge, X-ray stress topography 9-34983
- films on Ge, X-ray stress topography 9-32839
- fluid, parametric instability in alternating elec. field 9-23207
- frictional wear, probabilistic model 9-37270
- gas-solid interactions at ultra-high vacuum 9-39152
- gas-surface interactions, continuum and discrete lattice models 9-40836
- granulation phenomenon of laser illuminated scattering surface 9-43919
- graphite sliding against stainless steel, interface geometry rel. to wear 9-41036
- impurities effect on epitaxial processes 9-42721
- inert gas crystals, dynamical props. by molecular dynamics method 9-39191
- inert gas crystals, dynamical props. in quasiharmonic approximation 9-39190
- interface between metals, clean 9-36936
- interface distribution coeffs. during solidification of ideal binary syst. in presence of heat flow 9-37100
- interface monolayer thickness calc. from van der Waals gas constant a 9-23449
- interface reactions, press. effects 9-24531
- interface stability, solid-liq., of semi-transparent mats. 9-37057
- interface stability bet. liq.-solid phases in freezing of dil. binary alloy 9-36920
- interface stability of lamellar eutectics 9-36935
- interface stability of large facets on soln. grown cryst. 9-36984
- interfacial flow near two-phase boundary, critical wave length from linear theory 9-40633
- interparticle interference eff. in diff.-controlled growth, influence on morphological stability 9-37058
- kerosene, rheology near solid boundary 9-39069
- light scatt. obs. of interface props. 9-23503
- liquid, highly viscous, stimulated light scattering 9-42655
- liquid, shape of cavity formed by impinging air jet 9-40762
- liquid, simple, density change in transmission zone and surface tension obs. 9-46621
- liquid, stimulated light scattering, theory 9-26109
- liquid binary mixture, critical, diffuse interface, optical reflectivity obs. 9-39084
- liquid drop, coalescence at liq.-liq. interface, effect of surface active agent 9-36838
- liquid-solid interface, convective diffusion accel. by u.s. sound field 9-23615
- liquid-vapour interface in accel. container, large-amplitude irrotational motion 9-34711
- liquids, rheology near solid boundary 9-39069
- liquids levitation effect, u.s. imaging appl. for materials inspection 9-29292
- mat. surface, refl. of light, physical mechanism of the specular peak 9-41945
- melt/crystal interface, impurity encircled layer 9-48802
- metal, impedance in weak mag. field, field strength and electron surface reflection depend. 9-26514
- metal, laser-heated, time-resolved temp. meas. 9-32835
- metal, ordering of microcraters prod. by lasers rel. to purity 9-46715
- metal carbides, refractory, surface layer fracture due to giant laser pulses 9-44774
- metal interfaces, effective dielec. const. determ. 9-41230
- metal-semiconductor interface, interpretation of elec. props. meas. 9-43094
- metallic, clean surface maintenance in vacuum, charact. energy loss spectra methods 9-32832
- metals, tracer diffusion studies use of microtome 9-46843
- Mossbauer investigation using β spectra 9-30476
- nodal patterns of surface vibs, obs. by laser speckle 9-42710
- noise, low frequency, at barriers, spectral analysis by correlation methods 9-36521
- optical spin-waves in a Heisenberg ferromagnet 9-26628
- patchwise heterogeneous, heat of adsorpt. calcs. from condensation approx. 9-34999
- phase interface stability in isothermal ternary systems 9-36934
- physics of surfaces in rarefied gases, conference, Saclay, France (1968) 9-48747
- piezoelectric substrates, acoustic surface wave propag. 9-37320
- polymethylmethacrylate, molecular motion in surface layers, study by impulse NMR methods 9-23191
- polystyrene, molecular motion in surface layers, study by impulse NMR methods 9-23191
- porous electrode systems, effect of finite-contact-angle meniscus 9-31203
- porous mats., mutual attraction determination between two surfaces, method 9-39484
- quartz, cryst., acoustic surface wave propag., 30-800 MHz 9-37319
- quartz, surface conc. of broken bonds on fresh face 9-46734
- radiant heat transfer, effect of direction and wavelength depend. props. 9-22273
- radiation emission rel. to macroscopic roughness 9-41359
- rarefied gases, kinetic theory, and gas-solid interaction, book 9-44519
- sapphire-sapphire contact, thermal resistance 9-39544
- and self-fluidised layer, heat exchange mechanism 9-38316
- self-insulation of materials in a medium against intense light 9-27343
- semiconductor 9-43064
- semiconductor, n-type degenerate, plasma screening effect on electron energy spectrum 9-49099
- semiconductor, sensitizing-dye mol. regeneration 9-26553
- semiconductor-electrolyte interface, impedance meas. 9-43067
- silica gel, H-bonding in interaction of adsorbed mols. with surface OH groups 9-23650

Surface phenomena continued

- siliceous materials, surface conc. of broken bonds on fresh face 9-46734
 silicone resin films on Si, elec. props. and surface recomb. vel. 9-30959
 solid, clean, cohesion and adhesion, investig. methods 9-28203
 solid, contact area rel. to topographical, electrical, thermal and stress phenomena 9-28208
 solid-liquid interface, polar mol. orientation, i.r. absorpt. spectra obs. 9-46341
 solid-liquid interface impedance meas. 9-47467
 solid-liquid interface stability growth from stirred melts 9-37056
 solid-liquid interface stability of semi-transparent mats. during growth 9-37057
 solid-plasma interface polarization, theory 9-34976
 solid-solid London-Van der Waals force, temp. depend. 9-45934
 steel in water, self-insulation against intense light 9-27343
 substrate to N_2 nucleate pool boiling, effect of roughness and material 9-28189
 superconducting sheath, induced persistent currents 9-49035
 thermal conductance of imperfect contacts 9-41099
 thin films, surface vibration modes 9-48945
 vapour bubble growth on semi-infinite solid 9-28206
 water, flow on evaporating from capillaries 9-44533
 water with air flow over it, heat transfer obs., temp. instability obs. 9-34837
 waves, magnetostatic, amplification by interaction with drifting charge carriers in crossed elec. and mag. field 9-43816
 waves in presence of second sound 9-27186
 wires, sintering by surface diffusion 9-44783
 wires, sintering by surface diffusion 9-44782
 zeolite Y, interactions with adsorbed aromatic hydrocarbons from i.r. spectroscopy 9-24520
 Ag thin films, roughness, correl. with plasma reson. radiation 9-44621
 AgCl aqueous solution, space charge limited ionic transport at solution interface 9-32833
 Ag(111), scatt. of isotopic He and H_2 beams 9-42713
 Al, C or O impurities, identification of contamination by nuclear reaction analysis 9-26178
 Al, layer stress, effect on fatigue resistance and brittle fracture 9-23880
 Al_2O_3 particles-Cu matrix interface, dislocation generation, local shear stresses 9-30611
 Al foils, deform. markings, direct correlation of dislocation structures 9-23878
 Al-(2wt.%Cu), solid-liquid interface, microstructure and composition variation 9-34961
 Au on KCl crystal, surface diffusion rel. to temp., 130-500°C 9-40848
 BaTiO_3 , enhanced conc. of c-domains, X-ray diff. study 9-39683
 Bi, effect on magnetoresistance 9-30844
 CdS-fused quartz system, elastic surface wave structure and dispersion 9-45844
 CdS, discrete trapping levels, detection 9-28575
 Cu single crystals, markings, during early stages of fatigue 9-30637
 Cu surface atoms, Ar^+ bombard., charge exchange of scattered ions 9-48418
 CuAu(Al) alloy films, effective surface diffusion coeffs., vol. diffusion effect in electron diff. obs. 9-39379
 Fe-C alloy, contamination during H_2 annealing, effect on oxidation 9-36938
 Fe, Fe-Al and Fe-Cr oxides, effect of O chemisorption under high vacuum on surface conductivity 9-37822
 Ge, effect of atomic H on elec. props. 9-28515
 Ge, effect of quinone on surface props. 9-43093
 n-Ge, interaction with O 9-46718
 Ge, interface stability during growth from stirred melts 9-37056
 Ge, slow potential change mechanism 9-30927
 Ge, solid-liquid interface stability during growth from stirred melts 9-37056
 Ge, modified by alkylchlorosilane, adhesion and elec. charact. variation 9-48924
 Ge decoration of cleavage surfaces 9-48749
 Ge(Li), p-i-n detector reproducible method of chemically forming surface 9-46140
 n- and p-InSb, photoconductivity changes under X-irradiation 9-30993
 KBr, etching dislocations 9-23618
 KF, etching dislocations 9-23618
 LiF, etching dislocations 9-23618
 LiF cryst., He mol. scatt., theoretical 9-48751
 LiF transparency in the u.v. reduced by formation of surface film in air 9-33523
 LiF(001), preferential scatt. of Ar, correl. with lattice props. 9-42714
 Mo, interaction of O_2 on (100) surface, low-energy electron diff. 9-42732
 Na liquid interaction with 304 stainless steel, electron microscopy 9-28209
 NaCl, etching dislocations 9-23618
 NaF, etching dislocations 9-23618
 Nb superconducting layer, critical currents, nature 9-37472
 Ni film, diffusion of chemisorbed H 9-24547
 Pd-Ag alloy films, effective surface diffusion coeffs., vol. diffusion effect in electron diff. obs. 9-39379
 Pt- Al_2O_3 catalyst, surface transport of various gases 9-26195
 Re, obs. by field emission and field ion microscopes 9-46719
 Si, slow potential change mechanism 9-30927
 Si, surface resistivity of base region, method and suitable struct. 9-33336
 Si_3N_4 :P films, surface potential drifting 9-37579
 Si characts., eff. of Au doping 9-37535
 Si etched by H_2S gas 9-32837
 Si surface contamination, determination by large angle ion scattering 9-33333
 SiO_2 film on Si, and interface, charge density and electron donor sites 9-43099
 SiO_2 particles-Cu matrix interface, dislocation generation, local shear stresses 9-30611
 Sn-Zn eutectic, undercooling at the solid-liquid interface 9-46686
 Sn, surface active and inactive, effect on grain growth 9-48865
 W, catalytic activity distrib. in equilibration of $^{30}\text{N}_2$ - $^{28}\text{N}_2$ mixture 9-33662
 W, surface self-diffusion, 2,560-3,150°K, by atom process 9-44622
 W clean surface, thermal accommodation coeffs. of ^4He and ^3He 9-30501
 W layer formation by reactions with O and hydrocarbon, e emission microscope obs. 9-37127
 W ribbon at high temp. in low pressure O or ethylene atmosphere, anomalous reflection of rare gas atoms 9-40558

Surface phenomena continued

- W tip, morphology change by surface diffusion at 2500°K, obs. with scanning elec. microscope 9-48753
 ZnS polytypes, 2H-4H interface, electron microscope contrast effs. 9-28275
- Surface structure**
- alkali halides, topography change due to temp. effects (thermal attack) 9-30477
 atom location 9-42760
 dielectric single crystal substrates, real structure rel. to selective nucleation at surface local long range active centres 9-36990
 dislocations close to free surface, effect on electron microscopy contrasts 9-30605
 electron diff. examination, low energy 9-35044
 film with defects, electron scattering and conductivity 9-49016
 films, network growth morphology 9-23632
 glass, roughness rel. to light back scatter, inc. bulk scatt. effects 9-37692
 group IV-VI alloy epitaxial films, growth techniques and surface research 9-39157
 impurity equilib. conc. 9-23616
 interface, solid-melt, morphology obs. by technique using inert gas bubbles 9-39205
 ion-eroded electron microtopography obs. 9-35048
 LEED and energy analysis of scattered electrons determ. methods 9-42708
 Lummer-Gehrcke interferometer plates, error tolerance limits 9-34205
 metal, ordering of microcraters prod. by lasers rel. to purity 9-46715
 metallic surfaces in contact, effect of roughness and waviness on heat transfer 9-24037
 metals, roughness rel. to emissivity 9-43233
 mixed crystals, equilibrium form, surface composition and surface free energy 9-36931
 molecular layers on bulk substrate, lowering of m.p., n.m.r. meas. 9-40817
 Mossbauer investigation using β spectra 9-30476
 nuclear reaction analysis of impurities 9-28836
 opaque objects, interferometric generation of contour lines 9-36932
 opaque substance, porosity effect on emittance 9-49269
 optically rough, interferometric meas. using CO_2 laser source 9-45993
 orbital grinder-polisher for preparation of irradiated specimens 9-39465
 Permalloy films, roughness, effect on susceptibility 9-49211
 polyethylene, difference when crystallized in contact with Au or Teflon 9-23614
 polyethylene films, crystallinity rel. to substrate surface energy, i.r. obs. 9-34986
 preparation by cutting, lapping, polishing and etching 9-42711
 quartz, spires and terraces occurring on hydrothermally grown crystals 9-44642
 replica technique, two-stage using Bioten film 9-39151
 roughness, optical data processing obs. techniques 9-28204
 roughness, optical data processing obs. techniques 9-28204
 roughness effects on diffusion constants 9-42858
 semiconductor II-VI cpds., chem. polishing 9-44977
 semiconductor single crystal substrates, real structure rel. to selective nucleation at surface local long range active centres 9-36990
 solid, contact area, effects of topography under different loading and thermal conditions 9-28208
 step motion on crystal surfaces 9-36991
 targets for heavy ion channelling, proton scatt. etc., preparation 9-32882
 topography using Moiré patterns 9-39149
 vapour bubble growth on semi-infinite solid 9-28206
 zeolite Y, from i.r. spectra of adsorbed pyridine layers 9-24519
 Ag film, topography rel. to exposure to O_2 , N_2 , H_2O vapour or air during growth 9-34993
 Ag single crystal, atoms in (100) and (110) faces, mean displacement studies at low temps. 9-39248
 AgBr, influence on mechanism of Ag_2S formation 9-37024
 Al single crystal, pit formation during heat treatment 9-32946
 Al single crystals, under cyclic straining, microrelief changes, X-ray diff. method obs. 9-46777
 Al thin films, hillocks produced by annealing thermal cycling effect, electron micrographs 9-30705
 Ar (100), bulk-like and transformed, adsorpt. and diffusion of Ar atoms 9-35000
 Ar solid, equil. conc. of Ne and Kr atoms in (100) face 9-23616
 As (111) cleavage face vaporization pit growth at spiral dislocation site 9-30467
 Au, by large-angle Ar^+ scatt. on single crystal 9-48748
 Au film, topography rel. to exposure to O_2 , N_2 , H_2O vapour or air during growth 9-34993
 B,C rel. to cry. growth and two-dimens. nucleation at screw dislocations, obs. 9-28290
 BaTiO_3 , lattice deformations of (100) free surface 9-28210
 C deposits, structure and mech. strength, effect of deposition topography 9-26226
 CdS {0001} surfaces, LEED obs. 9-28211
 Co, defects due to chemisorbed layers in field ion microscope 9-26827
 Cr_2O_3 , sintered, metal content study by electron microprobe and elec. cond. probe 9-37279
 Cu, preferential deformation existence by dislocation density 9-41016
 Cu low energy e diff. meas. 9-35044
 Fe-Cr alloys polishing effects on pitting and anodic dissolution 9-24576
 Fe, defects due to chemisorbed layers in field ion microscope 9-26827
 Fe_2O_3 , sintered, metal content study by electron microprobe and elec. cond. probe 9-37279
 Fe low energy e diff. meas. 9-35044
 Ge, epitaxial grown by $\text{GeCl}_4\text{-H}_2$ reaction, surface morphology obs. 9-46761
 Ge epitaxial films from $\text{GeCl}_4\text{-H}_2$ system smooth surface conditions 9-36948
 Ge layer from thermodesorption and mass spectra obs. 9-36967
 Ge with Cs submonolayer on (111) and (100) plane, low energy diffraction obs. 9-30480
 Ge with K submonolayer on (111) and (100) plane, low energy diffraction obs. 9-30480
 Ge with Na submonolayer on (111) and (100) plane, low energy diffraction obs. 9-30480
 LiNO_3 , cryst. surface distortion, i.r. data 9-48750
 Mo, work-hardened, changes prod. by vacuum annealing 9-32932
 Mo-Re alloys, eff. of ht. treatment 9-24250

Surface structure continued

- NaCl, electrical relief by AgCl evaporation on C replica 9-32848
 NaCl, microstructure of growth surfaces, eff. of surface active impurities 9-23765
 NaCl cleavage surface, role of surface imperfections on selective nucleation of gold 9-37004
 NaNO₃, cryst. surface distortion, i.r. data 9-48750
 Nb, etch pits and sub-boundaries, optical microscopy obs., contribution to diffusion 9-32985
 Nb, work-hardened, changes prod. by vacuum annealing 9-32932
 Nd: glass, damage threshold improvement by chemical polishing 9-26171
 Ni, defects due to chemisorbed layers in field ion microscope 9-26827
 α -Pu, revealed by new electrolytic polishing and etching technique 9-39304
 Sb (111) cleavage face vaporization, pit growth at spiral dislocation site 9-30467
 Si, p-n junction, electrical structure imaging on C replica by AgCl evaporation 9-32847
 Si, stacking fault nucleation, growth and annihilation mechanisms 9-42844
 Si (111) and (100), by reflection high energy electron diffr. 9-48752
 Si single crystal, ion-implanted Au layer 9-39307
 Si single crystals, percussion marks on surface, divergent X-ray diffr. pattern 9-33037
 SiO₂, thermally oxidised, crystallographic symmetry of surface state density 9-23773
 Sn-Pb dilute alloys, electropolishing procedure to produce etched or polished surfaces 9-39959
 Sn, electropolishing procedure to produce etched or polished surfaces 9-39959
 Sn electrodeposited coatings 9-36933
 Sn treated with Br, investigation using Mossbauer β -spectra 9-30476
 W, bonding of surface atoms 9-26181
 W, C contamination, FEM-LEED studies 9-35071
 W, single cryst., thermal faceting rel. to O₂ adsorpt. and work function 9-35012
 W, work-hardened, changes prod. by vacuum annealing 9-32932
 W field emission tip, shape change obs. with electron microscope 9-39738
 W polycrystalline, defects rel. Cs absorption (thermionic converter electrode) 9-24254
 W ribbon, interaction of surface with inert gas beam 9-48754
 W tip, reshaping by surface diffusion at 2500°K, form. of solid drops 9-48753
 WSi₂-n-Si interface, rel. to barrier height reaction-process dependence 9-42715
 YFe garnet, chem. polishing 9-40835
 ZnO {0001} surfaces, LEED obs. 9-28211

Surface tension

see also Capillarity

- action on circular jet, finite amplitude effect on stability 9-39067
 n-alkoxy ethanol monomolecular films, surface viscosity at various temp. and pressures 9-23448
 bubbles, temperature dependent variations 9-32776
 contact angle and depth of free-energy minimum in thin liquid films 9-48689
 correction of master viscometer constant 9-28104
 critical pt., struct. and free energy of interface 9-42641
 critical tension under dynamic stress conditions 9-42618
 cyclohexane-methanol mixtures, near-critical, interfacial tension 9-34886
 detergent films, interface props. 9-23446
 electric and magnetic fields, external, effect 9-48692
 Eotvos expression deriv. from molecular model of classical liqs. 9-34869
 glasses, by capillary flow technique 9-36854
 ionic cryst. in presence of dipole moments 9-32831
 liquid, simple 9-46621
 liquid and its vapour, statistical calc. 9-31780
 liquid film, contact angle, meas. technique 9-36839
 metal surface wetting, effect of adsorbed water on critical surface tension 9-23437
 polyethylene, amorphous, significant structs. model 9-34887
 Rayleigh-Taylor instability, effect on linear and nonlinear phases 9-46598
 Shereshevsky's eqn. for binary mixtures checked experimentally 9-32743
 solid surface diffusion in thin liquid film flowing past in laminar motion, effect on rate 9-48668
 static meniscus in vertical circular cylinder, for range of Bond numbers and contact angles 9-34885
 thin liquid films, contact angle and depth of free-energy minimum 9-48689
 Ag, 1300-2200°K 9-28110
 Ar, solid, wetting, critical surface tension and contact angle meas. 9-23451
 Bi, 1300-2200°K 9-28110
³He, surface thickness, theoretical determination 9-39124
⁴He, surface thickness, theoretical determination 9-39124
³He-⁴He dilute soln. 9-30444
 Hg-rich binary and ternary alloys, reln. to work function 9-24246
 Hg, electrode, from electrocapillary curves 9-49384
 Hg, fatty acids on surface, test of two-dimensional scaled-particle theory 9-40782
 In-Pb system, temp. and conc. depend. 9-23471
 Kr, solid, wetting critical surface tension and contact angle meas. 9-23451
 Pb-Bi eutectic, and contact angle for drop on stainless steel, calc. from shape of drop 9-34867
 Pb, 1300-2200°K 9-28110
 Ti, 1300-2200°K 9-28110
 Xe, solid, wetting, critical surface tension and contact angle meas. 9-23451

Surface tension measurement

- from drops pendent shape, computer calc. 9-32775
 by isotope exchange, condensation coeff. elimination 9-39083
 sessile drops, and contact angle, from shape, by non-linear regression method 9-34867
 tensiometer, du Nouy, capabilities 9-36855

Surface texture *see Surface structure***Surveys** *see Reviews***Suspensions**

see also Aerosols; Sedimentation; Sols

- air-graphite, heat transfer agent, hydrodynamics, expt. 9-30437

Suspensions continued

- alcohol, with mineral particles, heterogeneous nucleation of polyamides 9-35030
 atmospheric lowest boundary layers, turbulent nonadiabatic diffusion 9-31304
 attapulgite, orientated, light scattering studies rel. to effect of alt. elec. fields 9-34929
 clay, plastic flow behaviour surface prop. dependence 9-23548
 colloid in gas, ionization-chamber detector and step-down amplifier, patent 9-34931
 colloidal, electrophoretic mobility in insulating liquids, apparatus for meas. 9-46662
 colloidal, with induced and permanent elec. particlemoments, electro-optical effects 9-42684
 concentration in (NH₄)₂SO₄, u.s. abs. technique 9-32802
 continuous media, asymmetric hydrodynamics 9-45806
 dilute orientated, constitutive eqns. 9-44603
 fluid-particle, flow induced by infinite rotating disk 9-26135
 gas-solid particle, distrib. of solid component in counterflow chamber by beta-raying 9-28160
 gas-solids, convective heat transfer coeff. at Reynolds no. 130,000 9-26136
 gaseous, statistical mechanics; dynamic and spectral eqns. 9-36902
 laser light scatt., spotted background structure 9-44602
 liquid-solid, heterogeneous, viscosity over whole range of solid conc. 9-28162
 orientation distrib. function of rigid particles suspended in fluid undergoing shear flow 9-46660
 polystyrene latex particles in air, elec. charge obs. 9-46661
 protein, electronic deposited of sprayed suspensions for e. microscopy 9-42686
 solid particles in viscous fluid, laminar flow 9-42624
 virus, absorpt. meas. with integrating photometer 9-31685
 viscoelastic spheres in steady laminar flow 9-44603
 BaO-Ar, as closed-cycle MHD working fluids, coagulation 9-30436
 C, colloidal, in insulating liq., electrophoretic development of electrostatic charge images 9-44604
 (NH₄)₂SO₄, concentration by u.s. absorption meas. 9-32802
 Na, liquid with high solid concentration, flow properties 9-23544

Suzuki atmospheres *see Crystal imperfections/dislocations***Switching time, ferroelectric** *see Ferroelectric materials; Ferroelectric phenomena***Switching time, ferromagnetic** *see Ferromagnetism; Magnetic properties of substances/ferromagnetic***Symbols** *see Nomenclature and symbols***Synchrocyclotrons** *see Particle accelerators/cyclotrons***Synchrotron radiation**

- amplification in stream-plasma system 9-25882
 cosmic, effect on electron propagation 9-43508
 from Crab nebula, model, and relativistic particle acceleration mechanism 9-49538
 electron energy distrib. calc. 9-29041
 electron moving spirally, theory 9-46062
 light sources calibration in ultraviolet range 9-36380
 losses in self-absorbed radio sources 9-27056
 magnetoactive plasma, single gyrating electrons 9-34758
 plasma, magnetoactive relativistic, transfer, and polarization of normal waves 9-27989
 in plasma by relativistic rotating electrons interact with magnetoactive plasma 9-25840
 polarised emission, generation and transfer in cosmic space 9-41650
 r.f., from trapped electrons above auroral zones 9-37961
 Scheuer luminosity meas. method queried for moving sources and quasars 9-27054
 solar radio bursts, h.f. cutoff due to anisotropic pitch angle distrib. electrons 9-45680
 spectra below Razin cutoff, asymptotic form, extragalactic radio sources 9-27060
 spectrum and polarization of a source of synchrotron emission with components flying apart at relativistic velocities 9-33916
 from supernovae galaxies and quasars 9-29042
 u.v., use in u.h. vacuum reflectometer 9-27396

Synchrotrons *see Particle accelerators/synchrotrons***Szillard-Chalmers reactions** *see Radiochemistry***Tables, mathematical**

No entries

Tables, physical *see Collections of physical data***Tachometers** *see Angular velocity measurement***Tandel** *see Dielectric devices***Tantalum**

- alloy with 10%W, emissive power and specific resistivity above 400°K, relationship 9-39547
 blocking patterns detection in solids, scanning 9-25529
 capacitor, improvement in elec. characts. 9-49151
 capacitor, preparation from low-density film and device characts. 9-49152
 cavitation damage validity of hydrogen penetration mechanism 9-44746
 cold-worked, internal friction and cold-work-peaks obs. 9-23870
 diffusion coefficients of C 9-35133
 diffusion of isotopes in W, lattice coeffs. meas. 9-40989
 dislocation relaxation at low temp., max. in dissipation vs temp. curve, and Reierls stress 9-23816
 foil, insulating material for space flight, outgassing behaviour 100-1800°F obs. 9-38173
 hardness, refining effects; electron beam melting 9-33101
 hydride and deuteride solid solutions, interstitial ordering 9-23990
 imperfect structure in single crystal rods 9-32930
 integral hemispherical rad. power and elec. resistivity, 1200 to 2800°K 9-43018
 magnetoacoustic effect, l.f., stiffness and attenuation, mag. field depend. 9-35283
 photoelec. cross sections meas., E_p=280 keV 9-22945
 photoelectric cross-section bs. for 662 keV γ 9-29962
 photoelectric cross-section of atom obs. at 84, 100 kev. 9-44282
 plastic strain ageing, low temp., hardening obs. 9-44767
 reactions with Pu and U oxides at high temps. 9-28782
 resistance meas. during supercond.-normal transition 9-37476
 spectral emittance, i.r. 9-45327

Tantalum continued

- sphere, heat transfer to liquid sodium during forced convection 9-26092
- sputtering, reactive, in mixed Ar/O atmospheres, mechanism 9-42716
- vibrational spectrum, computation 9-33168
- work function and surface energy correlation 9-33414
- He diffusion below room temp. 9-23843
- O interstitial impurities, diffusion coeff. and activation energy 9-28284
- Ta-Al point contacts, radiative emission at Ta energy gap freq. 9-25300
- Ta-Ta₂O₅-Nb superconducting thin film tunneling junction, theoretical and exptl. investg., and applic. to e.h.f. 9-26536
- Vfilm, preparation for nuclear studies 9-48766

Tantalum compounds

- nuclear quadrupole constants interpretation in ¹⁸¹Ta cpds. 9-45258
- Al-Ta alloys, dil., ²⁷Al n.m.r. rel. to impurity-disloc. effects 9-24504
- alloys with V, Nb and Ta, electrical resistivity as a function of temperature 9-39584
- CaO-Ta₂O₅ system, phase diagram, equilib. and melting points 9-39494
- Cr-(2 wt.%)Ta-(0.5 wt.%)Si alloy guide vane specimens, thermal fatigue testing 9-33075
- HfC-TaC solid soln., thermal expansion 9-26430
- Nb-Ta alloys, normal state sp. ht. 9-33181
- Nb-Ta alloys, type II superconductors, anisotropic pinning and guided motion of vortices 9-43035
- Nb-Ta solid solutions, hardening eff. of Ta 9-28385
- Ta-(20 at.%)Mo alloy single crystal, thermionic emission of (100) face 9-47211
- Ta-N film, electrical and optical meas. and electron diffraction analysis 9-23625
- Ta-Nb, solid solution alloys, lattice thermal conductivity, normal and superconducting state 9-30797
- Ta-Nb alloys, spectral coeff. 1300 to 2000°K at 0.65 μ 9-40795
- Ta₂O₅ lattice energies, heat of atomization, bond energy and dissociation energies, rel. to fund. props. 9-30494
- Ta₂O₅, emission spectra intensity struct. modifications influence 9-33560
- Ta₂O₅, film thickness meas. by electroreflectance interferometry 9-30486
- β-Ta₂O₅, unit cell meas. 9-39309
- Ta₂O₅ films, negative photocond. 9-24235
- Ta₂Si cryst., prod. by vapour transport react. 9-28231
- Pt₈₅Ta₁₅, superconducting behaviour 9-24163
- TaC, electron emission, second., total yield and charact. energy losses 9-31008
- TaC_{0.76}, ordering in struct., neutron diffraction obs. 9-40913
- TaC₂, magnetic susceptibility, temp. and comp. depend., 20-300°K, $\chi = 0.73-0.97$ 9-43153
- TaC emissivity and elect. conductivity obs. 9-37374
- TaF₅, liquid, Raman spectra rel. to possible polymerization 9-26119
- TaH, limiting composition, dissociation processes and lattice transforms 9-31185
- TaO capacitor films, Mo additive mass spectrometry 9-39968
- TaSe₂, structure of a new polymorph, X-ray diffraction 9-35011
- TaX_n anions (X=Cl, Br or I), electronic absorption spectra 9-30060
- Ta-N system, ordering phases and intrusion superstructures 9-46794
- Ta-O system, ordering phases and intrusion superstructures 9-46794

Targets see *Nuclear bombardment targets*

Teaching

- astronomers training in Britain 9-25016
- atomic physics, college textbook 9-48370
- atomic physics textbook 9-48371
- beats, frequency of occurrence 9-41810
- centripetal force magnitude, elementary derivation 9-43710
- conductivity, elec., of metals at low temp., temp. depend. 9-44902
- cosmological Friedman-Lemaître models, simplified treatment using observer's view 9-40113
- the deaf, turbulent consonants pronunciation, joint distrib. indicator device 9-38136
- education of physicists for work in industry 9-41721
- educational requirements of physicists in industry 9-41722
- electricity and magnetism college level textbooks 9-31866
- electric fields outside conductors carrying steady currents 9-45724
- electron optics, textbook 9-29165
- electronics experiments, laboratory manual 9-29143
- e.m. induction, various approaches 9-45722
- e.m.f. and p.d. 9-22037
- equilibrium producing molecular collisions and the expansion of phase space 9-45777
- equipotential and field line plots of 2-charge system for the student 9-47716
- Faraday's law, demonstration of teaser 9-45887
- Feynman course, exercises complementary to pt. I 9-47717
- Fresnel zone plate problem, soln. 9-43916
- general physics, in science faculty of U.N.A.M. (Universidad Nacional Autónoma de México) 9-36098
- group theory, applications for physicists 9-31750
- heat, definitions, review 9-45721
- holography and coherent imaging, review for undergraduates 9-25321
- holography in undergraduate course 9-38389
- informal teaching project tried at Northeastern University Boston, USA 9-45713
- introductory American physics textbook 9-34001
- isomer production by ⁶⁰Co irradiation, laboratory teaching expt. 9-48261
- laboratory as place of research 9-36097
- laboratory course treated as series of small research projects rather than demonstrations 9-38186
- magnetic monopoles in elec. field, quantization model 9-45888
- manual, programmed, to accompany American physics text 9-31736
- materials science at U.N.A.M. (Universidad Autónoma de México) 9-29146
- mechanical equilibrium of an isolated system without thermal equilibrium 9-36206
- middle level physics, scheme for new plan 9-29145
- molecular symmetry models for undergraduate chemistry course 9-48447
- Newton's third law, need for clarification 9-41789
- Newtonian mechanics textbook 9-36155
- nuclear models 9-22036
- nuclear theory, graduate level textbook 9-22039
- optics, undergraduate lab. facilities 9-27155
- orbital angular momentum, why it cannot be half-integral 9-43739
- physicists education for industry, specialist versus generalist 9-41725
- physicists extramural, post-graduate, and refresher courses, responsibilities of industry and universities 9-41726

Teaching continued

- physics American college textbook, introductory 9-36104
- physics college textbook for non-scientist 9-31735
- physics in biological sciences 9-29147
- physics textbook, American college, produced by physical science study committee 9-41730
- physics US college textbook, introductory 9-31734
- plasma display for computer controlled system, influence of gas composition and signal waveform 9-29136
- point groups, key to classification 9-45737
- Poisson statistics of nuclear instruments analyzed 9-46129
- practical physics, new techniques 9-22033
- prism, minimum deflection for symmetric ray paths, elementary proof 9-36338
- quantum mechanical theory of scattering from real multipoles 9-47761
- quantum mechanics, first introductory textbook 9-40239
- quantum mechanics, infinite tilted well problem and appl. 9-43748
- relativistic system in equilibrium, torques and angular momentum 9-38213
- relativistic two-particle collision kinematics, convenient 4-vector eqn. 9-36123
- relativistic velocity addition formula, representation in circular functions 9-38212
- relativity, special, four new approaches, survey 9-43707
- relativity, special, relationship between rest mass and pot. field 9-47715
- rotation operators in quantum mechanics 9-43705
- satellites, artificial, 16, orbital parameters and plots 9-45725
- scattering analyzer, macroscopic 9-45715
- school microscope 9-27399
- seminar, 'Perspective on science' 9-27154
- sound (complex) identification, training techniques 9-31696
- statistical mechanics, canonical distribution and Archimedes principle 9-27178
- textbook, undergraduate on waves and fields 9-38188
- university cooperation with industry, effect on physicists career 9-41723
- university courses adaptation to industrial needs for physicists 9-41724
- University of Flinders, Australia, 2nd year lab. course 9-25015
- X-rays, teaching aids and literature guide 9-45712
- α particle path length determ., energy loss in air meas. 9-45716

demonstrations

- air track gliders, recording 9-38187
- atomic superelastic collisions using linear air track 9-43701
- Atwood's machine, a simple frictionless rotation-free one 9-36101
- capacitor and inductor energy storage 9-43702
- centrifugal force 9-36102
- Curie point, ferromagnetism demonstration using Monel metal 9-22035
- Doppler shift demonstration apparatus, X-band, single antenna 9-43709
- elastic and inelastic collisions using bouncing and non-bouncing balls 9-22030
- electrometer, vacuum tube, and test rig 9-29150
- electrostatic generator, principles 9-45904
- e.m. pulse dispersion, simple expt. 9-47711
- e.s.r., simple apparatus for low fields 9-45901
- ferroelectricity, expts. with Rochelle salt and triglycine sulphate 9-37590
- ferromagnet at Curie temp., hysteresis loop degeneration 9-43704
- film quality evaluation using optical particle detector 9-23623
- fluid flow in rotating system, spin-up problem 9-29152
- forced oscillations and magnetic resonance in the introductory laboratory 9-41727
- Fourier series solns. to oscillatory problems, demonstration using combination tones 9-43708
- Franhofer diffraction and interference 9-41729
- gnomonic projection production and viewing 9-36152
- Hamilton's least action principle, computer programme to produce graph to illustrate 9-36099
- harmonic oscillator, rotating, two-dimen. 9-45719
- holography table, inexpensive 9-36319
- Josephson effect, a.c., simple undergraduate apparatus for its obs. 9-47714
- Kundt's tube, temp. distrib., thermistor obs. 9-45723
- lecture auditoria design 9-29149
- microwave optical bench for undergraduate experiments 9-36218
- Miller indices demonstration model 9-22034
- moon radar ranging expt. for students 9-43706
- Mossbauer spectrometer for graduate laboratories 9-43712
- optical diffraction from monolayer of polymer spheres using He-Ne laser 9-47712
- oscillating spring and weight, spring forces analysed 9-36100
- parabolic reflector rays from off focal-point source 9-29161
- phase and group velocity by considering superposition of two plane waves 9-45720
- plasma prod. using reflex discharge 9-43711
- platform, adjustable, for laboratory 9-36103
- plucked string, theory 9-43703
- prism spectrometer experiment improved computer version 9-43700
- pumping on a swing, analogy using pendulum 9-45726
- radioactivity, graphical concepts 9-25017
- Ramshauer effect, classical analogy 9-47713
- relativistic expanding wavefronts demonstrated on computer-generated film 9-43698
- Rutherford α scattering with Al surface and ball bearings 9-22031
- shock waves, simple model 9-36200
- sound, speed meas. 9-45853
- spatial filtering experiments for the undergraduate laboratory 9-43699
- stereographic projection production and viewing 9-36152
- superconductivity and flux quantization, undergraduate experiment 9-27156
- temperature scales, stretched wire useful in experimental courses 9-36214
- time-of-flight neutron experiment for undergraduate laboratory 9-45718
- velocity of light, low freq. phase-shift method 9-48079
- Wulff-Bragg law for cm. e.m. waves, apparatus 9-46763
- Ge(Li) detector used to demonstrate meas. of photoelectric Compton and pair-production cross-sections 9-36522

Technetium

- TC I spectrum, energy levels and classified lines, tables 9-34551

Technetium compounds

- Tc complex, hexahalo, K and Cs salts, vibration spectra and force constants 9-32487
- TcF₆ spectrum, i.r., Jahn-Teller effect 9-34647

Tektites *see Meteorites***Telescopes**

- anastigmats, flat-field, distortion-free 9-29108
- γ ray, with large area wire spark chamber, balloon-borne 9-38128
- meson, meteorological effects and their correction 9-42116
- resolving power 9-22464
- Schmidt-Cassegrain system, afocal 400 mm, diffr. limited from 0.4 to 0.5 μ 9-40383
- scintillation counter, for cosmic ray studies, large area, high charge resolution 9-27571
- spectrographs on telescopes, research possibilities with moderate dispersion 9-31677
- X-ray, parallel concentration, Bragg diffr. application 9-27153

astronomical*see also Radioastronomy*

- balloon-borne, operating characts. 9-27111
- Cassegrain, flat-field 9-33959
- collection of review articles for the amateur 9-49597
- correctors, two-mirror, for improving effectiveness 9-27112
- for cosmic ray, equator points and vertical intensity measurements 9-46125
- errors in star and planet coincidence obs. 9-40195
- extra-terrestrial 30m instrument, possibilities 9-24933
- Hartmann test, appl. to telescope adjustment 9-43687
- mirror, segmented, with automatic figure control 9-27369
- mirror deformable, with automatic figure control 9-25339
- positioning depend. on atmospheric temp. fluctuations 9-31675
- radiotelescopes suitable for more detailed exam. of radio sources 9-33958
- satellite, coupled to crew compartment, attitude stabilization 9-26974
- Schmidt camera, image quality exam. using spot diagrams 9-49596
- solar, balloon-borne, guiding system 9-26975
- space-borne, programmes review 9-26973
- Universal Reflecting, 2m, Nova Delphini 1967 obs. 9-40151
- u.v., automated, for satellite observatory 9-28976
- X-ray, glancing incidence, opt. design and prototype flight test 9-29109
- He liquid cooled, rocket-borne, with i.r. detectors 9-38123

Tellurium

- crystal growth by Czochralski method 9-39214
- crystals, blade-like, growth from vapour 9-23668
- cyclotron reson. in p-type Te, quantum effects 9-44896
- cyclotron resonance, isoenergetic surfaces ellipsoids at low mag. field, obs. 9-30827
- cyclotron resonance expts., rel. to valence band and secondary lines at high freq. 9-35324
- Debye temp. by X-ray reflections from powders 9-28428
- defects in single cryst., X-ray topography 9-44709
- diffusion of Ag along thin film in Ag-Te couple 9-35135
- effect on quantum efficiency of ZnS:Mn phosphor luminescence 9-43261
- Fermi surface of holes, shape, Shubnikov-de Haas eff. meas. 9-26552
- film, conduction, effect of ferroelec. substrate 9-28502
- growth, hydrothermal 9-37027
- internal friction by electron-hole pair recombination 9-23871
- magnetoresistance, longit., rel. to impurity conc., 1.6 to 20.4°K 9-28457
- Mossbauer effect, anisotropy at 80°K 9-31090
- Mossbauer emission spectra of ^{125}Te following thermal neutron capture in ^{124}Te 9-37703
- optical activity in single crystal, interpret. 9-37686
- p-type, cyclotron reson., quantum effects 9-44896
- p-type, warm hole energy relax. time 9-49087
- paramagnetic chemical shift, anisotropic 9-43272
- piezoelectric const., strain-induced electronic displacement rel. to cores obs. 9-35493
- whiskers, simultaneous growth with CdTe crystals by vapour phase reaction 9-28232
- ^{125}Te , nuclear decay effects on electronic structure of decaying atom and its bondinb in cpds. from Mossbauer meas. 9-38769
- Bi-Te, second-harmonic generation by damped Alfvén waves and helicons 9-41160
- in Bi layered structure, helicon propag. rel. to carrier drift effects 9-43015
- GaAs:Te, stacking faults, electron micro. exam. 9-23822
- Te: ^{57}Fe , Mossbauer obs. of Fe ions 9-39819
- Te-Ag photovoltaic eff. obs. on contact 9-35511
- Te₂, high resolution emission spectra, giving rotl. constants suggesting $\Sigma-\Sigma$ transition 9-34644
- Te₂, photoionization 9-44484

Tellurium compounds

- chalcogenide thin films, amorphous, negative capacitance 9-33283
- chalcogenides A^{IV}B^{IV}C^{IV} with perovskite structure, synthesis 9-42755
- glasses, elec. conductivity and opt. absorpt. 9-30956
- minerals, isotopic anomalies of extracted Xe 9-42354
- Ag₂Te, thin films, struct. transforms compared with solid state 9-48927
- Bi-50-60at%Te, phase characterization by X-ray diffr. patterns 9-28394
- Bi₂O₃-TeO₂ films, optical absorption 9-35649
- bonding of decaying ^{125}Te atom from Mossbauer meas. of nuclear decay effects 9-38769
- Cd₂Hg_{1-x}Te alloys, photovoltaic effect assoc. with effective mass gradient 9-39730
- Cu₂Te, thin films, struct. transforms compared with solid state 9-48927
- (Hg,Cd)Te as i.r. detector material 9-47204
- (Hg,Cd)Te photodetectors for 1.5 μ 9-49160
- Hg_{1-x}Cd_xTe alloys, 1 eV band gap, photoconductivity 9-41267
- Hg_{1-x}Cd_xTe alloys, photoconductivity and material parameters 9-41266
- In-Te system, thin films, elec. and photoelec. props. rel. to conc. 9-30485
- In-Te system, thin films, phase composition rel. to conc. 9-30484
- Pb-Sn-Te system, phase diagram 9-36918
- PbTe, diffusion coeffs. of Pb and Te 9-44744
- Sb₂Se₃-Te alloy, liquid, thermal conductivity mechanisms 9-34900
- Se-Te mixed cryst., long wavelength optical lattice vibrs., i.r. reflectivity obs. 9-39826
- Se-Te solid solns., edge absorpt. and band gap obs. 9-43250
- Se-Te system, single cryst. growth phenomena 9-36997
- TeO₂-V₂O₅-BaO glass, spectral transmittance and microhardness 9-39847
- TeO₂, ^{125}Te Mossbauer emission spectra following thermal neutron capture in ^{124}Te 9-37703
- TeO₂ based glass, high refraction 9-41352

Temperature

see also High-temperature phenomena and effects; Low-temperature production

- in bodies of finite size, calc. via surface temp. without thermal props. of subst. 9-22297
- concept of temperature in international scales 9-45883
- control, automatic, for cryogenic systems 9-31864
- control, for e.p.r. samples, 10 to 80 K, automatic equipment 9-31882
- control of metallic targets in vacuo, electron beam and i.r. radiometry techniques 9-29329
- determining, in heat cond. problems, inc. of intergeometry of surfaces 9-27244
- electric furnace, linear controlled rise technique 9-36216
- field in nonlinear boundary problems, use of Lagrangian techs. 9-25115
- international practical temperature scale, interpolation of differences in resistance ratios of Pt thermometers 9-45884
- of lightning, calculation 9-31328
- logarithmic laws, validity study 9-45871
- relativistic transformation, covariant equilibrium distribution 9-45780
- solid, 1-dimens., thermally radiated, transient surface temp. and conduction soln. 9-22286
- transformation law in relativistic thermodynamics 9-22125
- turbulent liquid flow in pipe, temp. pulsation spectrum 9-26056

Temperature control *see Cryostats; Thermostats***Temperature distribution**

- age of heat distribution estimates, backward solution of heat equation 9-41843
- air flow, axial rotational with impulsive discharge 9-25976
- air-ocean interface, heat flux and temp. variation 9-47528
- in annulus with internal heat source and variable conditions 9-40286
- in arc with 1 mol % k in various gases, rel. to radiation 9-42583
- atmospheres, nongrey planetary 9-24848
- axisymmetric pulse discharge channel, temp. profile 9-38958
- bodies of finite size, calc. inside via surface temp. 9-22297
- bubble, surface tension variations 9-32776
- cement paste, drying under gradient, role of moisture diffusion 9-34950
- in channel bounded by two confocal elliptic cylinders 9-31863
- contacts, lubricated, rolling/sliding, calc. for range of operating conditions 9-31862
- convective rotating spherical shell 9-26922
- coolant in double sided cooling of tubular fuel element by boiling and superheating 9-22865
- Couette flow between parallel plates, profile rel. to boundary conds. 9-28090
- disc, finite; instantaneous pt. heat source on periphery, thermal shock 9-31839
- field in active medium of continuous solid lasers 9-22409
- field in multidirection conducting system 9-25120
- field in sample, role in thermal conductivity investigation 9-25121
- field of tube of finned radiation emitter 9-41844
- fluids, passive scalar properties, turbulent mixing, zero-gradient points and minimal gradient surfaces 9-30169
- in jet flows, turbulent, interferometric study 9-23373
- in Kundt's tube, thermistor obs. 9-45723
- near lake surface, effect of evaporation retarding monomol. layer, airborne i.r. obs. 9-47515
- in laminar incompressible flow at circular tube entrance 9-23419
- liquid flow in annulus, with const. heat flux at inner wall, variable at outer 9-23480
- in liquid turbulent flow in square channel 9-39095
- magneto-optic readout, transient effects 9-41872
- on Mars' surface, seasonal and latitudinal variations 9-24861
- moist material in contact with hot plate, during drying proc. 9-23586
- Moon 9-29064
- non-steady-state temp. field in long cylinder, quantitative analysis 9-22296
- ocean surface temp. patterns and their synoptic charges, satellite data optimal processing 9-49442
- optical single crystals, fields at high temps. 9-42964
- propane-air flame, electrically augmented in discharge zone 9-25131
- in reacting binary gas mixture, near-wall region, effect of reaction rate 9-28777
- ruby laser rod, during pumping 9-22418
- saturated pool boiling of pure and binary liqs., local fluctuations 9-26164
- steady state, in heat generating fluid flowing in circular tube with flat velocity profile 9-22284
- steady state in 30° right angled triangle 9-22298
- in stellar atmosphere, effect of line shifts 9-49544
- time-dependent, applic. to meas. of thermal props. 9-42963
- upper atm., optical apparatus for space vehicles 9-41542
- water, from covariance between acoustic signals travelling diverging paths meas. 9-27225
- water, non-steady penetrative convection, vertical profiles 9-34896
- water film, vertical flow, temp. profile meas. 9-30384
- water layer with variable coeff. of heat exchange absorbing solar radiation 9-45478
- Ar arc, cylindrically symmetrical column 9-25992
- H₂ cascade arc, radial distributions, meas. up to 27,000 °K 9-40728

Temperature measurement

see also Pyrometers; Thermocouples; Thermometers

- apparatus, new list 9-25112
- atmosphere, airborne surface measurements, influence of air layer between target and radiometer 9-33754
- atmosphere, upper, tungsten wire sensor 9-43409
- calibration standards, triple point temp. meas. system 9-22295
- contacts, lubricated, rolling/sliding, numerical method 9-31862
- Cosmos 149 determ. rad. surface temp. 9-40030
- in creep testing, and control 9-39420
- dew point dynamic determ. method suitable for use on radiosondes 9-26895
- film type detector, heat conduction time const. 9-25136
- flames, based on combustion products measured with α -particles 9-38320
- in gases, live-reversal method 9-26021
- gases, PVT meas. up to 10 kilobars, apparatus 9-30333
- gases containing CO₂, method using blue continuum emission, 3% accuracy up to 3000°K 9-38837
- insulators, h.v., electrically stressed surface temp. and pot. distrib., simultaneous meas. 9-47887
- of interface, solid-liquid, by thermoelec. probe 9-39210

Temperature measurement continued

- International practical Scale 1063-2700°C, by NPL photoelec. pyrometer 9-43803
 ionosphere, E-region, from radar Thomson scatter obs. 9-40088
 using i.r. detector scan, patent 9-47838
 nuc. reactors, ffs., ultrasonic system 9-36636
 plasma, by γ resonance scatt. 9-40689
 plasma, by resonant laser radiation absorption 9-38997
 plasma, by Stark broadening and displacement of spectral lines 9-25913
 plasma, electron, by absorption meas. of X-radiation 9-30260
 plasma, Stark-broadened H lines as probe 9-48589
 with pyrometers, visual, accuracy 9-41845
 scales, stretched wire useful in experimental courses 9-36214
 sea, variation at four points, meas. system 9-35809
 sediments, temp. grad. and thermal cond., heat flow probe design 9-35771
 at surface of microscopic specimens, equipment 9-40288
 thermistor applic. small vars., at high temp. 9-22302
 thin film substrates, laser techniques 9-25132
 underlying ocean surface, aircraft i.r. obs. method 9-35830
 u.s. method for high temp. 9-42966
 water, towed thermometer dynamic frequency response 9-34104
 water drops, strongly charged in nonuniform field 9-40822
 wells, small diameter, effect of convective flow on logging 9-35770
 CO₂ supercritical flow, turbulent temp. fluctuations, cold wire resist. thermometer obs. 9-28172
 Ce₂Mg₃(NO₃)₁₂·24H₂O, obs. antiferromagnetic in millekelvin range 9-45210
¹⁹F in MnF₂, n.m.r. freq. depend., 10-40°K 9-40291
 H₂ cascade arc, radial distributions, meas. up to 27,000°K 9-40728
 He vapour press. thermometry, thermomolecular press. corrections 9-47839
 O₂ solid, at transition points, using Pt resistance thermometers 9-40289
 Pt resistance thermometer, interpolation of differences in resistance ratios 14°-91°K 9-45884

spectral methods

- discharge, gas temp. determ. with hyperfine structure 9-28044
 flames, meas. by absorpt. method 9-45879
 flames, two path method, using mirror 9-45882
 flames meas. by emission method 9-45880
 metal surface, laser-heated, time-resolved 9-32835
 rapid scan spectrometer for H plasma in impulse tube 9-44419
 two-beam i.r. spectrometer, correction tech. for thermal background 9-36215
 two-colour method preparation of suitable tables 9-36208
 upper atm., optical apparatus for space vehicles 9-41542
 Ar arc plasma jet at atm. pressure 9-30251
 Ar plasma induction torch 9-25907
 H plasma in impulse tube, meas. by rapid scan spectrometer 9-44419
 O₃ in atmosphere, from solar spectrum obs. 9-31288

Tensile strength *see Mechanical strength/tensile***Tensors**

- conductivity tensor, nonlinear, of weakly interacting electron system in external elec. field 9-48984
 dielectric permittivity, of electron gas, determ. 9-41786
 dynamical, of lattices, electronic contrib. 9-24002
 e.m. field in anisotropic dispersive media, relativistic formulation 9-22306
 energy-momentum, of Klein-Gordon field 9-29514
 in Hilbert space 9-45732
 MHD stress, non-dissipative components 9-25830
 permeability, ferrites, in various coordinate systems 9-39775
 potential, source equation, Poisson's field equation and Maxwell equations 9-41850
 reflection, generalization 9-25352
 scattering, vibrational Raman effect 9-27831

Terbium

- atom, structure of spectrum, 4f⁹d²6s 9-38775
 electronic structure, relativistic augmented-plane-wave calcs. 9-24095
 ferromagnetic reson. at 2.5-3 mm., rel. to magnetoelastic effects 9-45158
 ferromagnetic resonance in for i.r. 9-49341
 growth of single crystals by three methods 9-37078
 Hall effect and mag. susceptibility, 90° to 400°K, fields up to 15 kOe 9-33258
 Hall effect anomalous and ordinary, in single crystal 9-45090
 hysteresis loop displacement due to mag. viscosity 9-41291
 irreversible phase transition from h.c.p., and compressibility 9-39501
 Lorenz functions, elec. resistivity and thermal conductivity 9-33195
 magnetocrystalline anisotropy, spin-wave theory 9-37655
 micro-eddy current damping 9-26319
 thermal conductivity, elec. resistivity and Lorenz functions 9-33195
 thermal conductivity of single crystal as function of temp 5° to 300°K 9-47009
 u.s. attenuation near mag. phase transitions freq. and temp. depend 9-48958
 u.s. scatt., critical, in paramag. region near Neel temp. 9-24027
¹⁵⁹Tb, hyperfine struct. and g_J values of low levels 9-48403
 Tb³⁺-Cr³⁺ pair emission in TbAlO₃:Cr³⁺ 9-39878
 Tb³⁺, 4f-5d excitation energy in solids 9-49320
 Tb³⁺, ferromagnetic resonance in Y-Fe-Ga garnet with Tb impurity 9-33619
 Tb³⁺, Luminesc. in CaWO₄-CdWO₄ system 9-39865
 Tb³⁺ afterglow lifetime and radiationless transitions in aqueous solns., deuterated and undeuterated 9-28141
 Tb³⁺ in aq. soln., electronic energy levels 9-36886
 Tb³⁺ in CaF₂ and SrF₂, luminescence, quanta summation processes 9-45342
 Tb³⁺ in CaWO₄, absorpt. and fluorescence spectra, 4.2-77°K rel. to crystal field parameters 9-33550
 Tb³⁺ in LaCl₃, emission yields and lifetimes of ³D₃ and ³D₄ levels rel. to temp. and conc. 9-35690
 Tb³⁺ in rare earth oxysulphates (Ln₂ SO₄), fluoresc., phosphors obs. 9-43258
 YVO₄:Dy,Tb, luminesc. 9-47398

Terbium compounds

- ferrite garnets, Faraday effect, mag. field effect 9-49216
 Tb-Y alloy, Hall effect and mag. susceptibility, 90° to 400°K, fields up to 15 kOe 9-33258
 Tb-Y paramag. susceptibility and Hall eff. meas. 9-37644
 Tb₂Fe₂O₁₂ garnets, Faraday effect, anisotropy in i.r. region 9-31081

Terbium compounds continued

- TbAl garnet, Faraday effect, Verdet const. freq. depend., obs. 9-28657
 TbAlO₃:Cr³⁺, emission of Cr³⁺-Tb³⁺ pairs 9-39878
 TbCl₃, n.g.r. of ³⁵Cl 9-49365
 TbCrO₃, antiferromagnetic transitions, rel. to mag. symmetry and ferroelec. 9-45208
 TbFe garnet, Faraday rot. 9-43214
 TbFe garnet, Faraday rotation at 1.15 μ , 100° to 450°K 9-49218
 TbFe garnet, Sn-substituted, critical mag. isotherm 9-43188
 TbFe garnets, exchange magnetostriction 9-24319
 TbFe garnets, substituted, volume magnetostriction 9-43155
 Tb(OH)₃, ferromagnetic optical fluorescence and absorpt spectra rel. to low temp. mag. an thermal props 9-47401

Terrestrial electricity *see Earth/electricity***Terrestrial heat** *see Earth/heat***Terrestrial magnetism** *see Earth/magnetic field; Magnetic storms***Tetraneutrons** *see Neutrons***Thallium**

- adsorbed in Tl₂HgGe₂O₁₆·4H₂O, n.m.r. obs. 9-33650
 atom, 6²P_{3/2} state, lifetime and effective quenching cross section, r.f. discharge obs. 9-29949
 atom, excited, depolarizing collision with inert gas, cross section meas. 9-22976
 atom, unexcited, collisions with excited Hg atoms 9-48421
 diffusion in noble metals, rapid, interstitial mechanism 9-28321
 fluorescence direct line type, excitation mechanism 9-48409
 slip modes 9-44770
 surface tension, 1300-2200°K 9-28110
 in Hg, effect on electrodiffusion of Bi 9-46623
 KI/Tl, F centre prod. by impurities, α and V_K centre motion importance 9-44718
 in KI intercentre luminescence, elec. field effects 9-39871
 in Sn, liq., effect on electrodiffusion of Bi 9-46623
 Tl⁺ centres in alkali halides, u.v. absorpt. spectra 9-43237
 Tl⁺ conc. in HCl, LiCl, HBr, LiBr, luminesc. meas., 77°K 9-33697
 Tl⁺ energy parameters in KCl 9-31052
 Tl⁺ in KCl:KBr-Tl crystal, symmetry of centres 9-42852
 (Tl⁺)₂ in KI, absorpt. bands of ion centres obs., electr. struct. 9-35111
 Tl spectrum, influence of electric field on level crossings 9-48404

Thallium compounds

- alloys, binary and ternary solid solns., supercond. transition temp. 9-23989
 Ag halide vapours, u.v. absorpt. cross-sections 9-46376
 In-Tl liquid alloy, Knight shift calc. from pseudopotential formalism 9-23532
 In-Tl alloys, thermal expansion in vicinity f.c.c.-f.c.t. transition 9-28434
 Pb-(1.6wt.%)Tl superconductor, type II, rectangular flux line lattice 9-28479
 Pb-Tl alloy, superconducting, fluxons, nucleation and propagation in thin cylindrical specimens 9-44933
 Pb-Tl dilute solid solutions, vibrational entropy, electronic influences 9-39508
 Sn-Tl alloys, liquid, density determ. rel. to atomic and ionic volumes 9-30370
 Tl-Pb-Bi alloys, superconductivity from tunneling meas. 9-24161
 Tl-Se system, immiscibility phase boundaries determ. from density meas. 9-40779
 Tl₂O-SiO₂ glasses, cation distrib. 9-48781
 Tl₂Hg₃O₁₆·4H₂O, adsorption of water and Tl, n.m.r. obs. 9-33650
 Tl₂IAS₆, elec., thermal, optical props., and lattice const., obs. 9-35070
 Tl₂Te polycrystal, temp. depend. of thermoelec. power, elec. cond. and sp. ht. 9-26598
 Tl₂Te polycrystal, temp. depend. of thermoelec. power, elec. cond. and sp. ht. 9-26598
 TlBr, optical absorpt. edge press. shifts 9-45312
 TlBr, photocarriers polaron mass and relax. time from cyclotron reson. obs. 9-39726
 TlCl, optical absorpt. edge press. shifts 9-45312
 TlCl, photocarriers polaron mass and relax. time from cyclotron reson. obs. 9-39726
 TlCl, photoconductive, band struct. and pollaron transport props. 9-41272
 TlCl, r.f. spectra h.f.s. 9-34645
 TlCl, vibr. spectrum, phonon freq. calc. using shell model, sp. ht. temp. depend. 9-30763
 TlF attractive interaction with rare gases, anisotropy factor and scattering cross section 9-44390
 TlFeF₃, crystal structure and mag. props. 9-35063
 TlFeF₃, crystal growth from soln., X-ray diffraction powder study 9-26207
 TlFeS₃, ruginite, new mineral, crystal struct. and reflection props. 9-30574
 TlI films, strain-reduced, optical absorpt. 9-43219
 TlInS₂(Se₂Te₂), struct., elec. conductivity, Hall effect, photocond. and optical props. 9-44969
 TlNO₃-alkali nitrate molten mixtures, elec. cond. and density 9-23520
 TlNO₃, pyroelectric props. rel. to crystal space group 9-30977
 TlNO₃ fused, vapour press. and density meas., 250-450°C, b.p. and transpiration method 9-34966
 TlNiF₃, perovskite-like struct., phase transf. and stability relations at high press. 9-35241
 p-TlSe:Pb, conductivity and thermoelec. power, rel. to valence-band structure 9-43059

Thermal conductivity *see Conductivity, thermal***Thermal decomposition** *see Chemical reactions***Thermal diffusion** *see Diffusion in gases/thermal; Diffusion in liquids/thermal; Diffusion in solids/thermal***Thermal diffusion columns** *see Diffusion in gases/thermal; Isotope separation***Thermal diffusivity** *see Conductivity, thermal; Heat conduction***Thermal expansion**

- anharmonic crystal, interatomic pot. theory 9-30759
 anomalous component near broad ferroelec. phase transition point 9-42972
 cast vitreous-crystalline materials in different compositions 9-39525
 crystals of lower symmetry, coeffs., explt. method 9-24053
 diffraction gratings, plastic, with restricted expansion, production method 9-25364
 dilatometer, capacitance type, for low temp. meas. 9-42970

Thermal expansion continued

- dilatometer, optical lever, for low temp. use 9-26429
 dilatometer for meas. liq. expansion at elevated temp. 9-46582
 elastic cylinder, constrained, stress analysis 9-37358
 electronic, phonon-enhancement contrib. to Gruneisen function 9-44838
 equations of state rel. to Gruneisen's parameter 9-28430
 in ferroelectric phase transition region, anomalies in coeff., calc. method 9-33383
 glass, mixed alkali, non-linear variation due to alkali oxide replacement 9-39148
 glass, nonoxide, low temp. obs. 9-42970
 glass, temp. dependence 9-26698
 Gruneisen coefficient determ. from shock wave flow in system of plates and spaces 9-48972
 Gruneisen parameters of cubic metals 9-24059
 Gruneisen parameters rel. to elastic moduli in low symmetry cryst. 9-39392
 Invar alloy, mag. anomaly, spontaneous vol. magnetostriction obs. w.r.t. band theory 9-43177
 Irtran-6 window, values 9-42971
 metals, calc. from eqns. of state 9-39090
 metals paramag. and elasticity rel. to ϵ struct. 9-40996
 methane, solid, at 21-61°K 9-40926
 mica, ruby muscovite, coeffs. anisotropy 9-44839
 Niromet-42 material 9-42971
 optical polycrystalline materials, low temp. obs. 9-42970
 in optical systems, differential, resulting internal stresses 9-36373
 polycapromide in ν -form 9-24058
 polyethylene, expansion of unit cell 9-48842
 polyethylene, from Gruneisen const. 9-46979
 polymers, crystalline and glassy, from Gruneisen const. 9-46979
 polymers, organic, Gruneisen parameter expressions from eqn. of state 9-37361
 polymethylmetacrylate plate, viscoelastic, contraction calc. 9-28334
 solids, transport constants determ. from linear dimens. change with temp. 9-41097
 spinel lattice parameters rel. to temp. 9-30784
 β -spodumene-silica solid solutions, lattice parameters of spodumene throughout composition range 9-26431
 steel, cold-rolled transformer, coefficient rel. to annealing temp. 9-39455
 temperature scales, stretched wire useful in experimental courses 9-36214
 triglycine sulphate, near ferroelec. transitions, Pippard scheme 9-30970
 two-phase composite, and shrinkage, rel. to aggregate at centre 9-28392
 two-phase materials, and shrinkage 9-42864
 water, eff. of anomalous thermal expansion from free convection obs. 9-23482
 Ag, at low temp. 9-33188
 AgNO₃, orthorhombic and rhombohedral 9-35287
 Al-Li alloys, linear coeff. increase with Li conc. 9-39395
 Al T-6 2014, fractional expansion 9-42971
 Ar, coeff., Gruneisen parameter determ. 1-25K 9-41092
 Ba₄(₁₀)Na₂₋₂₀Nb₁₀O₃₆, coeffs. and crystallog. data 9-37134
 BaF₂, Gruneisen parameter calc. in low-temp. limit from u.s. pulse-echo meas. of elastic constants 9-33016
 BaTiO₃, near ferroelec. transitions, Pippard scheme 9-30970
 Bi, linear, 200° to 4.5°K, Gruneisen parameters 9-33189
 Bi, linear coeffs., down to 2°K 9-24054
 CaF₂, Gruneisen parameter calc. in low-temp. limit from u.s. pulse-echo meas. of elastic constants 9-33016
 CaO, 12 to 300°K, weff. deriv. from lattice parameter data 9-28429
 CoSi single crystals, 25° to 1000°K 9-37075
 Cr, anomalous, cry. distortions due to antiferromag. ordering 9-39780
 CrTe, due to lattice vibr., exchange striction obs. 9-33466
 Cu, Gruneisen parameters 9-26429
 DyAl garnet, 1° to 4°K 9-44840
 Fe-Al system intermetallics 9-46890
 Fe₄(Ni_{1-x}Mn_x)₃ alloy, temp. depend. rel. to mag. ordering 9-41303
 Fe filings and whiskers, effect of H atmos. 9-44666
 Ga, 50-700°K, liq. Ga immersion dilatometer meas., rel. to anharmonic effects 9-47007
 GdFe garnet, 296-1400°K, from lattice const. 9-41093
 GdGa garnet, 296-1400°K, from lattice const. 9-41093
 GeO₂, rutile-type, X-ray determ. 9-24055
³He, liq., coeff. at zero temp. 9-34939
³He, liq., coeff. calc. using ground-state energy and quasiparticle energies and interaction function 9-34940
 HfB₂, and conductivity, rel. to thermal stress resistance 9-35183
 HfC-TaC solid soln. system 9-26430
 Hg-In alloys, liq., 20 to 160°K, and vol. change on formation 9-28115
 Hg, 50-700°K, liq. Ga immersion dilatometer meas., rel. to anharmonic effects 9-47007
 In-Sn fractional expansion 9-42971
 In-Tl alloys, near f.c.c.-f.c.t. transition 9-28434
 In, anisotropic expansion and lattice parameters temp. variation 9-30785
 In fractional expansion 9-42971
 InSb phases at high pressure and temps. 9-42922
 K₂O-GeO₂ system, thermal expansion data for crystalline compounds 9-26398
 K₂SO₄ cry., orthorhombic, α -values, exptl. method applic. 9-24053
 KCl, 50-700°K, liq. Ga immersion dilatometer meas., rel. to anharmonic effects 9-47007
 KH₂PO₄, near ferroelec. transitions, Pippard scheme 9-30970
 [(1-x)L_xCa]MnO₃, rel. to phase transformation behaviour 9-33127
 Li, Gruneisen parameters, pseudopotential calcs. 9-26410
 LiF cry., coeffs., exptl. method applic. and accuracy 9-24053
 LiH, 12 to 300°K, weff. deriv. from lattice parameters data 9-28429
 MgO 12 to 300°K, weff. deriv. from lattice parameter data 9-28429
 Mo, coeff., temp. depend., 80° to 1200°K 9-44842
 Mo, coeff. temp. depend., 412-300K 9-37359
 NH₄ClO₄, mechanism 9-42973
 NaCl, 50-700°K, 50-700°K, liq. Ga immersion dilatometer meas., rel. to anharmonic effects 9-47007
 NaCl, high-temps., X-ray diffraction study 9-30786
 NaCl, single cryst. X-ray diff. meas., temp. depend. rel. to Schottky defects conc. 9-37360
 NaNO₃, near ferroelec. transitions, Pippard scheme 9-30970
 NaNO₃ ferroelec. phase transition at -95°K 9-35486
 Nb-Mo alloy, coeff. temp. depend., 412-300K 9-37359
 Nb, coeff. temp. depend., 412-300K 9-37359
 Nd:YAl garnet rod laser 9-22412

Thermal expansion continued

- Ni-Rh alloy, paramagnetic, low-temp. anomalies, rel. to spin fluctuations 9-45086
 NiF₂ thermal expansion determ. from room temp. to 600°K 9-44841
 Pb calc. from eqns. of state 9-39090
 PbTiO₃, near ferroelec. transitions, Pippard scheme 9-30970
 Pd-Ag alloys, at low temp. 9-33188
 Pd-Ni alloy, paramagnetic low-temp. anomalies, rel. to spin fluctuations 9-45086
 Pd, at low temp. 9-33188
 RuO₄, X-ray determ. lattice constants, 30-702°K 9-24056
 S₈, fibrous, expansion between -170° to 70°K 9-39533
 Sb, linear, 200° to 8°K, Gruneisen parameters 9-33189
 Si, 20°-300°K, interferometric meas. up to 800°K 9-30787
 Si, Gruneisen parameters, temp. depend. 9-33190
 Ti, coeff., temp. depend., 80° to 1200°K 9-44842
 U, fission gas induced swelling, effects of hydrostatic press. 0-1000 bar 9-38735
 U₂C₃, linear thermal expansion at elevated temps. 9-24057
 UO₂, linear thermal expansion at elevated temps. 9-24057
 V, coeff., temp. depend., 80° to 1200°K 9-44842
 W, 1700-2300°K, obs. using electron bombard. furnace and extensometer 9-35288
 W, coeff., temp. depend., 80° to 1200°K 9-44842
 Xe, solid, vol. coeffs. 9-42974
 YAl garnet, 296-1400°K, from lattice const. 9-41093
 YFe garnet, 296-1400°K, from lattice const. 9-41093
 YGa garnet, 296-1400°K, from lattice const. 9-41093
 Zn single crystal, rel. to vacancy formation parameters 9-46811
 ZnO, 20°-300°K, interferometric meas. up to 800°K 9-30787
 ZnO, Gruneisen parameters, temp. depend. 9-33190
 ZrB₂, and conductivity, rel. to thermal stress resistance 9-35183

Thermal measurement

- see also Calorimeters; Calorimetry; Conductivity, thermal; measurement; Temperature measurement; Vapour pressure measurement; Entries describing measurement methods for specific thermal quantities and effects may also be found listed under the various headings for the subjects concerned*
 arc solar furnace, simulator power characts. using pyrometric chopper 9-40283
 australites, fission track etch pits studies, sample age correction and thermal history by annealing 9-45463
 dynamic properties of detector, probability analysis 9-45873
 emissivity of materials up to 100°K 9-28678
 film, solid, insulating, shock tube method 9-39524
 heat flux transducer, low temp. high sensitivity 9-45874
 heat transfer, wall to gas, for high wall-temp. 9-40748
 instruments for thermophysical invest. new, list 9-25112
 new thermophysical instruments, review 9-41846
 rock-magnetic parameters, determ. by differential analysis 9-28970
 satellites, thermal control, coating stability and Earth refl. sunlight obs. 9-24714
 thermoreceiver transient response calc. 9-47831
 from time-dependent temp. distrib. 9-42963

Thermal radiation *see Radiation/heat***Thermal spikes** *see Crystal imperfections; Physical effects of radiations***Thermal transformations** *see Boiling; Condensation; Crystallization; Freezing; Heat of transformation; Melting; Phase transformations; Sublimation; Vaporization***Thermionic emission** *see Electron emission/thermionic; Ion emission/thermionic; Ionization, surface***Thermionic generators** *see Electricity, direct conversion/thermionic; Electron tubes***Thermionic tubes** *see Electron tubes***Thermisotrs** *see Semiconducting devices***Thermochemistry** *see Heat of reaction, etc.***Thermocouples**

- chromel-alumel, in-pile radiation and temp. effects on Inconel sheathed lead wires 9-36637
 chromel-alumel and chromel-capel microthermocouples, heat inertia in air jet, determ. 9-22300
 chromel-P/Au-Fe annealed temperature calibration extended 9-47841
 irradiated, decalibration by self-annealing scatt. centres 9-22301
 manometric transducers, error evaluation 9-31741
 new instruments, review 9-41846
 psychrometer, 50-thermocouple with digital recorder 9-33732
 radiometer based on thermopile 9-22277
 thermopile and photoelec. multiplier applic. to i.r. thermograph 9-38397
 Au-Fe, reproducibility tests 9-22299
 Au-Ni thin film, vacuum-evaporated, thermoelec. power and Seebeck coeff. thickness depend. 9-45017
 Cu/Au-Fe annealed temperature calibration extended 9-47841
 (Sb₂Te₃-Bi₂Te₃)-(Bi₂Te₃-Bi₂Se₃), transient response of thermoelec. cooling 9-28569
 W-Re, type-VR 5/20, calibration characts. 9-34105
 W-Re for periodic checking of furnace melt temp. 9-38321

Thermodynamic properties*see also Critical constants, thermal; Entropy; Heat of reaction; Latent heat*

- ³He-⁴He mixture, heat of mixing disc. at 0.05°K 9-32810
 activation entropy, eff. on discrepancy in dislocation velocity-stress exponent temp. depend. 9-26285
 alcohols, normal, heats of mixing and thermodynamics 9-23484
 alkali metal plasmas, computation 9-36755
 alkali metals electrical and thermal resistivities calc. using Sharma-Joshi model for lattice dynamics 9-42995
 alkaline earth oxides and aluminates, stability in flame spectroscopy 9-33692
 anharmonic crystal, interatomic pot. theory 9-30759
 9,10-anthraquinone, heat capacity and content, free energy, entropy 9-46418
 antiferromagnets, uniaxial, Heisenberg model 9-28637
 p-azoxyanisole, nematic, thermal fluctuations identified by Rayleigh laser scatt. 9-40793
 benzene/benzene-d₆, excess enthalpy and volume of mixing 9-23485
 binary mixtures near critical point, kinetic phen. 9-48735
 Bose gas, compressibility at transition pt. 9-47783
 butyl alcohol, thermodynamic const. 9-36895

Thermodynamic properties continued

- t-butyl alcohol-water soln., excess vol., comparison with methyl cyanide-water 9-42651
 cementite, stability under α irradiation 9-47000
 chemical pot. in systems under non-hydrostatic stress 9-22272
 chloroacetyl halides, enthalpy differences of rot. isomers 9-30094
 combustion products of methane and oil with ionizing K seeds, MHD 9-36748
 crystal lattices, transport equations of correlation function for quasi-momentum density 9-30778
 crystals with zero defects 9-40927
 cyclohexane/cyclohexane- d_{12} , excess enthalpy and volume of mixing 9-23485
 dense fluids, molec. dynamics of microscopic props. 9-38937
 diamond, surface enthalpy, phonon contribution 9-23617
 dioxane binary soln., excess vol. of mixing 9-34881
 electrolyte melts, thermo-chains 9-30386
 elements, collection of data, book 9-22026
 energy, internal, of solid, depend. on temp. change rate 9-26423
 enthalpy and entropy var. for reactions, determination from exptl. equil. curves, method 9-37814
 enthalpy distribution for hot-core and cold-region of arc heater 9-23393
 enthalpy of gas calc. from shock waves propagation, press., density, temp., and speed meas. 9-31850
 ethyl alcohol, thermodynamic consts. 9-36895
 factors in heat flow concept 9-45875
 ferroelectric, uniaxial, singularity at phase transition point 9-43114
 film, solid, insulating, shock tube method of meas. 9-39524
 films, thin, anisotropy of kinetic phenomena w.r.t. thermodynamics 9-33289
 fluid heated from below 9-25799
 fluids, two-component, Monte Carlo calc. in isothermal-isobaric ensemble 9-32560
 free energy function from intensity meas. in microwave spectroscopy 9-27837
 free energy of a liquid, useful partition function for calc. 9-48678
 free energy of molecular fluid, Monte Carlo calc. 9-36738
 gas behind shock wave in Ar, parameters calc. 9-38974
 of gas mixtures, binary, enthalpy surplus determ. 9-46579
 of gases, liquids and solids, conference 9-26014
 high temperature physics and chemistry, bibliography 9-41718
 hydrated electrons, kinetic relations 9-39955
 of impure crystal at low temp., Fermi and Bose condensation of impurities 9-47037
 interfacial energy during heterogeneous nucleation, electrostatic contribution 9-30523
 ionic crystals with homopolar bonding, from lattice vibration spectrum 9-24009
 LaB₆ enthalpy and heat capacity, 1100-2200°K 9-26428
 Lennard-Jones fluid, hypernetted-chain approx. 9-29209
 liquids, C₆₀, entropy, free energy and enthalpy, square well with infinite walls calc. 9-30385
 liquids, thermodynamic props. in Hartree-Fock approx. 9-29216
 liquids, u.s. pulse-repetition technique 9-23483
 of magnetic minerals 9-30776
 metal magnetization and thermodynamic pot. for 2-dimens, case 9-45079
 metal film, quantum oscillations in weak mag. field 9-30812
 metals, high temp., complex thermal charact. meas. 9-24039
 methane and methane- d_4 , theory 9-44617
 methane and methane- d_4 , theory 9-39143
 methods for determ. of thermophysical props. of substs. 9-36209
 methyl alcohol, thermodynamic consts. 9-36895
 methyl cyanide-water soln., excess vol. study, comparison with t-butyl alcohol-water 9-42651
 mixture of two Lennard-Jones liquids, free energy and enthalpy, Monte Carlo calc. 9-34894
 multilayer walled media, thermal oscillations, theory and expt. 9-24033
 1,4-naphthoquinone, heat capacity and content, free energy, entropy 9-46418
 nonstoichiometric cpds, interac. between point defects, thermodynamic activity variation 9-37160
 organic compounds 12 in their ideal gas state 9-26024
 paramagnet with negative anisotropy const. at low temp. 9-31022
 plasma, free energy, density fluctuation energy in relativistic and collisional states 9-36753
 plasma, partially ionized, quantum statistical calc. 9-38957
 plate, bilayer, monotonically heated, temp. depend. 9-29323
 polyesters and polyamides in amorphous state, solubility and heat resistance 9-28191
 polyethylene dissolution in xylene and octadecane 9-46616
 propyl alcohol, thermodynamic consts. 9-36895
 propylene imine, molec. calc. 9-44369
 quartz thermal emission of phonons obs. 9-30761
 reactions, entropy and enthalpy var., determination from exptl. equil. curves, method 9-37814
 refractory cryst. prod. by vapour transport react., thermodynamic analysis, integral face energy diag. 9-28231
 rubber, internal-energy contribs. to elastic stress 9-46860
 salt melts, two-components, conc. var. of thermodyn. functions 9-48693
 sapphire, thermal emission of phonons obs. 9-30761
 semiconductors, anisotropy of kinetic phenomena in surface channels w.r.t. thermodynamics 9-33289
 silica glass, densified, activation energy spectrum rel. to annealing 9-46700
 solid soln., elastic free energy, microscopic theory 9-37288
 solid solutions, activities, determ. using point defect conc. 9-30714
 solids, anharmonic effects: heat capacities of NaCl, KCl and KBr 9-24047
 solids, anharmonic effects, data analysis for NaCl, KCl and KBr 9-24048
 solids containing defects 9-44681
 solutions, diluted, near solvent critical point 9-26093
 solutions, effect of external elec. fields 9-48692
 spin-1/2 Heisenberg ferromagnet 9-31026
 steam dissociation, 1000-5000°K, 0.001-100b 9-30458
 stimulated scatt. of laser beams in isotropic media 9-43813
 superconducting alloys in high mag. field 9-33263
 superconducting ellipsoid, finite jumps in specific heat 9-44922
 superconductors, two-band, influence of paramag. impurities 9-33264

Thermodynamic properties continued

- surface enthalpy, relationship with characteristic temp. 9-28205
 thermomagnetic effect, modulation and detection by second sound in He 9-39523
 water film, vertical flow, temp. profile meas. 9-30384
 water-methyl cyanide soln., excess vol. study, comparison with t-butyl alcohol-water 9-42651
 wustite, rel. to composition by coulometric titration in high temp. galvanic cell 9-44828
 ∞ gas phase reaction rate data at high temperature 9-49373
 Ag-In liq. alloy system, Knudsen cell and mass spectrometric obs. 9-36860
 Ag-Zn alloy, concentration effect of free electron concentration 9-26477
 AgCl, from lattice vibration spectrum 9-24009
 Al-Bi system, phase equil. obs., integral mixing enthalpies and excess entropies 9-46679
 Al-In, system, phase equil. obs., integral mixing enthalpies and excess entropies 9-46679
 Al liquid, density and surface energy polytherms 9-40781
 Ar-Kr liq. mixtures, excess enthalpy, Monte Carlo calc. in isothermal-isobaric ensemble 9-32560
 Ar-Kr liquid mixtures, excess props. analysis 9-42646
 Ar-N solid mixtures 9-39528
 Ar, ionizing, behind reflected shock wave, shock reflection process and thermal layer 9-48662
 Ar, liq. 9-39071
 Ar, liq., Monte Carlo calc. 9-39070
 Au-Co alloys, liquid ferromagnetic, near Curie and melting point 9-23531
 Bi₂O₃-B₂O₃-(R₂O) glass systems, molar volumes rel. to chem. struct. 9-46698
 C films, activation energies for annealing 9-23937
 COS, computed, 200-2000°K 9-23032
 CaF₂:Tr³⁺ (Tr³⁺=trivalent rare-earth), of optical centres 9-30614
 Cd-Hg alloys, enthalpy and entropy of mixing, rel. to phase equil. and transform. 9-48878
 CoSi₃ solid and liquid, enthalpy changes 9-39092
 Cs gas, by X-ray methods 9-26177
 Cu-Sn liq. alloy system, Knudsen cell and mass spectrometric obs. 9-36860
 Cu-Th system, phase equil. obs., integral mixing enthalpies and excess entropies 9-46679
 CuAu II alloy, entropy of disorder, phase transition from CuAu I 9-30750
 Fe-O system, e.m.f. meas. 9-30741
 Fe_{1-x}O_x, transitions in single phase region 9-28402
 Ge, anharmonic effects in entropy, heat capacity and Gruneisen function 9-47002
 GeO₂, cryst. energy calc. of bond types 9-30504
 H₂ solid, ($\partial P/\partial T$), meas. and related props. 9-26424
 He II, analytic expressions using expt. dispersion curve for elementary excitations 9-23564
 Hg-Ga liq. alloys, activities, excess entropies, form. enthalpies 9-30369
 Hg-Pb alloys, liquid, enthalpies and excess entropies 9-39091
 Hg-Sn liq. alloys, activities, excess entropies, form. enthalpies 9-30369
 Hg-Tl alloys, liquid, enthalpies and excess entropies 9-39091
 Hg, u.s. pulse-repetition technique 9-23483
 KCl-NaCl solid soln., enthalpies of crystallisation, anomalies in struct. obs. 9-37161
 KCl:Oh electrocaloric phenomena, paraelec. cooling 9-37588
 Kr-Ar liquid mixtures, excess props. analysis 9-42646
 La₂O₃ enthalpy and specific heat, 298.15 to 1600°K 9-41105
 LaB₆ in temp. range 1340 to 2300°K 9-40830
 Li₂ in ideal gas state, 100 to 10000°K 9-42609
 Lu₂O₃ enthalpy and specific heat, 298.15 to 1600°K 9-41105
 Mo enthalpy and specific heat near melting point. 9-37356
 NH₄ClO₄, 5°-350°K 9-48970
 Na-C-O system, three-phase equil., activities 9-39127
 NaCl:Ca(Cd), Na⁺ diffusion and ionic conductivity obs., heats of assoc. 9-39672
 NaNO₂-AgNO₃ melt, thermo-chains 9-30386
 Ni-Mo alloy, H solubility, conc. depend. of enthalpy and entropy of soln. 9-39478
 Ni-W alloy, H solubility, conc. depend. of enthalpy and entropy of soln. 9-39478
 Ni_{1.04}Si_{1.91} solid and liquid, enthalpy changes 9-39092
 O at temps. to 250 K and press. to 350 atm, along isochores 9-34899
 Pb(Tl_{1-x}Zr_x)O₃, from PbO vapour pressure meas. 9-23609
 Pd-Fe, γ solid solutions, activities, entropies and heats of mixing 9-30753
 Pd-Pt, γ solid solutions, activities, entropies and heats of mixing 9-30753
 Pt-Fe, γ solid solutions, activities, entropies and heats of mixing 9-30753
 PuN, heat of formation and thermal functions, 700 to 3040°K 9-26809
 Pu $\alpha \rightarrow \beta$ transform., differential enthalpic study 9-44801
 SnO₂, cryst. energy calc. of bond types 9-30504
 Ti-O system 9-23173
 Ti-O system 9-23172
 TiO₂, cryst. energy calc. of bond types 9-30504
 UO₂, enthalpy, from 2500°K melting pt. 9-26425
 UO_{2.12}, partial molar free energy of O 9-28775
 VSi₃ solid and liquid, enthalpy changes 9-39092

Thermodynamics

- see also *Atmosphere/thermodynamics; Entropy; Equations of state; Statistical mechanics*
 adiabatic surfaces, reversible, existence proved 9-47829
 adsorption, physical, virial expansion treatment 9-40847
 adsorption of gas mixtures 9-34996
 anharmonic oscillators, coupled, 2D, approach to thermal equilib., computer studies 9-31777
 binary mixtures, theory of gravitation eff. 9-23454
 biochemical reactions, stability criteria 9-45411
 blackbody radiation spectrum, derivation without quantum assumptions 9-47830
 boson system one-dimensional with δ junction interaction 9-47782
 Casimir-Onsager reciprocal relations, phenomenological derivation 9-43761
 charged particle equil. system 9-36737
 chemical transport of ternary oxides, thermodynamic aspects 9-36999
 classical and differential forms 9-38307
 classical and relativistic, foundations, space dynamics 9-38308

Thermodynamics continued

- cluster formation free energy in nucleation theory, rot. and translation contrib. 9-37101
- convexity of function, further remarks 9-38309
- critical exponents, renormalization by hidden variables 9-36144
- critical phenomena, dynamic, scaling laws 9-22127
- electrical connections at cryogenic temps., thermodynamic optimum 9-22271
- electrons in solutions diluted into liq. ammonia at -35°C 9-39956
- energy conversion, chemical to kinetic, by active stress 9-29318
- energy conversion, steady state, sinusoidal, unified treatment 9-27264
- equilibrium, applic. to supersaturated vapour nucleation theory 9-34959
- equilibrium state of system with adiabatic internal constraints 9-43799
- energy, available energy, redefinition 9-29320
- Fermi gas, magnetized, thermodynamic approach to eqn. of state 9-25054
- first law, rel. to nature of time 9-45729
- flow systems, heterogeneous, second law applic. 9-23225
- fluids, at critical point, singularities 9-26152
- free energy, quantum mechanical, of hard-sphere gas 9-45790
- free-energy of interacting many-particle systems, density depend. obtained with Bogoliubov inequality 9-31786
- gas, H-function at local Maxwellian state 9-39042
- Gibb's entropy law validity in strongly coupled systems 9-38251
- gravitodynamics, generalized statistical mechanics of violent agitation 9-41622
- heat, engines, relativistic, Plank's and Ott's formulation 9-43798
- identities, for relationships between and props. of incomplete eqns. of state 9-43759
- irreversible MHD processes, variational description 9-30185
- Ising model, self-consistent field near critical point 9-39758
- Ising model 3D, 27 point array 9-36142
- justification for real matter with Coulomb forces 9-22132
- linear systems of interacting molecules, decay of pair correlation functions 9-34700
- magnetic resonance lines saturation, reln. 9-49348
- magnetic resonance lines saturation, reln. 9-49349
- magnetic systems, anisotropic, scaling approach 9-41290
- magnetocaloric conversion, ideal 9-31857
- Massieu functions and potentials, convexity of functions 9-38309
- mechanical behaviour of solids, book 9-39431
- mechanical equilibrium of an isolated system without thermal equilibrium 9-36206
- model, hadron pair production rate calc. 9-42026
- model for pp collisions, energy, ang. distrib. and multiplicities of secondaries 9-42101
- non-equilibrium, applic. to solidification of ideal binary syst., distrib. coeffs. 9-37100
- non-irreversible, entropy existence 9-43762
- nonequilibrium, of two-phase media 9-46677
- nucleation, cluster formation free energy, rot. and translation contrib. 9-37101
- phase transition, second-order, exact relations and rigorous exponent equalities near transition line 9-23575
- phase transition, second-order, impurity effects near critical point 9-46678
- phase transition points, averaging of singularities 9-47775
- plastic deform., activation parameters evaluation, review 9-44765
- plastic material, rate sensitive 9-22217
- polymer gelation 9-41447
- pressure of ideal gas on moving piston, calc. 9-43757
- quantum, harmonic oscillators infinite system 9-22136
- quantum or classical nonrelativistic many-body syst., inequalities for free energy 9-25050
- regenerative cycles, Clapeyron theorem extension 9-29319
- relativistic, appl. of dynamics with variable rest mass 9-43731
- relativistic, heat transformation 9-22270
- relativistic, temperature transformation law 9-22125
- relativistic and classical, foundations, space dynamics 9-38308
- replacement free energy in small systems 9-27179
- second law 9-38310
- statistical foundations 9-22133
- statistical mech., equilb., high-temp. expansion and error bounds 9-45778
- temperature, log laws, validity study 9-45871
- textbook, undergraduate level 9-40244
- variational methods applic. to viscous heat conducting flows 9-23228
- CO₂ anomalies in critical region 9-26155
- ⁴He anomalies in critical region 9-26155
- Xe anomalies in critical region 9-26155

applications

- chemical transport between two states in closed tube, model 9-37817
- cumulus dynamics equation 9-41508
- electrochemical equilibrium diagram of mixed binary dissociable conductors 9-39609
- Fermi gas, magnetized, equations of state 9-25056
- light scatt. ley multicomponent fluids 9-39099
- MHD generator - compressor closed cycle 9-25168
- plasma, dense nondegenerate, stability 9-42555
- refrigeration process using vapour compression, efficiency 9-40825
- spinel phase, stability calc. 9-30784
- CO₂ molecular laser design 9-41898

Thermoelasticity

- asymmetric, generalization of Galerkin's functions 9-45835
- Biot's soln. to coupled problem, completeness proved 9-22222
- bonded materials containing cuts on interface, thermal stresses 9-38289
- coupled problems, approximate solns. 9-47818
- crack running in quasi-brittle material, anal. of stress field at tip 9-33087
- current-induced stress effects in solid cylindrical conductors 9-45837
- cylinder, hollow circular, axially symmetric plane strain problems 9-47814
- disc, finite, quasi-static thermal stresses due to instantaneous point heat source 9-31839
- electrodes in vacuum impulse discharge, strain and thermoelastic waves 9-48620
- element, 1 dimens., elastic plastic, ratcheting growth induced by thermal cycling 9-25086
- generalization arising from modified Fourier heat cond. law 9-47817
- image technique for soln. of uncoupled problems with spherical temp. distrib. 9-22223

Thermoelasticity continued

- infinite solid, steady state stress distribns. in vicinity of external crack 9-27211
- linear coupled theory, appl. to free vibr. modes of infinite plate 9-22237
- magneto-thermo-elastic plane waves, phase velocity and energy loss 9-25084
- Menabrea's theorem, appl. to non-isothermal transforms. of elastic body 9-22224
- micropolar, basic solutions for wave eqns. in unlimited medium 9-47803
- microstructural materials, constitutive eqns. using specific free energy function 9-38278
- plane coupled micropolar, Beltrami-Mitchell compatibility eqns. 9-45833
- plane coupled micropolar, integral eqns. for steady vibrations 9-45834
- polymeric networks in swelling equil. 9-23850
- quartz particles in whitewares, strain meas. by X-ray technique 9-23869
- reciprocity theorem for material with microstructure, applies. 9-47816
- reciprocity theorems for materials with microstructure 9-47815
- rubber, internal-energy contribs. to elastic stress 9-46860
- rubber networks swollen in n-dexane 9-23850
- solid with external circular crack, stresses 9-45836
- static problems with variable heat transfer, inversion transformation soln. 9-25085
- stress fields, interferometric determ. 9-29469
- stress in long cylinder containing penny-shaped crack 9-38288
- structural stresses, initial, in a two-dimensional medium with isotropic components 9-45817
- thermal shock in spherical shells, image technique soln. 9-22223
- thermoviscoelasticity, coupled, linear theory, theorems 9-40271
- triangular prism with circular hole under non-uniform heat generation, steady-state problem 9-38290
- α -Fe, flow analysis, 78° - 320°K 9-23883
- α -S thermoelastic constns. meas. 9-48882

Thermoelectric conversion see *Electricity/direct conversion***Thermoelectricity**see also *Thermocouples*

- AgCl-AgI, molten eutectic mixture 9-39089
- alkali metals, power parameter rel. to volume depend. electron-lattice interaction 9-33402
- alloys, magnetic, dilute, calc. of thermoelectric power 9-33401
- anisotropic materials, effect of impurities 9-26595
- cooling effect on thermoelement operation in nonstationary conditions 9-49153
- dielectric film, cryostat for thermally stimulated currents 9-45015
- electrodes, reversible molten metal, for thermoelec. power meas. of molten salts 9-28149
- ferroelectric materials, electrocaloric effect, influence on dynamic susceptibility 9-39674
- flame, thermo electric effect at thermodynamic equilibrium 9-36763
- generator, radiation coupling between heat source and collector plates, patent 9-22338
- generator, radio-isotope heat source, design, patent 9-25159
- glasses containing transition metal ions, thermopower 9-30964
- graphite single crystal, power, 300° to 7°K 9-26597
- liquid alkali metals, power, changes at melting point 9-40802
- magnon drag contrib. 9-24332
- magnon-drag power analysis, Mag. field eff., low temp. 9-33400
- metal, liq., thermopower, temp. depend. 9-39110
- metal, power, temp. depend., carrier density and mobility obs. 9-39580
- metal monocrystalline film with lattice defects power and conductivity 9-37434
- metals, power meas. at low temp. using superconducting galvanometer 9-30982
- noble metals, power, rel. to elastic deform. effect on Fermi surface 9-44884
- nuclear fuels, thermo-e.m.f., in-reactor meas. 9-28431
- oligonitronic, donor-acceptor complexes, props. 9-33225
- Peltier eff. in type II superconductors 9-49043
- Peltier meas. below 4°K 9-30983
- probe for temp. and vel. meas. of solid-liquid interface 9-39210
- Seebeck coeff., meas. apparatus, rel. to thermoelec. figure of merit 9-33191
- Seebeck effect utilization for steel composition determ. 9-37846
- semiconductor, anisotropic, effect of impurities 9-26595
- semiconductor polypphase alloys, calc. of thermal, elec. conductivities and thermoelec. e.m.f. 9-37609
- semiconductors, low-resistivity, trap determination technique 9-49094
- solar generator, air-cooled, weight and energy characts. optimization 9-31902
- solar generator with cylindrical collectors 9-31901
- superconductors, existence 9-37456
- thermally stimulated conductivity meas. in determ. traps concentration in low-resistivity semiconductors 9-49094
- thermoreistance circuits for gas flow control 9-36799
- triphenylmethylarsonium 7, -7, 8, 8-tetracyanoquinodimethan single cryst., anisotropy of power 9-33314
- Ag, power, rel. to elastic deform. effect on Fermi surface 9-44884
- Ag₂Te, solid and liq., power 9-37519
- AgSbTe₂, Peltier coeff. at boundary between solid and liq. phases, determ. 9-45019
- Al-Cu dilute alloy, thermopower, temp. and size depend. 9-43123
- Al-Fe dilute alloy, thermopower, temp. and size depend. 9-43123
- Au-Ni thin film thermocouples, vacuum-evaporated, thermoelec. power and Seebeck coeff. thickness depend. 9-45017
- Au, Seebeck coeff., 325 to 1225°K 9-26440
- Au₃Cu alloy, temp. depend. of thermoelec. power w.r.t. long- and short-range order 9-37610
- Bi, anomalous behaviour at low temps. and high mag. field, theoretical 9-47193
- Bi, thermo-e.m.f. and thermomag. props., 3° to 80°K 9-30984
- Bi₂Te₃-(20 mol.%)Bi₂Se₃ solid solns., conc. inhomogeneities influence 9-41252
- Bi₈₈Sb₁₂:Sn,Te alloy, thermoelectromag. props. 9-49154
- Bi₈₈Sb₁₂:Sn,Te alloy, thermoelectromag. props. 9-49154
- CaTiO₃, point defects formation, Seebeck coeff. study 9-28276
- Cd₃As₂, power depend. on mag. field and temp. for effective mass of electrons 9-35313
- n-CdCr₂Se₄:In Seebeck coeff. normal Hall coeff. and elec resistivity 9-45018
- CdS layers, thermostimulated currents 9-30985

Thermoelectricity continued

- CdSb, Peltier coeff. at boundary between solid and liq. phases, determ. 9-45019
- CoO₂ and CeO₂:Gd³⁺ single crystals, power, 500° to 1500°K and elec. conductivity and O diffusion coeff. 9-33246
- Co-(42-54 at.%)Al alloys, at room temp. 9-47069
- Co-Al alloys, power, elec. resistivity and magnetoresist, 1.4° to 300°K 9-44908
- Co_{1-x}Cu_xRh₂S₄, Seebeck coeff. 9-41164
- p-CoO:Li, Seebeck coeff., drift mobility obs. 9-37518
- Cu-Sn alloy from X-ray interference meas. 9-28098
- Cu, power, rel. to elastic deform. effect on Fermi surface 9-44884
- Cu₂O, power, temp. depend. 9-28496
- Cu₂Se films, obs. 9-35398
- Cu₂SeI, films, obs. 9-35398
- Cu₂SeS, films, obs. 9-35398
- Cu₂SbSe₄, Seebeck eff., effective mass of holes calc., dimensionless thermoelec. fig. of merit 9-26505
- EuO:Gd, power, dopant effect, temp. depend. indicating metallic conduction 9-33463
- Fe-Al, Fe-Cr, and Fe oxides, effect of O chemisorption on thermoelec. power 9-37822
- Fe-Au, power at low temps. and magnetic field dependence 9-35495
- α -Fe₂O₃, power, influence of hydrostatic pressure, 20-100°K 9-33300
- α -Fe₂O₄, power, influence of hydrostatic pressure, 20-100°K 9-33300
- n-GaAs, power meas. for Fermi energy calc. 9-33301
- Gd, thermo e.m.f. and thermomag. effect, mag. field strength depend., low temp. 9-39700
- n-Ge, influence of elastic deform. 9-37611
- Ge, power anisotropy, influence of deformation 9-35496
- GeTe, power, carrier energy spectrum changes due to solid solns. form. obs. 9-47113
- HfC, power, rel. to C content 9-47114
- HgTe-CdTe crystal, composition depend. rel. to lattice dynamics 9-26450
- HgTe, power, as function of press. at varying temp., rel. to band structure 9-48998
- n-HgTe, power, 4.2-200°K 9-33196
- n-HgTe, power and change in mag. fields, temp. depend. 9-35497
- In, Seebeck coeff., 77 to 350°K 9-41104
- InAs-ZnSe solid solns., e.m.f., and conductivity, carrier mobility and conc. 9-44962
- n-InAs, in fields up to 21 kOe at 90, 200 and 300°K 9-39622
- n-InSb, power, eff. of hydrostatic pressure up to 16 Katm. 9-28501
- KI:CdI single cryst., power 9-41253
- KI single cryst., power 9-41253
- KMnO₄ thermo-e.m.f., temp. depend 9-33282
- La-Ce dilute alloys, power meas. and Kondo temp. determ. 9-43152
- p-n-LaCoO₃, Seebeck coeff. w.r.t. resistivity 9-37527
- LaTe₂-LaSb solid soln., Sb substitution effect on power 9-39639
- Li₂V₂O₇, power obs. 9-35328
- LiF, pure and doped, X-ray excited, thermally stimulated conductivity obs. 9-45355
- Mg-Bi alloys, amorphous, power, and conductivity 9-30851
- Mg_{0.9}Mn_{0.1}Fe₂O₄, power, influence of hydrostatic pressure, 20-100°K 9-33300
- MnP metamag. single cryst., mag. field effs. on thermoelec. power 9-35498
- MnTe, magnon drag contrib. to thermoelec. power 9-24332
- NbC, thermo-e.m.f., 20°-2000°C, obs. 9-39588
- NbO, power meas., temp. depend 9-37448
- n-NbO₂, power meas., temp. depend 9-37448
- Ni-(49-51 at.%)Al alloys, at room temp. 9-47069
- Ni_{0.9}Fe_{0.1}O₄, power, influence of hydrostatic pressure, 20-100°K 9-33300
- Ni_{1-x}Zn_xFe₂O₄, Seebeck effect, 500-1000°K, influence of magnetic structure 9-33310
- β -NiAl, absolute thermoelec. power, Fermi surface obs. 9-37449
- NiO, Seebeck coeff., temp. and O partial press. depend. 9-44966
- Pb_{1-x}Sn_xTe, Seebeck coeff. hole conc. dependence rel. to band structure determ. 9-39632
- PbCl₂, PbI₂, PbBr₂, molten, thermoelec. power meas. 9-28149
- p-PbSe, power meas., depend. on carrier density and temp., indication of two valence bands 9-35409
- PbTe, thermoelec. material, chemical compatibility with alloys 9-26808
- α -Pu rel. to self-irradiation effs. 9-24072
- Sb, differential thermoelec.-e.m.f., 300-750°K 9-47076
- Sb, Peltier coeff. at boundary between solid and liq. phases, determ. 9-45019
- (Sb₂Te₃-Bi₂Te₃)-(Bi₂Te₃-Bi₂Se₃) thermocouple, transient response of cooling 9-28569
- Sb₂Te₃, Peltier coeff. at boundary between solid and liq. phases, determ. 9-45019
- Se, infl. of crystallization method on props., 250°-360°K 9-30986
- SnCl₂, SnI₂, SnBr₂, molten, thermoelec. power meas. 9-28149
- ThC-UC solid solutions, 3.8 and 15 metal % U 9-26510
- TiC, n-type power 9-28468
- TiC, power, rel. to C content 9-47114
- TiO₂-VO₂ sintered pseudobinary system, thermoelec. power meas. rel. to semiconductor-to-semiconductor transition 9-49088
- TiO₂-VO₂ sintered pseudobinary system, thermoelec. power meas. rel. to semiconductor-to-semiconductor transition 9-49088
- Ti₃TaS₄, and optical props., lattice const., obs. 9-35070
- Ti₃Te₂ polycrystal, temp. dependence 9-26598
- Ti₃Te₂ polycrystal, temp. dependence 9-26598
- p-TlSe:Pb, thermopower and conductivity, rel. to valence-band structure 9-43059
- UC_{1-x}N_x, elec. resist. and Seebeck coeff., 80-1000°K obs. 9-35330
- UO₂, nearly stoichiometric single cryst., thermoelec. power, activation energies obs. 170-1250°K 9-33403
- V₂O₅ and related oxides, power, and Hall const., rel. to nature of metallic state, up to 800°K 9-30836
- VO₂, thermoelec. power comp. dependence 9-28272
- Zn, quantum oscillations in power, Peltier effect obs. 9-43124
- ZnCl₂, ZnI₂, ZnBr₂, molten, thermoelec. power meas. 9-28149
- p-ZnSnSb₂, differential thermal e.m.f., electro-physical props. obs. 9-35410
- ZrC, power, rel. to C content 9-47114

Thermoluminescence

alkali halide scintillators, effect of elec. field 9-45354

Thermoluminescence continued

- calcite, thermoluminescence mechanisms following α and reactor irradiation 9-31147
- F colour center formation, inhibited by Mn impurities, thermoluminescent investigation 9-31148
- feldspar separated from sands, rel. to accident dosimetry 9-49609
- glow curves, eqns. for simple models of electron trap transitions 9-44881
- glow curves, kinetic order and acutation energy, empirical relation 9-49328
- glow curves method for electron trap parameters determ. 9-44880
- phosphor-terfion dosimeter for radioactive jewellery 9-34363
- phosphors, thermoluminescent, relative sensitivities obs. 9-24466
- radiation dosimeter of CaSO₄:Mn + impurity ions, preparation patent 9-27596
- Al₂O₃ films, 500 to 6000Å, γ irradiated, traps study using thermoluminescence glow curves, 30 to 300°K 9-33245
- α -Al₂O₃, activation energies obs. 9-39889
- CaF₂: rare-earth, thermal glow curves, analysis 9-47406
- CaF₂:Dy:Ce, γ -irrad. 9-41411
- CaF₂:Dy, γ -irrad. 9-41411
- CaS:Cu, thermal glow and phosphoresc. decay curves rel. to trap levels 9-35693
- CaS:Cu,Zr, rel. to Cu activation and trap level distrib. 9-35694
- CaSO₄, γ irradiated 9-41402
- CaSO₄(Mn) film phosphors, dosimetry applic. 9-27594
- CaWO₄, local trapping levels obs., rel. to X-ray luminesc. props. 9-39890
- CaWO₄ phosphors sintered in HCl stream 9-28722
- CdWO₄, local trapping levels obs., rel. to X-ray luminesc. props. 9-39890
- KBr:Cd, F centres formation obs. 9-33606
- KBr:Zn, F centres formation obs. 9-33606
- KBr, F centres formation obs. 9-33606
- KCl:Mn, temp. depend. 9-28303
- KCl, additively coloured, photostimulated, traps and trapping mechanism obs. 9-47408
- KN₃, trapping levels, 10°-525°K 9-47407
- LiCl, reactor-irrad. 9-28729
- LiF, effect of particle size 9-41412
- LiF, in ionising radiation meas., 10-250Mrad. 9-38621
- LiF, TLD, correl. with optical absorpt. 9-45323
- LiF, thermotreatment effect 9-33607
- LiF dosimeter, heat stable, patent 9-36529
- LiF pure and doped crystals, X-ray excited 9-45355
- LiF:Eu,Mg radiation dosimetry meas., patent 9-28730
- NaCl:Ca(Cd), F centres formation obs. 9-33606
- NaCl:Sr²⁺ glow curves and phosphoresc. centres form. obs. 9-37773
- NaCl, F centres formation obs. 9-33606
- NaCl, glow curves, kinetic order and actuation energy anal. 9-49328
- NaN₃, 15° to 300°K 9-43264
- SiO₂ films, 500 to 6000Å, γ irradiated, traps study 9-33245
- SiO₂ films, 500 to 6000Å, γ irradiated, traps study using thermoluminescence glow curves, 30 to 300°K 9-33245
- SrS:Cu, thermal glow and phosphoresc. decay curves rel. to trap levels 9-35693
- SrS:Cu,Zr, rel. to Cu activation and trap level distrib. 9-35694
- YVO₄:Eu, impurity effects 9-47409
- ZnS:Bi and thermally stimulated current 9-33608
- ZnS:Er³⁺, with additional alkali, Cu and halogen doping 9-37774
- ZnS glow curves, kinetic order and actuation energy anal. 9-49328
- ZnS single crystals, before and after electron beam irrad. 9-45356
- ZnS single crystals grown from Ga and In melts 9-37095
- ZnWO₄, local trapping levels obs., rel. to X-ray luminesc. props. 9-39890
- ZrO₂(Ti), X-irrad., glow curve, 100-350°K, and effect of Ti-doping 9-39891

Thermomagnetic effects *see* Magneto thermal effects**Thermometers***see also* Pyrometers; Thermocouples

- dew point using equilibration curves of pre-cooled thermometers 9-26895
- fixed points, use of superconductors 9-35381
- interferometric for air temp. 25-30 km 9-37910
- quartz, ranges, sensitivity and fidelity limits 9-25134
- semiconductor diode, for low temp. 9-26572
- sonic anemometer - thermometer for direct method of determ. turbulent transport of physical quantities 9-24644
- thermistor, remote sensing, magnetically recording, linear display 9-29328
- 1°K in MnF₂, n.m.r. depend. on temp., 10-40°K 9-40291
- H vapour pressure compared with Pt resistance thermometer 9-45885

resistance

- calibration at low temperatures using ALGOL computer program 9-34103
- potentiometer, a.c., for low temp. work 9-47840
- self-balancing bridge for low temp. meas. 9-41847
- Wheatstone bridge, self-balancing, for low temp. meas. 9-41847
- Ge, calibration to 0.4°K using metal of known ht. capacity 9-25133
- In, in calorimetric assembly for adiabatic meas. of specific heat at low temp. 9-25135
- pt, 91°K-14°K, interpolation of differences in resistance ratios, accuracy determ. 9-45884
- Pt, accuracy in determ. of temps. between 2 and 14 K 9-40290
- Pt film type, towed in water, dynamic frequency response 9-34104
- Pt, compared with H vapour-pressure thermometer 9-45885

Thermonuclear devices *see* Plasma devices**Thermonuclear reactions** *see* Elements/origin; Nuclear fusion*see also* Elements/origin; Nuclear fusion

- 'Tokamak' type mag. apparatus, possible future in reactor 9-44452
- fusion, plasma confinement, survey of USAEC'S program 9-23313
- reactor, pulsed, toroidal system for plasma compression 9-32628
- researches, progress reports 9-34467
- stellar explosive nucleosynthesis conditions for C burning and Si burning 9-49546
- stellar plasma, dense, nuclear Q values, correction using modified ionic cluster expansion 9-49550
- URCA process in stars with neutrino emission 9-31531
- C burning in stars, synthesis of elements and energy generation 9-40142
- Si burning in sun and stars 9-49549

Thermopiles *see* Thermocouples**Thermosphere** *see* Atmosphere/upper; Ionosphere**Thermostats***see also* Cryostats

No entries

Theta pinch *see Plasma/confinement*

Thickness measurement

see also Particle size

- austenitic alloy foils, irradi., and void size determ. 9-48755
- crustal, from SM wave spectral behaviour 9-47497
- crystal plates, birefringent, interferometry 9-41354
- earth layers, by inverse magnetotelluric sounding 9-37890
- epitaxial layer, i.r. interference method 9-30482
- film; by optical method 9-36941
- film, nonabsorbing, on similar substrate, ellipsometry 9-28212
- of film, optical 9-41360
- film, thin, interference microscopy, replication method 9-23622
- of films, protective, using β backscatter 9-39154
- films, thin, slightly absorbing, ellipsometric meas., optical const. 9-37678
- films, using electron back-scatt. 9-29166
- ice sheet, polar, radio echo equipment 9-26883
- metal films, thin, simultaneous complex index meas. in u.v. 9-27378
- metal thin film, continuous ellipsometric determination during deposition 9-32845
- metallic thin film, hill-climbing technique 9-39804
- oil film between rolling discs meas., variable-magnetic-reluctance technique 9-36841
- optical filter dielec. layers 9-48107
- plating on small balls 9-31738
- thin film, discontinuous and absorbing, ellipsometric eqns. 9-36940
- thin film on reflecting surface, meas. by ellipsometry 9-36939
- in, vacuum deposition of anti-reflecting coatings 9-38402
- Ag foil, optical props. and curves of constant transmission 9-23640
- Ag thin film, continuous ellipsometric determination during deposition 9-32845
- Al alloys, X-ray transmission gauging, composition effects 9-39156
- Nb₂O₅ films, by electroreflectance interferometry 9-30486
- SiO₂ film on Si, reflectivity corrections for variable angle monochromatic fringe obs. 9-34982
- Ta₂O₅ films, by electroreflectance interferometry 9-30486

Thin films *see Films; Films, solid*

Thirring model *see Elementary particles; Field theory, quantum*

Thixotropy

No entries

Thomas-Fermi method *see Atoms/structure*

Thomson effect *see Thermoelectricity*

Thorium

- Fermi surface theor. model, relativistic augmented-plane-wave calc. 9-24108
- ion, ionic solvation and growth of ThO₂ sols. 9-23549
- magnetoresistance, transverse, 4.2-60°K, in fields up to 22 kOe 9-41318
- photoelectric cross-sections of gamma-rays 30-100keV 9-24231
- in rocks, gamma spectrometer surface obs. 9-37893
- in Siemens-Argonaut reactor, D₂O moderated Th lattices 9-34500
- spectral lines, 2747 to 4572 Å interferometric obs. 9-46284
- thermionic emission in Cs vapour, report on various aspects 9-25170
- X-ray absorption spectra, M, comparison with ThO₂ 9-49305
- ²³²Th isotope, distribution in the ocean 9-47519
- Th I, Slater, configuration-interact. and dipole integrals 9-25700
- in YPO₄:Ce u.v. phosphor, sensitization 9-31140

Thorium compounds

- Bi-Th system, Bi dissoc. press. 9-39937
- Cu-Th system, phase equil. obs., thermodynamic props. 9-46679
- In-Th alloys, elastic and anelastic behaviour during martensitic transform. 9-42865
- oxychalcogenides, cryst. prep. 9-30519
- TlO₂, M absorption spectra, comparison with Th 9-49305
- Th-ThO₂, phase equilibria thermal, X-ray and microscopic techniques analysis 9-41061
- Th_{1-x}Er_x, spin correlations rel. to superconducting transition temp. comp. dependence 9-24160
- Th₂Co₁₇, intermetallic 2-17 stoichiometry 9-26248
- Th₂Fe₁₇, intermetallic 2-17 stoichiometry 9-26248
- ThP₄, preparation, mag. susceptibility, elec. resistivity, hardness 9-35035
- ThB₆, sp. ht., low temp. 9-47003
- ThC-ThN mixtures, melting point maximum in N₂ atmos. rel. to composition 9-40819
- ThC-UC solid solutions, elec. props. 9-26510
- ThC, chemical bonding and mag. susceptibility at various temp. 9-28224
- ThC, non-stoichiometric, substructure existence around 830°C 9-28270
- ThC₂, coated particles preparation fluidized Bed. by reaction and sintering 9-41053
- ThF, evaporated film, refractive index, influence 9-33503
- Th(NO₃)₃, solvation in H₂O-acetone, p.m.r. 9-42682
- ThO₂:Np⁴⁺, absorption spectrum, analysis of crystal field splitting of J levels 9-35665
- ThO₂, point defect form. energy calc. 9-44688
- ThO₂ gels, calcination process, electron microscope exam. 9-35221
- ThO₂ powders, calcination process, electron microscope exam. 9-35221
- ThO₂ sols, ionic solvation and growth 9-23549
- ThP-UP solid solutions, synthesis and props. 9-33123
- ThP, diamagnetic, ³¹P nuclear mag. relax. 9-24343
- ThP, preparation, mag. susceptibility, elec. resistivity, hardness 9-35035
- ThP, synthesis by reaction of Th with PH₃ gas, lattice parameter 9-33123
- ThSiO₄:Gd³⁺, e.s.r. ground-state splitting 9-33626

Thulium

- atom, X-ray L emission spectra, α region, three new diagram lines 9-22966
- vapour, i.r. laser lines 9-29947
- ¹⁵⁷Tm in YGa garnet, selection rules in absorpt. spectrum 9-24416
- ¹⁷¹Tm, preparation by irradiating ¹⁶⁹Tm, then leaving to allow ¹⁷⁰Tm to decay and separating Yb, patent 9-22905
- Tm²⁺ in CaF₂, SiF₄, acoustical phonon tunable detector 9-26403
- Tm²⁺, (f-f) absorption spectrum obs. in CaF₂ 9-28682
- Tm³⁺, coherent emission from electro-optic crystals, obs. 9-26738
- Tm³⁺, energy transfer with Er³⁺ in Y₃Al₅O₁₂ 9-31126
- Tm³⁺ in CaF₂, anomalous population distrib. in optically excited metastable level 9-31161
- Tm³⁺ in LiNbO₃, electro-optic crystals, second-harmonic radiation at 77°K 9-43203
- Tm³⁺ in soda-silica glasses, Mossbauer effect, crystalline elec. field parameters 9-37702
- Tm³⁺ photoluminesc. in Y₃Ga₅O₁₂ 9-49338

Thulium continued

- Tm³⁺(4f¹²), spin-spin interactions determ. from matrix element expression 9-38774
- Tm I spectrum, level lifetimes and crossings, Hanle effect meas. 9-29950

Thulium compounds

- TmAl₃ garnet, n.m.r. of ¹⁶⁹Tm and ²⁷Al 9-45407
- TmCl₃·6H₂O, recoilless nuclear resonance spectra, pseudoquadrupole shift and asymmetric line broadening 9-24509
- TmFeO₃, domain structure and wall energy temp. dependence 9-47275

Thunderstorms

see also Lightning

- clouds, elec. field and conductivity obs. 9-31324
- electrification, role of ice sphere collisions 9-41534
- lightning, ball, microwaves generation 9-43402
- lightning discharges, audio frequency pressure variations 9-37921
- vortices, convective, cellular structure 9-45489

Thyratrons *see Gas-discharge tubes*

Tides *see Atmosphere/movements; Ionosphere; Oceanography*

Time interval measurement

- astronomical and atomic standards, review 9-29168
- multichannel techniques 9-31740
- nanosecond delays and time scale calibration, techniques 9-22042
- pulse like signals, electronic circuit design 9-47888
- second, new definition on quantum basis 9-22041

Time measurement

- astronomical and atomic standards, review 9-29168
- atomic clock, national physical laboratory, improvements 9-43713
- atomic clock with sequential optical pumping, based on reson. freq. of ⁸⁷Rb 9-47720
- picosecond pulse measurement by two-photon excitation of photographic film 9-22482
- pulse like signals, cct. design for integral, duration and interval meas. 9-47888
- spark timer, solid state 9-27157
- standards for long-baseline interferometry 9-36107
- time of arrival in quantum mechanics, formal considerations 9-36127
- time of arrival in quantum mechanics, statistical aspects 9-31765
- time of arrival in quantum mechanics, suitable apparatus 9-31764
- Cs frequency standards, U-shaped resonators applic. 9-34004
- Ge(Li) detector signals, filter and discriminator techniques comparison 9-36519

Tin

- absolute viscosity as function of temp., liquidus to 500°C 9-30378
- acoustic surface impedance behaviour on e.m. excitation of standing wave and quantum oscillations obs. 9-46987
- atom total γ cross-sections, 40-80 keV, mean values, analysis 9-22949
- atomic spectrum, odd-even isotope shifts 9-34542
- dendrite growth in pure tin melts and in tin containing Pb, Bi and Sb 9-48815
- diffusion coeffs., partial, from conc. meas. in zone of contact liq. layer with Bi 9-33003
- diffusion in noble metals, rapid, interstitial mechanism 9-28321
- drop, liquid inert sessile, rel. to surface energy of Fe determ. 9-32836
- electrodeposited coatings, surface texture 9-36933
- electrodiffusion of Bi, effect of Tl additions 9-46623
- electron focusing by longit. mag. field 9-26519
- electropolishing procedure to produce etched or polished surfaces 9-39959
- e.m. excitation of sound waves 9-42956
- film, epitaxial, residual strains analysis 9-39160
- films, vac. deposition, crystal orientation rel. to pressure, deposition rate and thickness 9-39164
- films on W(110) face, (structure from LEED obs. 9-26184
- gamma ray scatt., 145 keV, differential elastic scatt. X-section 9-46263
- grain growth in presence of surface active and inactive impurities 9-48865
- granular films, superconducting fluctuations in 3-d regime causing excess conductivity 9-26527
- heat capacity, 1-30°K 9-47006
- impurities in Ni alloys and steels, determ. 9-28830
- internal friction anomalies near melting pt. 9-39399
- liquid, elec. resistivity, 235°-910°C 9-40803
- liquid, impurity states, localized, magnetic susceptibilities of 3d-transition metals 9-28150
- magnetoconductivity of 2-dimens. coherent network of coupled orbits, oscillations obs. 9-44919
- molten, electrical resistance meas. by rot. field method 9-39583
- Mossbauer thermal shift meas. of ¹¹⁹Sn in β -Sn, 3.6-90°K 9-24386
- n.m.r. spin-echo meas. of spin-spin interactions 9-47445
- nucleation, eff. of small addition of solute 9-28180
- nucleation, supercooling depend. on liq. drop size 9-28179
- oxidized surface, work function, contact potential difference method 9-31000
- P-T diagram interpretation 9-36914
- plasma oscillations in liquid and solid foils 9-41148
- solid and liquid equations of state calc. from low temp. mechanical obs. 9-39090
- solvent in solution growth of group II-VI compounds 9-37073
- sound wave e.m. excitation 9-42956
- superconducting films, conductivity temp. dependence at 20 GHz 9-43042
- superconducting films, upper critical field meas. 9-35368
- superconducting films, upper critical field rel. to deposition on substrates held at low temps. 9-28480
- superconducting films as high-speed radiation detectors 9-35367
- superconducting narrow thin-films, quantum phase correlations and fluctuations 9-24159
- superconducting thin films, microwave conductivity 9-28481
- superconducting thin films, strain effect on T_c 9-41177
- superconductivity of small particles, obs. in tunnel junctions 9-43045
- surface props. studied using spectrum of Mossbauer electrons 9-30476
- surfaces, electron reflection, specularly 9-37411
- texture studies by anisotropy of galvanomag. eff. at low temp. 9-32929
- template corrosion, eff. of CS₂ and dithiocarbamates 9-28803
- twinning speed studied with high speed photography 9-23659
- u.s. absorption in supercond. transition rel. to cryst. orientation 9-37336
- whisker, elastically bent, resistance increase below 20°K, rel. to electron mean free, path meas. 9-37453
- whisker growth on Ni-Cr films, conditions and mechanism 9-48816

Tin continued

- whiskers, formation by vapour deposition 9-39218
white, band structure and Fermi surface from de Haas-van Alphen data 9-47049
white, Mossbauer effect on ^{119}Sn , anisotropy of emission probability and temp. and angular depend. 9-49265
p, range and ionization energy losses, Bragg's curve method meas., $E_p=100$ -660 MeV 9-33213
 ^{119}Sn satellites in PMR spectrum of tetravinyltin, $J_{\text{Sn-H}}$ coupling const. 9-27917
 ^{119}mSn , u.s. meas. using Mossbauer eff. 9-37697
 ^{119}Sn satellites in PMR spectrum of tetravinyltin, $J_{\text{Sn-H}}$ coupling const. 9-27917
Bi:Sn, distrib. coeff. and acceptor valency determ. 9-43002
Ge:Sn, radiative recomb. 9-37762
in Hg, effect on electrodiffusion of Bi 9-46623
Nb $_3$ Sn cryst. growth, Sn-rich phase boundary 9-44648
Sn:Cd, lattice thermal conductivity, dopant-conc. dependence, rel. to normal and superconducting states 9-26452
Sn-Pb normal metal-superconductor junctions, proximity effect by electron tunneling 9-24166
 α -Sn, semicond., covalent bond in rel. to neutral pseudo atom concept 9-28507
Sn II laser c.w. transitions, 6453 and 6844 Å 9-47983

Tin compounds

- alloys, simple hexagonal, axial ratio rel. to total energy 9-40918
alloys polycryst. up to 5 at. %Sn, onset stress for deform. twins 9-32980
SnO $_2$ -TiO $_2$ system, spinodal decomposition 9-33144
solder whisker growth on Ni-Cr films, conditions and mechanism 9-48816
Ag-Sn h.c.p. alloys, stacking fault energies 9-40960
Au-Sn system, metastable γ -brass and non-equilib. Hume-Rothery phases 9-35255
Bi-Sn alloys, crystal structure and superconducting props. under high pressures 9-23752
Bi-Sn alloys, magnetoresistance anisotropy, carrier influence 9-41161
Bi-(0.3 at.%)Sn alloy, isoenergetic surfaces struct. at L-maximum 9-35312
Co-Sn dilute alloy, Mossbauer hyperfine field of ^{119}Sn and resistivity study 9-47335
Cu-(14.95 wt.%)Sn alloys, b.c.c. to orthorhombic γ_1' martensite transformation, crystallography 9-30739
Cu-Sn, martensitically transformed, Young's mod., yield stress and plastic deform. 9-35172
Cu-Sn alloy liquid, X-ray interference function thermoelectric power and electrical resistivity determ. 9-28098
 α -Cu-Sn alloys, polycryst., twinning 9-39189
Cu-Sn liq. alloy system, thermodynamics, Knudsen cell and mass spectrometric obs. 9-36860
Fe-Sn dilute alloys, Mossbauer hyperfine field of ^{119}Sn and resistivity study 9-47335
Hg-Sn liq. alloys, thermodynamic activities 9-30369
InGaSn alloy activation in generator elements of rad. loop in water reflector of IRT reactor 9-32384
InGaSn alloy in activity generator elements of rad. loop of IRT reactor, influence on active section of water reflector 9-32385
Mg-Sn alloys, solution hardening, room temp. 9-23984
Nb-Sn superconducting alloys, mag. hysteresis and alloy constitution 9-37659
Nb $_3$ Sn, growth by solid Nb-liq. Sn reaction, diffusion and soln./deposition mechanisms 9-48764
Nb $_3$ Sn alloy, supercond., mag. hysteresis and cryst. struct. 9-39769
Ni-Sn dilute alloys, Mossbauer hyperfine field of ^{119}Sn and resistivity study 9-47335
Pb-Sn-Te system, phase diagram 9-36918
Pb-Sn alloy electrodes, electrochem. behaviour in different soln., corrosion resistance and passivation mechanism 9-33673
Pb-Sn alloys, absolute viscosity as function of temp. and composition 9-30378
Pb-Sn alloys, liq., stress cracking of Cu and alloys 9-48941
Pb-Sn liquid alloy, Knight shift calc. from pseudopotential formalism 9-23532
Pb-Sn-Te alloy system, magneto-optical effects, band struct. and cyclotron reson. obs. 9-39807
PbO-SnO mixed cryst. layers, photoconductivity 9-41269
Pd-Co-Sn alloys, ferromag., mag. props., Mossbauer obs. 9-43179
Pt-Sn alloys, lattice spacing and solid solubility of Sn 9-30571
Sn-Au alloys, liquid, elec. resistivity, 235°-910°C 9-40803
Sn-Au liq. alloys, at. distrib. and elec. resist. 9-30423
Sn-Bi, thermal conductivity, solid and liquid states 9-24065
Sn-(0.5-8.0)Bi alloys, Sn dendrite growth as function of supercooling 9-48815
Sn-Cd eutectic, plane to cell transition on solidification 9-23585
Sn-Cd lamellar eutectic, fault structure 9-28299
Sn-Cu alloy, spectrochem. analysis of e evap. vacuum condensates, obs. 9-28832
Sn-Pb, dilute alloys, electropolishing procedure to produce etched or polished surfaces 9-39959
Sn-Sb(Cu, Ni) dil. alloys internal friction anomalies near melting pt. 9-39399
Sn-Tl alloys, liquid, density determ. rel. to atomic and ionic volumes 9-30370
Sn-Zn alloys, liquid, self diffusion coeffs. meas 9-28113
Sn-Zn eutectic, undercooling at the solid-liquid interface 9-46686
Sn-Zn eutectic alloy system, morphology changes 9-46681
Sn-(1.0-5.0wt.%)Pb alloys, Sn dendrite growth as function of supercooling 9-48815
Sn-(1.0-6.0wt.%)Sb alloys, Sn dendrite growth as function of supercooling 9-48815
Sn $_4$ As $_3$, supercond., carrier conc. and ionic model obs. 9-37474
Sn $_4$ P $_3$, supercond., carrier conc. and ionic model obs. 9-37474
Sn complex, dimethyltin dibenzoate, n.m.r. spectra and configurations 9-27875
Sn complex, Et $_3$ SnCl $_3$, Et $_3$ SnCl $_2$ and Et $_3$ SnCl liq. or soln., v. vib. spectra and normal coord. anal. 9-48484
Sn complex, of type cis-SnX $_2$ ·2L, Raman spectra 9-30057
Sn oxide-ceramic devices, field effect studies 9-35489
Sn Te, relativistic band structure 9-39629
SnCl $_2$, solid solutions in ice, Mossbauer spectra 9-33532

Tin compounds continued

- SnCl $_4$, ν_1 fundamentals, Cl isotopic splitting, using low temp. Raman cell 9-32068
SnCl $_4$, positron lifetimes in liquid 9-44583
SnCl $_4$, vibr. freqs. and stretching force consts., i.r. obs. 9-27874
SnHPO $_4$ · $\frac{1}{2}$ H $_2$ O, vibrational spectrum 9-28704
SnI $_2$, model for electronic states 9-42612
SnI $_2$ and SnI $_4$ vapour, optical absorpt. 9-42612
SnI $_4$, Mossbauer studies reveal nature of bond in molecular crystal 9-34643
SnO $_2$, bond type, cryst. energy calc. 9-30504
SnO $_2$, cassiterite, natural crystals, ferromagnetism and remanence origin 9-47264
SnO $_2$, electrical semiconducting properties, stoichiometric relationship 9-35329
SnO $_2$ films, negative magnetoresistance 9-33311
SnO $_2$ powders, i.r. absorpt. spectra, interpretation 9-31111
SnO $_2$ semiconducting layer, i.r. reflection depend. on surface resistivity 9-26729
SnO in Ar, Kr, Xe matrices at 20°K, absorpt. and fluoresc., D-X transition and intersystem crossing 9-49286
SnS, dipole moment from Stark components of microwave rotational transitions 9-30051
SnS, lattice dynamic anisotropy and line asymmetry obs., 60-320°K, Mossbauer effect investig. 9-39822
SnS $_2$, electronic band structure and optical constant calc. 9-26485
SnS in Ar, Kr, Xe matrices at 20°K, absorpt. and fluoresc., D-X transition and intersystem crossing 9-49286
SnSe $_2$, electronic band structure and optical constant calc. 9-26485
SnTe-As $_2$ Te $_3$ quasibinary system, investig. 9-42920
SnTe-GeTe alloy, ferroelectric phase transitions from Mossbauer effect obs. 9-26592
SnTe, band struct. and electronic props., APW calcs. 9-47050
SnTe, characteristic electron energy losses 9-39553
SnTe, ferroelectric phase transitions from Mossbauer effect obs. 9-26592
SnTe, ferroelectricity, evidence from phonon temp. dependence calcs. 9-39692
SnTe, fund. energy gap, press. coeffs. 9-33317
SnTe, k.p. band model 9-39628
SnTe, optical props., band structure and supercond. props. 9-39794
SnTe, relativistic band struct. and electr. props. 9-43057
(SnTe) $_x$ -(MnTe) $_x$ alloys, mag. props. 9-39771
SnTe degenerate semiconductor, review of exptl. data on superconductivity 9-41179
SnTe film epitaxial growth on collodion, rock salt and mica obs. by electron diffraction 9-30492
SnTe soft phonon k=0 TO mode, low temp. region 9-37318
Ti(5 wt.%)Al-(2.5 wt.%)Sn alloy, fracture toughness and mech. props. at cryogenic temps. 9-37253
- Titanium**
added to Fe-Mn-Ni alloys, ageing 9-48917
additive in Ceto alloy, adsorption props. 9-36965
in Alnico, mag. props. rel. to structure 9-24310
annealing n. irradi. commercially pure mat. at 17°K, effect on tensile props. 9-33112
atom, with electronic configurations 3d 3 and 3d 4 3p, energy spectra, theoretical investig. 9-29940
B3 HD 37058 star abundance determ., Wrubel's curve of growth 9-33903
b.c.c., elastic moduli determ., anisotropy 9-46867
b.c.c., elastic moduli determ., anisotropy 9-46866
corrosion, aqueous-stress, infl. of comp. and Ht. treatment 9-37833
corrosion, crevice attack 9-37834
corrosion, sea-water stress, metallurgical and mechanical aspects 9-37832
desorption of D $_2$ from Ti sponge 9-30499
deuteron back-scattering, energy distribution 9-39549
emissive power and specific resistivity above 400°K, relationship 9-39547
fatigue damage under cyclic stress, slip band extrusions and twin boundary filamentary growths 9-32981
film on various substrates, elec. props. 9-37452
liquid vapour pressure, 1953-2193°K 9-23604
lubricants and wear coating 9-37268
magnetic susceptibility, var. with temp. rel. to electronic struct. 9-35533
neutron irradi. commercially pure, low temp. annealing effects on tensile props. 9-33112
oxidation isotope shift, nucl. vol. and mass eff. 9-29988
oxidation kinetics, effect of annealing 9-33671
oxidation kinetics analysis rel. to phenomenological scheme for non-steady-state range 9-47462
oxidized surface, work function, contact potential difference method 9-31000
proton back-scattering, energy distribution 9-39549
proton energy losses 9-30807
sorption of O $_2$ study at 273, 195 and 7°K 9-48772
spectra, neutral, odd configurations 9-29948
stable nuclides in iron meteorites, surface ionization mass spectrometric obs. 9-38089
surface energy, 'zero creep' method, 1600°C 9-23621
thermal diffusivity and conductivity at high temperatures 9-41109
thermal expansion coeff., temp. depend., 80-1200°K 9-44842
thermally activated deformation parameters from stress relaxation 9-28350
valence in titanobarium glass and ceramic, from X-ray emission spectra K α_1 line position 9-41398
X-ray spectra obs. of inner level shifts and band struct. 9-45340
Al-Al alloy addition, eff. on strain-induced solute disposition stability control of mech. strength 9-28360
in Al $_2$ O $_3$ far i.r. absorpt. spectrum in applied mag. field, Zeeman splitting of lines, single d electron obs. 9-31100
O concentration by fast neutron activation analysis 9-26851
 β -Ti foils, preparation for transmission electron microscopy 9-46772
Ti-Zr film in getter-ion pump, residual gas analysis 9-38176
 α -Ti, coarsened grained, fatigue behaviour and twin formation 9-33083
 α -Ti, deformation mechanism below 0.4 T $_m$, comments 9-28351
 α -Ti, relaxation spectrum, effect of H content, comment 9-30647
 α -Ti, relaxation spectrum, effect of H content, comment 9-30648
Ti $^{3+}$, spin relaxation through modulating the orientation 9-47295
Ti $^{3+}$ formation in barium silicate glass due to gamma irradi. 9-37693
Ti $^{4+}$ coordination in glasses in RO-TiO $_2$ system 9-32827

Titanium continued

- Ti II, line strengths for the transition array ($3d^3+3d^4s$)– $3d^4p$, calc. 9–34522
in ZrO_2 , effect on thermoluminescent glow curves 9–39891

Titanium compounds

- alloys, commercial grade, fracture toughness and mech. props. 9–37253
alloys, crack tolerance, influencing factors, review 9–37263
Alloys, crack tolerance influencing factors, review 9–37264
alloys, crevice corrosion 9–37834
alloys, fatigue 9–23924
alloys, high strength, structural ductility 9–37243
alloys, hot-salt stress corrosion cracking initiation 9–37265
alloys, mechanical properties, effect of low temps. 9–23905
alloys, mechanical strength and toughness rel. to fine structure 9–37252
alloys, sheet, elastic props. 9–23849
alloys, stress corrosion in methanolic solution 9–23922
alloys, stress-corrosion cracking in aq. NaCl at room temp. 9–23921
alloys, texture strengthening, cryogenic temps. 9–37254
alloys, texture strengthening and fracture toughness 9–37255
alloys, thermal conductivity meas. apparatus at cryogenic temps. 9–26454
 β -alloys, work-hardened, dislocation struct. and mech. props. rel. to initial state 9–41031
anatase grown by reactive vacuum evaporation, optical props. and struct. determ. 9–42729
charge transfer, electron spectroscopic meas. 9–44636
hydride lattice, H and D vibr. and thermal n cross-sections 9–30767
oxide inclusions in Fe-Cr, Fe-Ni alloys, X-ray microanalysis of emission spectra fine structure 9–37752
oxides, family of ordered phases, and nature of slightly-reduced rutile 9–44675
rutile, reduced, microwave acoustic relaxation 9–35280
rutile grown by reactive vacuum evaporation, optical props. and struct. determ. 9–42729
rutile single crystals, nature of defects formed during chemical reduction 9–32945
titanate materials, lattice defects and colour centres 9–32942
Al(<0.22at.%)Ti solid solution, lattice parameter comp. dependences 9–42918
Cl–Ti alloys, ageing kinetics, decomposition activation energies 9–23941
Co-Ni-Al-Cu-Ti-Fe alloys, magnetost. analysis 9–47251
Co(7.45 wt.%)Ti solid soln., γ -phase, precip. during ageing, neutron diff. and chem. analysis 9–41065
Cr(49wt.%)Ni(1wt.%)Ti alloy, corrosion on exposure to pyrolysis conditions of sodium-base spent pulping liquors 9–28800
Cr(49wt.%)Ni(1wt.%)Ti alloy, corrosion on exposure to pyrolysis conditions of Na base spent pulping liquors 9–28799
Cu-Ti-Al alloys, decomp. nature, struct. changes on ageing electron microscopy 9–46938
Cu-Ti-Al alloys, dispersion-hardened, mechanical twinning 9–23926
Cu-Ti alloys, decomp. nature, struct. changes on ageing electron microscopy 9–46938
Cu-Ti alloys, dispersion-hardened, mechanical twinning 9–23926
Cu-(2.3 wt.%)Ti alloy, aluminium additions, effect on decomp. kinetics 9–37292
Fe-Ni-Al-Co-Ti alloys, thermomech. treatment effect on mag. props. 9–47259
Fe-Ni-Al-Ti alloys, thermomech. treatment effect on mag. props. 9–47259
Fe-Ni-Mn-Ti martensitic alloys, pre-precip. stage during ageing 9–37283
 $GeCl_4$, freqs. and stretching force consts., i.r. obs. 9–27874
Nb-Ti-Zr-Hf alloy system, constitution and supercond. props. 9–39597
Nb-Ti-N alloy thin films, supercond. critical current-field meas. in continuous mag. fields 9–35362
Nb-Ti alloys, supercond., cold working and precip. for effective flux pinning at high current densities 9–49053
Nb-Ti supercond. sheets as stabilizing walls for levitated rings, flux penetration obs. 9–37493
Nb-Ti supercond. tubes, steady-state flux jumping in superimposed a.c. and d.c. mag. fields 9–37471
Nb(25 at.%)Ti(10 at.%)Zr alloy, solution-treated, ageing rel. to recrystallization 9–33122
Nb(5 at.%)Ti alloy strip., supercond., peak effect in critical current w.r.t. temp. and field 9–39600
Nb(75 at.%)Ti quenched alloy, phases and crystal structure by e. microsc. and X-ray diffraction study 9–23767
Nb-(40wt.%)Zr-(10wt.%)TiNb-(40wt.%)Zr-(10wt.%)Ti superconducting hollow cylinders, mag. shielding in applied mag. fields at 4.2°K 9–43174
Ni-Si-Ti alloys, microstruct. and tensile props. 9–48902
Ni-Ti alloy, grain boundary deformation rel. to temp. under constant strain 9–23889
Ni-Ti alloys γ' phase, coherent solubilities 9–28403
 $Ni_3(TiAl)$ alloy hardened by coherent and ordered precip., yielding 9–39408
 $SnCl_4$, freqs. and stretching force consts., i.r. obs. 9–27874
Ti(5 wt.%)Al-(2.5 wt.%)Sn alloy, fracture toughness and mech. props. at cryogenic temps. 9–37253
Ti(6 at.%)Al(4 at.%)V alloy, plane-strain cyclic and sustained load flow growth charact. 9–30722
Ti(8 wt.%)Al(4 wt.%)Co alloy, mech. props. and structure 9–23956
Ti(8 wt.%)Al(4 wt.%)Co alloy, heat treatment rel. to mech. props. 9–40994
Ti(8 wt.%)Al(4 wt.%)Co alloy, microstruct. and heat treatment rel. to mech. props. 9–44747
Ti(6 wt.%)Al(4 wt.%)V alloy, surface treatment for impact fatigue and wear resistance 9–37259
Ti(6 wt.%)Al(4 wt.%)V alloy, two-phase microstructures, toughness 9–37251
Ti(6 wt.%)Al(4wt.%)V alloy, stress-corrosion cracking in anhydrous methanol, mechanism 9–48894
Ti-Al-Co alloy system, diagram for Ti-rich corner, struct. obs. 9–40919
Ti(8wt.%)Al(1wt.%)Mo(1wt.%)V alloy sheet, hot-salt-stress-corrosion cracking and effect on tensile props. 9–23923
Ti-Al alloy, equilb. diagram, study on Ti-rich region 9–26381
Ti-Al alloys, Ti_3Al precip., particle size line broadening 9–28400
Ti-Cr binary alloys, martensite react., morphology and substruct. 9–26393
Ti(8 wt.%) Mn alloy, heat-treated, microstruct., electron microscope obs. 9–35214
Ti(5 at.%) Mn alloy martensites, electron microscope obs. 9–39311

Titanium compounds continued

- Ti-Mo alloys, effect of ω -phase precipitates on superconductivity and sp. ht. 9–35370
Ti-Mo dil. alloys, martensitic, supercond. transition temp. enhancement 9–37477
Ti-Nb, multifilament, and Cu composites, magnetiz., coupling obs. 9–35369
Ti(50 wt.%)Nb alloy, struct., X-ray diff. and electron microscope obs. 9–42792
Ti-Nb supercond. alloy, magnetization, hysteretic loss and flux-jump stability obs. 9–35364
Ti(20 at.%) Nb alloy, supercond. props. correlation with metallurgical props. 9–39603
Ti-22 at.%)Nb alloy, superconducting, critical currents 9–37478
Ti-O alloys, magnetic susceptibility, var. with temp. and alloying rel. to electronic struct. 9–35533
Ti-Rh alloy, supercond. transition temp., determ. by sp. ht. meas. 9–30880
Ti-V alloys, ω -phase precip. 9–23987
Ti-base alloys, resistance to atmospheric corrosion 9–37835
 Ti_2O_3 :V, Fe, low-field magnetoresistance anomaly, Kondo condensation obs. 9–31018
 Ti_2O_3 :V $^{3+}$, negative magnetoresistance at 4.2°K 9–47070
 Ti_2O_3 , antiferromag., existence rel. to metal-semiconductor transition 9–45236
 Ti_2ZrO , crystal structure 9–26249
 Ti_3Al ordered and disordered alloys, low temp. electronic sp. ht. coeff. 9–30751
 Ti_3Al precip. in Ti-Al alloys, temp. eff. on growth, particle size line broadening 9–28400
 Ti_3O_3 , polymorphism 9–32860
 $Ti_{n-2}Cr_2O_{2n-1}$, ESR determ. of weak antiferromagnetism 9–49022
Ti complex, hexaurea Ti(III) trioxide, crystal spectra, Jahn-Teller effect 9–39848
Ti complex, TiX_4 bipy ($X=Cl$ or Br and bipy=2,2'-bipyridyl), Raman spectra 9–30057
Ti complex, $Ti(en)Cl_4$ and $Ti(en)Br_4$ partial normal coord. analysis 9–38871
 TiB_2 , X-ray spectra obs. of inner level shifts and band struct. 9–45340
TiC, conductivity, thermoelec. power, Hall coeff., rel. to C content 9–47114
TiC, X-ray emission K α band of C 9–26762
TiC, X-ray spectra obs. of inner level shifts and band struct. 9–45340
 $TiC_{0.67}$, diffusion of ^{14}C , anomalous 9–46858
TiC emissivity and elect. conductivity obs. 9–37374
TiC in austenitic steel, plastic deform. and recrystn. during creep of steel 9–33045
 $TiCO_2$, elec. resistivity, magnetic susceptibility, thermoelec. power 9–28468
 $TiCl_4$, freqs. and stretching force consts., i.r. obs. 9–27874
 TiF_3^{3-} octahedral ion, modified Wolfsberg-Helmholz molecular orbital calc. 9–36708
 $TiH_{1.6}$, p nuclear spin relaxation time 9–28761
 $Ti(H_2O)_6^{3+}$ octahedral ion, modified Wolfsberg-Helmholz molecular orbital calc. 9–36708
 TiH_3F , SCF calc. 9–42419
 TiH_4 cryst., internal motions, n.m.r. and use of relax. function 9–31168
TiN, X-ray spectra obs. of inner level shifts and band struct. 9–45340
TiNi-II complex structure existence 9–35069
TiO, elastic const. and Debye temp. calc. from force field 9–35142
TiO, Madelung potentials and ordering energy 9–30508
TiO, nonstoichiometric, defect complexes and microdomains 9–44685
TiO, X-ray spectra obs. of inner level shifts and band struct. 9–45340
 TiO_2 - Cr_2O_3 electric resistivity, freezing point, defects, mag. props. 9–49022
 TiO_2 - SnO_2 system, spinodal decomposition 9–33144
 TiO_2 -VO $_2$ interred pseudobinary system, semiconductor-to-semiconductor transition from elec. conductivity and thermoelectric power meas. 9–49088
 TiO_2 , bond type, cryst. energy calc. 9–30504
 TiO_2 , conduction, rel. to polaron theory 9–49009
 TiO_2 , crystallization under hydrothermal conditions 9–37044
 TiO_2 , defect controlled elec. props. 9–26512
 TiO_2 , diffusion of Fe, anisotropy of diffusion front 9–46859
 TiO_2 , dynamic spin Hamiltonian for Fe^{3+} impurity, eigenvalues 9–26667
 TiO_2 , e.s.r. of Cr^{3+} ions coupled with O vacancies 9–37801
 TiO_2 , Fe^{3+} spin-lattice relaxation for X- and F-band transitions 9–47300
 TiO_2 , final photocurrents, calc. by field emission concept 9–24236
 TiO_2 , phase transform. at high press. and temp., X-ray diff. obs. 9–23988
 TiO_2 , polymorphism under dynamic loading 9–39482
 TiO_2 , rutile, flux grown, dielec. meas. without contacting electrodes 9–45002
 TiO_{2-x} reduced rutile, ionic defects rel. to mech. and dielec. relax. of hopping electrons 9–44690
 TiO_2 , addition to discharge as aid to spectrochemical analysis of alkali elements 9–31229
 TiO_2 , elec. conductivity, field enhanced, rel. donor impurities 9–26511
 TiO_2 films, preparation and optical applies. 9–36962
 TiO_2 in barium silicate glass, gamma-induced absorpt. 9–37693
 TiO_2 plasma-grown crystals, elec. props. 9–39198
 TiO_2 powders, i.r. absorpt. spectra, interpretation 9–31111
 TiO_2 rutile, acoustic microwave absorption, temp. and freq. depend. 9–30773
 TiO_2 specially reduced single cry., dielec. const. and loss, elec. conductivity, variations 9–47159
 TiO_2 , rutile, slightly-reduced, nature, and family of titanium oxides 9–44675
 TiO bands, new, in one micron spectra of Mira variable stars 9–41644
 TiO mol., γ -system, rot. analysis of (0,0) band 9–40603
 TiO mol., spectra, four new bands in β system 1-0 sequence. 9–32489
 TiO_2 thermal emission obs., 10^{-8} – 10^{-9} torr. 9–41280
 $TiO(g)$, dissociation energy 9–23173
 $TiO(g)$, dissociation energy 9–23172
 $TiPO_4$, ion exchanger for Cs recovery from nuclear wastes, synthesis and performance 9–24593
 $Ti(Pt_{0.84}Ni_{0.16})_3$, crystal structure 9–39310
 VF_6^{2-} octahedral ion, modified Wolfsberg-Helmholz molecular orbital calc. 9–36708

Titanium compounds continued

Zr-(25 at.%) Ti alloy, ω phase, as-quenched form, electron diffr. and microscopy obs. 9-37307

Torquemeters *see* **Mechanical measurement****Torsion**

see also **Elastic constants**; **Stress analysis**
balances on moving bases for gravimetry 9-33703
of cylindrical elastic rod partially bonded to elastic half space 9-22215
elastic-plastic, of hollow bars, stress analysis by quadratic programming 9-36166
fracture, interpret. 9-26350
helicopter blade, flutter in forward flight 9-23387
liquid crystals, partially oriented, theory 9-36847
magnetoelastic, vibration of viscoelastic cylinder 9-29235
oscillations of elastic half-space 9-27214
pendulum, precision, with electronic resetting mechanism, period weight sensitivity 9-34058
polyurethane, nonlinear viscoelastic, stress relax., torsion creep 9-31838
steel, cyclic, rel. to low-endurance fatigue studies 9-23860
tube, polygonal, buckling under combined compression and torsion 9-27195
wires under axial tension, elastic torsional stiffness 9-34059
Al alloy, cyclic, rel. to low-endurance fatigue studies 9-23860
Cu polycrystalline, effect of torsional prestrain 9-46877

Total cross-sections *see* **under individual particles, no subheading****Townsend coefficient** *see* **Ionization/gases****Tracers**

see also **Radioactive tracers**; **Radiochemistry**
luminescent, durability on sand grains 9-41399
³⁹Ar, possible applications in earth sciences 9-45498

Transducers

see also **Acoustic generators**; **Acoustic receivers**; **Microphones**; **Sound reproduction**
acoustic, coupling losses 9-48956
acoustic, underwater, flexensional, basic principles 9-22261
acoustic, use of ferrofluids 9-27229
acoustic-surface-wave, 1.75 GHz, LiNbO₃ on quartz substrate, electron beam fabrication 9-48951
electroacoustic, in multibeam receiving arrays, effect of their interaction on directivity 9-47827
electrodynamic, use with vibr. plate viscosity meas technique 9-23467
ferromagnetic film, for magnetostrictive generation of transverse microwave phonons in nonpiezoelec. crystals 9-45272
heat flux, low temp. high sensitivity 9-45874
for high pressure infrared measurements 9-34005
interdigital, electrode, fabrication method 9-29286
metal testing, ultrasonic, for locating flaws or interfaces, patent 9-38303
piezoelectric, bonded, high performance, for freqs. beyond 100 MHz 9-36184
piezoelectric, non-uniform, elimination of resonant behaviour 9-34082
piezoelectric, nonhomogeneous, acoustic response w.r.t. piezoelec. stress 9-37348
piezoelectric, semicond., reson. freqs. 9-25105
piezoelectric, thin-film, electromech. coupling factors, elec. meas. tech. 9-37594
piezoelectric, video-pulsed excitation 9-47825
piezoelectric, surface elastic waves, excitation and detection 9-43784
piezomagnetic, dual forms of equivalent circuits 9-41828
plane piston, emitting sound field, integrated effect on traversing light beam 9-22249
pressure, capacitive 9-22045
pressure, strain-gauged diaphragm type 9-25024
pressure acting on transducer as function of radiator and receiver dimensions 9-22250
resonant elements design for endfire array 9-29288
in seismometer, optimum magnet size determ. 9-41468
solid state sensors, conference Minneapolis (1968) 9-49115
using stress phenomena in f.e.t. and bipolar transistors 9-49126
surface wave, h.f., fabrication method 9-29286
for thin film strain gauge, design 9-46861
thin-film piezoelec., development and results 9-30980
turbulent pressure fluctuations resolution, effect of transducer size 9-45862
u.s., depletion layer, amplitude-freq. characts. 9-47826
u.s. for nondestructive testing 9-36183
CdS:Ag shear-mode-evaporated u.s. transducers, preparation 9-42957
CdS, l.f., vapour deposition method 9-33984
LiNbO₃ on quartz substrate, acoustic-surface-wave transducer, 1.75 GHz, electron beam fabrication 9-48951
ZnO thin-film, prep. using vapour transport technique 9-48767

Transformations *see* **Phase transformations****Transformations, mathematical**

coordinate, application to two dimensional scattering and diffraction problems 9-34122
differential and S matrix operators, new classical dynamics formulation 9-29169
elementary particle beams, remarks on transformation rule 9-25408
Foldy-Wouthuysen, rel. to de Sitter group and Lorentz transforms. 9-41736
Fourier, fast, of large data arrays 9-25379
Fourier, spectroscopic analogue computer 9-29487
Fresnel, simplification of diffraction theory 9-27389
Fresnel reflection coeffs., generalized, and representation in Smith chart 9-32008
geodetic applications of conformal transformations in three dimensions 9-31243
holographic intensity pattern mapping, integral transform. 9-27352
integral transforms in composite one-dimens. space, derivation and applic. to physical problems 9-34009
Lagrangian, 2p-pole linear syst., irreducible representations 9-36154
Laplace, analysis of dynamic response of circular anisotropic cylinder undergoing forced vibrations 9-29238
Laplace, monoenergetic neutron transport eqn. for finite slab, soln. applic. 9-42316
Laplace, numerical inversion of discontinuous original, theoretical seismology applic. 9-36111
Laplace transform of transition matrix of linear system, tech. for writing straight from differential eqn. 9-22051
optical systems and transforms for engineering students, book 9-40377

Transformations, mathematical continued

quantum field theory, phase factors in discrete symmetry operations 9-40391
Schwartzschild and Tolman coordinate systems, reln. 9-25026
spectral analysis at surface barriers by correlation method 9-36521
spherical harmonics under change of reference frame 9-45733

Transistors *see* **Semiconducting devices/transistors****Transition metal compounds**

alloys, paramag. susceptibility, effect of spin-orbit interac., approx. band struct. 9-35536
alloys, paramag. susceptibility and elasticity rel. to e struct. 9-40996
azines, transition metal (II) complexes 9-34659
binary constitutional diagrams for groups IIIA-VIA, rel. to valence electrons and electronic config. 9-39469
borides, bond and band structure theory test from heat capacity meas., 1.5-18°K 9-28445
carbides, charge transfer, electron spectroscopic meas. 9-44636
carbides, diatomic, stability 9-32490
carbides, self-diffusion in interstitial phases 9-23832
carbides, thermal conductivity rel. to phonon scatt. by conduction electrons and lattice vacancies 9-47010
chalcogenides, crystal chemistry 9-26201
chalcogenides with Cr₃S₄ structure, susceptibility meas. 9-24329
complexes, K-absorpt. edges, molec. orbital theory 9-39854
complexes, octahedral, magnetic dipole transitions of transition metal ions 9-49230
complexes, one and more step reactions, extension of Woodward-Hoffmann rules of stereoelectronic control 9-39332
complexes, solid, overlap and Coulomb integral calcs. 9-45248
complexes, structural chem., bonding 9-23744
complexes with N-containing ligands, i.r. and Raman obs. of normal vibr. 9-32459
conductance of cpds. with ordered vacancies 9-44920
dichalcogenides, electron energy loss studies rel. to band structure 9-30804
difluorides, high press. transform. and stability obs. 9-37299
fluorides, electron delocalization and spectra 9-42379
fluorides, in ZnS Lumocen devices, electroluminesc. 9-35700
fluorocarbon derivatives, mononuclear, mass spectra 9-34514
-ion complexes, EPR spectra, vib. struct. study 9-23024
ion complexes, octahedral, paramag. susceptibility rel. to excited configs. 9-39752
metallic and non-metallic behaviour 9-41170
molybdates, anion co-ordination and vol. changes in high press. phase transforms. 9-35244
oxides, polaron theory including impurity induction 9-49009
oxides, present status of polaron, review 9-28454
oxides, semicond. metal-transition, model 9-33279
phosphides, solid solns., crystallographic and mag. props. 9-44676
pnictides, crystal chemistry 9-26201
pyridine-2-carboxamide chelates, far i.r. spectra, normal coord. treatments 9-25751
rare-earth-transition metal Laves phase, lattice parameters 9-35066
salts, electrostatic and exchange interactions, high degree 9-47227
spinel manganites, preparation condition, eff. of heat treatment on props. 9-28253
sulphides, rel. to itinerant d-electron ferromagnetism model 9-45094
superconducting alloys, transition temps. rel. to electron interaction in 3d band 9-24151
superconducting props. of thin films with rocksalt structure 9-36959
thionobates, synthesis and lattice constants on basis of hexagonal unit cell 9-39284
transition metal-Sn dilute alloys, Mossbauer hyperfine field ¹¹⁹Sn and resistivity study 9-47335

Transition metals

3d, in liquid Sn, mag. susceptibilities 9-28150
3d, K β , line appearance mechanism in X-ray spectrum 9-24433
absorption spectra in region of 3p transitions 9-33561
APW energy bands of 3d group, b.c.c. and f.c.c. 9-28447
band struct. 9-48991
band structures, approx. calc. 9-44892
band structures calc. method 9-33227
band-structure calc., energy-indepnd. model Hamiltonian 9-37392
b.c.c., paramag. susceptibility, effect of spin-orbit interac., approx. band struct. 9-35536
b.c.c., point defects, review 9-26274
central ions in complexes in solid-state, quantum calcs. 9-45248
chemisorption of H, self-consistent model 9-24548
dielectric screening of impurity pot. 9-43100
electronic structure, photoemission studies of optical densities of states 9-44891
films, galvanomagnetic phenomena 9-30848
impurities in GaAs, width of e.s.r. line 9-45384
ions, first row, in phosphate glasses, absorpt. spectra 9-33543
ions, in crystal, spin-orbit coupling eff. on ground state 9-24285
ions in complex, ⁵S state, in soln e.s.r. solvent induced fluctuations 9-30038
ions in crystals, e.p.r. investigation, techniques, book 9-38338
ions substituted in CdCr₂S₄ spinels, mag. props. 9-35551
liquid, electron transport, wave function model 9-48714
magnetic properties of b.c.c. metals from generalized susceptibility calcs. using electronic structure 9-26658
magnetic susceptibility 9-45083
Mossbauer effect, of ⁵⁷Fe, isomer shift 9-26718
in noble metal host, effective spin-orbit coupling 9-47303
oxides, first series, p-H₂ enrichment, hydrogen-deuterium equilibration 9-24524
paramagnetic susceptibility and elasticity rel. to e struct. 9-40996
phase diagram computation, review 9-48936
pseudopotentials 9-47018
Rayleigh scatt., 3d magnetized metal, scatt. amplitude and spin depend. determ. 9-41361
resonant states 9-37379
surface tension calc. using method of moments 9-49002
trivalent, in LaF₃, photo- and X-ray luminescence 9-31145
trivalent ions in MgO, effect on cryst. lattice cell dims. 9-32921
work function and surface energy correlation 9-33414
in AgCl single cryst., relax. of vacancy-dipoles 9-33372
in Fe alloys, effect on phase equil. 9-33148

Transmission

- direct of plane wave by transparent sphere 9-29177
 e.m. waves through metal slab, effect of boundary scatt. on helicon transmission near cut-off 9-26491
 radiowaves, i.f., in ionosphere, calc. 9-31387
 seismic waves, primary, 100 to 600 km 9-35774
 SH waves at solid-firmoviscous boundary in earth 9-35791
 of surface waves by movable strip, theory 9-30360
 of whistlers, 1-10 kHz, obs. rel. to theory 9-31386
 Au, 400keV protons, through thin crystals 9-42979

acoustic waves

- see also *Acoustic wave propagation*
 acoustic filter performance, transmission factor determination 9-43794
 layered medium synthesis from geophysical response 9-37878
 multilayer structures, transmission loss 9-41824
 multimode media responses, effect of frequency and space averaging 9-45864
 noise, from turbulent boundary layer through flexible plate into closed cavity 9-45866
 through partition, using statistical energy analysis 9-41825
 speech, narrowing of frequency band 9-29280
 walls, hollow and solid, between rooms 9-25107

acoustic waves, ultrasonic

- liquid metals by electrodynamic excitation 9-23492
 in ocular tissue, problems 9-38134
 water, temp. microstructure from covariance between diverging acoustic signals meas. 9-27225
 CdS:Ag shear-mode- evaporated transducers, preparation 9-42957
 LiNbO₃, microwave pulses, Brillouin scatt. obs. 9-35278

electromagnetic waves see *Electromagnetic wave propagation***light**

- see also *Absorption/light; Filters, optical*
 anisotropic transfer problems in thick layers, asymptotic fitting method for solution 9-34209
 p-azoxyanisole liq. cry., temp. depend. 9-26112
 bulk materials, transmittance data rel. to optical const. determ. 9-26695
 chlorophyll solns., eff. of laser light on optical transmission coeff. 9-28131
 collimated, through blood and milk 9-45703
 colloid, capillary-porous, rad. distrib. for bilateral irradiation 9-23546
 crystals, analogies with propag. of u.s. waves 9-37325
 dielectric three-layer medium 9-48099
 diffuse, of time-dependent collimated, by a finite inhomogeneous atm. 9-45582
 fiber elements, effect of interdiffusion of glass 9-34219
 films, thin, transmittance data rel. to optical const. determ. 9-26695
 glass, effect of false flashes 9-35630
 glass-ceramics, transparent 9-49234
 glasses, colourless, in range 300 to 400 n.m. 9-39792
 harmonic 1D cry., isotropically disordered, transmission props. 9-26280
 ice, extinction, absorpt. and scatt. rel. to mean grain size determ. 9-45464
 inhomogeneous medium, holographic penetration 9-45974
 intense beam through layer with 2-level molecules 9-40301
 i.r. 8-15 microns, by Se based glass, preparation, patent 9-24352
 laser, 0.63 μ , in artificial fogs, wood smokes and model media 9-28886
 laser beams through atmosphere 9-31322
 layer thickness selection for given spectral charact. 9-46016
 light pipes, cylindrical, with total internal refl. 9-34215
 liquid mixtures, binary, critical opalescence, light scatt. studies 9-34909
 metal films, self-supporting, covered by oxide layers, eff. of plasma oscills. 9-26672
 paraffins in β,β' -dichlorodiethyl ether, critical opalescence, light-scatt. studies 9-34909
 by photographic film, fluctuations rel. to r.m.s. density 9-34235
 phthalocyanine soln. phototropic laser shutters, obs. 9-36277
 plant leaves, spectral coeff. changes due to photon irradiation, dynamics 9-38133
 plastic fiber optics, off-axis charact. 9-36374
 plate, homogeneous plane parallel, rel. to reflectivity 9-41940
 polarized, monochromatic, through continuous media, random dipoles luminescence determ. 9-29461
 quartz, u.v., reduction on heating to boiling point 9-36880
 quartz fibres, fused, for u.v. region 9-48104
 snow, extinction, absorpt. and scatt. rel. to mean grain size determ. 9-45464
 TE-wave in nonlinear media, self-channeling rel. to dielec. permittivity 9-37676
 tetraerythroquinodimethan, meas., 0.29-2.5 μ rel. to absorpt. coeff. calc. 9-39796
 triglycine sulphate, i.r. spectra, optical const. and pyroelec., obs. 9-35615
 through turbulent medium 9-25350
 Ag foil, optical props. and curves of constant transmission 9-23640
 Ag thin evaporated films, percentage transmittance 9-47313
 Au thin evaporated films, percentage transmittance 9-47313
 BaTi₃-Ni₂O₃ single crystal, visible and i.r., and dielec. const. between -192° and +300°C 9-41362
 Bi₂GeO₂₀, 0.4 to 7 μ m, and crystal prep. 9-40864
 Bi₂GeO₂₀, i.r., and growth and props. 9-42751
 Bi₂O₃ layers, evaporated band gap obs. for optical and valence-conduction band transitions 9-39162
 Bi₂(GeO₄)₃, i.r., and growth and props. 9-42751
 CuAlS₂(Se₂), single cryst. prepared by vapour transport with iodine 9-48797
 EuO, i.r., mag. birefringence and Faraday rotation 9-45273
 n-GaAs, meas. in optical probing of inhomogeneities and acoustoelec. instabilities 9-49080
 GaP, p-n junction, reverse-biased, electro-optic and waveguide props. 9-24196
 H₂O vapour, rel. to absorption charact., between 0.5 and 36 cm⁻¹ 9-34620
 K₄Nb₆O₁₇, biaxial props. 9-26238
 LiYF₄, of cry.-grown from melt 9-23683
 PbTe, in band structure parameter determ. 9-39630
 SF₆ gas, transmission of coherent optical pulses 9-46574
 Sb₂O₃, spectra 0.4-0.06 eV 9-39825
 Sb₂S₃, Sb₂S₃, spectra 0.4-0.06 eV 9-39825
 SiO₂, GeO₂ glass, i.r. spectra 9-49267
 SiSe₂, single crystal filaments 9-28694
 Ti₁Ta₈, and elec. props., lattice const., obs. 9-35070
 ZnO, spectra for excitations exhibiting spatial dispersion 9-45309

Transmission continued**light continued**

- ZnP₂, characteristics, Energy range 1.2 to 2.0 eV 9-35609

Transmission lines, r.f. see *Electromagnetic wave propagation/guided waves***Transparency**

- see also *Optical constants; Transmission/light*
 atmospheric haze, 0.37 to 1.0 μ 9-40037
 atmospheric surface layer, to i.r. laser 9-40036
 epoxy resin film, changes due to u.v. irradiation 9-47328
 quartz, u.v., loss at boiling temp., causes 9-36880
 rubber adhesive film, changes due to u.v. irradiation 9-47328
 semiconductor, self-transparency effect of ultrashort pulse of coherent light 9-49252
 Ge, combination with reflection for elec. resistivity calc. 9-24190
 LiF, in the u.v. reduced by formation of surface film in air 9-33523
 PbTe thick layers, heat treatment effects 9-39625
 Si, combination with reflection for elec. resistivity calc. 9-24190

Transport processes

- see also *Diffusion; Kinetic theory; Liquids/theory; Radiative transfer; Solids/theory; Statistical mechanics*
 air, dissociating, collision integrals for components 9-23407
 air, subsonic flow in contraction section 9-28065
 alkali halides, f.c.c., mass transport 9-44729
 arc plasma, high pressure, coeff. determ. 9-32635
 atmosphere, turbulent transport of physical quantities, direct method 9-24644
 Benard convection, problem for geophysical model with vertically varying exchange processes 9-41481
 Boltzmann's H function convexity 9-47766
 Boltzmann chem.-kinetic eqn., variational soln. 9-39934
 Boltzmann collision integral approx. representation by Focke-Planck type operator 9-36148
 Boltzmann eqn., density scaling and applic. in reactor physics 9-22849
 Boltzmann eqn., inelastic scatt. prob. and collision freq. determ., slightly ionized gas 9-22150
 Boltzmann eqn. applic. to X-ray prod. and electron scatt. in electron-probe analysis 9-36092
 Boltzmann eqn. soln. for elec. props. of point defects in metals, utilization of symmetry 9-32943
 Boltzmann operator, generation of semigroups 9-34054
 C sphere, pulsed with neutrons (15 MeV), time spectra of emitted neutrons 9-34479
 charged particle beams, theor. and expt. optics 9-38348
 chemical transport, simplified models, review 9-37816
 chemical transport reactions, theory 9-37817
 classical liquids, appl. of molecular model 9-34869
 coefficients determ. for moderately dense gas, review 9-36802
 condensation, effect on transport of matter from vapour and noncondensable gas mixtures 9-23405
 correlation function equations for quasi-momentum density 9-30778
 cross sections for screened and cutoff Coulomb potentials 9-25848
 crystals, 1-dimen., propag. of thermal and mechanical disturbances 9-39515
 determinacy of phenomenological coeffs. for dependent fluxes 9-47788
 diffusion eqn. soln. 9-45799
 diffusion eqn. soln. 9-45800
 distribution function in any geometry, development in spherical harmonics 9-38731
 of drops moving relative to gas stream 9-34866
 eddy fluxes, meas. in lower atmosphere 9-24647
 electron gas, Maxwellian, relativistic Boltzmann eqn., for photon transport with noncoherent scatt. 9-31792
 electron-impurity model transport equations, deriv. methods 9-47777
 energy and mass transfer, soln. by elec. simulation 9-27191
 Fermi liquid in random scatt. centres, quasiparticle description in macroscopic and low-temp. limit 9-25055
 in fluid of orientable particles 9-31795
 fluids, at critical point, singularities 9-26152
 fluids (van der Waals) and fluid mixtures, transport processes near critical points, models 9-44392
 fluids under weightlessness conditions, influence of oscillations 9-23474
 in fuel cell electrolytes 9-22328
 gas, intermolecular collision processes and forces in dilute gases 9-36819
 gas, moderately dense, quantum corrections to classical Enskog collisional transfer corrections 9-34834
 gas mixture equations 9-26047
 gas-vapour mixture condensation, mass transfer in absence of forced convection 9-28185
 gaseous mixture, Boltzmann equations, 13-moment solutions 9-42606
 gases, binary mixtures, coefficients 9-46576
 gases, density depend. 9-23404
 gases, diatomic, Boltzmann eqn. for calc. h.f. effects in spin relax. 9-34603
 gases, dil. polyatomic, mag. dispersion relations in Senfleben-Beenakker effect 9-23406
 gases, many-body T matrix, application 9-40256
 gases, many-body T matrix, application 9-40257
 He, near λ -point transport coeffs. determ. by single frequency 9-26147
 integral evaluation 9-41787
 ion exchange, liquid-side mass transfer coefficients 9-31176
 ionosphere charged particle vertical transport velocity 9-43450
 ions across membrane, noise spectra and relax. times obs. 9-34892
 Kramers eqn., exact time-depend. analysis 9-43768
 laminar boundary layer, multicomponent, behaviour prediction by integral-matrix method 9-23216
 laminar boundary layer on plate, mass transfer rel. to variable suction or injection velocity 9-25998
 linear-response theory and irreversibility in strong mag. field, transport phenomena 9-36135
 liquid, stat. mech. approximate theories and models 9-26079
 liquid metals, electron transport, wave function model 9-48714
 liquid metals, electron transport using Boltzmann eqn. 9-48713
 liquids, theory 9-48679
 Lorentz gas diffusion coeff. density expansion 9-22165
 mass, 2-phase air-liquid system, redox method, coeff. determ. 9-34882
 mass and heat transfer, simultaneous, in laminar free convection from vertical plate 9-26085
 mass transfer, conference 9-34094
 mass transfer, gas-liquid and solid-liquid, to liquid films on inclined plane 9-34868

Transport processes continued

- mass transfer convective, from rot. disc, surface suction/injection effects 9-27248
- mass transfer in heterogeneous flow systems simultaneous with heat transfer 9-23225
- mass transfer in jet drying 9-25116
- mass transfer in oxides, conf. 9-44726
- mass transfer in packed beds or systems with turbulence promoters, effect of viscous forces 9-25804
- mass transfer in particulate systems, particle size and residence time distrib. effects 9-23539
- mass transfer in sublimation dehydration, mechanism 9-28183
- mass transfer method for surface heterodiffusion coeff. determination 9-37193
- mass transfer of bubble gas, in liquid phase, rel. to volume change and velocity of rise 9-26072
- mass transfer systems design; fluid velocity distributions in randomly packed beds 9-34716
- mass-transfer at walls in variable-area duct with steady flow, conservation eqns. 9-26050
- mass-transfer coeff., liquid-side, in ion exchange, Nernst-Planck model 9-24525
- master equation, reln. with density matrix eqn. 9-27175
- master equation in phase space formulation of quantum optics 9-31924
- master equation of laser system, time depend. soln. 9-29397
- through membrane, Onsager's reciprocal relation not always true in bulk flow theory 9-32779
- membranes, permeability characteristics 9-26087
- MHD-generator plasma 9-27982
- mixture, almost Lorentzian, coefficients calc. by perturbation method 9-25059
- mixture, binary, variational calc., of transport coefficients 9-27192
- moist material drying by contact with hot plate, moisture distrib. calc. 9-23586
- molecular slit flow, nearly-free, local and average mass flow rates 9-34820
- momentum transfer in atmosphere between air and water surface 9-24643
- monatomic fluids, second order constitutive equations 9-46128
- N₂ sphere, pulsed with neutrons (14 MeV), time spectra of emitted neutrons 9-34479
- neutron, Boltzmann eqn., 2-time doublet including delayed neutrons 9-27774
- neutron, boundary transients at core and reflector interface 9-22858
- neutron, equation, consistency of certain approximate solutions 9-22852
- neutron, integral transport calculations, polynomial approximation 9-22853
- neutron, two-group theory, full range completeness theorem 9-22857
- neutron energy spectra in U, polyethylene, graphite and Na 9-27783
- neutron leakage in small exponential cores, new means of analysis 9-27780
- neutron wave propagation, axial, in heterogeneous media 9-22855
- neutron wave propagation, one-speed, with source off interface 9-22843
- neutron waves, reln. with sound waves 9-29860
- neutron waves in moderators, limiting critical freq., physical criteria 9-27782
- neutron waves in moderators, limiting critical freq., physical criteria 9-27781
- neutron-wave propagation, application of Laguerre polynomials in analysis 9-22854
- neutrons, monoenergetic, time independent, 3 dimen. transport equation, elementary solns. 9-22848
- neutrons, slab geometry, monoenergetic initial-value transport problem 9-22856
- new method involving invariant imbedding and case eigenfunctions 9-38265
- particle system, coeffs from molecular dynamics 9-23394
- plane wave disturbances in thermal neutron distrib., propag. theory 9-22842
- plasma, Boltzmann equations, 13-moment solutions 9-42606
- plasma, calc. using cross-sections derived from collision term of Boltzmann equation 9-40664
- in plasma, coefficient calc. using quasi-particle concept 9-40656
- plasma, magnetically confined, low-beta collision dominated cross-field transport 9-25902
- plasma, many component, props. calc. 9-40661
- plasma, partially degenerated, transport theory 9-25853
- plasma properties, experimental and analytical studies 9-23274
- in plasma with microinstability 9-44416
- polyatomic gases, effect of internal mol. struct., applic. of Chapman-Enskog theory 9-46566
- powders, during spark excitation of filled C electrodes in spectrochemical anal. 9-48114
- probe, coded electrostatic in plasma, continuum theory extension 9-25912
- properties near mag. transition points 9-45040
- quantum syst. of interac. part., rigorous evolution eqn. for one-body density matrix, closing 9-34053
- reacting gas mixtures, coefficients by rigorous kinetic theory 9-26016
- rotating sphere sublimating in rarefied air, heat and mass transfer proc. 9-23607
- rough spheres, Rice-Allnatt theory 9-36147
- ruby, energy transport 9-45305
- solids, constants determ. from linear dimens. change with temp. 9-41097
- solutions, d.c. transport coeffs. 9-23519
- superconductor, transport eqns. and Fermi-liq. effects 9-35347
- time-dependent anisotropic transport for slab geom., eqn., exact soln., generating functions for transf. 9-22164
- transition metals, electron transport, wave function model 9-48714
- two-phase random medium, variational bounds on bulk props. 9-43754
- Van der Waals gas, critical anomalies of transport coeffs. 9-26041
- variational principle, applic. 9-40260
- water, deep, mass in long crested random gravity waves 9-28857
- A g colloidal particles, electron m.f.p. limitation, refractive index meas., absorption coeff. determ. 9-41115
- Ag halides, f.c.c., mass transport 9-44729
- AgCl aqueous solution, space charge limited ionic transport at solution interface 9-32833
- CaSO₄ aqueous solution, boiling, mass transfer characts. 9-23602
- H₂ and reactivity, control of nuclear reactor 9-22883

Transport processes continued

- H⁺/Cu²⁺-Cl⁻ ion exchange, liquid-side mass transfer coefficients 9-31176
- He, gas, thermal transpiration at low pressures, use of leached Pyrex tube 9-36820
- He liquid, viscosity, thermal conductivity and spin diffusion estimated 9-23559
- He plasma, partially ionized, coefficients 9-44417
- ⁴He, phonon-drag eff. in mobility of charged impurities, eff. on conductivity 9-30442
- K⁺ ion swarm in N₂, mobility, diffusion coeff. and reaction, determ. 9-23203
- Na, molten, spin-flip scatt. of conduction electrons from impurities 9-32793
- Ne plasma, partially ionized, coefficients 9-44417
- Pt-Al₂O₃ catalyst, surface transport of various gases 9-26195
- Rn decay products, transport proc. in air 9-32327
- Rn decay products transport proc. in air 9-22762
- Sb₂Se₃-Sb(Te) liquid alloy, carrier motion contribution to thermal conductivity 9-34900
- Sb₂Se₃ liquid, carrier motion contribution to thermal conductivity 9-34900
- Transport theory, neutron** *see* Neutron transport theory
- Trapped free radicals** *see* Free radicals
- Traps** *see* Crystal electron states/impurity states and effects; Crystal imperfections; Semiconductors
- Travelling wave tubes** *see* Electron tubes
- Triboelectric emission** *see* Electron emission
- Triboelectricity**
No entries
- Triboluminescence** *see* Luminescence
- Trions (³He, ³H)** *see* Helium-3; Tritons
- Triple point** *see* Critical constants, thermal
- Tritium**
atom, spatial wave func. from symmetry reln. 9-25718
atom reactions with methane 9-47474
 β -decay, probability of formation of [³He]⁺_{4s} 9-48432
in meteorites, stone and iron 9-24888
monitor based on scintillation 9-25593
³H, improved S-state wave function 9-40476
³H, improved S-state wave function 9-27623
- Tritium compounds** *see* Hydrogen compounds
- Tritons**
see also Nuclear reactions and scattering due to tritons
low energy neutron-deuteron scatt. parameters relationship 9-42115
- interactions**
No entries
- scattering**
No entries
- Troposphere** *see* Atmosphere
- Tungsten**
absorbed layer on W, tunneling of field emitted electrons 9-30960
accommodation coeffs. of ⁴He and ³He on clean surface 9-30501
adsorption and decomp. of NH₃ 9-48774
adsorption and decomp. of NH₃ 9-48773
adsorption lifetimes and binding energies of Ag and Au 9-39177
adsorption of ³He, small energy accommodation coeffs., classical theory 9-35004
adsorption of CO, field emission from single planes 9-39176
adsorption of Cs on single-cryst. planes 9-39175
adsorption of methanol, photoelectron spectroscopy rel. to orbitals involved in bonding 9-44634
adsorption of O₂, N₂, CO₂ and H₂ on (100) surface rel. to work function changes 9-42734
adsorption of O₂, N₂, H₂ and CO, surface potentials determ. 9-48775
adsorption of Sr on surface, field emission through atoms 9-24251
adsorption of U, multilayer, work function rel. to thickness and U phase transition 9-32850
adsorption of Y on (121), (111) and (021) faces, investig. using electron field-emission projector 9-44632
adsorption of Zr 2-d crystals, binding energy from temp. depend. of growth 9-23652
atom total ν cross-sections, 40-80 keV, mean values, analysis 9-22949
atoms, ionization coeffs. determ. on W and Pt surfaces 9-45034
bubble growth at grain boundaries 9-28300
cast, polycryst., tensile and compressive yield stresses, temp. and pressurization effects 9-44757
catalysis of ³⁰N₂-²⁸N₂ mixture equilibration, distrib. of active sites on surface 9-33662
channeling of ions, low energy, light and heavy, critical angle variations 9-24078
channeling of MeV He⁺, Rutherford scatt. and L and H X-ray yields obs. 9-41120
chemisorptive luminesc. 9-43326
cleavage velocity determ. with u.s. fractography 9-33094
cluster formation of diffusing metal adsorbates 9-40851
conductivity, elec., jump during melting 9-26156
controlled-fracture switching of elec. current 9-33068
crystal, electron diffraction determ. mean inner potential 9-28273
crystals, quantum-mechanical tunneling of dislocations 9-26288
defects due to deuteron irradi. in single cryst., ion microscope exam. 9-39358
defects in single crys. bombarded with deuterons of 0.1 MeV 9-37162
deformed struct., X-ray diff. topography 9-42815
desorption of Y in strong elec. field, 300° to 630°K 9-46733
diffusion mobility in high-speed cutting steel, role in carbide precip. kinetics 9-39383
diffusion of Nb, Ta and W isotopes, lattice coeffs. meas. 9-40989
dislocations, parallel array, impurity segregation obs. in neutron irradiated sample 9-28295
elastic bulk eff., infl. of point defects 9-30631
electrode erosion in high current discharge and cathode spot temp., obs. 9-34798
electrodes of variable current plasmotrons, emission 9-43141
electron ejection by inert-gas metastable atoms, adsorbate effects 9-31002
electron ejection ion induced, from gas covered single cryst. 9-41275
electron emission, secondary anisotropic, from single cryst. surface, temp. depend. 9-39743
equation of state of shock-loaded sample at 950°C 9-44829

Tungsten continued

- field emission, temp. depend., of single crystal planes 9-24252
 field emission tip, shape change obs. with electron microscope 9-39738
 field evaporation from edges of (111) plane and bonding of surface atoms 9-26181
 filament lifetime under constant-current heating 2000° to 2950°K 9-34222
 film, electrical conductivity and Hall consts. 9-30848
 fracture, brittle, of (100) axis single crystals, 77°K 9-33095
 growth, single crystal on glowing tips in N₂-H₂ mixture 9-26206
 inert gas thermal release from (110) and (211) surfaces 9-44633
 interstitial Stage-I behaviour after e. irradi. 9-26279
 ion entrapment observed through desorption spectra 9-36970
 isotope effect on W-B supercond. transition temp. 9-30872
 lamps, standard, rel. to errors in absolute intensity meas. 9-25388
 LEED intensities, multiple diffraction origin 9-23778
 micro-strain, temp. depend., and transition to macro-strain 9-23890
 neutron irradi., annealing rel. to vacancy clustering, obs. 9-44694
 Ohm's law verification up to 10⁹ A/cm² current densities 9-24126
 phonon dispersion relations calc. from Sharma-Joshi theory, specific heat calc. 9-48946
 polycrystalline, cold worked and annealed, preferred grain orientation from ion microscope exam. 9-40889
 powder, substruct. and block size distrib., X-ray diff. obs. 9-46796
 pyrolytic deposition from WF₆ 9-39199
 radiation defects in single cryst., ion microscope exam. 9-39358
 re-emission, ion-induced, of noble gas atoms 9-30799
 ribbon, high temp., refl. of rare gas atomic beam anomaly obs. 9-40558
 secondary electron emission, origin of angular depend. 9-37635
 shock-loaded at 950°C, eqn. of state 9-44829
 sintering of spherical particles under high press. 9-30728
 solid and liquid equations of state calc. from low temp. mechanical obs. 9-39090
 solubility of N₂, high temp. 9-35136
 spectral emissivity, discrepancies in measured data 9-26744
 spectral line transitions, probability determ. 9-46302
 sputtering of inert gas atoms during secondary ion bombardment 9-33207
 strip lamp as spectral radiance standard 9-25377
 substrate for Al, Mg and Sn films, LEED obs. of films structure on (110) face 9-26184
 substrate for ZnS films, epitaxy 9-28216
 as supporting structures for semiconducting devices 9-30935
 surface, C contamination, FEM-LEED studies 9-35071
 surface free energy anisotropy meas. with field ion microscope 9-34980
 surface layers, work-hardened, crystal structure changes prod. by vacuum annealing 9-32932
 surface of ribbon, interaction with inert gas beam 9-48754
 surface self-diffusion, 2,560-3,150°K, by adatom process 9-44622
 texture of deposits formed from vapour 9-37152
 thermal expansion, 1700-2300°C, obs. using electron bombard. furnace and extensometer 9-35288
 thermal expansion coeff., temp. depend., 80° to 1200°K 9-44842
 thermal facetting rel. to O₂ adsorpt., effect on work function 9-35012
 thermionic converter electrode, polycrystalline, electron mirror microscope study 9-24254
 thermionic work function changes following 100-600 eV inert gas ion bombardment 9-24257
 tip, morphology change by surface diffusion at 2500°K, obs. with scanning elec. microscope 9-48753
 wire sensor for upper atm. temp. meas. 9-43409
 work function and surface energy correlation 9-33414
 work functions of (110) and (100) surfaces of single cryst. and polycryst. foil, temp. coeffs. 9-35516
 X-ray Debye temp. meas. 9-35286
 yielding and fracture, effect of Rh alloying on ductile-brittle transition 9-39415
 electron emission microscope obs. of grain growth and formation of surface layers by reaction with hydrocarbons 9-37127
¹⁸³W 46.5 keV γ line MOssbauer absorpt., Debye-Waller f factor determ. 9-46795
 b.c.c. single crystal, temp. depend. of flow stress 9-41011
 Cs adsorbed layer electronic and lattice struct. 9-32849
 Cs and Ba coated, total energy distrib. of field-emitted electrons 9-45031
 Cu-W fibre-reinforced composite, stress-strain curve 9-42875
 Ge coated surfaces with oxygen adsorption, electron emission charact. stability 9-45030
 H₂ and N₂ simultaneous adsorption at 300°K, obs. 9-23651
 SiO₂ surface, vaporization of Sr atoms and ions 9-37637
 W-Re thermocouple, type-VR 5/20, calibration characts. 9-34105
 W-UO₂ cermet produced from coated particles, high temp. creep-rupture tests 9-23910
 W I spectrum, energy levels and classified lines, tables 2000→10500 Å 9-34552
 W I spectrum, even energy levels, theor. interpretation tables 9-34553
 W(111) and (110), electron ejection by metastable He and Ar atoms 9-31001

Tungsten compounds

- alloys, supporting structures for semiconducting devices 9-30935
 bronzes, supercond. 9-49034
 oxide secondary ions, sputtering probability with Ar⁺ 9-42982
 oxides, thermionic emission properties 9-33419
 tungstates, metal heteropolytungstates, n.m.r. obs. of state of H 9-43303
 tungsten-bronze crystal, properties and improvements 9-35490
 W₁₈O₄₉, reflectance spectra, specular and diffuse, rel. to electronic props. 9-31094
 Co-W alloy, stress rupture and superplasticity behavior, structural effects 9-26343
 Fe-W alloy precipitates, fine faults and cryst. struct., electron microscope obs. 9-42787
 Mo-W alloys, electrotransport and diffusion, tracer technique 9-28320
 Nb-W solid solutions, hardening eff. of W 9-28385
 Nb₂O₅-W₂O₃ system, non-periodic shear struct., electron microscope obs. and evaluation 9-39291
 Ni-W alloy, local ordering and elec. resistance annealing effect 9-33255
 Ni-W alloy, solubility of H 9-39478
 Ni₃(Fe, W) alloys, atomic ordering effects 9-39297
 W-(1wt.%Gd₂O₃) alloy, ion microscope exam. of matrix 9-41057
 W-Mo alloy, metal-metal carbide eutectic temp. determ. 9-34951
 W-Mo alloy, secondary ion emission under effect of slow ions 9-24259

Tungsten compounds continued

- W-(5 at.%)Re alloy single crystal, thermionic emission of (100) face 9-47211
 W-(5 at.%)Re single cryst., deform. prod. during ion microscope exam. 9-39235
 W-Rh alloy, metal-metal carbide eutectic temp. determ. 9-34951
 W-Rh alloys, yield stress and ductile-brittle transition temp. rel. to Rh concn. 9-39415
 W₂O₅, reflectance spectra, specular and diffuse, rel. to electronic props. 9-31094
 W-B, supercond. isotope effect 9-30872
 W-C rhombic modification, neutron diff. obs. 9-32933
 WF₆-UF₆ melting point and eutectic props 9-34953
 WF₆-UF₆ melting point and eutectic props 9-23580
 WO₃, activated fuel cell electrodes, mechanism and performance 9-47891
 WO₃, dipole field correction due to lattice deformation 9-28558
 WO₃, stopping of kV ¹²⁵Xe ions by elastic collisions 9-36678
 WO₃ single crystal, semiconducting, conduction mode study 9-49089
 WO₃ structures stable at room temp., symmetry and polymorphism 9-23655
 WS₂, orbital valence force field constants 9-32486
 W-Si₃-n-Si interface, barrier height reaction-process dependence rel. to interface structure 9-42715
 W(VI) dioxobis(acetylacetonate), i.r. spectrum 9-23076
 Zr-W system, high-temp. phase relations, m.p. and X-ray anal. 9-48940

Tuning forks see *Vibrating bodies*

Tunnel diodes see *Semiconducting devices/tunnel and interface devices*

Turbidimetry see *Chemical analysis*

Turbidity see *Scattering/light; Suspensions*

Turbulence

- see also *Cavitation; Flow; Vortices*
 atmosphere, 80 to 100 km, internal scale determ. from structure function of inhomogeneities 9-31347
 atmosphere, effect on laser beam, meas. 9-28890
 atmosphere, free, spectra in stable and convective layers 9-45488
 atmosphere, heat flux patterns, winter, over N.Atlantic 9-31290
 atmosphere, laser beam log-amplitude fluctuations 9-31320
 atmosphere, momentum, heat and water vapour transfer between air and water surface 9-24643
 atmosphere, turbulent nonadiabatic diffusion of suspensions 9-31304
 atmosphere, turbulent transport of physical quantities, direct method 9-24644
 atmosphere with thermal stratification, spectral characts. 9-45484
 atmospheric, diffusion calculations using Richardson's number and eddy diffusivity 9-43392
 atmospheric, rel. holographic image degradation 9-40366
 atmospheric, spectra 9-33760
 atmospheric, turbulent heat and moisture fluxes and turbulent friction stress 9-40016
 atmospheric boundary layer, turbulent region, influence of baroclinicity and nonstationarity 9-40018
 in atmospheric boundary layer above steppe and sea 9-37911
 atmospheric heat, flux near ground, negligible third moment term 9-31292
 atmospheric macroturbulent exchange, horizontal, coefficient 9-24651
 axisymmetric, stationary state 9-34713
 in beam-plasma, nonlinear effects 9-32677
 boundary layer, 3-d, calc., for swept wing in wind tunnel 9-39037
 boundary layer, compressible with pressure gradient 9-23218
 boundary layer, diffusion from line source 9-34842
 boundary layer flow, two-dimens., criteria for reverse transition 9-34824
 boundary layer flow on smooth wall, effect of press. gradient on law of wall 9-34725
 boundary layer on plate, heat transfer rel. to boundary conds. 9-27240
 boundary layer reverse transition, special cases of general criterion 9-34727
 boundary layers, compressible, study on coefficient of local skin friction 9-30181
 boundary layers, interaction of an oblique shock wave 9-22268
 boundary layers, pressure fluctuations resolution, effect of transducer size 9-45862
 boundary layers, three-dimensional, wall similarity 9-23217
 boundary layers, turbulent, influence of elastic plate on acoustic radiation 9-45861
 in boundary layers with injection, calculation 9-42601
 Burger's eqn. for dealing with Navier-Stokes eqn. 9-25806
 channel flow, incompressible turbulent boundary layers, study 9-25820
 compressible boundary layer with air injection, experiment 9-42586
 compressible boundary layers in 3-dimensional flow, approximate solutions 9-27950
 in conductive atmosphere 9-43388
 convection, thermal, at large Prandtl number, appl. statistical turbulence theories 9-27247
 convection boundary layer over heated surface, instability and disturbance amplification 9-34895
 Couette flow, rotating, periodic vortex struct. rel. to wave-forms and mean flow 9-34726
 diffusion, turbulent, effective coefficient magnitude 9-39064
 displacement effects on pitot tubes with rectangular mouths 9-38942
 downstream of grid of parallel rods, isotropic after approx. thirty mesh lengths 9-46591
 drag, reduction by viscoelastic fluids, fluid dynamics approach 9-42621
 eddy fluxes, meas. in lower atmosphere 9-24647
 eddy viscosity, concept and constraints 9-34717
 eddy viscosity, conference 9-34094
 effect on detonation 9-36203
 ensemble of weakly nonlinear dispersive systems, uniformly turbulent, time evolution of wave correl. 9-27959
 entrainment across density interface, molecular diffusivity effects 9-23473
 in flames, vel. in homogeneous gas media, theory and expt. comparison 9-27250
 flooding of stream of electrically conducting liquid in longitudinal magnetic field 9-30205
 flow, asymmetrical effects 9-45806
 flow, fully developed, in circular tube and parallel plate channel 9-34740
 flow, mean vel. meas., non-directional probe design 9-46437

Turbulence continued

- flow between rotating cylinders, oscillatory critical modes and onset of hydromag. instability 9-38953
- flow in low speed wind tunnel, diffusion characts. 9-36826
- flow noise, nearfield, from vehicle/water boundary layer 9-45865
- fluctuations in viscous sublayer 9-23212
- fluid, incompressible; functional integration theory, velocity-correlation tensor determ. 9-36739
- in fluid, incompressible, with time varying Wiener-Hermite basis 9-26058
- fluid flow, press. grad., vel. and temp. distrib. 9-34718
- fluid flow, structure meas. using c.w. lasers, S/N ratio and spectral broadening 9-46443
- fluid flow, transverse turbulent velocity fluctuations close to wall, limiting behaviour 9-42626
- fluid mixing, scalar fields fine structure, spectral theory 9-30170
- fluids, decay of proton spin echoes, rel. to Kolmogorov scaling laws 9-30178
- fluids mixing, passive scalar properties, zero-gradient points and minimal gradient surfaces 9-30169
- front structure of axisymmetric compressible wake 9-28070
- gas flow, intensity and freq. spectrum of longit. component, optical investigation. 9-28064
- grid, effect of small polymer additives to water 9-44536
- grid generated, energy spectra of longit. and lateral velocities 9-46556
- grid-generated, correlation meas. of longit. velocity fluctuations, using digital harmonic anal. 9-28066
- growing spiral wave instabilities in viscous flow in rotating pipe 9-34721
- heat transfer assoc. with controls, for separated or attached flow, at Mach 6 9-26006
- high-temperature flow, photoelec. meas. 9-36744
- homogeneous flow, one dimensional representation, pseudo-random function algebra 9-44391
- hydrodynamic for incompressible fluid, physical model 9-44537
- of incompressible viscous fluid at high Reynolds number 9-28085
- interplanetary plasma rel. to charged particle energy changes 9-43644
- in inviscid incompressible flow, decaying, spectrum at large Reynolds' number 9-48674
- ionosphere, lower, conditioning of mag. fluctuations, estimation 9-33826
- isotropic, energy spectrum at large wavenumbers 9-48529
- isotropic atmospheric, pressure on moving surface 9-46560
- jet flows, heat transfer and temp. distrib., interferometric study 9-23373
- jets and plumes, rotating fluid, similarity solutions 9-23213
- relation to laser beam scintillation magnitude saturation in near-earth propag. 9-31968
- laser Doppler meas. 9-43714
- layer, plane asymmetric flows, stress distrib. 9-40637
- layers, twinkling range 9-26905
- liquid flow, heat transfer in variable viscosity 9-40783
- liquid in pipe, time characts. and temp. pulsation spectrum 9-26056
- magnetic fields, weak, amplification in turbulent flow, calc. 9-48541
- measurement with inclined hot wires error eqns. 9-44400
- MHD, axially symmetric flow past fixed bodies, numerical approach 9-34746
- MHD, effect on Lorentz field strength and Hall coeff. 9-23260
- in MHD flow between parallel plates, in transverse field, mean velocity 9-27969
- MHD flow of liquid metals, laminar/ turbulent transition from resistance meas. 9-27962
- mixing under second-order chemical reactor, Lagrangian history direct interaction equations 9-30171
- model, nearly normal, equilibrium props. 9-44396
- noise transmission from turbulent boundary layer through flexible plate into closed cavity 9-45866
- nonhomogeneous, distribution function 9-32568
- ocean, energy dissipation at surface 9-35800
- ocean and tidal channel, spectra of temp. and velocity fluctuations 9-35805
- open sea, in and above thermocline, and temp., microstruct., meas. techs. 9-35806
- optical, incoherent object seen through turb. medium, detection and resolution 9-41531
- optical propag. through 9-25350
- overpressure shock at foot of vertical wall facing air blast 9-34823
- passage through peak wave, acoustic energy flux from unit area downstream of shock 9-34825
- patch formation in transition boundary layer 9-23425
- pipe flow, average vel. distrib. rel. to viscous sublayer 9-46590
- pipe flow outline of second-order theory 9-23423
- pipe flow through mired right-angle bend, prod. of downstream secondary circulation 9-27954
- in planetary boundary layer above surface roughness change, shear stress rel. to mean vel. field 9-41504
- in plasma 9-23325
- plasma, energy of e.m. and kinetic fluctuations 9-27973
- plasma, heating by current, energy loss and efficiency investig. 9-36752
- plasma, heating in toroidal system with current, diamagnetism, h.f. behaviour and radiation investig. 9-36751
- plasma, interstellar, cosmic ray acceleration 9-24728
- plasma, ion acoustic waves 9-42543
- plasma, one particle distribution function and elec. field spectrum 9-48546
- plasma, particle-wave interaction in mag. field, theory 9-34752
- in plasma, quantum mechanical interpretation 9-30213
- plasma, weakly, dielec. const., Langmuir freq. correction 9-32612
- in plasma collision-free shocks, lab. obs. rel. space data 9-25873
- plasma discharge magnetized positive column 9-42554
- plasma flow, electrical conductivity meas., problems 9-38968
- in plasma shock wave, role of ballistic term 9-32614
- plasma turbulent diffusion and ion heating during current instability 9-30289
- polyethylene oxide dilute solns., critical Taylor number rel. to conc. 9-44538
- polymer solution in tube, heat exchange, lowering during flow 9-40785
- preliminary study, in compressible turbulent boundary layers 9-30181
- due to prismatic bodies, aerodynamic resistance coefficient, initial effect 9-44516
- pseudoturbulence; statistical mechanics of gaseous suspensions 9-36902
- reversion to laminar flow in presence of severe favourable press. grad. 9-39036

Turbulence continued

- rotating fluid in mag. field, weakly conducting, asymptotic analysis 9-44401
- rotating fluid layer, convective flow transition to thermal turbulence 9-34735
- salt fingers instability rel. to internal gravity waves, and collective instability 9-33748
- sea, small scale, obs. 9-40001
- sea waters, special ref. to wave motion 9-49435
- in seawater, light scattering 9-44564
- shear flow, accelerations defining mean turbulent trajectories 9-40639
- shear flow, applic. of extended Wiener-Hermite expansion 9-32567
- in shear flow, nonstratified, spectral eqn. elementary soln. 9-32576
- shear flow, streamline curvature and buoyancy, analogy with meteorological parameters 9-41477
- in shear flows, phenomenological theory 9-32574
- shear layers, free, compressible, turbulent, initial development 9-32577
- of shock wave in plasma 9-32615
- shock waves interaction, acoustic waves production, experiment 9-42602
- slugs, vel. in transition pipe flow 9-25817
- solar, producing turbulent diffusion, effects 9-36029
- in solar flare plasma and accompanying phenomena, Petschek's model appl. 9-43674
- solar wind, long wavelength turbulence as heat source 9-36055
- sound generation and surfaces in arbitrary motion 9-25104
- spectral theory, Kovasznay, generalisation 9-32751
- in stratified flow over obstacle, rel. to validity of Long's model 9-40758
- supersonic wake, 2 dimens., mean-flow obs. 9-26008
- surge in bathtub vortex, speed, effect of circulation, geometry and viscosity 9-26060
- rat solution in tube, heat exchange, lowering during flow 9-40785
- three-dimensional boundary layers, surface-vel. grad., meas. tech. 9-30359
- of tidal current boundary layer 9-39996
- tracer injected into water flow in a pipe, obs. 9-28086
- track, friction and heat exchange in stationary turbulent stream, transverse magnetic field 9-30203
- transport, in numerical fluid dynamics 9-38939
- transverse perturbation velocities in rectangular duct, two-dimensional flow of compressible fluid 9-30204
- tropopause, clear air, energy dissipation 9-47535
- turbosphere, altitude variation of field 9-35836
- turbulent boundary layers on porous flat plate with injection 9-30330
- Vlasov turbulence, class of exact solns. 9-48549
- Vlasov turbulence, closure conditions 9-48548
- vorticity, direction of maximum in shear flow 9-25818
- wakes behind circular cylinders, one-dimens. spectra for Reynolds number 320-95000 9-46589
- wakes and waves in steady compressible m.h.d. flow with dissipative effects 9-25836
- water, thermal boundary layer, expt. study with forced convection 9-23424
- water flow in smooth walled pipe, wall press. field obs. 9-42627
- water with air flow over it onset depend. on vol. obs. 9-34837
- weak, plasma, conservation equations, inclusion of magnetic fields 9-38967
- wind, Doppler radar system meas., feasibility study 9-31308
- CO₂ supercritical flow, hot wire anemometer and cold wire resistance thermometer meas. 9-28172
- H₂O pipe flow, velocity and eddy viscosity distrib. in wall region 9-26054
- He flow, mixing of trace gas rel. to in-pile meas. on radioactive gases 9-25679
- NaK, liq., meas. of temp. fluctuations 9-23426
- S gas flow, heat content of plane layer 9-40750

Turbulent flow *see* Flow**Twilight**

- see also Atmospheric spectra; Zodiacal light*
- aerosol study by light scatt., photometric meas. 9-40053
- measurements, use in upper atmosphere exploration 9-49474
- zenith sky, second Umkehr obs. and interpretation 9-41555
- He 10830 Å emission, identification and photometric obs. 9-31363
- HeI emission, 1.083 μ resonance line obs., Feb. 1968-Feb. 1969 9-40052
- Na layer, evening-morning eff., Victoria, British Columbia Feb. 1967-Feb. 1968 9-26928
- O₂ stratospheric quantity, effect on polarization 9-41556
- OI 6300 Å airglow enhancement rel. to latitude 9-28924

Twinning *see* Crystals, twinning**Twistors** *see* Calculating apparatus; Magnetic devices**Two-phase flow** *see* Flow/two-phase**Type II superconductors** *see* Superconductivity/type II**Ultracentrifuges** *see* Centrifuges**Ultrasonics**

- see also separate headings, e.g. Absorption*
- anemometer u.s. for air-steam convection currents meas. 9-36794
- applic. high temp. solid state meas. 9-42966
- beam transmission within laser cavity, patent 9-47947
- composite interferometer, for velocity and temp. coeff. meas. in liquids 9-23494
- conference 9-31849
- dialysis, effect of ultrasound on diffusion rate 9-34893
- diffraction effects in high accuracy meas. 9-25099
- emission from materials, meas. and recording tech. 9-37324
- fountain effect, influence of static press. on height 9-23490
- generation in metals, direct 9-37321
- glass, molten, effect on adherence to metal surface during cooling 9-28388
- halography, liq. surface and scanned, refinements and variations 9-36197
- halography, limitations 9-36191
- halography, review mainly covering Gabor hologram 9-48066
- halography, scanned u.s., refinements and variations 9-36190
- halography, temporal reference 9-25146
- hydrolysis of sucrose solns., non-cavitating ultrasound effects 9-37821
- image converter, solid state, u.s. 9-34087
- images, 3-dimensional, using holographic techniques 9-27350
- imaging, holographic techniques for optically opaque structures 9-29295
- imaging system using diode switching 9-29294
- imaging system using liq. surface levitation effect, materials inspection appl. 9-29292
- imaging systems, appl. to nondestructive testing 9-27322

Ultrasonics continued

- kinetics of solid-state reactions, Cu and Cu-Be alloy, influence of intense ultrasonic energy 9-28380
- lenses, ceramic, for control of u.s. energy 9-36195
- light diffraction technique, rel. to photoelastic coeffs. determ. 9-26308
- liquid metals, electrodynamic excitation 9-23492
- liquids at high press., meas. method for eqn. of state 9-34872
- machining, application of rocket effect on bubbles 9-39068
- machining, with stepped tool, forces developed 9-36187
- measurement of elasto-optical constants, improved methods 9-36366
- measurement of pulses in liquids and solids, methods 9-30768
- in metal precision casting 9-37275
- mobility and for the blind, pulse refl. method 9-22265
- modulation of light, theory and expt. 9-32021
- in nondestructive testing 9-37324
- in nondestructive testing, transducer charact. 9-36183
- nuc. reactors, fis., temperature measuring system 9-36636
- in ophthalmology, problems 9-38134
- in phase transitions investigations of solids 9-37302
- pulse meas. of elastic wave propag. in rocks 9-37884
- radiator focusing, 60 MHz, using CdS crystal 9-22266
- speech components 9-38137
- technique for meas. of stresses in viscoelastic solids 9-37222
- testing of inhomogeneities in heterogeneous media 9-29279
- transducer for metal testing, patent 9-38303
- transducer used for phonic desorption of impurities from walls of a vacuum vessel 9-40217
- He bubble chamber, expansion techs, tests 9-34365
- KI solution, cavitation, relaxation phenomena 9-46629
- Ni-(1.18 at.%)Al alloys, effect on creep rate, 700°C 9-33047
- Sn, absorption in supercond. transition rel. to cryst. orientation 9-37336
- W, cleavage velocity determ. with u.s. fractography 9-33094

Ultraviolet detectors *see* Radiation detectors**Ultraviolet sources** *see* Light sources**Umklapp process** *see* Crystals/lattice mechanics**Uncertainty** *see* Indeterminacy; Probability**Undor** *see* Electron theory; Field theory, quantum**Unified field theory** *see* Relativity/unified field theories**Unimolecular layers** *see* Adsorbed layers**Units**

see also Constants; Dimensions. Nomenclature and symbols

- electricity and magnetism, systems, book 9-47718
- photometric 9-32027
- photometric, SI, and conversion tables 9-41948
- second, new definition on quantum basis 9-22041
- SI, introduction 9-22038

Upper atmosphere *see* Atmosphere/upper; Ionosphere**Uranium**

see also Nuclear fission/uranium

- adsorption on W, multilayer, work function rel. to thickness and phase transition 9-32850
- anisotropic grain growth and cavitation swelling, effect of alloying additions 9-33206
- atom, scattering factor calc. by WKB method 9-27824
- buckling of tubes enriched with ²³⁵U in light water 9-23913
- content of store meteorites, and Pu-Xe decay intervals 9-45675
- d.c. arc plasma of U matrix in air, distrib. of temp., voltage and elec. field 9-25918
- fission gas induced swelling, as function of external hydrostatic press., 0-1000 bar 9-38735
- foils <2000 Å, preparation for electron microscopy rel. to stress corrosion cracking 9-23777
- isotope analysis using X-ray fluorescence combined with α -activity meas. 9-24598
- isotope analysis using X-ray fluorescence combined with A-activity meas. 9-33690
- isotopes mass spectra 9-47914
- isotopic ratio, by Ge (Li) detector 9-27830
- laser microprobe analysis, impurity emission rel. to matrix effects, obs. 9-24604
- natural-D₂O lattices params., obs. 9-32378
- neutron spectra from spherical shell obs. 9-27783
- in rocks, gamma spectrometer surface obs. 9-37893
- self-diffusion in UO_{2.14} (0.005 $\leq x \leq 0.217$), 1275-1650°C 9-37215
- self-diffusion in UO_{2.14} rel. to comp., obs. review 9-37210
- self-diffusion in UO₂, UO_{2.14}, 1200-1600°C 9-37211
- self-diffusion in UO₂, sintering rel. to O/U ratio, obs. 9-37287
- intrabasic rocks and carbonates neutron activation analysis 9-45461
- void effect on neutron spectrum indices and fast fission ratio 9-38737
- X-ray absorption spectra, M, comparison with UO₂ 9-49305
- ²³³U ground ¹S₀ level, hyperfine struct., arc spectrum obs. 9-29952
- ²³³U, resonance self-shielding factors for energy groups 5 eV to 2 keV 9-22890
- in BaF₂, neutron-irrad. single cryst., diffusion of Kr and Xe 9-35127
- in SrF₂, neutron-irrad. single cryst., diffusion of Kr and Xe 9-35127
- U-D₂O lattice with Pu, epithelial cross-sections 9-25672
- U-H₂O reactor assembly, neutron flux distrib. in slab elements 9-22879
- U-Pu fuel systems, breeding gain in fast reactors, effects of spectral hardness 9-22866
- α -U, dislocation energy rel. to temp. and angular depend. 9-37181
- A-U, low-temp. phase transition 9-26394
- δ -U, neutron irrad. defects and Matthiessen's rule 9-46805
- U³⁺ in CaF₂, strongly polarized, e.p.r. obs. 9-39901
- U³⁺ in CaF₂, SrF₂ and BaF₂, spin lattice relaxation in paramagnetic resonance 9-35710
- U⁴⁺ in CaF₂, spin-phonon interaction from u.s. paramag. resonance 9-33623
- U⁴⁺ in CaF₂, superhyperfine interactions in EPR and UPR spectra 9-39905
- U II spark spectrum, A and B systems unification 9-29951
- U(IV) in Na silicate glass, paramag. susceptibility 9-33442

Uranium compounds

- alloyed tubes in EL 3 reactor, mechanical strength, creep resistance; neutron irradiation 9-34496
- alloys, cavitation swelling, temp./exposure thresholds for dilute concs. (<1000 ppm) 9-41117
- alloys, determ. of Fe and Al content by atomic absorption spectroscopy 9-26839

Uranium compounds continued

- oxides and Ta reactions at high temps. 9-28782
- alloys, type II twinning in martensitic transformations 9-30512
- oxychalcogenides, cryst. prep. 9-30519
- Th-Pu solid solutions, synthesis and props. 9-33123
- U-Al, alloy, morphology of precipitation 9-28377
- U-Al, alloy, of precipitation 9-28378
- U-C-O-N system, phase relations at 1700°C 9-26400
- U-Fe-Al, alloy, morphology of precipitation 9-28377
- U-Fe-Al, alloy, of precipitation 9-28378
- U-(1.5 wt.%)Mo alloy, high temp. anneal, rapid quench, UC precipitation in gamma phase 9-35260
- U-(0.45 wt.%)Mo, transform. kinetics rel. to cooling rates and overheating temp. 9-41069
- U-Nb system, monoclinic deform. of α -U lattice 9-40920
- U-Pu oxide fuel irradiated, solid fission product behaviour, neutron flux 9-41118
- U-(3.96 at.%)Si alloy, structure, effects of fabrication and heat treatment variables 9-33124
- U-UAl₂-Al₂Mo₃-Mo system, melting equil. 9-39133
- U-Zr alloys, specific heat meas. for various compositions 9-24052
- U-Zr alloys, specific heat meas. for various compositions 9-33185
- (U,Pu)O₂ fuel, thermal diffusion mechanisms rel. to stoichiometry 9-37213
- U₂C₃, linear thermal expansion at elevated temps. 9-24057
- U₃As₄ single cryst., mag. props. 9-37656
- S-U₂O₈, existence of δ phase 9-28271
- β -U₂O₈ monocrystals, growth and structure 9-28233
- U₂P₄ single cryst., mag. props. 9-37656
- U₂Sb₄, magnetic structure and ordering, neutron diff. investigation 9-47294
- U₂Si, irrad., X-ray diffraction patterns rel. to change in struct. 9-40921
- U₂Si, irradiation at 60°C, plastic deformation, phase change, X-ray diffraction analysis 9-35248
- U₂Si nuclear reactor fuel, corrosion tests in 300°C water 9-28804
- U₂O₃, electron absorpt. in transmission microscopy, and O sublattice stability obs. 9-39312
- U₂O₃, dielec. props. 9-41232
- U₂O₃, phase transition due to electronic ordering 9-41127
- U₂O₃, transmission electron microscopy, O sublattice stability obs. 9-39312
- U₂Fe, Mossbauer effect 9-39821
- UAs, antiferromagnetic ordering 9-33488
- UB₂ cryst., prod. by vapour transport react. 9-28231
- UBi, magnetic structure and ordering, neutron diff. investigation 9-47294
- UBi antiferromag. struct., neutron diff. obs. 9-39785
- UC-ThC solid solutions, elec. props. 9-26510
- UC-UN mixtures, melting point maximum in N₂ atmos. rel. to composition 9-40819
- UC, arc cast and sintered, thermal conductivity, radiation eff. 9-41111
- UC, bubble formation and swelling, nucleation time and temp. depend. 9-38736
- UC, chemical binding eff. on neutron scatt. of C atoms 9-23776
- UC, linear thermal expansion at elevated temps. 9-24057
- UC, release of Rn and fission Xe, obs. 9-37214
- UC, stability 9-32490
- UC, swelling calcs. using extrapolated Xe eqn of state 9-40742
- UC, synthesis by precipitation in liq. metal soln. 9-36630
- UC_{1-x}N_x, elec. resist. and Seebeck coeff., 80-1000°K obs. 9-35330
- UC_{1-x}O_x, heat of formation and heat capacity from thermochem. study 9-28783
- UC_{1.08}, compressive creep, 1200-1600°C, 3000-10,000 psi 9-23899
- UC, coated particles preparation fluidized Bed. by reaction and sintering 9-41053
- UC₂O₃, thermal conductivity rel. to O content, 100 to 1500°C 9-26458
- UC gamma phase precipitation in U-Mo 1.5% alloy, high temp. anneal, rapid quench 9-35260
- UC large dilute reactor cores, physical parameters 9-32391
- UC preparation from UF₄, Al and graphite 9-28772
- UC single cryst., Rn 220 recoil atoms interstitial diffusion 9-28325
- UC void effect on neutron spectrum indices and fast fission ratio 9-38737
- UC(P,S) powders, densification 9-35238
- UCl₄, n.g.r. of ³⁵Cl 9-49365
- UF₃, n.m.r. of ¹⁹F, dipolar broadening obs. 9-33651
- UF₄ prod. from UF₃ in fluidized bed reactor, 500-600°F, patent 9-22903
- UF₄-H₂, HF chem. laser, operation and chem. 9-36292
- UF₄-WF₆, melting point and eutectic props. 9-23580
- UF₄-WF₆, melting point and eutectic props. 9-34953
- UF₆, magnetic structure and spin density distrib. 9-45127
- UF₆O₄, magnetic structures and props. 9-45238
- UGa₃ (x=1,2,3), magnetic props. 9-33458
- UI₃, n.m.r. in para- and antiferromagnetic states, freq. and temp. depend. 9-39921
- U(IV)tetracyclopentadienide complex, isotropic ¹H-NMR shift, transferred hyperfine interac. mechanisms 9-27877
- UN_{2-x}, preparation in UC+NH₃+UN_{2-x}+CH₄+H₂ 9-31186
- UN paramag. state, ¹⁴N n.m.r. obs. 9-37807
- UO₂-Cu alloy, phase diagram and investigation of system 9-28395
- UO₂-Mo system, UO₂ cermet prod. by isostatic hot pressing, impact strength, thermal cond. meas. 9-35222
- UO₂-PuO₂ fuels, heat flux distrib. in rods rel. to fissile material segregation 9-36632
- UO₂-SiO₂ system, thermal conductivity, with varying UO₂ concentrations over the range 100-800°C 9-26456
- UO₂-UN mixtures, cintering behaviour, elec. conductivity, mech. props. 9-30730
- UO₂-metal cermets, preparation and thermic conductivity 9-26455
- UO₂, 6% enriched, -0.05 wt% B₄C irrad. stability, 1000 and 5000 MWd/te burnup 9-32389
- UO₂, α irrad., rel. to ²³⁸U fission, shadow pattern agn. distrib. of fragments 9-40524
- UO₂, density effect of thermal conductivity 9-41110
- UO₂, dielec. props. 9-41232
- UO₂, dislocation behaviour in {100}- {110}- and {111}-glide planes 9-40956
- UO₂, enthalpy, from 2500°K melting pt. 9-26425
- UO₂, fission gas bubbles and sintering pores irrad. stability, obs. 9-37187
- UO₂, fission gas release rel. to bubbles mobility, obs. 9-37190
- UO₂, ht. capacity, 300-1100°K 9-35285

Uranium compounds continued

- UO₂, irradiated, growth of fission gas bubbles 9-28152
 UO₂, irradiated, re-solution of fission gases 9-28326
 UO₂, laser microprobe analysis, impurity emission rel. to matrix effects, obs. 9-24604
 UO₂, M, absorption spectra, comparison with U 9-49305
 UO₂, neutron-irradiated, Pu isotopic analysis 9-43346
 UO₂, nonstoichiometric, defect complexes and microdomains 9-44685
 UO₂, O diffusion and comp. in temp. gradient, 1300-2500°C 9-37212
 UO₂, point defect form. energy calc. 9-44688
 UO₂, release of Rn and fission Xe, obs. 9-37214
 UO₂, sintered, thermal conductivity, radiation eff. 9-41111
 UO₂, sintered, thermal diffusivity and conductivity 9-26457
 UO₂, sintering, Dorn method in initial phase study, comment 9-26369
 UO₂, small gas bubbles stability, irradiation environment, thermal diffusion near 1000°C 9-34495
 UO₂, sublimation mechanism of bubble migration in temp. gradient 9-35134
 UO₂, surface diffusion, obs. review 9-37198
 UO₂, U self-diffusion, 1200-1600°C 9-37211
 UO₂, flow stress depend. on nonstoichiometry at high temp. 9-33049
 UO₂, O and U self-diffusion rel. to comp., obs. review 9-37210
 UO₂, partial molar free energy of O 9-28775
 UO₂, U self-diffusion, 1200-1600°C 9-37211
 UO₂, (0.005<x<0.217), U and O self-diffusion 780-1650°C 9-37215
 UO₂²⁺, fundamental bending freq. from far i.r. spectra 9-49287
 UO₂, deformed single crystal dislocation substructure, strain rate 10⁻³-10⁻¹ min, 750-1400°C 9-40957
 UO₂, deformed single crystal dislocation substructure, strain rate 10⁻³-10⁻¹ min, 750-1400°C 9-35095
 UO₂, electric multipole coupling via lattice 9-47227
 UO₂, fuel, thermal diffusion mechanisms rel. to stoichiometry 9-37213
 UO₂, fuel, vibration compacted., eff. of sinusoidal vib. on compacted density 9-34494
 UO₂, fuel coolant temperature effects in steam generating heavy water reactors 9-25674
 UO₂, fuel, irradi., U and Pu isotopic distrib., theory and expt. 9-25675
 UO₂, irradiated fuels, preferential edge breeding of ²³⁹Pu 9-22899
 UO₂, nearly stoichiometric single cryst., thermoelec. power and elec. conductivity, activation energies obs., 170-1250 °K 9-33403
 UO₂, porosity effect on kinetics of grain growth 9-26250
 UO₂, powders with high-surface-area, sintering, influence of atmosphere 9-33113
 UO₂, sintering rel. to O/U ratio, obs. 9-37287
 UO₂, void formation and migration in a single crystal subject to a temperature gradient 9-32950
 UO₂(NO₃)₂·6H₂O, i.r. spectra, rel. to bending fundamental freq. of UO₂²⁺ ion 9-49287
 UOS, thermochemistry 9-28774
 UOS, thermochemistry 9-33658
 UOSE, antiferromagnetic props. 9-33487
 UP-US solid solns., mag. props. 9-45117
 UP, low temp. magnetic transitions, neutron diff. study 9-28590
 UP, paramagnetic, ³¹P nuclear mag. relax. 9-24343
 UP_{0.75}Se_{0.25} powder, metomag. state obs. 9-33434
 UP_{1-x}S_x (x=0.05), antiferromagnetic structure 9-41342
 UP_{1-x}S_x system, (0<x≤1) magnetic phase diag., neutron diffraction investigation 9-45237
 US-UO₂ mixtures, evaporation 9-28774
 US-UO₂ mixtures, evaporation 9-33658
 USb, antiferromagnetic ordering 9-33488
 USb, magnetic structure and ordering, neutron diff. investigation 9-47294
 USb antiferromag. struct., neutron diff. obs. 9-39785
 UX₂ type, magnetic symmetry 9-37670
 W-UO₂, cermet produced from coated particles, high temp. creep-rupture tests 9-23910

Urey-Bradley forces see *Molecules/internal mechanics*

V-centres see *Colour centres*

V-particles see *Hyperons; Mesons*

Vacancies see *Crystal imperfections/vacancies*

Vacancy breakdown see *Diffusion in solids*

Vacuum apparatus

see also *Seals*

- automatic balance for heat and mass transfer study 9-22040
 chamber, large, performance during 10000 hour 2200°F test 9-38172
 chambers, elliptical, equations for stresses amd deflection 9-47708
 diode, prod. of very short X-ray pulses 9-33997
 electron probe explanation of phenomena based on law of temperature change 9-31726
 film deposition and in-situ galvanomag. meas. 9-39193
 filter deposition, multilayer, in high current vacuum system 9-36958
 flowmeters for meas. small gas inflow 9-38181
 gas distribution within a vacuum system 9-38174
 hot-press for toxic materials 9-25007
 induction heating power-lead coupling, demountable, for uhv 9-31725
 joint, using water paste of powdered glass solder, above m.p., high vacuum 9-33989
 leak detection and residual gas analysis, metastable mols. time-of-flight meas. 9-38170
 for linear accelerator, operation when subject to intense radiation 9-36547
 magnetron-type ion source, low-pressure, residual gas analysis 9-38182
 reflectometer, u.h. vacuum, for use with extreme u.v. synchrotron radiation 9-27396
 seal, for leading wires into vacuum system 9-33992
 stellarator sirius, vacuum system 9-46505
 tongs for remote control manipulation under high vacuum 9-33991
 zeolites, A and X, artificial, applic. in vacuum technology 9-25006
 Ba getter film activity determ., press. meas., pumping speed calc. 9-38169

Vacuum gauges

- Bayard-Alpert, hot filament ionization disturbance in mass spectrometry 9-27146
 Bayard-Alpert, ionization, improved sensitivity and reduced collector residual current 9-45710
 Bayard-Alpert, ionization, with or without modulators 9-47709
 Bayard-Alpert, magnetic field modulation to distinguish between true and residual ion currents 9-40222

Vacuum gauges continued

- Bayard-Alpert designed to meas. press. below 10⁻¹⁰ torr, protected from soft X-rays 9-25001
 calibration, three-chamber pressure-reduction system 9-25004
 dynamic calibration, pressure distrib. in calibration recipient 9-24998
 gas analysis in u.h.v. by mass spectrometer, no memory eff., max. 500°C 9-36647
 ion desorption, electron-induced, from Pt, Pt-Ir, Mb; u.h.v., mass spectrometric investigation 9-38178
 ionization, evaporation rate monitor and push-pull Miller op. amp. 9-43694
 ionization, for scatt. chamber 9-25005
 ionization, hot-cathode, electron-mol. collision theory 9-40223
 ionization, with quadrupole system to control electrons, pressure dependence 9-38180
 McLeod, contamination-free operation 9-47710
 McLeod, magnetic ball valve and condenser device to obstruct Hg vapour flow 9-40220
 Pirani and related gauges, design methods 9-27145
 Pirani-type with good zero stability and fast response time 9-40221
 resolution of randomized and non-randomized mols. 9-25002
 sensitivity of 10⁻¹⁴ torr, reduction of X-ray limit, patent 9-41719
 space charge ion focussing gauge 9-25003
 vacuumeter, membrane, differential 9-24999
 vane, Monte Carlo force-pressure correlation 9-25000

Vacuum polarization see *Quantum electrodynamics*

Vacuum pumps

- backstreaming of oil, use of liquid-nitrogen traps for elimination 9-40219
 cryogenic, applic. to Mo annealing 9-26367
 electron orbiting device, using coaxial electrodes for generating radial elec. field, patent 9-49617
 getter ion, suction performance improvement over wide range, patent 9-49618
 getter-ion, atomizing, description and performance 9-31727
 getter-ion, multicomponent getter films, residual gas analysis 9-38176
 getter-ion, of magnetron type, Penning discharge mechanism 9-24994
 getter-ion, sublimation, high capacity and rigid temp. conditions operation 9-38175
 getter-ion and sputter-ion, pumping techniques, conference 9-33990
 industrial, for removal of water, modification to rotary oil-sealed pump 9-38179
 sputter-ion diode pump, cathode post geometry, pumping speed depend. 9-40218
 sputter-ion pump, noble gas pumping enhancement depend. on cathode geometry 9-38177
 Ti-Zr film in getter-ion pump, residual gas analysis 9-38176

Vacuum technique

- condensation, potentialities as pumping technique for H₂ and D₂ in ultra-high vac. regime 9-48770
 contaminants on a surface, Auger electron spectrometer analysis 9-39150
 continuously pumped systems 9-24997
 crystallography, goniometer for ultra high vacuum 9-23643
 film deposition and in-situ galvanomag. meas., apparatus 9-39193
 hydrocarbon-free 10⁻⁹ torr procedure 9-25008
 ion pumped noble gases, pre-exponential factor in desorption from glass 9-39171
 metal oxide films, reactive sputtering 9-30487
 for metallic surface purity maintenance, characteristic energy loss spectra method 9-32832
 molecular leak, large conductance, for gas sampling at high press 9-40216
 multifoil insulation materials in sealed vacuum system, outgassing behavior obs., 100-1800°F 9-38173
 orthoclase, cloven in vacuum, electrostatic distrib. obs. on faces 9-37571
 phonic desorption of impurities from walls of a vacuum vessel 9-40217
 reduction of vacuum by laser sputtering of absorbent titanium oxide-magnesium oxide film at u.h.f. 9-43693
 residual gas analysis, mass spectrometer 9-24597
 superconducting resonating cavities, technology of prod. bright Pb layers 9-39607
 surface cryopumping, condensation coeff. meas. 9-40224
 thin-film deposition, substrate temp. meas., laser technique 9-25132
 tongs for remote control manipulation under high vacuum 9-33991
 ultimate pressure, feasibility of easily reaching 10⁻¹⁶ Torr 9-38171
 Cr, gettering effect, detection during evaporation and condensation in vacuum 9-30457
 H₂, solid, thin foil prod. for targets 9-27147
 Rb atomic beam, comparison meas. with UHV microbalance, quartz osc. and ionization foil 9-22988

Vacuum tubes see *Electron tubes*

Valence bands see *Crystal electron states/band structure*

Valency

- ions, of Ti oxide inclusion in Fe-Cr, Fe-Ni, X-ray microanalysis of emission spectra fine structure 9-37752
 ions and chemical bonding from X-ray microanalysis of emission spectra fine structure 9-37739
 rare-earth ethylsulphates, covalency eff. 9-35008
 Eu in compounds, states 9-32853
 FeCl₃ hydrates, covalency eff. from Mossbauer studies 9-28667
 Ti in titanobarium glass and ceramic, from X-ray emission spectra Kα₁ line position 9-41398
 Yb in compounds, states 9-32853

Valves, thermionic see *Electron tubes*

Van Allen radiation see *Atmosphere/radiation belts*

Van de Graaff generators see *High voltage techniques; Particle accelerators/linear*

van der Waals forces see *Atoms; Kinetic theory; Molecules/intermolecular mechanics; Solids*

Vanadium

- atom, with electronic configurations 3d³ and 3d³4p, energy spectra, theoretical investig. 9-29940
 degassing of wires by heating 9-35195
 diffusion coefficients of C 9-35133
 domain boundaries, lattice distortion formation 9-32960
 films, temp. coeff. resistance thickness dependence (60-900 Å) 9-47077
 hydride and deuteride solid solutions, interstitial ordering 9-23990
 Knight shift pressure dependence 9-24510

Vanadium continued

- neutron-irradiated, cylindrical damage cells, transmission electron microscopy 9-44698
 radiation induced defect clusters and loops, effect of annealing 9-39367
 stable nuclides in iron meteorites, surface ionization mass spectrometric obs. 9-38089
 superconducting anisotropy temp. dependence, 1.7-4.2°K 9-24154
 thermal expansion coeff., temp. depend., 80-1200°K 9-44842
 wires, degassing by heating 9-35195
 in Al_2O_3 far i.r. absorpt. spectrum in applied mag. field, Zeeman splitting of lines, single d electron obs. 9-31100
 in Al_2O_3 single cryst., low temp. thermal conductivity meas. 9-35086
 V^{+} ion spectrum, new lines 2500-8800 Å 9-38777
 V^{3+} , ground-state splitting in hexaurea complexes 9-35654
 V^{3+} , V^{2+} , spectra in CdF_2 9-47385
 V^{3+} impurity ion in CaF_2 , spin-lattice coupling consts. 9-31054
 $^{50}\text{V}/^{51}\text{V}$ abundance ratio in chondrites and terrestrial matter 9-41681
 $\text{V}(100)$, gas adsorp., low-energy electron diffraction 9-30500
 Vfilm, preparation for nuclear studies 9-48766

Vanadium compounds

- charge transfer, electron spectroscopic meas. 9-44636
 ferrite, mag.-acoustic resonance 9-37346
 metalline cpds., Fermi levels, density of states determ. from X-ray spectra 9-37753
 oxy-carbonate, new, formation 9-28236
 sandwich complexes, hyperfine coupling consts. and covalency 9-42420
 vanadates, n.m.r. powder patterns 9-43293
 vanadyl phthalocyanine, e.s.r. 9-41430
 Al-V dil. solid soln., mag. susceptibility and sp. ht. w.r.t. localized d-state props. 9-33269
 alloys with V, Nb and Ta, electrical resistivity as a function of temperature 9-39584
 Au-V dilute alloys, n.m.r. low-temp. mag. props. obs. 9-45395
 Au-V dilute magnetic alloys, specific heat, temp. depend. below Kondo temp. 9-24050
 Co-Fe-V alloys, high strength, high ductility, rel. to partially-recrystallized structure 9-44790
 Co-V binary alloys, σ -phase, mag. props. 9-43158
 Fe-(49wt.%Cr-(2wt.%V), brittle fracture, slip mode effects 9-26356
 Fe-V binary alloys, σ -phase, mag. props. 9-43158
 Hf-V binary system, phase equilib. diag. 9-33149
 Nb-V solid solutions, hardening eff. of V 9-28385
 Ni-V alloys, ferromagnetic resonance absorption, g-value temp. depend. 9-24477
 Ni-V binary alloys, σ -phase, mag. props. 9-43158
 Ti-(6 at.%Al-(4 at.%V) alloy, plane-strain cyclic and sustained load flaw growth charact. 9-30722
 Ti-(6 wt.%Al-(4 wt.%V) alloy, surface treatment for impact fatigue and wear resistance 9-37259
 Ti-(6 wt.%Al-(4 wt.%V) alloy, two-phase microstructures, toughness 9-37251
 Ti-(6 wt.%Al-(4wt.%V) alloy, stress-corrosion cracking in anhydrous methanol, mechanism 9-48894
 Ti-(8wt.%Al-(1wt.%Mo)-(1wt.%V) alloy sheet, hot-salt-stress-corrosion cracking and effect on tensile props. 9-23923
 Ti-V alloys, ω -phase precip. 9-23987
 TiO_2 - VO_2 sintered pseudobinary system, semiconductor-to-semiconductor transition from elec. conductivity and thermoelectric power meas. 9-49088
 V-Cr alloys, ^{51}V resonance, Knight shift and Neel temp. 9-24324
 V-O solid soln., degassing kinetics 9-39942
 $\text{V}_{1-x}\text{Ni}_x$, superconducting behaviour 9-24163
 V_2O_3 , positron lifetime spectra rel. to semiconductors to metal transition 9-47063
 V_2O_3 and related oxides, Hall const. and thermopower, rel. to nature of metallic state, up to 800°K 9-30836
 V_2O_3 metal-semiconductor transitions on excitonic phase change, pressure depend. studies 9-30892
 V_2O_3 , conductivity, d.c., model, and Hall effect meas. 9-33247
 V_2O_3 , flame photometry determ. of Li, suitable acid for quenching Li rad. 9-37857
 V_2O_3 , solubility of YVO_4 and rare earth vanadates, crystn. conditions and structure 9-40777
 V_2V_3 , metal-semiconductor transition, critical pressure 9-44921
 V_3Au , normal, quadrupole and anisotropic Knight shift effects, obs. 9-39923
 V_3Ga , supercond., critical fields temp. depend. from magnetiz. obs. 9-44945
 V_3Pd , superconducting behaviour 9-24163
 V_3Si , cubic-to-tetragonal transformation, volume changes 21°K 9-35249
 V_3Si , hydrostatic pressure effect on superconductive transitions 9-49052
 V_3Si , n.m.r. of ^{51}V , quadrupole effects of second-order 9-49361
 V_3Si , superconducting critical current density change on structural transformation suppression by uniaxial stress 9-24162
 V_3Sn , type II supercond., V^{3+} nucl. spin-lattice relax. time, temp. variation 9-35371
 V_3C , coherence with α -Fe matrix, critical magnitude meas. 9-32931
 V_3Te , struct. study 9-37151
 V_6C_3 , ordered, radiation damage by electron microscope beam bombardment 9-26468
 V complex, hexaurea $\text{V}(\text{III})$ ion in crystals, spectra and mag. props. 9-35654
 V phthalocyanide, laser pulse length reduction in forced Mandel'shtam-Brillouin scatt. 9-28129
 VAu_4 and related cpds., magnetiz. and susceptibility meas. rel. to ferromagnetism 9-45128
 VC precipitation during tempering of martensite, mechanism 9-33121
 VC single cryst. growth by floating zone tech. 9-37090
 $\text{V}(\text{CO})_6$, vibrational and electronic spectra and bonding 9-32491
 VCl_4 , n.m.r. of liquid 9-39118
 VCl_4 , static Jahn-Teller distortion of ground state 9-30059
 VF_3 single crystal and powdered samples, magnetic structure, neutron diff. study 9-45074
 $\text{V}(\text{NCS})_3$, $\text{V}(\text{NCS})_6^{2-}$, $\text{V}(\text{N}_3)_3$, complexes, electronic spectra 9-40593
 VO_2 , growth and elec., conductivity transition 9-28230
 VO_2 , growth of single cryst. by chem. transport reaction using TeCl_4 9-32872
 VO_2 , addition to discharge as aid to spectrochem. analysis of alkali elements 9-31229
 VO_2 films, photoemission rel. to electronic structure 9-24255

Vanadium compounds continued

- VO_2 single-cryst. growth by isothermal flux evap. 9-28236
 VO_2 thin films, structure rel. to elec. props. 9-23629
 VO_2 , structural and elec. props. composition dependence 9-28272
 VO^{2+} chelates, in-plane g values 9-31163
 VO^{2+} in Rb_2SO_4 , e.s.r. spectrum 9-41429
 VOF_3 , E-species force consts. 9-30050
 $\text{VO}(\text{NCS})_3$, $\text{VO}(\text{NCS})_6^{2-}$, $\text{VO}(\text{N}_3)_6^{2-}$ complexes, electronic spectra 9-40593
 VS_2 , orbital valence force field constants 9-32486
 VSe_2 system, NiAs-like struct. cpds. obs. 9-30575
 VSi , enthalpy changes at high temp. 9-39092
 VTe_x system, NiAs-like struct. cpds. obs. 9-30575
- Vaporization**
 see also Boiling; Condensation; Distillation; Evaporation; Heat of vaporization; Vapour pressure
 arc spectrochemical analysis sample, servocontroller 9-28827
 of drops moving relative to gas stream 9-34866
 entropy of inorganic gas, b.p. molecular weight and volume meas. 9-34965
 exploding wires, expansion vel. of discharge plasma 9-25852
 exploding wires causing inductive ignition of surface-discharge 9-25970
 graphites, by laser evap., mass spectr. anal. 9-23601
 laser, of solid materials, coupling technique with mass spectrometer 9-22922
 propane, meas. of latent heat of vaporization 9-36818
 refractory metals, by laser-microscope system, microsampling applic. 9-24594
 solids, spectroscopic study of high temp. mats. 9-28190
 water, film boiling on horizontal Pt wire, heat transfer and growth rate 9-28188
 AlP, thermodynamics 9-36927
 As-Se system, laser-induced, mass spectra 9-28187
 C, and heat of sublimation and vapour composition and pressure 9-48740
 C, and structure, mech. props., growth and gasification studies, book 9-46695
 Ce-C system, thermodynamics 9-32821
 Cs in liquid-vapor transition up to 2000°C and 100 to 320 atm., elec. cond. 9-40801
 K/Hg amalgam, equilibrium vapor compressibility factor 9-36926
 KCl single cryst. mass spectrum 9-48741
 NH_4Cl , stability of gaseous mol. 9-36726
 Na, subcond., at surfaces of hot spheres, rel. to heat transfer rates 9-28116
 NbC from open surface in vacuum, 2453-3428°K 9-26167
 Sr atoms and ions from SrO surface on W and Re 9-37637
 Ti-O system 9-23172
 Ti-O system 9-23173
 ZrTe_3O_8 , characts., and fusion 9-26159

Vapour density see Density/gases**Vapour pressure**

- see also Humidity; Vaporization
 carbon tetrachloride, and cohesion energy and molar vol., obs. 9-28094
 Freon 22, meas. 9-36805
 methane, halogen substituted saturated, calc. 9-26030
 methane and methane- d_4 , theory 9-39143
 methane and methane- d_4 , theory 9-44617
 monosilane, halogen substituted, saturated, calc. 9-26030
 n-nonane, and cohesion energy and molar vol., obs. 9-28094
 pyridine, and cohesion energy and molar vol., obs. 9-28094
 solid and liquid elements, data 9-46689
 tetrachloroethylene, and cohesion energy and molar vol., obs. 9-28094
 water, anomalous, lower than normal water 9-40771
 water, saturation press. eqn., 0-374.15°C 9-32819
 Ar, correction of tables 9-39144
 Ba 9-42702
 BiF_3 , over liquid, derivation 9-30021
 BiF_3 , over solid, transpiration method 9-30021
 Cm metal 9-48742
 Fe, liquid, 1813-1973°K 9-23604
 K/Hg amalgam at 20 compositions and up to 10 atm. pressure 9-36926
 K, const. vol. piezometer obs. 9-40829
 Kr, between 72° and 91°K 9-39144
 LaB₆ partial press. of La vapour 9-40830
 Li saturated, 1200-2160°K 9-26170
 $\text{Pb}(\text{Ti}_{1-x}\text{Zr}_x)\text{O}_3$, of PbO , Knudsen effusion meas. 9-23609
 PuO_{2-x} , hypostoichiometric, 2070° to 2380°K 9-28169
 S, during heat treatment of CdS, rel. to dark conductivity 9-49076
 Ti, liquid, 1953-2193°K 9-23604
 TiNO_3 fused, b.p. and transpiration meas. method, m.p. entropy of vaporization, 250-450°C 9-34966

Vapour pressure measurement

- by atomic absorption spectrophotometry 9-23608
 encapsulation technique for metal and semiconductor melts 9-32820
 Knudsen effusion, Monte Carlo analyses of thin-edged and channel orifices 9-30466
 metals, by atomic absorpt. spectrophotometry 9-23608
 Cd, torsional and Knudsen techniques, comparison 9-39146
 of Cs expt. determ. 9-42700
 K, using const. vol. piezometer 9-40829
 Zn, torsional and Knudsen techniques, comparison 9-39146

Variable stars see Stars**Variational calculus** see Mathematics**Variational method** see Quantum theory/application methods**Vavilov-Cherenkov radiation** see Cherenkov radiation**Vectons (vector mesons)** see Mesons**Vectors**

- Green's dyads, eigenvector expansion 9-24626
 reflection of, an illustration 9-22050

Velocity

- bubbles, gas, flowing into fluid 9-40766
 particle trajectories in gas-particle flow in nozzles 9-34819
 shock waves in gas mixtures, separation of components 9-34826
 surge in bathtub vortex, effect of circulation, geometry and viscosity 9-26060
 water droplets, effects on collision, coalescence and disruption 9-46604

Velocity continued**acoustic waves**

see also *Dispersion, acoustic; Helium/liquid, sound propagation; Shock waves*

alkanes, liq., mol. vel. temp. and press. depend. 9-42650
alkanes, liq., molecular sound vel., variation with temp. and press. 9-34904

anomalous change near mag. critical pts. 9-46989

n- and iso-butyl alcohol, temp. depend. 9-30401

films, thin, meas. tech. 9-37323

gas, dissociating and diffusing, propagation theory with particular cases 9-23398

in gases, low pressure, confined to tubes of circular cross section 9-46571
n-hexane, near saturation line 9-23466

inert gases, internol. potential parameters obs. 9-36733

invar, temp. and mag. field depend. 9-44817

isentropic sound vel. thermodynamics near 4 He superfluid transition 9-46674

liquids, meas. by resonance method 9-34901

liquids, relation with compression and density, expt. verification 9-42647
measurement method 9-45853

methane, liq., mol. vel. temp. and press. depend. 9-40789

in ocean, fluctuations, spatial correl. with ocean movements 9-31280

n-octane, liq., at const. density mol. vel. 9-40790

$\text{Pd}_{1-x}\text{Ag}_x$, doped with transition elements, torsional speed of sound obs. 9-30771

n-pentane, liq., at const. density mol. vel. 9-40790

photoconducting materials, electron-hole plasma interactions with lattice vibrations 9-26415

piezoelectric materials, electron-hole plasma interactions with lattice vibrations 9-26415

in plasma, multitemp. 9-23267

polycapromide fibres, temp. depend., infl. of processing method 9-24024

polyethylmethacrylate, press. and temp. depend. 9-35276

Rao's constant and molecular compressibility in liquids and their mixtures 9-30398

renormalisation at Curie point 9-39514

resonance method for meas. in liquids 9-34901

in saturated vapour, for critical temp. determ. 9-39128

toluene, at constant density 9-46633

toluene, liq., at const. density mol. vel. 9-40790

toluene, meas. along saturation line 9-44561

in water, distilled and sea, comments on previous determs. 9-29271

water, pure and sea 9-28120

m-xytol, at constant density 9-46633

$\text{Bi}_{12}\text{Ge}_{20}$, piezoelec., elasto-optic matrix elements for longit. waves 9-33394

$\text{Bi}_{12}\text{SiO}_{20}$, piezoelec., elasto-optic matrix elements for longit. waves 9-33394

Cd, ultrapure, mag. field dependence 9-35274

Cr steels, hardened, rel. to struct. 9-23755

Cs vapour, speed-of-sound meas. 9-32736

Cu, ultrapure, mag. field dependence 9-35274

He solid 9-23573

Kr, liquid, isotherms and effective at. radii, obs. 9-30396

MnF₂, near Neel pt. 9-44818

$\text{Rh}_x\text{Pd}_{1-x}$ doped with transition elements, torsional speed of sound obs. 9-30771

$\text{Sr}_x\text{Ba}_{1-x}\text{Nb}_2\text{O}_6$, ferroelec., elasto-optic matrix elements for longit. waves 9-33394

Xe, liquid, isotherms and effective at. radii, obs. 9-30396

acoustic waves, ultrasonic

see also *Dispersion, acoustic/ultrasonic*

alkali halides containing CN^- , and attenuation 9-37329

anthracene, elastic constants determs. 9-35143

electrolyte solns., molal compressibilities determ. 9-48696

ferroelectric solid solns. with perovskite struct., temp. depend. 9-41084

formic acid, temp. coeff. meas. with composite interferometer 9-23494

gases, temp. depend. of rot. relax. time 9-23397

gases temp. depend. of rot. relax time 9-23396

in human teeth 9-37327

in liquid metals, obs. from melting point to 900-1000°C 9-30395

in liquid, pulse-echo meas. and computer program 9-42649

liquids, hypersonic, temp. coeff. 9-30393

in liquids, modified method using u.s. interferometer 9-26095

liquids, speed meas. by semi-automatic method 9-46630

in plates, temp. depend., pulsed elec. interferometer obs. 9-46988

propionic acid, temp. coeff. meas. with composite interferometer 9-23494

1,2-propylene glycol, liq., hypersonic propag. obs. from stimulated Mandelstam-Brillouin scatt. 9-30399

quartz, fused, plates, temp. depend. 9-46988

in resonance absorption region, low-pulse, 10 GHz 9-25098

salts, inorganic, molar sound vel. evaluation 9-36868

$(\text{Sr},\text{Bi})_2\text{TiO}_5$ solid solns., polycrystalline temp. depend. 9-41084

steel, carbon, polycryst., total refl. technique meas. 9-35275

in steel, hardened ball bearing, rel. to residual austenite determ. 9-42911

stilbene, acoustic impedance calc., use as high temp. acoustic bond 9-26416

triacetin, liq., hypersonic propag. obs. from stimulated Mandelstam-Brillouin scatt. 9-30399

urea, sq. solns. 9-30400

water, distilled, 23° to 75°C, u.s. echo technique 9-29261

AgCl , velocity of ultrasound, eff. of pressures up to 100 kbar 9-24023

Al plates, temp. depend. 9-46988

Ar, 60-17000 MHz/atm., u.s. interferometer appl. 9-46572

$(\text{Ba},\text{Sr})\text{TiO}_5$ solid solns., polycrystalline, temp. depend. 9-41084

$\text{Ba}(\text{Ti},\text{Zr})\text{O}_3$ solid solns., polycrystalline temp. depend. 9-41084

$\text{Ba}(\text{Ti},\text{Zr})\text{O}_3$ solid solns., polycrystalline temp. depend. 9-41084

EuO , near mag. phase transition, vel. change with const. attenuation 9-24030

GaAs , temp. depend., determ. of effective mass of carriers 9-46999

GeTe-GaTe system, conc. depend. of propagation velocity 9-28417

^4He , velocity of sound at 1 MHz near critical point 9-36913

KCl, KBr and KI containing CN^- , and attenuation 9-37329

KTaO_3 temp. and freq. depend., interpret. w.r.t. soft optic phonon mode interac. 9-37328

NH_4Br , high-press. elastic const. and phase transitions determ. 9-30633

NaCl containing CN^- , and attenuation 9-37329

Nb plates, temp. depend. 9-46988

SbSI , dispersion along ferroelec. C axis at 10-30 Mc/s, 16-24°C 9-42960

Velocity continued**acoustic waves, ultrasonic continued**

$(\text{Sr},\text{Bi})_2\text{TiO}_5$ solid solns., polycrystalline temp. depend. 9-41084

light

faster-than-light particles, popular article 9-45748

Fizeau's results and the invariance of speed of light 9-25337

Fizeau's results and the invariance of the speed of light 9-27367

invariability, expt. to test validity of Einstein's second postulate 9-41744

laser interferometric experiment, JILA/NASA/NBS 9-25357

superluminal systems, violation of causality 9-47744

transparent media, moving, comment from speed of light invariance 9-29449

in vacuo, from laser wavelength and freq. meas. in i.r. and far i.r. 9-36281

wavelength independence in space, from meas. on Crab Nebula pulsar 9-41665

Velocity analysis, particles see Particle velocity analysis**Velocity measurement**

see also *Angular velocity measurement; Stroboscopes*

by Doppler effect combined with Schlieren method 9-38191

Doppler shifts method using optical radiation 9-47722

drift of structure with internal rearrangement, cross-correl. and cross-spectral methods 9-22044

droplets in water spray, rel. to concentration, Fabry-Perot obs. 9-42685

electron, low-energy, apparatus, patent 9-38611

electrons in annular beams 9-31913

in flows, high-speed 9-23834

galactic H spectral line source (r.f.), radial vel., astronomical unit determ. 9-29100

gas flow by elec. discharge 9-32718

holographic, of rapidly moving objects 9-31984

of interface, solid-liquid, by thermolec. probe 9-39210

meter to measure velocity on an air track 9-22043

plasma, Doppler determ. with photoelec. recording 9-40692

plasma flow, nonuniform, determination by measurement of induced potential 9-25854

three-dimensional flow-field velocity components, holographic meas. 9-48538

turbulent flow, non-directional probe design 9-46437

vector, 3D, and turbulence, laser Doppler method 9-43714

velocimetry, holographic, data processing methods 9-48539

CO_2 supercritical flow, turbulent vel. fluctuations, hot wire anemometer obs. 9-28172

acoustic waves

diffraction corrections from mean pressure acting on transducer as function of radiator and receiver dimensions 9-22250

in distilled water, for study of structure change 9-40772

elastic, in medium with random inhomogeneity distrib., accuracy 9-26874

in gases, confined, const. geometry amplitude detect. method 9-30347

in Kundt's tube, thermistor obs. 9-45723

relative vel. changes of GHz waves at low temp., meas. tech. 9-36178

in seawater, accurate eqns. development 9-47521

acoustic waves, ultrasonic

in liquids, interferometric method, effect of diffraction 9-46631

changes in vel., high loss materials, pulse transmission technique 9-22255

c.w. technique for automatic meas. 9-43786

differential method using u.s. and clock impulse coincidences 9-43785

diffraction effects 9-47822

echo phase comparison technique, results for water 9-29261

guided wave propag., multimode, interference with phase delay meas., remedy 9-36179

high-precision velocimeter 9-48696

interferometer, for rarefied gases, up to 20000 MHz/atm. 9-46572

liquids, elec. interference method at 0.7-30 MHz 9-46628

pulse-echo-overlap, modified method, for vel. and attenuation in solids 9-30769

pulses, in presence of noise, coherent detect. and signal averaging techniques 9-29272

solids, pulse-echo-overlap modified method 9-30769

light

Kerr cell phase-shift method using low modulating freq. and simple circuitry 9-48079

Venus see Planets**Verdet constant see Magneto-optical effects****Verneuil process see Crystals/growth****Vertex functions see Elementary particles; Field theory, quantum; Functions****Vibrating bodies**

see also *Crystals/lattice mechanics; Elastic waves; Pendulums; Piezoelectric oscillations*

beam, centrally loaded, nonlinear free vib. 9-29251

beam, ends elastically restrained, finite transform soln. 9-22238

beam, thin-walled elastic, dynamic stability of flexural vibrations 9-40274

beam grid, infinite, free and forced vibrs. anal. 9-25088

beams, compressed, bending frequencies 9-29250

beams, ends clamped and supported, nonlinear free vibrs. 9-31840

beams, nonuniform, orthonormal props. of mode forms 9-31841

beams, uniform, response to homogeneous random press. fields 9-29247

beams, uniform, transverse freq., effect of non-homogeneity 9-22234

beams response under concentrated moving masses 9-31828

cantilever laminated beam, energy dissipation due to slip theor. 9-25090

chin, hanging, three lowest natural freqs., derivation 9-27216

circular rigid, on infinite elastic stratum, torsional 9-41812

column, axially loaded, dynamic stability under stochastic excitations 9-22228

crystal, neutron diff. obs. 9-48823

crystal, spectral characts. rel. to direction of exciting elec. field 9-41251

crystals, X-ray diff., theory 9-35041

cylinder, viscoelastic, under magnetoelastic torsion 9-29235

cylindrical shell on three supports, method of minimizing Lagrangian 9-34076

cylindrical shells, axisymmetrical motions, anal. inc. rotary inertia and shear correction factor 9-22227

elastic beams natural frequencies analysis, with random imperfections 9-43782

electrodes, electrochem., ionic mass transfer obs. 9-47465

excited by solid CO_2 , determ. of resonant frequencies by recording and comparing to oscillator 9-29240

Vibrating bodies continued

- excited by sound sources in their neighbourhood 9-29239
framed structure, existence of dual with same natural frequencies 9-22239
fuselage panel with fatigue crack, characts. 9-40273
girders, continuous, natural freq. and critical axial load 9-34062
helicopter blade, flutter in forward flight 9-23387
Helmholtz integral, vanishing of surface-press. contrib. 9-29243
interactive method of soln. to relevant eqn 9-38291
interference holograms, stroboscopy method 9-31843
lipid-cholesterol spherical, normal mode vibrs. 9-41816
membranes, skew, natural freqs. and modes 9-29249
normal modes of masses connected by springs, symm. props. 9-22232
oscillators, weakly anharmonic, for pulse amplification 9-34114
piezoelectric plates, electromech. coupling const. rel. to fundamental material const. 9-37593
plate, infinite, free vibr. modes based on linear coupled theory of thermoe-
lasticity 9-22237
plate, infinite, isotropic, elastic, with vertical harmonic load 9-45842
plate, rectangular, with attached mass constraints, freq. and mode shapes
determ. 9-34078
plate, rectangular orthotropic, flexural vib. sine series soln. 9-31842
plate, square, degenerate modes, influence of nonlinearities 9-29241
plate damping, h.f., due to gas pumping in riveted joints 9-29245
plates, laminated, vibr. characts, calc. using transform. matrix 9-25089
plates, loss factor meas. 9-40275
plates, loss factor meas. 9-41815
plates, quartz, AT-cut, beveled, thickness-twist vibrs. 9-29259
plates, rib stiffened, flexural vibrs., shear and rotary inertia effects
9-29242
plates, transverse normal modes, excitation methods 9-22225
plucked string, theory 9-43703
quartz plate, AT-cut, with metallic electrode strip, shear-flexure-twist
vibrs. 9-22236
rigid-viscoplastic strain hardening annular plate, impulsively loaded
9-22240
rod, edge vibrs. effect on propag. of strain transient 9-29248
rods, aluminium, square and circular cross sections, vel. dispersion
9-27218
roller bearings, axial testing method for noise qualities determ. 9-29299
sandwich panels in supersonic gas flow, dynamic stability 9-22231
shaker, piezoelec. for calib. of vibr. pickups 9-38295
shell, thin, cylindrical, end response to extensional waves 9-29244
shells, conical, ring- and stringer-stiffened, resonant frequency determ.
9-45840
shells, cylindrical, thin, with thickness discontinuity 9-41813
shells, spherical, of deolotropic mats, stresses due to radial and rotary vibrs.
9-22230
shells, spherical fluid-filled; frequency spectra 9-45841
solids, damping props. by a nonlinear viscoelastic law 9-47819
spherical shell, fluid-filled, axially symmetric vibrations 9-27213
spring-mass system, non-linear, subject to const. force excitation, response
9-41814
steel, microcracks initiated by 17.8 kc/sec 9-35190
stiffened cylinders with symmetrically distributed stringers, comp. pro-
gram. 9-22241
string stretched, large amplitude damped free vibr. 9-27217
surface displacement phas meas. using Michelson interferometer with laser
source 9-43781
tapered cantilever beams and shafts, characteristics by lumped inertia force
method 9-38294
turbine blades, possible meas. with laser Doppler system 9-41811
viscoelastic rod excited by linear oscillator, longit. and transverse vibrs.
9-40272
wing in transonic flight, calc. of forces 9-23388
Fe microcracks initiated by 17.8 kc/sec oscillations 9-35190

Vibration, molecular *see Molecules/vibration*

Vibrations

- see also Acoustics; Damping; Oscillations; Vibrating bodies; Waves*
anharmonic oscillators, coupled, 2D, approach to thermal equilib., com-
puter studies 9-31777
beams, transverse vibrs., natural freq. evaluation using Timoshenko theory
9-36170
bubbles in blood subject to fluctuating pressure 9-46603
cylindrical shell, nonlinear flexural vibrations, modal eqns. 9-22174
cylindrical shells, axisymmetrical motions, anal. inc. rotary inertia and
shear correction factor 9-22227
damped mechanical systems, book 9-25087
elastic bending in bars, propag. 9-34079
elastic layer, displacement and freq. expansion, asymptotic analysis
method 9-34077
flexible shell, anal. using concept of finite elements 9-31807
flexural, of thin-walled elastic beam, dynamic stability 9-40274
forced, of anisotropic cylinders 9-29238
forced tangential and rotatory, of rigid circular disc on semi-infinite solid
9-22233
insulation, flexural wave transmission across elastic spacers at plate junc-
tions 9-22242
interactive method of soln. to relevant eqn 9-38291
magnetospheric, resonant with 300 sec. period, Explorer 26 obs. 9-43419
music, basis for its concept in the vibrating string 9-40199
plastic plate, reinforced, input impedance determ. 9-37227
plates, freq. calc. using finite element method 9-22235
quartz, thickness-shear, Bechmann's number for harmonic overtones
9-31848
random, of thin elastic plates 9-29252
relaxation effect on shock wave limiting layer 9-45869
steady plane coupled micropolar thermoelastic, integral eqns. 9-45834
thickness-twist, in quartz, AT-cut, beveled plates 9-29259
vibration, torsional, of rigid circular body on infinite elastic stratum
9-41812
viscoelastic rod excited by linear oscillator, longit. and transverse vibrs.
9-40272
excitation
column under axial stochastic load, dynamic stability, Lyapunov-type
anal. 9-22228
longitudinal, two-material cable system, dynamic stress and displacements
9-45843
plates, transverse normal modes, surface or end excitation, investigation
9-22225

Vibrations continued**excitation** continued

- vibrator, piezoelec., remotely controlled, for low temp. region of cryostat.
9-34080
vibrator, tubular, with lumped masses at ends, use as viscometer 9-22226
in CdS, elastic, for elec. conducting sample 9-44763
measurement
see also Seismology
combination mode vibr. patterns, meas. by hologram interferometry
9-38292
displacement phase meas. using Michelson interferometer with laser
source 9-43781
holographic, using Powell and Stetson fringes 9-22434
interference holograms, stroboscopy method 9-31843
for internal friction, strain depend. of transverse vibrs., calc. method
9-31810
laser interferometry with heterodyne detection 9-31970
laser technique 9-45839
mechanical admittance, modified rapidly converging modal series
representation 9-29237
Mossbauer velocity drive, vibration detector 9-36169
phase meas. by rot.-stroke holography 9-43792
shells, conical, ring- and stringer-stiffened, resonant frequency determ.
9-45840
surface modal patterns, obs. by laser speckle 9-42710
turbine blades, by laser Doppler system 9-41811
CO₂ excited, determ. of resonant frequencies by recording and comparing
to oscillator 9-29240
by He-Ne laser speckle pattern obs. 9-38293

Vibronic states *see Molecules/electronic structure; Molecules/vibration*

Vidicons *see Electron tubes*

Virial coefficients *see Equations of state*

Virtuons (virtual phonons) *see Crystals/lattice mechanics*

Viscoelasticity

see also Plasticity

- additive in liquid flow rel. to turbulent drag, reduction, mechanism
9-42621
adhesion of materials to rigid substrates, peeling force meas. 9-35239
bar, cyclic loading, a second order strain accumulation 9-27207
binary mixtures of pure liquids, relaxation obs. 9-26064
bitumens in rubber transition zone, u.s. absorption and dispersion
9-30450
columns, parametric resonance, analytical and expt. 9-45831
composite systems, dynamic moduli, bounds for real and imaginary parts
9-31836
Couette viscometer pseudo-flow curve, transformation into real curve
9-31835
creep buckling of beam column, isothermal conditions, soln. bounds, com-
puter determ. 9-38287
cylinder, hollow circular, axially symmetric plane strain problems
9-47814
cylinder, magnetoelastic torsional vibration 9-29235
elasto-viscoplastic solid, effect of time rate of change of temp. on behavi-
our 9-25066
fluid, boundary-layer flow, equation 9-36836
fluid, macromolecular, network model 9-38940
fluid flow in wavy cyl. tube, heat transfer obs. 9-27953
fluid flow near stagnation point 9-23431
Foigt and Maxwell media, relative deform. and stress due to temp. changes
9-28334
Green-Rivlin representation for nonlinear materials, accuracy 9-45832
Hertzian frictional contacts, behaviour under ramp-type loads 9-41003
inelastic inclusion in elastic or viscoelastic matrix 9-31819
linear viscoelastic materials, creep and relax, tests, error functions
9-33019
liquid, balance rheometer theory for meas. of complex viscosity 9-32755
liquid, high-viscosity, distinction from plastic solid by microscopic flow
processes 9-28353
Maxwell fluid, flow bet. torsionally oscillating discs 9-25814
Maxwell fluid, flow due to torsional oscillations of plane 9-23239
Maxwell solid, disturbances due to mag. field 9-29236
network model for viscoelastic macromolecular fluid 9-27948
non-Newtonian media, hydrodynamic equations investigation 9-36829
nonlinear viscoelastic bodies with hidden parameters, deform. uniqueness
9-27209
poly-n-butylacrylates, four, relax. obs., -40 to 148°C 9-23430
polyethylacrylates, four, relax. obs., -40 to 148°C 9-23430
polymer solutions and melts, nonlinear model 9-23432
polymers, crosslinked, effect of blending sol. and gel fractions 9-46708
polymers, high, storage and loss moduli, meas. method 9-33020
polyurethane, nonlinear viscoelastic, stress relax., torsion creep 9-31838
properties of heterogeneous media 9-31837
rings, dynamic load factors rel. to solid viscosity 9-29234
Rivlin-Ericksen fluids, conditions for validity Squire's theorem for stability
of parallel flow 9-40757
rod excited by linear oscillator, longit. and transverse vibrs. 9-40272
rubber, styrene-butadiene, nonlinear non-isothermal behaviour 9-28333
rubber vulcanizates, stress relax., simple model 9-30645
rubber-sulphur systems, comparison of viscoelastic and dielectric props.
9-33376
stress analysis, numerical method 9-27210
stress meas. in solid, u.s. technique 9-37222
stress waves, thermodynamic influences 9-22221
thermoviscoelasticity, coupled, linear theory, theorems 9-40271
Volterra operators algebra applic. 9-22220
wave propag. solns. from superposition principle 9-27208
Al subject to tensile creep with stress variation 9-39422

Viscometers

- absolute, for use in systems with limited access to liquid 9-23468
coiled capillary, helical, 200 foot stainless steel 9-36825
correction to constant for master viscometer on account of surface ten-
sions 9-28104
cylindrical, for viscosity of road binders, 10⁸-10¹¹ poises 9-44551
high press. for viscosities between 1 and 10⁴ P 9-30377
for highly viscous heterogeneous liquids 9-42638
horizontal plate conductivity meas. app. modified to find conduction/con-
vection transition 9-36813
low-shear-rate, press. <120000 lb-in² 9-36740
Newtonian fluids, review of meas. methods 9-36822

Viscometers continued

- oscillating disc method giving different results from capillary flow method 9-36823
- plate, undamped lengthwise vibr., meas. theory, technique and appl. 9-23467
- for powder flow characteristics meas. 9-23610
- quartz-crystal, resonant freq. changes with pressure to 8000 atm. 9-41809
- vibrator, tubular, with lumped masses at ends 9-22226

Viscoplasticity *see Plasticity***Viscosity**

- binary mixtures near critical point, kinetic phen. 9-48735
- bubbles in blood, vibrating, effect on resonance frequency curves 9-46603
- coefficients tensor statistical determination 9-36746
- composite viscoelastic systems, shear and bulk, bounds for real and imaginary parts 9-31836
- cylindrical tube obeying Stokes' law, hydrodynamic field of ellipsoid of revolution 9-32565
- dissipation effects in natural convection at high Prandtl numbers 9-25127
- in Earth's mantle, effect on thermal convection 9-24613
- eddy, concept and constraints 9-34717
- eddy, conference 9-34094
- effective magnetic viscosity field, physical meaning 9-33875
- electron gas in metals, shear, corat.-function calcs. 9-49011
- film, adsorbed, with slowly rotating disc, velocity field meas. 9-34714
- fluid, macromolecular, network model 9-38940
- fluid oscillations in viscous incompressible sphere, own gravitation and surface stress 9-23214
- glass, high pressure effects 9-28193
- glass, mixed alkali, non-linear variation due to alkali oxide replacement 9-39148
- heat and mass transfer in systems with turbulence promoters or packed beds, effect of forces 9-25804
- laminar flow near the entrance and exit of a pipe 9-34715
- latex particles, sulfonated, secondary electroviscous effect calc. from zeta pot. 9-32801
- lubricated contacts, rolling/sliding, viscosity variations calc. 9-31862
- magnetic, of magnetite, rel. to demagnetizing field 9-38011
- magnetic fluid in mag. field 9-48532
- measurements on various substs, conference 9-26014
- mixture, binary, variational calc. of coefficient 9-27192
- negative, introduced and applied to the earth's atmosphere and galaxies, book 9-32564
- non-Newtonian media, hydrodynamic equations investigation 9-36829
- poly(diethylene glycol methacrylate) and its copolymers, effect of hydroxyl endgroups 9-32547
- poly(ethylene glycol methacrylate) and its copolymers, effect of hydroxyl endgroups 9-32547
- polystyrene, plasticized with esters of aromatic dicarboxylic acids, viscosity and glass temp. 9-23901
- polyvinyl chloride, unplasticized, 100-180°C 9-30652
- silica, Brazil quartz, 1600-2480°C 9-30470
- skin friction in laminar Couette flow near critical point, with heat transfer 9-23374
- slab of fluid, depth depend., free boundary soln. rel. to isostatic adjustment 9-47504
- sublayer, turbulent fluctuations 9-23212
- turbulence of incompressible viscous fluid at high Reynolds number 9-28085
- turbulent variation, effect of generation, diffusion and convection 9-32574
- variable pseudoviscosity, one-dimensional hyperbolic difference schemes 9-34708
- variational methods applic. to viscous heat conducting flows 9-23228
- viscometers, high viscosity meas., for non-Newtonian fluids and semi-solids 9-42476
- Hg annular cylinder, current carrying, rel. stability 9-23250
- O₂, liquid, rel. to press. and temp. 9-46619

gases

- calculation techniques in dilute gases 9-36819
- in canals, narrow, viscous flow with heat transfer, integral correlation method 9-32721
- rel. to collisions, inelastic, 10⁴°K 9-34841
- data discrepancies for simple gases 9-26043
- dilute gases at low temp. 9-44529
- dilute polar gases, averaged potentials 9-42615
- dipolar, initial press. depend. 9-34835
- drag correlations for hypersonic low-density spheres and cores 9-26005
- flow, axisymmetric hypersonic, over slender body, theory incl. power-law variation 9-25999
- flow through porous materials 9-26042
- heat transfer from hypersonic, laminar flow to blunt cone 9-36800
- lar, by oscillating disc method, exp.6 exponential-6 potential preferred 9-36823
- linear polar molecule gas, electric Senftleben-Beenakker effect 9-48644
- mixtures, compressed nonreacting at high temp., calc. 9-40754
- Newtonian fluids, review of meas. methods 9-36822
- plasma, approximate calc. methods 9-42486
- polar (mixed) gases, used to determ. coeffs. of mutual diffusion 9-36827
- polyatomic gas in mag. field, 5 shear viscosity coeffs. determ. 9-46577
- quantum corrections to shear viscosity in moderately dense gas 9-34834
- rarefied gas, extrapolation to moderately high temperatures 9-36821
- Senftleben-Beenakker effect, for linear polar molecule gas 9-48644
- Van der Waals gas near critical pt., anomalous bulk and shear viscosity behaviour 9-26041
- Ar, calc. by eqn. 9-30355
- Ar at atmospheric pressure, determ. over 3500 to 8500°K 9-26044
- Ar plasma, obs. up to 12×10¹⁰°K 9-38964
- CO₂, meas. by oscillating disc method, Lennard-Jones potential fit 9-36823
- D, 20.4°K to 300°K, constant density 9-36824
- He-CO₂ gas mixture, absolute viscosity determ. using 200 foot stainless steel capillary 9-36825
- He, Lennard-Jones (6-9) potential calc. 9-26045
- He meas. by oscillating disc method, Lennard-Jones potential fit 9-36823
- Kr, potential parameters from viscosity and second virial data 9-34838
- Kr calc. by eqn. 9-30355
- Kr meas. by oscillating disc method, Morse pot. fit 9-36823
- N₂, in mag. field, 5 shear viscosity coeffs. determ. 9-46577

Viscosity continued**gases continued**

- N₂ meas. by oscillating disc method, exp.6 pot. fit 9-36823
- N plasma, calculation 9-36754
- Ne calc. by eqn. 9-30355
- SO₂, dimethyl ether and ethyl chloride binary and ternary mixtures 9-36817
- Xe calc. by eqn. 9-30355

liquids

- see also Lubrication; Superfluidity*
- alkali-metal chloride aq. solns., rel. to nuclear spin-lattice relax. 9-44593
- p-azoxyanisole nematic liquid crystal, Leslie's coeffs, calc. from scatt. of laser light 9-40793
- behaviour near critical point 9-36852
- boundary layers, anomalies 9-48685
- bulk viscosity, model 9-36850
- classical, expression deriv. from molecular model 9-34869
- cyclohexane-aniline mixture, shear viscosity obs. near critical point 9-32771
- detergent films, effect on flow props. 9-23446
- drag, 2 dimens. bodies near free surface 9-26081
- drag experienced by sphere with vel. depend. on single time scale 9-26080
- elastico-viscous liq., balance rheometer theory for meas. of complex viscosity 9-32755
- of elastoviscous liquids, superposed, rel. to stability of Couette flow 9-32747
- electrolytes in system of capillaries, viscosity meas. 9-26832
- fused salts, effect of internal Coulomb field 9-32770
- hydrate melts, temp. depend. meas. 9-28105
- isobutynic acid-water binary mixture at critical conc., anomalous shear viscosity 9-48687
- kinetic theory in local equilibrium model 9-23486
- Langevin eqn. for shear viscosity in monatomic liquids 9-34883
- liquid-solid heterogeneous system, over whole range of solid conc. 9-28162
- long waves, non-linear, viscosity effect 9-34859
- magnetic colloids, magnetoviscosity 9-48722
- measurement, for highly viscous heterogeneous media 9-42638
- metals, shear and bulk, rel. to isotopic mass and classical theory 9-30376
- Newtonian fluids, review of meas. methods 9-36822
- oil, index improver by alkyl acrylate and fluoroalkyl acrylate copolymer, patent 9-23192
- organic, effect of ultrasound 9-42637
- paraffins, linear and cyclic, rel. to mol. structure 9-25776
- pipe flow, turbulent, average vel. distrib. rel. to viscous sublayer 9-46590
- poly(propylene oxide) solutions, conc. depend. of viscosity 9-28109
- poly-N-isobutylmaleinimide, monomeric units per segment 9-23193
- polybutadienes, stereoregular Ziegler rel. to mol. wt., microactivity, obs. 9-30379
- polyelectrolytes, intrinsic 9-32772
- polyisoprene, solns., meas. 9-48524
- polymer chains with excluded vol. effects 9-36731
- polymer coil, non-draining dil. soln., depend. of shear rate 9-28107
- polymer melt, hydrostatic press. depend., extrusion rheometer, 190°C 9-39082
- polymer melts, cone and plate rheometer for meas. 9-46618
- polymer solns., dilute, rel. to molecular entanglement and relaxation time 9-46615
- polymer solns., excluded-vol. effects on limiting viscosity number 9-36849
- polymer solns., solvent depend. of rheological behaviour 9-28108
- polymer solns., wormlike chains 9-27927
- polymer solns. intrinsic value, theory and expt. 9-48684
- polymer solns. intrinsic viscosity and Huggins const., extrapolation calcs. comparison 9-34884
- polymer solutions, extension of Zimm's theory 9-32773
- polymers, intrinsic value in mixed solvents 9-46620
- polymers, low mol. wt., intrinsic viscosity, obs. 9-28106
- polymers, properties acoustic meas. 9-36835
- polymethylmethacrylate soln., minimum in shear stress depend. of viscosity 9-32774
- polystyrene sol, electroviscous effects in dispersions of monodisperse latices 9-23551
- polystyrene solns., 23-300 MHz 9-48688
- polystyrene-polybutadiene block copolymers, dilute soln., 34.2°C 9-39086
- rotations, non-stationary, linearized 9-32744
- shear viscosity in monatomic liq., Langevin eqn. derivation 9-34883
- shear viscosity of simple liq. mixtures, model 9-36851
- shell-liquid impact, relative importance in anal. compared with compressibility, gravity and shell density 9-22186
- silica, Brazil quartz, 1600-2480°C 9-30470
- silicone gum viscous sphere on flat surface, from flow due to gravity 9-32745
- stratification role in two-layer flow down an incline 9-23420
- stratified, hydrodynamic stability of free-surface flows 9-26051
- styrene-butyl methacrylate graft copolymer 9-32553
- styrene-methyl methacrylate graft copolymer 9-32553
- surge in bathtub vortex, effect on speed 9-26060
- temperature and volume, independent variables of state 9-42640
- temperature dependent, velocity profiles and heat transfer for laminar flow 9-26083
- tetrapropylammonium tetrakisfluoroborate, anomalies of analogues 9-42640
- toluene, effect of ultrasound 9-42637
- viscous flow in canal bounded by two porous concentric circular arcs 9-26082
- water, anomalous, higher than normal water 9-40771
- water, temp. depend. obs. 9-39081
- water dynamic viscosity eqn. 9-36853
- Ar-Kr simple mixtures, shear viscosity 9-36851
- B₂O₃, pressure depend., 380° to 465°C 9-26084
- BeF₂-LiF molten solns. 9-42639
- Cd(NO₃)₂-glycine-water system, cpd. existence from viscometric and densimetric obs. 9-23461
- D₂O, 0-150°C, 1-1200 kg/cm² pressure range 9-23470
- Ga, melting process, viscometric investigation 9-40818
- H₂O, 0-150°C, 1-1200 kg/cm² pressure range 9-23470
- H₂O, eddy distrib. and velocity in wall region of turbulent pipe flow 9-26054

Viscosity continued
liquids continued

- He, by sound meas. 9-26141
 He changes due to ion size increase near gas-liquid critical point 9-46672
 He II, roton-roton contribution calc. 9-44607
³He, calc. using ground-state energy and quasiparticle energies and interaction function 9-34940
³He in ⁴He, dilute solutions, 0.1-1.2°K 9-26143
⁴He, 2-50°K 9-46665
 Hg, coeff., temp. depend. 9-32762
 Hg, Tl₂, melting process, viscometric investigation 9-40818
 K-NH₃ solns., vacancy calc. 9-48686
 K up to 1500°C 9-40780
 Kr-Ar simple mixtures, shear viscosity 9-36851
 Li up to 1500°C 9-40780
 Na borosilicate glasses, phase-separated, viscosity and transform. temp. 9-46680
 Na up to 1500°C 9-40780
 Pb-Sn alloys, absolute, as function of temp. and composition 9-30378
 Pb, absolute viscosity as function of temp., liquidus to 500°C 9-30378
 Se-Te system, single cryst. growth phenomena 9-36997
 Sn, absolute viscosity as function of temp., liquidus to 500°C 9-30378

Viscosity *see Atmospheric optics***Vision**

- see also Colour vision; Eye*
 after-image of square, fragmentation 9-33966
 auditory thresholds during stroboscopic visual stimulation 9-38142
 background light and intense field after effect do not act in same way 9-24979
 binocular, coordination and convergence 9-33965
 brightness, apparent., effect of surround field to which observer is preadapted 9-24977
 brightness function, psychophysical, linearity 9-24978
 brightness of background variation with angle at which light impinges on retina 9-24976
 cat, effects of bilateral frontal lesions 9-24986
 contrast threshold meas. with sine-wave gratings 9-36086
 cortical response to checkerboard seen through various lenses 9-24970
 detection and identification of compound stimuli, spatial interactions 9-24975
 discrimination of two-pulse-interval differences, data 9-38154
 electroretinographic response to light stimulus 9-31713
 electroretinographical variability rel. to b wave duration 9-29127
 energetic theory aspects, review 9-31715
 extrafoveal, partial and full accommodation thresholds 9-40211
 eye pathology rel. to pictorial art 9-31714
 field of view, elliptical geometry and parallel postulate 9-33971
 flicker temporal summation 9-27135
 flickered stabilized retinal image, visibility 9-24972
 foveal acuity-luminance relns. for grating test object, effect of wavelength 9-27133
 head movements, translational during steady fixation 9-29129
 high luminance aversion 9-29132
 human, size detecting mechanisms, obs. 9-29130
 human pupil contraction, latency var. due to stimulus and/or adaptation level 9-27131
 iguana, props. of parietal eye 9-24987
 image formation, review 9-29125
 luminance change, visibility in presence or absence of boundary 9-29128
 Moire expt. with random dots 9-47701
 monocular fixation, target size effect 9-36085
 monocularly perceivable symmetry, suppression during binocular fusion 9-38156
 neurons, cortex, response to stimuli during rapid eye movements 9-29134
 orientation of lines, perceived relative to real 9-24969
 pattern recognition, model 9-31718
 perception of an octave 9-27132
 perception of moving, spatially periodic, intensity distributions 9-24965
 peripheral glare, role in narrowing pupil and improving focus 9-24973
 Pulfrich effect with minimal differential adaptation of eyes 9-24966
 quantitative models, discussion 9-29126
 real and apparent movement 9-45706
 response of dark adapted retina, time changes 9-33968
 response to time step of luminance 9-31717
 retinal sensitivity, perimetric, in young children 9-24980
 S-potential and receptor potential, physiological basis 9-24974
 scaling optic nerve impulse rel. increment thresholds 9-41717
 scotopic thresholds, meas. methods comparison 9-31716
 sensitivity, differences in individual sine wave response 9-29131
 stabilized image, visibility rel. to freq. and amplitude of luminance variation 9-33969
 stereoscopic acuity and horizontal angular distance from fixation 9-45705
 stroboscopic movement perception difference between monocular and binocular 9-24968
 tempered resolution, two-pulse meas. method factors 9-24967
 threshold for black barred pattern, rel. to that of homogeneous field 9-24971
 threshold suppression due to saccades 9-33970
 thresholds, absolute, rating scale expt. 9-33967
 transfer function of eye, sine wave gratings tests 9-49611
 vernier acuity and intersaccadic interval, relationship 9-27134
 visibility of sinusoidal diff. gratings modulation thresholds rel. to spatial freq. 9-34206
 visual threshold, rel. to size of surrounding field 9-24964
- Vitreous state**
see also Glass
 anthracene solidified solns., absorpt. spectra, aggregates existence obs. 9-46701
 cast vitreous-crystalline materials in different compositions, thermophysical properties 9-39525
 chalcogenide glasses, elastic consts., softening temp. and struct. 9-48744
 cyano-(19) anthracene solns., absorpt. spectra, aggregates struct. obs. 9-46702
 ice, short ordering range and transform. to diamond cubic struct. 9-46699
 metastable oxide phases obtained by rapid quenching, expt. and theory 9-23612
 polymers, high elastic state, friction depend. on temp. 9-27931
 porcelain enamels, TiO₂ opacified, reflectance and colour 9-37687
 silica, acoustoelastic effect 9-35141

Vitreous state continued

- silica, Brazil quartz, viscosity 9-30470
 silica, metastability of high cristobalite 9-48932
 silica, Stokes-Raman spectrum, temp. depend. 9-49297
 vitreous-crystalline materials based on ferroelectrics, props. 9-39676
 water, vitrification temp. estimate 9-23584
 B₂O₃-PbO-Al₂O₃ system, spinodal decomposition 9-39492
 C. combustion kinetics in low O₂ press. 9-26815
 C. glassy, deformation-induced anisotropy 9-39147
 C monofilaments, glassy, struct. isotropy 9-28195
 CS, solid polymer, structural and elec. props. investigation 9-34975
 C₆(NO₂)₆, KNO₃ melts, high-press. elec. cond. 9-39113
 GeO₂, neutron diffraction patterns 9-28269
 GeO₂, vibrational analysis using i.r. absorpt. and reflection spectra 9-28196
 K₂O-SiO₂ system, elec. conduction and phase separation by electron microscopy 9-41156
 Se, hole Hall mobility and trap parameters determ. in multiple trapping case 9-39668
 SiO₂, H⁺ transport during H₂ permeation 9-46856
 SiO₂, neutron diffraction patterns 9-28269
 SiO₂, pile-exposed, ionization expansion 9-35175
 ZnO-B₂O₃ syst., lamellar glass-cryst. structures from eutectic solidification 9-36930

Vlasov equation *see Plasma***Vocoders** *see Speech***Voigt effect** *see Magneto-optical effects***Volta effect** *see Contacts, electrical***Volume measurement**

- gases, PVT meas. up to 10 kilobars, apparatus 9-30333
 Hg-In alloys, liquid, vol. change on formation 9-28115
 ND₂Br specific vol. determ. by hydrostatic weighing dilatometer, 20°-140°C 9-33141
 NH₃Br specific vol. determ. by hydrostatic weighing dilatometer, 20°-140°C 9-33141

Vortices

- see also Cavitation; Turbulence*
 atmospheric, mesoscale with vertical axis, non-stationary problem 9-35814
 atmospheric, small-scale eddy momentum processes in westerly wind field 9-41498
 in atmospheric shear flow with friction, motion 9-41500
 bathtub, speed of surge, effect of circulation, geometry and viscosity 9-26060
 convective, cellular structure 9-45489
 Couette flow, rotating, periodic structure and wavelengths rel. to wave-forms and mean flow 9-34726
 cyclone development, potential vorticity field 9-47536
 electrical, in plasma, induced by e.m. field 9-27995
 flow, viscous, around circular cylinders, vorticity and stream functions 9-26061
 incompressible, breakdown flow field 9-32752
 liquid, elec. current effect on cavitating street, cylinder-wake 9-48676
 MHD radial-vortex motion 9-38952
 pattern, symmetrical, at edge of rotating disk in liquid 9-32753
 plasma MHD vortex flows, double, axially traversing multipole fields 9-32607
 quantized vortex lines, detection in rotating He II 9-28166
 rotation generated, in Rayleigh's problem 9-48536
 supersonic trail behind blunt bodies 9-42590
 tangled vortex lines, degree of knottedness 9-34712
 Taylor, with eccentric rotating cylinders, torque and crit. speed meas. 9-30177
 Taylor, in rotating couette flow, wave-number selection 9-34724
 transport in shock tubes, rel. to boundary layers 9-45868
 turbulent vorticity, direction of maximum in shear flow 9-25818
 vortex shedding and wake form. behind inclined flat plate, low R obs. 9-34845
 He films, surface effects 9-26142
 He II, rotating, quantized vortex lines, detection 9-28166
 He II film, vorticity associated with flow 9-48733
 *He, vortex ring creation in presence of ³He impurities 9-23558

Water

- see also Ice; Seawater; Steam*
 α -irradiated vapour, ion-mol. reactions 9-45428
 acoustic wave propag. in shallow isovelocity water 9-30390
 acoustic waves, u.s., vel., 23° to 75°C 9-29261
 adsorbed, effect on wetting props. of borosilicate glass, quartz and sapphire by hydrophobic liq. 9-34978
 adsorbed in Ti₃HGeO₁₆·4H₂O, n.m.r. obs. 9-33650
 adsorbed layers on critical surfaces, effect on critical surface tension of wetting 9-23437
 with AgI contained, rate of mass loss and freezing expt. rel. to droplet temp. determ. 9-40822
 air-water mixtures, concurrent flow down vertical pipes, expt. 9-26001
 anomalous, in capillaries, props. and struct. study 9-40771
 atmospheric, surface evaporation minus precipitation 9-49450
 atmospheric vapour, rot. structure in solar absorption spectra 9-24642
 binary mixtures with organic liquids, molecular motion from n.m.r. meas. 9-46654
 boiling, emission bands, phase transition luminescence 9-40797
 boiling, heat transfer depend. on e.m. field 9-23597
 bubbles, gas, in long-standing and tap water, size distrib. 9-46607
 t-butyl alcohol mixture, X-ray scatt. conc. and temp. depend. 9-28101
 carbon tetrachloride, electron scatt., cross section and spin polarization meas., E₀=60-1600 eV 9-23167
 cavitation, acoustic method of determining the distribution of air nuclei responsible 9-22264
 cavitation noise spectra from rot. bars. 9-26059
 cavitation scale formulae for reaction type turbines 9-34857
 cavitation threshold lowering by fast neutrons 9-46592
 cavities, empty spherical collapsing, flow field behind 9-23429
 chloride-containing high temp., effect on stress corrosion cracking susceptibility of austenitic stainless steels 9-26355
 cloud content, radio-astronomical meas. 9-24655
 clusters in vapour phase, H-bond energy determ. 9-44616
 condensation coeff., estimation from heat transfer meas. in dropwise condensation 9-23594
 conductivity and ionic dissoc., 100 kbar and 1000°C 9-44585

Water continued

- continuum model, interpretation 9-39074
 convection, natural, during turbulent flow at supercritical press. 9-26090
 convection in layer continuously formed by melting ice, onset 9-32781
 critical heat flux modeling, comparison with Freon-22 9-34736
 deep, long crested random gravity waves, mass transport 9-28857
 dielectric medium in Cherenkov counter for relativistic muons 9-22643
 dielectric permittivity and loss angle meas., industrial water 9-44580
 dielectric props., changes during adsorption by solids 9-48716
 diffusion coeffs. of inert gases 9-28112
 diffusion coeffs. of Ne, Kr, Xe, Co and No, 10° to 60°C 9-26086
 diffusion in apophyllite (KFCa₈Si₆O₂₀·8H₂O), p.m.r. study 9-47447
 diffusion in soda-lime glass near and within transform range 9-46854
 dimeric molecules in atmosphere, presence shown by sub. mm absorpt. expts. 9-33755
 dimethylsulphoxide-water system, phase diagram and stable hydrate form 9-32815
 discrete molecules in the vicinity of two oppositely charged ions 9-23462
 distilled, structure change using measurement of sound velocity 9-40772
 drop, in electric field, deformation and discharge 9-28146
 drop, on water surface, supported by air layer 9-30364
 drop producer giving uniform size drops at controlled intervals 9-47704
 droplets, collision, coalescence and disruption 9-46604
 droplets, intensity and polarization of scattered radiation 9-28888
 droplets freezing in free fall, shattering rel. to possible rotation 9-28181
 drops, 100 μ charged in nonuniform a.c. field, temp. estimation 9-40822
 drops, collisional charging wind tunnel expt. 9-31325
 drops, freezing, fragmentation in free fall 9-26898
 drops, large, containing AgI crystals, freezing temp. 9-42697
 drops, max. size on jet injection into N₂ or He gas streams 9-34864
 drops, nucleation at deep supercooling in He, H₂, O₂, Ar and CO₂ 9-26075
 electric breakdown, trigger spark effect 9-32709
 electrolysis in electrolytic cell with permeable electrodes, patent 9-28813
 electrolysis in electrolytic cell with porous electrodes patent 9-31207
 electron scatt., cross section and spin polarization meas., E_e=60-1600 eV 9-23167
 equation of state, 350-650°C, 165.37-1000 bar 9-30448
 equations of state, analytical and experimental, isothermal data fit, review 9-36844
 evaporation from soil 9-34854
 evaporation rate, retardation by hexadecanol monolayers 9-23591
 fast neutron spectrum obs. 9-22896
 field ionization 9-32691
 filtering through nonhomogeneous stratified soil 9-43364
 flow, cooling of power station pump, meas. by ²⁴Na tracer 9-28084
 flow, laminar, in vertical tubes, heat transfer studies 9-28114
 flow, Reynolds similarity, exactness investigation 9-25996
 flow, turbulent, in smooth walled pipe, wall press. field obs. 9-42627
 flow, turbulent at supercritical press., natural convection, heat transfer study 9-26090
 flow, vertical, temp. profile meas. along film 9-30384
 flow forced laminar, free convection influence in circular tube, uniform heat flux 9-25128
 flow in pipe turbulent, velocity and eddy viscosity distrib. in wall region 9-26054
 flow in square channel, turbulent, space-time temp. pulsations 9-39095
 flow in surface layers when evaporating from capillaries 9-44533
 flow past smooth wall with single projection, wall press. fluctuations, spectral characts. 9-46583
 flow speed in nuclear reactor, meas. by thermocouple noise cross-correlation 9-38740
 flowing through rock fracture, temp. 9-43353
 freezing of drops in hydrophobic liquid 9-34963
 freezing of hot and cold, comparison 9-42695
 gas chromatography detection using β -ionization detectors 9-33689
 gravity waves, scattering by circular dock 9-26069
 heat transfer in supercritical forced flow through curvilinear channels 9-26089
 heat transfer phenomena in natural circulation supercritical press. system 9-26091
 heavy, for deuterization of non-volatile compounds by isotope exchange 9-26804
 heavy, isotope content determ. by photometry 9-49392
 heavy water, i.r. laser irradi., Stark spectrum obs. 9-25766
 ice-water interfacial free energy and morphological stability theory 9-37102
 i.f. sound absorpt. in Lake Superior 9-28124
 industrial, dielectric permittivity and loss angle meas. 9-44580
 injection into compressed air, flow and temp. levelling rel. to droplet size 9-23435
 interface with air, effect of hydration on CO₂ exchange 9-30453
 interstellar, detection by its microwave rad. 9-41649
 ionization equilibria, 25°C, pressure eff. 9-42676
 ionospheric D region, cluster ions origin due to vapour reactions, lab. obs. 9-43457
 jet, turbulent, in still gas, core length rel. to nozzle config., obs. 9-42632
 lake surface temp. with and without monomol layer, airborne i.r. obs. 9-47515
 lasers, vapor population inversion mechanism in discharges, explanation of laser action, laser line data 9-22394
 i.f. molec. motions in ionic solns., neutron inelastic scatt. 9-44547
 light pulses, short, propag. 9-39101
 light scattering, enhanced, in Kerr cell under r.f. excitation 9-40792
 light scattering, small-angle multiple, loss of resolution in images 9-36878
 lower-lying excited states, ab initio calc. 9-23046
 lunar subsurface, distrib. rel. to sinuous rilles 9-36019
 mixture, isobutyric acid-water, at critical conc., anomalous shear viscosity 9-48687
 moderating system, pulsed with thermal neutrons, extrapolation length 9-34497
 modification at high pressure and temp. 9-26076
 molecular g value determ. and hyperfine structure 9-34618
 molecule, Coulomb and exchange integrals anal. using SCF expansion 9-23019
 molecule ground state, Hartree-Fock SCF minimal basis calc. 9-38844
 molecules, isotope-substituted, force constants determ. by known ratio of frequencies 9-48445
 molecules vibr. spectra in CaSO₄·2H₂O rel. to pot. environment, obs. 9-24391

Water continued

- Moon surface erosion, evidence 9-24843
 natural circulation, supercritical press. system, heat transfer phenomena 9-26091
 neutron diffusion, temp.-depend. on geometric parameter, meas. by pulse method 9-46251
 neutron diffusion length and age 9-22891
 neutron diffusion meas., 18-280°C 9-30380
 neutron scatt., slow inelastic 9-48681
 neutron scatt. in water cylinder, distrib. junction calc. 9-22841
 neutron wave propagation 9-34478
 oscillations in boundary layer, meas. by obs. tension in fibre suspended at right angles 9-32750
 penetrative convection, non-steady, simulating atm. inversion 9-34896
 phenol-water mixture, light scatt. meas. of conc. fluctuations near critical point 9-40794
 photolysis, rot. distrib. of OH*(² Σ^+) radicals 9-38867
 in polycaprolactam, effect on elastic relax. 9-33027
 radio occultation meas. from Mariner 9-49464
 radiolysis, charge separation and ionic processes 9-31214
 radiolysis, nanosecond pulse expts., nonhomogeneous kinetics rel. to [H₂O] behaviour 9-35756
 rainwater, salinity meas. by elec. cond., effects of temp., dust and de-ionization 9-34879
 Raman spectrum, stimulated 9-34911
 reaction of vapour with graphite single cry. in He, e. microscopic investig. 9-24537
 removal during industrial processes by high vacuum pump 9-38179
 in Rochelle salt, molecule dynamics from n.m.r. exam. in ferroelec. state 9-28765
 salt, stably stratified, laminar flow plast flat plate 9-26055
 saturation press. eqn., 0-374.15°C 9-32819
 scattering law for 0.05 eV neutrons, multiple scatt. and fit to McMurry-Russell model 9-27559
 self-diffusion and spin-lattice relax., temp. depend. 9-32778
 in solids, content determ. by neutron moderation 9-39972
 solvation of nitrate ion, i.r. spectroscopic evidence 9-42661
 sorption by crystalline nylon, mechanism 9-32851
 sound speed absolute meas., pure and sea water 9-28120
 specific heat at constant press., maxima fitting neither Ehrenfest's nor thermodynamic stability theory 9-36861
 spectrum, 22 GHz line, foreign-gas broadening 9-23045
 -steam heat transfer loop at Harwell, description 9-27242
 structurally modified, drop density meas. method 9-23464
 structure, effect of dimethylsulphoxide and dimethylsulphone in soln. 9-32763
 structure, Monte Carlo calc. using Rowlinson's intermolecular pair pot 9-34874
 structure at 25°C, X-ray diff. study and radial distrib. function 9-28099
 structure in urea solns. 9-30400
 supercooled, ice nucleation, time lag, activation energy, formation probability 9-32814
 supercooled, in hailstones, cavitation induced by u.s. waves 9-45491
 supercooled, induced freezing by physical stimuli 9-34957
 supercooled drops, AgI particle de-activation 9-42696
 supercooling and nucleation of droplets rel. to shock waves, pre-heating, aeration and elec. field, obs. 9-39134
 surface, ripple damping coeff. 9-36837
 surface waves, variable tangential stress effect 9-32756
 surface with air flow heat transfer coefficient, surface instability, temp. and vel. depend 9-34837
 temperature profile of thermal sublayer on Cu horizontal surface during pool boiling 9-23598
 temperature variation, daily, due to solar radiation absorpt 9-45478
 thermal conductivity and dynamic viscosity eqns. 9-36853
 thermal desorption from Ge in ultra high vac. rel. to surface states 9-35425
 thermal diffusivity, -40° to +60°C 9-42965
 thermal free convection from ice spheres, in water flow and heat transfer phen. obs. 9-23482
 thermal-neutron diffusion coeffs., from relax. lengths in poisoned samples and pulsed decay const. 9-27776
 toughening effect on MgO crystals 9-42906
 transient film boiling on horizontal submerged wire 9-28188
 turbulent flow in pipe, time characts. and temp. pulsation spectrum 9-26056
 turbulent flow of water in a pipe, tracer mixing obs. 9-28086
 turbulent thermal boundary layer, expt. study with forced convection 9-23424
 two-state model versus continuum model 9-39073
 vacuum u.v. spectrum of liquid 9-36884
 vapour, absorption between 0.5 and 36 cm⁻¹, line parameters and transmittance paths 9-34620
 vapour, absorpt. rel. to atm. anomaly, 337, 311 μ m 9-47547
 vapour, atmospheric, anomalous dispersion calculations 9-33774
 vapour, charge exchange with H ion beam, energies 1 to 60 keV 9-44493
 vapour, effect on e.s.r. of evaporated C film 9-39904
 vapour, excited H atoms prod. by electron impact 9-30151
 vapour, ν_2 band, twenty lines, strength meas. 9-36699
 vapour, penetration into photon counters, gas filters and gas discharge tubes used in vacuum u.v. 9-22368
 vapour, react. with graphite single cry. in He, e. microscope investig. 9-24537
 vapour, vibrational-rotational energy levels quantum mechanical calc., spectrum fine structure obs. 9-23049
 vapour absorption and wettability of high polymers and silica glasses 9-42736
 vapour absorption background, near 3811 cm⁻¹ 9-38845
 vapour absorption band, correl. between terrestrial radiation intensities, Cosmos 45 obs. 9-31315
 vapour absorption lines, 475-692 cm⁻¹ position, intensity and width 9-36701
 vapour adsorption as pore struct. analysis method, t-curves 9-35052
 vapour effect on sintering of glass powder compacts 9-33129
 vapour influence on ionization prod. in air 9-46534
 vapour ions, charge transfer cross sections 9-25967
 vapour laser, pulsed, undulation in output waveforms 9-25260
 vapour line, Venus, effect of cloud scattering 9-41679
 Venus, vapour variations, high-dispersion spectroscopic studies 9-27083
 Venus and Earth, vapour escape mechanisms 9-24876

Water continued

- Venus atmosphere, vapour microwave spectroscopy 9-24878
viscosity, 0-150°C, 1-1200 kg/cm² pressure range 9-23470
viscosity measurements, temp. depend., reported anomalies not obs. 9-39081
vitrification temperature estimate 9-23584
water hydronium ion system, isotopic abundances 9-48437
water vapour radiolysis by fission fragments, obs. 9-33684
water-glycol solutions of CuSO₄, u.s. absorpt. rel. to temp. 9-34903
waves, long standing, in curved canal, dynamics 9-26068
waves, shallow, directional variation due to arbitrary periodic surface press. 9-34858
wedge, 60°, collapse, path of particle 9-23376
X-ray forward scatt. coeff. 9-40770
Ar-water two-phase flow, adiabatic, phase and vel. distrib., obs. 9-46558
CO₂-H₂O mixtures emissivity, analytical calc. 9-26028
CO₂-N₂-He-H₂O glow discharge, spectra 2800-6500 Å, 3-7 torr 9-25979
D₂O-H₂O mixture, poisoned, scatt. kernels test by thermal neutron spectra 9-27788
D₂O-potassium oleate soln., n.m.r. study of smectic liq. cryst. phase 9-40775
D₂O, inelastic neutron scatt. at 300°K for energies to 0.65eV, energy-transfer cross-sections 9-28096
D₂O, molecular g value determ. 9-34618
D₂O, thermal-neutron diffusion coeffs., from relax. lengths in poisoned samples and pulsed decay consts. 9-27776
D₂O, vacuum u.v. spectrum of liquid 9-36884
D₂O, viscosity, 0-150°C, 1-1200 kg/cm² pressure range 9-23470
D₂O⁺, bombardment of D₂ gas, reaction kinetics 9-49374
D₂O circulation loop at MZFR Karlsruhe reactor, fuel pins irradiation facility 9-38739
D₂O moderated Th lattices in Siemens-Argonaut reactor 9-34500
D₂O moderator, local boiling risk study via thermal exchanges 9-25673
D₂O reactors, steam generating coolant temp. effects in fuels 9-25674
D₂O vapour, laser oscillations, far i.r., correlation 9-27322
H₂¹⁸O, lab-spectra rel. to features in atm. absorption 9-44331
H₂¹⁶O, ν_1 and ν_2 bands, 2.5-3.0 μ m, rotational structure 9-34624
H₂¹⁸O, ν_1 and ν_2 bands, 2.5-3.0 μ m, rotational structure 9-34623
H₂O, in lowest obs. state, rot. transitions rel. to features in atm. absorpt. 9-44331
H₂O+D₂O=2HDO equilib., zero-point energy 9-31179
H₂O+H⁺→OH⁺+H₂, 0.3 eV obs. 9-46430
H₂S⁺ bombardment of D₂ gas, reaction kinetics 9-49374
HDO, vibrational band envelopes rel. to molec. struct. 9-34622
HDO¹⁷, h.f.s. by beam maser 9-44329
HDO vapour, lab. spectra rel. to weak features in atm. absorpt. 9-44331
U-D₂O lattice with Pu, epithermal cross-sections 9-25672
U-H₂O nuclear reactor assembly, neutron flux distrib. in slab elements 9-22879

Wave equations, quantum theory see *Quantum theory/wave equations*

Wave functions see *Quantum theory/wave equations*

Wave mechanics see *Quantum theory*

Wavefront-reconstruction imaging see *Diffraction/light; Holography; Optical images*

Waveguides see *Electromagnetic wave propagation/guided waves*

Waxes

- see also *Acoustic waves; Elastic waves; Electromagnetic waves; Liquid waves; Magnetohydrodynamics; Seismic waves; Shock waves*
accelerated, in nonlinear field, no shock, ray velocity, covariant formulation 9-36118
in annular two-phase flow, disturbance waves coalescence 9-23227
atmospheric, characteristic parameters 9-40022
atmospheric, in baroclinic zonal flow, effect of horizontal shear on structure 9-41499
beats, frequency of occurrence 9-41810
cyclotron harmonic, propag. in hot plasma in uniform mag. field 9-23285
cylindrical shell, circumferentially travelling wave flutter, limiting amplitudes, nonlinear anal. 9-22243
in discharge positive column, ionic and drift 9-48629
in elastic rod, solution of large amplitude longit. propag. rel. to end velocity 9-27221
gravity, attenuation, turbulent conditions 9-30182
gravity, in an upper half-space, modelling by an induced current 9-35768
gravity, in rotating, homogeneous ideal fluid 9-27957
gravity, internal, for inhomogeneous atmosphere 9-40019
gravity, internal, in fluid with spatially varying mean flows, ray tracing 9-42478
gravity, ionospheric F region during mag. storm 9-49505
gravity, multiple, due to shallow water interaction with submerged bars 9-45470
gravity in thermosphere, 10⁻³ to 10⁻² Hz, calc. 9-41585
hydrodynamic formulation, classical and relativistic, for particle without spin 9-45742
hydromagnetic in magnetosphere, amplification 9-47558
internal gravity waves in stratified fluids with shear, reflectivity of critical levels 9-27958
Kelvin, in tropical stratosphere, evidence 9-24671
in kinetic theory, propagation and other spectral problems 9-22107
Korteweg-de Vries and Burgers eqn. derivation, nonlinear Galilean-invariant system 9-36110
lee wave generation in stratified flow over semi-elliptical obstacle 9-34730
lee waves in stratified flow over obstacle, perturbation approx. 9-34731
longitudinal, two-material cable system, dynamic stress and displacements 9-45843
MHD in upper atmosphere, excitation by finite source 9-49470
in modern media, averages of various props. 9-40249
neutron, in moderators, limiting critical freq., physical criteria 9-27781
neutron in moderators, limiting critical freq., physical criteria 9-27782
nonlinear, weakly, periodic soln. of eqn. in E₃, with spherical symmetry 9-34015
nonplanar oscillating surface problem, used complex cross-flow representation 9-22229
normal, in spherically-laminar anisotropic media, wave number calc. by impedance-scaling method 9-22065
periodic, in cold plasma in magnetic field, stabilities 9-30283
phase and group velocity demonstration 9-45720
plane, disturbances in thermal neutron distrib., propag. theory 9-22842
plane, reflection from stratified medium 9-22066

Waves continued

- plane, totally refl., pulse shape, rel. to Cagniard spherical wave soln. 9-29175
plane harmonic, scatt. in infinite elastic solid by 2 dimens. obstacles 9-36121
plane shear-pressure wave in elastic-plastic half-space, closed form solution 9-22218
planetary Rossby, vertical propag. through atmosphere with Newtonian cooling 9-31302
pressure, in gas, plane harmonic propagation in infinite uniform media 9-42596
propagation in medium with random inhomogeneities, one-dimensional problem 9-41741
quasi-stationary ultra-long, interaction with zonal flow 9-34844
in radnom medium, general method for velocity and attenuation determ. 9-36119
resonant four wave processes, general weak turbulence theory 9-27959
Rossby, time periodic, effect of radnom currents 9-43377
scattering by transparent sphere, third term of Debye expansion 9-29178
solitary at interface of, two fluid system is channel of arbitrary cross section 9-48537
spherical, Cagniard soln., rel. to totally refl. plane wave pulse shapes 9-29175
spherical, refl. and refr. from fluid interface, pulse shape determ. 9-30183
stationary, of finite amplitude, caused by pressure distrib. on flow surface of infinitely deep heavy fluid 9-23245
stress, transient, in shells and plates, effective applic. regions of three-dim. and two-dim. analysis 9-41801
surface, in piezoelectric materials, no counterpart in elastic homogenous materials 9-24224
surface, in presence of second sound 9-27186
temperature, diurnal, propagation, thermal interaction between atmosphere and earth 9-26460
theory, uniform approximation 9-48247
tidal, harmonic constants 9-43374
undergraduate text 9-38188
viscous fluid waves, harmonic components 9-25813
wave equation, reduced, subject to mixed boundary value conditions, uniqueness of soln. 9-22068
Hg surface waves, influence of axial magnetic field 9-30358

Waxes

- carnauba, eff. of ionic additives on heterocharge 9-37573
magnetoelectret state 9-30979
shellac, thermo- or magneto-electret depend. on conditions 9-37607
stearyl methacrylate-cetyl methacrylate copolymer i.r. spectrum. determ. 9-37860

Weak interactions see *Elementary particles/interactions, weak; Field theory, quantum/interactions, weak*

Wear

- cavitation in non-aqueous liquid 9-36834
conference, Plymouth, May (1967) 9-40991
diamond, on metal machining, adhesive interaction 9-23930
diamond, on metal machining, contact etecting melting process 9-26358
erosive rupture due to friction and fluid flow around surface, mechanism 9-23912
fatigue nature, physical confirmation from cyclic nature of accumulation of distortions of second kind in surface layer 9-23929
fluctuation model 9-37269
graphite sliding against stainless steel, rel. to interface geometry 9-41036
law, geometric method for determination 9-23928
metals, cavitation erosion, effect of elec. current 9-48676
Nylon-6, and friction, γ irradi. effects, obs. 9-39444
polyethylene, and friction, γ irradi. effects, obs. 9-39444
steel, unlubricated surfaces, variation 9-41037
of surfaces in friction, probabilistic model 9-37270
testing of dry and lubricated systems, review 9-37267
Al sintered powders, control of fretting wear 9-41035
Cu and steel surfaces, unlubricated sliding at high speeds 9-41038
Ti-(6 wt.%)Al-(4 wt.%)V alloy, resistance, surface treatment 9-37259
Ti, coatings 9-37268

Weather

see *Meteorology*

Weighing see *Balances; Mechanical measurement*

Weissenberg cameras see *Cameras; X-ray crystallography/apparatus*

Welding see *Forming processes*

Wentzel-Kramers-Brillouin method see *Quantum theory*

Wertheim effect see *Magnetomechanical effects*

Wetting

- see also *Capillarity*
alumina, recrystallized, by molten Al, alloys, Cu and Au, contact angle meas., sessile drop technique 9-34977
glass, borosilicate, by hydrophobic liqs., effect of adsorbed water on props. 9-34978
metal surface, critical surface tension, effect of adsorbed water 9-23437
quartz, by hydrophobic liqs., effect of adsorbed water on props. 9-34978
ruby, by molten Al, alloys, Cu and Au, contact angle meas., sessile drop technique 9-34977
sapphire, by hydrophobic liqs., effect of adsorbed water on props. 9-34978
sapphire, by liquid Cu-O alloys 9-26179
sapphire, by molten Al, alloys, Cu and Au, contact angle meas., sessile drop technique 9-34977
Ar, solid, contact angle meas. 9-23451
Kr, solid, contact angle meas. 9-23451
SiC fibres, critical of wetting, rel. to interact. with resins and coupling agents 9-23620
Xe, solid, contact angle meas. 9-23451

Whiskers see *Crystals/whiskers*

Whistlers see *Atmospherics; Ionosphere*

White dwarfs see *Stars*

Wiedemann effect see *Magnetomechanical effects; Magnetostriction*

Wiedemann-Franz law see *Conductivity, electrical/solids; Conductivity, thermal/solids*

Wien effect see *Conductivity, electrical/liquids, electrolytic*

Wigner coefficients see *Quantum theory*

Wigner effect see *Physical effects of radiations*

Wilson cloud chambers see *Cloud chambers*

Wind

- air flow over ridge, lee waves, numerical calc. 9-37912
- air flow over ridge, lee waves, numerical calc. 9-43389
- angular momentum transfer between hemispheres 9-40023
- rel. to atmospheric ground-pressure waves from nuclear explosion, models 9-24645
- components, longitudinal and vertical, 2.5 to 37 m above steppe 9-40005
- cyclone development, potential vorticity field 9-47536
- cyclone problem, history of models of cyclonic storm 9-31310
- dynamo, structure deduced from geomag. variation with solar flares 9-35915
- E_h ionization rel. to wind shear rocket obs. 9-47580
- eddy fluxes, meas. in lower atmosphere 9-24647
- F2 asymmetries rel. to world-wide neutral air winds and electrodynamic drift 9-47582
- F-region, neutral-air winds for asymmetric global press. system 9-47586
- friction of air currents over inhomogeneous souls 9-31301
- in Gauss-Argand diagram, rel. to friction 9-49452
- geostrophic field, northern hemisphere, zonal harmonic analysis 9-33765
- hurricanes, thermodynamics, recent advances in theoretical studies 9-31309
- hurricanes Gladys and Gloria, Apollo 7 obs. 9-33764
- in ionosphere, dynamics 9-40077
- ionosphere, lower, strong vertical component 9-49492
- ionosphere, lower, tidal semi-diurnal, seasonal phase changes 9-49491
- in ionospheric F layer, rel. to polar F2 layer control by Universal Time 9-43472
- isallobaric, divergence calc. from vector analysis 9-41506
- jet stream, mesoscale press. fluctuations rel. to distance from core 9-28869
- N. Hemisphere W-E wind. latit. profile and atm. angular momentum 9-47537
- in neutral atmosphere, 150-400 km, calc. 9-40045
- ocean circulation, wind-driven, three-dimensional model 9-26889
- oscillations spectra for near-water layer 9-40008
- planetary boundary layer above surface roughness change 9-41504
- Saharan dust transported by winds, falling in Britain, July 1968 9-26900
- sea, surface oscillations caused by wind 9-49434
- sea-air interactions, long range prediction of large scale motion, simplified model 9-24648
- sea-air interface, stress and surface roughness 9-31307
- sonic anemometer - thermometer for direct method of determ. turbulent transport of physical quantities 9-24644
- speed, correl. with geomag. variations 9-45487
- spiral model applic. planetary boundary layer flow with neutral thermal stability 9-41501
- stratified-atmosphere, vertical energy flux due to ground disturbance 9-35816
- stratospheric, hazard of wind shears during parachute recovery of instruments 9-31305
- stratospheric, structure and influence on suspended instrument package 9-28873
- stratospheric observations in tropics 9-31311
- stress coefficients at air-water interface, Froude number scaling 9-41503
- structure, from persistent radio meteor echoes amplitude fluctuations 9-37933
- surface and mid-troposphere, rel. to water vapour 9-49450
- tangential stress on sea surface 9-26891
- thermospheric, F region, diurnal and seasonal vars. from Thomson scatt. obs. 9-49504
- tidal, contribs. to the ionospheric Sq current system 9-47574
- tropospheric vector period comparison with rot. fluctuation and polar movement 9-31306
- tunnel, particle motion 9-39040
- turbulence meas. using Doppler radar system, feasibility study 9-31308
- upper, near 100 km altitude, irregular 9-28911
- upper atm. obs. by means of meteor trails 9-41547
- variations rel. to see level forced oscills., S. Baltic 9-37900
- velocity, Doppler radar determ. 9-41507
- velocity, mean vertical profiles, rel. to turbulence parameters in near-surface layer 9-24643
- velocity fluctuations in upper troposphere, vertical distribution 9-40024
- velocity rel. to daytime sky brightness 9-40025
- velocity remote probing using stellar scintillations 9-33758
- velocity vector, remote sensing by optical heterodyne measurement of Doppler shifts 9-33766
- vertical spectra rel. to atm. stability 9-41526
- westerly field, small-scale eddy momentum and heat diffusion processes 9-41498
- zonal, temperate latit. 200 mb, S. Hemisphere GHOST balloon obs. 9-41505

WKB method see *Quantum theory***Wolfram** see *Tungsten***Wood**

- tree bark, reflectivity, diffuse near i.r. 9-39800

Work functionsee also *Electron emission*

- alkali metals, correlation energy contribution using pseudopotential model 9-35515
- electron, variation with particle size, theoretical 9-49155
- exoelectron glow curves intensity depend. 9-33415
- measured using field emission 9-37628
- metal, free-electron model calc. 9-41276
- metal surface, self-consistent calc. for semi-infinite electron gas model 9-47052
- metal surface, static-field penetration and atomic polarization effects 9-43137
- metal-CdS contacts at higher current densities 9-39733
- oxide cathodes, reduction, electric field effects 9-30999
- photoelectric, computation by Fowler analysis 9-26610
- semiconductor surface, photoelec. emission determ. 9-43142
- transition metals, correlation with surface energy 9-33414
- of two contacting spherical particles of different size 9-39019
- Al, correlation energy contribution using pseudopotential model 9-35515
- Au thermionic emission changes due to inert gas ion bombardment 9-24257
- Cd, oxidized surfaces, contact potential differences method 9-31000
- CdS-metal contacts at higher current densities 9-39733
- CdS with blocking Au contacts, reduction with increasing photocurrent 9-39732

Work function continued

- n-GaAs single cryst., external photoemission meas. 9-41283
- n-GaAs single cryst., external photoemission meas. 9-41283
- GaP, giant temp. depend. 9-35514
- n-Ge, increase due to 50 keV ion irradi. 9-47124
- Hg-rich binary and ternary alloys, reln. to surface tension 9-24246
- Mg, correlation energy contribution using pseudopotential model 9-35515
- Mg, oxidized surface, contact potential difference method 9-31000
- Nb, oxidized surface, contact potential difference method 9-31000
- Ni (100), rel. to adsorption of N₂O, NO or CO₂ 9-35003
- PbS (100) surface, O₂ chemisorption effects 9-39949
- Re, oxidation effects rel. to positive surface ionization of Na, Na halides and LiCl 9-35522
- SbSI, eff. of O₂ adsorption 9-30496
- Sn, oxidized surface, contact potential difference method 9-31000
- Ti, oxidized surface, contact potential difference method 9-31000
- W, from single planes with adsorbed CO 9-39176
- W, rel. to thermal faceting and O₂ adsorption 9-35012
- W, with U adsorbed to twelve monolayers, rel. to thickness and U phase transition 9-32850
- W (100) surface, changes as O₂, N₂, CO₂ and H₂ adsorbed 9-42734
- W single crystal, (121), (111) and (021) faces, effect of Y adsorption 9-44632
- W single-cryst. planes with adsorbed Cs 9-39175
- W single cryst. (110) and (100) surfaces and polycryst. foil, temp. coeffs. 9-35516
- W thermionic emission, changes due to inert ion bombardment 9-24257
- W (111) and (110), effect on electron ejection by metastable He and Ar atoms 9-31001
- Zr-O solid solns., sintered, electron function 9-39734

Work hardeningsee also *Cold working; Surface structure*

- rel. to edge dislocations pair in perpendicular slip planes 9-44786
- kinetics, intense u.s. energy influence 9-28380
- metals, deform. processes 9-35196
- metals b.c.c., at low temp. theory 9-46924
- rigid-viscoplastic strain hardening annular plate, impulsively loaded 9-22240
- superconductor alloys, for effective flux pinning at high current densities 9-49053
- Ag single cryst., rel. of stored energy due to deform. 9-26325
- Ag single crystals, stage III quantitative analysis 9-39459
- Ag single crystals, between 77 and 1200°K, three stage curve 9-46926
- Al-Ag alloys, strength increase by strain-induced solute disposition stability control, eff. of additions 9-28360
- Al, polycryst., curve obs. for tensile deform. 9-41014
- Cu-Ga solid solns. 9-41045
- Cu-Ge solid solns. 9-41045
- CuAu, tensile axis initial orientation and domain size effects, rel. to tensile props. in single crystals 9-30710
- Cu microhardness when failed by 17.8 kc/sec oscillations 9-35190
- Cu single cryst., cyclic hardening 9-30709
- Fe, microhardness when failed by 17.8 kc/sec oscillations 9-35190
- Fe single cryst., temp. depend. of hardening rate 9-35197
- Fe single crystals, orientation depend. 9-26370
- Fe single crystals deformed at -75°C, yield drop orientation dependence 9-33028
- Mo surface layers, crystal structure changes prod. by vacuum annealing 9-32932
- Nb, single crystal of high purity in compression, effect of specimen dimensions 9-46885
- Nb surface layers, crystal structure changes prod. by vacuum annealing 9-32932
- Pb, stress strain curves and injected dislocation density determ. 9-41046
- W surface layers, crystal structure changes prod. by vacuum annealing 9-32932

X and gamma-ray astronomy

- γ ray telescope with large area wire spark chambers, balloon-borne 9-38128
- Cassiopeia A, supernova remnant, search for energetic γ emission 9-29055
- Centaurus XR-2, nova model 9-41646
- Compton scatt., as p source analyzed 9-29054
- cosmic γ due to microwave Compton scatt. on cosmic ray electrons 9-27070
- Crab Nebula, pulsed hard X-ray flux, attempt at detection 9-41669
- Crab nebula and the diffuse background near the Galactic anticentre 9-28995
- Crab nebula γ detection by digitized spark chamber 9-35962
- Cyg X-1, intensity and spectral distrib. of high energy X-rays 9-38061
- Cyg XR1 source, upper limit on ang. diameter in energy range 25 to 100 keV 9-45655
- Cyg XR-1, spectra, 1.5-13 keV 9-38060
- Cyg XR-2, spectra, 1.5-13 keV 9-38060
- Cygnus X-2, search for radio emission at 4.5 cm, unsuccessful 9-41670
- data analysis and reporting, general procedure 9-32241
- dilute image transform applic. to star camera 9-29141
- discrete gamma sources as origin of 100 MeV flux 9-45656
- discrete X-ray sources and diffuse background rad., characts. 9-33921
- enhanced gamma flux in direction of galactic disc. defect. with balloon flights 9-45594
- extra-galactic X-ray sources, evolutionary effects rel. to diffuse background 9-40169
- galactic gamma-rays, origin from collisional mechanisms with interstellar gas 9-43608
- gamma rays, high energy, from pulsars, implications 9-41661
- GX3+1, hard X-ray source, Sagittarius-Scorpio region, spectral data, 1-8 keV 9-43602
- hard radiation from Galactic centre, balloon obs. 9-49573
- intergalactic bremsstrahlung and diffuse X-ray background 9-24833
- metagalactic, γ -ray spectrum from secondary particle prod. 9-47663
- metagalactic gamma flux from secondary pi meson decay, estimation 9-29056
- metagalactic gamma intensities, corrections and implications 9-45657
- modulation collimators, review 9-47690
- moon, gamma investigation, spectra and intensity 9-33933
- optical identification of X-ray sources 9-47661
- polarization of X-rays in Sco X-1, search 9-27028
- pulsar NP 0532, existence of strong pulsed X-ray signal 9-43605

X and gamma-ray astronomy continued

- pulsar CPl133 pulsar, search for high energy γ rays using atmos. Cherenkov tech. 9-29047
- SCO X-1, five nights of continual monitoring of optical flux 9-40166
- SCO X-1, obs. of black-body with var. temp. 9-43601
- SCO X-1, polarization of X-rays, search 9-27028
- SCO X-1, X-ray source, position and proper motion 9-31583
- SCO X-1 X-ray source, long term periodicity in optical intensity 9-43607
- SCO XR-1, spectra, 1.5-13 keV 9-38060
- sky background of soft X-rays, galactic origin 9-27069
- sky-scan for discrete sources of γ -rays, 240-7000 KeV 9-24834
- solar flare soft X-rays, Explorer 33 and 35 obs. (8 July 1968) 9-43673
- solar X-ray activity, peak characts. (Mar-Apr 1966) 9-41692
- solar X-ray spectrum, obs. from OSO-II 9-40188
- source location using rotating modulation collimator 9-47662
- spectrometer, scintillation, rocket borne, for cosmic ray obs. 9-31584
- supernova remnant, Cassiopeia A, search for energetic γ emission 9-29055
- Tau X-1, intensity and spectral distrib. of high energy X-rays 9-38061
- techniques in X-ray astronomy, review 9-29107
- telescope, X-ray, glancing incidence, opt. design and prototype flight test 9-29109
- upper limits to gamma fluxes from three pulsating radio sources 9-33923
- Vir XR-1, point source of X-rays, possible identification and emission mechanism 9-43606
- X radiation spectrum isotropic determ. by single mechanism 9-49564
- X-ray background, soft, recent meas. 9-47615
- X-ray bremsstrahlung associated with suprathermal protons 9-43603
- X-ray diffuse background, origin and break in spectrum, cosmological implications 9-43604
- X-ray source in optically thick environment, physical conditions 9-36014
- X-ray source in optically thin environment, physical conditions 9-36013
- X-ray sources, absence of pulsar characts. 9-40168
- X-ray sources, model involving matter accretion onto a white dwarf 9-40167
- X-ray sources and interstellar gas densities, correl. 9-38064
- X-ray sources in energy range 4-8 keV, planetary nebulae possibility 9-33922
- X-ray stars, model 9-38062
- X-rays, cosmic, absolute intensity, rocket obs. 9-38063
- X-rays, high-energy, from Magellanic clouds, search 9-29053
- γ -radiation, high energy, apparatus and obs. from OSO-III (1967) satellite 9-24730
- γ -ray distrib., energy >50 MeV, OSO-III (1967) satellite obs. 9-24731
- O III and V III lines from galaxies explaining soft X-ray sky background 9-27069

X-ray absorption

- see also *X-ray spectra/absorption*
- calculation from simplified orders-of-scattering 9-46059
- gases, optically thick, surrounding X-ray source, physical conditions 9-36014
- gases, optically thin, surrounding X-ray source, physical conditions 9-36013
- in plasma diagnostics of electron temp. 9-30260
- Ar gas flow boundary layer $\leq 1500^\circ\text{C}$, investigation method 9-40735
- Cu film, density meas., compared with bulk Cu 9-30483
- Cu K α by Pb in brass, depend. on particle size in multiphase syst. 9-24440
- Ge, absorpt. coeff., oscillator strength for K-electrons 9-32916
- Ge, amonalous, 203-5°K and Debye-Waller factor 9-23758
- Si, anomalous transmission, 100° to 650°K 9-33573

X-ray analysis see *Chemical analysis/X-ray; Crystal structure, atomic; X-ray crystallography***X-ray astronomy** see *X and gamma-ray astronomy***X-ray characteristic temperature** see *Specific heat***X-ray crystallography**

- For results of structure analysis see *Crystal structure, atomic*
- absorpt. factors, spherical 9-35039
- charge and momentum density, theory and expt. 9-23693
- Debye-Waller factors, anharmonic contribs. 9-26404
- diffraction line profiles rel. to stacking faults in h.c.p. and f.c.c. polycrystals, general theory 9-23817
- dislocations, scatt. dynamic theory, derivation 9-39224
- distorted cryst., dynamical theory 9-42767
- graphite, diffraction studies 9-48822
- line profile analysis (Warren-Averback), applic. 9-35040
- mounting for Welch-Bragg apparatus 9-23702
- multiple diffraction effects, intensity meas. 9-23707
- orientation of single crystals 9-23719
- phase determ. using two-beam interferometry 9-26217
- real crystals, effect of specimen-dependent props. on accuracy of intensity meas. 9-23711
- reflection intensities, Bragg's paper, 1914 9-23704
- rocking curves for single crystal, anomalous absorpt. effect on shape 9-35043
- scattered beam broadening, ang. factors influence, exptl. data correction methods 9-46766
- scattering, diffuse, correlation of intensity meas. 9-37123
- size effects, linear and quadratic, in polycrystalline diffuse scattering, calc. 9-40880
- small-angle scatt., collimational distortion calc., correction for slit height 9-46768
- spherical absorpt. factors 9-35039
- tetragonal space groups, phase relations of reflections 9-23697
- C, diffraction studies 9-48822
- Ge, Debye-Waller factor and anomalous absorpt., 293-5°K 9-23758
- ND₂Br transition and lattice parameters determ., -192 to 196°C 9-30743
- NH₄Br III-IV transition and lattice parameters determ., -192 to 196°C 9-30743
- Si Laue reflected and refracted beams, rocking curve oscillations 9-32928
- apparatus**
- see also *X-ray monochromators; X-ray spectrometers*
- alignment using photographs, design 9-37122
- automatic diffractometers, off-line, three and four circle, significance of specifications 9-28243
- camera for diff. study at very high pressure and for meas. of compressibility of β -SiC 9-48820
- densitometer, digital scanning system for diff. films processing 9-32080

X-ray crystallography continued

- apparatus continued**
- diffractometers, electronic and mechanical sources of error 9-23699
- diffractometers, single-crystal, for precision intensity meas. 9-23706
- focusing monochromators 9-23705
- image intensifier for time-resolved study of dynamic events 9-48821
- Manenc's double focusing device, geometrical aberrations 9-37121
- mounting for Welch-Bragg apparatus 9-23702
- powder specimen accurate relative intensity meas. 9-23700
- scanning device, automatic, for double crystal spectrometer 9-32883
- specimen holder, single crystal, 77-1300°K 9-30539
- calculation apparatus**
- Camera for large and small-angle diffraction photographs 9-25009
- computers in error evaluation, cost aspects 9-23726
- diffractometer with inclined photographs, integral intensity meas. 9-42770
- calculation methods**
- absorption correction rel. to transmission surface props. 9-23733
- absorption corrections calc. for photographic data 9-40873
- accuracy indicators in structure factor meas. 9-23734
- attenuation coeff. estimation for elements and cpds. 9-23728
- α -bromine-anthraquinone, Patterson function rel. to cryst. and molecular struct. 9-42799
- cell parameter determ. in hexagonal and tetragonal crystals, rational choice of reflections 9-46774
- collimation corrections, slit-length for small angle scatt. data from Kratky camera, computer program 9-48827
- computer fitting of diff. profiles, least squares method 9-39239
- computer program for least squares method of phase determ. for estriol structure 9-39332
- differential synthesis method, modification 9-42769
- diffraction line profile correction by deconvolution 9-23740
- diffraction line profile correction by deconvolution applic. to effect of receiving slit on profile recording 9-23741
- diffraction profile correction for instrumental broadening in transmission geometry 9-42766
- diffraction structure results compared with neutron diff. results, error analysis methods 9-23712
- domain size from tails of diff. profiles 9-40879
- error analysis methods rel. to structure results comparison with neutron diff. technique 9-23712
- error evaluation versus 'on line' correction 9-23726
- extinction corrections in structure factor meas. 9-23730
- free-atom form factor model as cause of errors in calculated structure factors 9-23735
- h.c.p. crystals with double faults, diff. theory 9-23819
- indexing with modified computer programme for IBM360 9-40894
- integrated Bragg intensities, contrib. of thermal diffuse scatt. 9-48825
- intensity measurement error-sources, investigation projects 9-23739
- inverse images and their role in resolution 9-26221
- least-squares, filtering for structure refinement 9-39237
- least-squares refinement, accidentally absent reflexions treatment 9-30535
- line broadening analysis by Rachinger separation and Stokes correction 9-40895
- line profile, harmonic analysis, optimum design of expt. 9-40897
- line-profile parameters, statistical variance 9-40874
- Neskuchae's technique for interpreting powder patterns, by a BECM-4 computer 9-39242
- Neskuchae's technique for interpreting powder patterns, by a BECM-4 computer 9-39241
- optimization process for least-squares weighting schemes of diffractometer-collected data 9-39238
- Patterson function projections, arbitrary, interpret. using superposition method 9-40896
- photographic data, absorpt. corrections calc. 9-40873
- pole figure evaluation by IBM 1800 9-40893
- polymorphic layer sequence determ. in close-packed structures, Patterson method applic. 9-23743
- powder intensity meas., accuracy assessment 9-23737
- powder patterns, cubic, thermal diffuse scatt. contrib. to integrated intensities 9-32885
- profile analysis in single-crystal diffractometry 9-23725
- reflection by plane and bent cry., duration of coherent emission 9-37120
- satellite reflections analysis, atomic ordering arrangements determ. 9-39225
- scalar wave dynamical diff. theory, matrix formalism 9-23701
- scattered beam broadening, ang. factors influence, exptl. data correction methods 9-46766
- small angle scatt., collimational distortion calc., digital computer programme and expt. verification of theory 9-46769
- structure factor, accuracies of expt. values 9-23738
- structure factor determ. by intensity meas. from large single-crystals 9-40892
- structure factors, significance 9-23691
- structure functions, selective, for Patterson distrib., spurious maxima 9-42768
- texture determination, quantitative, automatic conversion of data to pole figures 9-30550
- thermal diffuse scatt. contrib. to integrated Bragg scatt. intensities 9-23716
- thermal diffuse scattering contrib. to integrated intensities of cubic powder patterns 9-32885
- thermal diffuse scattering corrections in structure factor meas. 9-23729
- thermal diffuse scattering in comparing neutron and X-ray diff. data 9-30537
- twinning, pseudo-merohedral, treatment of overlapped data 9-30510
- twinning, pseudo-merohedral, Weissenberg photographs, chart for use in interpretation 9-30511
- undistorted Fourier maps, alphabetic plotting by computer 9-39240
- unit cell determ. from powder data, fully automatic program 9-48826
- weighted periodic vector set extractions from Patterson function 9-23742
- structures** see *Crystal structure, atomic*
- technique**
- absolute scale for intensity meas., determ. from relative intensities 9-23713
- absorption corrections, experimental determ. 9-23733
- acicular crystal studies by axial scanning, two expt. methods 9-23717
- diffraction topography with vidicon TV image system 9-23718

X-ray crystallography continued
technique continued

- divergent X-ray method, principle technique and applics. 9-32888
 extinction factor determ. using polarized X-rays 9-23709
 high-speed diffraction spectrography 9-23720
 integrated intensity meas., geometrical aspects and errors due to non-monochromatic radiation 9-23727
 intensity meas., history 9-23703
 intensity meas. from large single crystals, accuracy 9-23731
 intensity measurement error-sources, investigation projects 9-23739
 intensity precision meas. by single-crystal diffractometers 9-23706
 Lang method, radiographs and topographs of perfect crystals 9-40877
 macromolecular crystals, rapid parallel meas. of reflections 9-23710
 for particle size distrib. determ., small-angle scatt. 9-40878
 Pendellosung fringes in structure factor determ. 9-23708
 photographic means of accurate intensity measurement 9-40875
 photographic means of intensity meas. 9-40876
 photographic means of rapid parallel meas. of reflections from macromol. crystals 9-23710
 powder intensity meas., I.U.Cr. project 9-23714
 powder intensity meas., survey of results of structure factors for metals, alloys and covalent compounds 9-23715
 powder meas. of electron states and charge distrib. in ionic crystals, metallic oxides, carbides and nitrides 9-23692
 powder specimen accurate relative intensity meas. 9-23700
 random-layer lines, profile analysis 9-28260
 refraction effects on radiographs and topographs of perfect crystals 9-40877
 structure factor determ. by intensity meas. from large single-crystals 9-40892
 structure factor determ. from pendellosungs fringes in Lang topography 9-46765
 Al, cold-worked, Debye-Scherrer line broadening meas. 9-46776

X-ray diffraction

- see also X-ray crystallography; X-ray scattering*
 ageing alloys, diff. eff. rel. to elastic lattice distortions 9-23746
 alkali metal solid samples, reactive, protection method 9-46767
 anthracene thin film, new crystalline phase obs. 9-35689
 automatic diffractometers, off-line, three and four circle, significance of specifications 9-28243
 bicrystal containing translation fault, theory 9-32982
 β -brass solid soln., static atomic displacements influence on diffuse intensity 9-37132
 crystallography, high-speed technique 9-23720
 d.h.c.p. cryst. with deform. stacking faults, diff. pattern 9-30612
 distorted cryst., dynamical theory 9-42767
 double crystal method for microstrain analysis of BeO single crystals 9-42765
 dynamical theory 9-23690
 electron density distrib. multiple diff. effects in determ. 9-28263
 f.c.c. cryst. with intrinsic and extrinsic stacking faults, model 9-32887
 f.c.c. metal film, oriented, line broadening rel. to particle size and strain 9-44657
 Fraunhofer hologram, image reconstruction with visible light 9-46003
 Fresnel zone plate, image formation in visible and soft X-ray region 9-27385
 grating reflectivity in ultrafast region 9-36351
 h.c.p. crystals with double faults, theory 9-23819
 image intensifier for time-resolved study of dynamic events 9-48821
 instrumental broadening of profiles in transmission geometry, correction 9-42766
 intensity, integral, in single crystal diffractometer with inclined photographs, meas. geometry 9-42770
 intensity precision meas. by single-crystal diffractometers 9-23706
 line breadth analysis of cubic polycrystals 9-39227
 line profile, harmonic analysis, optimum design of expt. 9-40897
 line profile analysis (Warren-Averbach), applic. 9-35040
 line profile correction by deconvolution 9-23740
 line profile correction by deconvolution applic. to effect of receiving slit on profile recording 9-23741
 liquid alloys, pattern prediction from Percus-Yevick partial structure factors 9-40768
 in magnetic domains and boundaries visualiz. of ferromag. and antiferromag. samples 9-28612
 Microstrain analysis of GeO single crystals, double crystal method 9-42765
 molecular form factors from ab initio wave functions applic. to struct. analysis 9-32884
 multiple effects, intensity meas. 9-23707
 and neutron diff. data, joint refinement 9-30551
 and neutron diff. data comparison, role of thermal diffuse scatt. 9-30537
 noncentrosymmetric cryst., perfect, ratio of integrated intensities obs. 9-35042
 Photographs, large- and small-angle use of X-ray camera 9-25009
 pole figure integrator for fibres 9-44652
 polymer disordered cryst. 9-35072
 powder patterns, cubic, thermal diffuse scatt. contrib. to integrated intensities 9-32885
 powder samples, photographic recording using ^{55}Fe sources prod. in reactor 9-40907
 profile analysis in single-crystal diffractometry 9-23725
 satellite reflections analysis, atomic ordering arrangements determ. 9-39225
 scalar wave dynamical diff. theory, matrix formalism 9-23701
 scattered beam broadening, ang. factors influence, expd. data correction methods 9-46766
 scattering by structures with random distribution of defects 9-28244
 Schulz method determ. of subgrain misalignment 9-32886
 stacking fault, deformation, in h.c.p. crystals, rel. to solute segregation effects in alloys 9-23818
 by stacking faults in h.c.p. and f.c.c. cryst. 9-42842
 steel, retained austenite determ. 9-23953
 topography for u.s. vibr. modes in resonating crystal 9-39226
 topography with vidicon TV image system 9-23718
 vibrating cryst., scatt. amplitude 9-35041
 Weissenberg photographs of pseudo-merohedral twins, chart for use in interpretation 9-30511
 Ag-Au layered struct. static atomic displacements influence on diffuse intensity 9-37132
 Ag-Mn molten alloys, elec. resist. from partial interf. functions 9-30422

X-ray diffraction continued

- Al-Ag alloy, δ phase formation studied 9-23947
 Au-Sn liq. alloys, at. distrib. and elec. resist. 9-30423
 BaTiO₃, Berg-Barrett determ. of tilt angles of twin components in various lattice planes 9-37145
 BeO single crystals, analyses of microstrains using double-crystal 9-42765
 α -Cu-Ge evaporated film faulting meas. 9-23820
 Cu, extinction changes during annealing 9-44662
 Cu, Au solid soln. static atomic displacements influence on diffuse intensity 9-37132
 Mg₂Si, single crystals, multiple diff. effects on determ. of electron density distrib. 9-28263
 Na intensities, temp. depend. in range 115-353°K 9-23766
 NiO, Berg-Barrett determ. of tilt angles of twin components in various lattice planes 9-37145
 Si bicornst., ion-bombarded, contrast and geometry of fringes in topographs 9-32982
 TiO₂ phase transform. at high press. and temp., obs. 9-23988
 W, X-ray Debye temp. meas. 9-35286
 YFe garnet, dense ferrimagnetic perovskite allotropic form, existence 9-26252
 YFe garnet, multiple, crystal struct. study 9-37153

X-ray diffractometers *see X-ray crystallography/apparatus***X-ray examination of materials**

- see also Chemical analysis/X-ray; Radiography*
 alloy E1437B, effect of ageing on lattice parameters 9-41047
 alloys, structure factors from powder intensity meas. 9-23715
 alnico alloy, solid solution decomposition obs. by the Laue and rotating cry. methods 9-39473
 aluminium methylammonium alum., lattice dimensions, 78° to 291°K 9-42927
 bicrystal containing translation fault, diff. theory 9-32982
 binary solid solutions, coherency loss during ageing 9-30711
 colour images of inclusions obtained with microprobe 9-48851
 copper trichite whiskers, refraction effect on radiograph and topograph 9-40877
 covalent cpds., structure factors from powder intensity meas. 9-23715
 cubic polycrystals, line breadth analysis 9-39227
 dendrites in solid solns., distrib. of dissolved element 9-48814
 3-deoxy-2-C-hydroxymethyl-D-erythro-pentate, crystal structure 9-39345
 d.h.c.p. cryst. with deform. stacking faults, diff. pattern 9-30612
 diamond, Debye temp. meas. at low temps. 9-24043
 diamond, natural, with garnet inclusion 9-42804
 diffraction and fluorescence techniques in pathology 9-29112
 diffractometer, high resolution at small and wide angle 9-40881
 dolomite, cryst. defects, topographic obs. 9-32958
 electron state band struct. determ. with ultra-soft X-rays 9-30811
 electron-probe microanalysis, X-ray prod. and electron scatt. predictions using Boltzmann eqn. 9-36092
 f.c.c. cryst., diff. by stacking faults 9-42842
 f.c.c. cryst. with intrinsic and extrinsic stacking faults, diff., model 9-32887
 ferritin macromol., diff. obs. of inorg. core, comparison with Fe hydroxides 9-37139
 fibres, pole figure integrator for use with diffractometers 9-44652
 films on Ge, stress topography 9-34983
 films on Ge, stress topography 9-32839
 garnets, flux-grown, topography of internal growth defects 9-32937
 glasses, alkali-ion movement, electron-probe microanalysis 9-34968
 grain size effect on scatt. 9-49399
 gramicidin C bromohydrate, and synthesis 9-42800
 graphite-B, neutron irradi., lattice parameters as function of B conc., rel. to defect clustering 9-30597
 graphite, chem. structure and graphitization, samples from polynuclear aromatics 9-39257
 graphite, diffraction studies 9-48822
 h.c.p. cryst., diff. by stacking faults 9-42842
 henritermierite, Ca₂(Mn_{1-x}Al_x)₂(SiO₄)₂(OH)₂ 9-32906
 hexaiodobenzene, crystal and molecular struct. 9-46799
 hexamethylenetetramine joint refinement of X-ray and neutron diff. data 9-30551
 image analysis by computer for bone density meas. 9-47700
 interferometer, transmission 9-44651
 ionic crystals, survey of results of powder meas. rel. to electron states and charge distrib. 9-23692
 kimrite (hydrated Ba feldspar), at. struct., satellite occurrence in inverse lattice 9-46782
 koninkite, cry. symmetry obs. 9-37140
 liquid, compression processes near elec. discharge 9-32767
 of liquid dielec. breakdown compression headwaves 9-32768
 liquid metals and alloys, review 9-36846
 liquids, lattice structure 9-36845
 magnesite, cryst. defects, topographic obs. 9-32958
 martensites, Co- and Cr-bearing, decomposition kinetics of martensites extracted by anodic dissolution from steels 9-37274
 metallic oxides, carbides, nitrides, survey of results of powder meas. rel. to electron states and charge distrib. 9-23692
 metals, pure, size of crater prod. by laser beam 9-48909
 metals, structure factors from powder intensity meas. 9-23715
 metals magnetic, density of state X-ray photoelec. spectroscopy study 9-44886
 meteorites, stony, composition by sample preparation and fluorescence method 9-45661
 methane, crystal struct. and thermal expansion 4.2-75°K 9-40926
 Mossbauer effect, film recording 9-26716
 mounanaite, PbFe₂(VO₄)₂(OH)₂, powder diff. 9-32925
 1-p-nitrobenzenazo-2-naphthol (Para Red), twinning 9-32863
 non-metallic substances 9-39223
 noncentrosymmetric cryst., perfect, ratio of integrated intensities obs. 9-35042
 particle size distrib. determ., small-angle scatt. 9-40878
 polycapraamide, cracks, submicroscopic, formation under load 9-33096
 polycapraamide, stressed, cracks, submicroscopic, charact. features of growth 9-33097
 polymer coating for protection of reactive samples 9-46767
 polymer disordered crystal, scatt., theory 9-35072
 polymers, stressed, cracks, submicroscopic, charact. features of growth 9-33097

X-ray examination of materials continued

- polypropylene, cracks, submicroscopic, formation under load 9-33096
 polyvinyl butyral, cracks, submicroscopic, formation under load 9-33096
 polyvinyl butyral, stressed, cracks, submicroscopic, charact. features of growth 9-33097
 polyvinyl chloride, cracks, submicroscopic, formation under load 9-33096
 polyvinyl chloride, stressed, cracks, submicroscopic, charact. features of growth 9-33097
 polyvinylcyclopropane, crystalline, oriented fibre and film samples, unit cell determ. 9-46804
 powder patterns, cubic, thermal diffuse scatt., contrib. to integrated intensities 9-32885
 probe microanalysis, sample preparation techniques for reducing errors from surface effects 9-39234
 quartz, lattice displacement meas. by moire topography 9-26287
 quartz particles in whitewares, strain meas. 9-23869
 rancieite, powder diff. obs. 9-32922
 secondary ammonium halides, long-chain, crystal structure 9-37154
 size effects, linear and quadratic, in polycrystalline diffuse scattering, calc. 9-40880
 solute atom position, by X-ray fluoresc. scatt. 9-23797
 β -spodumene, thermal expansion 9-26431
 β -spodumene-silica solid solutions, thermal expansion, spodumene lattice parameters 9-26431
 steel, Fe-Mn-C, austenite-martensite transform., lattice axes variation and cryst. struct. obs. 9-46948
 steel, inclusion analysis by colour X-ray images obtained with a microscope 9-48851
 steel, martensite transf. 9-39495
 steel, retained austenite determ. by diff. 9-23953
 steel, χ -martensite rel. to carbon content 9-37294
 structure functions, selective, spherulites maxima 9-42768
 tetraphenylcyclobutadiene molybdenum dicarbonyl bromide, cry. struct. determ. 9-48841
 1, 4 thallous benzoate-thiourea complex, crystal structure 9-39319
 2, 4, 6-tribromonitroaniline, crystal structure 9-39318
 triglycine sulphate, ferroelec. domains boundaries, X-ray topography obs. 9-28556
 twinning, pseudo-merohedral, Weissberg photographs, chart for use in interpretation 9-30511
 water, forward scatt. coeff. 9-40770
 water, structure at 25°C 9-28099
 wustite, ordered struct. obs. 9-26232
 Ag-Ca alloys, determ. of phase diagram 9-48937
 Ag-Pd alloys, stacking fault densities from diff. line profiles 9-40961
 Ag₂Te, phase diagram determ. from diff. meas. 9-46956
 Ag halides, B1-type press.-induced phase transform., diff. obs. 9-41063
 AgBiSe₂-AgBiS₂ system, high-temp. β -phase, rel. to cryst. structure order 9-42782
 γ -AgI, diff. obs. of cryst. struct. 9-33379
 AgNO₃, orthorhombic and rhombohedral, thermal expansion meas. 9-35287
 Al-($<0.22\text{at.}\%$)Ti solid solution, lattice parameter comp. dependences 9-42918
 Al-Cu-Cr supersaturated solid solns., decomp. kinetics, diff. obs. 9-46937
 Al-(3-15wt.%)Mg alloys, dislocation struct. determ. 9-40946
 Al-Mn-Zn alloys, lattice parameters rel. to ageing during pre-precipitation 9-41049
 Al-(30 at.%)Zn alloys, Debye-Scherrer patterns, sidebands 9-46936
 Al-(40 wt.%)Zn alloys, structural changes during ageing 9-23943
 Al-Zn alloys, of spinodal struct. formation, stability and decomp. 9-37290
 Al, absolute structure factors from transmission meas. on powder sample 9-28254
 Al, atomic scatt. factors from thermal diffuse intensities meas. 9-32900
 Al, dislocation configurations at 350°C, topographical investig. 9-46820
 Al alloys, transmission for thickness gauging, composition effects 9-39156
 Ar-methane, phase diagram 9-44803
 As, amorphous, intensity curves rel. to dimensions of struct. element 9-32824
 As single of high purity, struct. determ. at 4.2, 78 and 299°K 9-39254
 Au/Pb supercond. layered films, phase composition and transition obs. 9-26528
 Au-(50 at.%)Cd alloy, influence of plastic deformation on martensite transform. 9-39491
 Au-(46 at.%)Cu-(4 at.%)Ni alloy, order transform. of type $\alpha_{\text{disorder}} \rightarrow \beta_{\text{order}}$ 9-37304
 β' -Au-Zn alloy, long-range order, diff. meas. 9-28256
 AuCu₃, diffuse scatterings and superlattice reflections, new type 9-23750
 AuCu₃, order transform. of type $\alpha_{\text{disorder}} \rightarrow \beta_{\text{order}}$ 9-37304
 BaOFe₂O₃, cry. struct., diff. obs. 9-47283
 BaTiO₃, ferroelec. domains boundaries, X-ray topography obs. 9-28556
 BaTiO₃, ferroelec. domain walls, visibility on diff. topographs and comparison with Fe-Si ferromag. walls 9-39682
 Bi₂O₃ layers, evaporated, diff. obs. 9-39162
 Bi (50-60at.%) Te, phase characterization by diff. patterns 9-28394
 BiFeO₃, atomic struct., diff. obs. 9-37135
 C, diffraction studies 9-48822
 C, from heated polyacrylonitrile, profile anal. of random layers 9-28260
 C, saccharose, (hard coke), heat treatment effects 9-37277
 C, structure, and vaporization, mech props., growth and gasification studies, book 9-46695
 CS₂ solid polymer, structural studies 9-34975
 CaF₂-AlF₃ system, phase diagram, powder patterns obs. 9-44805
 CaO-Mn₂O₃-Zn₂Fe₂O₄ system, diff. obs. 9-46958
 CaTiSiO₄ monoclinic cell dimensions, space group 9-39209
 Cd, Bragg reflections from powders for Debye temp. 9-28428
 Cd complex, bis(selenourea)cadmium (II) thiocyanate, powder data rel. to crystal structure 9-26227
 Cd whiskers, lattice imperf. 9-37109
 CdFe₂O₄, oxygen parameter and degree of inversion meas. 9-44660
 CdI₂ single cryst., arcs formation on photographs due to tilt boundaries of dislocations 9-30606
 CdI₂ single cryst., closed rings formation on photographs due to tilt boundaries of dislocations 9-30607
 CdO films prepared by d.c. reactive sputtering 9-48756
 CdS, acousto-electric phonon generation, diff. microscopy obs. 9-46997

X-ray examination of materials continued

- Ce structural analysis, transition to tetravalent state under press., 50 kbar 9-41072
 Co-Ni alloys, transform. kinetics 9-37298
 Co complex, bis(selenourea)cobalt (II) thiocyanate, powder data rel. to crystal structure 9-26227
 Co complex, bis(tricarbonyl enneacarbonyl) acetone, crystal and mol. structure 9-39264
 CoCr₂S₄ ferrimagnetic spinel, lattice const. from powder diff. 9-39196
 Co(KSO₄)₂·2H₂O, powder data rel. to probable struct. 9-35056
 CrSb₂, marcasite-type, mag. props. obs. 9-35581
 Cs gas, thermodynamic props. 9-26177
 Cu-Al martensite cryst. struct. stability, solute content effect, diff. obs. 9-42929
 α -Cu-Cu evaporated film faulting meas. 9-23820
 Cu-Mn-Al phase formation on heat treatment and ageing 9-37293
 Cu, strain centres topograph obs., correl. with etch-pit technique 9-32939
 Cu deformed, monocrystalline struct. defects exam. by X-ray diffraction 9-40939
 Fe-Al alloys, phase relations, diff. obs. 9-44664
 Fe-Al alloys, short-range order, diffuse scatt. obs. 9-44665
 Fe(40 at.%) Al alloy, ordering and struct. diff. obs. 9-42784
 Fe(32 at.%)Pt alloy, quenched, fine struct., diff. obs. 9-46787
 Fe-Ru h.c.p. alloys, ϵ -phase, diff. obs. of mag. props. 9-43159
 Fe(3 wt.%)Si, ferromag. domains, X-ray topographic obs., diff. contrast on walls 9-26643
 Fe-Si, ferromag. domain walls, image contrast, origin, X-ray topography obs. 9-28614
 Fe-Si ferromag. domain walls, visibility on diff. topographs and comparison with BaTiO₃ ferroelec. walls 9-39682
 Fe-Si single cryst., topographic contrast due to 90° ferromag. domain wall 9-33460
 Fe(3 wt.%)Si alloys of different impurities, recryst. textures 9-39474
 Fe, electrolytically deposited under different electrolysis conditions, fine crystal structure 9-44663
 Fe alloys, growth morphology and solute segregation during solidification 9-23952
 Fe cold-worked, diffraction line broadening correlation with mag. permeability 9-45146
 Fe single crystals hardness anisotropy 9-35192
 FeCr₂S₄ ferrimagnetic spinel, lattice const. from powder diff. 9-39196
 FeLiO₂, disordered phase, short range order and local displacement of ions determ. 9-48935
 (FeMn)₂, precipitated during ageing of Fe-Al alloy, diff. obs. 9-33139
 Ga, liquid, atomic radial distrib. meas. over wide range of temps. 9-30371
 γ -Ga, powder data for crystal structure 9-39277
 GaAs_{1-x}P_x cryst. of solid soln. grown from Ga-rich soln., atomic struct. and lattice distortions 9-35206
 GaAs, covalent charge transfer obs., from electron density synthesis of diff. data 9-33302
 GaP films, vacuum-deposited, structural props. 9-42719
 GaSb, covalent charge transfer obs. from electron density synthesis of diff. data 9-33302
 Ge, atomic scattering factor 9-40902
 Ge, Debye-Waller factor and anomalous absorpt., 293.5°K 9-23758
 Ge, internal recontacted splits 9-42846
 Ge dislocation loops prod. by scratches on surface (III), loop vel. temp. depend. 9-32970
 GeO₂, rutile-type, thermal expansion meas. 9-24055
 H₂Fe(CN)₆ cryst. struct. 9-23756
 H₂Fe(CN)₆ cryst. struct., H-bonds and isotope eff. obs. 9-23756
 Hg, liq. struct., diff. obs. 9-32762
 HgS Cinnabar monocryst. grown by hydrothermal method 9-44647
 In₇Cu₁₂Cr₂X₄ (X=S or Se), ionic ordering on A-sites 9-28588
 InAs, covalent charge transfer obs. from electron density synthesis of diff. data 9-33302
 K_{0.99}MoPO₄, diff. obs. of struct., elec. resistivity anisotropy considerations 9-37446
 KCl, lattice defects 9-46815
 KCl, structure factor determ., anharmonicity and thermal diffuse scatt. corrections 9-24014
 KCuF₃ single cryst., polytype struct., diff. obs. 9-32917
 KH₂PO₄, ferroelec. domains boundaries, X-ray topography obs. 9-28556
 KHgBr₃·H₂O, crystal structure 9-39280
 KNbO₃, ferroelec. cry. struct. 9-46788
 (KPO₃)₂, phase transform., Weissberg photographs obs. 9-35245
 K₂TiCl₆ lattice defects 9-46815
 Li-Ag (Cd,Al) alloys, parameters 9-42789
 Li-Mg alloys, lattice parameters 9-42789
 Li₂O-SiO₂ glass, metastable precipitate formation on heat treatment 9-24215
 LiH, Compton profile analysis rel. to valence-electron wave functions 9-46789
 MnAlGe ternary alloy, atomic and ferromagnetic structure 9-35560
 MnF₂, polymorphism at high temp. and press., phase diagram and transform. diff. obs. 9-39184
 MnTO₃(T=Y, Ho, Er, Tm, Lu), hysteresis cycles and ferroelec. domains obs., method 9-26590
 MnTiO₃, II high press. phase, struct. obs. 9-44667
 Mo-Zn alloys prepared by reduction of volatile halides, phase diagram obs. 9-39466
 Mo single crystals, rolling texture exam. 9-41040
 3(NH₄)₂·0.7MoO₃·4H₂O thermal decomposition intermediate phases 9-30745
 NH₄F, wurtzite type struct., space group P6₃mc, h.c.p. sublattices displacement, N-H bond distances 9-32923
 Na, diffraction, intensities, temp. depend. in range 115-353°K 9-23766
 NaCl, deformed, single cryst., dislocation density, diff. obs. 9-32974
 NaCl, thermal expansion at high-temp., diffraction study 9-30786
 NaCl single cryst., thermal expansion, diff. obs. 9-37360
 NaLa(MoO₄)₂ and NaLa(MoO₄)₃·H₂O, structure, and prep. 9-40912
 NaNiF₃, two forms obs. 9-44670
 Nb-Ti-Zr-Hf alloy system, constitution, obs. 9-39597
 Nb-(75 at.%)Ti quenched alloy, phases and crystal struct. 9-23767
 Nb₂Cr₂Si₃, θ -phase in Nb-Cr-Si system, cry. struct. 9-46790
 Nb₂O₅, struct. modifications influence on emission spectra intensity 9-33560
 NbSe₂, lamellar struct., supercond., occupation of sublattice sites rel. to critical temp. 9-41181
 Nd₂(MoO₄)₃-Nd₂(WO₄)₃ system, phase struct., diff. obs. 9-37305

X-ray examination of materials continued

- Ni, initial stages of plastic deformation 9-23888
 Ni, polycrystalline, structure after plastic deformation, X-ray diff. 9-23768
 Ni complex, bis(selenourea)nickel (II) thiocyanate, powder data rel. to crystal structure 9-26227
 NiCrO₃, crystal and mag. structure obs. form powder diffraction analysis 9-43160
 Pb₂Ti₂O₇F₂ pyrochlore, diff. pattern 9-40914
 PbF₂-AlF₃ system, phase diagram, powder patterns obs. 9-44805
 PbZr_{1-x}Ti_xO₃, perovskitic ferroelec. atomic struct. for x=0.9, 0.58 diff. obs. 9-44673
 Pu-Ga alloy, delta stabilized, % of α -Pu 9-39479
 PuO₂, thermal expansion from precision determ. of lattice constants, 30-702°C 9-24056
 Sb₂S₃ film, crystallization process 9-42726
 Se, amorphous, intensity curves rel. to dimensions of struct. element 9-32824
 Si:O single crystals, periodicity by X-ray transmissions 9-32926
 Si, absolute scatt. factor determ. 9-23771
 Si, deformed by thermal gradient 9-23772
 Si, dislocations quantitative relation determ. in 14 mm slice 9-40954
 Si, internal recontacted splits 9-42846
 Si, lattice deform. due to high-energy ion implantation, topography 9-35103
 Si, lattice imperfections induced by P deep diffusion, diff. topography 9-32975
 Si bicryst., ion-bombarded, diff. topographs, fringe contrast and geometry 9-32982
 Si films with SiO₂ diffusion mask, topographic investigation of strain 9-26246
 Si Laue reflected and refracted beams, rocking curve oscillations 9-32928
 Si single cryst. wafers, thermal stresses prod. by electron beam melting, source image distortion obs. 9-35164
 Si single crystals, percussion marks on surface, divergent X-ray diff. pattern 9-33037
 SiC diffraction line intensities, revised, for polytypes 6H, 4H and 15R 9-40916
 SiC thermal reactions with oxides and compounds of Ti, Zr, V, Ta, Mo and W, product exam. 9-49372
 β -SiC whiskers, structure from relative peak intensities, comments 9-32927
 SnTe-As₂Te₂ quasibinary system 9-42920
 Sr₂CuSi₂O₇, akermanite analogue, distorted tetrahedra of Cu²⁺ obs. 9-35010
 Ta₂O₅, struct. modifications influence on emission spectra intensity 9-33560
 Tb, after irreversible transform., struct. interpretation 9-39501
 Te, Bragg reflections from powders for Debye temp. 9-28428
 Ti-(50 wt.%)Nb alloy, struct., diff. obs. 9-42792
 Ti₂ZrO₃ crystal structure 9-26249
 Ti₂O-SiO₂ glasses, cation distrib., scatt. obs. 9-48781
 TlInS₇(Se₂,Te₂) single cryst., struct. obs. 9-44969
 U₂Si, irradi., patterns show no change of struct. 9-40921
 W, X-ray Debye temp. meas. 9-35286
 YFe garnet, multiple diffraction study of crystal. struct. 9-37153
 ZnS polytypes of 10l, 22l and 26l families, oscillation photographs 9-32861

liquids

- p-azoxyanisole crystals, structure study in alternating elec. fields 9-42634
 t-butyl alcohol-water mixtures, small angle scatt. and molecule clusters 9-28101
 dimethylsulphoxide and dimethylsulphone aq. solns. 9-32763
 CoCl₂ conc. solns. in water and alcohols 9-44548
 Hg-Ga system (0.96 and 0.02 mole fraction Hg), radial distrib. functions and co-ord. numbers 9-28100

microstructures

- see also Crystal structure/microstructure*
 crystallite size distrib. in coarse-grained samples, method using interference spots on Debye-Scherrer rings 9-26218
 graphitized C fibres, fine struct. 9-30557
 ice single cryst. growth from melt, dislocation struct., diff. topographs 9-37080
 Mo, deformed and annealed, diff. topography 9-42815
 polyethylene, crystallites mol. and textural orientation, applied stress eff. 9-30584
 polypropylene, on pressure-crystallization 9-46711
 quartz, Brazil twin boundaries, topography, diff. contrast effects 9-42845
 quartz, diffraction contrast of Dauphine twin boundaries 9-30572
 Schulz method determ. of subgrain misalignment 9-32886
 steel, (Cr,Fe), C₃ identification and transform. obs. 9-48831
 Ag-Cu alloys, liq. and vapour quenched, metastable struct. obs. 9-40899
 Ag-Ge film, domains and phase particles anal. 9-28213
 Al single cryst., cyclically strained, surface microrelief changes, diff. method obs. 9-46777
 Al single cryst., dislocation configurations produced by annealing in air and vacuum, comparison 9-37171
 B filaments, vapour-deposited, crystal structure 9-46780
 C, non-graphitizable, small angle scattering, micropore system 9-37136
 Ca-3wt.%Al-0.6wt.%Cu alloy, structural changes during precipitation of hard soln. 9-44789
 CaF₂, diffraction profiles broadening due to pile irradiation 9-46784
 Cu, extinction changes in diff. lines during annealing 9-44662
 Cu films, vacuum evaporated, structure defects 9-30488
 Fe-Al alloys, domain struct. and short range order, depend on Al conc. 9-23757
 Fe-Ni-Mn-Ti martensitic alloys, diff. obs. of pre-precip. stage during ageing 9-37283
 Fe-(40 at.%)Ni alloy oxidized at high temp., scale struct. and chem. composition 9-33669
 Fe rod, crystalline structure under surface electron beam bombardment melting and quick cooling 9-33110
 Ga_{1-x}In_xSb solid soln., growth by temp.-gradient zone melting 9-30719
 Ge, neutron-irrad., diff. obs. of struct. effects 9-44695
 Ge dislocation on bending, by X-ray topography 9-40953
 Ge dislocation orientation by X-ray transmission topography 9-42830
 Mg-Mn alloys, creep specimens and thermally aged, α -Mn precipitate, e. microprobe exam. 9-28265
 Mn-Ni constitutional diagram 9-39502

X-ray examination of materials continued

- microstructures continued**
 Mo, large helical dislocations, equilibrium vacancy conc. derivation 9-35094
 NaCl grown from H₂O soln. with Mn⁺⁺, diff. topographs 9-37144
 Se single cryst., defects topography 9-44709
 Si, defect detection, applic. in integrated circuit fabrication 9-30604
 Ta, imperfect structure in single crystal rods, investigation 9-32930
 Te single cryst., defects topography 9-44709
 TeSe₂, new polymorph. structure 9-35011
 Ti-Al-Co alloy system, Ti-rich corner struct. obs. 9-40919
 TiO₂, polymorphism 9-32860
 U₂Si, irradiation at 60°C, plastic deformation, phase change, diffraction analysis 9-35248
 W, deformed and annealed, diff. topography 9-42815
 W powder, substruct. and block size distrib., diff. obs. 9-46796
 Zn single cryst., diff. topography of imperfections 9-35096
 Zr-Nb system, $\alpha/(\alpha+\beta)$ boundary, microprobe determ. 9-28406
- molecular structure**
 p-bromobenzoyl derivative of ϵ' -caesalpin 9-39324
 3,4^{bis}-bisoxazole, intermolecular and bond distances and angles 9-39338
 2-chlorobiphenyl-4-carboxylic acid, diff. obs. 9-35073
 2-chlorotropone-cycloheptatriene adduct 9-39327
 citric acid, anhydrous, diff. obs. 9-35074
 citric acid, anhydrous, diff. obs. 9-44677
 3,4-dihydro-2,4,6-triphenyl-s-tetrazin-1(2H)-yl 9-48516
 form factors from ab initio wave functions, applic. to diff. struct. analysis 9-32884
 lead stearate, multilayer films 9-39349
 methyl cephalonate bromoacetate 9-39340
 4-methyl-3-(p-bromophenyl)-1,2,5-oxadiazole, 2-oxide, diff. obs. 9-44678
 4-methyl-3-(p-bromophenyl)-1,2,5-oxadiazole, 5-oxide, diff. obs. 9-40924
 3-phenylisoxazolin-5-one, cryst. and mol. struct., X-ray obs. 9-35077
 3-phenylisoxazolin-5-one, cryst. and mol. struct., X-ray obs. 9-42801
 terpenoids, C₂₅ heavy atom derivative, methyl cephalonate bromoacetate 9-39340
 trioxane, low-temp. 9-44679
 yugawaralite, Ca₂Al₆Si₂O₃₂·8H₂O 9-39258
 BaOFe₂O₃, diff. obs. 9-47283
 Ca₂Al₆Si₂O₃₂·8H₂O, yugawaralite 9-39258
 CIOF cry. growth by hydrolysis of ClF₃, X-ray diffraction study 9-26205
 CsBr₃, diff. obs., Br₂⁻ and I₃⁻ systems comparison 9-35057
 Fe complex thio-p-toluoxydisulfidobis (dithio-p-toluato) iron (III), 3-dimen. diff. obs. 9-42785
 NH₄F, form factors of NH₄⁺, diff. obs. 9-32884
 NH₄FeF₆, crystal growth from soln., powder study 9-26207
 NiSO₄·6H₂O 9-39294
 RbFeF₆, crystal growth from soln., powder study 9-26207
 S₂(NH₂), three isomers 9-39305
 Sb complex, tetraphenylantimony hydroxide 9-42418
 TlFeF₆, crystal growth from soln., powder study 9-26207
 Zn (II) complex, n-butylphenylphosphinate polymer, monoclinic and orthorhombic forms, diff. obs. 9-39315

X-ray fluorescence *see Luminescence; X-ray spectra/emission***X-ray measurement**

- see also Dosimetry*
 6KeV with resolution 355eV using Si detector with low-noise preamplifier 9-29660
 C_K values at high energies 9-27150
 calorimeter, total absorption 9-27151
 dosimeter, solid state, digital integrating 9-25533
 Farmer-Baldwin and Victrometer ionization chambers for dosimetry at high energies 9-25511
 fluorescence analyser using avalanche detector, planetary geochemical exploration 9-37863
 intensity measurement, pulses of ns. duration and 10¹⁰ to 10¹¹ roentgens/s range 9-46130
 ionization chamber, inflated balloon for low-level meas. 9-27152
 LET dependence of thermally stimulated exoelectron emission 9-37634
 low energy, general considerations 9-27149
 open multipliers, mag. and channel, 1.5-44 Å 9-48225
 proportional counter with automatic gain control 9-25509
 recording by secondary e multipliers 9-38606
 telescope to concentrate parallel X-rays, using Bragg diffraction 9-27153
 FeSO₄ dosimeter 9-25011
 NaI(Tl) scintillation counter, ratio of 'escape-peak' to 'photo-peak' 9-25514

X-ray microscopes *see Microscopes***X-ray monochromators**

- polarisation scattering factor, including extinction 9-42771

- LiF, double bent, for CuK α radiation diffuse scatter meas. 9-40225

X-ray photoeffect *see Electron emission/photoelectric***X-ray reflection**

- Bragg, from ideal absorbing cryst., integral coeff. 9-42764
 interference expts. with single quanta 9-30540
 kimrite (hydrated Ba feldspar), at. struct., satellite occurrence in inverse lattice 9-46782

X-ray scattering

- see also Compton effect; X-ray diffraction*
 β -brass solid soln., static atomic displacements influence on diffuse intensity 9-37132
 colloidal particle size distribution determ. 9-36904
 crystal with dislocations, derivation of dynamic theory 9-39224
 n-decane- β , β' dichloroethyl critical opalescence investigated by light and X-ray scatt. 9-36877
 diffuse, correlation of intensity meas. 9-37123
 diffuse, meas. using LiF monochromator 9-40225
 in distorted crystals, theoretical study 9-37119
 ferroelectric crystals, critical, rel. to lattice dynamics, and dielec. props. 9-49141
 due to free electrons, increase by applic. of laser rad., no observable eff. 9-22529
 grain size effect 9-49399
 by irregular densely packed systems 9-37124
 polarisation factor including extinction of monochromator 9-42771
 polymer disordered cryst. 9-35072

X-ray scattering continued

- quartz near α - β transition, small-angle scatt. 9-39931
 small angle, collimational distortion calc., digital computer programme and expt. verification of theory 9-46769
 small-angle, collimational distortion calc., correction for slit height 9-46768
 small-angle, for particle size distris. 9-40878
 small-angle, from randomly oriented plane laminas, theory 9-26137
 structure factor determ., lattice vibrations corrections 9-24014
 thermal gradient deformation of perfect crystal, effect on X-ray propag. 9-23772
 Ag-Au layered struct. static atomic displacement influence on diffuse intensity 9-37132
 Al-Zn-Mg alloys, small-angle scatt., preprecip. obs. 9-23979
 Al, absolute structure factors from transmission meas. on powder samples 9-28254
 BaTiO₃, anomalies from lattice dynamical model 9-35267
 BaTiO₃ crystals, critical, rel. to lattice dynamics, and dielec. props. 9-49141
 C, non-graphitizable, small-angle, rel. to micropore system 9-37136
 Cu₂Au solid soln., static atomic displacements influence on diffuse intensity 9-37132
 from Fe₃Al, critical scatt., stat. analysis of data 9-26715
 Ge, atomic factor 9-40902
 H atoms, for transitions between arbitrary atomic shells 9-46326
 KCl, structure factor determ., anharmonicity and thermal diffuse scatt. corrections 9-24014
 KH₂PO₄ crystals, critical, rel. to lattice dynamics, and dielec. props. 9-49141
 NaNO₂ crystals, critical, rel. to lattice dynamics, and dielec. props. 9-49141
 Ni, diffuse, anomalously high intensities near Curie point 9-24304
 O in crystals, anomalous, rel. to determ. of absolute configurations 9-30538
 Si, deformed by thermal gradient 9-23772

X-ray spectra

- see also *Atmospheric spectra; Chemical analysis/X-ray*
 3d transition metals, K β_1 lines, appearance mechanism 9-24433
 analysis by differential reflecting filters, optics 9-36337
 atoms, L-series satellites, $30 \leq Z \leq 50$ 9-22928
 cosmic, and absolute intensity, rocket obs. 9-38063
 diamond, luminescence, electron vibratory series 9-43263
 emission, energy band calc. 9-44877
 heavy elements, L₂- and L₃-subshell fluorescence yields 9-34525
 K α X-ray energies, π , μ , meas. for elements Z=3 to Z=6, including nuclear force shifts 9-27803
 of machines, various, transportable spectrometer 9-25012
 of muonic atoms, rel. to nuclear charge distribution 9-38632
 rare earth metals, K α_1 lines, chem. shifts during oxidation, role of f-electrons 9-37750
 satellite spectra, formation of screening and spin doublets 9-42325
 satellite theory based on sudden approx. only. exptl. evidence against 9-35676
 screening consts, over entire range of Z values 9-44249
 solar, below 20 Å, spatial variability 9-24904
¹⁴¹Pr, muonic X-rays magnetic h.f.s. parameter meas. 9-36575
²⁵²Cf, fission, obs. of KX-rays in association with long-range α 9-38727
²³⁷Th, charge distrib., intrinsic quadrupole moment, radius studied by obs. of muonic X-rays 9-38677
²⁴³Am γ emission by $\alpha\gamma$ coincidences 9-46226
²³⁸U charge distrib., intrinsic quadrupole moment, radius studied by obs. of muonic X-rays 9-38677
 B, scatt. of Cu K α and β_1 rad. 9-45338
 Be and cpds., scatt. of Cu K α and β_1 rad. 9-45338
 C, scatt. of Cu K α and β_1 rad. 9-45338
 Ca, optical isotope shift obs. 9-29988
 Cr, optical isotope shift obs. 9-29988
 Cr metal and some valence II and III halides, K α doublet 9-27807
 Fe-(30 wt.%)Ni alloy, f.c.c. and b.c.c., electron energy spectra, sensitivity to α - γ transform. 9-39856
 Fe, optical isotope shift obs. 9-29988
 Gd, M_{IV} and M_V absorption and emission bands 9-28707
 Gd₂O₃, M_{IV} and M_V absorption of Gd and emission bands 9-28707
 Ge(Li), X-ray escape simultaneous with photopeak obs. 9-29661
 Ho, satellite reflections due to aspherical 4f charge density, theory and expt. 9-24441
 LiF integral refl. coeff., 0.7 to 2.1 Å, obs. and comparison with graphite 9-47384
 Mo, optical isotope shift obs. 9-29988
 Ni, optical isotope shift obs. 9-29988
 RbBr single cryst., K-line yield by positrons, anisotropic penetration obs. 9-35300
 Si, satellite theory based on sudden approx. only exptl. evidence against 9-35676
 Sr, optical isotope shift obs. 9-29988
 Ti, optical isotope shift obs. 9-29988
 V metalline cpds., Fermi levels, density of states determ. 9-37753
 ZnS-Cu luminescence, nonadditivity changes 9-28727
 Zr, optical isotope shift obs. 9-29988

absorption

- absorber thickness and tube voltage effects on fine structure 9-39857
 ferrites, spinel and garnet type, study of composition and different states 9-37743
 K-absorpt. edges, molec. orbital theory 9-39854
 metals, singularities, first-order parquet calcs. 9-24435
 metals, singularities, one-body theory exact solution 9-28706
 metals, soft-X-ray, threshold behaviour 9-49302
 rare earth metals, X-ray absorpt. coeff. determ. for 4d e, N_{IV}, γ e studied, 50-500 Mev 9-37744
 transition-metal complexes, K-absorpt. edges, molec. orbital theory 9-39854
 tube voltage and absorber thickness effects on fine structure 9-39857
 Ag, K and L fine structure investigation 9-39855
 Ag M spectra, in ultrasoft region, abs. coeff. depend. 17-200 Å 9-37754
 CaCO₃, calcite, Ca K-absorpt. fine structure obs. 9-24437
 CaCO₃, limestone, Ca K-absorpt. fine structure obs. 9-24437
 CaMg(CO₃)₂, dolomite Ca K-absorpt. fine structure obs. 9-24437
 CaSO₄·2H₂O, gypsum, Ca K-absorpt. fine structure obs. 9-24437
 CdS, wurtzite structure, K-absorpt. of S. obs. 9-31121
 CdS, zincblende structure, K-absorpt. of S. obs. 9-31121

X-ray spectra continued**absorption continued**

- Cr-Mn alloys, K-absorption edges 9-24439
 Cu randomly and preferentially oriented thin films, fine struct. of K absorpt. edge 9-47383
 Fe-Al alloy, K-absorpt. edges of Fe, position investig. 9-33571
 Fe-Mo alloy, K-absorpt. edges of Fe, position investig. 9-33571
 In, uni-, and trivalent in halides, L_{III} abs. obs. 9-37746
 K₂(Ni(CN)₄)·H₂O, fine structure of Ni K X-ray absorpt. obs. 9-37747
 Mn in Mn cpds. crystals, K lines obs., effective co-ordination charges 9-37745
 Mo M spectra, in ultrasoft region, abs. coeff. depend. 17-200 Å 9-37754
 Na halides, Na⁺La_{2,3} absorpt. 9-41385
 Nb M spectra, in ultrasoft region, abs. coeff. depend. 17-200 Å 9-37754
 nD in Nd cpds. crystals, K lines obs., effective co-ordination charges 9-37745
 Ni(CN)₄·4H₂O, fine structure of Ni K X-ray absorpt. obs. 9-37747
 NiCl₂·6H₂O, fine structure of Ni K X-ray absorpt. obs. 9-37747
 Ni(NH₃)₆Cl₂, fine structure of Ni K X-ray absorpt. obs. 9-37747
 NiO, fine structure of Ni K X-ray absorpt. obs. 9-37747
 NiSO₄·6H₂O, fine structure of Ni K X-ray absorpt. obs. 9-37747
 Pd L_{III} region, white line obs., band structure filling 9-37749
 Pd L series obs., e states studied 9-37748
 Pd M spectra, in ultrasoft region, abs. coeff. depend. 17-200 Å 9-37754
 Rh L series obs., e states studied 9-37748
 Ru, L series obs., e states studied 9-37748
 Th and TlO₂, M spectra, comparison 9-49305
 Ti K absorpt. from TiC, TiN, TiO, TiB₂ and Ti inner level shifts and band struct. obs. 9-45340
 U and UO₂, M spectra, comparison 9-49305
 Y K-absorpt., fine struct. 9-39859
 ZnS, wurtzite, K-absorpt. of S. obs. 9-31121
 ZnS, zincblende, K-absorpt. of S. obs. 9-31121
 Zr M spectra, in ultrasoft region, abs. coeff. depend. 17-200 Å 9-37754

emission

- alloys, dilute, impurity spectrum, effect of localized states 9-49301
 analysis, high A elements, gamma source for excitation 9-29953
 atomic, due to α bombard., cross-section meas. for various atoms 9-46267
 auroral, intensity pulsations, rel. to auroral electrojet development 9-31369
 diamond, K α band of C 9-26762
 energy band calc. 9-44877
 graphite, K α band of C 9-26762
 from hot dense plasma by conversion of focused laser radiation 9-42517
 intensity distrib. in massive anode 9-36675
 ion valence, chemical bonding in cpds. from X-ray microanalysis of fine structure 9-37739
 ion valence from fine structure microanalysis, Ti oxide inclusion in Fe-Cr, Fe-Ni 9-37752
 K lines from fragments of ²⁵²Cf spontaneous fission, yield and emission time meas. 9-38724
 K α satellites, rel. intensities and chem. bonding for elements 12 ≤ Z ≤ 18 9-37740
 K α satellites fine structure calc. for L-S and j-j coupling 9-36650
 metals, behaviour near high-energy Fermi edge, theory 9-31119
 metals, electron- interaction effects on soft X-ray spectrum, formalism and first-order theory 9-24434
 metals, light energy band calcs. 9-44877
 metals, singularities, first-order parquet calcs. 9-24435
 metals, singularities, one-body theory exact solution 9-28706
 metals, singularities, self-consistent treatment of divergences 9-26760
 metals, soft-X-ray, threshold behaviour 9-49302
 muonic atoms, low-Z, K and L series, discrepancies removed 9-46339
 oxides, O K-spectra, investigation of chem. bonding 9-49304
 primary L and M intensity evaluation method for heavy elements 9-36652
 soft, coax, discharge, dominant source determ. 9-25010
 solar, during flares, OSO-III satellite (1967) obs. 9-24906
 solar, quiescent, rocket and satellite obs. 9-45679
 structure depend. on atomic no., 1st large period elements 9-36651
 targets, various metals, 100-1000 eV electron bombard. obs. 9-25013
 Z=17 to 92, K-meson spectra meas., transitions cutoff determ. 9-34530
 Σ-hyperon atom, K-meson spectra peak 9-34530
²¹⁰Pb-²⁰⁹Bi, L-subshell X-ray fluorescence yield and Coster-Kronig transition prob. 9-25602
²⁰⁹Bi e capture decay, L-subshell fluorescence yield, ²⁰⁹Pb Coster-Kronig transition prob. 9-27678
 α - and γ -Al₂O₃, O K-spectra, investigation of chem. bonding 9-49304
 Al atom, with simultaneous emission of L shell shell electron 9-40553
 Al co-ordination number in titanobarium glass and ceramic determ. from line positions 9-41398
 Al in minerals, K lines obs., chemical bonds covalence and ionicity determ. 9-37741
 Al K-shell, ionization by H, He ions, cross section and yield meas., E=25-200 keV 9-22940
 Ar K series, e collision excitation cross sections, 3-16 keV 9-34539
 B₂O₃, K-emission spectra of B 9-24436
 B₄C, K-emission spectra of B 9-24436
 B amorphous, ultrasoft region, energy diagrams determ. 9-37742
 B in BN ultrasoft region, energy diagrams determ. 9-37742
 BN, K-emission spectra of B 9-24436
 BN X-ray emission spectra in ultrasoft region, energy diagrams determ. 9-37742
 Be, K emission spectra of Be 9-26761
 BeO, K emission spectra of Be 9-26761
 C-Cu ionized atoms, K α type lines, theoretical wavelengths, for stars 9-24432
 CU piezo soft x-ray rel. to determination of deformation potential, critical points and Fermi energy 9-49303
 (Ca, Cd)₁₀(PO₄)₆FCl structural and optical props., Pb and Mn activated 9-47382
 Cr-Mn alloys, K β_1 -emission bands 9-24439
 Cu, L_{II} and L_{III} bands, struct. of 3d band 9-45339
⁶⁰Dy, L spectrum forbidden transitions, obs. 9-38766
⁶⁰Dy L-spectrum s-line, 2023.4 XU 9-48392
 Eu, muonic atom isotopes, K and L L-rays meas. 9-29997
⁶¹Ga₂O₃, O K-spectra, investigation of chem. bonding 9-49304
⁶⁴Gd, L-spectrum, new quadrupole transitions 9-22951

X-ray spectra continued**emission continued**

- ⁶⁴Gd L emission, new forbidden lines 9-22953
 In₂O₃, O K α -spectra, investigation of chem. bonding 9-49304
 K in KCl cry., K emission obs., lattice defects determ. 9-36693
 Lu muonic atom isotopes, K and L X-rays meas. 9-29997
 Mg₅Cd, ordered and disordered, L_{2,3} edge-breadth 9-43248
 Mg atom, with simultaneous emission of L shell electron 9-40553
 Mo, electronic structure determ. from fluorescence spectra 9-37755
 N in BN ultrasoft region, energy diagrams determ. 9-37742
 Ni, electronic structure determ. from fluorescence spectra 9-37755
 Pd band shape anal., valence e level diagram determ. 9-36665
 Rh band shape anal., valence e level diagram determ. 9-36665
 S, K $\alpha_{1,2}$ lines chem. shift in cpds. 9-37751
 S atom, with simultaneous emission of L shell electron 9-40553
 Si atom, with simultaneous emission of L shell electron 9-40553
 Ti K emission from TiC, TiN, TiO, TiB₂ and Ti, inner level shifts and band struct. obs. 9-45340
 Ti valence in titanobarium glass and ceramic determ. from Ti K α_1 line positions 9-41398
 TiC, K α band of C 9-26762
 Tm, L emission, α region, three new diagram lines 9-22966
 W, L and M yields w.r.t. channeling of MeV He⁺ 9-41120
 Zr, electronic structure determ. from fluorescence spectra 9-37755
 ZrB₂, K-emission spectra of B 9-24436

X-ray spectrometers

- see also Gamma-ray spectrometers; X-ray crystallography/apparatus*
 astronomical objectives, design and manufacture 9-29140
 double crystal, automatic scanning device 9-32883
 double crystal spect., design and use 9-26177
 fluorescence, using spherically curved crys., sensitivity 9-33993
 radioisotope fluorescence, with high-resolution semicond. detector, sensitivity 9-49397
 source scanning type grating spectrometer, design method 9-36093
 spectra from various X-ray machines, transportable 9-25012
 spectrograph, total reflection, for fluorescent analysis of light elements 9-31235
 twisted crystal 9-31729
 Ge(Li), ultra-high resolution, for low and high energy meas., characts. 9-36523

X-ray spectroscopy

- see also X-ray crystallography; X-ray diffraction*
 analytical fluorescence spectrometry, improved calc. methods 9-47482
 fluorescence spectrometers, thin windows for flow proportional counters 9-32066
 large-area modular focusing system 9-36094
 metals, magnetic, photoelec. study of density-of-states 9-44886
 microdensitometer, computer-linked for analysis of X-ray plates 9-32031
 multichannel quantometer for computerized analysis 9-45433
 trace elements, slope-ratio technique, matrix problems 9-37862

X-ray tubes

- field emission, for cineradiography 9-32097
 flash discharge emission, pinhole camera exposures 9-25014
 flash timing improvement 9-33994
 four-electrode, design for intensive soft and supersoft radiation 9-31730
 generator, new type 9-49619
 multi-stage coaxial surge generator 9-33995
 six-gap device for soft radiation 9-33996
 spectral distributions for quantitative fluorescence analysis 9-31232

X-rays

- see also Cosmic rays/X-rays; Gamma-rays*
 auroral pulsations, damping rel. to primary particle velocity 9-35846
 auroral zone intensity pulsations rel. to electron precipitation 9-31370
 collimator, improved 9-48103
 leakage radiation from 6 MV source 9-24944
 production, use of 5 MeV electron linac 9-48239
 production and electron scatt. in electron-probe microanalysis, Boltzmann eqn. applic. 9-36092
 pulse prod. with vacuum diodes 9-33997
 solar, 8-12 Å, ion chamber photometer obs. 9-24907
 teaching aids and literature guide 9-45712
 ultrafast reproducible pulse from exploding wire 9-31731
 F muonic atom, 2p pionic levels population determ. 9-44301
 N muonic atom, 2p pionic levels population determ. 9-44301
 Na muonic atom, 2p pionic levels population determ. 9-44301
 Na₂SO₄, paramagnetic colour centres identified by e.s.r. 9-30616
 O₂ density distributions, photometric determinations of latitudinal and temporal variations in 70 to 150 km region of atmosphere 9-31341
 O K-shell X-ray prod. in Al₂O₃ thin films by 20-100 keV protons, calc. 9-24073
¹⁶O muonic atom, 2p pionic levels population determ. 9-44301
¹⁸O muonic atom, 2p pionic levels population determ. 9-44301

effects

- see also Nuclear reactions and scattering due to photons*
 alkaline earth fluorides, self-trapped hole and exciton obs. 9-46831
 alkaline-earth fluorides, H and F bands 9-28302
 dibenzocyclohexadienyl radical in anthracene single crystal, radiation induced, ENDOR studies 9-39913
 F centres creation by ionizing radiation above 77K, interpretation w.r.t. recomb. model of interstitials and vacancies 9-40968
 ice crystals, OH radicals 9-47436
 liquid ionization, free ion yield determ. by clearing field 9-23527
 phosphors, luminous efficiency, reflectance and glow curves 9-28721
 Rochelle salt, Barkhausen effect in irradiated crystal 9-47180
 secondary, due to 6 MV X-ray source 9-24943
 triglycine sulphate, Barkhausen effect in irradiated crystal 9-47180
 BaF₂, center formation due to X-ray irradiation with and without H doping 9-26293
 Ca₁₀(PO₄)₆F₂, colour and paramag. centres form. from OH and oxide ion impurities 9-40933
 CaF₂: rare earth ions, irradiation effect on absorption spectrum 9-49271
 CaF₂, trapped electron and H atom centres only produced if there is H doping 9-26293
 CdS X-ray conductivity 9-24173
 n-p-InSb, irradi. elec. and thermal conductivity changes 9-49086
 n- and p-InSb, surface eff. of photoconductivity changes 9-30993
 K₂SO₄ crystal irradiated, e.p.r. spectra obs. 9-24491
 KBr, interstitial centres form. 9-42849

X-rays continued**effects continued**

- KBr, ionizing rad. induced vacancies and interstitials, prod. rate at low temp. 9-32948
 KCl-Ag, irradi., photostimulated luminesc. due to hole release from V_K-centres 9-39897
 KCl, defect production at 20°K, electron-hole recombination mechanism 9-26276
 KCl, interstitial centres form. 9-42849
 KCl, simultaneous optical bleaching and X-irrad., e.s.r. obs. 9-42848
 KCl fracture surface energy changes 9-28372
 KClO₃, irradi. at low temp., e.p.r. of ClO₂ ($\Delta M_3=1$, $\Delta M_1=\pm 1$ or ± 2) 9-49352
 KBr:Na⁺, interstitial centres form. 9-42849
 LiCl, irradi., e.s.r. of Cu²⁺ centres 9-43281
 LiF:Si, X-irrad., e.p.r. rel. to paramag. fault 9-49353
 LiF:U colour centres, formation obs. 9-35115
 LiF, F centres creation, 77-600K 9-40974
 LiF, irradiated, effect on physical props. 9-28546
 LiF colour center formation obs. 9-32986
 LiF thermoluminescence and thermally stimulated conductivity 9-45355
 NH₃OHCl, irradi. optical and thermal conversion of V₂ centres 9-32995
 NH₄Cl:CO²⁺, Ni²⁺, VO²⁺, F-centres, e.p.r. obs. 9-32994
 NaCl:Ag, irradi., photostimulated luminesc. due to hole release from V-k-centres 9-39897
 NaCl:Ca²⁺, V-centre production, effect of irradi. at different temps., e.s.r. obs. 9-30618
 NaCl, defect production at 20°K, electron-hole recombination mechanism 9-26276
 SrF₂, with and without H doping, rate of center formation 9-26293
 ZrO₂:(Ti), thermoluminescence, effect of Ti-doping 9-39891

protection *see Radiation protection***Xenon**

- adsorbed on LiF films, u.v. spectra 9-44630
 adsorption on cleaved faces of absorbers with lamellar struct., formation of first condensed layer 9-48776
 arc emission in far i.r. obs. 9-28059
 arcs, high pressure, stable, radiation portion, indirect determination 9-30323
 atom, electron scatt., neutral bremsstrahlung cross section, shock tube obs. 9-29965
 atom, photoionization, cross-sections for Xe⁺, Xe²⁺ and Xe³⁺ production, 28-83 eV 9-40551
 atoms, charge state change for proton interaction, 5-50 keV 9-44483
 atoms, long-lived autoionization states, mass spectra 9-38782
 breakdown, dye laser-induced, wavelength dependence 9-46543
 breakdown pot. obs., secondary ionization coeffs. calc., mild steel electrodes 9-34811
 bubble chamber, accuracy for determ. of energy of γ 40-2400 MeV 9-22681
 conductivity ratio of electrons meas. in microwave resonant cavity discharge, 2.7 GHz 9-23288
 decays and Lande factors of 7p^{3/2}_{1/2} and 7p^{1/2}_{1/2} levels, mag. reson. meas. 9-46285
 diffusion from UC, UO₂, obs. 9-37214
 diffusion in CsI, trapping rel. to defects, obs. 9-37202
 diffusion in CsI, use of fission recoil doping techniques 9-23837
 diffusion in Cu, influence on gas release of implanted ions, implantation energy and dose 9-35129
 diffusion in H₂O, coeffs., 10° to 60°C 9-26086
 diffusion in irradiated UO₂, from fission bubble growth kinetics 9-28152
 diffusion in NaCl, after irradi. by 10⁸ to 2×10¹⁶ ions/cm² 9-48875
 diffusion in SrF₂ and BaF₂, neutron-irrad. single cryst. 9-35127
 discharge, 1s and 2p level population, electronic temp., conc. meas., 9500 MHz 9-32702
 discharge, electrodeless h.f., characts. 9-40717
 discharge electrodeless, relationship between radiation power and thermal loss at high pressures 9-39027
 discharges, column resistance as function of tube dimensions 9-32613
 electron elastic scattering from ³p metastable state, calc. 9-46307
 equation of state, extrapolation to higher temp. and press., use in fuel swelling calcs. 9-40742
 excited levels, mag.-reson. expts. 9-29955
 extracted from Te minerals, isotopic anomalies 9-42354
 fission, search for n prod. 9-40527
 flash tube performance analysis 9-32043
 fluid, critical region chemical pot. function of density and temp. 9-26155
 gas, viscosity calc. by eqn. 9-30355
 gas, viscosity calc. by eqn. 9-30355
 He-Xe mixture, laser stimulated conc. scatt. of light 9-46286
 intermolecular potential calcs. rel. to thermal-diffusion column operation 9-34843
 ionized partially, elec. conductivity 9-26037
 isotopes, shift meas. in i.r. laser lines 9-29991
 isotopic variation (132, 130) of thirteen i.r. laser lines, relative isotopic displacement 9-48438
 lamp, pulsed, radiation rel. energy supplied 9-41969
 laser field, highly saturated, zero-field level-crossing effects in cascade process 9-32415
 liquid, sound vel. isotherms and effective at. radii, obs. 9-30396
 liquid and solid, refractive indices 9-44562
 magnetic depolarization expts. on ²P_{1/2} and ²P_{3/2} levels under laser irradi. 9-46288
 in meteorites, anomalous isotopic composition 9-41682
 meteorites (chondrites), isotopic composition 9-49393
 optical pumping of ³P₂ state and subsequent collisional depolarization 9-22973
 optical pumping of atoms in ³P₂ metastable state 9-27814
 perturbation theory, eqn. of state and free energy 9-46610
 phase transitions, u.s. investigations 9-37302
 photoionization continua, 40-60 Å region, discrete structure 9-34531
 plasma, absorpt. coeffs in continuum, obs. 9-34766
 plasma, electrostatic ion waves in mag. field due to He contamination, Landau damping 9-30279
 plasma, laser radiation absorpt., transparency effect 9-25888
 plasma beam from coaxial gun, fast neutrals obs. 9-32606
 pulse discharges, discharge pressure and spatial radiation dist. meas. 9-30307
 resonance beam at 1295 Å, disturbances by inert gases and H₂ 9-44265
 shock waves, spectral distrib. of u.v. and visible radiation 9-48654

Xenon continued

- solid, electron drift velocity saturation 9-26587
 solid, thermal expansion 9-42974
 solid, wetting, critical surface tension and contact angle meas. 9-23451
 supersonic jet, intermolecular binding 9-23035
 thermal conductivity calc. from shock heated gas heat transfer rates, 650-5000°K 9-26026
 thermal-diffusion column operation rel. to intermol. pot. calcs. 9-34843
 unexpected intensity obs. in ^{252}Cf fission 9-38727
 u.v. absolute spectral energy distrib. 9-36666
 ^{252}Cf fission yield obs., by examination of Al foils 9-40526
 ^{136}Xe ions in WO_3 , stopping by elastic collisions 9-36678
 ^{136}Xe , hyperfine struct. of i.r. laser lines, interpretation on visible and i.r. 9-29954
 in Cu, vacancy defect clusters 9-32947
 I $^+$ -Xe 0.5-6 MeV with large angle scatt., evidence for prod. of inner shell vacancies 9-32428
 K-Xe collisions, cross-sections 9-27823
 KCl irradi. damage stabilization by trapped Xe, obs. 9-37205
 Xe-Ne system, thermal diffusion factors 9-42616
 Xe-methane charge exchange obs. by ion-cyclotron double reson. 9-44495
 Xe-methane ionic reactions 9-42566
 Xe $^+$, symmetric charge transfer, ($2p_{3/2} \rightarrow 2p_{1/2}$) 9-44261
 Xe $^+$ in very pure Xe, mobility and diffusion cross section 9-44492
 Xe I, radiative lifetimes and collision cross-sections 9-48405
 Xe II, radiative lifetimes of excited states 9-48405
 Xe $^{2+}$ 5353 Å line, pulsed mode, high-power output 9-22405

Xenon compounds

- fluorides, ^{129}Xe - ^{19}F coupling constant as function of ^{19}F chemical shift 9-34646
 oxyfluorides, ^{129}Xe - ^{19}F coupling constant as function of ^{19}F chemical shift 9-34646
 XeF $_2$, mag. shielding of ^{19}F 9-31172
 XeF $_4$ -H $_2$, methane mixtures photolysis, HF chem. laser emission, obs. 9-31944
 XeF $_6$, n.m.r., back of observed coupling, empirical explanation 9-34646

Xerography see Photography**Y-particles see Hyperons/resonances****Yield see Elastic limit; Plastic deformation; Plastic flow****Young's modulus see Elastic constants****Ytterbium**

- electrical resistivity between 4.2-300°K, hysteresis effect, martensitic transform. near room temp. 9-46953
 isotopes, stable, 6s 6 $1p_{1/2}$ level h.f.s. determ., level-crossing and anticrossing spectroscopy 9-22967
 metal-insulator transition, resistance meas. 9-41171
 in NH $_3$, conc. >6 MPM, electrical conductivity meas., 200-300°K 9-23521
 phase transformation near room temp. from elec. resistivity meas. 9-46953
 valence states in compounds 9-32853
 vapour, i.r. laser lines 9-29947
 $^{171}\text{Yb}^{3+}$ endor in CaF $_2$, obs. 9-35732
 $^{173}\text{Yb}^{3+}$ endor in CaF $_2$, obs. 9-35732
 Yb $^{3+}$ doped glass laser, patent 9-48046
 Yb $^{3+}$ excitation in silica glass laser, by Cr $^{3+}$ energy transfer, obs. 9-29430
 Yb $^{3+}$ in CaF $_2$, ENDOR on $^{173}\text{Yb}^{3+}$, electronic shielding by closed shells obs. 9-35731
 Yb $^{3+}$ in CaF $_2$, optical spectra and lifetimes of $2F_{5/2}$ energy level 9-31091
 Yb $^{3+}$ in CaF $_2$ and SrF $_2$, luminescence, quanta summation processes 9-45342
 Yb $^{3+}$ in CaF $_2$ at different site symmetries, Zeeman effect in absorpt. spectra 9-31103
 Yb $^{3+}$ in GaF $_3$, spin-lattice relax. times, nucl. dynamic polarization obs. 9-47297
 Yb $^{3+}$ ions in disordered systems, e.p.r. line shapes 9-28742
 Yb $^{3+}$ trigonal centre in CeO $_2$, ENDOR studies of charge compensation mechanisms 9-33652
 Yb $^{3+}$ -o $^{2-}$ -Fe $^{3+}$ system, superexchange integrals 9-45076
 Yb I, absorpt. spectra 9-44270

Ytterbium compounds

- o-ferrite, e.m. propag. 9-45262
 germanides Mossbauer spectra obs. of oxidation states and chem. bond charact. 9-37696
 silicides, Mossbauer spectra obs. of oxidation states and chem. bond charact. 9-37696
 YbAl garnet, Raman spectra, laser excited 9-49298
 Ca-Yb system, b.c.c. and f.c.c. solid soln. characts. 9-30716
 Yb $_2$ O $_3$, mag. struct. 9-45075
 Yb $_2$ Fe $_{1-x}$ Ga $_x$ O $_{12}$ ($x=0.5-4.0$), crystallization from PbO/PbF $_2$ solvent 9-37047
 Yb Fe garnet, cooling by adiabatic magnetization 9-45194
 YbB $_6$, sp. ht., low temp. 9-47003
 YbFe garnet: Lu, supertransferred hyperfine field, temp. depend. 9-35607
 YbFe garnet, angled spin configs., spectroscopic study 9-45193
 YbFe garnet, canted spin config. 9-47277
 YbFe garnet, magnetic torques consistent with canted sublattice configuration, 4.2°K 9-35576

Yttrium

- adsorption on (121), (111) and (021) faces of W single crystal, investig. using electron field-emission projector 9-44632
 atomic spectrum, a bibliography 9-38765
 in compounds, L level shifts and width changes 9-48400
 desorption from W in strong elec. field, 300° to 630°K 9-46733
 Hall effect and mag. susceptibility, 90° to 400°K, fields up to 15 kOe 9-33258
 heat capacity, 1-30°K 9-47006
 impurity in F, colour centre formed under u.v. irradi., e.s.r. identification 9-40971
 magnetic susceptibility between 0.36-300°K 9-49190
 paramagnetic susceptibility, 20.4° to 293°K 9-31024
 X-ray K-absorpt. spectrum, fine structure 9-39859
 Y $^{2+}$ colour centre in γ -irrad. CaF 9-39373
 CdF $_2$:Y, semicond., resistivity and Hall coeff. 9-49077
 in CdF $_2$, donor conc. effects on i.r. absorpt. rel. to trapped electron theories 9-47354
 Fe-Cr alloy, effect on oxidation 9-24559

Yttrium compounds

- ethyl sulphate single cryst., Gd $^{3+}$ e.s.r. spin Hamiltonian parameters 9-43290
 ferrite, ferromagnetic, mag. extinction of neutrons 9-41308
 garnet, elastic anisotropy, investigation by magnetoelastic interac. 9-37221
 Y:Gd dil alloy, at 1000 ppm, mag. saturation moment 9-49190
 YAl garnet:Nd $^{3+}$, optical transition props. using Jarrell-Ash 1m Ebert scanning spectrometer 9-26751
 Al $_2$ O $_3$ /Y $_3$ Al $_5$ O $_{12}$ system, eutectic solidification 9-34960
 Al $_2$ O $_3$ -Y $_3$ Al $_5$ O $_{12}$ system, eutectic point position, microstruct. obs. 9-35254
 Ce-Y alloys, nondil., resistance minima, spin-compensated mag. state and Neel temp. obs. 9-35337
 Dy-Y alloy, Hall effect and mag. susceptibility, 90° to 400°K, fields up to 15 kOe 9-33258
 Dy-Y paramag. susceptibility and Hall eff. meas. 9-37644
 Gd-Y alloys, magnetic structure props. 4° to 300°K 9-45125
 Tb-Y alloy, Hall effect and mag. susceptibility, 90° to 400°K, fields up to 15 kOe 9-33258
 Tb-Y paramag. susceptibility and Hall eff. meas. 9-37644
 Y-Ni system, role of YNi $_3$ cell in struct. determ. of other cpds. 9-30567
 Y $_3$ Ca $_2$ Fe $_3$ V $_3$ O $_{12}$, Mossbauer spectra of ^{57}Fe , non-equivalency of Fe $^{3+}$ octahedral-site 9-24387
 Y $_1$ - $_x$ Eu $_x$ VO $_4$:Tb luminescence brightness and instability control by doping, patent 9-24450
 Y $_{2-x}$ - $_x$ Bi $_x$ Ca $_x$ Fe $_x$ -Si $_x$ O $_{12}$ ($x=0.6-1.3$), crystallization from PbO/B $_2$ O $_3$ solvent 9-37047
 Y $_2$ O $_3$, high pressure synthesis and superconducting props. 9-35372
 Y $_2$ O $_3$:S:Eu $^{3+}$, luminescence spectra, satellite lines due to ion-pairs 9-24449
 Y $_2$ O $_3$:Bi $^{3+}$, luminescence 9-31125
 Y $_2$ O $_3$:Eu $^{3+}$ emission spectrum, Eu $^{3+}$ emission from two symmetry sites 9-33562
 Y $_2$ O $_3$:ThO $_2$ sintered optical ceramic, prep., props. and applic. 9-33501
 Y $_2$ O $_3$ analysis using YVO $_4$ lanthanide phosphors 9-28714
 Y $_2$ O $_3$ polycryst., cation self-diffusion coeffs. 9-42860
 Y $_2$ SiB $_6$ O $_7$, crystal structure and refinement 9-39314
 Y $_{3-x}$ Tb $_x$ Fe $_x$ Ga $_x$ O $_{12}$, ferromag. reson. of Tb $^{3+}$ and Ga $^{3+}$, anisotropy of reson. field and line width 9-33619
 Y $_3$ Al $_5$ O $_{12}$, Cr $^{3+}$ and Nd $^{3+}$ impurity distribution, rel. to trivalent oxide solubility and cry. growth 9-36980
 Y $_3$ Al $_5$ O $_{12}$, Cr $^{3+}$ and Nd $^{3+}$ impurity distribution, rel. to trivalent oxide solubility and cry. growth 9-36980
 Y $_3$ Al $_5$ O $_{12}$, crystal growth, free from strained central core 9-28235
 Y $_3$ Al $_5$ O $_{12}$, energy transfer between Er $^{3+}$ and Tm $^{3+}$, and Er $^{3+}$ and Ho $^{3+}$ 9-31126
 Y $_3$ Al $_5$ O $_{12}$, luminescence of Nd $^{3+}$, conc. quenching 9-31126
 Y $_3$ Al $_5$ O $_{12}$, optical absorpt., 10- to 55000 cm $^{-1}$ wave no. 9-35666
 Y $_3$ Al $_5$ O $_{12}$ habit changes of single crystals grown from a PbO-PbF $_2$ flux 9-40922
 Y $_3$ Fe $_5$ O $_{12}$, ferrimag. reson., linewidth, independent grain and dipole narrowing theories comparison 9-45373
 Y $_3$ Ga $_5$ O $_{12}$:Tm $^{3+}$, photoluminesc., optical transitions obs. 9-49338
 Y $_3$ Ga $_5$ O $_{12}$, luminescence of Nd $^{3+}$, conc. quenching 9-31126
 Y $_3$ Ga $_5$ O $_{12}$ habit changes of single crystals grown from a PbO-PbF $_2$ flux 9-40922
 Y $_3$ Mn $_5$ O $_{12}$ Fe $_4$ O $_{12}$ mag. anisotropy and magnetostriction at 300°K 9-49219
 Y $_3$ OCl $_2$:Yb $^{3+}$, Er $^{3+}$ phosphors for i.r. to visible conversions 9-49324
 Y $_3$ OCl $_2$, i.r.-pumped visible and u.v. emission from Yb $^{3+}$ -Er $^{3+}$ and Yb $^{3+}$ -Ho $^{3+}$ ions, mechanisms 9-48110
 Y $_4$ Co $_3$, crystal structure 9-39313
 Y Fe garnet slab, transversely magnetised, surface magnetostatic waves, boundary conditions 9-47860
 YAl garnet: Nd $^{3+}$ (Er $^{3+}$) crystal struct. and lum. props. studied 9-33596
 YAl garnet:Nd, imperfection assessment and control in crystals used for laser devices 9-37157
 YAl garnet:Nd, optical pumping using K-Hg discharge lamp 9-25201
 YAl garnet:Nd $^{3+}$, quasicontinuous giant pulse emission of $^4F_{3/2} \rightarrow ^4I_{3/2}$ transitions at 1.32 μ m 9-22420
 YAl garnet:Nd laser, 100 W output, 3% efficiency 9-48031
 YAl garnet:Nd laser, feedback-controlled, dynamics 9-48030
 YAl garnet:Nd laser, Kr lamp pumping, 105 W output 9-48033
 YAl garnet:Nd laser, Q-switched, coherence length corresp. to pulse length 9-48035
 YAl garnet:Nd laser, repetitively Q-switched, pulse-to-pulse stability 9-48032
 YAl garnet:Nd lasers, diode pumped, c.w. operation, 46 mW output at 1.0614 μ m with 1% efficiency 9-48034
 YAl garnet, e.p.r. spectra and relax. processes of Nd $^{3+}$ 9-24498
 YAl garnet, etch figures, rel. to point defects, dislocations and orientation 9-44641
 YAl garnet, growth by hollow cathode floating-zone method 9-37091
 YAl garnet, Raman spectra, laser excited 9-49298
 YAl garnet, thermal expansion at 296-1400°K 9-41093
 YAl garnet: Nd $^{3+}$ laser, self-Q-switching at 77°K 9-36309
 YAl garnet: Nd laser, continuous operation by injection luminescent pumping 9-25301
 YAl garnet single crystals, optical quality, incorporation of increased conc. of rare earth activator ions 9-37093
 YAl garnets, synthetic cryst., inhomogeneities, optical investig. 9-37165
 YAlO $_3$:TR $^{3+}$, as active laser medium 9-48015
 YAlO $_3$, growth by hollow cathode floating-zone method 9-37091
 YAsO $_4$:Gd $^{3+}$ e.p.r. spectra obs. 9-43286
 YAsO $_4$ rare-earth doped, crystal growth and lattice parameters determ. 9-39215
 YB $_{66}$, crystal structure 9-26251
 YCl $_3$.6H $_2$ O:Gd $^{3+}$, e.s.r. 9-28747
 YCO $_3$, ferromag., press. effect on curie point 9-45154
 YCO $_3$, YCO $_3$ and Y $_2$ CO $_3$ single crystals, mag. moments, polarized-neutron diffraction study 9-47250
 YCrO $_3$, absorption and fluorescence spectrum of Cr $^{3+}$ magnon-assisted 9-49321
 YCrO $_3$, antiferromagnetic, Davydov splitting direct obs. 9-24335
 YCrO $_3$, Cr $^{3+}$ fluorescence spectrum, magnon sideband emission 9-31136
 YF $_3$, lattice vibr. and i.r. props. 9-42951
 YFe garnet: Cu $^{2+}$, ferrimag. reson. 9-45374
 YFe garnet: Si, i.r. sensitive ferrimag., relax. and mag. anneal of anisotropy 9-45191
 YFe garnet:Co, magnetocrystalline anisotropy and ferrimag. reson. 9-33480

Yttrium compounds continued

- YFe garnet:Ho, ferrimagnetic resonance linewidth and fine structure 9-26790
 YFe garnet, (Ca, V, In)-substituted, anisotropy and magnetostriction meas. 9-45192
 YFe garnet, and Ca-V-substituted, effective linewidth due to porosity and anisotropy, field depend., microwave freqs. 9-45371
 YFe garnet, Ca-V-substituted, effective linewidth due to porosity, relax. obs. 9-31055
 YFe garnet, chem. polishing 9-40835
 YFe garnet, dense ferrimagnetic perovskite allotropic form, existence 9-26252
 YFe garnet, dislocation effects on magnetiz. process, direct investigation 9-47276
 YFe garnet, effective linewidth due to porosity, relax. obs. 9-31055
 YFe garnet, electrostatic and exchange interactions high degree 9-47227
 YFe garnet, Faraday rot. 9-43214
 YFe garnet, Faraday rotation at 1.15μ 100° to 450°K 9-49218
 YFe garnet, i.r. radiation scattering by two magnon processes 9-45337
 YFe Garnet, InSb hybrid structure, interaction between spin waves and electrons 9-24230
 YFe garnet, longit. magnon-phonon interaction in obliquely magnetized rods 9-35574
 YFe garnet, magnetoelastic pulse prod. by Schlomann method, pulse sequences 9-43178
 YFe garnet, no 2-magnon scatt., ferromag. resonance linewidth, 9.3 GHz. 4.2-300 K 9-41420
 YFe garnet, optical absorpt. and emission studies of Ho³⁺ ions 9-45331
 YFe garnet, partially magnetized bar, generation and propagation of magnetoelastic waves 9-33479
 YFe garnet, preparation, improvement in yield 9-37092
 YFe garnet, relaxation processes investigation with propagating magnetostatic spin waves 9-45241
 YFe garnet, seeded growth from molten salts 9-37045
 YFe garnet, Si doped, optical dichroism and photoinduced magnetic anisotropy 9-24307
 YFe garnet, Sn-substituted, critical mag. isotherm 9-43188
 YFe garnet, spontaneous magnetisation rel. to temp. in range 4.2-290°K 9-41328
 YFe garnet, thermal expansion at 296-1400°K 9-41093
 YFe garnet, thermal transport, effect of magnons 9-44847
 YFe garnet, two-magnon scatt of i.r. radiation 9-24421
 YFe garnet axially magnetized rod, magnetoelastic wave instability threshold 9-37668
 YFe garnet epitaxial films, ferromag. reson. 9-45372
 YFe garnet films, epitaxial, on YAl garnet and GdGa garnet, microwave phonon generation 9-44816
 YFe garnet films with narrow ferrimagnetic resonance linewidth, epitaxial growth 9-36952
 YFe garnet rod, axially magnetized, magnetoelastic wave instability threshold 9-45190
 YFe garnet rod, axially magnetized, magnetostatic mode instabilities 9-45189
 YFe garnet rods, (110) oriented, magnetoelastic wave propag. 9-45187
 YFe garnet rods containing turning point, magnetostatic mode excitation 9-45188
 YFe garnet single crystal, resonant absorpt. of elastic waves in absence of external mag. field 9-30649
 YFe garnet single crystals, X-ray multiple diffraction study, structure 9-37153
 YFe garnet single crystals, flux growth 9-37046
 YFe garnet single crystals, effect of pressure on homogeneous distribution of gallium 9-36979
 YFe garnet with Tb admixture, meas. of domain wall mobility 9-41327
 YFe garnets: Ca²⁺(Si⁴⁺), microwave dielec. loss and permittivity 9-33374
 YFe garnets, Ga-substituted, cation distrib. by Mossbauer effect spectroscopy 9-45303
 YFeO₃ h.f. lattice vibrs. deduced from absorpt. and refl. spectra 9-41080
 YFeO₃ orthoferrite, exchange interaction and g factor determ. 9-45182
 YFeO₃ weak ferromagnet, susceptibility tensor, temp. depend. 9-43187
 YGa garnet:Sm³⁺ (Dy³⁺), crystal-field energy levels of ⁶H and ⁶F multiplets 9-45254
 YGa garnet: Tm³⁺, selection rules in absorpt. spectrum 9-24416
 YGa garnet: Yb, ²F_{7/2} levels Raman-Zeeman obs. 9-49300
 YGa garnet:Co, spin reson. in single cryst. 9-35575
 YGa garnet, double ferromag. reson. obs. 9-49343
 YGa garnet, optical absorpt. and emission studies of Ho³⁺ ions 9-45331
 YGa garnet, Raman spectra, laser excited 9-49298
 YGa garnet, thermal expansion at 296-1400°K 9-41093
 YMnO₃ hexagonal, far i.r. antiferromag. reson. 9-45377
 Y(NO₃)₃, solvation in H₂O-acetone, p.m.r. 9-42682
 YOCl:lanthanides, cathodo and photo-luminesc., obs. 9-28732
 YOCl: rare earth activated, fluoresc. under u.v. irradi., photo- and cathodo luminesc. 9-37768
 YPO₄:Ce, u.v. phosphor, sensitized by Th ions 9-31140
 YPO₄:Gd³⁺ e.p.r. spectra obs. 9-43286
 YPO₄, rare-earth doped, crystal growth and lattice parameters determ. 9-39215
 YVO:lanthanides, luminesc. 0.7-1.1 μ and luminesc. Y₂O₃ analysis appls. 9-28714
 YVO₄:Dy, luminescence, effect of Eu and Tb impurities 9-47398
 YVO₄:Eu, phosphor, method of preparation, patent 9-28715
 YVO₄:Eu, photo-, cathodo- and thermo- luminesc., impurity effects 9-47409
 YVO₄:Gd³⁺ e.p.r. spectra obs. 9-43286
 YVO₄:In, photo- and cathodo-luminesc. 9-47397
 YVO₄:Nd³⁺, absorption, luminescence and stimulated emission spectra 9-26746
 YVO₄, solubility in Na₂VO₄, Li₂VO₄ and V₂O₅, crystn. conditions and structure 9-40777
 YVO₄, rare-earth doped, crystal growth and lattice parameters determ. 9-39215
 Yal garnet: Sm³⁺ (Dy³⁺), crystal-field energy levels of ⁶H and ⁶F multiplets 9-45254
 Y₁₃Gd₃-₁₃Al₁₁(In/Sc)₁₂Fe₅₋₁₁₋₁₂O₁₂, isomagnetization lines 9-39778

Yukawa potential see *Field theory, quantum/meson field; Nuclear forces; Scattering***Zeeman effect**

- alkali vapour, Zeeman transitions, saturation. eff. on h.f. spectrum 9-27806

Zeeman effect continued

- p-bromophenol, ²I_B n.q.r. 9-39929
 carriers trapped by dislocation, anomalous effect 9-33533
 p-chlorophenol, ³⁵Cl n.q.r. 9-39929
 electronic impurity states interact. with Jahn-Teller coupling 9-31057
 ethylene oxide, molec. g values and mag. anisotropy 9-42431
 ethylene sulfide rotational transitions, mol. g values and mag. susceptibility anisotropies obs. 9-40612
 fluoroacetylene, obs. mag. susceptibility anisotropy and mol. quadrupole moment 9-25764
 fluorobenzene, molec. g values and mag. anisotropy 9-44359
 interstellar clouds of neutral H, mag. fields determ. from Zeeman effect obs. 9-36001
 interstellar magnetic field meas. by splitting of 21 cm line by HI clouds 9-36002
 ions in crystals, symmetries 9-24388
 ketene, g values, mag. susceptibilities anisotropy 9-30126
 stars, metallic-line, Zeeman observations 9-43545
 stars, metallic-line, Zeeman observations 9-43546
 symmetries, for ions in crystals 9-24388
²⁰¹Hg atoms disturbed by imaginary elec. field, diagram 9-46278
 Al₂O₃:Ti(V,Cr) far-i.r. absorpt. spectrum in applied mag. field, line splitting, single d electron obs. 9-31100
 CaF₂:Yb³⁺, in absorpt. spectra rel. to different site symmetries of Yb³⁺ 9-31103
 CaO:Bi, splitting in absorption and emission spectra 9-33549
 CdS, donor-acceptor pair lines obs. 9-49273
 CeF₃:Nd³⁺ single cryst., far i.r. electronic and vibronic transitions obs. 9-35653
 CeF₃:Nd³⁺ oriented single cryst., far i.r. electr. and vibronic transitions 9-39843
 CuCl, of bound excitons, absorpt. and emission obs. 9-37721
 Er I, 4P⁰6s² and 4P¹5d6s² configurations 9-46277
 ErGa garnet, ⁴I_{15/2}-⁶S_{3/2} transition, Er³⁺ g-tensor anisotropy determ. 9-23040
 F, ²P_{1/2} level, (1,0)-(1,-1) transition, g factor calc. 9-32411
 GaP:Bi, splitting of recomb. radiation from excitons 9-45347
 Gd configuration identification 9-44262
 Ge, splittings of shallow acceptor states 9-41378
 I, 5s² sp² ²P_{3/2}-5s² 5p² ²P_{1/2} obs. at 7603°K 9-29935
 KH₂PO₄, rotary saturation and spin calorimetry 9-28757
 LaF₃:Nd³⁺ oriented single cryst., far i.r. electr. and vibronic transitions 9-39843
 LaF₃:Nd³⁺ single cryst., far i.r. electronic and vibronic transitions obs. 9-35653
 MgF₂:Co²⁺, far-i.r. spectra, exchange interactions obs. 9-41384
 MnF₂, antiferromag., critical Zeeman effect anisotropy 9-35642
 N¹⁵N¹⁵O¹⁶, mag. anisotropy, molec. g value and quadrupole moment 9-38862
¹⁵NH₃, first order at 25 kG, rel. to g-values of levels 9-42408
 NO₂, near-i.r. high-resolution 9-36702
 Nd I arc spectrum, parametric calc. for electronic config. 9-29943
 NdF₃ oriented single cryst., far i.r. electr. and vibronic transitions 9-39843
 NdF₃ single cryst., far i.r. electronic and vibronic transitions obs. 9-35653
 OCS, g value and mag. susceptibility anisotropy 9-30046
 PrF₃:Nd³⁺ oriented single cryst., far i.r. electr. and vibronic transitions 9-39843
 PrF₃:Nd³⁺ single cryst. far i.r. electronic and vibronic 9-35653
 Rb nonlinear hyperfine pressure shift induced by optical pumping 9-36664
 YGa garnet:Yb, electronic Raman scatt. to crystal field levels of ²F_{7/2} manifold 9-49300
 ZnS:Cu in absorption spectrum line at 1.44 μ m 9-24417
- Zener diodes** see *Semiconducting devices/diodes*
- Zener effect** see *Metals; Semiconducting materials; Semiconductors*
- Zeta-potential** see *Electrokinetic effects*
- Zinc**
- ³P, state, collision broadening of double resonance line empirical formula for resonance curve 9-34554
 atom, energy transfer to 4¹D₂ level from ⁷S₁ level of Hg in discharge, process 9-48422
 atomic spectrum, bibliography 9-38765
 atoms, photoionization cross sections wavelength dependences, 247-1242 A 9-34562
 Bauschinger effect in twinning of crystals 9-42880
 bicrystals, grain-boundary crack formation during deform. at high temp. 9-30698
 bicrystals, grain-boundary slide-hardening 9-42889
 brittle fracture in liquid Hg, effects of alloying 9-23916
 cleavage planes 9-48786
 cleavage surface energy of basal plane 9-30481
 corrosion, atmospheric, effect of 1% Cu addition 9-37836
 corrosion, literature review 9-26830
 corrosion in water, NaOH and other decinormal solns. 9-28805
 corrosion of rolled zinc, effect of atmospheric factors 9-37837
 creep of single cryst., activation vol. determ. 9-39426
 creep of single cryst., γ quanta irradi. effect anisotropy 9-39425
 critical shear stress, dislocation forest density depend. 9-46878
 crystal, thermal etching of dislocations in vapour grown mat. 9-48864
 deformation of single crystals at high strain rates 9-23891
 diffusion in AlSb, chemical and isoelectronization conc. depend. 9-35124
 diffusion in AlSb, GaAs and GaSb, chemical and isoelectronization, Longini's interstitial/substitutional model 9-35125
 diffusion in Cu whiskers, coeff. depend. on diameter 9-26300
 diffusion in GaAs, 1000°C 9-28327
 diffusion of Ag and self-diffusion Ag conc. dependence 9-23845
 dislocation contrib. to u.s. attenuation 9-39521
 elastic shear constants, band structure contribution, model potential theory validity test 9-30630
 electrode, spectral lines in nearby region, dynamics in pulsed discharge 9-36791
 electrodeposited from aqueous KOH soln. with zincate ions, electrolyte flow effect on morphology 9-33679
 electromigration 9-23844
 electrotransfer in Bi 9-48873
 epitaxial growth of electrodeposits on Cu single crystals 9-30490
 etching, selective, at dislocations mechanism 9-40856

Zinc continued

- fatigue damage under cyclic stress 9-32981
 film preparation by high-vac. evaporation 9-36963
 in flames, absorpt. line profile, atm. and reduced press., Zeeman scanning 9-28786
 grain boundary relax. 9-44715
 grain boundary sliding anisotropy in bicryst. grown from melt 9-40965
 grain boundary sliding anisotropy in bicryst. grown from melt 9-40964
 grain growth after deformation 9-26363
 growth form, alteration as result of diffusion non-homogeneity of supersaturation 9-37013
 growth of single cryst. from vapour in H atmosphere, cavities form. abs. 9-48799
 growth of spherical single cryst. from supersaturated vapour just below melting pt. 9-48798
 Hall coeff. at -196-100°C 9-47071
 heat capacity, 1-30°K 9-47006
 hexagonal, vibrational spectrum 9-42946
 ingots, rolling, patent 9-35203
 interfacial energy of (0001) plane in contact with liq. Hg, 298°K 9-40837
 internal friction anomalies near melting point 9-39399
 ion polarization via Penning collisions with optically pumped metastable He 9-38803
 ionic spectra, new classifications and corrected wavelengths of selected lines 9-34549
 isoelectronic series, oscillator strengths energy eigenvalues, mean radii, calcs. 9-44271
 liquid, density meas. up to 700°C 9-30375
 liquid, neutron diff. anal. for ion-ion pot. determ. 9-23459
 metallization of plastic dielectrics for capacitors 9-39698
 in minerals, spectrochem. analysis using C cavity electrodes, obs. 9-28828
 optical constants 9-31070
 plasticity, extended in commercial purity sample 9-28352
 recrystallization during thermal cycling 9-32879
 rolled, atmospheric corrosion, eff. of 1% Cu addition 9-37836
 rolled, eff. of atmosphere on corrosion 9-37837
 single crystals, X-ray diff. topography 9-35096
 stacking fault formation in {1012} twins, from slip dislocation-deform. twin interactions 9-26289
 Stark effect, shifts in 3P, excited states 9-36660
 stopping power for 0.6-2.4 MeV protons 9-33212
 strength loss due to adsorption, anisotropy 9-23911
 sublimation, enthalpy and entropy correlation, torsional and Knudsen vapour pressure meas. methods 9-39146
 superconducting, microwave absorpt. obs., mag. field depend. 9-47094
 superconducting transition temp. 9-35358
 thermodynamic activity in Ag-Zn alloys, effect of free electron conc. 9-26477
 thermoelectric power, quantum oscillations, Peltier effect obs. 9-43124
 twinning speed studied with high speed photography 9-23659
 u.s. absorpt., quantum oscillations, rel. to Fermi surface 9-44822
 u.s. attenuation at low temp. in single cryst. 9-33174
 u.s. attenuation in normal and supercond. state 9-37338
 vacancy formation parameters from thermal expansion meas. on single crystals 9-46811
 whisker, elastically bent, resistance increase below 6°K, rel. to electron mean free path meas. 9-37453
 whiskers, galvanomagnetic props., size effects 9-30853
 whiskers, size effect on resistivity 9-37454
 band structure in magnetic fields, calc. using single band effective Hamiltonian 9-24096
 in Cd, Hall resistivity and magnetoresistance rel. to small-angle intersheet scatt. 9-26515
 in Cd, Hall resistivity and magnetoresistance 9-41165
 GaAs:Zn, noise spectra in thermal equil. and under optical excitation, electron fluctuations obs. 9-41198
 in GaAs, luminescence, broad-band emission near 1.38 eV, temp., excitation-intensity and stress dependences 9-24447
 in GaAs, surface resistivity, average mobility and carrier conc. obs., post-implantation annealing depend. 9-33320
 GaP:Zn, resistivity and Hall coeff. variation with dopant conc. 9-44954
 in GaP, epitaxial growth, carrier and Zn conc. obs. 9-30529
 in p-GaP, red emission, config. coordinates applic. 9-37761
 in GaP soln.-grown, red luminesc. generation obs. 9-33321
 in KBr, thermoluminesc. and optical absorpt., F centres formation 9-33606
 Mn-Zn ferrite production from MnCO₃-ZnO-Fe₂O₃ calcination 9-35742
 Si-Zn photoconductors, noise and changing recomb. traffic obs. 9-41270
 in SiO₂-Si m.o.s. struct., effects on C-V characts. 9-33362
 Zn:Ag, diffusion of ⁶⁵Zn and ¹¹⁰Ag, effect of dopant 9-40990
 Zn:Li single cryst., space charge limited currents between asymmetric contacts 9-33378
 Zn/O secondary battery, use of fluidized bed Zn anode to overcome dendrite form. 9-37839
 Zn-Hg-Kr, discharge, excitation energy transfer from Hg to Zn in afterglow, process 9-48422
 Zn II laser c.w. transitions, 7479 and 7588 Å 9-47983
 Zn IV, elec. dipole transition configs. obs. 9-48398
⁶⁵Zn, diffusion in Zn:Ag, effect of Ag 9-40990
⁶⁵Zn in GaP, vapour-grown, substrate orientation effect on dopant incorporation 9-30920
 ZnI absorption spectrum obs. in vacuum u.v. 9-27798

Zinc compounds

- β_1 -brass, metastable, martensitic transformations, heat treatment, n. irradiation and deformation effects 9-23981
 β -brass, ordered, energy bands using Green's function 9-48990
 α -brass, rolled, orientation distrib. of crystallites, electron microscopy determ. 9-48830
 brass, Young's modulus and torsion modulus calcs. by different methods 9-30629
 β -brass single cryst., creep behaviour near T_g 9-30668
 chalcogenides, 'e.p.r.' of rare-earth ions, rel. to atomic environment 9-47430
 chalcogenides, solution growth using tin as solvent 9-37073
 phthalates, luminesc. 9-47399
 rare earth-Zn cpds. with CsCl struct., mag. obs. 9-35556
 sulfates, infrared absorpt. spectra 9-47368
 Zn₃(BO₃)₂, pure cubic, electron trap distrib. obs. in phosphorescence 9-45353

Zinc compounds continued

- ZnSe:Xu,I, electro-, photoluminesc. temp. depend. rel. to centres, obs. 9-35701
 Al-(10 wt.%)Zn alloy, irradiated at 78°K, pre-precipitation rate 9-30715
 Ag-(31 at.%)Zn alloy, elastic after-effect kinetics, resistance meas. 9-35161
 Ag-Zn alloys, thermodynamic activity of Zn, effect of free electron concentration 9-26477
 Ag-Zn equiatomic alloy, $\beta_1 \rightarrow \beta_2$ transform., stress effect 9-30737
 Ag-Zn equiatomic alloys, $\beta_1 \rightarrow \beta_2$ and $\beta_1 \rightarrow \beta_3$ transform. 9-33145
 Ag-Zn system, mag. susceptibility of ϵ and η phase alloys 9-43150
 Ag-Zn β -phase alloys, order-disorder transf., Hall coeffs., elec. resistivity 9-35253
 Al-Mg-Zn alloy, recrystn., dislocation arrangement influences 9-37276
 Al-Mg-Zn alloys, ageing and plastic deform. 9-37280
 Al-Mg-Zn pre-precipitation, lattice parameters rel. to ageing 9-41049
 Al-(30 at.%)Zn alloys, side-bands in Debye-Scherrer patterns 9-46936
 Al-Zn-Mg-Cu alloys, deformed, substructure and susceptibility to intergranular stress corrosion cracking 9-23811
 Al-Zn-Mg alloys precipitation near grain boundaries 9-39489
 Al-Zn-Mg 1 type alloy, blue tint of glossy anodized extruded profiles 9-39833
 Al-Zn-Mg alloy, fatigue props., effect of shot peening 9-26315
 Al-Zn-Mg alloy, weldable, stress-corrosion resistance, effect of quench rate, rel. to microstruct. changes 9-46919
 Al-Zn-Mg alloys, preprecip., hardness and small-angle X-ray scatt. meas. 9-23979
 Al-Zn-Mg properties rel. to natural ageing and ageing between 100-340°C 9-37281
 Al-(40 at.%)Zn alloy, aged at 240° to 250°C, stacking fault formation 9-23979
 Al-(40 wt.%)Zn alloy, structural changes during ageing 9-23943
 Al-Zn alloys, spinodal decomp. effect on yield and tensile strengths and ductility 9-37289
 Al-Zn alloys, spinodal struct. decomp. by Zn precip., dislocation struct. 9-37291
 Al-Zn alloys, spinodal struct. study by X-ray diff. stability and breakdown with ageing 9-37290
 Al-Zn dilute solid solutions, vibrational entropy, electronic influences 9-39508
 Al-Zn eutectoid, superplastic behaviour, rel. to grain boundary sliding and grain rotation 9-23900
 Al-Zn solid soln. and precip. hardened alloy cryst., plastically deformed, dislocation distrib. 9-39364
 Al-(4.4 wt.%)Zn alloy, Be atoms influence on elec. resistivity changes due to clustering 9-40932
 Al-(6wt.%)Zn(2wt.%)Mg alloy, precipitate nature and morphology 9-28390
 Al-2at.%Zn-2at.%Mg: reversion and reaging 9-41048
 AlZnMg 1 alloy, annealing effect on microstruct., susceptibility to stress and layer corrosion 9-46779
 Au-Cu-Zn alloys, β phase stability and elastic anisotropy 9-46957
 Au-(10 at.%)Zn, specific heat meas. at 3°K, nuclear terms obs., crystal electric field studied 9-30780
 β' -Au-Zn, long-range order, X-ray diff. meas. 9-28256
 Cd-Zn alloys, Hall resistivity meas., below 77°K, scattering phenomenon 9-37440
 Cd,Zn_{1-x}S mixed semicond., phonon vibr. spectrum 9-42947
 Cu-(39.8wt.%) Zn, alloy, precipitation, effect of uniaxial tensile stress 9-46939
 Cu-Zn, laser pulsed discharges, elimination of effects of tertiary elements 9-27297
 Cu-(36wt.%) Zn alloys, stress-corrosion cracking, electrochem. factors 9-23920
 Cu-(26 wt.%)Zn alloys, ZnO establishment and growth 9-26191
 α -Cu-Zn alloy, Hall effect meas. and phonon drag effects, 4.2° to 300°K 9-43026
 β_1 -Cu-Zn alloy, martensitic transform., effect of neutron irradiation 9-37296
 Cu-Zn alloy single cryst., positron annihilation, Fermi surface change with increasing electrons per atom 9-33241
 α -Cu-Zn alloys, activation vol. analysis at yield point w.r.t. dislocation intersection processes 9-39413
 Cu-Zn alloys, dislocation phonon scattering values from thermal conductivity and dislocation density meas. 9-41078
 Cu-Zn alloys, dispersion relations for lattice vibrations from neutron scatt. 9-30766
 α -Cu-Zn alloys polycryst., 10 and 15 at.%Zn onset stress for deform. twins 9-32980
 Cu-Zn β -phase alloys, order-disorder transf., Hall coeffs., elec. resistivity 9-35253
 Cu-Zn dilute alloys, ⁶⁹Cu n.m.r. lines conc. depend., 1st order quadrupole effect obs. 9-35724
 Cu-Zn surface alloy, rel. to fatigue strength of Cu 9-33058
 Cu-Zn system phases, interdiffusion coeff., conc. depend. 9-46850
 Cu-(0.06-5.2 at.%)Mn alloys elec. resist. at 2-300°K, max. value 9-47068
 Cu(9.5 at.%)Be-(0.2 at.%)Zn alloys, neutron irradi., ageing characts. from resistivity meas. 9-33115
 Cu(36wt.%)Zn, Fe and P influence on recrystn., grain growth inhibition 9-30718
 Cu(36wt.%)Zn, solubility of Fe and P, max. saturation and precipitation 9-30717
 Cu-(12.6wt.%) Be-(0.2wt.%) Co-(0.1wt.%) Zn, alloy, Mossbauer eff. 9-45288
 HgTe-ZnTe, conduction band struct. and electron scatt. mechanism 9-35307
 Mg-(5.1 wt.%) Zn alloy, deform. twinning inhibition by precipitates 9-46827
 Mg-Zn-Mn alloy, age hardening, patent 9-48942
 Mg-Zn-Mn alloy, heat treated, patent 9-46960
 Mg-Zn-Zr alloy, strain-rate hardening, grain-size depend. 9-39443
 Mg-Zn-Zr cast alloy system, dendritic growth forms, non-equilib., of phase ZnZr, conversion 9-41056
 Mg-Zn alloy, single-cryst. growth by stationary mould solidification technique 9-32877
 Mn-Zn ferrite, coarse-grained, permeability and harmonic distortion increase with induction 9-35573
 MnCO₃-ZnO-Fe₂O₃, calcination, Mn-Zn ferrite production 9-35742
 Mo-Zn alloys prepared by reduction of volatile halides, phase diagram obs. 9-39466

Zinc compounds continued

- Ni-Zn:Co²⁺ ferrites, Fe-rich, temp. spectra, mag. after-effects 9-28632
 Ni-Zn-Si system, phase equilibria at 800°C 9-35209
 Ni-Zn alloys, ferro- and paramagnetic props., comparison 9-35539
 Ni-Zn ferrite thin film, prep. and mag. props. 9-45184
 Ni₂Zn₃Si phase, cubic Ti₂Ni struct. and interatomic distance calc. 9-32924
 Sn-Zn alloys, liquid, self diffusion coeffs. meas 9-28113
 Sn-Zn eutectic, undercooling at the solid-liquid interface 9-46686
 Sn-Zn eutectic alloy system, morphology changes 9-46681
 Sn-Ag alloys in solid soln., cold-worked state, X-ray diff. study 9-46935
 Zn-Ag dilute alloys, relax. time meas. from de Haas-van Alphen studies 9-37424
 Zn-Al alloy, superplasticity 9-26330
 Zn-Al alloys, liquid, density meas. up to 700°C 9-30375
 Zn-Cd alloy, single cryst. growth, orientation depend. of solute partition coeff. 9-37104
 Zn-Cd alloys, solute trapping by rapid solidification 9-26160
 η-Zn-Cu alloys, Hall coeffs. at -196-100°C 9-47071
 Zn-Cu alloys, liquid, density meas. up to 700°C 9-30375
 Zn-(2 wt.%)Cu alloy, grain boundary reaction type precipitation from obs. of cracking in Cu films deposited on alloy surface 9-23957
 Zn-(0.005at.%)Mn alloy, anisotropy of Kondo scatt., obs by de Haas-van Alphen effect 9-24109
 Zn-Mg alloy, liq. with dissolved U and suspended Cd, prep. by UC by precipitation 9-36630
 Zn-Mn dilute alloys, relax. time meas. from de Haas-van Alphen studies 9-37424
 Zn-Pb alloys, liquid, density meas. up to 700°C 9-30375
 Zn-Zr phase, dendritic growth forms, non-equilib., in Mg-Zn-Zr cast alloy system, conversion 9-41056
 Zn_{0.87}Mn_{0.13}Fe₂O₄, mag. struct., neutron diff. obs. 9-43189
 Zn_{0.9}Mn_{0.1}S crystals, 0.004<δ<0.4, magnetic susceptibility changes, photo-induced, 77° to 400°K 9-45279
 Zn_{1-x}Cd_xCr₂Se₄, mixed phase syst., susceptibilities and moments 9-31035
 Zn₃PtO₄, synthesis and unit cell const. 9-32868
 Zn₂SiO₄:Mn phosphors, film deposition by vapour phase reaction and vacuum evaporation 9-30493
 Zn₃P₂, solid, n.m.r. resolution of chemical shift 9-35729
 α-Zn₃(VO₄)₂:Co²⁺, crystal field studies 9-26668
 Zn₃(VO₄)₂, luminesc. in sintered oxides and salts, obs. 9-35687
 Zn₃Cd_{1-x}Te ternary system, photovoltaic effect 9-24242
 Zn₃Hg_{1-x}Te solid solutions, givanomagnetic props., 77°-400°K, 250-10000 Gs 9-30913
 Zn₃Ni_{1-x}Fe_xO₄ ferrite system, Yafet-Kittel mag. ordering 9-41329
 n-Zn_{0.95}Cd_{0.05}Sb effect of oxygen and conduction 9-49098
 Zn (II) complex, n-butylphenylphosphinate polymer, monoclinic and orthorhombic forms, cryst. struct., X-ray diff. 9-39315
 Zn (II) complex, o-phenanthroline, Raman and i.r. spectra, vib. freq. determ. 9-23052
 Zn base alloy ingots, rolling, patent 9-35203
 Zn complex, 1:1 Zn(II)-malate geometry of ligand, n.m.r. study 9-46400
 Zn complex, bis (L-aminoacid) (II), circular dichroism and far U.V. spectra 9-23077
 Zn complex, zinc (II) acetylacetonate, matrix-isolated spectrum, rel. to struct., 650-2200 cm⁻¹ 9-27870
 Zn complexes with o-phenylenebisdimethylarsyls, i.r. spectra 9-23078
 Zn Fe₂O₄, atomic vibration, mean square amplitude determ. 9-41081
 Zn II tetrahalo-anions, Raman spectra rel. to vibrs. obs. 9-44327
 ZnAl₂O₄, e.s.r. and optical absorpt. meas. of Cr³⁺ and Fe³⁺ rel. to single-ion mag. interactions 9-45080
 ZnBr, band spectrum in near u.v., vibr. const. 9-46377
 ZnBr₂, emission spectrum in visible region, analysis and vib. const. of B^{2Σ}X^{2Σ} syst. 9-32492
 Zn(BrO₃)₂·6H₂O:Cu²⁺, relaxation behaviour, e.p.r. and electron-spin-echo obs. 9-31159
 ZnCr₂O₄, antiferromag.-paramag. transform. of first order 9-49224
 ZnCr₂S₄(Se₄) single crystals growth 9-44646
 ZnF₂, Mn²⁺ ion axial field splitting, ⁵⁵Si ion spin Hamiltonian explanation 9-45247
 ZnF₂, phase transitions at pressures up to 160 bar 9-44800
 ZnFe₂O₄, electric field gradient sign at octahedral site from Mossbauer spectrum 9-35633
 ZnFe₂O₄, oxygen parameter by neutron diffraction 9-30576
 ZnGa₂O₄, e.s.r. and optical absorpt. meas. of Cr³⁺ and Fe³⁺ rel. to single-ion mag. interactions 9-45080
 ZnGeP₂, energy zone structure 9-30822
 ZnIn₂S₄, growth of single cryst. 9-35024
 ZnO:Co²⁺, e.s.r. 9-28752
 ZnO:Cu, ligand-field-band theory of Cu 9-37673
 ZnO:Cu, microwave acoustic amplification 9-37344
 ZnO:Cu, tetrahedrally coordinated Cu²⁺ obs. 9-35599
 ZnO:Cu single cryst., e.p.r., ⁶³Cu hyperfine lines obs. 9-35718
 ZnO:Fe³⁺, g tensor anisotropy from e.s.r. meas. 9-26795
 ZnO:Gd³⁺, e.p.r., hyperfine interaction with odd Gd isotopes 9-33636
 ZnO:Li, u.s. wave attenuation, temp. and freq. depend. 9-37339
 ZnO:Ni, emission process mechanisms w.r.t. activator excitation energy transfer to electrons in traps 9-39874
 ZnO-CdSe alloy systems, electroluminesc. 9-47415
 ZnO, {0001} surfaces, LEED obs. 9-28211
 ZnO, absorption edge 9-37719
 ZnO, acoustic shear-waves generated by supersonic electrons, Brillouin scattering study 9-46996
 ZnO, dielectric dispersion, 10⁻¹⁰ Hz 9-45001
 ZnO, excitons spatial dispersion, refl. and transmission spectra 9-45309
 ZnO, flow stress increase under illumination 9-26329
 ZnO, growth of single crystals by vapour phase reaction method 9-37012
 ZnO, i.r. electroabsorption in multi-photon region 9-33565
 ZnO, i.r. electrorreflectance, elec. Gruneisen const. calc. 9-33540
 ZnO, luminescence, parametric, involving polariton excitation 9-49317
 ZnO, mechanism of dye-sensitized photocond., use of rhodamine B dye 9-49163
 ZnO, polarity, chem. etching behaviour obs. 9-32858
 ZnO, polarity, ion bombardment obs. 9-32857
 ZnO, refr. index press. depend. 9-47317
 ZnO, ruby laser irradiated, luminescence 9-35686
 ZnO, sintering studies rel. to surface area 9-35234
 ZnO, surface states, assoc. with chemisorbed species 9-43008
 ZnO, thermal expansion, 20°-300°K, interferometric meas. up to 800°K 9-30787

Zinc compounds continued

- ZnO, thermal expansion, Gruneisen parameters 9-33190
 ZnO, wurtzite-type, 1st-order Raman scatt. 9-47373
 ZnO added to borolanthanum glasses immiscibility and catalytic crystallization 9-34971
 ZnO attenuation of compressional and shear piezoelectrically active u.s. waves, freq. depend. 9-37340
 ZnO crystals, polar surfaces, elec. conductivity and light reflectance meas. 9-42741
 ZnO e.s.r. of Cu²⁺ 9-33637
 ZnO electrophotographic layers, photodischarge kinetics, influence of trapping and capture 9-39727
 ZnO electrophotographic layers, space charge density, effect of elec. field 9-30963
 ZnO film deposition by triode sputtering, crystallographic orientation 9-39187
 ZnO films establishment and growth on 74:26 brass 9-26191
 ZnO on Ag support, photosensitized CO oxidation 9-28796
 ZnO single-cryst. basal faces, nonequilibrium vaporization rates 9-46690
 ZnO single crystals, high electric field effects 9-47116
 ZnO thin film transducer prep. using vapour transport technique 9-48767
 ZnO thin film sputtered on CdS, sapphire; perfection depend. on deposition rate, substrate polish, temp. 100-500°C 9-36953
 ZnO-B₂O₃ syst., eutectic solidification forming lamellar glass-cryst. structures 9-36930
 ZnP₂, electrical and optical characteristics 9-35609
 ZnS:Cl:Cl, photoelectric 9-24237
 ZnS:Cu luminesc. damage due to incident ions. 9-45349
 ZnS/Cu, luminesc. decay times after proton-excitation 9-49318
 ZnS-CdS:Mn, u.v. and visible photoluminesc., i.r. reinforcement 9-47416
 Zn(S₁₀₀,Se₀):Cu:Li Gudden-Pohl effect and phosphoresc. spectra rel. to emission centres, obs. 9-35696
 ZnSO₄:Mn²⁺, e.p.r., fine struct. and cryst.-field interac. obs. 9-33635
 ZnSO₄ mixture in H₂O-ethylene glycol, u.s. absorpt. obs. 9-39097
 ZnSb:Te, effect of doping of crystn. process and elec. props. 9-42757
 n-ZnSb, prep. and props. 9-39612
 ZnSe:Al, Li, i.r. absorption of localized vibration 9-47369
 p-ZnSe:Cu, photoelectronic props. 9-49164
 ZnSe:Ge(Pb) impurities as hole traps, EPR meas. 9-35706
 ZnSe:V, incorporation mechanisms of donors 9-37531
 ZnSe, band struct. and reflectivity 9-49268
 ZnSe, barrier heights and contact props. 9-43069
 ZnSe, e.p.r. of defect centres 9-37803
 ZnSe, energy band models, self-consistent orthogonalized-plane-wave and empirically refined orthogonalized-plane-wave calcs. 9-39567
 ZnSe, epitaxial, high purity preparation 9-36954
 ZnSe, epitaxy on Ge, close-spaced HCl process 9-37114
 ZnSe, etchants 9-46750
 ZnSe, Gunn effect 9-49090
 ZnSe, in hollow cathode or d.c. arc² spectral anal. of excess Zn or Se 9-37859
 ZnSe, mixing of CO₂ and He:Ne laser radiation 9-26694
 ZnSe, oscillatory photoconduction and exciton spectra 9-39713
 ZnSe, pair spectra and edge emission 9-24451
 ZnSe, Raman scattering intensities 9-47377
 ZnSe, Se X-ray K-absorpt. edges, shifts 9-39858
 ZnSe, synthesis and crystal growth 9-37074
 ZnSe as-grown cryst. with Cu impurity, luminesc. excitation spectra 9-43254
 ZnSe coated NaCl beam-splitter for CO₂ laser 9-48099
 ZnSe electrically conducting photoluminescent films, prep. 9-31127
 ZnSe epitaxial films, optical props. and struct. 9-37684
 ZnSe epitaxial layers on Ge, elec. and photoelec. props. 9-35417
 ZnSe epitaxial layers on Ge, prep. 9-34991
 ZnSe film refl. as NaCl and CO₂ laser beam splitter 9-48099
 ZnSe films, longit. cathode conductivity under e. bombardment 9-41155
 ZnSe valence band structure, spin-orbit corrections 9-37403
 ZnSiAs₂, energy zone structure 9-30822
 ZnSiF₆·6H₂O:Fe²⁺, Mn²⁺, single cryst., spin-lattice relax. of ¹H and ¹⁹F 9-35594
 ZnSiP₂, recombination radiation spectrum, eff. of different impurities and preparation techniques 9-26770
 ZnSnP₂, optical constants and vibrational frequencies from i.r. reflection spectra 9-35614
 p-ZnSnSb₂, electro-photoelectric props. 9-35410
 ZnTe:Li(P), luminescence rel. to shallow acceptor centres 9-26769
 ZnTe:Pb, photo-induced paramagnetic resonance of Pb³⁺ 9-47439
 ZnTe-GaSb heterojunction, fabrication and props. 9-49067
 ZnTe, Er³⁺ and acceptor co-doped, e.p.r. and photoluminesc. obs. 9-41431
 ZnTe, excitons and absorption edge 9-37733
 ZnTe, ion-implanted, type conversions and p-n junction formation 9-26571
 ZnTe, Raman scattering intensities 9-47377
 ZnTe, semicond., Pockels' coeff., refr. index and absorpt. coeff., dispersion 9-39811
 ZnTe, synthesis and crystal growth 9-37074
 ZnTe, thermoelec. material, chemical compatibility with alloys 9-26808
 ZnTe crystals, use as nonlinear mixer for submillimeter-wave generation with ruby laser lines 9-24353
 ZnWO₄:Co(Ni), optical absorpt. spectra 9-37731
 ZnWO₄:Cr³⁺, absorpt., i.r. emission and excitation spectra 9-33563
 ZnWO₄, Cr³⁺ optical and e.p.r. obs. of anisotropic spin-orbit coupling 9-33564
 ZnWO₄, e.s.r. spectra of Cu²⁺ and Ni²⁺ 9-37802
 ZnWO₄, local trapping levels, thermal activation energies and recomb. kinetics, thermoluminesc. props. rel. to X-ray luminesc. props. 9-39890
 ZnWO₄, single crystals, colouring 9-39378

zinc sulphide

- afterglow due to tunneling 9-37763
 band struct. and reflectivity 9-49268
 blende, cleaved faces, diffuse patterns in slow electron diffraction 9-28274
 coating on ferromagnetic materials to enhance domain study by Kerr reflection 9-35558
 crystal growth, cubic, molten flux method 9-37094
 crystals, needlelike and large single, preparation 9-48795
 electro- and photoluminesc. spectra, comparison 9-26787
 electroluminescence, impact ionization and tunnel effect 9-43265
 use in electroluminescent devices 9-41413

Zinc compounds continued
zinc sulphide continued

- electrooptical effects, absorption shift and high-field domain development 9-26711
- electroluminescence, a.c., and polytypism 9-24468
- energy band models, self-consistent orthogonalized-plane-wave and empirically refined orthogonalized-plane-wave calcs. 9-39567
- epitaxial growth of films evaporated on NaCl 9-32844
- epitaxial layers on Si, defects obs. by transmission electron microscopy 9-34994
- epitaxy on W or Mo substrates 9-28216
- e.p.r. of defect centres 9-37803
- films, electroluminescent, low temp. elec. props. in strong fields 9-28461
- films, epitaxial, optical props. and struct. 9-37684
- films, evaporated, Cu, Mn or Cl doped; d.c. electroluminescence and photoluminescence 9-33612
- films, longit. cathode conductivity under e. bombardment 9-41155
- growth from Ga and In melts, optical and electrical properties 9-37095
- Lumocen devices, rare-earth and transition-metal fluoride doped, electroluminesc. 9-35700
- oxidation, electron microscope obs. 9-49379
- phosphor, i.r. stimulable, use in gamma dosimeter with time lapse indication 9-27597
- phosphors, luminescence spectra, effect of prep. method 9-24470
- phosphors, simultaneous electro- and photo-excitation investig. 9-47414
- photocapacitive effects 9-37625
- photoconductivity of cryst. excited by ruby laser 9-47199
- photodiodes, Schottky barrier, as u.v. detectors 9-33347
- polytypes, 2H-4H interface, electron microscope contrast effs. 9-28275
- polytypes of 10L, 22L and 26L families 9-32861
- polytypism 9-36982
- powder, activation energies of glow curves, numerical calc. 9-27834
- powder, triboluminesc., jet powder technique 9-26788
- powders, crystal structure and phase transitions, effect of point defects 9-40923
- raman scatt., 1st-order 9-47373
- Raman scatt. by Mn impurities, vibr. resonant modes obs. 9-43247
- Raman scattering intensities 9-47377
- Raman spectrum of cubic crystals, electro-optic and lattice dynamic effects 9-47376
- reflectivity and band struct. 9-49268
- self-activated, i.r. induced photoconductivity, correl. with luminesc. obs. 9-41273
- stacking fault periodicity and polytypism rel. to growth conditions, correl. with luminesc. 9-35099
- stacking faults distrib. in cryst. grown from vapour, rel. of polytypism 9-37184
- thermoluminescence glow curves, kinetic order and actuation energy anal. 9-49328
- thermoluminescence of single crystals before and after electron beam irradi. 9-45356
- travelling wave light modulator, improved efficiency, 40 MHz to 15 GHz 9-27362
- valence band structure, spin-orbit corrections 9-37403
- wurtzite structure, X-ray K-absorpt. of S. obs. 9-31121
- zincblende, X-ray K-absorpt. of S. obs. 9-31121
- ZnS, hexagonal-cubic phase transition, kinetics 9-23970
- Ag activated, scintillation decay due to α particles and fission fragments 9-47410
- CsCl structures, i.r. localized modes, shell models 9-23800
- Cu activated, ruby laser induced luminescence 9-35686
- electro-absorption in single cryst. 9-39812
- phosphors, containing Mn, luminesc. and Gudden-Pohl effect 9-45348
- Zn activated, ruby laser induced luminescence 9-35686
- ZnS:Ag, thermal recrystallization effects on particle size and morphology 9-30555
- ZnS:Bi, electronic struct. of luminesc. centre 9-24462
- ZnS:Bi, thermoluminescence and thermally stimulated current 9-33608
- ZnS:Cu, electroluminescence, shallow trap participation, variable temp. above liq. nitrogen temp. 9-33611
- ZnS:Cu, Gudden-Pohl effect, intensity of flashes and temp. depend. 9-39893
- ZnS:Cu, i.r. luminescence, modulation and excitation by a.c. fields 9-35702
- ZnS:Cu, ligand-field-band theory of Cu 9-37673
- ZnS:Cu, tetrahedrally coordinated Cu^{2+} obs. 9-35599
- ZnS:Cu, trap analysis by frequency study of electroluminescence 9-49334
- ZnS:Cu, Zeeman effect in absorpt. spectrum 9-24417
- ZnS:Cu $^{2+}$, absorption and excitation spectra, correlation with valence band structure 9-37732
- ZnS:Er $^{3+}$, thermoluminescence and photoluminescence 9-37774
- ZnS:Mn, Cu electroluminescent cell, d.c., efficiency of i.r. emitting phosphors 9-41415
- ZnS:Mn,Cu,Cl powder phosphors, preparation and d.c. electroluminescent props. 9-37781
- ZnS:Mn,Li, spin-lattice relaxation time of Mn^{2+} 9-47301
- ZnS:Mn films, electroluminescence processes, non-stationary, polarization effects 9-24469
- ZnS:Mn phosphor photoluminescence, effect of Te on quantum efficiency 9-43261
- ZnS:Ni $^{2+}$, mag. susceptibility and spin-orbit coupling 9-33435
- ZnS:Pb, Gudden-Pohl effect, intensity of flashes and temp. depend. 9-39893
- ZnS/ZnSe mixed crystal, e.p.r. of defect centres 9-37803
- ZnS-CdS-Cu phosphors excited with 365 nm line, i.r. quenching of luminescence 9-41408
- ZnS-Cu, photoluminescence, eff. of coactivator conc. 9-24473
- ZnS-Cu phosphor, electro and X-ray luminescence, nonadditivity changes 9-28277
- ZnS-Cu phosphors excited with 365 nm line, i.r. quenching of luminescence 9-41408
- ZnS-Mn sublimate, electroluminescence during pulsed excitation 9-49335
- ZnS-Sm, ZnS-Tu and ZnS-Eu phosphors, radical recombination characs. 9-31141
- ZnS, e.p.r. of paramagnetic centres 9-28751
- α -ZnS, refr. index press. depend. 9-47317
- ZnS.CdS-Ag cathodoluminescence depend. on Cu impurity 9-24474

Zirconium

adsorbed layer on W, tunneling of field emitted electrons 9-30960

Zirconium continued

- adsorption on 2-d crystals on W and Nb, binding energy from temp. depend. of growth 9-23652
- atomic spectrum, a bibliography 9-38765
- damage, rate and distribution, effect of fast neutron spectrum 9-26469
- electronic structure determ. from X-ray emission spectra 9-37755
- energy levels in V, VI and VII spectra 9-46287
- film on various substrates, supercond. obs. 9-37452
- nuclear reaction analysis of surface impurities 9-28836
- optical isotope shift, nucl. vol. and mass eff. 9-29988
- oxidation kinetics, effect of gas flow rate 9-45420
- polymorphs, stability of high-pressure phases, effect of neutron irradiation 9-35250
- single crystal, {10 $\bar{1}$ 7} hydride habit plane 9-35013
- spectral emissance, i.r. 9-45327
- X-ray M absorpt. spectra in u.s. region, absorpt., coeff. depend. 17-200 Å 9-37754
- Al-Ag alloy addition, eff. on strain-induced solute disposition stability control of mech. strength 9-28360
- SrTiO $_3$:Zr, supercond., transitions from large to nearly-small polarons 9-47056
- in SrTiO $_3$ superconducting ceramic, effective masses determ. 9-26532
- Ti-Zr film in getter-ion pump, residual gas analysis 9-38176
- α -Zr, O $_2$ diffusivity and parabolic oxidation kinetics 9-26306
- β -Zr, thermomigration and electromigration 9-39388
- Zr-ZrO $_2$ -metal structure, I.V. characts. 9-30954
- Zirconium compounds**
- alloy, breakdown of oxide film 9-40839
- hydride lattice, H and D vibr. and thermal n cross-sections 9-30767
- internal friction at low temps. 9-41005
- oxidation of alloys at high temps. 9-41451
- oxide (carbide, chloride) mixture with HF oxide (Carbide chloride), X-ray fluorescence analysis 9-41461
- zircalloy-4, radiation enhanced relaxation 9-41006
- Zircalloys, aqueous corrosion at low temp. 9-26831
- Zircaloy, creep during neutron irradi., rel. to strain rates and defect form. 9-41023
- Zircaloy, creep props. during irradi. 9-28356
- Zircaloy, pre-transition oxidation behaviour of individual piece, comments 9-37826
- Zircaloy tubes, hydride orientation rel. to deform., texture and stresses 9-39188
- Zircaloy-2, diffusion of H up thermal gradient 9-28310
- Zircaloy-2, fracture in BWR and PWR conditions, obs. 9-37258
- Zircaloy-2, laser microprobe analysis, impurity emission rel. to matrix effects, obs. 9-24604
- Zircaloy-2 tubes, failure rel. to neutron irradi., hydride precip. and stress 9-39435
- Zircaloy-4, non-linear irradi. growth mechanism 9-37375
- Zircaloy-4, tensile props. at low strain rates, in-pile, un- and post-irradi. obs. 9-37256
- zircalloys, post-transition corrosion by steam at 300 and 340°C rel. to deuterium absorpt. and heat treatment 9-28806
- zircon, sintered, compressive creep characs. 9-37244
- zirconia, stabilized particles, prep. by sol-gel process 9-30731
- zirconia, struct. transform., high temp. 9-30736
- zirconia, yttria-stabilized, as high-temp. electrodes, conductivity 9-33248
- zirconia with rare-earth oxides additions, effects and phase relationships of solid soln. formed 9-30723
- zirconia-rare-earth oxide solid solns., preheating products obs. 9-30724
- Zr $_2$ Co-Zr $_2$ Ni mixed cryst., supercond. transition temp. and mag. susceptibility 9-33276
- Zr-C system, phase range and lattice parameters 9-30754
- Al-Zr-Si alloys, recryst. and age hardening, influence of Si 9-42910
- Al-(0.5wt.%)Zr, alloy precipitation eff. on plastic deformation and recrystallization 9-44794
- Al-Zr alloys, quenched superheating melt effect on struct. and props. 9-39450
- Cd-Zr system, crystal structure of intermetallic compounds 9-39266
- Cu-(2.5 wt. %)Zr-(0.5 wt.%)Nb alloy, radiation enhanced relaxation 9-41006
- Mg-Al-Zr-Be, alloy, correlation of orientation and polarized etching facets 9-39186
- Mg-Zr alloy, strain-rate hardening, grain-size depend. 9-39443
- Mg-Zn-Zr cast alloy system, dendritic growth forms, non-equilib., of phase Zr $_2$ Nb, conversion 9-41056
- Mg-Zr alloy, creep curve anal. in const. load tests 9-30673
- Nb-Ti-Zr-Hf alloy system, constitution and supercond. props. 9-39597
- Nb-(25 at.%) Ti-(10 at.%)Zr alloy, solution-treated, ageing rel. to recrystallization 9-33122
- Nb-(25 wt.%)Zr alloy, supercond., fluxoid pinning by second phases 9-49049
- Nb-Zr alloy, supercond., cellular decomp. and precipitation 9-39499
- Nb-Zr alloys, supercond., cold working and precip. for effective flux pinning at high current densities 9-49053
- Nb-(25 at.%) Zr alloy, a.c. energy losses around H $_2$ 9-35361
- Pu-(0.10at.%)Zr, equilib. phase diagram 9-37306
- U-Zr alloys, specific heat meas. for various compositions 9-24052
- U-Zr alloys, specific heat meas. for various compositions 9-33185
- Zr-(1.2wt.%) Cr-(0.1wt.%) Fe alloy, quench hardening behaviour, cooling rate dependence 9-41034
- Zr-Al, N diffusion, pumping speed meas., 10 $^{-6}$ -1 Torr, 300 and 500°C 9-37197
- Zr-Co alloy, magnetic moments, localised of Co, e.p.r. investig. 9-33634
- Zr-Cu reactor fuel claddings, oxidation and cracking in CO $_2$, obs. 9-37266
- Zr-Nb alloy, $\alpha(\alpha+\beta)$ boundary 9-41062
- Zr-Nb system, $\alpha(\alpha+\beta)$ boundary, microprobe determ. 9-28406
- Zr-O solid solns., sintered, electron work function 9-39734
- Zr-Si binary system, phase equilib. diag. 9-35258
- Zr-(25 at.%) Ti alloy, ω phase, as-quenched form, electron diff. and microscopy obs. 9-37307
- Zr-W system, high-temp. phase relations, m.p. and X-ray anal. 9-48940
- (Zr $_1$ -Nb $_2$)Fe $_2$ with cubic Laves structure pressure depend. of Curie temp. 9-45129
- (Zr $_1$ -Ti $_2$)Fe $_2$ with cubic Laves structure, pressure depend. of Curie temp. 9-45129
- (Zr $_1$ -Ti $_2$)Zn, magnetization, ferromag. Curie temp. and lattice parameter 9-26650
- Zr $_2$ Co $_2$ Ge $_2$, V-phase crystal structure 9-26253

Zirconium compounds continued

- Zr complex, tetrafluoride adducts of p-subst. pyridine-N-oxides, vibrational spectra 9-32493
 ZrB₂, growth and characterization of single crystals 9-37096
 ZrB₂, hot-pressed, bending strength, fracture mode and thermal stress resistance 9-35183
 ZrB₂, hot pressing, densification 9-30708
 ZrB, K-emission spectra of B 9-24436
 ZrC, elec. conductivity, thermoelec. power, Hall coeff., rel. to C content 9-47114
 ZrC, hemispherical and monochromatic emissive, power and specific resistivity, 1200-3500°K 9-39548
 ZrC emissivity and elect. conductivity obs. 9-37374
 ZrCo₂, elastic constants, 4.2-300°K 9-42866
 Zr(Fe_{1-x}Co_x)₂ with cubic Laves structure, pressure depend. of Curie temp. 9-45129
 Zr(Fe_{1-x}Co_x)₂ with cubic Laves structure, pressure depend. of Curie temp. 9-45129
 ZrH, neutron single differential cross-section at 296 and 700°K 9-22901
 ZrH₄:U fueled, thermal conductivity 9-26459
 Zr(HPO₄)₂·H₂O, crystal structure rel. to ion exchange mechanism 9-23779
 Zr(HPO₄)₂, crystalline, prep., model structs., and ion-exchange props. 9-26208
 Zr(HPO₄)₂·2H₂O, crystalline, prep., model structs., and ion-exchange props. 9-26208
 ZrO₂-CaO:Bi, luminescence following exposure to Hg illumination, depend. on CaO conc. 9-39875
 ZrO₂-CaO.SiO₂-2CaO.SiO₂ system, phase equilibria 9-33147
 ZrO₂, crystallization under hydrothermal conditions 9-37044
 ZrO₂, lattice energies, heat of atomization, bond energy and dissociation energies, rel. to fund. props. 9-30494
 ZrO₂, monoclinic, e.p.r. of Fe²⁺ 9-33627
 ZrO₂, phase diagram determination 9-23991
 ZrO₂, recrystallization kinetics during sintering 9-33105
 ZrO₂ stabilized, oxygen ion conductivity by electrolysis in Cu solutions 9-35754
 ZrO₂CeO₂ binary system, solvated electron study 9-39957
 Zr(PO₄)₂ gels, ion exchange and sorption rel. to comp., obs. 9-28789
 ZrSiO₄:Gd³⁺, e.s.r. ground-state splitting 9-33626
 ZrSiO₄, high pressure transformations 9-44799
 ZrTe₂O₈, vaporization and fusion characts. 9-26159
 ZrX₆²⁻ anions (X=halogen), electronic absorption spectra 9-30060

- Zr-(1 at.%)Nb alloy, oxidation kinetics and corrosion behaviour in pressurized steam and air 9-35747

Zodiacal light

- brightness and polarization, suggested meas. from space probes 9-45510
 evening spectrum, Doppler shifts rel. to orbital parameters of interplanetary dust particles 9-31362
 review paper 9-38096

Zonal heating *see Atmosphere/thermodynamics***Zone melting and refining**

- alloy, binary, cylindrical rods, conc. distrib. calc. from variable length of melted zone 9-39470
 anthracene, crystal scintillator, effect of zone refining on pulse height and shape 9-42136
 apparatus, patent 9-30521
 floating zone apparatus design, and characts. of ring-shaped electron gun 9-38350
 floating zone technique, applic. to VC single cryst. growth 9-37090
 method and apparatus, patent 9-48803
 naphthalene, effect on delayed fluoresc. lifetime 9-24459
 p-quaterphenyl, crystal scintillator, effect of zone refining on pulse height and shape 9-42136
 steel, mild, electron beam floating zone-melting 9-33109
 techniques and applications, review 9-23674
 trans-stibene, crystal scintillator, effect of zone refining on pulse height and shape 9-42136
 AgCl, zone refining indicating that blue lum. band is due to defects 9-35679
 Cd₂Hg_{1-x}Te cryst. prep. 9-46755
 CdGeAs₂, single crystal preparation 9-37071
 CdSe, rapid non-detonative synthesis 9-37074
 Fe, high purity prod. 9-39448
 Ga₂In_{1-x}Sb solid soln. 9-30719
 Rh single cryst., by electron-beam 9-48807
 Si:Au p-n junctions, prep. conditions rel. to breakdown voltage 9-43080
 VC single cryst. growth by floating zone tech. 9-37090
 ZnSe, rapid non-detonative synthesis 9-37074
 ZnTe, rapid non-detonative synthesis 9-37074

Zone plates *see Diffraction/light***Zoology**

9-28183

- CO₂ atmosphere, Monte Carlo calc. of H₂ escape rate 9-12747
 CO₂ content in Venus atmosphere 9-2056

SCIENCE ABSTRACTS SUBSCRIPTION RATES

Information retrieval

Produced by computer-controlled phototypesetting, these abstracts journals cover the world's periodical, conference and book literature and are extending into the fields of reports and patents. Alphabetical author and subject indexes are given twice yearly. Concurrent microfiche

Physics Abstracts (PA), fortnightly, covers the whole field of physics.

***Electrical & Electronics Abstracts (EEA)** specialises in electrical and electronics engineering. Published monthly.

***Computer & Control Abstracts (CCA)**, monthly, covers computer science and technology, control and automation.

£80 (\$US 192) p.a.

£65 (\$US 156) p.a.

£35 (\$US 84) p.a.

* Combined subscription to EEA/CCA: £80 (\$US 192) p.a.

Current awareness

Each 'Current Papers' publishes the full bibliographic reference of every abstract in the corresponding abstract journal and is produced by computer-controlled phototypesetting. Individual members of the IEE, AIP, IEEE,

IPPS and IERE, wherever they reside, can obtain Current Papers at special privilege prices if they order through their own society.

Current Papers in Physics (CPP), Fortnightly.

£12 (\$US 28.80) p.a.

Current Papers in Electrical & Electronics Engineering (CPE), Monthly.

£12 (\$US 28.80) p.a.

Current Papers on Computers & Control (CPC), Monthly.

£10 (\$US 24) p.a.

CUMULATIVE INDEXES

Physics Abstracts—author index for the five years 1955–59 inclusive, bound in one volume, stiff covers and buckram cloth, 750 pp.

£20

in preparation

Physics Abstracts—subject index for the five years 1955–59 inclusive, bound in one volume, stiff covers and buckram cloth 800 pp.

£20

Physics Abstracts—author index for the five years 1960–64 inclusive, bound in four parts, stiff covers and buckram cloth, 2300 pp.

£17 set

Members: £10 set

Physics Abstracts—subject index for the five years 1960–64 inclusive, bound in two parts, stiff covers and buckram cloth, 2550 pp.

£40 set

Physics Abstracts—author index for the four years 1965–68 inclusive, bound in two parts, stiff covers and buckram cloth, 2000 pp.

£25 set

Physics Abstracts—subject index for the four years 1965–68 inclusive, bound in three parts, stiff covers and buckram cloth, 3300 pp.

£60 set

Electrical Engineering Abstracts—author index for the five years 1955–59 inclusive, bound in one volume, stiff covers and buckram cloth, 389 pp.

£20

Electrical Engineering Abstracts—subject index for the five years 1955–59 inclusive, bound in one volume, stiff covers and buckram cloth, 320 pp.

£15

Members: £9

Electrical Engineering Abstracts—author index for the five years 1960–64 inclusive, bound in two volumes, stiff covers and buckram cloth, 970 pp.

£12 10s. set

Members: £7 10s. set

Electrical Engineering Abstracts—subject index for the five years 1960–64 inclusive, bound in one volume, stiff covers and buckram cloth, 950 pp.

£20

Members: £12

Electrical Engineering Abstracts—author index for the four years 1965–68 inclusive, bound in one volume, stiff covers and buckram cloth, 1000 pp.

£20

Electrical Engineering Abstracts—subject index for the four years 1965–68 inclusive, bound in two parts, stiff covers and buckram cloth, 1800 pp.

£35

Control Abstracts—author and subject index combined for the three years 1966–68 inclusive, bound in one volume, stiff covers and buckram cloth, 380 pp.

£15

Subscription renewals, orders, inquiries and changes of address should be sent as follows:

(1) For **Physics Abstracts** and **CPP** from AIP members, wherever they reside, and from the public in the Americas, to the Subscription Department, American Institute of Physics, 335 East 45th Street, New York, NY 10017, USA. Please allow six weeks' notice for changes of address. Send both old and new addresses and include an address label from a recent issue.

(2) For **Electrical & Electronics Abstracts**, **Computer & Control Abstracts**, **CPE** and **CPC** from IEEE members, wherever they reside, and from the public in the Americas, to the Fulfillment Manager, Institute of Electrical & Electronics Engineers Inc., 345 East 47th Street, New York, NY 10017, USA.

(3) For all subscriptions not covered by (1) and (2) above, and for all **Cumulative indexes**, to IEE, Savoy Place, London WC2, England. Telephone 01-240 1871, Telex 261176, Telegrams Voltampere London WC2.

All other correspondence should be sent to: IEE Publishing Department, PO Box 8, Southgate House, Stevenage, Herts., England. Telephone Stevenage 3311 (s.t.d. 0438 3311), Telex 261176, Telegrams Voltampere Stevenage.

Periodicals

Proceedings IEE, published monthly, contains papers of industrial and technological interest from engineers and scientists the world over. Each issue comprises three self-contained groups of papers on Electronics; Power; and Control and Electrical Science, and these can be ordered as separate publications—*Electronics Record*, *Power Record*, and *Control & Science Record*.

Subscriptions to *Proceedings IEE*:

£30 p.a. IEE Associates and Associate Members under 28 and IEE Students: £2 10s. Other IEE members: £5

Separate copies of individual papers are available when they have been published in the *Proceedings*. Price 2s. each

Electronics Record is published every two months, the papers being taken from the two previous issues of *Proceedings IEE*.

£15 p.a. IEE Associates and Associate Members under 28 and IEE Students: 25s. Other IEE members: £2 10s.

Power Record, quarterly, takes its material from the three preceding issues of *Proceedings IEE*.

£9 p.a. IEE Associates and Associate Members under 28 and IEE Students: 15s. Other IEE members: 30s.

Control & Science Record, quarterly, includes papers on control and automation and electrical science taken from the three previous issues of *Proceedings IEE*.

£9 p.a. IEE Associates and Associate Members under 28 and IEE Students: 15s. Other IEE members: 30s.

Electronics Letters, published fortnightly, is an international journal offering speedy dissemination of research and development results in electronics, control and allied subjects, in the form of communications up to about 1200 words in length. Publication is within two to six weeks of receipt, giving the engineer an immediate picture of the latest developments in the field.

£10 p.a. IEE members: £3

Electronics & Power, published monthly, is a wide-ranging magazine covering the complete field of interest of electrical, electronics, and control technology by means of articles, product reviews, correspondence, editorial comment and book reviews.

Electronics & Power: £8 p.a.
IEE members: free

IEE News is a twice-monthly tabloid newspaper for the professional electrical, electronics and control-systems engineer.

IEE News: £2
IEE members: free

Students' Quarterly Journal is received free of further subscription by all IEE Students, Associates and Associate Members under the age of 30. It caters particularly for the younger member, and specialises in concise, topical articles on the latest advances in electrical, electronics and control engineering.

20s. p.a. Senior members: 10s. p.a.

IEE Conference Publications

Each conference is organised by one or more of the IEE Divisions, Power, Electronics or Control & Automation, or by the Science & Education Joint Board. The conferences thus survey the whole ambit of electrotechnology and control.

IEE Conference Publications are internationally recognised as up-to-date, authoritative reviews of development and progress in the various branches of electrotechnology and control with which they deal.

Conference
Publication
No.

- 49 **Applications of microelectronics**
80 pp. 7 papers. 1968. price £2 10s. members 25s.
- 50 **Performance of electrified railways**
571 pp. 21 papers. 1968. price £6 10s. members £4 5s.
- 51 **Computer-aided design**
683 pp. 69 papers. 1969. price £11; members £7 10s.
- 52 **Switching techniques for telecommunication networks**
482 pp. 103 papers. 1969. price £11 10s.; members £7 10s.
- 53 **Power thyristors & their applications**
Part 1. 543 pp. 68 papers. 1969. price £11 10s.; members £7 10s.
Part 2. 198 pp. 1969. price £6 1s.; members £4 1s.
Inclusive price Part 1 and Part 2 £14; members £9 4s.
- 54 **Microelectronics**
69 pp. 33 papers. 1969. price £5 10s.; members £3 12s.
- 55 **Computer Science & technology**
324 pp. 39 papers. 1969. price £8 10s.; members £5 13s.
- 56 **Measurement education**
167 pp. 32 papers. 1969. price £7; members £4 13s.
- 57 **Industrial applications of dynamic modelling**
227 pp. 23 papers. 1969. price £6 10s.; members £4 7s.
- 59 **Digital satellite communication**
558 pp. 46 papers. 1969. price £11 9s.; members £7 13s.
- 60 **Reliability in electronics**
187 pp. 30 papers. 1969. price £5 18s.; members £3 19s.

Copies and information may be obtained from the
Publications Department
IEE, Savoy Place, London WC2



3 8198 307 023 505
THE UNIVERSITY OF ILLINOIS AT CHICAGO

**THIS BOOK IS FOR USE
ONLY IN THE LIBRARY
IT DOES NOT CIRCULATE**



